CRC HANDBOOK OF

Organic Photochemistry and Photobiology

SECOND EDITION

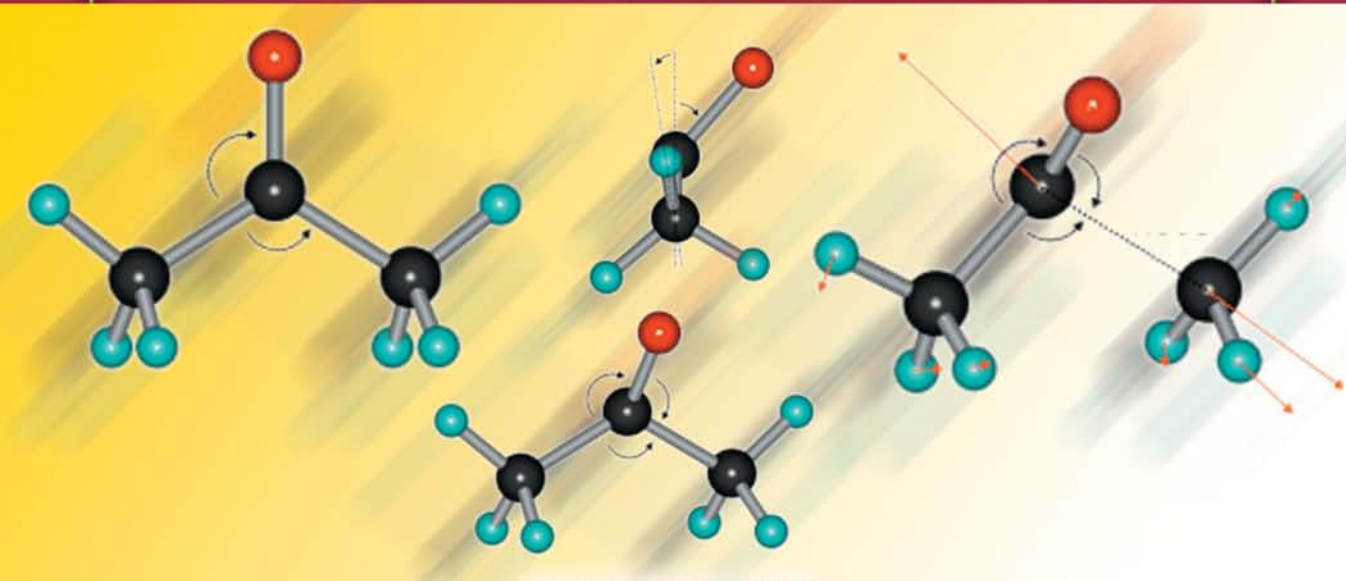

EDITED BY

William Horspool

Francesco Lenci

CRC PRESS

CRC HANDBOOK OF

Organic Photochemistry and Photobiology

SECOND EDITION

CRC HANDBOOK OF

Organic Photochemistry and Photobiology

SECOND EDITION

EDITED BY
William Horspool
Francesco Lenci

CRC PRESS

Boca Raton London New York Washington, D.C.

Library of Congress Cataloging-in-Publication Data

CRC handbook of organic photochemistry and photobiology / edited by William M. Horspool, Francesco Lenci.--2nd ed.
p. cm.
Includes bibliographical references and index.
ISBN 0-8493-1348-1 (set : alk. paper)
1. Photochemistry--Handbooks, manuals, etc. 2. Photobiology--Handbooks, manuals, etc. I. Horspool, William M. II. Lenci, Francesco.

QD719.C73 2003
547′.135--dc21

2003055212

Visit the CRC Press Web site at www.crcpress.com

International Standard Book Number 0-8493-1348-1
Library of Congress Card Number 2003055212
Printed in the United States of America 1 2 3 4 5 6 7 8 9 0
Printed on acid-free paper

Foreword

The second edition of the *Handbook of Organic Photochemistry and Photobiology* has sought to give extensive coverage within the broad area of organic photochemistry and photobiology. Although the cover is not encyclopedic, the editors have ensured that the articles included will give a good idea of the advances that are being made within the various subject headings. The authors who have contributed are all international authorities at the forefront of their research areas and they all have produced well-written articles that are extensively referenced and should be of value to the beginner or to the specialist.

From its humble beginnings more than a century ago organic photochemistry has become an interdisciplinary science. In its early days the studies could only examine what happened on the exposure of organic molecules to light. Now, with the added sophistication of photophysics, the breadth of our understanding has increased dramatically. Our knowledge of what can be achieved from a given reaction has increased dramatically over the last decade. This has led us to situations where control can be exercised on the outcome of many photoprocesses. Many of the articles included in this Handbook deal with these new methods such as photoelectron transfer, irradiation of compounds in the solid, as crystals or contained with supramolecular cages. All of these techniques have changed the specificity of the reactions being studied. The use of chiral auxiliaries has also provided paths to molecules with high enantio or diastereoselectivity. All of these techniques provide more ammunition to the synthetic organic chemist. Indeed there is every hope that the new techniques will open more doors to the development of reactions that will provide new paths to molecules of biological and pharmacological interest.

Such a handbook could not have been compiled without the good will and cooperation of all the contributors and I am truly indebted to everyone who has given of their valuable time in writing for this text. I express my sincere thanks to Professor Francesco Lenci for his unstinting help in identifying and securing manuscripts from the authors for the photobiology section. I would also like to thank the members of the editorial staff at CRC Press for their great help and encouragement throughout the compilation of this magnum opus.

William M. Horspool
Dundee, Scotland

Introduction to Photobiology Section

This second edition of the *CRC Handbook of Organic Photochemistry and Photobiology* reports updated and extended chapters on topics already described and discussed in the first edition as well as chapters on new emerging subjects. As Pill-Soon Song mentioned in his foreword to the first edition, photobiology is a profoundly interdisciplinary science, and to properly face any photobiological problem a variety of skills and professional qualifications are needed: from photophyscis and photochemistry to biochemistry and molecular biology, from optical spectroscopy to genetic engineering, from structural biology to medicine and biomedicine to environmental sciences. This makes clear why most research groups active in photobiology include physicists, biologists, and chemists. The synergistic connection of different cultural backgrounds, in fact, not only allows the research group to successfully use different theoretical and experimental approaches, but also contributes to the form of photobiology as a new frontier of science. All photobiological phenomena originate from a single first act, the absorption of a photon, but the cascades of molecular, cellular, and biological events following this step end in a variety of phenomena, which is as large as life itself. Indeed, without light, life as we know it on our planet would not exist. Solar radiation, in fact, is a fundamental source of energy for all photosynthetic organisms and microorganisms, and photosynthesis is one of the most important biological processes on earth, which, by consuming carbon dioxide and liberating oxygen, has made the world into the livable place we know today. Light is also a sensory stimulus which provides vital information on the environment to all living beings, terrestrial and aquatic, diurnal and nocturnal, preys and predators, to creatures provided with "eyes" and nervous system as well as to aneural life forms like plants, fungi, and unicellular microorganisms. Both ultraviolet and visible radiation are also responsible for a number of damaging effects on biological systems and the deep knowledge of these processes has allowed us to develop promising concepts and set up efficient procedures in photomedicine. Last, but not least, the detailed understanding of the molecular mechanisms operating in biological photoreceptors has brought about studies in biomolecular electronics with the aim of using biological molecules or biomimetic systems in electronic or photonic devices by taking advantage of the fact that natural selection has already evolved materials with key properties desired for device applications.

Not all fields of photobiology have been covered in this book and I do apologize for not being able to cover all the vast area of modern photobiological sciences. All the authors are among the most active and authoritative researchers in the different fields and I hope this Handbook will serve to advance our understanding in some areas of photobiology. Working and corresponding with Professor William Horspool has always been a pleasure and a great experience, both from the cultural and the human point of view. I wish to sincerely thank all the authors for their efforts and patience and gratefully acknowledge the precious collaboration of all the CRC staff, with specially warm thanks to Debbie Vescio, Editorial Assistant, for her long-lasting support and graciousness.

Certainly editing a large book like this is a special experience: I had the opportunity of staying in touch and corresponding with colleagues from different countries and different cultures. I think and I hope that our common work has favored cooperation, mutual confidence and trust, not only among us, but also among the many different countries in which we live, thus giving a small contribution toward making our world closer to the open world Niels Bohr called for.

Francesco Lenci
Pisa, Italy

Dedication

In memory of all those whom we have loved and who have donated to us the precious gift of their love and friendship.

Francesco Lenci

The Editors

William M. Horspool was a reader in organic chemistry in the Department of Chemistry at the University of Dundee in Scotland, where he taught from 1965 up to his retirement in 2001.

He obtained his Ph.D. from the University of Glasgow in 1964 and his D.Sc. from Dundee University in 1976. His undergraduate studies were carried out at the University of Strathclyde in Glasgow.

Dr. Horspool has carried out research in organic photochemistry for his entire professional career and has published extensively in this area. He has been a regular contributor (for the past 34 years) to *Photochemistry,* a publication of the Royal Society of Chemistry. In addition to these reviews, he has written two textbooks on the subject and has edited another, in addition to editing the first edition of this Handbook.

He is a Fellow of the Royal Society of Edinburgh and of the Royal Society of Chemistry.

Francesco Lenci, a physicist working in biophysics, is research director of National Research Council (CNR). From October 1990 to April 2002, he was director of the Istituto Biofisica in Pisa. His research specialties are in photosensory biology/photobiophysics, with particular attention to photosensory transduction in microorganisms, spectroscopic studies of natural and synthetic photoreceptor pigments, and photochemical reactivity of natural pigments. He has served as associate editor for *J. Photochem. Photobiol. B: Biol.* (1989–1995) and for *Photochem. Photobiol* (2000–present). He is a member of the Italian (SIFB), European (ESP), and American (ASP) Societies for Photobiology and has served as SIFB president (1992–1998), as a member of the ASP Council (1998–2001), as chairman of the ESP Education Committee (1999–present), and as one of the vice-presidents of the International Union for PhotoBiology (IUPB). Organizer and chair of several symposia at international congresses and conferences and director of NATO-ASIs, in 2001 Francesco Lenci was awarded the Medal of the European Society for Photobiology.

Contributors

Aboel-Magd A. Abdel-Wahab
Assiut University
Assiut, Egypt

Manabu Abe
Osaka University
Osaka, Japan

Zsolt Ablonczy
Medical University of South Carolina
Charleston, South Carolina

Waldemar Adam
University of Würzburg
Würzburg, Germany

Antonia R. Agarrabeitia
Universidad Complutense
Madrid, Spain

Saleh A. Ahmed
Assiut University
Assiut, Egypt

Motoko Akita
Kyushu University
Hakozaki, Fukuoka, Japan

Angelo Albini
University of Pavia
Pavia, Italy

Diego Armesto
Universidad Complutense
Madrid, Spain

Donald R. Arnold
Dalhousie University
Halifax, Nova Scotia, Canada

Thorsten Bach
Technische Universität München
Garching, Germany

Costanza Bagnoli
Istituto di Biofisica CNR
Pisa, Italy

Laura Barsanti
Istituto di Biofisica CNR
Pisa, Italy

Anna Bartoscheck
University of Cologne
Köln, Germany

Dario M. Bassani
Laboratoire de Chimie Organique dt Organometallique

Fabio Beltram
NEST-INFM Scuola Normale Superiore
Pisa, Italy

Lise Bertram
Università di Pisa
Pisa, Italy

Seong Hee Bhoo
Kyung Hee University
Suwon, South Korea

Robert R. Birge
University of Connecticut
Storrs, Connecticut

Gonzalo Blay
Universitat de València
València, Spain

Samir Bondock
University of Cologne
Köln, Germany

Francisco Boscá
Universidad Politécnica de Valencia
Valencia, Spain

Sara Bosio
University of Würzburg
Würzburg, Germany

Vladimir A. Bren
Rostov State University
Rostov on Don, Russia

Gerald O. Brown
Georgetown University
Washington, D.C.

Götz Bucher
Ruhr-Universität Bochum

Nigel J. Bunce
University of Guelph
Guelph, Ontario, Canada

Jens Otto Bunte
Universität Bielefeld
Bielefeld, Germany

Luis M. Campos
University of California, Los Angeles
Los Angeles, California

Thomas Carell
Philipps-Universität
Marburg, Germany

Tevye C. Celius
John Hopkins University
Baltimore, Maryland

Giovanni Checcucci
Istituto di Biofisica CNR
Pisa, Italy

Alexander K. Chibisov
Russian Academy of Sciences
Moscow, Russia

Michaela K. Cichon
Philipps-Universität
Marburg, Germany

Lenuta Cires
Al. I. Cuza University
Romania

Giuliano Colombetti
Istituto di Biofisica CNR
Pisa, Italy

Peter G. Conrad
University of Kansas
Lawrence, Kansas

Thomas P. Coohill
Siena College
Loudonville, New York

Elizabeth M. Crompton
Northwestern University
Evanston, Illinois

Rosalie K. Crouch
Medical University of South Carolina
Charleston, South Carolina

Peter I. Dalko
CNRS, Laboratoire de Chimie Organique, ESPCI
Paris, France

Francesco Dall'Acqua
University of Padova
Padova, Italy

Thomas J. Dougherty
Roswell Park Cancer Institute
Buffalo, New York

Alexander D. Dubonosov
Rostov State University
Rostov on Don, Russia

Ian R. Dunkin
University of Strathclyde
Strathclyde, Scotland

Heinz Dürr
University of Saarland
Saarbrücken, Germany

Thomas Ebrey
University of Washington
Seattle, Washington

Tamer T. El-Idreesy
University of Cologne
Köln, Germany

Valtere Evangelista
Istituto di Biofisica CNR
Pisa, Italy

Maurizio Fagnoni
University of Pavia
Pavia, Italy

Marcus G. Friedel
Philipps-Universität
Marburg, Germany

Masaki Furuya
University of Tokyo
Tokyo, Japan

Francisco Galindo
Universidad Jaume I de Castellon

Paul Galland
Philipps-Universität
Marburg, Germany

Miguel A. Garcia-Garibay
University of California, Los Angeles
Los Angeles, California

Francesco Ghetti
Istituto di Biofisica CNR
Pisa, Italy

Subrata Ghosh
Indian Association for the Cultivation of Science
Jadavpur, Kolkata, India

Andrew Gilbert
The University of Reading
Reading, United Kingdom

Sadanand Gite
AmberGen, Inc.
Boston, Massachusetts

Richard S. Givens
University of Kansas
Lawrence, Kansas

John H. Golbeck
Pennsylvania State University
University Park, Pennsylvania

Sandra O. Gollnick
Roswell Park Cancer Institute
Buffalo, New York

Norberto C. Gonzalez
University of Kansas Medical Center
Kansas City, Kansas

Charles M. Gordon
University of Strathclyde
Glasgow, Scotland

Helmut Görner
Max-Planck-Institut für Strahlenchemie
Mülheim an der Ruhr, Germany

Axel G. Griesbeck
University of Cologne
Köln, Germany

James Grimshaw
Queen's University of Belfast
Belfast, Ireland

Benjamin Grosch
Technische Universität München
Garching, Germany

Paolo Gualtieri
Istituto di Biofisica CNR
Pisa, Italy

Murthy S. Gudipati
University of Maryland
College Park, Maryland

Donat-P. Häder
Institut für Botanik und
Pharmazeutische Biologie
Erlangen, Germany

Naoki Haga
Tokyo University of Agriculture and
Technology
Tokyo, Japan

George S. Hammond
University of Hawaii
Honolulu, Hawaii

Eietsu Hasegawa
Niigata University
Niigata, Japan

Tadashi Hasegawa
Tokyo Gakugei University
Tokyo, Japan

Klaas J. Hellingwerf
University of Amsterdam
Amsterdam, the Netherlands

Barbara W. Henderson
Roswell Park Cancer Institute
Buffalo, New York

Johnny Hendriks
University of Amsterdam
Amsterdam, the Netherlands

Norbert Hoffmann
Université de Riems Champagne-
Ardenne
France

Felix T. Hong
Wayne State University
Detroit, Michigan

C. Akira Horiuchi
Rikkyo University
Tokyo, Japan

Nathalie Huther
University of York
Heslington, York, United Kingdom

Siddik Icli
Ege University
Turkey

Yoshiaki Inaki
Osaka University
Osaka, Japan

Seiichi Inokuma
Gunma University
Kiryu, Japan

Yoshihisa Inoue
Osaka University and ICORP/JST
Osaka, Japan

Masahiro Irie
Kyushu University
Hakozaki, Fukuoka, Japan

Shun-Jun Ji
Suzhou University
People's Republic of China

T. Wade Johnson
Pennsylvania State University
University Park, Pennsylvania

Graham B. Jones
Northeastern University
Boston, Massachusetts

Giulio Jori
University of Padova
Padova, Italy

Kwang-Hwan Jung
University of Texas
Houston, Texas

Lakshmi S. Kaanumalle
Tulane University
New Orleans, Louisiana

Masaki Kamata
Niigata University
Niigata, Japan

Canan Karapire
Ege University
Turkey

Tsugio Kitamura
Saga University
Honjomachi, Saga, Japan

Petr Klán
Masaryk University
Brno, Czech Republic

Andreas Kleineweischede
Universität Bielefeld
Bielefeld, Germany

Daniel Knapp
Medical University of South Carolina
Charleston, South Carolina

Helmut Knoll
Universität Leipzig
Leipzig, Germany

Ken Kokubo
Osaka University
Toyonaka, Osaka, Japan

Mahmut Köse
Zonguldak Koraelmas University

Oliver Krebs
University of Würzburg
Würzburg, Germany

Paul J. Kropp
University of North Carolina
Chapel Hill, North Carolina

Norihito Kuno
Hitachi Ltd.
Tokyo, Japan

Jon-Ill Lee
University of Kansas
Lawrence, Kansas

Francesco Lenci
Istituto di Biofisica CNR
Pisa, Italy

Bartolomeo Lercari
Università di Pisa
Pisa, Italy

Julia G. Levy
QLT, Inc.
Vancouver, British Columbia, Canada

Frederick D. Lewis
Northwestern University
Evanston, Illinois

Chun-Chen Liao
National Tsing Hua University
Hsinschu, Taiwan

Chultack Lim
Kyushu University
Hakozaki, Fukuoka, Japan

Edward D. Lipson
Syracuse University
Syracuse, New York

Robert S.H. Liu
University of Hawaii
Honolulu, Hawaii

Sabina Lucia
Istituto di Biofisica CNR
Pisa, Italy

Matthew Lukeman
University of Victoria
Victoria, British Columbia, Canada

D. Madhavan
Madurai Kamaraj University
Madurai, India

Hajime Maeda
Osaka Prefecture University
Sakai, Osaka, Japan

Dino Mangion
McMaster University
Hamilton, Ontario, Canada

Sergey Mamaev
AmberGen, Inc.
Boston, Massachusetts

Roberto Marangoni
Istituto di Biofisica CNR
Pisa, Italy

Paul Margaretha
University of Hamburg
Hamburg, Germany

Patrick S. Mariano
University of New Mexico
Albuquerque, New Mexico

María Luisa Marín
Universidad Politécnica de Valencia
Valencia, Spain

Paul Mathis
Service de Bioénergétique
CEA-Saclay, France

Albert R. Matlin
Oberlin College
Oberlin, Ohio

Jochen Mattay
Universität Bielefeld
Bielefeld, Germany

Vladimir I. Minkin
Rostov State University
Rostov on Don, Russia

Miguel Angel Miranda
Universidad Politécnica de Valencia
Valencia, Spain

David L. Mitchell
M.D. Anderson Cancer Center
Smithville, Texas

Kazuhiko Mizuno
Osaka Prefecture University
Sakai, Osaka, Japan

Tadashi Mori
Osaka University and ICORP/JST
Osaka, Japan

Yosuke Nakamura
Gunma University
Kiryu, Japan

Arunkumar Natarajan
Tulane University
New Orleans, Louisiana

Jun Nishimura
Gunma University
Kiryu, Japan

Takehiko Nishio
University of Tsukuba
Tsukuba, Ibaraki, Japan

Rika Nogita
Kyushu University
Hakozaki, Fukuoka, Japan

Michael Oelgemöller
Bayer Crop Science Japan
Yuki-City, Ibaraki, Japan

Kazue Ohkura
Health Sciences University of Japan
Ishikari-Tobetsu, Hokkaido, Japan

Jerzy Olejnik
AmberGen, Inc.
Boston, Massachusetts

Maria J. Ortiz
Universidad Complutense
Madrid, Spain

Takumi Oshima
Osaka University
Toyonaka, Osaka, Japan

Akihiko Ouchi
National Institute of Advanced
Industrial Science and Technology
Tsukuba, Ibaraki, Japan

Richard M. Pagni
University of Tennessee
Knoxville, Tennessee

Ravindra K. Pandey
Roswell Park Cancer Institute
Buffalo, New York

Andrew F. Parsons
University of York
Heslington, York, United Kingdom

Vincenzo Passarelli
Istituto di Biofisica CNR
Pisa, Italy

James W. Pavlik
Worcester Polytechnic Institute
Worcester, Massachusetts

Rama Krishna Peddinti
National Tsing Hua University
Hsinschu, Taiwan

Vittorio Pellegrini
NEST-INFM Scuola Normale Superiore
Pisa, Italy

Alicia B. Peñéñory
Universidad Nacional de Córdoba
Córdoba, Argentina

Jean-Pierre Pete
Université de Reims Champagne Ardenne
France

James A. Pincock
Dalhousie University
Halifax, Nova Scotia, Canada

K. Pitchumani
Madurai Kamaraj University
Madurai, India

Olivier Piva
Université Claude Bernard Lyon I
France

V. Ramamurthy
Tulane University
New Orleans, Louisiana

Carlos Rivas
Instituto Venezolano de Investigaciones Cientificas

S.M. Roberts
University of Liverpool
Liverpool, England

Roberto A. Rossi
Universidad Nacional de Córdoba
Ciudad Universitaria, Córdoba, Argentina

Kenneth J. Rothschild
Boston University
AmberGen, Inc.
Boston, Massachusetts

Mordecai B. Rubin
Technion — Israel Institute of Technology
Haifa, Israel

Keith C. Russell
Northern Kentucky University
Highland Heights, Kentucky

Masami Sakamoto
Chiba University
Yayoi-cho, Inagae-ku, Chiba, Japan

Jack Saltiel
Florida State University
Tallahassee, Florida

Aziz Sancar
University of North Carolina School of Medicine
Chapel Hill, North Carolina

Hugo Scheer
Universität München
München, Germany

John R. Scheffer
University of British Columbia
Vancouver, British Columbia, Canada

David I. Schuster
New York University
New York, New York

Leah Schutt
University of Guelph
Guelph, Ontario, Canada

Carl Scott
University of British Columbia
Vancouver, British Columbia, Canada

Koh-ichi Seki
Health Sciences University of Japan
Ishikari-Tobetsu, Hokkaido, Japan

Antonella Sgarbossa
Istituto di Biofisica CNR
Pisa, Italy

Yoshinori Shichida
Kyoto University and Core Research for Evolutional Science and Technology (CREST)
Kyoto, Japan

Toshio Shimizu
Tokyo Metropolitan University
Tokyo, Japan

Tetsuro Shimo
Kagoshima University
Kagoshima City, Japan

Terou Shinmyozu
Kyushu University
Hakozaki, Fukuoka, Japan

Scott McN. Sieburth
Temple University
Philadelphia, Pennsylvania

Vishwakarma Singh
Indian Institute of Technology
Bombay, India

Kenichi Somekawa
Kagoshima University
Kagoshima City, Japan

David E. Somers
Ohio State University
Columbus, Ohio

Pill-Soon Song
Kumho Life and Environmental Science Laboratory
Kwangiu, South Korea
University of Nebraska
Lincoln, Nebraska

Yoriko Sonoda
National Institute of Advanced Industrial Science and Technology
Tsukuba, Ibaraki, Japan

John L. Spudich
University of Texas
Houston, Texas

Zhuoyi Su
University of New Mexico
Albuquerque, New Mexico

Hiroshi Suginome
Hokkaido University
Sapporo, Japan

Kunio Sugiyama
Nihon University
Narashino, Chiba, Japan

Merrill Tarr
University of Kansas Medical Center
Kansas City, Kansas

Carol L. Thompson
University of North Carolina School of Medicine
Chapel Hill, North Carolina

Katsumi Tokumaru
International Institute for Advanced Studies

John P. Toscano
John Hopkins University
Baltimore, Maryland

Valentina Tozzini
NEST-INFM Scuola Normale Superiore
Pisa, Italy

Alexei V. Trofimov
University of Würzburg
Würzburg, Germany

Takashi Tsuno
Nihon University
Narashino, Chiba, Japan

Shiao-Chun Tu
University of Houston
Houston, Texas

Andrzej M. Turek
Jagiellonian University
Cracow, Poland

Kingo Uchida
Ryukoku University
Seta, Otsu, Japan

Dennis Paul Valenzeno
University of Kansas Medical Center
Kansas City, Kansas

Franklin Vargas
Instituto Venezolano de Investigaciones Cientificas

Daniela Vedaldi
University of Padova
Padova, Italy

Giampietro Viola
University of Padova
Padova, Italy

Peter J. Wagner
Michigan State University
East Lansing, Michigan

Peter Wan
University of Victoria
Victoria, British Columbia, Canada

Yuhong Wang
John Hopkins University
Baltimore, Maryland

Masakatsu Watanabe
National Institute for Basic Biology
Okazaki, Japan

Richard G. Weiss
Georgetown University
Washington, D.C.

Pablo Wessig
Humboldt University
Berlin, Germany

Frederick G. West
University of Alberta
Alberta, Canada

Kevin J. Wise
University of Connecticut
Storrs, Connecticut

John G. Wood
University of Kansas Medical Center
Kansas City, Kansas

Shigeru Yamago
Osaka City University
Osaka, Japan

Takuzo Yamakazi
Gunma University
Kiryu, Japan

Yasushi Yokoyama
Yokohama National University

Minjoong Yoon
Chungnam National University
Daejeon, Korea

Ung Chan Yoon
Pusan National University
Pusan, Korea

Jun-ichi Yoshida
Kyoto University
Kyoto, Japan

Toru Yoshizawa
Kyoto University and Core Research for Evolutional Science and Technology (CREST)
Kyoto, Japan

Abraham L. Yousef
University of Kansas
Lawrence, Kansas

Howard E. Zimmerman
University of Wisconsin
Madison, Wisconsin

Contents

1

Photobehavior of Alkyl Halides

Paul J. Kropp
University of North Carolina

1.1 Photochemical Behavior

Principal Pathways

Alkyl iodides afford mixtures of radical- and ion-derived photoproducts in solution, with the latter usually predominating. Indeed, this is a powerful method for generating carbocations, including many that cannot be readily prepared by other methods. Alkyl bromides display similar photobehavior, but with a lower proportion of ionic products. Analogous behavior has also been observed for phenyl thioethers and selenoethers,[1] as well as some organosilicon iodides.[2] In a process related to the formation of ionic intermediates, irradiation of dihalomethanes in the presence of alkenes results in cyclopropanation, a synthetically useful procedure that complements traditional methods. This chapter, which is concerned with alkyl halides, is a major expansion of an earlier review.[3] The solution-phase photobehavior of aryl, benzylic, and homobenzylic halides has been reviewed, along with that of alkyl systems.[4] The photobehavior of alkyl halides in the gas phase has also been reviewed.[5]

Spectroscopic Properties

Alkyl iodides have a long wavelength absorption arising from an $n \rightarrow \sigma^*$ transition that is red-shifted with increasing substitution about the iodine-bearing carbon atom, ranging in λ_{max} in hydrocarbon solvents from 258 nm for CH_3I to 269 nm for tertiary iodides (ε 375–675).[6] It is slightly blue-shifted with increasing solvent polarity, ranging in λ_{max} from 254 nm for CH_3I to 267 nm for tertiary iodides in CH_3OH (ε 380–735). There is also a strong shorter wavelength band at 194 nm arising from an $n \rightarrow R(6s)$ transition. The $n \rightarrow \sigma^*$ absorption in bromides is less intense and occurs at much shorter wavelengths, ranging in λ_{max} from 202 nm for CH_3Br to 215 nm for tertiary bromides in hydrocarbon solvents (ε 200–300). Alkyl chlorides have little or no absorption above 200 nm, rendering them difficult to study photochemically. The absorption spectra of geminal dihalides are more complex and extend to longer wavelengths due to mutual interaction of the two halogen atoms. For example, CH_2I_2 has absorptions at 212 (ε 1580), 240 (ε 600), and 290 (ε 1300) nm. These arise from four $n \rightarrow \sigma^*$ transitions, with the highest wavelength absorption consisting of two unresolved peaks.

0-8493-1348-1/04/$0.00+$1.50

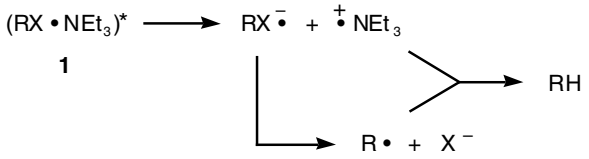

SCHEME 1

Irradiation Procedures

Since alkyl iodides have maximum absorption near the principal mercury line at 254 nm, they can be easily irradiated with a low-pressure mercury lamp and quartz or Vycor optics. Bromides, on the other hand, require light of shorter wavelengths, such as that emitted by a medium-pressure mercury arc.

The byproduct HX can frequently influence the course of reaction, by both re-adding to elimination products and serving as an efficient hydrogen atom donor, and is best removed from the irradiation mixture as it is formed. Triethylamine can be used as a scavenger in nonpolar solvents. In polar solvents, however, it leads to increased formation of the reduction product RH because of competing reaction via the amine–halide exciplex **1** (Scheme 1). The poorer electron donor HO^- has been found to be a suitable HX scavenger in alcoholic solvents.[7]

1.2 Mechanisms

It has long been recognized that absorption of light by the carbon–halogen chromophore results in homolytic cleavage of the bond. Not only is the antibonding sigma orbital occupied in the lowest lying excited singlet state, but also more than sufficient energy is available for bond cleavage. For example, the 0,0 energy levels of a typical tertiary iodide and bromide, estimated from the onsets of absorption at 315 and 250 nm, are 380 and 476 kJ/mol, respectively — substantially higher than the bond dissociation energies of 226 and 284 kJ/mol, respectively. It should be noted, however, that although the excited state is dissociative, it does not cleave with unit efficiency. The quantum yield for dissociation of ethyl iodide, for example, has been determined to be 0.30–0.32 in the gas phase, in the pure liquid, and in hexane.[8]

Early studies on the photobehavior of alkyl halides were usually conducted in the gas phase and interpreted in terms of radical intermediates.[5] Similar thinking carried over to early solution-phase studies.[4a] However, several "anomalous" products appeared in the solution phase that require skeletal rearrangements appropriate for carbocations but not typical of radical intermediates. These include the formation of (*E*)-2-butene (**3**) from iodide **2**[9] and the rearranged alkene **5** from iodide **4**,[10] which could readily arise via the ionic intermediates shown. In view of the formation of such products, an extensive study of the solution-phase photobehavior of alkyl iodides was undertaken, which provided firm evidence for the involvement of cationic intermediates and led to the proposal that they arise via initial homolytic cleavage followed by electron transfer within the resulting radical pair cage (**6**), as outlined in Scheme 2.[11] As discussed below, the resulting carbocations display behavior typical of other "free" cations generated by high-energy processes with little or no solvent participation.[12]

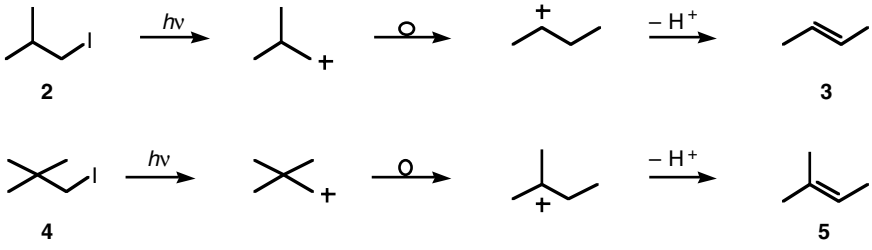

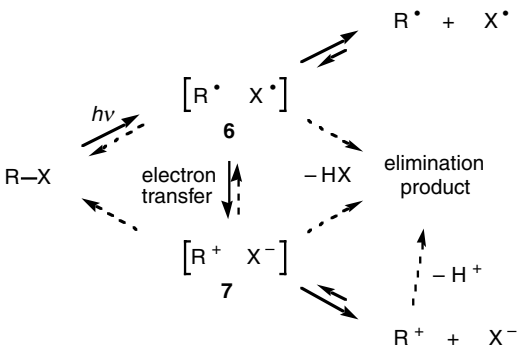

SCHEME 2

The initial studies centered on the 1-norbornyl halides **8**. On irradiation in CH_3OH, they afford a mixture of the reduction product norbornane (**9**) and the ether **10**, with the former predominating from bromide **8b** and the latter from iodide **8a**.[11,13] The reduction product **9** arises via abstraction of a hydrogen atom by 1-norbornyl radical from the medium and ether **10** via nucleophilic trapping of the 1-norbornyl cation. Irradiation of either halide in CH_3OD afforded ether **10** with no detectable incorporation of deuterium, indicating that it does not arise via acid-catalyzed addition of the alcohol to an initially formed unsaturated intermediate such as the bridgehead alkene **12** or the propellane **13**.

The higher ratio of ionic to radical products from iodide **8a** has proven to be general for iodides compared with the corresponding bromides. It is surprising since the more electronegative Br• might be expected to undergo electron transfer to the ion pair more readily than I• (Scheme 2). The observed trend apparently reflects a higher rate of diffusion from the radical pair cage relative to the rate of electron transfer for the lighter bromine atom.

As expected, the ratio of ionic to radical products is also dependent on the ionization potential of the alkyl radical R•. For example, in contrast with 1-iodonorbornane (**8a**), the 3-hydroxy derivative **14** afforded more of the reduction product **15** than ionic product **16** in CH_3OH.[14] Apparently the electron-withdrawing OH group impedes electron transfer. It has been proposed that the ionization potential of R• must be ≤200 kcal/mol for electron transfer to occur.[15]

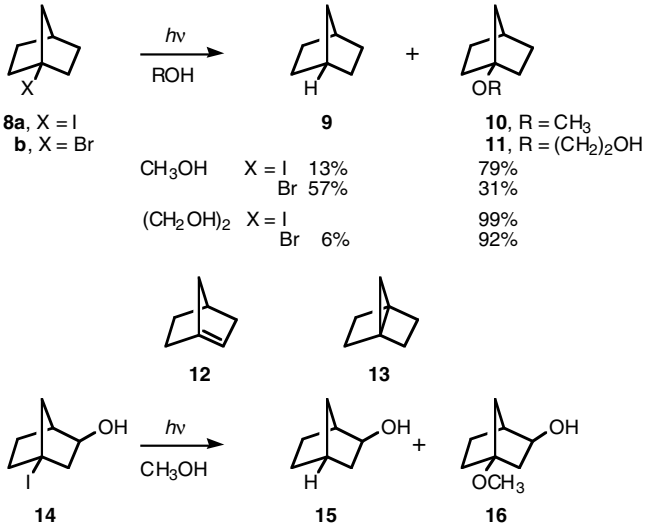

Consistent with the proposed mechanism, the ratio of ionic to radical product is dependent on the viscosity of the medium. Thus irradiation of halides **8** in $(CH_2OH)_2$, which is only slightly more polar than CH_3OH but is substantially more viscous, resulted in almost exclusive formation of the nucleophilic trapping product **11** from both the bromide and the iodide.[11,13] The extended lifetime of the radical pair in the more viscous medium permits electron transfer to compete more effectively with diffusion of the radical components from the cage.

The quantum yield for disappearance of iodide **8a** in CH_3OH at 254 nm is 0.10.[13] The low value is probably due, at least in part, to recombination of the radical and ion pairs **6** and **7**. The quantum yield was somewhat higher in CH_3OH saturated with O_2, with formation of the radical product **9** almost totally quenched and that of the ionic product **10** substantially reduced.[13] This was accompanied by the formation of a new product, hydroperoxide **17**, arising from trapping of R·. Bromide **8b** displayed similar behavior except that formation of norbornane (**9**) was not totally quenched. Quenching of the ionic product **10** by O_2 is consistent with the proposed coupling of the radical and ionic pathways by electron transfer (Scheme 2).

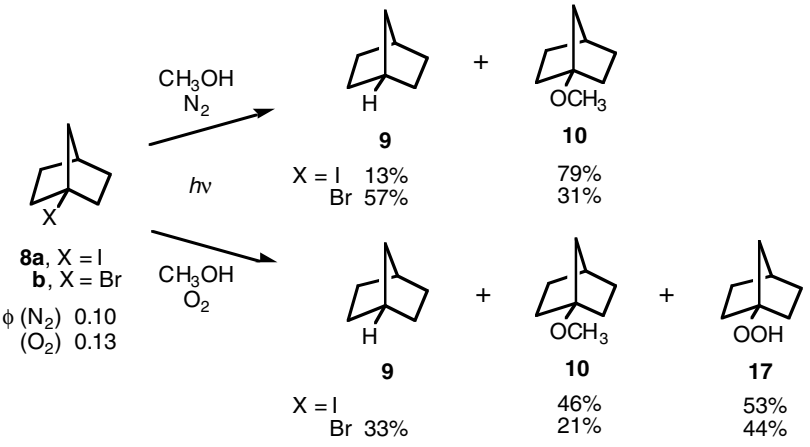

1.3 Examples

Monohalides

The photobehavior of alkyl halides varies with structure, depending on the ease of β-elimination.

Bridgehead and Related Halides: Nucleophilic Trapping vs. Reduction

Irradiation of bridgehead halides is thus a convenient method for generating bridgehead carbocations, which are readily trapped nucleophilically. Even though tertiary, these cations are difficult to form by conventional methods because bridgehead carbon atoms are structurally inhibited from relaxing to a planar geometry to provide the sp^2 hybridization preferred by carbocations. Thus iodide **8a** was recovered quantitatively from treatment with CH_3OH in the dark for 24 h — even in the presence of silver ion, which normally facilitates solvolysis of alkyl iodides.[13] By contrast, a methanolic solution of **8a** readily afforded ether **10** on exposure to ultraviolet light.

Since they are difficult to form, bridgehead cations are highly reactive. Irradiation of halides **8** in a variety of media provided a convenient means of exploring the remarkable reactivity of the 1-norbornyl cation (**18**).[13] It was efficiently trapped by diethyl ether and THF to afford the ethers **19** and **20**. Even in aqueous THF, a substantial portion of the butenyl ether **20** was obtained. Trapping by *t*-butyl alcohol afforded some of the ditertiary ether **21** but was accompanied by formation of 1-norbornanol (**22**) and 2-methylpropene. Cation **18** was trapped by CH_2Cl_2 to afford chloride **23**, and in aqueous CH_3CN the Ritter product **24** was formed. It should be noted that radical abstraction from CH_2Cl_2 occurs at H and ionic abstraction at Cl.

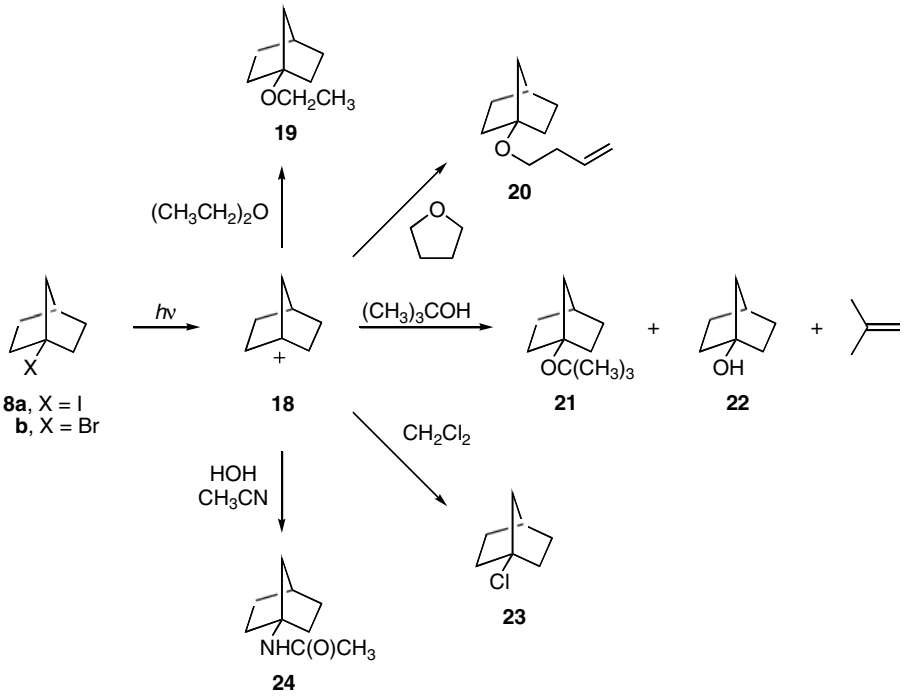

Interestingly, the 1,4-diiodide **25a** afforded mainly the acetal **28** rather than the dimethoxy product **27**.[16] Acetal **28** apparently arises from fragmentation of the 4-methoxy cation **29** prior to trapping with CH_3OH since it was also the principal product from separate irradiation of the 4-methoxy iodide **26a**. In contrast with diiodide **25a**, the 1,4-dibromide **25b** afforded predominantly the reduction product **8b**.

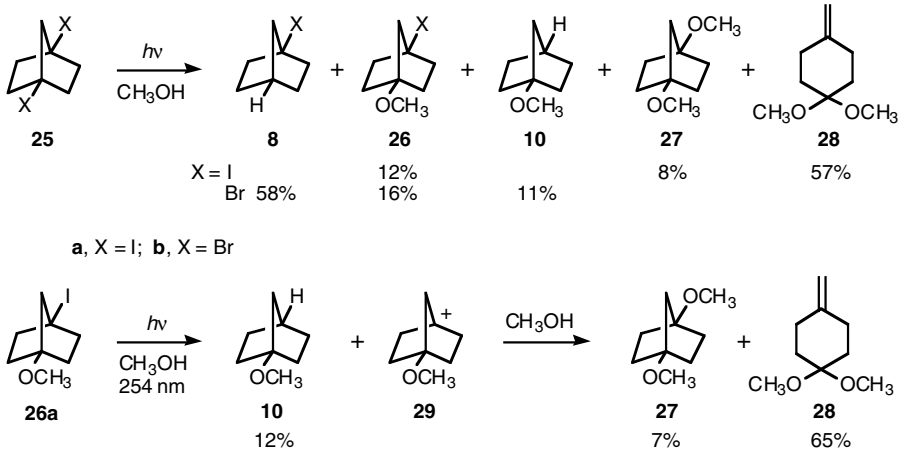

In analogy with 1-iodonorbornane (**8a**), the bridgehead iodides **30** afforded the corresponding ethers **32**, along with small amounts of the reduction products **31**.[17] Once again, irradiation in CH_3OD afforded ethers **32** with no detectable deuterium incorporation. The bicyclo[2.2.2]- and bicyclo[3.2.1]octyl cations were also obtained by irradiation of 1-(iodomethyl)norbornane (**33**) in CH_3OH to afford ethers **32a** and **32b** in a ratio approaching the kinetic ratio of 1:2.[13] By contrast, silver ion assisted methanolysis of iodide **33** afforded predominantly ether **32a**, arising from the thermodynamically more stable bicyclo[2.2.2]octyl cation, along with small amounts of the bicyclo[3.2.1]octyl ether **32b** and unrearranged ether **34**.

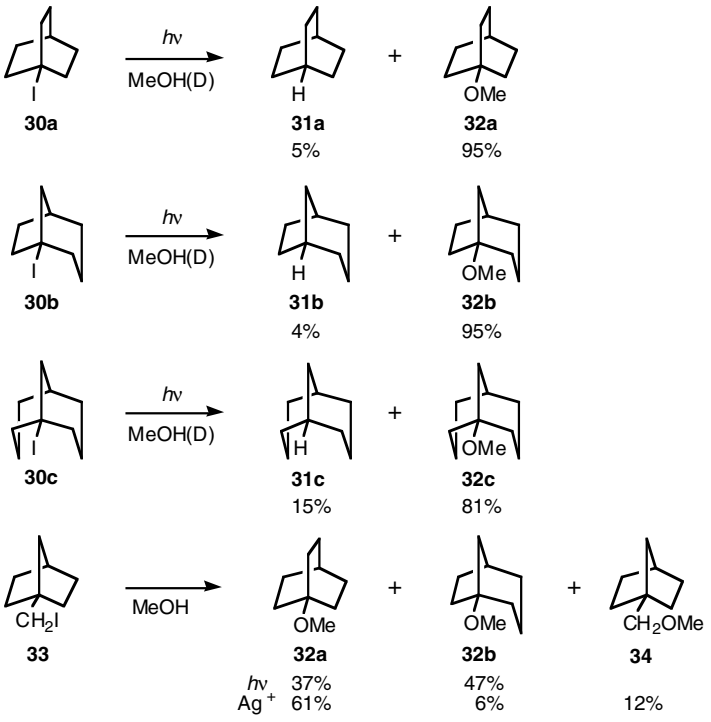

Irradiation of iodocubane (**35**) afforded the methyl ether **37** accompanied by a small amount of the reduction product cubane (**36**).[18] The high ratio of ionic to radical product indicates that the cubyl cation is easier to form than the 1-norbornyl cation, in agreement with solvolysis data and *ab initio* calculations showing stabilization of cubyl cation by cross-ring bonding to the β carbon atoms.[19] The 1,4-diiodide **38** afforded the mono- and disubstituted derivatives **39** and **40** in CH_3OH and wet CH_3CN.

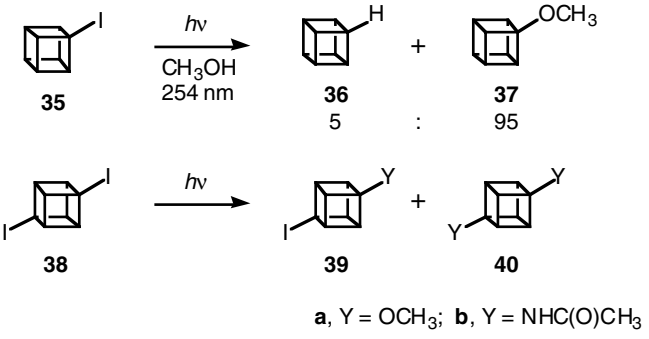

Irradiation of the 1-adamantyl halides **41** in a variety of alcohols afforded the ethers **43** along with a small amount of the reduction product adamantane (**42**).[13,20] The greater ease of forming the 1-adamantyl, compared with the 1-norbornyl, cation is reflected in the higher ratio of ionic to radical product from both the iodide and bromide. Once again, use of the viscous solvent $(CH_2OH)_2$ greatly increased the amount of ionic product **43** from the bromide **41b** compared with CH_3OH.[13] Adamantyl bromides are significantly more sensitive to the presence of electron-withdrawing substituents than are the corresponding iodides. Thus the 1,3-diiodides **44a** and **45a** afforded the corresponding diethers **44c** and **45c** in high yield, whereas the dibromides **44b** and **45b** afforded principally the corresponding monoether **43** (R = OCH_3) and its 3,5-dimethyl derivative.[20] Similarly, the tribromide **46** afforded mainly the diether **44c** in CH_3OH,[20] and the tetrabromide **47b** afforded only 1-acetamido-3,5,7-tribromoadamantane in wet

CH_3CN.[21] By contrast, the tetraiodide **47a** afforded the tetraamide **47c** in 51–60% yield under similar conditions.[21]

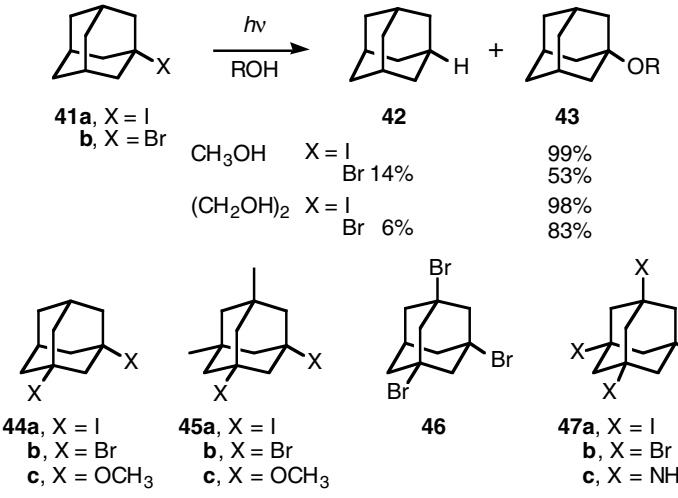

Nonbridgehead Halides: Elimination vs. Nucleophilic Trapping and Reduction

Except for systems such as the preceding bridgehead halides that are strongly inhibited from undergoing elimination, alkyl halides undergo competing elimination and trapping in nucleophilic solvents. The product ratio depends on the degree of structural inhibition to elimination and the nucleophilicity of the solvent, but there is a strong propensity for undergoing elimination that is characteristic of "free" cations formed by high-energy processes without substantial solvent participation.[12] Cationic rearrangements frequently precede elimination and nucleophilic trapping. Competing radical behavior is also usually observed.

1,2- and 1,3-Elimination

Irradiation of the 2-adamantyl halides **48** in CH_3OH afforded principally the 2-adamantyl ether **51**, along with the reduction product adamantane (**42**).[13,20] However, when the irradiation was conducted in the presence of NH_4OH as a HX scavenger, the 1,3-elimination product **49** and rearranged elimination product **50** were also obtained.[7,22] In the absence of scavenging, these latter products undergo addition of HX to reform the starting halides **48**. Irradiation of iodide **48a** in the nonnucleophilic solvent ether containing triethylamine as a scavenger afforded principally the 1,3-elimination product **49**.[22]

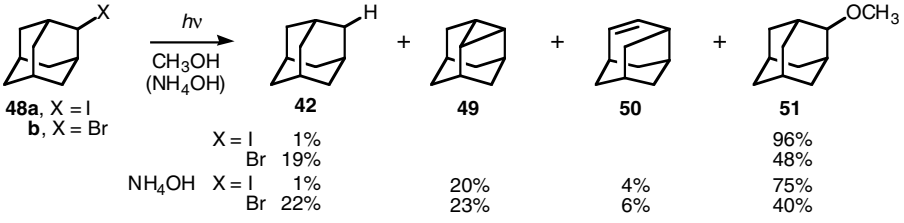

Another cation that, like bridgehead cations, is difficult to form by conventional methods is the 7-norbornyl cation. The problem in this case is angle strain. Thus, extended treatment of 7-iodonorbornane (**52**) with methanolic $AgNO_3$ afforded only a trace of ether **53** (R = CH_3).[23] By contrast, irradiation in CH_3OH readily afforded ether **53** (R = CH_3), along with smaller amounts of the reduction product norbornane (**9**), the unprecedented 1,3-elimination product **54** and the rearrangement products **55**–**57**. The 2-chloro derivatives **58** underwent *syn,anti* interconversion in competition with formation of the reduction product **60**, the ethers **61** and **63**, and the 1,3-elimination product **62**. By contrast, treatment

with methanolic $AgNO_3$ resulted in ionization of the more reactive chlorine substituent to afford ethers **59**. Thus, irradiation at 254 nm is a simple method for inducing selective reaction by the iodine substituent.

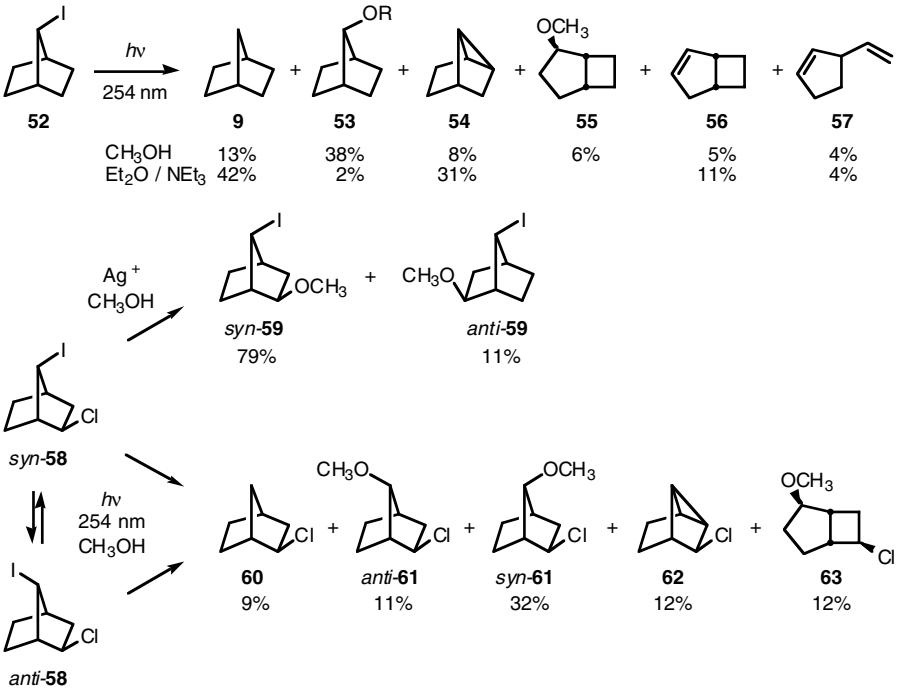

By contrast, the 2-norbornyl cation is easily formed. Moreover, the 2-norbornyl system can readily undergo elimination. On irradiation in CH_3OH or $(CH_3)_3COH$, the 2-norbornyl iodides **64a** underwent *exo,endo* equilibration and afforded the 1,2- and 1,3-elimination products **66** and **67**, along with the nucleophilic trapping product **68**.[7,24] The corresponding bromides **64b** each afforded the same products, along with small amounts of the radical products **65** and **9**, but underwent no detectable interconversion.

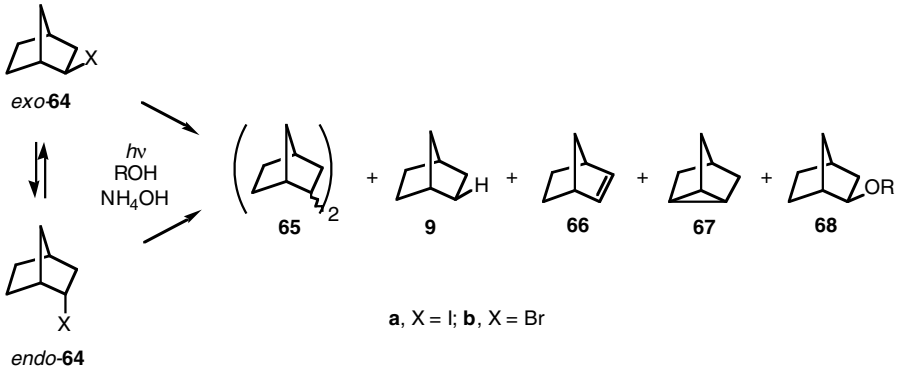

Clearly, the ethers **68** and the 1,3-elimination product nortricyclene (**67**) are ionic in origin. However, the 1,2-elimination product 2-norbornene (**66**) might, in principle, arise via either hydrogen atom transfer within the radical pair **6** or proton transfer within the ion pair **7** (Scheme 2). Deuterium labeling studies revealed that it arises by both paths, with the percent ionic pathway being 36% for iodides **64a** and 64–69% for bromides **64b**.[7] These distributions, combined with the yields of the ionic products

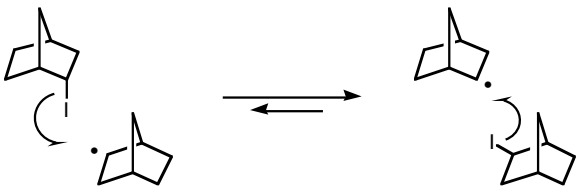

SCHEME 3

nortricyclene (**67**) and the ether **68** (R = CH_3), afford a ratio of in-cage radical to total ionic products of 1:3 for iodides **64a** but only 1:8 for bromides **64b**. Thus, of the material that is not lost by diffusion from the radical pair cage (**6**), a higher percentage is converted to products via ionic intermediates when X = Br, as expected based on the relative electronegativities of bromine and iodine.

Once out of the cage, the alkyl radical can abstract a hydrogen atom from the solvent or undergo combination/disproportionation with a second alkyl radical. Another available pathway in the case of iodides is transfer of an iodine atom from a molecule of unreacted starting material. Halogen atom transfer occurs readily for alkyl iodides ($k \approx 2 \times 10^5$ mol^{-1} sec^{-1})[25] and accounts for the observed interconversion of iodides **64a** (Scheme 3). In the more viscous solvent $(CH_3)_3COH$, in which escape from the radical cage (**6**) occurs more slowly, there is substantially less epimerization. In contrast with that for iodides, halogen atom transfer is much slower for alkyl bromides ($k \approx 6 \times 10^2$ mol^{-1} sec^{-1}),[25] permitting combination/disproportionation to compete. Hence bromides **64b** undergo no detectable epimerization.

Analogously with the parent 2-norbornyl iodides **64a**, the iodo ethers **69a** underwent *exo,endo* equilibration, accompanied by formation of the reduction product **70a**, the rearranged elimination product **73a**, the 1,3-elimination product **74a**, and the ethers **75a** and **76a**.[17] Also formed was the acetal **72**, which deuterium labeling studies surprisingly showed arises via elimination to the bridgehead alkene **71** followed by addition of CH_3OH. In the presence of furan, the bridgehead alkene **71** was trapped by cycloaddition. Formation of the highly strained intermediate **71** underscores the strong driving force for elimination exhibited by alkyl halides on irradiation.

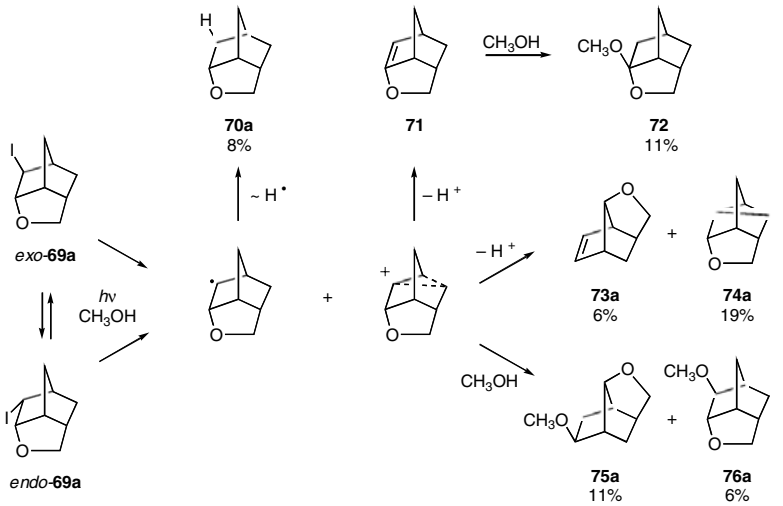

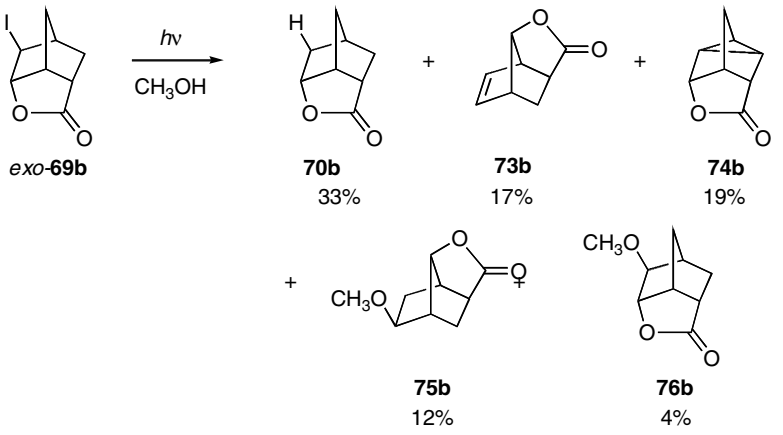

By contrast, the corresponding lactone **69b** underwent no detectable epimerization and afforded, principally, the reduction product **70b.**[17] The added inductive effect of the carbonyl oxygen atom apparently both retards electron transfer and renders the radical intermediate more reactive toward hydrogen abstraction from the medium, decreasing its lifetime and competing with the iodine exchange that leads to epimerization of iodo ether *exo*-**69a** (Scheme 3). The analogous elimination and trapping products **73b**–**76b** were formed, but there was no detectable formation of a product corresponding to acetal **72**, presumably because the increased strain introduced by the sp^2-hybridized carbonyl carbon atom precludes elimination to a bridgehead alkene.

The analogous iodo ethers **77** similarly underwent *exo,endo* equilibration, along with formation of the elimination product **78** and rearranged elimination product **79.**[26] In CH_3OH, the rearranged acetal **80** was also formed.

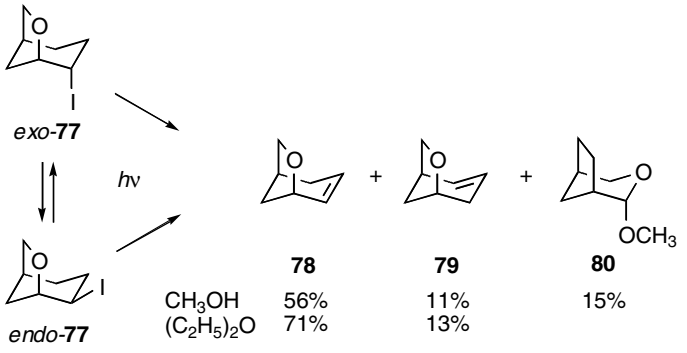

Epimerization was also observed in the interconversion of the deoxy iodo sugars **81** and **82.**[27] Interconversion occurred from either isomer with a quantum yield greater than unity, consistent with a mechanism analogous to that of Scheme 3. Also formed was the reduction product **83.** Similarly, the deoxy iodo sugar **84** afforded the reduction product **85.**[27] Irradiation of deoxy halo sugars is a useful synthetic application of the radical photobehavior of alkyl halides, affording the corresponding deoxy sugars in high yield under mild conditions.[28] Ionic products are not formed, even in nucleophilic solvents. Except at the anomeric position, carbohydrates form carbocations with difficulty because of the large number of electron-withdrawing oxygen atoms.

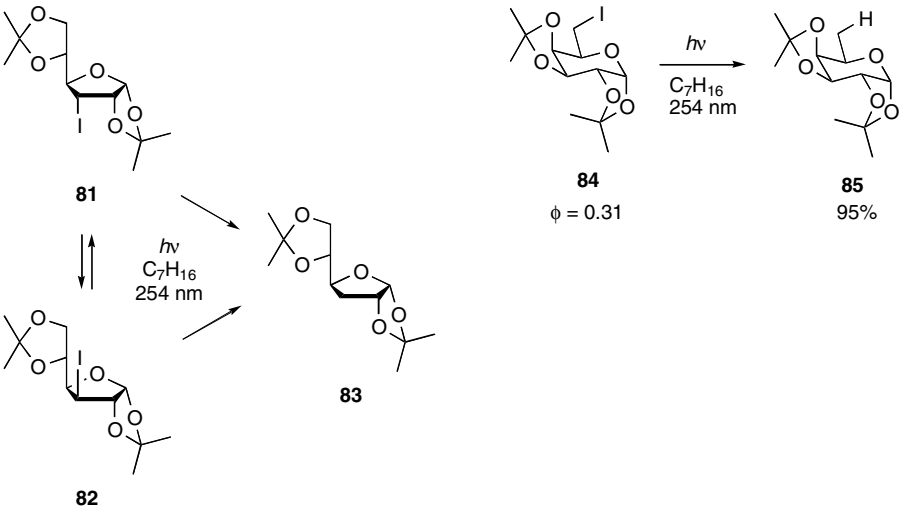

The *endo*-2-norbornyl analog longibornyl iodide (**86**) afforded principally the elimination products longifolene (**87**) and longicyclene (**88**), accompanied by a small amount of alkene **89** resulting from a transannular hydride shift.[29] Solvolysis of iodide **86** afforded only longifolene (**87**) and longicyclene (**88**), with none of the transannular elimination product **89**. Formation of this product on irradiation once again illustrates the high reactivity of "free" cationic intermediates generated photolytically from alkyl halides. Another example is the formation of the strained alkene **91** from the 2-(iodomethyl)norbornane **90**.[30]

Irradiation of 9-iodocamphor (**92**) in CH_3OH afforded the ring-expanded elimination products **93** and **94**, accompanied by a mixture of ethers **95**.[31] Thus, the CI chromophore can be selectively irradiated at 254 nm in the presence of a ketone carbonyl group. Under similar conditions (iodomethyl)trimethylsilane (**96**) afforded, principally, the silyl ether **99**, resulting from rearrangement of the α-silyl cation **97**.[32] By contrast, silver ion assisted methanolysis of iodide **96** afforded only the unrearranged ether **98** via S_N2 displacement, avoiding involvement of the α-silyl cation **97**.

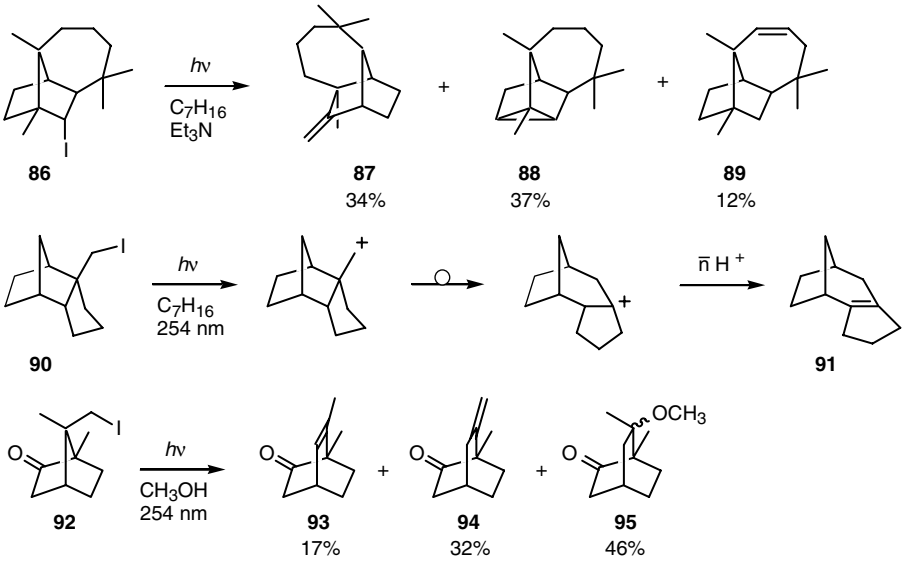

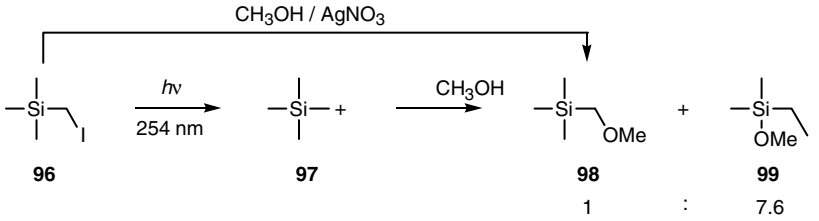

Even highly stabilized allylic cations undergo substantial elimination in a nucleophilic solvent when generated photochemically. Thus the allylic iodide **100a** and bromide **100b** afforded principally the elimination product **102**, along with the methyl ethers **103** and **104**, on irradiation in CH_3OH.[33] Similar behavior was exhibited by the tetramethyl derivative **106**. By contrast, the chloride **100c** simply underwent equilibration with the allylic isomer **105**, presumably via the radical pair.

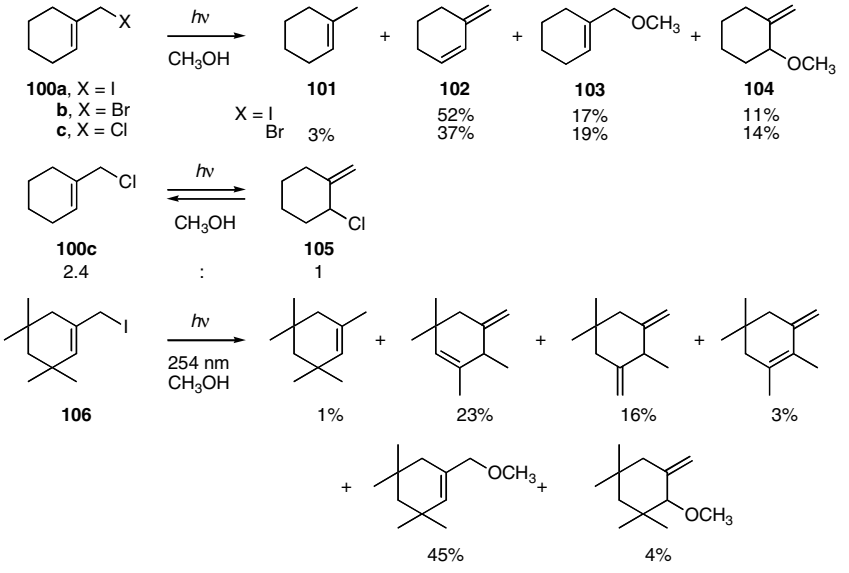

The 1-halooctanes **107** and iodocyclohexane (**114**) show once again the propensity of alkyl halides for photoelimination, giving primarily the elimination products 1-octene (**110**) and cyclohexene (**116**) in CH_3OH and only small amounts of the ethers **113** and **117**.[11,13,34] As is typical, bromide **107b** gave appreciable amounts of the out-of-cage radical products **108** and **109**. The *t*-butylcyclohexyl iodide **118** afforded substantial amounts of the rearranged elimination product **121**.[26]

In a dramatic application of the propensity of alkyl halides to undergo photoelimination, irradiation of the diiodosulfone **122a** proved to be the method of choice for effecting elimination to diene **123**, which was formed in good yield.[35] By contrast, the dihalosulfones **122** were either inert toward conventional elimination conditions or gave mainly methyl ethers on treatment with methanolic KOH. Irradiation of the dibromosulfone **122b** gave mainly reduction and no detectable formation of the elimination product **123**.

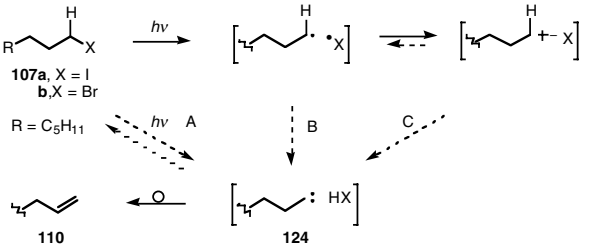

SCHEME 4

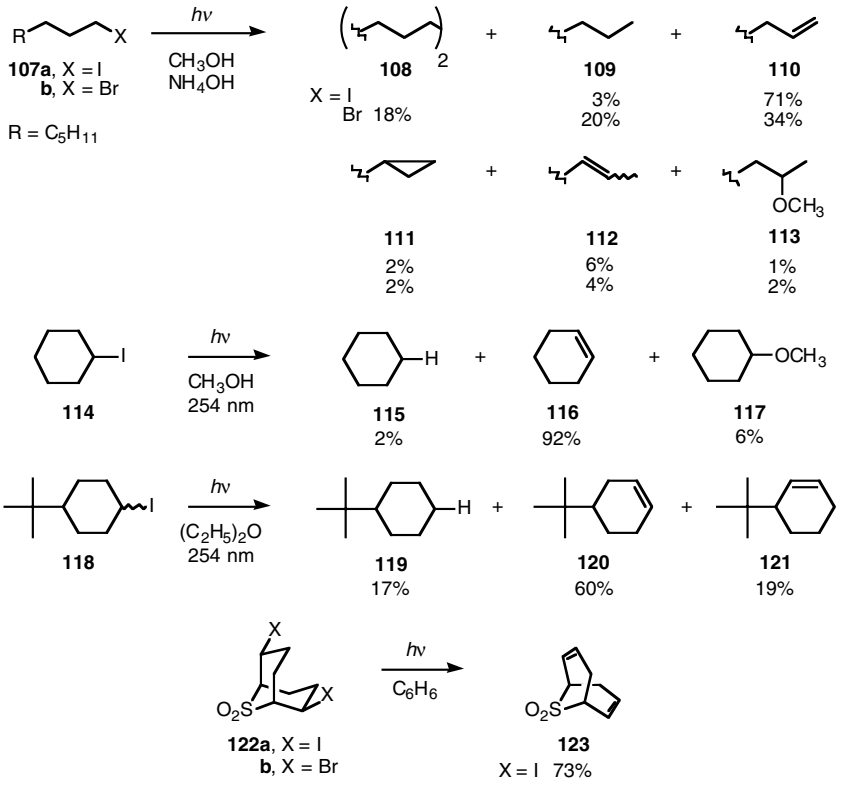

α-*Elimination: A Secondary Pathway to Unsaturated Products*

In the preceding discussion, it was assumed that elimination products such as 1-octene (**110**) are formed via transfer of a β-hydrogen atom or a β-proton from the corresponding radical or carbocation, respectively. However, deuterium labeling studies with 1-iodooctane (**107a**) showed that 17–29% of the 1-octene (**110**) is formed via α-elimination to the carbene intermediate **124**, depending on the solvent and irradiation conditions (Scheme 4).[34] Similarly, 27–30% of the cyclohexene (**116**) from 1-iodocyclohexane (**114**) arises via α-elimination. However, only 7% of the 1-octene (**110**) from bromide **107b** arises via α-elimination.[7]

As shown in Scheme 4 using the 1-halooctane system **107** as a model, the caged carbene-HX pair **124** may undergo undetected insertion to regenerate halide **107** in competition with rearrangement of the carbene to 1-octene (**110**). Thus, α-elimination may occur more extensively than reflected by the deuterium labeling results. Three possible routes to the carbene intermediate are outlined. The most obvious,

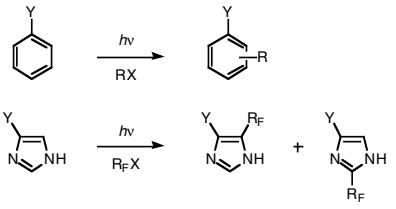

SCHEME 5

direct formation via concerted loss of HX (path A) is inconsistent with the observed lack of a deuterium isotope effect on the relative involvement of α-elimination in the formation of 1-octene (**110**). It is not clear which of the other two paths is involved in carbene formation. There is, however, precedent for the formation of carbene intermediates via transfer of α protons from carbocations.[36]

Trapping by Aromatic Solvents

Alkyl halides typically undergo slow elimination on irradiation in aromatic solvents, accompanied by the formation of alkylated aromatic products in low-to-moderate yields (Scheme 5).[37] These latter products were obtained in higher yields with methyl,[38] trifluoromethyl,[39] and allyl[40] iodides, which are incapable of undergoing competing elimination. Similarly, irradiation of 1-iodonorbornane (**8a**) in toluene afforded a mixture of 1-tolylnorbornanes (**8**, X = $C_6H_4CH_3$) in good yield.[13] Imidazole and its derivatives underwent facile trifluoromethylation or perfluoroalkylation on irradiation of perfluoroalkyl iodides in their presence in CH_3OH solution.[41] However, when the photolyses of simple alkyl halides were performed in CH_3OH or CH_3CN solutions containing aromatic substrates, nucleophilic trapping products (alkyl methyl ethers or *N*-alkylacetamides) were formed at the expense of aromatic substitution products.[37]

Since the absorption spectra of the CI and aryl chromophores have extensive overlap, it is not clear whether photoreaction involves direct absorption by the alkyl halide or whether the light is being absorbed by the aromatic substrate, followed by either energy or electron transfer with the alkyl halide. It is also not clear whether the aromatic substrates are capturing radical or cationic intermediates. Simple alkyl iodides afforded mixtures of toluene adducts having o:m:p ratios consistent with cationic attack.[37] This was reinforced by the formation of ethers or acetamides at the expense of aryl substitution products in the presence of CH_3OH or CH_3CN. On the other hand, the 1-tolylnorbornanes (**8**, X = $C_6H_4CH_3$) from 1-iodonorbornane (**8a**) were formed in a ratio typical of that for homolytic substitution.[13] It would be expected that methyl and trifluoromethyl iodides would afford only radical intermediates. However, they exhibited a lower reactivity at the ortho position than is generally typical of homolytic substitution reactions.[38,39] Similar results were afforded by allyl iodide.[40] Either competing trapping of radical and cationic intermediates is involved, or the mechanism is more complex than is apparent.

Cyclization

Trapping of the radical or cationic intermediates resulting from irradiation of alkyl halides can also occur intramolecularly. The 4-phenyl-1-butyl halides **125** afford the cyclized product **126** along with the additional products **127–130**.[7,42] As usual, elimination predominates over aryl substitution. The allylic analog **131**, which is structurally incapable of undergoing elimination, afforded the cyclization product **132**, along with the amide **133**, in CH_3CN.[42a] By contrast, the 2-phenyl-1-ethyl iodide **134a** gave only the ether **136**, whereas the bromide **134b** gave a mixture of ether **136** and the out-of-cage radical product **135**.[42b] Analogous behavior was exhibited in other alcoholic solvents. The olefinic analogs **137** afforded the cyclized products **140–142**, along with the reduction product **138** and elimination product **139**.[33]

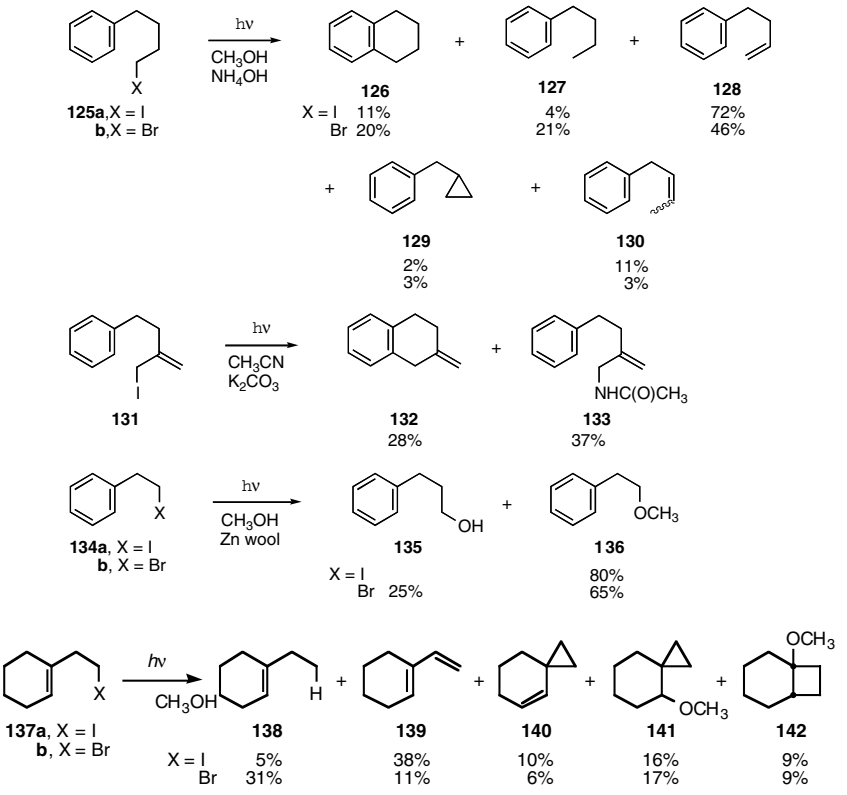

Charge-Transfer Irradiation: Radical Products

Irradiation of alkyl halides in the presence of amines proceeds via an amine–halide charge-transfer complex (**1**) to afford principally radical-derived products (Scheme 1). Thus citronellyl iodide (**143**) afforded a mixture of elimination (**145**) and cyclization products (**146**) accompanied by a small amount of reduction product **144**.[29,43] For reasons not clear, cyclization was somewhat more favored relative to elimination with increasing temperature and on going to the more polar solvent THF. Analogous behavior was exhibited by the 2,3-dihydrofarnesyl iodides **147**, which underwent competing elimination and cyclization.[43] Neryl iodide [(*Z*)-**148**] similarly afforded substantial amounts of both the elimination and cyclization products.[44] The isomeric geranyl iodide [(*E*)-**148**], which is structurally inhibited from undergoing cyclization, afforded a small amount of the cyclization product limonene (**149**), apparently via initial $E \rightarrow Z$ isomerization. Likewise, the farnesyl iodide (2*Z*)-**150** underwent principally cyclization, whereas the isomeric (2*E*)-**150** predominantly underwent elimination.[44]

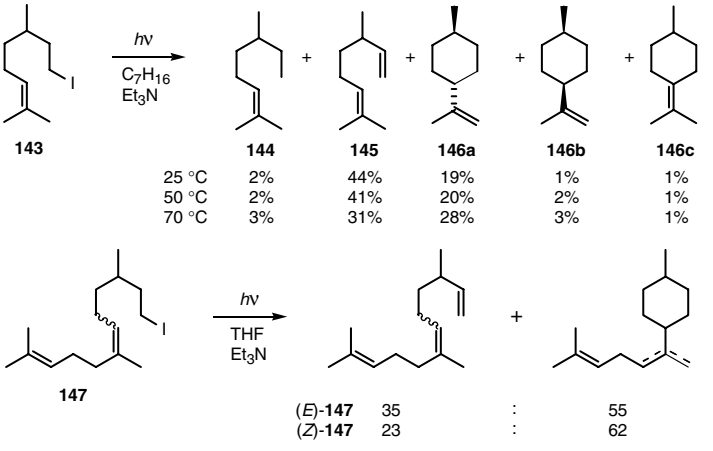

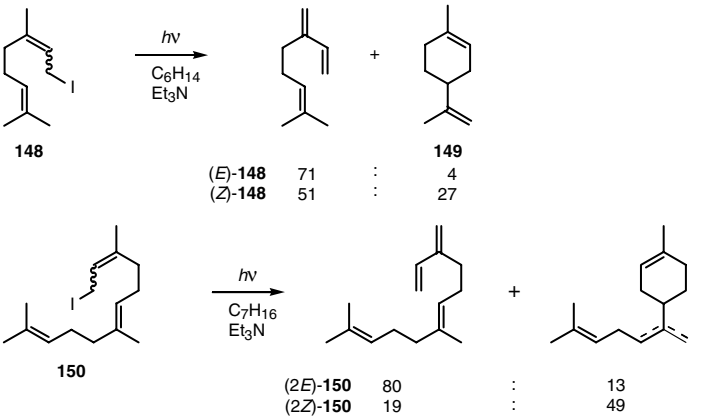

Irradiation of alkyl halides in the presence of amines is a synthetically useful method for generating radical-derived products that avoids the troublesome purification problems associated with the conventional method of using trialkyltin halides to generate radicals from alkyl halide precursors. This is illustrated by the bromides and iodides **151–153**, which afforded cyclization products in good to excellent yields.[45]

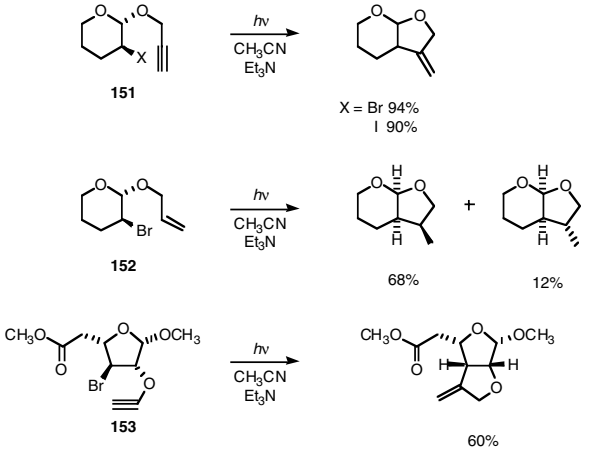

Irradiation of a number of alkyl iodides in the presence of CO and a variety of alcohols afforded the corresponding esters in good yield (59–87%) via trapping of the alkyl radical and alcoholysis of the resulting acyl iodide (Scheme 6).[46] Carboxylation occurred selectively at the carbon atom to which the iodine atom had been attached, and a wide range of aliphatic iodides, including tertiary, was effective. 2-Iodooctane (**154**) afforded the ester **155** in 72% yield, along with a mixture of 1- and 2-octenes (16%) as minor products. However, long irradiation times (12–50 h) and moderately high pressures (20–55 atm) were employed. Since irradiations were conducted through Pyrex (cutoff 280 nm) in polar solvents in the presence of a base, and no reaction occurred in the absence of base, the alkyl radicals were apparently formed via weak absorption of a charge-transfer complex (Scheme 1) rather than direct excitation of the C–I chromophore.

SCHEME 6

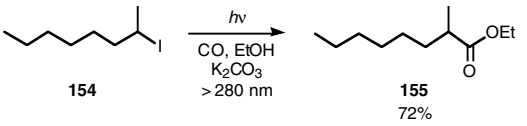

154 **155** 72%

An exception to the usual formation of radical-derived products in the presence of amines is a recent report that irradiation of 1-bromo- (**41b**) and 1-chloroadamantane (**41c**) and 1-chloronorbornane (**8c**) in the presence of primary amines afforded the substitution products **156** and **157**, along with the radical products adamantane (**42**) and an adamantyl dimer or norbornane (**9**) and a norbornyl dimer.[20b] However, the quantum yields were very small ($2–4 \times 10^{-7}$ for chloride **41b** and 6×10^{-9} for chloride **8c**), and neither the chemical yields of the products nor the relative yields of substitution and radical products were reported. Likewise, no comment was provided on the formation of monoalkyl amine intermediates. Since these amines are primary, electron transfer within the charge-transfer complex may occur less readily.

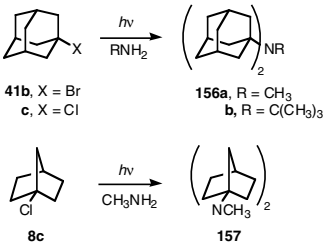

41b, X = Br
c, X = Cl

156a, R = CH_3
b, R = $C(CH_3)_3$

8c **157**

Vinyl Halides

The photobehavior of vinyl iodides closely parallels that of their saturated alkyl analogs in solution, serving as a convenient and powerful method for the generation of vinyl cations that can be effected even at low temperature and in solvents of widely varying polarity. Once again, however, there is a strong propensity for elimination.

As with that of their saturated analogs, the photobehavior of vinyl iodides was initially interpreted exclusively in terms of radical intermediates. One of the first to be studied in solution, 1-iodopropene (**158**), was observed to undergo *E,Z*-isomerization accompanied by elimination to propyne, reduction to propene, and fragmentation to ethyne and CH_3I.[47,48] The radical pair **159** was proposed as the sole intermediate, even though elimination of HI could equally well involve the corresponding ion pair. The behavior of 4-iodo-3-heptene (**160**), which afforded the additional elimination product allene **163** besides the reduction products **161** and the alkyne **162**, was similarly interpreted as radical in character.[49]

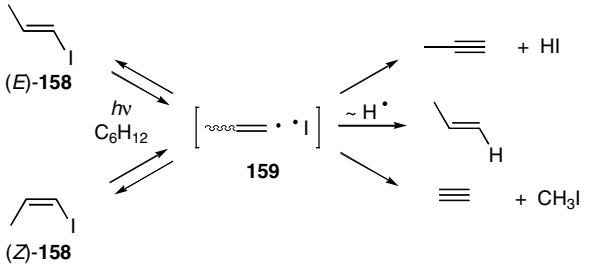

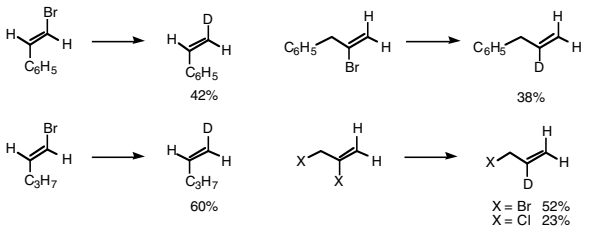

SCHEME 7

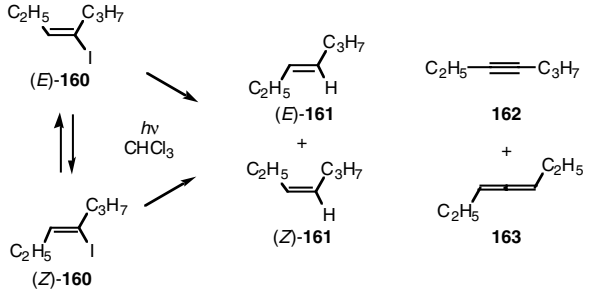

Advantage was taken of the formation of reduction products, which are undoubtedly of radical origin, to prepare specifically deuterated alkenes (Scheme 7).[50] It is interesting that substitution of a vinyl halogen atom by deuterium can be effected selectively in the presence of allylic bromides or chlorides, which normally are much more reactive, because they do not absorb strongly under the irradiation conditions. This was also seen in the irradiation of the insecticide bromodan (**164**), which afforded a mixture of the reduction products **165** and **167** in CH_3OH and **166** and **167** in C_6H_{14}.[51] It is not clear why the chlorine substituent at C2 or C3 is more reactive in CH_3OH or C_6H_{14}, respectively.

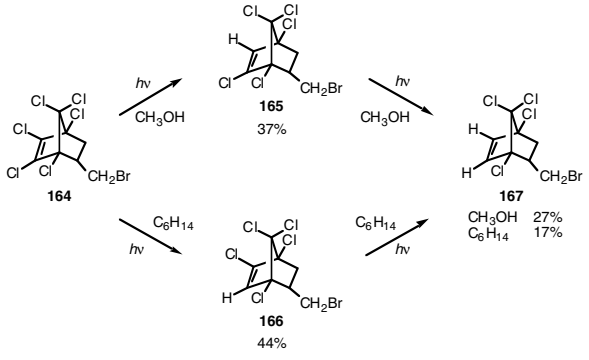

Evidence for the competing involvement of ionic intermediates in the photobehavior of vinyl halides was obtained by incorporating the chromophore in a cyclic environment, in which elimination is structurally inhibited. Thus, 1-iodocyclohexene (**168a**) afforded the nucleophilic trapping products **172–174** in high yields, clearly showing involvement of the vinyl cation **170**.[52] Irradiation in CH_3OH containing Zn as an acid scavenger afforded the vinyl ether **171** (65% yield) instead of the acetal **172**. As is typical, irradiation of bromide **168b** in CH_3OH afforded principally the reduction product cyclohexene (**116**) accompanied by smaller amounts of the acetal **172**.

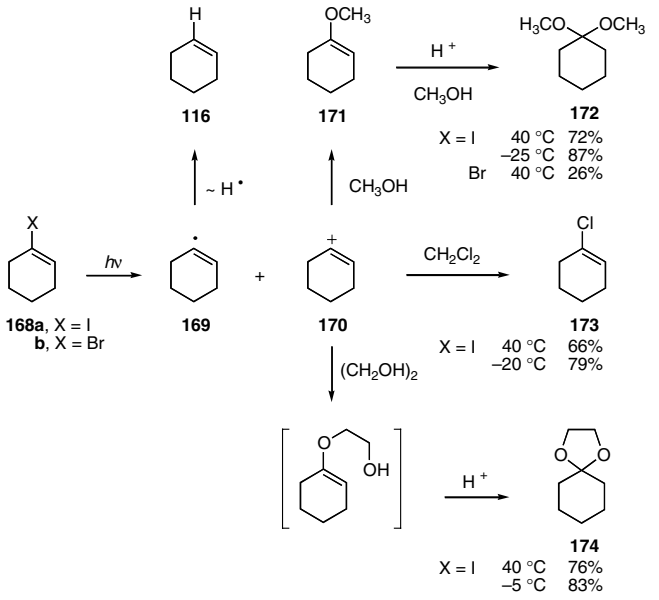

There was a moderate increase in the formation of the nucleophilic trapping products **172–174** relative to the reduction product cyclohexene (**116**) with decreasing temperature. The origin of this effect, which is general for vinyl iodides, is not clear. It does not appear to be due principally to the increased viscosity of the medium at lower temperatures, since vinyl halides show no significant increase in the yield of ionic products on going from CH_3OH to the highly viscous solvent $(CH_2OH)_2$. Saturated alkyl halides, which exhibit increased ionic behavior in more viscous solvents, do not exhibit a similar temperature effect.[33]

The cyclopentenyl analog **175** afforded principally the reduction product **176** accompanied by only a small amount of the trapping product **177** or **178** in CH_3OH or CH_2Cl_2, respectively, presumably because of the increased strain associated with incorporating an sp-hybridized center in a five-membered ring.[52] Nonetheless, these were the first unequivocal examples of the generation of a 1-cyclopentenyl cation from a cyclopentenyl precursor. The even more highly constrained cyclohexenyl halides **179** and **180** afforded exclusively the reduction product isolongifolene (**179c**) or neoisolongifolene (**180c**), respectively, on irradiation in CH_3OH.[53]

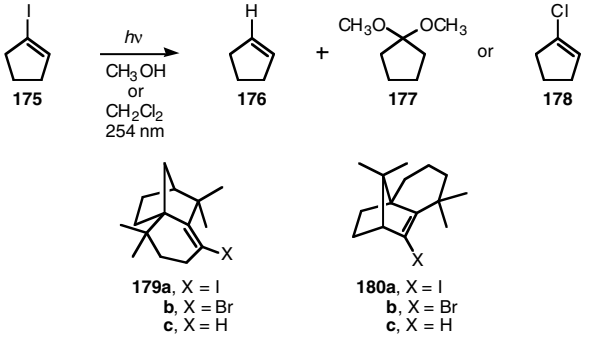

In the higher homolog, 1-iodocycloheptene (**181a**), the nucleophilic trapping product **184a** (Y = OCH_3 or Cl) predominated but was accompanied by the secondary products **185a** and **187a**, arising from competing elimination to the strained allene **183a**.[52] In 1-iodocyclooctene (**181b**), elimination to allene **183b**, leading to the secondary products **185b–187b**, predominated over nucleophilic trapping in CH_3OH and occurred exclusively in CH_2Cl_2. In each case, some of the reduction product **182** was also obtained.

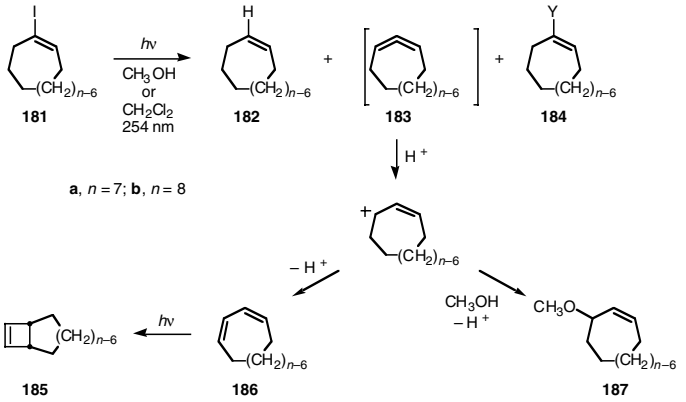

In the acyclic analog **188**, elimination occurred exclusively even in CH_3OH to give the secondary products **191** and **192** along with the reduction product **189**.[52] In CH_3OD, the allylic ether **192** was formed with deuterium incorporation as expected from protonation of the allene intermediate **190**. In marked contrast with its facile photoelimination, iodide **188** is totally inert toward methanolic $AgNO_3$.[52]

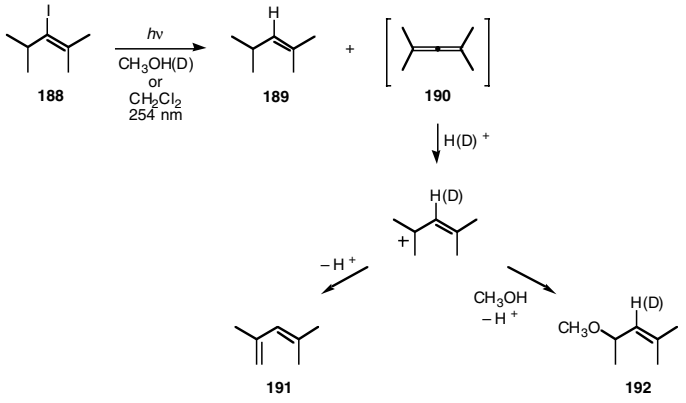

The exocyclic analog **193** similarly displays competing radical and ionic photobehavior. This is significant since vinyl cations generally require stabilization by an α substituent. Except for (halomethylene)cyclopropanes and β-aryl systems, which gain special stabilization from the β substituents, α-unsubstituted vinyl cations have not been generated solvolytically. Interestingly, the resulting vinyl cation **194**, which can assume the preferred linear geometry of an sp-hybridized center, undergoes rearrangement to the cyclohexenyl cation **170**, which is α-substituted but cannot be linear. Thus, irradiation of iodide **193** in CH_2Cl_2 or $(CH_2OH)_2$ afforded the reduction product **195** and either the vinyl chloride **173** or acetal **174**, respectively.[52]

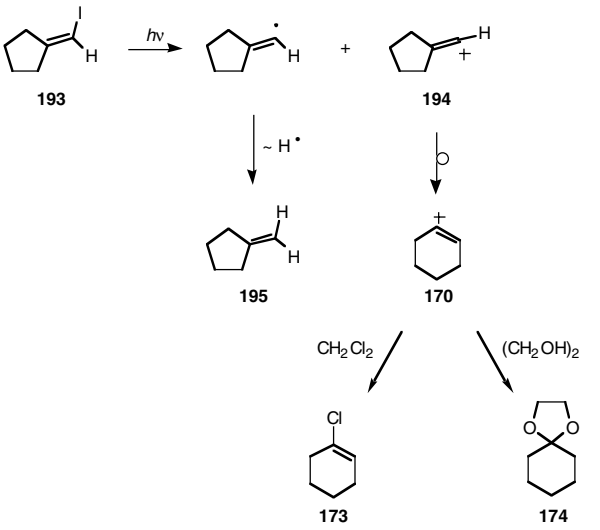

Analogous behavior was exhibited by the higher homolog (iodomethylene)cyclohexane.[52] The smaller homolog **196**, however, proved to be a poor precursor to the highly strained cyclopentenyl cation **201**. Irradiation in CH_2Cl_2 afforded principally the enyne **202**, along with small amounts of the reduction product **197** and vinyl chlorides **198** and **178**.[52] It is not clear whether enyne **202** arises from fragmentation of the radical **199** or cation **200**.

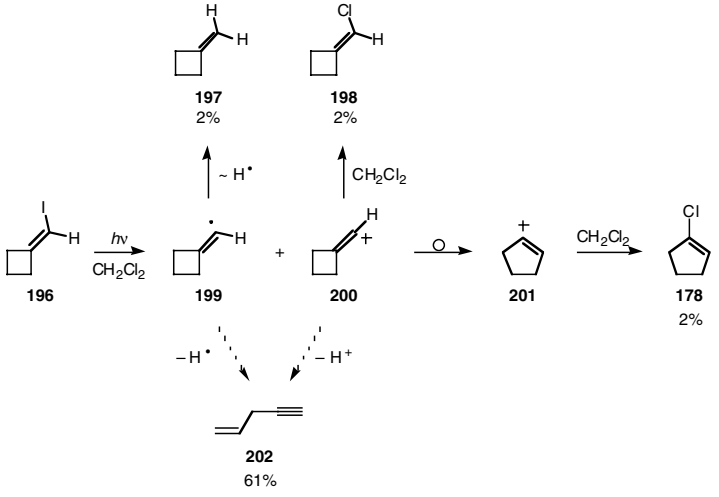

The exocyclic vinyl halides **203** clearly show the strong effect of α substituents on vinyl cations. The α-unsubstituted derivatives **203** (R = H), which are inert toward methanolic $AgNO_3$, afforded only the reduction product camphene [**204** (R = H)] on irradiation in CH_3OH.[54] Ring expansion as exhibited by the exocyclic iodide **193** would afford a highly strained bicyclo[3.2.1]octenyl cation. By contrast, the methyl derivatives **203** (R = CH_3) afforded a mixture of the reduction products **204** (R = CH_3) and the allene **205**, and the phenyl derivatives **203** (R = C_6H_5) afforded principally the ethers **206** (R = CH_3) in CH_3OH.[54] The ratio of ethers **206** to reduction products **204** (R = C_6H_5) from bromide **203b** (R = C_6H_5) was 3.2:1.5:0.1:0.9 for the solvent series CH_3OH, CH_3CH_2OH, $(CH_3)_2CHOH$, and $(CH_3)_3COH$, respectively.[55] This follows the decreasing polarity of these solvents except for $(CH_3)_2CHOH$, which is an excellent hydrogen atom donor.

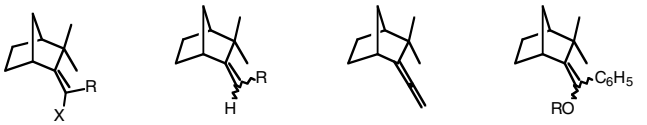

203a, X = I
b, X = Br

204 **205** **206**

The research groups of Taniguchi, Zupan, and Lodder have extensively studied the photobehavior of aryl-substituted vinyl halides.[56] Numerous examples of competing radical and ionic photobehavior have been observed; detailed review is beyond the scope of this report. Two of the earliest studies involved the 2,2-diarylvinyl halides **207**, which underwent predominant rearrangement–elimination to the tolans **208**, along with competing formation of several radical products.[57,58]

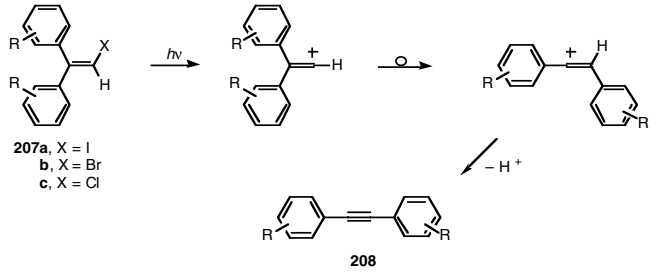

207a, X = I
b, X = Br
c, X = Cl

208

Alkynyl Halides

Early studies concentrated mostly on phenylethynyl halides and were interpreted in terms of radical intermediates.[59] Specific attempts to induce ionic photobehavior from the 1-halo-1-hexynes **209** in polar media, including the use of low temperature and viscous solvents, afforded almost exclusively radical-derived products.[15] This is consistent with the high ionization potentials of 1-alkynyl radicals.

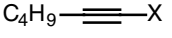

209a, X = I
b, X = Br

Iodocyclopropane

Irradiation of iodocyclopropane (**210**) in benzene solution afforded allyl iodide (**211**).[60] In the presence of TEMPO, products from trapping of both cyclopropyl radical and allyl radical were obtained. Since the ratio of the two products was not dependent on the concentration of TEMPO, the allyl radical is apparently a direct photoproduct rather than a secondary product from rearrangement of cyclopropyl radical. *Ab initio* calculations suggested that allyl radical arises via two crossings between open-shell and closed-shell surfaces; the $^1(n\sigma^*)$ state of iodocyclopropane (**210**) experiences a symmetry-allowed intersection with the closed-shell ion pair. The cyclopropyl cation thus generated undergoes a barrierless ring opening to generate allyl cation. In a second surface crossing, the resulting ion pair undergoes back electron transfer, by way of the same symmetry-allowed conical intersection, to generate allyl radical and an iodine atom. It is not clear how general such surface crossings may be in alkyl halides.

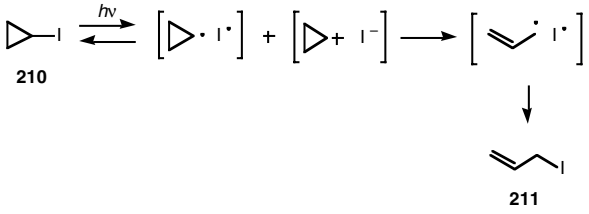

210 **211**

Alkyl Chlorides

Alkyl chlorides have been little studied because they absorb only at very short wavelengths. However, they form charge-transfer complexes with alcohols and amines that absorb at more accessible wavelengths. Irradiation of alkyl chlorides in the presence of amines is discussed above. Direct irradiation of 1-chloroadamantane (**41c**) and -norbornane (**8c**) in alcoholic solvents afforded ethers **43a–b** and **10** with quantum yields of 0.9–1.4 × 10^{-7} and 1.5 × 10^{-9}, respectively, in unstated chemical yields.[20b] Extended irradiation of (1*R*,2*S*,5*R*)-menthyl chloride (**212**) in CH_3OH afforded ether **213** in unstated yield.[20b] Interestingly, the 1*R*,2*S*,5*R* isomer was the only observed substitution product, although the C-5 epimer was apparently not specifically looked for.

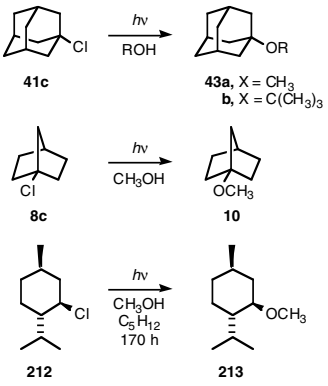

Dihalides

Dihalides undergo photocleavage of a single carbon–halogen bond and, like monohalides, exhibit competing radical and ionic behavior. In the case of geminal diiodides, the α-iodo substituent stabilizes the adjacent cation, facilitating ionic behavior.

Vicinal Dihalides

Laser flash photolysis of 1,2-dibromoethane (**214**) afforded two bromine atoms per photon absorbed.[61] Irradiation of dihaloketones **215** in CH_3OH afforded the (*E*)-enones **216**.[62] Competing ionic behavior resulted in accompanying formation of the dimethoxy derivatives **217**. The corresponding dibromoesters **218** gave a mixture of the *E*- and *Z*-unsaturated esters **219**.[62] Absorption by the phenyl group was apparently critical under the reaction conditions, since the aliphatic analog **220** afforded bromides **221** and **222** instead of the enones **223**.[62] This problem was avoided by irradiation in the presence of $(C_2H_5)_3N$, which presumably involves radical anion formation (Scheme 1). Under these conditions, a wide variety of vicinal dihalides undergo dehalogenation in moderate to excellent yields.[59,63]

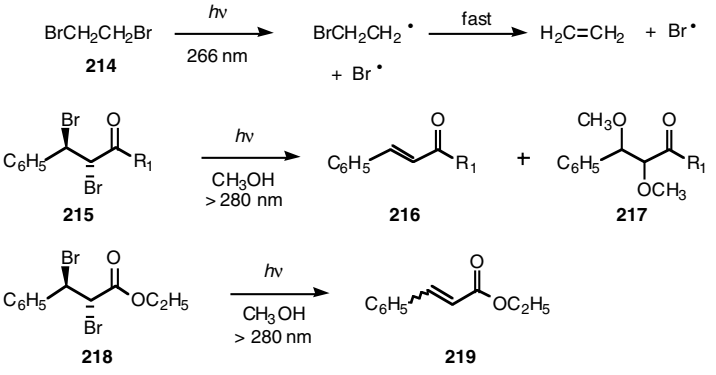

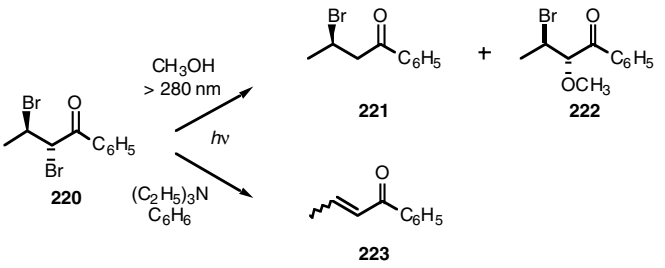

Geminal Dihalides

Appropriate dihalomethanes effect cyclopropanation of alkenes, whereas their higher homologs, which are capable of undergoing elimination, exhibit intramolecular behavior.

Dihalomethanes: Cyclopropanation of Alkenes

H.E. Simmons, co-discoverer of the cyclopropanation of alkenes with CH_2I_2 and Zn(Cu) couple, and co-workers observed early on that irradiation of CH_2I_2 in the presence of cyclohexene (**116**) afforded norcarane (**224**).[64] Because there was an accompanying formation of a mixture of the methylcyclohexenes **225**, which appeared to result from indiscriminate insertion into CH bonds as well as the π bond, it was concluded that the main product-forming intermediate is an excited state of CH_2I_2 accompanied by free CH_2**:**.[64] However, subsequent studies showed that the methylcyclohexenes **225** are secondary products that can be avoided by stirring the irradiation mixture with a scavenger solution to remove I_2 and HI.[10,65] Under these conditions, norcarane (**224**) is the exclusive product and can be isolated in excellent yield.[65] The procedure has proved effective for the cyclopropanation of a number of alkenes — especially sterically hindered ones such as **226**, which give little or no addition by the traditional Zn(Cu) couple procedures.[65,66] Addition occurs stereoselectively, with retention of stereochemistry. The relative rates of addition to the cyclohexenes **116**, **225a**, and **228** increase with increasing substitution — in contrast to the Zn(Cu) couple method, in which steric effects result in a decreased rate for the tetrasubstituted alkene **228**.[67]

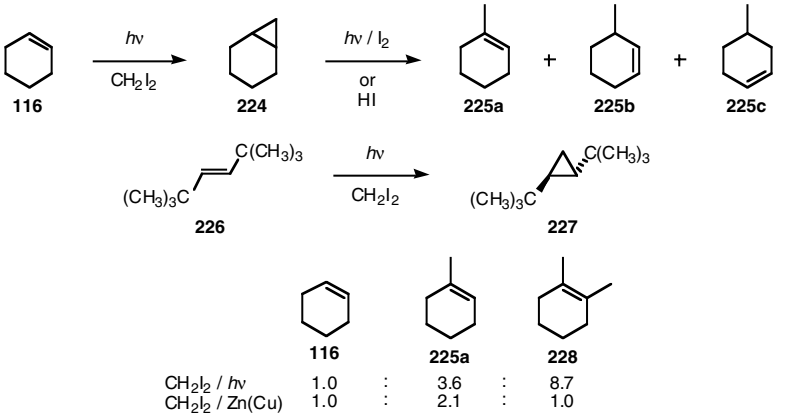

Cyclopropanation has also been observed on irradiation of CH_2Br_2 in the presence of alkenes, although in low yield.[68] However, irradiation of diiodo- or dibromohalomethanes in the presence of alkenes affords halocyclopropanes in good yield, as exemplified by formation of the 7-halonorcaranes **229**.[68,69]

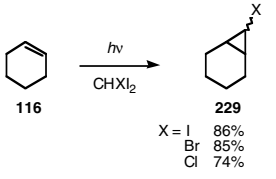

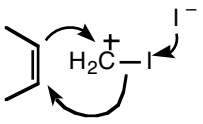

SCHEME 8

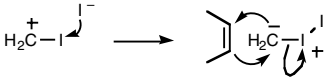

SCHEME 9

Based on the electrophilic nature of the reactive intermediate and on the photobehavior of higher homologs of CH_2I_2 described in the following section, it was proposed that photocyclopropanation involves attack of the ion pair $^+CH_2I\ I^-$ on the alkene (Scheme 8).[65] In support of this, irradiation of CH_2I_2 in the presence of LiBr afforded CH_2IBr and CH_2Br_2. Also, 1,2-dimethylcyclobutene (**230**) afforded the vinyl iodides **231**, as expected from initial addition of ^+CHXI followed by rearrangement.[69]

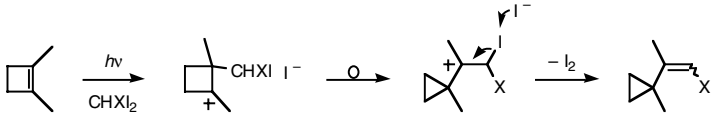

230 **231**

a, X = I; **b**, X = Cl

However, an isomeric intermediate, referred to as isodiiodomethane, has been observed on irradiation of CH_2I_2 in an argon or nitrogen matrix[70] or in solution,[71] for which the iodo-iodonium methylide structure (**232**) has been assigned.[72] Analogous intermediates have been observed for a number of other polyhalomethanes[73] except for CH_2FI, which showed no detectable isomerization.[73b] Isodiiodomethane (**232**) has been shown to react with cyclohexene (**116**) to afford I_2 and, presumably, norcarane (**224**), but no organic product was reported.[74] It has been proposed that isodiiodomethane (**232**) is the methylene transfer agent mainly responsible for cyclopropanation of alkenes on irradiation of CH_2I_2.[74,75] This is equivalent to involvement of the ion pair if the reaction occurs stepwise, since an initial attack of I^- on I would afford isodiiodomethane (**232**) (Scheme 8). Moreover, the ion pair may simply be regarded as a resonance form of isodiiodomethane (**232**).

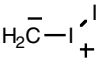

232

Higher Homologs

Elimination dominates the photobehavior of higher homologs. Early studies involved diiodide **233**, which on irradiation afforded the reduction and elimination products **234** and **158**.[10] The dimethyl derivative **235**, which is incapable of undergoing elimination, afforded the reduction product **4** almost exclusively.[10] However, it was more recently found that irradiation of diiodide **235** in the more polar solvent $(CH_2Cl)_2$ gives principally the alkene **5**, and irradiation in the polar but nucleophilic solvent CH_3OH affords the acetal **236**.[76,77]

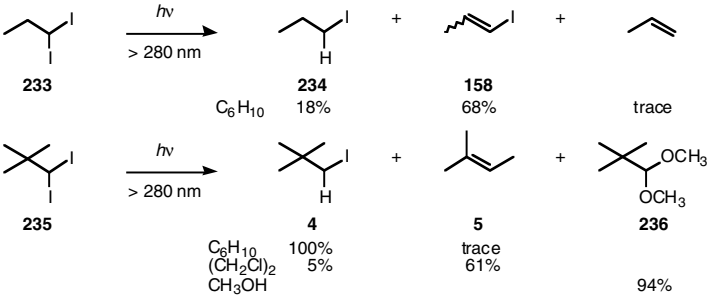

More detailed studies were conducted with the diiodide **237**.[76] Irradiation in a variety of solvents afforded predominantly the vinyl iodide **240**, which can arise from either the radical pair **238** or ion pair **239**. It was obtained from the labeled diiodide **237**-d_1 with complete loss of deuterium. In solvents having a dielectric constant ≥7.5, vinyl iodide **240** was accompanied by methylenecyclohexane (**242**). This is not a secondary product from photoreduction of vinyl iodide **240**, since the latter does not absorb under the irradiation conditions. The labeled diiodide **237**-d_1 afforded alkene **242**-$\boldsymbol{d_1}$, with almost complete retention of deuterium, which was located at the methylene position as expected from hydride rearrangement of the ion pair **239** followed by loss of I_2. Polar solvents apparently facilitate rearrangement of the ion pair **239**. Although shown here as stepwise, rearrangement and loss of I_2 may occur concertedly, in analogy with the mechanism for the cyclopropanation of alkenes (cf **227**). In the polar, but nucleophilic, solvent CH_3OH, trapping afforded the α-iodo ether **241a**, which underwent subsequent methanolysis to acetal **241b** as the principal product to the exclusion of methylenecyclohexane (**242**).

The bromo iodo derivative **243a** afforded mainly the elimination product **245**, whereas the dibromide **243b** gave mainly the reduction product **244** in the solvents $(C_2H_5)_2O$, CH_2Cl_2, and CH_3OH.[76] The cyclopentyl analog **246** displayed behavior analogous to that of diiodide **237** except for giving a mixture of methylenecyclopentane (**195**) and the ring-expanded cyclohexene (**116**), along with the vinyl iodide **193**, in CH_2Cl_2.[76] The cyclobutyl analog **248** afforded only the ring-expanded cyclopentene **250** and the vinyl iodide **249**.[76] Citronellal iodide (**251**) gave a mixture of products **143** and **252**–**254**.[76] Iodide **253** apparently arises from intramolecular trapping of the α-iodo cation **255** and carane (**254**) from competing intramolecular cyclopropanation analogous to that described above for CH_2I_2. It is interesting, however, that intermolecular addition of CH_2I_2 to alkenes gave no trapping analogous to the formation of iodide **253**.

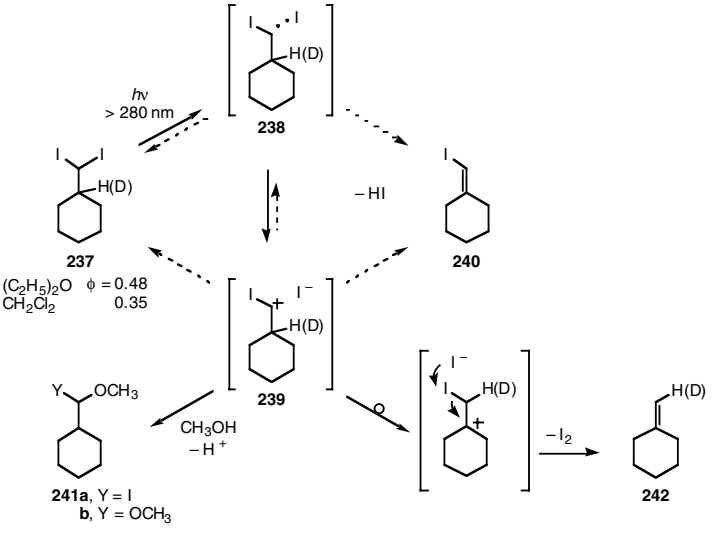

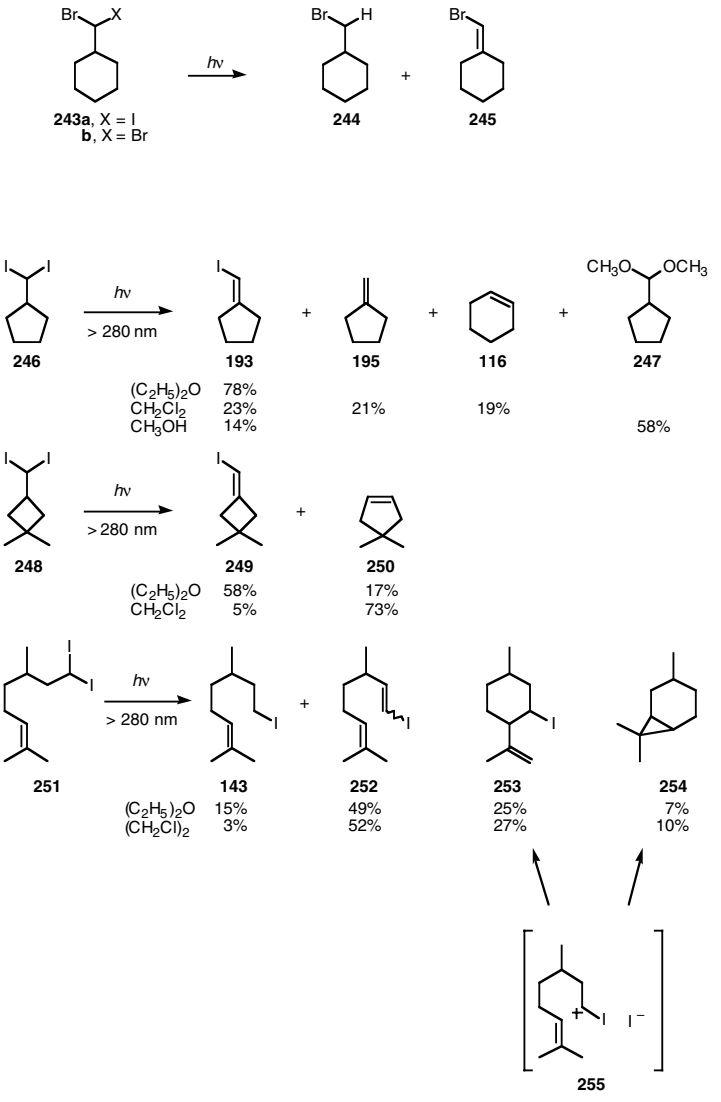

Advantage has been taken of the predominant radical behavior of bromides to effect reduction of the dibromocyclopropanes **256** to the corresponding monobromides **257**.[78] Weak absorption by the monobromides **257** under the irradiation conditions permits the selective removal of a single halogen atom.

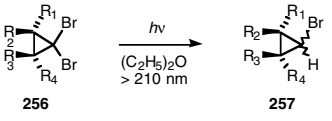

Vinylidene Dihalides

In accord with the trends observed in other systems, the dichloride **258c** gave only the reduction products **260** and **242**, while the dibromide **258b** gave a small amount of the nucleophilic trapping product **259b**, and the diiodide **258a** gave somewhat more of it.[52b] Similar behavior was exhibited by the norbornyl analogs **261**, with the dibromide **261b** affording only the reduction product **203b** and the diiodide **261a**

giving a mixture of iodide **203a** and the ether **262a**.[79] At –10°C, diiodide **261a** gave almost exclusively the ether **262a.** On further irradiation, the vinyl halides **203** underwent secondary conversion to camphene [**204** (R = H)], as described above.

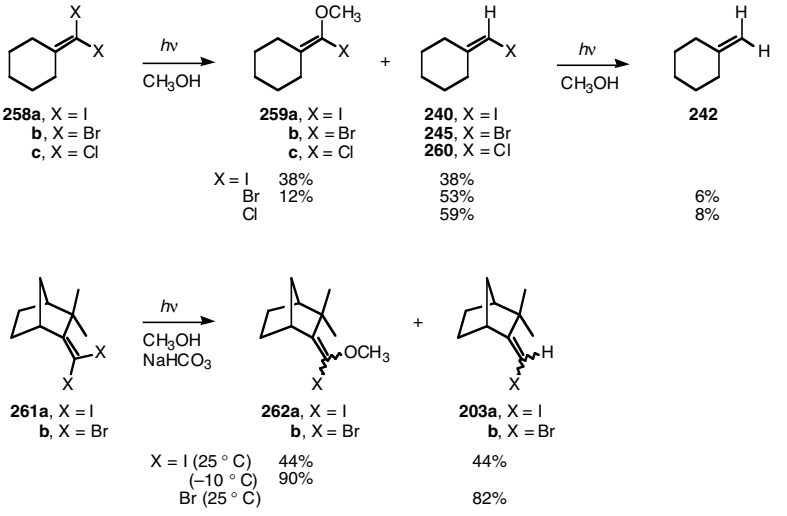

References

1. Kropp, P.J., Fryxell, G.E., Tubergen, M.W., Hager, M.W., Harris, G.D., Jr., McDermott, T.P., Jr., and Tornero-Velez, R., Photochemistry of phenyl thioethers and phenyl selenoethers. Radical vs. ionic behavior, *J. Am. Chem. Soc.,* 113, 7300, 1991.
2. Eaborn, C., Safa, K.D., Ritter, A., and Binder, W., Photoinduced ionic and free-radical reactions of some organosilicon iodides, *J. Chem. Soc., Perkin Trans. 2,* 1397, 1982.
3. Kropp, P.J., Photobehavior of alkyl halides in solution: radical, carbocation and carbene intermediates, *Acc. Chem. Res.,* 17, 131, 1984.
4. (a) Sammes, P.G., Photochemistry of the C–X group, in *Chemistry of the Carbon–Halogen Bond,* Patai, S., Ed., Wiley, London, 1973, chap, 11; (b) Grimshaw, J. and de Silva, A.P., Photochemistry and photocyclization of aryl halides, *Chem. Soc. Rev.,* 10, 181, 1981; (c) Lodder, G., Recent advances in the photochemistry of the carbon–halogen bond, in *The Chemistry of Functional Groups, Supplement D,* Patai, S. and Rappoport, Z., Eds., Wiley, London, 1983, chap. 29; (d) Cristol, S.J. and Bindel, T.H., Photosolvolyses and attendant photoreactions involving carbocations, *Org. Photochem.,* 6, 327, 1983; (e) Lodder, G. and Cornelisse, J., Recent advances in the photochemistry of the carbon–halogen bond, in *Chemistry of Halides, Pseudo-Halides and Azides, Pt. 2,* Patai, S., Ed., Wiley, London, 1995, p. 861.
5. (a) Majer, J.R. and Simons, J.P., Photochemical processes in halogenated compounds, *Adv. Photochem.,* 2, 137, 1967; (b) Okabe, H., *Photochemistry of Small Molecules*, Wiley-Interscience, New York, 1978.
6. (a) Kimura, K. and Nagakura, S., n $\rightarrow \sigma^*$ Absorption spectra of saturated organic compounds containing bromine and iodine, *Spectrochim. Acta,* 17, 166, 1961; (b) Balasubramanian, A., Substituent & solvent effects on the n $\rightarrow \sigma^*$ transition of alkyl iodides, *Indian J. Chem.,* 329, 1963.
7. Kropp, P.J. and Adkins, R.L., Photochemistry of alkyl halides. 12. Bromides vs. iodides, *J. Am. Chem. Soc.,* 113, 2709, 1991.
8. Shepson, P.B. and Heicklen, J., Photooxidation of ethyl iodide at 22°C, *J. Phys. Chem.,* 85, 2691, 1981.

9. McCauley, C.E., Hamill, W.H., and Williams, R.R., Jr., Isomerization in the photolysis of alkyl iodides, *J. Am. Chem. Soc.,* 76, 6263, 1954.
10. Neuman, R.C., Jr. and Wolcott, R.G., Photochemistry of 1,1-diiodoalkanes, *Tetrahedron Lett.,* 6267, 1966.
11. Poindexter, G.S. and Kropp, P.J., Photochemistry of alkyl halides. II. Support for an electron transfer process, *J. Am. Chem. Soc*., 96, 7142, 1974.
12. For a discussion of the concept of "free" cations, see: Keating, J.T. and Skell, P.S., Free carbonium ions, in *Carbonium Ions,* Vol. 2, Olah, G.A. and Schleyer, P.v.R., Eds., Wiley-Interscience, New York, 1970, chap. 15.
13. Kropp, P.J., Poindexter, G.S., Pienta, N.J., and Hamilton, D.C., Photochemistry of alkyl halides. 4. 1-Norbornyl, 1-norbornylmethyl, 1- and 2-adamantyl and 1-octyl bromides and iodides, *J. Am. Chem. Soc.,* 98, 8135, 1976.
14. Leuf, W. and Keese, R., Synthese von 1-hydroxynorbornen aus norcampher, *Chimia,* 36, 81, 1982.
15. Inoue, Y., Fukunaga, T., and Hakushi, T., Direct photolysis of 1-halo-1-hexynes. Lack of ionic behavior, *J. Org. Chem.,* 48, 1732, 1983.
16. Pienta, N.J., The Photochemistry of Alkyl Dihalides. Part I: Geminal Dihalides. Part II: 1,4-Dihalonorbornanes, Ph.D. dissertation, University of North Carolina, Chapel Hill, 1978.
17. Kropp, P.J., Worsham, P.R., Davidson, R.I., and Jones, T.H., Photochemistry of alkyl halides. 8. Formation of a bridgehead alkene, *J. Am. Chem. Soc.,* 104*,* 3972, 1982.
18. Reddy, D.S., Sollott, G.P. and Eaton, P.E., Photolysis of cubyl iodides: access to the cubyl cation, *J. Org. Chem.,* 54, 722, 1989.
19. See: Hrovat, D.A. and Borden, W.T., *Ab initio* calculations find that formation of cubyl cation requires less energy than formation of 1-norbornyl cation, *J. Am. Chem. Soc.,* 112, 3227, 1990.
20. (a) Perkins, R.R. and Pincock, R.E., Photochemical substitution reactions of adamantyl halides, *Tetrahedron Lett.,* 943, 1975; (b) Miller, J.B. and Salvador, J.R. Photoinduced electron-transfer substitution reactions via unusual charge-transfer intermediates, *J. Org. Chem.,* 67, 435, 2002.
21. Sollott, G.P. and Gilbert, E.E., A facile route to 1,3,5,7-tetraaminoadamantane. Synthesis of 1,3,5,7-tetranitroadamantane, *J. Org. Chem.,* 45, 5405, 1980.
22. See also: Kropp, P.J., Gibson, J.R., Snyder, J.J., and Poindexter, G.S., Photochemistry of alkyl halides. 5. 2,4-Dehydroadamantane and protoadamantene from 2-bromo- and 2-iodoadamantane, *Tetrahedron Lett.,* 207, 1978.
23. Davidson, R.I., Tise, F.P., McCraw, G.L., Underwood, G.A., and Kropp, P.J., Unpublished results.
24. Kropp, P.J., Jones, T.H. and Poindexter, G.S., Photochemistry of alkyl halides. 1. Ionic vs. radical behavior, *J. Am. Chem. Soc.,* 95*,* 5420, 1973.
25. Newcomb, M., Sanchez, R.M., and Kaplan, J., Fast halogen abstractions from alkyl halides by alkyl radicals. Quantitation of the processes occurring in and a caveat for studies employing alkyl halide mechanistic probes, *J. Am. Chem. Soc.,* 109, 1195, 1987.
26. Worsham, P.R., The Photochemistry of β-Iodoethers and -esters, Ph.D. dissertation, University of North Carolina, Chapel Hill, 1977.
27. Roth, R.C. and Binkley, R.W., A mechanistic study of the photoreactions of deoxy iodo sugars, *J. Org. Chem.,* 50, 690, 1985.
28. For a review, see: Binkley, R.W., Photochemical reactions of carbohydrates, *Adv. Carbohydr. Chem. Biochem.,* 38, 105, 1981.
29. Gokhale, P.D., Joshi, A.P., Sahni, R., Naik, V.G., Damodaran, N.P., Nayak, U.R., and Dev, S., Photochemical transformations. I. Reactions of some terpene iodides, *Tetrahedron*, 32, 1391, 1976.
30. Takaishi, N., Miyamoto, N., and Inamoto, Y., Ring enlargement of the photochemically generated *endo*-2,3-trimethylenenorborn-*exo*-2-ylcarbinyl cation. Occurrence of a different reaction pathway from that in sulfuric acid, *Chem. Lett.,* 1251, 1978.
31. Brown, D.M., Underwood, G.A., and Kropp, P.J., Unpublished results.
32. Bloom, J.A., Tise, F.P., Suddaby, B.R., and Kropp, P.J., Unpublished results.

33. McNeely, S.A., The Photobehavior of Unsaturated Alkyl Halides, Ph.D. dissertation, University of North Carolina, Chapel Hill, 1976.
34. Kropp, P.J., Sawyer, J.A., and Snyder, J.J., Photochemistry of alkyl halides. 11. Competing reaction via carbene and carbocationic intermediates, *J. Org. Chem.,* 49, 1583, 1984.
35. McCabe, P.H., de Jenga, C.I., and Stewart, A., Photochemical and assisted cleavages of halo-9-thiabicyclononanes, *Tetrahedron Lett.,* 22, 3681,1981.
36. (a) Olofson, R., Walinsky, S.W., Marino, J.P., and Jernow, J.L., Carbenes from carbonium ions. I. Dithiomethoxymethyl cation and its conversion to tetrathiomethoxyethylene, *J. Am. Chem. Soc.,* 90, 6554, 1968; (b) Curtin, D.Y., Kampmeier, J.A., and O'Connor, B.R., Possible divalent carbon intermediates, *J. Am. Chem. Soc.,* 87, 863, 1965.
37. (a) Kurz, M. and Rodgers, M., Photochemical aromatic cyclohexylation, *J. Chem. Soc., Chem. Commun.,* 1227, 1985; (b) Kurz, M.E., Noreuil, T., Seebauer, J., Cook, S., Geier, D., Leeds, A., Stronach, C., Barnickel, B., Kerkemeyer, M., Yandrasits, M., Witherspoon, J., and Frank, F.J., Photochemical aromatic alkylation, *J. Org. Chem.,* 53, 172, 1988.
38. Ogata, Y., Tomizawa, K., and Furuta, K., Photochemical reactions of methyl iodide with aromatic compounds, *J. Org. Chem.,* 46, 5276, 1981.
39. Birchall, J.M., Irvin, G.P., and Boyson, R.A., Reactions of trifluoromethyl radicals. Part I. The photochemical reactions of trifluoroiodomethane with benzene and some halogenobenzenes, *J. Chem. Soc., Perkin Trans. 2,* 435, 1975.
40. Camaggi, C.M., Leardini, R., and Zanirato, P., Photolysis of allyl iodide in aromatic solvents, *J. Org. Chem.,* 42, 1570, 1977.
41. (a) Kimoto, H., Fujii, S., and Cohen, L.A., Photochemical perfluoroalkylation of imidazoles, *J. Org. Chem.,* 47, 2867, 1982; (b) Kimoto, H., Fujii, S., and Cohen, L.A., Photochemical trifluoromethylation of some biologically significant imidazoles, *J. Org. Chem.,* 49, 1060, 1984.
42. (a) Charlton, J.L., Williams, G.J., and Lypka, G.N., The photochemistry of 4-phenyl-1-iodobutane and 4-phenyl-2-iodomethyl-1-butene, *Can. J. Chem.,* 58, 1271, 1980; (b) Bhalerao, V.K., Nanjundiah, B.S., Sonawane, H.R., and Nair, P.M., Photolysis of 2-phenylethyl and 4-phenyl-1-butyl halides in alcoholic solvents, *Tetrahedron,* 42, 1487, 1986; (c) Subbarao, K.V., Damodaran, N.P., and Dev, S., Photochemical transformations—V. Organic iodides (part 4): Solution photochemistry of 4-phenyl-1-iodobutane and 4-phenyl-1-bromobutane, *Tetrahedron,* 43, 2543, 1987.
43. Saplay, K.M., Sahni, R., Damodaran, N.P., and Dev, S., Photochemical transformations — II. Organic iodides—II: cetronellyl iodide, 2,3-dihydro-6(*Z*)-farnesyl and 2,3-dihydro-6(*E*)-farnesyl iodides, *Tetrahedron,* 36, 1455, 1980.
44. Saplay, K.M., Damodaran, N.P., and Dev, S., Photochemical transformations — III. Organic iodides (part 3): geranyl and neryl iodides and 2(*E*),6(*E*)- and 2(*Z*),6(*E*)-farnesyl iodides, *Tetrahedron,* 39, 2999, 1983.
45. Cossy, J., Ranaivosata, J.-L., and Bellosta, V., Formation of radicals by irradiation of alkyl halides in the presence of triethylamine, *Tetrahedron Lett.,* 35, 8161, 1994.
46. (a) Nagahara, K., Ryu, I., Komatsu, M., and Sonoda, N., Radical carboxylation: ester synthesis from alkyl iodides, carbon monoxide and alcohols under irradiation conditions, *J. Am. Chem. Soc.,* 119, 5465, 1997; (b) Ryu, I., Radical carboxylations of iodoalkanes and saturated alcohols using carbon monoxide, *Chem. Soc. Rev.,* 30, 16, 2001.
47. Neuman, R.C., Jr., Photochemistry of *cis*- and *trans*-1-iodopropene, *J. Org. Chem.,* 31, 1852, 1966.
48. For analogous behavior by iodoethene, see: Roberge, P.C. and Herman, J.A., Photolyse de l'iodure de vinyle en solution dans le tetrachlorure de carbone, *Can. J. Chem.,* 42, 2262, 1964.
49. Neuman, R.C., Jr. and Holmes, G.D., Photolytic formation of isomeric vinyl radicals from *cis*- and *trans*-vinyl iodides, *J. Org. Chem.,* 33, 4317, 1968.
50. Müller, J.P.H., Parlar, H., and Korte, F., Einfache photochemische Methode zur deuterierung von Olefinen und Aromaten, *Synthesis,* 524, 1976.
51. Walia, S., Dureja, P., and Mukerjee, S.K., Photoreductive dehalogenation of 5-bromomethyl-1,2,3,4,7,7-hexachloro-2-norbornene (bromodan) — a cyclodiene insecticide, *Tetrahedron*, 43, 2493, 1987.

52. (a) McNeely, S.A. and Kropp, P.J., Photochemistry of alkyl halides. 3. Generation of vinyl cations, *J. Am. Chem. Soc.,* 98, 4319, 1976; (b) Kropp, P.J., McNeely, S.A., and Davis, R.D., Photochemistry of alkyl halides. 10. Vinyl halides and vinylidene dihalides, *J. Am. Chem. Soc.,* 105, 6907, 1983.
53. Sonawane, H.R., Nanjundiah, B.S., and Rajput, S.I., Photochemistry of vinyl halides: Part II. Reactions of some conformationally rigid vinyl halides derived from isolongifolene & neoisolongifolene, *Indian J. Chem.,* 23B, 339, 1984.
54. Sonawane, H.R., Nanjundiah, B.S., and Rajput, S.I., Photochemistry of vinyl halides: Part I. Radical versus ionic photobehavior of some vinyl halides based on camphene, *Indian J. Chem.,* 23B, 331, 1984.
55. Sonawane, H.R., Nanjundiah, B.S., Udaykumar, M., and Panse, M.D., Photochemistry of vinyl halides: Part III — Photolysis of ω-bromo-ω-phenylcamphene in different solvents & its mechanistic implications, *Indian J. Chem.,* 24B, 202, 1985.
56. (a) For an extensive compilation of references, see: van Ginkel, F.I.M., Cornelisse, J., and Lodder, G., Photoreactivity of some α-arylvinyl bromides in acetic acid. Selectivity toward bromide versus acetate ions as a mechanistic probe, *J. Am. Chem. Soc.,* 113, 4261, 1991. See also: (b) Kitamura, T., Kabashima, T., Kobayashi, S., and Taniguchi, H., Isolation and alcoholysis of an ipso adduct, vinylidenecyclohexadiene, from photolysis of 1-(*p*-ethoxyphenyl)vinyl bromide, *Tetrahedron Lett.,* 29, 6141, 1988; (c) Kitamura, T., Nakamura, I., Kabashima, T., Kobayashi, S., and Taniguchi, H., A novel spiro adduct from intramolecular *ipso* substitution in the photolysis of an α-[*p*-(2-hydroxyalkoxy)phenyl]vinyl bromide, *J. Chem. Soc., Chem. Commun.,* 1154, 1989; (d) Kitamura, T., Kobayashi, S., and Taniguchi, H., Photolysis of vinyl halides. Reaction of photogenerated vinyl cations with cyanate and thiocyanate ions, *J. Org. Chem.,* 55, 1801, 1990; (e) Hori, K., Kamada, H., Kitamura, T., Kobayashi, S., and Taniguchi, H., Theoretical and experimental study on the reaction mechanism of photolysis and solvolysis of aryvinyl halides, *J. Chem. Soc., Perkin Trans. 2,* 871, 1992.
57. Suzuki, T., Sonoda, T., Kobayashi, S., and Taniguchi, H., Photochemistry of vinyl bromides: a novel 1,2-aryl group migration, *J. Chem. Soc., Chem. Commun.,* 180, 1976.
58. (a) Sket, B., Zupan, M., and Pollak, A., The photo-Fritsch-Buttenberg-Wiechell rearrangement, *Tetrahedron Lett.,* 783, 1976; (b) Sket, B. and Zupan, M., Photochemistry of 2-halogeno-1,1-diphenylethylenes. The photo-Fritsch-Buttenberg-Wiechell rearrangement, *J. Chem. Soc., Perkin Trans. 1,* 752, 1979.
59. See ref 15 for a compilation of references.
60. Arnold, P.A., Cosofret, B.R., Dylewski, S.M., Houston, P.L., and Carpenter, B.K., Evidence of a double surface crossing between open and closed-shell surfaces in the photodissociation of cyclopropyl iodide, *J. Phys. Chem. A.,* 105, 1693, 2001.
61. Scaiano, J.C., Barra, M., Calabrese, G., and Sinta, R., Photochemistry of 1,2-dibromomethane in solution. A model for the generation of hydrogen bromide, *J. Chem. Soc., Chem. Commun.,* 1418, 1992.
62. Izawa, Y., Takeuchi, M., and Tomioka, H., Photo-dehalogenation of vicinal dihalide to olefin, *Chem. Lett.,* 1297, 1983.
63. Takagi, K. and Ogata, Y., Ultraviolet light induced dechlorination of vicinal polychlorocyclohexanes with triethylamine, *J. Org. Chem.,* 48, 1966, 1983.
64. Blomstrom, D.C., Herbig, K., and Simmons, H.E., Photolysis of methylene iodide in the presence of olefins, *J. Org. Chem.,* 30, 959, 1965.
65. Kropp, P.J., Pienta, N.J., Sawyer, J.A., and Polniaszek, R.P., Photochemistry of alkyl halides — VII. Cyclopropanation of alkenes, *Tetrahedron,* 37, 3229, 1981.
66. Kropp, P.J. and Tise, F.P., Photochemistry of alkenes. 8. Sterically congested alkenes, *J. Am. Chem. Soc.,* 103, 7293, 1981.
67. Rickborn, B. and Chan, J.H.-H., Conformational effects in cyclic olefins. The relative rates of iodomethylzinc addition, *J. Org. Chem.,* 32, 3576, 1967.
68. Marolewski, T. and Yang, N.C., Photochemical addition of polyhalogenomethanes to olefins, *J. Chem. Soc., Chem. Commun.,* 1225, 1967.

69. Yang, N.C. and Marolewski, T.A., The addition of halomethylene to 1,2-dimethylcyclobutene, a methylene–olefin reaction involving a novel rearrangement, *J. Am. Chem. Soc.,* 90, 5644, 1968.
70. Maier, G. and Reisenauer, H.P., Photoisomerization of dihalomethanes, *Angew. Chem.,* 98, 829, 1986.
71. (a) Tarnovsky, A.N., Alvarez, J.-L., Yartsev, A.P., Sundstrom, V., and Akesson, E., Photodissociation dynamics of diiodomethane in solution, *Chem. Phys. Lett.,* 312, 121, 1999; (b) Zheng, X. and Phillips, D.L., Solvation can open the photoisomerization pathway for the direct photodissociation reaction of diiodomethane: transient resonance Raman observation of the isodiiodomethane photoproduct from ultraviolet excitation of diiodomethane in the solution phase, *J. Phys. Chem. A,* 104, 6880, 2000; (c) Kwok, W.M., Ma, C., Parker, A.W., Phillips, D., Towrie, M., Matousek, P., and Phillips, D. L., Picosecond time-resolved resonance Raman observation of the iso-CH_2I-I photoproduct from the "photoisomerization" reaction of diiodomethane in the solution phase, *J. Chem. Phys.,* 113, 7471, 2000.
72. (a) Glukhovtsev, M.N. and Bach, R.D., Methylene-iodonium ylide: an isomer of diiodomethane, *Chem. Phys. Lett.,* 269, 145, 1997.
73. (a) Maier, G., Reisenauer, H.P., Hu, J., Hess, B A., Jr., and Schaad, L. J., Photoisomerization of tetrachloromethane in an argon matrix, *Tetrahedron Lett.,* 30, 4105, 1989; (b) Maier, G., Reisenauer, H.P., Hu, J., Hess, B.A., Jr., and Schaad, L.J., Photochemical isomerization of dihalomethanes in argon matrixes, *J. Am. Chem. Soc.,* 112, 5117, 1990; (c) Zheng, X. and Phillips, D.L., Photoisomerization reaction of CH_2BrI following A-band and B-band photoexcitation in the solution phase: transient resonance Raman observation of the iso-CH_2I-Br photoproduct, *J. Chem. Phys.,* 113, 3194, 2000; (d) Zheng, X., Kwok, W.M., and Phillips, D.L., Solvation effects on the A-band photodissociation of dibromomethane: turning a photodissociation into a photoisomerization, *J. Phys. Chem. A,* 104, 10464, 2000; (e) Zheng, X., Fang, W.-H., and Phillips, D.L., Transient resonance Raman spectroscopy and density functional theory investigation of iso-polyhalomethanes containing bromine and/or iodine atoms, *J. Chem. Phys.,* 113, 10934, 2000; (f) Zheng, X. and Phillips, D.L., Solvation effects on the ultraviolet direct photoisomerization reaction: opening the photoisomerization channel, *Chem. Phys. Lett.,* 324, 175, 2000; (g) Kwok, W.M., Ma, C., Parker, A.W., Phillips, D., Towrie, M., Matousek, P., Zheng, X., and Phillips, D.L., Picosecond time-resolved resonance Raman observation of the iso-CH_2Cl-I and iso-CH_2I-Cl photoproducts from the "photoisomerization" reactions of CH_2ICl in the solution phase, *J. Chem. Phys.,* 114, 7536, 2001; (h) Zheng, X., Lee, C.W., Li, Y.-L., Fang, W.-H., and Phillips, D.L., Transient resonance Raman spectroscopy and density functional theory investigation of iso-$CHBr_2Cl$ and iso-CCl_3Br photoproducts produced following ultraviolet excitation of $CHBr_2Cl$ and CCl_3Br, *J. Chem. Phys.,* 114, 8347, 2001; (i) Li, Y.-L., Chen, D.M., Wang, D., and Phillips, D.L., Time-resolved resonance Raman and density functional theory investigation of iodocyclopropanation and addition reactions with alkenes after ultraviolet photolysis of iodoform, *J. Org. Chem.,* 67, 4228, 2002.
74. Li, Y.-L., Leung, K H., and Phillips, D.L., Time-resolved resonance Raman study of the reaction of isodiiodomethane with cyclohexene: implications for the mechanism of photocyclopropanation of olefins using ultraviolet photolysis of diiodomethane, *J. Phys. Chem. A,* 105, 10621, 2001.
75. Phillips, D.L., Fang, W.-H., and Zheng, X., Isodiiodomethane is the methylene transfer agent in cyclopropanation reactions with olefins using ultraviolet photolysis of diiodomethane in solutions: a density functional theory investigation of the reactions of isodiiodomethane, iodomethyl radical and iodomethyl cation with ethylene, *J. Am. Chem. Soc.,* 123, 4197, 2001.
76. Kropp, P.J. and Pienta, N.J., Photochemistry of alkyl halides. 9. Geminal dihalides, *J. Org. Chem.,* 48, 2084, 1983.
77. Moret, E., Jones, C.R., and Grant, B., Photochemistry of organic geminal diiodides, *J. Org. Chem.,* 48, 2090, 1983.
78. Shimizu, N. and Nishida, S., Photochemical reduction of gem-dibromocyclopropanes, *Chem. Lett.,* 839, 1977.
79. Sonawane, H.R., Nanjundiah, B.S., and Panse, M.D., Photochemistry of organic halides: some interesting features of the photobehaviour of vinyl halides and vinylidene dihalides derived from camphene, *Tetrahedron Lett.,* 26, 3507, 1985.

2

Photochemical Generation of Glycosyl Radicals and Its Applications in Carbohydrate Synthesis

Shigeru Yamago
Osaka City University

Jun-ichi Yoshida
Kyoto University

2.1 Introduction

Addition of glycosyl radicals to alkenes is a key process in the synthesis of *C*-glycosides, which are well known to have potent antiviral, antibacterial, and antitumor activities. While various methods for the synthesis of *C*-glycosides under ionic conditions have been developed, the importance of radical-mediated synthesis should be stressed because of the mild reaction conditions employed. As radicals are neutral species, various polar functional groups in carbohydrate molecules are compatible under the reaction conditions, and the reaction is sometimes carried out without protecting the hydroxyl and amino groups.

Glycosyl radicals can be generated both thermally and photochemically. While the thermal generations using radical initiators are more popular than the photochemical methods to date, the photochemical path will become increasingly important from the viewpoint of selectivity and "green" chemistry. For example, the photochemical method allows radical generation at low temperature, and such mild conditions would be advantageous for chemo- and stereoselective reactions. In addition, radical generation by direct photolysis enables atom-economical reactions without using radical initiators or promoters. Furthermore, the absence of radical promoters can prevent undesirable competing side reactions of chain-carrying radicals, such as reduction of the glycosyl radical by tin hydride. Because of the importance of glycosyl radicals in organic synthesis, several reviews on this subject have been published recently.[1] However, no systematic reviews that focus on the photochemical reactions have been published. This

0-8493-1348-1/04/$0.00+$1.50

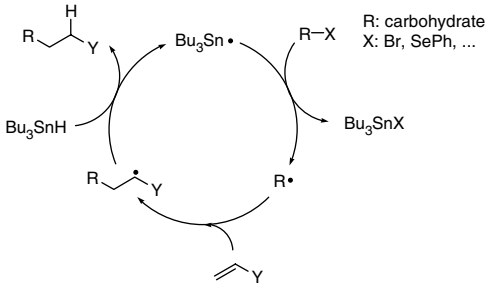

SCHEME 1

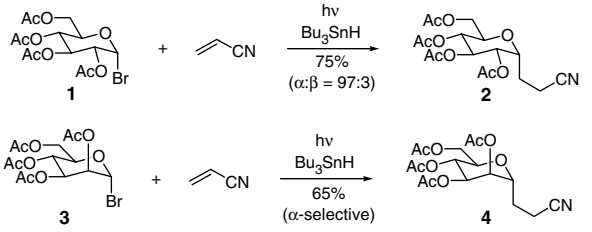

SCHEME 2

review, therefore, will survey the photochemical generation of glycosyl radicals and applications to *C*-glycoside syntheses. This review also includes the photochemical generation of glycosyl carbenes, which are potentially important neutral and reactive species in *C*-glycoside synthesis.

2.2 Intermolecular Carbon–Carbon Bond Formation

Tin Hydride–Mediated Reaction

The tin hydride–mediated radical coupling reaction has been widely utilized in carbon–carbon bond formation under both thermal and photochemical conditions after the seminal reports from Giese's group. Among various haloglycosides and chalcogenoglycosides, bromo- and selenoglycosides have been widely utilized due to their stability under reaction conditions as well as the ease of preparation. The reaction is promoted by a tributyltin radical generated from tributyltin hydride through the radical chain mechanism shown in Scheme 1. Thus, the tributyltin radical reduces haloglycosides or chalcogenoglycosides to produce glycosyl radical R, which adds to alkenes. The subsequent hydride abstraction of the resulting radical species from tributyltin hydride gives the coupling product with the regeneration of the tributyltin radical.

Specific examples starting from bromoglycosides are shown in Scheme 2. Giese et al., reported that the glycosyl radical generated from the α-bromoglucopyranoside **1** by photolysis in the presence of tributyltin hydride and an excess of acrylonitrile gives the *C*-glycoside **2** in 75% yield.[2,3] The reaction predominantly gives the α-isomer, but a small amount of the β-isomer is also formed (α:β = 97:3). Bromomannoside **3** also reacts with acrylonitrile under similar conditions and exclusively gives the α-isomer of *C*-glycoside **4** in good yield.

Giese rationalized the observed high α-stereoselectivity in terms of the stereoelectronic effects of radical species, namely the radical anomeric effects, by electron spin resonance (ESR) spectroscopy, as shown in Scheme 3.[4] The ESR of the glucopyranosyl radical **5** suggests that **5** adopts a boat rather than a chair conformation. This is attributed to the strong stabilizing interactions between the singly occupied molecular orbital (SOMO) of the radical and both the *n*-orbital of the adjacent pyranose oxygen and the

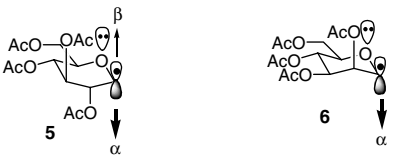

SCHEME 3

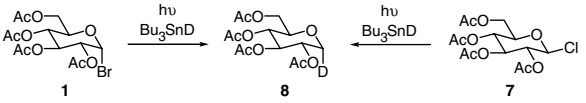

SCHEME 4

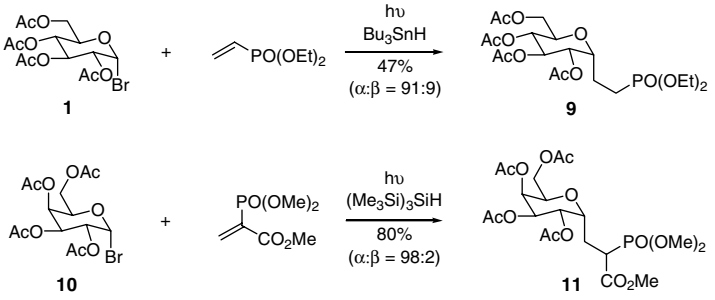

SCHEME 5

σ^*-orbital of the C2 carbon–oxygen bond. The reaction with alkene takes place preferentially from the more sterically accessible α-face (equatorial-like attack) in this conformation. This face selectivity is also electronically favored because the interaction of SOMO and the *n*-orbital is maintained during the bond-forming process. The mannosyl radical **6**, on the other hand, does not undergo conformational change and adopts a chair conformation due to the favorable stereoelectronic effects within this conformation. The reaction with alkene takes place exclusively from the sterically and electronically favored α-face.

The conformational change from the chair form in the radical precursors to the boat form in the anomeric glycosyl radicals is so rapid that stereochemical memory is lost upon the generation of the radical. Thus, the reduction of β- and α-haloglycosides **1** and **7** by tributyltin deuteride afforded α-deuterated product **8** regardless of the stereochemistry of the starting materials (Scheme 4).[5]

The reactivity of glycosyl radicals is unaffected by photo irradiation, but the photochemical method also suffers the following problems similar to those involved in the thermal method. First, since the anomeric glycosyl radicals are nucleophilic in character due to the interaction of the SOMO and the *n*-orbital of the pyranose oxygen, the alkene acceptors can only be electron deficient. Second, because the glycosyl radicals, e.g., R radical in Scheme 1, competitively react with tin hydride to form the reduced product, e.g., RH, a large excess of alkenes (usually 5- to 20-fold excess) is required to avoid undesirable side reactions. Third, because the tin radical must react much faster with the glycosyl radical precursors than with alkenes, the precursors must be sufficiently reactive towards tin radicals. Despite these disadvantages, this method has been widely used in *C*-glycoside synthesis.

Vinyl phosphates are electron-deficient alkenes sufficiently reactive to anomeric glycosyl radicals. Fessner et al. has applied this type of reaction to the synthesis of *C*-glycosyl phosphate derivatives (Scheme 5). Bromoglycoside **1** undergoes *C*-glycosylation with diethyl vinylphosphonate in the presence of tributyltin hydride to give **9** with high α-selectivity.[6] The use of tris(trimethylsilyl)silane, which is an

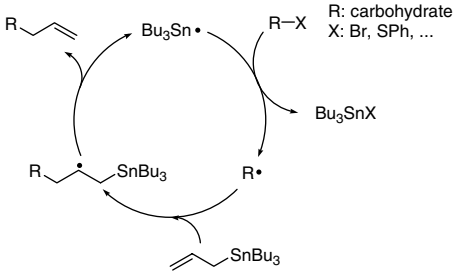

SCHEME 6

environmentally benign analogue of tributyltin hydride,[7] is also effective, and the *C*-glycosylation of bromoglycosides **10** with highly electron-deficient methyl 2-(dimethoxy-phosphoryl)-acrylate in the presence of tris(trimethylsilyl)silane gives **11** in good yield with excellent α-selectivity.[8] Anomeric sugar phosphates possess various important biological functions, and the *C*-glycosyl phosphate analogues can be used as hydrolytically stable mimics of naturally occurring sugar phosphates after hydrolysis of the protecting groups. In addition, the alkyl phosphonate esters are important building blocks as Horner–Wadsworth–Emmons reagents, and the phosphonate ester functional groups in the products can be used for further carbon–carbon bond formations.

Allyltin Method

As a result of the seminal report from Keck's group, the addition of glycosyl radicals to allyltributyltin provides a general method for the preparation of *C*-allyl glycosides. The reaction is also promoted by tin radicals as in the tin hydride–mediated *C*-glycosylation, which reduces haloglycosides and chalcogenoglycosides to generate glycosyl radicals (Scheme 6). The radicals thus generated add to allyltributyltin, followed by the β-elimination of a tributyltin radical from the resulting radical intermediate to give the allylated products with the regeneration of tin radicals. This allylation has two advantages over the tin hydride method. Though the same R radical is generated by the tin hydride method, no competing reduction pathway of the R radical exists in the allylation method. Therefore, the use of a large excess of allyltributyltin is unnecessary. Second, while the alkene functionality is lost in the tin hydride method upon the addition of glycosyl radicals to alkenes, the double bond is retained in the products by the β-elimination of the tin radicals in the allylation reaction. The alkene functionality in the products can be used for further synthetic transformations.

Haloglycosides can be used as radical precursors in certain cases, but they are usually unstable under the reaction conditions. Instead, thioglycosides are more stable, and pyranoside- and furanoside-derived phenylthioglycosides are known to serve as excellent glycosyl radical precursors. The photochemical reaction is usually conducted at room temperature, while the thermal reaction requires elevated temperature, e.g., 80°C, in the presence of a radical initiator (AIBN). Hexabutylditin is sometimes used as a photo-labile radical initiator. The reaction exhibits similar stereoselectivity to that seen with electron-deficient alkenes and is controlled by the radical anomeric effects as discussed earlier in this chapter. Specific examples starting from thioglycosides are shown in Scheme 7.[9] Keck et al. has reported that the photochemical allylation of lyxose-derived thioglycosides **12** with allyltributyltin proceeds to give **13** as a single isomer. Furanose-derived thioglycoside **14** also undergoes stereoselective allylation to give **15** in excellent yield.

Bednarski has reported that this allylation reaction has been used for the key step in the synthesis of *C*-glycoside derivatives of sialic acids, which are the carbohydrate groups found at the terminal sites of cell-surface glycoproteins and glycolipids. Thus, the allylation of glycosyl chloride **16** with allyltributyltin under photo irradiation in the presence of hexabutylditin followed by hydrolysis gives an approximate 1:1 mixture of the α- and β-isomers. It is worth mentioning that while several synthetic approaches by

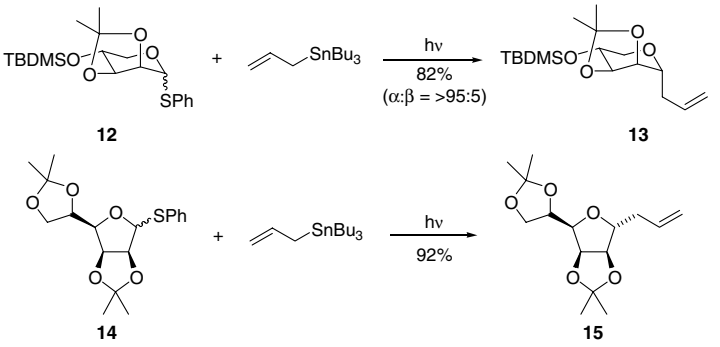

SCHEME 7

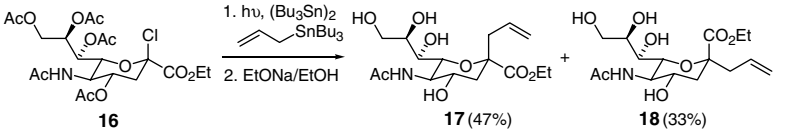

SCHEME 8

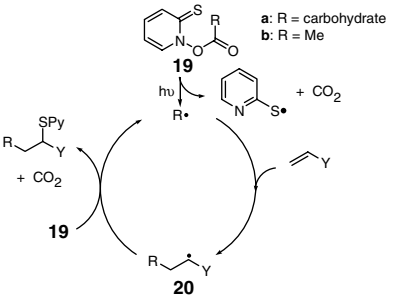

SCHEME 9

ionic reactions, e.g., Lewis acid-mediated allylation reactions, fail, only the radical method is successfully applicable for the synthesis of this highly functionalized allylated product.[10]

Photochemical Fragmentation of Barton Esters

Photochemical decarboxylation of carboxylic acids of 2-thioxo-2*H*-pyridin-1-yl ester **19** (Barton esters) can be applied successfully to *C*-glycosylation reactions according to a radical chain reaction (Scheme 9). The requisite Barton esters are easily prepared from the corresponding carboxylic acid through several synthetic routes by condensation with *N*-hydroxy-2-thiopyridone or its derivatives.[11] Photolysis of Barton ester **19a** generates 2-pyridylthiyl radical, carbon dioxide, and glycosyl radical R, which react with electron deficient alkenes to give **20**. Radical **20** then reacts with the sulfur moiety of **19a** to give the desired coupling product with the regeneration of radical R. The reaction proceeds by a 2-thiopyridyl group transfer, and the thiopyridyl group can be used for further synthetic transformations. For example, tin hydride–mediated radical reduction of the carbon–sulfur bond gives the corresponding reduced products, and oxidation of sulfur gives rise to β-elimination to give alkenes.

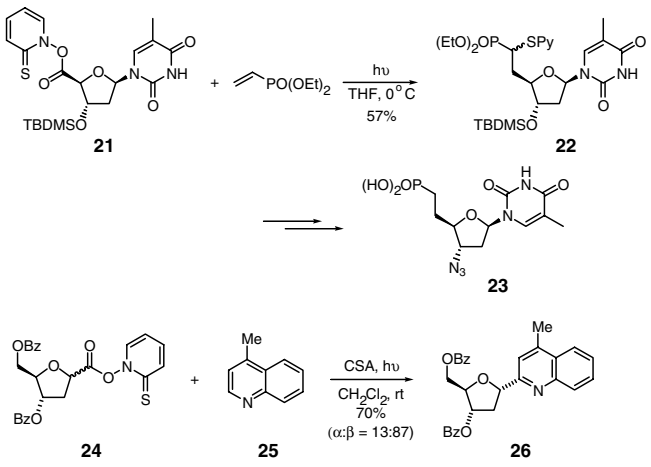

SCHEME 10

Specific examples are shown in Scheme 10. Barton et al. have reported that addition of a furanosyl radical generated from Barton ester **21** to diethyl vinylphosphonate takes place stereoselectively to give group-transfer product **22**. The high stereoselectivity is caused by introducing the bulky *t*-butyldimethylsilyl protecting group (TBDMS) for the C3′ hydroxyl. Radical-mediated reduction of the 2-pyridylthio group in **22** followed by synthetic transformation of the C3′ hydroxyl group to an azide enables the synthesis of the isostere of AZT-5′ monophosphate **23**.[12] Togo et al. have also used Barton esters for the direct synthesis of *C*-nucleosides based on the addition of anomeric glycosyl radicals to activated π-systems of electron-deficient heteroaromatic compounds. For example, the ribofuranosyl radicals generated from **24** add to 4-methylquinoline in the presence of acid to afford **26** in good yield.[13] The addition of an equal amount of acid is required to activate the heteroaromatic compounds.

Barton et al. have reported that a combination of Barton ester **19b** (R = Me) and telluroglycosides under photochemical conditions also generates glycosyl radicals, which initiate *C*-glycosylation via radical chain reaction. Thus, methyl radicals generated by the photolysis of **19b** undergo homolytic substitution with aryltelluroglycosides to generate the resulting anomeric glycosyl radicals and methyl aryl telluride. The glycosyl radicals thus generated react with electron-deficient alkenes followed by 2-pyridylthio-group transfer with **19b** to give *C*-glycosides with the regeneration of a methyl radical. Specific examples starting from pyranose- or furanose-derived telluroglycosides are shown in Scheme 11.[14] Telluroglycoside **27** undergoes *C*-glycosylation with methyl vinyl ketone in the presence of **19b** under photo irradiation to give the group-transfer product **28**. The addition of ribofuranosyl radicals, generated from ribofuranosyl telluride **29**, to maleimide, followed by the oxidative elimination of the 2-pyridylthio group of the coupling product affords **30** as a single product. Deprotection of **30** under acidic conditions provides showdomycin, which belongs to the biologically active *C*-nucleosides. The stereoselective nature of the *C*-glycosylation provides a highly efficient synthetic route.

Direct Photolysis of Cobaloximes

Giese et al. have reported that the alkylcobaloxime complex **31** can act as a radical precursor because irradiation promotes the homolytic cleavage of the Co–C bond (Scheme 12). In the absence of radical traps, the radical R recombines with the Co(II) complex **32** to reform the starting material **31**. Dimerization and disproportionation reactions between the alkyl radicals occur only to a small extent. This feature may be explained by considering that the Co(II) complex **32** serves as a persistent radical.[15] The reversibility of the radical generation process in the current alkylcobaloxime system has advantages over radical chain reactions because competing side reactions involving radical promoters can be minimized.[16,17] In the presence of radical acceptors, such as alkenes, the glycosyl radical R generated from **31** undergoes group-transfer

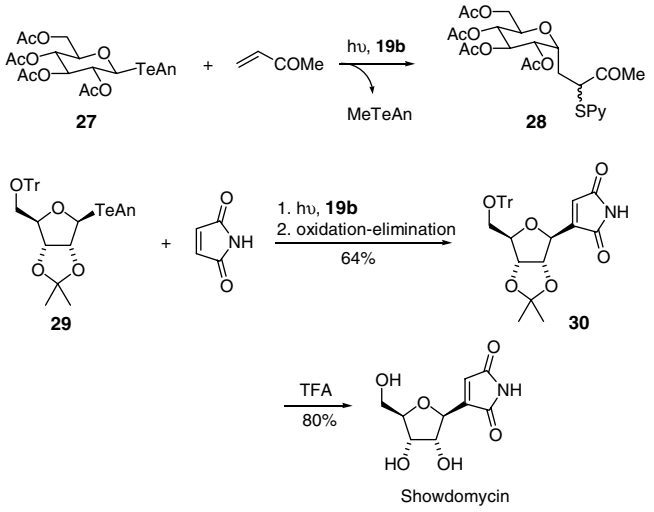

SCHEME 11

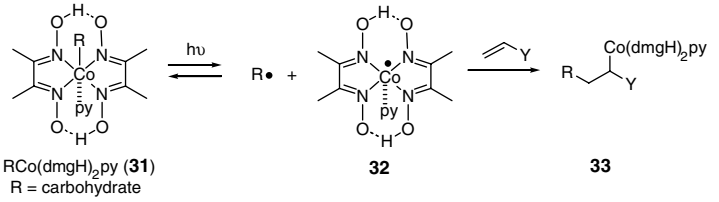

SCHEME 12

addition to alkenes, and the resulting alkylcobaloxime **33** either hydrolyzes or undergoes β-elimination to form alkenes.

Specific examples are shown in Scheme 13. Giese et al. have reported that mannosyl cobalt complex **35**, which can be prepared from bromoglycosides **34** and Co(I) complexes generated from $[Co(dmgH)_2py]_2$ and sodium borohydride, reacts with alkenes under photo irradiation. The initially formed group-transfer product subsequently undergoes solvolysis in methanol or β-hydride elimination to give **36** or **37**, depending on the substituents on the alkenes. Nitrous oxide is a persistent radical and an excellent radical trapping agent, and the trapping of the mannosyl radical generated from cobalt complex **35** by nitrous oxide gives glycosyl oxime **38** with high efficiency.[18]

Direct Photolysis of Organotellurium Compounds

Yamago et al. have reported that direct photolysis of telluroglycosides also generates the corresponding anomeric glycosyl radicals and telluranyl radicals.[19] The radical generation is reversible as is the case with the cobaloximes. As the generated radicals recombine with the starting telluroglycosides in the absence of radical acceptors, isomerization of the anomeric carbon is observed. In the presence of radical acceptors, such as alkynes, the glycosyl radicals group transfer addition reactions.[20] This method offers several advantages. First, telluroglycosides are easily prepared from haloglycosides and are storable for a long period.[21] Second, the current method is free from the problems inherent in the tin hydride methods, such as the addition of tin radical to alkynes[22] or the simple reduction of glycosyl radicals. Finally, because the reaction proceeds via a group transfer, the carbon–tellurium bond in the products can be used for further synthetic transformations.

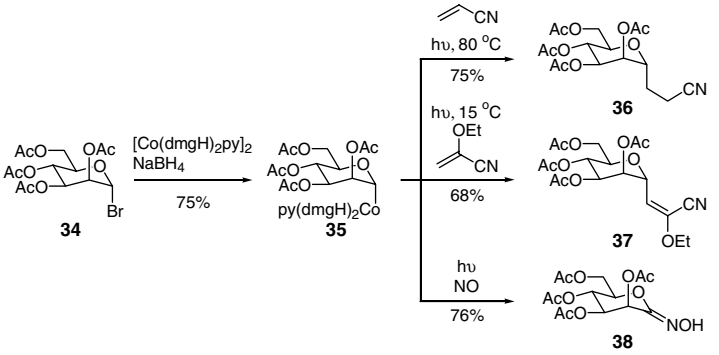

SCHEME 13

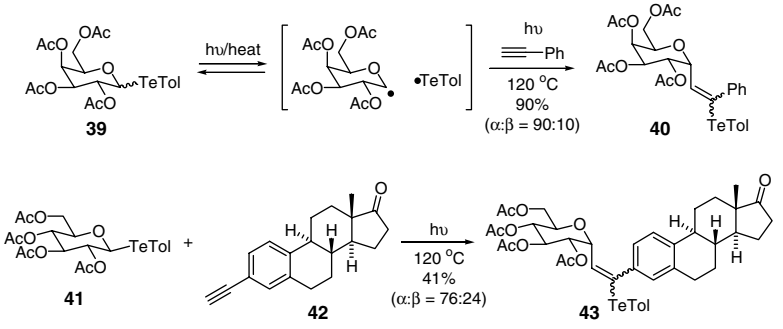

SCHEME 14

Specific examples for the synthesis of vinylic *C*-glycosides are shown in Scheme 14. Conjugated alkynes are excellent acceptors, and the photolysis of galactose-derived telluroglycoside **39** with phenylacetylene at 120°C affords the group transfer product **40** in excellent yield. While the same reaction proceeds in the dark, photo irradiation considerably increases the coupling efficiency. The reaction mainly gives the α-isomer (α:β = 90:10), and the anomeric stereoselectivity is somewhat lower than that in the conventional *C*-glycosylation with alkenes. This method can be applied to the synthesis of the sugar–steroid hybrid molecule **43** by the coupling of telluroglycoside **41** with the steroidal alkyne **42**.

Yamago et al. have also reported that isonitriles serve as excellent glycosyl radical trapping reagents in conjunction with the C1 homologation reaction. Therefore, the reaction of telluroglycoside **41** with xylylisonitrile under photo irradiation at 100°C affords group-transfer coupling product **44** in good yield (Scheme 15).[23] It is worth mentioning that carbon monoxide, which possesses an isoelectronic structure with isonitriles, is a totally inefficient reagent. The reaction proceeds with complete stereoselectivity and gives the α-isomer **44** as the sole product. The observed stereoselectivity is consistent with the anomeric radical effects as discussed earlier in this chapter. The complete α-selectivity is a general trend, and all pyranose-derived telluroglycosides afford the α-anomer with a single exception; the reaction of 2-phthaloyl protected aminoglycoside **48** gives the β-isomer **49** exclusively. The origin of the observed β-selectivity is suggested by the intramolecular participation of the polar C2 phthaloyl (Phth) group to the glycosyl radical to shield the α-face. The imidoylations also take place with complete *syn* selectivity with respect to the stereochemistry of the imine moiety. This is due to the predominant participation of thermodynamically stable *anti* imidoyl radicals in the tellurium-group transfer step.

The imidoylated products serve as important building blocks for the synthesis of a variety of *C*-glycosides through carbon–tellurium bond modifications (Scheme 15). For example, radical-mediated

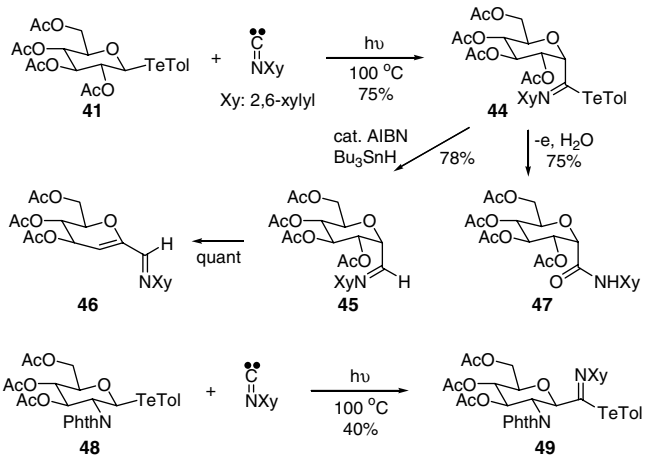

SCHEME 15

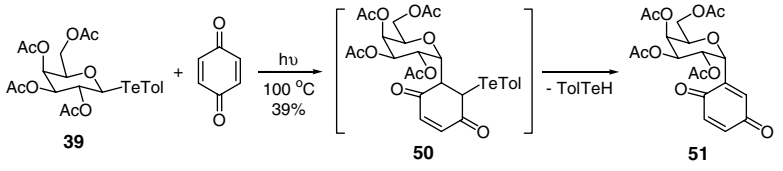

SCHEME 16

reduction of the carbon–tellurium bond in **44** with tributyltin hydride affords glycosyl imine **45**, which is further converted quantitatively to glycal **46**. Oxidative hydrolysis of **44** gives 1-acylglycosides **47**.

Yamago et al. have also reported that quinones serve as excellent acceptors for glycosyl radicals.[24] Therefore, heating a solution of telluroglycoside **39** and 1,4-benzoquinone under photo irradiation affords galactose-substituted 1,4-benzoquinone **51** (Scheme 16). While the reaction also takes place in the dark, photo irradiation considerably accelerates the rate of conversion. The reactions can be carried out both in polar protic and nonpolar aprotic solvents, and the lack of solvent effects is consistent with the involvement of neutral radical species. The reaction initially gives group-transfer product **50**, which subsequently eliminates tellurol to give **51**.

Miscellaneous

Giese et al. have reported that irradiation of the dimeric iron complex **52** generates the monomeric iron radical **53**, which abstracts halogen atoms from bromoglycosides to give the corresponding glycosyl radicals and $Cp(CO)_2FeBr$ (Scheme 17). Therefore, irradiation of bromoglycoside **1** with **52** in the presence of acrylonitrile in methanol gives *C*-glycoside **2** in 60% yield. The reaction is believed to proceed through an organoiron-transfer reaction, followed by solvolysis of the organoiron intermediate in methanol in an ionic manner.[25]

Vasella et al. have reported that glycosyl radicals generated by direct photolysis from 1-*C*-nitroglycosyl halides undergo additions to an anion of nitroalkanes. For example, irradiation of the 1-*C*-nitromannosyl bromide **54** with the lithium salt of 1-deoxy-nitromannose **55** gives dimeric glycoside **56** in good yield (Scheme 18).[26]

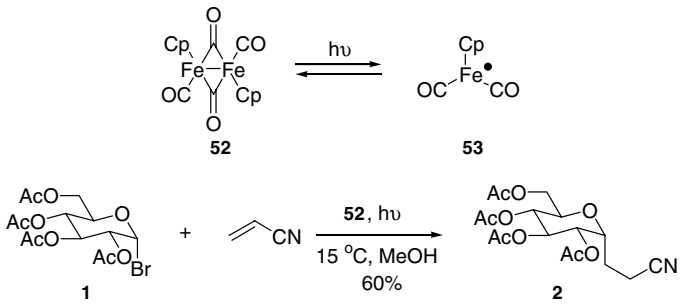

SCHEME 17

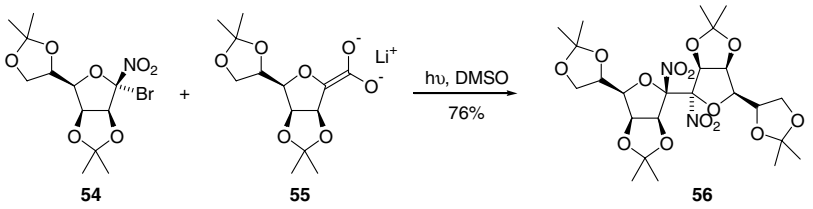

SCHEME 18

2.3 Intramolecular Carbon–Carbon Bond Formation

C-Glycosides can also be prepared by intramolecular addition of an anomeric glycosyl radical to an acceptor, which is tethered to a suitable hydroxyl group of the glycoside. Because intramolecular cyclizations such as the 5-*exo*-trig process take place very rapidly compared to intermolecular additions, the intramolecular reactions do not require activation of the alkenes by electron-withdrawing substituents. In addition, while the intermolecular addition predominantly gives α-glycoside, the stereochemistry of the intramolecular reaction is controlled by the conformational constraint of the tether to give either α- or β-glycosides selectively. De Mesmaeker et al. reported that the configuration of C2 is transformed to the stereochemistry of the products in the case of C2 hydroxyl-linked allylic acceptors (Scheme 19).[27] Thus, the 2-*O*-allyl-1-selenogalactopyranoside **57**, possessing a C2-equatorial substituent, affords the α-*C*-isomers **58** and **59**, whereas the 2-*O*-allyl-1-selenomannoside **60,** possessing a C2-axial substituent, affords the β-*C*-glycosides **61** and **62**. It is also worth noting that the decrease of reaction temperature caused by using photochemical radical generations increases stereoselectivity, and virtually a single stereoisomer is formed at temperatures below –30°C.

2.4 Stereoselective Reduction

Because of the inherent stereoselectivity in the reaction of anomeric glycosyl radicals with radical acceptors, the β-*O*-glycosides can be successfully synthesized by stereoselective reduction of 1-substituted anomeric glycosyl radicals. Kahn et al. reported that the reduction of 1-methoxy substituted methylthioglycoside **63** with tributyltin hydride in the presence of AIBN preferentially occurs from the axial direction to give the β-glycoside **64** as the major isomer (Scheme 20). The formation of the β-isomer **64** increases on decreasing the temperature, and photochemical radical generation at 30°C shows the highest selectivity (**64**:**65** = 12:1) compared to thermal generation at 80°C and 110°C.[28]

The drawback of this strategy lies in the tedious synthetic procedures for the formation of the requisite 1-substituted thioglycosides. Crich et al. have developed a more general protocol mediated by Barton esters and has applied this to the synthesis of the β-isomer of 2-deoxy glycosides and mannosides.[29,30]

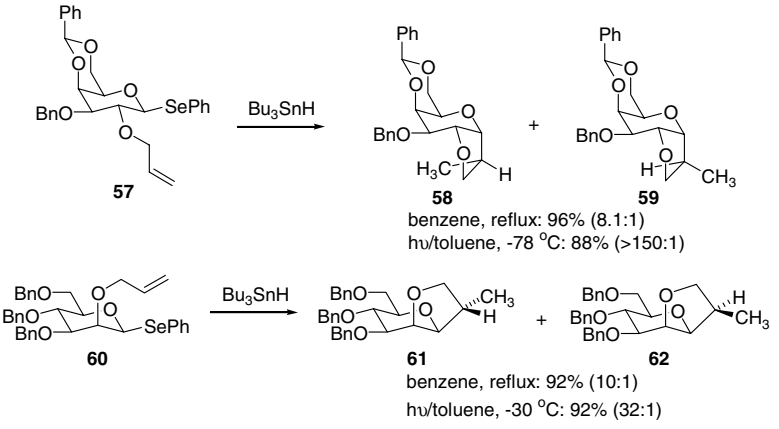

SCHEME 19

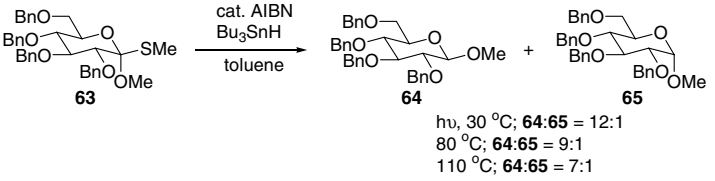

SCHEME 20

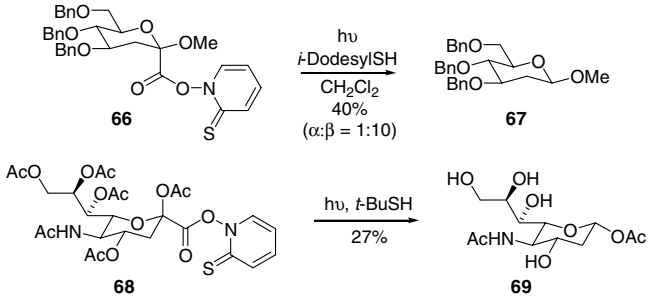

SCHEME 21

Although many biologically active natural products possess the β-linkage of 2-deoxy glycosides and mannosides, stereoselective synthesis is problematic under conventional ionic reactions. Specific examples for the synthesis of the β-isomer of 2-deoxyglycosides are shown in Scheme 21. Photolysis of the Barton ester **66** in the presence of *t*-dodecyl mercaptan gave the 2-deoxy-β-D-glycoside **67** with high stereoselectivity. Wong et al. have also utilized the same protocol for the synthesis of the decarboxylated analogue of 3-deoxy-D-*manno*-2-octulosonic acid, which is a vital component of the outer membrane lipopolysaccharide of Gram-negative bacteria.[31]

Crich et al. have used the radical translocation method for the generation of anomeric glycosyl radicals and has also applied this to the stereoselective synthesis of β-mannoside (Scheme 22).[32] Photolysis of the readily available α-mannoside **70**, which possesses a C2-bromoethoxy group, with tributyltin hydride in the presence of a catalytic amount of AIBN affords β-mannoside **71** as a major product after acid hydrolysis of the resulting C2-acetal group. The reaction proceeds through the formation of radical **72**

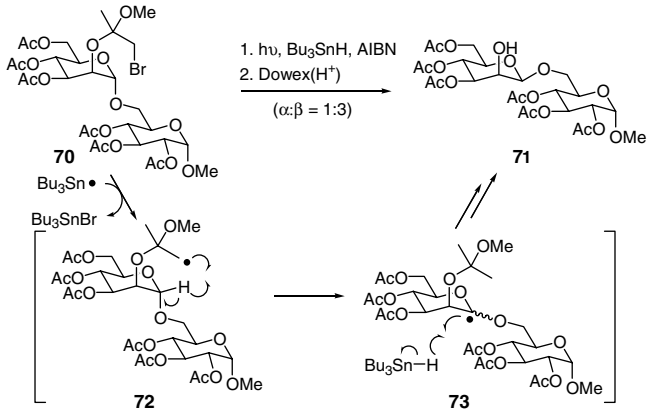

SCHEME 22

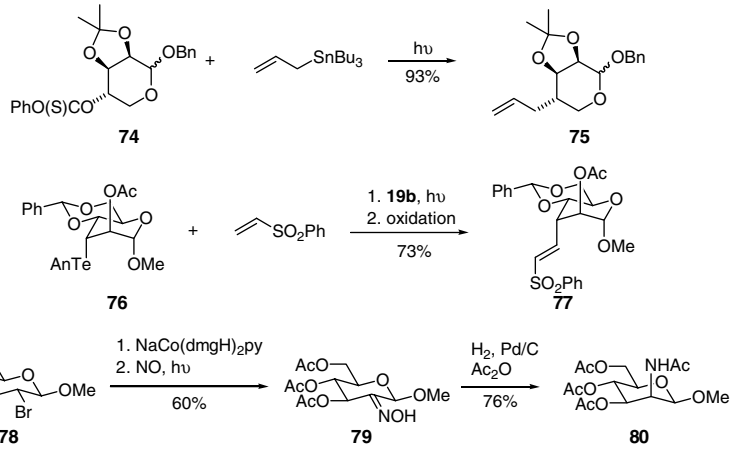

SCHEME 23

from **70** by bromine atom abstraction by the tributyltin radical. Subsequent intramolecular 1,5-hydrogen atom transfer generates the anomeric glycosyl radical **73**, which undergoes α-face selective hydrogen atom abstraction from tributyltin hydride to give the β-mannoside **71**.

2.5 Nonanomeric Glycosyl Radicals

A major strategy for the preparation of branched-chain sugars is the intermolecular addition of nonanomeric carbohydrate-based radicals to a π-system. Since no special electronic factors, such as radical anomeric effects, are present, the stereoselectivity is controlled sterically, and the stereochemistry of the substituents adjacent to the radical center mainly governs the stereochemical control. Representative results are summarized in Scheme 23.

The allyltin method developed by Keck et al. also provides a general method for the preparation of allyl branched carbohydrates through nonanomeric radicals. For example, irradiation of L-lyxose derivative **74** in the presence of allyltributyltin gives the corresponding allylated product **75**, which was transformed into pseudomonic acid C.[33] Barton esters have also been applied to the synthesis of branched carbohydrates. Barton et al. have reported that telluroglycoside **76** generates the corresponding glycosyl radical by the treatment of Barton ester **19b** under photo irradiation, and the trapping of the resulting

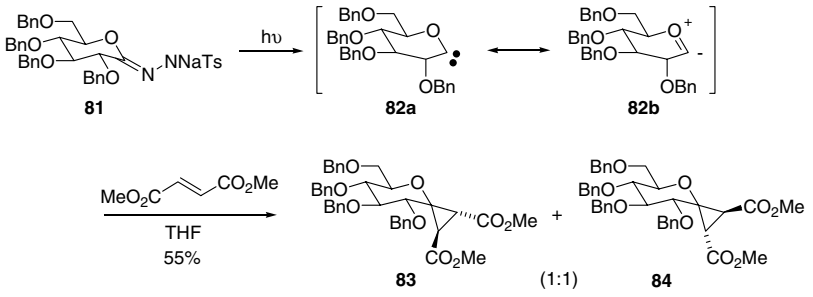

SCHEME 24

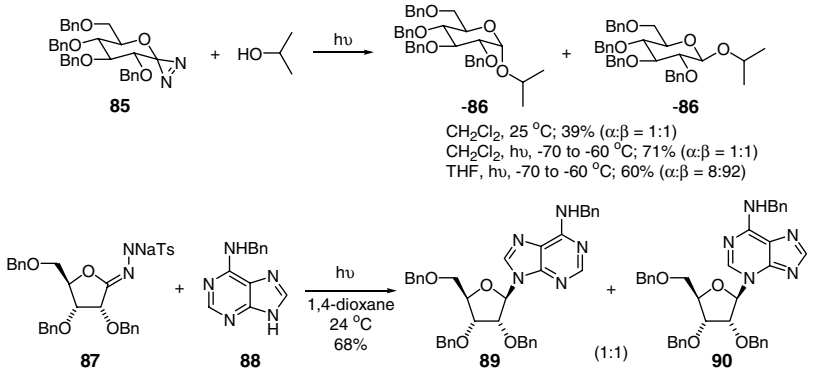

SCHEME 25

radical with vinyl sulfone followed by oxidation of the group-transfer product affords **77** in good yield.[14] Giese et al. have applied the cobaloxime method for the synthesis of 2-deoxy-2-amino-mannoside synthesis. Therefore, trapping of glycosyl radicals generated from cobaloximes derived from **78** and Co(I) species with nitrous oxide gives oxime **79** efficiently. Stereoselective hydrogenation of the oxime moiety in **79** affords 2-deoxy-2-amino-mannoside **80**.[18]

2.6 Glycosylidene Carbenes

Anomeric glycosylidene carbenes are neutral and nucleophilic species, and their additions to electron-deficient π-acceptors provide a valuable method for the synthesis of functionalized carbohydrate molecules. Vasella has reported that the sodium salts of glycosyl tosylhydrazones, e.g., **81**, and glycosyl diazenes, e.g., **85**, are excellent precursors for glycosylidene carbenes under photochemical conditions, whereas glycosyl diazenes also generate glycosyl carbenes under thermal conditions. Photolysis of **81** generates glycosylidene carbene **82a**, which can also be considered as the zwitterionic resonance structure **82b** due to the interaction of one of the *p*-orbitals of the carbene and the *n*-orbital of the adjacent pyranose oxygen (Scheme 24). In the presence of electron-deficient alkenes, such as dimethyl fumarate, **82** adds to alkenes to give a mixture of the cyclopropane products **83** and **84**.[34]

Vasella has also reported that, because of the zwitterionic character of **82**, the glycosylidene carbenes insert into the polar oxygen–hydrogen bond in hydroxyl groups or the nitrogen–hydrogen bond in pyrrole derivatives. Specific examples are shown in Scheme 25. While the diazene **85** generates the glycosylidene carbene under thermal conditions, photochemical reaction under low temperature remarkably increases the efficiency of the insertion reaction and affords the desired *O*-glycoside **86** in good yield.[35] The solvent considerably affects the stereoselectivity, and the reaction in tetrahydrofuran (THF) predominantly gives

the β-isomer of **86**, whereas the reaction in dichloromethane gives a 1:1 mixture of the α- and β-isomers of **86**. The glycosylidene carbene derived from furanosyl tosylhydrazone **87** reacts with *N*-benzyladenine (**88**) under photochemical conditions to generate a 1:1 mixture of two nucleotides, **89** and **90**.[36] The formation of **89** is due to the insertion of the glycosylidene carbene into the nitrogen–hydrogen bond, and that of **90** is due to the addition of the carbene to the nucleophilic N(3) position of **88**.

References

1. Postema, M.H.D., C-*Glycoside Synthesis*, CRC Press, Boca Raton, FL, 1995; Giese, B. and Zeitz, H.-G., Synthesis of *C*-glycosyl compounds, in *Comprehensive Carbohydrate Chemistry,* Hanessian, S., Ed., Marcel Dekker, New York, 1997, p. 507; Skrkdstrup, T., Vauzeilles, B., and Beau, J.-M., Synthesis of *C*-oligosaccharides, in *Carbohydrates in Chemistry and Biology*, Vol. 1, Ernst, B., Hart, G.W., and Sinaÿ, P., Eds., Wiley-VCH, Weinheim, 2000, p. 495; Pearce, A.J., Mallet, J.-M., and Sinaÿ, P., Radicals in carbohydrate chemistry, in *Radicals in Organic Synthesis*, Vol. 2, Renaud, P. and Sibi, M.P., Eds., Wiley-VCH, Weinheim, 2001, p. 538; Togo, H., He, W., Waki, Y., and Yokoyama, M., *C*-Glycosidation technology with free radical reactions, *Synlett,* 700, 1998; Giese, B., Stereoselective syntheses with carbohydrate radicals, *Pure Appl. Chem.,* 60, 1655, 1988.
2. Dupius, J., Giese, B., Hartung, J., and Leising, M., Electron transfer from trialkyltin radicals to nitrosugars: the synthesis of *C*-glycosides with tertiary anomeric carbon atoms, *J. Am. Chem. Soc.,* 107, 4332, 1985.
3. Giese, B. and Dupuis, J., Diastereoselective synthesis of *C*-glycopyranosides, *Angew. Chem. Int. Ed. Engl.*, 22, 622, 1983; Giese, B., Dupuis, J., and Nix, M., 1-Deoxy-2,3,4,6-tetra- *O*-acetyl-1-(2-cyanoethyl)-α-D-glycopyranose, *Org. Synth.,* 65, 236, 1987.
4. Descotes, G., Radical anomeric chemistry, *J. Carbohydr. Chem.,* 7, 1, 1988.
5. Praly, J.-P., Reduction stereoselective d'halogenures de glycosyles par le deuteriure de tributyletain, *Tetrahedron Lett.,* 24, 3075, 1983; Giese, B. and Dupuis, J., Anomeric effect of radicals, *Tetrahedron Lett.,* 25, 1349, 1984.
6. Junker, H.-D. and Fessner, W.-D., Diastereoselective synthesis of *C*-glycosylphosphonates via free-radical glycosylation, *Tetrahedron Lett.,* 39, 269, 1988.
7. Chatgilialglu, C., Organosilanes as radical-based reducing agents in synthesis, *Acc. Chem. Res.,* 25, 188, 1992.
8. Junker, H.-D., Phung, N., and Fessner, W.-D., Diastereoselective free-radical synthesis of α-substituted *C*-glycosyl phosphonates and their use as building blocks in the HWE-reaction, *Tetrahedron Lett.,* 40, 7063, 1999.
9. Keck, G. and Yates, J.B., Carbon–carbon bond formation via the reaction of trialkylallylstannanes with organic halides, *J. Am. Chem. Soc.,* 104, 5829, 1982; Keck, G.E., Enholm, E.J., Yates, J.B., and Wiley, M.R., One electron C-C bond forming reaction via allylstannanes: scope and limitations, *Tetrahedron,* 41, 4079, 1985.
10. Nagy, J.O. and Bednarski, M.D., The chemical–enzymatic synthesis of a carbon glycoside of *N*-acetyl neuranic acid, *Tetrahedron Lett.,* 32, 3953, 1991.
11. Barton, D.H.R., Crich, D., and Motherwell, W.B., The invention of new radical chain reactions. Part VIII. radical chemistry of thiohydroxamic esters: a new method for the generation of carbon radicals from carboxylic acids, *Tetrahedron,* 41, 3901, 1985.
12. Barton, D.H.R., Bero, S.D., Quinclet-Sire, B., and Samadi, M., New synthesis of sugar, nucleoside and α-amino acid phosphonates, *Tetrahedron,* 48, 1627, 1992; Barton, D.H.R., Géro, S.D., Quinclet-Sire, B., and Samadi, M., Stereocontrolled radical reactions in carbohydrate and nucleoside chemistry, *Tetrahedron Assym.,* 5, 2123, 1994.
13. Togo, H., Ishigami, S., Fujii, M., Ikuma, T., and Yokoyama, M., Synthesis of *C*-nucleosides via radical coupling reaction, *J. Chem. Soc., Perkin Trans. 1,* 2931, 1994.

14. Barton, D.H.R. and Ramesh, M., Tandem nucleophilic and radical chemistry in the replacement of the hydroxyl group by a carbon–carbon bond. a concise synthesis of showdomycin, *J. Am. Chem. Soc.,* 112, 891, 1990.
15. Fischer, H., The persistent radical effects, *Chem. Rev.,* 101, 3581, 2001.
16. Ghosez, A., Göbel, T., and Giese, B., Synthesis and reaction of glycosylcobaloximes, *Chem. Ber.,* 121, 1807, 1988.
17. Yu, C.-X., Tyler, D.R., and Branchaud, B.P., Thermal and photochemical epimerization/equilibration of carbohydrate cobaloximes, *J. Org. Chem.,* 66, 5687, 2001.
18. Veit, A.V. and Giese, B., Synthesis of mannosamine via cobaloximes, *Synlett,* 166, 1990.
19. Yamago, S., Miyazoe, H., and Yoshida, J., Reversible generation of glycosyl radicals from telluroglycosides under photochemical and thermal conditions, *Tetrahedron Lett.,* 40, 2339, 1999.
20. Yamago, S., Miyazoe, H., and Yoshida, J., Synthesis of vinylic *C*-glycosides from telluroglycosides. Addition of photochemically and thermally generated glycosyl radicals to alkynes, *Tetrahedron Lett.,* 40, 2343, 1999.
21. Yamago, S., Kokubo, K., Masuda, S., and Yoshida, J., Practical synthesis of telluroglycosides, *Synlett,* 929, 1996.
22. Araki, Y., Endo, T., Tanji, M., Nagasawa, J., and Ishido, Y., Synthesis of *C*-glycosyl compounds by the addition of glycosyl radicals to olefins, *Tetrahedron Lett.,* 28, 5853, 1987.
23. Yamago, S., Miyazoe, H., Goto, R., and Yoshida, J., Radical mediated imidoylation of telluroglycosides. Insertion of isonitriles into glycosidic carbon–tellurium bond, *Tetrahedron Lett.,* 40, 2347, 1999; Yamago, S., Miyazoe, H., Goto, R., Hashidume, M., Sawazaki, T., and Yoshida, J., Synthetic and theoretical studies on group-transfer imidoylation of organotellurium compounds. Remarkable reactivity of isonitriles in comparison with carbon monoxide in radical-mediated reactions, *J. Am. Chem. Soc.,* 123, 3697, 2001.
24. Yamago, S., Hashidume, M., and Yoshida, J., A new synthetic route to substituted quinones by radical-mediated coupling of organotellurium compounds with quinones, *Tetrahedron,* 58, 6805, 2002.
25. Thoma, G. and Giese, B., Generation and synthetic use of alkyl radicals with $[CpFe(CO)_2]_2$ as mediator, *Tetrahedron Lett.,* 30, 2907, 1989.
26. Aebischer, B., Meuwly, R., and Vasella, A., Chain elongation of 1-*C*-nitroglycosyl halides by substitution with some weakly basic carbanions, *Helv. Chim. Acta,* 67, 2236, 1984.
27. De Mesmaeker, A., Waldner, A., Hoffmann, P., Hug, P., and Winkler, T., C(5)-Epimerization in glycopyranosides during the cyclization of anomeric radicals: a comparison with glycofuranosides, *Synlett,* 285, 1992.
28. Kahne, D., Yang, D., Lim, J.J., Miller, R., and Paguaga, E., The use of alkoxy-substituted anomeric radicals for the construction of β-glycosides, *J. Am. Chem. Soc.,* 110, 8716, 1988.
29. Crich, D. and Ritchie, T.J., Stereoselective free radical reactions in the preparation of 2-deoxy-β-D-glycosides, *J. Chem. Soc., Chem. Commun.,* 1461, 1988; Crich, D. and Ritchie, T.J., Diastereoselective free-radical reactions. Part 1. Preparation of 2-deoxy-β-glycosides by synthesis and reductive decarboxylation of 3-deoxyulosinoc acid glycosides, *J. Chem. Soc., Perkin Trans. 1,* 945, 1990; Crich, D. and Hermann, F., Sequential diastereoselective free radical reactions: synthesis of an advanced olivomycin A C-D disaccharide, *Tetrahedron Lett.,* 34, 3385, 1993. Crich, D., Hwang, J.-T., and Yuan, H., Chemistry of 1-alkoxy-1-glycosyl radicals: formation of β-mannopyranosides by radical decarboxylation and decarbonylation of *manno*-heptulosonic acid glycoside derivatives, *J. Org. Chem.,* 61, 6189, 1996.
30. Crich, D. and Lim, L.B.L., Synthesis of 2-deoxy-β-*C*-pyranosides by diastereoselective hydrogen atom transfer, *Tetrahedron Lett.,* 31, 1897, 1990; Crich, D. and Lim, L.B.L., Diastereoselective free-radical reactions. Part 2. Synthesis of 2-deoxy–β–*C*-pyranosides by diastereoselective hydrogen-atom transfer, *J. Chem. Soc., Perkin Trans. 1,* 3953, 1991.
31. Sugai, T., Shen, G.-J., Ichikawa, Y., and Wong, C.-H., Synthesis of 3-deoxy-D-*manno*-2-octulosonic acid (KDO) and its analogs based on KDO aldolase-catalyzed reactions, *J. Am. Chem. Soc.,* 115, 413, 1993.

32. Crich, D., Sun, S., and Brunckova, J., Chemistry of 1-alkoxy-1-glycosyl radicals: formation of β-mannopyranosides by radical decarboxylation and decarboxylation of *manno*-heptulosonic acid glycoside derivatives, *J. Org. Chem.,* 61, 605, 1996.
33. Keck, G.E., Kachensky, D.F., and Enholm, E.J., Pseudomonic acid C from L-lyxose, *J. Org. Chem.,* 50, 4317, 1985.
34. Mangholz, S.E. and Vasella, A., Glycosyl carbenes, Part 5. Synthesis of glycono-1,5-lactone tosylhydrazones as precursors of glycosylidene carbenes, *Helv. Chim. Acta,* 74, 2100, 1991.
35. Briner, K. and Vasella, A., Glycosylidene carbenes, Part 6. Synthesis of alkyl and fluoroalkyl glycosides, *Helv. Chim. Acta,* 75, 621, 1992.
36. Mangholz, S.E. and Vasella, A., Glycosylidene carbenes, Part 21. Synthesis of *N*-tosylglycono-1,4-lactone hydrazones as precursors of glycofuranosylidene carbenes, *Helv. Chim. Acta,* 78, 1020, 1995.

3

Comparison between Reactions Induced by UV/Vis Photons and Ionizing Radiation in Hydrocarbon-like Media

Gerald O. Brown
Georgetown University

Richard G. Weiss
Georgetown University

3.1 Introduction

A review of selected chemical and physical transformations of systems in hydrocarbon mixtures and solid polymer media induced by high-energy (keV–MeV range) radiation (i.e., "ionizing" radiation[1]) is presented. Where literature data are available, these results are compared with processes induced by eV range photons in the near UV and visible range of the electromagnetic spectrum. Radiation chemistry has been investigated primarily in aqueous media.[2] For instance, about 200 publications in the 1970s alone dealt with aqueous systems.[5] However, a considerable amount of work has been performed in organic liquids[3] and solid organic media, also.[4]

The most common ionizing radiation sources are γ-rays, x-rays, neutrons, and charged particles such as fast electrons, protons, and alpha particles. Unlike photochemistry, which relies on absorption of individual UV/Vis photons by single chromophores (i.e., distinct functional groups within molecules),

0-8493-1348-1/04/$0.00+$1.50

initial interactions of ionizing radiation with matter are much less discriminating; each quantum of ionizing radiation can cause formation of many ionized and/or electronically excited species.[5] Only secondary or tertiary interactions of ionizing radiation with matter lead to *distinct* electronic excitation or ionization of chromophores with the lowest energetic thresholds.

Comparative Terms and Units in UV/Vis Photon and High-Energy Radiation Chemistry

Quantum yield (Φ_x) (Equation 3.1) is the accepted expression of efficiency for formation of a species **X** or the occurrence of a process **X** in photochemistry.[6]

The G-value ($\mathbf{G_x}$) (Equation 3.2) is used to express the efficiency of reactions or processes induced by ionizing radiation.[6] Although Φ_x and $\mathbf{G_x}$ are quantitative measures of efficiency, the former is based on the number of quanta absorbed (but not their energy), and the latter relies on the total energy absorbed (but not the number of quanta). Neither considers the radiation flux or depends on the mechanism for formation of **X**.

$$\Phi_X = \frac{\text{number of species X formed or processes X followed}}{\text{number of photons absorbed by the system}} \tag{3.1}$$

$$G_X = \frac{\text{number of } \mu\text{moles of species X formed}}{\text{Joules per kg material}} \tag{3.2}$$

The denominator of Equation 3.2, the dose in Grays (Gy),[7] can be obtained from Equation 3.3 for charged particles, where **F** is the fluence in cm^{-2}, **E** is the energy of an Avogadro's number of particles in MeV, ρ is the density of the material in g/cm^3, and **R** is the maximum depth of particle penetration in cm (i.e., particle range) calculated by the Transport of Ions in Materials (TRIM) code.[8] Fast neutrons deposit their energy in organic matrices through nuclear collisions. As a result, the dose they impart is calculated on the basis of fluence and a probability function for collisions.[9]

$$\text{Dose}(\text{Gy}) = \left(1.60 \times 10^{-10}\right) \text{FE}/\text{R}\rho \tag{3.3}$$

Energy Deposition by Ionizing Radiation

The rate of energy transfer from quanta of ionizing radiation (as charged particles) to a material can be calculated from linear energy transfer (LET) equations.[10] The LET depends on the depth of penetration and the degree of deceleration of the ionizing radiation. The dominant initial interaction between high-energy radiation and a material is inelastic collisions with electrons in atoms.[5] The ejected electrons emit photons as they decelerate (i.e., Bremsstrahlung),[5] and the energies of the emitted photons are reduced further via Compton scattering (in which inelastic collisions between the Bremsstrahlung photons and loosely bound or free electrons lead to other photon emissions). These primary events create energy "tracks" within the material. Electronically excited states and ions of specific chromophores are created via interactions with ejected electrons along "spurs" of tracks. At penetrations near the stopping distances, the Bragg maximum where LET is highest, the spatial density of spurs is greater, and they have a larger probability of overlapping.[11] Consequently, the concentrations of ions and electronically excited chromophores are highest in these regions. An energy deposition profile for protons of three different kinetic energies is shown in Figure 3.1.

Sources of High-Energy Radiation

Decay of ^{60}Co from thermal neutron bombardment of ^{59}Co is accompanied by emission of 1.2 MeV γ-rays, and decay of ^{137}Cs provides 0.66 MeV γ-rays.[12] Broad-band x-ray sources, as Bremsstrahlung, can

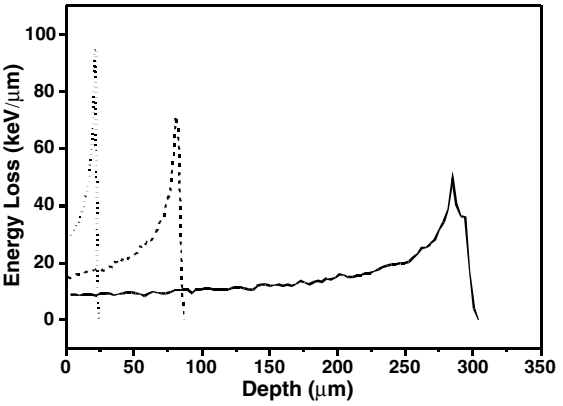

FIGURE 3.1 Profile for loss of energy by 1.0 (L), 2.2 (---), and 4.5 MeV (—) protons to a polyethylene matrix calculated by the TRIM code.[8]

be generated when electrons in a beam (from particle accelerators, for instance) are slowed as they pass through a target material composed of high atomic number nuclei such as tungsten, gold, or lead.[13] Intense beams of a wide range of x-rays are also emitted in synchrotrons as high-energy particles are accelerated along a circular path in the storage ring.[14] Monochromators can select narrow energy ranges of x-rays for sample bombardment.

Van de Graaf accelerators are good sources of electron beams.[24] A positive or negative electrostatic charge is carried to a high-voltage electrode by a rapidly moving belt, and the difference in potential between the electrode and the ground accelerates electrons or positive ions to high velocities. Emitted electrons from a cathode source that is placed at the high potential end of the tube are accelerated at 2–5 MeV energies and then directed towards the target sample. Febetrons, consisting of a bank of capacitors charged in parallel, are another source of fast electrons.[12] A high potential is created when a spark gap switches the capacitors from parallel to series. A very large pulse of electrons with a wide distribution of energies is then discharged through a cathode tube. Electron beams can also be produced using a linear accelerator (LINAC) or a radio-frequency photocathode electron gun (RFPE).[12] Both use traveling waves of electromagnetic radiation (in the radio or microwave frequency range) to accelerate charged particles, and both are capable of producing short pulses of electrons that are particularly useful in time-dependent radiolysis studies.

A variety of positively charged ion beams can be accelerated by tandem Van de Graaf accelerators.[15] Negative-ion sources permit production of ions from most elements in the periodic table. Gaseous and solid elements are normally ionized using radio frequency sources and sputtered cesium, respectively. Negative ions from the source are injected into the low-energy side of the tandem accelerator by an injector magnet and accelerated towards the positive terminal, where (some) electrons are removed by a nitrogen stripper gas or thin carbon foils. The positive ions are accelerated from the terminal and exit from the high-energy end of the tandem accelerator. A 90° analyzing magnet selects ions within narrow mass-energy ranges.

Radiolyses in Liquid Organic Media

Lipsky has investigated ionization processes by high-energy photons and electrons in the liquid phases of alkanes and the subsequent geminate ion-pair states induced.[16] In particular, he and others examined the influence of applied magnetic and electric fields on the fluorescence that accompanies recombination of the ion pairs and found that it depends on initial geminate ion-pair separation distances.[17,18]

Early studies by Thomas et al. demonstrated that large yields of excited singlet and triplet states are formed upon pulsed radiolyses of aromatic molecules in liquid and solid solutions of cyclohexane or benzene.[19] Ion recombination and direct excitation by secondary, low-energy electrons were suggested

TABLE 3.1 Comparison of Radiostationary States and Photostationary States Established with Acetophenone and Benzophenone Sensitizers

	cis Content at Stationary States	
Initial Alkene	Radio	Photo
cis- or *trans*-Stilbene	58.8	59.4
cis- or *trans*-Diphenylpropene	54.65	54.75
trans-1,3-Pentadiene	42.5	43.5

Source: Caldwell, R.A., Whitten, D G., and Hammond, G.S., *J. Am. Chem. Soc.,* 88, 2659, 1966.

$$C_6H_6 \xrightarrow{\gamma\text{-rays}} (C_6H_6)^3 \quad (4)$$

$$(C_6H_6)^3 + \underset{\textit{cis} \text{ or } \textit{trans}}{RCH{=}CHR} \longrightarrow C_6H_6 + RCH{=}CHR^3 \quad (5)$$

$$RCH{=}CHR^3 \longrightarrow \textit{cis}\text{-}RCH{=}CHR \quad (6)$$

$$RCH{=}CHR^3 \longrightarrow \textit{trans}\text{-}RCH{=}CHR \quad (7)$$

SCHEME 1 γ-Radiolysis-induced isomerization of alkenes in benzene.[23]

as the major sources of solute excited states in cyclohexane, while energy transfer from excited solvent molecules was cited as the probable mechanism for formation of solute excited states in benzene and toluene.[20] In the latter, very rapid ion-recombination reactions lead to both excited singlet and triplet states of the solvent molecules.

Seminal studies by Hammond and co-workers compared γ–radiolyses and photolyses of several types of molecules in liquid organic media. For instance, γ-radiolyses and triplet-sensitized photolyses resulted in very similar steady-state *cis–trans* compositions of a series of alkenes, including stilbenes, 1,2-diphenylpropenes, and piperylenes in benzene solutions (Table 3.1).[21,22] The high **G** values for triplet state formation during γ-radiolyses were attributed to rapid energy transfer to the alkenes, which competes with triplet-triplet annihilation reactions within spurs (where the local density of excited state solvent molecules is high) (Scheme 1).[23]

Radiolyses of "Simple" Alkanes

γ–Radiolyses of *n*-alkanes cause random cleavage of both CC and CH bonds, leading to the evolution of molecular hydrogen and lower molecular weight hydrocarbons. Chain shortening becomes less important as the length of the *n*-alkane increases, and the major products from long *n*-alkanes have more carbon atoms than their parents do.[24] The long *n*-alkanes are gelled at higher doses and their melting points are increased. As indicated by electron paramagnetic resonance (EPR) analyses of frozen alkane samples, CC bond cleavage by high-energy radiation occurs preferentially at tertiary centers and is least probable at primary ones.[24]

Hydrogen, cyclohexene, and bicyclohexyl are the major products from radiolyses of cyclohexane.[25] Scission of a CH bond is a major reaction mode. At high doses, polymeric species are formed upon secondary reaction of cyclohexyl radicals with cyclohexene molecules.

The specific nature of γ-radiation–induced reactions of solid *n*-alkanes depends on details of the layered molecular packing[26,27] of the matrix. Toriyama et al. found that the centers of the initially formed radicals of long *n*-alkanes are at terminal carbon atoms (R_I•; i.e., $-CH_2$· a primary radical).[28,29] *n*-Alkanes with an even number of carbon atoms and shorter than tetracosane (≤24 carbon atoms) form triclinic crystals, where the hydrogen atom of a neighboring molecule closest to a terminal radical center of R_I• is at C2 or C3. As a result, there is a higher probability of *nondegenerate* intermolecular hydrogen abstraction to

form either $R_{II}\bullet(-\dot{C}HCH_3)$ or $R_{III}\bullet(-\dot{C}HCH_2CH_3)$, secondary radicals, than in long *n*-alkanes with an odd number of carbon atoms. Their layers are orthorhombically ordered so that the closest *intermolecular* hydrogen atom to an $R_I\bullet$ center is at C1; intermolecular hydrogen abstraction, if it occurs, should be degenerate because the probability of hydrogen abstraction (and radical center migration) decreases as the distance from the initial radical center to the nearest intermolecular hydrogen atom increases. In addition, the distances between $R_I\bullet$ centers and the nearest H-atom on a neighboring chain are intrinsically longer in orthorhombic than in triclinic crystals.

Pyrene and Perylene Doped Alkane Matrices

Lamotte et al. have examined the reactivity of upper electronically excited states of pyrene and perylene in liquid and solid alkane solutions.[30]At low temperatures, irradiation of pyrene at 185 or 248 nm in both methane and cyclohexane matrices leads to four detected photoproducts, including high yields of 1-substituted pyrenyl derivatives. Several substituted perylenes were obtained upon 185 or 248 nm irradiation in liquid and solid alkane solutions. A mechanism for alkylation of the aromatic solutes involving sequential absorption of two photons at 248 nm or one photon at 185 nm has been proposed.

Recently, the photochemical attachment of *n*-alkanes with 8,19, 20, 21, 24, and 28 carbon atoms and 1-eicosene to pyrene has been investigated.[31] The dependence of attachment selectivity (based on the degree of retention of the pyrenyl aromatic system in the products and the fraction of them in which attachment is at the 1-position of the *n*-alkane and the 1-position of pyrene) and efficiency (based on the relative yields of attached products when irradiations were performed under conditions of constant flux) on solvent phase, pyrene concentration, radiation wavelength (above and below 300 nm), and alkane chain length was explored. Without exception, attachment was more efficient and selection was greater in the solid than in the liquid phases of the alkanes. Also, the efficiency decreased significantly when initial pyrene concentrations were $> 10^{-5}$ *M*. Reactions in the solid state of solid *n*-alkanes with ≥21 carbon atoms yielded 1-(*n*-alkyl)pyrenes almost exclusively when the radiation wavelength was >300 nm. This behavior was attributed, in part, to the location of the pyrene molecules at the interfaces between alkane lamellae.

Degassed cyclohexane and *n*-alkane solutions of pyrene have also been exposed to <1.3> MeV x-rays.[32] Although the major products, 1-alkypyrenes, suggest a mechanism of attachment similar to that initiated by eV range photons, this does not appear to be the case (Scheme 2). Whereas eV range photons excite pyrene chromophores selectively in a sea of nonabsorbing C-H and C-C bonds from the alkane solvent, the initial interaction of MeV range x-rays is predominantly with the solvent matrix.[24]

The vertical (gas phase) ionization potential of pyrene is *ca.* 6.2 eV.[33] If the same ionization potential applies in alkane solutions, absorption of 185 nm photons (6.7 eV) can produce highly excited (i.e., "high-Rydberg") singlet states ($^1PyH^{**}$),[30,34] and cation radicals. However, excitations with >240 nm (<5.1 eV) yield lower-lying excited singlet states which undergo efficient intersystem crossing to the longer-lived lowest triplet state ($\Phi_{ST} = 0.37$ and $\tau_T = 180$ μsec at 25°C in cyclohexane[35]) that subsequently can absorb another photon under the high-flux conditions employed.[30,36,37] The highly energetic $^3PyH^{**}$ and $^1PyH^{**}$ states initiate the photochemistry of attachment by transferring their excitation energy to neighboring solvent molecules (RH), which dissociate to radicals (or ions) via CH or CC cleavage reactions.[30] The so-formed alkyl radicals then can add preferentially to their ground-state pyrene donors provided diffusion is slower than reaction. Finally, the 1-alkylpyrenes are produced after formal loss of H• (step 16 in Scheme 2).

Due to the rather indiscriminate mode of initial interaction of ionizing radiation with matter and the much higher population of CH or CC bonds of the alkane chains of the solvent matrix (than pyrene molecules), the primary loci of energy deposition for secondary radiation evolved from x-rays or MeV range protons reside in the solvent. In principle, therefore, attachment can occur *without* formation of $^1PyH^{**}$, $^3PyH^{**}$ (steps 8 through 11 in Scheme 2), or any other pyrene-based excited states; step 18 of Scheme 3 is a mechanistic departure point when films are bombarded by ionizing radiation. However, there is strong experimental evidence to support step 18, also.[38–40]

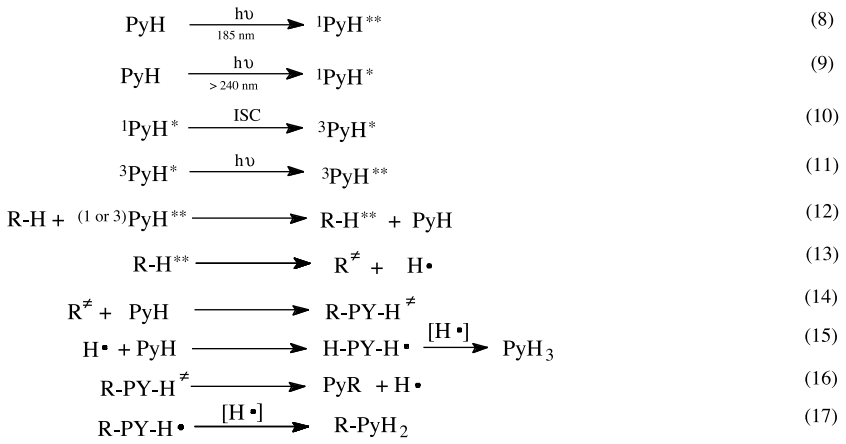

SCHEME 2 Proposed mechanism for attachment of pyrene (PyH) to polyethylene/alkanes using eV range photons. For 185 nm excitations, steps 9 through 11 are omitted (one photon process). Steps 9–17 are presumed to occur using >240 nm radiation (two photon process). When an intermediate has a ≠ sign (symbolizing · or +) on one side of an equation only, an electron (from pyrene, the polyethylene/alkane matrix, or a species derived from them) must be added to balance charges/electrons.

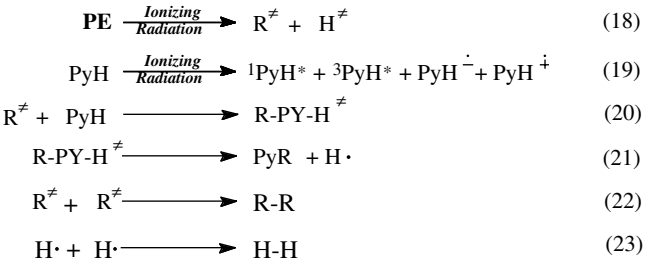

SCHEME 3 Proposed mechanism for attachment of pyrene to polyethylene using high-energy radiation. When an intermediate has a ≠ sign (symbolizing · or +) on one side of an equation only, an electron (from pyrene, the polyethylene/alkane matrix, or a species derived from them) must be added to balance charges/electrons.

3.2 Radiolyses in Block Polymers

Polyethylene (PE)

The degree of crystallinity in a PE sample is strongly dependent on the degree of chain branching that is incorporated at the time of polymerization. Highly branched polyethylenes have very small, distorted crystallites and low overall crystallinities. Their melting points and densities are lower than those of polyethylenes with higher degrees of crystallinity. Less branched polyethylenes have much larger crystallites and higher melting points and are much stiffer, more brittle, higher density materials.

High-energy radiation induces similar effects in polyethylene and low molecular weight paraffins.[41] Molecular hydrogen and low molecular weight hydrocarbons are formed, as well as insoluble polymer networks from chain cross-linking. Loss of crystallinity, associated with PE radiation damage, increases with increasing dose, and yellowing from oxidation is frequently observed during irradiations of PE in the presence of oxygen.

$$\mathbf{PE} \xrightarrow[radiolysis]{pulsed} \mathbf{PE}^{+} + e^{-} \quad (24)$$

$$e^{-} + PyH \longrightarrow PyH^{-} \quad (25)$$

$$\mathbf{PE}^{+} + PyH \longrightarrow PyH^{+} + \mathbf{PE} \quad (26)$$

$$PyH^{-} + PyH^{+} \longrightarrow {}^{3}PyH^{*} \quad (27)$$

SCHEME 4 Proposed mechanism for pulsed γ-radiolysis of pyrene-doped PE.[52]

Molecular Hydrogen Formation during Heavy-Ion Bombardment of Polyethylene and Other Polymer Films

LET dependence has been related to hydrogen yields in PE, polypropylene (PP), poly(methyl methacrylate) (PMMA), and polystyrene (PS) when their films were exposed to γ-rays, MeV range protons, and MeV range carbon ions.[42–44] The number of hydrogen molecules formed per incident particle, when each is stopped within a film, increases with particle energy and charge, but the G values decrease.

The yields of molecular hydrogen generally increased with particle LET in a dose range from 0.2 eV/nm of film thickness for γ-rays to 800 eV/nm for 30 MeV $^{12}C^{+4}$ ions.[42] PMMA and PS samples exhibited lower yields of molecular hydrogen than PE and PP when exposed to γ–rays. Although the four polymers approach a common value in the high LET region, the rate of increase in yields of molecular hydrogen with increasing LET was larger for PMMA and PS than for PE and PP in the lower LET region.

The relatively high yields of molecular hydrogen suggest that homolytic CH scissions and hydrogen atom abstraction reactions are a major reaction pathway during γ–radiolyses of PE and PP. Consistent with this hypothesis, the yields of molecular hydrogen are usually large when aliphatic hydrocarbons are exposed to ionizing radiation and the mechanisms involve homolytic cleavage of CH bonds.[45–47]

Degradation and Cross-Linking of Polyethylene Films by Ionizing Radiation

The effects of electron beams, fast neutron beams, and γ-rays on the crystallinity of low- and high-density PE films have been analyzed by x-ray diffraction (XRD) and differential scanning calorimetry (DSC).[48] The melting point of PE is known to decrease as the sizes of its crystallites and the organization of chains within them decrease.[3] Thus, lowered melting temperatures of low-density PE with higher γ-ray doses[48] are consistent with increased chain disorganization (from shortened chains) and frequency of chain branches that accompany CC and CH bond scissions. Their effect on polymer morphology outweighs that of increased cross-linking, another consequence of polymer chain scissions. In addition, increased intensities and shifts in position of x-ray peaks of low-density PE samples were observed as doses of γ-radiation were increased. They were interpreted as another indication of the greater importance of degradation at lower doses and more cross-linking at higher doses.[48]

Pulsed Radiolyses of Pyrene-Doped PE

Pulsed radiolyses with electrons of pyrene doped polyethylene samples have been examined over a wide temperature range.[49,50] Time-dependent changes in concentration of pyrenyl excited states and ions were used to study mechanisms of energy- and charge-transfer within the polymer matrix. Fast exciton migration is followed by molecular ion rearrangement and recombination to form pyrene excited states (step 28 in Scheme 4).[51–53]

These mechanistic pathways were inferred previously by Thomas et al. based on results from pulsed radiolyses (using 0.4 MeV electrons) of pyrene-doped aromatic polymers such as PS.[54] Especially in the absence of strong electron acceptors, ionizing radiation induces efficient charge separation via electronic hopping and molecular diffusion. In addition, the formation of excited singlet and triplet states of

$$\mathbf{PS} \xrightarrow[\textit{Electrons}]{\textit{0.4 MeV}} \mathbf{PS^+} + e^- \quad (28)$$

$$\mathbf{PS^+} + e^- \longrightarrow {}^{1,3}\mathbf{PS^*} \quad (29)$$

$$PyH + e^- \longrightarrow PyH^- \quad (30)$$

$$\mathbf{PS^+} + PyH \longrightarrow PyH^+ \quad (31)$$

$$\mathbf{PS^+} + PyH^- \longrightarrow {}^{1,3}PyH^* \quad (32)$$

$$PyH^+ + PyH \longrightarrow {}^{1,3}PyH^* \quad (33)$$

SCHEME 5 Proposed mechanism for formation of intermediates upon bombardment of pyrene (PyH) in PS with 0.4 MeV electrons.

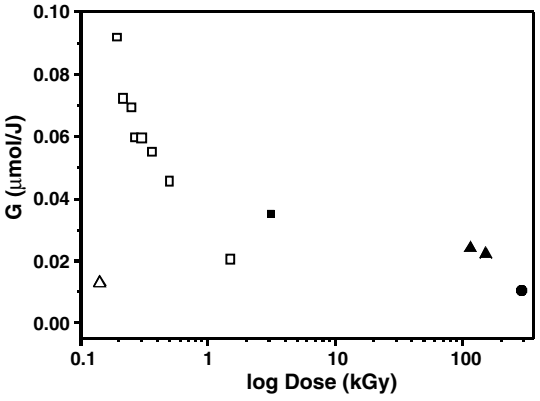

FIGURE 3.2 Plot of G versus log (dose) for 10^{-2} mol/kg pyrene in PE42 films bombarded with 4.5 MeV protons (□),1.0 MeV protons (●), 32 MeV electrons (■), 7.0 MeV alpha particles (▲), <2.0> MeV neutrons (△).

aromatic groups was observed in the polymers, primarily by geminate recombinations of polymer-based radical-cations and displaced electrons (Scheme 5).[54,55]

Bombardment of Pyrene-Doped Polyethylene Films with Neutrons, Electrons, Protons, and Alpha Particles

As an extension of studies in *n*-alkanes (Scheme 1), pyrene-doped polyethylene films have also been exposed to ionizing radiation.[56,57] Polyolefins with fluorescent probes such as pyrenyl groups,[58] selectively labeled at interior positions, have permitted the micromorphological consequences of several macro perturbations (e.g., film stretching) to be investigated.[59]

The influences of variables such as the type of ionizing radiation, the amount of kinetic energy of the bombarding particle, dose, polymer crystallinity, and initial pyrene concentration on the efficiency and selectivity of attachment of pyrene molecules to chains of PE films have been examined.[56,57] Irrespective of the type of ionizing radiation, selectivity and attachment efficiency (G) increased with decreasing particle dose (Figure 3.2). At higher doses, the dependence of G on initial pyrene concentrations was smaller because the number of polyethylene-based radicals and ions probably exceeded the (depleted) concentration of pyrene molecules. As expected, the damage to the polymer matrices, as determined from differential scanning calorimetry thermograms, also increased with increasing dose. Attachment efficiency (G) decreases as PE crystallinity increases under otherwise identical experimental conditions.

Interestingly, the efficiency of attachment is more or less independent of the kinetic energy of the particles (Table 3.2).[60] Due to the manner by which fast neutrons interact with polyethylene films, no penetration range can be calculated.[9]

TABLE 3.2 Comparison of 1-Pyrenyl Attachment Efficiencies (G) upon Bombardment of 10^{-2} mol/kg Pyrene in PE42 Films by Different High Energy Particles

Particle Type	Kinetic Energy (MeV)	Penetration Range (cm)	Dose (kGy)	G (μmol/J)
Electrons	32	12.8	3180	0.035
Protons	2.2	81×10^{-4}	0.344	0.3
Alphas	7.0	54×10^{-4}	0.247	0.9
Neutrons	<2.0>[a]	[b]	0.141	<0.05[c]

[a] Average value.
[b] Cannot be calculated; see text for details.
[c] Assuming an upper limit of 7×10^{-6} mol/kg for 1-pyrenyl attachment.
Source: Brown, G.O., Guardala, N.A., Price, J.L., and Weiss, R.G., unpublished results.

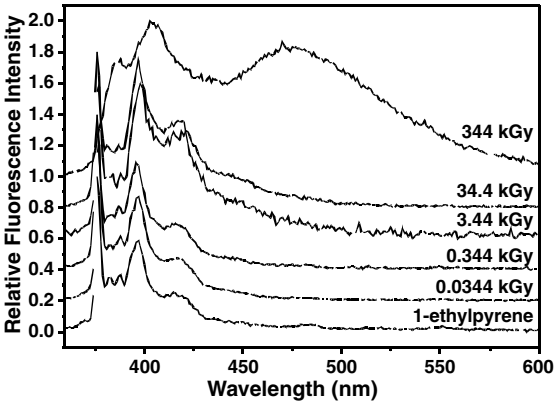

FIGURE 3.3 Emission spectra (λ_{ex} 343 nm) of 42% crystallinity PE films doped with 10^{-2} mol/kg pyrene after bombardment with 2.2 MeV protons (and removal of unreacted pyrene) as a function of dose at constant fluence and the emission spectrum of 10^{-6} mol/kg 1-ethylpyrene in 42% crystallinity PE. Spectra are normalized for intensity at 377 nm except that from 344 kGy dose. Spectra are offset for clarity.[56]

Attachment selectivity was independent of proton and alpha particle kinetic energies within the ranges (1–4.5 MeV for protons; 3–7 MeV for alpha particles) explored. However, the selectivity decreased with increasing doses of electrons, protons, or alpha particles (Figure 3.3). Higher doses generate more radicals and ions in a unit volume within a film and increase the probability of secondary events through track overlaps.[61]

A mechanism to describe the high-energy, radiolysis-initiated attachment of pyrene molecules to PE chains has been proposed by Biscoglio and Thomas.[62] Its principal claim, that preformed carbon-centered PE radicals or cations add to ground-state pyrene molecules, is supported by transient absorption spectra. Signals ascribed to electronically excited singlet and triplet states ($^1Py^*$, $^3Py^*$), and radical ions ($Py^{+\bullet}$, $Py^{-\bullet}$) of pyrene were detected initially after initiation of reactions by a pulse of 0.4 MeV electrons, but decayed to undetectable levels within 4 msec. However, polymer-centered radicals remained 4 msec after pulsed excitation and are presumed to decay according to step 19 of Scheme 3. Another transient absorption, consistent with a PE-bound 1-pyrenyl radical (RPyH•), persisted up to 3 sec after the excitation pulse.

Excitation and emission spectra from pyrenyl groups attached to polyethylene films upon exposure to low doses of eV-range photons and MeV-range particles cannot be distinguished, and both are very selective. As mentioned, the attachment selectivity does decrease with increasing photon or MeV-range

TABLE 3.3 Comparison of G Values for UV Photolysis (313 nm) and γ-Radiolysis of Symmetrical Aliphatic Ketones at 35°C

	G (Photolysis)[a]			G (Radiolysis)		
Ketone	$CO_{(I)}$	Methyl $Ketone_{(II)}$	Ratio (G_I/G_{II})	$(Alkane/2)_{(I)}$[b]	Methyl $Ketone_{(II)}$	Ratio (G_I/G_{II})
4-Heptanone	0.44	3.8	0.12	0.71	0.49	1.45
5-Nonanone	0.025	2.8	0.0090	0.43	0.51	0.88
6-Undecanone	0.020	2.4	0.0083	0.28	0.45	0.62
7-Tridecanone	0.017	2.0	0.0085	0.18	0.26	0.69
8-Pentadecanone	0.015	1.7	0.0088	0.065	0.092	0.71
12-Tricosanone	0.012	1.5	0.0080	0.040	0.081	0.69

Note: The subscripts I and II refer to products from Norrish Type I and Type II reactions, respectively.

[a] In the photolyses, $\mathbf{G} = \phi(100/\varepsilon_p)$, where ϕ is the quantum efficiency for a process and ε_p is the energy of the photons in eV.

[b] In the radiolyses, the **G** value of $CO_{(I)}$ = the **G** value of $(alkane/2)_{(I)}$.[64b]

Source: Slivinskas, J.A. and Guillet, J.E., *J. Polym. Sci. Polym. Chem. Ed.,* 11, 3043, 1973; Ausloos, P. and Paulson, J.F., *J. Am. Chem. Soc.,* 80, 5117, 1958.

particle dose. The lowest and highest photon doses employed for pyrene attachment were ~$(2–7) \times 10^3$ kGy and $(2–9) \times 10^4$ kGy, respectively, as estimated by fulgide actinometry.[56] The magnitude of the corresponding G value is significantly lower than most of those found upon particle bombardments despite the fact that all of the energy is deposited initially only into the pyrene molecules. Clearly, the vast majority of pyrene molecules in their singlet and triplet excited states (steps 10 and 11 in Scheme 2) must return radiatively or radiationlessly to their ground state without reacting.

Comparative Effects of UV photons and γ-Rays on the Degradation and Cross-Linking of Model Ketone-Containing Polymers

Guillet et al. have compared the effects of ^{60}Co γ-radiolysis and UV photons on the reactions of a series of model polymers containing ketone functional groups under vacuum.[63–65] A quantum yield for chain scission in a styrene-methyl vinyl ketone copolymer (containing 0.5% methyl vinyl ketone) was calculated to be 0.002 from the G values for γ-radiolysis;[63] the quantum yield for UV photolysis was 0.2, two orders of magnitude greater. The much lower efficiency of the γ-radiolysis can be attributed to the phenyl rings of the polymer, which are high energy sinks. No such protective effect occurs when the carbonyl groups are excited directly by UV photons.

The excited states of symmetrical aliphatic ketones produced upon γ-radiolyses are largely localized in the same n,π^* excited states that are produced upon excitation by UV photons.[64] In addition, the molecular weights of PE and copolymers of ethylene and carbon monoxide were increased by γ-radiolyses because cross-linking was more favorable than main chain scissions.[65] UV irradiation of the copolymer resulted in significant decreases in molecular weight as a result of the dominance of main chain scissions via a Norrish Type II processes.

Pitts and Osborne have compared the γ-radiolyses and UV photolyses of low molecular weight methyl ketones, which undergo both Norrish Type I and II processes.[66] They were unable to formulate a detailed mechanism for the γ-radiolyses due to the multiplicity of excitation processes and the large number of possible excited species present. However, the gross pathway of reaction appears to be similar to that initiated by UV photons (i.e., predominantly Norrish Type I and II processes). From the product ratios, the authors estimated that carbonyl groups are ~4 times more reactive than methylene groups when exposed to γ-rays (Table 3.3).

Diarylethene (DA) Doped Polymers as Dosimeters

Recently, thermally irreversible photochromic heterocyclic diarylethenes,[67] such as DA, have been examined as radiation dosimeters.[68,69]

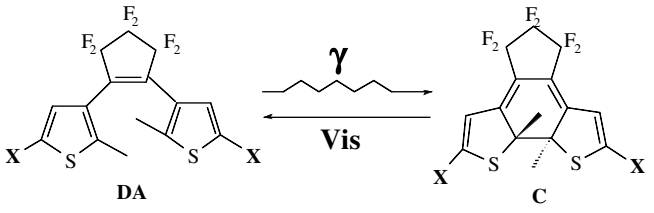

X = CH_3 or C_6H_5 (34)

DA, both neat and in colorless single crystals[68] and doped at 0.1–30 wt% into PMMA or PS films, changes from colorless (DA form) to red (closed form C), when DA (X = CH_3) is exposed to γ-radiation.[69] A visible absorbance from PS films containing 2.0 wt% DA was detected after doses as low as 100 Gy, and the absorbance increased linearly with dose to 3000 Gy. Greater sensitivity was achieved by increasing film thickness: at 2 wt% DA**,** the color change induced in a 7.5 mm-thick film by 100 Gy was equivalent to that observed in a 0.75-mm thick film after exposure to 1000 Gy.

Coloration efficiency, defined as the magnitude of the absorbance from C at 600 nm, was also found to depend on DA (X = C_6H_5) concentration, and saturation (i.e., nonlinear response) was noted at 25 wt% at a total dose of 1000 Gy. From a plot of coloration intensity versus DA concentration in PS films of constant thickness, an energy transfer distance, $R_0 \cong 14$ Å, from an aromatic group of PS to a molecule of DA could be calculated using a modified Perrin expression (Equation 3.36).[70] $\mathbf{A_\infty}$ and $\mathbf{A_D}$ are absorbances extrapolated to infinite concentration and at known concentrations of DA, respectively. N is Avogadro's number and V is the reaction volume, assumed to be $4/3\ \pi\ \mathbf{R_o}^3$, where $\mathbf{R_o}$ is the distance at which 50% of the PS* transfer their excitation energy to molecules of DA.

$$\ln\left(\frac{A_\infty}{A_\infty - A_D}\right) = VN[DA] \tag{3.35}$$

In the initial step of the proposed mechanism for energy transfer (Scheme 6),[69] the PS matrix transfers some of the energy from a γ-ray to form highly excited states localized on the phenyl groups, PS**, that rapidly undergo internal conversion to low-lying excited states, PS*. The excitation energy of the PS* groups is transferred to nearby DA molecules, allowing formation of C and film coloration.

$$\mathbf{PS} \xrightarrow{\gamma\text{-}rays} \mathbf{PS^{**}} \tag{36}$$

$$\mathbf{PS^{**} + PS} \longrightarrow \mathbf{PS + PS^{*}} \tag{37}$$

$$\mathbf{PS^{*} + DA} \longrightarrow \mathbf{PS + DA^{*}} \tag{38}$$

$$\mathbf{DA^{*}} \longrightarrow \mathbf{C} \tag{39}$$

SCHEME 6 Proposed mechanism of γ-ray induced coloration of DA in PS films.[69]

3.3 Conclusions

This review has compared how energy from high-energy particles (i.e., ion beams, neutrons, γ-rays, x-rays, and fast electrons in the MeV range) and low-energy radiation (i.e., photons in the eV range) is deposited in liquid and solid hydrocarbon-like media and the experimental consequences of the differences. Exposure of a sample to high-energy radiation results in rather indiscriminate energy deposition initially, leading subsequently to the creation of highly excited species that are normally unattainable via

irradiation with eV range photons. Deciphering how energy flows within the sample matrices and to added photo-reactive species provides insights into how various high-energy quanta deposit energy in materials. Where possible, the photoprocesses suffered by solute molecules under conditions of UV/Vis and high-energy particle bombardment has been compared. The examples included here demonstrate that very selective photochemical processes with relatively high efficiencies are possible when the particle type, dose, medium ,and solute molecule are carefully controlled.

Acknowledgment

This work was supported by the National Science Foundation.

References

1. Kircher, J.F. and Bowman, R.E., *Effect of Radiation on Materials and Components,* Chapman & Hall, London, 1964.
2. (a) Saenger, D. and von Sonntag, C.Z., Radiation chemistry of alcohols. XIV. Intermolecular hydrogen elimination in the UV photolysis of tert-butyl alcohol, *Naturforsch. B,* 25, 1491, 1970; (b) von Sonntag, C.Z. and Thoms, E.Z., Radiation chemistry of alcohols. XV. γ-Radiolysis of ethylene glycol in aqueous solution, *Naturforsch. B,* 25, 1405, 1970; (c) von Sonntag, C.Z., Irradiation chemistry of alcohols. XII. Formation of methane in γ-radiolysis of 2-propanol, *Naturforsch. B,* 25, 645, 1970; (d) von Sonntag, C.Z., Radiation chemistry of alcohols. X. UV photolysis, λ 185 nm, of liquid ethanol and ethanol–water mixtures, *Phys. Chem.,* 69, 292, 1970.
3. Chapiro, A., *Radiation Chemistry of Polymeric Systems*, John Wiley & Sons, London, 1962.
4. Charlesby, A., Effects of radiation on behavior and properties of polymers, in *Effects of Radiation on Materials*, Harwood, J.J., Hausner, H.H., Morse, J.G., and Rauch, W.G., Eds., Chapman & Hall, London, 1958, pp. 261–286.
5. Hughes, G., *Radiation Chemistry,* Oxford University Press, London, 1973.
6. Verhoeven, J.W., Glossary of terms used In photochemistry, *Pure Appl. Chem.,* 68, 2223, 1996.
7. Patterson, L.K., Instrumentation for measurement of transient behavior in radiation chemistry, in *Radiation Chemistry: Principles and Applications*, Farhataziz and Rogers, M.A.J., Eds., VCH Publishers, New York, 1987, p. 68.
8. Ziegler, J.F. and Manoyan, J.M., The stopping of ions in compounds, *Nucl. Instrum. Methods Phys. Res.,* B35, 215, 1988.
9. Grigoriev, I.S. and Meilikhov, E Z., Eds., *Handbook of Physical Quantities*, CRC Press, Boca Raton, FL, 1997, pp. 1356–1359.
10. Chatterjee, A., Interaction of ionizing radiation with matter, in *Radiation Chemistry: Principles and Applications*, Farhataziz and Rogers, M.A.J., Eds., VCH Publishers, New York, 1987, p. 17.
11. Schuler, R.H., Radiolysis of benzene by heavy ions, *Trans. Faraday Soc.,* 61, 100, 1965.
12. Wishart, J.F. and Nocera, D.G., *Photochemistry and Radiation Chemistry, Complementary Methods for the Study of Electron Transfer,* Oxford University Press, London, 1998.
13. Christophorou, L.G., *Atomic and Molecular Radiation Physics*, Wiley, London,1971.
14. Weaver, J.H. and Margaritondo, G., Solid-state photoelectron spectroscopy with synchrotron radiation, *Science*, 206, 151, 1979.
15. Price, J.L., Land, D.J., Stern, S.H., Guardala, N.A., Cady, P.K., Simons, D.G., Brown, M.D., Brennan, J.G., and Stumborg, M.F., An overview of the ion-beam analysis laboratory at White Oak, *Nucl. Instrum. Methods Phys. Res.,* B56–57, 1014, 1991.
16. Lipsky, S., Ionization and excitation in non-polar liquids, *J. Chem. Edu.*, 58, 93, 1981.
17. Krishna, T.S.R., Low concentration anomalies in the electronic energy transfer behavior of saturated hydrocarbon liquids, *J. Phys. Chem. A,* 102, 496, 1998.
18. Saik, V.O. and Lipsky, S., Magnetic field effects on recombinant fluorescence: comparison of VUV and fast electron excitation, *Chem. Phys. Lett.,* 264, 649, 1997.

19. Thomas, J.K., Johnson, K., Klippert, T., and Lowers, R., Nanosecond pulse radiolysis studies of the reaction of ions in cyclohexane solutions, *J. Chem. Phys.*, 48, 1608, 1968.
20. Hunt, J.W. and Thomas, J.K., Pulse radiolysis studies of the formation of triplet excited states in cyclohexane solutions of naphthalene and anthracene, *J. Chem. Phys.,* 46, 2954, 1967.
21. Caldwell, R.A., Whitten, D.G., and Hammond, G.S., Triplet states in radiation chemistry. Radiochemical *cis–trans* isomerization, *J. Am. Chem. Soc.,* 88, 2659, 1966.
22. Penner, T.L., Whitten, D.G., and Hammond, G.S., Radiation-induced reactions of 1,3-cyclohexadiene, *J. Am. Chem. Soc.,* 92, 2861, 1970.
23. Hammond, G.S., Caldwell, R.A., King, J.M., Kristinsson, H., and Whitten, D.G., *Photochem. Photobiol.,* 7, 695, 1968.
24. Spinks, J.W.T. and Woods, R.J., *An Introduction to Radiation Chemistry*, Wiley, New York, 1964.
25. Barker, R. and Hill, M.R.H., Polymer production in the radiolysis of liquid cyclohexane, *Nature*, 194, 277, 1962.
26. Crissman, J.M., Passaglia, E., Eby, R.K., and Colson, J.P., Crystal data on *n*-eicosane ($C_{20}H_{42}$), *J. Appl. Crystallogr.*, 3, 174, 1970.
27. Small, D.M., *The Physical Chemistry of Lipids,* Plenum, New York, 1986.
28. Toriyama, K., Iwasaki, M., and Fukaya, M., Even-odd alteration of the formation of chain end alkyl radicals in irradiated crystalline alkanes: ESR evidence, *J. Chem. Soc., Chem. Commun.,* 1293, 1982.
29. Toriyama, K., Nunome, K., and Iwasaki, M., Structures and reactions of radical cations of some prototype alkanes in low temperature solids as studied by ESR spectroscopy, *J. Chem. Phys.*, 77, 5891, 1982.
30. (a) Lamotte, M., Joussot-Dubien, J., Lapouyade, R., and Pereyre, J., Reactions following the excitation in upper excited states of pyrene and perylene in alkane solutions, in *Photophysics and Photochemistry above 6eV,* Lahmani, F., Ed., Elsevier, Amsterdam, 1985; (b) Lamotte, M., Pereyre, J., Lapouyade, R., and Joussot-Dubien, J., Multiphotonic photolysis of perylene and pyrene in liquid cyclohexane, *J. Photochem. Photobiol. A: Chem.,* 58, 225, 1991.
31. Zimerman. O.E. and Weiss, R.G., Pyrene photochemistry in solid *n*-alkane matrices: comparisons with liquid phase reactions, *J. Phys. Chem. A.,* 103, 9794, 1999.
32. Brown, G.O., Guardala, N.A., Price, J.L., and Weiss, R.G., Comparison of energy deposition modes in polyethylene films by MeV range neutrons, electrons, protons, and alpha particles. Covalent attachment of doped pyrene molecules, *J. Phys. Chem.,* **A**, 107, 3343, 2003.
33. Boschi, R. and Schmidt, W., Photoelectron spectra of delocalized π-systems. 2. Photoelectron spectra of polycyclic aromatic hydrocarbons. pyrene and coronene, *Tetrahedron Lett.,* 25, 2577, 1972.
34. Freund, R.S., High-Rydberg molecules, in *Rydberg States of Atoms and Molecules*, Stebbings, R. F. and Dunning, F.B., Eds., Cambridge University Press, Cambridge, 1983, Chapt. 10.
35. Slifkin, M.A. and Walmsley, R.H., Triplet states of polycyclic aromatic hydrocarbons in fluid solution and in the solid state, *Photochem. Photobiol.,* 13, 57, 1971.
36. Sun, Y.P., Ma, B., Lawson, G.E., Bunker, C.E., and Rollins, H.W., Effects of photochemical reactions of pyrene in alcohol and aqueous solvent systems on spectroscopic analyses, *Anal. Chim. Acta,* 319, 379, 1996.
37. (a) Pandey, S. and Acree, W.E., Jr., Comments concerning "Effects of photochemical reactions of pyrene in alcohol and aqueous solvents on spectroscopic analysis," *Anal. Chim. Acta,* 343, 155, 1997; (b) Sun, Y.P., Ma, B., Lawson, G.E., Bunker, C.E., and Rollins, H.W., A response to the comments of S. Pandey and W.E. Acree, Jr. on "Effects of photochemical reactions of pyrene in alcohol and aqueous solvents on spectroscopic analysis", *Anal. Chim. Acta*, 343, 159, 1997.
38. Warman, J.M., Asmus, K.D., and Schuler, R.H., Electron scavenging processes in the radiolysis of hydrocarbon solutions, *Adv. Chem. Ser.,* 82, 29, 1968.
39. Hagerman, R.J. and Schwarz, H.A., A pulse radiolysis study of solutions of α-chlorotoluene in cyclohexane, *J. Phys. Chem.,* 71, 2694, 1967.
40. Thomas, J.K., Johnson, K., Lippert, T.K., and Lowers, R., Nanosecond pulse radiolysis studies of the reaction of ions in cyclohexane solutions, *J. Chem. Phys.,* 48, 1608, 1968.

41. Charlesby, A., Ed., *Atomic Radiation and Polymers*, Pergamon Press, New York, 1960.
42. Chang, Z. and LaVerne, J.A., Hydrogen production in the heavy ion radiolysis of polymers. 1. Polyethylene, propylene, poly(methylmethacrylate) and polystyrene, *J. Phys. Chem. B,* 104, 10557, 2000.
43. Chang, Z. and LaVerne, J.A., Molecular hydrogen production in the radiolysis of high-density polyethylene, *J. Phys. Chem. B,* 103, 8267, 1999.
44. Chang, Z. and LaVerne, J.A., Hydrogen production in gamma-ray and helium-ion radiolysis of polyethylene, polypropylene, poly(methyl-methacrylate) and polystyrene, *J. Polym. Sci. A,* 38, 1656, 2000.
45. Burns, W.G. and Reed, C.R.V., Effects of L.E.T. (linear energy transfer) and temperature in the radiolysis of cyclohexane. 1. Experimental results and comparisons with predictions of diffusion kinetic models, *Trans. Faraday Soc.,* 66, 2159, 1970.
46. LaVerne, J.A., Schuler, R.H., and Foldiak, G., Intratrack reactions of cyclohexyl radicals in the heavy ion radiolysis of cyclohexane, *J. Phys. Chem. A,* 96, 2588, 1992.
47. LaVerne, J.A., Pimblott, S.M., and Wojnarovits, L., Diffusion kinetic modeling of the γ-radiolysis of liquid cycloalkanes, *J. Phys. Chem. A,* 101, 1628, 1997.
48. Badr, Y., Ali, Z., Zahran, A., and Khafagy, R., Characterization of gamma irradiated polyethylene films by DSC and x-ray diffraction techniques, *Polym. Int.,* 49, 1555, 2000.
49. Szadkowska-Nicze, M., Mayer, J., and Kroh, J., Excimer formation in irradiated high density polyethylene doped with aromatics, *J. Photochem. Photobiol. A: Chem.,* 54, 389, 1990.
50. Szadkowska-Nicze, M., Kroh, J., and Mayer, J., Excited state formation in pulse irradiated polyethylene doped with aromatics, *Radiat. Phys. Chem.,* 45, 87, 1995.
51. Szadkowska-Nicze, M., Kroh, J., and Mayer, J., Pulse radiolysis study of charge transfer processes in polyethylene film containing two solutes, *J. Photochem. Photobiol. A: Chem.,* 91, 241, 1995.
52. Szadkowska-Nicze, M., Mayer, J., and Kroh, J., Pulse radiolysis of solid polyethylene in the presence of pyrene, *Radiat. Phys. Chem.,* 39, 23, 1992.
53. Szadkowska, M. and Mayer, J., Ion recombination in PMMA doped with pyrene as observed by wavelength selected radiothermoluminescence, *Res. Chem. Intermed.,* 27, 823, 2001.
54. Zhang, G. and Thomas, J.K., Energy transfer via ionic processes in polymer films irradiated by 0.4 MeV electrons, *J. Phys. Chem.,* 100, 11438, 1996.
55. Zhang, G. and Thomas, J.K., spectroscopic investigation of photoinduced charge separation and recombination in solid polymers, *J. Phys. Chem. A,* 102, 5465, 1998.
56. Brown, G.O., Guardala, N.A., Price, J.L., and Weiss, R.G., Selectivity and efficiency of pyrene attachment to polyethylene films by bombardment with MeV range protons, *J. Phys. Chem. B,* 106, 3375, 2002.
57. Brown, G.O., Guardala, N.A., Price, J.L. and Weiss, R.G., Pyrenyl attachment to polyethylene is more selective with MeV-range protons than with eV-range photons, *Polymer Preprints,* 41, 1536, 2000.
58. Yamazaki, I., Winnik, F.M., Winnik, M.A., and Tazuke, S., Excimer formation in pyrene labelled hydroxypropyl cellulose in water: picosecond fluorescence studies, *J. Phys. Chem.,* 91, 4213, 1987.
59. He, Z., Hammond, G.S., and Weiss, R.G., Novel methods for the determination of dopant site distributions and dopant rates of diffusion in low–density polyethylene films with covalently attached anthryl groups: fluorescence quenching by *N,N*-dimethylaniline in unstretched, stretched and swelled films, *Macromolecules*, 25, 1568, 1992.
60. Brown, G.O., Guardala, N.A., Price, J.L., and Weiss, R.G., unpublished results.
61. Bol'bit, N M., Taraban, V.B., Shelukhov, I.P., Klinshpont, E.R., and Milinchuk, V., A new type of plastic scintillator with excellent radiation resistance, *Instrum. Exp. Tech.,* 43, 460, 2000.
62. Biscoglio, M. and Thomas, J.K., Radiolysis of polyethylene films containing arenes: bromopyrene dissociation and pyrene binding in polymer films, *J. Phys. Chem. B,* 104, 475, 2000.
63. Slivinskas, J.A. and Guillet, J.E., γ-Radiolysis of ketone polymers. II. γ-Irradiation of styrene-methyl vinyl ketone copolymers, *J. Polym. Sci. Polym. Chem. Ed.,* 11, 3057, 1973.

64. (a) Slivinskas, J.A. and Guillet, J.E., γ-Radiolysis of ketone polymers. I. Studies of symmetrical aliphatic ketones as model compounds, *J. Polym. Sci. Polym. Chem. Ed.,* 11, 3043, 1973. (b) Ausloos, P. and Paulson, J.F., Radiolysis of simple ketones, *J. Am. Chem. Soc.,* 80, 5117, 1958.
65. Slivinskas, J.A. and Guillet, J.E., γ-Radiolysis of ketone polymers. III. Copolymers of ethylene and carbon monoxide, *J. Polym. Sci. Polym. Chem. Ed.,* 12, 1469, 1974.
66. Pitts, J.N. and Osborne, A.D., Structure and reactivity in the radiolysis of ketones, *J. Am. Chem. Soc.,* 83, 3011, 1961.
67. Irie, M., Diarylethenes for memories and switches, *Chem. Rev.,* 100, 1685, 2000.
68. Irie, S., Yamaguchi, T., Nakazumi, H., Kobatake, S., and Irie, M., Radiation-induced coloration of photochromic dithienylethene derivatives, *Bull. Chem. Soc. Jpn.,* 72, 1139, 1999.
69. Irie, S. and Irie, M., Radiation-induced coloration of photochromic dithienylethene derivatives in polymer matrices, *Bull. Chem. Soc. Jpn.,* 73, 2385, 2000.
70. Birks, J.B., *Photophysics of Aromatic Molecules*, Wiley, London, 1970.

4

Oxidative Single Electron Transfer (SET) Induced Fragmentation Reactions

Angelo Albini
University of Pavia

Maurizio Fagnoni
University of Pavia

4.1 Introduction

The excited states of organic molecules present, as demonstrated throughout this book, a rich and diverse chemistry. However, a property that is common to all excited states is that of being both much better oxidants and much better reductants than the corresponding ground states. This makes redox processes involving organic molecules, a rare occurrence in ground state chemistry, a frequent path in excited state chemistry.[1–5] When the light-absorbing molecule is relatively stable as a radical ion, it functions as an electron transfer sensitizer, and the chemical reaction of the oppositely charged radical ion can be exploited. In this chapter, the use of electron accepting sensitizers is considered. Aromatic nitriles or esters, quinones, and aromatic ketones are used. These satisfy the requirement of chemical stability in the reduced state and are strong oxidants indeed [e.g., 1,4-dicyanonaphthalene, DCN (S_1), E_{red} 2.17 V vs. SCE; 1,2,4,5-tetracyanobenzene, TCB (S_1), 3.44 V; tetrachloro-*p*-benzoquinone (T_1), 3.33 V; α,α,α,–trifluoroacetophenone (T_1), 1.65 V]. The radical cation formed in the photoinduced Single Electron Transfer (SET) process may undergo addition or rearrangement processes. In the following, however, attention will be concentrated on reactions involving the fragmentation of the substrate RX.

$$\text{Sens} + h\nu \rightarrow \text{Sens}^{\star} \tag{4.1}$$

$$\text{Sens}^{\star} + \text{R-X} \rightarrow \text{Sens}^{-\bullet} + \text{R-X}^{+\bullet} \tag{4.2}$$

$$\text{R-X}^{+\bullet} \rightarrow \text{R}^{\bullet} + \text{X}^{+} \rightarrow \text{Products} \tag{4.3}$$

0-8493-1348-1/04/$0.00+$1.50

In the key step, a mesolytic process, as it has been dubbed, cleavage of a σ bond yields a radical and a cation.[6–13] The same result may be obtained through nonphotochemical means, such as anodic oxidation or ground state oxidation by an inorganic reagent. Excitation through light absorption generates the actual oxidant (the excited state) in a very low steady state concentration and in solution, thus differing from electrochemistry, where holes are concentrated on the electrode, and from oxidation with inorganic species, where a relatively high concentration of the oxidant must be added. Therefore, photosensitization is a much milder method, where e.g., over-oxidation of the radical formed initially to a cation, a common occurrence with the other two methods, is easily avoided. On the other hand, the strongly positive reduction potential of many organic molecules in the excited state (compare the examples above) makes redox sensitization an effective process also for quite modest donors, for which no thermal counterpart exists, and photosensitization is a much more flexible method than γ radiation. The range of application of photosensitized (by A*, in the singlet or triplet state) oxidation of organic molecules (RX) is pictorially represented in Equation 4.4.

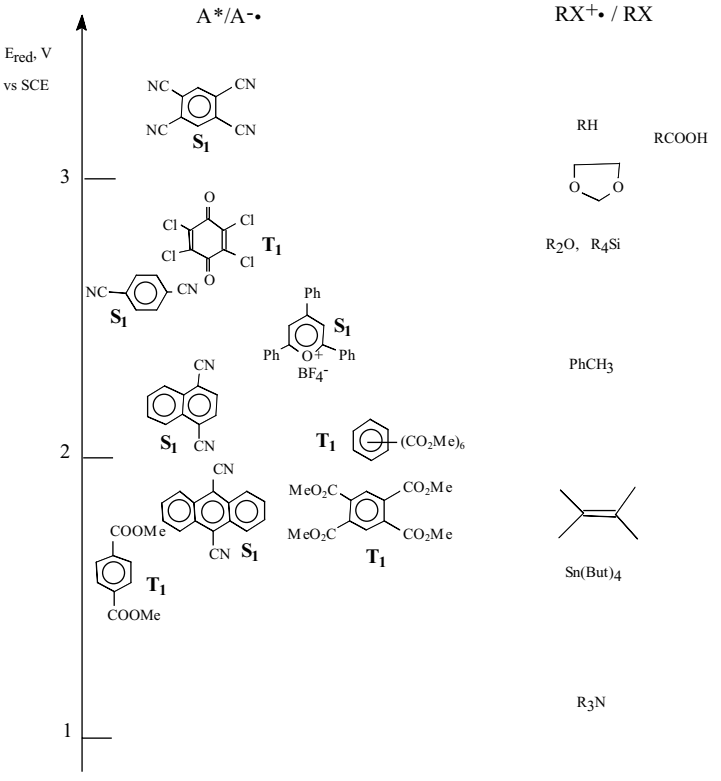

(4.4)

The efficiency and mildness characteristic of this method have led to the widespread use of electron transfer photosensitized oxidation followed by fragmentation as a novel method for the generation of radicals (and, generally less importantly from the synthetic point of view, of cations) from unusual precursors. The sensitizers initiate the process and at some stage of the following chemistry give back to some intermediate the electron initially accepted, so that it is not consumed during the process, and the sensitizing cycle continues. Alternatively, they function as the radical trap (see an example for the case of TCB in Equation 4.5).

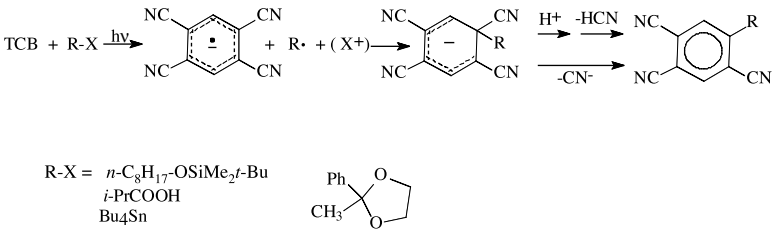

(4.5)

Typical reactions of the thus formed (usually alkyl) radicals (R·) are trapping by electrophilic alkenes (EWG = electron-withdrawing substituent), resulting in conjugate alkylation, or by oxygen, leading to oxidation, besides the above mentioned coupling with the radical anion of the sensitizer, giving addition or substitution products (see Equation 4.6).

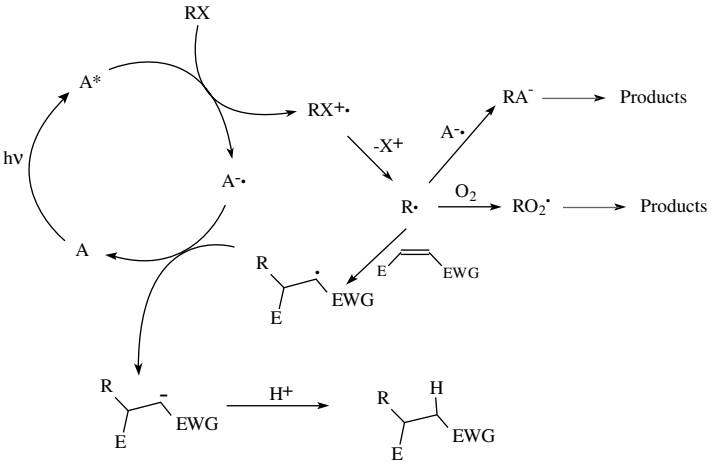

(4.6)

In this chapter, attention is given to the fragmentation step, and thus, after an introductory section on the scope of the method, the material is organized according to the structure of the donor and, within each category, according to the structure of the electrofugal group cleaved in the key chemical step.

4.2 Scope of Radical Cation Fragmentation

The feasibility of the fragmentation can be assessed through thermochemical cycles (see Equation 4.7).[9,14–17]

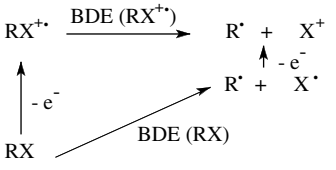

(4.7)

Some examples are presented in Table 4.1, where it is apparent both that many organic substrates can undergo photoinduced oxidation with the sensitizers mentioned above and that one electron oxidation dramatically weakens σ bonds. In fact, it has been shown above that the reduction potential of excited

TABLE 4.1 Oxidation Potential of Some Organic Substrates and Evaluated Free Energy for the Fragmentation of the Corresponding Radical Cations in a Polar Solvent

Substrate	E_{ox}, V	Cleavage	ΔG, kcal/mol
$PhCH_3$	2.4	$PhCH_2^{\cdot}$ + H^+	–14.0
$Ph_2CHCHMePh$	2.15	$PhCH_2^{\cdot}$ + $PhMeCH^+$	12.7
Cis-2-butene	2.17	$MeCH{=}CHCH_2^{\cdot}$ + H^+	–9.9
Me_3N	1.15	$Me_2NCH_2^{\cdot}$ + H^+	6
Me_2O	3.18	$MeOCH_2^{\cdot}$ + H^+	13
Me_4Si	3	$Me^{\cdot}$ + Me_3Si^+	15

TABLE 4.2 Rates of Fragmentation of Some 4-Methoxybenzyl Derivatives 4-$MeOC_6H_4CH_2X$ at 298 K in MeCN

X	Fragmentation	k_1[a] (sec^{-1})	k_2[b] ($mol^{-1}sec^{-1}$)
CMe_2OMe	C-C	3.6×10^4	
CPh_2OMe	C-C	2.8	
1,3-dioxolanyl-2-yl-	C-C	8.5	
2-methyl-1,3-dioxolanyl-2-yl	C-C	152.8	
$SiMe_3$	C-Si	215.0	
H	C-H		0.67×10^8
COOH	O-H, then C-C[c]		19.0
CH_2OMe	C-H		0.77
COOMe	C-H		8.8

[a] The radical cation fragmentation occurs unimolecularly.

[b] The radical cation fragmentation involves assistance by cerium ammonium nitrate (0.15 *mM*), the photochemical precursor of the oxidant used in this case, the nitrato radical.

[c] The process is assumed to involve deprotonation from the radical cation of the acid, followed by C-C bond fragmentation at the neutral radical level.

sensitizers is usually larger than 1.5 V vs. SCE and can be in excess of 3 V. Thus both π donors such as aromatics and alkenes and n donors can be oxidized. Indeed, very strong oxidants such as TCB in the singlet-excited state oxidize alkanes, also. Furthermore, the energy involved in single electron transfer is often in the same order as bond energy, and fragmentation becomes in many cases close to thermo neutral or even conspicuously exothermal. On the other hand, the thermochemical data are not per se an indication of which cleavage path(s) are sufficiently fast to compete with back electron transfer (BET, see Equation 4.8)

$$Sens^{-\cdot} + R\text{-}X^{+\cdot} \rightarrow Sens + R\text{-}X \tag{4.8}$$

or with other reactions of the radical cation, the competition being at any rate strongly dependent on the choices of the sensitizer and the medium (see below some hints about the dynamics of the process). A number of direct measurements of the cleavage rate are now available. As an example, one may refer to a recent determination of the fragmentation rates of some 4-methoxybenzyl derivatives in order to appreciate the variety of electrofugal groups and also to highlight the kinetic difference between them (see Table 4.2).[18]

As it appears from Table 4.2, CC bond fragmentation is a very fast process with electrofugal groups such as disubstituted α-alkoxy cation or (substituted) α,α-dialkoxy cations, and the CSi bond cleaves very quickly. CH bond cleavage is a much slower process, in the cases discussed occurring only as a nucleophile-assisted (in this case by cerium ammonium nitrate) process. Notice that the data refer to

the highly stabilized radical cation of anisole derivatives. With poorer donors, and thus higher energy radical cations, the same processes may be orders of magnitude faster, but the scale of reactivity remains as illustrated, e.g., for benzylic donors the relative rate of cleavage remains in the order k_{cl} ($-SiMe_3^+$) > 10 k_{cl} ($-CO_2 - H^+$) > 10 k_{cl} ($-H^+$).[19] It may be noted that deprotonation is in most cases predicted to be the most exothermic process by thermochemical considerations (see Table 4.1). Nevertheless, less exothermic or even slightly endothermic processes involving different fragmentations, e.g., CC bond breaking, often compete successfully, possibly due to the more important change in the solvation sphere imposed by deprotonation. Some kind of assistance by a purposely added nucleophile, the sensitizer, or the solvent can in fact strongly affect competition between alternative fragmentation processes and between these and BET. Several studies have been devoted to the determination of the detailed mechanism for the (nucleophile-assisted) fragmentation of radical cations, always among benzylic derivatives. These are by far the best-studied class.[20–23]

From the point of view of synthetic application, the most important point is the type of radical generated. In most instances the electron-donating moiety, whether a π donor (aromatic or olefin) or an n donor (a heteroatom), is located in the part of the molecule that forms the radical R·, usually in the α–position with respect to the cleaving σ bond (see Equation 4.3). Splitting of cation X thus gives an α-substituted (and stabilized) radical, such as benzyl, allyl, or α-heteroatom substituted. In other cases, however, the donating moiety is part of the electrofugal cation X^+, as is the case with tetraalkylsilanes or with ketals (vide infra). In this case a nonstabilized alkyl radical is generated, just as when an alkane is directly oxidized and deprotonates from the radical cation. The chemistry of the radicals formed follows the patterns indicated in Equation 4.6. An exception is strongly stabilized radicals (e.g., benzhydryl) that usually dimerise or undergo electron transfer steps (see the following section and Equation 4.12).

Furthermore, the above presentation has been grossly oversimplified. Actually, association between the radical ions and solvation has an important influence on the various steps of the reaction. Thus, fragmentation of the radical cation may take place either when it is still more or less strongly associated with the oppositely charged radical ion (from the sensitizer) or when it is a free solvated ion. This has a role not only in the fragmentation efficiency but also in the probability that the resulting radical can be trapped by an addend that is different from the sensitizer radical ion. This point has been the subject of in-depth investigations, as it appears in several of the references that will be mentioned where appropriate. A general idea of the kinetics involved has been obtained, for aliphatic donors, by using rearranging radicals (radical clocks, see Equation 4.9).[24]

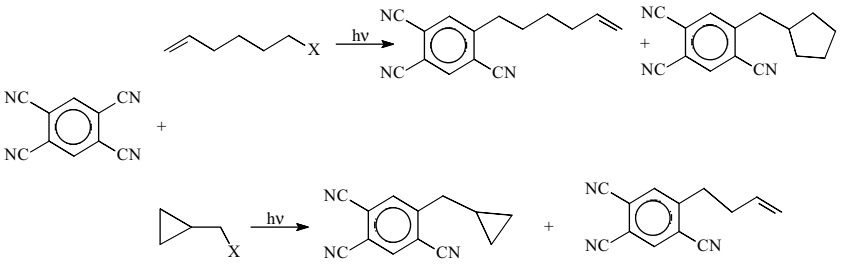

X = Electrofugal group (4.9)

4.3 Aromatic Donors — Benzylic Cleavage

Deprotonation

Aromatic donors form the largest class of substrates fragmentable by electron transfer in view of their accessible oxidation potential and the easy cleavage at the benzylic position. Pioneering work by Nicholas and Arnold[14] demonstrated the high acidity of the toluene radical cation. The process has been extended

over the years to the cleavage of bonds different from CH, in particular CC, CSi, CSn, and others, and these will be dealt with in this order in the following discussion. However, from the preparative point of view, deprotonation is often fast enough to generate benzyl radicals with reasonable efficiency by loss of a proton from the α–site and obtain benzylation reactions. Typical examples are substitution or addition reactions to the sensitizer, e.g., a cyanoaromatic (see Equation 4.10),[25–30] phthalimides,[31] quinones,[32] and immonium salts.[33,34]

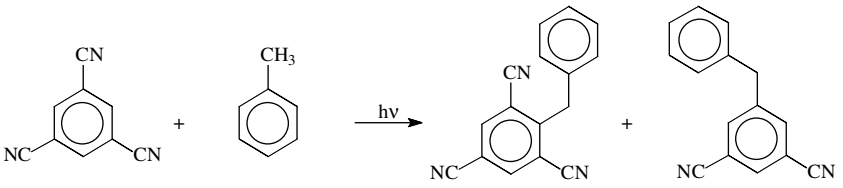

(4.10)

Evidence that stereoelectronic effects are important has been obtained by studying the intramolecular deprotonation selectivity in asymmetric polymethylbenzenes, which is the same in photoinduced SET and in activation by inorganic oxidants,[26,35] or the methyl vs. *iso*-propyl selectivity in cymenes.[36] When the benzyl radicals are highly stabilized, they undergo dimerization.[37] More interestingly from the synthetic point of view, these may be used for the photoinduced benzylation of electrophilic alkenes both by using molecular sensitizers such as DCN (1,4-dicyanonaphthalene, see Equation 4.11)[38] and by using titanium dioxide powder photocatalysis,[39] as well as for selective oxidation at the benzylic position[40–45] and photoinduced nitration with tetranitromethane.[46]

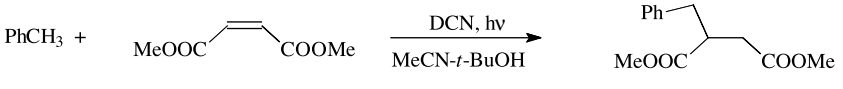

(4.11)

Other Fragmentations

Benzyl radicals are likewise obtained from radical cations by fragmentation of other electrofugal cations, in particular carbon–carbon bond fragmentation with various C-centered cations as leaving groups, such as a benzyl cation in bibenzyl derivatives,[47–49] stabilized alkyl groups,[50,51] e.g., the *t*-butyl cation in neopentylbenzene, proton and carbon dioxide in phenylacetic acids,[19,52] as well as heteroatom stabilized cations such as α-alkoxy[53–57] or α,α-dialkoxy cations and α-amino cations.[58,59] The radical cation of triarylmethylarylketones gives the triarylmethyl cation and the benzoyl radical upon triphenylpyrylium-sensitized oxygenation, but that of less heavily substituted benzylarylketones appears to cleave both ways.[60] Also in this case, benzyl radicals are trapped by the sensitizer or other additives, or otherwise couple. The recombination of the radical and cation sites leads to isomerization in some phenylcycloalkanes.

Several classes of such fragmentation reactions have been studied in detail in order to understand the effect of substituents, the stereoelectronic requirements, and the effects of the medium and of nucleophiles. The mesolytic fragmentation of bibenzyls with the reduction of the radical and nucleophilic trapping of the cation is the main process for stabilized fragments, typical examples being cumyl or benzhydryl (see Equation 4.12). The relative stability of radical and cation makes the cleavage selective for Ar ≠ Ar′.[17,61–63]

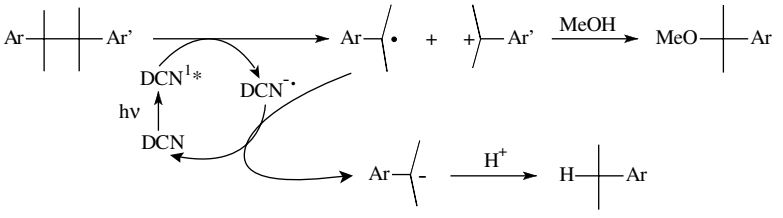

(4.12)

Another extensively investigated class, besides that of 2-phenylethyl ethers mentioned above, is that of 1,2-diarylpinacols, aminoalcohols, and diamines.[64] A variety of electron transfer sensitizers have been used with these substrates: besides aromatic acceptors, chloranil and related benzoquinones (in some cases by specific irradiation in the absorption band of the charge transfer complex formed with these donors)[65] have been used. Also, singlet oxygen is an effective SET agent with good donors.[66] With diphenylpinacol and 1,2-diphenyl-2-aminoethanols the chemical reaction, viz. oxidative (retropinacol) cleavage, is clean but the quantum yield is low, though it increases under co-sensitized (by biphenyl) conditions[67–70] because the unimolecular fragmentation of the radical cation competes unfavorably with back electron transfer. The process occurring actually involves proton transfer to the sensitizer radical anion as the rate-determining step followed by CC bond cleavage at the alkoxy radical level (see Equation 4.13).

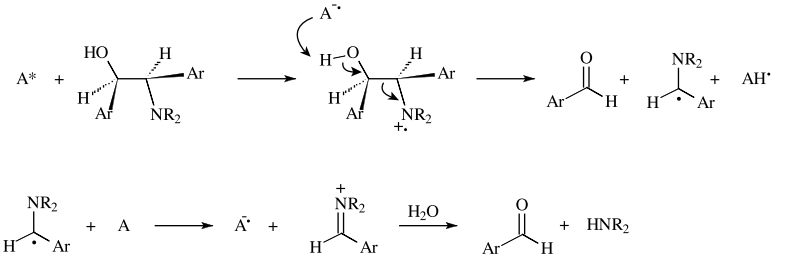

(4.13)

However, in the case of benzopinacol and with methylviologen as the sensitizer, unimolecular fragmentation of the radical cation has been detected ($\tau \approx 10$ psec).[71] With ring electron donating substituted pinacols[72] and with 1,2-diphenyldiamines,[73] unassisted fragmentations are much faster (up to 10^6–10^8 sec^{-1}). An important application is the co-fragmentation of such radical cations and of fragmentable radical anions, such as those of alkyl halides (see Equation 4.14)[74,75] or those of electron-deficient pinacols.[76]

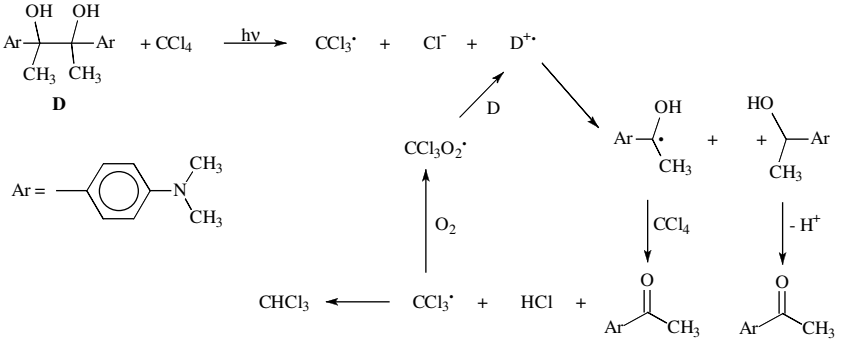

(4.14)

A particular class of benzylic CC bond cleaving radical cations is that of arylated cyclopropanes and their heterocyclic analogues. Thus, 1,2-diarylcyclopropanes[77–81] as well as 2,3-diaryloxiranes[77,82–84] and 2,3-diarylaziridines (2-monophenyl aziridine derivatives have also been studied)[77,85,86] undergo CC fragmentation upon photoinduced electron transfer sensitization. This results, after back electron transfer, in *cis-trans*-isomerization or trapping, unless a further fragmentation intervenes.[85] Trapping, whether it occurs at the radical cation level or at the ylide level after back electron transfer, has some synthetic interest. Additions to electrophilic alkenes,[82] to oxygen[77,79,80,83,84] or to nitrogen oxide (see Equation 4.15),[81] as well as to the sensitizer,[78] have been observed.

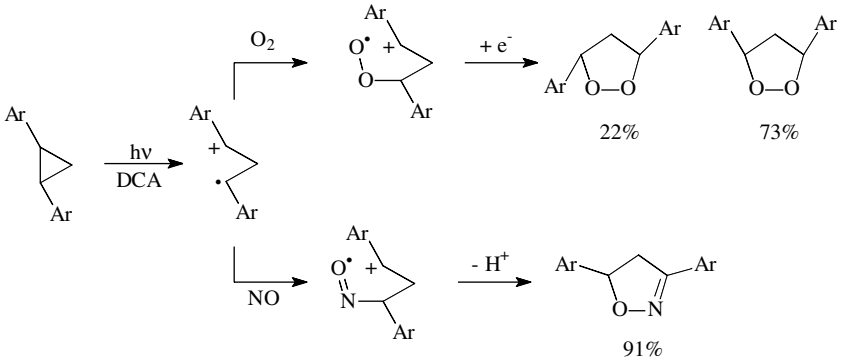

(4.15)

Diphenylazirines also cleave and the open form can be trapped to yield imidazoles and heterophanes (see Equation 4.16).[12]

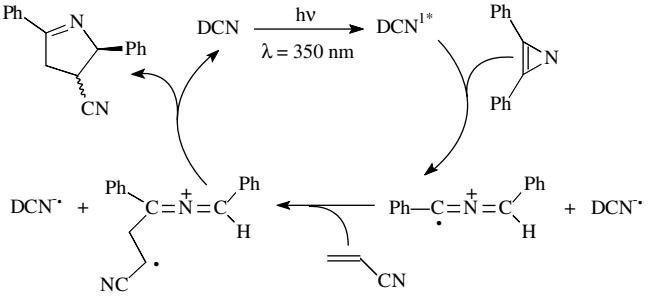

(4.16)

Among heteroatom centered leaving groups, an efficient reaction is the fragmentation in benzylsilanes, germanes, and stannanes, which has been largely exploited for benzylation reactions both with organic sensitizers (see Equation 4.17) [87–92] and through photocatalysis (see Equation 4.18).[39]

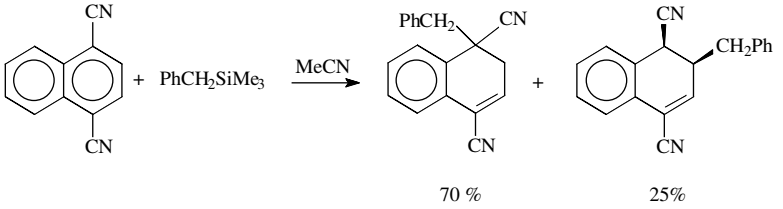

(4.17)

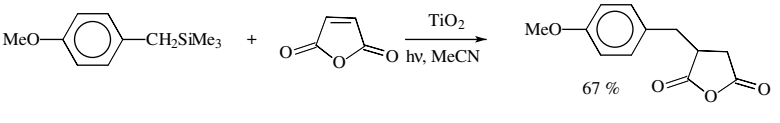

(4.18)

Di- and triphenylmethylphenyl sulfides cleave in the opposite direction giving benzyl cations and phenylthiyl radical,[93] and the same applies to benzylphenyl selenides.[94]

4.4 Olefinic Donors — Allylic Cleavage

Alkenes are reasonably good donors. Allylic deprotonation from the radical cation is usually a slow process, but it does occur to some extent as indicated by the allylation of aromatic nitriles used as electron transfer sensitizers, which takes place to a variable extent (see Equation 4.19).[95–98]

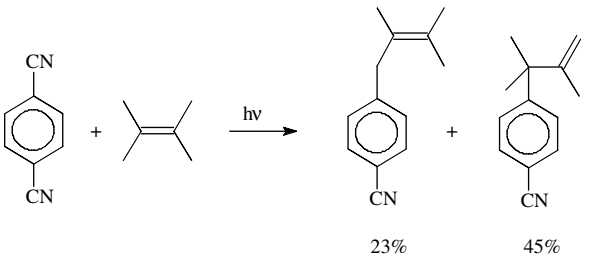

(4.19)

Solvent addition to the alkene radical cation is often preferred to fragmentation in nucleophilic media such as alcohols (this gives rise to another useful photosubstitution process on aromatics, the photo-NOCAS reaction discussed elsewhere in this Handbook).[99]

Allylic carbon–carbon bond cleavage occurs more effectively: examples are the stereospecific Cope rearrangement observed with 2,5-diary-1,5-hexadienes upon electron transfer sensitization (see Equation 4.20)[100,101] and the cleavage of the four-membered ring in pinenes at the radical cation stage.[102]

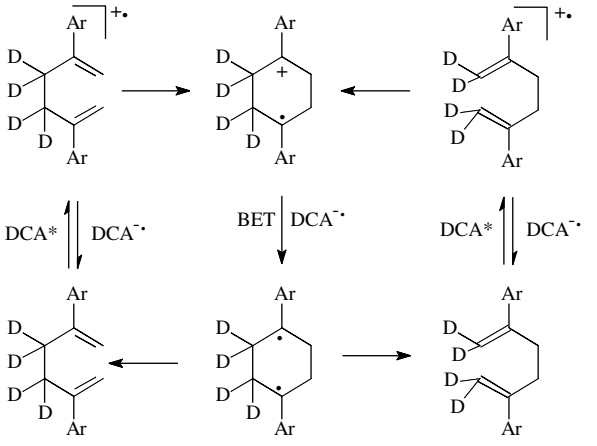

(4.20)

Allylic silanes, germanes, and stannanes have been found to fragment smoothly in the presence of various acceptors, leading to the allylation of ketones,[103–106] imminum salts,[107] and aromatics.[108,109]

4.5 Aliphatic Donors

Nitrogen-Containing Donors

Amines form relatively stable radical cations, and back electron transfer often overrides chemical reactions, except in the presence of good electrofugal groups in the α–position. Nevertheless, α-deprotonation (or alternatively a proton or hydrogen transfer process within an exciplex) may be fast enough to cause addition to unsaturated esters and ketones,[110–113] aromatics,[114] and arylalkenes.[115,116] Deprotonation and further oxidation of some tertiary amines appear to produce aminium salts that are then allylated by allyl radicals simultaneously produced by fragmentation of allylsilane. Both processes are brought about by photosensitized electron transfer.[117]

Carbon–carbon bond cleavage is important in the retro-aldol fragmentation of 2-aminoethanol and in the decarboxylation of α-aminoacids. As an example, decarboxylation in α-anilinocarboxylic acid has been shown to be an unusually fast process (10^6 to 10^7 sec^{-1}) and to occur unimolecularly, differently from deprotonation and desilylation from structurally related anilines.[20] The decarboxylation of the *N*-phthaloyl derivatives of α-amino acids has been extensively investigated (see e.g., Equation 4.21).[118–122]

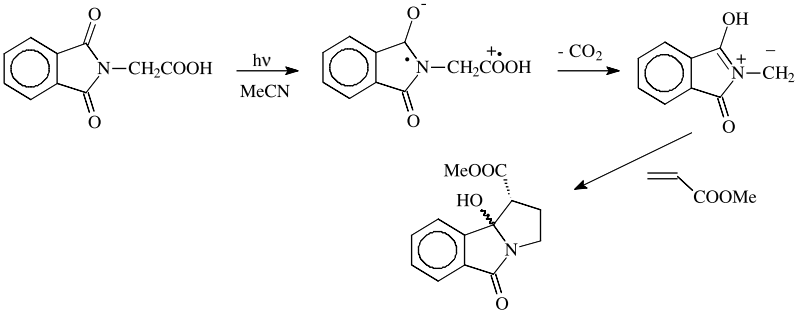

(4.21)

With aliphatic amines, the silyl cation has been shown once again to be an excellent electrofugal group, and α–silylamines have proved to be convenient precursors for the generation of alkyl radicals and the alkylation of cyanoaromatics[123,124] and of unsaturated ketones (see Equation 4.22).[125–131] The latter reaction has a wide synthetic potential.

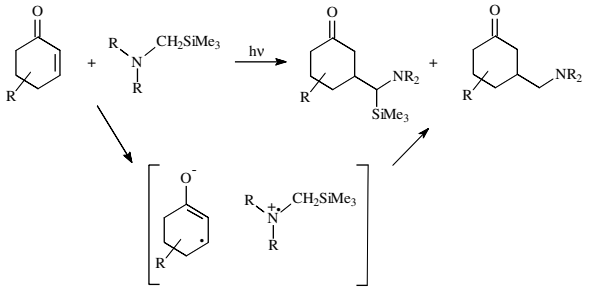

(4.22)

Electron transfer photosensitization of spiro-diaziridines with aromatic ketones is a method for the generation of carbenes initiated by CN bond fragmentation at the cation radical stage.[132]

Aliphatic azo derivatives extrude nitrogen upon photosensitized electron transfer, and this is a smooth entry to distonic radical cations, the chemistry of which has been studied in a number of cases. As an example, the cationic character of the intermediate in the photolysis of 7,7-dimethyl-2,3-diazabicyclo[2,2,1]hept-2-ene is clearly demonstrated by the Wagner–Meerwein rearrangement leading to 2,3-dimethylcyclopentene (see Equation 4.23).[133–135]

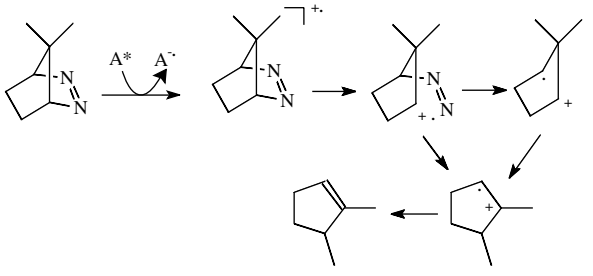

(4.23)

Oximes are deprotected to ketones by photosensitization with chloranil, apparently via proton transfer from the radical cation to the radical anion of the acceptor.[136]

With particularly strong acceptors, such as singlet excited tri- and tetracyanobenzenes, weak donors such as aliphatic nitriles can deprotonate from the α-position (see Equation 4.24)[137,138] and alkylate the sensitizer.

Oxygen- and Sulfur-Containing Donors

Photosensitized oxidation of ethers causes α-deprotonation; in the case of methyl neopentyl ether, CC and CH fragmentation compete.[139] The resulting radicals react with the sensitizer, viz. an aromatic nitrile[139–143] or an iminium salt.[144] As in the case of amines, α-trimethylsilyl ethers and thioethers are excellent precursors for the corresponding α-heteroatom-substituted alkyl radicals.[123,124] The potassium salts of α–oxoalkyl and α-thioalkyl carboxylic acid decarboxylate upon photosensitization by phthalimides.[145] Alcohols undergo, as expected, α-CH and no OH deprotonation, via the radical cation formed with sensitizers such as tetracyanobenzene (see Equation 4.24)[124] and pyrrolinium salts.[144]

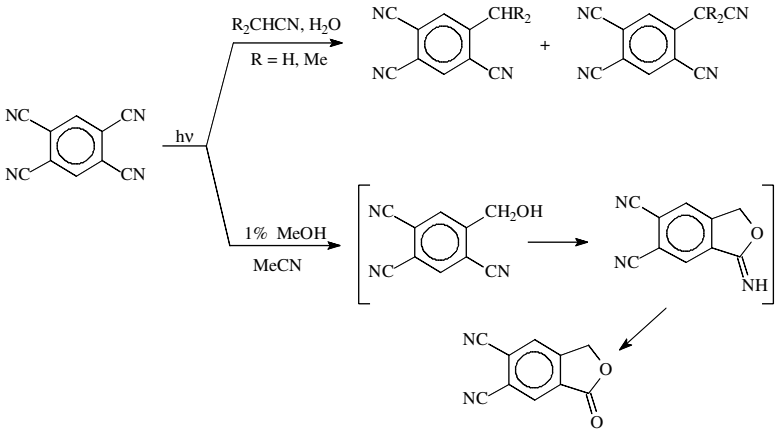

(4.24)

Acetals and ketals cleave to yield alkyl radicals and α,α-dioxo substituted cations. This is one of the cases where the electron-donating moiety is incorporated in the electrofugal group, and a nonstabilized alkyl radical is formed. This is an efficient process, and such substrates, in particular 2-alkyl and 2,2-dialkyl-1,3-dioxolanes, serve as useful precursors for the mild generation of alkyl radicals that can be trapped by the sensitizer (see Equation 4.5)[146] or, more usefully from the synthetic point of view, by electrophilic alkenes. In the latter case, the resulting adduct radical may in turn enter into a substitution process on the aromatic nitrile (the ROCAS process, Radical Olefin Combination Aromatic Substitution)[147] or be reduced by the radical anion of the sensitizer and be protonated. In the last case, the sensitizer is regenerated and conjugate radical alkylation results (see Equation 4.25).

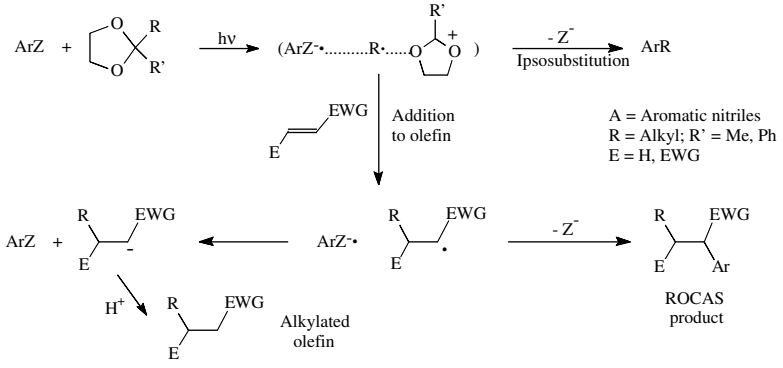

(4.25)

The thermodynamic conditions governing this partitioning have been defined,[148,149] and acetals and further radical precursors have been extensively applied for conjugate alkylation.[150–153] Photosensitized conjugate addition is particularly effective when using aromatic esters in the place of nitriles as the

sensitizers, since the former compounds are consumed at a lower rate and their turnover number is particularly favorable.[154] Fragmentation of acetals and thioacetals serves also as a mild procedure for deprotection of carbonyls[155–157] (including fragmentation of the glucoside bond in aryl glycosides),[158,159] and some useful chemistry can be carried out also via transformations of the electrofugal cation, as shown for the case of some carbohydrate ketals (see Equation 4.26).[160]

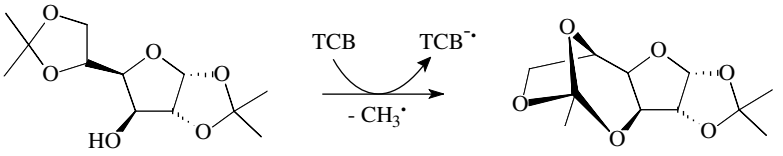

(4.26)

Among other sulfur containing donors, thiocarbonates also cleave,[161] and electron transfer from cysteine leading to decarboxylation involves the sulfur atom at all pHs.[162] Electron transfer photosensitization of some 2,2-diarylthietanes causes retrocycloaddition and yields 1,1-diarylethylenes (see Equation 4.27, DCA = 9,10-dicyanoanthracene).[163]

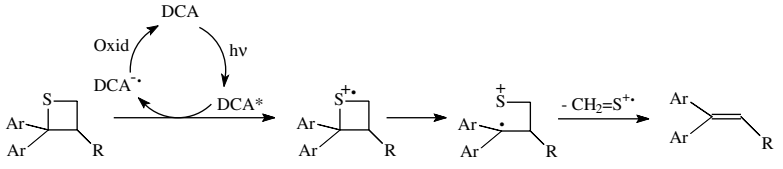

(4.27)

Silylethers also give alkyl radicals (see Equation 4.5),[124] and siloxycyclopropanes yield β-keto radicals.[164] Arylpinacol silyl ethers can be used to silylate tetrachloro-*p*-benzoquinone.[165]

Organometallic Donors

Tetralkyl-silanes, -germanes, and –stannanes,[24,166,167] as well as disilanes[168] and distannanes,[166] have been successfully used as alkyl radical precursors. The use of alkyl radicals is closely parallel to that presented above starting from ketals for the substitutive alkylation of aromatics and the conjugate addition to alkenes and alkynes (see Equations 4.5 and 4.28). Notice, however, that the final result depends on the sensitizer-trap used. Thus, *N*-methylacridinium perchlorate is reductively alkylated by hexamethyldisilane[168] but undergoes reductive dimerization with the corresponding digermanes and distannanes.[169]

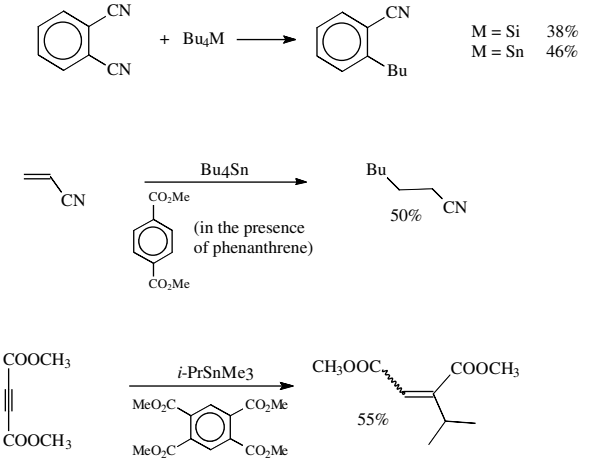

(4.28)

Alkylborates likewise generate alkyl radicals efficiently that alkylate the sensitizer (an aromatic nitrile).[170,171] On the other hand, disilanes may undergo cleavage of the SiSi bond and act as silylating agents, as is the case for the silylation of tetrachloro-*p*-benzoquinone[172] and (in low yield) of polycyanobenzenes[173] by hexamethyldisilane. Polysilanes containing a terminal hydroxyl group have been found to undergo SiSi bond fragmentation followed by intramolecular trapping to yield cyclic siloxanes upon photosensitization by DCA.[174]

No Donating Moiety

Strong acceptors such as tetracyanobenzene can oxidize and decarboxylate aliphatic acids (see Equation 4.5)[175] as well as *t*-butyl esters.[176] Indeed, simple alkanes also undergo photosensitized oxidation and are deprotonated via the radical cation under these conditions. The radicals are identified from the alkylation of the sensitizer (in this case, TCB, see Equation 4.29).[177–180]

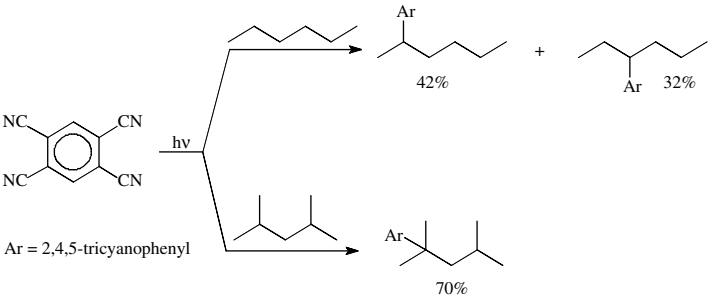

(4.29)

Ring opening and rearrangement have been observed with strained hydrocarbons such as bicyclo[2.2.0]hexane,[181] cubane (see Equation 4.30),[182] and other cage hydrocarbons.[183]

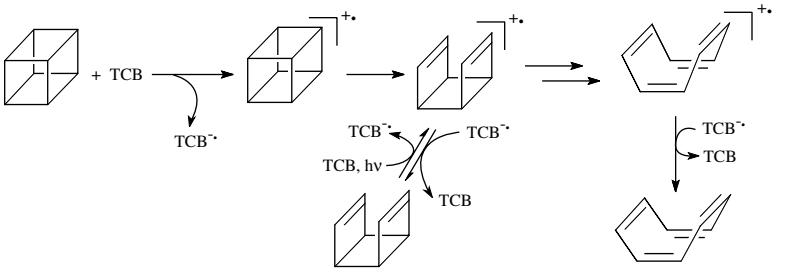

(4.30)

References

1. Fox, M.A. and Chanon, M., *Photoinduced Electron Transfer,* Elsevier, Amsterdam, 1988.
2. Kavarnons, G.J. and Turro, N.J., Photosensitization by reversible electron transfer: theory, experimental evidence and examples, *Chem. Rev.,* 86, 401, 1986.
3. Mattay, J. and Vondenhof, M., Contact and solvent separated radical ion pairs in organic chemistry, *Top. Curr. Chem.,* 159, 219, 1991.
4. Albini, A., Fagnoni, M., and Mella, M., Photoinduced electron transfer: perspectives in organic synthesis, in *Chemistry at the Beginning of the Third Millennium*, Fabbrizzi, L. and Poggi, A., Eds., Springer, Berlin, 2000, p. 83.
5. Mattay, J., Charge transfer and radical ions in photochemistry, *Angew. Chem. Int. Ed. Engl.,* 26, 825, 1987.
6. Saeva, F.D., Photoinduced electron transfer (PET) bond cleavage reactions, *Top. Curr. Chem.,* 156, 59, 1990.

7. Maslak, P., Fragmentations by photoinduced electron transfer. Fundamentals and practical aspects, *Top. Curr. Chem.,* 168, 1, 1993.
8. Albini, A., Mella, M., and Freccero, M., A new method in radical chemistry: generation of radicals by photo-induced electron transfer and fragmentation of the radical cation, *Tetrahedron,* 50, 575, 1994.
9. Albini, A., Fasani, E., and d'Alessandro, N., Radical cation: generation by photoinduced electron transfer and fragmentation, *Coord. Chem. Rev.,* 125, 269, 1993.
10. Gaillard, E.R. and Whitten, D.G., Photoinduced electron transfer bond fragmentations, *Acc. Chem. Res.,* 29, 292, 1996.
11. Mella, M., Fagnoni, M., Freccero, M., Fasani, E., and Albini, A., New synthetic methods via radical cation fragmentation, *Chem. Soc. Rev.,* 27, 81, 1998.
12. Albrecht, E., Averdung, J., Bischof, E.W., Heidbreder, A., Kirschberg, T., Müller, F., and Mattay, J., Photoinduced electron transfer (PET) in organic synthesis. [3 + 2]-Type cycloaddition, cyclization and C-C bond cleavage reactions, *J. Photochem. Photobiol. A: Chem.,* 82, 219, 1994.
13. Schmittel, M. and Burghart, A., Understanding reactivity patterns of radical cations, *Angew. Chem. Int. Ed. Engl.,* 36, 2550, 1997.
14. Nicholas, A.M.P. and Arnold, D.R., The estimation of the pKa of radical cations based on thermochemical calculations, *Can. J. Chem.,* 60, 2165, 1982.
15. Du, X., Arnold, D.R., Boyd, R.J., and Shi, Z., Cleavage of the radical cations of alkenes; 1-butene and 4,4-dimethyl-1-pentene, *ab initio* calculations on the interaction between the allyl and alkyl radical and cation moieties, *Can. J. Chem.,* 69, 1365, 1991.
16. Wayner, D.D.M., McPhee, D.J., and Griller, D., Oxidation and reduction potential of transient free radicals, *J. Am. Chem. Soc.,* 110, 132, 1988.
17. Popielartz, R. and Arnold, D.R., Carbon–carbon bond cleavage of radical in solution: theory and application, *J. Am. Chem. Soc.,* 112, 3068, 1992.
18. Freccero, M., Pratt, A., Albini, A., and Long, C., A kinetic evaluation of carbon–hydrogen, carbon–carbon, and carbon–silicon bond activation in benzylic radical cations, *J. Am. Chem. Soc.,* 120, 284, 1998.
19. d'Alessandro, N., Albini, A., and Mariano, P.S., Methylbenzene cation radical α-fragmentation selectivities revealed in SET photoaddition of *p*-xylene derivatives to 1,4-dicyanonaphthalene, *J. Org. Chem.,* 58, 937, 1993.
20. Su, Z., Mariano, P.S., Falvey, D.E., Yoon, U.C., and Oh, S.W., Dynamics of anilinium radical α–heterolytic fragmentation processes. Electrofugal group, substituent and medium effects on desilylation, decarboxylation and retro-aldol cleavage pathways, *J. Am. Chem. Soc.,* 120, 10676, 1998.
21. Su, Z., Falvey, D.E., Yoon, U.C., and Mariano, P.S., The dynamics of α–anilinocarboxylate and related cation radical α–heterolytic fragmentation processes, *J. Am. Chem. Soc.,* 119, 5261, 1997.
22. Zhang, X., Yeh, S.R., Hong, S., Freccero, M., Albini, A., Falvey, D.E., and Mariano, P.S., Dynamics of α-CH deprotonation and α-desilylation reaction of tertiary amine cation radicals, *J. Am. Chem. Soc.,* 116, 4211, 1994.
23. Dinnocenzo, J.P., Farid, S., Goodman, J.L., Gould, I.R., Todd, W.P., and Mattes, S.L., Nucleophile-assisted cleavage of silane radical cation, *J. Am. Chem. Soc.,* 111, 8973, 1989.
24. Fagnoni, M., Mella, M., and Albini, A., Scope and mechanism of the electron transfer photoinduced alkylation of an aromatic nitrile, *Tetrahedron*, 50, 6401, 1994.
25. Albini, A., Fasani, E., and Freccero, M., The photochemical reaction between arenenitriles and benzylic donors, *Adv. El. Tr. Chem.,* 5, 103, 1996.
26. Lewis, F.D. and Petisce, J.R., Proton transfer reactions of photogenerated cyanoaromatics or methylaromatics radical ion pairs, *Tetrahedron*, 42, 2975, 1984.
27. Yoshino, A., Yamasaki, K., Yonezawa, T., and Ohashi, M., Photosubstitution of 1,2,4,5-tetracyanobenzene by toluene, *J. Chem. Soc., Perkin Trans. 1,* 735, 1975.

28. Ohashi, M., Aoyagi, N., and Yamada, S., Photoreaction of 1,3,5-tricyanobenzene by toluene, *J. Chem. Soc., Perkin Trans. 1,* 1335, 1990.
29. Albini, A., Fasani, E., and Sulpizio, A., On the mechanism of the photochemical reaction between 1,4-naphthalenedicarbonitrile and methylbenzenes, *J. Am. Chem. Soc.,* 106, 3562, 1984.
30. d'Alessandro, N., Fasani, E., Mella, M., and Albini, A., On the mechanism of the photoreaction between 1,4-dicyanonaphthalene and benzylic derivatives, *J. Chem. Soc., Perkin Trans. 2,* 1977, 1991.
31. Freccero, M., Fasani, E., and Albini, A., Photochemical reaction of phthalimides and dicyanophthalimides with benzylic donors, *J. Org. Chem.,* 58, 1740, 1993.
32. Jones, G., Haney, W.A., and Phan, X.T., Photoaddition and photoreduction of chloranil via singlet and triplet excited complexes: effect of irradiation wavelength and radical ion pair multiplicity, *J. Am. Chem. Soc.,* 110, 1922, 1988.
33. Stavinoha, J. and Mariano, P.S., Electron transfer induced photocyclization reactions of arene-iminium salts system. Effect of cation diradical deprotonation and desilylation on the nature and efficiency of the pathways followed, *J. Am. Chem. Soc.,* 109, 2738, 1987.
34. Borg, R.M., Heuckenroth, R.O., Lan, A.J.Y., Quillen, S.L., and Mariano, P.S., Arene–iminium salt electron transfer photochemistry. Mechanistically interesting photoaddition processes, *J. Am. Chem. Soc.,* 109, 2728, 1987.
35. Baciocchi, E., Mandolini, L., and Rol, C., Intramolecular selectivity in the side-chain oxidation of *p*-ethyltoluene and isodurene by cobalt (III), cerium (IV) and manganese (III), *J. Org. Chem.*, 45, 3906, 1980.
36. Sulpizio, A., Mella, M., and Albini, A., Hydrogen abstraction from the isomeric cymenes, *Tetrahedron*, 45, 7545, 1989.
37. Boggeri, E., Fasani, E., Mella, M., and Albini, A., The photochemical reaction between acenaphthene and arenecarbonitriles, *J. Chem. Soc., Perkin Trans. 2,* 2097, 1991.
38. Mella, M., Fagnoni, M., and Albini, A., Benzyl radicals from toluene by photosensitization with naphthalene-1,4-dicarbonitrile. Benzylation and hydroxymethylation of unsaturated compounds, *Eur. J. Org. Chem.,* 2137, 1999.
39. Cermenati, L., Mella, M., and Albini, A., Titanium dioxide photocatalyzed alkylation of maleic acid derivatives, *Tetrahedron*, 54, 2575, 1998.
40. Albini, A. and Spreti, S., Photoinduced oxygenation of methylbenzenes, bibenzyls and pinacols in the presence of 1,4-dicyanonaphthalene, *J. Chem. Soc., Perkin Trans. 2,* 1175, 1987.
41. Santamaria, J. and Ouchabane, R., 9,10-dicyanoanthracene-sensitized photooxygenations. Formation of $O_2^{-\bullet}$ and $^1O_2$, *Tetrahedron,* 42, 5559, 1986.
42. Julliard, M. and Chanon, M., Activation of aromatics towards oxygen by oxidative or reductive photosensitization, *Bull. Soc. Chim. Fr.,* 242, 1992.
43. Santamaria, J. and Jroundi, R., Electron transfer activation — a selective photooxidation method for the preparation of aromatic aldehydes and ketones, *Tetrahedron Lett.,* 32, 4291, 1991.
44. Bokobza, L. and Santamaria, J., Exciplex and radical ion intermediates in electron transfer reactions. Solvent effect on the photo-oxygenation of 1,4-dimethylnaphthalene sensitized by 9,10-dicyanoanthracene, *J. Chem. Soc., Perkin Trans. 2,* 269, 1985.
45. Akaba, R., Kamata, M., Itoh, H., Nakao, A., Goto, S., Saito, K., Negishi, A., Sakuragi, H., and Tolumaru, K., Photoinduced electron-transfer oxygenation of arylalkanes. Generation and oxygenation pathways of benzylic-type free radicals from the cation radical deprotonation, *Tetrahedron Lett.,* 33, 7011, 1992.
46. Masnovi, J.M., Sankararaman, S., and Kochi, J.K., Direct observation of the kinetic acidities of transient aromatic cation radicals. The mechanism of electrophilic side-chain nitration of methylbenzenes, *J. Am. Chem. Soc.,* 111, 2263, 1989.
47. Okamoto, A., Snow, M.J., and Arnold, D.R., Photosensitized (electron transfer) carbon–carbon bond cleavage of radical cations. The diphenylmethyl system, *Tetrahedron,* 42, 6175, 1986.

48. Kochi, J.K., Sankaraman, S., and Perrier, S., Effective charge transfer photochemistry via fragmentable cation radicals with variable lifetimes. Direct comparison with chloranil, *J. Am. Chem. Soc.,* 111, 6448, 1989.
49. Albini, A., Fasani, E., and Mella, M., Photochemical reactions of 1,4-naphthalenedicarbonitrile with alkylbenzenes and bibenzyls, *J. Am. Chem. Soc.,* 108, 4119, 1986.
50. Sulpizio, A., Albini, A., d'Alessandro, N., Fasani, E., and Pietra, S., The photochemical reaction between 1,4-naphthalenedicarbonitrile and α-substituted benzylic derivatives, *J. Am. Chem. Soc.,* 111, 5773, 1989.
51. Bardi, L., Fasani, E., and Albini, A., Photoinduced SET reactions of bibenzyl and some of its derivatives, *J. Chem. Soc., Perkin Trans. 1,* 545, 1994.
52. Libman, J., The photochemical behavior of 1-cyanonaphthalene in the presence of phenylacetic acid derivatives, *J. Am. Chem. Soc.,* 97, 4139, 1975.
53. Arnold, D.R. and Lamont, L.J., Photosensitized (electron transfer) carbon–carbon bond cleavage of the 2-phenyl ether and acetal system, *Can. J. Chem.,* 67, 2119, 1989.
54. Arnold, D.R., Lamont, L.J., and Perrot, A.L., 1,n–cation radicals. Photosensitized (electron transfer) carbon–carbon bond cleavage. Formation of 1,6 radical cations, *Can. J. Chem.,* 69, 2119, 1991.
55. Perrot, A.L., de Lijser, H.J.P., and Arnold, D.R., The importance of conformational effects on the carbon–carbon bond cleavage of β-phenethyl ether radical cations, *Can. J. Chem.,* 75, 384, 1997.
56. Arnold, D.R., Du, X., and Hensleit, K.M., The effect of *meta*- and *para*-methoxy substitution on the reactivity of the radical cations of arylalkenes and alkanes, *Can. J. Chem.,* 69, 839, 1991.
57. Arnold, D.R., Du, X., and Chen, J., The effect of *meta*- and *para*-cyano substitution on the reactivity of the radical cations of arylalkenes and alkanes, *Can. J. Chem.,* 73, 307, 1995.
58. Ohashi, M., Akiyama, S., and Yamada, S., Design and mass spectrometric mimetic reactions in solution. Cleavage of C-C bonds in the radical cations of *N,N*-dimethyl-2,2-diphenylamine, *Nippon Kagaku Kaishi,* 1386, 1989.
59. Yamada, S., Tanaka, T., Akiyama, S., and Ohashi, M., Fragmentation of laudanosine by single electron transfer reactions, *J. Chem. Soc., Perkin Trans. 2,* 449, 1992.
60. Akaba, R., Niimura, Y., Fukushima, T., Kawai, Y., Tajima, T., Kuragami, T., Negishi, A., Kamata, M., Sakuragi, H., and Tokumaru, K., Photoinduced electron transfer carbon–carbon bond cleavage of radical cations of carbonyl compounds in solution. 2,4,6-Triphenylpyrylium salt-sensitized oxygenation of aralkyl ketones and aldehydes, *J. Am. Chem. Soc.,* 114, 4460, 1992.
61. Ishiguro, K., Osaki, T., and Sawaki, Y., A novel role of methanol in in-cage reaction of radical cations during photosensitized C-C bond cleavage of 1,1,2,2-tetraphenylethane, *Chem. Lett.,* 743, 1992.
62. Maslak, P. and Chapman, W.H., Dicyanobenzene sensitized carbon–carbon bond cleavage in methoxybicumenes. Products and mechanistic studies, *Tetrahedron,* 46, 2715, 1990.
63. Maslak, P. and Chapman, W.H., Mesolytic scission of C-C bonds as a probe for photoinduced electron transfer reactions of quinones, *J. Org. Chem.,* 61, 2647**,** 1996.
64. Gan, H., Kellet, M.A., Leon, J.W., Kloeppner, L.R., Leinhos, U., Gould, I.R., Farid, S., and Whitten, D.G., Novel intermolecular and intramolecular photochemical reactions initiated by excited state single electron transfer processes, *J. Photochem. Photobiol. A: Chem.*, 82, 211, 1994.
65. Perrier, S., Sankararaman, S., and Kochi, J.K., Photoinduced electron transfer in pinacol cleavage with quinones via highly labile cation radicals. Direct comparison of charge-transfer excitation and photosensitization, *J. Chem. Soc., Perkin Trans. 2,* 825, 1993.
66. Haugen, C.M., Bergmark, W.R., and Whitten, D.G., Singlet oxygen mediated fragmentation of amino alcohols, 1,2-diamines and amino ketones, *J. Am. Chem. Soc.,* 114, 10293, 1992.
67. Albini, A. and Mella, M., The photochemical reaction of 1,4-naphthalenedicarbonitrile with aromatic pinacols and pinacol ethers, *Tetrahedron*, 42, 6219, 1986.
68. Ci, X. and Whitten, D.G., Photoinduced dehydrofragmentation reactions: importance of donor and acceptor structure in determining the reactivity in radical ion pairs formed in electron transfer reactions, *J. Am. Chem. Soc.,* 109, 7215, 1987.

69. Ci, X., Kellet, M.A., and Whitten, D.G., Oxidative fragmentation of α, β-amino alcohols via single electron transfer: cooperative reactivity of donor and acceptor ion radicals in photogenerated contact radical ion pairs, *J. Am. Chem. Soc.,* 113, 3893, 1991.
70. Lucia, L.A., Burton, R.D., and Schanze, K.S., Direct observation of carbon–carbon bond fragmentation in α-amino alcohol radical cations, *J. Phys. Chem.,* 97, 9078, 1993.
71. Bockman, T.M., Hubig, S., and Kochi, J.K., Direct measurement of ultrafast carbon–carbon cleavage rates via the subpicosecond charge transfer activation of pinacols, *J. Am. Chem. Soc.,* 120, 6542, 1998.
72. Gan, H., Leinhos, U., Gould, I.R., and Whitten, D.G., Photoinduced electron transfer oxidative fragmentation of aminopinacols. Factors governing reaction rates and quantum efficiencies of C-C bond fragmentation, *J. Phys. Chem.,* 99, 3566, 1995.
73. Lucia, L.A., Wang, Y., Nafisi, K., Netzel, T.L., and Schanze, K.S., Direct observation of ultrafast carbon–carbon bond fragmentation in a diamine radical cation, *J. Phys. Chem.,* 99, 11801, 1995.
74. Chen, L., Farahat, M.S., Gaillard, E.R., Farid, S., and Whitten, D.G., Photoinduced electron transfer double fragmentation: an oxygen-mediated radical chain process in the co-fragmentation of substituted pinacol donors with carbon tetrachloride, *J. Photochem. Photobiol. A: Chem.,* 95, 21, 1996.
75. Zhang, W., Yang, L., Wu, L.M., Liu, Y.C., and Liu, Z.L., Photoinduced electron transfer retropinacol reaction of 4-(*N,N*-dimethylamino)phenyl pinacols in chloroform, *J. Chem. Soc., Perkin Trans. 2,* 1189, 1998.
76. Chen, L., Lucia, L., and Whitten, D.G., Cooperative electron transfer fragmentation reactions. Amplification of a photoreaction through a tandem chain fragmentation of acceptor and donor pinacols, *J. Am. Chem. Soc.,* 120, 439, 1998.
77. Schaap, A.P., Siddiqui, S., Pradad, G., Palomino, E., and Lopez, L., Cosensitized electron transfer photo-oxygenations. The photochemical preparation of 1,2,4-trioxolanes, 1,2-dioxolanes and 1,2,4-dioxazolidines, *J. Photochem.,* 25, 167, 1984.
78. Mizuno, K., Ichinose, N., and Otsuji, Y., Photochemistry of the 9,10-dicyanoanthracene–1,2-diarylcyclopropane system. Photocycloaddition and photoisomerization, *J. Org. Chem.,* 57, 1855, 1992.
79. Mizuno, K., Kamiyama, N., Ichinose, N., and Otsuji, Y., Photooxygenation of 1,2-diarylcyclopropanes via electron transfer, *Tetrahedron,* 41, 2207, 1985.
80. Ichinose, N., Mizuno, K., Tamai, T., and Otsuji, Y., Photooxygenation of 1-alkyl-2,3-diarylcyclopropanes via photoinduced electron transfer: stereoselective formation of 4-alkyl-3,5-diaryl-1,2-dioxolanes and their conversion to 1,2-diols, *J. Org. Chem.,* 55, 4079, 1990.
81. Mizuno, K., Ichinose, N., Tamai, T., and Otsuji, Y., Insertion of nitrogen oxide and nitrosonium ion in the cyclopropane ring: a new route to 2-isoxazolidines and its mechanistic studies, *J. Org. Chem.,* 57, 4669, 1992.
82. Albini, A. and Arnold, D.R., The photochemical ring opening of aryloxiranes, *Can. J. Chem.,* 56, 2985,1978.
83. Schaap, A.P., Lopez, L., and Gagnon, S.D., Formation of an ozonide by electron transfer photooxygenation of tetraphenyloxirane. Cosensitization by 9,10-dicyanoanthracene and biphenyl, *J. Am. Chem. Soc.,* 105, 663, 1983.
84. Schaap, A.P., Siddiqui, S., Prasad, G., Rahman, A.F.M.N., and Oliver, J.P., Stereoselective formation of *cis*-ozonides by electron transfer photooxygenation of naphthyl-substituted epoxides. Stereochemical assignment of ozonides by x-ray crystallography and chromatographic resolution, *J. Am. Chem. Soc.,* 106, 6087, 1984.
85. Gaebert, C. and Mattay, J., [3 + 2] Cycloaddition and nucleophile additions of aziridines under C-C and C-N bond cleavage, *Tetrahedron,* 53, 14297, 1997.
86. Hasegawa, E., Koshii, S., Horaguchi, T., and Shimizu, T., Photoinduced electron transfer reaction of 1-substituted 2,3-diphenylaziridines with 9,10-dicyanoanthracene and chloranil, *J. Org. Chem.,* 57, 6342, 1992.

87. Mizuno, K., Ikeda, M., and Otsuji, Y., A novel photosubstitution of dicyanobenzenes by allylic and benzylic silanes, *Tetrahedron Lett.,* 26, 461, 1985.
88. Baciocchi, E., Del Giacco, T., Elisei, F., and Ioele, M., Chloranil-sensitized photolysis of benzyltrimethylsilanes. Solvent effect on the competition between carbon–hydrogen and carbon–silicon cleavage, *J. Org. Chem.,* 60, 7974, 1995.
89. Cermenati, L., Freccero, M., Venturello, P., and Albini, A., SET and exciplex pathway in the photochemical reactions between aromatic ketones and benzylsilanes and stannanes derivative, *J. Am. Chem. Soc.,* 117, 7869, 1995.
90. Nakanishi, K., Mizuno, K., and Otsuji, Y., Photosubstitution of dicyanobenzenes by allylic silanes, germanes, and stannanes via photoinduced electron transfer, *Bull. Chem. Soc. Jpn.,* 66, 2731, 1993.
91. Tamai, T., Mizuno, K., Hashida, I., and Otsuji, Y., Photoinduced electron transfer reactions of arylmethyl-substituted 14 group compounds: photoarylmethylation and photooxygenation, *Bull. Chem. Soc. Jpn.,* 66, 3747, 1993.
92. Azarani, A., Berinstain, A.B., Johnston, L.J., and Kazanis, S., Electron transfer reactions between excited diarylmethyl and triarylmethyl carbocations and aromatic donors, *J. Photochem. Photobiol. A: Chem.,* 57, 175, 1991.
93. Adam, W., Arguello, J.E., and Penenory, A.B., Photochemical electron-transfer reactions between sulfides and tetranitromethane. Oxidation vs. fragmentation of the sulfide radical-cation intermediate, *J. Org. Chem.,* 63, 3905, 1998.
94. Pandey, G. and Sekhar, B.B.V.S., Photoinduced electron transfer initiated activation of organoselenium substrates as carbocation equivalents: sequential one-pot selenylation and deselenylation reaction, *J. Org. Chem.,* 59, 7367, 1994.
95. Torriani, R., Mella, M., Fasani, E., and Albini, A., On the mechanism of the photochemical reaction between 1,4-dicyanobenzene and 2,3-dimethylbutene, *Tetrahedron,* 53, 2573, 1997.
96. Borg, R.M., Arnold, D.R., and Cameron, T.S., The photosubstitution reaction between dicyanobenzene and alkyl olefins, *Can. J. Chem.,* 62, 1785, 1984.
97. McCullough, J.J., Miller, R.C., and Wu, W.S., Photoreaction of 1- and 2-naphthalenenitriles with tetramethylethylene, *Can. J. Chem.,* 55, 2909, 1977.
98. de Lijser, H.J.P. and Arnold, D.R., Interconversion and rearrangement of radical cations. Part 2. Photoinduced electron transfer and electrochemical oxidation of 1,4-bis(methylene)cyclohexane, *J. Chem. Soc., Perkin Trans. 2,* 1369, 1997.
99. Arnold, D.R. and Snow, M.S., The photochemical nucleophile-olefin combination, aromatic substitution reaction. Part 2. Cyclic olefins, methanol, 1,4-dicyanobenzene, *Can. J. Chem.,* 66, 3012, 1988.
100. Ikeda, H., Takasaki, T., Takahashi, Y., Konno, A., Matsumoto, M., Hoshi, Y., Aoki, T., Suzuki, T., Goodman, J., and Miyashi, T., Photoinduced electron-transfer Cope rearrangements of 3,6-diaryl-2,6-octadienes and 2,5-diaryl-3,4-dimethyl-1,5-hexadienes: stereospecificity and an unexpected formation of the bicyclo[2.2.0]hexane derivatives, *J. Org. Chem.,* 64, 1640, 1999.
101. Ikeda, H., Minegishi, T., Abe, H., Konno, A., Goodman, J.L., and Miyashi, T., Photoinduced electron-transfer degenerate Cope rearrangement of 2,5-diaryl-1,5-hexadienes: a cation radical cyclization–diradical cleavage process, *J. Am Chem. Soc.,* 120, 87, 1998
102. Arnold, D.R. and Du, X., The photochemical nucleophile-olefin combination, aromatic substitution (photo-NOCAS) reaction. Part 5 methanol-monoterpenes (α- and β-pinene, tricyclene, and nopol), 1,4-dicyanobenzene, *Can. J. Chem.,* 72, 403, 1994.
103. Takuwa, A., Nishigaichi, Y., Yamashita, K., and Iwamoto, H., Allylation of α-diketones by photochemical reaction with allylstannanes. Regiochemistry of the introduced allyl group, *Chem. Lett.,* 639, 1990.
104. Takuwa, A., Nishigaichi, Y., Yamaoka, T., and Iihama, K., A highly stereospecific allylation of benzil using *(E)* and *(Z)* allyl stannanes via photoinduced electron transfer, *J. Chem. Soc., Chem. Commun.,* 1359, 1991.

105. Takuwa, A., Nischigaichi, Y., and Iwamoto, H., Conjugate addition of allylic groups to α, β–enones via photoinduced electron transfer reaction of allyl stannanes, *Chem. Lett.,* 1013, 1991.
106. Hasgawa, E., Ishigama, K., Horaguchi, T., and Shimizu, T., Free radical trapping of α-keto radicals derived from α, β-epoxyketones via photoinduced electron transfer, *Tetrahedron Lett.,* 32, 2029, 1991.
107. Ohga, K., Yoon, U.C., and Mariano, P.S., Exploratory and mechanistic studies on electron transfer initiated photoaddition reaction of the allylsilane–iminium salt system, *J. Org. Chem.,* 49, 213, 1984.
108. Mella, M., Fasani, E., and Albini, A., The photochemical reaction between aromatic nitriles and allylsilane, *J. Org. Chem.,* 57, 6210, 1992.
109. Nakanishi, K., Mizuno, K., and Otsuji, Y., Photosubstitution of dicyanobenzene by allylic silanes, germanes and stannanes via photoinduced electron transfer, *Bull. Chem. Soc. Jpn.,* 66, 2371, 1993.
110. Bertrand, S., Hoffmann, N., Humbel, S., and Pète, J.P., Diastereoselective tandem addition–cyclization reactions of unsaturated tertiary amines initiated by photochemical electron transfer (PET), *J. Org. Chem.,* 65, 8690, 2000.
111. Cookson, R.C., Hudec, J., and Mirza, N.A., Photochemical addition of amines to conjugated olefins, *J. Chem. Soc., Chem. Commun.,* 180, 1968.
112. Schuster, D.I. and Insogna, A.M., A reinvestigation of the reaction occurring upon photoexcitation of cyclohexenone in the presence of triethylamine, *J. Org. Chem.,* 56, 1879, 1991.
113. Pienta, N.J. and McKinney, J.E., Competitive 2-cyclohexenone dimerization and adduct formation with triethylamine, *J. Am. Chem. Soc.,* 104, 5501, 1982.
114. a) Ohashi, M., Miyake, K., and Tsujimoto, K., Photochemical reactions of dicyanobenzenes with aliphatic amines, *Bull. Chem. Soc. Jpn.,* 53, 1683, 1980. b) Bellas, M., Bryce-Smith, D., Clarke, M.T., Gilbert, A., Klunkin, G., Krestonovisich, S., Manning, C., and Wilson, S., The photoaddition of aliphatic amines to benzene, *J. Chem. Soc., Perkin Trans. 1,* 2571, 1977.
115. Lewis, F.D., Ho, T.I., and Simpson J.T., Photochemical addition of tertiary amines to stilbene. Free radical and electron transfer mechanism for amine oxidation, *J. Am. Chem. Soc.,* 104, 1924, 1982.
116. Hub, W., Schneider, S., Doerr, F., Oxman, J.D., and Lewis, F.D., *Trans*-stilbene amine exciplexes. Behavior of the exciplex, solvent separated radical ion pair and free radical ions, *J. Am. Chem. Soc.,* 106, 708, 1984.
117. Pandey, R.S., Rani, K.S., and Lakshmaiah, G., Direct carbon–carbon bond strategy at the α-position of tertiary amines by photoinduced electron transfer process, *Tetrahedron Lett.,* 33, 3201, 1992.
118. Griesbeck, A.G., Henz, A., Hirt, J., Ptaschek, V., Engel, T., Loffler, D., and Schneider, F.W., Photochemistry of *N*-phthaloyl derivatives of electron-donor substituted amino-acids, *Tetrahedron*, 50, 701, 1994.
119. Griesbeck, A.G., Photochemical activation of amino acids. From the synthesis of enantiomerically pure β, γ-unsaturated amino acids to macrocyclic ring systems, *Liebigs Ann.,* 1951, 1996.
120. Yoon, U.C. and Mariano, P.S., The synthetic potential of phthalimide SET photochemistry, *Acc. Chem. Res.,* 34, 523, 2001.
121. Takahashi, Y., Miyachi, T., Yoon, U., Oh, S.W., Mancheno, M., Su, Z., Falvey, D.F., and Mariano, P.S., Mechanistic studies on the azomethine ylide-forming photoreactions of *N*-(silylmethyl)phthalimides and *N*-phthaloylglycine, *J. Am. Chem. Soc.,* 121, 3926, 1999.
122. Sato, Y., Nakai, H., Mizoguchi, T., Kawanishi, M., Hatanaka, Y., and Kanaoka, Y., Photochemistry of the phthalimide system. 20. Photodecarboxylation of *N*-phthaloyl-α-amino acids, *Chem. Pharm. Bull.,* 30, 1263, 1982.
123. Hasegawa, E., Brumfield, M., Mariano, P.S., and Yoon, U.C., Photoaddition of ethers, thioethers and amines to 9,10-dicyanoanthracene by electron transfer pathways, *J. Org. Chem.,* 53, 5435, 1988.
124. Mella, M., d'Alessandro, N., Freccero, M., and Albini, A., Photochemical reaction of arenenitriles in the presence of alkylsilanes, silyl ethers, and silyl amines, *J. Chem. Soc., Perkin Trans. 2,* 515, 1993.
125. Hasegawa, E., Xu, W., Mariano, P.C., Yoon, U.C., and Kim, J.U., Electron transfer induced photoaddition of the silylamine Et_2NCH_2TMS to α,β-unsaturated cyclohexanones. Dual reaction pathways leading to a ion-pair–selective cation-radical chemistry, *J. Am. Chem. Soc.,* 110, 8099, 1988.

126. Yoon, U.C., Kim, Y.C., Choi, J.J., Kim, D.W., Mariano, P.S., Cho, I.S., and Jeon, Y.T., Photoaddition reaction of acenapthylendione with silyl n-electron donors via triplet single electron transfer and triplet hydrogen abstraction pathways, *J. Org. Chem.,* 57, 1422, 1992.
127. Xu, W. and Mariano, P.S., Substituent effects on amine cation radical acidity in regiocontrol of β-(aminoethyl)cyclohexenones photocycloaddition, *J. Am. Chem. Soc.,* 113, 1431, 1991.
128. Xu, W., Zhang, X.M., and Mariano, P.S., Single electron transfer promoted photocyclization reactions of (aminoethyl)cyclohexenones. Mechanistic and synthetic features of process involving the generation and reaction of amine cations and α-amine radicals, *J. Am. Chem. Soc.,* 113, 8863, 1991.
129. Jeon, Y.T., Lee, C.P., and Mariano, P.S., Radical cyclization reaction of α-silyl amine α, β-unsaturated ketones and esters promoted by single electron transfer sensitization, *J. Am. Chem. Soc.,* 113, 8847, 1991.
130. Zhang, X.M. and Mariano, P.S., Mechanistic details for single electron transfer promoted cyclization of amines to enones arising from studies of aniline-cyclohexenones photoreactions, *J. Org. Chem.,* 56, 1655, 1991.
131. Yoon, U.C. and Mariano, P.S., Mechanistic and synthetic aspect of amine-enone photochemistry, *Acc. Chem. Res.,* 25, 233, 1992.
132. Post, A.J. and Morrison H., Generation of carbenes via the photosensitization of spirodiaziridines with ketones, *J. Org. Chem.,* 61, 1560, 1996.
133. Adam, W., Denninger, U., Finzel, R., Kita, F., Platsc, H., Walter, H., and Zang, G., Comparative study of the pyrolysis, photoinduced electron transfer (PET), and laser-jet and 185-nm photolysis of alkyl-substituted bicyclic azoalkanes, *J. Am. Chem. Soc.,* 114, 5027, 1992.
134. Slugget, G., Turro, N.J., and Roth, H.D., Electron transfer induced deazatization of cyclic azo derivatives of quadricyclane and norbornadiene, *J. Am. Chem. Soc.,* 117, 9982, 1995.
135. Adam, W. and Sendelbach, J., Photosensitized electron transfer form azoalkanes: generation, fragmentation, and rearrangement of radical cations structurally related to dicyclopentadiene, *J. Org. Chem.,* 58, 5310, 1993.
136. De Lijser, H.J.P., Fardoun, F.H., Sawyer, J.R., and Quant, M., Photosensitized regeneration of carbonyl compounds from oximes, *Org. Lett.,* 4, 2325, 2002.
137. Fagnoni, M., Vanossi, M., Mella, M., and Albini, A., Limits to oxidation of organic substrates. SET oxidative processes of commonly used solvents as revealed through the photochemical reactions with 1,2,4,5-benzenetetracarbonile, *Tetrahedron*, 52, 1785, 1996.
138. Freccero, M., Mella, M., and Albini, A. The photochemical reaction of 9,10-anthracenedicarbonitrile and 1,4-naphthalenedicarbonitrile in acetonitrile in the presence of bases, *Tetrahedron,* 50, 2115, 1994.
139. Fasani, E., Mella, M., and Albini, A., Aliphatic radicals from ethers via photoinduced electron transfer: selective formation and chemistry, *J. Chem. Soc., Perkin Trans. 2,* 449, 1995.
140. Hasegawa, E., Brumfield, M., Mariano, P.S., and Yoon, U.C., Photoadditions of ethers, thioethers and amines to 9,10-dicyanoanthracene, *J. Org. Chem.,* 53, 5435, 1988.
141. Ohashi, M., Tsujimoto, K., and Furukawa, Y., Photosubstitution of 1,2,4,5-tetracyanobenzene by aliphatic ethers, *J. Chem. Soc., Perkin Trans. 1,* 1147, 1979.
142. Al-Fakhri, K. and Pratt, A.C., Photoreaction of tetrahalogenophthalonitriles with ethers, *J. Chem. Soc., Chem. Comm.,* 484, 1976.
143. Kyushin, S., Masuda, Y., Matsushita, K., Nadaira, Y., and Ohashi, M., Novel alkylation of aromatic nitriles via photoinduced electron transfer of group 14 metal carbon σ-donors *Tetrahedron Lett.,* 31, 6395, 1990.
144. Mariano, P.S., Stavinoha, J., and Bay, E., Photochemistry of iminium salt. Electron transfer mechanism for singlet quenching and photoaddition of n-donating ethers and alcohols, *Tetrahedron,* 37, 3385, 1981.
145. Griesbeck, A.G. and Oelgemoller, M., Decarboxylative photoadditions of heteroatom-substituted carboxylates to phthalimides, *Synlett*, 71, 2000.

146. Mella, M., Freccero, M., and Albini, A., The photochemical reaction of benzene-1,2,4,5-tetracarbonitrile with the acetals of cyclic and bicyclic ketones, *J. Org. Chem.,* 59, 1048, 1994.
147. Mella, M., Fagnoni, M., and Albini, A., Radicals through photoinduced electron transfer. Addition to olefin and addition to olefin-aromatic substitution reactions, *J. Org. Chem.,* 59, 5614, 1994.
148. Fagnoni, M., Mella, M., and Albini, A., Alkylation of alkenes via electron transfer photosensitization, *Tetrahedron,* 51, 859, 1995.
149. Fagnoni, M., Mella, M., and Albini, A., Radical addition to alkenes by radicals generated through photoinduced electron transfer, *J. Am. Chem. Soc.,* 117, 7877, 1995.
150. Gonzalez-Cameno, A.M., Mella, M., Fagnoni, M., and Albini, A., Photochemical alkylation of ketene dithioacetals *S,S*-dioxides. An example of capto-dative olefin functionalization, *J. Org. Chem.,* 65, 297, 2000.
151. Campari, G., Mella, M., Fagnoni, M., and Albini, A., Diastereoselective photosensitized radical addition to fumaric acid derivatives bearing oxazolidine chiral auxiliaries, *Tetrahedron Assym.,* 11, 1891, 2000.
152. Fagnoni, M., Mella, M., and Albini, A., Tandem energy transfer–electron transfer in the photosensitized alkylation of α,β-unsaturated ketones, *J. Phys. Org. Chem.,* 10, 777, 1997.
153. Courtney, M. and Albini, A., Photochemistry of some trialkylsilyloxybenzylidenmalonic acids, *J. Chem. Soc., Perkin Trans. 2,* 1105, 1997.
154. Fagnoni, M., Mella, M., and Albini, A., Electron transfer photosensitized conjugate alkylation, *J. Org. Chem.,* 63, 4026, 1998.
155. Fasani, E., Freccero, M., Mella, M., and Albini, A., The role of SET in the deprotection of (thio)ketals under photosensitization by π acceptors, *Tetrahedron,* 53, 2219, 1997.
156. Kamata, M., Kato, Y., and Hasegawa, E., Photoinduced single electron transfer reactions of 1,3-dithianes and 1,3-dithiolanes sensitized by triphenylpyrylium salt in the presence of molecular oxygen, *Tetrahedron Lett.,* 32, 4349, 1991.
157. Epling, G.A. and Wang, Q., Photosensitized cleavage of the dithio protecting group by visible light, *Tetrahedron Lett.,* 40, 5909, 1992.
158. Davis, H.F., Das, P.K., Griffin, G.W., and Timpa, J.D., Mechanistic aspects of 1,4-dicyanonaphthalene-sensitized phototransformation of arylglycopyranosides, *J. Org. Chem.,* 48, 5256, 1983.
159. Timpe, J.D., Legendre, M., Griffin, G.W., and Das, P.K., Photoinduced, electron transfer reactions of arylglycosides, *Carbohydr. Res.,* 117, 69, 1983.
160. Mella, M., Fagnoni, M., and Albini, A., Selective transformation of acetonides to orthoesters as an application of a photoinduced electron transfer process, *Tetrahedron*, 57, 555, 2001.
161. Barton, D.H.R., Dalko, P.I., and Géro, S., Radical cation reaction associated with the thiocarbonyl group, *Tetrahedron,* 33, 1883, 1992.
162. Goez, M., Rozwadowski, J., and Marciniak, B., Photoinduced electron transfer, decarboxylation and radical fragmentation of cysteine derivatives: a chemically induced dynamic nuclear polarization study, *J. Am. Chem. Soc.,* 118, 2882, 1996.
163. Shima, K., Sazaki, A., Nakabayashi, K., and Yasuda, M., Ring-splitting reaction of 2,3-diarylthietane by electron transfer photosensitization by 9,10-dicyanoanthracene, *Bull. Chem. Soc. Jpn.,* 65, 1472, 1992.
164. Rinderhagen, H., Grota, J., and Mattay, J., PET-oxidative generation of β-keto radicals. Optimization of intermolecular radical addition reactions, *J. Inf. Rec.,* 25, 229, 2000.
165. Sankararaman, S., Perrier, S., and Kochi, J.K., Effective charge transfer photochemistry via fragmentable cation radical with variable lifetimes. Direct comparison with chloranil sensitization, *J. Am. Chem. Soc.,* 111, 6448, 1989.
166. Minisci, F., Fontana, F., Caronna, T., and Zhao, L., A novel substitution reaction via photoinduced electron transfer between pyridine derivatives and alkyltin compounds, *Tetrahedron Lett.,* 33, 3201, 1992.
167. Kyushin, S., Nakadaira, Y., and Ohashi, M., Photoalkylation of pyrylium salts with group 14 metal-carbon σ donors via electron transfer, *Chem. Lett.,* 2191, 1990.

168. Fukuzumi, S., Kitano, T., and Mochida, K., Photoinduced hydride reduction of an NAD^+ analogue with permethyl polysilanes acting as electron sources and water as proton source, *Chem. Lett.,* 2177, 1989.
169. Fukuzumi, S., Kitano, Y., and Mochida, K., Photochemical one-electron reduction of 10-methylacridinium ion with group 14 dimetallic compounds with visible irradiation, *J. Chem. Soc., Chem. Commun.,* 1236, 1990.
170. Lan, J.Y. and Schuster, G.B., Photoalkylation of dicyanoarenes with alkyltriphenylborates, *J. Am. Chem. Soc.,* 107, 6710, 1985.
171. Lan, J.Y. and Schuster, G.B., Free radical formation in the photooxidative alkylation of dicyanonaphthalene with alkyltriphenylborate salts, *Tetrahedron Lett.,* 27, 4261, 1986.
172. Igarashi, M., Uedo, T., Wasaka, M., and Sakaguchi, Y., Photoinduced electron transfer reaction between hexamethyldisilane and quinones as studied by CIDNP technique, *J. Organomet. Chem.,* 421, 9, 1991.
173. Kyushin, S., Ehara, Y., Nakadaira, Y., and Ohashi, M., Novel silylation of aromatic nitriles via photoinduced electron transfer, *J. Chem. Soc., Chem. Commun.,* 279, 1989.
174. Nakadaira, Y., Otami, S., Kyushin, S., Ohashi, M., Sakurai, H., Funada, Y., Takamoto, K., and Sekiguchi, A., Mass spectral fragmentation of polysilanylalkanols. The analogies between mass spectrometry and photoinduced electron transfer, *Chem. Lett.,* 601, 1991.
175. Tsujimoto, K., Nakao, N., and Ohashi, M., Electron-donating behavior of aliphatic carboxylic acids in the photoreaction with 1,2,4,5-tetracyanobenzene, *J. Chem. Soc., Chem. Commun.,* 366, 1992.
176. Fasani, E., Mella, M., and Albini, A., Aliphatic radicals from *t*-butyl esters via photoinduced electron transfer, *Tetrahedron Lett.,* 35, 9275, 1976.
177. Mella, M., Frecccero, M., and Albini, A., Photoinduced SET for the functionalisation of alkanes, *J. Chem. Soc., Chem. Commun.,* 41, 1995.
178. Mella, M., Freccero, M., and Albini, A., The photochemical approach to the functionalisation of open-chain and cyclic alkanes. 1. Single electron transfer oxidation, *Tetrahedron,* 52, 5523, 1996.
179. Mella, M., Freccero, M., Soldi, T., Fasani, E., and Albini, A., Oxidative functionalisation of adamantane and some of its derivatives in solution, *J. Org. Chem.,* 61, 1413, 1996.
180. Mella, M., Freccero, M., Fagnoni, M., Fasani, E., and Albini, A., The photochemical approach to the functionalisation of alkanes, in *Free Radicals in Biology and Chemistry*, Minisci, F., Ed., Kluwer, Dordrecht, 1997, p. 161.
181. Tsuji, T., Miura, T., Sugiura, K., Matsumoto, M., and Nishida, S., Photoinduced electron transfer reaction of some 1,4-dialkylbicyclo[2.2.0]hexanes. Generation of cyclohexane-1,4-diyl radical cations in boat form and their stereospecific [σ^1s + σ^2s] cleavage, *J. Am. Chem. Soc.,* 115, 482, 1993.
182. Schreiner, P.R., Wittkopp, A., Gunchenko, P.A., Yaroshinsky, A.I., Peleshanko, S.A., and Fokin, A.A., The rearrangement of the cubane radical cation in solution, *Chem.-Eur. J.,* 7, 2739, 2001.
183. Fokin, A.A., Gunchenko, P.A., Peleshanko, S.A., Schleyer, P.V.R., and Schreiner, P.R., Common radical cation intermediates in cage hydrocarbon activation, *Eur. J. Org. Chem.,* 855, 1999.

5

Photochemistry in Ionic Liquids

Richard M. Pagni
University of Tennessee

Charles M. Gordon
University of Strathclyde

5.1 Introduction

A molten salt is a liquid consisting of a compound or mixture of compounds in which all, or virtually all, of the components are ionic. Liquid NaCl (m.p. 801°C), KSCN (m.p. 173.2°C), and pyridinium chloride (m.p. 146.0°C) are thus one-component molten salts. On the other hand, an ionic liquid, a term also used to refer to a salt solution, is a molten salt that is a liquid at or near room temperature. Although organic chemistry in molten salts has been known for decades,[1] molten salts were and continue to be used primarily in the study of inorganic chemistry and electrochemistry. With the fairly recent development of ionic liquids, however, the study of organic and organometallic chemistry in ionic media has come to the fore.[2] Surprisingly, many ionic compounds and their mixtures are liquids at room temperature. Consider the following three examples:

Ethylammonium nitrate, with a melting point of 4°C, has been used successfully as a medium for the Diels–Alder reaction.[3]

Lithium perchlorate in diethyl ether (LPDE), which is used widely in organic synthesis,[4] is an ionic liquid when the lithium perchlorate concentration is greater than 4.25 *M* because all of the ether is complexed to Li^+.[5] The primary means by which LPDE operates is via Li^+ catalysis.[6,7]

"Almost anhydrous" tetrabutylammonium fluoride, prepared by heating the corresponding hydrate at 40–45°C, is an excellent source of naked fluoride in organic synthesis.[8]

Even though the above three ionic liquids have considerable utility and interest, they do not represent the mainstream. The ionic liquids that are the most widely used, and the ones used in photochemical studies to date, contain 1-alkylpyridinium or 1,3-dialkylimidazolium ions. The first of these to be prepared was the two-component ionic liquid consisting of mixtures of crystalline 1-butylpyridinium chloride ([bp][Cl]) and aluminum chloride that are liquids at 40°C over a wide range of BPC to $AlCl_3$ ratios.[9] The second consists of mixtures of 1-ethyl-3-methyl-imidazolium chloride ([emim][Cl]) and $AlCl_3$ that are liquids at room temperature and below over a wide range of [emim][Cl] to $AlCl_3$ ratios.[10] These conducting media, which have been used extensively in electrochemical studies, have interesting acid–base properties. When the heterocyclic chloride is in excess, the medium is basic because of the presence of Cl^- (and $AlCl_4^-$). When aluminum chloride is in excess, the ionic liquid is acidic because of the presence of $Al_2Cl_7^-$, a powerful Lewis acid. HCl in acidic [emim][$Cl/AlCl_3$] has superacidic properties and is the strongest chlorine-containing Brønsted acid known.[11,12] These ionic liquids are not particularly

0-8493-1348-1/04/$0.00+$1.50

viscous, have very little vapor pressure at room temperature, and readily dissolve an array of organic and inorganic compounds. Because the ionic liquids contain $AlCl_3$, however, they must be prepared and handled on vacuum lines and in glove boxes. Furthermore, products are generally removed from them by extraction only after they are quenched with water which, of course, destroys the ionic liquid.

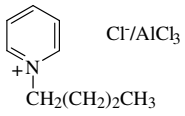

BPC/$AlCl_3$

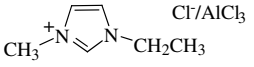

emimCl/$AlCl_3$

Many imidazolium and pyridinium salts are liquids at room temperature, even in the absence of $AlCl_3$. 1-Ethyl-3-methylimidazolium tetrafluoroborate ([emim][BF_4]) and acetate ([emim][OAc]) are both liquids at room temperature.[13] By systematically varying the size of the alkyl chains of the heterocyclic cations and the nature of the anion, it is possible to synthesize a large number of salts that are liquids at room temperature. 1-Butyl-3-methylimidazolium hexafluorophosphate ([bmim][PF_6]), which is insoluble in both water and alkanes, is perhaps the most widely used of the neutral, air stable ionic liquids. Because these ionic liquids have virtually no vapor pressure and have large liquidus ranges, they have found wide application in the field of green chemistry.[2,14,15] Procedures to remove products from the ionic liquids and to clean up ionic liquids for reuse (they are often expensive and cannot be distilled) are still being developed.

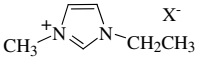

X = BF_4 ($emimBF_4$)
X = OAc (emimOAc)

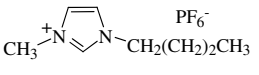

bmimPF_6

Because they are ionic in nature, ionic liquids (IL) should have large cohesive energy densities and solubility parameters; this is the case for the few ILs examined to date.[16] Generally, nonelectrolyte solutes are soluble in solvents in which the solute and solvent have similar solubility parameters.[17] One would thus expect solutes with low solubility parameters, the majority of solutes, to be poorly soluble in ionic liquids that have high values. As attested by the large number of reactions taking place in these media, this is not the case.[2] Perhaps the correlation breaks down because ionic liquids themselves are ionic.

Because they have no hydroxyl groups and are polar, ionic liquids should be categorized as aprotic dipolar solvents. Anions in typical aprotic solvents such as dimethyl sulfoxide are poorly solvated and, as a result, function as good bases and nucleophiles. In the S_N2 reaction of benzyl bromide with the nucleophile 2-naphtholate, products arise with the phenolate oxygen and C1 of the naphthalene ring functioning as nucleophiles. In protic solvents such as ethanol, where hydrogen bonding with the phenolate oxygen occurs, large amounts of C-alkylation occur.[18] In aprotic solvents such as dimethyl sulfoxide, however, mostly O-alkylation occurs.[18] In the ionic liquids (n-Bu)$_4$NBr[19], (n-Bu)$_4$PBr[19], and bmimPF_6,[20] the reaction gives mostly O-alkylation. These results are consistent with the ionic liquids acting as aprotic dipolar solvents.

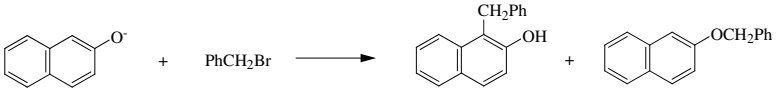

Although the above results are qualitatively consistent with ionic liquids being aprotic dipolar media, they are not definitive. The best currently available methods for characterization of solvents, including ionic liquids, involve the use of photophysical data and are the topic of the next section.

5.2 Photophysical Investigations in Ionic Liquids

Photophysical investigations of the behavior of solvatochromic probes have been widely used to give information about the properties of reaction media. The use of ionic liquids as reaction solvents dates back several years, as has been outlined in the preceding section. Despite this, only recently have photophysical measurements been extensively employed to determine their properties as solvents. Probably the most important feature to bear in mind, when considering the use of solvatochromic probe molecules in ionic liquids, is the purity of the solvent. While conventional organic solvents may be purified by distillation, the lack of vapor pressure means that ionic liquids cannot be purified in this manner. It has been shown that the presence of even small quantities of impurities such as halide ions and water can have a large effect on physical properties such as viscosity of ionic liquids.[21] Similarly, the presence of even small amounts of impurity can have drastic effects on the interactions with solvatochromic probe molecules. Bearing this in mind, some investigations into the polarity of ionic liquids have used mixtures with known quantities of other co-solvents, most commonly water.

The vast majority of photophysical investigations have focused on the widely used 1,3-dialkylimidazolium cation–based ionic liquids. Therefore, the major part of this section will consider these salts. Previously, a few workers looked at the behavior of solvatochromic probe molecules in other ionic liquids. In 1991, Herfort and Schneider reported the behavior of Reichardt's dye in ethylammonium nitrate (EAN) and its mixtures with water, methanol, *t*-butanol, dimethyl sulfoxide (DMSO) and dimethoxyethane (DME).[22] Reichardt's dye has been widely used as a probe of solvent polarity, and the molar transition energy $E_T(30)$ is a widely used polarity scale [molar transition energy $E_T(30) = 28592/\lambda_{max}$ (kcal mol^{-1})].[23] The value of $E_T(30)$ for pure EAN was reported to be in the range 59.8–60.3 kcal mol^{-1}, not much lower than the value obtained for water (62.0 kcal mol^{-1}). Even small quantities (ca. 5×10^{-3} mole fraction) of EAN added to organic co-solvents resulted in large increases in the value of $E_T(30)$, suggesting strong specific hydrogen bonding interactions between Reichardt's dye and EAN. This hypothesis was tested by comparison with the effect of added tetraethylammonium salts to DMSO, which resulted in little change in $E_T(30)$ at salt concentrations up to 0.14 *M*.

Prior to this, Poole et al. reported a Kamlet–Taft analysis of a range of alkylammonium salts using the Reichardt's dye and a series of nitroaromatic compounds to calculate the parameters π^*, α, and β.[24] The $E_T(30)$ values reported for tetraalkylammonium salts were generally in the range 45–51 kcal mol^{-1}, significantly lower than those for salts containing at least one proton directly attached to the quaternary nitrogen atom on the cation, such as EAN. As a result, the α parameters (a measure of solvent hydrogen bond donor acidity) for the latter salts were significantly higher. There also appeared to be little dependence of $E_T(30)$ or α on the anion present. Parameter π^* (a measure of dipolarity/polarizability) was similar in all cases, being close to unity (the standard reference value for DMSO). Fewer examples of parameter β (solvent hydrogen bond basicity) were quoted, but these appeared more dependent on the anion than the cation present.

In 1994, Bart et al. reported the solvation dynamics of coumarin 153 in a range of molten tetraalkylammonium salts.[25] Since these salts have melting points in the range 105–170°C, they do not qualify as ionic liquids by the current definition (usually melting point <100°C), but the results gained are of relevance to those discussed below. It was found that the emission maxima of the salts decreased steadily with increasing alkyl chain length, indicating decreasing polarity. A correlation of the emission maxima with the $E_T(30)$ gave estimated values for the latter parameter ranging from 60 kcal mol^{-1} for tetrapropylammonium hydrogen sulfate (TPAHS), close to the value for water, to 38 kcal mol^{-1} for tetradodecylammonium perchlorate (TDDAPCl), close to the value for THF. The time-resolved emission showed biphasic solvent dynamics. The short-lived component lifetime ranged from 35 psec for TPAHS to 200 psec for TDDAPCl, while the longer-lived component lifetime ranged from 125 to 2000 psec for the same salts. The dynamic behavior was tentatively explained in terms of separate contributions from the cation and anion.

The first paper to describe measurements on the 1,3-dialkylimidazolium salts was that of Bonhôte et al. in 1996, in which the emission spectra of 1-pyrenecarboxaldehyde (PyCHO), pyrene, and 1-bromonaphthalene in [emim][Tf_2N] were reported.[26] Perhaps surprisingly, the measurements using PyCHO

were similar to those obtained for solvents of low dielectric constant ($\varepsilon < 10$). The same study noted that the position of λ_{em} was very sensitive to the addition of methanol. Thus, the addition of 10% w/w methanol resulted in a shift in λ_{em} from 431 nm in pure [emim][Tf_2N] to 440 nm. The measurements using pyrene indicated a ratio of $I_1/I_3 = 1.54$ (not 1.18 as reported in the paper), approximately halfway between the values for CH_3OH (1.33) and CH_3CN (1.85). The emission lifetime of pyrene was 300 nsec in degassed [emim][Tf_2N], as against 145 nsec in aerated solutions. These data were used to estimate the saturation O_2 solubility to be ca. 6×10^{-3} *M*. Finally, the observation of room temperature phosphorescence in Ar-purged [emim][Tf_2N] suggested that the high viscosity of the reaction medium allowed considerable stabilization of triplet states. Probably the most significant conclusion to be drawn from these results was that one must be careful when considering the nature of ionic liquids as solvents. In the first instance, they appear to be low dielectric liquids (based on the measurements with PyCHO) but also solvents of relatively high polarity (as determined using pyrene).

Since that time, the number of papers reporting the solvent properties of ionic liquids as measured by solvatochromic probes has increased greatly, and these will be summarized below. The first papers specifically reporting the polarity of 1-alkyl-3-methylimidazolium based ionic liquids used the solvatochromic dyes Nile Red[27] and Reichardt's dye,[28] the solvatochromic salt [Cu(acac)(tmen)][BPh_4] (acac = acetoacetonate, tmen = *N,N,N′,N′*-tetramethyleneethylenediamine),[28] and the fluorescent probe molecules 4-aminophthalimide (AP) and 4-(*N,N*-dimethylamino)phthalimide (DAP).[29] The study using Nile Red was carried out on ionic liquids containing a range of $[Rmim]^+$ cations (R = butyl, hexyl, octyl, and decyl) and anions ($[NO_2]^-$, $[NO_3]^-$, $[BF_4]^-$, $[PF_6]^-$, and $[Tf_2N]^-$), with results as indicated in Table 5.1. Little difference in λ_{max} was observed between the different salts, the range being 556.0 nm (for [bmim][NO_2]) to 545.7 nm (for [C_{10}mim][BF_4]). These values equate to molar transition energies (E_{NR}) in the range 51.4–52.4 kcal mol^{-1}, close to that obtained for ethanol (52.1 kcal mol^{-1}) or other short-chain alcohols. Salts based on the [bmim] cation gave similar $E_T(30)$ values regardless of anion, generally close to those obtained for short chain primary alcohols (see Table 5.1).[28] A slight decrease in $E_T(30)$ was obtained on increasing the length of the alkyl chain at the 1-position to octyl. A more significant decrease in $E_T(30)$ was observed when an extra methyl group was present at the 2-position of the imidazolium ring. Aki et al. reported $E_T(30)$ values for four ionic liquids determined indirectly from the emission maximum, quantum yield, and fluorescence lifetime of DAP.[29] The values gained for [bmim][PF_6] appeared initially to be very similar to that obtained directly using Reichardt's dye (52.4 kcal mol^{-1} as compared to 52.2 kcal mol^{-1}), although rigorous drying of the liquid by heating at 75°C *in vacuo* for 24 h resulted in a decrease in the estimated value of $E_T(30)$ to 49.0 kcal mol^{-1}. A similar value was obtained for [bmim][NO_3], but for [C_8mim][PF_6], it was 46.8 kcal mol^{-1}. The other ionic liquid studied was 1-butylimidazolium tetrafluoroborate, which gave a value of $E_T(30)$ that was lower still (44.9 kcal mol^{-1}). These data seem to show that, although care must be taken in the interpretation of small data sets, families of ionic liquids show distinct trends in their interactions with different probe molecules.

One important observation from these data is that, using the probe molecules mentioned above, the apparent polarity of the ionic liquids studied was almost entirely dependent on the cation. The role of the anion in the properties of ionic liquids was probed using [Cu(acac)(tmen)][BPh_4] (acac = acetylacetone, tmen = *N,N,N′,N′*-tetramethyleneethylenediamine).[28] This square planar salt exhibits large shifts in the position of its lowest energy d-d band depending on the donor properties of its environment. The position of λ_{max} was found to vary considerably depending on the anion present, from 516.5 nm in [bmim][PF_6] to 601.5 nm in [bmim][TfO]. No significant shift in λ_{max} was observed for salts with the same anion but different cations, however.

Soon after these studies, Fletcher et al. reported the behavior of a number of solvatochromic probes (Reichardt's dye, pyrene, dansylamide, Nile Red, and 1-pyrenecarbaldehyde) in [bmim][PF_6].[30] The results gained using pyrene indicated a value of $I_1/I_3 = 1.84$, close to that of acetonitrile (1.88) and considerably higher than that of ethanol (1.37). The dansylamide results compared both the value of λ_{max}^{flu} and also the Stokes shift ($\nu_{max}^{abs} - \nu_{max}^{flu}$). The position of λ_{max}^{flu} was close to that obtained in ethylene glycol, while the Stokes shift result was closer to that for acetonitrile. For Nile Red, instead of the absorbance spectrum as in reference 27, the emission and excitation maxima were reported. The

TABLE 5.1 Values of E_{NR} and $E_T(30)$ Recorded in a Range of Ionic Liquids

Solvent	λ_{max}/nm (E_{NR}/kcal mol^{-1})	λ_{max}/nm ($E_T(30)$/kcal mol^{-1})
[C_4mim][PF_6]	547.5 (52.2)[a]	546.5 (52.3)[b]
[C_6mim][PF_6]	551.7 (51.7)[a]	—
[C_8mim][PF_6]	549.8 (52.0)[a]	558.0 (51.2)[b]
[C_4mim][BF_4]	550.8 (51.9)[a]	545.0 (52.5)[b]
[C_6mim][BF_4]	551.9 (51.8)[a]	—
[C_8mim][BF_4]	549.5 (52.0)[a]	—
[C_{10}mim][BF_4]	545.7 (52.4)[a]	—
[C_3mim][Tf_2N]	547.0 (52.3)[c]	550.5 (51.9)[c]
[C_4mim][Tf_2N]	548.7 (52.1)[a]	555.5 (51.5)[b]
[C_8mim][Tf_2N]	—	559.0 (51.1)[b]
[C_4mim][TfO]	—	547.0 (52.3)[b]
[C_4dmim][Tf_2N]	—	588.0 (48.6)[b]
[C_8dmim][Tf_2N]	—	599.5 (47.7)[b]
[C_8dmim][BF_4]	—	592.0 (48.3)[b]
[$C_6H_5CH_2$mim][Tf_2N]	552.0 (51.8)[c]	546.0 (52.4)[c]
[$CH_3O(CH_2)_2$mim][Tf_2N]	561.0 (51.0)[c]	528.0 (54.1)[c]
[$HO(CH_2)_2$mim][Tf_2N]	565.0 (50.6)[c]	470.0 (60.8)[c]

[a] Reference 27.
[b] Reference 28.
[c] Reference 32.

position of both was very close to those observed for water, indicating a significant deviation from the absorbance spectrum results. Finally, the emission maximum of pyrenecarbaldehyde in [bmim][PF_6] was observed at 428 nm, close to the value of 431 nm reported for the same probe molecule in [emim][Tf_2N].[26] The authors concluded that, overall, [bmim][PF_6] showed a polarity most closely related to acetonitrile or DMSO. They did stress, however, that the wide range of interactions that contribute to "polarity" meant that such a comparison must be treated with care.

A recent paper by Baker et al. reports the results of a study on [bmim][PF_6] to determine the Kamlet–Taft parameters π, α, and β.[31] The authors also discuss the temperature dependence of $E_T(30)$ and the influence of water. The value of $E_T(30)$ in dry [bmim][PF_6] shows a linear correlation with temperature over the range 10–70°C. As noted by previous workers, the presence of water not only results in a small increase in the value of $E_T(30)$ but also in a near doubling of the temperature dependence of this parameter. It should be noted that for the study using "wet" [bmim][PF_6], a dichloro-analogue of Reichardt's dye was used because of problems with protonation of the standard molecule. The Kamlet–Taft parameters were assembled by combining the Reichardt's dye data with those obtained using 4-nitroaniline and *N,N*-diethyl-4-nitroaniline. Based on these, at 20°C the parameters for dry [bmim][PF_6] were $\pi^* = 0.92$, $\beta = 0.21$, and $\alpha = 0.76$. The values of π^* and β were little affected by the addition of water, whereas α increased to 0.88 in the presence of 2% v/v water. This is to be expected as α is the solvent hydrogen bond donating acidity. Furthermore, the temperature dependence of α was much greater in the wet liquid.

Dzyuba and Bartsch have recently reported a study of the polarity of ionic liquids containing nonalkyl substituents.[32] They found that the presence of an ether linkage in one of the side-chains and especially a hydroxide group gives a significant increase in polarity as determined by $E_T(30)$ values (Table 5.1). Nile Red gave a similar behavior trend, although the variation in E_{NR} values was rather smaller. In the same study, it was reported that the water content of the ionic liquids made little difference to the values of $E_T(30)$ or E_{NR}. For example, [pmim][Tf_2N] gave an $E_T(30)$ value of 52.0 kcal mol^{-1} with a water content of 3810 ppm, which decreased only slightly to 51.9 when the water content was reduced to 160 ppm. A more significant effect of water content was noted by Wasserscheid et al. for [bmim][PF_6].[33] In this case, the presence of 0.15 *M* water in [bmim][PF_6] increased the value of $E_T(30)$ to 52.9 kcal mol^{-1} from 52.3 kcal mol^{-1} for the dried (water content ca. 6.0×10^{-3} *M*) liquid.

Fletcher et al. have reported a study on the fluorescence quenching of several polyaromatic hydrocarbons (PAHs) in [bmim][PF_6].[34] The emission spectra of all probe molecules indicated more favorable interactions between the excited state PAH and [bmim][PF_6] than with acetonitrile, although the exact cause of this observation was not determined. Fluorescence quenching by nitromethane indicated the interesting observation that alternant PAHs (i.e., those with fully conjugated aromatic systems such as pyrene) were selectively quenched in [bmim][PF_6] compared with nonalternant PAHs (disrupted aromaticity). For example, effectively no quenching of the fluorescence of fluoranthene was observed in [bmim][PF_6] containing up to 0.123 *M* nitromethane, whereas a Stern–Volmer quenching constant (K_{SV}) of 2.4 M^{-1} was obtained for anthracene in the same solvent/quencher mixture. This result can be compared with K_{SV} = 21.1 M^{-1} in acetonitrile/nitromethane mixtures. The much lower value of K_{SV} in the ionic liquid was attributed to the much higher viscosity of [bmim][PF_6].

Three recent papers report the results of solvation dynamics in ionic liquids as probed by fluorescence lifetimes of a range of probe molecules. Baker et al. have reported a study of the local microenvironment (cybotactic region) surrounding pyrene, PRODAN (6-propionyl-2-dimethylaminonaphthalene), and BTBP [*N,N′*-bis(2,5-di-*tert*-butylphenyl)-3,4,9,10-perylenedicarboximide] in [bmim][PF_6].[35] One notable observation was the fact that the Ham effect for pyrene in [bmim][PF_6], I_1/I_3, was 2.079 in dry [bmim][PF_6] and 2.080 in the same solvent after exposure to the atmosphere for 5 h. Note that this is a higher value than that reported in reference 30. Since such treatment is known to result in the uptake of ca. 1% w/w water, it appears that the solvation of pyrene in [bmim][PF_6] is not affected by the presence of water. Similarly, the fluorescence lifetimes (251 nsec "dry" and 247 nsec "wet" [bmim][PF_6]) were not affected by the presence of water and were significantly longer than that previously reported for pyrene dissolved in water. The addition of CO_2 up to a pressure of 130 bar to a solution of pyrene in [bmim][PF_6] was found to result in only a decrease of approximately 10% in the value of I_1/I_3 up to the critical pressure (ca. 70 bar), and thereafter no further change was observed. This suggests that the intermolecular interactions between pyrene and [bmim][PF_6] are disrupted relatively little by the presence of CO_2. The multifrequency phase modulated behavior of the emission spectrum of PRODAN was used to probe the dipolar relaxation of [bmim][PF_6] surrounding the probe molecule. The results gained indicated that two separate nanosecond relaxation processes were occurring. A combination of the pyrene and PRODAN results was used to estimate values of 11.4 ± 1.0 for the dielectric constant ε and 1.523 ± 0.025 for the refractive index *n* of [bmim][PF_6]. Finally, the rotational reorientation dynamics (ϕ) of BTBP in [bmim][PF_6] were reported to show an activation energy of 9.3 ± 0.45 kcal mol^{-1}, very close to the activation energy for viscous flow (9.28 ± 0.2 kcal mol^{-1} in this study). In this case a fivefold decrease in the value of ϕ was observed between 0 and 150 bar CO_2.

A recent study reports the solvation dynamics of coumarin 153 and 6-propionyl-2-dimethylaminonaphthalene (PRODAN) in [emim][BF_4] and [bmim][BF_4].[36,37] The fluorescence decay profiles showed biphasic solvation dynamics as was observed for molten tetraalkylammonium salts.[25] The results were interpreted as indicating a short-lived component resulting from the motion of the anion, followed by a longer-lived component resulting from the motion of both the anion and the cation. In the same papers, estimates of the value of $E_T(30)$ were made for these solvents based on comparisons of the λ_{em} values for each probe molecule in conventional solvents. The values obtained (48.9 from coumarin 153 and 47.1 kcal mol^{-1} from PRODAN for [bmim][BF_4]) were somewhat lower than those measured directly using Reichardt's dye.[28]

The studies reported above can probably be summarized by two general comments. First, although a wide range of photophysical measurements has been carried out in the most widely used ionic liquids, many gaps remain in our understanding of these materials. Such studies are still required to be carried out on salts with a wider range of structural variations in order to give a better understanding of how these affect solvent properties. Second, it is clear from the contrasting results gained using different probe molecules that ionic liquids cannot generally be portrayed as being "like a short chain alcohol" or "like a dipolar aprotic solvent." That they are generally polar materials is clear, but their basicity is very dependent on the anion present, and it also appears that they have low dielectric constants. The considerable variation in properties among different ionic liquids suggests that they do indeed live up to the

TABLE 5.2 Arrhenius Parameters for the Reaction between ^{3}Bp* and N in a Range of Ionic Liquids and Conventional Solvents, along with Andrade Parameters for the Same Solvents

Solvent	η/cP[a]	ln η	E_η	k_q/mol^{-1}dm^{3}sec^{-1}[a]	ln A	E_a/kcal mol^{-1}
[omim][PF_6]	690.6	–18.79	45.6	1.10×10^8	38.09	11.6
[bmim][PF_6]	257.1	–16.52	37.6	1.26×10^8	33.87	8.9
[omim][Tf_2N]	92.7	–14.62	30.3	2.96×10^8	33.23	8.1
[bmmim][Tf_2N]	97.1	–14.91	31.2	2.39×10^8	31.28	7.1
[bmim][Tf_2N]	51.5	–13.21	25.4	3.83×10^8	29.41	5.7

[a] At 298 K.

title of "designer solvents." It is probably best to avoid using the traditional definitions of polarity such as "dipolar aprotic" and better to consider the specific interactions any particular ionic liquid is likely to engage in with particular solute molecules.

5.3 Reactive Intermediates in Ionic Liquids

The study of mechanistic processes and more specifically reactive intermediates in room temperature ionic liquids has lagged considerably behind their use as reaction solvents. Recently, however, a number of reports have appeared on the study of intermediate species formed using laser flash photolysis and pulse radiolysis. The first report of laser flash photolysis in room temperature ionic liquids (RTILs) was by Gordon and McLean, who studied the electron transfer reaction between photoexcited $[Ru(bpy)_3]^{2+}$ and methylviologen dication (MV^{2+}) in [bmim][PF_6].[38] The Arrhenius activation energy was calculated as 9.9 kcal mol^{-1}, slightly higher than the activation energy for viscous flow in the same liquid of 9.0 kcal mol^{-1}. Thus, the electron transfer process is effectively diffusion controlled, although the additional 1 kcal mol^{-1} might indicate a small extra contribution from electrostatic repulsion. Another interesting observation was that the cage escape yield (η_{ce}) for the formation of $MV^{\cdot+}$ was much higher than expected based on the high viscosity of the ionic liquids. More recently, the same authors have reported the behavior of triplet excited state benzophenone (^{3}BP*) in a range of ionic liquids. The quenching reaction with naphthalene (N) was studied for five ionic liquids based around the 1-alkyl-3-methylimidazolium cation and the $[PF_6]^-$ and $[Tf_2N]^-$ anions.[39] In all cases, it was found that the rate of quenching was diffusion controlled; the values of E_a were almost identical to the activation energy for viscous flow. Thus, the bimolecular rate constants reported in this paper represent the limiting values for diffusion-controlled processes between neutral reactants of this type in the ionic liquids. Examples of the bimolecular rate constants obtained are illustrated in Table 5.2.

An isokinetic relationship between pre-exponential factors and E_a was also reported. In the absence of quenchers, it was found that the degree of hydrogen abstraction from 1-alkyl-3-methylimidazolium–based ionic liquids was considerably lower than that observed for conventional solvents such as toluene or butan-1-ol.[40] Furthermore, the activation energy for this process was similar in all ionic liquids studied (ca. 6 kcal mol^{-1}) and roughly 2.4 kcal mol^{-1} higher than the values obtained in the conventional solvents.

Pulse radiolysis has also been used to generate reactive intermediates in ionic liquids. The products formed have been studied at low temperatures in frozen ionic liquid glasses, and their kinetics have also been investigated at higher temperatures. Two similar studies were reported almost simultaneously in 2001.[41,42] In both of these, the reaction of $[bmim]^+$ with e_{aq} to form the equivalent radical species was reported in aqueous solution (Equation 5.1).

$$\left[\text{bmim}\right]^+ + e_{aq} \rightarrow \left[\text{bmim}\right]\cdot \tag{5.1}$$

Identification of the main product as [bmim]· was confirmed by its λ_{max} value of 320 nm. Similar values for the bimolecular rate constant of this reaction were reported in the two studies (1.9×10^{10} l mol^{-1} sec^{-1} in reference 41 and 1.5×10^{10} l mol^{-1} sec^{-1} in reference 42). In reference 41, the reaction of [bmim]$^+$ with ·OH and $SO_4^{\cdot-}$ was also reported, the latter resulting in the formation of [bmim]$^{\cdot 2+}$ (Equation 5.2).

$$\left[\text{bmim}\right]^+ + SO_4^{\cdot-} \rightarrow \left[\text{bmim}\right]^{\cdot 2+} + SO_4^{2-} \tag{5.2}$$

Pulse radiolysis of neat ionic liquids was also reported to give [bmim]· and [bmim]$^{\cdot 2+}$, although Behar et al. suggested that other radical adducts might also be formed. One notable feature was that the transient spectra measured on radiolysis of [bmim][PF_6] and [bmim][Tf_2N] were effectively identical, while the spectra recorded on radiolysis of [bmim]Br showed clear evidence for the formation of $Br_2^{\cdot-}$.[43]

Both investigations also reported the pulse radiolysis of solutes dissolved in ionic liquids. Behar et al. studied the effect of the presence of O_2 and CCl_4 in [bmim][PF_6]; their results suggested that the latter was a more effective radical scavenger. They also looked at the formation of the radical cations of chlorpromazine (ClPz·$^+$) and *N,N,N′,N′*-tetramethyl-*p*-phenylenediamine (TPMD·$^+$) in the same solvent. Finally, the kinetics of oxidation of ClPz in [bmim][PF_6] were studied. The experimentally determined bimolecular rate constant values were corrected for the high viscosity of the ionic liquid by estimation of the values of k_{diff}, the diffusion-controlled rate constant, using Equation (5.3),

$$k_{diff} = 8000\,RT/3\eta \tag{5.3}$$

where R is the gas constant, T is the absolute temperature, and η the viscosity in Pa sec.* The activation-controlled rate constants thus gained were reported to be in the range 2.6×10^7 to 1.12×10^8 l mol^{-1} sec^{-1} over the temperature range 22 to 75°C. The value at 22°C is comparable to that obtained for secondary alcohols such as 2-propanol. The study by Marcinek et al.[42] also reported the formation of naphthalene radical cation and the radical anion of tetracyanoquinodimethane (TCQM$^{\cdot-}$) in glassy [bmim][Tf_2N]. In the case of TCQM$^{\cdot-}$, it appeared that the solute trapped the majority of electrons generated, probably because of the low reducibility of [bmim]$^+$. Under cryogenic conditions these radical ions were completely stable, only decaying when the solid glasses melted. One interesting feature was the demonstration that both radical cations and anions may be formed simultaneously in ionic liquids. Finally, the ionic liquids were used as media for the characterization of previously unobserved radical cations formed in the radiolysis of 1-methyl-1,4-dihydronicotinamide (MNAH), a structural analogue of nicotinamide adenine dinucleotide reduced form (NADH). The low solubility of this molecule in organic solvents conventionally used for pulse radiolysis experiments had previously hindered this investigation. Using a glassy [bmim][PF_6] matrix, the intermediates *keto*- and *enol*-MNAH$^{\cdot+}$ shown in Scheme 1 were identified for the first time.

Since this time, further pulse radiolysis results have been reported in the ionic liquids methyltributylammonium *bis*(trifluoromethylsulfonyl)imide ([mtba][Tf_2N]), *N*-butylpyridinium tetrafluoroborate ([bupy][BF_4]), and *N*-butyl-4-methylpyridinium hexafluorophosphate ([bupic][PF_6]).[43] The former liquid was chosen because radiolysis produces solvated electrons that do not react with the parent ions and can thus be scavenged by reactive solutes (Equation 5.4).

$$[R_4N][Tf_2N] \quad \sim\sim\rightarrow \quad e_{solv}, H^+, [R_4N]^{\bullet 2+}, [NTf_2]^{\bullet}, R^{\bullet} \tag{5.4}$$

The *N*-alkylpyridinium-based cations do react with solvated electrons, producing a pyridinyl radical that can transfer an electron to many solutes (Equations 5.5 and 5.6).

$$[bupy][BF_4] \quad \sim\sim\rightarrow \quad e_{solv}, H^+, [bupy]^{\bullet 2+}, [BF_4]^{\bullet} \tag{5.5}$$

*It should be noted that the work reported in reference 37 suggests that this approximation may not be valid for solvents of such high viscosity.

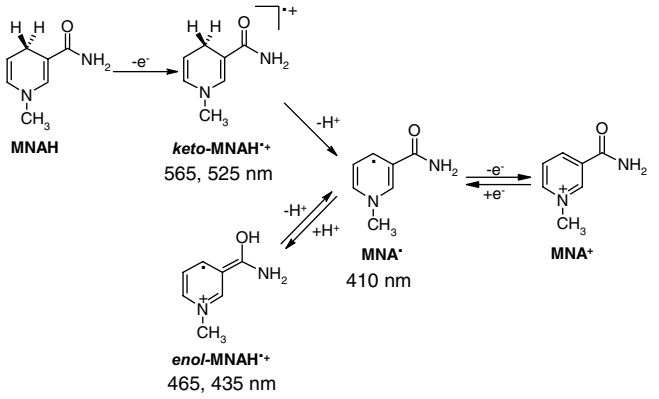

SCHEME 1 (Taken from reference 42 © American Chemical Society)

$$\left[\text{bupy}\right]^{+} e_{\text{solv}} \rightarrow \left[\text{bupy}\right]^{\cdot} \tag{5.6}$$

Radiolytic reduction reactions have been carried out on substrates such as quinones, benzophenone, methyl viologen, and nitroaromatic compounds. In [mtba][Tf_2N], the principal reactions were reduction of the substrates by solvated electrons and organic radicals derived from the solvent. For example, irradiation of benzoquinone (BQ) or duroquinone (DQ) resulted in the formation of the protonated semiquinone radical, with the proton formed by radiolysis of [mtba][Tf_2N] (Equation 5.7). The addition of triethylamine to capture the protons resulted instead in the formation of the semiquinone radical anions (Equation 5.8).

$$\text{BQ} + e^{-}_{\text{solv}} + \text{H}^{+} \rightarrow \text{BQH}\cdot \tag{5.7}$$

$$\text{BQ} + e^{-}_{\text{solv}} \rightarrow \text{BQ}^{\cdot -} \tag{5.8}$$

When the same reaction was carried out with benzophenone (BP), the first product formed was the radical anion $BP^{\cdot -}$ (λ_{max} = 700 nm), which was converted within 10 μsec into BPH· (λ_{max} = 545 nm). The measured absorbance of BPH· was used to estimate the radiolytic yield of solvated electrons (0.9×10^{-7} mol J^{-1} in the absence of amine and approximately twice as much when amine was present).

Solutes in [bupy][BF_4] and [bupic][PF_6] were reduced by butylpyridinyl radicals ([bupy]·) formed on radiolysis of these salts instead of solvated electrons. Bimolecular rate constants were reported for the reaction of [bupy]· with a number of solutes. Comparison of these values with calculated values of k_{diff} for the ionic liquids (calculated using Equation 5.3) gave the surprising result that the rate of reaction was an order of magnitude higher than k_{diff}. This was explained by an electron transfer mechanism involving hopping of the electron between solvent cations, thus preventing the need for direct diffusion of [bupy]· to the substrate. It should be noted, however, that k_{diff} values calculated using Equation 5.3 are significantly lower than those measured by McLean et al.,[39] perhaps suggesting that this approximation may not be particularly accurate for these relatively viscous RTILs.

The secondary electron transfer between $MV^{\cdot +}$ and DQ (Equation 5.9) was also studied in [bupy][BF_4] containing varying amounts of water.

$$\text{MV}^{+} + \text{DQ} \rightleftharpoons \text{MV}^{2+} + \text{DQ}^{\cdot -} \tag{5.9}$$

In this case, the bimolecular rate constant in the absence of water was k_q 1.4 (± 0.2) × 10^5 l $mol^{-1}sec^{-1}$, approximately two orders of magnitude lower than the estimated value of k_{diff}. The addition of even small

quantities of water resulted in a large increase in k_q. It was also found that the driving force of this reaction is in fact to the left, as is also found with 2-propanol. The reaction could be driven to the right, however, by protonation of $DQ^{-\bullet}$.

The same study reported radiolytic oxidation of both TPMD and ClPz in neat ionic liquids and also the oxidation of ClPz and Trolox by $CCl_3O_2\cdot$ radicals formed in the presence of CCl_4. Unlike the similar study in [bmim][PF_6] reported above, in [mtba][Tf_2N], oxidation of both TPMD and ClPz to their corresponding radical cations occurred even in the absence of CCl_4. The yield of $ClPz^{\cdot+}$ was small, but its formation even in the absence of oxygen indicates that oxidizing species are formed in this IL. Experimental rate constants for the oxidation of ClPz by $CCl_3O_2\cdot$ in all ionic liquids were found to be within an order of magnitude of 1×10^7 l mol^{-1}sec^{-1}, but always lower than the calculated values of k_{diff} by a factor of 1.5 to 2. Rate constants for the oxidation of Trolox were slightly lower than those for the oxidation of ClPz.

Most recently, Grodkowski and Neta have reported a pulse radiolysis study of the reaction kinetics of $\cdot CF_3$ in the ionic liquid [mtba][Tf_2N].[44] Radiolysis of CF_3Br resulted in the formation of $\cdot CF_3$ (identified by a peak at $\lambda = 405$ nm), although there was also evidence for the formation of this radical as a breakdown product of the $[Tf_2N]^-$ anion. Radiolysis of pyrene in the same solvent gave the pyrene radical anion and cation (identified by peaks at λ = 495 and 450 nm), which decayed rapidly, as well as the protonated pyrene radical anion, which had a longer lifetime. Pulse radiolysis of a pyrene solution that was saturated with CF_3Br gave an intense peak at $\lambda = 405$ nm. This product was assigned as $\cdot PyrCF_3$, formed by reaction of the preferentially formed $\cdot CF_3$ with pyrene. The rate constants for the reaction of $\cdot CF_3$ with pyrene and phenanthrene were reported in [mtba][Tf_2N] containing either CF_3Br or 0.2 mol l^{-1} $HClO_4$. Effectively identical bimolecular rate constants were observed for each substrate in both media. In some cases, the absolute rate constants determined for the reaction of $\cdot CF_3$ with pyrene or phenanthrene were used to determine rate constants for reactants that did not form readily observable species (crotonic acid, valeric acid and 2-propanol) using competition kinetics. The overall conclusion of these studies was that experimental rate constants for hydrogen abstraction and addition reactions of $\cdot CF_3$ in [mtba][Tf_2N] were slightly lower than in water or acetonitrile, while those for electron transfer reactions were generally an order of magnitude or more lower in the RTIL than in water or alcohols.

5.4 Product and Mechanistic Studies

Although photochemistry in ionic liquids is a relatively new subject, photochemistry in salt solutions is well known.[45,46] Added salts will, of course, alter the polarity of a solvent and thus may affect the energetics of electronic transitions. Adding a salt such as $LiClO_4$, $NaClO_4$, $Mg(ClO_4)_2$, or Bu_4NClO_4 to a solvent often enhances the quantum yield of a photoinduced electron transfer reaction. This occurs by exchanging ions in the initially formed ion pair with ions in the salt, thus inhibiting back electron transfer that regenerates the donor (D) and acceptor (A). Similar effects could take place in ionic liquids.

$$D \xrightarrow{h\nu} D^*$$

$$D^* + A \longrightarrow [D^{+\bullet} A^{-\bullet}]$$

$$[D^{+\bullet} A^{-\bullet}] + LiClO_4 \rightleftharpoons [D^{+\bullet} ClO_4^-] + Li^+, A^{-\bullet}$$

$$[D^{+\bullet} ClO_4^-] \longrightarrow \text{Products}$$

Photochemistry in ionic liquids to date has been carried out exclusively with pyridinium and imidazolium salts. Pyridinium[47,48] and imidazolium[49,50] salts dissolved in conventional solvents are known to be photoactive. The ionic liquid [bmim][PF_6] yields as yet uncharacterized photoproducts when photolyzed below 300 nm.[51] Because the pyridinium- and imidazolium-based ionic liquids have little absorption above 300 nm, photodegradation of the solvent will be minimized when a photoreaction is initiated with light of wavelength >300 nm. The substrate must have, of course, an absorption band above 300 nm.

Even here, the heterocyclic cation may participate in the subsequent chemistry. Most of the reactions described below are initiated by photoinduced electron transfer, whose energetics are determined using the Rehm–Weller equation.[52] In most instances, the equation contains a Coulombic term due to the attraction of the radical cation ($D^{+\cdot}$) and radical anion ($A^{-\cdot}$) in the initially formed ion pair. If the acceptor is a pyridinium or imidazolium ion of the ionic liquid, however, the Coulombic term is zero because the reduced acceptor has no charge.

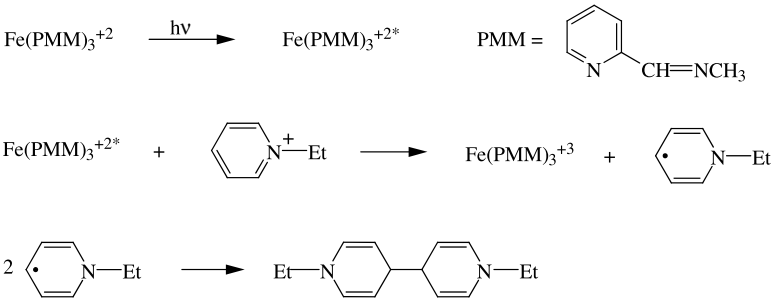

The first photochemical experiments in an ionic liquid were those of Osteryoung and co-workers,[53] who investigated the behavior of 10 Fe(II) tris complexes including $Fe(PMM)_3^{+2}$, where PMM = 2-pyridinecarboxaldehyde *N*-methylimine, in Lewis acidic *N*-ethylpyridinium bromide/$AlCl_3$ (1:2) using visible light. UV/vis spectroscopy showed that the Fe(II) complexes were converted cleanly into the corresponding Fe(III) complexes, which were also made independently. The appearance of a band at 680 nm, independent of the complex used, was attributed to the reduction product, a dimer of the *N*-ethylpyridinyl radical. That these reactions occurred by photoinduced electron transfer from the iron complex to the pyridinium cation was verified by comparing the relative rate of disappearance of the 10 complexes to their oxidation potentials. Complexes that were calculated to undergo the electron transfer exothermically according to the Rehm–Weller equation had quantum yields of disappearance close to one. When the electron transfer became endothermic, the quantum yield fell off linearly with increasing $E_{1/2}$ values of the complexes. In a second inorganic example, the substrate is reduced and the ionic liquid cation oxidized.[54] UCl_6^-, which is stable in acidic [emim][Cl]/$AlCl_3$ (43:57), has a ligand-to-metal charge transfer band at 457 nm. Photolysis into this band afforded uranium(IV) chloride and a transient chlorine atom that reacted in turn with the imidazolium cation to afford unknown products. Interestingly, UCl_6^- is photo inert in acidic NaCl/$AlCl_3$ (45:55) at 320°C. Here there is no chemical outlet for the chlorine atom.

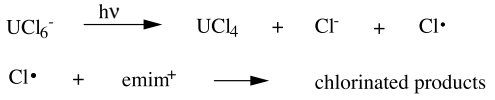

The photochemistry of anthracene (AN) has been studied for close to 150 years. In fact, it was the first substrate whose photochemistry was studied in a laboratory. It is now well established that in virtually every solvent in which it has been studied, AN reacts in the same way.[55] In degassed or deoxygenated solution, the reaction proceeds through the singlet excited state of AN, AN^{*1}, which reacts with ground state AN to form an excimer, which in turn collapses to a [4 + 4]-dimer. In water, on the other hand, the complex chemistry is initiated by electron transfer from AN^{*1} to water.[56] In oxygenated solvent the reaction proceeds differently. AN^{*3}, formed by intersystem crossing of AN^{*1}, on collision with O_2 yields AN and singlet O_2, $^1O_2$. Reaction of $^1O_2$ with AN affords the [4 + 2]-*endo* peroxide. In degassed basic [emim][Cl]/$AlCl_3$ (55:45), the photochemistry of AN occurs in the normal manner, yielding the [4 + 4]-dimer quantitatively, in spite of the fact that the electron transfer from AN^{*1} to $emim^+$ is exothermic by more than 5 kcal mol^{-1}.[57] In oxygenated basic [emim][Cl]/$AlCl_3$ of the same composition, the photoreaction affords anthrone, anthraquinone, 9-chloroanthracene, 9,10-dichloroanthracene, and the [4 + 4]-dimer.[58] One may

assume that the [4 + 4]-dimer is formed by the mechanism previously described. The formation of the chlorinated products may be rationalized as follows: AN^{*1} undergoes electron transfer with O_2 to form a radical cation, $AN^{+\cdot}$ and superoxide, $O_2^{-\cdot}$. $AN^{+\cdot}$ then reacts with Cl^-, a component of the IL, to form a radical that eventually yields 9-chloroanthracene (9-ClAN). 9-Chloroanthracene then affords 9,10-dichloroanthracene by an identical mechanism. The mode by which the oxygenated products are formed is not known but may involve the reaction of $AN^{+\cdot}$ with $O_2^{-\cdot}$.

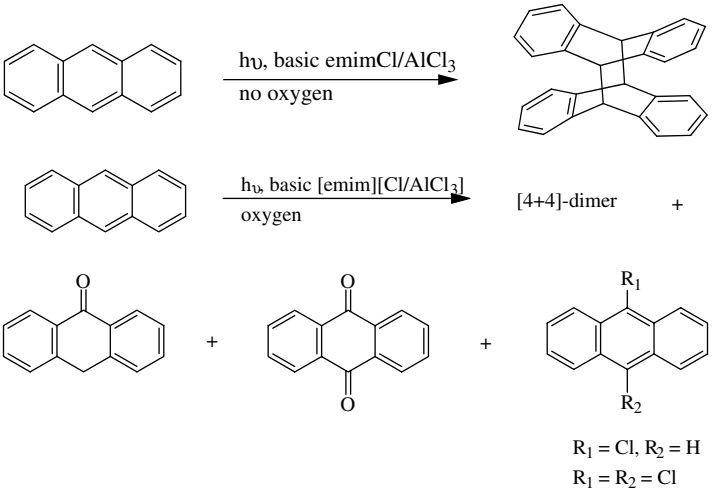

Unlike the basic solution of AN, which is colorless, the acidic [emim][Cl]/$AlCl_3$ (45:55), which contains the powerful Lewis acid, $Al_2Cl_7^-$, is green due to the presence of about 3% of protonated anthracene, ANH^+. Even the most rigorously purified IL contains traces of HCl, a very strong acid, in the acidic IL.[11,12] Photolysis of the degassed green solution afforded an array of reduced, neutral, and oxidized monomeric and dimeric products. At 13% conversion, the products were 9,10-dihydroanthracene, 2,9′-bianthracene, 9′,10′-dihydro-2,9′-bianthracene, 9,10-dihydro-2,9′-bianthracene, anthra[2,1-a]aceanthrylene, and an unidentified hydrocarbon with a structure similar to the aceanthrylene.

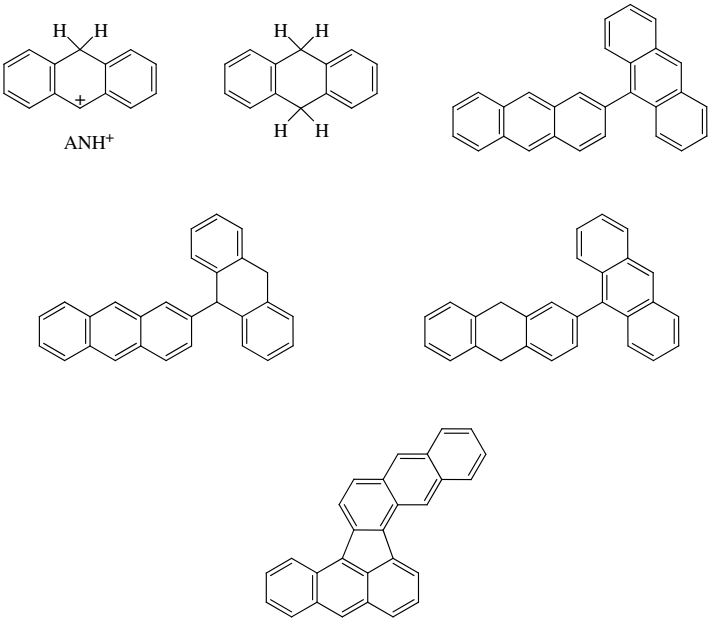

By seeing how the product distribution is affected by deliberately adding HCl to the AN solution or removing it by adding methylaluminum sesquichloride, a mechanism for the photoreaction could be formulated involving $AN^{+\cdot}$. The photoreaction is initiated by photoinduced electron transfer, AN^{*1} to ANH^+ and/or AN to ANH^{+*}, as both AN and ANH^+ absorb the light to form $AN^{+\cdot}$ and ANH·. When $AN^{+\cdot}$ is generated photochemically in water, it reacts with the water.[56] No bases with which $AN^{+\cdot}$ can react are present in the acidic IL. The species $AN^{+\cdot}$ and ANH· thus undergo a series of electron transfer, hydrogen transfer, and coupling reactions to yield the observed products. It was possible to mimic the behavior of AN in acidic [emim]Cl/$AlCl_3$ by using CF_3SO_3H and CF_3COOH instead.[59] In the very strong acid, CF_3SO_3H (H_o = –14.0), AN is completely protonated, and it did not react photochemically. In the much weaker acid, CF_3COOH (H_o = –2.7), AN is unprotonated, and it reacted to yield the 4 + 4 dimer quantitatively. In a mixture of 2% CF_3SO_3H in CF_3COOH (w/w) with H_o = –8.1, where AN and ANH^+ are both present, the photochemistry yielded the same products and in approximately the same amounts as seen in the acidic IL.

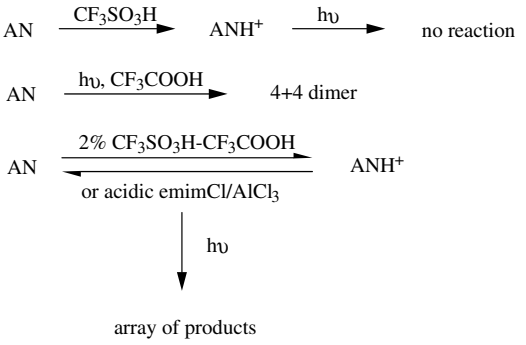

It is clear that the photochemistry of polyaromatic hydrocarbons (PAHs) in strong acid solutions, especially when the hydrocarbon and its conjugate acid are present, has synthetic potential. It may be possible to prepare previously unknown PAHs or ones difficult to prepare by known methodology by the photochemical method. Unlike AN, 9-methylanthracene (9-CH_3AN) does undergo photoinduced electron transfer in degassed basic [emim][Cl]/$AlCl_3$ and also *N*-butylpyridinium chloride [bp][Cl]/$AlCl_3$.[60] The electron transfer from 9-CH_3AN^{*1} to the heterocyclic cation in each IL is exothermic in each case, and the resulting radical cation, 9-$CH_3AN^{+\cdot}$, has a chemical outlet by its reaction with Cl^-, an IL component, to form the 9-anthrylmethyl radical, 9-$ANCH_2$·, and HCl. Radical cations of methylarenes are known to be very acidic.[61] Not only HCl but also $emim^+$ serve as a proton donor in [emim][Cl]/$AlCl_3$. Alder and co-workers had previously shown that imidazolium cations have appreciable acidity.[62] Interestingly, deprotonation of $emim^+$ yields a heterocyclic carbene, a species of current interest.[63] 9-$ANCH_2$· has many potential outlets including dimerization, hydrogen atom abstraction, addition to 9-CH_3AN, and reduction. Reduction is possible because of the presence of emim· (or bp·), a potential electron donor formed in the initial electron transfer step.

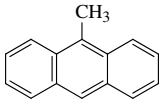

9-CH_3AN

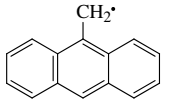

9-$ANCH_2$•

HCl and emim$^+$ - potential proton donors

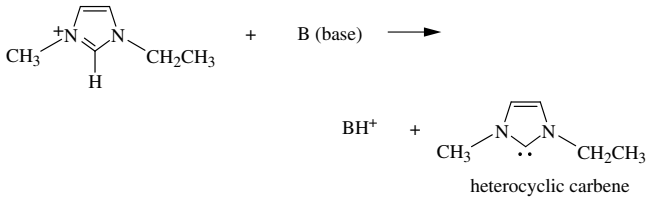

emim$^\bullet$ and bp $^\bullet$- potential reductants

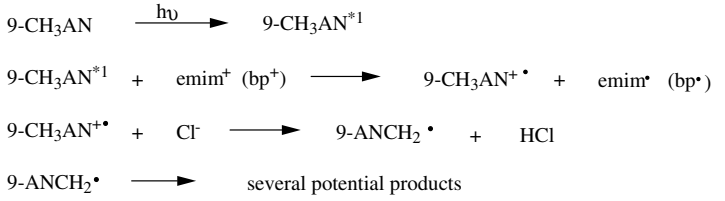

The photochemistry of 9-CH_3AN in degassed basic [emim][Cl]/$AlCl_3$ (55:45) afforded seven products, none of which was chlorinated. The major product was the *anti* [4 + 4]-dimer, presumably formed by the mechanism described early for the photodimerization of AN, which does not involve electron transfer. In addition, two dimers of 9-$ANCH_2$·, the head-to-head 1,2-bis(9-anthrylmethyl)ethane formed in trace amounts and the head-to-tail lepidopterene, were formed. The unusual lepidopterene having C_{2h} symmetry has two adjacent quaternary carbon atoms. There were also two isomeric products, both in small amounts, resulting from the addition of 9-$ANCH_2$· to the 9 and 10 positions of 9-CH_3AN followed by hydrogen abstraction. The last two products were identified as 9-methylene-9,10-dihydroanthracene in trace amounts and 9,10-dihydroanthracene.

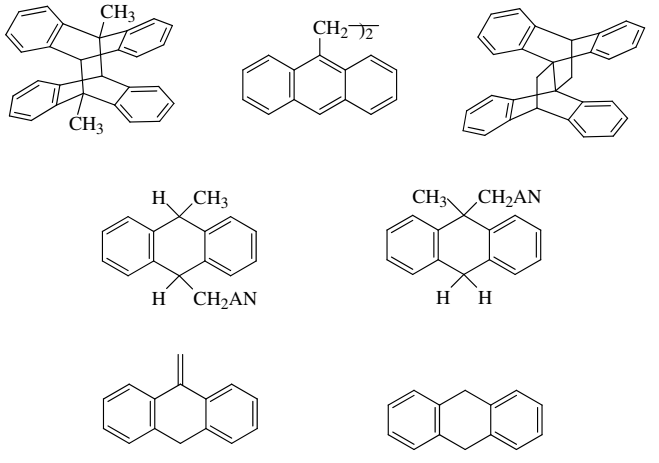

The formation of 9-methylene-9,10-dihydroanthracene is unexpected. Although one would assume that it arises by carbon 10 of 9-$ANCH_2$· abstracting a hydrogen atom from another species, this is not the case. Photolysis of 9-chloromethylanthracene in the IL, for example, yielded 9-CH_3AN and the two dimers of 9-$ANCH_2$·, but none of the methylene compound. Likewise, reduction of 9-chloromethylanthracene with AIBN/Bu_3SnH yielded 9-CH_3AN exclusively. The isomer of 9-CH_3AN is formed in two

steps from 9-$ANCH_2$·. In the first, 9-$ANCH_2$· is reduced by emim· to yield the carbanion 9-$ANCH_2^-$, and in the second, carbon 10 of the anion abstracts a proton. 9-$ANCH_2^-$ is known to be protonated at carbon 10.[64] Deuterium labeling experiments clearly showed that both HCl and $emim^+$ served as proton sources in this last reaction.

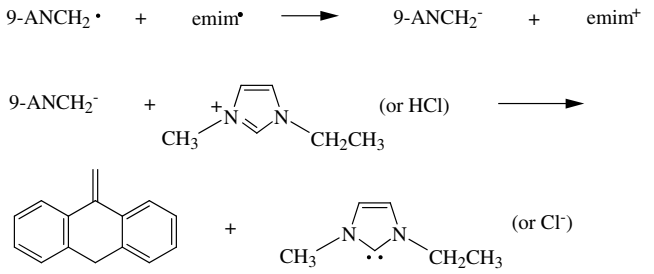

9,10-Dihydroanthracene is also formed in an interesting fashion. The initial step is the reduction of 9-CH_3AN by emim·, a reaction exothermic by 9 kcal mol^{-1} in the IL, to form the radical anion 9-$CH_3AN^{-\bullet}$ and $emim^+$. Proton transfer from HCl and $emim^+$ (deuterium labeling experiments) followed by further reduction yields the observed product.

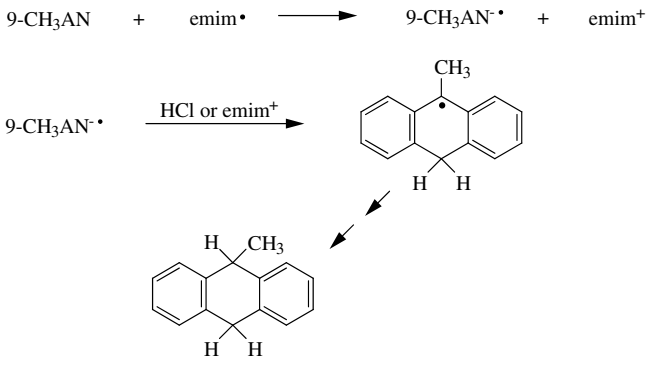

That the reaction, surprisingly, proceeds through 9-$CH_3AN^{-\cdot}$ was demonstrated by repeating the photochemistry in [bp][Cl]/$AlCl_3$. The cation bp^+ is more easily reduced than $emim^+$, but its reduction product bp· is a much poorer reducing agent than emim·. In fact, the reaction bp· + 9$CH_3AN \rightarrow bp^+$ + 9-$CH_3AN^{-\cdot}$ is endothermic by 10 kcal mol^{-1}. The photochemistry here yielded the [4 + 4]-dimer and the head-to-head and the head-to-tail dimers of 9-$ANCH_2$·, which was the major product; no 9,10-dihydroanthracene was formed. In addition, the photoreaction yielded several products not seen in [emim][Cl]/$AlCl_3$ including pyridine, 9-pentylanthracene, 9-butyl-10-methylanthracene, and *N*-butyl-1,4-dihydropyridine. Clearly, the first three of these new products arise by reaction of 9-$ANCH_2$· with bp·.

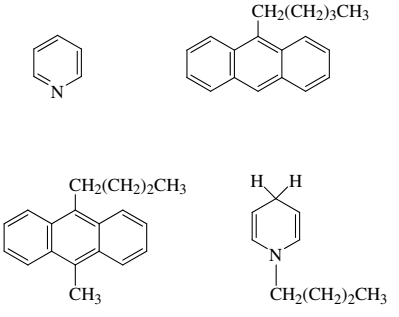

The most unusual feature in the rather complicated photochemistry of 9-CH_3AN in [emim][Cl]/$AlCl_3$ is the formation of both 9-$CH_3AN^{+\cdot}$ and 9-$CH_3AN^{-\cdot}$ at different stages of the reaction. Although this is rare, there are undoubtedly other methylarenes for which this is possible. ILs are well placed to probe for this chemistry.

The photoisomerization of *cis*- and *trans*-stilbene (S_c and S_t) has been studied quite extensively and occurs by several different mechanisms depending on reaction environment and conditions.[65] Two of these relevant to ionic liquids will now be described. In most solvents, direct irradiation of S_c and S_t results in isomerization by the singlet mechanism in which the singlet excited states of the substrates, S_c^{*1} and S_t^{*},[1] twist about their ethylene double bonds to form a common perpendicular excited state, p^{*1}. The excited state p^{*1} in turn undergoes radiationless transition to yield p on the ground state surface, which decays to S_c and S_t. The photostationary state (PS) that results depends on the extinction coefficients of S_c and S_t and their respective quantum yields of interconversion. If light of $\lambda > 300$ nm is used, the PS should be rich in S_c unless something about the quantum yields is unusual.

In the Electron Transfer Mechanism, the radical cations of the substrates, $S_c^{+\cdot}$ and $S_t^{+\cdot}$, are involved in the isomerization.[66] S_c^{*1} and S_t^{*1} formed on direct irradiation transfer an electron to a suitable acceptor to form $S_c^{+\cdot}$ and $S_t^{+\cdot}$. Here the isomerization is essentially one way, $S_c^{+\cdot} \rightarrow S_t^{+\cdot}$, while $S_t^{+1\cdot}$ serves as a conduit for the formation of more S_c^{+} in the reaction $S_t^{+\cdot} + S_c \rightarrow S_t + S_c^{+\cdot}$. At some later stage, back electron transfer regenerates S_c and S_t. The electron transfer mechanism will yield a PS very rich in S_t. In CH_3CN, the PS contains 98.8% S_t, for example.[66]

The *cis,trans*-photoisomerization of S_t and S_c does indeed take place in ILs.[51,67] Ozawa and Hamajuchi showed, for example, that S_t photoisomerizes to S_c in bmimPF_6,[51] almost certainly by the singlet mechanism. Transient fluorescent measurements showed that S_t isomerizes to S_c with a rate constant of 6.6×10^9 sec^{-1}. This is almost seven times faster than what is expected based on the polarity and viscosity of [bmim][PF_6].

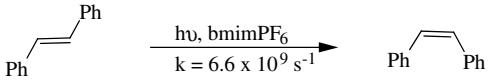

S_t and S_c interconvert photochemically in basic emimCl/$AlCl_3$ and bpCl/$AlCl_3$, but by different mechanisms.[67] The photoisomerization could not be studied in the Lewis acidic ionic liquids because this results in the very large Brønsted acidity of traces of HCl in the media; S_t, for instance, underwent an acid-catalyzed dimerization in acidic [emim][Cl]/$AlCl_3$. In basic [bp][Cl]/$AlCl_3$, both S_c and S_t photoisomerize cleanly to give a PS containing ~99% S_t. In addition, the electron transfers from S_t^{*1} and S_c^{+1} to bp^+ are quite exothermic (electron transfers from the triplet states are endothermic). Thus, the isomerizations in [bp][Cl]/$AlCl_3$ occur by the Electron Transfer mechanism.

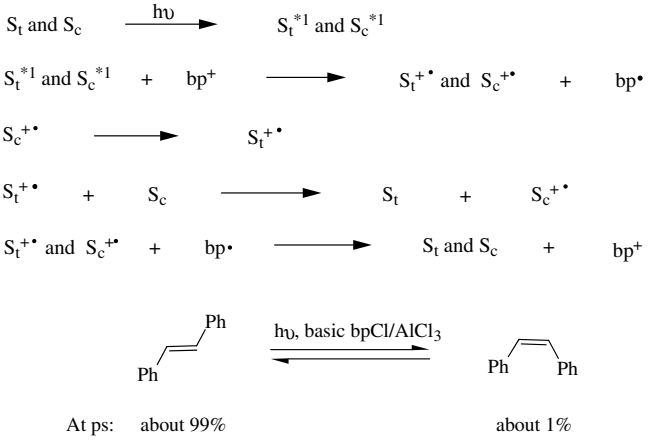

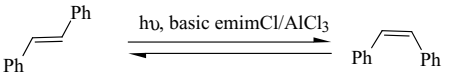

At ps: about 55% about 45%

The stilbenes S_t and S_c isomerize photochemically in basic emimCl/$AlCl_3$, but not by the electron transfer mechanism. S_t and S_c do interconvert but, in addition, yield small amounts of unidentified products. As a result, it is not possible to calculate the PS exactly. An estimate of 55% S_t and 45% S_c at the PS seems reasonable. The low value of S_t at the PS clearly rules out the electron transfer mechanism even though electron transfer from both S_t^{*1} and S_c^{*1} to $emim^+$ is calculated by the Rehm–Weller equation to be exothermic. The PS is unusual for the isomerization occurring by the singlet mechanism, however. With >300 mm, which was used here, the PS should have been rich in S_c unless there is something unusual about the quantum yields of interconversion, $\Phi_{t\rightarrow c}$ and $\Phi_{c\rightarrow t}$.

A different type of photoreaction in ILs has been studied by Jones and co-workers: the photoreduction of benzophenones by primary amines.[68] Prior work by Cohen demonstrated that photolysis of benzophenone in benzene in the presence of *sec*-butylamine afforded benzopinacol (and an imine).[69] This reaction proceeds through a radical pair formed by hydrogen-atom abstraction by the triplet excited state benzophenone from the amine. In the much more polar environment of an IL, the radical pair may instead undergo single electron transfer to form an iminium cation and a hydroxyl-substituted carbanion. Proton transfer from the cation to the anion will yield benzhydrol and an imine.

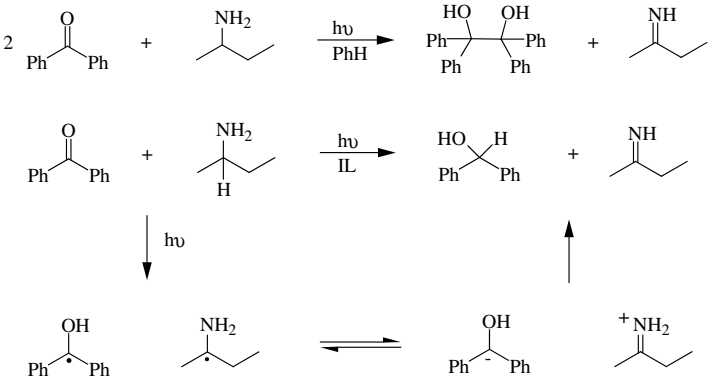

Which reduction product, benzopinacol or benzhydrol, is formed depends on the IL used and the substituents on the benzophenone. In the ILs, *sec*-butylammonium trifluoroacetate with added *sec*-butylamine and isopropylammonium nitrate with added isopropylamine, benzophenone afforded benzopinacol exclusively. On the other hand, benzophenone yielded benzhydrol exclusively in several emim and bmim ILs. The origin of this difference in behavior is unclear. Benzophenones with electron-withdrawing substituents (2-CO_2CH_3, 3-CO_2CH_3, 4,4-diCl) afforded the corresponding benzhydrol quantitatively in $bmimBF_4$. These substituents, of course, stabilize the hydroxyl-substituted carbanions. 4-Methoxy- and 4,4-dimethoxybenzophenone gave mixtures of benzopinacol and benzhydrol in $[emim]^+$ and $[bmim]^+$ ILs, with the dimethyoxy compound giving more benzopinacol than the monomethoxy compound. There appears to be a correlation between the product distribution and the electron-donating ability of the aryl rings. Interestingly, when 4,4-dimethoxybenzophenone is reduced in eight$[emim]^+$ and $[bmim]^+$ ILs, the benzhydrol to benzopinacol ratio varies from 30:70 ([bmim][OTf]) to 75:25 ([bmim][NO_3]). There is no obvious property of the ILs that accounts for these differences.

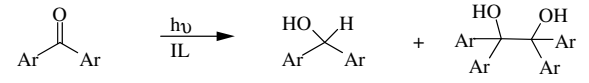

Ar = 4-MeOPh bmimOTf: 30 70

bmimNO3: 75 25

References

1. Pagni, R.M., Organic and organometallic reactions in molten salts and related melts, in *Advances in Molten Salt Chemistry*, vol. 6, Mamantov, G., Mamantov, C.B., and Braunstein, J., Eds., Elsevier, Amsterdam, 1987, p. 211.
2. Welton, T., Room-temperature ionic liquids. Solvents for synthesis and catalysis, *Chem. Rev.,* 99, 2071, 1999.
3. Jaeger, D.A. and Tucker, C., Diels–Alder reactions in ethylammonium nitrate, a low-melting fused salt, *Tetrahedron Lett.,* 40, 793, 1989.
4. Grieco, D.A., Organic chemistry in unconventional solvents, *Aldrichim. Acta,* 24, 59, 1991.
5. Pocker, Y. and Ciula, J.C., Electrostatic catalysis by ionic aggregates. 7. Interactions of dipolar indicator molecules with ionic clusters, *J. Am. Chem. Soc.,* 111, 4728, 1989 and six earlier papers in the series.
6. Springer, G., Elam, C., Edwards, A., Bowe, C., Boyles, D., Bartmess, J., Chandler, M., West, K., Williams, J., Green, J., Pagni, R.M., and Kabalka, G.W., Chemical and spectroscopic studies related to the Lewis acidity of lithium perchlorate in diethyl ether, *J. Org. Chem.,* 64, 2202, 1999.
7. Kumar, A. and Pawar, S.S., Rate acceleration and subsequent retardation of Diels–Alder reactions in $LiClO_4$ diethyl ether: an experimental investigation, *J. Org. Chem.,* 66, 7646, 2001.
8. Cox, D.P., Perpinski, J., and Lawrynowicz, W., "Anhydrous" tetrabutylammonium fluoride: a mild but highly efficient source of nucleophilic fluoride ion, *J. Org. Chem.,* 49, 3216, 1984.
9. Robinson, J. and Osteryoung, R.A., An electrochemical and spectroscopic study of some aromatic hydrocarbons in the room temperature molten salt system aluminum chloride-n-butylpyridinium chloride, *J. Am. Chem. Soc.,* 101, 323, 1979.
10. Wilkes, J.S., Levisky, J.A., Wilson, R.A., and Hussey, C.L., Dialkylimidazolium chloroaluminate melts: a new class of room-temperature ionic liquids for electrochemistry, spectroscopy and synthesis, *Inorg. Chem.,* 21, 1263, 1982.
11. Smith, G.P., Dworkin, A.S., Pagni, R.M., and Zingg, S.P., Brønsted superacidity of HCl in a liquid chloroaluminate. $AlCl_3$–1-ethyl-3-methyl-1*H*-imidazolium chloride, *J. Am. Chem. Soc.,* 111, 525, 1989.
12. Smith, G.P., Dworkin, A.S., Pagni, R.M., and Zingg, S.P., Quantitative study of the acidity of HCl in a molten chloroaluminate system ($AlCl_3$/1-ethyl-3-methyl-1*H*-imidazolium chloride) as a function of HCl pressure and melt composition (51.0–66.4 mol% $AlCl_3$), *J. Am. Chem. Soc.,* 111, 5075, 1989.
13. Wilkes, J.S. and Zaworotko, M.J., Air and water stable 1-ethyl-3-methylimidazolium based ionic liquids, *J. Chem. Soc., Chem. Commun.,* 965, 1992.
14. Earle, M.J. and Seddon, K.R., Ionic liquids. Green solvents for the future, *Pure Appl. Chem.,* 72, 1391, 2000.
15. Wasserscheid, P. and Keim, P., Ionic liquids — new "solutions" for transition metal catalysis, *Angew. Chem. Int. Ed. Engl.,* 39, 3772, 2000.
16. Barton, A.F.M., *Handbook of Solubility and Other Cohesive Parameters,* 2nd ed., CRC Press, Boca Raton, FL, 1991.
17. Reichardt, C., *Solvents and Solvent Effects in Organic Chemistry,* 2nd ed., VCH, Weinheim, 1988, p. 191.
18. Jones, R.A.Y., *Physical and Mechanistic Organic Chemistry,* 2nd ed., Cambridge, Cambridge, 1984, p. 165.
19. Badri, M., Brunet, J.-J., and Perron, R., Ionic liquids as solvents for the regioselective O-alkylation of C/O ambident nucleophiles, *Tetrahedron Lett.,* 33, 4435, 1992.
20. Earle, M.J., McCormac, P.B., and Seddon, K., Regioselective alkylation in ionic liquids, *J. Chem. Soc., Chem. Commun.,* 2245, 1998.
21. Seddon, K.R., Stark, A., and Torres, M.-J., Influence of chloride, water and organic solvents on the physical properties of ionic liquids, *Pure Appl. Chem.,* 72, 2275, 2000.

22. Herfort, I.-M. and Schneider, H., Spectroscopic studies of the solvent polarities of room-temperature liquid ethylammonium nitrate and its mixtures with polar solvents, *Liebigs Ann. Chem.,* 27, 1991.
23. Reichardt, C., Solvochromatic dyes as solvent polarity indicators, *Chem. Rev.,* 94, 2319, 1994.
24. Poole, S.K., Shetty, P.H., and Poole, C.F., Chromatographic and spectroscopic studies of the solvent properties of a new series of room-temperature liquid tetraalkylammonium sulfonates, *Anal. Chim. Acta,* 218, 241, 1989.
25. Bart, E., Meltsin, A., and Huppert, D., Solvation dynamics of coumarin 153 in molten salts, *J. Phys. Chem.,* 98, 3295, 1994.
26. Bonhôte, P., Dias, A.P., Papageorgiou, N., Kalyanasundaram, K., and Grätzel, M., Hydrophobic, highly conductive ambient-temperature molten salts, *Inorg. Chem.,* 35, 1168, 1996.
27. Carmichael, A.J. and Seddon, K.A., Polarity study of some 1-alkyl-3-methylimidazolium ambient-temperature ionic liquids with the solvatochromic dye Nile Red, *J. Phys. Org. Chem.,* 13, 591, 2000.
28. Muldoon, M.J., Gordon, C.M., and Dunkin, I.R., Investigations of solvent–solute interactions in room temperature ionic liquids using solvatochromic dyes, *J. Chem. Soc., Perkin Trans. 2,* 433, 2001.
29. Aki, S.N.V.K., Brennecke, J.F., and Samanta, A., How polar are ionic liquids? *J. Chem. Soc., Chem. Commun.,* 413, 2001.
30. Fletcher, K.A., Storey, I.A., Hendricks, A.E., Pandey, S., and Pandey, S., Behavior of the solvatochromic probes Reichardt's dye, pyrene, dansylamide, Nile Red, and 1-pyrenecarbaldehyde within the room-temperature ionic liquid bmimPF_6, *Green Chem.,* 3, 210, 2001.
31. Baker, S.N, Baker, G.A., and Bright, F.V., Temperature-dependent microscopic solvent properties of "dry" and "wet" 1-butyl-3-methylimidazolium hexafluorophosphate: correlation with E_T (30) and Kamlet–Taft polarity scales, *Green Chem.,* 4, 165, 2002.
32. Dzyuba, S.V. and Bartsch, R.A., Expanding the polarity range of ionic liquids, *Tetrahedron Lett.,* 43, 4657, 2002.
33. Wasserscheid, P., Gordon, C.M., Hilgers, C., Muldoon, M.J., and Dunkin, I.R., Ionic liquids: polar, but weakly coordinating solvents for the first biphasic oligomerization of ethene to higher α-olefins with cationic Ni-complexes, *J. Chem. Soc., Chem. Commun.,* 1186, 2001.
34. Fletcher, K.A., Pandey, S., Storey, I.A., Hendricks, A.E., and Pandey, S., Selective fluorescence quenching of polycyclic aromatic hydrocarbons by nitromethane within room temperature ionic liquid 1-butyl-3-methylimidazolium hexafluorophosphate, *Anal. Chim. Acta,* 453, 89, 2002.
35. Baker, S.N., Baker, G.A., Kane, M.A., and Bright, F.V., The cybotactic region surrounding fluorescent probes dissolved in 1-butyl-3-methylimidazolium hexafluorophosphate: effects of temperature and added carbon dioxide, *J. Phys. Chem. B,* 105, 9663, 2001.
36. Karmakar, R. and Samanta, A., Solvation dynamics of coumarin-153 in a room-temperature ionic liquid, *J. Phys. Chem. A,* 106, 4447, 2002.
37. Karmakar, R. and Samanta, A., Steady-state and time-resolved fluorescence behavior of C153 and PRODAN in room-temperature ionic liquids, *J. Phys. Chem. A,* 106, 6670, 2002.
38. Gordon, C.M. and McLean, A.J., Photoelectron transfer from excited-state ruthenium(II) tris(bipyridyl) to methylviologen in an ionic liquid, *J. Chem. Soc., Chem. Commun.,* 1395, 2000.
39. McLean, A.J., Muldoon, M.J., Gordon, C.M., and Dunkin, I.R., Bimolecular rate constants for diffusion in ionic liquids, *J. Chem. Soc., Chem. Commun.,* 1880, 2002.
40. Muldoon, M.J., McLean, A.J., Gordon, C.M., and Dunkin, I.R., Hydrogen abstraction from ionic liquids by benzophenone triplet excited states, *J. Chem. Soc., Chem. Commun.,* 2364, 2001.
41. Behar, D., Gonzalez, C., and Neta, P., Reaction kinetics in ionic liquids: pulse radiolysis studies of 1-butyl-3-methylimidazolium salts, *J. Phys. Chem. A,* 105, 7607, 2001.
42. Marcinek, A., Zielonka, J., Gebicki, J., Gordon, C.M., and Dunkin, I.R., Ionic liquids: novel media for characterization of radical ions, *J. Phys. Chem. A,* 105, 9305, 2001.
43. Behar, D., Neta, P., and Schultheisz, C., Reaction kinetics in ionic liquids as studied by pulse radiolysis: redox reactions in the solvents methyltributylammonium bis(trifluoromethylsulfonyl)-imide and *N*-butylpyridinium tetrafluoroborate, *J. Phys. Chem. A,* 106, 3139, 2002.

44. Grodkowski, J. and Neta, P., Reaction kinetics in the ionic liquid methyltributylammonium bis(trifluoromethylsulfonyl)imide. Pulse radiolysis of $\cdot CF_3$ radical reactions, *J. Phys. Chem. A,* 106, 5468, 2002.
45. Loupy, A. and Tchoubar, B., *Salt Effects in Organic and Organometallic Reactions,* VCH, Weinheim, 1992, p. 233.
46. Kavarnos, G.J., *Fundamentals of Photoinduced Electron Transfer,* VCH, New York, 1993.
47. King, R.A., Luthi, H.P., Schaefer, H.F., III, Glarner, F., and Burger, V., The photohydration of *N*-alkylpyridinium salts: theory and experiment, *Chem.-Eur. J.,* 7, 1734, 2001.
48. Ogata, Y., Takagi, K., and Tanabe, Y., Photo-induced reduction of pyridinium ions catalyzed by zinc (II) tetraphenylporphyrin, *J. Chem. Soc., Perkin Trans. 2,* 1069, 1979.
49. Byun, Y.-S., Jung, C.-H., and Park, Y.-T., Synthesis of 5*H*-imidazo[5,1-a]isoindole: photocyclization of *N, N′*-bis(o-chlorobenzyl)imidazolium chloride and *N*-(*o*-chlorobenzyl)imidazole, *J. Heterocyclic Chem.,* 32, 1835, 1995.
50. Dohrmann, J.K. and Krohn, H., Radicals from the reaction of photochemically generated α-hydroxyalkyl radicals with some imidazoles. An *in situ* ESR study, *Radiat. Res.,* 77, 242, 1979.
51. Ozawa, R. and Hamaguchi, H., Does photoisomerization proceed in an ionic liquid? *Chem. Lett.,* 736, 2001.
52. Rehm, D. and Weller, A., Kinetics of fluorescence quenching by electron and hydrogen-atom transfer, *Isr. J. Chem.,* 8, 259, 1970.
53. Chum, H.L., Koran, D., and Osteryoung, R.A., Photochemistry of iron(II) diimine complexes in a room temperature molten salt, *J. Am. Chem. Soc.,* 100, 310, 1978.
54. Dai, S. and Toth, L.M., Photochemistry of uranium(V) hexachloride complex in acidic room temperature molten salts, *Proc. Electrochem. Soc.,* 98–11, 261, 1998.
55. Cowan, D.O. and Drisko, R.L., *Elements of Organic Photochemistry,* Plenum Press, New York, 1976, chap. 2.
56. Sigman, M.E., Zingg, S.P., Pagni, R.M., and Burns, J. H., Photochemistry of anthracene in water, *Tetrahedron Lett.,* 32, 5737, 1991.
57. Hondrogiannis, G., Lee, C.W., Pagni, R.M., and Mamantov, G., Novel photochemical behavior of anthracene in a room temperature molten salt, *J. Am. Chem. Soc.,* 115, 9828, 1993.
58. Pagni, R.M., Mamantov, G., Lee, C.W., and Hondrogiannis, G., The photochemistry of anthracene and its derivatives in room temperature molten salts, *Proc. Electrochem. Soc.,* 94–13, 638, 1994.
59. Pagni, R.M., Mamantov, G., Hondrogiannis, G., and Unni, A., Photoinduced electron transfer reactions of anthracene in CF3503H-CF3COZH, *J. Chem. Res. (S),* 486, 1999.
60. Lee, C., Winston, T., Unni, A.l., Pagni, R.M., and Mamantov, G., Photoinduced electron transfer chemistry of 9-methylanthracene. Substrate as both electron doner and acceptor in the presence of the 1-ethyl-3-methylimidazolium ion, *J. Am. Chem. Soc.,* 118, 4919, 1996.
61. Bordwell, F.G. and Cheng, J.-P. Radical-cation acidities in solution and in the gas phase, *J. Am. Chem. Soc.,* 111, 1792, 1989.
62. Alder, R.W., Allen, P.R., and Williams, S.J., Stable carbenes as strong bases, *J. Chem. Soc., Chem. Commun.,* 1267, 1995.
63. Bourissou, D., Guerret, O., Gabbai, F.P., and Bertrand, G., Stable carbenes, *Chem. Rev.,* 100, 39, 2000.
64. Rigaundy, J., Seuleiman, A.M., and Guong, N.K., Tele-substitution in anthracenyl series I. Behavior of 9-bromo-10-methylanthracene with phenoxide or alkoxide anions, *Tetrahedron,* 38, 3143, 1982.
65. Gorner, H. and Kuhn, H.J., *Cis–trans* photoisomerization of stilbenes and stilbene-like molecules, in *Advances in Photochemistry*, Neckers, D.C., Volmun, D.H., and von Bunan, G., Eds., Wiley and Sons, New York, 1995, vol. 19, chap. 1.
66. Lewis, F.D., Petisce, J.R., Oxman, J.D., and Nepras, M.J., One-way photoisomerization of *cis*-stilbene via a cation radical chain mechanism, *J. Am. Chem. Soc.,* 107, 203, 1985.
67. Lee, C., Mamantov, G., and Pagni, R.M., The photoisomerization of *cis*- and *trans*- stilbene in ionic liquids, *J. Chem. Res. (S),* 122, 2002.

68. Reynolds, J.L., Erdner, K.R., and Jones, P.B., Photoreduction of benzophenones by amines in room temperature ionic liquids, *Org. Lett.,* 4, 917, 2002.
69. Cohen, S.G. and Stein, N.G., Kinetics of photoreduction of benzophenones by amines. Deamination and dealkylation of amines, *J. Am. Chem. Soc.,* 93, 6542, 1971.

6

Photochemically Induced Alkylation Reactions

Nathalie Huther
University of York

Andrew F. Parsons
University of York

6.1 Introduction

A considerable number of photochemical reactions are widely utilized in modern organic synthesis. Light-induced reactions have been shown to afford a mild and efficient approach to a variety of complex target molecules.[1] These reactions can offer a chemo-, regio-, and stereoselective approach to molecules, which can be difficult or impossible to achieve using other synthetic methods. Reactants can be irradiated with light of a particular energy so that only certain bonds are broken. This means that photolysis can be a cleaner method of synthesis than thermolysis, where heating to high temperatures can lead to the cleavage of a variety of bonds. The use of high-energy ultraviolet light also allows the cleavage of even strong bonds at low temperatures, and this has found application in classical hydrocarbon chlorination and nitrosation reactions, which have been carried out on a large scale in industry.[2,3]

Of particular importance in organic synthesis is the construction of carbon–carbon bonds, and this can be achieved using a variety of intra- and inter-molecular photochemical processes. Whereas acidic or basic conditions are required for ionic carbon–carbon bond-forming reactions, the corresponding photochemical reactions can be conducted under neutral conditions, and thus a variety of sensitive functional groups can be tolerated in both the reactants and products. This review will aim to briefly survey some of the different photochemical methods that are now available for the formation of carbon–carbon bonds by alkylation reactions involving free radical intermediates. A number of strategies have been developed ranging from initiation of radical chain reactions by photolysis of azo compounds or peroxides to the excitation of carbonyl compounds in Norrish type II reactions. Of particular recent interest has been the development of photoinduced electron-transfer reactions (often in the presence of photosensitizers), and the use of this method to prepare carbon–carbon bonds is also highlighted. A number of different functional groups can be employed to generate radicals in alkylation reactions, and these groups are discussed individually.

0-8493-1348-1/04/$0.00+$1.50

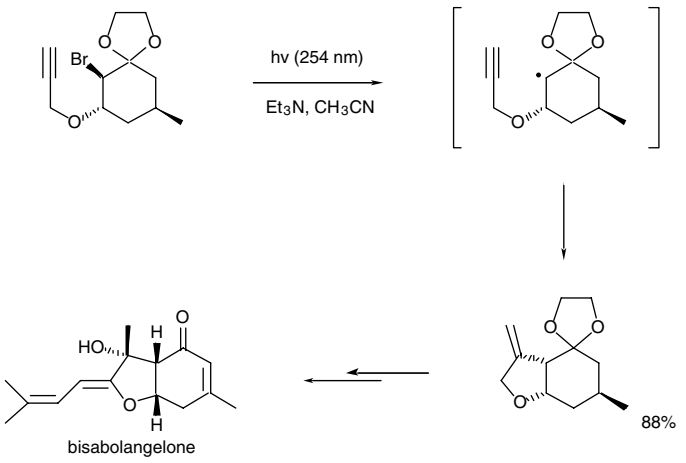

SCHEME 1

6.2 Photochemical Alkylations

Organohalides

The direct photolysis of alkyl or aryl halides in solution to form carbon-centered radicals is rarely used in organic synthesis.[4] Alkyl iodides usually afford mixtures of radical and ionic products, while alkyl bromides can produce radical-derived products but in low yield. A notable exception is the photocyclization of haloarenes, which has been shown to produce carbon-centered radicals that can add to aromatic rings. A similar reaction has recently been observed on irradiation of iodoheterocycles, with substituted benzenes or electron-poor alkenes, to form arylated or alkylated heterocycles in good yield.[5] Related reactions have also been reported on irradiation of 4-chloroanilines in the presence of (electron-rich) alkenes, although in this case, the alkylations appear to involve the formation of a phenyl cation.[6] An alternative approach to form carbon-centered radicals is to irradiate the alkyl iodide or bromide in the presence of triethylamine; this is proposed to form an amine–halide exciplex, which cleanly breaks down to give a carbon-centered radical and a halide anion. Cossy and co-workers have shown this to be a fast, convenient, and chemoselective method of radical generation, which has recently been used to prepare the bicyclic core of (±)-bisabolangelone (Scheme 1).[7]

Organoditin Compounds and Dimanganese Decacarbonyl

Irradiation of hexaalkylditin or hexaarylditin compounds ($R_3Sn–SnR_3$) can lead to homolysis of the weak tin–tin bond to form tin-centered radicals ($R_3Sn^{\cdot}$).[8] Absorption of UV light (for Bu_6Sn_2, λ_{max} = 236 nm) can produce a $\sigma \rightarrow \sigma^*$ transition to give an excited state with a weaker Sn–Sn bond. Photolysis of ditin compounds in the presence of triplet sensitizers (including acetone) has also been reported to afford a particularly mild approach to tin-centered radicals.[9] It should be noted that dimers of other group 14 elements can also undergo homolysis, and for hexamethyl compounds (Me_6M_2; where M = group 14 element), the strength of the M–M bond decreases as the size of the element increases; lead-centered radicals are therefore more easily formed than tin-centered radicals.

The resulting tin-centered radicals can react with a variety of organohalides (or related compounds) to efficiently form carbon-centered radicals; this type of reaction has played a central role in the development of synthetic and mechanistic organic radical chemistry.[10,11] Halogen-atom abstraction from alkyl or aryl halides allows the controlled formation of a variety of carbon-centered radicals, which can undergo a number of intra- or intermolecular carbon–carbon bond forming reactions. This includes cascade (or

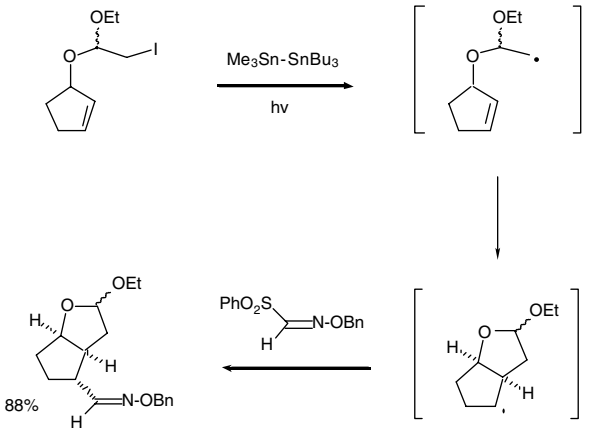

SCHEME 2

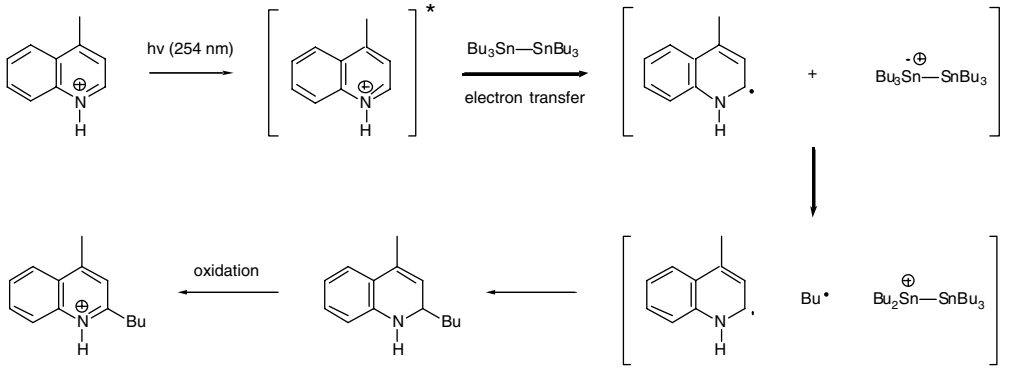

SCHEME 3

domino) reactions, as illustrated by the intra- followed by intermolecular radical reaction sequence shown in Scheme 2.[12]

Electron transfer reactions[13] involving hexabutylditin have also been reported, and these types of reactions have been shown to lead to the alkylation of protonated pyridine derivatives including lepidine (Scheme 3).[14] Similar reactions using tetraalkyltin compounds are also possible, as outlined in the next section of this chapter.

It should be noted that the majority of radical reactions involving tin-centered radicals involve the use of tin hydrides, especially ^{n}tributyltin hydride, Bu_3SnH. This reagent can be used to reduce a variety of organohalides via radical intermediates, and the reactions can be initiated by photolysis of peroxides or azo compounds (chiefly azobisisobutyronitrile, AIBN).[15]

Other organometallic dimers can produce metal-centered radicals, and dimanganese decacarbonyl $[Mn_2(CO)_{10}]$ can undergo efficient homolytic cleavage of the relatively weak Mn–Mn bond on photolysis using visible light.[8] The resulting manganese pentacarbonyl radical $[^{\cdot}Mn(CO)_5]$, like tin-centered radicals, can abstract halogen atoms from organohalides to form carbon-centered radicals under mild reaction conditions. This has been successfully exploited in a number of dimerization, cyclization, and intermolecular addition reactions, including an enantioselective approach to the pyrrolizidine alkaloid (–)-trachelanthramidine (Scheme 4).[16,17]

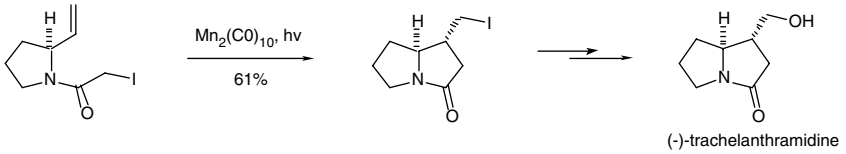

SCHEME 4

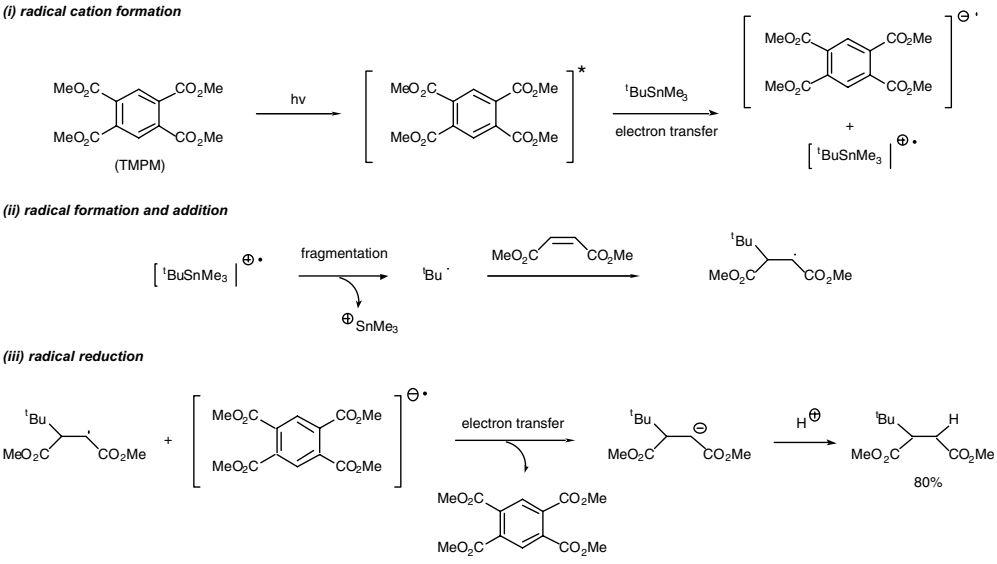

SCHEME 5

Tetraalkylstannanes and -silanes

The facile photosensitized oxidation of tetraalkylstannanes (R_4Sn) and related group-14 compounds has been widely exploited by Mella and co-workers to form carbon-centered radicals.[18] Photoinduced electron transfer from tetraalkylstannanes to a sensitizer, such as aromatic nitriles and esters (including tetramethyl pyromellitate, TMPM), affords a radical cation $[R_4Sn]^{+\cdot}$ that can fragment to form an alkyl radical ($R^{\cdot}$) together with the R_3Sn^+ cation. The alkyl radicals can then react with electron-poor alkenes, alkynes, aromatics, or the radical anion formed from the photosensitizer to form new carbon–carbon bonds. Careful choice of the photosensitizer can ensure that the radical anion selectively reduces the radical adduct (derived from addition to a double bond) rather than the first-formed alkyl radical (Scheme 5).

Similar reactions can occur using tetraalkylsilanes including benzyl- and allyl-silanes and, for example, photo-induced electron transfer in the presence of aromatic nitriles can afford alkylated products.[13a] These reactions can lead to the regioselective replacement of a cyano substituent with an alkyl group as shown in Scheme 6.[19] Mechanistic studies support the unimolecular fragmentation of the intermediate radical cation $[Bu_4Si]^{+\cdot}$ followed by radical–radical combination.[18c]

Related alkylation reactions involving electron-transfer have also been observed using silyl amines (including $Et_2NCH_2SiMe_3$) and silyl amides. Photolysis of these types of compound in the presence of conjugated cyclohexenones and the sensitizer 9,10-dicyanoanthracene (DCA) can lead to carbon–carbon bond formation in modest to very good yields. Electron-transfer forms α-amino radical cations, which fragment to form nucleophilic carbon-centered radicals, and examples of intermolecular[20] and intramolecular (Scheme 7)[21] addition reactions have been documented (see also the section "Amines and Alcohols" in this chapter).

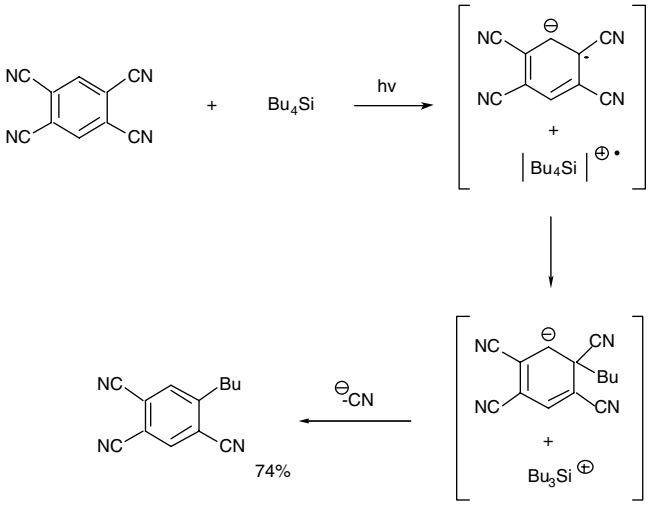

SCHEME 6

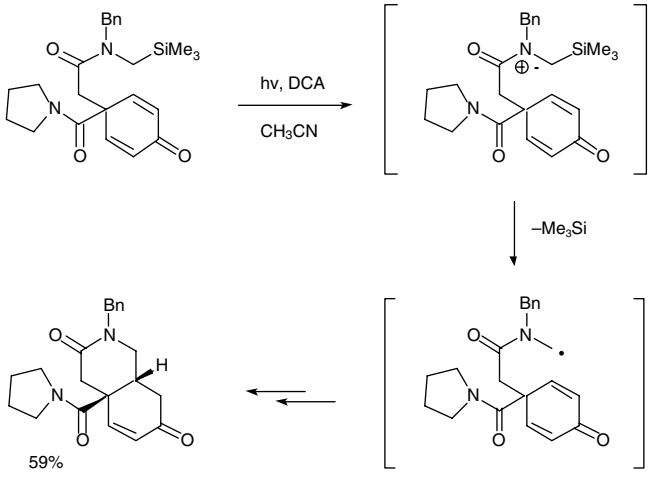

SCHEME 7

Organoborates

Photoinduced alkylation of aromatic compounds has been reported using alkyltriphenylborates.[22] Irradiation of acetonitrile solutions of dicyanoarenes with methyl- or benzyl-triphenylborate ($MeBPh_3^-$ or $BnBPh_3^-$) gave good yields of alkylcyanoarenes (cf. Scheme 6). The reaction is believed to be initiated by a photoinduced electron-transfer from the alkyltriphenylborate to the excited dicyanoarene followed by a fast cleavage of the alkyltriphenylborane radical ($RBPh_3^{\cdot}$) to form an alkyl radical. Coupling between the radical anion (derived from the dicyanoarene) and the alkyl radical produces a new carbon–carbon bond. Similar reactions have been reported using butyltriphenylborate and anthracene,[23] and more recently, using pyridinium tetraalkylborates (Py^+, BR_4^-).[24] For example, the efficient transfer of a methyl group (involving radical–radical coupling within a solvent cage) from tetramethylborate to pyridinium cations affords adducts in good yield (Scheme 8).

It should also be noted that 1,3-diketonatoborinates derived from 9-borabicyclo[3.3.1]nonane and 1,3-diketones have been shown to undergo a photo-rearrangement leading to an intramolecular alkylation and the formation of aldol products.[25]

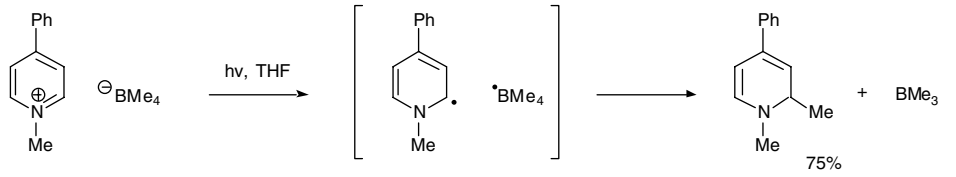

SCHEME 8

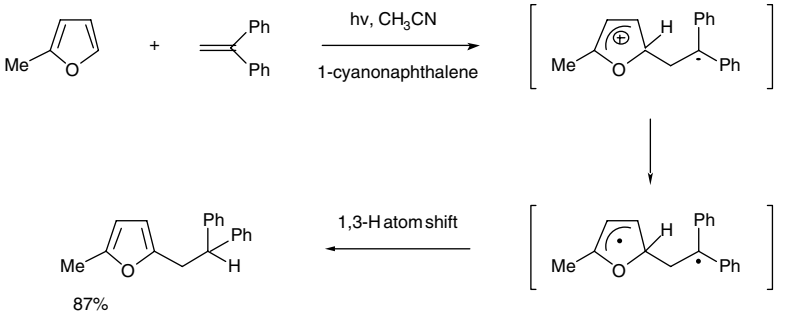

SCHEME 9

Heteroaromatics

A variety of photoinduced electron transfer reactions leading to the alkylation of heteroaromatic compounds are known. A typical example involves the reaction of five-membered heterocycles with electron-rich alkenes as illustrated in Scheme 9.[26] Thus, photolysis of furans in the presence of 1,1-diarylethenes and a sensitizer (such as 1-cyanonaphthalene) gives alkylated products in good yield following an unusual 1,3-hydrogen atom shift.

Related intramolecular alkylation reactions are possible, and the use of chloroacetamides as substrates for photocyclization has been shown to be an important method for making heterocyclic compounds, particularly medium-ring lactams (Scheme 10).[27]

Toluene

The formation of benzyl radicals from toluene can be achieved by photosensitization in the presence of 1,4-naphthalenedicarbonitrile (DCN). Photoinduced electron-transfer from toluene to DCN is followed by proton transfer and radical coupling or addition to electrophilic alkenes (including dimethyl maleate) to form new carbon–carbon bonds (Scheme 11).[28]

It should also be emphasized that benzyl radicals can be formed from toluene by hydrogen atom abstraction reactions. This may involve, for example, reaction with reactive oxygen-centered radicals derived from the photolysis of peroxides (see "Amino Acids and Peptides" later in this chapter).

Phthalimides and Ketones

The photoinduced cyclization of *N*-substituted phthalimides has proved an effective method for the synthesis of medium- to large-membered rings. These alkylation reactions can involve either electron-transfer or hydrogen-atom abstraction reactions.[29] For example, irradiation of *N*-(2-hydroxyethyl)-4,5,6,7-tetrachlorophthalimide in the presence of 1,1-diphenylethene leads to electron transfer and the formation of a tricyclic derivative in good yield (Scheme 12).[30] The regioselectivity of this reaction can be explained by the positive charge in the intermediate radical cation being largely concentrated at the terminal carbon atom; this cation is susceptible to nucleophilic attack by the primary alcohol to form a

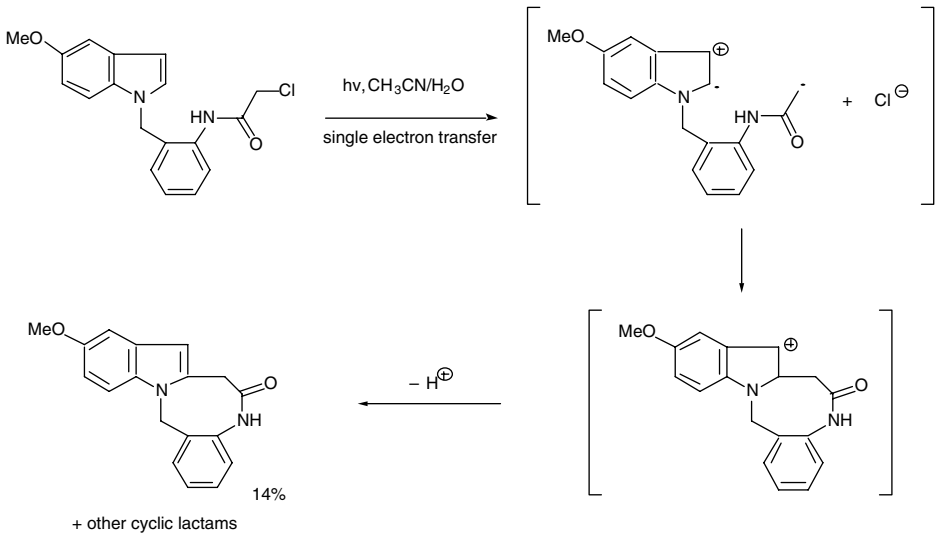

SCHEME 10

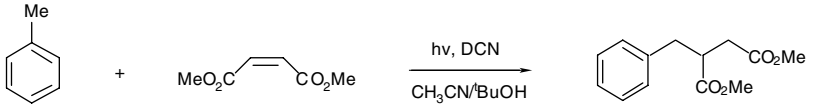

SCHEME 11

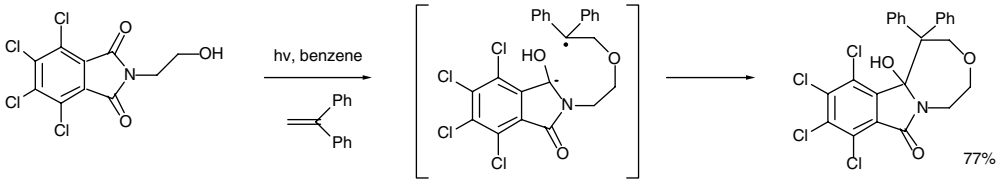

SCHEME 12

new C–O bond. Related intermolecular single electron-transfer reactions involving the alkylation of *N*-methyl phthalimide by α-keto carboxylates have also been reported.[31]

A variety of photochemical reactions involving phthalimides can be attributed to reaction of the excited state of the phthalimide group by 1,5-hydrogen atom transfer in a Norrish Type II reaction. Following abstraction of a hydrogen atom from the γ-CH position, the resulting 1,4-biradical can undergo Norrish type I fragmentation or alternatively, Yang cyclization. Steric factors play a large part in determining the ratio of fragmentation to ring closure. As shown in Scheme 13, a tricyclic product can be isolated from a remarkable phthalimide reaction involving two Yang-type cyclizations (Scheme 13).[32]

As with phthalimides, photolysis of alkyl aryl ketones can give rise to hydrogen atom abstraction reactions leading to the formation of cyclic products. Although 1,5-hydrogen atom abstraction is generally preferred (because of stereoelectronic/geometric requirements),[1,33] reactions involving 1,6-hydrogen atom abstraction have also been reported.[34] Examples of these types of reaction include the photocyclization of γ-ketoamides to form 6-membered lactams, the photocyclization of 2-alkoxybenzophenones to form dihydrobenzofuranols (Scheme 14), the photochemical cyclization of a glyoxylate ester to form coumestrol (Scheme 14), and the diastereoselective cyclization of *o*-benzylaminophenylketones to form

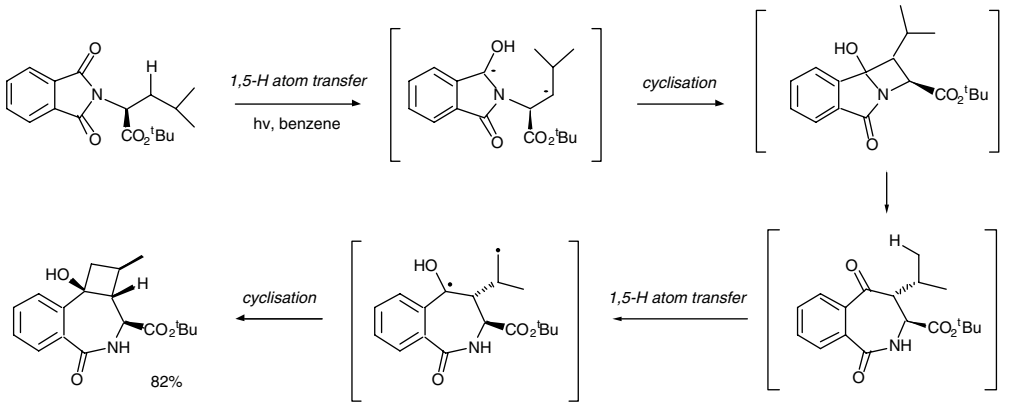

SCHEME 13

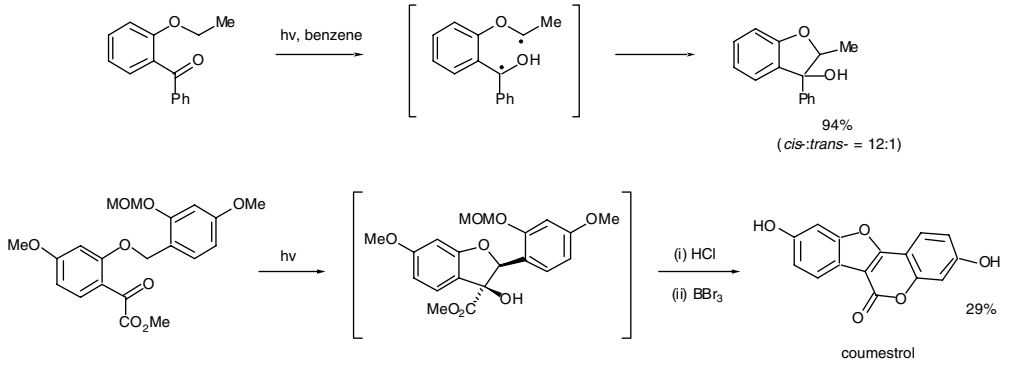

SCHEME 14

dihydroindolinols.[35] Intermolecular hydrogen atom abstraction reactions are very common; indeed, aromatic ketones (and also quinones) are often employed as sensitizers in photochemical alkylations (as illustrated in the sections "Amines and Alcohols" and "Amino Acids and Peptides" later in this chapter). This includes, for example, mediating the cyclization of aldehydes onto acceptor double bonds by generation of intermediate acyl radicals (RCO·).[36]

Novel photo-induced electron-transfer reactions have recently been reported using α,β-unsaturated ketones. Photolysis in the presence of an electron acceptor (such as 9,10-dicyanoanthracene, DCA) and a sacrificial electron donor (triphenylphosphine) leads to the formation of carbon-centered radicals, which can cyclize to form carbocycles as shown in Scheme 15.[37]

1,3-Dioxolanes

Irradiation of 1,3-dioxolanes in the presence of a sensitizer such as benzophenone (Ph_2CO), leads to the abstraction of an acetal hydrogen atom (by the triplet state ketone) to generate 1,3-dioxolanyl radicals, together with the resonance-stabilized diphenyl ketyl radical (Scheme 16). These nucleophilic 1,3-dioxolanyl radicals have been shown to add to a variety of alkenes to form adduct radicals, which can then accept a hydrogen atom from the diphenyl ketyl radical to give the desired alkylated product.[38] The diastereoselective addition of 1,3-dioxolanyl radicals to alkenes bearing chiral auxiliaries has also recently been reported,[38b] while the photochemical alkylation of diketene with 2-undecyl-1,3-dioxolane has been utilized as a key step in the synthesis of (–)-tetrahydrolipstatin (Scheme 17).[39]

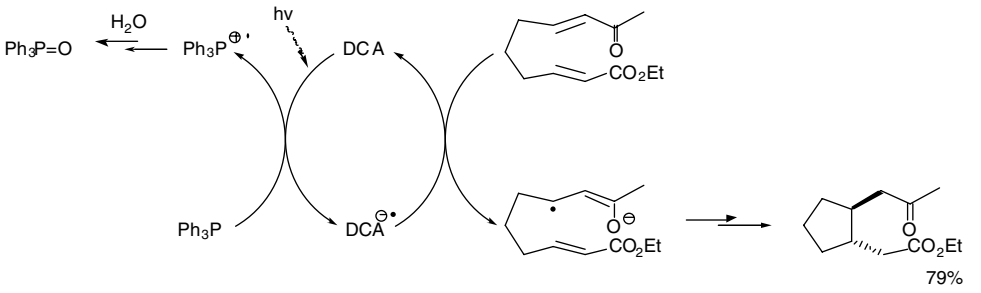

SCHEME 15

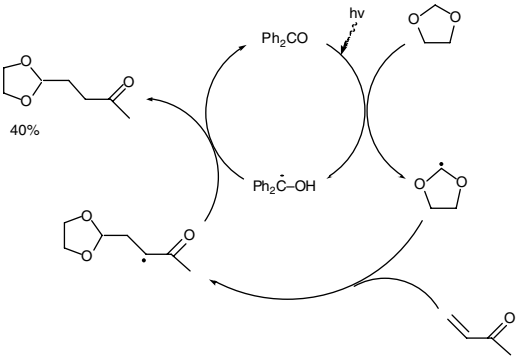

SCHEME 16

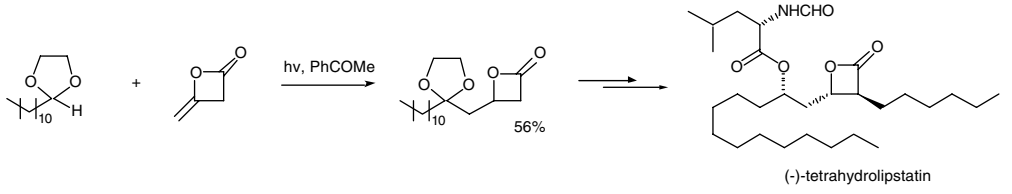

SCHEME 17

Amines and Alcohols

α-Aminoalkyl radicals [$R_2(R_2N)C^{\cdot}$] can be generated from amines [$R_2(R_2N)CH$] via photoinduced electron transfer reactions in the presence of sensitizers (including aromatic ketones). These nucleophilic radicals have been shown to add to electron-poor alkenes, leading to the efficient construction of carbon–carbon bonds adjacent to nitrogen. This has proved to be an effective method for the formation of lactams from, for example, reaction of *N*-allylamines with α,β-unsaturated esters.[40] The diastereoselective addition of tertiary amines to a chiral furanone derivative has also been reported (Scheme 18), as has a related intramolecular cyclization reaction to form the indolizidine alkaloid skeleton (Scheme 19).[41]

Similar intermolecular alkylation reactions can occur by irradiation of primary or secondary alcohols in the presence of sensitizers. The resulting α-hydroxyalkyl radicals [$R_2(HO)C^{\cdot}$] have been shown to add to a range of double bond acceptors. Recent examples, which lead to the formation of new carbon–carbon bonds, include addition to maleimides,[42] a dihydropyrrole,[43] and a 2,2-difluorovinyl carbamate.[44]

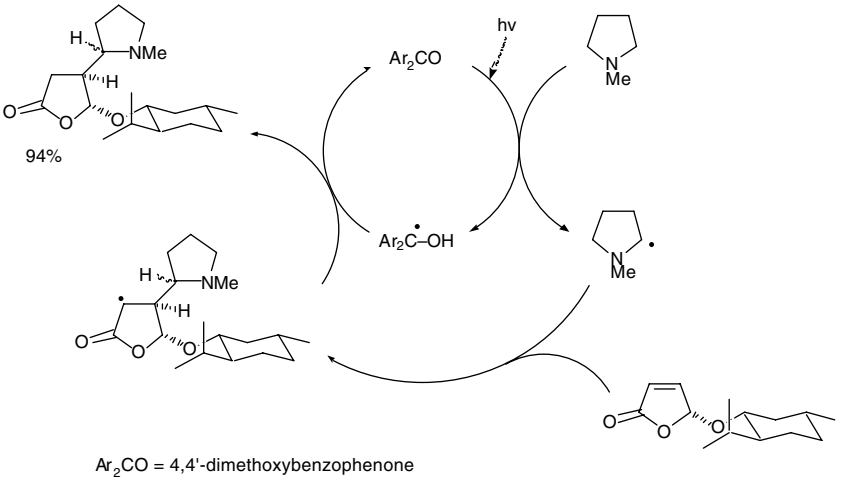

SCHEME 18

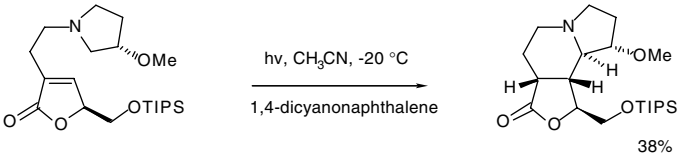

SCHEME 19

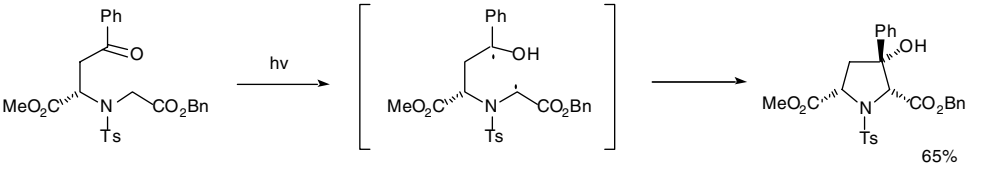

SCHEME 20

Amino Acids and Peptides

A variety of photochemical methods have been reported for α-alkylation of amino acids and in particular glycine derivatives.[45] Norrish-Yang photocyclization reactions have been used extensively to prepare nitrogen heterocycles, particularly proline derivatives (Scheme 20), from acyclic glycine derivatives bearing an aromatic ketone.[34,35] Related photocyclizations of oligopeptide-linked anthraquinones have also been reported, and interestingly, these radical coupling reactions resulted in the formation of a C–O rather than a C–C bond.[46]

Intermolecular radical reactions have also been reported, including selective radical–radical coupling reactions. These reactions involve the formation of α-amino acid radicals (stabilized by the captodative effect), which can couple to, for example, benzyl radicals to form phenylalanine derivatives (Scheme 21).[47] The benzyl radicals are generated by hydrogen-atom abstraction from toluenes using alkoxyl radicals derived from peroxides and/or aromatic ketone sensitizers.

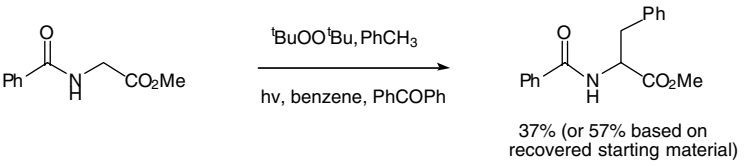

SCHEME 21

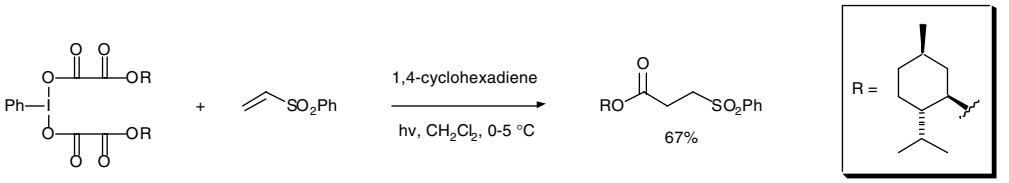

SCHEME 22

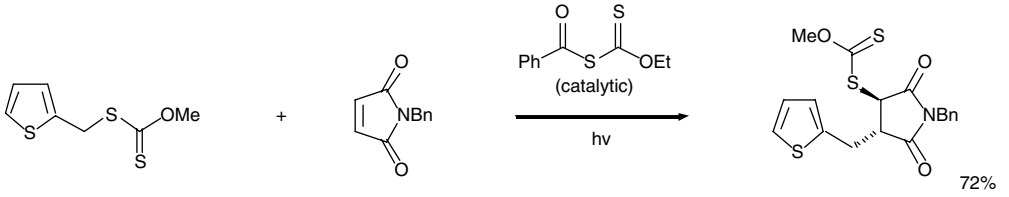

SCHEME 23

6.3 Summary and Outlook

This short review has highlighted a diverse range of mild and efficient photochemical methods for the formation of carbon–carbon bonds. These intra- or intermolecular free radical reactions have been shown to afford a versatile and controlled synthetic approach to a wide variety of organic products. Many of the photochemical methods can be thought of as offering "clean" (or "green") synthetic approaches to compounds — an active area of current research. Bearing in mind the versatility of radical reactions and the relatively small number of radical-generating systems currently available, it is expected that future research will lead to the development of new environmentally friendly photochemical alkylation reactions. Recent examples of particularly interesting alkylation methods include the use of organohypervalent iodine compounds[48] as a route to carbon-, oxygen-, or nitrogen-centered radicals (Scheme 22), and chain reactions involving xanthates, which can be initiated by using catalytic amounts of *S*-benzoyl xanthates (Scheme 23).[49] The development of these and related free-radical methods should help to promote the more widespread use of photochemical alkylations in both academia and industry in the future.

References

1. De Keukeleire, D. and He, S-L., Photochemical strategies for the construction of polycyclic molecules, *Chem. Rev.,* 93, 359, 1993.
2. Fischer, M., Industrial applications of photochemical syntheses, *Angew. Chem. Int. Ed. Engl.,* 17, 16, 1978.
3. Clements, A.D., Photochemistry in commercial synthesis, *Chem. Br.*, 16, 464, 1980.
4. Kropp, P.J., Photobehavior of alkyl halides in solution: radical, carbocation, and carbene intermediates, *Acc. Chem. Res.,* 17, 131, 1984.

5. (a) D'Auria, M., Ferri, R., Poggi, G., Mauriello, G., and Racioppi, R., Photochemical behavior of iodoheterocyclic derivatives in the presence of electron-poor olefins, *Eur. J. Org. Chem.,* 1653, 2000; (b) D'Auria, M., De Luca, E. Mauriello, G., Racioppi, R., and Sleiter, G., Photochemical substitution of halogenopyrrole derivatives, *J. Chem. Soc., Perkin Trans. 1,* 2369, 1997.
6. Coppo, P., Fagnoni, M., and Albini, A., Photochemical conversion of 4-chloroaniline into 4-alkylanilines, *Tetrahedron Lett.,* 42, 4271, 2001.
7. (a) Cossy, J., Ranaivosata, J-L., and Bellosta, V., Formation of radicals by irradiation of alkyl halides in the presence of triethylamine, *Tetrahedron Lett.,* 35, 8161, 1994; (b) Cossy, J., Bellosta, V., Ranaivosata, J-L., and Gille, B., Formation of radicals by irradiation of alkyl halides in the presence of triethylamine. Application to the synthesis of (±)-bisabolangelone, *Tetrahedron,* 57, 5173, 2001.
8. Gilbert, B.C. and Parsons, A.F., The use of free radical initiators bearing metal–metal, metal–hydrogen and non-metal–hydrogen bonds in synthesis*, J. Chem. Soc., Perkin Trans. 2,* 367, 2002.
9. Harendza, M., Junggebauer, J., Leβmann, K., Neumann, W.P., and Tews, H., Mild photochemical generation of stannyl radicals $Bu_3Sn\cdot$ from hexabutyl distannane for organic synthesis*, Synlett,* 286, 1993.
10. Parsons, A.F., *An Introduction to Free Radical Chemistry,* Blackwell Science, Oxford, 2000.
11. Renaud, P. and Sibi, M., Eds., *Radicals in Organic Synthesis*, Wiley-VCH, Weinheim, 2001.
12. (a) Kim, S., Lee, I.Y., Yoon, J-Y., and Oh, D.H., Novel radical reaction of phenylsulfonyl oxime ethers. A free radical acylation approach, *J. Am. Chem. Soc.,* 118, 5138, 1996; (b) Kim, S., Kim, N, Yoon, J-Y., and Oh, D.H., Preparation of cycloalkanone oxime ethers via a free radical acylation approach, *Synlett,* 1148, 2000.
13. (a) Albini, A., Mella, M., and Freccero, M., A new method in radical chemistry: generation of radicals by photo-induced electron transfer and fragmentation of the radical cation, *Tetrahedron,* 50, 575, 1994; (b) Dalko, P.I., Redox induced radical and radical ionic carbon–carbon bond forming reactions, *Tetrahedron*, 51, 7579, 1995; (c) Mella, M., Fagnoni, M., Freccero, M., Fasani, E., and Albini, A., New synthetic methods via radical cation fragmentation, *Chem. Soc. Rev.,* 27, 81, 1998.
14. Minisci, F., Fontana, F., Caronna, T., and Zhao, L., A novel substitution reaction by photoinduced electron-transfer between pyridine derivatives and alkyltin compounds, *Tetrahedron Lett.,* 33, 3201, 1992.
15. (a) Jasperse, C.P., Curran, D.P., and Fevig, T.L., Radical reactions in natural product synthesis, *Chem. Rev.,* 91, 1237, 1991; (b) Neumann, W.P., Tri-n-butyltin hydride as reagent in organic synthesis, *Synthesis,* 665, 1987.
16. (a) Gilbert, B.C., Kalz, W., Lindsay, C.I., McGrail, P.T., Parsons, A.F., and Whittaker, D.T.E., Initiation of radical cyclisation reactions using dimanganese decacarbonyl. a flexible approach to preparing 5-membered rings, *J. Chem. Soc., Perkin Trans. 1,* 1187, 2000; (b) Huther, N., McGrail, P.T., and Parsons, A.F., Biphasic manganese carbonyl reactions: a new approach to making carbon–carbon bonds, *Tetrahedron Lett.,* 43, 2535, 2002.
17. Friestad, G.K. and Qin, J., Intermolecular alkyl radical addition to chiral *N*-acylhydrazones mediated by manganese carbonyl, *J. Am. Chem. Soc.,* 123, 9922, 2001.
18. (a) Fagnoni, M., Mella, M., and Albini, A., Radical addition to alkenes via electron transfer photosensitization, *J. Am. Chem. Soc.,* 117, 7877, 1995; (b) Fagnoni, M., Mella, M., and Albini, A., Alkylation of alkenes by radicals generated through photoinduced single electron transfer, *Tetrahedron*, 51, 859, 1995; (c) Fagnoni, M., Mella, M., and Albini, A., Scope and mechanism of the electron transfer photoinduced alkylation of an aromatic nitrile, *Tetrahedron,* 50, 6401, 1994; (d) Fagnoni, M., Mella, M., and Albini, A., Electron-transfer-photosensitized conjugate alkylation, *J. Org. Chem.,* 63, 4026, 1998; (e) Fagnoni, M., Mella, M., and Albini, A., Tandem energy transfer–electron transfer in the photosensitised alkylation of α,β-unsaturated ketones, *J. Phys. Org. Chem.,* 10, 777, 1997.
19. Kyushin, S., Masuda, Y., Matsushita, K., Nakadaira, Y., and Ohashi, M., Novel alkylation of aromatic nitriles via photo-induced electron transfer of group 14 metal-carbon σ donors, *Tetrahedron Lett.,* 31, 6395, 1990.

20. Hasegawa, E., Xu, W., Mariano, P.S., Yoon, U-C., and Kim, J-U., Electron-transfer-induced photoadditions of the silyl amine Et_2NCH_2TMS to α,β–unsaturated cyclohexenones. Dual reaction pathways based on ion-pair-selective cation-radical chemistry, *J. Am. Chem. Soc.,* 110, 8099, 1988.
21. (a) Jung, Y.S., Swartz, W.H., Xu, W., Mariano, P.S., Green, N.J., and Schultz, A.G., Exploratory studies of α-silylamido 2,5-cyclohexadien-1-one SET photochemistry. Methodology for synthesis of functionalised hydroisoquinolines, *J. Org. Chem.,* 57, 6037, 1992; (b) Khim, S-K., Cederstrom, E. Ferri, D.C., and Mariano, P.S., SET-Photosensitized reactions of α-silylamino-enones and ynones proceeding by 6-endo α-amino radical cyclisation pathways, *Tetrahedron,* 52, 3195, 1996.
22. Lan, J.Y. and Schuster, G.B., Free radical formation in the photooxidative alkylations of dicyanonaphthalene with alkyltriphenylborate salts, *Tetrahedron Lett.,* **2**7, 4261, 1986.
23. Lund, T., Photoinduced alkylation of anthracene by butyltriphenylborate ion. A comparison between products from the photochemical and electrochemical butylation of anthracene, *Acta Chem. Scand.,* 50, 64, 1996.
24. Zhu, D. and Kochi, J.K., Alkylation of pyridinium acceptors via thermal and photoinduced electron transfer in charge-transfer salts with organoborates, *Organometallics,* 18, 161, 1999.
25. Ishiyama, J-I., and Chow, Y.L., A novel photorearrangement of 1,3-diketonatoborinate: a photoinduced intramolecular alkylation on a conjugated carbonyl system, *Can. J. Chem.,* 77, 1374, 1999.
26. (a) Mizuno, K., Ishii, M., and Otsuji, Y., Photoinduced alkylation of five-membered heteroaromatic compounds via electron-transfer reaction: heterodimer cation radical intermediacy, *J. Am. Chem. Soc.,* 103, 5570, 1981; (b) Nakagawa, K., Photoinduced alkylation reaction of benzo[f]indole-4,9-dione with arylalkenes, *Bull. Chem. Soc. Jpn.,* 64, 1031, 1991.
27. Bremner, J.B., Russell, H.F., Skelton, B.W., and White, A.H., Novel indole-fused medium-sized ring heterocycles via chloroacetamide photochemistry, *Heterocycles*, 53, 277, 2000.
28. Mella, M., Fagnoni, M., and Albini, A., Benzyl radicals from toluene by photosensitization with naphthalene-1,4-dicarbonitrile – benzylation and hydroxymethylation of unsaturated compounds, *Eur. J. Org. Chem.,* 2137, 1999.
29. Easton, C.J. and Hutton, C.A., Recent developments in the use of *N*-phthaloyl-amino acid derivatives in synthesis, *Synlett,* 457, 1998.
30. Xue, J., Zhu, L., Fun, H-K., and Xu, J-H., Synthesis of medium and large ring heterocycles by photoinduced intermolecular and intramolecular electron transfer reactions of tetrachlorophthalimides with alkenes, *Tetrahedron Lett.,* 41, 8553, 2000.
31. Griesbeck, A.G., Oelgemöller, M., and Lex, J., Photodecarboxylative additions of α-keto carboxylates to phthalimides. Alkylation, acylation and ring expansion, *Synlett,* 1455, 2000.
32. Griesbeck, A.G., Henz, A., Kramer, W., Wamser, P., Peters, K., and Peters, E-M., Stereo- and spinselectivity of primary (singlet) and secondary (triplet) Norrish type II reactions, *Tetrahedron Lett.,* 39, 1549, 1998.
33. Griesbeck, A.G. and Heckroth, H., Stereoselective synthesis of 2-aminocyclobutanols via photocyclization of α-amido alkylaryl ketones: mechanistic implications for the Norrish/Yang reaction, *J. Am. Chem. Soc.,* 124, 396, 2002.
34. (a) Wessig, P., Wettstein, P., Giese, B., Neuburger, M., and Zehnder, M., Asymmetric synthesis of 3-hydroxyprolines by photocyclisation of *N*-(2-benzoylethyl)glycinamides, *Helv. Chim. Acta,* 77, 829, 1994; (b) Steiner, A., Wessig, P., and Polborn, K., Asymmetric synthesis of 3-hydroxyprolines by photocyclisation of C(1′)-substituted *N*-(2-benzoylethyl)glycine esters, *Helv. Chim. Acta,* 79, 1843, 1996; (c) Wyss, C., Batra, R., Lehmann, C., Sauer, S., and Giese, B., Selective photocyclization of glycine in dipeptides, *Angew. Chem. Int. Ed. Engl.,* 35, 2529, 1996.
35. (a) Lindemann, U., Reck, G., Wulff-Molder, D., and Wessig, P., Photocyclisation of 4-oxo-4-phenyl-butanoyl amines to γ-lactams, *Tetrahedron,* 54, 2529, 1998; (b) Griesbeck, A.G., Heckroth, H., and Schmickler, H., Regio- and stereoselective 1,6-photocyclization of aspartic acid–derived chiral γ-ketoamides, *Tetrahedron Lett.,* 40, 3137, 1999; (c) Sharshira, E.M., Okamura, M., Hasegawa, E., and Horaguchi, T., Photocyclisation reactions. Part 6. Solvent and substituent effects in the synthesis of dihydrobenzofuranols using photocyclisation of 2-alkoxybenzophenones and

ethyl 2-benzoylphenoxyacetates, *J. Heterocyclic Chem.,* 34, 861, 1997; (d) Seiler, M., Schumacher, A., Lindemann, U., Barbosa, F., and Giese, B., Diastereoselective photocyclisation to dihydroindolinols, *Synlett,* 1588, 1999; (e) Kraus, G.A. and Zhang, N., Hydrogen-atom abstraction/cyclisation in synthesis. Direct syntheses of coumestan and coumestrol, *J. Org. Chem.,* 65, 5644, 2000.

36. Brown, D., Drew, M.G.B., and Mann, J., Intramolecular photocyclisation reactions of 5-*tert*-butyldimethylsiloxymethyl-3-(3-formylpropyl)furan-2(5*H*)-one: formation of bicyclic and spirocyclic lactones, *J. Chem. Soc., Perkin Trans. 1,* 3651, 1997.
37. (a) Pandey, G., Hajra, S., Ghorai, M.K., and Kumar, K.R., Designing photosystems for harvesting photons into electrons by sequential electron-transfer processes: reversing the reactivity profiles of α,β–unsaturated ketones as carbon radical precursor by one electron reductive β-activation, *J. Am. Chem. Soc.,* 119, 8777, 1997.
38. (a) Manfrotto, C., Mella, M., Freccero, M., Fagnoni, M., and Albini, A., Photochemical synthesis of 4-oxobutanal acetals and of 2-hydroxycyclobutanone ketals, *J. Org. Chem.,* 64, 5024, 1999; (b) Campari, G., Fagnoni, M., Mella, M., and Albini, A., Diastereoselective photosensitised radical addition to fumaric acid derivatives bearing oxazolidine chiral auxiliaries, *Tetrahedron: Asymm.,* 11, 1891, 2000; (c) Mosca, R., Fagnoni, M., Mella, M., and Albini, A., Synthesis of monoprotected 1,4-diketones by photoinduced alkylation of enones with 2-substituted-1,3-dioxolanes, *Tetrahedron,* 57, 10319, 2001.
39. Parsons, P.J. and Cowell, J.K., A rapid synthesis of (–)-tetrahydrolipstatin, *Synlett,* 107, 2000.
40. Das, S., Kumar, J.S.D., Shivaramayya, K., and George, M.V., Formation of lactams via photoelectron-transfer catalyzed reactions of *N*-allylamines with α,β-unsaturated esters, *Tetrahedron,* 52, 3425, 1996.
41. (a) Bertrand, S., Glapski, C., Hoffmann, N., and Pete, J-P., Highly efficient photochemical addition of tertiary amines to electron deficient alkenes. Diastereoselective addition to (5*R*)-5-menthyloxy-2[5*H*]-furanone, *Tetrahedron Lett.,* 40, 3169, 1999; (b) Bertrand, S., Hoffmann, N., and Pete, J-P., Stereoselective radical addition of tertiary amines to (5*R*)-5-menthyloxy-2[5*H*]-furanone: application to the enantioselective synthesis of (–)-isoretronecanol and (+)-laburnine, *Tetrahedron Lett.,* 40, 3173, 1999; (c) Farrant, E. and Mann, J., Novel synthesis of the indolizidine alkaloid skeleton with appropriate functionality and stereochemistry for use as a "chiral scaffold," *J. Chem. Soc., Perkin Trans. 1,* 1083, 1997.
42. Al-Amoudi, M.A.S. and Vernon, J.M., Photochemical addition of secondary alcohols to maleimides, *J. Chem. Soc., Perkin Trans. 2,* 2667, 1999.
43. Drew, M.G.B., Harrison, R.J., Mann, J., Tench, A.J., and Young, R.J., Photoinduced addition of methanol to 5(*S*)-5-triisopropylsiloxymethyl-*N*-boc-dihydropyrrole-2(5*H*)-one: a new route to 4(*S*),5(*S*)-disubstituted pyrrolidin-2-ones, *Tetrahedron,* 55, 1163, 1999.
44. Okano, T., Nakajima, A., and Eguchi, S., Preparation of masked 2,2-difluoro-1,3-diols and 2,2-difluoro-1,3,4-butanetriol via photochemical and thermal addition of oxygenated radicals to 2,2-difluorovinyl carbamate, *Synlett,* 1449, 2001.
45. Easton, C.J., Free-radical reactions in the synthesis of α-amino acids and derivatives, *Chem. Rev.,* 97, 53, 1997.
46. (a) Maruyama, K., Hashimoto, M., and Tamiaki, H., Intramolecular photoreaction of synthetic oligopeptide-linked anthraquinone molecules, *J. Org. Chem.,* 57, 6143, 1992; (b) Tamiaki, H., Hashimoto, M., and Maruyama, K., Intramolecular photocyclisation in quinone-bearing oligopeptides, *Bull. Chem. Soc. Jpn.,* 67, 1987, 1994.
47. (a) Knowles, H.S., Hunt, K., and Parsons, A.F., Photochemical alkylation of glycine leading to phenylalanines, *Tetrahedron Lett.,* 41, 7121, 2000; (b) Knowles, H.S., Hunt, K., and Parsons, A.F., A photochemical approach to phenylalanines and related compounds by alkylation of glycine, *Tetrahedron,* 57, 8115, 2001.
48. (a) Togo, H. and Katohgi, M., Synthetic uses of organohypervalent iodine compounds through radical pathways, *Synlett,* 565, 2001; (b) Togo, H., Aoki, M., and Yokoyama, M., Reductive addition to electron-deficient olefins with trivalent iodine compounds, *Tetrahedron,* 49, 8241, 1993.
49. Zard, S.Z., On the trail of xanthates: some new chemistry from an old functional group, *Angew. Chem. Int. Ed. Engl.,* 36, 672, 1997.

7

SET Addition of Amines to Alkenes

Frederick D. Lewis
Northwestern University

Elizabeth M. Crompton
Northwestern University

7.1 Introduction

Amines are good electron donors that participate in a wide variety of electron transfer reactions.[1–3] The free energy for a photochemical electron transfer quenching process can be estimated from the singlet energy and reduction potential of the excited state, the oxidation potential of the amine, and the solvent polarity using Weller's equation [$\Delta G_{et} = E^* - (E^{ox} - E^{red}) - (e^2_o/\varepsilon R)$].[4] Amine oxidation potentials decrease in the order tertiary > secondary > primary amines and aromatic > aliphatic amines. However, the irreversible nature of the oxidation of aliphatic amines results in considerable uncertainty in their oxidation potentials and hence in the calculated free energy for a photochemical single electron transfer (SET) process.[5]

Quenching of singlet state reactants by tertiary amines can result in the formation of fluorescent exciplex or radical ion pair intermediates, which can be detected by transient absorption spectroscopy or other spectroscopic techniques such as chemically induced dynamic nuclear polarization (CIDNP).[6] These intermediates can either undergo charge recombination, resulting in regeneration of the ground state reactants, or chemical reactions leading to product formation. Amine oxidation results in a dramatic increase in the acidity of the α-CH bonds, and thus proton transfer is the expected chemical reaction for tertiary amine cation radicals, except in the case of α-trimethylsilylamines, which can undergo nucleophilic displacement of the silyl group in competition with deprotonation. Secondary and primary amines undergo either α-CH or NH deprotonation reactions, depending upon the proton acceptor. Deprotonation and desilylation of the amine cation radicals yield free radical intermediates and hence,

0-8493-1348-1/04/$0.00+$1.50

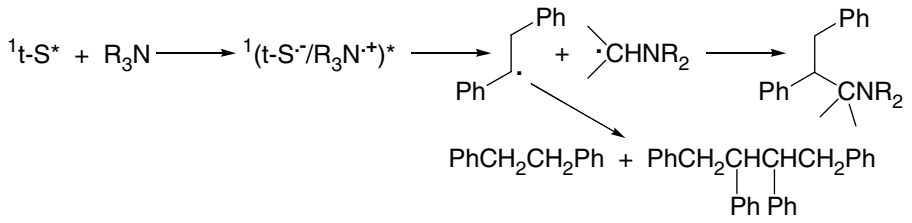

SCHEME 1

the ultimate products of photoinduced SET reactions of amines typically result from radical pair combination or radical–neutral addition reactions.

Several comprehensive reviews of photochemical SET reactions of amines are available,[1–3] as are more specialized reviews of the reactions of amines with specific classes of excited states.[6–8] These include reviews of the photochemical reactions of amines with arenes and iminium ions, which appeared in the first edition of this Handbook. The present article provides an overview of the photochemical addition reactions of amines with alkenes. Detailed information about the mechanisms and dynamics of these reactions is provided in the original literature and the comprehensive reviews.

7.2 Additions of Stilbenes with Amines

Irradiation with Tertiary Amines

From a historical perspective, investigations in the 1970s and 1980s of the addition reactions of the excited singlet state of *trans*-stilbene with alkylamines provided the basis for our current mechanistic understanding of SET addition reactions involving amines. These reactions have been the topic of several reviews, and thus a brief review will suffice.[1–3,6,9–11] The direct irradiation of stilbene with symmetric trialkylamines such as Et_3N in acetonitrile solution affords a single adduct and other products characteristic of radical pair intermediates (Scheme 1).[12] The preparative yields of stilbene–amine adducts are modest (<50%), as expected for a radical pair process. Radical pair formation was proposed to occur via electron transfer followed by proton transfer from the α-carbon of the amine cation radical to the stilbene anion radical. The formation of a radical ion pair as a putative intermediate in these reactions is supported by the observation in nonpolar solvents of stilbene–amine exciplex fluorescence without adduct formation,[12] by the presence of the stilbene anion radical observed by time-resolved Raman spectroscopy,[13] and by a CIDNP study of the reaction products.[14]

The addition reactions of singlet stilbene with nonsymmetrical tertiary amines yield addition products resulting from proton transfer from each of the nonequivalent α-carbons (Scheme 2).[15] The adduct resulting from proton transfer from the *less substituted* carbon of simple trialkylamines, such as *N,N*-dimethylisopropylamine, is formed selectively. In contrast, the adduct resulting from proton transfer from the *more substituted* carbon is formed selectively in the case of *N,N*-dimethylallylamine and other amines possessing a radical-stabilizing α-substituent.[16] The former result was attributed to a stereoelectronic effect on the proton transfer process and the latter result to the effects of substituents upon the kinetic acidity of the α-protons.[3] Similar trends have been reported for other amine photooxidation reactions. The selectivity pattern is dependent upon the identity of the proton acceptor.

The addition reactions of ring-substituted stilbenes with Et_3N are nonregioselective.[17] (Aminoalkyl)stilbenes in which a trialkylamine is appended to the stilbene ortho position with a mono-, di-, or trimethylene linker form fluorescent intramolecular exciplexes but fail to undergo intramolecular addition, even in polar solvents.[18] It is possible that the exciplex or radical ion pair geometry is not suitable for a least-motion proton transfer process.

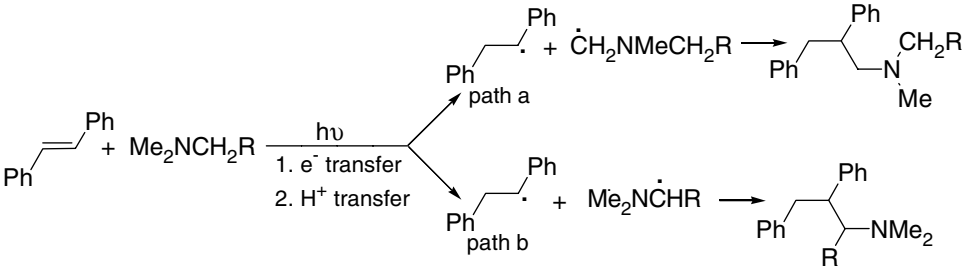

SCHEME 2

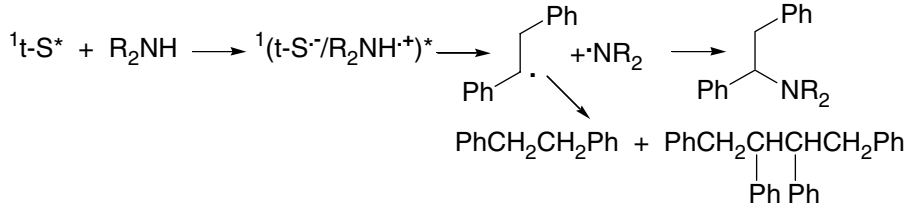

SCHEME 3

Irradiation with Secondary Amines

The reactions of singlet stilbene with secondary amines such as Et_2NH yield a single adduct and other products characteristic of radical pair intermediates in both polar and nonpolar solvents (Scheme 3).[12] Selective NH proton transfer has been attributed to either greater NH vs. α-CH cation radical acidity or to NH-stilbene hydrogen bonding in an exciplex or radical ion pair intermediate.[19] The addition of singlet ring-substituted stilbenes with Et_2NH is also nonregioselective.[18]

(Aminoalkyl)stilbenes **1** and **2**, in which a *N*-methylamine is appended to the stilbene ortho position with a di- or trimethylene linker, undergo intramolecular addition reactions, yielding 3-benzazepine and 2-benzazepine products **1a** and **2a**, respectively (Scheme 4).[18] Note that the NH proton transfer occurs regioselectively to the end of the stilbene double bond proximal to the point of attachment of the ethylene linker, but distal to the point of attachment of the propylene linker. This selectivity was attributed to a least-motion pathway for intramolecular exciplex proton transfer. The (aminoalkyl)stilbenecarboxamides **3** and **4** also undergo regioselective intramolecular addition (Scheme 5) to form the medium-ring azalactams **3a** and **4a**, respectively, in moderate yield (ca. 40%).[20] Singlet stilbenes fail to undergo either inter- or intramolecular reactions with primary amines, reflecting the inability of primary amines to quench stilbene fluorescence.

Irradiation with Heterocyclic Amines

Irradiation of stilbene in *N*-methylimidazole results in the formation of the α-CH adduct **5a**.[21] Adduct formation is proposed to occur via a 1,4-biradical intermediate (Scheme 6). Similarly, irradiation of stilbene in pyrrole yields two CH adducts, **6a** and **6b**.[22] Irradiation of stilbene with indole or carbazole in acetonitrile solution results in the formation of both NH and CH adducts in low yield. However, irradiation of polycrystalline mixtures of stilbene and these heterocycles yields predominantly the NH adducts in moderate yield (ca. 50%). The role of electron transfer in these reactions has not been established; however, exciplex fluorescence is observed upon quenching of stilbene by *N*-methylpyrrole in cyclohexane solution.

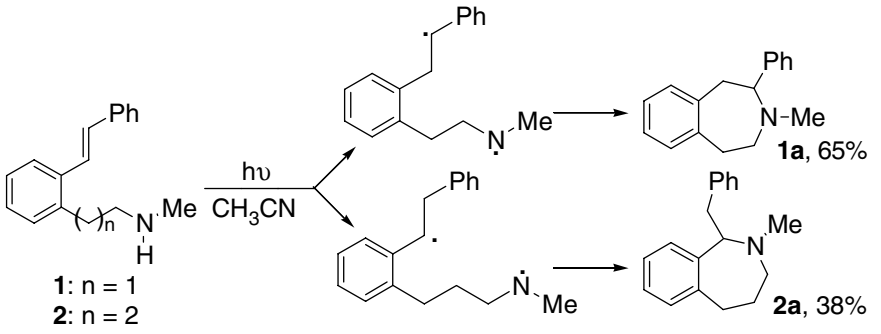

SCHEME 4

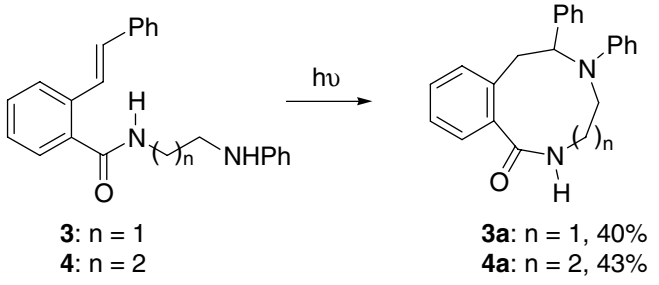

SCHEME 5

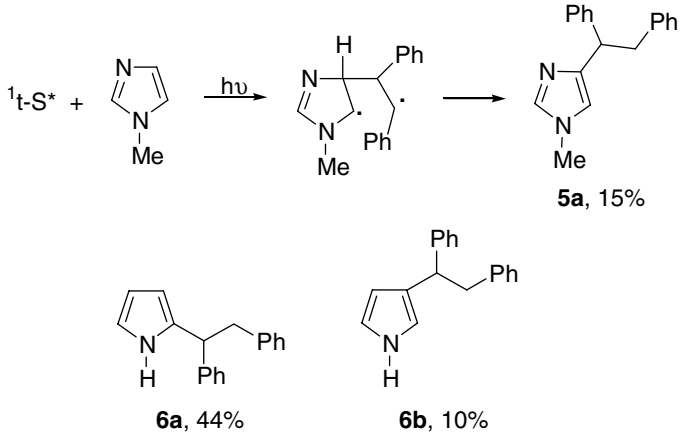

SCHEME 6

ET-Sensitized Irradiation with Ammonia and Primary Amines

Whereas singlet stilbene fails to react with primary amines or ammonia, irradiation in the presence of the electron acceptor *p*-dicyanobenzene (DCNB) in acetonitrile–water solution results in efficient addition via an ET-sensitized mechanism.[23] The mechanism of this reaction involves nucleophilic addition of the amine to the stilbene cation radical, which is generated via stilbene photooxidation by singlet DCNB (Scheme 7). The yields, in some cases, are excellent — exceeding 90%. DCNB-sensitized addition of stilbenes and secondary amines is not successful, a consequence of more facile oxidation of the

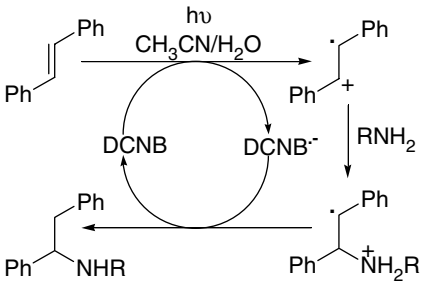

SCHEME 7

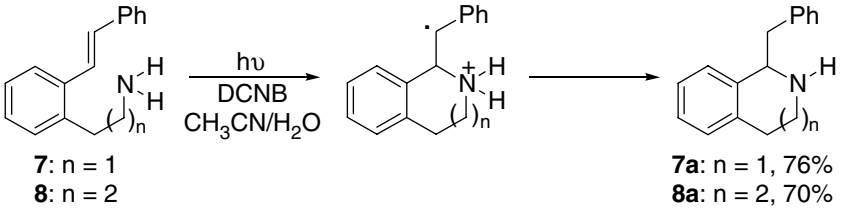

SCHEME 8

secondary amines vs. stilbene. The DCNB-sensitized addition reactions of ring-substituted methyl- and chlorostilbenes display modest regioselectivity. However, addition of ammonia to *p*-methoxystilbene is highly regioselective, reflecting localization of the positive charge on the benzylic carbon stabilized by the methoxyphenyl group. This selectivity has been exploited in the photochemical synthesis of intermediates, which were converted nonphotochemically to isoquinolines and other alkaloids.[24]

(Aminoalkyl)stilbenes **7** and **8**, in which a primary amine is appended to the stilbene ortho position with a di- or trimethylene linker, undergo DCNB-sensitized intramolecular addition reactions, yielding isoquinoline and benzazepine products **7a** and **8a**, respectively (Scheme 8).[18] In both cases, ring formation occurs via intramolecular nucleophilic addition to the end of the stilbene double bond proximal to the point of attachment of the aminoalkyl group. Addition to the distal end of the double bond presumably would form a less stable distonic cation radical intermediate.

7.3 Additions of Styrenes with Amines

Irradiation with Tertiary Amines

The photochemical behavior of singlet styrenes in the presence of tertiary alkylamines has received far less attention than the behavior of singlet stilbene. However, the behavior of styrene and 1- and 2-phenylpropene is qualitatively similar to that of singlet stilbene.[25–28] As is the case for stilbene, the formation of fluorescent exciplexes are observed upon quenching of singlet styrenes by tertiary but not by secondary amines. One operational difference is the formation of styrene–amine adducts in both polar and nonpolar solvents. The addition reaction of 1-phenylpropene with Me_3N is regioselective, yielding only the α-substituted adducts (Scheme 9).[25] This is indicative of α-CH proton transfer to form a benzyl radical, which then undergoes radical pair combination.

The intramolecular addition reactions of aminoalkylstyrenes have proven to be a particularly fruitful subject of investigation. Photocyclization reactions of the *N,N*-diethyl α-aminoalkylstyrenes **9** and **10** yield the pyrrolidine **9a** and piperidine **10a**, respectively (Scheme 10), as mixtures of diastereoisomers.[29,30] Similarly, the cyclic amines **11** and **12** yield the bicyclic adducts **11a** and **12a**, respectively (presumably as mixtures of diastereoisomers), in good preparative yield. These reactions are assumed to occur via

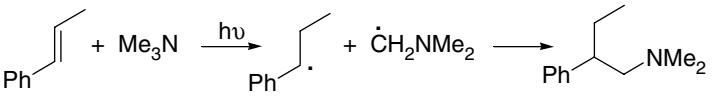

SCHEME 9

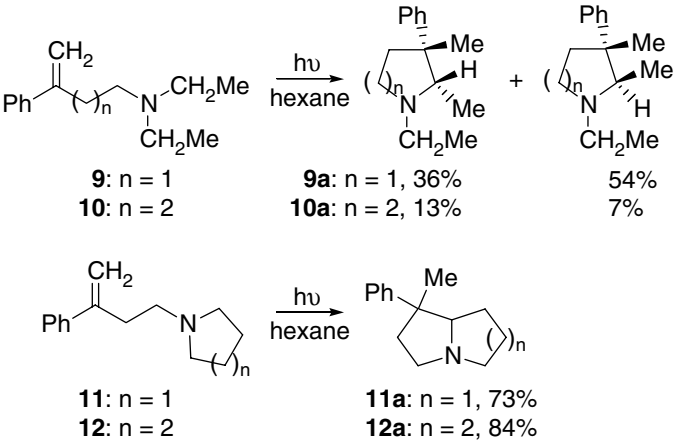

SCHEME 10

biradical intermediates formed by the regioselective transfer of an amine α-CH to the unsubstituted end of the styrene double bond.

The effect of alkyl chain length on the photochemical behavior of the *N,N*-dimethyl α-aminoalkylstyrenes **13–15** and the β-aminoalkylstyrenes **16–18** is summarized in Scheme 11, which includes the putative biradical intermediates in these reactions.[31] Mechanistic studies indicate that the biradical intermediates are formed via proton transfer in a fluorescent exciplex intermediate. There are several noteworthy features of the chain-length dependence of these reactions. First, the aminopropyl systems **14** and **17** form stable exciplex intermediates, which are chemically unreactive. Second, the aminoethyl system **13** forms the more stable benzylic radical, whereas **16** forms the less stable 2-phenylalkyl radical. Finally, both aminobutyl systems **15** and **18** form α-aminoalkyl radicals rather than α-aminomethyl radicals. The latter would have been expected on the basis of the selective formation of the less substituted α-aminoalkyl radicals in the reactions of singlet stilbene with *N,N*-dimethylalkylamines.[15] The chain-length-dependent behavior of **13–18** has been ascribed to the geometry of their intramolecular exciplexes, which are assumed to optimize overlap of the amine lone pair and styrene double bond while minimizing nonbonded repulsion. The resulting exciplex geometries permit least motion α-CH transfer leading to formation of the biradical intermediates shown in Scheme 11. Evidently, no least motion pathway is available for the aminopropyl systems **14** and **17**.

Irradiation with Secondary and Primary Amines

The intermolecular reactions of singlet styrenes with secondary amines have also received relatively little attention. Reaction of either 1-phenylpropene or 2-phenylpropene with Et_2NH yields a single adduct and other products characteristic of a radical pair intermediate (Scheme 12).[25,27,28] Presumably, regioselective NH proton transfer in a nonfluorescent exciplex intermediate yields the radical pair. Adduct formation between singlet styrenes and primary amines has not been reported.

The intramolecular reactions of the secondary α-(aminoalkyl)styrenes and β-(aminoalkyl)styrenes are dependent upon both the alkyl chain length and its point of attachment. The products of direct irradiation of the α-(aminoalkyl)styrenes **19–21** are shown in Scheme 13 along with their putative

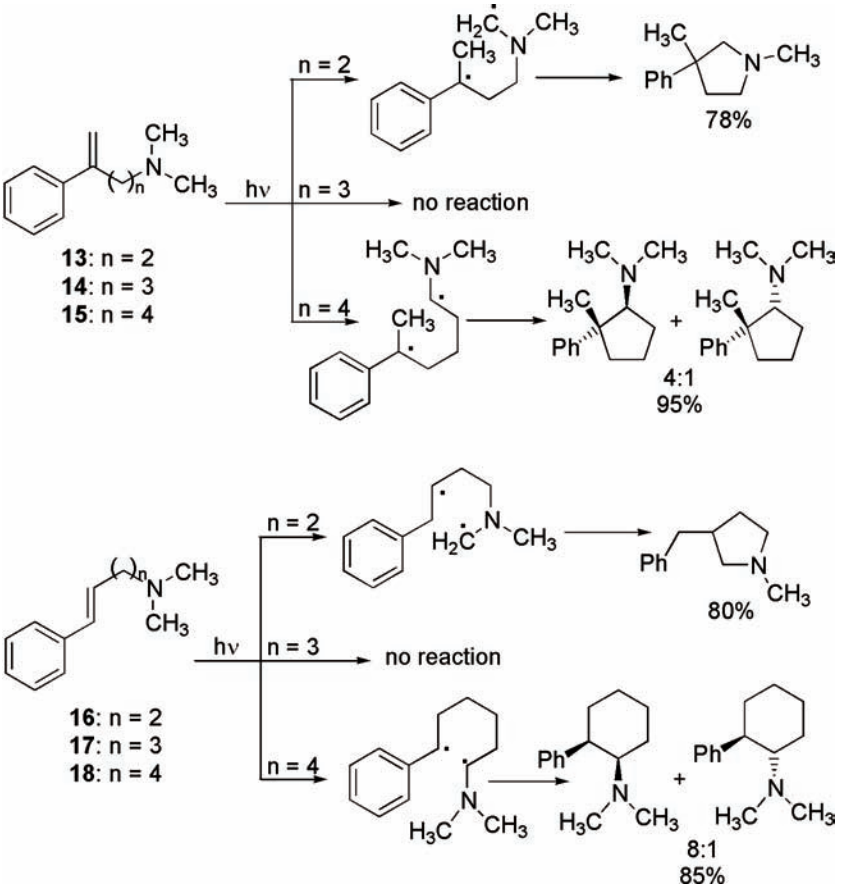

SCHEME 11

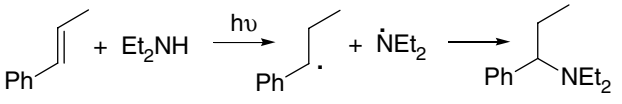

SCHEME 12

biradical intermediates.[28] The 1,n-biradical intermediates (n = 5 or 6) undergo combination to afford **19a–21a** in 70–80% yield. In all of these reactions, the NH proton transfer process selectively yields the more stable benzyl radical, as is the case in the intermolecular reactions of styrenes with secondary amines (Scheme 12).

The intramolecular reactions of β-(aminoalkyl)styrenes **22–24** yield more complex product mixtures, resulting from NH transfer to either end of the styrene double bond (Scheme 14).[27] The aminoethylstyrene **22** selectively forms adduct **22b** via the 2-phenylalkyl radical intermediate, whereas the aminobutylstyrene **24** selectively forms adduct **24a** via the benzyl radical intermediate. The aminopropylstyrene **23** affords the two regioisomeric adducts **23a** and **23b** in a 1:2.4 ratio. Formation of the less stable biradical intermediate is attributed to the similar energies of the folded conformations required for 1,5- vs. 1,6-proton transfer (Scheme 15). Intramolecular addition is also observed for the primary (aminoalkyl)styrene analog of **23**, affording the analogous adducts in a 1:1.4 ratio. This is the only example of which we are aware of addition of a primary amine to a singlet styrene.

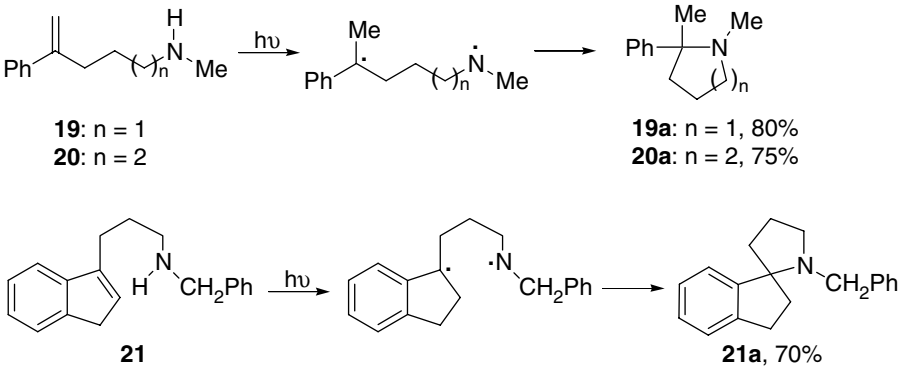

SCHEME 13

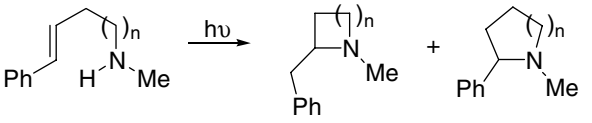

SCHEME 14

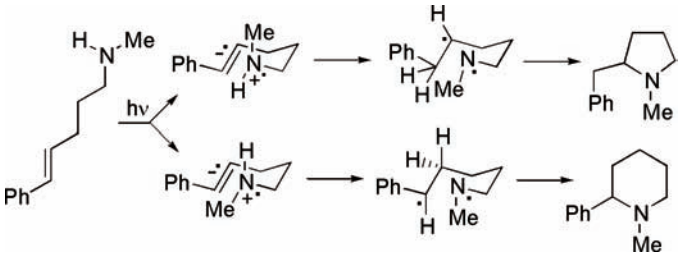

SCHEME 15

In most studies of styrene–amine photochemical addition reactions, the singlet styrene interacts with a ground state amine. The roles of styrene and amine are reversed in a study of the photochemical behavior of the (styrylalkyl)anilines **25–27**, in which the aniline singlet state lies slightly below the styrene singlet state.[32] Irradiation of **25** and **26** affords the intramolecular adducts **25a** and **26a**, respectively, as the major products, whereas **27** affords mainly adduct **27b** (Scheme 16). Presumably, electron transfer quenching of singlet aniline by ground state amine yields the same exciplex intermediate that would be formed by the reverse process.

An interesting mechanistic variant of styrene–amine addition upon direct irradiation is presented by the reaction of the *o*-hydroxystyrene **28** with $MeNH_2$ to yield the adduct **28a** in 62% yield (Scheme 17).[33] The initial step in the reaction mechanism is deprotonation of the acidic singlet state of **28** by the amine to yield a phenolate–ammonium ion pair. Reprotonation of the phenolate ion yields a zwitterion, which is trapped by the nucleophilic amine. Thus, the amine serves both as a base and as a nucleophile in this reaction.

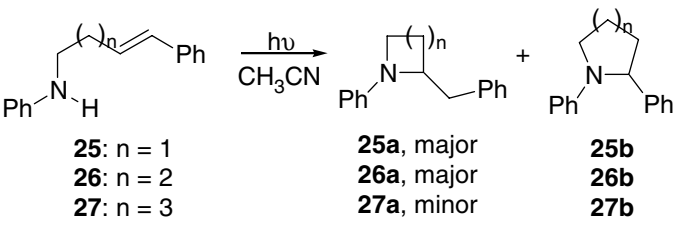

25: n = 1 **25a**, major **25b**
26: n = 2 **26a**, major **26b**
27: n = 3 **27a**, minor **27b**

SCHEME 16

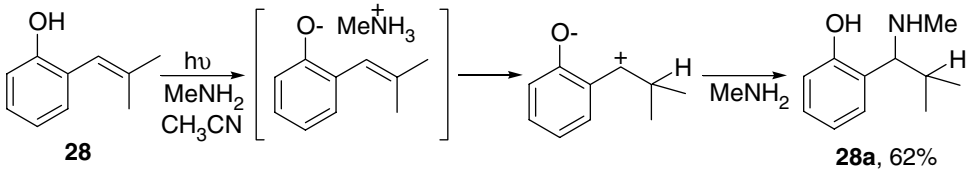

28 **28a**, 62%

SCHEME 17

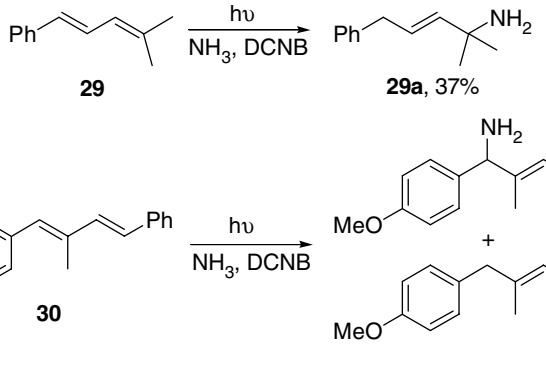

29 **29a**, 37%

30a, 58%

30

30b, 13%

SCHEME 18

ET-Sensitized Irradiation with Ammonia and Primary Amines

The DCNB-sensitized addition reactions of 1,1-diarylethylenes with ammonia or primary amines yield the *anti*-Markovnikov adducts.[34] The mechanism is analogous to that shown in Scheme 7 for addition to stilbene. The regioselectivity is determined by nucleophilic attack of the amine on the alkene cation radical to yield the more stable benzyl radical intermediate. The mechanism and dynamics of the reactions of *p*-methoxystyryl radical cations with amines have been investigated.[35] Aniline and Et_3N are found to react as electron donors with rate constants near the diffusional limit. Primary amines react as nucleophiles, with somewhat slower rate constants.

The DCNB-sensitized addition of ammonia to the 1-arylbutadiene **29** occurs selectively to afford the allylamine **29a** (Scheme 18).[36] The locus of amine addition is determined, as expected, by formation of the most stable radical intermediate, in this case the 1-phenylallyl radical. Reduction of this radical by $DCNB^{-}\cdot$ yields the 1-phenylallyl anion, which is selectively protonated at the locus of highest charge density, adjacent to the phenyl ring. The nonsymmetric 1,4-diphenylbutadiene **30** affords a 5:1 mixture of the adducts **30a** and **30b**.

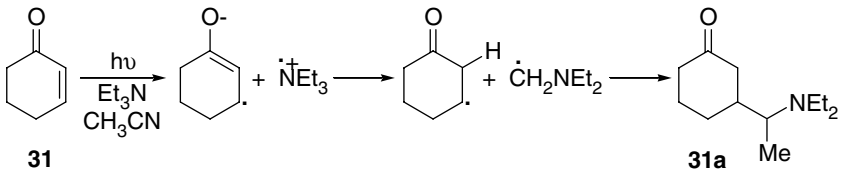

SCHEME 19

7.4 Additions of α,β-Unsaturated Carbonyl Compounds with Amines

Irradiation with Tertiary Amines

The direct and sensitized irradiations of several α,β-unsaturated carbonyl compounds with tertiary amines have been the subject of several recent reviews.[1–3,37] Direct irradiation with Et_3N is reported to yield the products of amine α-CH addition across the conjugated carbon–carbon double bond. For example, the reaction of cyclohexenone **31** with Et_3N in acetonitrile solution affords the adduct **31a** (Scheme 19), as well as the products of reduction and dimerization of **31**.[38] Investigation of the mechanism led to the proposal that electron transfer quenching of the triplet enone by a ground-state amine yields the radical ion pair, which undergoes regioselective proton transfer to form the radical pair precursor of the addition and reduction products. The yields of adducts between enones and tertiary amines are generally poor.[38,39] No reports exist of photochemical reactions of triplet enones with secondary or primary amines. The intramolecular addition of a secondary aniline to an unsaturated ester, ethyl 5-(phenylamino)-2-pentenoate, has been reported.[32] This reaction presumably involves reduction of the acrylate by the singlet aniline.

Irradiation of the cyclohexenone **32** with the tertiary α-silylamine $Et_2NCH_2SiMe_3$ affords two adducts **32a** and **32b** in a product ratio that is solvent dependent (Scheme 20).[40,41] In acetonitrile solution, the formation of **32a** as major product can be attributed to selective α-CH deprotonation adjacent to the silyl substituent, whereas the formation of **32b** as the major product in methanol solution can be attributed to nucleophilic displacement of the silyl group followed by addition of the radical $EtNCH_2$· to either the neutral enone or its anion radical. Intramolecular analogs of this reaction have also been studied for substrates **33** and **34** and display highly selective α-CH deprotonation adjacent to the silyl substituent in acetonitrile solution to yield **33a** and **34a** and desilylation in methanol solution to yield **33b** and **34b** (Scheme 21).[42,43] Intramolecular addition can also compete with *trans,cis* isomerization of acyclic enones, whereas intermolecular addition is too slow to do so.[41,42]

The effects of α-substituents on the amine cation radical kinetic acidities were probed by determining the product ratios for intramolecular enone–amine cyclization of several nonsymmetically substituted β-(aminoethyl)cyclohexenones (Scheme 22).[43,44] The observed trend, C≡CH > $CH{=}CH_2$ > Ph > CO_2Et > $SiMe_3$ > Me ~ H, is similar to that observed for the addition of substituted tertiary amines to singlet stilbene.[16] The dynamics of deprotonation of the corresponding tertiary anilines have been investigated by means of time-resolved spectroscopy.[45]

ET-Sensitized Irradiation with Tertiary Amines

Irradiation of methyl methacrylate or acrylonitile with Et_3N in the presence of either anthraquinone or 9,10,-dicyanoanthracene (DCA) sensitizers results in the formation of complex mixtures of adducts containing one or more conjugated alkenes.[46] ET-sensitized addition reactions of *N*-alkylpyrrolidines to a variety of electron deficient alkenes have recently been reported to occur with high yields.[47] For example, addition of *N*-methylpyrrolidine to methyl acrylate **38** affords adduct **38a**. The proposed mechanism of this reaction is outlined in Scheme 23. Addition to the furanone **39**, which possesses a chiral auxiliary,

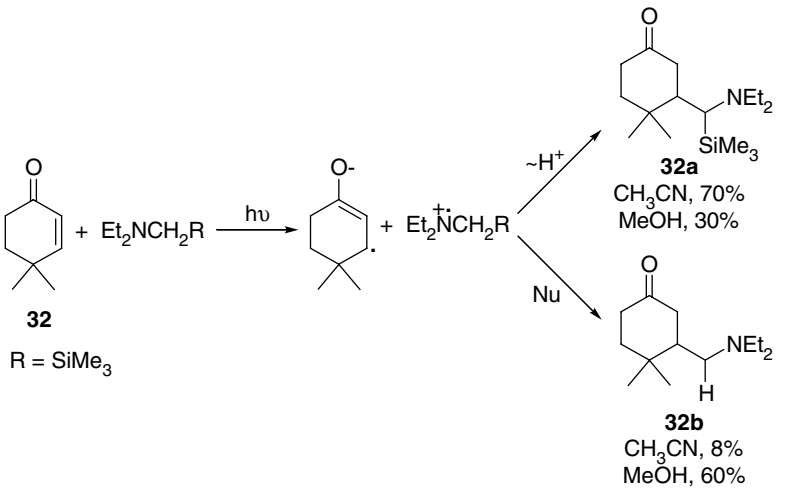

SCHEME 20

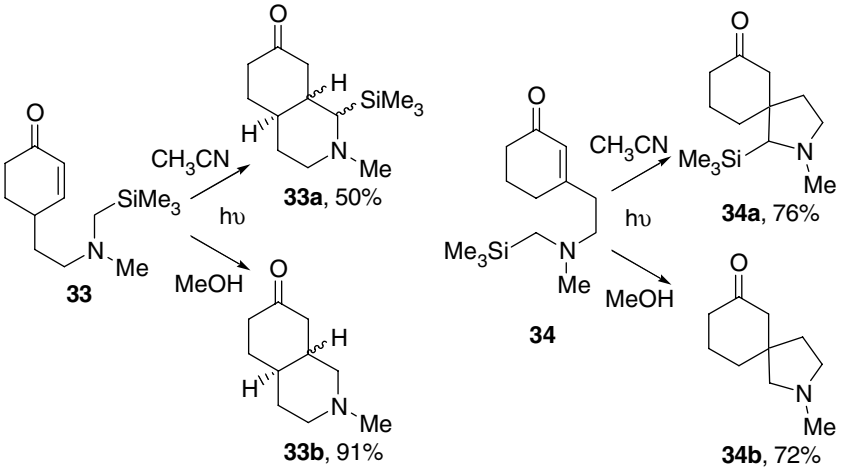

SCHEME 21

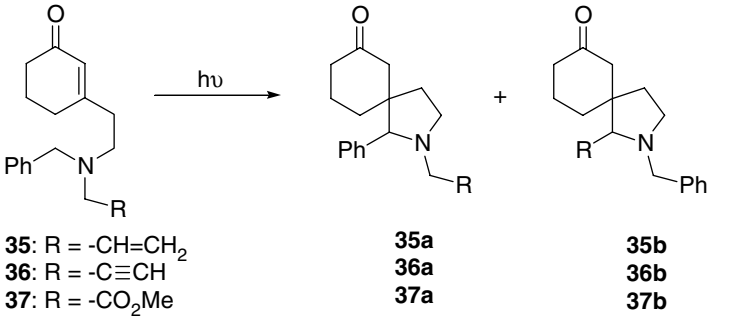

SCHEME 22

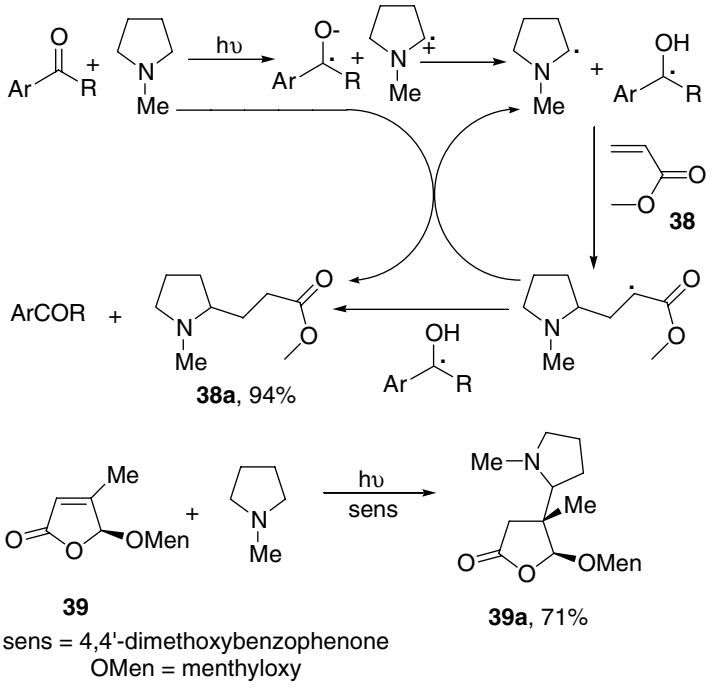

SCHEME 23

displays high facial selectivity in the formation of **39a**. High yields require the use of an unusual ET sensitizer, 4,4′dimethoxybenzophenone, which selectively deprotonates the more substituted α-CH bond of the amine cation radical. Furthermore, the resulting ketyl radical reduces the intermediate radical adduct rather than undergoing pinacol formation (Scheme 23). This methodology has been extended to the tandem addition reactions of **39** with *N,N*-dialkylanilines and with *N*-allyl- and *N*-propargylpyrrolidines.[48] These addition reactions can also be sensitized by TiO_2.[49]

Irradiation of cyclohexenone **32** with the tertiary α-silylamine $Et_2NCH_2SiMe_3$ in methanol solution in the presence of the electron acceptor 9,10-dicyanoanthracene (DCA) yields predominantly the desilylated adduct **32b**. The product ratios depend on amine concentration.[41] The mechanism proposed for adduct formation is outlined in Scheme 24. Oxidation of the tertiary amine by singlet DCA yields the amine cation radical, which undergoes desilylation upon nucleophilic reaction with the solvent. Addition of the α-aminoalkyl radical to the neutral enone affords the radical adduct, which is reduced by $DCA^{-}\cdot$ and protonated by solvent.[50] Intramolecular trapping of the radical adduct can compete with reduction by $DCA^{-}\cdot$, as seen in the reaction of **32** with an α-silylaniline, which yields the tandem addition product **32c** (Scheme 24).[51]

The DCA- and 1,4-dicyanonaphthalene (DCN)-sensitized intramolecular reactions of both acyclic and cyclic enones with acyclic and cyclic α-silylamines have been studied extensively, from both mechanistic and synthetic perspectives.[42,43] As examples (Scheme 25), DCA-sensitized irradiation of the acyclic enone **40** affords the piperidine **40a**,[50] irradiation of the γ-silylaminoethylcyclohexanone **41** affords the hydroisoquinolones **41a** and **41b** in a 6:1 ratio,[43] and irradiation of the unsaturated ester **42** affords a mixture of the hydroquinolizines **42a** and **42b** in a 5:1 ratio.[52] DCA-sensitized reactions of α-silylamines have been used to synthesize key intermediates in the total synthesis of several natural products.[1,3]

ET-Sensitized Irradiation with Secondary and Primary Amines

Anthraquinone (AQ)-sensitized irradiation of methyl acrylate **43** with the secondary amines diisopropylamine or pyrrolidine affords the lactams **43a–c** (Scheme 26).[46,53] The use of reduced reaction temperatures

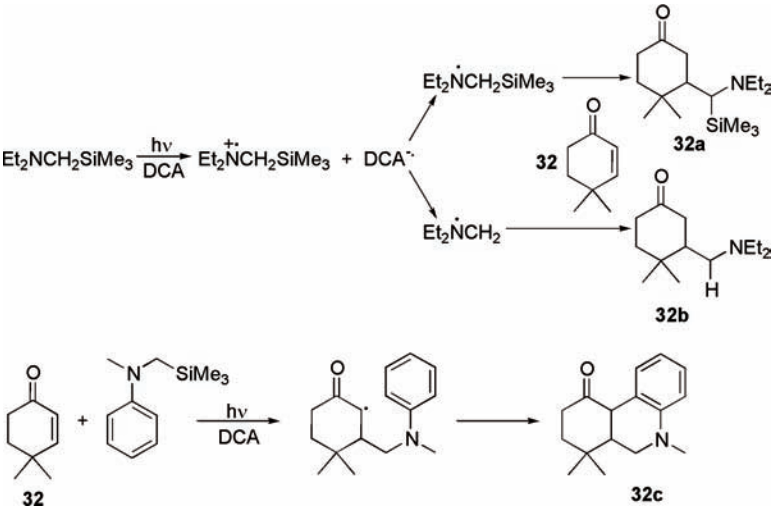

SCHEME 24

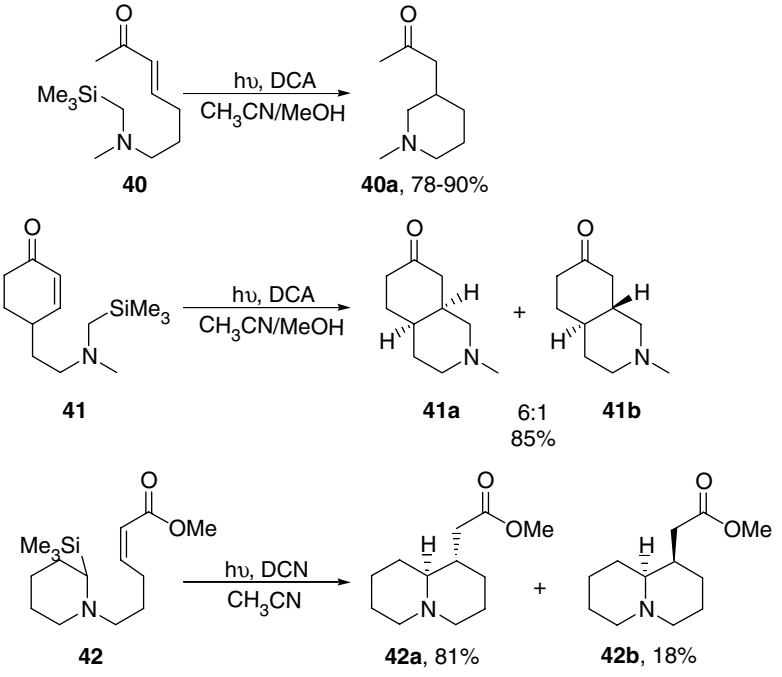

SCHEME 25

(0°C) is necessary for the photochemical reaction to compete with thermal Michael addition. The mechanism of the reaction is presumed to involve ET-sensitized addition to yield β-aminoesters, followed by thermal cyclization to yield the lactams. The use of acrylonitrile in place of methyl acrylate affords more complex product mixtures, resulting from trapping of the intermediate radical adducts by acrylonitrile.

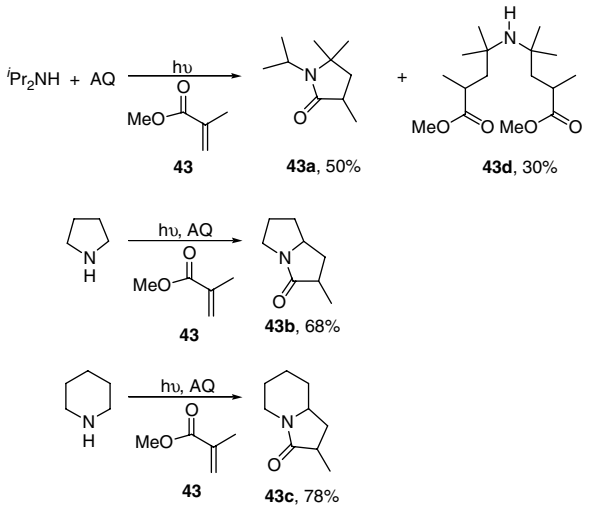

SCHEME 26

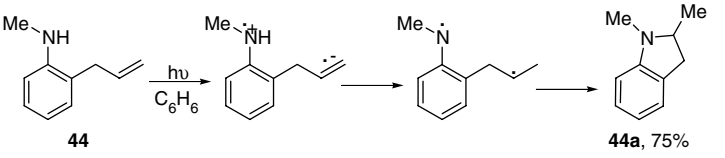

SCHEME 27

7.5 Additions of Unactivated Alkenes and Fullerenes with Amines

There have been relatively few reports of photochemical addition reactions of unactivated alkenes with amines, under either conditions of direct irradiation or ET sensitization. Direct irradiation of the *o*-allylaniline **44** is reported to yield the indoline **44a** (Scheme 27).[54] Electron transfer from singlet aniline to the ground state alkene followed by NH proton transfer would yield the biradical precursor of **44a**. Similar intramolecular addition reactions occur for the *N*-phenyl and primary anilines. Intramolecular aniline–alkene addition is not observed for *N*-phenyl-5-hexene-1-amine.[32]

Intramolecular addition of unactivated alkenes and α-silylamines can be sensitized by DCN.[55] For example, irradiation of **45** or **46** results in regioselective formation of the adduct **45a** or **46a** (Scheme 28). The addition reaction is proposed to occur via cyclization of the α-silylmethyl radical cation prior to desilaytion, on the basis of the absence of products expected from the aminoalkyl radical intermediate.

Direct irradiation of [60]fullerene **47** in the presence of trimethylamine is reported to yield the adducts **47a** and **47b** as primary and secondary products (Scheme 29).[56,57] Only small amounts of these adducts are isolated from complex product mixtures. Formation of **47a** is proposed to occur via an electron transfer, proton transfer, radical coupling mechanism similar to that for addition of stilbene and trialkylamines.[56] Formation of **47b** is found to require oxidation of **47a** by singlet fullerene. Direct irradiation of **47** with dimethylamine in the presence of air is reported to result in the formation of the tetra(amino)fullerene epoxide **47c** (Scheme 29).[58] Isolated yields as high as 98% are reported for the reaction of *N*-methylpiperazine. More hindered secondary amines such as Et_2NH and primary amines fail to undergo this extraordinary reaction.

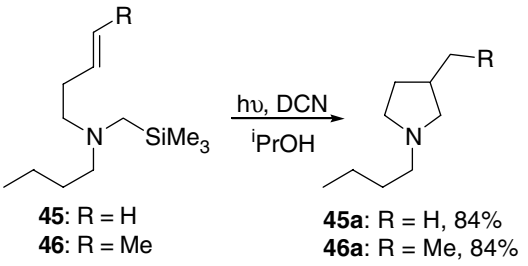

45: R = H
46: R = Me

45a: R = H, 84%
46a: R = Me, 84%

SCHEME 28

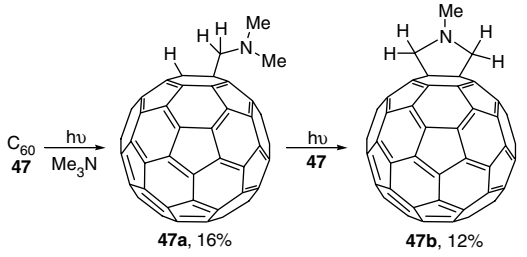

47a, 16%

47b, 12%

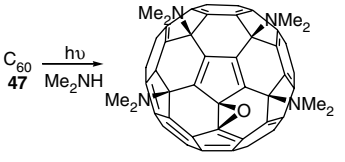

47c, 42%

SCHEME 29

7.6 Concluding Remarks

The photochemical addition reactions of amines to alkenes have provided a remarkably fertile area for synthetic and mechanistic investigations for over three decades. Each decade has brought the discovery of significant new reactions. Much of the body of work described in this review now appears to be complete, including the authors' own work on stilbene–amine and styrene–amine reactions. Thus, as we pause to take stock of what has been accomplished, we look forward to discoveries of new reactions and mechanistic insights.

References

1. Das, S. and Suresh, V., Electron-transfer reactions of amines, *in Electron Transfer in Chemistry,* Vol. 2, Balzani, V., Ed., Wiley-VCH, Weinheim, Germany, 2001, p. 379.
2. Ho, T.I. and Chow, Y.L., Photochemistry of amines and amino compounds, in *Supplement F2: The Chemistry of Amino, Nitroso, Nitro and Related Groups,* Part 2, Patai, S., Ed., John Wiley & Sons, New York, 1996, p. 683.
3. Yoon, U.C., Mariano, P.S., Givens, R.S., and Atwater, B.W., III, Photoinduced electron transfer chemistry of amines and related electron donors, in *Advances in Electron Transfer Chemistry,* Vol. 4, Mariano, P.S., Ed., JAI Press Inc., Greenwich, CT, 1994, p. 117.

4. Weller, A., Photoinduced electron transfer in solution: exciplex and radical ion pair formation free enthalpies and their solvent dependence, *Z. Phys. Chem. (Wiesbaden),* 133, 93, 1982.
5. Jacques, P., Burget, D., and Allonas, X., On the quantitative appraisal of the free energy change ΔG_{et} in photoinduced electron transfer, *New J. Chem.,* 20, 933, 1996.
6. Lewis, F.D., Photoaddition reactions of amines with aryl olefins and arenes, in *Advances in Electron Transfer Chemistry,* Vol. 5, Mariano, P.S., Ed., JAI Press Inc., Greenwich, CT, 1996, p. 1.
7. Bunce, N.J., Photochemical reactions of arenes with amines, in *CRC Handbook of Organic Photochemistry and Photobiology,* Horspool, W.M. and Song, P.-S., Eds., CRC Press, Inc., Boca Raton, FL, 1995, p. 266.
8. Mariano, P.S., SET-Induced inter- and intramolecular additions to iminium cations, in *CRC Handbook of Organic Photochemistry and Photobiology,* Horspool, W.M. and Song, P.-S., Eds., CRC Press, Inc., Boca Raton, FL, 1995, p. 867.
9. Lewis, F.D., Bimolecular photochemical reactions of the stilbenes, in *Advances in Photochemistry, Vol. 13,* Volman, D.H., Hammond, G.S., and Gollnick, K., Eds., John Wiley & Sons, New York, 1986, p. 165.
10. Lewis, F.D., Bassani, D.M., and Reddy, G.D., Styrene–amine and stilbene–amine intramolecular addition reactions, *Pure Appl. Chem.,* 64, 1271, 1992.
11. Lewis, F.D., Reddy, G.D., Bassani, D., Schneider, S., and Gahr, M., Photophysical and photochemical behavior of intermolecular and intramolecular styrene–amine exciplexes, *J. Photochem. Photobiol., A: Chem.,* 65, 205, 1992.
12. Lewis, F.D. and Ho, T.-I., *trans*-Stilbene–amine exciplexes. Photochemical addition of secondary and tertiary amines to stilbene, *J. Am. Chem. Soc.,* 99, 7991, 1977.
13. Hub, W., Schneider, S., Doerr, F., Oxman, J.D., and Lewis, F.D., *trans*-Stilbene–amine exciplexes. Behavior of the exciplex, solvent-separated radical ion pair, and free radical ions, *J. Am. Chem. Soc.,* 106, 708, 1984.
14. Klaukien, H. and Lehnig, M., ^{1}H CIDNP study of the photoinduced electron transfer reaction between trans-stilbene and triethylamine, *J. Photochem. Photobiol. A: Chem,* 84, 221, 1994.
15. Lewis, F.D., Ho, T.-I., and Simpson, J.T., Photochemical addition of tertiary amines to stilbene. Stereoelectronic control of tertiary amine oxidation, *J. Org. Chem.,* 46, 1077, 1981.
16. Lewis, F.D., Ho, T.I., and Simpson, J.T., Photochemical addition of tertiary amines to stilbene. Free-radical and electron-transfer mechanisms for amine oxidation, *J. Am. Chem. Soc.,* 104, 1924, 1982.
17. Mai, J.C., Lin, Y.C., and Ho, T.I., Stilbene–amine exciplexes. Substituent effects, *J. Photochem. Photobiol., A: Chem,* 54, 299, 1990.
18. Lewis, F.D., Bassani, D.M., Burch, E.L., Cohen, B.E., Engleman, J.A., Reddy, G.D., Schneider, S., Jaeger, W., Gedeck, P., and Gahr, M., Photophysics and photochemistry of intramolecular stilbene–amine exciplexes, *J. Am. Chem. Soc.,* 117, 660, 1995.
19. Lewis, F.D., Zebrowski, B.E., and Correa, P.E., Photochemical reactions of arenecarbonitriles with aliphatic amines. 1. Effect of arene structure on aminyl vs. α-aminoalkyl radical formation, *J. Am. Chem. Soc.,* 106, 187, 1984.
20. Lewis, F.D. and Kultgen, S.G., Photochemical synthesis of medium-ring azalactams from *N*-(aminoalkyl)-2-stilbenecarboxamides, *J. Photochem. Photobiol. A: Chem,* 112, 159, 1998.
21. Kaupp, G. and Grueter, H.W., Known and new types of reactions in the photoreaction of stilbenes with cyclic imines, *Chem. Ber.,* 114, 2844, 1981.
22. Kubota, T. and Sakurai, H., Photoaddition of stilbene to pyrrole, *Chem. Lett.,* 923, 1972.
23. Yasuda, M., Isami, T., Kubo, J., Mizutani, M., Yamashita, T., and Shima, K., Regiochemistry on photoamination of stilbene derivatives with ammonia via electron transfer, *J. Org. Chem.,* 57, 1351, 1992.
24. Yasuda, M., Hamasuna, S., Yamano, K., Kubo, J., and Shima, K., Application of photoamination to synthesis of benzylisoquinolines, aporphines, and isopavines, *Heterocycles,* 34, 965, 1992.

25. Mai, J.-C., Lin, Y.-C., Hseu, T.-M., and Ho, T.-I., Styrene–amine exciplexes: substituent effects, *J. Photochem. Photobiol. A: Chem,* 71, 237, 1993.
26. Lewis, F.D. and Bassani, D.M., Formation and behavior of 1-arylpropene–amine exciplexes, *J. Photochem. Photobiol. A: Chem,* 81, 13, 1994.
27. Lewis, F.D., Reddy, G.D., Schneider, S., and Gahr, M., Photophysical and photochemical behavior of intramolecular styrene–amine exciplexes, *J. Am. Chem. Soc.,* 113, 3498, 1991.
28. Lewis, F.D., Bassani, D.M., and Reddy, G.D., Intramolecular photoaddition of secondary α-(aminoalkyl)styrenes, *J. Org. Chem.,* 58, 6390, 1993.
29. Aoyama, H., Arata, Y., and Omote, Y., Photocyclization of γ,δ- and δ,ε-unsaturated amines. Hydrogen transfer reactions via eight-membered cyclic transition states, *J. Chem. Soc., Chem. Commun.,* 1381, 1985.
30. Aoyama, H., Sugiyama, J., Yoshida, M., Hatori, H., and Hosomi, A., Photocyclization of 4-(dialkylamino)-2-aryl-1-butenes, *J. Org. Chem.,* 57, 3037, 1992.
31. Lewis, F.D., Reddy, G.D., Bassani, D.M., Schneider, S., and Gahr, M., Chain-length- and solvent-dependent intramolecular proton transfer in styrene–amine exciplexes, *J. Am. Chem. Soc.,* 116, 597, 1994.
32. Lewis, F.D., Wagner-Brennan, J.M., and Miller, A.M., Formation and behavior of intramolecular *N*-(styrylalkyl)aniline exciplexes, *Can. J. Chem.,* 77, 595, 1999.
33. Yasuda, M., Sone, T., Tanabe, K., and Shima, K., Photochemical reactions of *o*-alkenylphenols and 1-alkenyl-2-naphthol with alkylamines: amination via photoinduced proton transfer, *J. Chem. Soc., Perkin Trans. 1,* 459, 1995.
34. Yamashita, T., Shiomori, K., Yasuda, M., and Shima, K., Photoinduced nucleophilic addition of ammonia and alkylamines to aryl-substituted alkenes in the presence of *p*-dicyanobenzene, *Bull. Chem. Soc. Jpn.,* 64, 366, 1991.
35. Johnston, L.J. and Schepp, N.P., Laser flash photolysis studies of the reactivity of styrene radical cations, *Pure Appl. Chem.,* 67, 71, 1995.
36. Kojima, R., Yamashita, T., Tanabe, K., Shiragami, T., Yasuda, M., and Shima, K., Regioselective 1,4-addition of ammonia to 1-aryl-1,3-alkadienes and 1-aryl-4-phenyl-1,3-butadienes by photoinduced electron transfer, *J. Chem. Soc., Perkin Trans. 1,* 217, 1997.
37. Yoon, U.C. and Mariano, P.S., Mechanistic and synthetic aspects of amine–enone single electron transfer photochemistry, *Acc. Chem. Res.,* 25, 233, 1992.
38. Pienta, N.J. and McKimmey, J.E., Photoreactivity of α,β–unsaturated carbonyl compounds. Competitive 2-cyclohexenone dimerization and adduct formation with triethylamine, *J. Am. Chem. Soc.,* 104, 5501, 1982.
39. Mattay, J., Banning, A., Bischof, E.W., Heidbreder, A., and Runsink, J., Radical ions and photochemical charge transfer phenomena. 36. Photoreactions of enones with amines. Cyclization of unsaturated enones and reductive ring opening by photoinduced electron transfer (PET), *Chem. Ber.,* 125, 2119, 1992.
40. Yoon, U.C., Kim, J.U., Hasegawa, E., and Mariano, P.S., Electron-transfer photochemistry of α-silylamine–cyclohexenone systems. Medium effects on reaction pathways followed, *J. Am. Chem. Soc.,* 109, 4421, 1987.
41. Hasegawa, E., Xu, W., Mariano, P.S., Yoon, U.C., and Kim, J.U., Electron-transfer–induced photoadditions of the silyl amine, $Et_2NCH_2SiMe_3$, to α,β-unsaturated cyclohexenones. Dual reaction pathways based on ion pair–selective cation-radical chemistry, *J. Am. Chem. Soc.,* 110, 8099, 1988.
42. Xu, W., Jeon, Y.T., Hasegawa, E., Yoon, U.C., and Mariano, P.S., Novel electron-transfer photocyclization reactions of α-silyl amine α,β–unsaturated ketone and ester systems, *J. Am. Chem. Soc.,* 111, 406, 1989.
43. Xu, W., Zhang, X.M., and Mariano, P.S., Single electron transfer promoted photocyclization reactions of (aminoalkyl)cyclohexenones. Mechanistic and synthetic features of processes involving the generation and reactions of amine cation and α-amino radicals, *J. Am. Chem. Soc.,* 113, 8863, 1991.

44. Xu, W. and Mariano, P.S., Substituent effects on amine cation radical acidity. Regiocontrol of β-(aminoethyl)cyclohexenone photocyclizations, *J. Am. Chem. Soc.,* 113, 1431, 1991.
45. Zhang, X., Yeh, S.-R., Hong, S., Freccero, M., Albini, A., Falvey, D.E., and Mariano, P.S., Dynamics of α-CH deprotonation and α-desilylation reactions of tertiary amine cation radicals, *J. Am. Chem. Soc.,* 116, 4211, 1994.
46. Das, S., Kumar, J.S.D., Thomas, K.G., Shivaramayya, K., and George, M.V., Photocatalyzed multiple additions of amines to α,β–unsaturated esters and nitriles, *J. Org. Chem.,* 59, 628, 1994.
47. Bertrand, S., Hoffmann, N., and Pete, J.-P., Highly efficient and stereoselective radical addition of tertiary amines to electron-deficient alkenes. Application to the enantioselective synthesis of necine bases, *Eur. J. Org. Chem.,* 2227, 2000.
48. Bertrand, S., Hoffmann, N., Humbel, S., and Pete, J.P., Diastereoselective tandem addition–cyclization reactions of unsaturated tertiary amines initiated by photochemical electron transfer (PET), *J. Org. Chem.,* 65, 8690, 2000.
49. Marinkovic, S. and Hoffmann, N., Efficient radical addition of tertiary amines to electron-deficient alkenes using semiconductors as photochemical sensitizers, *J. Chem. Soc., Chem. Commun.,* 1576, 2001.
50. Jeon, Y.T., Lee, C.P., and Mariano, P.S., Radical cyclization reactions of α-silyl amine α,β-unsaturated ketone and ester systems promoted by single electron transfer photosensitization, *J. Am. Chem. Soc.,* 113, 8847, 1991.
51. Zhang, X.M. and Mariano, P.S., Mechanistic details for SET-promoted photoadditions of amines to conjugated enones arising from studies of aniline–cyclohexenone photoreactions, *J. Org. Chem.,* 56, 1655, 1991.
52. Hoegy, S.E. and Mariano, P.S., Indolizidine and quinolizidine ring formation in the SET-photochemistry of α-silyl amines, *Tetrahedron Lett.,* 35, 8319, 1994.
53. Das, S., Kumar, J.S.D., Shivaramayya, K., and George, M.V., Anthraquinone-photocatalyzed addition of amines to α,β-unsaturated esters: a novel route to indolizidone, pyrrolizidone and related ring systems, *J. Chem. Soc., Perkin Trans. 1,* 1797, 1995.
54. Koch-Pomeranz, U., Schmid, H., and Hansen, H.J., Photoreactions. 52. Photochemical cyclization of *o*-, *m*-, and *p*-allylanisoles and *o*-allylanilines, *Helv. Chim. Acta,* 60, 768, 1977.
55. Pandey, G., Reddy, G.D., and Kumaraswamy, G., Photoinduced electron transfer (PET) promoted cyclizations of 1-[*N*-alkyl-*N*-(trimethylsilyl)methyl]amines tethered to proximate olefin: mechanistic and synthetic perspectives, *Tetrahedron,* 50, 8185, 1994.
56. Liou, K.-F. and Cheng, C.-H., Photoinduced reactions of tertiary amines with [60]fullerene; addition of an α-C-H bond of amines to [60]fullerene, *J. Chem. Soc., Chem. Commun.,* 1423, 1996.
57. Lawson, G.E., Kitaygorodskiy, A., and Sun, Y.-P., Photoinduced electron-transfer reactions of [60] fullerene with triethylamine, *J. Org. Chem.,* 64, 5913, 1999.
58. Isobe, H., Tomita, N., and Nakamura, E., One-step multiple addition of amine to [60]fullerene. Synthesis of tetra(amino)fullerene epoxide under photochemical aerobic conditions, *Org. Lett.,* 2, 3663, 2000.

8

Ene-Reactions with Singlet Oxygen

Axel G. Griesbeck
Univeristy of Cologne

Tamer T. El-Idreesy
University of Cologne

Waldemar Adam
University of Würzburg

Oliver Krebs
University of Würzburg

8.1 Introduction and Definition of the Reaction

The active species in Type II photooxygenation reactions is molecular oxygen in its first excited singlet state, as already postulated by Kautsky et al.[1] This has been unambiguously proven by the elegant experiments performed by Foote et al., in which reactions of photochemically generated singlet molecular oxygen were compared with the corresponding reactions of the active oxygen formed in the hypochlorite/hydrogen peroxide system.[2] The results from these allylic oxidations with singlet molecular oxygen ($^1O_2$) are clearly different from those of autoxidative (triplet oxygen) pathways.[3] Several reaction modes of $^1O_2$ with unsaturated organic molecules are known ([4 + 2]- and [2 + 2]-cycloaddition, ene and silyl-ene-reaction, physical quenching) and have been summarized in excellent reviews.[4] For the allylic activation of CC double bonds in the presence of allylic hydrogen atoms, the ene-reaction is the most prominent path. G.O. Schenck first described the reaction in a patient in 1943, and hence it is known as the Schenck reaction.[5] In the course of this reaction, $^1O_2$ attacks one center of a CC double bond with abstraction of an allylic hydrogen atom or an allylic silyl group (bound to oxygen) and simultaneous allylic shift of the double bond. As the result of this reaction, allylic hydroperoxides or O-silylated α-hydroperoxy carbonyl compounds are formed.

8.2 Mechanism of the Singlet Oxygen Ene-Reaction

Theoretical Models

In the last 20 years, several mechanisms have been postulated for this reaction with concerted or "concerted two-stage" mechanisms,[6] as well as 1,4-biradicals,[7] 1,4-zwitterions,[8] or perepoxides[9] as intermediates. A series of semiempirical and *ab initio* calculations has been published, but the exact mechanism of this reaction type is still doubtful.[10] The suprafacial reaction course (see Section 8.4), the lack of

0-8493-1348-1/04/$0.00+$1.50

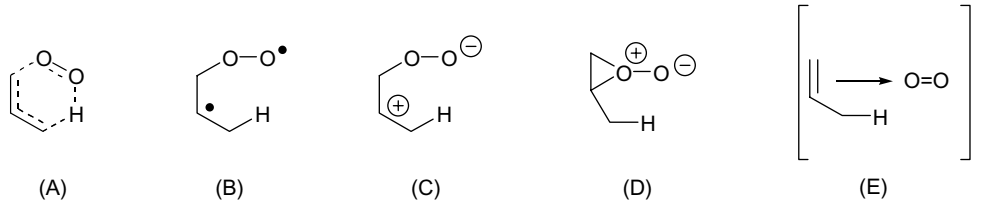

FIGURE 8.1

Markovnikov effects, and the results of Stephenson's intramolecular and intermolecular isotope effect test[11] provide evidence for the formation of the perepoxide D (first proposed by Sharp in 1960)[12] or a similar enophile–substrate encounter complex (exciplex E) as intermediate (Figure 8.1). In a recent report by Leach and Houk, the ene-reaction of singlet oxygen with alkenes is described to proceed "through a highly asynchronous concerted mechanism, involving regions of the potential surface with both perepoxide and polarized biradical character. Although both biradical and perepoxide intermediates can be located on the potential energy surface, both are bypassed by way of a valley ridge inflection, and the reaction is concerted."[13]

Experimental Conditions

Singlet molecular oxygen ($^1O_2$) may be generated by several methods.[14] From an experimental point of view, however, the most convenient process is the photochemical route. Photosensitization is advantageous because of its flexibility in regard to reaction temperature, solvent, sensitizer, and light source. In solution, $^1O_2$ is efficiently deactivated not only by chemical reactions with appropriate acceptor molecules but also physically by the solvent and the sensitizer and in many cases even by the acceptor itself. Therefore, $^1O_2$ has to be generated repeatedly, and only photosensitization can do this. Nevertheless, selectivity problems arise from incorrectly chosen parameters such as solvent and sensitizer, because competing reaction modes ("physical" quenching, electron-transfer reactions, cycloadditions) are influenced differently by the solvent polarity and the nature of the sensitizer.[15] The lifetime of $^1O_2$ is also very sensitive to changes of the solvent structure.[16] An additional problem comes from changing the type of the oxygen activation, i.e., "type II" and "type III." When powerful electron acceptors such as 9,10-dicyanoanthracene (DCA) or methylene blue (MB) are used as sensitizers, a photoinitiated electron-transfer processes may be initiated, which may lead to a different reactivity and product pattern.[17] In many cases, the superoxide anion radical, which is also produced from singlet oxygen, is important in these reactions. The solvent polarity again plays an extremely important role in these "polar reactions."[18] For $^1O_2$-selective reactions, some experimental rules should be considered (these considerations are also valid for [4 + 2]- and [2 + 2]-cycloadditions of singlet oxygen):

- Nonpolar solvents (halogenated, at best fluorinated hydrocarbons) suppress electron transfer and increase the lifetime of singlet oxygen. In polar solvents, [2 + 2]-cycloadditions are considerably faster than in nonpolar solvents.
- Weak electron acceptors [tetraphenylporphyrin (TPP), metalloporphyrins, haematoporphyrin (HP)] with low triplet energies [MB: 33.5; TPP: 34.0; HP: 37.2; RB: 39.2–42.2 kcal/mol][19] should be used as sensitizers. Octachlorinated TPP has been reported as a superior sensitizer and shows largely improved turnover numbers.[20] The use of Rose Bengal (RB) is advantageous in polar solvents, but in some cases even RB may undergo electron-transfer photooxygenations.[21] Methylene Blue (MB) should be avoided due to competing electron transfer. Recently, fullerenes have been described as excellent sensitizers for singlet oxygen formation,[22] and so has lumiflavin (LF).[23]
- Long-wavelength light should be used ($\lambda > 400$ nm). If high-pressure mercury lamps are utilized, filters should be employed to exclude high-energy UV light.[24] Medium-pressure mercury lamps and tungsten lamps[25] have also been applied without the need of filters. Sodium (street) lamps are most convenient and inexpensive.

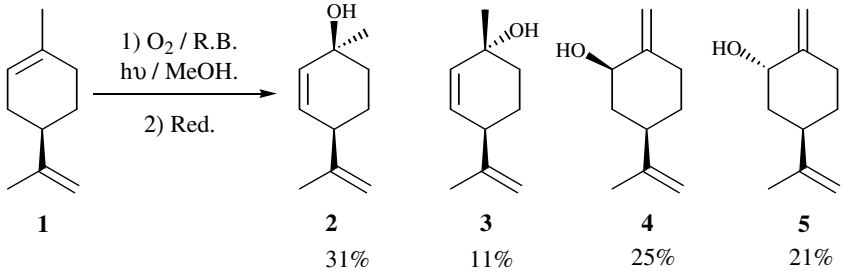

SCHEME 1

- In most cases, only a little activation energy is necessary for the described transformations (1–5 kcal/mol),[26] which accounts for the insensitivity of the rates of singlet-oxygen photooxygenations to reaction temperature, i.e., the reactions may be also carried out at low temperatures (in order to circumvent secondary reactions of the peroxidic products).
- (+)-Limonene (**1**) is a singlet-oxygen acceptor with a very characteristic pattern of regioisomeric and stereoisomeric allylic hydroperoxides **2–5** as products (Scheme 1). Under autoxidative conditions, this pattern is changed completely, and additional products without allylic shift of the CC double bond are formed.[27]
- The regio- and stereoselectivity of a particular transformation should be determined directly at the stage of the peroxidic product. A number of examples are known in which further transformations (reduction, rearrangement, cleavage) change the regioisomeric as well as the stereoisomeric composition of the products.
- Addition of radical-scavenging reagents, e.g., 2,6-di-*t*-butylphenol, inhibits radical autoxidation reactions[28] but does not alter the singlet oxygen reaction. As a test for the involvement of singlet oxygen, an efficient quencher such as DABCO (1,4-diazabicyclo[2.2.2]octane) may be added.[29]

8.3 Selectivity

Chemoselectivity

Electron-rich monoalkenes interact with singlet oxygen in three ways: physical quenching, [2 + 2]-cycloaddition, and ene-reaction. Which reaction mode dominates depends on the ionization potential of the double bond, the appropriate alignment of allylic hydrogens, and the polarity of the solvent.[30] Methyl-substituted acyclic enol ethers, for example, give ene products in a multitude of solvents,[31] whereas the corresponding cyclic enol ethers (2,3-dihydrofurans) give mixtures of allylic hydroperoxides (ene products) and 1,2-dioxetanes ([2 + 2]-cycloaddition) with notable solvent dependency.[32] While the photooxygenation of alkenyl arenes within thionin-supported zeolite Na-Y surprisingly afforded the ene products in a highly chemoselective manner, these ene products were less favored compared to [4 + 2]- and [2 + 2]-cycloadducts when the reaction was carried out in solution.[33]

Locoselectivity

In polyolefins, the locoselectivity of singlet-oxygen ene-reactions may be predicted by considering the ionization potentials of the corresponding model monoolefins.[34] Steric and electronic effects operate, moderating the reactivity of the double bond or influencing the trajectory of the incoming enophile. As a rule of thumb, each additional alkyl group increases the ene-reactivity by a factor of about 10 to 20.[35]

Regioselectivity

Alkenes with different allylic hydrogens may yield various regioisomeric products on reaction with singlet oxygen. For controlling the regioselectivity of such allylic oxidations by $^1O_2$, several general effects are

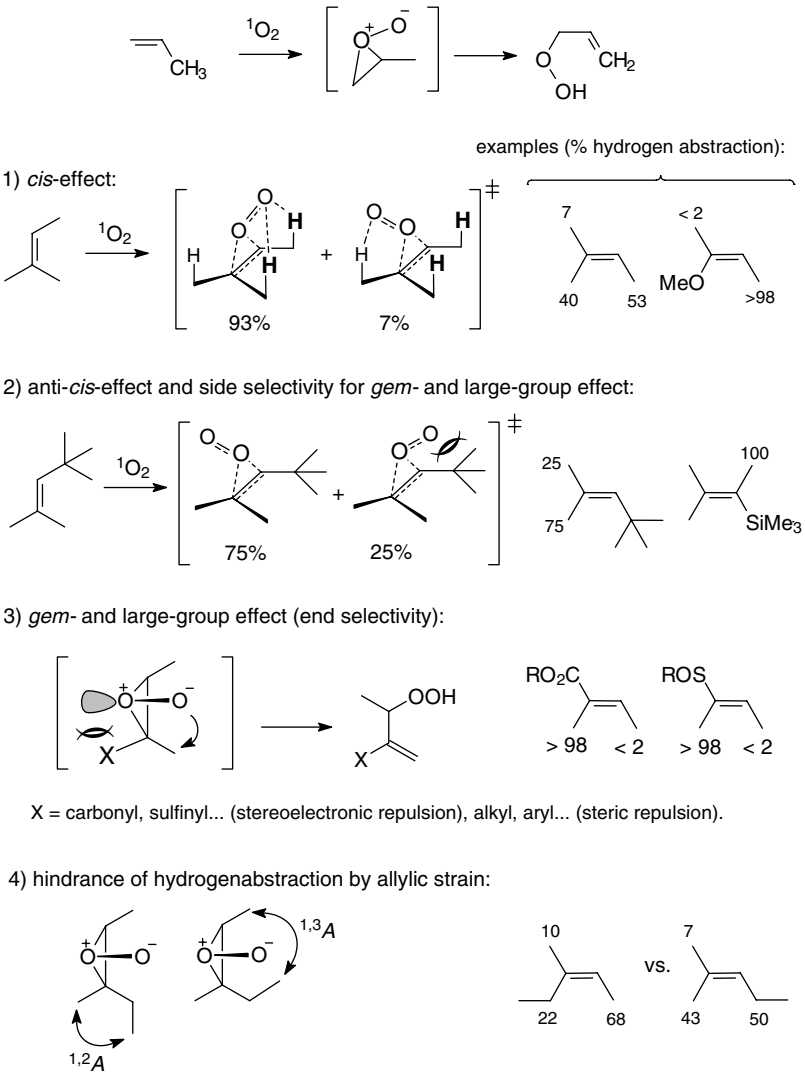

SCHEME 2

known that help in designing appropriate compounds for the regioselective introduction of hydroperoxy groups: the *cis* (or *syn*) effect, the *gem* effect, and the large-group effect (Scheme 2)**.**

The *cis* (or *syn*) effect promotes highly selective hydrogen abstraction from the higher substituted *side* of a trisubstituted CC double bond, when both substituents bear allylic hydrogens (*twix* and *lone*)[36] or one substituent is alkoxy (*lone*).[37] The *gem* effect leads to highly selective abstraction of an allylic hydrogen from a substituent at the α position of an α,β-unsaturated carbonyl compound (*twix*).[38] The large-group effect leads to selective (moderate) abstraction of an allylic hydrogen from the substituent with a large group at the same carbon atom of the CC double bond.[39] For example, a R_3Si substituent at the *twin* site of the CC double bond directs singlet oxygen towards the geminal position (*twix*).[40] The termini *twix*, *twin,* and *lone* are defined as follows: attention is focused on the central alkyl substituent, which is defined as the *twixt* group (R_{twix}, for simplification the last "t" has been dropped); "*twixt*" comes from old English and means "between," i.e., R_{twix} is between a geminal and a vicinal alkyl group. The other geminal substituent is then designated as the *twin* group (R_{twin}) and the remaining vicinal substituent as the *lone* group (R_{lone}).

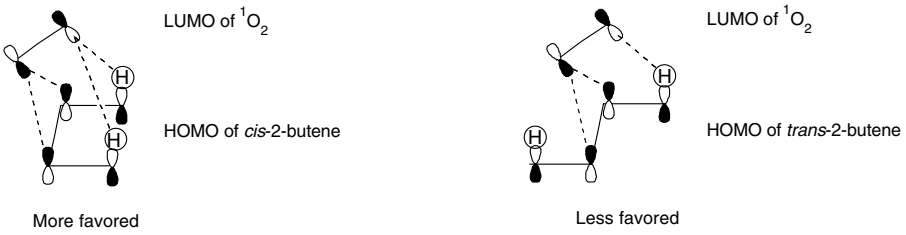

FIGURE 8.2

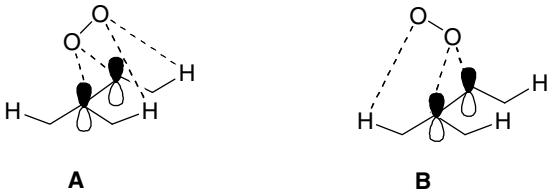

FIGURE 8.3

Two detailed reviews have covered the regioselectivity in the singlet-oxygen ene-reaction.[41]

Analogies to the ene reaction of triazolinedione and nitrosoarene are helpful to understand the steric and electronic effects, which control the regioselectivity.[42] The mechanistic rationalization is not simple, since the regioselection occurs at different stages of the reaction. In the first step, namely the formation of the three-membered ring structure, the side of the double bond for hydrogen abstraction is determined. Here, the *cis* as well as anti-*cis* effects[43] and the side selectivity for the *gem* or the large-group effect operate. Once the enophile is fixed in the perepoxide-type geometry and points to one side of the double bond, there is a second choice between the *cis*-positioned allylic hydrogens for abstraction. The steric or stereoelectronic response of a substituent X weakens the C(1)-O^+ bond and pushes the free electron pair of O^+ towards the unsubstituted corner of the double bond, which results in a *skew* line arrangement of the enophile toward the double bond · to afford the major product by hydrogen abstraction at the geminal substituent (*vide infra*). Another steering effect is the hindrance of hydrogen abstraction. When the CH bond assumes a conformation perpendicular to the double bond for abstraction, unfavorable allylic strain may build up, which favors abstraction at the other *cis*-positioned substituent.

The different effects are now discussed separately in detail.

Several models have been proposed to explain the *cis* effect: in one of these Houk and co-workers[44] postulated that the lower the rotational barrier of a specific alkyl group at the double bond, the higher the reactivity of this group toward hydrogen abstraction by singlet oxygen. The respective hydrogen atoms adopt more readily the favored perpendicular conformation with respect to the double bond; however, several recent results contradict this computational analysis.[45] Stephenson suggested that orbital interaction between the HOMO of the olefin and the LUMO of singlet oxygen stabilizes the transition state for the perepoxide-like exciplex formation.[46] This interaction is favored in the case of *cis*-2-butene, in which the allylic σ orbitals and the HOMO of the olefin generate a system similar to π_3 of butadiene; hence, the ene-reaction of singlet oxygen with *trans*-2-butene is less favorable (Figure 8.2).

Frimer and Barlett et al.[47,48] assumed that the formation of the CO bond requires a closer approach to the alkene carbons compared to the CH bond cleavage; consequently, transition state **A** is less hindered and energetically preferred relative to transition state **B** (Figure 8.3).

The fact that singlet oxygen ene-reactions with *cis*-olefins have less negative activation entropies and about 2–8 times larger reaction rates (e.g., for *cis*-2-butene: $\Delta S^{\#} = -32$ e.u., $\Delta H^{\#} = 1.6$ kcal/mol; for *trans*-2-butene: $\Delta S^{\#} = -42$ e.u., $\Delta H^{\#} = 0.3$ kcal/mol) than with *trans*-olefins implies that the transition states

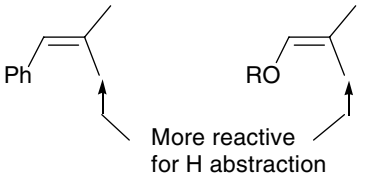

FIGURE 8.4

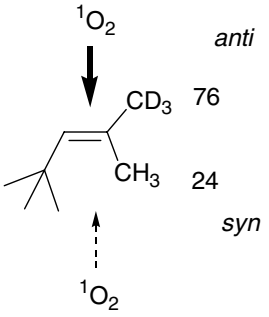

FIGURE 8.5

for the ene-reaction are "more organized" or further along the reaction coordinate for *trans*-olefins than it is for *cis*-olefins. The possibility for simultaneous interaction of $^1O_2$ with two allylic hydrogens in *cis*-olefins reduces the activation entropy.[49,50] In conclusion, the simultaneous interaction between singlet oxygen and two allylic hydrogen atoms on the more substituted side of the double bond stabilizes the transition state that leads to the perepoxide-like exciplex, and abstraction of these hydrogens is favored.

In analogy, trisubstituted styrenes and enol ethers exhibit similar *cis* effects (*syn* effect or *syn* selectivity), resulting from the simultaneous interaction of the incoming singlet oxygen with one allylic hydrogen and either a phenyl or an alkoxy group, which stabilizes the transition state for the perepoxide-like structure (Figure 8.4).

The regioselectivity that results from the large-group nonbonded interaction may be rationalized in the case of trisubstituted alkenes with bulky *cis*-alkyl groups;[51] the steric repulsion between singlet oxygen and the bulky group directs the enophilic attack. The absence of the stabilizing interaction of singlet oxygen with the allylic hydrogen atoms on the same side of the double bond in the transition state additionally accounts for the observed anti-*cis* effect with abstraction of the hydrogen atom at the *lone* site (Figure 8.5).

Hydrogen abstraction from the alkyl group geminal to the bulky vinylic or allylic substituent in alkenes may be rationalized by repulsive large-group nonbonded steric interactions between the O^+ atom in the perepoxide-like structure and the large-group at the *lone* site (Scheme 3). Consequently, the CO bond next to the bulky substituent (*lone* site) is lengthened and thereby weakened in comparison to the CO bond at the less substituted end of the alkene. Since hydrogen abstraction at the "large group" is hindered by allylic strain, hydrogen abstraction is preferred from the alkyl group geminal to the bulky substituent (*trix*).[52–54]

The geminal regioselectivity is also observed for alkenes with carbonyl groups (carboxylic acids,[55] aldehydes,[56] ketones,[57] amides,[58] or esters[59]) and other functionalities at the α position (Figure 8.6) (cyano, sulfinyl,[60] iminyl,[61] silyl,[62] or stannyl[63] groups). This is rationalized in terms of the 1,3-nonbonding interaction already used to explain the large-group effect; additionally, a resonance effect is proposed that stabilizes the transition state that leads to the conjugated products. Stereoelectronic effects were used to explain the geminal selectivity observed for vinylsilanes and vinylstannanes.[64]

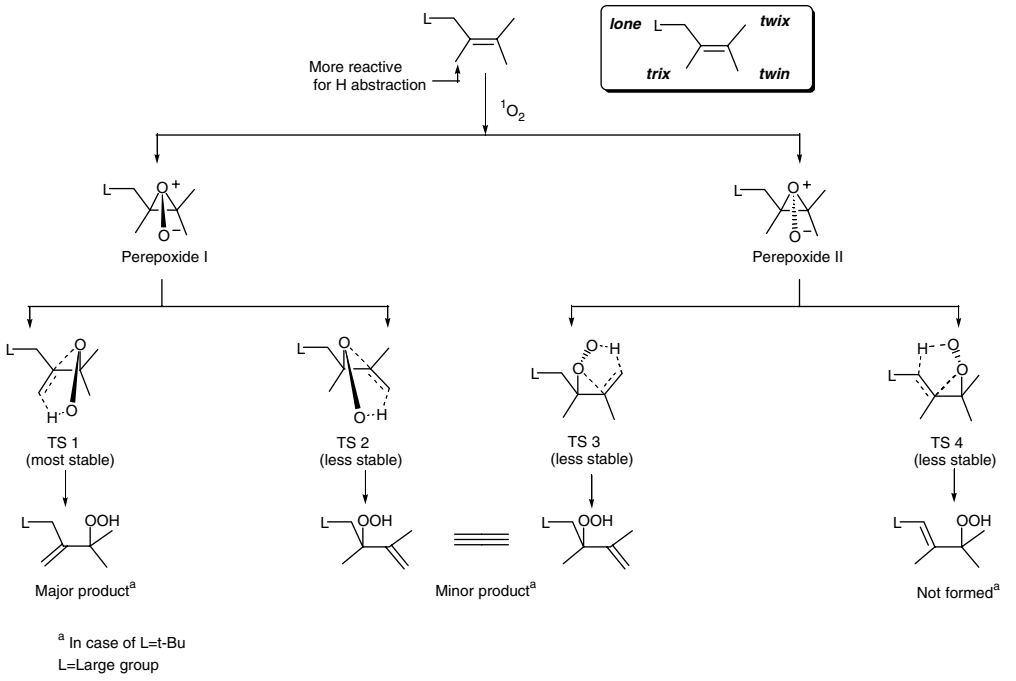

SCHEME 3

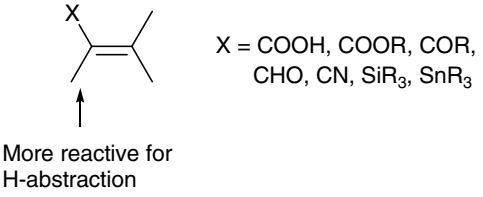

FIGURE 8.6

Stereoselectivity

The stereoselectivity of the singlet oxygen ene-reaction has been investigated in detail in the last decade.[41b,65] The singlet oxygen attacks in a suprafacial process, and hydrogen abstraction occurs from the same π face of the olefinic double bond.[66] In principle, there are two means for stereoselectivity control, namely steric as well as stereoelectronic and electronic (hydrogen bonding) interactions, both of which direct the incoming enophile to one π-face of the double bond. In view of the small size of the singlet-oxygen enophile, the electronic influence is more effective. Remarkable steering effects of the diastereoselectivity for the ene-reaction were discovered with chiral allylic alcohols (Scheme 4).[67]

The hydroxy group is conformationally aligned by 1,3-allylic strain, and hydrogen bonding coordinates the incoming enophile with preferential formation of the *threo*-configured ene product. By the use of chiral auxiliaries, which also coordinate the singlet oxygen through hydrogen bonding, diastereomerically pure, optically active hydroperoxides or alcohols may be synthesized.[68] As shown in Scheme 5, the coordination through hydrogen bonding may also control the regioselectivity.

For the ene-reaction of tiglic acid derivative **6** (Figure 8.7), a low diastereoselectivity was achieved even at –60°C (*de* 64%). The naphthyl group aligns parallel and next to the tiglate ester group and hence, one of the alkene diastereotopic faces is shielded.[69] From the tiglic amides **7**, no diastereoselectivity control

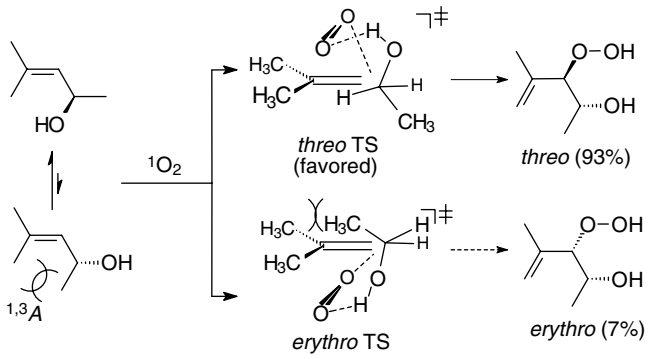

SCHEME 4

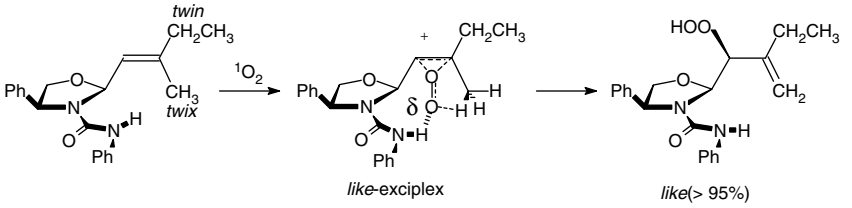

SCHEME 5

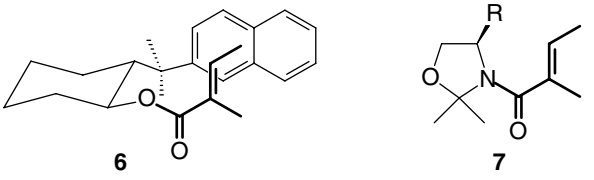

FIGURE 8.7

was achieved with $^1O_2$, although these substrates react with triazolinedione to afford one diastereoisomer.[70]

8.4 Substrates for Ene-Reactions

Acyclic Substrates

Alkenes and Alkadienes

Stephenson et al. have shown, with optically active monodeuterated olefin **8**, that the ene-reaction is a highly stereoselective suprafacial process in which the proper arrangement of the allylic hydrogens controls the stereochemical course.[71] In the model reaction with the stereolabeled substrate **8**, no isotope discrimination was found: the allylic hydroperoxide **7** with (R)-configuration and deuterium migration was formed in equal amounts as the corresponding (S)-hydroperoxide **10** with hydrogen migration (Scheme 6).

Similar results were obtained in the photooxygenation of silyl cyanohydrins of α,β-unsaturated aldehydes.[56] The trimethylsilyl and *t*-butyldimethylsilyl cyanohydrins of senecioaldehyde **11** react with low regioselectivity (because of the *cis*-effect) but high diastereoselectivity (Scheme 7). In both cases, the two

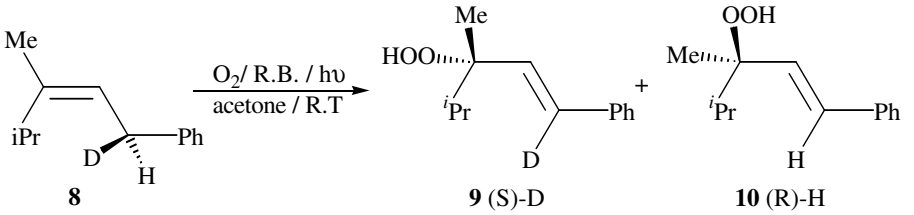

SCHEME 6

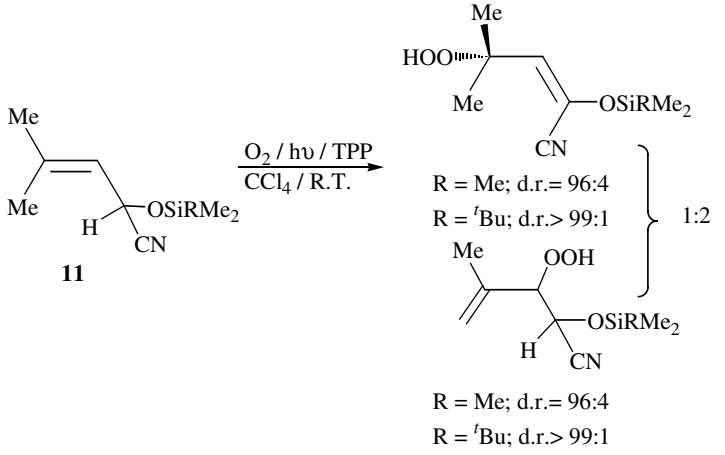

SCHEME 7

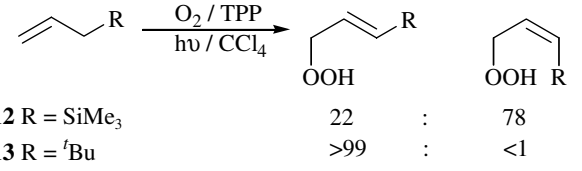

SCHEME 8

regioisomeric allylic hydroperoxides were formed with identical diastereomeric ratios, which clearly demonstrates the necessity for a common symmetrical intermediate, presumably with perepoxide-type geometry. The relative configuration of the photooxygenation products, to assess the π-facial preference, was not determined.

Shimizu et al. have shown that certain allylsilanes react with singlet oxygen *Z*-selectively.[72] They compared the reaction of allyltrimethylsilane **12** (d.r. = 22.78) with that of the corresponding hydrocarbon, 3-*tert*-butyl-1-propene **13**, for which a diastereomeric ratio of >99:1 in favor of the *trans*-diastereomer was found (Scheme 8).

Kropf and Reichwaldt have investigated chiral trisubstituted monoalkenes.[73] Diastereomeric ratios from 1:4.4 to 1:5.3 (*threo:erythro*) were obtained. In one case, two regioisomeric products were formed with identical d.r. values, which again validates that a stereoselective, suprafacial mechanism applies. Dang and Davies[74–77] have reported that the reaction of singlet oxygen with allylic stannanes **14** affords metal-ene, hydrogen-ene, and cycloaddition products (Scheme 9). The amount of the metal-ene product may be enhanced by using substrates with electropositive tin centers (attached to electron withdrawing groups).

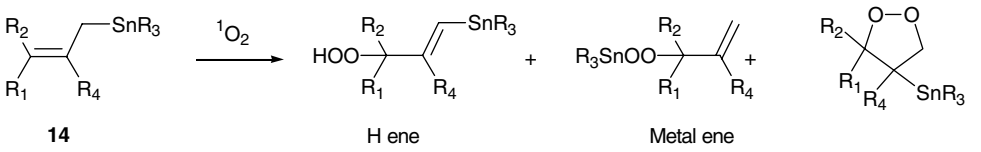

SCHEME 9

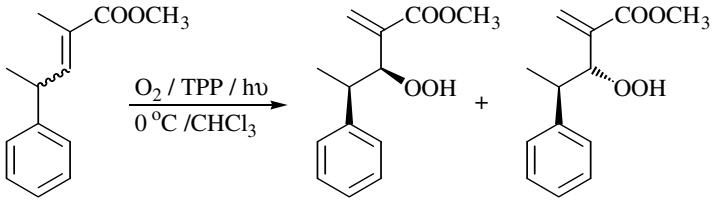

SCHEME 10

α,β-Unsaturated Carbonyl Compounds and Derivatives

The photooxygenation of α,β-unsaturated esters **15** with a stereogenic center at the γ–position leads to allylic hydroperoxides with > 99% regiocontrol ("*gem* effect" operates) and the preferred formation of the R*S* (unlike, *ul*)-products (Scheme 10).[78]

The diastereoselectivity was modest (d.r. = 65:35) when the *Z*-**15** substrate was used and substantial (d.r. = 80:20) for the *E*-**15** diastereomer, which again demonstrates the importance of secondary orbital effects as postulated in the perepoxide mechanism. For chiral allylic alcohols, a remarkably high diastereoselectivity for acyclic substrates was obtained,[79] called the "hydroxy-directing" effect, in which the incoming singlet oxygen is associated with the allylic hydroxy group through hydrogen bonding. A large number of substrates with a variety of allylic substituents have been investigated and classified as either having attractive (as OH, NH_2, $^+NH_3$) or repulsive (HNAc, HNBoc, *t*-Bu, Cl^-) interactions with the pendant oxygen atom in the perepoxide-like structure.[80] Substituents with attractive interactions (H-bonding) direct *threo*-selectively whereas those with repulsive interactions (steric or electrostatic) direct *erythro*-selectively.[81]

Cycloalkenes

Exocyclic CC Double Bonds

The diastereofacial differentiation in *exo*-alkylidenenorbornenes was investigated for 2-ethylidenebicyclo[2.2.1]hept-5-ene (**16**).[82] The *exo*- and *endo*-2-hydroxy-2-vinylnorborn-5-enes **17** and **18** were formed as main products in a 35:12 ratio with the regioisomeric 2-(1-hydroxyethyl)-norbornadiene **19** (23%) as a third component; traces of two ketones could be detected as secondary products (Scheme 11).

Schmid and Hofheinz described an important application of this reaction to the total synthesis of the antimalarial drug artemisinin.[83] The key step in the (–)-isopulegol-based synthesis is the ene-reaction of singlet oxygen with an enol ether (Scheme 12). This reaction leads to an allylic hydroperoxide **20** when the reaction is performed in the nonpolar solvent, CH_2Cl_2. The use of the more polar, protic methanol inverts the regioselectivity, and the α-hydroperoxy acetal **21** is formed (presumably by trapping of an intermediary 1,4-zwitterion), which is cyclized to the target molecule **22** by acid catalysis.

The photooxygenation of 7-isopropylidinenorbornene discloses a preference for the attack of singlet oxygen on the *anti* face of the isopropylidine double bond (Scheme 13).[84] The stereoselectivity for a series of 7-isopropylidinebenzonorbornenes[85,86] was found to be sensitive to the electronic properties of the

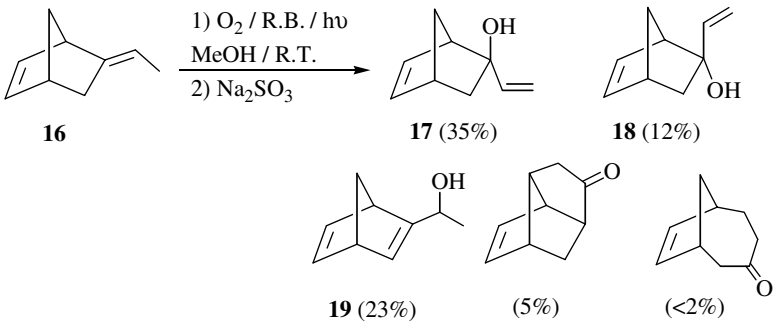

16 **17** (35%) **18** (12%) **19** (23%) (5%) (<2%)

SCHEME 11

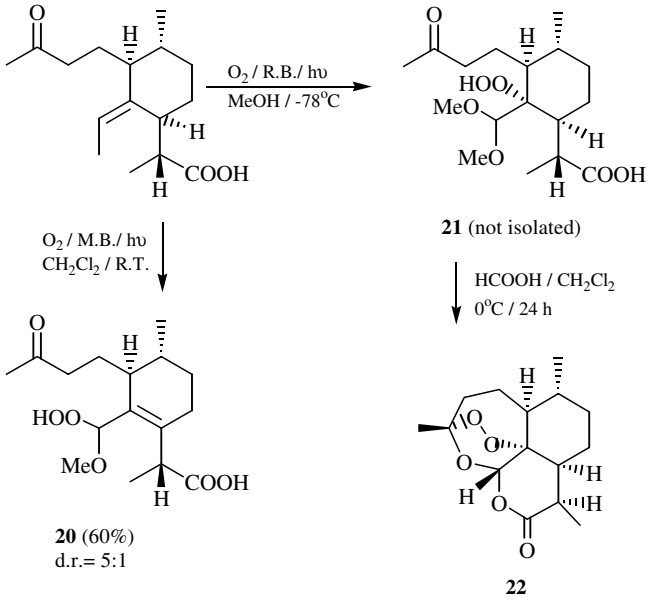

21 (not isolated)

20 (60%)
d.r.= 5:1

22

SCHEME 12

annulated arene ring, which suggests an anchimeric assistance through π–electron donation from the aryl ring to the perepoxide-like structure.

Endocyclic CC Double Bonds

When 2-substituted (methyl or trimethylsiloxy) norborn-2-enes and 1,7,7-trimethylnorborn-2-enes are treated with $^1O_2$, ene products are formed efficiently.[87] In case of the trimethylsiloxy-substituted derivative **23**, migration of the trimethylsilyl group occurs, and O-silylated α-hydroperoxy ketones **24**, which are readily reduced to O-silylated α-hydroxy ketones **25** (Scheme 14) are isolated. High *exo* selectivity is observed for the 7,7-unsubstituted substrates and *endo* selectivity for the 7,7-dimethyl ones. The steric demand seems to be higher for the silyl-ene reaction, for which *endo/exo* ratios from 0:100 to 94:6 were observed, whereas 2-methylnorborn-2-ene shows a 98.5:1.5 *exo* diastereoselectivity.[88]

Anellation of cyclopropane rings to cycloalkenes alters the ground-state geometry of the ring system, which may lead to considerable diastereotopic differentiation in the ene-reaction when singlet oxygen attacks the CC double bond. Several model systems were tested by Paquette and co-workers.[89] The photooxygenation of cholesterol (**26**) and cholest-5-en-3-one (**27**) has been investigated in detail by

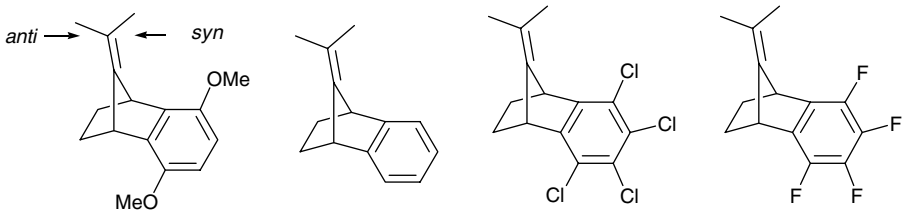

anti / syn	79 / 21	80 / 20	48 / 52	46 / 54
k ($M^{-1}s^{-1}$) x 10^{-4}	428	13.6	9.63	5.24

SCHEME 13

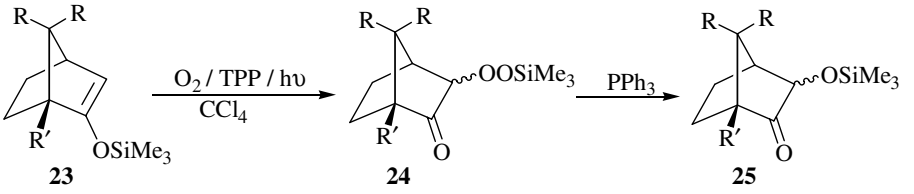

23 **24** **25**

	exo / endo:
R=R′= H	100 : 0
R=Me, R′=H	6 : 94
R=R′= Me	6 : 94

SCHEME 14

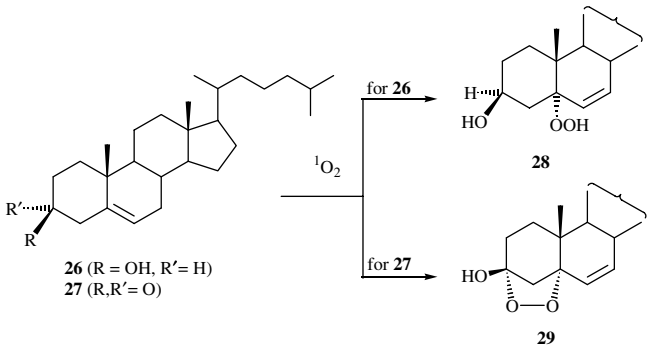

28 **29**

SCHEME 15

Schenck and Davies[90] (Scheme 15). While the reaction of $^1O_2$ with **26** results exclusively in the 5α-hydroperoxy product **28**, **26** gives a complex mixture with the hemiperketal **29** as major product from 5α-attack.

exo-Methylene functionalities may readily be generated from the corresponding substrates with endocyclic double bonds when allowed to react with singlet oxygen.[91] This is an important application because the stereochemistry of the newly formed chirality center is perfectly controlled, and the resulting products are synthetically valuable. Since bridgehead hydrogens cannot be abstracted, these ene-reactions are also highly regioselective. Ene-reactions with bicyclic systems are not limited to monoolefins; 1,3 dienes with suitable stereogenic centers react in this fashion, as shown for the photooxygenation of hexahydronaphthalene **30**. No [4 + 2]-cycloadducts were found in the reaction of the diene **30** with $^1O_2$

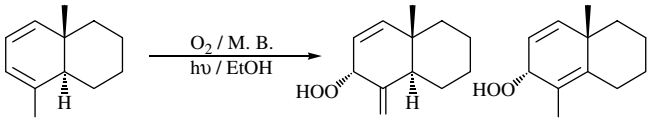

30 10-15% 85-90%

SCHEME 16

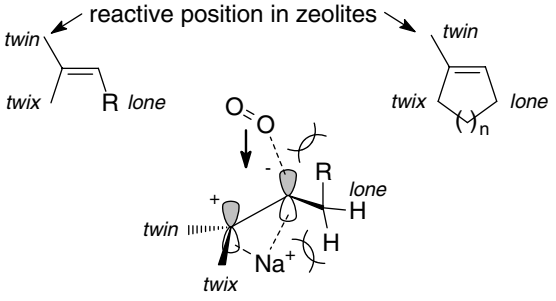

FIGURE 8.8

(Scheme 16). As major product, the allylic hydroperoxide from bridgehead-hydrogen abstraction was isolated.[92]

8.5 Photooxygenation in Zeolites

In 1996, Li and Ramamurthy reported the use of zeolites to enhance the regioselectivity in the $^1O_2$ ene-reaction.[93] In contrast to the reaction in solution, in which the *cis* effect applies,[26] a remarkable *twin* selectivity is observed in zeolites.[94] This was mechanistically rationalized in terms of coordination of the double bond to the Na^+ ion in the zeolite (cation-π interaction), which polarizes the double bond for Markovnikov selectivity and induces conformational constraint in the allylic *cis* substituents (Figure 8.8). The latter effect disfavors sterically the formation of the *cis* perepoxide-like structure or prevents a perpendicular orientation of the *cis*-hydrogens for coordination and abstraction.[93,95] Complications may arise from the formation of tertiary hydroperoxides from *lone*-hydrogen abstraction, which may selectively decompose on prolonged irradiation; this falsifies the regioselectivity.[96]

Furthermore, an increase in asymmetric induction, in cases where the stereogenic center in the substrate resides at remote positions with respect to the double bond, can also be observed within the zeolite cavity.[97] A thorough experimental reexamination and mechanistic interpretation have recently been published.[41b]

8.6 Further Transformations of Ene Products

Allylic hydroperoxides are easily reduced with a variety of reducing agents, of which sodium sulfite or sodium iodide are convenient for substrates that are not sensitive to water and further oxidation. For more sensitive hydroperoxides, dialkyl or aryl alkyl sulfides in organic solvents may be used. Triphenylphosphine and triethyl- or triphenylphosphite also have been employed successfully. These reductions all preserve the configuration at the hydroperoxy-substituted carbon atom. The resulting allylic alcohols are valuable building blocks for organic synthesis. The compounds obtained may be transformed to a multitude of highly useful target molecules. An efficient synthetic access to epoxy alcohols is the "one-pot" synthesis of epoxy alcohols in the photooxygenation of alkenes **31** in the presence of transition-metal complexes derived from Ti, V, and Mo (Scheme 17).[98]

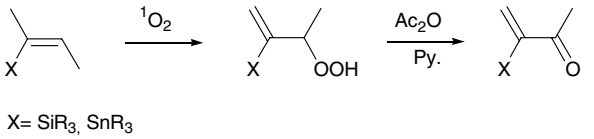

SCHEME 18

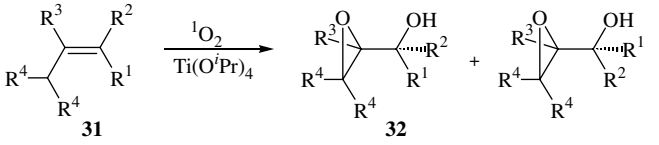

SCHEME 17

The products are formed in good chemical yields and high diastereoselectivity, analogous to the Sharpless-method; from acyclic substrates, R*S* (unlike, *ul*)-products **32** were formed preferentially. The allylic hydroperoxides obtained from the photooxygenation of vinylic silanes or stannanes are readily dehydrated to α,β-unsaturated carbonyl products with a silyl or stannyl group at the α carbon (Scheme 18).

Two carbonyl fragments could also be formed on acid-catalyzed hydrolysis of the allylic hydroperoxides that mostly proceeds through Hock-type fragmentation. Allylic alcohols obtained by reduction of the corresponding allylic hydroperoxides are versatile building blocks with diverse synthetic utility;[99] they could also be either regioselectively dehydrated to 1,3-dienes[100] or oxidized to α,β-unsaturated ketones.[101] The ene-reaction was also utilized in the synthesis of some natural products[102] and diastereoselective allene derivatives.[103]

References

1. Kautsky, H., de Bruijn, H., Neuwirth, R., and Baumeister, W., Photo-sensibilisierte Oxydation als Wirkung eines aktiven, metastabilen Zustandes des Sauerstoff-Moleküls, *Chem. Ber.,* 66, 1588, 1933.
2. (a) Foote, C.S., Wexler, S., and Ando, W., Chemistry of singlet oxygen. III. Product selectivity, *Tetrahedron Lett.,* 4111, 1965. (b) Foote, C.S., Photosensitized oxygenations and the role of singlet oxygen, *Acc. Chem. Res.,* 1, 104, 1968.
3. Schenck, G.O., Gollnick, K., Buchwald, G., Schroeter, S., and Ohloff, G., Zur chemischen und sterischen Selektivität der photosensibilisierten O_2-Übertragung auf (+)-Limonen und (+)-Carvomenthen, *Justus Liebigs Ann. Chem.,* 674, 93, 1964.
4. (a) Wasserman, H.H. and Murray, R.W., Eds., *Singlet Oxygen*, Academic Press, New York, 1979; (b), Rodgers, M.A.J. and Powers, E.L., Eds., *Oxygen and Oxy-Radicals in Chemistry and Biology,* Academic Press, New York, 1981; (c) Frimer, A.A., Ed., *Singlet O_2*, Vol. II and IV, CRC Press, Boca Raton, FL, 1985.
5. Schenck, G.O., Eggert, H., and Denk, W., *Liebigs Ann. Chem.,* 584, 177, 1953.
6. (a) Yamaguchi, K., Fueno, T., Saito, I., and Matsuura, T., On the mechanism of the ene reaction of electron-rich olefins with singlet oxygen. *Ab-initio* MO calculations, *Tetrahedron Lett.*, 21, 4087, 1980; (b) Yamaguchi, K., Fueno, T., Saito, I., Matsuura, T., and Houk, K.N., On the concerted mechanism of the ene reaction of singlet molecular oxygen with olefins. An *ab-initio* MO study, *Tetrahedron Lett.,* 22, 749, 1981.
7. Harding, L.B. and Goddard, W.A., III, The mechanism of the ene reaction of singlet oxygen with olefins, *J. Am. Chem. Soc.,* 102, 439, 1980.
8. Jefford, C.W., Kohmoto, S., Boukouvalas, J., and Burger, U., Reaction of singlet oxygen with enol ethers in the presence of acetaldehyde. Formation of 1,2,4-trioxanes, *J. Am. Chem. Soc.,* 105, 6498, 1983.

9. (a) Dewar, M.J.S. and Thiel, W., MINDO/3 study of reactions of singlet oxygen with carbon–carbon double bonds, *J. Am. Chem. Soc.,* 97, 3978, 1975; (b) Harding, L.B. and Goddard, W.A., III, The mechanism of the ene reaction of singlet oxygen with olefins, *J. Am. Chem. Soc.,* 102, 439, 1980; (c) Hotokka, M., Roos, B., and Siegbahn, P., CASSCF study of reaction of singlet molecular oxygen with ethylene. Reaction paths with C^{2v} und C^{s} symmetries, *J. Am. Chem. Soc.,* 105, 5263, 1983.
10. e.g., Yamaguchi, K., Takada, K., Otsuji, Y., and Mizuno, K., Theoretical and general aspects of organic peroxides, in *Peroxides*, Ando, W., Ed., Wiley, Chichester, NY, 1992, p. 65.
11. (a) Grdina, M.J., Orfanopoulos, M., and Stephenson, L.M., Stereochemical dependence of isotope effects in the singlet oxygen–olefin reaction, *J. Am. Chem. Soc.,* 101, 3111, 1979; (b) Stephenson, L.M., Grdina, M.J., and Orfanopoulos, M., Mechanism of the ene reaction between singlet oxygen and olefins, *Acc. Chem. Res.,* 13, 419, 1980.
12. Sharp, P.R., abstract, 138th Nat. Meet. Am. Chem. Soc., New York, 1960, p. 79.
13. Leach, A.G. and Houk, K.N., Diels–Alder and ene reactions of singlet oxygen, nitroso compounds and triazolinediones: transition states and mechanisms from contemporary theory, *J. Chem. Soc., Chem. Commun.,* 12, 2002.
14. Rosenthal, I., Chemical and physical sources of singlet oxygen, in *Singlet* O_2, Vol I, Frimer, A.A., Ed., CRC Press, Boca Raton, FL, 1985, p. 13.
15. (a) Gollnick, K. and Griesbeck, A., Solvent dependence of singlet oxygen/substrate interactions in ene-reactions, [4 + 2]- and [2 + 2]-cycloaddition reactions, *Tetrahedron Lett.,* 25, 725, 1984; (b) Gollnick, K. and Griesbeck, A., Interactions of singlet oxygen with 2,5-dimethyl-2,4-hexadiene in polar and non-polar solvents. Evidence for a vinylog ene-reaction, *Tetrahedron,* 40, 3235, 1984.
16. Monroe, B.M., Singlet oxygen in solution: lifetimes and reaction rate constants, in *Singlet* O_2, Vol I, Frimer, A.A., Ed., CRC Press, Boca Raton, FL, 1985, p. 177.
17. (a) Manring, L.E., Eriksen, J., and Foote, C.S., Electron-transfer photooxygenation. 4. Photooxygenation of *trans*-stilbene sensitized by methylene blue, *J. Am. Chem. Soc.*, 102, 4275, 1980; (b) Casarotto, M.G. and Smith, G.J. Methylene-blue–sensitized photooxidation of terpenes, *Photochem. Photobiol.,* A40, 87, 1987.
18. Rehm, D. and Weller, A., Kinetics of fluorescence quenching by electron and H-atom transfer, *Isr. J. Chem.,* 8, 259, 1970.
19. Pförtner, K.H., Alkenes: photo-oxidation, in *Photochemistry in Organic Synthesis*, Coyle, J.D., Ed., Special publication, The Royal Society of Chemistry, 57, 189, 1986.
20. Quast, H., Dietz, T., and Witzel, A., Tetra(2,6-dichlorophenyl)porphyrin: a superior sensitizer for the singlet-oxygen ene reaction (Schenck reaction), *Liebigs Ann.,* 1495, 1995.
21. Akasaka, T. and Ando, W., Stereospecific oxygenation of 3-adamantylidenetricyclo-[3.2.1.$0^{2,4}$]octane: singlet oxygen vs. electron-transfer oxygenations, *J. Am. Chem. Soc.,* 109, 1260, 1987.
22. Arbogast, J.W., Darmanyan, A.O., Foote, C.S., Rubin, Y., Diederich, F.N., Alvarez, M.M., Anz, S.J., and Whetten, R.L., Photophysical properties of C_{60}, *J. Phys. Chem.,* 95, 11, 1991.
23. Shuping, W., Zhiqin, J., Heting, L., Li, Y., and Daixun, Z., Sensitized photooxygenation of cholesterol and pseudocholesterol derivatives via singlet oxygen, *Molecules*, 6, 52, 2001.
24. Calvert, J.G. and Pitts, J.N., *Photochemistry,* Wiley, New York, 1966.
25. Murtinho, D., Pineiro, M., Pereira, M.M., Gonsalves, A.M.d'A.R., Arnaut, L.G., Miguel, M.D.G., and Burrows, H.D., Novel porphyrins and a chlorin as efficient singlet oxygen photosensitizers for photooxidation of naphthols or phenols to quinones, *J. Chem. Soc., Perkin Trans. 2,* 2441, 2000.
26. Hurst, J.R., Wilson, S.L., and Schuster, G.B., The ene reaction of singlet oxygen: kinetic and product evidence in support of a perepoxide intermediate, *Tetrahedron*, 41, 2191, 1985.
27. Schenck, G.O., Neumüller, O.-A., Ohloff, G., and Schroeter, S., Zur Autoxydation des (+)-Limones, *Justus Liebigs Ann. Chem.,* 687, 26, 1965.
28. (a) Foote, C.S., Photosensitized oxidation and singlet oxygen: consequences in biological systems, in *Free Radicals in Biology*, Vol. II, Pryor, W.A., Ed., Academic Press, New York, 1976; pp. 85, 101; (b) Frimer, A.A., Singlet oxygen in peroxide chemistry, in *The Chemistry of Peroxides,* Patai, S., Ed., Wiley, New York, 1983, pp. 201–234.

29. Ouannes, C. and Wilson, T., Quenching of singlet oxygen by tertiary amines. Effect of DABCO, *J. Am. Chem. Soc.,* 90, 6527, 1968.
30. Griesbeck, A.G., Fiege, M., Gudipati, M.S., and Wagner, R., Photooxygenation of 2,4-dimethyl-1,3-pentadiene: solvent dependence of the chemical (ene reaction and [2 + 4] cycloaddition) and physical quenching of singlet oxygen, *Eur. J. Org. Chem.,* 2833, 1998.
31. Rousseau, G., LePerchec, P., and Conia, J.M., A novel synthesis of α,β-unsaturated aldehydes and esters by dye-photooxygenation of methyl enol ethers, *Synthesis,* 67, 1978.
32. Adam, W., Griesbeck, A.G., Gollnick, K., and Knutzen-Mies, K., 1,2-Dioxetanes derived from 4,5-dimethyl-2,3-dihydrofuran: synthesis via photooxygenation, activation parameters and excitation properties*, J. Org. Chem.,* 53, 1492, 1988.
33. Stratakis, M. and Rabalakos, C., Chemoselective hydroperoxidation of alkenylarenes within thionin-supported zeolite Na-Y, *Tetrahedron Lett.,* 42, 4545, 2001.
34. Paquette, L.A., Liotta, D.C., and Baker, A.D., Frontier molecular orbital basis for the structurally dependent regiospecific reactions of singlet oxygen with polyolefins, *Tetrahedron Lett.,* 2681, 1976.
35. (a) Denny, R.W. and Nickon, A., Sensitized photooxygenation of olefins, *Org. Reactions,* 20, 133, 1973; (b) Gollnick, K., Ene-reaction with singlet oxygen, in *Singlet Oxygen,* Wasserman, H H. and Murray, R.W., Eds., Academic Press, New York, 1979, chap. 8.
36. (a) Schulte-Elte, K.H., Muller, B.L., and Rautenstrauch, V., Preference for syn ene additions of $^1O_2$ to trisubstituted, acyclic olefins, *Helv. Chim. Acta,* 61, 2777, 1978; (b) Orfanopoulos, M., Grdina, M.B., and Stephenson, L.M., Site specificity in the singlet oxygen–trisubstituted olefin reaction, *J. Am. Chem. Soc.,* 101, 275, 1979; (c) Frimer, A.A. and Roth, D., Reaction of $^1O_2$ with strained olefins. 3. Photooxidation of vinylcyclopropanes, *J. Org. Chem.,* 44, 3882, 1979; (d) Jefford, C.W. and Rimbault, C.G., *Syn* regioselectivity of the hydroperoxidation of cycloalkenes with singlet oxygen, *Tetrahedron Lett.,* 22, 91, 1981; (e) Rautenstrauch, V., Thommen, W., and Schulte-Elte, K.H., Singlet oxygen ene reactions of (E)-4-propyl[1,1,1-$^2H_3$]oct-4-ene, *Helv. Chim. Acta,* 69, 1638, 1986.
37. (a) Rousseau, G., Le Perchec, P., and Conia, J.M., Stereochemical course in the addition of singlet oxygen to vinylcyclopropane derivatives, *Tetrahedron Lett.,* 2517, 1977; (b) Jefford, C.W., The role of zwitterionic peroxides in controlling hydroperoxidation, *Tetrahedron Lett.,* 985, 1979.
38. (a) Ensley, H.E., Balakrishnan, P., and Ugarkar, B., Reaction of singlet oxygen with ß-alkoxyenones, *Tetrahedron Lett.,* 24, 5189, 1983; (b) Orfanopoulos, M. and Foote, C.S., Regioselective reaction of singlet oxygen with α,ß-unsaturated esters, *Tetrahedron Lett.*, 26, 5991, 1985; (c) Adam, W. and Griesbeck, A., Regioselective synthesis of 2-hydroperoxy-2-methylene-butanoic acid derivatives via photooxygenation of tiglic acid derivatives, *Synthesis*, 1050, 1986; (d) Akasaka, T., Misawa, Y., Goto, M., and Ando, W., Singlet oxygen and triazolinedione additions to α,ß-unsaturated sulfoxides, *Tetrahedron,* 45, 6657, 1989; (e) Kwon, B.M., Kanner, R.C., and Foote, C.S., Reaction of singlet oxygen with 2-cyclopenten-1-ones, *Tetrahedron Lett.,* 30, 903, 1989.
39. (a) Clennan, E.L. and Chen, X., Reactions of an allylic sulfide, sulfoxide and sulfone with singlet oxygen. The observation of a remarkable diastereoselective oxidation, *J. Am. Chem. Soc.,* 111, 5787, 1989; (b) Orfanopoulos, M., Stratakis, M., and Elemes, Y., Geminal selectivity of singlet oxygen ene reactions. The nonbonding large group effect, *J. Am. Chem. Soc.,* 112, 6417, 1990.
40. Fristad, W.E., Bailey, T.R., Paquette, L.A., Gleiter, R., and Böhm, M.C., Regiospecific photosensitized oxygenation of vinylsilanes. A method for converting saturated ketones to 1,2-transposed allylic alcohols. Possible role of silicon in directing the regioselectivity of epoxysilane cleavage reactions, *J. Am. Chem. Soc.,* 101, 4420, 1979.
41. (a) Orfanopoulos, M. and Stratakis, M., Regioselectivity in the ene reaction of singlet oxygen with alkenes, *Tetrahedron,* 56**,** 1595, 2000; (b) Clennan, E.L., New mechanistic and synthetic aspects of singlet oxygen chemistry, *Tetrahedron,* 56, 9151, 2000.
42. Adam, W., Bottke, N., and Krebs, O., The new skew and the established *cis* and *gem* regioselectivities in the ene reaction of trisubstituted olefins: comparison of the singlet oxygen, triazolinedione and nitrosoarene enophiles, *J. Am. Chem. Soc.,* 122, 6791, 2000.

43. Orfanopoulos, M. and Stratakis, M., Anti "cis effect" selectivity in the reaction of singlet oxygen with trisubstituted alkenes, *Tetrahedron Lett.,* 36, 4291, 1995.
44. Houk, K.N., Williams, J.C., Jr., Mitchell, P.A., and Yamaguchi, K., Conformational control of reactivity and regioselectivity in the singlet oxygen ene reactions: Relationship to the rotational barriers of acyclic alkylethylenes, *J. Am. Chem. Soc.,* 103, 949, 1981.
45. Orfanopoulos, M., Stratakis, M., Elemes, Y., and Jensen, F., Do rotational barriers dictate the regioselectivity in the ene reactions of singlet oxygen and triazolinedione with alkenes? *J. Am. Chem. Soc.,* 113, 3180, 1991.
46. Stephenson, L.M., The mechanism of the singlet oxygen ene reaction, *Tetrahedron Lett.,* 21, 1005, 1980.
47. Frimer, A.A., Barlett, P.D., Boschung, A.F., and Jewett, J.G., Reaction of singlet oxygen with 4-methyl-2,3-dihydro-γ-pyrans, *J. Am. Chem. Soc.,* 99, 7977, 1977.
48. Barlett, P.D. and Frimer, A.A., The reaction of singlet oxygen with 1-methoxycyclohexene, *Heterocycles,* 11, 419, 1978.
49. Hurst, J.R., McDonald, J.D., and Schuster, G.B., Lifetime of singlet oxygen in solution directly determined by laser spectroscopy, *J. Am. Chem. Soc.,* 104, 2065, 1982.
50. Hurst, J.R., Wilson, S.L., and Schuster, J.B., The ene reaction of singlet oxygen: kinetic and product evidence in support of a perepoxide intermediate, *Tetrahedron,* 41, 2191, 1985.
51. Stratakis, M. and Orfanopoulos, M., Anti *cis* effect selectivity in the reaction of singlet oxygen with trisubstituted alkenes, *Tetrahedron Lett.,* 36, 4291, 1995.
52. Clennan, E.L., Chen, X., and Koola, J.J., Steric and electronic effects on the conformations and singlet oxygen ene regiochemistries of substituted tetramethylethylenes, *J. Am. Chem. Soc.,* 112, 5193, 1990.
53. Brünker, H.-G. and Adam, W., Diastereoselective and regioselective singlet oxygen ene oxyfunctionalization (Schenck reaction): photooxygenation of allylic amines and their acyl derivatives, *J. Am. Chem. Soc.,* 117, 3976, 1995.
54. Stratakis, M. and Orfanopoulos, M., Regioselective formation of cyclic and allylic hydroperoxides, *Synth. Commun.,* 23, 425, 1993.
55. Adam, W. and Griesbeck, A., Synthesis of the first α-methylene-β-peroxylactone: regioselective ene reaction of singlet oxygen with α,β-unsaturated carboxylic acids, *Angew. Chem. Int. Ed. Engl.,* 24, 1070, 1985.
56. Adam, W., Catalani, L.H., and Griesbeck, A., Diastereoselective ene reaction in the photooxygenation of the silyl cyanohydrins of α,β-unsaturated aldehydes: necessity for a common symmetrical intermediate of the perepoxide type, *J. Org. Chem.,* 51, 5494, 1986.
57. (a) Kwon, B.-M., Kanner, R.C., and Foote, C.S., Reactions of singlet oxygen with 2-cyclopenten-1-ones, *Tetrahedron Lett.,* 30, 903, 1989; (b) Ensley, H.E., Balakrishnan, P., and Ugarkar, B., Reactions of singlet oxygen with β-alkoxyenones, *Tetrahedron Lett.,* 24, 5189, 1983.
58. Adam, W. and Griesbeck, A., Regioselective synthesis of 2-hydroperoxy-2-methylene-butanoic acid derivatives via photooxygenation of tiglic acid derivatives, *Synthesis,* 1050, 1986.
59. Orfanopoulos, M. and Foote, C.S., Regioselective reaction of singlet oxygen with α,β-unsaturated esters, *Tetrahedron Lett.,* 26, 5991, 1985.
60. Akasaka, T., Misawa, Y., Goto, M., and Ando, W., Singlet oxygen and triazolinedione additions to α,β–unsaturated sulfoxides, *Tetrahedron,* 45, 6657, 1989.
61. (a) Akasaka, T., Takeuchi, K., Misawa, Y., and Ando, W., Reaction of singlet oxygen with α,β-unsaturated aldimines: novel formation of 3-amino-4-methylene-1,2-dioxolanes, *Heterocycles,* 28, 445, 1989; (b) Akasaka, T., Takeuchi, K., and Ando, W., Reaction of singlet oxygen with α,β-unsaturated aldimines, *Tetrahedron Lett.,* 28, 6633, 1987.
62. (a) Fristad, W.E., Bailey, T.R., and Paquette, L.A., 1,2-Transposition of ketones via vinylsilanes, *J. Org. Chem.,* 43, 1620, 1978; (b) Fristad, W.E., Bailey, T.R., Paquette, L.A., Gleiter, R., and Böhm, M.C., Regiospecific photosensitized oxygenation of vinylsilanes. A method for converting saturated

ketones to 1,2-transposed allylic alcohols. Possible role of silicon in directing the regioselectivity of epoxysilane cleavage reactions, *J. Am. Chem. Soc.,* 101, 4420, 1979; (c) Fristad, W.E., Bailey, T.R., and Paquette, L.A., Silanes in organic synthesis. Enesilylation as a method for 1,2-carbonyl migration within ketones and for conversion to 1,2-transposed allylic alcohols, *J. Org. Chem.,* 45, 3028, 1980; (d) Adam, W. and Richter, M.J., Regioselectivity of the singlet oxygen ene reaction (Schenck reaction) with vinylsilanes, *J. Org. Chem.,* 59, 3335, 1994.

63. (a) Adam, W. and Klug, P., Photooxygenation of vinylstannanes: tin-substituted allylic hydroperoxides through the regio- and diastereoselective ene reaction with singlet oxygen, *J. Org. Chem.,* 58, 3416, 1993.
64. Adam, W. and Klug, P., β-Stannyl allylic alcohols through photooxygenation (Schenck reaction) of vinylstannanes and reduction of the resulting allylic hydroperoxides: synthesis and selected transformations, *J. Org. Chem.,* 59, 2695, 1994.
65. (a) Adam, W. and Prein, M., The Schenck ene reaction: diastereoselective oxyfunctionalization with singlet oxygen in synthetic applications, *Angew. Chem.,* 108, 519, 1996; *Angew. Chem. Int. Ed. Engl.,* 35, 477, 1996; (b) Adam, W. and Wirth, T., Hydroxy group directivity in the epoxidation of chiral allylic alcohols: control of diastereoselectivity through allylic strain and hydrogen bonding, *Acc. Chem. Res.,* 32, 703, 1999.
66. Orfanopoulos, M. and Stephenson, L.M., Stereochemistry of singlet oxygen olefin-ene reaction, *J. Am. Chem. Soc.,* 102, 1417, 1980.
67. (a) Adam, W. and Nestler, B., Hydroxy-directed regio- and diastereoselective ene reaction of singlet oxygen with chiral allylic alcohols, *J. Am. Chem. Soc.,* 115, 5041, 1993; (b) Adam, W. and Brünker, H.-G., Diastereoselective and regioselective singlet oxygen ene oxyfunctionalization (Schenck reaction): photooxygenation of allylic amines and their acyl derivatives, *J. Am. Chem. Soc.,* 117, 3976, 1995; (c) Adam, W., Brünker, H.-G., Kumar, A.S., Peters, E.-M., Peters, K., Schneider, U., and von Schnering, H.G., Diastereoselective singlet oxygen ene reaction (Schenck reaction) and diastereoselective epoxidations of heteroatom-substituted acyclic chiral olefins: a mechanistic comparison, *J. Am. Chem. Soc.,* 118, 1899, 1996.
68. (a) Adam, W., Peters, K., Peters, E.-M., and Schambony, S.B., Diastereoselective and regioselective singlet-oxygen ene reaction of oxazolidine-substituted alkenes: control through hydrogen bonding mediated by the urea functionality of chiral auxiliaries, *J. Am. Chem. Soc.,* 122, 7610, 2000; (b) Adam, W., Peters, K., Peters, E.-M., and Schambony, S.B., Efficient control of the diastereoselectivity and regioselectivity in the singlet-oxygen ene reaction of chiral oxazolidine-substituted alkenes by a remote urea NH functionality. Comparison with dimethyldioxirane and *m*-chlorobenzoic acid epoxidations, *J. Am. Chem. Soc.,* 123, 7228, 2001.
69. Dussault, P.H., Woller, K.R., and Hillier, M.C., Stereoselective dioxygenation of enoates, *Tetrahedron,* 50, 8929, 1994.
70. Adam, W., Wirth, T., Pastor, A., and Peters, K., Dramatic diastereoselectivity differences in the asymmetric ene reactions of triazolinediones and singlet oxygen with chiral 2,2-dimethyloxazolidine derivatives of tiglic acid, *Eur. J. Org. Chem.,* 501, 1998.
71. (a) Stephenson, L.M., McClure, D.E., and Sysak, P.K., Stereochemistry of the singlet oxygen ene reaction with olefins, *J. Am. Chem. Soc.,* 95, 7888, 1973; (b) Orfanopoulos, M. and Stephenson, L.M., Stereochemistry of the singlet oxygen olefin-ene reaction, *J. Am. Chem. Soc.,* 102, 1417, 1980.
72. Shimizu, N., Shibata, F., Imazu, S., and Tsumo, Y., The ene reaction of allylsilanes with singlet oxygen. Unusual product stereoselectivity, *Chem. Lett.,* 1071, 1987.
73. Kropf, H. and Reichwaldt, R., Photooxygenation of phenyl-substituted propenes, but-2-enes and pent-2-enes: reactivity, regioselectivity and stereoselectivity, *J. Chem. Res. (S),* 412, 1987.
74. Dang, H.-S. and Davies, A.G., Ene reaction of allylic tin compounds with 4-phenyl-1,2,4-triazoline-3,5-dione, *J. Chem. Soc., Perkin Trans. 2,* 2011, 1991.
75. Dang, H.-S. and Davies, A.G., Ene reactions of allylic tin compounds with singlet oxygen, *Tetrahedron Lett.,* 32, 1745, 1991.

76. Dang, H.-S. and Davies, A.G., Ene reaction of allylically stannylated cholestenes: singlet oxygenation of 7α-triphenylstannylcholest-5-en-3β-oland of 7-α-triphenylstannyl- and 7α-tributylstannylcholest-5-en-3-one and the rearrangement of 5α-tributylstannylperoxy-3β-benzoyloxycholest-6-ene and of 7α-tributylstannylperoxy-3β-benzoyloxycholest-5ene, *J. Chem. Soc., Perkin Trans. 2,* 1095, 1992.
77. Dang, H.-S. and Davies, A.G., The effect of ligands, solvent and temperature on the reactions of allyltin(IV) compounds with singlet oxygen, *J. Organomet. Chem.,* 430, 287, 1992.
78. Adam, W. and Nestler, B., Regio- and diastereoselective ene reactions of singlet oxygen with dialkyl-substituted acrylic esters, *Liebigs Ann. Chem.,* 1051, 1990
79. Adam, W. and Nestler, B., Photooxygenation of chiral allylic alcohols: hydroxy-directed regio- and diastereoselective ene reaction of singlet oxygen, *J. Am. Chem. Soc.,* 114, 6549, 1992.
80. Brünker, H.-G. and Adam, W., Diastereoelective and regioselective singlet oxygen ene oxyfunctionalization (Schenck reaction): photooxygenation of allylic amines and their acyl derivatives, *J. Am. Chem. Soc.,* 117, 3976, 1995.
81. Linker, T. and Fröhlich, L., Regioselective and diastereoselective photooxygenation of chiral 2,5-cyclohexadiene-1-carboxylic acids, *Angew. Chem. Int. Ed. Engl.,* 33, 1971, 1994.
82. Adams, W.R. and Trecker, D.J., The dye-sensitized photooxygenation of 2-ethylidene bicyclo[2.2.1]hept-5-ene, *Tetrahedron*, 28, 2361, 1972.
83. Schmid, G. and Hofheinz, W., Total synthesis of qinghaosu, *J. Am. Chem. Soc.,* 105, 624, 1983.
84. Okada, K. and Mukai, T., Stereoselective addition of singlet oxygen to 7-isopropylidenenorbornene derivatives. Possibility of π-orbital distortion in the homoconjugated system, *J. Am. Chem. Soc.,* 100, 6509, 1978.
85. Paquette, L.A., Hertel, L.W., Gleiter, R., and Böhm, M., Electronic control of stereoselectivity. 1. Singlet oxygen and related electrophilic additions to aryl-substituted 7-isopropylidenebenzonorbornenes, *J. Am. Chem. Soc.,* 100, 6510, 1978.
86. Hetel, L.W. and Paquette, L.A., Electronic control of stereoselectivity. 2. A stereochemical method for qualitatively assessing the relative electrophilicity of various electron-deficient species, *J. Am. Chem. Soc.,* 101, 7620, 1979.
87. (a) Jefford, C.W. and Rimbault, C.G., Reaction of singlet oxygen with norbornenyl ethers. Characterization of dioxetanes and evidence for zwitterionic precursors, *J. Am. Chem. Soc.,* 100, 6437, 1978; (b) Jefford, C.W. and Boschung, A.F., Reaction of singlet oxygen with 2-methylnorborn-2-ene, 2-methylidenenorbornane, and their 7,7-dimethyl derivatives. The transition state geometry for hydroperoxidation, *Helv. Chim. Acta,* 57, 2242, 1974.
88. Jefford, C.W., Laffer, M.H., and Boschung, A.F., Exo-endo steric impediment in norbornene. Specification of the transition state for the reaction of singlet oxygen with 2-methylnorborn-2-ene and 2-methylenenorbornane, *J. Am. Chem. Soc.,* 94, 8904, 1972.
89. (a) Paquette, L.A. and Kretschmer, G., Stereoreversed electrophilic additions to 3-norcarenes. Insight into the relative steric demands of singlet oxygen in the ene reaction, *J. Am. Chem. Soc.,* 101, 4655, 1979; (b) Paquette, L.A. and Detty, M.R., Synthesis and protonation studies of syn- and anti-2,4-bishomotropone. Comparison with the behavior of epimeric 2,4-bishomocycloheptatrienols under long- and short-lived ionization conditions, *J. Am. Chem. Soc.,* 100, 5856, 1978.
90. (a) Schenck, G.O., Neumüller, O.-A., and Eisfeld, W., Æ^5-Steroid-7α-hydroperoxide und -7-ketone durch Allylumlagerung von Æ^6-Steroid-5α-hydroperoxiden, *Liebigs Ann. Chem.,* 618, 202, 1958; (b) Dang, H.-S., Davies, A.G., and Schiesser, C.H., Allylic hydroperoxides formed by singlet oxygenation of cholest-5-en-3-one, *J. Chem. Soc., Perkin Trans. 1,* 789, 1990.
91. (a) Piozzi, F., Nenturella, P., Bellino, A., and Marino, M.L., Partial synthesis of ent-kaur-16-ene-15ß,18-diol and ent-kaur-16-ene-7α,15ß,18-triol, *J. Chem. Soc., Perkin Trans. 1,* 1973, 1164; (b) Büchi, G., Hauser, A., and Limacher, J., The synthesis of khusimone, *J. Org. Chem.,* 42, 3323, 1977.
92. Sasson, I. and Labovitz, J., Synthesis, photooxygenation and Diels–Alder reactions of 1-methyl-4a,5,6,7,8,8a-trans-hexahydronaphthalene and 1,4a-dimethyl-4a,5,6,7,8,8a-trans-hexahydronaphthalene, *J. Org. Chem.,* 40, 3670, 1975.

93. Li, X. and Ramamurthy, V., Selective oxidation of olefins within organic dye cation-exchanged zeolites, *J. Am. Chem. Soc.,* 118, 10666, 1996.
94. Stratakis, M. and Froudakis, G., Site specificity in the photooxidation of some trisubstituted alkenes in thionin-supported zeolite Na-Y. On the role of the alkali metal cation, *Org. Lett.,* 2, 1369, 2000.
95. Ramamurthy, V., Lakshminarasimhan, P., Grey, C.P., and Johnston, L.J., Energy transfer, proton transfer and electron transfer reactions within zeolites, *J. Chem. Soc., Chem. Commun.,* 2411, 1998.
96. Shailaja, J., Sivaguru, J., Robbins, R.J., Ramamurthy, V., Sunoj, R.B., and Chandrasekhar, J., Singlet oxygen mediated oxidation of olefins within zeolites: selectivity and complexities, *Tetrahedron*, 56, 6927, 2000.
97. Stratakis, M. and Kosmas, G., Enhanced diastereoselectivity of an ene hydroperoxidation reaction by confinement within zeolite Na-Y; a stereoisotopic study, *Tetrahedron Lett.,* 36**,** 4291, 1995.
98. (a) Adam, W., Griesbeck, A., and Staab, E., Ein einfacher Zugang zu 2-Epoxyalko-holen: Titan(IV)-katalysierter Sauerstofftransfer von allylhydroperoxiden, *Angew. Chem.,* 98, 279, 1986; (b) Adam, W., Griesbeck, A., and Staab, E., A convenient "one-pot" synthesis of epoxy alcohols via photooxygenation of olefins in the presence of titanium(IV) catalyst, *Tetrahedron Lett.,* 27, 2839, 1986; (c) Adam, W., Braun, M., Griesbeck, A.G., Lucchini, V., Staab, E., and Will, B., Photooxygenation of olefins in the presence of titanium(IV) catalyst: a convenient "one-pot" synthesis of epoxy alcohols, *J. Am. Chem. Soc.,* 111, 203, 1989.
99. (a) Adam, W. and Richter, M.J., Metal-catalyzed direct hydroxy-epoxidation of olefins, *Acc. Chem. Res.,* 27, 57, 1994. (b) Prein, M. and Adam, W., The Schenck ene reaction: diastereoselective oxyfunctionalization with singlet oxygen in synthetic applications, *Angew. Chem. Int. Ed. Engl.,* 35, 477, 1996.
100. Wenkert, E. and Naemura, K., Synthesis of the himachalenes by an intramolecular Diels–Alder reaction route, *Synth. Commun.,* 3, 45, 1973.
101. Ireland, R.E., Baldwin, S.W., Dawson, D.J., Dawson, M.I., Dolfini, J.E., Newbould, J., Johnson, W.S., Brown, M., Crawford, R.J., Hudrlik, P.F., Rasmussen, G.H., and Schmiegel, K.K., The total synthesis of an unsymmetrical pentacyclic triterpene DL-germanicol, *J. Am. Chem. Soc.,* 92, 5743, 1970.
102. (a) Adam, W. and Brünker, H.-G., Diastereoselective synthesis of merucathin: the singlet oxygen ene reaction (Schenck reaction) as a key step towards an *E*-configured β-amino allylic alcohol, *Synthesis*, 1066, 1995; (b) Adam, W. and Klug, P., (*Z*)-3-Alkylidine-4,5-dihydro-4-hydroxy-5-methyl-2-(3H)-furanones by regio and diastereo-selective ene reaction of singlet oxygen (Schenck reaction) with γ-hydroxy vinylstannanes: an enantioselective synthesis of dihydromahubanolide B, *Synthesis,* 567, 1994.
103. Hajime, M., Takafumi, M., Kanako, Y., and Shigeo, K., Novel diastereoselective allene formation by an ene reaction of significantly twisted 1,3-dienes with singlet oxygen, *Tetrahedron Lett.,* 40, 6461, 1999.

9

Photoreactions of Alkenes in Protic Media

Paul J. Kropp
University of North Carolina

9.1 Photochemical Behavior

Principal Pathways

On sensitized irradiation, alkenes undergo principally *E,Z*-isomerization, unless it is structurally inhibited. In weakly protic media, the highly strained *E*-isomers arising from cyclohexenes, cycloheptenes, and cyclooctenes undergo protonation. Similar behavior is exhibited on direct irradiation. In addition, on direct irradiation styrenes undergo protonation whether they are cyclic or acyclic, and alkenes undergo nucleophilic trapping in hydroxylic solvents to afford alcohols or ethers. This chapter is concerned principally with this latter process, as well as photoprotonation of cycloalkenes. Emphasis is given to developments since the topic was reviewed extensively in 1979.[1] The photobehavior of alkenes on direct irradiation in nonhydroxylic media is discussed in Chapter 13.

Spectroscopic Properties

The ultraviolet absorption spectra of simple alkenes in solution typically consist of single, featureless bands with maxima at 185–195 nm ($\varepsilon = 5\text{–}10 \times 10^3$) and tails extending to 210–255 nm.[2] Absorption extends to longer wavelengths with increasing degrees of substitution. Hydroxylic solvents, which are frequently used as proton sources, have cutoffs at 205–210 nm. Highly substituted alkenes can be irradiated in such media with medium-pressure mercury lamps and quartz optics, but less highly substituted alkenes do not absorb light under these conditions. Since alkenes do not undergo intersystem crossing, sensitized irradiation is required to induce triplet photobehavior. Best results are obtained using aromatic sensitizers such as *p*-xylene or phenol, which have maximum absorption in the region 250–270 nm. For this either a low- or medium-pressure arc and quartz or Vycor optics can be used. A preparative procedure has been described.[3] Phenol can serve as both the sensitizer and a proton source.[4] It has the added advantage of being easily removed from the irradiation mixture by extraction with base.

In the triplet manifold of alkenes one excited state, $\pi\pi^*$, is clearly low lying, separated from the πR(3s) Rydberg triplet by approximately 2 eV.[5] By contrast, as is detailed in Chapter 13, two or more excited states are low lying and close in energy in the singlet manifold — including the $\pi\pi^*$ and πR(3s) Rydberg states, which do not communicate effectively. Hence, the sensitized photobehavior of alkenes is usually much simpler than that resulting from direct irradiation.

0-8493-1348-1/04/$0.00+$1.50

9.2 Examples and Mechanisms

Sensitized Irradiation

On sensitized irradiation, acyclic and large-ring cyclic alkenes having a nine-membered ring or larger undergo only *E,Z*-isomerization, whether in protic or aprotic media.[6] By contrast, sensitized irradiation of cyclohexenes, cycloheptenes, and cyclooctenes in protic media results in photoprotonation.[7] Thus, for example, *p*-xylene-sensitized irradiation of 1-methylcyclohexene [(*Z*)-**1b**] in methanol affords a mixture of the exocyclic isomer **3b** and the ether **4b**.[8] The cycloheptyl and cyclooctyl analogs (*Z*)-**1c** and **-1d** afford principally the corresponding ethers **4c–d**, accompanied by small amounts of the exocyclic isomers **3c–d**. Similar behavior is exhibited by the unsubstituted analogs (*Z*)-**5b–d**, which afford the ethers **6b–d**.

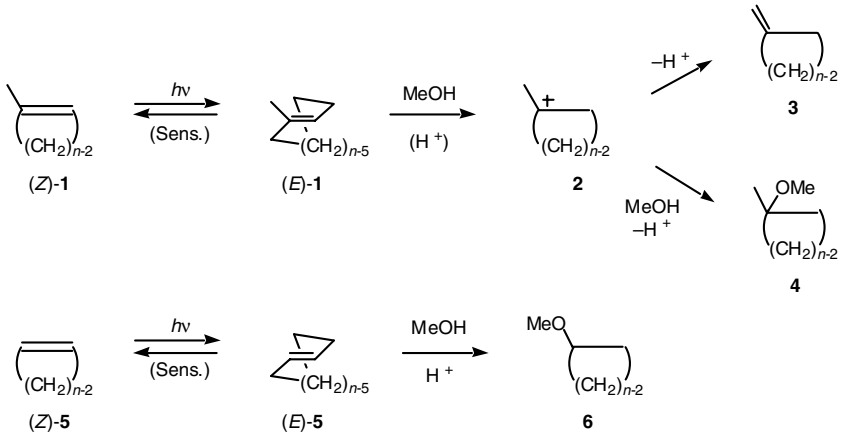

a, *n* = 5; **b**, *n* = 6; **c**, *n* = 7; **d**, *n* = 8

It was proposed that photoprotonation of cyclohexenes, cycloheptenes, and cyclooctenes involves initial formation of the corresponding *E*-isomers, which are much more easily protonated than the starting *Z*-isomers because of the attendant reduction in strain.[6a] A fine balance exists between the reactivity of the *E*-isomers and the acidity of the alcoholic medium. The highly strained and alkyl-substituted *(E)*-1-methylcyclohexene [*(E)*-**1b**] is readily protonated in neutral methanol. However, the higher homologs *(E)*-**1c–d**, as well as the unsubstituted analogs *(E)*-**5b–d**, require the presence of small amounts of mineral acid (e.g., 0.3–0.6% H_2SO_4), conditions under which the *E*-isomers are protonated but the *Z*-isomers are stable.

Cyclooctenes

Substantial support for the proposed formation of (*E*)-cycloalkene intermediates on sensitized irradiation and their involvement in photoprotonation has been obtained. Irradiation of (*Z*)-cyclooctene [(*Z*)-**5d**] with the triplet sensitizers benzene, toluene, or xylene afforded a mixture of the *E*- and *Z*-isomers with a photostationary *E:Z* ratio of 0.05.[9] The use of methyl benzoate as the sensitizer, which involves the formation of a singlet exciplex followed by decay to the twisted $\pi\pi^*$ singlet excited state, gave a higher *E:Z* ratio of 0.36:1.[10] The decay ratio to the *E* vs. *Z* isomer is higher for the singlet than for the triplet-excited state, providing a simple method for the preparation of moderate amounts of the *E*-isomer. The highly strained (*E*)-**5d** was found to undergo acid-catalyzed addition of methanol 3000 times more rapidly than the *Z* isomer.[11]

Cycloheptenes

Methyl benzoate sensitized irradiation of (*Z*)-cycloheptene [(*Z*)-**5c**] in neutral methanol at –78°C similarly afforded a mixture of the *E*- and *Z*-isomers with an estimated *E*:*Z* photostationary ratio of 0.25:1.[12] The *E*-isomer is stable in methanol at –78°C but, on being warmed to room temperature in the absence of dioxygen, underwent unimolecular decay to the *Z*-isomer quantitatively with E_a = 17.4 ± 0.7 kcal/mol, $\Delta G^{\ddagger}_{266}$ = 19.4 ± 1.4 kcal/mol, $\Delta H^{\ddagger}_{266}$ = 17.0 ± 0.7 kcal/mol, and $\Delta S^{\ddagger}_{266}$ = –9 ± 8 kcal/K mol. The lifetime in methanol at –10°C was 38.3 min. In the presence of air, isomerization occurs by an alternative mechanism involving a termolecular complex between triplet dioxygen and two molecules of (*E*)-**5c**.[13]

Irradiation of (*Z*)-cycloheptene [(*Z*)-**5c**] in acidic methanol at –78°C afforded ether **6c**. When an irradiation was conducted in neutral methanol and the resulting irradiation mixture allowed to stand in the dark at –78°C for 24 h before the addition of acid, ether **6c** was obtained in a similar yield. This clearly rules out the protonation of an excited state in the formation of ether **6c**. A kinetic study showed that (*E*)-cycloheptene [(*E*)-**5c**] undergoes protonation 7.7 × 10^8 times faster than its *Z*-isomer and 3.3 × 10^5 times faster than its higher homolog, (*E*)-cyclooctene [(*E*)-**5d**].

Generation of (*E*)-cycloheptene [(*E*)-**5c**] by methyl benzoate irradiation has also permitted its ^{1}H NMR and UV spectra to be obtained.[14] The UV maximum is shifted 40–50 nm to the red compared with the *Z*-isomer, suggesting substantial twist about the double bond, but the vinyl proton coupling shows that these atoms have a dihedral angle very close to 180°. Apparently, the vinyl carbon atoms mainly pyramidalize, rather than twist, to accommodate the strained ring.

Evidence has also been obtained for the intermediacy of the (*E*)-cycloheptene (*E*)-**7** in the formation of methyl ethers **8** and **9** on direct, *p*-xylene-sensitized and methyl benzoate–sensitized irradiation of the 3,7-disilacycloheptene (*Z*)-**7** in acidified methanol.[15] Sensitized irradiation of (*Z*)-**7** in methylcyclohexane solution at –75°C followed by siphoning of the irradiation mixture into acidified methanol similarly afforded ethers **8** and **9**, showing that a long-lived intermediate is involved. Addition of cyclopentadiene to the cold irradiation mixture in the dark afforded a Diels–Alder adduct shown to have a trans ring juncture.

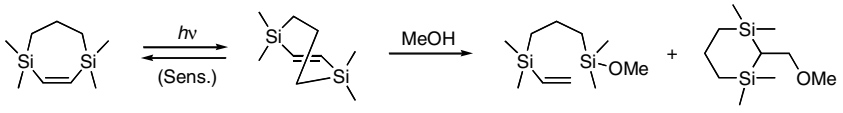

(*Z*)-**7** **8** (*E*)-**7** **9**

Cyclohexenes

Although they have much shorter lifetimes because of their higher strain, a number of (*E*)-cyclohexene derivatives have been observed on direct or photosensitized irradiation of the *Z*-isomers using flash spectroscopic techniques. The first observation of an (*E*)-cyclohexene derivative involved 1-phenylcyclohexene (*cis*-**10**), which afforded a transient having a lifetime of 9 μsec in methanol at 25°C.[16] Either direct or sensitized irradiation in methanol of *cis*-**10** affords the ether **12**.[17] On direct irradiation, a diastereomeric mixture of the cyclobutane dimers **11** is also formed.[18] Kinetic studies showed that ether **12** is formed on direct and sensitized irradiation via a common intermediate having the same lifetime as the spectroscopic transient.[19] The proposed trans stereochemistry for the transient was supported by the finding that direct or sensitized irradiation of *cis*-**10** in neutral methanol at –75°C afforded dimer **13**, which was shown to have a trans juncture by x-ray crystallographic analysis.[20] Time-resolved photoacoustic calorimetry has shown that the enthalpy of isomerization to the highly strained *trans*-isomer is 45 kcal/mol.[21]

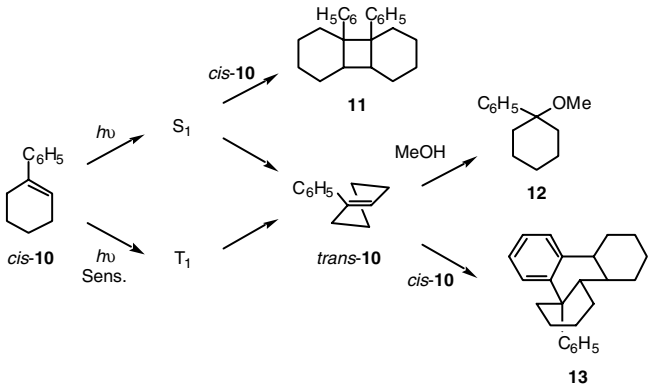

Either direct or triplet-sensitized irradiation of diene (*E,E*)-**14** in methanol affords the *cis*-cyclobutene **15** and the methyl ethers **16** and **17**.[8b,22] Laser flash spectroscopy revealed the formation of a ground-state intermediate having λ_{max} = 360 nm and a lifetime of 0.8 μsec at 23°C in methanol.[22] Based on the change of the quantum yields for the formation of ethers **16** and **17** with E_T for a variety of sensitizers, it was concluded that cyclobutene **15** and ether **16** arise from the *s-Z*-conformation of isomer (*E,Z*)-**14** and ether **17** from the *s-E*-conformation.[23] In view of large deuterium isotope effects, k_H/k_D, of 8 ± 1 and 10 ± 2, that were observed for the formation of ethers **16** and **17**, respectively, in CH_3OD, concerted formation of the CH and CO bonds in the transition states for ether formation was proposed.

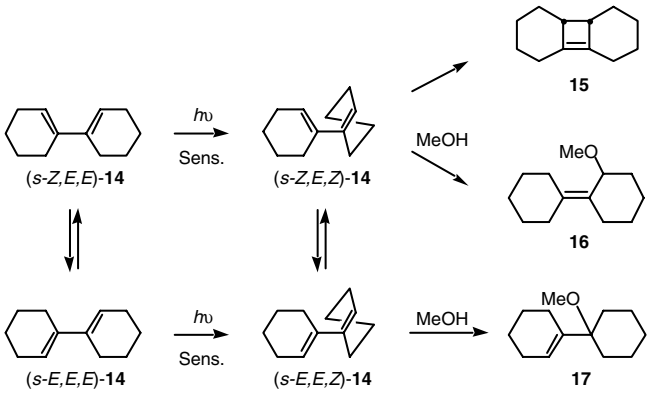

The spectroscopic and kinetic properties of five additional (*E*)-cyclohexene derivatives have recently been determined.[24] The properties of all of the (*E*)-cyclohexene derivatives that have been reported are remarkably constant: the ππ* maxima of the *E*-isomers are generally shifted to the red by about 15,000 cm^{-1} relative to the *Z*-forms; the activation energy for the thermal *E*→*Z* isomerization is about 10 kcal/mol, the corresponding pre-exponential factor is in the range 10^{12}–10^{13} sec^{-1}, and they undergo extremely efficient protonation by acid. *Ab initio* calculations have confirmed that the parent (*E*)-cyclohexene [(*E*)-**5b**] corresponds to a local minimum, although the activation energy for its isomerization to the *Z*-isomer is small.[25]

Support for the involvement of (*E*)-cyclohexenes in photoprotonation has also come from the stereochemistry of protonation.[26] Direct or sensitized irradiation of (*Z*)-bicyclo[3.3.1]non-1-ene [(*Z*)-**18**] in neutral methanol afforded ether **19**.[2a] On irradiation in CH_3OD the labeled ether **19**-*endo*-2*d* was obtained, whereas reaction of (*Z*)-**18** with CH_3OD catalyzed by DCl gave ether **19**-*exo*-2*d*. These results are consistent with preferential protonation of alkenes (*Z*)- and (*E*)-**18** from their less hindered faces. Protonation of (*E*)-**18** was found to have a large kinetic isotope effect, k_H/k_D, of eight, indicating that proton transfer is about half completed in the transition state.

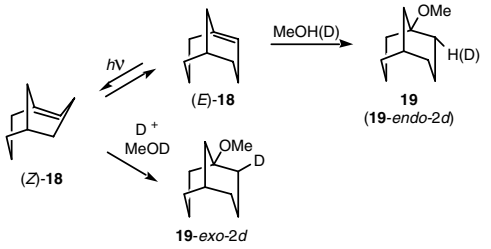

Cyclopentenes

In contrast with their higher homologs, cyclopentenes display no ionic behavior on sensitized irradiation in protic media. For example, sensitized irradiation of 1-methylcyclopentene [(*Z*)-**1a**] in either neutral or acidified methanol affords a mixture of the exocyclic isomer **3a**, the saturated product **21**, and ethane-1,2-diol — as expected from initial abstraction of a hydrogen atom from the solvent by the $\pi\pi^*$ excited state followed by disproportion of the resulting radical **20**.[8] In CH_3OD, the photoproducts **3a** and **21** are formed with no detectable incorporation of deuterium. Thus, cyclohexene is apparently the smallest-sized cycloalkene that can accommodate an *E* double bond. Being unable to relax to an orthogonal conformation, the $\pi\pi^*$ triplet intersystem crosses to the ground state more slowly and has a sufficiently long lifetime to undergo intermolecular reaction, in which it displays radical behavior.

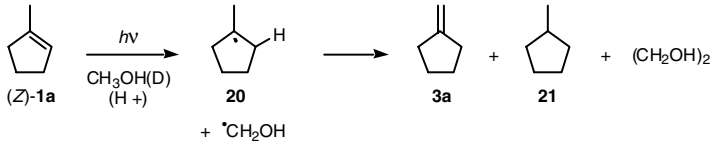

Direct Irradiation

Alkenes

Alkenes undergo *E,Z*-isomerization on direct, as well as sensitized, irradiation. However, since there are two or more low-lying excited states in the singlet manifold, the singlet photobehavior of alkenes is complex. On direct irradiation in hydroxylic solvents, tetrasubstituted alkenes afford, in addition to *E,Z*-isomerization, mixtures of saturated and unsaturated alcohols or ethers.[8b,27] Thus, for example, 2,3-dimethyl-2-butene (**22**) affords a mixture of the alcohols or ethers **28** and **29**, which apparently arise via nucleophilic trapping of the πR(3s) Rydberg excited state (**23**) followed by disproportionation of the resulting radical **25**.[8b] Small amounts of the hydrocarbons **26** and **27** are also formed, apparently via trapping of hydrogen atoms formed by attack of free electrons on the solvent. Since formation of the πR(3s) state involves promotion of one of the π electrons to an orbital having approximately the size and shape of a 3s helium orbital, it has an electron-deficient core with radical cation character. Undergoing nucleophilic trapping in hydroxylic media was the first chemical property of this state to be established. In nonnucleophilic media, it rearranges to carbene intermediates, as detailed in Chapter 13.

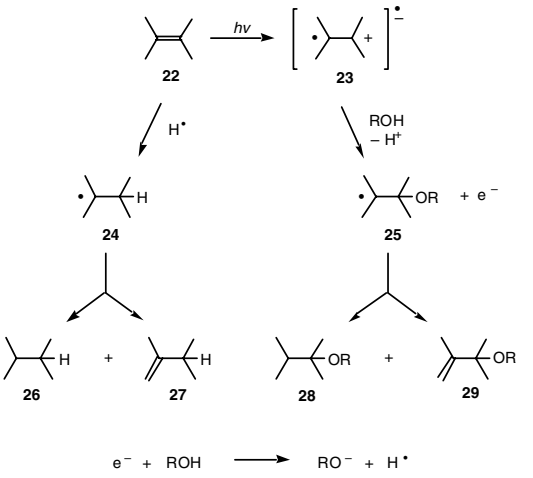

The cyclic analog (*Z*)-**30**, which on *p*-xylene-sensitized irradiation in methanol gives the epimeric ethers **31** and the exocyclic isomer **32**, affords in addition the unsaturated ethers **34** on direct irradiation.[8b] There is apparently competing protonation of the *E* isomer [(*E*)-**30**] and nucleophilic trapping of the πR(3s) excited state (**33**). This is consistent with the ππ* and πR(3s) states being close lying and both readily populated in tetrasubstituted alkenes. The cyclobutene analog **35**, which is incapable of *E,Z*-isomerization, afforded principally a mixture of the saturated and unsaturated ethers **36** on irradiation in methanol at 228 nm, along with small amounts of the ring opening and fragmentation products that are formed in the gas phase and hydrocarbon media.[28] The latter products increased relative to the ethers **36** at 214 nm, which is overlapped more effectively by the ππ* rather than the πR(3s) absorption band. This wavelength dependence supports the proposed involvement of the πR(3s) excited state in nucleophilic trapping.

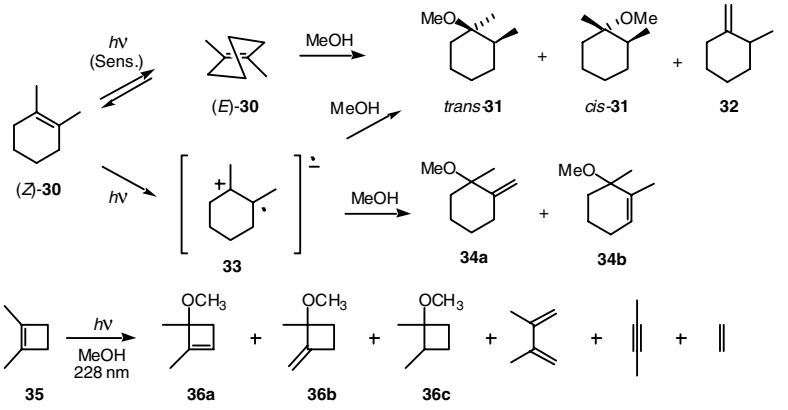

The trisubstituted alkene **37** similarly affords a mixture of the saturated and unsaturated ethers **38** and **39** and hydrocarbons **40–41** in methanol, but only on extended irradiation.[8b] By contrast, the cyclic analog 1-methylcyclohexene [(*Z*)-**1b**] affords only the exocyclic isomer **3b** and the saturated ether **4b** on direct irradiation in methanol.[8b] Similarly, the higher homologs (*Z*)-**1c–d** afford ethers **4c–d**, accompanied by small amounts of the exocyclic isomers **3c–d**, in acidified methanol. Apparently the πR(3s) excited state, which is significantly more sensitive to alkyl substitution, is higher lying than the ππ* state in trisubstituted alkenes. Disubstituted alkenes do not have sufficient absorption above the cutoffs of hydroxylic solvents to give photoproducts in these media.

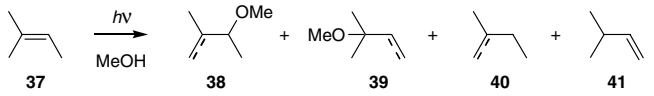

Styrenes

Acyclic styrenes (**42**) undergo Markovnikov addition on direct, but not sensitized, irradiation in water or methanol.[29] The reaction is acid catalyzed but employs considerably lower acid concentrations or weaker acids than required for ground-state addition. The proposed mechanism is protonation of the first excited singlet state, which is estimated to occur 10^{11}–10^{14} times more rapidly than protonation of the ground sate. Similar behavior is exhibited by the cyclic analog **43**, which on direct irradiation in aqueous or alcoholic media affords principally the alcohol or ether **44**, accompanied by smaller amounts of an epimeric mixture of the reduction products **45**.[30] Labeling studies showed that both types of products are formed via initial 3-*exo* protonation. Again, no reaction occurs on photosensitized irradiation. However, as noted above, the larger-ring analog *cis*-1-phenylcyclohexene (*cis*-**10**) undergoes addition of methanol on either direct or sensitized irradiation, with protonation in both cases involving the *trans*-isomer.[19] Thus, in contrast with acyclic and small-ring cyclic styrenes, in which the first singlet excited state undergoes protonation, the highly strained isomers of medium-ring cyclic styrenes are apparently more rapidly protonated.

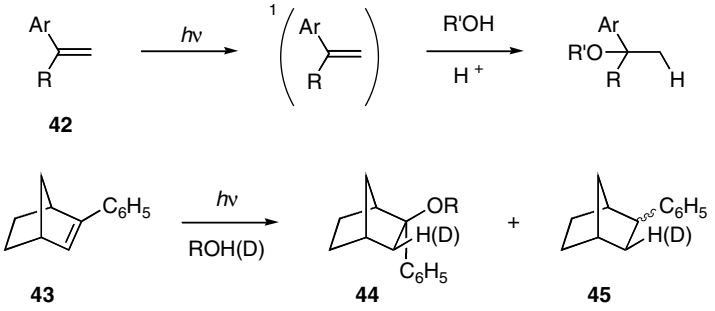

Synthetic Applications of Photoprotonation

There are several synthetically useful applications of the photoprotonation of cycloalkenes:

1. *Irradiation of 1-alkylcyclohexenes, cycloheptenes, and cyclooctenes in non-nucleophilic, protic media is a useful method for effecting contra thermodynamic isomerization to the exocyclic isomer.* For example, sensitized irradiation of 1,2-dimethylcyclohexene [(*Z*)-**30**] in ether containing a trace of sulfuric acid afforded the exocyclic isomer **32** in excellent yield.[31] In the absence of competing nucleophilic trapping, the cycloalkyl cation **46** resulting from photoprotonation simply undergoes deprotonation to afford a mixture of exocyclic and endocyclic alkenes. Any endocyclic alkene formed undergoes photoprotonation again and is recycled. The exocyclic isomer, on the other hand, is photo inert under these conditions except for *E,Z*-isomerization, which simply involves interchanging the positions of the vinyl hydrogen atoms and does not produce a strained *E* intermediate. Hence, there is a net isomerization of the double bond to the thermodynamically less stable exocyclic position.

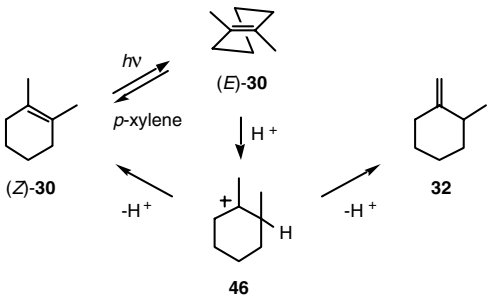

2. *Photoprotonation is a convenient method for effecting complete addition of water or an alcohol to a cyclohexene, cycloheptene, or cyclooctene.* Acid-catalyzed addition is reversible and does not go to completion, whereas the photochemical method proceeds until all of the alkene has been consumed. Moreover, since photoprotonation can be effected at low acid concentrations, even less highly substituted cycloalkenes, which are not readily protonated in the ground state, undergo photoprotonation readily. In many cases, photoprotonation affords addition when acid-catalyzed addition fails. For example, sensitized irradiation of cyclohexene [(*Z*)-**5b**] in methanol containing 0.6% sulfuric acid affords ether **6b** in excellent yield; in a preparative procedure it was isolated in 70% yield.[32] By contrast, treatment of cyclohexene in the dark with methanol containing 10 times the concentration of acid afforded no detectable ether formation.

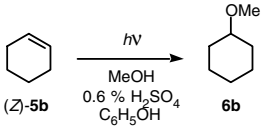

3. *The photochemical method permits the selective protonation of a cyclohexene, cycloheptene, or cyclooctene in the presence of a second double bond located in an acyclic, exocyclic, or larger ring cyclic environment.* For example, light-induced addition of methanol to *(R)*-(+)-limonene (**b**) afforded specifically a mixture of the epimeric ethers **49**, along with the exocyclic isomer **48**.[3,33] Acid-catalyzed, nonphotochemical additions to limonene (**47**) generally afford a mixture of products resulting from competing protonation of both double bonds. The selective photoreactivity stems from the fact that *E,Z*-isomerization of the cyclohexene moiety affords a strained alkene whereas isomerization of the second double bond does not.

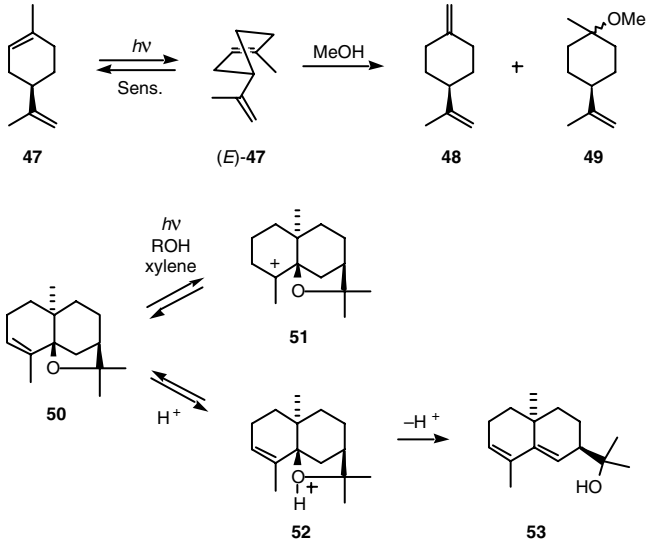

A similar type of selectivity is seen in the xylene-sensitized irradiation of the sesquiterpene α-agarofuran (**50**) in alcoholic media, which affords products resulting from selective protonation of the double bond to afford the cationic intermediate **51**.[34] By contrast, treatment with standard methods of protonation in the dark resulted in attack at oxygen (**52**) and opening of the oxide ring to afford alcohol **53** without rearrangement.[35]

These are just a few of the ways that a creative chemist can make use of the photoprotonation of cycloalkenes to induce selective reactivity in synthesis.

References

1. Kropp, P.J., Photochemistry of alkenes in solution, *Org. Photochem.,* 4, 1, 1979.
2. For some examples, see: (a) Wiseman, J.R. and Kipp, J.E., (*E*)-Bicyclo[3.3.1]non-ene, *J. Am. Chem. Soc.,* 104, 4688, 1982; (b) Clark, K.B. and Leigh, W.J., Cyclobutene photochemistry. Involvement of carbene intermediates in the photochemistry of alkylcyclobutenes, *Can. J. Chem.,* 66, 1571, 1988; (c) Wen, A.T., Hitchcock, A.P., Werstiuk, N.H., Nguyen, N., and Leigh, W.J., Studies of electronic excited states of substituted norbornenes by UV absorption, electron energy loss and HeI photoelectron spectroscopy, *Can. J. Chem.,* 68, 1967, 1990; (d) Leigh, W.J., Zheng, K., and Clark, K.B., Cyclobutene photochemistry. Substituent and wavelength effects on the photochemical ring opening of monocyclic alkylcyclobutenes, *Can. J. Chem.,* 68, 1988, 1990; (e) Leigh, W.J., Zheng, K., and Clark, K.B., Cyclobutene photochemistry. The photochemistry of *cis*- and *trans*-bicyclo[5.2.0]non-8-ene, *J. Org. Chem.,* 56, 1574, 1991; (f) Leigh, W.J., Zheng, K., Nguyen, N., Werstiuk, N.H., and Ma, J., Cyclobutene photochemistry. Identification of the excited states responsible for the ring-opening and cycloreversion reactions of alkylcyclobutenes, *J. Am. Chem. Soc.,* 113, 4993, 1991.
3. Tise, F.P. and Kropp, P.J., Photoprotonation of cycloalkenes: limonene to *p*-menth-8-en-1-yl methyl ether, *Org. Synth.,* 61, 112, 1983.
4. Guénard, D. and Beugelmans, R., Rôle du phénol dans les réactions photochimiques de type ionique subies par les alcools allyliques et homoallyliques en série stéroïde, *C.R. Seances Acad. Ser. C,* 280, 1033, 1975.
5. For a detailed treatment of the excited states of alkenes, see: Merer, A.J. and Mulliken, R.S., Ultraviolet spectra and excited states of ethylene and its alkyl derivatives, *Chem. Rev.,* 69, 639, 1969.
6. See, for example: Snyder, J.J., Tise, F.P., Davis, R.D., and Kropp, P.J., Photochemistry of alkenes. 7. *E*,*Z* isomerization of alkenes sensitized with benzene and derivatives, *J. Org. Chem.*, 46, 3609, 1981.
7. (a) Kropp. P.J., Photochemical behavior of cycloalkenes, *J. Am. Chem. Soc.,* 88, 4091, 1968; (b) Marshall, J.A. and Carroll, R.D., The photochemically initiated addition of alcohols to 1-menthene. A new type of photochemical addition to olefins, *J. Am. Chem. Soc.,* 88, 4092, 1966.
8. (a) Kropp, P.J. and Krauss, H.J., Photochemistry of cycloalkenes. 3. Ionic behavior in protic media and isomerization in aromatic hydrocarbon media, *J. Am. Chem. Soc.,* 89, 5199, 1967; (b) Kropp, P.J., Reardon, E.J., Jr., Gaibel, Z.L.F., Willard, K.F., and Hattaway, J.H., Jr., Photochemistry of alkenes. 2. Direct irradiation in hydroxylic media, *J. Am. Chem. Soc.,* 95, 7058, 1973.
9. Inoue, Y., Takamuku, S., and Sakurai, H., Direct and sensitized cis-trans photoisomerisation of cyclooctene. Effects of spin multiplicity and vibrational activation of excited states on the photostationary trans/cis ratio, *J. Phys. Chem.,* 71, 3104, 1967.
10. Inoue, Y., Takamuku, S., Kunitomi, Y., and Sakurai, H., Singlet photosensitization of simple alkenes. Part 1. *cis-trans* Photoisomerisation of cyclooctene sensitized by aromatic esters, *J. Chem. Soc., Perkin Trans. 2,* 1672, 1980.
11. Inoue, Y., Ueoka, T., and Hakushi, T., Relative rate of acid-catalyzed addition of methanol to *cis*- and *trans*-cyclooctenes, *J. Chem. Soc., Chem. Commun.,* 1076, 1982.
12. Inoue, Y., Ueoka, T., Kuroda, T., and Hakushi, T., Singlet photosensitization of simple alkenes. Part 4. *cis-trans* Photoisomerisation of cycloheptene sensitized by aromatic esters. Some aspects of the chemistry of *trans*-cycloheptene, *J. Chem. Soc., Perkin Trans. 2,* 983, 1983.

13. Inoue, Y., Ueoka, T., and Hakushi, T., A novel oxygen-catalyzed *trans-cis* thermal isomerization of *trans*-cycloheptene, *J. Chem. Soc., Perkin Trans. 2,* 2053, 1984.
14. Squillacote, M., Bergman, A., and De Felippis, J., *trans*-Cycloheptene: spectral characterization and dynamic behavior, *Tetrahedron Lett.,* 30, 6805, 1989.
15. Steinmetz, M.G., Seguin, K.J., Udayakumar, B.S., and Behnke, J.S., Evidence for a metastable *trans*-cycloalkene intermediate in the photochemistry of 1,1,4,4-tetramethyl-1,4-disilacyclohept-2-ene, *J. Am. Chem. Soc.,* 112, 6601, 1990.
16. Bonneau, R., Joussot-Dubien, J., Salem, L., and Yarwood, A.J., A trans cyclohexene, *J. Am. Chem. Soc.,* 98, 4329, 1976.
17. Kropp, P.J., Photochemistry of cycloalkenes. 5. Effects of ring size and substitution, *J. Am. Chem. Soc.,* 91, 5783, 1969.
18. Rosenberg, H.M. and Servé, M.P., The photolysis of 1-phenylcyclohexene in methanol, *J. Org. Chem.,* 37, 141, 1972.
19. Dauben, W.G., van Riel, H.C.H.A., Robbins, J.D., and Wagner, G.J., Photochemistry of *cis*-1-phenylcyclohexene. Proof of involvement of trans isomer in reaction processes, *J. Am. Chem. Soc.,* 101, 6383, 1979.
20. Dauben, W.G., van Riel, H.C.H.A., Hauw, C., Jeroy, F., Joussot-Dubien, J., and Bonneau, R., Photochemical formation of *trans*-1-phenylcyclohexene. Chemical proof of structure, *J. Am. Chem. Soc.,* 101, 1901, 1979.
21. Goodman, J.L., Peters, K.S., Misawa, H., and Caldwell, R.A., Use of time-resolved photoacoustic calorimetry to determine the strain energy of *trans*-1-phenylcyclohexene and the energy of the relaxed 1-phenylcyclohexene triplet, *J. Am. Chem. Soc.,* 108, 6803, 1986.
22. Saltiel, J., Marchand, G.R. and Bonneau, R., *cis,trans*-1,1′-Bicyclohexenyl: A strained ground state intermediate in the photocyclization of 1,1′-bicyclohexenyl to its isomeric *cis*-cyclobutene, *J. Photochem.,* 28, 367. 1985.
23. Saltiel, J. and Marchand, G.R., *cis,trans*-1,1′-Bicyclohexenyl: conformer-dependent chemistry in benzene and in methanol, *J. Am. Chem. Soc.,* 113, 2702, 1991.
24. Bonneau, R., Some new examples of "trans" cyclohexenes: properties characteristic of these species, *J. Photochem.,* 36, 311, 1987.
25. Verbeek, J., van Lenthe, J.H., Timmermans, P.J.J.A., Mackor, A., and Budzelaar, P.H.M., On the existence of *trans*-cyclohexene, *J. Org. Chem.,* 52, 2955, 1987.
26. For a review of some earlier studies on the stereochemistry of photoprotonation, see: Marshall, J.A., Photosensitized ionic additions to cyclohexenes, *Acc. Chem. Res.,* 2, 33, 1969.
27. Fravel, H.G., Jr. and Kropp, P.J., Photochemistry of alkenes. 4. Vicinally unsymmetrical olefins in hydroxylic media, *J. Org. Chem.,* 40, 2434, 1975.
28. Leigh, W.J. and Cook, B.H.O., Stereospecific (conrotatory) photochemical ring opening of alkylcyclobutenes in the gas phase and in solution. Ring opening from the Rydberg excited state or by hot ground state reaction? *J. Org Chem.,* 64, 5256, 1999.
29. For a review, see: Wan, P. and Yates, K., Photogenerated carbonium ions and vinyl cations in aqueous solution, *Rev. Chem. Intermed.,* 5, 157, 1984; See also: McEwen, J. and Yates, K., Photohydration of styrenes and phenylacetylenes. General acid catalysis and Brønsted relationships, *J. Am. Chem. Soc.,* 109, 5800, 1987; 3-Nitrostyrenes undergo anti-Markovnikov addition: Wan, P., Davis, M.J. and Teo, M.-A., Photoaddition of water and alcohols to 3-nitrostyrenes. Structure-reactivity and solvent effects, *J. Org. Chem.,* 54, 1354, 1989.
30. Kropp, P.J., Photochemistry of cycloalkenes. 8. 2-Phenyl-2-norbornene and 2-phenyl-2-bornene, *J. Am. Chem. Soc.,* 95, 4611, 1973.
31. Kropp, P.J., Fields, T.R., Fravel, H.G., Jr., Tubergen, M.W., and Crotts, D.D., Unpublished results.
32. Tise, F.P. and Kropp, P.J., Unpublished results.

33. Shim, S.C., Kim, D.S., Yoo, D.J., Wada, T., and Inoue, Y., Diastereoselectivity control on photosensitized addition of methanol to (*R*)-(+)-limonene, *J. Org. Chem.,* 67, 5718, 2002. The trans isomer of ether **49** was formed with high diastereoselectivity (>96%) using 0.5 *M* methanol in ether solution at –75°C and either methyl benzoate or dimethyl phthalate as sensitizer. However, chemical yields were low.
34. (a) Marshall, J.A. and Pike, M.T., A stereoselective synthesis of α- and β-agarofuran, *J. Org. Chem.,* 33, 435, 1968; (b) Thomas, A.F. and Ozainne, M., A photoinitiated Wagner–Meerwein rearrangement, *Helv. Chim. Acta,* 59, 1243, 1976.
35. Asselin, A., Mongrain, M., and Deslongchamps, P., Syntheses of α-agarofuran and isodihydroagarofuran, *Can. J. Chem.,* 46, 2817, 1968.

10

Silyl Enol Ether Radical Cations: Generation and Recent Synthetic Applications

Jens Otto Bunte
Universität Bielefeld

Jochen Mattay
Universität Bielefeld

10.1 Introduction

Silyl enol ethers are a class of electron-rich, nonaromatic compounds that easily form reactive radical cations on one electron oxidation. The silyl enol ether functional group is closely related to the carbonyl function and consequently, syntheses of silyl enol ethers generally make use of enolates. In addition, silyl enol ethers can be described as masked enols or enolates since their reactions often yield ketones.[1] A number of oxidation reactions of silyl enol ethers making use of oxygen[2] or oxygen-containing reagents such as peroxides,[3] peracids (known as Rubottom oxidation),[4] dioxirane,[5] osmium tetraoxide,[6] or triphenyl phosphite ozonide[7] have been described in the literature. In all cases either α-hydroxy-ketones or the silyl enol ether epoxides are formed.

This chapter reviews recent advances in the chemistry of radical cations of silyl enol ethers, focusing on their photochemical generation and usage in intramolecular reactions. Only oxidants that do not react via inner-sphere electron transfer are discussed as oxidants for the silyl enol ethers. In general, one electron oxidation leads to the formation of radical cations, and therefore this process can be regarded as an umpolung reaction.[8] The former nucleophilic silyl enol ether now acts as an electrophile. The synthetic possibilities resulting from this change in reactivity and the underlying mechanistic features of the oxidation process will be discussed in the following sections.

10.2 One Electron Oxidation of Silyl Enol Ethers

An assessment of the electron donor properties of silyl enol ethers can be made by comparison of their ionization potentials and anodic oxidation potentials with those of related compounds. Scheme 1 summarizes selected examples.

0-8493-1348-1/04/$0.00+$1.50

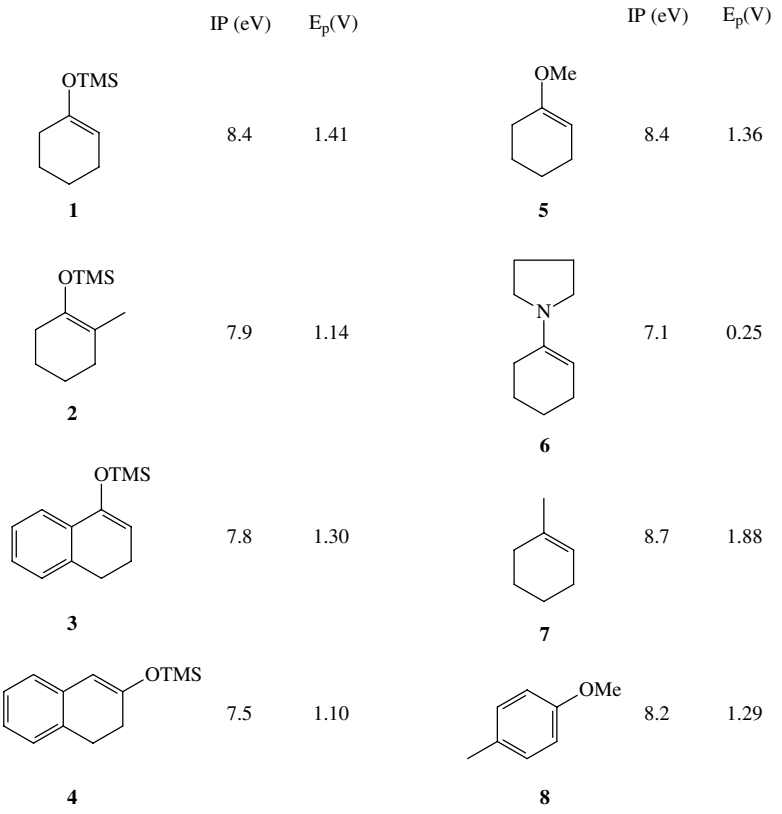

SCHEME 1 Ionization potentials (IP) and anodic potentials (E_p vs. SCE) of silyl enol ethers and related compounds.[9] (References for **6** (E_p),[10] **7**, **8** (IP),[11] **7** (E_p)[12] and **8** (E_p)[13]).

Silyl enol ethers such as **1** can be more easily oxidized than the corresponding alkenes, as seen in comparison with methyl-cyclohexene (**7**). In general, their electron donor properties are comparable to those of electron-rich arenes such as anisoles **8**, but are clearly lower than, for example, the heteroanalogue enamines, such as **6**. A significant change in the redox properties of silyl enol ethers can be achieved by increasing the degree of substitution at the double bond (as in **2**) or by incorporation of the double bond into a mesomeric system (as in **3** or **4**). In contrast, variation of the silyl group or changing to an alkyl enol ether does not significantly influence the oxidation potential (as seen with **5**).

Removal of an electron in solution can be accomplished in different ways, for example by use of chemical oxidants, electrochemical (anodic) oxidation, or photoinduced electron transfer (PET). However, oxidations involving chemical oxidants should be assessed carefully with respect to inner sphere oxidation mechanisms, which are known for several common metal ion oxidants.[14]

Although relatively short-lived, radical cations are the primary products of the electron transfer (ET) step. Evidence for the formation of radical cations has been presented for silyl enol ether systems that form stabilized radical cations. Kochi and coworkers investigated the photoinduced electron transfer between different silyl enol ethers and chloranil in detail.[15,16] In a system suitable for the spectroscopic study of the radical cation intermediate, chloranil (CA) is electronically excited to its triplet state ^{3}CA* (**10**). Subsequent electron transfer generates the corresponding radical ion pair (**11/12**). All these transient species have been observed by time-resolved spectroscopy.

Schmittel et al. investigated highly stabilized silyl enol ethers such as **13** by cyclic voltammetry (CV).[17] They found irreversible first oxidation potentials for their substances at low scan rates, which is consistent with findings for other silyl enol ethers and consistent with a mechanism including a fast follow-up

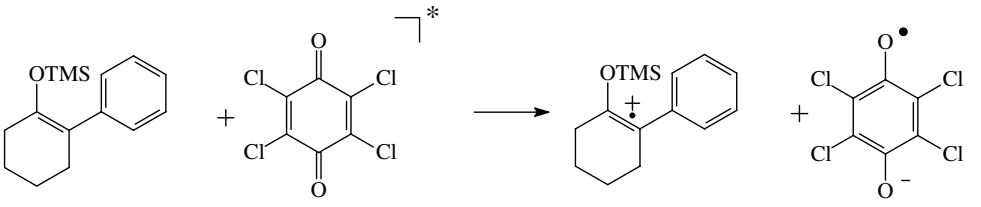

9 **10** **11** **12**

SCHEME 2 Formation of silyl enol ether radical cation **11** via electron transfer.

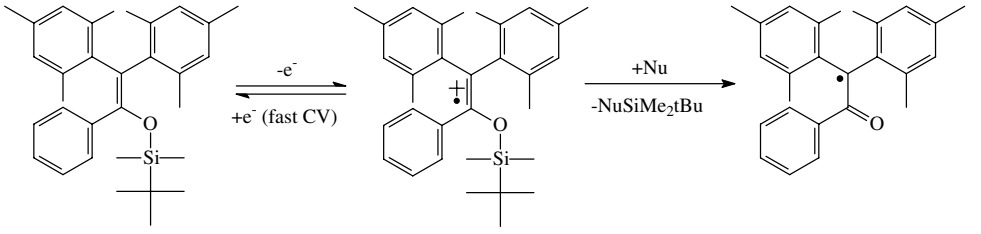

13 **14** **15**

SCHEME 3 Reversible oxidation of **13** vs. loss of the silyl cation.

reaction after electrochemical oxidation. In fast scan CV experiments (scan rates up to 2000 V sec^{-1}), they were able to reduce reversibly the generated radical cation **14**. The authors reported a strong solvent dependence on the conditions for reaching a reversible CV, indicating differences in the rate constants for the follow-up reactions. For example, in acetonitrile this reaction proceeded significantly faster than in dichloromethane, whereas addition of nucleophiles increased the rate constant for the process as well. These facts are interpreted as a nucleophile-assisted cleavage of the silicon–oxygen bond leading to the α-carbonyl radical **15**.

In PET reactions, the choice of solvent is crucial, but not only due to the possibility of SiO bond cleavage. Even the fate of the contact radical ion pair (CIP) formed by electron transfer is determined by the solvent applied (Scheme 4). Kochi and coworkers assigned different reaction pathways for the radical ion pair generated from excited chloranil (**10**) and the silyl enol ether **16** in dichloromethane and acetonitrile.[15,16] In the less polar solvent dichloromethane, the contact ion pair (**17,12**) decays to the radical pair (**18,19**) by interionic proton transfer. Oxidative elimination yields the enone **20** and tetrachlorohydroquinone-mono-trimethylsilyl ether (**21**).

A different reaction takes place with acetonitrile as solvent. The initially formed contact ion pair (**17,12**) undergoes diffusive separation to the corresponding solvent-separated ion pair (SSIP). The Si-O bond is cleaved by assistance of the nucleophilic solvent, and the resulting α-carbonyl radical **22** combines with the chloranil radical anion **12** to yield the final product **23**.

The two reaction channels described represent the most important steps following the generation of the initial radical cation and can be directly incorporated into synthetic applications involving silyl enol ether radical cations. Deprotonation of the radical cation is a way to conduct a ketone–enone transformation via the silyl enol ether. Other synthetic applications utilizing the radical cation or the α-carbonyl radical are coupling reactions of silyl enol ethers, intramolecular addition to double bonds, or introduction of substituents other than carbon at the α-carbonyl position, respectively. Examples for these synthetic transformations will be presented in the following sections.

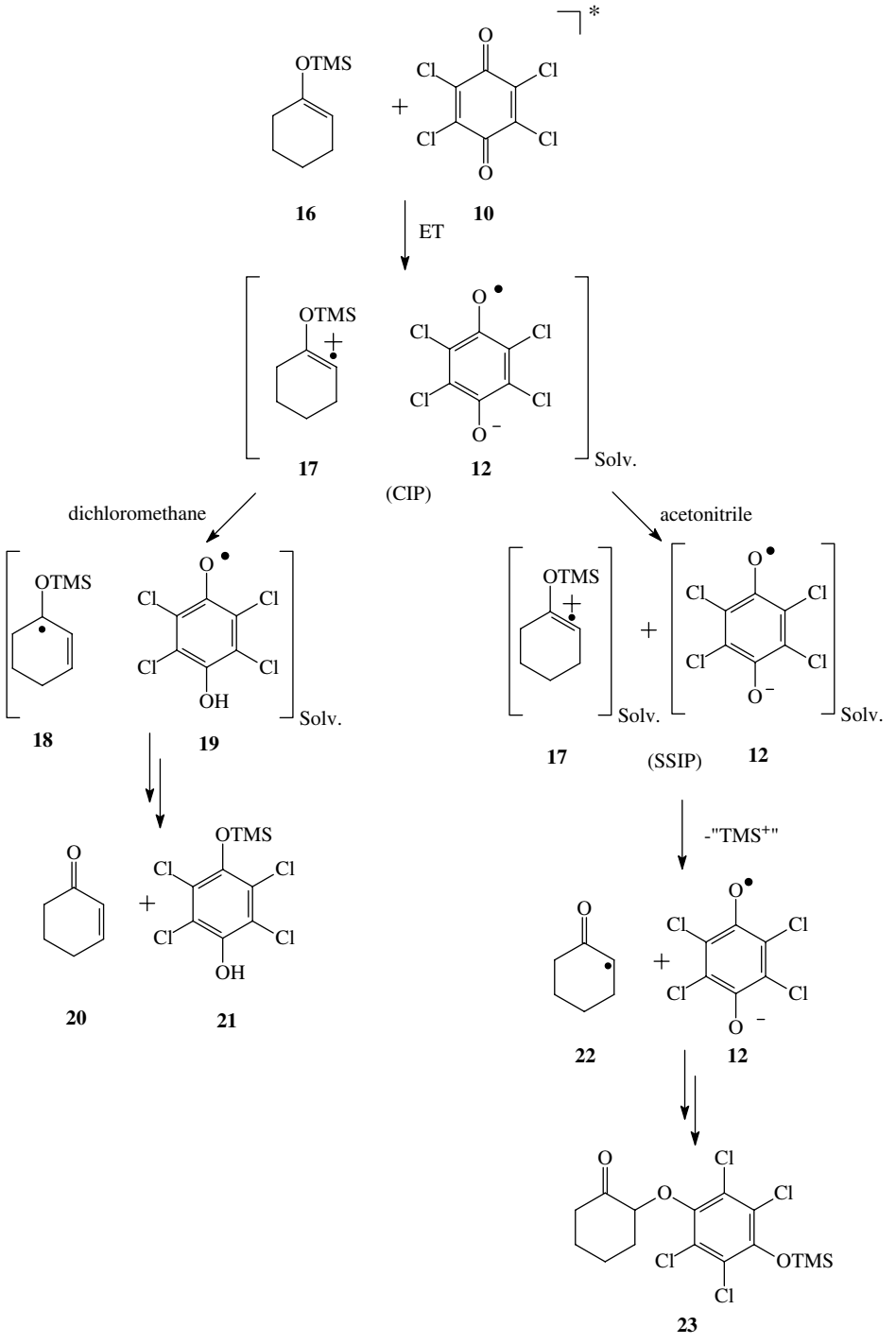

SCHEME 4 Different reaction pathways in dichloromethane and acetonitrile.

10.3 Transformation of Silyl Enol Ethers into Enones

The conversion of ketones to the corresponding α,β-unsaturated carbonyl compounds is an important transformation in organic synthesis. Methods utilizing the silyl enol ether became important because of

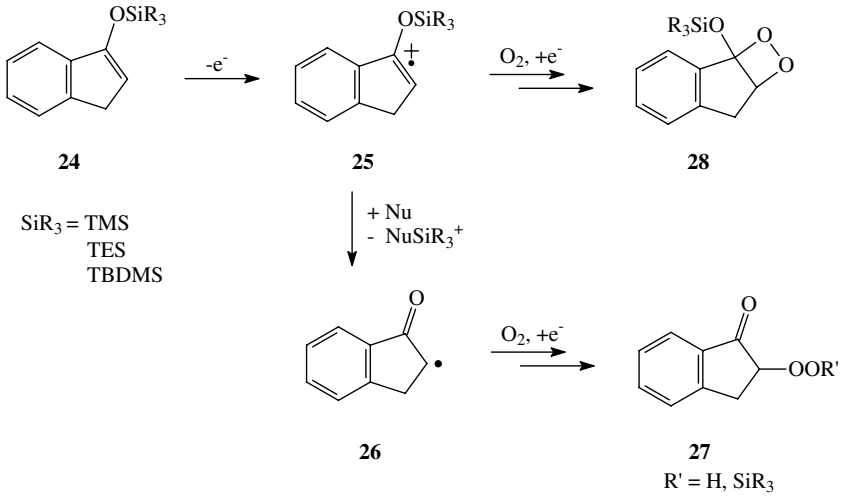

SCHEME 5 Photooxygenation of silyl enol ethers via radical cations.

the possibility of regioselective formation of the silyl enol ether and consequently the enone double bond. Several methods to conduct this transformation are available; procedures using singlet oxygen,[18] palladium catalysis,[19,20] or dichlorodicyanoquinone (DDQ)[21,22] have been described. The reaction mechanism involving quinones as oxidizing agent has been investigated by Kochi et al. (Scheme 4).[23] Recently, Nicolaou et al. presented an oxidation of silyl enol ethers by *o*-iodoxybenzoic acid (IBX), for which they also postulated an electron transfer as the key step.[24]

10.4 Introduction of Noncarbon Substituents at the α-Carbonyl Position

Before describing one of the most important synthetic aspects, i.e., the addition to carbon–carbon double bonds (see Sections 10.5 and 10.6), we will briefly discuss functionalization reactions leading to α-heterosubstituted carbonyl compounds. However, although several of the oxidation reactions of silyl enol ethers with oxygen-containing compounds lead to α-hydroxy-carbonyl compounds as α-carbonyl functionalization, radical cations are not involved in these reactions.[2–7]

Photooxygenations of silyl enol ethers via electron transfer oxidation have been investigated by Abe and coworkers.[25] They obtained two different oxidation products depending on the nucleophilicity of the solvent and the bulkiness of the silyl group. Using 9,10-dicyanoanthracene (DCA) as sensitizer and the silyl enol ethers **24** (TMS = trimethylsilyl, TES = triethylsilyl, TBDMS = *t*-butyldimethylsilyl) as starting material, they generated the corresponding radical cations **25**. Nucleophilic solvents and less sterically hindered silyl groups lead to products derived from the α-carbonyl radicals **26**, whereas less nucleophilic solvents underwent dioxetane (**28**) formation resulting from a postulated addition of oxygen to the radical cation. as shown in Scheme 5.

The simplest way of introducing a "functional group" at the α-carbonyl position is the addition of a hydrogen atom. Although there is no increase in molecular complexity, this is one of the most fundamental applications of PET-reactions involving silyl enol ethers. Gassman et al. showed that trimethylsilyl enol ethers **30** can be selectively deprotected in the presence of trimethylsilyl ethers by PET-induced cleavage of the SiO bond in a methanol/acetonitrile mixture (Scheme 6). Saturation of the resulting α-carbonyl radical leads to the formation of the final ketone **31**.[26]

Kochi and co-workers presented a synthesis of α–nitroketones involving silyl enol ether radical cations as key intermediates.[27] Remarkably, the reaction of silyl enol ethers with tetranitromethane yielded α-nitroketones under both thermal and photochemical conditions.

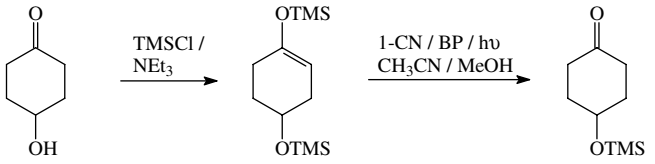

29 **30** **31**

SCHEME 6 ET-induced deprotection of silyl enol ethers.

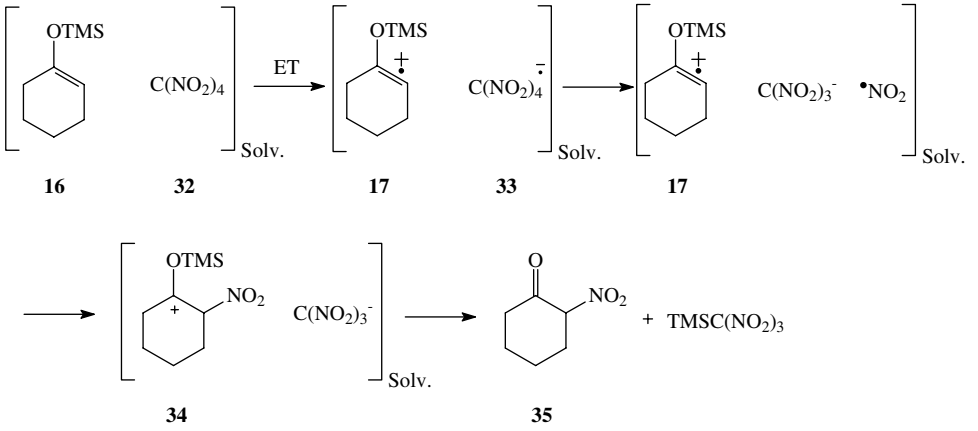

16 **32** **17** **33** **17** **34** **35**

SCHEME 7 α-Nitration of ketones.

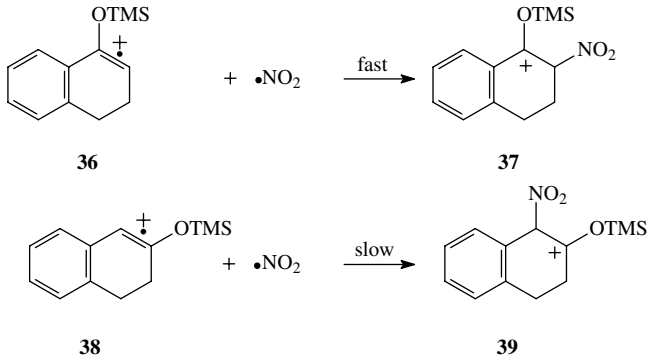

36 **37** **38** **39**

SCHEME 8 Stabilizing effects in tetralone based silyl enol ether radical cations.

The same authors also observed an interesting difference in the behavior of the α- and β-tetralone silyl enol ethers **3** and **4**, providing a further indication for the presence of radical ions as reactive intermediates in this reaction.[27] The α-tetralone silyl enol ether radical cation **36** reacted with nitrogen dioxide to form cation **37**, whereas the β-tetralone based radical cation **38** reacted much more slowly and gave a mixture of products (Scheme 8). Due to the mesomeric stabilization of the radical cation **38,** its lifetime increased dramatically as observed by time resolved spectroscopy. This favors a cage escape of the radical cation and opens the possibility for further reactions.

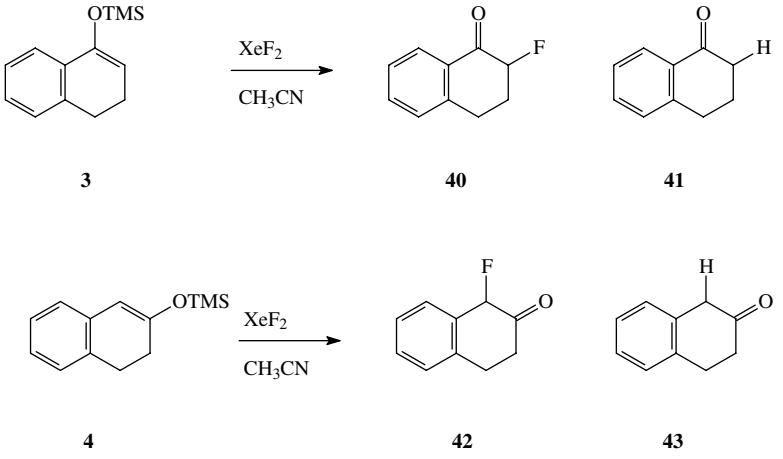

SCHEME 9 Fluorination of tetralone silyl enol ethers **3** and **4**.

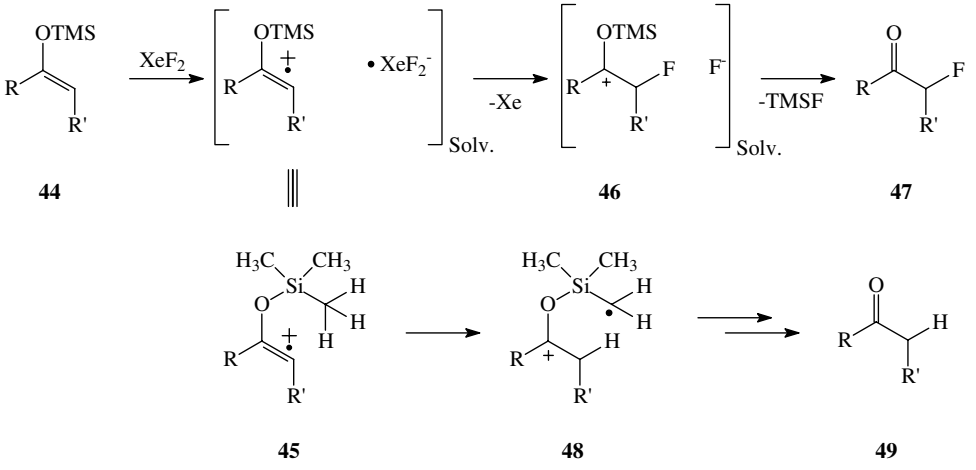

SCHEME 10 Mechanism of the reaction between silyl enol ethers and xenon difluoride.

Ramsden et al. have obtained similar results for tetralone silyl enol ether radical cations.[28] They investigated the reaction of various silyl enol ethers with xenon difluoride in acetonitrile and found a new method for the selective preparation of α-fluoroketones (Scheme 9).

The reaction of the α-tetralone silyl enol ether **3** with xenon difluoride gave fluoroketone **40** in a high yield of 90%. Ketone **41** was obtained as a byproduct in 4% yield. In contrast, the β-tetralone based silyl enol ether **4** formed fluoroketone **42** in 14% yield and ketone **43** as main product in 52% yield. The reaction mechanism proposed is shown in Scheme 10.

One electron oxidation of silyl enol ether **44** leads to the formation of a radical ion pair of **45** and the xenon difluoride radical anion. Subsequent transfer of a fluoride radical yields cation **46**, which reacts by loss of the trimethylsilyl cation to yield the fluoroketone **47**. The formation of ketone **49** is explained by a [1,5]-hydrogen migration from the trimethylsilyl group to the radical cationic moiety of **45**, leading to the formation of **48**.

The high yield of ketone **43** was based on a longer lifetime of the corresponding radical cation due to the stabilizing effect of the conjugated aromatic system. The increased lifetime allows a separation of the radical ions, and an intramolecular hydrogen abstraction becomes favored. This out-of-cage scenario

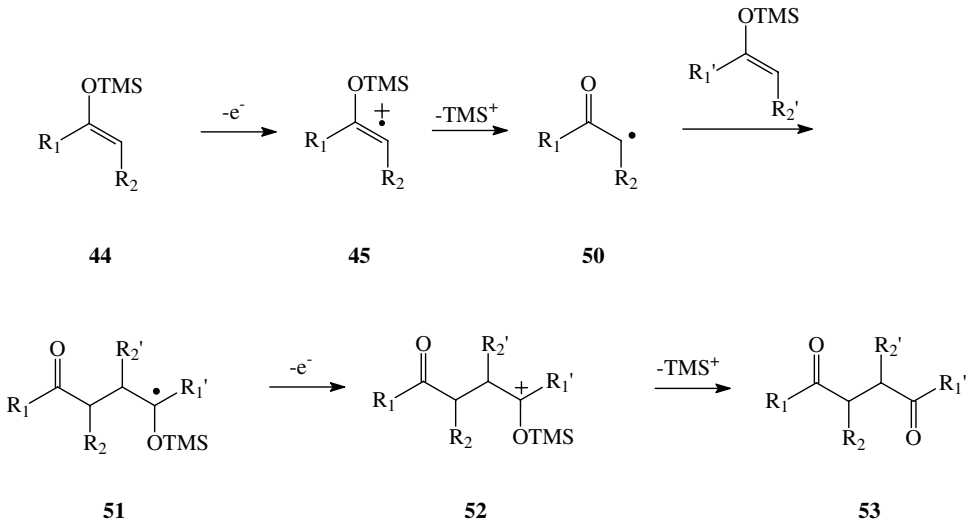

SCHEME 11 Coupling of silyl enol ether via radical cations.

also becomes obvious from the product composition. The combined yield of **42** and **43** is 66%, whereas the remaining 34% comprises products incorporating the solvent molecules.

10.5 Coupling Reactions of Silyl Enol Ethers

The general mechanistic scenario of the silyl enol ether coupling (**44**→**53**) can be described as formation of a silyl enol ether radical cation **45** and its corresponding α-carbonyl radical **50**, addition of this electrophile to a second silyl enol ether double bond, a second one electron oxidation of the intermediate radical **51,** and a final desilylation to **53** (Scheme 11). Ceric (IV) ammonium nitrate (CAN),[29,30] dichloro-ethoxy-oxyvanadium(V),[31] and dichloro(2,2,2-trifluoroethoxy)-oxovanadium(V)[32] have been applied as suitable one electron oxidants for the described transformation.

When identical silyl enol ethers are used in the coupling reaction ($R_1 = R_1'$, $R_2 = R_2'$), homocoupling to symmetrical 1,4-diketones can be achieved (Scheme 11).[31] For the synthesis of unsymmetrical 1,4-diketones, the two silyl enol ethers must differ significantly in terms of their oxidation potentials. This can be realized by selecting monosubstituted silyl enol ethers (R_2' = H) and 1,2-disubstituted silyl enol ethers for the coupling reaction.[29,31,32] Another possible way to reduce the oxidation potential is by the use of mesomeric stabilization (*vide supra*).[30] In the coupling reactions presented so far, the reactivity of silyl enol ethers is twofold. The component that is more easily oxidized forms the radical cation and consequently the α-carbonyl radical. In contrast, the second component acts as an electron-rich double bond in the radical addition reaction.

Electron-rich compounds with an oxidation potential lower than that of silyl enol ethers can be oxidized in the presence of silyl enol ethers, and in this case the silyl enol ether behaves as an electron-rich double bond. This strategy has been realized with enamines,[33] benzylsilanes,[34] organoselenium compounds,[35] and alkoxy-substituted arenes.[36]

Coupling reactions of silyl enol ether radical cations with double bonds other than silyl enol ethers have been investigated as well. Reactions with butadiene,[37] ethyl vinyl ether,[38] and allylic silanes[39] have been reported.

For the more important coupling reaction of silyl enol ethers, the Mukaiyama Aldol reaction, electron transfer reactions of silyl enol ethers have to be taken into account. As commonly used catalysts, transition metal complexes can be deactivated by electron transfer reduction, leading to a significant change in Lewis acidity as has been shown by Bosnich and co-workers.[40] Setsune et al. reported another connection

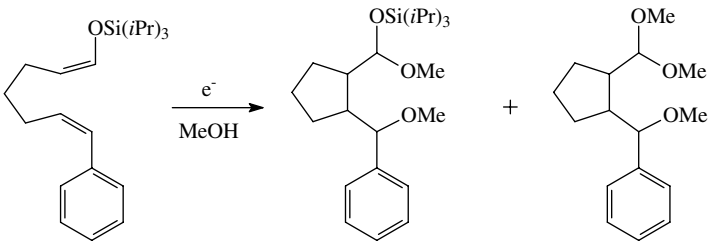

54 **55** **56**

SCHEME 12 Oxidative cyclization by anodic oxidation.

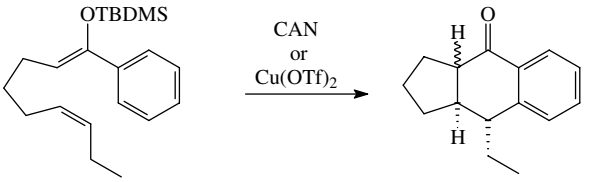

57 **58**

SCHEME 13 Oxidative cyclization by oxidation with metal salts.

between the Mukaiyama Aldol reaction and the electron transfer processes. They investigated PET catalysis of the Mukaiyama Aldol reaction using modified porphyrins.[41]

10.6 Intramolecular Addition of Silyl Enol Ether Radical Cations to Double Bonds

In this important area of silyl enol ether chemistry, similar transformations have been realized by transition metal catalysis; for example, silyl enol ethers carrying suitable olefinic side chains have been cyclized in the presence of palladium(II) complexes.[42,43]

Moeller and co-workers published the electron transfer cyclization of silyl enol ethers initiated by anodic oxidation.[44] The *in situ* generated radical cation of **54** intramolecularly attacks the double bond. The resulting benzylic radical position is further oxidized and attacked by a solvent molecule as well as the remaining cationic center to yield **55**. Cleavage of the SiO bond leads to the formation of **56** (Scheme 12).

Snider et al. investigated the oxidative cyclization of silyl enol ethers by use of CAN or cupric triflate.[45]

The transformation **57**→**58** includes two consecutive ring closure steps, two single electron oxidations, the desilylation step, and a deprotonation and can be regarded as a domino cyclization (Scheme 13).[46]

As can be seen from the reactions described so far, desilylation of the primary radical cation is a major pathway in silyl enol ether chemistry. Thus, it becomes important to know whether the reactive intermediate of the cyclization reaction is indeed the primary radical cation or its corresponding α-carbonyl radical. Curran et al. investigated the free radical atom transfer reaction of several α-iodo carbonyl compounds with hexabutylditin.[47] The reaction with **62** led to the formation of products resulting from both the 6-*endo* closed radical **63** and the 5-*exo* closed radical **64**. In contrast, the CAN-induced cyclization of **60** solely gave products resulting from a 6-*endo* ring closure reaction. In this context, Snider et al. proposed a reaction mechanism with the radical cation as the reactive key-intermediate in the cyclization step leading to exclusive 6-*endo* ring closure.[45]

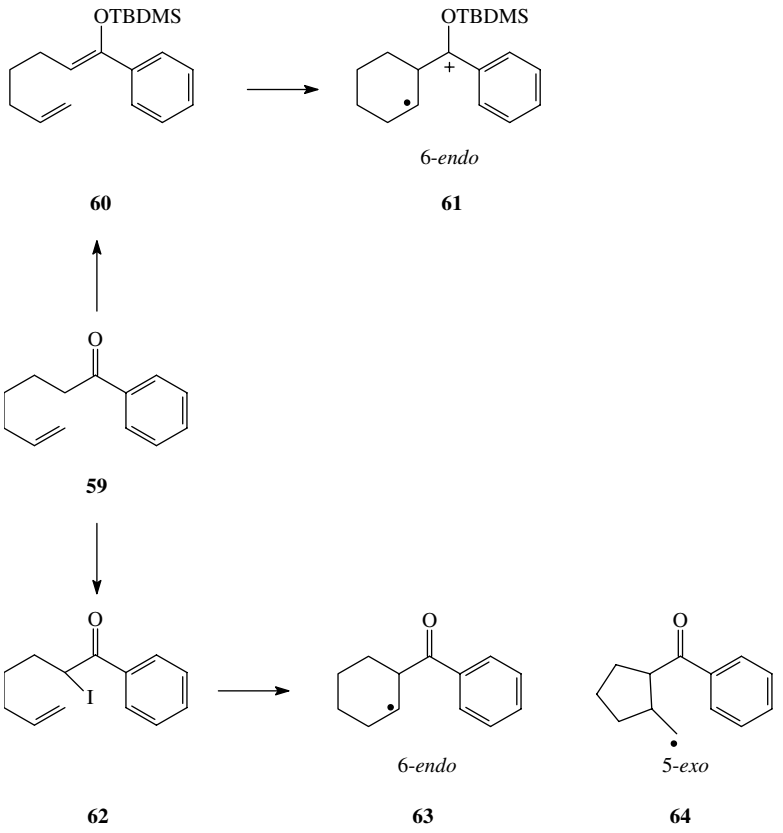

SCHEME 14 Comparison between radical and radical cationic ring closure selectivity.

The corresponding trimethylsilyl enol ether **65**, which is unstable under CAN oxidation conditions, has been successfully cyclized by Mattay and co-workers via PET with 9,10-dicyanoanthracene (DCA) as sensitizer (Scheme 15).[48] The selective formation of the 6-*endo* cyclization products was explained through the radical cation **66** as the reactive intermediate in the ring closure step. Loss of the trimethylsilyl cation is assumed to occur from radical cation **67** after cyclization. However, the source of the required hydrogen transfer step has not been clarified in detail.

The introduction of substituents at the olefinic double bond (as in **69**, **71**) leads to the stereoselective formation of the corresponding cyclization products **70** and **72**, respectively. The cyclization of the radical cation of **69** directly leads to the *trans* orientation of the substituents in **70**, whereas the high stereoselectivity in the formation of **72** results from a selective saturation of the intermediate radical moiety (Scheme 16).[48]

Analogous to the double cyclizations found by Snider and co-workers, a change to the bulkier triisopropylsilyl group as realized in **73** resulted in the additional formation of the tricyclic ketone **74** (Scheme 17).[45]

Introduction of an alkyne side chain (as in **75**), exclusively led to the formation of **76** via a double cyclization sequence (Scheme 18).[49]

A further extension of this work to silyl enol ethers derived from cyclic ketones not only confirmed the strong preference for the 6-*endo* ring closure, but additionally revealed a high diastereoselectivity shown in the exclusive formation of *cis*-junctions between the ring constructed in the cyclization and the ketone ring. Thus, this procedure can be seen as a useful tool for the construction of fused carbocycles (Scheme 19).[50]

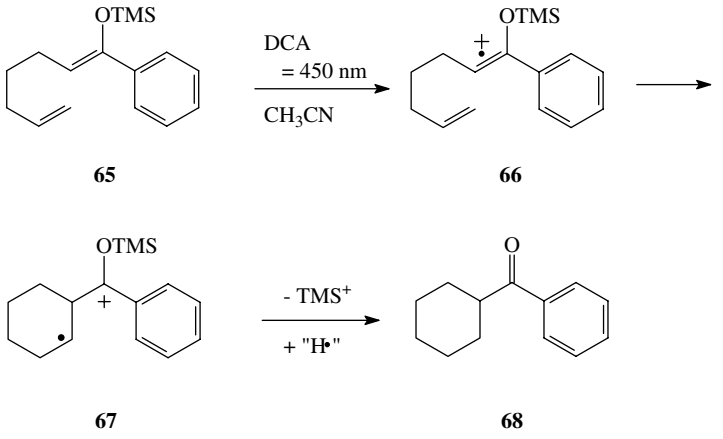

SCHEME 15 PET-induced cyclization of **65**.

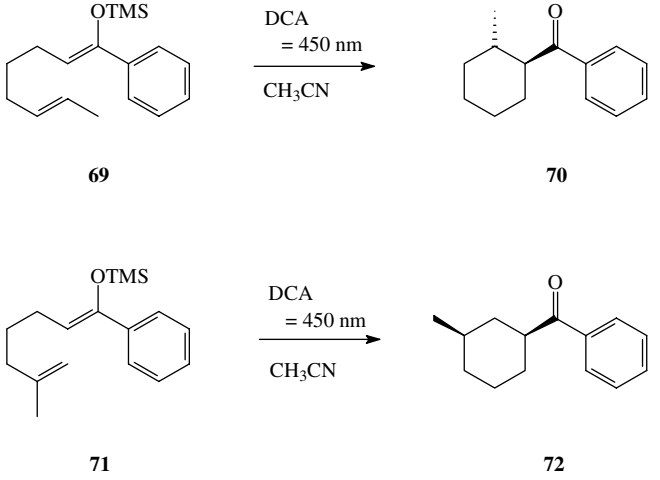

SCHEME 16 Introduction of substituents at the olefinic double bond.

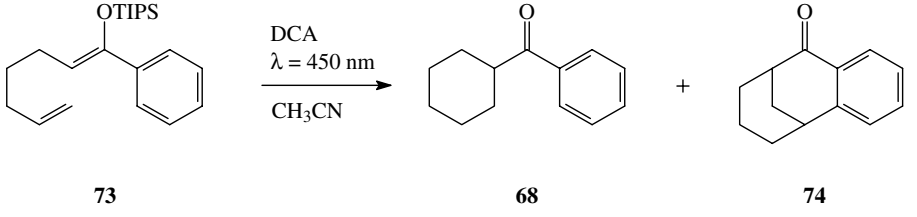

SCHEME 17 Double cyclization of **73**.

The silyl enol ether **83** represents an exception from the 6-*endo* cyclization rule. The reason for this differing behavior can be seen in the stability of the tertiary radical intermediate and the bulkiness of the trisubstituted double bond. The alkyne substituted silyl enol ether **85** resulted in the formation of the isomeric olefins **86** and **87** in a 1:1 ratio.

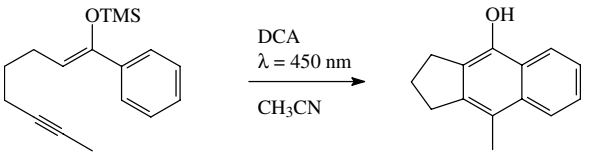

75 **76**

SCHEME 18 Double cyclization with alkyne side chain.

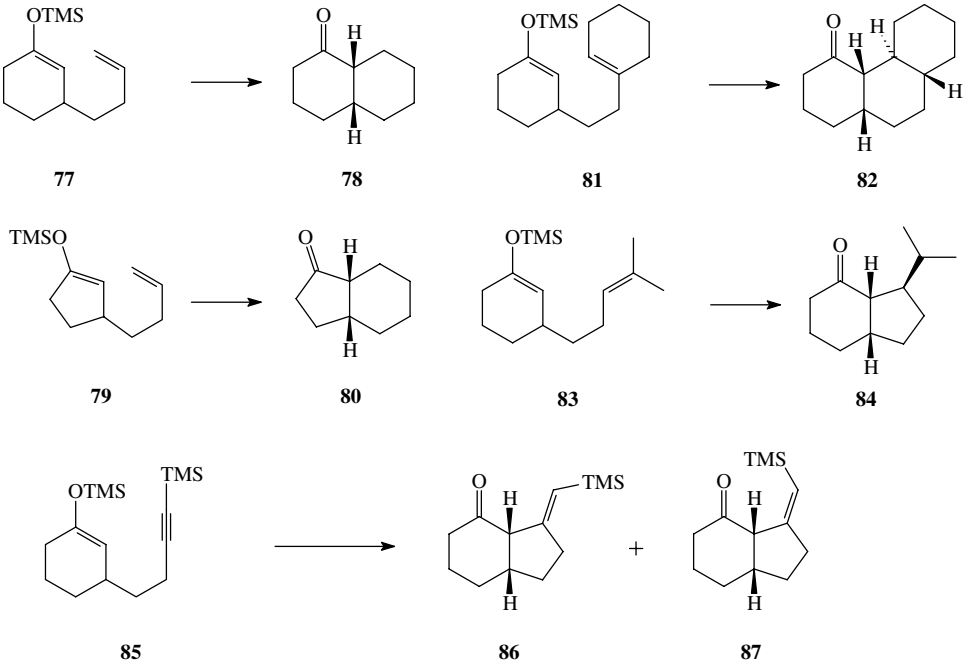

SCHEME 19 PET cyclizations in acetonitrile with DCA as sensitizer.

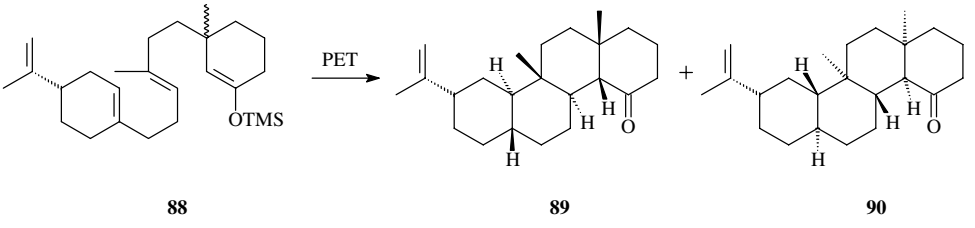

SCHEME 20 Cascade cyclization of silyl enol ether **88**.

In order to explore the scope and limitations of this reaction for the synthesis of complex carbocycles, the silyl enol ether **88** has been synthesized and efficiently cyclized in the anticipated way.[51] The cyclization reaction of **88** further revealed a remarkable stereoselectivity (Scheme 20). Besides a complete 6-*endo* selectivity, the five new stereogenic centers are built-up in an *anti:trans*-fashion, yielding solely one configuration of the bridgehead carbon atoms from the diastereomeric mixture of **88**.

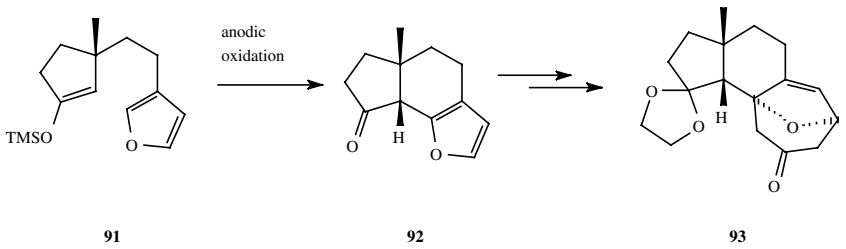

SCHEME 21 Synthesis of the cyathin skeleton **93**.

An elegant access to natural product synthesis was realized by Wright and co-workers, who obtained a *cis*-junction through the cyclization reaction of **91**.[52] The silyl enol ether **91** is electrochemically oxidized and subsequently cyclizes to yield compound **92**. In three further steps, the cyathin core **93** can be prepared.

Acknowledgments

Financial support of our own research was provided by the Ministerium für Schule, Wissenschaft und Forschung des Landes Nordrhein-Westfalen (MSWF-NRW), the Deutsche Forschungsgemeinschaft (DFG), the Fonds der Chemischen Industrie, the Volkswagen-Stiftung, the AG-Solar project of NRW, and the Innovationsfonds der Universität Bielefeld and is gratefully acknowledged. We also thank the state of Nordrhein-Westfalen for granting a predoctoral scholarship for J.O.B. and Michael Oelgemöller (Bayer CropScience K.K.) for his help in the preparation of the manuscript.

References

1. (a) Brownbridge, P., Silyl enol ethers in synthesis — Part I, *Synthesis*, 1, 1983; (b) Brownbridge, P., Silyl enol ethers in synthesis —Part II, *Synthesis*, 85, 1983; (c) Fleming, I., Barbero, A., and Walter, D., Stereochemical control in organic synthesis using silicon-containing compounds, *Chem. Rev.,* 97, 2063, 1997.
2. (a) Rubottom, G.M. and Lopez Nieves, M.I., The photosensitised singlet oxygen addition to a silyl enol ether, *Tetrahedron Lett.,* 24, 2423, 1972; (b) Friedrich, E. and Lutz, W., Sensibilisierte Photooxygenierung von Silylenolethern cyclischer Ketone, *Chem. Ber.,* 113, 1245, 1980.
3. (a) Sakaguchi, S., Yamamoto, Y., Sugimoto, T., Yamamoto, H., and Ishii, Y., Dehomologation of aldehydes via oxidative cleavage of silyl enol ethers with aqueous hydrogen peroxide catalysed by cetylpyridinium peroxotungstophosphate under two-phase conditions, *J. Org. Chem.,* 64, 5954, 1999; (b) Stankovic, S. and Espenson, J.H., Facile oxidation of silyl enol ethers with hydrogen peroxide catalysed by methyltrioxorhenium, *J. Org. Chem.,* 63, 4129, 1998; (c) Kaneda, K., Nobuyoshi, K., Jitsukawa, K., and Teranishi, S., Double bond cleavage reaction of silyl enol ethers using $MoO_2(acac)_2$-^{t}BuOOH, *Tetrahedron Lett.,* 22, 2595, 1981.
4. (a) Rubottom, G.M., Gruber, J.M., Boeckman, R.K., Jr., Ramaiah, M., and Medwid, J.B., Clarification of the mechanism of rearrangement of silyl enol ether epoxides, *Tetrahedron Lett.,* 19, 4603, 1978; (b) Zoretic, P.A., Wang, M., Zhang, Y., Shen, Z., and Ribeiro, A.A., Total synthesis of *d,l*-isospongiadiol: an intramolecular radical cascade approach to furanoditerpenes, *J. Org. Chem.,* 61, 1806, 1996; (c) Horiguchi, Y., Nakamura, E., and Kuwajima, I., Double hydroxylation of silyl enol ethers. A single-step synthesis of α, α′-dihydroxy ketones, *Tetrahedron Lett.,* 30, 3323, 1989.
5. Adam, W., Fell, R.T., Saha-Möller, C.R., and Zhao, C.-G., Synthesis of optically active α-hydroxy ketones by enantioselective oxidation of silyl enol ethers with a fructose-derived dioxirane, *Tetrahedron Assym.,* 9, 397, 1998.
6. McCormick, J.P., Tomasik, W., and Johnson, M.W., α-Hydroxylation of ketones: osmium tetroxide/*N*-methylmorpholine-*N*-oxide oxidation of silyl enol ethers, *Tetrahedron Lett.,* 22, 607, 1981.

7. Iwata, C., Takemoto, Y., Nakamura, A., and Imanishi, T., Oxidation of 2-trimethylsiloxy-1,3-dienes with triphenyl phosphite ozonide. A regioselective α′-hydroxylation of α,β-unsaturated ketones, *Tetrahedron Lett.,* 26, 3227, 1985.
8. Schmittel, M., Umpolung of ketones via enol radical cations, in *Topics in Current Chemistry,* Mattay, J., Ed., Springer-Verlag, Berlin, 1994, p. 169.
9. Rathore, R. and Kochi, J.K., Quantitative assessment of electron-donor properties of enol silyl ethers: charge-transfer complex formation, photoelectron spectra and transient electrochemical oxidation, *Tetrahedron Lett.,* 35, 8577, 1994.
10. Renaud, P. and Schubert, S., Radical reductive alkylation of enamines with chloromethyl *p*-tolyl sulfone, a chain radical process, *Angew. Chem. Int. Ed. Engl.,* 29, 433, 1990; *idem.,* Radikalische reduktive Alkylierung von Enaminen mit Chlormethyl-*p*-tolylsulfon, *Angew. Chem.,* 102, 416, 1990.
11. Baidin, V.N., Timoshenko, M.M., and Chizov, Y.V., Photoelectron spectra and the structure of organomercury compounds, *J. Organomet. Chem.,* 292, 55, 1985.
12. Patz, M., Mayr, H., Maruta, J., and Fukuzumi, S., Reactions of carbocations with π nucleophiles: polar mechanism and no outer sphere electron transfer processes, *Angew. Chem. Int. Ed. Engl.,* 34, 1225, 1995; *idem.,* Reaktionen von Carbokationen mit π-Nukleophilen: polarer Mechanismus statt Outersphere-Elektronentransfer, *Angew. Chem.,* 107, 1351, 1995.
13. Arisawa, M., Ramesh, N.G., Nakajima, M., Tohma, H., and Kita, Y., Hypervalent iodine(III)-induced intramolecular cyclization of α-(aryl)alkyl-β-dicarbonyl compounds: a convenient synthesis of benzannulated and spirobenzannulated compounds, *J. Org. Chem.,* 66, 59, 2001.
14. Eberson, L., Reaction between organic and metal ion species, in *Electron Transfer Reactions in Organic Chemistry,* Reactivity and Structure, Vol. 25, Hafner, K., Lehn, J.-M., Rees, C.W., von Ragué-Schleyer, P., Trost, B.M., and Zahradnik, R., Eds., Springer-Verlag, Berlin, 1987, chap. 7.
15. Bockman, T.M., Shukla, D., and Kochi, J.K., Photoinduced electron transfer from enol silyl ethers to quinone. Part 1. Pronounced effects of solvent polarity and added salt on the formation of α-enones, *J. Chem. Soc., Perkin Trans. 2,* 1623, 1996.
16. Bockman, T.M. and Kochi, J.K., Photoinduced electron transfer from enol silyl ethers to quinone. Part 2. Direct observation of ion-pair dynamics by time-resolved spectroscopy, *J. Chem. Soc., Perkin Trans. 2,* 1633, 1996.
17. Schmittel, M., Keller, M., and Burghart, A., Silyl enol ether cation radicals in solution: nucleophile assisted Si-O bond cleavage, *J. Chem. Soc., Perkin Trans. 2,* 2327, 1995.
18. Friedrich, E. and Lutz, W., Synthesis of chiral α,β-unsaturated cyclic ketones by sensitized photooxidation of silylenol ethers, *Angew. Chem. Int. Ed. Engl.,* 16, 413, 1977; *idem.,* Synthese chiraler α,β-ungesättigter cyclischer Ketone durch sensibilisierte Photooxidation von Silylenolethern, *Angew. Chem.,* 89, 426, 1977.
19. Ito, Y., Hirao, T., and Saegusa, T., Synthesis of α,β-unsaturated carbonyl compounds by palladium(II)-catalyzed dehydrosilylation of silyl enol ethers, *J. Org. Chem.,* 43, 1011, 1978.
20. Larock, R.C., Hightower, T.R., Kraus, G.A., Hahn, P., and Zheng, D., A simple, effective, new, palladium-catalyzed conversion of enol silanes to enones end enals, *Tetrahedron Lett.,* 36, 2423, 1995.
21. Ryu, I., Murai, S., Hatayama, Y., and Sonoda, N., A ketone–enone conversion via the reaction of silyl enol ethers with DDQ, *Tetrahedron Lett.,* 37, 3455, 1978.
22. Fleming, I. and Paterson, I., A simple synthesis of carvone using silyl enol ethers, *Synthesis,* 736, 1979.
23. Bockman, T.M., Perrier, S., and Kochi, J.K., Dehydrosilylation versus α-coupling in the electron-transfer of silyl enol ethers to quinones. Strong effect on photogenerated ion pairs, *J. Chem. Soc., Perkin Trans. 2,* 595, 1993.
24. Nicolaou, K.C., Gray, D.L.F., Montagnon, T., and Harrison, S.T., Oxidation of silyl enol ethers by using IBX and IBX·*N*-oxide complexes: a mild and selective reaction for the synthesis of enones, *Angew. Chem. Int. Ed. Engl.,* 41, 996, 2002; *idem., Angew. Chem.,* 114, 1038, 2002.
25. Einaga, H., Nojima, M., and Abe, M., Photooxygenation (*electron transfer*) of silyl enol ethers derived from 1-indanone: silyl group and medium effects on the competitive formation of 3-siloxy-1,2-dioxetane and α-peroxy ketone, *Main Group Metal Chem.,* 22, 539, 1999.

26. Gassman, P.G. and Bottorf, K.J., Electron transfer induced desilylation of trimethylsilyl enol ethers, *J. Org. Chem.,* 53, 1097, 1988.
27. Rathore, R. and Kochi, J.K., α-Nitration of ketones via enol silyl ethers. Radical cations as reactive intermediates in thermal and photochemical processes, *J. Org. Chem.,* 61, 627, 1996.
28. Ramsden, C.A. and Smith, R., Reaction of silyl enol ethers with xenon difluoride in MeCN: evidence for a nonclassical radical cation intermediate, *Org. Lett.,* 1, 1591, 1999.
29. Baciocchi, E., Casu, A., and Ruzziconi, R., Synthesis of unsymmetrical 1,4-diketones by the ceric ammonium nitrate promoted cross-coupling of trimethylsilyl enol ethers, *Tetrahedron Lett.,* 30, 3707, 1989.
30. Belli Paolobelli, A., Latini, D., and Ruzziconi, R., γ-Selectivity in the ceric ammonium nitrate promoted oxidative addition of silyl dienol ethers to silyl enol ethers, *Tetrahedron Lett.,* 34, 721, 1993.
31. Fujii, T., Hirao, T., and Ohshiro, Y., Oxovanadium-induced oxidative desilylation for the selective synthesis of 1,4-diketones, *Tetrahedron Lett.,* 33, 5823, 1992.
32. Ryter, K. and Livinghouse, T., Dichloro(2,2,2-trifluoroethoxy)oxovanadium(V). A remarkably effective reagent for promoting one-electron oxidative cyclization and unsymmetrical coupling of silyl enol ethers, *J. Am. Chem. Soc.,* 120, 2658, 1998.
33. Narasaka, K., Okauchi, T., Tanaka, K., and Murakami, M., Generation of cation radicals from enamines and their reactions with olefins, *Chem. Lett.,* 2099, 1992.
34. Hirao, T., Fujii, T., and Ohshiro, Y., Selective cross coupling via oxovanadium(V)-induced oxidative desilylation of benzylic silanes, *Tetrahedron Lett.,* 35, 8005, 1994.
35. Pandey, G. and Sochanchingwung, R., Photoinduced electron transfer (PET) promoted cross coupling of organoselenium and organosilicon compounds: a new carbon–carbon bond formation strategy, *J. Chem. Soc., Chem. Commun.,* 1945, 1994.
36. (a) Pandey, G., Krishna, A., Girija, K., and Karthikeyan, M., Intramolecular addition of silylenol ether to photosensitised electron transfer (PET) generated arene radical cations: a novel non-reagent based carboannulation reaction, *Tetrahedron Lett.,* 34, 6631, 1993; (b) Pandey, G., Karthikeyan, M., and Murugan, A., New intramolecular α-arylation strategy of ketones by the reaction of silyl enol ethers to photosensitised electron transfer generated arene radical cations: construction of benzospiroannulated compounds, *J. Org. Chem.,* 63, 2867, 1998; (c) Pandey, G., Murugan, A., and Balakrishnan, M., A new strategy towards the total synthesis of phenanthridone alkaloids: synthesis of (+)-2,7-dideoxypancratistatin as a model study, *J. Chem. Soc., Chem. Commun.,* 624, 2002.
37. Belli Paolobelli, A., Seccherelli, P., Pizzo, F., and Ruzziconi, R., Regio- and stereoselective synthesis of unsaturated carbonyl compounds based on ceric ammonium nitrate–promoted oxidative addition of trimethylsilyl enol ethers to conjugated dienes, *J. Org. Chem.,* 60, 4954, 1995.
38. (a) Baciocchi, E., Casu, A., and Ruzziconi, R., Synthesis of 4-oxoaldehydes by the ceric ammonium nitrate promoted oxidative addition of trimethylsilyl enol ethers to ethyl vinyl ether, *Synlett,* 679, 1990; (b) Lupattelli, P., Ruzziconi, R., Scafato, P., Alunni, S., and Belli Paolobelli, A., A new synthetic approach to substituted 1(2*H*)-phenanthrenones based on the ceric ammonium nitrate-promoted oxidative addition of 3-aryl-1-[(trimethylsilyl)oxy]-cyclohexenes to ethyl vinyl ether, *J. Org. Chem.,* 63, 4506, 1998; (c) Belli Paolobelli, A., Ruzziconi, R., Lupatelli, P., Scafato, P., and Spezzacatena, C., A facile access to polycyclic homo- and heteroaromatic hydrocarbons based on the ceric ammonium nitrate–promoted oxidative addition of 3-aryl-1-[(trimethylsilyl)oxy]cyclohexenes to ethyl vinyl ether, *J. Org. Chem.,* 64, 3364, 1999; (d) Gourvès, J.-P., Ruzziconi, R., and Vilarroig, L., Oxidative coupling of *O*-silyl and *O*-alkyl eneethers: application of the novel annulation sequence to the synthesis of fluorinated naphthaldehydes and naphthyl ketones, *J. Org. Chem.,* 66, 617, 2001.
39. Hirao, T., Fujii, T., and Ohshiro, Y., Versatile desilylative cross-coupling of silyl enol ethers and allylic silanes via oxovanadium-induced chemoselective one-electron oxidation, *Tetrahedron,* 50, 10207, 1994.

40. Odenkirk, W., Whelan, J., and Bosnich, B., Homogeneous catalysis. A transition metal based catalyst for the Mukaiyama crossed-aldol reaction and catalyst deactivation by electron transfer, *Tetrahedron Lett.,* 33, 5729, 1992.
41. Wada, K., Yamamoto, M., and Setsune, J., Photosensitized electron transfer catalysis of the Mukaiyama aldol reaction by monocationic N^{21},N^{22}-bridged porphyrins, *Tetrahedron Lett.,* 40, 2773, 1999.
42. (a) Ito, Y., Aoyama, H., Hirao, T., Mochizuki, A., and Saegusa, T., Cyclization reactions via oxo-π-allylpalladium(II) intermediates, *J. Am. Chem. Soc.,* 101, 494, 1979; (b) Ito, Y., Aoyama, H., and Saegusa, T., Palladium(II)-promoted cyclizations of olefinic silyl enol ethers. Preparations of σ-(1-substituted 3-oxocyclopentyl)methylpalladium(II) complexes and their oxidative rearrangements, *J. Am. Chem. Soc.,* 102, 4519, 1980.
43. (a) Kende, A.S., Roth, B., and Sanfilippo, P.J., Facile, palladium(II)-mediated synthesis of bridged and spirocyclic bicycloalkenones, *J. Am. Chem. Soc.,* 104, 1784, 1982; (b) Kende A.S., Roth, B., Sanfilippo, P.J., and Blacklock, T.J., Mechanism and regioisomeric control in palladium(II)-mediated cycloalkenylations. A novel total synthesis of (±)-quadrone, *J. Am. Chem. Soc.,* 104, 5808, 1982.
44. (a) Moeller, K.D., Marzabadi, M.R., New, D.G., Chiang, M.Y., and Keith, S., Oxidative organic electrochemistry: a novel intramolecular coupling of electron-rich olefins, *J. Am. Chem. Soc.,* 112, 6123, 1990; (b) Hudson, C.M., Marzabadi, M.R., Moeller, K.D., and New, D.G., Intramolecular anodic olefin coupling reactions: a useful method for carbon–carbon bond formation, *J. Am. Chem. Soc.,* 113, 7372, 1991.
45. (a) Snider, B.B. and Kwon, T., Oxidative cyclization of δ,ε- and ε,ζ-unsaturated enol silyl ethers, *J. Org. Chem.,* 55, 4786, 1990; (b) Snider, B.B. and Kwon, T., Oxidative cyclization of δ,ε- and ε,ζ-unsaturated enol silyl ethers and unsaturated siloxycyclopropanes, *J. Org. Chem.,* 57, 2399, 1992.
46. (a) McCarroll, A.J. and Walton, J.C., Programming organic molecules: design and management of organic syntheses through free-radical cascade processes, *Angew. Chem. Int. Ed. Engl.,* 40, 2224, 2001; *idem.,* Programmierung organischer Meloküle: Design und Management organischer Synthesen über radikalische Kaskaden, *Angew. Chem.,* 113, 2282, 2001; (b) Tietze, L.F., Domino reactions in organic synthesis, *Chem. Rev.,* 96, 115, 1996; (c) Malacria, M., Selective preparation of complex polycyclic molecules from acyclic precursors via radical mediated- or transition metal-catalyzed cascade reactions, *Chem. Rev.,* 96, 289, 1996.
47. Curran, D.P. and Chang, C.-T., Atom transfer cyclization reactions of α-iodo esters, ketones and malonates: examples of selective 5-exo, 6-endo, 6-exo and 7-endo ring closures, *J. Org. Chem.,* 54, 3140, 1989.
48. (a) Heidbreder, A. and Mattay, J., PET-Oxidative cyclization of unsaturated enol silyl ethers, *Tetrahedron Lett.,* 33, 1973, 1992; (b) Ackermann, L., Heidbreder, A., Wurche, F., Klärner, F.-G., and Mattay, J., Mechanistic studies on PET-oxidative cyclization of unsaturated silyl enol ethers: Dependence of the regioselectivity on alcohol addition and pressure effects, *J. Chem. Soc., Perkin Trans. 2,* 863, 1999.
49. (a) Heidbreder, A. and Mattay, J., PET-Oxidative cyclization of unsaturated enol silyl ethers, *J. Inf. Rec. Mats.,* 21, 575, 1994; (b) Heidbreder, A., Cyclisierungsreaktionen nichtkonjugiert-ungesättigter Silylenolether durch photoinduzierten Elektronentransfer, Ph.D. thesis, University of Münster, 1994.
50. (a) Hintz, S., Fröhlich, R., and Mattay, J., PET-Oxidative cyclization of unsaturated silyl enol ethers. Regioselective control by solvent effects, *Tetrahedron Lett.,* 37, 7349, 1996; (b) Hintz, S., Mattay, J., van Eldik, R., and Fu, W.-F., Regio- and stereoselective cyclization reactions of unsaturated silyl enol ethers by photoinduced electron transfer — mechanistic aspects and synthetic approach, *Eur. J. Org. Chem.,* 1583, 1998.
51. Bunte, J.O., Rinne, S., Schäfer, C., Neumann, B., Stammler, H.-G., and Mattay, J., Synthesis and PET oxidative cyclization of silyl enol ethers: build-up of steroidal carbocycles, *Tetrahedron Lett.,* 44, 45, 2003.
52. Wright, D.L., Whitehead, C.R., Sessions, E.H., Ghiviriga, I., and Frey, D.A., Studies on inducers of nerve growth factor: synthesis of the cyathin core, *Org. Lett.,* 1, 1535, 1999.

11

C–X Bond Fission in Alkene Systems

Tsugio Kitamura
Saga University

11.1 Introduction

This chapter describes the photochemical C-X bond fission in alkene systems that have halogen atoms bonded to the carbon–carbon double bond. The substitution of halogen atoms in alkenes results in a red shift of the π,π^* absorption band because of the interaction between the lone pair on the halogen atom and the π-orbitals.[1,2] However, the UV absorption of aliphatic alkenyl halides, except for the iodides, lies in a region of short wavelength less than 254 nm (Table 11.1). Therefore, the majority of the alkenyl halides studied in these photolyses are the iodides.

Introduction of aromatic substituents to the carbon–carbon double bond leads to considerable π-conjugation causing the absorption to move to longer wavelength (>254 nm) with a concomitant increase in the extinction coefficient. 1,2-Diaryl- and triarylvinylhalides, including the bromides and chlorides, have absorptions at wavelengths around 300 nm. Therefore, these systems have been used mostly for synthetic applications because the secondary photochemical reactions can be eliminated by the use of a suitable filter.

The excitation energy obtained by absorption of light is consumed chemically by isomerization, extrusion of small molecules, and bond fission. In this chapter, the bond fission aimed at synthetic application is discussed. The ease of bond fission is proportional to the bond strength of the C-X bond. As shown in Table 11.2, the bond strength of the C-X bond in alkenyl halides is much higher than that of alkyl halides and is intermediate between those of the corresponding ethyl and phenyl halides. The C-X bond increases in strength in the order: I < Br < Cl < F. The bond dissociation energy of vinyl fluoride (479 kJ mol^{-1}) is higher than the energy of the light from low-pressure Hg lamps (254.7 nm = 472 kJ per Einstein) and accordingly, the direct photochemical cleavage of a carbon–fluorine bond is extremely rare.

11.2 Mechanism for C-X Bond Fission in Alkene Systems

Previously, Sammes[2] and Lodder[18] have reviewed the photochemistry of the carbon–halogen bond. Photolysis of alkenyl halides is well known, but little attention has been paid to the synthetic applications.

0-8493-1348-1/04/$0.00+$1.50

TABLE 11.1 UV Properties of Alkenyl Halides

Compound	λ_{max}, nm (log ε)	Solvent	Ref.
1-Chlorocyclohexene	200 (3.64)	EtOH	3
1-Bromocyclohexene	207.3 (3.65)	95% EtOH	4
1-Iodocycloheptene	263 (2.55)	EtOH	3
E-4-Iodo-3-heptene	249 (~2.60)	—	5
N-[*E*-(2-Iodoacryloyl)]-2,6-dimethylpyrolidine	249 (4.06)	95% EtOH	6
E-β-Bromostyrene	257 (~4.04)	95% EtOH	7
1-Fluoro-2,2-diphenylethene	244 (4.07)	Cyclohexane	8
1-Chloro-2,2-diphenylethene	255 (4.10)	95% EtOH	9
1-Bromo-2,2-diphenylethene	259 (4.12)	95% EtOH	9
1-Iodo-2,2-diphenylethene	263 (4.15)	95% EtOH	9
1-Bromo-2,2-bis(*p*-methoxyphenyl)ethene	212 (4.54), 252 (4.32), 270 (4.27)	MeOH	10
E-1-Bromo-1,2-diphenylethene	260 (4.0), 300sh (3.7)	MeOH	11
Z-1-Bromo-1,2-diphenylethene	285 (4.2)	MeOH	11
1-Bromo-1,2,2-triphenylethene	231 (4.3), 295 (5.0)	EtOH	12
1-Bromo-1-(*p*-methoxyphenyl)-2,2-diphenylethene	239 (4.34), 302 (4.06)	Cyclohexane	13
1-Bromo-1,2,2-tris(*p*-methoxyphenyl)ethene	249 (4.36), 310.5 (4.11)	Cyclohexane	13
1-Bromo-1-[*p*-(2-hydorxyethoxy)phenyl]-2,2-diphenylethene	213 (4.36), 239 (4.27), 301 (4.01)	EtOH	14
1-Bromo-2,2-bis(*o*-methoxyphenyl)-1-phenylethene	284 (4.02)	Cyclohexane	15

TABLE 11.2 Comparison of Bond Dissociation Energies of the C–X Bond among Ethyl, Vinyl, and Phenyl Halides

Ethyl halide[16]	D (C–X) (kJ mol^{-1})	Vinyl halide[17]	D (C–X) (kJ mol^{-1})	Phenyl Halide[16]	D (C–X) (kJ mol^{-1})
CH_3CH_2–F	452	CH_2=CH–F	497	Ph–F	527
CH_3CH_2–Cl	335	CH_2=CH–Cl	372	Ph–Cl	402
CH_3CH_2–Br	285	CH_2=CH–Br	320	Ph–Br	339
CH_3CH_2–I	222	CH_2=CH–I	260	Ph–I	272

One advantage for synthetic application of alkenyl halide photochemistry is that the reactions that alkenyl halides undergo allow for the introduction of a C-C double bond into the product molecule.

The well-known principal example in solution is the homolysis of the C-X bond, affording a radical pair composed of a vinyl radical and a halogen atom, as represented by the photolysis of alkenyl iodides (Equation 11.1).[2]

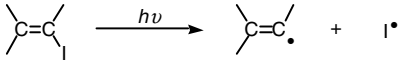

(11.1)

The main reaction of the vinyl radical is abstraction of a hydrogen or halogen atom. The dimerization of the vinyl radical is extremely rare because of its high reactivity.

A novel aspect of the photochemical behavior of alkenyl halides is the generation of vinyl cations.[18,19] The detailed mechanism of the formation of the vinyl cations has not yet been fully established. Two possible paths for cation formation have been postulated:

1. Homolytic cleavage of the C-X bond and subsequent electron transfer within the radical pair[20–23]
2. Direct heterolysis of the C-X bond[24] (Equation 11.2)

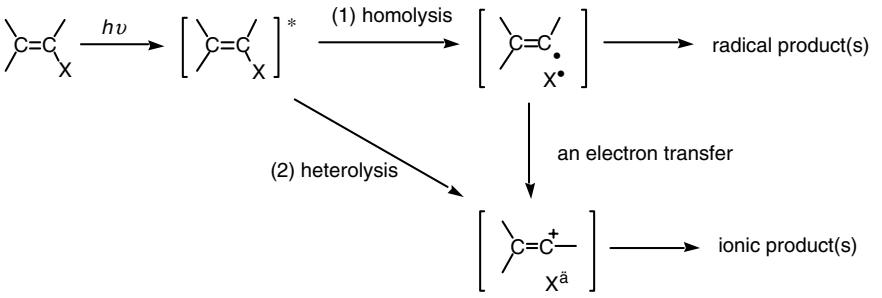

(11.2)

Recent studies by laser-flash photolysis showed that vinyl cations are formed quite rapidly after excitation of alkenyl halides, suggesting that photolysis of aromatic alkenyl halides induces both heterolysis and homolysis of the C-X bond. The synthetically interesting and useful characteristics of these processes are:

1. The generation of unstable vinyl cations, e.g., α-unsubstituted or cyclic vinyl cations
2. The mild reaction conditions
3. The use of aprotic solvents or less polar solvents

The reactions that the vinyl cations can undergo are nucleophilic substitution and rearrangement, similar to those of solvolytically generated vinyl cations[25] (Equation 11.3). The photolysis procedures have the advantage that they can be applied to a wide variety of substrates.

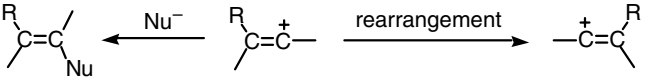

(11.3)

Some general rules can be used to predict the outcome of irradiation of alkenyl halides. Thus, the photolysis of α-arylvinylhalides leads to stable α-arylvinyl cations, and the vinyl cation route is followed predominantly. A nucleophilic reagent can capture such intermediates. Conversely, in the cases that produce unstable vinyl cations, vinyl radicals are formed preferentially, or else the formation of radical and cation intermediates competes. Clearly, the nature of the substituent is important in predicting the reactions of the vinyl cations. Results indicate that the nucleophilic trapping of the vinyl cations follows the order:[26] H << alkyl << Ph < *p*-MeC_6H_4 < *p*-$MeOC_6H_4$. The halogen employed is also important, with chlorides and bromides better than iodides at undergoing fission. Fluorides, as mentioned previously, are inactive in photolysis.[27a] In aliphatic alkenyl halides,[3] conversely, iodides afford ionic intermediates more preferentially than do bromides or chlorides. However, capture by nucleophiles is restricted to the nucleophilic solvent employed.

11.3 Synthetic Applications

Reduction: Abstraction of a Hydrogen Atom

As described above, synthetic applications using alkenyl halides are divided into two classes: radical and ionic reactions. The most common reaction of the alkenyl radical is abstraction of a hydrogen atom.[5] Although this reaction is useful for reduction of organic halides, its synthetic usefulness is low since most alkenyl halides are prepared from the corresponding alkenes, and replacement of the halogen by hydrogen simply reforms the starting material. However, deuteration can be carried out successfully by the photochemical reaction. Several alkenyl bromides and chlorides are transformed to the deuterated alkenes in good to high yields (Equation 11.4 and Equation 11.5).[27] An interesting feature of this deuteration is

that only the site to which the halogen is attached is deuterated. This procedure can also be applied effectively to aryl halides.[27]

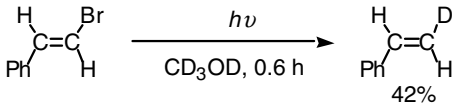

(11.4)

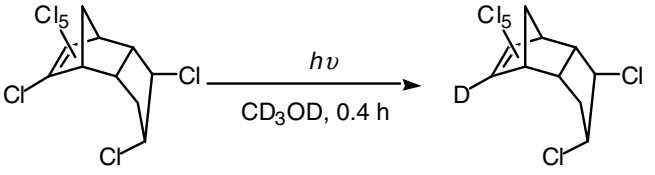

(11.5)

Other interesting reactions involve the photolysis of β-iodoacrylamides (Equation 11.6), which brings about an intramolecular hydrogen abstraction and subsequent dealkylation, i.e., ring opening of the amine moiety.[6]

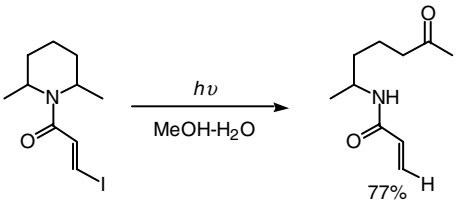

(11.6)

Intramolecular Cyclization

Intramolecular cyclization by radicals is one of the strategies used to synthesize cyclic compounds or heterocycles. One such example is the intramolecular attack of vinyl radicals at sulfur, which is reported to be an efficient synthesis of benzo[b]thiophenes[21g,28] (Equation 11.7).

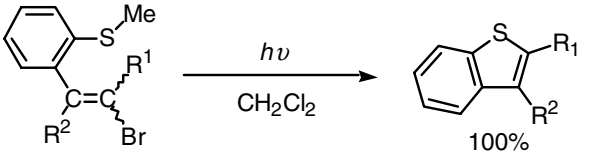

R^1, R^2 = H, Me, Ph

(11.7)

Dimerization

Tadros et al.[29] reported the dimerization of 1-bromo-2,2-bis(*p*-methoxyphenyl)ethene in acetic acid under sunlight irradiation. However, recent reports concerning this type of compound, 1,1-diaryl-2-haloethenes,[21a,b,g,22a,b] present a more complex reaction system with several processes taking place such as hydrogen abstraction, rearrangement, dimerization, and capture of the solvent.

Substitution by Solvents

Ionic reactions occur preferentially when aliphatic alkenyl iodides and aromatic alkenyl chlorides and bromides are irradiated. The trapping of the vinyl cations generated by irradiation readily takes place in nucleophilic solvents such as alcohols. In these cases, enol ethers or acetals are the main products (Equation 11.8 and Equation 11.9).[3,20,24,30]

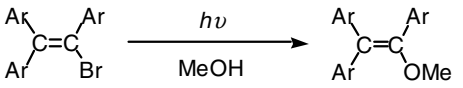

(11.8)

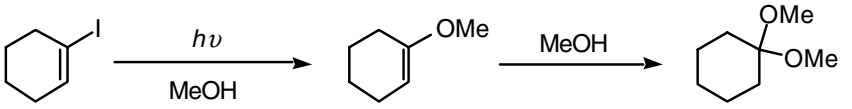

(11.9)

When nitriles such as acetonitrile are used as the solvent, a Ritter-type reaction is observed, in which the photogenerated vinyl cation is trapped to yield an intermediate nitrilium ion. This ion cyclizes, when there is an aryl group at the β-position of the vinylnitrilium ion, to give isoquinolines in good yield (Equation 11.10).

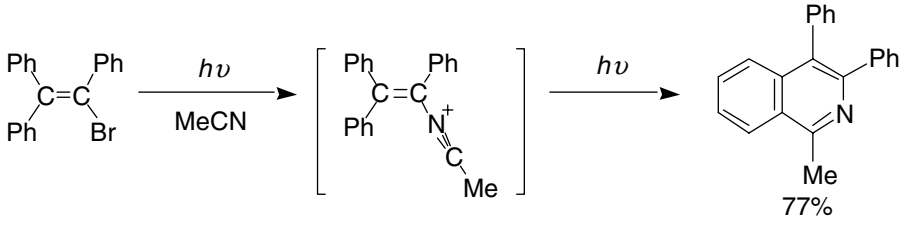

(11.10)

Substitution by Nucleophiles

Other reactions of synthetic utility can be observed when suitable nucleophiles are added to the reaction system. Typical examples of these nucleophiles are azide,[26,32] cyanate,[33] thiocyanate,[33] and cyanide anions and thioanisole.[34,39] Reactions using these nucleophiles provide a reaction path to functionalized vinyl derivatives. The transformations are successfully achieved by using triaryl-substituted alkenyl halides. The reactions with such nucleophiles provide an efficient path to heterocyclic compounds, among others. Some examples, such as the pyrrolines, isoxazolines, isoquinolones, and thio derivatives, are prepared by this method and are shown in Equation 11.11.

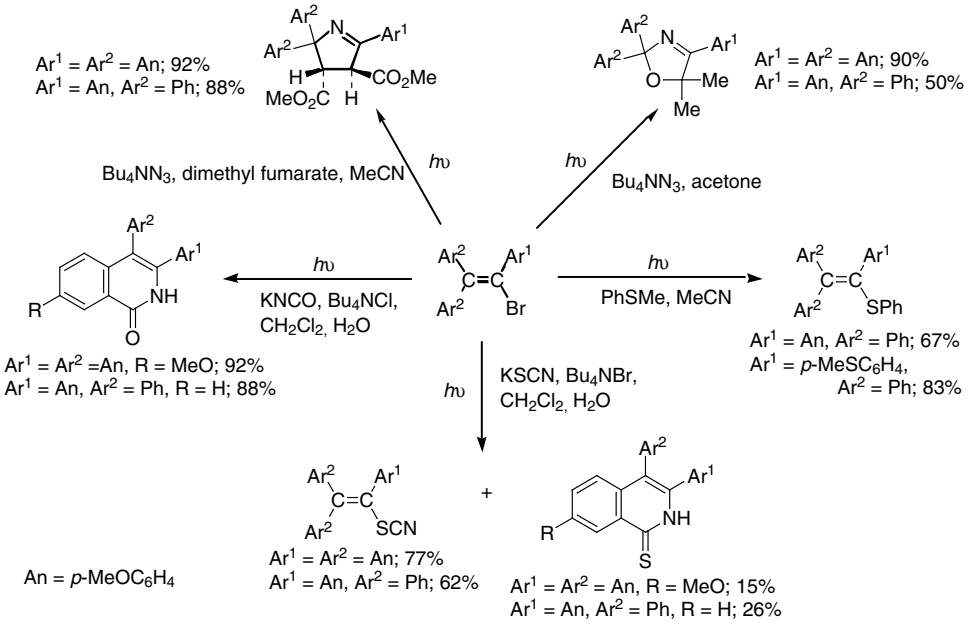

(11.11)

ipso-Substitution

Substitution at the aromatic ring (*ipso*-substitution) is also observed, but only in the cases of *p*-alkoxyphenylvinylhalides.[34,35] The *ipso*-substitution process was first observed in the reaction with cyanide anion as the nucleophile. The irradiation illustrated in Equation 11.12 brings about double substitution followed by a *cis*-stilbene type photocyclization to afford the dicyanophenanthrene shown.[34]

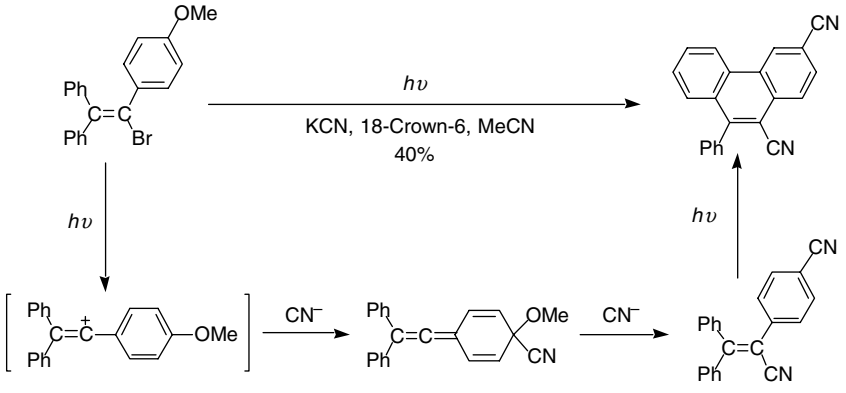

(11.12)

The intermediate *ipso*-adduct can be isolated in high yield when alkoxide anions are used as the nucleophile and the reaction temperature is controlled between 0 and 5°C (Equation 11.13).[35b] The *ipso*-adduct is obtained by intramolecular trapping by a pendant alkoxy chain at the *para*-position (Equation 11.14). The resulting spiro *ipso*-adducts are stable at room temperature.[36]

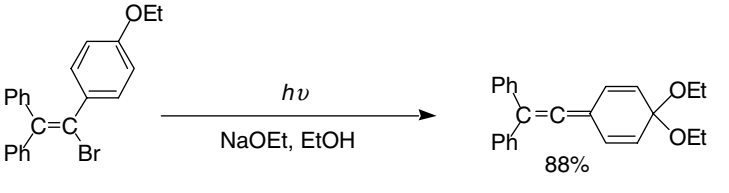

(11.13)

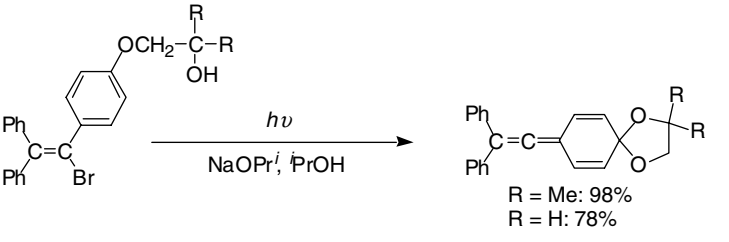

(11.14)

Intramolecular Cyclization

Intramolecular trapping of the vinyl cations provides a useful synthetic approach to several classes of molecule. The presence of an *ortho*-substituted aryl group at the β-position facilitates the cyclization. Benzofurans[21c] and dibenz[b,f]oxepines[37] can be prepared by this method (Equation 11.15 and Equation 11.16). The β-*p*-oxidophenyl group participates to give spiro cyclopropenes[38] (Equation 11.17).

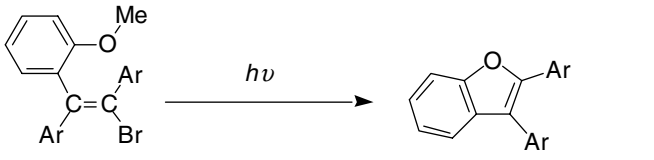

(11.15)

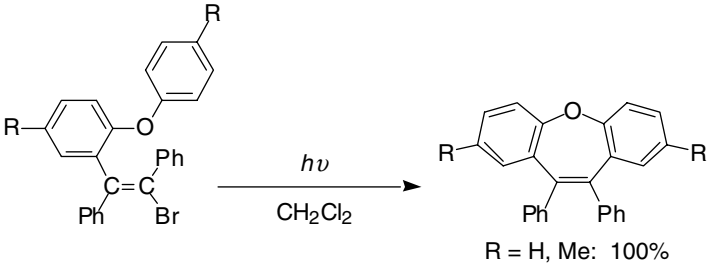

(11.16)

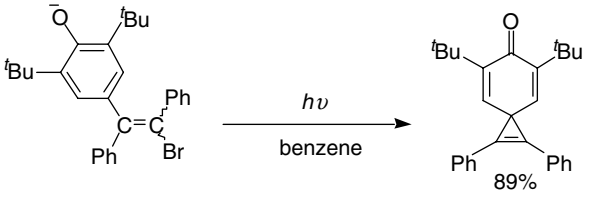

(11.17)

References

1. Majer, J.R. and Simons, J.P., Photochemical processes in halogenated compounds, *Adv. Photochem.,* 2, 137, 1964.
2. Sammes, P.G., Photochemistry of the C-X group, in *Chemistry of the Carbon–Halogen Bond,* Patai, S., Ed., Wiley, New York, 1973, chap. 11.
3. Kropp, P.J., McNeely, S.A., and Davis, R.D., Photochemistry of alkyl halides. 10. Vinyl halides and vinylidene dihalides, *J. Am. Chem. Soc.,* 105, 6907, 1983.
4. Chiurdoglu, G., Ottinger, R., Reisse, J., and Toussaint, A., Etudes spectroscopiques de quelques derives halogenes du cyclohexene, *Spectrochim. Acta,* 18, 215, 1962.
5. Newman, R.C., Jr. and Holmes, G.C., Photolytic formation of isomeric vinyl radicals from *cis*- and *trans*-vinyl iodides, *J. Org. Chem.,* 33, 4317, 1968.
6. Wilson, R.M. and Commons, T.J., Photochemistry of β-iodoacrylamides, *J. Org. Chem.,* 40, 2891, 1875.
7. Grovenstein, E., Jr. and Lee, D.E., The stereochemistry and mechanism of the transformation of cinnamic acid dibromide to β-bromostyrene, *J. Am. Chem. Soc.,* 75, 2639, 1953.
8. Bodenstein, J. and Borden, M.R., Rearrangement accompanying the addition of fluoride to 1,1-diphenylethylene, *Chem. Ind. (London),* 441, 1958.
9. Pritchard, J.G. and Bothner-By, A.A., Base-induced dehydrohalogenation and rearrangement of 1-halo-2,2-diphenylethylenes in *t*-butyl alcohol. The effect of deuterated solvent, *J. Phys. Chem.,* 64, 1271, 1960.
10. Beltame, P. and Favini, G., Reaction of halodiphenylethylenes with sodium ethoxide. II, *Gazz. Chim. Ital.,* 93, 757, 1963.
11. Drefahl, G. and Zimmer, C., Untersuchugen über Stilbene, XXXII. Halogenewasserstoff-Addition on Acetylene- und Äthylene-Bindungen, *Chem. Ber.,* 93, 505, 1960.

12. Apelgot, S., Cheutin, A., Mars, S., and Bergers, R., Microsynthesis of radiobromotriphenylethylene, *Bull. Soc. Chim. Fr.,* 533, 1952.
13. Rappoport, Z. and Apeloig, Y., Vinylic cations from solvolysis. II. The stereochemistry of the S_N1 reaction of 1,2-dianisyl-2-phenylvinyl halides, *J. Am. Chem. Soc.,* 91, 6734, 1969.
14. Kitamura, T., Nakamura, I., and Taniguchi, H., unpublished data, 1990.
15. Sonoda, T., Kobayashi, S., and Taniguchi, H., Studies of carbenium ion on unsaturated carbon. II. Exclusive formation of benzofurans via vinyl cations in the solvolytic reactions of 1-aryl-2,2-bis(*o*-methoxyphenyl)vinyl halides, *Bull. Chem. Soc. Jpn.,* 49, 2560, 1976.
16. Kerr, J.A., Strengths of chemical bonds, in *CRC Handbook of Chemistry and Physics,* CRC Press, Boca Raton, FL, 1987–1988, F-184.
17. Egger, K.W. and Cocks, T.T., Homopolar and heteropolar bond dissociation energies and heats of formation of radicals and ions in the gas phase. I. Data on organic molecules, *Helv. Chim. Acta,* 56, 1516, 1973.
18. (a) Lodder, G., Recent advances in the photochemistry of the carbon–halogen bond, in *The Chemistry of Functional Groups, Supplement D,* Patai, S. and Rappoport, Z., Eds., John Wiley & Sons, Chichester, 1983, chap. 29; (b) Lodder, G., Photochemical generation and reactivity, in *Dicoordinated Carbocations,* Rappoport, Z. and Stang, P.J., Eds., John Wiley & Sons, Chichester, 1997, chap. 8.
19. Kropp, P.J., Photobehavior of alkyl halides in solution: radical, carbocation and carbene intermediates, *Acc. Chem. Res.,* 17, 131, 1984.
20. McNeely, S.A. and Kropp, P.J., Photochemistry of alkyl halides. 3. Generation of vinyl cations, *J. Am. Chem. Soc.,* 98, 4319, 1976.
21. (a) Suzuki, T., Sonoda, T., Kobayashi, S., and Taniguchi, H., Photochemistry of vinyl bromides: a novel 1,2-aryl group migration, *J. Chem. Soc., Chem. Commun.,* 180, 1976; (b) Kitamura, T., Kobayashi, S., and Taniguchi, H., Copper(II) salt-enhanced vinyl cation formation in the photolysis of vinyl bromides, *Chem. Lett.,* 1223, 1978; (c) Suzuki, T., Kitamura, T., Sonoda, T., Kobayashi, S., and Taniguchi, H., Photochemistry of vinyl halides. Formation of benzofurans by photolysis of β-(*o*-methoxyphenyl)vinyl bromides, *J. Org. Chem.,* 46, 5234, 1981; (d) Kitamura, T., Muta, T., Kobayashi, S., and Taniguchi, H., A novel *ortho*-substituent effect on formation of vinyl cations in the photolysis of vinyl bromides, *Chem. Lett.,* 643, 1982; (e) Kitamura, T., Kobayashi, S., and Taniguchi, H., Photochemistry of vinyl halides. Vinyl cation from photolysis of 1,1-diphenyl-2-halopropenes, *J. Org. Chem.,* 47, 2323, 1982; (f) Kitamura, T., Muta, T., Tahara, T., Kobayashi, S., and Taniguchi, H., Photolysis of cyclic arylvinyl halides. Formation of 1,2-benzo-1,3-cycloalkadienyl cations and their rearrangement, *Chem. Lett.,* 759, 1986; (g) Kitamura, T., Kawasato, H., Kobayashi, S., and Taniguchi, H., Exclusive cyclization at sulfur in photolysis of β-[*o*-(arylthio)phenyl]vinyl bromides, *Chem. Lett.,* 839, 1986; (h) Kitamura, T., Kobayashi, S., and Taniguchi, H., Photolysis of vinyl halides. Preferential formation of vinyl cations by copper(II) salts, *J. Am. Chem. Soc.,* 108, 2641, 1986.
22. (a) Sket, B., Zupan, M., and Pollak, A., The photo-Fritsch-Butternberg-Wiechell rearrangement, *Tetrahedron Lett.,* 783, 1976; (b) Sket, B. and Zupan, M., Photochemistry of 2-halogeno-1,1-diphenylethylenes. The photo-Fritsch-Buttenberg-Wiechell rearrangement, *J. Chem. Soc., Perkin Trans. 1,* 752, 1979; (c) Zupanic N. and Sket, B., The influence of metal(II) salts and solid supports on the nature of the photochemical reaction of 1,1-diphenyl-2-haloethene, *J. Photochem. Photobiol. A: Chem.,* 60, 361, 1991.
23. Sonawane, H.R., Nanjundiah, B.S., and Panse, M.D., Photochemistry of organic halides: some interesting features of the photobehaviour of vinyl halides and vinylidene dihalides derived from camphene, *Tetrahedron Lett.,* 3507, 1985.
24. (a) van Ginkel, F.I.M., Visser, R.J., Varma, C.A.G.O., and Lodder, G., Nanosecond laser flash photolysis of 1-anisyl-2,2-diphenylvinyl bromide in acetonitrile and acetic acid, *J. Photochem.,* 30, 435, 1985; (b) Verbeek, J.M., Cornelisse, J., and Lodder, G., Photolysis of the vinyl bromide 9-(α-bromobenzylidene)fluorene in methanol. Effect of wavelength of irradiation, sodium methoxide

and oxygen, *Tetrahedron,* 42, 5679, 1986; (c) van Ginkel, F.I.M., Cornelisse, J., and Lodder, G., Photoreactivity of some α-arylvinyl bromides in acetic acid. Selectivity toward bromide versus acetate ions as a mechanistic probe, *J. Am. Chem. Soc.,* 113, 4261, 1991; (d) Van Ginkel, F.I.M., Cornelisse, J., and Lodder, G., Kinetic treatment of photochemically induced concurrent isotope exchange and product formation, *J. Photochem. Photobiol. A: Chem.,* 61, 301, 1991; (e) Kobayashi, S. and Schnabel, W., Reactions of substituted vinyl cations in acetonitrile solution as studied by flash photolysis. Part II, *Z. Naturforsh. B: Chem. Sci.,* 47, 1319, 1992; (f) Krijnen, E.S. and Lodder, G., Photochemical generation of destabilized vinyl cations, *Tetrahedron Lett.,* 34, 729, 1993; (g) Verbeek, J.-M., Stapper, M., Krijnen, E.S., van Loon, J.-D., Lodder, G., and Steenken, S., Photochemical formation and electrophilic reactivities of vinyl cations. Influence of substituents, anionic leaving groups, solvents and excitation wavelength on photoheterolysis and photohomolysis of 1-(*p*-R-phenyl)-2-(2,2′-biphenyldiyl)vinyl halides, *J. Phys. Chem.,* 98, 9526, 1994; (h) Krijnen, E.S., Zuilhof, H., and Lodder, G., Electronic and conformational effects in the photochemistry of α-alkenyl-substituted vinyl halides, *J. Org. Chem.,* 59, 8139, 1994; (i) Galli, C., Gentili, P., Guamieri, A., Kobayashi, S., and Rappoport, Z., Competition of mechanisms in the photochemical cleavage of the C-X bond of aryl-substituted vinyl halides, *J. Org. Chem.,* 63, 9292, 1998.

25. (a) Stang, P.J., Rappoport, Z., Hanack, M., and Subramanian, L.R., *Vinyl Cations,* Academic Press, New York, 1979; (b) Rappoport, Z., Vinyl cations, in *Reactive Intermediates,* Vol. 3, Abramovitch, R.A., Ed., Plenum Press, New York, 1983, chap. 7; (c) Hanack, M., *Carbokationen, Carbokation-Radikale,* Georg Thieme Verlag, Stuttgart, 1990.
26. Kitamura, T., Kobayashi, S., and Taniguchi, H., Photochemistry of vinyl halides. Heterocycles from reaction of photogenerated vinyl cations with azide anion, *J. Org. Chem.,* 49, 4755, 1984.
27. Müller, J.P.H., Parlar, H., and Korte, F., Einfache Photochemische Methode zur Deuterierung von Olefinen und Aromaten, *Synthesis,* 524, 1976.
28. Kitamura, T., Kobayashi, S., and Taniguchi, H., Photolysis of β-(*o*-methylthiophenyl)vinyl bromides. A versatile synthesis of benzo[b]thiophenes, *Chem. Lett.,* 1637, 1988.
29. Tadros, W., Skla, A.B., and Akhookh, Y., Butadienes and related compounds. III. Further study of the factors bearing the formation of 1,1,4,4-tetraarylbuta-1,3-dienes, *J. Chem. Soc.,* 2701, 1956.
30. Kitamura, T., Kobayashi, S., Taniguchi, H., Fiakpui, C.Y., Lee, C.C., and Rappoport, Z., Degenerate β-aryl rearrangements in photochemically generated triarylvinyl cations, *J. Org. Chem.,* 49, 3167, 1984.
31. Kitamura, T., Kobayashi, S., and Taniguchi, H., Isoquinoline derivatives from the Ritter-type reaction of vinyl cations, *Chem. Lett.,* 1351, 1984.
32. Kitamura, T., Kobayashi, S., and Taniguchi, H., Photolysis of vinyl bromides in the presence of tetrabutylammonium azide: trapping of a vinyl cation with azide ion, *Tetrahedron Lett.,* 1619, 1979.
33. (a) Kitamura, T., Kobayashi, S., and Taniguchi, H., Reaction of photogenerated vinyl cations with ambident anions, *Chem. Lett.,* 1523, 1984; (b) Kitamura, T., Kobayashi, S., and Taniguchi, H., Photolysis of vinyl halides. Reaction of photogenerated vinyl cations with cyanate and thiocyanate ions, *J. Org. Chem.,* 55, 1801, 1990.
34. Kitamura, T., Murakami, M., Kobayashi, S., and Taniguchi, H., *ipso*-Substitution by cyanide anion in photolysis of 1-(*p*-methoxyphenyl)vinyl bromides, *Tetrahedron Lett.,* 27, 3885, 1986.
35. Kitamura, T., Kabashima, T., Kobayashi, S., and Taniguchi, H., Drastic base dependence of products in photolysis of 1-(*p*-methoxyphenyl)-2,2-diphenylvinyl bromide. *ipso*-Substitution by alkoxide anions, *Chem. Lett.,* 1951, 1988; (b) Kitamura, T., Kabashima, T., Kobayashi, S., and Taniguchi, H., Isolation and alcoholysis of an *ipso* adduct, vinylidenecyclohexadiene, from photolysis of 1-(*p*-ethoxyphenyl)vinyl bromide, *Tetrahedron Lett.,* 29, 6141, 1988; (c) Kitamura, T., Nakamura, I., Kabashima, T., Kobayashi, S., and Taniguchi, H., *ipso*-Substitution by alkoxide ions in photolysis of triarylvinyl halides. Firm evidence of intervention of vinyl cations, *Chem. Lett.,* 9, 1990; (d) Kitamura, T., Kabashima, T., Nakamura, I., Fukuda, T., Kobayashi, S., and Taniguchi, H., *ipso* Substitution of triarylvinyl cations by alkoxide anions, *J. Am. Chem. Soc.,* 113, 7255, 1991.

36. (a) Kitamura, T., Nakamura, I., Kabashima, T., Kobayashi, S., and Taniguchi, H., A novel spiro adduct from intramolecular *ipso* substitution in the photolysis of an α-[*p*-(2-hydroxyalkoxy)phenyl]vinyl bromide, *J. Chem. Soc., Chem. Commun.,* 1154, 1989; (b) Kitamura, T., Soda, S., Nakamura, I., Fukuda, T., and Taniguchi, H., Importance of β-phenyl group in *ipso* substitution of arylvinyl cations, *Chem. Lett.,* 2195, 1991.
37. (a) Kitamura, T., Kobayashi, S., and Taniguchi, H., Formation of dibenz[b,f]oxepins from β-(*o*-aryloxyphenyl)vinyl bromides, *Chem. Lett.,* 547, 1984; (b) Kitamura, T., Kobayashi, S., Taniguchi, H., and Hori, K., Photolytic and solvolytic reactions of β-[*o*-(aryloxy)phenyl]vinyl bromides. Intramolecular arylation of vinyl cations into dibenzoxepins, *J. Am. Chem. Soc.,* 113, 6240, 1991.
38. Ikeda, T., Kobayashi, S., and Taniguchi, H., A new route to spiro[2.5]octa-1,4,7-trien-6-ones, *Synthesis,* 393, 1982.
39. Kitamura, T., Kabashima, T., and Taniguchi, H., Phenylthiolation of arylvinyl bromides by photolysis, *J. Org. Chem.,* 56, 3739, 1991.

12

Low Temperature Matrix Photochemistry of Alkenes

Ian R. Dunkin
University of Strathclyde

12.1 Introduction

This chapter covers photochemical studies of alkenes and cycloalkenes isolated in very low temperature matrices, typically solidified noble gases or nitrogen at temperatures of 10–20 K. Under the conditions of such *matrix isolation,* trapped species are prevented from diffusing and are therefore prevented from undergoing bimolecular reactions. As a result, extremely reactive species can be stabilized and investigated by a variety of normal spectroscopic methods, of which IR spectroscopy usually provides the most useful structural information. A brief description of the matrix-isolation technique and an account of its applications in several areas of organic photochemistry are given in a later chapter.

The matrix stabilization of reactive species has been exploited in a number of ways in the investigation of alkene photochemistry. Examples include the identification of reactive products, such as radicals, resulting from alkene photolysis, the direct observation of the dimerizations and rearrangements of carbenes to alkenes, the generation of strained alkenes, and studies of alkene oxidation resulting from irradiation of contact charge-transfer complexes between alkenes and NO_2. Sometimes, the principal advantage of matrix isolation derives not from the ability to stabilize reactive species but simply from the fact that the IR bands of matrix-isolated species tend to be very narrow. As a consequence, overlap between the IR bands of different compounds in product mixtures is minimized. This facilitates identification of the individual species present. Moreover, matrix IR frequencies are generally not greatly shifted from gas-phase frequencies, so calculated and experimental spectra can be expected to be in good agreement. In recent years, density functional theory (DFT) has been conspicuously successful in predicting the IR spectra of matrix-isolated species.[1]

Related topics that lie outside the scope of this chapter include thermal reactions in matrices between alkenes and reactive species such as F atoms and NH, even when these have been generated photochemically, the photochemistry of alkene radical cations, and matrix studies of azaalkenes, silaalkenes, and other alkene analogues.

0-8493-1348-1/04/$0.00+$1.50

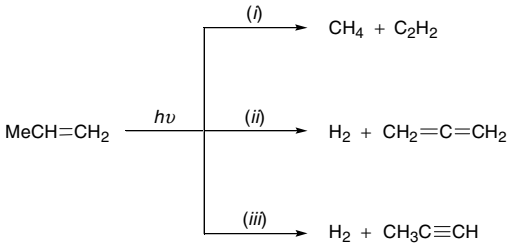

SCHEME 1

12.2 Photolysis of Alkenes in Matrices

Monoenes

The lowest energy absorptions of simple monoenes lie well into the vacuum-ultraviolet region of the spectrum, and the high-energy reactions, which result from absorption at these wavelengths, tend to be nonspecific. In fact, very few matrix-isolation studies of the photolysis of simple alkenes have been conducted.

Propene has been photolyzed in Ar and N_2 matrices with microwave powered hydrogen, bromine, and nitrogen discharge lamps as the light sources.[2] It was found that propene decomposition occurred most efficiently by absorption of the 121.5 nm hydrogen emission. Although the energy at this wavelength lies above the ionization threshold, no evidence of propene ionization was obtained. The major products, identified by IR spectroscopy, were methylacetylene, allene, methane, and acetylene. These were presumed to arise in the three primary processes shown in Scheme 1, with process (*i*) predominating. It is noteworthy that neither ethene nor the methyl radical was formed in sufficient amounts to be detected. Moreover, in additional experiments, propene was photolyzed in CO and CO-doped Ar matrices in order to probe for the generation of H atoms or methylene (CH_2). These species would have reacted with CO to give the formyl radical (HCO) or ketene, respectively, both with easily recognized IR spectra. Neither of these CO-trapping products was detected, however. Thus, the matrix-isolation experiments provided good evidence that the primary photoprocesses occurred by extrusion of methane [process (*i*)] or molecular hydrogen [processes (*ii*) and (*iii*)] and not via radical or ionic fragmentations.

Similar studies were made of the vacuum ultraviolet (VUV) photolysis of fluoroethene[3] and all three difluoroethenes.[4] A major pathway in these reactions was the extrusion of molecular HF, yielding acetylene and fluoroacetylene, respectively. In contrast to the behavior of propene, however, a significant radical-fragmentation pathway was also observed, which gave $C_2H_2F\cdot$ from fluoroethene and $C_2HF_2\cdot$ from the difluoro compounds. Interconversion of the difluoroethenes was observed to a minor extent.

The absorptions of chloro-, bromo-, or iodo-substituted monenes are accessible to longer wavelength light sources than those of unsubstituted or fluoro-substituted analogues. Photolysis of 3-chloro-, 3-bromo-, and 3-iodopropene was carried out in Ar matrices with a medium pressure mercury arc.[5] In each case, the matrix IR spectra indicated that the major product was a complex between allene and the photoextruded hydrogen halide. Propyne and cyclopropyl halides were produced by secondary photolysis of the allene complexes. More recently, it was found that similar matrix photolyses of vinyl bromide and vinyl iodide gave hydrogen halide–acetylene complexes as the primary products and the corresponding haloacetylenes as secondary products.[6]

An interesting matrix effect was discovered for the photolysis of 1,2-dichloroethenes, the products of which differed in xenon and krypton matrices.[7] In Xe, photolysis of *E*- and *Z*-1,2-dichloroethene at 237 nm resulted in elimination of both Cl_2 and HCl, whereas in Kr, only HCl elimination and isomerization were observed. The results indicated that a triplet pathway operated in Xe but not in Kr, and this difference was attributed to intersystem crossing aided by the heavy-atom effect of the Xe matrix.

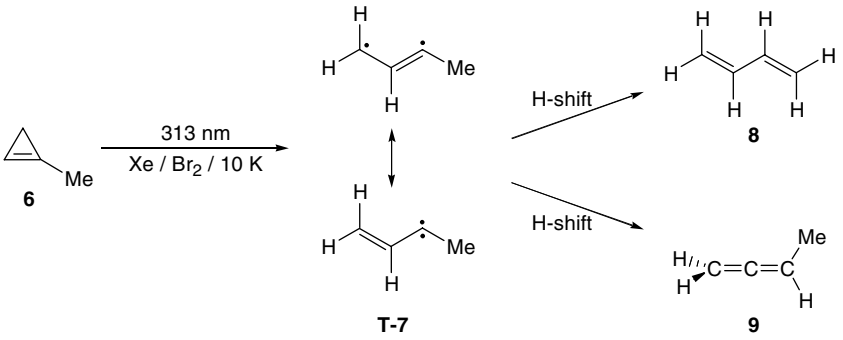

SCHEME 3

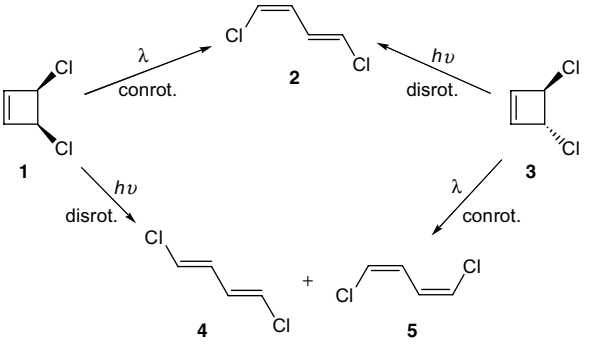

SCHEME 2

A second type of matrix effect has been observed for the photochemical ring opening of *cis*-3,4-dichlorocyclobutene (**1**) and *trans*-3,4-dichlorocyclobutene (**3**) (Scheme 2).[8] The thermally induced ring opening of **1** and **3** occurred with high stereospecificity via a conrotatory pathway, in accordance with the Woodward–Hoffman rules. On the other hand, direct excitation (193 nm) of **1**, matrix isolated in Ar or Xe, gave rise to products from the allowed disrotatory pathway (**4** and **5**) and also from the forbidden conrotatory route (**2**). IR bands of all the products increased at about the same rates, thus excluding the likelihood that **2** was formed in a secondary isomerization process. The stereoisomers **1** and **3** have no significant absorption at $\lambda > 230$ nm and were found to be photostable to light of $\lambda > 254$ nm in Ar matrices. Remarkably, however, both compounds were rapidly photolyzed by light of $\lambda > 270$ nm in Xe matrices, and both underwent *conrotatory* ring opening, the expected pathway for the thermal reaction. Under these conditions, the light was apparently absorbed by the solid xenon in a cooperative process with the dichlorocyclobutene molecules, and the reaction probably occurred via vibrationally excited molecules in the electronic ground state. Although no reactive species were observed in these experiments, matrix isolation brought the advantage of very narrow bandwidths in the product IR spectra. Thus, with minimal overlap of bands and also in conjunction with DFT computations, the products and their various conformations could be readily identified.

The addition of halogens, e.g., bromine, to Xe matrices is a refinement of the technique for photochemically inducing reactions of vibrationally excited electronic ground-state molecules, which has been developed in the last few years. Thus, 1-methylcyclopropene (**6**) was found to be stable towards light of 248, 254, or 313 nm in Ar matrices but was photolyzed by 313 nm light in Br_2-doped Xe matrices (Scheme 3).[9] The stable products were identified by their IR absorptions as buta-1,3-diene (**8**) and methylallene (**9**), but an additional set of IR bands was also observed in the product spectra. These absorptions decreased in intensity rapidly on subsequent irradiation at 313 or 366 nm, while the absorptions of **6**, **8**, and **9**

increased. A thorough DFT study showed that the additional IR bands belonged to triplet but-2-ene-1,3-diyl (**T-7**), which could therefore be identified as the primary photoproduct. The formation of this biradical from **6** corresponds to the theoretically calculated lowest energy ground-state pathway. In parallel experiments, propene-1,3-diyl was seemingly formed from cyclopropene under similar conditions, although the identification of the biradical was less certain in this case.

An alternative use of matrix isolation is to stabilize highly reactive species generated thermally, which can then serve as the starting materials for photochemical studies. A good example of this approach is provided by the highly strained, doubly pyramidalized alkene **11**, which has been generated by flash vacuum pyrolysis of the β-lactone **10** and isolated in Ar matrices by co-condensation of the pyrolysate with argon.[10,11] The strained alkene was found to have a broad UV absorption with λ_{max} = 245 nm, and irradiation with the 248 nm line of a KrF laser or with a low pressure Hg arc caused a gradual conversion of **11** into **12** in a reverse of the usual vinylcyclopropane rearrangement. Analogous attempts were made to generate alkene **14**, which is even more strained than **11**, by pyrolysis of the corresponding β-lactone.[12] These failed because the lactone was much more resistant than **10** to pyrolysis. Nevertheless, **14** was successfully matrix isolated by reaction of the diiodo precursor **13** with potassium or cesium vapor, followed by condensation with excess argon. Computations suggested that alkene **14** has a nearly tetrahedral geometry at the olefinic carbon atoms. On photolysis at 248 nm, **14** was converted into a new product, which was tentatively identified as **15** on the basis of the similarity of its matrix IR spectrum to that of **12**.

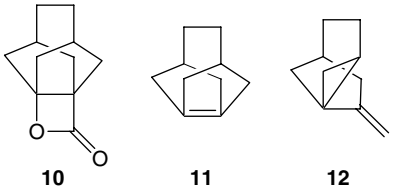

10 **11** **12**

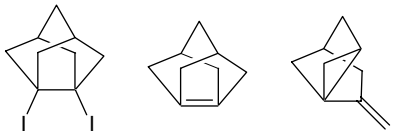

13 **14** **15**

Dienes, Trienes, and Higher Polyenes

The photolyses of cyclohexa-1,3-diene,[13] cycloocta-1,3,5-triene,[14] and bicyclo[4.2.0]octa-2,4-diene[14] were investigated by matrix-isolation techniques at a relatively early date and certainly before reliable computational methods for IR transitions were available. As an example, both IR and UV-visible spectroscopy were employed to monitor the photoreaction of cyclohexa-1,3-diene at 240–270 nm in Ar matrices at 20 K.[13] It was discovered that the diene photolyzed irreversibly to *Z*-hexa-1,3,5-triene, which photolyzed more slowly but still irreversibly to *E*-hexa-1,3,5-triene and several other thermally unstable products. The latter could not be identified with certainty, but hexa-1,2,4-triene and *exo*-2-vinylbicyclo[1.1.0]butane were proposed as possibilities.

When *E*-2,5-dimethyl-1,3,5-hexatriene (**16**) was isolated in Ar matrices, it was found to exist almost exclusively as the *tEt* rotamer, but UV irradiation led to the formation of thermodynamically less stable rotamers (Scheme 4).[15] The various rotamers could be identified by comparison of their experimental and computed IR transitions. When the *Z* triene (**17**) was isolated in Ar matrices, it existed predominantly as the *cZt* rotamer, but it could also be generated in the *cZc* form by matrix photolysis of 1,4-dimethylcyclohexa-1,3-diene (**18**). In contrast to the *E* isomer, the *Z* isomer underwent photo-induced double bond isomerization, generating rotamers of the *E* form. It should be noted that matrix isolation provides

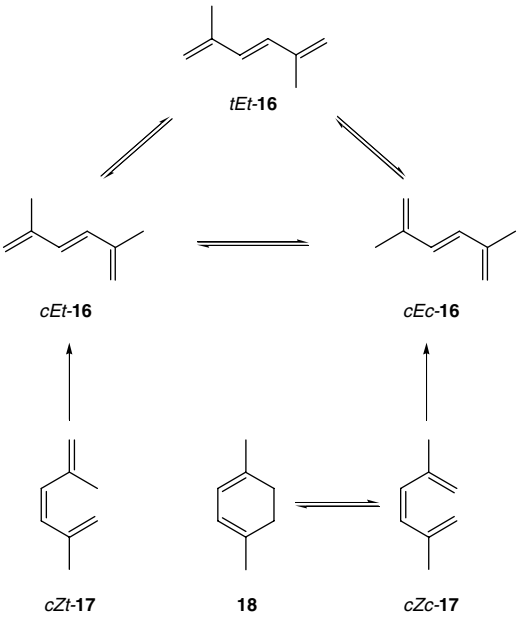

SCHEME 4

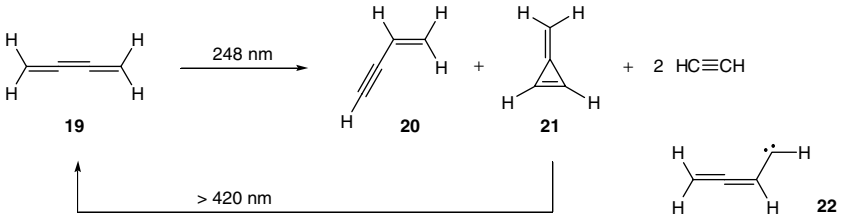

SCHEME 5

a generally applicable means of stabilizing the individual rotamers of flexible molecules and is thus an ideal way to identify their spectra and study their interconversions.

The 248 nm photolysis of butatriene (**19**) in Ar matrices at 10 K produced vinylacetylene (**20**), methylenecyclopropene (**21**), and acetylene (as a dimeric complex) (Scheme 5).[16] The rearrangement of **19** to **21** could be reversed by irradiation at long wavelengths ($\lambda > 420$ nm). The conversion of **19** to **21** was most likely to have proceeded by a [1,2]-H migration, forming allenylcarbene (**22**), and theoretical calculations suggest that this species is an energy minimum on both the singlet and triplet potential energy surfaces. Careful analysis of the matrix IR spectra revealed two sets of absorptions that could be attributed either to the *syn* or *anti* forms of singlet **22** or to a mixture of singlet and triplet **22**. Thus, the rearrangement of **19** to **21** appeared to proceed in a stepwise manner on either the singlet or triplet energy surface, with **22** as the intermediate.

Tetrafluoro-*p*-xylylene **23** has been matrix isolated by flash vacuum pyrolysis of the corresponding octafluoro[2.2]paracyclophane followed by condensation at 30 K with a large excess of argon.[17] This is a further example of the use of matrix isolation to stabilize a highly reactive species produced in a thermal reaction, which then becomes the starting material for photochemical studies. Irradiation of **23** at 248 nm resulted in partial conversion to a new species, which was identified as the tetrafluoroheptafulvene **24** by comparison of the experimental and computed IR transitions. Several possible reaction mechanisms for this rearrangement were proposed, but no intermediate species was detected in the matrix photolysis experiments, so a final conclusion as to the mechanism could not be drawn.

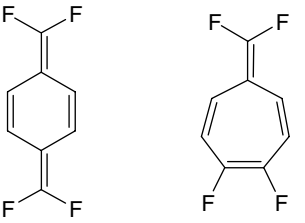

23 **24**

The UV photolysis of the [2,2]paracyclophan-ene **25** in Ar at 10 K resulted in cleavage of the ethano bridge and formation of **26**, which was identified by means of its IR and UV-visible absorption spectra.[18] The absence of an electron paramagnetic resonance (EPR) signal showed that the new species had a singlet ground state, while comparison of the IR and UV-visible spectra with those of *p*-xylylene and the benzyl radical suggested that the electronic structure of the photoproduct was predominantly quinonoid (**26a**) but with a substantial biradical contribution (**26b**). Related studies of a benzoannelated analogue of **25** gave similar results.

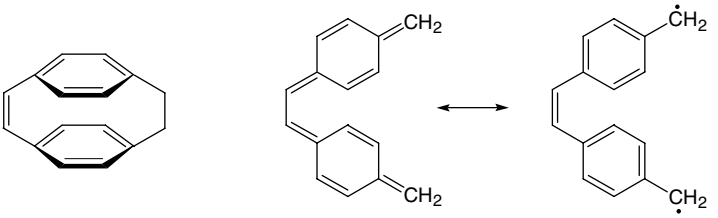

25 **26a** **26b**

12.3 Photochemical Generation of Alkenes in Matrices

Cyclobutadiene

The story of the generation, detection, and determination of the structure of cyclobutadiene isolated in low temperature matrices is one of the most celebrated and long running in the history of matrix isolation, and it illustrates both the strengths and pitfalls of the technique.

The generation of cyclobutadiene (**30**) by matrix photolysis of α-pyrone (**27**) (Scheme 6) was reported independently in 1972–73 by two research groups.[19,20] Irradiation of matrix-isolated **27** with 313 nm light[21] or with $NiSO_4$-filtered[19] or Pyrex-filtered[22] Hg arcs resulted quickly in a reversible ring-opening to the aldehyde-ketene **28** and its rotamers, which could be interconverted photochemically. More prolonged irradiation, however, gave the β-lactone **29**, recognized by its characteristic high frequency ν(C=O) bands at 1850 and 1826 cm^{-1}. After a sufficiently long period of irradiation, quite high conversion of **27** into **29** could be achieved. Prolonged further irradiation, or irradiation with the filter removed, caused the disappearance of the IR bands of **29** and the appearance of those of CO_2 and another species, presumed to be cyclobutadiene (**30**). IR absorptions at or near 3040, 1240, 650, and 570 cm^{-1} were attributed to the latter species, which decomposed to acetylene on even more prolonged photolysis. A weak electronic absorption with λ_{max} at 405 nm was also attributed[19] to **30**. These experiments provided for the first time an IR spectrum of cyclobutadiene on which to base discussions of its structure. The crucial first question was whether the ring is square or rectangular.

Symmetry considerations predict four infrared-active fundamental vibrations for a square planar (D_{4h}) structure for **30** and seven for a rectangular planar (D_{2h}) structure. The simplicity of the observed IR spectrum, with only four absorptions, led one group[20] to the tentative conclusion that **30** has a square planar structure, in contradiction to nearly all previous theoretical predictions. The difficulty, of course,

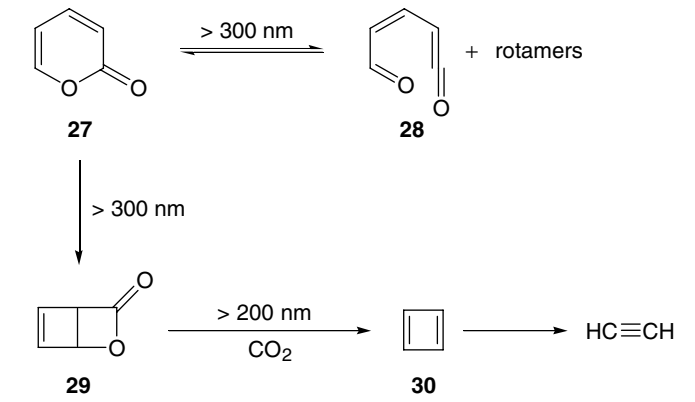

SCHEME 6

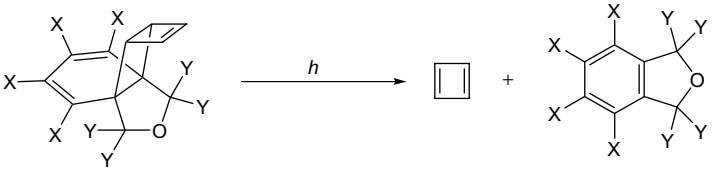

31a: X = Y = H
31b: X = D, Y = H
31c: X = H, Y = D
31d: X = Y = D

32a: X = Y = H
32b: X = D, Y = H
32c: X = H, Y = D
32d: X = Y = D

SCHEME 7

was that some fundamental IR bands might have remained undetected simply because they were too weak. In an effort to gain more structural information, mono- and dideuteriocyclobutadienes were generated in matrices by photolysis of the appropriate deuteriated α-pyrones,[23,24] but these experiments still left the question of the geometry of **30** unresolved. The uncertainty intensified when, a few years later, cyclobutadiene was generated in matrices from several different precursors,[25,26] in particular **31a**, from which cyclobutadiene was obtained along with phthalan (**32a**) but without the simultaneous formation of CO_2 (Scheme 7). In these studies, it was shown that the IR band at 650 cm^{-1} did not belong to **30** but was rather due to a complex between molecules of **30** and CO_2, which had remained together in the matrix cage after the photolysis of **29**. The 650 cm^{-1} band was apparently due to the bending mode of CO_2 perturbed slightly by interaction with **30**. This assignment of the 650 cm^{-1} band was confirmed by matrix photolysis of α-pyrone isotopically labeled with ^{13}C at the carbonyl carbon.[27] The product band normally at 650 cm^{-1} exhibited a substantial isotope shift to 636 cm^{-1}, showing that it belonged to CO_2 and not to the diene. Furthermore, after photolysis of α-pyrone ^{13}C-labelled at the 6-position, the 650 cm^{-1} IR band had no detectable isotope shift, whereas the 1240 cm^{-1} band of **30** was shifted to lower frequency by about 4 cm^{-1}. These observations left only three IR bands that could be reliably attributed to cyclobutadiene, and the inevitable conclusion was that at least one IR band of this compound had not been detected. If one such band, why not more than one?

The main question concerning the geometry of cyclobutadiene was eventually resolved when two additional IR bands of this molecule were observed at 1523 and 723 cm^{-1}, thus demonstrating that the molecule is not square.[28] The diene was generated by photolysis of precursors **31a-d** in argon matrices at 7 K. Although the IR absorptions of the byproduct, phthalan (**32a**), masked several regions of the matrix IR spectra, the IR bands of the isotopomers **32b-d** were significantly shifted, thus permitting careful scrutiny of the entire mid-IR region from 4000 to 400 cm^{-1}.

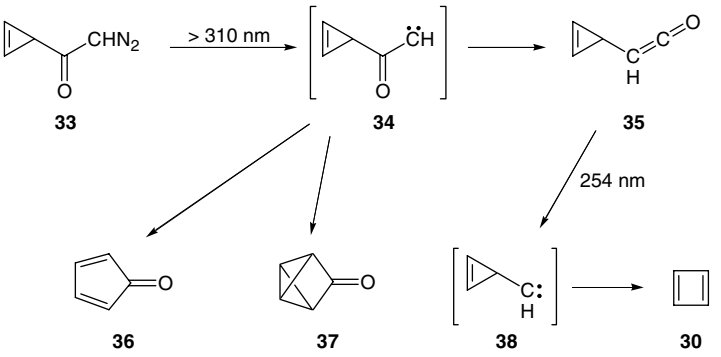

SCHEME 8

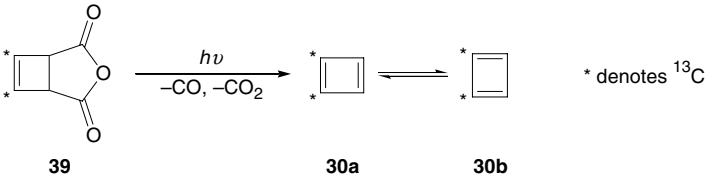

SCHEME 9

A thorough and critical review of cyclobutadiene chemistry[29] was published in 1980. A theoretical study of possible interactions between cyclobutadiene molecules and the various byproducts formed when **30** is generated photolytically in matrices appeared later.[30] Weak complexes between **30** and CO, CO_2, HCN, benzene, and phthalan (**32a**) were predicted, but no attempt was made to evaluate the effects of such complex formation on the IR absorptions of **30**.

Since the early work, the matrix chemistry of cyclobutadiene has attracted less attention, although some interesting results have been obtained. Diazoketone **33** gave cyclopropenylketene **35**, cyclopentadienone (**36**), and tricyclopentanone **37** when photolyzed at >310 nm in argon matrices, presumably via the ketocarbene **34**, which was not, however, observed directly (Scheme 8).[31] Ketene **35** was then further photolyzed at 254 nm, yielding cyclobutadiene (**30**), presumably via carbene **38**. At this shorter wavelength, **36** was photostable, but the tricyclopentanone **37** also gave mainly **30**, but in a very slow reaction.

Once it appeared certain that cyclobutadiene had a rectangular structure with alternating single and double bonds, it became interesting to consider the interconversion of the two valence tautomers. This was first probed by polarized IR spectroscopy coupled with one of the rare examples of the use of ^{13}C NMR spectroscopy of matrix isolated species.[32] Linearly polarized UV light was used to generate a matrix sample of partially oriented **30** from the unlabelled version of anhydride **39**, and the resulting matrices were then probed with linearly polarized IR light to determine the linear dichroism of each product IR band.[33] These studies were made with Ne and Ar matrices at temperatures down to 2.8 K. Although persistent IR dichroism was observed for six IR bands of **30**, the pattern of dichroism did not allow a conclusion to be drawn with regard to the rate of interconversion of the valence tautomers. On the other hand, ^{13}C NMR spectra of the matrix photolysis products of the vicinally ^{13}C-dilabelled anhydride **33** showed that the rate of interconversion of the two cyclobutadiene tautomers **30a** and **30b** exceeded 10^3 sec^{-1} at 25 K (Scheme 9). It was not possible to distinguish between thermally activated and tunneling interconversion, but the theoretically predicted energy barrier for the reaction (40–60 kJ mol^{-1}) was consistent only with a tunneling process.

A subsequent investigation using matrix Raman spectroscopy confirmed the submillisecond timescale for tautomer interconversion but led to the conclusion that even this was slow compared to theoretical expectations.[34] It was therefore suggested that the matrix environment, including the CO and CO_2

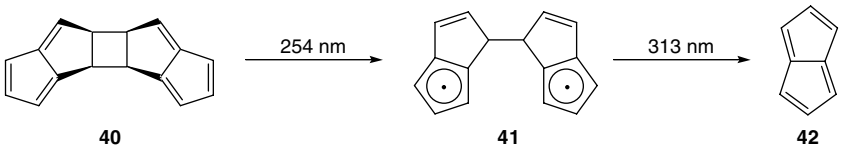

SCHEME 10

byproducts, might have a hindering effect on the tunneling process. In a further study of the UV and polarized IR spectra of matrix isolated cyclobutadiene and its *1-d*-, *1,2-*d_2-, *1,4-*d_2-, *1*–^{13}C-, *1,2*–$^{13}C_2$-, and *1,4*–$^{13}C_2$-labelled derivatives,[35] it was found that the two tautomers interconverted on a time scale of minutes even at 10 K. It was moreover discovered that the presence of CO_2 in the same matrix site inhibited the photodecomposition of cyclobutadiene to acetylene, probably because the CO_2 molecules enhanced the rate of vibrational relaxation in competition with fragmentation.

Pentalene

Although sterically shielded or electronically stabilized derivatives of pentalene (**42**) had been characterized previously, the first convincing spectroscopic evidence for the parent molecule was obtained when the *syn-cis* dimer **40** was photolyzed in argon and N_2 matrices (Scheme 10).[36] The cleavage took place in two steps: the first with 254 nm light leading apparently to the biradical **41**, while the subsequent cleavage to **42** occurred with 313 nm light. Pentalene was thus observed for the first time by electronic and vibrational absorption spectroscopy and was identified positively by an excellent agreement between the experimental IR spectrum and IR transitions computed by DFT theory. A C_{2h} structure for **42**, with pronounced alternation of single and double bonds, was indicated by both theory and experiment. In addition, a reinterpretation of the previously reported electronic spectra of pentalene derivatives emerged from this work.

Carbene Dimerizations

In principle, the dimerization of a carbene or the addition reaction of two different carbenes should provide a fundamental method for double bond formation. In practice such reactions are rare, primarily because carbenes are highly reactive species and are seldom generated in concentrations high enough to favor dimerization; they therefore usually undergo reactions with other species present, e.g., solvent or precursor molecules. The matrix-isolation technique, however, provides a means of generating carbenes in high concentration before the matrix is allowed to warm sufficiently to allow diffusion. This should permit the observation of genuine carbene dimerizations, and some such cases have been reported.

The simplest of all carbenes, methylene (CH_2), initially proved difficult to observe in low temperature matrices, owing to its small size and high mobility. One of the first indications that methylene had been generated in matrices was the observation of the supposed chemiluminescence of ethene following photolysis of diazomethane in solid argon or nitrogen.[37] The luminescence exhibited a distinct isotope effect when CD_2N_2 was photolyzed and was presumed to arise from excited ethene molecules formed by the dimerization of methylene. Nevertheless, a reinvestigation of this reaction[38] led to the conclusion that the excited ethene could have arisen either from the dimerization of CH_2 or from the reaction of CH_2 with the precursor CH_2N_2.

One of the first unequivocal examples of carbene dimerization in matrices seems to have been that of cyclopentadienylidene (**44**) (Scheme 11).[39,40] Photolysis of diazocyclopentadiene (**43**) in N_2 matrices produced the carbene **44**, which could be detected directly through both its UV and IR absorptions, provided that very dilute matrices were employed. When matrices containing **44**, but little or no **43**, were warmed to 20–25 K, fulvalene (**45**) was produced, which was recognized by its highly structured and distinctive UV absorption spectrum. Several carbenes analogous to **44**, e.g., tetrachloro- and tetrabromocyclopentadienylidene and fluorenylidene,[41,42] failed to undergo similar dimerizations even at 30–35 K.

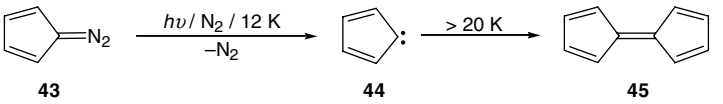

SCHEME 11

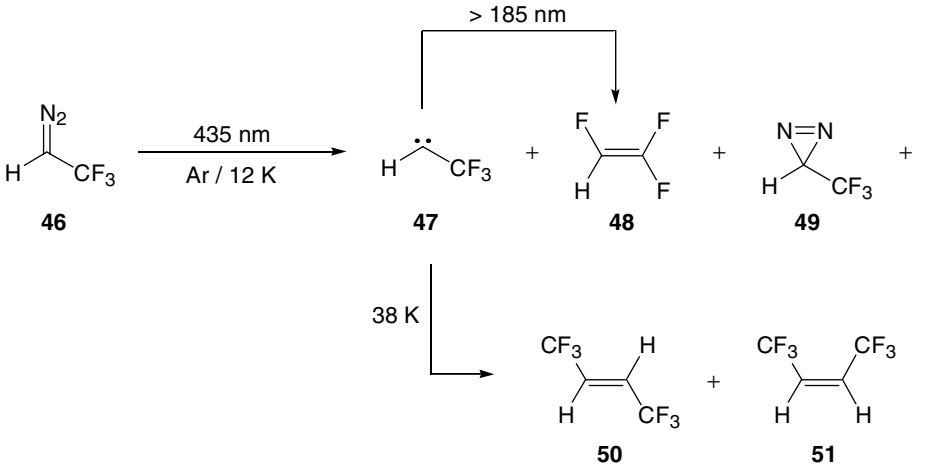

SCHEME 12

This was assumed to be a result of the increased size of the molecules compared with **44**, which would hinder diffusion within the matrix and also increase the energies of the transition states leading to the corresponding fulvalenes through unfavorable steric interactions.

Many carbenes undergo rapid isomerizations when generated in matrices, especially via hydrogen or alkyl shifts. These unimolecular reactions compete very favorably with the bimolecular carbene dimerizations unless suppressed, e.g., by fluorine substitution. For example, 435 nm photolysis of 2,2,2-trifluorodiazomethane (**46**) in Ar matrices at 12 K generated significant amounts of the triplet carbene **47** as well as trifluoroethene (**48**) and small amounts of diazirine **49** and the hexafluorobut-2-enes **50** and **51** (Scheme 12).[43] Shorter-wavelength irradiation converted the carbene into trifluoroethene, whereas warming the matrix to 35–38 K increased the yields of the hexafluorobut-2-enes **50** and **51**, with a concomitant decrease in the concentration of the carbene.

Carbene Rearrangements

The rearrangements of carbenes via CC bond shifts have afforded routes to a number of matrix isolated strained bi- and tricycloalkenes of the *anti*-Bredt type. The inherently high energy of the carbene provides the driving force for the rearrangement to the strained product. As an example, the moderately strained bridgehead alkene bicyclo[3.2.2]non-1-ene (**54**) was generated in low temperature matrices and in fluid solutions by photolysis of the diazo precursor **52** and its diazirine isomer **53** (Scheme 13).[44] The diazo compound **52** was matrix isolated in argon by flash vacuum pyrolysis of the corresponding tosylhydrazone, followed by condensation of the pyrolysate in an excess of argon at 28 K. UV irradiation of **52** at 248 or 254 nm resulted in rapid decomposition, but slower and more selective photolysis occurred with visible light (488 or 514 nm). Under the latter conditions, **52** was converted into a mixture of products, which were identified as the diazirine isomer **53** (major) and the bridgehead alkene **54** (minor). The diazo compound and the diazirine could be photochemically interconverted by suitable choice of irradiation wavelength: 308 nm light favoring **52**, while 514 nm light favored **53**. Alternate irradiation of the

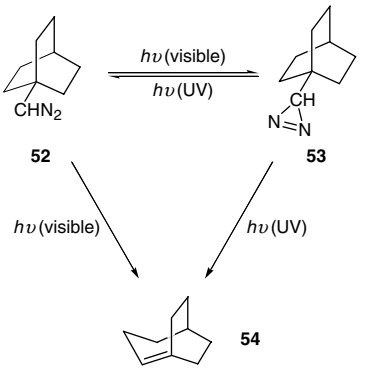

SCHEME 13

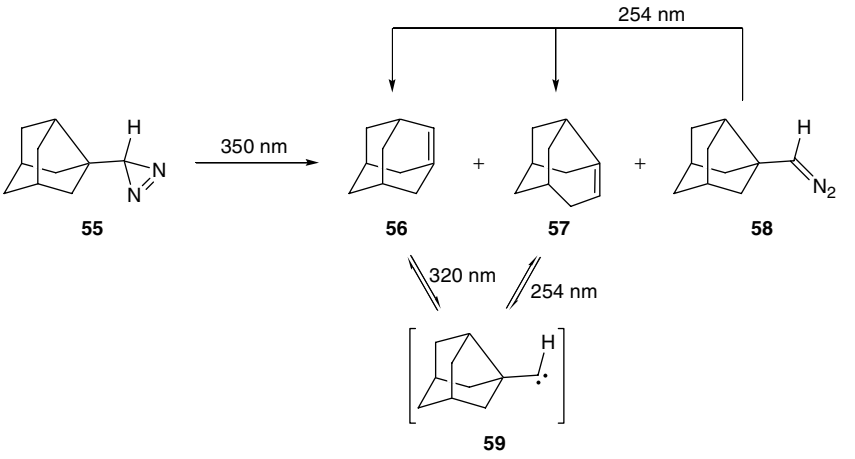

SCHEME 14

matrix sample at 514 and 308 nm eventually caused all the UV and IR absorptions of **52** and **53** to disappear, leaving an IR spectrum that could be assigned to **54** by comparison with a calculated spectrum.

Matrix photolysis of 3-noradamantyldiazirine **55** at 350 nm produced adamantene **56** and protoadamant-3-ene (**57**), together with some of the diazo isomer **58**, which gave the same two bridgehead alkenes when irradiated at 254 nm (Scheme 14).[45] The two alkenes **56** and **57** could be photochemically interconverted with 320 and 254 nm light. The intermediacy of the carbene **59** was proposed for these processes, but the carbene was not detected directly, either in low temperature matrices or in parallel flash-photolysis studies. In an earlier investigation,[46] it had been found that 2-adamantylidene (**60**) rearranged to the tetracyclic tautomer **61** rather than the bridgehead alkene **62**. Computations suggested that formation of **61** from **60** is a much more exothermic process than formation of **62** and that the [1,2]-hydrogen shift that would lead to **62** is effectively prevented by the geometry of the carbene, which keeps the empty *p* orbital perpendicular to the migrating CH bond.

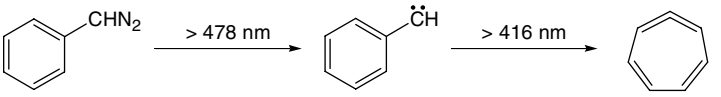

65 **66** **67**

SCHEME 15

The triplet carbene **T-63** was generated in argon matrices by photolysis of the corresponding diazo precursor and characterized by UV-visible and IR spectroscopy.[47] On further irradiation with light of $\lambda > 515$ nm, this carbene rearranged irreversibly to the strained cyclopropene **64**. This reaction most probably occurred on the singlet energy surface, after excitation of **T-63** to the singlet state via excited triplet states.

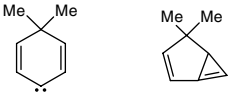

T-63 **64**

Matrix isolated aryl carbenes have yielded routes to a number of strained polyenic systems, including strained cyclopropenes and cyclic cumulenes. For example, photolysis of phenyldiazomethane (**65**) with visible light ($\lambda > 478$ nm) gave phenylmethylene (**66**), which was characterized by its highly structured UV absorptions and its IR spectrum (Scheme 15).[48] Further irradiation of **66** at shorter wavelengths ($\lambda > 416$ nm) produced a new species with a broad UV absorption with $\lambda_{max} = 271$ nm and IR absorptions which seemed considerably more complex than those usually encountered with phenyl groups. It was concluded that the new species was the cyclic allene cyclohepta-1,2,4,6-tetraene (**67**), and IR bands at 1824 and 1816 cm^{-1} were identified as belonging to the $\nu(C{=}C{=}C)_{as}$ stretch of the strained allenic system. In a detailed extension of this first study,[49] the identity of **67** was further supported by deuterium labeling and photolysis of fluoro and chloro derivatives of **65**, which ruled out the bicycloheptatriene **68** and the carbene **69** as alternative possibilities for the photoproduct of **66**. It was also discovered that diazobicycloheptadiene **70**, rather surprisingly, gave **67** as the sole product when photolyzed in argon matrices, and neither the corresponding carbene nor bicycloheptatriene **71** was detected. The diazoketone **72** also yielded **67** as a matrix photoproduct, along with CO and other carbonyl-containing species. The cyclic allene **67** is thus a readily accessible species. A theoretical study of substituent effects on the interconversions of phenylmethylene (**66**), cyclohepta-1,2,4,6-tetraene (**67**), and bicyclo[4.1.0]hepta-2,4,6-triene (**68**) has been published very recently.[50]

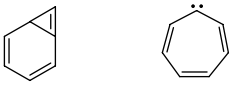

68 **69**

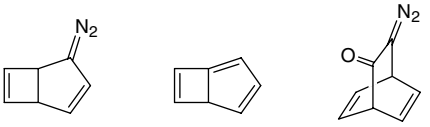

70 **71** **72**

In contrast to phenyldiazomethane, matrix photolysis of the naphthyldiazomethanes produced benzobicyclo[4.1.0]heptatrienes in photoequilibrium with the corresponding carbenes, rather than cyclic allenes.[51–53] For example, photolysis of 2-naphthyldiazomethane (**73**) ($\lambda > 300$ or $\lambda = 480$ nm) in argon at 10 K gave a mixture of the carbene **74** and the benzobicycloheptatriene **75**, which could be interconverted photochemically by choice of suitable irradiation wavelengths (Scheme 16).[52] Broadly similar

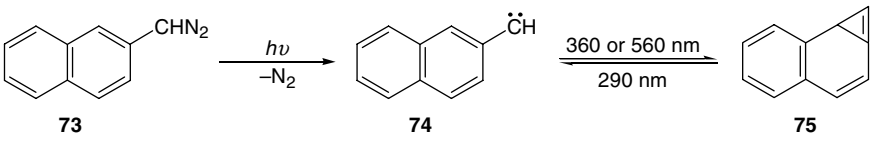

SCHEME 16

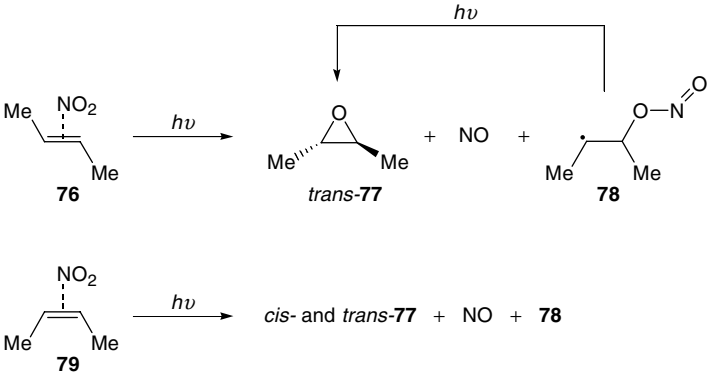

SCHEME 17

results were obtained in an examination of the matrix photolysis of 1-naphthyldiazomethane and its diazirine isomer.[53] Cyclic allenes analogous to **67** were not observed in any of these matrix-isolation studies of naphthylmethylenes.

12.4 Matrix Photochemistry of Alkene Complexes

Alkene Complexes with NO_2

Charge transfer complexes between alkenes and NO_2 in low temperature matrices can be photolyzed with long-wavelength light, resulting in mild and selective oxidation of the alkene. For example, *E*-but-2-ene–NO_2 pairs (**76**) isolated in solid Ar were photolyzed with red, yellow, and green light, yielding *trans*-but-2-ene oxide (*trans*-**77**) and NO (Scheme 17).[54] In this reaction, the epoxide was formed with complete retention of stereochemistry. An addition product was also observed, and this was identified as the butyl nitrite radical **78**. With the isotope mixture $N^{16}O_2/N^{16}O^{18}O/N^{18}O_2$, the product IR spectrum revealed that the radical had nonequivalent O atoms, and this ruled out the analogous nitro radical, in which the O atoms would be identical. Analysis of the photolysis-wavelength dependence of the growth kinetics of *trans*-**77** + NO and the radical **78** showed that the epoxide was formed in two processes. In one, the epoxide, NO, and the radical **78** were generated upon absorption of a single photon by each reactant pair; in the other, *trans*-**77** arose by secondary photolysis of **78**. With *Z*-but-2-ene–NO_2 pairs (**79**) at low matrix concentrations, only 85% of the product epoxide retained the original stereochemistry, and this proportion decreased at higher concentrations.[55] Two conformers of the butyl nitrite radical **78** were also identified in these experiments: one *syn* and the other *anti* with respect to the position of the methyl groups about the central CC bond. Interestingly, on photolysis the *anti* conformer gave *trans*-**77** and NO at a threshold wavelength of 613 nm, while the *syn* conformer gave 2-methylpropanal and NO at 573 nm and shorter wavelengths.

Similar studies have been made of matrix isolated cyclohexene- and cyclopentene–NO_2 pairs.[56] At wavelengths greater than the dissociation threshold of NO_2 (398 nm), the corresponding cycloalkene oxides were the only final oxidation products, although two diastereomeric nitrite radicals were detected

as intermediates in the cyclohexene oxidation, and a single nitrite radical in the cyclopentene case. Comparable results have also been obtained for matrix-isolated complexes of NO_2 with propene.[57] With ethene- and tetradeuterioethene–NO_2 pairs, however, acetaldehyde was formed as well as ethylene oxide at wavelengths greater than 398 nm, and at wavelengths just above this NO_2 dissociation limit (385 and 355 nm), a new pathway leading to ketene was observed.[58] A carbonyl product, pinacolone, was also formed in the matrix photolysis of 2,3-dimethylbut-2-ene–NO_2 complexes alongside tetramethyloxirane.[59]

From these studies of the matrix photolysis of alkene–NO_2 pairs, it has been concluded that the primary process is a large amplitude O-atom transfer from NO_2 to the alkene, which occurs at photon energies below the dissociation threshold of NO_2. This transfer reaction is assumed to give biradicals **80**, which can undergo ring closure to the epoxides, rearrange to carbonyl products, or react with NO within the matrix cage to generate the nitrite radicals. So far, no example of a biradical of the type **80** seems to have been observed directly. In view of the retention of stereochemistry (partial or complete) observed in some of the reactions, it is likely that such biradicals have lifetimes that are short compared to rotation about CC bonds, so any difficulty encountered in detecting them spectroscopically would not be surprising.

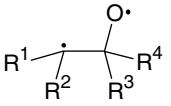

80

The matrix photochemistry of the 2,3-dimethylbut-2-ene complex with N_2O_4 (the NO_2 dimer) has also been investigated.[60] In this case the major product was 2,3-dimethyl-3-nitroso but-2-yl nitrate, a nitroso nitrate, and the minor product 2,3-dimethyl-3-nitrobut-2-yl nitrite, a nitro nitrite. The mechanism by which the observed products were formed appeared to be distinct from that previously suggested for the thermal reaction of alkenes with N_2O_4 in solution.

Other Alkene Complexes

There have been a few studies of the matrix photolysis of complexes between alkene molecules and species other than NO_2. The charge transfer complex between O_2 and 2,5-dimethylhexa-2,3,4-triene (**81**) has been photolyzed in Ar matrices containing various amounts of O_2 and in pure O_2 matrices.[61] Oxidation products were formed even with visible light (543 nm), and these included the trisdioxetane **82**, which decomposed on further irradiation (slowly at $\lambda > 500$ nm, rapidly at $\lambda > 300$ nm) to acetone and CO_2. Identification of **82** was assisted by interpretation of its IR spectrum and the use of oxygen isotopes. At O_2 concentrations between 10 and 100%, the trisdioxetane was almost the sole product in these matrix reactions. At lower O_2 concentrations, a second product was observed, which was identified as dimethylpropadienone (**83**) and was probably formed from dioxetane **84**.

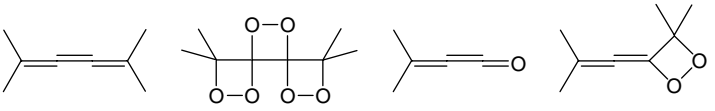

81 **82** **83** **84**

When 2,3-dimethylbut-2-ene was isolated in pure O_2 matrices, a broad charge-transfer band was observed, which tailed into the visible region to about 550 nm.[62] Irradiation of the matrices with visible light ($\lambda > \sim 520$ nm) gave a single product, which was tentatively identified as the tetraoxane **85** on the basis of the IR spectrum obtained with $^{18}O_2$. No product characteristic of the reaction of alkenes with singlet O_2 was detected. Two reaction mechanisms were proposed for the formation of **85**: one involved

stepwise addition of the two O_2 molecules via a triplet biradical, the other was a concerted mechanism in which two O_2 molecules participate in the excitation. The experimental results did not discriminate between these alternatives, however.

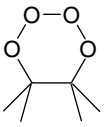

85

The complexes of ethene and cyclopropene with bromine were generated in argon matrices by co-condensation of alkene–argon and bromine–argon mixtures.[63] The structures of the complexes were determined by IR spectroscopy in conjunction with theoretical computations as complexes with the Br–Br bond perpendicular to the CC double bond, e.g., **86**. On photolysis with $\lambda > 300$ nm, the ethene–Br_2 complex gave 1,2-dibromoethane as the only detectable product, but apparently with an unusually high proportion of the normally disfavored *gauche* conformation. Similar photolysis of the cyclopropene complex **86** gave *cis*-1,2-dibromocyclopropane (**87**), 3-bromocyclopropene (**88**), and 1,3-dibromopropene (**89**) as the main products. The experimental results for both complexes fit well with a reaction mechanism in which initial cleavage of the Br–Br bond was followed by addition of one Br atom to the alkene to yield an intermediate monobromo radical.

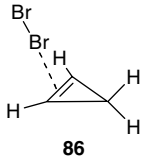

86

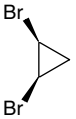

87

88

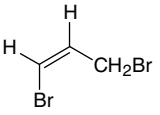

89

References

1. For an up-to-date discussion of the merits of DFT computations, including a comparison of methods for computing IR transitions, see Koch, W. and Holthausen, M.C., *A Chemist's Guide to Density Functional Theory,* Wiley-VCH, Weinheim, 2000.
2. Guillory, W.A. and Thomas, S.G., Jr., Condensed-phase photochemistry of propylene, *J. Phys. Chem.,* 79, 692, 1975.
3. Guillory, W.A. and Andrews, G.H., Primary photochemical processes in the vacuum-ultraviolet photolysis of fluoroethylene, *J. Chem. Phys.,* 62, 4667, 1975.
4. Guillory, W.A. and Andrews, G.H., The vacuum-ultraviolet photolysis of the difluoroethylenes, *J. Chem. Phys.,* 62, 3208, 1975.
5. Barnes, A.J. and Holroyd, S., Photochemistry of 3-halopropenes in argon matrices, *Spectrochim. Acta Part A,* 39, 579, 1983.
6. Paolucci, D.M., Gunkelman, K., McMahon, M.T., McHugh, J., and Abrash, S.A., Photochemistry and dynamics of vinyl bromide and vinyl iodide in rare gas matrices, *J. Phys. Chem.,* 99, 10506, 1995.
7. Laursen, S.L. and Pimentel, G.C., Matrix-induced intersystem crossing in the photochemistry of the 1,2-dichloroethenes, *J. Phys. Chem.,* 93, 2328, 1989.
8. Maier, G. and Bothur, A., The thermally and photochemically induced ring opening of *cis*-3,4-dichlorocyclobutene and *trans*-3,4-dichlorocyclobutene: new insights from a matrix-spectroscopic study, *Eur. J. Org. Chem.,* 2063, 1998.
9. Maier, G., Lautz, C., and Senger, S., Ring opening of 1-methylcyclopropene and cyclopropene: matrix infrared spectroscopic identification of 2-butene-1,3-diyl and propene-1,3-diyl, *Chem.-Eur. J.,* 6, 1467, 2000.

10. Radziszewski, J.G., Yin, T.-K., Miyake, F., Renzoni, G.E., Borden, W.T., and Michl, J., A doubly pyramidalized olefin: matrix isolation spectroscopy of tricyclo[3.3.2.0^{3,7}]dec-3(7)-ene, *J. Am. Chem. Soc.,* 108, 3544, 1986.
11. Yin, T.-K., Radziszewski, J.G., Renzoni, G.E., Downing, J.W., Michl, J., and Borden, W.T., Thermal reorganization of two pyramidalized alkenes by reverse vinylcyclopropane rearrangements, *J. Am. Chem. Soc.,* 109, 820, 1987.
12. Radziszewski, J.G., Yin, T.-K., Renzoni, G.E., Hrovat, D.A., Borden, W.T., and Michl, J., Matrix isolation of tricyclo[3.3.1.0^{3,7}]non-3(7)-ene, a doubly pyramidalized alkene predicted to have a nearly tetrahedral geometry at the olefinic carbons, *J. Am. Chem. Soc.,* 115, 1454, 1993.
13. Datta, P., Goldfarb, T.D., and Boikess, R.S., Photolysis of matrix isolated 1,3-cyclohexadiene, *cis*-1,3,5-hexatriene and *trans*-1,3,5-hexatriene, *J. Am. Chem. Soc.,* 93, 5189, 1971.
14. Datta, P., Goldfarb, T.D., and Boikess, R.S., Photolysis of matrix-isolated 1,3,5-cyclooctatriene and bicyclo[4.2.0]octa-2,4-diene. Spectra of their transient photolysis products, *J. Am. Chem. Soc.,* 91, 5429, 1969.
15. Brouwer, A.M. and Jacobs, H.J.C., Photochemistry of 2,5-dimethyl-1,3,5-hexatrienes in argon matrices. Formation of isomers and rotamers, *Recl. Trav. Chim. Pays-Bas,* 114, 449, 1995.
16. Wrobel, R., Sander, W., Cremer, D., and Kraka, E., Photochemistry of butatriene — spectroscopic evidence for the existence of allenylcarbene, *J. Phys. Chem. A,* 104, 3819, 2000.
17. Wenk, H.H., Sander, W., Leonov, A., and de Meijere, A., Matrix isolation and photochemistry of tetrafluoro-*p*-xylylene, *Eur. J. Org. Chem.,* 3287, 1999.
18. Marquardt, R., Sander, W., Laue, T., and Hopf, H., Photochemistry of [2,2]paracyclophan-enes — a matrix-isolation study, *Liebigs Ann. Chem.,* 2039, 1996.
19. Lin, C.Y. and Krantz, A., Matrix preparation of cyclobutadiene, *J. Chem. Soc., Chem. Commun.,* 1111, 1972.
20. Chapman, O.L., McIntosh, C.L., and Pacansky, J., Cyclobutadiene, *J. Am. Chem. Soc.,* 95, 614, 1973.
21. Pong, R.G.S. and Shirk, J.S., Photochemistry of α-pyrone in solid argon, *J. Am. Chem. Soc.,* 95, 248, 1973.
22. Chapman, O.L., McIntosh, C.L., and Pacansky, J., Photochemistry of α-pyrone in argon at 8 K, *J. Am. Chem. Soc.,* 95, 244, 1973.
23. Chapman, O.L., De La Cruz, D., Roth, R., and Pacansky, J., Mono- and dideuteriocyclobutadienes, *J. Am. Chem. Soc.,* 95, 1337, 1973.
24. Krantz, A., Lin, C.Y., and Newton, M.D., Cyclobutadiene. II. On the geometry of the matrix-isolated species, *J. Am. Chem. Soc.,* 95, 2744, 1973.
25. Maier, G., Hartan, H.-G., and Sayrac, T., Cyclobutadiene — a square singlet molecule? *Angew. Chem. Int. Ed. Engl.,* 15, 226, 1976; *Angew. Chem.,* 88, 252, 1976.
26. Masamune, S., Sugihara, K., Morio, K., and Bertie, J.E., [4]Annulene. Comments on its infrared spectrum, *Can. J. Chem.,* 54, 2679, 1976.
27. Pong, R.G.S., Huang, B.-S., Laureni, J., and Krantz, A., Cyclobutadiene. 3. Photolysis of matrix-isolated ^{13}C-labeled bicyclopyranones, *J. Am. Chem. Soc.,* 99, 4153, 1977.
28. Masamune, S., Souto-Bachiller, F.A., Machiguchi, T., and Bertie, J.E., Cyclobutadiene is not square, *J. Am. Chem. Soc.,* 100, 4889, 1978.
29. Bally, T. and Masamune, S., Cyclobutadiene, *Tetrahedron*, 36, 343, 1980.
30. Fraga, S., Possible interactions of cyclobutadiene with by-products in inert matrix isolation studies, *Tetrahedron Lett.,* 22, 3343, 1981.
31. Maier, G., Hoppe, M., Lanz, K., and Reisenauer, H.P., Neue Wege zum Cyclobutadien und Methylencyclopropen, *Tetrahedron Lett.,* 25, 5645, 1984.
32. Orendt, A.M., Arnold, B.R., Radziszewski, J.G., Facelli, J.C., Malsch, K.D., Strub, H., Grant, D.M., and Michl, J., ^{13}C NMR and polarized IR spectra of vicinally labeled [$^{13}C_2$]cyclobutadiene in an argon matrix: interconversion of valence tautomers, *J. Am. Chem. Soc.,* 110, 2648, 1988.

33. For a detailed account of the generation of oriented samples and linearly polarized spectroscopy, see Michl, J. and Thulstrup, E.W., Spectroscopy with Polarized Light: Solute Alignment by Photoselection, *in Liquid Crystals, Polymers and Membranes,* VCH, New York, 1986. For a shorter account of the applications of linearly polarized photolysis and spectroscopy to matrix-isolation studies, see Dunkin, I.R., *Matrix-Isolation Techniques: A Practical Approach,* Oxford University Press, Oxford, 1998, chap. 5.
34. Arnold, B.R., Radziszewski, J.G., Campion, A., Perry, S.S., and Michl, J., Raman spectrum of matrix-isolated cyclobutadiene. Evidence for environmental hindrance to heavy-atom tunneling? *J. Am. Chem. Soc.,* 113, 692, 1991.
35. Arnold, B.R. and Michl, J., Ultraviolet and polarized infrared spectroscopy of matrix-isolated cyclobutadiene and its isotopomers, *J. Phys. Chem.,* 97, 13348, 1993.
36. Bally, T., Chai, S., Neuenschwander, M., and Zhu, Z., Pentalene: formation, electronic and vibrational structure, *J. Am. Chem. Soc.,* 119, 1869, 1997.
37. Goldfarb, T.D. and Pimentel, G.C., Chemiluminescence of ethylene formed probably from methylene in an inert matrix, *J. Chem. Phys.,* 33, 105, 1960.
38. Lee, Y.-P. and Pimentel, G.C., Chemiluminescence of ethylene in an inert matrix and the probable infrared spectrum of methylene, *J. Chem. Phys.,* 75, 4241, 1981.
39. Baird, M.S., Dunkin, I.R., and Poliakoff, M., Thermal dimerization and carbonylation of a carbene in low-temperature matrices, *J. Chem. Soc., Chem. Commun.,* 904, 1974.
40. Baird, M.S., Dunkin, I.R., Hacker, N., Poliakoff, M., and Turner, J.J., Cyclopentadienylidene. A matrix isolation study exploiting photolysis with unpolarized and plane-polarized light, *J. Am. Chem. Soc.,* 103, 5190, 1981.
41. Bell, G.A. and Dunkin, I.R., Tetrachlorocyclopentadienylidene, indenylidene and fluorenylidene in low-temperature matrices: ultraviolet and infrared spectra and reactions with carbon monoxide, *J. Chem. Soc., Faraday Trans. 2,* 81, 725, 1985.
42. Dunkin, I.R. and McCluskey, A., Tetrabromocyclopentadienylidene: generation and reaction with CO in low temperature matrices, *Spectrochim. Acta Pt. A,* 49, 1179, 1993.
43. O'Gara, J.E. and Dailey, W.P., Matrix-isolation and *ab initio* molecular orbital study of 2,2,2-trifluoroethylidene, *J. Am. Chem. Soc.,* 116, 12016, 1994.
44. Gudipati, M.S., Radziszewski, J.G., Kaszynski, P., and Michl, J., Bicyclo[3.2.2]non-1-ene: matrix isolation and spectroscopic characterization of a moderately strained bridgehead olefin, *J. Org. Chem.,* 58, 3668, 1993.
45. Tae, E.L., Zhu, Z., and Platz, M.S., A matrix isolation, laser flash photolysis and computational study of adamantene, *J. Phys. Chem. A,* 105, 3803, 2001.
46. Bally, T., Matzinger, S., Truttmann, L., Platz, M.S., and Morgan, S., Matrix spectroscopy of 2-adamantylidene, a dialkylcarbene with singlet ground state, *Angew. Chem. Int. Ed. Engl.,* 33, 1964, 1994; *Angew. Chem.,* 106, 2048, 1994.
47. Albers, R., Sander, W., Ottosson, C.-H., and Cremer, D., 4,4-Dimethylbicyclo[3.1.0]hexa-1(6),2-diene — a highly strained 1,3-bridged cyclopropene, *Chem.-Eur. J.,* 2, 967, 1996.
48. West, P.R., Chapman, O.L., and LeRoux, J.-P., Cyclohepta-1,2,4,6-tetraene, *J. Am. Chem. Soc.,* 104, 1779, 1982.
49. McMahon, R.J., Abelt, C.J., Chapman, O.L., Johnson, J.W., Kreil, C.L., LeRoux, J.-P., Mooring, A.M., and West, P.R., 1,2,4,6-Cycloheptatetraene: the key intermediate in arylcarbene interconversions and related C_7H_6 rearrangements, *J. Am. Chem. Soc.,* 109, 2456, 1987.
50. Geise, C.M. and Hadad, C.M., Substituent effects in the interconversion of phenylcarbene, bicyclo[4.1.0]hepta-2,4,6-triene and 1,2,4,6-cycloheptatetraene, *J. Org. Chem.,* 67, 2532, 2002.
51. West, P.R., Mooring, A.M., McMahon, R.J., and Chapman, O.L., Benzobicyclo[4.1.0]hepta-2,4,6-trienes, *J. Org. Chem.,* 51, 1316, 1986.

52. Albrecht, S.W. and McMahon, R.J., Photoequilibration of 2-naphthylcarbene and 2,3-benzobicyclo[4.1.0]hepta-2,4,6-triene, *J. Am. Chem. Soc.,* 115, 855, 1993.
53. Bonvallet, P.A. and McMahon, R.J., Photoequilibration of 1-naphthylcarbene and 4,5-benzobicyclo[4.1.0]hepta-2,4,6-triene, *J. Am. Chem. Soc.,* 121, 10496, 1999.
54. Nakata, M. and Frei, H., Stereoselective photooxidation of *trans*-2-butene to epoxide by nitrogen dioxide excited with red light in a cryogenic matrix, *J. Am. Chem. Soc.,* 111, 5240, 1989.
55. Nakata, M. and Frei, H., Stereocontrol of the red light induced photoepoxidation of 2-butenes by nitrogen dioxide in solid Ar, *J. Phys. Chem.,* 93, 7670, 1989.
56. Fitzmaurice, D.J. and Frei, H., Photochemistry of cycloalkene·NO_2 collisional pairs in a cryogenic matrix: chemical trapping of cycloalkene oxirane biradical conformers and comparison of product control for excitation above and below the NO_2 dissociation threshold, *J. Phys. Chem.,* 95, 2652, 1991.
57. Nakata, M., Somura, Y., Takayanagi, M., Tanaka, N., Shibuya, K., Uchimaru, T., and Tanabe, K., Visible light-induced reaction of NO_2 with propene in low-temperature argon and xenon matrices, *J. Phys. Chem.,* 100, 15815, 1996.
58. Fitzmaurice, D.J. and Frei, H., Photoinduced oxygen transfer from NO_2 to ethylene in the vicinity of the NO_2 dissociation threshold. A laser photochemical study on reactant pairs isolated in solid argon, *J. Phys. Chem.,* 96, 10308, 1992.
59. Nakata, M., Red light-induced reaction of NO_2 with 2,3-dimethyl-2-butene in a low-temperature argon matrix, *Spectrochim. Acta Pt. A,* 50, 1455, 1994.
60. Blatter, F. and Frei, H., Visible-light–induced photochemistry of 2,3-dimethyl-2-butene·N_2O_4 charge-transfer complexes in solid inert matrices at 75 K, *J. Phys. Chem.,* 97, 1178, 1993.
61. Sander, W. and Patyk, A., Photooxidation of 2,5-dimethyl-2,3,4-hexatriene — matrix isolation of a trisdioxetane, *Angew. Chem. Int. Ed. Engl.,* 26, 475, 1987; *Angew. Chem.,* 99, 495, 1987.
62. Hashimoto, S. and Akimoto, H., Visible light photooxygenation of 2,3-dimethyl-2-butene at the contact charge-transfer band in the cryogenic oxygen matrix, *J. Phys. Chem.,* 90, 529, 1986.
63. Maier, G. and Senger, S., Bromine complexes of ethylene and cyclopropene: matrix-IR-spectroscopic identification, photochemical reactions, *ab initio* studies, *Liebigs Ann. Chem.,* 317, 1997.

13

Photorearrangement and Fragmentation of Alkenes

Paul J. Kropp
University of North Carolina

13.1 Photochemical Behavior

On direct irradiation in nonhydroxylic solvents, alkenes typically undergo several competing photoreactions. In addition to *E,Z*-isomerization, which is also exhibited on triplet sensitization, several processes occur that are usually observed only on direct irradiation: rearrangement via carbene intermediates, double bond migration, alkyne formation, and hydrogen atom abstraction. This chapter is concerned with these latter processes. Emphasis is given to developments since the topic was reviewed extensively in 1979.[1] Portions of this material are covered in reviews that have appeared since then.[2,3] The photobehavior of alkenes in hydroxylic media is discussed in Chapter 9.

Spectroscopic Properties

The ultraviolet absorption spectra of simple alkenes in solution typically consist of single, featureless bands with maxima at 185–195 nm ($\varepsilon = 5\text{–}10 \times 10^3$) and tails extending to 210–255 nm.[4] Absorption extends to longer wavelengths with increasing degrees of substitution. The spectra are deceptively simple, as they consist of several overlapping bands arising from close-lying transitions, two of which are generally accepted as being $\pi \rightarrow \pi^*$ and $\pi \rightarrow R(3s)$.[5] Weak absorptions attributed to $\pi \rightarrow \sigma^*$ transitions have also been reported for alkenes in the liquid state,[5c] although their presence has not been independently confirmed. Gas-phase absorption spectra are generally similar to those in solution except for the presence of some structure in the bands and somewhat longer absorption tails. Due to the diffuseness of Rydberg orbitals, bands corresponding to Rydberg transitions are severely reduced in intensity and blue-shifted in the condensed phase compared to the gas phase at low pressure.

0-8493-1348-1/04/$0.00+$1.50

Alkenes exhibit only weak fluorescence, which is thought to involve emission from the π,R(3s) state.[6] On excitation at 185 nm, the emission maximum moves from 231 to 263 nm with increasing alkyl substitution, and the fluorescence quantum yield increases from 1×10^{-6} to 1.5×10^{-4}. Ethene itself does not fluoresce. The excitation maximum increases with increasing wavelength, moving from 195 nm for disubstituted to 229 nm for tetrasubstituted alkenes. The fluorescence lifetime is estimated at 15 psec.

Owing to the large energy gap between the singlet and triplet manifolds, alkenes do not readily undergo intersystem crossing. Thus, their behavior on direct irradiation arises from singlet-excited states. The vertical excitation energy of the π,R(3s) singlet is generally below that of the ππ* singlet. Having a somewhat electron-deficient core, the ππ* excited state moves to lower energy with increasing alkyl substitution. But due to the large size of the 3s Rydberg orbital, the π,R(3s) state has an even more electron-deficient core and responds more strongly to alkyl substitution. Thus, the separation between the ππ* and π,R(3s) vertical levels increases with increasing substitution. However, the ππ* state undergoes substantial relaxation through pyramidalization and/or rotation about the central CC bond. Thus, in alkenes that are not highly substituted, the vertical levels are close, and the relaxed ππ* level is close to, if not lower than, that of the π,R(3s) state. With increasing substitution, there is increasing likelihood that the π,R(3s) state is lower lying. However, analysis of the ultrafast dynamics following irradiation of several alkenes in the gas phase has recently implied the presence of yet a third excited state somewhat lower lying than these two: the zwitterionic Z state (π^{*2}), which involves excitation of two π electrons.[7]

Principal Pathways

Irradiations of alkenes are generally conducted with a low-pressure mercury lamp (185 nm), an ArF excimer laser (193 nm), or a zinc resonance lamp (214 nm). Highly substituted alkenes can also be irradiated with a medium-pressure lamp and quartz optics (>200 nm). Because of the presence of two or more close-lying singlet excited states, irradiation of alkenes usually results in several competing photoprocesses. Thus, for example, irradiation of 2,3-dimethyl-2-butene (**1**) in hydrocarbon or ether solvent results in rearrangement to the carbene-derived products **4** and **5** and the double bond isomer **9**.[8] *E,Z*-Isomerization also occurs but is not apparent in this case because of the symmetry of alkene **1**. Similar behavior is exhibited in the gas phase.[9] In alcoholic or aqueous media, the nucleophilic trapping products **8** are formed in competition with the carbene-derived products **4** and **5**.[10]

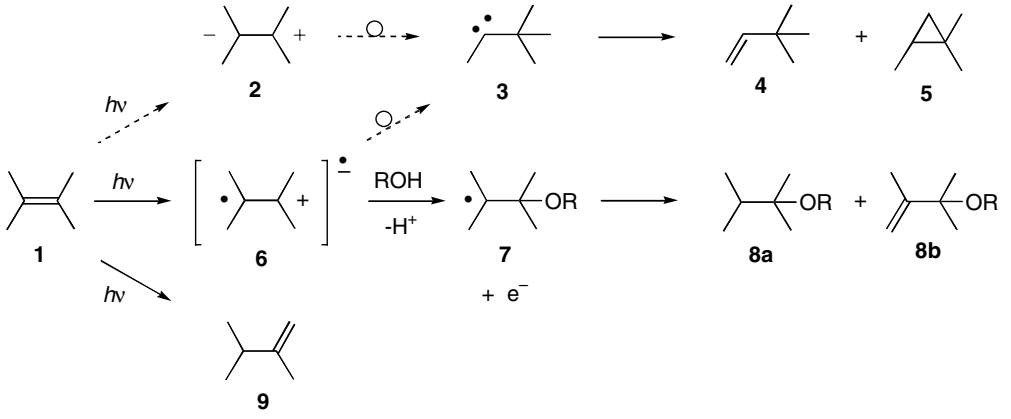

The monosubstituted alkene 1-octene (**10**), on the other hand, affords the double bond migration products *E*- and *Z*-2-octene (**11**) but no products obviously derived from a carbene intermediate.[11] However, a new type of product, alkyne **12**, is formed, along with a small amount of the reduction product **13**. In addition to these general types of photobehavior, some alkenes exhibit behavior that is specific to particular systems, as outlined below.

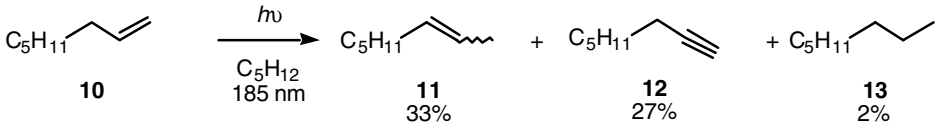

13.2 Mechanisms

Rearrangement via Carbene Intermediates

There is general agreement with the proposal that products such as the rearranged alkene **4** and the cyclopropane **5** arise via competing 1,2 and 1,3 insertion of a carbene intermediate (**3**).[8] The involvement of carbene intermediates is supported by formation of the same products in similar ratios on independent generation of the corresponding carbenes for a wide range of alkenes. Formation of the carbene-derived products **4** and **5** relative to the double bond migration product **9** is wavelength dependent, being favored at higher wavelengths.[9,12]

2-Norbornene (**14**) affords products (**17** and **18**) derived from two carbene intermediates (**15** and **16**), along with small amounts of the radical-derived products **20–22**.[13,14] In the case of cyclohexene (**27**), deuterium-labeling studies showed that products **30** and **31** arise from carbenes **28** and **29**.[13] It was concluded that these intermediates are formed in a ratio of 14:1, respectively, but this does not take into account any reformation of starting material. Thus, in alkenes that are not fully substituted, hydrogen migration can compete with alkyl migration in carbene formation. However, hydrogen migration to form cyclopentylidene is at most a minor process in the photobehavior of cyclopentene (**32**), which affords the carbene-derived products **36** and **37** along with the radical-derived products **34** and **35**.[14,15]

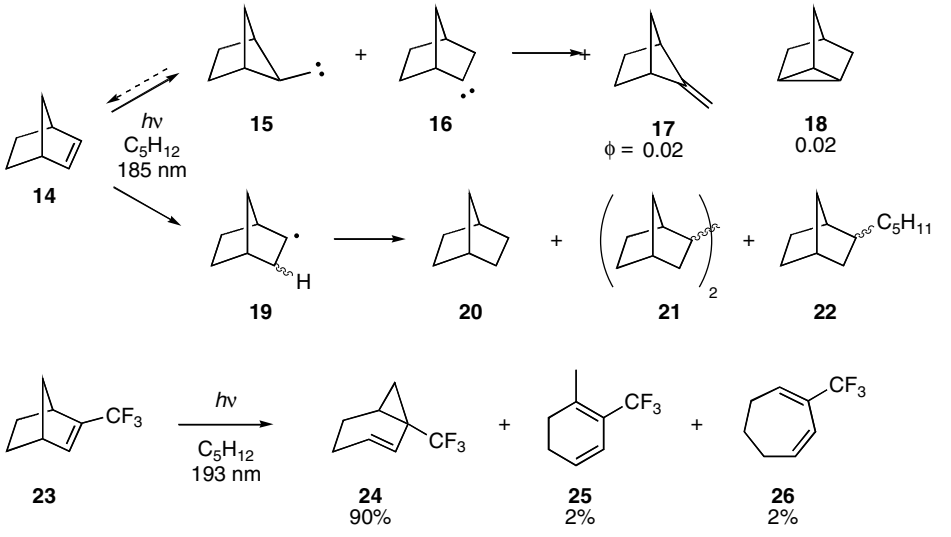

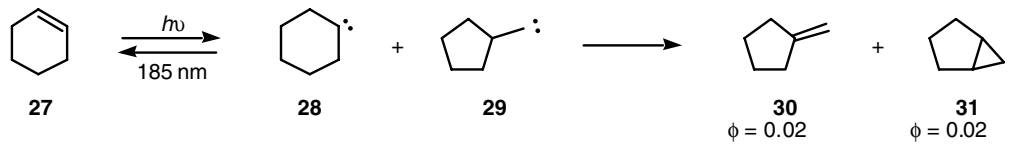

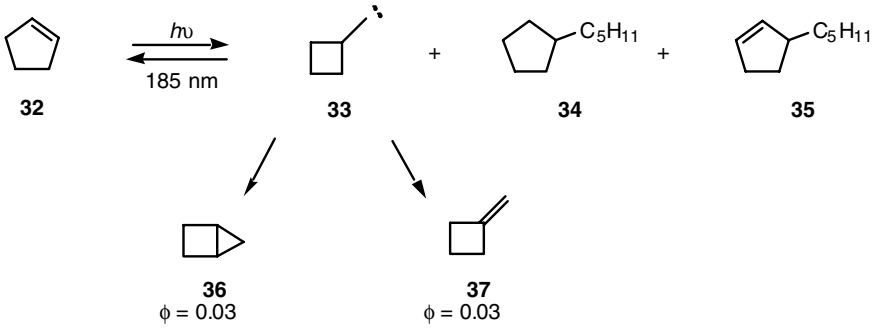

In contrast with 2-norbornene (**14**), the 2-CF_3 derivative **23** afforded no carbene-derived products but gave instead principally the 1,3-alkyl migration product **24** along with the related minor products **25** and **26**.[16] Spectroscopic studies of **23** showed that the strongly electron-withdrawing CF_3 substituent raises the energy of the π,R(3s) state, rendering the ππ* state lower lying in solution.[4b] The absence of carbene-derived products from **23** suggests that they normally arise from the π,R(3s) state. This would also be consistent with the preferred formation of the carbene-derived products **4** and **5** from alkene **1** at higher wavelengths, since the π,R(3s) state is lower lying than the ππ* state in tetrasubstituted alkenes. The electron-deficient core of the π,R(3s) state (**6**) could readily undergo [1,2]-sigmatropic rearrangement to a carbene. However, from analysis of the ultrafast dynamics following irradiation of 2-norbornene (**14**) and cyclohexene (**27**) in the gas phase, it was recently proposed that the carbene intermediates arise instead from the zwitterionic state Z (**2**), which crosses the ππ* surface.[7,17]

Labeling studies on the related homobrexene (**38**), which afforded the carbene-derived products **40** and **42**, revealed that the migrating hydrogen atom had a 2.3:1 preference for assuming the axial position.[18] Interestingly, deuterium had an even greater preference (10.2:1) for the axial pathway. Some scrambling of labeled **38** occurred, presumably because of competing return of one or both of the carbene intermediates **39** and **41**. On independent generation, carbene **39** afforded an approximately 3:1 mixture of the insertion product **40** and homobrexene (**38**).

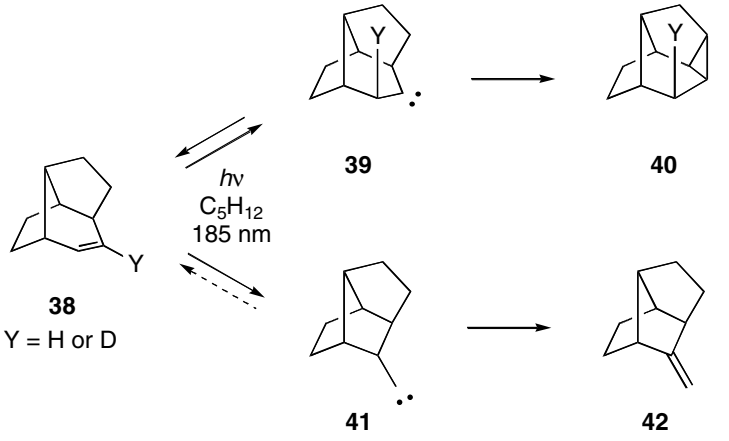

[1,3]-Sigmatropic Rearrangements

Double bond migration generally competes with *E,Z*-isomerization and the formation of carbene-derived products, unless it is structurally inhibited as in 2-norbornene (**14**) and homobrexene (**38**). It presumably occurs in cyclohexene (**27**) and cyclopentene (**32**) but is not observable. In an alkene such as **43**, in which the double bond is exocyclic to a five-membered ring, migration is the dominant photoprocess and occurs

preferentially into, rather than away from, the ring.[19] Labeling studies with 43-d_4 showed that double bond migration involves an intramolecular [1,3]-sigmatropic migration of an allylic hydrogen atom and exhibits a deuterium isotope effect of 2.7.

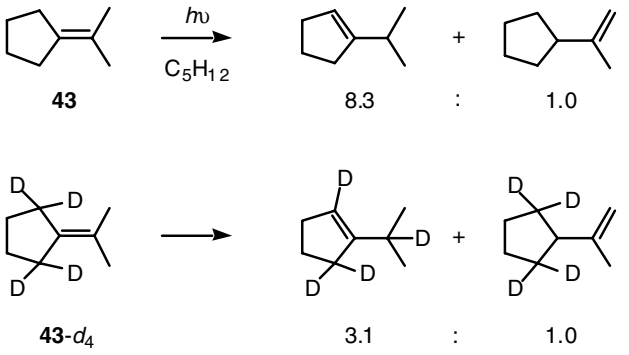

No current agreement exists as to which excited state is responsible for [1,3]-hydrogen migration. As noted above, the ratio of double bond migration to formation of carbene-derived products from alkene **1** is wavelength dependent, being favored at shorter wavelengths. Thus, the π,R(3s) state is apparently not involved in [1,3]-hydrogen migration. Similarly, irradiation of *Z*-2-octene (*Z*-**11**) at 185 nm afforded competing *E,Z*-isomerization and rearrangement to a mixture of the double isomers **10** and *E*- and *Z*-**44**, whereas at wavelengths >200 nm only *E,Z*-isomerization was observed.[12] It was thus concluded that [1,3]-hydrogen migration does not involve the ππ* state either, and the $\sigma_\pi(CH_2)$,π* or π(C=C),σ_π*(CH_2) charge-transfer state was suggested as an alternative. However, it has been noted that the latter wavelength effect merely indicates that double bond migration does not involve the ππ* state in the case of a disubstituted alkene such as **11**.[16] It is conceivable that the double bond isomers **10** and **44** arise via the carbene intermediates **45** in this case and are thus derived from the π,R(3s) excited state, which is higher lying than the ππ* state in a disubstituted alkene.

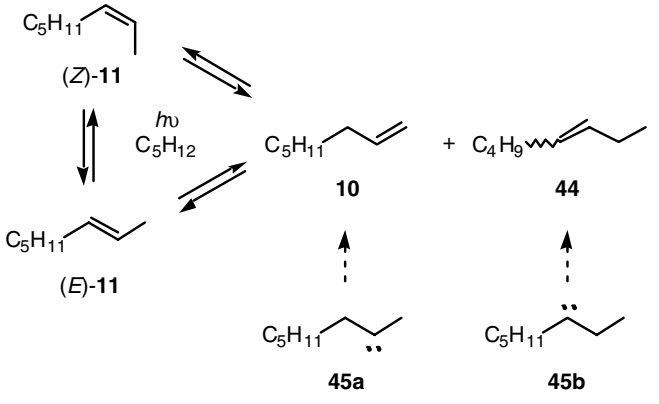

This leaves the possible involvement of the ππ* state in the direct [1,3]-hydrogen migrations in alkenes such as **1** and **43**. Some support for this assignment is provided by the formation of the analogous [1,3]-alkyl migration product **15** by the CF_3-substituted norbornene **23**, which has a low-lying ππ* state.[4b,16] Similar behavior was exhibited by the nitrile **46**, which afforded a 20:1 mixture of the [1,3]- and [1,2]-alkyl shift products **47** and **48**, respectively.[20] Since the lowest-lying excited singlet state of the conjugated alkene **46** is π,π*, it has been proposed that 1,3-alkyl migration in norbornene **23** also involves the ππ* state.[16]

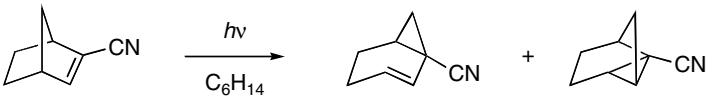

46 **47** 20 : **48** 1

Alkyne Formation

As noted above, irradiation of 1-octene (**10**) afforded a substantial amount of 1-octyne (**12**).[11] Similarly, the principal photobehavior of ethene is formation of ethyne and H_2.[21] Since the 1,1-d_2 derivative **10**-d_2 afforded alkyne **12** with an isotope effect ϕ_H/ϕ_D of 1.9 and almost complete loss of deuterium, the principal route to **12** apparently involves the vinylidene **49** as an intermediate. Alkyne formation is also a major pathway for the keto analog **55**.[22] Interestingly, the γ,δ-unsaturated ketones **55**, **59**, and **62** exhibit photobehavior typical of alkenes at 185 nm. Similar to alkene **10**-d_2, the terminally labeled derivative of enone **55** afforded alkyne **57** with 90% loss of deuterium. The 2,2-disubstituted alkene **50** afforded a mixture of the alkyne **52** and 1-methylcyclopentene (**53**), expected products from the vinylidene intermediate **51**, along with the double bond migration product **54**, and the keto analog **59** similarly afforded alkyne **61** and the double bond migration product **60**. Alkyne formation has also been observed in the 1,2-disubstituted analog **62**, which afforded a mixture of alkynes **64** and **65**, along with the double bond migration product **63** and the 1,3-acyl migration product **66**. It has been proposed that alkyne formation involves the ππ* excited state, since it has not been observed for highly substituted alkenes, in which the π,R(3s) state is lowest lying.[11,22]

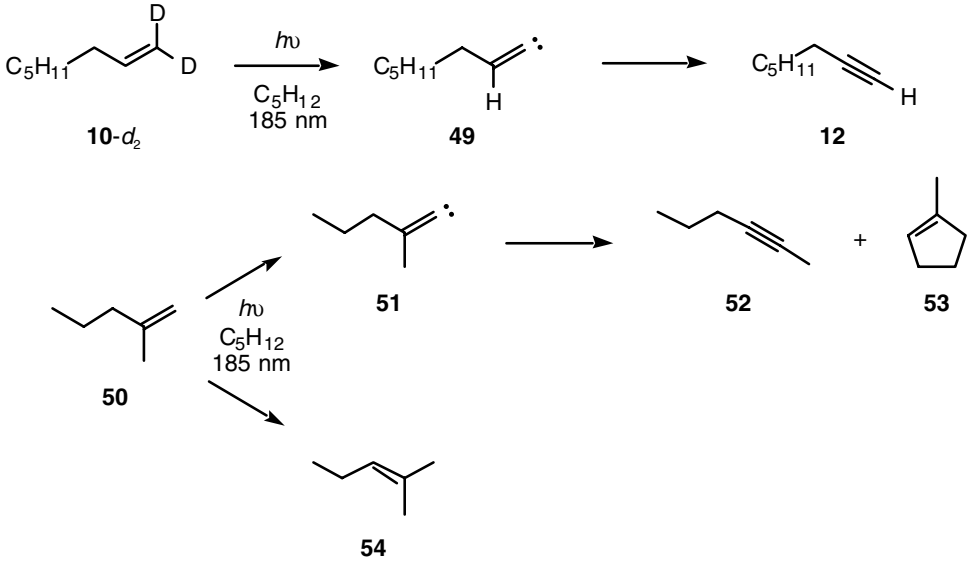

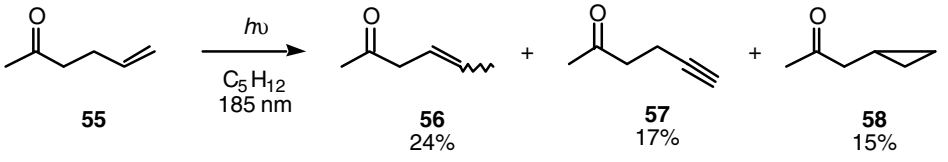

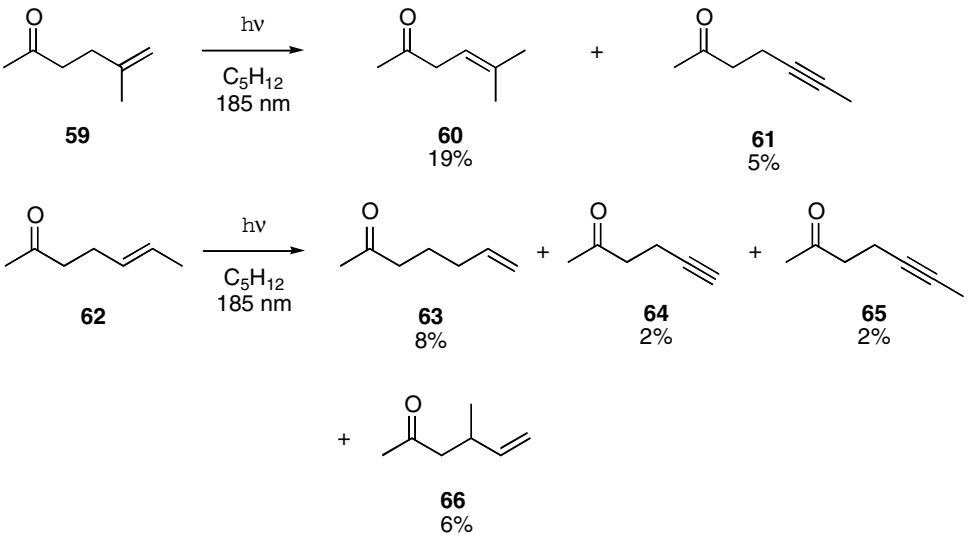

Hydrogen-Atom Abstraction

As noted above, irradiation of 2-norbornene (**14**) in pentane afforded, in addition to the carbene-derived products **17** and **18**, a mixture of alkanes **20–22**, which appear to be derived from the radical **19**, formed by hydrogen atom abstraction from the solvent.[14] Analogous behavior was observed for 1-octene (**10**), which afforded the reduction product octane (**13**), and cyclopentene (**32**), which afforded the radical-derived products **34** and **35**.[11,14] In each case, a mixture of branched decanes arising from coupling of solvent-derived pentyl radicals was also obtained. Hydrogen-atom abstraction has also been attributed to the $\pi\pi^*$ excited state.[14]

13.3 Further Examples

Medium and Large Cycloalkenes

Medium- and large-ring systems are noted for undergoing transannular reactions. This is seen in the cycloalkenes **67**, which afforded, in addition to *E,Z*-isomerization, the *cis*-bicyclo[*n*.3.0]alkanes **70** resulting from 1,5-transannular insertion of the corresponding cycloalkylidene intermediates **68**.[23] Only the smallest member of the series of cyclic alkenes, **67a**, afforded a product, which was identified as (**72a**). Apparently, this product arises from a ring-contracted cycloalkylmethylene intermediate (**69a**). The largest members of the series, **67d** and **67e**, gave small amounts of the fragmentation products **74** and **75**. Double bond migration presumably also occurs but is an identity process in these cases. When generated independently, cycloalkylidenes **68** undergo substantial 1,2-insertion to form cycloalkenes **67**. This is particularly true for the two largest members of the series, **68d** and **68e**, which give only a small amount of transannular insertion when generated independently. Transannular insertion is magnified when the cycloalkylidene intermediates are generated by irradiation of the corresponding cycloalkenes, since any 1,2-insertion simply regenerates the cycloalkene, which is recycled, whereas the bicyclic products **70** are photostable and accumulate in the irradiation mixture.

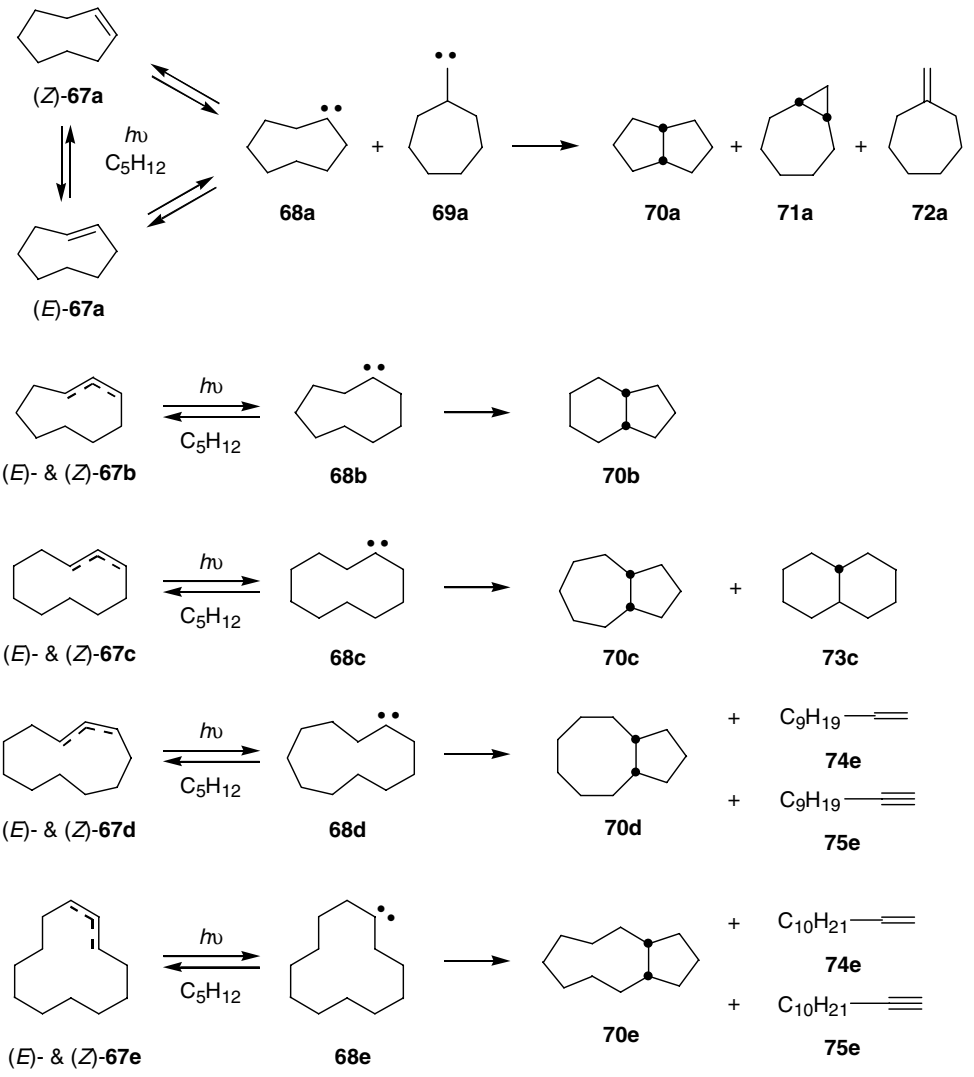

Cyclobutenes

Leigh and co-workers have studied the photochemical reactions of cyclobutenes. A rather complex picture has emerged, which may not yet be fully understood. Irradiation of cyclobutene (**76**) itself afforded principally the ring opening product 1,3-butadiene (**77a**), accompanied by smaller amounts of methylenecyclopropane (**78**) and the fragmentation products ethene and ethyne.[24] Under the irradiation conditions, 1,3-butadiene (**77**) underwent a small amount of reversion to cyclobutene (**76**), and methylenecyclopropane (**78**) underwent secondary conversion to 1,3-butadiene (**77a**) and the fragmentation products ethene and ethyne. It was proposed that 1,3-butadiene (**77a**) arises via electrocyclic ring opening of the $\pi\pi^*$ excited singlet state and that the minor products are derived from the carbene intermediates **79** and **80** formed by rearrangement of the π,R(3s) state.

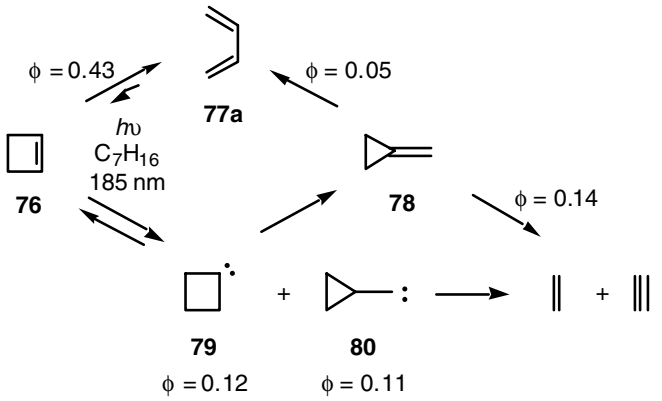

Similar behavior was exhibited by the bicyclo[*n*.2.1]alkenes **81**, except that the highly strained methylenecyclopropane **83a** was not formed.[25] Surprisingly, **81b** and **81c** afforded an *E,Z*-mixture of the 1,3-dienes **82b** and **82c** under conditions in which the dienes do not undergo interconversion.[4c,25b,26] Thus, ring opening of cyclobutenes is not stereospecific.

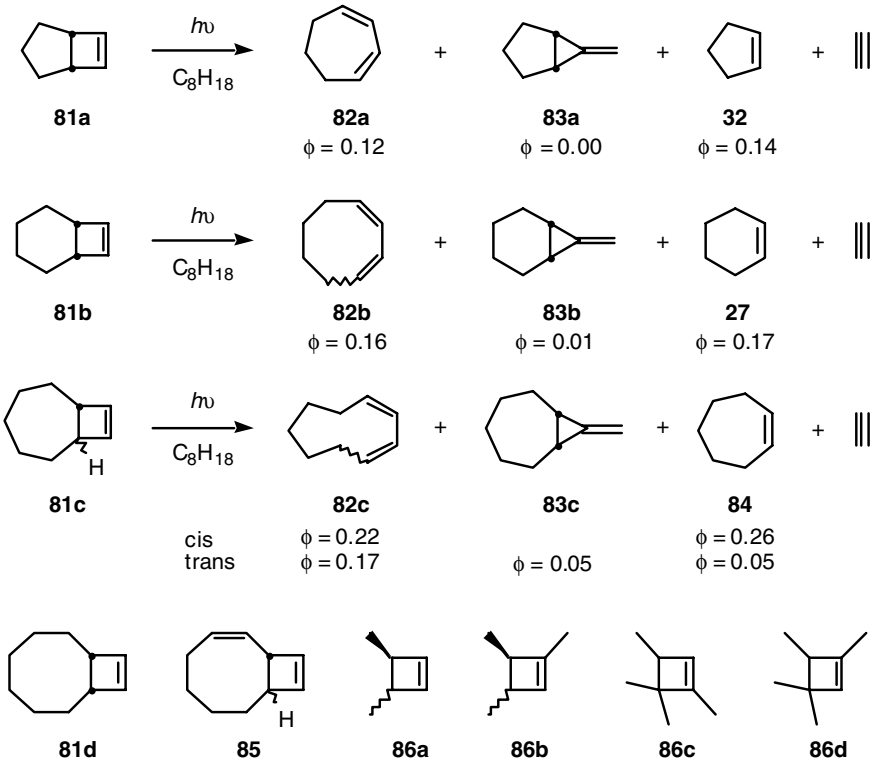

Similar lack of specificity has been observed for the bicyclo[6.2.1]octenes **81d** and **85**,[26] as well as the *cis*- and *trans*-isomers of cyclobutenes **86a–b** and the pair of tetrasubstituted cyclobutenes **86c–d**.[4a,4c,25b] On irradiation at 214 nm, the 1,2-dimethylcyclobutenes **87** also afforded all possible stereoisomers of the ring-opening products **77** (combined quantum yields 0.05–0.26), along with the usual fragmentation products (combined quantum yields 0.010–0.032).[27]

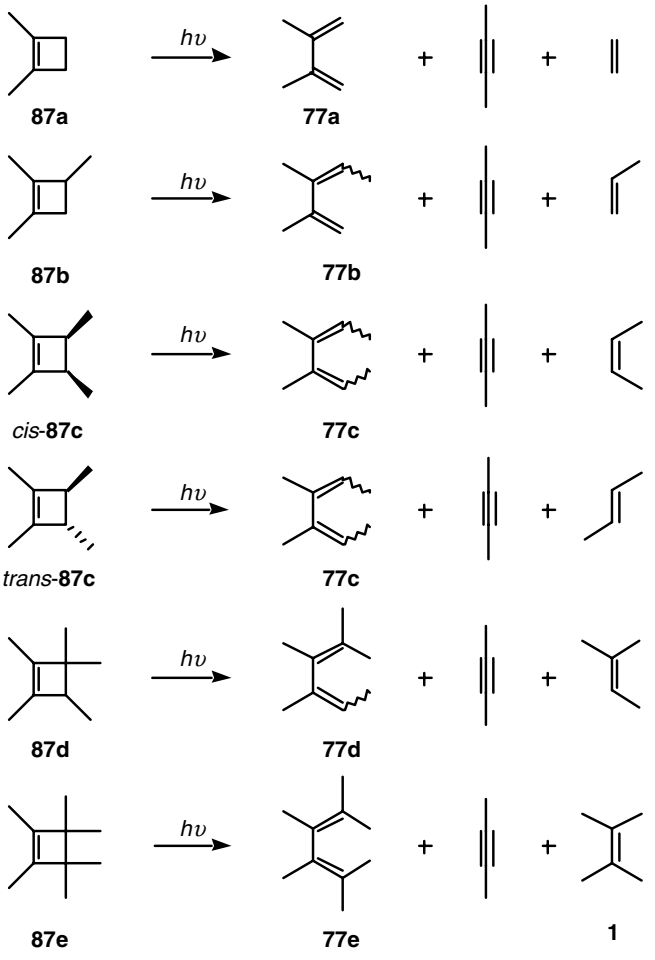

The bicyclo[4.2.0]oct-1(6)-ene system **88** comes closest to affording the disrotatory opening expected by orbital symmetry, with the *cis*-isomer giving mainly diene *E,E*-**89** and the *trans*-isomer even more predominantly diene *E,Z*-**89**.[28] Similarly, cyclobutene *cis*-**90** undergoes ring opening to diene *E,E*-**91** with a substantially higher quantum yield than *trans*-**90**, which would have to afford the highly strained *E,Z*-isomer of diene **91** to open in a disrotatory fashion.[29] Indeed, the *E,Z*-isomer may be formed initially and undergo rapid isomerization to *E,E*-**91**. These observations suggest that orbital symmetry plays a role in the photochemical ring opening of cyclobutenes. From analysis of steric effects on the efficiency of ring opening of the 1,2-dimethylcyclobutenes **87**, along with time-resolved resonance Raman studies of cyclobutene,[30] it was concluded that ring opening begins with disrotatory stereochemistry, as orbital symmetry selection rules predict for an excited-state process, but that stereospecificity is lost because ring opening proceeds adiabatically, yielding the disrotatory diene in an excited state, from which it decays by *E,Z*-isomerization.[27]

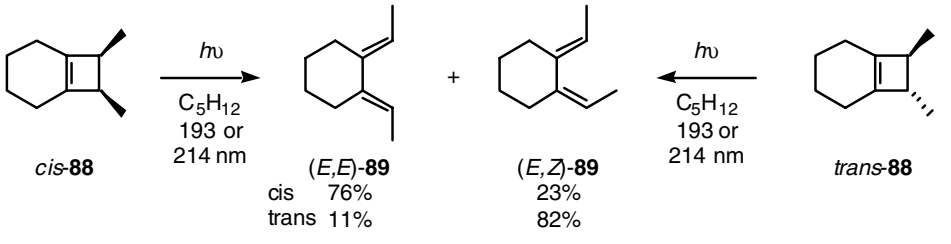

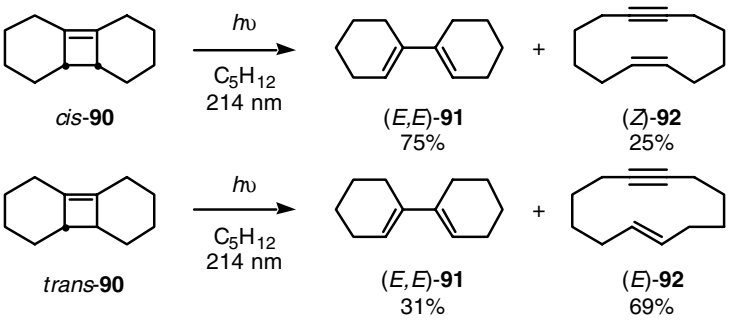

The assignment of the ππ* singlet excited state for ring opening has been supported by a study of the bicyclo[4.2.0]octenes **81b**.[4e] Spectroscopic studies indicate that the ππ* singlet excited state is higher lying than the π,R(3s) excited state in the parent **81b** (R = H) and the methyl derivative **81b** (R = CH_3) but the π,R(3s) excited state is raised to a higher energy than the ππ* state in the trifluoromethyl derivative **81b** (R = CF_3). Accordingly, fragmentation predominates over ring opening for the methyl and unsubstituted derivatives, whereas ring opening is more efficient for the trifluoromethyl-substituted derivative. Moreover, ring opening is enhanced over fragmentation on going from 214 to 193 nm for the first two compounds but is favored at the longer wavelength for the trifluoromethyl derivative.

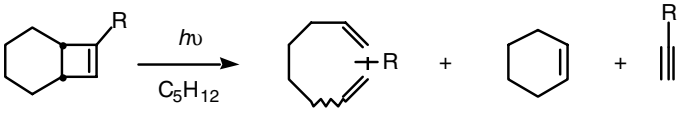

R = CH_3	193	1	:	1.49
	214	1	:	2.84
H	193	1	:	0.80
	214	1	:	1.10
CF_3	193	1	:	0.10
	214	1	:	0.06

However, it has recently been found that the stereochemical course of ring opening is wavelength dependent. The 1,2-dimethylcyclobutenes **87c** undergo stereospecific conrotatory ring opening at 228 nm, in contrast with the almost complete lack of stereospecificity at 193 and 214 nm.[31] The *cis*-isomer (***cis*-87c**) afforded stereospecifically the conrotary product (*E,Z*-**77c**), whereas the trans isomer (***trans*-87c**) afforded a mixture of the two conrotatory products *E,E*-**77c** and *Z,Z*-**77c** — those that would be allowed by thermal electrocyclic opening. The quantum yields for electrocyclic ring opening were significantly higher than those estimated for ring opening via a hot ground-state mechanism, suggesting that ring opening at 228 nm is a true excited state process.[30] Thus, ring opening proceeds by at least two mechanisms depending on excitation wavelength. The first, which dominates at short wavelengths, involves the ππ* excited state and occurs nonstereospecifically, as discussed above. Since absorption by the cyclobutenes **87c** at 228 nm involves the π,R(3s) excited singlet state, this state is apparently responsible for the observed stereospecific conrotatory opening.

In contrast with ring opening, fragmentation is consistently stereospecific. For example, the *cis*- and *trans*-epimers of cyclobutene **90** afford exclusively the *Z*- and *E*-isomers of enyne **92**, respectively.[27,29] Similarly, the *cis*-isomers of cyclobutenes **86a–b** afford *Z*-2-butene and the *trans*-isomers afford *E*-2-butene with >90% stereospecificity.[4c] Moreover, cyclobutenes **88**, which would have to afford the highly strained cyclohexyne, give only ring-opening products.[28] Although fragmentation is formally a retro [2 + 2]-cycloaddition, it apparently occurs, at least in part, stepwise via a cyclopropylmethylene intermediate, as noted above for cyclobutene (**76**). Some evidence that the required carbene intermediates are indeed formed has come from cyclobutenes **86c–d**, which undergo some interconversion on

irradiation.[4a] Presumably the cyclopropylmethylenes **93** and/or **94** are involved in the interconversion as well as in fragmentation. As noted above, since fragmentation predominates when the π,R(3s) excited state is low lying and at wavelengths at which absorption involves principally the π,R(3s) band, it has been assumed that fragmentation involves this state. However, the recent proposal that carbene intermediates arise instead via rearrangement of the zwitterionic state Z must now be evaluated as an alternative pathway for fragmentation.

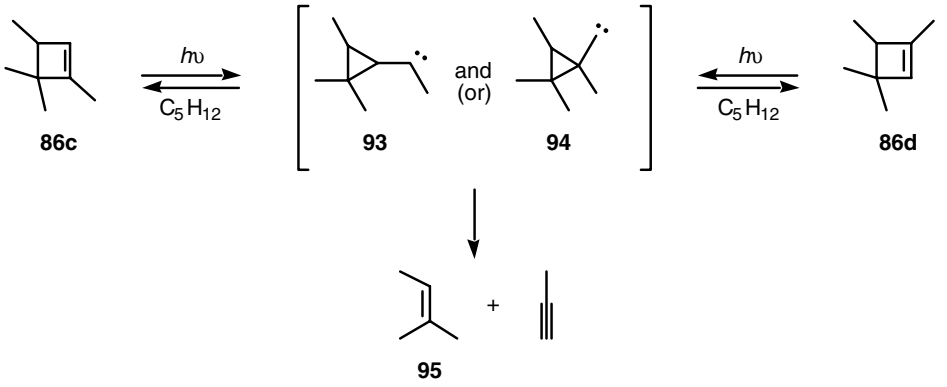

3-Oxacycloalkenes

The oxacycloalkenes **96** afforded aldehydes **98** and **99**, which apparently arise from the diradical intermediate **97** formed via cleavage of the allylic OC bond.[32] The dihydropyran analog **96b** also afforded the carbene-derived product **100**. It was suggested that bond cleavage involves a πσ* excited state.

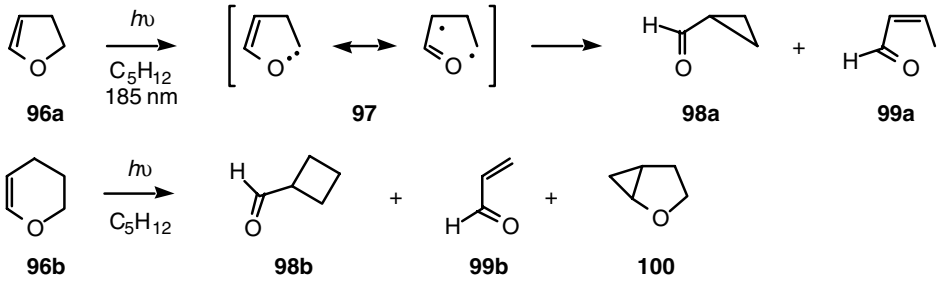

Homoallylic Alcohols

The homoallylic alcohols **101** afforded a mixture of aldehydes **103** and **104**.[33] Deuterium labeling showed that rearrangement occurs intramolecularly, presumably via the diradical **102**. Since in each case the endo epimer afforded an excess of the Δ^3 isomer **103**, it was proposed that the *endo*-epimers undergo a competing concerted rearrangement as shown for *endo*-**101a**.

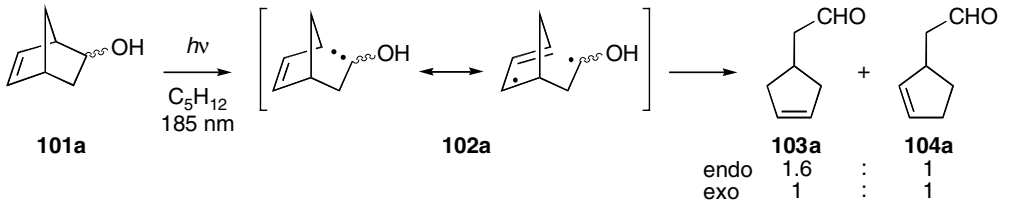

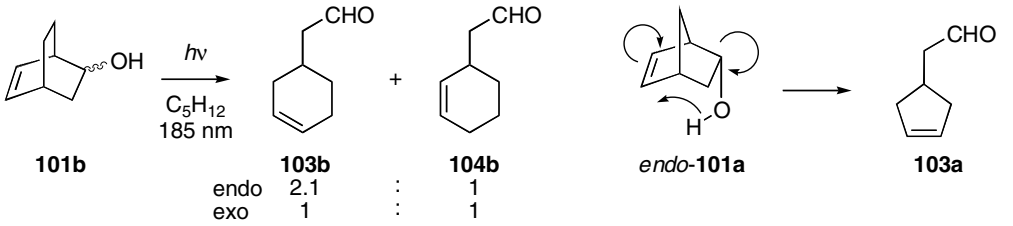

13.4 Summary

The photochemistry of alkenes is exceptionally rich, arising from two or more closely lying excited states that appear not to communicate well between themselves. In addition to undergoing nucleophilic trapping in hydroxylic media (Chapter 9),[10,34] the π,R(3s) singlet excited state has been implicated in stereospecific long-wavelength ring opening of cyclobutenes,[29c,31] as well as undergoing rearrangement to carbene intermediates, although the closely related Z state has also been proposed for this latter process.[7,17] The resulting carbene intermediates, in turn, undergo intramolecular insertion to afford isomers of the starting alkene or, in the case of cyclopropylmethylenes derived from cyclobutenes, fragmentation to an alkene and alkyne. A variety of behavior has been ascribed to the π,π* singlet excited state. In addition to its widely recognized role in *E,Z*-isomerization, the π,π* state has been implicated in 1,3-alkyl migration,[16] alkyne formation,[11,22] hydrogen-atom abstraction,[14] and nonstereospecific ring opening of cyclobutenes.[4e] By analogy to 1,3-alkyl migration, 1,3-hydrogen migration may also involve this state. However, much remains to be done to place these assignments on a firmer basis.

References

1. Kropp, P.J., Photochemistry of alkenes in solution, *Org. Photochem.,* 4, 1, 1979.
2. For reviews of the photobehavior of alkenes in solution, see: (a) Adam, W. and Oppenländer, T., 185-nm photochemistry of olefins, strained hydrocarbons and azoalkanes in solution, *Angew. Chem. Int. Ed. Engl.,* 25, 661, 1986; (b) Steinmetz, M.G., Photochemistry with short UV light, *Org. Photochem.,* 8, 67, 1987.
3. For reviews of the photobehavior of alkenes in the gas phase, see: (a) Collin, G.J., Ring contraction of cyclic olefins: chemical processes specific to electronically excited states? *J. Photochem.,* 38, 205, 1987; (b) Collin, G.J., Photochemistry of simple olefins: chemistry of electronic excited states or hot ground state? *Adv. Photochem.,* 14, 135, 1988.
4. For some examples, see: (a) Clark, K.B. and Leigh, W.J., Cyclobutene photochemistry. Involvement of carbene intermediates in the photochemistry of alkylcyclobutenes, *Can. J. Chem.,* 66, 1571, 1988; (b) Wen, A.T., Hitchcock, A.P., Werstiuk, N.H., Nguyen, N., and Leigh, W.J., Studies of electronic excited states of substituted norbornenes by UV absorption, electron energy loss and HeI photoelectron spectroscopy, *Can. J. Chem.,* 68, 1967, 1990; (c) Leigh, W.J., Zheng, K., and Clark, K.B., Cyclobutene photochemistry. Substituent and wavelength effects on the photochemical ring opening of monocyclic alkylcyclobutenes, *Can. J. Chem.,* 68, 1988, 1990; (d) Leigh, W.J., Zheng, K., and Clark, K.B., Cyclobutene photochemistry. The photochemistry of *cis*- and *trans*-bicyclo[5.2.0]non-8-ene, *J. Org. Chem.,* 56, 1574, 1991; (e) Leigh, W.J., Zheng, K., Nguyen, N., Werstiuk, N.H., and Ma, J., Cyclobutene photochemistry. Identification of the excited states responsible for the ring-opening and cycloreversion reactions of alkylcyclobutenes, *J. Am. Chem. Soc.,* 113, 4993, 1991; (f) Wiseman, J.R. and Kipp, J.E., *E*-Bicyclo[3.3.1]non-ene, *J. Am. Chem. Soc.,* 104, 4688, 1982.
5. (a) Merer, A.J. and Mulliken, R.S., Ultraviolet spectra and excited states of ethylene and its alkyl derivatives, *Chem. Rev.,* 69, 639, 1969; (b) Watson, F.H., Jr., Armstrong, A.T., and McGlynn, S.P., Electronic transitions in mono-olefinic hydrocarbons. I. Computational results, *Theor. Chim. Acta,* 16, 75, 1970; (c) Watson, F.H., Jr. and McGlynn, S.P., Electronic transitions in mono-olefinic

hydrocarbons. II. Experimental results, *Theor. Chim. Acta,* 21, 309, 1971; (d) Robin, M.B., *Higher Excited States of Polyatomic Molecules,* Vol. II, Academic Press, New York, 1975, p. 22; (e) Wiberg, K.B., Hadad, C.M., Foresman, J.B., and Chupka, W.A., Electronically excited states of ethylene, *J. Phys. Chem.,* 96, 10756, 1992.

6. (a) Hirayama, F. and Lipsky, S., Fluorescence of mono-olefinic hydrocarbons, *J. Chem. Phys.,* 62, 576, 1975; (b) Wickramaaratchi, M.A., Preses, J.M., and Weston, R.E., Jr., Lifetime and quenching rate constants for a fluorescent excited state of tetramethylethylene, *Chem. Phys. Lett.,* 120, 491, 1985; (c) Inoue, Y., Daino, Y., Tai, A., Hakushi, T., and Okada, T., Synchrotron-radiation study of weak fluorescence from neat liquids of simple alkenes: anomalous excitation spectra as evidence for wavelength-dependent photochemistry, *J. Am. Chem. Soc.,* 111, 5584, 1989.
7. (a) Fuss, W., Schmid, W.E., and Trushin, S.A., Ultrafast dynamics of cyclohexene and cyclohexene-d_{10} excited at 200 nm, *J. Am. Chem. Soc.,* 123, 7101, 2001; (b) Fuss, W., Pushpa, K.K., Schmid, W.E., and Trushin, S.A., Ultrafast rearrangement of norbornene excited at 200 nm, *J. Phys. Chem. A,* 105, 10640, 2001.
8. Fields, T.R. and Kropp, P.J., Photochemistry of alkenes. 3. Formation of carbene intermediates, *J. Am. Chem. Soc.,* 96, 7559, 1974.
9. (a) Collin, G.J., Deslauriers, H., and Wieckowski, A., Photolysis of gaseous tetramethylethylene between 185 and 230 nm, *J. Phys. Chem.,* 85, 944, 1981; (b) Collin, G.J. and Deslauriers, H., Photoisomerization of gaseous tetramethylethylene in the far ultraviolet, *Can. J. Chem.,* 61, 1510, 1983.
10. Kropp, P.J., Reardon, E.J., Jr., Gaibel, Z.L.F., Willard, K.F., and Hattaway, J.H., Jr., Photochemistry of alkenes. 2. Direct irradiation in hydroxylic media, *J. Am. Chem. Soc.,* 95, 7058, 1973.
11. Inoue, Y., Mukai, T., and Hakushi, T., Direct photolysis at 185 nm of 1-alkenes in solution. Molecular elimination of terminal hydrogens, *Chem. Lett.,* 1725, 1084.
12. Inoue, Y., Mukai, T., and Hakushi, T., Wavelength-dependent photochemistry of 2,3-dimethyl-2-butene and 2-octene in solution, *Chem. Lett.,* 1665, 1983.
13. Srinivasan, R. and Brown, K.H., Organic photochemistry with high level (6.7 eV) photons: duality of carbene intermediates from cyclic olefins, *J. Am. Chem. Soc.,* 100, 4602, 1978. (Quantum yields quoted from this report have been adjusted to reflect the subsequently revised value for the *E,Z* isomerization of cyclooctene: Schuchmann, H.-P., von Sonntag, C., and Srinivasan, R., Quantum yields in the photolysis of *cis*-cyclooctene at 185 nm, *J. Photochem.,* 15, 159, 1981.)
14. Inoue, Y., Mukai, T., and Hakushi, T., Direct photolysis at 185 nm of cyclopentene and 2-norbornene. A novel reaction channel for π,π^* excited singlet alkene, *Chem. Lett.,* 1045, 1982.
15. Adam, W., Oppenländer, T., and Zang, G., 185-nm photochemistry of bicyclo[2.1.0]pentane and cyclopentene, *J. Am. Chem. Soc.,* 107, 3924, 1985.
16. Nguyen, N., Harris, B.E., Clark, K.B., and Leigh, W.J., The solution-phase photochemistry of 2-trifluoromethylnorbornene, *Can. J. Chem.,* 68, 1961, 1990.
17. Ohmine, I., Mechanisms of nonadiabatic transitions in photoisomerization processes of conjugated molecules: role of hydrogen migrations, *J. Chem. Phys.,* 83, 2348, 1985.
18. Nickon, A., Ilao, M.C., Stern, A.G., and Summers, M.F., Hydrogen trajectories in alkene to carbene rearrangements. Unequal deuterium isotope effects for the axial and equatorial paths, *J. Am. Chem. Soc.,* 114, 9230, 1992.
19. (a) Kropp, P.J., Fravel, H.G., Jr., and Fields, T.R., Photochemistry of alkenes. 4. Vicinally unsymmetrical olefins in hydroxylic media, *J. Am. Chem. Soc.,* 98, 840, 1976; (b) Kropp, P.J., Fields, T.R., Fravel, H.G., Jr., Tubergen, M.W., and Crotts, D.D., Unpublished results.
20. Akhtar, I.A., McCullough, J.J., Vaitekunas, S., Faggiani, R., and Lock, C.J.L., Photorearrangement of 2-cyanobicyclo[2.2.1]hept-2-ene. Observation of 1,2- and 1,3-sigmatropic shifts, *Can. J. Chem.,* 60, 1657, 1982.
21. For a list of references and a theoretical treatment, see: Evleth, E.M. and Sevin, A., A theoretical study of the role of valence and Rydberg states in the photochemistry of ethylene. *J. Am. Chem. Soc.,* 103, 7414, 1981.

22. Leigh, W.J. and Srinivasan, R., Organic photochemistry with 6.7-eV photons: γ,δ-unsaturated ketones, *J. Am. Chem. Soc.,* 104, 4424, 1982.
23. (a) Kropp, P.J., Mason, J.D., and Smith, G.F.H., Photochemistry of alkenes. 9. Medium-sized cycloalkenes, *Can. J. Chem.,* 63, 1845, 1985; (b) Haufe, G., Tubergen, M.W., and Kropp, P.J., Photochemistry of alkenes. 10. Photocyclization of cyclononene and cycloundecene, *J. Org. Chem.,* 56, 4292, 1991.
24. Adam, W., Oppenländer, T., and Zang, G., 185-nm photochemistry of cyclobutene and bicyclo[1.1.0]butane, *J. Am. Chem. Soc.,* 107, 3921, 1985.
25. (a) Inoue, Y., Sakae, M., and Hakushi, T., Direct photolysis at 185 nm of simple cyclobutenes. Molecular elimination of acetylene, *Chem. Lett.,* 1495, 1983; (b) Clark, K.B. and Leigh, W.J., Cyclobutene photochemistry. Nonstereospecific photochemical ring opening of simple cyclobutenes, *J. Am. Chem. Soc.,* 109, 6086, 1987.
26. Dauben, W.G. and Haubrich, J.E., The 193-nm photochemistry of some fused-ring cyclobutenes: absence of orbital symmetry control, *J. Org. Chem.,* 53, 600, 1988.
27. Leigh, W.J. and Postigo, J.A., Cyclobutene photochemistry. Steric effects on the photochemical ring opening of alkylcyclobutenes, *J. Am. Chem. Soc.,* 117, 1688, 1995.
28. Leigh, W.J. and Zheng, K., Cyclobutene photochemistry. Partial orbital symmetry control in the photochemical ring opening of a constrained cyclobutene, *J. Am. Chem. Soc.,* 113, 4019, 1991 and 114, 796, 1992.
29. (a) Saltiel, J. and Lim, L.-S.N., Stereospecific photochemical fragmentation of cyclobutenes in solution, *J. Am. Chem. Soc.,* 91, 5404, 1969; (b) Leigh, W.J. and Zheng, K., Cyclobutene photochemistry. Reinvestigation of the photochemistry of *cis*- and *trans*-tricyclo[6.4.0.$0^{2,7}$]dodec-1-ene, *J. Am. Chem. Soc.,* 113, 2163, 1991; (c) Cook, B.H.O., Leigh, W.J. and Walsh, R., Conrotatory photochemical ring opening of alkylcyclobutenes in solution. A test of the hot ground-state mechanism, *J. Am. Chem. Soc.,* 123, 5188, 2001.
30. Lawless, M.K., Wickham, S.D., and Mathies, R.A., Direct investigation of the photochemical ring-opening dynamics of cyclobutene with resonance Raman intensities, *J. Am. Chem. Soc.,* 116, 1593, 1994.
31. Leigh, W.J. and Cook, B.H.O., Stereospecific (conrotatory) photochemical ring opening of alkylcyclobutenes in the gas phase and in solution. Ring opening from the Rydberg excited state or by hot ground state reaction? *J. Org Chem.,* 64, 5256, 1999.
32. Inoue, Y., Matsumoto, N., Hakushi, T., and Srinivasan, R., Photochemistry of 3-oxacycloalkenes, *J. Org. Chem.,* 46, 2267, 1981.
33. Studebaker, J., Srinivasan, R., Ors, J.A., and Baum, T., Organic photochemistry with 6.7-eV photons: Rigid homoallylic alcohols. An inverse Norrish type II rearrangement, *J. Am. Chem. Soc.,* 102, 6872, 1980.
34. Fravel, H.G., Jr. and Kropp, P.J., Photochemistry of alkenes. 4. Vicinally unsymmetrical olefins in hydroxylic media, *J. Org. Chem.,* 40, 2434, 1975.

14

Matrix Photochemistry

Ian R. Dunkin
University of Strathclyde

14.1 Introduction

In matrix-isolation experiments, stable molecules or reactive species are trapped as *guests* in rigid *host materials* and then examined spectroscopically. A common way of generating reactive species in matrices is by photolysis of photolabile precursors (Figure 14.1). The resulting matrix-isolated species are prevented from diffusing and undergoing bimolecular reactions (except with the host). They are therefore stabilized and can usually be characterized by standard spectroscopic techniques, such as IR or UV-visible absorption spectroscopy. Matrix isolation thus provides one of the many methods for the study of reactive intermediates.

The host material can be a crystalline solid, a polymer, or a glass formed by freezing a liquid or solidifying a gas. The term *matrix isolation* is, however, most commonly used in a more restricted sense to refer to the technique of trapping guest species in solidified inert gases, such as neon, argon, krypton, or nitrogen. In this form, the technique requires very low temperatures — typically 4 to 20 K. Occasionally, when it is desired to observe specific host–guest reactions, reactive gases such as methane, carbon monoxide, or oxygen are utilized as matrix hosts.

This chapter provides a brief description of the matrix-isolation technique and then gives some examples of its applications in the study of organic photochemistry. The topics that have been included have been selected from areas of photochemical research to which matrix isolation has made an important and sustained contribution. The choices have been made from among many possibilities and inevitably reflect the author's personal interests, but, in addition to this more general chapter, two specific areas of matrix photochemistry, alkenes and small ring compounds, are covered in Chapters Y and Z, respectively.

Although the technique of matrix isolation was first reported nearly fifty years ago[1] and has been employed in the study of organic photochemistry for at least the last thirty years, the contribution made by matrix studies to our understanding of structure, bonding, and reaction mechanisms is probably still

0-8493-1348-1/04/$0.00+$1.50

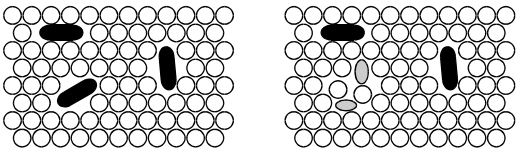

FIGURE 14.1 (a) Precursor molecules (shown in black) matrix isolated in an excess of the host material (white circles). (b) The same matrix after photolysis of one of the precursor molecules, and the formation of fragment species (grey ellipses).

not as well known among organic chemists as it should be. Perhaps this is due to the fact that specialized equipment is required, which is not very widely available, or that many key papers have been published in journals of physical chemistry or chemical physics.

A comprehensive review of matrix-isolation studies of organic photochemistry is not possible in a work of this type, because it would run to many hundreds — possibly thousands — of references. Fortunately, two useful bibliographies have been published: the first[2] covers the literature from the invention of the technique up to about 1985, while the second[3] extends this period to about 1997. These bibliographies are not free of omissions and errors, nor will they be found in every library, but both contain formula and author indexes and are valuable sources of information on matrix-isolation research. An earlier bibliography, which covered IR spectra at sub-ambient temperatures, including matrix-isolation IR spectra.[4] and an associated review of IR spectra of reactive species trapped in matrices[5] give useful entry points to the literature up to about 1968. Also, various aspects of matrix studies in organic photochemistry have been reviewed.[6–16]

14.2 The Matrix-Isolation Technique

Solidified Gas Matrices

Polymers or frozen solvents have several disadvantages as trapping media for the spectroscopic study of reactive species. First, they are often not chemically inert to very reactive species, such as metal atoms and carbenes. Second, they absorb strongly over large regions of the IR spectrum. Since much more structural information about trapped molecules can usually be derived from IR than from UV-visible or electron paramagnetic resonance (EPR) spectroscopy, the latter is a severe problem.

Solidified noble gases and nitrogen have three advantages when used as trapping media for reactive species: chemical inertness, complete transparency throughout the normal IR-visible-UV regions of the spectrum, and a tendency to form clear glasses. To make rigid matrices from the noble gases and nitrogen, very low temperatures are necessary — typically 4–20 K — and nowadays these are usually attained by means of closed-cycle helium refrigerators.

Matrices are formed by deposition from the gas phase onto a cold window. Any species that is to be trapped in a matrix must therefore be volatile, at least to a small extent. The guest species can be mixed with the host gas in either of two ways. If the guest has a high enough vapor pressure, it can be mixed with the host gas on a vacuum line by standard manometric techniques. This produces a gas mixture of guest and host, usually of known proportions; the ratio of host to guest is known as the *matrix ratio*. The gas mixture is then allowed into the vacuum chamber of the cold cell at a controlled rate and is deposited as a solid matrix. Figure 14.2 shows the important features of a suitable cold cell.

If the guest has low volatility, it is usual to evaporate it from a side arm attached to the vacuum chamber of the cold cell, while the host gas is deposited simultaneously. It is difficult to measure the matrix ratio in these conditions. To assist volatilization, the host gas can be passed directly over the solid or liquid guest material in the side arm and the guest can be heated, provided it does not decompose thermally at the necessary temperature.

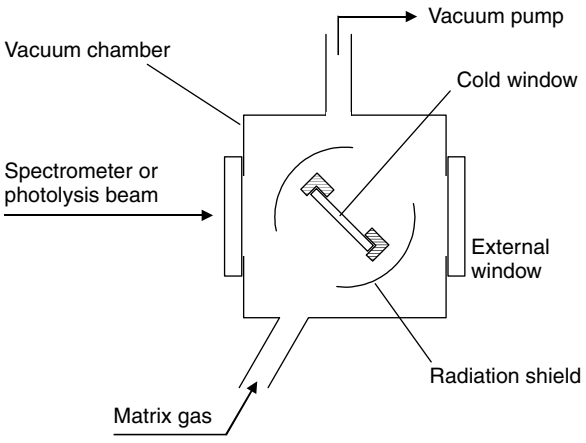

FIGURE 14.2 Top view of a cold cell for matrix isolation. The cold window in a metal holder is located inside a vacuum chamber fitted with an inlet port for the matrix gas, external windows, and a port for connection of the vacuum pump. The cold window can be rotated to face the inlet port or the external windows, and it is usual to incorporate a metal radiation shield around it (cooled to *ca.* 80K) to minimize warming. Matrices are formed by allowing a gas mixture to enter the vacuum chamber through the inlet port, whereupon it will condense on the cold window.

After matrix deposition, the vacuum chamber is maintained at very low pressure — typically 10^{-6} mbar or less. This provides a *Dewar vacuum,* which thermally insulates the matrix and cold window from the atmosphere outside and also prevents the deposition of appreciable amounts of extra material on top of the matrix.

The material from which the cold window is made is chosen to suit the spectroscopic techniques to be employed. For IR studies, CsBr or CsI are preferred. These are softer and less prone to cracking than NaCl or KBr and can better withstand repeated cooling and warming cycles. Although also transparent in the UV and visible regions of the spectrum, CsBr and CsI tend to deform and become scratched, which results in scattering of the shorter wavelengths. For this reason, CaF_2 or sapphire windows are often preferred for UV-visible studies. The external windows of the vacuum chamber do not have to be cooled, so KBr, which is inexpensive, is a popular choice for both IR and UV-visible experiments.

In principle, there could be another approach to forming matrices: first dissolving the guest material in a liquefied gas, such as argon or nitrogen, and then freezing the resulting solution. Usually, this does not work well. Liquefied gases at their normal boiling points are poor solvents for most organic materials, so only extremely dilute solutions can be prepared in this way. Moreover, when the solutions are cooled and frozen, guest molecules can aggregate or even crystallize out, so proper isolation of the molecules is unlikely. Until techniques like this can be utilized reliably, however, really involatile materials such as polypeptides or polysaccharides cannot be studied by the matrix chemist or spectroscopist.

Generation of Reactive Species in Matrices

As a consequence of the way in which matrices are deposited, the generation of reactive species can be carried out either (a) by photolysis or radiolysis of precursors already trapped in the matrices or (b) by gas-phase or surface (gas-solid) reactions prior to deposition. The second category can include flash vacuum pyrolysis, microwave excitation, or reactions of organic precursors with metals. After the reactants have passed through the region where the reaction takes place, the resulting product mixture is diluted with a large excess of the host gas and condensed as quickly as possible on the cold window as a matrix.

In whatever way reactive species are generated and trapped in the matrix, further reactions can be induced by photolysis or by annealing the matrix, i.e., warming to allow softening and then re-cooling.

TABLE 14.1 Strengths and Limitations of Matrix Isolation in Comparison with Flash Photolysis

Matrix Isolation	Flash Photolysis
Solid-phase reactions only, but precursor must be volatile	Reactions in gas, liquid or solid phases
Reactive species stabilized in the abnormal conditions of a matrix cage	Reactive species observed in the normal conditions of a reaction medium
Reactive species long lived — often indefinitely	Reactive species transient, and lifetimes can be measured
Spectra recorded normally, and in favorable cases, different types of spectra can be recorded for the same matrix	Spectra usually recorded at one wavelength per flash; multiple flashes are needed
Many types of spectroscopy applicable including far-, mid-, and near-IR absorption, Raman, UV-visible absorption, ESR, and various type of emission spectroscopy	Detection of transient species by UV-visible or IR absorption, but only part of the IR region is accessible at present
Reactive species can be generated by a range of methods including photolysis, vacuum pyrolysis, microwave discharge, and chemical reaction	Reactive species generated by photolysis

Spectroscopic Techniques for Matrix Studies

A wide range of spectroscopic techniques can be used with low-temperature matrices, and fairly routine spectrometers will usually suffice. Nevertheless, NMR spectroscopy is, for all practical purposes, unavailable. A few research groups have developed special forms of NMR for matrices, but the solid-state spectra obtained are of low resolution, lacking the coupling information that makes conventional NMR in liquids such a powerful structural tool. Usually, matrix chemists make do with IR and UV-visible spectroscopy, supplemented where appropriate with less common techniques such as Raman spectroscopy, laser-induced emission, and EPR.

Throughout the history of matrix-isolation studies of reactive intermediates, IR spectroscopy has undoubtedly played the most important part in the identification of reactive species and the determination of their structures. Recently, the interpretation of matrix IR spectra has been greatly enhanced by the development of reliable computational methods for predicting vibrational transitions — both frequencies and intensities — and then by the incorporation of these methods in commercially available software packages such as Gaussian and Spartan. In general, matrix IR frequencies are not greatly shifted from gas-phase values, so experimental and computed spectra usually agree well. Density functional theory (DFT) seems to have been particularly successful in predicting the IR spectra of matrix isolated species.[17]

The Matrix Isolation Laboratory

The preceding paragraphs have given a brief description of the essential features of matrix-isolation equipment and the way in which matrix experiments are conducted. It is hoped that this will assist readers previously unfamiliar with matrix isolation to understand the experimental constraints.

The use of matrix isolation on a preparative scale has been advocated by several workers and is an attractive idea for reactions that follow different pathways in low-temperature matrices and normal, ambient conditions. In these cases, matrix isolation could result in greater selectivity or even completely different products. There is no great difficulty in scaling up a cold cell to handle hundreds of milligrams or even gram quantities of guest materials, nor is it hard to monitor the progress of the reactions or to recover stable products from scaled-up matrix reactions.[18] Nevertheless, matrix isolation for synthesis has not yet become established and nearly all the studies reported in this chapter involved spectroscopic investigations carried out on a small scale, usually to characterize reactive intermediates. The strengths and limitations of matrix isolation as a technique for studying reaction mechanisms are summarized in Table 14.1, where there is also a comparison with flash photolysis.

A practical guide to the matrix-isolation technique has been published fairly recently.[19] This should be consulted for more details about cold cells, the scope of the technique, and how to carry out matrix experiments.

14.3 Radicals

The term *radicals* will here be applied exclusively to molecular fragments with single unpaired electrons, e.g., alkyl radicals (R·) and alkoxy radicals (RO·), as distinct from other hypovalent species such as carbenes and nitrenes. Radicals are conveniently studied by means of EPR spectroscopy, a sensitive technique that can, for example, be applied to photochemical reactions occurring in flow cells or in frozen organic glasses. Although there have been numerous matrix-isolation studies of radicals utilizing EPR, an important advantage of matrix hosts such as argon or nitrogen is the opportunity that they provide to obtain IR spectra of reactive species. This section will therefore concentrate on matrix IR studies of radicals. Not only have IR spectra been obtained for a range of radicals, but it has also been possible to investigate the photochemical reactions of some of these species. IR spectroscopy, unlike EPR, has the advantage of allowing both radical and non-radical products to be detected and characterized.

An obvious route to matrix-isolated radicals is by photo-induced bond homolysis of a suitable precursor. Such a reaction, however, will generate a pair of radicals within the same matrix cage, and in many cases efficient recombination can occur, resulting in a very low persistent yield of the desired radical. For instance, near-UV-photolysis of methyl iodide in matrices does not normally result in a sufficient concentration of methyl radicals to be detected by IR spectroscopy. Fortunately, as described below, several ways of circumventing this problem have been found.

Matrix IR Spectra of Radicals

Photolysis of haloalkanes or alkanes with vacuum-UV light, which has considerably higher photon energies than near-UV light, seems to produce radicals with enough thermal energy to escape the matrix cage. This is particularly true when one of the radical fragments is a hydrogen atom, which has high mobility. Thus, the out-of-plane deformation IR band of the methyl radical at 611 cm^{-1} and the equivalent bands for several isotopomers ($^{13}CH_3$, $^{12}CH_2D$, $^{12}CHD_2$, $^{12}CD_3$ and $^{13}CD_3$), were observed following photolysis of normal and isotopically substituted methane in Ar and N_2 matrices with light from Kr-He or H_2-He helium discharge lamps.[20] Similar studies with halomethanes as the precursors provided the matrix IR spectra of a range of halomethyl radicals, e.g., CH_2F from CH_3F,[21] CH_2Cl from CH_3Cl,[22] and CF_3 from CHF_3, CF_3Br, and other precursors.[23] As an illustration of the value of matrix IR spectroscopy in giving structural information, two IR bands of CF_3 were found in the ν(C–F) region, and this indicated that CF_3 is nonplanar. Nevertheless, these high-energy photolyses did not produce the radicals cleanly, and other products, such as carbenes and dimeric species, were formed as well. Only with simple molecules such as methane derivatives was there much chance of disentangling the matrix IR spectra, so this approach was likely to encounter difficulties with much larger radicals.

Nonetheless, various isotopomers of the vinyl radical (CH_2=CH·) have since been generated in Ar matrices by vacuum-UV photolysis of D- and ^{13}C-substituted ethenes and detected by IR spectroscopy.[24] These were identified through their ν_7 IR absorptions near 900 cm^{-1}; *ab initio* computations satisfactorily accounted for the observed isotope shifts in the frequencies.

An alternative method of minimizing radical recombination in matrices is to generate a pair of radicals separated by one or more inert molecules. For example, photolysis of acetyl benzoyl peroxide (**1**) in Ar matrices resulted in elimination of CO_2, producing methyl benzoate (**2**), but also phenyl radicals (**3**) and methyl radicals (**4**) in sufficient amounts to be detected by IR spectroscopy (Scheme 1).[25] The radicals were apparently kept apart by the eliminated molecules of CO_2. On warming the matrix to 30 K, the matrix softened, allowing diffusion of the radicals and the formation of toluene (**5**). The matrix photolysis of diacyl peroxides such as **1** proved a rich vein of research, and in analogous experiments matrix IR spectra were obtained for a range of alkyl radicals, e.g., ethyl,[26–28] isopropyl,[28] *n*-butyl,[29] isobutyl,[30] *n*-pentyl,[29] and neopentyl.[30] Enough data were collected in these investigations to permit the identification of characteristic differences in the IR spectra of primary, secondary, and tertiary alkyl radicals.[30,31]

Much more recently, the use of solid parahydrogen as a matrix host has been advocated for spectroscopic studies of radicals.[32] Its extreme softness, compared with the more usual matrix materials, allows

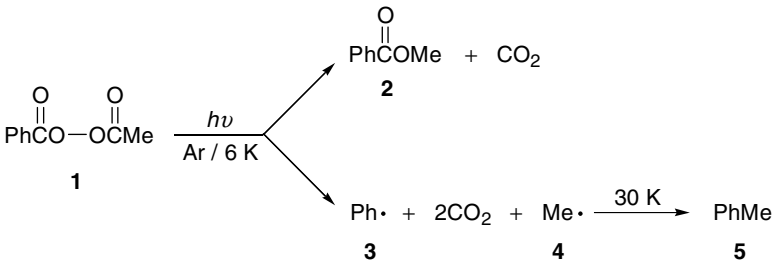

SCHEME 1

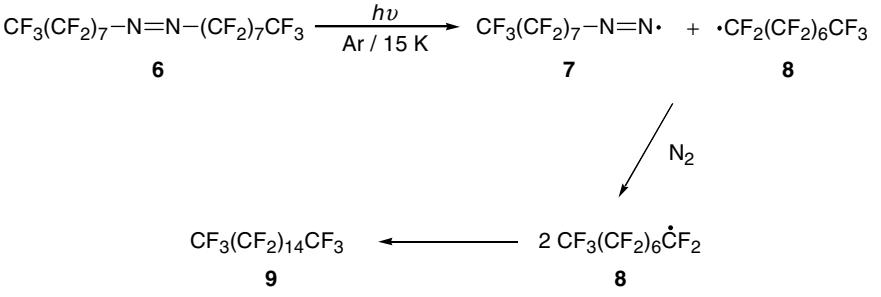

SCHEME 2

easy separation of radical pairs and, for example, photolysis of ethyl iodide in a parahydrogen matrix afforded the ethyl radical in amounts quite sufficient for IR detection.[32]

It might be thought that the photolysis of azoalkanes should also generate alkyl radical pairs, separated, in this case, by extruded N_2 molecules. There do not appear to have been many matrix-isolation studies of azoalkane photochemistry, but a recent example showed a more complicated and more interesting pattern of behavior. Photolysis of *cis*-enriched perfluoroazooctane (**6**) (Scheme 2) in argon matrices with a low-pressure Hg arc led to the IR and EPR observation of perfluorooctyl radicals (**8**), as expected, but a second reactive species was also detected.[33] This disappeared on warming to 30 K, accompanied by an increase in the yield of **8**. The thermally labile species was identified as the diazenyl radical **7**, thus confirming the view that azo photolyses normally proceed in a stepwise fashion. In this study, *cis*-enriched **6** was used as the starting material in order to avoid complications in the interpretation of IR spectra due to *cis-trans* isomerization of the *trans* isomer.

In addition to the photolysis of benzoyl peroxides (see Scheme 1), the phenyl radical (**3**) has also been generated by matrix photolysis of nitrosobenzene monomer.[34] Nitrosobenzene (PhNO) exists as a yellow *cis*-dimer (PhN(O)=N(O)Ph) in the solid state at room temperature but forms the blue monomer when sublimed and trapped in solid argon. Irradiation with light of $\lambda > 300$ nm of matrices containing the monomer decomposed the nitroso compound, while new species were formed. Among these were the phenyl radical and its triplet radical-pair complex with NO. On warming the matrix, PhNO was regenerated. Photolysis of PhNO provided an IR spectrum of the phenyl radical, which was less obscured by the absorptions of other species (principally CO_2, $PhCO_2Me$, and the methyl radical) than was the case in the earlier study of the matrix photolysis of **1**. Thus, seven previously unreported IR bands belonging to Ph· could now be observed for the first time.

The value of generating a reactive species by several independent routes is well illustrated in the case of the phenyl radical. Very recently, a thorough matrix-isolation and theoretical study has been made of the electronic absorption spectrum[35] and IR spectrum[36] of Ph·, in which the radical was generated by photolysis (193 or 248 nm) of phenyl iodide and other precursors, as well as by thermolysis reactions. Several D-substituted isotopomers of the radical were also investigated, and polarized light was used to

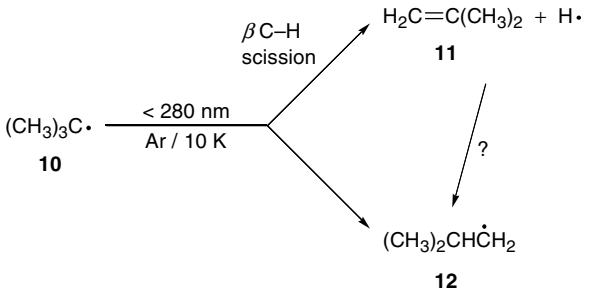

SCHEME 3

produce oriented samples from which band symmetries could be derived. The result was an impressively full description of the IR spectrum of the phenyl radical, with experiment and DFT calculations in good agreement.

In addition to alkyl and phenyl radicals, IR spectra of certain oxygen-centered radicals have also been obtained by matrix isolation. As an example, the trifluoroperoxy radical ($CF_3OO\cdot$), with IR absorptions at 1174 and 1094 cm^{-1}, was identified amongst the products of the UV-photolysis of CF_3OOF and bistrifluoromethyl trioxide (CF_3OOOCF_3) in Ar matrices.[37] Isotopic labeling experiments with $CF_3{}^{16}O^{16}O^{16}OCF_3$, $CF_3{}^{16}O^{18}O^{16}OCF_3$, $CF_3{}^{18}O^{16}O^{18}OCF_3$ and $CF_3{}^{18}O^{18}O^{18}OCF_3$ demonstrated the non-equivalence of the two O atoms in $CF_3OO\cdot$ through the observation of four distinct isotopic absorptions for the ν(O–O) band at 1094 cm^{-1}. This helped to confirm the identity of $CF_3OO\cdot$ by ruling out the possibility that the IR bands assigned to this radical belonged instead to its F-atom loss product, difluorodioxirane (CF_2O_2), in which the two O atoms are equivalent. More recently, the phenoxyl radical ($PhO\cdot$) has been matrix isolated in argon by photolysis of several different precursors, including phenol and diphenyl carbonate.[38] All but one of the IR-active fundamentals of $PhO\cdot$ were identified, and with the aid of DFT computations, a detailed assignment of its vibrational spectrum was made. Significant shifts of vibrational frequency were noted compared with previous data obtained from resonance Raman studies in polar solutions. In particular, the ν(C–O) frequency was found to be very susceptible to the polarity of the environment, apparently owing to an increase in quinoidal character of the radical in more polar media.

Photochemistry of Matrix-Isolated Radicals

Matrix isolation provides the chance of investigating the photochemistry of radicals, irrespective of their mode of generation – thermal or photochemical. When the ethyl radical was formed in matrices, along with CO_2, by photolysis at $\lambda > 280$ nm of dipropionyl peroxide (*cf.* Scheme 1), subsequent photolysis at $\lambda < 280$ nm produced ethyl propionate, propionic acid, ethane, and ethyne.[39] It thus appeared that, upon excitation, $Et\cdot$ either reacted with CO_2 to yield propionic acid and ethyl propionate, or lost a hydrogen atom, or a hydrogen molecule and a hydrogen atom, to give ethene and ethyne, respectively. Similar behavior was observed for the isopropyl radical, which gave isobutyric acid, isopropyl isobutyrate, and propene, when photolysed under analogous conditions.[40]

The matrix photochemistry of the *t*-butyl radical (**10**) was examined following generation of this radical by flash vacuum pyrolysis of a gaseous mixture of azoisobutane and argon and subsequent condensation of the pyrolysate as a matrix.[41] Irradiation of the resulting sample with light of $\lambda < 280$ nm yielded two major photoproducts: isobutene (**11**) and the isobutyl radical (**12**) (Scheme 3). The former apparently arose in a β C–H scission reaction, eliminating a hydrogen atom; the latter probably was the result of a photoinduced rearrangement, but the possibility of a recombination of **12** and an H atom could not be completely ruled out. Since H atoms were being produced, it was also thought possible that some isobutene might have been produced in a disproportionation reaction of H atoms and the *t*-butyl radical.

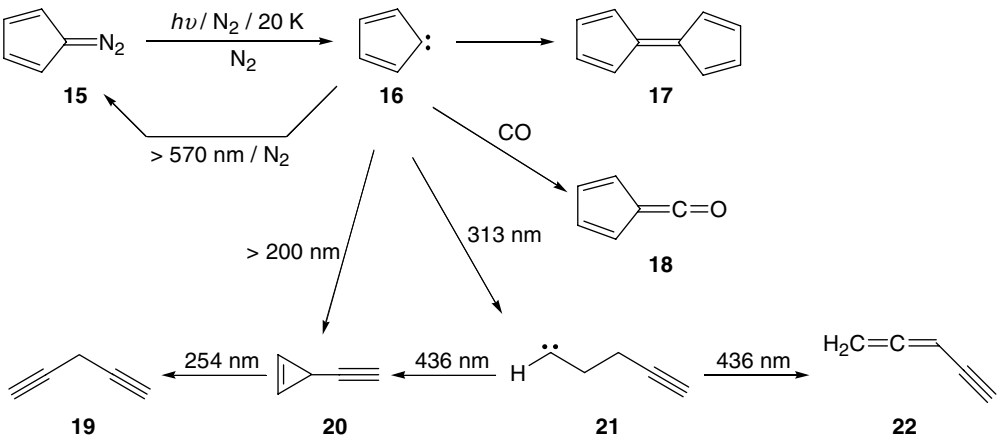

SCHEME 4

Methylperoxy radicals (MeOO·) were formed when methyl radicals, generated by the gas-phase pyrolysis of azomethane or methyl iodide, were trapped in Ar matrices containing a few percent of oxygen.[42] Subsequent 254 nm irradiation resulted in destruction of these radicals, while IR absorptions of H_2O, CO, CO_2, formaldehyde, and probably HO_2 were seen to grow in intensity. A theoretical study suggested that the primary photochemical step was likely to have been O–O bond cleavage to give MeO· and an oxygen atom, but the experimental reaction pathways were not fully elucidated. Allylperoxy radicals (**13**) have been similarly trapped in Ar matrices and photolyzed.[43] The vinylacyl radical **14**, with a characteristically high ν(C=O) frequency at 1823 cm^{-1}, was identified in the product IR spectrum, seemingly resulting from elimination of H_2O from **13**.

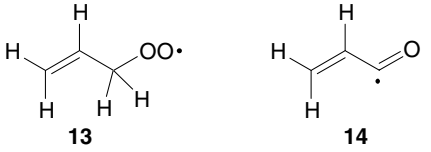

Carbenes and Their Reactions

Of the various types of reactive organic species, carbenes have been the most extensively studied by matrix-isolation techniques. A comprehensive review of carbenes in matrices, with more than 400 references, was published in 1993 and is an excellent entry point into the literature on this subject.[44]

Methylene (CH_2) was generated from diazomethane in some of the earliest matrix studies of organic reactions, and its dimerization to ethene was observed, although its IR spectrum proved somewhat elusive.[45–47] Various halomethylenes were also observed among the products from the vacuum-UV irradiation of halomethanes in matrices. Examples are CHF from photolysis of methyl fluoride[21] and CCl_2 from dichloromethane.[22]

Simple carbenes such as the halomethylenes were comparatively easy to identify by IR spectroscopy, even when present in mixtures of photoproducts. With larger carbenes, however, identification often had to rely on the observation of characteristic reactions, e.g., dimerization or addition of CO to give ketenes. Cyclopentadienylidene (**16**) was one of the first carbenes to be investigated in this way.[48,49]

Cyclopentadienylidene and Related Carbenes

When diazocyclopentadiene (**15**) was photolyzed in N_2 matrices at 12–20 K, the product that was first identified was fulvalene (**17**) (Scheme 4), which has a highly structured and easily recognizable UV

spectrum.[48,49] Only in exceptionally dilute matrices (matrix ratio N_2/**15** = 1.5×10^6) was formation of fulvalene completely suppressed, and then UV and IR absorptions of another photoproduct were observed. This species was identified as the carbene, cyclopentadienylidene (**16**) on the basis of its reactions. Thus, warming matrices containing **16** (but little or none of the diazo precursor) to 30 K, produced fulvalene; also, when **16** was generated in matrices containing CO, warming to 24 K gave a ketene, assumed to be **18**.

In the original investigation, an attempt was made to observe the back reaction of the carbene with N_2 to regenerate diazocyclopentadiene: unlabelled **15** was photolyzed in a $^{15}N_2$ matrix, but no $^{15}N_2$-substituted **15** was formed. It was therefore concluded that the elimination of N_2 from **15** was irreversible. It was also observed that, on photolysis of the carbene **16** with an unfiltered medium-pressure Hg arc, a secondary photoproduct appeared with IR absorptions near 3315 cm^{-1}, characteristic of a terminal alkyne. The secondary product was shown not be either ethyne or penta-1,4-diyne (**19**), but no further identification could be made at that time.

A later study, benefiting from DFT computations and the skilful use of various irradiation wavelengths, has considerably extended our knowledge of the photochemistry of cyclopentadienylidene.[50] First, it was shown that the back reaction of **16** with N_2 could be induced with long-wavelength light ($\lambda > 570$ nm). Second, several products from the photolysis of **16** at shorter wavelengths were identified. These included the ring-opened carbene **21**, a minor amount of ethynylallene (**22**), 3-ethynylcyclopropene (**20**), and penta-1,4-diyne (**19**). The photoreactions are summarized in Scheme 4.

Several other cyclopentadienylidenes have been similarly investigated, including the tetrachloro[51] and tetrabromo[52] derivatives (**23**: R = Cl, Br), indenylidene (**24**),[51] and fluorenylidene (**25**).[51] These carbenes all reacted thermally with CO in matrices, generating the corresponding ketenes, but none could be induced to dimerize to the corresponding fulvalenes. The greater bulk of the carbene molecules compared with the unsubstituted parent **15** could inhibit diffusion within the matrix or simply prevent dimerization through adverse steric effects.

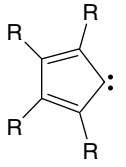

23

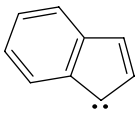

24

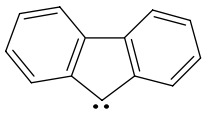

25

Interesting parallels with the photochemistry of cyclopentadienylidene have been discovered for some heterocyclic analogues. 2*H*-Imidazol-2-ylidene (**26**), for example, was trapped in argon matrices by photolysis of the corresponding diazo precursor, 2-diazo-2*H*-imidazole.[53] As with other carbenes, **26** reacted with CO in CO-doped matrices, yielding the corresponding ketene. Upon photolysis with light of $\lambda > 570$ nm, **26** was transformed into 1-cyano-1*H*-azirine (**27**), which in turn was efficiently converted into *N*-cyanoketenimine (**28**) by 254 nm irradiation. Interestingly, carbene **26** could not be trapped under thermal conditions, and flash vacuum pyrolysis of 2-diazo-2*H*-imidazole gave only imidazole.

26

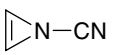

27

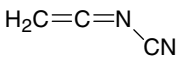

28

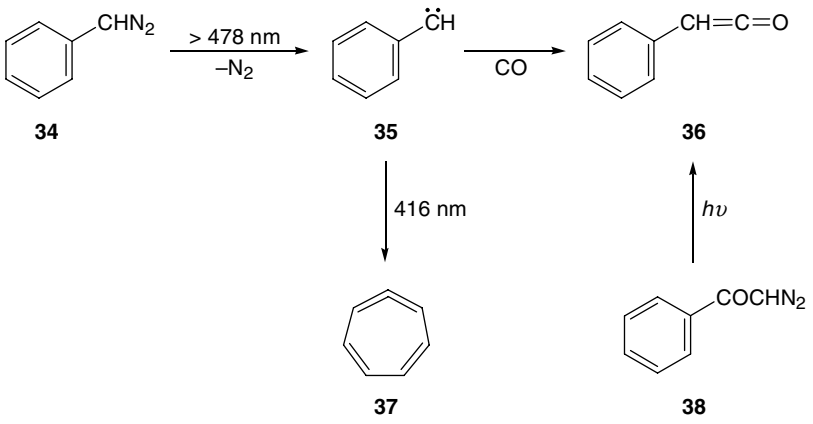

SCHEME 5

4*H*-Imidazol-4-ylidene (**29**) was similarly generated in argon matrices by photolysis of 4-diazo-4*H*-imidazole and was converted into the ring-opened carbene **30** when irradiated at >570 nm.[54] Further photolysis of **30** at > 310 nm produced 2-cyano-2*H*-azirine (**31**), which decomposed when irradiated at 254 nm to products with IR absorptions at 2067 and 2155 cm^{-1}. These were thought to belong to ketenimine **32** and isocyanoacetonitrile (**33**), respectively.

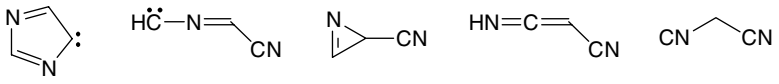

29 **30** **31** **32** **33**

Carbenes **26** and **29** both underwent facile reactions with N_2 to regenerate their diazo precursors, and neither could be detected when the diazo compounds were photolyzed in N_2 matrices. Moreover, when 2-diazo-2*H*-imidazole, the precursor of **26**, was photolyzed in a matrix of ^{15}N-labelled nitrogen, IR bands due to [$^{15}N_2$]-2-diazo-2*H*-imidazole were observed to arise after a very short irradiation time, providing a positive demonstration of the recapture of nitrogen from the matrix material.

Aryl Carbenes

The triplet ground state of phenylcarbene (**35**) was first observed by EPR spectroscopy, but a matrix-isolation study of the photolysis of phenyldiazomethane (**34**) provided IR and UV spectra of this species and allowed an investigation of its photochemistry (Scheme 5).[55,56] When generated in matrices containing CO, carbene **35** gave phenylketene (**36**) on warming. The same ketene was also generated by photolysis of diazoacetophenone (**38**), thus confirming its identity. Irradiation of carbene **35** with light of $\lambda > 416$ nm produced a new species with a considerably altered IR spectrum, including bands at 1824 and 1816 cm^{-1}. This species did not react with CO to give a ketene and was therefore not another carbene. After the exclusion of other possibilities, such as bicyclo[4.1.0]hepta-2,4,6-triene (**39**), with the help of deuterium-labeling studies, it was identified as the cyclic allene, cyclohepta-1,2,4,6-tetraene (**37**). Subsequently, **37** was generated from a number of other precursors, including 2-diazobicyclo[3.2.0]hepta-3,6-diene (**40**) and 8-diazobicyclo[2,2,2]octa-2,5-diene (**41**). Several substituted derivatives of **37** were also investigated.[56] It was moreover shown that cyclic allene **37** and phenylcarbene (**35**) could be interconverted photochemically by appropriate choice of wavelengths. Thus, irradiation of matrix isolated **37** with light of $\lambda > 279$ nm produced a small, steady-state concentration of **35**.

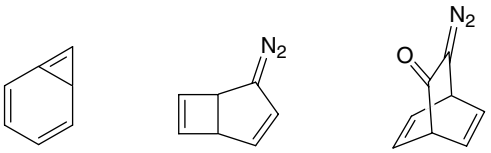

39 **40** **41**

The mechanism for the formation of **37** is not completely clear, however. There is a question of whether it is formed directly from carbene **35** or via the bicyclic triene **39** as an intermediate. So far, the triene has not been detected, and calculations have suggested that it may not correspond to a local energy minimum on the ground-state singlet C_7H_6 energy surface.[57] On the other hand, in matrix studies of naphthylcarbenes, cyclopropene derivatives analogous to **39** have been observed, but not the corresponding cyclic allenes.[58–60]

In contrast to phenyl- and naphthyl carbenes, which have triplet ground states, 1- and 2-naphthylchlorocarbenes (**42** and **43**) exist as ground-state singlets; their matrix IR and UV-visible spectra were reported recently.[61] In the case of **43**, two distinct conformations were observed, and these could be interconverted by selective irradiation. Both **42** and **43** underwent cyclization upon prolonged UV-irradiation, yielding the chlorotricycloheptatrienes **44** and **45**, respectively. No ring-expanded cyclic allene products were detected. It therefore seems that both triplet and singlet naphthyl carbenes have similar photochemistry, which contrasts with that of phenylcarbenes.

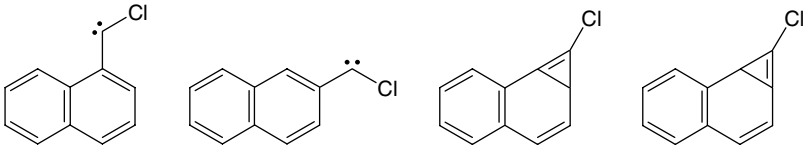

42 **43** **44** **45**

Matrix photolysis of methyl α-diazo-(2-naphthyl)acetate (**46**) at 450 nm gave primarily the triplet ground-state carbene **47**, which was characterized by its UV-visible, IR, and EPR spectra and by its reactions with carbon monoxide and oxygen.[62] Bleaching the weak visible bands of triplet **47** ($\lambda > 515$ nm) led to the disappearance of the triplet EPR signals, while a new absorption arose in the near-UV. Thereafter, however, the spectra of triplet **47** were almost fully recovered in the dark at 12 K. The species generated by visible irradiation of triplet **47** had IR and UV spectra consistent with singlet **47** and not a tricyclic cyclopropene analogous to **45**. Theoretical exploration of the potential energy surfaces for triplet and singlet **47** showed that a barrier between the two states is created by a pronounced change in conformation of the methoxycarbonyl group; for singlet–triplet interconversion, the necessary conformational change is likely to be hindered in the matrix environment.

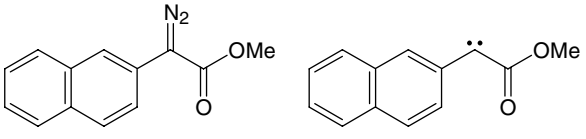

46 **47**

Carbonyl Oxides

The reaction of matrix-isolated carbenes with carbon monoxide, as noted above, gives ketenes, even if the ground state of the carbene is a triplet. For triplet carbenes, the process is formally spin-forbidden;

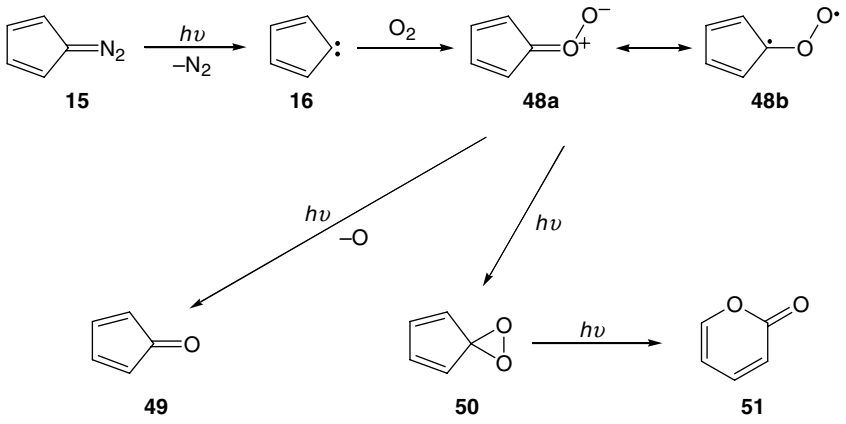

15 **16** **48a** **48b** **49** **50** **51**

SCHEME 6

so it is remarkable that it proceeds readily in the temperature range 20–30 K. It might be supposed that the reaction of triplet carbenes with dioxygen, which also has a triplet ground state, would be even more favorable than the reaction with CO. This indeed appears to be the case and has provided a convenient means of investigating carbonyl oxides (R^1R^2COO), reactive species that were first proposed as intermediates in the ozonolysis of alkenes.

The first IR spectrum of a carbonyl oxide was obtained when diazocyclopentadiene (**15**) was photolysed in Ar or N_2 matrices containing O_2 (Scheme 6).[63] Under these conditions, a new species was observed to arise, either directly or on annealing the matrices, which appeared to be an adduct of the carbene **16** and O_2 and which was supposed to be the carbonyl oxide **48**. The matrix photolysis of **15** was reported independently by two research groups, and at first there was a discrepancy between the two IR spectra attributed to the carbonyl oxide.[63,64] This was resolved by studies utilizing mixtures of $^{16}O_2$, $^{18}O_2$, and $^{16}O^{18}O$ as the source of oxygen.[63,65] These showed that the initial product had nonequivalent oxygen atoms and could be identified as **48**, but that this species was very photolabile, either losing an O atom to give cyclopentadienone (**49**) or rearranging to α-pyrone (**51**) via the dioxirane **50**, which has equivalent O atoms.

Several analogues of **48** were also investigated soon after the initial study. These included the tetrachloro derivative[66] of **48** and the adducts of O_2 with the carbenes, indenylidene and fluorenylidene.[67] In each case, both the O-atom loss and the rearrangement reactions (*cf.* Scheme 6) were observed to occur on further photolysis of the carbonyl oxides. Subsequently, many other examples were generated in similar fashion, and the formation and photolysis of carbonyl oxides, exemplified by **48**, turned out to be reasonably general.[68–70] Moreover, the trapping of an α–carbonylcarbene[71] and an α-sulfonylcarbene[72] by reaction with O_2 competed efficiently with the Wolff or hetero-Wolff rearrangements of these species, thus confirming the intermediacy of discrete carbenes in these reactions.

Before these matrix-isolation studies, it had been usual to denote carbonyl oxides as zwitterions (*cf.* **48a**), but the experimental IR spectra of **48** and its analogues did not exhibit absorptions that could be assigned to C=O bonds. It was therefore concluded that carbonyl oxides are better represented as polar singlet biradicaloids (*cf.* **48b**).[68]

Other Carbenes

Matrix-isolation studies of carbenes have been numerous and their scope extensive. Many interesting results have, of necessity, been left out of this review.

A notable case, which does not fit into the reaction types discussed in the earlier parts of this section, is that of the extremely electrophilic carbene difluorovinylidene (**53**), which has recently been isolated in argon matrices by 193 nm photolysis of difluoroethyne (**52**) (Scheme 7).[73,74] Carbene **53** thermally

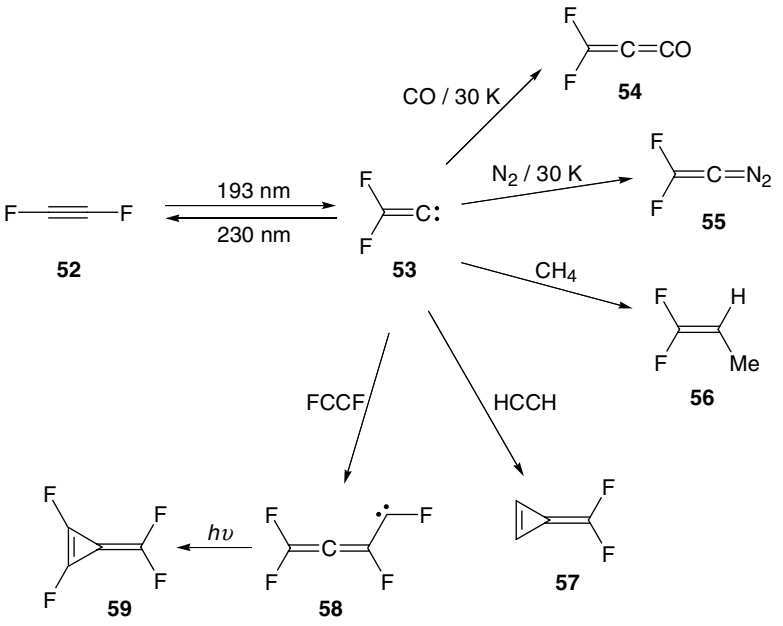

SCHEME 7

added CO and N_2 to give ketene **54** and diazoethene **55**, respectively. These reactions occurred so efficiently that carbene **53** could not be trapped in matrices by photolysis of either **54** or **55**. Carbene **53** also inserted into CH_4 at temperatures below 40 K to give **56** and added to ethyne to give cyclopropene **57** and to difluoroethyne to give the allenyl carbene **58**, which rearranged to the cyclopropene **59** when irradiated with visible light. Difluorovinylidene even underwent a thermal reaction with Xe to produce a distinct charge-transfer complex with characteristic IR absorptions.

The careful selection of suitable precursors is obviously needed for the study of such reactive species as vinylidenes, which rearrange to the corresponding alkynes very easily. Dimethylvinylidene ($Me_2C{=}C{:}$) has recently been trapped in matrices by photolysis of the bisperoxyester **60** and was identified by its reaction with CO and by comparison of the matrix IR spectrum with DFT computations of the IR transitions.[75] It was suggested that this approach could provide a convenient and general route to other vinylidenes in low-temperature matrices.

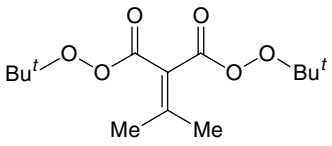

60

Matrix isolated α-carbonylcarbenes generated by photolysis of various α-diazocarbonyl compounds in low-temperature matrices have been investigated, among other reasons, in the hope of detecting oxirenes. A very interesting variation has been found in the photochemistry of **61**, which has two nonequivalent diazo groups.[76,77] Photolysis of **61** was investigated in Ar matrices and in liquid solutions. The product distribution was found to be remarkably dependent on irradiation wavelength. In Ar matrices, photolysis of **61** with light of $\lambda > 350$ nm produced mainly **62**, by selective elimination of N_2 from C2, whereas light of $\lambda > 420$ resulted mainly in N_2 elimination from C4, to give **63**. It was proposed that the wavelength effect in these photoreactions was probably due to selective excitation of **61** into the lowest excited singlet state (S_1) at longer wavelengths and the participation of higher excited states at

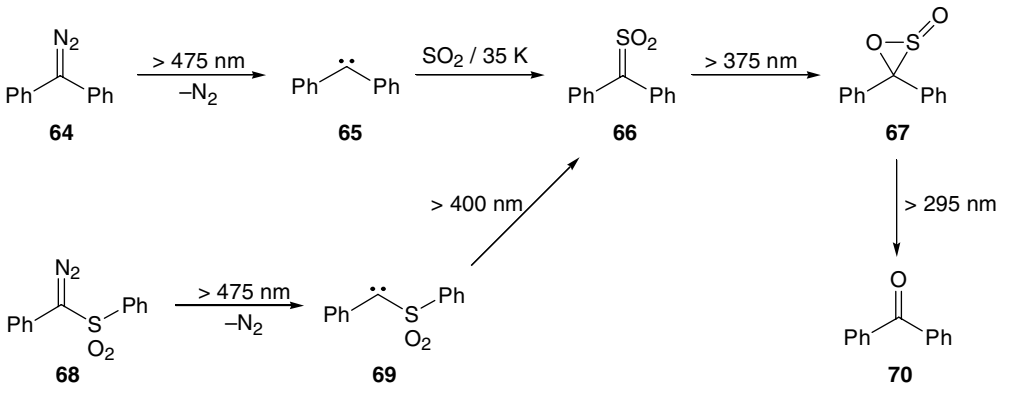

SCHEME 8

shorter wavelengths. Nevertheless, the involvement of different vibrational states of S_1 could not be ruled out.

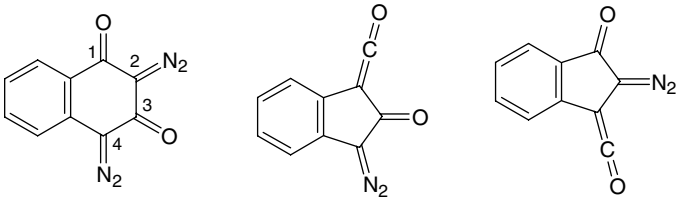

Matrix investigations of sulfur and phosphorus analogues of αcarbonylcarbenes have also been reported. For example, diphenylsulfene (**66**) and diphenyl-α-sultine (**67**) were isolated in low-temperature matrices following the thermal reaction of SO_2 and diphenylcarbene (**65**) and the stepwise photolysis of phenyl(phenylsulfonyl)diazomethane (**68**), as summarized in Scheme 8.[72] The ultimate photoproduct was benzophenone (**70**).

For a series of bis(sulfonyl)diazomethanes (**71**: R = Me, cyclohexyl, Ph, 4-MeC_6H_4, 4-ClC_6H_4), the corresponding carbenes could be trapped chemically in solution, but attempts to isolate them in Ar matrices were unsuccessful, and only sulfenes and other rearranged products were observed.[78] This failure, however, was in accord with theoretical computations, which predicted that the singlet carbenes correspond to saddle points on the potential energy surfaces, while the triplet carbenes lie at higher energies and are therefore not expected to have prolonged lifetimes even in matrices.

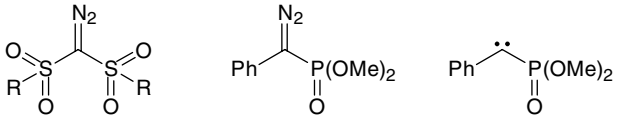

Photolysis of dimethyl α-diazobenzylphosphonate (**72**) in Ar matrices gave the corresponding carbene **73**.[79] Prolonged irradiation of **73**, even with short-wavelength light (254 nm), did not result in any appreciable photoreaction, but it underwent the normal thermal reactions with CO and O_2 in appropriately doped matrices.

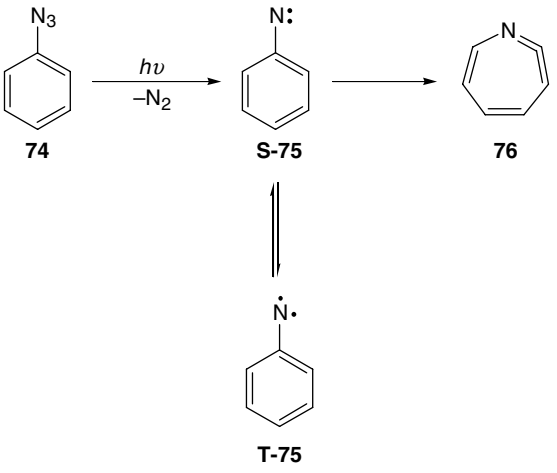

SCHEME 9

14.5 Nitrenes

Phenyl Nitrenes

The matrix photochemistry of phenylnitrene (PhN) has many similarities to that of phenylcarbene, but also some significant differences. A comparison between the two, including flash-photolysis as well as low-temperature, matrix-isolation studies, can be found in a 1995 review.[57]

Any account of matrix studies of aryl nitrenes should begin with some early reports of the photolysis of aryl azides in frozen organic solvents, in which UV-visible absorptions of the photoproducts were assigned to the corresponding nitrenes.[80–82] It was therefore expected that IR spectra of the nitrenes should be readily obtainable by similar photolyses in Ar or other similar matrices. However, the nitrenes proved more elusive.

When phenyl azide (**74**) was photolyzed in Ar matrices, phenylnitrene (**75**) was not detected in the resulting IR spectrum, but a product with an intense absorption at 1895 cm^{-1} was formed.[83] It was concluded that the only plausible candidate for the observed product was the strained cyclic ketenimine **76** (Scheme 9), with the 1895 cm^{-1} IR band corresponding to the $\nu(C{=}C{=}N)_{as}$ vibration. The identity of **76** received further support when it was found that the ^{15}N-isotopomer had this IR band shifted to lower frequency by about 15 cm^{-1}.[84] At the same time, it was found that a series of 3- and 4-substituted phenyl azides gave the same type of ketenimine products when photolyzed in Ar and N_2 matrices, all with IR bands in the 1910–1880 cm^{-1} region.[84]

It was next discovered that when the *ortho* positions were substituted, the ring-expansion reaction was suppressed, and the direct observation of an aryl nitrene by matrix IR spectroscopy became possible. The first two examples were pentafluorophenylnitrene (**77**)[85] and 2,6-dimethylphenylnitrene (**78**).[86] Both these nitrenes underwent reaction with CO to give the corresponding isocyanates (ArNCO), but, unlike the situation with carbenes, the addition of CO did not proceed thermally at temperatures up to 35 K, requiring instead further irradiation ($\lambda > 330$ nm). The fluorinated nitrene **77** showed no tendency to undergo ring expansion to the corresponding keteninime on further irradiation, but the dimethylphenylnitrene **78** seemed to undergo an inefficient rearrangement on prolonged irradiation to give the corresponding ketenimine, with an IR absorption at 1899 cm^{-1}. The effect of *o*-fluorine substitution in suppressing the ring expansion of phenylnitrene has been examined theoretically.[87] The increase in energy barrier seems to derive principally from steric repulsion in the transition state when nitrogen approaches the fluorine-bearing ring carbon.

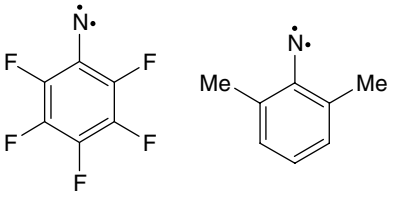

77 **78**

The question now arose as to why aryl nitrenes were apparently the major products when aryl azides were photolyzed in frozen organic solvents, but cyclic ketenimines were the major products in Ar and N_2 matrices, unless the ring expansion was suppressed by *ortho* substitution. One possible explanation lay in the differing abilities of the two types of media to dissipate excess vibrational energy following excitation of the precursor azides and generation of the nitrenes. Organic solvents with many molecular vibrations could couple more effectively with the initial, vibrationally hot, nitrene and cool it quickly, thus minimizing further reaction. On the other hand, matrices such as Ar or N_2 would probably be less effective in removing excess vibrational energy, so that further reaction of the nitrene would be more likely.[88] This idea has received some support from a comparison of the rates of disappearance of phenyl azide (**74**) and formation of ketenimine **76** in Ar, CH_4, and 3-methylpentane matrices.[89] With 280 nm light, the rate of appearance of **76** was significantly less than the rate of disappearance of **74** in both CH_4 and 3-methylpentane, but not in Ar. This indicated that an intermediate — presumably the triplet phenynitrene (**T-75**) — was accumulating in the hydrocarbon but not in the Ar matrices. This intermediate then required a second photon to rearrange to the ketenimine.

In fact, the key to obtaining a matrix IR spectrum of triplet phenylnitrene was the careful choice of photolysis wavelength, not of matrix host material. It was found that photolysis of phenyl azide in Ar or N_2 matrices with 334 nm light produced only a small amount of ketenimine **76**, and the IR bands of another species were then observable.[90] These disappeared on further irradiation with light of $\lambda > 450$ nm, while the IR absorptions of **76** increased. Clearly, **76** was being formed in a two-step process. It was concluded that **76** could be formed directly only from the singlet nitrene **S-75** and that the observed intermediate species was the triplet nitrene **T-75**, which required further excitation to the singlet manifold, presumably via higher triplet excited states, before being converted into **76**. A fuller study of phenyl azide photolysis, utilizing organic glasses at 77 K in conjunction with a variety of spectroscopic techniques, revealed that the preferred reaction pathway at ambient temperatures was different from that at 77 K and provided further examples of *ortho,ortho´*-disubstituted phenyl nitrenes.[88] It was concluded from this study that rearrangement of singlet phenylnitrenes to cyclic ketenimines is strongly dependent on temperature and substituent effects and that the competing process of intersystem crossing to the triplet nitrene is favored at low temperatures. In matrix-isolation conditions, it is quite possible that all the ketenimine observed comes from secondary photolysis of the triplet nitrene.

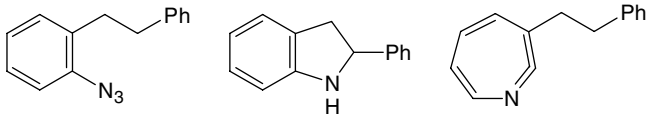

79 **80** **81**

The matrix photochemistry of phenyl nitrenes becomes more complex when substituents are present that can take an active part in the reactions. For instance, irradiation of azide **79** in Ar matrices gave a product (**80**) from nitrene insertion into an adjacent CH bond as well as the ring-expanded ketenimine **81**.[91] The nitrene center can also react by attack on oxygen. Thus, the photolysis of 2-(methoxycarbonyl)phenyl azide (**82**) in Ar matrices gave rise to at least five major products: nitrene **83**, cyclic ketenimine **84**, the two geometrical isomers of ketene-oxime **86**, and *N*-methoxyazetinone **87** (Scheme 10).[92] Products

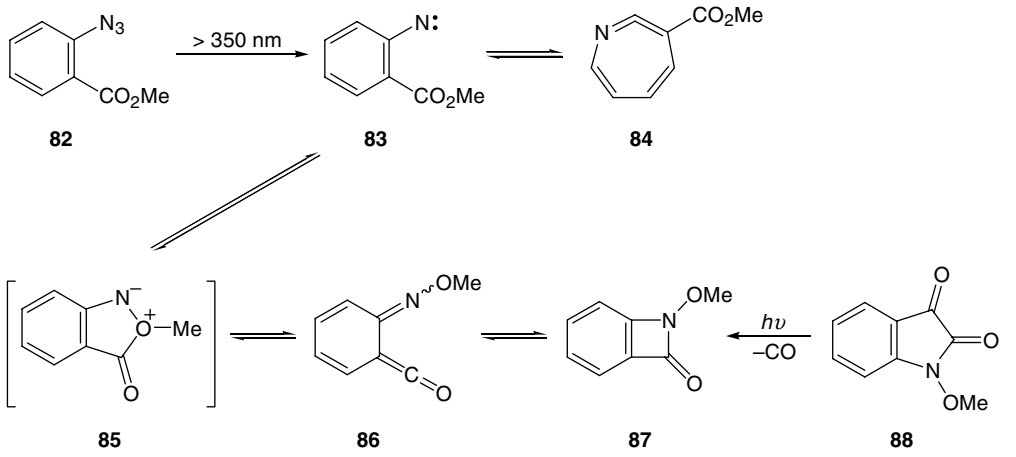

SCHEME 10

86 and **87** were proposed to arise via the oxonium ylide **85**, which was not itself directly detected. All the observed products were shown to be photochemically interconvertible, and the same mixtures could be generated by photodecarbonylation of *N*-methoxyisatin (**88**).

When 4-azidophenols such as **89** (X = Y = Cl) were photolyzed in N_2 matrices, azepin-4-ones (**91**) were the major products, presumably arising by tautomerization of the corresponding hydroxy-substituted cyclic ketenimines (**90**).[93,94] In some cases, the ketenimine was observed directly in the IR spectra. Tautomerization to give the azepinones was favored in more concentrated matrices, suggesting that this process involved intermolecular proton transfer between pairs or aggregates of ketenimine molecules. Matrix photolysis of 4-azidophenols held out the promise of a synthetic route to the elusive azepin-4-ones under exceptionally mild conditions and was tried on preparative scales up to 50 mg or more in a specially constructed matrix-isolation cell. Unfortunately, the azepinones did not survive warm-up at the end of the experiments, and only polymeric products were ultimately obtained.

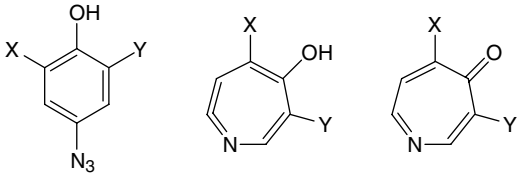

Azirine Intermediates

As with phenylcarbene (**35**) (*cf.* Scheme 5), the ring expansion of phenylnitrene (**75**) could occur directly on the singlet potential energy surface or via a bicyclic intermediate, in this case azirine **92**. Such azirines were first detected in the matrix photolysis of 1- and 2-azidonaphthalene.[95] For example, photolysis of **93** generated a photoproduct with an IR absorption at 1730 cm^{-1}, which in turn gave a cyclic ketenimine [ν(C=C=N)$_{as}$ at 1926 cm^{-1}] on further photolysis. It was proposed that the intermediate with the 1730 cm^{-1} IR band was the tricyclic azirine **94**, which subsequently rearranged to **95**. At the time of these experiments, however, reliable computations of IR transitions were not available, so a definitive identification of the azirines was scarcely possible. Nevertheless, a clear parallel was found here with the behavior of aryl carbenes, which give detectable cyclopropenes in the naphthalene series (*cf.* **44** and **45**) but not with the monocyclic carbenes (see the brief discussion of this point in Section 14.4).

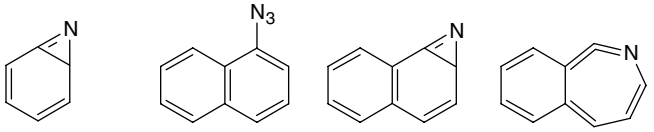

92 **93** **94** **95**

It was later discovered that azirines **96** (R = H, F) could be generated in amounts sufficient for IR detection when the corresponding phenyl nitrenes were photolyzed with 444 nm light.[96] The azirines had prominent IR absorptions in the range 1680–1660 cm^{-1}, which could be assigned as ν(C=C + C=N) vibrations. Theoretical calculations of the IR transitions were in reasonable agreement with experimental results. Both of these azirines reverted to the corresponding nitrenes when irradiated at 366 nm but showed no tendency to rearrange to the seven-membered cyclic ketenimines.

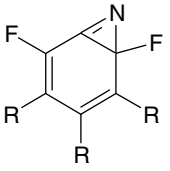

96

Heterocyclic Nitrenes

Matrix-isolation studies of the photochemistry of heterocyclic analogues of phenylnitrene have been reported at various times. The following are some recent examples.

A number of trifluoromethyl-substituted 2-pyridyl azides, e.g., **97**, have been matrix-isolated and photolyzed in Ar at 12–18 K.[97] Like other 2-pyridyl azides, **97** exists in equilibrium with the tetrazole valence tautomer **98**, but sublimation for the purpose of matrix isolation usually causes significant ring opening to the azido forms. In any case, the tetrazole forms as well as the azides eliminate N_2 when photolyzed. All the 2-pyridyl azides or tetrazoles investigated underwent conversion into the corresponding 1,3-diazacyclohepta-1,2,4,6-tetraenes, e.g., **99** from **97**, and these ring expanded products, which are cyclic carbodiimides, had $\nu(N{=}C{=}N)_{as}$ bands at about 2000 cm^{-1} in their IR spectra. In the case of **97**, the triplet nitrene was also observed by both IR and EPR spectroscopy, and it was seen to give **99** on further photolysis.

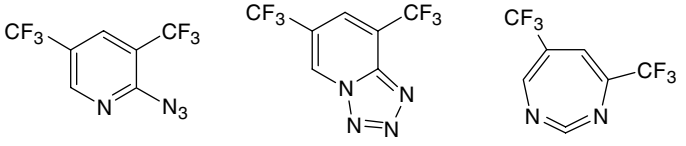

97 **98** **99**

Triplet ground-state 2-pyrimidylnitrene (**100**) has similarly been observed by EPR and UV-visible absorption spectroscopy in ethanol glasses at 77 K and by UV-visible and IR spectroscopy in Ar matrices, following 254 nm photolysis of the equilibrium mixture of 2-azidopyrimidine and its tetrazole tautomer.[98] The matrix IR spectrum of **100** was in good agreement with that predicted by DFT theory. The matrix IR spectra also revealed that a second, unidentified product, which might have been a photoproduct of the tetrazole tautomer of the starting azide, accompanied **100**. On continued exposure of the matrix to 254 nm light, the IR bands of **100** and the unidentified product disappeared and a new band arose at 2045 cm^{-1}, which was assigned to the carbodiimide **101**. In accord with theoretical predictions, no

benzodiazirine, analogous to **96**, was detected. In a comparable reaction, 2-azido-4,6-dichloro-*s*-triazine (**102**) yielded both the corresponding triplet nitrene and the cyclic carbodiimide **103** when photolyzed in Ar matrices.[99]

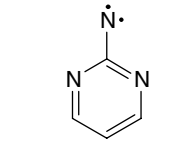

100

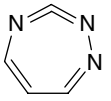

101

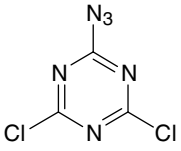

102

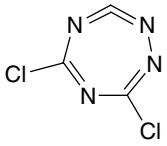

103

Di- and Trinitrenes and Carbenonitrenes

In the past few years, a growing interest in the investigation of reactive species with more than one nitrene or carbene center has developed.

Photolysis of *p*-diazidobenzene in Ar matrices led to the IR detection of *p*-phenylenebisnitrene (**104**), which decomposed to **105** and then to ethyne and 1-cyano-2-isocyanoethene, most probably in its *Z* form (**106**), on further irradiation.[100] The identification of the reaction products from the matrix IR spectra relied greatly on DFT computations of IR transitions. The dinitrene **104** was predicted to have a singlet ground state with a small S–T splitting, which is in accord with the experimental results and is best described as a bisiminyl diradical. Owing to its high symmetry, only one C=N bond stretch of **104** is IR active, and this was observed at 1576 cm^{-1} with a weak intensity.

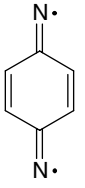

104

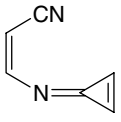

105

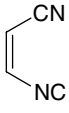

106

Related studies of the photolysis of 1,4-diazidonaphthalene[101] and 1,5-diazidonaphthalene[101,102] have afforded UV-visible, IR, and EPR spectra of the corresponding bisiminyl diradicals (dinitrenes), **107** and **108**, respectively. These also seem to have singlet ground states with quinonoidal character rather than aromatic dinitrene structures.

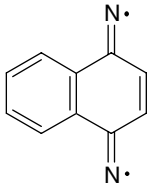

107

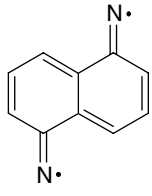

108

Matrix photolysis of 3,5-dichloro- and 3-chloro-5-cyano-2,4,6-triazidopyridines (**109**: X = Cl, Y = Cl, CN) gave in rapid succession mono-, di-, and trinitrenopyridines, which were identified by agreement of the matrix IR spectra with DFT calculations.[103] The 3,5-dicyano analogue (**109**: X = Y = CN), however, did not yield an identifiable trinitrene. The quintet dinitrenes and septet trinitrenes in this series have also been examined by EPR spectroscopy.[104]

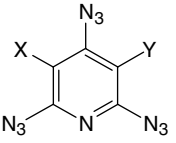

109

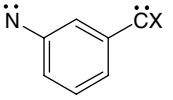

110

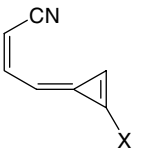

111

As a final example, *m*-phenylene–coupled carbenonitrenes **110** (X = H, F, Cl, Br) have recently been the subject of theoretical and experimental studies, the latter utilizing matrix IR, UV, and EPR spectroscopy.[105] At the highest level of theory, the unsubstituted species (**110**: X = H) should have a quintet ground state, whereas the halogen derivatives should have triplet ground states. Attempts to detect **110** (X = H) by matrix photolysis of 3-azidophenyldiazomethane did not yield detectable amounts of the carbenonitrene. Instead, an excellent match was found between the photoproduct IR spectrum and the cyclopropene derivative **111** (X = H). In the case of the three halogen derivatives, however, the triplet carbenonitrenes were detected and characterized. The matrix IR spectra indicated that all three isomerized to cyclopropenes **111** (X = F, Cl, Br) on further irradiation.

14.6 Arynes

o-Benzynes

An account of the matrix-isolation studies of *o*-benzyne (**112**) provides a cautionary tale. This species was first isolated in matrices by the stepwise photochemical elimination of two molecules of CO_2 from **113** or two molecules of CO from **114**, and its IR spectrum was thereby observed.[106] IR bands at 1627, 1607, 1451, 1053, 1038, 849, 736, and 469 cm^{-1} were attributed to **112**. Although none of these bands appeared in the ν(C≡C) region of the spectrum and although the experimental band at 1672 cm^{-1} proved troublesome to fit, force-field calculations based on the matrix IR spectrum of **112** suggested that this molecule had a cycloalkyne structure, i.e., with a genuine triple bond.[107] On the basis of the force field, it was predicted that **112** should have IR absorptions with ν(C≡C) character at 2450 and 2083 cm^{-1}. In further experiments, an IR band at 2085 cm^{-1} was observed and assigned to **112**, in excellent agreement with the predicted ν(C≡C) band at 2083 cm^{-1}, thus seeming to provide firm confirmation of the triple bond character of **112**.[108] No band near 2450 cm^{-1} was observed, but it seemed likely that this other ν(C≡C) band could have very low intensity.[107]

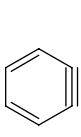

112

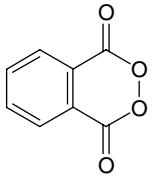

113

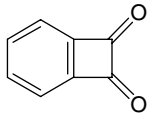

114

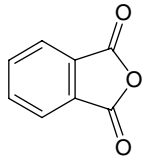

115

It was later found that *o*-benzyne could also be generated in matrices by photoelimination of CO and CO_2 from phthalic anhydride (**115**), a more convenient precursor than **113** or **114**.[109] This provided an alternative route to **112** and also the matrix IR spectrum of its tetradeuterio isotopomer. The problematical IR band at

1627 cm^{-1} was not present in the matrix spectrum of **112** produced from **114** and was therefore due to a byproduct. Otherwise, the agreement in the IR spectra of **112** obtained from different precursors remained good, including the 2085 cm^{-1} band assigned to the C≡C stretch. On the other hand, the IR spectrum of tetradeuterio-*o*-benzyne did not fit as well as expected with predictions made from the force-field calculations for **112**. Some doubts as to the bonding in *o*-benzyne therefore remained, especially with respect to the surprising conclusion that the bond between C1 and C2 had full triple bond character.

Only much later, with the help of more modern theory, did the true picture emerge.[110] It was shown that the 2085 cm^{-1} band, previously assigned as ν(C≡C), belonged not to *o*-benzyne but to cyclopentadienylideneketene (**116**), which was formed in a remarkable, reversible photochemical reaction of *o*-benzyne with CO. A complete set of vibrational frequencies was obtained for *o*-benzyne and two of its isotopomers, C_6D_4 and 1,2–$^{13}C_2C_4H_4$, and symmetries were assigned for most of the transitions from the linear dichroism exhibited by matrices containing photo-oriented *o*-benzyne. From these results, the ν(CC) IR absorption of the bond between C1 and C2 in **112** was identified at 1846 cm^{-1}, indicating a bond somewhere between a double and a triple bond. Later, the ^{13}C NMR spectrum of *o*-benzyne isolated in Ar matrices was reported.[111] Simulation of the spectrum gave an estimated bond length of 124 ± 2 pm for the bond between C1 and C2, in good agreement with geometry optimizations carried out by *ab initio* methods and with the qualitative finding of a bond lying somewhere between double and triple in character. The introduction sections of these definitive IR[110] and NMR[111] papers should be read for their excellent critiques of the numerous previous investigations of *o*-benzyne.

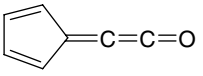

116

Recently, tetrafluoro-*o*-benzyne (**117**) has been isolated in Ar matrices, together with CO and CO_2, by photolysis of tetrafluorophthalic anhydride.[112] On subsequent irradiation at 350 nm, **117** was carbonylated to give the cyclopropenone **118**. The C≡C stretching vibration in **117** could not, however, be identified. DFT computations predicted that the ν(C≡C) IR band should be found at 1936 cm^{-1}, but with very low intensity.

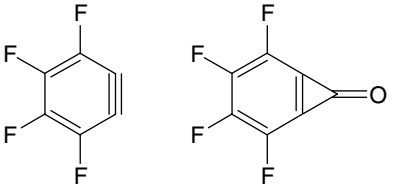

117 **118**

Benzdiynes and Analogues

The convenience of aromatic dicarboxylic anhydrides as precursors for benzynes has encouraged the search for benzdiynes. So far these efforts have provided some, but by no means universal, success. Much interesting chemistry has emerged, nonetheless.

Sequential photolysis of dianhydride **119** in Ar matrices, as shown in Scheme 11, resulted first in the elimination of CO_2 and then CO from one of the anhydride groups, giving cyclopropenone **120** and benzyne **121**.[113] The identity of benzyne **121** was confirmed by generating this species in argon matrices containing furan, allowing the argon to evaporate by gentle warming and finally analyzing the residue by GC-MS, which revealed the presence of the furan adduct of **121** (M^+ = 350). Further irradiation of matrices containing **121** at 248 nm led to a decrease in its IR absorptions, increases in the IR absorptions of CO and CO_2, and the appearance of a new species with IR bands at 1466, 1183, 1127, and 798 cm^{-1}.

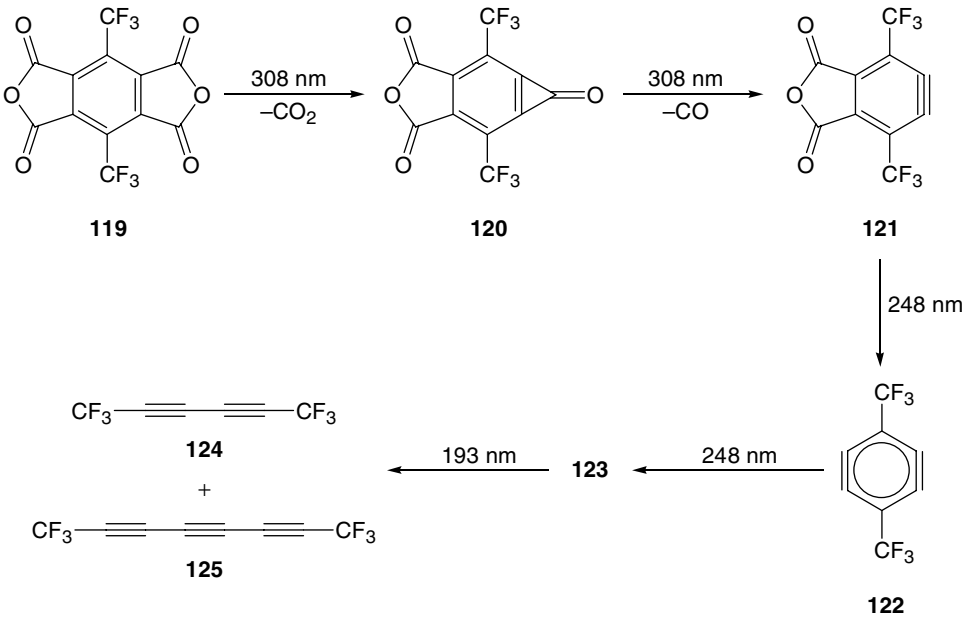

SCHEME 11

On the basis of its IR spectrum and subsequent photochemistry, this new species was identified as the 1,4-benzdiyne **122**. With 248 nm light, **122** decomposed to an intermediate **123**, which could not be identified, but which in turn was transformed by 193 nm light into diyne **124** and triyne **125**.

Attempts to observe unsubstituted 1,4- and 1,3-benzdiynes (**126** and **127**) by similar wavelength-selective photolyses of 1,2:4,5- and 1,2:3,4-benzenetetracarboxylic dianhydrides were unsuccessful.[114] The corresponding cyclopropenone and benzyne photoproducts (*cf.* **120** and **121**) were observed in the initial stage in each case, but only ring-opened final products, such as hexa-1,3,5-triyne, were detected thereafter. Comparable results were obtained in attempts to observe naphthdiynes such as **128**.[115,116] Most recently, a second example of a 1,4-benzdiyne has been identified: the 3,6-difluoro derivative, which like the 3,6-bis(trifluoromethyl) analogue **122**, was converted into a hexatriyne on secondary photolysis.[117]

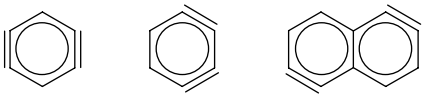

126 **127** **128**

References

1. Whittle, E., Dows, D.A., and Pimentel, G.C., The matrix isolation method for the experimental study of unstable species, *J. Chem. Phys.,* 22, 1943, 1954.
2. Ball, D.W., Kafafi, Z.H., Fredin, L., Hauge, R.H., and Margrave, J.L., *A Bibliography of Matrix Isolation Spectroscopy: 1954–1985,* Rice University Press, Houston, 1988.
3. Ochsner, D.W., Ball, D.W., and Kafafi, Z., *A Bibliography of Matrix Isolation Spectroscopy: 1985–1997,* Naval Research Laboratory, Washington, 1998.
4. Hermann, T.S. and Harvey, S.R., Infrared spectroscopy at sub-ambient temperatures: I. Literature review, *Appl. Spectrosc.,* 23, 435, 1969.
5. Hermann, T.S., Infrared spectroscopy at sub-ambient temperatures: III. Molecules and molecular fragments within matrices, *Appl. Spectrosc.,* 23, 461, 1969.
6. Chapman, O.L., Low temperature and photochemical studies, *Pure Appl. Chem.,* 40, 511, 1974.

7. Chapman, O.L., Photochemistry of diazo compounds and azides in argon, *Pure Appl. Chem.,* 51, 331, 1979.
8. Dunkin, I.R., The matrix isolation technique and its application to organic chemistry, *Chem. Soc. Rev.,* 9, 1, 1980.
9. Perutz, R.N., Photochemistry of small molecules in low-temperature matrices, *Chem. Rev.,* 85, 97, 1985.
10. Sheridan, R.S., Matrix isolation photochemistry, *Org. Photochem.,* 8, 159, 1987.
11. Dunkin, I.R., Reactive organic species in matrices, in *Chemistry and Physics of Matrix Isolated Species,* Andrews, L. and Moskovits, M., Eds., North-Holland, Amsterdam, 1989, chap. 8, pp. 203–237.
12. Tomioka, H., Photochemistry of reactive intermediates within inert gas matrices, *Photochemistry,* 17, 21, 1991.
13. Vancik, H., Matrix isolation and vibrational spectroscopy of carbocations, *Pure Appl. Chem.,* 67, 761, 1995.
14. Sander, W., Marquardt, C., Bucher, G., and Wandel, H., Chemistry and spectroscopy of aromatic diradicals in cryogenic matrices, *Pure Appl. Chem.,* 68, 353, 1996.
15. Tomioka, H., Matrix isolation study of reactive o-quinoid compounds: generation, detection and reactions, *Pure Appl. Chem.*, 69, 837, 1997.
16. Wentrup, C., Reisinger, A., Qiao, G.G., and Visser, P., Photochemistry of pyridyl azides and diazoketones in matrix and solution, *Pure Appl. Chem.,* 69, 847, 1997.
17. For a recent and thorough treatment of density functional theory, including its applications in predicting vibrational transitions, see Koch, W. and Holthausen, M.C., *A Chemist's Guide to Density Functional Theory,* Wiley-VCH, Weinheim, 2000.
18. See, for example, Dunkin, I.R. and Gallivan, S.L., The use of diffuse reflectance infrared Fourier transform spectroscopy to monitor reactions in low-temperature films and matrices, *Vib. Spectrosc.,* 9, 85, 1995.
19. Dunkin, I.R., *Matrix-Isolation Techniques: A Practical Approach,* Oxford University Press, Oxford, 1998.
20. Milligan, D.E. and Jacox, M.E., Infrared and ultraviolet spectroscopic study of the products of the vacuum-ultraviolet photolysis of methane in Ar and N_2 matrices. The infrared spectrum of the free radical CH_3, *J. Chem. Phys.,* 47, 5146, 1967.
21. Jacox, M.E. and Milligan, D.E., Matrix-isolation study of the vacuum-ultraviolet photolysis of methyl fluoride. The infrared spectra of the free radicals CF, HCF and H_2CF, *J. Chem. Phys.,* 50, 3252, 1969.
22. Jacox, M.E. and Milligan, D.E., Matrix-isolation study of the vacuum-ultraviolet photolysis of methyl chloride and methylene chloride. Infrared spectra of the free radicals CCl, H_2CCl and CCl_2, *J. Chem. Phys.,* 53, 2688, 1970.
23. Milligan, D.E., Jacox, M.E., and Comeford, J.J., Infrared spectrum of the free radical CF_3 isolated in inert matrices, *J. Chem. Phys.,* 44, 4058, 1966.
24. Shepherd, R.A., Doyle, T.J., and Graham, W.R.M., A Fourier transform infrared study of the D and ^{13}C substituted C_2H_3 vinyl radical in solid argon, *J. Chem. Phys.,* 89, 2738, 1988.
25. Pacansky, J. and Bargon, J., Low temperature photochemical studies on acetyl benzoyl peroxide. The observation of methyl and phenyl radicals by matrix isolation infrared spectroscopy, *J. Am. Chem. Soc.,* 97, 6896, 1975.
26. Pacansky, J., Gardini, G.P., and Bargon, J., Low temperature studies on propionyl benzoyl peroxide and propionyl peroxide. The ethyl radical, *J. Am. Chem. Soc.,* 98, 2665, 1976.
27. Pacansky, J. and Coufal, H., On the barrier for rotation about the C–C bond of the ethyl radical, *J. Chem. Phys.,* 72, 5285, 1980.
28. Pacansky, J. and Coufal, H., Infrared spectroscopic studies on the ethyl and isopropyl radicals, *J. Mol. Struct.,* 60, 255, 1980.
29. Pacansky, J. and Guiterrez, A., Infrared spectra of the *n*-butyl and *n*-pentyl radicals, *J. Phys. Chem.,* 87, 3074, 1983.

30. Pacansky, J., Brown, D.W., and Chang, J.S., Infrared spectra of the isobutyl and neopentyl radicals. Characteristic spectra of primary, secondary and tertiary alkyl radicals, *J. Phys. Chem.,* 85, 2562, 1981.
31. Pacansky, J., Horne, D.E., Gardini, G.P., and Bargon, J., Matrix isolation studies of alkyl radicals. The characteristic infrared spectra of primary alkyl radicals, *J. Phys. Chem.,* 81, 2149, 1977.
32. Sogoshi, N., Wakabayashi, T., Momose, T., and Shida, T., Infrared spectroscopic studies on photolysis of ethyl iodide in solid parahydrogen, *J. Phys. Chem. A,* 101, 522, 1997.
33. Nakamura, T., Ohana, T., and Koga, Y., Photolysis of perfluoroazooctane in an argon matrix, *Phys. Chem. Chem. Phys.,* 2, 2535, 2000.
34. Hatton, W.G., Hacker, N.P., and Kasai, P.H., The photochemistry of nitrosobenzene: direct observation of the phenyl radical–nitric oxide triplet radical pair in argon at 12 K, *J. Chem. Soc., Chem. Commun.,* 227, 1990.
35. Radziszewski, J.G., Electronic absorption spectrum of phenyl radical, *Chem. Phys. Lett.,* 301, 565, 1999.
36. Friederichsen, A.V., Radziszewski, J.G., Nimlos, M.R., Winter, P.R., Dayton, D.C., David, D.E., and Ellison, G.B., The infrared spectrum of matrix-isolated phenyl radical, *J. Am. Chem. Soc.,* 123, 1977, 2001.
37. Smardzewski, R.R., De Marco, R.A., and Fox, W.B., Argon matrix infrared spectra of CF_3OOF and CF_3OOOCF_3 and their photolysis products. Spectroscopic evidence for the CF_3OO radical, *J. Chem. Phys.,* 63, 1083, 1975.
38. Spanget-Larsen, J., Gil, M., Gorski, A., Blake, D.M., Waluk, J., and Radziszewski, J.G., Vibrations of the phenoxyl radical, *J. Am. Chem. Soc.,* 123, 11253, 2001.
39. Pacansky, J. and Coufal, H., Photochemical studies on the ethyl radical, *J. Chem. Phys.,* 71, 2811, 1979.
40. Pacansky, J. and Coufal, H., The photochemistry and infrared spectrum of the isopropyl radical, *J. Chem. Phys.,* 72, 3298, 1980.
41. Pacansky, J., Brown, D.W., and Chang, J.S., Photochemical studies on the tertiary butyl radical isolated in argon matrices, *Tetrahedron*, 38, 257, 1982.
42. Ase, P., Bock, W., and Snelson, A., Alkylperoxy and alkyl radicals.1. Infrared spectra of CH_3O_2 and $CH_3O_4CH_3$ and the ultraviolet photolysis of CH_3O_2 in argon + oxygen matrices, *J. Phys. Chem.,* 90, 2099, 1986.
43. Baskir, E.G. and Nefedov, O.M., IR spectroscopic study of allylperoxy radical and products of its phototransformations in the Ar matrix, *Russ. Chem. Bull.,* 45, 99, 1996; *Izv. Akad. Nauk Ser. Khim.,* 109, 1996.
44. Sander, W., Bucher, G., and Wierlacher, S., Carbenes in matrices — spectroscopy, structure and reactivity, *Chem. Rev.,* 93, 1583, 1993.
45. Goldfarb, T.D. and Pimentel, G.C., Chemiluminescence of ethylene formed probably from methylene in an inert matrix, *J. Chem. Phys.,* 33, 105, 1960.
46. Jacox, M.E. and Milligan, D.E., Infrared study of the reactions of CH_2 and NH with C_2H_2 and C_2H_4 in solid argon, *J. Am. Chem. Soc.,* 85, 278, 1963.
47. Lee, Y.-P. and Pimentel, G.C., Chemiluminescence of ethylene in an inert matrix and the probable infrared spectrum of methylene, *J. Chem. Phys.,* 75, 4241, 1981.
48. Baird, M.S., Dunkin, I.R., and Poliakoff, M., Thermal dimerization and carbonylation of a carbene in low-temperature matrices, *J. Chem. Soc., Chem. Commun.,* 904, 1974.
49. Baird, M.S., Dunkin, I.R., Hacker, N., Poliakoff, M., and Turner, J.J., Cyclopentadienylidene. A matrix isolation study exploiting photolysis with unpolarized and plane-polarized light, *J. Am. Chem. Soc.,* 103, 5190, 1981.
50. Maier, G. and Endres, J., Photochemistry of matrix-isolated cyclopentadienylidene revisited, *J. Mol. Struct.,* 556, 179, 2000.
51. Bell, G.A. and Dunkin, I.R., Tetrachlorocyclopentadienylidene, indenylidene and fluorenylidene in low-temperature matrices: ultraviolet and infrared spectra and reactions with carbon monoxide, *J. Chem., Soc. Faraday Trans. 2*, 81, 725, 1985.

52. Dunkin, I.R. and McCluskey, A., Tetrabromocyclopentadienylidene: generation and reaction with CO in low temperature matrices, *Spectrochim. Acta Part A,* 49, 1179, 1993.
53. Maier, G. and Endres, J., 2*H*-Imidazol-2-ylidene: new insights from a matrix-spectroscopic study, *Chem.–Eur.J.,* 5, 1590, 1999.
54. Maier, G. and Endres, J., Photochemistry of matrix-isolated 4-diazo-4*H*-imidazole: IR-spectroscopic identification of 4*H*-imidazol-4-ylidene, *Eur. J. Org. Chem.,* 2535, 2000.
55. West, P.R., Chapman, O.L., and LeRoux, J.-P., Cyclohepta-1,2,4,6-tetraene, *J. Am. Chem. Soc.,* 104, 1779, 1982.
56. McMahon, R.J., Abelt, C.J., Chapman, O.L., Johnson, J.W., Kreil, C.L., LeRoux, J.-P., Mooring, A.M., and West, P.R., 1,2,4,6-Cycloheptatetraene: the key intermediate in arylcarbene interconversions and related C_7H_6 rearrangements, *J. Am. Chem. Soc.,* 109, 2456, 1987.
57. Platz, M.S., Comparison of phenylcarbene and phenylnitrene, *Acc. Chem. Res.,* 28, 487, 1995.
58. West, P.R., Mooring, A.M., McMahon, R.J., and Chapman, O.L., Benzobicyclo[4.1.0]hepta-2,4,6-trienes, *J. Org. Chem.,* 51, 1316, 1986.
59. Albrecht, S.W. and McMahon, R.J., Photoequilibration of 2-naphthylcarbene and 2,3-benzobicyclo[4.1.0]hepta-2,4,6-triene, *J. Am. Chem. Soc.,* 115, 855, 1993.
60. Bonvallet, P.A. and McMahon, R.J., Photoequilibration of 1-naphthylcarbene and 4,5-benzobicyclo[4.1.0]hepta-2,4,6-triene, *J. Am. Chem. Soc.,* 121, 10496, 1999.
61. Rempala, P. and Sheridan, R.S., Matrix isolation and photochemistry of 1- and 2-naphthylchlorocarbene, *J. Chem. Soc., Perkin Trans. 2,* 2257, 1999.
62. Zhu, Z., Bally, T., Stracener, L.L., and McMahon, R.J., Reversible interconversion between singlet and triplet 2-naphthyl(carbomethoxy)carbene, *J. Am. Chem. Soc.,* 121, 2863, 1999.
63. Bell, G.A. and Dunkin, I.R., Cyclopentadienone *O*-oxide: a highly labile intermediate in the matrix reaction between cyclopentadienylidene and oxygen, *J. Chem. Soc., Chem. Commun.,* 1213, 1983.
64. Chapman, O.L. and Hess, T.C., Cyclopentadienone *O*-oxide: spectroscopic observation and photochemistry of a carbonyl oxide, *J. Am. Chem. Soc.,* 106, 1842, 1984.
65. Dunkin, I.R. and Shields, C.J., The photo-isomerization of cyclopentadienone *O*-oxide isolated in low temperature matrices, *J. Chem. Soc., Chem. Commun.,* 154, 1986.
66. Dunkin, I.R., Bell, G.A., McCleod, F.G., and McCluskey, A., An infrared study of the formation and photochemical decomposition of tetrachlorocyclopentadienone *O*-oxide in low temperature matrices, *Spectrochim. Acta Part A,* 42, 567, 1986.
67. Dunkin, I.R. and Bell, G.A., The generation and photochemistry of indenone *O*-oxide and fluorenone *O*-oxide in low temperature matrices, *Tetrahedron,* 41, 339, 1985.
68. Sander, W., Carbonyl oxides: zwitterions or diradicals? *Angew. Chem. Int. Ed. Engl.,* 29, 344, 1990; *Angew. Chem.,* 102, 362, 1990.
69. Dunkin, I.R. and McCluskey, A., Carbonyl cyanide *O*-oxide, the adduct of dicyanomethylene and dioxygen in argon matrices at 12 K, *Spectrochim. Acta Part A,* 50, 209, 1994.
70. Wierlacher, S., Sander, W., Marquardt, C., Kraka, E., and Cremer, D., Propinal O-oxide, *Chem. Phys. Lett.,* 222, 319, 1994.
71. McCluskey, A. and Dunkin, I.R., Suppression of the Wolff rearrangement of the unstrained α-carbonyl carbene by CO and O_2 in low-temperature matrices, *Aust. J. Chem.,* 48, 1107, 1995.
72. Sander, W., Kirschfeld, A., and Halupka, M., Matrix isolation of diphenylsulfene and diphenyl-α-sultine, *J. Am. Chem. Soc.,* 119, 981, 1997.
73. Breidung, J., Bürger, H., Kötting, C., Kopitzky, R., Sander, W., Senzlober, M., Thiel, W., and Willner, H., Difluorovinylidene, $F_2C{=}C{:}$, *Angew. Chem. Int. Ed. Engl.,* 36, 1983, 1997; *Angew. Chem.* 109, 2072, 1997.
74. Sander, W. and Kötting, C., Reactions of difluorovinylidene — a super-electrophilic carbene, *Chem.–Eur. J.,* 5, 24, 1999.
75. Reed, S.C., Capitosti, G.J., Zhu, Z., and Modarelli, D.A., Photochemical generation and matrix-isolation detection of dimethylvinylidene, *J. Org. Chem.,* 66, 287, 2001.

76. Murata, S., Kobayashi, J., Kongou, C., Miyata, M., Matsushita, T., and Tomioka, H., Photochemistry of 2,4-bis(diazo)-1,2,3,4-tetrahydronaphthalene-1,three-dimensionalione: selective photodecomposition of one of the two inequivalent diazo groups, *J. Am. Chem. Soc.,* 120, 9088, 1998.
77. Murata, S., Kobayashi, J., Kongou, C., Miyata, M., Matsushita, T., and Tomioka, H., Remarkable wavelength-dependent photoreactions of the bis(diazo)ketone having inequivalent diazo groups: studies in fluid solutions and in low-temperature matrixes, *J. Org. Chem.,* 65, 6082, 2000.
78. Sander, W., Strehl, A., and Winkler, M., Photochemistry of bis(sulfonyl)diazomethanes, *Eur. J. Org. Chem.,* 3771, 2001.
79. Tomioka, H., Komatsu, K., and Shimizu, M., The photochemistry of matrix-isolated (α–diazobenzyl)phosphonate. Observation and reactions of phosphonylphenylcarbene, phosphonyl phenyl ketone oxide and phenylphosphonyldioxirane, *J. Org. Chem.,* 57, 6216, 1992.
80. Reiser, A., Bowes, G., and Horne, R.J., Photolysis of aromatic azides. Part 1. — Electronic spectra of aromatic nitrenes and their parent azides, *Trans. Faraday Soc.,* 62, 3162, 1966.
81. Reiser, A., Wagner, H.M., Marley, R., and Bowes, G., Photolysis of aromatic azides. Part 2. — Formation and spectra of dinitrenes, *Trans. Faraday Soc.,* **63**, 2403, 1967.
82. Reiser, A. and Marley, R., Photolysis of aromatic azides. Part 3. — Quantum yield and mechanism, *Trans. Faraday Soc.,* 64, 1806, 1968.
83. Chapman, O.L. and Le Roux, J.-P., 1-Aza-1,2,4,6-cycloheptatetraene, *J. Am. Chem. Soc.,* 100, 282, 1978.
84. Donnelly, T., Dunkin, I.R., Norwood, D.S.D., Prentice, A., Shields, C.J., and Thomson, P.C.P., Didehydroazepines from the photolysis of phenyl azide and 3- and 4-substituted phenyl azides in low-temperature matrices, *J. Chem. Soc., Perkin Trans. 2,* 307, 1985.
85. Dunkin, I.R. and Thomson, P.C.P., Pentafluorophenyl nitrene: a matrix isolated aryl nitrene that does not undergo ring expansion, *J. Chem. Soc., Chem. Commun.,* 1192, 1982.
86. Dunkin, I.R., Donnelly, T., and Lockhart, T.S., 2,6-Dimethylphenylnitrene in low-temperature matrices, *Tetrahedron Lett.,* 26, 359, 1985.
87. Karney, W.L. and Borden, W.T., Why does *o*-fluorine substitution raise the barrier to ring expansion of phenylnitrene? *J. Am. Chem. Soc.,* 119, 3347, 1997.
88. Leyva, E., Platz, M.S., Persy, G., and Wirz, J., Photochemistry of phenyl azide: the role of singlet and triplet phenylnitrene as transient intermediates, *J. Am. Chem. Soc.,* 108, 3783, 1986.
89. Dunkin, I.R., Lynch, M.A., McAlpine, F., and Sweeney, D., A medium effect in the photolysis of phenyl azide in low-temperature matrices, *J. Photochem. Photobiol. A: Chem.,* 102, 207, 1997.
90. Hayes, J.C. and Sheridan, R.S., Infrared spectrum of triplet phenyl nitrene. On the origin of didehydroazepine in low-temperature matrices, *J. Am. Chem. Soc.,* 112, 5879, 1990.
91. Murata, S., Yoshidome, R., Satoh, Y., Kato, N., and Tomioka, H., Reactivities of nitrenes generated by photolysis of 2-(ω-phenylalkyl)phenyl azides, *J. Org. Chem.,* 60, 1428, 1995.
92. Tomioka, H., Ichikawa, N., and Komatsu, K., Photochemistry of 2-(methoxycarbonyl)phenyl azide studied by matrix-isolation spectroscopy. A new slippery energy surface for phenyl nitrene, *J. Am. Chem. Soc.,* 115, 8621, 1993.
93. Dunkin, I.R., El Ayeb, A., and Lynch, M.A., A synthetic approach to azepin-4-ones exploiting azide photolysis in low temperature matrices, *J. Chem. Soc., Chem. Commun.,* 1695, 1994.
94. Dunkin, I.R., El Ayeb, A.A., Gallivan, S.L., and Lynch, M.A., 4*H*-Azepin-4-ones from azidophenols in low-temperature matrices, *J. Chem. Soc., Perkin Trans. 2,* 1419, 1997.
95. Dunkin, I.R. and Thomson, P.C.P., Infrared evidence for tricyclic azirines and didehydrobenzazepines in the matrix photolysis of azidonaphthalenes, *J. Chem. Soc., Chem. Commun.,* 499, 1980.
96. Morawietz, J. and Sander, W., Photochemistry of fluorinated phenyl nitrenes: matrix isolation of fluorinated azirines, *J. Org. Chem.,* 61, 4351, 1996.
97. Evans, R.A., Wong, M.W., and Wentrup, C., 2-Pyridylnitrene 1,3-diazacyclohepta-1,2,4,6-tetraene rearrangements in the trifluoromethyl-2-pyridyl azide series, *J. Am. Chem. Soc.,* 118, 4009, 1996.
98. Cerro-Lopez, M., Gritsan, N.P., Zhu, Z., and Platz, M.S., A matrix isolation spectroscopy and laser flash photolysis study of 2-pyrimidylnitrene, *J. Phys. Chem. A,* 104, 9681, 2000.

99. Bucher, G., Siegler, F., and Wolff, J.J., Photochemistry of 2-azido-4,5-dichloro-*s*-triazine: matrix isolation of a strained cyclic carbodiimide containing four nitrogen atoms in a seven-membered ring, *J. Chem. Soc., Chem. Commun.,* 2113, 1999.
100. Nicolaides, A., Tomioka, H., and Murata, S., Direct observation and characterization of *p*-phenylenebisnitrene. A labile quinoidal diradical, *J. Am. Chem. Soc.,* 120, 11530, 1998.
101. Serwinski, P.R., Walton, R., Sanborn, J.A., Lahti, P.M., Enyo, T., Miura, D., Tomioka, H., and Nicolaides, A., Connectivity effects in isomeric naphthalenedinitrenes, *Org. Lett.,* 3, 357, 2001.
102. Sato, T., Niino, H., Arulmozhiraja, S., Kaise, M., and Yabe, A., Preparation of 1,5-dinitrenonaphthalene in cryogenic matrices, *J. Chem. Soc., Chem. Commun.,* 749, 2001.
103. Chapyshev, S.V., Kuhn, A., Wong, M.W., and Wentrup, C., Mono- di- and trinitrenes in the pyridine series, *J. Am. Chem. Soc.,* 122, 1572, 2000.
104. Chapyshev, S.V., Walton, R., Sanborn, J.A., and Lahti, P.M., Quintet and septet state systems based on pyridylnitrenes: effects of substitution on open-shell high-spin states, *J. Am. Chem. Soc.,* 122, 1580, 2000.
105. Enyo, T., Nicolaides, A., and Tomioka, H., Halogen derivatives of *m*-phenylene(carbeno)nitrene: a switch in ground-state multiplicity, *J. Org. Chem.,* 67, 5578, 2002.
106. Chapman, O.L., Mattes, K., McIntosh, C.L., Pacansky, J., Calder, G.V., and Orr, G., Benzyne, *J. Am. Chem. Soc.,* 95, 6134, 1973.
107. Laing, J.W. and Berry, R.S., Normal coordinates, structure and bonding of benzyne, *J. Am. Chem. Soc.,* 98, 660, 1976.
108. Chapman, O.L., Chang, C.C., Kolc, J., Rosenquist, N.R., and Tomioka, H., A photochemical method for the introduction of strained multiple bonds: benzyne C≡C stretch, *J. Am. Chem. Soc.,* 97, 6586, 1975.
109. Dunkin, I.R. and MacDonald, J.G., Matrix photolysis of unsaturated cyclic anhydrides and the infrared spectrum of tetradeuteriobenzyne, *J. Chem. Soc., Chem. Commun.,* 772, 1979.
110. Radziszewski, J.G., Hess, B.A., Jr., and Zahradnik, R., Infrared spectrum of *o*-benzyne: experiment and theory, *J. Am. Chem. Soc.,* 114, 52, 1992.
111. Orendt, A.M., Facelli, J.C., Radziszewski, J.G., Horton, W.J., Grant, D.M., and Michl, J., ^{13}C dipolar NMR spectrum of matrix-isolated *o*-benzyne-*1,2*–$^{13}C_2$, *J. Am. Chem. Soc.,* 118, 846, 1996.
112. Wenk, H.H. and Sander, W., Matrix isolation and spectroscopic characterization of perfluorinated *ortho*- and *meta*-benzyne, *Chem.–Eur. J.,* 7, 1837, 2001.
113. Moriyama, M., Ohana, T., and Yabe, A., Direct observation of benzdiyne: photolysis of 1,4-bis(trifluoromethyl)-2,3,5,6-benzenetetracarboxylic dianhydride in an argon matrix, *J. Am. Chem. Soc.,* 119, 10229, 1997.
114. Moriyama, M., Sato, T., Uchimaru, T., and Yabe, A., Multi-step photolysis of benzenetetracarboxylic dianhydrides in low-temperature argon matrices: exploration of reactive intermediates containing benzdiynes produced stepwise during photochemical reactions, *Phys. Chem. Chem. Phys.,* 1, 2267, 1999.
115. Sato, T., Niino, H., and Yabe, A., Generation of $C_{10}H_4$ species in a low-temperature argon matrix: consecutive photolysis of 1,2:5,6-naphthalenetetracarboxylic dianhydride, *J. Chem. Soc., Chem. Commun.,* 1205, 2000.
116. Sato, T., Niino, H., and Yabe, A., Reactive intermediates formed by the consecutive photolyses of naphthalenetetracarboxylic dianhydrides: direct observation of reactive intermediates generated by laser-induced reaction in low-temperature argon matrices, *J. Photochem. Photobiol. A: Chem.,* 145, 3, 2001.
117. Sato, T., Arulmozhiraja, S., Niino, H., Sasaki, S., Matsuura, T., and Yabe, A., Benzdiynes (1,2,4,5-tetradehydrobenzenes): direct observation by wavelength-selective photolyses of benzenetetracarboxylic dianhydrides in low-temperature nitrogen matrices, *J. Am. Chem. Soc.,* 124, 4512, 2002.

15

Matrix Photochemistry of Small Ring Compounds

Ian R. Dunkin
University of Strathclyde

15.1 Introduction

This chapter covers photochemical studies of three- and four-membered ring compounds isolated in very low temperature matrices, typically solidified noble gases or nitrogen at temperatures of 10–20 K. Under the conditions of such *matrix isolation*, reactive species are stabilized because they are prevented from diffusing and therefore from undergoing bimolecular reactions. Matrix-isolated species can be characterized by a variety of normal spectroscopic methods; IR spectroscopy usually provides the greatest amount of structural information. In the study of small ring compounds, the matrix-isolation technique has allowed the characterization and identification of previously elusive compounds such as thiirenes and highly reactive small ring species such as cyclopropenylidenes.

In addition to the stabilization of reactive species, an important advantage of matrix isolation is that IR bands tend to be very narrow. This means that overlap between the IR bands of different compounds in product mixtures is minimized, which facilities identification of the individual species present. Moreover, matrix IR frequencies are generally not greatly shifted from gas-phase frequencies, so experimental IR spectra can be expected to be in good agreement with IR spectra predicted theoretically. In recent years, density functional theory (DFT) has been highly successful in predicting the IR spectra of matrix-isolated species and has extended the scope of matrix isolation as a technique for the study of organic photochemistry.[1]

0-8493-1348-1/04/$0.00+$1.50

Although in a handbook of this type, comprehensive coverage of each topic is rarely possible, this chapter endeavors to represent the scope of matrix-isolation studies of the photochemistry of small-ring compounds over an extended period of time. In addition, attempts have been made to give examples of work by most of the research groups that are, or have been, active in the area and to give a sufficient number of key references to facilitate further searches.

15.2 Photochemical Generation of Three-Membered Rings in Matrices

Three-membered ring compounds have been generated photochemically in low-temperature matrices using three general reaction types:

1. Addition of reactive species, such as NH or an oxygen atom, to double or triple bonds, i.e., [1 + 2]-cycloaddition reactions
2. Elimination of small molecules, most commonly N_2, from suitable precursors
3. Photorearrangement, e.g., of carbenes and nitrenes or of compounds with larger rings

[1 + 2]-Cycloadditions

The reactions of ethene and ethyne with imidogen (NH) from photolysis of HN_3 and of ethyne with methylene (CH_2) from CH_2N_2 were among the first organic systems to be studied by the matrix-isolation technique.[2] The IR spectra for argon matrices at 4 K showed that the [1 + 2]-cycloadduct, aziridine (ethyleneimine), was the main product from NH and ethene, but no other cyclic products were detected. Instead, allene was formed from CH_2 and ethyne, and probably ketenimine from NH and ethyne. It was suggested that at least some of the NH and CH_2, generated initially as singlets, underwent deactivation to the triplet ground states before reaction.

Similar studies have been made of the reactions of various unsaturated compounds with atomic oxygen, generated by the photolysis of ozone in argon matrices. It is generally assumed that the reactions involve ground-state O (^3P) atoms. The primary products from ethene included the [1 + 2]-cycloadduct, oxirane (ethylene oxide), along with acetaldehyde, ketene, and vinyl alcohol.[3] In similar conditions, benzene gave phenol, benzene oxide (**1**) (the [1 + 2]-cycloadduct), cyclohexa-2,4-dienone (**2**), and a ring-opened product, hexa-1,3,5-trienone (**3**).[4] The reaction mechanism shown in Scheme 1 was proposed to account for these observations. In contrast, the alkynes, dimethylacetylene[5] and hexafluorobut-2-yne,[6] did not give the corresponding [1 + 2]-cycloadducts, which would have been oxirenes. (See below for further attempts to generate and characterize these species.)

The photolysis of matrix-isolated complexes of alkenes with NO_2 has provided an alternative method for adding oxygen atoms to alkenes, thus generating oxiranes.

An interesting variation in the addition of oxygen atoms to alkenes in low-temperature matrices has been discovered for allenes. Photoinduced transfer of O atoms to allene (**4a**), either from ozone[7] or in a separate study,[8] from N_2O, gave cyclopropanone (**6a**) and methyleneoxirane (allene oxide) (**8a**) (Scheme 2), along with CO, formaldehyde, acrolein, and ketene. Similarly, tetramethylallene (**4b**), with ozone, gave **6b** and **8b**, together with acetone and dimethylketene.[9] It seemed possible that the initial attack of the O atom could occur either at the central carbon of the allene, to give biradical **5**, leading to a cyclopropane, or at a terminal carbon of the allene, to give an allenoxy biradical **7** and ultimately an allene oxide. Biradicals such as **5** and **7** were not observed directly, however. Moreover, generation of the biradical **5b** in an independent reaction from a pyrazolinone[9] (see below), led to the production of both tetramethylcyclopropanone (**6b**) and the allene oxide **8b**. The latter product could conceivably arise from **5b** by attack of one radical center on the carbonyl oxygen. Some questions still remain, therefore, over the exact mechanism of the addition of O atoms to allenes.

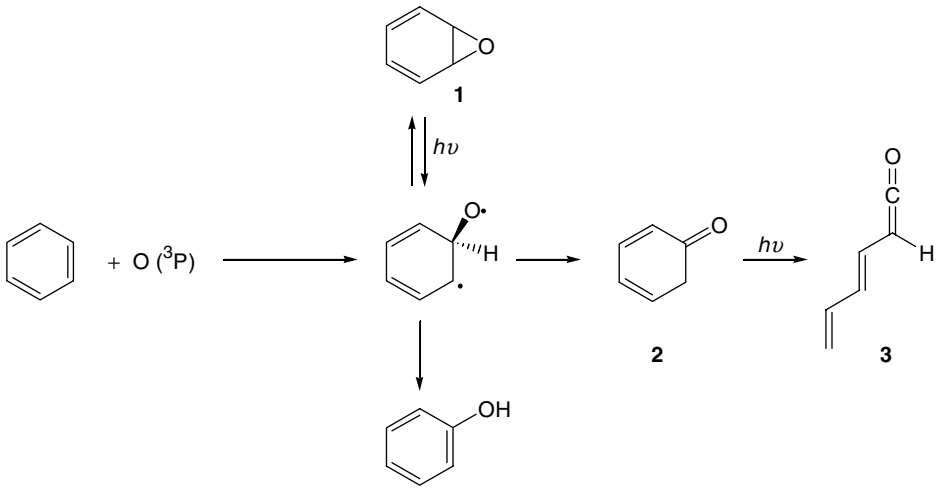

SCHEME 1

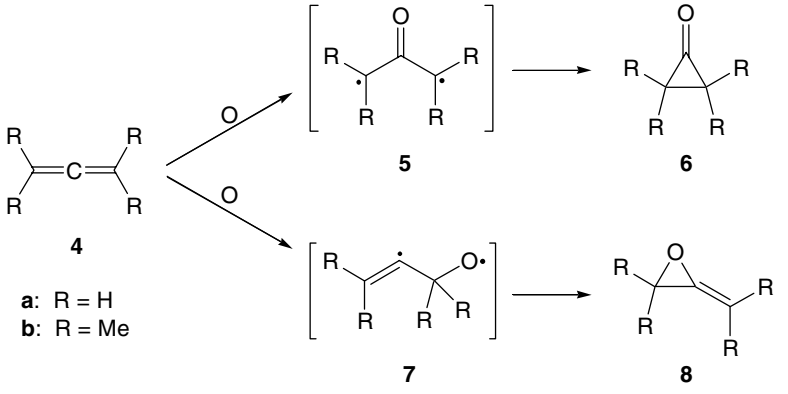

SCHEME 2

Complexes of sulfur monoxide (SO) with allene and dimethylacetylene in Ar matrices have been irradiated with near-infrared light.[10] Two novel episulfoxides (**9** and **10**, respectively) were the products identified by IR spectroscopy. No such 1 + 2 cycloadducts were detected in earlier studies of triplet reactions of SO; hence, it was concluded that **9** and **10** were formed in reactions of singlet-state SO. Near-infrared light apparently excites the reactant complexes to an electronic energy surface different from that of the ground state, while the long wavelength of the exciting photons ensures that the products, once formed, carry the least possible amount of excess vibrational energy, thus minimizing the chances of ring opening.

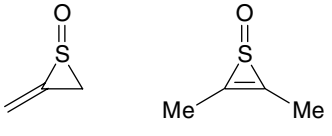

9 **10**

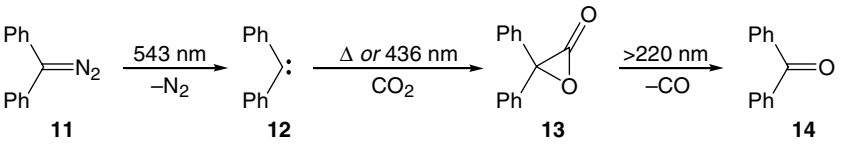

SCHEME 3

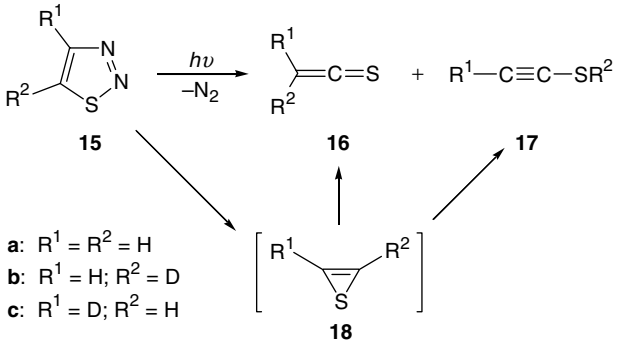

SCHEME 4

Photolysis at 543 nm of diphenyldiazomethane (**11**) in Ar or Xe matrices containing CO_2 resulted in the cycloaddition of the carbene **12** and CO_2, yielding the oxiranone (α-lactone) **13**, which was identified by means of strong ν(C=O) absorptions at 1890 and 1878 cm^{-1} (Scheme 3).[11] The IR assignments were supported by isotopic labeling studies utilizing [1–^{13}C]-**11**, $^{13}C^{16}O_2$, and $^{12}C^{18}O_2$. On further photolysis at wavelengths >220 nm, **13** lost CO to give benzophenone (**14**). Carbene **12** was not carboxylated thermally at 10 K and only slowly at higher temperatures, but irradiation into the long wavelength $\pi \rightarrow \pi^*$ (triplet-triplet) absorption of **12** (λ_{max} = 454 nm) gave **13** in a rapid reaction, even at 10 K. Since the formation of **13** from triplet **12** and CO_2 is formally spin forbidden, this provided evidence that excited triplet carbene **12** reacts like a singlet carbene, a possibility that had first been noted for **12** in alcohols at 77 K.

Photoeliminations

Only a few photoeliminations yielding three-membered ring products have been investigated by matrix-isolation techniques. Nonetheless, one of these — the generation of thiirene and its selenium analogue — was probably one of the most significant contributions made by matrix isolation to the study of organic reactive intermediates.

Photolysis of 1,2,3-thiadiazole (**15a**) in argon or nitrogen matrices gave thioketene (**16a**) and ethynyl mercaptan (**17a**) as the main products (Scheme 4).[12] When the singly labeled deuterium isotopomers **15b** and **15c** were similarly photolyzed, the two isotopomers of ethynyl mercaptan, **17b** and **17c**, were formed in the same ratio from each precursor. Since the isomeric deuterium labeled mercaptans were not interconverted under the matrix photolysis conditions, it was concluded that an intermediate was involved in their formation — probably thiirene (**18b,c**) — in which the deuterium label became scrambled. The same conclusion was reached when ^{13}C labeled isotopomers of **15a** were also photolyzed in matrices.[13] In this second study, a new species was detected that arose on initial photolysis of the thiadiazole at 300 nm and decomposed on further photolysis, with concomitant production of ethynyl mercaptan. It seemed likely that this species was thiirene (**18a**), but an unequivocal identification could not be made on the basis of the few IR bands observed.

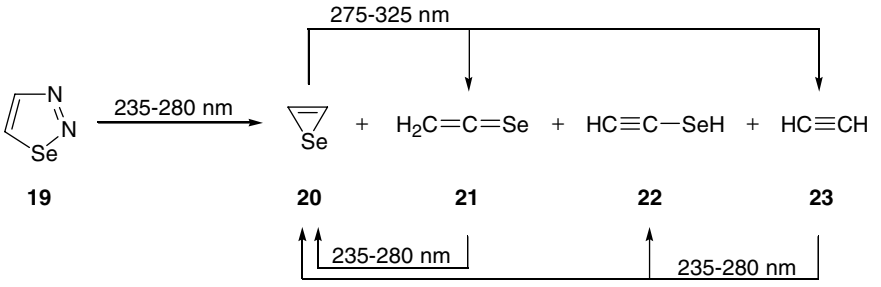

19 **20** **21** **22** **23**

SCHEME 5

The definitive identification of thiirene was eventually made following careful matrix studies involving a number of isotopically labeled precursors and a range of substituted derivatives.[14–17] From the scrambling of ^{13}C labels, it was shown that the formation of both thioketenes (**16**) and ethynyl mercaptans (**17**) probably involved the same intermediate thiirenes (**18**). This work was carried out before reliable methods for theoretically predicting IR spectra became available, but it provided the IR spectra of a number of thiirenes, which could be analyzed and compared in detail. Convincing identifications of **18a** and some analogues were then possible. It was found that thiirene itself, trifluoromethylthiirene, and benzothiirene were all highly unstable, but ethoxycarbonylmethylthiirene (**18**: $R^1 = CO_2Et$, $R^2 = Me$) appeared to be relatively stabilized by the electron withdrawing substituent and persisted in Xe matrices up to at least 73 K, the softening point of the matrix. A thiirene with two ester groups, bis(methoxycarbonyl)thiirene (**18**: $R^1 = R^2 = CO_2Me$), proved to be even more stable.[18] This species was generated almost quantitatively from the corresponding thiadiazole by irradiation at 254 or 265 nm and was itself photolyzed only slowly and at short wavelength (210 nm). Moreover, the secondary photolysis resulted mainly in extensive fragmentation rather than the formation of bis(methoxycarbonyl)thioketene. A more detailed discussion of the chemistry of thiirene, including matrix-isolation studies, can be found in a 1980 review.[17]

In parallel with the matrix isolation investigations of thiirene, more limited studies of the selenium analogue, selenirene, were also carried out.[13,14] In its details, the matrix photochemistry of 1,2,3-selenadiazole differed significantly from that of 1,2,3-thiadiazole. The various reactions are summarized in Scheme 5. Photolysis of 1,2,3-selenadiazole (**19**) at 235–280 nm in argon at 8 K gave a mixture of products, which were identified by their IR absorptions as selenoketene (**21**), ethynyl selenol (**22**), acetylene (**23**), and a species with an IR spectrum strikingly similar to that of thiirene, which was therefore concluded to be selenirene (**20**). Further photolysis of this mixture at 275–325 nm led to the decomposition of selenirene,while the IR bands of **21** and **22** grew. Thereafter, if irradiation was continued at 235–280 nm, the IR bands of **21** and **23** were reduced in intensity, while those of selenirene (**20**) reappeared and those of **22** were enhanced. It was suggested that the conversion of acetylene back into **20** and **22** could have occurred by reaction of acetylene with photoexcited Se atoms. Following this initial study of selenirene, the analogue, benzoselenirene (**24**), was observed in matrices following 254 nm photolysis of 1,2,3-benzoselenadiazole.[19] On further irradiation, **24** rearranged to fulvene-6-selone (**25**).

24 **25**

The photolysis at 310 or 335 nm of *N*-substituted 1,2,4-triazoline-3,5-diones **26** (R = Me, Ph) in Ar matrices gave the corresponding isocyanates (RNCO) as the most abundant products, resulting from the elimination of N_2 and CO.[20] Nevertheless, aziridine-2,three-dimensionaliones (**27**: R = Me, Ph) were also detected as minor products. These were identified by their IR absorptions, interpreted with the assistance

of *ab initio* calculations. The aziridinediones **27** were further photolyzed with light of $\lambda \geq 230$ nm to give the isocyanates (RNCO) and CO.

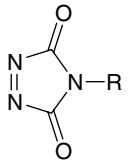

26

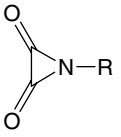

27

Matrix photolysis of the dimethyltetrazolinone **28** (X = O) gave the diaziridinone **29** (X = O) and methyl isocyanate (MeNCO).[21] The isocyanate was seemingly produced by the elimination of methyl azide (MeN_3) from **28**, in a process that had not been previously observed for the photolysis in solution. The *t*-butylvinyl derivative **30** also gave the corresponding diaziridinone and *t*-butyl isocyanate when photolyzed in matrices, even though in solution the imidazolone **31** was the sole isolable product. In the same study, it was also found that the imino analogue **28** (X = NMe) similarly gave the iminodiaziridine **29** (X = NMe) and the carbodiimide MeN=C=NMe. Analogous thiones, such as **28** (X = S), however, did not give diaziridinethiones, but rather eliminated sulfur atoms to yield the corresponding carbodiimides, e.g., MeN=C=NMe from **28** (X = S).

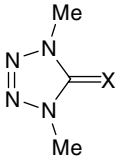

28

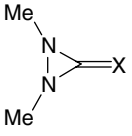

29

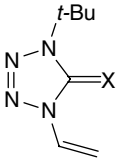

30

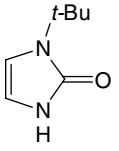

31

Photolysis of the tetramethylpyrazolinone **32** at 193 nm in Ar matrices resulted in high yields of tetramethylcyclopropanone (**6b**) (see Scheme 2) and allene oxide **8b**, the same products observed from the addition of O atoms to tetramethylallene (**4b**).[9] The primary photoproduct was presumably the biradical **5b**, so it seems likely that the allene oxide and the cyclopropanone arose from a common intermediate. In the case of **32**, a minor amount of the ketazine **33** was also formed, a result of the elimination of CO.

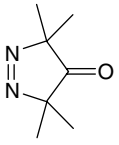

32

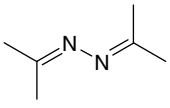

33

Although thermolysis of thiadiazolines **34a-c** gave the corresponding thiiranes **37a-c** exclusively, matrix photolysis in an organic glass at 77 K or in argon at 10 K allowed detection of the thiocarbonyl ylides **36a-c** (Scheme 6).[22] Surprisingly, in the photochemical reaction these ylides did not appear to arise directly from the thiadiazolines by elimination of N_2, but instead were formed via initial elimination of diazomethane (CH_2N_2), yielding thioketones **35a-c**. Photolysis of the diazomethane then gave methylene (CH_2), and this carbene reacted with the thioketones to give the thiocarbonyl ylides **36a-c**. Finally, the thiiranes **37a-c** could be produced from the thiocarbonyl ylides by further irradiation at 366 nm.

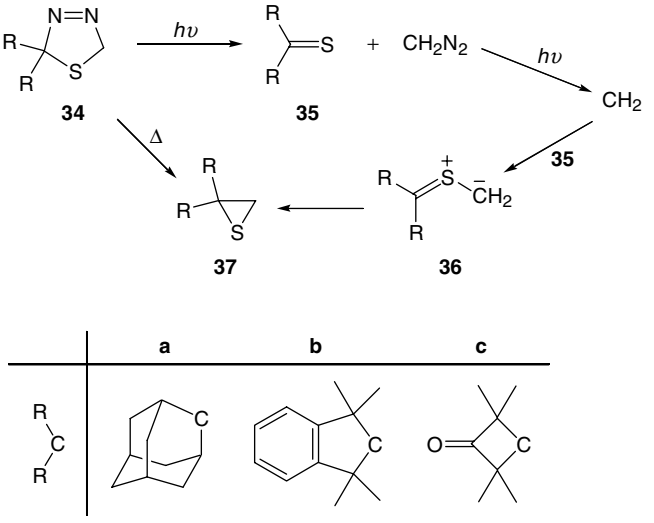

SCHEME 6

For an unusual generation of the CC double bond in a cyclopropenone by double photoelimination of nitrogen from an α,α'-bis diazoketone, see Scheme 12 in Section 15.3. Examples of photoeliminations of CO from a cyclobutanedione (**109**) and a cyclobutenedione (**112**), to afford a cyclopropanone and a cyclopropenone, respectively, are given in Section 15.4. The latter reaction appeared to proceed by a two-step mechanism involving an initial ring opening,

Photorearrangements

Several types of carbenes undergo rearrangements to cyclopropenes when generated photolytically in low-temperature matrices, either immediately or upon further irradiation. Early examples were found when naphthyldiazomethanes were photolyzed at 15 K in argon matrices.[23] For example, 1-naphthyldiazomethane (**38**) produced the cyclopropene derivative, 4,5-benzobicyclo[4.1.0]hepta-2,4,6-triene (**39**), when irradiated with light of $\lambda > 510$ nm (slowly) or $\lambda > 336$ nm (more rapidly), together with a small amount of the cyclobuta[*de*]naphthalene **40**. This behavior contrasted with the flash vacuum thermolysis of **39**, which gave mainly **40**. Both **39** and **40** were presumed to arise by rearrangement of the carbene resulting from the photoelimination of N_2 from **38**, but the carbene itself was not detected in the early studies. In a more recent study, utilizing DFT calculations of IR spectra, the original identifications were confirmed and the triplet carbene identified by IR and UV-visible spectroscopy.[24] It was moreover shown that the carbene and **39** could be interconverted photochemically. The analogous formation of azirines from aryl nitrenes has also been observed in certain cases.

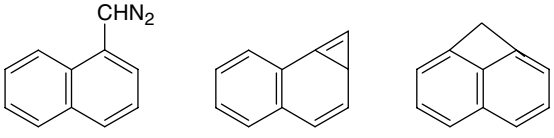

38 **39** **40**

The interconversion of vinylcarbenes and cyclopropenes has been directly observed in the case of the 4-oxocyclohexa-2,5-dienylidenes **42**, several examples of which were generated in Ar matrices by photolyzing the corresponding quinone diazides **41** (Scheme 7).[25] On irradiation into their longest wavelength absorption bands (420–700 nm), the carbenes **42** rearranged to the corresponding bicyclo[3.1.0]hexadienones **43**. This

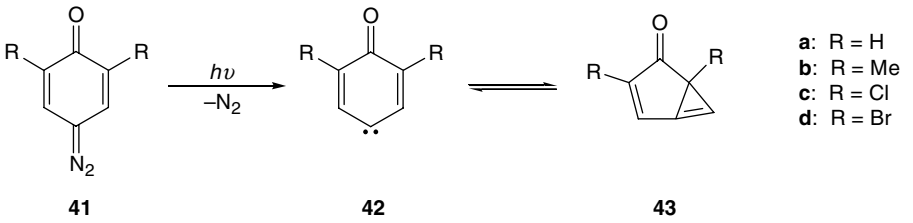

41 **42** **43**

SCHEME 7

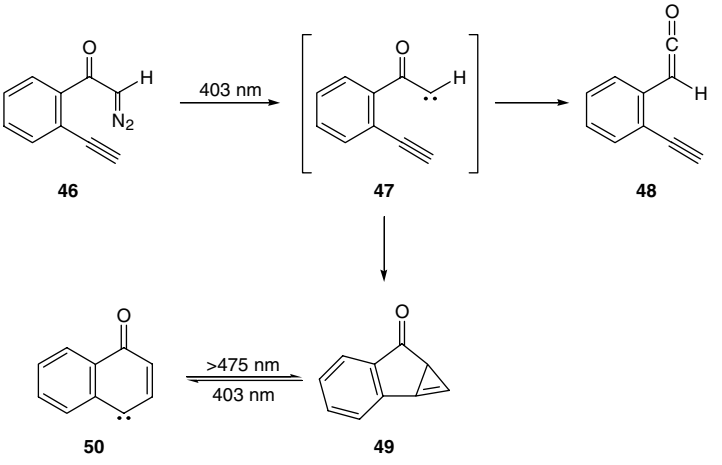

46 **47** **48** **50** **49**

SCHEME 8

rearrangement could be reversed by IR irradiation or by visible light with $\lambda > 470$ nm. The related carbene **44** rearranged to the bicyclohexadiene **45** when irradiated at $\lambda > 515$ nm in Ar matrices, but in this case the rearrangement was irreversible.[26]

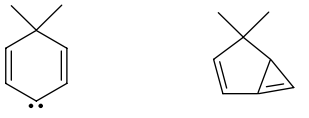

44 **45**

An intriguing alternative entry into this type of cyclohexadienylidene chemistry has been provided by matrix isolation studies of the photolysis of α-diazo-2-ethynylacetophenone (**46**) (Scheme 8).[27] Irradiation of **46** at 403 nm in solid argon gave the ketene **48** as the major product but also the carbene **50** as a minor product. Carbene **50** was reversibly converted into **49** on irradiation at $\lambda > 475$ nm. Thus, the Wolff rearrangement of ketocarbene **47**, which was not observed directly, competed with the intramolecular addition of the carbene center to the triple bond.

One of the main interests in matrix ketocarbene chemistry has been the quest for oxirene (**52**: $R^1 = R^2 = H$) and its derivatives. In principle, an oxirene should lie on the energy surface linking the two α-carbonylcarbenes **51** and **53** (Scheme 9), but whether as an intermediate or as a transition state has been much debated. Photolysis of diazoacetaldehyde (**51**: $R^1 = R^2 = H$) and ethyl diazoacetate (**51**: $R^1 = H$, $R^2 = CO_2Et$) in argon matrices was the first reported attempt to observe oxirenes.[28] Only the corresponding

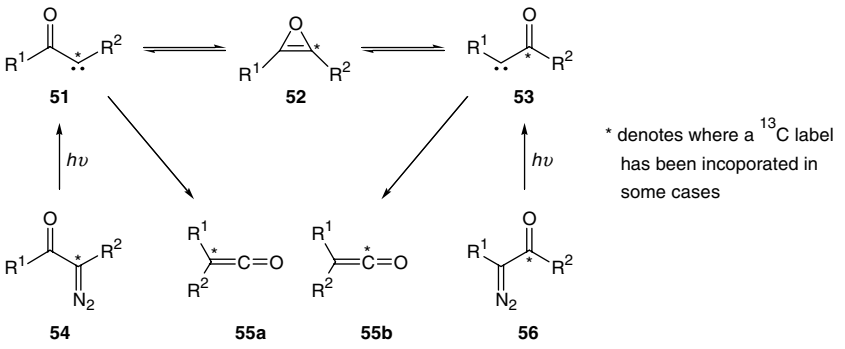

SCHEME 9

ketenes (**55**) were detected as products, however. Interestingly, the yield of ethoxyketene from ethyl diazoacetate was substantially reduced in methane, ethane, and ethylene matrices. This was taken as evidence that intermolecular reactions of the corresponding α-carbonylcarbene could compete with the intramolecular Wolff rearrangement, a conclusion that has since been drawn for other α-carbonylcarbenes, e.g., **47**.

Evidence for the involvement of oxirenes in the photolysis and thermolysis of α-carbonyldiazo compounds (**54, 56**) was obtained from the fate of isotopic labels, as indicated in Scheme 9.[17] Nevertheless, the goal of detecting an oxirene directly proved elusive. The problem was dealt with in a study of the matrix photolysis of diazoketones, from which it was concluded that oxirenes were, at best, intermediates lying in very shallow energy wells.[29]

Soon after, however, the detection and characterization of bis(trifluoromethyl)oxirene (**52**: $R^1 = R^2 = CF_3$) and perfluoromethylethyloxirene (**52**: $R^1 = CF_3$, $R^2 = CF_3CF_2$) in Ar matrices were reported, following photolysis of the corresponding diazoketones.[30] The species identified as oxirenes could be converted into the corresponding ketenes by irradiation at 360 nm and, in accord with predictions of very low stabilization energies for oxirenes, their spectra decayed substantially when the matrices were warmed to 35 K. In a later investigation of the matrix photolysis of the diazoketones **51** ($R^1 = R^2 = CH_3, CD_3$), the ketenes were always found to be more abundant, but species identified as oxirenes were detected as minor but well-defined products.[31] These were stable at temperatures below 25 K and isomerized to the ketenes when irradiated with light of $\lambda > 230$ nm.

Despite these seemingly reliable reports of oxirenes, doubts have recently been raised that any oxirene has been observed under matrix isolation conditions.[32] Most significantly, the computed IR spectrum of bis(trifluoromethyl)oxirene (**52**: $R^1 = R^2 = CF_3$) differed significantly from the experimental spectrum previously assigned to this species. Extraordinarily accurate agreements between experimental matrix IR spectra and those computed by modern theoretical methods are now routinely achieved. In view of this, a significant discrepancy has to be taken seriously. Therefore, the existence of oxirenes as reaction intermediates, which can be trapped in matrices, is still open to question.

The vinylcarbene–cyclopropene rearrangement, leading to cyclopropenes such as **39** and **43**, can be regarded formally as an addition of the carbene center across a flanking double bond. In contrast, (3-thienyl)methylene **57** (X = S) did not yield an analogous bicyclic compound, such as **58** (X = S), as the main product when generated in matrices, but underwent a more deep-seated rearrangement to give the methylenecyclopropene **59** (X = S).[33] It was plausibly suggested that **59** (X = S) arose by secondary rearrangement of **58** (X = S) and, indeed, a few weak IR absorptions in the matrix product spectra could be tentatively assigned to the latter species. Similarly, (3-furyl)methylene (**57**: X = O) gave α-formylmethylenecyclopropene (**59**: X = O); but no cyclopropene product was detected from the isomeric (2-furyl)methylene.[34]

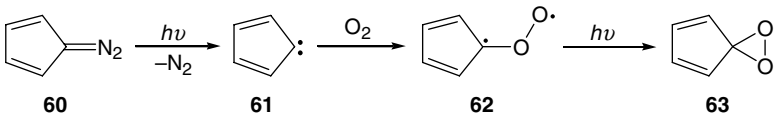

60 **61** **62** **63**

SCHEME 10

57 **58** **59**

Although carbene rearrangements form the most numerous class of photorearrangements leading to three-membered rings, some other reaction types have been reported. The transformation of carbonyl oxides into dioxiranes is an example. This was first established for the photolysis of diazocyclopentadiene (**60**) in N_2 or Ar matrices doped with O_2 (Scheme 10).[35,36] Carbene **61** reacted readily with O_2 to give initially the carbonyl oxide **62**, which on subsequent irradiation with light of $\lambda > 420$ nm isomerized to the dioxirane **63**. The reaction with $^{16}O^{18}O$ demonstrated, from splittings in the IR spectra, that the two oxygen atoms were nonequivalent in **62** and equivalent in **63**. Subsequently, it has been discovered that this is a quite general reaction of carbenes.[37]

Matrix IR spectra of bicyclo[2.1.0]pent-2-ene (**64**: X = CH_2) and the heterocyclic analogues, Dewar furan (**64**: X = O) and Dewar thiophene (**64**: X = S), were obtained after UV-irradiation of cyclopentadiene, furan, and thiophene, respectively, in Ar matrices.[38] All three spectra contained a strong absorption in the region 700–800 cm^{-1}. Identifications on the basis of the matrix IR spectra alone would probably have remained somewhat tentative, but in the cases of cyclopentadiene and thiophene, the matrix products were distilled off the cold window at the end of the experiments, and ^1H NMR spectra were obtained. Dewar furan and Dewar thiophene were both produced along with other products, but **64** (X = CH_2) appeared to be the sole product of the matrix photolysis of cyclopentadiene. On further photolysis, Dewar furan gave cyclopropene-3-carboxaldehyde (**65**), whereas Dewar thiophene and the bicyclopentene **64** (X = CH_2) reverted to thiophene and cyclopentadiene, respectively.

64 **65**

15.3 Matrix Photolysis of Three-Membered Ring Compounds

Cyclopropane, Cyclopropene, and Derivatives

Cyclopropane does not absorb in the UV-visible region of the spectrum, but it has been discovered that cyclopropane isolated in a xenon matrix doped with a halogen, such as bromine, undergoes ring opening when irradiated at 254 or 270 nm.[39] The products have been identified by IR spectroscopy. At 254 nm, the main products were propene and the allyl radical, with allene, propyne, and small amounts of ethyne and methane appearing at high conversion. At 270 nm, however, propene was produced exclusively. It was suggested that the ring opening occurred in the vibrationally excited electronic ground state of cyclopropane, by energy transfer from Xe-halogen exciplexes.

In much the same way, triplet but-2-ene-1,3-diyl (**67**: R = Me) was generated on UV-irradiation of 1-methylcyclopropene (**66**: R = Me) in bromine-doped Xe matrices and was characterized by IR spectroscopy.[40] Under similar conditions, cyclopropene seemed to yield propene-1,3-diyl (**67**: R = H), although the interpretation of the spectral data was less certain in this case. Theoretical calculations accorded with the experiments in predicting that formation of the diyls is the lowest energy ground-state pathway for ring opening of each of the cyclopropenes.

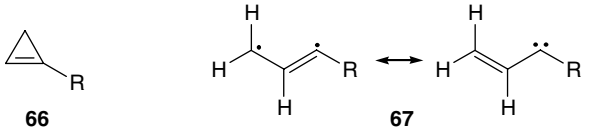

66 **67**

The IR spectrum of the non-Kekulé hydrocarbon trimethylenemethane (**69**) was observed for the first time when methylenecyclopropane (**68**) was irradiated with a low-pressure Hg arc (254 nm) in solid Xe doped with Cl_2, Br_2, or I_2.[41] The conversion of **68** into **69** was even more efficient when carried out in Xe matrices doped with bromine or iodine *atoms*, prepared by heating Br_2 or I_2 with Xe at 750°C, followed by the simultaneous condensation of the pyrolysate and a gaseous mixture of **68** and Xe at 10 K. Previous attempts to generate **69** from several alternative precursors had produced only enough to allow detection by electron paramagnetic resonance (EPR) spectroscopy. Under similar conditions, 1-methylene-2-vinylcyclopropane (**70**) afforded 4-methylene-2-pentene-1,5-diyl (**71**).[42] The results for bicyclopropylidene (**72**), however, were considerably more complicated.[43] Irradiation of **72** in Xe matrices doped with Br_2 at 313 nm led to the formation of 1,2-dimethylenecyclobutane (**76**) almost exclusively, with a small amount of methylenespiropentane (**74**). The initial photolysis product was probably the biradical **73**, but this species was not detected spectroscopically. Likewise, there was no indication of the presence of tetramethyleneethane (**75**), although this was likely to be an intermediate in the pathway leading to **76**. On further irradiation at 254 nm, 3-methylenecyclopentene (**78**) was formed. The rationalization of these experimental observations is summarized in Scheme 11.

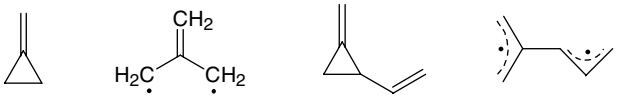

68 **69** **70** **71**

The photoextrusion of CO from cyclopropenones provides a convenient route to strained cycloalkynes. This approach seems to have been first exploited in low-temperature matrices in the formation of acenaphthyne (**83**) from cyclopropenone **82**, which was itself generated photolytically from the bisdiazoketone **81** by elimination of two nitrogen molecules (Scheme 12).[44] The ν(C≡C) IR bands of cycloalkynes are expected to be of low intensity, but a weak band at 1930 cm^{-1} was observed in the matrix IR spectrum of **83** and this was tentatively assigned to the C≡C stretch. The frequency is considerably lower than that for most normal disubstituted alkynes (2250–2200 cm^{-1}),[45] presumably as a result of the strain imposed by the distortion of the C–C≡C–C system from the ideal linear geometry. A number of other cycloalkynes have since been generated in matrices by photoelimination of CO from cyclopropenones. Examples are cycloheptyne [ν(C≡C) 2121 cm^{-1}] and the tetramethylcyclohexyne **84** [ν(C≡C) 2107 and 2116 cm^{-1}].[46] It is noteworthy that the ν(C≡C) frequencies reported for the six- and seven-membered ring cycloalkynes are appreciably higher than that for the more strained five-membered ring cycloalkyne **83**, but still lower than for unstrained alkynes. Note also that without the distortion of the C–C≡C–C moiety from linearity in cycloalkynes such as **83** and **84**, the ν(C≡C) vibration would be infrared inactive; the bent structure ensures that there is a small change of dipole moment during the vibration, *perpendicular* to the C≡C bond.

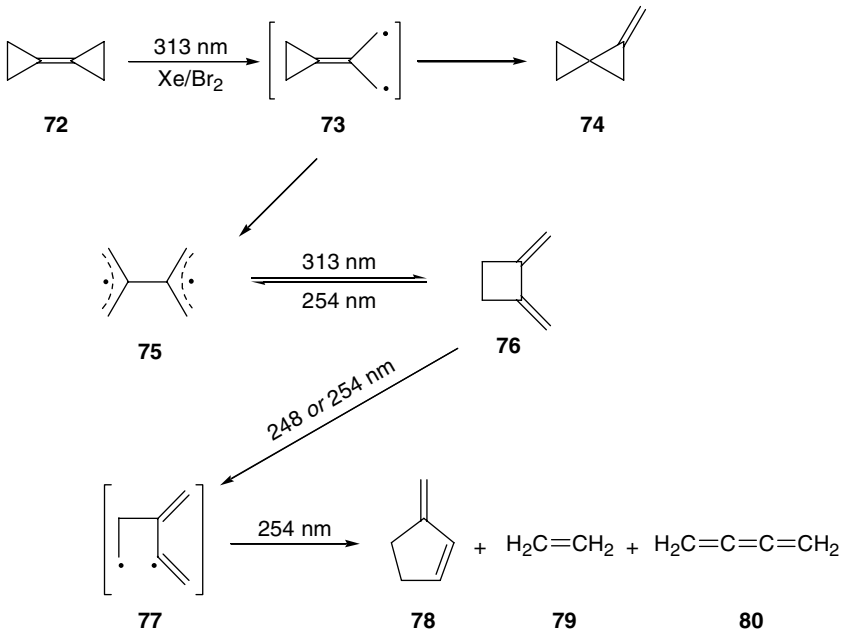

72 **73** **74** **75** **76** **77** **78** **79** **80**

SCHEME 11

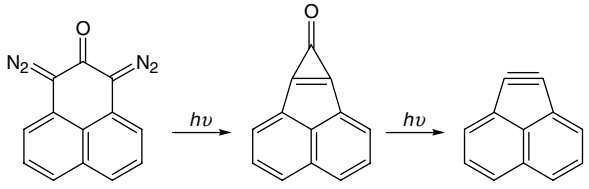

81 **82** **83**

SCHEME 12

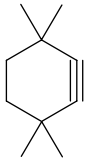

84

The carbene cyclopropylidene (**87**) has been generated in Ar matrices by the route shown in Scheme 13.[47] UV-irradiation ($\lambda \geq 230$ nm) of the acid chloride **85** resulted first in the elimination of HCl, yielding ketene **86**, which then underwent reversible photoelimination of CO. The ultimate products of this process were identified by IR spectroscopy as chlorocyclopropane (**88**) and allene (**89**), but an intermediate in their formation was also detected. This intermediate was identified as cyclopropylidene (**87**), primarily on the basis of its further reactions to give **88** and **89**.

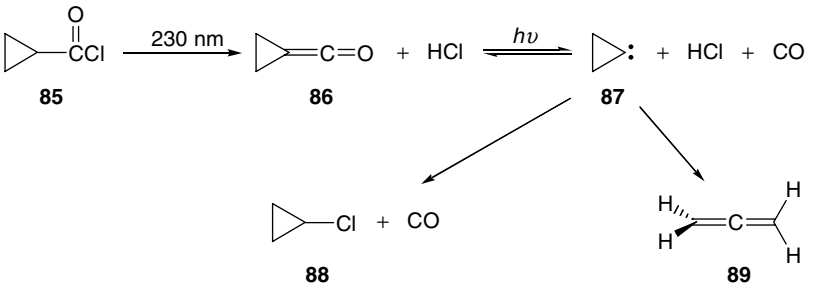

85 **86** **87** **88** **89**

SCHEME 13

Cyclopropenylidenes and Related Species

One of the advantages of the matrix-isolation technique is that it affords opportunities to study photochemical reactions not only of stable compounds but also of highly reactive species. A good example is provided by the carbene, cyclopropenylidene (**91**), which was first trapped in Ar matrices, together with benzene, following gas-phase pyrolysis of the quadricyclane **90**.[48] Four IR bands of the carbene were observed, and these were in good agreement in both frequency and intensity with the computed IR transitions of **91**. When matrices containing carbene **91** were irradiated at >360 nm, only these four IR bands disappeared, while the IR bands of propynylidene (**92**) arose. Later, it was found that both propynylidene (**92**) and its isomer, vinylidenecarbene (**93**), were produced in the photorearrangement of **91**, with **93** arising from **92** in a secondary photolysis step.[49] By changing the wavelength, the back reaction of **93** to **92** could be induced.

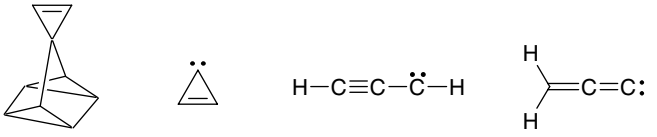

90 **91** **92** **93**

Mono- and dichlorocyclopropenylidene have been generated by flash pyrolysis of di- and trichlorocyclopropenes and trapped in argon matrices.[50] As with the parent carbene **91**, subsequent photolysis (254 nm) of the carbenes, e.g., **94**, led to the formation of the corresponding propynylidenes, e.g., **95**, and the isomeric vinylidenecarbenes, e.g., **96**. The photochemical back reaction (**95**, **96** → **94**) could be induced by changing the irradiation wavelength to 280–310 nm.

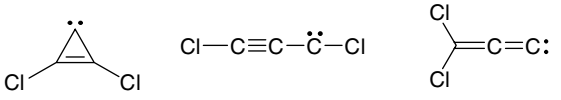

94 **95** **96**

In a later study utilizing ^{13}C labeling, the mixture of C_3H_2 isomers was accessed via the direct generation of propynylidene (**92**) by photolysis of the corresponding diazo precursor, diazopropyne (**97**).[51] Three ^{13}C-isotopomers of **97**, with each carbon singly labeled, were photolyzed in argon matrices at 8 K, and the experimental investigations were accompanied by theoretical computations of the geometries, energies, and IR transitions of the various species of interest. The products identified by IR spectroscopy included triplet propynylidene (**92**), singlet vinylidenecarbene (**93**), and singlet cyclopropenylidene (**91**). At 313 nm, **91** and **92** photoequilibrated, but the process did not seem to occur by a simple ring-closure or ring-opening mechanism because hydrogen migration accompanied the interconversion. At $\lambda > 444$ nm, isotopomers of **93**, $H_2C{=}C{=}{}^{13}C$: and $H_2C{=}{}^{13}C{=}C$: rapidly equilibrated; it was suggested, on

the basis of the parallel theoretical studies, that this equilibration could involve a cyclopropyne transition state.

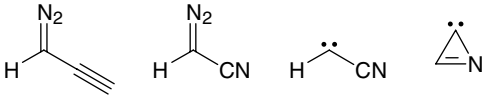

97 **98** **99** **100**

Azacyclopropenylidene (**100**), as well as cyanocarbene **99** and its isocyano isomer, were produced when diazoacetonitrile (**98**) was photolyzed in matrices.[52] Ring opening of **100** to regenerate **99** occurred on irradiation with light of $\lambda > 345$ nm.

Matrix isolated 1-silacyclopropenylidene (**101**) was generated by pulsed flash pyrolysis of 2-ethynyl-1,1,1-trimethyldisilane ($HC{\equiv}CSiH_2SiMe_3$).[53] Upon 254 nm photolysis, **101** first isomerized to ethynylsilanediyl (**102**) and then, on more prolonged irradiation, to vinylidenesilanediyl (**103**) and silacyclopropyne (**104**). Identifications were made by comparison of experimental and calculated IR spectra and the employment of ^{13}C labeling. On irradiation with longer wavelength light ($\lambda > 395$ nm), silacyclopropyne (**104**) regenerated **101**. Calculations suggested that the bonding in silacyclopropyne is unusual, having one electron pair in a CC nonbonding orbital. This molecule was an unexpected product because the all-carbon analogue cyclopropyne is unstable. A subsequent high-level theoretical study confirmed the identification of **104** and also indicated that this molecule has a relatively high energy barrier to isomerization, whereas cyclopropyne corresponds to a high-lying saddle point on the C_3H_2 potential energy surface.[54]

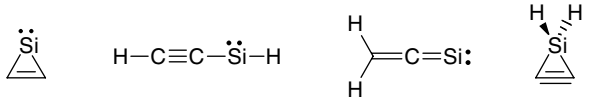

101 **102** **103** **104**

Silacyclopropylidene **101** has also been generated by evaporation of silicon atoms and co-condensation of these with acetylene and an excess of argon.[55] Similar reaction of Si atoms with hydrogen cyanide gave a mixture of CHNSi and CNSi isomers.[56] The product IR spectra, in comparison with computations, showed that the initial species formed was (silaisocyano)carbene (**105**). This rearranged to 2-aza-1-silacyclopropenylidene (**106**) and a small amount of cyanosilylene (**107**), when irradiated with light of $\lambda > 700$ nm.

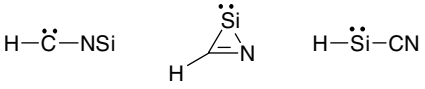

105 **106** **107**

15.4 Matrix Photochemistry of Four-Membered Ring Compounds

Cyclobutanes, Cyclobutenes, and Derivatives

As in the case of cyclopropane (see Section 15.3), cyclobutane does not absorb at wavelengths in the normally accessible UV region of the spectrum and is photostable in argon matrices. Nevertheless, cyclobutane was found to undergo photoinduced reactions in bromine-doped xenon matrices when irradiated with a low-pressure Hg arc (254 nm) and even in undoped xenon, provided a KrF laser (248 nm) was used.[57] The main products were found to be but-1-ene and ethene, although in the doped

matrices, 1-methylallyl radical was also detected. In these reactions, the energy of irradiation was absorbed by the matrix host material and transferred to the cyclobutane molecules.

When cyclobutanone was photolyzed in Ar, CO, and N_2 matrices with UV or vacuum-UV light, photodecomposition occurred by at least two and possibly three primary processes.[58] Photolysis with the 302 nm Hg line produced only CO and cyclopropane, while photolysis with the full Hg arc, with major lines at 302, 297, 289, and 280 nm, gave ketene and propene as IR detectable products, as well. It was concluded that the processes operating were (1) *c*-$C_3H_6CO \rightarrow$ *c*-C_3H_6 + CO, (2) *c*-$C_3H_6CO \rightarrow C_2H_4$ + CH_2=C=O, and possibly (3) *c*-$C_3H_6CO \rightarrow CH_3CH{=}CH_2$ + CO. Additional secondary photolysis products were detected when the matrices were irradiated in the vacuum-UV.

3-Methylenecyclobutanone (**108**) gave a small yield of trimethylenemethane (**69**) when irradiated at 300 nm in argon at 10 K, but a more efficient source of **69** was later found in the photolysis of methylenecyclopropane (**68**) in halogen-doped xenon matrices (see Section 15.3).[41] As also noted earlier in this chapter, 1,2-dimethylenecyclobutane (**76**) was amongst the products observed in the matrix photolysis of bicyclopropylidene (**72**). When incorporated into matrices independently, **76** afforded an alternative entry into the photoprocesses summarized in Scheme 11 and gave both tetramethyleneethane (**75**) and 3-methylenecyclopentene (**78**) when irradiated at 248 nm.[43] When **76** rather than **72** was employed as the starting material, tetramethyleneethane (**75**) could be detected directly in the IR spectrum, although only through a single absorption near 790 cm^{-1}.

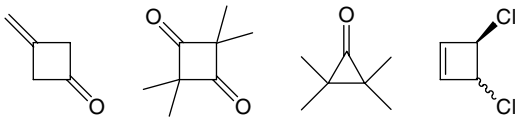

108 **109** **110** **111**

The photolysis of tetramethylcyclobutane-1,3-dione (**109**) was followed by IR spectroscopy in N_2 matrices at 4 K in one of the earliest matrix isolation studies of an organic photochemical reaction.[59,60] The products identified included tetramethylcyclopropanone (**110**), from elimination of CO, and dimethylketene, from [2 + 2]-cycloreversion.

The stereochemistry of the thermally and photochemically induced ring opening of *cis*- and *trans*-3,4-dichlorocyclobutene (**111**) has been studied using matrix isolation.[61] Dichlorocyclobutenedione (**112**) also underwent ring opening when irradiated in matrices with light of $\lambda > 335$ nm, giving the dichlorobisketene **113** as the primary photoproduct.[62] On further photolysis, **113** eliminated CO and gave dichlorocyclopropenone (**114**) and dichloropropadienone (**115**) in a ratio of 93:7, probably via a common intermediate carbene. Both **114** and **115** finally gave dichloroacetylene when irradiated with light of $\lambda > 230$ nm.

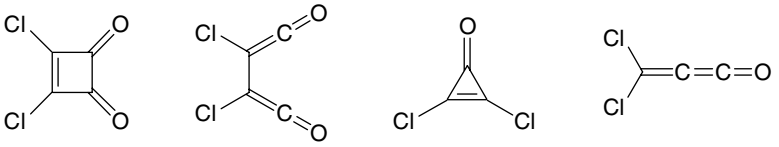

112 **113** **114** **115**

Cyclobutadiene

Cyclobutadiene (**118**) has been the subject of numerous matrix isolation investigations over a long period. It was first generated in matrices from α-pyrone (**116**), which gave β-lactone **117** on photolysis, from which CO_2 was subsequently eliminated to yield cyclobutadiene.[63,64] At first, an insufficient number of IR bands of **118** were observed to settle the question of whether the molecule has a square or rectangular geometry, but eventually a fuller spectrum was obtained, which contained too many bands to be consistent

with a square structure.[65] The history of matrix isolation studies of cyclobutadiene is presented in more detail in another chapter, and a 1980 review of cyclobutadiene chemistry gives a very full account of the literature up to that time.[66]

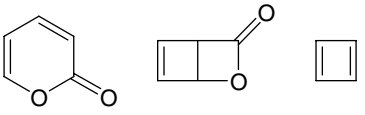

116 **117** **118**

Heterocyclic Four-Membered Rings

In Ar or N_2 matrices containing SO_2, ketene underwent a [2 + 2]-cycloaddition reaction when irradiated with Pyrex-filtered light from a medium-pressure Hg arc ($\lambda > 300$ nm), affording 1,2-oxathietan-4-one 2-oxide (**119**: $R^1 = R^2 = H$).[67,68] On further irradiation with an unfiltered arc lamp ($\lambda > 200$ nm), **119** underwent a retrocycloaddition in the opposite sense, to give CO_2 and, presumably, the sulfine **120** ($R^1 = R^2 = H$). The latter, however, was not detected directly, but decomposed to formaldehyde (CH_2O) and sulfur atoms, which were evident from an intense blue chemiluminescence when the matrix was warmed at the end of each experiment. The retrocycloaddition of **119** was taken as reasonable evidence for the regiochemistry of the addition of SO_2 to ketene, but this work was carried out before the era of reliable computations of IR transitions, which might have settled the question more satisfactorily. Exactly similar reactions were observed for other ketenes ($R^1 = Me$, $R^2 = H$; $R^1 = Ph$, $R^2 = Et$; and $R^1 = R^2 = Ph$).[68]

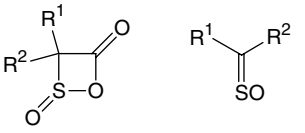

119 **120**

The trisdioxetane (**121**) was an observed product of the addition of dioxygen to 2,5-dimethylhexa-2,3,4-triene ($Me_2C{=}C{=}C{=}CMe_2$), when the latter compound was irradiated with visible light in Ar matrices containing O_2.[69] At O_2 concentrations between 10 and 100%, the trisdioxetane was almost the sole product. It decomposed on further irradiation to acetone and CO_2. Identification of **121** from its matrix IR spectrum was aided by the use of oxygen isotopes.

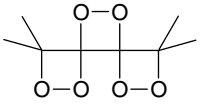

121

The Dewar isomer, **123**, of 3-methyl-4(3*H*)-pyrimidinone (**122**) was generated in argon matrices by 308 nm irradiation of the parent molecule and identified by comparison of the experimental matrix IR spectrum with spectra computed for **123** and other possible products.[70] For several 4(3*H*)-pyrimidinones not methylated at N3, two other types of matrix photoreactions were observed in addition to the isomerization to the Dewar isomer: phototautomerism and ring opening. Somewhat later, matrix isolated Dewar pyridine (**124**) was produced by UV-irradiation of pyridine in solid argon and was identified with the aid of DFT computations.[71] On further photolysis, **124** produced cyclobutadiene (**118**) and HCN.

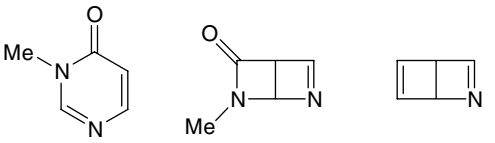

122 **123** **124**

Photolysis of phthaloyl peroxide (**125**) in argon at 8 K resulted in the elimination of CO_2 and produced a mixture of benzpropiolactone (**126**) and the *o*-quinoid ketoketene **127**.[72] The two product species could be interconverted photochemically, with long-wavelength light ($\lambda > 340$ nm) favoring **126** and shorter wavelengths ($\lambda > 310$ nm) favoring **127**. Subsequently, there have been periodic attempts to generate benzannelated four-membered ring compounds (**128**), which could be interconverted with their *o*-quinoid isomers (**129**), particularly if the latter could be generated easily, thus providing convenient routes to the four-membered ring compounds.

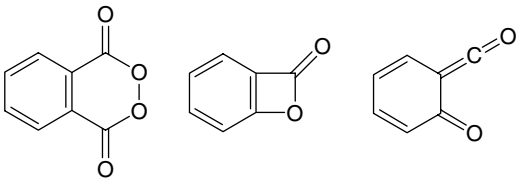

125 **126** **127**

A fruitful approach has been to generate phenylcarbenes or -nitrenes with suitable *ortho* substituents, from which a hydrogen atom can be transferred intramolecularly. For example, 6-methylene-2,4-cyclohexadien-1-imine (**129**: X = CH_2, Y = NH) was generated in low-temperature matrices by intramolecular H-transfer in either (2-aminophenyl)carbene (**130**) or 2-tolylnitrene (**131**), following flash vacuum pyrolysis or matrix photolysis of the corresponding diazo and azido precursors, respectively.[73] The imine **129** (X = CH_2, Y = NH) was converted into benzoazetine (**128**: X = CH_2, Y = NH) when irradiated with light of $\lambda > 385$ nm, and the reverse, ring-opening reaction occurred at shorter wavelengths ($\lambda > 280$ nm). Similarly, benzoxete (benzoxetene) (**128**: X = CH_2, Y = O) and its photointerconversion with *o*-quinone methide (**129**: X = CH_2, Y = O) have been observed in Ar matrices, following photoelimination of CO from benzofuran-2-one (isophthalide) (**132**) or the generation of (2-hydroxyphenyl)carbene (**133**) from 2-(diazomethyl)phenol.[74] It has subsequently been shown that the methyl groups in 4,6-dimethylbenzoxete (**134**) stabilize this molecule to the extent that it could be observed to persist when warmed to room temperature in the solid state.[75]

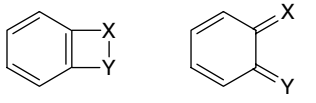

128 **129**

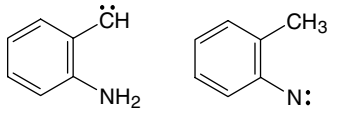

130 **131**

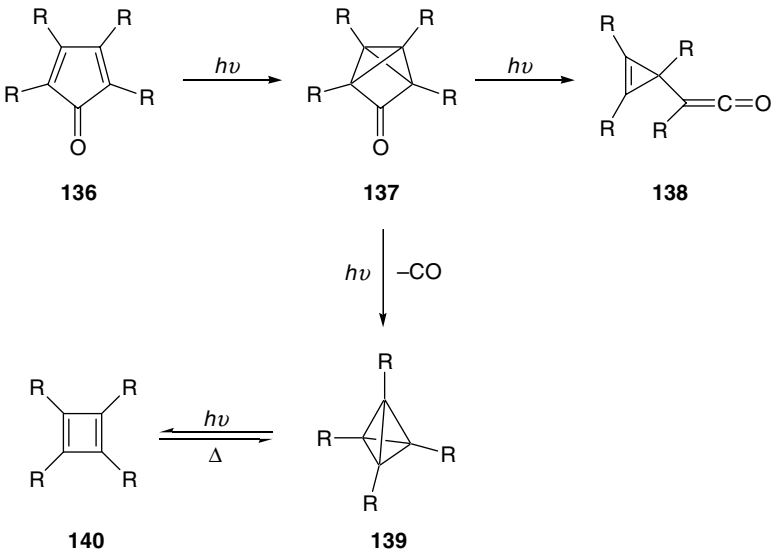

136 **137** **138** **140** **139**

SCHEME 14

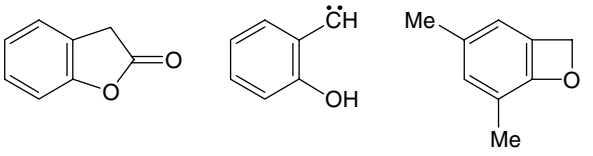

132 **133** **134**

At the present time, it seems that ring closure of *o*-quinoids (**129**) can be achieved only when one of the terminal groups (X or Y) is a CH_2 group.[76] Thus, neither *o*-benzoquinone imine (**129**: X = NH, Y = O) nor *o*-benzoquinone diimine (**129**: X = Y = NH) forms the corresponding ring closed compounds (**128**) when photolyzed in matrices; instead, they undergo ring opening to compounds of structure **135**.

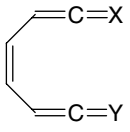

135

15.5 Tetrahedrane Derivatives and Related Compounds

The quest for tetrahedrane and its derivatives forms a fascinating chapter in the history of organic chemistry in which matrix isolation played a crucial part, at least in the initial stages. In spite of discouraging theoretical predictions of the instability of tetrahedranes and earlier failures, an example of a tetrahedrane was eventually generated photochemically in low-temperature matrices.[77,78] Photolysis of tetra-*t*-butylcyclopentadienone (**136**: R = *t*-Bu) in solid argon gave exclusively the criss-cross adduct **137** (R = *t*-Bu) (Scheme 14). On further photolysis, the criss-cross adduct rearranged to the cyclopropenylketene **138** (R = *t*-Bu) or lost a molecule of CO to give tetra-*t*-butyltetrahedrane **139** (R = *t*-Bu).

Matrix IR spectra would not have been sufficient to identify the tetrahedrane, but fortunately and perhaps surprisingly, the same photochemistry could be carried out in frozen solvents at 77 K and in liquid solutions up to room temperature, so the processes could also be monitored by ^{1}H and ^{13}C NMR spectroscopy. Even more surprisingly, it was found that tetra-*t*-butyltetrahedrane could be isolated from the solution product mixture by chromatography and was stable up to about +135°C. At this temperature, it was isomerized to tetra-*t*-butylcyclobutadiene (**140**: R = *t*-Bu), UV-irradiation of which, in Ar at 10 K or in solution at room temperature, regenerated **139** (R = *t*-Bu).

The possibility of isolating tetra-*t*-butyltetrahedrane as a stable compound allowed its full characterization by ^{1}H and ^{13}C NMR, IR, Raman, and photoelectron spectroscopy, by mass-spectrometry,[79–82] and ultimately by means of an x-ray crystal structure.[83] Nevertheless, related attempts to directly observe other tetrahedranes with smaller or fewer substituents, e.g., dimethyltetrahedrane,[84] tetramethyltetrahedrane,[85–87] bis(trimethylsilyl)tetrahedrane,[88] and tetrahedrane itself,[89,90] were uniformly unsuccessful. With bulky substituents, however, as in the case of the recently reported tetrakis(trimethylsilyl)tetrahedrane (**139**: R = $SiMe_3$),[91] tetrahedrane derivatives seem stable enough to be studied without the need for low-temperature matrix isolation techniques. This is not to say that such chemistry is easy. The photoisomerization of tetrakis(trimethylsilyl)cyclobutadiene (**140**: R = $SiMe_3$) to the corresponding tetrahedrane was achieved only after many unsuccessful experiments, with variations of wavelength, temperature, and solvent. Nearly all attempts led to fragmentation of the cyclobutadiene into two molecules of bis(trimethylsilyl)acetylene, but one set of conditions — prolonged 254 nm irradiation in deuteriated methylcyclohexane at −130°C — eventually afforded the desired tetrahedrane.

Two recent theoretical studies, one of the C_4H_4 isomers[92] and the other of tetramethyl- and tetra-*t*-butyl-substituted cyclobutadiene and tetrahedrane,[93] give further insights into the stabilities of tetrahedrane derivatives.

References

1. For an up-to-date discussion of the merits of DFT computations, including a comparison of methods for computing IR transitions, see Koch, W. and Holthausen, M.C., *A Chemist's Guide to Density Functional Theory,* Wiley-VCH, Weinheim, 2000.
2. Jacox, M.E. and Milligan, D.E., Infrared study of the reactions of CH_2 and NH with C_2H_2 and C_2H_4 in solid argon, *J. Am. Chem. Soc.,* 85, 278, 1963.
3. Hawkins, M. and Andrews, L., Reactions of atomic oxygen with ethene in solid argon. The infrared spectrum of vinyl alcohol, *J. Am. Chem. Soc.,* 105, 2523, 1983.
4. Parker, J.K. and Davis, S.R., Photochemical reaction of ozone and benzene: an infrared matrix isolation study, *J. Am. Chem. Soc.,* 121, 4271, 1999.
5. Parker, J.K. and Davis, S.R., Photochemical reaction of ozone and dimethylacetylene: an infrared matrix isolation and *ab initio* investigation, *J. Phys. Chem. A,* 103, 7280, 1999.
6. Singmaster, K.A., Jonnalagadda, S., and Chan, S., Photolysis of hexafluoro-2-butyne/ozone mixtures in cryogenic matrices, *J. Am. Chem. Soc.,* 122, 9078, 2000.
7. Singmaster, K.A. and Pimentel, G.C., Photolysis of allene–ozone mixtures at 647 nm. Part 1. Formation of allene oxide, *J. Mol. Struct.,* **194**, 215, 1989.
8. Nakata, M. and Frei, H., Chemical trapping of electronically excited biradicals upon visible light-induced oxygen-atom transfer from NO_2 to allene and dimethylacetylene in a cryogenic matrix, *J. Am. Chem. Soc.,* 114, 1363, 1992.
9. Sander, W., Wrobel, R., Komnick, P., Rademacher, P., Muchall, H.M., and Quast, H., Flash vacuum pyrolysis and photolysis of 3,3,5,5-tetramethylpyrazolin-4-one: a matrix isolation study, *Eur. J. Org. Chem.,* 91, 2000.
10. Salama, F. and Frei, H., Near-infrared-light-induced reaction of singlet SO with allene and dimethylacetylene in a rare gas matrix. Infrared spectra of two novel episulfoxides, *J. Phys. Chem.,* 93, 1285, 1989.

11. Sander, W.W., Reaction of diphenylmethylene with carbon dioxide. Matrix isolation of diphenyloxiranone, *J. Org. Chem.,* 54, 4265, 1989.
12. Krantz, A. and Laureni, J., Matrix photolysis of 1,2,3-thiadiazole. On the possible involvement of thiirene, *J. Am. Chem. Soc.,* 96, 6768, 1974.
13. Laureni, J., Krantz, A., and Hadju, R., Photolysis of isotopically labelled 1,2,3-selenadiazole and 1,2,3-thiadiazole. Symmetry properties of the paths leading to ethynyl mercaptan and selenol. Evidence for thiirene, *J. Am. Chem. Soc.,* 98, 7872, 1976.
14. Krantz, A. and Laureni, J., A methodology for the preparation and characterization of three membered, potentially antiaromatic molecules. Preparation of matrix-isolated thiirene and selenirene, *J. Am. Chem. Soc.,* 99, 4842, 1977.
15. Torres, M., Clement, A., Bertie, J.E., Gunning, H.E., and Strausz, O.P., Low-temperature matrix isolation of thiirenes, *J. Org. Chem.,* 43, 2490, 1978.
16. Krantz, A. and Laureni, J., Characterization of matrix-isolated antiaromatic three-membered heterocycles. Preparation of the elusive thiirene molecule, *J. Am. Chem. Soc.,* 103, 486, 1981.
17. Torres, M., Lown, E.M., Gunning, H.E., and Strausz, O.P., 4n-π Electron antiaromatic heterocycles, *Pure Appl. Chem.,* 52, 1623, 1980.
18. Torres, M., Clement, A., and Strausz, O.P., Argon-matrix isolation of bis(carbomethoxy)thiirene: formation of acyl- and carbalkoxythioketenes, *Z. Naturforsch. Teil B,* 38, 1208, 1983.
19. Schulz, R. and Schweig, A., Photolysis and gas phase pyrolysis of 1,2,3-benzoselenadiazole: matrix isolation of benzoselenirene, *Tetrahedron Lett.,* 25, 2337, 1984.
20. Risi, F., Pizzala, L., Carles, M., Verlaque, P., and Aycard, J.-P., Photolysis of matrix-isolated 4-R-1,2,4-triazoline-3,5-diones: identification of aziridine-2,three-dimensionalione transients, *J. Org. Chem.,* 61, 666, 1996.
21. Dunkin, I.R., Shields, C.J., and Quast, H., The photochemistry of 1,4-dihydro-5*H*-tetrazole derivatives isolated in low-temperature matrices, *Tetrahedron*, 45, 259, 1989.
22. Mloston, G., Romanski, J., Schmidt, C., Reisenauer, H.P., and Maier, G., Photochemische und thermische Erzeugung von Thiocarbonylyliden aus 2,5-Dihydro-1,3,4-thiadiazolen, *Chem. Ber.,* 127, 2527, 1994.
23. West, P.R., Mooring, A.M., McMahon, R.J., and Chapman, O.L., Benzobicyclo[4.1.0]hepta-2,4,6-trienes, *J. Org. Chem.,* 51, 1316, 1986.
24. Bonvallet, P.A. and McMahon, R.J., Photoequilibration of 1-naphthylcarbene and 4,5-benzobicyclo[4.1.0]hepta-2,4,6-triene, *J. Am. Chem. Soc.,* 121, 10496, 1999.
25. Bucher, G. and Sander, W., Direct observation of the cyclopropene–vinylcarbene rearrangement. Matrix isolation of bicyclo[3.1.0]hexa-3,5-dien-2-ones, *J. Org. Chem.,* 57, 1346, 1992.
26. Albers, R., Sander, W., Ottosson, C.-H., and Cremer, D., 4,4-Dimethylbicyclo[3.1.0]hexa-1(6),2-diene — a highly strained 1,3-bridged cyclopropene, *Chem.–Eur. J.,* 2, 967, 1996.
27. Komnick, P. and Sander, W., Intramolecular carbene addition to a triple bond: matrix photochemistry of α-diazo-2-ethynylacetophenone, *Liebigs Ann. Chem.,* 7, 1996.
28. Krantz, A., Matrix photolysis of diazoacetaldehyde, *J. Chem. Soc., Chem. Commun.,* 670, 1973.
29. Maier, G., Reisenauer, H.P., and Sayraç, T., Oxiren: Zwischenprodukt oder Übergangszustand? – Matrixbestrahlung von Diazoketonen, *Chem. Ber.,* 115, 2192, 1982.
30. Torres, M., Bourdelande, J.L., Clement, A., and Strausz, O.P., Argon matrix isolation of bis(trifluoromethyl)oxirene, perfluoromethylethyloxirene and their isomeric ketocarbenes, *J. Am. Chem. Soc.,* 105, 1698, 1983.
31. Bachmann, C., N'Guessan, T.Y., Debû, F., Monnier, M., Pourcin, J., Aycard, J.-P., and Bodot, H., Oxirenes and ketocarbenes from α-diazoketone photolysis: experiments in rare gas matrices. Relative stabilities and isomerization barriers from MNDOC-BWEN calculations, *J. Am. Chem. Soc.,* 112, 7488, 1990.
32. Delamere, C., Jakins, C., and Lewars, E., On the generation of oxirene and dimethyloxirene by retro-Diels–Alder reactions and reactions of dimethyloxirene: a computational study, *Can. J. Chem.,* 80, 94, 2002.

33. Albers, R. and Sander, W., Photolysis of diazo(3-thienyl)methane: a simple synthesis of a methylenecyclopropene, *J. Org. Chem.,* 62, 761, 1997.
34. Albers, R. and Sander, W., Rearrangements of 2- and 3-furfurylidene, *Liebigs Ann. Chem.,* 897, 1997.
35. Bell, G.A. and Dunkin, I.R., Cyclopentadienone *O*-oxide: a highly labile intermediate in the matrix reaction between cyclopentadienylidene and oxygen, *J. Chem. Soc., Chem. Commun.,* 1213, 1983.
36. Dunkin, I.R. and Shields, C.J., The photo-isomerization of cyclopentadienone *O*-oxide isolated in low temperature matrices, *J. Chem. Soc., Chem. Commun.,* 154, 1986.
37. Sander, W., Carbonyl oxides: zwitterions or biradicals? *Angew. Chem. Int. Ed. Engl.,* 29, 344, 1990; *Angew. Chem.,* 102, 362, 1990.
38. Rendall, W.A., Clement, A., Torres, M., and Strausz, O.P., Dewar furan and Dewar thiophene: low-temperature matrix photolysis of furan and thiophene, *J. Am. Chem. Soc.,* 108, 1691, 1986.
39. Maier, G. and Senger, S., Ring opening of cyclopropane at 10 K, *Angew. Chem. Int. Ed. Engl.,* 33, 558, 1994; *Angew. Chem.,* 106, 605, 1994.
40. Maier, G., Lautz, C., and Senger, S., Ring opening of 1-methylcyclopropene and cyclopropene: matrix infrared spectroscopic identification of 2-butene-1,3-diyl and propene-1,3-diyl, *Chem.–Eur. J.,* 6, 1467, 2000.
41. Maier, G., Reisenauer, H.P., Lanz, K., Tross, R., Jürgen, D., Hess, B.A., Jr., and Schaad, L.J., Detection of trimethylenemethane by IR spectroscopy: the result of an unexpected photoisomerization of methylenecyclopropane in a halogen-doped Xe matrix, *Angew. Chem. Int. Ed. Engl.,* 32, 74, 1993; *Angew. Chem.,* 105, 119, 1993.
42. Maier, G. and Senger, S., 2-Vinylmethylenecyclopropane/3-methylenecyclopentene rearrangement: matrix infrared spectroscopic identification of 4-methylene-2-pentene-1,5-diyl (1,2-bisallyl biradical), *J. Am. Chem. Soc.,* 119, 5857, 1997.
43. Maier, G. and Senger, S., Photoisomerization of bicyclopropylidene and 1,2-dimethylenecylobutane in rare-gas matrices: towards the IR-spectroscopic identification of tetramethyleneethane (2,three-dimensionalimethylenebutane-1,4-diyl), *Eur. J. Org. Chem.,* 1291, 1999.
44. Chapman, O.L., Gano, J., West, P.R., Regitz, M., and Maas, G., Acenaphthyne, *J. Am. Chem. Soc.,* 103, 7033, 1981.
45. See, for example, Lin-Vien, D., Colthup, N.B., Fateley, W.G., and Grasselli, J.G., *The Handbook of Infrared and Raman Characteristic Frequencies of Organic Molecules,* Academic Press, Boston, 1991, Table 7–4 on p. 99 and pp. 101–2.
46. Krebs, A., Cholcha, W., Müller, M., Eicher, T., Pielartzik, H., and Schnöckel, H., Erzeugung von Sieben- und Sechsring-Alkinen durch Photolyse und Thermolyse von Cyclopropenonen, *Tetrahedron Lett.,* 25, 5027, 1984.
47. Monnier, M., Allouche, A., Verlaque, P., and Aycard, J.-P., Photolysis of matrix-isolated cyclopropylidene ketene: kinetic and theoretical studies of the cyclopropylidene formation, *J. Phys. Chem.,* 99, 5977, 1995.
48. Reisenauer, H.P., Maier, G., Riemann, A., and Hoffmann, R.W., Cyclopropenylidene, *Angew. Chem. Int. Ed. Engl.,* 23, 641, 1984; *Angew. Chem.,* 96, 596, 1984.
49. Maier, G., Reisenauer, H.P., Schwab, W., Čársky, P., Hess, B.A., Jr., and Schaad, L.J., Vinylidenecarbene: a new C_3H_2 species, *J. Am. Chem. Soc.,* 109, 5183, 1987.
50. Maier, G., Preiss, T., Reisenauer, H.P., Hess, B.A., Jr., and Schaad, L.J., Chlorinated cyclopropenylidenes. Vinylidenecarbenes and propargylenes: identification by matrix isolation spectroscopy, *J. Am. Chem. Soc.,* 116, 2014, 1994.
51. Seburg, R.A., Patterson, E.V., Stanton, J.F., and McMahon, R.J., Structures, automerizations and isomerizations of C_3H_2 isomers, *J. Am. Chem. Soc.,* 119, 5847, 1997.
52. Maier, G., Reisenauer, H.P., and Rademacher, K., Cyanocarbene, isocyanocarbene and azacyclopropenylidene: a matrix-spectroscopic study, *Chem.–Eur. J.,* 4, 1957, 1998.
53. Maier, G., Pacl, H., Reisenauer, H.P., Meudt, A., and Janoschek, R., Silacyclopropyne: matrix spectroscopic identification and *ab initio* investigations, *J. Am. Chem. Soc.,* 117, 12712, 1995.

54. Sherrill, C.D., Brandow, C.G., Allen, W.D., and Schaefer H.F., III, Cyclopropyne and silacyclopropyne: a world of difference, *J. Am. Chem. Soc.,* 118, 7158, 1996.
55. Maier, G., Reisenauer, H.P., and Egenolf, H., Reaction of silicon atoms with acetylene and ethylene: generation and matrix-spectroscopic identification of C_2H_2Si and C_2H_4Si, *Eur. J. Org. Chem.,* 1313, 1998.
56. Maier, G., Reisenauer, H.P., Egenolf, H., and Glatthaar, J., Reaction of silicon atoms with hydrogen cyanide: generation and matrix-spectroscopic identification of CHNSi and CNSi isomers, *Eur. J. Org. Chem.,* 1307, 1998.
57. Maier, G. and Senger, S., Fragmentation of cyclobutane in a bromine-doped and undoped xenon matrix, *Liebigs Ann. Chem.,* 45, 1996.
58. Thomas, S.G. and Guillory, W.A., Condensed-phase photochemistry of cyclobutanone, *J. Phys. Chem.,* 78, 1461, 1974.
59. Haller, I. and Srinivasan, R., Primary processes in the photochemistry of tetramethyl-1,3-cyclobutanedione, *J. Am. Chem. Soc.,* 87, 1144, 1965.
60. Haller, I. and Srinivasan, R., Infrared study of the photochemistry of tetramethylcyclobutane-1,3-dione, *Can. J. Chem.,* 43, 3165, 1965.
61. Maier, G. and Bothur, A., The thermally and photochemically induced ring opening of *cis*-3,4-dichlorocyclobutene and *trans*-3,4-dichlorocyclobutene: new insights from a matrix-spectroscopic study, *Eur. J. Org. Chem.,* 2063, 1998.
62. Mincu, I., Hillebrand, M., Allouche, A., Cossu, M., Verlaque, P., Aycard, J.P., and Pourcin, J., Photolysis of the dichlorocyclobutenedione in rare gas at 10 K. Infrared spectral analysis and *ab initio* calculations of vibrational frequencies. First identification of two new species (dichloro-substituted bisketene and dichloropropadienone). Kinetics and reaction mechanism, *J. Phys. Chem.,* 100, 16045, 1996.
63. Lin, C.Y. and Krantz, A., Matrix preparation of cyclobutadiene, *J. Chem. Soc., Chem. Commun.,* 1111, 1972.
64. Chapman, O.L., McIntosh, C.L., and Pacansky, J., Cyclobutadiene, *J. Am. Chem. Soc.,* 95, 614, 1973.
65. Masamune, S., Souto-Bachiller, F.A., Machiguchi, T., and Bertie, J.E., Cyclobutadiene is not square, *J. Am. Chem. Soc.,* 100, 4889, 1978.
66. Bally, T. and Masamune, S., Cyclobutadiene, *Tetrahedron*, 36, 343, 1980.
67. Dunkin, I.R. and MacDonald, J.G., Matrix isolated 1,2-oxathietan-4-one 2-oxide: a $2\pi + 2\pi$ adduct of sulphur dioxide and keten, *J. Chem. Soc., Chem. Commun.,* 1020, 1978.
68. Dunkin, I.R. and MacDonald, J.G., Photochemical 2 + 2-cycloadditions of sulphur dioxide and ketenes in low-temperature matrices, *J. Chem. Soc., Perkin Trans. 2,* 2079, 1984.
69. Sander, W. and Patyk, A., Photooxidation of 2,5-dimethyl-2,3,4-hexatriene: matrix isolation of a trisdioxetane, *Angew. Chem. Int. Ed. Engl.,* 26, 475, 1987; *Angew. Chem.,* 99, 495, 1987.
70. Lapinski, L., Nowak, M.J., Leś, A., and Adamowicz, L., *Ab initio* calculations of IR spectra in identification of products of matrix isolation photochemistry: Dewar form of 4(3*H*)-pyrimidinone, *J. Am. Chem. Soc.,* 116, 1461, 1994.
71. Kudoh, S., Takayanagi, M., and Nakata, M., Dewar pyridine studied by matrix isolation infrared spectroscopy and DFT calculation, *J. Photochem. Photobiol. A: Chem.,* 123, 25, 1999.
72. Chapman, O.L., McIntosh, C.L., Pacansky, J., Calder, G.V., and Orr, G., Benzpropiolactone, *J. Am. Chem. Soc.,* 95, 4061, 1973.
73. Morawietz, J., Sander, W., and Träubel, M., Intramolecular hydrogen transfer in (2-aminophenyl)carbene and 2-tolylnitrene. Matrix isolation of 6-methylene-2,4-cyclohexadien-1-imine, *J. Org. Chem.,* 60, 6368, 1995.
74. Tomioka, H. and Matsushita, T., Benzoxetene. Direct observation and theoretical studies, *Chem. Lett.,* 399, 1997.
75. Qiao, G.G., Lenghaus, K., Solomon, D.H., Reisinger, A., Bytheway, I., and Wentrup, C., 4,6-Dimethyl-*o*-quinone methide and 4,5-dimethylbenzoxete, *J. Org. Chem.,* 63, 9806, 1999.

76. Tomioka, H., Matrix isolation study of reactive o-quinoid compounds: generation, detection and reactions, *Pure Appl. Chem.,* 69, 837, 1997.
77. Maier, G., Pfriem, S., Schäfer, U., and Matusch, R., Tetra-*tert*-butyltetrahedrane, *Angew. Chem. Int. Ed. Engl.,* 17, 520, 1978; *Angew. Chem.,* 90, 552, 1978.
78. Maier, G., Pfriem, S., Schäfer, U., Malsch, K.-D., and Matusch, R., Tetra-*tert*-butyltetrahedran, *Chem. Ber.,* 114, 3965, 1981.
79. Maier, G., Pfriem, S., Malsch, K.-D., Kalinowski, H.-O., and Dehnicke, K., Spektroskopische Eigenschaften von Tetra-*tert*-butyltetrahedran, *Chem. Ber.,* 114, 3988, 1981.
80. Heilbronner, E., Jones, T.B., Krebs, A., Maier, G., Malsch, K.-D., Pocklington, J., and Schmelzer, A., A photoelectron spectroscopic investigation of tetra-*tert*-butyltetrahedrane and tetra-*tert*-butylcyclobutadiene, *J. Am. Chem. Soc.,* 102, 564, 1980.
81. Loerzer, T., Machinek, R., Lüttke, W., Franz, L.H., Malsch, K.-D., and Maier, G., Tetra-*tert*-butyltetrahedrane: ^{13}C–^{13}C coupling constants and hybridization, *Angew. Chem. Int. Ed. Engl.,* 22, 878, 1983; *Angew. Chem.,* 95, 914, 1983.
82. Maier, G., Tetrahedrane and cyclobutadiene, *Angew. Chem. Int. Ed. Engl.,* 27, 309, 1988; *Angew. Chem.,* 100, 317, 1988.
83. Irngartinger, H., Goldmann, A., Jahn, R., Nixdorf, M., Rodewald, H., Maier, G., Malsch, K.-D., and Emrich, R., Tetra-*tert*-butyltetrahedrane: crystal and molecular structure, *Angew. Chem. Int. Ed. Engl.,* 23, 993, 1984; *Angew. Chem.,* 96, 967, 1984.
84. Maier, G. and Reisenauer, H.P., Versuche zur Darstellung von Dimethyltetrahedran, *Chem. Ber.,* 114, 3916, 1981.
85. Maier, G., Schneider, M., Kreiling, G., and Mayer, W., Versuche zur Darstellung von Tetramethyltetrahedran aus heterocyclischen Vorstufen, *Chem. Ber.,* 114, 3922, 1981.
86. Maier, G., Mayer, W., Freitag, H.-A., Reisenauer, H.P., and Askani, R., Versuche zur Darstellung von Tetramethyltetrahedran von alicyclischen Vorstufen, *Chem. Ber.,* 114, 3935, 1981.
87. Maier, G. and Reisenauer, H.P., Weitere Versuche zur Matrixisolierung von Tetramethyltetrahedran, *Chem. Ber.,* 114, 3959, 1981.
88. Maier, G., Hoppe, M., Reisenauer, H.P., and Krüger, C., Synthesis and properties of [2,3-bis(trimethylsilyl)-2-cyclopropen-1-yl]diazomethane, *Angew. Chem. Int. Ed. Engl.,* 21, 437, 1982; *Angew. Chem.,* 94, 445, 1982.
89. Lage, H.W., Reisenauer, H.P., and Maier, G., Trimethylsilylated bicylobutane-2,4-dicarboxylic-acid-anhydrides, *Tetrahedron Lett.,* 23, 3893, 1982.
90. Maier, G., Hoppe, M., and Reisenauer, H.P., Tricyclo[2.1.0.$0^{2,5}$]pentan-3-one, *Angew. Chem. Int. Ed. Engl.,* 22, 990, 1983; *Angew. Chem.,* 95, 1009, 1983.
91. Maier, G., Neudert, J., and Wolf, O., Tetrakis(trimethylsilyl)cyclobutadiene and tetrakis(trimethylsilyl)tetrahedrane, *Angew. Chem. Int. Ed. Engl.,* 40, 1674, 2001; *Angew. Chem.,* 113, 1719, 2001.
92. Jursic, B.S., Theoretical study of structural properties, infrared spectra and energetic properties of C_4H_4 isomers, *J. Mol. Struct. (Theochem),* 507, 185, 2000.
93. Balci, M., McKee, M.L., and Schleyer, P. von R., Theoretical study of tetramethyl- and tetra-*tert*-butyl-substituted cyclobutadiene and tetrahedrane, *J. Phys. Chem. A,* 104, 1246, 2000; *J. Phys. Chem. A,* 104, 6338, 2000.

16

Photochemical Isomerization of Cycloalkenes

Tadashi Mori
Osaka University

Yoshihisa Inoue
Osaka University and ICORP/JST

16.1 Introduction

A number of reviews have been devoted to the photoisomerism of alkenes,[1–4] with the photochemistry of cycloalkenes treated as a subcategory.[5–10] The geometrical photoisomerization of alkenes was reviewed also in the previous edition.[11] However, the photobehavior of cycloalkenes is not a simple extension of that of acyclic alkenes, particularly in the cases of small- and medium-sized cycloalkenes. Medium-sized (*E*)-cycloalkenes produced photochemically are highly constrained and rapidly react with alcohols in the presence, or even in the absence, of dilute acid. An account of the photoprotonation-driven cationic reactions, such as addition, isomerization, rearrangement, and fragmentation of cyclohexenes and cycloheptenes, in protic solvents has been published.[12] The protonation of strained (*E*)-cycloalkenes was also reviewed in the previous edition.[13]

In this review, we will concentrate on the *E-Z*-photoisomerization and subsequent (photo)chemical transformations of cycloalkenes caused by direct and sensitized excitation. Valence isomerization, rearrangement, and fragmentation, observed upon irradiation of cyclopropene, cyclobutene, and cyclopentene, are only briefly described, as they have been extensively reviewed elsewhere.[3,4,8,9] Although the photochemistry of acyclic alkenes will not be included in this chapter, we will refer to the photobehavior of conjugated cycloalkenes, such as cyclic dienes, enones, and styrenes, as far as it relates to the cycloalkene functionality. As the photochemical formation of labile (*E*)-cycloalkenes is one of the major topics in this chapter, the physical properties of the (*E*)-isomers will be tabulated and discussed in detail. Recent studies on enantiodifferentiating photoisomerization of cycloalkenes are summarized in one section in view of the rapidly growing interest in asymmetric photochemistry.[14]

0-8493-1348-1/04/$0.00+$1.50

16.2 Simple Cycloalkenes

Direct Irradiation

In direct photolysis of cycloalkenes, rearrangement and decomposition are the major reactions observed. Spiro-substituted cyclopropene (**1**) undergoes rearrangement upon direct irradiation to afford allene (**2**), acetylene (**3**), and vinylcyclopentene (**4**).[15,16] Cyclobutene (**5**) gives a ring-opening product, 1,3-butadiene (**6**), as the major product, and decomposition products, ethylene (**7**) and acetylene (**8**), together with rearranged methylenecyclopropane (**9**).[17–20] Cyclopentene (**10**) and cyclohexene (**13Z**) give the ring-contracted rearrangement products, i.e. methylenecyclobutene (**11**) plus bicyclo[2.1.0]pentane (**12**) from **10** and methylenecyclopentane (**14**) plus bicyclo[3.1.0]hexane (**15**) from **13Z**.[21,22] Most of the products are considered to be derived from the carbene intermediates.[3,4,8,9]

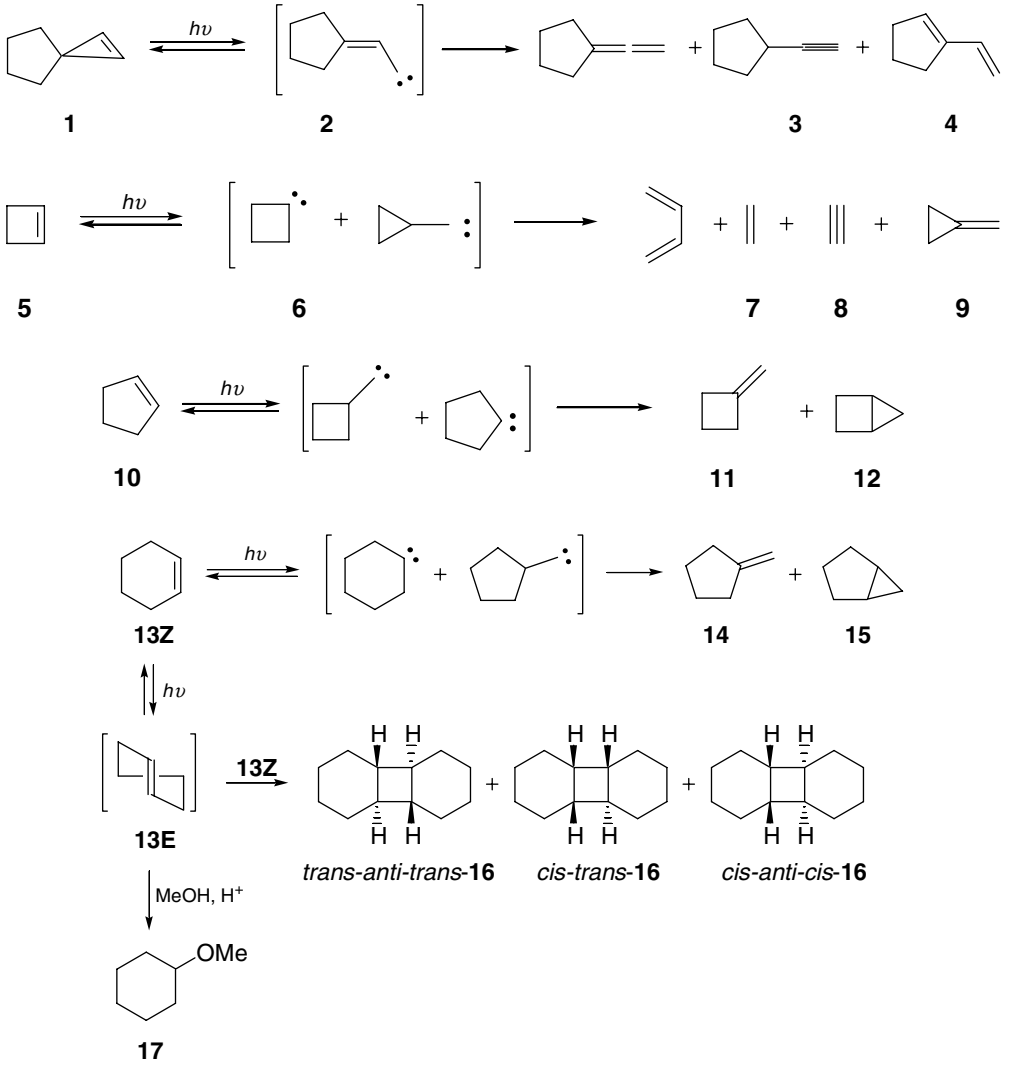

As is the case with acyclic alkenes, cycloalkenes undergo geometrical isomerization upon direct excitation. Thus, irradiation at ~200 nm of cyclohexene (**13Z**) in aprotic media affords a stereoisomeric mixture of [2 + 2]-cyclodimers (**16**), in 1.6:2.3:1 ratio.[23] This photocyclodimerization is interpreted in

terms of a successive photo/thermochemical process, which involves the initial photo-induced *Z*-to-*E* isomerization of **13Z** and the subsequent ground-state cycloaddition of photo produced **13E** to **13Z**.[23] Highly strained **13E** can be trapped by acidic methanol to give adduct **17**.

The photobehavior of cyclohexene (**13Z**), cycloheptene (**18Z**), and cyclooctene (**20Z**), upon direct irradiation at 185 nm, was studied comparatively in vapor and liquid phases.[24] In the vapor phase, direct excitation leads to decomposition and rearrangement reactions, affording those products that are obtained upon pyrolysis of each cycloalkene. This coincidence indicates that the excited singlet π,π^* state produced suffers rapid internal conversion to give hot (vibrationally excited) ground-state molecules, which in turn undergo thermal decomposition and rearrangement in the absence of effective collisional deactivations in the vapor phase.[13,24] In solution, the formation of these pyrolysis products is completely suppressed, and carbene-derived rearrangement products (see below) and the (*E*)-isomer become the major products.

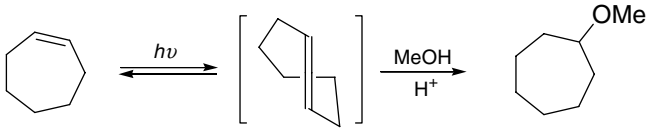

18Z **18E** **19**

Formation of highly constrained (*E*)-cyclohexene (**13E**) and (*E*)-cycloheptene (**18E**) upon direct irradiation has been claimed and/or proven as precursors to the corresponding methanol adducts, **17** and **19**, in acidic methanol.[24]

(*E*)-Cyclooctene (**20E**) is the smallest member of the (*E*)-cycloalkene series that can survive at room temperature. Hence, the conventional synthesis of **20E**, though tedious, has long been known.[25,26] Direct irradiation at 185 nm of (*Z*)-cyclooctene (**20Z**) in pentane or methanol affords **20E**, together with small amounts of *cis*-bicyclo[3.3.0]octane (**21**), *cis*-bicyclo[5.1.0]octane (**22**), and methylenecycloheptane (**23**). The latter three products are derived from the carbene intermediate(s) formed via the π,Rydberg(3s) excited state.[27] The direct photoisomerization of **20Z** has been compared with the sensitized one. A high photostationary-state *E/Z* ratio of 0.96 is obtained upon irradiation at 185 nm,[28,29] while the sensitization by benzenepolycarboxylates gives *E/Z* ratios of <0.32.[30] The formation of **20E** upon direct irradiation of **20Z** involves the π,π^* singlet.[31] The direct photoisomerization of **20Z** in pentane can be used as a chemical actinometer at 185 nm;[32] the photoisomerization quantum yield of **20Z** to **20E** is 0.32, while that of **20E** to **20Z** is 0.44.[33] This direct photoisomerization can be used for the practical synthesis of (*E*)-cycloalkene that is thermally stable and isolable. Thus, in a typical preparative-scale photoisomerization, a pentane solution (350 ml) of **20Z** (0.12 *M*) is irradiated at 185 nm for 6 h under a nitrogen atmosphere, and the irradiated solution is concentrated and extracted with aqueous silver nitrate. The aqueous extract is washed with pentane and then added to ammonium hydroxide to give **20E** of 99.6% purity in 26% yield.[29]

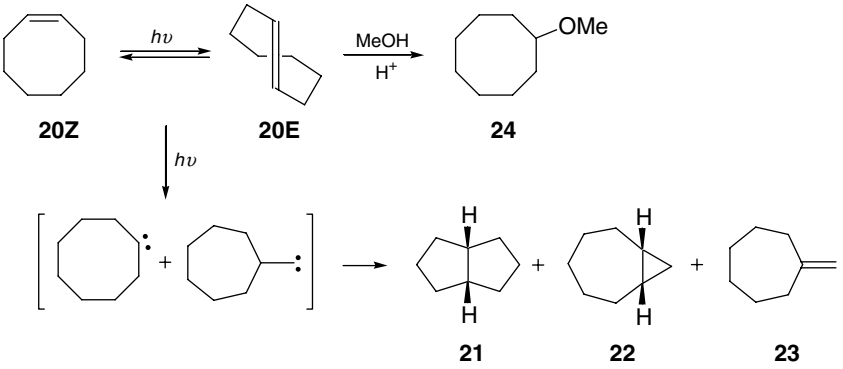

20Z **20E** **24**

21 **22** **23**

In the vapor-phase photolysis of larger (*Z*)-cycloalkenes, the photoisomerization to the (*E*)-isomer has not been described explicitly in the literature.[34] It is believed, however, that, analogous to **20Z**, cyclononene (**25Z**), cyclodecene (**27Z**), cycloundecene (**30Z**), and cyclododecene (**34Z**) afford not only the carbene-derived products but also the (*E*)-isomers (though not yet isolated) as intermediates upon irradiation in solution. Direct irradiation of (*Z*)-cycloundecene (**30Z**) in pentane affords *cis*-bicyclo[6.3.0]undecane (**31**) as the major photoproduct, together with ring-opened products **32** and **33**, and the *Z-E* isomerization appears to occur during the photolysis. (*Z*)-Cyclononene (**25Z**) is also believed to undergo the *Z-E* isomerization upon irradiation in solution, but the final product, after prolonged irradiation, is the carbene-derived *cis*-ocathydro-1*H*-indene (**26**).[35] Direct irradiation of (*Z*)-cyclodecene (**27Z**) and (*Z*)-cyclododecene (**34Z**) give similar carbene-derived products (**2829** and **3537**). The *E-Z* photoisomerization of these cycloalkenes is reported to occur, although no further examinations have been made.[27]

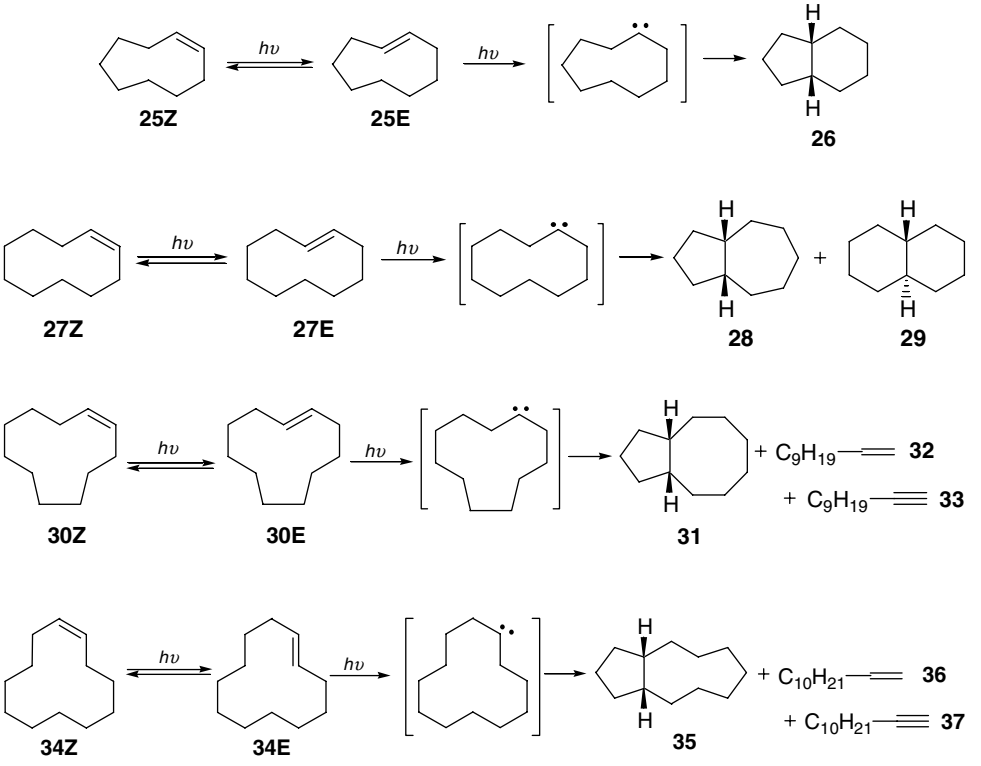

Sensitized Irradiation of Cycloalkenes

Cyclohexenes

A more commonly employed photochemical procedure to obtain (*E*)-cycloalkenes is the photosensitized isomerization of the (*Z*)-isomers, where conventional light sources can be used. Although (*E*)-cyclohexene (**13E**) has never been isolated, various chemical and spectroscopic observations strongly support its formation as a labile intermediate upon direct and sensitized irradiations of cyclohexenes. Thus, the triplet-sensitization of (*Z*)-cyclohexene (**13Z**) with benzene derivatives in aprotic media gives a stereoisomeric mixture of [2 + 2]-cyclodimers (**16**) via the initial *Z-E* photoisomerization.[23,36] A longer-wavelength irradiation of **13Z** in the presence of copper(I) leads to the formation of the same cyclodimers but in a quite different ratio. 1-Methylcyclohexene (**38a**) and *p*-menth-1-ene (**38b**) are converted to the corresponding exocyclic isomer (**39**) and the methanol adduct (**40**) upon alkylbenzene sensitization in methanol. In aromatic hydrocarbons used as sensitizing solvents, only the exocyclic isomer is obtained.[37]

Xylene sensitization of limonene (**38c**) in the presence of acidic methanol leads to photoprotonation, affording a mixture of (*Z*)- and (*E*)-*p*-menth-8-en-1-yl methyl ether (1.6:1) in 56% yield.[38–41] Cyclohexene (**13Z**) and 1-phenylcyclohexene also undergo photoinduced addition of methanol in the presence of acid.[42] In the photoreaction of (*E*)-1-phenylcyclohexene (**41E**)* in methanol at 30°C, 1-methoxy-1-phenylcyclohexane (**42**) and three [2 + 2]-cyclodimers (**43**) in a 55:40:5 ratio are formed. At –75°C, the [4 + 2]-cyclodimer (**44**) is obtained upon direct and/or acetophenone-sensitized irradiation, which is taken as evidence for the formation of the highly strained "*trans*" or (*Z*)-isomer (**41Z**).[43] X-ray crystallographic analysis of **44** supports the mechanism that involves **41Z**, as the stereochemistry is consistent with the addition of photogenerated **41Z** to **41E** as allowed by the Woodward–Hoffmann rule.[44] The quantum yield (Φ) of disappearance of **41E** at 300 nm amounts to 0.12,[45] whereas the intersystem crossing of **41E** is very inefficient (Φ = 0.001).[46] Hence, the singlet-excited state is most plausible as the precursor to **41Z** in the direct photoisomerization. A flash photolysis study of **41E** in methanol clearly reveals the intervention of **41Z** as a transient species.[47] In deuterium-labeling experiments, an exceptionally large secondary kinetic isotope effect (k_H/k_D) of up to two was observed upon thermal isomerization of **41Z** to **41E**. This was attributed to the changes in the torsion angle around the C=C bond and also in the bending angles of vinylic CH (or CD), both of which are seriously deformed during the geometrical isomerization.[48]

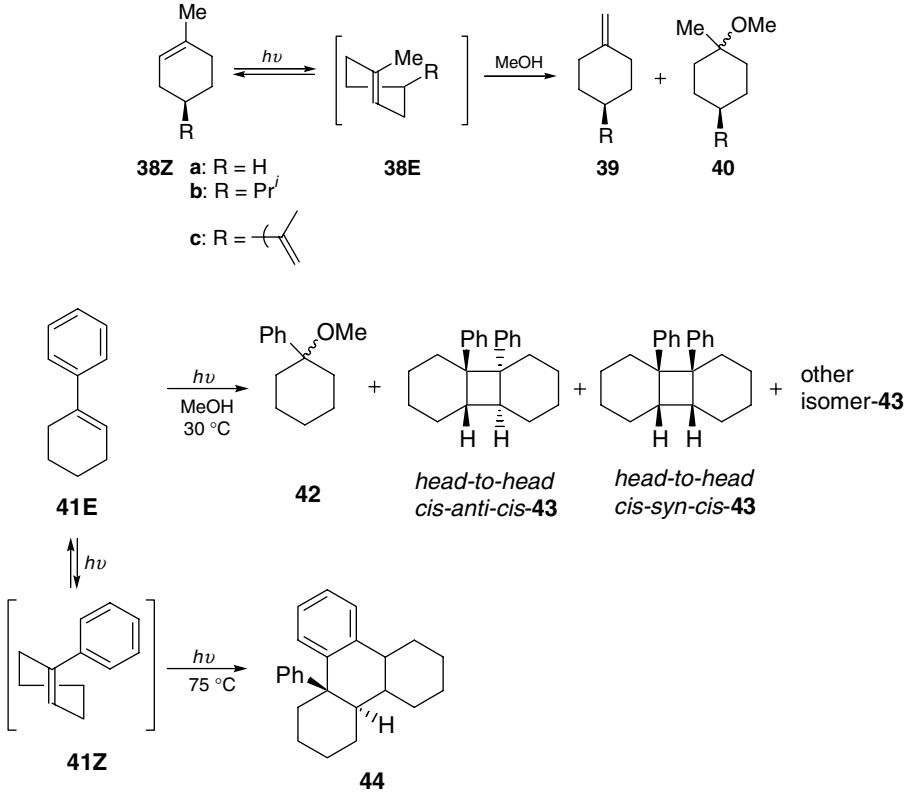

Cycloheptenes

(*Z*)-Cycloheptene (**18Z**) and (*E*)-1-phenylcycloheptene (**45a**) both undergo photoinduced methanol addition in the presence of acid, suggesting the intervention of (*E*)-cycloheptene (**18E**) and (*Z*)-1-phenylcycloheptene, respectively.[42] In sharp contrast to (*E*)-cyclohexene (**13E**), which has never been

* Note that the prefix (*E*)" represents the *cis* configuration in this compound.

isolated, **18E** has been identified and characterized by several spectroscopic methods. Irradiation of **18Z** in the presence of methyl benzoate as sensitizer in dimethyl ether-d_6 at −90°C affords the (*E*)-isomer **18E**, which has been characterized *in situ* by ^{1}H NMR spectroscopy. Upon warming to −30°C, **18E** quickly reverts to **18Z** with an energy barrier of 10 kcal/mol.[49] Upon irradiation of **18Z** at −78°C in the presence of methyl benzoate, **18E** is produced in the high *E/Z* ratio of 0.24. Triplet sensitization with toluene or xylenes affords **18E** in low yield with *E/Z* ratios of 0.065 or 0.094.[50,51] (*Z*)-1-Methylcycloheptene (**45b**) gives the exocyclic isomer (**46b**) and the methanol adduct (**47b**), both of which are derived from the (*E*)-isomer, upon alkylbenzene sensitization in methanol.[37] Low-temperature laser flash photolysis of (*E*)-1-phenylcycloheptene affords the transient absorption ascribable to the (*Z*)-isomer.[52] Irradiation of (*E*)-1-methoxycarbonylcylcoheptene (**45c**) in pentane gives the *head-to-head* cyclodimer (**48c**) in high stereoselectivity of 86:14 (the *trans-anti-cis* isomer is dominant), suggesting the intermediacy of the (*Z*)-isomer produced photochemically.[53]

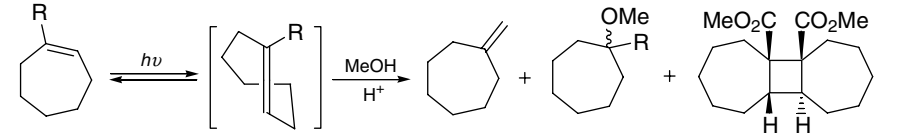

45 **a**: R = Ph
b: R = Me
c: R = CO_2Me
d: R = COMe

46b **47a**, **b** *head-to-head trans-anti-cis* and other isomers, **48c**

Cyclooctenes

Since (*E*)-cyclooctene (**20E**) is the smallest member of the (*E*)-cycloalkenes isolable under ambient conditions, its photochemical behavior has been studied intensively as a prototype or model system of the cycloalkene family; selected results are summarized in Table 16.1. When (*Z*)-cyclooctene (**20Z**) is irradiated with an equimolar amount of benzene or naphthalene, 1:1 sensitizer–substrate adducts rather than the (*E*)-isomer are produced.[54–56] Upon xylene sensitization, however, the adduct formation is retarded and the geometrical isomerization dominates to afford **20E** in an acceptable isolated yield.[57] The triplet-sensitized photoisomerization of **20Z** has been studied in some detail and has established that the *E/Z* ratio depends on the alkene concentration. The concentration dependence observed is attributed to the involvement of the excited singlet state, which tends to give arene–cyclooctene adducts such as **49** and **50**.[58] Temperature and solvent-viscosity effects upon triplet-sensitized photoisomerization of cyclooctene have been studied in detail.[59] In the alkylbenzene-sensitized isomerization of **20Z** in pentane, the photostationary-state *E/Z* ratio is substantially affected by temperature, being doubled when the temperature is lowered from 20 to −78°C. This result is in contrast with the photoisomerization behavior of acyclic 2-octene.

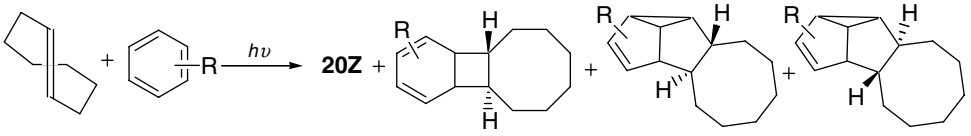

20E **49** **50**

Singlet sensitization performs better, as the photostationary-state *E/Z* ratios of 0.250.34 obtained from singlet sensitization with benzenepolycarboxylates are appreciably higher than those from triplet sensitization with alkylbenzenes.[30] Furthermore, benzenecarboxylates with electron-withdrawing group(s), such as trifluoromethyl, give much higher photostationary-state *E/Z* ratios of up to 0.6.[60,61] Singlet energies of the sensitizers employed are in a range 95–100 kcal/mol.[62]

The photobehavior of cycloalkene is significantly altered by the substituent introduced at the C-1; the alkyl substituent causes severe steric hindrance, and the aromatic functions as a built-in sensitizer. Direct irradiation of (*Z*)-1-methylcyclooctene (**50a**) at 214 nm leads to a photostationary-state *E/Z* ratio of 0.30,

while triplet-sensitization with alkylbenzenes affords smaller ratios of 0.03 to 0.26, which are slightly larger than those obtained with the parent cyclooctene. In contrast, singlet sensitization with alkyl benzoates gives *E/Z* ratios of 0.01 to 0.24, which are smaller than those for cyclooctene. This is attributable to the steric hindrance within the singlet exciplex.[63]

Irradiation of (*E*)-1-nitrocycloctene (**50b**) gives the (*Z*)-isomer, which is trapped by Diels–Alder reaction with cyclopentadiene to give an adduct (**51b**) in 40% yield; the (*Z*)-isomer content is estimated to be >28% at the photostationary state.[64] Irradiation at 337 nm of (*E*)-1-acetylcyclooctene (**50c**) in acetonitrile-d_3 affords a photostationary-state *E/Z* mixture in a ratio of 12:88; the strained (*Z*)-isomer produced is trapped by cyclopentadiene.[65] Irradiation of (*E*)-1-methoxycarbonylcyclooctene (**50d**) in pentane leads to the formation of deconjugated (*Z*)-3-methoxy derivative (**52d**) in 70% yield, along with the reduced and hydrated products (**53d** and **54d**) in 4 and 1% yields, respectively.[53] It is plausible that the reaction proceeds through the (*Z*)-isomer, in which the allylic hydrogen at C3 is readily accessible in space to the ester carbonyl.

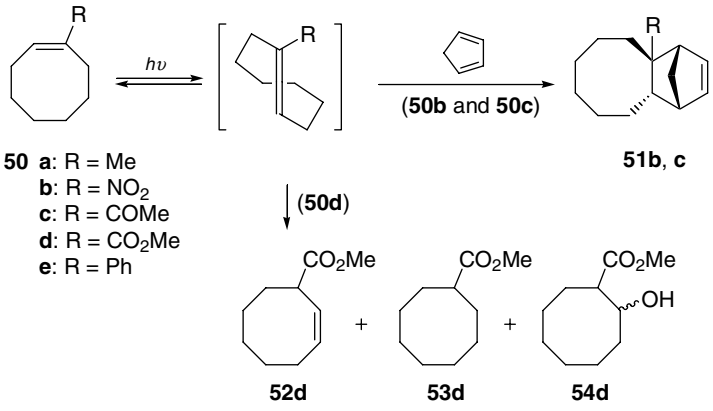

16.3 Miscellaneous Cycloalkenes

Benzene-sensitized photoisomerization of (*Z*)-cyclododecene (**34Z**) affords **34E** in a 39:61 *E/Z* ratio at the photostationary state. Other triplet sensitizers such as benzophenone, acetophenone, and acetone, as well as copper salts, can also be used.[66] Sensitized photoisomerization of 1,5,9-cyclododecatriene has also been studied.[66] Direct irradiation of (*E*)-3-methylenecyclodecene (**55E**) affords **55Z**, which further photoisomerizes to yield **56**, **57**, and **58**. Triphenylene sensitization of **55E** affords a photostationary-state mixture of **55E** and **55Z** in a ratio of 94:6.[67] Doubly-bridged ethylene derivatives **59Z** (n = 8, 10), i.e., (*Z*)-bicyclo[8.8.0]octadec-1(10)-ene and (*Z*)-bicyclo[10.8.0]eicos-1(12)-ene, isomerize to the (*E*)-isomers upon xylene-sensitized or direct irradiation. An *E/Z* ratio of 0.42 is given upon sensitization of the latter,[68] while much higher *E/Z* ratios of 9 and 2 are attained upon direct irradiation at 254 nm of (*Z*)-bicyclooctadecene and (*Z*)-bicycloeicosene, respectively.[69]

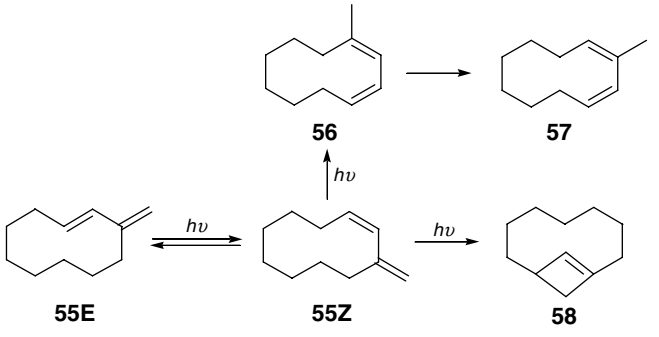

TABLE 16.1 Geometrical Photoisomerization of (*Z*)-Cyclooctene

Sensitizer	[Sensitizer]	[Cyclooctene]	Solvent	Temperature (°C)	*E:Z*	*E/Z* ratio	Ref.
(Direct irradiation at 185 nm)	—	—	—	17	49.0:51.0	0.96	28
Benzene	3 torr	3 torr	Vapor phase	—	16.5:83.5	0.198	31
Toluene	3 torr	3 torr	Vapor phase	RT	13.3:86.7	0.154	28
Fluorobenzene	3 torr	3 torr	Vapor phase	—	14.4:85.6	0.168	31
p-Xylene	3 torr	3 torr	Vapor phase	—	8.6:91.4	0.094	31
Benzonitrile	1 torr	3 torr	Vapor phase	—	2.5:97.5	0.026	28
Benzene	0.4 *M*	80 m*M*	Pentane	17	4.6:95.4	0.048	31
Benzene	0.1 *M*	80 m*M*	Pentane	RT	6.5:93.5	0.07	58
Benzene	0.1 *M*	10 m*M*	Pentane	RT	11.5:88.5	0.13	58
Benzene	0.1 *M*	0.2 m*M*	Pentane	RT	17.4:82.6	0.21	58
Benzene	0.1 *M*	2 m*M*	Pentane	25	16.7:83.3	0.2	61
Benzene	0.1 *M*	2 m*M*	Hexane	25	20.0:80.0	0.25	59
Benzene	0.1 *M*	2 m*M*	Cyclohexane	25	20.6:79.4	0.26	59
Benzene	0.1 *M*	2 m*M*	Cyclohexane	75	17.4:82.6	0.21	59
Benzene	0.1 *M*	2 m*M*	Pentane	−78	32.4:67.6	0.48	61
Benzene	0.1 *M*	2 m*M*	Pentane	−123	36.7:63.3	0.58	59
Benzene	0.1 *M*	2 m*M*	Ethylene glycol	25	>27:73	0.37	59
Toluene	0.5 *M*	80 m*M*	Pentane	17	5.0:95.0	0.053	28
Toluene	0.1 *M*	2 m*M*	Pentane	25	13.8:86.2	0.16	61
Toluene	0.1 *M*	2 m*M*	Pentane	−100	30.6:69.4	0.44	59
Toluene	0.1 *M*	2 m*M*	Acetonitrile	25	15.3:84.7	0.18	59
p-Xylene	0.4 *M*	80 m*M*	Pentane	17	4.5:95.5	0.047	31

p-Xylene	0.1 *M*	2 m*M*	Pentane	25	8.2:91.8	0.089	61
p-Xylene	0.1 *M*	2 m*M*	Pentane	−100	18.0:82.0	0.22	59
Durene	0.25 *M*	80 m*M*	Pentane	17	3.9:96.1	0.041	31
Acetophenone	0.4 *M*	80 m*M*	Pentane	17	3.1:96.9	0.032	31
Benzophenone	0.25 *M*	80 m*M*	Pentane	17	0.5:99.5	0.005	31
Benzoic acid	36 m*M*	70 m*M*	Pentane	20	20.6:79.4	0.26	30
Methyl benzoate	0.40 *M*	70 m*M*	Pentane	20	20.0:80.0	0.25	30
Methyl benzoate	10 m*M*	70 m*M*	Methanol	20	26.5:73.5	0.36	30
Methyl benzoate	10 m*M*	70 m*M*	Acetonitrile	20	25.9:74.1	0.35	30
Ethyl benzoate	70 m*M*	70 m*M*	Pentane	20	20.6:79.4	0.26	30
t-Butyl benzoate	28 m*M*	70 m*M*	Pentane	20	19.4:80.6	0.24	30
Methyl *o*-methoxylbenzoate	35 m*M*	70 m*M*	Pentane	20	4.8:95.2	0.05	30
Methyl *o*-methylbenzoate	37 m*M*	70 m*M*	Pentane	20	8.3:91.7	0.09	30
Methyl *p*-methylbenzoate	61 m*M*	70 m*M*	Pentane	20	9.9:90.1	0.11	30
Methyl *p*-cyanobenzoate	5 m*M*	70 m*M*	Pentane	20	10.7:89.3	0.12	30
Dimethyl phthalate	31 m*M*	70 m*M*	Pentane	20	6.5:93.5	0.07	30
Dimethyl isophthalate	20 m*M*	70 m*M*	Pentane	20	25.4:74.6	0.34	30
Dimethyl terephthalate	6 m*M*	70 m*M*	Pentane	20	21.3:78.7	0.27	30
Tetramethyl pyromellitate	5 m*M*	70 m*M*	Pentane	20	9.1:90.9	0.1	30
1,4-Dicyanobenzene	4 m*M*	70 m*M*	Pentane	20	2.0:98.0	0.02	30
Methyl *o*-trifluoromethylbenzoate	10 m*M*	30 m*M*	Pentane	25	10.7:89.3	0.12	60
Methyl *m*-trifluoromethylbenzoate	10 m*M*	30 m*M*	Pentane	25	29.6:70.4	0.42	60
Methyl *p*-trifluoromethylbenzoate	10 m*M*	30 m*M*	Pentane	25	31.5:68.5	0.46	60
Methyl 3,5-bis(trifluoromethyl)benzoate	10 m*M*	10 m*M*	Cyclohexane	25	37.1:62.9	0.59	60
Methyl 3,5-bis(trifluoromethyl)benzoate	10 m*M*	0.2 *M*	Cyclohexane	25	>35:65	0.55	60
Methyl 3,5-bis(trifluoromethyl)benzoate	0.1 *M*	0.8 *M*	Cyclohexane	25	>32:68	0.47	60

Note: RT = room temperature.

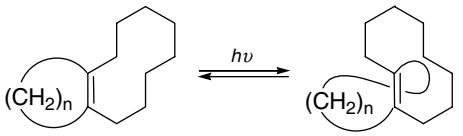

59Z (n = 8, 10) **59E**

Irradiation of (*Z,Z*)-1,3-cyclooctadiene (**60ZZ**) affords the (*E,Z*)-isomer (**60EZ**), together with small amounts of bicyclo[4.2.0]oct-7-ene (**61**) and (*Z,Z*)-1,4-cyclooctadiene (**62**).[70] Upon direct irradiation of **60ZZ** and (*Z,Z*)-1,3-cycloheptadiene (**63ZZ**), the product distributions do not depend on the irradiation wavelength. (*E,Z*)-1,3-Cyclooctadiene **60EZ** is produced from **60ZZ** in 62 to 89% yields.[71] Low-temperature irradiation of **63ZZ** in a glassy matrix at −196°C affords the (*E,Z*)-isomer (**63EZ**), which is stable at that temperature and has been characterized spectroscopically.[72] Direct and triphenylene-sensitized irradiation of **63ZZ** in pentane or in neutral methanol at room temperature affords bicyclo[3.2.0]hept-6-ene (**64**) in excellent yields. In contrast, irradiation in acidic methanol gives 3-methoxycycloheptene (**65**) and 7-methoxybicyclo[4.1.0]heptane (**66**). All of these products are derived from the photochemically produced (*E,Z*)-isomer **63EZ**. Direct photolysis of (*Z,Z,Z*)-1,3,5-cycloheptatriene (**67**) affords bicyclo[3.2.0]hepta-2,6-diene (**68**) in an excellent yield. However, no experimental evidence for the *Z-E* photoisomerization has been obtained in this particular case; instead, the direct photocyclization allowed by the Woodward–Hoffmann rule appears to be operative.[73] Singlet photosensitization of (*Z,Z*)-1,5-cyclooctadiene (**69ZZ**) in pentane gives **69EZ**, along with tricyclo[3.2.0.0^{2,6}]octane (**70**), which arises from the thermal cyclization of **69EZ**.[74]

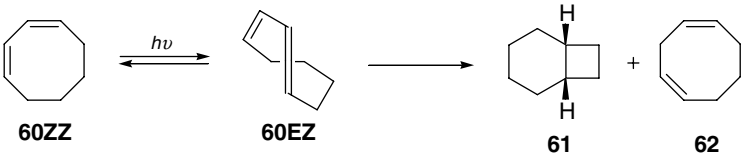

60ZZ **60EZ** **61** **62**

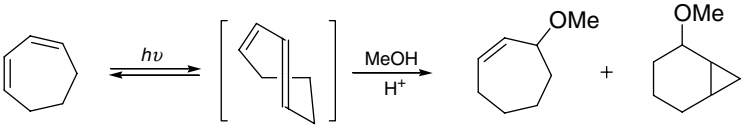

63ZZ **63EZ** **65** **66**

64

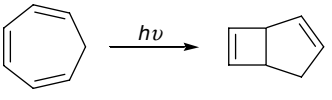

67 **68**

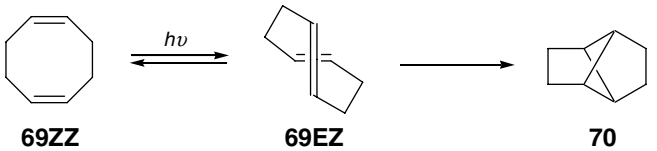

69ZZ **69EZ** **70**

(*Z*)-2-Cyclooctenone (**71Z**) isomerizes to (*E*)-isomer upon irradiation at 300 nm, affording an 80:20 *E/Z* mixture. The (*E*)-isomer **71E** can be trapped by **71Z** or by 5,5-dimethoxy-1,2,3,4-tetrachlorocyclopentadiene at room temperature to afford adducts **72** or **73**, respectively.[75] Similarly, (*E*)-2-cycloheptenone (**74E**) is produced upon irradiation of **74Z** at −50°C and trapped by cyclopentadiene to yield adduct **75**.[76] The formation of **74E** as a transient species has been proven by IR spectroscopy at −160°C, although this species is not stable above −120°C.[77] Laser flash photolysis revealed that **74E** has a lifetime of 45 sec in cyclohexane at room temperature.[78] A variety of alcohols and amines are known to add to the photochemically produced (*E*)-cycloheptenone, (*E*)-cyclooctenone, and (*E*)-cyclononenone.[79] Smaller-sized (*Z*)-cyclohexenone affords a similar adduct only in low yield (0.7%) upon irradiation in methanol, implying inefficient formation and/or trapping of the (*E*)-isomer. Photoinduced methanol additions to 2-cycloheptenone, 2-cyclooctenone, and 2,3-benzo-2,6-cycloheptadienone are also considered to involve the corresponding (*E*)-isomers as reactive intermediates on the basis of a deuterium-labeling experiment.[80]

Photochemical isomerization of cycloalkenes via copper(I) complexes is only briefly described here, as practically no additional studies have been published since the previous edition.[10] In copper(I) trifluoromethanesulfonate-sensitized photodimerizations of (*Z*)-cyclopentene, (*Z*)-cyclohexene, and (*Z*)-cycloheptene, the major products are a stereoisomeric mixture of cyclodimers, which may be derived from the initial *Z-E* isomerization of cycloalkenes.[81] Irradiation at 254 nm of (*Z*)-cyclooctene with copper(I) chloride affords the (*E*)-isomer in 19% isolated yield, the photostationary-state *E/Z* ratio being 20:80 after 24 h irradiation.[82] Photobehavior of (*Z*)-cyclohexene and (*Z*)-cycloheptene in the presence of copper(I) trifluoromethanesulfonate has also been examined.[83] Copper(I)-catalyzed photoreaction of cyclohexene in the presence of 1,3-butadiene affords Diels–Alder adducts.[84] Irradiation of the (*Z*)-cycloheptene-copper(I) triflate complex in hexane affords a stable (*E*)-cycloheptene-copper(I) complex, which can be isolated and identified by conventional analyses.[85] The xylene-sensitization of cycloheptene gives the 1:1 arenecycloheptene adduct in good yield; the cycloheptene dimer is obtained in 57% yield upon irradiation at 254 nm in the presence of copper(I)-benzene complex.[81] Mercury-sensitized photolyses of cyclohexene,[86] 3-methylcyclohexene,[86] and cycloheptene[87] in vapor phase lead to decomposition via biradicals.

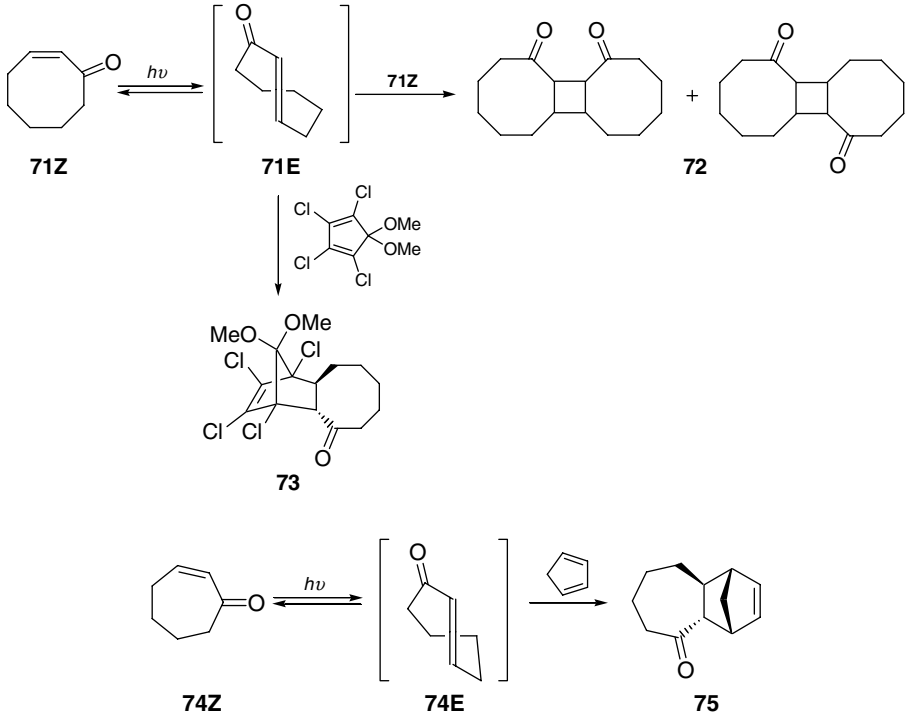

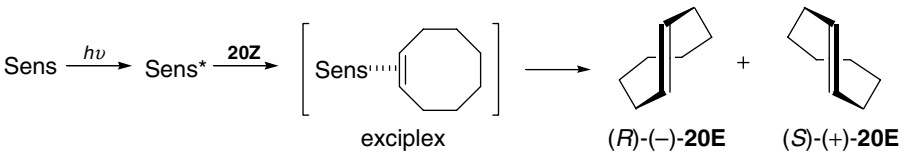

16.4 Physical Properties of (*E*)-Cycloalkenes

Highly constrained (*E*)-cycloalkenes, generated readily through the photoisomerization of (*Z*)-isomers, are known to possess unique physical and (chir)optical properties. These properties are of particular interest and importance from both the experimental and theoretical points of view. For example, the experimental barriers of thermal *E*-to-*Z* isomerization of cycloalkenes are compared with the theoretical values obtained by semiempirical calculations. Among the calculations reported, the PM3 method appears to give good fits to the experimental results; e.g., the experimental strain energy of (*Z*)-cyclooctene (**20Z**) is 11.37 kcal/mol, which is close to the value (10.55 kcal/mol) obtained by PM3.[88] The relevant experimental (chir)optical properties, such as specific rotations and absorption maxima and thermodynamic parameters for isomerization, are summarized in Table 16.2.

16.5 Asymmetric Photoisomerization of Cycloalkenes

Cyclooctene

Enantiomeric (*E*)-cyclooctene (**20E**) was first resolved in 1963 through its diastereomeric platinum(II) complex.[89] Synthesis of optically active **20E** has been the subject of intensive study since 1968.[90] The first preparation involves the treatment of enantiopure (*E*)-cyclooctane-1,2-thiocarbonate with triisooctyl phosphate or of (*E*)-cyclooatane-1,2-trithiocarbonate with 1,3-dibenzyl-2-methyl-1,3,2-diazaphospholidine.[91] Following analogous synthetic routes, enantiomeric (*E*)-cycloheptene (**18E**) can be produced and trapped by 2,5-diphenyl-3,4-isobenzofuran as an optically active adduct. In 1973, the circular dichroism spectrum of enantiopure **20E** vapor was recorded in the vacuum UV region down to 150 nm.[92] The first enantiodifferentiating *Z-E* photoisomerization of cyclooctene sensitized by chiral benzenecarboxylates appeared in 1978.[93] Transfer of chiral information from sensitizer to substrate occurs within the exciplex intermediate.[30]

A few comprehensive reviews on asymmetric photochemistry in solution[94,95] and on asymmetric photosensitization[96,97] have been published. An account of the multidimensional control of asymmetric photoreaction by environmental factors appeared recently.[98]

Enantiodifferentiating *Z-E* photoisomerization of cyclooctene (**20Z**) sensitized by chiral polyalkyl benzenepolycarboxylates has been extensively studied; some of the results are summarized in Table 16.3.[99] The crucial enantiodifferentiating step is the rotational relaxation of prochiral **20Z** to enantiomeric perpendicular singlets within the exciplex of the chiral sensitizer with **20Z**. In order to elucidate the detailed mechanism and to obtain higher enantiomeric excess (*ee*), the steric and electronic effects of the sensitizer and its chiral substituent as well as the involvement of the intra/intermolecular triplex have been studied extensively. Thus, the sensitizations with bulky 8-phenylmenthyl and 8-cyclohexylmenthyl 1,2,4,5-benzenetetracarboxylates afford good *ee*s of up to 50% even at room temperature. The *ee* is improved at lower temperatures to reach 64% at −89°C.[62] In contrast, chiral triplet sensitizers afford much lower *ee*s, which are not appreciably improved even at low temperatures (at least in this system).[100] The enantiodifferentiating photoisomerization can also be effected by chiral aromatic amides,[101] phosphoryl esters,[102] and phosphoramides.[103]

Temperature effects do not appear to have been seriously considered or examined in the studies of photoisomerization, except for the purpose of stabilizing strained (*E*)-cycloalkenes, before the recent finding of the dramatic inversion of product chirality by changing temperature in the enantiodifferentiating

photoisomerization of cyclooctene **20Z** sensitized by chiral benzenepolycarboxylates.[104] More recent studies demonstrate that not only temperature[105] but also other entropy-related factors such as pressure,[106] magnetic/electronic fields,[107,108] and solvent[109] play vital roles in determining the product's *ee* and chiral sense in the excited-state interactions within the exciplex. Indeed, the chiral sense of photoproduct **20E** is switched from *R* to *S* either by lowering the temperature under atmospheric pressure (0.1 MPa) or by increasing pressure at 25°C in the enantiodifferentiating photosensitization of **20Z** with tetra-(−)-menthyl 1,2,4,5-benzenetetracarboxylate. When saccharide esters are used as the chiral sensitizer, the product chirality is inverted by simply changing the solvent from nonpolar to polar. In fact, the major product is (*S*)-(+)-**20E** in pentane but is switched to (*R*)-(−)-**20E** in diethyl ether in the photosensitization of **20Z** with tetrakis(diacetoneglucosyl) 1,2,4,5-benzenetetracarboxylate at low temperatures.[109]

Supramolecular asymmetric photoisomerization of cyclooctene has also been performed in native[110] and modified cyclodextrin cavities,[111,112] in zeolite supercages modified with chiral sensitizers,[113] and in DNA grooves.[114]

Cyclooctene Derivatives

Photoisomerization of (*Z*)-1-methylcyclooctene (**50a**) sensitized by hindered chiral benzene(poly)carboxylates affords photostationary-state *E/Z* ratios much lower than those obtained for unsubstituted cyclooctene, probably as a consequence of the steric hindrance of the 1-methyl functional group. However, the steric hindrance does not enhance the product *ee* in this particular case.[115]

Enantiodifferentiating photoisomerization of (*Z,Z*)-1,3-cyclooctadiene (**60ZZ**) is sensitized by chiral benzene(poly)carboxylates.[116] Upon sensitization with hexa-(−)-menthyl benzenehexacarboxylate in pentane at −40°C, the (*E,Z*)-isomer (**60EZ**) is obtained in 18% *ee*. Photoisomerization of (*Z,Z*)-1,5-cyclooctadiene (**69ZZ**) sensitized by (−)-menthyl benzoate affords (−)-(*E,Z*)-isomer (**69EZ**) in only 1.6% *ee*.[74]

Self-sensitized photoisomerization of (*Z*)-3-benzoyloxycyclooctene (**76Z**) affords diastereomeric (1*R**,3*R**)- and (1*S**,3*R**)-**76E** in moderate diastereomeric excess (*de*). Intriguingly, the product chirality is switched by changing the substrate concentration. Thus, irradiation of a 1 m*M* pentane solution of **76Z** at 25°C gives (1*R**,3*R**)-**76E** in 17% *de*, but the product *de* gradually decreases with increasing substrate concentration to ~0% at 10 m*M*, and eventually the epimeric (1*S**,3*R**)-**76E** becomes dominant at higher concentrations to give 11% *de* at 100 m*M*.[117] This unprecedented observation is rationalized in terms of the competing intra- and intermolecular sensitization mechanism, provided that each process gives the opposite product. In contrast, diastereodifferentiating photoisomerizations of 4- and 5-benzoyloxycyclooctenes (**77Z** and **78Z**) do not show such concentration dependence.[118] For the 4-benzoyl derivative, both intra- and intermolecular sensitizations give the same diastereomers, while essentially no intramolecular sensitization occurs in the 5-benzoyloxycyclooctene case due to the steric inaccessibility.

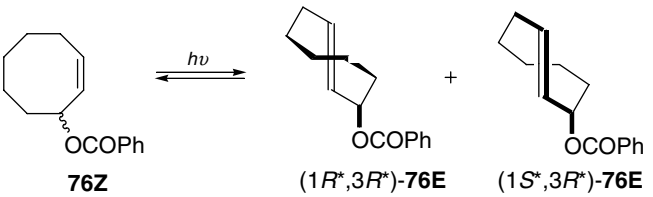

76Z (1*R**,3*R**)-**76E** (1*S**,3*R**)-**76E**

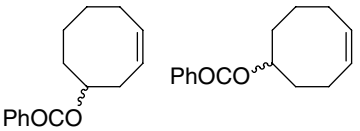

77Z **78Z**

TABLE 16.2 Physical and Spectral Properties of (*E*)- and (*Z*)-Cycloalkenes

Cycloalkene	Physical and (Chir)optical Properties	*cis*-Isomer	*trans*-Isomer	Ref.
Cyclooctene (**20**)	UV spectra, λ_{max}, nm	(*Z*):~185	(*E*):196	92
	Strain energy, kcal mol^{-1}	(*Z*):7.4	(*E*): 16.7	51
	Oxidation potential, V vs. SCE	(*Z*):2.01	(*E*):1.81	74
	k(MeOH), M^{-1} sec^{-1}	(*Z*):1.7×10^{-8}	(*E*):5.1×10^{-5}	51
	Vertical ionization potential, eV	(*Z*):8.98		125
	Strain energy (PM3 calcd), kcal mol^{-1}		11.37 (10.55)	88
	Specific rotation $[\alpha]_D$, °	(*E*):412 (CH_2Cl_2, *c* 1.11, 28°C)		126
1-Methylcyclooctene (**50a**)	Specific rotation $[\alpha]_D$, °	(*E*): 106 (CH_2Cl_2, *c* 0.549, 25°C)		115
1-Phenylcyclooctene (**50e**)	Strain energy (PM3 calcd), kcal mol^{-1}		13.3 (14.18)	88
1,3-Cyclooctdiene (**60**)	τ (*cis* to *trans*: 90°C) = 50 min; cyclizes to bicyclo[4.2.0]oct-7-ene. (stable at 60°C)			127
	Specific rotation $[\alpha]_D$, °	(*Z*),*trans*: 1380 (CH_2Cl_2, *c* 1.07, 25°C)		116
1,5-Cyclooctdiene (**69**)	Oxidation potential, V vs. SCE	(*Z*):2.07	(*E*):0.73	74
	Specific rotation $[\alpha]_D$, °	(*Z*),*trans*: 152 (CH_2Cl_2, *c* 0.87, 10°C)		128
Cycloheptene (**18**)	k(MeOH), M^{-1} sec^{-1}	(*Z*):2.2×10^{-8}	(*E*):17	51
	Strain energy, kcal mol^{-1}	(*Z*):6.7	(*E*):27	51
	Vertical ionization potential, eV	(*Z*): 9.04		125
	Kinetic parameters for isomerization, E_a = 17.4 kcal mol^{-1}, log A = 11.1 (under nitrogen) E_a = 9.0 kcal mol^{-1}, log A = 7.8 (under air)			129
	τ ((*E*), methanol, −10°C) = 38.3 min			51
	τ ((*E*), pentane, −10°C) = 23 min			24

1-Phenylcycloheptene (**45a**)	UV spectra, λ_{max}, nm	(*E*):248	(*Z*):300	52
	k(MeOH), M^{-1} sec^{-1}		(*Z*):103	52
	τ((*Z*), cyclohexane, RT) = 250 sec			52
	Strain energy (PM3 calcd) / kcal mol^{-1}		29 (30.29)	88, 130
1,3-Cycloheptdiene (**63**)	τ(Isopentane–methylcyclohexane =3:1, –78°C) = 7.1 min			72
	τ(methanol, –78°C) = 6.5 min			73
2-Cycloheptenone (**74**)	UV spectra, λ_{max}, nm	(*Z*):222	(*E*):265	78
	τ ((*E*), cyclohexane, RT) = 45 sec, major decay process is the reaction with substrate			78
	τ ((*E*), methanol, RT) = 0.033 sec, major decay process is the reaction with solvent			78
1-Acetylcycloheptene (**45d**)	UV spectra, λ_{max}, nm	(*E*):236	(*Z*):282	131
1,1,4,4-Tetramethyl-1,4-disila-2-cycloheptene	Half-life ((*E*), methylcyclohexane, 20°C) = 101 min			132
1,1,3,3,6,6-Hexamethyl-1-sila-4-cycloheptene (**79**)	Half-life ((*E*), 123°C) = 5.7 d			119
Cyclohexene (**13**)	Strain energy, kcal mol^{-1}	(*Z*):2.5		51
	Vertical ionization potential, eV	(*Z*):9.12		133
	k(MeOH), M^{-1} sec^{-1}	(*Z*):4.4×10^{-8}		51
1-Methylcyclohexene (**36a**)	Strain energy, kcal mol^{-1}	(*Z*):1.7		51
1-Phenylcyclohexene (**41**)	UV spectra, λ_{max}, nm	(*E*):248	(*Z*):385	47
	Vertical ionization potential, eV	(*E*):8.29		134
	k(MeOH), M^{-1} sec^{-1}	(*E*):3.1×10^{-4}		51
	Kinetic parameters for isomerization, E_a = 12.1 kcal mol^{-1}, log *A* = 14.1			48
	Strain energy (PM3 calcd), kcal mol^{-1}		47 (54.42)	88
	Strain energy, kcal mol^{-1}		44.7	135

Note: RT = room temperature.

TABLE 16.3 Photosensitized Enantiodifferentiating Isomerization of (*Z*)-Cyclooctene (**20Z**)

Sensitizer	Solvent	Temperature (°C)	*E/Z*	% ee (% op)	Ref.
(−)-Menthyl benzoate	Pentane	20	—	−3.1	93
Cholesteryl benzoate	Pentane	20	—	−0.3	93
Di-(−)-menthyl isophthalate	Pentane	20	—	−4.0	93
(−)-Menthyl benzoate	Pentane	25	—	−2.7	99
Di-(−)-menthyl phthalate	Pentane	25	—	+3.8	99
Di-(−)-menthyl isophthalate	Pentane	25	—	−4.4	99
Di-(−)-menthyl terephthalate	Pentane	25	—	−6.0	99
Tri-(−)-menthyl 1,2,3-benzenetricarboxylate	Pentane	25	—	−9.4	99
Tri-(−)-menthyl 1,3,5-benzenetricarboxylate	Pentane	25	—	−3.4	99
Tetra-(−)-menthyl 1,2,4,5-benzenetetracarboxylate	Pentane	25	—	−9.6	99
Tetra -(−)-menthyl 1,2,4,5-benzenetetracarboxylate	Heptane	25	—	−8.8	99
Tetra-(−)-menthyl 1,2,4,5-benzenetetracarboxylate	Heptane	−87	—	+30.7	99
Tetra-(−)-menthyl 1,2,4,5-benzenetetracarboxylate	Decane	25	—	−8.7	99
Tetra-(−)-menthyl 1,2,4,5-benzenetetracarboxylate	Cyclohexane	25	—	−16.1	99
Tetra-(−)-menthyl 1,2,4,5-benzenetetracarboxylate	Methylcyclohexane	25	—	−12.9	99
Tetra-(−)-menthyl 1,2,4,5-benzenetetracarboxylate	Hexane	−85	—	+3.8	99
Tetra-(−)-menthyl 1,2,4,5-benzenetetracarboxylate	Isopentane	25	—	−13.1	99
Tetra-(−)-menthyl 1,2,4,5-benzenetetracarboxylate	Isooctane	25	—	−14.2	99
Tetra-(−)-menthyl 1,2,4,5-benzenetetracarboxylate	Ether	25	—	−7.4	99
Tetra-(−)-menthyl 1,2,4,5-benzenetetracarboxylate	Acetonitrile	25	—	−8.4	99
Tetra-(−)-menthyl 1,2,4,5-benzenetetracarboxylate	Ethanol	25	—	−7.1	99
Tetra-(−)-menthyl 1,2,4,5-benzenetetracarboxylate	Methanol	25	—	−6.0	99
Tetra-(−)-bornyl 1,2,4,5-benzenetetracarboxylate	Pentane	25	—	+11.5	99
Tetra-(+)-1-methylpropyl 1,2,4,5-benzenetetracarboxylate	Pentane	25	—	−0.0	99
Tetra-(+)-1-methylpentyl 1,2,4,5-benzenetetracarboxylate	Pentane	25	—	+1.8	99
Tetra-(+)-1-methylheptyl 1,2,4,5-benzenetetracarboxylate	Pentane	25	—	+1.5	99
Tetra-(+)-1-methylnonyl 1,2,4,5-benzenetetracarboxylate	Pentane	25	—	+1.2	99
Tetra-(+)-1,2-dimethylpropyl 1,2,4,5-benzenetetracarboxylate	Pentane	25	—	+3.1	99
Tetra-(+)-1,2,2-trimethylpropyl 1,2,4,5-benzenetetracarboxylate	Pentane	25	—	+11.6	99
Tetra-(+)-isopinocamphyl 1,2,4,5-benzenetetracarboxylate	Pentane	25	—	+4.2	99
Tetra-(−)-fenchyl 1,2,4,5-benzenetetracarboxylate	Pentane	25	—	−0.9	99
Tetra-(+)-isomenthyl 1,2,4,5-benzenetetracarboxylate	Pentane	25	—	+6.0	99
Hexa-(+)-neomenthyl benzenehexacarboxylate	Pentane	25	—	−8.4	99
Hexa-(+)-1-cyclohexylethyl benzenehexacarboxylate	Pentane	25	—	+1.8	99
Hexa-(+)-cedryl benzenehexacarboxylate	Pentane	25	—	−22.5	99

(−)-Menthyl benzoate	Pentane	25	—	−2.7	62
Di-(−)-menthyl phthalate	Pentane	25	—	+3.8	62
Di-(−)-menthyl phthalate	Pentane	−60	—	+10.3	62
Di-(−)-menthyl terephthalate	Pentane	25	—	−6.0	62
Di-(−)-menthyl terephthalate	Pentane	−40	—	−8.2	62
Tetra-(−)-menthyl 1,2,4,5-benzenetetracarboxylate	Pentane	25	—	−9.6	62
Tetra-(−)-menthyl 1,2,4,5-benzenetetracarboxylate	Pentane	−87	—	+28.9	62
(−)-(1*R*,2*S*,5*R*)-8-phenylmenthyl benzoate	Pentane	25	—	−0.5	62
(−)-(1*R*,2*S*,5*R*)-8-phenylmenthyl benzoate	Pentane	−40	—	−1.6	62
(−)-Bis-[(1*R*,2*S*,5*R*)-8-phenylmenthyl] phthalate	Pentane	25	—	+18.3	62
(−)-Bis-[(1*R*,2*S*,5*R*)-8-phenylmenthyl] phthalate	Pentane	−87	—	+8.5	62
(−)-Tetrakis-[(1*R*,2*S*,5*R*)-8-phenylmenthyl] 1,2,4,5-benzenetetracarboxylate	Pentane	25	—	+49.5	62
(−)-Tetrakis-[(1*R*,2*S*,5*R*)-8-phenylmenthyl] 1,2,4,5-benzenetetracarboxylate	Pentane	−87	—	+16.1	62
(−)-Tetrakis-[(1*R*,2*S*,5*R*)-8-cyclohexylmenthyl] 1,2,4,5-benzenetetracarboxylate	Pentane	25	—	+49.2	62
(−)-Tetrakis-[(1*R*,2*S*,5*R*)-8-cyclohexylmenthyl] 1,2,4,5-benzenetetracarboxylate	Pentane	−89	—	+63.5	62
(−)-Tetrakis-[(1*R*,2*S*,5*R*)-5-methyl-2-diphenylmethylcyclohexyl] 1,2,4,5-benzenetetracarboxylate	Pentane	25	—	+14.3	62
(−)-Tetrakis-[(1*R*,2*S*,5*R*)-2-(dicyclohexylmethyl)-5-methylcyclohexyl] 1,2,4,5-benzenetetracarboxylate	Pentane	−86	—	−14.8	62
Tetrakis-(−)-(1,2:5,6-di-*O*-isopropylidene-α-D-glucofranyl) 1,2,4,5-benzenetetracarboxylate	Pentane	25	—	−5.5	109
Tetrakis-(−)-(1,2:5,6-di-*O*-isopropylidene-α-D-glucofranyl) 1,2,4,5-benzenetetracarboxylate	Pentane	−78	—	−40.4	109
Tetrakis-(−)-(1,2:5,6-di-*O*-isopropylidene-α-D-glucofranyl) 1,2,4,5-benzenetetracarboxylate	Methylcyclohexane	25	—	−5.7	109
Tetrakis-(−)-(1,2:5,6-di-*O*-isopropylidene-α-D-glucofranyl) 1,2,4,5-benzenetetracarboxylate	Methylcyclohexane	−78	—	−57.2	109
Tetrakis-(−)-(1,2:5,6-di-*O*-isopropylidene-α-D-glucofranyl) 1,2,4,5-benzenetetracarboxylate	Diethyl ether	25	—	−5.5	109
Tetrakis-(−)-(1,2:5,6-di-*O*-isopropylidene-α-D-glucofranyl) 1,2,4,5-benzenetetracarboxylate	Diethyl ether	−78	—	+50.3	109
Tetrakis-(−)-(1,2:5,6-di-*O*-isopropylidene-α-D-glucofranyl) 1,2,4,5-benzenetetracarboxylate	Tetrahydrofuran	25	—	−0.2	109
Tetrakis-(−)-(1,2:5,6-di-*O*-isopropylidene-α-D-glucofranyl) 1,2,4,5-benzenetetracarboxylate	Tetrahydrofuran	−78	—	+47.6	109
Tetrakis-(−)-(1,2:5,6-di-*O*-isopropylidene-α-D-glucofranyl) 1,2,4,5-benzenetetracarboxylate	Acetonitrile	25	—	+11.3	109
Tetrakis-(−)-(1,2:5,6-di-*O*-isopropylidene-α-D-glucofranyl) 1,2,4,5-benzenetetracarboxylate	Acetonitrile	−40	—	+34.9	109
Tetrakis-(−)-menthyl 1,2,4,5-benzenetetracarboxylate (0.1 MPa)	Pentane	25	0.21	−11.2	106
Tetrakis-(−)-menthyl 1,2,4,5-benzenetetracarboxylate (100 MPa)	Pentane	25	0.32	−3.6	106
Tetrakis-(−)-menthyl 1,2,4,5-benzenetetracarboxylate (200 MPa)	Pentane	25	0.36	+5.7	106
Tetrakis-(−)-menthyl 1,2,4,5-benzenetetracarboxylate (300 MPa)	Pentane	25	0.020	+12.4	106
Tetrakis-(−)-menthyl 1,2,4,5-benzenetetracarboxylate (400 MPa)	Pentane	25	0.050	+17.9	106
Tetrakis-(−)-menthyl 1,2,4,5-benzenetetracarboxylate (0.1 MPa)	Pentane	−9	0.018	−12.3	106
Tetrakis-(−)-menthyl 1,2,4,5-benzenetetracarboxylate (100 MPa)	Pentane	−9	0.032	−15.3	106
(−)-Menthyl benzoate	Pentane	25	0.22	−2.7	100
(−)-Menthyl benzoate	Pentane	−25	—	−3.0	100
Di-(−)-menthyl phthalate	Pentane	25	0.058	+3.8	100
Di-(−)-menthyl phthalate	Pentane	−60	—	+10.3	100
Di-(−)-menthyl terephthalate	Pentane	25	0.22	−6.0	100

TABLE 16.3 Photosensitized Enantiodifferentiating Isomerization of (*Z*)-Cyclooctene (**20Z**) (continued)

Sensitizer	Solvent	Temperature (°C)	*E/Z*	% ee (% op)	Ref.
Di-(−)-menthyl terephthalate	Pentane	−40	0.22	−8.2	100
Benzyl (−)-menthyl ether	Pentane	25	0.015	−1.3	100
Benzyl (−)-menthyl ether	Pentane	−78	0.014	+1.0	100
(−)-1,2-Bis(menthyloxymethyl)benzene	Pentane	25	0.021	+0.5	100
(−)-1,2-Bis(menthyloxymethyl)benzene	Pentane	−78	0.018	−0.4	100
(−)-1,4-Bis(menthyloxymethyl)benzene	Pentane	25	0.013	−1.3	100
(−)-1,4-Bis(menthyloxymethyl)benzene	Pentane	−60	0.008	−0.6	100
(2*R*,5*R*)-Di(methoxymethyl)-pyrrolidine benzamide	Pentane	25	0.10	+0.3	101
Bis-(2*R*,5*R*)-di(methoxymethyl)-pyrrolidine phthalamide	Pentane	25	0.10	+0.5	101
Di-(−)-menthyl phenyl phosphate	Pentane	25	0.112	−0.4	102
Di-(−)-bornyl phenylphosphonate	Pentane	25	0.179	−1.4	102
(−)-Menthyl diphenylphosphinate	Pentane	25	0.143	−0.7	102
(1*R*,2*R*)-(+)-Cyclohexane-1,2-bis(diphenylphosphoramide)	Pentane	25	0.086	+8.3	103
(1*R*,2*R*)-(+)-Cyclohexane-1,2-bis(diphenylphosphoramide)	Pentane	−56	0.090	+20.0	103
(1*R*,2*R*)-(+)-Cyclohexane-1,2-bis(diphenylthiophosphoramide)	Pentane	25	0.086	+10.3	103
(1*R*,2*R*)-(+)-Cyclohexane-1,2-bis(diphenylthiophosphoramide)	Pentane	56	0.090	+28.0	103
(*R*)-1-Methylheptyl benzoate, immobilized in NaY zeolite	Pentane slurry	25	0.021	−4.5	113
Di-(*R*)-1-methylheptyl phthalate, immobilized in NaY zeolite	Pentane slurry	25	0.057	−2.5	113
Di-(*R*)-1-methylheptyl terephthalate, immobilized in NaY zeolite	Pentane slurry	25	0.049	−3.5	113
ct-DNA	Water	5	0.008	−15.2	114
ct-DNA	Water	25	0.014	−9.2	114
Thymidine	Water	25	0.66	+5.2	114
Uridine	Water	25	0.33	+3.1	114
β-Cyclodextrin (1:1 complex)	Solid	25	0.47	+0.24	110
β-Cyclodextrin 6-*O*-benzoate (host occupancy: 17%)	Methanol	25	0.22	−0.9	112
β–Cyclodextrin 6-*O*-benzoate (host occupancy: 42%)	75% Aq. methanol	25	0.57	−3.1	112
β-Cyclodextrin 6-*O*-benzoate (host occupancy: 73%)	50% Aq. methanol	25	0.76	−5.0	112
β-Cyclodextrin 6-*O*-benzoate (host occupancy: 91%)	25% Aq. methanol	25	0.06	−10.7	111
β–Cyclodextrin 6-*O*-benzoate (host occupancy: 91%)	25% Aq. methanol	25	0.58	−4.0	112
β-Cyclodextrin 6-*O*-benzoate (host occupancy: 98%)	Water	25	0.14	−5.7	112
α-Cyclodextrin 6-*O*-benzoate	50% Aq. methanol	25	0.73	+1.7	112
γ-Cyclodextrin 6-*O*-benzoate	50% Aq. methanol	25	0.54	+3.0	112
β-Cyclodextrin 6-*O*-(2′-methoxycarbonyl)benzoate (host occupancy: 33%)	50% Aq. methanol	55	0.44	+12.0	112
β-Cyclodextrin 6-*O*-(2′-methoxycarbonyl)benzoate (host occupancy: 60%)	50% Aq. methanol	25	0.42	+17.5	112
β-Cyclodextrin 6-*O*-(2′-methoxycarbonyl)benzoate (host occupancy: 98%)	50% Aq. methanol	−40	0.29	+23.5	112

In the presence of (+)-ephedrine, (*E*)-1-acetylcyclooctene (**50d**) photoisomerizes to enantiomeric (*Z*)-isomer, which is trapped by cyclopentadiene to give a Dies-Alder adduct in 22 %ee.[65] A stable sila analogue of (*E*)-cycloheptene (**79E**) was prepared,[119] and its enantiomers were resolved by chiral HPLC.[120] However, direct and sensitized asymmetric photoisomerizations afford the (*E*)-isomer in low chemical and optical yields.[121] Direct irradiation at >280 nm of doubly bridged (*Z*)-D_{2h}-1(10)-bicyclo[8.8.0]octadecen-2-one (**80Z**) in diethyl (+)-tartrate as solvent affords the levorotatory (*E*)-isomer with an *E/Z* ratio of 7.[122,123]

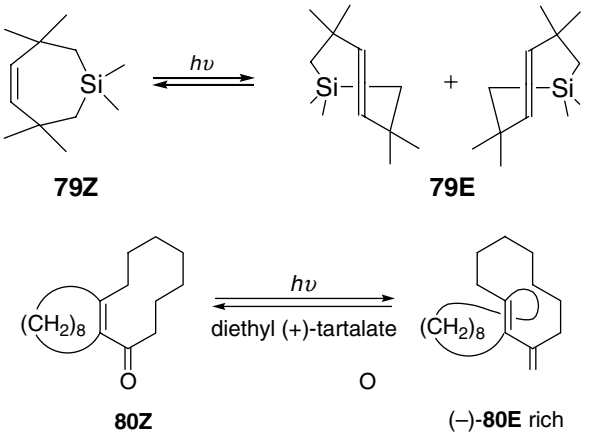

Cyclohexene and Cycloheptene

In spite of the thermal instability of the (*E*)-isomers, the enantiodifferentiating photoisomerization of smaller-sized cycloalkenes has been investigated to some extent. Photosensitization of (*Z*)-cyclohexene (**13Z**) with chiral benzene(poly)carboxylates affords *trans-anti-trans*-, *cis-trans*-, and *cis-anti-cis*-[2 + 2]-cyclodimers (**16**). Interestingly, only the *trans-anti-trans* product is optically active, and the *ee* reaches up to 68% *ee*, for which the enantiodifferentiating photoisomerization of **13Z** to optically active (*E*)-isomer **13E** and the subsequent stereospecific concerted addition to **13Z** are responsible. In contrast, the *cis-trans* photoadduct is formed through the stepwise cyclization via a biradical intermediate, losing the original chiral information in **13E**.[36]

Enantiodifferentiating photoisomerization of (*Z*)-cycloheptene (**18Z**) was also studied in detail.[124] Low-temperature irradiation of **18Z** in the presence of a chiral aromatic ester as sensitizer gives the labile (*E*)-isomer **18E**, which is trapped by 1,3-diphenylisobenzofuran or oxidized by osmium tetraoxide to afford adduct **81** or diol **82**, respectively. The *ee* of **18E** can be evaluated from that of the adduct. The photostationary state is reached after 25–40 min irradiation, giving an *E/Z* ratio of ca. 0.1, which is comparable to or slightly lower than that obtained for the singlet-sensitized photoisomerization of cyclooctene **20Z**. The *ee* of **18E**, which is higher than that of **20E** obtained under the comparable conditions, is sensitive to the solvent polarity and reaction temperature. Upon sensitization with tetra-(–)-bornyl 1,2,4,5-benzenetetracarboxylate in hexane at –80°C, **18E** is obtained in 77% *ee*, the highest value ever obtained for enantiodifferentiating photosensitization.

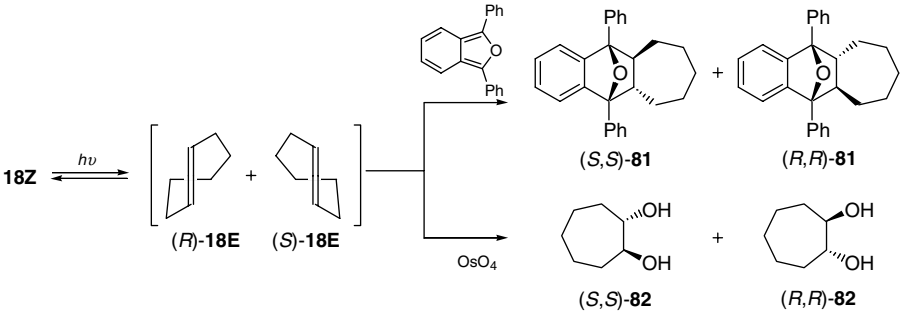

16.6 Conclusions

As can be recognized from the above discussion, the photochemistry of cycloalkenes is not a simple extension or subcategory of the photochemistry of acyclic alkenes, but rather constitutes a distinct new area that provides a variety of mechanistic insights, novel reactivities, and useful synthetic methodologies. Direct irradiation of (*Z*)-cycloalkenes, mostly in or near the vacuum UV region, leads to a broad spectrum of photoreactions, including valence and geometrical isomerization, rearrangement, cyclization, and decomposition reactions through the π,π^* and π,R(3s) excited states. Both singlet and triplet sensitizations are useful strategies for effecting the photoisomerization of cycloalkenes. However, the singlet manifold is more advantageous in obtaining high photostationary-state *E/Z* ratios, particularly when the *trans* isomer is highly constrained. Environmental factors, such as temperature, pressure, solvent, and phase, can affect the photostationary-state *E/Z* ratio in the sensitized photoisomerization of cyclooctene.

Recent studies on enantiodifferentiating photoisomerization reveal that the photosensitization of C_6C_8 (*Z*)-cycloalkenes with optically active aromatic esters affords chiral (*E*)-cycloalkenes in good to excellent *ee*s. The mechanism involves enantiodifferentiating rotational relaxation within the exciplex intermediate formed from the excited singlet state of chiral sensitizer and prochiral substrate. The exciplex structure and hence the stereochemical outcome are very sensitive not only to the *internal* factors, such as sensitizer energy and structure, but also to the *external* entropy-related factors such as temperature, pressure, and solvent. This leads to a novel idea of multidimensional control of product chirality by several environmental factors. The asymmetric photosensitization can be applied to the photochemical asymmetric synthesis and also be used as a powerful tool for exploiting the reaction mechanisms in the excited-state chemistry.

References

1. Kropp, P.J., Photochemistry of alkenes in solution, *Pure Appl. Chem.,* 24, 585–598, 1970.
2. Saltiel, J. and Charlton, J.L., *Cis–trans* isomerization of olefins, in *Rearrangements in Ground and Excited States,* de Mayo, P., Ed., Academic Press, New York, 1980, pp. 25–89.
3. Collin, G.J. and De Mare, G.R., Ring contraction of cyclic olefins: chemical processes specific to electronically excited states? *J. Photochem.,* 38, 205–215, 1987.
4. Kropp, P.J., Photorearrangement and fragmentation of alkenes, in *CRC Handbook of Organic Photochemistry and Photobiology,* Horspool, W.M. and Song, P.-S., Eds., CRC Press, Boca Raton, FL, 1995, pp. 16–28.
5. Horspool, W.M., Photochemistry of olefins, acetylenes and related compounds, *Photochemistry* 2, 427–488, 1971.
6. Saltiel, J., D′Agostino, J., Megarity, D.E., Metts, L., Neuberger, K.R., Wrighton, M., and Zafiriou, O.C., The *cistrans* photoisomerization of olefins, *Org. Photochem.,* 3, 1–113, 1973.
7. Kropp, P.J., Photobehavior of alkenes in solution, *Mol. Photochem.,* 9, 39–65, 1978–1979.
8. Kropp, P.J., Photochemistry of alkenes in solution, *Org. Photochem.,* 4, 1–142, 1979.
9. Steinmetz, M.G., Photochemistry with short UV light, *Org. Photochem.,* 8, 67–158, 1987.
10. Langer, K. and Mattay, J., Copper(I)-catalyzed intra- and intermolecular photocycloaddition reaction of alkenes, in *CRC Handbook of Organic Photochemistry and Photobiology,* Horspool, W.M. and Song, P.-S., Eds., CRC Press, Boca Raton, FL, 1995, pp. 105–114.
11. Saltiel, J., Sears, D.F., Jr., Ko, D.-H., and Park, K.-M., *Cis–trans* isomerization of alkenes, in *CRC Handbook of Organic Photochemistry and Photobiology,* Horspool, W.M. and Song, P.-S., Eds., CRC Press, Inc., Boca Raton, FL, 1995, pp. 3–15.
12. Marshall, J.A., Photochemically induced ionic reactions of cycloalkenes, *Science,* 170, 137–141, 1970.
13. Kropp, P.J., Photoreactions of alkenes in protic media, in *CRC Handbook of Organic Photochemistry and Photobiology,* Horspool, W.M. and Song, P.-S., Eds., CRC Press, Boca Raton, FL, 1995, pp. 105–114.
14. *Photochirogenesis, 2001: 1st International Symposium on Asymmetric Photochemistry (ISAP)*, Osaka, Sept. 4–6, 2001.

15. Padwa, A., Chou, C.S., Rosenthal, R.J., and Terry, L.W., Photochemistry of cyclopropene derivatives. Intramolecular hydrogen transfer reaction of some 1-(alkyl-substituted)cyclopropenes, *J. Org. Chem.,* 53, 4193–4201, 1988.
16. Zimmerman, H.E. and Bunce, R.A., Cyclopropene photochemistry. Part 4. Mechanistic and exploratory organic photochemistry. Part 134, *J. Org. Chem.,* 47, 3377–3396, 1982.
17. Leigh, W.J., Postigo, J.A., and Venneri, P.C., Orbital symmetry and the photochemical ring opening of cyclobutene, *J. Am. Chem. Soc.,* 117, 7826–7827, 1995.
18. Leigh, W.J. and Postigo, J.A., Cyclobutene photochemistry. Steric effects on the photochemical ring opening of alkylcyclobutenes, *J. Am. Chem. Soc.,* 117, 1688–1694, 1995.
19. Lawless, M.K., Wickham, S.D., and Mathies, R.A., Direct investigation of the photochemical ring-opening dynamics of cyclobutene with resonance Raman intensities, *J. Am. Chem. Soc.,* 116, 1593–1594, 1994.
20. Leigh, W.J., 1992 Merck–Frosst award lecture: orbital symmetry and the photochemistry of cyclobutene, *Can. J. Chem.,* 71, 147–155, 1993.
21. Inoue, Y., Mukai, T., and Hakushi, T., Direct photolysis at 185 nm of cyclopentene and 2-norbornene. A novel reaction channel for π,π^* excited singlet alkene, *Chem. Lett.,* 1045–1048, 1982.
22. Adam, W. and Oppenlaender, T., The 185-nm photochemistry of bicyclo[2.1.0]pentane and cyclopentene, *J. Am. Chem. Soc.,* 107, 3924–3928, 1985.
23. Kropp, P.J., Snyder, J.J., Rawlings, P.C., and Fravel, H.G., Jr., Photochemistry of cycloalkenes. 9. Photodimerization of cyclohexene, *J. Org. Chem.,* 45, 4471–4474, 1980.
24. Inoue, Y., Takamuku, S., and Sakurai, H., Direct photolysis of cycloalkenes, *J. Chem. Soc., Perkin Trans. 2,* 1635–1642, 1977.
25. Ziegler, V.K. and Wilms, H., Über vielgliedrige Ringsysteme XIII: Ungesätige Kohlenwasserstoff-8-ring, *Justus Liebigs Ann. Chem.,* 567, 143, 1950.
26. 26. Cope, A.C., Pike, R.A., and Spencer, C.F., Cyclic polyolefins. XXVII. *cis*- and *trans*-Cyclooctene from *N,N*-dimethylcyclooctylamine, *J. Am. Chem. Soc.,* 75, 3212–3215, 1953.
27. Kropp, P.J., Mason, J.D. and Smith, G.F.H., Photochemistry of alkenes. 9. Medium-sized cycloalkenes, *Can. J. Chem.,* 63, 1845–1849, 1985.
28. Inoue, Y., Takamuku, S., and Sakurai, H., An anomalously high *trans:cis* photostationary ratio on the direct photoisomerization of cyclo-octene, *J. Chem. Soc., Chem. Commun.,* 423–424, 1976.
29. Inoue, Y., Takamuku, S., and Sakurai, H., Direct *cis–trans* photoisomerization of cyclooctene. A convenient method for preparing *trans*-cyclooctene, *Synthesis,* 111, 1977.
30. Inoue, Y., Takamuku, S., Kunitomi, Y., and Sakurai, H., Singlet photosensitization of simple alkenes. Part 1. *Cis–trans* photoisomerization of cyclooctene sensitized by aromatic esters, *J. Chem. Soc., Perkin Trans. 2,* 1672–1677, 1980.
31. Inoue, Y., Takamuku, S., and Sakurai, H., Direct and sensitized *cis–trans* photoisomerization of cyclooctene. Effects of spin multiplicity and vibrational activation of excited states on the photostationary *trans/cis* ratio*, J. Phys. Chem.,* 81, 7–11, 1977.
32. Srinivasan, R. and Brown, K.H., Organic photochemistry with high energy (6.7 eV) photons: cis↔ trans isomerism in cyclooctene, *J. Am. Chem. Soc.,* 100, 2589–2590, 1978.
33. Schuchmann, H.P., von Sonntag, C., and Srinivasan, R., Quantum yields in the photolysis of *cis*-cyclooctene at 185 nm, *J. Photochem.,* 15, 159–162, 1981.
34. Inoue, Y., Takamuku, S., and Sakurai, H., Vapor-phase photolysis of *cis*-cyclononene, *Bull. Chem. Soc. Jpn.,* 49, 1147–1148, 1976.
35. Haufe, G., Tubergen, M.W., and Kropp, P.J., Photocyclization of cyclononene and cycloundecene, *J. Org. Chem.,* 56, 4292–4295, 1991.
36. Asaoka, S., Horiguchi, H., Wada, T. ,and Inoue, Y., Enantiodifferentiating photocyclodimerization of cyclohexene sensitized by chiral benzenecarboxylates, *J. Chem. Soc., Perkin Trans. 2,* 737–747, 2000.
37. Kropp, P.J. and Krauss, H.J., Photochemistry of cycloalkenes. III. Ionic behavior in protic media and isomerization in aromatic hydrocarbon media, *J. Am. Chem. Soc.,* 89, 5199–5208, 1967.

38. Kropp, P.J., Photochemistry of cycloalkenes. VII. Limonene, *J. Org. Chem.,* 35, 2435–2436, 1970.
39. Tise, F.P. and Kropp, P.J., Photoprotonation of cycloalkenes: limonene to *p*-menth-8-en-1-yl methyl ether, *Org. Synth.,* 61, 112–116, 1983.
40. Kim, D.S., Shim, S.C., Wada, T., and Inoue, Y., Highly diastereoselective photoaddition of methanol to limonene, *Tetrahedron Lett.,* 42, 4341–4344, 2001.
41. Shim, S.C., Kim, D.S., Yoo, D.J., Wada, T., and Inoue, Y., Diastereoselectivity control in photosensitized addition of methanol to (*R*)-(+)-limonene, *J. Org. Chem.,* 67, 5718–5726, 2002.
42. Kropp, P.J., Photochemistry of cycloalkenes. V. Effects of ring size and substitution, *J. Am. Chem. Soc.,* 91, 5783–5791, 1969.
43. Dauben, W.G., Van Riel, H.C.H.A., Robbins, J.D., and Wagner, G.J., Photochemistry of *cis*-1-phenylcyclohexene. Proof of involvement of *trans* isomer in reaction processes, *J. Am. Chem. Soc.,* 101, 6383–6389, 1979.
44. Dauben, W.G., Van Riel, H.C.H.A., Hauw, C., Leroy, F., Joussot-Dubien, J., and Bonneau, R., Photochemical formation of *trans*-1-phenylcyclohexene. Chemical proof of structure, *J. Am. Chem. Soc.,* 101, 1901–1903, 1979.
45. Rosenberg, H.M., The photolysis of 1-phenylcyclohexene, *J. Org. Chem.,* 37, 141–142, 1972.
46. Zimmerman, H.E., Kamm, K.S., and Werthemann, D.P., Mechanisms of electron demotion. Direct measurement of internal conversion and intersystem crossing rates. Mechanistic organic photochemistry, *J. Am. Chem. Soc.,* 97, 3718–3725, 1975.
47. Bonneau, R., Joussot-Dubien, J., Salem, L., and Yarwood, A.J., A *trans* cyclohexene, *J. Am. Chem. Soc.,* 98, 4329–4330, 1976.
48. Caldwell, R.A., Misawa, H., Healy, E.F., and Dewar, M.J.S., An unusually large secondary deuterium isotope effect. Thermal *trans–cis* isomerization of *trans*-1-phenylcyclohexene, *J. Am. Chem. Soc.,*109, 6869–6870, 1987.
49. Squillacote, M., Bergman, A., and De Felippis, J., *Trans*-cycloheptene: spectral characterization and dynamic behavior, *Tetrahedron Lett.,* 30, 6805–6808, 1989.
50. Inoue, Y., Ueoka, T., Kuroda, T., and Hakushi, T., *trans*-Cycloheptene. Photochemical generation and thermal *trans–cis* isomerization, *J. Chem. Soc., Chem. Commun.,* 1031–1033, 1981.
51. Inoue, Y., Ueoka, T., Kuroda, T., and Hakushi, T., Singlet photosensitization of simple alkenes. Part 4. *cis–trans* Photoisomerization of cycloheptene sensitized by aromatic esters. Some aspects of the chemistry of *trans*-cycloheptene, *J. Chem. Soc., Perkin Trans. 2,* 983–988, 1983.
52. Bonneau, R., Joussot-Dubien, J., Yarwood, J., and Pereyre, J., Spectre electronique de la forme "*trans* du phenyl-1 cycloheptene, *Tetrahedron Lett.,* 235–238, 1977.
53. Gibson, T.W., Majeti, S., and Barnett, B.L., Photochemistry of esters. II. Effects of ring size on the photochemical behavior of α,β–unsaturated esters, *Tetrahedron Lett.,* 4801–4802, 1976.
54. Bryce-Smith, D., Gilbert, A., and Orger, B.H., Photochemical 1,3-cycloaddition of olefins to aromatic compounds, *J. Chem. Soc., Chem. Commun.,* 512–514, 1966.
55. Bryce-Smith, D., Photoaddition and photoisomerization reactions of the benzene ring, *Pure Appl. Chem.,* 16, 47–63, 1968.
56. Bryce-Smith, D., Photoaddition to the benzene ring, *Pure Appl. Chem.,* 34, 193–212, 1973.
57. Swenton, J.S., Photoisomerization of *cis*-cyclooctene to *trans*-cyclooctene, *J. Org. Chem.,* 34, 3217–3218, 1969.
58. Inoue, Y., K]obata, T., and Hakushi, T., Reinvestigation of triplet-sensitized *cis–trans* photoisomerization of cyclooctene. Alkene-concentration and sensitizer-E_T dependence of photostationary *trans/cis* ratio, *J. Phys. Chem.,* 89, 1973–1976, 1985.
59. Inoue, Y., Yamasaki, N., Tai, A., Daino, Y., Yamada, T., and Hakushi, T., The temperature- and viscosity-dependent photostationary *E/Z* ratio in triplet-sensitized photoisomerization of cyclooctene, *J. Chem. Soc., Perkin Trans. 2,* 1389–1394, 1990.
60. Yamasaki, N., Inoue, Y., Yokoyama, T., and Tai, A., High photostationary state *trans/cis* ratios upon aromatic ester-sensitized photoisomerization of cyclooctene, *J. Photochem. Photobiol. A: Chem.,* 48, 465–467, 1989.

61. Inoue, Y., Yamada, T., Daino, Y., Kobata, T., Yamasaki, N., Tai, A., and Hakushi, T., Temperature-dependent photostationary *trans/cis* ratio in photosensitized isomerization of cyclooctene, *Chem. Lett.,* 1933–1934, 1989.
62. Inoue, Y., Yamasaki, N., Yokoyama, T., and Tai, A., Highly enantiodifferentiating photoisomerization of cyclooctene by congested and/or triplex-forming chiral sensitizers, *J. Org. Chem.,* 58, 1011–1018, 1993.
63. Tsuneishi, H., Inoue, Y., Hakushi, T., and Tai, A., Direct and sensitized geometrical photoisomerization of 1-methylcyclooctene, *J. Chem. Soc., Perkin Trans. 2,* 457–462, 1993.
64. Yokoyama, K., Kato, M., and Noyori, R., Photo-induced cycloaddition of 1-nitrocyclooctene and cyclopentadiene, *Bull. Chem. Soc. Jpn.,* 50, 2201–2202, 1977.
65. Henin, F., Muzart, J., Pete, J.P. and Rau, H., Asymmetric catalysis: kinetic resolution of the photochemically-produced *trans*-1-acetylcyclooctene, *Tetrahedron Lett.,* 31, 1015–1016, 1990.
66. Nozaki, H., Nishikawa, Y., Kawanisi, M., and Noyori, R., The *cis–trans* isomerization of twelve-membered cyclic olefins, *Tetrahedron,* 23, 2173–2179, 1967.
67. Dauben, W.G., Poulter, C.D. and Suter, C., Photoisomerizations of *cis*- and *trans*-3-methylenecyclodecene, *J. Am. Chem. Soc.,* 92, 7408–7412, 1970.
68. Nakazaki, M., Yamamoto, K., and Yanagi, J., *trans* Doubly-bridged ethylene. Preparation of (±)-*trans*-bicyclo[10.8.0]eicos-1(12)-ene, *J. Chem. Soc., Chem. Commun.,* 346347, 1977.
69. Nakazaki, M., Yamamoto, K., and Yanagi, J., Synthesis of *trans* doubly bridged ethylenes. (±)-C*2*-Bicyclo[10.8.0]eicos-1(12)-ene and (±)-D*2*-bicyclo[8.8.0]octadec-1(10)-ene, *J. Am. Chem. Soc.,* 101, 147151, 1977.
70. Nebe, W.J. and Fonken, G.J., Photolysis of *cis,cis*-1,3-cyclooctadiene, *J. Am. Chem. Soc.,* 91, 1249–1251, 1969.
71. Inoue, Y., Daino, Y., Hagiwara, S., Nakamura, H., and Hakushi, T., Direct photolysis at 185–254 nm of cycloocta-1,3-diene and cyclohepta-1,3-diene. Wavelength-independent photobehavior, *J. Chem. Soc., Chem. Commun.,* 804–805, 1985.
72. Inoue, Y., Hagiwara, S., Daino, Y., and Hakushi, T., *cis,trans*-Cyclohepta-1,3-diene as a transient intermediate in the photocyclization of *cis,cis*-cyclohepta-1,3-diene, *J. Chem. Soc., Chem. Commun.,* 1307–1309, 1985.
73. Daino, Y., Hagiwara, S., Hakushi, T., Inoue, Y., and Tai, A., Photochemistry of cyclohepta-1,3-diene and cyclohepta-1,3,5-triene. Photochemical formation and chemical reactivity of the strained *trans*-isomer, *J. Chem. Soc., Perkin Trans. 2,* 275–282, 1989.
74. Goto, S., Takamuku, S., Sakurai, H., Inoue, Y., and Hakushi, T., Singlet photosensitization of simple alkenes. Part 2. Photochemical transformation of cyclo-octa-1,5-dienes sensitized by aromatic ester, *J. Chem. Soc., Perkin Trans. 2,* 1678–1682, 1980.
75. Eaton, P.E. and Lin, K., *trans*-2-Cyclooctenone, *J. Am. Chem. Soc.,* 86, 2087–2088, 1964.
76. Corey, E.J., Tada, M., LaMahieu, R., and Libit, L., *trans*-2-Cycloheptenone, *J. Am. Chem. Soc.,* 87, 2051–2052, 1965.
77. Eaton, P.E. and Lin, K., *trans*-2-Cycloheptenone, *J. Am. Chem. Soc.,* 87, 2052–2054, 1965.
78. Bonneau, R., de Violet, P.F., and Joussot-Dubien, J., *trans*-Cycloheptenone: a flash photolytic study of the reactive intermediate in the photochemistry of 2-cycloheptenone, *Nouv. J. Chim.,* 1, 31–34, 1976.
79. Noyori, R. and Kato, M., Photo-induced addition of protic solvents to cycloalkenones. Evidence for the ground-state *trans* isomers as chemically reactive intermediates, *Bull. Chem. Soc. Jpn.,* 47, 1460–1466, 1974.
80. Hart, H. and Dunkelblum, E., Stereochemistry of the photoinduced and Michael addition of methanol to seven- and eight-membered 2-cycloalkenones, *J. Am. Chem. Soc.,* 100, 5141–5147, 1978.
81. Salomon, R.G., Folting, K., Streib, W.E. and Kochi, J.K., Copper(I) catalysis in photocycloadditions. II. Cyclopentene, cyclohexene and cycloheptene, *J. Am. Chem. Soc.,* 96, 1145–1152, 1974.
82. Deyrup, J.A. and Betkouski, M.F., Alkene isomerization. Improved one-step synthesis of *trans*-cyclooctene, *J. Org. Chem.,* 37, 3561–3562, 1972.

83. Evers, J.T.M. and Mackor, A., Photocatalysis III. Photochemical isomerization of cyclohexenes and cycloheptene in the presence of copper(I) trifluoromethanesulfonate. Identification and acid-catalyzed isomerisation of the products, *Tetrahedron Lett.,* 2321–2324, 1978.
84. Evers, J.T.M. and Mackor, A., Photocatalysis II. Photochemical cycloadditions of cyclohexenes and cycloheptene with conjugated dienes catalyzed by copper(I) trifluoromethane sulphonate, *Tetrahedron Lett.,* 2317–2320, 1978.
85. Evers, J.T.M. and Mackor, A., Photocatalysis IV. Preparation and characterization of a stable copper(I) triflate *trans*-cycloheptene complex, *Recl. Trav. Chim. Pays-Bas,* 98, 423–424, 1979.
86. de Mare, G.R., Strausz, O.P., and Gunning, H.E., The Hg $6(^3P_1)$ photosensitized decomposition of cyclohexene vapor, *Can. J. Chem.,* 43, 1329–1337, 1965.
87. Gibbons, W.A., Allen, W.F., and Gunning, H.E., Ring contraction in the mercury-photosensitized decomposition of cyclopentene, *Can. J. Chem.,* 40, 568–569, 1962.
88. Strickland, A.D. and Caldwell, R.A., Thermochemistry of strained cycloalkenes: experimental and computational studies, *J. Phys. Chem.,* 97, 13394–13402, 1993.
89. Cope, A.C., Ganellin, C.R., Johnson, H.W., Jr., Van Auken, T.V., and Winkler, H.J.S., Molecular asymmetry of olefins. I. Resolution of *trans*-cyclooctene, *J. Am. Chem. Soc.,* 85, 3276–3279, 1963.
90. Corey, E.J. and Shulman, J.I., The direct synthesis of optically active *trans*-cyclooctene. Optically active *trans*-bicyclo[6.1.0]nonane, *Tetrahedron Lett.,* 3655–3658, 1968.
91. Corey, E.J., Carey, F.A., and Winter, R.A.E., Stereospecific syntheses of olefins from 1,2-thionocarbonates and 1,2-trithiocarbonates. *trans*-Cycloheptene, *J. Am. Chem. Soc.,* 87, 934–935, 1965.
92. Mason, M.G. and Schnepp, O., Absorption and circular dichroism spectra of ethylenic chromophores-*trans*-cyclooctene, α- and β-pinene, *J. Chem. Phys.,* 59, 1092–1098, 1973.
93. Inoue, Y., Kunitomi, Y., Takamuku, S., and Sakurai, H., Asymmetric *cis–trans* photoisomerization of cyclooctene sensitized by chiral aromatic esters, *J. Chem. Soc., Chem. Commun.,* 1024–1025, 1978.
94. Rau, H., Asymmetric photochemistry in solution, *Chem. Rev.,* 83, 535–547, 1983.
95. Inoue, Y., Asymmetric photochemical reactions in solution, *Chem. Rev.,* 92, 741–770, 1992.
96. Inoue, Y., Asymmetric synthesis through photosensitization: state of the art, *J. Synth. Org. Chem. Jpn.,* 53, 348–357, 1995.
97. Everitt, S.R.L. and Inoue, Y., Asymmetric photochemical reactions in solution, in *Organic Molecular Photochemistry,* Ramamurthy, V. and Schanze, K.S., Marcel Dekker, New York, 1999, pp. 71–130.
98. Inoue, Y., Wada, T., Asaoka, S., Sato, H., and Pete, J.-P., Photochirogenesis: multidimensional control of asymmetric photochemistry, *J. Chem. Soc., Chem. Commun.,* 251–259, 2000.
99. Inoue, Y., Yamasaki, N., Yokoyama, T., and Tai, A., Enantiodifferentiating *Z–E* photoisomerization of cyclooctene sensitized by chiral polyalkyl benzenepolycarboxylates, *J. Org. Chem.,* 57, 1332–1345, 1992.
100. Tsuneishi, H., Hakushi, T., and Inoue, Y., Singlet- versus triplet-sensitized enantiodifferentiating photoisomerization of cyclooctene: remarkable effects on spin multiplicity upon optical yield, *J. Chem. Soc., Perkin Trans. 2,* 1601–1605, 1996.
101. Shi, M. and Inoue, Y., Enantiodifferentiating photoisomerization of (*Z*)-cyclooctene and (*Z,Z*)-cycloocta-1,3-diene sensitized by chiral aromatic amides, *J. Chem. Soc., Perkin Trans. 2,* 1725–1729, 1998.
102. Shi, M. and Inoue, Y., Geometrical photoisomerization of (*Z*)-cyclooctene sensitized by aromatic phosphate, phosphonate, phosphinate, phosphine oxide and chiral phosphoryl esters, *J. Chem. Soc., Perkin Trans. 2,* 2421–2428, 1998.
103. Shi, M. and Inoue, Y., Enantiodifferentiating photoisomerization of (*Z*)-cyclooctene sensitized by chiral C_2-symmetric phosphoramide, *Aust. J. Chem.,* 54, 113–115, 2001.
104. Inoue, Y., Yokoyama, T., Yamasaki, N., and Tai, A., An optical yield that increases with temperature in a photochemically induced enantiomeric isomerization, *Nature,* 341, 225–226, 1989.
105. Inoue, Y., Yokoyama, T., Yamasaki, N., and Tai, A., Temperature switching of product chirality upon photosensitized enantiodifferentiating *cis–trans* isomerization of cyclooctene, *J. Am. Chem. Soc.,* 111, 6480–6482, 1989.

106. Inoue, Y., Matsuyama, E., and Wada, T., Pressure and temperature control of product chirality in asymmetric photochemistry. Enantiodifferentiating photoisomerization of cyclooctene sensitized by chiral benzenepolycarboxylates, *J. Am. Chem. Soc.,* 120, 10687–10696, 1998.
107. Raupach, E., Rikken, G.L.J.A., Train, C., and Malezieux, B., Modeling of magneto-chiral enantioselective photochemistry, *Chem. Phys.,* 261, 373–380, 2000.
108. Rikken, G.L.J A. and Raupach, E., Enantioselective magnetochiral photochemistry, *Nature,* 405, 932–935, 2000.
109. Inoue, Y., Ikeda, H., Kaneda, M., Sumimura, T., Everitt, S.R.L., and Wada, T., Entropy-controlled asymmetric photochemistry: switching of product chirality by solvent, *J. Am. Chem. Soc.,* 122, 406–407, 2000.
110. Inoue, Y., Kosaka, S., Matsumoto, K., Tsuneishi, H., Hakushi, T., Tai, A., Nakagawa, K., and Tong, L.-H., Vacuum UV photochemistry in cyclodextrin cavities. Solid state *Z-E* photoisomerization of a cyclooctene-β-cyclodextrin inclusion complex, *J. Photochem. Photobiol. A: Chem.,* **71**, 61–64, 1993.
111. Inoue, Y., Dong, F., Yamamoto, K., Tong, L.-H., Tsuneishi, H., Hakushi, T., and Tai, A., Inclusion-enhanced optical yield and *E/Z* ratio in enantiodifferentiating sensitized by β-cyclodextrin monobenzoate, *J. Am. Chem. Soc.,* 117, 11033–11034, 1995.
112. Inoue, Y., Wada, T., Sugahara, N., Yamamoto, K., Kimura, K., Tong, L.-H., Gao, X.-M., Hou, Z.-J., and Liu, Y., Supramolecular photochirogenesis. 2. Enantiodifferentiating photoisomerization of cyclooctene included and sensitized by 6-*O*-modified cyclodextrins, *J. Org. Chem.,* 65, 8041–8050, 2000.
113. Wada, T., Shikimi, M., Inoue, Y., Lem, G., and Turro, N.J., First photosensitized enantiodifferentiating isomerization by optically active sensitizer immobilized in zeolite supercages, *J. Chem. Soc., Chem. Commun.,* 1864–1865, 2001.
114. Wada, T., Sugahara, N., Kawano, M., and Inoue, Y., First asymmetric photochemistry with nucleosides and DNA: enantiodifferentiating *Z-E* photoisomerization of cyclooctene, *Chem. Lett.,* 1174–1175, 2000.
115. Tsuneishi, H., Hakushi, T., Tai, A., and Inoue, Y., Enantiodifferentiating photoisomerization of 1-methylcyclooct-1-ene sensitized by chiral alkyl benzenecarboxylates: steric effects upon stereodifferentiation, *J. Chem. Soc., Perkin Trans. 2,* 2057–2062, 1995.
116. Inoue, Y., Tsuneishi, H., Hakushi, T., and Tai, A., Optically active (*E,Z*)-1,3-cyclooctadiene: first enantioselective synthesis through asymmetric photosensitization and chiroptical property, *J. Am. Chem. Soc.,* 119, 472–478, 1997.
117. Inoue, T., Matsuyama, K., and Inoue, Y., Diastereodifferentiating *Z-E* photoisomerization of 3-benzoyloxycyclooctene: diastereoselectivity switching controlled by substrate concentration through competitive intra- vs intermolecular photosensitization processes, *J. Am. Chem. Soc.,* 121, 9877–9878, 1999.
118. Matsuyama, K., Inoue, T., and Inoue, Y., Self-sensitized diastereodifferentiating *Z–E* photoisomerization of 3-, 4- and 5-benzoyloxycyclooctenes: intra- versus intermolecular photosensitization, *Synthesis,* 1167–1174, 2001.
119. Krebs, A., Pforr, K.-I., Raffay, W., Thölke, B., König, W.A., Hardt, I., and Boese, R., A stable hetero-*trans*-cyclopentene, *Angew. Chem. Int. Ed. Engl.,* 36, 159160, 1997.
120. Krebs, A.W., Thölke, B., Pforr, K.-I., König, W.A., Scharwächter, K., Grimme, S., Vögtle, F., Sobanski, A., Schramm, J., and Hormes, J., Synthesis of enantiomerically pure (*E*)-1,1,3,3,6,6-hexamethyl-1-sila-4-cycloheptene and its absolute configuration, *Tetrahedron: Asym.,* 10, 3483–3492, 1999.
121. Kaneda, M., Wada, T., Inoue, Y., and Krebs, A.,W., Unpublished data.
122. Nakazaki, M., Yamamoto, K., and Maeda, M., Asymmetric synthesis of an optically active *trans* doubly bridged ethylene, (−)-(*R*)-D_2-Bicyclo[8.8.0]octadec-1(10)-ene, *J. Chem. Soc., Chem. Commun.,* 294–295, 1980.
123. Nakazaki, M., Yamamoto, K., and Maeda, M., Asymmetric synthesis of an optically active *trans* doubly bridged ethylene. (−)-(*R*)-D_2-Bicyclo[8.8.0]octadec-1(10)-ene, *J. Org. Chem.,* 45, 3229–3232, 1980.

124. Hoffmann, R. and Inoue, Y., Trapped optically active (*E*)-cycloheptene generated by enantiodifferentiating *Z–E* photoisomerization of cycloheptene sensitized by chiral aromatic esters, *J. Am. Chem. Soc.,* 121, 10702–10710, 1999.
125. Bischof, P. and Heilbronner, E., Photoelectron spectra of cycloalkenes and cycloalkadienes, *Helv. Chim. Acta,* 53, 1677–1682, 1970.
126. Cope, A.C. and Mehta, A.S., Molecular asymmetry of olefins. II. The absolute configuration of *trans*-cyclooctene, *J. Am. Chem. Soc.,* 86, 5626–5630, 1964.
127. Bloomfield, J.J., McConaghy, J. S., Jr., and Hortmann, A.G., The conrotatory ring opening of *cis*-bicyclo[4.2.0]oct-7-ene to *cis,trans*-1,3-cyclooctadiene, II. A kinetic treatment, *Tetrahedron Lett.,* 3723–3726, 1969.
128. Cope, A.C., Hecht, J.K., Johnson, H.W., Jr., Keller, H., and Winkler, H.J.S., Molecular asymmetry of olefins. V. Resolution of *cis,trans*-1,5-cyclooctadiene, *J. Am. Chem. Soc.,* 88, 761–763, 1966.
129. Inoue, Y., Ueoka, T., and Hakushi, T., A novel oxygen-catalyzed *trans–cis* thermal isomerization of *trans*-cycloheptene, *J. Chem. Soc., Perkin Trans. 2,* 2053–2056, 1984.
130. Brennan, C.M. and Caldwell, R.A., Photoacoustic calorimetry of cycloheptene derivatives. Relaxed triplet energies of 1-phenylcycloheptene and 1,3-cycloheptadiene and the energetics of ground-state *cis–trans* isomerization, *Photochem. Photobiol.,* 53, 165–168, 1991.
131. Eaton, P.E., Photochemical reactions of simple alicyclic enones, *Acc. Chem. Res.,* 1, 50–57, 1968.
132. Steinmetz, M.G., Seguin, K.J., Udayakumar, B.S., and Behnke, J.S., Evidence for a metastable *trans*-cycloalkene intermediate in the photochemistry of 1,1,4,4-tetramethyl-1,4-disilacyclohept-2-ene, *J. Am. Chem. Soc.,* 112, 6601–6608, 1990.
133. Clary, D.C., Lewis, A.A., Morland, D., Murrell, J.N., and Heilbronner, E., Ionization potentials of cycloalkenes, *J. Chem. Soc., Faraday Trans. 2,* 70, 1889–1894, 1974.
134. Hohlneicher, G., Mueller, M., Demmer, M., Lex, J., Penn, J.H., Gan, L.X., and Loesel, P.D., 1,2-Diphenylcycloalkenes: electronic and geometric structures in the gas phase, solution and solid state, *J. Am. Chem. Soc.,* 110, 4483–4494, 1988.
135. Goodman, J.L., Peters, K.S., Misawa, H., and Caldwell, R.A., Use of pulsed time-resolved photoacoustic calorimetry to determine the strain energy of *trans*-1-phenylcyclohexene and the energy of the relaxed 1-phenylcyclohexene triplet, *J. Am. Chem. Soc.,* 108, 6803–6805, 1986.

17

The Photochemical Reactivity of the Norbornadiene–Quadricyclane System

Alexander D. Dubonosov
Rostov State University

Vladimir A. Bren
Rostov State University

Vladimir I. Minkin
Rostov State University

17.1 Introduction

Photochemical valence isomerization involving the intramolecular (2 + 2)-cycloaddition that converts bicyclo[2.2.1]hepta-2,5-diene **1** (norbornadiene, N) to tetracyclo[3.2.0.0.^{2,7}0^{4,6}]heptane **2** (quadricyclane, Q) has been the subject of much investigation from a mechanistic point of view.[1–4] The N/Q system has found diversified applications as an efficient abiotic system for solar energy storage,[5–7] in molecular switching,[8–10] in optoelectronic devices,[11–14] as a data storage material,[15,16] as a photodynamic chemosensor for metal cations,[17,18] as a potential photoresponsive organic magnet,[19–21] and as an energetic binder for solid rocket propellants.[22]

0-8493-1348-1/04/$0.00+$1.50

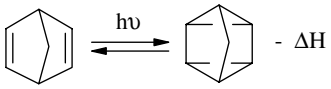

1 **2**

The principal drawback of the N/Q system is a very low (~0.05) quantum yield (**Φ**) of the direct photoconversion **1**→**2**.[6,16] It has been established that the N→Q rearrangement occurs via the triplet state of N.[23,24] Consequently, this reaction can be photoinitiated by various sensitizers (S). Electron-donating and electron-withdrawing substituents attached to one or both double bonds of N can also increase the **Φ** value, providing a long-wavelength shift of the edge of the N absorption (λ_e, $\varepsilon \sim 1$).[25–27] The reverse Q→N reaction is thermally forbidden by the Woodward–Hoffmann rules, but this transformation can be readily accomplished via a radical-cation chain reaction pathway[24] initiated by chemical, electrochemical, or photosensitized single-electron oxidations.[4] The metastable Q structure contains a highly strained cyclobutane and two cyclopropane rings, and the enthalpy of the **2**→**1** isomerization in the pure liquid state has the value of $\Delta H = -89$ kJ mol^{-1}, as obtained from direct calorimetric measurement.[28] Results of other experiments and computed values vary in the range of –81 to –112 kJ mol^{-1}.[3,29,30]

17.2 Photosensitization of the Norbornadiene–Quadricyclane Rearrangement

Two distinct mechanisms are conceivable for the photosensitized N→Q isomerization.[31–35] The first one is characterized by the formation of ground-state adducts of S with N that can be selectively irradiated to release Q:

$$S + N \rightarrow \left[S\text{---}N\right] \xrightarrow{h\nu} S + Q$$

The alternative pathway involves interaction of excited S with ground state N either via formation of excited-state charge-transfer complexes (exciplexes) that collapse to Q:

$$S \xrightarrow{h\nu} {}^*S \rightarrow {}^*\left[S^{\delta-}\text{---}N^{\delta+}\right] \rightarrow S + Q$$

or via triplet–triplet energy transfer:

$$S \xrightarrow{h\nu} {}^1S \rightarrow {}^3S + N \rightarrow S + {}^3N \rightarrow Q.$$

Triplet–Triplet Energy Transfer

As mentioned in the Introduction, triplet photosensitizers can be used to increase efficiency of the **1**→**2** reaction.[2,23,24,34,36] This process is considered to consist of the following stages:

1. Photoexcitation of S into the singlet state: $S \xrightarrow{h\nu} {}^1S$
2. The intersystem crossing: ${}^1S \rightarrow {}^3S$
3. Triplet-triplet energy transfer: ${}^3S + N \rightarrow S + {}^3N$
4. Adiabatic isomerization of N to the triplet state of Q: ${}^3N \rightarrow {}^3Q$
5. Formation of the ground state of quadricyclane: ${}^3Q \rightarrow Q$

The energy levels of the electronic excited states[2,23,37] of N are relatively high, for which reason this mechanism of energy transfer is thermodynamically favorable (exothermic) only when the energy level of ${}^3S$ is higher than that of ${}^3N$, i.e., $E_T > 257$ kJ mol^{-1}, and even a small value of the singlet–triplet splitting of S corresponds to $\lambda_e \leq 400$ nm.[38] Only a small number of sensitizers S meet this condition; the range of sensitizers is mainly limited to carbonyl-containing compounds such as acetophenone, propiophenone,

TABLE 17.1 Quantum Yields of the Isomerization **1**→**2** in Acetonitrile

Sensitizer	E_T, kJ mol^{-1}	$\Phi_{1\rightarrow2}$	Ref.
Acetophenone	309.6	>0.9[a]	34
4,4′-Dimethylbenzophenone	290.1	0.59	43
4-Methylbenzophenone	289.7	0.50	43
Benzophenone	289.7	0.45	43
4-Cyanobenzophenone	280.5	0.33	43
1,2,4,5-Tetracyanobenzene	271.3	0.34[a]	34
Michler's ketone	259.6	0.04	43
2-Naphtaldehyde	249.1	0.06	6, 36
10-Methylacridinone	246.0	0.11[b]	42
2,7-Dibromo-10-methylacridinone	231.0	0.06[b]	42
Benzil	227.3	0.009	43
Benzoquinone	221.9	0.0[a]	34

[a] In CH_2Cl_2.
[b] In DMF.

benzophenone and its derivatives, benzoylpyridines, triphenylene, Michler's ketone, and some others.[34,37,39–43] (Table 17.1). The highest values of Φ for the N/Q transformation were found with acetophenone and benzophenone. This is due to the high values of E_T of these sensitizers, with λ_e equal to 366 and 388 nm, respectively. In the cases of other sensitizers, the classical triplet energy transfer mechanism is coupled with the formation of exciplexes. Formation of the ^{3}N species with a lifetime of about 7 nsec in the presence of triplet acetophenone as sensitizer was detected by photoacoustic calorimetry.[34] By contrast, reaction of N with the triplet benzoquinone does not yield ^{3}N, as no energy transfer was found to occur.

Adducts of Norbornadiene with Sensitizers

Due to the presence of two double bonds in norbornadiene and its derivatives, these compounds readily form π-complexes with transition metal salts and coordination compounds. The latter may serve as photosensitizers S for the N/Q transformation and can also be designated as photocatalysts.[32] Photoexcitation of the stable ground state adducts [S---N], results in the formation of quadricyclanes:

$$\left[\text{S}\text{---}\text{N}\right] \xrightarrow{h\nu} \text{S} + \text{Q}.$$

A suitable metal-containing photosensitizer S should satisfy the following requirements:[44]

1. The metal center in S must be in its low oxidation state with only one coordination site available for binding N in order to avoid undesirable dimerization processes.
2. The [S---N] complex must absorb in the visible region.
3. The compound S must be resistant to oxidative addition reactions and must not catalyze the reverse Q → N reaction.
4. The whole catalytic system must not promote side reactions.

Although many transition metals are capable of forming complexes with N, only univalent copper compounds comply with the above requirements.[31–33,45,46] The initial ligand N and copper salts S (CuX, X = Cl, Br, I, OCOMe) do not absorb light with $\lambda > 300$ nm, whereas their adducts [S---N] display an intense charge-transfer absorption band with $\lambda_e \sim 370$ nm. Irradiation of these complexes by light of $\lambda =$ 313 nm results in the formation of Q as the sole product with reasonably high quantum yields ($\Phi =$ 0.2–0.4).

Photoexcitation ($\lambda = 313$ nm) of the charge-transfer adducts of N with $CuBr(Py)(PPh_3)$ or $Cu[HB(Pz)_3]$ in hexane (Py = pyridine, Pz = 1-pyrazolyl) gives rise to Q with $\Phi = 0.37$–0.65.[47,48] The photorearrangement of the complexes of N with halo(ferrocenyl-diphenylphosphine)copper(I) tetramers

$[CuX(PFcPh_2)]_4$ (X = Cl, Br) under irradiation (λ = 366 nm) in tetrahydrofuran (THF) solutions occurs with lower quantum efficiency ($\Phi \sim 0.01$).[49] With chloro(tertiary phosphine)copper(I) oligomers[32] $[CuCl(PR_3)]_n$ (R = 2-MeC_6H_4, 4-EtC_6H_4Me) as photocatalysts, the N $\rightarrow$ Q transformation (THF, λ = 366 nm) is characterized by quantum yields in the range of 0.11–0.49.

The highest value of $\lambda_e \leq 405$ nm has been achieved in the case of dinuclear complexes of norbornadiene $[Cu_2L_2(\mu\text{-N})]$, $[Cu_2L'_2(\mu\text{-N})]$, $[Cu_2L''_2(\mu\text{-N})]$, and $[Cu_2L'''_2(\mu\text{-N})]$ [L = 2-methyl-8-oxoquinolinato, L′ = 2-methyl-5,7-dichloro-8-oxoquinolinato, L″ = 4-oxoacridinato, L‴ = 2-(2-oxo-3,5-di-*tert*-butylphenyl)benzothiazole)],[31] whose structures were determined by x-ray crystallography. Absorption spectra of these adducts show metal-to-ligand charge-transfer bands in the visible region. Their photoisomerization (λ_{irr} = 405 nm) in methanol solution results in the formation of Q with Φ = 0.029. The **1**$\rightarrow$**2** turnover number (moles of Q produced by a mole of S) of 5000 was obtained. An increase in the temperature of the solution leads to significant enhancement of the quantum yield.

To gain insight into the energy and geometric characteristics of the experimentally studied $[Cu_2(2\text{-methyl-8-oxoquinolinato})_2(\mu\text{-N})]$ system, *ab initio* (the B3LYP hybrid exchange-correlation functional) calculations on the model ground state adduct [Cu(8-oxoquinolinato)N] **3** have been performed.[50]

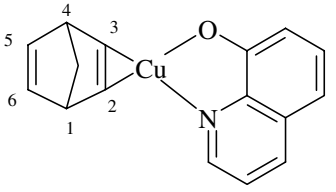

3

The computed C2=C3 distance of 1.409 Å in **3** is strongly elongated compared with 1.339 Å in uncomplexed N. Complexation with S reduces the HOMO-LUMO gap in N due to donation of electron density from the metal center to the π^*-antibonding orbital of N. The decrease in the HOMO-LUMO gap is the main factor that causes narrowing of the gap between the ground and the first excited singlet state of [S---N]. This makes it possible to initiate the **1**$\rightarrow$**2** photoisomerization under irradiation with λ_{irr} = 405 nm.

Complexes of Norbornadiene with Photosensitizers in Their Excited Electronic States

Most metal salts and complexes do not form stable adducts with N, and for a large number of the triplet sensitizers with E_T < 257 kJ mol^{-1}, the energy transfer from ^{3}S to N is thermodynamically unfavorable (endothermic). Another way of promoting **1**$\rightarrow$**2** photoisomerization is to accomplish it in the complexes formed by N with photosensitizers S in their excited states.[24,34,35] Such a process includes the following stages:

1. Photoexcitation of S to the singlet excited state ^{1}S
2. The intersystem crossing: $^1S \rightarrow {}^3S$
3. Formation of the excited-state complexes [^{3}S ---N] (usually of charge-transfer or exciplex nature)
4. The dark reaction that leads to formation of Q in its ground state

Carbonyl-containing compounds or transition metal complexes used as photosensitizers must meet the following requirements:[44]

1. Metal-containing S must be inert towards ligand substitution and must not coordinate with N.
2. S must intensely absorb light in the visible region.
3. The lifetime of the excited state ^{3}S must be long enough for the bimolecular reaction to proceed.
4. S must not promote any reverse or side photoreactions.

Substituted acridinones act by this type of mechanism (E_T = 239–260 kJ mol^{-1}) and absorb in the long-wavelength region (λ_e = 360–420 nm). They bring about the **1**→**2** rearrangement to yield Q with Φ = 0.4–0.7.[42] A number of Cu(I) complexes do not react with N in the ground state and are capable of sensitizing the Q formation. The values of λ_e 330 nm and Φ 0.56–0.88 were achieved for the N → Q transformation in benzene with $Cu[PPh_2Me]_3BH_4$, $Cu[PPh_3]_2BH_4$, and Cu(prophos)BH_4 (prophos = 1,3-bis(diphenylphosphino)propane) as photosensitizers.[51,52]

The use of copper(I)-nitrogen ligand complexes, such as Ph_3PCuXL (X = Cl, Br; L = 2,2′-bipyridine, 1,10-phenantroline, phthalazine, pyridine) enables the **1**→**2** isomerization to occur upon irradiation of the solutions of the components in the spectral region $\lambda > 350$ nm (Φ 0.008–0.011 in THF and 0.03–0.13 in ethanol).[53] With another group of photosensitizers $[Cu(PPh_3)_2(dpk)]NO_3$, $[Cu_2I_2(PPh_3)_2(dpk)]$, $[Cu_4I_4(dpk)_3]$ (dpk = di-2-pyridyl ketone) (Φ 0.17–0.36 in CH_2Cl_2), it is possible to conduct the **1**→**2** photoreaction on exposure to light with wavelengths $\lambda_e \leq 600$ nm.[46]

Some of the compounds S are capable of forming adducts with N in both their excited and ground states. A high quantum yield (Φ = 0.75) for the **1**→**2** conversion was achieved upon illumination of concentrated chloroform solutions of N containing $Cu_2Br_2(AsPh_3)_3$ and $[CuCl(AsPh_3)]_4$[54] as the sensitizers of the reaction. Sensitization with the complexes $(Ph_2PCH_2CH_2PPh_2)CuCl$, $(Ph_3P)_3CuX$ and $(MePh_2P)_3CuX$ (X = Cl, Br, I) made it possible to achieve the maximum value Φ = 1.0 in a highly concentrated solution.[55] Dilution sharply reduced the quantum yield.

Transition metal complexes of other than Cu(I) metals are less frequently used for sensitizing the **1**→**2** transformation: $[Ru(bpy)_3]^{2+}$, $[Ru(phen)]^{2+}$, $[cis\text{-}Ir(phen)_2Cl_2]^+$, $[Ir(bpy)_3OH]^{2+}$, $[Rh(phen)_3]^{2+}$, $[Rh(phen)_3]^{3+}$, and $[Rh(phi)_2(phen)]^{3+}$ (bpy = 2,2′-bipyridine, phen = 1,10-phenanthroline, phi = 9,10-phenanthrenequinone diimine).[44,56–59] However, in these cases quantum yields of the conversion are rather low. An exception is the use of $[Ir(bpy)_2(bpy')]^{2+}$, in which case Φ = 0.72.[57]

A triplex electron-transfer mechanism involving interaction of dibenzoylmethanatoboron difluoride (DMB) and an aromatic co-sensitizer (A — toluene, ethylbenzene, biphenyl, and durene) with N was suggested based on the results from a chemically induced dynamic nuclear polarization study of the reaction:

$$\mathrm{DMB} \xrightarrow{h\nu} {}^1\mathrm{DMB} + \mathrm{A} \rightarrow {}^1\left[\mathrm{DMB\ A}\right] + \mathrm{N} \rightarrow {}^1\left[\mathrm{DMB}^{-\cdot}\left(\mathrm{A\ N}\right)^{+\cdot}\right] \rightleftharpoons$$

$$ {}^3\left[\mathrm{DMB}^{-\cdot}\left(\mathrm{A\ N}\right)^{+\cdot}\right] \rightarrow \mathrm{DMB} + \mathrm{A} + {}^3\mathrm{N} \rightarrow \mathrm{Q}.$$ [60]

An efficient electron-transfer mechanism of the **1**→**2** photoisomerization without intermediate formation of the triplet ^{3}N was shown to be involved in the presence of 3,3′,4,4′-benzophenonetetracarboxylic dianhydride (BTDA):

$$\mathrm{BTDA} \xrightarrow{h\nu} {}^1\mathrm{BTDA} \rightarrow {}^3\mathrm{BTDA} + \mathrm{N} \rightarrow {}^3\left[\mathrm{BTDA}^{-\cdot}\,\mathrm{N}^{+\cdot}\right] \xrightarrow{\mathrm{BCET}} \mathrm{BTDA} + {}^3\mathrm{Q} \rightarrow \mathrm{Q}.$$

The abbreviation BCET (bond coupled electron transfer) has been employed to describe such a mechanism.[34]

N-(α-Naphthyl)carbazole (N-C) has been shown to form a twisted intramolecular charge transfer (TICT) excited singlet state. It was used as a sensitizer to produce Q by the following mechanism:

$$\text{N-C} \xrightarrow{h\nu} {}^1\left[\text{N-C}\right] \rightarrow {}^1\left[\text{N}^{-\cdot}\text{-C}^{+\cdot}\right]\left(\text{TICT}\right) \rightarrow {}^3\left[\text{N-C}\right] + \text{N} \rightarrow {}^3\left[\text{N-C}\cdots\text{N}\right] \rightarrow \text{N-C} + \text{Q}.$$ [61]

Photoinitiated Quadricyclane and Norbornadiene Cycloaddition Reactions and Rearrangements

The reverse photochemical conversion **2**→**1** can be efficiently brought about via a radical-cation chain reaction $Q^{+\cdot}\rightarrow N^{+\cdot}$.[3,4] The stability of the two distinct isomeric radical cations with energy differences between $N^{+\cdot}$ and $Q^{+\cdot}$ of about 35.6–46.1 kJ mol^{-1} was confirmed by various experimental methods and theoretical calculations.[3, 62–66]

Carbonyl-containing compounds such as acetophenone, benzophenone, and chloranil can sensitize not only the **1**→**2** rearrangement but also the back reaction, though quantum yields for the latter (Φ 0.05–0.10) are much less than those for the direct photoreaction.[36,43,67,68] Photogenerated catalysis of the **2**→**1** reaction with some metal complexes is a more effective process, since a single photon may produce several molecules of N according to the sequence

$$S \xrightarrow{h\nu} {}^{*}S \xrightarrow{Q} S^{-} + Q^{+\cdot} \rightarrow S^{-} + N^{+\cdot} \xrightarrow{Q} N + Q^{+\cdot};\ Q^{+\cdot} + S^{-} \rightarrow Q + S.$$

This mechanism operates upon irradiation of solutions Q and $Ru(bpy)_3^{2+}$ (bpy = 2,2′-bipyridine) or $PdCl_2(\eta^4\text{–N})$ with 436 nm light and produces N with quantum yields above 1.0 and a turnover number greater than 10^2.[69,70]

Such efficiency is the result of the intermolecular redox process in which Q reductively quenches the metal-to-ligand charge-transfer (MLCT) excited state of the palladium complex. The resulting radical cation $Q^{+\cdot}$ rearranges to its most stable isomer $N^{+\cdot}$, which then oxidizes another molecule Q to restart the cycle.

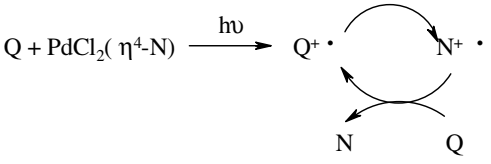

In the presence of methylviologen MV^{2+}, the $Ru(bpy)_3^{2+}$ complex is oxidized to $Ru(bpy)^{3+}$, which serves as a catalyst for the Q→N conversion, with the quantum yield (Φ) > 1.0.

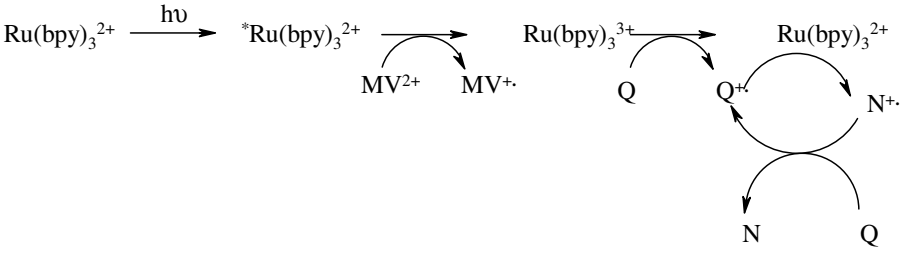

When the bipyridine ligands in the ruthenium complex are replaced by 1,10-phenanthroline analogues, the quantum yield of the reaction is drastically decreased to <0.01.[35]

Much like the **1**→**2** photoisomerization, the back **2**→**1** reaction may be catalyzed by complexation of Q with *N*-(α-naphthyl)carbazole (NC) in its TICT excited state. The following reaction scheme was suggested[61]:

$$N\text{-}C \xrightarrow{h\nu} {}^{1}N\text{-}C \rightarrow {}^{1}\left[N^{-\cdot}\text{-}C^{+\cdot}\right]\left(TICT\right) + Q \rightarrow \left[N^{-\cdot}\text{-}C\cdots Q^{+\cdot}\right] \rightleftharpoons \left[N^{-\cdot}\text{-}C\cdots N^{+\cdot}\right] \rightarrow N\text{-}C + N$$

The main disadvantage of using carbonyl-containing compounds for sensitization of the **1**→**2** or **2**→**1** photoreactions is the formation of products of the side reaction of their photoaddition to N and Q.[71–73]

Irradiation of a benzene solution of benzophenone and N affords the adducts **4–6**[74] even though, in the triplet state, the ketone was shown to add only to Q.[75]

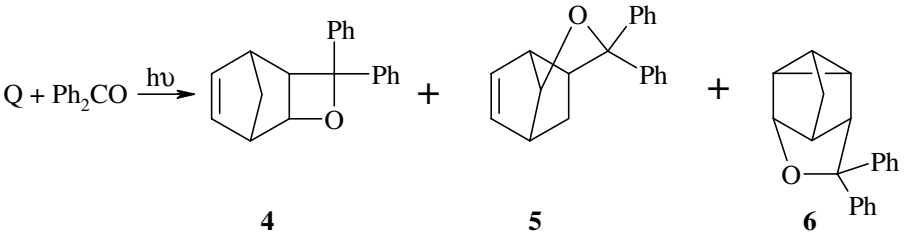

4 **5** **6**

Photoreaction of N with *p*-benzoquinone in benzene yielded a mixture of four isomeric 1:1 adducts **7–10**, whereas Q, under similar conditions, afforded only two *exo* adducts **7** and **8**.[76]

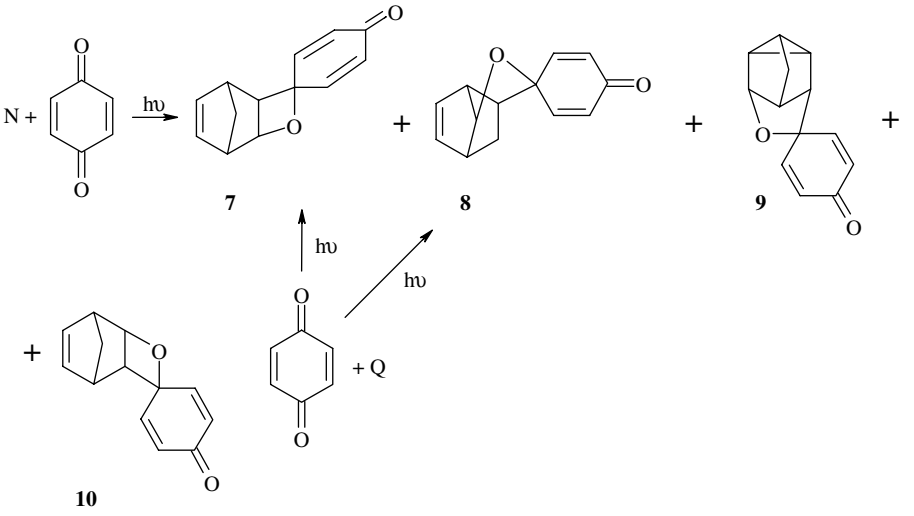

7 **8** **9** **10**

Photolysis of a benzene solution of chloranil and N gave rise to the norbornene analogues of **7**, **8**, and **10** and the tricyclene derivative **9**. By contrast, in acetonitrile solution, formation of only small amounts of type **8** and **9** adducts was detected.[71] The photoreaction of chloranil and Q gave rise to the type **7** adduct as the sole product. Irradiation of Q in acetone or methanol solution under Rose Bengal–sensitized (RB) conditions generated about 70% of N and adducts **11** and **12**.[77]

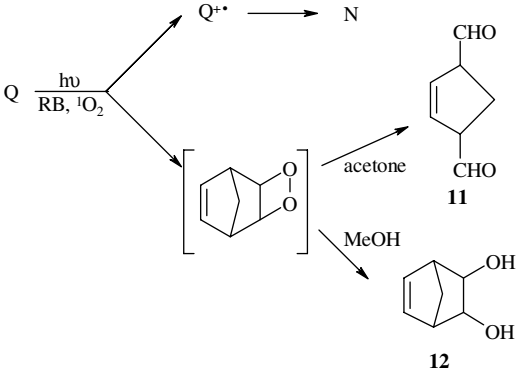

11 **12**

When a methanol solution of Q and RB was irradiated in the presence of NaOMe in an oxygen atmosphere, the epimeric pairs of methoxynorbornenols **13**, **14** and methoxynortricyclanols **15**, **16** were obtained along with the bis-aldehyde **11**.

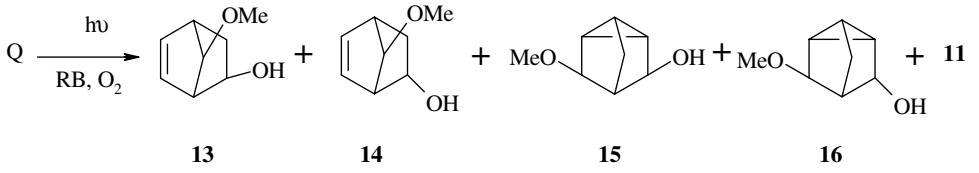

13 **14** **15** **16**

The photoinduced charge-transfer reactions between N or Q and 1,4-dicyanobenzene (DB) in acetonitrile/methanol lead to adducts **17** and **18**, photoinduced nucleophile-olefin-combination-aromatic-substitution (NOCAS) products **19–22** and two acetonitrile adducts, **23** and **24**, which are formed only from N.[78]

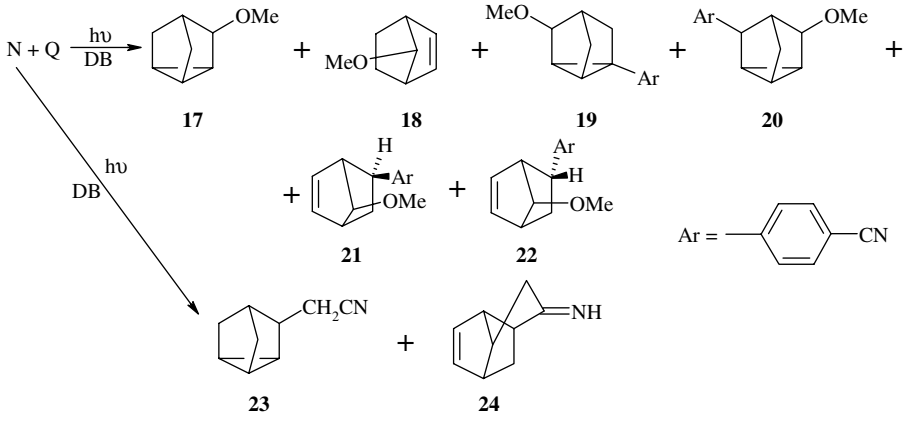

17 **18** **19** **20** **21** **22** **23** **24**

The photocycloaddition of methyl 2,4-dioxopentanoate (DOP) **25** to N afforded the esters **26** and **27**, the adduct **28**, the 7-substituted norbornene **29**, and the norbornadiene **30**. The analogous reaction of **25** with Q gave **26**, **27**, and the oxetane **31**.[72] The presence of **27** in the reaction mixture is evidence for the formation of zwitterions arising via single electron transfer.

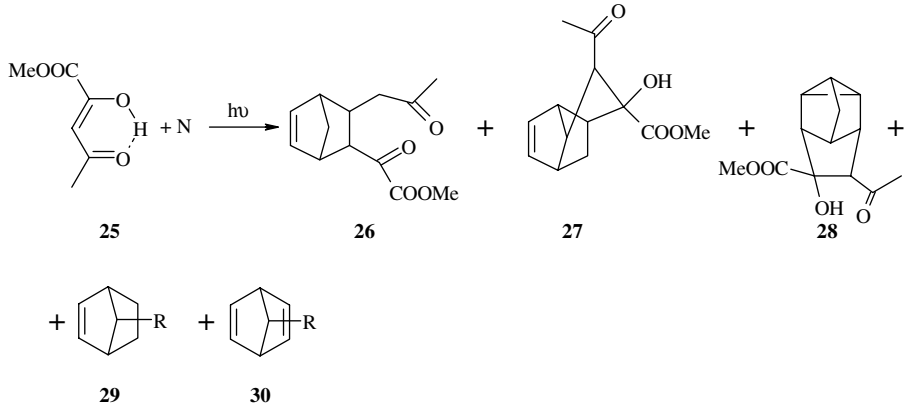

25 **26** **27** **28** **29** **30**

R = 3-DOP

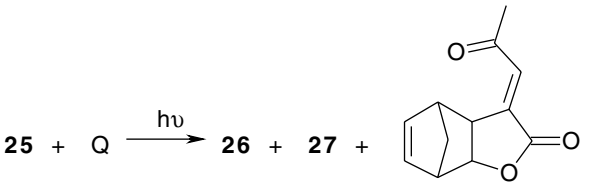

31

No photosensitized processes **1**→**2** and **2**→**1** took place in the presence of DOP, although dibenzoylmethanatoboron difluoride (DMB) readily sensitized the conversion of Q to N via an electron transfer mechanism.[60]

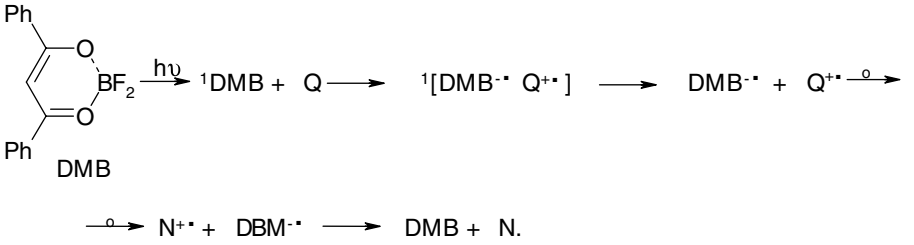

In the presence of durene (D), the participation of triplexes in the co-sensitized reaction is possible.[79]

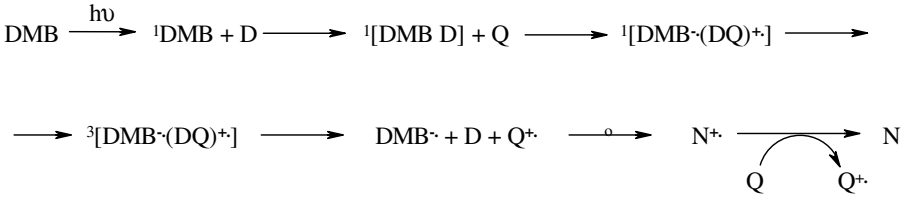

Cobaltadithiolenes (CDT) and rhodiadithiolenes react with Q to give adducts **32** in which the norbornadiene-5,7-diyl group bridges the metal atom to one of the sulfur atoms. UV-irradiation of the complex **32** in acetonitrile solution gives rise to the formation of the free metaladithiolene and norbornadiene in almost 100% yield.[80]

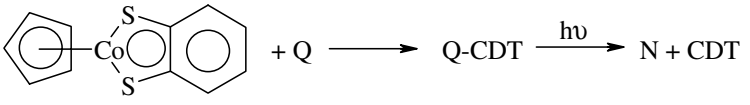

CDT **32**

Photosensitizers Covalently Bonded to Norbornadiene

In order to avoid undesirable photoreactions, some of the suitable sensitizers S may be covalently linked to the norbornadienyl moieties N. Intramolecular photosensitized isomerization of norbornadienes **33** containing a carbazole (CZ) fragment produces the Q derivative **34** through a photoinduced electron transfer between the CZ ring and the olefinic fragment of N ($\lambda_{irr} \geq 350$ nm).[81]

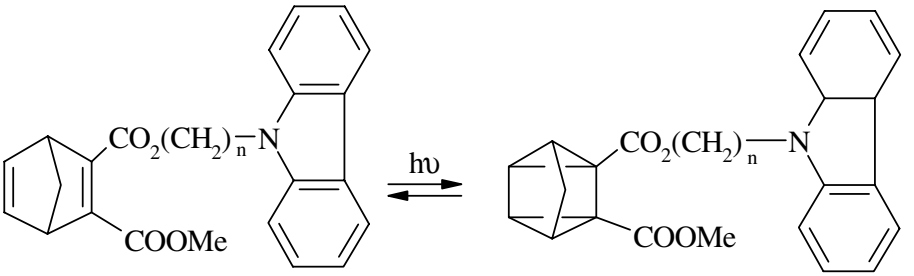

33 **34**

n = 2, 6

Intramolecular energy transfer from the second triplet of the anthracene moiety in **35** is exemplified by the **35**→**36** valence isomerization initiated by the stepwise two-color two-photon excitation method.[82] The energy transfers from the first excited singlet and triplet states of the anthryl group are highly endothermic, whereas that from the second triplet is exothermic. The quantum yield (Φ) of the reaction performed under argon has been determined to be 0.029.

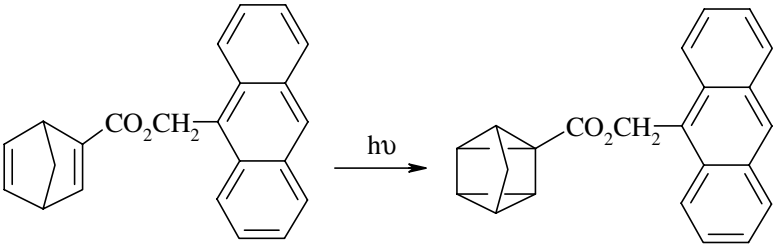

35 **36**

The photophysical and photochemical characteristics of the norbornadiene-steroid-sensitizer systems **37** were investigated by steady-state and time-resolved techniques.[83–86]

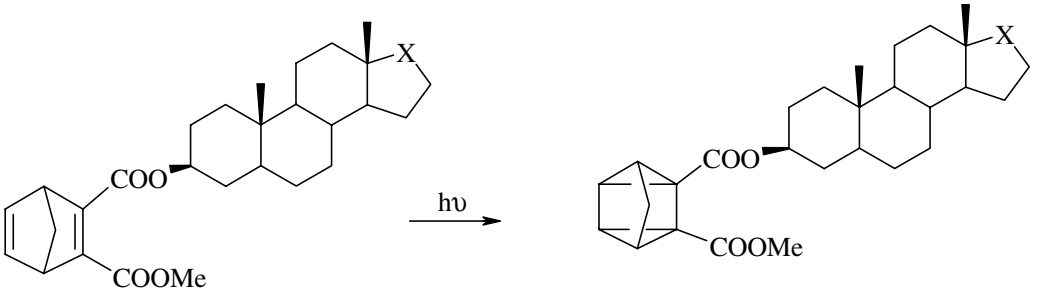

37 **38**

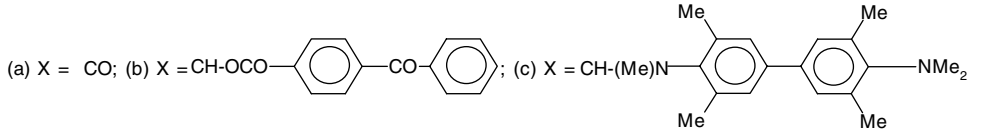

Selective excitation of the benzophenone or benzidine chromophores results in **37**→**38** isomerization. The long-distance intramolecular triplet-energy transfer is proposed to proceed via a through-bond exchange mechanism. For the benzophenone derivative **37b** (BP-ST-N), this process involves the following steps:

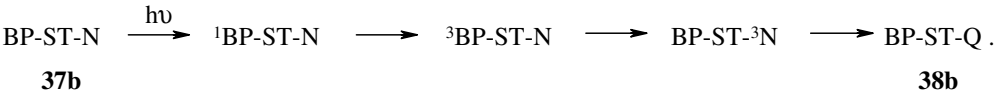

37b **38b**

For the benzidine derivative **37c** (B-ST-N), the photorearrangement occurs via one long-distance triplet energy transfer process and two long-distance electron transfer processes (the electron transfer from the singlet benzidine and the recombination of the radical-ion pair).

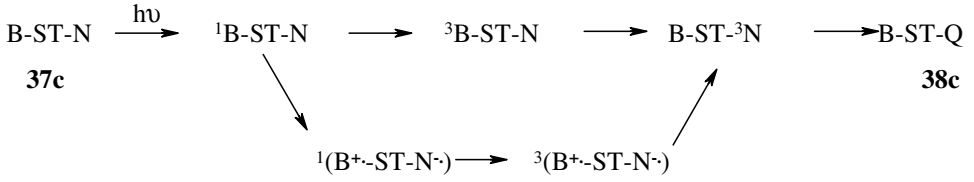

37c **38c**

17.3 Valence Photoisomerization of Derivatives of Norbornadiene

An alternative way of increasing the quantum yield (Φ) of the **1**→**2** photoreaction, as well as achieving a bathochromic shift of the long wavelength edge of N absorption λ_e, is by the substitution of the hydrogen atoms at one or both double bonds of N by suitable electron-withdrawing and electron-donating substituents. The push–pull type of substitution is required due to the well-established fact that for the majority of N derivatives with simple electron-withdrawing groups (COOH, COOMe, CN, SO_2Bu^t) at the 2- and 3-positions, λ_e is not greater than 365 nm.[87–90] The only known exception[8] is that of the bis[pentaammineruthenium(II)] complex of 2,3-dicyanonorbornadiene **39,** which absorbs at $\lambda_e \leq$ 700 nm; the quantum yield of the **39**→**40** rearrangement is, however, very low (8.3×10^{-4}).

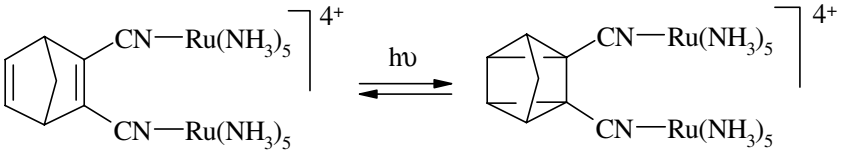

39 **40**

Mono- and 2,3-Disubstituted Norbornadienes

The process of synchronous enantiomeric enrichment of both reactant and product using circularly polarized light (CPL), for which the term new absolute asymmetric synthesis (NAAS) has been coined, was studied in detail for the case of methyl norbornadiene-2-carboxylate **41**.[91–93] This photorearrangement (irreversible NAAS) of racemic **41** produces the chiral product **42**. When **41** was irradiated with *r*-CPL at 290 nm, enantiomeric enrichment by (+)-**41** and (+)-**42** occurs. The inverse process was observed for *l*-CPL. The enantiomeric enrichment of **41** increases up to 100% enantiomeric excess (*ee*) at nearly 100% conversion, and the *ee* of **42** gradually decreases to zero at the end of reaction. These results suggest that one can obtain about 40% *ee* of **41** and **42** at 50% conversion if a starting material with an anisotropy factor *g* ($g = \Delta\varepsilon/\varepsilon$) of unity is used.

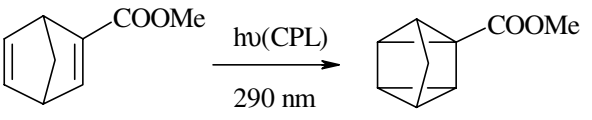

41 **42**

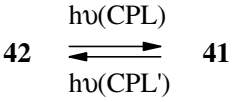

For the reversible photoisomerization, it was found that the *ee* of **41** and **42** concurrently increased by using CPL irradiation in such a way that if the *g* factors of **41** and **42** are large enough, the sign of the *g* factor of **41** is opposite to that of **42**, and the photochemical equilibrium constant is less than unity.[93]

With the aim of developing photoresponsive organomagnets, norbornadienes **43** with tetramethyl piperidine oxide (TEMPO) radical substituents were prepared and investigated.[19–21] Antiferromagnetic behavior was observed in the *bis*-amide-substituted valence isomers **43a** and **44a**. Intermolecular ferromagnetic interactions in the lower temperature region manifest themselves in **43b**. However, no substantial difference in magnetic properties of **43b** and **44b** has been found in spite of the difference in their Weiss temperatures.

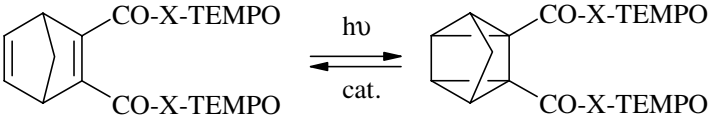

43 **44**

(a) X = NH (b) X = O; TEMPO =

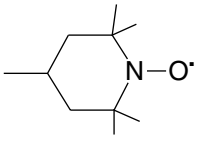

2-Aroyl-3-arylnorbornadienes **45**,[94] in which charge transfer occurs from the aryl to the aroyl group, thus helping to increase Φ and long-wavelength shifting λ_e, absorb at $\lambda_e \leq 450$ nm. Irradiation of their solutions with light of $\lambda_{irr} = 350$ nm yields the corresponding quadricyclanes **46** in high quantum yields ($\Phi = 0.30–0.60$). Electron-donating groups in the aroyl moiety favor an increase in both λ_{max} and Φ values, while a nitro group, although such substitution increases the λ_{max}, markedly reduces the quantum efficiency of the photoisomerization.

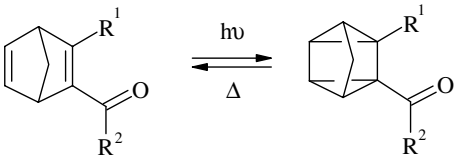

45 **46**

R^1 = Ph or 4-$R^3C_6H_4$, R^3 = Me, OMe, Cl or NO_2; R^2 = Ph or 4-$R^3C_6H_4$, R^3 = Cl or NO_2

The photoisomerization of aromatic derivatives of N **47** into **48** was studied in different solvents.[95,96] These compounds absorb at λ_e < 360 nm, and quantum yields (Φ) are in the range of 0.18 to 0.36. The increase in fluorescence intensity during the irradiation of **47** was found and attributed to the formation of Q derivatives **48**. This peculiarity is probably due to the intramolecular or intermolecular self-quenching of the phenyl-ester fluorophore emission provoked by the N cycle.

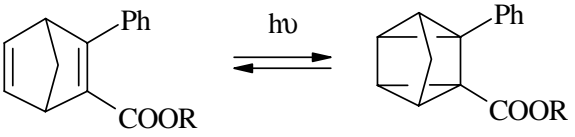

47 **48**

R = H, $PhCH_2$, 4-$MeOC_6H_4CH_2$ or 4-$MeOC_6H_4(CH_2)_6$

2-Trifluoroacetyl-3-phenylnorbornadiene **49** absorbs at $\lambda_e \leq 460$ nm, and the photoinitiated reaction **49**→**50** proceeds quantitatively in benzene with quantum yields of 0.62–0.86, depending on the concentration of the initial compound.[97]

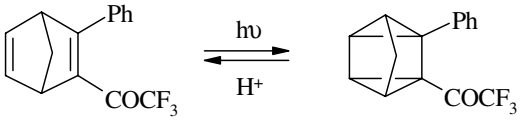

49 **50**

The presence of amide and carboxyl groups at the 2- and 3-positions of N in **51** shifts λ_e up to the 365–415 nm range. The photoisomerization **51**→**52** can be performed not only in organic solvents but also in weakly alkaline aqueous solutions.[26,98–101] *N*-Alkylamides absorb at longer wavelengths than do *N,N*-dialkylamides. On irradiation of **51** in aqueous solutions, quadricyclanes **52** are formed with quantum yields of 0.1–0.6. An important photochemical behavioral principle[26] was postulated based on the study of the **51**→**52** photorearrangement: displacement of λ_e to longer wavelengths in the spectrum results in the decrease in quantum yields (Φ) of the photocyclization.

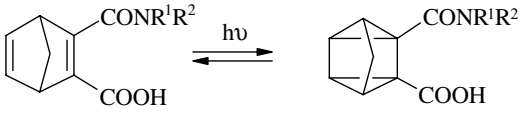

51 **52**

R^1 = H, Me, Ph CH_2, Ph, Ar, *t*-Bu; R^2 = H, Me, Ph; R^1-R^2 = -$(CH_2)_4$-, or 2-$(CH_2)_2C_6H_4$

The amides of 3-phenylnorbornadiene-2-carboxylic acid **53** absorb in the 280–305 nm spectrum region (λ_e = 375–435 nm).[27,102] Irradiation of their solutions with light of 313 nm results in the formation of **54**. Quantum yields for this photoisomerization (Φ = 0.15–0.71) depend on the nature of substituents in the amide fragment of **53**. Their values are increased for compounds with electron-withdrawing

substituents and decreased for those containing electron-donating groups in the phenyl ring, when compared with unsubstituted *N*-phenyl-3-phenylnorbornadiene-2-carboxamide.

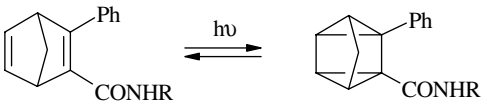

53 **54**

R = Ph, 4-MeC_6H_4, 2-MeC_6H_4, 4-$MeOC_6H_4$, 4-AcC_6H_4, 4-$CO_2EtC_6H_4$, 3-$NO_2C_6H_4$, α-$C_{10}H_7$ or β-$C_{10}H_7$

The carbonyl-containing norbornadienes **55** readily convert into the corresponding quadricyclanes **56** under irradiation with either light of 313 nm or 365 nm.[27,103–106] The compounds **55** have $\lambda_e \leq 500$ nm, and the quantum yields (Φ) of the **55**→**56** interconversion vary from 0.12 to 0.60. Of all these compounds, aroylvinylnorbornadienes **55** (R^1 = H, X = CHCOAr) possess the most suitable spectral characteristics for application to solar energy storage. At the same time, the unsubstituted 2-phenyl-3-(2-benzoylvinyl)norbornadiene **55** (R^1 = H, X = CHCOPh) (λ_{max} = 377 nm, λ_e = 450 nm) exhibits a low quantum efficiency (Φ 0.1) for the photocyclization. Substituents in the phenyl groups have little influence on the position of λ_{max} but significantly affect the values of the quantum yields. Thus, an electron-donating methyl substituent decreases Φ whereas introduction of electron-withdrawing substituents (Cl, Br, NO_2) increase Φ up to the value of 0.25. The quadricyclanes **56** easily revert to starting material **55** in the presence of homogeneous (CF_3COOH) and heterogeneous (MoO_3) catalysts.

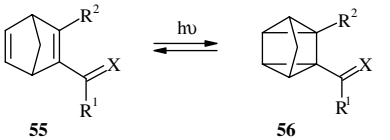

55 **56**

R^1 = H, Me, OMe, CH=CHPh; R^2 = Br, 4-$R^3C_6H_4$, R^3 = H, Br, NO_2, NH_2; X = O, $CHCOC_6H_4R^4$-4, R^4 = H, Me, Cl, Br, NO_2, Ph

The long-wavelength absorption bands of 3-arylnorbornadiene-2-carbaldehyde derivatives **57** are shifted to the 340–505 nm region ($\lambda_e \leq 620$ nm).[27,104,106,107] Quadricyclanes **58** are readily formed by irradiation of isopropanol or acetonitrile solutions of **57** with light of 313, 365, or 436 nm (Φ = 0.10–0.75). The reverse reaction of the oximes **58** (X = NOH, NOMe) proceeds spontaneously at 293 K in the absence of catalysts. On the contrary, other compounds **58** are stable and form norbornadienes **57** only in the presence of MoO_3 ($k = 5 \times 10^{-3}$–10^{-3} sec^{-1}).

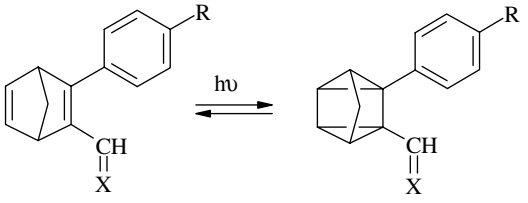

57 **58**

R = H, NO_2, NH_2; X = NOH, NOMe, NAr, N-NHPh, $C(CN)_2$, C(CN)COOEt, $C(COOEt)_2$

Irradiation of the imine **59** in methanol solution (λ_{irr} = 356 nm) causes oxidative photocyclization to give 2-(3-arylnorbornadien-2-yl)-benzo-1,3-oxazole **60**, which then converts to the quadricyclane isomer **61**.[108] The back thermal reaction **61**→**60** proceeds on heating the solution. Under prolonged UV-irradiation further (2 + 2 + 2)-photocyclization of **61**, followed by a 1,5-sigmatropic migration of a hydrogen atom, occurs. The resulting photoproduct **62** possesses intense fluorescence (λ^{fl}_{max} = 390 nm).

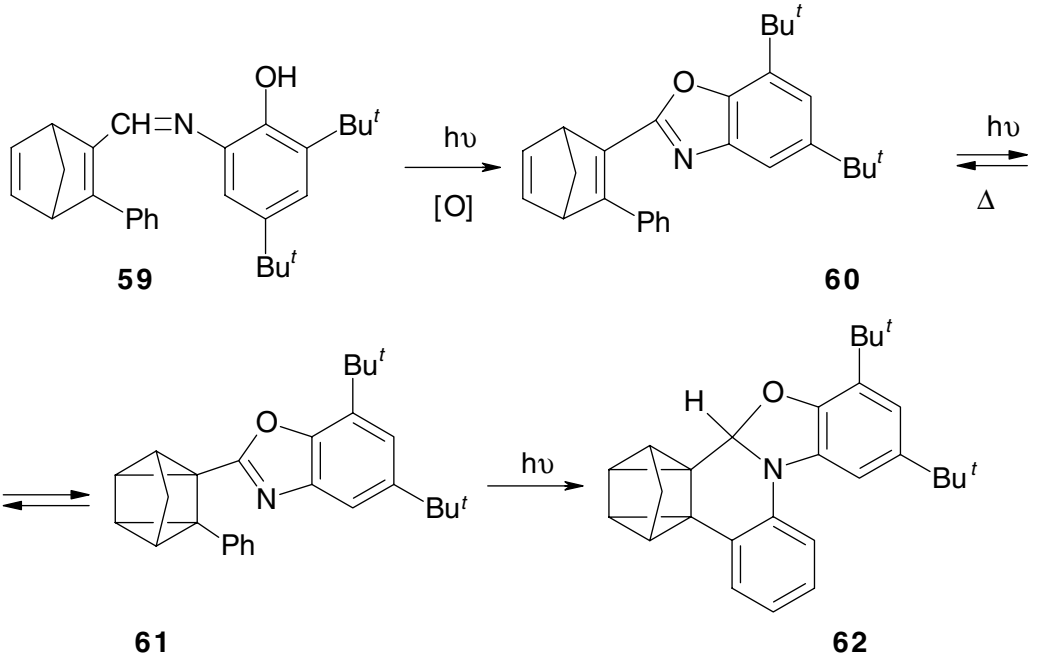

In order to study the influence of substituents on the geometry of the norbornadienyl moiety, x-ray structures of the compounds **63**, **64** have been investigated[109] and compared with the literature data for the parent norbornadiene **1**[4] and for 2-(2,2-diphenylvinyl)norbornadiene-3-carboxylic acid **65**.[110]

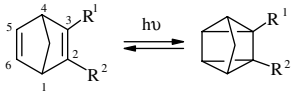

1, 63, 64, 65 **2, 66, 67, 68**

$R^1 = R^2 = H$ (**1**, **2**); R^1 = Ph, R^2 = CH=NPh (**63**, **66**); R^1 = Ph, R^2 = C=C(CN)$_2$ (**64**, **67**); R^1 = COOH, R^2 = CH=CPh$_2$ (**65**, **68**)

In **63**, the single bonds have normal lengths (average value 1.57 Å), whereas the C2=C3 double bond is lengthened to 1.342 Å, and the C5=C6 bond is shortened to 1.310 Å, as compared with the C=C bonds in unsubstituted norbornadiene **1** (1.339 Å). The C2=C3 double bond in **64**, to which a strong electron-withdrawing group C=C(CN)$_2$ is attached, shows additional lengthening up to 1.38(1) Å accompanied by shortening the C5=C6 bond to 1.29(2) Å. In accordance with these data, the quantum yields increase in the following sequence: 0.05 (**1**) < 0.15 (**63**) < 0.74 (**64**). Similar results were obtained earlier for **65**: the C2=C3 double bond is lengthened to 1.359(4) Å due to the π-conjugation with the substituent, and the C5=C6 double bond is shortened to 1.271(4) Å.[110]

The presence of two electron-withdrawing substituents attached to one of the ethylenic bonds of N (**69**, **70**) has a substantially less pronounced effect on the bond lengths.[111,112] For example, in **69**, the lengths of C2=C3 and C5=C6 double bonds are 1.341(3) Å and 1.285(4) Å, respectively. It may be assumed that push–pull substitution of hydrogens in one of the ethylenic bonds with electron-donating and electron-withdrawing substituents causes lengthening of the bond accompanied by the increasing of Φ and λ_e values of the corresponding N/Q system.

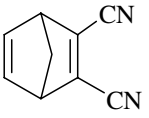

69

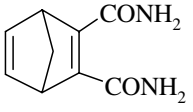

70

Norbornadienes Possessing Cationic Electron-Withdrawing Groups

In accordance with the above conclusion, organic cationic substituents in N cause significant changes in spectral and photochemical properties of the N/Q system. Quaternary salts of dipyridylnorbornadienes **71** absorb up to $\lambda_e \leq 470$ nm.[113,114] However, the **71**→**72** conversion is incomplete. Upon irradiation of solutions of **71** in acetonitrile with the light of $\lambda_{irr} = 350$ nm, a photostationary state is established between **71** and **72** containing about 70–88% Q. In the presence of water and methanol, the adduct **73** is obtained as the sole product of the photoreaction.

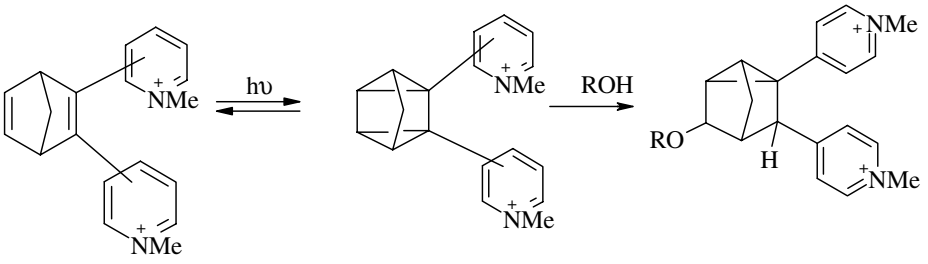

71 **72** **73** (R = H, Me)

In some instances, there is instability of the cyclopropane rings in the quadricyclanes. This instability manifests itself when strong electron-withdrawing groups are attached to the system. Thus, the photorearrangement of norbornadienes **74** with pyrylium cation substituents[114] follows the usual path, but the product **75** is unstable and undergoes ring-opening to yield **76.** The value of λ_e reaches 580 nm, and the quantum yields (Φ) are 0.10–0.50. The reaction **74**→**75** is very sensitive to traces of moisture.

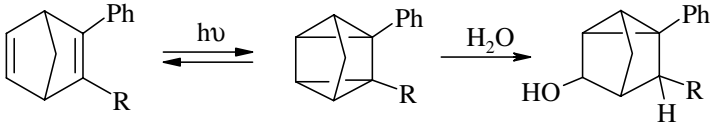

74 **75** **76**

R = 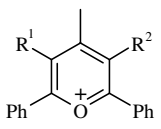 ; R^1, R^2 = H, Me

Benzoxazolyl derivative **77a** exhibits irreversible photoisomerization into the quadricyclane **78a**. The presence of an electron-donating NMe-group in the heterocyclic fragment of **77b** makes this process reversible.[27,115] The value of λ_e reaches 410 nm (**77b**), and Φ = 0.41–0.45. The reverse reaction **78b**→**77b** takes place upon heating the solution at 70°C.

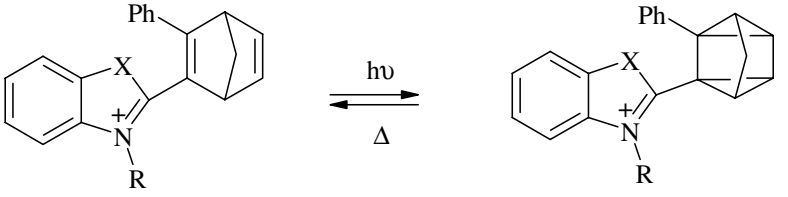

77 **78**

(a) X = O, R = H (b) X = NMe, R = Me

Biphotochromic Norbornadiene Derivatives

Compounds **79** containing two norbornadiene chromophores absorb at different wavelengths (a: λ_e = 370 nm; b: λ_e = 430 nm; c: λ_e = 475 nm). Upon irradiation with the light of the long-wavelength absorption band, they undergo stepwise isomerization first to monoquadricyclanes **80** and then to diquadricyclanes **81**.[26] N and Q moieties in all these systems do not interact with each other in either the ground or in the excited states. The quantum yields (λ_{irr} = 313 nm) of **79**→**80** and **80**→**81** decrease in the following order: **a** (0.58 and 0.56) > **b** (0.16 and 0.19) > **c** (0.035 and 0.034).

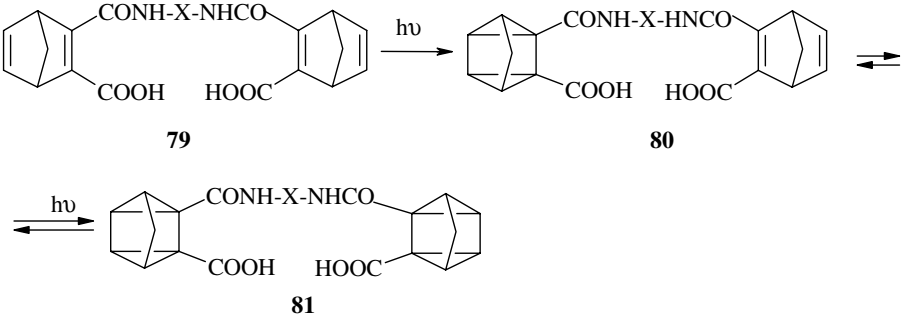

79 **80**

81

(a) X = $-(CH_2)_2-$; (b) X = 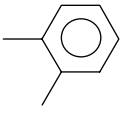 ; (c) X = 

Dinorbornadienes **82** absorb at long-wavelength spectral region $\lambda_e \leq 560$ nm. On irradiation of solutions of **82** in isopropanol with light of 365 nm (a) and 436 nm (b–e), valence isomerization into corresponding monoquadricyclanes **83** and then into the diquadricyclanes **84** occurs. The two-stage character of this reaction, postulated for the compounds **79**, is exemplified by the evolution of the UV spectra of **82b** as well as the NMR spectra. A new absorption band appearing at 380 nm characterizes the mono product **83b**. On prolonged irradiation with light of 365 nm, the formation of diquadricyclane **84b** (λ_{max} = 300 nm) is observed. The total quantum yields of **82**→**84** conversion are rather low, in the range 0.011–0.039.

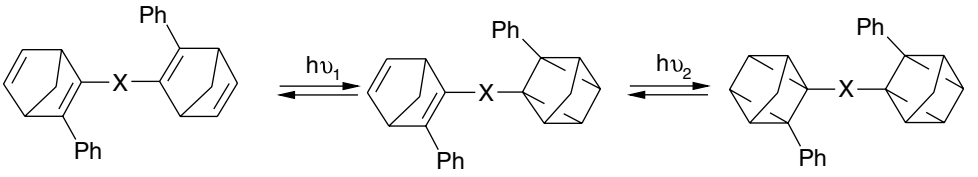

82 **83** **84**

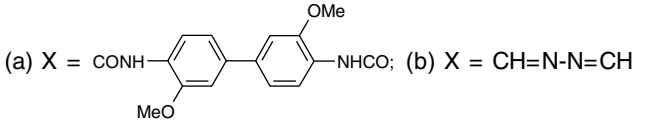

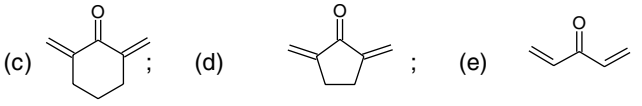

Two types of photochemical processes were found in dinorbornadienes **85**: *E/Z*-isomerization and valence isomerization into the diquadricyclanes **86**.[106] Quantum yields of the formation of **86** are about 0.025. The electronic absorption spectrum of **86** (λ_{max} = 340 nm) resembles that of 4,4′-dimethylazobenzene.[117] Diquadricyclanes **86** can revert into **85** with the aid of the heterogeneous catalyst MoO_3.

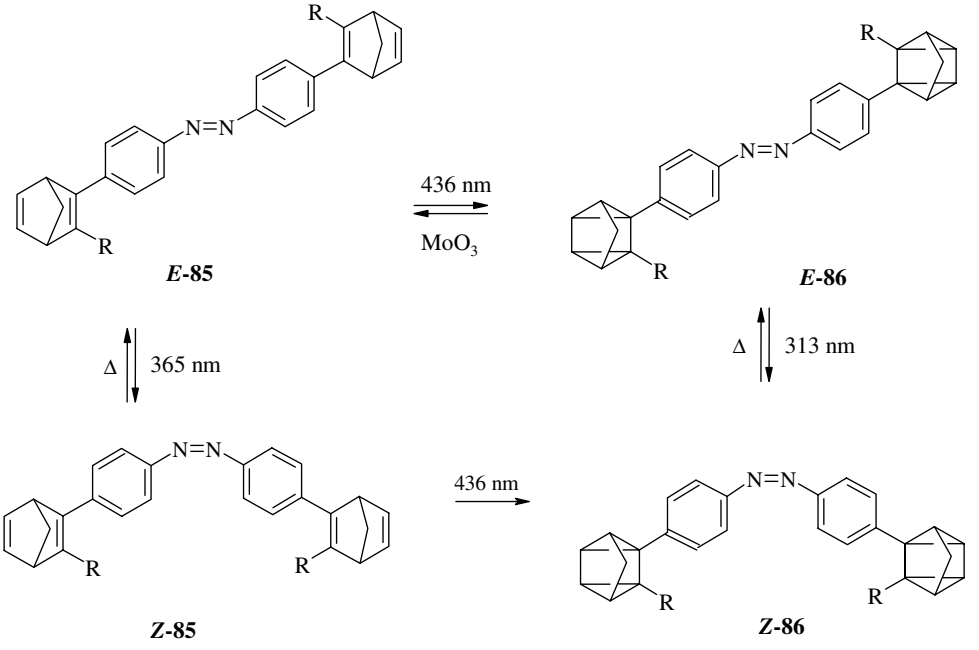

***E*-85** ***E*-86**

***Z*-85** ***Z*-86**

(a) R = CHO, (b) R = CH=C(CN)$COOC_2H_5$

2,3,5,6-Tetrasubstituted Norbornadienes

Due to steric strain, the double bonds in N are pulled close together, which leads to the through-space interaction of their π-orbitals. This results in a considerable convergence of the energy levels of the frontier molecular orbitals.[1,118,119] This interaction manifests itself in the notably longer wavelength

absorption than that expected for a compound with two isolated C=C bonds. A similar interaction is seen with electron-donating substituents attached to one of the double bonds of N, while electron-withdrawing substituents on the another C=C bond can lead to the appearance of a charge-transfer band in the visible spectral region. Such molecular systems as **87** have been called "donor–acceptor" norbornadienes.[25]

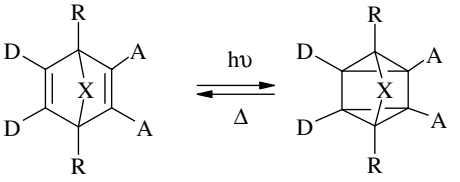

87 **88**

R = H, Me; X = CH_2, CMe_2; D = H, Me, Ph, C_6H_4OMe-4; A = CN, COOMe, COOEt, CONHPh

Depending on the nature of the substituents D and A in **87**, λ_e can vary from 345 to 558 nm, but the quantum yields of the N/Q photorearrangement remain high (0.26–0.96). Bathochromic shift of the long-wavelength absorption band of **87** is observed[16,25,120] with the increase of the electron-donating and electron-withdrawing capacities of D and A. The most important characteristic of "donor–acceptor" norbornadienes is that this shift of λ_e is not usually accompanied by a significant decrease in the quantum yield of the photoreaction **87**→**88**. The thermally reversible valence isomerization **87** $\rightleftharpoons$ **88** can be carried out in polymethylmethacrylate films, and the number of the cycles occurring without tangible changes in the initial absorption approaches 10^3. In solution, however, about 20% of **87** is decomposed.[16] However, despite the high Φ values, the visible light absorption is of low optical density with an extinction coefficient of the long-wave charge-transfer band of ε ~ 1000. Some of the quadricyclanes **88** are not stable enough at room temperature and gradually revert to the starting material. In order to stabilize "donor–acceptor" systems, trifluoromethyl substituted norbornadienes **89** were prepared and investigated.[121–123] The CF_3-substituted compounds **89** possess larger absorption coefficients (ε = 5000–20000) in the visible spectral region as compared with **87** and have $\lambda_e \leq 580$ nm. The absorption maxima of **89** tend to be red-shifted with increase in the electron-donating capacities of R^1 and R^2 groups, and the corresponding quadricyclanes **90** are thermally stable at 293 K. Due to these properties, "donor–acceptor" norbornadienes represent useful materials for energy and optical data storage.

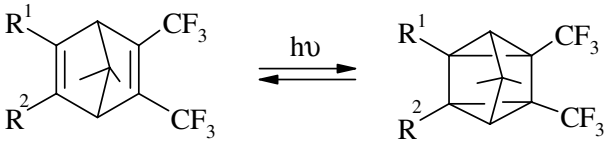

89 **90**

R^1, R^2 = 4-$MeOC_6H_4$, 4-$NMe_2C_6H_4$, 2-thiophenyl or 2-benzofuryl

Another application of 2,3,5,6-tetrasubstituted norbornadienes is their design as photoresponsive sensors for metal cations. The complexing ability of **91** is relatively low, but the corresponding quadricyclanes **92** with long-chain ether ligands containing six or eight oxygen donor atoms are able to extract Na^+ and K^+ from the aqueous phase into chloroform due to a grab or pincer-like movement of ligands

upon photoisomerization.[17,18] The systems **91b/92b** and **91c/92c** can be viewed as photochemically switchable polypodants.

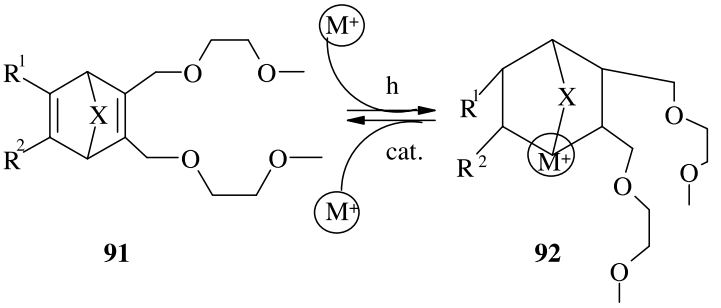

91 **92**

(a) X = C=CMe$_2$; R^1 = H, R^2 = H;

(b) R^1 = CH$_2$O(CH$_2$)$_2$OMe, R^2 = H;

(c) R^1 = R^2 = CH$_2$O(CH$_2$)$_2$OMe

17.4 Photoresponsive Polymers Containing Norbornadiene and Photosensitizer Moieties

The N/Q isomerizations were studied for various polymeric materials containing norbornadienyl fragments in the main chain of the macromolecules or pendant N moieties and photosensitizers. These materials are designed mainly for solar energy storage and also for optical waveguides[11–14] and energetic binders for solid rocket propellants.[22]

Polymers Containing Photosensitizer Units

Immobilized benzophenone or acetophenone molecules can be used as effective photosensitizers of the **1**→**2** conversion.[124,125] However, photostability of such polymeric systems is rather low. A new type of multifunctional polymeric photosensitizers **93** containing both pendant nitroaryloxy group functioned as the interposed sensitizer, and pendant ammonium or phosphonium salts as the substrate-attracting groups were applied for initiating the photoconversion of substituted N **94**→**95**.[126] Quantum yields of this reaction occurring in water solution under irradiation with 366 nm light were found to be 0.19 and 0.42 in the absence and in the presence of the sensitizers **93**, respectively. This result indicates that the energy transfer occurs effectively from the multifunctional S **93** to **94**.

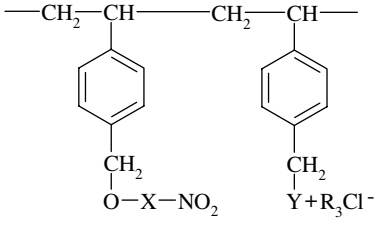

93

X = 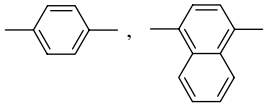 ; Y = P, N; R = Pr, Bu, Hex

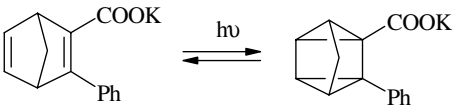

94 **95**

When irradiated with visible light (λ_{irr} > 350 nm), polymeric systems **96** containing N and carbazole pendants (S) undergo the valence N→Q isomerization.[127] The electron transfer mechanism: S–N (**96**) $\xrightarrow{h\nu}$ ^{1}S–N → ^{1}[S$^+$–N$^-$] ⇌ ^{3}[S$^+$–N$^-$] → S–^{3}N → S–Q (**97**) was proposed for this transformation. The reverse reaction proceeded smoothly under the action of catalytic amounts of cobalt porphyrin or trifluoroacetic acid.

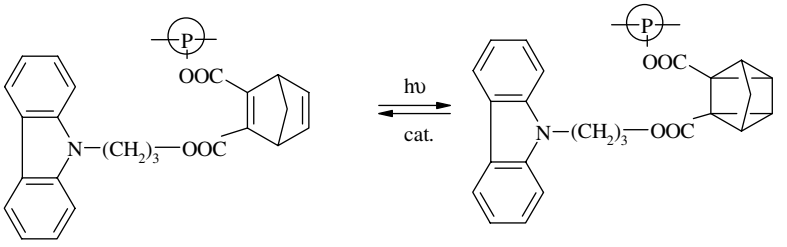

96 **97**

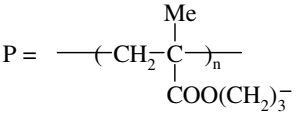

The valence isomerization **98**→**99** photosensitized by energy transfer from the benzophenone groups proceeds smoothly and in high quantum yields (Φ = 0.62–0.84) not only in polymeric films, but also in dichloromethane solution.[128] All the compounds **99** had good stability and can release about 90 kJ mol^{-1} of stored thermal energy.

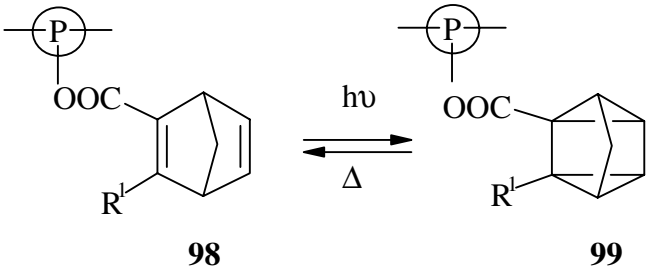

98 **99**

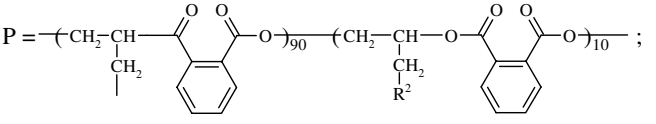

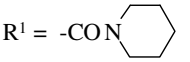

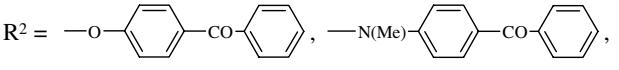

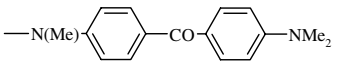

Polymers Containing Norbornadiene Residues in the Main Chain

The photoconversion of N residues in polyamides **100** occurs selectively without any side reactions in the polymeric film as well as in a dichloromethane solution.[129–131] 4-(*N*,*N*-Dimethylamino)benzophenone and Michler's ketone strongly sensitize this photoreaction in the films.

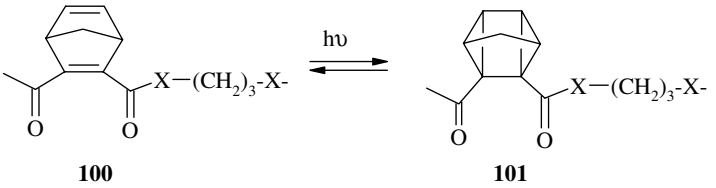

100 **101**

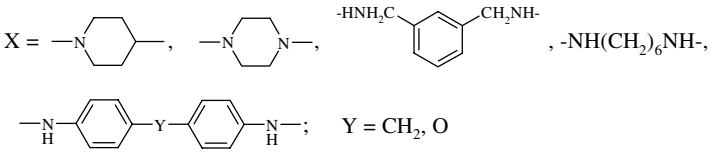

The photochemical valence isomerization of N residues in poly(ester-amide)s **102** occurs smoothly to give the corresponding quadricyclane-containing polymer **103** upon irradiation with sunlight in films or in THF solution.[132] The back-photochemical reaction proceeds also in the polymeric films **103** under irradiation with 272 nm light. The value of the stored thermal energy in such systems is about 84 kJ mol^{-1}.

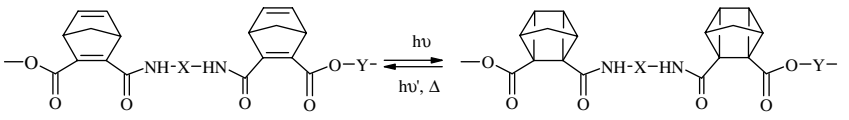

102 **103**

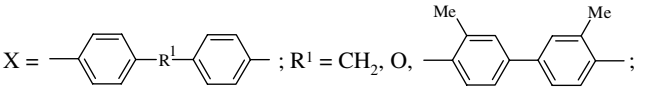

Y = -CH_2-CH(OH)-CH_2-O-R^2-O-CH_2-CH(OH)-CH_2-;

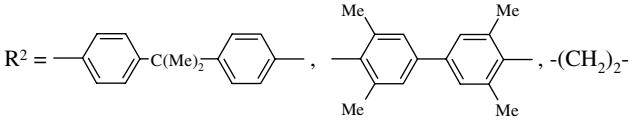

Photoresponsive polyesters containing donor–acceptor norbornadienyl residues in the main chain of the macromolecule were obtained and investigated.[133,134] The long-wavelength absorption of the compounds **104** with λ_e at nearly 500 nm is due to the appearance of the charge-transfer absorption band.[134] The back dark reaction proceeds at room temperature, and its rate can be controlled by structure of the polymer.

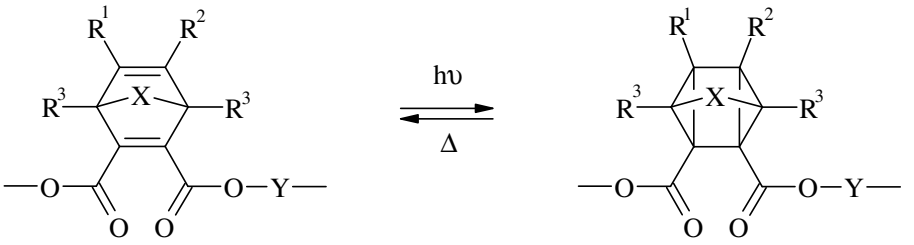

104 **105**

X = CMe_2; R^1 = 4-$MeOC_6H_4$; R^2 = Me, 4-$MeOC_6H_4$; R^3 = H, Me;

Y = -CH_2-CH(OH)-CH_2-O-R^4-O-CH_2-CH(OH)-CH_2-;

R^4 = 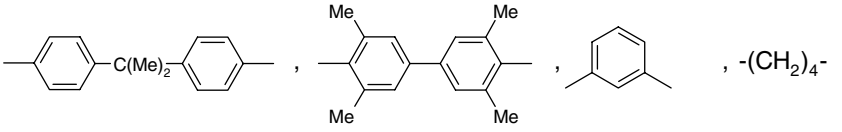

Polymers Containing Pendant Norbornadiene Moieties

The poly-isoprene derivative **106** readily undergoes photochemical isomerization to quadricyclane **107** in the presence of $(PPh_3)_2CuBr$ in benzene solution.[22] The reaction in the solid state is thermally reversible at 180°C.

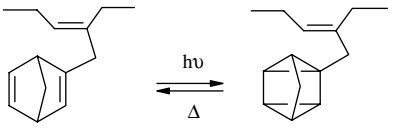

106 **107**

Under irradiation with 313 nm light, polymers **108** bearing 3-phenylnorbornadiene-2-carboxylic acid residues readily isomerize into the corresponding quadricyclanes **109**.[135–137] For **109b**, the back photoreaction (λ_{irr} = 248 nm) also occurs on heating the polymeric films at 100°C or in the presence of (5,10,15,20-tetraphenyl-21H,23H-porphine)cobalt(II) catalyst (Co-TPP) in a dichloromethane solution.

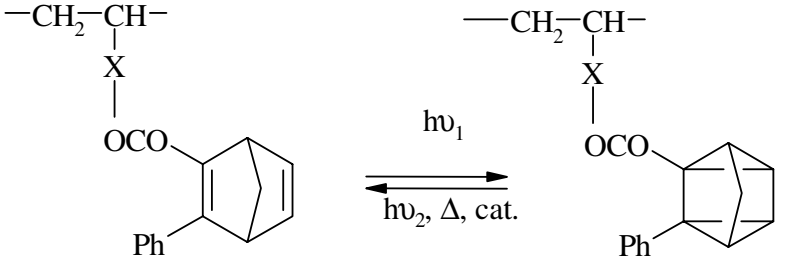

108 **109**

(a) X = 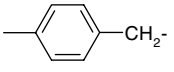

(b) X = -O-$(CH_2)_2$-

The red shift of λ_e up to 425 nm is achieved for the polymers **110** in comparison with **108**.[138] The rate of the **110**→**111** conversion is strongly affected by *para*-substituents in the benzene rings in the order of rate constants: **110e** < **110d** ≤ **110a** < **110b** < **110c**. The storage energy of Q moieties in **111** was determined to be about 60 kJ mol^{-1}. By replacing the carbamoyl group in the 3-position of N moieties of **111** by *N,N*-disubstituted amide groups, the stored energy can be increased up to 80–86 kJ mol^{-1}.[139] Poly(glycidyl methacrylate-co-methylmethacrylate)s containing the same pendant N moieties as in **108** and **110** produce under UV-irradiation the corresponding Q derivatives, which can gradually release thermal energy when Co-TPP is present in the solid films.[140]

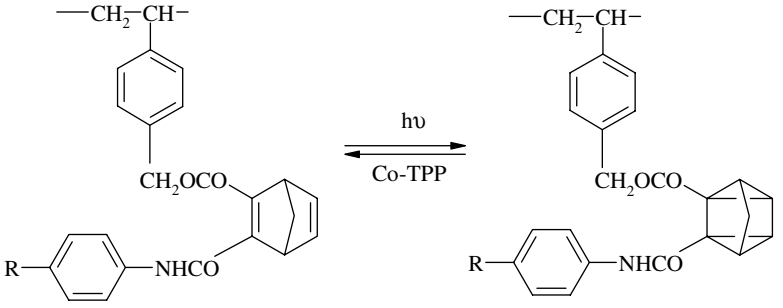

110 **111**

(a) R = H, (b) R = Me, (c) R = OMe, (d) R = Cl, (e) R = COMe, (f) R = NO_2

Under UV-irradiation, polyesters **112** with N moieties readily form the photoproduct **113** with quantum yields in the 0.33–0.41 range.[141] The reverse reaction occurs thermally. The stored thermal energy is about 90 kJ mol^{-1}.

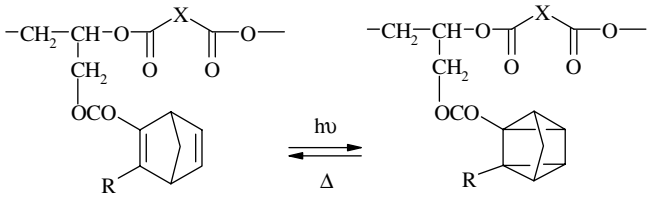

112 **113**

X = 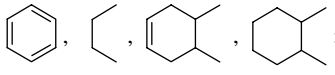 ; R = Ph, $CONPr_2$, COOMe

Enhancement of the photoreactivity and cyclicity of the N/Q transformations of N-containing polymers is very important for their use in solar energy storage processes. With this purpose in mind, the polymers **114** with pendant donor–acceptor type N moieties were prepared.[142] Unexpectedly, these compounds were found to absorb light only up to $\lambda_e \leq 350$ nm. The polymers **114** isomerize quantitatively to **115** and show good repeatability of the N/Q interconversion. Methyl groups in the N moieties decrease the durability of the N-containing polymers **114**. Heating of the polymers **115** releases 55–74 kJ mol^{-1} of thermal energy.

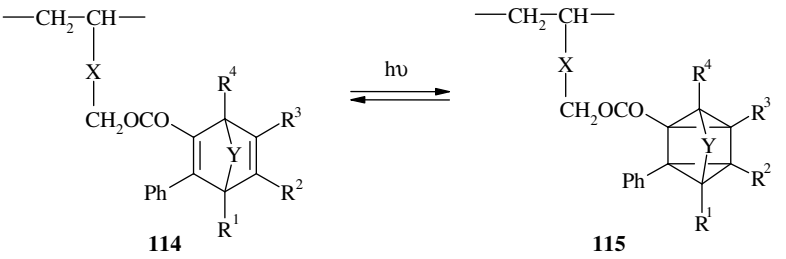

X = 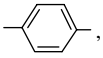 , -O-CH_2- ; Y = CH_2, CHMe; $R^1 = R^2 = R^3 = R^4$ = H, Me

Excellent values of $\lambda_e \leq 505$ nm were achieved in the polymers **116** containing trifluoromethyl substituents in the N moieties.[143]

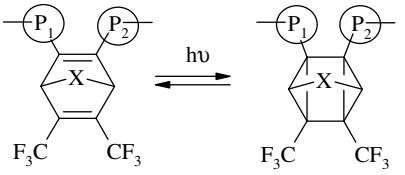

P_1 = 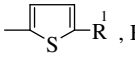 , R^1 = H, CO-; P_2 = 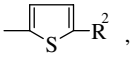 ,

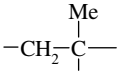

R^2 = CO-$(CH_2)_6$-O-, 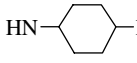 , CO-O-CH_2-CH(OH)-CH_2-OCO,

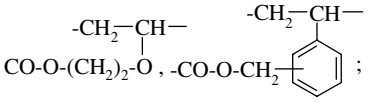

; X = CMe_2

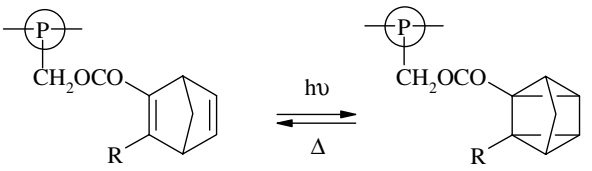

118 **119**

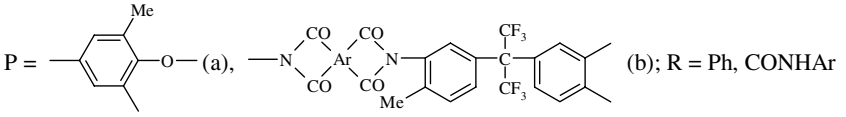

Polymers for Optical Devices

The highly efficient and low-cost procedures for the direct production of channel polymeric wave guides utilizing photochromic reactions have many advantages since such systems do not need to use photoresists and etching.[11–14] The requirements for a suitable material are substantial change in the refractive index triggered by irradiation with light and high transparency as well as thermal and chemical stability. The polymer **120** meets these requirements. The **120**→**121** valence photoisomerization occurs with 50% quantum yield.[147]

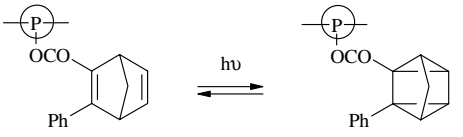

120 **121**

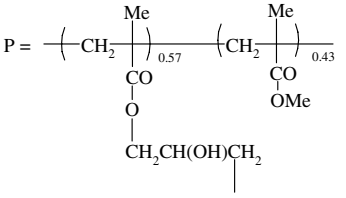

The refractive index change produced by this rearrangement is about 0.01 in the spectral region far outside of the absorption band (~ 633 nm). The polymer **120** has a good potential for application in channel wave guides and photo-optical switching devices.

Acknowledgement

The authors are grateful to the Russian Foundation for Basic Research (grant 02–03–32527), RF Ministry of Education (grant E02-5.0-2Y2), RF Ministry of Science (grant NSh.945.2003.3), and to CRDF/RF Ministry of Education (grant REC-004) for financial support. V.I.M. is grateful to the Foundation for the Support of Russian Science.

References

1. Fuß, W., Pushpa, K.K., Schmid, W.E., and Trushin, S.A., Ultrafast [2 + 2]-cycloaddition in norbornadiene, *Photochem. Photobiol. Sci.,* 1, 60–66, 2002.
2. Helms, A.M. and Caldwell, R.A., Triplet species from norbornadiene. Time-resolved photoacoustic calorimetry and *ab initio* studies of energy, geometry, and spin-orbit coupling, *J. Am. Chem. Soc.,* 117, 358–361, 1995.

3. Bach, R.D., Schilke, I.L., and Schlegel, H.B., The energetics of valence isomerization in the norbornadiene–quadricyclane system, *J. Org. Chem.,* 61, 4845–4847, 1996.
4. Inadomi, Y., Morihashi, K., and Kikuchi, O., Theoretical study of the thermal interconversion mechanism between the norbornadiene and quadricyclane radical cations, *J. Mol. Struct. (Theochem),* 434, 59–66, 1998.
5. Hautala, R.R., King, R.B., and Kutal, C., *Solar Energy: Chemical Conversion and Storage*, Humana, Clifton, NJ, 1979, p. 333.
6. Bren, V.A., Dubonosov, A.D., Minkin, V.I., and Chernoivanov, V.A., Norbornadiene–quadricyclane — an effective molecular system for the storage of solar energy, *Russ. Chem. Rev.,* 60, 451–469, 1991.
7. Cox, A., Photochemical aspects of solar energy conversion, *Photochemistry*, 30, 389–397, 1999.
8. Laine, P., Marvaud, V., Gourdon, A., Launnay, J.-P., Argazzi, R., and Bignozzi, C.-A., Electron transfer through norbornadiene and quadricyclane moieties as a model for molecular switching, *Inorg. Chem.,* 35, 711–714, 1996.
9. Bonfantini, E.E. and Officer, D.L., The synthesis of norbornadiene conjugatively linked to tetraphenylporphyrin and anthracene: towards a norbornadiene-derived molecular electronic device, *J. Chem. Soc., Chem. Commun.,* 1445–1446, 1994.
10. Fraysse, S., Coudret, C., and Launay, J.-P., Synthesis and properties of dinuclear complexes with a photochromic bridge: an intervalence electron transfer switching "on" and "off," *Eur. J. Org. Chem.,* 1582–1590, 2000.
11. Takahashi, S., Samata, K., Muta, H., Machida, S., and Horie, K., Refractive index pattering using near-field scanning optical microscopy, *Appl. Phys. Lett.,* 78, 13–15, 2001.
12. Horie, K., Nishikubo, T., Kinoshita, K., Morino, S., Machida, S., and Yamashita, S., Material for making polymer optical waveguide, Jpn. Kokai Tokkyo Koho JP 10448727 A2, 1998.
13. Morino, S., Watanabe, T., Magaya, Y., Horie, K., and Nishikubo, T., Photo-optical effect of polymers containing norbornadiene moieties, *J. Photopolymer. Sci. Technol.,* 7, 121–126, 1994.
14. Morino, S. and Horie, K., Photoinduced refractive index changes of polymer films containing photochromic dyes and evaluation of the minimal switching energy, *ACS Symp. Ser.,* 672**,** 260–279, 1997.
15. Nishino, H. and Inoue, Y., Chiral norbornadiene–quadricyclane derivative and reversible optical recording material using it, Jpn. Kokai Tokkyo Koho JP 2000086588, 2000.
16. Miki, S., Asako, Y., and Yoshida, Z., Photochromic solid films prepared by doping with donor–acceptor norbornadienes, *Chem. Lett.,* 195–198, 1987.
17. Starck, F., Jones, P.G., and Herges, R., Synthesis of photoresponsive polyethers, *Eur. J. Org. Chem.,* 2533–2539, 1998.
18. Herges, R. and Reif, W., Photoresponsive carboxylic acids, *Liebigs Ann. Chem.,* 761–768, 1996.
19. Nakatsuji, S., Takeuchi, S., Ojima, T., Ogawa, Y., Akutsu, H., and Yamada, J., Preparation and properties of photofunctional systems with nitroxide radicals, *Mol. Cryst. Liq. Cryst. Sci. Technol. Sect. A,* 356, 23–32, 2001.
20. Takeuchi, S., Ogawa, Y., Naito, A., Sudo, K., Yasuoka, N., Akutsu, H., Yamada, J., and Nakatsuji, S., Preparation and properties of some photo-responsive compounds with TEMPO radical, *Mol. Cryst. Liq. Cryst. Sci. Technol. Sect. A,* 345, 167–172, 2000.
21. Nakatsuji, S., Ogawa, Y., Takeuchi, S., Akutsu, H., Yamada, J., Naito, A., Sudo, K., and Yasuoka, N., Novel photo-responsive organic spin systems: preparation and properties of norbornadienes and spiropyrans with TEMPO radical substituents, *J. Chem. Soc., Perkin Trans. 2,* 1969–1975, 2000.
22. Wright, M.E., Allred, G.D., Wardle, R.B., and Cannizzo, L.F., New monomers and polymers based on cyclopropane, norbornadiene, and quadricyclane, *J. Org. Chem.,* 58, 4122–4126, 1993.
23. Turro, N.J., Cherry, W.R., Mirbach, M.F., and Mirbach, V.J., Energy acquisition, storage, and release. Photochemistry of cyclic azoalkanes as alternative entries to the energy surface interconnecting norbornadienes and quadricyclanes, *J. Am. Chem. Soc.,* 99, 7388–7390, 1977.
24. Kavarnos, G.J. and Turro, N.J., Photosensitization of reversible electron transfer: theories, experimental evidence, and examples, *Chem. Rev.,* 86**,** 401–449, 1986.

25. Yoshida, Z., New molecular energy storage systems, *J. Photochem.,* 29, 27–40, 1985.
26. Maruyama, K., Tamiaki, H., and Kawabata, S., Development of a solar energy storage process. Photoisomerization of a norbornadiene derivative to a quadricyclane derivative in an aqueous alkaline solution, *J. Org. Chem.,* 50, 4742–4749, 1985.
27. Chernoivanov, V.A., Dubonosov, A.D., Bren, V.A., Minkin, V.I., Suslov, A.N., and Borodkin, G.S., Photoinitiated rearrangement of 3-phenylnorbornadiene with conjugated substituents in 2-position, *Mol. Cryst. Liq. Cryst. Sci. Technol. Sect. A,* 297, 239–245, 1997.
28. An, X. and Xie, Y., Enthalpy of isomerization of quadricyclane to norbornadiene, *Thermochim. Acta,* 220, 17–25, 1993.
29. Wiberg, K.B. and Connon, H.A., Enthalpy of the metal catalyzed isomerizations of quadricyclane and of tricyclo[4.1.0.0.^{2,7}]heptane, *J. Am. Chem. Soc.,* 98, 5411–5412, 1976.
30. Maruyama, K., Tamiaki, H., and Kawabata, S., Exothermic isomerization of water-soluble quadricyclanes to norbornadienes by soluble and insoluble catalysts, *J. Chem. Soc., Perkin Trans. 2,* 543–548, 1986.
31. Franceschi, F., Guardigli, M., Solari, E., Floriani, C., Chiesi-Villa, A., and Rizzoli, C., Designing copper(I) photosensitizers for the norbornadiene–quadricyclane transformation using visible light: an improved solar energy storage system, *Inorg. Chem.,* 36, 4099–4107, 1997.
32. Onishi, M. and Hiraki, K., Phosphine steric effects on the catalytic activities of a few chloro(tertiary phosphine) copper(I) oligomers in photoisomerizations of norbornadiene and *trans*-stilbene, *Inorg. Chim. Acta,* 202, 27–30, 1992.
33. Kutal, C., Photochemistry of transition metal-organic systems, *Coord. Chem. Rev.,* 64, 191–206, 1985.
34. Cuppoletti, A., Dinnocenzo, J.P., Goodman, J.L., and Gould, I.R., Bond-coupled electron transfer reactions: photoisomerization of norbornadiene to quadricyclane, *J. Phys. Chem. A,* 103, 11253–11256, 1999.
35. Sluggett, G.W., Turro, N.J., and Roth, H.D., Rh(III)-Photosensitized interconversion of norbornadiene and quadricyclane, *J. Phys. Chem. A,* 101, 8834–8838, 1997.
36. Barwice, A.J.G., Gorman, A.A., Leyland, R.L., Smith, P.G., and Rodgers, M.A.J., A pulse radiolysis study of the quenching of aromatic carbonyl triplets by norbornadienes and quadricyclanes. The mechanism of interconversion, *J. Am. Chem. Soc.,* 100, 1814–1820, 1978.
37. Hammond, G.S., Wyatt, P., De Boer, C.D., and Turro, N.J., Photosensitized isomerization involving saturated centers, *J. Am. Chem. Soc.,* 86, 2532–2533, 1964.
38. Kutal, C., Chemical storage of energy in organic photoisomers, *Sci. Pap. Inst. Phys. Chem. Res. (Jpn),* 78, 186–192, 1984.
39. Ristic, G.S., Marincovic, M.D., Comor, J.J., Vasic, V.M., Ristic, M.S., and Nicolic, R.M., Possibility of photochemical energy storage in norbornadiene–quadricyclane system, *J. Mol. Struct.,* 267, 7–12, 1992.
40. Gorman, A.A., Hamblett, I., and McNeeney, S.P., Sensitization of the norbornadiene to quadricyclane conversion by substituted benzophenones: evidence against biradical intermediacy, *Photochem. Photobiol.,* 51, 145–149, 1990.
41. Taoda, H., Hayakawa, K., and Kawase, K., Photosensitized isomerization of norbornadiene for solar energy storage and suppression of side reaction, *J. Chem. Eng. Jpn.,* 20, 335–338, 1987.
42. Tinnemans, A.H.A., den Ouden, B., Bos, H.J.T., and Mackor, A., Photochemical conversion of norbornadiene and quadricyclane in the presence of acridinone-type sensitizers, *Recl. Trav. Chim. Pays-Bas,* 104, 109–116, 1985.
43. Arai, T., Oguchi, T., Wakabayashi, T., Tsuchiya, M., Nishimura, Y., Oishi, S., Sakuragi, H., and Tokumaru, K., Mechanistic approach to the sensitization process of aromatic ketones in the isomerization between norbornadiene and quadricyclane, *Bull. Chem. Soc. Jpn.,* 60, 2937–2943, 1987.
44. Juris, A., Sandrini, D., and Rancati, E., New coordination compounds as tentative photosensitizers for the valence isomerization of norbornadiene to quadricyclane, *Chim. Ind.,* 62, 837–842, 1980.
45. Schwendiman, D.P. and Kutal, C., Transition metal photoassisted valence isomerization of norbornadiene. An attractive energy-storage reaction, *Inorg. Chem.,* 16, 719–721, 1977.

46. Basu, A., Saple, A.R., and Sapre, N.Y., Di-2-pyridil ketone complexes of copper (I): efficient photocatalysts for norbornadiene–quadricyclane conversion, *J. Chem. Soc., Dalton Trans.,* 1797–1799, 1987.
47. Borsub, N., Chang, S., and Kutal.C., Ligand control of the mechanism of photosensitization by copper(I) compounds, *Inorg. Chem.,* 21, 538–543, 1982.
48. Sterling, R.S. and Kutal, C., Photoconversion of norbornadiene to quadricyclane in the presence of a copper(I) carbonyl compound, *Inorg. Chem.,* 19, 1502–1505, 1980.
49. Onishi, M., Hiraki, K., Itoh, H., Eguchi, H., and Abe, S., Synthesis of new ferrocenylphosphinecopper(I) complexes and their application to the valence isomerization of norbornadiene to quadricyclane, *Inorg. Chim. Acta,* 145, 105–109, 1988.
50. Rosi, M., Sgamelotti, A., Francheschi, F., and Floriani, C., Use of norbornadiene in solar energy storage: theoretical study of a copper(I) photosensitizer for the norbornadiene–quadricyclane transformation, *Inorg. Chem.,* 38, 1520–1522, 1999.
51. Orchard, S.W. and Kutal, C., Photosensitization of the norbornadiene to quadricyclane rearrangement by an electronically excited copper(I) compound, *Inorg. Chim. Acta,* 62, 95–96, 1982.
52. Liaw, B., Orchard, W., and Kutal, C., Role of the triplet state of (arylphosphine)copper(I) complexes in the photosensitized isomerization of dienes, *Inorg. Chem.,* 27, 1311–1316, 1988.
53. Maruyama, K., Terada, K., Naruta, Y., and Yamamoto, Y., Photoisomerization of norbornadiene to quadricyclane in the presence of copper(I)–nitrogen ligand catalysts, *Chem. Lett.,* 1259–1262, 1980.
54. Sakaki, S., Ohkubo, K., Fudjiwara, H., and Ohyoshi, A., Photoisomerization of norbornadiene with some Cu(I)-triphenylphosphine and -triphenylarsine complexes, *J. Mol. Catal.,* 16, 181–186, 1982.
55. Fife, D.J., Moore, W.M., and Morse, K.W., Photosensitized isomerization of norbornadiene to quadricyclane with (arylphosphine)copper(I) halides, *J. Am. Chem. Soc.,* 107, 7077–7083, 1985.
56. Ikezawa, H., Kutal, C., Yasufuki, K., and Yamazaki, H., Direct and sensitized valence photoisomerization of a substituted norbornadiene. Examination of the triplet-state reactivities, *J. Am. Chem. Soc.,* 108, 1589–1594, 1986.
57. Grutsch, P.A. and Kutal, C., Charge-transfer sensitization of the valence isomerization of norbornadiene to quadricyclane by an orthometallated transition-metal complex, *J. Am. Chem. Soc.,* 108, 3108–3110, 1986.
58. Kutal, C., Use of transition metal compounds to sensitize an energy storage reaction, *Adv. Chem. Ser.,* 168, 158–173, 1978.
59. Grutsch, P.A. and Kutal, C., A silica-supported inorganic photosensitizer, *J. Chem. Soc., Chem. Commun.,* 893–894, 1982.
60. Liu, Z., Zhang, M., Yang, L., Liu, Y., Chow, Y.L., and Johansson C.I., Electron transfer photoisomerization of norbornadiene to quadricyclane cosensitized by dibenzoylmethanatoboron difluoride and aromatic hydrocarbons, *J. Chem. Soc., Perkin Trans. 2,* 585–590, 1994.
61. Jiwan, J.L.H. and Soumillion, J.P., Electron transfer photochemistry initiated from a twisted intramolecular charge transfer state used as an electron donor and as an acceptor, *J. Photochem. Photobiol. A: Chem.,* 64, 145–158, 1992.
62. Clark, T., The quadricyclane to norbornadiene radical cation rearrangement: an *ab initio* and density functional study, *Acta Chem. Scand.,* 51, 646–652, 1997.
63. Ishiguro, K., Khudyakov, I.V., McGarry, P.F., and Turro, N.J., Time-resolved ESR study of the quadricyclane radical-cation, *J. Am. Chem. Soc.,* 116, 6933–6934, 1994.
64. Barnabas, M.V., Werst, D.W., and Trifunac, A.D., Quadricyclane and norbornadiene radical cations in silicalite: comparison with freon matrices, *Chem. Phys. Lett.,* 206, 21–24, 1993.
65. Raghavachari, K., Haddon, R.C., and Roth, H.D., Theoretical study in the norbornadiene–quadricyclane system, *J. Am. Chem. Soc.,* 105, 3110–3114, 1983.
66. Haselbach, E., Bally, T., Lanyiova, Z., and Baertschi, P., The type C valence–isomeric system quadricyclane radical cation/norbornadiene radical cation, *Helv. Chim. Acta,* 62, 583–588, 1979.
67. Nakabayashi, K. and Takamuki, S., Triplet sensitized quadricyclane–norbornadiene valence isomerization of methyl 5-(4-biphenyl)tetracyclo[3.2.0.^{2,7}0.^{4,6}]heptane-1-carboxylate, *Bull. Chem. Soc. Jpn.,* 65, 3177–3179, 1992.

68. Meng, Q., Yamakage, Y., Aizawa, T., Maeda, K., and Azumi, T., Studies of photochemical reaction by CIDNP-detected ESR spectrum, *Proc. Indian Acad. Sci. (Chem. Sci.),* 105, 619–628, 1993.
69. Kutal, C., Photosensitive metal-organic systems: an overview, in *Photosensitive Metal-Organic Systems. Mechanistic Principles and Applications*, Kutal, C. and Serpone, N., Eds., American Chemical Society, Washington, D.C., 1993, pp. 1–25, chap. 1.
70. Kutal, C., Kelley, C.K., and Ferraudi, G., Catalyzed valence isomerization of quadricyclane to norbornadiene via photochemical generation of a strong ground-state oxidant, *Inorg. Chem.,* 26, 3258–3261, 1987.
71. Braun, M., Christl, M., Deeg, O., Rudolph, M., Peters, E.-M., and Peters, K., Photocycloaddition of chloranil to homobenzvalene, norbornadiene, and quadricyclane, *Eur. J. Org. Chem.,* 2093–2101, 1999.
72. Hatsui, T., Hayashi, K., and Takeshita, H., Photoaddition of methyl 2,4-dioxopentatoate to norbornadiene and quadricyclane, *J. Photochem. Photobiol. A: Chem.,* 87, 209–213, 1995.
73. Goez, M. and Frisch, I., Rearrangements of photogenerated 1,5-biradicals in the Paterno–Buchi reaction of quinones with norbornadiene or quadricyclane, *J. Inf. Rec.,* 25, 287–293, 2000.
74. Kubota, T., Shima, K., and Sakurai, H., The photocycloaddition of benzophenone to norbornadiene, *Chem. Lett.,* 343–346, 1972.
75. Gorman, A.A. and Leyland, R.L., The reaction of benzophenone triplets with norbornadiene and quadricyclene, *Tetrahedron Lett.,* 5345–5348, 1972.
76. Fehnel, E.A. and Brokaw, F.C., Photocycloaddition reactions of norbornadiene and quadricyclane with *p*-benzoquinone, *J. Org. Chem.,* 45, 578–582, 1980.
77. Hatsui, T. and Takeshita, H., Rose Bengal–sensitized photooxidation of quadricyclane. A [$2\sigma + 2\sigma + 2\pi$] cycloaddition of singlet oxygen, *Chem. Lett.,* 129–132, 1993.
78. Weng, H. and Roth, H.D., Electron transfer photochemistry of norbornadiene and quadricyclane. Nucleophilic capture of radical cations, free-radical rearrangements, and hydrogen abstraction, *J. Org. Chem.,* 60, 4136–4145, 1995.
79. Yang, L., Zhang, M., Liu, Y., Liu, Z., and Chow, Y.L., Triplex promoted intersystem crossing of ion-radical pairs in the photosensitized valence isomerization of quadricyclane: chemically induced dynamic nuclear polarization (CIDNP) evidence, *J. Chem. Soc., Chem. Commun.,* 1055–1056, 1995.
80. Kajitani, M., Fujita, T., Hisamatsu, N., Hatano, H., Akiyama, T., and Sugimori, A., Photochemical reactions of several adducts of metalladithiolenes and metalladithiazoles. Dissociation and rearrangement, *Coord. Chem. Rev.,* 135, 175–180, 1994.
81. Wu, Q.H., Zhang, B.W., Ming, Y.F., and Cao, Y., Inter- and intramolecular electron transfer isomerization of norbornadiene derivatives, *J. Photochem. Photobiol. A: Chem.,* 61, 53–63, 1991.
82. Okada, K., Sakai, H., Oda, M., and Kikuchi, K., Intramolecular T_2-energy transfer from anthryl group studied by stepwise two-color two-photon excitation: a *cis* to *trans* isomerization and a valence isomerization, *Chem. Lett.,* 977–978, 1995.
83. Cao, H., Akimoto, Y., Fujiwara, Y., Tanimoto, Y., Zhang, L.P., and Tung, C.H., A laser flash photolysis study of the intramolecular energy transfer reaction from benzophenone to norbornadiene covalently bonded by a rigid steroid bridge, *Bull. Chem. Soc. Jpn.,* 68, 3411–3415, 1995.
84. Tung, C.H., Zhang, L.P., Li, Y., Cao, H., and Tanimoto, Y., Benzophenone-initiated photoisomerization of the norbornadiene group in a benzophenone-steroid-norbornadiene system via long-distance intramolecular triplet energy transfer, *J. Phys. Chem.,* 100, 4480–4484, 1996.
85. Tung, C.H., Zhang, L.P., and Li, Y., Photoisomerization of norbornadiene group in a rigid bichromophoric compound initiated by remote keto chromophore: long-distance through-bond triplet energy transfer, *Chin. J. Chem.,* 14, 377–380, 1996.
86. Tung, C.H., Zhang, L.P., Li, Y., Cao, H., and Tanimoto, Y., Intramolecular long-distance electron transfer and triplet energy transfer. Photophysical and photochemical studies on a norbornadiene-steroid-benzidine system, *J. Am. Chem. Soc.,* 119, 5348–5354, 1997.
87. Gleiter, R. and Ohlbach, F., Photochemical experiments with 2,3-bis(tert-butylsulfonyl)bicyclo[2.2.2]octa-2,5-diene and related systems, *J. Chin. Chem. Soc.,* 43, 117–122, 1996.

88. Kaupp, G. and Prinzbach, H., Zur Kinetick der Norbornadiene-Quadricyclan-Photocycloaddition, *Helv. Chim. Acta,* 52, 956–966, 1969.
89. Edman, J.R., 2,3-Dicyanoquadricyclane. Synthesis and isomerization, *J. Org. Chem.,* 32, 2920–2921, 1967.
90. Cristoll, S.J. and Snell, R.L., The photoisomerization of bicyclo[2.2.1]hepta-2,5-diene-2,3-dicaboxylic acid to quadricyclo[2,2,1,0,^{2,6}0^{3,5}]heptane-2,3-dicarboxylic acids, *J. Am. Chem. Soc.,* 80, 1950–1952, 1958.
91. Nishino, H., Nakamura, A., and Inoue, Y., Theoretical and experimental verification of the asymmetric photoisomerization of methyl norbornadiene-2-carboxylate to methyl quadricyclane-1-carboxylate, *J. Chem. Soc., Perkin Trans. 2,* 1693–1700, 2001.
92. Nakamura, A., Nishino, H., and Inoue, Y., Verification of the validity of assuming first-order kinetics upon deriving the equation for the relationship between conversion and enantiomeric excess, *J. Chem. Soc., Perkin Trans. 2,* 1701–1705, 2001.
93. Nishino, H., Nakamura, A., Shitomi, H., Onuki, H., and Inoue, Y., Numerical simulation and experimental verification of the reversible symmetric photoisomerization between methyl norbornadiene-2-carboxylate and methyl quadricyclane-1-carboxylate, *J. Chem. Soc., Perkin Trans. 2,* 1706–1713, 2001.
94. Toda, T., Hasegawa, E., Mukai, T., Tsuruta, H., Hagiwara, T., and Yoshida, T., Photochemical reaction of 2-aroyl-3-arylnorbornadienes, *Chem. Lett.,* 1551–1554, 1982.
95. Maafi, M., Lion, C., and Aaron, J.J., Synthesis, photophysical properties and valence photoisomerization of new fluorescent aromatic norbornadienes, *New. J. Chem.,* 20, 559–570, 1996.
96. Maafi, M., Aaron, J.J., and Lion, C., Direct valence isomerization of newly synthesized norbornadiene aromatic derivatives. A kinetic and photophysical study, *Chem. Lett.,* 1865–1868, 1994.
97. Proskurnina, M., Kazmin, A.G., Zenova, A.Y., Lermontov, S.A., Borisenko, A.A., and Zefirov, N.S., Photoinitiated valence isomerization of 2-(trifluoroacetyl)-3-phenylbicyclo[2.2.1]hepta-2,5-diene, *Zh. Org. Khim. (Russ.),* 32, 146–147, 1996.
98. Tamiaki, H. and Maruyama, K., A water-stable quadricyclane derivative, *Chem. Lett.,* 1875–1876, 1988.
99. Maruyama, K., Tamiaki, H., and Yanai, T., Valence isomerization between water-soluble norbornadiene and quadricyclane derivative, *Bull. Chem. Soc. Jpn.,* 58, 781–782, 1985.
100. Maruyama, K. and Tamiaki, H., A water-soluble solar energy storage system, *Chem. Lett.,* 1699–1702, 1982.
101. Maruyama, K., Terada, K., and Yamamoto, Y., Highly efficient valence isomerization between norbornadiene and quadricyclane derivatives under sunlight, *Chem. Lett.,* 839–842, 1981.
102. Chernoivanov, V.A., Dubonosov, A.D., Popova, L.L., Galichev, S.V., Borodkin, G.S., Bren V.A., and Minkin V.I., Valence isomerization of 3-phenylnorbornadiene-2-carboxamides, *Zh. Org. Khim. (Russ.),* 29, 2148–2152, 1993.
103. Chernoivanov, V.A., Dubonosov, A.D., Bren, V.A., Minkin, V.I., Galichev, S.V., and Suslov, A.N., Valence isomerization of carbonyl-containing norbornadienes, *Zh. Org. Khim. (Russ.),* 28, 1647–1651, 1992.
104. Minkin, V.I., Bren, V.A., Chernoivanov, V.A., Dubonosov, A.D., and Galichev, S.V., Photochromic behaviour of 2,3-substituted norbornadienes, *Mol. Cryst. Liq. Cryst. Sci. Technol. Sect. A,* 246, 151–154, 1994.
105. Dubonosov, A.D., Chernoivanov, V.A., Popova, L.L., Bren, V.A., and Minkin, V.I., Synthesis and photoinitiated isomerization of 2-phenyl-3-(2-aroylvinyl)norbornadiene, *Zh. Org. Khim. (Russ.),* 30, 148–149, 1994.
106. Dubonosov, A.D., Galichev, S.V., Chernoivanov, V.A., Bren, V.A., and Minkin, V.I., Synthesis and photoinitiated isomerization of 3-(4-nitrophenyl)- and 3-(4-aminophenyl)bicyclo[2.2.1]hepta-2,5-diene-2-carbaldehyde and –2-carboxylic acid derivatives, *Russ. J. Org. Chem.,* 37, 67–71, 2001.
107. Chernoivanov, V.A., Dubonosov, A.D., Minkin, V.I., Bren, V.A., and Lyubarskaya, A.E., Photoisomerization of 3-phenylnorbornadiene-2-carbaldehyde and its imines, *Zh. Org. Khim. (Russ.),* 25, 443–444, 1989.

108. Ivakhnenko, E.P., Makarova, N.I., Knyazhansky, M.I., Bren, V.A., Chernoivanov, V.A., Shiff, A.I., and Borodkin, G.S., Photochemical generation, photochromism and photocyclization of 2-norbornadienyl substituted benzo-1,3-oxazoles, *Mol. Cryst. Liq. Cryst. Sci. Technol. Sect A,* **297**, 233–237, 1997.
109. Aldoshin, S.M., Bren, V.A., Dubonosov, A.D., Kozina, O.A., Minkin, V.I., Chernoivanov, V.A., and Chuev, I.I., Molecular and crystal structure of 3-phenylnorbornadiene-2-(N-phenyl)carbaldimine and 3-phenyl-2-(2,2-dicyano-vinyl)norbornadiene, *Izv. Acad. Nauk Ser. Khim. (Rus.),* 504–508, 1995.
110. Browne, N.R., Brown, R.F., Eastwood, F.W., and Fallon, G.D., The chemistry of ethyl 2-ethoxycarbonyl-5,5-diphenylpenta-2,3,4-trienoate, a potential precursor of $Ph_2C{=}C{=}C{=}C{=}C{=}O$, *Aust. J. Chem.,* 40, 1675–1686, 1987.
111. Ingartinger, H., Oeser, T., Jahn, R., and Kallfaß, D., Pyramidalization of the sp^2-hybrized carbon atoms in 1,4-bridged 2,5-cyclohexadienes, *Chem. Ber.,* 125, 2067–2073, 1992.
112. Gourdon, A. and Laine, P., Bicyclo[2.2.1]hepta-2,5-diene-2,3-dicarboxamide, $C_9H_{10}N_2O_2$, *Acta Cryst.,* 50, 414–415, 1994.
113. Yamashita, Y., Hanaoka, T., Takeda, Y., Mukai, T., and Miyashi, T., Synthesis and properties of dipyridylnorbornadienes, *Bull. Chem. Soc. Jpn.,* 61, 2451–2458, 1988.
114. Koblik, A.V., Muradyan, L.A., Dubonosov, A.D., and Zolotovskova, G.P., Diene synthesis with 4-phenylethynylpyrylium salts, *Khim. Geterotsikl. Soedin. (Russ.),* 307–311, 1990.
115. Suslov, A.N., Chernoivanov, V.A., Dubonosov, A.D., Kozina, O.A., Bren, V.A., and Minkin, V.I., Reversible photoisomerization of 2-benzimidazolyl-3-phenylnorbornadienes into corresponding quadricyclanes, *Zh. Org. Khim. (Russ.),* 31, 1255–1256, 1995.
116. Bren, V.A., Minkin, V.I., Dubonosov, A.D., Chernoivanov, V.A., Rybalkin, V.P., and Borodkin, G.S., Biphotochromic norbornadiene systems, *Mol. Cryst. Liq. Cryst. Sci. Technol. Sect A,* 297, 247–253, 1997.
117. Fanghanl, D., Timpe, C., and Orthman, V., Photochromic compounds with N=N and C=N chromophores, in *Organic Photochromes,* Eltsov, A., Ed., Plenum, New York, 1990, chap. 3.
118. Roos, B.O., Merchan, M., McDiarmid, R., and Xing, X., Theoretical and experimental determination of the electronic spectrum of norbornadiene, *J. Am. Chem. Soc.,* 116, 5927–5936, 1994.
119. Xing, X., Gedanken, A., Sheybani, A.-H., and McDiarmid, R., The 198–225 nm transition of norbornadiene, *J. Phys. Chem.,* 98, 8302–8309, 1994.
120. Hirao, K., Ando, A., Hamada, T., and Yonemitsu, O., Valence isomerization between coloured acylnorbornadienes and quadricyclanes as a promising model for visible (solar) light energy storage, *J. Chem. Soc., Chem. Commun.,* 300–302, 1984.
121. Nagai, T., Fujii, K., Takahashi, I., and Shimada, M., Trifluoromethyl-substituted donor-acceptor norbornadiene, useful solar energy material, *Bull. Chem. Soc. Jpn.,* 74, 1673–1678, 2001.
122. Nagai, T., Takahashi, I., and Shimada, M., Trifluoromethyl-substituted norbornadiene, useful solar energy material, *Chem. Lett.,* 897–898, 1999.
123. Hirao, K. and Yamashita, A., Fluoroalkylnorbornadienes and their corresponding valence isomer quadricyclanes. A light energy storage system, *J. Fluorine Chem.,* 36, 293–305, 1987.
124. Hautala, R.R., Little, J., and Sweet, E., The use of functionalized polymers as photosensitizers in an energy storage reaction, *Sol. Energy,* 19, 503–508, 1977.
125. Asai, N. and Neckers, D.C., Poly(p-(triflurovinyl)benzophenone) and poly(p-(trifluorovinyl)acetophenone). Photostable polymeric triplet energy transfer donors, *J. Org. Chem.,* 45, 2903–2907, 1980.
126. Nishikubo, T., Kawashima, T., Inomata, K., and Kameyama, A., Design of multifunctional polymeric photosensitizers containing pendant (nitroaryl)oxy groups and quaternary onium salts for photochemical valence isomerization of potassium 3-phenyl-2,5-norbornadiene-2-carboxylate, *Macromolecules,* 25, 2312–2318, 1992.
127. Wang, X.S., Zhang, B.W., and Cao, Y., Valence isomerization of norbornadiene in polymer systems for solar energy storage, *J. Photochem. Photobiol. A: Chem.,* 96, 193–198, 1996.

128. Nishimura, I., Kameyama, A., and Nishikubo, T., Synthesis of self-photosensitizing polyesters carrying pendant norbornadiene (NBD) moieties and benzophenone groups and their photochemical reactions, *Macromolecules,* 31, 2789–2796, 1998.
129. Nishikubo, T., Kameyama, A., Kishi, K.A., and Nakajima, T., Synthesis of new photoresponsive polyamides containing norbornadiene residues in the main chain, *Macromolecules,* 27, 1087–1092, 1994.
130. Nishikubo, T., Kameyama, A., Nakajima, T., and Kishi, K., Synthesis of new photoresponsive polyamides containing norbornadiene residues in the main chain, *Polym. J.,* 24, 1165–1168, 1992.
131. Kamogawa, H., Goucho, S., and Nakahara, M., Synthesis and photo valence isomerization of polyamide bearing norbornadiene unit, *Bull. Chem. Soc. Jpn.,* 65, 2306–2308, 1992.
132. Tsubata, A., Uchiyama, T., Kameyama, A., and Nishikubo, T., Synthesis of poly(ester-amide)s containing norbornadiene (NBD) residue by the polyaddition of NBD dicarboxylic acid derivatives with bis(epoxide)s and their photochemical properties, *Macromolecules,* 30, 5649–5654, 1997.
133. Konno, Y., Kameyama, A., Nishikubo, T., and Nagai, T., Synthesis of new photoresponsive polyesters containing norbornadiene residues by the polyaddition of donor–acceptor norbornadiene carboxylic acid diglycidyl ester with dicarboxylic acids and their photochemical properties, *J. Polym. Sci. Part A: Polym. Chem.,* 39, 2683–2690, 2001.
134. Ikeda, A., Kameyama, A., Nishikubo, T., and Nagai, T., Synthesis of new photoresponsive polyesters containing donor-acceptor norbornadiene (D-A NBD) residues by the polyaddition of D-A NBD dicarboxylic acids with bis(epoxide)s and their photochemical properties, *Macromolecules,* 34, 2728–2734, 2001.
135. Nishikubo, T., Kameyama, A., Kishi, K., Kawashima, T., Fujiwara, T., and Hijikata, C., Synthesis of new photoresponsive polymers bearing norbornadiene moieties by selective cationic polymerization of 2-[[(3-phenyl-2,5-norbornadienyl)-2-carbonyl]oxy]ethyl vinyl ether and photochemical reaction of the resulting polymers, *Macromolecules*, 25, 4469–4475, 1992.
136. Nishikubo, T., Shimokawa, T., and Sahara, A., Successful synthesis of polymers containing pendant norbornadiene moieties and norbornadiene photochemical valence isomerization, *Macromolecules*, 22, 8–14, 1989.
137. Nishikubo, T., Hijikata, C., and Iizawa, T., Photochemical property of the polymer-bearing pendant norbornadiene moiety and storage stability of the resulting quadricyclane group in the polymer, *J. Polym. Sci. Part A: Polym. Chem.,* 29, 671–676, 1991.
138. Iizawa, T., Hijikata, C., and Nishikubo, T., Synthesis and solar energy storage property of polymers containing norbornadiene moieties, *Macromolecules*, 25, 21–26, 1992.
139. Nishikubo, T., Kameyama, A., Kishi, K., and Mochizuki, Y., Synthesis and photochemical properties of solar energy storage-exchange polymers containing pendant norbornadiene moieties, *J. Polym. Sci. Part A: Polym. Chem.,* 32, 2765–2773, 1994.
140. Nishikubo, T., Kawashima, T., and Watanabe, S., Synthesis of polymers bearing pendant norbornadiene moieties by addition reaction of poly(glycidyl methacrylate-co-methyl methacrylate)s with 2,5-norbornadiene-2-carboxylic acids, *J. Polym. Sci., Part A: Polym. Chem.,* 31, 1659–1665, 1993.
141. Nishimura, T., Kameyama, A., Sakurai, T., and Nishikubo, T., Synthesis of polyesters carrying norbornadiene (NBD) moieties by the ring-opening copolymerization of glycidic esters containing NBD moieties with carboxylic anhydrides and their photochemical reactions, *Macromolecules*, 29, 3818–3825, 1996.
142. Kawashima, N., Kameyama, A., Nishikubo, T., and Nagai, T., Synthesis and photochemical property of polymers with pendant donor-acceptor-type norbornadiene moieties, *J. Polym. Sci. Part A: Polym. Chem.,* 39, 1764–1773, 2001.
143. Nagai, T., Shimada, M., and Nishikubo, T., Synthesis of new photoresponsive polymers containing trifluoromethyl-substituted norbornadiene moieties, *Chem. Lett.,* 1308–1309, 2001.
144. Iizava, T., Suyeoshi, T., Hijikata, C., and Nishikubo, T., Synthesis of rigid polymer containing pendant norbornadiene moieties and its photochemical valence isomerization, *J. Polym. Sci. Part A: Polym. Chem.,* 32, 3091–3098, 1994.

145. Iizava, T., Ono, H., and Matsuda, F., Synthesis of rigid polyimides containing pendant norbornadiene moieties and their valence isomerization between norbornadiene and quadricyclane, *React. Funct. Polym.,* 30, 17–25, 1996.
146. Nishikubo, T., Kameyama, A., Kishi, K., and Hijikata, C., Synthesis and photochemical properties of insoluble poly(styrene) beads containing pendant norbornadiene moieties, *React. Polym.,* 24, 65–72, 1994.
147. Kinoshita, K., Horie, K., Morino, T., and Nishikubo, T., Large photoinduced refractive index changes of a polymer containing photochromic norbornadiene groups, *Appl. Phys. Lett.,* 70, 2940–2942, 1997.

18

Copper(I)-Catalyzed Inter- and Intramolecular [2 + 2]-Photocycloaddition Reactions of Alkenes

Subrata Ghosh
Indian Association for the Cultivation of Science

18.1 Introduction

Photoinduced [2 + 2]-cycloaddition of alkenes to form cyclobutanes is one of the most well-studied and synthetically useful reactions among all the photochemical processes. The utility of this reaction in organic synthesis stems from its ability to create in a single step a complex multicyclic carbon network[1,2] with up to four asymmetric centers on the cyclobutane ring in a regio- and stereoselective fashion. The scope of this photoreaction has been widened further by the proclivity of the cyclobutane ring to undergo facile ring expansion and carbon–carbon bond fragmentation. A sequence of [2 + 2]-photocycloaddition and ring expansion or C-C bond fragmentation has been extensively employed for the construction of five-[3] to eight[4]-membered rings.

The generally accepted mechanism[5] that accounts for the majority of the $2\pi + 2\pi$ photocycloaddition reactions involves excitation of the alkene on UV irradiation either directly or sometimes with sensitizer to the triplet-excited state. Quenching of the triplet-excited state by a ground-state alkene leads to an excited-state complex or exciplex that either directly or through biradical intermediates gives rise to cyclobutanes. The actual mechanism involved in a cycloaddition process depends on the substrates and the reaction conditions employed. Alkenes conjugated to a π-system, such as enones having UV absorption maxima around 300 nm, easily lead to triplet-excited states on direct irradiation, and these add to a ground state alkene to give cyclobutanes. A classic example of enone–olefin cycloaddition[6] is the addition of isobutylene to cyclohexenone **1** to produce the adduct **2** (Scheme 1).

0-8493-1348-1/04/$0.00+$1.50

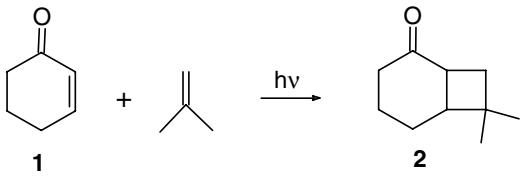

1 **2**

SCHEME 1

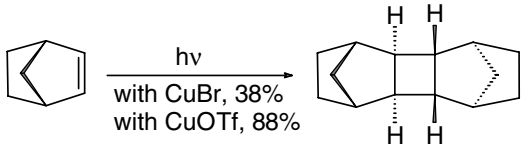

3 **4**

SCHEME 2

Nonconjugated alkenes have UV absorption maxima at 190–200 nm and thus require high energy for excitation not available from conventional photochemical equipment. Triplet energies are also relatively high. Thus, photocycloaddition between simple alkenes is difficult to attain through direct irradiation or sensitization. However, in the presence of transition metal salts, such alkenes exhibit UV absorption maxima around 240 nm. Thus, nonconjugated alkenes can be raised to the excited state when irradiated in the presence of transition metal salts[7] and undergo [2 + 2]-photocycloaddition. Although there are reports of the use of several transition metals,[7] copper(I) salts, especially copper(I) trifluoromethane sulfonate(CuOTf), first reported by Salomon and Kochi[8] as the 2CuOTf C_6H_6 complex, has been found to be the most efficient and selective for [2 + 2]-cycloaddition. The remarkable feature of the Cu(I)-catalyzed photocycloaddition reaction of the alkenes is the stereochemical outcome that leads preferentially to a single diastereoisomer especially in case of intramolecular reactions. A brief account of the mechanism, stereochemical aspects, and synthetic applications of Cu(I)-catalyzed [2 + 2]-photocycloaddition reactions is presented here.

18.2 Mechanism of Catalysis

Copper(I)-catalyzed [2 + 2]-photocycloaddition between two nonconjugated alkenes involves coordination of both the reacting alkene units in their ground states with a single copper(I). Photoexcitation of this bis-alkene-Cu(I) complex leads to a cyclobutane with regeneration of the Cu(I) catalyst. That Cu(I) forms complexes with alkenes was evidenced by isolation of several olefin-Cu(I) complexes.[8–10] The involvement of a bis-alkene-Cu(I) complex in [2 + 2]-photocycloaddition was obtained from dimerization of norbornene **3** when irradiated in the presence of CuCl or CuBr to afford mainly the dimer **4** in 38% yield (Scheme 2).[11] While norbornene and CuBr separately are almost transparent in the UV, an intense UV absorption band at 239 nm was observed for a solution containing norbornene and CuBr. A 1:1 norbornene-Cu(I) complex was also isolated. No dimer formation was observed on irradiation of this complex in ether solution. However, irradiation of the complex in the presence of excess norbornene provided[12] the dimer **4**. Thus, dimer formation presumably involves a complex having one Cu bonded to two norbornene units. Irradiation of norbornene in the presence of CuOTf affords the dimer **4** in 88% yield.[13] NMR investigations[14] have shown that with CuOTf, both 1:1 and 1:2 Cu(I)-alkene complexes with the same UV absorption spectra are formed. Quantum yield experiments confirmed that it is the 1:2 complex that leads to dimer production. Thus, copper(I)-catalyzed [2 + 2]-photocycloaddition of alkenes requires ground-state coordination of both reacting alkene bonds with a single Cu(I).[7] The requirement of a 1:2 Cu(I)-alkene complex is confirmed further by the almost exclusive formation of the

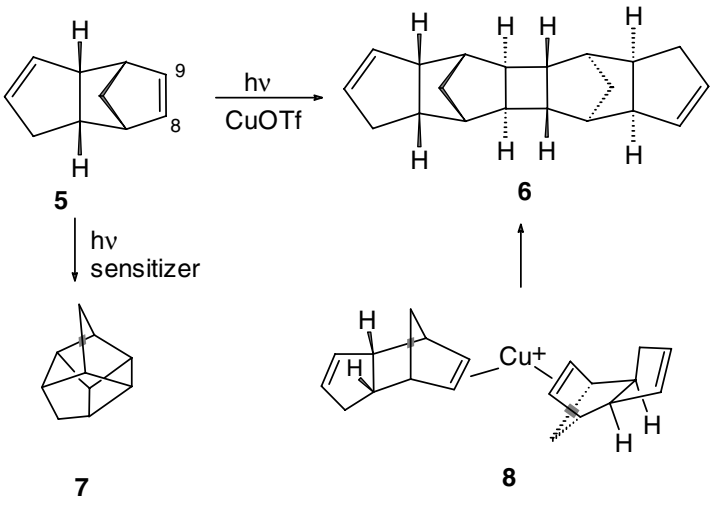

SCHEME 3

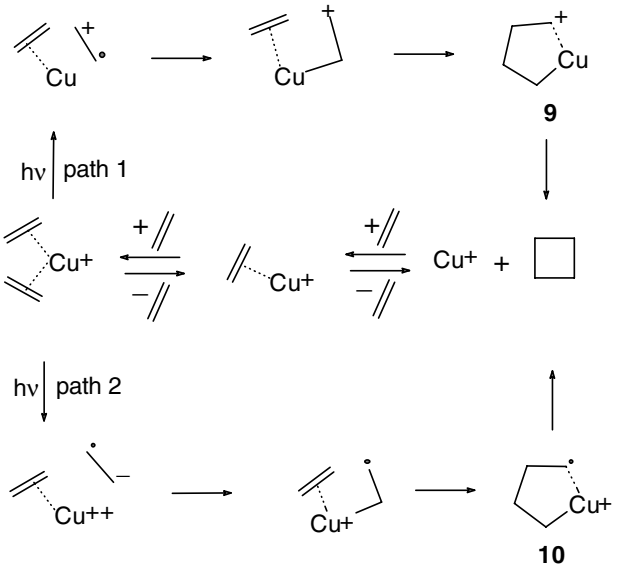

SCHEME 4

dimer **6**[14] from CuOTf-catalyzed photocycloaddition of *endo*-dicyclopentadiene **5**, which on sensitized irradiation[15] undergoes intramolecular cycloaddition to afford **7** (Scheme 3). A 1:2 Cu(I)-dicyclopentadiene complex **8** involving the more strained $\Delta^{8,9}$-bond has also been isolated.

The CuOTf-norbornene complex shows two UV absorption maxima at 236 nm (ε 3400) and 272 nm (ε 2000). The shorter wavelength absorption possibly arises through a metal-to-alkene ligand charge transfer (MLCT) excitation[16], while the longer wavelength absorption is assumed to be due to an alkene ligand-to-metal charge transfer (LMCT) excitation. The relative contribution of these two interactions is dependent on the olefin involved, as determined by NMR investigation[17,18] of the metal–alkene complex. Assuming bond formation to be a sequential process, LMCT (Path 1) and MLCT (Path 2) (Scheme 4)

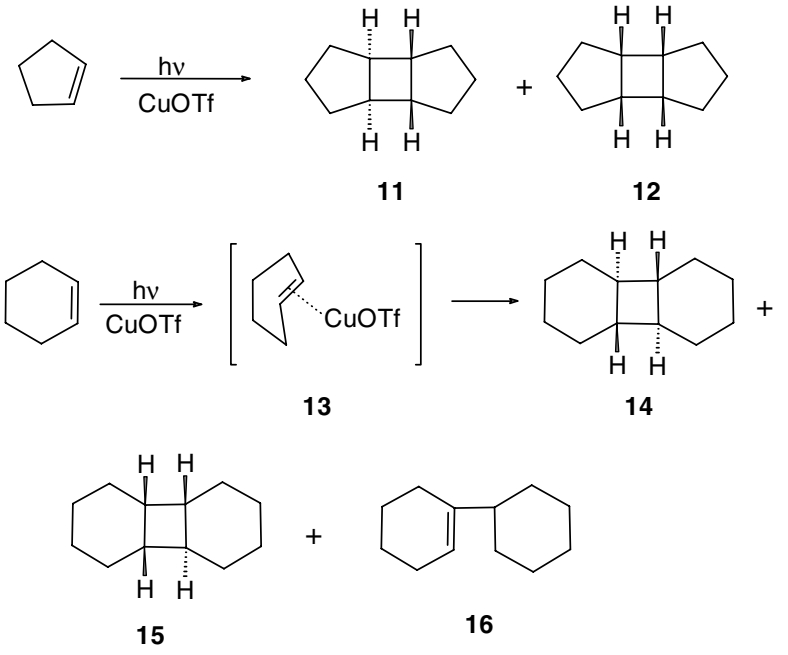

SCHEME 5

excitation may proceed through cyclization of either cationic or radical alkyl copper intermediates **9** or **10**, respectively. It has not yet been settled which of these processes actually leads to photocycloaddition. There is evidence in support of both radical[19] and cationic paths.[14,20,21] A concerted pathway[22] has also been supported by intermolecular cycloaddition studies.

Catalyst for [2 + 2]-Photocycloaddition

It is now well established that Cu(I)-catalyzed [2 + 2]-photocycloaddition of alkenes requires formation of a complex in which one copper is coordinatively linked with two alkene units. Among the various copper salts (CuCl, CuBr, CuOTf) used, the triflate anion in CuOTf has exceptional weak coordinating ability compared to halide ions, which compete with alkene for coordination with copper. Thus, CuOTf exhibits a strong tendency to form 1:2 Cu-alkene complexes compared to CuCl or CuBr. This is reflected in improved yields of adducts obtained with CuOTf rather than CuCl or CuBr (*vide infra*). In addition, CuOTf is soluble in most organic solvents and is stable under the photochemical reaction conditions. Hence, CuOTf is the catalyst of choice for [2 + 2]-photocycloaddition between two nonconjugated alkenes.

18.3 Intermolecular Photocycloadditions

Copper(I)-catalyzed intermolecular photocycloaddition requires that one of the reacting alkenes must be highly strained and reactive. It was already stated that norbornene **3** undergoes intermolecular addition to form the dimer **4** (Scheme 2) in 38% yield with CuBr and in 88% yield[13] with CuOTf as the catalyst. This is the first example of copper(I)-catalyzed intermolecular [2 + 2]-photocycloaddition.[11] Similarly, *endo*-dicyclopentadiene **5**, on irradiation in the presence of CuOTf, undergoes [2 + 2]-addition at the more stained 8,9-double bond to form the dimer **6**[14] (Scheme 3). Cyclopentene does not undergo dimerization with CuBr, while with CuOTf it forms the dimers **11** (30%) and **12** (2%) (Scheme 5).[22]

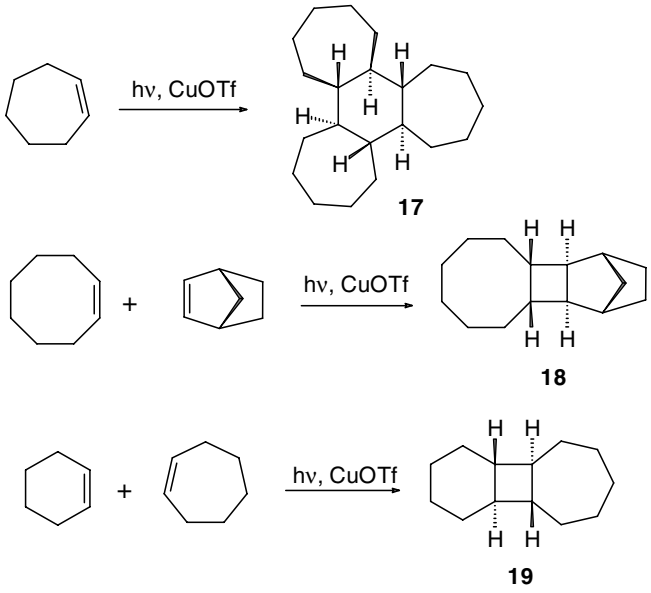

SCHEME 6

Irradiation of cyclohexene in the presence of CuOTf produces the dimers **14** (49%) and **15** (8%), along with the cyclohexylcyclohexene **16** (24%) (Scheme 5).[22] The stereochemical outcome in Cu(I)-catalyzed dimerization of cyclohexene may be the result of *cis-trans* isomerization on irradiation of the initially formed Cu(I)-cyclohexene complex to the *trans*-cyclohexene-CuOTf complex **13**, followed by a concerted ground state $2_{\pi a} + 2_{\pi s}$ cycloaddition of the highly strained *trans*-cyclohexene to another cyclohexene. Cycloheptene, on the other hand, produces the all *trans*-fused trimer **17** (Scheme 6) as the sole product.[23] A 1:3 CuOTf-*trans*-cycloheptene complex has been proposed to be the precursor of this product. No dimerization reaction has been observed for cyclooctene[14] and acyclic olefins.[22] However, mixed photocycloaddition occurs with cyclooctene if the other olefin is sufficiently reactive. Thus, cyclooctene adds to norbornene to produce the cyclobutane derivative **18** in 40% yield.[14] Codimerization was also observed when a mixture of cyclohexene and cycloheptene was irradiated in the presence of CuOTf to yield the adduct **19** (Scheme 6).[24]

Photocycloaddition of alkenes having allylic functional groups is of special significance, as the resulting cyclobutanes provide scope for further synthetic transformations. Allyl alcohol has been found to add to strained cycloalkenes only. Thus norbornene and *endo*-dicyclopentadiene, when irradiated in the presence of CuOTf with allyl alcohol as solvent, produce a pair of the cyclobutanes **20**, **21** and **22**, **23**, respectively (Scheme 7).[25] It is reasonable that the equilibrium between the complex **8** required for dimerization of dicyclopentadiene and the complex **24** required for the formation of **22** and **23** strongly favors the complex **24** in allyl alcohol due to additional coordinative interaction by the OH group of the allyl alcohol. No intermolecular cycloaddition between cyclohexene and allyl alcohol was observed, as the required mixed ligand complex having Cu(I) linked to both cyclohexene and allyl alcohol is not formed due to weak coordinating ability of cyclohexene with copper. Even cycloaddition between two units of allyl alcohol was not observed. However, irradiation of a dilute solution of allyl alcohol in dioxane in the presence of CuOTf does lead to photocycloaddition yielding 3-oxabicyclo[3.2.0]heptane **26** through intramolecular cycloaddition of *in situ* generated diallyl ether **25** (Scheme 8).[26] Interestingly, while acyclic olefins fail to undergo intermolecular [2 + 2]-photocycloaddition,[22] intramolecular cycloaddition of acyclic dienes proceeds smoothly. This observation has added a new dimension to copper(I)-catalyzed [2 + 2]-photocycloaddition of alkenes.

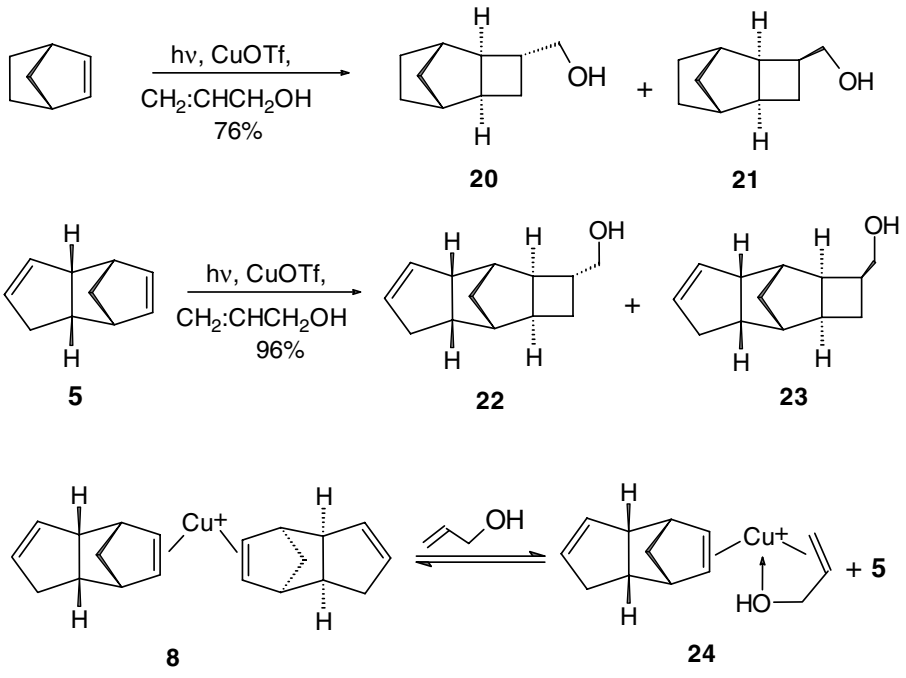

SCHEME 7

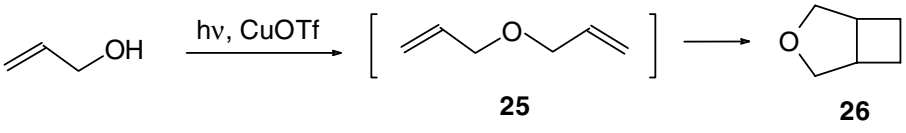

SCHEME 8

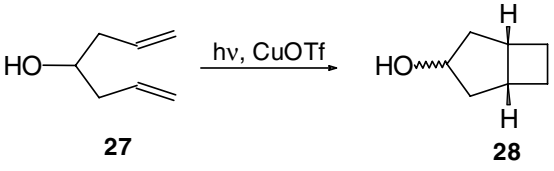

SCHEME 9

18.4 Intramolecular [2 + 2]-Photocycloadditions

Copper (I)-catalyzed intramolecular photocycloaddition between two acyclic double bonds was first observed by Evers and Mackor in 1978.[26] They demonstrated that although 3-oxabicyclo[3.2.0]heptane **26** is formed from diallyl ether **25** (Scheme 8), 4-hydroxy-1,6-heptadiene **27** produces an *endo,exo* (3:2) mixture of 3-hydroxy bicyclo[3.2.0]heptanes **28** (Scheme 9) on irradiation in presence of CuOTf. The generality and scope of this reaction were investigated in great detail by Salomon et al.[27] The acyclic dienes

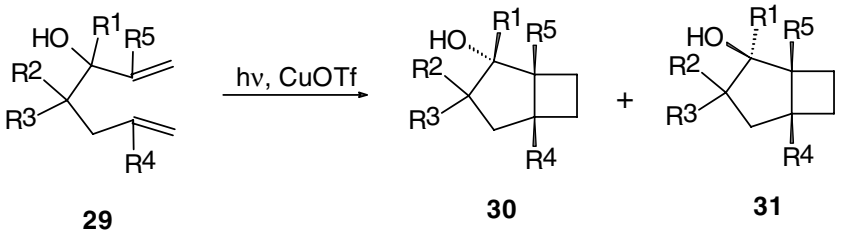

29 **30** **31**

a, $R^1 = R^2 = R^3 = R^4 = R^5 = H$; **b**, $R^1 = R^2 = R^3 = R^4 = H$, $R^5 = Me$;
c, $R^1 = R^4 = R^5 = H$, $R^2 = R^3 = Me$; **d**, $R^1 = R^4 = H$, $R^2 = R^3 = R^5 = Me$;
e, $R^1 = R^2 = R^3 = H$, $R^4 = R^5 = Me$; **f**, $R^1 = R^2 = R^3 = R^5 = H$, $R^4 = Me$;
g, $R^1 = Me$, $R^2 = R^3 = R^4 = R^5 = H$

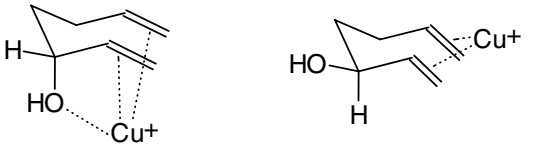

32 **33**

SCHEME 10

TABLE 18.1 Copper(I)-Catalyzed Photocycloaddition of 1,6-Heptadiene-3-ols

Entry	Diene	Bicyclo[3.2.0]heptanes	*endo*:*exo*	Yield (%)
1	**29a**	**30a, 31a**	9:1	86
2	**29b**	**30b, 31b**	6:1	81
3	**29c**	**30c, 31c**	9:1	91
4	**29d**	**30d, 31d**	3:2	83
5	**29e**	**30e, 31e**	>20:1	[a]
6	**29f**	**30f, 31f**	5:1	78
7	**29g**	**30g, 31g**	>20:1	89

[a] 40% conversion after 24 h.

investigated so far include 1,6-heptadienes, diallyl ethers, homoallyl vinyl ethers, and *N,N*-diallyl carbamates.

[2 + 2]-Cycloaddition of 1,6-heptadienes

Copper(I)-catalyzed intramolecular photocycloaddition of 1,6-heptadiene-3-ols **29** provides an efficient route for the synthesis of bicyclo[3.2.0]heptan-2-ols **30** and **31** (Scheme 10).[27–30] Generally, a great preference for stereoselective generation of the thermodynamically less stable *endo*-2-hydroxy diastereoisomer **30** (Table 18.1) was observed. The observed selectivity is attributed to the behavior of the dienols **29** acting preferentially as a tridentate ligand shown in structure **32** rather than a bidentate ligand as in structure **33**. In contrast to the strong preference for *endo*-selectivity in the photocycloaddition of the dienes **29**, the dienol **34** produces *endo*-**35** and *exo*-**36** in a ratio of 3:4 (Scheme 11). The complex **34x** producing the *exo*-alcohol **36** is favored over the tri-coordinated Cu(I)-complex **34n** due to unfavorable steric interference by a Me substituent in the 5-position. The Cu(I)-catalyzed photocycloaddition of 1,6-

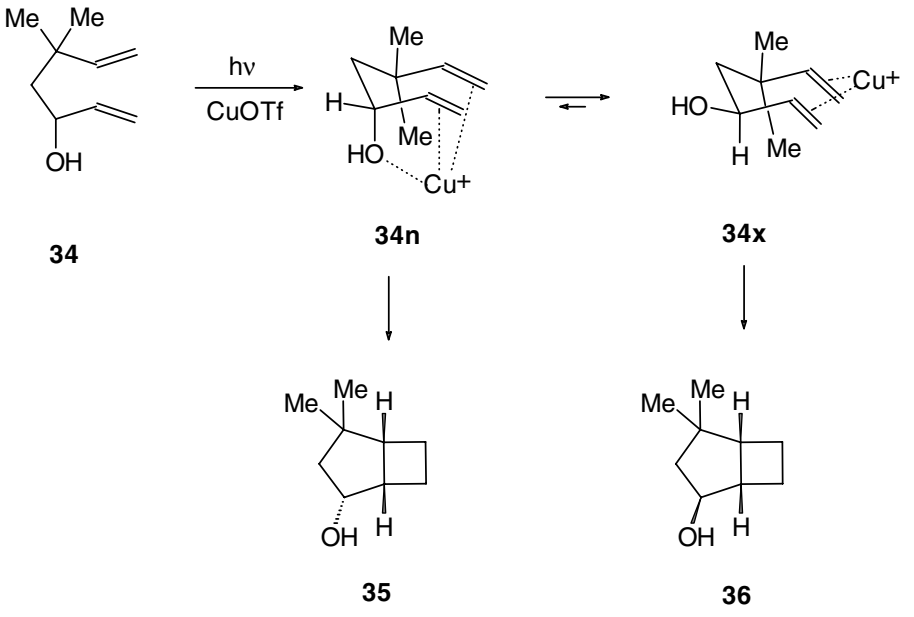

SCHEME 11

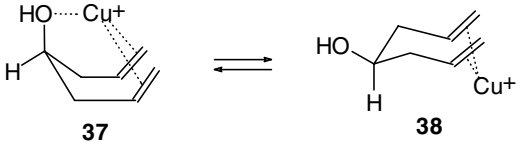

SCHEME 12

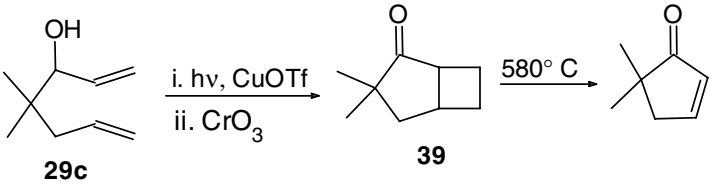

SCHEME 13

heptadien-4-ol **27**, with the OH group at the homoallylic position, is nonstereoselective producing a 3:2 *endo-exo* mixture of bicyclo[3.2.0]heptane-3-ols **28** (Scheme 9). In this case the *exo*-alcohol formation requires a tri-coordinated complex **37**[28] having a boat-like conformation that is disfavored in comparison to the chair-like arrangement in the complex **38** (Scheme 12). Thus, the presence of a hydroxyl group at the allylic position in 1,6-heptadiene plays a crucial role in determining the stereochemical outcome during the photocycloaddition.

The copper(I)-catalyzed photocycloaddition of 1,6-heptadien-3-ols **29**, in conjunction with oxidation of the resulting bicyclic alcohols to bicyclo[3.2.0]heptan-2-ones, as illustrated by the transformation of **29c** to **39** (Scheme 13), provides an alternative route to $2\pi + 2\pi$ intermolecular photocycloaddition of

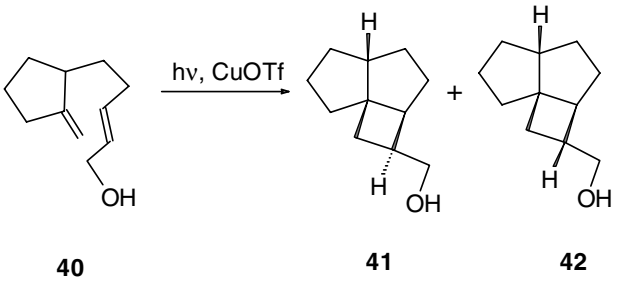

40 **41** **42**

SCHEME 14

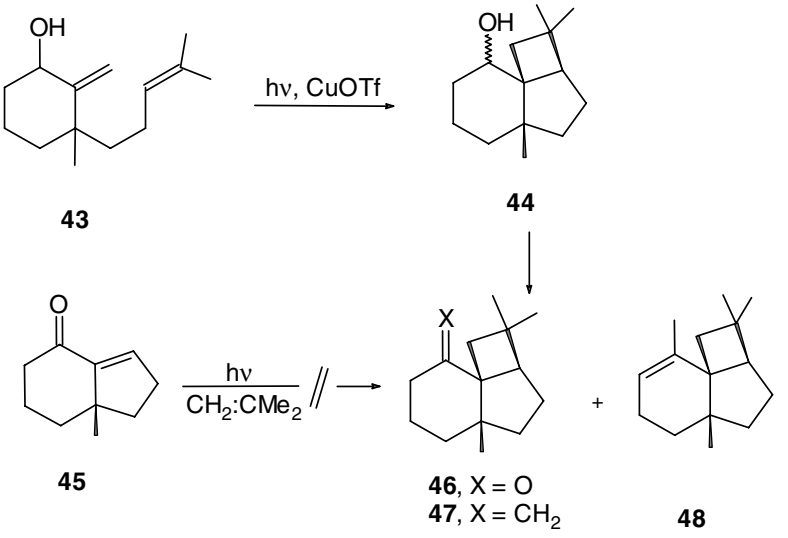

43 **44** **45**

46, X = O
47, X = CH_2 **48**

SCHEME 15

olefins to cyclopent-2-en-1-ones. Pyrolysis of the bicyclo[3.2.0]heptan-2-ones provides a new route to cyclopentenones also.[27] For example, the bicyclic ketone **39** on pyrolysis provides 6,6-dimethylcyclopent-2-en-1-one (Scheme 13).

Tricyclic ring systems can also be constructed when one of the alkene units of the 1,6-heptadiene is part of a ring. For example, the dienol **40** leads to the tricyclic products **41** (68%) and **42** (23%) (Scheme 14).[29] The loss of stereospecificity in the products probably arises due to competing copper(I)-catalyzed geometric isomerization of the *trans*-allylic alcohol during photocycloaddition.

Stereoselective copper(I)-catalyzed [2 + 2]-photocycloaddition of 1,6-heptadienols has been used as a key step in the synthesis of several natural products. The total synthesis of the sesquiterpenes α-panasinsene **47** and β-panasinsene **48** has been achieved by CuOTf catalyzed photocycloaddition of the dienol **43** as the key step (Scheme 15).[31] The resulting bicyclo[3.2.0]heptanol **44** was then converted to the natural products through the ketone **46**. It is noteworthy that direct access to the requisite intermediate **46** involving photoaddition of isobutylene to the enone **45** failed, illustrating the importance of the copper(I)-catalyzed photocycloaddition of 1,6-heptadienols.

The bicyclo[3.2.0]heptanols obtained through this cycloaddition process can be exploited for the stereocontrolled synthesis of 1,2-disubstituted cyclobutanes. The concept is demonstrated by the synthesis of grandisol **53** (Scheme 16), the pheromone of the male cotton boll weevil. Rosini et al. have described

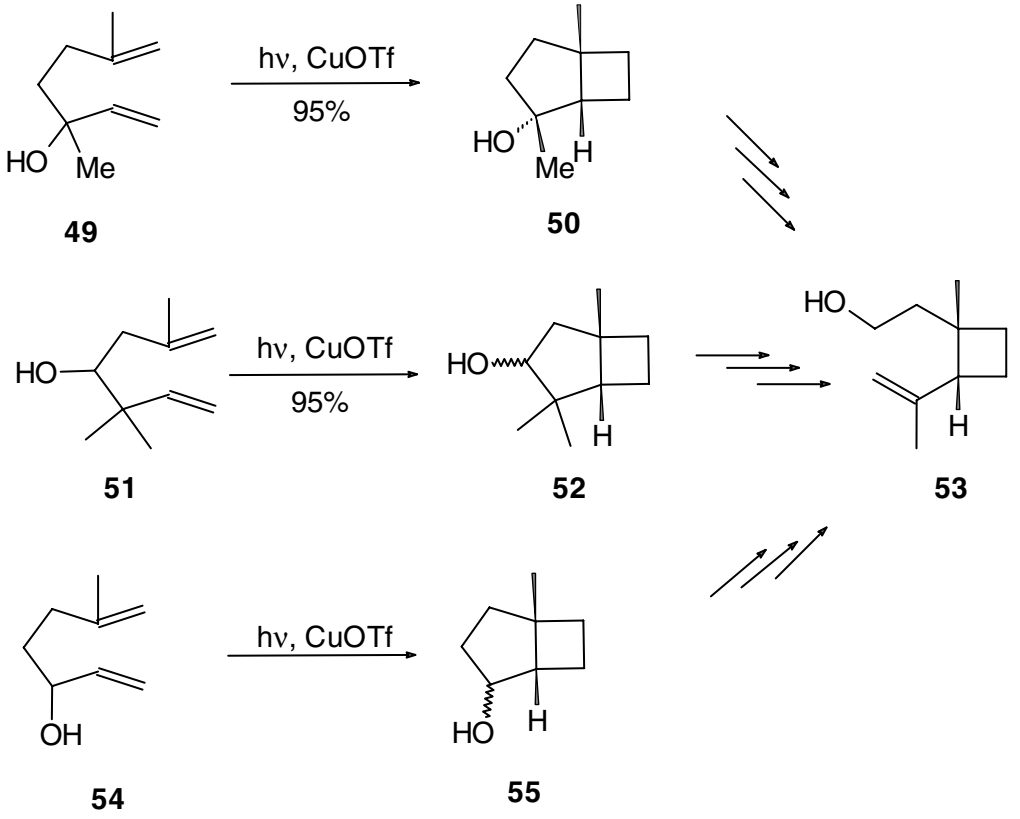

SCHEME 16

two stereoselective routes involving bicyclo[3.2.0]heptanols **50** and **52** as the intermediates.[32,33] These were obtained in excellent yields from CuOTf catalyzed photocycloaddition of the 1,6-heptadienols **49** and **51**, respectively. The functionalized cyclopentane ring in **50** and **52** was then cleaved to provide, finally, (±)-grandisol. Rosini et al.[34,35] have also achieved enantiomerically pure compound (EPC) synthesis of both enantiomers of grandisol through resolution of the bicyclo[3.2.0]heptanol **50**. Langer et al.[36] have also accomplished a racemic synthesis of grandisol through the bicyclo[3.2.0]heptanol **55** obtained through copper(I)-catalyzed photocycloaddition of the 1,6-heptadien-3-ol **54**. Later, this group completed enantioselective synthesis of (+)- and (–)- grandisol using enantiomerically pure dienol **54**.

In connection with the enantioselective synthesis of grandisol, Langer and Mattay[37] explored several different approaches for asymmetric induction during [2 + 2]-photocycloaddition of 1,6-heptadienols. One of these approaches involves the use of chiral Cu(I)-complexes as the catalyst. This has resulted in photoadducts with very low enantiomeric excess (ee) (<5%). The low *ee*s have been attributed to the poor coordinating ability of the Cu(I) of the chiral Cu-complexes with alkenes. The other approach investigated involves photocycloaddition of dienes having a chiral auxiliary. Thus, reaction of 1,6-heptadien-3-ol having a chiral auxiliary attached to the 3-hydroxy group afforded bicyclo[3.2.0]heptan-2-ols with *ee*s of up to 15%. In another approach, the diene **56**, having a ketal made of a chiral diol, gives on CuOTf catalyzed photocycloaddition and auxiliary removal from the photoadduct **57**, the bicyclic ketone **58** with *ee*s of up to 60% (Scheme 17).

The Cu(I)-catalyzed photocycloaddition of 1,6-heptadien-4-ol **59** (Scheme 18) was employed by Lal and co-workers[38,39] for the synthesis of the sesquiterpenes robustadials for which the structures **61** were proposed. The bicyclo[3.2.0]heptane **60** obtained from this reaction was converted to three of the four

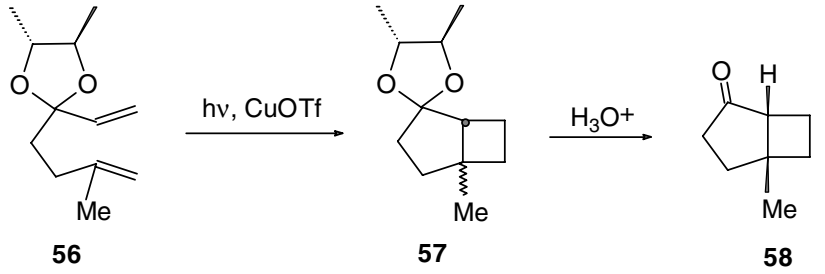

56 **57** **58**

SCHEME 17

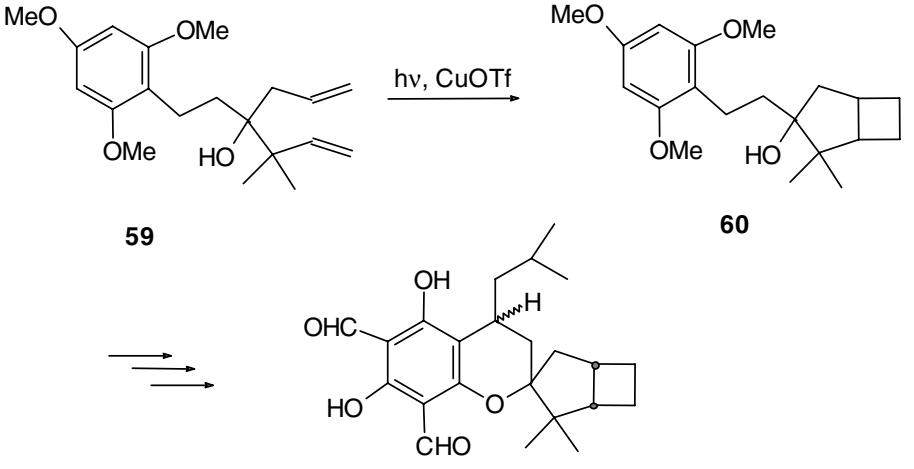

59 **60** **61**

SCHEME 18

possible diastereoisomers of the structure **61**. None of these structures corresponds to the natural product, disproving the proposed structure.

A sequence of Cu(I)-catalyzed [2 + 2]-photocycloaddition–cyclobutyl carbinyl cation rearrangement has been employed for the construction of novel carbocyclic compounds. Thus, cycloaddition of the dienol **40** to the hydroxymethyl cyclobutane **41** followed by solvolysis of its tosylate **62** afforded the triquinane **63** after reduction (Scheme 19).[29] An efficient route[40] to *exo*-1,2-polymethylene-7-hydroxy norbornanes **66** has also been developed based on this protocol. Photocycloaddition of an epimeric mixture of the dienols **64** to 2-hydroxybicyclo[3.2.0]heptanes **65** followed by treatment with trifluoroacetic acid (TFA) affords the 7-hydroxynorbornanes **66** in overall good yields.

Ghosh et al[41] have recently demonstrated that the CuOTf-catalyzed [2 + 2]-photocycloaddition can be successfully carried out when 1,6-heptadienes are incorporated in a carbohydrate derivative, thus widening the scope of the Cu(I)-catalyzed photocycloaddition. The diene **67a**, on irradiation in the presence of CuOTf, afforded the thermodynamically less stable *cis-syn-cis* adduct **68a** (Scheme 20). Initially, this unexpected stereochemical outcome was thought to arise through the tri-coordinated Cu(I) complex **69**. However, photocycloaddition of the analogous diene **67b** (with benzophenone as sensitizer) in the absence of a Cu(I) catalyst also produced the *cis-syn-cis* adduct **68b**, excluding the possibility of the involvement of the Cu(I)-complex **69**. Possibly, the observed stereoselectivity arises through the Cu(I)-

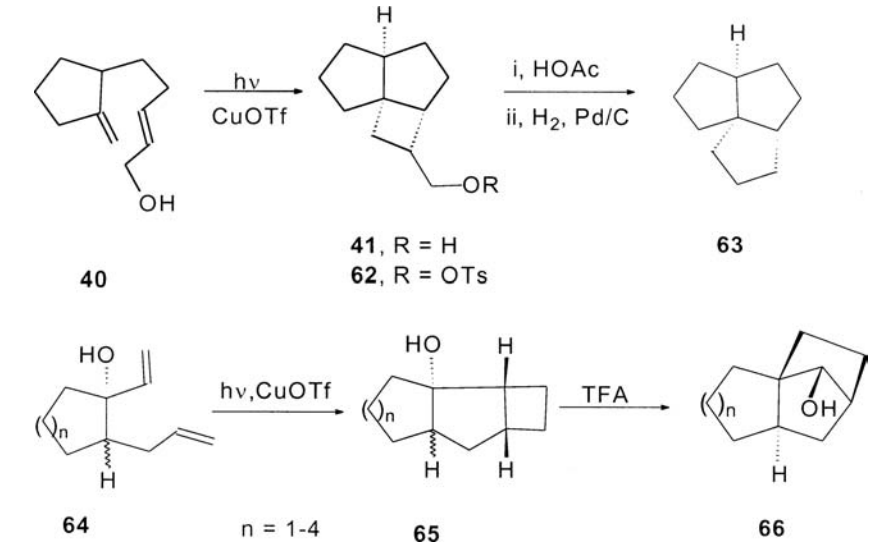

40 **41**, R = H; **62**, R = OTs **63** **64** **65** **66**

SCHEME 19

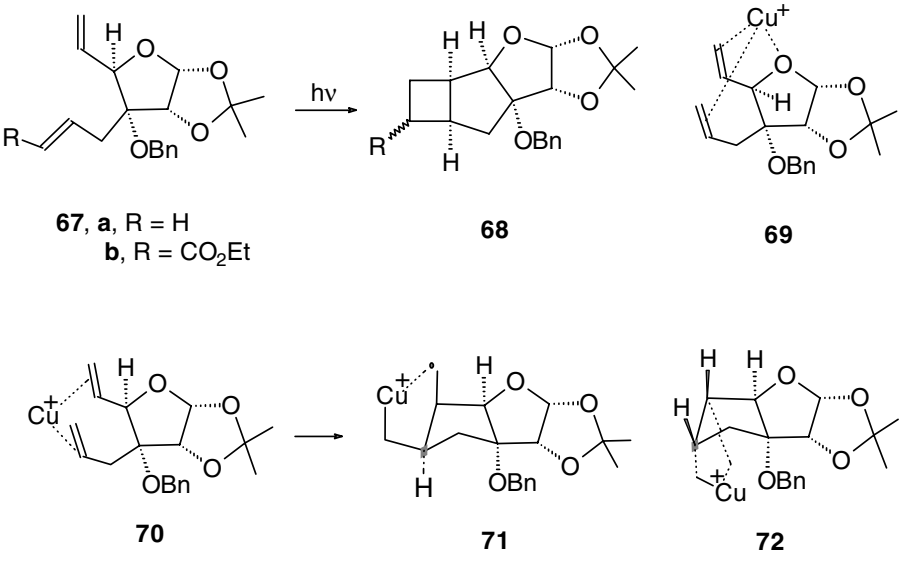

67, **a**, R = H; **b**, R = CO_2Et **68** **69** **70** **71** **72**

SCHEME 20

alkyl radical intermediate **71** rather than the more sterically crowded intermediate **72** derived from the Cu(I)-complex **70**. In contrast to this observation, irradiation of the 1,6-heptadienes **73** and **75** incorporated in a pyranosugar produced the expected adducts **74** and **76**, respectively (Scheme 21)[42], in accord with Salomon's earlier observation on photocycloaddition of 1,6-heptadien-3-ols.

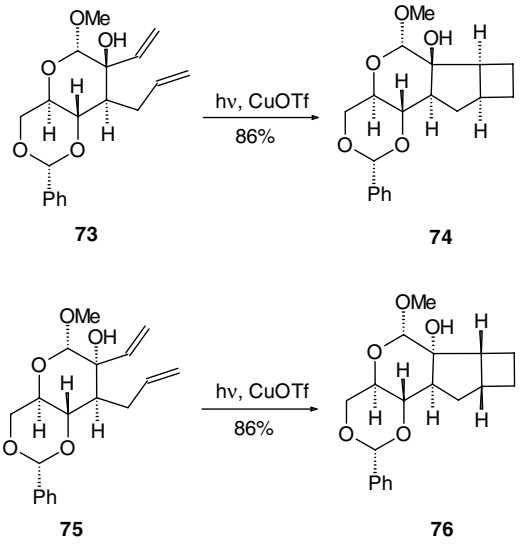

73 **74** **75** **76**

SCHEME 21

[2 + 2]-Photocycloaddition of Diallyl Ethers and Homoallyl Vinyl Ethers

Copper(I)-catalyzed intramolecular [2 + 2]-photocycloaddition of diallyl ethers and homoallyl vinyl ethers provides a new route to 3-oxabicyclo- and 2-oxabicyclo[3.2.0]heptanes, respectively.[43,44] Different structural variants of diallyl ethers have been investigated. UV irradiation of diallyl ethers **77a–f** in the presence of CuOTf catalyst produces 3-oxabicyclo[3.2.0]heptanes **78a–f** in moderate to excellent yields (Scheme 22). The diallyl ethers **77c** and **77d** having alkyl substitution at the allylic position produce exclusively the 2-*exo*-alkyl-3-oxabicyclo[3.2.0]heptanes **78c** and **78d**, respectively. The observed stereoselectivity arises through photocycloaddition of the Cu(I)-diene complex **80,** which is sterically less crowded than the complex **81** with an axial alkyl group. The bicyclic ethers **78** can be oxidized smoothly to the lactones **79** with RuO_4. Cu(I)-catalyzed photocycloaddition of homoallyl vinyl ethers **82** also proceeds smoothly, producing 2-oxabicyclo[3.2.0]heptanes **83** (Scheme 22).

Using the sequence of Cu(I)-catalyzed photocycloaddition of diallyl ethers or homoallyl vinyl ethers and RuO_4 oxidation, a variety of novel multicyclic compounds such as **86** and **89** can be synthesized (Scheme 23) starting with the dienes **84** and **87**, respectively.

Copper(I)-catalyzed intramolecular [2 + 2]-photocycloaddition is selective for 1,6-dienes only. The 1,5- and 1,7-dienes do not react. Thus, the trienes **90, 92**, and **94** produce only the adducts **91**,[43] **93**,[45] and **95**[43] (Scheme 24), arising from reactions of 1,6-dienes only.

CuOTf-catalyzed photocycloaddition of the tetraene **96** produces a mixture of the compounds **98**, **99**, and **100** (Scheme 25).[46] The 1,2-divinyl cyclobutanes **97** initially formed from [2 + 2]-addition of the tetraene **96** undergo further reaction on prolonged irradiation in the presence of CuOTf to form these products. The tricyclic compound **100** arises from intramolecular $2\pi + 2\pi$ addition of cyclooctadiene derivative **99**. In fact, the transformation of *cis,cis*-1,5-cyclooctadiene **101** to the tricyclic compound **102** on irradiation in the presence of CuCl was the first example of an intramolecular Cu(I)-catalyzed photocycloaddition reaction.[47,48]

Panda and Ghosh[49] have recently reported the Cu(I)-catalyzed $2\pi + 2\pi$ addition of 1,6-dienes, where the alkene units are tethered through an acetal oxygen. For example, the mixed acetal **103** produces stereoselectively the bicyclic lactol **104** in 50% yield (Scheme 26). Chromic acid oxidation of the lactol **104** produces the lactone **105**. The advantage of this protocol is the exclusive synthesis of the lactone **105**, which was obtained as a mixture with its regioisomeric lactone **79e** by using the protocol involving

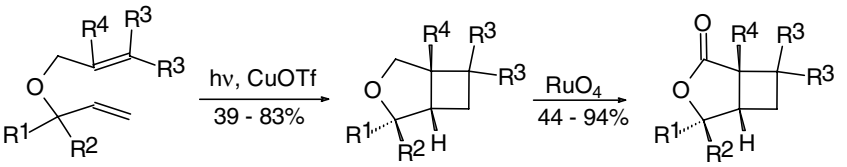

77 **78** **79**

a, $R^1 = R^2 = Me$, $R^3 = R^4 = H$; **b**, $R^1 = R^2 = R^4 = Me$, $R^3 = H$
c, $R^1 = R^3 = R^4 = H$, $R^2 = Me$; **d**, $R^1 = R^3 = R^4 = H$, $R^2 = Bu$
e, $R^1 = R^2 = R^4 = H$, $R^3 = Me$; **f**, $R^1 = R^2 = R^3 = H$, $R^4 = Me$

80 **81**

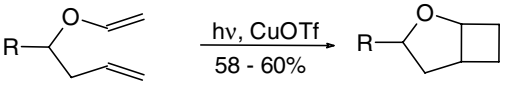

82 R = H, CH:CH$_2$ **83**

SCHEME 22

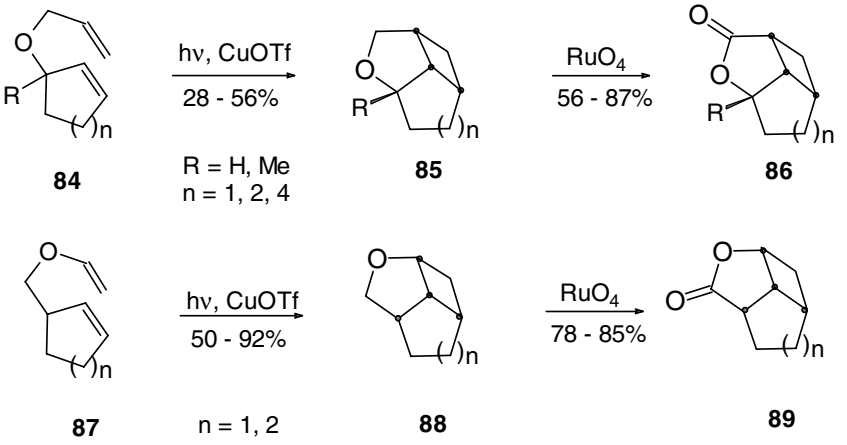

84 R = H, Me; n = 1, 2, 4 **85** **86**

87 n = 1, 2 **88** **89**

SCHEME 23

photocycloaddition of the diallyl ether **77e** followed by RuO_4 oxidation (Scheme 22). This protocol has been employed for a formal synthesis of grandisol (Scheme 27), beginning with the mixed acetal **106**.[49] Very recently, a synthesis of cyclobut-A **111**, an inhibitor of HIV, has been accomplished,[50] using the CuOTf catalyzed $2\pi + 2\pi$ addition of the acetal **109** (Scheme 28) as the key step.

CuOTf catalyzed $2\pi + 2\pi$ addition of diallyl ethers to form 3-oxabicyclo[3.2.0]heptanes has been elegantly employed for a novel stereoselective approach to the construction of vicinally substituted

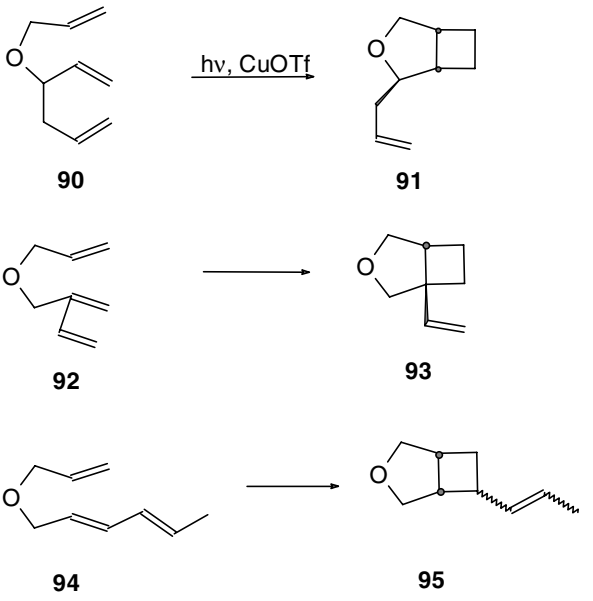

SCHEME 24

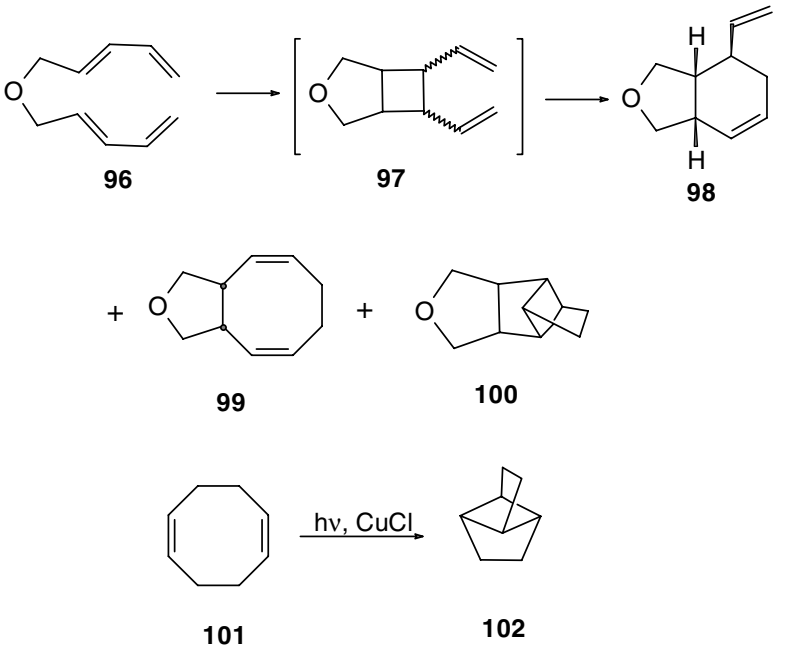

SCHEME 25

cyclopentanones with a quaternary Me, rudimentary synthons for the synthesis of complex natural products. The protocol[51–53] involves (Scheme 29) intramolecular $2\pi + 2\pi$ addition of the diene **113**, derived from reaction of the ketone **112** with ethoxyvinyl lithium followed by allylation of the resulting carbinol. CuOTf catalyzed photocycloaddition of the dienes **113** then provides the cyclobutane derivatives **114**. The strategic placement of the alkoxy group on the oxabicyclo[3.2.0]heptanes **114** permits facile rear-

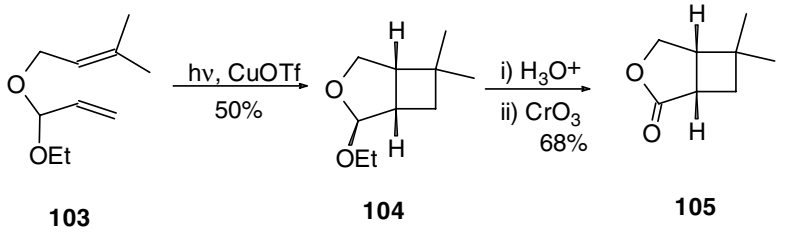

103 **104** **105**

SCHEME 26

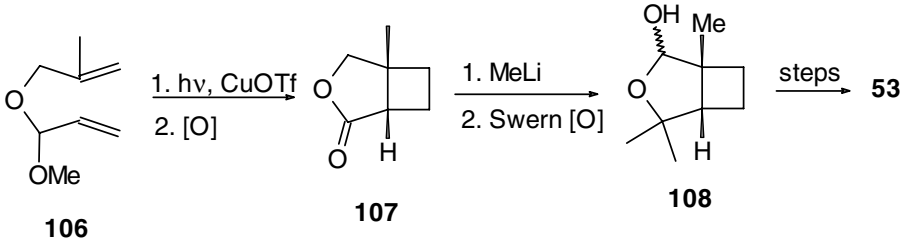

106 **107** **108**

SCHEME 27

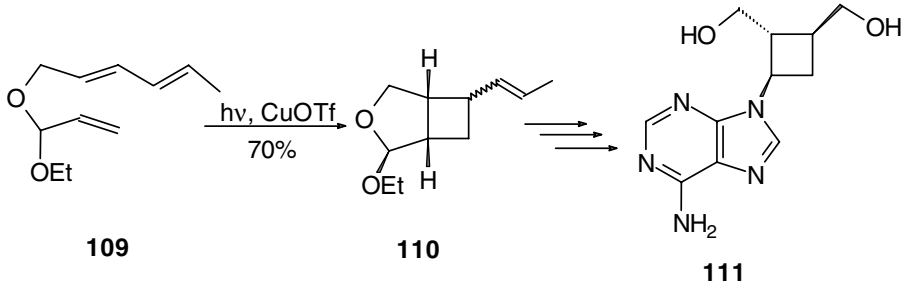

109 **110** **111**

SCHEME 28

rangement, on treatment with trifluoromethane sulfonic acid (TfOH), to the substituted cyclopentanones **115**. During photocycloaddition, a strong preference for the formation of the adduct **114** with the alkyl group R occupying an *exo* position increases with an increase in the bulk of the substituent R (Table 18.2).[53] Cycloaddition takes place through the less sterically crowded Cu(I)-diene complex **116** in preference to the more crowded complex **117** with a bulky substituent (R) in the axial position. Thus, any acyclic ketone can be converted to a cyclopentanone through this protocol.

The cyclopentanone derivative **115a** (R = Me) has been used as an intermediate in the total synthesis of β-necrodol **118**,[52] an insect repellent isolated from the defensive spray of the red-lined carrion beetle, *Necrodes surinamensis,* and the sesquiterpene herbertene **119**.[54]

This methodology has also been extended to the construction of cyclopentanones with substituents at three contiguous centers.[55] Thus, the diene **120a** afforded the photoadduct as a mixture of *exo*-**121a** and its *endo*-isomer in a ratio of 2.5:1 (Scheme 30). In contrast, the diene **120b** afforded exclusively the *exo*-cyclobutane **121b**. The difference in stereochemical outcome in the photocycloaddition of the dienes **120a** and **120b** is explained as follows. Cycloaddition of these dienes is expected to proceed through the

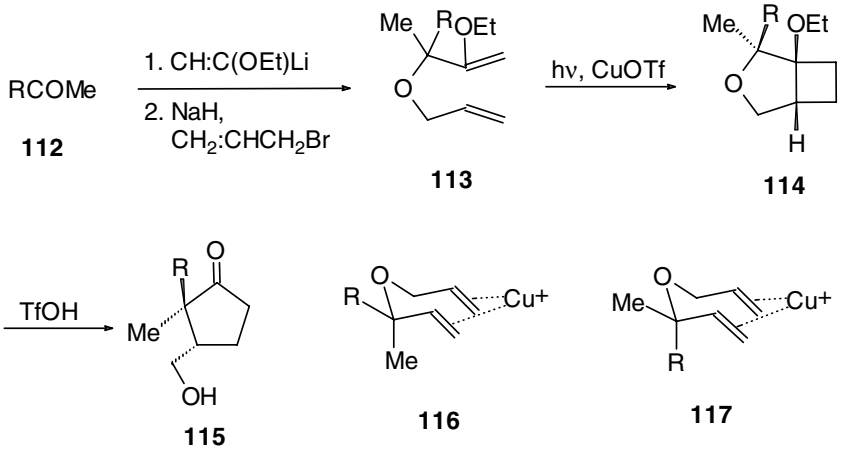

SCHEME 29

TABLE 18.2 Synthesis of Vicinally Substituted Cyclopentanones

Ketones	R	Photoadducts[a] (%)	*exo:endo*	Cyclopentanones (%)
112a	Me	**114a** (88)	—	**115a** (88)
112b	Et	**114b** (53)	3.8:1	**115b** (62)
112c	CH_2CH_2Ph	**114c** (61)	5:1	**115c** (66)
112d	CH_2Ph	**114d** (54)	19:1	**115d** (30)
112e	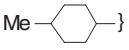	**114e** (71)	>99:1	**115e** (75)
112f	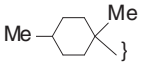	**114f** (60)	>99:1	**115f** (25)

[a] Photoadducts with R occupying *exo* position.

Cu(I)-diene complex **123**, as well as the complex **124** arising from the competing geometric olefin isomerization. In case of the diene **120b**, photocycloaddition takes place only through the Cu(I)-diene complex **123b**, as the alternative complex **124b** is sterically crowded due to the bulky Ph group, producing exclusively the *exo*-adduct **121b**. Acid treatment of the cyclobutanes **121** then leads to the cyclopentanones **122**. A synthesis of the diquinane **125**, an intermediate in the synthesis of the sesquiterpene $\Delta^{9,12}$-capnellene, has also been accomplished from the cyclobutane derivative **121c** obtained from photocycloaddition of the diene **120c** (Scheme 30).[56]

Employing this protocol, spirocyclopentanones can be obtained when cyclic ketones are used, as illustrated in Scheme 31.[57,58] The spirocyclopentanone **129**, obtained from 4-methylcyclohexanone **126**, has been converted to the spiro ketone **130**, which was earlier transformed to the sesquiterpene α-cedrene **131** (Scheme 31). Thus, CuOTf catalyzed photocycloaddition of 1,6-heptadienes provides a novel route to spiro cyclopentanones, also.

The Cu(I)-catalyzed $2\pi + 2\pi$ addition of diallyl ethers in conjunction with cyclobutyl carbinyl cation rearrangement has also been used for the construction of densely functionalized substituted cyclopentanones **135** from the ketones **132**, as illustrated in Scheme 32.[59]

An interesting application of CuOTf-catalyzed intramolecular $2\pi + 2\pi$ addition is the synthesis of isomers not formed in the corresponding intermolecular process. For example, the tricyclo[5.2.1.$0^{2,6}$]decene **136** undergoes dimerization when irradiated in the presence of CuOTf to form only

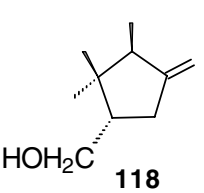

118

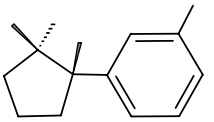

119

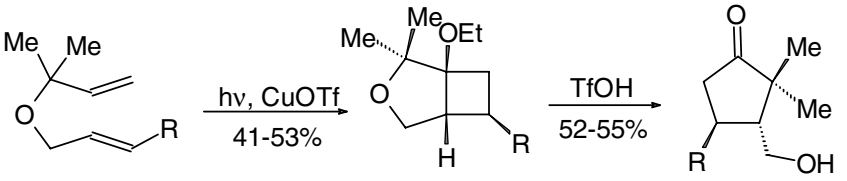

120

a, R = Me
b, R = Ph
c, R = CH:CHMe

121

exo:endo(2.5:1)
only exo

122

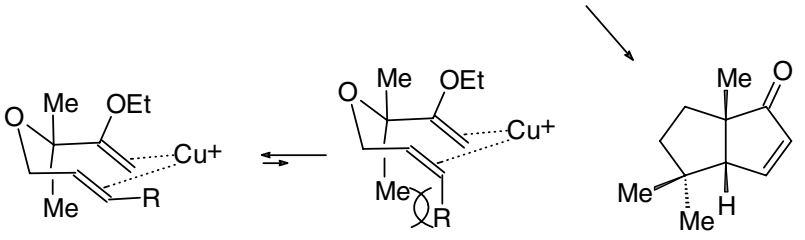

123 **124** **125**

SCHEME 30

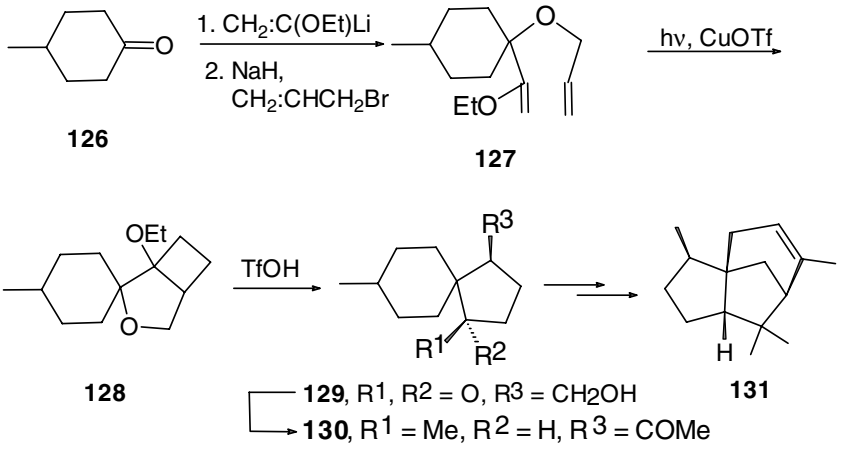

126 **127**

128

129, R1, R2 = O, R3 = CH_2OH
130, R1 = Me, R2 = H, R3 = COMe

131

SCHEME 31

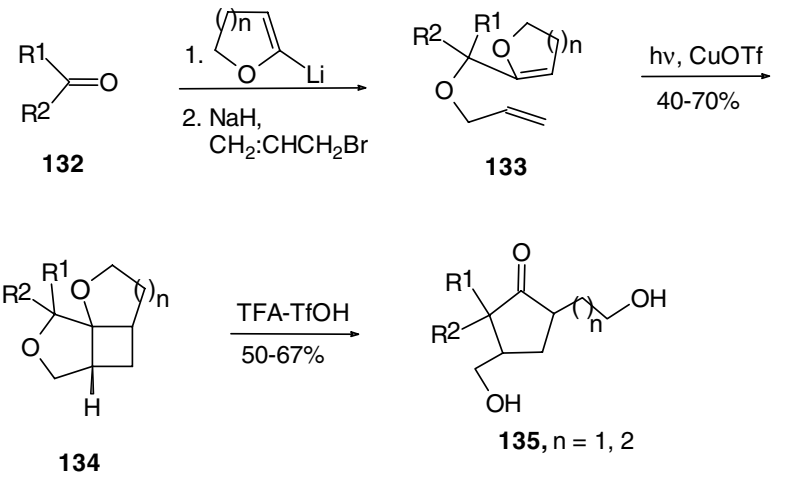

SCHEME 32

the *exo-trans-exo* isomers **137** and **138** (Scheme 33). However, when two such units are linked through tethers such as the diester **139**, photoreaction under identical conditions produces a 1:1 mixture of the unknown *exo,cis,exo*-dimer **141**[60] originating from the (R,S/S,R) diastereoisomer of the diester **139** and the *exo,trans,exo*-isomer **140** originating from the (R,R/S,S) diastereoisomer (Scheme 33).

The efficiency of this reaction depends on the length and rigidity of the tether. The tether can be removed easily through $LiAlH_4$ reduction to provide the dimers.

[2 + 2]-Photocycloaddition of Diallyl Carbamates

The *N,N*-diallyl carbamates **142a–c** undergo smooth $2\pi + 2\pi$ photocycloaddition in the presence of CuOTf catalyst to produce 3-azabicyclo[3.2.0]heptanes **143a–c** in excellent yields.[61] *exo*-Selectivity was observed for photocycloaddition of **142c** with a Me group at an allylic position to produce exclusively **143c**, as observed in photocycloaddition of the corresponding diallyl ethers. Multicyclic compounds **145** containing a N atom in the ring can also be prepared from $2\pi + 2\pi$ addition of the carbamates **144**. It is important to note that *N,N*-diallyl acetamide and *N,N*-diallyl formamide do not undergo [2 + 2]-photocycloaddition under these conditions. The failure of these photoreactions is possibly due to excitation of the amide functional groups rather than photoactivation of the Cu(I)-diene complex.

18.5 Conclusion

Copper(I)-catalyzed [2 + 2]-photocycloaddition of alkenes yields cyclobutanes in high yields in regio- and stereoselective fashion. A variety of functional groups are tolerant to the reaction conditions. Both carbo- and heterocyclic rings can be easily constructed. This reaction has been used as a key step in the synthesis of several natural products and molecules of novel architecture. The synthetic utility of this reaction would be greatly enhanced if asymmetric induction during cycloaddition could be achieved. Further investigation in this direction is greatly needed.

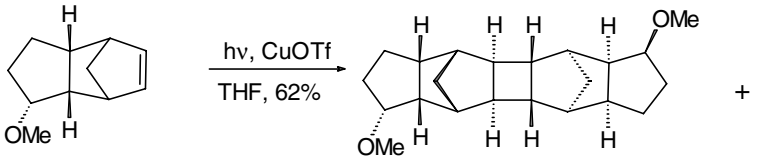

136 **137**

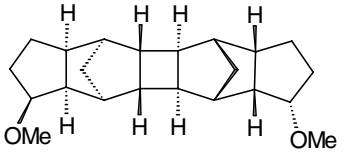

138

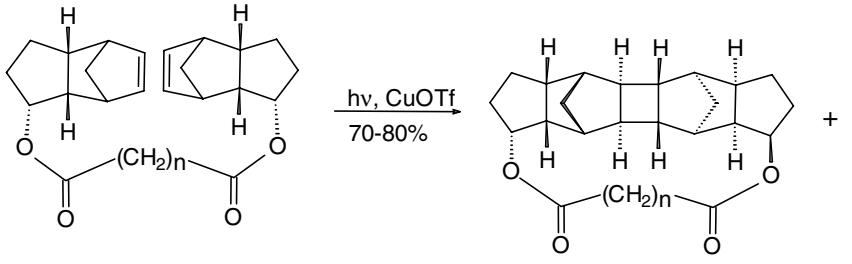

139 **140**

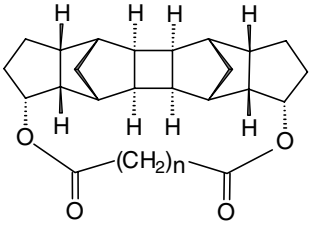

141

SCHEME 33

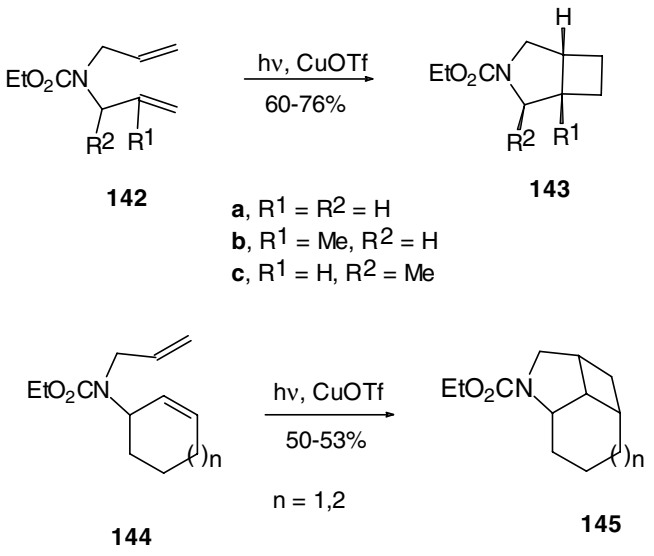

SCHEME 34

References

1. Crimmins, M.T., Synthetic applications of intramolecular enone–olefin photocycloadditions, *Chem. Rev.,* 88, 1453, 1988.
2. Bach, T., Stereoselective intermolecular [2 +2]-photocycloaddition reactions and their application in synthesis, *Synthesis,* 683, 1998.
3. Ramaiah, M., Cyclopentaannellation reaction in organic synthesis, *Synthesis*, 529, 1984.
4. Mehta, G. and Singh, V., Progress in the construction of cyclooctanoid systems: new approaches and applications to natural product syntheses, *Chem. Rev.,* 99, 881, 1999.
5. Wender, P.A., Alkenes: cycloaddition, in *Photochemistry in Organic Synthesis,* Coyle, J.D., Ed. The Royal Society of Chemistry, London, 1986, chap. 9, p. 163.
6. Corey, E.J., Mitra, R.B., and Uda, H., Total synthesis of *d,l*-caryophyllene and *d,l*-isocaryophyllene, *J. Am. Chem. Soc.,* 86, 485, 1964.
7. Salomon, R.G., Homogeneous metal-catalysis in organic photochemistry, *Tetrahedron,* 39, 485, 1983.
8. Salomon, R.G. and Kochi, J.K., Cationic benzene and olefin complexes of copper(I) trifluoromethane sulphonate, *J. Chem. Soc., Chem. Commun.,* 559, 1972.
9. Van den Hende, J.H. and Baird, W.C., The structure of the cuprous chloride-cyclooctadiene-1,5 complex, *J. Am. Chem. Soc.,* 85, 1009, 1963.
10. Ishino, Y., Ogura, T., Noda, K., Hiroshima, T., and Manabe, O., Copper(I) perchlorate complexes of allyl, 2-methylallyl and *cis*- and *trans*-2-butenyl alcohols, *Bull. Chem. Soc. Jpn.,* 45, 150, 1972.
11. Trecker, D.J., Henry, J.P., and McKeon, J.E., Photodimerization of metal-complexed olefins, *J. Am. Chem. Soc.,* 87, 3261, 1965.
12. Trecker, D.J., Foote, R.S., Henry, J.P., and McKeon, J.E., Photochemical reactions of metal-complexed olefins. II. Dimerization of norbornene and derivatives, *J. Am. Chem. Soc.,* 88, 3021, 1966.
13. Salomon, R.G. and Kochi, J.K., Copper(I) triflate: A superior catalyst for olefin photodimerization, *Tetrahedron Lett.,* 2529, 1973.
14. Salomon, R.G. and Kochi, J.K., Copper(I) catalysis in photocycloaddition. I. Norbornene, *J. Am. Chem. Soc.,* 96, 1137, 1974.

15. Schenck, G.O. and Steinmetz, R., Photofragmentierung von dehydronorcampher in cyclopentadien und keten und photosensibilisierte synthese des pentacyclo[5.2.1.0.^{2,6}0^{4,8}]decans, *Chem. Ber.,* 96, 520, 1963.
16. Hurst, J.K. and Lane, R.H., Binuclear ions of copper(I) and certain transition metal complexes and kinetics of electron transfer between metal centers, *J. Am. Chem. Soc.,* 95, 1703, 1973.
17. Salomon, R.G. and Kochi, J.K., Cationic olefin complexes of copper(I). Structure and bonding in group Ib metal-olefin complexes, *J. Am. Chem. Soc.,* 95, 1889, 1973.
18. Salomon, R.G. and Kochi, J.K., Structure and bonding in cationic olefin complexes of copper(I) by NMR, *J. Organomet. Chem.,* 43, C7, 1972.
19. Geiger, D. and Ferraudi, G., Photochemistry of Cu-olefin complexes: a flash photochemical investigation of the reactivity of Cu(ethylene)$^{+}$ and Cu(*cis,cis*-1,5-cyclooctadiene)$_2^{+}$, *Inorg. Chim. Acta.,* 101, 197, 1985.
20. Salomon, R.G. and Salomon, M.F., Copper(I) catalysis of olefin photoreactions. Photorearrangement and photofragmentation of 7-methyleno-carane, *J. Am. Chem. Soc.,* 98, 7454, 1976.
21. Salomon, R.G., Sinha, A., and Salomon, M.F., Copper(I) catalysis of olefin photoreactions. Photorearrangement and photofragmentation of methylenecyclopropanes, *J. Am. Chem. Soc.,* 100, 520, 1978.
22. Salomon, R.G., Folting, K., Streib, W.E., and Kochi, J.K., Copper(I) catalysis in photocycloadditions. II. Cyclopentene, cyclohexene and cycloheptene, *J. Am. Chem. Soc.,* 96, 1145, 1974.
23. Evers, J.T.M. and Mackor, A., Photocatalysis. V. Cyclotrimerization of cycloheptene, *Tetrahedron Lett.,* 21, 415, 1980.
24. Timmermans, P.J.J.A., de Ruiter, G.M.J., Tinnemans, A.H.A., and Mackor, A., Photocatalysis VIII. (Stereo)selective photochemical codimerization of cyclohexene and cycloheptene, catalyzed by copper(I)triflate, *Tetrahedron Lett.,* 24, 1419, 1983.
25. Salomon, R.G. and Sinha, A., Copper(I) catalyzed $2\pi + 2\pi$ photocycloaddition of allyl alcohol, *Tetrahedron Lett.,* 1367, 1978.
26. Evers, J.T.M. and Mackor, A., Photocatalysis I. Copper(I) trifluorfomethane sulphonate catalyzed photochemical reactions of unsaturated ethers and alcohols, *Tetrahedron Lett.,* 821, 1978.
27. Salomon, R.G., Coughlin, D.J., and Easler, E.M., Copper(I) catalysis of olefin photoreactions 8. A stepwise olefin metathesis synthesis of cyclopent-2-en-1-ones via photobicyclization of 3-hydroxyhepta-1,6-dienes, *J. Am. Chem. Soc.,* 101, 3961, 1979.
28. Salomon, R.G., Coughlin, D.J., Ghosh, S., and Zagorski, M.G., Copper(I) catalysis of olefin photoreactions. 9. Photobicyclization of α,β- and γ-alkenylallyl alcohols, *J. Am. Chem. Soc.,* 104, 998, 1982.
29. Salomon, R.G., Ghosh, S., Zagorski, M.G., and Reitz, M.T., Copper(I) catalysis of olefin photoreactions. 10. Synthesis of multicyclic carbon networks by photobicyclization, *J. Org. Chem.,* 47, 829, 1982.
30. Salomon, R.G. and Ghosh, S., Copper(I) catalyzed photocycloaddition: 3,3-dimethyl-*cis*-bicyclo[3.2.0]heptan-2-one, *Org. Synth.,* 62, 125, 1984.
31. McMurry, J.E. and Choy, W., Total synthesis of α- and β-panasinsene, *Tetrahedron Lett.,* 21, 2477, 1980.
32. Rosini, G., Marotta, E., Petrini, M., and Ballini, R., Stereoselective total synthesis of racemic grandisol. An improved convenient procedure, *Tetrahedron*, 41, 4633, 1985.
33. Rosini, G., Geier, M., Marotta, E., Petrini, M., and Ballini, R., Stereoselective total synthesis of racemic grandisol via 3-oximino-1,4,4-trimethylbicyclo[3.2.0]heptane. An improved practical procedure, *Tetrahedron,* 42, 6027, 1986.
34. Rosini, G., Carloni, P., Carmela, M., and Marotta, E., Resolution, specific rotation and absolute configuration of 2,6,6-trimethylbicyclo[3.2.0]heptan-*endo*-2-ol and of 2,5-dimethylbicyclo[3.2.0]heptan-*endo*-2-ol, key intermediate in the synthesis of grandisol, *Tetrahedron Assym.,* 1, 751, 1990.

35. Rosini, G., Marotta, E., Raimondi, A., and Righi, P., Resolution and EPC synthesis of both enantiomers of 2,5-dimethylbicyclo[3.2.0]heptan-*endo*-2-ol, key intermediate in the synthesis of grandisol, *Tetrahedron Assym.,* 2, 123, 1991.
36. Langer, K., Mattay, J., Heidbreder, A., and Möller, M., A new stereoselective synthesis of grandisol, *Liebigs Ann. Chem.,* 257, 1992.
37. Langer, K. and Mattay, J., Stereoselective intramolecular copper(I) catalyzed [2 + 2]-photocycloaddition. Enantioselective synthesis of (+)- and (–)-grandisol, *J. Org. Chem.,* 60, 7256, 1995.
38. Lal, K., Zarate, E.A., Youngs, W.J., and Salomon, R.G., Total synthesis necessitates revision of the structure of robustadials, *J. Am. Chem. Soc.,* 108, 1311, 1986.
39. Lal, K., Zarate, E.A., Youngs, W.J., and Salomon, R.G., Robustadials. 2. Total synthesis of the bicyclo[3.2.0]heptane structure proposed for robustadials A and B, *J. Org. Chem.,* 53, 3673, 1988.
40. Salomon, R.G. and Avasthi, K., A copper(I) catalyzed photobicyclization route to *exo*-1,2-polymethylene- and 7-hydroxynorbornanes. Nonclassical 2-bicyclo[3.2.0]heptyl and 7-norbornyl carbenium intermediates, *J. Org. Chem.,* 51, 2556, 1986.
41. Ghosh, S., Banerjee, S., Chowdhury, K., Mukherjee, M., and Howard, J.A.K., Intramolecular [2 + 2]-photocycloaddition of 1,6-dienes incorporated in a furanose ring. Unusual formation of *cis-syn-cis* 6-oxatricyclo[6.2.0.$0^{3,7}$]decanes, *Tetrahedron Lett.,* 42, 5997, 2001.
42. Holt, D.J., Barker, W.D., Jenkins, P.R., Ghosh, S., Russell, D.R., and Fawcett, J., The copper(I) catalysed [2 + 2]-intramolecular photoannulation of carbohydrate derivatives, *Synlett*, 1003, 1999.
43. Ghosh, S., Raychaudhuri, S.R., and Salomon, R.G., Synthesis of cyclobutanated butyrolactones via copper(I) catalyzed intermolecular photocycloadditions of homoallyl vinyl or diallyl ethers, *J. Org. Chem.,* 52, 83, 1987.
44. Raychaudhuri, S.R., Ghosh, S., and Salomon, R.G., Copper(I) catalysis of olefin photoreactions. 11. Synthesis of multicyclic furans and butyrolactones via photobicyclization of homoallyl vinyl and diallyl ethers, *J. Am. Chem. Soc.,* 104, 6841, 1982.
45. Avasthi, K., Raychaudhuri, S.R., and Salomon, R.G., Synthesis of vinyl cyclobutanes via copper(I) catalyzed intramolecular $2\pi + 2\pi$ photocycloadditions of conjugated dienes to alkenes, *J. Org. Chem.,* **49**, 4322, 1984.
46. Hertel, R., Mattay, J., and Runsink, J., Copper(I) catalyzed intramolecular diene–diene cycloaddition reactions and rearrangements, *J. Am. Chem. Soc.,* 113, 657, 1991.
47. Srinivasan, R., Use of an olefin as a photochemical catalyst, *J. Am. Chem. Soc.,* 85, 3048, 1963.
48. Srinivasan, R., Photochemical transformations of 1,5-cyclooctadiene, *J. Am. Chem. Soc.,* 86, 3318, 1964.
49. Panda, J. and Ghosh, S., Intramolecular [2 + 2]-photocycloaddition for the direct stereoselective synthesis of cyclobutane fused γ-lactols, *Tetrahedron Lett.,* 40, 6693, 1999.
50. Panda, J., Ghosh, S., and Ghosh, S., A new stereoselective route to the carbocyclic nucleoside cyclobut-A, *J. Chem. Soc., Perkin Trans. 1,* 3013, 2001.
51. Ghosh, S. and Patra, D., A convenient route to vicinally substituted cyclopentanones via pinacol type rearrangement of cyclobutanes, *Tetrahedron Lett.,* 34, 4565, 1993.
52. Samajdar, S., Ghatak, A., and Ghosh, S., Stereocontrolled total synthesis of (±)-β-necrodol, *Tetrahedron Lett.,* 40, 4401, 1999.
53. Patra, D. and Ghosh, S., Regioselectivity and stereospecificity in a contrastereoelectronically controlled pinacol rearrangement of alkoxycyclobutane derivatives. A novel route to vicinally substituted cyclopentanones, *J. Org. Chem.,* 60, 2526, 1995.
54. Nayek, A. and Ghosh, S., Enantiospecific synthesis of (+)-herbertene, *Tetrahedron Lett.,* 43, 1313, 2002.
55. Ghosh, S., Patra, D., and Samajdar, S., Intramolecular [2 +2]-photocyclo-addition-cyclobutane rearrangement. A novel stereocontrolled approach to highly substituted cyclopentanones, *Tetrahedron Lett.,* 37, 2073, 1996.
56. Samajdar, S., Patra, D., and Ghosh, S., Stereocontrolled approach to highly substituted cyclopentanones. Application in a formal synthesis of $\Delta^{9(12)}$-capnellene, *Tetrahedron,* 54, 1789, 1998.

57. Ghosh, S., Patra, D., and Saha, G., A novel route to usefully functionalised spiro[n.4]systems; application to a formal synthesis of (±)-α-cedrene, *J. Chem. Soc., Chem. Commun.,* 783, 1993.
58. Patra, D. and Ghosh, S., Photocycloaddition-cyclobutane rearrangement to spiro cyclopentanones: application in a formal synthesis of (±)-α-cedrene, *J. Chem. Soc., Perkin Trans. 1,* 2635, 1995.
59. Haque, A., Ghatak, A., Ghosh, S., and Ghoshal, N., A facile access to densely functionalised substituted cyclopentanes and spiro cyclopentanes. Carbocation stabilization directed bond migration in rearrangement of cyclobutanes, *J. Org. Chem.,* 62, 5211, 1997.
60. Galoppini, E., Chebolu, R., Gilardi, R., and Zhang, W., Copper(I)-catalyzed [2 + 2]-photocycloadditions with tethered linkers: synthesis of *syn*-photodimers of dicyclopentadienes, *J. Org. Chem.,* 66, 162, 2001.
61. Salomon, R.G., Ghosh, S., Raychaudhuri, S.R., and Miranti, S.R., Synthesis of multicyclic pyrrolidines via copper(I) catalyzed photobicyclization of ethyl *N,N*-diallyl carbamates, *Tetrahedron Lett.,* 25, 3167, 1984.

19

Photochemical Synthesis of Cyclophanes

Jun Nishimura
Gunma University

Yosuke Nakamura
Gunma University

Takuzo Yamazaki
Gunma University

Seiichi Inokuma
Gunma University

19.1 Introduction

In 1949, [2.2] paracyclophane[1] was prepared by the pyrolysis of *p*-xylene.[2] This intriguing event highlighted the birth of cyclophane chemistry, a name that was coined by Cram.[3] Recently, a member of the cyclophane family that has some cytotoxicity to LoVo tumors was isolated from a species of marine blue-green algae.[4,5] This general field of cyclophane chemistry was extended to host–guest chemistry, again coined by Cram,[6] applying the rigidity and planarity of the arene rings in cyclophanes as shaping or building blocks.[7]

In this chapter, the term cyclophane is used as the family name or general name for phanes as well as for the standard phanes composed of benzene nuclei.

Unless they have considerable strain in their ring systems, cyclophanes can be formed by most conventional bond-forming reactions. The first photochemical approach was applied by Schönberg et al. to prepare cage compound **1**, a cyclophane, in 1968.[8] Moreover, styrene photocyclodimerization (Scheme 1) was also published in the same year,[9,10] although it took almost two decades before we first successfully applied the reaction to cyclophane synthesis.[11] The mechanism (Scheme 1) of [2 + 2] cycloaddition with direct photoirradiation of vinylarenes and their derivatives has been published.[12]

Since then, several phanes have been prepared by photoirradiation as a key step for CC bond formation (Table 19.1).[13–15] Until the mid-1980s, stilbene, vinyl ether, and cinnamic acid moieties were used for the [2 + 2] cycloaddition, avoiding the use of labile vinylarenes. Thus, the phanes formed had some additional substituents at the tethers. This sometimes made their characterization complex. Other techniques were developed for the photochemical transformation of the simplest starting materials with vinyl groups directly attached to arene nuclei.

0-8493-1348-1/04/$0.00+$1.50

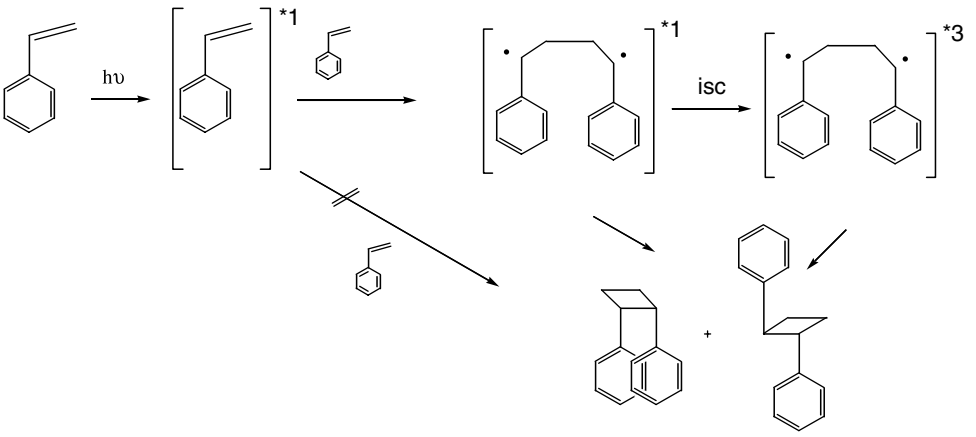

SCHEME 1

TABLE 19.1 Cyclophanes Prepared from Stilbene, Vinyl Ether, and Cinnamic Acid Derivatives in Solution and Solid-State Reactions

Cyclophane	Reaction Conditions	Yield, %	Isomer Ratio	Ref.
1	In benzene	—	—	9
2 (**X** = **O**)	In benzene	70	—	16
3 + **4**	In benzene	30	—	13,14
5	In benzene	47	—	17
6	Solid state	100	—	18
7 + **8**	In acetonitrile; sensitized by DCA	n = 4, 25 n = 20, 66	n = 4, 96: 4 n = 20, 42:58	15

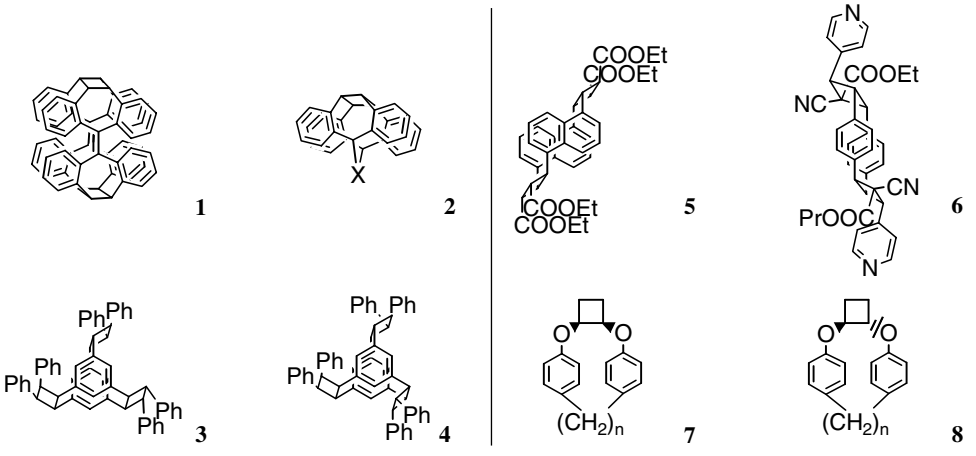

In 1986, it was recognized for the first time that the [2 + 2] photocycloaddition of styrene moieties was efficient if proper conditions were chosen.[11] After this discovery, many simple phanes were prepared from styrene derivatives or from vinylarenes by using the [2 + 2] photocycloaddition in solution.[19,20] This photochemical approach to cyclophanes is reviewed in this chapter, which focuses on the scope and limitations of the process.

19.2 Experimental

The vinylarenes are prepared from the corresponding bromides and from 1-arylethanols, such as phenethol, using Pd-catalyzed vinyl couplings including the Kosugi–Migita–Stille reaction[21] and dehydration methods including the acid-DMSO (dimethyl sulfoxide) system.[22]

Irradiation at around 300 nm under a nitrogen atmosphere is achieved using a high-pressure mercury lamp. A Pyrex filter that also serves as the reaction vessel is recommended to eliminate wavelengths <280 nm. Short wavelength irradiation sometimes forms undesired complex products via other reaction processes occurring before and/or after the [2 + 2] cycloaddition. In most cases, the polymerization of vinylarenes accompanies the cycloaddition. This affords polymers that do not have cyclobutane units in the main chains. Moreover, the phanes produced are generally photoreactive and can be degraded on prolonged irradiation. It is important to monitor the reaction to ensure maximum yields of the desired products.

Sensitizers and/or electron acceptors are not always necessary for the [2 + 2] cycloaddition of vinylarenes, which generally react from their excited singlet states. If sensitizers are used, the isomer ratios obtained are often different, and the process can yield more of the stable isomers. This occurs because of the intervention of longer-lived less active species such as triplet biradicals and ion radicals.[23]

Many different solvents can be used, although nonpolar benzene is recommended for most purposes. Generally speaking, simple distillation is adequate for the purification of solvents when singlet excited states are involved. Metal ion templates for the synthesis of crown-type phanes or crownophanes help to increase product stabilities but do not necessarily increase the efficiency of the cyclization.[24] The concentration of substrates should be in the 10^{-4} to 10^{-1} *M* range. The intermolecular reaction needs more concentrated solutions to raise the yield of adduct, but the intramolecular reaction occurs efficiently in more dilute conditions.

Products are isolated with a combination of column chromatography, GPC, and HPLC. Most isomers can be separated easily by HPLC. The most difficult cases may require recycled GPC and HPLC to achieve separation.[25] The phanes formed are stable if they are stored in a refrigerator or in a dark cool place in the solid or the crystalline state.

Structures are determined by many spectroscopic methods including ^{1}H NMR.[26] Methine proton signals around $\delta 4$ to $\delta 5$, as well as the high-field shifted aromatic proton signals, are used for the structural determination. So far only *cis*- and *trans*-1,2-diarylcyclobutane moieties have been found in the cyclophane structures obtained in solution, although 1,3-diarylcyclobutane moieties are often formed in solid-state addition reactions.[27]

19.3 Scope and Limitations of [2 + 2] Photocycloaddition as a Cyclophane Synthetic Method

The photochemical method has been successfully carried out in solution to make cyclophanes,[11] biphenylophanes,[11] cyclonaphthalenophanes,[11] naphthalenophanes,[11,21] binaphthylophanes,[28] phenanthrenophanes,[25,29–32] biphenylophenanthrenophane,[33] thiophenophanes,[34] and carbazolophanes.[35] Although the cycloaddition approach is quite general, some limitations exist as a result of strain and other competitive photoprocesses.[19,20]

In the following sections, the scope is summarized for inter- and intramolecular reactions. The limitations are discussed as a whole, combining some solid-state photoreactions listed in Table 19.1.

Intermolecular Reactions

Details of the yields of cyclophanes, naphthalenophanes, and phenanthrenophanes are summarized in Table 19.2. All phanes possess more than two cyclobutane rings, although they are described simply as [2.2]- and [2_n]phanes in this chapter.[1]

TABLE 19.2 Intermolecular Cyclization to Prepare Cyclophanes from Polyvinylarenes

Cyclophane	Yield, %	Isomer Ratio	Ref.
9	11		36
10 + **11** + **12**	5	56:28:16	37
13 + **14**	1	74:26	38
15	0.6		36
16	8		21
17	18		21
18 + **19**	15	65:35	21
20 + **21**	18	65:35	21
22 + **23**	33	60:40	25
24 + **25** + **26**	46	54:41:5	25

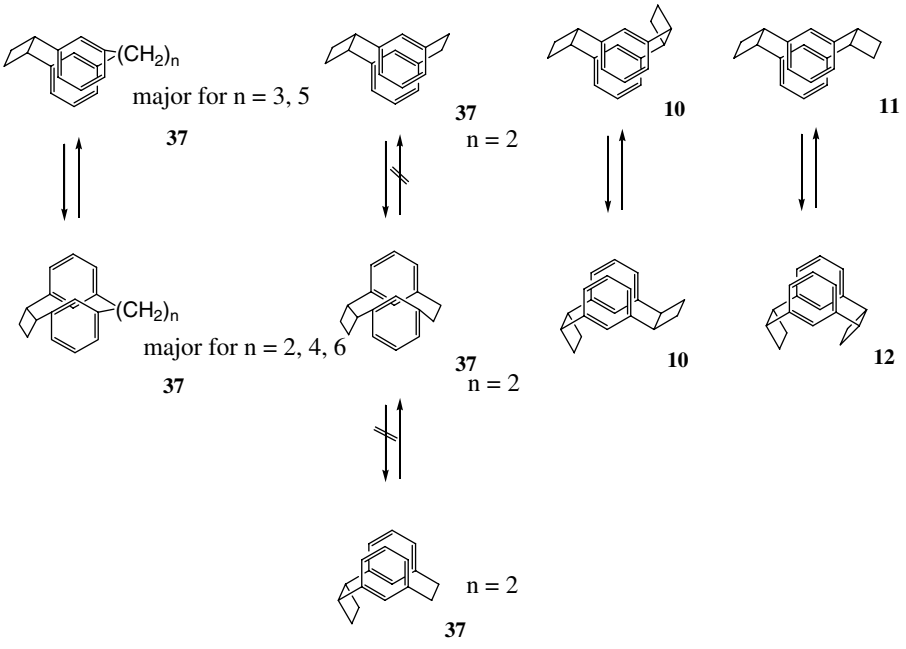

SCHEME 2

[2_n]Cyclophanes

[2.2]Orthocyclophane **9**,[36] [2.2]metacyclophane **10–12**,[37] [2_3](1,3,5)cyclophane **13–14**,[38] and [2_4](1,2,4,5)-cyclophane **15**[36] were successfully prepared by irradiation through a Pyrex filter of the appropriate di-, tri-, and tetravinylbenzene in benzene solution at room temperature. The yields obtained were not optimized at that time (Table 19.2). It is clear that the more strained the cyclophane is, the less product is formed. [2.2]Paracyclophane was not obtained by this route, although [2_4](1,2,4,5)cyclophane **15**, which contains the paracyclophane moiety, was prepared. It is likely that a zipper effect could be operative in this cycloaddition following the first metacyclophane formation.[36]

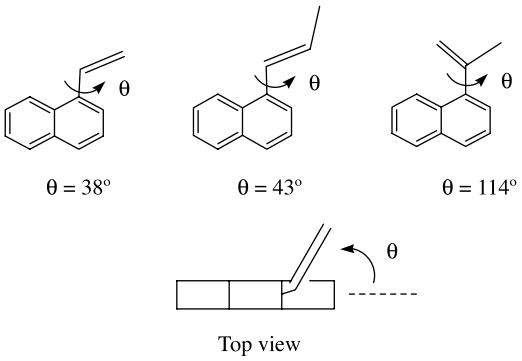

FIGURE 19.1

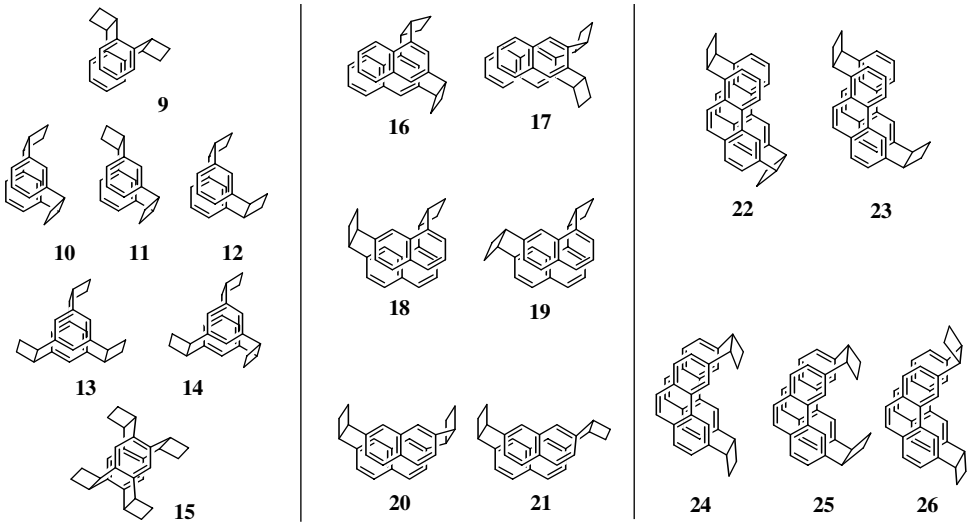

The [2.2]orthocyclophane formed has a pair of considerably tilted benzene nuclei, but the $[2_4](1,2,4,5)$cyclophane has a perfectly stacked pair. The difference in structure is seen in the UV-Vis spectra; i.e., the latter shows a bathochromic shift of 40 nm from durene, but the former is similar to *o*-xylene.[36]

[2.2]Naphthalenophanes

Many regioisomeric divinylnaphthalenes were examined, and some were found to produce [2.2]naphthalenophanes (Table 19.2).[21] They are the 1,3- **16**, 2,3- **17**, 1,7- **18–19**, 1,8-, 2,6-, and 2,7-isomers **20–21**. Again, the method failed to produce any [2.2](1,4)naphthalenophane, whose structural elements are the same as those of [2.2]paracyclophane.

A 1:1 mixture of two different divinylnaphthalenes was irradiated, but only homocycloadducts **16–21** were obtained in yields that were similar to those obtained by irradiation of the pure divinylnaphthalene.[21]

The synthetic route possesses an interesting stereochemical character: i.e., if the vinyl group is attached at the α-position of the naphthalene (and the 1- or 8-position of the phenanthrene) nucleus, the molecule is conformationally rigid because of the steric hindrance of the peri-hydrogen. The vinyl group always faces the *exo*-direction. This fact has been verified by ^{1}H NMR spectroscopy (Figure 19.1).[39] As a consequence, the naphthalenophane produced always has *exo*-cyclobutane ring(s), and moreover, a *syn*-conformation around the naphthalenophane (see **16**, **18**, **19**).[11] This selectivity had not been attained using

TABLE 19.3 Fluorescence Spectroscopic Data of [2.n]Phenanthrenophanes

Phenanthrenophane	Conformation	Origin of Emission	Emission, λ_{max}, nm	Ref.
23	*syn*	Excimer	410	25
27	*syn*	Excimer	405	30
29	*syn*	Excimer	420	31
31	*syn*	Excimer	420	32
33	*syn*	Excimer	395	31
28	*anti*	Excimer	395	30
30	*anti*	Excimer	407	31
26	*syn*	Monomer	—	25
32	*anti*	Monomer	—	32
34	*anti*	Monomer	—	31

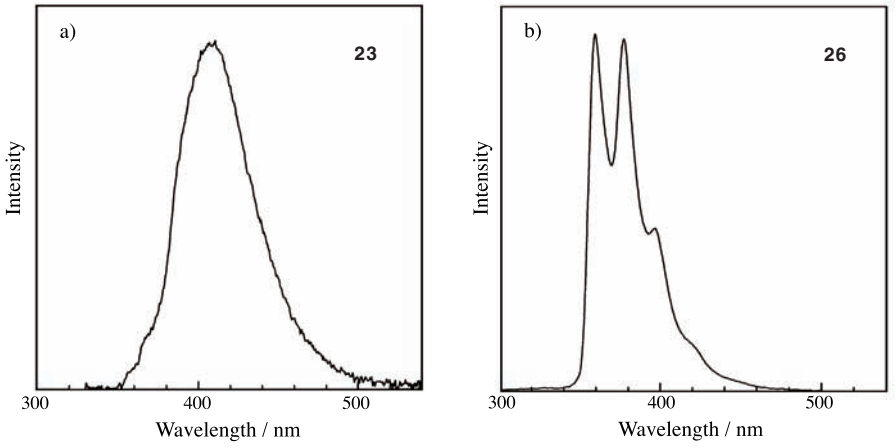

FIGURE 19.2

other synthetic methods reported previously.[21] Generally speaking, most CC bond formations used for the synthesis of naphthalenophanes are apt to give *anti*-isomers exclusively or largely with a minimal yield of the *syn*-isomer. When α-(2-propenyl)naphthalene is used, the situation is changed completely, and the *endo,cis,syn*-isomer is obtained as the major product.[17]

[2.2]Phenathrenophanes

Several phenanthrenophanes listed in Table 19.2 were prepared after a structural examination of strain within the molecule using molecular mechanics (MM2) calculations.[25,29–32] Their predicted three-dimensional structures look much the same, but they actually are considerably different in reality. Evidence for the structural differences can be seen in the excimer emission behavior that is summarized in Table 19.3. Two typical fluorescence spectra are depicted in Figure 19.2.

The same stereochemical control as that for the naphthalenophane mentioned above is operative in this synthesis. The vinyl groups attached at the 1- and 8-positions are conformationally rigid due to the peri-hydrogen, and therefore yield the phenanthrenophane stereoselectively to some extent, as seen for **22** and **23**.

Intramolecular Reactions

The yields of cyclophanes, naphthalenophanes, and phenanthrenophanes synthesized by the intramolecular photocyclization are summarized in Table 19.4. Again, although all the phanes have at least one cyclobutane ring, they are described here as [2.n]phanes for simplicity.

TABLE 19.4 Intramolecular Cyclization to Prepare Cyclophanes from Polyvinylarenes

Cyclophane	Yield, %	Isomer Ratio	Ref.
35	0-61		11
36	65		40
37	61–80		23
38	33–35		11
39	29–38		11
40	45–47		28
27 + 28	44	1:1.3	30
29 + 30	44	1:6	31
31 + 32	42	6:1	32
33 + 34	40	1:3	31
41	38–49		25
42 + 43	4	1:0.6	34
44 + 45	39–77	1:0.3–5	35
46	48–95		24
47	25–50		45

TABLE 19.5 Quantum Yield Dependence on Tether Length and Flexibility

Cyclophane	Quantum Yield	Cyclophane	Quantum Yield
35 (n = 3)	0.05	**46 (n = 1)**	0.34
35 (n = 4)	0.36	**46 (n = 4)**	0.34
35 (n = 5)	0.38	**47 (n = 5)**	0.34
35 (n = 6)	0.26	**47 (n = 14)**	0.10

Note: For intramolecular reactions of vinylnaphthalene moieties ($\phi = 0.26$), see References 43 and 44.

[2.n]Cyclophanes

Unless much strain will be induced by the cycloaddition, the [2.n]paracyclophanes **35**, **36** ($n \geq 3$)[11] and metacyclophanes **37** ($n \geq 2$)[23,41,42] are easily prepared by intramolecular photocycloaddition. The quantum yield is usually as high as 0.4,[43–45] and sometimes the cyclophanes are isolated in quantitative yield. As shown in Table 19.5, the quantum yield tends to decrease with the increase of tether length, with the exception of the flexible oligooxyethylene unit (see **46** and **47**).[45]

While the paracyclophanes synthesized have little stereochemical diversity, the metacyclophanes can be obtained as *syn*- and *anti*-isomers on the cyclophane substructure and *cis*- and *trans*-isomers around the cyclobutane ring system. When the [2.n]metacyclophanes where $n \geq 4$ ring flipping of the benzene moiety occurs. At the flipping equilibrium, [2.4]-, [2.5]-, and [2.6] phanes **37** possess mainly *anti*-, *syn*-, and *anti*-conformations, respectively. This is dependent to some extent on the tether conformation. The smaller [2.2]- and [2.3]metacyclophanes **37** showed no ring flipping and were obtained as *cis,anti*- and *trans,anti*-isomer mixtures. Note that the *cis,anti*-[2.2]metacyclophane was formed instead of the *cis,syn*-isomer. It is believed that the photocycloaddition gives initially the *cis,syn*-isomer, which then converts irreversibly to the more stable *cis,anti*-isomer.[46] This result, together with the conformation of bisethano[2.2]metacyclophane **10**, **11**, and **12** implies that a single cyclobutane linkage is insufficient to maintain the cyclophane in *syn*-conformation (see Scheme 2).

[2.n](4,4′)Biphenylophanes ($n \geq 3$) are also produced by the general method and usually in reasonable yields.[11,28]

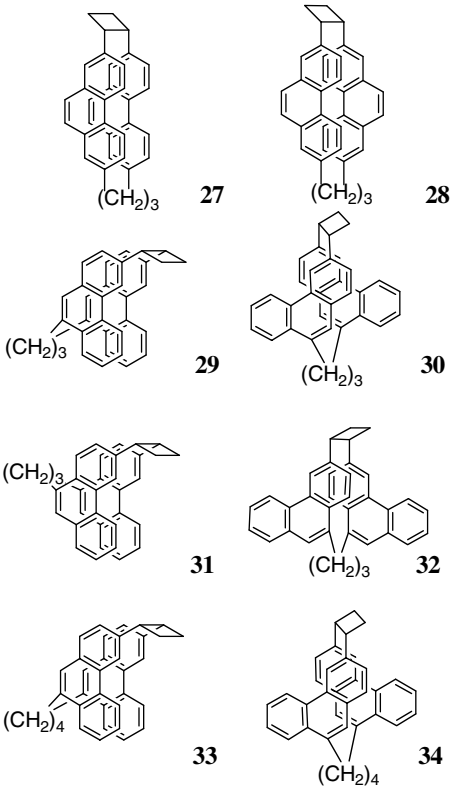

[2.n]Naphthalenophanes

The intramolecular cycloaddition path can afford phanes with different aromatic nuclei. In fact, [2.3]paracyclo(1,4)naphthalenophane was prepared in 8% yield.[11] The method has been applied to prepare [2.n](1,4)- **38**, -(1,5)- **39**, and –(2,7)naphthalenophanes (n ≥ 3) in reasonable yields. [2.2](1,4)Naphthalenophane cannot be synthesized by this route.

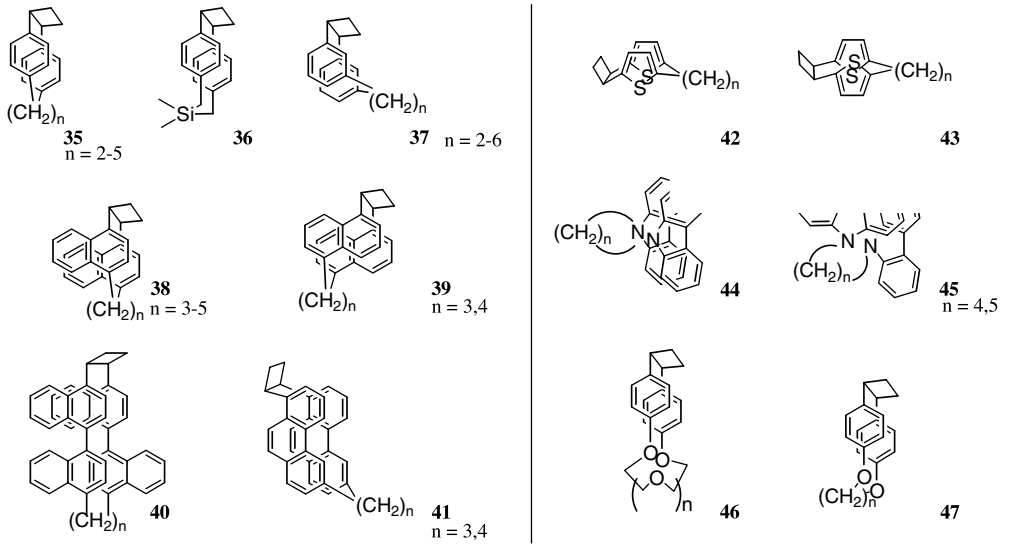

It is important to note that the conformational rigidity of the α-vinyl group referred to earlier makes the reaction stereoselective. This control is also operative in the preparation of [2.n](4,4′)binaphthylophanes **40**, where a pair of naphthalene moieties is adjacent to the vinyl groups. Moreover, it is possible to synthesize the [2.6](4,4′)phane due to lessening of molecular strain, while the synthesis of the [2.5]phane fails. The length of the methylene tether (n ≥ 6) is important.[28]

[2.n]Phenanthrenophanes

Some phenanthrenophanes cannot be prepared by the intermolecular photocyclization pathway, mainly because of strain induced by the two carbon linkage (n = 2). However, some were prepared using longer methylene chains (-$(CH_2)_n$-, n ≥ 3). This is typically seen in the synthesis of [2.n](2,7)phenanthrenophanes **27** and **28**.

The same stereochemical selectivity induced by the α-vinyl group again operates in the reaction, and [2.n](1,6)phenanthrenophanes **41** are obtained.[25,29]

[2.n]Heterophanes

Among heterophanes, some thiophenophanes and carbazolophanes were successfully synthesized. Some [2.2]phanes with relatively small frameworks are too strained to be synthesized by this method. However, the photocycloaddition can afford some [2.n](2,5)thiophenophanes **42–43** (n ≥ 3),[34] [2.n](3,9)carbazolophanes **44–45** (n ≥ 4),[35] with the limitations shown in parentheses. These syntheses are also dependent on the large atomic radii of the hetero elements and on the electrostatic repulsive interaction between two co-facially arranged heteroatoms.

Conformationally stable *cis,exo,syn*- **42** (n = 3) and *cis,anti*-[2.3](2,5) thiophenophane **43** (n = 3) were obtained as shown in Scheme 3. However, the [2.4](2,5)thiophenophane **43** (n = 4) exists as a mixture of two *anti*-conformers that rapidly interconvert. It is believed that even larger [2.n](2,5)thiophenophanes (n ≥ 4) are first formed as *exo,syn*-isomers and then undergo a ring flip to the more stable and flexible *anti*-isomer.

[2.4]Carbzolophane **44–45** (n = 4) was produced as a mixture of *syn*- and *anti*-isomers. These did not undergo interconversion due to the short linkage. Interconversion occurs at a slow rate with the larger [2.5]carbazolophane.

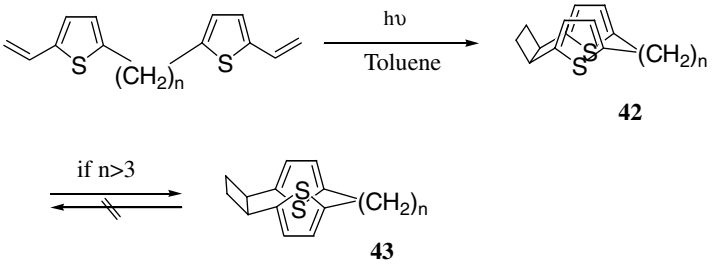

SCHEME 3

Limitations: Competing Photochemical Processes and the Influence of Strain at the Transition State

As mentioned above, the photochemical method has some limitations. These limitations are due to the variety of different photochemical processes involved and the strain at the transition state.

Vinylarenes can undergo several reactions on irradiation depending on the substitution involved. Sometimes the photoreactive compound is bichromophoric, with the possibility of interaction between the vinyl group and another substituent. In some instances, supramolecular techniques can be applicable. An example of this is shown in Scheme 4. The excited singlet styrene moiety could react with the tertiary- or

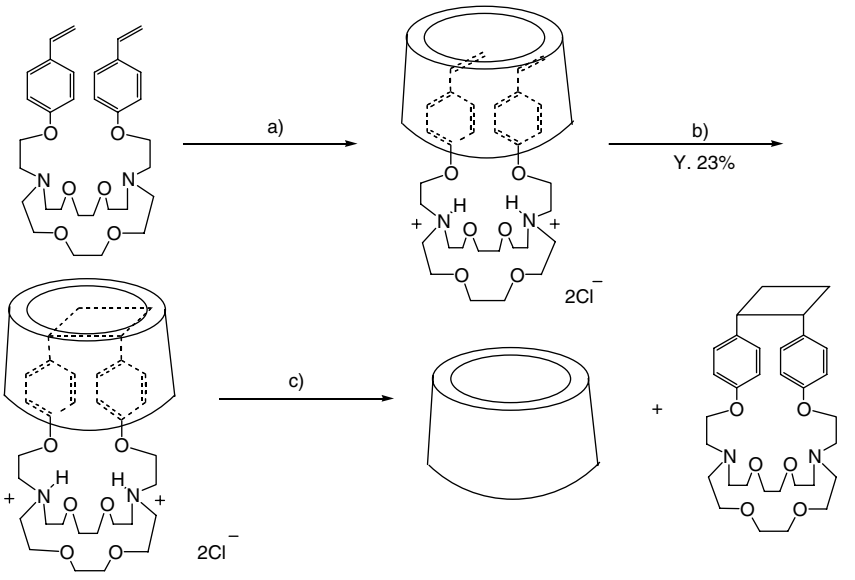

a) 1) HCl/H_2O, 2) γ-CD. b) hυ (>280 nm). c) $NaOH/H_2O$

SCHEME 4

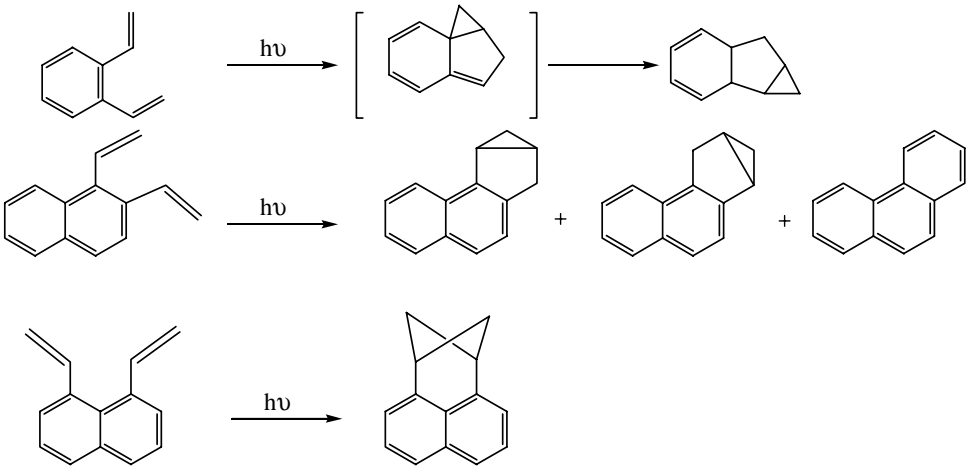

SCHEME 5

secondary-amino groups. To minimize this side reaction, γ-cyclodextrin is used to complex the vinylarene moieties. Under these conditions, the cycloaddition occurs normally.[47]

The two neighboring vinyl groups have to be in the proper conformational arrangement to react with each other. This type of reaction affords the cyclized compounds shown in Scheme 5.[48] However, the *exo,endo*-vinyl group arrangement shown for *o*-divinylbenzene is not preferred under thermal equilibrium conditions. The arrangement is present in ground-state 1,2-divinylnaphthalene, and irradiation of this gives, exclusively, the phenanthrene and its derivatives without any intermolecular cycloadditions leading to naphthalenophanes. In order to compete with these intramolecular reactions, the concentration of starting polyvinylarenes has to be increased to several hundred m*M*. Such a concentrated system easily produces polymeric byproducts.[36]

TABLE 19.6 Strain Energy of 1,2-Ethano[2.n]paracyclophanes

	1,2-Ethano[2.n]paracyclophane **35**	
n	Strain Energy (kcal/mol)[a]	Remarks[b]
2	52.0	Not obtained by the reaction
3	41.1	14% yield
4	33.9	61% yield

[a] Calculated by HDE method.
[b] Ref. 11.

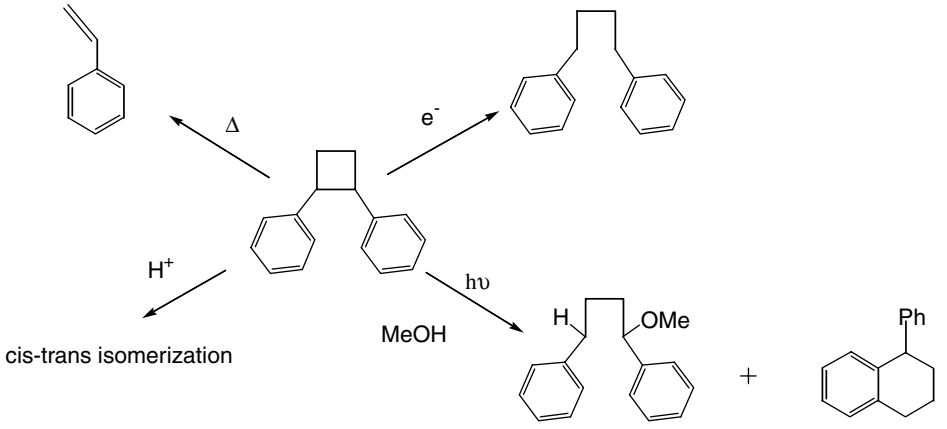

SCHEME 6

A typical cyclophane with short linkages, [2.2]paracyclophane, could not be prepared by this photochemical method in solution even though the strain calculated by the HDE (homodesmic destabilization energy) method at the *ab initio* (PM3) level is not too high, as shown in Table 19.6.[49] It was supposed that the wavelength used (300 nm) could supply sufficient energy to *p*-divinylbenzene. In fact, as shown in Table 19.1, a solid-state photoreaction successfully gave [2.2]paracyclophane in quantitative yield.[18,50,51] Therefore, it is proposed that in solution, monocyclized species are formed and undergo second photon excitation. However, the excited species may undergo bond fission or internal conversion before a second bond is made between the two free vinyl groups. Thus the cyclization fails. In the solid state, however, two molecules are arranged parallel and are constrained, and both cyclobutane rings can be formed. The limitation due to the strain can be seen in the syntheses of metapara-, orthopara-, and metaorthocyclophanes and several naphthalenophanes and phenanthrenophanes in which the two nuclei are connected with each other at different positions.

19.4 Transformation of Products

Diphenyl cyclobutanes can react in several ways, as shown in Scheme 6. The thermal ring cleavage of cyclobutane is not efficient unless there is considerable strain.[52] The most labile [2.2]metacyclophane among the phanes examined undergoes ring opening to the corresponding styrene derivative at 200°C with a rate constant of 1.0×10^{-1} sec^{-1}. Others do not ring open as fast as this and are in the range 1 to 50×10^{-5} sec^{-1}.

Yamamoto and coworkers have reported a photochemical ring-opening using electron transfer and the production of cation radical species.[53] One of the electron transfer reactions of this sort is the Birch reduction. This is quite useful to bring about ring enlargement. When it is applied to the phane systems,

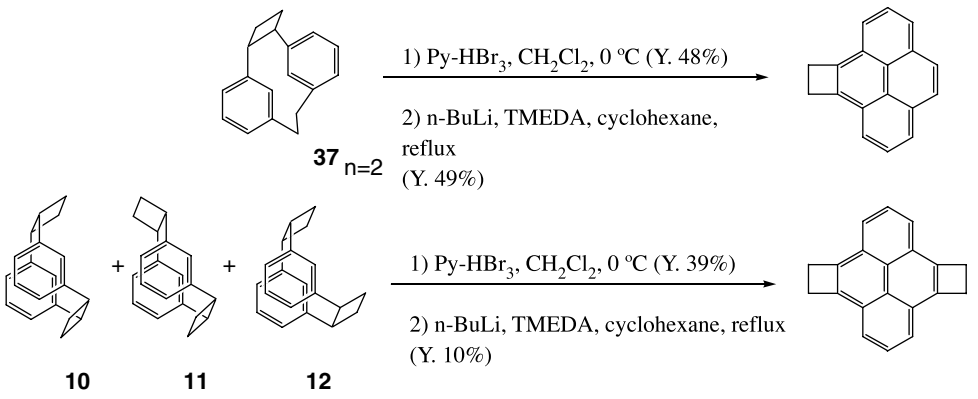

SCHEME 7

the products obtained have linkages two methylene groups larger than the starting materials, i.e., [2.n]-phanes become [4.n]phanes.[54]

Cyclobutane rings can be converted to arene-fused cyclobutene rings as shown in Scheme 7. It should be noted that the largest homologue of benzocyclobutene was prepared for the first time by this transformation.[55]

19.5 Future Prospects

Many photoreactions on phane skeletons have not been included in this chapter, such as reports related to ring construction via sulfides and esters.[3,56] Several phanes have been examined as photochromic materials, but these molecules usually do not exhibit reversible photochromicity and decompose on repeated irradiation. It may be possible to carry out some asymmetric-induced formation of phanes. These studies are of value for practical and theoretical reasons.[44] Other work has used a supramolecular catalyst for the preorganization of vinylarenes.[47] The technique could be of considerable value.[57] Some additional photochemical syntheses of phanes have been described for the formation of sterically strained systems.[58] In order to make such highly strained phanes, solid-state reactions could play a key role.

The intramolecular photochemical synthesis of phanes can be applied to the construction of covalent templates. Moreover, the cyclobutane ring(s) formed by the cycloaddition reaction can act as a stereochemical control forcing the phane conformation to one side similar to a caliper system. Other work has been directed towards the synthesis of receptors and ionophores applicable to host–guest chemistry.[59]

19.6 Conclusion

The [2 + 2] photocycloaddition of vinylarenes in solution was successfully carried out to make cyclophanes, biphenylophanes, cyclonaphthalenophanes, naphthalenophanes, binaphthylophanes, phenantherenophanes, thiophenophanes, carbazolophanes, and other related systems.

Unless the reacting system leads to a highly strained molecule, phanes are easily prepared by inter- and intramolecular photocycloaddition.[21] The intramolecular method can afford phanes with different aromatic nuclei. It is stressed that the conformational rigidity of the vinyl group and/or the apparent difference of the product stability makes the reaction stereoselective.

Those [2.n]phanes possessing cyclobutane ring(s) can be transformed into [4.n]phanes by Birch reduction and can also be transformed into benzocyclobutene analogs.

References

1. Vögtle, F. and Neumann, P., Zur Nomenklatur der Phane-II, *Tetrahedron Lett.,* 5847, 1970.
2. Brown, C.J. and Farthing, A.C., Preparation and structure of di-*p*-xylylene, *Nature (London),* 164, 915, 1949.
3. Cram, D.J. and Cram, J.M., Cyclophane chemistry: bent and battered benzene rings, *Acc. Chem. Soc.,* 4, 204, 1971 and references cited therein.
4. Moore, B.S., Chen, J.-L., Patterson, G.M.L., and Moore, R.E., [7.7]Paracyclophanes from blue-green algae, *J. Am. Chem. Soc.,* 112, 4061, 1990.
5. Smith, A.B., III., Adams, C.M., Kozmin, S.A., and Paone, D.V., Total synthesis of (–)-cylindrocyclophanes A and F exploiting the reversible nature of the olefin cross metathesis reaction, *J. Am. Chem. Soc.,* 123, 5925, 2001 and references cited therein.
6. Cram, D.J. and Cram, J.M., Host-guest chemistry: Complexes between organic compounds simulate the substrate selectivity of enzymes, *Science,* 183, 803, 1974.
7. Vögtle, F., *Cyclophane Chemistry,* John Wiley & Sons, Chichester, 1993.
8. Schönberg, A., Sodtke, U., and Praefcke, K., Über die Photochemische Dimersierung des 2.3;6,7;2′3′;6′,7′-Tetrabenzo-heptafulvalenes zu einer Käfigverbindung (cage compound), *Tetrahedron Lett.,* 3669, 1968.
9. Mayo, F.R., The dimerization of styrene, *J. Am. Chem. Soc.,* 90, 1289, 1968.
10. Brown, W.G, Cyclodimerization of styrene, *J. Am. Chem. Soc.,* 90, 1916, 1968.
11. Nishimura, J., Doi, H., Ueda, E., Ohbayashi, A., and Oku, A., Efficient intramolecular [2 + 2] photocycloaddition of styrene derivatives towards cyclophanes, *J. Am. Chem. Soc.,* 109, 5293, 1987.
12. Lewis, F.D. and Kojima, M., Photodimerization of singlet *trans*- and *cis*-anethole. Concerted or stepwise, *J. Am. Chem. Soc.,* 110, 8660, 1988.
13. Juriew, J., Skorochodowa, T., Merkuschew, J., Winter, W., and Meier, H., A simple route to a new type of cyclophane, *Angew. Chem. Int. Ed. Engl.,* 20, 269, 1981.
14. Winter, W., Langiahr, U., Meier, H., Merkuschew, J., and Juriew, J., Photochemie des 1,3,5-Tristyrylbenzols, *Chem. Ber.,* 117, 2452, 1984.
15. Mizuno, K., Kagano, H., and Otsuji, Y., Regio- and stereoselective intramolecular photocycloaddition: synthesis of macrocyclic 2,ω-dioxabicyclo[n.2.0] ring system, *Tetrahedron Lett.,* 24, 3849, 1983.
16. Rokach, J., Girard, Y., and Atkinson, J.G., A new heterocyclic cage ring system: preparation of the *cis*-cyclobutane dimer of dibenz[*a,d*]cyclohepten-5-one, *J. Chem. Soc., Chem. Commun.,* 602, 1975.
17. Nishimura, J., Takeuchi, M., Koike, M., Yamashita, O., Okada, J., and Takaishi, N., Intramolecular [2 + 2]-photocycloaddition. 17. Effects of the linkage length and substituents on the photochemical reaction courses of vinylnaphthalene derivatives and cycloreversion of a naphthalenophane-photoproduct, *Bull. Chem. Soc. Jpn.,* 66, 598, 1993.
18. Maekawa, Y., Kato, S., and Hasegawa, M., Quantitative formation of a highly strained tricyclic [2.2]paracyclophane derivative from a mixed crystal of ethyl and propyl α-cyano-4-[2-(4-pyridyl)ethenyl]cinnamates through a topochemical reaction, *J. Am. Chem. Soc.,* 113, 3867, 1993.
19. Nishimura, J., Okada, Y., Inokuma, S., Nakamura, Y. and Gao, S.-R., Intramolecular [2 + 2] photocycloaddition of vinylarenes: synthesis of cyclophanes, *Synlett,* 884, 1994.
20. Nishimura, J., Nakamura, Y., Hayashida, Y., and Kudo, T., Stereocontrol in cyclophane synthesis: photochemical method to overlap aromatic rings, *Acc. Chem. Res.,* 33, 679, 2000.
21. Takeuchi, M., Tuihiji, T., and Nishimura, J., Synthesis of [2.2]naphthalenophanes from divinylnaphthalenes, *J. Org. Chem.,* 58, 7388, 1993 and references cited therein.
22. Nishimura, J., Ishida, Y., Mimura, M., Nakazawa, N., and Yamashita, S., C3 Cyclopolymerization. III. Preparation of α,ω-bis(*p*-vinylphenyl)alkane and 1,3-bis(4-vinylnaphthyl)propane, *Polym. J.,* 13, 635, 1981.

23. Nishimura, J., Ohbayashi, A., Doi, H., Nishimura, K., and Oku, A., Intramolecular [2 + 2] photocycloaddition. 3. Synthesis of 1,2-ethano[2.n]metacyclophanes from styrene derivatives, *Chem. Ber.,* 121, 2019, 1988.
24. Inokuma, S., Yamamoto, T., and Nishimura, J., Efficient intramolecular [2 + 2] photocycloaddition of styrene derivatives toward new crown ethers, *Tetrahedron Lett.,* 31, 97, 1990.
25. Nakamura, Y., Tsuihiji, T., Mita, T., Minowa, T., Tobita, S., Shizuka, H., and Nishimura, J., Synthesis, structure, and electronic properties of *syn*-[2.2]phenanthrenophanes: first observation of their excimer fluorescence at high temperature, *J. Am. Chem. Soc.,* 118, 1006, 1996.
26. Ernst, L., NMR studies of cyclophanes, *Prog. NMR Spectroscopy,* 37, 47, 2000.
27. Ramamurthy, V. and Venkatesan, K., Photochemical reactions of organic crystals, *Chem. Rev.,* 87, 433, 1987.
28. Hayashida, Y., Nakamura, Y., Chida, Y., and Nishimura, J., Synthesis and structure of novel [2.n](4,4′)binaphthylophanes: a new family in cyclophane chemistry, *Tetrahedron Lett.,* 40, 6435, 1999.
29. Takeuchi, M. and Nishimura, J., Intramolecular [2 + 2] photocycloaddition. 19. 1,2-Ethano-*syn*-[2.n](1,6)phenanthrenophanes; first isolated *syn*-phenanthrenophane, *Tetrahedron Lett.,* 33, 5563, 1992.
30. Nakamura, Y., Fujii, T., Sugita, S., and Nishimura, J., Excimer fluorescence from *anti*-[2.3](2,7)phenanthrenophane, *Chem. Lett.,* 1039, 1999.
31. Nakamura, Y., Fujii, T., and Nishimura, J., Synthesis and fluorescence emission behavior of novel *anti*-[2.n](3,9)phenanthrenophanes, *Tetrahedron Lett.,* 41, 1419, 2000.
32. Nakamura, Y., Fujii, T., and Nishimura, J., Synthesis and fluorescence emission behavior of *anti*-[2.3](3,10)phenanthrenophane: overlap between phenanthrene rings required for excimer formation, *Chem. Lett.,* 970, 2001.
33. Nakamura, Y., Mita, T., and Nishimura, J., Synthesis and properties of [2.2](3,3′)biphenylo(3,6)phenanthrenophane, *Tetrahedron Lett.,* 37, 3877, 1996.
34. Nakamura, Y., Kaneko, M., Shinmyozu, T., and Nishimura, J., Synthesis of [2.*n*]thiophenophanes by intramolecular [2 + 2]-photocycloaddition, *Heterocycles*, 51, 1059, 1999.
35. Nakamura, Y., Kaneko, M., Yamanaka, N., Tani, K., and Nishimura, J., Synthesis and photophysical properties of *syn*- and *anti*-[2.*n*](3,9)carbazolophanes, *Tetrahedron Lett.,* 40, 4693, 1999.
36. Nakamura, Y., Hayashida, Y., Wada, Y., and Nishimura, J., Synthesis of paddlanes possessing cyclophane shaft and cyclobutane blades, *Tetrahedron,* 53, 4593, 1997.
37. Nishimura, J., Horikoshi, Y., Wada, Y., Takahashi, H., and Sato, M., Intramolecular [2 + 2]-photocycloaddition. 10. Conformationally stable *syn*-[2.2]metacyclophanes, *J. Am. Chem. Soc.,* 113, 3485, 1991.
38. Wada, Y., Ishimura, T., and Nishimura, J., 1,2;9,10;17,18-Triethano[2_3](1,3,5)cyclophanes; paddlanes with cyclophane shaft and cyclobutane blades, *Chem. Ber.,* 125, 2155, 1992.
39. Anderson, J.E., Barkel, D.J.D., and Parkin, J.E., Conformations and internal rotation of simple 1-alkenylnaphthalenes, studied by dynamic nuclear magnetic resonance spectroscopy, nuclear Overhauser effects, and molecular mechanics calculation, *J. Chem. Soc., Perkin Trans. 2,* 955, 1987.
40. Nakanishi, K., Mizuno, K., and Otsuji, Y., Intramolecular [$2_\pi + 2_\pi$] photocycloaddition of group 14 organometallic compounds bearing a styrene chromophore: a route to sila- and germa-cyclophanes and spiro compounds, *J. Chem. Soc., Perkin Trans. 1,* 3362, 1990.
41. Okada, Y., Ishii, F., and Nishimura, J., Stereoselective synthesis of dimethoxy[2.n]metacyclophanes, *Bull. Chem. Soc. Jpn.,* 66, 3828, 1993.
42. Okada, Y., Mabuchi, S., Kurahayashi, M., and Nishimura, J., Synthesis and structural analysis of dimethoxy[2.n]metacyclophanes, *Chem Lett.,* 1345, 1991.
43. Nishimura, J., Ohbayashi, A., Wada, Y., Oku, A., Ito, S., Tsuchida, A., Yamamoto, M., and Nishijima, Y., Intramolecular [2 + 2] photocycloaddition. 2. Mechanism of intramolecular photocyclization of α,ω-bis(*p*-vinylphenyl)alkanes, *Tetrahedron Lett.,* 29, 5375, 1988.

44. Wulff, G., Krieger, S., Kühneweg, B., and Steigel, A., Occurrence of strong circular dichroism during measurement of CD spectra due to intramolecular cyclization, *J. Am. Chem. Soc.,* 116, 409, 1994.
45. Nakamura, Y., Fujii, T., Inokuma, S., and Nishimura, J., Effects of oligooxyethylene linkage on intramolecular [2 + 2] photocycloaddition of styrene derivatives, *J. Phys. Org. Chem.,* 11, 79, 1998.
46. Mitchell, R.H., Vinod, T.K., and Bushell, G, W., *syn*-[2.2]Metacyclophane: synthesis and facile isomerization to *anti*-[2.2]metacyclophane. The use of (arene)chromium carbonyl complexes to control the stereochemistry of cyclophanes, *J. Am. Chem. Soc.,* 107, 3340, 1985.
47. Inokuma, S., Kimura, K., and Nishimura, J., Synthesis and complexation of azacrownophanes: the cyclodextrin catalysis of the photochemical cyclization reaction, *J. Inclusion Phenomena,* 39, 35, 2001.
48. Meinwald, J. and Mazzocchi, P.H., Photoisomerization of *o*-divinylbenzene, *J. Am. Chem. Soc.,* 89, 696, 1967.
49. George, P., Trachtman, M., Bock, C.W., and Brett, A.M., An alternative approach to the problem of assessing destabilization energies (strain energies) in cyclic hydrocarbons, *Tetrahedron,* 32, 317, 1976.
50. Hasegawa, M., Nohara, M., Saigo, K., Mori, T., and Nakanishi, H., Photodimerization of 1,4-dicinnamoylbenzene crystal via a topochemical process, *Tetrahedron Lett.,* 25, 561, 1984.
51. Takeuchi, A., Komiya, H., Tsutsumi, T., Hashimoto, Y., Hasegawa, M., Iitaka, Y., and Saigo, K., Photochemical reaction of 2,3-di[*(E)*-styryl]pyrazine derivatives in the crystalline state and in solution, *Bull. Chem. Soc. Jpn.,* 66, 2987, 1993.
52. Nishimura, J., Wada, Y., and Sano, Y., Intramolecular [2 + 2] photocycloaddition. 14. Cycloreversion of cyclophanes possessing a cyclobutane ring at their tether, *Bull. Chem. Soc. Jpn.,* 65, 618, 1992.
53. Gotoh, T., Kato, M., Yamamoto, M., and Nishijima, Y., Cation-radical transfer: transfer efficiency photosensitized isomerization reaction, *J. Chem. Soc., Chem. Commun.,* 90, 1981.
54. Nishimura, J., Ohbayashi, A., Ueda, E., and Oku, A., Intramolecular [2 + 2] photocycloaddition, 4. Synthesis of [4.n]cyclophanes by [2 +2] photocycloaddition and Birch reduction. A rare fragmentation of tetramethylene radical anion, *Chem. Ber.,* 121, 2025, 1988.
55. Wada, Y., Sugata, K., Tago, T., and Nishimura, J., Synthesis and Diels–Alder reaction of cyclobuteno[*e*]pyrene and biscyclobuteno[*e,l*]pyrene, *J. Org. Chem.,* 57, 5955, 1992.
56. Kaplan, M.L. and Truesdale, E.A., [2.2]Paracyclophane by photoextrusion of carbon dioxide from a cyclic diester, *Tetrahedron Lett.,* 3665, 1976.
57. Bassani, D.M., Darcos, V., Mahony, S., and Desvergne, J.-P., Supramolecular catalysis of olefin [2 + 2] photodimerization, *J. Am. Chem. Soc.,* 122, 8795, 2000.
58. Greiving, H., Hopf, H., Jones, P.G., Bubenitschek, P., Desvergne, J.P., and Bouas-Laurent, H., Synthesis, photophysical and photochemical properties of four [2.2] "cinnamophane" isomers; highly efficient stereospecific [2 + 2] photocycloaddition, *J. Chem. Soc., Chem. Commun.,* 1075, 1994.
59. Inokuma, S., Takezawa, M., Satoh, H., Nakamura, Y., Sasaki, T., and Nishimura, J., Efficient and selective synthesis of crownopaddlanes possessing two cyclobutane rings and exclusive complexation of lithium, *J. Org. Chem.,* 63, 5791, 1998.

20

The Dimerization of Cinnamic Acid Derivatives

Dario M. Bassani
Laboratoire de Chimie Organique et Organometallique

20.1 Background

The photoinduced dimerization of cinnamic acid and its derivatives has sparked continued interest since its initial reports, nearly one hundred years ago.[1,2] The reasons for such a privileged position in the annals of photochemistry surely lie in its intriguing solid-state behavior and its versatility in a number of industrial applications, ranging from cosmetics to polymers for photoresists and lithography. With so much interest, an exhaustive review of all the pertinent literature would be overly lengthy and beyond the scope of this book. Therefore, greater emphasis is placed on more recent advances, particularly those dealing with reactions in complex or organized media (polymers, aggregates, and supramolecular architectures).

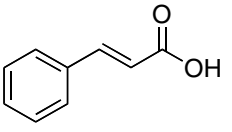

E-Cinnamic acid

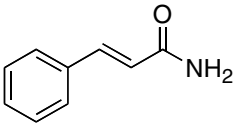

E-Cinnamamide

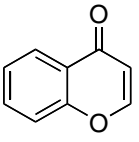

Coumarin

Hydroxycinnamic acids are present in plants, where they play an important role in controlling the structure of cell walls.[3] It should come as no surprise, therefore, that cyclodimerization products of naturally occurring cinnamate and coumarin derivatives, such as *p*-coumaric acid and ferrulic acid, have been isolated from a variety of plants.[4] It has been postulated that dimers are formed by a photoinduced mechanism, causing cross-linking of the polysaccharide chains.[5,6] For example, sagerinic acid isolated from sage (*Salvia officinalis*) was identified as the uncommon μ-truxinate dimer **2**, presumably the result of the [2 + 2]-cyclodimerization of rosmarinic acid **1** present in the plant.[7]

0-8493-1348-1/04/$0.00+$1.50

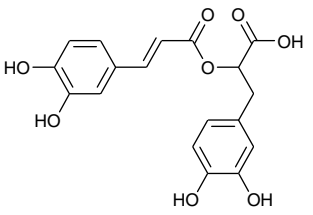

Rosmarinic acid (**1**)

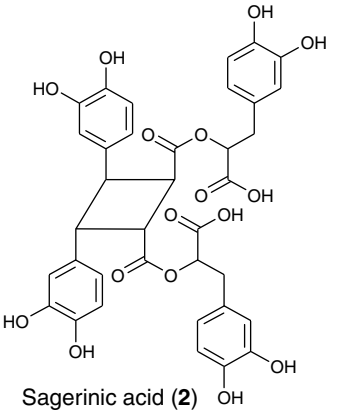

Sagerinic acid (**2**)

In principle, the [2 + 2]-cyclodimerization of cinnamates can proceed to yield 11 different products, commonly divided between those arising from a head-to-head dimerization (truxinates) and those from a head-to-tail dimerization (truxillates).

Truxinates

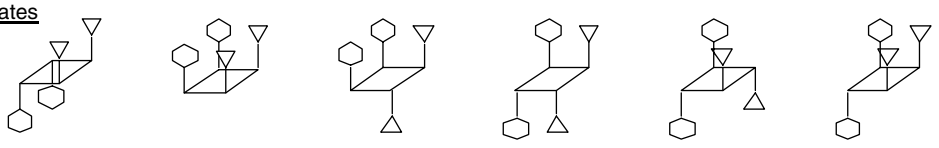

β ω neo μ δ ξ

Truxillates

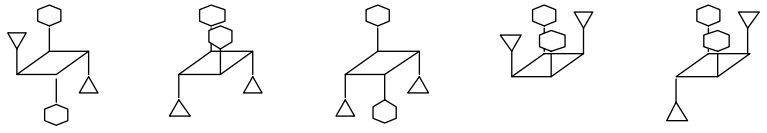

α ε γ peri epi

Whereas the preparation of the α- and β-truxinic acids from the solid-state irradiation of the corresponding crystals is straightforward,[8–10] the remaining cyclobutane structures are more complicated to prepare. The cross-photocycloaddition of stilbene to diethylfumarate can be used to prepare the μ-truxinate isomer,[11] and a similar procedure was used to prepare diethyl ξ-truxinate.[12] The preparation of the ε- and γ-isomers was described by Stoermer and Emmel.[13] To prepare the δ-isomer in good yields, a tetramethylene tether can be used to temporarily connect two cinnamoyl units during irradiation.[14]

The situation is considerably simplified in the case of coumarin due to the absence of *cis* and *trans* isomers of the exocyclic double bond. Only four isomers are possible, resulting from the head-to-head or head-to-tail dimerization in a *syn* or *anti* approach. Optically active coumarin dimers have found applications as chiral derivatizing agents for amines and alcohols.[15]

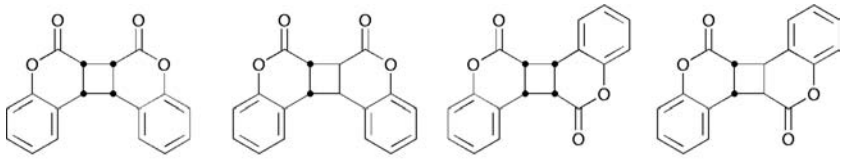

syn head-to-head anti head-to-head syn head-to-tail anti head-to-tail

20.2 Photodimerization in Solution

The photochemistry of cinnamate derivatives in solution has received comparatively less attention than in the solid state. In solution, dimerization must compete with fast *E,Z*-isomerization, and long irradiation times are required to achieve significant conversions. Reiser and co-workers[12] investigated the dimerization of thin films of neat ethyl cinnamate both as a liquid and as an amorphous solid. Their findings dispelled remaining doubts on the possibility of photodimerization outside of ordered crystalline matrices. High yields (>90%) of photodimers, predominantly the δ- and β-truxinate, were obtained in all cases, with the formation of the α-truxillate dimer favored at lower temperatures. Overall quantum yields for the photodimerization of ethyl cinnamate of 0.08 (neat) and $< 10^{-4}$ (0.2 *M* dichloromethane solution) were later determined by Lewis et al.[16,17] In this work, the authors also reported a significant increase in photodimerization efficiency through the use of Lewis acid catalysts such as BF_3 and $SnCl_4$, which is accompanied by a reduction in regiospecificity. In contrast, Cu(I) complexes of cinnamates were found to only undergo *E,Z*-isomerization without dimerization.[18] The photodimerization of a number of hydroxycinnamic acids,[19] methoxy-cinnamate esters,[20] and *p*-nitrocinnamate esters[21] has also been reported.

The low efficiency of photoinduced dimerization of cinnamates is in agreement with the short (< 3ps) fluorescent lifetime of methyl cinnamate estimated by Lewis et al.[22] using picosecond time-resolved spectroscopy. Inefficient intersystem crossing from the lowest $n\pi^*$ singlet excited state excludes the possibility that the photoinduced isomerization and dimerization reactions observed upon direct excitation originate from the excited triplet. Consistent with these observations, Herkstroeter and Farid[23] measured a bimolecular rate constant for the dimerization of triplet methyl cinnamate of $8.8 \times 10^6\ M^{-1}s^{-1}$ and a triplet lifetime of 10.6 ns (E_T = 229 kJ mol^{-1}), giving a limiting quantum yield of 0.5 — considerably higher than observed for dimerization from the excited singlet state. The isolated photoproducts were found to consist mainly of the δ–truxinate dimer (63%), with smaller proportions of the β-truxinate dimer (25%). Many other examples of sensitized dimerization of cinnamates have been reported (see, for example, refs. 20, 24) and more recently, the use of electron transfer sensitization has also been reported.[25]

Positive identification of the cycloadducts has vastly improved, thanks to advances in modern spectroscopy. Generally, ^{1}H-NMR provides the most information regarding the geometry of the cyclobutane ring (detailed NMR data of photoproducts may be found in refs. 17, 19, 21, and 26; for detailed analysis of cyclobutane NMR spectra, see references 27–29). This is frequently complemented by mass spectroscopy to identify the fragmentation pattern characteristic of truxinates, which, unlike truxillates, may fragment along one of two possible pathways to give stilbene and dicarboxylate fragments.[30]

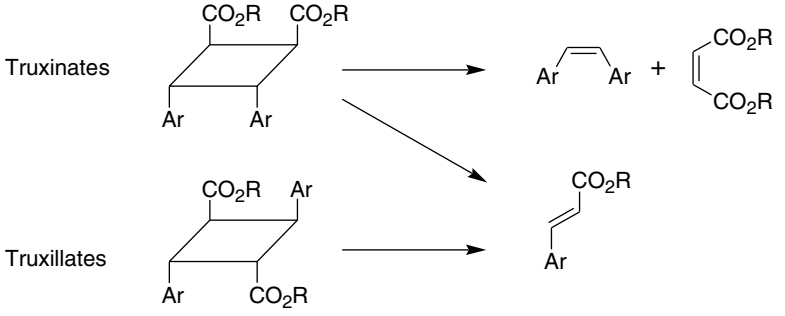

Moderately efficient photochemical scission of truxinates and truxillates is also possible via direct,[31,32] benzene-sensitized irradiation[33] and via an electron transfer mechanism[34] (γ irradiation in 2-methyltetrahydrofuran matrix).

Like cinnamate esters, coumarin also dimerizes slowly under direct irradiation conditions to give a mixture of photodimers composed of the *syn* head-to-head (major product) and *syn* head-to-tail

dimers.[35–37] At low coumarin concentrations, intersystem crossing competes with dimerization to generate excited triplet coumarin, which undergoes dimerization to yield the *anti* head-to-head dimer.[38] Coumarin dimerization in the presence of BF_3 has been investigated in detail by Lewis et al.,[22] revealing uncommon complexity even under long-wavelength (313 nm) irradiation. Thiocoumarin also undergoes dimerization in solution, which, in marked contempt to all topological principles, is cleaner than in the solid, yielding principally the *anti* head-to-head dimer.[39,40]

Connection of two cinnamate chromophores has frequently been used to attain high local concentrations of reactants, thereby circumventing the inefficiency of the above-mentioned bimolecular dimerization reactions. An extreme example of this approach is embodied in the cyclophane structures **3**, in which two cinnamate moieties undergo photodimerization to give quantitatively the β-truxinate dimer with a quantum yield of 0.55.[41,42] Similarly, the bis-cinnamamide **4** furnished 48% of β-truxinimide upon irradiation through Pyrex.[43] Other cyclophanes have been prepared, including highly strained multibridged tricyclic phanes.[44,45]

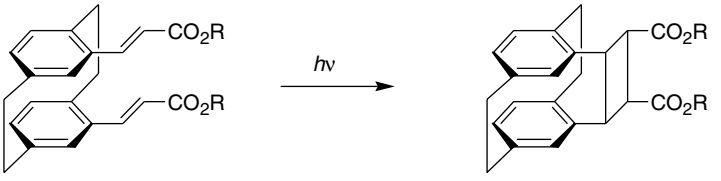

3, R = H, Me

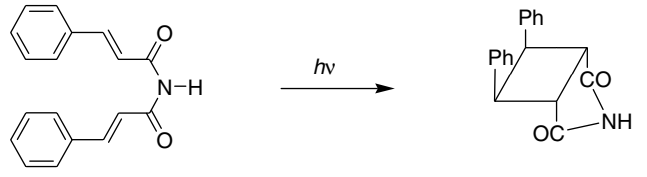

4

Many macrocyclic compounds have been prepared by the irradiation of α,ω-dicinnamates[46–48] and dicoumaryl derivatives (130, 130–16).[49,50] When the tether is a polyglycol unit, the photodimerization is sensitive to alkali metal ions, and crown-ether-like structures can be prepared.[51] Intramolecular dimerization reactions can find preparative importance as, for instance, in the preparation of the β- and δ-truxinate dimers from the irradiation of propylene-1,3-dicinnamate and *n*-butylene-1,4-dicinnamate, respectively.[14,52] The tether may also function as a chiral auxiliary, such as in the irradiation of L-erythritol 1,4-dicinnamate or mannitol hexacinnamate.[53,54] In the latter case, an excess of the (+)-δ–truxinate isomer was observed, along with several other isomers.

20.3 Photodimerization in the Solid

The solid-state photoreactivity of cinnamic acids is one of the most explored areas in organic solid-state photochemistry and holds considerable potential for preparative applications.[55] In a series of papers published in 1964, Schmidt and co-workers[56–59] elegantly established the principle of topochemical control of reactivity first expressed by Kohlshütter et al.[60] and Hertel et al.[61] The observation that one could relate the relative orientation of molecules in crystals to the geometry of the reaction products has since governed solid-state photochemistry. Cinnamic acid is the archetypical example of such processes, crystallizing in one of three morphologies. The stable α and metastable β forms are photoreactive, yielding the α- and β-truxinic acid dimers, respectively, with similar quantum yields of 0.7.[62] (Cohen,[63] however, has cast some doubts on this value.) The γ form, in which the olefinic double bonds are separated by a distance >4.7 Å, is unreactive. These findings are general for the wide variety of substitution patterns examined by Schmidt and co-workers and lead to the conclusion that the reactive double bonds must

be within ca. 4.2 Å for photodimerization.[64] Keating and Garcia-Garibay[65] have recently reviewed the physical aspects of several photochemical solid-to-solid reactions, including cinnamates.

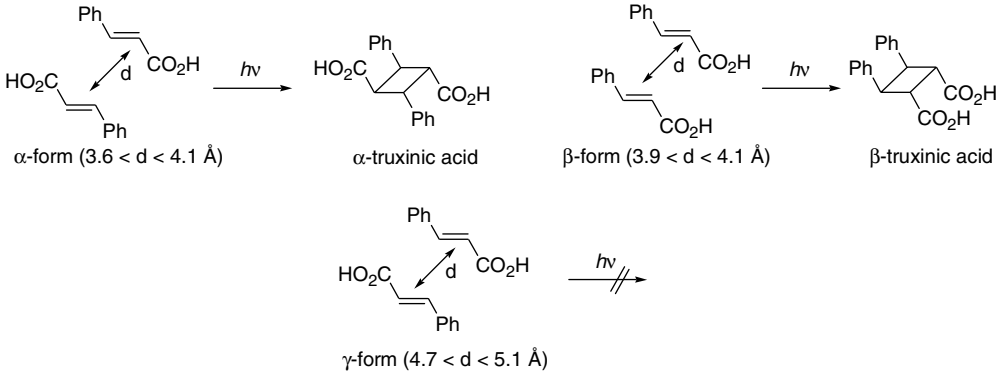

In cases where irradiation of photoreactive crystals proceeded without destroying the crystal lattice, it has been possible to investigate the dimerization process by x-ray diffraction. Data from single crystal–to–single crystal transformations provide invaluable insight to the atomic movement during the cycloaddition step[66] and have been obtained for several cinnamate derivatives, including α-cinnamic acid[67] and its α-acetylamino derivative,[68] various cinnamamides,[69] co-crystals of *trans*-cinnamamide with phthalic acid,[70] coumarins in chiral hosts,[71] and cinnamic acid in clays.[72] In some cases, the presence of water[73,74] or hydrocarbons[75] in the crystal lattice has been noted. The dimerization of cinnamic acids in crystals has also been investigated by the use of atomic force microscopy,[76] scanning near-field optical microscopy,[77] and vibrational microspectroscopy.[78] It has been the subject of Monte Carlo simulation[79] and detailed mathematical analysis.[80]

Irradiation of cinnamate derivatives in chiral host environments has long attracted attention as a gateway to asymmetric photochemical synthesis.[53,54,81–84] The use of a nonchiral host induced to crystallize in a chiral space group represents an example of absolute asymmetric synthesis, as described by Vaida et al.[85] for the cinnamamide/cinnamic acid host/guest system and by Hasegawa et al.[86,87] for the cross dimerization of **5** (which spontaneously crystallizes in a chiral space group). It should be noted that even apparently minor modifications, at times, have a profound impact on the outcome of solid-state reactions. In the previous example, the methyl ester derivative of **5** gives, upon irradiation, linear polymers.

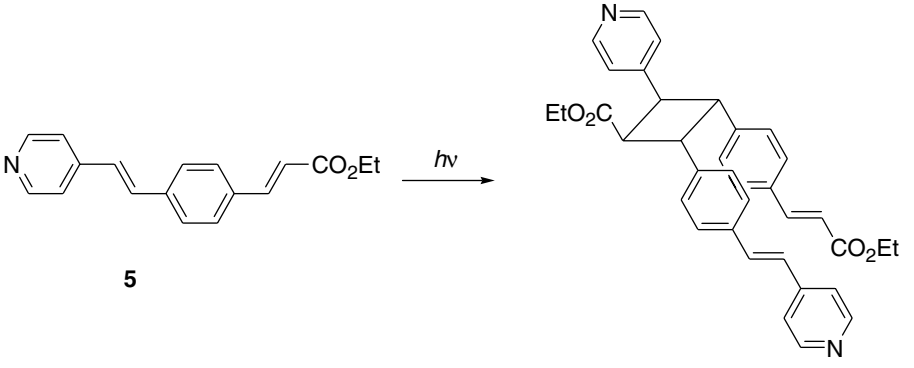

5

Noncovalent interactions, principally hydrogen bonding and electrostatics, have also been used in conjunction with mixed crystal environments in view of directing the outcome of the dimerization process.[88] This approach, which borders on the fields of supramolecular chemistry and crystal engineering, has at times proven very successful. Noteworthy examples include the use of linear or conformationally restricted diamines

such as **6** to induce variation in the mutual orientation of cinnamic acid during crystallization.[89,90] Here, electrostatic interactions form the basis for driving the formation of 1:2 adducts in the solid phase. Hydrogen bonding between cinnamamides and dicarboxylic acids has also been used to achieve similar results.[91]

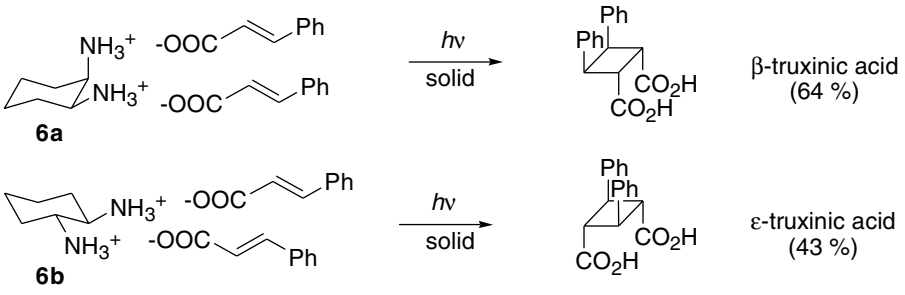

Electrostatic interactions probably also play a role in directing the unusual cross photocycloaddition between tryptamine (**7**) and 3-nitrocinnamic acid (**8**) in the solid as reported by Ito and Fujita.[92]

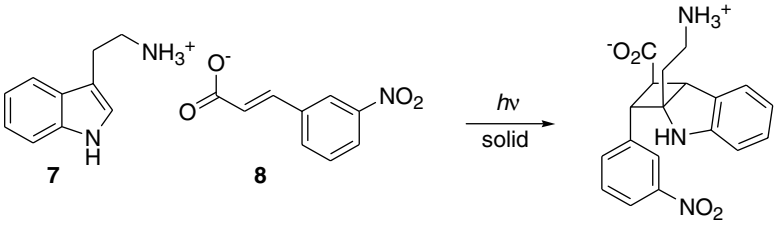

Coates et al.[93] used stacking interactions in the phenyl–perfluorophenyl system[93] to direct co-crystallization of mixed stilbene and cinnamic acid co-crystals, thereby directing the formation of the mixed β-truxinic acid derivative in very high yield. Ito has recently reviewed the solid-state organic photochemistry of mixed crystals.[94]

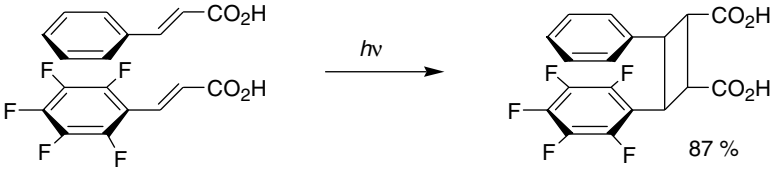

Many examples of dimerization of cinnamate derivatives in the solid exist, including thiocinnamate esters,[40,95–97] α-cyano-cinnamates,[98,99] and in the presence of BF_3.[16,17] It is frequently admitted that the outcome of the dimerization reflects the "prereaction" ordering of the chromophores.[12] This seems to hold true, with a few exceptions where rearrangement or isomerization (as in the case of crystalline *Z*-cinnamic acid) takes place prior to photodimerization.

The solid-state chemistry of coumarin has also received considerable attention, mainly due to the biological importance of coumarin derivatives, and has been summarized in several reports.[35,100,101] In a comprehensive study of nearly 30 coumarin derivatives in the solid state, Venkatesan, Ramamurthy, and co-workers[102] discuss the criteria for topochemical reactivity in the solid set forth 20 years earlier by Schmidt. Their results, though not invalidating previous guidelines for solid-state reactivity, indicate that caution, rather than rigor, is recommended in their application. The irradiation of coumarin within chiral inclusion complexes has also been used as a means to achieve enantioselective dimer synthesis.[71,103–105]

20.4 Polymer Systems

Photoresponsive polymers, in which light is used to bring about a change in a sample's physical or chemical properties, have found numerous commercial applications. A wealth of fundamental research has accompanied these developments, with the aim to shed light on the many parameters that influence the behavior and properties of such advanced materials. One of the most commercially successful examples in the field involves the use of pendant cinnamate moieties to induce cross-linking of polymer chains upon exposure to light. Discovered nearly 50 years ago,[106] polymers such as poly(vinyl cinnamate) function as negative photoresists in lithographic materials[14,107] and can also be used in photocurable coatings.[108] Photoreactive polymers combining crown ether and cinnamate units were shown to be active toward cation transport in liquid membranes.[109] Often, the progress of the photodimerization process can be conveniently followed by UV absorption spectroscopy by monitoring the disappearance of the cinnamate chromophore; this approach has often been used to obtain valuable kinetic data (see, for example, reference 110).

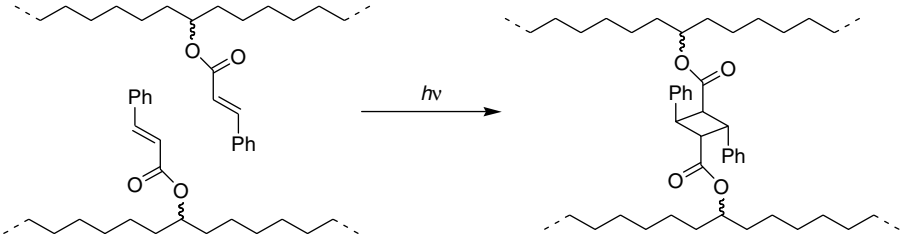

The photoinduced cross-linking of a number of polyacrylates and polymethacrylates containing substituted cinnamoyl groups has been reported.[111,112] Controlling the competition between intra- and interstrand dimerization is of paramount importance in achieving high degrees of cross-linking, as only the latter is productive. Blends of electron donor and electron acceptor substituted vinyl cinnamate polymers were shown to possess superior sensitivity, presumably as a result of the preordering of reactant pair sites due to donor–acceptor interactions.[113]

A photochemical template effect (footprinting) was demonstrated by Damen and Neckers[114] through the use of polystyrene networks that were prepared in the presence of monomers appended with truxinic or truxillic acids. Treatment of the hydrolyzed polymers with cinnamoyl chloride, followed by irradiation and hydrolysis, yielded dimers whose composition was biased in favor of the photoproduct with which the polymer had been molded.

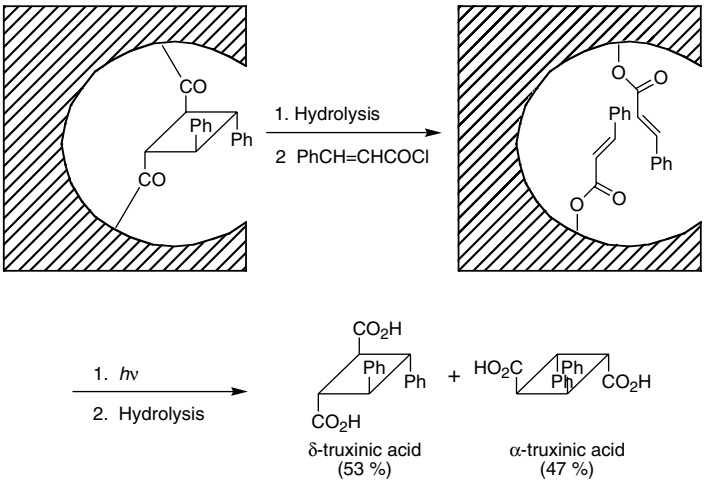

Another promising application of photo-crosslinkable polymers is in the stabilization of nanospheres and other micellar assemblies formed from block copolymers.[115–117] Typically, the photosensitive cinnamates are included in one of the polymer blocks, and a block-selective solvent is used to induce its micellation. Irradiation causes photo-dimerization of nearby chromophores, thus covalently linking the aggregated polymer blocks. In their investigation of chiral bifunctional photopolymers, Bernstein et al.[118] showed that the chiral sugar ester **9** yields polymeric material incorporating exclusively α-truxillate linkages when irradiated in the solid state. In contrast, irradiation in benzene solution affords mixtures of mainly the β- and δ-truxinate isomers.

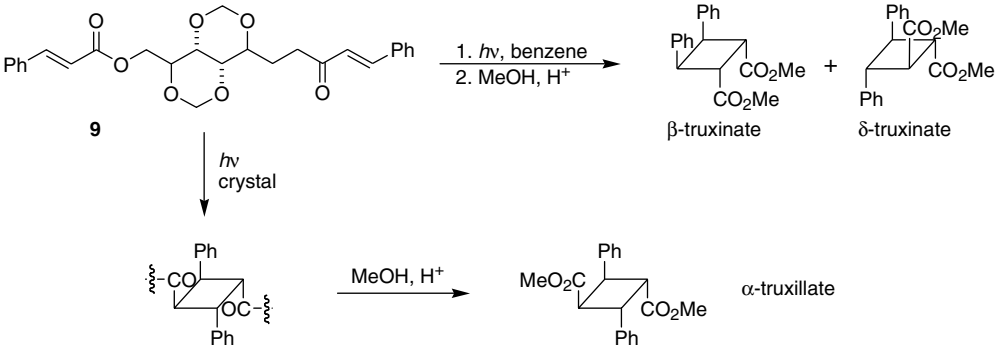

Numerous derivatives of arylethenylcinnamate ester **10** (Ar = 2- or 4-pyridine, pyrimidine; X = H, CN; R = alkyl) have been investigated by Hasegawa and co-workers.[87,119–121] These compounds are remarkable in their versatility, undergoing hetero- and homo-dimerization processes that are very sensitive to their environment. Various dimer and polymer structures can be formed, sometimes with high enantioselectivity.

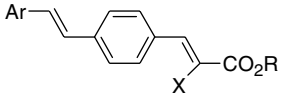

10

Ar = pyridine, pyrimidine
X = H, CN
R = Me, Et, Pr

An important breakthrough in the area of photoresponsive polymers came from the discovery that the use of polarized light in the cross-linking step results in birefringent materials that could be used to induce alignment of liquid crystals.[122] This provides an appealing alternative to the rubbing technique used in polyimide films. In addition to the extensive work on the use of azobenzene-containing polymers for such applications, much effort has focused on polymers containing photodimerizable units such as cinnamates and coumarins which, compared to azobenzene derivatives, can exhibit superior long-term thermal stability. Although it is generally assumed that the induced alignment is a result of the anisotropy of the cinnamoyl groups on the polymer chains, the mechanism by which this is brought about remains a topic of debate. Schadt et al.[123] proposed that alignment is a result of preferential dimerization perpendicular to the plane of the incident linearly polarized light.[124–127] This view has been questioned by Ichimura and co-workers, who proposed that both *E,Z*-isomerization and dimerization are, in fact, responsible for the observed photo-induced anisotropy.[128,129] This dual reactivity of the cinnamate chromophore was also evidenced by Olenik et al.,[130] using surface second harmonic generation. Other investigations of the photoinduced molecular orientation and liquid crystal alignment in cinnamate and coumarin thin films include phase-modulated IR[131,132] and Raman spectroscopy.[133] Coumarins have also been applied to the generation of photoinduced anisotropy.[134,135]

Yet another promising application of cinnamate- and coumarin-containing polymers is in the field of biocompatible or biodegradable materials. Due to their costs, these find use predominantly in medical applications, such as drug delivery systems and as scaffolds for tissue engineering. Thus, coumarin-containing peptides display photoresponsive behavior in their gelling ability.[136] Direct incorporation of *E*-4-hydroxycinnamic acid in poly(lactic acid) affords a polyester that is reported to be photoresponsive towards both *E,Z*-isomerization and dimerization, as evidenced by UV absorption spectroscopy.[137]

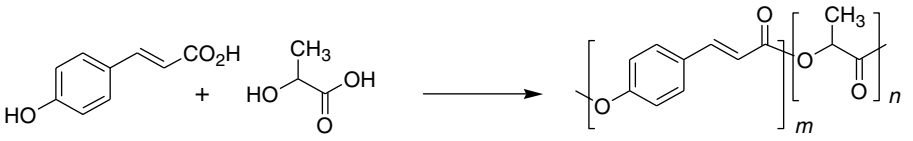

20.5 Organized Assemblies and Supramolecular Systems

For simplicity, the irradiation of cinnamate derivatives in various organized assemblies, ranging from self-assembled monolayers and micelles to discrete multi-component architectures, is grouped together. Whether all such structures are indeed "supramolecular" is left to the reader to decide, but it should be noted that many of the preceding examples, particularly those dealing with solid-state crystal engineering, could also belong here. Many photochemical reactions have been revisited in self-organized aggregates such as micelles or monolayers, sometimes with surprising results.[138–140] Cinnamate derivatives are no exception and present the added quality of supplying information on the morphological structure of the assembly, provided the results can be rationalized in terms of topochemical control set forth above.

In its deprotonated form, cinnamic acid already presents some prerequisites of surfactants and is easily incorporated in reversed micelles, as demonstrated by Sawaki and co-workers[141,142] and others.[143,144] Their results support the view that increased local concentration and alignment can be achieved at micellar interfaces. Substantially higher conversion of cinnamate to its photodimers is observed upon irradiation of reversed micelles formed by laurylammonium or hexadecyltrimethylammonium cinnamate in carbon tetrachloride.[142] The photoproducts are mainly the β- and δ-truxinates, consistent with the requirements imposed by the assembly for the formation of contact ion pairs. Unfortunately, these are also the main products observed by Reiser upon irradiation of ethyl cinnamate (albeit in different proportions).[12] Interestingly, however, the observed dimer distribution varies as a function of added water that is proposed to lie near the ion pair interface. Similar results were also obtained for indene-2-carboxylate[145] and using sodium dodecyl sulfate microemulsions in water.[146] The photodimerization of coumarin in micelles has been investigated by Ramamurthy and co-workers.[147–149]

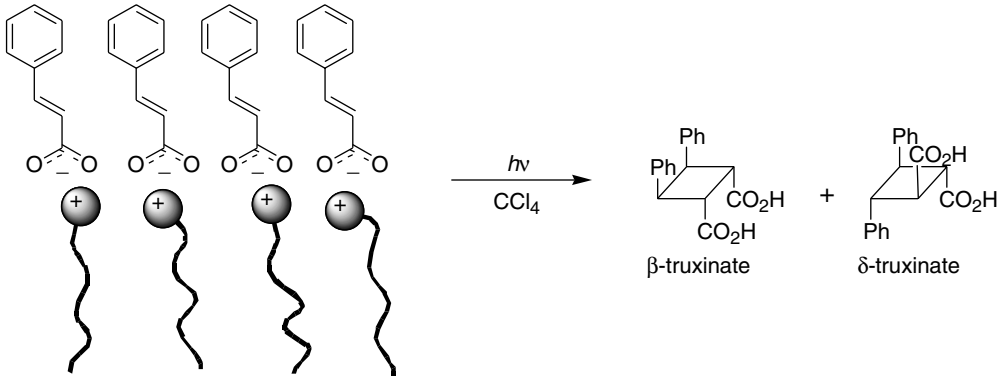

Interest in the study of photoresponsive liquid crystals has expanded tremendously with the advent of flat-panel displays, and the use of cinnamates and coumarin derivatives to orient liquid crystalline

materials has already been discussed (see also Mukkamala et al.[150] and Ramesh and Weiss[151]). It is also possible to use the photoinduced cycloaddition process to crosslink liquid crystalline polymers, thus imparting orientational anisotropy to the entire assembly. This, in turn, can be used to significantly improve such parameters as the viewing angle and contrast of the display.[134] The application of cinnamate derivatives to liquid crystalline polymers has been recently reviewed by Creed et al.,[152,153] who also established the presence of aggregates absorbing in the long-wavelength region,[154,155] and compared the temperature and phase dependence of photocycloaddition products upon triplet sensitization of arylcinnamate liquid crystalline polymers.[156] The photoreactivity of cholesteryl cinnamate in isotropic and mesomorphic phases[157–159] and of liquid crystals based on cinnamate-containing poly(methylmethacrylate)[160] have also been reported.

The irradiation of cinnamic acid and cinnamamides at the air/water interface was used by Lahav and co-workers to obtain structural information during the early stages of crystal growth.[161,162] Additionally, Langmuir–Blodgett (L-B) films also provide a facile means of controlling packing structures in two-dimensional assemblies, which can be used to direct dimerization.[163] A limiting factor, in some cases, occurs from disruption of the close packing of the molecules in the film from product formation.[164,165] Comprehensive studies of cinnamate dimerization in L-B films have also been undertaken by the group of Nakanishi[166–168] and by Itoh and co-workers.[169]

Since the mid-eighties, the term supramolecular chemistry has come to signify the programmed self-assembly of complex architectures through the interplay of noncovalent interactions.[170] In the case of the dimerization of cinnamate derivatives, Beak and Ziegler[171] presented, over 20 years ago, the first example of the use of hydrogen bonding in solution to accelerate the usually inefficient cycloaddition reaction. In their work, the self-complementary pyridone unit was used to direct the head-to-head dimerization of the appended cinnamate moieties.

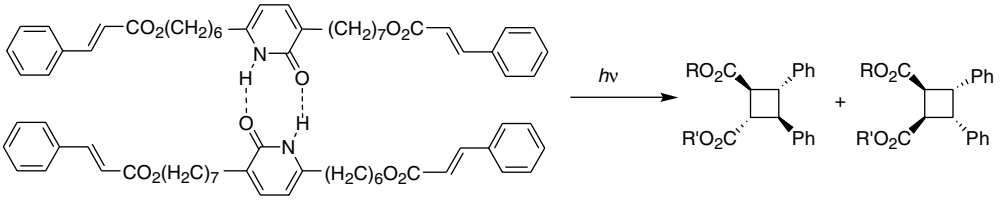

In their communication, however, the authors only reported overall yields of photoproducts, and no kinetic or binding data are available to characterize the intervention of the supramolecular assembly during the photocycloaddition step. In this regard, the choice of ethyl cinnamate as a model compound is also unfortunate, as it cannot be ruled out that the enhancement in yield results from an increase in the single state lifetime of the cinnamate chromophore due to hindered *E,Z*-isomerization. Although the observed products are the β- and δ-truxinate dimers, which are usually the major products from solution photodimerization,[12] the presence of methylene tethers of different lengths could, in principle, be used to provide evidence for the proposed hydrogen-bonded assembly.

Along similar lines, Feldman et al.[172] used a naphthalene scaffold to construct hydrogen-bonded assemblies in the solid state. Their results, which border on the field of crystal engineering, indicate that the dimerization occurs in a quasi-unimolecular fashion to afford the α-truxillate dimer in near-quantitative yield. The reported lack of photoreactivity in tetrahydrofuran (THF) solutions may be due to the weakness of the hydrogen-bonding interactions in those solvents suitable for solubilizing such compounds.

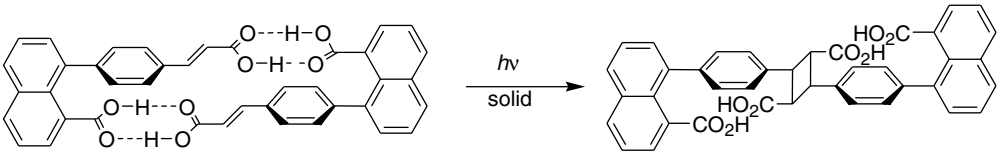

Recently, Bassani et al.[173] reported the use of hydrogen-bonded tape-like structures to assemble cinnamate derivatives in solution. In this work, a dialkylbarbiturate derivative serves to bind two diaminotriazine units appended with cinnamate chromophores. Of the several structures that may be formed, one places the reactive double bonds in close proximity. A nearly 100-fold enhancement in the dimerization rate constant with respect to solution (at identical concentration) is calculated based on the experimentally determined quantum yields and binding constants. The formation of the ε-truxillate dimer — unusual in solution — and control experiments in the absence of template or using a di-*N*-methylated barbiturate substantiate the proposed supramolecular control of photoreactivity.

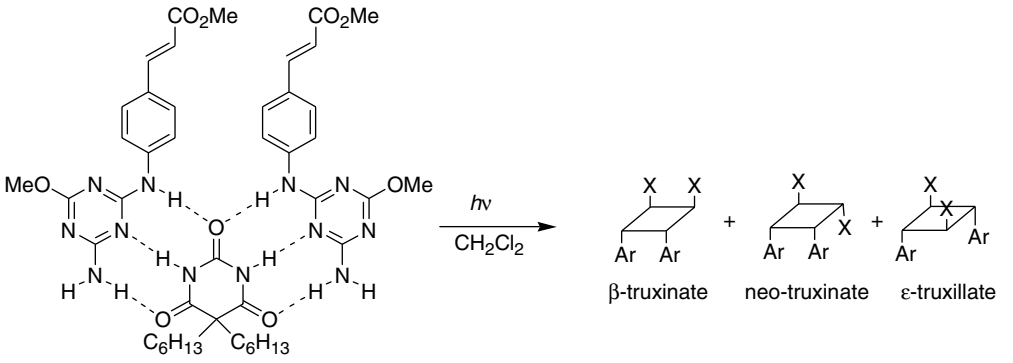

Dendrimers decorated with peripheral cinnamoyl groups have been prepared to impart photoreactivity to the assembly. Boiko et al.[174] reported the synthesis and investigation of a liquid crystalline carbosilane dendrimer (second generation) containing eight *p*-methoxycinnamate ester chromophores. Irradiation of thin films results in *E,Z*-isomerization and cycloaddition between dendrimers to generate a covalent three-dimensional structure. Wang et al.[175] have shown that intra-dendrimer cycloaddition of the appended cinnamate units is possible upon irradiation of dilute solutions (ca. 10^{-4} *M*) of the dendrimers. Regrettably, in both examples only UV-Vis absorption was used to characterize the formation of photoproducts, and further structural characterization appears complicated due to the dendritic assembly.

An elegant example of the use of supramolecular interactions (hydrophobic forces in this case) to accelerate and direct photochemical cycloaddition reactions is embodied in the use of β-cyclodextrins as a reaction vessel in which to assemble two coumarin molecules in a geometry adequate for dimerization.[37] In the case of 4,7-dimethylcoumarin, recent investigations by Brett et al.[176] using x-ray crystallography to determine the structures of the inclusion complex before irradiation and of the photoproduct reveal that the latter is not the expected *syn* head-to-tail or *anti* head-to-head, but rather the *anti* head-to-tail photodimer. Single crystal–to–single crystal photoreaction was observed for the β-cyclodextrin-4-hydroxy-7-methylcoumarin complex and, in this case, the observed photoproduct is correctly predicted from the topochemical principles set forth by Schmidt[64] over 30 years earlier.

References

1. Stobbe, H., Constitution of the truxillic acids and of truxone, *Ber. Dtsch. Chem. Ges.,* 8, 1021, 1919.
2. Stoermer, R. and Laage, E., Natural and artificial truxinic and truxillic acids, *Ber. Dtsch. Chem. Ges.,* 54B, 77, 1921.
3. Faulds, C.B. and Williamson, G., The role of hydroxycinnamates in the plant cell wall, *J. Sci. Food. Agric.,* 79, 393, 1999.
4. Hartley, R.D., Morrison, W.H., III, Himmelsbach, D.S., and Borneman, W.S., Cross-linking of cell wall phenolic arabinoxylans in graminaceous plants, *Phytochemistry,* 29, 3705, 1990.
5. Dimberg, L.H., Andersson, R.E., Gohil, S., Bryngelsson, S., and Lundgren, L.N., Identification of a sucrose diester of a substituted β–truxinic acid in oats, *Phytochemistry,* 56, 843, 2001.
6. Ishi, T., Structure and functions of feruloylated polysaccharides, *Plant Sci.,* 127, 111, 1997.

7. El-Ansari, M.A., Nawwar, M.A., and Saleh, N.A.M., Stachysetin, a diapigenin-7-glucoside-*p,p′*-dihydroxy-truxinate from *Stachys aegyptiaca*, *Phytochem.,* 40, 1543, 1995.
8. Schmidt, G.M.J., Photodimerization in the solid state, *Pure Appl. Chem.,* 27, 647, 1971.
9. Bernstein, H.I. and Quimby, W.C., The photochemical dimerization of *trans*-cinnamic acid, *J. Am. Chem. Soc.,* 65, 1845, 1943.
10. Nishikubo, T., Takahashi, E., Miyaji, T., and Iizawa, T., Convenient synthesis of β-truxinic acid via photodimerization of *p*-nitrophenyl cinnamate in the crystalline state, *Bull. Chem. Soc. Jpn.,* 58, 3399, 1985.
11. Green, B.S. and Rejto, M., μ-Truxinic acid, *J. Org. Chem.,* 39, 3284, 1974.
12. Egerton, P.L., Hyde, E.M., Trigg, J., Payne, A., Beynon, P., Mijovic, M.V., and Reiser, A., Photocycloaddition in liquid ethyl cinnamate and in ethyl cinnamate glasses. The photoreaction as a probe into the micromorphology of the solid, *J. Am. Chem. Soc.,* 103, 3859, 1981.
13. Stoermer, R. and Emmel, E., Truxillic acids. II, *Chem. Ber.,* 53B, 497, 1920.
14. Williams, J.L.R., Farid, S.Y., Doty, J.C., Daly, R.C., Specht, D.P., Searle, R., Borden, D.G., Chang, H.J., and Martic, P.A., The design of photoreactive polymer systems for imaging processes, *Pure Appl. Chem.,* 49, 523, 1977.
15. Saigo, K., Sekimoto, K., Yonezawa, N., Ishii, F., and Hasegawa, M., Optically active head-to-head coumarin dimer. A new agent for the determination of enantiomeric excess of amines and alcohols, *Bull. Chem. Soc. Jpn.,* 58, 1006, 1985.
16. Lewis, F.D., Oxman, J.D., and Huffman, J.C., Photodimerization of lewis acid complexes of cinnamate esters in solution and the solid state, *J. Am. Chem. Soc.,* 106, 466, 1984.
17. Lewis, F.D., Quillen, S.L., Hale, P.D., and Oxman, J.D., Lewis acid catalysis of photochemical reactions. 7. Photodimerization and cross-cycloaddition of cinnamic esters, *J. Am. Chem. Soc.,* 110, 1261, 1988.
18. Lorain, C., Bolte, M., and Lemaire, J., Study on the photoreactivity of copper(I) carboxylates. Part I. Study on copper(I) cinnamate, *Nouv. J. Chim.,* 5, 643, 1981.
19. Russell, W.R., Hanley, A.B., Burkitt, M.J., and Chesson, A., Effect of substitution on the 2 + 2 cycloaddition reaction of phenylpropanoids, *Bioorg. Chem.,* 27, 339, 1999.
20. D'Auria, M. and Vantaggi, A., Photochemical dimerization of methoxy substituted cinnamic acid methyl esters, *Tetrahedron,* 48, 2523, 1992.
21. Ishigami, T., Murata, T., and Endo, T., The solution photodimerization of (*E*)-*p*-nitrocinnamates, *Bull. Chem. Soc. Jpn.,* 49, 3578, 1976.
22. Lewis, F.D., Quillen, S.L., Elbert, J.E., Schneider, S., and Geiselhart, P., The singlet states of methyl cinnamate and methyl indenoate, *J. Photochem. Photobiol. A: Chem.,* 47, 173, 1989.
23. Herkstroeter, W.G. and Farid, S., Photodimerization-relevant triplet state parameters of methyl cinnamate, diethyl 1,4-phenylenediacrylate and methyl 1-naphthylacrylate, *J. Photochem.,* 35, 71, 1986.
24. Curme, H.G., Natale, C.C., and Kelley, D.J., Photosensitized reactions of cinnamate esters, *J. Phys. Chem.,* 71, 767, 1967.
25. Galindo, F. and Miranda, M.A., Pyrylium and thiopyrylium salts as electron transfer photosensitizers for the [2π + 2π] cyclodimerization of poly(vinyl cinnamate) in solution, *J. Photochem. Photobiol. A: Chem.,* 113, 155, 1998.
26. Montaudo, G., Caccamese, S., and Librando, V., Photodimers of cinnamic acid and related compounds. Stereochemical study of NMR, *Org. Magn. Reson.,* 6, 534, 1974.
27. Ben-Efraim, D.A. and Green, B.S., Use of mid-points or average nmr chemical shifts in stereochemical assignments, *Tetrahedron,* 30, 2357, 1974.
28. Ben-Efraim, D.A. and Arad-Yellin, R., A dynamic nmr study of restricted rotation of two substituted phenyl groups in a *cis*-1,2-diphenylcyclobutane, *Tetrahedron,* 44, 6175, 1988.
29. Ben-Efraim, D.A. and Arad-Yellin, R., Remarkable dynamic nmr spectra and properties of a sterically congested *cis*-1,2-diarylcyclobutene, *J. Chem. Soc., Perkin Trans. 2,* 853, 1994.

30. Stewart, D., Robertson, G.W., and Morrison, I.M., Identification of cyclobutane-type dimers of substituted cinnamic acids by gas chromatography/mass spectrometry, *Rapid Commun. Mass Spectrom.,* 6, 46, 1992.
31. Aloisi, G.G., Mazzucato, U., Bartocci, G., Cavicchio, G., Maravigna, P., and Montaudo, G., Luminescence and photolytic cycloreversion of cyclobutane derivatives: cinnamic acid dimers and their diamides, *Z. Phys. Chem.,* 138, 207, 1983.
32. Rennert, J. and Grossman, D., Photochemical scission of cinnamic acid dimers. α-truxillic and β-truxinic acids, *J. Photochem.,* 3, 163, 1974.
33. Rennert, J. and Grossman, D., Benzene photosensitized depolymerization of α-truxillic acid, *J. Photochem.,* 3, 171, 1974.
34. Takamuku, S., Kigawa, H., Suematsu, H., Toki, S., Tsumori, K., and Sakurai, H., Pulse radiolysis and 77 k matrix γ irradiation of dimethyl truxinates and *trans*-methyl cinnamate in 2-methyltetrahydrofuran, *J. Phys. Chem.,* 86, 1861, 1982.
35. Anet, R., The photodimers of coumarin and related compounds, *Can. J. Chem.,* 40, 1249, 1962.
36. Hammond, G.S., Stout, C.A., and Lamola, A.A., Mechanisms of photochemical reactions in solution. XXV. The photodimerization of coumarin, *J. Am. Chem. Soc.,* 86, 3103, 1964.
37. Moorthy, J.N., Venkatesan, K., and Weiss, R.G., Photodimerization of coumarins in solid cyclodextrin inclusion complexes, *J. Org. Chem.,* 57, 3292, 1992.
38. Hoffman, R., Wells, P., and Morrison, H., Organic photochemistry. XII. Further studies on the mechanism of coumarin photodimerization; observation of an unusual "heavy atom" effect, *J. Org. Chem.,* 36, 102, 1971.
39. Klaus, C.P., Thiemann, C., Kopf, J., and Margaretha, P., Solid-state photocyclodimerization of 1-thiocoumarin, *Helv. Chim. Acta,* 78, 1079, 1995.
40. Margaretha, P., Photochemistry of (*S*-hetero)cyclic unsaturated carbonyl compounds, in *Molecular and Supramolecular Photochemistry,* Vol. 1, Ramamurthy, V. and Schanze, K.S., Eds., Marcel Dekker, New York, 1997, p. 85.
41. Meyer, U., Lahrahar, N., Marsau, P., Hopf, H., Greiving, H., Desvergne, J.P., and Bouas-Laurent, H., Photoactive phanes. Part II. X-ray structure and photoreactivity of pseudo-gem cinnamophanedicarboxylic acid {bis-4,15-(2′-hydroxycarbonylvinyl)[2.2]paracyclophane}, *Liebigs Ann. Chem.,* 381, 1997.
42. Hopf, H., Greiving, H., Jones, P.G., and Bubenitschek, P., Topochemical reaction control in solution, *Angew. Chem. Int. Ed. Engl.,* 34, 685, 1995.
43. LaLonde, R.T. and David, C.B., Photolysis and mass spectra of *trans*-cinnamimide, *Can. J. Chem.,* 47, 3250, 1969.
44. Maekawa, Y., Kato, S., and Hasegawa, M., Quantitative formation of a highly strained tricyclic [2.2]paracyclophane derivative from a mixed crystal of ethyl and propyl α-cyano-4-[2-(4-pyridyl)ethenyl]cinnamates through a topochemical reaction, *J. Am. Chem. Soc.,* 113, 3867, 1991.
45. Okada, Y., Kaneko, M., and Nishimura, J., The formylation of *syn*-[2.N]metacyclophanes and application to multi-bridged cyclophane synthesis, *Tetrahedron Lett.,* 42, 1919, 2001.
46. Jiang, X., Hui, Y., and Fei, Z., The effect of hydrophobic–lipophilic interactions on chemical reactivity. Part 13. A successful application of the concept of making use of hydrophobic forces to prepare large-ring compounds, *J. Chem. Soc., Chem. Commun.,* 689, 1988.
47. Ors, J.A. and Sprinivasan, R., Synthesis of macrocyclic rings by internal photocycloaddition of α,ω-dicinnamates, *J. Chem. Soc., Chem. Commun.,* 400, 1978.
48. Ors, J.A. and Srinivasan, R., Internal photocycloaddition between chromophores separated by 17 bonds, *J. Am. Chem. Soc.,* 100, 315, 1978.
49. Leenders, L.H., Schouteden, E., and De Schryver, F.C., Photochemistry of nonconjugated bichromophoric systems. Cyclomerization of 7,7′-polymethylenedioxycoumarins and polymethylenedicarboxylic acid 7-coumarinyl diesters, *J. Org. Chem.,* 38, 957, 1973.

50. Tung, C.-H., Yuan, Z.-Y., Wu, L.-Z., and Weiss, R.G., Enhancement of intramolecular photocycloaddition of bichromophoric compounds via inclusion in low-density polyethylene films, *J. Org. Chem.,* 64, 5156, 1999.
51. Kimura, M., Shimoyama, M., and Morosawa, S., The formation of aryltetralin derivatives in the photolysis of two *trans*-cinnamoyl moieties at both ends of a polyethylene glycol chain in the presence of lithium perchlorate, *J. Chem. Soc., Chem. Commun.,* 375, 1991.
52. Freedman, M., Mohadger, Y., Rennert, J., Soloway, S., and Waltcher, I., β- and δ-truxinic acids, *Org. Prep. Proced.,* 1, 267, 1969.
53. Green, B.S., Hagler, A.T., Rabinsohn, Y., and Rejto, M., Photochemical asymmetric synthesis. Irradiation of ring and open-chain derivatives of L-erythritol 1,4-dicinnamate, *Isr. J. Chem.,* **15**, 124, 1977.
54. Green, B.S., Lahav, M., and Schmidt, G.M.J., Reactions in chiral crystals. Principles governing asymmetric synthesis via topochemically controlled solid-state photodimerization, *Mol. Cryst. Liq. Cryst.,* 29, 187, 1975.
55. Scheffer, J.R. and Scott, C., Perspectives: solid state organic chemistry: stepping it up, *Science,* 291, 1712, 2001.
56. Cohen, M.D. and Schmidt, G.M.J., Topochemistry. I. A survey, *J. Chem. Soc.,* 1996, 1964.
57. Cohen, M.D., Schmidt, G.M.J., and Sonntag, F.I., Topochemistry. II. The photochemistry of *trans*-cinnamic acids, *J. Chem. Soc.,* 2000, 1964.
58. Schmidt, G.M.J., Topochemistry. III. The crystal chemistry of some *trans*-cinnamic acids, *J. Chem. Soc.,* 2014, 1964.
59. Bregman, J., Osaki, K., Schmidt, G.M.J., and Sonntag, F.I., Topochemistry. IV. The crystal chemistry of some *cis*-cinnamic acids, *J. Chem. Soc.,* 2021, 1964.
60. Kohlschutter, V. and Haenni, P., Graphitic carbon and graphitic acid, *Z. Anorg. Allgem. Chem,* 105, 121, 1919.
61. Hertel, E. and Schneider, K., Transformations in crystal lattices, *Z. Elektrochem.,* 37, 536, 1931.
62. Rennert, J., Ruggiero, E.M., and Rapp, J., Nonradiative dissipation of excitation energy in solid cinnamic acid by dimer formation, *Photochem. Photobiol.,* 6, 29, 1967.
63. Cohen, M.D., Solid-state photochemical reactions, *Tetrahedron,* 43, 1211, 1987.
64. Hasegawa, M., Photopolymerization of diolefin crystals, *Chem. Rev.,* 83, 507, 1983.
65. Keating, A.E. and Garcia-Garibay, M.A., Photochemical solid-to-solid reactions, in *Molecular and Supramolecular Photochemistry,* Vol. 2, Ramamurthy, V. and Schanze, K.S., Eds., Marcel Dekker, New York, 1998, p. 195.
66. Osaki, K. and Schmidt, G.M.J., Single-crystal diffraction experiments in a search for direct structural evidence for solid-state reactions, *Isr. J. Chem.,* 10, 189, 1972.
67. Enkelmann, V., Wegner, G., Novak, K., and Wagener, K.B., Single-crystal–to–single-crystal photodimerization of cinnamic acid, *J. Am. Chem. Soc.,* 115, 10390, 1993.
68. Iwamoto, T. and Kashino, S., Topochemical studies. XVI. Direct observation of the solid-state photoreaction of α-(acetylamino)cinnamic acid dihydrate by single crystal x-ray diffraction, *Bull. Chem. Soc. Jpn.,* 66, 2190, 1993.
69. Hosomi, H., Ito, Y., and Ohba, S., Crystal-to-crystal photodimerization of *trans*-cinnamamides, Ohba, S., Hosomi, H., and Ito, Y., *In situ* x-ray observation of pedal-like conformational change and dimerization of *trans*-cinnamamide in cocrystals with phthalic acid, *J. Am. Chem. Soc.,* 123, 6349, 2001.
70. Tanaka, K., Mochizuki, E., Yasui, N., Kai, Y., Miyahara, I., Hirotsu, K., and Toda, F., Single-crystal–to–single-crystal enantioselective [2 + 2] photodimerization of coumarin, thiocoumarin and cyclohex-2-enone in the inclusion complexes with chiral host compounds, *Tetrahedron,* 56, 6853, 2000.
71. Shichi, T., Takagi, K., and Sawaki, Y., Stereoselectivity control of [2 + 2] photocycloaddition by changing site distances of hydrotalcite interlayers, *J. Chem. Soc., Chem. Commun.,* 2027, 1996.

72. Nakanishi, F., Nakanishi, H., Tsuchiya, M., and Hasegawa, M., Water participation in the crystalline-state photodimerization of cinnamic acid derivatives. A new type of organic photoreaction, *Bull. Chem. Soc. Jpn.,* 49, 3096, 1976.
73. Nakanishi, F., Nakanishi, H., Tasai, T., Suzuki, Y., and Hasegawa, M., Water participation in the crystalline state photoreaction, photodimerization of *p*-formylcinnamic acid, *Chem. Lett.,* 525, 1974.
74. Nakanishi, F., Yamada, S., and Nakanishi, H., Participation of hydrocarbons in the photodimerization of 3,4-dichlorocinnamic acid, *J. Chem. Soc., Chem. Commun.,* 247, 1977.
75. Kaupp, G., Photodimerization of cinnamic acid in the crystal: new results from atomic force microscopy, *Angew. Chem. Int. Ed. Engl.,* 31, 592, 1992.
76. Kaupp, G., Herrmann, A., and Haak, M., Near-field optical microscopy with uncoated tips: calibration, chemical contrast on organic crystals and photolithography, *J. Vac. Sci. Technol. B,* 15, 1521, 1997.
77. Allen, S.D.M., Almond, M.J., Bruneel, J.L., Gilbert, A., Hollins, P., and Mascetti, J., The photodimerization of *trans*-cinnamic acid and its derivatives: a study by vibrational microspectroscopy, *Spectrochim. Acta A,* 56A, 2423, 2000.
78. Even, J. and Bertault, M., Monte Carlo simulations of chemical reactions in molecular crystals, *J. Chem. Phys.,* 110, 1087, 1999.
79. Harris, K.D.M., Thomas, J.M., and Williams, D., Mathematical analysis of intra-stack dimerizations in reactive crystalline solids, *J. Chem. Soc., Faraday Trans.,* 87, 325, 1991.
80. Green, B.S., Lahav, M., and Rabinovich, D., Asymmetric synthesis via reactions in chiral crystals, *Acc. Chem. Res.,* 12, 191, 1979.
81. Green, B.S., Rabinsohn, Y., and Rejto, M., Photochemical asymmetric synthesis. Irradiation of mannitol hexacinnamate, *J. Chem. Soc., Chem. Commun.,* 313, 1975.
82. Griesbeck, A.G. and Fiege, M., Stereoselectivity of photocycloadditions and photocyclizations, in *Molecular and Supramolecular Photochemistry,* Vol. 6, Ramamurthy, V. and Schanze, K.S., Eds., Marcel Dekker, New York, 2000, p. 33.
83. Addadi, L. and Lahav, M., Towards the planning and execution of an "absolute" asymmetric synthesis of chiral dimers and polymers with quantitative enantiomeric yield, *Pure Appl. Chem.,* 51, 1269, 1979.
84. Vaida, M., Shimon, L.J.W., Van Mil, J., Ernst-Cabrera, K., Addadi, L., Leiserowitz, L., and Lahav, M., Absolute asymmetric photochemistry using centrosymmetric single crystals. The host/guest system (*E*)-cinnamamide/*E*-cinnamic acid, *J. Am. Chem. Soc.,* 111, 1029, 1989.
85. Hasegawa, M., Chung, C.M., Muro, N., and Maekawa, Y., Asymmetric synthesis through the topochemical reaction in a chiral crystal of a prochiral diolefin molecule having a "cisoid" molecular structure and amplification of asymmetry by a seeding procedure, *J. Am. Chem. Soc.,* 112, 5676, 1990.
86. Hasegawa, M., Stereo- and enantioselective topochemical photoreactions. A model of the generation of chiral homogeneity in nature, *Proc. Jpn. Acad. Ser. B,* 68, 9, 1992.
87. Gamlin, J.N., Jones, R., Leibovitch, M., Patrick, B., Scheffer, J.R., and Trotter, J., The ionic auxiliary concept in solid state organic photochemistry, *Acc. Chem. Res.,* 29, 203, 1996.
88. Ito, Y., Borecka, B., Olovsson, G., Trotter, J., and Scheffer, J.R., Control of the solid-state photodimerization of some derivatives and analogs of *trans*-cinnamic acid by ethylenediamine, *Tetrahedron Lett.,* 36, 6087, 1995.
89. Ito, Y., Borecka, B., Trotter, M., and Scheffer, J.R., Control of solid-state photodimerization of *trans*-cinnamic acid by double salt formation with diamines, *Tetrahedron Lett.,* 36, 6083, 1995.
90. Ito, Y., Hosomi, H., and Ohba, S., Compelled orientational control of the solid-state photodimerization of *trans*-cinnamamides: dicarboxylic acid as a non-covalent linker, *Tetrahedron,* 56, 6833, 2000.

91. Ito, Y. and Fujita, H., Unusual [2 + 2] photocycloaddition between tryptamine and 3-nitrocinnamic acid in the solid state, *Chem. Lett.,* 288, 2000.
92. Coates, G.W., Dunn, A.R., Henling, L.M., Ziller, J.W., Lobkovsky, E.B., and Grubbs, R.H., Phenyl-perfluorophenyl stacking interactions: topochemical [2 + 2] photodimerization and photopolymerization of olefinic compounds, *J. Am. Chem. Soc.,* 120, 3641, 1998.
93. Ito, Y., Solid-state organic photochemistry of mixed molecular crystals, in *Molecular and Supramolecular Photochemistry,* Vol. 3, Ramamurthy, V. and Schanze, K.S., Eds., Marcel Dekker, New York, 1999, p. 1.
94. Karbe, C. and Margaretha, P., Photocycloadditions to 1-thiocoumarin, *J. Photochem. Photobiol. A: Chem.,* 57, 231, 1991.
95. Kinder, M.A., Kopf, J., and Margaretha, P., Solid state photochemistry of isocoumarins and isothiocoumarins, *Tetrahedron,* 56, 6763, 2000.
96. Schwebel, D., Soltau, M., and Margaretha, P., Photochemical synthesis of cyclopenta[*c*]-anellated benzopyrans and benzothiopyrans, *Synthesis*, 1111, 2001.
97. Kato, S., Nakatani, M., Harashina, H., Saigo, K., Hasegawa, M., and Sato, S., Hetero head-to-head dimer by topochemical photoreaction of methyl α-cyano-4-[2-(2-pyridyl)ethenyl]cinnamate, *Chem. Lett.,* 847, 1986.
98. Chimichi, S., Sarti-Fantoni, P., Coppini, G., Perghem, F., and Renzi, G., Solid-state photoreactivity of ethyl (*E*)-α-cyano-2-methoxycinnamate, *J. Org. Chem.,* 52, 5124, 1987.
99. Gnanaguru, K., Ramasubbu, N., Venkatesan, K., and Ramamurthy, V., A study on the photochemical dimerization of coumarins in the solid state, *J. Org. Chem.,* 50, 2337, 1985.
100. Murthy, G.S., Arjunan, P., Venkatesan, K., and Ramamurthy, V., Consequences of lattice relaxability in solid state photodimerizations, *Tetrahedron,* 43, 1225, 1987.
101. Gnanaguru, K., Ramasubbu, N., Venkatesan, K., Ramamurthy, V., Theocharis, C.R., Jones, W., Thomas, J.M., Motevalli, M., and Hursthouse, M.B., A study on the photochemical dimerization of coumarins in the solid-state photodimerization of 2,5-dibenzylidenecyclopentanone (dbcp): a topochemical reaction that yields an amorphous product, *J. Org. Chem.,* 50, 2337, 1985.
102. Moorthy, J.N. and Venkatesan, K., Stereospecific photodimerization of coumarins in crystalline inclusion complexes. Molecular and crystal structure of 1:2 complex of (s,s)-(–)-1,6-bis(*o*-chlorophenyl)-1,6-diphenyl-hexa-2,4-diyne-1,6-diol and coumarin, *J. Org. Chem.,* 56, 6957, 1991.
103. Tanaka, K. and Toda, F., Selective photodimerizations of coumarin in crystalline inclusion compounds, *J. Chem. Soc., Perkin Trans. 1,* 943, 1992.
104. Tanaka, K. and Toda, F., Cd spectral study on chiral arrangement and enantioselective reaction of thiocoumarin in inclusion crystal, *Mol. Cryst. Liq. Cryst. A,* 313, 179, 1998.
105. Minsk, L.M., Smith, J.G., Van Deusen, W.P., and Wright, J.F., Photosensitive polymers. I. Cinnamate esters of poly(vinyl alcohol) and cellulose, *J. Appl. Polym. Sci.,* 2, 302, 1959.
106. Specht, D.P., Martic, P.A., and Farid, S., Ketocoumarins. A new class of triplet sensitizers, *Tetrahedron,* 38, 1203, 1982.
107. Reiser, A., *Photoreactive Polymers — The Science and Technology of Resists,* Wiley, New York, 1989.
108. Anzai, J., Suzuki, Y., Ueno, A., and Osa, T., Cation transport through liquid membranes mediated by photoreactive crown ethers. Effects of alkali metal cations on their photoreactivities and transporting properties, *Isr. J. Chem.,* 26, 60, 1985.
109. Coqueret, X., Photoreactivity of polymers with dimerizable side-groups. Kinetic analysis for probing morphology and molecular organization, *Macromol. Chem. Physic.,* 200, 1567, 1999.
110. Reddy, A.V.R., Subramanian, K., Krishnasamy, V., and Ravichandran, J., Synthesis, characterization and properties of novel polymers containing pendant photocrosslinkable chalcone moiety, *Eur. Polym. J.,* 32, 919, 1996.
111. Reddy, A.V.R., Subramanian, K., and Sainath, A.V.S., Photosensitive polymers: synthesis, characterization and photocrosslinking properties of polymers with pendant α,β-unsaturated ketone moiety, *J. Appl. Polym. Sci.,* 70, 2111, 1998.

112. Lin, A.A., Chu, C.F., Huang, W.Y., and Reiser, A., Reactant preordering in solid photopolymers, *Pure Appl. Chem.,* 64, 1299, 1992.
113. Damen, J. and Neckers, D.C., Stereoselective syntheses via a photochemical template effect, *J. Am. Chem. Soc.,* 102, 3265, 1980.
114. Henselwood, F. and Liu, G., Water-soluble nanospheres of poly(2-cinnamoylethyl methacrylate)-block-poly(acrylic acid), *Macromolecules,* 30, 488, 1997.
115. Ding, J. and Liu, G., Polyisoprene-block-poly(2-cinnamoylethyl methacrylate) vesicles and their aggregates, *Macromolecules,* 30, 655, 1997.
116. Tao, J. and Liu, G., Polystyrene-block-poly(2-cinnamoylethyl methacrylate) tadpole molecules, *Macromolecules,* 30, 2408, 1997.
117. Bernstein, J., Green, B.S., and Rejto, M., Solid-state photooligomerization of an extended chiral bifunctional monomer, (+)-2,4:3,5-di-*o*-methylene-*d*-mannitol 1,6-di-trans-cinnamate, *J. Am. Chem. Soc.,* 102, 323, 1980.
118. Chung, C.M. and Hasegawa, M., "Kaleidoscopic" photoreaction behavior of alkyl 4-[2-(4-pyridyl)ethenyl]cinnamate crystals: a crystalline linear high polymer from the methyl ester, an "absolute" asymmetric reaction of the ethyl ester and two types of dimer formation from the propyl ester, *J. Am. Chem. Soc.,* 113, 7311, 1991.
119. Chung, C.M., Kunita, A., Hayashi, K., Nakamura, F., Saigo, K., and Hasegawa, M., Topochemical induction to an alternating zigzag-linear and *syndiotactic* chain structure in the course of [2 + 2] photoreaction of alkyl α-cyano-4-[2-(2-pyridyl)ethenyl]cinnamate crystals, *J. Am. Chem. Soc.,* 113, 7316, 1991.
120. Hasegawa, M., Endo, Y., Aoyama, M., and Saigo, K., Topochemical photopolymerization and photocopolymerization of the crystals of unsymmetrically substituted diolefin compounds having pyrimidine ring, *Bull. Chem. Soc. Jpn.,* 62, 1556, 1989.
121. Gibbons, W.M., Kosa, T., Palffy-Muhoray, P., Shannon, P.J., and Sun, S.T., Continuous gray-scale image storage using optically aligned nematic liquid crystals, *Nature,* 377, 43, 1995.
122. Schadt, M., Schmitt, K., Kozinkov, V., and Chigrinov, V., Surface-induced parallel alignment of liquid crystals by linearly polymerized photopolymers, *Jpn. J. Appl. Phys. Part 1,* 31, 2155, 1992.
123. Galabova, H.G., Allender, D.W., and Chen, J., Orientation and surface anchoring of nematic liquid crystals on linearly polymerized photopolymers, *Phys. Rev. E,* 55, 1627, 1997.
124. Ionescu, A.T., Barberi, R., Giocondo, M., Iovane, M., and Alexe-Ionescu, A.L., Order distribution function of a linear polymerized photopolymer orienting a nematic liquid crystal, *Phys. Rev. E,* 58, 1967, 1998.
125. Kim, H.-T., Lee, J.-W., Sung, S.-J., and Park, J.-K., Mechanism of photoinduced liquid crystal alignment on a poly(vinyl cinnamate) thin layer, *Polym. J.,* 33, 9, 2001.
126. Kim, H.-T., Lee, J.-W., Sung, S.-J., and Park, J.-K., Synthesis, photoreaction and photoinduced liquid crystal alignment of soluble polyimide with pendant cinnamate group, *Liq. Cryst.,* 27, 1343, 2000.
127. Obi, M., Morino, S.Y., and Ichimura, K., Reversion of photoalignment direction of liquid crystals induced by cinnamate polymer films, *Jpn. J. Appl. Phys. Part 2,* 38, L145, 1999.
128. Ichimura, K., Akita, Y., Akiyama, H., Kudo, K., and Hayashi, Y., Photoreactivity of polymers with regioisomeric cinnamate side chains and their ability to regulate liquid crystal alignment, *Macromolecules,* 30, 903, 1997.
129. Olenik, I.D., Kim, M.W., Rastegar, A., and Rasing, T., Characterization of unidirectional photopolymerization in poly(vinyl cinnamate) by surface optical second-harmonic generation, *Phys. Rev. E,* 60, 3120, 1999.
130. Perny, S., Le Barny, P., Delaire, J., Buffeteau, T., and Sourisseau, C., Molecular orientation and liquid crystal alignment properties of new cinnamate-based photocrosslinkable polymers, *Liq. Cryst.,* 27, 341, 2000.

131. Perny, S., Le Barny, P., Delaire, J., Buffeteau, T., Sourisseau, C., Dozov, I., Forget, S., and Martinot-Lagarde, P., Photoinduced orientation in poly(vinyl cinnamate) and poly(7-methacryloyloxycoumarin) thin films and the consequences on liquid crystal alignment, *Liq. Cryst.,* 27, 329, 2000.
132. Barbet, F., Bormann, D., Warenghem, M., Kurios, Y., Reznikov, Y., and Khelifa, B., Raman spectroscopy evidence of phototransformation in poly(vinyl 4-fluorocinnamate), *Mol. Cryst. Liq. Cryst. A,* 320, 405, 1998.
133. Schadt, M., Seiberle, H., and Schuster, A., Optical patterning of multi-domain liquid-crystal displays with wide viewing angles, *Nature,* 381, 212, 1996.
134. Obi, M., Morino, S.Y., and Ichimura, K., The reversion of photoalignment direction of a liquid crystal induced by a polymethacrylate with coumarin side chains, *Macromol. Rapid Comm.,* 19, 643, 1998.
135. Ohkawa, K., Shoumura, K., Yamada, M., Nishida, A., Shirai, H., and Yamamoto, H., Photoresponsive peptide and polypeptide systems, 14a: biodegradation of photocrosslinkable copolypeptide hydrogels containing *l*-ornithine and δ-7-coumaryloxyacetyl-*l*-ornithine residues, *Macromol. Biosci.,* 1, 149, 2001.
136. Matsusaki, M., Kishida, A., Stainton, N., Ansell, C.W.G., and Akashi, M., Synthesis and characterization of novel biodegradable polymers composed of hydroxycinnamic acid and *d,l*-lactic acid, *J. Appl. Polym. Sci.,* 82, 2357, 2001.
137. Ramamurthy, V., Organic photochemistry in organized media, *Tetrahedron,* 42, 5753, 1986.
138. Ramamurthy, V., Photochemical reactions in oriented systems, *ACS Symp. Ser.,* 278, 267, 1985.
139. Ramamurthy, V., Weiss, R.G., and Hammond, G.S., A model for the influence of organized media on photochemical reactions, *Adv. Photochem.,* 18, 67, 1993.
140. Nakamura, T., Takagi, K., and Sawaki, Y., Photodimerization of *trans*-cinnamic acid in a bilayer of dimethyldioctadecylammonium bromide, *Bull. Chem. Soc. Jpn.,* 71, 909, 1998.
141. Takagi, K., Fukaya, H., Miyake, N., and Sawaki, Y., Organized photodimerization of cinnamic acid in cationic reversed micelle, *Chem. Lett.,* 1053, 1988.
142. Nakamura, Y., Regioselective photodimerization of cinnamic acid in a micellar solution, *J. Chem. Soc., Chem. Commun.,* 477, 1988.
143. Ohtani, O., Sasai, R., Adachi, T., Hatta, I., and Takagi, K., Self-assembled thin solid films of dioctadecyldimethylammonium cinnamate lamella units that control the photostationary state of *E-Z* photoisomerizations, *Langmuir,* 18, 1165, 2002.
144. Takagi, K., Itoh, M., Usami, H., Imae, T., and Sawaki, Y., Organized photodimerization of unsaturated carboxylates. Selectivity control by normal and reversed micelles, *J. Chem. Soc., Perkin Trans. 2,* 1003, 1994.
145. Amarouche, H., De Bourayne, C., Riviere, M., and Lattes, A., Chemical and photochemical reactivity in micellar media and microemulsions. VIII. Photoreactivity of cinnamate derivatives in microemulsions, *C. R. Acad. Sci. Ser. 2,* 298, 121, 1984.
146. Muthuramu, K., Ramnath, N., and Ramamurthy, V., Photodimerization of coumarins in micelles: limitations of alignment effect, *J. Org. Chem.,* 48, 1872, 1983.
147. Muthuramu, K. and Ramamurthy, V., Selectivity in chemical reactions in micellar media: photodimerization of substituted coumarins in micelles, *Indian J. Chem. Soc. Sect. B,* 23B, 502, 1984.
148. Ramnath, N. and Ramamurthy, V., Photochemical reactions in constrained systems: changes in mode of solubilization due to long-chain hydrophobic groups, *J. Org. Chem.,* 49, 2827, 1984.
149. Mukkamala, R., Burns, C.L., Jr., Catchings, R.M., III, and Weiss, R.G., Photopolymerization of carbohydrate-based discotic mesogens. Syntheses and phase properties of 1,2,3,4,6-penta-*o*-(*trans*-3,4-dialkoxycinnamoyl)-(*d*)-glucopyranoses and their oligomers*, J. Am. Chem. Soc,* 118, 9498, 1996.
150. Ramesh, V. and Weiss, R.G., Liquid-crystalline solvents as mechanistic probes. 20. Crystalline and smectic B solvent control over the selectivity of photodimerization of *n*-alkyl cinnamates*, J. Org. Chem.,* 51, 2535, 1986.
151. Creed, D., Photochemistry and photophysics of liquid crystalline polymers, in *Molecular and Supramolecular Photochemistry,* Vol. 2, Ramamurthy, V. and Schanze, K.S., Eds., Marcel Dekker, New York, 1998, p. 129.

152. Creed, D., Cozad, R.A., Griffin, A.C., Hoyle, C.E., Jin, L., Subramanian, P., Varma, S.S., and Venkataram, K., Photochemistry of liquid-crystalline polymers, *ACS Symp. Ser.,* 579, 13, 1994.
153. Creed, D., Griffin, A.C., Hoyle, C.E., and Venkataram, K., Chromophore aggregation and concomitant wavelength-dependent photochemistry of a main-chain liquid crystalline poly(aryl cinnamate), *J. Am. Chem. Soc.,* 112, 4049, 1990.
154. Creed, D., Griffin, A.C., Hoyle, C.E., and Venkataram, K., The role of aggregates in the wavelength dependent photochemistry of a main-chain liquid crystalline polyaryl cinnamate, *Proc. SPIE-Int. Soc. Opt. Eng.,* 1213, 184, 1990.
155. Creed, D., Hoyle, C.E., Jin, L., Peeler, A.M., Subramanian, P., and Krishnan, V., Triplet-sensitized irradiation of a main-chain liquid crystalline poly(aryl cinnamate) in three different phases, *J. Polym. Sci. Part A,* 39, 134, 2000.
156. Tanaka, Y. and Suzuki, M., Photoreaction of cholesteryl cinnamate in multilayers, *Springer Ser. Chem. Phys.,* 11, 350, 1980.
157. Tanaka, Y. and Tsuchiya, H., Photoreaction of cholesteryl cinnamate, *J. Phys., Colloq.,* 41, 1979.
158. Tanaka, Y., Tsuchiya, H., Suzuki, M., Tsuda, K., Takano, J., and Kurihara, H., Photoreaction of cholesteryl *trans*-cinnamate in mesomorphic states, *Mol. Cryst. Liq. Cryst.,* 68, 113, 1981.
159. Whitcombe, M.J., Gilbert, A., and Mitchell, G.R., Synthesis and photochemistry of side-chain liquid crystal polymers based on cinnamate esters, *J. Polym. Sci. Part A: Polym. Chem.,* 30, 1681, 1992.
160. Weissbuch, I., Leiserowitz, L., and Lahav, M., Structured self-aggregates of 4-methoxy-(*E*)-cinnamic acid at the air/solution interface as detected by $2\pi + 2\pi$ photodimerization and their role in the control of crystal polymorphism, *J. Am. Chem. Soc.,* 113, 8941, 1991.
161. Weissbuch, I., Popovitz-Biro, R., Wang, J.L., Berkovic, G., Leiserowitz, L., and Lahav, M., Structure and dynamics of amphiphilic aggregates at air/solution interfaces en route to crystal formation, *Pure Appl. Chem.,* 64, 1263, 1992.
162. Weissbuch, I., Bouwman, W., Kjaer, K., Als-Nielsen, J., Lahav, M., and Leiserowitz, L., Two-dimensional crystalline structures and photochemical behavior of cinnamate monolayers on water surfaces, *Chirality,* 10, 60, 1998.
163. Nakanishi, F., Photoreaction of amphiphilic diolefins in monolayers formed on an air-water interface, *J. Polym. Sci. Part C: Polym. Lett.,* **26**, 159, 1988.
164. Nakanishi, F., Okada, S., and Nakanishi, H., Photopolymerization of amphiphilic diolefins in mono- and multilayers, *Polymer,* 30, 1959, 1989.
165. Zhao, J., Hafiz, H.R., Akiyama, H., Tamada, K., and Nakanishi, F., Kinetics of photoreaction of *p*-phenylenediacrylic acid derivative in LB films: an infrared spectroscopic study, *Mol. Cryst. Liq. Cryst. A,* 322, 233, 1998.
166. Zhao, J., Akiyama, H., Abe, K., Liu, Z., and Nakanishi, F., Studies on the molecular environment and reaction kinetics of photo-oligomerization in Langmuir-Blodgett films of 4-(4-(2-(octadecyloxycarbonyl)vinyl)- cinnamoylamino)benzoic acid, *Langmuir,* 16, 2275, 2000.
167. Zhao, J., Abe, K., Akiyama, H., Liu, Z., and Nakanishi, F., Photoinduced dimerization of a *p*-phenylenediacrylic acid derivative in a Langmuir monolayer mixed with stearic-d35 acid on a water surface, *Langmuir,* 15, 2543, 1999.
168. Yamamoto, M., Furuyama, N., and Itoh, K., Hydrogen bonding and photochemical processes of a cinnamic acid derivative in Langmuir-Blodgett films, *J. Phys. Chem.,* 100, 18483, 1996.
169. Lehn, J.-M., *Supramolecular Chemistry — Concepts and Perspectives*, VCH, Weinheim, 1995.
170. Beak, P. and Zeigler, J.M., Molecular organization by hydrogen bonding: juxtaposition of remote double bonds for photocyclization in a 2-pyridone dimer, *J. Org. Chem.,* 46, 619, 1981.
171. Feldman, K.S., Campbell, R.F., Saunders, J.C., Ahn, C., and Masters, K.M., Toward covalently linked organic networks: model studies and connector syntheses, *J. Org. Chem.,* 62, 8814, 1997.
172. Bassani, D.M., Darcos, V., Mahony, S. and Desvergne, J.-P., Supramolecular catalysis of olefin [2 + 2] photodimerization, *J. Am. Chem. Soc.,* 122, 8795, 2000.
173. Boiko, N., Zhu, X., Bobrovsky, A., and Shibaev, V., First photosensitive liquid crystalline dendrimer: synthesis, phase behavior and photochemical properties, *Chem. Mater.,* 13, 1447, 2001.

174. Wang, J., Jia, X., Zhong, H., Wu, H., Li, Y., Xu, X., Li, M., and Wei, Y., Cinnamoyl shell-modified poly(amidoamine) dendrimers, *J. Polym. Sci. Part A: Polym. Chem.,* 38, 4147, 2000.
175. Brett, T.J., Alexander, J.M., and Stezowski, J.J., Chemical insight from crystallographic disorder — structural studies of supramolecular photochemical systems. Part 2. The β-cyclodextrin-4,7-dimethylcoumarin inclusion complex: a new β-cyclodextrin dimer packing type, unanticipated photoproduct formation and an examination of guest influence on β-cd dimer packing, *J. Chem. Soc., Perkin Trans. 2,* 1095, 2000.
176. Brett, T.J., Alxander, J.M., and Stezowski, J.J., Chemical insight from crystallographic disorder — structural studies of supramolecular photochemical systems. Part 3. The β-cyclodextrin-7-hydroxy-4-methylcoumarin inclusion complex: direct observation of photodimerization by x-ray crystallography, *J. Chem. Soc., Perkin Trans. 2,* 1105, 2000.

21

Photochemical Dimerization of Acenaphthylene and Related Compounds

Naoki Haga
Tokyo University of Agriculture and Technology

Katsumi Tokumaru
International Institute for Advanced Studies

21.1 Introduction

Acenaphthylene (ACN), which forms bright yellowish plates with a melting point of 93–94°C, is one of the simplest nonalternant aromatic hydrocarbons. Since its discovery by Dziewonski and Rapalski in 1912, the photochemical conversion of ACN into two isomeric dimers (*cisoid*-**1** and *transoid*-**1**) has been studied because of its unique photophysical properties and mechanistic interest.[1] ACN is very weakly fluorescent both from the S_1[2–6] and the S_2 states[5] and has an extremely low intersystem crossing efficiency, $\Phi_{S1\rightarrow T1}$.[6] Distortion in the S_1 state would lead to a large Frank–Condon overlap with higher vibrational levels of the S_0 state, resulting in rapid nonradiative decay from the S_1 state to the S_0 state with a very short lifetime (e.g., 1.2 nsec in *n*-hexane,[4] 3.5 nsec in cyclohexane,[5] 0.6 nsec in toluene[6]). Moreover, ACN is not phosphorescent at low temperatures.[7] Therefore, the S_1 state of ACN undergoes efficient internal conversion as a major pathway and is expected to be poorly reactive on irradiation. However, upon irradiation with UV or visible light, the alkene CC double bond of ACN undergoes various photochemical processes, including dimerization, as is the case with many other simple alkenes.

0-8493-1348-1/04/$0.00+$1.50

TABLE 21.1 Photophysical and Electrochemical Properties of ACN, NP, and ACE

	ACN	NP[a]	ACE[a]
E_S (kJ mol^{-1})[b]	256.1[c]	384	376
	257 ± 13[d]		
	257.1[e]		
τ_{S1} (nsec)[f]	1.2[l]	105	46
	0.6[d]		
	0.36[g]		
Φ_F[h]	6×10^{-4} [g]	0.19	0.39
	$(1.0 \pm 0.02) \times 10^{-3}$ [d]		
$\Phi_{S1\rightarrow T1}$	0.00 ± 0.02[d]	0.21	0.58
τ_{S2} (nsec)[i]	< 0.04[g]		
$\Phi_{S2\rightarrow T1}$[j]	0.03[k]		
E_T (kJ mol^{-1}) [l]	193–197	255	332
	189 ± 6[d]		
τ_{T1}(μsec)[m]	4.0[n]	1800	3300
	2.15[o]		
Φ_p[p]	0[q]	0.039	0.05
$E_{1/2}^{Ox}$ (V)[r]	1.58[s]	1.54	1.21

[a] From Ref. 69.
[b] Energy of the S_1 state.
[c] From Ref. 4; in *n*-hexane.
[d] From Ref. 6; in toluene.
[e] From Ref. 70; in ethanol.
[f] Lifetime of the S_1 state.
[g] From Ref. 5; in cyclohexane.
[h] Fluorescence quantum yield from the S_1 state.
[i] Lifetime of the S_2 state.
[j] Quantum yield for ISC from the S_1 to the T_1 state.
[k] From Ref. 71; in cyclohexane.
[l] Energy of the T_1 state.
[m] Lifetime of the T_1 state.
[n] From Ref. 72; in cyclohexane with ethyl iodide.
[o] From Ref. 22.
[p] Phosphorescence quantum yield from the T_1 state.
[q] From Ref. 7.
[r] Oxidation potential vs. standard calomel electrode (SCE) in acetonitrile.
[s] From Ref. 73.

In this review, we will first describe the photochemical dimerization of ACN in solution, summarizing studies that have been carried out over the past 30 years, focusing on the mechanistic aspects and the reactivity of the S_1 and the T_1 states and of radical ions generated by photochemical electron transfer. Thereafter, reactions in the solid state and constrained media, including the crystalline state, silica gel surfaces, micelles, liquid crystals, zeolite, and other heterogeneous media will be described.

21.2 Physical Properties of Excited States of Acenaphthylene

The photophysical and electrochemical properties of ACN are summarized in Table 21.1. Data for naphthalene (NP) and acenaphthene (ACE), congeners of ACN with a naphthalene moiety, are included in the same table to emphasize the peculiarly short lifetime of the ACN S_1 state, the low efficiency of fluorescence, the low quantum yield for intersystem crossing (ISC), and the low efficiency for phosphorescence.

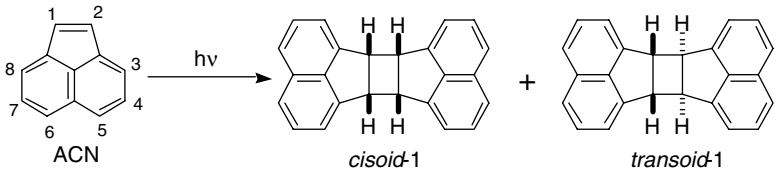

SCHEME 1

21.3 Photochemical Dimerization in Isotropic Solutions

Formation of the Two Isomeric Dimers of Acenaphthylene

The first report on dimerization of ACN described its exposure to sunlight and its conversion into two dimeric products with higher melting point (305°C) for *transoid*-**1** and a lower melting point (233°C) for *cisoid*-**1** (Scheme 1).[1] Chemical conversion of these compounds into 1,2,3,4-tetracarbomethoxycyclobutanes by ozonolysis followed by esterification with diazomethane allowed the verification of their structures.[8] Direct evidence for the structure of *cisoid*-**1**[9] and *transoid*-**1**[10] was obtained from x-ray crystallographic analysis, where space group, lattice parameters, Z value, and observed density were determined, though lacking the atomic positions for the latter. The use of a nitrogen laser as a light source was also reported in the literature to give the dimers **1** on irradiation of ACN in methanol. This report lacked chemical yields and the *cisoid/transoid* ratio of **1**.[11]

Mechanism of Dimerization from the S_1 and T_1 States of ACN

In 1947, Bowen and Marsh determined quantum yields of the dimerization reaction of ACN at 436 nm (direct excitation of ACN) in toluene, varying the concentration of ACN in the range of 0.16 ~ 1.13 M, and suggested that the mechanism is probably not of a collisional type, but is dependent on the existence of van der Waals complexes in solution.[12] Schenck and Wolgast found that the dimerization can be sensitized by Rose Bengal on irradiation with light of $\lambda > 590$ nm and gives the dimers **1** in a *cisoid/transoid* ratio of 2.64 in methanol. The dimerization was inhibited by O_2 and cyclooctatetraene as triplet quenchers. The authors concluded that the dimers **1** were, for the most part, derived from the T_1 state of ACN.[13] Formation of the T_1 state of ACN by sensitization was also demonstrated in later work by White et al. They generated triplet states of simple ketones by thermolysis of trimethyl-1,2-dioxetane at 100°C and used these excited state ketones to transfer energy to the ground state of ACN. This afforded the dimers **1** from the T_1 state of ACN in a *cisoid/transoid* ratio similar to that mentioned above.[14]

Hartmann et al. studied the effect of ACN concentration [ACN] and the presence of cyclooctatetraene on direct or Rose Bengal–sensitized excitation in 16 solvents of varying polarity.[15] The logarithmic *cisoid/transoid* ratio of **1** showed a linear relationship with the dielectric constant of the solvent. Cyclooctatetraene suppresses the formation of *transoid*-**1**, whereas sensitization by Rose Bengal results in a decreased *cisoid/transoid* ratio. In line with these results, the authors made some important inferences on the reaction mechanism that have currently been proven to be correct in essence. Thus, an association of two ground state ACN molecules can form a molecular complex (van der Waals complex), which is stabilized in more polar solvents. The S_1 state of the molecular complex (an excimer) may give *cisoid*-**1** exclusively; this is in contrast to the T_1 state of the uncomplexed ACN molecule, which leads to both *cisoid*- and *transoid*-**1**, whose distribution depends on the nature of the solvent.

Livingston and Wei irradiated ACN at various concentrations in methanol and benzene (0.05 ~ 1.5 M) and found that both the quantum yield and the chemical yield of *cisoid*-**1** increase with the increase of [ACN] in degassed solutions.[16] Only *cisoid*-**1** was found in oxygen-saturated solutions. They determined the apparent

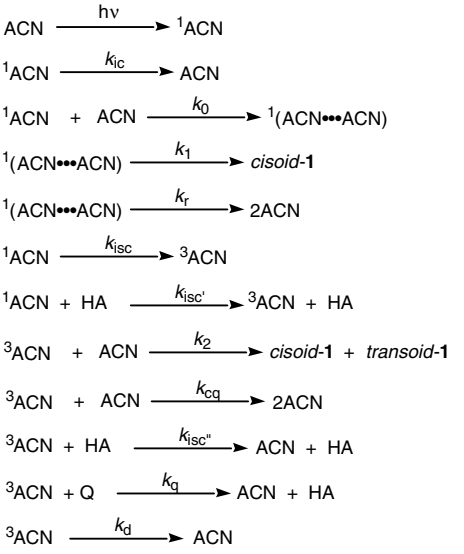

SCHEME 2

molecular weight of ACN in *n*-hexane as 154 using a differential vapor pressure method to give a value slightly higher than the formula weight of 152. This result was taken to support the proposal by Hartmann et al. that two ACN molecules in the ground state form a van der Waals dimer in a face-to face manner. Exclusive excitation of this molecular complex gives *cisoid*-**1** by a unimolecular reaction of an excimer, whereas excitation of the monomeric ACN affords both *cisoid*-**1** and *transoid*-**1**.[15]

A more detailed insight into the mechanism has been contributed by Cowan and Drisco.[17,18] Their results showed that both the quantum yield at 436 nm for the dimer formation and the *cisoid/transoid* ratio increased linearly with increase of [ACN] in the high concentration range of 0.22 ~ 1.34 *M*. Formation of *cisoid*-**1** was more dominant in polar methanol than in nonpolar cyclohexane and benzene. Ferrocene and O_2 quenched the precursor of *transoid*-**1** but only slightly reduced *cisoid*-**1** formation.[18] Sensitized dimerization experiments were utilized to bracket the energy of the T_1 state: E_T, as 170 ~ 180 kJ mol^{-1}.[18] Thus, energy transfer from excited sensitizer to the ground state ACN was successful with Rose Bengal (E_T = 187.0 kJ mol^{-1}) but failed with Crystal Violet (E_T = 163.2 kJ mol^{-1}). These results are also in accord with the mechanism proposed by Hartmann et al.[15]

Cowan et al., furthermore, investigated the dimerization of ACN from the T_1 state.[19–21] In studies that employed solvents that include heavy atoms such as chlorine, bromine, iodine, antimony, and tin, the chemical yields and the *cisoid/transoid* ratio of the dimers **1** were determined in each solvent; the relative quantum yields, **Φ**, for **1** were also determined. These solvents were found to promote formation of products originating from the T_1 state in comparison with solvents without heavy atoms, such as benzene and cyclohexane. Correlation of the yields of *transoid*-**1** with the square of the spin-orbit coupling parameters of these heavy atoms indicates that the heavy atom solvent effect is a result of spin-orbit coupling to enhance ISC from the S_1 state of ACN to the T_1 state.[19] Plots of 1/**Φ** increased linearly with increase of concentration of ethyl iodide [EtI] and [ACN]$^{-1}$.[20,21] Ethyl iodide apparently enhanced ISC from the S_1 to the T_1 state leading to predominant dimerization from the T_1 state with preference for *transoid*-**1** (*cisoid/transoid* ratio of 0.28) in cyclohexane. However, higher [EtI] resulted in a decrease of **Φ**, indicating a smaller but significant effect of the heavy atom to accelerate ISC from the T_1 to the S_0 state. On the basis of elegant analysis of kinetic data including Stern–Volmer quenching plots by ferrocene, the mechanism shown in Scheme 2 has been proposed, where ^{1}(ACN•••ACN) = singlet excimer, HA = EtI, Q = ferrocene. The triplet lifetime of ACN, τ_{T1}, the rate constant for dimerization from the T_1 state, k_2, the rate constant for concentration quenching, k_{cq}, the rate constant for unimolecular decay, k_d, and

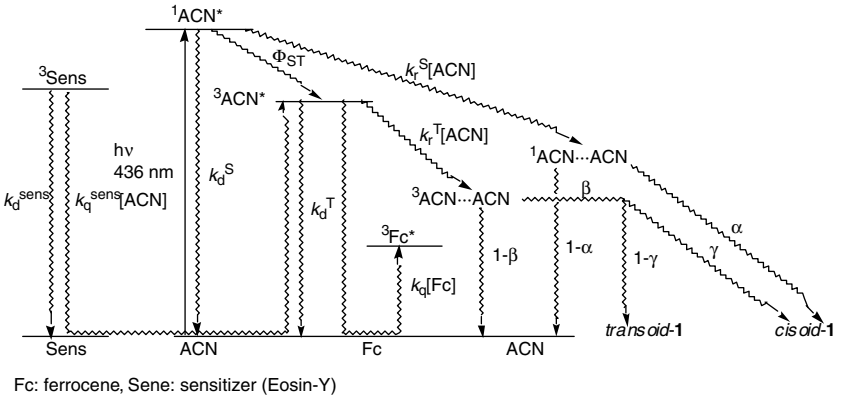

Fc: ferrocene, Sene: sensitizer (Eosin-Y)

SCHEME 3

the rate constant for quenching by EtI, k_{isc}, were reported to be 2.15×10^{-6} sec, 6.58×10^5 M^{-1} sec^{-1}, 1.58×10^6 M^{-1} sec^{-1}, 9.20×10^4 sec^{-1}, and 6.71×10^4 sec^{-1}, respectively.[21]

Later studies by Koser and Liu also demonstrated that the heavy atom effect promoted the formation of **1** derived from the T_1 state of ACN in the presence of *p*-X-bromobenzenes (X = OCH_3, CH_3, H, CHO, CF_3) in methanol; however, the *cisoid/transoid* ratio does not vary linearly with Hammett's substituent constant, σ.[22]

According to the valid mechanism pictured in Scheme 2, the singlet excimer, whether coming from an encounter between the S_1 state of ACN and the ground state ACN or from the van der Waals dimer formed in the ground state, is converted into *cisoid*-**1**, while excitation of a monomeric ACN molecule leads to the T_1 state of ACN, which results in the formation of both of the isomeric dimers with a preference for *transoid*-**1**. Actually, the larger Mulliken electronic overlap population at the 1,1′ positions for the *cis* configuration of an excited molecular pair than for the *trans* configuration with a shorter distance of 3.5 ○ between the alkene moieties of ACN explains the preferred formation of *transoid*-**1** in the absence of aggregation of two ACN molecules prior to excitation.[23] Taking the electronic overlap population at the 6,6′ positions of ACN for excimer formation from an aggregated molecular complex in the ground state, the *cis* configuration can be favored over the *trans* configuration.

The above conclusions derived from the studies Hartmann et al.,[15] Livingston and Wei,[16] and Cowan et al.[17–21] were confirmed by the recent studies of Haga et al.[24] For the purpose of strict elucidation of the roles of the S_1 and the T_1 state of ACN, they scrutinized the dimerization under irradiation of a highly diluted solution. The quantum yields at 435.8 nm, Φ_R, and the *cisoid/transoid* ratios in several solvents over a wide range of concentration ($2.0 \times 10^{-4} \sim 2.0$ *M*) in the absence of additives and in the presence of 1,2-dibromoethane (a heavy atom solvent), Eosin-Y (a triplet sensitizer), and ferrocene (a triplet quencher) were measured. In dilute solution, where ISC from the S_1 state occurs in competition with rapid internal conversion because reaction from the S_1 state can be considerably suppressed, the resultant T_1 state reacts with ground state ACN to give the dimers **1** with the *cisoid/transoid* ratio depending on the solvent. In more concentrated solutions, the S_1 state reacts with ACN prior to ISC into the T_1 state leading to exclusively *cisoid*-**1**. In line with the mechanism depicted in Scheme 3, they have determined the following values (see Table 21.2):

Fraction survival from the singlet excimer leading to *cisoid*-**1**, α
Fraction survival from the T_1 state of ACN to **1**, β
Distribution between *cisoid*- and *transoid*-**1** from the T_1 state, γ
The rate constant from the singlet excimer to afford *cisoid*-**1**, k_r^S
Quantum yields from the S_1 into the T_1 state with and without the heavy atom solvent dibromoethane, Φ_{ST} and Φ_{ST}^{DBE}, respectively

TABLE 21.2 Selected Data for the Photochemical Process from the S_1 and the T_1 States

	1,2-Dichloroethane	Acetonitrile	Cyclohexane
α	0.257	0.286	0.385
k_r^S (M^{-1} sec^{-1})[a]	6.3×10^9	2.6×10^9	1.6×10^9
β[b]	0.85	1.05	0.75
Φ_{ST}	0.18	0.029	0.045
Φ_{ST}^{DBE}	0.37	0.13	0.17
k_r^T (M^{-1} sec^{-1})[c]	2.13×10^6	1.78×10^6	2.94×10^6
τ_T (sec)[c]	2.93×10^{-6}	2.24×10^{-6}	3.94×10^{-6}
γ^c	0.337	0.618	0.361
γ^b	0.393	0.615	0.367

[a] Estimated from $\tau_S = 3.6 \times 10^{-10}$ sec.
[b] Determined by Eosin-Y–sensitized irradiation at 546.1 nm.
[c] Determined by quenching with ferrocene.

The rate constant from the T_1 state to afford **1**, k_r^T
The lifetime of the T_1 state, τ^T

It is clearly demonstrated that the small but nevertheless significant Φ_{ST} of 0.029 in acetonitrile and 0.045 in cyclohexane is the origin of *transoid*-**1**. The 10,000-fold longer lifetime of the T_1 state of 10^{-6} sec than that of the S_1 state of 10^{-10} sec, together with the larger β than α in each solvent, contributes to the higher Φ_R from the T_1 state at low [ACN]. The γ value depends on the solvent used, with preference for *transoid*-**1** in 1,2-dichloroethane (0.337) and in cyclohexane (0.361), but for *cisoid*-**1** in more polar acetonitrile (0.618).

Preferred formation of *cisoid*-**1** from the T_1 state in polar solvents was observed in the reaction in aqueous solution. Sigman et al. irradiated very dilute solutions of ACN (5×10^{-5} *M*) in water both by direct excitation ($\lambda > 350$ nm) of ACN and by Rose Bengal–sensitization ($\lambda > 540$ nm).[25] It is worthy of note that the quantum yield for formation of **1** was greater in water than in methanol. Also, the *cisoid/transoid* ratio by direct excitation at lower conversion of ACN showed a small excess of *cisoid*-**1** (*cisoid/transoid* = 1.5), and upon further conversion the ratio changed to favor *transoid*-**1** (*cisoid/transoid* = 0.6). Rose Bengal sensitization afforded a large excess of *cisoid*-**1**. Moreover, irradiation at elevated temperatures gave rise to increased *cisoid*-**1** but with a lower quantum yield. The authors interpreted these unique phenomena as follows: not only the S_1 but also the T_1 state preferentially yields *cisoid*-**1** in water. On the other hand, *transoid*-**1** comes from crystalline ACN produced by co-precipitation on seed crystals of *cisoid*-**1** produced in the early stage of the irradiation. The enhanced quantum yield in water compared to that in organic solvents was due to the hydrophobic effect by co-precipitation of ACN with *cisoid*-**1** produced. High temperature will prevent the co-precipitation leading to the reduced quantum yield and increased *cisoid/transoid* ratio.

Ichimura and Watanabe also addressed the question of ISC to the T_1 state and found that, under 13 kG of magnetic field in benzene, the *cisoid/transoid* ratio of the dimers **1** increased from 0.05 to 0.10.[26] They attributed the increase of the *cisoid/transoid* ratio to the effect of the magnetic field in promoting ISC or to relaxation of complexes produced from the T_1 state.

Gáplovsky et al. conducted ultrasound irradiation of ACN.[27] Sonication at 35 or 20 kHz of ACN (0.09 *M*) solutions in benzene using reactors designed to allow simultaneous irradiation by UV light and ultrasound resulted in preferred formation of *cisoid*-**1** (*cisoid/transoid* = 45). This is marked contrast to the silent process (*cisoid/transoid* = 25). This fact showed that ultrasound did not affect the dimerization from the S_1 state of ACN but affected the dimerization from the T_1 state by quenching.

Dimerization in the Presence of an Electron Acceptor or Electron Donor

Shields et al. reported the reaction of ACN with maleic anhydride in dioxane, acetone, acetonitrile, dichloromethane, dibromoethane, and iodomethane.[28] On irradiation of the solution of ACN ($\lambda >$

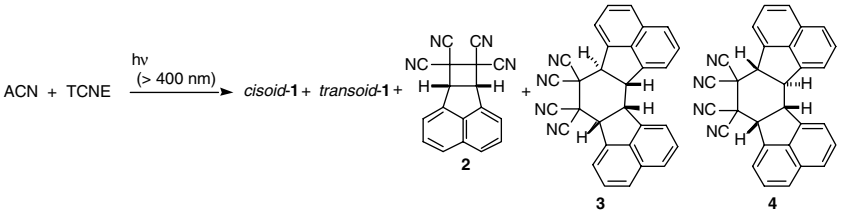

SCHEME 4

330 nm), a 1:1-adduct between maleic anhydride and ACN with a cyclobutane ring was produced stereoselectively, along with the dimers **1** (no data for the *cisoid/transoid* ratio were reported), and the distribution among these products depended on the solvent used. They stated that both the S_1 and T_1 states of ACN undergo exergonic electron transfer to maleic anhydride to generate the radical cation $ACN^{+\cdot}$, which subsequently leads to dimerization with a neutral (ground state) ACN. No reference was made regarding the detailed mechanism for formation of **1**.

Recently, Jiang et al. conducted photochemical reactions of ACN sensitized by cyanoanthracene or dicyanoanthracene in the presence of O_2.[29] Irradiation ($\lambda > 300$ nm) of ACN (4×10^{-2} *M*) in the presence of the sensitizers (4×10^{-4} *M*) in acetonitrile or benzene gave *cisoid*-**1** as well as acenaphthone and acenaphthenequinone as primary photochemical products. It is quite obvious that the key intermediate leading to these primary products is $ACN^{+\cdot}$ produced by electron transfer to the sensitizers. Though the authors attributed this result to quenching of the T_1 state of ACN by O_2 and did not refer to participation of $ACN^{+\cdot}$, preferential formation of *cisoid*-**1** is in accord with the recent findings of Haga et al. involving $ACN^{+\cdot}$, as described below.[30]

Haga et al. have clearly demonstrated contrasting reactivities between different modes of photoinduced electron transfer from ACN to tetrcyanoethylene (TCNE).[30] That is, ACN and TCNE form a tan-brown charge transfer (CT) complex in equilibrium in acetonitrile or 1,2-dichloroethane. This complex has an absorption at wavelengths longer than 500 nm. Excitation of the CT complex ($\lambda > 500$ nm) did not give any reaction product. On the contrary, direct excitation of ACN ($\lambda > 400$ nm) in the presence of TCNE gave the dimers **1** as the major products as well as addition products (**2, 3, 4**) to TCNE as minor products (Scheme 4). This result is consistent with an early report by Shirota et al., who found that excitation of ACN in the presence of TCNE in 1,2-dichloroethane with $\lambda > 320$ nm light yielded the 1:1-adduct (**2**), but excitation of the CT complex with light of wavelengths in the 500 ~ 600 nm range failed to yield any product.[31]

On direct excitation of ACN, the resultant excited state of ACN acts on TCNE to undergo electron transfer affording the solvent separated radical ion pair (SSIP) of $ACN^{+\cdot}$ and $TCNE^{-\cdot}$, which subsequently undergoes diffusion from the pair to give free radical ions (FRIs) of $ACN^{+\cdot}$ and $TCNE^{-\cdot}$, competing with back electron transfer, BET, reverting to the ground state of ACN and TCNE (Scheme 5). The $ACN^{+\cdot}$ that escapes from the SSIP either adds to the ground state of ACN to give the dimeric radical cation, $ACN_2^{+\cdot}$, which then accepts an electron from $TCNE^{-\cdot}$ to produce the dimers **1** and regenerate TCNE, or encounters with $TCNE^{-\cdot}$ to produce the 1:1-adduct (**2**).

On the contrary, selective excitation of the CT complex affords the contact radical ion pair (CIP) of $ACN^{+\cdot}$ and $TCNE^{-\cdot}$, which undergoes charge separation by the way of SSIP competing with BET between $ACN^{+\cdot}$ and $TCNE^{-\cdot}$ within the CIP. Because SSIP undergoes BET much more slowly than CIP does, SSIP produced by direct excitation of ACN can dissociate to FRIs with a higher proportion leading to the dimers **1**, whereas CIP generated from selective excitation of the CT complex prefers deactivating BET without chemical change rather than dissociation to FRIs via SSIP.

Data pertinent to the mechanism of direct excitation of ACN are obtained from the effect of concentration of TCNE on quantum yields for products (Φ_R) and the *cisoid/transoid* ratio of **1**. These data rationalize the involvement of the singlet SSIP (^{1}SSIP) under high [ACN] and the triplet SSIP (^{3}SSIP) under low [ACN]; the former tends to undergo BET but the latter undergoes dissociation to FRIs leading to **1** (Scheme 5). The rate constant for electron transfer from the T_1 state of ACN to TCNE (k_{ET}^T), the

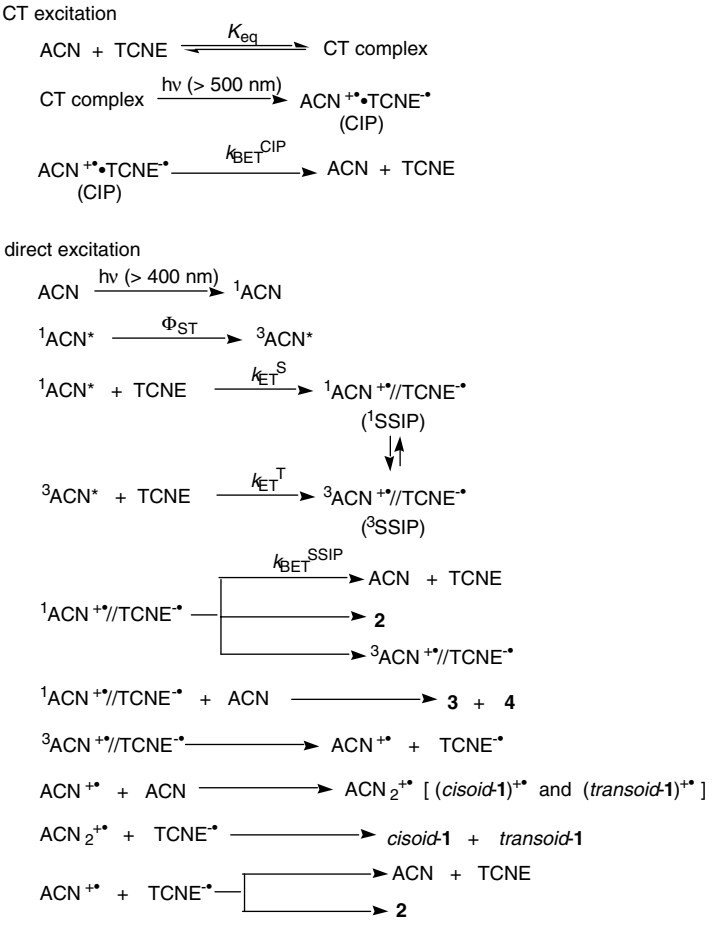

SCHEME 5

TABLE 21.3 Selected Data Relating to the Dimerization of ACN on Excitation in the Presence of TCNE

	1,2-Dichloroethane	Acetonitrile
k_{ET}^{T} (M^{-1} sec^{-1})	2.3×10^8	3.4×10^8
k_{ET}^{S} (M^{-1} sec^{-1})	3.3×10^{11}	5.8×10^{11}
x_T	0.023	0.11
x_S	0.017	0.015

fraction survival from the T_1 state of ACN to afford **1** (x_T), the rate constant for electron transfer from the S_1 state of ACN to TCNE (k_{ET}^{S}), and the fraction survival from the S_1 state leading to **1** (x_S) were established both in 1,2-dichloroethane and in acetonitrile (Table 21.3).

Haga et al. have subsequently studied photochemical reactions of CT complexes of ACN with a series of acceptors, including nitriles, acid anhydrides, and 1,4-benzoquinones (BQs), with varying reduction potential ($E_{1/2}^{Red}$), with the intention of quantitatively estimating the effect of the ease of BET from CIP on the efficiency of production of reaction products.[32,33] They found a clear trend indicating that the quantum yields for the formation of the dimers **1** by CT excitation (Φ_{CT}^{dimers}) tended to decrease with the decrease of the energy gap between the ground state and CIP ($-\Delta G_{BET}$) and finally became zero when

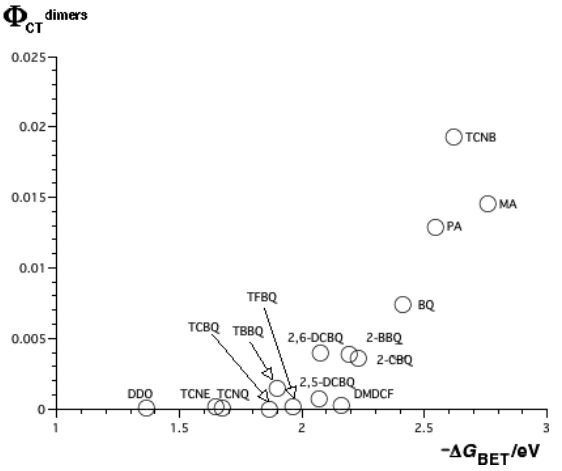

FIGURE 21.1

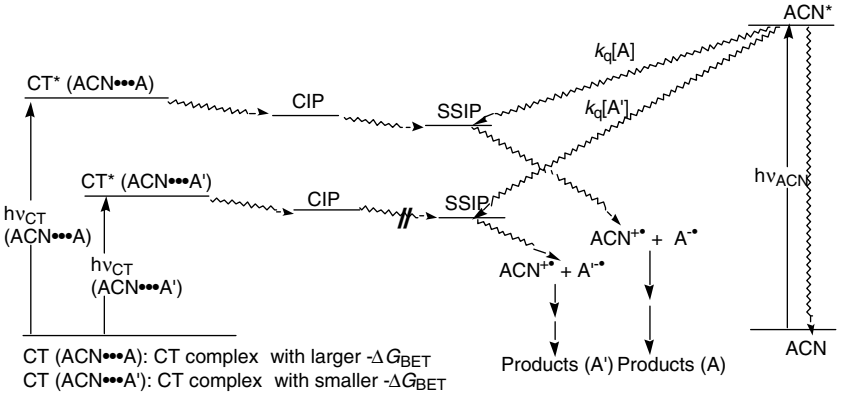

SCHEME 6

$-\Delta G_{BET}$ was smaller than a threshold of ca. 1.8 ~ 1.9 eV (Figure 21.1). On the contrary, direct excitation of ACN afforded products irrespective of the acceptor. It is undoubtedly clear that dissociation from CIP is almost nonexistent when $-\Delta G_{BET}$ is smaller than the threshold value referred to above, and dissociation from CIP to FRIs via SSIP tends to be enhanced with increase of $-\Delta G_{BET}$ and therefore enhances Φ_{CT}^{dimers} (Scheme 6). This is in keeping with the results of the transient spectroscopy by Mataga and co-workers showing that CIP produced by excitation of CT complexes of various aromatic hydrocarbons with nitriles or acid anhydrides tend to deactivate more rapidly with decrease of $-\Delta G_{BET}$.[34]

Compared to the production of $ACN^{+\cdot}$, the formation of the radical anion $ACN^{-\cdot}$ by photoinduced electron transfer has seldom been mentioned in the literature. Davidson has carried out irradiation of ACN in the presence of tertiary amines such as *N,N*-dimethylaniline and triethylamine in benzene and acetonitrile.[35] Reaction in benzene affords **1** in the *cisoid/transoid* ratio of 1.0. On the other hand, in acetonitrile *cisoid*-**1** was formed, as well as acenaphthene (ACE), without affording *transoid*-**1**. Interpretation for the solvent-dependent product distribution is that the T_1 state of ACN, produced from interaction

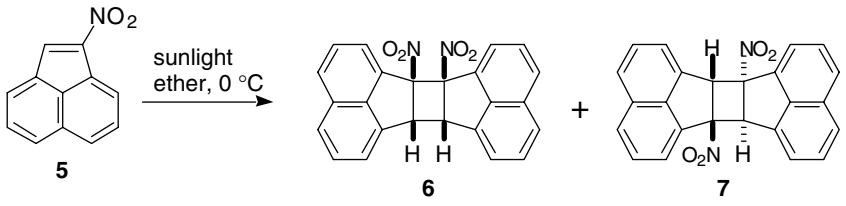

SCHEME 7

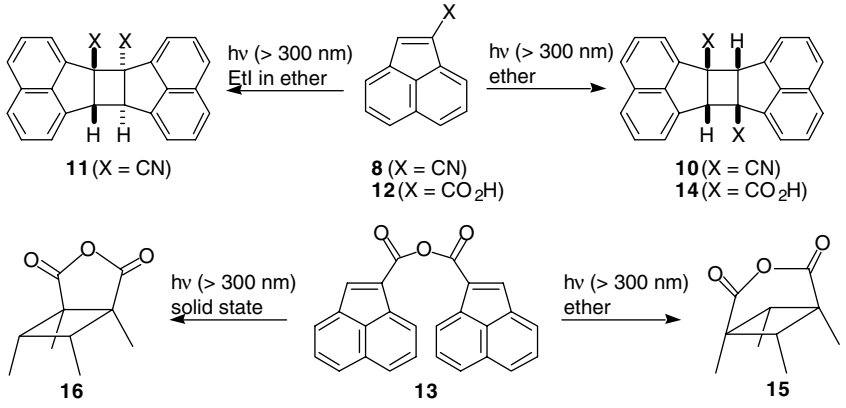

SCHEME 8

between the S_1 state of ACN with electron donors such as amines in benzene, is responsible for formation of both of the dimers, whereas the S_1 state can be produced in acetonitrile, which then undergoes dimerization with ground state ACN leading to *cisoid*-**1** or electron transfer with the amines to give $ACN^{-\cdot}$, followed by its further reduction to ACE.

Dimerization of Substituted ACN

Photochemical dimerization of substituted ACN is a relatively unexplored field, presumably in part due to synthetic difficulty. Substrates studied so far are limited to derivatives of ACN substituted at the alkene carbons (position 1 and 2); those with substituents on the aromatic rings have not been investigated. Cantrell and Shechter irradiated 1-nitroacenaphthylene (**5**), which was obtained by reaction of ACN with dinitrogen tetroxide (N_2O_4).[36] Sunlight irradiation of **5** in ether solution (0.046 *M*) at 0°C gave the *syn-cisoid*-dimer (**6**) and the *anti-transoid*-dimer (**7**) in isolated yields of 35 and 3.8%, respectively (Scheme 7). The stereochemistry of the two products was deduced on the basis of measured dipole moments of 5.82 ± 0.2 and 0.00 D for **6** and **7**, respectively. Castellan et al. performed irradiation of 1-cyanoacenaphthylene (**8**) and 1,2-dicyanoacenaphtylene (**9**) in the presence and the absence of a sensitizer such as Eosin-Y or ethyl iodide in methanol or benzene.[4] The E_S of **8** and **9** were determined to be 251.5 and 244.8 kJ mol^{-1}, respectively. Direct excitation of **8** in ether in the absence of ethyl iodide gave the *anti-cisoid*-dimer (**10**) predominantly, which shows that **10** arises from the S_1 state of **8** (Scheme 8). To the contrary, the T_1 state of **8**, produced in the presence of ethyl iodide or by sensitization, resulted in exclusive formation of the *syn-transoid*-dimer (**11**). The stereoselectivity and regioselectivity of these reactions are discussed in terms of a biradicaloid transition state stabilized by the ACN ring and the cyano group.

21.4 Photochemical Dimerization in Organized and Constrained Media

Dimerization of Acenaphthylene in the Crystalline or Solid State

Wei and Livingston published the first report of the photochemical dimerization of ACN in the solid state in 1969. They irradiated molten or crystalline ACN at 436 nm at 0 ~ 70°C.[37] At 0 ~ 25°C, *transoid*-**1** was exclusively produced with a low quantum yield (Φ_{trans} = 0.0029 at 0°C); however, at elevated temperatures over 60°C. both the Φ and the *cisoid/transoid* ratio gradually increased (Φ_{cis} = 0.0405, Φ_{trans} = 0.0041 at 70°C). These results allow us to estimate the activation energy, E_{act}, for formation of *transoid*-**1** and *cisoid*-**1** as 10.0 and 167 kJ mol^{-1}, respectively. Cohen et al. irradiated ($\lambda > 300$ nm) crystalline ACN at 0°C and also found *transoid*-**1** as the sole product.[38] Photomicrography of thin single crystals of ACN showed dislocation arrays within the monomer crystal; however, selective formation of *transoid*-**1** was not rationalized.

Attempts to elucidate the detailed crystal structure of ACN by x-ray diffraction, a crucial issue for exclusive formation of *transoid*-**1** at low temperature, have largely been unsuccessful[39,40] due to the high degree of disorder in the crystal at ambient temperatures.[41] It has been pointed out by pulse NMR technique that ACN undergoes an order–disorder phase transition at 130 K.[42] Furthermore, He and Welberry have demonstrated, using semiempirical potential energy calculations, that 10 out of 12 possible ordered structures of crystalline ACN with various molecular orientations had total potential energies within 2.5 kJ mol^{-1} of each other.[43] Therefore, poorer selectivity among the dimers **1** at room or higher temperature agrees well with promoted disorder of ACN molecules in the crystalline state with many different molecular orientations. A detailed crystal structure of ACN was accomplished by neutron diffraction at 80 K;[44] however, topochemical evidence for preferential formation of *transoid*-**1** at low temperature is, at present, not available.

In the recent work on photoinduced electron transfer of CT complex between ACN and TCNE by Haga et al., the crystalline CT complex with a 1:1 composition, ACN•TCNE, was prepared as tan-brown prisms.[30,45] Irradiation of ACN•TCNE either by CT excitation ($\lambda > 500$ nm) or by direct excitation of ACN moiety ($\lambda > 400$ nm) at 25°C afforded the 1:1-adduct **2** as the sole product in yields higher than 70% based on ACN consumed without giving the dimers **1**. X-ray crystallography shows, in the CT crystalline lattice, that the two alkene parts of ACN and TCNE are aligned parallel with the interatomic distances within 3.7 Å, which satisfies the requirements for the [2 + 2]-cycloaddition of ACN to TCNE in the solid state under the topochemical control in the crystalline lattice (Figure 21.2).[46] On the other hand, those of two ACN molecules are aligned unfavorably for the dimerization to give **1** with interatomic distances longer than 6 Å. This is reflected in no formation of **1** by irradiation of ACN•TCNE CT crystal. Instead of irradiation of the CT crystal, irradiation of the tan-brown ground powder of an equimolar mixture of ACN and TCNE with $\lambda > 500$ nm light (CT excitation) afforded **2** (75.8%) and **1** (12.5%) with a *cisoid/transoid* ratio of 0.71, which is much larger than the ratio, 0.19, from the irradiation of crystalline ACN without TCNE.[30] Production of both **1** and **2** from this mixed powder is attributed to the formation of microcrystalline ACN•TCNE by pulverization of the mixture, which under irradiation undergoes electron transfer to give $ACN^{+\cdot}$ leading to not only **2**, by coupling with $TCNE^{-\cdot}$, but also **1** by reaction with a proximate ground state ACN molecule in looser and randomly arranged molecules in the mixed powder. Furthermore, direct excitation of ACN ($\lambda > 400$ nm) in the mixed powder resulted in a decrease in the yield of **2** (12.2%) and an increase in **1** (78.7%) with a *cisoid/transoid* ratio of 0.20, which is close to that for the direct irradiation of crystalline ACN without TCNE. Therefore, in the mixed powder excited ACN dimerizes by reaction with neighboring ACN molecules and preferentially gives *transoid*-**1** without participation of $ACN^{+\cdot}$ competing with electron transfer to TCNE due to disordered arrangement of molecules.

Bouas-Laurent et al. undertook irradiation of 1-substituted ACN (**8**, **12**: X = CO_2H, **13**: X = CO-O-CO) in solution and in the solid state (Scheme 8).[47] Irradiation ($\lambda > 300$ nm) of **8**, **12**, **13** in ether at

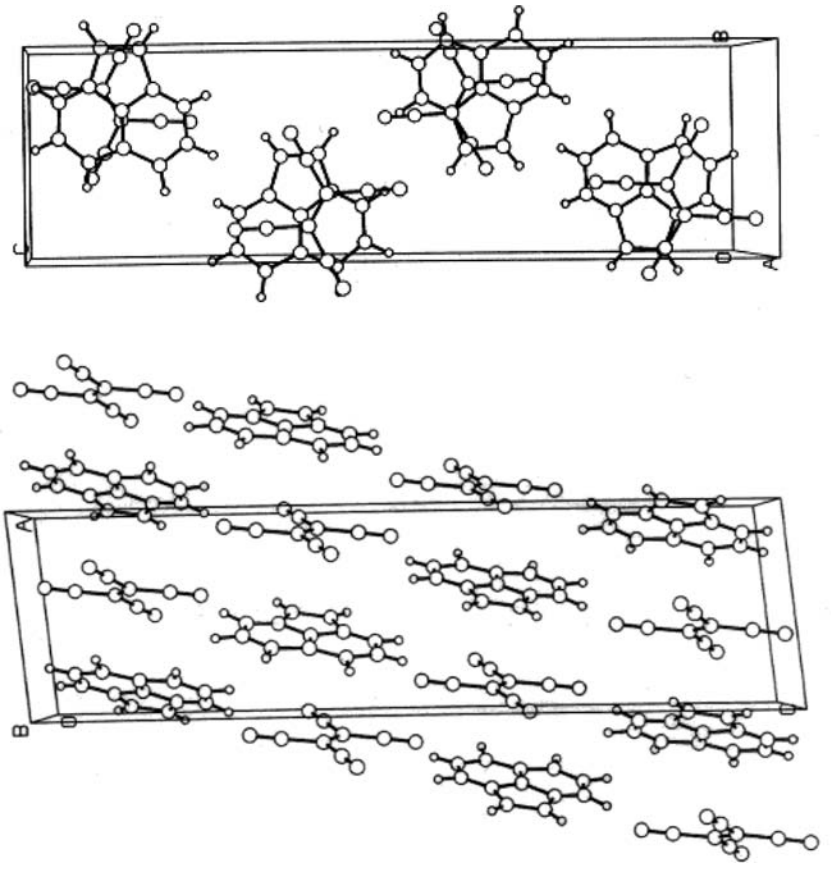

FIGURE 21.2

25°C leads to the *anti-cisoid* dimers (**10, 14, 15**) as major products in yields of 92, 35, and 40%, respectively. Compounds **10** and **15** were hydrolyzed to **14**, and final confirmation of the structure of **10** came from x-ray crystallographic analysis.[48] The dipole moments of **10** and **11** were determined to be 5.90 and 3.65 D, respectively, in benzene at 25°C. On the other hand, irradiation of **13** in both the crystalline and the molten state gave the *syn-cisoid*-dimer (**16**) as the sole product in a yield of 65%. X-ray crystallographic analysis of the monomer **13**[49] demonstrated stereo- and regioselective formation of **16** in the solid state irradiation of **13** according to the topochemical rules.

Dimerization on Silica Gel Surfaces

Photochemistry of ACN adsorbed on a silica gel surface has been reported by de Mayo and coworkers.[50–52] ACN with coverage of 0 ~ 100% on silica gel in the presence or absence of additives (alcohols, ACE, Rose Bengal) was irradiated with a xenon lamp under suitable filters. The major results are abridged as follows.[50,51] The *cisoid/transoid* ratio increased linearly with increase of ACN coverage up to 20%. At above 40%, the curve flattened to about 21 of the ratio. Stern–Volmer plots using ferrocene as a triplet quencher revealed that the formation of *transoid*-**1** is inhibited by the quencher, while efficiency for the formation of *cisoid*-**1** is independent of quencher concentration. Rose Bengal–sensitization produces **1** even at low coverage (0.1%) of the sensitizer. Intergranular movement of ACN molecules adsorbed on the silica gel surface across silica gel particles was directly demonstrated by elaborate experiments using two groups of silica gel particles with different particle sizes.

Essentially, photochemical dimerization on a silica gel surface proceeds by an identical mechanism to that in solution, the short-lived S_1 state leading to the *cisoid*-**1,** and the T_1 state, with a relatively long lifetime, leading to *cisoid*- and *transoid*-**1** with a preference for the latter; however, comparison of quantum yields for the dimerization in solution is not available. Three possible courses leading to **1** from excited ACN proposed by de Mayo et al. are: (a) bimolecular intragranular process, (b) reaction of nearest neighbors (reaction with ACN molecules on neighboring particle), and (c) molecular intergranular encounter. Reactions (a) and (b) could depend on the coverage and proceed mainly via the S_1 state of ACN, whereas reaction (c) comes from the T_1 state because interparticle migration of ACN molecules is sufficiently slow to permit S_1 to T_1 intersystem crossing. An increase in the coverage brings about increased contributions from both reactions (a) and (b), resulting in linear increases of the *cisoid/transoid* ratio. The plateau value of the ratio reflects saturated contribution from reactions (a) and (b) due to a sufficiently high concentration of ACN to allow dimerization from the S_1 state at a diffusion-controlled rate. Sensitization at low coverage (0.1%) of Rose Bengal suggests intra- and intergranular movement of the T_1 state of the sensitizer molecules to allow energy transfer to ground state ACN.

The effect of co-adsorbates such as alcohols and ACE was scrutinized by direct or sensitized excitation of ACN.[51,52] In the direct excitation, the *cisoid/transoid* ratio was reduced from 8.78 with additives to 1.6 ~ 2.8 without additives. In the Rose Bengal sensitization, the ratio remained relatively constant at 0.34 ~ 0.61. Co-adsorption of alcohols increased ACN mobility on the silica gel surface because of blocking of stronger binding sites and reduced the *cisoid/transoid* ratio because increased mobility by solvent molecules would be advantageous for dimerization from the T_1 state, rather than the S_1 state, over a longer time span. Moreover, the co-adsorbed alcohols would result in diminished formation of preferred pairs of ACN that would lead to *cisoid*-**1** from the S_1 state owing to the occupation of sites for pair formation by the co-adsorbate. When ACN is diluted with ACE as an inert counterpart, a hybrid pair of ACN with ACE that is unable to dimerize may be created, and therefore the *cisoid/transoid* ratio reflects the diffusional dimerization via the T_1 state.

Later, Barbas et al. performed irradiation ($\lambda > 350$ nm) of ACN on a dry silica gel–air interface with monolayer coverage of 0.3 ~ 9%.[53] The dimers **1** were produced along with oxidation products of ACN. These products included 1,2-acenaphthenedione, 2-hydroxy-1-acenaphthenone, 1,8-naphthalenedicarboxaldehyde, and 1,8-naphthalic anhydride. For formation of **1**, results derived by Barbas et al. support the validity of de Mayo's results. Thus, the yield of *cisoid*-**1** increased much more dramatically than that of *transoid*-**1** and rose from 2.4 to 13.2 as the surface coverage was increased from 0.3 to 8.6%, which indicates that the contribution from the S_1 state to *cisoid*-**1** formation is more significant than that from the T_1 state.

Dimerization in Micelles

In a pioneering study, Nakamura et al. have pointed out enhancement of photochemical dimerization of ACN in micelles compared to dimerization in solution phase.[54] They employed sodium dodecyl sulfate (SDS) as an ionic surfactant and polyoxyethylene–polyoxypropylene cetyl ether (PBC-34) as a nonionic surfactant. In general, the dimerization occurred efficiently in both of the micelles even with concentrations of ACN as low as 1.9 mmol, whereas dimerization in benzene solution was nil. Under concentrations of 5 ~ 30 mmol of ACN, the *cisoid/transoid* ratio in PBC-30 was ca. 0.8 and independent on the initial concentration of ACN, while that in SDS was as high as 2.7, showing dependence of the ratio on the surfactant used.

The presence of oxygen and the use of surfactants with heavy atoms in micellar systems show similar effects as in homogeneous solution.[55] Mayer and Sauer irradiated ($\lambda > 400$ nm) ACN and 1-substituted ACN (**8**: X = CN, **12**: X = CO_2H, **17**: X = CO_2CH_3, **18**: X = $CO_2C_4H_9$, **19**: X = $CO_2C_8H_{17}$) in the micellar systems of SDS and dodecyltrimethylammonium fluoride, chloride, bromide, and iodide with and without O_2. The reaction of ACN in the SDS micelle resulted in a higher *cisoid/transoid* ratio of ca. 9 under O_2 than that of ca. 1.5 under argon. The ratio decreased with increase of the atomic number of the

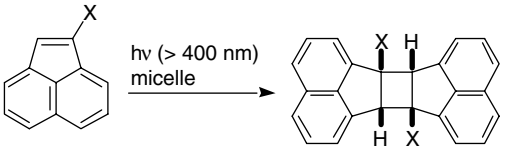

8 (X = CN)
12 (X = CO_2H)
17 (X = CO_2CH_3)
18 (X = $CO_2C_4H_9$)
19 (X = $CO_2C_8H_9$)

10 (X = CN)
14 (X = CO_2H)
20 (X = CO_2CH_3)
21 (X = $CO_2C_4H_9$)
22 (X = $CO_2C_8H_9$)

SCHEME 9

counterion of the dodecyltrimethylammonium salts: fluoride 3.54, chloride 2.57, bromide 1.12, and iodide 1.12. As in the case of reaction in homogeneous solutions, the effect of O_2 can be attributed to quenching of the T_1 of ACN leading to preferential dimerization from the S_1 state. Acceleration of ISC by spin-orbit coupling is apparently responsible for the lower *cisoid/transoid* ratio in the reactions in micelles with bromide or iodide anions. Irradiation of **8**, **12**, **17**, **18**, and **19** afforded an *anti-cisoid*-dimer (**10**, **14**, **20**, **21**, **22**) as a major product for each substitution (Scheme 9), the structures of which were deduced by means of ^{1}H- and ^{13}C-NMR.[56] Regio- and stereoselective formation of **10** from **8** and **14** from **12** is essentially identical to the results obtained from irradiation in solution.[47] The same authors compared the *cisoid/transoid* ratio in the reactions in micelles by direct excitation of ACN and by Rose Bengal sensitization with that in solutions with varying polarity of solvent.[57] The ratio in micelles (1.0 ~ 1.1) was independent of [ACN] (8.3 ~ 40.1 mmol) 1.04 and 0.48 for direct and sensitized excitation, respectively. The former ratio corresponds to that in polar solvents such as MeCN and DMF.

Tamura and Aida reported the unique influence of shape and volume of inner micellar space on product distribution.[58] They irradiated ACN in aqueous sodium octyl sulfate, decyl sulfate, dodecyl sulfate, and hexadecyltrimethylammonium bromide under pressures up to 150 MPa. Pressure enhanced the dimerization reaction in all micellar systems due to the formation of a van der Waals dimer in the ground state. Plots of the consumed ACN vs. concentration of micelles exhibited a minimum under constant concentration (9.7 mmol kg^{-1}) of ACN. Thus, the number of micelles in the solution increases with increase of surfactant concentration and, as a result, the number of ACN molecules solubilized per micelle decreases. This leads to a decrease of probability of collision between ACN molecules that undergo bimolecular reaction. Viscosity measurements indicate that spherical micelles start to aggregate and form rod-shaped micelles with larger volumes at ca. 9 wt% of micelle, which exactly coincides with the minimum concentration of micelles. At concentrations of micelles higher than the minimum, the number of ACN molecules included in a micelle increases due to aggregation of spherical micelles into rod-shaped micelles, leading to enhanced dimerization of ACN.

Ramesh and Ramamurthy demonstrated a dependency of the *cisoid/transoid* ratio on the mean occupancy number (S), which refers to number of ACN molecules per micelle.[59] Under constant concentration (0.05 *M*) of aqueous surfactant SDS, the *cisoid/transoid* ratio decreased with decrease of [ACN]; that is, the ratio was 4.6, 4.6, 4.0, 3.6, 2.0, and 1.7 under S of 9.0, 7.0, 6.0, 3.0, 2.0, and 1.0, respectively. When cetyltrimethylammonium bromide (CTAB) was employed in place of SDS, the ratio decreased from 4.6 to 1.3 at S of ca. 9. These results can be interpreted as follows. With a decrease of [ACN], the S value decreases. Since the probability for formation of S_1-derived *cisoid*-**1** increases at high [ACN], *cisoid*-**1** is favored under conditions of high S. With a decrease of S, the probability for the S_1 state to encounter a ground state ACN prior to ISC to the T_1 state decreases, and hence the *cisoid/transoid* ratio decreases. In CTAB micelles, the heavy atom effect of the bromide ion leads to promoted formation of T_1-derived *transoid*-**1**, whereas in micelles with atoms lighter than bromine, the S_1-derived *cisoid*-**1** predominates.

Dimerization in Liquid Crystals

Nerbonne and Weiss demonstrated that upon irradiation ($\lambda > 340$ nm), dimerization of ACN is enhanced in a 1:1 mixture of 5α-cholestan-3β-yl acetate and 5α-cholestan-3β-yl nonanoate as a cholesteric liquid crystal (LC), compared to that in isotropic solution such as benzene.[60] Thus, the quantum yield (Φ) for formation of the dimers **1** at 366 nm under 0.08 *M* of ACN in the LC was 0.23 ~ 0.28 in the temperature range of 10 ~ 40°C when the LC was in a cholesteric phase; however, above 50°C, when the ester was in an isotropic phase, the Φ dropped to 0.03, which is comparable to that in isotropic solution and in smectic phase such as *n*-butyl stearate. The enhanced Φ for the dimerization in the cholesteric LC can be ascribed to an ordering effect induced by alignment of LC molecules on collisions between excited and ground state ACN molecules. The *cisoid/transoid* ratio was, however, generally constant (0.7 ~ 1.0) in the concentration range 0.02 ~ 0.08 *M* of [ACN]. This is in contrast to the results by Nakano and Hirata described below.[61]

Nakano and Hirata found that the *cisoid/transoid* ratio of **1** increased from ca. 0.3 to 0.7 with an increase of [ACN] from ca. 7×10^{-3} to 7×10^{-2} *M* in cholesteric LC (cholesteryl oleyl carbonate, cholesteryl linolate, and cholesteryl oleate), whereas nematic LC or benzene as the reaction medium did not affect the ratio. These results suggest that the cholesteric LC structure makes the ACN molecules align in a phase-to-phase manner. For dimerization of ACN in the nematic phase, Oh-hashi et al. reported briefly the effect of electric fields on the *cisoid/transoid* ratio.[62] Upon irradiation ($\lambda > 300$ nm) of ACN in nematic LC (4-hexyloxyphenyl 4′-butylbenzoate, LC1), application of an electric field up to 5 kV cm^{-1} decreased the *cisoid/transoid* ratio from 0.33 to 0.15. They attributed this effect to the preferred formation of the T_1 state of ACN by "molecular stirring" under dynamic scattering of the nematic phase.

Dimerization in Zeolites

Like other constrained media, supercages in zeolites can offer reactivity and selectivity for products in photochemical reactions that cannot be expected in homogeneous solutions. Ramamurthy et al. have undertaken photochemical reactions in dry cation-exchanged Y zeolite (LiY, NaY, KY, RbY, CsY, TlY).[63] On irradiation ($\lambda > 300$ nm) of ACN, formation of *cisoid*-**1** was favored in zeolites with lower atomic number metals (Li and Na) and with a higher occupancy number (S). The *cisoid/transoid* ratios in NaY and CsY, for example, were 25 and 4.2, respectively, at S = 0.5 and decreased to 22 and 2.8 at S = 0.25. It is apparent that a higher S value is favorable for formation of *cisoid*-**1** derived from the S_1 state with a short lifetime, while heavy atom cations accelerate ISC from the S_1 to the T_1 state of ACN in the cage. Transient absorption of the T_1 state was observed at 470 nm with higher relative yield with the use of heavier cations.

Furthermore, the same authors compared the reactions in hexane slurry with those in the dry solid.[64] Employing LiY and NaY zeolites with occupancy numbers of 0.2 ~ 0.9, they showed that irradiation of ACN in slurry zeolite led to formation of **1** with *cisoid/transoid* ratios of 2.3, 3.5, and 7.2 for S of 0.2, 0.5, and 0.9, while the ratios in the solid zeolite were 0.6, 1.7, and 2.0 for the corresponding S values. Higher *cisoid/transoid* ratios in the slurry compared to the solid were interpreted in terms of mobility of ACN molecules between the zeolite supercage: that is, ACN molecules in single occupancy cages should migrate between cages to give **1** from the T_1 state with a long lifetime, which is comparable to the time for migration between cages, whereas ACN molecules in double occupancy cages react in the cages, affording *cisoid*-**1** from the short-lived S_1 state. Because the solvent inhibits or blocks migration of ACN molecules between cages, predominant migration of ACN molecules between supercages in the absence of solvents results in preferred production of the T_1 state, leading to a decrease in the *cisoid/transoid* ratio.

Dimerization in Miscellaneous Heterogeneous Systems

Recently, the nonpolar and flexible sites available between the alkyl chains of surfactant-intercalated graphite oxide were used as a noble reaction medium.[65] Matsuo et al. irradiated ($\lambda > 330$ nm) ACN in

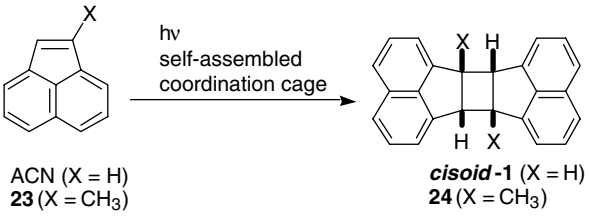

SCHEME 10

graphite oxide as a layered material intercalated with myristyltrimethylammonium bromide $[C_{14}H_{29}N(CH_3)_3Br]$ as a surfactant. X-ray diffraction patterns of powdered ACN-surfactant graphite oxide before and after UV irradiation showed broadening of the interlayer spacing (d = 2.7 to 3.2 nm) because **1** is bulkier than ACN and this prevents dense packing of surfactant and **1**. The authors did not refer to the origin for the notably high *cisoid/transoid* ratio of 8.8 obtained in relation to molecular configuration in the layer of graphite oxide and nature of excited state of ACN, however.

Also quite recently, Yoshizawa et al. found that self-assembled coordination cages containing palladium can function as a medium of dimerization of alkenes.[66] Irradiation of ACN or 1-methyl-ACN (**23**) in coordination cages in D_2O resulted in efficient formation of the dimers with high stereoselectivity and regioselectivity with a preference for *cisoid*-**1** of > 49 (ACN) and the *anti-cisoid*-dimer of > 49 (**23**), which is in contrast with the less efficient reaction in benzene with the ratio of 1.1 (ACN) and no reactivity (**23**) (Scheme 10).

Tong and Zeng applied cyclodextrins, one of the most widespread microenvironmental media, to the photochemical dimerization of ACN and found an effect of cavity size on reactivity.[67] Thus, upon irradiation ($\lambda > 340$ nm) of ACN in γ-cyclodextrin, the formation of the dimers **1** was promoted, whereas no dimerization occurred in β–cyclodextrin. The distinction between γ- and β-cyclodextrin may be due to number of the guest molecules accommodated; γ-cyclodextrin includes two ACN molecules that may lead to **1** within the cage, while escape from the cage should be necessary for encounter of singly occupied ACN molecules in β-cyclodextrin.

Behymer and Hites carried out photolysis of ACN from the viewpoint of the polycyclic hydrocarbons formed by combustion of fuel and their transportation in the vapor phase and adsorption on particulate matter.[68] Using a rotary photoreactor to simulate environmental conditions in the atmosphere, they carried out irradiation ($\lambda > 300$ nm) on ACN adsorbed on 16 kinds of fly ashes with varying chemical and physical compositions. The half-life of ACN was determined as 1 ~ 125 h depending on the properties of the fly ash; however, no product analysis was performed.

21.5 Conclusions

In conclusion, this chapter details the photochemical dimerization of ACN. This reaction proceeds with relatively low quantum yields, since the S_1 state is short lived (ca. 1 nsec) and undergoes ISC to the T_1 state with low efficiency. On excitation of ACN in solution, the resultant S_1 state produces *cisoid*-**1** in competition with very fast internal conversion from the S_1 both in solution and in constrained media as far as movement of molecules is permitted. An excimer, where two ACN molecules are aligned in the same direction, is responsible for regioselective formation of the *cisoid*-dimer, whether the excimer originated from a van der Waals dimer in the ground state or from action of an S_1 state of ACN on ground state ACN. High concentration or aggregation of ACN molecules in a limited space is advantageous for dimerization from the S_1 state. In contrast, the T_1 state produces both *cisoid*- and *transoid*-**1**, whose ratio is seriously affected by polarity of the media of reaction. Because the T_1 state is produced in a low efficiency from the S_1 state and has a relatively longer lifetime (2 ~ 4 μsec) than the S_1 state, low concentrations or separated circumstances where long-distance migration is necessary for contact

between two ACN molecules are advantageous for dimerization from the T_1 state. Sensitized formation of the T_1 state, therefore, enhances efficiency of the dimerization. In the crystalline state under topochemical control, *transoid*-**1** is preferentially produced, presumably due to unfavorable arrangement of the ACN molecules in the crystalline lattice for formation of the *cisoid*-**1**. Properties and reactions of radical ions, especially radical anions of ACN generated by photoinduced electron transfer, are areas for future development from the viewpoint of reaction mechanisms and synthetic application.

Acknowledgement

The authors would like to thank Professor Hiroaki Takayanagi, School of Pharmaceutical Sciences, Kitasato University, Japan, for his valuable assistance with x-ray diffraction measurements.

References

1. (a) Dziewonski, K. and Rapalski, G., Über die Photochemische Umwandlung des Acenaphthylens.I., *Chem. Ber.,* 45, 2491, 1912; (b) Dziewonski, K. and Rapalski, G., Über die Photochemische Umwandlung des Acenaphthylens. II, *Chem. Ber.,* 46, 1986, 1913; (c) Dziewonski, K. and Rapalski, G., Über die Photochemische Umwandlung des Acenaphthylens und Synthese einiger hö chstmolecularer Kolenwasserstoffe., *Chem. Ber.,* 47, 1679, 1914.
2. Brown, E.J., The photochemistry of aromatic hydrocarbon solutions, in *Advances in Photochemistry,* Vol. 1, Noyes, W.A. Jr., Hammond, G., and Pitts, J.N. Jr., Eds., John Wiley and Sons, New York, 1963, p. 23.
3. Plummer, B.F., Hopkinson, M.J., and Zoeller, J.K., Dual wavelength fluorescence from acenaphthylene and derivatives in fluid media, *J. Am. Chem. Soc.,* 101, 6779, 1979.
4. Castellan, G., Dumartin, G., and Bouas-Laurent, H., Photocycloaddition des hydrocarbures aromatiques polynucleaires en solution — IV, *Tetrahedron*, 36, 97, 1980.
5. Samanta, A., Devadoss, C., and Fessenden, R.W., Picosecond time-resolved absorption and emission studies of the singlet excited states of acenaphthylene, *J. Phys. Chem.,* 94, 7106, 1990.
6. Dunsbach, R. and Schmidt, R., Photophysical properties of some polycyclic conjugated hydrocarbons containing five-membered rings, *J. Photochem. Photobiol. A: Chem.,* 83, 7, 1994.
7. Ferree, W.I., Jr., and Plummer, B.F., Photochemical heavy-atom effect. IV. External and internal heavy-atom effects upon the reaction of acenaphthylene with cyclopentadiene, *J. Am. Chem. Soc.,* 95, 6709, 1973.
8. Griffin, G.W. and Veber, D.F., Tetracarbomethoxycyclobutane; structure of β-heptacyclene, *J. Am. Chem. Soc.,* 82, 6467, 1960.
9. Welberry, T.R., The crystal and molecular structure of the *cis*-dimer of acenaphthylene, *Acta Cryst.,* B27, 360, 1971.
10. Dunitz, J.D. and Weissman, L., The constitution of the dimer of acenaphthylene, *Acta. Cryst.,* 62, 1949.
11. Sahoo, N. and Galagari, R.J., Nitrogen laser photochemistry, *Nat. Acad. Sci. Lett.,* 11, 145, 1988.
12. Bowen, E.J. and Marsh, J.D.F., The photochemical dimerization of acenaphthylene, *J. Chem. Soc.,* 109–110, 1947.
13. Schenck, G.O. and Wolgast, R., Durch Rose Bengal–photosensibilisielte Cyclodimerisation von Acenaphthylen und Mechanismus der Energieübertragung, *Naturwiss.,* 49, 36, 1962.
14. (a) White, E.H., Wiecko, J., and Wei, C-C., Utilization of chemically generated excited states, *J. Am. Chem. Soc.,* 92, 2167, 1970; (b) White, E.H., Wildes, P.D., Wiecko, J., Doshan, H., and Wei, C-C., Chemically produced excited states. Energy transfer, photochemical reactions and light emissions, *J. Am. Chem. Soc.,* 95, 7050, 1973.
15. Hartmann, I.-L., Hartmann, W., and Schenck, G.O., Zum Mechanismus der sensibilisierten und unsensibilisierten Photodimerisation von Acenaphthylen in Lösung, *Chem. Ber.,* 100, 3146, 1967.
16. Livingston, R. and Wei, K.S., Reversible photochemical dimerization of acenaphthylene. I. The reaction in liquid solutions, *J. Phys. Chem.,* 71, 541, 1967.

17. Cowan, D.O. and Drisco, R.L.E., Solvent effect of photodimerization of acenaphthylene, *Tetrahedron Lett.,* 1255, 1967.
18. Cowan, D.O. and Drisco, R.L.E., The photodimerization of acenaphthylene. Mechanistic studies, *J. Am. Chem. Soc.,* 92, 6286, 1970.
19. Cowan, D.O. and Drisco, R.L.E., The photodimerization of acenaphthylene. Heavy-atom solvent effects, *J. Am. Chem. Soc.,* 92, 6281, 1970.
20. Cowan, D.O. and Koziar, J.C., Effect of iodide on the photodimerization of acenaphthylene, *J. Am. Chem. Soc.,* 96, 1229, 1974.
21. Cowan, D.O. and Koziar, J.C., Heavy-atom effects on the spin-forbidden processes of acenaphthylene, *J. Am. Chem. Soc.,* 97, 249, 1975.
22. Koser, G.F. and Liu, V.-S., Heavy-atom effect on the photodimerization of acenaphthylene: substituent analysis on the efficiency of external aromatic perturbers, *J. Org. Chem.,* 43, 478, 1978.
23. Muszkat, K.A. and Sharafi-Ozeri, S., Electronic overlap population as reactivity measure. The photodimerization of acenaphthylene, *Chem. Phys. Lett.,* 38, 346, 1976.
24. Haga, N., Takayanagi, H., and Tokumaru, K., Mechanism of photodimerization of acenaphthylene, *J. Org. Chem.,* 62, 3734, 1997.
25. Sigman, M.E., Chevis, E.A., Brown, A., Bravas, J.T., Dabestani, R., and Burch, E.L., Enhanced photoreactivity of acenaphthylene in water: a product and mechanism study, *J. Photochem. Photobiol. A: Chem.,* 94, 149, 1996.
26. Ichimura, K. and Watanabe, S., External magnetic field effect on chemical reactions (I). Photodimerization of acenaphthylene, *Seni Kobunshi Zairyo Kenkyusho Kenkyu Hokoku,* 108, 29, 1975.
27. Gáplovsky, A., Donovalová, J., Toma, S., and Kubinec, R., Ultrasound effects on photochemical reactions. 2. A study of ultrasound effects on some monomolecular and bimolecular photochemical reactions, *J. Photochem. Photobiol. A: Chem.,* 115, 13, 1998.
28. Shields, J.E., Gavrilovic, D., Kopecky, J., Hartmann, W., and Heine, H.-G., Photochemical cycloadditions of maleic anhydride and some derivatives to acenaphthylene. A new route to pleiadienes, *J. Org. Chem.,* 39, 515, 1974.
29. (a) Jiang, Z.-Q. and Liu, J.-F., Photooxidations. V. Cyanoanthracene-sensitized electron transfer photooxidation of acenaphthylene, *Huaxue Xuebuo,* 46, 96, 1988; (b) Jiang, Z-Q., Liu, J.-F., Wu, S.-P., Yu, Q., and Ye, J-P., Sensitized electron transfer photooxygenation of acenaphthylene via competing sequential processes, *J. Photochem. Photobiol. A: Chem.,* 128, 57, 1999.
30. Haga, N., Nakajima, H., Takayanagi, H., and Tokumaru, K., Photoinduced electron transfer between acenaphthylene and tetracyanoethylene. Effect of irradiation mode on reactivity of the charge-transfer complex and the resulted radical ion pair in solution and crystalline state, *J. Org. Chem.,* 63, 5372, 1998.
31. Shirota, Y., Nagata, J., and Mikawa, H., The photocycloaddition of acenaphthylene with tetracyanoethylene, *Chem. Lett.,* 49, 1972.
32. Haga, N., Takayanagi, H., and Tokumaru, K., Control of reaction course of the excited state of charge-transfer complexes by free energy for backward electron transfer, *J. Chem. Soc., Chem. Commun.,* 2093, 1998.
33. Haga, N., Takayanagi, H., and Tokumaru, K., Photoinduced electron transfer between acenaphthylene and 1,4-benzoquinones. Formation of dimers of acenaphthylene and 1:1-adducts and effect of excitation mode on reactivity of the charge-transfer complexes, *J. Chem. Soc., Perkin Trans. 2,* 734, 2002.
34. (a) Asahi, T. and Mataga, N., Charge recombination process of ion pair state produced by excitation of charge-transfer complex in acetonitrile solution. Essentially different character of its energy gap dependence from that of geminate ion pair formed by encounter between fluorescer and quencher, *J. Phys. Chem.,* 93, 6576, 1989; (b) Ojima, S., Miyasaka, H., and Mataga, N., Femtosecond–picosecond laser photolysis studies on the dynamics of excited charge-transfer complexes in solution. 2. Ion pair formation processes in the excited state of 1,2,4,5-tetracyanobenzene–aromatic hydrocarbon complexes in polar solvents, *J. Phys. Chem.,* 94, 5834, 1990; (c) Asahi, T. and Mataga, N.,

Femtosecond–picosecond laser photolysis studies on the dynamics of excited charge-transfer complexes: aromatic hydrocarbon-acid anhydride, -tetracyanoethylene and -tetracyanoquinodimethane systems in acetonitrile solutions, *J. Phys. Chem.,* 95, 1956, 1991; (d) Miyasaka, H., Nagata, T., Kiri, M., and Mataga, N., Femtosecond–picosecond laser photolysis studies on reduction process of excited benzophenone with *N*-methyldiphenylamine in acetonitrile solution, *J. Phys. Chem.,* 96, 8060, 1992; (e) Asahi, T., Ohkohchi, M., and Mataga, N., Energy gap dependence of charge recombination processes of ion pairs produced by excitation of charge-transfer complexes: solvent polarity effects, *J. Phys. Chem.,* 97, 13132, 1993; (f) Mataga, N. and Miyasaka, H., Photoinduced charge transfer phenomena: femtosecond–picosecond laser photolysis studies, *Progr. React. Kinetics,* 19, 317, 1994; (g) Miyasaka, H., Kotani, S., Itaya, A., Schweizer, G., DeSchryver, F.C., and Mataga, N., Temperature effect on the energy gap dependence of charge recombination rates of ion pairs produced by excitation of charge-transfer complexes adsorbed on porous glass, *J. Phys. Chem. B,* 101, 7978, 1997.

35. Davidson, R.S., The photoreactions of aromatic hydrocarbons in the presence of amines, *J. Chem. Soc. Chem. Commun.,* 1450, 1969.
36. Cantrell, T.S. and Shechter, H., Reaction of dinitrogen tetroxide with acenaphthylene. Diels–Alder reactions and photodimerizations of 1-nitro- and 2-nitroacenaphthylenes, *J. Org. Chem.,* 33, 114, 1968.
37. Wei, K.S. and Livingston, R., Reversible photochemical dimerization of acenaphthylene. II. The reaction in the molten and crystalline phase, *J. Phys. Chem.,* 71, 548, 1967.
38. Cohen, M.D., Ron, I., Schmidt, G.M.J., and Thomas, J.M., Photochemical decoration of dislocations inside crystals of acenaphthylene, *Nature*, 224, 167, 1969.
39. Cser, F., Crystal structure study on acenaphthylene, *Acta Chim. (Budapest),* 80, 317, 1974.
40. Gordon, R.D. and Yang, R.F., The electronic spectrum of acenaphthylene, *J. Mol. Spectrosc.,* 34, 266, 1970.
41. Bree, A., Kydd, R.A., Vilkos, V.V.B., and Williams, R.S., The vibrational spectra and crystal structure of acenaphthylene, *Can. J. Chem.,* 51, 402, 1973.
42. Sanford, R.D., Kupferschmidt, G.J., Fyfe, C.A., Boyd, R.K., and Ripmeester, J.A., The dynamic structure of acenaphthylene in the solid state: pulse nuclear magnetic resonance measurements, *Can. J. Chem.,* 58, 906, 1980.
43. He, H. and Welberry, T.R., A study of the disordered low-temperature structure of acenaphthylene, $C_{12}H_8$, using semi-empirical potential energy calculations, *J. Chem. Soc., Perkin Trans. 2,* 1947, 1988.
44. Wood, R.A., Welberry, T.R., and Rae, A.D., Crystal structure of acenaphthylene, $C_{12}H_8$, at 80 K by neutron diffraction, *J. Chem. Soc., Perkin Trans. 2,* 451, 1985.
45. Haga, N., Nakajima, H., Takayanagi, H., and Tokumaru, K., Exclusive production of a cycloadduct from selective excitation of charge-transfer complex between acenaphthylene and tetracyanoethylene in crystalline state in contrast to failure of reaction in solution, *J. Chem. Soc., Chem. Commun.,* 1171, 1997.
46. Venkatesan, K. and Ramamurthy, V., Bimolecular reactions in crystals, in *Photochemistry in Organized and Constrained Media,* Ramamurthy, V., Ed., VCH Publishers, New York, 1991, p. 133.
47. (a) Bouas-Laurent, H., Castellan, A., Desvergne, J.P., Courseille, C., and Hauw, C., Photodimerization of 1-substituted acenaphthylenes in solution and in the solid state, *J. Chem. Soc., Chem. Commun.,* 1267, 1972; (b) Castellan, A., Dumartin, G., Gaultier, J., and Bouas-Laurent, H., Photocycloaddition des hydrocarbures aromatiques polynucléaires en solution. III. — Photodimérisation de dérivés acénaphthyléniques; structure des photodiméres, *Bull. Soc. Chim. Fr.,* 217, 1976.
48. Courseille, C., Busetta, B., Hospital, M., and Castellan, A., Head-to-tail *cis* photodimer of 1-cyano acenaphthylene, $C_{14}H_{14}N_2$, *Cryst. Struct. Comm.,* 1, 337, 1972.
49. Bouas-Laurent, H., Desvergne, M., Gaultier, J., and Hauw, C., Acenaphthylene 1-carboxylic acid, $C_{13}H_8O_2$, *Cryst. Struct. Comm.,* 2, 547, 1973.
50. (a) de Mayo, P., Okada, K., Rafalska, M., Weedon, A., and Wong, G.S.K., Surface photochemistry: the photodimerization of acenaphthylene on dry silica gel, *J. Chem. Soc., Chem. Commun.,* 820,

1981; (b) Bauer, R.K., Borenstein, R., de Mayo P., Okada, K., Rafalska, M., Ware W.R., and Wu, K.C., Surface photochemistry: translational motion of organic molecules adsorbed on silica gel and its consequences, *J. Am. Chem. Soc.,* 104, 4635, 1982.
51. de Mayo, P., Superficial photochemistry, *Pure Appl. Chem.,* 54, 1623, 1982.
52. Bauer, R.K., de Mayo, P., Okada, K., Ware, W.R., and Wu, K.C., Surface photochemistry. The effects of coadsorbed molecules on pyrene luminescence and acenaphthylene dimerization on silica gel, *J. Phys. Chem.,* 87, 460, 1983.
53. Barbas, J., Dabestani, R., and Sigman, M.E., A mechanistic study of photodecomposition of acenaphthylene on a dry silica surface, *J. Photochem. Photobiol. A: Chem.,* 80, 103, 1994.
54. Nakamura, Y., Imakura, Y., Kato, T., and Morita, Y., *J. Chem. Soc., Chem. Commun.,* 887, 1977.
55. Mayer, H. and Sauer, J., Photodimerization of acenaphthylene derivatives in solutions and micelles, *Tetrahedron Lett.,* 24, 4091, 1983.
56. Mayer, H. and Sauer, J., Structure and configuration of the photodimers of 1-substituted acenaphthylenes, *Tetrahedron Lett.,* 24, 4095, 1983.
57. Mayer, H., Schuster, F., and Sauer, J., Photochemically induced 2 + 2-cycloaddition in micelles: a comparison of the product spectra with reactions in solution, *Tetrahedron Lett.,* 27, 1289, 1986.
58. Tamura, K. and Aida, M., Effects of pressure of the photodimerization of acenaphthylene in micellar systems, *J. Chem. Soc., Faraday Trans. 2,* 82, 1619, 1986.
59. Ramesh, V. and Ramamurthy, V., Reactive state selectivity in photodimerization through micellar counter-ion effects: photodimerization of acenaphthylene, *J. Photochem.,* 24, 395, 1984.
60. (a) Nerbonne, J.M. and Weiss, R.G., Effects of liquid crystal solvents on the photodimerization of acenaphthylene, *J. Am. Chem. Soc.,* 100, 2571, 1978; (b) Nerbonne, J.M. and Weiss, R.G., Liquid crystalline solvents as mechanistic probes. 3. The influence of ordered media on the efficiency of the photodimerization of acenaphthylene, *J. Am. Chem. Soc.,* 101, 402, 1979.
61. Nakano, T. and Hirata, H., Liquid crystals as reaction media. I. Photochemical dimerization of acenaphthylene in cholesteric liquid crystal, *Bull. Chem. Soc. Jpn.,* 55, 947–948, 1982.
62. Oh-hashi, M., Tsujimoto, K., and Yamada, S., Organic photochemistry using a mediator, *Kokagaku*, 12, 102, 1988.
63. Ramamurthy, V., Corbin, D.R., Kumar, C.V., and Turro, N.J., Modification of photochemical reactivity by zeolites: cation controlled photodimerization of acenaphthylene within faujasites, *Tetrahedron Lett.,* 31, 47, 1990.
64. Ramamurthy, V. and Corbin, D.R., Modification of photochemical reactivity by zeolites. A comparison between zeolite-solvent slurry and dry solid photolyses, *J. Org. Chem.,* 56, 255, 1991.
65. Matsuo, Y., Fukutsuka, T., and Sugie, Y., Photochemical dimerization of acenaphthylene in surfactant-intercalated graphite oxide, *Carbon,* 40, 955, 2002.
66. Yoshizawa, M., Takeyama, Y., Kusukawa, T., and Fujita, M., Cavity-directed, highly stereoselective 2 + 2 photodimerization of olefins within self-assembled coordination cages, *Angew. Chem. Int. Ed. Engl.,* 41, 1347, 2002.
67. Tong, Z. and Zeng, Z., Microenvironmental effects of cyclodextrins. II. Effects of cyclodextrins on photodimerization of acenaphthylene, *Youji Huaxue,* 44, 1986.
68. Behymer, T.D. and Hites, R., Photolysis of polycyclic hydrocarbons adsorbed on fly ash, *Environ. Sci. Technol.,* 22, 1311, 1988.
69. Murov, S.L., Carmichael, I., and Hug, G.L., *Handbook of Photochemistry,* 2nd ed., Marcel Decker, Inc., New York, 1993.
70. Heilbronner, E., Weber, J.P., Michl, J., and Zahradnik, R., The electronic spectra of acenaphthylene and fluoranthene. A comment on the classification of electronic spectra, *Theoret. Chim. Acta,* 6, 141, 1966.
71. Samanta, A., Direct evidence for intersystem crossing involving higher excited states of acenaphthylene, *J. Am. Chem. Soc.,* 113, 7427, 1991.
72. Samanta, A. and Fessenden, R.W., Sensitized and heavy atom induced production of acenaphthylene triplet: a laser flash photolysis study, *J. Phys. Chem.,* 93, 5823, 1989.

73. (a) Santa Cruz, T.D., Akins, D.L., and Birke, R.L., Chemiluminescence and energy transfer in systems of electrogenerated aromatic anions and benzoyl peroxide, *J. Am. Chem. Soc.,* 98, 1677, 1976; (b) Tanimoto, I., Kushioka, K., and Maruyama, K., Binary phase chlorination of aromatic hydrocarbons with solid copper (II) chloride: reaction mechanism, *Bull. Chem. Soc. Jpn.,* 52, 3586, 1979.

22

Photochemical Synthesis of Cage Compounds

Teruo Shinmyozu
Kyushu University

Rika Nogita
Kyushu University

Motoko Akita
Kyushu University

Chultack Lim
Kyushu University

Interest in alicyclic highly strained cage molecules has accelerated greatly during the past decade, and these compounds continue to fascinate chemists since their synthesis is a major challenge. These molecules also have useful physical and chemical properties and biological activity. The extensive efforts devoted to the synthesis of these molecules are described in this chapter. One of the most important components of the cage compounds is a highly strained cyclobutane ring (strain energy 26.4 kcal/mol). The first synthetic approach to a cyclobutane ring via a photochemical reaction was reported by Ciamician and Silber in 1908.[1] They found that exposure of an alcohol solution of carvone **1** to sunlight provided carvone camphor **2** via [2 + 2]-photocyclization of the carbon–carbon double bonds (Scheme 1). Since then, formation of a cyclobutane ring by a photochemical [2 + 2]-process has been one of the most important and useful methods for the synthesis of cage compounds. Accumulated experimental data on the synthesis of cage compounds indicate that the best method to construct highly strained molecules is to use photochemical reactions.

Light is one of the cleanest energy sources, and various light sources are now available for different types of reactions. In the [2 + 2]-photochemical reaction, the most widely used light source is the mercury (Hg) arc lamp. Three main types are designated as low, medium, and high pressure, and each has different spectral characteristics. The low pressure Hg lamp operates at room temperature and emits mainly 253.7 nm and weak 184.9 nm light. The so-called sterilizing lamps are coated with special filters and cut off below 200 nm to obtain only 253.7 nm light.

Monochromatic 253.7 nm light can be obtained from the low pressure Hg lamp using a Vycor filter. The spectral lines at 265.4, 313, and 365 nm have reasonably high relative intensity in the medium pressure Hg lamp. A stronger continuum is obtained with broadening of these emission lines in the high pressure Hg lamp.

0-8493-1348-1/04/$0.00+$1.50

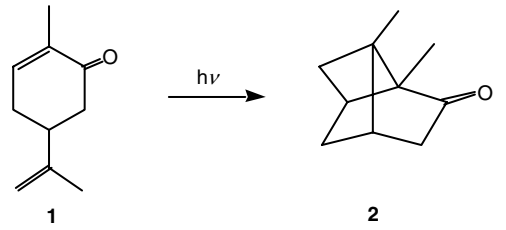

SCHEME 1 The first report of the photochemical [2+2]-addition by Ciamician et al.

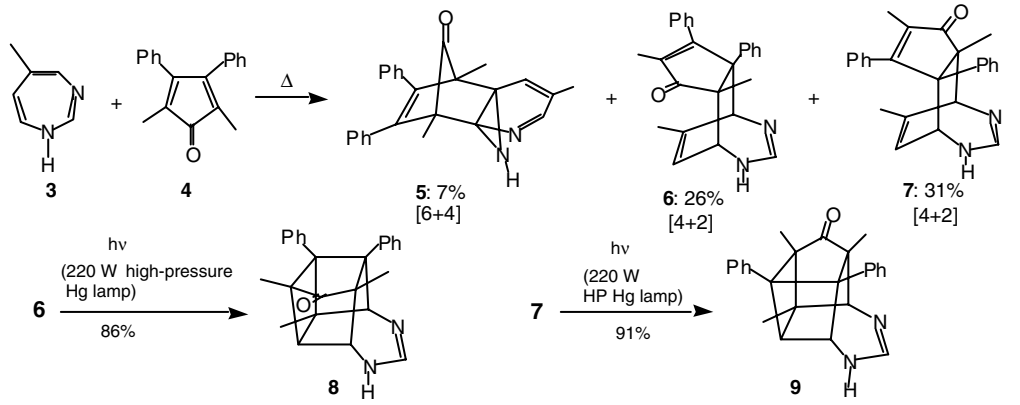

SCHEME 2 Photocycloadditions of the Diels-Alder adducts with cyclopentadienone and 1H-1,3-diazepine.

In this chapter, prototypes of the photochemical reactions useful for the synthesis of cage compounds are outlined first, and then photochemical approaches towards the synthesis of [n]prismanes as representative cage compounds are reviewed.

22.1 Prototypes of the Photochemical Reactions for the Synthesis of Cage Compounds

Prototypes of the photochemical reactions for the synthesis of cage compounds are classified as shown in Table 22.1. The most predominant examples are [2 + 2]-reactions of Diels–Alder adducts with an *endo*-configuration. Intramolecular photochemical [2 + 2]-, [6 +2]- and [6 + 6]-reactions in the rigid polycyclic framework have been increasingly employed for the synthesis of polycyclic cage compounds. Other photochemical reactions, such as [4 + 4]-cycloaddition and related processes, are also important. According to this arrangement, prototypes of the photocycloadditions and their important applications are described.

Photochemical [2 + 2]-Reactions of Diels–Alder Adducts

Diels–Alder Adducts of Cyclopentadiene and Cyclopentadienone with Cyclopentadienone and Cyclopentene-3,5-dione.

The cycloaddition reaction of 1*H*-1,3-diazepine **3** and 2,4-dimethylcyclopentadienone **4** in refluxing xylene resulted in the formation of three adducts: **5** ([6 + 4]), **6** ([4 + 2]), and **7** ([4 + 2]).

Irradiation (220 W high-pressure Hg lamp) of **6** in benzene for 30 min afforded cage compound **8** (86%) via intramolecular [2 + 2]-photocycloaddition. Similarly, the adduct **7** gave the regio-isomeric cage compound **9** (91%).[2]

TABLE 22.1 Prototypes of the Photochemical [2+2]- and Related Reactions for the Synthesis of Cage Compounds

diene	dienophile	Diels-Alder adduct	cyclobutane

1.1. Photochemical [2+2]-reactions of the Diels-Alder adduct.

(1) The Diels-Alder adducts of cyclopentadiene and cyclopentadienone with cyclopentadienone and cyclopentene-3,5-dione.

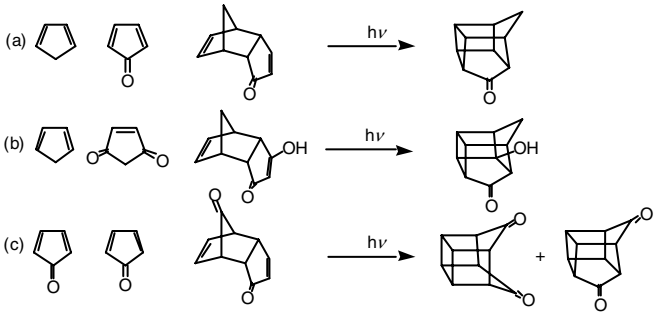

(2) The Diels-Alder adducts of cyclopentadiene and cyclopentadienone with *p*-benzoquinone and 2,4-cyclohexadienone.

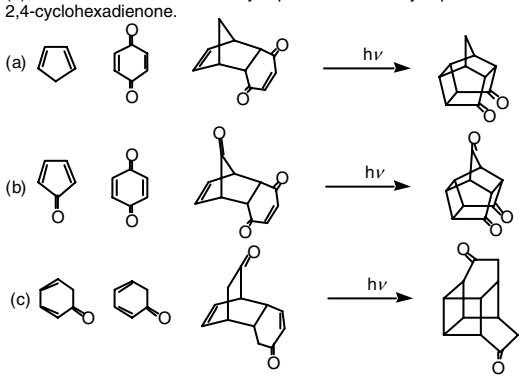

1.2. Photochemical [2+2]-, [6+2]-, and [6+6]-reactions in the rigid polycyclic compounds.

(1) [2+2]-reactions

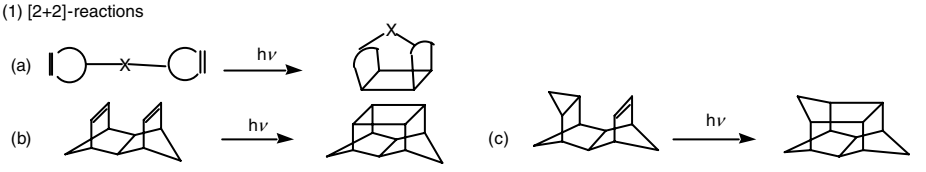

(2) [6+2]-and [6+6]-reactions

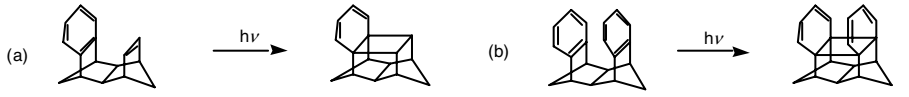

1.3. Photochemical [4+4]- and related reactions.

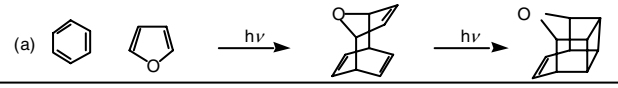

1,3-Bishomocubane acetate **12** was synthesized conveniently by the photocycloaddition of the Diels–Alder adduct **11** of cyclopentadiene with cyclopentene-3,5-dione **10**. Base induced homoketonization of the acetal of **12** led to the thermodynamically favored half-cage skeleton **13**.[3]

The Diels–Alder dimerization of 2-bromo-2,4-cyclopentadienone ethylene acetal **15** gave *endo*-2,7-dibromodicyclopentadiene-1,8-dione 1,8-bis(ethylene acetal) **16** as a minor product (4.5%), along with the major product **17** (91.5%). Adduct **17** is an important synthetic intermediate for the synthesis of cubane. Irradiation of the mono-acetal of the minor product **18** with a high-pressure Hg lamp in CH_2Cl_2

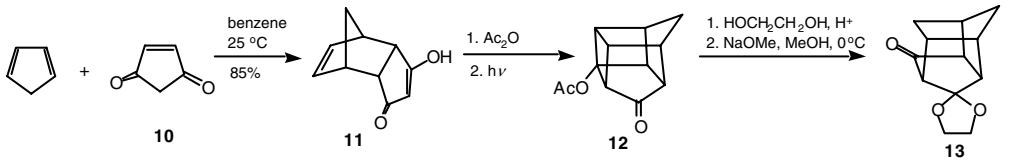

SCHEME 3 Photocycloaddition of the Diels-Alder adduct from cyclopentadiene and cyclopenta-3,5-dione.

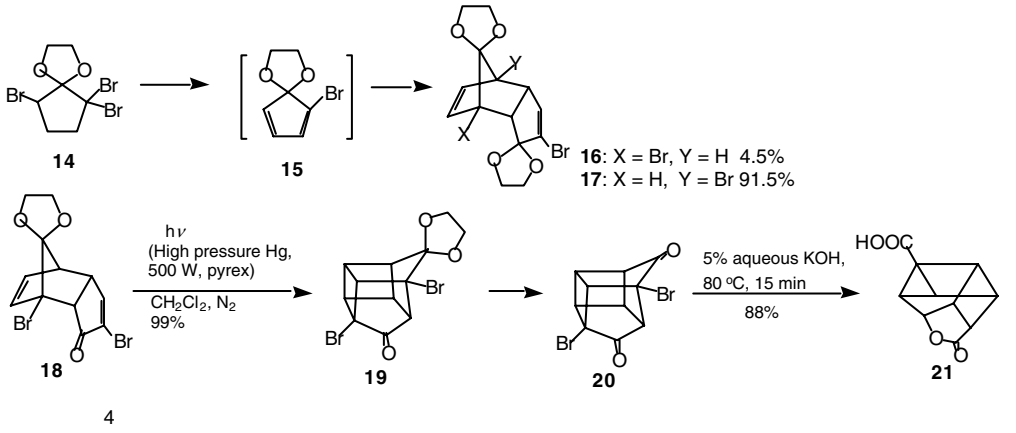

4

SCHEME 4 Photocycloaddition of the Diels-Alder dimer of 2-bromo-2,4-cyclopentadienone ethylene acetal.

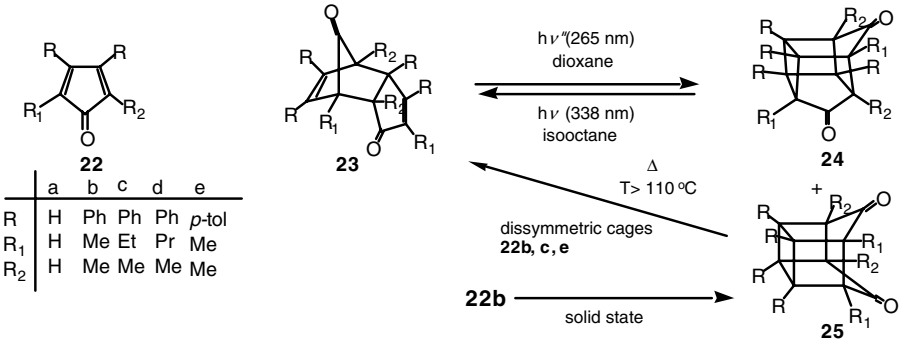

SCHEME 5 Photochemistry of cyclopentadienone dimers.

provided cage compound **19** (99%). Unexpectedly, Favorskii contraction of the diketone **20** in 5% aqueous KOH solution at 80°C gave lactone-carboxylic acid **21** with the pentacyclo[5.3.0.^{2,4}0.^{3,6}0^{5,8}]octane skeleton in place of the expected cubane-dicarboxylic acid (Scheme 4).[4]

The cyclopentadienones **22** are primarily known as building blocks of interesting structures, e.g., the dimers **23,** which are known to exist as reversibly dissociating or nondissociating dimers depending on whether or not the starting monomers bear substituents in both the 2- and the 5-positions; the effect is largely steric. The parent cyclopentadienone **22a** exists as a monomer at –196°C and dimerizes above –80°C to give the *endo*-dimer **23a**.[5] Fuch et al. first isolated the monomers **22b,c,d** bearing aryl substituents in the 3 and 4 positions and alkyl substituents in the 2 and 3 positions by sublimation *in vacuo* of the corresponding dimers **23** (Scheme 5).[6]

Direct irradiation ($\lambda > 290$ nm) of **23b** in dioxane for 94 h provided the dissymmetric cage **24b** (1%) and the symmetric cage **25b** (48%) at 67% conversion. The amount of **24b** was enhanced (**24b**: **25b** =

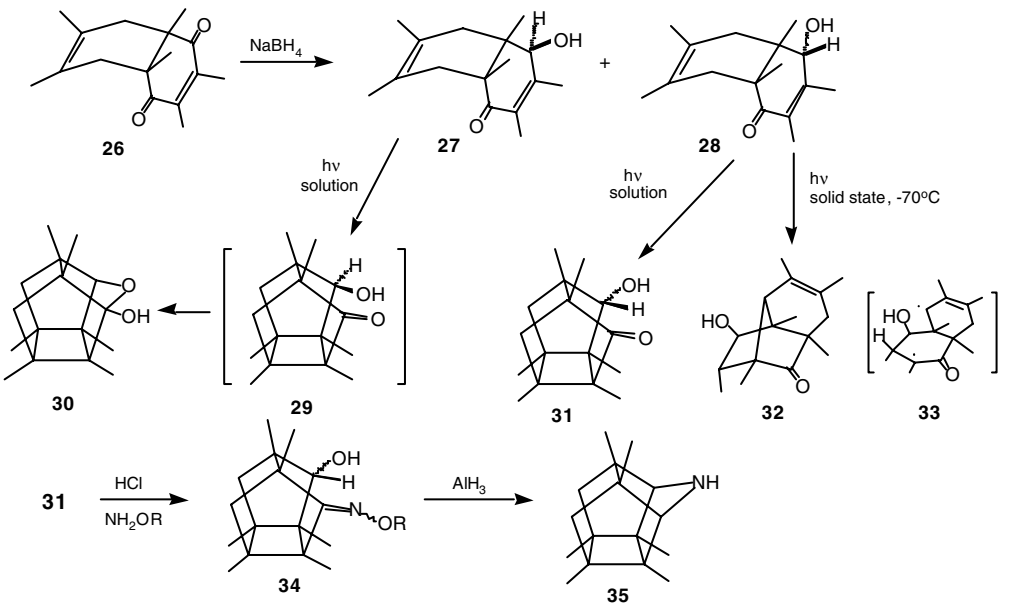

SCHEME 6 Differences in cyclohexenone photochemistry in solution and the solid state.

11:42) when the reaction was discontinued after 48 h of irradiation. Under similar conditions, **23e** gave a mixture of **24e** (22%) and **25e** (21%), whereas **23c** and **23d** did not afford photoproducts. Interestingly, irradiation of crystals of the monomer **22b** into any of its absorption bands resulted in efficient and quantitative cycloaddition to give **25b**.[6] The dissymmetric cages (**24b,c,e**) ring open on irradiation ($\lambda >$ 300 nm) back to the dimer **23**, whereas the symmetric cages **25** do not. While **24** is thermally stable, the symmetric dimer **25** undergoes a thermal reversion to **23**.

Diels–Alder Adducts of Cyclopentadiene and Cyclopentadienone with *p*-Benzoquinone and 2,4-Cyclohexadienone

p-Benzoquinones are potent dienophiles in the Diels–Alder reaction. The strong preference for *endo*-addition, together with the long-wavelength absorption of the enedione chromophore, has made these adducts very suitable for photocycloaddition. Scheffer et al. reported the photocycloaddition of the epimeric hydroxycyclohexenones (**27**, **28**), which were readily obtained from the tetrahydro-1,4-naphthoquinone derivatives **26**. Direct or benzophenone-sensitized irradiation ($\lambda >$ 330 nm) of **27** and **28** in benzene afforded a high yield of the [2 + 2]-cycloaddition products with the tetracyclo[5.3.0.0.^{2,6}0^{4,9}]decane skeleton (**30** and **31**). However, irradiation ($\lambda >$ 330 nm) of crystalline samples of **28** gave **32** via intermediate **33**, while no reaction was observed with the isomer **27**. Scheffer et al. concluded that solid phase photoreactions are crystal lattice–controlled, least motion processes, and the solid state/solution reactivity differences are the results of reaction from different conformational isomers in the two media.[7] The ketol **31** is a useful synthetic intermediate to the synthesis of a variety of cage compounds with bridging nitrogen atoms such as 11-azapentacyclo[6.2.1.0.0.^{2,7}0.^{4,10}0^{5,9}]decane **35**, which has antiviral activity.[8]

Cookson et al. first reported prior to 1965 that photochemical reaction of the Diels–Alder *endo*-adducts of cyclopentadiene or cyclohexa-1,3-diene with *p*-benzoquinone gave cage compounds by formation of a cyclobutane ring from the two double bonds.[9] Irradiation of an ethyl acetate solution of the cyclopentadiene adduct **36** with a medium pressure Hg lamp for 6 h afforded cage **37** (90%). This photoreaction proceeded even in the solid state, and the cage compound **37** was obtained in 80% yield after 80 h irradiation. Similarly, the 1:1 adduct **38** of cyclohexa-1,3-diene and *p*-benzoquinone was converted into cage **39** by irradiating the ethyl acetate solution for 10 h (80%) or the solid state for 90 h (90%). This reaction was successfully applied to the adduct **40** of cyclooctatetraene (COT) and *p*-benzoquinone (92%

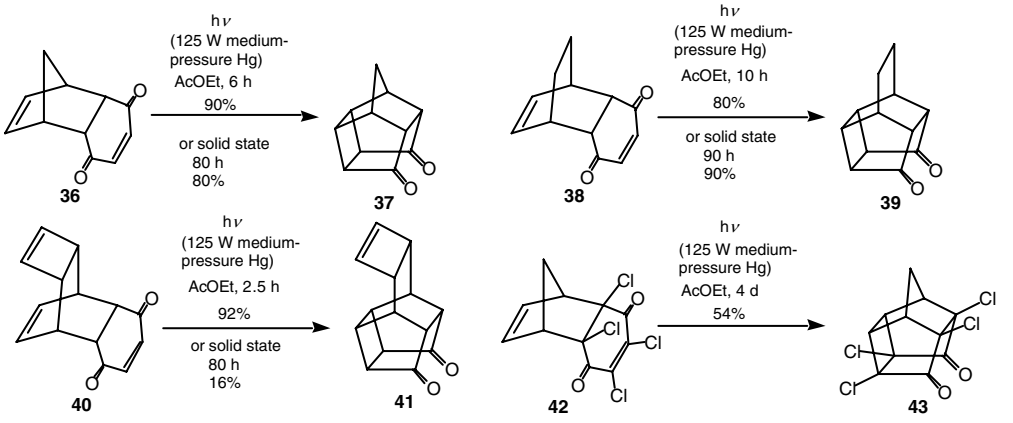

SCHEME 7 Photocycloaddition of cyclodiene-*p*-benzoquinone adducts.

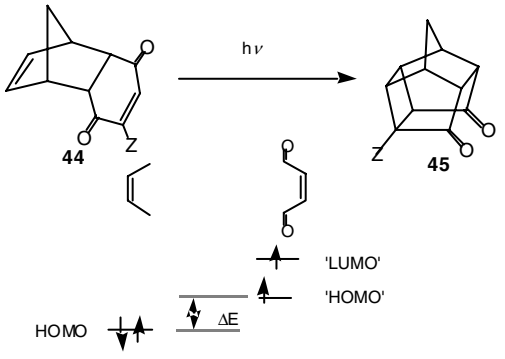

Table 2. Relative quantum yields and energy level differences between the interacting double bonds.

Z		Φ_{rel}	ΔE/eV
44a	OMe	0.71	0.06
44b	*p*-$NO_2C_6H_4S$	0.51	0.32
44c	OPh	0.39	0.42
44d	SMe	0.45	0.43
44e	SPh	0.44	0.48
44f	*p*-ClC_6H_4S	0.35	0.49
44g	SePh	0.06	0.67
44h	*p*-MeC_6H_4S	0.00	0.78
44i	NHPh	0.00	0.96
44j	H	1.00	0.00

SCHEME 8 The importance for cage compound formation of the oxidation potential of the enedionic system in *p*-benzoquinone-cyclopentadiene adducts.

of **41** in ethyl acetate solution or 16% in the solid state) and **42** of cyclopentadiene and chloranil (54% of **43** in ethyl acetate solution). γ–Irradiation (^{60}Co) was used in place of a UV lamp for similar conversions (**36** to **37**, 33%).[10]

Wladislaw et al. examined the reactivity–substituent effect relationship in the photo-cyclization of the adducts **44** of cyclopentadiene with *p*-benzoquinone. Some substituted adducts **44h** and **44i** do not undergo photocyclization. Table 22.2 shows the quantum yield (Φ_{rel}) for photocyclization of the mono-substituted adducts **44a–i**, relative to that of the unsubstituted adduct **44j** for which Φ was assumed to be 1.00. These data show not only that the adducts **44h,i,j** do not photocyclize but also that adduct **44g** photocyclizes inefficiently. It is proposed that the factor that determines the photocyclization efficiency is the difference between the energy levels of the two interacting orbitals (HOMO-′HOMO′) since the cyclization is most probably initiated by a photochemical electron transfer (PET).[11]

The photocyclization of the Diels–Alder *endo*-adducts of cyclic dienes with *p*-benzoquinone has been successfully applied to the construction of polycyclic cages. Nair et al. reported that the photocyclization of the 2,5-bis(bromomethyl) compound **47** gave the unexpected cage compound **49** as a major product along with the anticipated product **48** (Scheme 9).[12] The formation of **49** can be explained through the initial photolytic cleavage of the bromine–allylic carbon bond (**50**) followed by radical reorganization and final bromine radical capture.

Fessner et al. developed a high yield route to the triene **53,** a new unsaturated member of the $(CH)_{14}$ family (Scheme 10 from the COT-*p*-benzoquinone adduct **41** described above [Scheme 7]).[13] This, upon

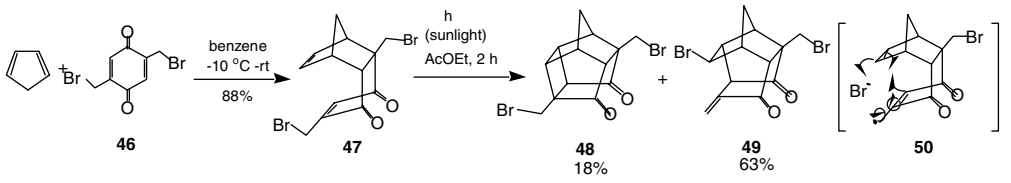

SCHEME 9 Photocycloaddition of a cyclopentadiene-*p*-benzoquinone adduct.

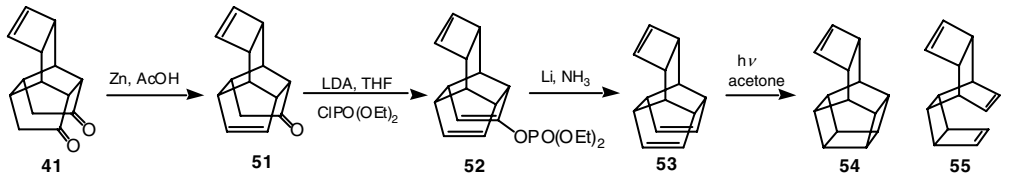

SCHEME 10 Synthesis and interconversion of new $(CH)_{14}$ isomers.

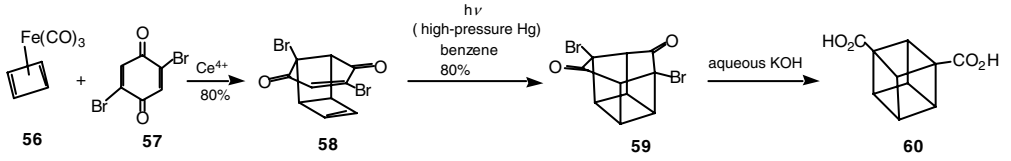

SCHEME 11 The covenient synthesis of the cubane system.

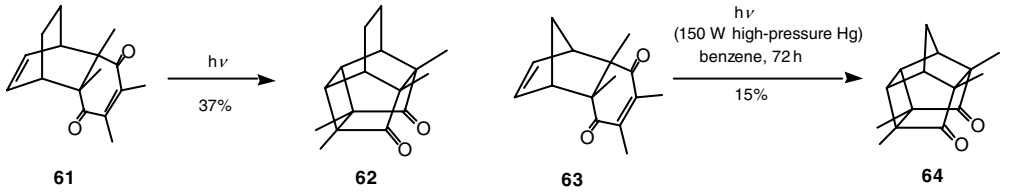

SCHEME 12 Photocycloaddition of the cyclohexa-1,3-diene and cyclopentadiene-duroquinone adducts.

triplet-sensitized photolysis (acetone) of **53** gave the cage **54**, while heating in solution to above 80°C induced a quantitative, regiospecific [3.3]-shift to **55**.

A convenient synthesis of a cubane system, in which the cyclobutadiene transfer reaction plays a key role, was reported by Pettit et al. (Scheme 11).[14] By the oxidative decomposition of cyclobutadiene-iron tricarbonyl **56** with Ce^{4+} ion in the presence of a dienophile, a molecule of cyclobutadiene can be transferred from the iron to the dienophile. Decomposition of **56** in the presence of 2,5-dibromobenzoquinone **57** yielded the Diels–Alder adduct **58** with *endo*-configuration. Irradiation of **58** in benzene with a high-pressure Hg lamp afforded the bishomocubane derivative **59**, which gave cubane-1,3-dicarboxylic acid **60** (80%) by treatment of **59** with aqueous KOH at 100°C.

Schenck et al. studied the photochemical reactions of the adducts of duroquinone with unsaturated compounds such as cyclic dienes, acenaphthylene, coumarin, and styrene (Scheme 12).[15,16] Formation of both oxetanes[17] and cyclobutanes was observed, depending on the substituents present in the quinone. From the theoretical and experimental investigations, *p*-benzoquinone reacts from its triplet $n\pi^*$ excited state to yield exclusively oxetane adducts, while its tetramethyl or tetrachloro derivatives, duroquinone

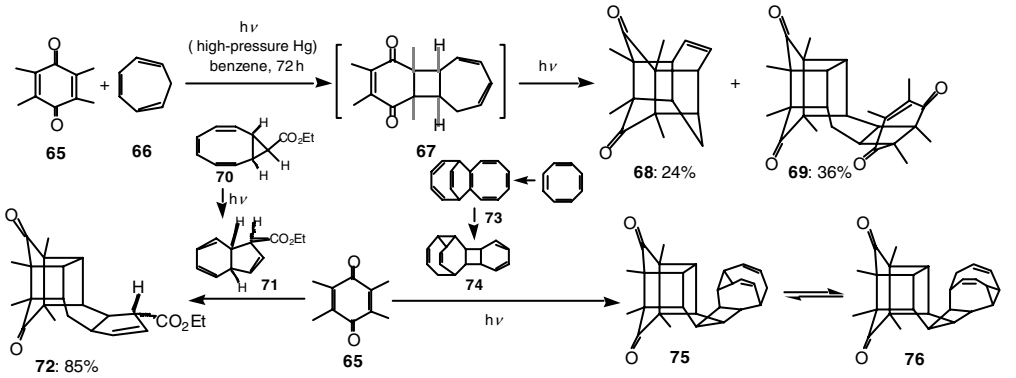

SCHEME 13 Photocycloaddition of duroquinone-cyclic polyene adducts.

or chloranil, whose lowest triplet should be $\pi\pi^*$, afford only cyclobutanes. These photocyclizations are one of the most convenient methods for the synthesis of cage compounds. For example, Ogino et al. reported the photoreaction of duroquinone with cyclic trienes.[18]

On irradiation of a benzene solution of duroquinone **65** and cyclohepta-1,3,5-triene **66** (**65**:**66** = 1:2), 1:1 adduct **68** (24%) and 2:1 adduct **69** (36%) were formed via the [2 + 2]-photoadduct **67** as the intermediate (Scheme 13).

Although only the formation of the dimer of tropone and the recovery of duroquinone were observed in the photoreaction of duroquinone and tropone, the photoreaction of ethyl bicyclo[6.1.0]nona-2,4,6-triene-9-carboxylate **70** with duroquinone afforded the 1:1 adduct **72** (85%). When a solution of duroquinone and COT in benzene was irradiated under similar conditions, a single product **75** was obtained in low yield (3–5%). COT is known to thermally dimerize to afford **73** and/or **74**, and these dimers should be reactive compounds for the photoaddition with duroquinone. In fact, duroquinone reacted with **74** to afford photoproduct **75** under similar conditions (63%). No reaction was detected with **73**. A Cope rearrangement of the dihydrobullvalene moiety interconverts **75** and **76**.

p-Benzoquinone behaves only as a weak dienophile in the Diels–Alder reaction and is rather inert to homodienes, conjugated medium-ring polyenes such as norbornadiene, cycloheptatriene, and tropone even under drastic conditions. Kanematsu et al. developed *p*-benzoquinone-2,3-dicarboxylic anhydride **77a** and *N*-phenylimide **77b** as powerful electron-withdrawing dienophiles for the cycloadditions. The reactions with 6,6-dimethylfulvene and cycloheptatriene gave the corresponding 1:1 adducts (**80** or **78**) with *endo*-configurations in quantitative yields.[19]

Irradiations of the adducts **80** and **78** in acetone solution (100 W high-pressure Hg lamp, Pyrex filter) afforded the cage compounds **81** and **79,** respectively, in quantitative yields. Tropone also reacted with **77b** smoothly to give adduct **82**, which was converted into cage compound **83** on irradiation. Kanematsu et al. also developed the site-selective Diels–Alder reactions of 1,4,5,8-naphthoquinone **84** with anthracene; the reaction of **84** with anthracene exclusively afforded the adduct **85** attached to the internal double bond.[20] Irradiation of the adduct **86** of **85** with cyclopentadiene in chloroform with a high-pressure Hg lamp (400 W) through a Pyrex filter resulted in the smooth formation of a cage compound **87**. By using this methodology, Kanematsu et al. also prepared caged crown ethers.[21]

2,5-Dimethyl-3,4-diphenylcyclopenta-2,4-dienone **88a** and related 1,4-dimethyl-2,diphenylcyclopenta-1,3-diene **88b** readily formed adducts **89a** and **89b** on reaction with *p*-benzoquinone in refluxing chloroform. Irradiation of the adduct **89a** in benzene with a high-pressure Hg lamp (400 W) through a Pyrex filter afforded cage compound **90a** as a major product along with oxetane **91** (21%), while solid state irradiation with sunlight gave **90a** as single product (Scheme 15).[22] The cyclopentadiene **88b** was far less reactive than the dienone **88a** toward *p*-benzoquinone, the reaction requiring heating under reflux in benzene to yield the single adduct **89b**. The cage compound **90b** was formed in quantitative yield by high-pressure Hg lamp–irradiation of **89b** both in the solid state and in benzene solution. The oxetane

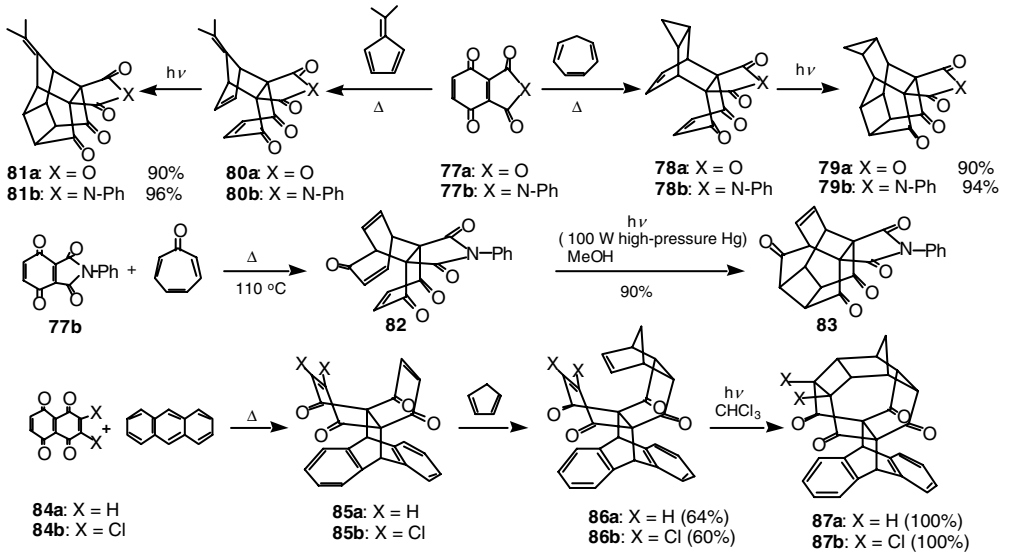

SCHEME 14 Photocycloaddition of highly reactive *p*-benzoquinone-tropone or cycloheptadiene adducts.

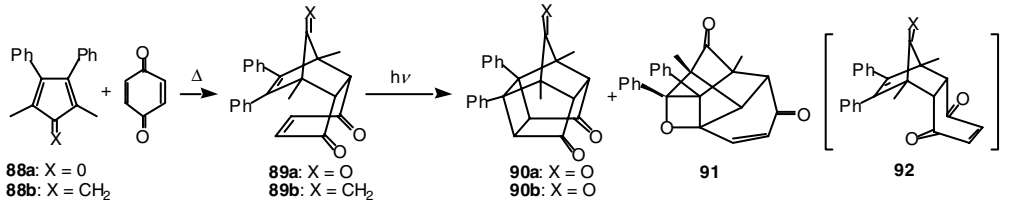

SCHEME 15 An unusual oxetane formed by intramolecular photocyclization within an enedione.

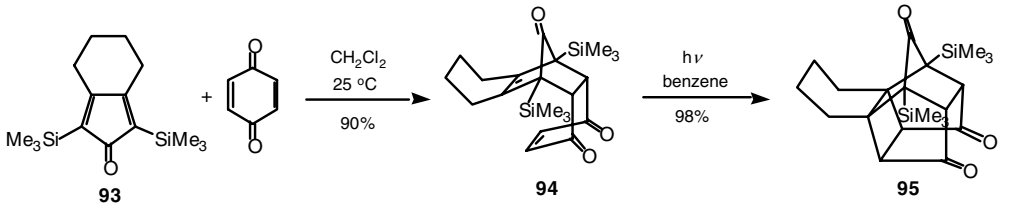

SCHEME 16 Cycloadditions of annulated 2,5-bis(trimethylsilyl)cyclopentadienones.

formation may be explained by the photochemical [2 + 2]-reaction between the CC and CO double bonds within a suitable conformation **92.**

The use of annulated 2,5-bis(trimethylsilyl)cyclopentadienone **93** in this reaction gave the hexacyclic cage compound **95** in high yield via consecutive [4 + 2]- and photochemical [2 + 2]-cycloaddition with *p*-benzoquinone (Scheme 16).[23]

Becker et al.[24] and Yonemitsu and co-workers[25] independently found that dimerization of 2,4-cyclohexadienone **96** gave the adduct **97**, which upon photoirradiation ($\lambda > 300$ nm) in MeOH (91%) or ethyl acetate (64%) yielded cage **98** (Scheme 17).

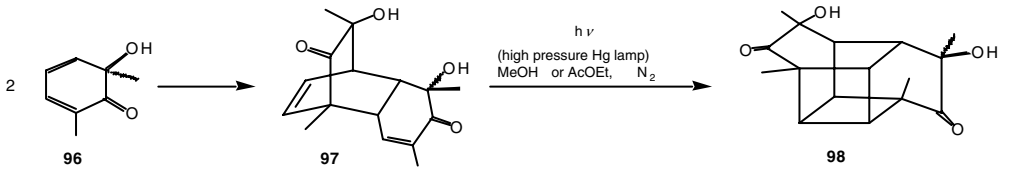

SCHEME 17 Photochemical intramolecular cycloaddition of 2,4-cyclohexadienone Diels-Alder dimers.

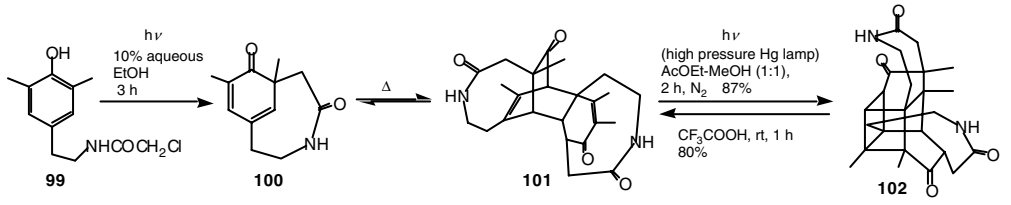

SCHEME 18 The photocyclization of a pharmacodynamic amine.

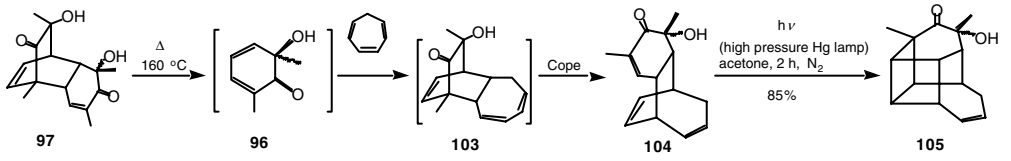

SCHEME 19 A novel periselective cycloaddition of cycloheptatriene with cyclohexa-2,4-dienones.

Yonemitsu et al. found that irradiation of the *N*-chloroacetyl derivative of dimethyltyramine **99** gave the dimeric cage compound **102** (Scheme 18). The presence of cyclohexa-2,4-dienone **100** as a transient species and its thermal dimerisation to the dimer **101** were proven by flash photolysis and also by trapping the intermediate with *N*-ethylmaleimide by a Diels–Alder addition. On treatment with trifluoroacetic acid, the cage compound **102** easily reverted to **101**.[26]

The highly periselective cycloaddition reaction of cycloheptatriene and cyclohexa-2,4-dienones to yield *endo*-tricyclic systems followed by their photocyclization to cage compounds have been reported.[27] The cyclohexa-2,4-dienones **96** were generated by pyrolysis (160°C) of the dimer **97**. Subsequent trapping with cycloheptatriene gave adduct **104** with *endo*-configuration as the exclusive product. The formation of the adduct **104** was ascribed to Cope rearrangement of the initially formed [4 + 2]-adduct **103**. Acetone-sensitized [2 + 2]-photocycloaddition of **104** gave the cage **105**.

22.2 Photochemical [2 + 2]-, [6 + 2]-, and [6 + 6]-Reactions in Rigid Polycyclic Compounds

[2 + 2]-Reactions

The [2 + 2]-photocycloaddition of activated alkenes is the most useful route to cyclobutane derivatives, but the main impediment to the use of photoannelations in synthesis remains the generally poor regio- and stereochemical control. Some simple approaches to a *cis,cis,cis*-tetrasubstituted cyclobutane backbone have been reported. Although the photochemical dimerization of dibenzo[a,d]cycloheptane-5-one **109** yielded *trans*-cyclobutane dimer **110**[28], *cis*-cyclobutane dimer **108** can be prepared through a novel heterocyclic ring cage system **107** (Scheme 20).[29] Irradiation of **106a** in benzene with a high-pressure Hg

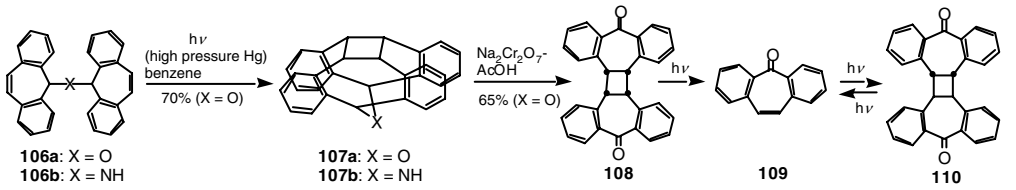

SCHEME 20 A new heterocyclic cage ring system; the preparation of the *cis*-cyclobutane dimer of benzo[a,d]cyclohepten-5-one.

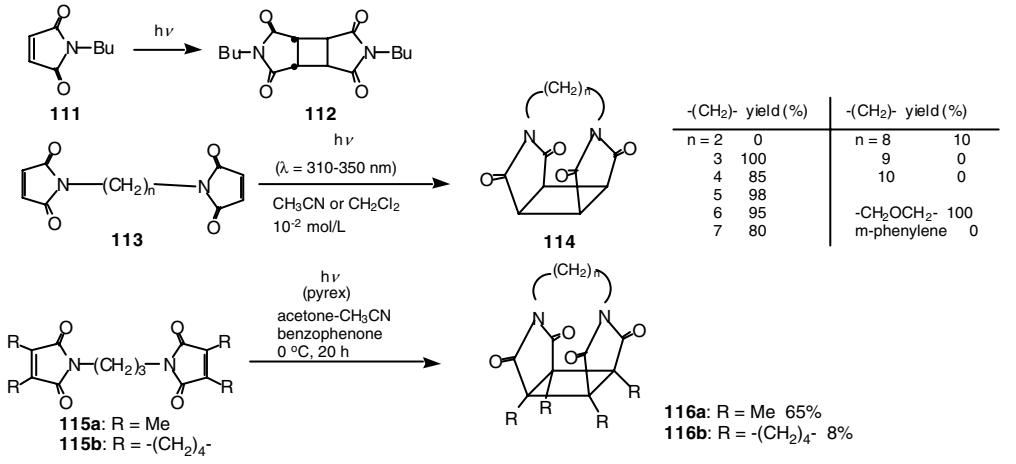

SCHEME 21 Intramolecular photocycloaddition of *N,N′*-alkylenedimaleimides.

lamp through a Pyrex filter gave the new cyclobutane cage **107a** (70%). Similarly, irradiation of **106b** (X = NH) in benzene gave *cis*-**107b**. Oxidation of the cage ether **107a** afforded *cis*-diketone **108**. The *cis*- and *trans*-diketones **108** and **110** reverted to **109** on photoirradiation ($\lambda > 200$ nm).

The biacetyl-sensitized photoreaction of *N*-butylmaleimide **111** in methylene chloride afforded only the *trans*-isomer **112** in which the two rings lie *anti* to each other (Scheme 21). Upon irradiation of dimaleimide **113**, an intramolecular cycloaddition to tetracyclic compound **114** occurs.[30] The reactions were carried out in solution in acetonitrile or methylene chloride at a concentration of 10^{-2} mol/l using 310 or 350 nm light. Almost quantitative intramolecular reactions occur for dimaleimides with three to six methylene units. Increasing the chain length from seven to eight methylene units causes a marked drop in the yield of products. With chain lengths longer than eight methylene units, no reaction is observed. Sensitized irradiation of dimaleimide **115** affords the cage diimide **116**.[31]

Photochemical [2 + 2]-reactions of two olefinic double bonds in rigid polycyclic compounds have been widely examined. The photocycloaddition of the isodrin-type compound **117** to give the cage compound **118** was studied in detail by Jones et al.[32] Both direct irradiation and triplet-sensitized reaction of **117** gave **118** exclusively (Scheme 22). In addition, on irradiation in polar solvents in the presence of an electron acceptor sensitizer, **117** gave **118** with quantum yield greater than unity. It is suggested that the formation of a polar exciplex between the sensitizer (e.g., 2-cyanonaphthalene; electron affinity EA = 0.68 eV) and **117** is the first step of this reaction, and the resulting exciplex finally gives **118** by excitation energy transfer from naphthalene to the diene.

Chou et al. successfully applied this [2 + 2]-photocycloaddition to the synthesis of hexacyclotetradecadiene **125** (30% overall yield from **119**).[33] On irradiation (450 W medium-pressure Hg lamp, 130 h) of an acetone solution of the diene **120**, the reaction proceeds slowly but efficiently to give the photoproduct **121**. Decarboxylation of **121** and subsequent ring expansion of **123** afforded the desired novel cage

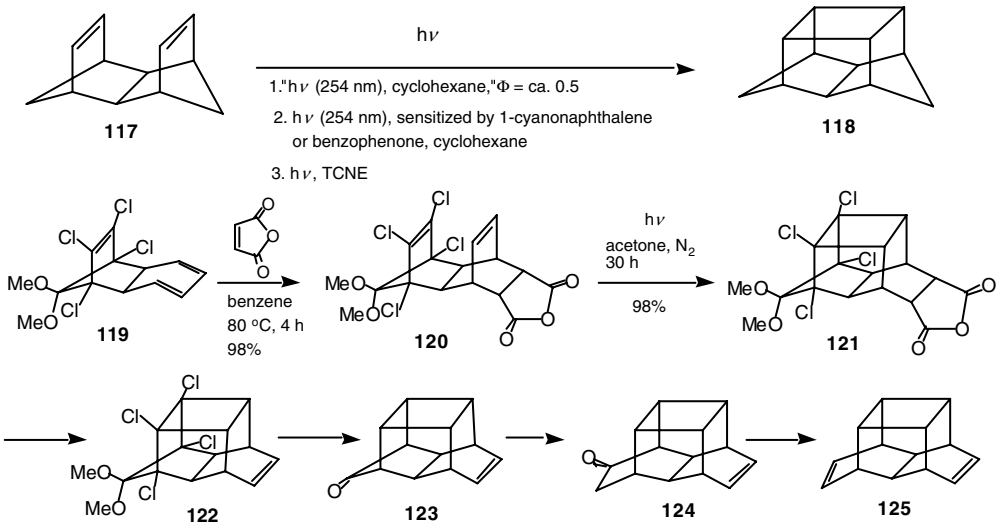

SCHEME 22 Photochemical enelene cycloaddition reactions: The synthesis of hexacyclo[6.5.1.$0^{2,7}$, $0^{3,11}$, $0^{4,9}$, $0^{10,14}$]tetradeca-5,12-dienes.

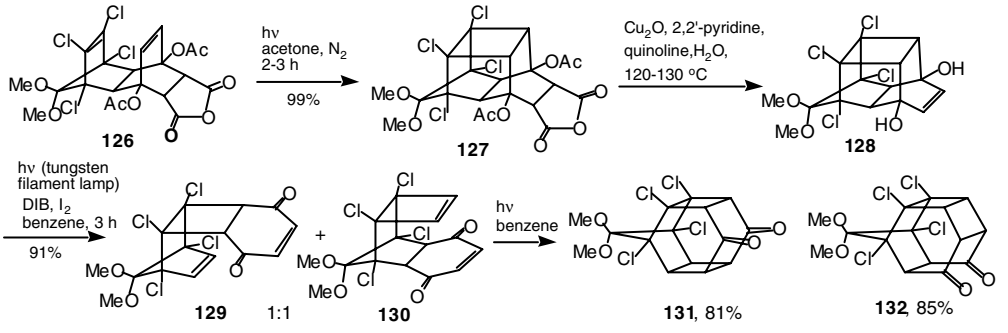

SCHEME 23 A fragmentation-photocyclization approach to the homosecoprismane skeleton.

compound **125**. Similar [2 + 2]-photocycloaddition of **126** and decarboxylation of the photoproduct **127** give the diol **128**, which is converted to tetracyclic dienes **129** and **130** by oxidative fragmentation. [2 + 2]-Photoreaction of the mixture of **129** and **130** affords the hexacyclic cage compounds **131** and **132** with homosecohexaprismane skeleton (Chou et al., Scheme 23).[34]

Mehta et al. also employed this type of [2 + 2]-photocycloaddition for the synthesis of novel, caged, nona-cyclic $C_{20}H_{24}$-hydrocarbon of D_{2d} symmetry, golcondane **138**, named after the old name for Hyderabad.[35] On irradiation of **134** with a 450 W high-pressure Hg lamp through a Pyrex filter, smooth intramolecular [2 + 2]-ring closure takes place to give the nona-cyclic annulated bishomocubane dione **136**. Finally acetone-sensitized photocyclization of **137** affords golcondane **138**.

Behr et al. studied the photoreaction of tetracyclic trienedione **139**,[36] which was prepared by the thermal addition of *o*-benzoquinone to barrelene (15%). Irradiation of **139** in deoxygenated methylcyclohexane (MCH) or chloroform with benzophenone at 366 nm afforded the cage compound **140** (25%). The first step of this cycloaddition may be the formation of a biradical by a pathway similar to that of the oxa-di-π-methane rearrangement from the lowest $^3(n\,\pi^*)$ state (Scheme 25). Since the excitation energy of the α-dicarbonyl unit in **139** [EA (biacetyl) = 0.72 eV] is similar to that of 2-cyanonaphthalene, intramolecular excitation energy transfer from dione to diene similar to that from 2-cyanonaphthalene

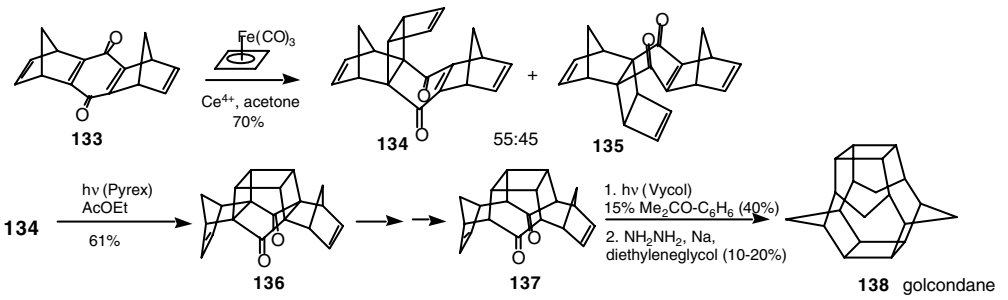

SCHEME 24 Golcondane: novel, caged, nonacyclic $C_{20}H_{24}$-hydrocarbon of D_2d symmetry.

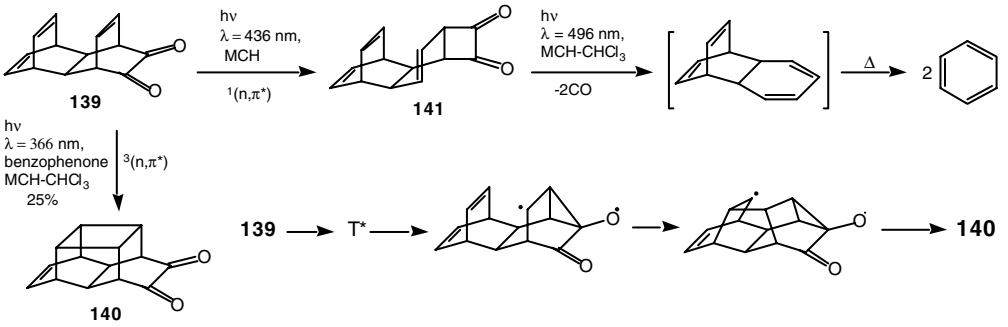

SCHEME 25 Photoreaction of trienedione.

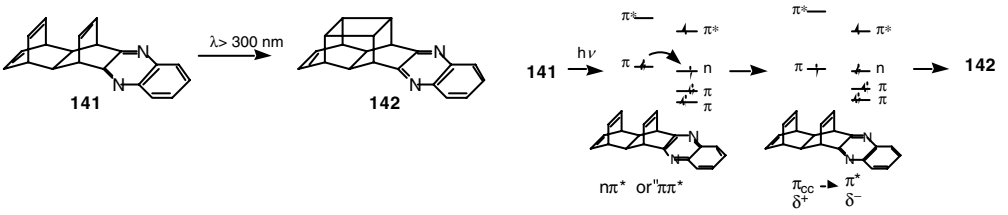

SCHEME 26 Photoreaction of multichromophoric polycyclic compound in which the dicar bonyl moiety of **139** is replaced by the quinoxaline.

to **117** might occur. Irradiation of **139** at 436 nm ($n\pi^*$ excitation) in MCH gave the rearrangement product **141**. Subsequent irradiation of **141** at 496 nm or with broad spectrum light in MCH at room temperature resulted in bisdecarbonylation and formation of benzene. The intramolecular [2 + 2]-cycloaddition did not occur within the excited $^1(n\pi^*)$ state of **139** since intramolecular energy transfer might be possible; the process does not seem to able to compete with the faster 1,3-acyl shift and rearrangement of **139** to **141**.

In consideration of the above results, Behr et al. examined the photoreaction of the multichromophoric compound **141** in which the dicarbonyl moiety of **139** was replaced by the quinoxaline (Scheme 26).[37] The irradiation of **141** with $\lambda > 300$ nm, which brings about $n\pi^*$ or $\pi\pi^*$excitation localized in the quinoxaline chromophore, afforded the cage compound **142** as the sole product in high yield.

It is suggested that intramolecular [2 + 2]-cycloaddition of **141** is sensitized by the quinoxaline chromophore, since the π_{cc},π_{cc}^* isodrin transition of **141** is presumably not excited by $\lambda > 300$ nm by analogy with the corresponding transition of **117**. Behr et al. proposed two reaction mechanisms. The

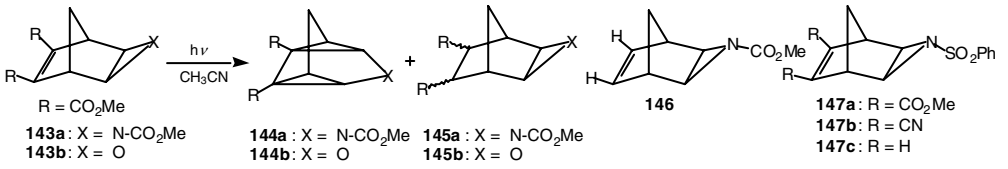

SCHEME 27 Intramolecular photocycloaddition between an alkene double bond and a three-membered ring.

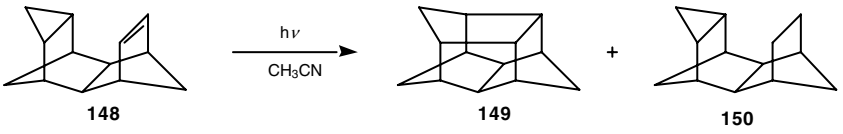

SCHEME 28 Photocycloaddition between an ethylene moiety and a three-membered ring.

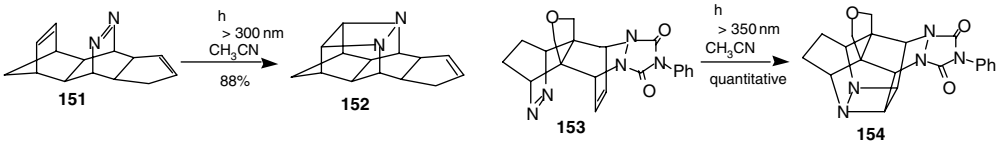

SCHEME 29 Photocycloaddition of C=C and N=N double bonds.

intramolecular cycloaddition is induced by the energy transfer from $n\pi^*$ or $\pi\pi^*$-excited quinoxaline to isodrin. The other possible mechanism would involve singlet–triplet intersystem crossing followed by an aza-di-π-methane rearrangement similar to the oxo-di-π-methane rearrangement of **139** to **140**.

Intramolecular $[2\pi + 2\sigma]$-photocycloaddition between an ethylene unit and a three-membered ring for the construction of a cyclopentane ring is a valuable synthetic step. Klaus and Prinzbach reported that the direct irradiation of **143** resulted in the formation of the cage compounds **144** (Scheme 27).[38] Irradiation of the aziridine derivative **143a** with Vycor-filtered light in oxygen-free acetonitrile at –20°C afforded the cage compound **144a** (50–55%) along with a small amount of hydrogenated product **145a** and polymeric material. Under similar irradiation conditions, the oxirane **143b** afforded cage compound **144b** as a major product (16–20%) along with hydrogenated analogue of **145b**. No cage compound such as **144** was formed in ether, cyclohexane, or acetone. Since the unsubstituted **146** does not undergo $[2\pi + 2\sigma]$-cycloaddition, it was suggested that this reaction was initiated by excitation of the maleic acid ester chromophore of **143**. Analogous results were reported by Umano et al. from the photoreaction of **147**.[39] Compounds **147a** and **147b** gave the corresponding cage compounds in moderate yields, while unsubstituted **147c** afforded no cage product.

Prinzbach et al. reported the formation of a cyclopentane ring via photochemical alkene–cyclopropane cycloaddition (Scheme 28). Direct irradiation of **148** in acetonitrile in a quartz vessel resulted in the formation of the cage product **149** (65%) along with the hydrogenated product **150** and polymeric material.[40] In the photoreaction of rigid polycyclic compounds, a CC double bond can be replaced by a NN double bond, and this change constitutes a remarkable extension of the intramolecular photocycloaddition system. Photocycloaddition between parallel CC and NN double bonds in a rigid polycyclic framework gives the corresponding cage compounds. For example, irradiation of **151** in acetonitrile brings about ring closure to give **152** in a [2 + 2]-process (Scheme 29).[41] Because of its rigid framework, this reaction proceeds without elimination of nitrogen. In a similar way, propellane **153** gave **154** quantitatively.[42]

Similar to the CC double bonds mentioned above, the cycloaddition reactions between NN double bonds and three-membered rings takes place and gives the corresponding cage compounds. On irradiation of **155** at 254 nm ($\pi\pi^*$ excitation) in methanol, the cycloaddition between three-membered rings

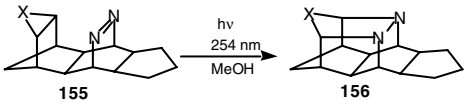

155 **156**

substrate	irradiation time (min)	product (yield %)	
155a<X = CH_2	120	**156a**<X = CH_2	63%+
155b<X = NH	120	**156b**<X = NH	80%+
155c<X = O	360	**156c**<X = O	30%+[a)]

a) in addition to **156c** , transannular product was obtained in 35%.

SCHEME 30 Photocycloaddition between a three-membered ring and an azo group.

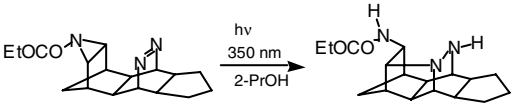

157 **158**

solvent	irradiation time (min)	product (%)
MeOH	600	**158** (75%)
2-PrOH	180	**158** (<10%) + **157** (>90%)
2-PrOH:acetone (1:1)	270	**158** (90%)
2-PrOH + piperylene(1.7 mmol)	180	**157** (100%)

SCHEME 31 Photoreaction between an aziridine and an azo group.

(cyclopropane, aziridine, and oxirane) and the azo groups proceeded and yielded the corresponding cage compounds **156** in a [σ2s + π2s]-process (Scheme 30).[43] These cycloadditions proceeded without elimination of nitrogen. The reactivity order of the three-membered rings toward photocycloaddition at 254 nm, i.e., aziridine > cyclopropane >> oxirane, corresponds well with the energy order of the e_s orbitals measured from their photoelectron spectra, –8.50, –9.15, and –9.40 eV. This order is also reflected in the solvent dependence of the photoreaction. Cycloaddition of **157** (X = N–CO_2Et) occurred smoothly in solvents less polar than acetonitrile and even occurred in hexane, whereas the cycloaddition of **155a** or **155c** did not take place under the same conditions. On irradiation at 350 nm ($n\pi^*$ excitation), these cyclizations did not occur. Irradiation at 350 nm in methanol gave the transannular product **158** instead of cage compounds. The slow transformation of **157** into **158** in 2-propanol (a better proton donor than methanol) by irradiation at 350 nm was accelerated dramatically by the addition of acetone (triplet sensitizer) or suppressed by the addition of piperylene (triplet quencher). These observations clearly show that the transannular reaction occurs via the $^3(n\pi^*)$ state of the azo group and not by the $^1(n,\pi^*)$ state. In contrast, on irradiation at $\lambda > 300$ nm, [2 + 2]-cycloaddition of an olefin to azo bridges occurred smoothly. In aprotic solvents, this type of reaction does not occur on $n\pi^*$ excitation.

[6 + 2]- and [6 + 6]-Cycloaddition Reactions

Irradiation of a cyclohexane solution of the adduct **159**, formed by addition of cyclopentadiene to 1,4-naphthoquinone, led to a photostationary 1:3 mixture of **159** and **160** (Scheme 32). This reaction was sensitized by xanthone, benzophenone, and di-4-pyridyl ketone.[44] Direct irradiation of the adduct **159** in benzene for 1 h afforded **160** (80%) along with recovered **159** (15%).[45]

Prinzbach et al. reported that direct irradiation with monochromatic 254 nm light from a low-pressure Hg lamp or sensitized excitation (acetone or xanthone) produced ca. 2:1, 4:1, and 1:3 photoequilibrium mixtures of **161** and **163**, respectively. The cage compound **163** was stable up to 250°C in benzene solution (Scheme 33).[46] The [6 + 2]-cycloaddition between the *o*-phenylene bridge and a NN double bond also takes place. Irradiation of **164** at $\lambda > 300$ nm afforded cycloadduct **165** quantitatively. In contrast,

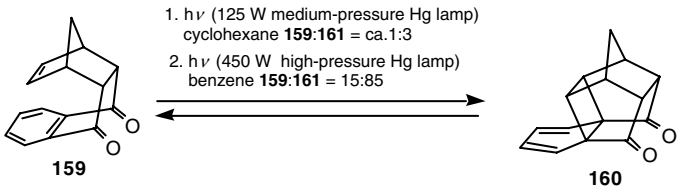

SCHEME 32 Photochemical [6+2]-cycloaddition.

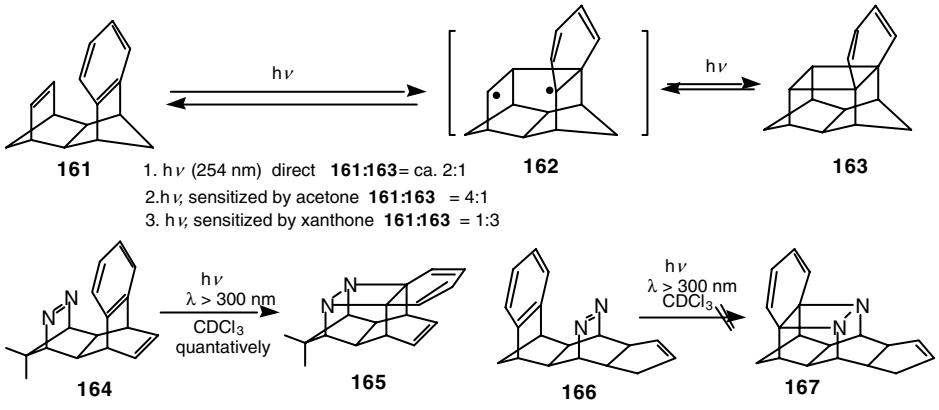

SCHEME 33 Photochemical [6+2]-cycloadditions.

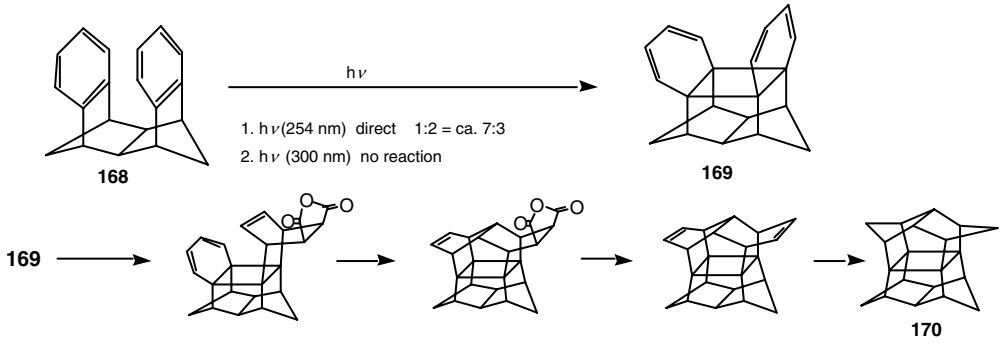

SCHEME 34 Photochemical [6+6]-cycloadditions.

compound **166**, in which the chromophores are interchanged, failed to cyclize under the same irradiation conditions. The difference in photochemical behavior of **164** and **166** is due to the different interaction between parallel π systems observable in the UV spectrum; the interaction of the NN double bond and the *o*-phenylene bridge is stronger in **164** than in **166**.

The dibenzo compound **168** was inert toward acetone-sensitized excitation, probably because the triplet energy for the isolated chromophoric xylene units is too high, whereas irradiation of **168** with monochromatic 254 nm light slowly gave a ca. 7:3 equilibrium mixture of **168** and the [6 + 6]-photoaddition product **169**.[47] The key step for the successful synthesis of "Pagodane," the $C_{20}H_{20}$ polyquinane, is this type of benzo/benzo [6 + 6]-photocycloaddition and a domino Diels–Alder reaction.

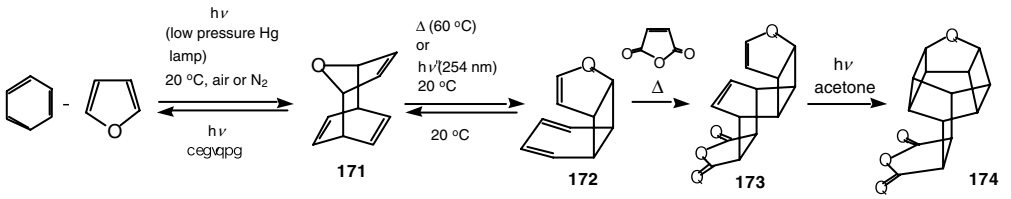

SCHEME 35 Photocycloaddition of furan to benzene.

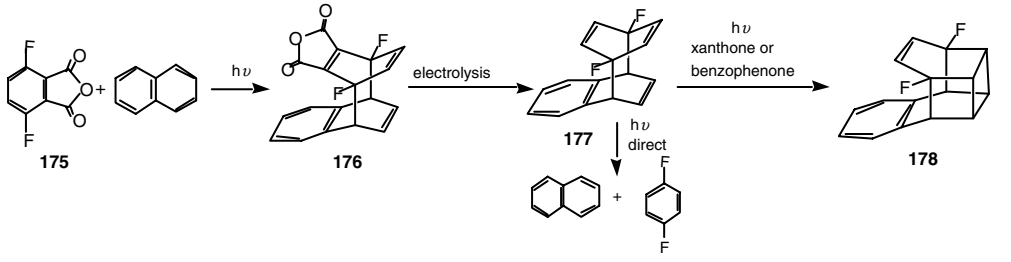

SCHEME 36 Synthesis and adiabatic photochemistry of a 1,4-difluorobenzene-naphthalene biplanemer.

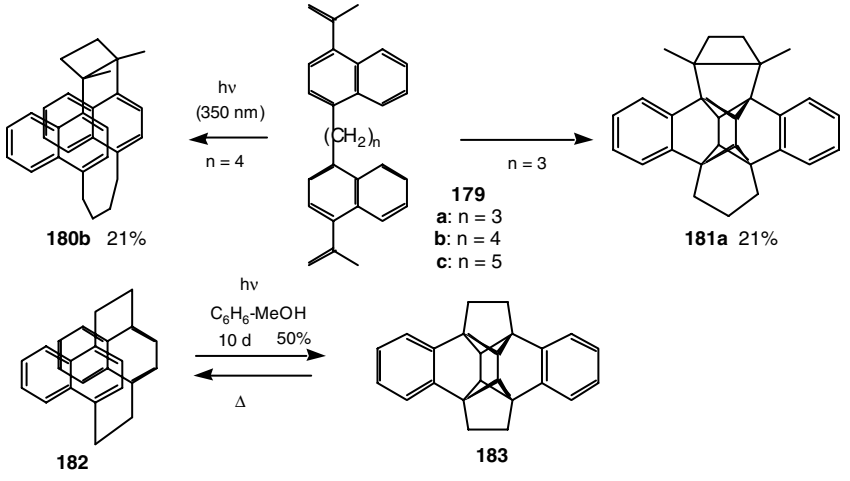

SCHEME 37 Photocycloaddition of naphthalenophanes.

Photochemical [4+4]-Cycloadditions and Related Reactions

Irradiation (low-pressure Hg lamp) of an equimolar mixture of benzene and furan gives fulvene together with a mixture of five 1:1 photoadducts and some material of higher molecular weight. The major component has the 2,5–1′,4′-structure **171**, which rearranged very cleanly both photochemically and thermally to the isomeric adduct **172**. This compound proved to be identical to the second most abundant component of the original mixture of photoproducts. Thermal Cope rearrangement of **171** to **172** occurred readily at 60°C. Acetone-sensitized photochemical cyclization of the maleic anhydride adduct **173** gave the cage compound **174**.[48]

Kimura et al. prepared the naphthalene-1,4-difluorobenzene adduct **177** by a [4 + 4]-photocyclization followed by oxidative decarboxylation of **176**. They named this type of [4 + 4]-adduct "biplanemer."[49] The direct irradiation of **177** gave 1,4-difluorobenzene and excited naphthalene in both singlet and triplet

states at 77 K in EPA. In the triplet-sensitized reaction, **177** underwent an intramolecular [2 + 2]-reaction to give the cage compound **178** instead of forming triplet naphthalene.

Through their studies on the synthesis of naphthalenophanes via [2 + 2]-photocycloaddition,[50] Nishimura et al. found that the irradiation of diolefin **179a** gave cage compound **181a**,[51] structurally similar to dibenzoquinene **183**, which was obtained from *anti*-[2.2](1,4)naphthalenophane **182** by photoirradiation.[52] Interestingly, the diolefin **179b,c** having longer tethers showed different photochemical behaviors from those of **179a**. Under the same irradiation condition, **179b** gave the expected [2 +2]-photocycloadduct (naphthalenophane) **180b**. On the other hand, **179c** gave no photoproduct. It is assumed that **181a** is formed through twofold [π4s + π2s]-photocycloaddition during the [π2s + π2s]-photocycloaddition of 2-propenyl groups, although there is no conclusive evidence on whether this reaction occurs by a concerted or a stepwise mechanism. This reaction is an uncommon examples of the photochemical reactions of naphthalenophanes, which tend to give a [π4s + π4s]-cycloadduct by irradiation. The [4 + 4]-photochemical cycloaddition and related reactions of cyclophanes have been the subject of a review by Misumi.[53]

References

1. Ciamician, G. and Silber, P. *Ber. Dtsch. Chem. Ges.,* 41, 1928, 1908.
2. Kurita, J., Kojima, H., and Tsuchiya, T., Cycloaddition reaction of 1H-1,3-diazepine with 2,4-dimethyl-3,4-diphenylcyclopentadienone, *Chem. Pharm. Bull.,* 34, 4866, 1986.
3. de Valk, W.C.G.M., Klunder, A.J.H., and Zwanenburg, B., Directive effect of β-functionalization of the regiochemistry of the base induced homoketalization of bridgehead substituted 1,3-bishomocubane acetates, *Tetrahedron Lett.,* **21**, 971, 1980.
4. Nigo, T., Hasegawa, T., Kuwatani, Y., and Ueda, I., Base-promoted rearrangement of 1,5-dibromopentacyclo[5.3.0.^{2,5}0.^{3,9}0^{4,8}]decane-6,10-dione: easy entry to a novel cage system, 10-oxa-9-oxopentacyclo[5.3.02,4.03,6.05,8]decane, *Bull. Chem. Soc. Jpn.,* 66, 2068, 1993.
5. Chapman, O.L. and McIntosh, C.L., Cyclopentadienone, *J. Chem. Soc., Chem. Commun.,* 770, 1971.
6. (a) Fuchs, B. and Pasternak, M., Isolation, spectral properties and photochemistry of unstable substituted cyclopentadienones, *J. Chem. Soc., Chem. Commun.,* 537, 1977; (b) Fuchs, B., Pasternak, M., and Pazhenchevsky, B., Irradiation induced transformations of reversibly dissociating cyclopentadienone-dimers and their monomers, *Tetrahedron,* 36, 3443, 1980; (c) Fuchs, B. and Pasternak, M., Dimers of 3,4-(o,o′-biphenylene)cyclopentadienones: thermal and photochemical behaviour, *Tetrahedron,* 37, 2501, 1981.
7. (a) Appel, W.K., Greenhough, T.J., Scheffer, J.R., Trotter, J., and Walsh L., Crystal lattice control of unimolecular photorearrangements. Differences in cyclohexenone photochemistry in solution and the solid state, *J. Am. Chem. Soc.,* 102, 1158, 1980; (b) Appel, W.K., Greenhough, T.J., Scheffer, J.R., Trotter, J., and Walsch L., Crystal lattice control of unimolecular photorearrangements. Differences in cyclohexenone photochemistry in solution and the solid state. Solid-state results, *J. Am. Chem. Soc.,* 102, 1160, 1980.
8. Sacks, S.L. Scheffer, J.R., Teh, C.-Z., and Tse, A., Synthesis and antiviral activity of 11-azapentacyclo[6.2.1.02,7.04,10.05,9]decane, *J. Med. Chem.,* 28, 819, 1985.
9. (a) Cookson, R.C., Crundwell, E., and Hudec, J., Synthesis of cage like molecules by irradiation of Diels–Alder adducts, *Chem. Ind.,* 1003, 1958; (b) Cookson, R.C., Hill, R.R., and Hudec, J., The stereochemistry of the adducts of *p*-benzoquinone with two molecules of cyclopentadiene. Charge transfer from olefinic double bonds to *p*-benzoquinone and ene-1,4-dione groups, *J. Chem. Soc.,* 3043, 1964; (c) Cookson, R.C., Crundwell, E., Hill, R.R., and Hudec, J., Photochemical cyclization of Diels–Alder adducts, *J. Chem. Soc.,* 3062, 1964.
10. Krauch, C.H. and Metzner, W., Lösungsmittelsensibilisierte isomerisierung von DielsAlder-Addukten des *p*-benzochinons mit ^{60}Co-γ-strahlen, *Chem. Ber.,* 98, 2106, 1965.
11. Wladislow, B., Marzorati, L., Campos, I.P.A., and Viertler, H., The importance for cage compound formation of the oxidation potential of the enedionic system in benzoquinonecyclopentadiene adducts, *J. Chem. Soc., Perkin Trans. 2,* 475, 1992.

12. Nair, M.S., Sudhir, U., Joly, S., and Rath, N.P., Two fascinating rearrangements through selective placement of bromine substituents. Photochemical synthesis of 3-bromo-7-(bromomethyl)tetracyclo[5.3.1.02,6.04,8]undec-10(12)-ene-9,11-dione and its rearrangements with amines, *Tetrahedron,* 55, 7653, 1999.
13. Fessner, W-D. and Rodriguez, M., Synthesis and interconversion of new $(CH)_{14}$ isomers, *Angew. Chem. Int. Ed. Engl.,* 30, 1020, 1991.
14. Barborak, J.C., Watts, L., and Pettit, R., The convenient synthesis of the cubane system, *J. Am. Chem. Soc.,* 88, 1328, 1966.
15. Bruce, J.M., Photochemistry of quinones, in *The Chemistry of the Quinonoid Compounds,* Patai, S. Ed., Wiley-Interscience, New York, 1974, Part 1, p. 478.
16. (a) Schenck G.O., Hartman, I., and Metzner, W., Photochemische carbocyclopolymerization von durochinon mit olefine, *Tetrahedron Lett.,* 347, 1965; (b) Koltzenburg, G., Kraft, K., and Schenk, G.O., Photochemische carbocyclopolymerization von durochinon mit dienen, *Tetrahedron Lett.,* 353, 1965.
17. (a) Bryce-Smith, D., Fray, G.I., and Gilbert, A., 1:1 and 2:1 Photoaddition of cyclooctene and cycloocta-1,5-diene to chloranil, *Tetrahedron Lett.,* 3471, 1964; (b) Zimmerman, H.E. and Craft, L., Photochemical reaction of benzoquinone with tolan, *Tetrahedron Lett.,* 2131, 1964.
18. (a) Ogino, K., Minami, T., and Kozuka, S., Photoreactions of duroquinone with cyclic polyenes. Entry into new cage compounds, *J. Chem. Soc., Chem. Commun.,* 480, 1980; (b) Ogino, K., Minami, T., Kozuka, S., and Kinoshita, T., Photochemical reactions of duroquinones with cyclic polyenes. Synthesis of new cage compounds, *J. Org. Chem.,* 45, 4694, 1980.
19. Kanematsu, K., Morita, S., Fukushima, S., and Osawa, E., Reagent design and study of *p*-benzoquinone derivatives as highly reactive electron-attracting dienophiles. A promising class of reagents (synthons) for cycloaddition, *J. Am. Chem. Soc.,* 103, 5211, 1981.
20. Hayakawa, K., Aso, M., and Kanematsu, K., Site-selective Diels–Alder reaction of 1,4,5,8-naphthodiquinones with anthracenes and successively with cyclopentadiene: electronic effects vs. steric effects, *J. Org. Chem.,* 50, 2036, 1985.
21. Hayakawa, K., Kido, K., and Kanematsu, K., Synthesis and characterization of crowned 1,4-benzoquinones as ionophore-dienophile (redox) combined systems: double interaction with catecholamines and tryptamine, *J. Chem. Soc., Perkin Trans. 1,* 511, 1988.
22. Warrener, R.N., McCay, I.W., and Paddon-Row, M.N., An unusual caged oxetane formed by intramolecular photocyclization onto the carbonyl group of a polyalicyclic enedione, *Aust. J. Chem.,* 30, 2189, 1977.
23. Knolker, H.-J., Baum, E., and Heber, J., Cycloadditions of annulated 2,5-bis(trimethylsilyl)cyclopentadienones, *Tetrahedron Lett.,* 42, 7647, 1995.
24. (a) Becker, H.-D. and Konar, A,, Photochemical intramolecular cycloaddition of 2,4-cyclohexadienone Diels–Alder dimers, *Tetrahedron Lett.,* 5177, 1972; (b) Becker, H.-D., Ruge, B., and Westlof, T., Photochemistry of oxirane-substituted 2,4-cyclohexadienone Diels–Alder dimers, *Tetrahedron Lett.,* 253, 1975.
25. Iwakuma, T., Hirao, K., and Yonemitsu, O., Photocyclization of *N*-chloroacetyltyramines. II. Flash photolysis and substituent effect studies on the formation of dimeric cage compounds and novel acid-catalyzed reversion, *J. Am. Chem. Soc.,* 96, 2570, 1974.
26. (a) Iwakuma, T., Nakai, H., Yonemitsu, O., Jones, D.S., Karle, I.L., and Witkop, B., Photocyclization of pharmacodynamic amines. VII. Photorearrangements and roentgen-ray analyses of novel tyramine dimers, *J. Am. Chem. Soc.,* 94, 5136, 1972; (b) Iwakuma, T., Yonemitsu, O., Kanamori, N., Kimura, K., and Witkop, B., Transient cyclohexadienones by novel reversal reactions from cage photodimers derived from *N*-chloroacetyltyramines, *Angew. Chem. Int. Ed. Engl.,* 12, 72, 1973.
27. Singh, V. and Porinchu, M., A novel periselective cycloaddition of cycloheptatriene with cyclohexa-2,4-dienones, *Tetrahedron Lett.,* 34, 2817, 1993.
28. Kopecky, J. and Shields, J.E., Photochemical behavior of dibenzo derivatives of tropone, tropylidene and heptafulvene, *Tetrahedron Lett.,* 24, 2821, 1968.

29. Rokach, J. and Atkinson, J.G., A new heterocyclic cage ring system: preparation of the *cis*-cyclobutadiene dimer of benzo[a,d]cyclohepten-5-one, *J. Chem. Soc., Chem. Commun.,* 602, 1975.
30. (a) De Schryver, F.C., Bhardway, I., and Put, J., Intramolecular photocycloaddition of *N,N′*-alkylenedimaleimides, *Angew. Chem. Int. Ed. Engl.,* 8, 213, 1969; (b) Put, J. and Schryver, F.C., Photochemistry of nonconjugated bichromophoric systems. Intramolecular photocycloaddition of *N,N′*-alkylenedimaleimides in solution, *J. Am. Chem. Soc.,* 95, 137, 1973.
31. Laurenti, D., Santelli-Rouvier, C., Repe, G., and Santelli, M., Synthesis of *cis, cis, cis*-tetrasubstituted cyclobutanes. Trapping of tetrahedral intermediates in intramolecular nucleophilic addition, *J. Org. Chem.,* 65, 6418, 2000.
32. Jones, G., II., Becker, W.G., and Chiang, S.-H., Variations in mechanism for photoinduced valence isomerization of an electron-donor nonconjugated diene, *J. Am. Chem. Soc.,* 105, 1269, 1983.
33. Chou, T.-C., Chuang, K.-S., and Lin, C.-T., Synthesis of hexacyclo[6.5.1.0.^{2,7}0.^{3,11}0.^{4,9}0^{10,14}]tetradeca-5,1,2-diene, *J. Org. Chem.,* 53, 5168, 1988.
34. Chou, T.-C., Yeh, Y.-L., and Lin, G.-H., A fragmentation–photocyclization approach towards homosecohexaprismane skeleton, *Tetrahedron Lett.,* 37, 8779, 1996.
35. Mehta, G. and Reddy, S.H. K., Golcondane: novel, caged, nonacyclic $C_{20}H_{24}$-hydrocarbon of D_{2d} symmetry, *Angew. Chem. Int. Ed. Engl.,* 32, 1160, 1993.
36. Behr, J., Braun, R., Grimme, S., Kummer, M., Martin, H.-D., Mayer, B., Rubin, M.B., and Ruck, C., Multichromophoric systems by Diels–Alder reaction of barrelene with *o*-benzoquinones: tetracyclo[6.2.2.2.^{3,6}0^{2,7}]tetradaca-9,11,13-triene-4,5-diones, *Eur. J. Org. Chem.,* 2339, 1998.
37. Behr, J., Br'aun, R., Martin, H.-D., Rubin, M.B., and Steigel, A., Photorearrangement of polycyclic quinoxalines, isomerization of isodrin-type aza-di-π-methane chromophores, *Chem. Ber.,* 124, 815, 1991.
38. (a) Klaus, M. and Prinzbach, H., Photochemical olefin–oxirane cyclodimerization, *Angew. Chem. Int. Ed. Engl.,* 8, 276, 1969; (b) Klaus, M. and Prinzbach, H., Photochemical olefin–aziridine cycloaddition, *Angew. Chem. Int. Ed. Engl.,* 10, 273, 1971.
39. Umano, K., Koura, H., and Inoue, H., Photochemical isomerization of 6,7-dicyano- and 6,7-bis(methoxycarbonyl)-3-phenylsulfonyl-(2,4-*exo*)-3-azatricyclo[3.2.1.0^{2,4}]oct-6-ene, *Bull. Chem. Soc. Jpn.,* 54, 2827, 1981.
40. Prinzbach, H., Sedelmeier, G., and Martin, H.-D., Geometrical dependence of [2π + 2σ]-photocycloaddition, *Angew. Chem. Int. Ed. Engl.,* 16, 103, 1977.
41. Berning, W. and Hünig, S., Photochemical [2 + 2]-cycloaddition between parallel CC and NN double bonds, *Angew. Chem. Int. Ed. Engl.,* 16, 777, 1977.
42. Kettenring, J. and Ginsburg, D., A [2 + 2]-photocycloaddition of a N = N bond to a C = C bond, *Tetrahedron*, 40, 5269, 1984.
43. (a) Hünig, S. and Schmitt, M., Laticyclische 1,5-Konjugation in Azoverbindungen mit parallel Benachbarten dreiringeinheiten, *Tetrahedron Lett.,* 28, 4251, 1987; (b) Hünig, S. and Schmitt, M., Intramolecular [σs^2 + πs^2]-photocycloaddition reaction of parallel three-membered ring with azo group, *Liebigs. Ann.,* 575, 1996.
44. Filipescu, N. and Menter, J.M., Cage formation subsequent to intramolecular triplet-energy transfer, *J. Chem. Soc. B.,* 616, 1969.
45. Kushner, A.S., Photoisomerization of the 1,4-naphthoquinone-cyclopentadiene adduct. A novel intramolecular [6 + 2]-cycloaddition, *Tetrahedron Lett.,* 3275, 1971.
46. (a) Prinzbach, H., Sedelmeier, G., Krüger, C., Goddart, R., Martin, H.-D., and Gleiter, R., An unusual benzene/benzene through space interaction, *Angew. Chem. Int. Ed. Engl.,* 17, 271, 1978; (b) Wollenweber, M., Hunkler, D., Keller, M., Knothe, L., and Prinzbach, H., Photochemical transformations, 77. En route to isopagodanes — exploration into arene/alkene and arene/arene photocycloaddition reactions, *Bull. Soc. Chim. Fr.,* 130, 32, 1993.
47. Fessner, W.-D., Sedelmeier, G., Spurr, P.R., Rihs, G., and Prinzbach, H., "Pagodane": the efficient synthesis of a novel, versatile molecular framework, *J. Am. Chem. Soc.,* 110, 4626, 1989.

48. Berridge, J., Bryce-Smith, D., and Gilbert, A., Photoaddition of furan to benzene, *J. Chem. Soc., Chem. Commun.,* 964, 1974.
49. Okamoto, H., Kimura, M., Satake, K., and Morosawa, S., Synthesis and adiabatic photochemistry of a 1,4-difluorobenzene-naphthalene biplanemer, *Bull. Chem. Soc. Jpn.,* 66, 2436, 1993.
50. Nishimura, J., Nakamura, Y., Hayashida, Y., and Kudo, T., Stereocontrol in cyclophane synthesis: a photochemical method to overlap aromatic rings, *Acc. Chem. Res.,* 33, 679, 2000.
51. Nishimura, J., Takeuchi, M., Takahashi, H., and Sato, M., Intramolecular [2 + 2]-photocycloaddition. 9. Stereoselective synthesis of naphthalenophanes and effects of the tether length and substituents on the photochemical reaction courses of vinylnaphthalenes, *Tetrahedron Lett.,* 31, 2911, 1990.
52. Wasserman, H.H. and Keehn, P.M., Dibenzoequinene. A novel heptacyclic hydrocarbon from the photolysis of [2.2]paracyclonaphane, *J. Am. Chem. Soc.,* 89, 2770, 1967.
53. Misumi, S., Cycloaddition reactions of cyclophanes, *Pure Appl. Chem.,* 59, 1627, 1987.

23

Photochemical Approaches to the Synthesis of [n]Prismanes

Terou Shinmyozu
Kyusha University

Rika Nogita
Kyusha University

Motoko Akita
Kyusha University

Chultack Lim
Kyusha University

23.1 Synthesis of [n]Prismanes (n = 3–5)

Prismanes constitute an infinite family of $(CH)_n$ polyhedra that chemists find aesthetically appealing because of their molecular architecture (Figure 23.1).[1] Notwithstanding their structural regularity, many years of effort were needed before the first three members, prismane ([3]prismane) **1**,[2] cubane ([4]prismane) **2**,[3] and pentaprismane ([5]prismane) **3**,[4] could be successfully synthesized. Recently, attention has been focused on the challenging objective of constructing the higher prismanes, in particular, hexaprismane ([6]prismane) **4**. The molecules in the prismane family are highly strained due to their unusual structural features, extended CC bond lengths, and deformed bond angles. Their strain energies are estimated to be 140–178 kcal/mol based on *ab initio* MO calculations (6–31G*).[5] Pentaprismane has the smallest strain energy, while hexaprismane has the highest. Although several approaches have been tried, hexaprismane **4** has eluded synthesis so far. In this section, strategies for the synthesis of [n]prismanes (n = 3–5) are outlined, where the key steps of the synthesis are the [2 + 2]-photocyclization and Favorskii contraction. In the next section, photochemical synthetic approaches toward hexaprismane and its derivatives are introduced as a hot topic in this area.

Scheme 1 illustrates the synthesis of prismane ([3]prismane) **1** by Katz and Acton[2] Benzvalene **5** reacts with the powerful dienophile, 4-phenyltriazolinedione **6**, in diethyl ether–dioxane to give the 1:1 adduct **7** (60–70%). Refluxing **7** with KOH in MeOH/H_2O, followed by treatments with acidic $CuCl_2$ and aqueous NaOH, gives azo compound **8**. Irradiation of **8** through Pyrex in isobutane at 35°C affords prismane **1** (1.8%) as an explosive colorless liquid. Prismane is stable at room temperature. One of the key steps of this synthesis is a photochemical nitrogen extrusion (Scheme 1).

The ethylene ketal of 2-bromocyclopentadienone undergoes spontaneous dimerization to give the dimeric adduct **10**, which is converted to the cage compound **11** by ultraviolet irradiation in benzene (95%). The bishomocubane system **11** is contracted to the homocubane system **12** by the Favorskii rearrangement. Decarboxylation of **12** via perester **13** gives **14**, and subsequent similar ring contraction (**14** to **15**) and decarboxylation of **15** provide the desired cubane **2** as glistening rhombs (mp 130–131°C).[3] In this synthesis, the critical steps are the [2 + 2]-photochemical reaction and subsequent Favorskii ring contractions (Scheme 2).

0-8493-1348-1/04/$0.00+$1.50

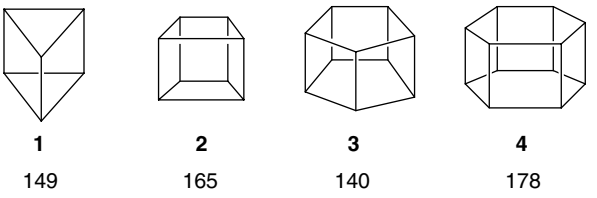

FIGURE 23.1 Strain energies of the [*n*]prisanes. Strain energies (kcal/mol) (*ab initio,* MO 6-31G*) (From Disch, R.L. and Shulman, J.M., *J. Am. Chem. Soc.,* 110, 2102, 1988.)

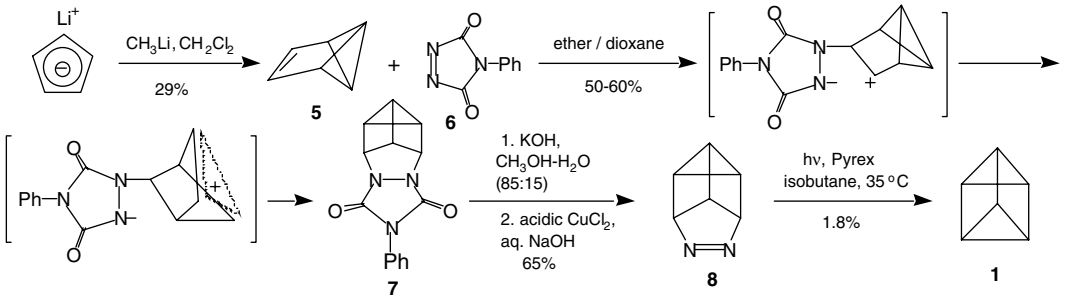

SCHEME 1 Synthesis of [3]prismane. (From Katz, T.J. and Acton, N., Synthesis of prismane, *J. Am. Chem. Soc.,* 95, 2738, 1973.)

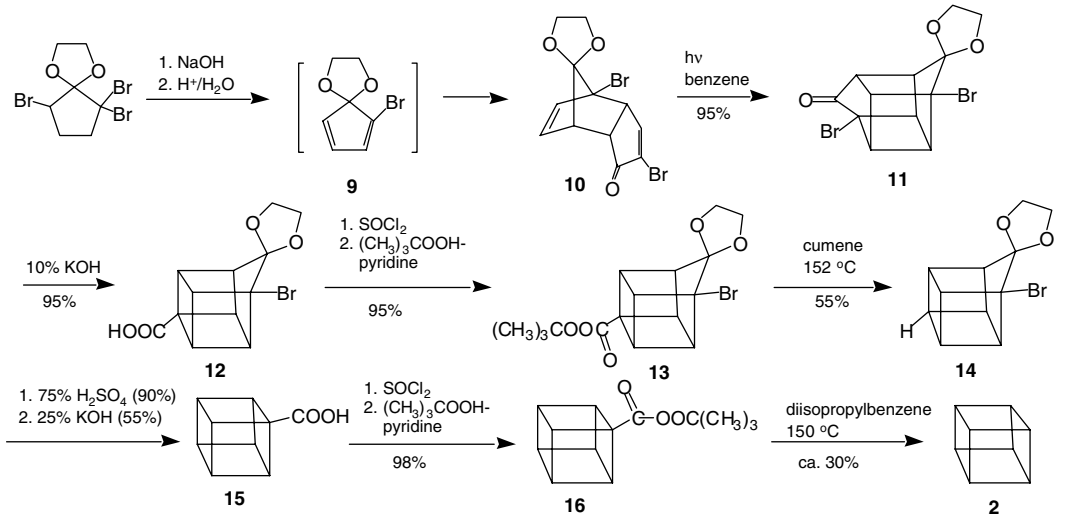

SCHEME 2 Synthesis of [4]prismane (cubane). (From Reference 3.)

Acetone-sensitized [2 + 2]-photocycloaddition of the adduct **17** of 1,2,3,4-tetrachloro-5,5-dimethoxycyclopentadiene with *p*-benzoquinone gives the cage compound **18** effectively (95%) (Scheme 3). Dechlorination and reduction of the carbonyl groups of **18** with Li in liquid NH_3 and tosylation of the *endo-endo*-diol **19**, is followed by treatment with NaI to give a mixture (1:3) of diiodide and iodotosylate **20**. Reaction of the mixture with *t*-butyl lithium gives dimethoxyhomohypostrophene **21**, which is photocyclized to give homopentaprismanone **22**. A tosyl group is introduced α to the bridging carbonyl

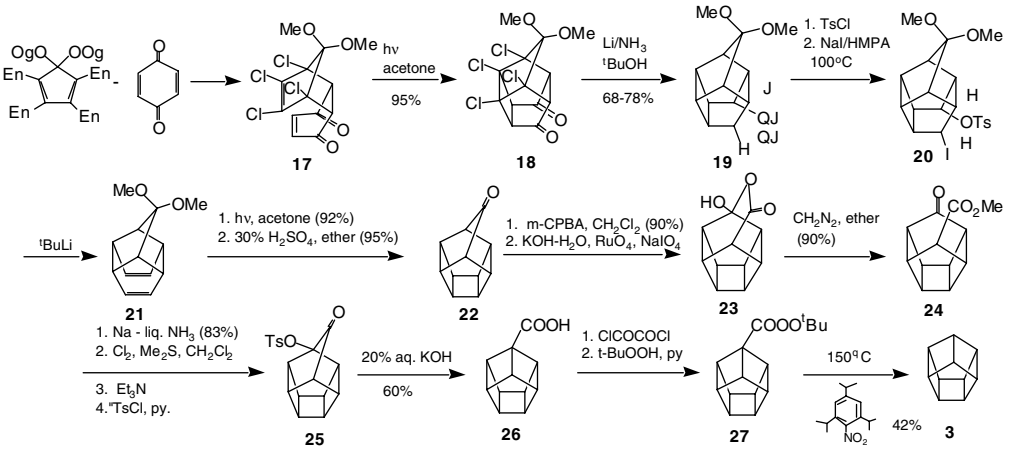

SCHEME 3 Synthesis of [S] prismane (pentaprismane). (From Reference 4.)

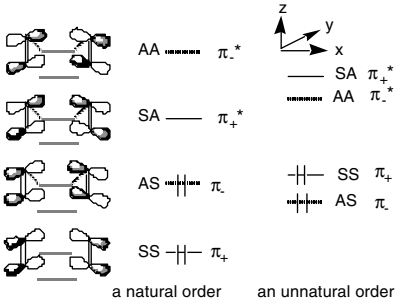

FIGURE 23.2 In a diene with juxtaposed double bonds, the natural frontier molecular orbitals (FMO) in the absence of through bond interaction is $\pi^{+} < \pi^{-} < \pi^{+*} < \pi^{-*}$.

group (**22** to **25**), and the Favorskii ring contraction of **25** followed by decarboxylation of **26** affords the desired pentaprismane **3** as glistening crystals (mp 127.5–128.5°C).[4,6]

Gleiter et al. suggested an alternative simple approach to the synthesis of cubane derivatives. Osawa et al. reported that the failure to produce the cubane skeleton from *syn*-tricyclo[4.2.0.0^{2,5}]octa-3,7-diene **28** was rationalized by assuming that the sequence of the frontier orbitals was π_{+} above π_{-} and π_{+}^{*} above π_{-}^{*} as a result of strong through-bond interaction between the cyclobutene ring and the π orbitals (an unnatural order). As a result of this orbital sequence, photochemical [2 + 2]-cycloaddition of **28** to cubane is a symmetry-forbidden process (Figure 23.2).[7]

However, Polesi and Miller reported in 1976 that irradiation (450 W high-pressure Hg lamp) of a perfluoro-derivative of *anti*-tricyclo[4.2.0.0^{2,5}]octa-3,7-diene in a fluorocarbon solution yielded perfluorooctamethylcubane **30** (ca. 20%) and perfluorooctamethylcuneane **31** (15%) (Scheme 4). They postulated that the cubane **30** and cuneane **31** were formed from the *syn*-isomer **29** and the semibullvalene **32**, respectively.[8]

Gleiter et al. found that the alkyl-substituted *syn*-tricyclo[4.2.0.0^{2,5}]octa-3,7-dienes **33**, **36**, **41**, and **43** afforded the cubane derivatives **34**, **37**, **42**, and **44** via photoirradiation (high-pressure Hg lamp) of the pentane solution.[9] In the case of octamethyl-diene **36**, six different photoproducts were isolated, but the main product was octamethylcuneane **38**. The cubane **37** may be formed directly via photoirradiation, whereas a mechanism involving either a biradical intermediate or the triene **40** was proposed for the formation of other products (**38**, **39**). Although the parent **28** is photochemically inactive, Gleiter et al. revealed that its octaalkyl derivatives have a rich photochemistry.

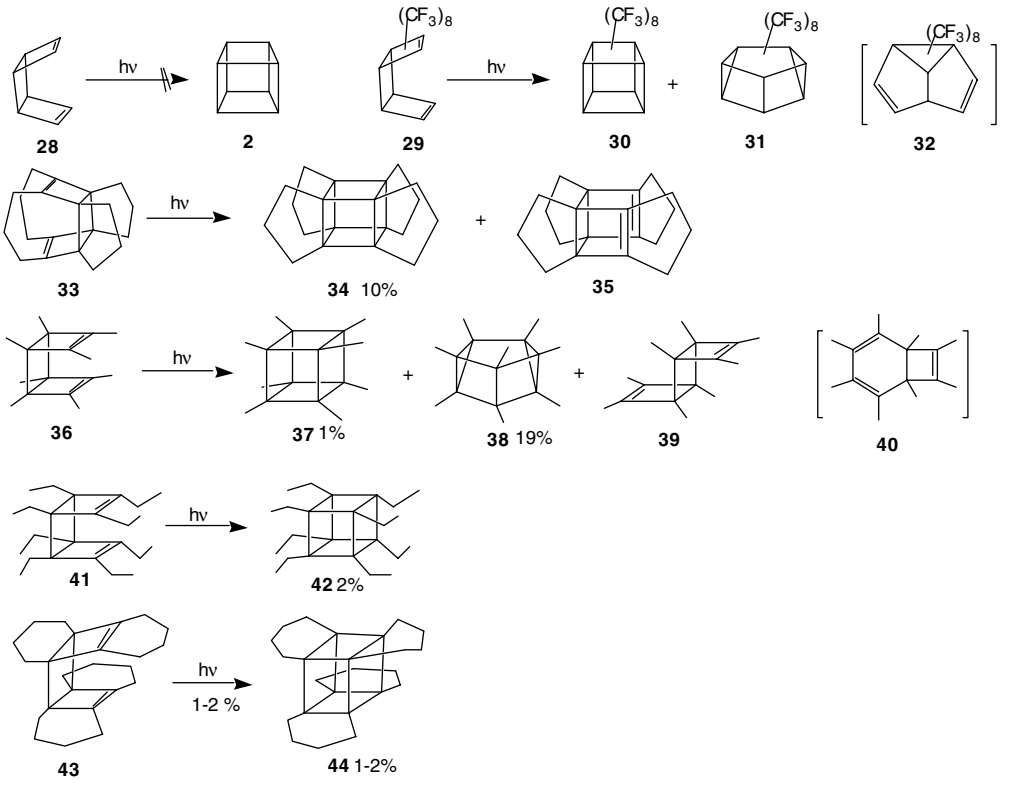

SCHEME 4 Photochemistry of *syn*-tricyclo[4.2.0.0^{2,5}]-octa-3,7-dienes.

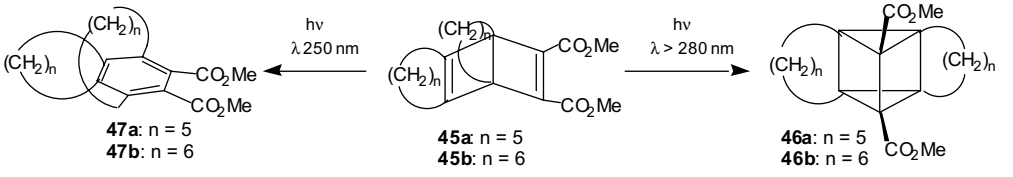

SCHEME 5 Synthesis of doubly bridged prismanes.

Gleiter and Treptow reported the synthesis of the first doubly bridged prismane derivatives **46a** (n = 5) and **46b** (n = 6).[10] Irradiation (500 W high-pressure Hg lamp) of the Dewar benzene derivatives **45a** (n = 5) at 250 nm in diethyl ether under Ar yields only polymeric material because of the instability of the initially formed [5]paracyclophane **47a**, whereas irradiation at 280 nm gives the prismane **46a** (15%, 72 h). When **45b** (n = 6) was irradiated at 250 nm, rapid isomerization to the [6]paracyclophane **47b** (100%, 1 h) took place; increasing the wavelength to 280 nm led to the prismane **46b** (30%, 24 h).

23.2 Photochemical Approaches to the Synthesis of Hexaprismane and Its Derivatives

Many diverse synthetic strategies have been developed, and significant progress toward the synthesis of hexaprismane has been made. Through these efforts, bissecohexaprismane **48** (Eaton and Chakraborty),[11] secohexaprismane **49** (Mehta and Padma)[12] 1,4-bishomohexaprismane (garudane) **50** (Mehta and Padma),[13] 1,4-bishomohexaprismane dione **51** (Dailey and Golobish),[14] and homosecohexaprismane skeleton **52** (Chou et al.)[15] have been synthesized (Figure 23.3).

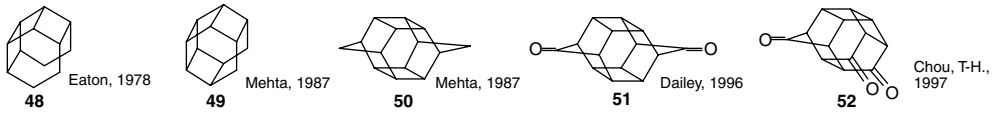

FIGURE 23.3

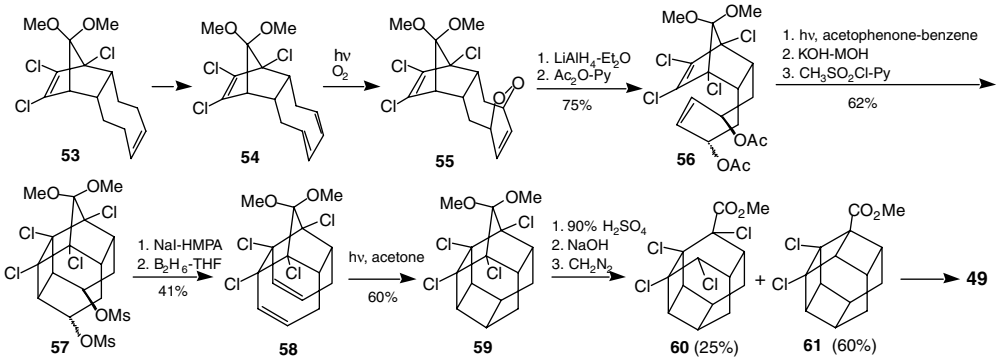

SCHEME 6 Synthesis of secohexaprismane. (From Reference 12.)

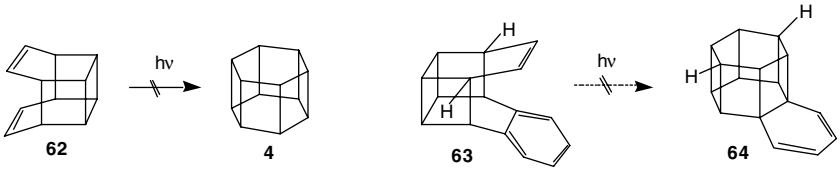

SCHEME 7 Photochemistry of pentacyclo[6.4.0.0^{2,7}.0^{3,12}.0^{6,9}]dodeca-4-10-dienes.

The synthesis of secohexaprismane **49** is outlined in Scheme 6.[12] The Diels–Alder adduct **53** of 1,5-cyclooctadiene and 5,5-dimethoxy-1,2,3,4-tetrachlorocyclopentadiene was readily available. It was converted into the diacetate **56** via the cyclic peroxide **55**, which was formed through stereoselective [4 + 2]-addition of singlet oxygen to the diene moiety of **54**. Acetophenone-sensitized photocyclization gave the caged pentacyclic *endo,endo*-diacetate, which was converted into the diene **58** by conventional methods (Scheme 3, **19** to **21**) via the dimesylate **57**. Acetone-sensitized photocyclization provided **59**, and deprotection of the carbonyl group of **59** and Favorskii ring contraction gave a 2:5 mixture of **60** and **61**. Alkaline hydrolysis, Hunsdiecker reaction, and reductive dehalogenation of **61** provided secohexaprismane **49** as a highly volatile waxy solid (mp > 250°C). It should be noted that the [2 + 2]-photocyclization of the Diels–Alder adduct and Favorskii contraction play pivotal roles in the synthesis of these cage compounds. However, hexaprismane and its derivatives have not yet been synthesized.

An alternative approach is the photochemical dimerization of benzene and its equivalent. Yang and Horner synthesized pentacyclododecanediene **62** as a logical precursor of hexaprismane **4**,[16] but the [2 + 2]-photocyclization did not occur (Scheme 7). A similar approach was reported by Kimura et al. Acetone-sensitized irradiation of the benzene solution of diene **63** did not give the desired hexaprismane derivative **64**; only naphthalene and *p*-difluorobenzene were formed.[17] In principle, the [2 + 2]-photocyclization of the pentacyclododecanediene skeletons **62** and **63** may be a symmetry-forbidden process.[7]

Misumi and co-workers reported the first example of photodimerization of benzene rings incorporated into a *syn*-quadruple-layered diheteracyclophane **65**. A benzene solution of **65a** (X = O) was irradiated with a high-pressure Hg lamp under N_2 for 30 min to give the cage compound **66a** (Scheme 8).[18] In a

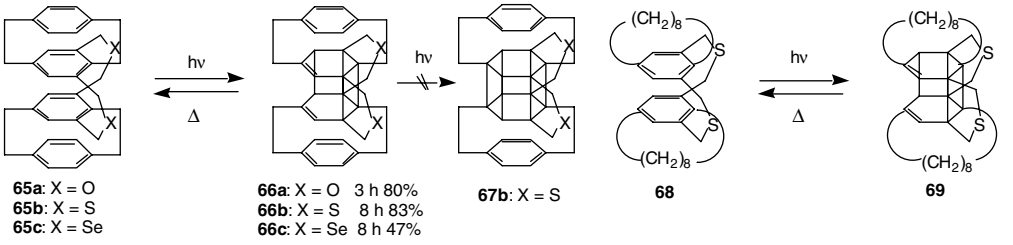

SCHEME 8 A novel photodimerization of benzene moieties in the *syn*-quadruple-layered diheteracyclophanes.

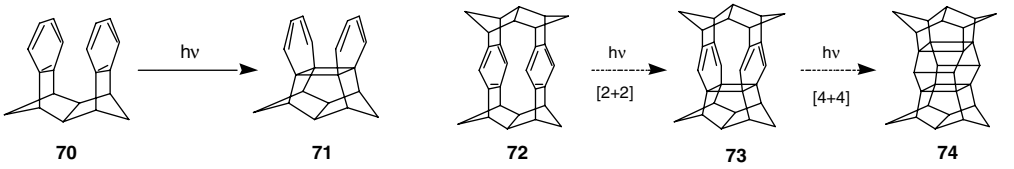

SCHEME 9 Benzo/benzo [6+6]-photocycloaddtion.

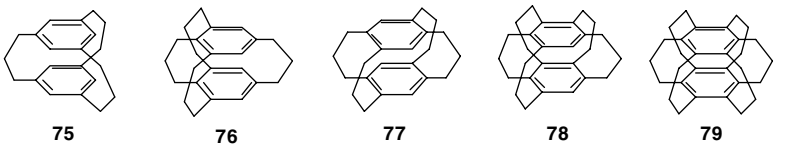

FIGURE 23.4 [3_n]cyclophanes (n = 3-6).

similar manner, **65b** (X = S) and **65c** (X = Se) were converted into the cage compounds **66b** and **66c**, respectively. These cage compounds reverted thermally to the starting cyclophanes. In dithia compounds with an [n]paracyclophane framework, the compound **68** (n = 8), which is as strained as **65b**, also gave the photoisomer **69** (17% at room temperature, 31% at –78°C), whereas no photoisomer was obtained with the compound (n = 10), with much less strain. A [2 + 2]photocycloaddition of the remaining two double bonds of **66b** was attempted by irradiating with a low-pressure Hg lamp at various temperatures, but only formation of a small amount of dimethyl[2.2]-paracyclophane was observed. They concluded that the face-to-face stacking of two fairly strained benzene nuclei is responsible for the photodimerization, and the two outer benzenes are required for effective interconversion between quadruple-layered diheteracyclophanes and their isomeric cage compounds.

As already described (Chapter 22, Scheme 34), Prinzbach et al. reported benzo/benzo [6 + 6]-photodimerization of benzene rings (**70** to **71**), and this is the second example of the photodimerization of benzene rings.[19] Recently, they proposed a possible synthetic route of pagodane-condensed prismane derivatives **74** via a photochemical benzo/benzo [6 + 6]-photoreaction of **72** followed by a photochemical [4 + 4]-cycloaddition reaction of **73** (Scheme 9).[20]

Recently, we discovered a third example of the photodimerization of the benzene rings. In our photochemical approach to the construction of hexaprismane derivatives, we used the [3_n]cyclophanes ([3_n]CPs) **75–79** (n = 3–6)[21], in which two benzene rings are stacked at 3.0–3.2 Å transannular distances (Figure 23.4), as precursors.[22] We expected that the photocyclization of the [3_n]CP would proceed via the first [4 + 4]-photoreaction (**79** to **80**), followed by successive [2 + 2]-reactions (**80** to **81** then **81** to **82**) (Scheme 10). We describe here the photochemical reactions of [3_3](1,2,3)CP **75** and [3_4](1,2,3,5)- and (1,2,4,5)CPs **76** and **77**.

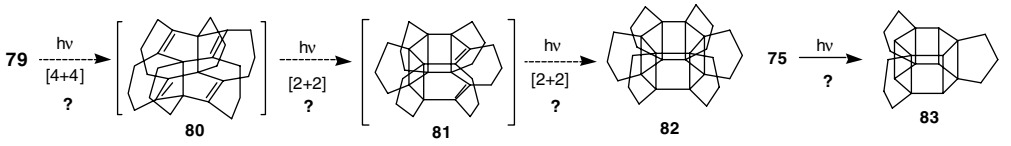

SCHEME 10 Expected photochemical isomerizations.

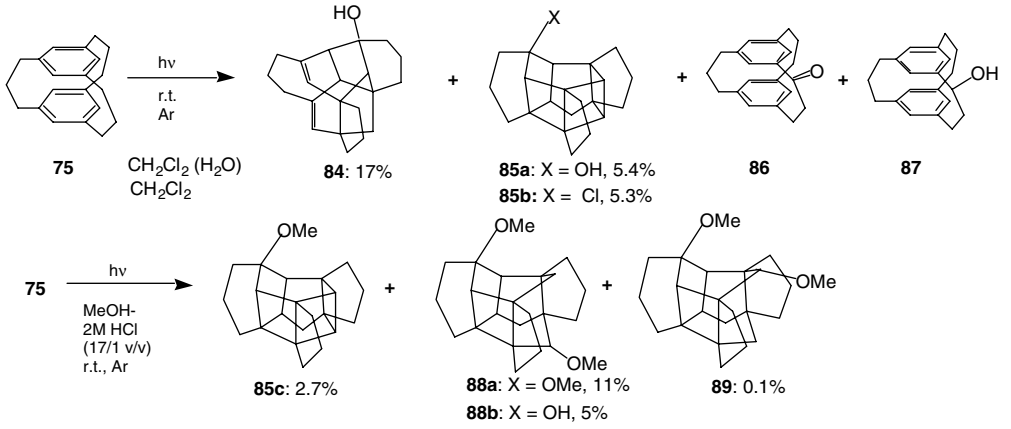

SCHEME 11 Photochemical reactivity of [3_3](1,3,5)cyclophane.

Irradiation of the [3_3]CP **75** by a sterilizing lamp (254 nm) in cyclohexane, methanol, or benzene left **75** intact although some polymerization occurred. However, two types of products were formed when methylene chloride was used as a solvent. A dry methylene chloride solution of **75** (4.90 mmol/l) in a quartz vessel was irradiated by a sterilizing lamp for 2.5 h at room temperature under Ar to give a new cage compound, the bridged hexacyclic chlorododecane **85b** (5.3%), with a bishomopentaprismane skeleton and the recovery of the starting compound **75** (40%) (Scheme 11).[23a] Irradiation of **75** under the same conditions, but in a methylene chloride solution saturated with water (14.5 mmol/l), for 2.5 h under Ar gave, in addition to **75** (18%), two photoproducts: diene–alcohol **84** and caged alcohol **85a** with the same skeleton as **85b**.[23a,24]

In order to examine the photochemical reaction mechanism, photolysis in acidic and basic conditions was examined. A d_4 methanol or d_3 acetonitrile solution of **75** containing 2 mol/l aqueous HCl solution in a quartz NMR tube was irradiated with a sterilizing lamp for 2.5 h at room temperature under Ar. The reaction proceeded in acidic conditions, whereas the reaction in dideuterio methylene chloride in the presence of triethylamine failed. In a preparative scale reaction, a mixture of MeOH and 2 mol/l aqueous HCl solution (17:1 v/v) (10.2 mmol/l) of **75** was irradiated with a sterilizing lamp in a quartz vessel for 80 min at room temperature under Ar to give recovered **75** (11%) and the methoxy compound **85c** (2.7%), as well as the dimethoxy and methoxy–hydroxy compounds **88a** (11%) and **88b** (5.9%), with a new cage skeleton. Prolonged irradiation gave the dimethoxy compound **88a** as a major product (57%).

In completely degassed nonpolar solvents such as hexane, pentane, and cyclohexane, no reaction apparently took place even on prolonged irradiation. On the other hand, in the presence of dissolved oxygen in the solvent, trace amounts of the photoproducts **86** and **87**, formed by oxidation at the benzylic carbon, were isolated.

The photochemical reactions of the [3_4](1,2,3,5)CP **76** and [3_4](1,2,4,5)CP **77** were also examined. A water-saturated methylene chloride solution of **76** or **77** was irradiated with a sterilizing Hg lamp for 1.5 h at room temperature under Ar to afford a new cage compound **90** (4.5%)[25] or **91** (7%),[26] respectively, along with the starting material (Scheme 12). We have failed to gather conclusive evidence for the reaction mechanism, but a proposal is shown in Scheme 13. The [3_3]CP **75**, on irradiation in methylene chloride,

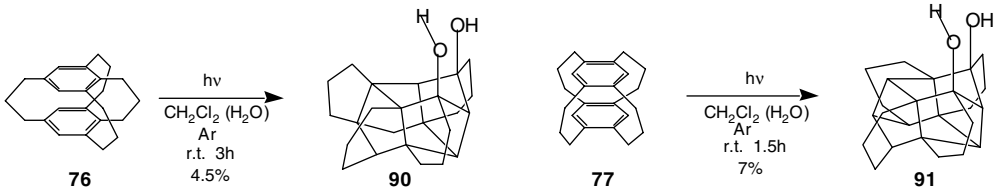

SCHEME 12 Photochemical reactions of the $[3_4](1,2,3,5)$cyclophane and $[3_4](1,2,4,5)$ cyclophane.

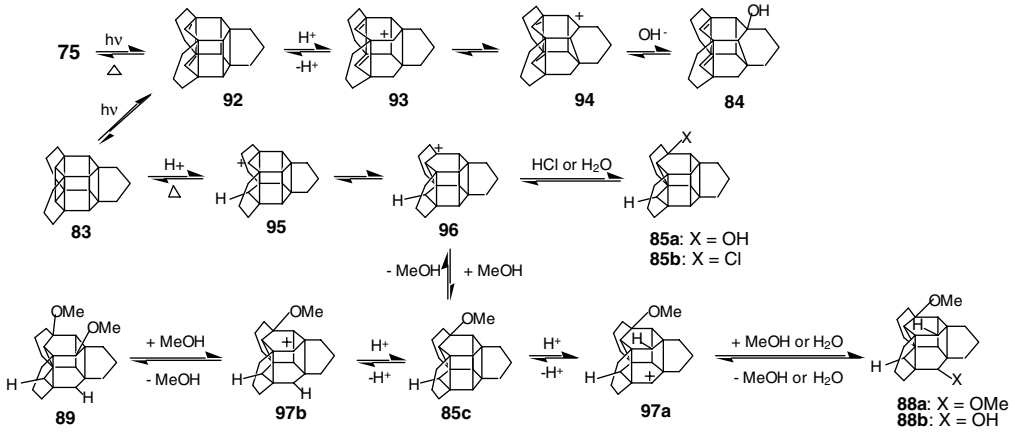

SCHEME 13 Expected mechanism for the formation of the photoproducts.

first gives the highly strained hexaprismane derivative **83**. Protonation occurs at the unbridged carbon atom of a cyclobutane ring to give the secondary carbocation **95**, which rearranges to the more stable tertiary carbocation **96**. Finally, **96** is trapped by chloride or hydroxide ions to give the products **85b** (X = Cl) or **85a** (X = OH).

One of the driving forces in this series of reactions must be release of the steric strain. The formation of the diene–alcohol **84** is explained in a similar way. The protons may be generated upon photoirradiation of methylene chloride. In fact, the pH of the reaction mixture was ca. 2 after irradiating in the wet methylene chloride solution. The photochemical reaction of **75** did proceed in methanol in the presence of a proton source to give **85c**, as was the case in methylene chloride. Subsequent protonation to the unbridged carbon atom of the central bicyclo[2.2.0]hexane skeleton of **85c** from the upper side may give the secondary carbocation **97**, which is intercepted by MeOH or H_2O to give the products **88a** and **88b**, respectively. This trapping of the secondary carbocation occurred preferentially on the lower face. This preference is the result of a variety of factors such as steric hindrance by the methoxy group and repulsion by the lone pair of electrons on the oxygen atoms between the flagpole bonds if attack occurred on the upper face. In this reaction, isolation and characterization of the highly strained propella$[3_3]$prismane **83**, a possible intermediate, is impossible because **83** may be protonated under the acidic conditions.

Although we have not yet succeeded in the isolation of **83**, these photochemical reactions provide useful one-step synthetic methods leading to new polycyclic cage compounds with novel skeletons **98–101** from the $[3_3]$CP **75** and $[3_4]$CPs **76**, **77** (Figure 23.5). Further investigation of the photochemical reaction conditions via the excited singlet state of **75**, and modification of the benzene ring of **75** in order to stabilize the hexaprismane skeleton, may lead to the isolation of the hexaprismane derivative. The photochemical reactions of $[3_6]$CP **79** and fluorinated $[3_3](1,3,5)$CPs[27] are in progress. We believe that a successful synthesis of hexaprismane or hexaprismane derivatives will be realized in the near future.

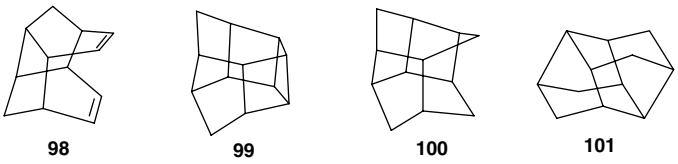

FIGURE 23.5 Skeleta of the new cage compounds.

References

1. For recent reviews, see (a) Dodziuk, H., Unusual saturated hydrocarbons: interaction between theoretical and synthetic chemistry, in *Topics in Stereochemistry,* Vol. 21, Eliel, E.L. and Wilen, S.H., Eds, John Wiley & Sons, Inc., New York, 1994; (b) Dodziuk, H., *Modern Conformational Analysis* elucidating novel exciting molecular structures, VCH Publishers, Inc., Weinheim, Germany, 1995.
2. Katz, T.J and Acton, N., Synthesis of prismane, *J. Am. Chem. Soc.,* 95, 2738, 1973.
3. (a) Eaton, P.E. and Cole, T.W., Jr., The cubane system, *J. Am. Chem. Soc.,* 86, 962, 1964; (b) Eaton, P.E. and Cole, T.W., Jr., Cubane, *J. Am. Chem. Soc.,* 86, 3157, 1964; (c) Eaton, P.E., Cubanes: starting materials for the chemistry of the 1990s and the new century, *Angew. Chem. Int. Ed. Engl.,* 31, 1421, 1992.
4. (a) Eaton, P.E., Or, Y.S., and Branca, S.J., Pentaprismane, *J. Am. Chem. Soc.,* 103, 2134, 1981; (b) Eaton, P.E., Or, Y.S., Branca, S.J., and Shankar, B.K.R., The synthesis of pentaprismane, *Tetrahedron,* 42, 1621, 1986.
5. Disch, R.L. and Shulman, J.M., *Ab initio* heats of formation of medium-sized hydrocarbons, *J. Am. Chem. Soc.,* 110, 2102, 1988.
6. Dauben, W.G. and Cunningham, A.F., Jr., Formal syntheses of pentaprismane, *J. Org. Chem.,* 48, 2842, 1983.
7. (a) Cha, O.J., Osawa, E., and Park, S., Design of bridged polycyclic diolefin precursors for prismane using FMO order as criteria. Interbridged distance as a new factor for controlling the intramolecular [$\pi 2 + \pi 2$]cycloaddition, *J. Mol. Struct.,* 300, 73, 1993; (b) Osawa, E., Rudzinski, J.M., and Xun, Y.-M., Strain, orbital interaction and conformation of propella[3_4]prismane and its precursor diolefin. Analysis of orbital interactions of cycloacta-1,5-diene and cyclodeca-1,6-diene with AM1 molecular orbital method, *Struct. Chem.,* 1, 333, 1990.
8. Polesi, L.F. and Miller, W.T., Syntheses from perfluoro-2-butyne. 2. Perfluorooctamethylcubane, perfluorooctamethylcuneane and perfluorooctamethylcyclooctatetraene, *J. Am. Chem. Soc.,* 98, 4311, 1976.
9. (a) Gleiter, R. and Karcher, M., Synthesis and properties of a bridged *syn*-tricyclo[4.2.0.$0^{2,5}$]octa-3,7-diene: detection of propella[3_4]prismane, *Angew. Chem. Int. Ed. Engl.,* 27, 840, 1988; (b) Gleiter, R. and Brand, S., Photochemistry of bridged and unbridged octaalkyl-substituted *syn*-tricyclo[4.2.0.$0^{2,5}$]octa-3,7-diene derivatives, *Chem.-Eur. J.,* 4, 2532, 1998; (c) Brand, S. and Gleiter, R., Synthesis of a propella[4_4]prismane with averaged S_4 symmetry, *Tetrahedron Lett.,* 38, 2939, 1997; (d)Gleiter, R., Cycloalkadiynes from bent triple bonds to strained cage structures (review), *Angew. Chem. Int. Ed. Engl.,* 31, 27, 1992.
10. Gleiter, R. and Treptow, B., Doubly bridged prismanes, Dewar benzene and benzene derivatives from cyclooctyne and 1,8-cyclotetradecadiyne: en route to propella[n_3]prismanes, *Angew. Chem. Int. Ed. Engl.,* 27, 840, 1988.
11. Eaton, P.E. and Chakraborty, U.R., Octahydro- and perhydro[0.0]paracyclophane, *J. Am. Chem. Soc.,* 100, 3634, 1978.
12. (a) Mehta, G. and Padma, S., Secohexaprismane, *J. Am. Chem. Soc.,* 109, 2212, 1987; (b) Mehta, G. and Padma, S., Synthetic studies towards prismanes: seco-[6]-prismane, *Tetrahedron,* **47**, 7783, 1991.

13. (a) Mehta, G. and Padma, S., D_{2h}-Bishomohexaprismane ("garudane"). Design of the face-to face 2+2 dimer of norbornadiene, *J. Am. Chem. Soc.,* 109, 7230, 1987; (b) Mehta, G. and Padma, S., Synthetic studies towards prismanes: 1,4-bishomo-[6]-prismane ("garudane"), *Tetrahedron,* 47, 7783, 1991.
14. Dailey, W.P. and Golobish, T.D., Synthesis and structure of bishomohexaprismane-dione, *Tetrahedron Lett.,* 37, 3239, 1996.
15. (a) Chou, T.-C., Lin, G.-H., Yeh, Y.-L., and Lin, K.-J., Synthetic approach towards hexaprismane. A. Novel entry to homosecohexaprismane skeleton by cage enlargement, *J. Chin. Chem. Soc.,* 44, 477, 1997; (b) Chou, T.-C., Yeh, Y.-L., and Lin, G.-H., A fragmentation–photocyclization approach towards homosecohexaprismane skeleton, *Tetrahedron Lett.,* 37, 8779, 1996,.
16. Yang, N.C. and Horner, M.G., The synthesis of pentacyclo[6.4.0.0.^{2,7}0.^{3,12}0$^{6.9}$]dodeca-4,10-diene, *Tetrahedron Lett.,* 27, 543, 1986.
17. (a) Kimura, M., Kura, H., Nukada, K., Okamoto, H., Satake, K., and Morosawa, S., Syntheses and photochemistry of 3,6-difluoro-10,11-benzopentacyclo[6.4.0.0.^{2,7}0.^{3,12}0$^{6.9}$]-dodeca-4,10-diene, *J. Chem Soc., Perkin Trans. 1,* 3307, 1988; (b) Okamoto, H., Kimura, M., Satake, K., and Morosawa, S., Syntheses and adiabatic photochemistry of a 1,4-difluorobenzene-naphthalene biplanemer, *Bull. Chem. Soc. Jpn.,* 66, 2436, 1993.
18. (18) (a) Higuchi, H., Takatsu, K., Otsubo, T., Sakata, Y., and Misumi, S., Photodimerization of benzene- photochromism of layered dithiacyclophane, *Tetrahedron Lett.,* 23, 671, 1982; (b) Higuchi, H., Kobayashi, E., Sakata, Y., and Misumi, S., Photodimerization of benzenes in strained dihetera[3.3]metacyclophanes, *Tetrahedron* 42, 1731, 1986.
19. Prinzbach, H., Sedelmeier, G., Krüger, C., Goddard, R., Martin, H.-D., and Gleiter, R., An unusual benzene/benzene through space interaction, *Angew. Chem. Int. Ed. Engl.,* 17, 271, 1978.
20. Wollenweber, M., Etzkorn, M., Reinbold, J., Wahl, F., Voss, T., Melder, J.-P., Grund, C., Pinkos, R., Hunkler, D., Keller, M., Wörth, J., Knothe, L., and Prinzbach, H., Photochemical transformations. 85. [2.2.2.2]/[2.1.1.1]Pagodanes and [1.1.1.1]/[2.2.1.1]/[2.2.2.2]-isopagodanes: syntheses, structures, reactivities — benzo/ene and benzo/benzo-photocycloadditions, *Eur. J. Org. Chem.,* 3855, 2000.
21. (a) Sakamoto, Y., Miyoshi, N., and Shinmyozu, T., Synthesis of a "molecular pinwheel": [3.3.3.3.3.3]-(1,2,3,4,5,6)cyclophane, *Angew. Chem. Int. Ed. Engl.,* 35, 549, 1996; (b) Sakamoto, Y., Miyoshi, N., Hirakida, M., Kusumoto, S., Kawase, H., Rudzinski, J.M., and Shinmyozu, T., Synthesis, structure and transannular π–π interactions of multibridged [3^n]cyclophanes, *J. Am. Chem. Soc.,* 118, 12267, 1996; (c) Sakamoto, Y. and Shinmyozu, T., Synthesis, structure and transannular π–π interactions of multibridged [3^n]cyclophanes, *Rec. Res. Dev. Pure Appl. Chem.,* 2, 371, 1998; (d) Meno, T., Sako, K., Suenaga, M., Mouri, M., Shinmyozu, T., Inazu, T., and Takemura, H., Conformational analysis of [3.3.3]cyclophane systems, *Can. J. Chem.,* 68, 440, 1990. (e) Sentou, W., Satou, T., Yasutake, M., Lim, C., Sakamoto, Y., Itoh, T., and Shinmyozu, T., Improved synthesis, structure and cycloaddition reaction of [3$_4$](1,2,4,5)cyclophane, *Eur. J. Org. Chem.,* 1223, 1999.
22. (a) Yasutake, M., Sakamoto, Y., Onaka, S., Sako, K., Tatemitsu, H., and Shinmyozu, T., Crystal structural properties of a pinwheel compound: [3.3.3.3.3.3]-(1,2,3,4,5,6)cyclophane *Tetrahedron Lett.,* 41, 7933, 2000; (b) Yasutake, M., Koga, T., Sakamoto, Y., Komatsu, S., Zhou, M., Sako, K., Tatemitsu, H., Aso, Y., Inoue, S., and Shinmyozu, T., An improved synthetic route of [3$_5$](1,2,3,4,5)cyclophane and structural and electric properties of charge transfer complexes of multibridged [3$_n$]cyclophanes (n = 3–6) in the solid state, *J. Am. Chem. Soc.,* 124, 10136, 2002; (c) Yasutake, M., Araki, M., Zhou, M., Nogita, R., and Shinmyozu, T., Structural and electric properties of the charge transfer complexes of 5,7,9-trimethyl-and 2,11,20-trithia[3$_3$](1,3,5)-cyclophanes, *Eur. J. Org. Chem.,* 1343, 2003; (d) Yasutake, M., Koga, T., Lim, C., Zhou, M., Matsuda-Sentou, W., and Shinmyozu, T., Solid state structural properties of multibridged [3$_n$]cyclophanes and their charge transfer complexes, in *Cyclophane Chemistry for the 21st Century,* Takemura, H., Ed., Research Signpost, Kerana, India, 2002, pp. 265–300.

23. (a) Sakamoto, Y., Kumagai, T., Matohara, K., Lim, C., and Shinmyozu, T., Formation of novel cage compounds via photoreaction of [3.3.3](1,3,5)cyclophane, *Tetrahedron Lett.,* 40, 919, 1999; (b) Matohara, K., Lim, C., Yasutake, M., Nogita, R., Koga, T., Sakamoto, Y., and Shinmyozu, T., Formation and structural features of novel cage compounds with pentacyclo-[6.4.0.0.^{3,7}0^{4,11}.0^{5,10}]dodecane skeleton via photolysis of [3.3.3](1,3,5)cyclophane, *Tetrahedron Lett.,* 41, 6803, 2000.
24. Nogita, R., Matohara, K., Yamaji, M., Oda, T., Sakamoto, Y., Kumagai, T., Lim, C., Yasutake, M., Shimo, T., Jefford, C.W., and Shinmyozu, T., A photochemical study of [3_3](1,3,5)cyclophane and emission spectral properties of [3_n]cyclophanes (n = 2–6), submitted to *J. Am. Chem. Soc.,* in press.
25. Lim, C., Yasutake, M., and Shinmyozu, T., Photolysis of [3_4](1,2,3,5)cyclophane: formation of a pentacyclo[6.3.1.1.^{6,10}0.^{3,7}0^{4,10}]dodecane skeleton with abnormally elongated C-C single bonds, *Tetrahedron Lett.,* 40, 6781, 1999.
26. Lim, C., Yasutake, M., and Shinmyozu, T., Formation of a novel cage compound with a pentacyclo[6.3.0.1.^{4,11}0.^{2,6}0^{5,10}]dodecane skeleton by photolysis of [3_4](1,2,4,5)cyclophane, *Angew. Chem. Int. Ed. Engl.,* 39, 578, 2000,.
27. Koga, T., Yasutake, M., and Shinmyozu, T., Synthesis and crystal structural properties of fluorinated [3_3](1,3,5)cyclophanes, *Org. Lett.,* 3, 1419, 2001.

24

Photochemistry of Allenes

Toshio Shimizu
Tokyo Metropolitan University

24.1 Introduction

Allenes are frequently used as building blocks for the synthesis of cyclic compounds by inter- and intramolecular photochemical cyclization reactions with ketones, thiones, enones, and related compounds. Most of the reactions, however, proceed between the ground state of the allenes and the excited state of the other reactants. Over the past 40 years, many photochemical reactions of allenes have been reported, and theoretical studies of the excited states have been conducted.[1–6] In this chapter, the fundamental photochemical reactions of allenes will be described.

24.2 Photochemical Reactions of Acyclic Allenes

In 1957, Collin and Lossing reported that the mercury-photosensitized decomposition of allene in the vapor phase leads to the formation of a C_3H_3 radical, which was detected by mass spectrometry. This radical affords the corresponding dimer.[7] They proposed two modes of decomposition for the mercury-photosensitized decomposition of 1,2-butadiene: one is decomposition giving H_2 and C_4H_4, and the other path yields CH_3 and C_3H_3 radicals. Later, Doepker and co-workers studied the direct photochemical reaction of 1,2-butadiene.[8,9] Vacuum-ultraviolet photolysis (1470 and 1236 Å) of 1,2-butadiene **1** affords vinylacetylene **2**, methylacetylene **3**, acetylene **4**, 1,3-butadiene **5**, butatriene **6**, and ethylene **7**. Ward and Karafiath reported the photochemical reaction of 1,2-hexadiene.[10] Benzene-sensitized vapor-phase photolysis (2537 Å) of 1,2-hexadiene **8** leads to the formation of 1,3-butadiene **5** ($\phi = 0.16$), ethylene **7** ($\phi = 0.15$), vinylcyclobutane **9** ($\phi = 0.07$), and bicyclo[3.1.0]hexane **10** ($\phi = 0.005$) as the primary products, whereas direct vacuum-ultraviolet photolysis (1600–2100 Å) of **8** yields **5**, **7**, **9** and a further nine products. Products **5**, **7**, and **9** are suggested to be formed via the intermediate biradical species **11**, which is generated by a pathway similar to that of the Norrish type II reaction of ketones. The bicyclic product **10** may be formed by an allene–cyclopropylidene rearrangement followed by insertion into a CH bond. Chapman reported the photochemical reaction of the simplest allene.[11] Irradiation of allene **12** matrix-isolated in argon at 8 K affords cyclopropene **13** and methylacetylene **3**.

0-8493-1348-1/04/$0.00+$1.50

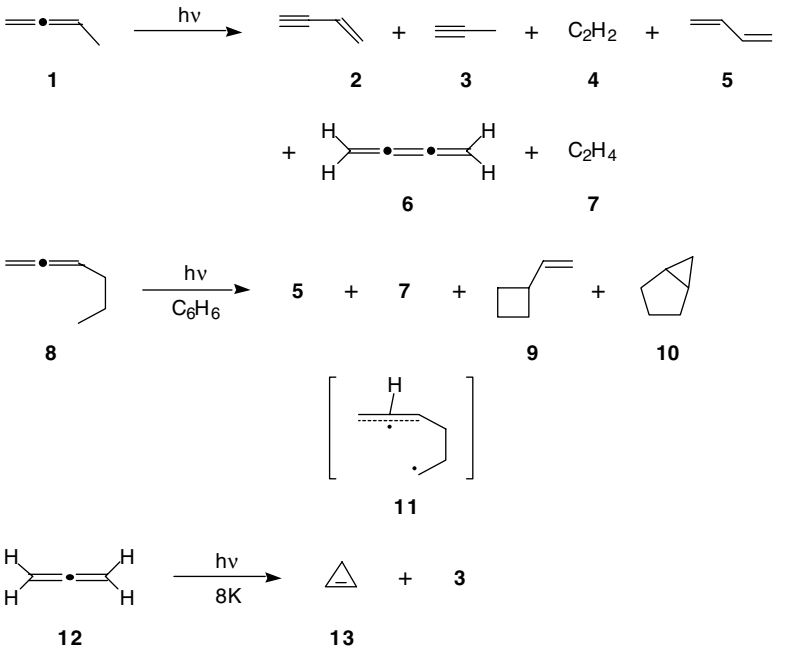

Fujita and co-workers reported the photochemical reaction of allenes in acetic acid.[12] Irradiation (254 nm) of **14a–e** affords the respective enol acetates **15**. In the reaction of **14b**, a triplet mechanism is proposed on the basis of quenching experiments. In methanol solution, on the other hand, the photochemical reaction of tetraphenylallene **16,** using Corex or Pyrex filters, was reported by Klett and Johnson to yield the allylic methyl ether **17** as the major photoproduct along with **18** and **19** (in ratios of 10:1:1).[13] Similar reactions of triphenylallene **20** and 1,3-diphenylallene **21** also afford allyl ethers **22**, **23** (5:1), and **24**, respectively. In these reactions, a mechanism involving a strongly polarized planar singlet excited state is proposed on the basis of triplet sensitization experiments.

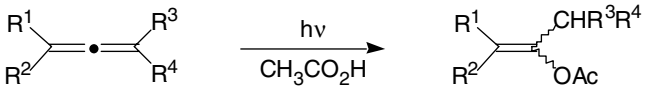

14a $R^1 = n\text{-}C_6H_{13}$; $R^2 = R^3 = R^4 = H$ **15a**
14b $R^1 = Ph$; $R^2 = Me$; $R^3 = R^4 = H$ **15b**
14c $R^1 = Ph$; $R^2 = R^3 = Me$; $R^4 = H$ **15c**
14d $R^1 = m\text{-}MeOC_6H_4$; $R^2 = Me$; $R^3 = R^4 = H$ **15d**
14e $R^1 = m\text{-}CF_3C_6H_4$; $R^2 = Me$; $R^3 = R^4 = H$ **15e**

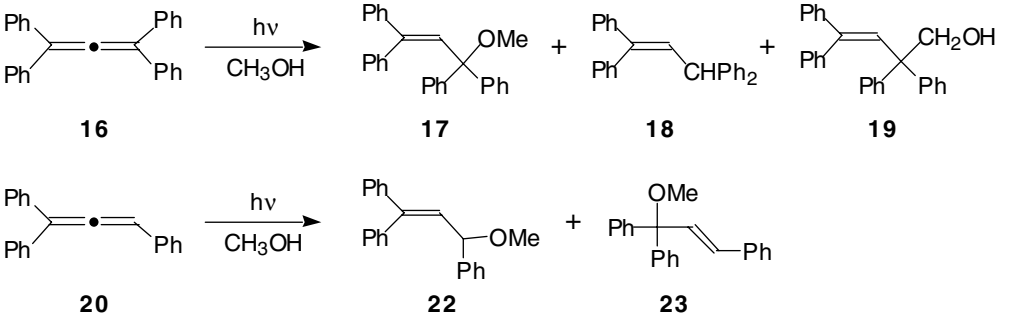

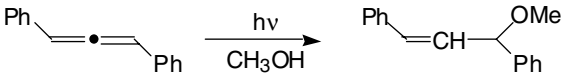

21 **24**

Several cyclopropene-forming reactions from allenes have been reported. Steinmetz and co-workers reported that the direct irradiation of 1,1-diphenylallenes **25** through a Vycor filter in *t*-butanol produces 3,3-diphenylcyclopropenes **26** and diphenylpropynes **27**, along with indenes **28**, as the major products.[14,15] The mechanism is proposed as follows. Vertical allene excited state **25*** forms the vinylmethylene biradical species **29** via 1,2-hydrogen migration. Further hydrogen migration within **29** affords propynes **27**. On the basis of deuterium labeling experiments, it is suggested that the second 1,2-hydrogen shift is the rate-determining step. Due to unfavorable steric interactions from bulky terminal substitution, the stereoisomerization of **29** to *anti*-**30** would provide a pathway for the formation of cyclization products **26** and **28**. An additional pathway for the formation of products **26** and **28** involving equilibration from **30** to vinylcarbene followed by cyclization is suggested on the basis of theoretical calculations.[16] Klett and Johnson also reported that irradiation (254 nm) of triphenylallene **20** in pentane at –10°C (to prevent thermal dimerization) rapidly forms **31–33** as the primary photoproducts.[17,18]

Irradiation (>220 nm) of tetraphenylallene **16** in cyclohexane very slowly yields indene **34** as the primary product, and no cyclopropene derivative is formed. In this reaction, triplet sensitization (xanthone, benzene, wavelengths >330 nm) gives unreacted **16** and the sensitizer. In these reactions in hydrocarbons, vinylcarbenes are proposed as the common intermediates. The direct photolysis of vinylidenecyclobutane **35** in pentane or hexane at 185 nm was reported by Steinmetz and co-workers to afford spiro[2.3]hex-1-ene **36**, ethynylcyclobutane **37**, 3-methylenecyclopentene **38**, butatriene **6**, and ethylene **7** as the primary products in quantum yields of 0.054, 0.044, 0.078, 0.12, and 0.14, respectively.[19] The reaction path to compounds **36** and **37** is thought to involve the biradical **39** generated by the 1,2-hydrogen shift of **35**. Compound **38** is formed via biradical **40** generated by 1,2-carbon migration. The reverse reaction from spiro compound to allene at 185 nm was also reported in the case of spiro[2.4]hept-1-ene **41** to yield vinylidenecyclopentane **42**.[20]

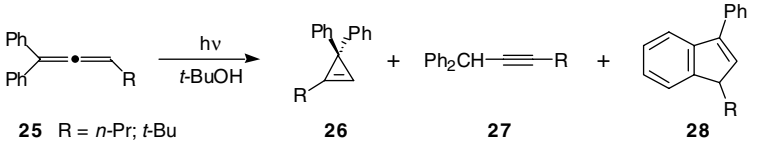

25 R = *n*-Pr; *t*-Bu **26** **27** **28**

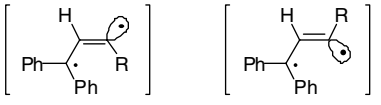

29 **30**

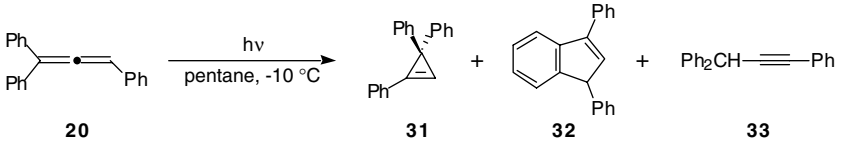

20 **31** **32** **33**

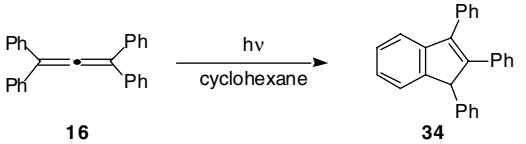

16 **34**

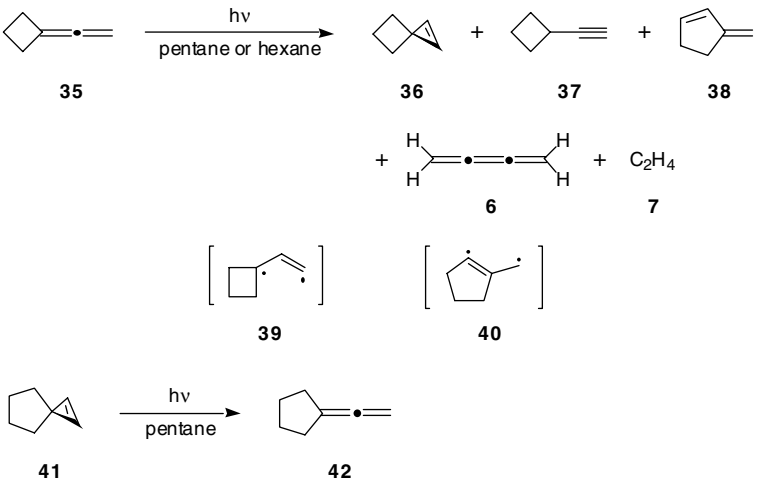

The photochemical reactions of allenes via an electron-transfer pathway have also been reported. The triplet-sensitized reaction of tetraphenylallene **16** in the presence of xanthone was reported by Klett and Johnson to afford only vinyl ether **43**.[13] They also reported that the photochemical reaction (λ >330 nm) of triphenylallene **20** in methanol in the presence of 1,4-dicyanonaphthalene (1,4-DCN) yields vinyl ethers **44–46** via an electron-transfer pathway, together with allyl ether **47** and alkyne **33**.[21] In this reaction, the radical cation of allene **48** is assumed to be the key intermediate.

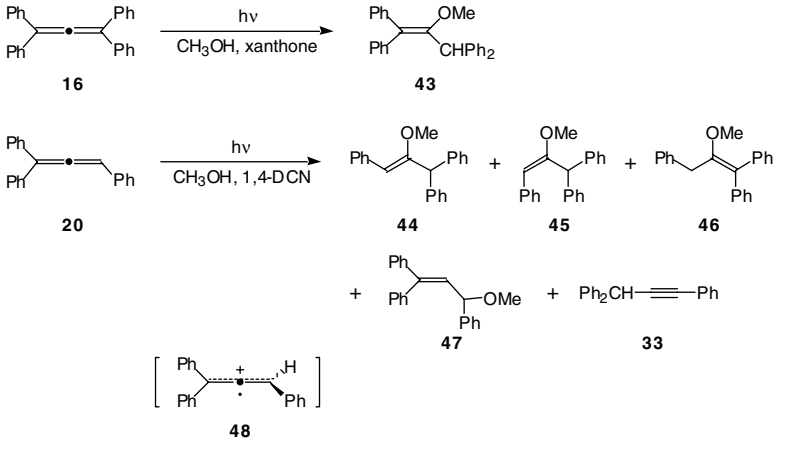

Mariano and co-workers also reported the photochemistry of allenes using an electron-transfer sensitizer.[22,23] Irradiation of allenes **12**, **49**, and **50** in the presence of 2-phenylpyrrolinium perchlorate affords adducts **51** and **52**, **53** to **55**, and **56**, respectively. In these reactions, the radical cation of allene **57** and pyrrolidinyl radical **58** are assumed to be the key intermediates. Mangion and co-workers reported the photochemical reactions of allenes with cyanoarenes.[6] For example, irradiation of 1,2,4,5-tetracyanobenzene **59** and tetramethylallene **50** in acetonitrile–methanol (3:1) through a Pyrex filter leads to 1:1:1 arene–allene–methanol adduct **60**. Similar reaction of 1,1-dimethylallene **49** also affords adducts **61** and **62**.

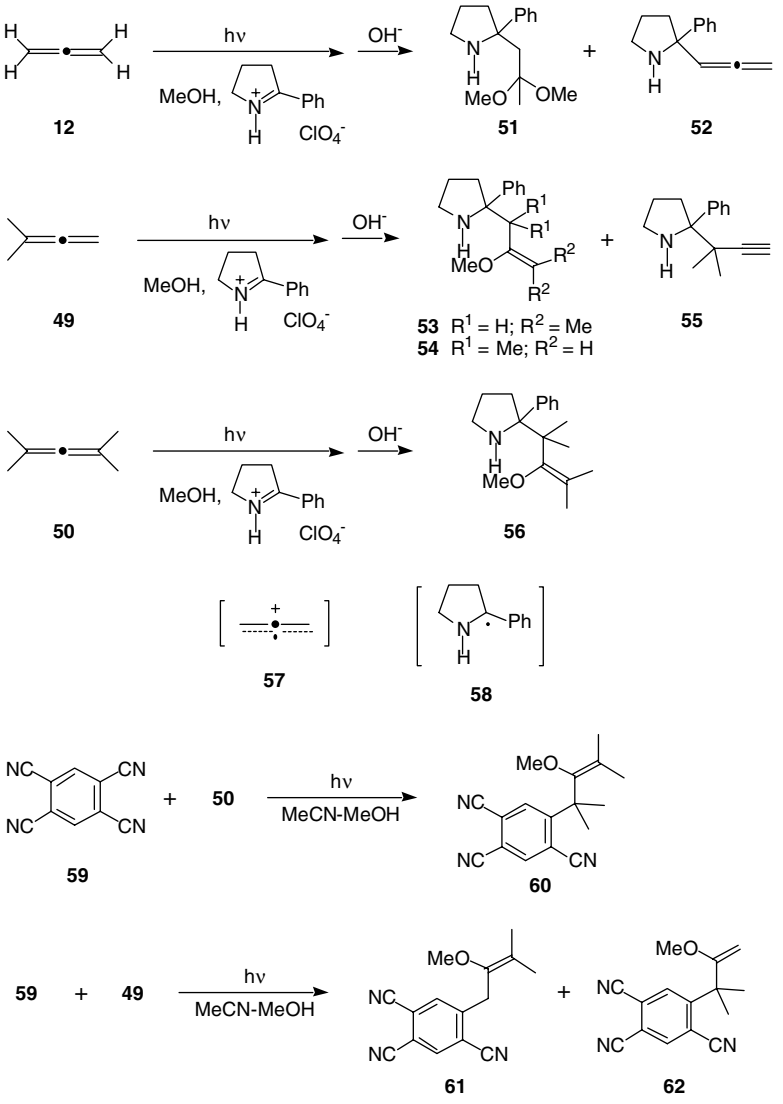

Slobodin reported the photodimerization reaction of allene.[24] Irradiation of 1,1-dimethylallene **49** affords dimers **63** and **64**. The ring-opening reaction of cyclic bisallene **65** was reported by Kaupp to yield butatriene **66** on irradiation in a low-temperature matrix,[25] and the reverse reaction from butatriene **67** to cyclic bisallene **68** in the solid state was also reported by Berkovitch-Yellin and co-workers.[26] The photochemical racemization of optically active penta-2,3-diene **69** in hexane was reported by Rodriguez and Morrison.[27] Kuhn and Schulz reported the photochemical *cis,trans*-isomerization reaction between *cis*-butatriene **70** and *trans*-butatriene **71** and also reported a 39.5%:60.5% *cis-trans* ratio at equilibrium upon irradiation at 313 nm.[28]

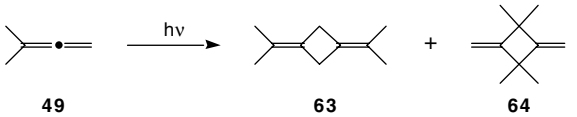

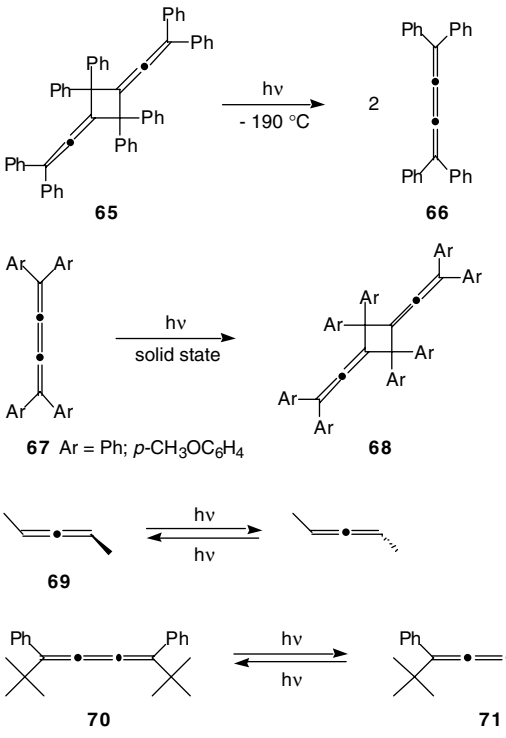

24.3 Photochemical Reactions of Cyclic Allenes

Cyclic allenes are also interesting subjects for photochemistry. In the late 1960s, Ward and Karafiath reported the photolysis of 1,2-cyclononadiene.[29] Benzene-sensitized photolysis (2537 Å) of 1,2-cyclononadiene **72** in the vapor phase affords tricyclo[4.3.0.0^{2,9}]nonane **73** as the primary product ($\phi = 0.17$). The closing of the allene to form the cyclopropylidene and the subsequent transannular insertion of the species into a C–H bond are surmised to be the most reasonable pathway for the formation of **73**. Direct irradiation of **72** in the vacuum-ultraviolet region also forms **73** along with three other isomers.[10] Later, Stierman and Johnson investigated the photochemistry of this system in solution.[30,31] Irradiation ($\lambda > 220$ nm) of a dilute pentane solution of **72** affords tricyclic compound **73**, bicyclo[6.1.0]non-1(9)-ene **74**, and cyclononyne **75** as the primary photoproducts in ratios of 3:94:3. In the formation of **74** from **72**, the authors propose a concerted [$\sigma 2_a + \pi 2_a$] electrocyclization process. Direct irradiation ($\lambda > 220$ nm) of a dilute pentane solution of the larger cyclic allene, 1,2-cyclodecadiene **76**, also yields a cyclopropene derivative **77** and cyclodecyne **78** (5:1) as the primary photoproducts at low conversion (<1%).[32] At high conversions, a complex mixture is obtained from the secondary reactions of **77**. On the other hand, benzene-sensitized irradiation (254 nm) of **76** in the vapor phase yields five major tricyclic products **79–83**. The photochemical reaction of a chiral cyclic allene was also reported.[31] Irradiation of optically active 1,2-cyclononadiene (R)-(+)-**72** or (S)-(–)-**72** yields racemic **72**.

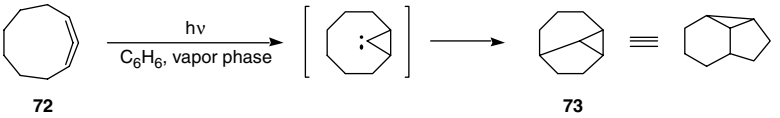

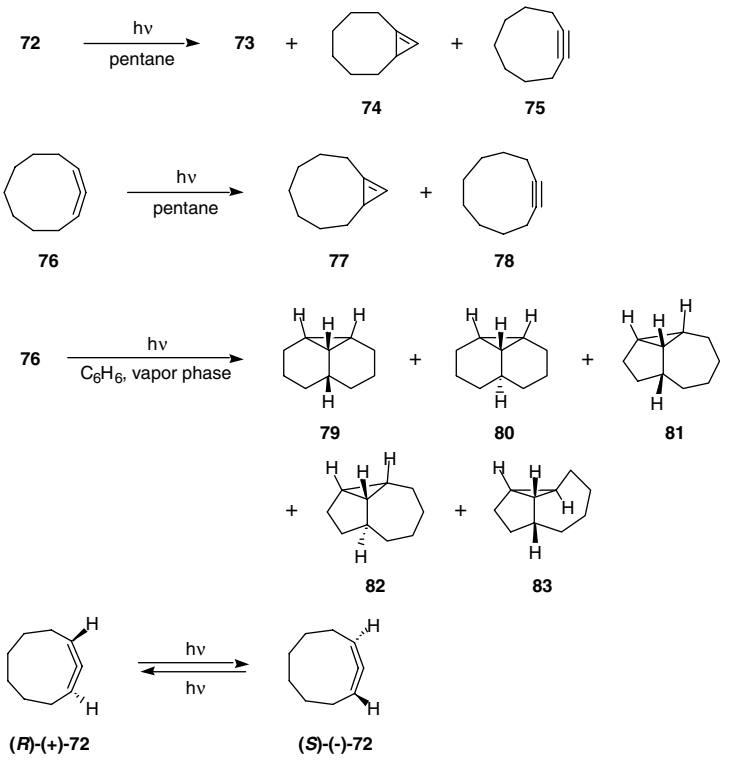

The photochemical reactions of substituted 1,2-cyclononadiene, 1-methyl-1,2-cyclononadiene **84**, were also reported by Stierman and co-workers.[33] Direct irradiation ($\lambda > 220$ nm) of **84** in pentane solution affords seven isomers **85–91** as the primary products, along with the secondary product **92**. Methyl derivative **84** seems to favor vinylcarbene intermediates, in contrast to the concerted reaction of **72**. Benzene-sensitized irradiation of strained 1-*t*-butyl-1,2-cyclooctadiene **93** affords the spiro compound **94** in the vapor phase, and irradiation (254 nm) of a dilute benzene solution of **93** yields 3-*t*-butylbicyclo[3.3.0]oct-2-ene **95** and 2-*t*-butyl-1,3-cyclooctadiene **96** in a 1:1 ratio.[34] The difference in reactivity between the vapor phase and the solution is explained as follows: the vapor-phase reaction proceeds through biradical **97**, whereas selective hydrogen abstraction from C7 yields biradical **98** in solution. On the other hand, direct irradiation (254 nm) of **93** in cyclohexane solution affords five photoproducts: **95**, **96**, and **99–101**.

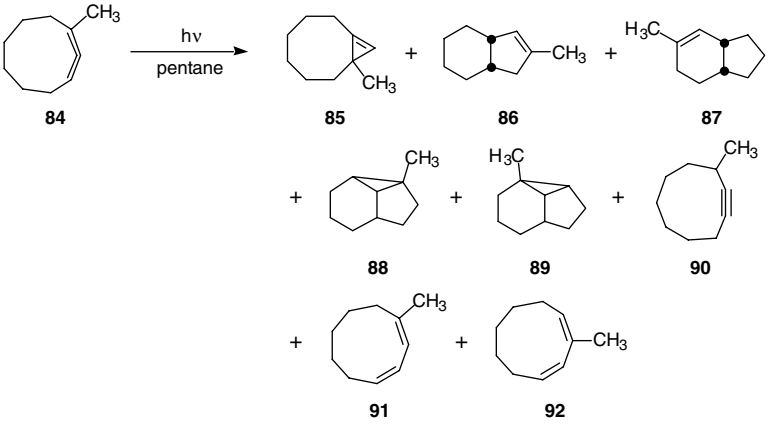

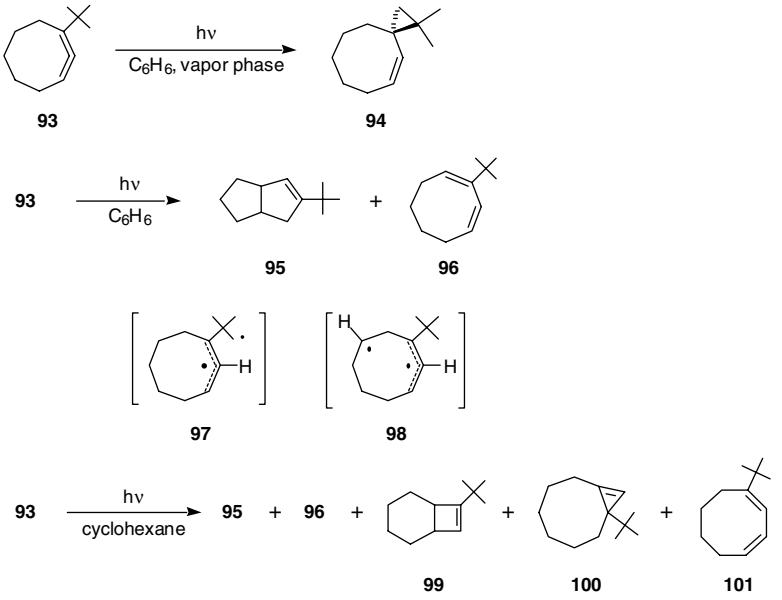

24.4 Intra- and Intermolecular Photochemical Reactions between Allenes and Olefins

1,2,6-Heptatriene **102** was reported by Ward and Karafiath to afford the Cope rearrangement product, 3-methylene-1,5-hexadiene **103** ($\phi = 0.24$), as the primary product by benzene photosensitization at 2537 Å in the vapor phase.[10,35] This rearrangement is not reversible. Similarly, 2,3-divinylcyclopentene **105** is also obtained from 1,2,6-cyclononatriene **104** ($\phi = 0.02$). 1,2-Cyclononadiene is known to give tricyclo[4.3.0.$0^{2,9}$]nonane via the cyclopropylidene intermediate under similar conditions.[29,30] However, in this reaction, the compound that is expected to be obtained from the cyclopropylidene is not produced. The gas-phase benzene-sensitized photolysis (2537 Å) of *cis*-1,2,6-octatriene **106** was reported by Karan to lead to the formation of the *trans*-isomer **107** and six other primary products **108–113** with quantum yields of 0.150, 0.013, 0.023, 0.006, 0.007, 0.042, and 0.011, respectively.[36] At higher conversion, compounds **108–110** become the major products. One reasonable reaction pathway from **106** to **108** and **109** is proposed to proceed in a stepwise manner through an α,δ–biradical intermediate **114** formed from the excited state of the starting material. The intermediate **114** undergoes ring closure to form **108** and **109**. 2-Methyltricyclo[4.1.$0^{1,3}$]heptane **110** is considered to be formed via cyclopropylidene **115**.

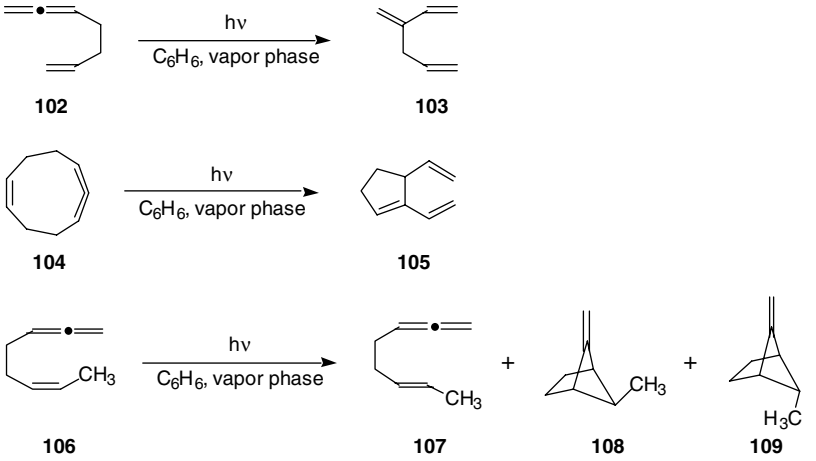

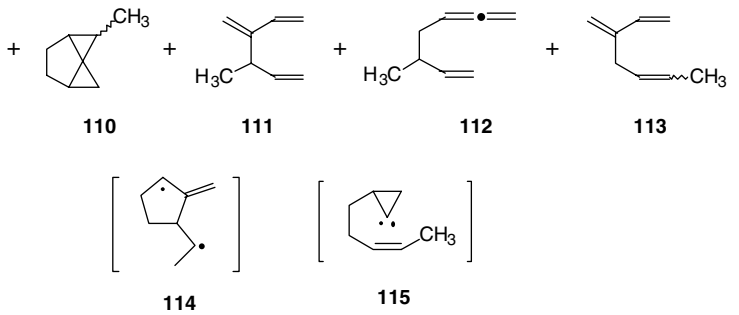

110 **111** **112** **113** **114** **115**

Lankin and co-workers reported the photochemical reaction of allylallene.[37,38] Direct irradiation (254 nm) of *trans*-7-phenyl-2,5,5-trimethylhepta-2,3,6-triene **116** in *t*-butyl alcohol leads to the formation of methylene bicyclo[2.1.0]pentane **117** and allenic cyclopropane **118**, along with *trans,cis*-isomerization product **119**. Similarly, the irradiation of the *cis*-isomer **119** also affords **117** and **120** with *cis,trans*-isomerization product **116**. No di-π-methane rearrangement to cyclopropanes is observed in these reactions. On the basis of quenching studies, the triplet states of *trans*- and *cis*-trienes **116** and **119** are indicated to be chemically significant excited states in the formation of bicyclo[2.1.0]pentane **117**. The photochemical reaction of vinylallene **121** was reported by Maier and co-workers to afford intramolecular cyclization product **122**, and **122** also yields allene **121** photochemically.[39]

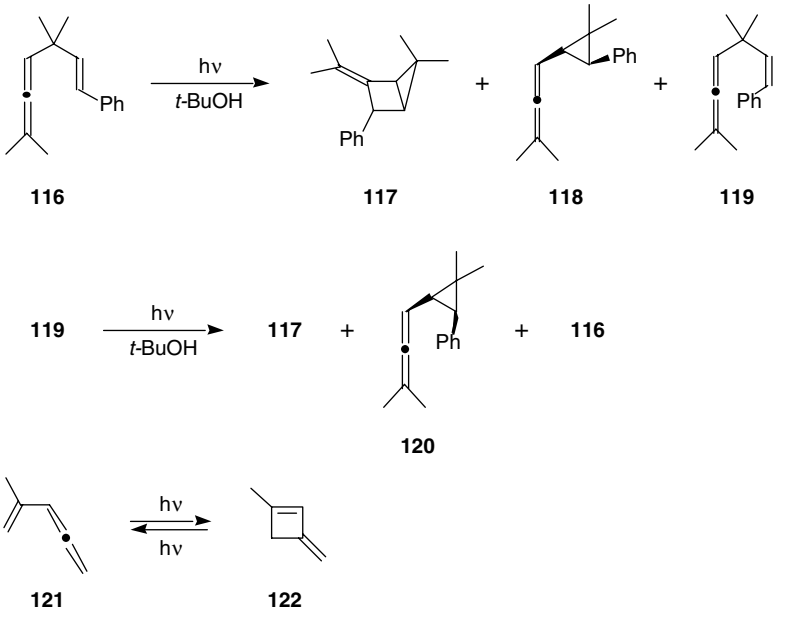

The intermolecular photochemical reaction of allene and olefin was also reported by Schneider and co-workers.[40] The benzophenone-sensitized reaction of 1,2,4-pentatriene **123** in pentane leads to the formation of cyclobutane derivatives **124–126** as the primary photoproducts. These products are suggested to be formed via biradical intermediate **127** followed by intermolecular addition to **123**.

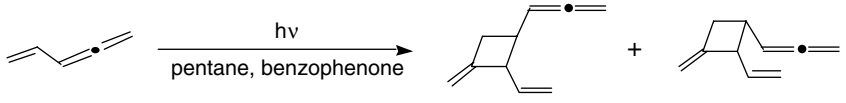

123 **124** **125**

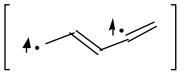

127

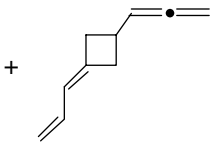

126

24.5 Photochemical Reactions of Allenes Containing Heteroatoms

α-Allenic halides **128** were reported by Troyanowsky and co-workers to undergo photorearrangement in solution to yield 1,3-dienes **129**.[41–43] A mechanism involving a free radical derived from the cleavage of carbon–heteroatom bonds is proposed, and the reactions proceed via bimolecular rearrangement on the basis of crossover experiments. Ueda and Toda reported the photochemical reaction of bromoallene.[44] Irradiation of a benzene solution of bromoallene **130** affords intermolecular cyclization product **131**, whereas the fluorenone-sensitized reaction of **130** yields **132**. In this sensitized reaction, radical **133** is thought to be the intermediate.

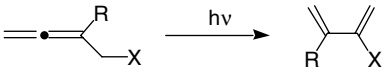

128 R = alkyl
X = Cl, Br, OH, OAc

129

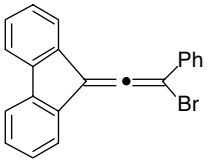

130

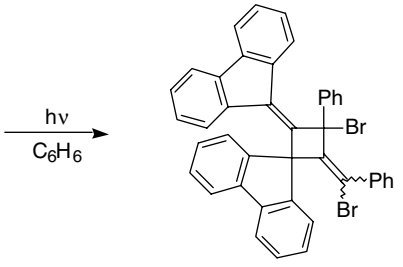

131

130

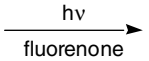

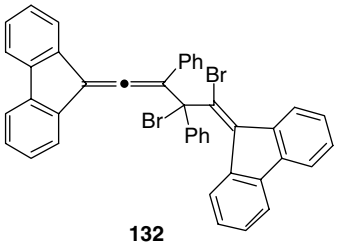

132

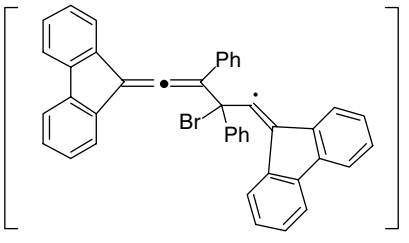

133

Recently, we reported the photochemical reactions of sulfur- and selenium-substituted allenes. Irradiation (λ >300 nm) of benzene solutions of 1,3-bis(alkylthio)allenes **134** affords rearrangement products **135** together with secondary products **136**.[45] A mechanism involving photoinduced 1,2-rearrangement of the alkylthio group to yield carbene **137** via biradical **138** is suggested. Irradiation (λ >300 nm) of cyclic bisallenes *dl*- and *meso*-**139** also causes similar rearrangement to give products **140** and **141**, together with the stereoisomer of the starting materials. The photoisomerization of **139** is assumed to be a result of a reverse reaction from the carbene or the biradical. In the case of selenium-substituted allenes, on the other hand, irradiation (λ >300 nm) of 1,3-bis(methylseleno)allene **142** affords enediynes **143** and **144**, along with rearrangement product **145**.[46] In this reaction, enediynes **143** and **144** are secondary products of propyne **145**. Irradiation (λ >300 nm) of 1,3-bis(benzylseleno)allene **146** also yields enediynes **143** and **144** together with dibenzyldiselenide **147**. Cyclic allenes **148** also form enediynes **143** and **144** with rearrangement product **149**.

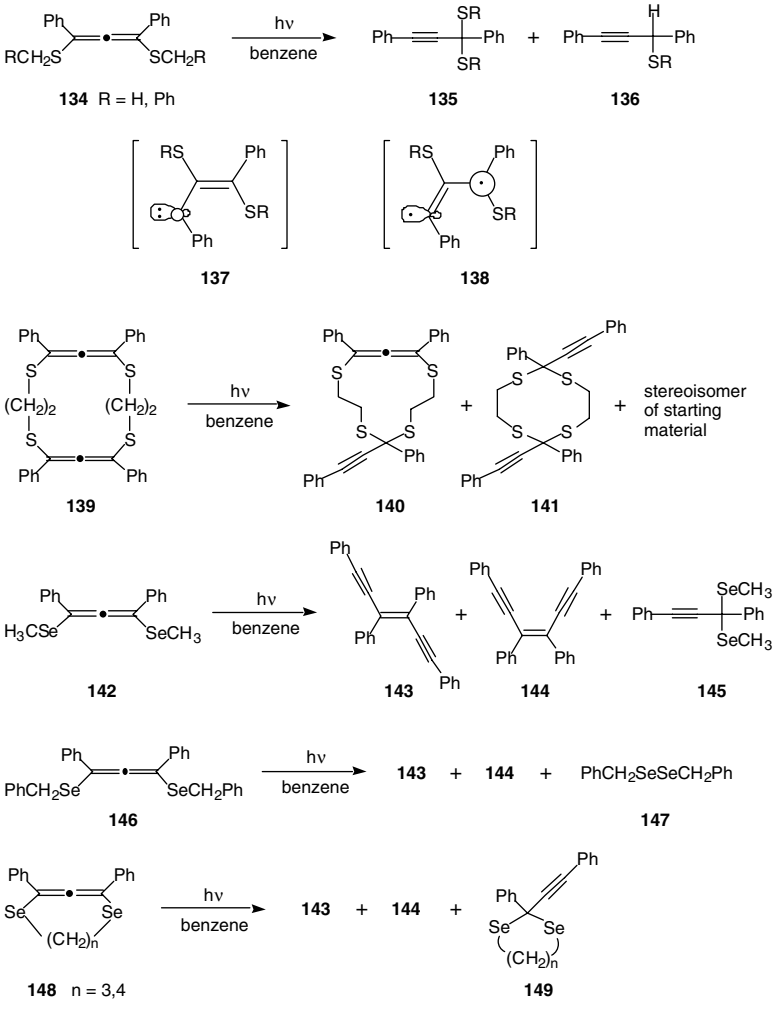

References

1. Johnson, R.P., Cumulene photochemistry, *Org. Photochem.,* 7, 75, 1985.
2. Horspool, W.M., Ed., *Synthetic Organic Photochemistry,* Plenum, New York, 1984.
3. Schuster, H.F. and Coppola, G.M., Eds., *Allenes in Organic Synthesis,* Wiley, New York, 1984.
4. Huntsman, W.D., Rearrangements involving allenes, in *The Chemistry of Ketenes, Allenes and Related Compounds*, Patai, S., Ed., Wiley, New York, 1980, part 2, chap. 15, p. 521.
5. Leigh, W.J., Techniques and applications of far-UV photochemistry in solution. The photochemistry of the C_3H_4 and C_4H_6 hydrocarbons, *Chem. Rev.,* 93, 487, 1993.
6. Mangion, D., Arnold, D.R., Cameron, T.S., and Robertson, K.N., The electron transfer photochemistry of allenes with cyanoarenes. Photochemical nucleophile–olefin combination, aromatic substitution (photo-NOCAS) and related reactions, *J. Chem. Soc., Perkin Trans. 2,* 48, 2001 and references cited therein.
7. Collin, J. and Lossing, F.P., Free radicals by mass spectrometry. XIII. The mercury photosensitized decomposition of allene and butadiene: the C_3H_3 radical, *Can. J. Chem.,* 35, 778, 1957.
8. Doepker, R.D. and Hill, K.L., Vacuum-ultraviolet photolysis of the C_4H_6 isomers. II. 1,2-Butadiene, *J. Phys. Chem.,* 73, 1313, 1969.
9. Diaz, Z. and Doepker, R.D., Gas-phase photolysis of 1,2-butadiene at 147.0 nm, *J. Phys. Chem.,* 81, 1442, 1977.
10. Ward, H.R. and Karafiath, E., The photolysis of allenes, *J. Am. Chem. Soc.,* 91, 7475, 1969.
11. Chapman, O.L., Low temperature photochemical studies, *Pure Appl. Chem.,* 40, 511, 1974.
12. Fujita, K., Matsui, K., and Shono, T., Novel polar photochemical additions of acetic acid to phenylallenes, *J. Am. Chem. Soc.,* 97, 6256, 1975.
13. Klett, M.W. and Johnson, R.P., Cumulene photochemistry: photoaddition of neutral methanol to phenylallenes, *Tetrahedron Lett.,* **24**, 1107, 1983.
14. Steinmetz, M.G., Mayes, R.T., and Yang, J.-C., Interconversions among the C_3H_4 hydrocarbons: photoisomerization of allenes to cyclopropenes and methylacetylenes, *J. Am. Chem. Soc.,* 104, 3518, 1982.
15. Steinmetz, M.G. and Mayes, R.T., Mechanisms for interconversions among C_3H_4 hydrocarbons: deuterium isotope effects and independent generation of vinylmethylene intermediates in photoisomerizations of allenes and cyclopropenes, *J. Am. Chem. Soc.,* 107, 2111, 1985.
16. Sevin, A. and Arnaud-Danon, L., Theoretical investigation of the photochemical unimolecular reactions of cyclopropene, *J. Org. Chem.,* 46, 2346, 1981.
17. Klett, M.W. and Johnson, R.P., Cumulene photochemistry: phenyl and hydrogen migration in phenylallene photoreactions, *Tetrahedron Lett.,* 24, 2523, 1983.
18. Klett, M.W. and Johnson, R.P., Cumulene photochemistry: photorearrangements of tetraphenyl and triphenyl C_3 isomers, *J. Am. Chem. Soc.,* 107, 3963, 1985.
19. Steinmetz, M.G., Stark, E.J., Yen, Y.-P., and Mayes, R.T., Far-UV (185-nm) photochemistry of allenes: photoisomerization and cycloreversion reactions of vinylidenecyclobutane, *J. Am. Chem. Soc.,* 105, 7209, 1983.
20. Steinmetz, M.G., Yen, Y.-P., and Poch, G.K., Comparison between ground and excited state reactivity of cyclopropenes: thermolysis and far-U.V. (185 nm) photolysis of spiro[2.4]hept-1-ene, *J. Chem. Soc., Chem. Commun.,* 1504, 1983.
21. Klett, M.W. and Johnson, R.P., Photogeneration of triphenyl C_3 radical cations: deprotonation and nucleophilic addition as competitive pathways, *J. Am. Chem. Soc.,* 107, 6615, 1985.
22. Somekawa, K., Haddaway, K., Mariano, R.S., and Tossell, J.A., Electron-transfer photochemistry of allene–iminium salt systems. Probes of allene cation radical structure by theoretical and chemical techniques, *J. Am. Chem. Soc.,* 106, 3060, 1984.
23. Haddaway, K., Somekawa, K., Fleming, P., Tossell, J.A., and Mariano, P.S., The chemistry of allene cation radicals probed by the use of theoretical and electron-transfer photochemical methods, *J. Org. Chem.,* 52, 4239, 1987.

24. Slobodin, Y.M., Photodimerization of 3-methyl-1,2-butadiene, *Zh. Org. Khim.,* 24, 1556, 1988.
25. Kaupp, G., Photochemische Umlagerungen und Fragmentierungen von Alkenen und Polyenen, *Angew. Chem.,* 90, 161, 1978.
26. Berkovitch-Yellin, Z., Lahav, M., and Leiserowitz, L., Photochemistry of crystalline cumulenes. Reassignment of the structure of the solid-state photodimer of tetraphenylbutatriene, *J. Am. Chem. Soc.,* 96, 918, 1974.
27. Rodriguez, O. and Morrison, H., Photosensitized racemization of an optically active allene, *J. Chem. Soc., Chem. Commun.,* 679, 1971.
28. Kuhn, R. and Schulz, B., Über *cis-trans*-isomere Butatrien-Kohlenwasserstoffe, *Chem. Ber.,* 98, 3218, 1965.
29. Ward, H.R. and Karafiath, E., The photolytic conversion of an allene to a cyclopropylidene. The photolysis of 1,2-cyclononadiene, *J. Am. Chem. Soc.,* 90, 2193, 1968.
30. Stierman, T.J. and Johnson, R.P., Cumulene photochemistry: photorearrangement of 1,2-cyclononadiene to a bicyclic cyclopropene, *J. Am. Chem. Soc.,* 105, 2492, 1983.
31. Stierman, T.J. and Johnson, R.P., Cumulene photochemistry: singlet and triplet photorearrangements of 1,2-cyclononadiene, *J. Am. Chem. Soc.,* 107, 3971, 1985.
32. Price, J.D. and Johnson, R.P., Cumulene photochemistry: evidence for *cis-* and *trans*-cyclopropylidene intermediates in triplet photoreactions of 1,2-cyclodecadiene, *J. Am. Chem. Soc.,* 107, 2187, 1985.
33. Stierman, T.J., Shakespeare, W.C., and Johnson, R.P., Cumulene photochemistry: substituent effects on the mechanism of 1,2-cyclononadiene photochemistry, *J. Org. Chem.,* 55, 1043, 1990.
34. Price, J.D. and Johnson, R.P., Cumulene photochemistry: photoreactions of a strained 1,2-cyclooctadiene, *J. Org. Chem.,* 56, 6372, 1991.
35. Ward, H.R. and Karafiath, E., Photosensitized Cope rearrangements of 1,2,6-trienes, *J. Am. Chem. Soc.,* 91, 522, 1969.
36. Karan, H.I., Photolysis of *cis*-1,2,6-octatriene, *J. Org. Chem.,* 46, 2186, 1981.
37. Lankin, D.C., Chihal, D.M., Griffin, G.W., and Bhacca, N.S., The photochemistry of a phenylpropenyl allene; suppression of the di-π-methane rearrangement in an allenic system, *Tetrahedron Lett.,* 4009, 1973.
38. Lankin, D.C., Chihal, D.M., Bhacca, N.S., and Griffin, G.W., The photochemistry of phenylpropenyl allenes. Suppression of the di-π-methane rearrangement in an acyclic system through involvement of the triplet excited state, *J. Am. Chem. Soc.,* 97, 7133, 1975.
39. Maier, G., Reisenauer, H.P., and Freitag, H.-A., Photospaltung von Überbrückten Bicyclobutan-Derivaten — Ein Weg zu Tetrahedranen?, *Tetrahedron Lett.,* 121, 1978.
40. Schneider, R., Siegel, H., and Hopf, H., Thermische und photochemische Dimerisierung von 1,2,4-Pentatrien (Vinylallen), *Liebigs Ann. Chem.,* 1812, 1981.
41. Raffi, J. and Troyanowsky, C., Photochimie – transposition photochimique de composés α–alléniques, *Comptes Rend. Acad. Sci.,* 271C, 533, 1970.
42. Michel, E., Raffi, J., and Troyanowsky, C., Proof of a radical mechanism in the photochemical rearrangement of α–allenic halides, *Tetrahedron Lett.,* 825, 1973.
43. Raffi, J. and Troyanowsky, C., The photorearrangement mechanism of α–allenic compounds: its specific character, *Tetrahedron*, 32, 1751, 1976.
44. Ueda, K. and Toda, F., Photodimerization of 3,3-biphenylene-1-bromo-1-phenylallene, *Chem. Lett.,* 257, 1975.
45. Shimizu, T., Sakamaki, K., Miyasaka, D., and Kamigata, N., Preparation and reactivity of 1,3-bis(alkylthio)allenes and tetrathiacyclic bisallenes, *J. Org. Chem.,* 65, 1721, 2000.
46. Shimizu, T., Miyasaka, D., and Kamigata, N., Synthesis and reactivity of allenes substituted by selenenyl groups at 1- and 3-positions, *J. Org. Chem.,* 66, 1787, 2001.

25

Photooxygenation of 1,3-Dienes

Waldemar Adam
University of Würzburg

Sara Bosio
University of Würzburg

Anna Bartoschek
University of Cologne

Axel G. Griesbeck
University of Cologne

25.1 Introduction and Definition of the Reaction

Since the early period of steroid chemistry, when the first photooxygenation of a 1,3-diene was reported by Windaus and Brunken[1] with an ergosteryl derivative as substrate, hundreds of examples of this reaction type have been described. Similar to the (thermal) reaction of 1,3-dienes with electron-deficient dienophiles, the Diels–Alder reaction mode ([4 + 2]-cycloaddition) is one of several possibilities when 1,3-dienes are subjected to photooxygenation conditions (light, oxygen, a dyestuff, and the substrate). In contrast to ground-state reactions, physical quenching of the electronically excited species (the dyestuff or singlet oxygen) may compete. The electronically excited dyestuff interacts with the diene to produce an electronically excited diene (energy transfer), a diene radical cation (electron transfer), or a pentadienyl radical (hydrogen abstraction) that subsequently is trapped by triplet oxygen. Another possibility is energy transfer from the excited dye (the sensitizer) to triplet oxygen with formation of singlet oxygen. The subsequent reaction of singlet oxygen with an acceptor molecule is termed a Type II process, whereas oxygenation reactions through an activated substrate molecule (radicals) are called Type I processes. In addition to this historically valuable nomenclature,[2] electron-transfer processes that involve alkene radical cations or superoxide radical anion have been designated as Type III photooxygenation reactions.[3] Most reactions discussed in this chapter are Type II reactions of singlet oxygen, the latter in its first electronically excited singlet state ($^1\Delta_g$).

Numerous alternatives exist for performing photooxygenation reactions with respect to solvent, sensitizer, and reaction temperature. Some of the most useful sensitizers for singlet oxygen generation are rose bengal (RB), polymer-bound RB, methylene blue (MB), and eosine for aqueous or alcoholic solvents and haematoporphyrin (HP) or tetraphenylporphin (TPP) for nonpolar organic solvents; recently, C_{60}[4] was also introduced as an efficient sensitizer for nonpolar organic solvents. The triplet energy of these sensitizers is low enough to guarantee selective energy transfer to molecular oxygen; however, in some cases the use of methylene blue may be critical because of electron transfer reactions. As light sources, sodium lamps are most convenient, but "traditional" light sources such as high-pressure mercury lamps

0-8493-1348-1/04/$0.00+$1.50

may be employed if appropriate filters are used to cut off the short-wavelength region ($\lambda >$ ca. 400 nm). Radical scavengers such as 2,5-di-*t*-butyl-phenol may be added in order to suppress radical reactions. Furthermore, typical singlet oxygen quenchers such as DABCO (diazobicyclo[2.2.2]octane) are useful as indicators for the nature of the reactive electronically excited species. Important reviews, which cover recent developments in a greater detail, are helpful for the reader as background material.[5]

25.2 Mechanism of the Singlet Oxygen Diene Photooxygenation

Theoretical Models

Several possibilities exist for the primary interaction of singlet oxygen with 1,3-dienes. As with monoalkenes, the reversible formation of an exciplex possibly precedes product formation. This exciplex collapses to a perepoxide, a 1,4-biradical, or a 1,4-zwitterion. Alternatively, the formation of the [4 + 2]-cycloadduct may take place in a concerted fashion without the involvement of an intermediate. Should intermediates such as those mentioned above participate, other reaction pathways such as hydrogen transfer to give allylic hydroperoxides (ene reaction) or cycloaddition to give 1,2-dioxetanes ([2 + 2]-cycloaddition) compete. MINDO/3 calculations suggested that a stable perepoxide intermediate for the butadiene/singlet oxygen reaction is feasible.[6] Orbital correlations characterize the [4 + 2]-cycloaddition reaction of singlet oxygen with 1,3-dienes as a stepwise process.[7] The role of charge-transfer (CT) interactions in these reactions and a detailed discussion of the various theoretical aspects are given in the review by Yamaguchi.[8]

Sevin and McKee[9] have computed the reaction of singlet oxygen with 1,3-cyclohexadiene at the B3LYP76–31G(d) and CASPT2(12e,10o) levels. They found a stepwise biradical pathway, in which a biradical is formed in the first step with an activation barrier of 6.5 kcal/mol (experimental value: 5.5 kcal/mol). The second transition structure has a lower energy than the biradical intermediate and for this reason the reaction could also be considered as a nonsynchronous concerted reaction. Bobrowski et al.[10] studied the 1,4-cycloaddition of singlet oxygen with both s-*cis*-1,3-butadiene and benzene by CAS MCSCF/CAS MCQDPT2 *ab initio* methods with a 6–31G* basis set. They propose a biradical intermediate on the lowest energy pathway (MCQDPT2/6–31G(d)) of the reaction of singlet oxygen with s-*cis*-butadiene to the endoperoxide. In the case of benzene, the reaction occurs in a concerted manner with an activation energy of 25.3 kcal/mol.

Experimental Results

Rigaudy et al. originally investigated the stereoselectivity of addition of the singlet oxygen to 1,3-dienes[11] with the s-*cis*-1,3-diene **1**. In agreement with the high degree of stereoselectivity observed in this case, Gollnick and Griesbeck[12] have found that *trans,trans*-2,4-hexadiene **4** reacts with singlet oxygen chemo- and stereoselectively to yield the *cis*-disubstituted endoperoxide **5**. The stereoisomeric *cis,trans*-2,4-hexadiene **6**, however, gave a mixture of the *trans*-endoperoxide **7** and its *cis*-isomer **5**. This result was confirmed by NMR studies that clearly showed that singlet oxygen induces *cis-trans* isomerization of the starting 1,3-diene.[13] Such isomerization was also observed for the *cis,cis*-2,4-hexadiene isomer. A time profile of the photooxygenation of the (*E,Z*)-1-aryl-1,3-pentadiene showed that singlet oxygen adds exclusively to the (*E,E*)-isomer that is generated from the (*E,Z*)-isomer by photoinduced isomerization; the rates of both isomerization and photooxygenation increased with increasing electron-donating ability of the aryl ring.[14]

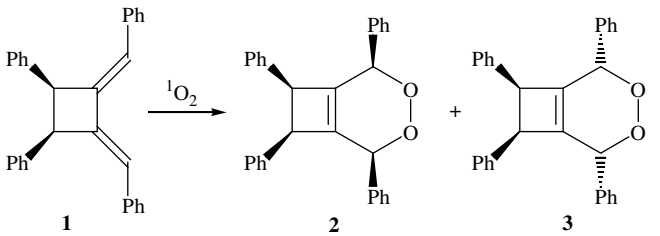

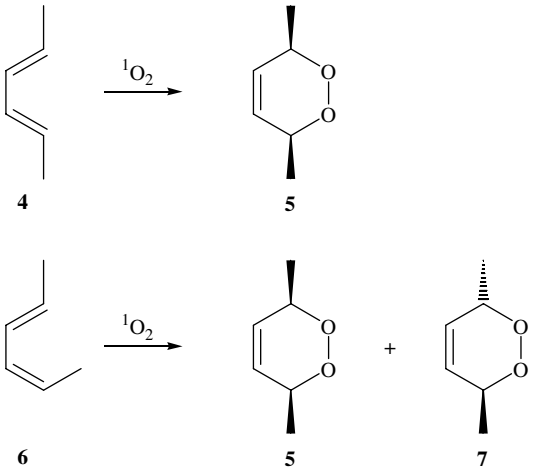

Clennan has investigated two s-*cis*-fixed 1,3-dienes.[15] These compounds, the *trans,trans*- and the *cis,trans*-dioxolanes **8** and **9**, reacted with a high degree of stereoselectivity, besides appreciable amounts of dioxetane formation (*vide supra*). Therefore, it may be deduced that the interaction between singlet oxygen and 1,3-dienes with conformationally flexible 2,3 single bonds leads to intermediary 1,4-biradicals or 1,4-zwitterions. These may undergo retrocleavage to triplet oxygen (physical quenching) with concomitant *cis-trans* isomerization, whereas s-*cis*-fixed 1,3-dienes give endoperoxides highly stereoselectively. From a detailed investigation of the kinetics for a series of Diels–Alder reactions between singlet oxygen and symmetrically and unsymmetrically substituted furans, it was concluded that these reactions proceed concertedly but asynchronously (at least for unsymmetric substrates), with an exciplex involved as the primary reaction intermediate.[16]

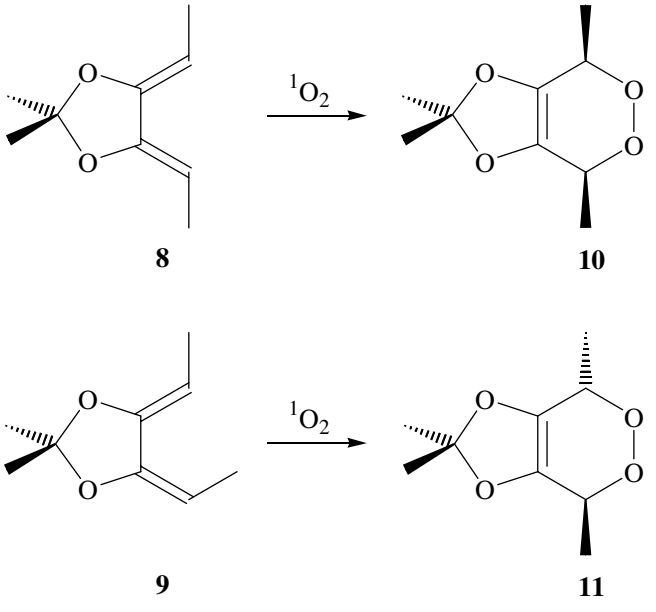

The intervention of an exciplex is in agreement with the nearly zero activation energies for the singlet oxygen [4 + 2]-cycloadditions[17] and with the solvent insensitivity of the reaction rates.[18] Paquette and

TABLE 25.1 Photooxygenation of Unsubstituted 1,3-cyclodienes

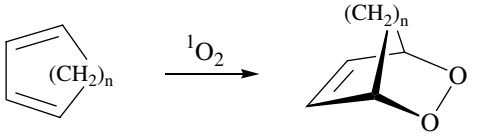

n =	$k_r x 10^{-6}$ ($M^{-1}s^{-1}$)	yield (%)
1	100[a], 32[b]	86[c]
2	7.1[a]	21[d]
3	1.1[a]	29[e]
4	0.065[a]	53[f]

[a]in chloroform, lit.21; [b]in toluene, lit.17;
[c]MeOH,RB,-100°, lit.22; [d]iPrOH,MB, lit.23;
[e]EtOH,eosin, lit.24; [f]CH_2Cl_2,MB, lit.25.

coworkers have shown that the facial selectivity for the [4 + 2]-reaction with tricyclic cyclopentadiene derivatives is unusual compared to other [4 + 2]-cycloadditions, which indicates that the mechanism may be different from that of most Diels–Alder reactions.[19] De Lucchi and co-workers have shown that the cycloaddition of $^1O_2$ to 3,3′,4,4′-tetrahydro-1,1′-binaphthalene occurs with a preference for antarafacial addition, which is consistent with the intermediacy of a perepoxide.[20]

25.3 Substrates for Diene Photooxygenation

Carbocyclic Substrates

Unsubstituted Compounds

One of the most reactive substrates for endoperoxide formation is 1,3-cyclopentadiene. Rate constants of 1×10^8 (in chloroform)[21] and 3.9×10^7 (in toluene)[17] mol^{-1} sec^{-1} have been determined. The kinetics and the solvent dependence of the singlet oxygen [4 + 2]-cycloaddition with 1,3-cyclohexadiene have been investigated in detail.[18,21] The rate constant decreases about tenfold when the ring size is increased by one methylene unit (Table 25.1).

Except for the endoperoxide from 1,3-cyclopentadiene,[22] the higher homologues are thermally stable compounds, which have been isolated in moderate to good yields under various photooxygenation conditions.[23–25] Cyclic 1,3,5-trienes, which can undergo valence tautomerization, give the respective cycloaddition products (Table 25.2).

From 1,3,5-cycloheptatriene[26] and 1,3,5-cyclooctatriene,[27] the respective bicyclic and tricyclic endoperoxides were obtained in 93:7 and 80:20 ratios, respectively. From cyclooctatetraene, no adduct with the bicyclic valence tautomer was obtained, but 26% of the bicyclic [4 + 2]-adduct was isolated.[28] The valence tautomer of cyclooctatetraene, however, could be prepared independently and afforded the expected tetracyclic endoperoxide with singlet oxygen.[29]

Substituted Compounds

Electron-donating substituents activate the 1,3-cyclodiene towards electrophilic attack by singlet oxygen, which clearly demonstrates that the [4 + 2]-cycloaddition is controlled by HOMO (diene)–LUMO (singlet oxygen) interaction. For 1,3-cyclopentadiene derivatives, alkylation or arylation at positions 1 to 4 did

TABLE 25.2 Photooxygenation of Unsubstituted 1,3,5-cyclotrienes

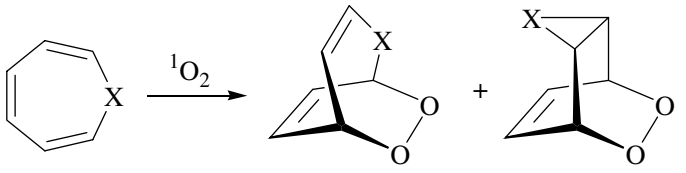

X =	yields (%)	
CH_2	40[a]	3
$(CH_2)_2$	20[b]	5
CH=CH	26[c]	-

[a]CCl_4,TPP, lit.26; [b]CH_2Cl_2,TPP, lit.27; [c]acetone,TPP, lit.28.

not change the chemoselectivity, i.e., only bicyclic endoperoxides were formed.[30] This was not the case for the higher homologues: even α-terpinene **12**, a classical singlet oxygen acceptor[31] and of similar reactivity as 1,3-cyclopentadiene,[21] led to 90% of the [4 + 2]-cycloadduct ascaridole **13** and about 5% of ene products **14–16** (besides 5% *p*-cumene).[32]

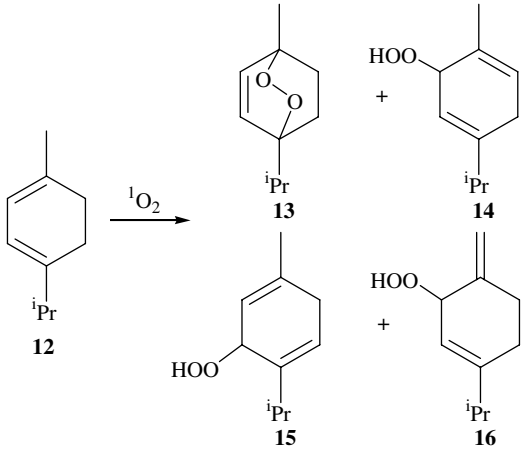

13 /14 /15 /16 = 90 / 2.2 / 2.2 / 0.5

More illustrative was the photooxygenation of the optically active terpene R-(–)-α-phellandrene **17**.[33] In this case, a 3:2 facial selectivity (*cis* predominates) was observed for all products, namely for 65% of the [4 + 2]-cycloadduct **18** and 30% of the ene products **19–21**.[34] The methyl group at position 2 is only marginally involved (ene product **20**) in the reaction but activates the trisubstituted double bond towards the ene reaction (ene product **19**). Alkoxy substituents have been reported to have the same effect.[35]

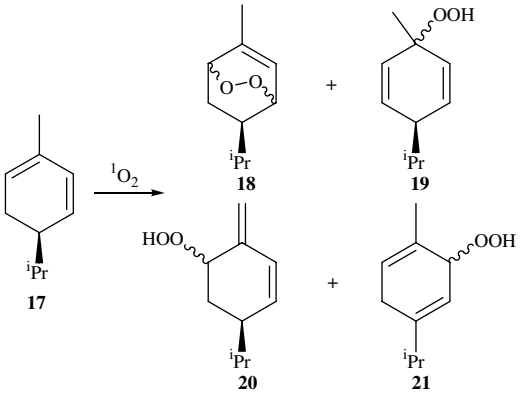

18 /19 / 20 /21 = 65 / 23 / 3.0 / 5.8

An extreme example is the photooxygenation of a hexahydronaphthalene **22** from which only the ene products **23** and **24** were isolated.[36] The latter case constitutes a combination of steric shielding and substituent activation that leads to high loco- and stereoselectivity. The photooxygenation of chiral 1,2-dihydronaphthalene derivatives with additional allylic hydroxy groups proceeds with moderate chemoselectivity ([4 + 2] versus ene reaction) but a high degree of stereoselectivity, which may be rationalized in terms of attractive interactions between the terminal oxygen of $^1O_2$ and the allylic hydroxy group in an intermediate with perepoxide geometry.[37]

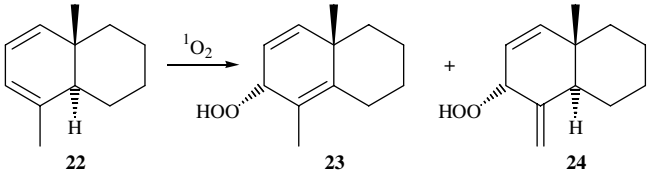

A synthetically useful example for perfect regioselective control was reported for furan photooxygenation in the presence of a tricarbonyliron-protected cyclohexadiene.[38] Numerous examples are known for terpene and steroid substrates with 1,3-cyclohexadiene subunits in which endoperoxides have been isolated in good to excellent yields, e.g., dehydro-ß-ionone **25** gives the endoperoxide **26** in 50% yield by using rose bengal as the sensitizer in methanol.[39]

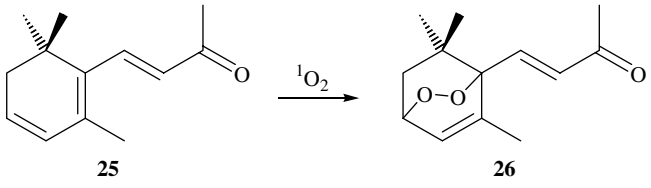

Substituted 1,3,5-cycloheptatrienes and 1,3,5-cyclooctatrienes afford mixtures of bicyclic and tricyclic endoperoxides in ratios that are highly dependent on the electronic nature of the substituent.[27,28,40,41] Indene[42] and 1,2-dihydronaphthalene[43] derivatives were shown to add two equivalents of singlet oxygen to give rise to *bis*-endoperoxides or their corresponding rearrangement products.[44] The photooxygenation of 6-methyl-5-phenylindene **27** in Freon 11/TPP gave the *bis*-endoperoxide **28** in 82% yield.[42]

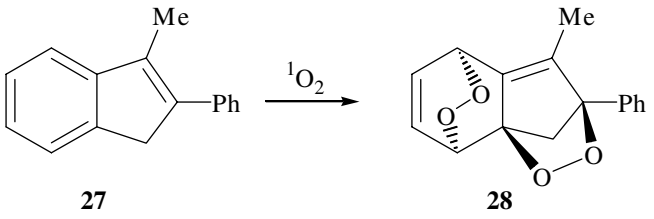

27 **28**

Photooxygenation of pentafulvenes afforded the corresponding endoperoxides[45] as primary products (which rearrange subsequently to allene oxides). The 6,6-dialkoxy-substituted pentafulvene **29** generates the [4 + 2]-cycloadduct **30** and, after further photooxygenation, the diastereoisomeric oxetanes **31** are prepared by subsequent [2 + 2]-cycloaddition.[46]

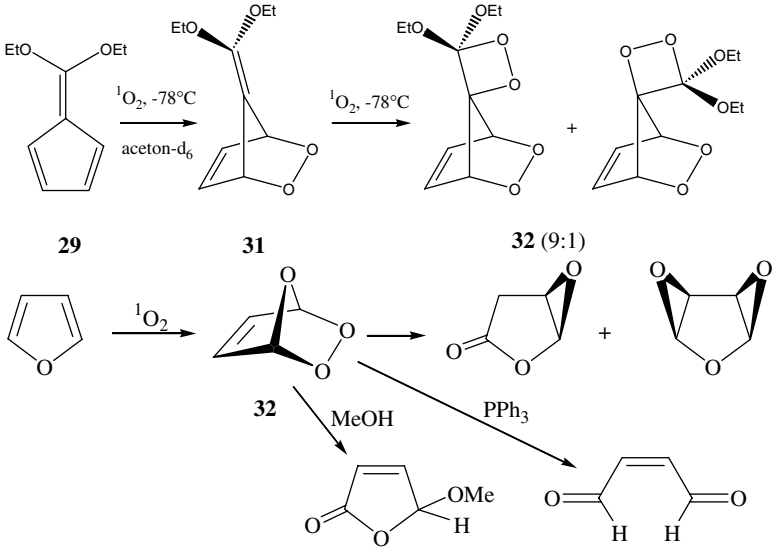

Heterocyclic Substrates

The photooxygenation of furans was investigated initially by Schenck in the mid-forties.[47] A crystalline and highly explosive material **32** was isolated from the parent furan by Schenck and Koch.[48] This secondary ozonide rearranges thermally to an epoxybutanolide and a *bis*-epoxide; reduction with triphenylphosphine leads to maleic dialdehyde, methanolysis to a methoxy butenolide.

The rate constants of singlet oxygen reactions have been determined for a series of substituted furans by Koch,[49] Clennan et al.,[16] and Gollnick and Griesbeck.[50] Only a moderate solvent dependence was observed, which implies a concerted (possibly asynchronous) [4 + 2]-cycloaddition. More thermally persistent endoperoxides were obtained from alkyl-substituted furans, e.g., 2,5-dimethylfuran[51] or furans with electron-withdrawing substituents.[52] A few representative examples of furan endoperoxides together with their thermal stability are given in Table 25.3.

TABLE 25.3 Photooxygenation of Furans

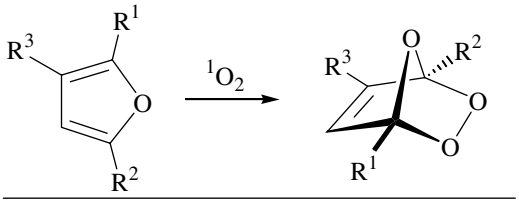

R^1	R^2	R^3	decomp. temp. (°C)
H	H	H	- 15[a]
Me	Me	H	+ 20[b]
Me	Me	COOEt	+ 78[c]

[a] lit.50; [b] lit.51; [c] lit.52.

These furan endoperoxides are valuable building blocks for the synthesis of di- and tetrahydrofuran derivatives, e.g., *bis*-epoxides, epoxy lactones, ene diones, *cis*-diacyloxiranes, enol esters, butenolides,[53] and others. Furthermore, the primary [4 + 2]-cycloadducts may rearrange into 1,2-dioxetanes[54] or 1,2-dioxolenes.[55]

Unlike furan, thiophene was found to be unreactive under photooxygenation conditions. The alkylated derivative 2,5-dimethylthiophene **33**, however, is reactive[56] and the structure of the endoperoxide **34** was unambiguously proven by low-temperature NMR studies,[57] as well as by diimide reduction to the saturated thermally persistent endoperoxide **35**.[58]

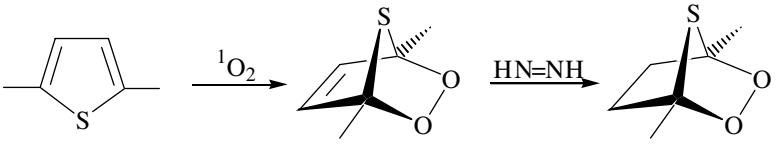

33 **34** **35**

The heterocyclic 1,3-dienes such as pyrroles,[59] thiazoles,[60] and oxazoles[61] are also reactive and afford endoperoxides on photooxygenation. Most of these ozonide-type cycloadducts have neither been isolated nor detected but have been postulated as plausible reaction intermediates.

Acyclic/Cyclic Substrates

Mode Selectivity

As mentioned in the introduction, two main pathways compete with the singlet oxygen [4 + 2]-cycloaddition, the ene reaction and [2+2]-cycloaddition. The formation of carbonyl products during the photooxygenation of dienes is due to the decomposition of the intermediary dioxetane in many cases. Another route to these fragments is a Hock-type cleavage of the allylic hydroperoxides formed by the ene reaction.[62] Three predominant factors control the mode selectivity in the photooxygenation of substrates that possess one (or more) endocyclic C=C double bond(s) and one conjugated exocyclic C=C double bond: (i) the amount of s-*cis* conformer in the equilibrium necessary for a *concerted* [4 + 2]-cycloaddition, (ii) the relative reactivity difference of the C=C double bonds, e.g., an alkoxy substituent activates an exocyclic double bond strongly for [2 + 2]-addition, and (iii) the appropriate alignment of the allylic hydrogens for the competing ene reaction. Even a small amount of the s-*cis* conformer in the conformational equilibrium may give rise to an appreciable amount of endoperoxide due to the very low activation energy of this reaction mode.

TABLE 25.4 Photooxygenation of 1-vinylcycloalkenes[a]

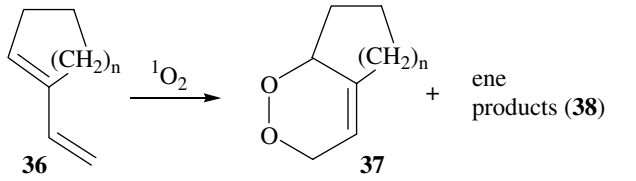

36 **37**

n =	**37** : **38** ([4+2] vs. ene reaction)
1	16 : 84
2	77 : 23
3	22 : 78
4	50 : 50
5	47 : 53
6	67 : 33

[a] 5% MeOH / CH_2Cl_2 mixture, RB as sensitizer, lit. 63.

Substituted Compounds

A series of 1-vinylcycloalkenes **36** with ring sizes from 3 to 8 has been investigated.[63] For these substrates, factor (iii) controls the ratio of [4 + 2] versus ene product (**37/38**) (Table 25.4). It may be safely assumed that the s-*cis*/s-*trans* ratio is similar for all starting materials, and the decisive difference comes from the alignment of the allylic hydrogens in the central ring. Analogous to the ene reactions of singlet oxygen with cyclopentene and cyclohexene, the ene path is largely preferred for the five-membered versus the six-membered ring.

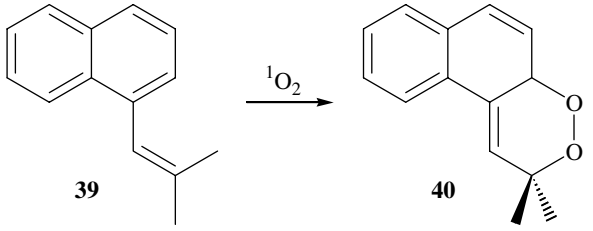

39 **40**

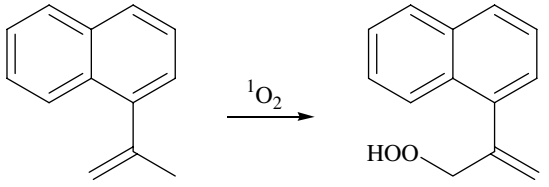

41 **42**

1-Vinylnaphthalenes preferentially undergo [4 + 2]-cycloadditions when alkyl-substituted at the vinylic positions,[64] e.g., the dimethyl substrate **39** gives **40** in 78% yield.[65] In contrast, the geminally dimethyl-substituted substrate **41** is prone to ene reaction because of steric (*peri*) interactions that depopulate the s-*cis* conformer. In this case, controlled by factor (i), the allylic hydroperoxide **42** is formed in 90% yield.[64]

An example in which the relative reactivity of the C=C double bond (factor ii) depends on the population of the s-*cis* conformer (factor i) is the photooxygenation of the *E*- and *Z*-2′-methoxy-1-vinylnaphthalenes **43** and **44**. The *Z*-isomer affords the [4 + 2]- and [2 + 2]-cycloaddition/cleavage products **46** and **47** in nearly equal amounts, whereas the *E*-diastereomer **43** generates, nearly quantitatively,

the endoperoxide **45**.[66] Presumably, the s-*cis* conformer of **44** is present only in small amounts, and even the rapid [4 + 2]-cycloaddition does not compensate for this disadvantageous situation.

For similar substrates, such as substituted styrenes,[67] stilbenes,[68] or 1-vinylthiophenes,[69] in some cases *bis*-endoperoxides have been isolated similar to the indene and dihydronaphthalene cases (*vide infra*). Also, terpene derivatives are a treasure house of polyfunctional substrates for which all types of reaction modes have been observed.[70] Substituted 3-vinylindoles **48** without allylic hydrogens give with $^1O_2$ the endoperoxides **49** by [4 + 2]-cycloaddition unless the s-*cis* conformation is disfavored due to the substituent pattern.[71] Product **50** is formed presumably by [2 + 2]-cycloaddition of singlet oxygen and subsequent 1,2-dioxetane cleavage.

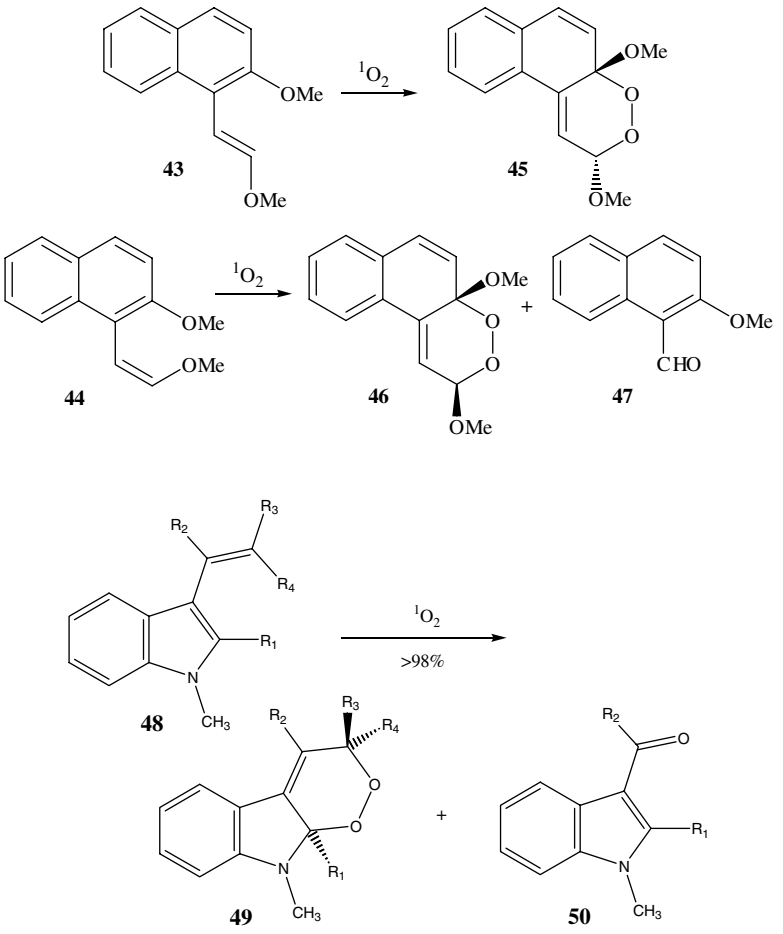

Acyclic Substrates

Mode Selectivity and Regioselectivity

According to the guidelines described previously, the mode selectivity and regioselectivity of singlet oxygen reactions with acyclic 1,3-dienes may be controlled and predicted. The parent compound, 1,3-butadiene, leads to the endoperoxide in 20% yield.[72] Electron-donating substituents activate 1,3-butadienes in the reaction with the electrophilic singlet oxygen. As already discussed, alkyl substituents with allylic hydrogens favor ene reactions with singlet oxygen, whereas alkoxy substituents activate the diene for [2 + 2]-cycloadditions. A fact that is often ignored is that in many cases the main reaction pathway is efficient physical quenching of singlet oxygen by the diene.[73]

Another way to control mode selectivity is by solvent polarity. The photooxygenation of 2,4-dimethyl-1,3-pentadiene in different polar and nonpolar solvents gave in all cases the [4 + 2]-cycloaddition product as the major product. In CCl_4, the [4 + 2]-mode selectivity is as high as 97%, but it drops in polar and especially in protic solvents such as methanol to 65%.[74] From the dependence of the [4 + 2]-cycloaddition of substituted naphthalenes on the solvent structure and polarity, exciplex formation was suggested especially in the highly polar solvent dimethylformamide (DMF).[75]

Substituted Compounds

As a model substrate, 2,5-dimethyl-2,4-hexadiene **51** has been intensively investigated by several research groups.[73,76–79] Depending on the solvent polarity, five peroxidic products have been isolated in varying relative yields: the endoperoxide **52** (from [4 + 2]-cycloaddition), the allylic hydroperoxide **53** (from ene reaction), the 1,2-dioxetane **54** (from [2 + 2]-cycloaddition), the diene hydroperoxide **55** (either from a vinylogous ene reaction or a radical-induced rearrangement of **53**),[78] and the methoxy-substituted hydroperoxide **56** (a methanol trapping product) were observed. A maximum of 23% of the [4 + 2]-cycloaddition product **52** was detected in tetrachloromethane, whereas the dioxetane **54** dominated in polar acetonitrile.

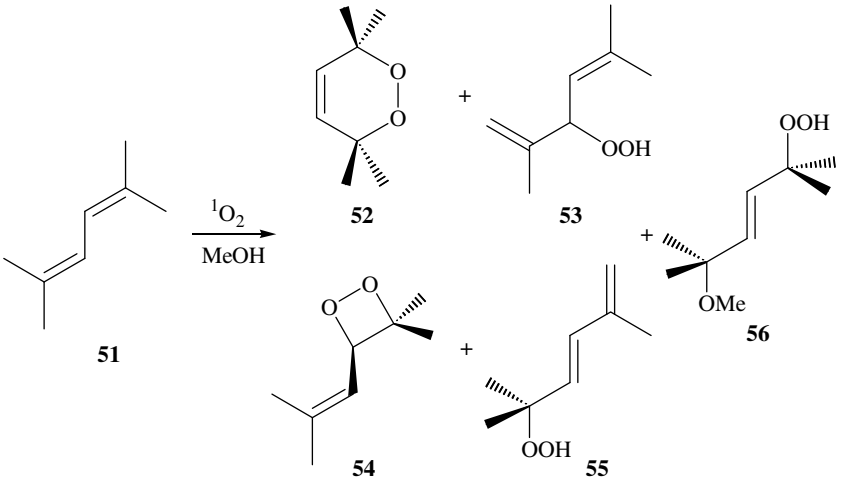

For a series of methyl- and phenyl-substituted 1,3-butadienes, the proportion of [4 + 2]-cycloaddition to ene products was shown to be determined by the factors mentioned previously (Table 25.5).[79] The relative amount of [4 + 2]-cycloaddition products may be explained by assessing the number of appropriate allylic hydrogens and the s-*cis*/s-*trans* ratio for the 1,3-diene system.

The terpenes α- and ß-myrcene are classical examples of substrates controlled by factor (ii). In these polyenes the relative reactivity of the nonconjugated C=C double bond (di- versus trisubstituted) controls the first reaction event. ß-Myrcene, a monoterpene triene with a trisubstituted nonconjugated double bond, undergoes preferentially the ene reaction with subsequent [4 + 2]-cycloaddition,[80] whereas α-myrcene **57** solely reacts in a [4 + 2]-mode to give the endoperoxide **58**.[81] Alkoxy-substituted 1,3-dienes, which cannot undergo ene reaction, have been shown to be excellent substrates for [2 + 2]-cycloaddition.[82,83] The 1,4-di-*t*-butoxy-1,3-butadienes were the first substrates that showed nonstereoselective [2 + 2]-cycloaddition reactions. Formation of the endoperoxide **60** was observed only from the *E,Z*-isomer **59**, which indicates a pronounced activation effect by the alkoxy groups for dioxetane formation.

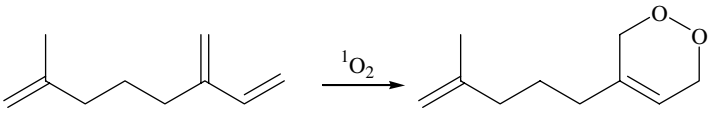

TABLE 25.5 Photooxygenation of Acyclic 1,3-dienes[a]

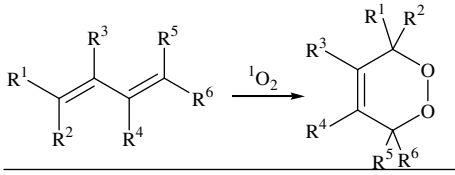

	yield (%)
R^1-R^6= H	20
R^1 = Me	31
R^3= Me	50
$R^{1,5}$ = Me	56
$R^{1,4}$ = Me	58
$R^{3,4}$ = Me	10
$R^{1,2,4}$ = Me	41
$R^{1,5}$ = Ph	92

[a] CCl_4, TPP as sensitizer, lit. 79.

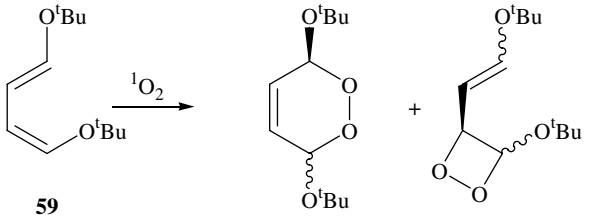

59 **60** (3 diastereomers)

25.4 Diastereoselectivity in the [4 + 2]-Cycloaddition Reaction with Singlet Oxygen

The diastereoselectivity of the [4 + 2]-cycloaddition may be controlled with chiral auxiliaries, by directing the singlet oxygen attack from the less hindered side of the diene (steric control) through conformational effect of the substrate or by using electrostatic interactions between the substrate and the incoming singlet oxygen (electronic control). High facial selectivity (d.r. = 95:5 like versus unlike attack) has been achieved for the reaction of singlet oxygen with a 1,3-diene derived from 2,2-dimethyloxazolidine-substituted amides of sorbic acid **61**; such stereochemical control derives from the steric interactions between singlet oxygen and the shielding substituent in the chiral auxiliary.[84]

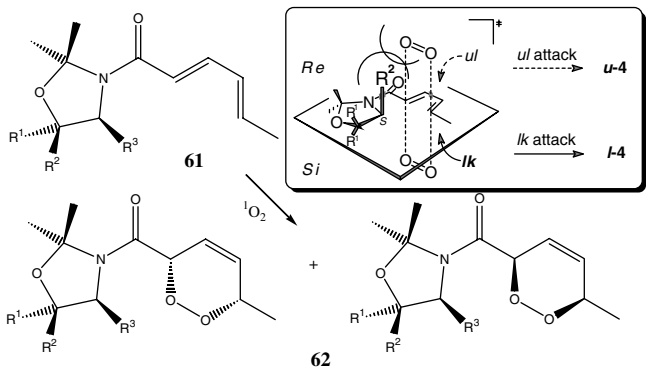

61 **62**

In the photooxygenation of chiral dienol ethers, the facial selectivity (maximum d.r. achieved was 74:26) depends both on the conformational preference of the dienol ether and on the ability of the chiral auxiliary to shield one face of the diene substrate. The modest diastereoselectivity that is observed for most cases is due to the lack of conformational control in the substrate.[85] The reaction of the isopropyl-substituted cyclohexadiene with singlet oxygen gave an endoperoxide that is derived from preferential attack on the sterically *more* hindered diastereotopic face of the diene. It was suggested that the less hindered face undergoes ene reaction preferentially rather than [4 + 2]-cycloaddition through a common perepoxide intermediate.[86] A surprising result was described for the photooxygenation of the 1,3-diene **63,** for which *E*/*Z*-isomerization of the enone double bond is not possible: a mixture of the diastereoisomeric 1,4-endoperoxides **64** (expected configuration) and **65** was isolated. This nonselective [4 + 2]-addition reaction was rationalized in terms of a two-step process through a perepoxide intermediate.[87]

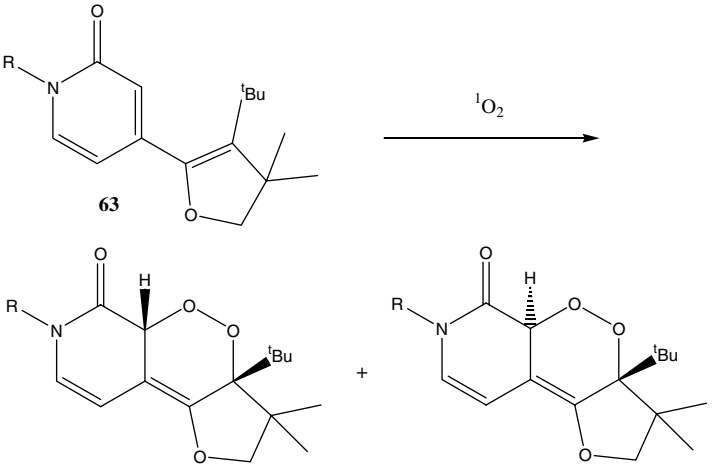

Hydrogen-bonding substituents strongly influence the facial selectivity of the singlet oxygen [4 + 2]-cycloaddition, as shown by the hydroxy-directing effect with chiral naphthyl alcohols.[88] For facially unsymmetric dienes, e.g., the hexacyclo-[7.5.1.0.^{1,6}0.^{6,13}0.^{8,12}0.^{10,14}]pentadeca-2,4-diene-7,15-diones, the facial diastereoselectivity of the [4 + 2]-cycloaddition with singlet oxygen may be modulated by modification of protecting groups.[89]

25.5 Applications of the Photooxygenation of 1,3-Diene

Primary Products

The peroxide products obtained in the photocycloaddition of 1,3-dienes with singlet oxygen are of interest either as pharmaceutically active compounds, e.g., the legendary ascaridole **13**, or as model compounds for biochemical studies, e.g., prostaglandin biosynthesis,[90] allocolchicinoids synthesis.[91] These compounds were prepared directly from fatty acid precursors[92] or from 1,3-cyclopentadienes, followed by reduction of the resulting C=C double bond.[93] Other attractive target structures were antitumor-active cyclic peroxy ketals chondrillin and plakorin synthesis.[94] For most preparative purposes, however, the photooxygenation reactions have been designed in such a way that either *in situ* or by subsequent treatment of the initially formed peroxides synthetically valuable products and/or building blocks have been obtained for organic synthesis, e.g., the preparation of hydroxycodeinone from thebaine.[95]

Secondary Products

Endoperoxides (also 1,2-dioxetanes) are versatile starting materials for further transformations. In view of the weak O-O bond, these peroxides are thermally sensitive to homolytic cleavage, a feature that makes most of them **hazardous**. Ring opening opens up attractive opportunities for selective transformations that include reductions (diols), oxidations (dicarbonyl products), rearrangements (hydroxy carbonyl compounds, epoxy carbonyl compounds, *bis*-epoxides, ene diones, etc.) and additions (polycyclic dioxanes[96] or trioxanes,[97] some of which display antimalarial activity). The synthesis and the subsequent reactions of the 2,3-dioxabicyclo[2.2.2]oct-7-en-5-one skeleton have been studied by Adam et al.[98] An impressive number of chemical transformations and examples for applications in organic synthesis have been collected in several reviews.[5c,59,99]

References

1. Windaus, A. and Brunken, J., Über die photochemische Oxydation des Ergosterins, *Liebigs Ann.Chem.,* 460, 225, 1928.
2. Gollnick, K., Type II photooxygenation reactions in solution, *Adv. Photochem.,* 6, 1, 1968.
3. See however: Foote, C.S., Definition of type I and type II photosensitized oxidation, *Photochem. Photobiol.,* 54, 659, 1991.
4. Tokuyama, H. and Nakamura, E., Synthetic chemistry with fullerenes. Photooxygenation of olefins, *J. Org. Chem.,* 54, 1135, 1994.
5. (a) Leach, A.G. and Houk, K.N., Diels–Alder and ene reactions of singlet oxygen, nitroso compounds and triazolinediones: transition states and mechanisms from contemporary theory, *J. Chem. Soc. Chem. Commun.,* 1243, 2002; (b) McCullough, K.J. and Nojima, M., Recent advances in the chemistry of cyclic peroxides, *Curr. Org. Chem.,* 5, 601, 2001; (c) Clennan, E.L., Synthetic and mechanistic aspects of 1,3-diene photooxidation, *Tetrahedron*, 47, 1343, 1991; (d) Bloodworth, A.J. and Eggelte, H.J., Endoperoxides, in *Singlet* O_2, Vol. II, Frimer, A.A., ed., CRC Press, Boca Raton, FL, 1985, p. 93; (e) Gollnick, K. and Schenck, G.O., Oxygen as a dienophile, in *1,4-Cycloaddition Reactions,* Hamer, J., Ed., Academic Press, Orlando, 1967, p. 255; (f) Frimer, A.A., The reaction of singlet oxygen with olefins: the question of mechanism, *Chem. Rev.,* 79, 359, 1979; (g) Kearns, D.R., Physical and chemical properties of singlet molecular oxygen, *Chem. Rev.,* 71, 395, 1971.
6. Dewar, M.J.S. and Thiel, W., MINDO/3 study on the addition of singlet oxygen ($^1\Delta_g$) to 1,3-butadiene, *J. Am. Chem. Soc.,* 99, 2338, 1977.
7. McCarrick, M.A., Wu, Y.-D., and Houk, K.N., Hetero-Diels–Alder reaction transition structures: reactivity, stereoselectivity, catalysis, solvent effects and the exo-lone-pair effect, *J. Org. Chem.,* 58, 3330, 1993.
8. Yamaguchi, K., Theoretical calculations of singlet oxygen reactions, in *Singlet* O_2, Vol. III, Frimer, A.A. ed., CRC Press, Boca Raton, FL., 1985, p. 119.
9. Sevin, F. and McKee, M.L., Reaction of 1,3-cyclohexadiene with singlet oxygen. a theoretical study, *J. Am. Chem. Soc.,* 123, 4591, 2001.
10. Bobrowski, M., Liwo, A., Oldziej, S., Jeziorek, D., and Ossowski, T., CAS MCSCF/CAS MCQDPT2 study of the mechanism of singlet oxygen addition to 1,3-butadiene and benzene, *J. Am. Chem. Soc.,* 122, 8112, 2000.
11. Rigaudy, J., Capdevielle, P., Cambrisson, S. and Maumy, M., Ouverture concertee des adduits du *bis* benzylidene-1,2 (E,E) diphenyl-3,4 cyclobutane cis. Rectification des structures des produits derives, *Tetrahedron Lett.,* 2757, 1974.
12. Gollnick, K. and Griesbeck, A., [4 + 2]-Cycloaddition of singlet oxygen to conjugated acyclic hexadienes: evidence of singlet oxygen induced *cis-trans*-isomerization, *Tetrahedron Lett.,* 24, 3303, 1983
13. O'Shea, K.E. and Foote, C.S., Chemistry of singlet oxygen. 51. Zwitterionic intermediates from 2,4-hexadienes, *J. Am. Chem. Soc.,* 110, 7167, 1988.

14. Motoyoshiya, J., Okuda, Y., Matsuoka, I., Hayashi, S., Takaguchi, Y., and Aoyama H., Tetraphenylporphine-sensitized photooxygenation of (*E,E*)- and (*E,Z*)-1-aryl-1,3-pentadienes generating *cis*-endoperoxides, *J. Org. Chem.,* 64, 493, 1999.
15. Clennan, E.L. and Nagraba, K., Reactions of singlet oxygen with alkoxy-substituted dienes. Formation of dioxetanes in the singlet oxygenations of s-*cis* fixed dienes (*Z,Z*)- and (*E,Z*)-4,5-diethylidene-2,2-dimethyl-1,3-dioxolanes, *J. Org. Chem.,* 52, 294, 1987.
16. (a) Clennan, E.L. and Mehrsheikh-Mohammadi, M.E., Addition of singlet oxygen to conjugated dienes. The mechanism of endoperoxide formation, *J. Am. Chem. Soc.,* 105, 5932, 1983; (b) Clennan, E.L. and Mehrsheikh-Mohammadi, M.E., Mechanism of endoperoxide formation. 2. Possibility of exciplexes on the reaction coordinates, *J. Org. Chem.,* 49, 1321, 1984; (c) Clennan, E.L. and Mehrsheikh-Mohammadi, M.E., Mechanism of endoperoxide formation. 3. Utilization of the Young and Carlsson kinetic techniques, *J. Am. Chem. Soc.,* 106, 7112, 1984.
17. Gorman, A.A., Lovering, G. and Rodgers, M.A.J., The entropy-controlled reactivity of singlet oxygen ($^1\Delta_g$) towards furans and indols in toluene. A variable-temperature study by pulse radiolysis, *J. Am. Chem. Soc.,* 101, 3050, 1979.
18. Gollnick, K. and Griesbeck, A., Solvent dependence of singlet oxygen/substrate interactions in ene reactions, [4 + 2]- and [2 + 2]-cycloaddition reactions, *Tetrahedron Lett.,* **25**, 725, 1984.
19. Paquette, L.A., Carr, R.V.C., Arnold, E., and Clardy, J., Electronic control of stereoselectivity. 5. Stereochemistry of singlet oxygen capture by cyclopentadiene rings fused to norbornyl and norbornenyl frameworks, *J. Org. Chem.,* 45, 4907,1980.
20. Fabris, F., Sbrogió, F., De Lucchi, O., Delogu, G., Fabbri, D., and Valle, G., Cycloadditions of dienophiles to bisdialine and stereochemistry of the adducts, *Gazz. Chim. Ital.,* 127, 393, 1997.
21. Monroe, B.M., Rate constants for the reaction of singlet oxygen with conjugated dienes, *J. Am. Chem. Soc.,* 103, 7253, 1981.
22. (a) Schenck, G.O. and Dunlap, D.E., Photosynthese von Cyclopentadien-endoperoxyd bei –100°C und Hydrierung von Endoperoxyden mit Thioharnstoff-Verwendung von Na-Dampflampen in der präparativen Photochemie, *Angew. Chem.,* 68, 248, 1956; (b) Schulte-Elte, K.H., Willhalm, B., and Ohloff, G., Eine neue Peroxidumlagerung: *cis*-4,5-Epoxy-2-pentenal aus 1,4-Epidioxy-2-cyclopenten, *Angew. Chem.,* 81, 1045, 1969.
23. Schenck, G. O., Probleme präparativer Photochemie, *Angew. Chem.,* 64, 12, 1952.
24. Cope, A.C., Liss, T.A., and Wood, G.A., Proximity effects, X. *cis*-1,4-cycloheptanediol from solvolysis of cycloheptene oxide, *J. Am. Chem. Soc.,* 79, 6287, 1957.
25. Horinaka, A., Nakashima, R., Yoshikawa, M., and Matsuura, T., Photosensitized oxygenation of unconjugated cyclic dienes, *Bull. Chem. Soc. Jpn.,* 48, 2095, 1975.
26. Adam, W. and Balci, M., Photooxygenation of 1,3,5-cycloheptatriene: isolation and characterization of endoperoxides, *J. Am. Chem. Soc.,* 101, 7537, 1979.
27. (a) Adam, W. and Erden, I., Cyclic peroxides. 85. Singlet oxygenation of cycloocta-1,3,5-triene: formation of [4.2.2] and [2.2.2] cycloadducts, *Tetrahedron Lett.,* 2781, 1979; (b) Adam, W., Gretzke, N., Hasemann, L., Klug, G., Peters, E.-M., Peters, K., von Schnering, H.G., and Will, B., Cycloaddition of singlet oxygen and 4-phenyl-4H-1,2,4-trizole-3,5-dione to 7-substituted 1,3,5- cyclooctatrienes, *Chem. Ber.,* 118, 3357, 1985.
28. Adam, W., Klug, G., Peters, E.-M., Peters, K., and von Schnering, H. G., Synthesis of endoperoxides derived from cyclooctatetraenes via singlet oxygenation, *Tetrahedron*, 41, 2045, 1985.
29. Adam, W., Cueto, O., DeLucchi, O., Peters, K., Peters, E.-M., and von Schnering, H.G., Synthesis of the endoperoxide *anti*-7,7-dioxatricyclo[4.2.2.$0^{2,5}$]deca-3,9-diene via singlet oxygenation of the bicyclic valence tautomer of cyclooctatetraene and its transformations, *J. Am. Chem. Soc.,* 103, 5822, 1981.
30. Rio, G., Charifi, M., Le diphényl-1,2 cyclopentadiène et ses dérivés substitués en 4 par un méthyle ou un carboxyle. Photoxydation, *Bull. Soc. Chim. Fr.,* 3585, 1970.
31. Schenck, G.O. and Ziegler, K., Die Synthese des Ascaridols, *Naturwiss.,* 32, 157, 1944.

32. Matusch, R. and Schmidt, G., Konkurrenz von Endoperoxid- und Hydroperoxidbildung bei der Reaktion von Singulettsauerstoff mit cyclischen, konjugierten Dienen, *Angew. Chem.,* 100, 729, 1988.
33. Schenck, G.O., Kinkel, K.G. and Mertens, H.-J., Photochemische Reaktionen I. Über die Photosynthese des Askaridols und verwandter Endoperoxyde, *Liebigs Ann. Chem.,* 584, 125, 1953.
34. Matusch, R. and Schmidt, G., Konkurrenz von Endoperoxid- und Hydroperoxid-Bildung bei der Umsetzung von Singulett-Sauerstoff mit cyclischen, konjugierten Dienen, *Helv. Chim. Acta,* 72, 51, 1989.
35. Clennan, E.L. and L'Esperance, R.P., The addition of singlet oxygen to alkoxy and trimethylsilyloxy butadienes. The synthesis of novel new peroxides, *Tetrahedron Lett.,* 24, 4291, 1983.
36. Sasson, I. and Labovitz, J., Synthesis, photooxygenation and Diels–Alder reactions of 1-methyl-4a,5,6,7,8,8a-*trans*-hexahydronaphthalene and 1,4a-dimethyl-4a,5,6,7,8,8a-*trans*-hexahydro-naphthalene, *J. Org. Chem.,* 40, 3670, 1975.
37. Linker, T., Rebien, F., and Toth, G., Highly diastereoselective photooxygenation of chiral 1,2-dihydronaphthalenes: evidence for a common intermediate in the ene reaction and the [4 + 2] cycloaddition, *J. Chem. Soc., Chem. Commun.,* 2585, 1996.
38. Adam, W. and Schuhmann, R.M., Selective oxyfuncionalization of (tricarbonylcyclohexadiene) iron-substituted furans with singlet oxygen and dimethyldioxirane, *Liebigs Ann.,* 635, 1996.
39. Mousseron-Canet, M., Mani, J.C., Dalle, J.P., and Olivé, J.L., Photoxydation sensibilisée de quelques composés apparentés à la déhydro ß-ionone, synthèse de l´ester méthylique de la (±) abscisine, *Bull. Soc. Chim. Fr.,* 3874, 1966.
40. Adam, W., Adamsky, F., Klärner, F.-G., Peters, E.-M., Peters, K., Rebollo, H., Rüngeler, W., and von Schnering, H.G., Stereochemistry and product distribution in the singlet oxygen cycloaddition with 7,7-disubstituted 1,3,5-cycloheptatrienes, *Chem. Ber.,* 116, 1848, 1983.
41. Dastan, A., Saracoglu, N., and Balci, M., A new method for the synthesis of stipitatic acid isomers: photooxygenation of ethyl 6*h*-cyclohepta[*d*][1,3]dioxole-6-carboxylate, *Eur. J. Org. Chem.,* 3519, 2001.
42. (a) Jefford, C.W., Hatsui, T., Deheza, M.F., and Bernardinelli, G., Photooxygenation of indene and 1,2-dihydronaphthalene: formation of 1,2-dioxetanes and 1,2,4-trioxanes, *Chimia*, 46, 114, 1992; (b) Boyd, J.D. and Foote, C.S., Chemistry of singlet oxygen. 32. Unusual products from low-temperature photooxygenation of indenes and trans-stilbene, *J. Am. Chem. Soc.,* 101, 6758, 1979.
43. Burns, P.A. and Foote, C.S., Chemistry of singlet oxygen, XXIV. Low temperature photooxygenation of 1,2-dihydronaphthalenes, *J. Org. Chem.,* 41, 908, 1976.
44. (a) Burns, P.A., Foote, C.S., and Mazur, S., Chemistry of singlet oxygen. XXIII. Low temperature photooxygenation of indenes in aprotic solvent, *J. Org. Chem.,* 41, 899, 1976; (b) Jiancheng, Z. and Foote, C.S., Photooxygenation of substituted indenes at low temperature, *Tetrahedron Lett.,* 27, 6153, 1986.
45. Erden, I., Drummond, J., Alstad, R., and Xu, F., Chemistry of singlet oxygen: isolation and characterisation of a stable allene oxide from a fulvene endoperoxide, *Tetrahedron Lett.,* 34, 1255, 1993.
46. Zhang, X., Lin, F., and Foote, C.S., Sensitized photooxygenation of 6-heteroatom-substituted fulvenes: primary products and their chemical transformation, *J. Org. Chem.,* 60, 1333, 1995.
47. Schenck, G.O., Autoxydation von Furan und anderen Dienen (Die Synthese des Ascaridols), *Angew. Chem.,* 56, 101, 1944.
48. Koch, E. and Schenck, G.O., Zur photosensibilisierten O_2-Übertragung auf Furan: Isolierung und Eigenschaften des ozonidartigen Furanperoxids bei –100°C, *Chem. Ber.,* 99, 1984, 1966.
49. Koch, E., Zur photosensibilisierten Sauerstoffübertragung. Untersuchung der Terminationschritte urch Belichtungen bei tiefen Temperaturen, *Tetrahedron,* 24, 6295, 1968.
50. Gollnick, K. and Griesbeck, A., Singlet oxygen photooxygenation of furans: isolation and reactions of [4 + 2]-cycloaddition products (unsaturated sec.-ozonides), *Tetrahedron,* 41, 2057, 1985.
51. Gollnick, K. and Griesbeck, A., [4 + 2]-Cycloaddition von Singulett-Sauerstoff an 2,5-Dimethylfuran: Isolierung und Reaktionen des monomeren und dimeren Endoperoxids, *Angew. Chem.,* 95, 751, 1983.

52. Graziano, M.L., Iesce, M.R., and Scarpati, R., Photosensitized oxidations of furans. Part 4. Influence of the substituents on the behaviour of the endoperoxides of furans, *J. Chem. Soc., Perkin Trans. 1,* 2007, 1982.
53. Onitsuka, S., Nishino, H., and Kurosawa, K., Photooxygenation of 3-acetyl-5-aryl-2-methylfurans via endoperoxide intermediate and the following reactions, *Tetrahedron,* 57, 6003, 2001
54. Adam, W., Ahrweiler, M., and Sauter, M., Photosensitized oxygenation of a keto furan: isolation of the first furan dioxetane by rearrangement of its endoperoxide and selected chemical transformations, *Angew. Chem.,* 105, 104, 1993.
55. Graziano, M.L., Iesce, M.R., Cimminiello, G., and Scarpati, R., Photosensitized oxidation of furans. Part 14. Nature of intermediates in thermal rearrangement of some *endo*-peroxides of 2- alkoxyfurans: new rearrangement pathway of furan *endo*-peroxides, *J. Chem. Soc., Perkin Trans. 1,* 241, 1989
56. Skold, C.N. and Schlessinger, R.H., The reaction of singlet oxygen with a simple thiophene, *Tetrahedron Lett.*, 791, 1970.
57. Gollnick, K. and Griesbeck, A., Thiaozonide formation by singlet oxygen cycloaddition to 2,5-dimethylthiophene, *Tetrahedron Lett.,* 25, 4921, 1984.
58. Adam, W. and Eggelte, H.J., 2,3-Dioxa-7-thiabicyclo[2.2.1]heptan: Ein neues heterocyclisches System mit Thiaozonid-Struktur, *Angew. Chem.,* 90, 811, 1978.
59. Matsumoto, M., Synthesis with singlet oxygen, in *Singlet* O_2, Vol. II, Frimer, A.A., Ed., CRC Press, Boca Raton, FL, 1985, p. 250.
60. Ando, W. and Takata, T., Photooxidation of sulfur compounds, in *Singlet* O_2, Vol. III, Frimer, A.A., Ed., CRC Press, Boca Raton, FL, 1985, p. 94.
61. (a) Wasserman, H.H., McCarthy, K.E., and Prowse, K. S., Oxazoles in carboxylate protection and activation, *Chem. Rev.,* 86, 845, 1986; (b) Gollnick, K. and Koegler, S., [4 + 2]-Cycloaddition of singlet oxygen to oxazoles — formation of oxazole endoperoxide, *Tetrahedron Lett.,* 29, 1003, 1988.
62. Sheldon, R.A., Synthesis and uses of alkyl hydroperoxides and dialkyl peroxides, in *The Chemistry of Peroxides,* Patai, S., ed., Wiley, New York, 1983, p. 162.
63. Herz, W. and Juo, R.-R., Photooxygenation of 1-vinylcycloalkenes. The competition between "ene" reaction and cycloaddition of singlet oxygen, *J. Org. Chem.,* 50, 618, 1985.
64. Matsumoto, M. and Kondo, K., The 1,4-cycloaddition of singlet oxygen to 1-vinylnaphthalenes, *Tetrahedron Lett.,* 3935, 1975.
65. Matsumoto, M. and Kuroda, K., Solvent effect in reaction of singlet oxygen with conjugated dienes, *Synth. Commun.,* 11, 987, 1981.
66. Matsumoto, M., Kuroda, K., and Suzuki, Y., The 1,4-addition of singlet oxygen to 2,6-dimethoxy-1-(2-methoxyethenyl)benzene and 2-methoxy-1-(2-methoxyethenyl)naphthalene. The 1,4-endoperoxides as equivalents of 6-oxo-2,4-cyclohexadienylidenacetates, *Tetrahedron Lett.,* 22, 3253, 1981.
67. Matsumoto, M., Dobashi, S., and Kondo, K., Sensitized photooxygenation of ß,ß-dimethylstyrenes; synthesis of (±)-crotepoxide, *Tetrahedron Lett.,* 3361, 1977.
68. Matsumoto, M., Dobashi, S., and Kondo, K., The 1,4-cycloaddition of singlet oxygen to stilbenes and ß-methylstyrenes, *Tetrahedron Lett.,* 2329, 1977.
69. Matsumoto, M., Dobashi, S., and Kondo, K., The 1,4-cycloaddition of singlet oxygen to 2-vinylthiophenes, *Tetrahedron Lett.,* 4471, 1975.
70. Gollnick, K. and Kuhn, H., Ene reactions with singlet oxygen, in *Singlet Oxygen,* Wasserman, H.H., and Murray, R.W., Eds., Academic Press, New York, 1979.
71. Zhang, X., Khan, S.K. and Foote, C.S., Sensitized photooxygenations of 3-vinylindole derivatives, *J. Org. Chem.,* 58, 7839, 1993.
72. Kondo, T., Matsumoto, M., and Tanimoto, M., Microwave and NMR studies of the structure and the conformational isomerization of 3,6-dihydro-1,2-dioxin, *Tetrahedron Lett.,* 3819, 1978.
73. Gollnick, K. and Griesbeck, A., Interactions of singlet oxygen with 2,5-dimethyl-2,4-hexadiene in polar and non-polar solvents. Evidence for a vinylog ene-reaction, *Tetrahedron,* 40, 3235, 1984.

74. Griesbeck, A.G., Fiege, M., Gudipati, M.S., and Wagner, R., Photooxygenation of 2,4-dimethyl-1,3-pentadiene: solvent dependence of the chemical (ene reaction and [4 + 2]-cycloaddition) and physical quenching of singlet oxygen, *Eur. J. Org. Chem.,* 2833, 1998.
75. Aubry, J.-M., Mandard-Cazin, B., Rougee, M., and Benasson, R.V., Kinetic studies of singlet oxygen [4 + 2]-cycloadditions with cyclic 1,3-dienes in 28 solvents, *J. Am. Chem. Soc.,* 117, 9159, 1995.
76. Hasty, N.M. and Kearns, D.R., Mechanisms of singlet oxygen reactions. Intermediates in the reaction of singlet oxygen with dienes, *J. Am. Chem. Soc.,* 95, 3380, 1973.
77. (a) Manring, L.E., Kanner, R.C., and Foote, C.S., Chemistry of singlet oxygen. 43. Quenching by conjugated olefins, *J. Am. Chem. Soc.,* 105, 4707, 1983; (b) Manring, L.E. and Foote, C.S., Chemistry of singlet oxygen. 44. Mechanism of photooxidation of 2,5-dimethylhexa-2,4-diene and 2-methyl-2-pentene, *J. Am. Chem. Soc.,* 105, 4710, 1983.
78. Adam, W. and Staab, E., Regio-controlled functionalization of 2,5-dimethyl-2,4-hexadiene into epoxy alcohols by photooxygenation in the presence of titanium(IV) or vanadium(V), *Tetrahedron Lett.,* 29, 531, 1988.
79. Matsumoto, M., Dobashi, S., Kuroda, K., and Kondo, K., Sensitized photo-oxygenation of acyclic conjugated dienes, *Tetrahedron,* 41, 2147, 1985.
80. Kenney, R.L. and Fisher, G.S., Photosensitized oxidation of myrcene, *J. Am. Chem. Soc.,* 81, 4288, 1959.
81. Matsumoto, M. and Kondo, K., Sensitized photooxygenation of linear monoterpenes bearing conjugated double bonds, *J. Org. Chem.,* 40, 2259, 1975.
82. Clennan, E.L. and L'Esperance, R.P., The unusual reactions of singlet oxygen with isomeric 1,4-di-*tert*-butoxy-1,3-butadienes. A 2_s-2_a cycloaddition, *J. Am. Chem. Soc.,* 107, 5178, 1985
83. Clennan, E. L. and Nagraba, K., Additions of singlet oxygen to alkoxy-substituted dienes. The mechanism of the singlet oxygen 1,2-cycloaddition reaction, *J. Am. Chem. Soc.,* 110, 4312, 1988.
84. Adam, W., Güthlein, M., Peters, E.M., Peters, K., and Wirth, T., Chiral-auxiliary-induced diastereoselectivity in the [4 + 2]-cycloaddition of optically active 2,2-dimethyloxazolidine derivatives of sorbic acid: a model study with singlet oxygen as smallest dienophile, *J. Am. Chem. Soc.,* 120**,** 4091, 1998.
85. Dussault, P.H., Han, Q., Sloss, D.G., and Symonsbergen, D.J., Photooxygenation of chiral dienol ethers: asymmetric synthesis of alkoxydioxines, *Tetrahedron*, 55, 11437, 1999.
86. Davis, K.M. and Carpenter B.K., Unusual facial selectivity in the cycloaddition of singlet oxygen to a simple cyclic diene, *J. Org. Chem.,* 61, 4617, 1996.
87. Matsumoto, M., Nasu, S., Takeda, M., Murakami, H., and Watanabe, N., Singlet oxygenation of 4-(4-*tert*-butyl-3,3-dimethyl-2,3-dihydrofuran-5-yl)-2-pyridone: non-stereospecific 1,4-addition of singlet oxygen to a 1,3-diene system and thermal rearrangement of the resulting 1,4-endoperoxides to stable 1,2-dioxetanes, *J. Chem. Soc., Chem. Commun.,* 821, 2000.
88. Adam, W., Peters, E.M., Peters, K., Prein, M., and von Schnering, H.G., Diastereoselective photooxygenation of chiral naphthylalcohols — the hydroxy group directing effect in singlet oxygen [4 + 2]-cycloaddition to arenes, *J. Am. Chem. Soc.,* 117, 6686, 1995.
89. (a) Mehta, G. and Uma, R., Diastereofacial control in cycloadditions to a dissymmetric cyclohexa-1,3-diene moiety in a polycyclic framework. Distal protective groups as stereodirectors, *Tetrahedron Lett.,* 36, 4873, 1995; (b) Mehta, G. and Uma, R., Role of heteroatoms in diastereofacial control in cycloaddition to a dissymmetric cyclohexa-1,3-diene moiety in a polycyclic framework. Remarkable stereodirecting influence of distal protective groups, *J. Org. Chem.,* 65, 1685, 2000.
90. Hamberg, M. and Samuelson, B., On the mechanism of the biosynthesis of prostaglandins E_1 and $F_{1\alpha}$, *J. Biol. Chem.,* 242, 5336, 1967.
91. Brecht, R., Büttner, F., Böhm, M., Seitz, G., Frenzen, G., Pilz, A., and Massa, W., Photooxygenation of the helimers of (–)-isocolchicine: Regio- and facial selectivity of the [4 + 2]- cycloaddition with singlet oxygen and surprising endoperoxide transformations, *J. Org. Chem.,* 66, 2911, 2001.
92. Mihelich, E.D., Structure and stereochemistry of novel endoperoxides isolated from the sensitized photooxidation of methyl linoleate. Implications for prostaglandin biosynthesis, *J. Am. Chem. Soc.,* 102, 7141, 1980.

93. Adam, W. and Eggelte, H.J., Prostanoid endoperoxide model compounds: 2,3-dioxabicyclo[2.2.1] heptane via selective diimide reduction, *J. Org. Chem.,* 42, 3987, 1977.
94. Snider, B.B. and Shi, Z., Total synthesis of (±)-chondrillin, (±)-plakorin and related peroxy ketals. Development of a general route to 3,6-dihydro-1,2-dioxin-3-ols, *J. Am. Chem. Soc.,* 114, 1790, 1992.
95. Lopez, D., Quinoa, E., and Riguera, R., The [4 + 2]-addition of singlet oxygen to thebaine: new access to highly functionalized morphine derivatives via opioid endoperoxides, *J. Org. Chem.,* 65, 4671, 2000.
96. Jefford, C.W., Eschenhof, H., and Bernardinelli, G., Synthesis of polycyclic 1,2-dioxanes from endoperoxides, *Heterocycles,* 47, 283, 1998.
97. Jefford, C.W., Jin, S., Rossier, J.-C., Kohmoto, S., and Bernardinelli, G., *Cis*-fused dihydrofurano-1,2,4-trioxanes, *Heterocycles*, 44, 367, 1997.
98. Adam, W., Balci, M., and Kiliç, H., 2,3-dioxabicyclo[2.2.2]oct-7-en-5-one: synthesis and reactions of the keto endoperoxide of phenol, *J. Org. Chem.,* 65, 5926, 2000.
99. (a) Wasserman, H.H. and Ives, J.L., Singlet oxygen in organic synthesis, *Tetrahedron*, 37, 1825, 1981; (b) Balci, M., Bicyclic endoperoxides and synthetic applications, *Chem. Rev.,* 81, 91, 1981; (c) Saito, I. and Nittala, S.S., Endoperoxides, in *The Chemistry of Peroxides,* Patai, S., ed., Wiley, New York, 1983, p. 311; (d) Kropf, H., ed., *Organische Peroxoverbindungen,* Houben-Weyl E13/2, Thieme Verlag, Stuttgart, New York, 1988, pp. 991–1122.

26

Hula-Twist: A Photochemical Reaction Mechanism Involving Simultaneous Configurational and Conformational Isomerization

Robert S.H. Liu
University of Hawaii

George S. Hammond
University of Hawaii

26.1 The Need for New Mechanisms for Photoisomerization

A well-known generalized observation for photochemical reactions of conjugated systems is the absence of conformational changes during photoexcitation. It is known as NEER, or nonequilibration of excited rotamers. Havinga and colleagues formulated the concept through an incisive examination of structural properties of reactants and photoproducts of compounds in the vitamin D series.[1] Later, the same concept was demonstrated with the simpler *cis*-1,3,5-hexatriene as shown below. Only products retaining the original conformation were observed.[2] (It should be pointed out that the same group was aware of the fact that ground state product analysis may not produce unambiguous information related to the excited species.[2,3])

Independently, from product analyses of triplet-sensitized dimerization of dienes, Hammond and Liu recognized the absence of interconversion of conformers in the triplet state. Thereby, the term isomeric triplets was coined.[4]

However, the NEER behavior was not without exceptions. As early as 1975, Squillacote et al. showed that butadiene, under argon matrix isolation conditions, undergoes ready s-*trans*,s-*cis* photo-equilibration.[5] Also, for several larger arylethenes where the excitation energy was largely localized in the aryl ring,

0-8493-1348-1/04/$0.00+$1.50

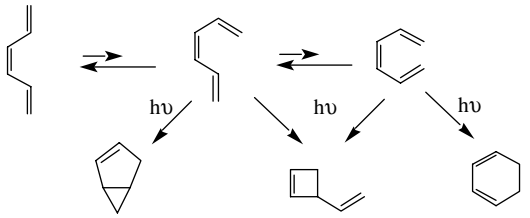

conformational reorganization was detected in the excited singlet state[6] as well as the longer lived triplet state.[7]

Ever since the first picosecond time-resolved spectroscopic study was carried out in 1972,[8] the question how the seemingly volume-demanding 11-*cis* to all-*trans* isomerization of the retinyl chromophore can take place within 6 psec was raised. The question is particularly relevant when one considers that photochemical isomerization is highly sensitive to medium viscosity. Thus, in the typical case of *trans*-stilbene, the quantum yield of isomerization under direct irradiation decreases with an increase of solvent viscosity and with a simultaneous increase in fluorescence efficiency.[9] This trend is attributed to the presence of a viscosity-dependent barrier that impedes the volume-demanding torsional relaxation (or the one-bond-flip, OBF) process. Fluorescence, being relatively insensitive to solvent viscosity, becomes the only observable deactivation process in a frozen medium. Also, it is known that rhodopsin formation is a stereospecific reaction — only one of 16 possible isomers of retinal is known to give the visual pigment.[10] Hence, there must be close interaction between a well-defined protein pocket and the centrally bent 11-*cis* retinyl chromophore (**1**). How, then, can the volume-demanding isomerization process take place within 100 fsec (based on the better time-resolved apparatus that have since become available),[7,11] a time scale clearly too short for protein reorganization?

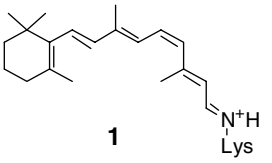

1

26.2 Volume-Conserving Mechanisms for Photoisomerization

Warshel first postulated the bicycle-pedal (BP) mechanism as a volume-conserving mechanism for photoisomerization.[12] In it, two alternating double bonds rotate concertedly with only the two CH units turning in and out of the plane of the molecule.

However, the stereochemical consequence of one-photon–two-bond isomerization for this model is not in agreement with experimental fact. Subsequently, the model was modified to one that involved small twists at various double and single bonds (none greater than 90°),[13] thus leading to one-bond isomerization only. The revised model appears to us a refined OBF process (i.e., a modified version of the conventional torsional relaxation) rather than a modified BP, as claimed.

In 1985, Liu and Asato proposed the Hula-twist (HT) concept, in which two adjacent double and single bonds are rotated concertedly.[14] The motion involves only one CH unit moving in and out of the plane of the molecule, with the remaining parts of the molecule sliding roughly in the original plane. It is also a volume-conserving process. The stereochemical consequence is simultaneous isomerization of a double bond and an adjacent single bond. In 1998, this concept met direct experimental confirmation when Fuss et al. reported the observation that photoisomerization of pre-vitamin D in an organic glass

at liquid nitrogen temperature takes place with simultaneous double bond and single bond isomerization[15] (for structures, see below). What was evident to us was its disagreement with the NEER phenomena when products with altered conformation were obtained. A quick survey of the literature revealed three more cases of photoreactions in apparent contradiction of NEER: the photochemical interconversion of s-*trans* and s-*cis* conformers of 1,3-butadiene (**2**) in an argon matrix,[4] the photochemical interconversion of all-s-*trans* and 2-s-*cis* 1,3,5,7-octatetraene (**3**) in a *n*-octane matrix at 3.5 K,[16] and the postulated HT process for the primary process of rhodopsin.[14,17,18]

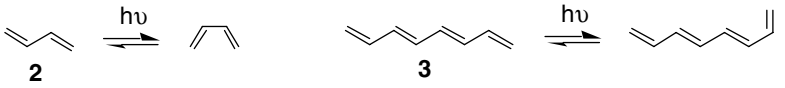

2 **3**

None of these papers referred to each other or to their apparent deviation from NEER. However, since they were the only exceptions to NEER (not counting the large aryl systems mentioned above), we suspected that there must be a shared common feature. After much deliberation, it suddenly dawned on us that these four examples share common reaction conditions in that all four photoisomerization studies were conducted in rigid media. This feature differs from numerous other photoisomerizations that obeyed NEER and were carried out either in fluid solutions or under other unconstrained conditions.[19]

Following this line of thought, we postulated the following generalization for all photoisomerization reactions.[19]

> Under unconstrained conditions (e.g., in fluid solutions or gaseous conditions), the conventional one-bond-flip (OBF) process is the dominant process with the HT being an undetectable higher energy ($\Delta G^{\dagger}$) process. Under confined conditions (whether in a solid matrix or solution or in a protein binding cavity), the additional viscosity-dependent barrier makes OBF a less favorable process, allowing the volume-conserving HT to be the dominant process for photoisomerization.

26.3 Examples of Hula-Twist

A subsequent survey of literature revealed many previously unexplained photoisomerization examples that can now be explained by this generalization.[20,21] The number of such examples has continued to increase.[22] However, they can be categorized into two groups.

Conjugated Polyenes

Possible photoisomerization of compounds in the vitamin D series in organic glass at liquid nitrogen temperature was first reported by Havinga more than 40 years ago.[23] Stereospecific photoisomerizations of pre-vitamin D (**4a, b**) in an organic glass were demonstrated only recently.[15] The results are consistent with HT at the vinylic centers shown below.

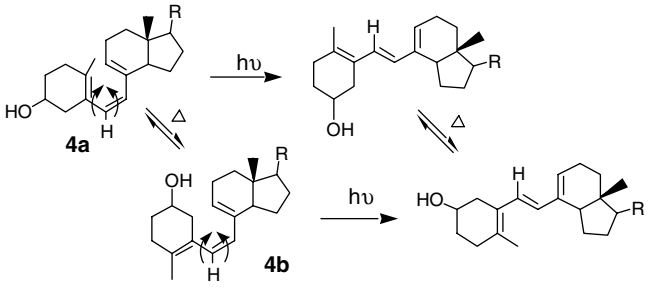

The ready interconversions of s-*trans*,s-*cis* conformers of 1,3-butadiene[5] and 1,3,5,7-octatetraene[16] in argon or *n*-octane matrix are consistent with HT-2. In the case of the octatetraene, the absence of products derived from HT at central carbons must be due to incompatibility of such products with the cavity provided by the host. For example, HT-4 would lead to the highly bent structure (3-*cis*-4-s-*cis*-**3**) shown, one not likely to fit in the linear *n*-octane matrix.

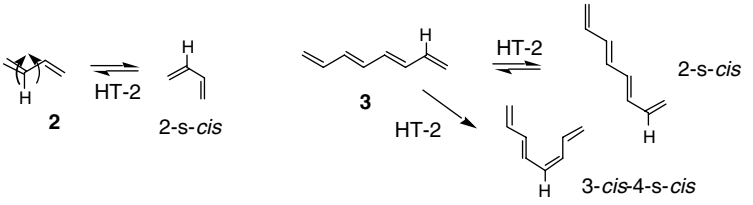

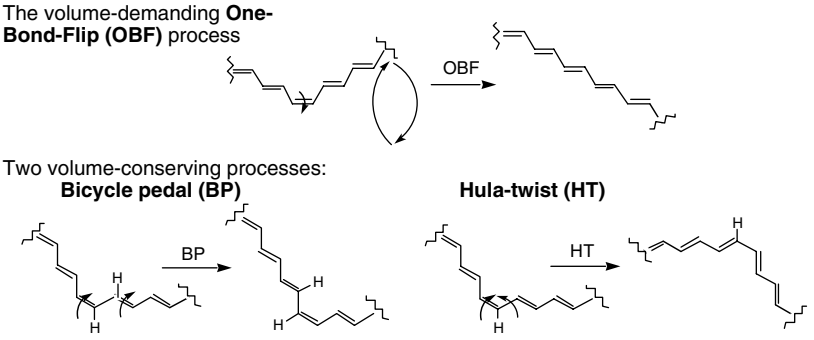

This leaves the interesting possibility of HT-1. Such a reaction is observable only after selective isotope labeling. In fact, a relevant experiment was carried out years ago. Irradiation *of trans,trans*-1,4-dideutero-2,3-dimethylbutadiene (**5**) in an argon matrix was reported not to result in any conformational changes around the central single bond.[24] Rather, the only facile reaction observed was *trans* to *cis* isomerization at the 1 or 4 centers. These results can be readily accounted for by the HT mechanism. Conformational changes at the 2,3-bond would involve HT of a CCH_3 unit, a much more hindered process than flipping a CH unit as in butadiene. Instead, the molecule will likely channel its excitation energy to the HT-1 process where either flipping of the CH or the CD unit leads to the observed products. Alternatively, a diene molecule might be all along undertaking a competing OBF at the terminal carbons by rotating a small methylene unit.[24] Only when HT-2 is hindered and D-labels are introduced can this process reveal itself.

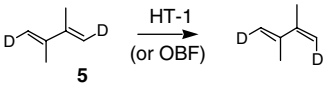

Additionally, conformational equilibrations upon irradiation in argon matrix were reported for 2-methyl-1,3-butadiene (isoprene) **6a** and 2-isopropylbutadiene, **6b**.[25] These results suggest that the size of the 2-substituent is not an important factor in controlling HT while the retention of at least one vinyl hydrogen (at C3) apparently is. However, there appear to be other limitations because conformational equilibration was not observed for *trans,trans*-2,4-hexadiene, **7**.[26] The latter observation suggests that

under these very stringent reaction conditions (low temperature and argon matrix), the sideways movement of the remaining portions of the molecules is also sensitive to steric hindrance. Apparently, methyl groups at the two ends are sufficiently bulky to stop the HT motion. On the other hand, in another matrix isolation study on isomers of 2,5-dimethyl-1,3,5-hexatriene (**8**), two-bond isomerized products were not detected, although IR analysis for this triene system is obviously more complex than for the dienes.[3]

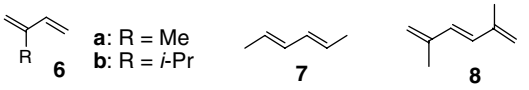

6 **7** **8**

1,2-Diarylalkenes

For diarylalkenes, the *trans* to *cis* isomerization is either completely inhibited or becoming very inefficient in low-temperature organic glasses. However, the *cis* to *trans* conversions remain moderately efficient.[27] (Photocyclization products are usually not observed in low temperature glasses.) However, in general the product *trans* isomers are formed as high-energy conformers. While no explanation was offered for formation of the unstable conformers, the method is widely recognized as a photochemical procedure for preparation of high-energy conformers of the *trans* isomer.[28]

These observations are now understandable within the context of the HT mechanism.[19–21] Two examples are illustrated below.

cis-1,2-α,α′-Binaphthylethene (**9**) should be conformationally homogeneous when cooled to liquid nitrogen temperature, existing in the least congested conformation shown. Photoisomerizations by way of HT and OBF are expected to lead to different conformers of the *trans* isomer as shown below. Of the two, only HT gives the less stable conformer that is in agreement with the low temperature photochemical results.[27] Therefore, one might muse at the conclusion that HT was, in fact, first detected in 1983,[27a] two years before postulation of the concept.[14]

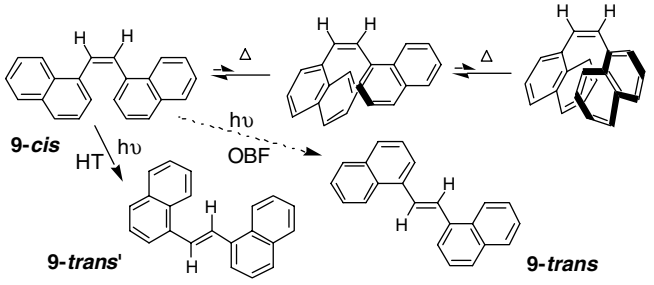

When conformational homogeneity is not ensured in a *cis*-diarylethene, the photoisomerization pathways could be rather complex. For example, for 1,2-β,β′-dinaphthylethene (**10**), the *cis* isomer should exist in three possible conformations (*cis*-**10a**, *cis*-**10b**, *cis*-**10c**), as shown below. HT of these conformers should lead to three conformers of the *trans* products (*trans*-**10a**, -**10b**, and -**10c**) (solid lines) with comparable internal steric strain. The same conformer products are also expected from OBF processes (dashed line), albeit not from the same starting conformers as in HT processes. While it is clear that the product ratio is dependent on a number of factors, this ambiguity renders such systems uninformative for elucidation of the exact nature of their photoisomerization pathways. On the other hand, it should be clear that photoisomerization, e.g., by HT, is not likely to produce the same equilibrated mixture of conformers of the *trans* isomer as in the equilibrated mixture, i.e., obtained from irradiation at room temperature. Thus, the claim of possible preparation of a nonequilibrated *trans* isomer in organic glass is also consistent with, but not a proof for, involvement of HT.

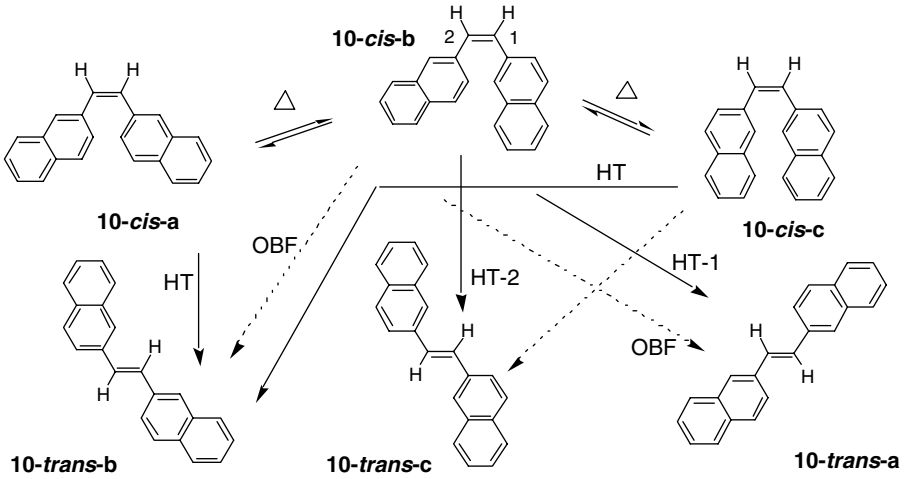

Other *cis*-diarylethene systems reported to give nonequilibrated *trans* products at low temperature in organic glasses[28] were: 1-naphthyl-2-phenylethenes,[27] 1-α-naphthyl-2-β-naphthylethene and 1-β-naphthyl-3-phenanthrylethene.[27b] But, none of these *cis* reactants is likely to be conformationally homogeneous.

With the new mechanistic insight on photoisomerization under confined conditions, we can now rationally design new systems for differentiation of HT from OBF. Several examples have been outlined in the literature.[19,20] Preliminary photochemical results have already been obtained for the stilbene analog **11**.[29] The additional fused 6-ring not only reduces the number of possible conformers, but also introduces sufficient steric strain making the *E* to *Z* isomerization also a facile process detectable at liquid nitrogen temperature. In an organic glass, photoirradiation led to an unstable product that differed from the *cis* (*Z*) product obtained from irradiation in solution at room temperature, but they become identical after the glass solution was warmed to room temperature. These observations are in agreement with the postulated dual mechanisms for photoisomerization. Interestingly, while the *Z* to *E* isomerization was also readily detected, the *Z* isomer apparently was not conformationally homogeneous even at low temperatures. Hence its photochemistry is more complex.

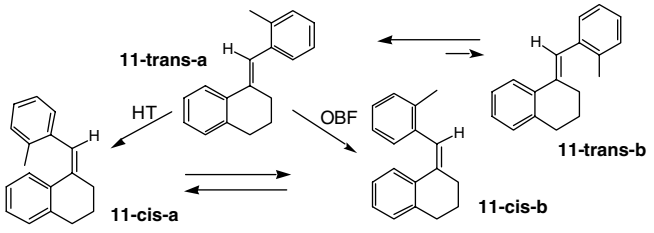

In other more complex diaryl systems, including the stilbene paracyclophane (**12**)[30] and stilbene dendrimers (**13**),[3] OBF is structurally impossible, yet efficient *trans* to *cis* photoisomerizations have been reported. The presence of vinylic hydrogens should allow the volume-conserving HT process to proceed, thereby initiating the *trans* to *cis* conversion. For dibenzoylethene (**14**), the *trans* to *cis* isomerization could be carried out with the *trans* crystals only.[32] An analysis of the shape of the crystal cavity of the starting *trans* isomer revealed that its dimensions are not sufficiently large for a OBF process, but an HT process is possible. The crystals of the *cis* isomer do not have a cavity sufficiently large for either the HT or the OBF process. Therefore, the relative photochemical reactivities of *cis* and *trans* isomers are different from those in frozen glass.

It is also interesting to recall that the ring-fused stilbene analog **15** behaves differently photochemically (obeying the Kramer equation throughout a wide range of solvent viscosity)[33] than *trans*-stilbene does (not obeying the Kramer equation at medium or high solvent viscosity).[34] This contrast is reminiscent of the difference between the indigo dye **16** (no photoisomerization)[35] and bilirubin **17** (efficient photoisomerization).[36] While both have constraints from internal hydrogen bonding, HT has been invoked for the latter, which contains key vinylic hydrogens[20,21] that are absent in **15** and **16**. The question is whether viscosity is a sufficient constraint to produce similar trends in stilbene and its ring-fused analog.

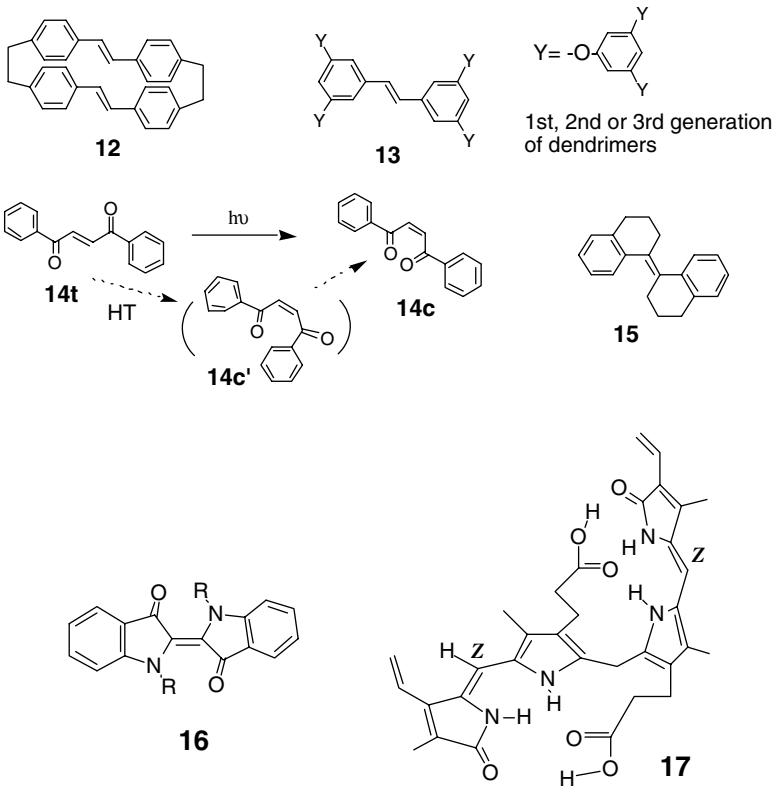

26.4 Theoretical Models Related to HT

A little-noticed theoretical paper interpreting the photochemistry of diazines recognized the concerted nature of the isomerization process.[37] However, somewhat bafflingly, it described the motion as a three-bond concerted twist process in the form of a "crank-shaft" motion. These inexact descriptions appeared to have distracted from what is distinctly an HT-like process as shown in an accompanying figure in the paper.

Interpreting photoisomerization of the visual chromophore, Seltzer[38] calculated the energy requirement of the isomerization process of the free retinyl chromophore by way of conventional torsional relaxation and the BP and the HT processes. BP was judged as an untenable, activated process while both the OBF and HT processes were considered energetically feasible.

The first direct connection of conical intersection (CI) calculations with HT was that of Fuss et al.[39] They pointed out that the geometry of the molecule at the CI in the minimum energy pathway of deactivation of an excited conjugated polyene corresponds to that from HT. Even though CI calculations are limited to isolated molecules, in a recent paper,[40] Fuss and co-workers argued that HT is general for all isomerization reactions including cases where one-bond isomerization is observed.

Recently, Wilsey and Houk[41] introduced a new detailed molecular reorganization process that more specifically describes the HT process and successfully accounts for formation of the observed products. It involves pyramidalization of a carbon and its bridging of the attached vinylic hydrogen with the adjacent carbon (in analogy with the minimized structure of excited ethene) for the CI structures of excited butadiene. They argued that pyramidal inversion of such a CI structure leads to the stereochemical consequence of HT.

25.5 A Word of Caution in Applying the HT Concept

The arguments presented above are applicable primarily to amorphous solids, where no or few specific interactions exist between the trapped molecule and the host system. If specific interactions are present, the energy required to break such interactions, rather than searching for empty space available for reaction, could become the controlling factor in determining directions of photoreactions. The situation is particularly acute when one considers a protein-bound substrate. It is usually anchored to the protein host at both ends. The motion associated with the isomerization reaction would have to be executed without moving (to any significant extent) the anchors within the short S_1 lifetime of the chromophore. Sometimes the movement is facilitated by the presence of a "rubber-band" (usually a saturated side chain of, e.g., a lysine residue to allow ready conformational reorganization) between the chromophore and the anchor(s).[42] The situation was first discussed in relation to the photochemistry of rhodopsin and recently elaborated in a discussion of the photoisomerization processes of photoactive yellow protein (PYP).[43]

Also, while conceptually it is easier to visualize HT as a higher energy process than OBF, we hasten to add that under confined conditions, the rate of HT does not necessarily have to be slowed. There could instead be specific medium assistance that might result in rate acceleration (e.g., through a favorable entropy factor). In this regard it is particularly relevant to point out that the 11-*cis*-retinyl chromophore when protein bound (i.e., in rhodopsin) isomerizes nearly 10 times faster[44] than the same free chromophore in solution.[45] Furthermore, the resonance Raman work of Mathies and Lugtenburg showed that the excess vibrational energy during relaxation of the Franck-Condon species produced immediately after light absorption of the 11-*cis* retinyl chromophore is largely localized in the hydrogen-out-of-plane (HOOP) vibrational mode of H_{12} of the first stable photoproduct, bathorhodopsin.[46] This appears to be a smoking gun for protein directed HT-12 for photoisomerization of rhodopsin as well as a mechanism for rate acceleration assisted by the surrounding protein residues. Whether the protein structure allows completion of the HT process, frequently involving substantial relocation of atoms associated with the expected change of the overall shape of the chromophore, remains a subject of further studies.[22]

We might also point out that our earlier thoughts on photochemical reactivity and radiationless transitions,[47] with the energy gap between the excited species and the corresponding ground state structure as a dominant factor, is not likely to be applicable to predicting HT reactivity. We suspect that the latter is controlled by kinetic factors such as entropy probability during relaxation of the Franck-Condon species. The latter topic will be dealt with in detail in a separate, future publication.[48]

25.6 Concluding Remarks

Hula-twist was postulated in 1985 to account for the unique photochemistry of the retinyl chromophore in retinal binding proteins.[14] In hindsight, it was probably too ambitious an attempt to tackle first the protein bound systems where direct experimental proof is difficult to obtain. The 1998 paper by Fuss and coworkers not only established unequivocally the first case of simultaneous configurational and conformational photoisomerization but also redirected our attention to molecules trapped in amorphous solids. The refocused thought process allowed the postulation of a simple generalization that led to rational design of new test systems. There is now a resurgence of interest and effort in examining scope and limitation of the hula-twist process, as indicated by the many publications that have appeared

recently.[22,26,31,32,40,41,43] Our recent activity in this area has also triggered our thoughts on factors controlling efficiency of diabatic processes such as HT.[48] But it is clear that the HT concept is still at a nascent stage awaiting new information from reliable experimental data and exact theoretical models. Nevertheless, we are hopeful that a more thorough understanding of the intricate details and scope and limitation of the process can be achieved in the near future.

Acknowledgment

This work was partially supported by a grant from the National Science Foundation (CHE01–32250).

References

1. (a) Havinga, E. and Schlatmann, J.L.M.A., Remarks on the specificities of the photochemical and thermal transformations in the vitamin D field, *Tetrahedron*, 16, 146, 1961; (b) Jacobs, H.J.C. and Havinga, E., Photochemistry of vitamin D and its isomers and of simple trienes, *Adv. Photochem.,* 11, 305, 1979.
2. Laarhoven, W.H.Y. and Jacobs, H.J.C., Photochemistry of acyclic 1,3,5-trienes and related compounds, in *Handbook of Photochemistry and Photobiology,* Horspool, W.M. and Song, P.S., Eds., CRC Press, Boca Raton, FL, 1995, p. 143.
3. Brower, A.M. and Jacobs, H.J.C., Photochemistry of 2,5-dimethyl-1,3,5-hexatrienes in argon matrices. Formation of isomers and rotamers, *Recl. Trav. Chim. Pays-Bas,* 114, 449, 1995.
4. Hammond, G.S. and Liu, R.S.H., Stereoisomeric triplet states of conjugated dienes, *J. Am. Chem. Soc.,* 85, 477, 1963.
5. Squillacote, M.E., Sheridan, R.S., Chapman, O.L., and Anet, F.A.L., Planar s-*cis*-1,3-butadiene, *J. Am. Chem. Soc.,* 97, 3657, 1975.
6. (a) Mazzucato, U. and Momicchioli, F., Ground state rotamers of 1,2-diarylethylenes detected by techniques involving electronic excitation limits to the validity of the NEER principle, *EPA Lett.,* March 1992, pp. 31–39; (b) Flom, R.S., Nagarajan, V., and Barbara, P.F., Dynamics solvent effects on large-amplitude isomerization rates. I. 2-Vinylanthracene, *J. Phys. Chem.,* 90, 2085, 1986.
7. Arai, T., Karatsu, T., Sakaraji, H., Tokumaru, K., Tamai, N., and Yamazaki, I., Highly selective rotational isomerization of 2-vinylanthracene in the excited state. Picosecond time-resolved fluorescence study, *Chem. Phys. Lett.,* 158, 429, 1989.
8. Busch, G.D., Applebury, M.L., Lamola, A.A. and Rentzepis, P., Formation and decay of prelumirhodopsin at room temperature, *Proc. Natl. Acad. Sci. USA,* 69, 2802, 1972.
9. Malkin, S. and Fischer, E., Temperature dependence of photoisomerization. III. Direct and sensitized photoisomerization of stilbenes, *J. Phys. Chem.,* 68, 1153, 1964.
10. (a) Liu, R.S.H., Matsumoto, H., Kini, A., Asato, A.E., Denny, M., and DeGrip, W.J., Seven new hindered isomeric rhodopsins. A reexamination of the stereospecificity of the binding site of bovine opsin, *Tetrahedron*, 40, 473, 1984; (b) Liu, R.S.H. and Mirzadegan, T., The shape of a three-dimensional binding site of rhodopsin based on molecular modeling analyses of isomeric and other visual pigment analogues, *J. Am. Chem. Soc.,* 110, 8617, 1988.
11. Mathies, R.A., Photons, femtoseconds and dipolar interactions: a molecular picture of the primary events in vision, in *Rhodopsins and Phototransduction,* John Wiley & Sons, New York, 1999, p. 70.
12. Warshel, A., Bicycle-pedal model for the first step in the vision process, *Nature (London),* 260, 679, 1976.
13. Warshel, A. and Barboy, N., Energy storage and reaction pathways in the first step of the vision process, *J. Am. Chem. Soc.,* 104, 1469, 1982.
14. (a) Liu, R.S.H. and Asato, A.E., The primary process of vision and the structure of bathorhodopsin: a mechanism for photoisomerization of polyenes, *Proc. Natl. Acad. Sci. USA,* 82, 259, 1985; (b) Liu, R.S.H. and Browne, D.T., A bioorganic view of the chemistry of vision: H.T.-n and B.P.-m,n mechanisms for reactions of confined, anchored polyenes, *Acc. Chem. Res.,* 19, 42, 1986.

15. Müller, A.M., Lochbrunner, S., Schmid, W.E., and Fuss, W., Low-temperature photochemistry of previtamin D: a hula-twist isomerization of a triene, *Angew. Chem. Int. Ed. Engl.,* 37, 505, 1998.
16. Ackerman, J.R., Forman, S.A., Hossain, M., and Kohler, B., S-*cis*-octatetraene — photoproduction and spectroscopic properties, *J. Chem. Phys.,* 80, 39, 1984.
17. Asato, A.E., Denny, M., and Liu, R.S.H., Retinal and rhodopsin analogues directed toward a better understanding of the H.T.-n model of the primary process of vision, *J. Am. Chem. Soc.,* 108, 5032, 1986.
18. Ishiguro, M., A mechanism of primary photoactivation reactions of rhodopsin: modeling of the intermediates in the rhodopsin photocycle, *J. Am. Chem. Soc.,* 122, 444, 2000.
19. Liu, R.S.H. and Hammond, G.S., The case of medium-dependent dual mechanisms for photoisomerization: one-bond-flip and hula-twist, *Proc. Natl. Acad. Sci. USA,* 97, 11153, 2000.
20. Liu, R.S.H., Photoisomerization by hula-twist: a fundamental supramolecular photochemical reaction, *Acc. Chem. Res.,* 34, 555, 2001.
21. Liu, R.S.H. and Hammond, G.S., Examples of hula-twist in photochemical *cis,trans* isomerization, *Chem.-Eur. J.,* 7, 4536, 2001.
22. Liu, R.S.H., Introduction to the symposium-in-print: photoisomerization pathways, torsional relaxation and the hula-twist, *Photochem. Photobiol.,* 76, 580, 2002.
23. deKock, R.J., van der Kuip, G., Verloop, A., and Havinga, E., Studies on vitamin D and related compounds. Irradiation of low temperatures, *Recl. Trav. Chim.,* 80, 20, 1961.
24. Squillacote, M.E., Semple, T.C., and Mui, P.W., The geometries of the s-*cis* conformers of some acyclic 1,3-dienes: planar or twisted? *J. Am. Chem. Soc.,* 107, 6842, 1985.
25. Squillacote, M.E. and Semple, T.C., Photochemistry of s-*cis* acyclic 1,3-dienes, *J. Am. Chem. Soc.,* 112, 5546, 1990.
26. Squillacote, M., Semple, T., Chen, J.W., and Liang, F., The low temperature photochemistry of s-*cis* acyclic 1,3-dienes, *Photochem. Photobiol.,* 76, 2002.
27. (a) Alfimov, M.V., Razumov, V.F., Rachinsky, A.G., Listvan, V.N., and Scheck, Y.B., Photochemical production of non-equilibrium conformers in glassy solutions at 77 K, *Chem. Phys. Lett.,* 101, 593, 1983; (b) Castel, N. and Fischer, E., Frozen-in non-equilibrium rotamers in 1,2-diarylethylenes obtained by low temperature irradiation, *J. Mol. Struct.,* 127, 159, 1985.
28. Mazzucato, U. and Momicchioli, F., Rotational isomerism in *trans*-1,2-diarylethylenes, *Chem. Rev.,* 91, 1679, 1991.
29. Imamoto, Y., Kuroda, T., Kataoka, M., Shavyakov, S., Krishnamoorthy, G., and Liu, R.S.H., Photoisomerization by Hula-twist. 2,2-Dimethylstilbene and a related ring-fused analog, *Angew. Chem.,* in press.
30. Tanner, D. and Wennerström, O., [2,2](4,4′) *Trans*-stilbenophane, *Tetrahedron Lett.,* 22, 2313, 1981.
31. Mizutani, T., Ikegami, M., Nagahata, R., and Arai, T., The first synthesis of stilbene dendrimers and their photochemical *trans-cis* isomerization, *Chem. Lett.,* 1014, 2001.
32. Kaupp, G. and Schmeyers, J., The solid-state *E/Z* photoisomerization of 1,2-dibenzoylethene, *J. Photochem. Photobiol. B; Biol.,* 59, 15, 2000.
33. Doany, F.E., Hochstrasser, R.M., and Greene, B.I., Isomerization intermediates in solution phase photochemistry of stilbenes, *Proc. SPIE Int. Soc. Opt. Eng.,* 533, 25, 1985.
34. Waldeck, D.H., Photoisomerization dynamics of stilbenes, *Chem. Rev.,* 91, 415, 1991.
35. Wyman, G.M., The *cis-trans* isomerization of conjugated compounds, *Chem. Rev.,* 55, 625, 1955.
36. Lightner, D. and McDonagh, A.E., Molecular mechanisms of phototherapy for neonatal jaundice, *Acc. Chem. Res.,* 17, 417, 1984.
37. Vettermann, S., Gustav, K., and Jungel, J., Quantum chemical studies on color and stereodynamics of cyclic azines, *J. Mol. Struct. THEOCHEM,* 104, 259, 1983.
38. Seltzer, S., MNDO barrier height for catalyzed bicycle-pedal hula-twist and ordinary *cis-trans* isomerizations of protonated retinal Schiff base, *J. Am. Chem. Soc.,* 109, 1627, 1987.

39. Fuss, W., Lochbrunner, S., Müller, A.M., Schikarki, T., Schmid, W.E., and Trushin, S.A., Pathway approach to ultrafast photochemistry: potential surfaces, conical intersections and isomerization of small polyenes, *Chem. Phys.,* 222, 161, 1998.
40. Ruiz, D.S., Cembran, A., Garavelli, M., Olivucci, M., and Fuss, W., Structure of the conical intersections driving the *cis-trans* photoisomerization of conjugated molecules, *Photochem. Photobiol.,* 76, 622, 2002.
41. Wilsey, S. and Houk, K., "H/Vinyl" conical intersections for dienes: a mechanism for the photochemical hula-twist, *Photochem. Photobiol.,* 76, 616, 2002.
42. Liu, R.S.H., Liu, C.W., Li, X.-Y., and Asato, A. E., Butyl conformational reorganization as a possible explanation for the longitudinal flexibility of the binding site of bacteriorhodopsin. The azulene and C-22 retinoid analogs, *Photochem. Photobiol.,* 54, 625–631, 1991.
43. Imamoto, Y., Kuroda, T., Kataoka, M., and Liu, R.S.H., Mechanistic pathways for the photoisomerization reaction of the anchored, tethered chromophore of the photoactive yellow protein and its mutants, *Photochem. Photobiol.,* 76, 584, 2002.
44. Chosrowjan, H., Mataga, N., Shibata, Y., Tachibana, S., Kandori, H., Shichida, Y., Okada, H., and Kouyama, T., Rhodopsin emission in real time: a new aspect of the primary event in vision, *J. Am. Chem. Soc.,* 120, 9706, 1998.
45. Kandori, H., Katsuta, Y., Ito, M., and Sasabe, H., Femtosecond fluorescence study of the rhodopsin chromophore in solution, *J. Am. Chem. Soc.,* 117, 2669, 1995.
46. Mathies, R.A. and Lugtenburg, J., The primary photoreaction of rhodopsin, in *Handbook of Biological Physics,* Vol. 3, Stavenga, D.G., deGrip, W.J. and Pugh, E.N., Jr., Eds., Elsevier Science, Amsterdam, 2000, p. 55.
47. Hammond, G.S., Reflections on photochemical reactivity, *Adv. Photochem.,* 7, 373, 1969.
48. Liu, R.S.H. and Hammond, G.S., Photochemical reactivity of polyenes. From dienes to rhodopsin; from microseconds to fentoseconds, *Photochem. Photobiol. Sci.,* in press.

27

Conformer-Specific Photochemistry in the Vitamin D Field

Jack Saltiel
Florida State University

Lenuta Cires*
Florida State University

Andrzej M. Turek**
Florida State University

27.1 Definition and Scope

Photochemistry in the vitamin D field has played a central role in the development of molecular photochemistry. Especially noteworthy have been the early contributions of Havinga[1] and Dauben[2] and their co-workers. Havinga introduced his principle of the nonequilibration of excited rotamers (NEER) to explain the excitation wavelength dependence of the photoproducts of the trienes previtamin D and tachysterol (Scheme 1).[3] The NEER principle is based on the idea, inspired by Hückel molecular orbital (MO) theory, that excitation of conjugated polyenes and related molecules to their lowest singlet or triplet excited states tends to reverse double/single bond character, preventing equilibration of ground state conformers. Thus, the ground state conformer equilibrium compositions, the individual spectra and excited state energies of the conformers, and the conformer-specific photochemical properties of the conformers control observed product quantum yields and distributions. The dependence of acyclic 1,3-diene photodimer distributions[4] and trans/cis photostationary states[5,6] on the triplet excitation energy of the sensitizer demonstrated by Hammond, Saltiel, and co-workers, soon thereafter, provided dramatic confirmation of this principle (Figure 27.1 and Schemes 2 and 3). Ground state conformer controlled photochemical ring opening of a substituted 1,3-cyclohexadiene to isomeric conjugated trienes was first reported in the case of α-phellandrene (Scheme 4).[7]

Demonstrations of photophysical manifestations of NEER include the resolution of the fluorescence of all-*trans*-1,6-diphenyl-1,3,5-hexatriene into s-*trans*,s-*trans* and s-*cis*,s-*trans* contributions[8] and analogous resolutions of fluorescence and absorption spectra of styrylarene conformers.[9,10] The conformer-specific adiabatic *cis*→*trans* photoisomerizations of 2-styrylnaphthalene[11] (*cis*- and *trans*-NPE) and 2-styrylanthracene[12] are especially striking examples. In each case, the more extended s-*trans*-like conformer undergoes adiabatic *cis*→*trans* photoisomerization whereas the less extended s-*cis*-like conformer undergoes selective photocyclization (Scheme 5).[13,14] In this sense, these *cis*-diarylethenes can be regarded as true previtamin D mimics.

*On leave from Al. I. Cuza University, Faculty of Chemistry, Bd. Carol I no 11, R-6600 Iasi-6, Romania.
**On leave from Jagiellonian University, Faculty of Chemistry, Cracow, Poland 30 060.

0-8493-1348-1/04/$0.00+$1.50

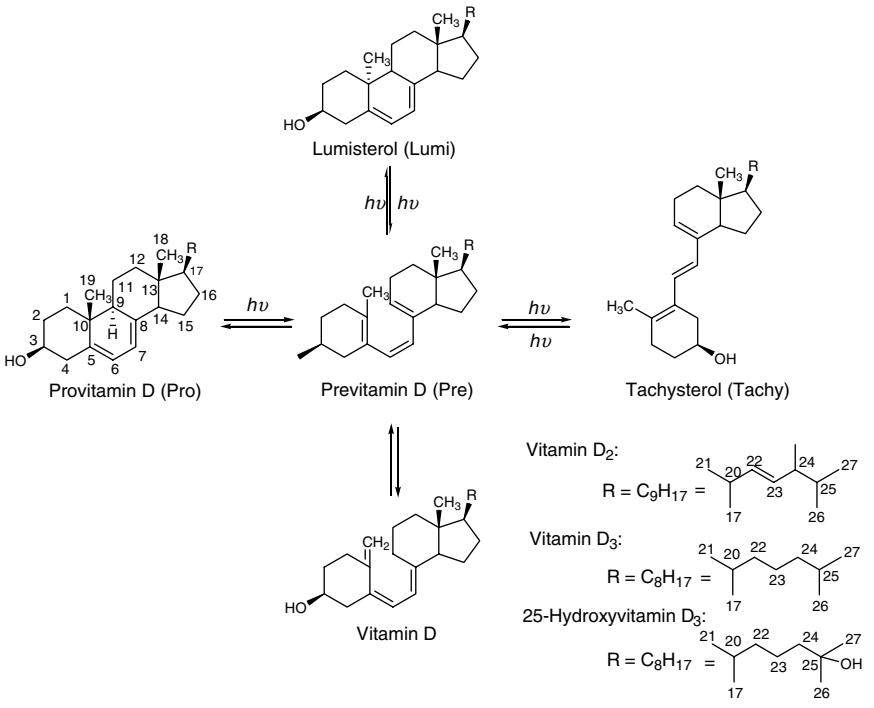

SCHEME 1 Major photochemical events in the vitamin D field.

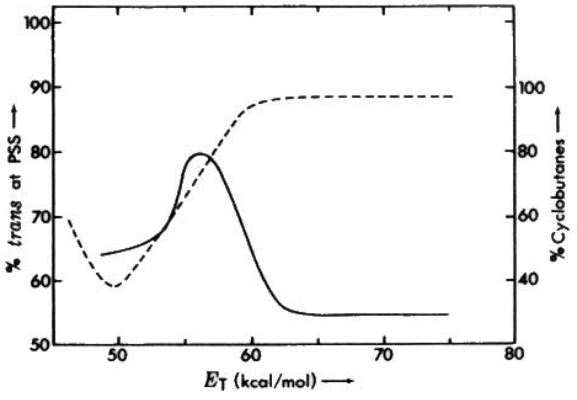

FIGURE 27.1 Saltiel plots of 1,3-butadiene dimer compositions (dashed line) and 1,3-pentadiene trans/cis photostationary states as a function of the triplet energy of the sensitizer (reproduced from Reference 6 with permission from the copyright owner, the American Chemical Society).

Adherence to the NEER principle is expected in molecules with relatively short-lived excited states in which the electronic excitation is delocalized extensively over the conjugated π-system. In such molecules, torsional barriers about essential ground state single bonds are enhanced in the lowest excited states. Conversely, molecules that have long excited state lifetimes and in which there is pronounced localization of electronic excitation in parts of the π-system are likely to violate the NEER principle. Alkenyl-substituted anthracenes provide well-documented examples.[9,15–17]

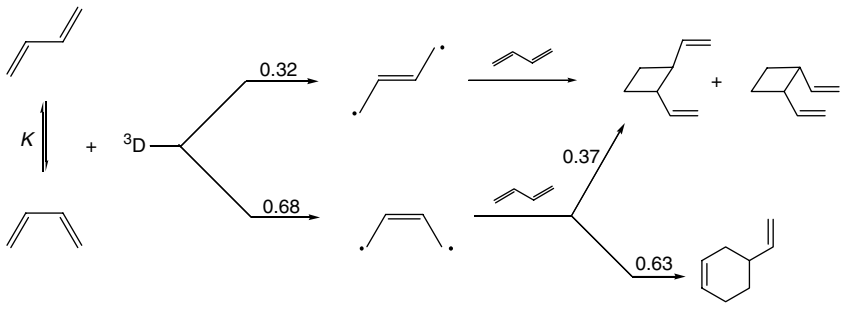

SCHEME 2 Fluorenone-sensitized 1,3-butadiene dimerization.

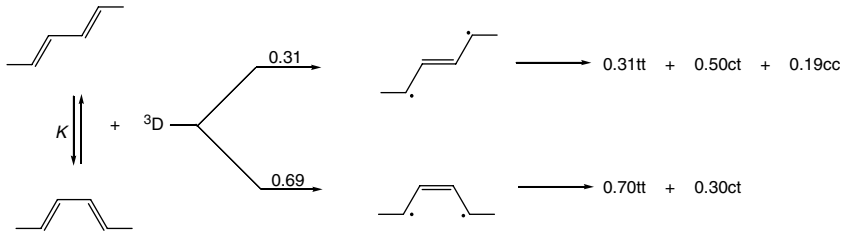

SCHEME 3 Fluorenone-sensitized isomerization of *trans,trans*-2,4-hexadiene.

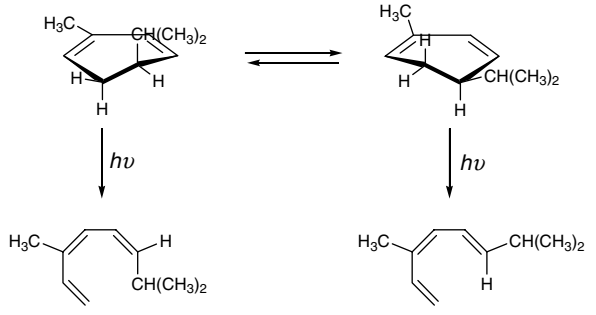

SCHEME 4 Conformer specific ring opening of α-phellandrene.

In recent years, it has been suggested that not all the excitation wavelength dependence of quantum yields in the vitamin D field can be accounted for by the NEER principle. We consider below the competing mechanisms that have been proposed to account for photochemical observations and describe some of the strategies that have been employed to improve the photochemical production of the previtamins from the provitamins. Optimization of the previtamin yields improves vitamin yields as the latter are formed thermally from the previtamins via 1,7-suprafacial hydrogen shifts.[18] Readers interested in the rich photochemistry leading to overirradiation products should consult previous reviews.[1a,2b]

27.2 Mechanism

Paradoxically, it was the dependence of product distributions and quantum yields in the interconversion of vitamin D precursors on the excitation wavelength that led Havinga to the postulation of the NEER principle and it was, subsequently, systematic confirmation of such dependence that led Dauben, Kohler, and co-workers and, more recently, Fuß and co-workers to propose alternative explanations.

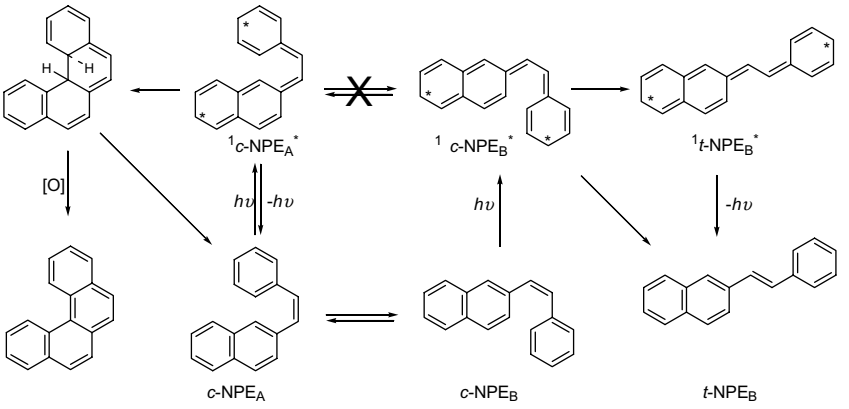

SCHEME 5 Conformer specific photochemistry of *c*-NPE.

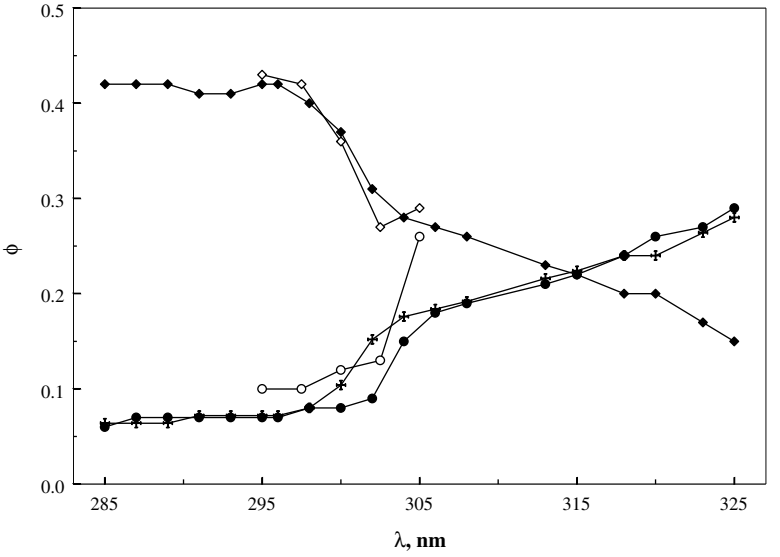

FIGURE 27.2 Excitation wavelength dependence of photocyclization (o,[19b] •[20]) and photoisomerization (◊,[19b] ♦[20]) quantum yields starting from previtamin D_2 in ether at 0°C; crosses designate calculated photocyclization quantum yields based on the NEER principle, see text.

The experimental data that have been presumed to be incompatible with the NEER principle derive from studies by Dauben and co-workers of the λ_{exc} dependencies of *cis-trans*-photoisomerization (to tachysterol, ϕ_T) and photocyclization quantum yields (to provitamin D_3 and lumisterol, ϕ_{PRO} and ϕ_{LUMI}, respectively) starting from pure previtamin D_3.[19,20] Quantum yields were measured in reference 20 (de-aerated anhydrous diethyl ether, 0°C). In reference 19 relative quantum yields were estimated from quasi-photostationary states and molar absorptivities and were converted to absolute quantum yields on the basis of Havinga's measurements at 254 and 302.5 nm.[21] Photocyclization quantum yields ($\phi_{PRO} + \phi_{LUMI}$) increase and photoisomerization quantum yields (ϕ_T) decrease as λ_{exc} is increased (Figure 27.2). A study of the effect of λ_{exc} in the 225–400 nm range on the formation of "potential vitamin D_2" found that 295-nm light is most effective,[22] in good agreement with the earlier findings of Havinga and co-workers[23] and a more recent study by Braun et al.[24] The "sudden" increase in the photocyclization quantum yields and decrease in the photoisomerization quantum yields in the narrow 302–305 nm λ_{exc} range (ϕ_{PRO} = 0.02, 0.04, ϕ_{LUMI}

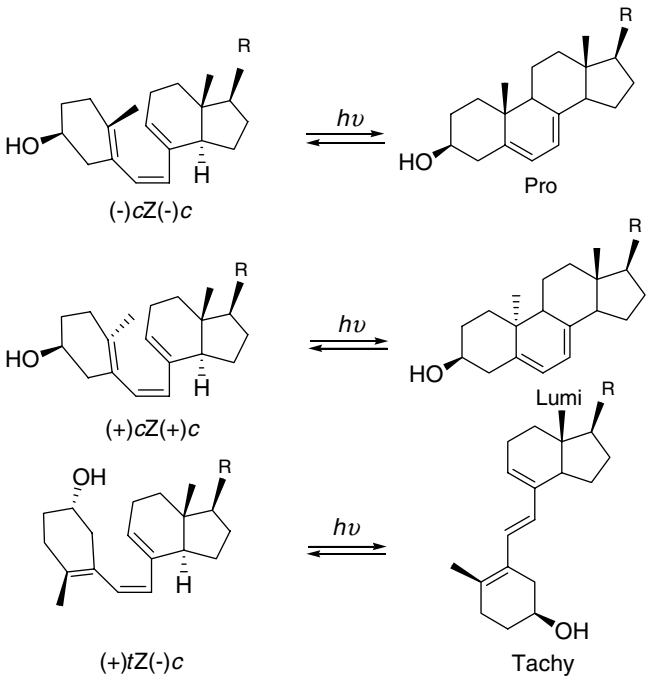

SCHEME 6 Conformer specific photochemistry of Pre in solution.

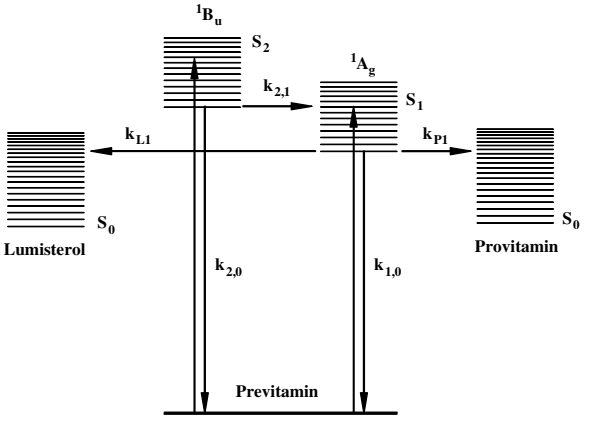

FIGURE 27.3 The Dauben-Kohler 1B/2A mechanism for *cZc*-previtamin D photochemistry (reproduced from Reference 19b with permission from the copyright owner, the American Chemical Society).[20]

= 0.07, 0.13, and ϕ_T = 0.31, 0.27 for 302 and 306 nm, respectively[20]) was judged to be inconsistent with changes in the absorption spectra of the previtamin conformers, potential specific precursors of the three photoproducts (Scheme 6).[19,20] It was suggested that $\lambda_{exc} \leq 302$ nm populates the lowest allowed 1B (S_2) excited state of the previtamin whose major reaction channel, photoisomerization, competes with internal conversion to 2A, the lowest (doubly) excited singlet state (S_1). Excitation at longer wavelengths, $\lambda_{exc} \geq$ 304 nm, directly populates S_1 whose major reaction channel, photocyclization, competes with radiationless decay to S_0 (Figure 27.3).[19,20] This interpretation was bolstered by low temperature (77 K) fluorescence measurements assigned to the $S_1 \rightarrow S_0$ transition in the previtamin that appeared to gain dramatically in intensity for $\lambda_{exc} > 300$ nm.[20] The latter result suggests poor communication between S_2 and S_1 excited

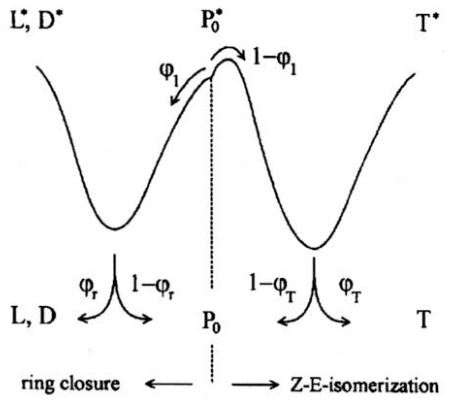

FIGURE 27.4 The Fuß hot excited state mechanism for *cZc*-previtamin D photochemistry in S_1 (2A) (reprinted from Reference 27, with permission from the copyright owner, Elsevier Science, Oxford, UK).

states in contrast to the very rapid $S_2 \rightarrow S_1$ in all-*trans*-1,6-diphenyl-1,3,5-hexatriene.[25,26] However, the relevance of the low temperature spectroscopic observations in a rigid medium to the interpretation of the high temperature photochemical observations in solution is questionable because different conformer equilibrium distributions are likely to be involved (see below).

Fuß and Lochbrunner have advanced an alternative interpretation of the λ_{exc} dependence of the quantum yields in Figure 27.2.[27] They retain Havinga's ground state conformer control at $\lambda_{exc} \leq 302$ nm but propose that the jumps in the quantum yields over the narrow wavelength range that follow are due to competing barrierless photocyclization and activated photoisomerization pathways in *cZc*-previtamin. Because of the short excited state lifetime, photoisomerization competes with vibrational relaxation, such that excitation over the torsional barrier favors cis→trans photoisomerization as a hot excited state reaction (Figure 27.4). Common features of the mechanisms in Figures 27.3 and 27.4 are that they attribute the sharp change in the quantum yields to the behavior of the excited states of a single conformer. Enhanced cis→trans photoisomerization efficiency with wavelengths shorter than 302 nm is assigned to the 1B state of the *cZc* (s-cis at C_5C_6, cis at C_6C_7, and s-cis at C_7C_8) conformer in the Dauben/Kohler mechanism and to a vibrationally hot S_1 (presumably 2A) state in the Fuß mechanism. Fuß argues in favor of his mechanism because it accounts for the monotonic increase in the overall cyclization quantum yield at the longer wavelengths that populate only S_1, whereas a constant quantum yield is predicted by the Dauben/Kohler mechanism.[27] However, the argument is not compelling because neither mechanism takes into account the fact that provitamin (Pro) and lumisterol (Lumi) have different (at least in a helical sense) *cZc*-previtamin (*cZc*-Pre) precursors. Thus, consideration of observed and expected changes in the spectra of the conformers of the previtamin indicates that the NEER principle still provides a viable explanation for the quantum yield variation in Figure 27.2,[28c] accounting also for the change in the ϕ_{LUMI}/ϕ_{PRO} ratio.[29]

Then, what is the relationship between photoisomerization and photocyclization quantum yields that would be predicted if the NEER principle were strictly adhered to throughout the λ_{exc} range? In view of the structural requirements of the two reactions, we assume that only cZc conformers undergo photocyclization and that the rest undergo only photoisomerization. For simplicity, we also assume that the cis→trans photoisomerization quantum yields of the cZc conformers are relatively small and can be neglected (this is not an essential assumption). Adopting the notation proposed by Fuß and Lochbrunner,[27] the previtamin conformers are divided into a set P that photoisomerizes and a set P_0 that photocyclizes. Since the sum $\phi_T + \phi_{PRO} + \phi_{LUMI}$ starts at 0.48 at the shorter wavelengths where ϕ_T dominates and decreases to 0.44 at the longer wavelengths where ϕ_{PRO} and ϕ_{LUMI} dominate (these are minimum values since back reaction corrections were not applied),[20] it is reasonable to assume maximum quantum yields of 0.50 and 0.40 for the photoisomerization of the P conformer set and the photocyclization of the P_0 conformer set,

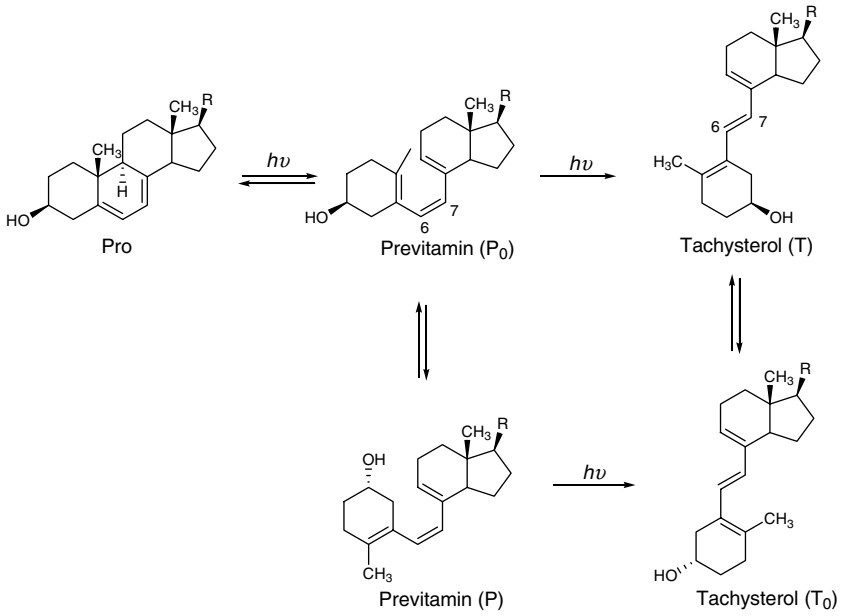

SCHEME 7 Proposed conformer specific Hula-Twist photoisomerization of Pre in a rigid medium.

respectively, independent of λ_{exc}. It follows that the fraction of absorbed light that excites P conformers is $f_P = \phi_T/0.50$, and the remainder, $f_{P0} = (1 - f_P)$, is the fraction that excites P_0 conformers. This allows calculation of the sum of cyclization quantum yields from the photoisomerization quantum yields: $(\phi_{PRO} + \phi_{LUMI}) = 0.40(1 - f_P)$. Cyclization quantum yields obtained in this way, Figure 27.2, are in excellent agreement with observed values at short and long wavelengths. The quantum yield "jump" is reproduced satisfactorily but is predicted to occur at shorter wavelengths by about 2 nm, in better agreement with results from the earlier study.[19] Application of this procedure separately on the experimental ϕ_{PRO} and ϕ_{LUMI} values can be used to divide f_{P0} into excitation fractions of cZc conformers that differ in helicity. In view of the large number of potentially accessible conformers and the low absorbance of the system above 300 nm (see below), a 2 nm lag between the fall in ϕ_T and the rise in $(\phi_{PRO} + \phi_{LUMI})$ could be caused by the drop of tZc conformer absorption initially coinciding with competing absorption by conformers that have low photoisomerization and photocyclization efficiencies. Clearly, the NEER principle accounts for the data over the entire wavelength range and predicts that absorption by the P_0 conformer set is shifted to the red of the absorption of the P conformer set, becoming important at the onset of the previtamin D spectrum (see below)

27.3 Conformer Spectra Energies and Populations

Experimental verifications of the conformational dependence of the UV absorption spectra of the triene moieties in tachysterol ($Tachy_3$) and previtamin D_3 (Pre_3) were obtained by excitation of Pre_3 at 92 K in a rigid EPA-type glass[28] (5/5/1 solution of ether/isopentane/ethyl alcohol) and of Pro_3 in EPA[27,30] (5/5/2 solution of ether/isopentane/ethyl alcohol), respectively. The current interpretation of these results, advanced by Fuß and co-workers, is shown in Scheme 7.[30] Irradiation of Pre_3 gives a red-shifted relatively structureless spectrum assigned to the *cEc* conformer of tachysterol because on warming the mixture to 100–105 K in the dark, the spectrum slowly shifts to the blue and develops the well defined vibronic progression of the equilibrium conformer mixture of tachysterol (mainly the *tEc* conformer), as shown in Figure 27.5.[28] On the basis of these observations, Havinga and co-workers proposed that *cEc*-Tachy forms from excited *cZc*-Pre.[28a,b] Fuß questioned this proposal because irradiation of the provitamin under

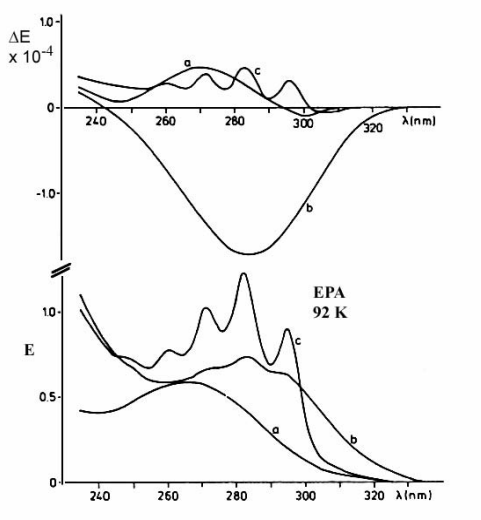

FIGURE 27.5 UV and CD spectra before (curves a) and after (curves b) irradiation of previtamin D_3 in EPA at 92 K. Curves c are for the irradiated sample after it was warmed to 105 K and re-cooled to 92 K (reproduced from Reference 28a with permission from the copyright owner, Wiley WCH Verlag GmbH, Weinheim, Germany).

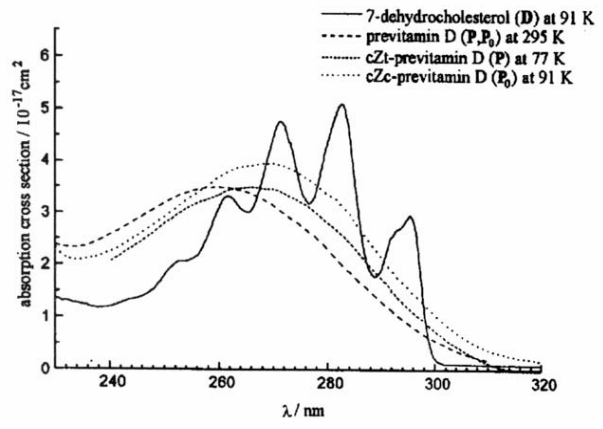

FIGURE 27.6 UV spectra of provitamin D_3 at 91 K, previtamin D_3 at 77 K (designated as conformer set P), previtamin D_3 formed *in situ* from provitamin D_3 at 91 K (designated as conformer set P_0), and previtamin D_3 at 295 K (designated as equilibrium P_0/P conformer mixture (reprinted from Reference 27, with permission from the copyright owner, Elsevier Science, Oxford, UK).

nearly identical conditions gives a red-shifted previtamin spectrum, presumed to be the cZc conformer, which, on further irradiation, gives the structured *tEc*-Tachy spectrum.[30]

The low temperature spectra of Pre[20] and of Pre formed photochemically from Pro are shown in Figure 27.6.[27] It was reasoned that the rigid medium prevents the nascent Pre from relaxing to an equilibrium conformer distribution and ensures that its initial geometry is retained, hence accounting for the red shift in the spectrum. Assignment of the red-shifted spectrum to the cZc conformer of Pre follows from least motion considerations in the highly viscous medium.[27,30] The conformer-specific photoisomerization outcomes in Scheme 7 are based on these spectroscopic structural assignments. No experimental mixture spectra have been published, and no clear description of the method used to derive

the pure component spectrum of the matrix-trapped *cZc*-Pre conformer, Figure 27.6, was provided. In accepting such assignments, it is important to establish that the initially observed transient arises from a one-photon process and that overirradiation was avoided. These precautions are essential because the sequence of light-induced s-trans to s-cis conformer equilibration followed by photochemical ring-closure of the s-cis conformer to the cyclobutene has been reported for Ar-matrix isolated 2,3-dimethyl-1,3-butadiene at 19.5 K.[31] Conformer interconversion under these conditions was first reported for 1,3-butadiene,[32] and Kohler et al. have shown that excitation of all-s-trans *trans,trans*-1,3,5,7-octatetraene in an *n*-octane matrix at 4.2 K leads to s-trans to s-cis conformer conversion[33] and that prolonged irradiation leads to formation of *cis,trans*-1,3,5,7-octatetraene even at this low temperature.[34]

If the assignments in Scheme 7 are correct, formation of the Tachy products involves rotations at adjacent double and single bonds, providing the first experimental verification of an outcome consistent with Liu's hula-twist mechanism for cis→trans photoisomerization.[30,35] They have stimulated the recent resurrection of this mechanism with special attention to the key role of the volume-conserving requirements of the rigid medium.[36]

Theoretical calculations at different levels of theory of the structures and energies of the ground state conformers of Pre have been carried out on the model compound with the side chain at the D ring replaced by a methyl group.[37–41] They generally predict a complex mixture of conformers in close energetic proximity. The order of conformer energies varies with the level of theory, but at least eight of them, four in the cZc family (P_0) and four in the tZc family (P), are predicted to lie within less than 2 kcal/mol of each other.[29] The *tZt* conformer set lies a little over 2 kcal/mol above the global minimum. Within each subset the conformers differ in helicity and in the quasi-axial or equatorial orientation of the OH group in the A ring. In such gas phase calculations, the interaction of the OH group in the axial orientation with the rest of the molecule has a pronounced stabilizing influence, which would be attenuated in solution.[41] At the B3LYP/6–31 G(d) level of theory, tZc conformers are generally predicted to lie roughly 1 kcal/mol below corresponding cZc conformers.[41]

In view of the above spectroscopic observations and theoretical predictions, Havinga's NEER principle appears to best account for the λ_{exc} dependence of the quantum yields of the products from Pre. The two competing mechanisms assign the change in the quantum yields at about 302 nm to the excited state behavior of the *cZc*-Pre conformers (P_0). The postulation of the 1B/2A origin of the effect[19b,20] by Dauben and Kohler was influenced by the finding that the 2A→1A fluorescence excitation spectrum of Pre_3 dissolved in a decalin/methylcyclohexane glass at 77 K extends well to the red of the absorption spectrum under the same conditions. However, although it is likely that this was correctly attributed to a strong fluorescence contribution by direct absorption into the highly forbidden 2A←1A transition in the 300–340 nm region,[20] the fact that the fluorescence intensity diminishes at shorter wavelengths where 1B←1A transitions are strongest cannot be taken as support for the conclusion of weak communication between 1B and 2A states of P_0. Transient spectroscopic observations have established that radiationless 1B→ 2A transitions occur in the fsec-timescale in trienes[25,26,42–44] and in cyclohexadienes,[42,45] including members of the vitamin D family.[45b] A much more likely interpretation is that the shorter excitation wavelengths are not effective because they excite the dominant tZc family of conformers (P), which do not fluoresce. Precisely such an interpretation applies to *cis*-NPE (Scheme 5).[46]

Fuß assigned the sharp quantum yield changes to hot excited state chemistry in P_0 because he also concluded, based on the spectra in Figure 27.6, that only P_0 absorbs above 300 nm. However, it seems to us difficult to predict from these spectra precisely where P absorption will stop and P_0 absorption will take over at 0°C. The low temperature spectra were taken in different solvents and at different temperatures. The spectrum assigned to the P set of conformers was measured at 77 K in a hydrocarbon glass[20] and that assigned to the P_0 set was for Pre prepared photochemically *in situ* from Pro in EPA glass at 91 K.[27] Not only are the spectra expected to shift to the blue with increasing *T*, but there is strong evidence in circular dichroism (CD) spectra that the conformer composition is strongly solvent dependent.[28] At the very least, the ethanol in EPA is expected to favor conformations with the 3-OH equatorial, whereas a hydrocarbon medium is expected to shift the equilibrium toward conformations with the 3-OH axial.[28c] We conclude that the Pre spectra in Figure 27.6 are consistent with strongly diminishing relative absorption

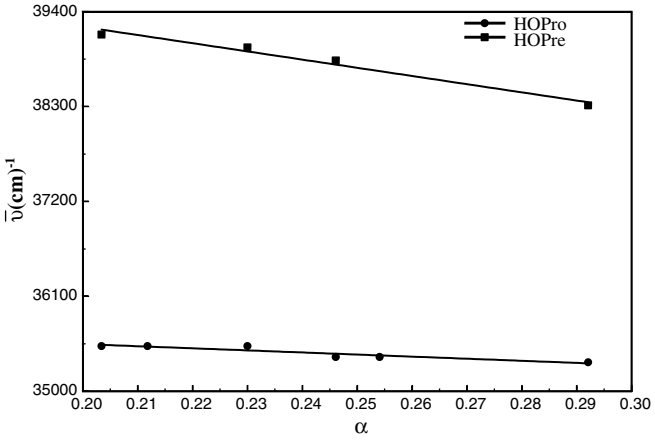

FIGURE 27.7 The dependence of the λ_{max} values of the UV spectra of HOPro and HOPre on solvent polarizability at 20°C;[48b] the solvents, in order of increasing polarizability are methanol, acetonitrile, isopropyl alcohol, tetrahydrofuran, dioxane, and toluene.

by P conformers (tZc) at 302 nm and substantial contribution at longer λ (the onset of the UV spectrum of Pre in ether at 0°C) by P_0 conformers (cZc). There is also the possibility, which may be remote due to the very viscous EPA medium, that following the ring opening of Pro, the hot Pre conformers equilibrate on the ground state surface, as has been reported for 1,3-cyclohexadiene in ethanol.[42]

27.4 Optimizing the Production of Vitamin D from Provitamin D

The production of vitamin Ds provides a rare example of an industrial scale synthesis in which, free radical chain reactions aside, photochemistry *in vitro* plays a crucial role.[47] The objective is to maximize the photochemical conversion of Pro to Pre and to follow this with the thermal rearrangement of the latter to the vitamin Ds (Vit). It is desirable to achieve optimum conversions to the Pre while minimizing the yields of the undesirable secondary photoproducts Lumi and Tachy.[1,2] Finally, the thermal Pre→Vit conversion must be carried out at an intermediate temperature in order to avoid competing thermal disrotatory cyclizations to pyro- and isopyrocalciferols, cyclohexadiene stereoisomers of the lumisterols and provitamins with cis ring B junctions, which occur at temperatures above 100°C.[47] The separation of photochemical and thermal steps is beneficial because it prevents formation of Vit photoproducts.[1,2]

Three strategies have been proposed to maximize the photochemical yields of Pre. They all have in common as a first step, roughly monochromatic UV-excitation of Pro in the absence of oxygen with the goal of approaching quasi-photostationary states (Q-PSS; Scheme 1). Overirradiation or even attainment of the Q-PSS is avoided because of slow, irreversible stoichiometric losses of the interconverting isomers to undesirable isomers transparent to the exciting light.[1,2] The success of the first strategy depends on the selection of an excitation wavelength that yields the largest previtamin contribution in the Q-PSS and employs no other photochemical step in the synthesis.[22–24] The optimum λ_{exc} selection has been based on the quantum yields of the interconversions and the absorption spectra of the contributing isomers. There is a general shift of the λ_{max} of the absorption spectra to the red with increasing solvent polarizability $\alpha = (n^2 - 1)/(n^2 + 2)$, where n is the index of refraction,[48] similar to that experienced by the α,ω-diphenylpolyenes.[49,50] More subtle changes are expected at the onsets of the absorption spectra due to the influence of solvent on the equilibrium distribution of the conformers.[28] Figure 27.7 shows the polarizability effect on the spectra of the Pro and Pre 25-OH analogues of vitamin D_3 ($HOVit_3$).[48] The effect is generally more pronounced for the trienes than for the cyclohexadienes.[48] The set of spectra for the 25-OH vitamin D_3 ($HOVit_3$) isomers in methanol, Figure 27.8,[48] is typical.

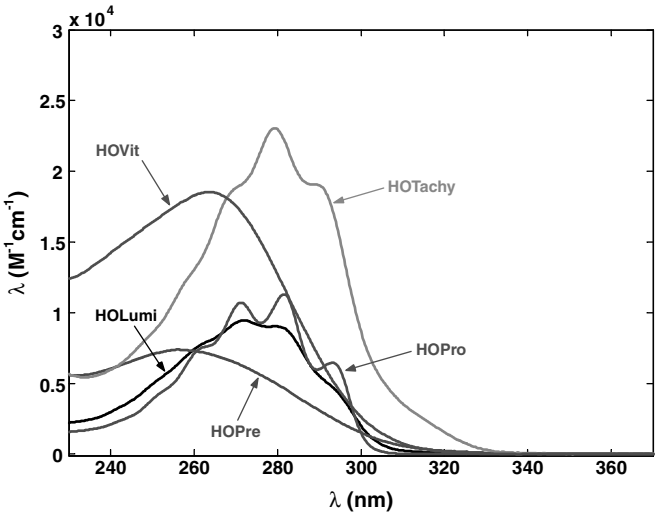

FIGURE 27.8 UV spectra of HOVit isomers in methanol at 20°C.[48]

Most quantitative determinations of the progress of the photochemical conversions, as Q-PSS relationships are approached, have been by high performance liquid chromatography (HPLC) analysis, a rather time-consuming method. The availability of an accurate set of absorption spectra, such as those in Figure 27.8, allows the product distribution to be conveniently determined directly from UV spectra of the reaction mixture taken during the course of the irradiation. Treatment of such spectral matrices by singular value decomposition (SVD) reveals the number of major components and stoichiometric losses due to the formation of photoproducts (i.e., toxisterols[1]) that do not contribute in the wavelength range of the spectra.[51,52] As an example, we present results from a 254 nm irradiation of HOPro (4.90×10^{-4} *M*) in methanol at 20°C. On the basis of the relative magnitude of the eigenvalues, the spectral matrix is a well-behaved three-component system (HOPro/HOPre/HOTachy). Pure component and mixture spectra are represented as linear combinations of the three major eigenvectors, and each is reduced to a point in the combination coefficient space. Figure 27.9 shows the time evolution of the spectra in the eigenvector combination coefficient space. Deviations from the stoichiometric plane defined by the combination coefficients of the three pure components (not obvious in Figure 27.9 but easily seen by rotating the plane to an edge view) are small. They reflect formation of very small amounts of HOLumi and HOVit (<1%) that are neglected in the analysis and stoichiometric losses to nonabsorbing products (≤3.3% at the end of this experiment). The results in Figure 27.9 correspond to the reaction profile in Figure 27.10.

Figure 27.11 shows the λ_{exc} dependence of Q-PSS compositions for the Vit_3 system in diethyl ether calculated by Braun et al.[24] based on absorption spectra and published quantum yields.[19a,53] The maximum contribution of the previtamin is predicted to occur for $\lambda_{exc} = 296$ nm,[24] in excellent agreement with the previous two studies[22,23] and in satisfactory agreement with experimental results (one glaring exception is the contribution of Lumi, which is found experimentally to be larger than that of Pro at nearly all wavelengths, and especially at wavelengths longer than 300 nm).[24] Excitation close to 296 nm is desirable in the one-step previtamin synthesis because it minimizes the formation of Tachy, the major undesirable secondary product for the $\lambda_{exc} \leq 296$ nm range. It was estimated that a 47% optimum conversion to Pre could be achieved by excitation of the provitamin at 296 nm. The process then requires separation of unreacted provitamin for recycling and of previtamin for the thermal conversion to the vitamin.

The other two strategies employ sequential photochemical steps. The excitation wavelength in the first step is chosen so as to maximize the conversion of Pro to Pre and Tachy, and a longer excitation wavelength, with or without an added triplet energy donor, is used in the second step to convert the initial Pre and Tachy mixture to a Pre-rich Q-PSS. The sequential direct excitation procedures mainly

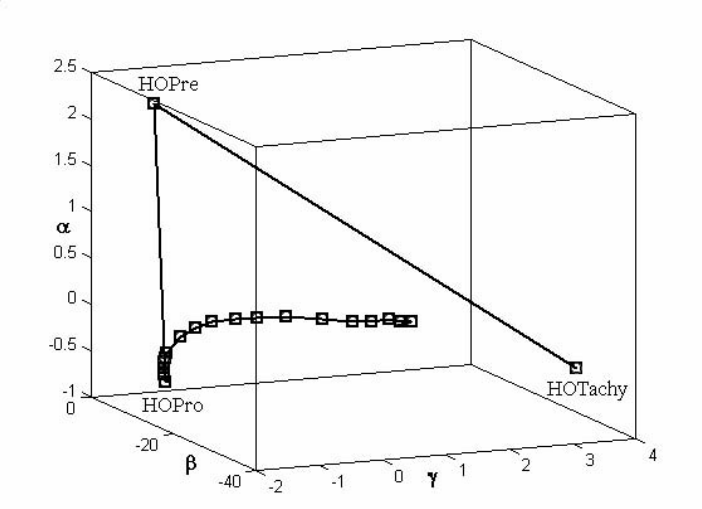

FIGURE 27.9 Stoichiometric plane (shown by the labeled pure component points) in SVD combination coefficient space for the 254 nm-irradiation of HOPro in methanol[48] (see text).

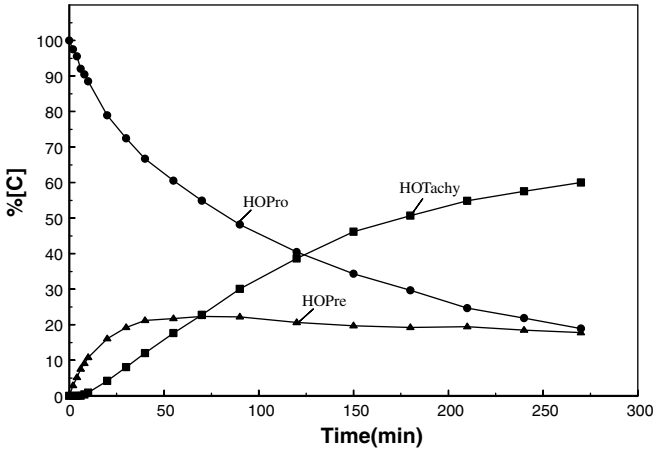

FIGURE 27.10 Product evolution according to Figure 27.9.

use a short wavelength (248 or 254 nm) for the Pro to Pre + Tachy step, followed by a second excitation wavelength in the 337–355 nm range to convert most of the Tachy to Pre.[54–56] These procedures have sought to take advantage of the fact that the Tachy UV spectrum extends to longer wavelengths than the Pre spectrum (Figure 27.8). However, the second wavelengths that have been suggested are barely absorbed by Tachy and, in addition, the desired selective excitation advantage is almost lost. For instance, the molar absorptivities of $Tachy_3$ and Pre_3 at 350 nm in diethyl ether are given as 100 and 25 $M^{-1}cm^{-1}$, respectively.[55] To make matters worse, wavelengths longer than 296 nm selectively excite *cZc*-Pre conformers (probably directly into the 2A state) and favor return to Pro and, especially, formation of Lumi (Figure 27.12).[19,20,24] Results from the Dauben and Phillips study are shown in Figure 27.12. They show that the Tachy→Pre conversion is the dominant process during the initial 350-nm irradiation period and that only when it is nearly complete do the Pre→Lumi and Pre→Pro photoreactions take over. The irradiation sequence in Figure 27.12 yielded up to 83% Pre at 95% Pro conversion.[55] The large Pre/Tachy Q-PSS ratios that were achieved with $\lambda_{exc} = 350$ nm indicate that the quantum yield in the Tachy→Pre

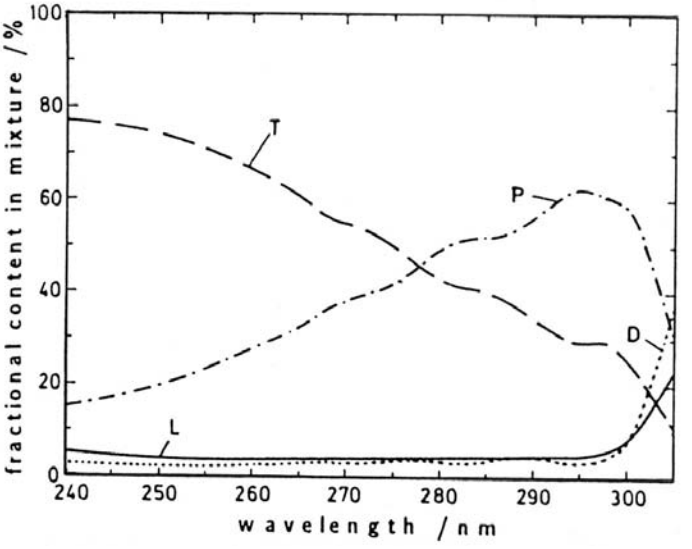

FIGURE 27.11 Calculated Q-PSS compositions for the Vit_3 isomers in ether as a function of excitation wavelength; T, P, L, and D are $Tachy_3$, Pre_3, $Lumi_3$, and Pro_3 (7-dehydrocholesterol), respectively (reprinted from Reference 24, with permission from the copyright owner, Elsevier Science, Oxford, UK).

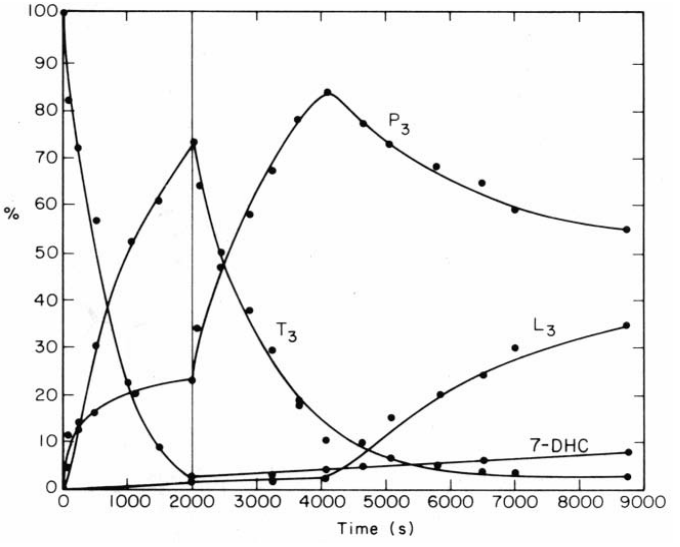

FIGURE 27.12 Product evolution from the irradiation of Pro_3 (7-DHC) in diethyl ether at 0°C at 254 and then (vertical line at 2000 min) at 350 nm (reproduced from Reference 55 with permission from the copyright owner, the American Chemical Society).

direction is at least four times larger than in the Pre→Tachy direction. Since, furthermore, Lumi becomes the major component in the Q-PSS at long irradiation times, it follows that the quantum yield trends in Figure 27.2 extend to longer wavelengths.

We have tested the use of the 313 nm Hg line to effect the HOTachy→HOPre conversion as an alternative wavelength in the second irradiation step.[48] This wavelength is absorbed more strongly and more selectively by the Tachy chromophore (Figure 27.8). Essentially identical Tachy→Pre quantum yields

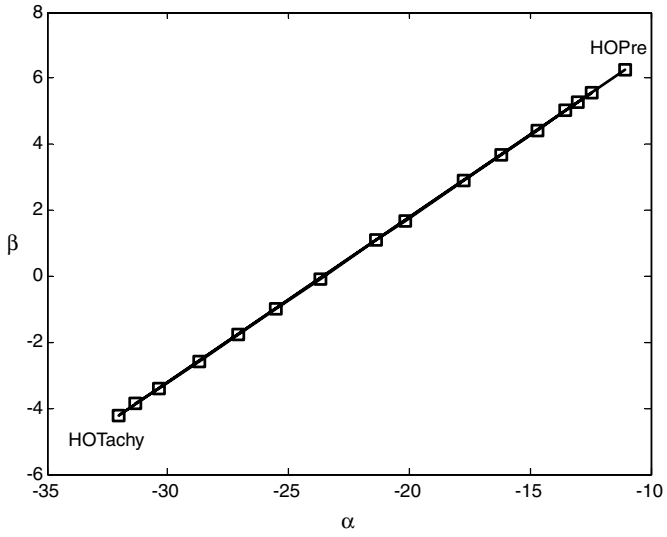

FIGURE 27.13 Stoichiometric line in 2-component SVD combination coefficient space for the 313 nm conversion of HOTachy to HOPre in methanol.[48]

of 0.10 at 254 and 313 nm in diethyl ether were reported by Jacobs and Havinga et al.[1a] Similar claims were made by Dauben and Phillips for 254 and 302 nm excitations,[19a] and by Gliesing and co-workers for excitation over the 254 to 313 nm range in ethanol.[57]

We used degassed methanol solutions and determined conversions by SVD analysis of UV spectra and by HPLC. The quantum yield for the HOTachy→HOPre direction in methanol at 20°C is 0.43. It is significantly larger than the 0.10 value at 254 nm[1a] (the 0.49 value for the Lumi→Pre quantum yield in ether at 313 nm[21] was assigned inadvertently to the Tachy→Pre process[47]).[48] Our value for the HOTachy→HOPre quantum yield in methanol at 254 nm is 0.14. The substantial λ_{exc} effect on the quantum yield for the Tachy→Pre process indicates that the two wavelengths excite different compositions of HOTachy conformers. SVD analyses of the UV spectra of product mixtures obtained in the course of the 313 nm irradiations of a degassed HOTachy solution in methanol are consistent with well-behaved 2-component systems. The excellent adherence of the combination coefficients points of individual spectra from the HOTachy/HOPre stoichiometric line in Figure 27.13 at up to an apparent 95% conversion to HOPre (see below) is typical. At the longer irradiation times, a three-component SVD analysis gives more accurate product compositions. The longer irradiation time spectra that were included in the two-component treatment in Figure 27.13, when treated as a three-component system give the product evolution shown in Figure 27.14. HPLC analysis of the final reaction mixture gave 5.7% (6.9%) HOTachy, 81.9% (82.4%) HOPre, 8.3% (7.8%) HOLumi, 2.4% HOPro, and 1.8% HOVit (values in parentheses are from the corresponding three-component SVD analysis). A filter solution was used to isolate the 313 nm Hg line, but nearly identical product compositions are attained much faster with the use of only Pyrex as the filter because 313 nm is the only transmitted Hg line that is absorbed significantly by the reaction mixture.[48]

Early discussions of the conformational equilibrium in Tachy have settled on the tEc and the tEt conformers as the most energetically favored, with the former being more abundant.[1a,58] A recent molecular mechanics-based (MMX) conformational search confirms the placing of tEc as the most abundant Tachy conformer (63%) but predicts cEc (18%) to be slightly more abundant than tEt (13%).[59] The weak structureless band at the onset of the UV spectrum of HOTachy, Figure 27.8, should then be assigned to either the cEc or the tEt conformer, or both, and 254 nm should favor *tEc*-HOTachy excitation (note that s-*cis* diene moieties normally absorb to the red of s-trans diene moieties).[60] The *s-cis*-butadiene moiety in *tEc*-HOTachy may explain the much lower HOTachy to HOPre quantum yield at 254 nm than

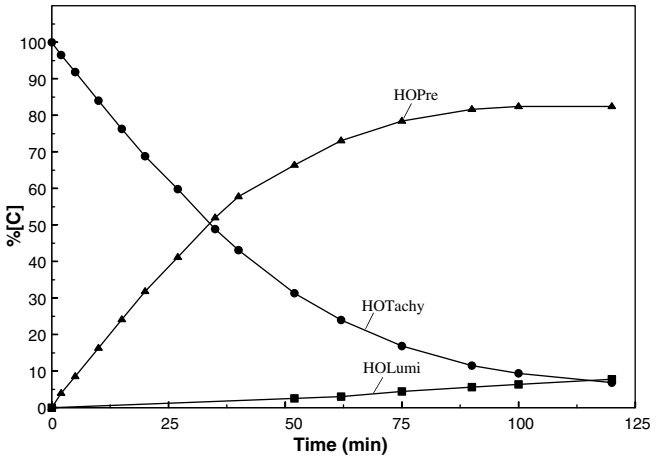

FIGURE 27.14 Product evolution for the 313 nm irradiation of HOTachy in methanol (2-component analysis up to 40 min and 3-component SVD analysis for longer times).[48]

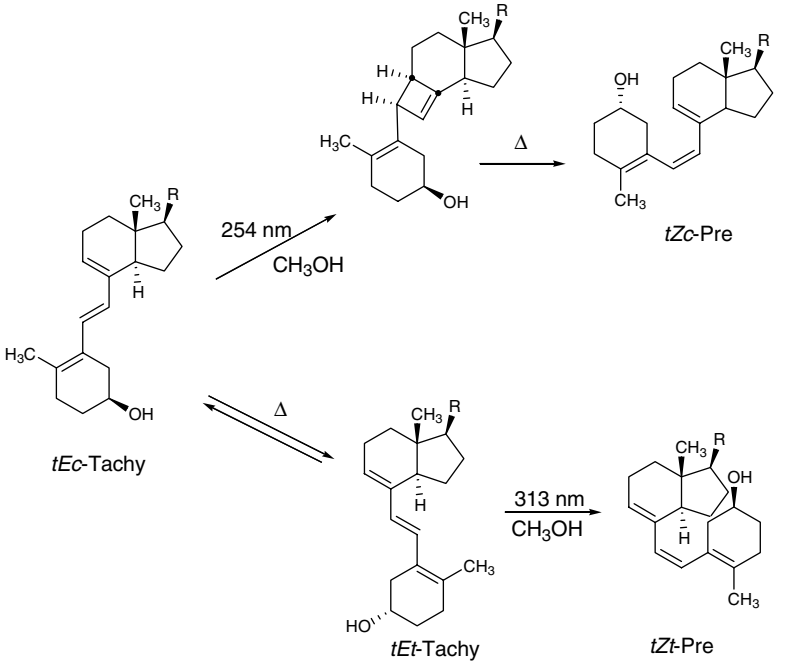

SCHEME 8 Proposed conformer specific photochemistry of HOTachy.

at 313 nm. Excited *tEc*-HOTachy has the potential of giving vinylcyclobutene[1a,61] (or deactivation along that reaction coordinate) in competition with trans→cis photoisomerization, whereas that reaction/deactivation channel is not available to excited *tEt*-Tachy, whose primary reaction may well be efficient trans→cis photoisomerization (Scheme 8).

The 254, 313 nm two-step sequence for Pro to Tachy conversion has advantages over the earlier sequences that employed longer wavelengths in the second step.[54–56] It achieves high, relatively clean Tachy to Pre conversion without requiring high excitation intensities or long irradiation times due to low absorbance in the second irradiation step and minimizes competing Pre photocyclizations to Pro and

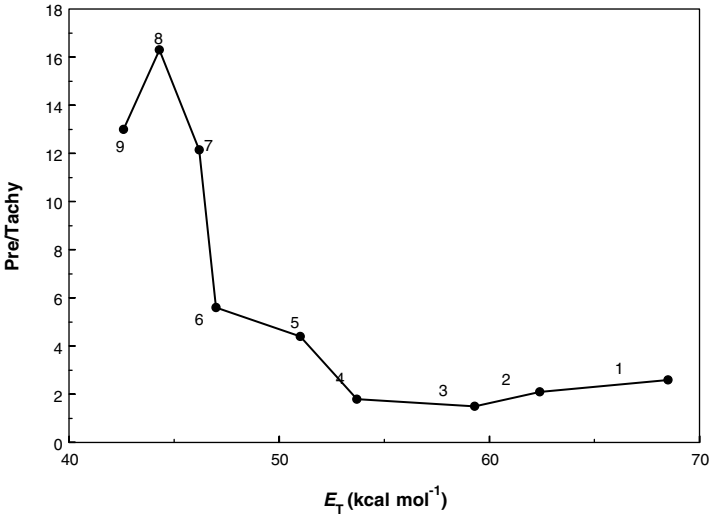

FIGURE 27.15 Saltiel plot for the sensitized Pre/Tachy interconversion. Photostationary Pre/Tachy ratios are given for benzophenone (1), anthraquinone (2), 2-naphthyl phenyl ketone (3), benzil (4), fluorenone (5), and benzanthrone (6) for the vitamin D_2 system,[66] 2-(6-hydroxy-3-oxo-3H-thioxanthene-9-yl)benzene-sulphonic acid[68] (7) and 7,12-dimethylbenzanthracene[70] (8), for the vitamin D_3 system, and anthracene (9) for both vitamin D_2 and D_3 systems.[67]

Lumi. The sequence employs a low-pressure Hg lamp for 254 nm irradiation in the first step, followed by the use of a medium pressure Hg lamp in the second step. Similar conversions to HOPre (82–84%) were attained starting from either HOTachy or HOPro.[48] In a variant of the sequential two excitation wavelength procedure, Reichenbächer and coworkers recommend simultaneous irradiation at 300 and 330 nm to enhance the conversion of Pro to Pre in a single photochemical step,[62] and they have recently refined this approach.[63]

Havinga and coworkers first reported the triplet sensitized Pre/Tachy interconversion for the trimethylsilyl ethers in the vitamin D_3 system,[64] and the idea of replacing the second direct excitation step with triplet sensitization using a sensitizer (fluorenone) to maximize the conversion to Pre was advanced by Eyley and Williams.[65] No side reactions compete in this second photochemical process, as efficient trans-cis interconversion is the only unimolecular triplet state reaction.[64] Efforts since then have been directed toward fine tuning the selection of the sensitizer.[66–70] The challenge here is to chose a triplet energy donor that yields a high PSS Pre/Tachy ratio by selectively exciting Tachy, is nontoxic, has no undesirable photochemistry of its own, and can be removed readily and completely from the reaction mixture. As is usually the case,[5,71] the cis/trans isomer ratio depends on the triplet energy of the sensitizer.[66–70] The Saltiel plot in Figure 27.15 is analogous to that shown in Figure 27.1 for the 1,3-pentadienes but is not as easily interpreted quantitatively due to the possibility of selectively exciting up to four different conformers of Pre and of Tachy in different sensitizer triplet energy regions. It is clear from the plot that very high conversions to Pre can be achieved with donors whose triplet energy is close to ~45 kcal/mol. The direct excitation of Pro followed by the sensitized conversion of Pre to Tachy has also been combined into a single step, simultaneous direct and triplet sensitized (fluorenone, benzanthrone) irradiation with promising results.[72]

Guillet and coworkers have reported very intriguing observations in a polymer medium (a "photozyme") in which the naphthalene chromophore is proposed to play a double role by sensitizing the singlet Pro→Pre→Tachy and the triplet Tachy→Pre conversions.[73] Aqueous solutions of poly(sodium styrenesulfonate-*co*-2-vinylnaphthalene irradiated at 313 nm or with solar light in the presence of Pro D_3 lead to very clean conversions of Pro to Pre. The proposed mechanism involves excitation of the polymer bound naphthyl groups followed by singlet excitation transfer to the polymer-solubilized Pro to effect the ring-opening reaction. Tachy is not observed, presumably due to its return to Pre via triplet sensitization

again from the pendant naphthyl group.[73] Extraction with chloroform separates the Pre-rich product mixture from the polymer-immobilized sensitizer. Formation of Pre, nearly free from Tachy, under these conditions is all the more remarkable when one considers that, based on Figure 27.15, the expected Pre/Tachy PSS ratio with a triplet energy donor having the triplet energy of naphthalene (61 kcal/mol) should be smaller than two. For the proposed Tachy→Pre conversion to be important, the polymer would have to control the conformational equilibria of Pre and of Tachy in ways that favor one-way triplet sensitization in the Tachy→Pre direction. In view of the fact that the Tachy UV spectrum extends well to the red of the Pro and Pre spectra, it is difficult to imagine why singlet energy transfer from naphthalene would not be enormously more efficient to Tachy than to Pro or Pre. Coupled with our finding of a significantly enhanced quantum yield for the trans→cis Tachy photoisomerization at 313 nm and the availability of 2A states that can be accessed directly with wavelengths as long as 355 nm,[54–56] we much prefer a singlet excitation transfer pathway for the proposed Tachy→Pre conversion. An alternative possibility is that excited naphthalene fails to sensitize the Pre→Tachy process in the first place. The selectivity achieved in an extension of this work using styrene-2-vinylnaphthalene copolymers in tetrahydrofuran to photosensitize the formation of Pre from Pro was again impressive, although less spectacular.[74] The observed 13:1 ratio of Pre:Tachy is again too high to be consistent with naphthalene triplet sensitized Pre/Tachy interconversion.

Differences between triplet-sensitized Tachy/Pre equilibration and analogous equilibrations of simpler conjugated trienes,[66,75] including the parent 1,3,5-hexatrienes,[76] are worth noting. In contrast to other acyclic trienes such as alloocimene,[75a] 1,3,5-hexatriene,[76] 1,6-diphenyl-1,3,5-hexatriene,[77] and 1,2-di-(1-cyclopentenyl)ethene,[65] there are no significant concentration or quencher effects on photoisomerization quantum yields or PSS ratios in the Pre/Tachy system.[65] Electronic and steric requirements of the steroid moieties apparently limit access to planar Tachy and Pre triplet states causing a shorter triplet lifetime and smaller effective T_1–S_0 energy gaps, effectively preventing their involvement as donors in excitation transfer steps.[65]

27.5 Conclusion

Its practical importance aside, photochemistry in the vitamin D field continues to claim its place at the forefront of the science. Its central role in the renewed interest in the hula-twist mechanism for trans-cis photoisomerization will no doubt prompt much research to test the validity and generality of that concept. Through it all, it provides a plethora of observations confirming Havinga's NEER principle.

Acknowledgment

This work was supported by a grant from Roche Vitamins and by NSF Grant No. CHE 9985895.

References

1. For reviews see (a) Jacobs, H.J.C. and Havinga, E., Photochemistry of vitamin D and its isomers and of simple trienes, *Adv. Photochem.,* 11, 305–373, 1979; (b) Jacobs, H.J.C. and Laarhoven, W.H., Photochemistry of vitamin D and related compounds, in *Handbook of Organic Photochemistry and Photobiology,* Horspool, W.M. and Song, P.-S., Eds., CRC Press, Boca Raton, FL, 1995, Section 1, pp. 155–164.
2. For reviews see (a) Dauben, W.G., Kellogg, M.S., Seeman, J.I., Vietmeyer, N.D., and Wendschuh, P.H., Steric aspects of the photochemistry of conjugated dienes and trienes, *Pure Appl. Chem.,* 33, 197–215, 1973; (b) Dauben, W.G., McInnis, E.L., and Michno, D.M., Photochemical rearrangements in trienes, in *Rearrangements in Ground and Excited States,* Vol III, de Mayo, P., Ed., Academic Press, New York, 1980, pp. 91–129.
3. (a) Havinga, E. and Schlatmann, J.L.M.A., Remarks on the specificities of the photochemical and thermal transformations in the vitamin D field, *Tetrahedron,* 16, 146–152, 1961; (b) Havinga, E., Über einige photochemische Reactionen, *Chimia*, 16, 145, 1962.

4. (a) Hammond, G.S. and Liu, R.S.H., Stereoisomeric triplet states of conjugated dienes, *J. Am. Chem. Soc.,* 85, 477–478, 1963; (b) Liu, R.S.H., Turro, N.J., and Hammond, G.S., Activation and deactivation of conjugated dienes by energy transfer, *J. Am. Chem. Soc.,* 87, 3406–3412, 1965.
5. Hammond, G.S., Saltiel, J., Lamola, A.A., Turro, N.J., Bradshaw, J.S., Cowan, D.O., Counsell, R.C., Vogt, V., and Dalton, C., Photochemical cis-trans isomerization, *J. Am. Chem. Soc.,* 86, 3197–3217, 1964.
6. Saltiel, J., Metts, L., Sykes, A., and Wrighton, M., The role of s-*cis*-1,3-diene triplets in sensitized cis-trans photoisomerization, *J. Am. Chem. Soc.,* 93, 5302–5303, 1971.
7. Baldwin, J.E. and Krueger, S.M., Stereoselective photochemical electrocyclic valence isomerizations of α-phellandrene conformational isomers, *J. Am. Chem. Soc.,* 91, 6444–6447, 1969.
8. Saltiel, J., Sears, D.F., Jr., Sun, Y.-P., and Choi, J.-O., Evidence for ground state s-*cis*-conformers in the fluorescence spectra of all-*trans*-1,6-diphenyl-1,3,5-hexatriene, *J. Am. Chem. Soc.,* 114, 3607–3612, 1992.
9. For reviews see (a) Scheck, Y.B., Kovalenko, N.P., and Alfimov, M.V., *J. Lumin.,* 15, 157–168, 1977; (b) Fischer, E., Emission spectroscopy evidence for the existence of rotamers in solutions of *trans*-diarylethylenes and related compounds, *J. Photochem.,* 17, 331–340, 1981; (c) Mazzucato, U. and Momicchioli, F., Rotational isomerism in *trans*-1,2-diarylethylenes, *Chem. Rev.,* 91, 1679–1719, 1991.
10. Saltiel, J., Sears, D.F., Jr., Choi, J.-O., Sun, Y.-P., and Eaker, D.W., The fluorescence, fluorescence-excitation and UV absorption spectra of *trans*-1-(2-naphthyl)-2-phenylethene conformers, *J. Phys. Chem.,* 98, 35–46, 1994.
11. Saltiel, J., Tarkalanov, N. and Sears, D.F., Jr., Conformer specific adiabatic cis to trans photoisomerization of *cis*-1-(2-naphthyl)-2-phenylethene. A striking application of the NEER principle, *J. Am. Chem. Soc.,* 117, 5586–5587, 1995.
12. Saltiel, J., Zhang, Y., and Sears, D.F., Jr., Temperature dependence of the photoisomerization of *cis*-1-(2-anthryl)-2-phenylethene. Conformer-specificity, torsional energetics and mechanism, *J. Am. Chem. Soc.,* 119, 11202–11210, 1997.
13. See the following reviews and references cited therein: (a) Muszkat, K.A., The 4a,4b-dihydrophenanthrenes, *Topics Curr. Chem.,* 88, 89–144, 1980; (b) Mallory, F.B. and Mallory, C.W., Photocyclization of stilbene and related molecules, *Org. React.*, 30, 1–456, 1984; (c) Laarhoven, W.H., 4n + 2 Systems. Molecules derived from *Z*-hexa-1,3,5-triene/cyclohexa-1,3-diene, in *Photochromism, Molecules and Systems*, Dürr, H., and Bouas-Laurent, H., Eds., Elsevier, Amsterdam, 1990, pp. 270–313.
14. Laarhoven, W.H., Cuppen, T.J.H.M., and Nivard, R.J.F., Photodehydrocyclizations in stilbene-like compounds. III. Effect of steric factors, *Tetrahedron,* 26, 4865–4881, 1970.
15. (a) Cherkasov, A.S., Spectral detection of s-*cis*- and s-*trans*-isomers of 2-vinylanthracene, *Dokl. Acad. Sci. USSR,* 146, 852, 1962; (b) Cherkasov, A.S. and Voldaykina, K.G., Absorption and fluorescence of vinylanthracenes and the change of molecular configuration in the excited state, *Bull. Acad. Sci. USSR Ser. Phys.,* 27, 628–633, 1963.
16. For a review see Tatsuo, A. and Tokumaru, K., Photochemical one-way adiabatic isomerization of aromatic olefins, *Chem. Rev.,* 93, 23–39, 1993.
17. (a) Brearly, A.M., Strandjord, A.J.G., Flom, S.R., and Barbara, P.F., Picosecond time-resolved emission spectra: techniques and examples, *Chem. Phys. Lett.,* 113, 43–48, 1985; (b) Flom, S.R., Nagarajan, V., and Barbara, P.F., Dynamic solvent effects on large-amplitude isomerization rates. 1. 2-Vinylanthracene, *J. Phys. Chem.,* 90, 2085–2092, 1986; (c) Brearly, A.M., Flom, S.R., Nagarajan, V., and Barbara, P.F., Dynamic solvent effects on large-amplitude isomerization rates. 2. 2-(2′-Propenyl)anthracene and (*E*)-2-(but-2′-en-2′-yl)anthracene, *J. Phys. Chem.,* 90, 2092–2099, 1986; (d) Barbara, P.F. and Jarzeba, W., Dynamic solvent effects on polar and nonpolar isomerizations, *Acc. Chem. Res.,* 21, 195–199, 1988.
18. Determination of the deuterium isotope effect on this [1,7]-sigmatropic shift is reported in Curtin, M.L. and Okamura, M.H., 1α,25-Dihydroxyprevitamin D_3: synthesis of the

9,14,19,19,19-pentadeuterio derivative and a kinetic study of its [1,7]-sigmatropic shift to 1α,25-dihydroxyprevitamin D_3, *J. Am. Chem. Soc.,* 113, 6958–6966, 1991.

19. (a) Dauben, W.G. and Phillips, R.B., Effects of wavelength on the photochemistry of provitamin D_3, *J. Am. Chem. Soc.,* 104, 5780–5781, 1982; (b) Dauben, W.G., Share, P.E., and Ollmann, R.R., Jr., Triene photophysics and photochemistry: previtamin D_3, *J. Am. Chem. Soc.,* 110, 2548–2554, 1988.
20. Dauben, W.G., Disanayaka, B., Funhoff, D.J.H., Kohler, B.E., Schilke, D.E., and Zhou, B., Polyene 2^1A_g and 1^1B_u states and the photochemistry of previtamin D_3, *J. Am. Chem. Soc.,* 113, 8367–8374, 1991.
21. Jacobs, H.J.C., Gielen, J.W.J., and Havinga, E., Effects of wavelength and conformation on the photochemistry of vitamin D and related conjugated trienes, *Tetrahedron Lett.,* 22, 4013–4016, 1981.
22. Kobayashi, T. and Yasamura, M., Studies on the ultraviolet irradiation of provitamin D and its related compounds. I. Effect of wavelength on the formation of potential vitamin D_2 in the irradiation of ergosterol by monochromatic ultraviolet rays, *J. Nutr. Sci. Vitaminol.,* 19, 123, 1973.
23. Havinga, E., de Kock, R.J., and Rappoldt, M.P., The photochemical interconversions of provitamin D, lumisterol, previtamin D and tachysterol, *Tetrahedron,* 11, 276–284, 1960.
24. Braun, M., Fuß, W., Kompa, K.L., and Wolfrum, J., Improved photosynthesis of previtamin D by wavelengths of 280–300 nm, *J. Photochem. Photobiol. A: Chem.,* 61, 15–26, 1991.
25. Hilinski, E.F., McGowan, W.M., Sears, D.F., Jr., and Saltiel, J., Evolutions of singlet excited-state absorption and fluorescence of all-*trans*-1,6-diphenyl-1,3,5-hexatriene in the picosecond time domain, *J. Phys. Chem.,* 100, 3308–3311, 1996.
26. Yee, W.A. O'Neil, R.H., Lewis, J.W., Zhang, J.Z., and Kliger, D.S., Femtosecond transient absorption studies of diphenylpolyenes. Direct detection of $S_2 \rightarrow S_1$ radiationless conversion in diphenylhexatriene and diphenyloctatetraene, *Chem. Phys. Lett.,* 276, 430–434, 1997.
27. Fuß, W. and Lochbrunner, S., The wavelength dependence of the photochemistry of previtamin D, *J. Photochem. Photobiol. A: Chem.,* 105, 159–164, 1997.
28. (a) Maessen, P.A., Jacobs, H.J.C., Cornelisse, J., and Havinga, E., Photochemistry of previtamin D_3 at 92 K: formation of an unstable $tachysterol_3$ rotamer, *Angew. Chem. Int. Ed. Engl.,* 22, 718–719, 1983; (b) Maessen, P.A., Jacobs, H.J.C., Cornelisse, J., and Havinga, E., Photochemistry of previtamin D at 92 K. Formation of an unstable tachysterol rotamer, *Angew. Chem. Suppl.,* 994–1004, 1983; (c) Maessen, P.A., The formation of toxisterols from previtamin D. Mechanistic studies, Ph.D. thesis, University of Leiden, Leiden, 1983; (d) Jacobs, H.J.C., Photochemistry of conjugated trienes: vitamin D revisited, *Pure Appl. Chem.,* 67, 63–70, 1995.
29. Dmitrenko, O., Frederick, J.H., and Reischl, W., Previtamin D conformations and the wavelength-dependent photoconversions of previtamin D, *J. Photochem. Photobiol. A: Chem.,* 139, 125–131, 2001.
30. Müller, A.M., Lochbrunner, S., Schmid, W.E., and Fuß, W., Low-temperature photochemistry of previtamin D: a hula-twist isomerization of a triene, *Angew. Chem. Int. Ed. Engl.,* 37, 505–507, 1998.
31. Squillacote, M.E., Semple, T.C., and Mui, P.W., The geometries of the high-energy conformers of some acyclic 1,3-dienes, *J. Am. Chem. Soc.,* 107, 6842–6846, 1985.
32. Squillacote, M.E., Sheridan, R.S., Chapman, O.L., and Anet, F.A.L., Planar *s-cis*-1,3-butadiene, *J. Am. Chem. Soc.,* 101, 3657–3658, 1979.
33. (a) Ackerman, J.R. and Kohler, B.E., *s-cis*-Octatetraene: ground state barrier for s-cis to s-trans isomerization, *J. Chem. Phys.,* 80, 45, 1984; (b) Ackerman, J.R., Forman, S.A., Hossain, M., and Kohler, B.E., *s-cis*-Octatetraene: photoproduction and spectroscopic properties, *J. Chem. Phys.,* 80, 39–44, 1984.
34. Kohler, B.E., Octatetraene photoisomerization, *Chem. Rev.,* 93, 41–54, 1993, and references cited therein.
35. (a) Liu, R.S.H. and Asato, A.E., The primary process of vision and the structure of bathorhodopsin: a mechanism for photoisomerization of polyenes, *Proc. Natl. Acad. Sci. U.S.A.,* 82, 259–263, 1985; (b) Liu, R.S.H., Mead, D., and Asato, A.E., Application of the H.T.-n mechanism of photoisomerization to the photocycles of bacteriorhodopsins. A model study, *J. Am. Chem. Soc.,* 107, 6609–6614, 1985.

36. (a) Liu, R.S.H. and Hammond, G.S., The case of medium-dependent dual mechanisms for photoisomerization: one-bond-flip and hula-twist, *Proc. Natl. Acad. Sci. U.S.A.,* 97, 11153–11158, 2000; (b) Liu, R.S.H., Photoisomerization by hula-twist: a fundamental supramolecular photochemical reaction, *Acc. Chem. Res.,* 34, 555–562, 2001.
37. Dauben, W.G. and Funhoff, D.J.H., Theoretical evaluation of the conformations of previtamin D_3, *J. Org. Chem.,* 53, 5070–5075, 1988.
38. Dmitrenko, O. and Reischl, W., Molecular mechanics-based conformational analysis of previtamin D and its A-ring analogues, *Monatsh. Chem.,* 127, 445–453, 1996.
39. Martinez-Nunez, E., Vazquez, S.A., and Mosquera, R.A., Conformational analysis of model compounds of vitamin D by theoretical calculations, *J. Comput. Chem.,* 18, 1647–1655, 1997.
40. Cholinski, J. and Kutner, A., Molecular modeling of three-dimensional structure of 1,25-dihydroxycholecalciferol and its A-ring analogs, *Pol. J. Chem.,* 71, 1321–1328, 1997.
41. Dmitrenko, O., Frederick, J.H., and Reischl, W., *Ab initio* study of conformational stability in previtamin D, vitamin D and related model compounds, *J. Mol. Struct. (Theochem.),* 530, 85–96, 2000 and references therein.
42. Fuß, W., Lochbrunner, S., Schmid, W.E., and Kompa, K.L., Electronic relaxation and ground-state dynamics of 1,3-cyclohexadiene and *cis*-hexatriene in ethanol, *J. Phys. Chem. A,* 102, 9334–9344, 1998.
43. Fuß, W., Schmid, W.E., and Trushin, S.A., Time-resolved dissociative intense-laser field ionization for probing dynamics: femtosecond photochemical ring opening of 1,3-cyclohexadiene, *J. Chem. Phys.,* 112, 8347–8362, 2000.
44. For a recent review of polyene photophysics see Fuß, W., Haas, Y., and Zilberg, S., Twin states and conical intersections in linear polyenes, *Chem. Phys.,* 259, 273–295, 2000.
45. (a) Pullen, S.H., Anderson, N.A., Walker, L.A., II, and Sension, R.J., The ultrafast photochemical ring-opening reaction of 1,3-cyclohexadiene in cyclohexane, *J. Chem. Phys.,* 108, 556, 1998; (b) Anderson, N.A., Shiang, J.J., and Sension, R.J., Subpicosecond ring opening of 7-dehydrocholesterol studied by ultrafast spectroscopy, *J. Phys. Chem. A,* 103, 10730–10736, 1999.
46. (a) Tarkalanov, N.D., Spectroscopic and photochemical properties of *cis*-1-(2-naphthyl)-2-phenylethene. Conformer specific photochemistry, Ph.D. dissertation, Florida State University, Tallahassee, 2001; (b) Saltiel, J. and Krishnamoorthy, V., Unpublished results.
47. Braun, A.M., Maurette, M.-T., and Oliveros, E., Vitamins, *Photochemical Technology*, Wiley, Chichester, 1991, chap. 12, pp. 500–523.
48. (a) Saltiel, J., Cires, L., and Turek, A., Conformer-specific photoconversion of 25-hydroxytachysterol to 25-hydroxyprevitamin D_3: role in the production of vitamin Ds, *J. Am. Chem. Soc.,* 125, 2866–2867, 2003. (b) Saltiel, J. and Cires, L., Unpublished observations.
49. For a review see Saltiel, J. and Sun, Y.-P., *Cis-trans* isomerization of C,C double bonds, in *Photochromism, Molecules and Systems,* Dürr, H. and Bouas-Laurent, H., Eds., Elsevier, Amsterdam, 1990, pp. 64–164.
50. Sklar, S.K., Hudson, B., Petersen, M., and Diamond, J., Conjugated polyene fatty acids as fluorescent probes: spectroscopic characterization, *Biochemistry,* 16, 813–819, 1977.
51. (a) Zimányi, L., Kulcsár, Á., Lanyi, J.K., Sears, D.F., Jr., and Saltiel, J., Singular value decomposition with self-modeling applied to determine bacteriorhodopsin intermediate spectra. Analysis of simulated data, *Proc. Natl. Acad. Sci. U.S.A.,* 96, 4408–4413, 1999; (b) Zimányi, L., Kulcsár, Á., Lanyi, J.K., Sears, D.F., Jr., and Saltiel, J., Intermediate spectra and photocycle kinetics of the Asp96Asn mutant bacteriorhodopsin determined by singular value decomposition with self-modeling, *Proc. Natl. Acad. Sci. U.S.A.,* 96, 4414–4419, 1999.
52. Alfimov, M.V., Gromov, S.P., Fedorov, Y.V., Fedorova, O.A., Vedernikov, A.I., Churakov, V., Kuz'mina, L.G., Howard, J.A.K., Bossmann, S., Braun, A., Woerner, M., Sears, D.F., Jr., and Saltiel, J., Synthesis, structure and ion selective complexation of trans and cis isomers of photochromic dithia-18-crown-6 ethers, *J. Am. Chem. Soc.,* 121, 4992–5000, 1999.
53. Jacobs, H.J.C., Gielen, J.W.J., and Havinga, E., Effects of wavelength and conformation on the photochemistry of vitamin D and related conjugated trienes, *Tetrahedron Lett.,* 22, 4013, 1981.

54. Malatesta, V., Willis, C., and Hackett, P.A., Laser photochemical production of vitamin D, *J. Am. Chem. Soc.,* 103, 6781–6783, 1981.
55. Dauben, W.G. and Phillips, R.B., Wavelength-controlled production of previtamin D_3, *J. Am. Chem. Soc.,* 104, 355–356, 1982.
56. Oppenländer, T. and Henning, T., Production of provitamin D_3 by longwave-selective dual irradiation of 7-dehydrocholesterol with noncoherent excimer UV radiators, *Chem. Ing. Tech.,* 67, 594–597, 1995.
57. Gliesing, S., Reichenbächer, M., Ilge, H.-D., and Faßler, D.E., Photokinetische Untersuchungen Zur Isomerisiezung von Provitamin D_3, *Z. Chem.,* 24, 150–151, 1984.
58. Sanders, G.M., Pot, J., and Havinga, E., Some recent results in the chemistry and stereochemistry of vitamin D and its isomers, *Prog. Chem. Org. Natl. Prod.,* 27, 131–157, 1969.
59. Dmitrenko, O. and Reischl, W., Ground-state conformational equilibrium of previtamin D and its *E*-isomer: effect on the absorption characteristics, *Res. Chem. Intermed.,* 23, 691–702, 1997.
60. Dmitrenko, O., Vivian, J.T., Reischl, W. and Frederick, J.H., Theoretical studies of the first strongly allowed singlet states of 3-desoxy analogs of previtamin D, vitamin D and their *E*-isomers, *J. Mol. Struct. (Theochem.),* 467, 195–210, 1999.
61. (a) Boomsma, F., Jacobs, H.J.C., Havinga, E., and van der Gen, A., The "over irradiation products" of previtamin D and tachysterol: toxisterols, *Recl. Trav. Chim. Pays-Bas,* 96, 104, 1977; (b) Boomsma, F., Jacobs, H.J.C., Havinga, E., and van der Gen, A., The photochemistry of previtamin D and tachysterol, *Recl. Trav. Chim. Pays-Bas,* 96, 113, 1977.
62. Gliesing, S., Ilge, H.-D., Reichenbächer, M., and Faßler, D.E., Wellenlängeneffecte auf die Quantenausbeuten der Photoisomerisiurung von Prävitamin D_3, *Z. Chem.,* 29, 21–22, 1989.
63. Reichenbächer, M., Gliesing, S., Lange, C., Gonschlor, M., and Schönecker, B., Ein effecktives Verfahren zur Herstellung von 1α,25-Dihydroxycholecalciferol (Calcitriol) aus 1α,3β,25-Trihydroxy-cholesta-5,7-dien (Procalcitriol), *J. Prakt. Chem.,* 338, 634–641,1996.
64. Snoeren, A.E.C., Daha, M.R., Lugtenburg, J., and Havinga, E., Studies of vitamin D and related compounds. Part 21. Photosensitized reactions, *Recl. Trav. Chim. Pays-Bas,* 89, 261–264, 1970.
65. Eyley, S.C. and Williams, D.H., Photolytic production of vitamin D. The preparative value of a photosensitizer, *J. Chem. Soc., Chem. Commun.,* 858, 1975.
66. Denny, M. and Liu, R.S.H., Photosensitized isomerization of previtamin D_2 and tachysterol and the related 1,2-bis-(1-cyclopentenyl) ethylene: torsional potential curves of triene triplets, *Nouv. J. Chim.,* 2, 637–641, 1978.
67. Stevens, R.D.S., Sensitized photochemical preparation of vitamin D, US Patent 4 686 023, 1987.
68. Pfoertner, K.-H., Novel photosensitizers for the *E/Z*-isomerization of trienes. Part 1. Syntheses and application, *J. Chem. Soc., Perkin Trans. 2,* 523–526, 1991.
69. Pfoertner, K.-H. and Voelker, M., Novel photosensitizers for the *E/Z*-isomerization of trienes. Part 2. Mechanistic and photophysical aspects, *J. Chem. Soc. Perkin Trans. 2,* 527–530, 1991.
70. Tatikolov, A.S., Dmitrenko, O., and Terenetskaya, L.P., Triplet–-triplet energy transfer in sensitized *cis-trans*-isomerization of previtamin D, *Chem. Phys. Reports,* 14, 461–466, 1995.
71. Saltiel, J. and Charlton, J.L., Cis-trans isomerization of olefins, in *Rearrangements in Ground and Excited States*, Vol III, de Mayo, P., Ed., Academic Press, New York, 1980, pp. 25–89.
72. Gliesing, S., Ilge, H.-D., Reichenbächer, M., and Faßler, D,E., Tripletsensibilisierte Photoisomerisierung von Provitamin D_3, *Z. Chem.,* 26, 207–208, 1986.
73. Nowakowska, M., Foyle, V.P., and Guillet, J.E., Studies of the antenna effect in polymer molecules. 24. Solar photosynthesis of previtamin D_3 in aqueous solutions of poly(sodium styrenesulfonate-co-2-vinylnaphthalene), *J. Am. Chem. Soc.,* 115, 5975–5981, 1993.
74. Nowakowska, M. and Guillet, J.E., Studies of the antenna effect in polymer molecules. 29. Isomerization of provitamin D_3 photosensitized by polymers containing pendant naphthalene groups, *J. Photochem. Photobiol. A: Chem.,* 107, 189–194, 1997.
75. (a) Liu, R.S.H. and Butt, Y.C.C., Photochemistry of polyenes. 1. A comparative study of *cis-trans* isomerization from the S1 and T1 states of a conjugated triene (alloocimene), *J. Am. Chem. Soc.,*

93, 1532–1534, 1971; (b) Liu, R.S.H., Recent studies on the photochemistry of conjugated trienes and higher polyenes, *Pure Appl. Chem., Suppl.,* 335–350, 1971; (c) Butt, Y.C.C., Singh, A.K., Baretz, B.H., and Liu, R.S.H., Photosensitized geometric isomerization of alloocimene. The triplet torsional potential surface of a conjugated triene, *J. Phys. Chem.,* 85, 2091, 1981.

76. Møller, S., Langkilde, F.W., and Wilbrandt, R., Sensitized triplet photochemistry of *E*- and *Z*-1,3,5-hexatriene, *J. Photochem. Photobiol. A: Chem.,* 62, 93–106, 1991.
77. (a) Saltiel, J., Wang, S., Ko, D.-H., and Gormin, D.A., Cis-trans photoisomerization of the 1,6-diphenyl-1,3,5-hexatrienes in the triplet state. The quantum chain mechanism and the structure of the triplet state, *J. Phys Chem. A.,* 102, 5383–5392, 1998; (b) Saltiel, J., Crowder, J.M., and Wang, S. Mapping the potential energy surfaces of the 1,6-diphenyl-1,3,5-hexatriene ground and triplet states, *J. Am. Chem. Soc.,* 121, 895–902, 1999.

28

Photochemical Reaction of Fullerenes and Fullerene Derivatives

Andreas Kleineweischede
Universität Bielefeld

Jochen Mattay
Universität Bielefeld

28.1 Introduction

In 1985, the existence of a form of elementary carbon with a definite number of carbon atoms became certain with the discovery of the fullerenes by Kroto, Smalley and co-workers.[1] The development of a simple procedure for making fullerenes available in macroscopic quantities by Krätschmer et al.[2] induced a veritable flood of investigations in the last two decades leading to molecules and materials with interesting behavior such as superconductivity,[3] ferromagnetism,[4] biological activity,[5,6,7] and nonlinear optics.[8,9,10] As a result, a great number of reports and reviews have been published describing the full scope of fullerene chemistry, including functionalization (thermally or photochemically) and physical properties.[11–19] Recently, two reviews dealing with the photochemical functionalization of fullerenes have been published.[20,21] This review will focus on the photochemistry of the two most prominent fullerenes, C_{60} and C_{70}, and their derivatives. Photochemistry of higher fullerenes will not be discussed. Before the different photochemical reactions of the fullerenes and derivatives are described, the photophysical properties of C_{60} and C_{70} will be briefly discussed in Section 28.2.

0-8493-1348-1/04/$0.00+$1.50

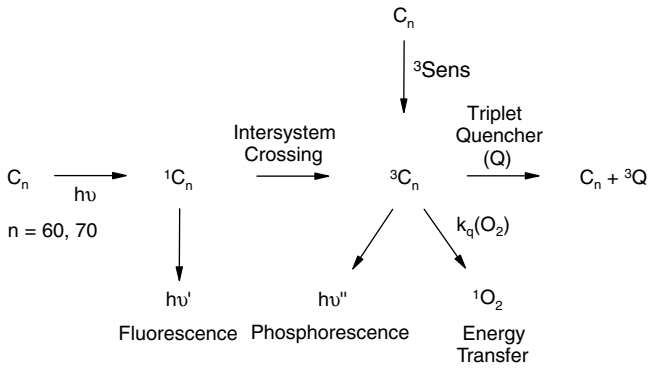

SCHEME 1 Photophysical processes in C_{60} and C_{70}.

TABLE 28.1 Photophysical Properties of C_{60} and C_{70}[22,23]

Property	C_{60}[a]	C_{70}[a]
E_S	46.1 kcal/mol[b]	44.1 kcal/mol[b]
E_T	37.5 ± 4.5 kcal/mol[c]	33.0 kcal/mol ≤ E_T < 42 kcal/mol[c]
ε_T (480 nm)	$(2.8 \pm 0.2) \times 10^3$ M^{-1} s^{-1}	$(1.4 \pm 0.1) \times 10^4$ M^{-1} s^{-1}
τ_T	40 ± 4 μs[d]	130 ± 10 μs[d]
k_q (O_2)	$(1.9 \pm 0.2) \times 10^9$ M^{-1} s^{-1}	$(9.4 \pm 1.5) \times 10^8$ M^{-1} s^{-1}
Φ $^1O_2$ (355 nm)	0.76 ± 0.05[e]	0.81 ± 0.15[e]
Φ $^1O_2$ (532 nm)	0.96 ± 0.04[f]	0.81 ± 0.15[f]
k_q ($^1O_2$)	$(5 \pm 2) \times 10^5$ M^{-1} s^{-1} [g]	not measurable[g]

[a] All measurements in C_6H_6 or C_6D_6 were taken at room temperature, with concentrations of $C_{60} \approx 3 \times 10^{-5}$ and 3×10^{-4} M (OD ≈ 0.5) at λ_{exc} = 355 and 532 nm; $C_{70} \approx 1 \times 10^{-5}$ and 4×10^{-5} M (OD ≈ 0.3) at λ_{exc} = 355 and 532 nm, respectively, unless otherwise noted. [b] Calculated from the presumed 0-0 band at 620 nm for C_{60}[24] and at 638 nm for C_{70}.[23] [c] Average of the triplet energy of TPP (33.0 kcal/mol) and anthracene (42 kcal/mol); however, the low quenching rate with TPP suggests the actual energy is closer to the level of TPP. [d] In argon-saturated solution. [e] C_{60}: average of the five determinations with TPP (Φ_Δ = 0.62) and acridine (Φ_Δ = 0.84)[22]; C_{70}: avarage of five determinations at varied laser energies (1-3 mJ/puls), OD = 0.3-0.5, with TPP (Φ_Δ = 0.62). [f] C_{60}: avarage of three determinations with TPP (Φ_Δ = 0.62); C_{70}: avarage of seven determinations, same conditions as for Φ^1O_2 (355 nm). [g] C_{60}: total of physical and chemical quenching of $^1O_2$ by C_{60} (TPP, 532nm). The maximum concentration of C_{60} was limited by saturation; C_{70}: No change in $^1O_2$ lifetime on adding C_{70} up to 4.9×10^{-4} M.[23]

28.2 Photophysical Properties of C_{60} and C_{70}

The first investigations of basic photophysical properties of pure fullerenes were carried out by Foote and co-workers in 1991.[22,23] Since then, research has led to an extensive knowledge about the photophysical behavior of the fullerenes in general.[24–91] Scheme 1 shows the main photophysical processes, and in Table 28.1 the most relevant photophysical properties are summarized.

UV/Vis-Absorption and Fluorescence

The electronic absorption spectra of both C_{60} and C_{70} show strong absorption bands in the UV region due to allowed $^1T_{1u} \rightarrow {}^1A_g$ transitions [$\varepsilon_{max} \sim 10^5$ M^{-1} cm^{-1}; λ_{max} (C_{60}) = 211, 256, 328 nm; λ_{max} (C_{70}) = 215, 236, 313].[24,25] The absorption in the visible region due to the low-lying electronic transitions is only weakly allowed because of the high degree of symmetry in the closed shell electronic configuration[28] (λ_{max} 540 nm, $\varepsilon_{max} \sim 710$ M^{-1} cm^{-1} for C_{60} and λ_{max} 468 nm, $\varepsilon_{max} \sim 15{,}000$ M^{-1} cm^{-1} for C_{70}).[24,25] The

longest wavelength absorption of C_{60} attributed to the $S_0 \rightarrow S_1$ transition appears at 620 nm.[24] The lower symmetry of C_{70} leads to stronger absorptions in the visible due to the fact that the longest wavelength transition is less forbidden.[23]

C_{60} shows very weak fluorescence with a low quantum yield (λ_{max} 720 nm, quantum yield $\Phi_F \sim 10^{-5}$–10^{-4}),[26–31] while fluorescence of C_{70} is somewhat stronger ($\Phi_F \sim 8.5 \times 10^{-4}$), and at 77 K structured fluorescence occurs with λ_{max} 682 nm.[22,32,34,35] It has been reported that fluorescence of C_{70} at 77 K strongly depends on the solvent matrix. This is most probably associated with deformations of the solute molecules.[33] The S_1–T_1 splitting of both C_{60} and C_{70} is small (~10 kcal/mol in C_{60}[49,51]; ~7 kcal/mol in C_{70}[31,33]). Surprisingly, the S_1–S_2 energy difference of C_{70} was found to be quite large, almost equal to the S_0–S_1 energy difference.[33] The low fluorescence of both C_{60} and C_{70} probably results from the short lifetime of the singlet excited state and from the symmetry forbiddeness of the lowest-energy transition. The decay rates k_F were determined to be 1.5×10^9 sec^{-1} for $^1C_{60}$* and 1.61×10^9 sec^{-1} for $^1C_{70}$*.[35,43] Both fullerenes display wavelength-independent photophysical properties both for absorption and emission and thus obey Kasha's rule.[52]

Excited State Spectroscopy and Phosphorescence

The singlet excited states (S_1) of C_{60} and C_{70} were characterized by transient absorption studies. The estimated lifetimes were 1.2 nsec for $^1C_{60}$* and 0.7 nsec for $^1C_{70}$*. The absorption maxima λ_{max} appear for C_{60} at 513, 759, and 885 nm and for C_{70} at 675 and 840 nm.[36–40] The reason for the very short singlet lifetimes of both C_{60} and C_{70} is related to the high intersystem crossing rate to the triplet excited state with triplet quantum yields close to 100%.[37,42–45] The intersystem crossing rates k_{ISC} for C_{60} and C_{70} are in good agreement with the values for the fluorescence decay rates [k_{ISC} (C_{60}): 1.5×10^9 sec^{-1}; k_{ISC} (C_{70}): 1.25×10^9 sec^{-1}].[35] These values were determined by spectroscopic and photothermal methods and agree with lower limits determined from singlet oxygen quantum yields.[22,23]

Triplet–triplet absorption spectra and extinction coefficients (C_{60}: λ_{max} = 330, 750 nm, ε_{max} 40,000, 20,000 M^{-1} cm^{-1}; C_{70}: λ_{max} = 335, 480, 690, 970 nm, ε_{max} 35,000, 12,000, 2250, 3800 M^{-1} cm^{-1}) were measured by several groups with varying details of the spectra because of difficulties of correcting the spectra for ground state depletion. The triplet lifetimes of both fullerenes in solution are quite short (50–100 μsec) due to triplet–triplet annihilation and ground state quenching.[22,23,35,38,40,44–48] However, Fraelich et al. reported significantly longer T_1 lifetimes of both fullerenes. For C_{60}, they determined a triplet lifetime of 133 μsec and for C_{70} 2.2 msec. In mixed solutions of C_{60} and C_{70}, they observed intermolecular energy transfer between nearly isoenergetic triplet states. The T_1–S_0 gap of C_{60} was estimated to be 102 ± 30 cm^{-1} greater than that of C_{70}.[41]

The triplet energy levels (E_T) of C_{60} and C_{70} were estimated to be close to 35 kcal/mol by triplet–triplet energy transfer.[22,23] Both compounds quench the triplet states of senzitizers with $E_T \geq 42$ kcal/mol with essentially diffusion-controlled rate constants. Quenching of the tetraphenylporphyrine (TPP) triplet (E_T = 33 kcal/mol)[49] is significantly slower (~2–4 – 10^7 M^{-1} sec^{-1}), probably because energy transfer with this sensitizer is slightly endothermic. Energy transfer from C_{60} and C_{70} triplets to acceptors with $E_T \leq 28$ kcal/mol is diffusion controlled. Despite the high quantum yield of triplet formation, no phosphorescence of C_{60} is observed, and C_{70} shows only weak phosphorescence at 77 K, which also confirmed the triplet energy of C_{70}.[39] Heavy-atom–induced phosphorescence can be observed and gives a triplet energy of 36.3 kcal/mol.[50] These values are in good agreement with those determined by photothermal [44,45,51] and spectroscopic methods.[25,38]

EPR studies of the triplet states of the fullerenes give much insight into rotational dynamics of the triplet. It could be shown that for both fullerenes two triplet states exist over a temperature range from T = 8 K to T = 213 K. The differences between them are in their relaxation rates, one type having a faster decay of magnetization (by one order of magnitude) than the other type. Additionally, a small difference exists in the resonance frequency (small shift in the g-value). The faster decaying triplet was found to have a stronger intensity. Also, triplet–triplet annihilation and quenching by nitroxide radicals was measured by EPR-technique.[39,53–61]

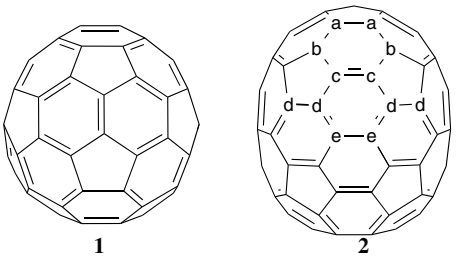

1 **2**

FIGURE 28.1 Different bond lengths in C_{60} and different bond types in C_{70}.

28.3 Photochemical Reactions of Fullerenes

In the early 1990s, the derivatization of fullerenes was based on thermal reactions, e.g., the Diels–Alder reaction of C_{60} with substituted dienes leading to cyclohexyl-fused fullerene derivatives, and only a few examples were known, where a fullerene adduct was obtained by photochemical reactions. The pioneering work in the field of photochemical derivatization of fullerenes was done by Wilson, Schuster, and colleagues who, for example, reported the [2 + 2]-photocycloaddition of enones to C_{60}. Nowadays, more and more fullerene derivatives are synthesized by photochemical reaction pathways.

The photoinduced functionalization of fullerenes can be achieved either by electron transfer activation leading to radical ions or by energy transfer processes, either by direct excitation of the fullerenes or the reaction partner (Equation 28.1). In the latter case both singlet and triplet species are involved. In the case of reactions proceeding via electronically excited fullerenes, the situation is somewhat different. As described in the previous section, the absorption features of fullerenes extend over the UV and visible region, and light of different wavelengths can be used for excitation. Depending on the frequency, various vibrational levels of singlet excited states are populated, followed by relaxation to the lowest vibrational level of S_1. This process is completed before efficient intersystem-crossing to the triplet excited state occurs.[19,35] Usually, the triplet excited state is then the starting point for the derivatization of the fullerenes. Before going into detail, a short summary of the principles of fullerene chemistry will be given.

Electron transfer activation:	Photochemical activation:	
$C_{60} \xrightarrow{+e^-} C_{60}^{\cdot -}$	$C_{60} \xrightarrow{hv} C_{60}* \xrightarrow{A} C_{60}A$	(28.1)
$C_{60} \xrightarrow{-e^-} C_{60}^{\cdot +}$	$A \xrightarrow{hv} A* \xrightarrow{C_{60}} C_{60}A$	

Principles of Fullerene Chemistry

The chemical behavior of C_{60} is largely governed by three properties attributable to the structure of C_{60}.[12,15,63] First, the bonds at the junctions of two hexagons ([6,6]-bonds) are shorter than the bonds at the junctions of a hexagon and a pentagon ([5,6]-bonds) (see Figure 28.1). Second, the highly pyramidalized sp^2 C-atoms in spherical C_{60} cause a large amount of strain energy within the molecule. Third, C_{60} is an electronegative molecule; it can easily be reduced, but it is difficult to oxidize.

The following rules of reactivity, which are based on these properties, can be deduced from the results obtained by the chemical transformation of fullerenes:

1. The reactivity of C_{60} is that of a fairly localized electron deficient polyolefin; thus, typical reactions are additions at a [6,6]-double bond.
2. The driving force is the relief of strain in the fullerene cage.
3. The regiochemistry of the addition reaction is governed by the minimization of [5,6]-double bonds within the fullerene framework.

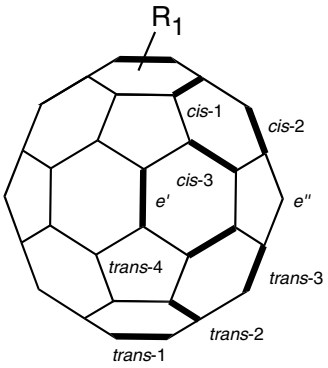

FIGURE 28.2 Positions of the ligand-carrying bonds in the eight possible regioisomers.

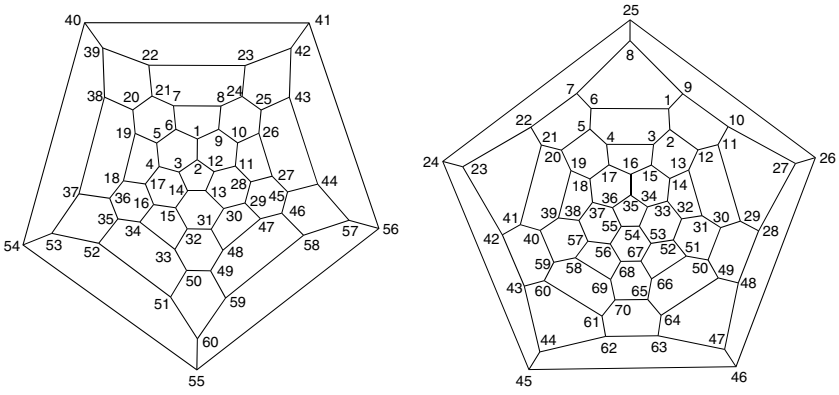

FIGURE 28.3 Schlegel diagrams with carbon atom numbering for C_{60} and C_{70}.

The chemical reactivity of C_{70} is very similar to that of C_{60}. While all positions in C_{60} are identical, and two different types of CC bonds exist, five sets of carbon atoms and eight distinct types of CC bonds are available in C_{70} (Figure 28.1). It can be anticipated that the different bonds will display different reactivity.[64]

Since there are up to 30 reactive double bonds in the C_{60} molecule, a great number of polyadducts are possible. For a description of the spatial arrangement of the addends, the C_{60} molecule is divided into three sections with regard to the location of the second attack.[65] The second attack can take place on the same hemisphere (*cis*), at the equator (*e*), or on the opposite hemisphere (*trans*). For example, for the addition of an identical second addend, eight regioisomeric bisadducts are possible, as shown in Figure 28.2. To identify modified fullerenes, a numbering system for the carbon atoms is necessary. According to the IUPAC nomenclature,[66] based on the proposal of Robert Taylor in 1993,[67] the carbon atoms are numbered as outlined for C_{60} and C_{70} in Figure 28.3.

Photochemical Synthesis of Substituted 1,2-Dihydro[60]fullerenes

As a first example, the photochemical synthesis of substituted 1,2-dihydro[60]fullerenes of type **3** (Scheme 2) should be discussed. These compounds can be synthesized via either oxidative or reductive photoinduced electron transfer (PET). Whereas the oxidation to the fullerene radical cation is difficult to achieve, reduction of the fullerenes leading to radical anions should be much easily performed due to their electronic features.

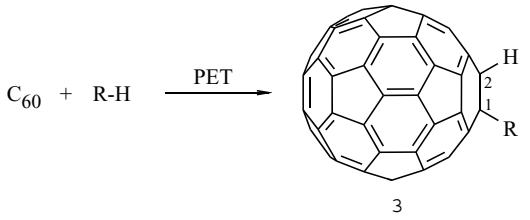

SCHEME 2 Formation of dihydro[60]fullerenes under PET conditions.

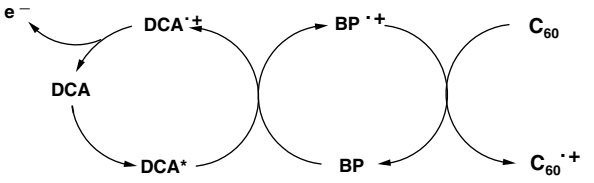

SCHEME 3 Generation of $C_{60}^{\bullet+}$ by cosensitization (hv: 419 nm, DCA, BP: biphenyl).

Synthesis of Substituted 1,2-Dihydro[60]fullerenes by Oxidative PET

The preparation of 1,2-dihydro[60]fullerenes via oxidative photoinduced PET was investigated by several research groups. In Scheme 2, the general formation of 1-substituted 1,2-dihydro[60]fullerenes is shown.

In 1995, Schuster, Wilson, and co-workers reported the formation of C_{60} radical cations by photosensitized electron transfer that were trapped by alcohols and hydrocarbons to yield alkoxy- or alkyl-substituted fullerene monoadducts as major products.[68] As a sensitizer for the generation of $C_{60}^{\bullet+}$, Schuster et al. used 1,4-dicyanoanthracene (DCA).

Following the conditions developed by Schuster et al., Mattay et al. also generated $C_{60}^{\bullet+}$ using different sensitizers such as *N*-methylacridinium hexafluorophosphate (NMA^+) and 2,4,6-triphenyl-pyrylium tetrafluoroborate (TPP^+) in the presence of biphenyl.[69,70] The assumed mechanism of formation of $C_{60}^{\bullet+}$ by this cosensitization is shown in Scheme 3.

Quenching of $C_{60}^{\bullet+}$ with H-donors such as *t*-butylmethylether, propionaldehyde, and alcohols results in the formation of 1:1 adducts. The product structures support a H-abstraction process[71,72] rather than nucleophilic addition. Some examples of the products generated by this method are summarized in Table 28.2 (products 4–12).

Time resolved laser flash photolysis and ESR spectroscopic investigations clearly demonstrate the formation of $C_{60}^{\bullet+}$ using PET conditions.[73–75] Upon addition of H-donors, the signal of $C_{60}^{\bullet+}$ is quenched.[74] The oxidation of C_{60} is followed by H-abstraction from the H-donor, as shown in Scheme 4. Nucleophilic addition can be excluded because no alkoxyfullerenes were detected.[69] After reduction of $H\text{-}C_{60}^{+}$, e.g., by electron transfer from the reduced sensitizer molecule, $H\text{-}C_{60}^{\bullet}$ might recombine with $R^{\bullet}$ to give the final product. Decay experiments of $C_{60}^{\bullet+}$ by the addition of alcohols support the proposed mechanism of H-abstraction as a first step. The involved radical products reveal $C_{60}^{\bullet+}$ as an electrophilic radical.

The authors reported the formation of some unexpected products in the above-mentioned reaction. For example, when aldehydes were used as the H-donor reactants, the products depended on the reactivity of the intermediate radical. Propionaldehyde as the starting material did not lead to decarbonylation because a primary alkyl radical is less stable than a benzyl radical. Consequently, the decarbonylation during the addition of phenylacetaldehyde leading to **10** (Table 28.2) strongly suggests that this reaction involves an acyl radical that undergoes decarbonylation.

In addition, the reaction of $C_{60}^{\bullet+}$ with glycol, propionic acid, and *t*-butanol could only be explained by loss of the hydrogen from an OH bond, either from the neutral or from the oxidized substrate. For example, the reaction of *t*-butanol with C_{60} leading to the dihydrofullerene **6** (path A in Scheme 5) and

TABLE 28.2 Selected Examples of 1-substituted 1,2-dihydro[60]fullerenes[69]

H-DONOR : FULLERENE PRODUCT	H-DONOR : FULLERENE PRODUCT
$HOCH_2CH_2OH$ 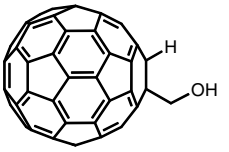 **4**	$CH_3OCH_2CH_2OH$ 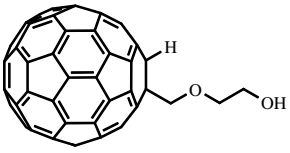 **9**
CD_3OD 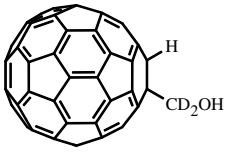 **5**	$PhCH_2CHO$ 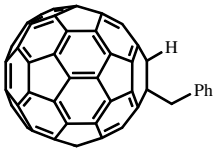 **10**
t-BuOH 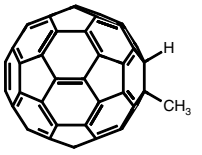 **6** + 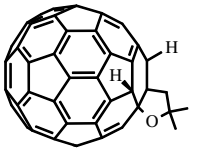 **7**	CH_3CH_2COOH 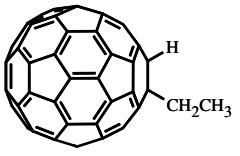 **11** $(CH_3)_2NCHO$ 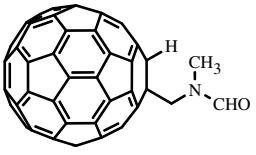 **12**
1,3-Dioxolane 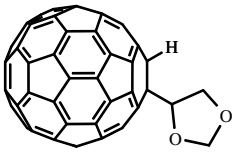 **8** + $C_{60}H_2$	$HCOOCH_3$ 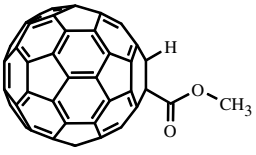 **13**

$$C_{60} \xrightarrow{PET} C_{60}^{\bullet +}$$

$$C_{60}^{\bullet +} + RH \longrightarrow H - C_{60}^{+} + \bullet R$$

$$H - C_{60}^{+} + \bullet R + e^{-} \rightleftharpoons H - C_{60} - R$$

SCHEME 4 Proposed mechanism of the addition of H-donors to C_{60}.

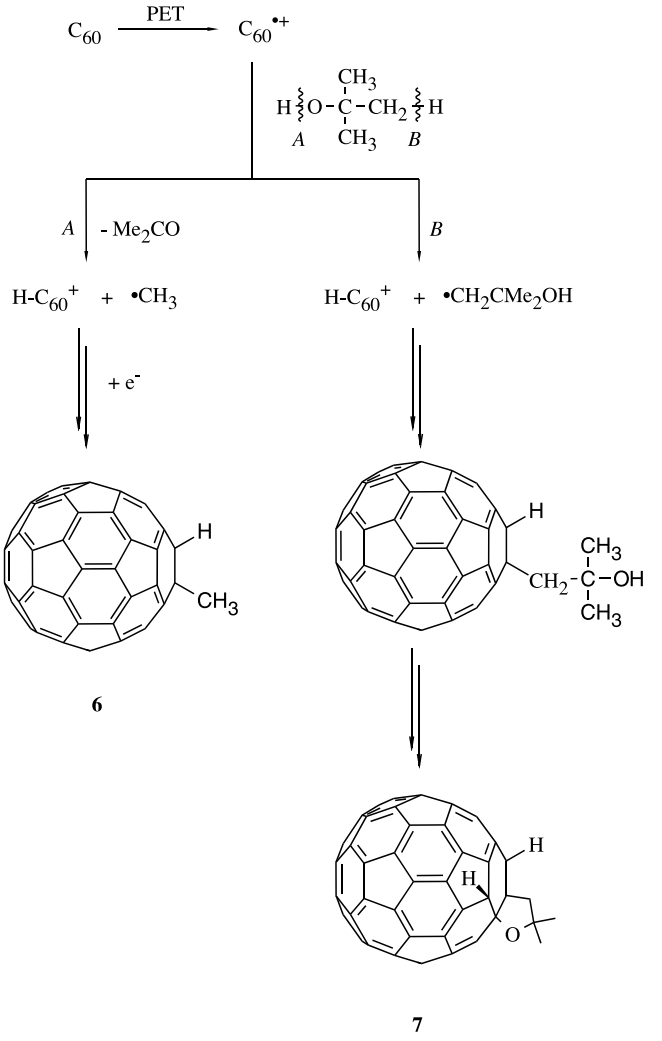

SCHEME 5 Reaction of *t*-butanol and C_{60} under PET conditions.

the tetrahydro[60]fullerene **7** (path B in Scheme 5) can be easily explained by homolytic bond breaking at the OH site in the former case and abstraction at the CH site in the latter. Reactions of alcohols and C_{60} under PET conditions yield hydroxylated dihydro[60]fullerenes. It was first considered that the α-centered hydroxyalkyl radicals were formed by direct abstraction of a hydrogen from a CH bond. Instead, it was shown that such radicals can be formed in a bimolecular process from O-centered radicals as a second step in a pseudo-[1,2]-shift reaction. Analogously, the product of the reaction with methoxyethanol can be explained. The primarily generated O-centered radical is transformed into the C-centered radical via a [1,5]-hydrogen shift in a six-membered transition state. Whether simple alcohols react with $C_{60}^{\bullet+}$ by direct H-abstraction from the α-position or via O-centered radicals in a two-step mechanism cannot finally be decided. Both reaction paths may operate.

Synthesis of Substituted 1,2-Dihydro[60]fullerenes by Reductive PET

Several examples are known in which formation of 1-substituted 1,2-dihydro[60]fullerenes occurs by reductive PET. In all these examples, single electron transfer between photoexcited $^3C_{60}$ and the electron donor to form the $C_{60}^{\bullet-}$-$D^{\bullet+}$ radical ion pair is suggested to be the key step in the synthesis of the 1,2-dihydro[60]fullerenes.

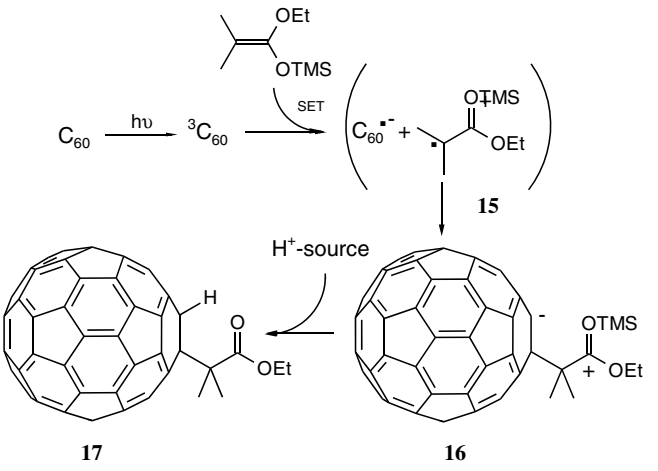

SCHEME 6 Reaction mechanism for the photo-induced CC bond formation of C_{60} with ketene silyl acetals.

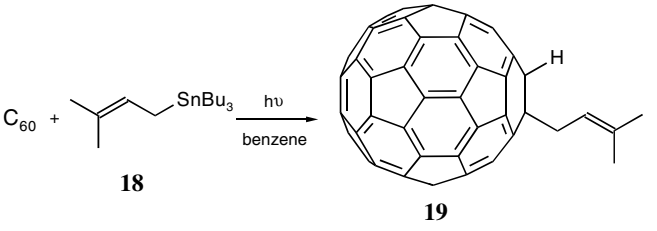

SCHEME 7 Reaction of prenyltributyltin 18 with C_{60} upon irradition.

As a first example, irradiation of C_{60} with ketene silyl acetals (KAs), first reported by Nakamura et al., will be discussed (Scheme 6).[76] Interestingly, when unstrained KAs were used, this reaction did not yield the expected [2 + 2]-cycloaddition product either by the thermal pathway, as observed by the use of highly strained ketene silyl acetals,[77] or by the photochemical pathway. As mentioned above, single electron transfer between photo-excited $^3C_{60}$ and the electron-rich ketene silyl acetal leads to the formation of the radical ion pair **15**, followed by coupling to a zwitterionic species **16**, which finally leads to product **17**.[78] The active role of water in the photoaddition in relation to the TMS/TBDMS-dependent reactivity difference indicates that the oxonium intermediate **16** is the direct precursor of the photoproduct **17**, which is formed by the water-assisted loss of the silyl group from **16**. The radical ion pair **15** is the most plausible precursor to **16**, in light of the high electron affinity of excited [60]fullerene[22] and the excellent single-electron donating ability of silyl KA.[79] No free radical species are involved in the reaction since addition of a radical trap (6 equiv. TEMPO) has no effect on the photoreaction. At least, the formation of the [2 + 2]-cycloadduct as an intermediate, which undergoes photoassisted heterolytic CC bond cleavage via **16**, cannot be excluded. Mikami et al. also investigated the addition of ketene silyl acetals. In further studies, they found that addition of the silyl enol ether of acetone and allylic silanes did not result in the synthesis of substituted 1,2-dihydro[60]fullerenes.[78a,80]

In 1997, Mikami, Fukuzumi, and co-workers[81] reported the photoaddition of allylic stannanes, which leads to mono-allylation of C_{60}. The CC bond formation of C_{60} with group 14 organometallic compounds is attained through photoinduced electron transfer from group 14 organometallic compounds acting as electron donors to the triplet excited state of C_{60}. When an unsymmetric allylic stannane such as γ,γ-dimethyl substituted allyl stannane **18** (Scheme 7) is employed,[82,83] the allylic group is introduced selectively at the α-position to yield C_{60}–1,2-$CH_2CH{=}CMe_2$ **19**. Since the allylic group is introduced selectively

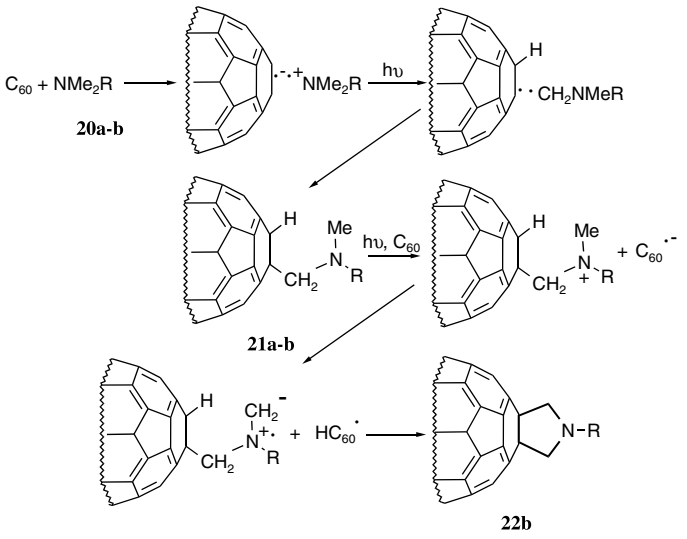

SCHEME 8 Mechanism for the reaction of C_{60} and tertiary amines $RN(Me)_2$ (R=CH_3, Ph) leading to monosubstituted 1,2-dihydro[60]fullerenes.

at the α-position and no γ-adduct has been formed, the SnC bond of the allylstannane radical cation formed in the photoinduced electron transfer may be nearly cleaved prior to the CC bond formation with $C_{60}^{\bullet-}$ in the radical ion pair.[83]

The reaction of fullerenes with amines has been the subject of considerable interest. Whereas primary and secondary amines readily add to C_{60} to give 1-H-2-(NR′R″)C_{60},[84] tertiary amines such as triethylamine, *N,N*-diethylaniline and *N,N*-dimethylaniline do not undergo the same type of addition due to the absence of an NH bond. Instead, weak charge transfer complexes with C_{60} are formed in the ground state.[85–87] Photoexcitation of amine [60]fullerene solutions leads to electron transfer from amines to the fullerene and the formation of C_{60}^{-} amine^{+} ion pairs.[22,31,53,88,89] For amines possessing α-hydrogens, proton transfer from amines to C_{60} is possible to give photochemical products.[90,91] When tertiary amines are reacted with C_{60} under PET conditions, these reactions usually result in the formation of pyrrolidinofullerenes (see the section below on [2 + 3]-photocycloaddition). Nevertheless, in some cases monosubstituted 1,2-dihydro[60]fullerenes are obtained. For example, Liou et al. reported the photochemical reaction of triethylamine and *N,N*-dimethylaniline with C_{60}.[92] Irradiation of C_{60} in the presence of an excess of amine **20a–b** in toluene slowly led to the isolation of **21a–b** (Scheme 8). No cycloadduct similar to the pyrrolidinofullerenes obtained from the irradiation of triethylamine and C_{60} was detected. In the case of **21b** (R = phenyl), further irradiation led to the pyrrolidinofullerene **22b** and a dihydrogen derivative, 1,2-H_2C_{60}, suggesting that **21b** is an intermediate for **22b**. Initial formation of the $C_{60}^{\bullet-}$-$D^{\bullet+}$ radical ion pair is followed by deprotonation of the amine cation by the fullerene anion to give an α-aminoalkyl and HC_{60} radical pair.[90] Subsequent combination of the radical pair leads to the final product. Formation of **22b** is likely to be initiated by PET from **21b** to C_{60}. This is then followed by successive intermolecular proton transfer, hydrogen abstraction, and ring closure to give 1,2-H_2C_{60} and **22** (Scheme 8).

Using diamines such as *N,N′*-dimethylethylenediamine or piperazine leads to the formation of heterocycle-fused fullerene derivatives **23** and **24** (Figure 28.4).[96] Again, the reaction proceeds via single elctron transfer to give the $C_{60}^{\bullet-}$-$D^{\bullet+}$ radical ion pair followed by successive intermolecular proton transfer, which completes the addition reaction with [60]fullerene.

Gan et al. used amino acids such as piperidino acetic acid or morpholino acetic acid in photochemical reactions with C_{60}.[93,94] Whereas the reaction of the ester derivatives of the amino acids results in the formation of pyrrolidine-fused C_{60} derivatives, the reactions of the free amino acids **25a–b** give the 1-substituted 1,2-dihydro[60]fullerenes **26a–b** (Scheme 9). The first step in the formation of the dihydrofullerenes is electron

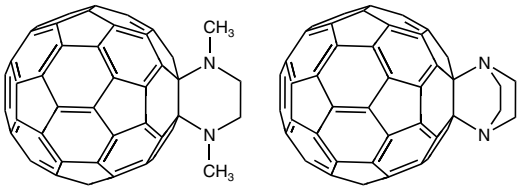

23 **24**

FIGURE 28.4 Different amino fullerene derivatives **23** and **24** upon irradiation of N,N′-dimethylenediamine or piperazine.

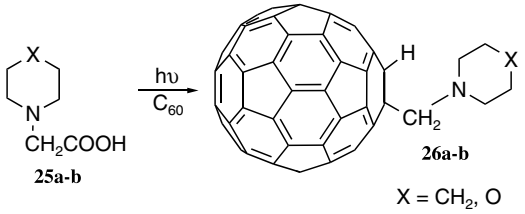

SCHEME 9 Formation of 1,2-dihydro[60]fullerenes **26a-b** upon irradiation of C_{60} and cyclic amino acids **25a-b** (a: X = CH_2, b: X = O).

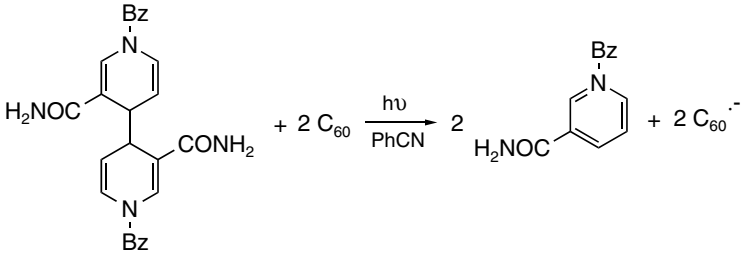

SCHEME 10 Generation of $C_{60}^{\bullet -}$ by selective one-electron reduction with $[(BNA)_2]$ in deaerated benzonitrile at $\lambda > 540$ nm.

transfer and proton loss. The CO_2 loss from carboxyl radicals is well known.[95] The aminomethyl radical formed by this path then adds to C_{60}. The final step is the abstraction of hydrogen from the environment.

The radical anion $C_{60}^{\bullet -}$ can also be easily obtained by photoinduced electron transfer from various strong electron donors such as tertiary amines (*vide supra*), ferrocenes, tetrathiafulvalenes, and thiophenes. In homogeneous systems, back electron transfer to the reactant pair plays a dominant role resulting in an extremely short lifetime of $C_{60}^{\bullet -}$. In these cases, no net formation of $C_{60}^{\bullet -}$ is observed. These problems were circumvented by Fukuzumi et al. by using NADH analogues as electron donors.[97,98] Selective one-electron reduction of C_{60} to $C_{60}^{\bullet -}$ takes place by the irradiation of C_{60} in a deaerated benzonitrile solution upon the addition of 1-benzyl-1,4-dihydronicotinamide (BNAH) or the corresponding dimer $[(BNA)_2]$ (Scheme 10).[97] The formation of $C_{60}^{\bullet -}$ is confirmed by the observation of the absorption band at 1080 nm in the NIR spectrum assigned to the fullerene radical anion.

As shown in Scheme 11, the triplet excited state $^3C_{60}^*$ is quenched by electron transfer from $[(BNA)_2]$, generating the radical ion pair $[(BNA)_2^{\bullet +}$ and $C_{60}^{\bullet -}]$, in competition with the decay to the ground state. However, back electron transfer is reduced by the fast cleavage of the CC bond in the dimer $[(BNA)_2^{\bullet +}]$. Finally, a second electron transfer from $BNA^{\bullet}$ occurs leading to two molecules of $C_{60}^{\bullet -}$. The photoreduction of C_{60} with BNAH also proceeds via photoinduced electron transfer. In this case, C_{60} is also reduced

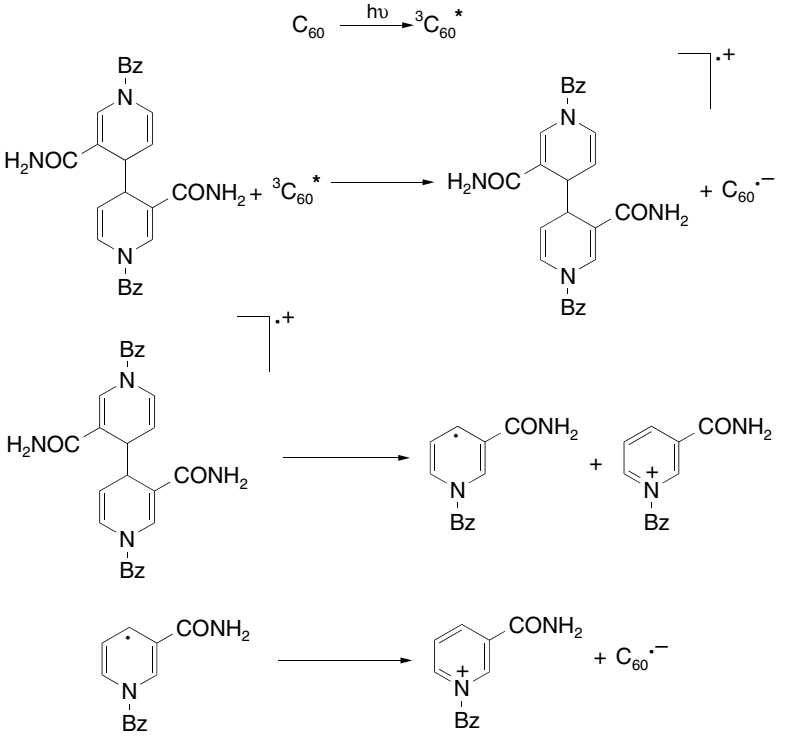

SCHEME 11 Mechanism for the generation of $C_{60}^{\bullet-}$ by selective one-electron reduction with [$(BNA)_2$].

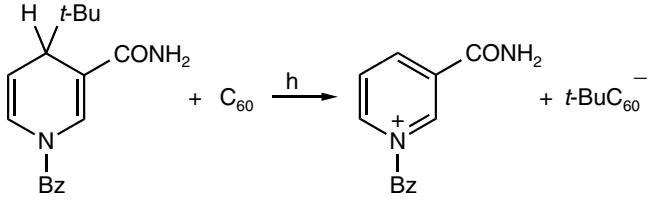

SCHEME 12 Selective two-electron reduction of C_{60} to t-BuC_{60}^-.

to the monoanion by $BNA^{\bullet}$, which is formed through deprotonation of $BNAH^{\bullet+}$. Formation of $C_{70}^{\bullet-}$ is also attained through photoinduced electron transfer from BNAH and [$(BNA)_2$] to the triplet excited state of C_{70}.[98]

In addition, Fukuzumi et al. observed selective two-electron reduction of C_{60} when BNAH is replaced by the 4-*t*-butylated BNAH (*t*-BuBNAH) in the above reaction, leading to the formation of *t*-BuC_{60}^- and the two-electron oxidation of BNAH to BNA^+ (Scheme 12). Subsequent trapping of initially formed t-BuC_{60}^- by CF_3COOH and $PhCH_2Br$ results in formation of the corresponding 1,2-substituted dihydrofullerene for the former and 1,4-substituted adduct for the latter.[99] The initial product of 1,4-*t*-$BuC_{60}H$ is rearranged to the 1,2-isomer during the isolation procedure to give the 1,2-adduct exclusively.[100]

Again, photoinduced electron transfer to the triplet excited state $^3C_{60}^*$ is the initial step to yield *t*-$BuBNAH^{\bullet+}$ and $C_{60}^{\bullet-}$. Upon C(4)-C bond cleavage of *t*-$BuBNAH^{\bullet+}$, the *t*-butyl radical is formed, which readily adds to the fullerene radical anion yielding *t*-BuC_{60}^-. In competition, back electron transfer takes place. Similar results are obtained in the photochemical reaction of C_{70} with the NADH analogues mentioned above. The reaction mechanism remains the same in the case of *t*-BuBNAH. However, there are some differences in the reaction mechanism for [$(BNA)_2$] and BNAH. After the photoinduced electron

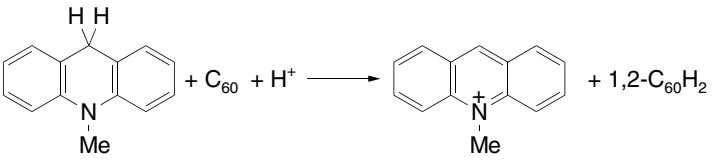

SCHEME 13 Selective two-electron reduction of C_{60} to 1,2-$C_{60}H_2$.

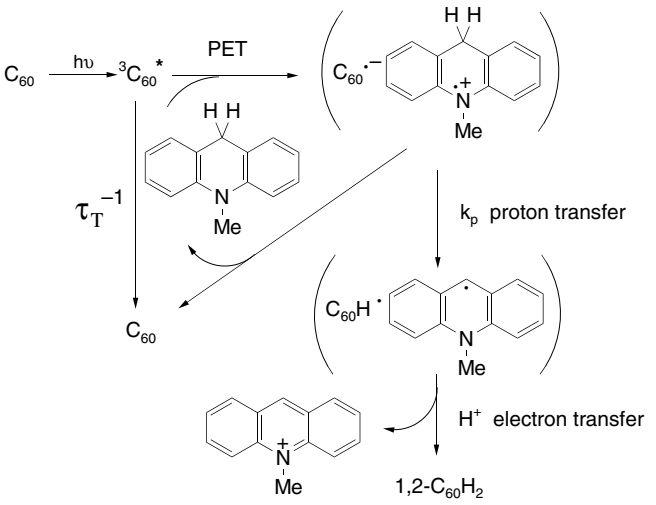

SCHEME 14 Mechanism for the selective two-electron reduction of C_{60} to 1,2-$C_{60}H_2$.

transfer reaction from [$(BNA)_2$] to C_{70}, resulting in the formation of the radical ion pair, CC bond cleavage of the dimer leads to C_{70}^{2-}, which is followed by facile electron transfer from C_{70}^{2-} to C_{70} to give two equivalents of $C_{70}^{\bullet -}$. In the case of BNAH, CH bond cleavage occurs to give HC_{70}^- and BNA^+. Subsequent electron transfer from C_{70}^{2-}, which is in equilibrium with HC_{70}^-, to C_{70} leads to the formation of two equivalents of $C_{70}^{\bullet -}$.

Using 10-methyl-9,10-dihydroacridine ($AcrH_2$) in the photochemical reaction with C_{60} in the presence of CF_3COOH, 1,2-$C_{60}H_2$ is formed exclusively (Scheme 13).[97] The reaction mechanism is shown in Scheme 14. Proton transfer from $AcrH_2^{\bullet +}$ to $C_{60}^{\bullet -}$ is significantly exergonic and occurs efficiently in the radical ion pair to give $C_{60}H^{\bullet}$. The product 1,2-$C_{60}H_2$ is obtained by fast electron transfer from $AcrH^{\cdot}$ in the presence of CF_3COOH. Protonation of $C_{60}^{\bullet -}$ by the acid and subsequent hydrogen transfer from $AcrH_2^{\bullet +}$ to $C_{60}H^{\bullet}$ yielding the final products, are also possible.

Photocycloaddition

Among the reactions applied in the synthesis of fullerene derivatives, cycloaddition reactions such as [2 + 1]-, [2 + 2]-, [3 + 2]- and [4 + 2]-cycloadditions play a dominant role. In these reactions, ring-fused fullerene derivatives are obtained, at least, with incorporation of heteroatoms such as oxygen or nitrogen. Such reactions will be the topics of the following sections.

[2 + 1]-Photocycloaddition

In general, by [2 + 1]-photocycloaddition reactions methanofullerenes, fullerene epoxide, and aziridinofullerenes as the corresponding oxygen and nitrogen analogues with a [6,6]-closed structure are obtained as shown in Figure 28.5.

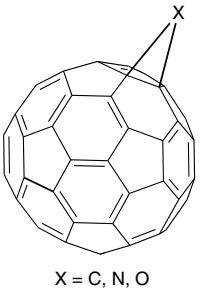

FIGURE 28.5 Fullerene derivatives obtained by [2+1]-photocycloaddition: methanofullerene, fullerene epoxide, and aziridinofullerene.

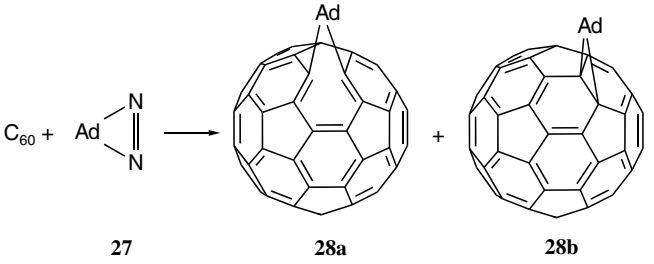

SCHEME 15 Photolysis of 2-adamantane-2,3′-[*3H*]-diazirine **27** and C_{60} with a high-pressure mercury lamp (cutoff <300 nm).

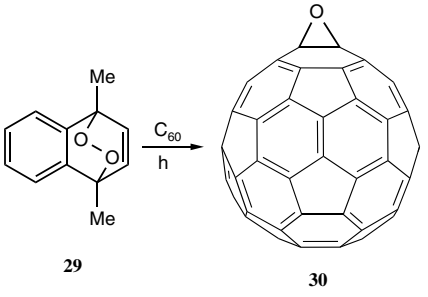

SCHEME 16 Irradiation of C_{60} and endoperoxide **29**.

Recently, Akasaka et al.[101] described the photochemical reaction of diazirine **27** with C_{60} resulting in the formation of a mixture of the isomers **28a** and **28b** in a ratio of 51:49 (Scheme 15). Structure elucidation by UV-vis spectroscopy and NMR investigations clearly demonstrates that isomer **28b** is the 6,6-adduct of C_{60} with C_{2v} symmetry, namely the methanofullerene. There is crucial evidence supported by ^{1}H and ^{13}C NMR that the isomer **28a** is the 5,6-adduct (fulleroid) of C_{60} with C_s symmetry. Isomerization of the pure fulleroid to the methanofullerene or *vice versa* upon photolysis, as reported by Wudl et al.,[102] is not observed; thus, the isomeric ratio of the two isomers reveals the formation ratio of carbene and diazo compound during the reaction.

Fullerene epoxide ($C_{60}O$, **30**), the oxygen analogue of the methanofullerene, can be obtained by the extended irradiation of C_{60} in an oxygen atmosphere as reported by Smith et al.[103] Irradiation of C_{60} with

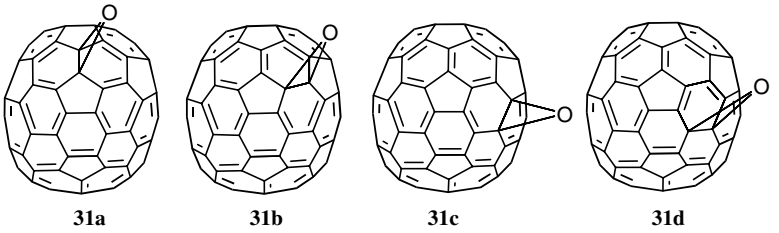

FIGURE 28.6 Possible C_{70} O isomers.

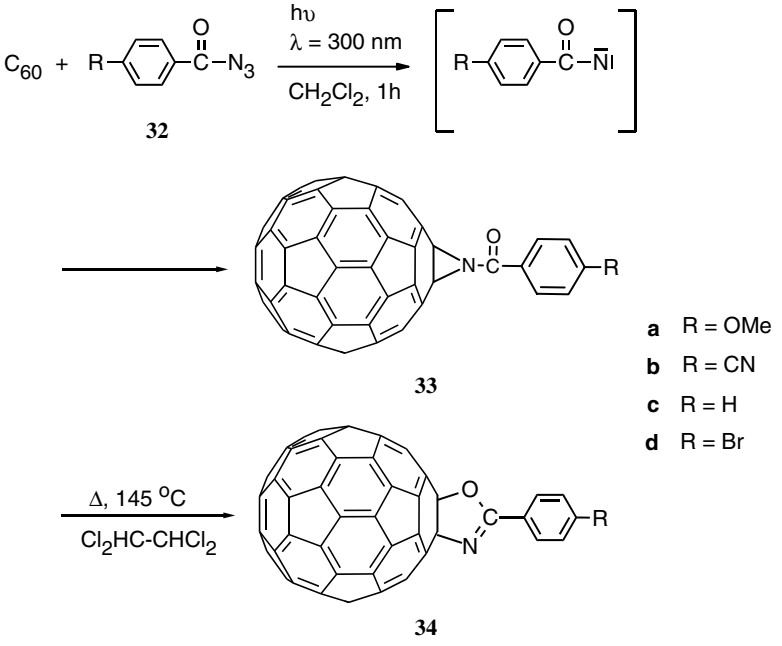

SCHEME 17 Photolysis of C_{60} and aroylazides **32a-d** in oxygen-free 1,1,2,2-tetra-chloroethane at $\lambda = 300$ nm.

endoperoxides **29**[104] leads to the formation of epoxide **30** in high yields (Scheme 16). Singlet oxygen $^1O_2$ released from the endoperoxides is the key species in the mechanism for fullerene oxide formation under photochemical reaction conditions and suggests that $C_{60}O$ results from reaction of $^1O_2$ with C_{60} triplet excited states as primarily suggested by Juha et al.[105]

Heymann et al.[106] as well as Smith et al.[107] reported the synthesis of $C_{70}O$ **31** by photo-oxygenation. Irradiation of an oxygenated toluene solution of C_{70} using rubrene as a sensitizer resulted in the formation of a nearly 1:1 mixture of two $C_{70}O$ isomers **31a** and **31b**, which cannot be separated (Figure 28.6). No evidence for the formation of isomers **31c** and **31d** was found.

The thermal reaction of nitrenes resulted in the formation of the nitrogen analogues of the fullerene epoxide, the aziridinofullerenes, and the 5,6-open azafulleroids.[108] Under photochemical reaction conditions, aziridinofullerenes are observed as the only addition product of nitrenes. Photochemical synthesis of aziridinofullerenes was first reported by Keana et al.[109] in low yields, probably due to the addition of the nitrene to the solvent chlorobenzene.[110] Averdung et al. also obtained several aziridinofullerenes by the reaction of C_{60} with acylnitrenes, generated by photolysis of aroylazides **32a–d**, leading to the fullerene adducts **33a–d** (Scheme 17).[111] The structures of the [6,6]-ring fused 1,2-dihydrofullerenes have been

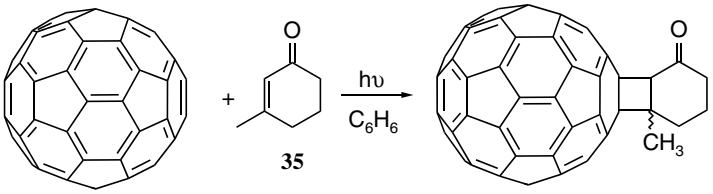

35 **36**

SCHEME 18 Reaction of C_{60} with cyclic enone **35**.

identified by standard spectroscopic methods. Irradiation at wavelengths >380 nm did not result in product formation. Thus, the formation of the acylnitrenes does not occur via excited C_{60}. The reaction of C_{60} and 4-cyanobenzoylazide **32b** in benzene at 300 nm did not lead to the expected fulleroaziridine **33b**. Instead, a 6,6-bridged dihydrofullerene was obtained as a main product. Mass spectral analysis and NMR spectroscopic investigations indicate an asymmetrical fullerene structure formed by reaction of the nitrene to C_{60} with incorporation of benzene, similar to the incorporation of benzene in the reaction of 1,8-dehydronaphthalene with C_{60}.[112] The exact structure still remains unknown. As a minor product, the fullerooxazole **34b** was observed. The formation of the corresponding fullerooxazoles **34a–d** was also observed by the thermal rearrangement of aziridinofullerenes.

[2 + 2]-Photocycloaddition

A very versatile method of formation of fullerene adducts is the [2 + 2]-photocycloaddition. The preparation and isolation of well-characterized [2 + 2]-monoadducts of C_{60} with alkynes,[113] arylalkenes,[114] dienes,[115] cycloenones,[116] acyclic enones,[117] and diones[118] has been reported. The pioneering work on this useful synthetic pathway was executed by Schuster and co-workers in 1993. In their first attempts, a crown-ether tagged fulleroid and various cyclohexen-2-one derivatives were used in the cycloaddition reaction.[62,119] Once the reaction was successfully performed, Schuster and co-workers synthesized cyclobutane–fullerene adducts by the irradiation of C_{60} (Scheme 18).[62] Up to seven enone units are incorporated on longer irradiation time. As shown by ^{1}H-NMR, IR and HPLC analysis, the isolated monoadducts consist of a mixture of two stereoisomers, the *cis*- and *trans*-isomers arising from the [2 + 2]-cycloaddition across the [6,6]-ring junction in C_{60}; the major product normally is *trans*. When 3-methyl-2-cyclohexen-1-one is used in the reaction, the obtained fullerene derivatives are chiral. Semipreparative HPLC analysis with a chiral stationary phase (*S,S*)-Whelk-O HPLC column results in the separation of the four stereoisomers.[118]

No product formation was observed upon irradiation at 532 nm where the fullerene is the only light-absorbing component. Thus, fullerene triplets do not undergo addition to ground-state enones. Instead, the reaction proceeds by the same mechanism operating in the photoaddition of enones to ordinary alkenes,[120] namely stepwise addition of enone triplet excited states to the fullerene via an intermediate triplet 1,4-biradical.

Orfanopoulos and co-workers studied the photochemical reaction of alkenes, aryalkenes, dienes, dienones, and acyclic enones with [60]fullerene to obtain various substituted cyclobutanofullerenes.[114,115,117,121] For example, the photocycloaddition of *cis*- and *trans*-1-(*p*-methoxyphenyl)-1-propene **37** to C_{60} gives only the *trans* [2 + 2]-adducts; thus, the reaction is stereospecific for the most thermodynamically stable cycloadduct (Scheme 19). A possible mechanism includes the formation of a common dipolar or biradical intermediate between $^3C_{60}$* and the arylalkene, followed by subsequent fast rotation of the aryl moiety around the former double bond leading to *trans*-**38**. Irradiation of this product yielded 90% *trans*-**37** and 10% *cis*-**37** as cycloreversion products. As the photocycloreversion is expected to give *trans*-**37** as the only product, a concerted mechanism can be excluded. Similarly, cycloreversion products from C_{60} and tetraalkoxyethylene adducts were also observed by Foote et al.[113b] As reported by this research group, the cycloreversion proceeds via the triplet excited state of the adduct because rubrene

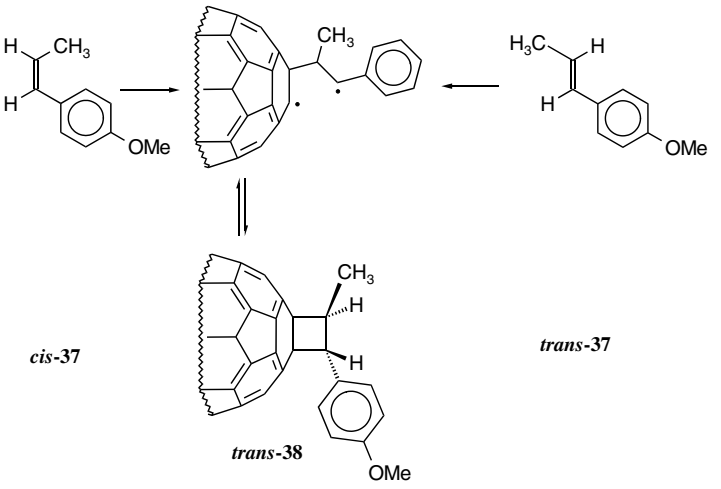

SCHEME 19 Reaction of C_{60} and *cis*-37/*trans*-37 at $\lambda > 530$ nm and proposed mechanism for this reaction.

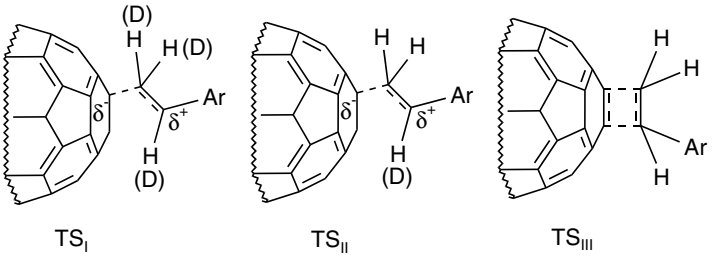

FIGURE 28.7 Possible transition states in the reaction of C_{60} with deuterated 1-(*p*-methoxyphenyl)ethylene.

and oxygen efficiently inhibit photocycloreversion. However, these results do not exclude an electron transfer or charge transfer mechanism with loss of stereochemical integrity.

Studies of the secondary isotope effect also confirmed the two-step mechanism, involving the formation of a dipolar or biradical intermediate in the rate-determining step. The observed isotope effects in the reaction of 1-(*p*-methoxyphenyl)-ethylene and its deuterated analogues 1-(*p*-methoxyphenyl)-ethylene-d_1 and 1-(*p*-methoxyphenyl)-ethylene-d_3 with C_{60}, when taken in conjunction, exclude the formation of transition state TS_{III} (concerted mechanism), because in that case substitution at either C_α or C_β would have given an inverse isotope effect (Figure 28.7).

Furthermore, addition reactions of alkyl-substituted 1,3-butadienes to C_{60}[115] supported the suggested two-step mechanism via a dipolar or biradical intermediate. The formation of this intermediate is responsible for the observed regioselectivity and the secondary isotope effects. The second step (collapse of the initial ion pair) dictates the diastereoselectivity that favors the more thermodynamically stable *trans*-cyclobutane products. The lifetime of the biradical intermediate is long enough to allow rotation around the C2C3 bond in the 1,3-butadienes, leading to loss of stereochemical integrity of the cycloadducts. However, the stereochemistry of the unreacted double bond of the dienes is retained, and this result is consistent with the known propensity of allylic radicals to resist rotation around the partial double bond. The regio- and stereoselectivity can also be observed in the reaction of acyclic enones to C_{60}.[117]

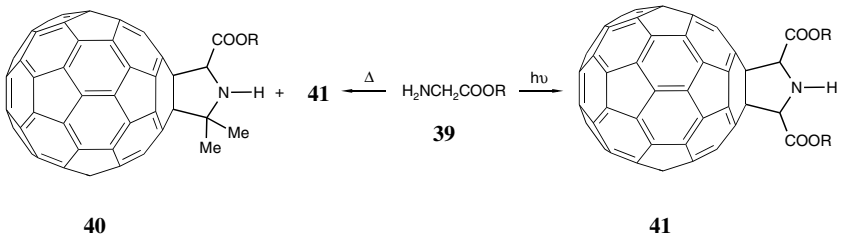

40 **41**

SCHEME 20 Thermal and photochemical reaction of glycine esters **39** with C_{60}.

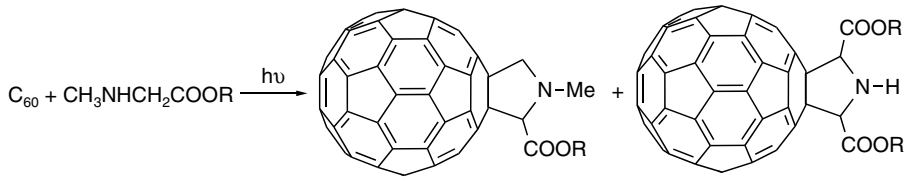

42

SCHEME 21 Photochemical reaction of sarcosine esters with C_{60}.

[2 + 3]-Photocycloaddition

The photochemical functionalization of fullerenes with amines leading to monosubstituted 1,2-dihydro[60]fullerenes has already been discussed in the section "Synthesis of Substituted 1,2-Dihydro[60]fullerenes by Reductive PET." In this context, formation of pyrrolidinofullerenes as the main reaction products, when tertiary amines are reacted with C_{60} under PET conditions, has already been mentioned. The synthesis of the pyrrolidinofullerenes via 1,3-dipolar cycloaddition of azomethine ylides has met a broad acceptance, probably due to the many ways to generate the reactive intermediates from a wide variety of easily accessible starting materials. The most successful approach has been the decarboxylation of iminium salts derived from condensation of α-amino acids with aldehydes.[122] An alternative way to pyrrolidinofullerenes was developed by Gan et al. using amino acid esters in both thermal and photochemical reactions with C_{60}.[123] For example, refluxing a mixture of C_{60} and glycine ethyl ester **39** afforded two products in a 4:1 ratio, with pyrrolidinofullerene **40** as the major product and **41** as the minor product, whereas upon photolysis **41** is the only isolated product indicating that the thermal and photochemical reactions follow different mechanisms (Scheme 20).

For the photochemical reaction, an air-assisted radical reaction mechanism was proposed, in which both CN bond breaking and bond formation processes are involved. Recently, Foote et al.[124] confirmed the involvement of singlet oxygen by a control experiment. The reaction of the glycine ester with C_{60} was performed thermally under the same reaction conditions using $DMNO_2$ as the singlet oxygen source, resulting in the formation of a product with identical ^{1}H-NMR and ^{13}C-NMR spectra to that reported by Gan et al.

When sarcosine esters are reacted with [60]fullerene, compounds **41**, bearing two ester functionalities, and **42**, containing only one ester functionality, are obtained (Scheme 21). Sarcosine has one more methyl group than glycine, which results in the amino group being more basic and also more crowded. Obviously, the electronic effect predominates leading to an increased rate compared to the glycine analogues.

The reaction mechanism for the sarcosine ester reaction is outlined in Scheme 22. In the first step three radicals are formed: the aminium radical cation (a) arising from single electron transfer from the amino group to C_{60} and the two carbon-centered radicals (b,c) produced by the interaction with $^1O_2$,

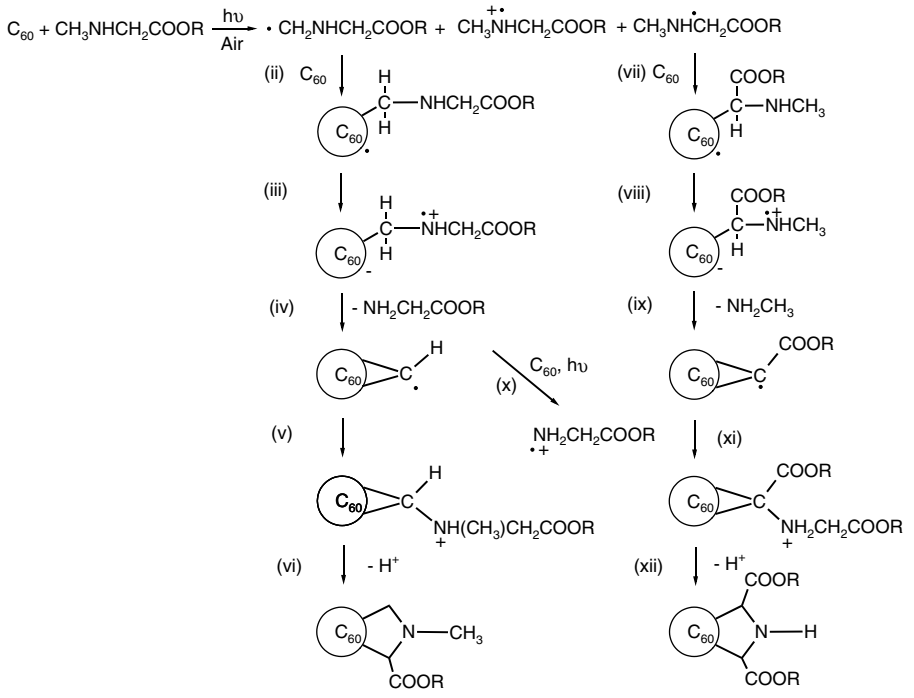

SCHEME 22 Mechanism for the photochemical reaction of sarcosine esters.

which is generated by C_{60} efficiently. Addition of the carbon-centered radicals to the fullerene is followed by electron transfer from the amine to the C_{60} fragment to form the zwitterionic radical (Step iii). The CN bond cleavage and the release of glycine at Step iv is unusual and may be due to the unique properties of C_{60}. Moderate heating is probably necessary due to the endothermic CN bond-breaking step. The driving force for the rearrangement in Steps vi and xii may be the more stable five-membered ring. Besides the main products **41** and **42**, several other products are possible, such as $C_{60}(CH_2)$, C_{60}(HCCOOR), and the amine addition product $C_{60}(H)(CH_3NCH_2COOR)$.

Photolysis of aminopolycarboxylates such as tetramethyl ethylenediaminetetraacetate (EDTA) **43** and pentamethyldimethylenetriaminepentaacetate (DTPA) **47** with C_{60} has been shown to be an effective method for the preparation of isomerically pure pyrrolidinofullerene derivatives, which can be used as complexones or polydentate ligands.[94] The presence of free acid functionalities leads to decarboxylation, and 1-alkylated 1,2-dihydro[60]fullerenes are formed as described by Zhang et al.[93] In case of esters, pyrrolidine-fused fullerenes are the major products. All reactions involve radicals as described for the photoaddition of glycine and sarcosine esters. Unlike primary amino acid esters, which undergo complicated bond-breaking and formation processes, amino acid esters with secondary and tertiary amino groups add to C_{60} simply by losing two H atoms. In comparison to the well-known synthesis of pyrrolidine ring-fused fullerene adducts in the above reaction, the use of aldehydes or ketones can be avoided. Table 28.3 gives a short overview of fullerene derivatives obtained by the photoreaction of EDTA and DTPA.

As a last example of fullerene functionalization leading to pyrrolidinofullerenes, the photoreaction of triethylamine (TEA) with C_{60} should be discussed. Fullerene C_{60} undergoes efficient photochemical reactions with TEA to form a complex mixture of addition products under ambient and deoxygenated conditions.[125] The reactions are initiated via photoinduced electron transfer between the excited singlet C_{60} and the amine. Three types of cycloadducts of fullerenes — **50**, **51**, and **52** — were obtained, whereas the formation of the mono-alkylated 1,2-dihydro[60]fullerene **53**, as described by Liou et al.[92] in the reaction of trimethylamine and *N*,*N*-dimethylaniline with C_{60}, was not observed (see Figure 28.8).

TABLE 28.3 Products of the Photolysis Aminopolycarboxylates with C_{60}[94]

STARTING MATERIAL	PRODUCTS
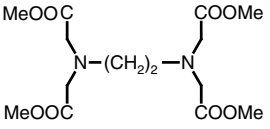 **43**	**41** 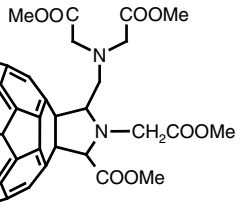 **44**
	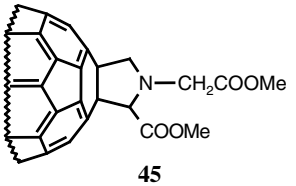 **45**
	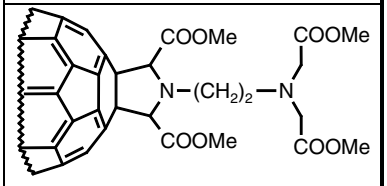 **46**
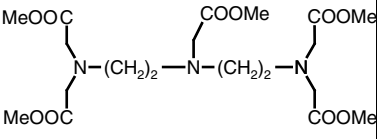 **47**	**41** **44** 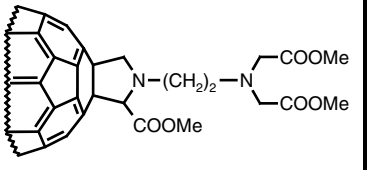 **48**
	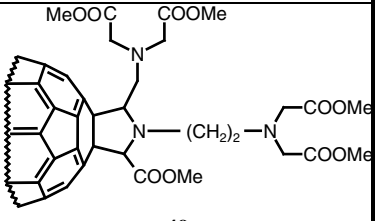 **49**

Compound **50** was formed in the deoxygenated solution, and compounds **51** and **52** were obtained by irradiation of air-saturated solutions. Sun and co-workers suggest that the simple adduct **53** should be the initial product formed in C_{60}-tertiary amine photochemical reactions regardless of whether the reaction is performed in deoxygenated or air-saturated solutions. The monoadducts isolated and identified by Sun et al. are completely different from those expected on the basis of the photoinduced

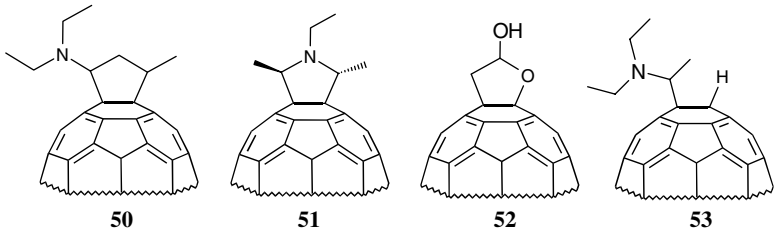

50 **51** **52** **53**

FIGURE 28.8 Structure of the products obtained upon irradiation of triethylamine and C_{60}.

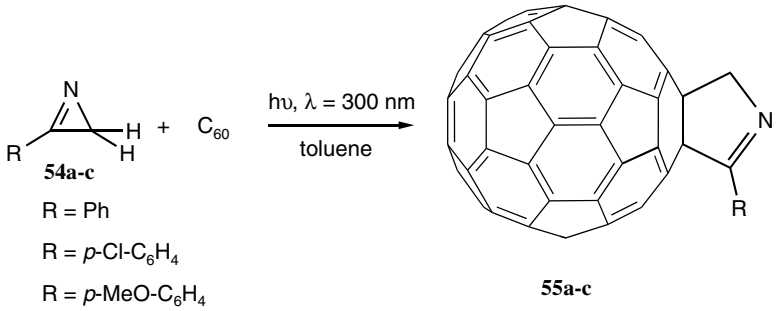

54a-c

R = Ph

R = *p*-Cl-C_6H_4

R = *p*-MeO-C_6H_4

55a-c

SCHEME 23 [3+2]-photocycloaddition of 2*H*-azirines and C_{60} in toluene at $\lambda = 300$ nm.

sequential electron transfer, proton transfer, and radical combination mechanism, which is well established in reactions of conventional aromatic molecules with tertiary amines. The complexity in the reactions involving fullerenes is attributed to the fact that the functionalized fullerenes remain electron acceptors for both inter- and intramolecular electron transfer reactions. The observed C_{60}-TEA photoadducts are likely from multistep processes, each of which may involve either inter- or intramolecular photoinduced electron transfer.

The photochemical [3 + 2]-cycloaddition of 2*H*-azirines with C_{60} has been intensively studied by Mattay et al.[126,127] Photolysis of a equimolar solution of C_{60} and **54a–c** leads to the corresponding monoadducts **55a–c**, which have a closed [6,6]-bridged 1,2-dihydrofullerene structure with C_1 symmetry as confirmed by UV spectroscopy and NMR investigations (Scheme 23). An open [1,6]-substituted [10]annulene structure can be excluded. Upon irradiation of a 10-fold excess of 2,3-substituted-2*H*-azirines **54a–c** with [60]fullerene, formation of mono- and oligoadducts is observed. In all cases a fraction of regioisomeric bisadducts can be obtained, which were not separated.

The formation of the [3 + 2]-cycloadduct **55** can be explained by two different reaction pathways (Scheme 24). Irradiation at 300 nm leads to ring opening of the azirine **54** to the nitrile ylide as an intermediate, which adds to C_{60} yielding the observed product **55**. No product formation is observed at wavelengths >400 nm. Instead, under photoinduced electron transfer conditions in the presence of 9,10-dicyanoanthracene (DCA), the [3 + 2]-cycloaddition reaction proceeds via the 2-azaallenyl radical cation.

[2 + 4]-Photocycloaddition

The thermal Diels–Alder reaction ([4 + 2]-cycloaddition) is widespread in the synthesis of fullerene derivatives. In contrast, only a few examples of photochemical Diels–Alder reactions in solution or in the solid state are known. Among the functionalization of C_{60}, Diels–Alder reactions with *o*-quinodimethanes as dienes are very versatile because they provide thermally stable adducts that are usually not subjected to cycloreversion to the original components. The photoirradiation of *o*-toluylaldehyde and related carbonyl compounds is known to give an *o*-quinodimethane species carrying a hydroxy group via the biradical generated by the intramolecular hydrogen abstraction of the carbonyl group in the excited triplet state ($n\pi^*$) from the neighboring methyl group.[128] Instead of the desired cyclohexyl-fused

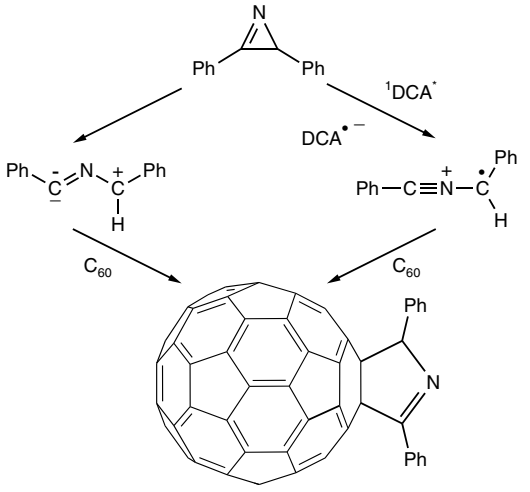

SCHEME 24 Mechanism for the [3+2]-photocycloaddition of 2*H*-azirines and C_{60}.

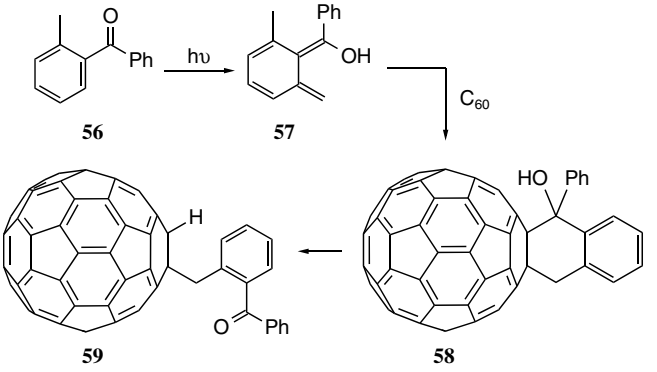

SCHEME 25 Irradiation of ketone **56** and C_{60} leading to monoalkyl-1,2-dihydro-[60]fullerene **59**.

fullerene derivative **58**, which is unexpectedly unstable, Tomioka et al. observed, in their study of the photoreaction of *o*-methylbenzophenone **56** with C_{60}, the formation of the monoalkyl-1,2-dihydrofullerene **59** by the cleavage of the CC bond connected to the fullerene core (Scheme 25).[129]

In contrast, Nishimura et al. obtained stable monoadducts **62a–g** possessing a hydroxy group suitable for further derivatization from the [2 + 4]-photocycloaddition of the corresponding carbonyl compounds **60a–g** and [60]fullerene (Scheme 26).[130] The adducts **62** were found to adopt one or both of two conformers **A** and **E**, which possess pseudoaxial and pseudoequatorial hydroxy groups, respectively (see Table 28.4). Two conformers existed for **62a**, **c**, **d**, and **f**, while **62b**, **e**, and **g** exclusively adopted **E**, **A**, and **E**, respectively. The comformer ratios remarkably depend on the bulkiness of the substituents attached to the aromatic nucleus and the cyclohexene ring.

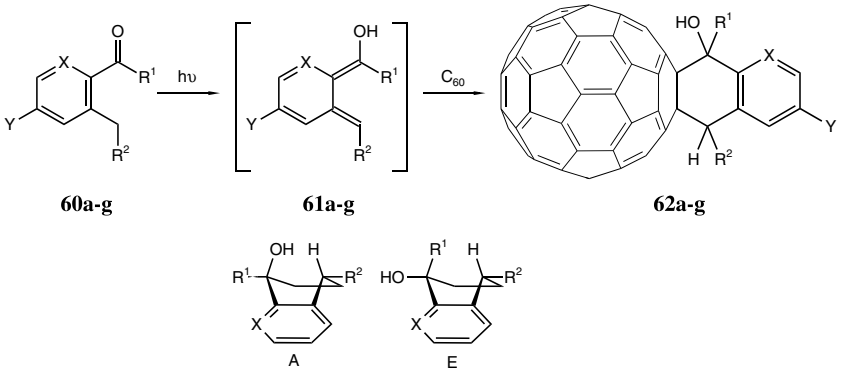

SCHEME 26 [4+2]-photocycloaddition of C_{60} with *o*-quinodimethane derivatives generated from carbonyl compounds.

Mikami et al. investigated the photochemical Diels–Alder reaction of anthracenes with C_{60} in the solid state.[131] Irradiation of a mixture of C_{60} and 9-methylanthracene led to the formation of mono- and bisadducts. No formation of 9-methylanthracene dimers as in solution was observed. The reaction did not work with less bulky anthracenes. The reaction rate depends on the ionization potential of the anthracenes. With decreasing ionization potential, the Diels–Alder reaction of C_{60} proceeds much more easily. Therefore, the reaction may proceed via photoinduced electron transfer from anthracenes to the triplet excited state of C_{60}. The energetics for the photoinduced electron transfer in the solid state are significantly different from those in solution where solvation plays an important role. Such a difference leads to the different reactivity of the anthracene derivatives in the solid state as compared to that in solution.

Recently, Fukuzumi et al. reported the photochemical Diels–Alder reaction with Danishefsky's diene.[132] A mixture of C_{60} and the stereochemically defined (1*E*,3*Z*)-1,4 disubstituted Danishefsky's diene **63** was irradiated for 9 h at –30°C to avoid the thermal reaction. After work-up, two desilylated adducts **65** were obtained, the major being the *trans*-product, the minor the *cis*-product (Scheme 27).

TABLE 28.4 Photoreaction of [60]fullerene with **60**[130b]

	X	R_1	R_2	Y	Adduct	Yield/%[a]	Conformer ratio **A/E**[b]
60a	CH	H	H	H	**62a**	32 (63)	4:6
60b	CH	H	Me	H	**62b**	17 (80)	0:10[c]
60c	CH	Me	H	H	**62c**	9 (87)	6:4
60d	CH	Ph	H	H	**62d**	29[d] (69)	6:4
60e	CMe	H	H	H	**62e**	33 (58)	10:0
60f	CH	H	H	OH	**62f**	5 (89)	5.5:4.5
60g	N	H	H	H	**62g**	15 (83)	0:10

[a] Isolated yields are shown, although not optimized. Recovery of C_{60} is also shown in parenthesis.

[b] The symbols A and E denote conformers possessing pseudoaxial or pseudo-equatorial hydroxy group, respectively.

[c] Only a single isomer was obtained in which both the hydroxy and methyl groups adopt pseudoequatorial conformations.

[d] A trace amount of the decomposition product is included.

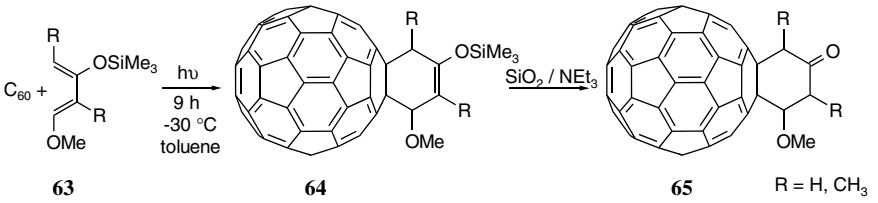

SCHEME 27 Irradiation of C_{60} and Danishefsky's diene **63**.

The same *trans*-product **65** is obtained as a single isomer after short irradiation, indicating that the *cis*-isomer may be formed by isomerization of the *trans*-adduct after a longer irradiation period, which is indicative of the Diels–Alder reaction proceeding by a stepwise mechanism rather than a concerted mechanism. Initially, the triplet radical ion pair (**A**) is formed by photoinduced electron transfer from **63** to triplet excited C_{60} (k_{et}) (Scheme 28), which then provides the singlet radical ion pair leading to a biradical intermediate (**B**) or a zwitterionic intermediate (**C**) in competition with back electron transfer to the reactant pair (k_b). In the latter case, the initial C–C bond formation should occur between the C4 carbon of **63**$^{\bullet+}$ and the $C_{60}^{\bullet-}$, while in the former it occurs betweenb the C1 carbon of **63**$^{\bullet+}$ and the $C_{60}^{\bullet-}$. Despite the fact that there are difficulties in distinguishing between the two possible reaction pathways, one can conclude that in any case the formation occurs stepwise, and thus there is no symmetry restriction for bond formation. Both *trans*-adduct and *cis*-adduct **65** are obtained as the final products.

28.4 Photochemistry of C_{60} and C_{70} Derivatives

Addition of Singlet Oxygen

The triplet excited state of C_{60} is formed with a quantum yield close to unity,[22] and by energy transfer to molecular oxygen, it produces large quantities of singlet oxygen (Equation 28.2). This useful photochemical property makes C_{60} a potent sensitizer for the mild photooxygenation of simple alkenes and dienes.[133]

$$^3C_{60/70}{}^* + {}^3O_2 \rightarrow C_{60/70} + {}^1O_2 \qquad (28.2)$$

As fullerene adducts with an oxidizable group are sensitive to oxygen and light,[134] a variety of oxygenated derivatives are available by self-sensitized photooxygenation. This is a simple synthetic strategy for oxo functionalization leading to fullerene compounds with better solubility in more polar solvents.[135] This useful observation has been applied successfully in photosensitized studies of biological systems.[6,136] Rubin et al. reported previously an unexpected regioselectivity in the self-sensitized ene photooxygenation of several adducts prepared by [4 + 2]-cycloaddition to C_{60} (Scheme 29).[137] In almost all cases, the reactions resulted in the formation of allylic alcohols **68** with endocyclic double bonds after reduction of the corresponding hydroperoxides **67** with PPh_3.[137]

In contrast, reaction of alkyl-substituted cyclohexenes yields a majority of products with an exocyclic double bond.[138] The unexpected regioselectivity is explained in conformational and electrostatic terms. The boat conformation of the C_{60}-fused cyclohexenes confers a rigid framework to the six-membered ring in which two of the 3,6 hydrogens are pseudoaxial. Because of favorable interactions between the incoming $^1O_2$ and these axial hydrogens, the *endo*-perepoxide resulting from transition state $\mathbf{TS_I}$ is formed, rather than the *exo*-isomer derived from transition state $\mathbf{TS_{II}}$ (Figure 28.9). Additional favorable electrostatic or electronic interactions may exist between the negative oxygen of the developing *endo*-perepoxide I and C_{60}, which is strongly electron deficient.

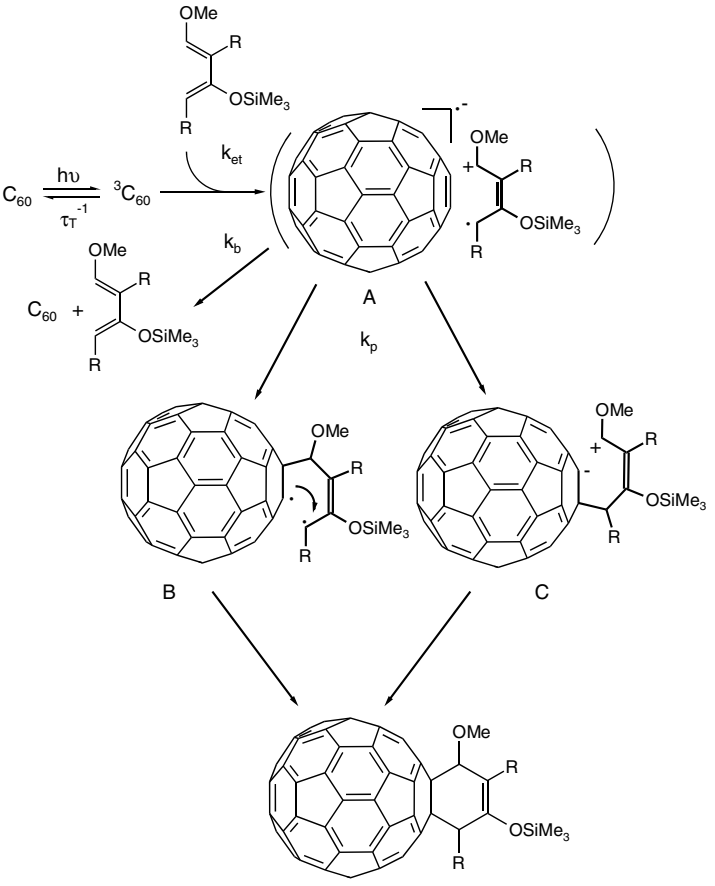

SCHEME 28 Proposed mechanism for the irradiation of C_{60} and Danishefsky's diene **63**.

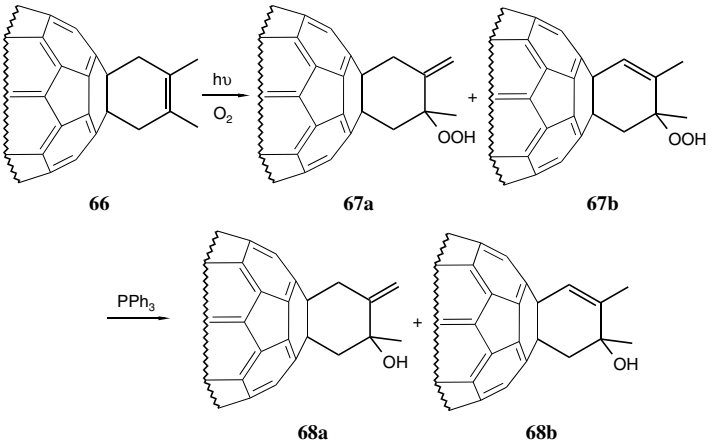

SCHEME 29 Self-sensitized ene photooxygenation of fullerene adduct **66** leading to allylic alcohols.

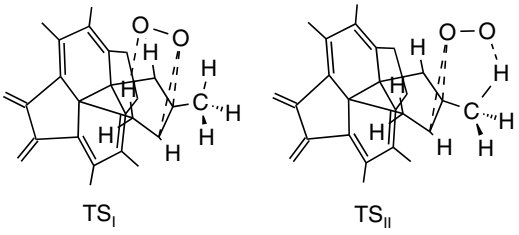

FIGURE 28.9 Transition states in the photooxygenation of C_{60}-fused cyclohexenes.

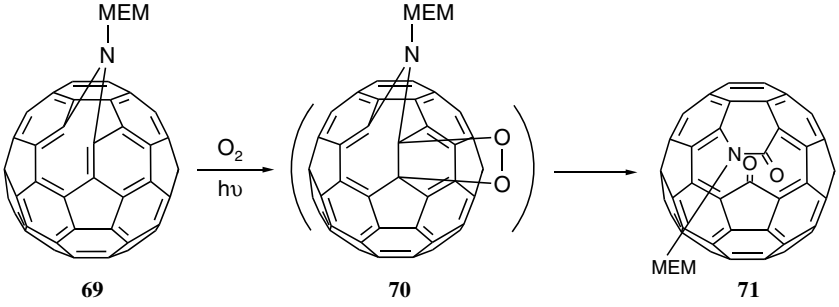

SCHEME 30 Self-sensitized photooxygenation of *N*-(MEM)-substituted [5,6]-azafulleroid **69**.

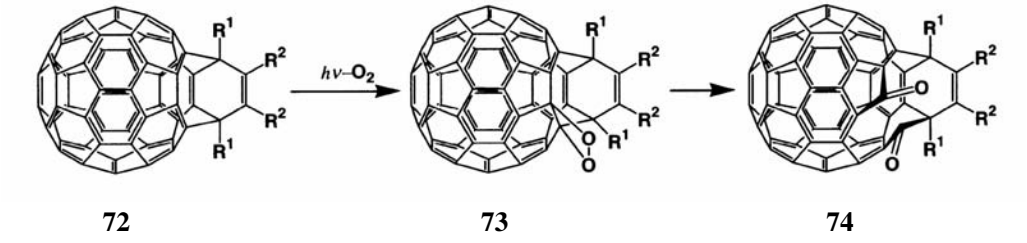

SCHEME 31 Self-sensitized photooxygenation of tetrasubstituted bis(fulleride) derivatives **72**.[146]

Self-sensitized photooxygenation of C_{60}-fused cyclobutanes containing an oxidizable alkene moiety[115] or alkenyl-substituted fullerene adducts[139] followed by reduction also results in the formation of allylic alcohols. Whereas in the former case formation of both the *threo* and *erythro* forms of the allylic alocohols is observed, in the latter case the reaction occurs regioselectively by the preferential abstraction of an allylic hydrogen next to the fullerene group. The hydrogen atom linked to the fullerene skeleton is unreactive under the reaction conditions.

Wudl et al. obtained the ring-opened *N*-MEM-ketolactam **71** by self-sensitized photo-oxygenation of *N*-methoxyethoxymethyl (MEM)-substituted [5,6]azafulleroid **69** (Scheme 30).[140] The reaction is highly regioselective, most likely because the anti-Bredt CC double bonds in **69** are more strained.

Similarly, irradiation of tetrasubstituted bis(fulleroid) derivatives **72** in the presence of oxygen affords a 12-membered ring diketone on the surface of the fullerene.[141] In spite of the same 60 π electronic structure as C_{60}, whose photooxygenation leads to the formation of the fullerene epoxide, [2 + 2]-cycloaddition of **72** with $^1O_2$ followed by symmetrical ring opening of the dioxetane **73** predominantly occured to give **74** (Scheme 31).[140,142] On the contrary, oxidation and Diels–Alder reaction of the mother compound ($R^1 = R^2 = H$) were reported to occur not at the fullerene skeleton but on the outside part.[143,144]

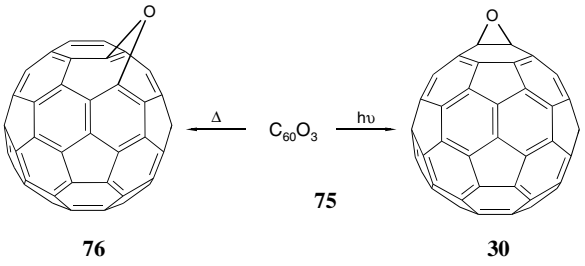

SCHEME 32 Photolysis of $C_{60}O_3$ leading to the [5,6] open fullerene oxide **76** (oxidoannulene).

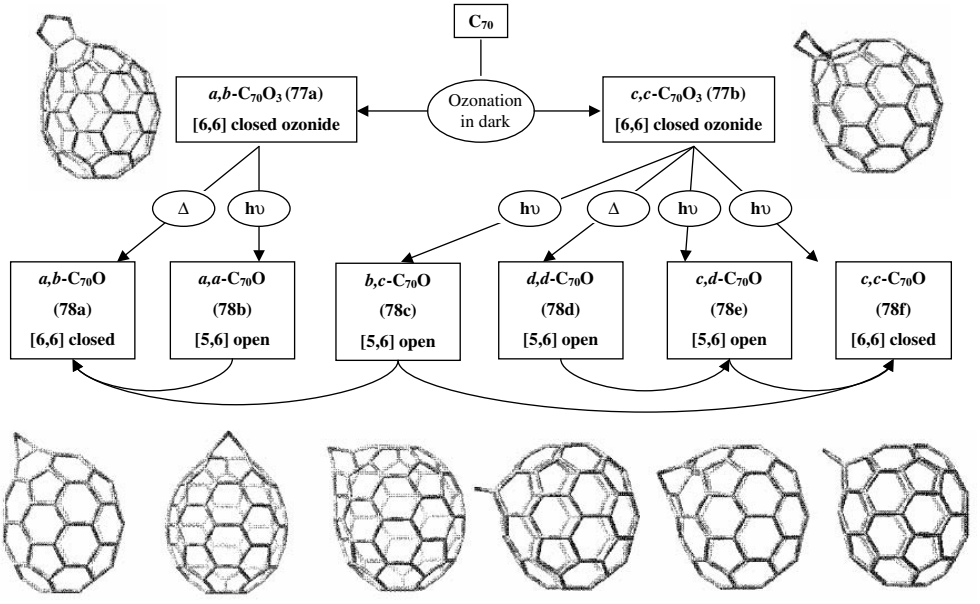

SCHEME 33 Thermolysis and photolysis of C_{70} ozonides **77a,b**.[146]

Photochemical Reactions Leading to Epoxides or Oxidoannulenes of C_{60}/C_{70}

The synthesis of fullerene epoxides via [2 + 1]-photocycloaddition of singlet oxygen has already been discussed (in the section "[2 + 1]-Photocycloaddition"). Alternatively, fullerene oxides can also be obtained by thermolysis or photolysis of the [6,6]-closed ozone adduct of C_{60} and C_{70}, namely $C_{60}O_3$ **75** and $C_{70}O_3$ **77**.[145,146] Thermolysis of $C_{60}O_3$ yields the fullerene epoxide with a [6,6]-closed structure. In contrast, photolysis resulted in the formation of the [5,6]-open oxidoannulene **76** with an ether structure (Scheme 32).[145]

In the case of the 1,3-diplar cycloaddition of ozone to C_{70}, formation of two isomeric forms of the [6,6]-closed C_{70} ozonide, *a,b*-$C_{70}O_3$ **77a** (C_1-symmetry) and *c,c*-$C_{70}O_3$ **77b** (C_s-symmetry), due to addition at the *a,b* or *c,c* bonds is observed (Scheme 33).[146] Upon thermolysis or photolysis of these ozonides, oxygen is released giving rise to the formation of different isomers of $C_{70}O$ by each route. The *a,b*-isomer of $C_{70}O_3$ resembles $C_{60}O_3$ in its unimolecular reactions, forming the epoxide **78a** through thermolysis and the oxidoannulene **78b** through photolysis. Extrusion of oxygen from the *c,c*-isomer **77b** leads to three isomeric oxidoannulenes, namely **78c**, **78d**, and **78e**, the latter arising from thermolysis, whereas the former are obtained by photolysis, showing that the dissociation pathways of *c,c*-$C_{70}O_3$ differ greatly from those of the *a,b*-isomer. In addition, epoxide **78f** is formed as a minor photoproduct. Photoisomerization of all the $C_{70}O$ oxidoannulenes to one of the C_{70} epoxides can be observed. Isomer *b,c*-$C_{70}O$

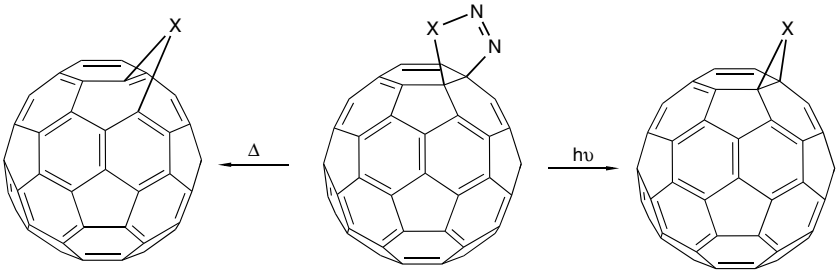

SCHEME 34 Thermolysis and photolysis of pyrazolino- (X = C) and triazolinofullerenes (X = N).

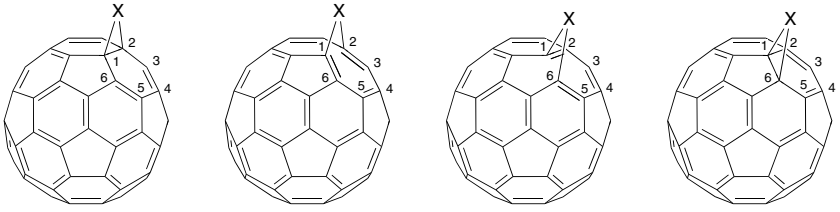

FIGURE 28.10 Possible and hypothetical structures of methano- and imino[60]fullerenes.

appears unique, as the photoisomerization leads directly to a mixture of both isomeric epoxides in similar amounts. Thus, in the presence of light, the two epoxides are the only stable monoadducts formed after ozonation of C_{70}.

Photochemical Reactions Leading to Methanofullerenes/Fulleroids and Aziridinofullerenes/Azafulleroids

Among various exohedral fullerene derivatives, fulleroid, a C_1 homologue with the [5,6]-open structure on C_{60}, has attracted much attention since the pioneering work of Wudl, Diederich and others[147] because of the ability to reform the original 60 π electron system and its mechanistically unique rearrangement to the methanofullerene (*vide infra*). Synthesis of fulleroids and their corresponding nitrogen analogues, the azafulleroids, can be achieved as the kinetic products by thermolysis of pyrazolino- or triazolinofullerenes obtained via thermal [3 + 2]-cycloaddition of diazo compounds or azides (Scheme 34). In contrast, the photochemical extrusion of N_2 leads preferably to the thermodynamically more stable [6,6]-closed isomers, namely, the methano- or aziridinofullerenes. The exclusive formation of cluster open [5,6]-bridged and closed [6,6]-bridged isomers is a consequence of the principle of the minimization of [5,6]-double bonds. Hypothetically open [6,6]- and closed [5,6]-bridged isomers would require the formation of three and two unfavorable [5,6]-bonds, respectively (Figure 28.10). No monoadduct with such a structure has yet been observed.

For example, irradiation of the C_{60} diazomethane adduct resulted in the formation of the [6,6]-closed cyclopropane $C_{61}H_2$, accompanied by the [5,6]-open fulleroid. The two isomers cannot be converted neither photochemically or thermally.[148] Upon photolysis and thermolysis of C_{70} pyrazolino derivatives **79a–c** synthesized by addition of diazomethane to C_{70}, four isomeric methylene derivatives of C_{70} are obtained. Irradiation of the pyrazolines leads to a mixture of the two isomeric [6,6]-bridged methanofullerenes **81a** and **81b**, while the thermal reaction gives rise to the formation of the [5,6]-bridged isomers **80a** and **80b** (Scheme 35).[147d]

Recent reports from Mattay's group have shown a fundamental equivalence in reactivity between pyrazolino- and triazolinofullerenes. Thermal extrusion of N_2 predominantly leads to the formation of the opened [5,6]-bridged azafulleroids, whereas the major products formed by photolysis of triazolinofullerenes are the closed [6,6]-bridged aziridinofullerenes.[149,150] In addition, upon photolysis, conversion

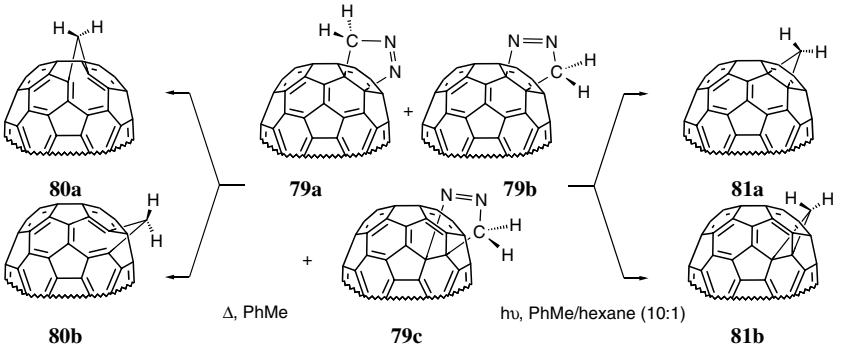

SCHEME 35 Thermolysis and photolysis of C_{70} pyrazolino derivatives **79**.

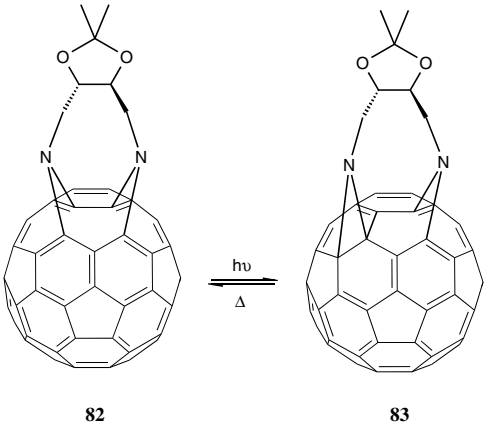

SCHEME 36 Conversion of bisazafulleroid **82** to the aza-aziridinofulleroid **83** upon irradiation.

of the azafulleroid to the aziridinofullerene was observed. Analogously, bistriazolinofullerenes can be converted to the corresponding aziridinofullerene and/or azafulleroid by thermal extrusion of nitrogen.[150,151] As the bisazafulleroids are thermally stable, no interconversion between the aziridinofullerene and the azafulleroid has been observed in general.[152] In contrast, a quantitative conversion of bisazafulleroid **82**, when exposed to light, leads to the aza-aziridinofulleroid **83**, in which the two imino groups add at both the [5,6]- and [6,6]-ring junctions (Scheme 36). Thermolysis of **83** resulted in conversion to **82**. These observations provided the first example of an interconversion between an aza- and an aziridinofulleroid.[153]

Similar rearrangements have been observed in the corresponding carbon analogues. For example, conversion of the fulleroids to the methanofullerenes upon thermolysis or photolysis was reported by Wudl et al. Irradiation of fulleroid **84** in deoxygenated *p*-xylene gives rise to a quantitative conversion to the methanofullerene **85** (Scheme 37).[102] Conversion of the methanofullerene to the fulleroid is not observed. Wudl proposed a di-π-methane rearrangement in the photochemical conversion of fulleroid **84** to the [6,6]-closed isomer **85** (Scheme 38).[102a] This was supported by the observations of Shevlin,[154] who demonstrated a photochemical step in the thermal rearrangement of a cyclopentylidene fulleroid to a methanofullerene. The photochemically induced azafulleroid–aziridinofullerene rearrangement also might be rationalized in terms of a di-π-methane rearrangement rather than a cleavage–cycloaddition process of a nitrene unit.[155]

Cheng et al. studied the nickel-promoted cycloaddition of bisalkynes to C_{60} in order to obtain cyclohexadiene derivatives of C_{60}.[143] Reports on the preparation of a cyclohexadiene ring via metal-catalyzed

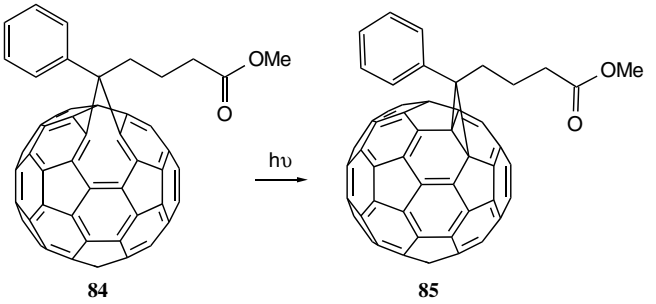

84 **85**

SCHEME 37 Conversion of fulleroid **84** to the methanofullerene **85** upon irradiation.

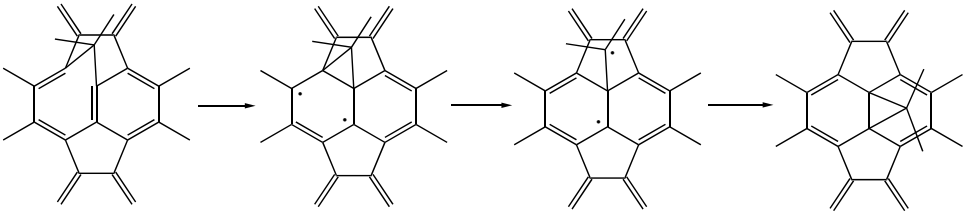

SCHEME 38 Mechanism for the conversion of fulleroids to methanofullerenes.

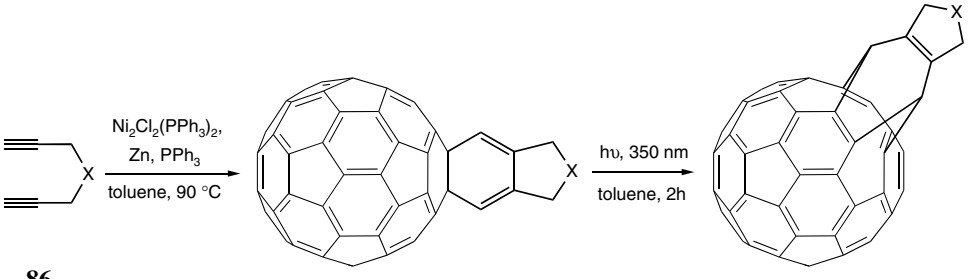

86 **87** **88**

SCHEME 39 Photolysis of cyclohexadiene-fused C_{60} derivatives.

cyclotrimerization of two alkynes with an alkene have appeared in the literature. Indeed, treatment of C_{60} with terminal 1,6-diynes **86a–e** afforded [2 + 2 + 2] bicyclohexadiene derivatives **87a–e**, which readily underwent photoinduced [4 + 4]-cycloaddition upon irradiation (350 nm) to give the corresponding bisfulleroids **88a–e** in excellent yields (Scheme 39). The formation of **88** is likely to proceed via an intramolecular photoinduced [4 + 4]-cycloaddition reaction of **87** to give an intermediate bismethanofullerene. This, upon subsequent CC bond cleavage and rearrangement, yielded the bisfulleroid product. It should be noted that the methano groups in the intermediate are across [5,6]-ring junctions of the C_{60} moiety. The rearrangement of the intermediate to **88** is expected in view of the fact that a bisfulleroid is generally more stable than the corresponding methanofullerene. Examples of such rearrangement are known.[147c]

Prior to the work of Cheng et al., Rubin et al. reported a similar [4 + 4]-photocyclization reaction.[156] Rubin has shown that a cyclohexadiene derivative underwent a very facile photochemically promoted rearrangement to the stable bridged bisfulleroid **92**. This process occurs via the initial [4 + 4]-photoadduct (not observed), which undergoes a thermally allowed [2 + 2 + 2]-cycloreversion to afford a bis-methano[12]annulene (Structure **92**). Alternatively, compound **92** can be obtained by photolysis of the allylic

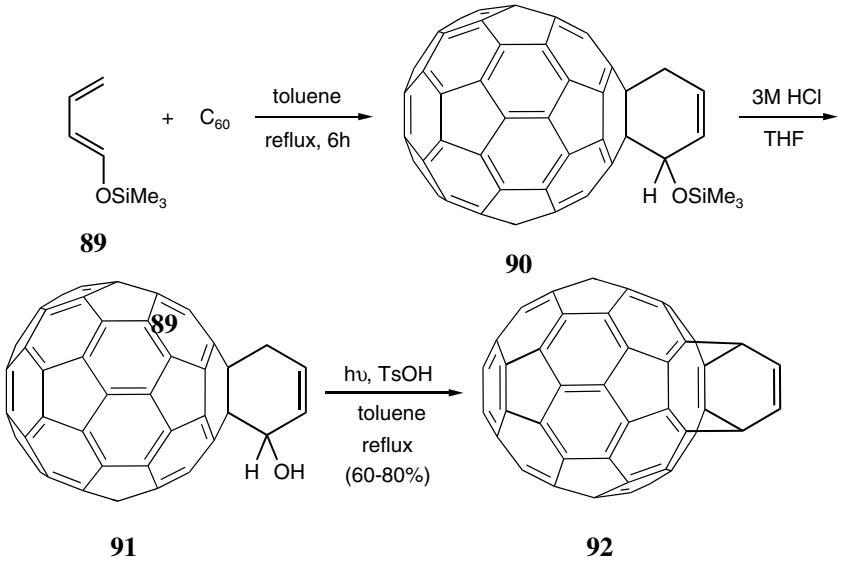

SCHEME 40 Double scission of a six-membered ring on the surface of C_{60} via [4+4]/[2+2+2] cycloaddition reactions.[156]

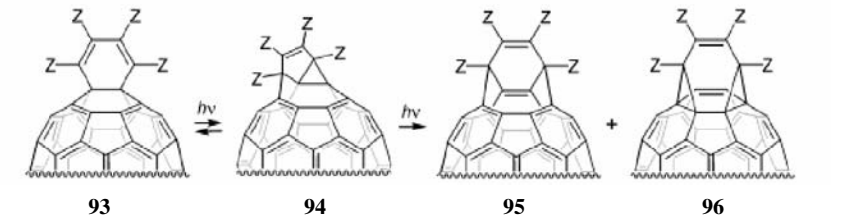

SCHEME 41 Photorearrangement of tetraakoxycarbonyl-substituted C_{60} cyclohexadiene derivatives **93** to bisfulleroids **95** and bismethanofullerenes **96**.[157]

alcohol **91** under reflux and acidic conditions in good yields (Scheme 40). The allylic alcohol is obtained by acidic work-up of the cycloadduct **90** formed by addition of a twofold excess of 1-((trimethylsilyl)oxy)-1,3-butadiene **89** to C_{60}. The structure of **92** was deduced from the high symmetry displayed by the ^{1}H and ^{13}C NMR spectra and the characteristic UV-vis spectrum. The x-ray structure of a cobalt complex formed by addition of $CpCo(CO)_2$ confirmed the suggested structure for compound **92**.[156]

Recently, Murata et al. described the photorearrangement of tetraalkoxycarbonyl-substituted cyclohexadiene derivatives of C_{60} **93**, yielding not only the well-known bisfulleroid **95** but also bismethanofullerene **96** (Scheme 41).[157] The existence of a labile and structurally new intermediate **94a** was observed in the reaction mixture. Although there still remained three possible structures as shown in Figure 28.11, only structure **94a** could be located as a local minimum. Furthermore, B3LYP chemical shifts of **94a** are in good agreement with the experimental values supporting this structure.

Formation of the unsymmetrical intermediate suggests that the rearrangement occurs *via* a different pathway than the previously described [4+4]/[2+2+2] mechanism. A possible mechanism includes the formation of an allylic biradical species bearing one [6,5]-closed structure. Then, isomerization from [6,5]-close to the [6,5]-open structure together with [6,6]-closed ring formation affords **94a**. Rearrangement of either the methanofullerene or fulleroid unit in **94a** into the other gives **95** and **96**.

Rubin et al.[158] also described the synthesis of C_{62}, a four-membered ring isomer of C_{60}. The dicarbonyl bridged bisfulleroid **100** seems to be a key precursor to C_{62}. Compound **100** was prepared by a stepwise

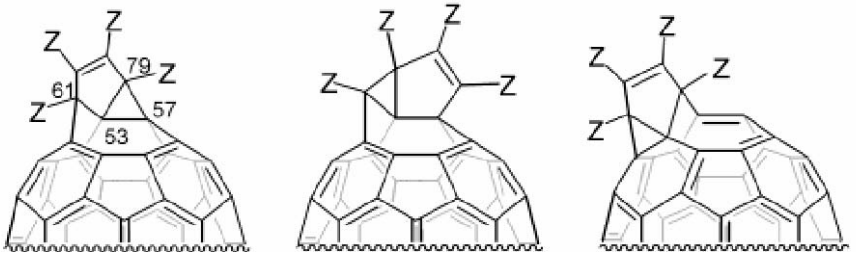

FIGURE 28.11 Possible structures for the intermediate **94** (Z = CO_2Me, $CO_2{}^tBu$).[157]

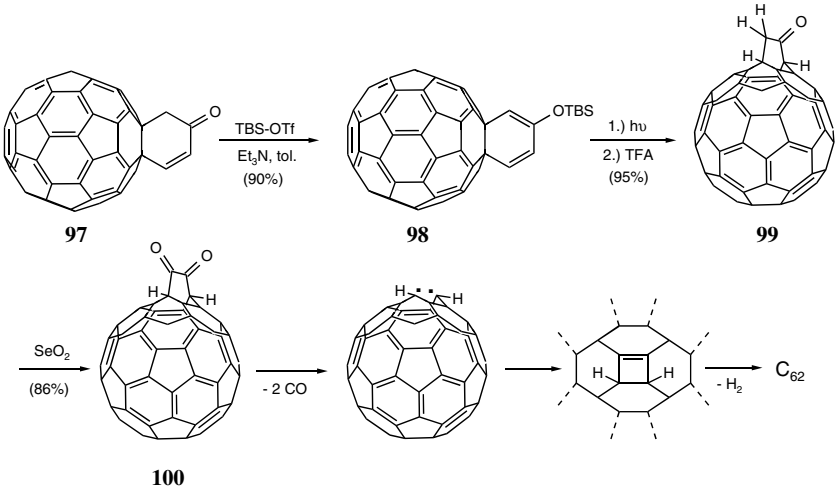

SCHEME 42 Formation of C_{62}.[158]

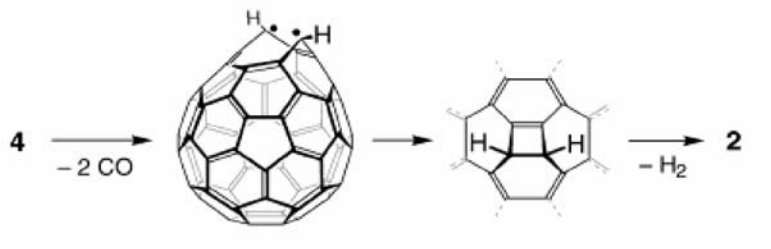

SCHEME 43

strategy (Scheme 42). Compound **97**[144] was converted to the corresponding silyl enol ether **98**. Visible light irradiation initiated its sequential [4 + 4]/[2 + 2 + 2] rearrangement to the bisfulleroid, which was deprotected with TFA to give the α-methylene ketone **99**. Oxidation of **99** results in the formation of the dicarbonyl compound **100**. Examples of photolytic α-fragmentation of 1,2-dicarbonyl compounds

with loss of two CO units have been described.[159] In the case of C_{62}, removal of both carbonyl groups under photochemical or thermal excitation should result in two adjacent radicals combining to the four-membered ring. Subsequently, facile dehydrogenation, which is characteristic for hydrofullerenes,[160] would give C_{62}.

28.5 Summary

In this review, we have given a brief summary of the photophysical behavior of C_{60} and C_{70}, followed by a detailed discussion of the photochemistry of these fullerenes and their derivatives. As shown in the last part of this review, photochemical reactions of C_{60}/C_{70} are very useful to obtain fullerene derivatives. In general, the photoinduced functionalization methods of C_{60}/C_{70} are based on electron transfer activation leading to radical ions or energy transfer processes either by direct excitation of the fullerenes or the reaction partner. In the latter case, both singlet and triplet species are involved, whereas most of the reactions of electronically excited fullerenes proceed via the triplet states due to their efficient intersystem crossing.

Acknowledgements

Financial support of our own research was provided by the Federal Department of Science, Research and Technology (BMBF) and the Deutsche Forschungsgemeinschaft (DFG). We also gratefully acknowledge the valuable contributions of Johannes Averdung, Christina Siedschlag, and Ingo Schlachter during their Ph.D. work and of Gregorio Torres-Garcia (Malaga University, Spain) and Waldemar Iwanek (University of Kielce, Poland) during their postdoctoral visits, as well as the helpful cooperation of the groups of Lothar Dunsch (IWF Dresden), Osamu Ito (Tohoku University, Sendai), Peter Luger (FU Berlin), Werner Abraham (HU Berlin), and Dirk M. Guldi (University of Notre Dame). Special thanks go to Heinrich Luftmann (University of Muenster), Matthias Letzel (University of Bielefeld), and Christian Wolff (University of Kiel) for their important contributions to mass spectrometry and NMR spectrometry, respectively. The support of Hoechst AG (now Aventis) during the early stages of our research is also gratefully acknowledged.

References

1. Kroto, H.W., Heath, J.R., O'Brien, S.C., Curl, R.F., and Smalley, R.E., C_{60}: buckminsterfullerene, *Nature*, 318, 162, 1985.
2. Krätschmer, W., Lamb, L.D., Fostiropoulus, K., and Huffmann, D.R., Solid C_{60}: a new form of carbon, *Nature*, 347, 354, 1990.
3. Hebard, A.F., Rosseinsky, M.J., Haddon, R.C., Murphy, D.W., Glarum, S.H., Palstra, T.T.M., Ramirez, A.P., and Kortan, A.R., Superconductivity at 18 K in potassium-doped fullerene (C_{60}), *Nature*, 350, 600, 1991.
4. Allemand, P.-M., Khemani, K.C., Koch, A., Wudl, F., Holczer, K., Donovan, S., Grüner, G., and Thompson, J.D., Organic molecular soft ferromagnetism in a fullerene C_{60}, *Science*, 253, 301, 1991.
5. Friedmann, S., DeCamp, D.L., Sijbesma, R., Srdanov, G., Wudl, F., and Kenyon, G.L., Inhibition of the HIV-1 protease by fullerene derivatives: model building studies and experimental verification, *J. Am. Chem. Soc.,* 115, 6506, 1993.
6. Boutorine, A.S., Tokuyama, H., Takasugi, M., Isobe, H., Nakamura, E., and Hélène, C., Fullerene–oligonucleotide conjugates — photoinduced sequence-specific DNA cleavage, *Angew. Chem. Int. Ed. Engl.,* 33, 2462, 1994.
7. Da Ros, T. and Prato, M., Medicinal chemistry with fullerenes and fullerene derivatives, *J. Chem. Soc., Chem. Commun.,* 663, 1999.
8. Signorini, R., Zerbetto, M., Meneghetti, M., Bozio, R., Maggini, M., De Faveri, C., Prato, M., and Scorrano, G., Optical limiting properties of soluble fullerene derivatives for incorporation in sol-gel materials, *J. Chem. Soc., Chem. Commun.,* 1891, 1996.

9. Sun, Y.-P. and Riggs, J.E., Non-linear absorptions in pendant [60]fullerene-polystyrene polymers, *J. Chem. Soc., Faraday Trans.,* 93, 1965–1970, 1997.
10. Sun, Y.-P., Riggs, J.E., and Bing, L., Optical limiting properties of [60]fullerene derivatives, *Chem. Mater.,* 9, 1268, 1997.
11. Taylor, R. and Walton, D.R.M., The chemistry of fullerenes**,** *Nature*, 363, 685, 1993.
12. Hirsch, A., *The Chemistry of the Fullerenes,* Georg Thieme, Stuttgart, 1994.
13. Diederich, F., Isaacs, L., and Philp, D., Synthesis, structures and properties of methanofullerenes, *Chem. Soc. Rev.,* 23, 243, 1994.
14. Hirsch, A., Addition-reactions of buckminsterfulllerene C_{60}, *Synthesis*, 895, 1995.
15. Hirsch, A., Ed., Fullerenes and related structures, *Top. Curr. Chem.,* 199, 1999.
16. Birkett, P.R., Fullerene chemistry, *Annu. Rep. Prog. Chem. Sect. A,* 95, 431, 1999.
17. Taylor, R., Surprises, serendipity and symmetry in fullerene chemistry, *Synlett*, 776, 2000
18. Reed, C.A. and Bolskar, R.D., Discrete fulleride anions and fullerenium cations, *Chem. Rev.,* 100, 1075, 2000.
19. Foote, C.S., Photophysical and photochemical properties of fullerenes, *Top. Curr. Chem.,* 169, 347, 1994.
20. Fukuzumi, S. and Guldi, D.M., Electron transfer chemistry of fullerenes, in *Electron Transfer in Chemistry,* Vol. II, Part. I, Balzani, V., Ed., Wiley-VCH, Weinheim, 2001, p. 270.
21. Mattay, J., Ulmer, L., and Sotzmann, A., Photophysics and photochemistry of fullerene and fullerene derivatives, in *Molecular and Supramolecular Photochemistry,* Vol. 8, Ramamurthy, V. and Schanze, K.S., Eds., Marcel Dekker, New York, 2001, p. 637.
22. Arbogast, J.W., Darmanyan, A.P., Foote, C.S., Rubin, Y., Diederich, F.N., Alvarez, M.M., Anz, S.J., and Whetten, R.L., Photophysical properties of C_{60}, *J. Phys. Chem.,* 95, 11, 1991.
23. Arbogast, J.W. and Foote, C.S., Photophysical properties of C_{70}, *J. Am. Chem. Soc.,* 113, 8886, 1991.
24. Ajie, H., Alvarez, M.M., Anz, S.J., Beck, D.R., Diederich, F.N., Fostiropoulos, K., Huffmann, D.R., Krätschmer, W., Rubin, Y., Schriver, K.E., Sensharma, D., and Whetten, R.L., Characterization of the soluble all-carbon molecules C60 and C70, *J. Phys. Chem.,* 94, 8630, 1990.
25. Leach, S., Vervloet, M., Desprès, A., Bréheret, E., Hare, J.P., Dennis, T.J., Kroto, H.W., Taylor, R., and Walton, D.R.M., Electronic spectra and transitions of the fullerene C_{60}, *Chem. Phys.,* 160, 451, 1992.
26. Sun, Y.P., Wang, P., and Hamilton, N.B., Fluorescence spectra and quantum yields of buckminsterfullerene (C_{60}) in room-temperature solutions. No excitation wavelength dependence, *J. Am. Chem. Soc.,* 115, 6378, 1993.
27. Catalán, J. and Elguero, J., Fluorescence of fullerenes (C_{60} and C_{70}), *J. Am. Chem. Soc.,* 115, 9249, 1993.
28. Ma, B. and Sun, Y.-P., Fluorescence spectra and quantum yields of [60]fullerene and [70]fullerene under different solvent conditions. A quantitative examination using a near-infrared–sensitive emission spectrometer, *J. Chem. Soc., Perkin Trans. 2,* 2157, 1996.
29. Kim, D., Lee, M., Suh, Y.D., and Kim, S.K., Observation of fluorescence emission from solutions of C_{60} and C_{70} and measurement of their excited-state lifetimes, *J. Am. Chem. Soc.,* 114, 4429, 1992.
30. Sibley, S.P., Argentine, S.M., and Francis, A.H., A photoluminescence study of the carbon sixty-atom and carbon seventy-atom molecules, *Chem. Phys. Lett.,* 188, 187, 1992.
31. Wang, Y., Characterization of the soluble all-carbon molecules C60 and C70**,** *J. Phys. Chem.,* 96, 764, 1992.
32. Sun, Y.P. and Bunker, C.E., Fluorescence of (5,6)-fullerene-C_{70} in room-temperature solutions — quantum yields and well-resolved spectra as a function of excitation wavelength, *J. Phys. Chem.*, 97, 6770, 1993.
33. Palewska, K., Sworakowski, J., Chojnacki, H., Meister, E.C., and Wild, U.P., A photoluminescence study of fullerenes: total luminescence spectroscopy of C60 and C70**,** *J. Phys. Chem.,* 97, 12167, 1993.

34. Williams, R.M. and Verhoeven, J.W., Fluorescence of fullerene C_{70} and its quenching by long-range intermolecular electron transfer, *Chem. Phys. Lett.,* 194, 446, 1992.
35. Watanabe, A., Ito, O., Watanabe, M., Saito, H., and Koishi, M., Excited states of C_{70} and the intersystem crossing process studied by picosecond time-resolved spectroscopy in the visible and near-IR region, *J. Phys. Chem.,* 100, 10518, 1996.
36. Ebbesen, T.W., Tanigaki, K., and Kuroshima, S., Excited-state properties of the carbon sixty-atom molecule, *Chem. Phys. Lett.,* 181, 501, 1991.
37. Tanigaki, K., Ebbesen, T.W., and Kuroshima, S., Picosecond and nanosecond studies of the excited-state properties of the carbon seventy-atom molecule, *Chem. Phys. Lett.,* 185, 189, 1991.
38. Lee, M., Song, O.-K., Seo, J.-C., Kim, D., Suh, Y.D., Jin, S.M., and Kim, S.K., *Chem. Phys. Lett.,* 196, 325, 1992.
39. Wasielewski, M.R., O'Neil, M.P., Lykke, K.R., Pellin, M.J., and Gruen, D.M., Triplet states of fullerenes C_{60} and C_{70}: electron paramagnetic resonance spectra, photophysics and electronic structures, *J. Am. Chem. Soc.,* 113, 2774, 1991.
40. Palit, D.K., Sapre, A.V., Mittal, J.P., and Rao, C.N.R., Photophysical properties of the fullenes, C_{60} and C_{70}, *Chem. Phys. Lett.,* 195, 1, 1992.
41. Fraelich, M.R. and Weismann, R.B., Triplet-states of C_{60} and C_{70} in solution — long intrinsic lifetimes and energy pooling, *J. Phys. Chem.,* 97, 11145, 1993.
42. Hung, R.R. and Grabowski, J.J., A precise determination of the triplet energy of carbon (C60) by photoacoustic calorimetry, *J. Phys. Chem.,* 95, 6073, 1991.
43. Sension, R.J., Phillips, C.M., Szarka, A.Z., Romanow, W.J., McGhie, A.R., McCauley, J.P., Jr., Smith, A.B., III, and Hochstrasser, R.M., Transient absorption studies of carbon (C60) in solution, *J. Phys. Chem.,* 95, 6075, 1991.
44. Kajii, Y., Nakagawa, T., Suzuki, S., Achiba, Y., Obi, K., and Shibuya, K., Transient absorption, lifetime and relaxation of the carbon sixty-atom molecule in the triplet state, *Chem. Phys. Lett.,* 181, 100, 1991.
45. Biczok, L., Linschitz, H., and Walter, R.I., Extinction coefficients of C_{60} fullerene triplet and anion radical and one-electron reduction of the triplet by aromatic donors, *Chem. Phys. Lett.,* 195, 339, 1992.
46. Dimitrijevic, N.M. and Kamat, P.V., Triplet excited state behavior of fullerenes: pulse radiolysis and laser flash photolysis of fullerenes (C60 and C70) in benzene, *J. Phys. Chem.,* 96, 4811, 1992.
47. Bensasson, R.V., Hill, T., Lambert, C., Land, E.J., Leach, S., and Truscott, T.G., Pulse radiolysis study of buckminsterfullerene in benzene solution. Assignment of the C_{60} triplet–triplet absorption spectrum, *Chem. Phys. Lett.,* 201, 326, 1993.
48. Bensasson, R.V., Hill, T., Lambert, C., Land, E.J., Leach, S., and Truscott, T.G., Triplet state absorption studies of C_{70} in benzene solution, *Chem. Phys. Lett.,* 206, 197, 1993.
49. McLean, A.J., McGarvey, D.J., Truscott, T.G., Lambert, C.R., and Land, E.J., Effect of oxygen-enhanced intersystem crossing on the observed efficiency of formation of singlet oxygen, *J. Chem. Soc., Faraday Trans.,* 86, 3075, 1990.
50. Zeng, Y., Biczok, L., and Linschitz, H., External heavy atom induced phosphorescence emission of fullerenes: the energy of triplet C60, *J. Phys. Chem.,* 96, 5237, 1992.
51. Gevaert, M. and Kamat, P., Photochemistry of fullerenes: excited-state behavior of C60 and C70 and their reduction in poly(methyl methacrylate) films. V. *J. Phys. Chem.,* 96, 9883, 1992.
52. Williams, R.M., Zwier, J.M., and Verhoeven, J.W., Photoinduced intramolecular electron transfer in a bridged C_{60} (acceptor)-aniline (donor) system. Photophysical properties of the first "active" fullerene diad, *J. Am. Chem. Soc.,* 117, 4093, 1995.
53. Closs, G.L., Gautam, P., Zhang, D., Krusic, P.J., Hill, S.A., and Wassermann, E., Steady-state and time-resolved direct detection EPR spectra of fullerene triplets in liquid solution and glassy matrixes: evidence for a dynamic Jahn–Teller effect in triplet C60, *J. Phys. Chem.,* 96, 5228, 1992.
54. Bennati, M., Grupp, A., Mehring, M., Dinse, K.-P., and Fink, J., Pulsed EPR on the photoexcited triplet state of C_{60} fullerene, *Chem. Phys. Lett.,* 200, 440, 1992.

55. Zhang, D., Norris, J.R., Krusic, P.J., Wassermann, E., Chen, C.C., and Lieber, C.M., Time-resolved EPR and Fourier transform EPR study of triplet fullerene C60: determinations of T1 and the carbon-13 hyperfine coupling constant, *J. Phys. Chem.,* 97, 5886, 1993.
56. Steren, C.A., Levsten, P.R., van Willigen, H., Linschitz, H., and Biczok, L., FT-EPR study of triplet state fullerene C_{60}. Spin dynamics and electron transfer quenching, *Chem. Phys. Lett.*, 204, 23, 1993.
57. Steren, C.A., van Willigen, H., and Dinse, K.-P., Spin dynamics of C60 triplets, *J. Phys. Chem.,* 98, 7464, 1994.
58. Bennati, M., Grupp, A., and Mehring, M., Pulsed EPR on the photoexcited triplet state of C_{60}, *Synth. Met.,* 86, 2321, 1997.
59. Terazima, M., Sakurada, K., Hirota, N., Shinohara, H., and Saito, Y., Dynamics of fullerene C70 in the lowest excited triplet state at low temperatures, *J. Phys. Chem.,* 97, 5447, 1993.
60. Goudsmit, G.-H. and Paul, H., Time-resolved EPR investigation on triplet state C_{60}. Triplet–triplet annihilation, CIDEP and quenching by nitroxide radicals, *Chem. Phys. Lett.,* 208, 73, 1993.
61. Levanon, H., Meiklayr, V., Michaeli, S., and Gamliel, D., Triplet state and dynamics of photoexcited C_{70}, *J. Am. Chem. Soc.,* 115, 8722, 1993.
62. Wilson, S.R., Kaprinidis, N., Wu, Y., and Schuster, D.I., A new reaction of fullerenes: [2 + 2] photocycloaddition of enones, *J. Am. Chem. Soc.,* 115, 8495, 1993.
63. Taylor, R., *The Chemistry of Fullerenes,* World Scientific, Singapore, 1995.
64. Karfunkel, H.R. and Hirsch, A., Prediction of the nucleophilic addition products of fullerene C_{70}, *Angew. Chem. Int. Ed. Engl.,* 31, 1468, 1992.
65. Hirsch, A., Lamparth, I., and Karfunkel, H.R., Fullerene chemistry in three dimensions: isolation of seven regioisomeric bisadducts and chiral trisadducts of C_{60} and di(ethoxycarbonyl)methylene, *Angew. Chem.,* 106, 453, 1994.
66. Taylor, R., Nomenclature and terminology of fullerenes: a preliminary survey, *Pure Appl. Chem.,* 69, 1411, 1997.
67. Taylor, R., C_{60}, C_{70}, C_{76}, C_{78} and C_{84}: numbering, π-bond order calculations and addition pattern considerations, *J. Chem. Soc., Perkin Trans. 2,* 813, 1993.
68. Schuster, D.I., Lem, G., Jensen, A.W., Courtney, S.H., and Wilson, S.R., Addition of alcohols and hydrocarbon to fullerenes by photosensitized electron transfer, in *Fullerenes, Recent Advances in the Chemistry and Physics of Fullerenes and Related Materials, Vol. 2,* Ruoff, R.S. and Kadish, K.M., Eds., The Eletrochemical Society, Pennington, NJ, 1995, p. 441.
69. Siedschlag, C., Luftmann, H., Wolff, C., and Mattay, J., Functionalization of [60]fullerene by photoinduced electron transfer (PET): synthesis of 1-substituted 1,2-dihydro[60]fullerenes, *Tetrahedron,* 53, 3587, 1997.
70. Siedschlag, C., Luftmann, H., Wolff, C., and Mattay, J., [60]Fullerene radical cation: reactions and mechanism, *Tetrahedron,* 55, 7805, 1999.
71. Schuster, D.I., Lem, G., Jensen, A.W., Hwang, E., Safanov, I., Courtney, S.H., and Wilson, S.R., New photochemical reactions of fullerenes in *Fullerenes, Recent Advances in Chemistry and Physics of Fullerenes and Related Materials,* Vol. 3, Ruoff, R.S. and Kadish, K.M., Eds., The Eletrochemical Society, Pennington, NJ, 1996, p. 287.
72. Mattay, J., Torres-Garçia, G., Averdung, J., Wolff, C., Schlachter, I., Luftmann, H., Siedschlag, C., Luger, P., and Ramm, M., Progress in fullerene chemistry: exohedral functionalization of first and second generation and a new approach to aza-heterofullerenes, *J. Phys. Chem. Solids,* 58, 1929, 1997.
73. Dunsch, L., Ziegs, F., Siedschlag, C., and Mattay, J., ESR spectroscopy of the C_{60} cation produced by photoinduced electron transfer, *Chem.-Eur. J.,* 6, 3547, 2000.
74. (a) Mattay, J., Siedschlag, C., Torres-Garçia, G., Ulmer, L., Wolff, C., Fujitsuka, M., Watanabe, A., Ito, O., and Luftmann, H., Photoreactions with fullerenes, in *Recent Advances in the Chemistry and Physics of Fullerenes and Related Materials,* Vol. 14, Ruoff, R.S. and Kadish, K.M., Eds., The Eletrochemical Society, Pennington, NJ, 1997, p. 326; (b) Siedschlag, C., Torres-Garçia, G., Wolff, C., Mattay, J., Fujitsuka, M., Watanabe, A., Ito, O., Dunsch, L., Ziegs, F., and Luftmann, H., Radical ions in fullerene chemistry, in *Recent Advances in Chemistry and Physics of Fullerenes and Related*

Materials, Vol. 42, Ruoff, R.S. and Kadish, K.M., Eds., The Electrochemical Society, 1997, p. 296; (c) Siedschlag, C., Torres-Garçia, G., Wolff, C., Mattay, J., Fujitsuka, M., Watanabe, A., Ito, O., Dunsch, L., Ziegs, F. ,and Luftmann, H., Radical ions in fullerene chemistry, *J. Inf. Rec.,* 24, 265, 1998.

75. Lem, G., Schuster, D.I., Courtney, S.H., Lu, Q., and Wilson, S.R., Addition of alcohols and hydrocarbons to fullerenes by photosensitized electron transfer, *J. Am. Chem. Soc.,* 117, 554, 1995.
76. Tokuyama, H., Isobe, H., and Nakamura, E., Photoaddition of silyl ketene acetal to [60]fullerene. Synthesis of α-fullerene-substituted carboxylic esters, *J. Chem. Soc., Chem. Commun.,* 2753, 1994.
77. Yamago, S., Takeichi, A., and Nakamura, E., Synthesis and [2 + 2] cycloaddition of dimethyleneketene acetals. Reaction with C_{60} and facile hydrolysis of the CC bond connected to C_{60}, *J. Am. Chem. Soc.,* 116, 1123, 1994.
78. (a) Mikami, K. and Matsumoto, S., Light-catalyzed carbon–carbon bond formation of C_{60} with ketene silyl acetals: fullerene functionalization chemistry, *Synlett*, 229, 1995; (b) Mikami, K., Matsumoto, S., Ishida, I., Takamuku, S., Suenobu, T., and Fukuzumi, S., Addition of ketene silyl acetals to the triplet excited state of C_{60} via photoinduced electron transfer leading to the fullereneacetates, *J. Am. Chem. Soc.,* 117, 11134, 1995.
79. Fukuzumi, S., Fujita, M., Otera, J., and Fujita, Y., Electron-transfer oxidation of ketene silyl acetals and other organosilanes. The mechanistic insight into Lewis acid mediated electron transfer, *J. Am. Chem. Soc.,* 114, 10271, 1992.
80. See refs. 4, 5 in Mikami, K., Matsumoto, S., Tonoi, T., Suenobu, T., Ishida, A., and Fukuzumi, S., *Synlett*, 85, 1997.
81. Mikami, K., Matsumoto, S., Tonoi, T., Suenobu, T., Ishida, A., and Fukuzumi, S., Addition reaction of allylic stannanes to the triplet excited state of C_{60} via photoinduced electron transfer process leading to asymmetric hybridization chemistry for fullerene terpenoid, *Synlett*, 85, 1997.
82. Fukuzumi, S., Fujita, M., and Otera, J., Regio-reversal in the thermal and photochemical reduction of 10-methylacridinium ion by allylic silanes and stannanes, *J. Chem. Soc., Chem. Commun.,* 1536, 1993.
83. Fukuzumi, S., Suenobu, T., Fujitsuka, M., Ito, O., Tonoi, T., Matsumoto, S., and Mikami, K., Addition of group 14 organometallic compounds to C_{60} via photoinduced electron transfer. Direct detection of radical ion pair intermediates, *J. Organomet. Chem.,* 574, 32, 1999.
84. (a) Wudl, F., Hirsch, A., Khemani, C., Suzuki, T., Allemand, P.-M., Koch, A., Eckert, H., Srdanov, G., and Webb, H.M., Survey of chemical reactivity of C_{60}, electrophile and dienopolarophile par excellence, in *Fullerenes: Synthesis, Properties and Chemistry of Large Carbon Clusters*, Hammond, G.S. and Kuck, V.J., Eds., American Chemical Society Symposium Series 481, 1992, p. 161; (b) Seshadri, R., Govindaraj, A., Nagarajan, R., and Rao, C.N.R., Addition of amines and halogens to fullerenes C_{60} and C_{70}, *Tetrahedron Lett.,* 33, 2069, 1992; (c) Hirsch, A., Li, Q., and Wudl, F., Hydrogen migration on the surface of the fullerene $C_{60}H_6(N(CH_2CH_2)_2O)_6$, *Angew. Chem. Int. Ed. Engl.,* 30, 1309, 1991.
85. Seshadri, R., Rao, C.N.R., Pal, H., Mukherjee, T., and Mittal, J.P., Interaction of C_{60} and C_{70} with aromatic amines in the ground and excited states. Evidence for fullerene–benzene interaction in the ground state, *Chem. Phys. Lett.,* 205, 395, 1993.
86. Sun, Y.-P., Ma, B., and Lawson, G.E., Electron donor–acceptor interactions of fullerenes C~6~0 and C~7~0 with triethylamine, *Chem. Phys. Lett.,* 95, 57, 1995.
87. Skiebe, A., Hirsch, A., Klos, H., and Gotschy, B., [DBU]C_{60}. Spin paring in a fullerene salt, *Chem Phys. Lett.,* 220, 138, 1994.
88. Sension, R.J., Szarka, A.Z., Smith, G.R., and Hochstrasser, R.M., Ultrafast photoinduced electron transfer to carbon sixty-atom molecule, *Chem. Phys. Lett.,* 185, 179, 1991.
89. (a) Sun, Y.P. and Ma. B., Solvent effects on formation and decay of electron donor–acceptor exciplex of C_{70} and *N,N*-diethylaniline — fluorescence quenching due to solvent polarity and polarizibality**,** *Chem Phys. Lett.,* 236, 285, 1995; (b) Wang, Y. and Cheng, L.-T., Nonlinear optical properties of fullerenes and charge-transfer complexes of fullerenes, *J. Phys. Chem.,* 96, 1530, 1992.

90. Ghosh, H.N., Pal, H., Sapre, A.V., and Mittal, J.P., Charge recombination reactions in photoexcited C_{60}-amine complexes studied by picosecond pump probe spectroscopy, *J. Am. Chem. Soc.,* 115, 11722, 1993.
91. Kajii, Y., Takeda, K., and Shibuya, K., Photochemical reaction of C_{60} in the presence of triethylamine in toluene, *Chem. Phys. Lett.,* 204, 140, 1993.
92. Liou, K.-F. and Cheng, C.-H., Photoinduced reactions of tertiary amines with [60]fullerene. Addition of an α-C-H bond of amines to [60]fullerene, *J. Chem. Soc., Chem. Commun.,* 1423, 1996.
93. Zhang, W., Su, Y., Gan, L., Jiang, J., and Huang, C., Photolysis of C_{60} with cyclic amino acids: preparation of dihydrofullerenes by decarboxylation, *Chem. Lett.,* 1007, 1997.
94. Gan, L., Jiang, J., Zhang, W., Su, Y., Shi, Y., Huang, C., Pan, J., Lü, M., and Wu, Y., Synthesis of pyrrolidine ring-fused fullerene multicarboxylates by photoreaction, *J. Org. Chem.,* 63, 4240, 1998.
95. Okada, K., Okubo, K., and Oda, M., A simple and convenient photo-decarboxylation method of intact carboxylic acids in the presence of aza aromatic compounds, *J. Photochem. Photobiol. A: Chem.,* 57**,** 265, 1991.
96. Wang, N.-X., Photochemical addition reactions of [60]fullerene with 1,2-ethylenediamine and piperazine, *Tetrahedron,* 58, 1017, 2002.
97. Fukuzumi, S., Suenobu, T., Patz, M., Hirasaka, T., Itoh, S., Fujitsuka, M., and Ito, O., Selective one-electron oxidation and two-electron reduction of C_{60} with NADH and NAD dimer analogues via photoinduced electron transfer, *J. Am. Chem. Soc.,* 120, 8060, 1998.
98. Fukuzumi, S., Suenobu, T., Hirasaka, T., Sakurada, N., Arakawa, R., Fujitsuka, M., and Ito, O., Enhanced reactivity of C_{70} in the photochemical reactions with NADH and NAD dimer analogues as compared to C_{60} via photoinduced electron transfer, *J. Phys. Chem. A,* 103, 5935, 1999.
99. (a) Hirsch, A., Soi, A., and Karfunkel, H.R., Titration of C_{60}: a synthesis of organofullerenes, *Angew. Chem. Int. Ed. Engl.,* 31, 766, 1992; (b) Kitagawa, T., Tanaka, T., Takata, Y., and Takeuchi, K., Regiospecific coordination of *tert*-butylfulleride ion and 1,4-dicyclopropyltropylium ion. Synthesis of a dialkyldihydrofullerene having a heterolytically dissociative carbon–carbon σ-bond, *J. Org. Chem.,* 60, 1490, 1995; (c) Tanaka, T., Kitagawa, T., Komatsu, K., and Takeuchi, K., Synthesis of a hydrocarbon salt having a fullerene framework, *J. Am. Chem. Soc.,* 119, 9313, 1997.
100. Banim, F., Cardin, D.J., and Heath, P., Proton migration on the [60]fullerene cage of 1-*tert*-butyl-1,4-dihydro[60]fullerene to yield the 1,2-isomer, *J. Chem. Soc., Chem. Commun.,* 60, 1997.
101. Akasaka. T., Liu, M.T.H., Niino, Y., Maeda, Y., Wakahara, T., Okamura, M., Kobayashi, K., and Nagase, S., Photolysis of diazirines in the presence of C_{60}: a chemical probe for carbene/diazomethane partitioning, *J. Am. Chem. Soc.,* 122, 7134, 2000.
102. (a) Jansen, R.A.J., Hummelen, J.C., and Wudl, F., Photochemical fulleroid to methanofullerene conversion via the di-π-methane (Zimmermann) rearrangement, *J. Am. Chem. Soc.,* 117, 544, 1995; (b) Gonzalez, R., Hummelen, J.C., and Wudl, F., The specific acid-catalyzed and photochemical isomerization of a robust fulleroid to a methanofullerene, *J. Org. Chem.,* 60, 2618, 1995.
103. Creegan, K.M., Robbins, J.L., Robbins, W.K., Millar, J.M., Sherwood, R.D., Tindall, P.J., Cox, D.M., Smith, A.B., III, McCauley, J.P., Jr., Jones, D.R., and Gallagher, R.T., Synthesis and characterization of $C_{60}O$, the first fullerene epoxide, *J. Am. Chem. Soc.,* 114, 1103, 1992.
104. Schuster, D.I., Baran, P.S., Hatch, R.K., Khan, A.U., and Wilson, S.R., The role of singlet oxygen in the photochemical formation of $C_{60}O$, *J. Chem. Soc., Chem. Commun.,* 2493, 1998.
105. Juha, L., Hamplová, V., Kodymová, J., and Spalek, A., Reacitvity of fullerenes with chemically generated singlet oxygen, *J. Chem. Soc., Chem. Commun.,* 1177, 1994.
106. Heymann, D. and Chibante, L.P.F., Photo-transformations of C_{60}, C_{70}, $C_{60}O$ and $C_{60}O_2$, *Chem. Phys. Lett.,* 207, 339, 1993.
107. Smith, A.B., III, Strongin, R.M., Brard, L., Furst, G.T., Atkins, J.H., Romanow, W.J., Saunders, M., Jiménez-Vázquez, H.A., Owens, K.G., and Goldschmidt, R.J., Synthesis and characterization of the first $C_{70}O$ epoxides. Utilization of ^{3}He NMR in analysis of fullerene derivatives, *J. Org. Chem.,* 61, 1904, 1996.

108. (a) Prato, M., Li, Q.C., Wudl, F., and Lucchini, V., Addition of azides to C_{60}: synthesis of azafulleroids, *J. Am. Chem. Soc.,* 115, 1148, 1993; (b) Banks, M.R., Cadogan, J.I.G., Gosney. I., Hodgson, P.K.G., Langridge-Smith, P.R.R., and Rankin, D.W.H., Bis-functionalization of C_{60} via thermal rearrangement of an isolable fulleroaziridine bearing a solubilizing supermesityl ester moiety, *J. Chem. Soc., Chem. Commun.,* 1365, 1994; (c) Kuwashima, S., Kubota, K., Kushida, K., Ishida, T., Ohashi, M., and Nogami, T., Synthesis and structure of nitrene-C_{60} adduct, C_{60}NPHTH (PHTH = phthalimido), *Tetrahedron Lett.,* 34, 4371, 1994; (d) Ishida, T., Tanaka, K., and Nogami, T., *Chem. Lett.,* 561, 1994.
109. Yan, M., Cai, S.X., and Keana, J.F.W., Photochemical and thermal reactions of C_{60} with *N*-succinimidyl 4-azido-2,3,5,6-tetrafluorobenzoate: a new method for functionalization of C_{60}, *J. Org. Chem.,* 59, 5951, 1994.
110. Poe, R., Schnapp, K., Young, M.J.T., Grayzar, J., and Platz, M.S., Chemistry and kinetics of singlet (pentafluorophenyl)nitrene, *J. Am. Chem. Soc.,* 114, 5054, 1992.
111. Averdung, J., Mattay, J., Jacobi, D., and Abraham, W., Cycloadditions 48. Addition of photochemically generated acylnitrenes to C_{60} — synthesis of fulleroaziridines and thermal rearrangement to fullerooxazoles, *Tetrahedron,* 51, 2543, 1995.
112. Averdung, J. and Mattay, J., Cycloadditions 47. Cycloaddition of 1,8-dehydro-naphthalene to [60]fullerene in benzene solution — a new functionalization of C_{60} by *in situ* generated 6b,10a-dihydrofluoranthene, *Tetrahedron Lett.,* 35, 6661, 1994.
113. (a) Zhang, X. and Foote, C.S., [2 + 2] Cycloaddition of fullerenes: synthesis and characterization of $C_{62}O_3$ and $C_{72}O_3$, the first fullerene anhydrides, *J. Am. Chem. Soc.,* 117, 4271, 1995; (b) Zhang, X., Fan, A., and Foote, C S., [2 + 2] Cycloaddition of fullerenes with electron-rich alkenes and alkynes, *J, Org. Chem.,* 61, 5456, 1996.
114. (a) Vassilikogiannakis, G. and Orfanopoulos, M., Stereochemistry and isotope effects of the [2 + 2] photocycloaddition of arylalkenes to C_{60}. A stepwise mechanism, *J. Am. Chem. Soc.,* 119, 7394, 1997; (b) Vassilkogiannakis, G. and Orfanopoulos, M., [2 + 2] Photocycloaddition of *cis/trans*-4-propenylanisole to C_{60}. A step-wise mechanism, *Tetrahedron Lett.,* 38, 4323, 1997.
115. Vassilikogiannakis, G., Chronakis, N., and Orfanopoulos, M., A new [2 + 2] functionalization of C_{60} with alkyl-substituted 1,3-butadienes: a mechanistic approach. Stereochemistry and isotope effects, *J. Am. Chem. Soc.,* 120, 9911, 1998.
116. Schuster, D.I., Cao, J., Kaprinidis, N., Wu, Y., Jensen, A., Lu, Q., Wang, H., and Wilson, S.R., [2 + 2] Photocycloaddition of cyclic enones to C_{60}, *J. Am. Chem. Soc.,* 118, 5639, 1996.
117. Vassilikogiannakis, G. and Orfanopoulos, M., Regio- and stereoselectivity of the [2 + 2] photocycloaddition of acyclic enones to C60, *J. Org. Chem.,* 64, 3392, 1999.
118. Jensen, A.W., Khong, A., Saunders, M., Wilson, S.R., and Schuster, D.I., Photocycloaddition of cyclic 1,3-diones to C_{60}, *J. Am. Chem. Soc.,* 119, 7303, 1997.
119. Wilson, S.R., Wu, Y., Kaprinidis, N.A., and Schuster, D.I., Resolution of enantiomers of *cis*- and *trans*-fused C_{60}-enone [2 + 2] photoadducts, *J. Org. Chem.,* 58, 6548, 1993.
120. For a recent review, see: Schuster, D.I., Lem, G., and Kaprinidis, N., New insights into an old mechanism: [2 + 2] photocycloaddition of enones to alkenes, *Chem. Rev.,* 93, 3, 1993.
121. Hatzimarinaki, M., Vassilikogiannakis, G., and Orfanopoulos, M., Stereochemistry and steric isotope effect on the [2 + 2] photocycloaddition of β,β-dimethyl-*p*-methoxystyrene to C_{60}: the nature of the transition state structures, *Tetrahedron Lett.,* 41, 4667, 2000.
122. (a) Maggini, M., Scorrano, G., and Prato, M., Addition of azomethine ylides to C_{60}: synthesis, characterization and functionalization of fullerene pyrrolidines, *J. Am. Chem. Soc.,* 115, 9798, 1993; (b) Novello, F., Prato, M., Da Ros, T., De Amici, M., Bianco, A., Toniolo, C., and Maggini, M., Stereoselective additions to [60]fullerene, *J. Chem. Soc., Chem. Commun.,* 903, 1996; (c) Prato, M., Maggini, M., Giacometti, C., Scorrano, G., Sandona, G., and Famia, G., Synthesis and electrochemical properties of substituted fulleropyrrolidines, *Tetrahedron,* 52, 5221, 1996.
123. (a) Zhou, D., Tan, H., Luo, C., Gan, L., Huang, C., Pan, J., Lu, M., and Wu, Y., Fullerene induced C-N bond breaking and formation: synthesis of fullerene pyrrolidine and methanofullerene sarcosine

derivatives by photochemical addition of sarcosine ester to C_{60}, *Tetrahedron Lett.,* 36, 9169, 1995; (b) Gan, L., Zhou, D., Luo, C., Tan, H., Huang, C., Lu, M., Pan, J., and Wu, Y., Synthesis of fullerene amino acid derivatives by direct interaction of amino acid ester with C_{60}, *J. Org. Chem.,* 61, 1954, 1996.

124. Bernstein, R. and Foote, C.S., Singlet oxygen involvement in the photochemical reaction of C60 and amines. Synthesis of an alkyne-containing fullerene, *J. Phys. Chem. A,* 103, 7244, 1999.
125. Lawson, G.E., Kitaygorodskiy, A., and Sun, Y.-P., Photoinduced electron-transfer reactions of [60]fullerene with triethylamine, *J. Org. Chem.,* 64, 5913, 1999.
126. Averdung, J., Albrecht, E., Lauterwein, J., Luftmann, H., Mattay, J., Mohn, H., Müller, W.H., and ter Meer, H.-U., Photoreactions with [60]fullerene. [3 + 2] photocycloaddition of 2,3-diphenyl-2*H*-azirine, *Chem. Ber.,* 127, 787, 1994.
127. Averdung, J. and Mattay, J., Exohedral functionalization of [60]fullerene by [3 + 2] cycloadditions: synthesis and chemical properties of triazolino[60]fullerenes and 1,2-(3,4-dihydro-2*H*-pyrrolo)[60]fullerenes, *Tetrahedron,* 52, 5407, 1996.
128. (a) Arnold, B.J., Mellows, S.M., Sammes, P.G., and Wallace, T.W., Photochemical reactions. II. Cycloaddition reactions of photoenols from 2-methylbenzaldehyde and realted systems, *J. Chem. Soc., Perkin Trans. 1,* 401, 1974; (b) Sammes, P.G., Photoenolization, *Tetrahedron,* 32, 405, 1976.
129. Tomioka, H., Ichihashi, M., and Yamamoto, K., Photolysis of *o*-methylbenzophenone in the presence of C_{60} — facile cleavage of the C-C bond connected to C_{60}, *Tetrahedron Lett.,* 36, 5371, 1995.
130. (a) O-kawa, K., Nakamura, Y., and Nishimura, J., Facile modification of [60]fullerene by photochemically generated hydroxy-*o*-quinodimethane derivatives, *Tetrahedron Lett.,* 41, 3103, 2000; (b) Nakamura, Y., O-kawa, K., Minami, S., Ogawa, T., Tobita, S., and Nishimura, J., Photochemical synthesis, conformational analysis and transformation of [60]fullerene-*o*-quinodimethane adducts bearing a hydroxy group, *J. Org. Chem.,* 67, 1247, 2002.
131. Mikami, K., Matsumoto, S., Tonoi, T., and Okubo, Y., Solid state photochemistry for fullerene functionalization: solid state photoinduced electron transfer in the Diels–Alder reaction with anthracenes, *Tetrahedron Lett.,* 39, 3733, 1998.
132. Mikami, K., Matsumoto, S., Okubo, Y., Fujitsuka, M., Ito, O., Suenobu, T., and Fukuzumi, S., Stepwise bond formation in photochemical and thermal Diels–Alder reactions of C_{60} with Danishefsky's dienes, *J. Am. Chem. Soc.,* 122, 2236, 2000.
133. (a) Tokuyama, H. and Nakamura, E., Synthetic chemistry with fullerenes. Photooxygenation of olefins, *J. Org. Chem.,* 59, 1135, 1994; (b) Orfanopoulos, M. and Kambourakis, S., Fullerene C_{60} and C_{70} photosensitized oxygenation of olefins, *Tetrahedron Lett.,* 35, 1945, 1994.
134. Zhang, X., Romero, A., and Foote, C.S., Photochemical [2 + 2] cycloaddition of *N,N*-diethylpropynylamine to C_{60}, *J. Am. Chem. Soc.,* 115, 11024, 1993.
135. Ruoff, R.S., Tse, D.S., Malhotra, R., and Lorents, D.C., Solubility of fullerene C_{60} in a variety of solvents, *J. Phys. Chem.,* 97, 3379, 1993.
136. An, Y.-Z., Anderson, J.L., Sigman, D.S., Foote, C.S., and Rubin, Y., Sequence-specific modification of guanosine in DNA by a C-60-linked deoxyoligonucleotide: evidence for a non-singlet oxygen mechanism, *Tetrahedron,* 89, 5179, 1996.
137. An, Y.-Z., Viado, A.L., Arce, M.-J., and Rubin, Y., Unusual regioselectivity in the singlet oxygen ene reaction of cyclohexenobuckminsterfullerene, Y. *J. Org. Chem.,* 60, 8330, 1995.
138. (a) Foote, C.S., Photosensitized oxygenations and the role of singlet oxygen, *Acc. Chem. Res.,* 1, 104, 1968; (b) Schulte-Elte, K.H. and Rautenstrauch, V., Preference for the syn ene additions of $^1O_2$ to 1-methylcycloalkenes. Correlation with ground-state geometry, *J. Am. Chem. Soc.,* 102, 1738, 1980.
139. Chronakis, N., Vougioukalakis, G.C., and Orfanopoulos, M., Synthesis and self-photooxygenation of alkenyl-linked [60]fullerene derivatives. A regioselective ene reaction, *Org. Lett.,* 4, 945, 2002.
140. Hummelen, J.C., Prato, M., and Wudl, F., There is a hole in my bucky, *J. Am. Chem. Soc.,* 115, 7003, 1995.

141. Inoue, H., Yamaguchi, H., Iwamatsu, S.-I., Uozaki, T., Suzuki, T., Akasaka, T., Nagase, S., and Mutata, S., Photooxygenative partial ring cleavage of bis(fulleroid): synthesis of a novel fullerene derivative with a 12-membered ring, *Tetrahedron Lett.,* 42, 895, 2001.
142. (a) Schick, G., Jarrosson, T., and Rubin, Y., Formation of an effective opening within the fullerene core of C_{60} by an unusual reaction sequence, *Angew. Chem. Int. Ed. Engl.,* 38, 2360, 1999; (b) Taliani, C., Ruani, G., Zamboni, R., Danieli, R., Rossini, S., Denisov, V.N., Burlakov, V.M., Nagri, F., Orlandi, G., and Zerbetto, F., Light-induced oxygen incision of C_{60}, *J. Chem. Soc., Chem. Commun.,* 220, 1993.
143. Hsiao, T.-S., Santhosh, K.C., Liou, K.-F., and Cheng, C.-H., Nickel-promoted first ene-diyne cycloaddition reaction on C_{60}: synthesis and photochemistry of the fullerene derivatives, *J. Am. Chem. Soc.,* 120, 12232, 1998.
144. An, Y.-Z., Ellis, G.A., Viado, A.L., and Rubin, Y., A methodology for the reversible solubilization of fullerenes, *J. Org. Chem.,* 60, 6353, 1995.
145. Weisman, R.B., Heymann, D., and Bachilo, S.M., Synthesis and characterization of the "missing" oxide of C_{60}: [5,6] open $C_{60}O$, *J. Am. Chem. Soc.,* 123, 9720, 2001.
146. Heymann, D., Bachilo, S.M., and Weisman, R.B., Ozonides, epoxides and oxidoannulenes of C_{70}, *J. Am. Chem. Soc.,* 124, 6317, 2002.
147. (a) Suzuki, T., Li, Q., Khemani, K.C., Wudl, F., and Almarsson, O., Systematic inflation of buckminsterfullerene C_{60}: synthesis of diphenyl fulleroids C_{61} to $C_{66,}$ *Science,* 254, 1186, 1991; (b) Wudl, F., The chemical properties of buckminsterfullerene (C60) and the birth and infancy of fulleroids, *Acc. Chem. Res.*, 25, 157, 1992; (c) Diederich, F., Isaacs, L., and Philp, D., Syntheses, structures and properties of methanofullerenes, *Chem. Soc. Rev.,* 243, 1994 and references therein; (d) Smith, A.B., III; Strongin, R.B., Brard, L., Furst, G.T., Romanow, W.J., Owens, K.G., Goldschmidt, R.J., and King, R.C., Synthesis of prototypical fullerene cyclopropanes and annulenes. Isomer differentiation via NMR and UV spectroscopy, *J. Am. Chem. Soc.,* 117, 5492, 1995.
148. Diederich, F., Isaacs, L., and Philp, D., Valence isomerism and rearrangement to methanofullerenes, *J. Chem. Soc. Perkin Trans.,* 2, 391, 1994.
149. Averdung, J., Torres-Garcia, G., Luftmann, H., Schlachter, I., and Mattay, J., Progress in fullerene chemistry: from exohedral functionalization to heterofullerenes, *Full. Sci. Techn.,* 4, 633, 1996.
150. Schick, G., Hirsch, A., Mauser, H., and Clark, T., Opening and closure of the fullerene cage in cis-1-bisimino adducts of C-60: the influence of the addition pattern and the addend, *Chem.-Eur. J.,* 2, 935, 1996.
151. (a) Shen, C.K.-F., Yu, H.-H., Juo, C.-G., Chien, K.-M., Her, G.-R., and Luh, T.-Y., Synthesis of 1,2,3,4-bisiminofullerene and 1,2,3,4-bis(triazolino) fullerene — on the mechanism of the addition reactions of organic azides to [60]fullerene, *Chem.-Eur. J.,* 4, 744, 1997; (b) Lamparth, I., Nuber, B., Schick, G., Skiebe, A., Grösser, T., and Hirsch, A., *Angew. Chem. Int. Ed. Engl.,* 35, 2257, 1995.
152. (a) Shiu, L.-L., Chien, K.-M., Liu, T.-Y., Lin, T.-I., Her, G.-R., and Luh, T.-Y., Bisazafulleroids, *J. Chem. Soc., Chem. Commun.,* 1159, 1995; (b) Shen, C.K.-F., Chien, K.-M., Juo, C.-G., Her, G.-R., and Luh, T.-Y., Chiral bisazafulleroids, *J. Org. Chem.,* 61, 9242, 1996.
153. Kanakamma, P.P., Huang, S.-H., Juo, C.-G., Her, G.-R., and Luh, T.-Y., Aza-aziridinofullerene: interconversion between aza-aziridinofullerene and bis-azafulleroid, *Chem.-Eur. J.,* 4, 2037, 1998.
154. Li, Z. and Shevlin, P.B., Why is the rearrangement of [6,5] open fulleroids to [6,6] closed fullerenes zero order? *J. Am. Chem. Soc.,* 119, 1149, 1997.
155. Ulmer, L., Torres-Garcia, G., Wolff, C., Mattay, J., and Luftmann, H., Mono- and bisfunctionalization of fullerenes with N-containing reactants, in *Recent Advances in the Chemistry and Physics of Fullerene and Related Materials,* Vol. 5, Kadish, K.M. and Ruoff, R.S., Eds., The Electrochemical Society, 1997, p. 306.
156. Arce, M.-J., Viado, A.L., An, Y.-Z., Khan, S.I., and Rubin, Y., Triple scission of a six-membered ring on the surface of C_{60} via consecutive pericyclic reactions and oxidative cobalt insertion, *J. Am. Chem. Soc.,* 118, 3775, 1996.

157. Iwamatsu, S.-I., Vijayalakshmi, P.S., Hamajima, M., Suresh, C.H., Koga, N., Suzuki, T., and Murata, S., A novel photorearrangement of a cyclohexadiene derivative of C_{60}, *Org. Lett.,* 4, 1217, 2002.
158. Qian, W., Bartberger, M.D., Pastor, S.J., Houk, K.N., Wilkins, C.L., and Rubin, Y., C_{62}, a non-classical fullerene incorporating a four-membered ring, *J. Am. Chem. Soc.,* 122, 8333, 2000.
159. (a) Chapman, O.L., Mattes, K., McIntosh, C.L., Pacansky, J., Calder, G.V., and Orr, G., Photochemical transformation. LII. Benzyne, *J. Am. Chem. Soc.,* 95, 6134, 1973; (b) Rubin, Y., Kahr, M., Knobler, C.B., Diederich, F., and Wilkins, J., The higher oxides of carbon $C_{8n}O_{2n}$ (n = 3–5): synthesis, characterization and x-ray crystal strucrure. Formation of cyclo[n]carbon ions C_n^+ (n = 18, 24), C_n^- (n = 18, 24, 30) and higher carbon ions including C_{60}^+ in laser desorption fourier transform mass spectormetric experiments, *J. Am. Chem. Soc.,* 113, 495, 1991.
160. Henderson, C.C., Rohlfing, C.M., Gillen, K.T., and Cahill, P.A. Synthesis, isolation, and equilibration of 1,9- and 7,8-$C_{70}H_2$, *Science,* 264, 397, 1994.

29

The Photo-Bergman Cycloaromatization of Enediynes

Graham B. Jones
Northeastern University

Keith C. Russell
Northern Kentucky University

29.1 Introduction

In 1986, a natural product was isolated from the soil bacterium *Micromonospora echinospora* ssp. *calichensis* and assigned the name calicheamicin.[1] Investigation of its biological profile revealed very high activity in a primary screen (prophage induction assay), and calicheamicin turned out to be one of the most potent antitumor agents (both *in vitro* and *in vivo*) ever evaluated.[2] This initial research, followed by subsequent structural identification, led to the realization of an apparently new and unprecedented class of antitumor agents collectively known as the "enediyne antibiotics."

calicheamicin γ_1

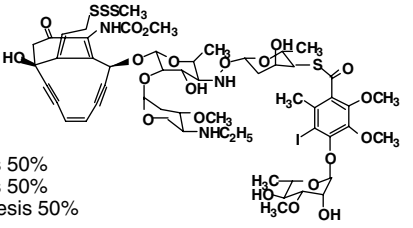

isol. *Micromonospora echinospora* ssp. calichensis

50 pg / ml inhibits DNA synthesis 50%
15 ng / ml inhibits RNA synthesis 50%
250 pg / ml inhibits protein synthesis 50%

	in vitro ED (ng / ml) Co-77	*in vivo* optimal dose (mg / kg) CD2F mice
calicheamicin 1	0.025	2.5
N-acetyl calicheamicin 1	0.25	40.0
vincristine	15.0	1000.0
mitomycin C	15.0	3000.0
adriamycin	200.0	8000.0

0-8493-1348-1/04/$0.00+$1.50

SCHEME 1 Thermal enediyne rearrangements that give rise to cytotoxic biradicals.

The history of the enediynes in fact dates back to 1965, with the discovery of neocarzinostatin.[3] Isolated as a chromoprotein complex, the structure of its enediyne-containing chromophore was finally determined in 1985,[4] and when the connection between it and the newly discovered calicheamicins and esperamicins was made, it sparked intense interest from research groups around the world. Over 20 discrete enediynes are now known, which fall into two distinct subcategories: those containing a 10-membered 3-hexene-1,5-diyne subunit [the calicheamicins, esperamicins and dynemicins] and those containing a nine membered enediyne, which are typically isolated as complexes with an associated apoprotein (neocarzinostatin, kedarcidin, C-1027, maduropeptin).[5]

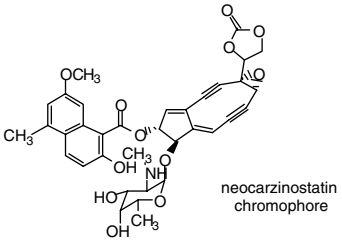

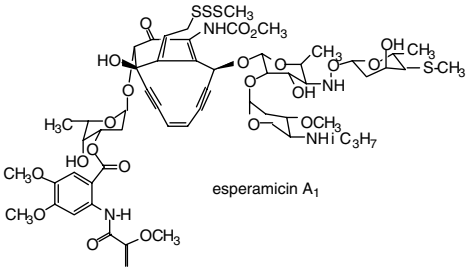

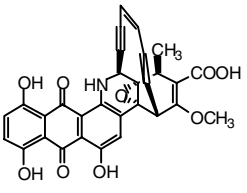

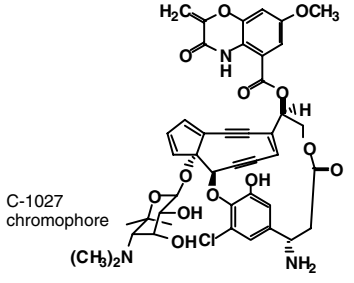

Clinical trials of neocarzinostatin derivatives continue in Japan, U.S. trials of a monoclonal antibody (MoAb) conjugate of calicheamicin have entered Phase III, and esperamicin has entered Phase II trials (Scheme 1).[6] Clinical interest in enediynes was heightened when it was found that a calicheamicin MoAb conjugate induced remission in up to 40% of patients with acute myeloid leukemia [AML] who had previously relapsed following other chemotherapies. It was demonstrated that calicheamicin, as well as other enediynes, are capable of causing single- and double-stranded DNA breaks at very low concentrations, and that the enediynes probably derive their biological activity from these events.[7] Enediynes *per se* are biologically inactive, but they undergo cycloaromatization reactions that give rise to cytotoxic diyl radicals, by either a Bergman-type cycloaromatization reaction[8] or, as in the case of neocarzinostatin, the Myers process (Scheme 1).[9]

In either case, the resulting biradicals [**2**/**4**] are highly reactive and undergo atom transfer chemistry in a bid to form stable arenes. Most typically, this involves hydrogen atom abstraction which, in the presence of biological targets, can inflict cellular damage, including DNA scission and, in specific cases,

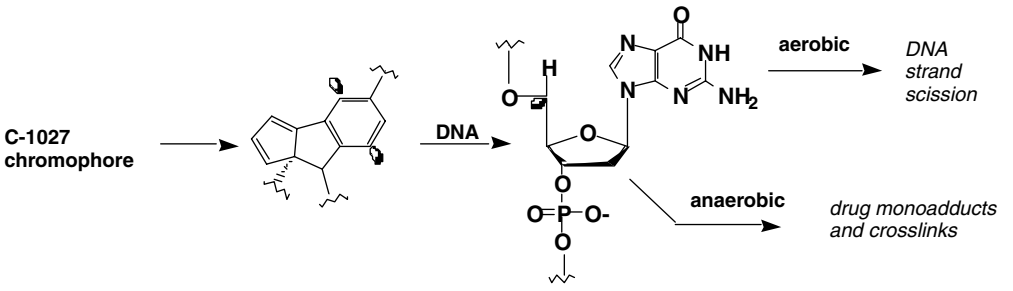

SCHEME 2 Fate of biradical-DNA interactions depends on environment.

other lesions.[10] The pathways by which the enediyne-derived biradicals inflict DNA damage and their sequence specificity has been extensively studied, and hydrogen abstractions from the C(5′), C(4′), and C(1′) positions have been proposed.[11] The resulting ribosyl radical is then typically intercepted by molecular oxygen, and the peroxide formed undergoes fragmentation resulting in cleavage. Specific enediynes are capable of inducing double-stranded lesions, whereas the more typical outcome is a single-stranded cut with limited sequence specificity. In the case of C-1027, Goldberg[5] demonstrated that adduction can occur under anaerobic conditions (Scheme 2), which may have ramifications for enediynes, which become activated in hypoxic regions, prevalent in solid tumors.[12]

While the *in vitro* and *in vivo* effectiveness of enediynes against certain cancers is firmly appreciated, the exact contribution of DNA cleavage to such biological activity remains to be resolved. Studies involving calicheamicin suggest that specific DNA strand scission is not directly related to cytotoxicity, but that subsequent promotion of the DNA suicide repair enzyme poly(ADP-ribose)polymerase results in cellular death by means of depleting cellular NAD^+ and ATP levels.[13] Additionally, compelling evidence now suggests that proteins may be the target of certain enediynes (*vide infra*). Nonetheless, it is the DNA-cleaving activity of enediynes that has guided the development of most analogs.

The typical half-lives of most unstrained 10-membered enediynes (for Bergman cyclization) are approximately 3 to 18 h at physiological temperature, making them ideal for *in vitro* and *in vivo* studies, and this in turn has fueled the quest for designed (synthetic) enediynes.[14] Nearly all of the natural enediynes possess chemical triggering units which, when activated, promote either Bergman or Myers type cycloaromatization of the core unit. Though chemical synthesis of triggered enediynes, which mimic the natural systems, can be accomplished, preparation of the parent enediyne core structures requires special care due to thermal instability. For this reason researchers have recently begun to investigate the possibility of using photochemical methods of activating otherwise thermally stable enediyne prodrugs (*vide infra*). Additional interest in enediynes has recently surfaced in materials chemistry. Examples include synthetic polymers and designed nanostructures.[15] Representative examples of enediyne materials include the (explosive) dehydroannulenes 5,[16] carbon-rod polydiacetylenes 6,[17] and the molecular switching device **7** (R = dihydroazulene).[18]

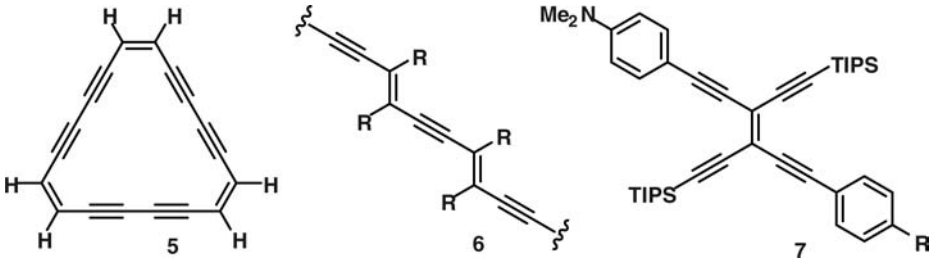

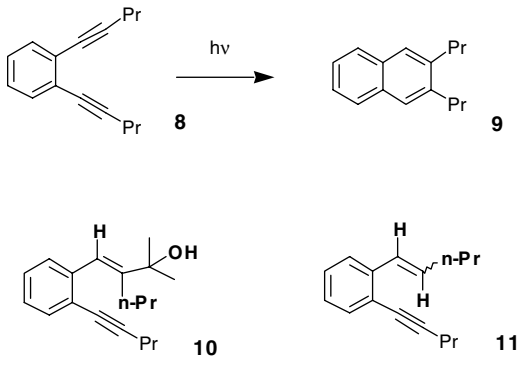

SCHEME 3 The prototypical Photo-Bergman rearrangement.

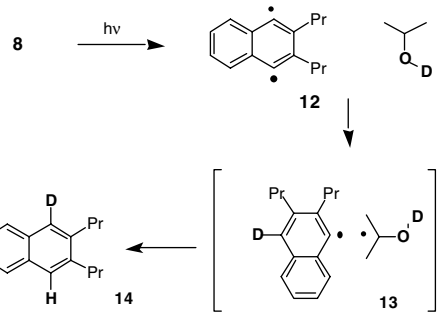

SCHEME 4 Mechanistic examination of Photo-Bergman.

29.2 Basic Overview of Photo-Bergman

Interest in a photochemical variant of the Bergman cyclization was stimulated by a report from the groups of Turro and Nicolaou in 1994.[19] They revealed that *n*-propylenediyne **8** underwent photochemical conversion to arene products following irradiation using a medium pressure Hg lamp, with cutoff at 313 nm. The choice of solvent plays a key role in both the efficiency of the process and the product distribution, as it plays a dual role as an atom transfer agent. Isopropanol, benzene, and hexane all gave variable yields of expected product **9**, but when benzene/1,4-cyclohexadiene mixture was employed, cyclohexadiene adducts were recovered. Of these combinations, isopropanol was most effective, at 50% conversion giving products **9:10:11** in ratios of 2:4:3 (2:1 *cis:trans* for **11**).[20] This corresponds to a 25% yield of **9**. Subsequent labeling studies, in which **8** was irradiated in the presence of deuteroisopropanol, suggested the intermediacy of diyl **12**, with isolation of arene **14** implying combination of radical pair **13** (Scheme 4).[19] Control experiments supported this pathway, since neither **14** irradiated with the labeled solvent nor the presence of sensitizers gave rise to additional D incorporation. Alternative outcomes are possible, however, depending on reaction conditions. Photolysis of substrate **15** in the presence of isopropanol gives arene **16**, implying the intermediate diyl **17** (Scheme 5).[20] Repeat irradiation in the presence of tetranitromethane, however, results in isolation of indene **18**, presumably via trapping of the radical cation **19**.[21] This implies the reversibility of the photoreaction, and competing ionic/radical pathways dictate product distribution, in stark contrast to the thermal process.

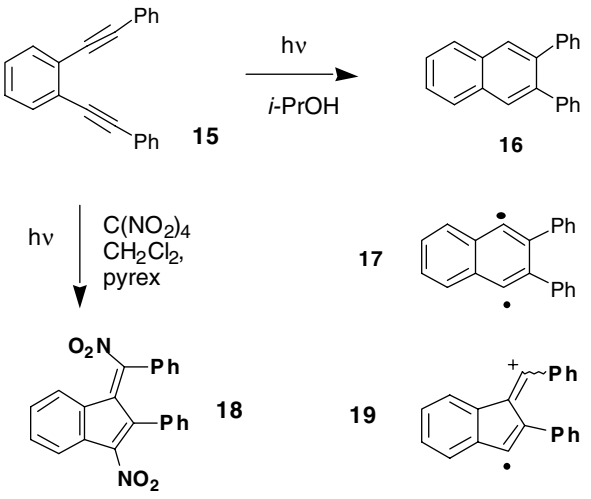

SCHEME 5 Divergent pathways reflect trapping agent.

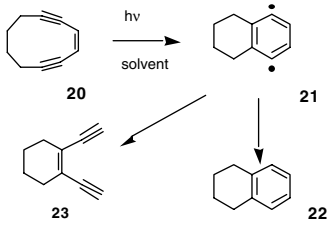

SCHEME 6 Cyclodec-1,5-diyn-3-ene.

TABLE 29.1 Photoconversion of Enediyne **20**[a]

Solvent	% Yield **22**	%Yield **23**
Hexane	29	6
Cyclohexane	26	20
CH_3CN	12	24
*i*PrOH	3	—

[a] 2.3 mmol, 3 h irradiation at 254 nm, 25°C

29.3 Cyclic Enediyne Substrates

With these results in hand, interest in the photo-Bergman cyclization increased, and a number of studies on the basic atom transfer chemistry and reversibility of cycloaromatization emerged. Hirama demonstrated that the C10 pharmacophore **20**, present in many of the naturally occurring enediyne antitumor agents, was capable of undergoing photo-Bergman cyclization, giving arene **22** and product **23**, which is derived from the reversed reaction of diyl **21** (Scheme 6).[22] The process was heavily influenced by solvent, with nonpolar solvents giving appreciable yields (Table 29.1).

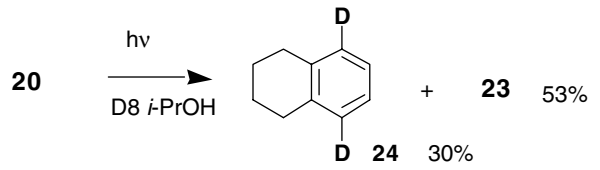

SCHEME 7 Reversed Bergman: Labeling Studies.

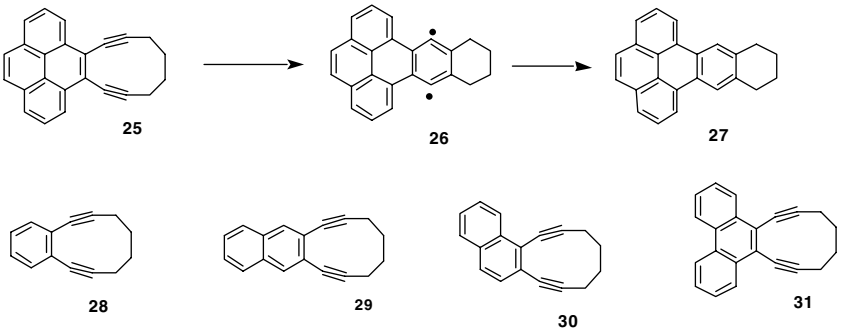

SCHEME 8 Pyrene enediyne Photo-Bergman cyclization.

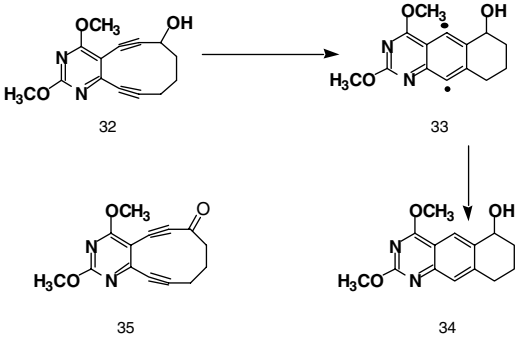

SCHEME 9 Heteroaryl substrates.

Subsequent labeling studies supported the reversed Bergman pathway, with isolation of the doubly labeled arene **24** in addition to enediyne **23** (Scheme 7).[22] It is interesting to note that the reversed pathway (isolation of enediyne **23**) has not been observed under thermal conditions.

Benzofused Systems

Following on from the initial reports of Turro,[19,20] a series of efficient substrates for photo-Bergman was reported by Funk and Williams (Scheme 8).[23] The most spectacular of these was pyrene enediyne **25**, which underwent smooth conversion to arene **27**, presumably via diyl **26**.[23] The template was later derivatized to allow DNA recognition, in part a consequence of the ability of the pyrene to intercalate (*vide infra*). The authors conducted systematic analysis of the prerequisites for efficient conversion, revealing that compounds **28**, **30**, and **31** (but not **29**) were good substrates.[23] An interesting heterocyclic variant was introduced by Russell and co-workers, involving fused systems e.g., **32** (Scheme 9).[24] The pyrimidine-fused enediyne **32** underwent highly efficient conversion to arene **34**, assuming the intermediacy

of diyl **33**. However, by contrast, ketone **35** gave only minimal conversion to the corresponding arene. It is interesting that compounds **32** and **35** showed a reversal in thermal and photochemical rates of reactivity. When cyclized thermally in toluene at 40°C, ketone **35** had a half-life of 5 h, while alcohol **35** had a half-life of 58 h. When treated photochemically in isopropanol for 2 h, again at 40°C, alcohol **32** underwent 83% conversion to arene **34**, with 4% **32** remaining. When ketone **34** was treated under identical conditions, only 10% of the corresponding Bergman cyclization product was produced, along with 34% starting material. The remaining mass resulted from other photochemical products of **34**. These results potentially point to subtle stereoelectronic effects in the transition state.[24] Compound **32** also demonstrated photochemically initiated DNA cleavage (*vide infra*).

Based partly on the success of benzofused enediynes such as **28**, **30**, **31**, and **34**, Wiest prepared highly strained enediynes **36** and **37** and subjected them to conditions suitable for photochemical Bergman cyclization.[25] These molecules proved stable to prolonged high-intensity irradiation. Based on calculations, it was suggested that the unexpected photochemical (and thermal) stability of **36** and **37** is the result of diyl intermediates that are unusually high in energy.

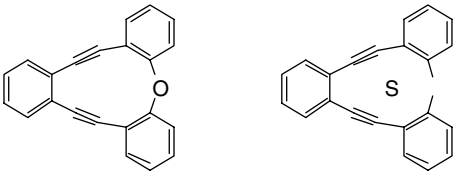

36 37

Carbocyclic Systems

Drawing analogy with the cyclopentane fused enediynes present in the naturally occurring chromoprotein enediyne antibiotic, Hirama has investigated the propensity for enediynes **38** to undergo photo-Bergman rearrangement (Scheme 10).[22] Surprisingly, the dialkyl enediyne was the most efficient (Table 29.2), and again the process had a strong solvent effect.[22] A labeling study was conducted, irradiating **38** (R = Me) in the presence of D_8 THF, which gave a 14% yield of labeled adduct with D_2:D_1:D_0 in ratios of 88:12:0.[22]

Based on the intriguing behavior of the alicyclic enediynes **38**, we sought to investigate the electronics and sterics of the photo-Bergman cyclization pathway. However, in order to be systematic, this would necessitate an entirely synthetic approach.

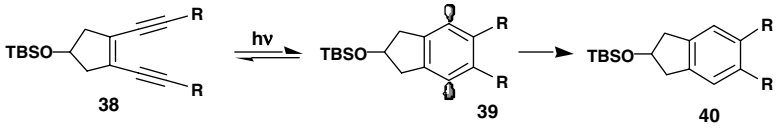

38 39 40

SCHEME 10 Photochemical Bergman cycloaromatization.

A *De Novo* Class of Photo-Enediynes

Based on **38** and the results from other laboratories involving diaryl enediynes, we wished to design enediyne systems where alkyne termini could be derivatized with variable functionality, and the photoactivity of the Bergman cycloaromatization could be tuned both in terms of electronics and strain energy. Specifically, since most photoactivated enediynes studied to date have the vinyl moiety embedded in an arene, we wished to design a family of differentially capped *alicyclic enediynes* **41** and investigate their photochemical activation to diyls **42** as a function of these effects (Scheme 11).

Commencing from commercially available acyl chlorides **43**, the corresponding diketones **44** were produced via the intermediate Weinreb amides (Scheme 12). Low valent Ti-mediated coupling gave **46** directly, but the yields were variable, in part due to problems recovering product from complex mixtures.

TABLE 29.2 Photoconversion of Enediynes **38**[a]

R	Solvent	Time (h)	%Yield **40**
H	Hexane	6	6
TMS	Hexane	18	0
Ph	Hexane	18	0
Me	Hexane	18	71
Me	MeOH	18	0
Me	Hexane[b]	18	41
Me	Cyclohexane	18	52
Me	THF	18	35
Me	CH_3CN	18	21[c]
Me	*i*PrOH	18	20
Me	CH_2Cl_2	18	—[d]

[a] 3.6 mmol irradiation at 254 nm, 25°C.
[b] Plus 1,4-CHD (20:1).
[c] Plus 8% solvent adduct.
[d] Plus 20% solvent adduct.

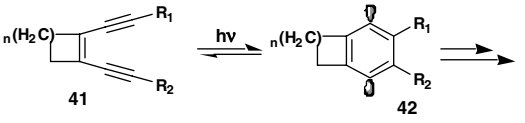

SCHEME 11 Photochemical Bergman cycloaromatization.

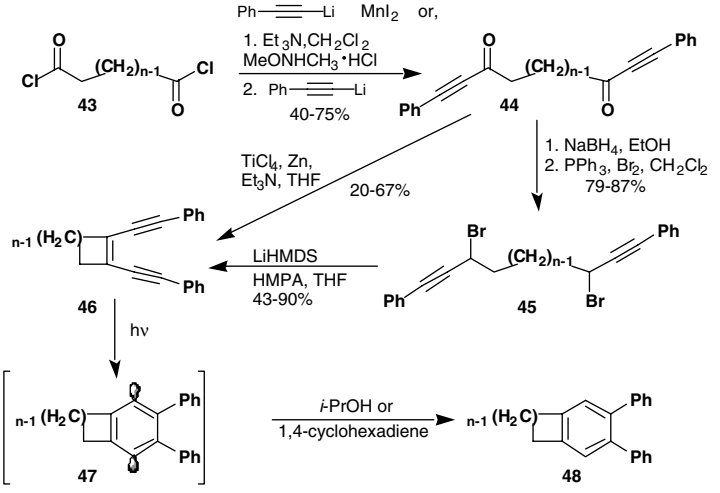

SCHEME 12 Synthesis of alicyclic Photo-Bergman candidates.

Alternatively, conversion to bromides **45** followed by carbenoid coupling gave **46** (n = 1–5) in good yield on a preparative scale.[26] Though stable at room temperature, photochemical Bergman cycloaromatization gave adducts **48** in moderate yield, presumably via diyls **48** (Table 29.3).[26]

As had been found previously, the nature of the hydrogen donor plays an important role in the conversion to arene adduct.[27] Thus, although consumption of enediyne was often rapid using 1,4-cyclohexadiene, optimal yields of cycloaromatization products were obtained using isopropanol, the balance of material typically composed of uncharacterized polymeric byproducts. Evidently, ring strain

TABLE 29.3 Synthesis and Cycloaromatization of Enediynes **46**

Entry	n	c-d (Å)[a]	Irradiation (h)[b]	Conversion[c]	%**48**[d] (based on **46**)
1	2	4.941	3	100e	0 (0)
2	3	4.284	3	97	13 (13)
3	4	4.018	3	49	15 (31)
4	4	4.018	12	95	21 (22)
5	5	3.947	12	70	11 (16)
6	6	3.893	12	66	9 (14)

[a] Equilibrium geometry calculated using PM3 (PC Spartan Pro).
[b] Reactions conducted at 0.4 g/l enediyne in 2-propanol in a quartz vessel, irradiated using a 450 W (Hanovia) lamp.
[c] Based on recovered starting material.
[d] Isolated yields.
[e] Decomposition and formation of polymeric adducts ensues in < 1 h.

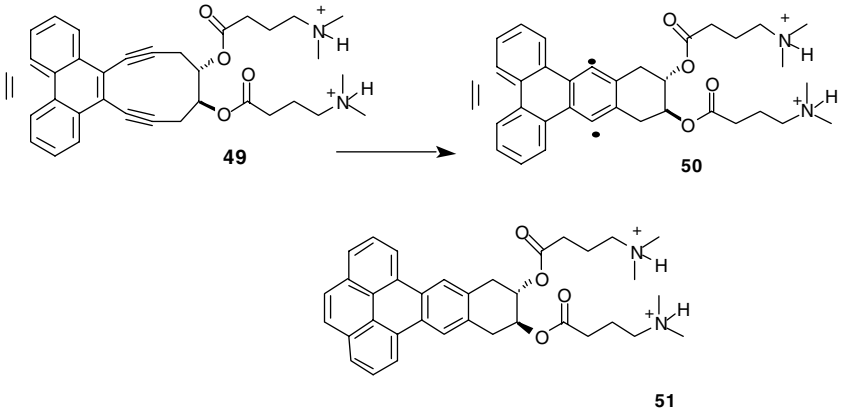

SCHEME 13 DNA targeted photo-Bergman substrates.

effects play a role in the cycloaromatization, with lower conversion efficiency observed with the C7 and C8 analogs despite the appreciable reduction in intramolecular "c-d" distances relative to the 6-membered analog (Table 29.3).[28] Though photo-Bergman cycloaromatization yields are modest, the synthesis of this class of enediynes (4- through 8-membered) is noteworthy and may lead to many new applications in materials and polymer chemistry.

29.4 Biological Applications

DNA Targeted

Since DNA is the predominant target of the natural enediynes, a natural extension of the photo-Bergman lies in the development of efficient enediyne-based photonucleases. Based on their model studies, Funk and Williams designed both a phenanthrene and pyrene enediyne **49**, which by virtue of the aminoalkyl side-chains had affinity for DNA (Scheme 13).[23]

Irradiation of these agents in the presence of supercoiled plasmid DNA (pUC19) resulted in single-stranded cleavage, with the pyrene-based substrate somewhat more efficient. Control studies supported the requirement of the enediyne structure for efficient cleavage, and it is implied that arene **51** is the terminal product, and the reactive species is diyl **50**.[23] This constituted the first example of an enediyne-based photochemical

nuclease, and the possibility for sequence specific variants clearly exists. It is not clear that compound **32** should possess significant DNA affinity, unlike **49** with its inherent ability to intercalate. Nonetheless, **32** did exhibit photochemically initiated DNA cleavage properties similar to those of **49**.[24] In this case, single-stranded cleavage was observed on the ΦX174 plasmid.

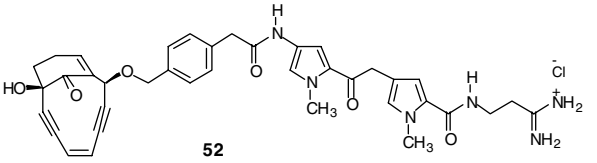

52

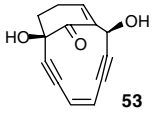

53

Protein Targets

While ongoing research will clarify their precise relevance, it is possible that DNA binding and/or DNA cleavage are not critical for antitumor activity of enediynes. Protein agglomeration induced by the enediyne *chromophores* of both C-1027[29] and kedarcidin[30] have been reported, but due to their unique architectures (which recognize DNA effectively), it is unlikely that this contributes to their biological effects. However, during development of the enediyne–netropsin conjugate **52**, researchers at Bristol-Myers Squibb noted the protein modulating ability of the enediyne core **53**[31] (related to the natural enediyne esperamicin), and this likely contributes to the observed *in vitro* and *in vivo* antitumor activity of the agent, whose affinity for DNA is low.[31] At physiological temperature, this agent induced damage to membrane extracts, tubulins, and histones, presumably via its derived diyl radicals. Spurred by these findings, we elected to study the viability of designing enediynes that (a) are targeted towards specific proteins[32] and (b) are substrates for the photo-Bergman reaction. Such a strategy could have far-reaching consequences. Excepting water, proteins are the most abundant constituents of cells and extracellular fluids by weight. Proteins govern the majority of events in a cell, and the ability to selectively inactivate or disrupt protein function in a tumor cell could be a valuable tool.

Bovine Serum Albumin

With a route to photoactivated enediynes **46** secure, we wished to investigate interaction of the intermediate diyl radicals **47** with protein targets and accordingly sought to prepare a hydrophilic variant, which was capable of recognizing protein architecture. Our design was influenced by the work of Kumar,[33] who reported that an alkyl pyrenyl derivative of phenylalanine (**54**) recognizes the proteins bovine serum albumin (BSA) and lysozyme, inducing photocleavage following irradiation in the presence an electron acceptor.[34] Molecular modeling studies indicated that diyl **55** would be a close mimic of this agent and could presumably be generated via irradiation of an enediyne precursor.

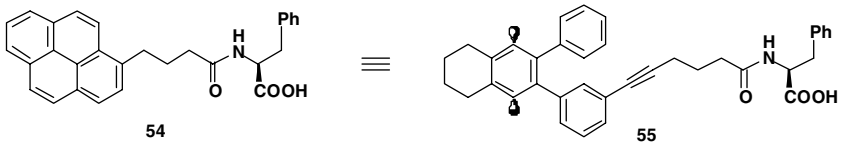

54 ≡ **55**

Accordingly, enediyne **60** became a logical candidate for proof-of-principle studies. First, diketone **56** was prepared from adipoyl chloride using a mixed coupling procedure. Subsequent functional group interconversion and carbenoid coupling gave the differentially functionalized C6-enediyne, which was unmasked to give **57**.[26] Photo-Bergman cycloaromatization of this enediyne (or the TIPS-protected precursor) gave <10% of the corresponding arene product, suggesting that the aryl groups play a key role in the (reversible) cyclization process. The alkyne was then coupled with methyl-3-(3-iododphenyl)hexynoate **58**, followed by hydrolysis to give carboxylate **59**, which was then coupled with L-phenylalanine methyl ester and subjected to saponification to give conjugate **60** in good yield. In contrast to the model series,

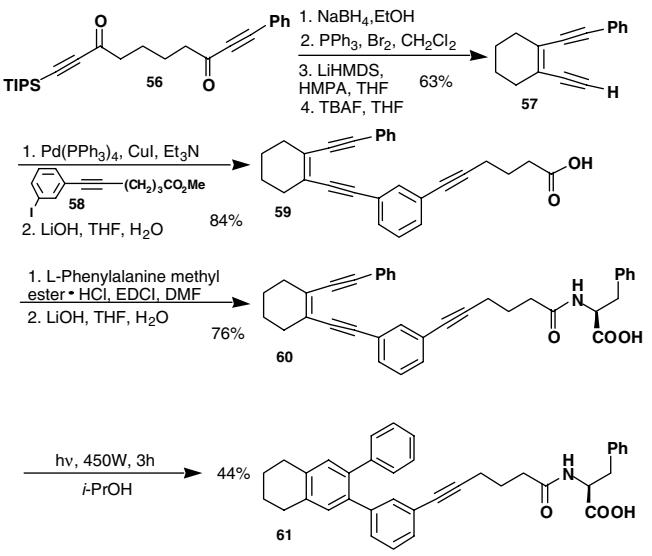

SCHEME 14 Preparation and Photo-Bergman cyclization of phe-enediyne hybrid.

FIGURE 29.1 10% SDS polyacrylamide gel of the reaction of bovine serum albumin (BSA) with **58** and **59**. All reactions were conducted in 50 mM Tris-HC1, pH 7.0 at 37°C. From right to left: lane 1, molecular weight markers (KDa); lane 2, BSA control (1.5 μM); lane 3, BSA (1.5 μM), **58** (150 μM), no irradiation; lane 4, BSA (1.5 μM), **59** (150 μM), 3h irradiation; lane 5, BSA (1.5 μM). **58** (7.5 μM), 3h irradiation.

photochemical activation (450 W, 3 h) of this enediyne gave arene product **61** in appreciable yield, together with unreacted starting material, underscoring the influence of the conjugated arene unit.[26]

Photochemically induced modification of BSA and lysozyme was examined by photolysing **60** in aqueous buffer, using **61** and enediynes **59, 57** as controls.[26] In the case of 66 kD protein BSA, subsequent analysis (SDS-PAGE) showed evidence of enediyne-induced degradation, with one principal fragment (~ 40 kDa) visible (Figure 29.1). Subsequent analysis by MALDI-TOF revealed the presence of fragments at 44.76 kDa, 11.28 kDa, and 10.22 kDa, suggesting the possibility of two sites of cleavage.[26,35] In the case of the 14 kDa protein lysozyme, dimerization to form a species with m/z 28.63 kDa was observed following irradiation (Figure 29.2), suggesting the possibility of intermolecular diyl-mediated cross coupling.[36] These initial findings led us to search for more specific photoproteases, and we were encouraged to use carboxylate **59** as a building block.

Histone H1

In the case of the naturally occurring chromoproteins kedarcidin, C-1027, and neocarzinostatin, the apoprotein component has proteolytic capacity. In the case of kedarcidin, studies have shown that the highly acidic apoprotein is capable of inducing selective degradation of histone H1.[37] As this is the most basic histone, a natural conclusion is that affinity plays a role. Following proteolysis of the histone, it has been suggested that the reactive enediyne chromophore is then more efficiently delivered to exposed DNA, contributing to the high efficiency of strand scission by kedarcidin. Based on our findings, we

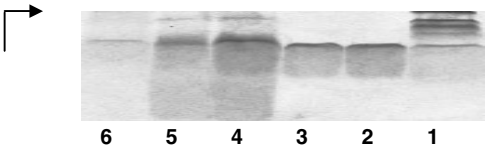

FIGURE 29.2 15% SDS polyacrylamide gel of the reaction of Lysozyme (Lyso) with **58** and **59**. All reactions were conducted in 50 mM Tris-HC1, pH 7.0. From right to left: lane 1, molecular weight markers (in KDa); lane 2, Lyso (0.15 μM); lane 3, Lyso (0.15 μM), 3h irradiation; lane 4, Lyso (0.15 μM, **58** (0.75 μM), 3h irradiation; lane 5, Lyso (0.15 μM), **58** (0.75 μM), 6h irradiation; lane 6, Lyso (0.15 μM), **59** (15 μM), 12h irradiation.

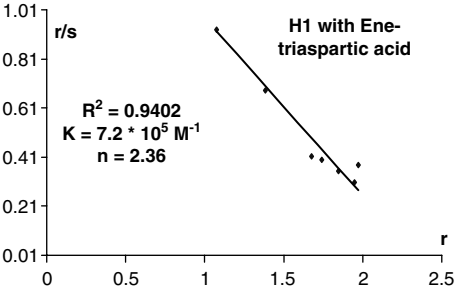

FIGURE 29.3 Scatchard plot of histone H1 with enediyne-triaspartic acid conjugate **61**.

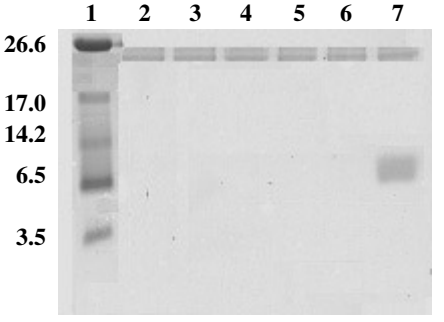

FIGURE 29.4 Histone agglomeration. 16.5% SDS polyacrylamide Tris-Tricine gel of the reaction Histone H1 (1 mg/ml). All reactions were conducted in 50 mM Tris-HC1, pH 7.0. From left to right: lane 1, molecular weight markers (KDa); lane 2, histone H1 no irradiation; lane 3, histone H1 after 3h irradiation; lane 4, histone H1 after 6h irradiation, lane 5 histone H1 + **61** no irradiation; lane 6 histone H1 after 3h irradiation; lane 7, histone H1 + **61** after 6h irradiation.

became interested in preparing an acidic enediyne–peptide conjugate to determine whether enediyne-mediated histone degradation could be achieved and if so, with what specificity. To investigate this, enediyne **59** was coupled with the triaspartic acid derivative **62.** Deprotection of the conjugate with LiOH gave the enediyne-tri-Asp conjugate **63** in good yield. As expected, this conjugate has appreciable solubility in aqueous buffer.[37] Binding of this agent to a variety of histones revealed that affinity, as expected, was greater for H1 versus others, and Scatchard analysis suggested that only one binding site is involved (Figure 29.3). More significantly, irradiation of **63** in the presence of histone H1 led to formation of **64** and degradation of the protein (Figure 29.4).[38]

Application of this concept towards other protein targets and subregional motifs within proteins would appear possible. Examples might include the SH2 and SH3 domains, which are important homology

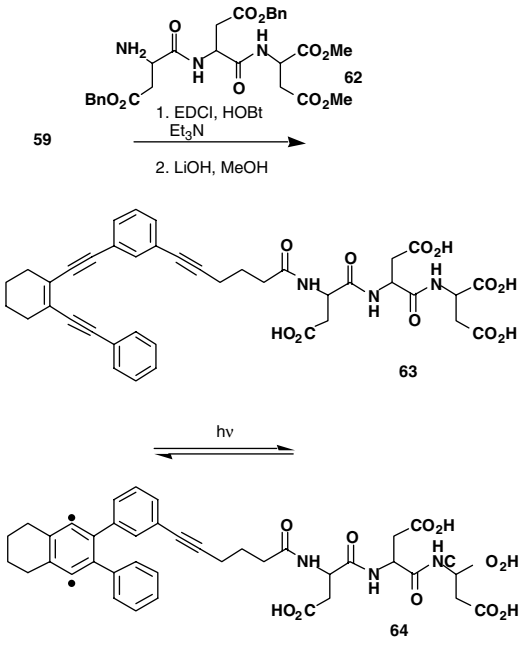

SCHEME 15 Synthesis of tri (asp) conjugate.

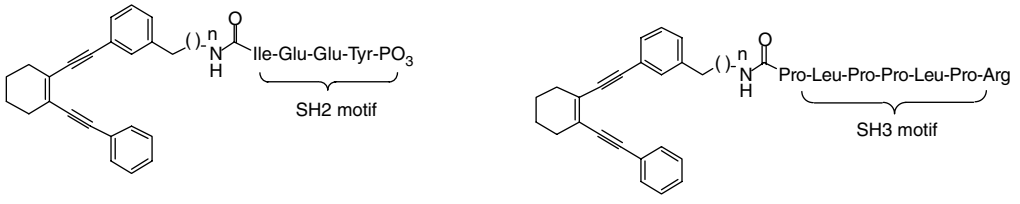

FIGURE 29.5 Possible protein targeted photoactivated enediyne candidates.

regions found in a diverse collection of proteins including signal transduction proteins, protein kinases, lipid kinases, protein phosphatases, phospholipases, and transcription factors.[39] Group I SH2 binders typically have a phosphorylated tyrosine flanked by hydrophilic–hydrophilic–hydrophobic amino acids; thus, the structure shown in Figure 29.5 would be predicted to have affinity.[40] In the case of SH3 binding peptides, a common motif is a proline-rich region P-X-X-P, present in class I ligands (consensus RXLP-PXP), e.g., the wild-type Src SH3 motif shown (Figure 29.5).[41]

Human Estrogen Receptor α

As a final example of application, we elected to study agents with the capability of degrading the human estrogen receptor (hER).[42] Though a multitude of substituted steroid templates are available via direct synthesis, we were particularly interested in commencing from a commercially available building block. Surveying numerous options, it was decided to utilize estrone, introducing the enediyne functionality at the 17α position. Through QSAR analysis it has been shown that 17α *alkynyl* derivatives of estradiol show comparable hER affinity to its endogenous ligand (estradiol), and we decided to construct a hybrid with an alkynyl linker between the enediyne and the steroidal template.[43] Accordingly, enediyne **57** was coupled to a protected (TBDMS) ether of estrone **65** via its organocerium derivative, then unmasked to give **66** (Scheme 16).

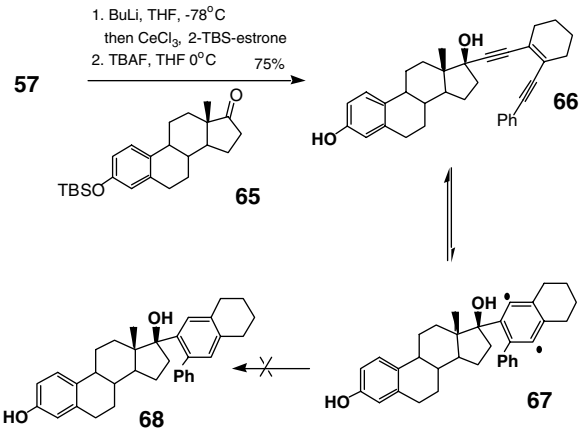

SCHEME 16 First generation photoenediyne-estrogens.

TABLE 29.4 Relative Binding Affinity of Steroid-Enediynes for hER[a]

Entry	Substrate	RBA (nmol)
1	**66**	103
2	**72**	14
3	**76**	12

[a] Candidate + ^{3}H β–estradiol incubated with cytosol at 4°C. Unbound agents removed (DCC) and bound ^{3}H β–estradiol measured by scintillation counter. RBA corresponds to concentration required to reduce hER bound ^{3}H β-estradiol by 50%.[47]

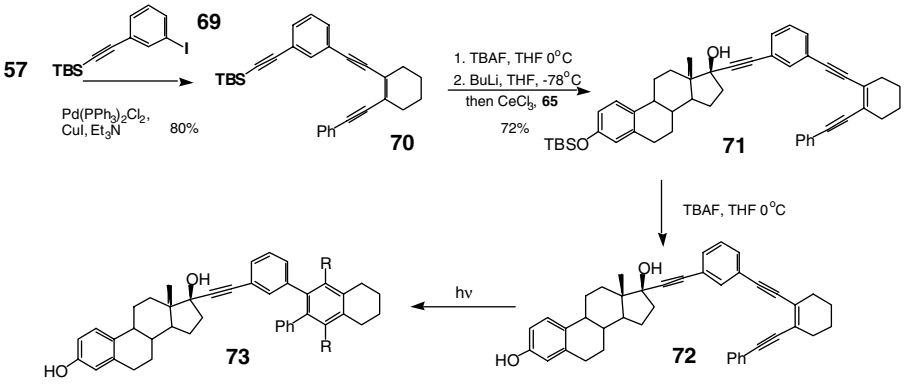

SCHEME 17 Spaced photoenediyne-estrogens.

Unfortunately, this compound, which had an RBA of >100 nmol (Table 29.4), proved stable at physiological temperature and did not undergo the expected photo-Bergman cycloaromatization to give **68** even on prolonged irradiation.[44] Following a strategy adopted previously, we elected to insert a spacer unit in the system between the enediyne and ligand and pursued *m*-disubstituted ligand **72** (Scheme 17). Coupling of **57** with iodoalkyne **69** gave **70**, which was unmasked and subjected to 1,2 addition to **65**, followed by phenolic deprotection to give **72**. To our surprise, the affinity of **72** was greatly superior to that of **66**, supporting the notion that the LBD of hERα has considerable tolerance for lipophilic

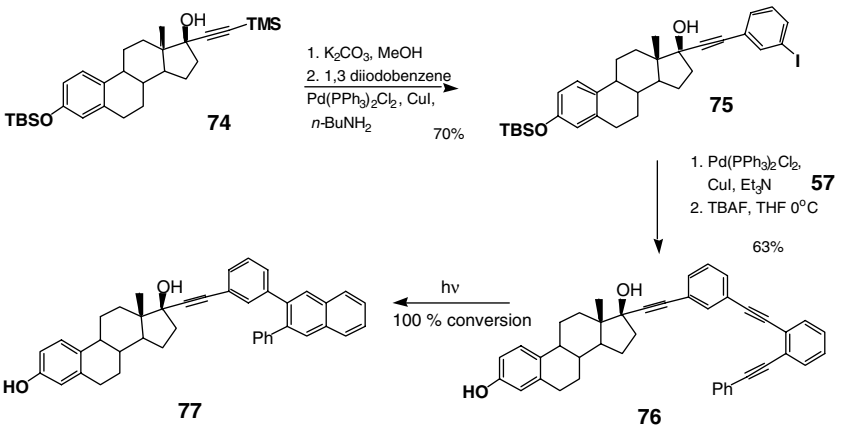

SCHEME 18 High affinity photoactivated enediyne-estrogens.

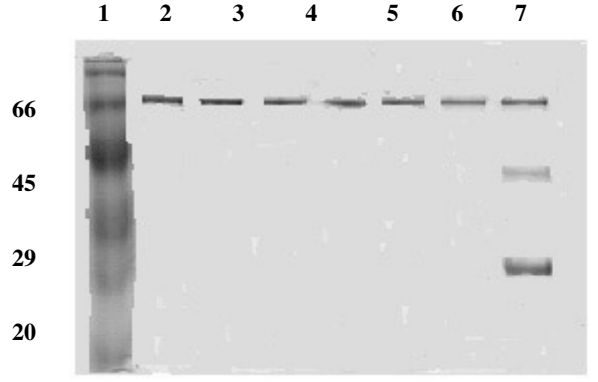

FIGURE 29.6 ER degradation. 10% SDS polyacrylamide gel of the reaction estrogen receptor (ER) (1.5 mg/ml) with the drug (550 μM). All reactions were conducted in 20 mM Tris-HCl buffer pH 8. From left to right: lane 1, molecular weight markers (KDa); lane 2, ER no irradiation; lane 3, ER after 6h irradiation; lane 4, ER after 12h irradiation, lane 5, ER + **72** no irradiation; lane 6, ER with control; lane 7, ER + **72** after 6h irradiation; and lane 8, ER + **72** after 12h irradiation.

functionality at the steroidal 17α position.[45] Though the binding affinity of **72** was spectacular, to our disappointment its photo-Bergman cycloaromatization profile was poor, giving only trace amounts of the expected cycloaromatization product **73** even after prolonged irradiation.[46] We elected to improve the efficiency of the critical process by extending the conjugation of the ligand and pursued **76** as a refined target. Though this required complete resynthesis, an efficient process was developed via pre-assembly of enediyne template **57** (Scheme 18).

This was coupled in turn to iodoarene **75**, produced by arylation of the unmasked alkyne derived from **74**, which could be produced either from **65** or the commercially available 17α-ethynyl estradiol. Though the binding affinity of **76** did not differ markedly from that of **72**, this ligand underwent smooth photocycloaromatization to give complete conversion to cycloaromatized product **77** within 3 h.[44] Irradiation in the presence of recombinant hER resulted in marked degradation, and control reactions confirmed the influence of the various constituents (Figure 29.6).[46]

Application of this strategy to other members of the hormone receptor superfamily would appear possible. The homology of the hormone receptor superfamily has been well studied, and endogenous small molecule ligands have been identified for most.[48] Examples include the progesterone and vitamin

D receptors and their associated coactivators[49] heat shock proteins.[50] Additional possibilities include the glucocortocoid and mineralcorticoid receptors and a number of orphan receptors, e.g., the aryl hydrocarbon receptor.[51] In the latter case, it has already been demonstrated that degradation can be effected by a thermally activated enediyne;[52] thus, a photochemical variant could be forthcoming.

In addition to the possibility of tethering enediynes to biological substrates for specific targeting is the concept of generating more intimate enediyne chimera, where the enediyne is fused with a biological substrate. One can envision photochemical activation of appropriate derivatives of uracil-enediyne **78**.[53] This compound already bears the hydrogen bonding pattern necessary for DNA duplex (AT) or triplex (TAT) formation. Such molecules could be incorporated into oligonulceotides for greater sequence specificity prior to photoactivation. Likewise, flavin–enediyne **79** might also be adapted for photochemical studies targeting selected flavoenzymes.[54] Studies have shown that many flavoenzymes can tolerate a number of different substituents at the flavin C7 and C8 positions.[55]

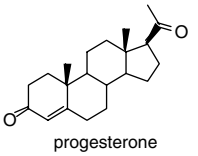

progesterone

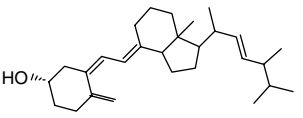

vitamin D

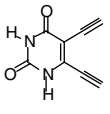

78

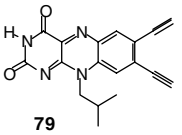

79

29.5 Theoretical Treatment of the Photochemical Bergman Cycloaromatization

Davidson and Zaleski have examined the photochemical Bergman cyclization computationally using spin-unrestricted density functional theory (UDFT) and multiconfigurational self-consistent field theory (MCSCF).[56] The ground states calculated using UB3LYP and CASSCF accurately reproduced the experimental geometry of *Z*-3-hexen-1,5-diyne (**80**). Other methods (UPBW91) overestimated some bond lengths. All of the methods used predicted a C_{2v} geometry strongly resembling a diradical for the transition state structure and a distorted benzene structure of D_{2h} symmetry when the intermediate (**81**) is completely formed. This is consistent with theoretical treatment of the thermal cyclization, where diyl formation has a late transition state.[57]

The excited states of the enediyne moiety were approximated by a weakly interacting ethylene acetylene model where the various states are expressed as linear combinations of the configurations for one ethylene and two acetylenes. The authors examined the first six excited states of **80**, three triplets and three singlets. All methods examined predicted that the spectroscopically forbidden triplet states (1^3B_2, 1^3B_1, and 1^3A_1, respectively) lie between the singlet ground state (S_0) and the first singlet excited state (1^1B_2).

The weakly interacting ethylene acetylene model indicates that the lowest energy triplet and singlet states of **80** are most closely related to the singlet and triplet states of ethylene. The model therefore predicts that symmetrical substitution at the enediyne alkyne termini will not affect the singlet–triplet energy gap (ΔE_{ST}), while substitution at the double bond will affect ΔE_{ST}. Indeed, enediynes with *n*-propyl or phenyl substituents at the triple bond termini have the same observed energy difference between fluorescent and phosphorescent states.[20] Other spectroscopic evidence supports this point of view when examining substituents on the carbon–carbon double bond.

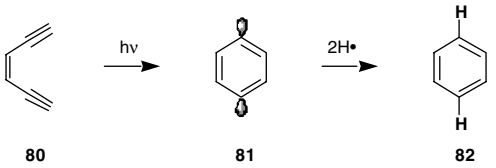

SCHEME 19 Theoretical examination of Photo-Bergman cyclization.

Bergman cyclization along the C_{2v} lowest energy triplet potential energy surface (PES) is not possible, as the symmetry constraints do not allow the necessary mixing of in-plane and out-of-plane orbitals (Woodward–Hoffmann forbidden). Cyclization along the symmetry-relaxed (C_2) lowest energy triplet PES is Woodward–Hoffmann allowed; however, two other possible mechanisms (isomerization or hydrogen abstraction from the alkyne termini) compete with the Bergman cyclization pathway.

When the lowest energy excited singlet state residing primarily on the triple bonds (1^1B_1) is examined, it is Woodward–Hoffman spin forbidden due to the C_{2v} symmetry of **80**. However, this excited state of **80** was found to relax through a second order Jahn–Teller distortion to a 2^1A state of C_1 symmetry. This state has two major reaction paths, deactivation to the S_0 state or Bergman cyclization, either of which result in Bergman cyclization products.

Even though the 1^3B path may seem preferable thermodynamically, the multiple non-Bergman pathways along the potential energy surface make it an unlikely source of photochemically generated Bergman cyclization reactions. The less exothermic 2^1A PES, while higher in energy, reduces in-plane repulsion between the approaching triple bonds, which is thought to facilitate cyclization. Interestingly, these calculations also indicated that the *p*-benzyne intermediate has unusual characteristics, combining singlet carbene and open-shell diradical features.

29.6 Summary and Outlook

Several research groups have successfully demonstrated the viability of the photo-Bergman cyclization. The efficiency of the process is influenced by several factors, but near-quantitative yields can be obtained under ideal circumstances, rivaling the thermal version of this pathway. The application of this process in molecular biology and molecular medicine would seem particularly attractive. Photoactivated enediynes have been successfully employed as chemical nucleases and as protein degrading agents, in both cases showing good correlation between affinity and cleavage activity. Based on these findings, coupled with expeditious synthetic routes to the core warheads of great diversity, enediyne reagents capable of inducing specific nucleic acid/protein modulation can now be designed. Such affinity cleavage systems may offer advantages over conventional methods since they do not function via metal ion redox chemistry.[58] It is anticipated that the scope and limitations of this field will be the focus of future reports.

Acknowledgments

We wish to acknowledge financial support from grants from NIH (5RO1GM57123), NSF (MCB98661), PRF (33920AC1), American Cancer Society, Elsa U. Pardee Foundation, Massachusetts Department of Health, and the GHS-CU Biomedical Cooperative research program (to GBJ); and from NSF (CHE0138640), NSF (CHE0211577), American Cancer Society, Petroleum Research Fund, and CINSAM (to KCR). KCR also wishes to thank C. Parrish for helpful discussions.

References

1. Lee, M.D., Dunne, T.S., Siegel, M.M., Chang, C.C., Morton, G.O., and Borders, D.B., Calichemicins, a novel family of antitumor antibiotics. 2. Chemistry and structure of calichemicin γ1, *J. Am. Chem. Soc.,* 109, 3464, 1987.

2. Lee, M.D., Durr, F.E., Hinman, L.H., Haman, P.R., and Ellestad, G.A., in *Advances in Medicinal Chemistry,* Vol. 2, Maryanoff, B.E. and Maryanoff, C.A., Eds., Jai Press, Greenwich, England, 1993.
3. Ishida, N., Miyazaki, K., Kumagai, K., and Rikimaru, M., Neocarzinostatin, an antitumor antibiotic of high molecular weight. Isolation, physiochemical properties and biological activities, *J. Antibiot.,* 18, 68, 1965.
4. Edo, K., Mizugaki, M., Koide, Y., Seto, H., Furihata, K., Otake, N., and Ishida, N., The chemical structure of antitumor polypeptide antibiotic neocarzinostatin chromophore, *Tetrahedron Lett.,* 26, 331, 1985.
5. Smith, A.L. and Nicolaou, K.C., The enediyne antibiotics, *J. Med. Chem.,* 39, 2103, 1996; Xi, Z. and Goldberg, I., DNA damaging enediyne compounds, in *Comprehensive Natural Products Chemistry,* Vol. 7, Barton, D.H.R. and Nakanishi, K., Eds. Pergamon, Oxford, 1999, p. 553.
6. For overviews of recent clinical findings, see: Schor, N.F., in *Cancer Therapeutics: Experimental and Clinical Agents,* Teicher, B., Ed., Humana Press, Totowa, NJ, 1996, pp. 229–240, Schmitt, D.A., Kisanuki, K., Kimura, S., Oka, K., Pollard, R.B., Maeda, H., and Suzuki, F., Antitumor activity of orally administered SMANCS, a polymer-conjugated protein drug, in mice bearing various murine tumors, *Anticancer Res.,* 12, 2219, 1992; Takahashi, T., Yamaguchi, T., Kitamura, K., Noguchi, A., Mitsuyo, H., and Otsuji, E., Follow-up study of patients treated with monoclonal antibody-drug conjugate: report of 77 cases with colorectal cancer, *Jpn. J. Cancer Res.,* 84, 976, 1993; Oda, M., Sato, F., and Maeda, H., Facilitated internalization of neocarzinostatin and its lipophilic polymer conjugate, SMANCS, into cytosol in acidic pH, *JNCI,* 79, 1205, 1987.
7. Kappen, L.S. and Goldberg, I.H., Activation and inactivation of neocarzinostatin-induced cleavage of DNA, *Nucleic Acids Res.,* 5, 2959, 1978.
8. Bergman, R.G., Reactive 1,4-dehydroaromatics, *Acc. Chem. Res.,* 6, 25, 1973.
9. Myers, A.G., Proposed structure of the neocarzinostatin chromophore-methyl thioglycolate adduct: a mechanism for the nucleophilic activation of neocarzinostatin, *Tetrahedron Lett.,* 28, 4493, 1987.
10. Zein, N., Solomon, W., Casazza, A.M., Kadow, J.F., Krishnan, B.S., Tun, M.M., Vyas, D.M., and Doyle, T.W., Protein damage caused by a synthetic enediyne core, *Bioorg. Med. Chem. Lett.,* 3, 1351, 1993; Lee, S., Bain, A., Sulikowski, G.A., Solomon, W., and Zein, N., Synthesis and biological evaluation of a bicyclo[7.4.1]enediyne, *Bioorg. Med. Chem. Lett.,* 6, 1261, 1996; Wittman, M.D., Kadow, J.F., Langley, D.R., Vyas, D.M., Rose, W.C., Solomon, W., and Zein, N., The synthesis and biological activity of enediyne minor groove binding hybrids, *Bioorg. Med. Chem. Lett.,* 5, 1049, 1995.
11. Dedon, P.C. and Goldberg, I.H., Free-radical mechanisms involved in the formation of sequence-dependent bistranded DNA lesions by the antitumor antibiotics bleomycin, neocarzinostatin, and calicheamicin, *Chem. Res. Toxicol.,* 5, 311, 1992.
12. Denny, W.A., in *Cancer Chemotherapeutic Agents*, Foye, W.O., Ed. *ACS Symp. Ser.,* 1995, pp. 483–500.
13. Durkacz, B.W., Omidiji, O., Gray, D.A., and Shall, S., (ADP-ribose)n participates in DNA excision repair, *Nature*, 283, 593, 1980; Zhao, B., Konno, S., Wu, J.M., and Oronsky, A.L., Modulation of nicotinamide adenine dinucleotide and poly(adenosine diphosphoribose) metabolism by calicheamicin γ1 in human HL-60 cells, *Cancer Lett.,* 50, 141, 1990.
14. Grissom, J.W., Gunawardena, G.U., Klingberg, D., and Huang, D., The chemistry of enediynes, enyne allenes and related compounds, *Tetrahedron,* 52, 6453, 1996.
15. Stang, P.J. and Diederich, F., Eds., *Modern Acetylene Chemistry,* VCH, Weinheim, 1995.
16. Okamura, W.H. and Sondheimer, F., 1,3,7,9,13,15 Hexadehydro[18]annulene, *J. Am. Chem. Soc.,* 89, 5991, 1967.
17. Anthony, J.A., Boudon, C., Diederich, F., Gisselbrecht, J.P., Gramlich, V., Gross, M., Hobi, M., and Seiler, P., Stable, soluble, conjugated carbon rods with a persilylethynylated polytriacetylene backbone, *Angew. Chem. Int. Ed. Engl.,* 33, 763, 1994.
18. Gobbi, L., Seiler, P., and Diederich, F., A novel three-way chromophoric molecular switch: pH and light controllable switching cycles, *Angew. Chem. Int. Ed. Engl.,* 38, 674, 1999.

19. Turro, N.J., Evenzahav, A., and Nicolaou, K.C., Photochemical analog of the Bergman cycloaromatization reaction, *Tetrahedron Lett.,* 35, 8089, 1994.
20. Evenzahav, A. and Turro, N.J., Photochemical rearrangement of enediynes: is a "photo-Bergman" cyclization a possibility? *J. Am. Chem. Soc.,* 120, 1835, 1998.
21. Ramakumar, D., Kalpana, M., Varghese, B., and Sankararaman, S., Cyclization of enediyne radical cations through chemical, photochemical, and electrochemical oxidation: the role of state symmetry, *J. Org. Chem.,* 61, 2247, 1996.
22. Kaneko, T., Takahashi, M., and Hirama, M., Photochemical cycloaromatization of non-benzenoid enediynes, *Angew. Chem. Int. Ed. Engl.,* 38, 1267, 1999.
23. Funk, R.L., Young, E.R.R., Williams, R.M., Flanagan, M.F., and Cecil, T.L., Photochemical cycloaromatization reactions of ortho dialkynylarenes: a new class of DNA photocleaving agents, *J. Am. Chem. Soc.,* 118, 3291, 1996.
24. Choy, N., Blanco, B., Wen, J., Krishan, A., and Russell, K.C., Photochemical and thermal Bergman cyclization of a pyrimidine enediynol and enediynone, *Org. Lett.,* 2, 3761, 2000.
25. Wardel, H. and Wiest, O., Enediynes in II-membered rights. Synthesis and structure of highly strained but unusually stable macrocycles, *J. Org. Chem.,* 67, 388, 2002.
26. Jones, G.B., Wright, J.M., Plourde, G.W., II, Hynd, G., Huber, R.S., and Mathews, J.E., A direct and stereocontrolled route to conjugated enediynes, *J. Am. Chem. Soc.,* 122, 1937, 2000; Jones, G.B., Wright, J., Plourde, G., Purohit, A., Wyatt, J., Hynd, G., and Fouad, F., Synthesis and photochemical activity of designed enediynes, *J. Am. Chem. Soc.,* 122, 9872, 2000.
27. Kim, C-S., Diez, C., and Russell, K.C., Tautomer-dependent Bergman cyclization of novel uracil-enediyne chimeras, *Chem.-Eur. J.,* 6, 1555, 2000.
28. Nicolaou, K.C., Zuccarello, G., Ogawa, Y., Schweiger, E.J., and Kumazawa, T., Cyclic conjugated enediynes related to calicheamicins and esperamicins: calculations, synthesis, and properties, *J. Am. Chem. Soc.,* 110, 4866, 1988; Magnus, P., Fortt, S., Pitterna, T., and Snyder, J.P., Synthetic and mechanistic studies on esperamicin A1 and calichemicin γ1. Molecular strain rather than π-bond proximity determines the cycloaromatization rates of bicyclo[7.3.1]enediynes, *J. Am. Chem. Soc.,* 112, 4986, 1990; Jones, G.B. and Warner, P.M., Electronic control of the Bergman cyclization: the remarkable role of vinyl substitution, *J. Am. Chem. Soc.,* 132, 2134, 2001.
29. Sakata, N., Tsuchiya, K.S., Moriya, Y., Hayashi, H., Hori, M., Otani, T., Nagai, M., and Aoyagi, T., Aminopeptidase activity of an antitumor antibiotic, C-1027, *J. Antibiot.,* 45, 113, 1992.
30. Zein, N. and Schroeder, D.R., in *Advances in DNA Sequence Specific Agents,* Vol. 3, Jones, G.B. Ed., JAI Press Inc., 1998, p. 201.
31. Zein, N., Solomon, W., Casazza, A.M., Kadow, J.F., Krishnan, B.S., Tun, M.M., Vyas, D.M., and Doyle, T.W., Protein damage caused by a synthetic enediyne core, *Bioorg. Med. Chem. Lett.,* 3, 1351, 1993; Lee, S., Bain, A., Sulikowski, G.A., Solomon, W., and Zein, N., Synthesis and biological evaluation of a bicyclo[7.4.1]enediyne, *Bioorg. Med. Chem. Lett.,* 6, 1261, 1996; Wittman, M.D., Kadow, J.F., Langley, D.R., Vyas, D.M., Rose, W.C., Solomon, W., and Zein, N., The synthesis and biological activity of enediyne minor groove binding hybrids, *Bioorg. Med. Chem. Lett.,* 5, 1049, 1995.
32. For early efforts using thermally activated enediynes see: Wang, J. and DeClercq, P.J., A new diyl precursor family derived from estradiol, *Angew. Chem. Int. Ed. Engl.,* 34, 1749, 1995; Py, S., Harwig, C.W., Banerjee, S., Brown, D.L., and Fallis, A.G., Taxamycin studies: synthesis of taxoid-calicheamicin hybrids, *Tetrahedron Lett.,* 39, 6139, 1998; Jones, G.B., Huber, R.S., Mathews, J.E., and Li, A., Target directed enediyne prodrugs: cytotoxic estrogen conjugates, *Tetrahedron Lett.,* 37, 3643, 1996; Jones, G.B., Wright, J.M., Hynd, G., Wyatt, J.K., Yancisin, M., and Brown, M.A., Protein-degrading enediynes: library screening of Bergman cycloaromatization products, *Org. Lett.,* 2, 1863, 2000.
33. Kumar, C.V., Buranaprapuk, A., Opiteck, G.J., Moyer, M.B., Jockusch, S., and Turro, N.J., Photochemical protease: site-specific photocleavage of hen egg lysozyme and bovine serum albumin, *Proc. Nat. Acad. Sci.,* 95, 10361, 1998.

34. Kumar, C.V. and Buranaprapuk, A., Tuning the selectivity of protein photocleavage: spectroscopic and photochemical studies, *J. Am. Chem. Soc.,* 121, 4262, 1999.
35. El-Shafey, A., Zhong, H., Jones, G.B., and Krull, I., Application of affinity capillary electrophoresis for the determination of binding and thermodynamic constants of enediynes with bovine serum albumin, *Electrophoresis,* 23, 945, 2002.
36. Brown, K.C., Yu, Z., Burlingame, A.L., and Craik, C.S., Determining protein–protein interactions by oxidative cross-linking of a glycine–glycine–histidine fusion protein, *Biochemistry*, 37, 4397, 1998; Yamamoto, O., in *Protein Cross Linking*, Part A, Friedman, M., Ed. Plenum Press, New York, 1977, pp. 519–547.
37. Zein, N., Reiss, P., Bernatowicz, M., and Bolgar, M., The proteolytic specificity of the natural enediyne-containing chromoproteins is unique to each chromoprotein, *Chem. Biol.,* 2, 451, 1995.
38. Plourde, G., El-Shafey, A., Fouad, F.S., Purohit, A.S., and Jones, G.B., Protein degradation with photoactivated enediyne-amino acid conjugates, *Bioorg. Med. Chem. Lett.,* 12, 2985, 2002.
39. Cohen, G.B., Ren, R., and Baltimore, D., Modular binding domains in signal transduction proteins, *Cell,* 80, 237, 1995.
40. Pascal, S.M., Singer, A.U., Gish, G., Yamazaki, T., Shoelson, S.E., Pawson, T., Kay, L.E., and Forman, K.J., Nuclear magnetic resonance structure of an SH2 domain of phospholipase C-gamma 1 complexed with a high affinity binding peptide, *Cell,* 77, 461, 1994.
41. Feng, S., Kasahara, C., Rickles, R.J., and Schreiber, S.L., Specific interactions outside the proline-rich core of two classes of Src homology 3 ligands, *Proc. Natl. Acad. Sci. U.S.A.,* 92, 12408, 1995.
42. O'Malley, B.W., The steroid receptor superfamily: more excitement predicted for the future, *Mol. Endocrinol.,* 4, 363, 1990; Evans, R.M., The steroid and thyroid hormone receptor superfamily, *Science*, 240, 889, 1988; Kumar, V., Green, S., Stack, G., Berry, M., Jin, J.-R., and Chambon, P., Functional domains of the human estrogen receptor, *Cell,* 51, 941, 1987.
43. Korach, K.S., Stilbestrol estrogens: molecular/structural probes for understanding estrogen action, in *Molecular Structure and Biological Activities of Steroids,* Bohl, W. and Duax, W.L., Eds., CRC Press, Boca Raton, FL, 1992, p. 210; Gao, H., Katzenellenbogen, J.A., Garg, R., and Hansch, C., Comparative QSAR analysis of estrogen receptor ligands, *Chem. Rev.,* 99, 723, 1999.
44. Jones, G.B., Purohit, A., Wright, J.W., Hynd, G., Wyatt, J., Swamy, N., and Ray, R., Chemical synthesis of hormone receptor probes: high affinity photoactivated enediyne–estrogens, *Tetrahedron Lett.,* 42, 8579, 2001.
45. Brzozowski, A.M., Pike, A.C.W., Dauter, Z., Hubbard, R.E., Bonn, T., Engstrom, O., Ohman, L., Greene, G.L., Gustafsson, J-A., and Carlquist, M., Molecular basis of agonism and antagonism in the estrogen receptor, *Nature,* 389, 753, 1997.
46. El-Shafey, A. and Jones, G.B., manuscript in preparation.
47. Scatchard, G., The attraction of proteins for small molecules and ions, *Ann. N.Y. Acad. Sci.,* 51, 660, 1949.
48. Ing, N.H., Beekman, J.M., Tsai, S.Y., Tsai, M.-J., and O'Malley, B.W., Members of the steroid hormone receptor superfamily interact with TFIIB (S300-II), *J. Biol. Chem.,* 267, 17617, 1992.
49. Chen, H., Lin, R.J., Xie, W., Wilpitz, D., and Evans, R.M., Regulation of hormone-induced histone hyperacetylation and gene activation via acetylation of an acetylase, *Cell,* 98, 675, 1999.
50. Dunn, D.K., Whelan, R.D., Hill, B., and King, R.J., Relationship of HSP27 and estrogen receptor in hormone sensitive and insensitive cell lines, *J. Steroid Biochem. Mol. Biol.*, 46, 469, 1993; Segnitz, B. and Gehring, U., Subunit structure of the nonactivated human estrogen receptor, *Proc. Natl. Acad. Sci. U.S.A.*, 92, 2179, 1995.
51. Chaloupka, K., Krishnan, V., and Safe, S., Polynuclear aromatic hydrocarbon carcinogens as anti-estrogens in MCF-7 human breast cancer cells: role of the Ah receptor, *Carcinogenesis*, 13, 2233, 1992; Wilhelmsson, A., Whitelaw, M.L., Gustafsson, J-A., and Poellinger, L., Agonistic and antagonistic effects of α-naphthoflavone on dioxin receptor function. Role of the basic region helix-loop-helix dioxin receptor partner factor Arnt, *J. Biol. Chem.,* 269, 19028, 1994; Merchant, M.,

Morrison, V., Santostefano, M., and Safe, S., Mechanism of action of aryl hydrocarbon receptor antagonists: inhibition of 2,3,7,8-tetrachlorodibenzo-*p*-dioxin-induced CYP1A1 gene expression, *Arch. Biochem. Biophys.,* 298, 389, 1992.

52. Jones, G.B., Kilgore, M.W., Pollenz, R.S., Li, A., Mathews, J.E., Wright, J.M., Huber, R.S., Tate, P.L., Price, T.L., and Sticca, R.P., Target directed enediyne prodrugs: hER and AhR degradation by a synthetic oxo-enediyne, *Bioorg. Med. Chem. Lett.,* 6, 1971, 1996.
53. Kim, C.-S., Diez, C., and Russell, K.C., Tautomer-dependent Bergman cyclization of novel uracil-enediyne chimeras, *Chem.-Eur. J.,* 6, 1555, 2000; Kumarasinghe, E.S., Peterson, M.A., and Robins, M.J., Synthesis of 5,6-bis(alkyn-1-yl)pyrimidines and related nucleosides, *Tetrahedron Lett.,* 41, 8741, 2000.
54. Choy, N., Russell, K.C., Alvarez, J., and Fider, A., Synthesis and redox properties of novel alkynyl flavins, *Tetrahedron Lett.,* 41, 1515, 2000.
55. Schopfer, L.M., Massey, V., and Claiborne, A., Active site probes of flavoproteins. Determination of the solvent accessibility of the flavin position 8 for a series of flavoproteins, *J. Biol. Chem.,* 256, 7329, 1981.
56. Clark, A.E., Davidson, E.R., and Zaleski, J.M., UDFT and MCSCF descriptions of the photochemical Bergman cyclization of enediynes, *J. Am. Chem. Soc.,* 123, 2650, 2001.
57. Lindh, R. and Persson, B.J., *J. Am. Chem. Soc.,* 116, 4963, 1994; Lindh, R., Lee, T.J., Bernhardsson, A., Persson, B.J., and Karlstrom, G., Extended *ab initio* and theoretical thermodynamics studies of the Bergman reaction and the energy splitting of the singlet *o*-, *m*-, and *p*-benzynes, *J. Am. Chem. Soc.,* 117, 7186, 1995; Kraka, E. and Cremer, D., CCSD(T) Investigation of the Bergman cyclization of enediyne. Relative stability of *o*-, *m*-, and *p*-didehydrobenzene, *J. Am. Chem. Soc.,* 116, 4929, 1994; Koga, N. and Morokuma, K., Comparison of biradical formation between enediyne and enyne-allene. *Ab initio* CASSCF and MRSDCI study, *J. Am. Chem. Soc.,* 113, 1907, 1991; Houk, K.N., Li, Y., and Evanseck, J.D., Transition structure in pericyclic reactions of hydrocarbons, *Angew. Chem. Int. Ed. Engl.,* 31, 682, 1992.
58. Rana, T.M. and Meares, C.F., Iron chelate mediated proteolysis: protein structure dependence, *J. Am. Chem. Soc.,* 113, 1859, 1991; Hoyer, D., Cho, H., and Schultz, P.G., New strategy for selective protein cleavage, *J. Am. Chem. Soc.,* 112, 3249, 1990; Cuenoud, B., Tarasow, T.M., and Schepartz, A., A new strategy for directed protein cleavage, *Tetrahedron Lett.,* 33, 895, 1992; Hegg, E.L. and Burstyn, J.N., Hydrolysis of unactivated peptide bonds by a macrocyclic copper(ii) complex: Cu([9]aneN3)Cl2 hydrolyzes both dipeptides and proteins, *J. Am. Chem. Soc.,* 117, 7015, 1995; Wu, J., Perrin, D.M., Sigman, D.S., and Kaback, H.R., Helix packing of lactose permease in *Escherichia coli* studied by site-directed chemical cleavage, *Proc. Nat. Acad. Sci.,* 92, 9186, 1995; Parac, T.N. and Kostic, N.M., Effects of linkage isomerism and of acid-base equilibria on reactivity and catalytic turnover in hydrolytic cleavage of histidyl peptides coordinated to palladium(II). Identification of the active complex between palladium(ii) and the histidyl residue, *J. Am. Chem. Soc.,* 118, 5946, 1996; Kumar, C.V. and Buranaprapuk, A., Tuning the selectivity of protein photocleavage: spectroscopic and photochemical studies, *J. Am. Chem. Soc.,* 121, 4262. 1999; Miyake, R., Owens, J.T., Xu, D., Jackson, W.M., and Meares, C.F., Site-directed photocleavage for mapping protein architecture, *J. Am. Chem. Soc.,* 121, 7453, 1999.

30

The Photochemical Reactivity of the Allenyl–Vinyl Methane System

Takashi Tsuno
Nihon University

Kunio Sugiyama
Nihon University

30.1 Introduction

The photochemistry of divinyl methane systems has been extensively examined on the base of energetic research by Zimmerman et al., and excellent published reports exist involving the reaction mechanism, multiplicities, and substituent effects.[1,2] These compounds mainly undergo a di-π-methane rearrangement (Scheme 1).[1,2] The divinyl methane systems in which one vinyl is an imine or carbonyl also undergo a di-π-methane rearrangement; the former is called an aza-di-π-methane rearrangement,[1a,3,4] and the latter is called an oxa-di-π-methane rearrangement[1a,5,6] (Scheme 1). Such structural photochemical rearrangements of the divinyl methane systems are important methods in organic syntheses.[1,3,5]

On the other hand, allenes are good alkenes and undergo intermolecular[7,8] and intramolecular [2 + 2]-cycloaddition[7–10] with enones to give *exo*-methylene–substituted fused cyclobutanes (Scheme 2). Because novel fused cyclic compounds or precursors of natural products can be formed from the resulting *exo*-methylene–substituted fused cyclobutanes, these reactions are also key reactions in organic syntheses.[8,9] Since 1,2-propadiene or alkyl-substituted allenes exhibit absorption maxima in the far-UV range and also show a shoulder absorption in the range of 200–250 nm, the enone moiety in the bichromophoric compounds is initially excited (>280 nm), and intramolecular [2 + 2]-cycloaddition then takes place. On the other hand, it has been found that excited allenes can undergo several intramolecular photochemical migrations and cleavage processes.[11,12] Thus, the photochemistry occurring from interaction between an excited state of the allene and the other chromophore in the ground state is also of considerable interest.

The allenyl and vinyl chromophores in allenyl–vinyl methanes are separated by a very short carbon chain: i.e., methylene; hence these compounds are expected to undergo interesting photoreactions within each of the excited states of the chromophores, multiplicities, substituent effects, etc. In 1973, Lankin et al.[13] communicated results dealing with the photochemistry of the allenyl–styryl methanes, and the

0-8493-1348-1/04/$0.00+$1.50

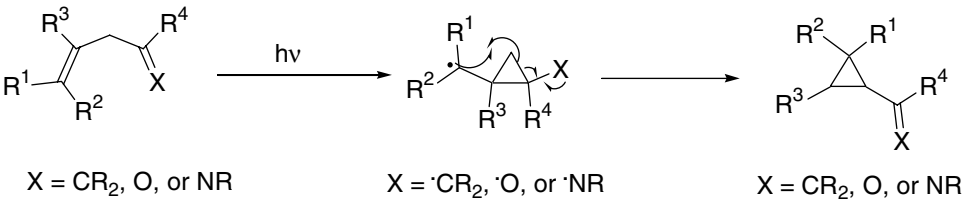

SCHEME 1

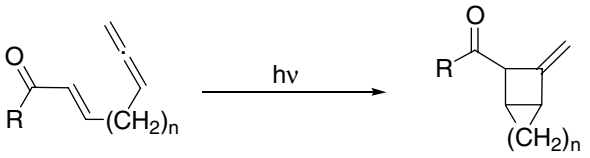

SCHEME 2

full report was published in 1975.[14] Although Jeger et al.[15] also reported the photochemistry of an allenyl–alkenoyl methane, the report is a mere note. Furthermore, several reports on the photochemistry of the allenyl–vinyl methanes substituted with an electron-withdrawing group(s) on the vinyl moiety have been published in the last decade by Tsuno et al.[16–27] In the following sections, we will discuss the observed photochemistry of the allenyl–vinyl methane systems.

30.2 Intramolecular [2 + 2]-Cycloaddition

Most of the divinyl methanes undergo mainly the di-π-methane rearrangement to give vinylcyclopropanes.[1,28] In contrast, there are quite a few examples of intramolecular [2 + 2]-cycloadditions during the direct and/or sensitized photolyses in spite of the substituents on the allenyl–vinyl methanes.[13–27]

Lankin et al. reported that allenyl–styryl methanes underwent an intramolecular [2 + 2]-cycloaddition upon both direct and acetone-sensitized photolyses (Scheme 3).[14] In the reinvestigation[16] of the allenyl–styryl methane systems, results similar to those in Lankin's report were obtained during the direct photolysis; however, the intramolecular [2 + 2]-cycloaddition by acetone-sensitization was not found, and *E,Z*-geometric isomerization proceeded to give an *E,Z*-equilibrium mixture. Sensitized photolyses of **1a** gave equilibrium ratios of **1a** to **2a** dependent upon the triplet energies of the sensitizers used (Figure 30.1).[29] Such a result is analogous to the photochemistry of 1-phenylpropene.[30] The photochemistry of allenyl *p*-substituent styryl methanes **1b–e** and **2b–e** has also been investigated, and Table 30.1 shows the quantum yields for the isomerization of these compounds. The values obtained from the quantum yield measurements show that the *E*-form **1a** prefers the intramolecular cycloaddition path rather than *E,Z*-geometric isomerization, whereas the *Z*-form **2a** reacts in the reverse manner. In the direct photolyses, **1c–e** and **2c–e**, which have an electron-withdrawing or electron-donating aromatic substituent, mainly undergo the *E,Z*-geometric isomerization.[16] Such tendencies indicate participation in barriers for twisting about the double bond on the singlet potential energy surface. In the photochemistry of 1-arylpropenes, the geometric isomerization of (*E*)-1-arylpropenes[31] occurs predominantly from the triplet excited state via intersystem crossing, whereas that of (*Z*)-1-arylpropenes occurs from the singlet state. Moreover, both the electron-donating and electron-withdrawing aromatic substituents of the (*E*)- and (*Z*)-1-arylpropenes have been found to have a low barrier for singlet state isomerization.[31] Hence, the singlet states of the allenyl–styryl methanes, except for **1a** and **1b**, can relax to a perpendicular singlet ($^1P^*$) to give either an *E*- or *Z*-form. The *E*-forms **1a** and **1b** undergo predominantly the intramolecular [2 + 2]-cycloaddition by the singlet state rather than undergoing the triplet geometric isomerization via intersystem crossing. In addition, within the triplet-sensitized reactions there can be relaxation

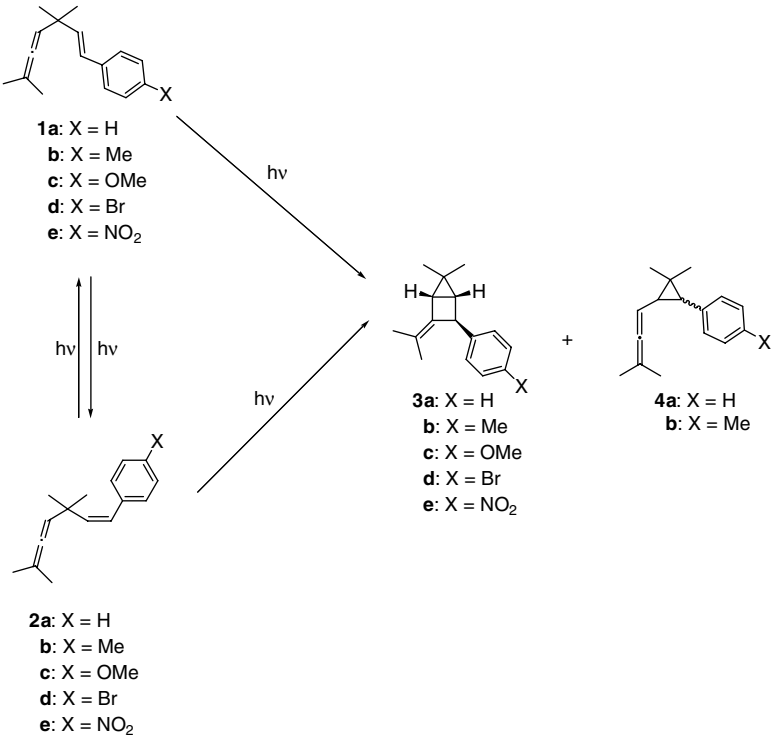

SCHEME 3

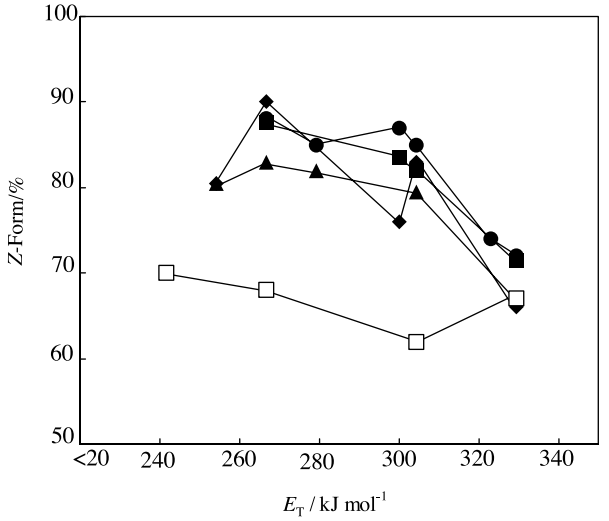

FIGURE 30.1 Compositions of the *Z*-forms in photostationary state by triplet sensitized isomerization of *p*-substituted styryl-allenyl methanes: (**2a**: ●), (**1b**: ■), (**2c**: ♦), **2d**: ▲), and **2e**: □).

to a perpendicular triplet ($^3P^*$) by a zero barrier energy surface. The decay to the ground state by intersystem crossing yields mixtures of the *E*- and *Z*-forms.

It has been reported that the divinyl methanes, in which one vinyl group is an electron-deficient alkene, undergo specific photochemistry: e.g., regioselective di-π-methane rearrangement[32] and an unusual diversion of the di-π-methane rearrangement.[2a] However, the allenyl–vinyl methanes **5–9**,

TABLE 30.1 Quantum Yields in the Direct Photolysis of the Allenyl-Styryl Methane Systems

Allene	Quantum Yields		
	$\Phi_{E\leftrightarrow Z}$[a]	Φ_{cy}[b]	Φ_{di}[c]
1a	0.044 (lit.[d] 0.059)	0.23 (lit.[d] 0.183)	0.059 (lit.[d] 0.044)
2a	0.22 (lit.[d] 0.14)	0.082 (lit.[d] 0.099)	0.025 (lit.[d] 0.043)
1b	0.062	0.24	0.024
2b	0.30	0.061	0.021
1c	0.21	0.028	
2c	0.34	0.021	
1d	0.30	<0.0001	
2d	0.23	<0.0001	
1e	0.28	<0.0001	
2e	0.36	0.067	

[a] Quantum yield for the geometric isomerization.
[b] Quantum yield for the intramolecular [2+2]-cycloaddition.
[c] Quantum yield for the di-π-methane rearrangement.
[d] See Reference 14.

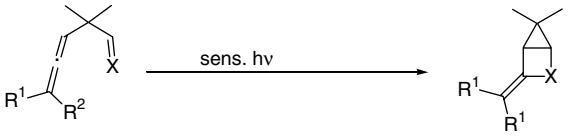

5: R^1, R^2 = H and/or Me, X = 

6: R^1, R^2 = H and/or Me, X = $C(COOMe)_2$

7: R^1, R^2 = H or Me, X = CHCOOMe

8: R^1, R^2 = H or Me, X = $C(CN)_2$

9: R^1, R^2 = H or Me, X = $C(COMe)_2$

10: R^1, R^2 = H and/or Me, X = 

11: R^1, R^2 = H and/or Me, X = $C(COOMe)_2$

12: R^1, R^2 = H or Me, X = CHCOOMe

13: R^1, R^2 = H or Me, X = $C(CN)_2$

14: R^1, R^2 = Me, X = $C(COMe)_2$

SCHEME 4

TABLE 30.2 Estimated Triplet Energies of Compounds 5-9

Compound	Energy/kJ mol^{-1}
5	250–290[a]
6	300[b]
7	300[b]
8	250[b]
9	260–280[c]

[a] See Reference 17.
[b] See Reference 19.
[c] See Reference 23.

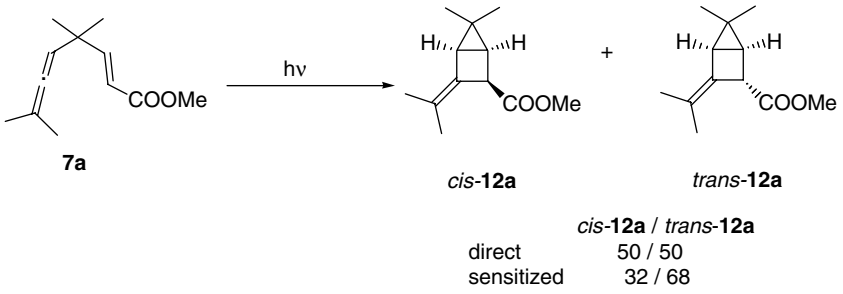

SCHEME 5

which have electron-withdrawing group(s) on the vinyl group, undergo predominantly the intramolecular [2 + 2]-cycloaddition by triplet sensitization (Scheme 4).[17–23] The triplet energies of these compounds were estimated from the energies of the sensitizers used, and the estimated values are shown in Table 30.2. The estimated energies reported are triplet energies of the vinyl moieties[32c,33,34] of the allenyl–vinyl methanes. Therefore, the intramolecular [2 + 2]-cycloaddition of **5–9** takes place, obviously, via the triplet-excited state of the vinyl chromophore.

These allenyl–vinyl methanes **5–9** also gave the housanes **10–14** as a main products or byproducts during direct photolyses.[17–23] From a consideration of triplet energies involved, it was expected that 2-methyl-1,3-butadiene could act as a quencher for intramolecular [2 + 2]-cycloaddition that occurs during direct photolyses. However, this effect was not observed. Thus, if intramolecular [2 + 2]-cycloaddition during the direct photolyses takes place via a triplet pathway only, the rate of its reaction is greater than that of diffusion control. Fortunately, the ratios of the resulting *cis*- and *trans*-housanes *cis*-**12a** and *trans*-**12a** from the direct and sensitized photolyses of **7a** were different (Scheme 5).[19] Therefore, the intramolecular [2 + 2]-cycloaddition of the allenyl–vinyl methanes **5–9** with electron-withdrawing substituents generally involves a singlet excited state pathway except where a triplet state has been definitely proven. Furthermore, because the formation of the *cis*- and *trans*-housane mixture indicates a biradical mechanism, the intramolecular [2 + 2]-cycloaddition involves either a pathway through the 1,4-biradical **15** or the cyclopentane-1,3-diyl radical **16** (Scheme 6). Hydrogen selenide is known to be a good radical hydrogenating reagent.[35–37] Weedon et al.[35–37] have reported the chemistry of trapping of a biradical intermediate for several ene–enone photocycloadditions. Their reports describe an experiment involving an intermolecular allene–cyclopentenone photocycloaddition. In this it has been found that the terminal carbon, rather than the central carbon of the allene, initially bonds to the α-carbon of the cyclopentenone.[35] If these allenyl–vinyl methanes undergo the intramolecular [2 + 2]-cycloaddition according to the mechanism proposed by them, the resulting intermediate would be the 1,4-biradical **15** (Scheme 6). However, we have observed that the path involving the "rule of five" for intramolecular [2 + 2]-cycloaddition of a cycloalkenone with a terminal alkene is involved, and the cyclopentane-1,3-diyl radical biradical intermediate was trapped with hydrogen selenide.[36] The intermediate of the intramolecular [2 + 2]-cycloaddition of the allenyl–vinyl methanes is the cyclopentane-1,3-diyl radical **16** on the basis of the "rule of five" (Scheme 6). If the bulk of the biradical intermediates was trapped with hydrogen selenide, each of the possible hydrogenated compounds **17–20** would be formed. From both the direct and sensitized photolyses of **7a** in the presence of hydrogen selenide, the formation of **17** and **18** by GCMS and GLC analyses was observed, but not that of **19** and **20**.[19] This result proves that the intermediate in the intramolecular [2 + 2]-cycloaddition is the cyclopentane-1,3-diyl radical **16**.

The photoreactivities for the intramolecular [2 + 2]-cycloaddition of the allenyl–vinyl methane systems increase with an increase in the number of methyl donating groups linked to the allene.[17–21,23,24] The results of PM3 MO calculations of the model chromophores **21–25** in the allenyl–vinyl methane systems are shown in Figure 30.2. The HOMOs of **22** and **23** lie at the C1-C2 position, whose coefficients have the same values. On the other hand, the HOMO of **21** lies at the C2-C3 position, and the MO coefficient of C3 has a larger value than that of C2. In addition, the MO coefficient of the β-carbon of **24** or **25** is

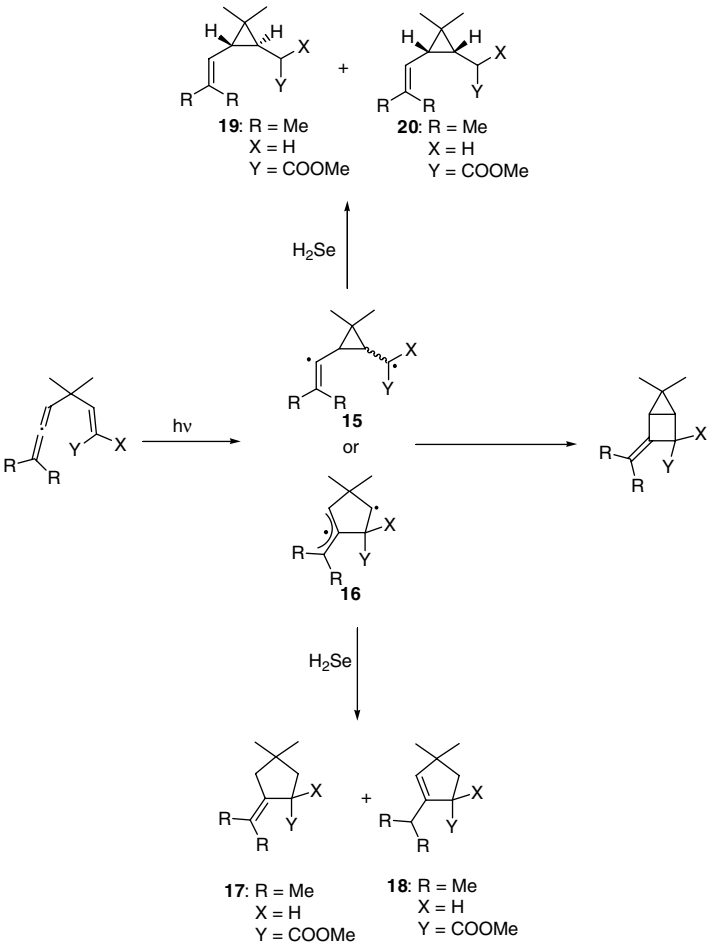

SCHEME 6

lower than that of the α-carbon. These coefficients also support the fact that the intramolecular [2 + 2]-cycloaddition apparently proceeds via the cyclopentane-1,3-diyl radical mechanism.

30.3 Formation of the Alkenylidenecyclopropanes

Because methylene Meldrum's acid is a very electron-deficient alkene,[38] the compounds **5a–c** form an intramolecular charge transfer (CT) complex and show CT bands in a range of 250 to 320 nm.[17,18] Each of the CTs (> 280 nm) and the local excitation (254 nm) of **5a–c** gave the alkenylidenecyclopropanes **26a–c** as main products (Scheme 7).[17,18] Triplet sensitization of these compounds brings about the intramolecular [2 + 2]-cycloaddition as mentioned above. Hence, these compounds are produced via a CT singlet excited state. This reaction mechanism is shown in Scheme 8. The 5-methine protons of a 5-alkyl-substituted Meldrum's acid act as a Brønsted acid.[26,38] These can possibly be exchanged with deuterium, and therefore deuteration under irradiation in methanol-O-*d* cannot fully prove the presence of the enol intermediate **27**.[17] However, when a solution of the monoester **7b** in methanol-O-*d* was irradiated, GCMS analysis showed the vinylidenecyclopropane with deuterium incorporated at the α-position (Scheme 9).[19] This strongly supports a reaction mechanism involving enol intermediates such as **27** or **28**.

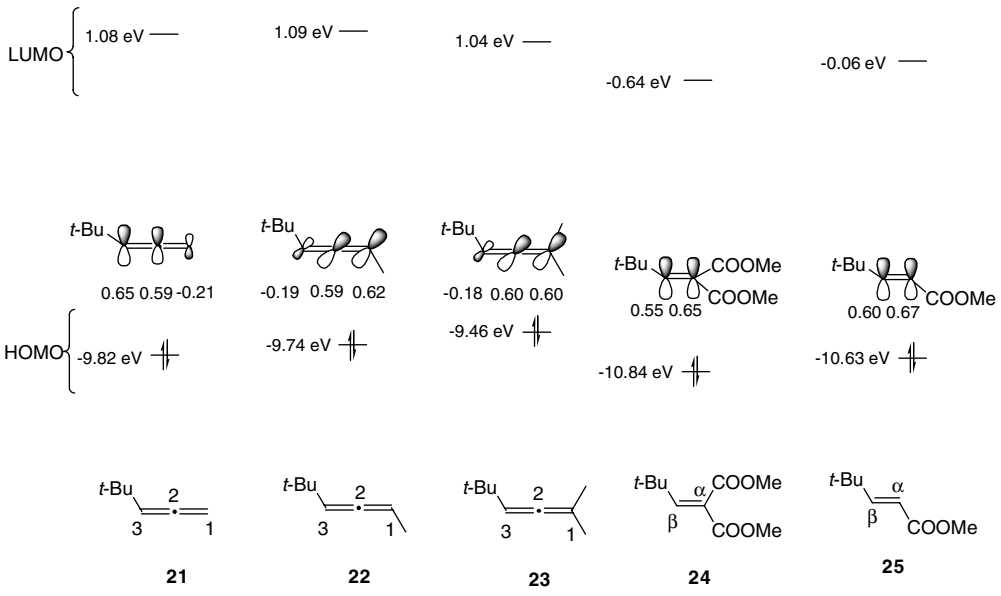

FIGURE 30.2 Molecular orbital correlation diagrams of **21–25**.

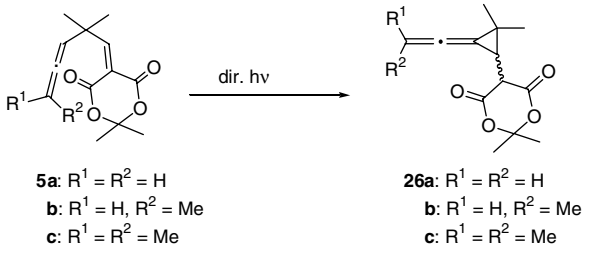

SCHEME 7

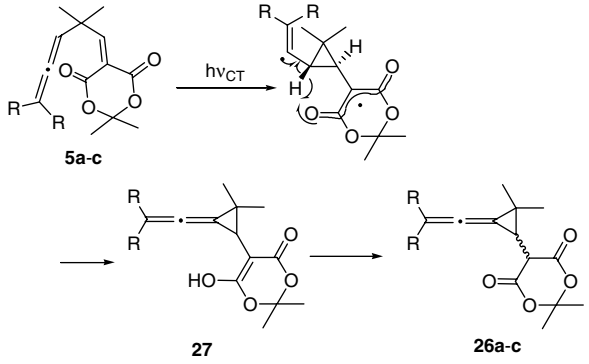

SCHEME 8

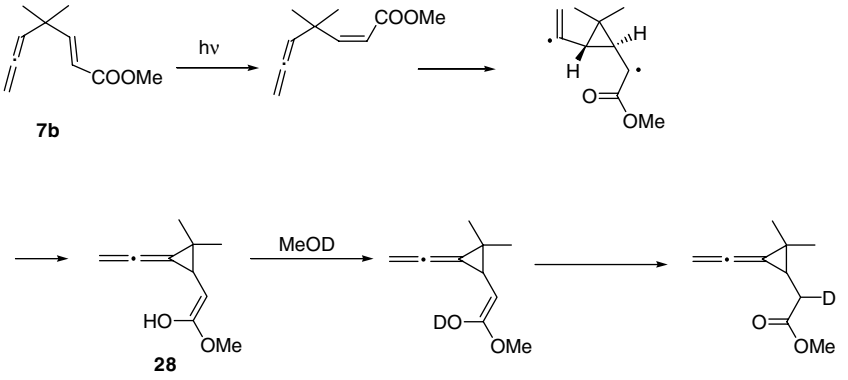

SCHEME 9

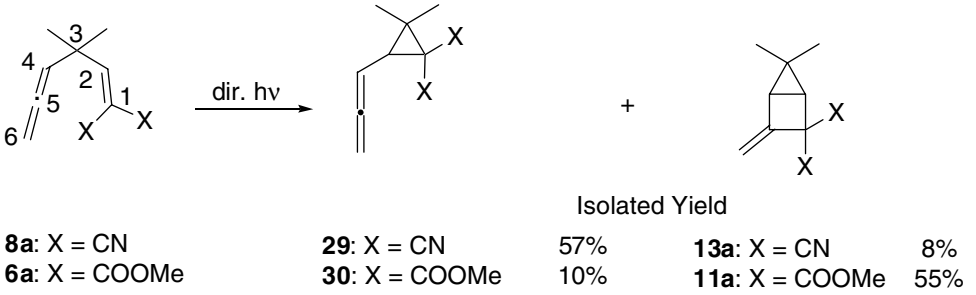

SCHEME 10

30.4 Di-π-Methane Rearrangement

Several allenyl–vinyl methanes undergo the di-π-methane rearrangement. All of the di-π-methane rearrangements observed take place regioselectively and lead to allenylcyclopropanes.[13,14,16,19–22] The allenyl-vinyl methanes, in which the allenyl is 1,2-propadiene, are apt to undergo the di-π-methane rearrangement. As shown in Figure 30.2, the MO coefficient of the C3 of allene **21** has a larger value than that of the C2; hence MO interaction between the C2 and C4 of the allenyl–vinyl methane brings about the di-π-methane rearrangement. Interestingly, the γ-1,2-propadienyl-substituted alkylidenemalononitrile **8a** gave the allenylcyclopropane **29** as the principal product,[21] while the γ-1,2-propadienyl-substituted alkylidenemalonate **6a** does not react by the di-π-methane pathway but prefers the intramolecular [2 + 2]-cycloaddition to give **11a** as a main product (Scheme 10).[19] The MO coefficient for the α-carbon of 2,2-dimethylpropylidenemalonate is larger than that of the β-carbon (Figure 30.2). Therefore, the principal MO interaction of the γ-1,2-propadienyl-substituted alkylidenemalonate **6a** is between C1 and C5, thus undergoing the intramolecular [2 + 2]-cycloaddition. On the other hand, the β-carbon of 2,2-dimethylpropylidenemalonitrile has a somewhat larger value: hence, the MO interaction between the C2 and C4 of the γ-1,2-propadienyl-substituted alkylidenemalononitrile **8a** is predominant, and this system undergoes the di-π-methane rearrangement.

30.5 Phenyl Migration

Phenyl migration and intramolecular [2 + 2]-cycloaddition occur in competition on direct and sensitized photolyses of phenyl-substituted allenyl–vinyl methanes.[21,22] The quantum yields for the isomerization of **31** and **32** upon the sensitized photolyses are shown in Table 30.3. Although the acetone, acetophenone, and benzophenone-sensitization of **31** yielded both **33** and, sensitizers with triplet energies < 280 kJ

TABLE 30.3 Quantum Yields for the Isomerization of **31** and **32** upon Triplet Sensitization

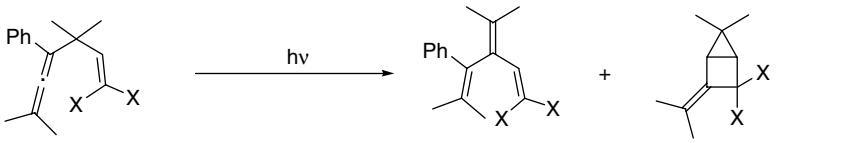

31: X = COOMe
32: X = CN

33: X = COOMe
35: X = CN

34: X = COOMe
36: X = CN

Substrate	Sensitizer (E_T/kJ mol^{-1})	Φ_{tri}[a]	Φ_{cy}[b]
31	Acetone (377-334)	0.25	0.027
	Acetophenone (310)	0.37	0.016
	Benzophenone (287)	0.29	0.0018
	2-Benzoylpyridine (279)	0.16	<0.0001
	Anthraquinone (259)	0.082	<0.0001
	4-Phenylacetophenone (254)	0.012	<0.0001
	1-Acenaphthone (236)	0.0031	<0.0001
32	Acetone (377-334)	0.15	0.039
	Acetophenone (310)	0.057	0.093
	Benzophenone (287)	0.14	0.29
	Thioxanthen-9-one (274)	0.051	0.14
	Michler's ketone (259)	<0.0001	0.11
	4-Phenylbenzophenone (249)	<0.0001	0.052

[a] Quantum yield for the formation of the cross-conjugated trienes **33** or **35**.
[b] Quantum yield for the formation of the intramolecular [2+2]-cycloadducts **34** or **36**.

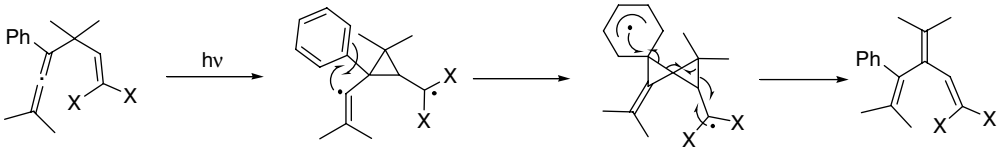

SCHEME 11

mol^{-1} did not affect the intramolecular [2 + 2]-cycloaddition. On the other hand, in the sensitized photolyses of **32**, acetone, acetophenone, benzophenone, and thioxanthen-9-one with triplet energies >270 kJ mol^{-1} show the formation of **35** and **36** from the triplet state, while Michler's ketone or 4-phenylbenzophenone gave only traces of **35**. The chemoselectivity of these compounds can be controlled by the correct choice of triplet sensitizer: e.g., the anthraquinone-sensitization of **31** gave **33**, while sensitization by Michler's ketone of **32** led to **36**.[21] These results indicate that there are two reaction pathways involving the triplet states of different chromophores. As mentioned above, the lowest triplet energies of the α,β-unsaturated ester and α,β-unsaturated nitrile have been estimated to be ca. 280 and 250 kJ mol^{-1}, respectively. The triplet energy of the phenyl-substituted allene has been estimated to lie in the range of 250–270 kJ mol^{-1}.[21,22] Hence, the triplet energies of the chromophores in **31** and **32** are in the order of $C = C(COOMe)_2 > PhC = C = CMe_2 > C = C(CN)_2$. The intramolecular [2 + 2]-cycloaddition of these compounds takes place above the estimated triplet energy level of the vinyl chromophore and further, when the triplet sensitizers over 260 kJ mol^{-1} were used, cross-conjugated trienes were produced. For the formation of the trienes **33** and **35**, it has been considered that the excited state of the allenyl chromophore bonds between the C3 and C5 yields a biradical, which undergoes a 1,2-phenyl migration to yield the trienes (Scheme 11).

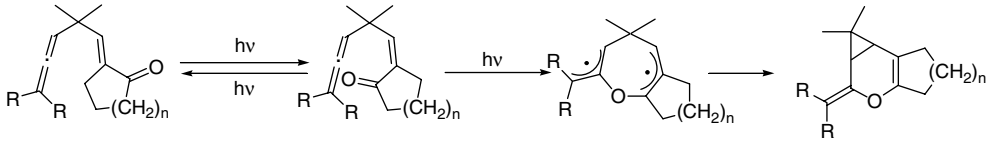

37a: R = H, n = 1
b: R = Me, n = 1
38a: R = H, n = 2
b: R = Me, n = 2

39a: R = H, n = 1
b: R = Me, n = 1
40a: R = H, n = 2
b: R = Me, n = 2

45

41a: R = H, n = 1
b: R = Me, n = 1
42: R = H, n = 2

SCHEME 12

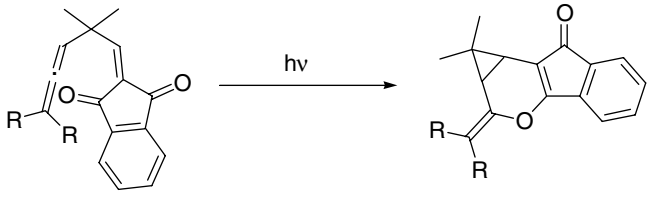

43a: R = H
b: R = Me

44a: R = H
b: R = Me

SCHEME 13

30.6 Intramolecular Oxa–Diels–Alder Reaction

The (*E*)-exo-methylenecycloalkanones **37a**, **b** and **38a**, **b** mainly undergo *E,Z*-geometric isomerization during direct photolysis to give the (*Z*)-isomers **39a**, **b** and **40a**, **b**, respectively (Scheme 12).[23,24] In the photolyses of **37a**, **b** and **38a**, pyrans **41a**, **b** and **42** formed slowly on prolonged irradiation.[23,24] It is obvious that the pyrans are derived from the photochemical intramolecular oxa-Diels–Alder reaction of the (*Z*)-*exo*-methylenecycloalkanones, and this is supported by GLC analyses of the reaction mixtures and by quantum yield measurements. Such intramolecular oxa-Diels–Alder reactions have also been found in the photochemistry of several other allenyl–vinyl methanes;[17,21–24,27] in particular, the photolyses of the γ-allenyl-substituted 2-alkylideneindan-1,3-diones **43a, b** gave the pyrans **44a, b** as a sole or main product (Scheme 13).[27] For the intramolecular oxa–Diels–Alder reaction, both the torsion angle and the *s-cis* conformation in the C=C-C=O are important factors: e.g., the intramolecular oxa–Diels–Alder reaction readily takes place with a small torsion angle. The initial pathway in the intramolecular oxa–Diels–Alder reaction parallels the Paternó–Büchi reaction of ketones with allenes,[15,39] although the resulting biradical **45** (Scheme 12) prefers the pathway for the formation of **41a, b** or **42** to that of oxetane formation.[40]

References

1. For reviews on the di-π-methane rearrangement: (a) Zimmerman, H.E. and Armesto, D., Synthetic aspects of the di-π-methane rearrangement, *Chem. Rev.,* 96, 3065–3112, 1996; (b) Zimmerman, H.E., The di-π-methane rearrangement, in *CRC Handbook of Organic Photochemistry and Photobiology,* Horspool, W.M. and Song, P.-S., Eds., CRC Press, Boca Raton, FL, 1995, pp. 184–193; (c) Zimmerman, H.E., The di-π-methane rearrangement, *Org. Photochem.,* 11, 1–36, 1991; (d) Zimmerman, H.E., Topics in photochemistry, *Top. Curr. Chem.,* 100, 45–73, 1982; (e) Zimmerman, H.E., Some theoretical aspects of organic photochemistry, *Acc. Chem. Res.,* 15, 312–317, 1982; (f) Zimmerman, H.E., Di-π-methane (Zimmerman) rearrangement, in *Rearrangement in Ground and Excited State,* Vol. 3, de Mayo, P., Ed.; Academic Press, New York, 1980, pp. 131–166.

2. Recent publications on the photochemistry of the divinyl methane systems: (a) Zimmerman, H.E. and Chen, W.S., The diverted di-π-methane rearrangement: mechanistic and exploratory organic photochemistry, *Org. Lett.,* 4, 1155–1158, 2002; (b) Zimmerman, H.E., Církva, V. ,and Jiang, L., A ground state tri-π-methane rearrangement, *Tetrahedron Lett.,* 41, 9585–9587, 2000; (c) Zimmerman, H.E. and Církva, V., The tri-π-methane rearrangement: mechanistic and exploratory organic photochemistry, *Org. Lett.,* 2, 2365–2367, 2000; (d) Zimmerman, H.E. and Církva, V., Excited- and ground-state versions of the tri-π-methane rearrangement: mechanistic and exploratory organic photochemistry, *J. Org. Chem.,* 66, 1839–1851, 2001.
3. For a review on the aza-di-π-methane rearrangement: Armesto, D., The aza-di-π-methane rearrangement, in *CRC Handbook of Organic Photochemistry and Photobiology,* Horspool, W.M. and Song, P.-S., Eds., CRC Press, Boca Raton, FL, 1995, pp. 915–930.
4. Recent publications on the aza-di-π-methane rearrangement: Ortiz, M.J., Agarrabeitia, A.R., Aparicio-Lara, S., and Armesto, D., The novel 1-aza-di-π-methane rearrangement of 1-substituted-1-aza-1,4-dienes promoted by DCA-sensitization, *Tetrahedron Lett.,* 40, 1759–1762, 1999; Armesto, D., Caballero, O., and Amador, U., Novel photorearrangements of 2-aza-1,4-dienes to produce vinylaziridines and cyclopropylimines, *J. Am. Chem. Soc.,* 119, 12659–12660, 1997; Armesto, D., Austin, M.A., Griffiths, O.J., Horspool, W.M., and Carpintero, M., A novel photochemical synthesis of 5,6-dihydro-4H-1,2-oxazines by DCA-sensitized irradiation of γ,δ-unsaturated oximes, *J. Chem. Soc., Chem. Commun.,* 2715–2716, 1996.
5. For a review on the oxa-di-π-methane rearrangement: Demuth, M., Synthetic aspects of the oxa-di-π-methane rearrangement, in *Organic Photochemistry,* Vol. 11, Padwa, A., Ed.; Marcel Dekker, New York, 1991, pp. 37–109.
6. Recent publications on oxa-di-π-methane rearrangement: Armesto, D., Ortiz, M.J., Agarrabeitia, A.R., and Martin-Fontecha, M., Di-π-methane reactions promoted by SET from electron-donor sensitizers, *J. Am. Chem. Soc.,* 123, 9920–9921, 2001; Armesto, D., Ortiz, M.J., Agarrabeitia, A.R., and Aparicio-Lara, S., New results on the triplet photoreactivity of β,γ-unsaturated aldehydes: diastereoselective synthesis of cyclopropanecarbaldehydes, *Synthesis,* 1149–1458, 2001; Armesto, D., Ramos, A., Ortiz, M.J., Horspool, W.M., Mancheno, M.J., and Caballero, O.M., Novel photochemical behavior of the oximes and hydrazones of β,γ-unsaturated carbonyl compounds, *J. Chem. Soc., Perkin Trans. 1,* 1535–1541, 1997; Armesto, D., Ortiz, M.J., Romano, S., Agarrabeitia, A.R., Gallego, M.G., and Ramos, A., Unexpected oxa-di-π-methane rearrangement of β,γ-unsaturated aldehydes, *J. Org. Chem.,* 61, 1459–1466, 1996.
7. Crimmins, M.T. and Reinhold, T.L., Enone olefin [2 + 2]-photochemical cycloadditions, *Org. React.,* 44, 297–588, 1993; Demuth, M. and Mikhail, G., New developments in the field of photochemical syntheses, *Synthesis,* 145–162, 1989; Schuster, H.F. and Coppola, G.M., Cycloaddition reaction of allenes, in *Allenes in Organic Synthesis,* Wiley, New York, 1984, chap. 9, pp. 286–330.
8. Crimmins, M.T., Synthetic applications of intramolecular enone–olefin photocycloadditions, *Chem. Rev.,* 88**,** 1453–1473, 1988.
9. Shepard, M.S. and Carreira, E.M., Enantioselective allene/enone photocycloadditions: the use of an inexpensive optically active 1,3-disubtituted allene, *Tetrahedron,* 53, 16253–16276, 1997; Hastings, C.A., Ringgenberg J.D., and Carreira, E.M., Mechanistic implications of stereospecific 1,5-hydrogen-atom transfer in the formation of an unusual allene/enone photoproduct, *Tetrahedron Lett.,* 38, 5789–8792, 1997; Tenaglia, A. and Barillé, D., Asymmetric induction in intramolecular [2 + 2]-photocycloaddition of alkyl hex-2-enopyronasid-4-uloses and further transformations of the cycloadducts, *Synlett,* 776–778, 1995; Carreira, E.M., Hastings, C.A., Shepard, M.S., Yerkey, L.A., and Millward, D.B., *J. Am. Chem. Soc.,* 116, 6622–6630, 1994; Dauben, W.G. and Shapiro, G., Photochemical synthesis of decipine diterpenes, *J. Org. Chem.,* 49, 4252–4258, 1984; Pirrung, M.C. and Thomson, S.A., Total synthesis of pentalenolactone G methyl ester, *J. Org. Chem.,* 53, 227–230, 1988; Pirrung, M.C. and Thomson, S.T., Intramolecular [2 + 2]-photocycloaddition of enone-acetals, *Tetrahedron Lett.,* 27, 2703–2706, 1986; Becker, D. and Haddad, N., About the stereochemistry of intramolecular [2 + 2]-photocycloadditions, *Tetrahedron Lett.,* 27, 6393–6396, 1986;

Dauben, W.G., Rocco, V.P., and Shapiro, G., Intramolecular [2 + 2]-photocycloaddition of 4-substituted cyclopent-2-en-1-ones, *J. Org. Chem.,* 50, 3155–3160, 1985; Dauben, W.G., Sapiro, G., and Luders, L., Intramolecular [2 + 2]-photocycloaddition of 4-(allenic-substituted)-2-cycloalken-1-ones. Ring size, length of side chain and temperature effects, *Tetrahedron Lett.,* 26, 1429–1432, 1985; Weisner, K., On the stereochemistry of photoaddition between α,β-unsaturated ketones and olefins, *Tetrahedron,* 31, 1655–1658, 1975; Weisner, K., Musil, V., and Weisner, K.J., Syntheses in the series of lycopodium alkaloids. IX. Two simple stereospecific syntheses of 12-epi-lycopodine, *Tetrahedron Lett.,* 5643–5646, 1968.

10. Becker, D., Nagler, M., Sahali, Y., and Haddad, N., Regiochemistry and stereochemistry of intramolecular [2 + 2]-photocycloadditions of carbon–carbon double bonds to cyclohexenones, *J. Org. Chem.,* 56**,** 4537–4543, 1991; Becker, D., Haddad, N., and Sahali, Y., Topological and steric effects in mechanism of intramolecular [2 + 2]-photocycloadditions, *Tetrahedron Lett.,* 30, 4429–4432, 1989; Dauben, W.G. and Shapiro, G., Stereochemistry of intramolecular [2 + 2]-cycloadditions of 4-(4,5-hexadimethyl)-2-cyclohexen-1-ones, *Tetrahedron Lett.,* 26, 989–992, 1985; Becker, D., Nagler, M., Harel, Z., and Gillon, A., Intramolecular photocycloaddition of substituted allenes to conjugated cyclohexenones, *J. Org. Chem.,* 48, 2584–2590, 1983; Becker, D., Harel, Z., Nagler, M., and Gillon, A., Intramolecular photoaddition of terminal allenes to conjugated cyclohexenones, *J. Org. Chem.,* 47, 3297–3306, 1982; Becker, D., Harel, Z., and Brinbaum, D., Intramolecular photocycloadditions of ketenes and allenes to cyclohexenones, *J. Chem. Soc., Chem. Commun.,* 377–378, 1975.
11. Steinmetz, M.G., Reactive intermediates in the interconversions of C_3H_4 hydrocarbons, *Rev. Chem. Intermed.,* 5, 57–105, 1984.
12. Kirmse, W. and Strehlke, I.K., Photochemistry of phenylallenes in protic media. Formation of allyl anions by way of vinylcarbenes, *J. Am. Chem. Soc.,* 117, 7007–7008, 1995; Duncan, J.A., Aki, L.Y., Absalon, M.J., Kwong, K.S., and Hendric, R.T., Photosensitized cope rearrangement of *syn*-7-(1,2-butadienyl)bicyclo[2.2.1]hept-2-ene [*syn*-7-(3-methylallenyl)norbornene], *J. Org. Chem.,* 53, 196–198, 1988; Trifonov, L.S., Orahovats, A.S., Prewo, R., Bieri, J.H., and Heimgartner, H., A novel photochemical rearrangement of allenic esters, *J. Chem. Soc., Chem. Commun.,* 708–709, 1986; Johnson, R.P., Cumulene photochemistry, *Org. Photochem.,* **7**, 75–147, 1985; Klett, M.W. and Johnson, R.P., Cumulene photochemistry: photorearrangements of tetraphenyl and triphenyl C_3 isomers, *J. Am. Chem. Soc.,* 107, 3963–3971, 1985; Price, J.D. and Johnson, R.P., Cumulene photochemistry: evidence for *cis*- and *trans*-cyclopropylidene intermediates in triplet photoreactions of 1,2-cyclodecadiene, *J. Am. Chem. Soc.,* **107**, 2187–2189, 1985; Stierman, T.J. and Johnson, R.P., Cumulene photochemistry: singlet and triplet photorearrangements of 1,2-cyclononadiene, *J. Am. Chem. Soc.,* 107, 3971–3980, 1985; Kitamura, T., Miyake, S., Kobayashi, S., and Taniguchi, H., Formation of allenyl cations by photolysis of triarylchloroallenes, *Chem. Lett.,* 929–930, 1985; Stierman, T.J. and Johnson, R.P., Cumulene photochemistry. Photorearrangement of 1,2-cyclononadiene to a bicyclic cyclopropene, *J. Am. Chem. Soc.,* 105, 2429–2493, 1983; Steinmetz, M.G., Stark, E.J., Yen, Y.-P., and Mayes, R.T., *J. Am. Chem. Soc.,* 105, 7209–7210, 1983; Klett, M.W. and Johnson, R.P., Cumulene photochemistry: phenyl and hydrogen migration in phenylallene photoreactions, *Tetrahedron Lett.,* 24, 2523–2526, 1983; Klett, M.W. and Johnson, R.P., *Tetrahedron Lett.,* 24, 1107–1110, 1983; Fujita, K., Matsui, K., and Shono, T., Novel polar photochemical additions of acetic acid to phenylallenes, *J. Am. Chem. Soc.,* 97, 6256–6257, 1975; Ward, H.R. and Karafiath, E., The photolysis of allenes, *J. Am. Chem. Soc.,* 91, 7475–7480, 1969.
13. Lankin, D.C., Chihal, D.M., Griffin, G.W., and Bhacca, N.S., Photochemistry of a phenylpropenyl allene; suppression of the di-π-methane rearrangement in allenic system, *Tetrahedron Lett.,* 4009–4012, 1973.
14. Lankin, D.C., Chihal, D.M., Bhacca, N.S., and Griffin, G.W., The photochemistry of phenylpropenyl allenes. Suppression of the di-π-methane rearrangement in an acyclic allenic system thorough involvement of the triplet excited state, *J. Am. Chem. Soc.,* 97, 7133–7141, 1975.

15. Kudrawcew, W., Frei, B., Wolf, H.R., and Jeger, O., Photolysis of homoconjugated allene ketones, *Heterocycles,* 17, 139–150, 1982.
16. Tsuno, T. and Sugiyama, K. Photochemical reaction of *p*-substituted styryl–allenyl methane compounds, Symposium on Photochemistry, Tokyo, Sep. 17–19, 1994, p. 145.
17. Tsuno, T. and Sugiyama, K., Allenyl(vinyl)methane photochemistry. Photochemistry of 5-[2-(1,2-propadienyl)-substituted alkylidene]-2,2-dimethyl-1,3-dioxane-4,6-diones, *Bull. Chem. Soc. Jpn.,* 68, 3175–3188, 1995.
18. Tsuno, T. and Sugiyama, K., Photochemistry of isopropylidene 3,3,6-trimethyl-1,4,5-heptatriene-1,1-dicarboxylate and its homologues, *Chem. Lett.,* 503–506, 1991.
19. Tsuno, T. and Sugiyama, K., Allenyl(vinyl)methane photochemistry. Photochemistry of methyl 4,4-dimethyl-2,5,6-heptatriennoate derivatives, *Bull. Chem. Soc. Jpn.,* 72, 519–531, 1999.
20. Sugiyama, K. and Tsuno, T., Photochemistry of dimethyl 1,4,5-hexatriene-1,1-dicarboxylate and its homologues, *Chem. Express,* 7, 929–932, 1992.
21. Tsuno, T. and Sugiyama, K., Allenyl(vinyl)methane photochemistry. Photochemistry of γ-(3-methyl-1-phenyl-1,2-butadienyl)-substituted α,β-unsaturated ester and nitrile derivatives, *Tetrahedron,* 57, 4831–4840, 2001.
22. Tsuno, T. and Sugiyama, K., Allenyl(vinyl)methane photochemistry. Photochemistry of 4,4,7-trimethyl-5-phenyl-2,5,6-octatrienoate derivatives, *Tetrahedron Lett.,* 38, 1581–1584, 1997.
23. Tsuno, T. and Sugiyama, K., Allenyl(vinyl)methane photochemistry. Photochemistry of γ-allenyl-substituted α,β-unsaturated enone derivatives, *Tetrahedron,* 58, 7681–7689, 2002.
24. Sugiyama, K., Yoshida, M., and Tsuno, T., Photochemistry of γ-allenyl-substituted conjugated alkylidenecycloalkanones, *Heterocycles,* 38, 1721–1726, 1994.
25. Tsuno, T. and Sugiyama, K., Allenyl(vinyl)methane photochemistry, in *Recent Research Developments in Organic Chemistry,* Vol. 2, Pandalai, S.G., Ed., Transworld Research Network, Trivandrum, 1999, pp. 435–453.
26. Tsuno T. and Sugiyama, K., Novel chemistry of 5-methylene-substituted 1,3-dioxane, 4,6-dione derivatives, in *Trends in Heterocyclic Chemistry,* Vol. 7, Ramchandran, U., Ed.; Research Trends, Trivandrum, 2001, pp. 91–106.
27. Tsuno T. and Sugiyama, K., Allenyl(vinyl)methane photochemistry. Photochemistry of 2-(3,4-pentadienylidene) indan-1,3-dione derivatives, *Heterocycles,* 57, 2129–2135, 2002.
28. It has been found that several divinyl methanes underwent the intramolecular [2 + 2]-cycloaddition as a main or minor photoreaction: Kueh, J.S.H., Mellor, M., and Pattenden, G., Synthetic photochemistry. Elaboration of the tricycle[6.3.0.$0^{2,6}$]undecane ("Hirsutane") carbon skeleton by intramolecular photocyclizations of dicyclopent-1-enylmethane, *J. Chem. Soc., Perkin Trans. 1,* 1052–1057, 1981; Barker, A.J., Kueh, J.S.H., Mellor, M., Otieno, D.A., and Pattenden, G., Divergent photoreactivity in intramolecular cycloadditions amongst prop-2-enylcyclopenenones, *Tetrahedron Lett.,* 1881–1884, 1979; Zimmerman, H.E., Baeckstrom, P., Johnson, T., and Kurtz, D.W., C-1 Stereochemistry of the di-π-methane rearrangement. Mechanistic and exploratory organic photochemistry, *J. Am. Chem. Soc.,* 96, 1459–1465, 1974; Zimmerman, H.E. and Pincock, J.A., σ + π Rearrangement of a di-π-methane systems. Central substitution and di-π-methane reactivity. Mechanistic and exploratory organic photochemistry LXXVI, *J. Am. Chem. Soc.,* 95, 2957–2963, 1973; Zimmerman, H.E., Baeckstrom, P., Johnson, T., and Kurtz, D.W., Stereochemistry of the di-π-methane rearrangement. Mechanistic and exploratory organic photochemistry LXIX, *J. Am. Chem. Soc.,* 94, 5504–5505, 1972; Zimmerman, H.E. and Pincock, J.A., An unexpected σ + π rearrangement of a di-π-methane reactant. Inhibition of the di-π-methane rearrangement. Mechanistic and exploratory organic photochemistry LXX, *J. Am. Chem. Soc.,* 94, 6208–6209, 1972; Block, E. and Orf, H., The photocyclization of 1,5-diphenyl-1,4-pentadiene. A simple synthesis of bicyclo[2.1.0]pentanes, *J. Am. Chem. Soc.,* 94, 8438–8446, 1972; Meinwald, J. and Smith, G.W., Mercury-photosensitized reactions of 1,4-dienes, *J. Am. Chem. Soc.,* 89, 4923–4932, 1967; Srinivasan R. and Carlough, K.H., Mercury ($^3P_1$) photosensitized internal cycloaddition reactions in 1,4-, 1,5- and 1,6-dienes, *J. Am. Chem. Soc.,* 89, 4932–4944, 1967.

29. Tsuno, T. and Sugiyama K., unpublished results.
30. Arai, T. and Tokumaru, K., Novel insight into the photochemical *cis-trans* isomerization of olefins, *Yuki Gosei Kagaku Kyoukaishi,* 44, 999–1009, 1986; Arai, T., Sakuragi, H., and Tokumaru, K., Photosensitized *cis-trans* isomerization of β-alkylstyrenes, *Bull. Chem. Soc. Jpn.,* 55, 2204–2007, 1982; Arai, T., Sakuragi, H., and Tokumaru, K., Unusual behavior of β-*tert*-alkylstyrenes in photosensitized *cis-trans* isomerization. Structural effects on triplet energy transfer, *Chem. Lett.,* 261–264, 1980; Caldwell, R.A., Sovocool, G.W., and Peresie, R.J., Secondary deuterium isotope effects on the transfer of triplet excitation, *J. Am Chem. Soc.,* 95, 1496–1502, 1973.
31. Lewis, F.D., Bassani, D.M., Caldwell, R.A., and Unett, D.J., Singlet state *cis, trans* photoisomerization and intersystem crossing of 1-arylpropenes, *J. Am. Chem. Soc.,* 116, 10477, 1994.
32. (a) Zimmermann, H.E. and Jonathan M.C., Unusual rearrangement in di-π-methane systems: mechanistic and exploratory organic photochemistry, *J. Org. Chem.,* 54, 3800–3816, 1989; (b) Zimmermann, H.E. and Factor, R.E., Di-π-methane hypersurfaces and reactivity; multiplicity and regioselectivity; relationship between the di-π-methane and bicycle rearrangements, *Tetrahedron,* 37 (Suppl. 1), 125–141, 1981; (c) Zimmerman, H.E., Armesto, D., Amezua, M.G., Gannet, T.P., and Johnson, R.P., Unusual organic photochemistry effected by cyano and methoxy substitution. Exploratory and mechanistic organic photochemistry, *J. Am. Chem. Soc.,* 101, 6367–6383, 1979; (d) Baeckström, P., Photochemical formation of chrysanthemic acid and cyclopropylacrylic acid derivatives, *Tetrahedron,* 34, 3331–3335, 1978; (e) Bullivant, M.J. and Pattenden, G., A photochemical di-π-methane rearrangement leading to methyl chrysanthemate, *J. Chem. Soc., Perkin Trans. 1,* 256–258, 1976.
33. Mirbach, M.J., Mirbach, M.F., and Saus, A., The triplet energies of butenedioic acid derivatives, *J. Photochem.,* 18, 391–393, 1982; Borrell, P. and Holmes, J.D., The photochemical *cis-trans* isomerization of 2-carbomethoxy-2-butene, *J. Photochem.,* 1, 433–441, 1972/73.
34. Schuster, D.I., Heibel, G.E., and Woning, J., The mechanism of interaction of triplet 3-methylcyclohex-2-en-1-one with maleo- and fumaronitrile: evidence for direct formation of triplet 1,4-biradicals in [2 + 2]-photocycloadditions without the intermediacy of exciplexes, *Angew. Chem., Int. Ed. Engl.,* 30, 1345–1347, 1991; Schuster, D.I., Heibel, G.E., Caldwell, R.A., and Tang, W., Determination of triplet excitation energies of cyclic enones by time-resolved photoacoustic calorimetry, *Photochem. Photobiol.,* 52, 645–648, 1990; Schuster, D.I., Photochemical rearrangement of enones, in *Rearrangement in Ground and Excited States,* Vol. 3, de Mayo, P., Ed., Academic Press, New York, 1980, pp. 167–279.
35. Maradyn, D.J., Sydnes, L.K., and Weedon, A.C., Origin of the regiochemistry in the photochemical cycloaddition reaction of 2-cyclopentenone with allene — trapping of triplet 1,4-biradical intermediates with hydrogen selenide, *Tetrahedron Lett.,* 34, 2413–2416, 1993.
36. Maradyn, D.J. and Weedon, A.C., Trapping of triplet 1,4-biradicals with hydrogen selenide in the intramolecular photochemical cycloaddition reaction of 3-(4′-pentenyl)cycloalk-2-enones – verification of the rule of five, *J. Am. Chem. Soc.,* 117, 5359–5360, 1995.
37. Andrew, D., Hastings, D.J., and Weedon, A.C., The mechanism of the photochemical cycloaddition reaction between 2-cyclopentenone and polar alkenes — trapping of triplet 1,4-biradical intermediates with hydrogen selenide, *J. Am. Chem. Soc.,* 116, 10870–10882, 1994; Maradyn, D.J. and Weedon, A.C., The photochemical cycloaddition reaction of 2-cyclohexenenone with alkenes — trapping of triplet 1,4-biradical intermediates with hydrogen selenide, *Tetrahedron Lett.,* 35, 8107–8110, 1994; Andrew, D., Hastings, D.J., Oldroyd, D.L, Rudolph, A., and Weedon, A.C., Triplet biradical intermediates in the photocycloaddition reactions of enones and *N*-acylindoles with alkenes, *Pure Appl. Chem.,* 64, 1327–1334, 1992; Hastings, D.J. and Weedon, A.C., Origin of the regioselectivity in the photochemical cycloaddition reactions of cyclic enones with alkenes — chemical trapping evidence for the structures, mechanism of formation and fates of 1,4-biradical intermediates, *J. Am. Chem. Soc.,* 113, 8525–8527, 1991; Hastings, D.J. and Weedon, A.C., The

origin of the regioselectivity in 2 + 2 photochemical cycloaddition reactions of *N*-benzoylindole with alkenes: trapping of 1,4-biradical intermediates with hydrogen selenide, *Tetrahedron Lett.,* 32, 4107–4110, 1991.

38. Tsuno, T., Sugiyama, K. and Ago, H., A facile epoxidation of 5-methylene-1,3-dioxane-4,6-diones with hydrogen peroxide without catalyst, *Heterocycles,* 38, 2631–2654, 1994; Tsuno, T. and Sugiyama, K., Addition reaction of photoenols from *o*-methyl-substituted aromatic ketones with 5-alkylidene-1,3-dioxane-4,6-dione derivatives, *Heterocycles,* 38, 859–876, 1994; Tsuno, T. and Sugiyama, K., Diels–Alder reaction of photoenol of 2-methylbenzaldehyde with 5-alkylidene-1,3-dioxane-4,6-dione derivatives, *Heterocycles,* 32, 1989–2004, 1991.
39. Gotthardt, H., Steinmetz, R., and Hammond, G.S., Mechanisms of photochemical reactions. LIII. Cycloaddition of carbonyl compounds to allenes, *J. Org. Chem.,* 33, 277–2780, 1968; Gotthardt, H., Steinmetz, R., and Hammond, G.S., Photocyclic addition of carbonyl compounds to allenes, *J. Chem. Soc. Chem. Commun.,* 480–482, 1967; Arnold, D.R. and Glick, A.H., The photocycloaddition of carbonyl compounds to allenes, *J. Chem. Soc., Chem. Commun.,* 813–814, 1966;
40. The photochemical intramolecular *oxa*–Diels–Alder reaction of several vinyl–alkenoyl methane compounds has been reported: Schneider, R.A. and Meinwald, J., Photochemical reactions of α,β-unsaturated carbonyl compounds with olefins, *J. Am. Chem. Soc.,* 89, 2023–2032, 1967; Meinwald, J. and Kobzina, J.W., Competing pathway in the photochemistry of a 2,5-pentadienone, *J. Am. Chem. Soc.,* 91, 5177–5178, 1969.

31

Photochemistry of Vinylidenecyclopropanes

Kazuhiko Mizuno
Osaka Prefecture University

Hajime Maeda
Osaka Prefecture University

31.1 Introduction

The photochemical and photophysical properties of small ring compounds such as cyclopropanes and cyclobutanes have been well investigated from the mechanistic and synthetic viewpoints.[1–11] The main reaction pathways of conjugated or activated cyclopropanes such as alkenyl- or aryl-substituted cyclopropanes, methylenecyclopropanes, and cyclopropyl ketones include *cis,trans*-photoisomerization, photorearrangement, photoaddition, and photocycloaddition. The photocycloaddition of allenes to carbonyl compounds[12–17] and the photoaddition of alcohols to aryl-substituted allenes[18–19] have also been reported by several groups. However, little has been reported about the photochemistry of vinylidenecyclopropanes, which have not only allene and cyclopropane units, but also a methylenecyclopropane unit. We have previously reported a convenient method for the synthesis of vinylidenecyclopropanes in good to high yields.[20] In this chapter, we will discuss the *cis,trans*-photoisomerization, photorearrangements, and [3 + 2]-photocycloaddition of 1-diarylvinylidenecyclopropanes **1**. It should be noted here that the reactive site in the excited states of **1** is the cyclopropane ring, and the regioselective bond cleavage occurs at the a-bond of **1** in Scheme 1.

31.2 *cis,trans*-Photoisomerization

Direct Photolysis

Direct photolysis of *cis*- and *trans*-1-(2′,2′-diphenylvinylidene)-2,3-dimethylcyclopropane (***c*-2a** and ***t*-2a**) in benzene caused *cis,trans*-photoisomerization to give a 1:1 photostationary state (PSS) mixture.[21]

0-8493-1348-1/04/$0.00+$1.50

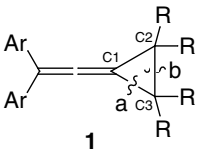

1

SCHEME 1

TABLE 31.1 The *cis-trans* Photoisomerization of Vinylidenecyclopropanes **2a-d**[a]

		cis : *trans* ratio on PSS[b]		
Entry	2	Direct irradn	Triplet-sensitizer	Triplet-sensitized irradn
1	***c*-2a**	50 : 50	MK[c]	30 : 70
2	***t*-2a**	50 : 50	MK	30 : 70
3	***c*-2a**		Acetophenone	30 : 70
4	***c*-2a**		Benzophenone	27 : 73
5	***c*-2a**		Pyrene	>99 : <1
6	***c*-2b**	50 : 50	MK	27 : 73
7	***c*-2c**	54 : 46	MK	27 : 73
8	***c*-2d**	46 : 54	MK	29 : 71

[a] [**2**] = 5×10^{-2} mol dm^{-3} in benzene. The PSS ratios were determined by 270 MHz ^{1}H NMR.
[b] Photostationary state.
[c] Michler's ketone.

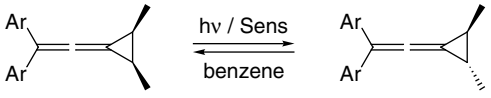

c-2 **t-2**

2a; Ar = Ph **2b**; Ar = *p*-$CH_3C_6H_4$
2c; Ar = *p*-ClC_6H_4 **2d**; Ar = *p*-$CH_3OC_6H_4$

SCHEME 2

Similar photoisomerization of ***c*-2a** and ***t*-2a** occurs in other solvents such as acetonitrile and ethyl acetate to afford the same PSS mixture as that in benzene. Direct irradiation of *p*-substituted vinylidenecyclopropanes **2b-d** also afforded 1:1 PSS mixtures. The results are summarized in Table 31.1. These photoisomerizations were not quenched by typical triplet quenchers such as molecular dioxygen, 2-methyl-1,3-butadiene, and cyclohexa-1,3-diene. Therefore, this photoreaction proceeds through a singlet mechanism.

Triplet Sensitization

The photoreaction of ***c*-2a** and ***t*-2a** in the presence of triplet sensitizers such as acetophenone (E_T = 309 kJ mol^{-1}), benzophenone (E_T = 288 kJ mol^{-1}), thioxanthen-9-one (E_T = 265 kJ mol^{-1}), Michler's ketone (MK; E_T = 259 kJ mol^{-1}), and 1-acetonaphthone (E_T = 236 kJ mol^{-1}) gave a 3:7 PSS mixture of ***c*-2a** and ***t*-2a**.[21] However, pyrene (E_T = 203 kJ mol^{-1}) did not sensitize this reaction. The photoisomerization of ***c*-2a** to ***t*-2a** in the presence of 9-fluorenone (E_T = 211 kJ mol^{-1}) does occur but only slowly. These results clearly show that the excited triplet state of **2a** is a reactive species in this photoisomerization, and the triplet energy of **2a** is estimated as 220–230 kJ mol^{-1}.

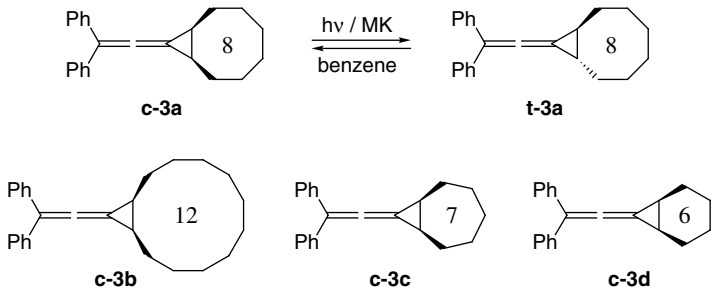

SCHEME 3

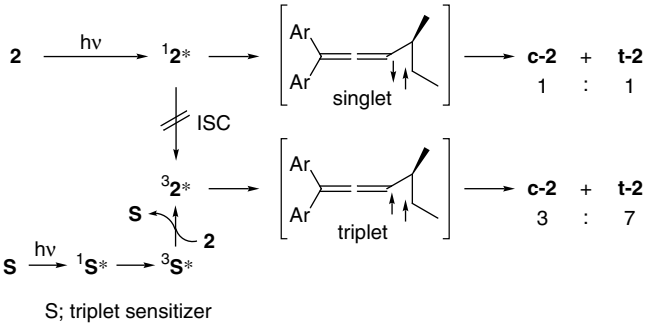

SCHEME 4

The triplet-sensitized photoisomerization occurs more efficiently than does isomerization by direct irradiation. The quantum yield from ***c*-2a** to ***t*-2a** in the presence of MK at 366 nm is 0.62. The triplet-sensitized photoisomerization of **2b-d** also takes place to give approximately 3:7 (*cis:trans*) PSS mixtures. The PSS ratios in both direct and triplet-sensitized photoreactions do not depend on the *p*-substituents on the aryl rings, but depend on the multiplicity of the reaction.

Bicyclic diphenylvinylidenecyclopropanes ***c*-3a** and ***t*-3a** with eight-membered rings in the presence of MK photoisomerized to give a 1:1 PSS mixture with high efficiency.[22] Similar irradiation of ***c*-3b** with a 12-membered ring in the presence of MK afforded ***t*-3b**. However, *cis*-diphenylvinylidenebicyclo[4.1.0]heptane and *cis*-diphenylvinylidenebicyclo[5.1.0]octane ***c*-3c-d** did not isomerize to the *trans*-isomers ***t*-3c** and ***t*-3d**.

The simplified mechanism is shown in Scheme 4. Both the excited singlet and triplet states of **2** smoothly bring about C1-C2 bond cleavage followed by isomerization to the PSS mixture depending on the excited state. Probably, the intersystem crossing (ISC) from the excited singlet state of **2** to the triplet state is quite slow or inefficient. The singlet 1,3-biradical reforms the cyclopropane ring before ISC to the triplet 1,3-biradical occurs. The cleaved bond in both the singlet and the triplet photoisomerizations is postulated from the results of photocycloaddition and photorearrangement discussed in later sections of this chapter.

Electron Transfer Sensitization

The 9,10-dicyanoanthracene (DCA)-sensitized *cis,trans*-photoisomerization of highly electron-rich 1,2-diarylcyclopropanes and diarylmethylenecyclopropanes efficiently proceeds via a radical cation chain transfer mechanism.[1,3,4] The photoisomerization of electron-rich 1-diarylvinylidene-*cis*-2,3-dimethylcyclopropane (***c*-2d**) in acetonitrile was also sensitized by DCA via photoinduced electron transfer.[23] The photoisomerization efficiently takes place to give a 3:7 PSS mixture of ***c*-2d** and ***t*-2d**. However, the less electron-rich 1-diarylvinylidenecyclopropanes ***c*-2a-c** under the same reaction conditions slowly isomerized

TABLE 31.2 Effects of Oxygen, Solvents, Additives, and Substituents in the *cis-trans* Photoisomerization of **c-2** to **t-2** in the Presence of DCA[a]

Entry	2	Solvent	Additive	Atmosphere	Φ^b
1	**c-2d**	CH_3CN	—	Degassed	0.17
2	**c-2d**	CH_3CN	—	Aerated	0.67
3	**c-2d**	CH_3CN	—	Argon	0.23
4	**c-2d**	CH_2Cl_2	—	Aerated	0.25
5	**c-2d**	C_6H_6	—	Aerated	0.017
6	**c-2d**	CH_3CN	$LiClO_4$[c]	Aerated	2.57
7	**c-2d**	CH_3CN	$MgClO_4$[c]	Aerated	13.7
8	**c-2d**	CH_3CN	Biphenyl[d]	Aerated	1.87
9	**c-2d**	CH_3CN	Phenanthrene[d]	Aerated	3.33
10	**c-2b**	CH_3CN	—	Aerated	0.01
11	**c-2a**	CH_3CN	—	Aerated	0.009

[a] $[\mathbf{2}] = 1 \times 10^{-2}$ mol dm^{-3}, $[DCA] = 5 \times 10^{-4}$ mol dm^{-3}. An aqueous $CuSO_4$-NH_3 filter solution (> 350 nm) was used.
[b] Quantum yields at > 400 nm irradiation.
[c] 5×10^{-3} mol dm^{-3}.
[d] 1×10^{-2} mol dm^{-3}.

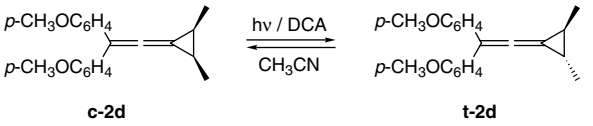

c-2d **t-2d**

SCHEME 5

to ***t*-2a-c**, respectively. The efficiency for the photoisomerization depends remarkably on the additives and solvents (Table 31.2). The photoisomerization is accelerated by molecular dioxygen and by some additives such as $Mg(ClO_4)_2$ and phenanthrene in a manner similar to the photoinduced electron transfer reaction of the DCA-1,2-diarylcyclopropane system.[1,3,24–26] The simplified mechanism is shown in Scheme 6. The first step is a photoinduced one-electron transfer from ***c*-2** to the excited singlet state of DCA, $^1DCA^*$, to generate the free radical ions via the radical ion pair $[DCA^{-\cdot} \cdots \boldsymbol{c}\text{-}\mathbf{2}^{+\cdot}]$. The key step of this photoisomerization is the dissociation from the radical ion pair to the free radical ions assisted by additives such as $Mg(ClO_4)_2$. The ring opening of $\boldsymbol{c}\text{-}\mathbf{2}^{+\cdot}$ generates ring opened radical cation $\mathbf{4}^{+\cdot}$ by cleavage of the C1-C2 bond. The rotation of the C2-C3 bond of $\mathbf{4}^{+\cdot}$ followed by a back-electron transfer from $DCA^{-\cdot}$ to the opened 1,3-biradical and rebonding process brings about *cis,trans*-photoisomerization. It is notably here that a chain mechanism in which an electron transfer from neutral ***c*-2d** to $\mathbf{4}^{+\cdot}$ takes place is included in the reaction. The back electron transfer (BET) from $DCA^{-\cdot}$ to $\boldsymbol{c}\text{-}\mathbf{2}^{+\cdot}$ was effectively suppressed by the addition of molecular dioxygen and $Mg(ClO_4)_2$. The enhancement of the reaction can be interpreted by the rapid electron-transfer from $DCA^{-\cdot}$ to molecular dioxygen to afford DCA and $O_2^{-\cdot}$ and/or by the interaction of $DCA^{-\cdot}$ with Mg(II) ion.

31.3 Generation of Vinylidenecarbenes

Photoirradiation of **2a** in methanol through a Pyrex filter did not give any methanol-incorporated product. On the other hand, irradiation of **2a** in the presence of a large excess of ethyl vinyl ether gave 2-ethoxy-1-(diphenylvinylidene)cyclopropane **6** in a 25% yield.[27] Similar irradiation of **2a** in the presence of cyclohexene gave the corresponding vinylidenecyclopropane, although in low yield. These results clearly demonstrate the formation of diphenylvinylidenecarbene, which is trapped by alkenes. The electrophilic character of this carbene was supported by the reactivity toward these alkenes. This carbene

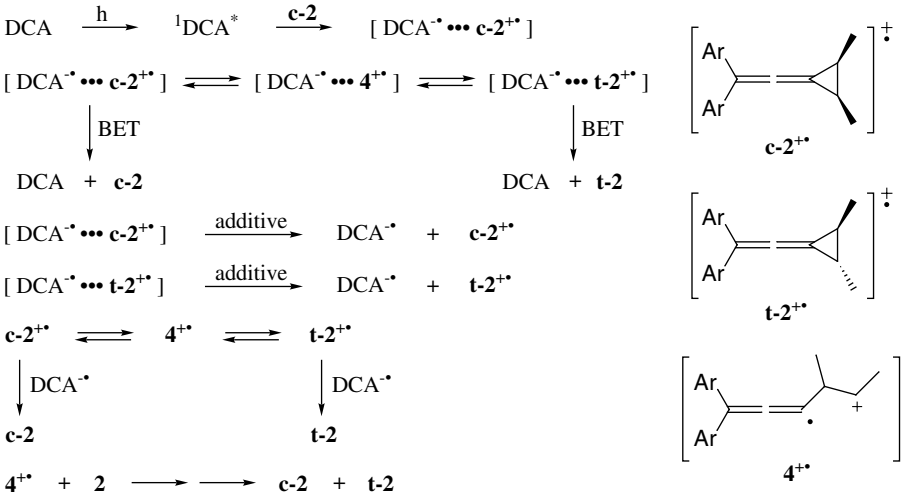

BET; back electron transfer

SCHEME 6

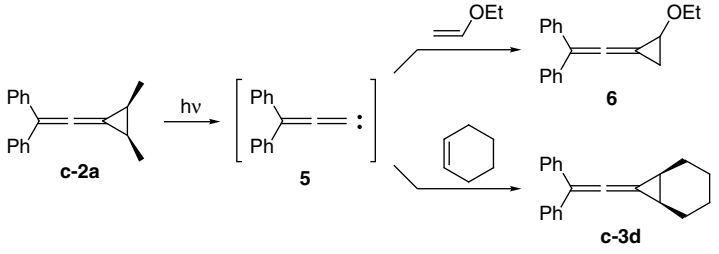

SCHEME 7

was not generated by triplet sensitization. Therefore, the vinylidenecarbene is produced as a competitive process with the formation of 1,2,3-butatriene from the excited singlet state of **2a**, as discussed in next section.

31.4 Photorearrangements

1,2,3-Butatriene

Irradiation of a benzene solution containing 1-diarylvinylidene-2,2,3,3-tetramethylcyclopropanes (**7a–d**) efficiently afforded 1,1-diaryl-4,5,5-tetramethyl-1,2,3-hexatrienes (**8a–d**) in high yields. The quantum yields for the formation of **8a–d** were not high ($\Phi = 0.01 \sim 0.02$) as shown in Table 31.3.[27] The photorearrangement of 2,2,3-trimethyl and 2,2-and 2,3-dimethyl derivatives **7e–f**, **2a** also took place, but the rates for the formation of the 1,2,3-butatrienes were quite slow and products were not isolated. The bicyclic vinylidenecyclopropanes **7g–h** also rearranged to the 1,2,3-butatriene derivatives **8e–g**. The structure of **8b** is confirmed by x-ray crystallography.

This photorearrangement was not sensitized by triplet sensitizers such as benzophenone and MK and was not quenched by molecular dioxygen and 2-methyl-1,3-butadiene, and thus a singlet mechanism is proposed. The homolysis of the C1-C2 bond of **7** from the excited singlet state of **7** generates the 1,3-singlet

TABLE 31.3 Photorearrangement of **7a-d** to **8a-d**[a]

Entry	Substrate	Ar	Product	Isolate yield / %	Φ[b]
1	**7a**	C_6H_5	**8a**	55	0.008
2	**7b**	*p*-ClC_6H_4	**8b**	85	0.016
3	**7c**	*p*-$MeOC_6H_4$	**8c**	45	0.008
4	**7d**	*p*-MeC_6H_4	**8d**	62	0.017

[a] [**7**] = 3.0×10^{-2} mol dm^{-3} in benzene.
[b] Quantum yield for the formation of **8** at 313 nm irradiation ([**7**] = 9.5×10^{-5} mol dm^{-3} in benzene).

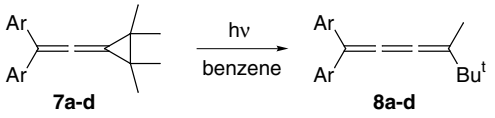

7a; Ar = Ph **7b**; Ar = *p*-ClC_6H_4
7c; Ar = *p*-$MeOC_6H_4$ **7d**; Ar = *p*-$CH_3C_6H_4$

SCHEME 8

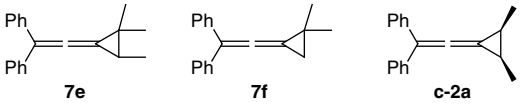

SCHEME 9

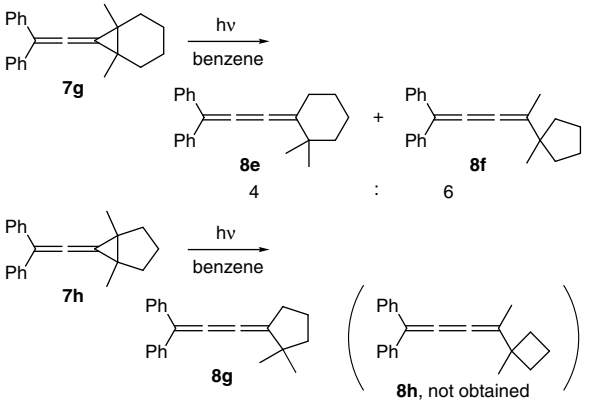

SCHEME 10

biradical intermediate, which rearranges to 1,2,3-butatriene by the migration of an alkyl group. A heterolytic cleavage seems unlikely, because the putative 1,3 dipolar intermediate **10** is not trapped by methanol under the reaction conditions.

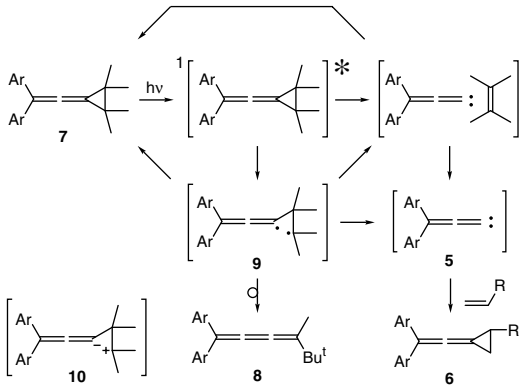

SCHEME 11

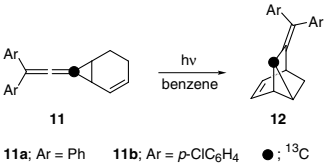

SCHEME 12

Carbon Skeleton Rearrangements

Irradiation of a benzene solution of 7-(2′,2′-diarylvinylidene)bicyclo[4.1.0]hept-2-enes **11a-b** gave 8-(diarylmethylene)tricyclo[2.2.2.0^{6,7}]oct-2-enes **12a-b** in good yields.[28] The structures of **12a-b** were determined from their spectral properties and from x-ray structure analysis of **12a**. The IR spectra showed the disappearance of the stretching vibration of the allenyl bond at 1990 cm^{-1}. The photorearrangement was not sensitized by triplet sensitizers such as benzophenone and MK. These results strongly suggest that this photorearrangement occurs from the singlet excited state. The photoreaction of ^{13}C-labeled compound gave the ^{13}C-labeled rearranged product when the ^{13}C was introduced exclusively into the position shown in Scheme 12. However, the detailed mechanism of the rearrangement is not clear at this stage.

Irradiation of a benzene solution of *exo*-3-(diarylvinylidene)tricyclo[3.2.1.0^{2,4}]oct-6-enes (**13a-b**) gave 4-(diarylvinylidene)bicyclo[3.2.1]octa-2,6-dienes (**14a-b**) in good yields (Scheme 13).[28] Similar irradiation of the *endo*-isomer and *exo*-3-(diphenylvinylidene)tricyclo[3.2.1.0^{2,4}]octane did not give the corresponding rearranged product. Irradiation by a low pressure lamp through a quartz glass filter of *exo*-3-(dimethylvinylidene)tricyclo[3.2.1.0^{2,4}]oct-6-ene also gave a rearranged product in low yield.

In contrast to the above photorearrangement in Scheme 12, the photoreaction of **13a-b** was sensitized by benzophenone and MK, suggesting that this photoreaction occurs from the excited triplet state. The photoreaction of ^{13}C-labeled compound clarified the mechanism as shown in Scheme 13.

31.5 [3 + 2]-Photocycloaddition with Unsaturated Compounds

Triplet-Sensitized Regioselective Photocycloaddition with Electron-Deficient Alkenes

Photoinduced [3 + 2]-cycloaddition of cyclopropanes and methylenecyclopropanes as C3-units with alkenes is a useful method for the one-step synthesis of five-membered ring compounds.[1] However, there is no

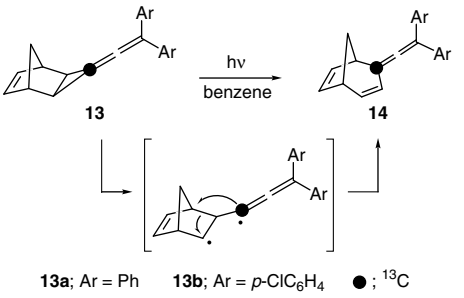

SCHEME 13

TABLE 31.4 (3+2) Photocycloaddition of Vinylidenecyclopropanes **7a-b**, **7f** with Alkenes[a]

	Cyclopropane			Alkene				Isolated
Entry		Ar	R^1		R^2	EWG	Product	yield / %
1	**7a**	Ph	Me	**15a**	H	CN	**16a**	85
2	**7a**	Ph	Me	**15b**	Me	CN	**16b**	44
3	**7a**	Ph	Me	**15c**	H	CO_2Et	**16c**	32
4	**7a**	Ph	Me	**15d**	Me	CO_2Me	**16d**	32
5	**7b**	*p*-ClC_6H_4	Me	**15b**	Me	CN	**16e**	32
6	**7f**	Ph	H	**15a**	H	CN	**16f**	71
7	**7f**	Ph	H	**15b**	Me	CN	**16g**	88

[a] Photoirradiation was conducted by a 300 W high pressure mercury lamp through Uranil filter (> 320 nm). Conditions: **7** (0.73 mmol), **15** (2 mL), MK (40 mg) in benzene (2 mL).

example of the photocycloaddition of vinylidenecyclopropanes with alkenes to give vinylidenecyclopentanes and related five-membered ring compounds. In this section, [3 + 2]-photocycloaddition of vinylidenecyclopropane derivatives with electron-deficient alkenes and cyano-substituted compounds is described.

Photoirradiation of a benzene solution containing **7a**, acrylonitrile **15a**, and MK under argon atmosphere gives 2-cyano-1-diphenylvinylidene-4,4,5,5-tetramethylcyclopentane **16a** in an 85% isolated yield.[29] Similar photoreactions of **7a-b,f** with electron-deficient alkenes **15a-d** under similar conditions afforded the corresponding vinylidenecyclopentane derivatives. The photocycloaddition occurs in a highly regioselective manner (Table 31.4). However, **7a** reacts neither with β-substituted alkenes such as crotononitrile, 1,2-dicyanoethene, and cyclo-2-hexenone, nor with electron-rich alkenes such as ethyl vinyl ether. In the case of **7f**, cycloaddition occurs with alkenes with high selectivity, and the corresponding cycloadducts **16f,g** are produced. The photoreaction did not proceed in the absence of a triplet sensitizer such as MK. Therefore, a triplet 1,3-biradical mechanism is proposed for the [3 + 2]-photocycloaddition of electron-deficient alkenes to 1-diarylvinylidenecyclopropanes. The C1-C2 bond cleavage of **7** occurs regioselectively (Scheme 14). This result is quite interesting because methylenecyclopropanes usually cleave at the 2,3-bond to generate trimethylenemethane intermediates as reactive species. The regioselective photocycloaddition can be reasonably explained by the nucleophilic attack of electron-deficient alkenes at the tertiary alkyl radical to give 1,5-biradicals, which cyclize to diarylvinylidenecyclopentanes.

Ritter-Type Photocycloaddition via Electron Transfer

Ritter-type nucleophilic photocycloaddition of a cyano group to the cationic carbon of the 1,3-radical cation of vinylidenecyclopropane generated by photoinduced electron transfer has been reported by Mizuno et al. (Table 31.5).[30] Irradiation of an acetonitrile solution containing electron-rich 1-[2′,2′-bis(4-methoxyphenyl)vinylidene]-2,2,3,3-tetramethylcyclopropane (**7c**) with aliphatic nitriles and benzonitriles in

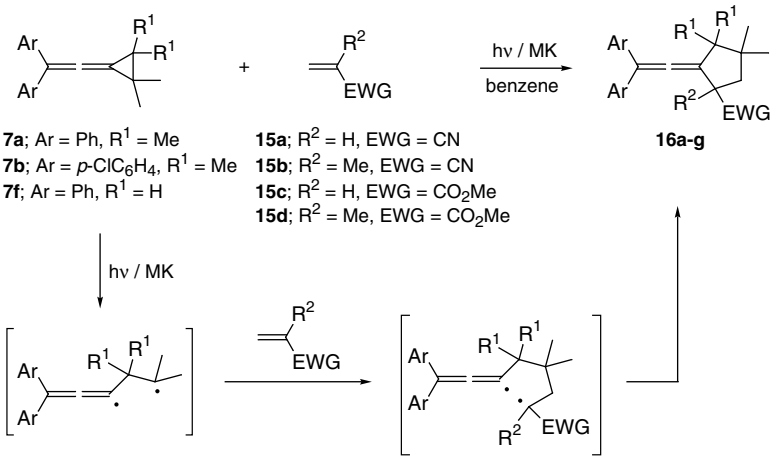

7a; Ar = Ph, R^1 = Me
7b; Ar = *p*-ClC_6H_4, R^1 = Me
7f; Ar = Ph, R^1 = H

15a; R^2 = H, EWG = CN
15b; R^2 = Me, EWG = CN
15c; R^2 = H, EWG = CO_2Me
15d; R^2 = Me, EWG = CO_2Me

16a-g

SCHEME 14

TABLE 31.5 (3+2) Photocycloaddition of Vinylidenecyclopropane **7c** with Organic Carbonitriles[a]

Entry	Cyclopropane	Ar	RCN	Product	Isolated yield / %
1	**7a**	Ph	MeCN	—	0
2	**7c**	*p*-$MeOC_6H_4$	MeCn	**17a**	86
3	**7c**	*p*-$MeOC_6H_4$	EtCN	**17b**	88
4	**7c**	*p*-$MeOC_6H_4$	PhCN	**17c**	90

[a] Photoirradiation was conducted by a 300 W high pressure mercury lamp through $CuSO_4$-NH_3 filter (> 400 nm). Conditions: [**7**] = 1×10^{-2} mol dm^{-3}, [$Mg(ClO_4)_2$] = 1×10^{-2} mol dm^{-3}, [DCA] = 5×10^{-4} mol dm^{-3} in acetonitrile.

the presence of DCA and $Mg(ClO_4)_2$ gives 2-alkyl or 2-phenyl substituted 3-[2′,2′-bis(4-methoxyphenyl)vinylidene]-4,4,5,5-tetramethyl-1-pyrroline **17a-c**.[30] The [3 + 2]-photocycloaddition hardly occurs in the absence of $Mg(ClO_4)_2$. The less electron-rich vinylidenecyclopropanes **7a-b,d** did not give the corresponding [3 + 2]-photocycloadducts. The photoreaction can be reasonably explained by a photoinduced electron-transfer mechanism. Organic carbonitriles attack the cation site of the ring-opened radical cation of **7c** followed by cyclization to give [3 + 2]-cycloadducts. The addition of $Mg(ClO_4)_2$ to the reaction system probably suppresses a back-electron transfer from $DCA^{-\cdot}$ to the radical cation of **7c**.

31.6 Photooxygenation

Photooxygenation of small ring compounds has received considerable attention from synthetic and mechanistic viewpoints in the past two decades. Recent progress in photooxygenation via photoinduced electron transfer has provided a new aspect in this area. DCA-sensitized photooxygenation of electron-rich 1,2-diarylcyclopropanes and diarylmethylenecyclopropanes afforded 1,2-dioxolanes in high yields via their radical cations. [1,3,24–25] However, little has been published about the photooxygenation of vinylidenecyclopropane derivatives. Akasaka et al. reported the formation of oxygenated products in the dye-sensitized photooxygenation of vinylidenecyclopropane derivatives.[31] On the other hand, the DCA-sensitized photooxygenation of 1-diarylvinylidenecyclopropanes in acetonitrile afforded benzophenone derivatives as a main product.[32]

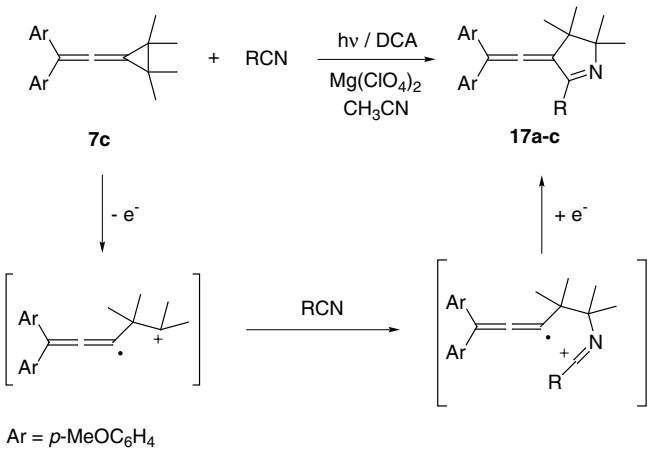

SCHEME 15

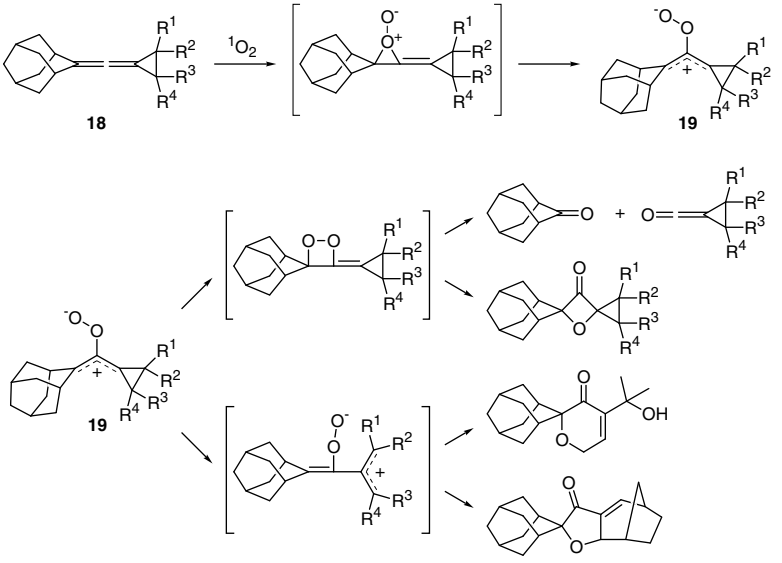

SCHEME 16

31.7 Photochemical Generation of Vinylidenecyclopropanes

Vinylidenecyclopropanes as photoproducts have been generated in some cases. Chapman et al. have reported the formation of unsubstituted vinylidenecyclopropane by the photolysis of 2,6-diazocyclohexanone in an argon matrix at 8 K.[33] The photolysis proceeds via several intermediates such as diazoketene, cyclopropenone, and cyclopentyne. The photolysis of allenyl(vinyl)methane derivatives produced the vinylidenecyclopropane derivatives as main products via intramolecular charge transfer complexes.[34–36] However, the photochemical behavior of these compounds has not been discussed.

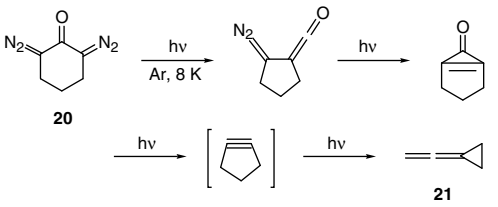

SCHEME 17

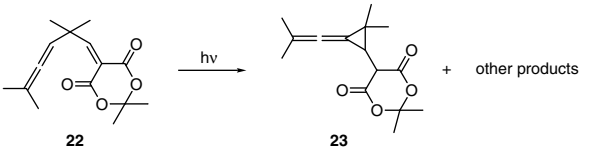

SCHEME 18

References

1. Mizuno, K., Ichinose, N., and Yoshimi, Y., Photochemistry of cyclopropanes, methylenecyclopropanes and vinylidenecyclopropanes, *J. Photochem. Photobiol. C: Photochem. Rev.,* 1, 167, 2000.
2. Hixson, S.S., Photochemistry of cyclopropanes, in *Organic Photochemistry,* Vol. 4, Padwa, A., Ed., Marcel Dekker, New York, 1979, p.191.
3. Mizuno, K. and Otsuji, Y., Addition and cycloaddition reactions via photoinduced electron transfer, in *Topics in Current Chemistry,* Vol. 169, Mattay, J., Ed., Springer-Verlag, Berlin, 1994, p. 301.
4. Miyashi, T., Ikeda, H., Takahashi, Y., and Akiyama, K., Photoinduced electron transfer reactions of cyclopropane derivatives, in *Advances in Electron Transfer Chemistry,* Vol. 6, Mariano, P.S., Ed., Jai Press Inc., Stamford, CT, 1999, p. 1.
5. Pac, C., Mechanism and structure–reactivity relationship in photosensitized reactions of some diarylcyclobutanes and quadricyclane by organic electron acceptor, *Pure Appl. Chem.,* 58, 1249, 1986.
6. Mizuno, K. and Pac, C., Cyclobutane photochemistry, in *Handbook of Organic Photochemistry and Photobiology,* Horspool, W.M. and Song, P.-S., Eds., CRC Press, Boca Raton, FL, 1995, p. 358.
7. Padwa, A., Photochemical transformation of cyclopropene derivatives, in *Organic Photochemistry,* Vol. 4, Padwa, A., Ed., Marcel Dekker, New York, 1979, p. 261.
8. Padwa, A., Photochemical transformation of small-ring carbonyl compounds, in *Organic Photochemistry*, Vol. 1, Padwa, A., Ed., Marcel Dekker, New York, 1967, p.91.
9. Chapman, O.L., Photochemistry of cyclic ketones, in *Organic Photochemistry,* Vol. 3, Padwa, A., Ed., Marcel Dekker, New York, 1973, p.197.
10. Roth, H.D., Organic radical cation, in fluid solution: unusual structures and rearrangements, *Acc. Chem. Res.,* 20, 343, 1987.
11. Roth, H.D., Structure and reactivity of organic radical cation, in *Topics in Current Chemistry*, Vol. 163, Mattay, J., Ed., Springer-Verlag, Berlin, 1992, p. 131.
12. Maradyn, D.J., Sydnes, L.K., and Weedon, A.C., Origin of the regiochemistry in the photochemical cycloaddition reaction of 2-cyclopentenone with allene: trapping of triplet 1,4-biradical intermediates with hydrogen selenide, *Tetrahedron Lett.,* 34, 2413, 1993.
13. Eaton, P.E., Photocondensation reactions of unsaturated ketones, *Tetrahedron Lett.,* 3695, 1964.
14. Sydnes, L.K. and Stensen, W., Regioselective photocycloaddition of 2-cyclopentenone to some allenes, *Acta Chem. Scand. Ser. B,* 40, 657, 1986.

15. Stensen, W., Svendsen, J.S., Hofer, O., and Sydnes, L.K., Photochemical [2 + 2] cycloadditions. LIII. Addition of 4-substituted 2-cyclopentenones to allene; configuration determination by lanthanide-induced shift studies, *Acta Chem. Scand. Ser. B,* 42, 259, 1988.
16. Gotthardt, H., Steinmetz, R., and Hammond, G.S., Mechanisms of photochemical reactions in solution. LIII. Cycloaddition of carbonyl compounds to allenes, *J. Org. Chem.,* 33, 2774, 1968.
17. Arnold, D.R. and Glick, A.H., Photocycloaddition of carbonyl compounds to allenes, *J. Chem. Soc., Chem. Commun.,* 813, 1966.
18. Klett, M.W. and Johnson, R.P., Cumulene photochemistry: photoaddition of neutral methanol to phenylallenes, *Tetrahedron Lett.,* 24, 1107, 1983.
19. Klett, M.W. and Johnson, R.P., Photogeneration of triphenyl C_3 radical cations: deprotonation and nucleophilic addition as competitive pathways, *J. Am. Chem. Soc.,* 107, 6615, 1985.
20. Isagawa, K., Mizuno, K., Sugita, H., and Otsuji, Y., General and convenient route to alkenylidenecyclopropanes: generation of alkenylidenecarbenes from 1,1-dibromocyclopropanes under phase-transfer conditions, *J. Chem. Soc., Perkin Trans. 1,* 2283, 1991.
21. Mizuno, K., Sugita, H., Hirai, H., and Maeda, H., A novel *cis-trans* photoisomerization of vinylidenecyclopropanes via excited singlet and triplet states, *Chem. Lett.,* 1144, 2000.
22. Maeda, H., Zhen, L., Hirai, T., and Mizuno, K., *cis-trans* Photoisomerization of bicyclic diphenylvinylidenecyclopropanes, *ITE Lett., Batt. New Tech. Med.,* 3, 485, 2002.
23. Mizuno, K., Nire, K., Sugita, H., and Maeda, H., A novel *cis-trans* photoisomerization of vinylidenecyclopropanes via an electron transfer chain process, *Tetrahedron Lett.,* 42, 2689, 2001.
24. Mizuno, K., Ichinose, N., and Otsuji, Y., *cis-trans* Photoisomerization and photooxygenation of 1,2-diarylcyclopropanes. Salt effects on the photoinduced electron transfer reactions, *Chem. Lett.,* 455, 1985.
25. Mizuno, K., Kamiyama, N., Ichinose, N., and Otsuji, Y., Photooxygenation of 1,2-diarylcyclopropanes via electron transfer, *Tetrahedron,* 41, 2207, 1985.
26. Mizuno, K., Ichinose, N., and Otsuji, Y., Photochemistry of 9,10-dicyanoanthracene-1,2-diarylcyclopropane systems. Photocycloaddition and photoisomerization, *J. Org. Chem.,* 57, 1855, 1992.
27. Mizuno, K., Maeda, H., Sugita, H., Nishioka, S., Hirai, T., and Sugimoto, A., Photorearrangement of vinylidenecyclopropanes to 1,2,3-butatriene derivatives, *Org. Lett.,* 3, 581, 2001.
28. Mizuno, K., Sugita, H., Isagawa, K., Goto, M., and Otsuji, Y., Novel photorearrangement of (2′,2′-diarylvinylidene)cyclopropanes, *Tetrahedron Lett.,* 34, 5737, 1993.
29. Mizuno, K., Sugita, H., Hirai, T., Maeda, H., Otsuji, Y., Yasuda, M., Hashiguchi, M., and Shima, K., A novel [3 + 2] photocycloaddition of electron-deficient alkenes to diarylvinylidenecyclopropanes: regioselective formation of vinylidenecyclopentanes, *Tetrahedron Lett.,* 42, 3363, 2001.
30. Mizuno, K., Nire, K., Sugita, H., and Otsuji, Y., A novel (3 + 2) photocycloaddition of (2′, 2-diarylvinylidene)cyclopropanes with organic carbonitriles via photoinduced electron transfer, *Tetrahedron Lett.,* 34, 6563, 1993.
31. Akasaka, T., Misawa, Y., and Ando, W., Reaction of singlet oxygen with alkenylidenecyclopropanes: implication for a peroxyallyl intermediate, *Tetrahedron Lett.,* 31, 1173, 1990.
32. Sugita, H., Synthesis and reactivities of vinylidenecyclopropane derivatives, Ph.D. dissertation, Osaka Prefecture University, Sakai, Japan, 1994.
33. Chapman, O.L., Gano, J., West, P.R., Regitz, M., and Maas, G., Acenaphthyne, *J. Am. Chem. Soc.,* 103, 7033, 1981.
34. Tsuno, T. and Sugiyama, K., Photochemistry of isopropylidene 3,3,6-trimethyl-1,4,5-heptatriene-1,1-dicarboxylate and its homologues, *Chem. Lett.,* 503, 1991.
35. Tsuno, T. and Sugiyama, K., Allenyl(vinyl)methane photochemistry. Photochemistry of 5-[2-(1,2-propadienyl)-substituted alkylidene]-2,2-dimethyl-1,3-dioxane-4,6-diones, *Bull. Chem. Soc. Jpn.,* 68, 3175, 1995.
36. Tsuno, T. and Sugiyama, K., Allenyl(vinyl)methane photochemistry. Photochemistry of methyl 4,4-dimethyl-2,5,6-heptatrienoate derivatives, *Bull. Chem. Soc. Jpn.,* 72, 519, 1999.

32

Photochemistry of Heteroarene-Fused Barrelenes

Chun-Chen Liao
National Tsing Hua University

Rama Krishna Peddinti
National Tsing Hua University

32.1 Introduction

The photochemistry of barrelenes and arene-fused barrelenes has been extensively explored, and several reviews have been published in recent years.[1–6] Barrelenes undergo facile photoisomerizations to the corresponding cyclooctatetraenes or semibullvalenes based on the irradiation conditions employed. It has been established[7] that upon direct irradiation of barrelene (**1**), cyclooctatetraene (COT) (**2**) is formed through a singlet-state pathway involving [2 + 2]-cycloaddition to quadricyclane-like intermediate **4** followed by isomerization, whereas the formation of semibullvalene (SB) (**3**) involves biradical intermediates **5** and **6** under triplet sensitization; this is known as the di-π-methane (DPM) rearrangement (Zimmerman rearrangement) (Scheme 1).[8]

When an arene is fused to barrelene, competition exists between vinyl–vinyl and arene–vinyl bridgings in the photorearrangement of arene-fused barrelenes leading to the formation of regio-isomeric photoproducts in the case of unsymmetrical reactants. The competition between the modes of bridging increases when two different arenes are fused to barrelene (vinyl–aryl 1 bridging, vinyl–-aryl 2 bridging, or aryl 1–aryl 2 bridging) or when an arene and a heteroarene are fused to barrelene (vinyl–aryl bridging, vinyl–heteroaryl bridging, or aryl–heteroaryl bridging). Unlike arene-fused barrelenes, heteroarene-fused barrelenes have received very little attention, apparently due to the lack of their easy accessibility. Only one example of the photorearrangement of heteroarene-fused barrelenes had been reported in the literature[9] when we commenced our work in this area. During our studies on masked *o*-benzoquinone Diels–Alder strategy, numerous Diels–Alder adducts that are immediate precursors for α-diketones of

0-8493-1348-1/04/$0.00+$1.50

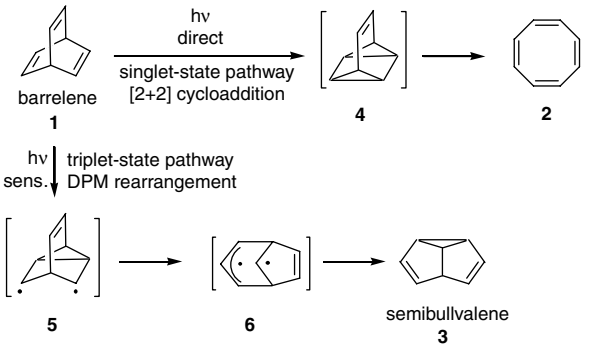

SCHEME 1

the bicyclic[2.2.2]system have been accessed.[10] Thus, an opportunity had arisen to synthesize heteroarene-fused barrelenes from the Diels–Alder adducts derived from masked *o*-benzoquinones. This article will focus mainly on the photochemistry of heteroarene-fused barrelenes, and comparison will be made with that of arene-fused barrelenes wherever possible; the photochemistry of dihydrobarrelenes and barrelenes with heteroatoms in the skeleton is beyond the scope of this chapter.

32.2 Synthesis of Heteroarene-Fused Barrelenes

Heteroarene-fused barrelenes are generally synthesized from α-diketones **7** and 1,2-diamines. Pyrazinobarrelenes[11–13] could be prepared either by condensation of α-diketones **7** with ethylenediamine followed by oxidative generation of the pyrazine ring or by direct condensation of **7** with diaminomaleonitrile (Scheme 2). Quinoxalinobarrelenes,[9,13–16] benzo[*g*]quinoxalinobarrelenes,[13,15] and dibenzo[*f,h*]-quinoxalinobarrelenes[17,18] are easily obtained by simple condensation of **7** with *o*-phenylenediamines, 2,3-diaminonaphthalene, and 9,10-diaminophenanthrene, respectively.

32.3 Photochemistry of Pyrazinobarrelenes

Pyrazinobarrelenes

The parent benzobarrelene upon direct irradiation produces benzocyclooctatetraene exclusively, whereas acetone-sensitized reaction affords the DPM rearrangement product benzosemibullvalene via a triplet-state pathway. Zimmerman's elegant studies on deuterated benzobarrelene (**8**) revealed that the benzo-vinyl bridging leading to **9a** is the predominant route on direct irradiation, and vinyl–vinyl bridging leading to **10a** is the predominant route in the sensitized reaction[19] (Scheme 3).

Our studies on the photochemistry of the pyrazinobarrelene **11** revealed that the pyrazinosemibullvalene **12** is the only product by either direct or acetone-sensitized reaction[20] (Equation 32.1). It is interesting to note that, in contrast to benzobarrelene, which upon direct irradiation undergoes [2 + 2]-cycloaddition followed by isomerization to furnish benzocyclooctatetraene, **11** affords no pyrazinocyclooctatetraene from the start of the irradiation. To distinguish the possible modes of rearrangement, *n*-propyl groups were substituted at bridgehead positions as shown in **13a,b**. Again, no pyrazinocyclooctatetraene is formed upon direct irradiation of **13a** in perdeuterated benzene; instead, almost equal amounts of the DPM product pyrazinosemibullvalene **14** (resulting from vinyl–vinyl bridging) and aza-di-π-methane (ADPM)[21] products **15a** and **16a** (resulting from pyrazino–vinyl bridging) are observed (Equation 32.2).[11] Nevertheless, in the case of pyrazinobarrelene **13b**, direct (in benzene or cyclohexane) irradiation results only in pyrazino–vinyl bridging products **15b** and **16b** in a 57:43 ratio, respectively. Even the acetone-sensitized reaction of **13b** affords **15b** and **16b** in a similar ratio.

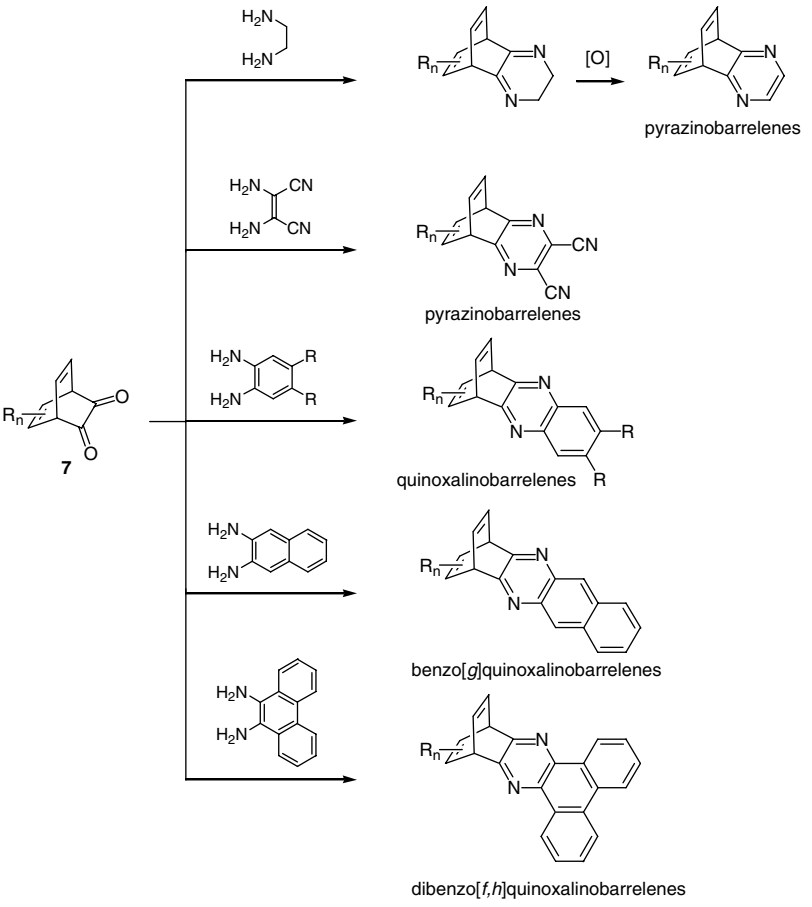

SCHEME 2

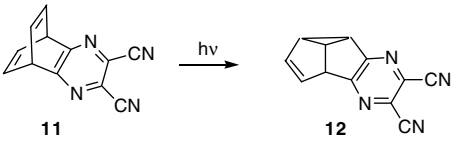

(32.1)

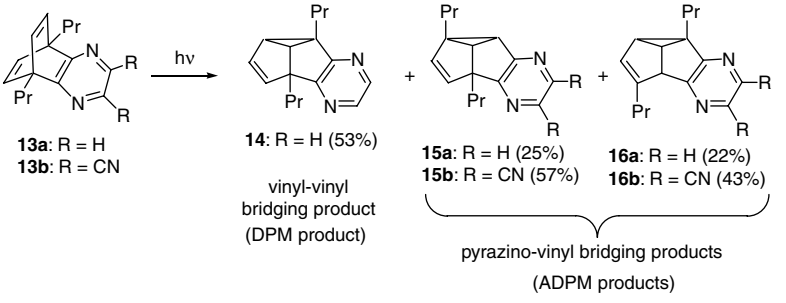

(32.2)

The pyrazinobarrelene **17** bearing three *t*-butyl groups (one on the bridgehead position and one on each vinylic double bond in a 1,3 and a 1,3′ manner) is a suitable substrate to ascertain the steric influence during the photorearrangement. Irradiation of a benzene solution of **17** gives pyrazinosemibullvalene **18**

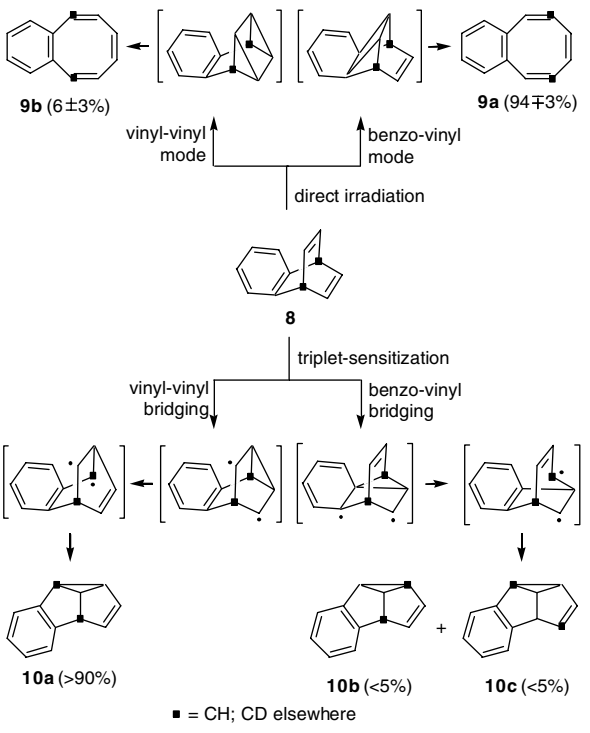

SCHEME 3

and **19** as a result of initial pyrazino-vinyl bridging in a 3:1 ratio[11] (Equation 32.3). The preferential formation of **18** (via a-a′ bridging) to **19** (via b-b′ bridging) may be attributed to the steric hindrance exerted by the *t*-butyl group at the b position.

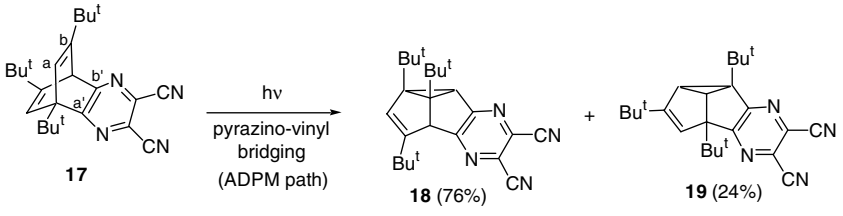

(32.3)

Obviously, owing to the presence of nπ* triplet-states in addition to ππ* triplet-states, the mechanisms of the photoisomerizations of **13** and **17** are even more complicated. It may be noted that the triplet energy of pyrazine[22a] [E_T(nπ*) = 74.3 kcal mol^{-1}; E_T(ππ*) = 75.3 kcal mol^{-1}] is lower than that of benzene[22b] (E_T = 84.3 kcal mol^{-1}), and the quantum yield of intersystem crossing of pyrazine[23a] (Φ_{isc} = 1.0) is greater than that of benzene[23b] (Φ_{isc} = 0.25) due to the presence of a nitrogen atom in the pyrazino moiety, which enhances the rate of intersystem crossing. The nitrogen atom in the pyrazine ring also stabilizes the radical-like intermediates, allowing **13a** to proceed at a higher percentage of pyrazino–vinyl bridging in contrast to benzo–vinyl bridging in the case of **8**. Furthermore, the cyano functionality greatly enhances the ADPM pathway in the reactions of **13b** and **17**.

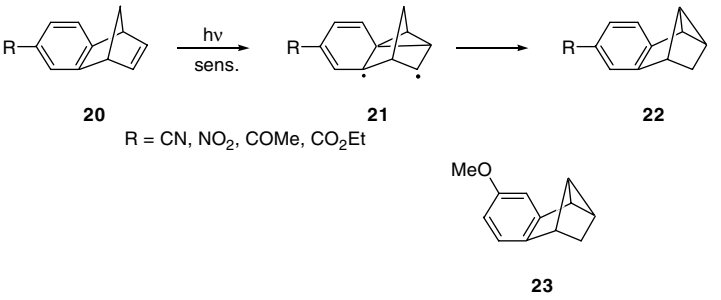

(32.4)

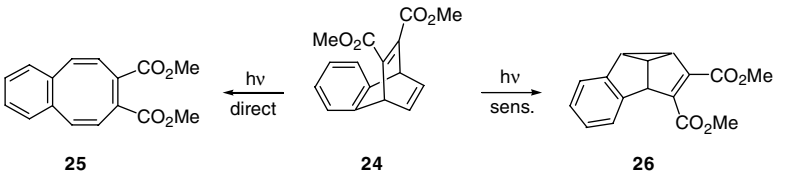

SCHEME 4

Paquette et al.[24] found that the acetophenone-sensitized photorearrangement of benzonorbornadienes **20** bearing electron-withdrawing groups proceeds with complete regiospecificity to afford tetracycloundecatrienes **22** as the sole products in each case (Equation 32.4). The reaction of methoxy compound **20** (R = OMe) produces the other regioisomer **23** as the major photoproduct. The formation of **22** occurs via the cyclopropyldicarbinyl biradical **21** as a result of exclusive benzo–vinyl bridging to the *para* position of the aryl ring. The excess negative charge of the carbinyl carbon of **21** is stabilized by the electron-withdrawing group.

The dimethyl dicarboxylate **24** upon direct excitation produces benzooctatetraene **25** via initial [2 + 2]-cycloaddition between vinyl and vinyldiester groups,[25a] whereas the acetone-sensitized reaction leads to the formation of the DPM rearrangement product **26** as the identified photoproduct. However, the mechanism of the process is not clear (Scheme 4).[25b]

The pyrazinobarrelene **27** bearing two-ester groups, upon irradiation in benzene, yields the ADPM rearrangement products **28–31**[18] (Scheme 5). The pyrazino–vinyldiester mode leading to pyrazinobullvalenes **28** and **29** is preferred over the pyrazino–vinyl mode leading to **30** and **31**. No products involving vinyl–vinyldiester bridging are observed. The bridging of pyrazino–vinyl/vinyldiester and the absence of vinyl–vinyldiester bridging may be attributed to the fact that the presence of nitrogen atoms in the pyrazino moiety coupled with the cyano functionalities on the pyrazine ring enhances the ADPM pathway. The distribution of products (**28** + **30** = 53% and **29** + **31** = 47%) from the two ADPM modes indicates that there is no profound effect due to the presence of the ester moieties in **27**, in comparison with the reaction of **13b**, in which the products **15b** and **16b** are obtained in 57 and 43%, respectively, from two ADPM modes (Equation 32.2).

Benzopyrazinobarrelenes

Within the barrelene system, the photochemistry of dibenzobarrelene and its derivatives have been extensively investigated, presumably due to their easy accessibility as well as the interesting mechanistic aspects. This material is covered in depth in other articles[3,5,26] and discussed here to the extent required for comparison with photochemical studies of heteroarene-fused barrelenes. Ciganek reported[27] that the acetone-sensitized reaction of dibenzobarrelene **32** results in the formation of dibenzosemibullvalene **34**.

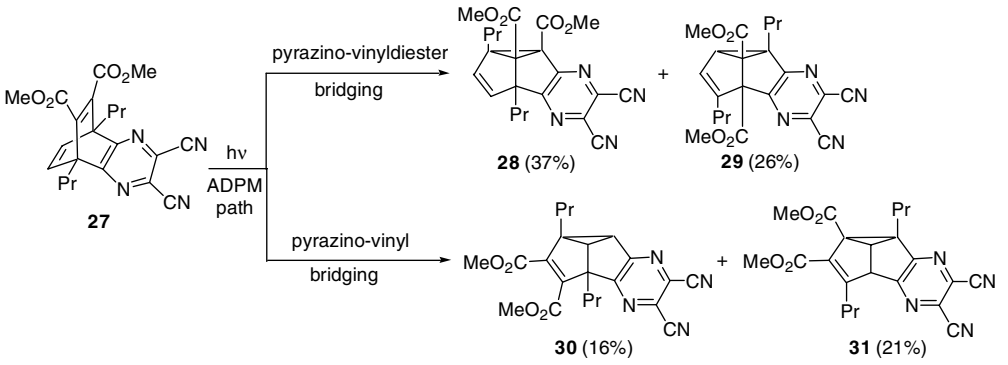

SCHEME 5

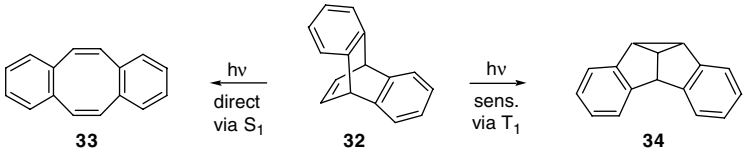

SCHEME 6

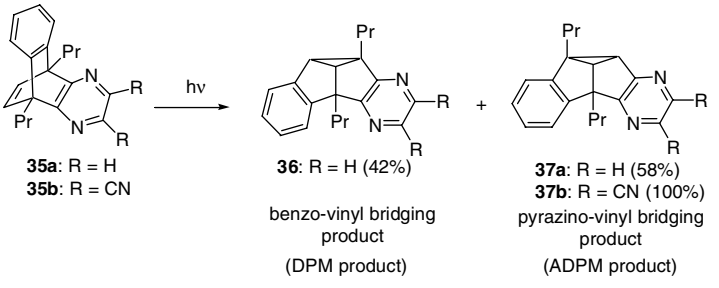

(32.5)

However, when a cyclohexane solution of **32** was irradiated, dibenzooctatetraene **33** was formed exclusively[19b] (Scheme 6).

Photoisomerization of several benzopyrazinobarrelenes was tested in this laboratory.[12] The irradiation of the parent benzopyrazinobarrelene (**35a**) in benzene produces the regioisomeric SBs **36** and **37a** via benzo–vinyl and pyrazino–vinyl bridgings, respectively; the latter is the major product. However, the reaction of the dicyano derivative **35b** undergoes ADPM rearrangement to furnish **37b** exclusively (Equation 32.5). Similarly, the *t*-butyl group substituted benzopyrazinobarrelenes **38a,b** afford SBs **39a,b** and **40a,b** via the ADPM process; the benzo-vinyl bridging products **41** and **42** are not observed (Scheme 7). Unlike **17**, the photolysis of **38** leads to the preferential formation of initial b-b′ bridging products **40**.

The hydroquinone-fused pyrazinobarrelene **43** did not undergo photoisomerization in methanol or benzene after prolonged irradiation (Equation 32.6).[28] Presumably, for the excited state of **43**, the proton transfer from a hydroxyl group of the hydroquinone moiety to a nitrogen atom of the pyrazine ring may be taking place to form an ammonium salt–like species, which may then go back to the ground state of **43** without undergoing any effective photochemical transformation. Subsequently, the free hydroxyl groups of **43** were protected as the dimethyl ether **44** and subjected to photolysis in benzene. The

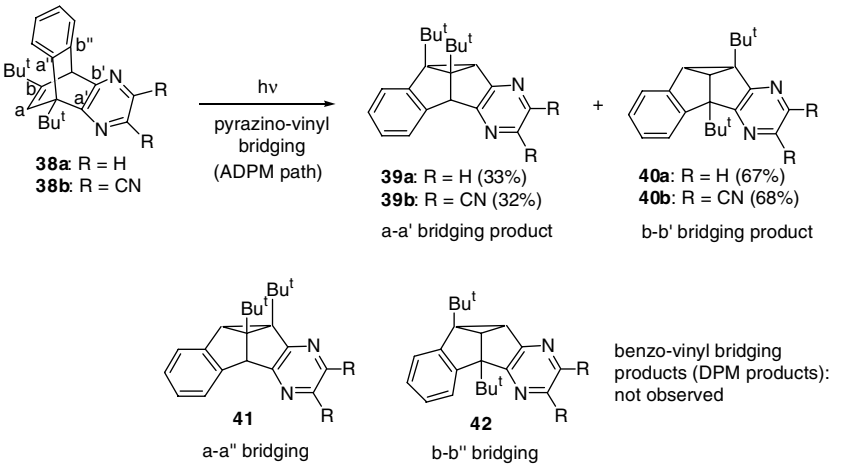

SCHEME 7

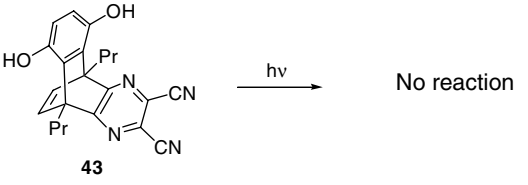

(32.6)

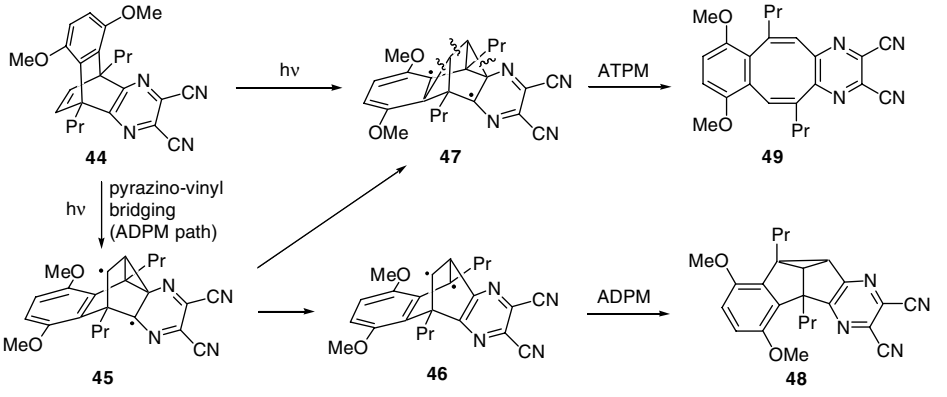

SCHEME 8

compound **44** undergoes photoisomerization and affords COT **49** and SB **48** in a ratio of 8:92 (Scheme 8). A plausible mechanism for the formation of **48** and **49** is outlined in Scheme 8. The compound **48** may be expected from the triplet state–mediated ADPM path via **45** and **46**. Interestingly, the product **49** might have arisen from **47** via an aza-tri-π-methane (ATPM) rearrangement directly from **44** or by the rearrangement of **45** or from both.

Interesting photochemistry involving the tri-π-methane rearrangement of bridgehead-substituted dibenzobarrelenes **50a,b** was reported earlier (Scheme 9).[29] When **50a** was irradiated in benzene, compounds **51a** and **52a** were obtained, whereas **51a** was the only product from acetone-sensitization, and

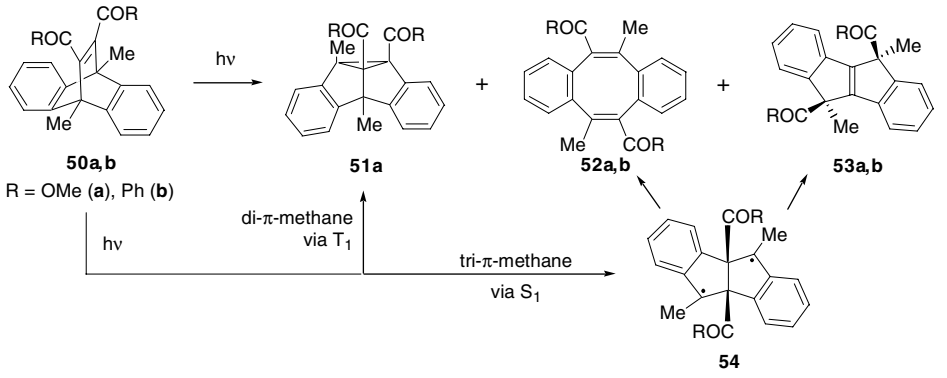

SCHEME 9

53a was observed in solid state reaction[29a]; the suggested mechanism is depicted in Scheme 9. The photoisomerization of **50b** in benzene yields **52b** and **53b**; the former is the major photoproduct.[29b]

Naphthopyrazinobarrelenes

The photoisomerization of benzo-2,3-naphthobarrelene **55** in cyclohexane was found to undergo the DPM rearrangement to provide SBs **56a** and **56b** in equal amounts via benzo-vinyl and 2,3-naphtho-vinyl bridgings, respectively (Equation 32.7).[30] However, in the case of pyrazino-2,3-naphthobarrelene **57**, the reaction affords SB **58** exclusively, resulting from the ADPM path[13] (Equation 32.8). Despite the fact that the triplet energy of pyrazine[22a] [E_T ($n\pi^*$) = 74.3 kcal mol^{-1}; E_T ($\pi\pi^*$) = 75.3 kcal mol^{-1}] is higher than that of naphthalene[31] [E_T = 60.9 kcal mol^{-1}], the reaction of **57** proceeds only via pyrazino–vinyl bridging. The stabilization effect of nitrogen atoms in the pyrazine moiety and the presence of cyano groups appear to be the driving forces for the enhancement of pyrazino–vinyl bridging.

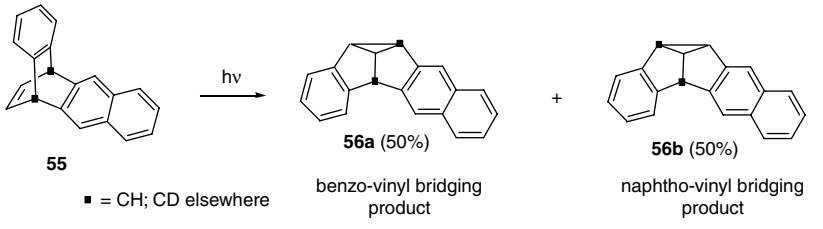

(32.7)

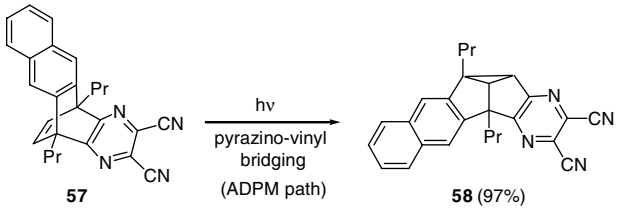

(32.8)

32.4 Photochemistry of Quinoxalinobarrelenes

Quinoxalinobarrelenes

Irradiation of 2,3-naphthobarrelene (**59**) under direct or sensitized conditions affords SB **60** by a vinyl–vinyl bridging route (Equation 32.9).[32] With a view to comparing their photochemical behavior with that of naphthobarrelenes, in this laboratory, several quinoxalinobarrelenes have been synthesized,

and their photoisomerization was carried out. The parent quinoxalinobarrelene (**61**) forms SB **62** exclusively upon direct or sensitized reaction[20] (Equation 32.10). To find out the possible modes of the rearrangement, bridgehead-substituted quinoxalinobarrelene **63** has been chosen as the starting material. Irradiation of **63** in benzene leads to the formation of DPM product **64** and ADPM products **65** and **66**. The major product **64** arises from initial vinyl–vinyl bridging, whereas the minor products **65** and **66** result from quinoxalino–vinyl bridging (Equation 32.11).[15]

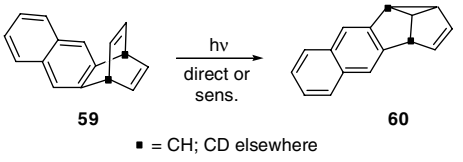

(32.9)

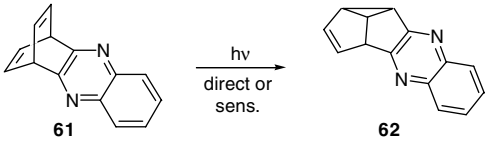

(32.10)

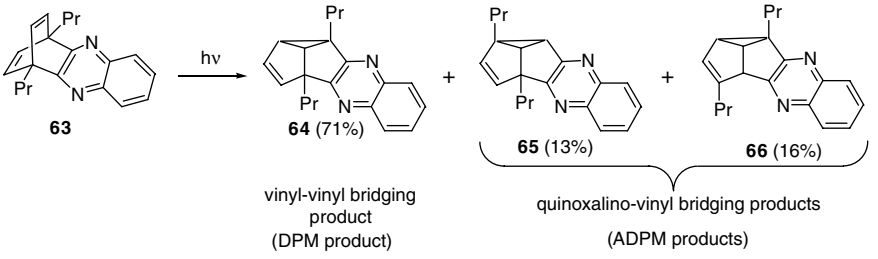

(32.11)

The phototransformation of the *t*-butyl group substituted quinoxalinobarrelene **67** in benzene gives **68** via the DPM mode and **69** and **70** as a result of the ADPM pathway[15] (Equation 32.12). The photoprocesses of **63** and **69** occur presumably via their triplet states, as the same reactions are sensitized by acetophenone. Furthermore, quinoxaline is known to undergo highly efficient intersystem crossing (ϕ_{isc} = 0.99).[33] Unlike naphthobarrelenes, where the vinyl–vinyl bridging is the only route, quinoxalinobarrelenes show enhancement in the quinoxalino–vinyl mode. As the triplet energies of naphthalene[31] and quinoxaline[34] are nearly the same (E_T = 60.9 and 60.6 kcal mol^{-1}, respectively), the increase in quinoxalino–vinyl bridging in **63** and **69** may be attributed to the stabilization effect of nitrogen atoms, which stabilize the biradical-like intermediate, as is evident in the case of the pyrazinobarrelenes. The enhanced quinoxalino–vinyl bridging for **69** over **63** and the preferential formation of the products derived from a-a and a-a′ bridging to b-b and b-b′ bridging in the case of **67** may be explained on steric grounds.

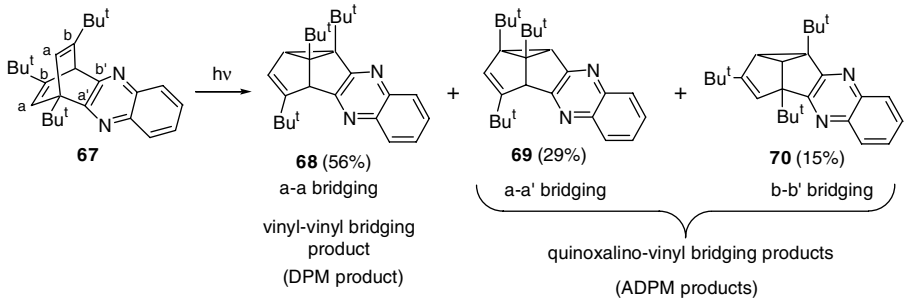

(32.12)

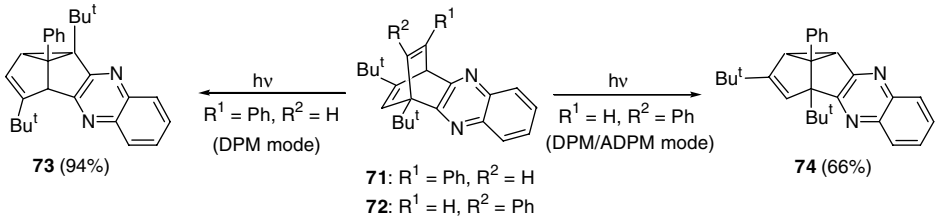

SCHEME 10

It is quite interesting to note that when a phenyl group replaces the *t*-butyl group at position b of **67**, the quinoxalinobarrelene **71** undergoes vinyl–vinyl bridging exclusively to furnish **73** as the sole product. The compound **72**, which is a regioisomer of **71**, photoisomerizes to SB **74** as a result of either a DPM or ADPM process (Scheme 10).[35]

The quinoxalinobarrelene **75** bearing ester functionalities affords SBs **76** and **77** in a 3:2 ratio via vinyl–vinyl mode exclusively (Equation 32.13). The enhanced vinyl–vinyl bridging in this reaction, in comparison to that of **63**, is presumably due to the stabilization of biradical-like intermediate by the ester group.[18]

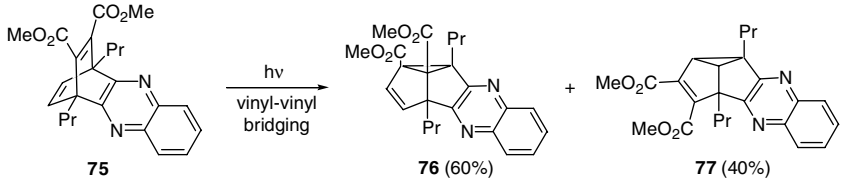

(32.13)

Benzoquinoxalinobarrelenes

Unlike benzo-2,3-naphthobarrelene, where the benzo–vinyl and the 2,3-naphtho–vinyl paths occur in equal proportions (Equation 32.7), the bridgehead substituted benzoquinoxalino-barrelenes **78a,b** predominantly undergo the ADPM process (Equation 32.14). In the case of chloro substituted **78c**, SB **80c** is formed as the sole product and occurs by the ADPM path.[14]

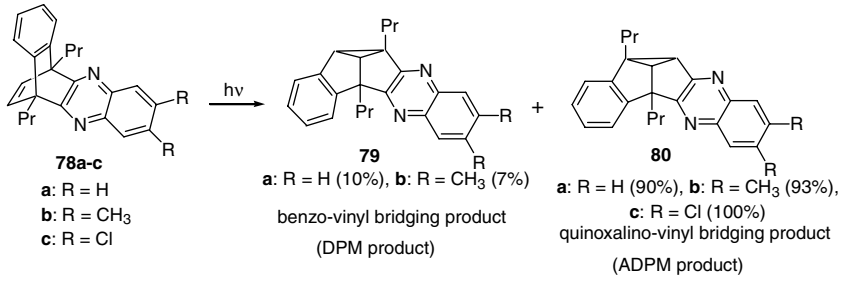

(32.14)

In the early seventies, it was reported[9] that irradiation of benzoquinoxalinobarrelene **81a** in furan affords SB **85a** via the DPM route. Contrarily, it was found upon re-examination of this reaction under similar conditions that ADPM products **82a** and **83a** arising from the initial quinoxalino–vinyl bridging are the only products.[14] The benzoquinoxalinobarrelenes **81b,c** also provide ADPM products **82b,c** and **83b,c** as the sole products in a similar ratio (Scheme 11). The enhanced quinoxalino–vinyl bridging observed in the reactions of **78a–c** and **81 a–c** in comparison with 2,3-naphtho-vinyl bridging in benzo-2,3-naphthobarrelene (**55**) may be a consequence of the lower triplet-state energy (60.6 kcal mol^{-1}) of

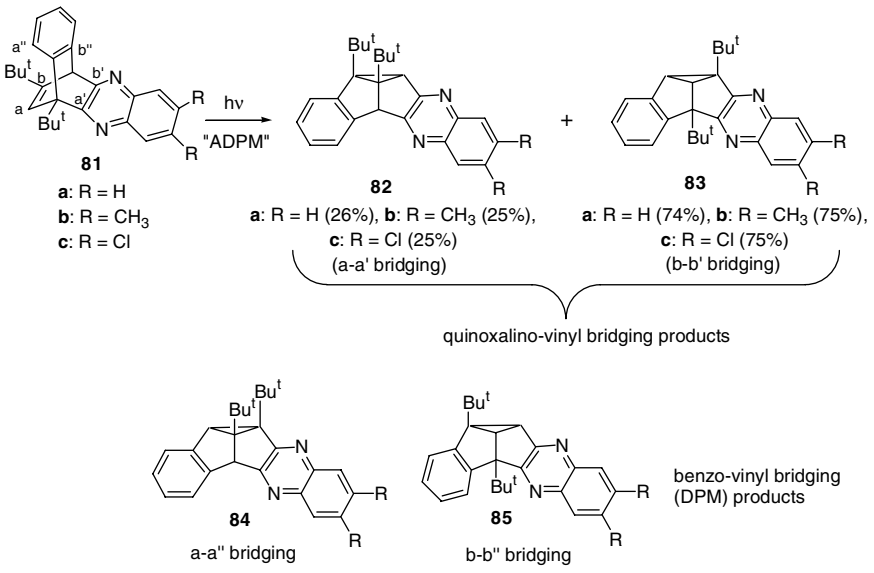

SCHEME 11

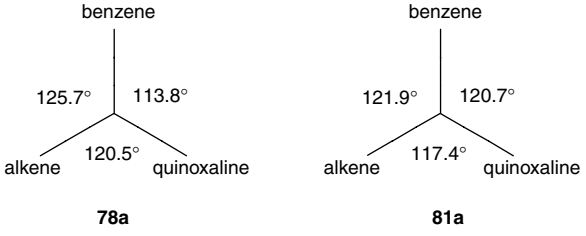

FIGURE 32.1

quinoxaline[34] than that of benzene[22b] (84.3 kcal mol^{-1}) coupled with the radical stabilizing effect of nitrogen atoms. The chlorine atoms also enhance the quinoxalino–vinyl bridging, as seen in the reactions of **78c** and **81c**.

As the barrelene is a rigid molecule, one can expect similar geometries in the ground state as well as the excited state. The crystal structures of heterobarrelenes **78a** and **81a** reveal that the dihedral angle between the quinoxaline and alkene moieties in **81a** is smaller than that in **78a** (Figure 32.1). The barrelene **81a** undergoes ADPM rearrangement exclusively owing to the relatively smaller distance between the quinoxaline and the alkene moieties, and the barrelene **78a** gives 10% benzo–vinyl bridging (DPM mode) product in addition to 90% ADPM product.

The benzoquinoxalinobarrelene **86** with methoxy functionalities at the 1,4-positions of the benzene moiety photorearranges to **87** and **88** in a 1:1 ratio, indicating that benzo and quinoxalino groups are in equal competition[28] (Equation 32.15). A fivefold enhancement of the DPM mode is observed in the reactions of **86** in comparison with those of **78** (see Equation 32.14). This enhancement arises from the introduction of methoxy groups in the benzene ring of **78**. As in the case of **43**, the hydroquinone-fused barrelene **89** did not undergo photoisomerization under direct or sensitized excitation (Equation 32.16).

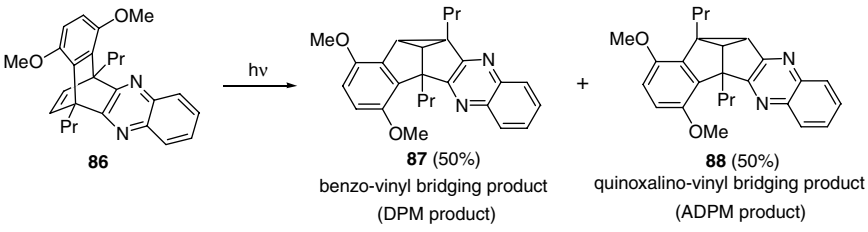

(32.15)

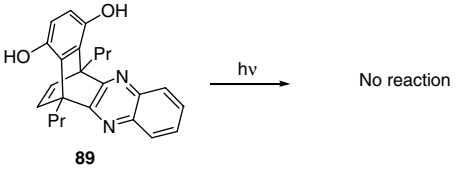

(32.16)

Naphthoquinoxalinobarrelenes

Recent research from this group revealed that the irradiation of 2,3-naphthoquinoxalinobarrelenes **90a–c** proceeds through an ADPM path to furnish SBs **91a–c** as the sole products as a result of quinoxalino–vinyl bridging (Equation 32.17).[13] The exclusive formation of ADPM products may be ascribed to the stabilization effect of nitrogen atoms of the quinoxaline ring, as evident in the phototransformation of 2,3-naphthopyrazinobarrelenes.

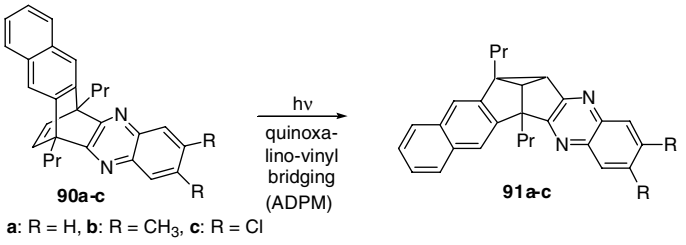

(32.17)

32.5 Photochemistry of Benzo[*g*]quinoxalinobarrelenes

Benzo[*g*]quinoxalinobarrelenes

2,3-Anthrabarrelene (**92**) undergoes the DPM rearrangement via initial vinyl–vinyl bridging under direct irradiation to form SB **93** (Equation 32.18). The reaction may proceed via the excited singlet-state (E_S = 76.3 kcal mol^{-1}) or the second excited triplet-state (E_{T2} = 74 kcal mol^{-1}), as the first excited triplet-state is unreactive owing to its low energy (E_{T1} = 43 kcal mol^{-1}).[36]

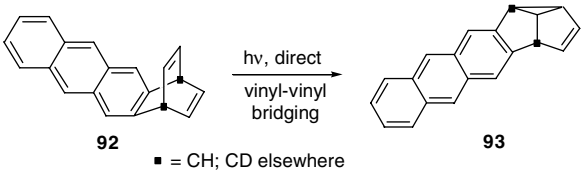

(32.18)

In contrast to **92**, the benzo[*g*]quinoxalinobarrelenes **94–97** failed to undergo photoisomerization under direct or sensitized excitation (Chart 1).[13,15,37] This may be attributed to the fact that the energy

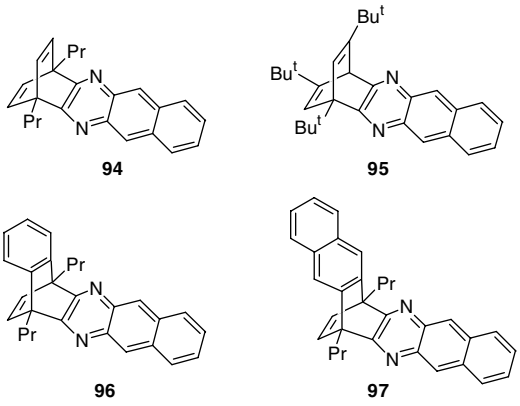

CHART 1

of the first excited triplet-state is too low to undergo photorearrangement and that the upper triplet-state is insufficiently long-lived for chemical reaction to occur. However, benzo[*g*]quinoxalinobarrelene **98** bearing ester groups gives the DPM products **99** and **100** almost in equal amounts via the vinyl–vinyl mode[18] (Equation 32.19). The success of this reaction is presumably due to the presence of the ester functionalities that lower the energy of the biradical-like intermediates.

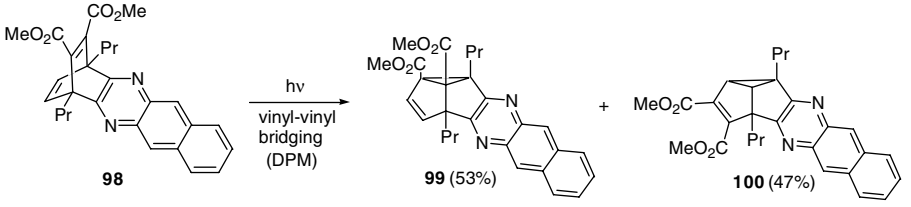

(32.19)

32.6 Photochemistry of Dibenzo[*f,h*]quinoxalinobarrelenes

Dibenzo[*f,h*]quinoxalinobarrelenes

As a further extension of the photochemistry of heteroarene-fused barrelenes, dibenzo[*f,h*]-quinoxalinobarrelenes have been subjected to photoisomerization in this laboratory. Upon direct irradiation of **101** in cyclohexane, the DPM product **102** and the ADPM products **103** and **104** are obtained. The vinyl–vinyl bridged product **102** is minor (Scheme 12).[18] Similarly, the reaction of heterobarrelene **105** under direct irradiation proceeds through both the DPM and the ADPM modes and produces SBs **106–108**. Again, the DPM product **106** is formed as a minor photoproduct (Scheme 13).[17]

In contrast to the reactions of **101** and **105**, heterobarrelene **109**, which has ester functionalities, affords DPM products **110** and **111** predominantly and a minor product **112**, which arises from the ADPM process[18] (Scheme 14).

32.7 Conclusions

While arene-fused barrelenes generally produce COTs on direct irradiation and SBs via DPM rearrangement under sensitized conditions, the DPM and/or ADPM rearrangements leading to SBs are the major reaction pathways in both direct irradiation and sensitized reactions of heteroarene-fused barrelenes. The percentage of heteroaryl–vinyl bridging is increased due to the stabilizing effect of nitrogen atoms

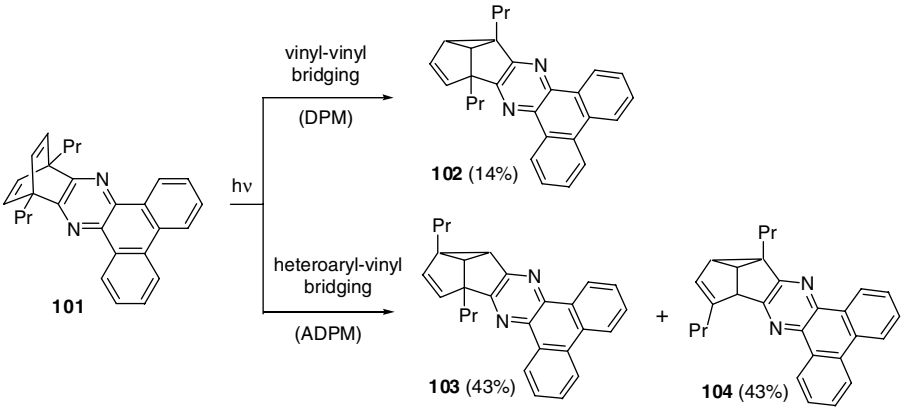

SCHEME 12

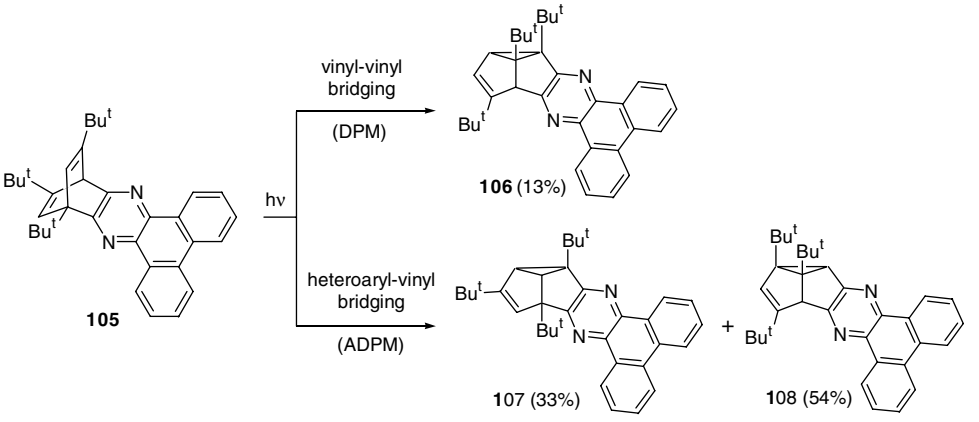

SCHEME 13

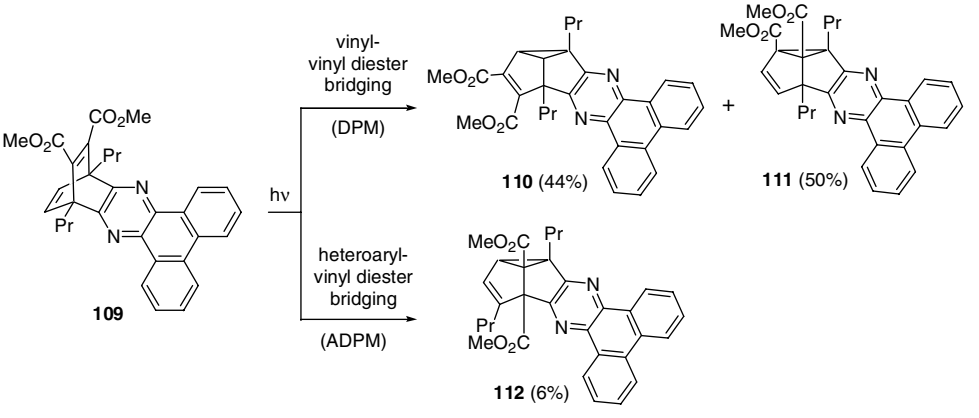

SCHEME 14

present in the heteroaromatic ring. The cyano and chloro groups at pyrazine and quinoxalino moieties increase the percentage of pyrazino–vinyl and quinoxalino–vinyl bridging (ADPM mode). Pyrazino– and quinoxalino–barrelenes fused with a hydroquinone moiety do not undergo (A)DPM rearrangement. Contrarily, their methyl derivatives undergo photochemical transformations, and the percentage of benzo–vinyl bridging is increased due to the presence of methoxy groups at the benzene moiety. It is unusual that an ATPM rearrangement occurs in addition to an ADPM rearrangement in the case of dimethoxybenzene-fused dicyanopyrazinobarrelene. Benzo[*g*]quinoxalinobarrelenes and their benzo and naphtho derivatives do not undergo photochemical transformations, whereas benzo[*g*]quinoxalinobarrelene bearing ester groups provides DPM product. Based on the findings documented here, the relative order of preferential bridgings can be shown as: dicyanopyrazino > vinyl > pyrazino > quinoxalino = dimethoxybenzo > benzo > naphtho.

References

1. Zimmerman, H.E., The di-π-methane (Zimmerman) rearrangement, in *Rearrangements in Ground and Excited States,* vol. 3, de Mayo, P., Ed., Academic Press, New York, 1980, pp 131–166.
2. Zimmerman, H.E., The di-π-methane rearrangement, in *Organic Photochemistry,* vol. 11, Padwa, A., Ed., Marcel Dekker, New York, 1991, pp 1–36.
3. Chen, J., Scheffer, J.R., and Trotter, J., Differences in photochemical reactivities of 9,10-ethenoanthracene derivatives in liquid and crystalline media, *Tetrahedron*, 48, 3251, 1992.
4. Liao, C.-C. and Yang, P.-H., Photorearrangements of benzobarrelenes and related analogues, in *Handbook of Photochemistry and Photobiology,* Horspool, W.M. and Song, P.-S., Eds., CRC Press, Boca Raton, FL, 1995, chap. 15.
5. Scheffer, J.R. and Yang, J., The Photochemistry of dibenzobarrelene (9,10-ethenoanthracene) and its derivatives, in *Handbook of Photochemistry and Photobiology,* Horspool, W.M. and Song, P.-S., Eds., CRC Press, Boca Raton, FL, 1995, chap. 16.
6. Zimmerman, H.E. and Armesto, D., Synthetic aspects of the di-π-methane rearrangement, *Chem. Rev.,* 96, 3065, 1996.
7. (a) Zimmerman, H.E. and Grunewald, G.L., The chemistry of barrelene. III. A unique photoisomerization to semibullvalene, *J. Am. Chem. Soc.,* 88, 183, 1966; (b) Zimmerman, H.E., Binkley, R.W., Givens, R.S., and Sherwin, M.A., Mechanistic organic photochemistry. XXIV. The mechanism of the conversion of barrelene to semibullvalene. A general photochemical process, *J. Am. Chem. Soc.,* 89, 3932, 1967; (c) Zimmerman, H.E., Binkley, R.W., Givens, R.S., Grunewald, G.L., and Sherwin, M.A., The barrelene to semibullvalene transformation. Correlation of excited-state potential energy surfaces with reactivity. Mechanistic and exploratory organic photochemistry. XLIV, *J. Am. Chem. Soc.,* 91, 3316, 1969; (d) Zimmerman, H.E., Sulzbach, H.M., and Tollefson, M.B., Experimental and theoretical exploration of the detailed mechanism of the rearrangement of barrelenes to semibullvalenes: diradical intermediates and transition states, *J. Am. Chem. Soc.,* 115, 6548, 1993.
8. For reviews on DPM rearrangement, see refs. 1, 2, 6 and (a) De Lucchi, O. and Adam, W., Di-π-methane photoisomerizations, in *Comprehensive Organic Synthesis,* Vol. 5, Trost, B.M., Fleming, I., and Paquette, L.A., Eds., Pergamon Press, Oxford, 1991, chap. 2.5; (b) Zimmerman, H.E., The di-π-methane rearrangement, in *Handbook of Photochemistry and Photobiology,* Horspool, W.M. and Song, P.-S., Eds., CRC Press, Boca Raton, FL, 1995, chap. 14.
9. Srinivasan, K.G. and Boyer, J.H., Photorearrangement of a benzoquinoxalinobicyclo[2.2.2]octatriene, *J. Chem. Soc. Chem. Commun.,* 1026, 1974.
10. (a) Liao, C.-C., Synthetic applications of masked benzoquinones, in *Modern Methodology in Organic Synthesis, Proceeding of the 1991 International Symposium of Organic Reactions, Kyoto*; Sheno, T. Ed., Kodansha, Tokyo, 1992, pp 409–424; (b) Liao, C.-C. and Peddinti, R.K., Masked *o*-benzoquinones in organic synthesis, *Acc. Chem. Res.,* 35, 856, 2002.

11. Liao, C.-C., Hsieh, H.-P., and Lin, S.-Y., Photorearrangement of some pyrazinobarrelenes, *J. Chem. Soc., Chem. Commun.,* 545, 1990.
12. Liao, C.-C. and Yang, P.-H., Photochemistry of some benzopyrazinobarrelenes, *J. Chem. Soc., Chem. Commun.,* 626, 1991.
13. Chou, C.-H., Peddinti, R.K., and Liao, C.-C., Photochemistry of pyrazino- and quinoxalino-fused naphthobarrelenes, *Heterocycles,* 54, 61, 2001.
14. Liao, C.-C. and Yang, P.-H., Photochemistry of benzoquinoxalinobarrelenes, *Tetrahedron Lett.,* 33, 5521, 1992.
15. Liao, C.-C., Lin, S.-Y., Hsieh, H.-P., and Yang, P.-H., Photochemistry of quinoxalinobarrelenes and (benzo[*g*]quinoxalino)barrelenes, *J. Chin. Chem. Soc.,* 39, 275, 1992.
16. Nair, V., Anilkumar, G., and Eigendorf, G.K., A facile synthesis of novel pyrazinoxalinobarrelenes from bicyclo[2.2.2]octenediones, *Ind. J. Chem.,* 36B, 65, 1997.
17. Hsieh, H.-P. and Liao, C.-C., Unpublished results.
18. Lin, S.-Y. and Liao, C.-C., Unpublished results.
19. (a) Zimmerman, H.E., Givens, R.S., and Pagni, R.M., Control of photochemical reaction pathways by excited-state multiplicity. Mechanistic and exploratory organic photochemistry. XXXIV, *J. Am. Chem. Soc.,* 90, 4191, 1968; (b) Rabideau, P.W., Hamilton, J.B., and Friedman L., Photoisomerization of mono- and dibenzobarrelenes, *J. Am. Chem. Soc.,* 90, 4465, 1968; (c) Zimmerman, H.E., Givens, R.S., and Pagni, R.M., The photochemistry of benzobarrelene. Mechanistic and exploratory organic photochemistry. XXXV, *J. Am. Chem. Soc.,* 90, 6096, 1968.
20. Chen, A.-C. and Liao, C.-C., Unpublished results.
21. For a review on ADPM rearrangement, see: Armesto, D., The aza-di-π-methane rearrangement, in *Handbook of Photochemistry and Photobiology,* Horspool, W.M. and Song, P.-S., Eds., CRC Press, Boca Raton, FL, 1995, chap. 73.
22. (a) Murov, S.L., Carmichael, I., and Hug, G.L. *Handbook of Photochemistry,* 2nd ed., Marcel Dekker, New York, 1991, p. 44; (b) p. 11 in ref. 22a.
23. (a) Madej, S.L., Gillespie, G.D., and Lim, E.C., Proximity effects in T_1–S_0 radiationless transitions of pyrazine and its methyl derivatives, *Chem. Phys.,* 32, 1, 1978; (b) Cundall, R.B. and Robinson, D.A., Primary photophysical processes in benzene. Part 2. Monomer studies, *J. Chem. Soc., Faraday Trans. 2,* 68, 1145, 1972.
24. Paquette, L.A., Cottrell, D.M., and Snow, R.A., Control by meta substituents of benzo-vinyl bonding options during triplet sensitized photorearrangement of benzonorbornadienes and *anti*-7,8-benzotricyclo[4.2.2.$0^{2,5}$]deca-3,7,9-trienes, *J. Am. Chem. Soc.,* 99, 3723, 1977.
25. (a) Bender, C.O. and Brooks, D.W., Polar substituents in pericyclic reactions: mechanistic course of 2π + 2π photocycloaddition of dimethyl 1,4-dihydro-1,4-ethenonaphthalene-2,3-dicarboxylate, *Can. J. Chem.,* 53, 1684, 1975; (b) Grovenstein, E., Jr., Campbell, T.C., and Shibata, T., Photochemical reactions of dimethyl acetylenedicarboxylate with benzene and naphthalene, *J. Org. Chem.,* 34, 2418, 1969.
26. Sajimon, M.C., Ramaiah, D., Kumar, S.A., Rath, N.P., and George, M.V., Substituent effects on regioselectivity in the photorearrangement of a few naphthobarrelenes, *Tetrahedron,* 56, 5421, 2000 and references therein.
27. Ciganek, E., The photoisomerization of dibenzobicyclo[2.2.2]octatrienes, *J. Am. Chem. Soc.,* 88, 2882, 1966.
28. Chen, J.-H. and Liao, C.-C., Unpublished results.
29. (a) Pokkuluri, P.R., Scheffer, J.R., and Trotter, J., Novel photorearrangements of bridgehead-substituted dibenzobarrelene derivatives in solution and the solid state, *J. Am. Chem. Soc.,* 112, 3677, 1990; (b) Asokan, C.V., Kumar, S.A., Das, S., Rath, N.P., and George, M.V., Novel phototransformations of bridgehead-dimethyl-substituted dibenzobarrelene. Structure of the photoproducts, *J. Org. Chem.,* 56, 5890, 1991.

30. Zimmerman, H.E. and Viriot-Villaume, M.-L., Competitive naphtho vs. benzo bridging in the di-π-methane rearrangement of benzo-2,3-naphthobarrelene. Mechanistic and exploratory organic photochemistry. LXXIV, *J. Am. Chem. Soc.,* 95, 1274, 1973.
31. p. 31 in ref. 22a.
32. Zimmerman, H.E. and Bender, C.O., The di-π-methane rearrangement of naphthobarrelenes. Mechanistic and exploratory organic photochemistry. L, *J. Am. Chem. Soc.,* 92, 4366, 1970.
33. Boldridge, D.W., Scott, G.W., and Spiglanin, T.A., Intersystem crossing and internal conversion from the lowest excited singlet state of diazanaphthalenes, *J. Phys. Chem.,* 86, 1976, 1982.
34. Loutfy, R.O. and Loutfy, R.O., The interrelation between polarographic half-wave potentials and the energies of electronic excited states, *Can. J. Chem.,* 54, 1454, 1976.
35. Nair, V., Anilkumar, G., Prabhakaran, J., Maliakal, D., Eigendorf, G.K., and Williard, P.G., Photochemical di-π-methane rearrangement of quinoxalinobarrelenes, *J. Photochem. Photobiol. A: Chem.,* 111, 57, 1997.
36. Zimmerman, H.E. and Amick, D.R., Photochemistry of anthrabarrelene. Mechanistic and exploratory organic photochemistry. LXXIX, *J. Am. Chem. Soc.,* 95, 3977, 1973.
37. Yang, P.-H. and Liao, C.-C., Unpublished results.

33

Cyclization of Stilbene and its Derivatives

Andrew Gilbert
The University of Reading

33.1 Introduction

The first report of the photoreactivity of stilbene appeared in 1934[1], but the product was not identified as phenanthrene until 1955.[2] It was, however, soon recognized that this type of process was common for many 1,2-diarylethenes and that the mechanism proceeded by photoinduced 6π-electrocyclization of the *cis*-isomer to give the *trans* 4a,4b-dihydrophenanthrene, which was readily oxidized by air or iodine to the arene (Figure 33.1).

The reaction was extensively reviewed in the 1980s,[3–6] and its potential as a convenient route to polynuclear aromatic compounds and as a reversible photochromic system continues to be exploited. In particular, the latter property for 1,2-dithienylethenes has attracted considerable interest in recent years in data storage and molecular switch applications.[7]

33.2 Substituted Stilbenes

The previous account of stilbene photocyclizations in this Handbook outlined the details of the mechanism of the process, including the factors that influence the arene positions between which the photocyclization may be expected to occur, as well as described the effects of substituents on the reaction.[8] This latter feature continues to attract attention and has been exploited in a number of synthetic applications. Examples to illustrate the variety of substituted stilbenes studied in recent years are given below. The amino *cis* stilbenes display differing photochemical reactivities.[9] The *meta* isomer undergoes photocyclization with the highest quantum yield of any reported monosubstituted *cis* stilbene and isomerizes with abnormally low efficiency, while the photochemistry of the *ortho* and *para* isomers is similar to that of many substituted stilbenes in being dominated by the *cis-trans* isomerization process. It is proposed that the marked differences in the photochemical behavior of the amino stilbenes results from perturbation of the excited state potential energy surface of the *meta* isomer. Not surprisingly, the acetamide **1** undergoes photocyclization to give the phenanthrene **2,** but it may be less expected that styryl-tetrahydroisoquinolines such as **3** can be converted by 6π-cyclization into the 1,2,3,4-dihydronaphtho[1,2-*f*]isoquinolines **4** in 60% yield.[10] Indeed, the photochemistry of the more flexible *trans* 2-(aminoalkyl)-stilbenes **5** reflects the propensity of stilbenes to undergo electron transfer and in this case yield the cyclized isomers **6** and **7** by a route involving intramolecular electron transfer followed by proton

0-8493-1348-1/04/$0.00+$1.50

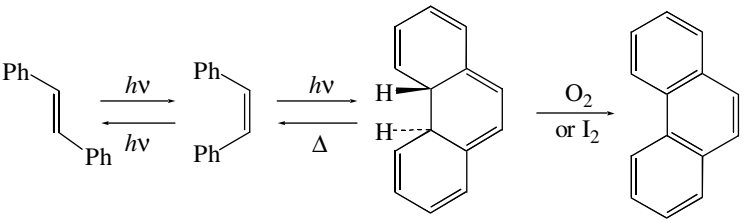

FIGURE 33.1 Stilbene photocyclization.

transfer and coupling of the biradical.[11] By a similar process, prolonged irradiation of the *N*-aminoalkyl-2-stilbenecarboxamides **8a–d** affords the 9- or 10-ring azalactams **9** in yields of 25–43%, while **10a–d** fluoresce with high quantum yields, and both series undergo *trans-cis* photoisomerization with similar efficiencies.[12] The radical cation of 1,2-distyrylbenzene, formed by intermolecular electron transfer to photoexcited *p*-dicyanobenzene, undergoes cyclization, and in the presence of ammonia yields 1-benzyl-3-phenyl-1,2,3,4-tetrahydroisoquinoline **11** and 1-amino-3-benzyl-2-phenylindan **12** (Figure 33.2).[13]

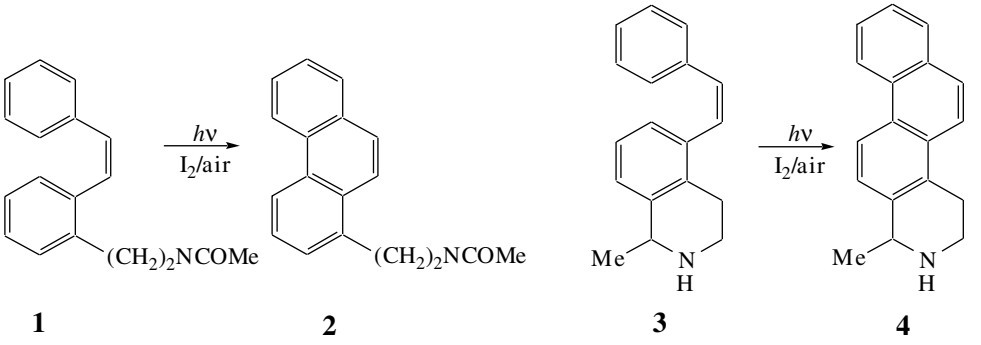

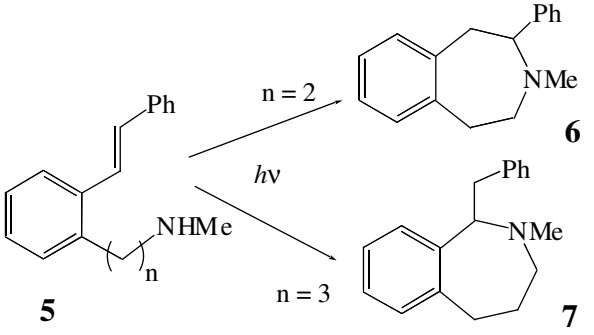

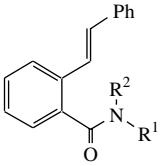

8a, R^1 = -$(CH_2)_2$-NHMe, R^2 = H
b, R^1 = -$(CH_2)_2$-NHPh, R^2 = H
c, R^1 = -$(CH_2)_2$-NHMe, R^2 = Me
d, R^1 = -$(CH_2)_3$-NHPh, R^2 = H
10a, R^1 = R^2 = Me
b, R^1 = -$(CH_2)_2$-NMe_2, R^2 = Me
c, R^1 = -$(CH_2)_3$-NHMe, R^2 = Me
d, R^1 = -$(CH_2)_3$-NMe_2, R^2 = Me

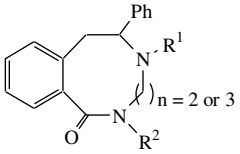

9, R^1 = H, Me, or Ph; R^2 = Me or Ph

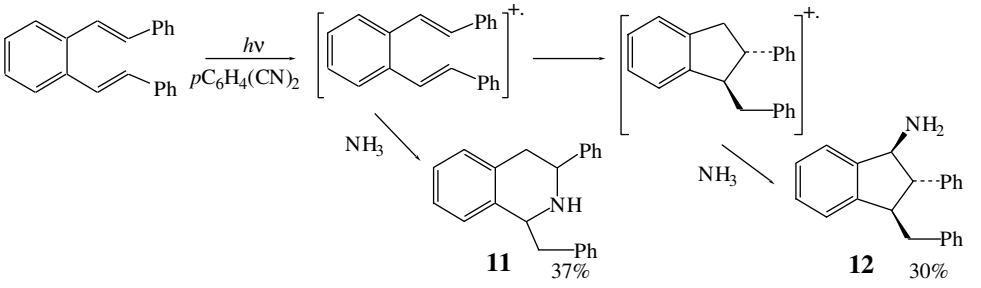

FIGURE 33.2 Photocyclization of the 1,2-distyrylbenzene radical cation.

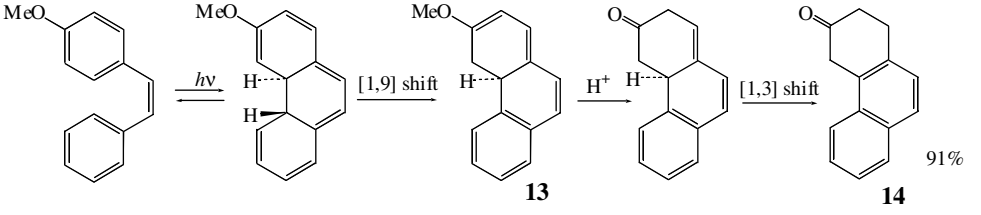

FIGURE 33.3 Photocyclization of 4-methoxystilbene in the presence of acid.

The 4a,4b-dihydrophenanthrene formed from the 6π-electrocyclization of 4-methoxy-stilbene undergoes a [1,9-H]-shift to give **13** which, in the presence of a protic acid, affords the ketone **14** in high yield (Figure 33.3).[14] The reaction has been extended to other methoxystyrylarenes, and evidently the ring closure is readily reversible since in a neutral degassed solution only geometrical isomerization is observed. The phenanthrenetetracarbonitriles **15** and **16**, required for use in phthalocyanine syntheses, can be obtained by irradiation of *cis*- or *trans*-1,2-bis(3,4-dicyanophenyl)ethene, but the more sterically crowded third possible isomer **17** is not formed.[15]

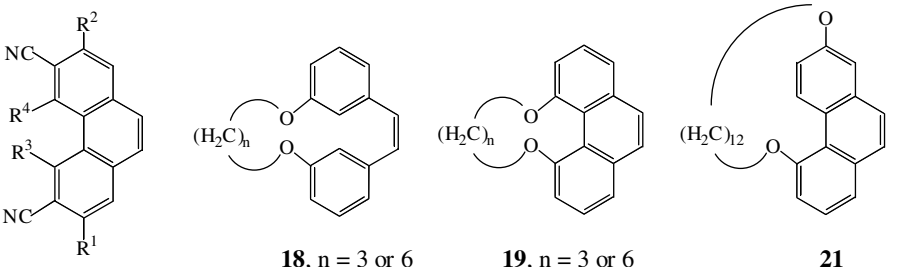

15, $R^1 = R^2 = CN$, $R^3 = R^4 = H$
16, $R^1 = R^4 = CN$, $R^2 = R^3 = H$
17, $R^1 = R^2 = H$, $R^3 = R^4 = CN$

18, n = 3 or 6
20, n = 12

19, n = 3 or 6

21

33.3 [n.2]Metacyclophanes

The influence on stilbene photochemistry of a bridge between the two aryl groups has been the subject of some interest. The ratio of *cis:trans* geometrical isomers of macrocyclic stilbenes **18** is, not surprisingly, dependent on the length of the bridge, but for n = 3 or 6, the sole product on irradiation in the presence of iodine is the 4,5-annulated phenanthrene **19**.[16] However, for **20**, which has a much longer bridge, the 6π-electrocyclic closure significantly favors the formation of the 2,5-bridged compound **21**. The photoreactivity of the stilbene unit in such [n.2]metacyclophanenes can be influenced by substituent interactions. In **22**, the steric repulsion between the methyl and methoxy groups forces the molecule into a *syn* conformation, whereas when the ethene bridge is unsubstituted, as in **23**, the *anti* conformation, typical of [3.2]cyclophanes, is preferred.[17] In the presence of iodine, both conformers undergo photocyclization, but the rate of reaction is appreciably greater for the *anti*-**23** than the *syn*-**22**. The *anti* isomer of 8-fluoro-16-methyl-[2.2]metacyclophane-1,9-diene **24** undergoes a 6π-electrocyclization-elimination process both thermally and photochemically to give pyrene and methyl pyrenes.[18] It is proposed that the reaction proceeds by the intermediate **25**, which yields the polynuclear arenes as outlined in Figure 33.4 by loss of fluoride ion and methyl shifts in the resulting carbocation **26**.

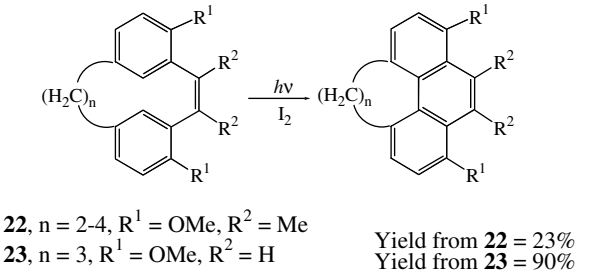

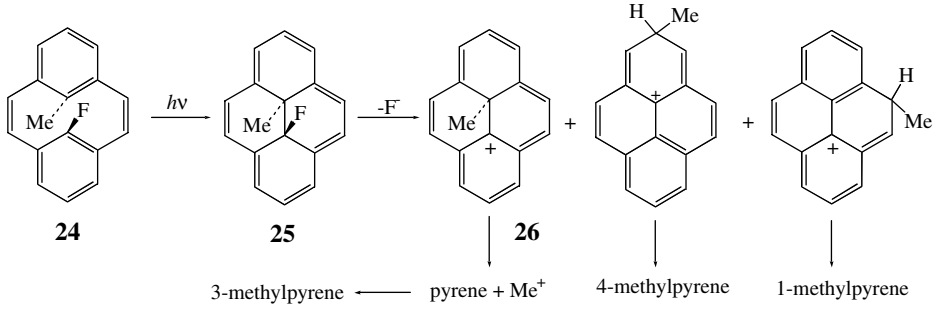

FIGURE 33.4 Formation of pyrenes from irradiation of **24**.

33.4 Formation of Polynuclear Arenes

In principle, the double photocyclization of 1,4-distyrylbenzenes offers a convenient route to dibenz[a,h]anthracenes and [5]helicenes dependent on the sites of reaction. In the first report of the photochemistry of 1,4-phenylene bis(phenylmaleic anhydride) **27**, the product was identified as the dibenz[a,h]anthracene **28**,[19] but more recently it has been shown that a mixture of isomers is formed (overall yield of 80%), in which **28** comprises less than 5%, with the [5]helicene **29** as the major product.[20] This approach towards the synthesis of polynuclear arenas, including helicenes, is complemented by the photocyclizations of styryl-naphthalenes, -phenanthrenes, etc. and of 1,2-dipolyarylethenes. Examples of these processes published during the review period are now considered.

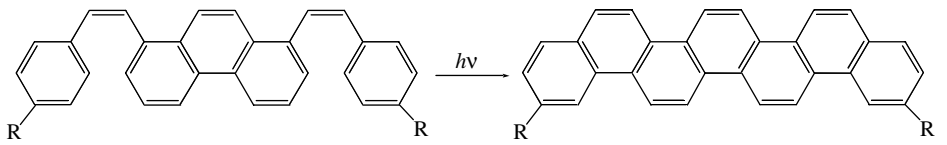

R = H, *n*-pentyl or *t*-butyl.

FIGURE 33.5 Formation of [7]phenacenes.

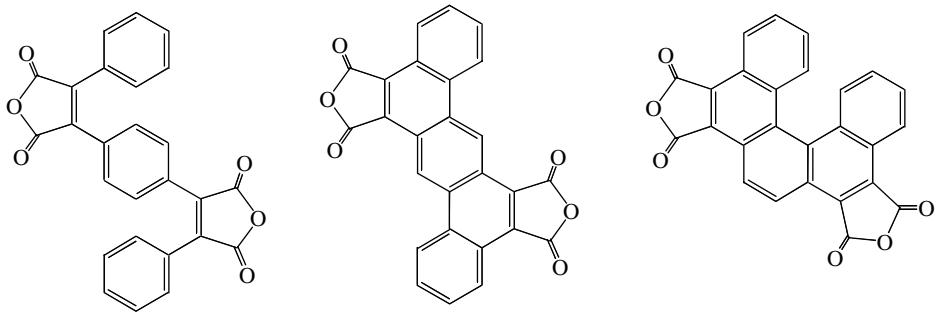

27 **28** **29**

1-Styrylanthracene undergoes photocyclization to yield 4a,4b-dihydrobenzo[b]chrysene **30**, which reverts to the starting material in deaerated solution and readily gives the fully aromatized compound under oxygen.[21] In contrast, although the *s-cis* rotomer **31** of 2-styrylanthracene does undergo 6π-electrocyclization, the 4a,4b-dihydroisomer undergoes ring opening appreciably faster than oxidation, and no 1,2-naphtho[a]anthracene is formed.[22] Phenacene is the name proposed for polynuclear arenes having an extended phenanthrene-like structure, and stilbene-type photocyclizations have been applied to the synthesis of both unsubstituted and 2,13-dialkyl[7]phenacenes, as outlined in Figure 33.5.[23] [6]Helicene **32** has a nonplanar structure due to overcrowding of the terminal rings, and hence there are two enantiomeric forms, designated P and M, of such compounds. Irradiation of 2-styryl-benzo[c]phenanthrene **33** provides an excellent access to these systems as yields are high (80–90%), and because of the very large optical rotation of P-**32** ($[\alpha]^{D}_{25}$ 3640°), even very small *ee* values can be determined accurately. The influence of circularly polarized light of the *ee* of **32** from **33** is of the order of 0.05%, but when the irradiations are carried out in chiral media, values on the order of 3% are achieved, which increase to around 6–7% on cooling the irradiated mixture to –26°C.[24] Iodine is frequently used as the oxidant in these photocycloaddition processes. From a study of the rate of formation of the polynuclear arenes produced on irradiation of di-2-naphthylethene, it has been shown that the yields of products are dependent on the concentration of I_2; it was concluded that complexation occurs between the *cis*-isomer and iodine.[25]

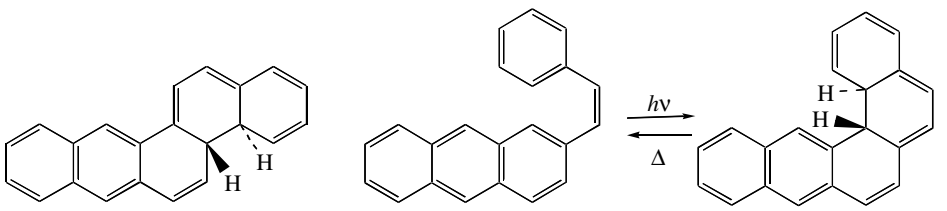

30 **31**

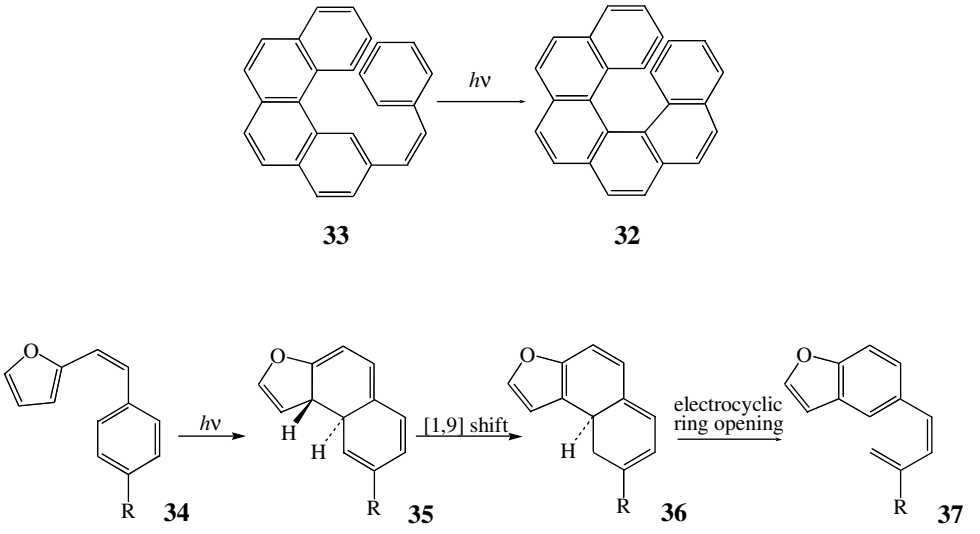

FIGURE 33.6 Photocyclization of 2-styrylfurans.

33.4 Heteroaryl Systems

It has long been known that the stilbene-type photocyclization occurs readily with styryl-heteroarenes and 1,2-diheteroaryl ethenes. Such processes not only provide a convenient access to novel as well as known polynuclear heteroarenes, but also in the latter series of these photoactive compounds, have been widely researched for a number of years as photochromic systems that have potential for development as the key element in data storage devices and as molecular switches.[7]

2-Styrylfurans **34** undergo photoinduced cyclization to the corresponding dihydroarenes **35** which yield **36** by a [1,9]-hydrogen shift.[26] This isomer undergoes thermal electrocyclic ring opening, initiated by aromatization, to give **37** in yields of 52–96% (Figure 33.6). In contrast, the dihydronaphtho[1,2-b]thiophene **38**, from photocyclization of 3-styrylthiophene, is readily converted into the heteroarene by air during the isolation procedure. However, when the photoreaction is carried out under oxygen, photo-oxidative cleavage and dimerization (in cyclohexane) also occur from a proposed complex of oxygen with the substrate (Figure 33.7).[27] The cyclization process of thienylethenes has been used by a number of research groups to synthesize novel sulfur-containing heteroarenes. For example, the double cyclization of tetra-substituted ethenes such as 1,1-bis(thiophen-2-yl)-2,2-diphenylethene **39** yields the sulfur heteroarene isoelectronic with dibenzo[g,p]chrysene.[28] In these systems, the intermediates isoelectronic with phenanthrene can be isolated, but the second ring closure is only efficient for those compounds with a thienyl group as one of the reacting arenes. A number of thiopyrone and pyrone derivatives have been synthesized using the photocyclization of 3-aryl-2-benzothienyl- and 2-naphthyl-3-thienyl-propenoic acids as the key step: for example, **40** is obtained in 73% yield from **41**.[29] In the absence of oxygen, 3-styrylpyridine and its 3′-amino derivative undergo highly regioselective photocyclization to give 2-azaphenanthrene products **42**.[30] As outlined in Figure 33.8, the reaction proceeds by a formal [1,7] hydrogen shift in the 4a,4b-dihydroazaphenanthrene intermediate to give the moderately stable 1,4-dihydropyridine **43**, which is converted into **42** in both the absence and presence of oxygen. However, when the reaction is carried out under oxygen, a mixture of **42** and the 4-azaphenanthrene **44** is formed. For some heteroarylethenes the photocyclization can be inefficient, but it has been reported that this limitation can be overcome by substitution of the ethene with a tosyl group, which promotes the formation of the cyclized product.[31]

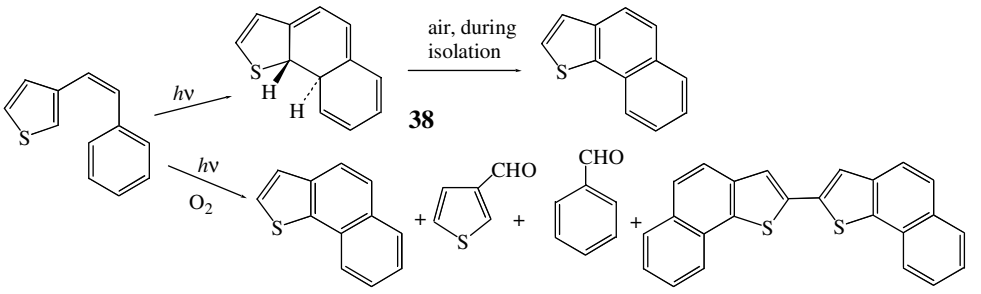

FIGURE 33.7 Photocyclization of 3-styrylthiophene.

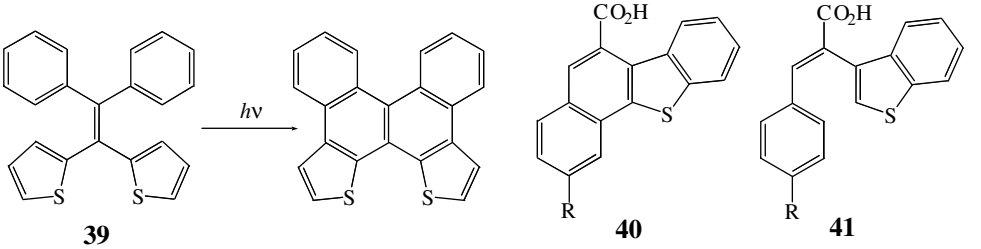

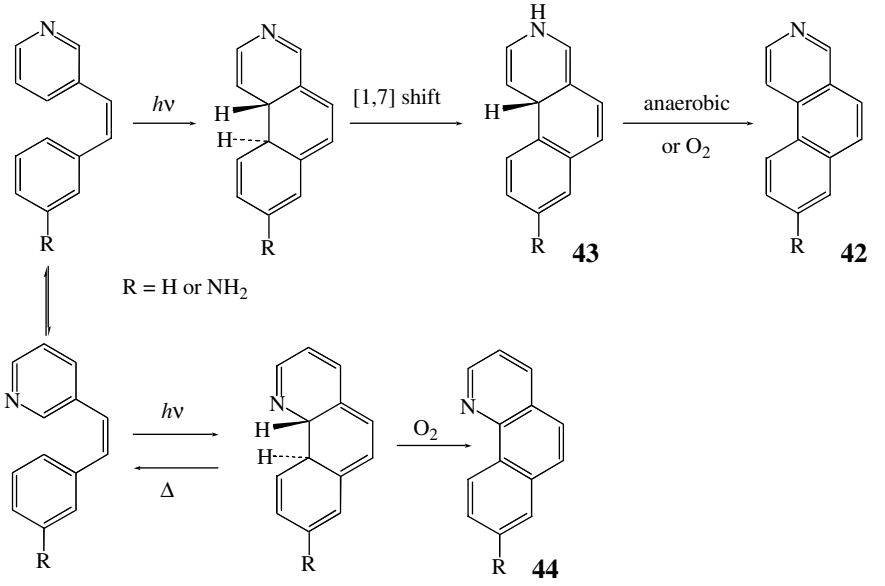

FIGURE 33.8 Photocyclization of 3-styrylpyridine and the 3′-amino derivative.

A huge variety of 1,2-diheteroarylethenes undergo photochemical 6π–electrocyclization, and much of this literature, particularly that of the photochromic reactions of 1,2-bis(methylthienyl)- and 1,2-bis(methylbenzothiophen-3-yl)-perfluorocyclopentenes, is reviewed elsewhere in this Handbook.[32] However, examples of these systems are presented here to illustrate the diversity of the molecular architectures that undergo this type of photochemical process. A variety of compounds derived from the basic 1,2-dithienylethene structure (e.g., **45**) undergo photochemical closure/ring opening in solution, films, and

the crystalline state. For derivatives such as **46**, the quantum yield of cyclization in aqueous solution can be increased appreciably by the presence of cyclodextrin, since the ratio of the photoreactive antiparallel conformer to the inactive parallel form is increased by its inclusion in the host cavity.[33] The open form of the derivative **47** uses the two crown ether moieties co-operatively like tweezers to capture large metal ions, which are then released from the photocyclized isomer[34]. The presence of an optically active substituent in the maleimide derivative **48** can lead to asymmetric photocyclization resulting in a diastereomeric excess as high as 86.6%.[35] Other photoactive systems in which the two heteroarenes are held in a *cis* geometry include 1,8a-dihydro-2,3-diarylazulenes such as **49**,[36] and the 2,3-bis(heteroaryl)quinones **50**.[37] As outlined in Figure 33.9, **49** undergoes both 6π-electrocyclization to **51** and conversion to the vinyl-heptafulvene **52** on irradiation, but when the 2,5-dimethyl-3-thienyl groups are replaced by phenyl, the photochromism only involves the latter process. Interestingly, the quinone derivatives **50** undergo cyclization both photochemically and by treatment with $AlCl_3$, $FeCl_3$, or CF_3SO_3H. The photocyclization of [2,3-a]quinolizinium salts (e.g., **53**) provides a convenient access to a series of novel hetero[5]helicenes having both thiophene and quinolizinium units.[38]

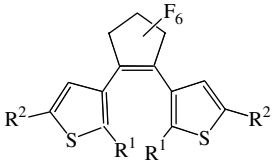

45 R's = alkyl *etc*

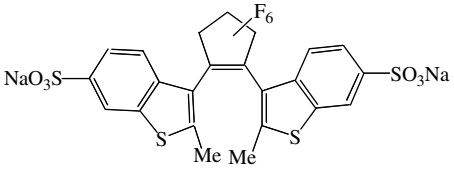

46

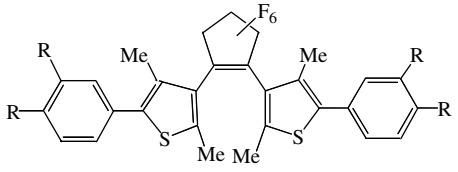

47 R-R = $O(CH_2CH_2O)_n$, n = 3-5

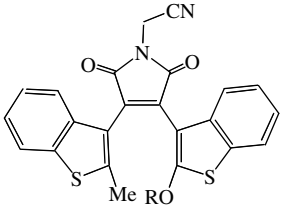

48 R = *l* or *d* menthyl

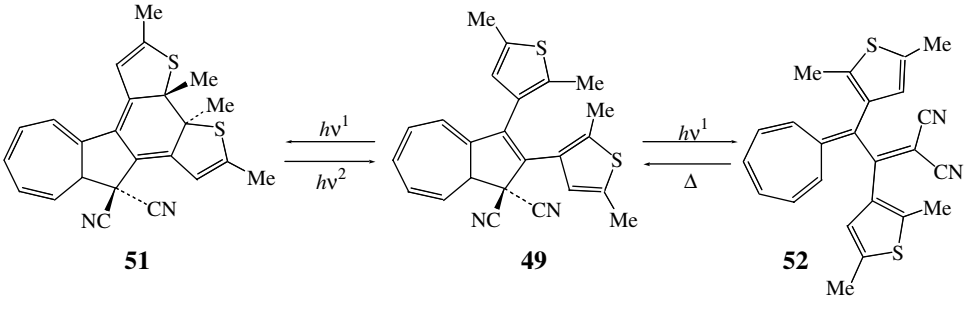

51 **49** **52**

FIGURE 33.9 Photochromism of 1,8a-dihydro-2,3-diarylazulenes.

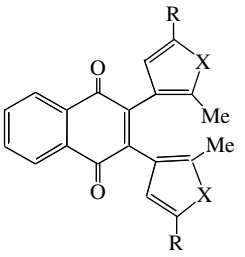

50 X = O, S or NMe
R = H, Me, Ph, thienyl, Br or I

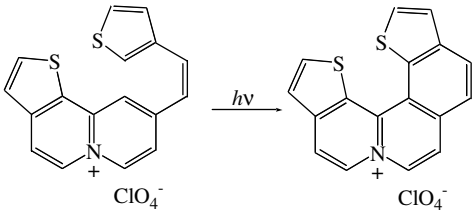

53

References

1. Smakula, A., Photochemical transformation of *trans*-stilbene, *Z. Phys. Chem.,* B25, 90, 1934.
2. Buckles, R.E., Illumination of *cis*- and *trans*-stilbenes in dilute solution, *J. Am. Chem. Soc.,* 77, 1040, 1955.
3. Laarhoven, W.H., Photochemical cyclizations and intramolecular cycloadditions of conjugated arylolefins. 1. Photocyclization with dehydrogenation, *Rec. Trav. Chim. Pays-Bas,* 102, 185, 1983.
4. Laarhoven, W.H., 2. Photocyclization without dehydrogenation and photocycloadditions, *Rec. Trav. Chim. Pays-Bas,* 102, 241, 1983.
5. Mallory, F.B. and Mallory, C.W., Photocyclization of stilbene and related molecules, *Org. Reactions,* 30, 1, 1984.
6. Laarhoven, W.H., Photocyclizations and intramolecular photocycloadditions of conjugated arylolefins and related compounds, *Organic Photochemistry,* Padwa, A., Ed., Marcel Dekker, New York, 1989.
7. Irie, M., Diarylethenes for memories and switches, *Chem. Rev.,* 100, 1685, 2000.
8. Gilbert, A., Cyclization of stilbene and its derivatives, in *CRC Handbook of Organic Photochemistry and Photobiology,* Horspool, W.M. and Song, P-S., Eds., CRC Press, Boca Raton, FL, 1995, p. 291.
9. Lewis, F.D. and Kalgutkar, R.S., The photochemistry of *cis-ortho-, meta-* and *para*-aminostilbenes, *J. Phys. Chem. A,* 105, 285, 2001.
10. Martinez, E., Estevez, J.J.C., Estevez, R.J.J., and Castedo, L., Photochemically induced cyclization of N-[2-(*o*-styryl) phenylethyl]acetamides and 5-styryl-1-methyl-1,2,3,4-tetrahydroisoquinolines: new total syntheses of 1-methyl-1,2,3,4-tetrahydronaphtho[2,1-f]isoquinolines, *Tetrahedron*, 57, 1981, 2001.
11. Lewis, F.D., Bassani, D.M., Burch, E.L., Cohen, B.E., Engleman, J.J.A., Reddy, G.D., Schneider, S., Jaeger, W., Gedeck, P., and Gahr, M., Photophysics and photochemistry of intramolecular stilbene–amine exciplexes, *J. Am. Chem. Soc.,* 117, 660, 1995.
12. Lewis, F.D. and Kultgen, S.G., Photochemical synthesis of medium-ring azalactams from *N*-(aminoalkyl)-2-stilbenecarboxamides, *J. Photochem. Photobiol. A: Chem.,* 112, 159, 1998.
13. Kojima, R., Shiragami, T., Shima, K., Yasuda, M., and Majima, T., Intramolecular cyclization of 1,2-distyrylbenzene via cation radical generated by photoinduced electron transfer, *Chem. Lett.,* 1241, 1997.
14. Ho, T.I., Ho, J.J.H., and Wu, J.J.Y., Novel acid-catalyzed hydrolysis of an intermediate from a photorearrangement of stilbenes, *J. Am. Chem. Soc.,* 122, 8575, 2000.
15. Leznoff, C.C., Terekhov, D.S., McArthur, C.R., Vigh, S., and Li, J., Multisubstituted phthalonitriles, naphthalenedicarbonitriles and phenanthrenetetracarbonitriles as precursors for phthalocyanine syntheses, *Can. J. Chem.,* 73, 435, 1995.
16. Dyker G., Korning J., and Stirner W., Synthesis and photocyclization of macrocyclic stilbene derivatives, *Eur. J. Org. Chem.,* 149, 1998.

17. Yamato, T., Fujita, K., Futatsuki, K., and Tsuzuki, H., Medium-sized cyclophanes. Part 53. Synthesis and conformational studies and photoinduced cyclization of *syn*-[n.2]metacyclophanenes, *Can. J. Chem.,* 78, 1089, 2000.
18. Lai, Y.H. and Zhou, Z.L., Synthesis, properties and conformational studies of *anti*-8-fluoro-16-methyl[2(2)]metacyclophane and anti-8-fluoro-16-methyl[2(2)]metacyclophane-1,9-diene, *J. Chem. Soc., Perkin Trans. 2,* 2361, 1994.
19. Fields, E.K., Behrend, S.J., Meyerson, S., Winzenburg, M.L., Ortega, B.R., and Hall, H.K., Diaryl-substituted maleic anhydrides, *J. Org. Chem.,* 55, 5165, 1990.
20. Frimer, A.A., Kinder, J.J.D., Youngs, W.J.J., and Meador, M.A.B., Reinvestigation of the photocyclization of 1,4-phenylene bis(phenylmaleic anhydride) — preparation and structure of [5]helicene 5,6–9,10-dianhydride, *J. Org. Chem.,* 60, 1658, 1995.
21. Karatsu, T., Kitamura, A., Zeng, H.L., Arai, T., Sakuragi, H., and Tokumaru, K., Photoisomerization and photocyclization reactions of 1-styrylanthracene, *Bull. Chem. Soc. Jpn.,* 68, 920, 1995.
22. Karatsu, T., Itoh, H., Nishigaki, A., Fukui, K., Kitamura, A., Matsuo, S., and Misawa, H., Picosecond time-resolved fluorescence spectroscopy of (*Z*)-1-(2-anthryl)-2-phenylethene and its model compounds: understanding the photochemistry by distinguishing between the *s-cis* and *s-trans* rotamers, *J. Phys. Chem. A,* 104, 6993, 2000.
23. Mallory, F.B., Butler, K.E., Evans, A.C. and Mallory, C.W., Phenacenes: a family of graphite ribbons. 1. Syntheses of some [7]phenacenes by stilbene-like photocyclizations, *Tetrahedron Lett.,* 37, 7173, 1996.
24. Prinsen, W.J.C. and Laarhoven, W.H., The influence of the chiral environment in the photosynthesis of enantiomerically enriched hexahelicene, *Recl. Trav. Chim. Pays-Bas,* 114, 470, 1995.
25. Veretennikov, A.V., Kazakov, S.P., and Razumov, V.F., Features of photocyclohydrogenation reaction of di-(2)-naphthylethylene in presence of molecular iodine, *Zh.. Nauch. Prikl. Fotogr.,* 41, 44, 1996.
26. Ho, T.I., Wu, J.Y., and Wang, S.L., Novel photochemical rearrangement of styrylfurans, *Angew. Chem. Int. Ed. Engl.,* 38, 2558, 1999.
27. Song, K., Wu, L.Z., Yang, C.H., and Tung, C.H., Photocyclization and photooxidation of 3-styrylthiophene, *Tetrahedron Lett.,* 41, 1951, 2000.
28. Fischer, E., Larsen, J., Christensen, J.B., Fourmigue, M., Madsen, H.G., and Harrit, N., Synthesis of new sulfur heteroaromatics isoelectronic with dibenzo[g,p]chrysene by photocyclization of thienyl- and phenyl-substituted ethenes, *J. Org. Chem.,* 61, 6997, 1996.
29. Tominaga, Y., Castle, L.W., and Castle, R.N., Photocyclization of 2-(naphth-1-yl)-3-(thien-2-yl)propenoic acid and the total assignment of the H-1- and C-13-NMR spectra of the product, *J. Heterocycl. Chem.*, 33, 1017, 1996; Sasaki, K., Satoh, Y., Hirota, T., Nakayama, T., Tominaga, Y., and Castle, R.N., Syntheses of thiopyrone and pyrone derivatives by photocyclization reaction of 3-aryl-2-([1]benzothien-3-yl)propenoic acids, *J. Heterocycl. Chem.,* 37, 959, 2000.
30. Lewis, F.D., Kalgutkar, R.S., and Yang, J.S., Highly regioselective anaerobic photocyclization of 3-styrylpyridines, *J. Am. Chem. Soc.,* 123, 3878, 2001.
31. Antelo, B., Castedo, L., Delamano, J., Gomez, A., Lopez, C., and Tojo, G., Photochemical ring closure of 1-tosyl-1,2-diarylethenes, *J. Org. Chem.,* 61, 1188, 1996.
32. Irie, M., in *CRC Handbook of Organic Photochemistry and Photobiology,* Horspool, W.M. and Song, P-S., Eds., CRC Press, Boca Raton, FL, 2003.
33. Takeshita, M., Kato, N., Kawauchi, S., Imase, T., Watanabe, J.J., and Irie, M., Photochromism of dithienylethenes included in cyclodextrins, *J. Org. Chem.,* 63, 9306, 1998.
34. Takeshita, M. and Irie, M., Photoresponsive tweezers for alkali metal ions. Photochromic diarylethenes having two crown ether moieties, *J. Org. Chem.,* 63, 6643, 1998.
35. Yamaguchi, T., Uchida, K., and Irie, M., Asymmetric photocyclization of diarylethene derivatives, *J. Am. Chem. Soc.,* 119, 6066, 1997.
36. Mrozek, T., Gorner, H., and Daub, J., Multimode-photochromism based on strongly coupled dihydroazulene and diarylethene, *Chem.-Eur. J.,* 7, 1028, 2001.

37. Deng, X.H. and Liebeskind, L.S., A contribution to the design of molecular switches: novel acid-mediated ring-closing-photochemical ring-opening of 2,3-bis(heteroaryl)quinines (heteroaryl = thienyl, furanyl, pyrrolyl), *J. Am. Chem. Soc.,* 123, 7703, 2001.
38. Sato, K., Yamagishi, T., and Arai, S., Synthesis of novel azonia[5]helicenes containing terminal thiophene rings, *J. Heterocycl. Chem.,* 37, 1009, 2000.

34

Synthesis of Heterocycles by Photocyclization of Arenes

Norbert Hoffmann
UMR CNRS et Université de Reims Champagne-Ardenne

34.1 Introduction

Heterocyclic compounds are important targets in organic synthesis. They possess numerous biological activities and can be used as intermediates for further transformations. Starting from readily accessible starting materials, various photochemical cyclization reactions provide convenient methods to build up to a large variety of heterocycles; several reviews deal with them.[1] In this context, the cyclization of aromatic compounds plays an important role. In these reactions, as in many ground state reactions of aromatic compounds, the aromatic character is momentarily suppressed. In this chapter, some of these reactions are discussed.

34.2 Electrocyclization

Electrocyclization provides an efficient way to synthesize a large variety of heterocyclic compounds. Among the many photocyclization reactions of aromatic compounds, electrocyclization is among the most frequently studied. An example of this is that illustrated in Scheme 1. This involves cyclization between the arene moieties of the protonated azobenzene **1**, which reacts from the $^1\pi\pi^*$ state reaction and is controlled by the Woodward–Hoffmann rules.[2] Six π-electrons are involved in the conrotatory cyclization. The reaction was not observed when unprotonated azobenzene was irradiated because in this case, the $^1n\pi^*$ state is populated. Since the photochemical electrocyclization is reversible, a consecutive trapping reaction is needed to obtain the final products in good yields. In the present case, as in many other reactions, a rearomatization step via oxidation took place to afford the final product **2**. In the same way, the imine **3** can be cyclized to the phenanthridine derivative **4**.[3] In this case, the oxidation of the

0-8493-1348-1/04/$0.00+$1.50

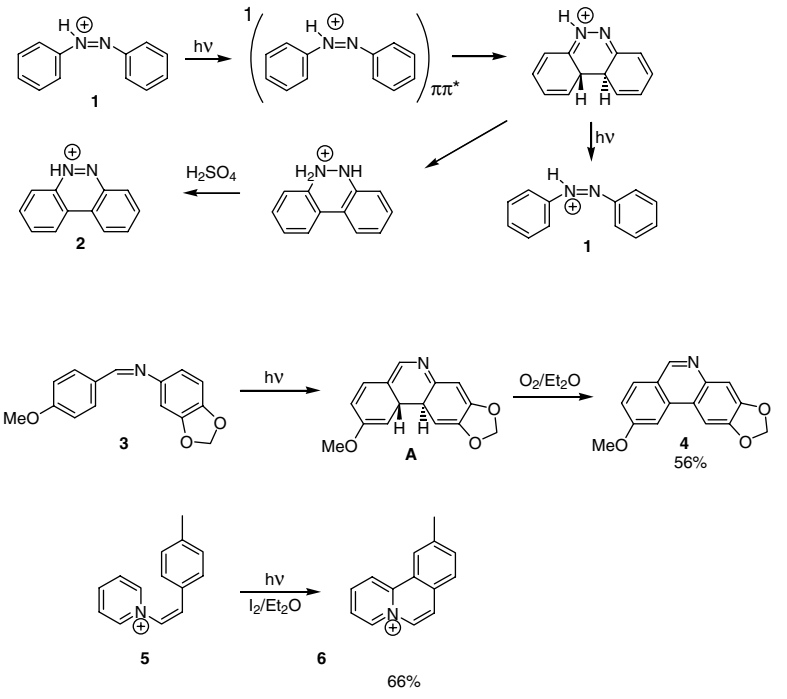

SCHEME 1

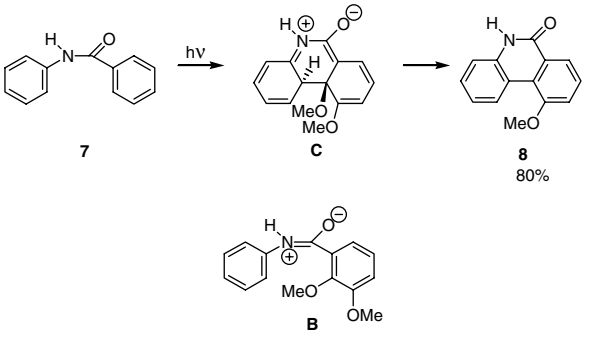

SCHEME 2

intermediate **A** was performed by oxygen. Phenanthridizinium derivatives **6** have been synthesized by photocyclization of styrylpyridinium **5** cations (Scheme 1) The rearomatization took place by oxidation with iodine.[4]

Cyclization of benzoanilide derivatives such as **7** is also possible (Scheme 2).[5] The 6π-electron system necessary for photochemical conrotatory cyclization is present due to the mesomeric structure **B**. In the present example, no oxidation was needed to regenerate the aromaticity in the final product **8**. In this case re-aromatization occurred via elimination of methanol from intermediate **C**.

Carbazoles,[6] dibenzofurans,[7] and dibenzothiophene[7] derivatives **10** have been obtained via photocyclization of the corresponding diphenylamine, diphenylether, or diphenylthioether precursors **9** (Scheme 3). In these reactions, the lone pair of heteroatoms contributes to the 6π–electrons engaged in the electrocyclization. The re-aromatization occurred under oxidative conditions in the presence of oxygen or iodine. When irradiated in acetonitrile solution containing aqueous HCl, compounds **11** were transformed into

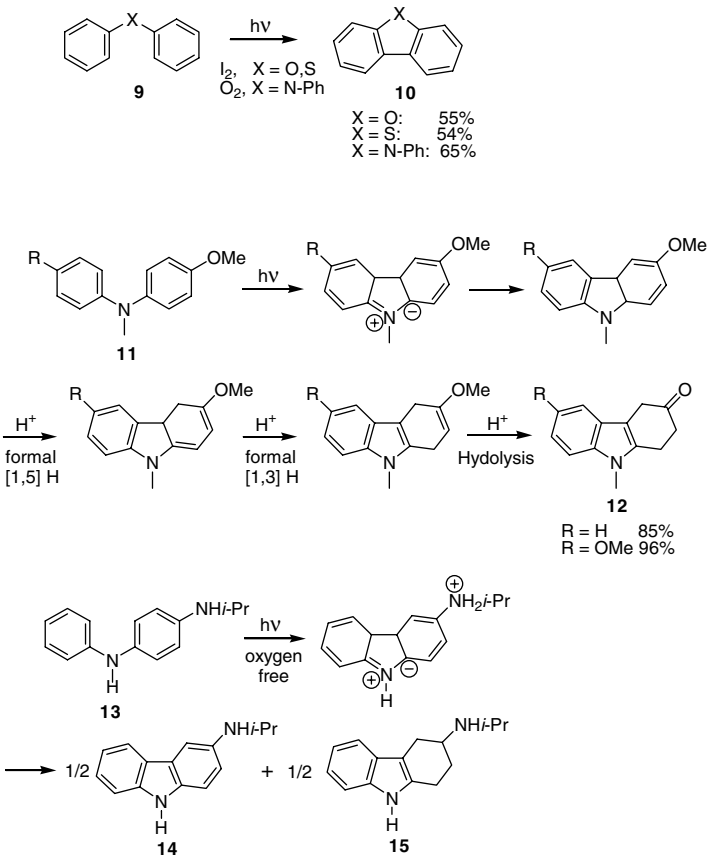

SCHEME 3

1,2,4-tetrahydro[4a*H*]carbazol-3-ones **12** with high yields.[8] Instead of aromatization through oxidation, acid-catalyzed rearrangements and hydrolysis took place. Under similar conditions and in the absence of oxygen the transformation of the corresponding amine derivative **13** yielded carbazole **14** and the tetrahydrocarbazole derivative **15**.[9]

Many photochemical electrocyclizations of compounds possessing an aromatic moiety and an olefinc substituent have been reported. Some examples are described here. Aromatic thioethers such as **16** afforded arenodihydrothiophene derivatives **17** (Scheme 4).[10] The presence of the ylide intermediate **D** was proven by its independent trapping in a 1,3-dipolar cycloaddition with *N*-phenylmaleimide. From this reaction, compound **18** was isolated in high yields. In the corresponding intramolecular reaction of **19**, product **20** was formed only in minor amounts.[11] However, the major product **21** resulted from an intramolecular trapping by a Michael reaction. A possible mechanism is indicated in structure **E**. Another minor product **22** resulted from simple cyclization. Under the same reaction conditions, the corresponding enol ether derivative **23** afforded product **24** resulting from an efficient intramolecular 1,3-dipolar addition of the alkene with the ylide intermediate of the photochemical cyclization.[12]

A large variety of *N*-benzoylenamines have been subjected to photochemical cyclization. Mostly *trans* fused ring systems were obtained from the cyclization of *N*-benzoylenamines such as **25** derived from cyclic amines, especially cyclohexylamines (Scheme 5).[13] The stereochemistry can be explained by a photochemical conrotatory cyclization leading to intermediate **F**. A thermal 1,5-suprafacial H shift leads then to the final product **26**. In this way, the aromaticity of the benzoyl moiety is reestablished. Frequently, the formation of a *cis*-isomer as a byproduct was observed. These products resulted from a consecutive photochemical or thermal isomerization of the *trans* product. When the reaction was carried out in the

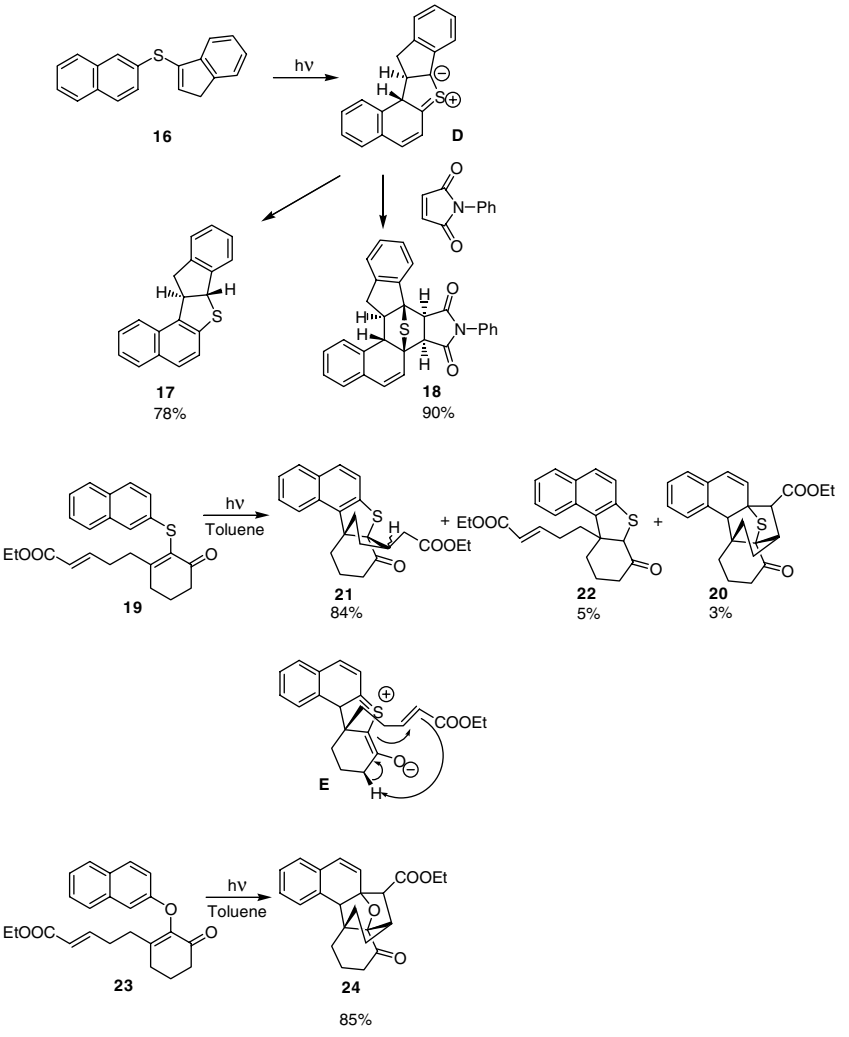

SCHEME 4

presence of oxygen or iodine, the double bond of the enamine moiety was reformed in the final product. This aspect was recently studied with the reaction of **27**.[14] Depending on the reaction conditions, the transformation of the intermediate **G** can be controlled, and unsaturated, nonaromatic products, **28** and **29**, can also be isolated. Compound **28** resulted from base-catalyzed rearrangements via intermediates **H** and **I**. Intermediate **H** was formed by deprotonation at H^a, and the final product **28** resulted from a base catalyzed rearrangement involving H^b. Compounds **30** and **31** were formed *via* oxidation and the 1,5 H shift path, respectively. Under reductive reaction conditions, **G** was reduced at the iminium moiety leading to **J**. This latter intermediate yielded **29** after protonation. The sequence of acid/base reactions was proven by isotopic labeling with deuterium.

Interesting carbocyclic systems such the spiro cyclic compound **32** can be formed from benzoenamides **33** (Scheme 6).[15] The same class of spirocyclic compounds was available from heterocyclic carboxamides.[16] Starting from the furan and thiophene derivatives **34**, the corresponding spirocyclic products **35** were obtained when the reaction was carried out in dry actonitrile. The intermediate **K** is generated by photochemical cyclization. A 1,5-[H] shift regenerates the aromaticity of the furan or thiophene ring. When the reaction was carried out in methanol as solvent, the intermediate **K** was trapped by addition of a solvent molecule to the iminium bond, and products **36** were obtained in high yields. The reaction

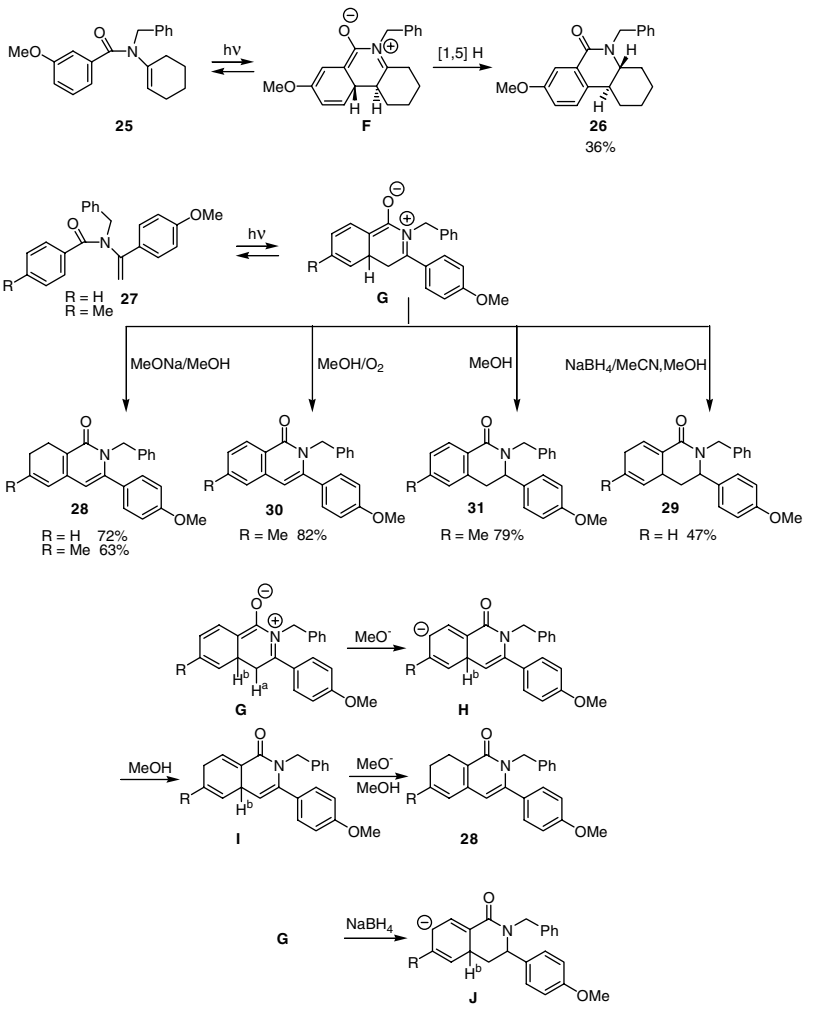

SCHEME 5

has been frequently applied to the synthesis of alkaloids. Thus, for example, irradiation of **37** in the presence of $NaBH_4$ yielded **38**, which was a convenient intermediate in the synthesis of the indole alkaloid, yohimbine.[17]

Aniline derivatives have been used to synthesize the indoline system. A large variety of indoline alkaloid substructures are available in a very efficient way. Enamine derivatives such as **39** bearing electron withdrawing substituents on the olefinic double bond were transformed in high yields (Scheme 7).[18] Two *syn/anti* isomers **41** and **42** were isolated. The isomeric ratio of the final products was influenced by a photostationary equilibrium between the substrates **39** and **40**. The reaction was applied to the synthesis of a variety of derivatives of the alkaloid aspidospermidine.[19] In this context, the cyclization products **43** were transformed into the polycyclic indole derivatives **44**, **45**, and **46**. Polycyclic indolone compounds **48** have been successfully produced by cyclization of enaminone derivatives **47** carrying a quinoline substituent.[20] In these cases and contrary to the examples **41**, **42,** and **43**, the products **48** resulted from an oxidation of the cyclization product (also compare the formation of **30** in Scheme 5).

The photochemical electrocyclization was also applied as key step in the synthesis of nitrogen-containing heterocycles possessing pharmaceutical activity such as, for example, the 5-$HT_{2C/2B}$ Receptor Antagonist **49**[21] or the nonsteroidal androgen receptor agonist **50** (Scheme 8).[22]

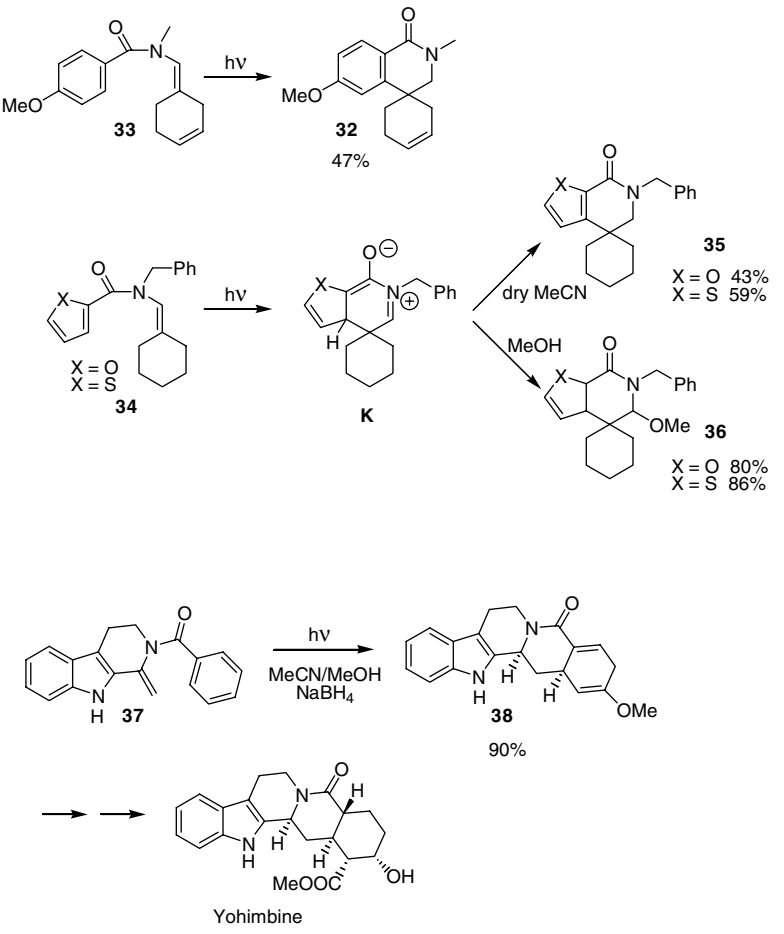

SCHEME 6

Higher functionalized aromatic compounds undergo photochemical electrocyclization as well. Two examples are presented in Scheme 9. When the benzoquinoxaline **51** was irradiated in an acidic medium, the indolo[1,2-a]quinoxaline **52** could be isolated in good yields.[23] The acid seems to have no significant influence on the photochemical cyclization, since the reaction can also be carried out in a neutral reaction medium. However, the acid might shift the equilibrium between the substrate **51** and the intermediate **L** towards the product side. The good yields resulted mainly from the fact that the protonated product **52** is more stable than the unprotonated form. The trifluoromethylated dihydroisoquinoline derivative **55** was obtained from the irradiation of benzamidine **53**.[24] Due to steric hindrance, the cyclization of the *Z*-isomer is unfavorable. However, the corresponding *E*-isomer **54** is formed in a photostationary equilibrium. After cylization hydrogen shifts lead to the final product **55**.

34.3 Chiral Induction in Electrocyclization Reactions

Few attempts have been made to induce chirality in these reactions. The cyclization of the homochiral enamide **56** was diastereoselective, and product **57** was obtained in good yield along with small amounts of the oxidation product **58** (Scheme 10).[25] Compound **57** was transformed into (–)-xylopinine. The exact mechanism of the chiral induction was not discussed. Most reasonably, the chirality was induced during the 6π-cyclization. The subsequent 1,5-[H] shift should be stereospecific. However, the diastereoselectivity was determined after several steps and revealed to be rather low. The stereoisomers **60a,b**

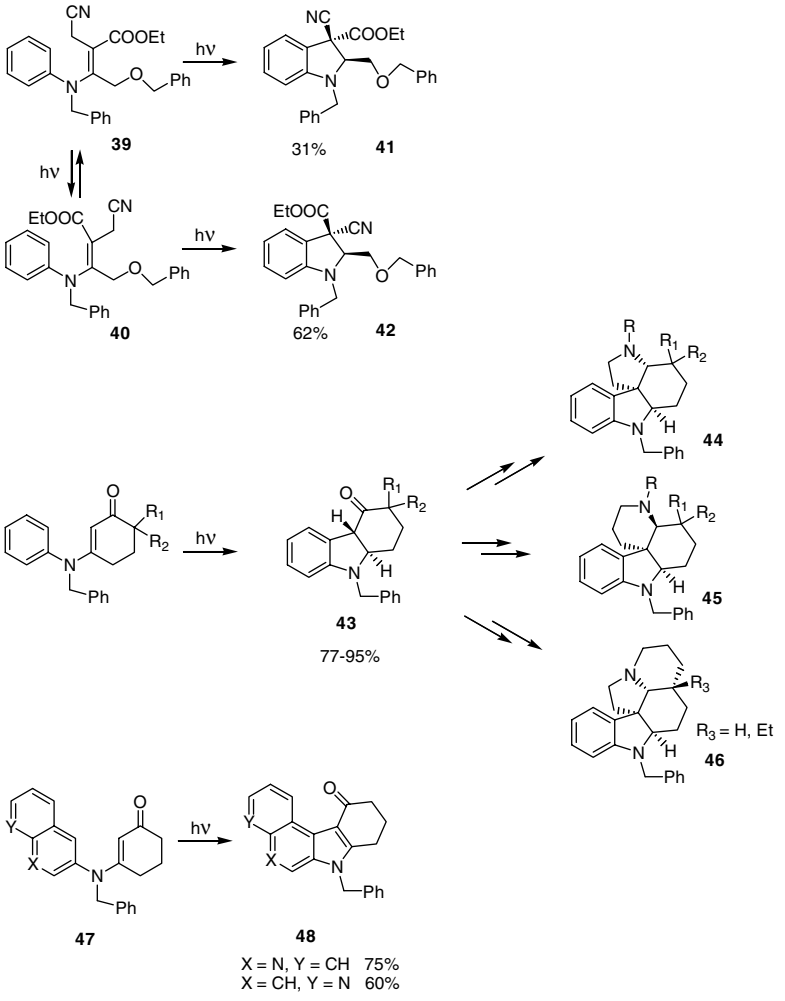

SCHEME 7

were isolated in a 3.7/1 ratio. It seems that during the transformations, partial epimerization occurred, especially when the lactam function was reduced to obtain **59**. For a similar derivative, the chiral induction in the photocyclization step was complete, but the products were obtained only in low yields.[26]

Absolute chiral induction was performed by irradiation with circularly polarized light with compound **61** (Scheme 11).[27] Using, for example, left-circularly-polarized light, the enantiomer of the cyclization product **62** possessing negative specific rotation was generated in a slight excess. Catalytical chiral induction in solution was carried out using the tartaric acid derivative **63** as inductor.[28] Complexation of intermediates of the substrate **64** with **63** led to the preferred formation of one enantiomer. The enantiomeric excess of the *trans*-isomer **65** was significantly higher than that of the *cis*-isomer **66**. Especially high chiral induction was observed when the substrate was co-crystallized with TADDOL derivatives.[29] TADDOLs are capable of forming crystal inclusion complexes with many organic compounds. The substrates are highly orientated and imobilized in the chiral environment, which favors one of the enantiotopic pathways. The sense of the chiral induction depends on the chiral cavity filled with the substrate molecule rather than on the configuration of the TADDOL derivative. Therefore, different enatiomers were favored when the cyclopentane- or the cyclohexane-derived TADDOL was used. When compound **64** was complexed with the cyclohexylidene TADDOL **67**, **ent-65** was isolated with almost complete enantioselectivity. However, when **64** was complexed with the corresponding cyclopentylidene TADDOL **68**, **65** was formed with only 70% enantiomeric excess.

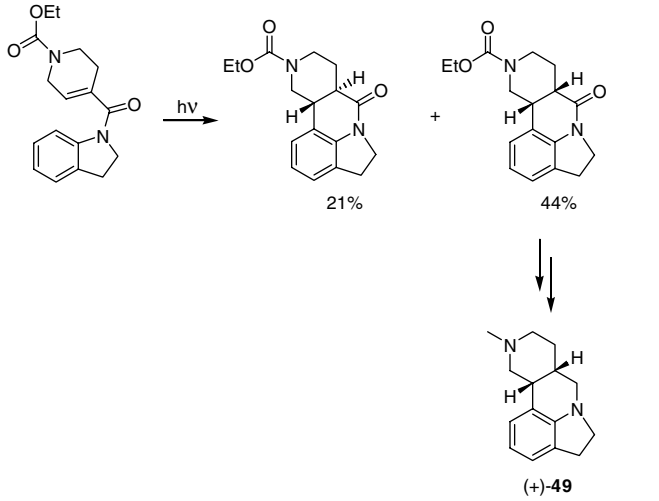

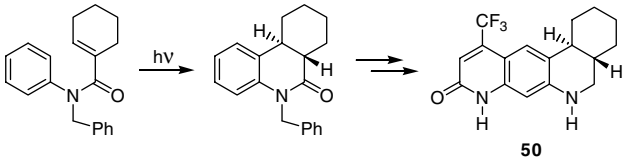

SCHEME 8

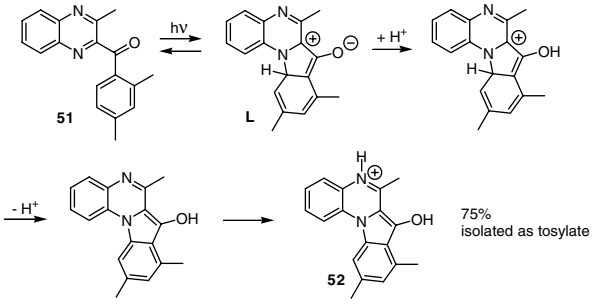

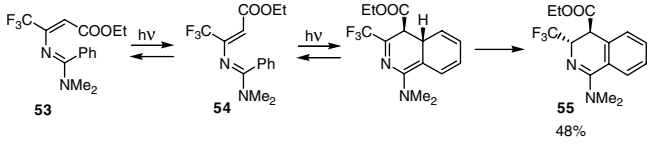

SCHEME 9

34.4 Photochemical Cyclization of Aromatic Compounds Involving Radical Species

Photochemically excited molecules often lose energy via production of radicals. Such intermediates are frequently involved in photochemical cyclizations. In this way, naphthylypyridylamine derivatives such

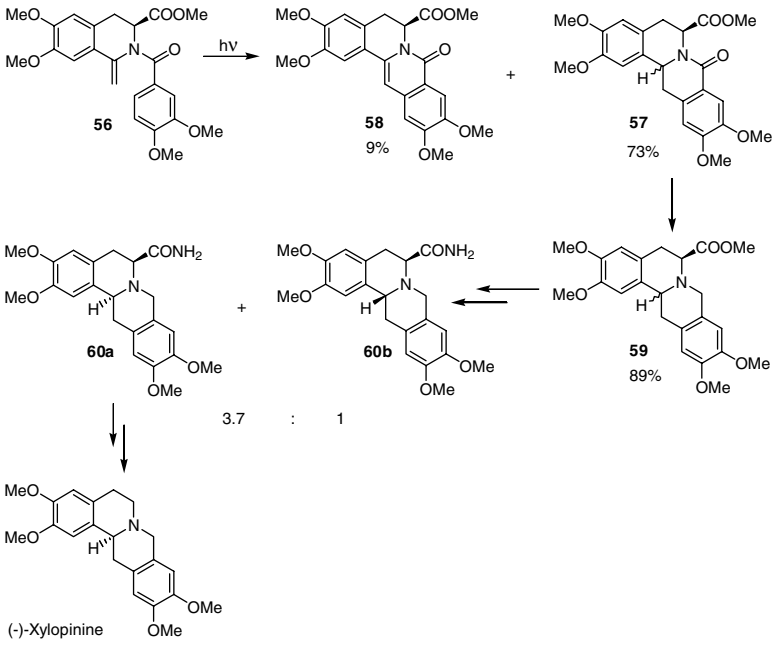

SCHEME 10

as **69** were successfully transformed into polycyclic compounds **70** and **71** (Scheme 12).[30] Cyclization was observed either at the ring nitrogen leading to **71** or at the 6-position of the pyridine ring leading to **70**. Benzo[*c*]naphthyridinones **73** were efficiently obtained by photocyclization of 2-halo-*N*-pyridinylbenzamides such as **72**.[31] Such photochemical cyclization of aromatic compounds carrying a halogen atom on the aromatic ring are frequently proposed to proceed via radical intermediates. However, in some cases, an electrocyclization followed by elimination of HX could explain the results as well. In the present case radical intermediates, especially n-complexes **M**, were identified by transient absorption spectra from laser flash photolysis of **72**. Polycyclic thiophene carbamides such as **74** yielded polycyclic lactams **75** in the same way.[32] This reaction was carried out with a large variety of such derivatives. Boron complexes of *N*-phenylbenzohydroxamic acids such as **76** were cyclized in high yields.[33] The complexation favorably orientates the two aromatic rings for cyclization. The presence of the bromine atom in the *ortho* position of the benzoyl moiety increased significantly the efficiency of the reaction. The corresponding bromine free boron complex, in the presence of iodine as oxidizing agent, needed 33 h for complete conversion instead of 2 h for the complex **76** (X = Br) to obtain the cyclization product **77**.

Mechanistic details were also discussed for the reaction of enamineones such as **78** (Scheme 13).[34] After photochemical excitation, single electron transfer took place. This transfer occurred in an intramolecular way leading to intermediate **N** or in an intermolecular way (in the presence of tertiary amines) leading to the radical ion pair **O**. After release of chloride, the latter intermediate yields the pyridyl radical **P**. Addition of the radical moiety to the enamineone double bond and loss of hydrogen led to the final product **79**. Hydrogen abstraction from a solvent molecule or addition with a solvent molecule (e.g., benzene) of **P** led to side products such as **80**. The same product could also result from the reaction of intermediate **N**. Under the described reaction conditions, **80** could not be isolated since under photochemical electrocyclization, it was transformed into **79** and **81**.

The enamine derivative **82** underwent photocyclization via intramolecular single electron transfer (Scheme14).[35] The favorable *E*-geometry **83** for the formation of the major product was generated by photochemical *cis/trans* isomerization. Electron transfer from the tertiary amine function on the side chain to the excited chromophore generated the radical ion pair **Q**. Consecutive hydrogen transfer from

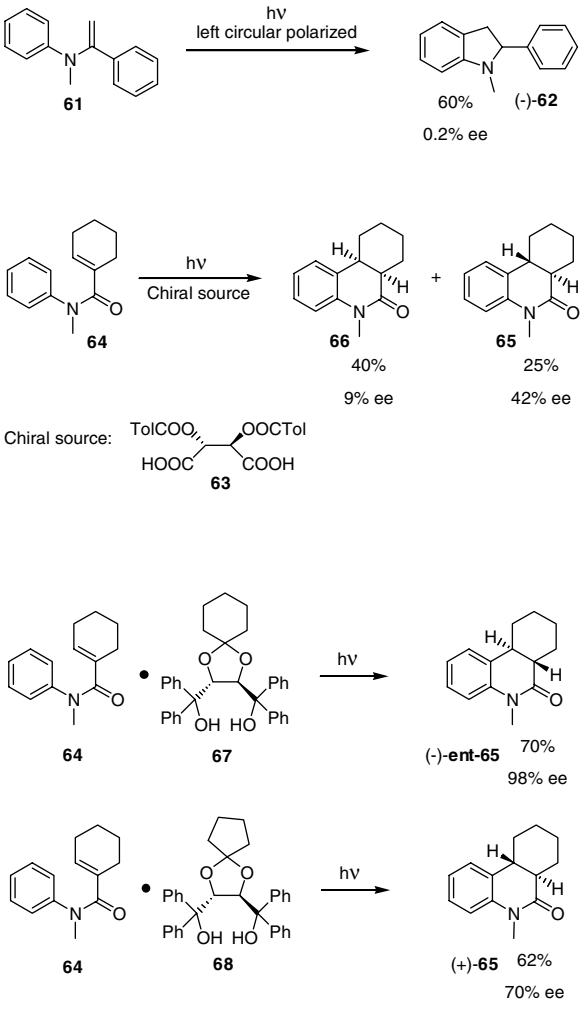

SCHEME 11

the amide nitrogen to the amide oxygen then led to the biradical **R**. Radical combination and tautomerization afforded the intermediate **S**. Finally, the main product **84** was formed via hydrogen shift. The side product **85** was formed by a cyclization/H shift/dehydration sequence of substrate **82**. A 4π–electrocyclization of the *trans*-isomer **83**, involving structure **T,** and followed by a H-shift and dehydration led to the didehydroazetidine derivative **86**.

A radical species can be generated on an aliphatic side chain. Intramolecular addition to the aromatic system then builds up a heterocycle. This strategy was applied to the synthesis of indanone derivatives (Scheme 15).[36] After photochemical excitation, intramolecular electron transfer in compound **87** took place leading to the intermediate **U**. Radical combination and deprotonation led to the final product **88**. In the present case, elimination of HBr occurred as a competing reaction and furnished the methacrylamide **89**. This compound underwent photochemical electrocyclization to yield **90**.

The photocyclization reactions of a large variety of aromatic chloroacetamide derivatives have been investigated. The cyclizations were applied to the synthesis of azepinoindol systems, which are not readily accessible by ground-state radical reactions.[37] The tricyclic azepine derivatives **92** were obtained from the cyclization of **91** (Scheme 16).[38] More complex azepine derivatives such as **93** could be synthesized in the same way.[39] The reaction of corresponding dichloroacetamides such as **94** is more efficient, especially

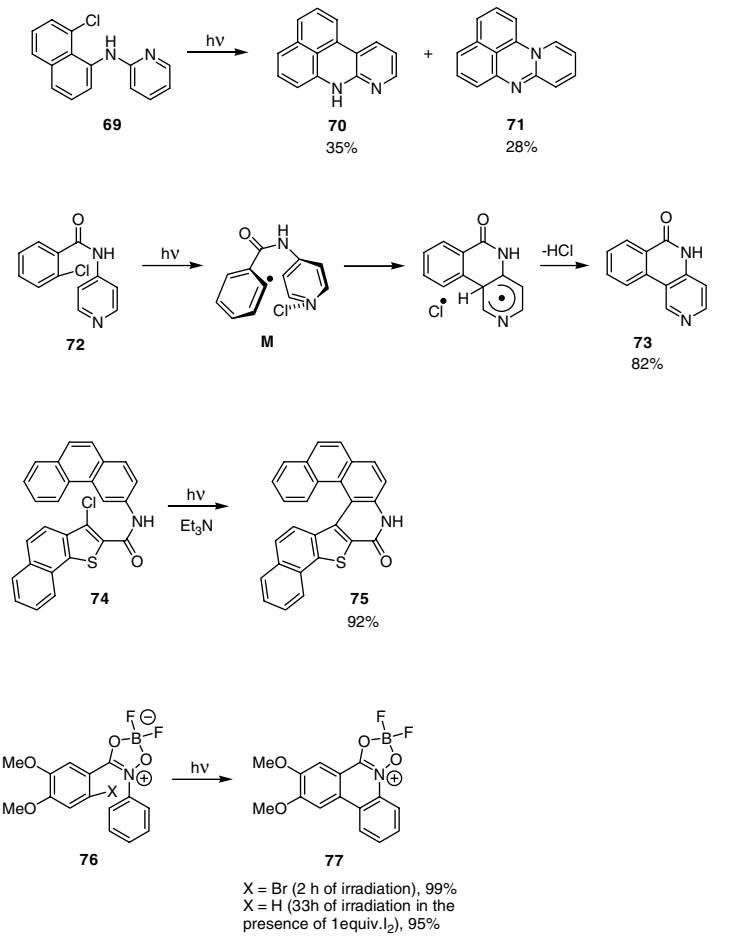

SCHEME 12

when the workup is carried out in the presence of nucleophiles such as methanol.[40] Eight-membered ring systems such as **95** were obtained in this way. The reaction of the indole derivatives **96** bearing a benzene ring in the *N*-sidechain was less selective.[41] Besides the eight-membered ring product **97**, a nine-membered lactam **98** and the pentacyclic product **99** were obtained from the cyclization.

Excited states of enones such as **100** can abstract hydrogen preferentially from the α position of alkyl ether or alkyl amines leading to the biradical intermediates **V**. Intramolecular addition to the benzene ring leads to dihydropyran or dihydropyridin derivatives **101** (Scheme 17).[42] Dibenzofuran derivatives **103** were obtained from polyfluorinated aryloxodihydronaphthalene compounds such as **102**.[43] Probably, in such cases, a photochemical electron transfer from the nonfluorinated aryl substituent to the fluorinated moiety takes place. When compound **104** was irradiated in the presence of $HClO_4$, the isoquinoline derivative **105** was isolated in good yields.[44]

The cyclization was followed by hydrolysis and oxidation. The transformation is a photochemical analogue of the Mannich or the Pictet–Spengler reaction. A photochemically sensitized cyclization was applied to the synthesis of the tetrahydroisoquinoline derivative **107**.[45] The reaction starts with an electron transfer from **106** to the photochemical excited sensitizer dicyanonaphthalene (DCN). The resulting radical cation **W** undergoes cyclization followed by the release of a trialkylsilyl cation. Intermediate **X** then yields the final product **107** by hydrogen loss.

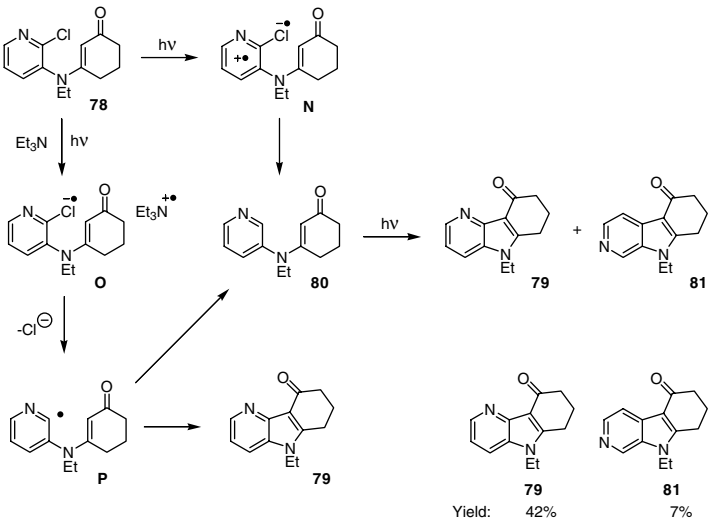

SCHEME 13

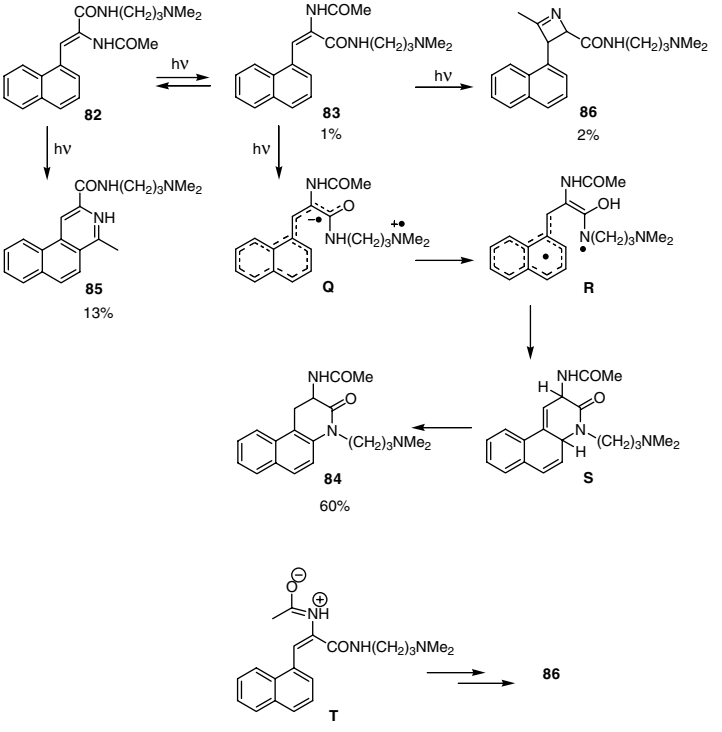

SCHEME 14

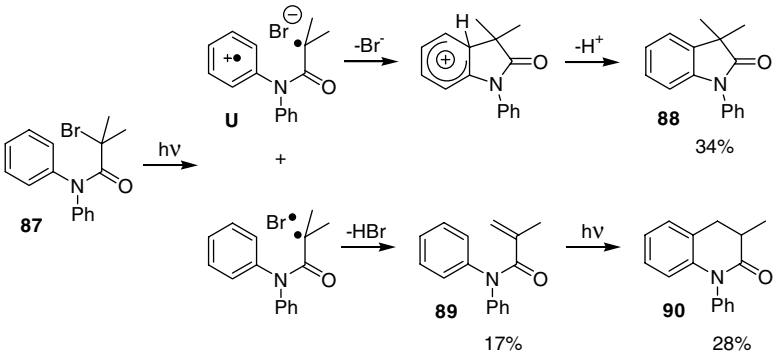

SCHEME 15

34.5 Photochemical Cyclization of Aromatic Compounds Involving Nitrenes and Other Reactive Intermediates

Electrocyclization of aromatic compounds involving temporary suppression of the aromatic character sometimes takes place in the context of photochemical rearrangements involving reactive centers other than radicals. The reaction of aromatic nitrenes has been particularly well studied. In addition to other methods, these intermediates were generated by photolysis of the corresponding azides. An example is depicted in Scheme 18. Under the indicated reaction conditions, the singlet nitrene **Y**, which was generated from the diphenylazide **108**, underwent cyclization to yield the carbazol **109**.[46] The concomitantly generated triplet nitrene (about 10%) yielded the side products, in particular the phenanthridine **110**. The yield of carbazole **109** was particularly high when the reaction was carried out at higher temperature. Control experiments have shown that thermolysis of the substrate **108** was negligible under these conditions. Singlet nitrenes obtained in the same way as described above could add to heterocyclic aromatic substitutents such as that illustrated in example **111**.[47] Upon irradiation, the azidophenylpyrazole **111** yielded the singlet nitrene **Z**, which cyclized to afford the pyrazolobenzotriazol **112**. The concomitantly generated triplet nitrene was at a minimum but still occurred to yield the pyrazolophenylamine **113** as a side product. 1,3-Dipolar intermediates **AA** were generated by irradiation of 2*H*-azirine derivatives **114**.[48] Cyclization followed by a 1,5-[H] shift afforded benzoazepine derivatives **155** in high yield. The corresponding naphthalene derivatives **116** and **117** were obtained in the same way and with the same efficiency.

34.6 Conclusion

Photochemical cyclization reactions provide an efficient route to a large variety of heterocyclic compounds starting from readily accessible substrates. Many of these heterocycles possess interesting biological activity. Aside from the halogen substrates, which are frequently used for cyclizations involving radical intermediates, no particular activation or derivatization or the use of metal reagents is necessary for C-C bond formation. This reflects the general advantage of photochemical reactions in the context of their application to organic synthesis.

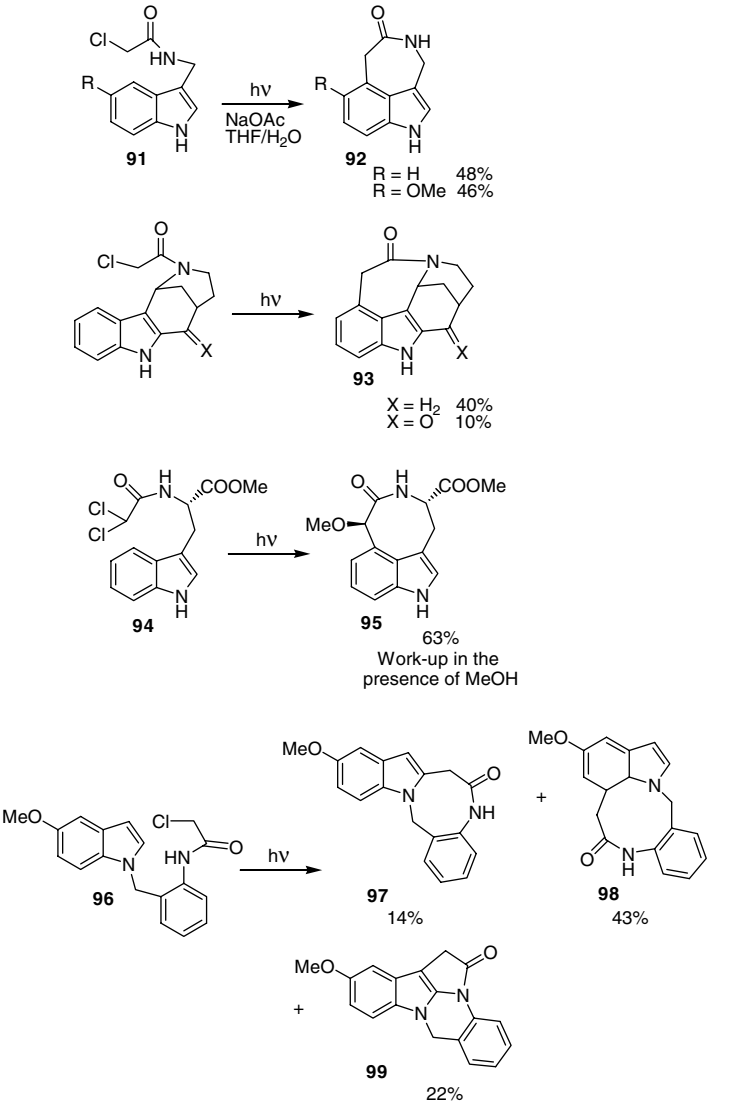
Cl
O
HN
R
N
H
91
hν
NaOAc
THF/H2O
NH
92
R = H 48%
R = OMe 46%
X
93
X = H2 40%
X = O 10%
COOMe
Cl
MeO
94
95
63%
Work-up in the
presence of MeOH
96
97
14%
98
43%
99
22%

SCHEME 16

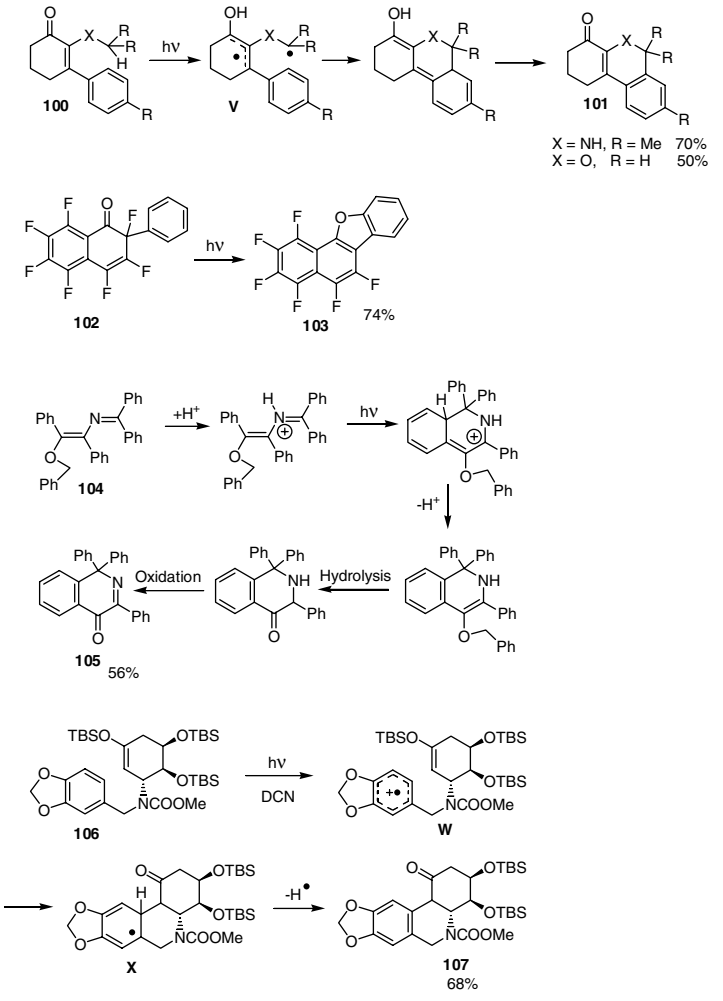
hν
100
V
101
X = NH, R = Me 70%
X = O, R = H 50%
102
103
74%
+H+
104
-H+
Oxidation
Hydrolysis
105
56%
DCN
106
W
X
-H•
107
68%

SCHEME 17

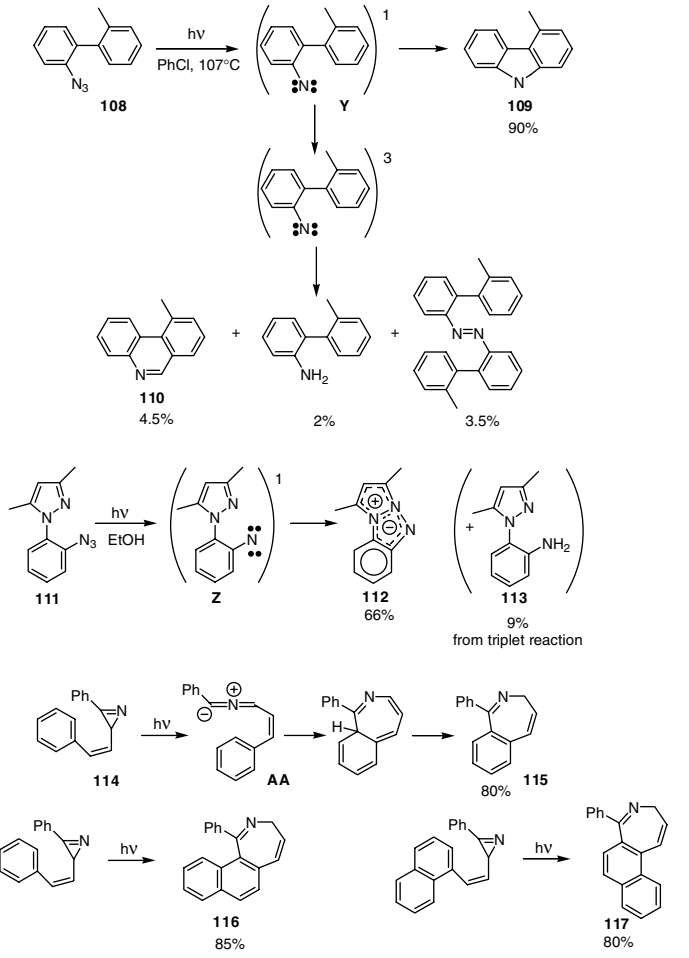

SCHEME 18

References

1. (a) Stermitz, F.R., The photocyclization of stilbenes, *Org. Photochem.,* 1, 247–282, 1967; (b) Lenz, G.R., The photochemistry of enamines, *Synthesis,* 489–518, 1978; (c) Kaupp, G., Photochemical rearrangements and fragmentations of benzene derivatives and annelated arenes, *Angew. Chem. Int. Ed. Engl.,* 19, 243–275, 1980; (d) Grimshaw, J. and de Silva, A.P., Photochemistry and photocyclization of aryl halides, *Chem. Soc. Rev.,* 10, 181–203, 1981; (e) Schultz, A.G., Photochemical six-electron heterocyclization reactions, *Acc. Chem. Res.,* 16, 210–218, 1983; (f) Schultz, A.G. and Motyka, L., Photochemical heterocyclizations of systems isoelectronic with the phentadienyl anion, *Org. Photochem.,* 6, 1–119, 1983; (g) Sundberg, R.J., Chloroacetamide photocyclization and other aromatic alkylations initiated by photo-induced electron transfer, *Org. Photochem.,* 6, 121–176, 1983; (h) Mallory, F.B. and Malory, C.W., Photocyclization of stilbenes and related molecules, *Org. React.,* 30, 1–456, 1984; (i) Ninomiya, I. and Naito, T., *Photochemical Synthesis,* Academic Press, London, 1989; (j) Ninomiya, I. and Kiguchi, T., Ergot alkaloids, *The Alkaloids,* Vol. 38, Brossi, A., Ed., Academic Press, San Diego, 1–156, 1990; (k) Armesto, D., Photochemistry of aza-substituted dienes, in *CRC Handbook of Organic Photochemistry and Photobiology,* Horspool, W.M. and Song, P.-S., Eds., CRC Press, Boca Raton, FL, 1995, pp. 901–914; (l) Tsuchiya, T., Nitrene formation by photoextrusion of nitrogen from azides, in *CRC Handbook of Organic Photochemistry and Photobiology,* Horspool, W.M. and Song, P.-S., Eds., CRC Press, Boca Raton, FL, 1995, pp. 984–991; (m)

Kitamura, T., C-X bond fission in alkene systems, *CRC Handbook of Organic Photochemistry and Photobiology,* Horspool, W.M. and Song, P.-S., Eds., CRC Press, Boca Raton, FL, 1995, pp. 1171–1180; (n) Beugelmans, R., The Photostimulated $S_{RN}1$ process: reactions of haloarenes with enolates, in *CRC Handbook of Organic Photochemistry and Photobiology,* Horspool, W.M. and Song, P.-S., Eds., CRC Press, Boca Raton, FL, 1995, pp. 1200–1217; (o) Kessar, S.V. and Singh Makotia, A.K., Photocyclization of haloarenes, in *CRC Handbook of Organic Photochemistry and Photobiology,* Horspool, W.M. and Song, P.-S., Eds., CRC Press, Boca Raton, FL, 1995, pp. 1218–1228; (p) Tominaga, Y. and Castle, R.N., Photocyclization of aryl- and heteroaryl-2-propenoic acid derivatives. Synthesis of polycyclic heterocycles, *J. Heterocyclic Chem.,* 33, 523–538, 1996; (q) Hazai, L. and Hornyak, G., Photochemical reactions of stilbenes and their heterocyclic derivatives — a review, *Models Chem.,* 135, 493–514, 1998; (r) Brousmiche, D.W., Briggs, A.G., and Wan, P., Photochemistry of hydroxyaromatic compounds, in *Molecular and Supramolecular Photochemistry, Vol. 6: Organic, Physical and Materials Photochemistry,* Ramamurthy, V. and Schanze, K.S., Eds., Marcel Dekker, Inc., New York, 2000, pp. 1–32, (s) Toda, F., Tanaka, K., and Miymoto, H., Enantioselective photoreactions in the solid state, in *Mol. Supramol. Photochem., Vol. 8: Understanding and Manipulating Excited-State Processes,* Ramamurthy, V. and Schanze, K.S., Eds., Marcel Dekker, Inc., New York, 2001, pp. 385–425.

2. Lewis, G.E., Photochemical reactions of azo compounds. I. Spectroscopic studies of the conjugate acids of *cis*- and *trans*-azobenzene, *J. Org. Chem.,* 25, 2193–2195, 1960.
3. Onaka, T., Kanda, Y., and Natsume, M., An application of the photocyclization reaction of Schiff Basses to the synthesis of a phenanthridine alkaloid, *Tetrahedron Lett.,* 1179–1180, 1974.
4. Doolittle, R.E. and Bradsher, C.K., Photochemical methods in the synthesis of heterocyclic compounds. I. Phenanthridizinium perchlorates, *J. Org. Chem.,* 31, 2616–2618, 1966.
5. Kanaoka, Y. and Itoh, K., Photocyclization of benzanilides to phenanthridones with elimination of the *ortho*-methoxy-group, *J. Chem. Soc., Chem Commun.,* 647–648, 1973.
6. Grellmann, K.-H., Sherman, G.M., and Linschitz, H., Photoconversion of diphenylamines to cabazoles and accompaning transient species, *J. Am. Chem. Soc.,* 85, 1881–1882, 1963; see also: Grellmann, K.-H., Kühnle, W., Weller, H., and Wolff, T., The photochemical formation of dihydrocarbazoles from diphenylamines and their thermal rearrangement and disproportionation reactions, *J. Am. Chem. Soc.,* 103, 6889–6893, 1981; Fox, M.A., Dulay, M.T., and Krosley, K. Comparison of oxidative and excited state cyclizations of *N*-benzyldiphenylamines to *N*-benzylcarbazoles, *J. Am. Chem. Soc.,* 116, 10992–10999, 1994.
7. (a) Zeller, K.-P. and Petersen, H., Photochemische Herstellung von Dibenzofuranen und Dibenzothiophenen, *Synthesis,* 532–533, 1975; (b) Zeller, K.-P. and Berger, S., Steric hindrance in substituted dibenzofurans, *J. Chem. Soc., Perkin II,* 54–58, 1977.
8. Ho, J.-H. and Ho, T.-I. Novel photoreaction of *N*-alkyl(*p*-methoxyl)arylamines assisted by protic acids, *J. Chem. Soc., Chem. Commun.,* 270–271, 2002.
9. Lopez, D., Boule, P., and Lemaire, J., Photochimie et environnement I. Comportement photochimique de la diphénylamine et d'antioxydants dérivés, en solution aqueuse diluée, *Nouv. J. Chim.,* 4, 615–620, 1980.
10. Schultz, A.G. and DeTar, M.B., Thiocarbonyl ylides. Photogeneration, rearrangement, and cycloaddition reactions, H., *J. Am. Chem. Soc.,* 98, 3564–3572, 1976.
11. Dittami, J.P., Nie, X.-Y., Buntel, C.J., and Rigatti, S., Photoinitiated intramolecular ylide-alkene cycloaddition reactions, *Tetrahedron Lett.,* 31, 3821–3824, 1990.
12. Dittami, J.P., Nie, X.Y., Nie, H., Ramanathan, H., Breining, S., Border, J., Decosta, D.L., Kiplinger, J., Reiche, P., and Ware, R., Intramolecular addition reactions of carbonyl ylides formed during photocyclization of aryl vinyl ethers, *J. Org. Chem.,* 56, 5572–5578, 1991.
13. Ninomiya, I., Kiguchi, T., Yamamoto, O., and Naito, T., Photocyclisation of enamides. Part 13. Substituent effects in the photocylisation of *N*-benzoylenamides, *J. Chem. Soc., Perkin I,* 1723–1728, 1979.
14. Couture, A., Grandclaudon, P., and Hooijer, S.O., Photocyclization in an alcohol solution containing dissolved base. A New development in enamide photochemistry, *J. Org. Chem.,* 56, 4977–4980, 1991.

15. Missoum, A., Sinibaldi, M.-E., Vallée-Goyet, D., and Gramain, J.-C., Photochemical synthesis of spirocyclohexylisoquinolines, Analogues of *rac*-galanthamine and *rac*-lycormaine, *Synth. Commun.,* 27, 453–466, 1997; see also: Gramain, J.-C., Mavel, S., Troin, Y., and Vallée-Goyet, D., Photocyclisation de *N*-Benzoylenamines. Synthèses de spirocyclohexanes en série isoquinoléine, *Tetrahedron,* 47, 7287–7300, 1991.
16. Gramain, J.-C., Troin, Y., and Vallée-Goyet, D., Photocyclisation de *N*-aroylenamines dérivées d'acides carboxyliques hétéroaromatiques. Synthèses de spirocyclohexyl pipéridines accolées à un hétérocycle, *Tetrahedron,* 47, 7301 - 7308, 1991.
17. Naito, T., Hirata, Y., Miyata, O., and Ninomiya, I., Photocyclisation of enamides. Part 27. Total synthesis of *rac*-yohimbine, *rac*-alloyohimbine, and *rac*-19,20-didehydroyohimbines, *J. Chem. Soc., Perkin Trans. I,* 2219–2225, 1988.
18. Ibrahim-Ouali, M., Sinibaldi, M.-E., Troin, Y., Guillaume, D., and Gramain, J.-C., Diastereoselective photochemical synthesis of 3,3′-disubstuted indolines, *Tetrahedron,* 53, 16083–16096, 1997.
19. (a) Dugat, D., Gramain, J.-C., and Dauphin, G., Structure, stereochemistry, and conformation of diastereoisomeric, *cis*- and *trans*-3-ethyl-1,2,3,4,4a,9a-hexahydrocarbazol-4-ones by means of ^{13}C and two-dimensional ^{1}H nuclear magnetic resonance spectroscopy. An example of diastereoselection in a photocylization reaction, *J. Chem. Soc., Perkin Trans. 2,* 605–611, 1990; (b) Gramain, J.-C., Husson, H.-P., and Troin, Y., A novel and efficient synthesis of aspidosperma alkaloid ring system: *N*(a)-benzyldeethylaspidospemidine, *J. Org. Chem.,* 50, 5517–5520, 1985; (c) Benchekroun-Mounir, N., Dugat, D., Gramain, J.-C., and Husson, H.-P., Stereocontolled formation of octahydro-1*H*-pyrrolo[2,3-*d*]carbazoles by reductive cyclization: total synthesis of rac-*N*-benzylaspidospermidine, *J. Org. Chem.,* 58, 6457–6465, 1993; (d) Dugat, D., Benchekroun-Mounir, N., Dauphin, G., and Gramain, J.-C., *J. Chem. Soc., Perkin Trans. 1,* 2145–2149, 1998.
20. Blache, Y., Benzech, V., Chezal, J.-M., Boule, P., Viols, H., Chavignon, O., Teulade, J.-C., and Chapat, J.-P., Reactivity of heterocyclic enaminones: regioselective synthesis of ployfused indolones, *Heterocycles,* 53, 905–916, 2000.
21. Nozulak, J., Kalkman, H.O., Floersheim, P., Hoyer, D., Schoeffter, P., and Buerki, H.R., (+)-*cis*-4,5,7a,8,9,10,11,11a-octahydro-7*H*-10-methylindolo[1,7-*bc*][2,6]-naphthyridine: A 5-$HT_{2C/2B}$ receptor antagonist with low 5-HT_{2A} receptor affinity, *J. Med. Chem.,* 38, 28–33, 1995.
22. Higuchi, R.I., Edwards, J.P., Caferro, T.R., Ringgenberg, J.D., Kong, J.W., Hamann, L.G., Arienti, K.L., Marschke, K.B., Davis, R.L., Farmer, L.J., and Jones, T.K., 4-Alkyl- and 3,4-dialkyl-1,2,3,4-tetrahydro-8-pyridono[5,6-*g*]quinolines: potent, nonsteroidal androgen receptor agonists, *Bioorg. Med. Chem. Lett.,* 9, 1335–1340, 1999.
23. Atfah, A., Abu-Shuheil, M.Y., and Hill, J., Photocyclisation of 2-aroylquinoxalines; formation of coloured indolo[1,2-a]quinoxalines, *Tetrahedron,* 46, 6483–6500, 1990.
24. Bouillon, J.-P., Maliverney, C., Janousek, Z., and Viehe, H.G., Reactions of triflouromethylated enamines with iminium chlorides and analogues. Synthesis of new 2-aza-1,3-dienes and pyridin-4-ones, *Bull. Soc. Chim. Fr.,* 134, 47–57, 1997.
25. Kametani, T., Takagi, N., Toyota, M., Honda, T., and Fukumoto, K., Total synthesis of the protoberberine alkaloid (–)-xylopinine by photochemical 1,3-asymmetric induction, *J. Chem. Soc., Perkin I,* 2830–2834, 1981.
26. Kametani, T., Takagi, N., Kanaya, N., Honda, T., and Fukumoto, K., Studies on the syntheses of heterocyclic and natural products. Part 979 (1). Attempted asymmetric synthesis of yohimbol by photocyclization of the enamide, *J. Heterocyclic Chem.,* 19, 1217–1219, 1982.
27. Nicoud, J.F. and Kagan, H.B., A new case of asymmetric synthesis using circularly polarized light, *Isr. J. Chem.,* 15, 78–81, 1976/77.
28. Naito, T., Tada, Y., and Ninomiya, I., Asymmetric photocyclization of *N*-α,β-unsaturated acylanilides, *Heterocycles,* 22, 237–240, 1984.
29. (a) Ohba, S., Hosomi, H., Tanaka, K., Miyamoto, H., and Toda, F., Enantioselective photocyclization of acrylanilides and *N*-ethyl-*N*-methylbenzoylformamide in inclusion crystals with (*R,R*)-(–)-[*trans*]-2,3-bis(α-hydroxydiphenylmethyl)-1,4-dioxaspiro[4.4]nonane and -[4.5]decane. Mechanistic

study based on x-ray crystal structure analyses, *Bull. Chem. Soc. Jpn.,* 73, 2075–2085, 2000; see also: (b) Toda, F., Miyamoto, H., Kanemoto, K., Tanaka, K., Takahashi, Y., and Takenaka, K.Y., Enantioselective photocyclization of *N*-alkylfuran-2-carboxyanilides to *trans*-dihydrofuran derivatives in inclusion crystals with optically active host compounds derived from tataric acid, *J. Org. Chem.,* 64, 2096–2102, 1999; (c) Toda, F., Miyamoto, H., Tamashima, T., Kondo, M., and Ohashi, Y., Enantioselective photochemical reactions of *N*-phenyl enaminones in inclusion complex crystals using a chiral host compound, *J. Org. Chem.,* 64, 2690–2693, 1999.

30. Frolov, A.N. and Baklanov, M.V., Unusual photocyclization of 1-(2-pyridylamino)-8-chloronaphthalene, *Mendeleev Commun.,* 22–23, 1992.
31. Park, Y.-T., Jung, C.-H., Kim, M.-S., and Kim, K.-W., Photoreaction of 2-halo-*N*-pyridinylbenzamide: intramolecular cyclization mechanism of phenyl radical assisted with n-complexation of chlorine radical, *J. Org. Chem.,* 66, 2197–2206, 2001.
32. (a) Luo, J.-K., Federspiel, R.F., and Castle, R.N., The synthesis of novel ploycyclic heterocyclic ring systems via photocyclization. 21 [1,2]. Naphtho[2′,1′:4,5]thieno[2,3-*c*]naphtho[1,2-*f*]quinoline, naphtho[2′,1′:4,5]thieno[2,3-*c*]naphtho[1,2-*f*][1,2,4]triazolo[4,3-*a*]quinoline and naphtho[2′,1′:4,5]thieno[2,3-*c*]naphtho[1,2-*f*]tetrazolo[1,5-*a*]quinoline, *J. Heterocyclic Chem.,* 37, 171 - 174, 2000. For other examples see references cited therein. See also: (b) Karminski-Zamaola, G., Pavličić, D., Bajić, M., and Blažević, N., The synthesis of new heterocyclic quinolone by twofold photocyclization: methoxycarbonylnaphtho[2″,1″:2′,3′-*b*]thieno[4′,5′:2,3]thieno[5,4-*c*]quinolin-6(5H)-one, *Heterocycles,* 32, 2323–2327, 1991.
33. Prabhakar, S., Lobo, A.M., and Tavares, M.R., Boron complexes as control synthons in photocyclizations: an improved phenanthridine synthesis, *J. Chem. Soc., Chem. Commun.,* 884–885, 1978.
34. (a) Blache, Y., Sinibaldi-Troin, M.-E., Voldoire, A., Chavignon, O., Gramain, J.-C., Teulade, J.-C., and Chapat, J.-P., Compared reactivity of heterocyclic enaminones: photochemical and palladium catalyzed synthesis of 3,7,8,9-tetrahydro-5*H*-pyrido[3,2-*b*]indol-9-ones, *J. Org. Chem.,* 62, 8553–8556, 1997. See also: (b) Iida, H., Yuasa, Y., and Kibayashi, C., Exploitation of intramolecular photochemical arylation of *N*-substituted enaminones. Efficient, general synthesis of heterocyclic compounds. *J. Org. Chem.,* 44, 1236–1241, 1979; (c) Blache, Y., Sinibaldi-Troin, M.-E., Hichour, M., Benezech, V., Chavignon, O., Gramain, J.-C., Teulade, J.-C., and Chapat, J.-P., Heterocyclic enaminones: photochemical synthesis of 6,7,8,9-tetrahydro-5*H*-pyrido[2,3-*b*]indol-9-ones, *Tetrahedron,* 55, 1959–1970, 1999. For the electron transfer from tertiary amines to halogen substituted arenes see: (d) Beecroft, R.A., Davidson, R.S., and Goodwin, D., The amine assisted photo-dehalogenation of halo-aromatic hydrocarbons, *Tetrahedron Lett.,* 24, 5673–5676, 1983.
35. Motohashi, T., Maekawa, K., Kubo, K., Igarashi, T., and Sakurai, T., An efficient transformation of substituted *N*-acyl-a-dehydro(1-naphthyl)alanines into 1,2-dihydrobenzo[f]quinolinone derivatives via photoinduced intramolecular electron transfer, *Heterocycles,* 57, 269–292, 2002.
36. Nishio, T., Asai, H., and Miyazaki, T., Photochemical reactions of *N*-(2-halogenoalkanoyl) derivatives of anilines, *Helv. Chim. Acta,* 83, 1475–1483, 2000.
37. Kaoudi, T., Quiclet-Sire, B., Seguin, S., and Zard, S.Z., An expedient construction of seven-membered rings adjoining aromatic systems, *Angew. Chem. Int. Ed. Engl.,* 39, 731–733, 2000.
38. (a) Klohr, S.E. and Cassady, J.M., An intramolecular photocyclization to form the azepino[3,4,5-cd]indol system, *Synth. Commun.,* 18, 671–674, 1988. For comparable examples see: (b) Naruto, S. and Yonemitsu, O., Photochemical synthesis of azepinoindoles and azocinoindoles from *N*-chloroacetylindolylethylamines, and a mechanistic study based on the correlation of between quantum yields and calculated frontier electron densities of indole radicals, *Chem. Pharm. Bull.,* 28, 900–909, 1980.
39. Bosch, J., Amat, M., Sanfeliu, E., and Miranda, M.A., Studies on the synthesis of pentacyclic strychnos indole alkaloids. photocyclization of *N*-chloroacetyl-1,2,3,4,5,6-hexahydro-1,5-methanoazocino[4,3-*b*]indole derivatives, *Tetrahedron,* 41, 2557–2566, 1985.

40. Beck, A.L., Mascal, M., Moody, C.J., Slawin, A.M.Z., Williams, D.J., and Coates, W.J., Synthesis of 3,4-bridged indoles by photocyclization reactions. Part 1. Photocyclization of halogenated tryptophan derivatives, *J. Chem. Soc., Perkin Trans. 1,* 797–811, 1992.
41. Bremner, J.B., Russell, H.F., Skelton, B.W., and White, A.H., Novel indole-fused, medium-sized hetercycles via chloroacetamide photochemistry, *Heterocycles,* 53, 277–290, 2000.
42. (a) Cossy, J. and Pete, J.-P., The photochemical cyclization of 2-alkylamino-3-aryl-2-cyclohexenones, *Heterocycles,* 22, 97–100, 1984; (b) Feigenbaum, A., Fort, Y., Pete, J.-P., and Scholler, D., Photochemical cyclization of 2-alkyl-3-aryl-2-cyclohexenones and 2-alkoxy-3-aryl-2-cyclohexenones, *J. Org. Chem.,* 51, 4424–4432, 1986; for comparable examples see: (c) Gupta, S.C., Sharma, S., Saini, A., and Dhawan, S.N., *J. Chem. Soc., Perkin Trans 1,* 2391–2395, 1999.
43. Kovtonyuk, V.N., Kobrina, L.S., Photochemical cyclization of polyfluorinated aryloxo-1,2-dihydronaphthalenes and 6-phenyl-3-phenoxy-2,4-cyclohexadienone, *J. Fluorine Chem.,* 66, 219–221, 1994.
44. (a) Armesto, D., Horspool, W.M., Ortiz, M.J., and Romano, S., Reaction of anions from monoimines of benzil with alkylating agents. photochemical reactivity of some 4-alkoxy-2-aza-1,3-dienes, *J. Chem. Soc. Perkin Trans.,* 1, 171–175, 1992. For similar examples see: (b) Armesto, D., Gallego, M. G., Ortiz, M.J., Romano, S.A, and Horspool, W.M., Synthesis of isoquinolinones by the photochemical cyclization of 2-azabuta-1,3-dienes in the presence of acids, *J. Chem. Soc., Perkin Trans. 1,* 1343–1347, 1989; (c) Armesto, D., Horspool, W.M., Ortiz, M.J., and Romano, S., Synthesis of 1*H*-isoindoles by a novel rearrangement of some isoquinolin-4(1*H*)-ones, *J. Chem. Soc., Perkin Trans. 1,* 2321–2324, 1992.
45. (a) Pandey, G., Murugan, A., Balakrishnan, M., A new strategy towards the total synthesis of phenanthridine alkaloids: synthesis of (+)-2,7-dideoxypancratistatin as a model study, *J. Chem. Soc., Chem. Commun.,* 624–625, 2002. For mechanistic details of the reaction see: (b) Pandey, G., Karthikeyan, M., and Murugan, A., New intramolecular α-arylation strategy of ketones by the reaction of silyl enol ethers to photosensitized electron transfer generated arene radical cations: construction of benzannulated and benzospiroannulated compounds, *J. Org. Chem.,* 63, 2867–2872, 1998.
46. Lindley, J.M., McRobbie, I.M., Meth-Cohn, O., Suschitzky, H., Competitive cyclisations of singlet and triplet nitrenes. Part 5. Mechanism of cyclisation of 2-nitrenobiphenyls and related systems, *J. Chem. Soc., Perkin I,* 2194–2204, 1977.
47. Albini, A., Bettinetti, G., and Minoli, G., Chemistry of nitrenes generated by the photocleavage of both azides and a five-membered heterocycle, *J. Am. Chem. Soc.,* 113, 6928–6934, 1991.
48. Padwa, A., Smolanoff, J., and Tremper, A., Intramolecular cycloaddition reactions of vinyl-substituted 2*H*-azirines, *J. Am. Chem. Soc.,* 97, 4682–4691, 1975.

35

Photochromism of Diarylethene Derivatives

Kingo Uchida
Ryukoku University

Masahiro Irie
Kyushu University

35.1 Introduction

Light-induced reversible transformation between two isomers having different absorption spectra is referred to as photochromism.[1,2]

$$A \underset{h\nu'}{\overset{h\nu}{\rightleftharpoons}} B$$

The two isomers differ from one another not only in the absorption spectra but also in refractive indices, dielectric constants, oxidation–reduction potentials, and geometrical structures. Therefore, upon irradiation with an appropriate wavelength of light, these properties can be reversibly switched.

Diarylethenes with heterocyclic aryl groups are newcomers to the photochromic field. They belong to the thermally irreversible (P-type) photochromic compounds. The most striking feature of the compounds is their fatigue resistance.[3] The coloration/decoloration cycle can be repeated more than 10^4 times while retaining the photochromic performance. Both properties, thermal stability of both isomers and fatigue resistance, are indispensable for application to optoelectronic devices, such as devices for memory and switches. In this chapter, recent research on diarylethene derivatives will be described.

35.2 Conformation of Diarylethenes

Diarylethenes with heterocyclic aryl groups have two conformations with the two rings in mirror (parallel) and C_2 (antiparallel) symmetries; the conrotatory photocyclization reaction can proceed only from

0-8493-1348-1/04/$0.00+$1.50

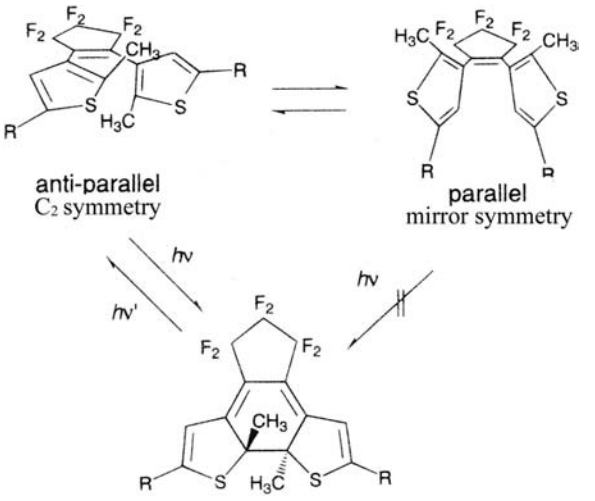

FIGURE 35.1 Anti-parallel and parallel conformations of diarylethene derivatives.

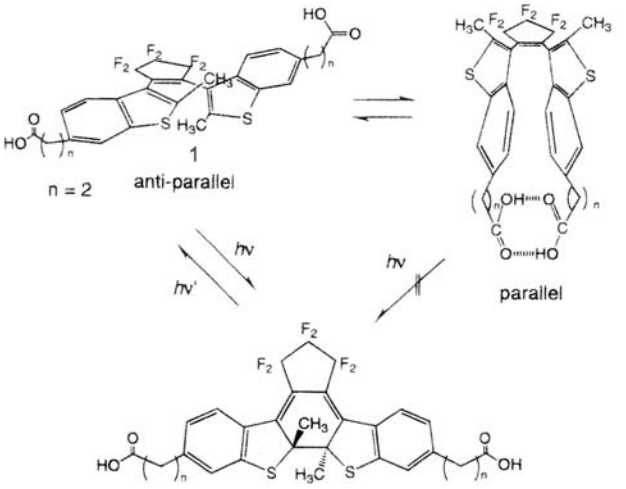

FIGURE 35.2 Locking of the conformations by intramolecular hydrogen bonds.

the C_2 symmetry,[4] as shown in Figure 35.1. The reactivity of the cyclization reaction can be controlled by controlling the conformations. A diarylethene **1** with terminal carboxylic acid moieties has no photoreactivity because the conformation is fixed in parallel by the intramolecular hydrogen bonds. The molecule becomes photoreactive by the addition of protic solvents or by elevating the temperature, which breaks the intramolecular hydrogen bonds. (Figure 35.2).[5]

The cyclization quantum yield can also be improved by controlling the conformations. When the ratio of the photoreactive antiparallel conformers is increased, the quantum yield is expected to increase. Introduction of bulky isopropyl groups at the 2 and 2′-positions of the benzothiophene rings enhanced the ratio of the conformers from 0.65 to 0.94 and increased the quantum yield of the cyclization reaction from 0.35 to 0.52. The increment of the population of photoreactive conformers accounts for the enhancement of the yield.[6]

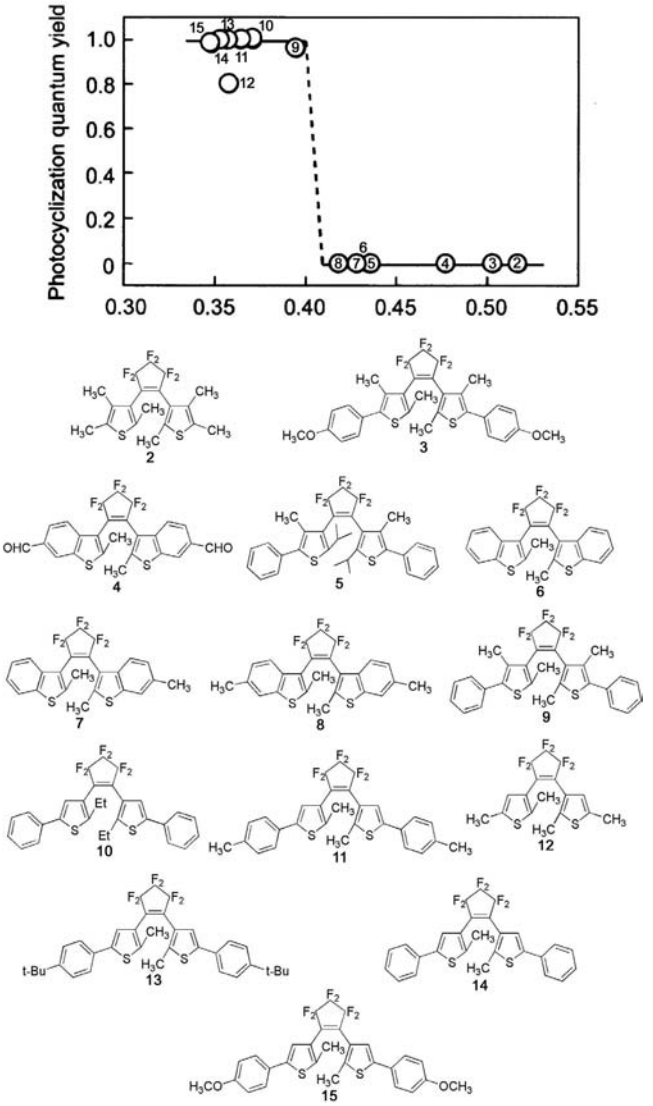

FIGURE 35.3 Relationship between the photocyclization quantum yields and the distances between the reacting carbons.

Another approach to increase the population of the photoreactive conformation is to include the compound into cyclodextrin cavities. α, β, and γ–Cyclodextrins were added to aqueous solutions containing 1,2-bis(2-methyl-1-benzothiophen-3-yl)perfluorocyclopentene having sulfonate groups, and the changes in the ratio of the two conformations were examined by NMR.[7–9] By the addition of 10 equivalents of β–cyclodextrin, the C_2 symmetry conformation ratio was increased from 0.64 to 0.94, and the cyclization quantum yield was increased from 0.32 to 0.49.

The most effective and ideal method to fix the compound into the appropriate photoreactive conformation is to use the crystal lattice. Some of the diarylethene derivatives exhibit photochromism even in the crystalline state.[10] X-ray crystallographic analysis revealed that the diarylethene molecules are packed in the crystal in the antiparallel photoreactive conformation. The reactivity in the crystals is dependent not only on the conformation but also on the distance between the reactive carbon atoms. Figure 35.3 shows the correlation of the cyclization quantum yields and the distance between the reactive carbon atoms in crystals. When the distance is shorter than 0.42 nm, the photocyclization quantum yield is unity (100%).[10,11]

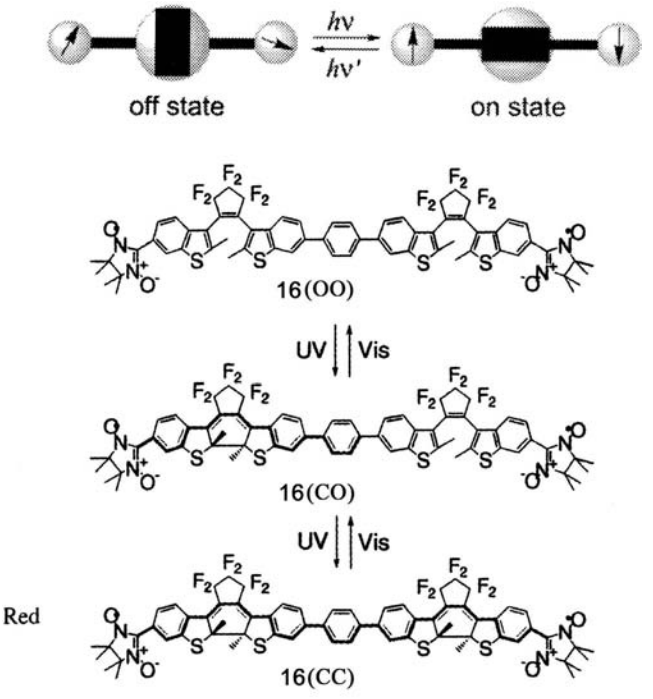

[a]Bold line indicates the connection of the bond alternation.

FIGURE 35.4 Photoswitching of the spin interaction (top) and the photochromic reaction of **16**[a] (bottom).

35.3 Photoswitching

Spin Interaction

Diarylethene derivatives can be used as molecular-scale photoswitching units. In the open-ring isomer, the aryl groups can freely rotate along the single bonds connecting them to the ethene moiety, and the two aryl groups are electrically independent. On the other hand, in the closed-ring isomer the two aryl groups are linked by the π-conjugation, and π-electrons delocalize throughout the molecule. When two unpaired electrons are placed at the ends of the π–conjugated chain, the spins of the unpaired electrons are expected to be switched upon photoirradiation.[12]

The exchange interaction between two nitroxide radicals, which are located at both ends of the diarylethene system **16(OO)**, was photoswitched reversibly by alternate irradiation with ultraviolet and visible light (Figure 35.4). The ESR spectra of isolated **16(OO)**, **16(CO)**, and **16(CC)** were measured in benzene at room temperature (Figure 35.5). The spectra of **16(OO)** and **16(CO)** show five lines, suggesting that the exchange interaction between the two nitronyl nitroxide radicals was much smaller than the hyperfine coupling constant ($2J/k_B < 3 \times 10^{-4}$ K). However, the spectrum of **16(CC)** showed nine well-defined lines, indicating that the exchange interaction between the two spins was much larger than the hyperfine coupling constant ($2J/k_B > 0.04$ K). The result indicates that each diarylethene chromophore served as a switching unit to control the magnetic interaction. The magnetic interaction between the terminal nitronyl nitroxide radicals was controlled by the switching units in series.

Launay et al., showed that the intramolecular electric coupling between two redox sites can be controlled upon photoirradiation. A dithienylethene derivative **17** (Figure 35.6) with cyclometallated $Ru(bpy)_2(pp)$ units via ethynyl spacers was synthesized.[13] Open-ring isomer **17a** can be reversibly photoisomerized to the closed isomer **17b**. Upon oxidation, a new band in the 1000–1500 nm range due to

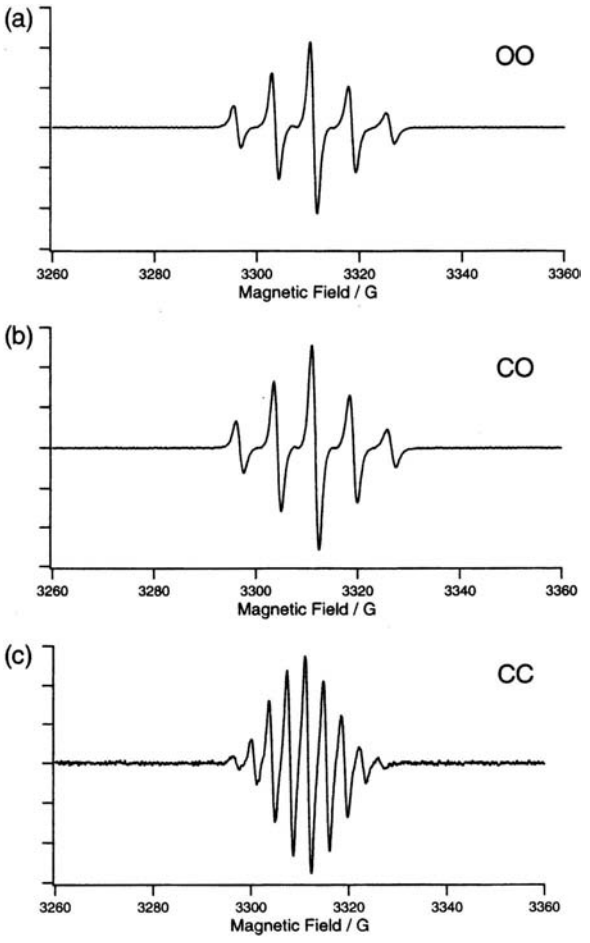

FIGURE 35.5 ESR spectra measured at room temperature in benzene (a) **16** (OO), (b) **16** (CO), and (C) **16** (CC).

the intervalence transition between ruthenium (II) and ruthenium (III) appeared in **17b** but was not observed in **17a**. The electric coupling parameter *V*ab was calculated to be 0.021 eV for closed-ring isomer **17b**, while it was 0.003 eV for **17a**. The former value is consistent with the observed coupling. *V*ab values in the 0.02 eV range have been observed for a π-conjugated system with four double bonds and a metal–metal distance of 20 Å. Compounds **17a** and **17b** allowed a fundamental study of switching in the electrical sense at the molecular level.

Fluorescence

Several methods to avoid destructive readout using fluorescence or infrared absorption as readout signals have been proposed. The fluorescence intensity change between the open- and closed-ring isomers makes it possible to use the change as the readout signal. When the fluorescence can be detected without influencing the ratio of the two isomers, the readout method becomes nondestructive.

Branda et al. reported the synthesis and optical characterization of a photochromic hybrid **18**, where porphyrin macrocycles are attached to the ends of the 1,2-bis(3-thienyl)cyclopentene backbone.[14] In the open ring isomer **18a**, the porphyrins exhibit significant fluorescence at 655 nm when excited at 430 nm. Upon irradiation with 313 nm light, **18a** converts to the nonfluorescent closed-ring isomer **18b**. The compound **18b** returns again to fluorescent **18a** upon irradiation with $\lambda > 480$ nm light. The intensity of the porphyrin fluorescence is conveniently regulated by alternate irradiation at 313 nm and >480 nm

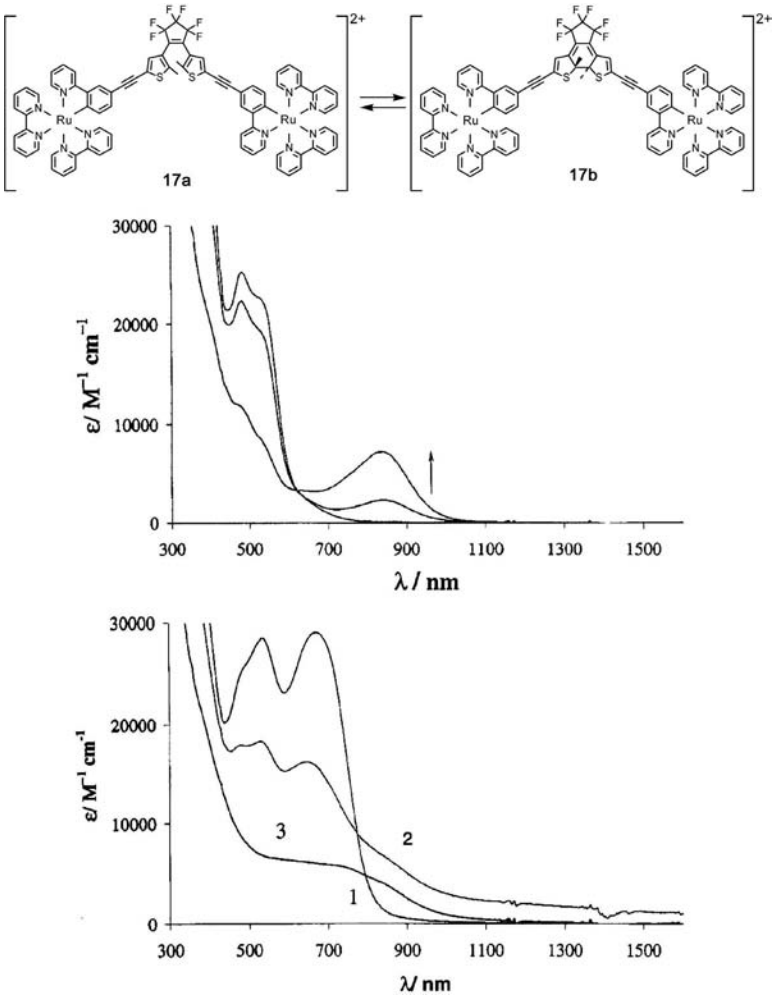

FIGURE 35.6 Spectra obtained during oxidation with bix(pyridyl)-phenyliodonium; top: open-ring isomer **17a**; bottom: closed-ring isomer **17b** exhibiting an intervalence absorption in the 1000–1500 range; 1: initial spectrum; 2: at half-oxidation; 3: spectrum of the fully oxidized solution.

(Figure 35.7). The molecule can be used as an optical memory medium with non-destructive readout capability.[14,15]

Branda et al. also reported the transition metal complexes coordinated to the ends of the pyridyl derivative of 1,2-dithienylethene **19**. The luminescence of the porphyrin macrocycle is dependent on whether the diarylethene moiety is in the open or closed state.[16] In this compound, ruthenium-based metalloporphyrins are axially coordinated to the Lewis-basic pyridyl ligands. Compound **20a** phosphoresces at 730 nm with varying intensities when excited throughout the UV region. The excitation wavelengths that yield the highest emission intensity exist in a narrow window of the visible spectrum between 400 and 480 nm. Irradiation with light at these wavelengths has little effect on the photochromic reaction of **20** in either direction. Therefore, the molecule can be used as a memory medium with nondestructive readout capability (Figure 35.8).

Another example of a metal complex of a diarylethene is shown in Figure 35.9.[17] In this case, the closed ring isomer **21b** shows the stronger fluorescence compared to the open-ring isomer **21a**. The emission quantum yield of **21b** was 0.15 (λ of excitation; 240 nm), while that of **21a** was 0.03 (240 nm). Excitation of this compound at 240 nm scarcely affects the photochemical reactivity. Therefore, the system can also be used potentially for nondestructive readout of optical memory.

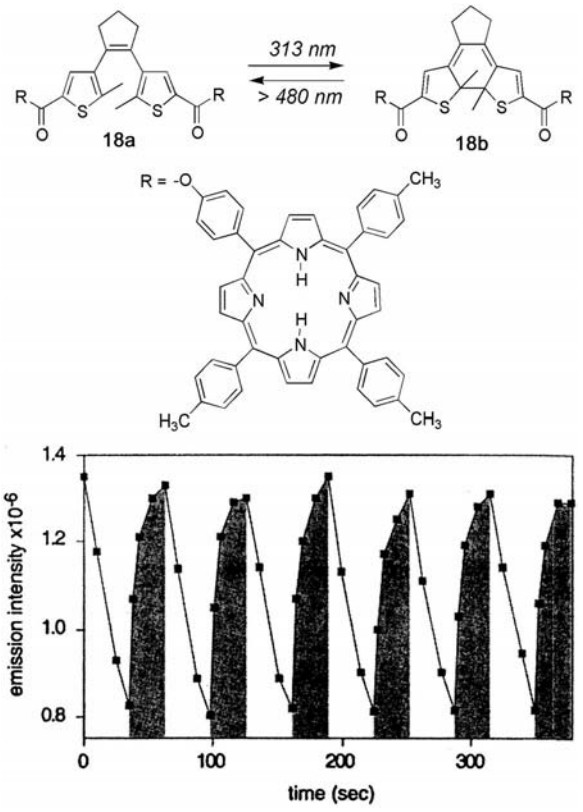

FIGURE 35.7 Modulated emission signal of a toluene solution of **18**(2×10^{-6} M) during alternating irradiation at 313 (unshaded areas) and >480 nm (shaded areas).

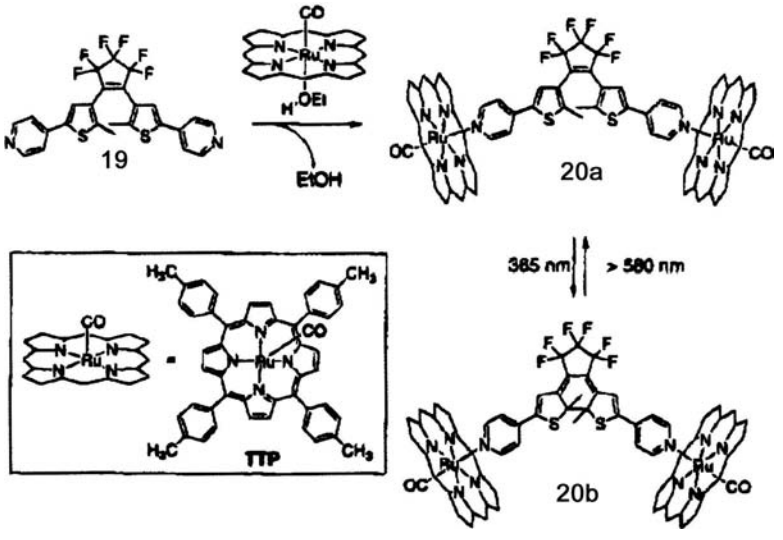

FIGURE 35.8 Photoisomerization of diarylethene complex **20**.

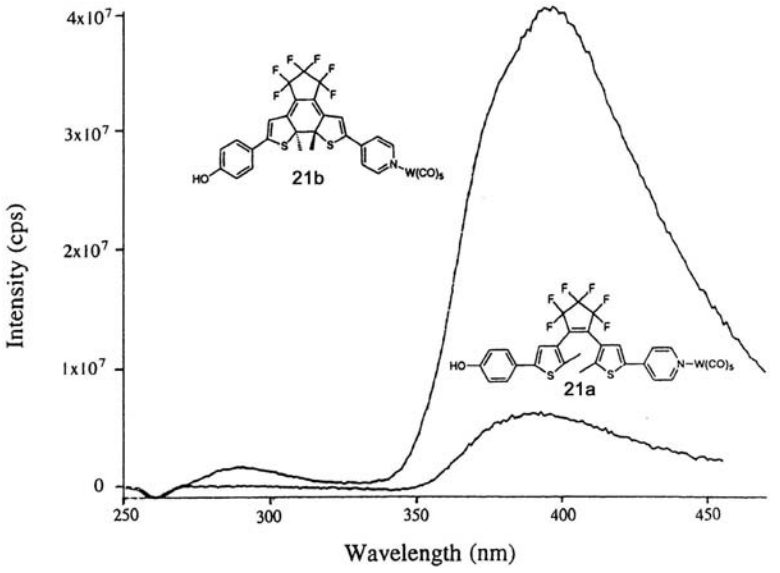

FIGURE 35.9 Fluorescence spectra of closed-ring isomer **21b** and open-ring isomer **21a** (excitation at 240 nm).

Another fluorescent diarylethene derivative is compound **22**, in which dithienylethene moieties are connected to fluorescent bis(phenylethynyl)anthracene. When the dithienylethene unit converted to the closed-ring isomer upon irradiation with 313 nm light, the fluorescence quantum yield decreased from 0.83 to 0.001.[18] The derivative exhibited a laser emission upon irradiation with 337.1 nm pulse laser, and the laser emission was controlled by the photochromic reaction of the dithienylethene units (Figure 35.10).

In diarylethenes with crown ether substituents, switching of the association with Ca^{2+} was observed.[19] The logarithm of the stability of the complex (log $K_{Ca}{}^{2+}$) of **23a** was 5.4 for Ca^{2+}, while that of **23b** was 1.7. These results indicate that the complexed cations can be released from **23a** by photocyclization. The open-ring isomer **23a** was fluorescent ($\Phi_f = 0.006$, $\lambda_{exe} = 390$ nm), while **23b** was nonfluorescent. The fluorescence intensity change suggests that photocyclization and binding-switch processes can be followed by fluorescence without perturbing the equilibrium (Figure 35.11).

35.4 IR Spectral Changes

Infrared (IR) spectral changes accompanied by photochromic reactions are useful for the nondestructive readout of the reactions. Zerbi et al. have demonstrated that the closed form **15b** shows the strongest band at 1495 cm^{-1} with an intensity of ~30,000 cm/mol. It turns out that this signal is highly selective for the closed-ring form as shown in Figure 35.12.[20]

35.5 Chiroptical Changes

Optical rotation changes accompanied by the photochromic reaction are a promising alternative for nondestructive readout. To enhance the readout signal intensity, two conditions must be satisfied:

1. The photochromic compounds should exhibit significantly contrasting optical rotating strengths between the two states.
2. The photochromic reactions should maximize the formation of only one stereoisomer.

Branda et al. reported self-assemblies of double-stranded copper (I) helicates with chiral ligands **24** and **25**.[21] When the chiral oxazoline auxiliaries on the periphery of the individual strands are brought into close proximity, chiral discrimination takes place. This orients the thiophene rings in a prochiral

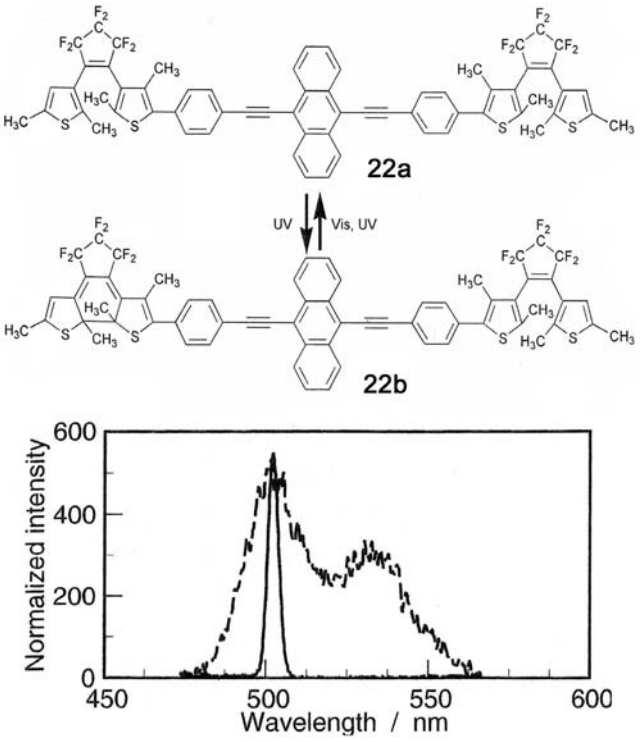

FIGURE 35.10 Fluorescence of **22a** inside (solid line) and outside (broken line) of the laser cavity.

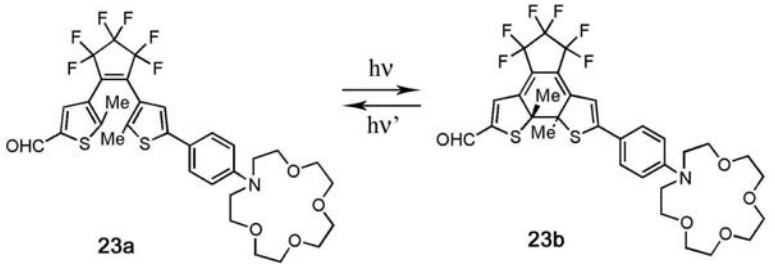

FIGURE 35.11 Photochromic reaction of diarylethene **23**.

conformation with respect to each other so that photocyclization yields a single diastereomer. The dramatic changes in optical rotation that accompany the stereoselective photochromic process can be used for nondestructive readout.

35.6 Control of the Liquid Crystalline Phases

The control of the structure and optical properties of liquid-crystalline (LC) phases by means of light is a major challenge in the development of molecular devices and optical data storage systems. Denekamp and Feringa[22] were first to report the induction of chirality by doping a diarylethene in nematic liquid crystals and effective photomodulation of LC phases. Doping of nematic LC materials ZLI-389 and K15 with (*S,S*)-**26a** resulted in stable cholesteric phases. When a mixture of **26a** in ZLI-389 was heated under a microscope slide and kept within the range of 51–54°C, the cholesteric phase was stable for many hours. When the mixture was irradiated with 300 nm light for 50 sec, the chiral nematic phase disappeared and

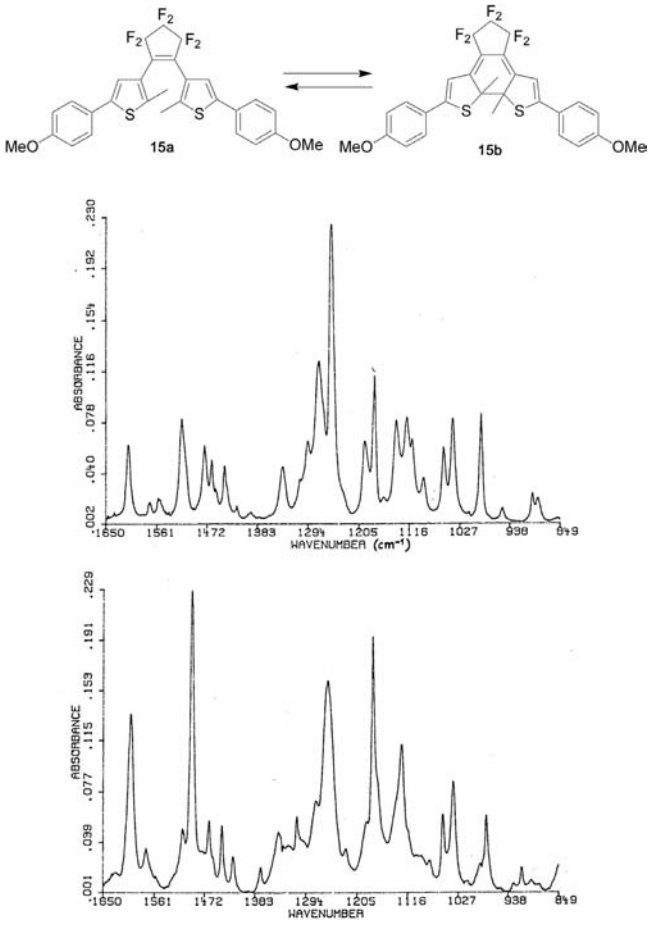

FIGURE 35.12 IR spectra of **15** in CCl_4 solution; the open-ring isomer **15a** (top), closed-ring isomer **15b** (bottom).

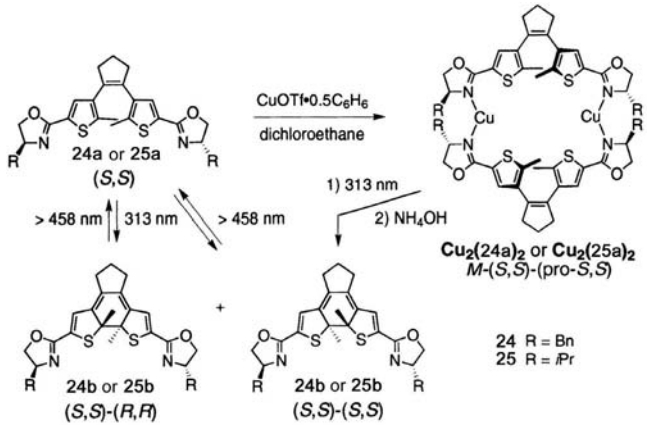

FIGURE 35.13 Formation of closed-ring products **24b** or **25b** from photochromes **24a** or **25a** and their complexes with copper.

TABLE 35.1 Conversions and Diastereoselectivities in the Photochromic Processes[a]

Entry	Photochrome	Concentration [M]	Conversion [%][b]	de [%]
1	(*S,S*)-**24a** + Cu(l)	0.001	95	98
2		0.0001	94	86
3	(*R,R*)-**24a** + Cu(l)	0.0001	92	89

[a] In a typical reaction, the ligand and CuOTf · 0.5 C_6H_6 were mixed in deoxygenated dichloroethane and exposed to 313-nm light for 20 minutes. After washing with excess NH_4OH to remove the metal, the conversions and *de* values of the products were measured by ^1H NMR spectroscopy in CD_2Cl_2.

[b] Based on the disappearance of the open isomers.

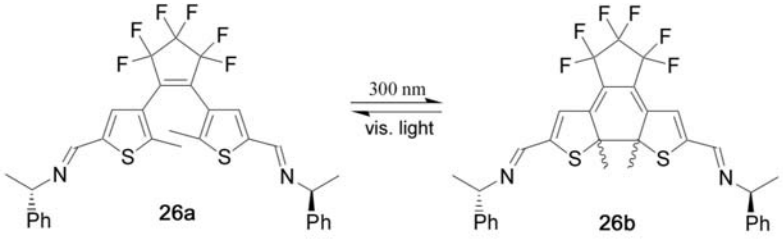

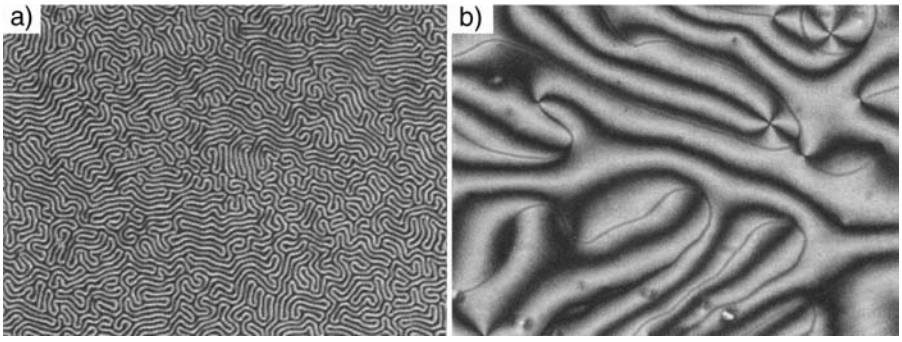

FIGURE 35.14 The texture of the nematic and twisted nematic liquid-crystalline phase; 1.4 wt.% of **26a** in ZLI-389 at 52°C. a)Cholesteric texture; b) nematic texture.

TABLE 35.2 Pitch Values, HTP, and Handedness of the Cholesteric Phases Formed by Doping Compound **26a** in K_{15} and ZLI-389, as Determined by the Cano-Grandjean Method

LC	wt.-% of **26**	Pitch [mm]	$\beta_m[\mu m^{-1}]$	Screw sense	Phase transition
ZLI-389	2.1	8.5	13	Negative[a]	N* 54 I
K_{15}	2.1	12	11	Negative	N* 33 I

[a] Doping with the cnantiomer of **26a** results in an opposite handedness.

changed to a nematic phase texture. Irradiation of the sample with visible light for 30 sec resulted in the reappearance of the cholesteric fingerprint texture (Figure 35.14).

Light-induced LC phase changes were also observed for a bisbenzothienylethene derivative with cholesterol units and a chiral binaphthyl derivative with two diarylethene moieties.[23,24]

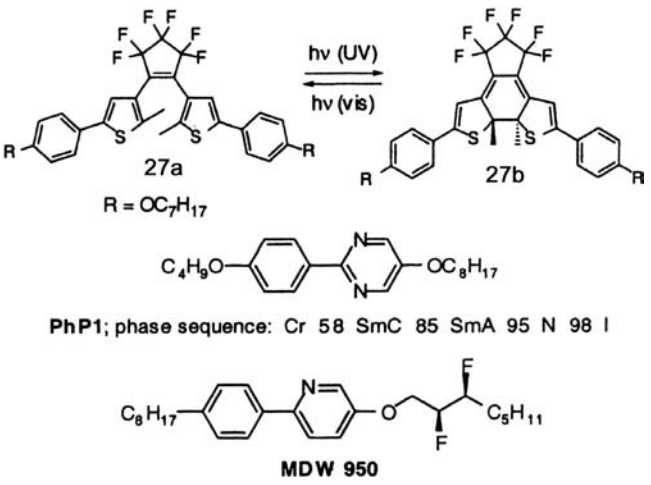

FIGURE 35.15 Structures of doped diarylethene and liquid crystal molecules.

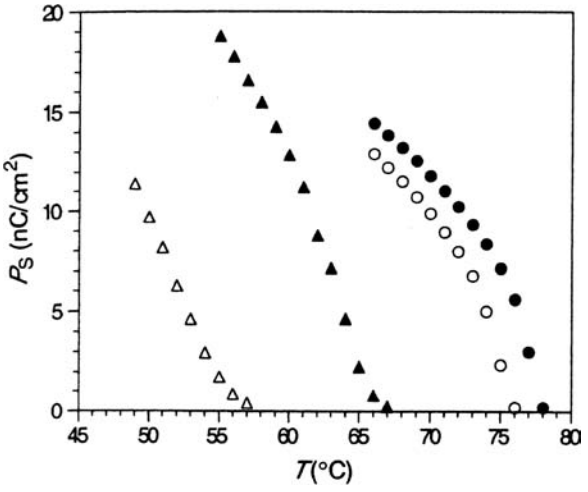

FIGURE 35.16 Spontaneous polarization P_s as a function of temperature T for FLC mixtures doped with **27a** at 1.0 mol % (circles) and 3.0 mol % (triangles) before and after irradiation with UV light (filled and open symbols, respectively).

Spontaneous electric polarization (*Ps*) of ferroelectric liquid crystal (FLC) can be modulated reversibly via photoisomerization of the dithienylethene dopant **27a**.[25] Compound **27a** was doped in a FLC host containing a 10 mol% mixture of the displaytech compound (*S,S*)-5-(2,3-difluorooctyl)-2-(4-octylphenyl)pyridine (**MDW950**) in the achiral SmC liquid crystal 2-(4-butyloxyphenyl)-5-octyloxypyrimidine (**PhP1**). *Ps* was measured as a function of temperature before and after irradiation of the FLC films with 365 nm light for a period of 3 min. As shown in Figure 35.16, photocyclization of the dopant causes the *Ps* vs. *T* plots to shift to lower temperatures. The shift indicates destabilization of the SmA* phase. The SmC*–SmA* transition temperature decreases by 2 K upon irradiation of the 1 mol% mixture and by 10 K upon irradiation of 3 mol% mixture. The spontaneous polarization can be fully restored by reversing the photocyclization by using visible light $\lambda > 455$ nm. The *Ps* photomodulation cycle can be repeated many times without any sign of photochemical degradation.

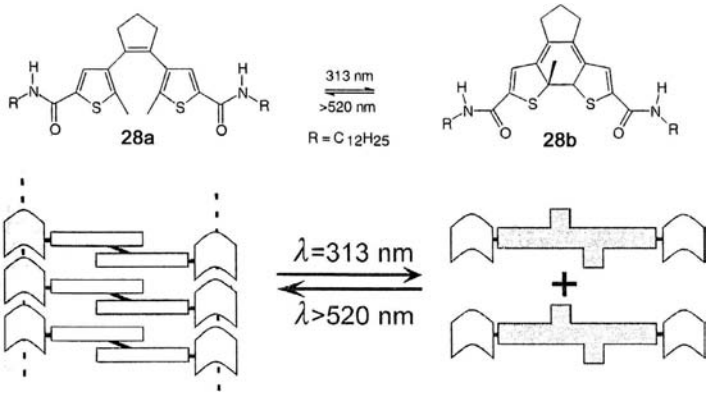

FIGURE 35.17 Photoswitching of diarylethene **28a** and **28b** and thereby controlling the extent of self-assembly of **28** by photochemical switching.

35.7 Self-Assembly

Feringa et al. reported the photocontrolled self-assembly of molecular switches using a diarylethene derivative. As shown in the Figure 35.17, the intermolecular interaction was found to change upon photoirradiation.[26] In the open-ring form **28a**, the two thienyl moieties can rotate along the bond connecting them to the ethene moiety, whereas in the closed-ring isomer **28b** the rotational freedom is lost and the molecule becomes planar. The geometrical change along with the photochemical transformation is expected to change the self-assembling properties of **28**. These researchers observed the viscosity change of the benzene solution containing **28** by alternative UV and visible light irradiation.

35.8 Conclusion

In this chapter we have described various types of diarylethene derivatives with different functionalities. The characteristic features of the photochromic reactions, such as switch of π-conjugation length, geometrical structure changes, and electric as well as vibrational structure changes, can find applications in various molecular photonics devices.

References

1. Bertelson, R.C., in *Photochromism,* Brown, G.H., Ed., John Wiley and Sons, New York, 1971.
2. Dürr, H. and Bouas-Laurent, H., *Photochromism Molecules and Systems*, Elsevier, Amsterdam, 1990,
3. Irie, M., Diarylethenes for memories and switches, *Chem. Rev.,* 100, 1685, 2000; Irie, M. and Mohri, M., Thermally irreversible photochromic systems. Reversible photocyclization of diarylethene derivatives, *J. Org. Chem.,* 53, 803, 1998; Irie, M. and Uchida, K., Synthesis and properties of photochromic diarylethenes with heterocyclic aryl groups, *Bull. Chem. Soc. Jpn.,* 73, 985, 1998; Tsivgoulis, G.M. and Lehn, J.M., Photoswitched and functionalized olifothiophenes: synthesis and photochemical and electrochemical properties, *Chem.-Eur. J.,* 2, 1399, 1996.
4. Uchida, K., Nakayama, Y., and Irie, M., Thermally irreversible photochromic systems. Reversible photocyclization of 1,2-bis(benzo[b]thiophen-3-yl)ethene derivatives, *Bull. Chem. Soc. Jpn.,* 63, 1311, 1990.
5. Irie, M., Miyatake, O., Uchida, K., and Eriguchi, T., Photochromic diarylethenes with intralocking arms, *J. Am. Chem. Soc.,* 116, 9894, 1994.
6. Uchida, K., Tsuchida, E., Aoi, Y., Nakamura, S., and Irie, M., Substitution effect on the coloration quantum yield of a photochromic bisbenzothienylethene, *Chem. Lett.,* 63, 1999.

7. Takeshita, M., Choi, C.N., and Irie, M., Enhancement of the photocyclization quantum yields of 2,2′-dimethyl-3,3′-(perfluorocyclopentene-1,2-diyl)bis(benzo[b]thiophene-6-sulfonate) by inclusion in a cyclodextrin cavity, *J. Chem. Soc., Chem. Commun.,* 2265, 1997.
8. Takeshita, M., Kato, N., Kawauchi, S., Imase, T., Watanabe, J., and Irie, M., Photochromism of dithienylethenes included in cyclodextrins, *J. Org. Chem.,* 63, 9306, 1998.
9. Takeshita, M. and Irie, M., Photoreversible circular dichroism change of 1,2-bis(1-benzothiophen-3-yl)perfluorocyclopentene modified cyclodextrin, *Tetrahedron Lett.,* 40, 1345, 1999.
10. Shibata, K., Muto, K., Kobatake, S., and Irie, M., Photocyclization/cycloreversion quantum yields of diarylethenes in single crystals, *J. Phys. Chem. A,* 106, 209, 2002.
11. Kobatake, S., Uchida, K., Tsuchida, E., and Irie, M., Single-crystalline photochromism of diarylethenes: reactivity-structure relationship, *J. Chem. Soc., Chem. Commun.,* 2804, 2002.
12. Matsuda, K. and Irie, M., Photoswitching of intramolecular magnetic interaction using a diarylethene dimer, *J. Am. Chem. Soc.,* 123, 9896, 2001.
13. Fraysse, S., Coudret, C., and Launay, J.P., Synthesis and properties of dinuclear complexes with a photochromic bridge: an intervalence electron transfer switching "on" and "off," *Eur. J. Inorg. Chem.,* 1581, 2000.
14. Norsten, T.B. and Branda, N.R., Photoregulation of fluorescence in a porphyrinic dithienylethene photochorom, *J. Am. Chem. Soc.,* 123, 1784, 2001.
15. Myles, A.J. and Branda, N.R., 1,2-Dithienylethene photochromes and non-destructive erasable memory, *Adv. Funct. Mater.,* 12, 167, 2002.
16. Norsten, T.B. and Branda, N.R., Axially coordinated porphyrinic photochromes for non-destructive information processing, *Adv. Mater.,* 13, 347, 2001.
17. Fernandez-Acebes, A. and Lehn, J.M., Optical switching and fluorescence modulation properties of photochromic metal complexes derived from dithienylethene ligands, *Chem.-Eur. J.,* 5, 3285, 1999.
18. Kawai, T., Sasaki, T., and Irie, M., A photoresponsive laser dye containing photochromic dithienylethene units, *J. Chem. Soc., Chem. Commun.,* 711, 2001.
19. Malval, J.P., Gosse, I., Morand, J.P., and Lapouyade, R., Photoswitching of cation complexation with a mono aza-crown dithienylethene photochrome, *J. Am. Chem. Soc.,* 124, 904, 2002.
20. Stellacci, F., Bertarelli, C., Toscano, F., Gallazzi, M.C., and Zerbi, G., Diarylethene-based photochromic rewritable optical memories: on the possibility of reading in the mid-infrared, *Chem. Phys. Lett.,* 302, 563, 1999.
21. Murguly, E., Norsten, T.B., and Branda, N.R., Non-destructive data processing based on chiroptical 1,2-dithienylethene photochromes, *Angew. Chem. Int. Ed. Engl.,* 40, 1752, 2001.
22. Denekamp, C. and Feringa, B.L., Optically active diarylethenes for multimode photoswitching between liquid-crystalline phases, *Adv. Mater.,* 10, 1080, 1998.
23. Uchida, K., Kawai, Y., Shimizu, Y., Vill, V., and Irie, M., An optically active diarylethene having cholesterol units: a dopant for photoswitching of liquid crystal phases, *Chem. Lett.,* 654, 2000.
24. Yamaguchi, T., Inagawa, T., Nakazumi, H., Irie, S., and Irie, M., Photoinduced pitch changes in chiral nematic liquid crystals formed by doping with chiral diarylethene, *J. Mater. Chem.,* 11, 2453, 2001.
25. Maly, K.E., Wand, M.D., and Lemieux, R.P., Bistable ferroelectric liquid crystal photoswitch triggered by a dithienylethene dopant, *J. Am. Chem. Soc.,* 124, 7898, 2002.
26. Lucas, L.N., van Esch, J., Kellogg, R.M., and Feringa, B.L., Photocontrolled self-assembly of molecular switches, *J. Chem. Soc., Chem. Commun.,* 759, 2001.

36

Photoprocesses in Polymethine Dyes: Cyanines and Spiropyrane-Derived Merocyanines

Helmut Görner
Max-Planck-Institut für Strahlenchemie

Alexander K. Chibisov
Russian Academy of Sciences

36.1 Introduction

Linear polyenes with push–pull groups are important synthetic organic dyes.[1] Their photophysics and photochemistry have attracted much attention and are the subject of many publications. The influence of the polymethine structure on the spectral-luminescent properties has been described elsewhere.[2–4] Recent work with polymethine dyes, carried out through the 1990s, has been reviewed by Mishra et al.[5] Among the various symmetric cyanine dyes, the classes of indocarbocyanine (**In**), thiacarbocyanine (**Tn**), oxacarbocyanine (**On**), and benzoimidocarbocyanine (**Bn**) in organic and aqueous solution have been intensively investigated. 1,3,3,1′,3′,3′-Hexaalkylindocarbocyanine (**I2**, n = 2), 3,3′-dialkylthiacarbocyanine (**T2**, n = 2), 3,3′-dialkyloxacarbocyanine (**O2**, n = 2) and 1,1′-dialkyl-2,2′-carbocyanine (**B2**, n = 2) are frequently used examples.

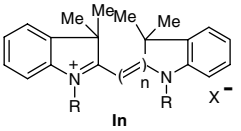

In

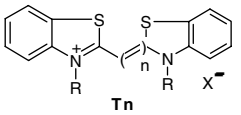

Tn

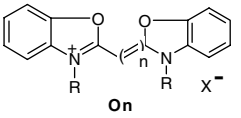

On

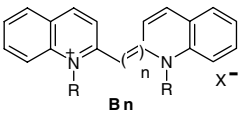

Bn

0-8493-1348-1/04/$0.00+$1.50

TABLE 36.1 Fluorescence Lifetime and Quantum Yields of Frequently Studied Cyanine Dyes[a]

Dye	Solvent	τ_f (nsec)	Φ_f	Φ_{isc}	$\Phi_{t\text{-}c}$	Ref.
I2	Benzene[b]	0.25	0.047			20, 21
	Propanol	0.15	0.03	<0.005		9, 22
	Ethanol	0.16	0.04	<0.001	0.6	22, 28
I3	Ethanol	0.6	0.14–0.2	0.003	0.04	27, 29
T2	Chloroform	0.3/0.5	0.10			25
	(M)ethanol	0.3	0.02–0.12	0.001	0.25	23, 25, 26, 28, 30
T3	(M)ethanol	1.4	0.36	<0.01	0.02–0.1	6, 18, 26
T4	Ethanol	1.3	0.22			30
O2	(M)ethanol	0.3	0.04		0.2	19, 23
O3	Ethanol	1.2	0.39	<0.005	0.08	6, 8, 26
O4	Ethanol		0.28			26
B2	Ethanol	0.04	0.007	<0.001		7

[a] All data in the chapter refer to room temperature unless otherwise indicated.
[b] Depending on the counterion.

Here we focus on the literature of photophysical processes and photochemical reactions of cyanine and merocyanine dyes in solution at ambient temperatures. Besides pioneering and fundamental articles,[6–15] mainly recent publications are discussed. This chapter does not include stilbazolium-type dyes and their crown ethers,[5] and data concerning films or adsorbed dyes[16,17] are not covered.

36.2 Photoprocesses of Cyanine Dyes in Organic Solvents

Polymethine dyes, unless they are sterically hindered, are generally present in their all-*trans* form.[18–43] The primary photoprocesses in nonaqueous fluid solution are fluorescence and rotation about a polymethine C-C bond prior to population of a *cis*-photoisomer.

Singlet and Triplet State Properties and *trans*→ *cis* Photoisomerization

The excited singlet state (S_1) of many cyanine dyes at room temperature is characterized by a relatively short lifetime (τ_f) and a low or moderate quantum yield of fluorescence (Φ_f).[2,11] A rather high quantum yield of *trans* → *cis* photoisomerization ($\Phi_{t\text{-}c}$) (Table 36.1) and a large rate constant for rotation about polymethine C-C bonds (k_{rot}) are typical for cyanine monomers.

The temperature dependence of fluorescence shows that *trans* → *cis* photoisomerization as a competing path is activated; the activation energy (E_{rot}) lies in the 15–30 kJ mol^{-1} range (Table 36.2). The viscosity dependence of k_{rot} was intensively studied by picosecond laser spectroscopy.[10,12–14] The relaxation rates of **I2** dyes were interpreted by assuming a viscosity dependence of E_{rot}.[33] The effect of viscosity on nonradiative processes in fluid solution was extended to high pressure.[22] For a homologous series of **T1–T4** dyes, k_{rot} increases with the chain length.[30] The quantum yield, $\Phi_{t\text{-}c,}$ is largest for n = 2 and decreases with increasing chain length. For 1,1′-diethyl-2,2′-dicarbocyanine (**B3**), $\Phi_{t\text{-}c}$ is 2×10^{-4}.[44] Upon high intensity excitation, another isomer becomes detectable for **T3**.[37]

The triplet lifetime (τ_T) of **T2** or **I2** in deoxygenated solution is in the 0.1–100 msec range; the triplet state is quenched by oxygen and the quenching rate constant is up to $3 \times 10^9 M^{-1}\text{sec}^{-1}$.[2,17,28,29] A low quantum yield of intersystem crossing (Φ_{isc}), $<5 \times 10^{-3}$ for several cases (Table 36.1), and a small rate constant (k_{isc}) are typical for monomeric dyes. A long-lived transient is often detected in addition to the triplet state. Its absorption difference spectrum is characteristic for a *cis*-isomer; the decay is temperature dependent and insensitive towards oxygen. The overlapping triplet and isomer spectra can be separated by appropriate conditions.

A frequently examined dye is 3,3′-diethyloxadicarbocyanine (**O3**); the iodide is commonly denoted as DODCI.[8] The activation energy ($E_{c\text{-}t}$) of the thermal *cis* → *trans* isomerization of cyanine dyes lies in the

TABLE 36.2 Activation Energies of Photoisomerization and Thermal Isomerization

Dye	Solvent	E_{rot} (kJ mol^{-1})	log A_{rot}	$E_{c\text{-}t}$ (kJ mol^{-1})	Ref.
I2	Ethanol			47	28
I3	Ethanol	27	14	51	26, 29
T2	CH_2Cl_2	19	13	65	23
	Ethanol	24	12.9	63	26, 28
T3	Ethanol	30	14	55	26
O2	CH_2Cl_2	17	13	74	23
	Ethanol	16–22	13	66	24, 26
O3	Ethanol	23	12	62	8, 26
O4	Ethanol	27	13	46	26

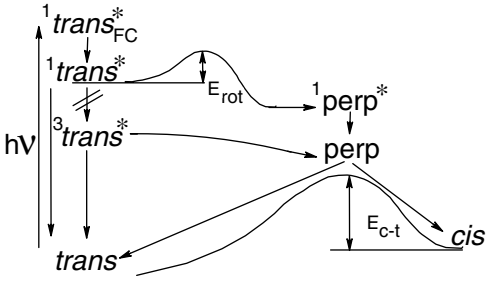

SCHEME 1

50–80 kJ mol^{-1} range (Table 36.2). The influence of the viscosity of the medium and molecular structure on the isomerization dynamics in several cyanines was investigated by Aramendía and co-workers.[26,27] For symmetric carbocyanines the experimental and theoretical data of the ground-state potential energy surface are in agreement.[38] In laser-induced optoacoustic spectroscopy studies, Braslavsky and her group found that the molecular volume change due to photoisomerization of **T2** in ethanol–water is 52 ml mol^{-1} and that of **O2** (iodide) is zero.[18,19] A combination with semiempirical calculations indicates mainly rearrangement of solvent molecules.[19]

There is agreement that the *trans* → *cis* photoisomerization in polymethine cyanines takes place via the S_1 state. The fluorescing ^{1}*trans** state is populated via the Franck Condon (FC) precursor and decays via the perpendicular state (^{1}*perp**) into *trans*- and *cis*-isomers (Scheme 1). The potential energies of the ground and excited singlet states as a function of the angle of rotation about polymethine C-C bonds have a respective maximum and minimum at about 90°.[8,13,14,38] Two theoretical models were presented for **O3** and **T3**; the experimental check reveals a common intermediate in the *cis* $\rightleftharpoons$ *trans* photoisomerization routes.[23,24] The deactivation routes were discussed for **I2**,[28,33,36] **I3**,[29,31,35,36] **T2**,[23,28] **T3**,[34,37] **O2**,[23] and **O3**.[6,32,34] For asymmetric **I2** and **I3** related dyes, *trans* → *cis* photoisomerization occurs about those bonds that have the highest bond order in S_0.[36] Isomerization dynamics of 1,1′-diethyl-4,4′-cyanine were studied by third-order nonlinear spectroscopy.[40] Photoisomerization via higher excited-state and intersystem crossing to T_1 was observed for **T3**.[32] To induce *trans* → *cis* isomerization via T_1, a sensitizer can be applied.[29]

Substituent Effects

Variations of the conjugated polymethine chain and the unconjugated alkyl chains have been examined. For **T2** and derivatives with a long chain (up to $C_{18}H_{37}$), the Φ_f, Φ_{isc}, and $\Phi_{t\text{-}c}$ values are rather similar.[25] Linking of two chromophores by one or two chains has substantial influences on the absorption, fluorescence, and other photorelaxation processes. The fluorescence decay of a bis-**T3** (two covalently linked

TABLE 36.3 Quantum Yields of **I2** and **T2** and bis-Cyanine Dyes

Dye	Φ_f	Φ_{isc}	$\Phi_{t\text{-}c}$
I2	0.04	<0.001	0.60
bis-**I2**	0.02	0.009	0.05
bis-**I2′**	0.07	0.03	<0.001
T2	0.03	0.001	0.25
bis-**T2**	0.03	0.03	0.12

Source: Chibisov, A.K., Zakharova, G.V., Görner, H., Sogulyaev, Y.A., Mushkalo, I.L., and Tolmachev, A.I., *J. Phys. Chem.*, 99, 886, 1995.

TABLE 36.4 Photophysical and Photochemical Properties of **I3** Dyes

9-R	Φ_{isc}	$\Phi_{t\text{-}c}$	$\tau_{c\text{-}t}$ (msec)	$E_{c\text{-}t}$ (kJ mol^{-1})
H	<0.003	0.04	0.9	53
Me	<0.01	0.25	0.4	53
Cl	0.04	0.4	0.17	49
Br	0.2	0.19	0.23	50
CN	<0.01	<0.06	0.015	45

Source: Chibisov, A.K., Zakharova, G.V., and Görner, H., *J. Chem. Soc. Faraday Trans.*, 92, 4917, 1996.

chains) has three fluorescence lifetime components, which originate from different structures.[39] The data for bis-**I2** (one link, L = C_2H_4), bis-**I2′** (two links, L = C_4H_8) and bis-**T2** (one link, L = C_5H_{10}) dyes show that Φ_{isc} is enhanced in ethanol at the expense of $\Phi_{t\text{-}c}$ (Table 36.3), while $E_{c\text{-}t}$ (47–64) kJ mol^{-1} remains essentially unchanged.[28] For bis-**I2** Φ_f is reduced and Φ_{isc} enhanced.[42]

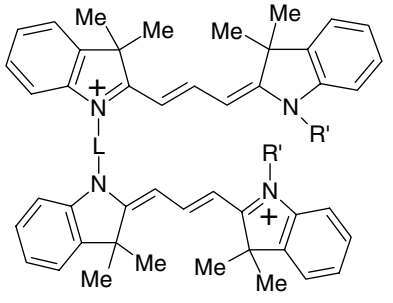

bis-**I2**

The effects of 9-substituents in the polymethine chain on the photoprocesses of **I3** in ethanol are compiled in Table 36.4. The quantum yield Φ_{isc} is largest when R is bromo, while $\Phi_{t\text{-}c}$ depends on charge-transfer and $E_{c\text{-}t}$ (47–64 kJ mol^{-1}) remains essentially unchanged. Bulky substituents in **I2**[43] or a 9-R-**T2**[45,46] force the molecule in organic solvents to adopt a sterically less hindered mono-*cis* form.

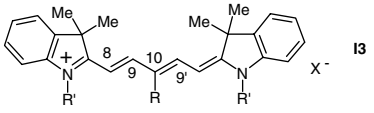

I3

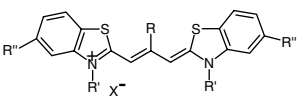

	R	R''	R'	X
T2a	H	H	Et	I^-
T2b	Me	H	C_2H_4OH	Cl^-
T2c	Et	OMe	$C_3H_6SO_3^-$	$C_5H_5NH^+$
T2'a	H	H	H	I^-
T2'b	Me	H	H	I^-
T2'c	Et	H	Cl	Cl^-

TABLE 36.5 Quantum Yields and Activation Energy of Thermal Isomerization of **T2** Dyes

Dye	Solvent	Φ_f	$\Phi_{t\text{-}c}^{rel}$	$\tau_{c\text{-}t}$ (msec)	$E_{c\text{-}t}$ (kJ mol^{-1})
T2a	Dioxane	0.07	0.7	3	61
	Acetone	0.04	1.0	3	60
T2b	Dioxane	0.065	0.8	0.3	60
	Ethanol	0.0025	<0.05		
T2c	Dioxane	0.1	0.6	0.1	58
	Acetone	0.009	0.4	0.4	65
	Acetonitrile	0.004	0.15	0.2	61
	Ethanol	0.003	0.05		

Source: Khimenko, V., Chibisov, A.K., and Görner, H., *J. Phys. Chem. A,* 101, 7304, 1997.

For **T2a–c** containing alkyl substituents in the polymethine chain, the equilibrium between two isomers is shifted from the all-*trans*-isomer in nonpolar media towards the mono-*cis*-isomer in polar media, thereby reducing Φ_f and $\Phi_{t\text{-}c}$ (Table 36.5).[47] The photophysics and subnanosecond relaxation dynamics of **T3** and its 9-Me derivative were studied.[48] Implications for the design of near-IR fluorochromes with high fluorescence efficiencies were found from steady-state and picosecond laser studies of a **I4** (IR 125) dye.[49]

Photoinduced Electron Transfer

The photochemistry of **I2** type ion-pairs in nonpolar solution was intensively studied by the group of Schuster.[20] Evidence was given for electronic and steric control of the rate for rotation about polymethine C-C bonds k_{rot} in the relaxation of **I2** in benzene.[20] For some salts, k_{rot} and τ_f or Φ_f are sensitive to the substitution on the aryl rings.[21] For **I2** alkyltriphenylborate salts, intra-ion-pair electron transfer occurs, a locally excited singlet state is formed, and boranyl radicals are involved; the relationship between the rate constant (k_{et}) and the free energy change (ΔG_{et}) has been outlined.[50] An influence over the k_{isc} value of iodide ion pairs and the external iodine atom was registered.[51] Bulky borate anions distort the structure of bis-**I2** (two links) and influences the deactivation processes.[52]

For **I2** and **I3** type dyes with various counterions in nonpolar media, electron transfers via singlet and triplet states were distinguished by flash photolysis.[53] The rate constant for electron transfer from the first excited singlet state of **O2** in methanol to benzoquinone and other suitable acceptors is $k_{et} = (1\text{–}3) \times 10^{10}$ $M^{-1}sec^{-1}$.[54] Electron transfer, involving the triplet state of **T2–T4**, was performed with benzoquinone and ascorbic acid in alcohols.[17] ESR results with various cyanine dyes were interpreted by electron transfer involving the superoxide radical anion.[55] Electron transfer competes with delayed fluorescence and *trans→cis* isomerization when induced by energy transfer from triplet anthracene to **I3** dyes.[56] Charge-transfer states were reported for cyanine–oxonol ion pairs.[57]

36.3 Merocyanines

Some properties of excited merocyanine dyes are compiled in Table 36.6. The most frequently studied is merocyanine 540 (**M1**). **M1** is readily soluble in alcohols and lipid membranes, making it attractive for many technical applications and biological activity studies.[58–66] The solvent polarity has a significant influence on τ_f and the related quantum yields.[59,60] An intrinsic barrier height of E_{rot} = 3 kJ mol^{-1} for isomerization in S_1 was determined from dynamical solvation effects on the rate k_{rot} of **M1** in polar solvents.[59] Environmental effects on radiative and nonradiative transitions have been studied for merocyanines in homogeneous and microheterogeneous systems.[67]

TABLE 36.6 Fluorescence Lifetime and Quantum Yields of Merocyanines

Dye	Solvent	τ_f (nsec)	Φ_f	Φ_{isc}	Φ_Δ	$\Phi_{t\text{-}c}$	Ref.
M1	1-Propanol	0.56	0.25	0.004		0.30	59, 60, 63
	Ethanol	0.3	0.16	0.003		0.40	58, 60, 62
	Methanol	0.2	0.14	0.04	0.002		60, 61
	1-Hepthanol	1.7	0.42				59, 60
M2	Methanol		0.15	0.015	0.001		61
M3	Ethanol	0.78	0.18	0.008		0.31	62
M4	Methanol		0.01	0.80	0.38		61
M5	Ethanol	0.48	0.16	0.38	0.045	0.03	62

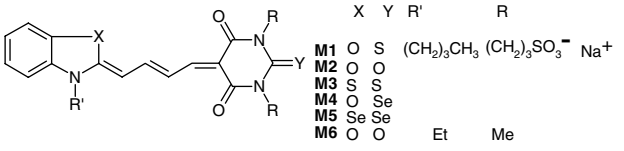

Structural modifications have implications on photophysical properties and biological activity. A correlation between Φ_{isc} and quantum yield of formation of molecular singlet oxygen (Φ_Δ) has been found.[61] Harriman and his group studied the photoisomerization of derivatives, e.g., with two sulfur (**M3**) and two selenium (**M5**) atoms; for **M5** Φ_{isc} is strongly enhanced (Table 36.6). The spin-orbital coupling for sterically hindered dyes is unaffected by substitution.[63] The role of a zwitterionic resonance form, where the barbiturate unit acts as an electron acceptor, was discussed.[64] Intersystem crossing from upper triplet levels was reported for parent **M1**.[65] Whitten and his group found for bis-**M6** type dyes with methylene spacers that exciton and charge-transfer interactions in nonconjugated merocyanine dye dimers cause novel solvatochromic behaviour for tethered bichromophores and excimers.[66] In liposomes, **M1** is incorporated into the lipid bilayer as monomer and Φ_{isc} is a few percent.[58] The parent **M1** has a high recognition potential for leukemia cells, but optimized photophysical and photochemical properties do not necessarily go along with therapeutic improvements. The phototoxicity was examined with Daudi cells[62] or clonogenic assays on L1210 cells.[61]

36.4 Cyanine Dyes in Aqueous Solution

The properties of dimers and aggregates have been discussed for various cyanine dyes in aqueous solution.[68–88] Aggregated cyanine dyes play a key role in spectral sensitization.[16,68,69] With increasing dye concentration, monomers are converted into dimers before higher aggregates are formed.[70] The equilibria depend also on the dye structure and the medium. J(Jelly)-aggregates and H-aggregates (H for hypsochromic) exhibit generally short- and long-wavelength peaks, respectively. Dimerization can be enhanced in the presence of salts or by the association with hydrophobic (borate) anions, thereby changing the luminescence features.[16] A face-to-face alignment was suggested for the non-fluorescent dimers of **T2d–g**.[72]

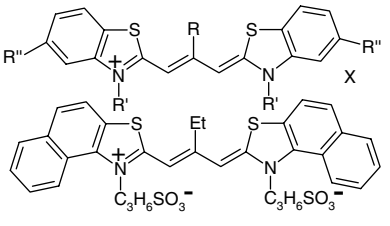

	R	R"	R'	X
T2d	H	H	$C_3H_6SO_3^-$	$C_5H_5NH^+$
T2e	Me	H	C_2H_4OH	Cl^-
T2f	Et	OMe	$C_3H_6SO_3^-$	$C_5H_5NH^+$
T2g				$C_5H_5NH^+$

TABLE 36.7 Absorption and Fluorescence Maxima and Yields of Fluorescence and Triplet Formation

Dye	Medium[a]	λ^M (nm)	λ^D (nm)	λ_f (nm)	Φ_f	Φ_{isc}
T1a	Ethanol	440		505	0.003	<0.002
	Water		416	510	0.06	≈0.2
T1b	Water		417, 480[b]	520	0.06	≈0.1
T1c	Water	460	421		0.055	≈0.1
T1d	Ethanol	448		512	0.004	
	Water		416	522	0.08	≈0.1
T2d	Ethanol	558		580	0.1	<0.001
	Water	556	512	573	≤0.07	<0.001
	CTAB	569	590[b]	583	0.4	
T2e	Water	545	503	572	≤0.002	<0.002
T2f	Ethanol	560		598	0.01	<0.02
	Water	560	520	586	≤0.004	0.15
	SDS	578		596	0.10	<0.002
	CTAB	587	(625, 650)[b]	600 (657)[b]	0.32	<0.002
T2g	Water	570	660[b]	536[b]	0.003	0.12

[a] Surfactant concentration = 4–24 m*M*.

[b] J-aggregate.

Sources: Chibisov, A.K., Zakharova, G.V., and Görner, H., *Phys. Chem. Chem. Phys.,* 1, 1455, 1999; Chibisov, A.K., Prokhorenko, V.I., and Görner, H., *Chem. Phys.,* 250, 47, 1999; Chibisov, A.K., Zakharova, G.V., and Görner, H., *Phys. Chem. Chem. Phys.,* 3, 44, 2001.

Ground State Equilibria

Self-association of dyes in solution is caused by van der Waals forces, hydrophobic interaction, and hydrogen bonding with the solvent or intermolecularly. For 4,5-benzo- (**T1a**) and 5,5′-dichlorothia-monomethincyaninebetaine, the thermodynamic parameters of photographic dimerization have been studied.[75] The monomethine dyes **T1a–d** were applied for spectral sensitization of emulsions, since the intrinsic sensitivity of AgCl grains is very low at 400–500 nm. They are mainly present as dimers in aqueous solution and as monomers in ethanol (Table 36.7). The dimerization constant is $K_D = 7 \times 10^5$ M^{-1} for **T1b** in water and lower in the presence of ethanol or in the case of **T1c**.[74] Pseudoisocyanine (**B1**, n = 1) is a frequently used water-soluble dye, denoted as PIC.[70,77,81]

Formation of dimers in water, due to hydrophobic interaction and hydrogen bonding, can be facilitated by the reduction of repulsion between similarly charged ions. In contrast, the dyes in alcohols, due to high solubility, are present as monomers. Moreover, dimer formation reduces hydrophobic interactions with water. Hydrogen bonding with water is the main driving force for dimerization of xanthene dyes, where the enthalpy (ΔH_D) and enthropy (ΔS_D) dimerization values are negative. The thermodynamic parameters for **T1a** in aqueous methanol are $\Delta H_D = -54$ kJ mol^{-1} and $\Delta S_D = -97$ J mol^{-1}K^{-1}.[74] Dimerization is characterized by an intense band at shorter and a weak band at longer wavelengths (Table 36.7), by the effects of temperature or concentration, and by an aggregation number of two. A distance of 1.0 nm between the centers of gravity of the two molecules and an angle of 55° between the polarization axes of the monomers in the dimer were estimated. The J-aggregate of **T1b** is formed in the presence of KCl and in heavy water. Anisotropic structures of aggregated dyes were found for pseudoisocyanine.[76] H- and J-Aggregates are formed when cyanine dyes are bound to DNA templates.[77]

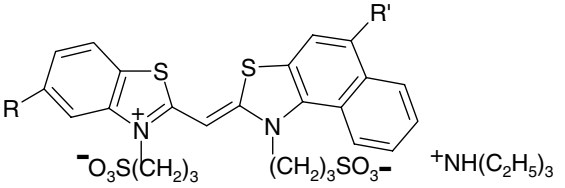

	R	R'
T1a	H	H
T1b	Cl	Cl
T1c	OMe	OMe
T1d	OMe	H

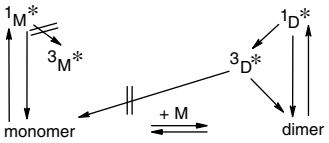

SCHEME 2

Photoprocesses of Dimers and Aggregates

The photoprocesses are determined by the state of aggregation. Aggregated molecules play an important role in photosynthesis in green plants and photosynthetic bacteria.[89,90] The dimers of **T1a–d** exhibit fluorescence with a yield 10–20 times larger than that of the monomers (Table 36.7). Lower Φ_f and Φ_{isc} values with respect to the dimers indicate efficient internal rotation of the naphthothiazolium residue about the monomethine chain. Φ_{isc} decreases with increasing temperature, supporting the hypothesis that the observed triplet state originates from the excited dimer (Scheme 2). Subnanosecond relaxation dynamics in monomers, dimers, and H- and J-aggregates were observed for **B1**[80] and **T2**.[82]

Fluorescence was observed for dimers of acridine orange and rhodamine 6G; whereas dimers of squaraine, Zn-phthalocyanine, and certain xanthene dyes do not fluoresce at ambient temperature.[74] Two aggregates were postulated on the basis of a fluorescence study of PIC.[78] $\Phi_f = 4 \times 10^{-4}$ was reported for J-aggregates from indocyanine green (**I4** type) in aqueous solution.[83] The dimers of **T2d–f** exhibit a lower Φ_f value than the monomers do (Table 36.7). This results from different orientations; i.e., an alignment other than face-to-face may be the reason for the fluorescence of the dimer of **T1**. Shifting the monomer–dimer equilibrium also changes Φ_{isc}. Triplet states of dimers were observed for methylene blue, acridine orange, rose bengal, triarylmethane dyes, triarylpyrylium salts, phthalocyanines, porphyrines, and **T2**, cf.[74] Photoinduced electron transfer takes place in J-aggregates when the dyes are adsorbed to a surface of an appropriate semiconductor, e.g., silver halide microcrystals.[17,69]

Surfactants

In the presence of surfactants, dyes can deaggregate. On the other hand, surfactants can influence aggregation, and ion-pairing is a prerequisite for this process. Dyes in microheterogeneous media, such as micelles, reveal a strong enhancement of Φ_f, e.g., for cyanine dyes (Table 36.7), and a higher photostability, e.g., for rose bengal, methyl orange, or **M1** cf.[74] These processes were studied using sodium dodecyl sulfate (SDS), cetyltrimethylammonium bromide (CTAB), or Triton X-100 as anionic, cationic, and nonionic surfactants, respectively. For similarly charged reactants and with increasing surfactant concentration, the monomer and dimer absorptions of **T2d–f** reach half of their maximum values ($conc_{1/2}$) at the critical micelle concentration (cmc).[73] This is in contrast to oppositely charged reactants, where aggregates appear at $conc_{1/2}$ values much smaller than the cmc (Table 36.8). Φ_f reflects the behavior of the monomer, whereas Φ_{isc} reflects that of the dimer.

For the cationic CTAB, the hydrophobic interaction between the monomer and the surfactant, which causes the deaggregation, is enhanced by the attracting Coulombic forces. The J-aggregates of **T2f**, due to association of the dye with the micelle in the cmc region and above, are converted into monomers. This system is characterized by three regimes, which are separated by the formation of ion pairs, formation of J-aggregates, and their conversion into solubilized monomers. For those dyes where J-aggregates are not formed, the $[CTAB]_{1/2}$ values in Table 36.8 refer to dimer splitting. Conversion into solubilized **T2d–f** monomers was suggested for [CTAB] higher than the cmc. Photoisomerization and fluorescence in micelles have also been studied for **O2** (iodide) and **T2d,g**.[87]

Polyanions

Aggregation phenomena are observable when cationic dyes are bound to anionic polyelectrolytes, such as polyacrylic acid (PAA), polymethacrylic acid (PMA), or polystyrene sulfonate (PSS).[91–98] Φ_f is strongly

TABLE 36.8 Half-Concentrations (m*M*) Obtained from Absorption and Fluorescence

Dye	Micelle	cmc	Abs (Monomer)	Abs (Dimer)	Fluorescence
T2d	SDS	—	8	8	8
T2e	SDS	—	7	<0.1	—
T2f	SDS	8.1	8	7.7	8/10[a]/8[b]
	CTAB	0.92	0.9/0.8[c]	0.017	0.02/0.8
	Triton X-100	0.26	2.7	2	2.7
	Brij 35	0.06	0.5	0.3	0.6

[a] Referring to Φ_{isc}^{rel}.
[b] For $\Phi_{t\text{-}c}^{rel}$.
[c] J-aggregate.

Source: Chibisov, A.K., Prokhorenko, V.I., and Görner, H., *Chem. Phys.,* 250, 47, 1999.

TABLE 36.9 Quantum Yields of Fluorescence, Intersystem Crossing and Isomerization

Dye	Polymer	r[a]	Φ_f	τ_T (msec)	Φ_{isc}	$\Phi_{t\text{-}c}$
T2′a		0	0.07	0.06	0.005	0.15
	PSS	10^4	0.19	0.6	0.008	0.11
	PAA	10^4	0.35	0.1	0.012	0.08
	PMA	10^4	0.29	0.1	0.016	0.10
T2′c		0	0.005	0.01	0.010	—
	PSS	10^4	0.12	0.005	0.014	—
	PAA	10^4	0.23	0.1	0.020	—

[a] Concentration ratio: r = [polyanion residue]/[dye].

Source: Slavnova, T.D., Chibisov, A.K., and Görner, H., *J. Phys. Chem. A,* 106, 10985, 2002.

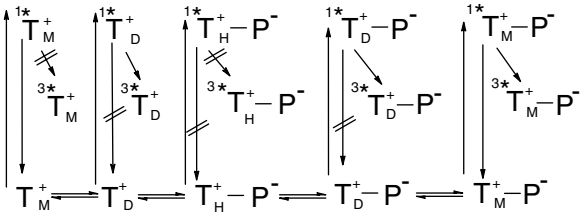

SCHEME 3

reduced when dimers and aggregates of **T2′a–c** are present (high dye loading conditions) and enhanced for bound monomers (low dye loading, Table 36.9). The ground state properties, the decay kinetics, and the Φ_f and Φ_{isc} values depend in specific manners on the ratio of polyanion residue to dye concentrations (r). **T2′a–c** in aqueous solution are present as cationic monomer and dimer (T_M^+ and T_D^+, respectively), and the amount of dimers is strongly enhanced with respect to organic solvents. The dye properties are changed by polyanions (P^-) due to their interactions. Higher aggregates (T_H^{+-} P^-) are formed at high dye loading, whereas dimers (T_D $^{+-}P^-$) are formed on increasing the concentration of polyanion residues, and at an even higher r monomers (T_M $^{+-}P^-$) are present (Scheme 3).

36.5 Spiropyran-Derived Merocyanines

Another class of merocyanines consists of ring-opened spiropyrans, such as spiro[2*H*-1-benzopyran-2,2′-indolines] (BIPS), especially of 6-nitro-substituted derivatives (NO_2BIPS). The photochromism of spiro

TABLE 36.10 Quantum Yields of Coloration, Intersystem Crossing, Singlet Oxygen Formation and Phosphorescence and Activation Energy

Dye	Solvent	Φ_{col}	Φ_{isc}	Φ_{Δ}	Φ_p/77 K	$E_{t\text{-}S}$ (kJ mol^{-1})
N1	Toluene	0.83	0.82	0.75 (0.60)[a]	0.05	80
	Acetonitrile	0.12	0.10	0.09		80
N2	Toluene	0.72	0.77	0.72	0.3	85
	Acetonitrile	0.22	0.25	0.19		95
	Ethanol	0.21	0.24	0.22	0.19	95
N3	Toluene	0.63	0.72	0.62	0.3	80
	Acetonitrile	0.16	0.16	0.13		90
N4	Toluene	0.6	0.5	0.45	0.3	90
	Acetonitrile	0.07	0.1	0.08		100

[a] In cyclohexane.[126]

Sources: Chibisov, A.K. and Görner, H., *J. Phys. Chem. A,* 101, 4305, 1997; Görner, H., *Chem. Phys.,* 222, 315, 1997; Görner, H., *Chem. Phys. Lett.,* 282, 381, 1998; Görner, H., *Phys. Chem. Chem. Phys.,* 3, 416, 2001; Chibisov, A.K. and Görner, H., *Phys. Chem. Chem. Phys.,* 3, 424, 2001.

compounds has been the subject of fundamental investigations,[99–102] and various features were reviewed by Bertelson[103] and Guglielmetti.[104,105] The spiropyrans and spirooxazines are versatile molecules widely used for technical[106,107] and biological[108] applications. Here, four NO_2BIPS (**N1–N4**)[109–127] and a spirooxazine (**SO**) were chosen as examples, and certain aspects are discussed.

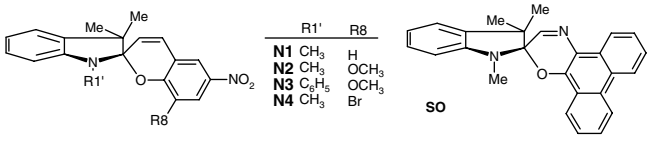

Photochromism of Spiropyrans

UV irradiation of spiropyrans enhances the coloration with maxima in the UV and in the red spectral range (λ_t). The major photoprocess at ambient temperature is ring opening, which takes place in the psec domain.[115–117] The eight possible merocyanines have a zwitterionic or quinoid character; four conformers with the central transoid segment can be expected after photochemical cleavage of the C-O bond (quantum yield: Φ_{col}); the most stable merocyanine isomer is indicated as *trans*.

When the light is removed, the absorbance in the red spectral range decreases and reaches its original stationary value. This rearrangement defines the thermal relaxation time ($\tau_{t\text{-}S}$), which depends on structure, solvent, and temperature.[113,114] In polar solvents generally a minor part of the *trans*-isomer remains after thermal relaxation, whereas in solvents of low polarity equilibrium (1) is completely shifted toward the Sp side. Indoline spiropyrans and their photomerocyanines are separated by an energy barrier, and the activation energy ($E_{t\text{-}S}$) lies in the 80–90 kJ mol^{-1} range (Table 36.10). The thermal relaxation of **N1** occurs also in polymer matrices.[123]

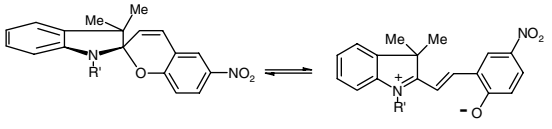

(1)

For NO_2BIPS, in contrast to BIPS and spirooxazines, intersystem crossing is dominant. In particular, a triplet state and a *cis*-isomer are involved in the photocoloration of **N1–N4**.[109–114] The triplet state with a typical τ_T of 10 μsec originates from an equilibrium between the perpendicular (^{3}perp*) and ^{3}*trans**

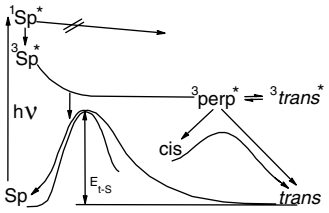

SCHEME 4

TABLE 36.11 Quantum Yields of Fluorescence and Activation Energies

Dye	Solvent	Φ_f	Φ_f/77 K	E_{rot} (kJ mol^{-1})	$E_{c\text{-}t}$ (kJ mol^{-1})
N1	MTHF	0.006	0.7	8	33
	Ethanol	0.012	0.7	10	33
N2	MTHF	0.005	0.7	11	36
	Acetonitrile	0.01			40
	Ethanol	0.016	0.7	13	39
N3	MTHF	0.004	0.7	10	
	Ethanol		0.7	8	33

Sources: Chibisov, A.K. and Görner, H., *J. Phys. Chem. A,* 101, 4305, 1997; Görner, H., *Chem. Phys.,* 222, 315, 1997.

forms (Scheme 4). This is concluded from the independence of the *cis*-isomer yield of oxygen.[109–114] Fluorescence from the $^1Sp^*$ state plays no role, but phosphorescence (Φ_p) is observable in rigid media; the energy level is E_T = 238 kJ mol^{-1} for **N2**.[118] The three yields Φ_{col}, Φ_{isc}, and Φ_Δ have rather large values in nonpolar media at room temperature and exhibit the same decrease with increasing solvent polarity (Table 36.10). In polar solvents, the major deactivation step of $^1Sp^*$ is internal conversion rather than reaction to *trans*-***N***. Significant spectral changes take place for **N1** in water, where the phenoxide moiety is sensitive to pH.[119] High switching reversibilities were found for **N1** in zeolites.[127]

The potential energy surface of the ground state along the reaction coordinate should have one major maximum with the activation barrier $E_{t\text{-}S}$ and at least one minor barrier. The potential energy surfaces of S_0 and S_1 have been calculated for BIPS[128] and NO_2BIPS.[129,130] MO calculations indicate that the dipole moment of the open form of **N1** is twice as large as for Sp.[130] A strong decrease of the potential energy of the relevant S_1 and T_1 states is expected on going from the Sp form via the *cis-cis-cis* (CCC) geometry to the TTC isomer or the most stable merocyanine. The mechanism for photochemical ring opening in BIPS and NO_2BIPS has also been interpreted on the basis of calculations.[128]

Photoprocesses of Spiropyran-Derived Merocyanines

The photoprocesses from *trans*-***N*** are weak fluorescence and weak intersystem crossing, i.e., the major path is internal conversion.[110,131–134] In particular, *trans* → *cis* photoisomerization takes place followed by thermal *cis* → *trans* isomerization (Table 36.11). In specific cases, such as **N2** in ethanol, a route into the Sp form is also opened.[131] The above-mentioned triplet state of **N1–N3** is likewise involved upon population of the ^{1}*trans** state (Scheme 5). The low values of Φ_f and Φ_{isc} at room temperature are in line with the 50- to 100-fold increase of both, when the viscosity is enhanced, e.g., at 77 K.[111] The activation energy, obtained from plots of Φ_f vs. 1/T, is $E_{rot} \approx 10$ kJ mol^{-1}; that for *cis* → *trans* isomerization is $E_{c\text{-}t} \approx 35$ kJ mol^{-1}.

Photoprocesses of Spiropyran Complexes with Metal Ions

In the presence of the metal salts (M^{n+} X^-, n = 2,3) the ground state equilibrium has to be extended towards complexes, *trans*-***N***-M^{n+} (Scheme 6), giving rise to modified spectroscopic and photophysical

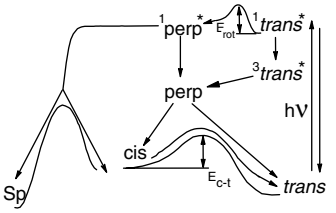

SCHEME 5

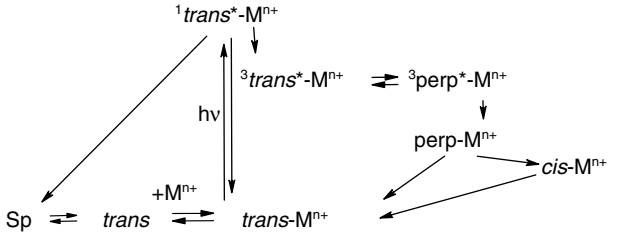

SCHEME 6

TABLE 36.12 Quantum Yields of Fluorescence, Intersystem Crossing, and Isomerization for Complexes with **N2**

Metal	Φ_f	Φ_{isc}^{rel}	$\Phi_{t\text{-}c}^{rel}$
Co^{2+}	0.001	<0.004	<0.05
Ni^{2+}	<0.001	<0.005	<0.005
Zn^{2+}	0.01	0.2	0.4
Pb^{2+}	0.01	1.0	1.0
Nd^{3+}	0.001	0.15	0.06
Tb^{3+}	0.002	<0.05	0.12

Source: Görner, H. and Chibisov, A.K., *J. Chem. Soc. Faraday Trans.*, 94, 2557, 1998.

features.[133–138] The absorption and fluorescence maxima are blue-shifted from 580–600 nm to 480–500 nm and from 660 nm to 580–640 nm, respectively, and the thermal relaxation times become longer. Photocolouration of Sp **N1–N3** yields the complexes via the above mentioned (noncomplexed) triplet state.[133,134] The photoprocesses of *trans-**N***-M^{n+} are fluorescence and intersystem crossing in modified yields; the latter initiates *trans* → *cis* photoisomerization. In addition, a photosubstitution of the ligand by solvent plays a role. Data in Table 36.12 show that Φ_{isc} and $\Phi_{t\text{-}c}$ are largest and smallest for complexes in acetone with Pb^{3+} and Ni^{2+}, respectively.

Photoprocesses of Spirooxazines

The photochromism of spirooxazines has been investigated by Chu,[139] Schneider,[140] and many other researchers.[141–151] Their application potential seems to be very powerful.[104–107] Ring opening of the Sp form of **SO** occurs via the S_1 state[105,144] and takes place in the psec domain.[150,151] The quantum yield Φ_{col} is rather large in solvents of either low or large polarity.[143,144] A biexponential thermal decoloration was observed, which is consistent with fully established equilibria between the Sp form and two photoisomers.[141] Therefore, two separate steps leading to the ring-closure were considered for **SO**. In addition, a more twisted isomer was spectroscopically and kinetically observed upon irradiation of the most stable

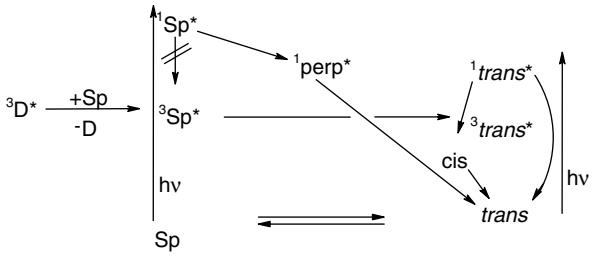

SCHEME 7

photomerocyanine in several solvents at lower temperatures.[142, 146] A triplet route (Scheme 7) can be initiated by energy transfer from an appropriate donor (D) to the Sp form.

To account for the finding that Φ_{col} is well below unity, there should be a deactivation pathway left of the maximum of the barrier in S_0, i.e., efficient internal conversion at the Sp geometry competes with ring opening via the singlet mechanism. From calculations of the energy levels of the stereoisomers, TTC was found to be the most stable form.[149] Whether or not the potential energy surface at the position of the CCC isomer has a minimum remains open as yet. The degree of zwitterionic and quinoid character in BIPS and spirooxazines is also an open question.[148]

Acknowledgments

We thank Wolfgang Lubitz for his support. A.K.C. is grateful to the Deutsche Forschungsgemeinschaft and the Russian Fund of Basic Researches (00–03–32300) for financial support.

References

1. (a) Tyutyulkov, N., Fabian, J., Mehlhorn, A., Dietz, F. and Tadjer, A., *Polymethine Dyes,* St. Kliment Ohridski Univ. Press, Sofia, 1991.
2. (a) Chibisov, A.K., Triplet states of cyanine dyes and reactions of electron transfer with their participation, *J. Photochem.,* 6, 199, 1976/77; (b) Korobov, V.E. and Chibisov, A.K., Primary photoprocesses in colorant molecules (*Usp. Khim.,* 52, 43, 1983), *Russ. Chem. Rev.,* 52, 27, 1983.
3. Kolesnikov, A.M. and Mikhailenko, F.A., The conformations of polymethine dyes (*Usp. Khim.,* 56, 466, 1987), *Russ. Chem. Rev.,* 56, 275, 1987.
4. Ishchenko, A.A., Structure and spectral-luminescent properties of polymethine dyes *(Usp. Khim.,* 60, 1708, 1991*), Russ. Chem. Rev.,* 60, 865, 1991.
5. Mishra, A., Behera, R.K., Behera, P.K., Mishra, B.K., and Behera, G.B., Cyanines during the 1990s: a review, *Chem. Rev.,* 100, 1973, 2000.
6. Dempster, D.N., Morrow, T., Rankin, R., and Thompson, G.F., Photochemical characteristics of cyanine dyes. Part I. 3,3′-Diethyloxadicarbocyanine iodide and 3,3′-diethylthiadicarbocyanine iodide, *J. Chem. Soc., Faraday Trans. II,* 68, 1479, 1972.
7. Dempster, D.N., Morrow, T., Rankin, R., and Thompson, G.F., Photochemical characteristics of the mode-locking dyes 1,1′-diethyl-4,4′-carbocyanine iodide (cryptocyanine, DCI) and 1,1′-diethyl-2,2′-dicarbocyanine iodide (DDI), *Chem. Phys. Lett.,* 18, 488, 1973.
8. Rullière, C., Laser action and photoisomerization of 3′-diethyloxadicarbocyanine iodide (DODCI): influence and temperature and concentration, *Chem. Phys. Lett.,* 43, 303, 1976.
9. Kuzmin, V.A. and Darmanyan, A.P., Study of sterically hindered short-lived isomers of polymethine dyes by laser photolysis, *Chem. Phys. Lett.,* 54, 159, 1978.
10. Sundström, V. and Gillbro, T., Viscosity dependent radiationless relaxation rate of cyanine dyes. A picosecond laser spectroscopy study, *Chem. Phys.,* 61, 257, 1981.
11. Sibbett, W., Taylor, J.R., and Welford, D., Substituent and environmental effects on the picosecond lifetime of the polymethine cyanine dyes, *IEEE J. Quantum Electron.,* 17, 500, 1981.

12. Waldeck, D.H. and Fleming, G.R., Influence of viscosity and temperature on rotational reorientation. Anisotropic absorption studies of 3,3′-diethyloxadicarbocyanine iodide, *J. Phys. Chem.,* 85, 2614, 1981.
13. Sundström, V. and Gillbro, T., Transient absorption spectra of pinacyanol and cyanine photoisomers obtained with a sync-pumped picosecond dye laser and independently tunable probe light, *Chem. Phys. Lett.,* 94, 580, 1983.
14. Åkesson, E., Sundström, V., and Gillbro, T., Isomerization dynamics in solution described by Kramers' theory with a solvent-dependent activation energy, *Chem. Phys.,* 106, 269, 1986.
15. Momicchioli, F., Baraldi, I., and Berthier, G., Theoretical study of *trans-cis* photoisomerism in polymethine cyanines. *Chem. Phys.,* 123, 103, 1988.
16. Herz, A.H., Dye-dye interactions of cyanines in solution and at AgBr surfaces, *Photogr. Sci. Eng*., 18, 323, 1974.
17. Chibisov, A.K., Zakharova, G.V., and Shapiro, B.I., Flash-photolysis study of dye positive holes in spectrally sensitized emulsions, *J. Inf. Recording.,* 22, 313, 1996.
18. Bilmes, G.M., Tocho, J.O., and Braslavsky, S.E., Photophysical processes of polymethine dyes. An absorption, emission, and optoacoustic study on 3,3′-diethylthiadicarbocyanine iodide, *J. Phys. Chem.,* 93, 6696, 1989.
19. Churio, M.S., Angermund, K.P., and Braslavsky, S.E., Combination of laser-induced optoacoustic spectroscopy (LIOAS) and semiemperical calculations for the determination of molecular volume changes: the photoisomerization of carbocyanines, *J. Phys. Chem.,* 98, 1776, 1994.
20. Yang, X., Zaitsev, A., Sauerwein, B., Murphy, S., and Schuster, G.B., Penetrated ion pairs: photochemistry of cyanine dyes within organic borates, *J. Am. Chem. Soc.,* 114, 793, 1992.
21. Murphy, S. and Schuster, G.B., Electronic relaxation in a series of cyanine dyes: evidence for electronic and steric control of the rotational rate, *J. Phys. Chem.,* 99, 8516, 1995.
22. Murphy, S., Sauerwein, B., Drickamer, H.G., and Schuster, G.B., Spectroscopy of cyanine dyes in fluid solution at atmospheric and high pressure: the effect of viscosity on nonradiative processes, *J. Phys. Chem.,* 98, 13476, 1994.
23. Ponterini, G. and Momicchioli, F., *Trans-cis* photoisomerization mechanism of carbocyanines: experimental check of theoretical models, *Chem. Phys.,* 151, 111, 1991.
24. Ponterini, G. and Caselli, M., Photoisomerization dynamics of 3,3′-diethyl oxacarbocyanine. Intramolecular and solvent viscosity effects, *Ber. Bunsenges. Phys. Chem.,* 96, 564, 1992.
25. Krieg, M. and Redmond, R.W., Photophysical properties of 3,3′-dialkylthiacarbocyanine dyes in homogeneous solution, *Photochem. Photobiol.,* 57, 472, 1993.
26. Aramendía, P.F., Negri, R.M., and San Román, E., Temperature dependence of fluorescence and photoisomerization in symmetric carbocyanines. Influence of medium viscosity and molecular structure, *J. Phys. Chem.,* 98, 3165, 1994.
27. Levitus, M., Negri, R.M., and Aramendía, P.F., Rotational relaxation of carbocyanines. Comparative study with the isomerization dynamics, *J. Phys. Chem.,* 99, 14231, 1995.
28. Chibisov, A.K., Zakharova, G.V., Görner, H., Sogulyaev, Y.A., Mushkalo, I.L., and Tolmachev, A.I., Photorelaxation processes in covalently linked indocarbocyanine and thiacarbocyanine dyes, *J. Phys. Chem.,* 99, 886, 1995.
29. Chibisov, A.K., Zakharova, G.V., and Görner, H., Effects of substituents in the polymethine chain on the photoprocesses in indodicarbocyanine dyes, *J. Chem. Soc., Faraday Trans.,* 92, 4917, 1996.
30. Sahyun, M.R.V. and Serpone, N., Photophysics of thiacarbocyanine dyes: relaxation dynamics in a homologous series of thiacarbocyanines, *J. Phys. Chem. A,* 101, 9877, 1997.
31. Bäumler, W. and Penzkofer, A., Fluorescence spectroscopic analysis of N and P isomers of DODCI, *Chem. Phys.,* 140, 75, 1990.
32. Reindl, S. and Penzkofer, A., Higher excited-state photoisomerization and singlet to triplet intersystem-crossing in DODCI, *Chem. Phys.,* 230, 83, 1998.

33. Korppi-Tommola, J.E.I., Hakkarainen, A., Hukka, T., and Subbi, J., An isomerization reaction of a cyanine dye in n-alcohols: microscopic friction and an excited-state barrier crossing, *J. Phys. Chem.,* 95, 8482, 1991.
34. Awad, M.M., McCarthy, P.K., and Blanchard, G.J., Photoisomerization of cyanines. A comparative study of oxygen- and sulfur-containing species, *J. Phys. Chem.*, 98, 1454, 1994.
35. Martini, I. and Hartland, G.V., Ultrafast investigation of vibrational relaxation in the S_1 electronic state of HITC, *J. Phys. Chem.,* 100, 19764, 1996.
36. Tatikolov, A.S., Derevyanko, N.A., Ishchenko, A.A., Baraldi, I., Caselli, M., Momicchioli, F., and Ponterini, G., Photoisomerization of asymmetric indobenzimidazolo cyanine dyes, *Ber. Bunsenges. Phys. Chem.,* 99, 763, 1995.
37. Vaveliuk, P., Scaffardi, L.B., and Duchowicz, R., Kinetic analysis of double photoisomerization of the DTDCI cyanine dye, *J. Phys. Chem.,* 100, 11630, 1996.
38. Rodríguez, J., Scherlis, D., Estrin, D., Aramendía, P.F., and Negri, R.M., AM1 study of the ground and excited state potential energy surfaces of symmetric carbocyanines, *J. Phys. Chem. A,* 101, 6998, 1997.
39. Sundström, V. and Gillbro, T., Excited state dynamics and photophysics of aggregated dye chromophores in solution, *J. Chem. Phys.,* 83, 2733, 1985.
40. Xu, Q.-H. and Fleming, G.R., Isomerization dynamics of 1,1′-diethyl-4,4′-cyanine (1144C) studied by different third-order nonlinear spectroscopic measurements, *J. Phys. Chem. A,* 105, 10187, 2001.
41. Shvedov, S.V. and Chibisov A.K., Conformational isomerism of dicarbocyanine dyes: semiemperical quantum-chemical calculations and kinetic spectroscopy, *Sci. Appl. Photo.,* 42, 521, 2001.
42. Ibrayev, N.K., Ishchenko, A.A., Karamysheva, R.K., and Mushkalo, I.L., Influence of interaction of chromophores, linked by the unconjugated chain, on the luminescence properties of biscyanine dyes, *J. Lumin.,* 90, 81, 2000.
43. Tatikolov, A.S., Shvedova, L.A., Derevyanko, N.A., Ishchenko, A.A., and Kuzmin, V.A., The influence of counterion on photochemistry of cationic indopolycarbocyanine dyes in ion pairs, *Chem. Phys. Lett.,* 190, 291, 1992.
44. Razumova, T.K. and Tarnovskii, A.N., Isomerization processes in the ground and first excited states of 1,1′-diethyl-2,2′-dicarbocyanine iodide (DDI) (*Optika Spektr.,* 78, 65, 1995), *Optics Spectr.,* 78, 56, 1995.
45. Noukakis, D., Van der Auweraer, M., Toppet, S., and De Schryver, F.C., Photophysics of a thiacarbocyanine dye in organic solvents, *J. Phys. Chem.,* 99, 11860, 1995.
46. Vranken, N., Jordens, S., De Belder, G., Lor, M., Rousseau, E., Schweitzer, G., Toppet, S., Van der Auweraer, M., and De Schryver, F.C., The influence of meso-substitution on the photophysical behavior of some thiacarbocyanine dyes in dilute solution, *J. Phys. Chem.,* 105, 10196, 2001.
47. Khimenko, V., Chibisov, A.K., and Görner, H., Effects of alkyl substituents in the polymethine chain on the photoprocesses in thiacarbocyanine dyes, *J. Phys. Chem. A,* 101, 7304, 1997 and references cited therein.
48. Serpone, N. and Sahyun, M.R.V., Photophysics of dithiacarbocyanine dyes: subnanosecond relaxation dynamics of a dithia-2,2′-carbocyanine dye and its 9-methyl-substituted meso analog, *J. Phys. Chem.,* 98, 734, 1994.
49. Soper, S.A. and Mattingly, Q.L., Steady-state and picosecond laser fluorescence studies of nonradiative pathways in tricarbocyanine dyes: implications to the design of near-IR fluorochromes with high fluorescence efficiencies, *J. Am. Chem. Soc.,* 116, 3744, 1994.
50. Chatterjee, S., Davis, P.D., Gottschalk, P., Kurz, M.E., Sauerwein, B., Yang, X., and Schuster, G.B., Photochemistry of carbocyanine alkyltriphenylborate salts: intra-ion-pair electron transfer and the chemsitry of boranyl radicals, *J. Am. Chem. Soc.,* 112, 6329, 1990.

51. Sauerwein, B. and Schuster, G.B., External iodine atoms influence over the intersystem crossing rate of a cyanine iodide ion pair in benzene solution, *J. Phys. Chem.,* 95, 1903, 1991.
52. Tolmachev, A.I., Zaitsev, A.K., Koska, N., and Schuster, G.B., Counter-ion effects in cationic dyes: photophysics and photochemistry of a macrocyclic dimer of dimethylindocarbocyanine, *J. Photochem. Photobiol. A: Chem.,* 77, 237, 1994.
53. Chibisov, A.K., Zakharova, G.V., Shapovalov, V.L., Tolmachev, A.I., Briks, Y.L., and Slominskii, Y.L., Flash photolysis of polymethine dyes with various counterions in nonpolar media (*Khim. Vys. Energ.,* 29, 211, 1995), *High Energy Chem.,* 29, 192, 1995.
54. Mialocq, J.C., Doizi, D., and Gingold, M.P., Picosecond study of an electron transfer in the first excited singlet state of DODCI, *Chem. Phys. Lett.,* 103, 225, 1983.
55. Chen, C., Zhou, B., Lu, D., and Xu, G., Electron transfer events in solutions of cyanine dyes, *J. Photochem. Photobiol. A: Chem.,* 89, 25, 1995.
56. Chibisov, A.K., Shvedov, S.V., and Görner, H., Photosensitized processes in dicarbocyanine dyes induced by energy transfer: delayed fluorescence, *trans→cis* isomerization and electron transfer, *J. Photochem. Photobiol. A: Chem.,* 141, 39, 2001.
57. Baraldi, I., Momicchioli, F., Ponterini, G., Tatikolov, A.S., and Vanossi, D., Exciton-like and charge-transfer states in cyanine-oxonol ion pairs. An experimental and theoretical study, *J. Phys. Chem. A,* 105, 4600, 2001.
58. Aramendía, P.F., Krieg, M., Nitsch, C., Bittersmann, E., and Braslavsky, S.E., The photophysics of merocyanine 540. A comparative study in ethanol and in liposomes, *Photochem. Photobiol.,* 48, 187, 1988.
59. Onganer, Y., Yin, M., Bessire, D.R., and Quitevis, E.L., Dynamical solvation effects on the *cis-trans* isomerization reaction: photoisomerization of merocyanine 540 in polar solvents, *J. Phys. Chem.,* 97, 2344, 1993.
60. Bessire, D.R. and Quitevis, E.L., Effect of temperature and viscosity on rotational diffusion of merocyanine 540 in polar solvents, *J. Phys. Chem.,* 98, 13083, 1994.
61. Redmond, R.W., Srichai, M.B., Bilitz, J.M., Schlomer, D.D., and Krieg, M., Merocyanine dyes: effect of structural modifications on the photophysical properties and biological activity, *Photochem. Photobiol.,* 60, 348, 1994.
62. Benniston, A.C., Gulliya, K.S., and Harriman A., Spin-orbital coupling effects on the photophysical properties and photocytotoxicity of merocyanine dyes, *J. Chem. Soc., Faraday Trans.,* 93, 2491, 1997.
63. Benniston, A.C., Harriman A., and McAvoy, C., Photoisomerization of sterically hindered merocyanine dyes, *J. Chem. Soc., Faraday Trans.,* 93, 3653, 1997.
64. (a) Benniston, A.C., Harriman, A., and McAvoy, C., Effect of resonance polarity on the rate of isomerization of merocyanine dyes, *J. Chem. Soc., Faraday Trans.,* 94, 519, 1998; (b) Mandal, D., Kumar, S., Sukul, D., and Bhattacharyya, K., Photophysical processes of merocyanine 540 in solutions and in organized media, *J. Phys. Chem. A,* 103, 8156, 1999.
65. Redmond, R.W., Kochevar, I.E., Krieg, M., Smith, G., and McGimpsey, W.G., Excited state relaxation in cyanine dyes: a remarkably efficient reverse intersystem crossing from upper triplet levels, *J. Phys. Chem. A,* 101, 2773, 1997.
66. Lu, L., Lachicotte, R.J., Penner, T.L., Perlstein, J., and Whitten, D.G., Exciton and charge-transfer interactions in nonconjugated merocyanine dye dimers: novel solvatochromic behavior for tethered bichromophores and excimers, *J. Am. Chem. Soc.,* 121, 8146, 1999.
67. Ortica, F. and Favaro, G., Environmental effects on radiative and nonradiative transitions of some merocyanine dyes in homogeneous and microheterogeneous systems, *J. Lumin.,* 68, 137, 1996.
68. Yuzhakov, V.I., Aggregation of dye molecules and its influence on the spectral luminescent properties of solutions, (*Usp. Khim., 61*, 1114, 1992), *Russ. Chem. Rev.,* 61, 613, 1992.
69. Shapiro, B.I., Aggregates of cyanine dyes: photographic problems (*Usp. Khim.,* 63, 243, 1994), *Russ. Chem. Rev.,* 63, 231, 1994.

70. Kopainsky, B., Hallermeier, J.K., and Kaiser, W., The first step of aggregation on PIC: the dimerization, *Chem. Phys. Lett.,* 83, 498, 1981.
71. Hayashi, Y., Ogawa, S., Sanada, M., and Hirohashi, R., Spectral sensitization of thermally processed silver film by cyanine dyes, *J. Imag. Sci.,* 33, 124, 1989.
72. Chibisov, A.K., Zakharova, G.V., and Görner, H., Photoprocesses in dimers of thiacarbocyanines, *Phys. Chem. Chem. Phys.,* 1, 1455, 1999 and references cited therein.
73. Chibisov, A.K., Prokhorenko, V.I., and Görner, H., Effects of surfactants on the aggregation behaviour of thiacarbocyanine dyes, *Chem. Phys.,* 250, 47, 1999.
74. Chibisov, A.K., Zakharova, G.V., and Görner, H., Photoprocesses of thiamonomethinecyanine monomers and dimers, *Phys. Chem. Chem. Phys.,* 3, 44, 2001 and references cited therein.
75. Zhang, Z., Hao, J., Wu, B., and Yuan, H., Thermodynamics of a blue-sensitizing cyanine dye in aqueous methanol solution, *J. Imag. Sci. Techn.,* 39, 373, 1995.
76. Stegemeyer, H. and Stöckel, F., Anisotropic structures in aqueous solutions of aggregated pseudoisocyanine dyes, *Ber. Bunsenges. Phys. Chem.,* 100, 9, 1996.
77. Wang, M., Silva, G.L., and Armitage, B.A., DNA-templated formation of a helical cyanine dye J-aggregate, *J. Am. Chem. Soc.,* 122, 9977, 2000.
78. Teuchner, K., Dähne, S., Dresner, J. and Prochorow, J., The anomalous blue fluorescence of pseudoisocyanine dyes, *J. Lumin.,* 23, 413, 1981.
79. Moll, J., Daehne, S., Durrant, J.R., and Wiersma, D.A., Optical dynamics of excitons in J aggregates of a carbocyanine dye, *J. Chem. Phys.,* 102, 6362, 1995.
80. De Rossi, U., Daehne, S., and Reisfeld, R., Photophysical properties of cyanine dyes in sol-gel matrices, *Chem. Phys. Lett.,* 251, 259, 1996.
81. Pawlik, A., Kirstein, S., De Rossi, U., and Daehne, S., Structural conditions for spontaneous generation of optical activity in J-aggregates, *J. Phys. Chem. B,* 101, 5646, 1997.
82. Khairutdinov, R.F. and Serpone, N., Photophysics of cyanine dyes: subnanosecond relaxation dynamics in monomers, dimers, and H- and J- aggregates in solution, *J. Phys. Chem. B,* 101, 2602, 1997.
83. Rotermund, F., Weigand, R., Holzer, W., Wittmann, M., and Penzkofer, A., Fluorescence spectroscopic analysis of indocyanine green J aggregates in water, *J. Photochem. Photobiol. A Chem.,* 110, 75, 1997.
84. (a) West, W., Some recent methods of investigation of spectral sensitivity, in *Dye Sensitization*, H. Berg, W.F., Mazzucato, U., Meier, H., and Semerano, G., Eds., The Focal Press, London, 1970, p. 105; (b) Armitage, B., Retterer, J., and O'Brien, D.F., Dimerization of cyanine dyes in water driven by association with hydophobic borate anions, *J. Am. Chem. Soc.,* 115, 10786, 1993.
85. (a) James, T.H., Ed., *The Theory of the Photographic Processes,* 4th ed., Macmillan, New York, 1977; (b) James, T.H., Chemical sensitization, spectral sensitization, and latent image formation in silver halide photography, *Adv. Photochem.,* 13, 329, 1986 .
86. Matsubara, T. and Tanaka, T., Dimerization and J-aggregation thermodynamics of an anionic oxacarbocyanine dye in solution, *J. Imag. Sci.,* 35, 274, 1991.
87. (a) Pal, S.K., Datta, A., Mandal, D., and Bhattacharyya, K., Photoisomerisation of diethyloxadicarbocyanine iodide in micelles, *Chem. Phys. Lett.,* 288, 793, 1998; (b) Tatikolov, A.S. and Costa, S.M.B., Photophysics and photochemistry of hydrophilic cyanine dyes in normal and reverse micelles, *Photochem. Photobiol. Sci.,* 1, 211, 2002.
88. Pal, M.K. and Ghosh, J.K., Energy transfer and formation of exciplexes between thiacyanine and acrdine orange facilitated by anionic biopolymers and synthetic polymers, *J. Photochem. Photobiol. A: Chem.,* 78, 31, 1994.
89. Katz, J.J., Long wavelength chlorophyll, *Spectrum,* 7, 1, 1994.
90. Miyatake, T., Tamiaki, H., Holzwarth, A.R., and Schaffner, K., Self-assembly of synthetic zinc chlorins in aqueous microheterogeneous media to an artificial supramolecular light-harvesting device, *Helv. Chim. Acta,* 82, 797, 1999.

91. (a) Chibisov, A.K. and Görner, H., Photophysics of aggregated 9-methylthiacarbocyanine bound to polyanions, *Chem. Phys. Lett.,* 357, 434, 2002; (b) Slavnova, T.D., Chibisov, A.K. and Görner, H., Photoprocesses of thiacarbocyanine monomers, dimers, and H-aggregates bound to polyanions, *J. Phys. Chem. A,* 106, 10985, 2002.
92. Zakharova, G.V. and Chibisov, A.K., Effect of poly(methacrylic acid) on photoinduced processes with cyanine dyes in aqueous solutions (*Khim. Vys. Energ.,* 35, 454, 2001), *High Energy Chem.,* 35, 417, 2001.
93. Horng, M.-L. and Quitevis, E.L., Excited-state dynamics of polymer-bound J-aggregates, *J. Phys. Chem.,* 97, 12408, 1993.
94. Jones, G., II and Oh, C., Photophysical and electron-transfer properties of pseudoisocyanine in the hydrophobic microdomain of an aqueous polyelectrolyte, *J. Phys. Chem.,* 98, 2367, 1994.
95. Lui, M., Kira, A., and Nakahara, H., Two-dimentional aggregation of a long-chain thiacarbocyanine dye monolayer on polyanion subphases, *J. Phys. Chem.,* 100, 20138, 1996.
96. Liu, M. and Kira, A., Fabrication of J aggregate films in synthetic polyanion matrix and their chemochromism, *Thin Solid Films,* 359, 104, 2000.
97. Fukumoto, H. and Yonezawa, Y., Layer-by-layer self-assembly of polyelectrolyte and water soluble cyanine dye, *Thin Solid Films,* 327, 748, 1998.
98. Peyratout, C., Donath, E., and Daehne, L., Electrostatic interactions of cationic dyes with negatively charged polyelectrolytes in aqueous solution, *J. Photochem. Photobiol. A: Chem.,* 142, 51, 2001.
99. Flannery, J.B., Jr., The photo- and thermochromic transients from substituted 1′,3′,3′ trimethylindolinobenzospiropyrans, *J. Am. Chem. Soc.,* 90, 5660, 1968.
100. Bercovici, T., Heiligman-Rim, R., and Fischer, E., Photochromism in spiropyrans. Part VI. Trimethylindolino-benzospiropyran and its derivatives, *Mol. Photochem.,* 1, 23, 1969.
101. Bercovici, T., Heiligman-Rim, R., and Fischer, E., Photochromism in spiropyrans. Part VIII. Photochromism in acidified solutions, *Mol. Photochem.,* 1, 189, 1969.
102. Kholmanskii, A.S. and Dyumaev, K.M., The photochemistry and photophysics of spiropyrans (*Usp. Khim.,* 56, 241, 1987), *Russ. Chem. Rev.,* 56, 136, 1987.
103. Bertelson, R.C., Photochromic processes involving heterolytic cleavage, in *Techniques in Chemistry, Vol. 3, Photochromism*, Brown, G.H., Ed., Wiley-Interscience, New York, 1971, p. 45.
104. Guglielmetti, R., 4n+2 Systems: spiropyrans in *Studies in Organic Chemistry, Vol. 40, Photochromism — Molecules and Systems,* Dürr, H. and Bouas-Laurent, H., Eds., Elsevier, Amsterdam, 1990, p. 314.
105. Crano, J.C. and Guglielmetti, R., Eds., *Organic Photochromic and Thermochromic Compounds,* Vol. 1 and 2, Plenum Press, New York, 1999.
106. Crano, J.C., Flood, T., Knowles, D., Kumar, A., and Van Gemert, B., Photochromic compounds: chemistry and application in ophthalmic lenses, *Pure Appl. Chem.,* 68, 1395, 1996.
107. (a) Berkovic, G., Krongauz, V., and Weiss, V., Spiropyrans and spirooxazines for memories and switches, *Chem. Rev.,* 100, 1741, 2000; (b) Raymo, M.F. and Giordani, S., Signal processing at the molecular level, *J. Am. Chem. Soc.,* 123, 4651, 2001.
108. Willner, I. and Willner, B., Molecular and bimolecular optoelectronics, *Pure Appl. Chem.,* 73, 535, 2001.
109. (a) Görner, H., Atabekyan, L.S., and Chibisov, A.K., Photoprocesses in spiropyran-derived merocyanines: singlet versus triplet pathway, *Chem. Phys. Lett.,* 260, 59, 1996; (b) Chibisov, A.K. and Görner, H., Singlet versus triplet photoprocesses in indodicarbocyanine dyes and spiropyran-derived merocyanines, *J. Photochem. Photobiol. A: Chem.,* 105, 261, 1997.
110. Chibisov, A.K. and Görner, H., Photoprocesses in spiropyran-derived merocyanines, *J. Phys. Chem. A,* 101, 4305, 1997.
111. Görner, H., Photoprocesses in spiropyrans and their merocyanine isomers: effects of temperature and viscosity, *Chem. Phys.,* 222, 315, 1997.

112. Görner, H., Photochemical ring opening in nitrospiropyrans: triplet pathway and the role of singlet molecular oxygen, *Chem. Phys. Lett.,* 282, 381 (cf. 288, 589), 1998.
113. Görner, H., Photochromism of nitrospiropyrans: effects of structure, solvent and temperature, *Phys. Chem. Chem. Phys.,* 3, 416, 2001.
114. Chibisov, A.K. and Görner, H., Photochromism of spirobenzopyranindolines and spironaphthopyranindolines, *Phys. Chem. Chem. Phys.,* 3, 424, 2001.
115. Krysanov, S.A. and Alfimov, M.V., Picosecond flash photolysis of photochromic spiropyrans, *Laser Chem.,* 4, 129, 1984.
116. (a) Ernsting, N.P., Dick, B., and Arthen-Engeland, T., The primary photochemical reaction step of unsubstituted indolino-spiropyrans, *Pure. Appl. Chem.,* 62, 1483, 1990; (b) Ernsting, N.P. and Arthen-Engeland, T., Photochemical ring-opening reaction of indolinospiropyrans studied by subpicosecond transient absorption, *J. Phys. Chem.,* 95, 5502, 1991.
117. Alfimov, M.V., Balakin, A.V., Gromov, S.P., Zaushitsyn, Yu.V., Fedorova, O.A., Koroteev, N.I., Pakulev, A.V., Resnyanskii, A. Y., and Shkurinov, A.P., Femtosecond spectrochronography of the reverse photochromic transition in derivatives of spiro compounds, (*Zh. Fiz. Khim.,* 73, 1871, 1999), *Russ. J. Phys. Chem.,* 73, 1685, 1999.
118. Appriou, P., Guglielmetti, R. and Garnier, F., Ètude du processus photochimique impliqué dans la réaction d'ouverture du cycle benzopyrannique des spiropyrannes photochromiques, *J. Photochem.,* 8, 145, 1978.
119. Drummond, C.J. and Furlog, D.N., Photochromism of a surface-active spirobenzopyran moiety in dioxane-water mixtures and self-assembled surfactant aggregates, *J. Chem. Soc., Faraday Trans.,* 86, 3613, 1990.
120. Tamaki, T., Sakuragi, M., Ichimura, K., and Aoki, K., Laser photolysis studies of nitrospiropyrans intramolecularly linked with a triplet quenching or sensitizing side group, *Chem. Phys. Lett.,* 161, 23, 1989.
121. Sakuragi, M., Aoki, K., Tamaki, T., and Ichimura, K., The role of triplet state of nitrospiropyran in their photochromic reaction, *Bull. Chem. Soc. Jpn.,* 63, 74, 1990.
122. (a) Pimienta, V., Lavabre, D., Levy, G., Samat, A., Guglielmetti, R., and Micheau, J.C., Kinetic analysis of photochromic systems under continuous irradiation. Application to spiropyrans, *J. Phys. Chem.,* 100, 4485, 1996; (b) Wetzler, D.E., Aramendía, P.F., Japas, M.L., and Fernández-Prini, R., Spectroscopy and thermal decay of a photomerocyanine in mixtures of polar and non-polar solvents, *Phys. Chem. Chem. Phys.,* 1, 4955, 1999.
123. Levitus, M., Talhavini, M., Negri, R.M., Atvars, T.D.Z., and Aramendía, P.F., Novel kinetic model in amorphous polymers. Spiropyran-merocyanine system revisited, *J. Phys. Chem. B.,* 101, 7680, 1997.
124. (a) Keum, S.-R.. Hur, M.-S., Kazmaier, P.M., and Buncel, E., *Can. J. Chem.,* 69, 1940, 1999; (b) Kieswetter, R., Pustet, N., Brandl, F., and Mannschreck, A., *Tetrahedron Asymm.,* 10, 4677, 1999; (c) Woityk, J.T., Wasey, A., Kazmaier, P., Hoz, S., and Buncel, E., Thermal reversion mechanism of N-functionalized merocyanines in spiropyrans: a solvatochromic, solvatokinetic, and semiempirical study, *J. Phys. Chem. A,* 104, 9046, 2000; (d) Raymo, F.M. and Giodani, S., Signal processing at molecular level, *J. Am. Chem. Soc.,* 123, 4651, 2001 .
125. Li, Y., Zhou, J., Wang, Y., Zhang, F., and Song, X., Reinvestigation on the photoinduced aggregation behavior of photochromic spiropyrans in cyclohexane, *J. Photochem. Photobiol. A: Chem.,* 113, 65, 1998.
126. Williams, R.M., Klihm, G., and Braslavsky, S.E., Time-resolved thermodynamic profile upon photoexcitation of a nitrospiropyran in cycloalkanes and of thecorresponding merocyanine in aqueous solutions, *Helv. Chim. Acta,* 84, 2557, 2001.
127. Schomburg, C., Wark, M., Rohlfing, Y., Schulz-Ekloff, G., and Wöhrle, D., Photochromism of spiropyran in molecular sieve voids: effects of host-guest interaction on isomer status, switching stability and reversibility, *J. Mater. Chem.,* 11, 2014, 2001.

128. Celani, P., Bernardi, F., Olivucci, M., and Robb, M.A., Conical intersection mechanism for photochemical ring opening in benzospiropyran compounds, *J. Am. Chem. Soc.,* 119, 10815, 1997.
129. Abe, Y., Nakao, R., Horii, T., Okada, S., and Irie, M., MNDO-PM3 MO studies on the thermal isomerization of photochromic 1′,3′,3′-trimethyl-6-nitrospiro[2H-1-benzopyran-2,2′-indoline], *J. Photochem. Photobiol. A: Chem.,* 95, 209, 1996.
130. Cottone, G., Noto, R., La Manna, G., and Fornili, S.L., *Ab initio* study on the photoisomers of a nitro-substituted spiropyran, *Chem. Phys. Lett.,* 319, 51, 2000.
131. Horie, K., Hirao, K., Mita, I., Takubo, Y., Okamoto, T., Washio, W., Tagawa, S., and Tabata, Y., Red fluorescence from the merocyanine form of spirobenzopyran, *Chem. Phys. Lett.,* 119, 499, 1985.
132. Lee, S.-K., Valdes-Aguilera, O., and Neckers, D.C., A low temperature luminescence study of the colored merocyanine form of substituted 6-nitrobenzospiropyrans, *J. Photochem. Photobiol. A: Chem.,* 67, 319, 1992.
133. Görner, H. and Chibisov, A.K., Complexes of spiropyran-derived merocyanines with metal ions: thermally activated and light-induced processes, *J. Chem. Soc., Faraday Trans.,* 94, 2557, 1998.
134. Chibisov, A.K. and Görner, H., Complexes of spiropyran-derived merocyanines with metal ions: relaxation kinetics, photochemistry and solvent effects, *Chem. Phys.,* 237, 425, 1998.
135. Winkler, J. D., Bowen, C.M., and Michelet, V., Photodynamic fluorescent metal ion sensors with parts per billion sensitivity, *J. Am. Chem. Soc.,* 120, 3237, 1998.
136. Zhou, J.-W., Li, Y.-T., and Song, X.-Q., Investigation of the chelation of a photochromic spiropyran with Cu(II), *J. Photochem. Photobiol. A: Chem.,* 87, 37, 1995.
137. Zhou, J., Zhao, F., Li, Y., Zang, F., and Song, X., Novel chelation of photochromic spironaphthoxazines to divalent metal ions, *J. Photochem. Photobiol. A: Chem.,* 92,193, 1995.
138. Filley, J., Ibrahim, M.A., Nimlos, M.R., Watt, A.S., and Blake, D.M., Magnesium and calcium chelation by a bis-spiropyran, *J. Photochem. Photobiol. A: Chem.,* 117, 193, 1998.
139. Chu, N.Y.C., Photochromism of spiroindolinonaphthoxazine. I. Photochemical properties, *Can. J. Chem.,* 61, 300, 1983.
140. Schneider, S., Investigation of the photochromic effect of spiro[indolino-naphthoxazine] derivatives by time-resolved spectroscopy, *Z. Phys. Chem. N. F.,* 154, 91, 1987.
141. Pottier, E., Dubest, R., Guglielmetti, R., Tardieu, P., Kellmann, A., Tfibel, F., Levoir, P., and Aubard, J., Effets de substituent, d'hétéroatome et de solvant sur les cinétiques de décolororation thermique et les spectres d'absorption de photomérocyanines en série spiro[indoline-oxazine], *Helv. Chim. Acta,* 73, 303, 1990.
142. Bohne, C., Fan, M.G., Li, Z.J., Liang, Y.C., Lusztyk, J., and Scaiano, J.C., Laser photolysis studies of photochromic processes in spirooxazines: solvent effects on photomerocyanine behavior, *J. Photochem. Photobiol. A: Chem.,* 66, 79, 1992.
143. Favaro, G., Masetti, F., Mazzucato, U., Ottavi, G., Allegrini, P., and Malatesta, V., Photochromism, thermochromism and solvatochromism of some spiro[indolinoxazine]-photomerocyanine systems: effects of structure and solvent, *J. Chem. Soc., Faraday Trans.,* 90, 333, 1994.
144. Favaro, G., Malatesta, V., Mazzucato, U., Ottavi, G., and Romani, A., Thermally reversible photoconversion of spiroindoline-naphthooxazines to photomerocyanines: a photochemical and kinetic study, *J. Photochem. Photobiol. A Chem.,* 87, 235, 1995.
145. (a) Wilkinson, F., Hobley, J., and Naftaly, M., Photochromism of spiro-naphthoxazines: molar absoption coefficients and quantum efficiencies, *J. Chem. Soc., Faraday Trans.,* 88, 1511, 1992; (b) Hobley, J. and Wilkinson, F., Photochromism of naphthoxazine-spiro-indolines by direct excitation and following sensitisation by triplet-energy donors, *J. Chem. Soc., Faraday Trans.,* 92, 1323, 1996.
146. Chibisov, A.K. and Görner, H., Photoprocesses in spirooxazines and their merocyanines, *J. Phys. Chem. A,* 103, 5211, 1999.

147. Nakamura, S., Uchida, K., Murakami, A., and Irie, M., *Ab initio* MO and ^{1}H NMR NOE studies of photochromic spironaphthoxazine, *J. Org. Chem.,* 58, 5543, 1993.
148. Malatesta, V., Neri, C., Wis, M.L., Montanari, L., and Millini, R., Thermal and photodegradation of photochromic spiroindolinenaphthooxazines and -pyrans: reaction with nucleophiles. Trapping of the merocyanine zwitterionic form, *J. Am. Chem. Soc.,* 119, 3451, 1997.
149. Horii, T., Abe, Y., and Nakao, R., Theoretical quantum chemical study of spironaphthoxazines and their merocyanines. Thermal ring-opening reaction and geometrical isomerization, *J. Photochem. Photobiol. A: Chem.,* 144, 119, 2001.
150. (a) Wilkinson, F., Worrall, D.R., Hobley, J., Jansen, L., Williams, S.L., Langley, A.J., and Matousek, P., Picosecond time-resolved spectroscopy of the photocolouration reaction of photochromic naphthoxazine-spiro-indolines, *J. Chem. Soc., Faraday Trans.,* 92, 1331, 1996; (b) Hobley, J., Malatesta, V., Hatanaka, K., Kajimoto, S., Williams, S.L., and Fukumura, H., Picosecond and nanosecond photo-dynamics of a naphthopyran merocyanine, *Phys. Chem. Chem. Phys.,* 4, 180, 2002.
151. Suzuki, M., Asahi, T., and Masuhara, H., Photochromic reactions of crystalline spiropyrans and spirooxazines induced by intense femtosecond laser excitation, *Phys. Chem. Chem. Phys.,* 4, 185, 2002.

37

Photochemical Aromatic Substitution

Canan Karapire
Ege University

Siddik Icli
Ege University

37.1 Introduction and Mechanism

The photochemical aromatic substitution reactions described within this article are mainly devoted to homocyclic aromatic compounds. The work described is focused on the mechanism of the various reactions described. An outstanding mechanistic feature of photochemical aromatic substitution is that, in contrast to thermal reactions, photochemical substitutions take place by nucleophilic paths.[1,2] There are numerous examples of photonucleophilic aromatic substitutions in the literature.[3] The aromatic nucleus is electron rich; therefore, electrophilic aromatic substitution is dominant in thermal reactions via the formation of an arenium σ-complex intermediate. Electrophilic aromatic substitution reactions are governed by thermodynamic factors rather than kinetic factors in ground-state chemistry, whereas the energetic nature of the photo-excited state of aromatic molecules brings about the different reaction paths seen in photochemical substitution reactions. Epiotis and Shaik[4] have shown that the regiochemistry of electrophilic and photonucleophilic substitution is controlled by the electron density of the highest occupied MO (molecular orbital) of the aromatic substrate, and the regiochemistry of nucleophilic and photoelectrophilic aromatic substitutions is controlled by the electron density of the lowest unoccupied MO of the aromatic substrate.[4] An electron is raised from the ground state HOMO to an excited state LUMO. This creates a susceptibility to nucleophilic attack on the half-filled HOMO level, and the electron in the half-filled LUMO level can undergo attack at an electrophile (Scheme 1).

Photosubstitution may proceed by direct attack of the nucleophile on the triplet (or singlet) excited state of the aromatic molecule with the formation of a σ-complex, S_N2Ar^* (Scheme 2).

Kuzmič and Souček proposed that the differences in the position of the photonucleophilic substitution of a methoxy group in 3,4-dimethoxybenzene and 3,4-dimethoxyacetophenone by cyano or hydroxide anion is due to the fact that the cyanide anion interacts with the singlet excited state of the aromatic ring (shown from fluorescence quenching studies) whereas hydroxyl anion does not.[5] Further evidence regarding the mechanism of photonucleophilic substitution is obtained from the fact that the reaction of 4,5-dinitroveratrole with amines also brings about photoreduction. This is the result of an electron transfer from the amine to the triplet state excited aromatic ring.[6–9]

Marquet et al. confirmed that differing photoreactivity is dependent on the excited state (singlet or triplet) involved. Thus, the photosubstitution of 4-nitroveratrole takes place through a singlet $S_N2^1Ar^*$ mechanism by elimination of a methoxy group, whereas 4,5-di-nitroanisole involves the triplet $S_N2^3Ar^*$ mechanism. This brings about the elimination of a nitro group in the presence of the amines as the

0-8493-1348-1/04/$0.00+$1.50

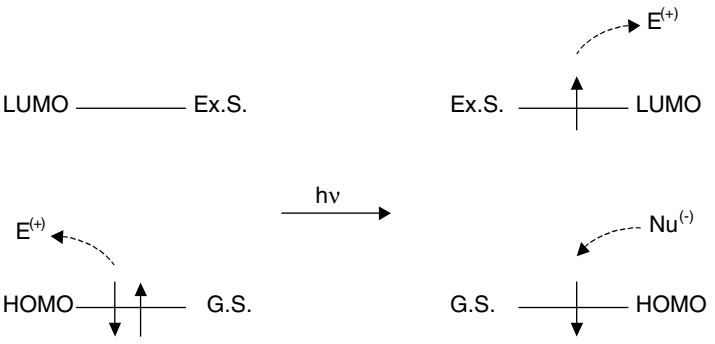

SCHEME 1

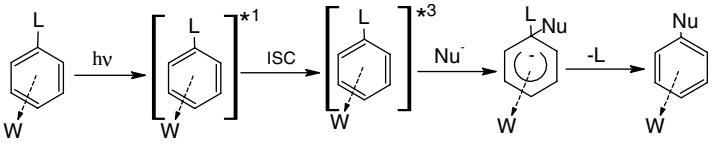

SCHEME 2

nucleophiles.[10] Marquet and co-workers have also compared the photochemistry of 4-nitroveratrole and 2-fluoro-4-anisole in polar solvents with nucleophiles such as cresol, sulfides, amines, and carboxylic acids. The reaction was also studied in aqueous methanol containing pancreatic bovine ribonuclease A. This particular study was designed to examine the applicability of nucleophilic aromatic substitution, S_N2Ar^*, as a method for labelling an enzyme. This would make use of nucleophilic centers within the peptide chain.[11] The nucleophilic aromatic substitution of 3-nitroanisole, 4-nitroanisole, and 4-nitroveratrole in the presence of phenethylamine was investigated in aqueous solution and in the solid state in a β-cyclodextrin complex.[12] In an aqueous solution of 4-nitroveratrole, the major product is 2-methoxy-5-nitrophenol, which arises from regioselective substitution of a methoxyl group. However, in the confined environment of β-cyclodextrin with phenethylamine as the nucleophile, the only product was identified as 4-nitrosoveratrole.

Bonilha et al. have studied the photonucleophilic substitution reaction between nitroaryl–alkyl ethers and hydroxide anions in water. The investigations of the quenching of nitroaryl ethers by anions led to the conclusion that the mechanism is a direct displacement within the triplet state, $S_N2^3Ar^*$.[13] Arnold and Snow [14] showed that in the photonucleophilic S_N2Ar^* aromatic substitution reaction, dicyanobenzene and a methanol–olefin combination are more efficient in the presence of an electron donor photosensitizer. Photochemical nucleophilic substitution with acenaphthylene and dicyanonaphthalene is found to be more complicated than with dicyanobenzene and tetracyanobenzene. In this system, photoelectron-transfer from a singlet exciplex resulted in the formation of numerous products.[15] Boggeri et al. have shown that aromatic nitriles can undergo photochemical nucleophilic substitution with acenaphthylene via electron-transfer in the singlet exciplex. This is evidence for the operation of a S_N2Ar^* mechanism.[16]

In the S_N1Ar^* mechanism, which is found in rare cases, a strong electron withdrawing group leaves the triplet excited state to form the cation of the aromatic moiety, This is followed by the addition of a nucleophile (Scheme 3). Havinga and Cornelisse and Spillane have recognized, in the photosubstitution of 2-nitrofurane with cyanide and water nucleophiles, that the quantum yield for the reaction is independent of the concentration of the nucleophile; a photodissociation (photoionization) to give an ion pair has been suggested.[17,18]

The photoionization of excited aromatic molecules would lead to $S_{RN}1Ar^*$ mechanisms by an electron-transfer from the nucleophile to the excited aromatic substrate with formation of the radical-anion

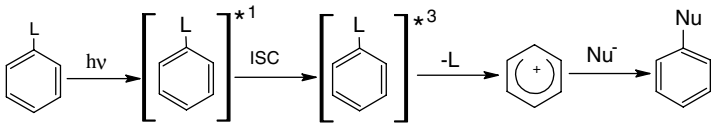

SCHEME 3

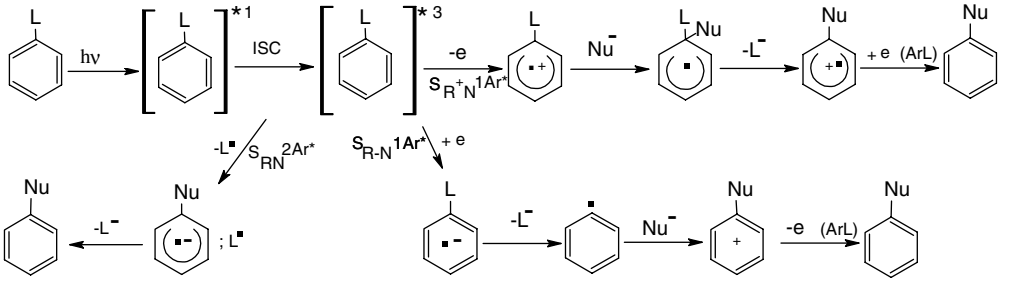

SCHEME 4

intermediate, $S_R{-}_N1Ar^*$, or by an electron-transfer from the excited aromatic substrate to an appropriate electron acceptor. This would be followed by the attack of the nucleophile on the resultant aromatic-cation, $S_R{+}_N1Ar^*$.[19] The radical cation intermediate within the $S_R{+}_N1Ar^*$ mechanism is formed only when an electron donating group is present on the aromatic substrate (Scheme 4). This $S_{RN}1Ar^*$ type of reaction was first reported by Kim and Bunnet[20] in the nucleophilic substitution of phenyl iodide by potassium iodide. The reactions of aryl halides with phosphonate anion,[21] carbanions,[22] aryl amides,[23] and phenoxide anions[24] have been studied extensively.[25] Photoreduction and nucleophilic photosubstitution of 4-bromonitrobenzene have been proven to be catalyzed by HCl in aqueous propanol solutions and involve radical intermediates.[26] The formation of a bimolecular exciplex via electron transfer from chloride anion to the $^3(n\text{-}\pi)^*$ state, following the protonation of the exciplex, proceeds by the $S_{RN}1Ar^*$ mechanism.

Photonucleophilic aromatic substitution reactions of phenyl selenide and telluride with haloarenes have also been proven to involve the $S_{RN}1Ar^*$ mechanism, with the formation of anion radical intermediates.[27] Another photonucleophilic substitution, cyanomethylation, proves the presence of radical cations in the reaction mechanism.[28] Liu and Weiss have reported that hydroxy and cyano substitution competes with photo substitution of fluorinated anisoles in aqueous solutions, where cation and anion radical intermediates have been shown to be the key factors for the nucleophilic substitution type.[29] Rossi et al. have proposed the $S_{RN}1Ar^*$ mechanism for photonucleophilic substitution of carbanions and naphthoxides to halo anisoles and 1-iodonaphthalene.[30,31] An anion radical intermediate photonucleophilic substitution mechanism has been shown for the reactions of triphenyl(methyl)stannyl anion with halo arenes in liquid ammonia.[32] Trimethylstannyl anion has been found to be more reactive than triphenylstannyl anion in the photostimulated electron- transfer initiation step.

37.2 Recent Studies on Photochemical Aromatic Substitutions

S_N2Ar^* Reactions

Photocyanation of deuterium-labelled 1-nitronaphthalenes with cyanide nucleophile has been proven to involve primarily an ipso attack followed by isomerizations.[33] The reaction of nucleophiles with halogenated aromatics proceeds via attack of the nucleophile on the nitroarene, generating an anionic σ-complex. This is followed by departure of the leaving group and rearomatization. Cervera et al. and Huertas et al. have shown a direct coupling of carbon nucleophiles with *m*-dinitrobenzene via fluoride promoted nucleophilic aromatic substitution (Scheme 5).[34,35] Amines, amides, ethyl acetate, acetonitrile, and acetone

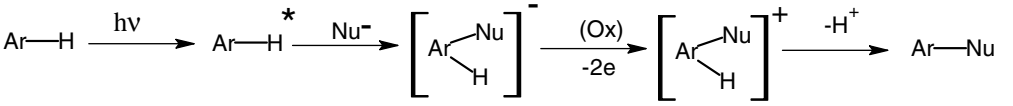

SCHEME 5

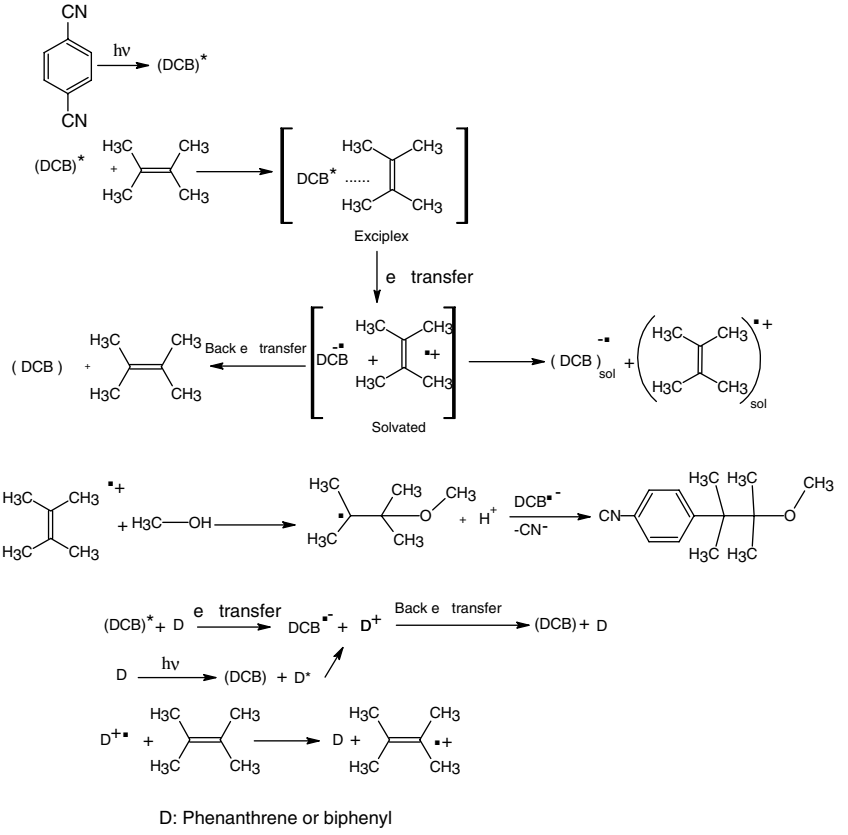

SCHEME 6

were used as nucleophiles to bring about regioselective nucleophilic substitution in the presence of *m*-dinitrobenzene and tetrabutylammonium fluoride in THF or DMF solutions.

The photo-NOCAS reaction was first described by McMahon and Arnold[15] and is a photonucleophilic S_N2Ar^* aromatic substitution between dicyanobenzene and an olefin in the presence of electron donor photosensitizers (phenanthrene or biphenyl) in acetonitrile–methanol solutions. This reaction system has been researched extensively in recent times. As shown in Scheme 6, the single electron transfer from olefin to photo-excited electron-deficient dicyanobenzene forms the cation radical of the olefin, which initiates a quenching reaction with nucleophile solvent methanol molecules and forms the methoxyalkyl radical. Addition of an electron transfer photosensitizer (phenanthrene or biphenyl) to the reaction mixture increases the efficiency of the reaction simply by absorbing more light. The excited state of the photosensitizer donates an electron to dicyanobenzene to give the photosensitizer radical cation and dicyanobenzene radical anion. The photosensitizer radical cation then oxidizes the olefin.

The reaction system discussed above was applied to optically pure α-pinene, β-pinene, tricyclene, and nopol.[36] 4-Cyanophenyl and/or methoxy substituted derivatives in optically pure or racemic mixture forms were isolated as products. Nucleophile-assisted cleavage of the radical cation has been proposed

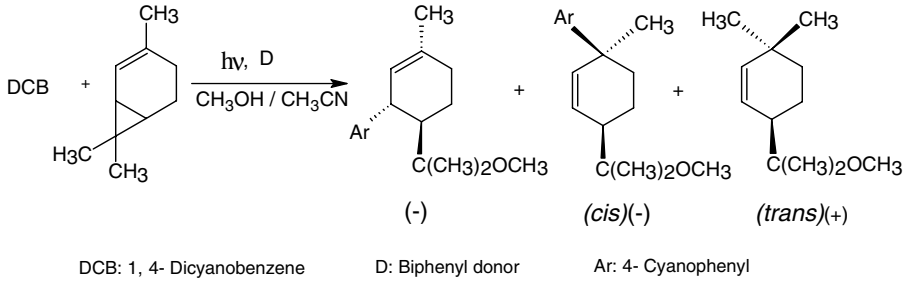

SCHEME 7

as the mechanism for the nucleophilic selectivity and the regio- and stereochemistry of the adducts. 1,5-Hexadiene and 2-methyl-1,5-hexadiene olefins also react with 1,4-dicyanobenzene under the same reaction conditions illustrated in Scheme 6. The photo-NOCAS products were also formed using 2-methyl-1,5-hexadiene as the alkene component. However, 1,5-hexadiene gave only *ortho* and *meta* cyclic adducts, and no photo-NOCAS products were found.[37] This result can be explained on the basis of the high oxidation potential of 1,5-hexadiene (>3 V vs. SCE), which precludes the single electron transfer from olefin to the 1,4-dicyanobenzene. The conjugated dienes, 1,3-butadiene, 2-methyl-1,3-butadiene, 2,3-dimethyl-1,3-butadiene, and 2,5-dimethyl-2,4-hexadiene, do not suffer this problem and yielded the regio- and stereoselective aryl and methoxy adduct products of the photo-NOCAS process.[38] High yields (80%) of the usual products were obtained with (+)-2-carene under the usual conditions (Scheme 7).[39] The oxidation potential of the (+)-2-carene was determined to be low, 1.39 V vs. SCE, and the calculated free energy change (ΔG_{ET} = –119.5 kJ mol^{-1}) for the electron transfer to the singlet excited state of dicyanobenzene was highest compared to the oxidation potentials and free energy change values of α-pinene, β-pinene, and 1-methylcyclohexene, respectively. The outcome of the reaction is illustrated in Scheme 7.

The photo-NOCAS reaction with 2,6-dimethyl-1,6-heptadiene gave two major cyclic aryl–methoxy adducts (a cyclohexane and a cycloheptane) as well as an acyclic heptene adduct.[40] Variation in concentration of the nucleophile, methanol, and co-donor, biphenyl, has been shown to affect the product ratios. Further applications of the photo-NOCAS S_N2Ar^* reactions with the alkyl-4-enols, α-terpineol, limonene, 2-methyl-2-butene, 2,3-dimethyl-2-butene, β-myrcene, and 1,4-bis (methylene) cyclohexene have been reported.[41–48] The aryl–methoxy adduct product ratios have been investigated and discussed in terms of the stability of radical intermediates and the factors controlling the regiochemistry of reaction with the nucleophiles alcohols, cyanide, and fluoride; attempts to justify the results by *ab initio* molecular orbital calculations have been made. The photo-NOCAS reaction with 2-methylpropene in the absence of methanol and a donor molecule has shown that solvent acetonitrile can act as a nucleophile. Under these conditions a tetrahydroisoquinoline product is formed, prior to HCN elimination, in high yield as illustrated in Scheme 8.[49] The adduct product formation was rationalized on the basis of the relatively high oxidation potential of the olefin.

Tetrahydroisoquinoline formation was reported earlier by Vanossi et al. following the S_N2Ar^* reaction of 1,2,4,5-tetracyanobenzene and 1-hexene in acetonitrile.[50] Photo-NOCAS mechanistic pathways were also operative when 1,4-dicyanobenzene was replaced with 1,2,4,5-tetracyanobenzene, 4-halobenzonitriles, 4-haloanisoles, and 1,4-dicyanonaphthalene as the electron acceptors.[51,52] A singlet excited state electron transfer reaction leading to nucleophilic aromatic substitution has been reported by Torriani et al. in the photolysis of 1,4-dicyanobenzene and 2,3-dimethyl-2-butene in the presence of CH_3OH, H_2O, and CF_3CH_2OH as the nucleophiles. These reactions gave adducts analogous to the previous examples discussed.[53] The quantum yields are in the range of 0.006–0.020 and reach the upper limit only in the presence of nucleophiles.

When nucleophilic aromatic substitution reactions of the S_N2Ar^* type are carried out in a protic solvent (i.e., water), the oxygen effect is neglected. Marquet has proven that aromatic radical anion intermediates

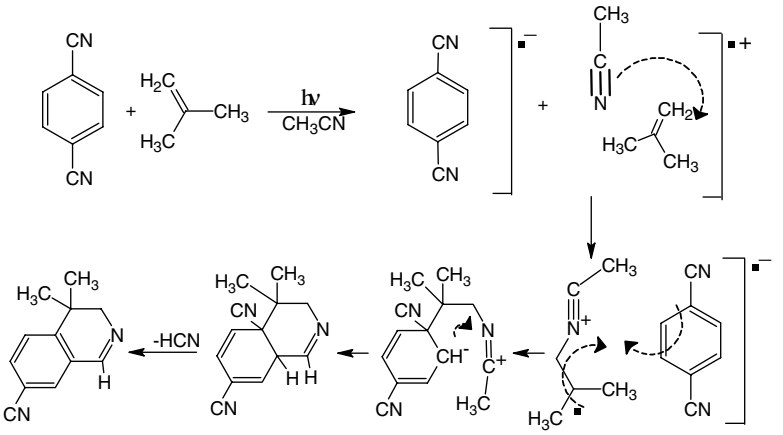

SCHEME 8

can form reactive superoxide anion radical via electron transfer, which then can form cyanide anion from acetonitrile and ethoxide anion from ethyl acetate. Hence it is proposed that the presence of oxygen in polar aprotic solvents should be avoided in nucleophilic aromatic photosubstitution reactions.[54]

Tedesco et al. have reported the nucleophilic aromatic substitution reactions of nitroaryl ethers with sodium hydroxide in aqueous solution contained in cationic micelles.[55] Quantum yields of the reactions were found to be dependent on the length of the *n*-alkyl chain of micelle (maximum for methyl, minimum for decyl). The dependence on surfactant concentration was in accord with the mechanistic model for aromatic nucleophilic photosubstitution. Intramolecular photoreactions were investigated with the bichromophoric *p*-nitroarylethers, $p\text{-}O_2NC_6H_4O(CH_2)_nNHC_6H_5$.[56] The lower homologues ($n \leq 6$) are found to undergo aromatic photochemical nucleophilic substitution of the S_N2Ar^*, which can be classified as a Smiles-type rearrangement. When the chain is sufficiently long ($n \geq 8$, i.e., $p\text{-}O_2NC_6H_4O(CH_2)_8NHC_6H_5$), the photorearrangement and the nucleophilic substitution are forbidden; instead, a photoredox reaction (reduction of nitro to nitroso and the oxidation of nitrogen bonded methylene to aldehyde) and the cleavage of the aniline molecule take place. Nakagaki and Mutai[56] have proposed that the photoredox reactions are the only accessible reaction processes for the higher homologues. The magnetic field effects on the end product distribution are due to changes in the intersystem crossings rate induced by hyperfine interaction within biradical intermediates.

$S_{RN}1Ar^*$ Reactions

Galli et al. have reported the calculation of the LUMO energy of the substitution product of the aromatic $S_{RN}1Ar^*$ reaction.[57] It is suggested that $S_{RN}1Ar^*$ reactivity can be predicted for structurally homogeneous compounds by calculation of the LUMO energy of the substituted product in relation to the MO energy of the aromatic radical anion intermediate. The photohydrolysis quantum yields were analyzed by the partial least square method, and it is predicted that the photohydrolysis quantum yields of substituted aromatic halides are dependent on the characters of the CX bonds being broken and the character of the halogen bonds to be replaced during photolysis.[58]

Almost quantitative radical nucleophilic aromatic substitution reactions were reported by Córsico and Rossi from the reaction of nucleophile trimethylstannyl ions with mono-, di- and trichloro-substituted aromatic substrates in liquid ammonia.[59] The chain process shown in Scheme 9 requires an initiation step, and it can be either light induced or be a spontaneous electron transfer from the nucleophile to the aromatic substrate.

Chen and Li have studied the photoinduced electron transfer reactions of perfluoroalkyl iodides both with a variety of nucleophiles and with electron-rich aromatic compounds.[60,61] A photoinduced electron

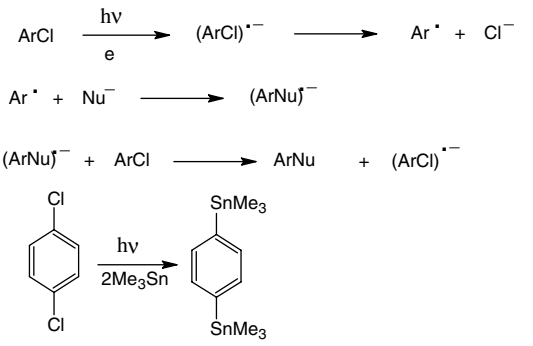

SCHEME 9

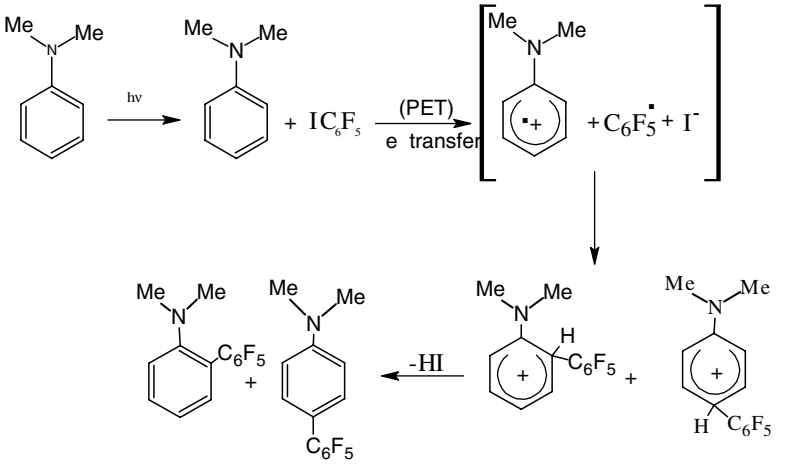

SCHEME 10

transfer (PET) mechanism was proposed for the photochemical reactivity of pentafluoroiodobenzene with anilines, pyrroles, indoles, aromatic ethers, and phenols (Scheme 10).[62]

Photobromination of naphthalene using molecular bromine gives tetrabromo-tetrahydronaphthalene as the only stereoisomer. This reaction is followed by dehydrobromination to give 1,3-dibromonaphthalene in high yield.[63] In a recent study by Mangion et al., the reaction of 1-methoxynaphthalene, 1,8-dimethoxynaphthalene, or 1,4-dimethoxynaphthalene with acrylonitrile in acetonitrile and methanol was found to have a distinct $S_R+_N1Ar^*$ mechanistic pathway. This has been called a photochemical electrophile-olefin combination, aromatic substitution abbreviated to a photo-EOCAS reaction.[64] The methoxynaphthalene forms a radical cation intermediate by the photoinduced electron transfer. This couples with the acrylonitrile radical (Scheme 11). The $S_R+_N1Ar^*$ reaction mode has been proposed to account for the nucleophilic photosubstitution of 1,4-dicyanobenzene with isobutylene in acetonitrile/methanol solutions.[65] A similar but reverse $S_R-_N1Ar^*$ reaction path, was suggested by Vanossi et al. for photoreactions of 1,2,4,5-benzenetetracarbonitrile with 1-hexene in acetonitrile.[66] The formation of aromatic anion radicals and allyl cation radicals were suggested,m and the allyl cation radical is trapped by methanol.

Nucleophilic aromatic photosubstitution reactions of furans and thiophenes substituted with iodo or bromo and electron withdrawing groups in the presence of aromatic compounds have been studied extensively.[67–71] The aryl nucleophilic substitution reaction mechanism of these compounds is illustrated in Scheme 12.

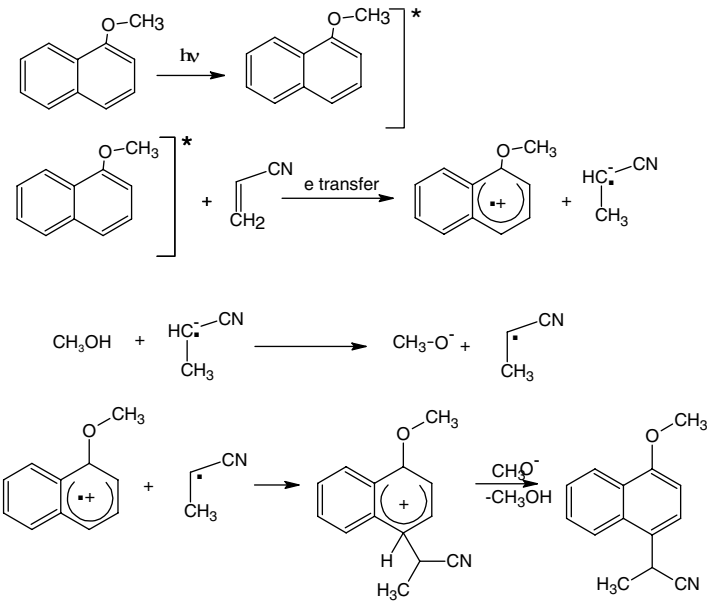

SCHEME 11

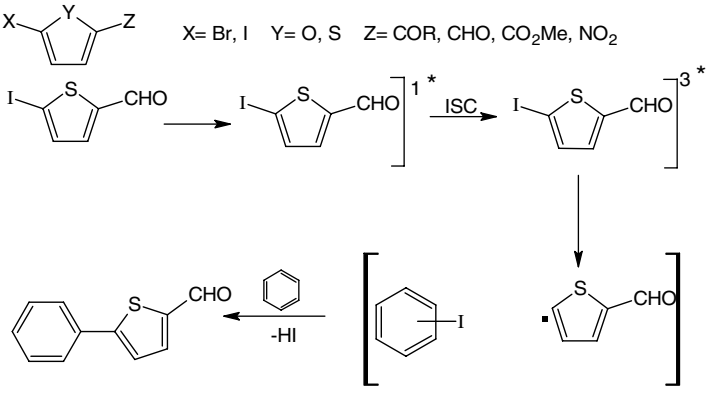

SCHEME 12

D'Auria proposes that the triplet n-π* excited state of furan and thiophene does not cleave the CI bond. The cleavage reaction would require a higher excited triplet state (π-σ*, n-σ*, or σ-σ*) mainly localized on the carbon–iodine bond. The interaction between this triplet state of the substrate and the aromatic compounds would lead to homolytic cleavage of the CI bond and the formation of a thienyl radical and a complex between the aromatic compound and the iodine atom. The formation of this complex was identified by the presence of a short-lived transient with $\lambda_{max} = 510$ nm, showing second order kinetics, $\tau \approx 0.4$ μsec, in laser flash photolysis. The thienyl radical then reacts rapidly with the aromatic compound to give the corresponding arylation product.[72] A recent study has proven that a similar $S_{RN}1Ar^*$ reaction mechanism is involved with mono and diiodopyrroles in the presence of various aromatic and heteroaromatic compounds.[73] The photochemical reaction between benzenecarbothioamide and substituted furans is reported to bring about β-benzoylation as a major reaction path. The mechanism appears to be more complex in this regioselective reaction.[74]

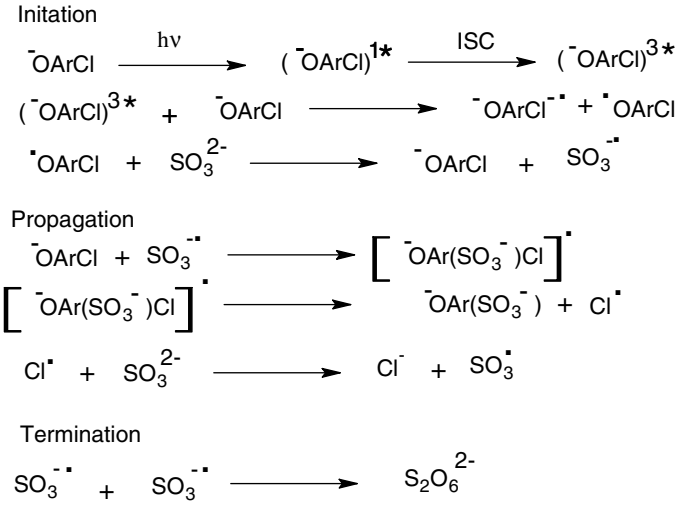

SCHEME 13

Photolysis of 4-chloro-1-hydoxynaphthalene in an aqueous solution of sodium sulfite results in replacement of chloride with sulfite. This is an example of an $S_{RN}1Ar^*$ mechanism. The chain reaction process is illustrated in Scheme 13.[75]

The presence of high concentrations of KI has been found to enhance the quantum yield of photosubstitution of chloride by sulfo groups on irradiation in the 313–365 nm band. The yields of aryl and heteroaryl products obtained by reactions of aryl and heteroaryl halides with a ketone enolate ion in Me_2SO are enhanced by catalysis with ferrous ion.[76] Photo-$S_{RN}1Ar^*$ reactions of chloro substituted *N*-methylpyridones with phenoxide have been reported.[77]

Photolysis of arylated digermanes is reported to involve germanium–germanium bond homolysis. This gives a pair of germyl radicals that abstract a hydrogen atom from a suitable source and either yield the corresponding hydromonogermanes or couple to afford digermanes as the main products. Irradiation of 1-(pentamethyldigerman)naphthalene yields 1-(dimethylgermyl)-8-(trimethylgermyl)naphthalene via the photochemical formation of a trimethylgermyl radical and a naphthyldimethylgermyl radical. Recombination at the 8 position of the latter followed by an intramolecular 1,4-hydrogen shift affords the final product.[78] Homolytic Ge-Ge bond scission within the singlet excited state is responsible for the germyl substitution on the naphthalene ring (Scheme 14).

$S_{RN}2Ar^*$ Reactions

Marquet et al. have proposed that if there is a direct reaction of the nucleophile on the aromatic substrate radical anion, an $S_{RN}2Ar^*$ mechanism is operative.[79] Such a mechanism was postulated by Hoz et al.[21,80] but was later rejected on experimental grounds. A few examples have appeared in the recent literature and have stimulated a reinvestigation of such a mechanism, which is shown in Scheme 15.[81,82]

The photoinduced photochemical substitution reactions of pentafluoronitrobenzene with several nucleophiles in aqueous media and the electrochemical detection of aromatic radical anions are taken as evidence for the presence of radical anion intermediates within the radical chain reaction steps.[79,83]

Acknowledgments

We thank Gül Koc-Weier for providing some of the literature data.

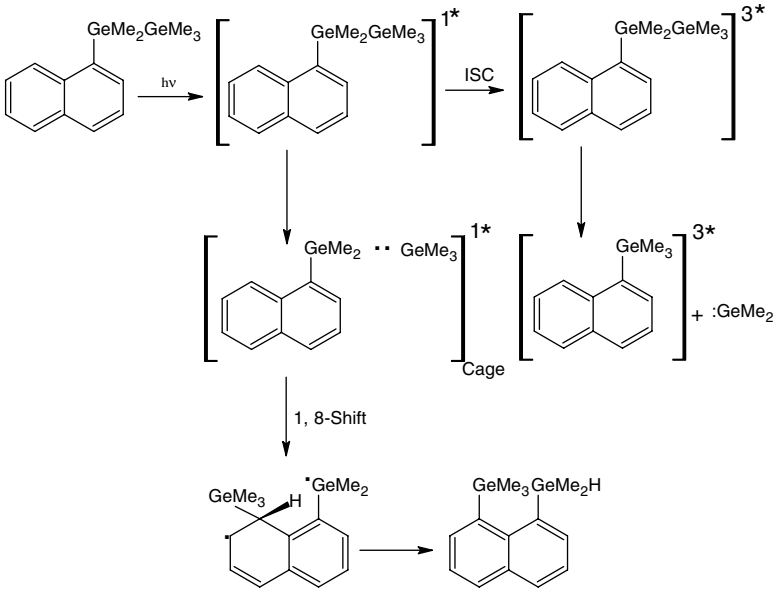

SCHEME 14

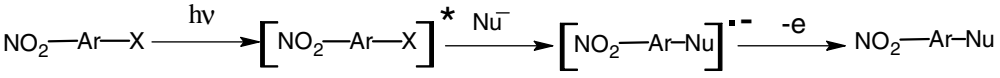

SCHEME 15

References

1. Coyle, J.D., *Introduction to Organic Photochemistry,* John Wiley & Sons, New York, 1986, 77.
2. Cornelisse, J., Photochemical Aromatic Substitution, in *CRC Handbook of Photochemistry and Photobiology,* CRC Press, Boca Raton, FL, 1994, 250.
3. Bryce-Smith, D. and Gilbert, A., Eds., *Specialist Periodical Reports, Photochemistry,* Vol. 1–25, The Royal Society of Chemistry, Cambridge, 1967–1992.
4. Epiotis, N.D. and Shaik, S., Qualitative potential energy surfaces. 4. Aromatic substitution, *J. Am. Chem. Soc.,* 100, 29, 1978.
5. Kuzmič, P. and Souček, M., Substituent effects in aromatic photochemistry. UV irradiation of 3,4-dimethoxybenzonitrile and 3,4-dimethoxyacetophenone in the presence of inorganic anions, *Coll. Czech. Chem. Commun.,* 52, 980, 1987.
6. Marquet, J., Moreno-Mañas, M., Vallriberia, A., Virgili, A., Bertran, J., Gonzales-Lafont, A., and Lluch, J.M., The nucleophilic aromatic photosubstitutions of 4,5-dinitroveratrole with amines. Photoreductions of aromatic dinitrocompounds, *Tetrahedron,* 43, 351, 1987.
7. Cantos, A., Marquet, J., and Moreno-Mañas, M., On the regioselectivity of the nucleophilic aromatic photosubstitution of 4-nitroanisole. A dual mechanistic pathway, *Tetrahedron Lett.,* 30, 2423, 1989.
8. Pleixats, R., Figueredo, M., Marquet, J., Moreno-Mañas, M., and Cantos, A., The search for new biochemical photoprobes. II.[1] The nucleophilic photosubstitution of 2-fluoro-4-nitroanisole, *Tetrahedron,* 45, 7817, 1989.

9. Cantos, A., Marquet, J., Moreno-Mañas, M. Gonzáles-Lafont, A., Lluch, J.M., and Bertrán, J., On the regioselectivity of 4-nitroanisole photosubstitution with primary amines. A mechanism and theoretical study, *J. Org. Chem.,* 55, 3303, 1990.
10. Marquet, J., Cantos, A., Moreno-Mañas, M., Cayón, E., and Gallardo, I., Singlet-triplet mechanistic duality in the photosubstitution of nitrophenyl ethers with ethyl glycinate. The role of single electron transfer, *Tetrahedron,* 48, 1333, 1992.
11. Marquet, J., Rafecas, L., Cantos, A., Moreno-Mañas, M., Cervera, M., Casado, F., Nogués, M.V., and Cuchillo, C.M., The search for biochemical photoprobes. III. The photoreactions of 4-nitroveratrole and 2-fluoro-4-nitroanisole with Bovine Pancreatic Ribonuclease A and with model nucleophiles, *Tetrahedron,* 49, 1297, 1993.
12. Mir, M., Marquet, J., and Cayón, E., Solid state photochemistry of ternary cyclodextrin complexes: total selectivity in the photoreduction of nitrophenyl ethers by 1-phenylethylamine, *Tetrahedron Lett.,* 33, 7053, 1992.
13. Bonilha, J.B.S., Tedesco, A.C., Nogueira, L.C., Diamantino, M.T.R.S., and Carreiro, J.C., Further evidence for the triplet mechanism in the photosubstitution of nitroaryl ethers in alkaline medium, *Tetrahedron,* 49**,** 3053, 1993.
14. Arnold D.R. and Snow, M.S., The photochemical nucleophile–olefin combination, aromatic substitution reaction (Part 2): methanol-cyclic olefins, 1,4-dicyanobenzene, *Can. J. Chem.,* 66, 3012, 1988.
15. McMahon, K. and Arnold, D.R., The photochemical nucleophile–olefin combination, aromatic substitution (photo-NOCAS) reaction (Part 4): methanol–olefins, methyl 4-cyanobenzoate, *Can. J. Chem.,* 71, 450, 1993.
16. Boggeri, E., Fasani, E., Mella, M., and Albini, A., Photochemical reaction between acenaphthene and arenecarbonitriles, *J. Chem. Soc., Perkin Trans. 2,* 2097, 1991.
17. Havinga, E. and Cornelisse, J., Aromatic photosubstitution reactions, *Pure Appl. Chem.,* 47, 1, 1976.
18. Spillane, W.J., Tritium in organic chemistry, in *Isotopes in Organic Chemistry,* Vol. 4, Buncel, E. and Lee, C.C., Eds., Elsevier, Amsterdam, 1978, p. 51.
19. Rossi, R.A. and Rossi, R.H., *Aromatic Substitution by SRN1 Mechanism,* ACS Monograph Series 178. American Chemical Society, Washington, D.C., 1983.
20. Kim, J.K. and Bunnet, J.F., Evidence for a radical mechanism of aromatic "nucleophilic" substitution, *J. Am. Chem. Soc.,* 92, 7463, 1970.
21. Hoz, S. and Bunnet, J.F., A quantitative study of the photostimulated reaction of iodobenzene with diethyl phosphite ion, *J. Am. Chem. Soc.,* 99, 4690, 1977.
22. Moon, M.P., Komin, A.P., Wolfe, J.F., and Morris G.F., Photostimulated reactions of 2-bromopyridine and 2-chloroquinoline with nitrile-stabilized carbanions and certain other nucleophiles, *J. Org. Chem,* 48, 2392, 1983.
23. Pierini, A.B., Baumgartner, M.T., and Rossi, R.A., Photostimulated reactions of haloarenes with 2-naphtyamide ions. A facile synthesis of 1-aryl-2-naphthylamines, *Tetrahedron Lett.,* 28, 4653, 1987.
24. Baumgartner M.T., Pierini, A.B., and Rossi R.A., The reactivity of oxygen nucleophiles with aryl radicals in the $S_{RN}1$ mechanism, *Tetrahedron Lett.,* 33**,** 2323, 1992.
25. Lablache-Combier, A., Heteroaromatics, in *Photoinduced Electron Transfer,* Fox, M.A. and Chanon, M., Eds., Elsevier, Amsterdam, 1988, Part C, p. 134.
26. Wubbels, G.G., Snyder, E.J., and Coughlin, E.B., HCl-catalysed photoreduction of 4-bromonitrobenzene as a concomitant of nucleophilic aromatic photosubstitution involving radical intermediates, *J. Am. Chem. Soc.,* 110, 2543, 1988.
27. Pierini, A.B. and Rossi, R.A., Photostimulated $S_{RN}1$ reactions of phenyl selenide and phenyl telluride ions with halo- and dihaloarenes in liquid ammonia, *J. Org. Chem.,* 44, 4667, 1979.
28. Kurz, M.E., Lapin, S.C., Mariam, K., Hagen, T.J., and Qian, X.Q., Photochemical aromatic cyanomethylation: aromatic substitution by way of radical cations, *J. Org. Chem.,* 49, 2728, 1984.

29. Liu, J.H. and Weiss, R.G., Anomalous effects during aromatic nucleophilic photosubstitutions of 2- and 4-fluoroanisoles in solvent mixtures of water and *tert*-butyl alcohol, *J. Org. Chem.,* 50, 3655, 1985.
30. Alonso, R.A., Austin, E., and Rossi, R.A., Photostimulated reaction of carbanions from α, β–unsaturated nitriles with aryl halides by the $S_{RN}1$ mechanism, *J. Org. Chem.,* 53, 6065, 1988.
31. Pierini, A.B., Baumgartner, M.T., and Rossi, R.A., Photostimulated reaction of aryl iodides with 2-naphthoxide ions by the $S_{RN}1$ mechanism, *Tetrahedron Lett.,* 29, 3429, 1988.
32. Yammal, C.C., Podestá, J.C., and Rossi, R.A., Reactions of triorganostannyl ions with haloarenes in liquid ammonia. Competition between halogen-metal exchange and electron transfer reactions, *J. Org. Chem.,* 57, 5720, 1992.
33. Lazaro, R., Bouchet, P., Sole, R., Alkorta, I., and Elguero, J., Aromatic photosubstitution, IV. Photocyanation of aromatic compounds: labeling experiments, *ACH-Models Chem.,* 136**,** 531, 1999.
34. Cervera, M. and Marquet, J., Direct coupling of carbon nucleophiles with *m*-dinitrobenzene: a novel fluoride promoted nucleophilic aromatic photosubstitution for hydrogen, *Tetrahedron Lett.,* 37, 7591, 1996.
35. Huertas, I., Gallardo, I., and Marquet, J., Direct formation of aromatic C-N bonds. Regioselective amination of *m*-dinitrobenzene via fluoride promoted nucleophilic aromatic photosubstitution for hydrogen, *Tetrahedron Lett.,* 41, 279, 2000.
36. Arnold, R.D. and Du, X., The photochemical nucleophile–olefin combination, aromatic substitution (photo-NOCAS) reaction. Part 5: methanol-monoterpenes (α- and β-pinene, tricyclene and nopol), 1,4-dicyanobenzene, *Can. J. Chem.,* 72, 403, 1994.
37. Arnold, D.R., McManus, K.A., and Du, X., Photochemical nucleophile– olefin combination, aromatic substitution (photo-NOCAS) reaction. Part 6: methanol-nonconjugated dienes and 1,4-dicyanobenzene, *Can. J. Chem.,* 72, 415, 1994.
38. McManus, K.A. and Arnold, D.R., Photochemical nucleophile–olefin combination, aromatic substitution (photo-NOCAS) reaction. Part 7: methanol-conjugated dienes and 1,4-dicyanobenzene, *Can. J. Chem.,* 72, 2291, 1994.
39. Arnold, D.R., Du, X., and de Lijser, H.J.P., The photochemical nucleophile–olefin combination, aromatic substitution (photo-NOCAS) reaction. Part 8: methanol-2-carene and 1,4-dicyanobenzene, *Can. J. Chem.,* 73, 522, 1995.
40. Connor, D.A., Arnold, D.R., Bakshi, P.K., and Cameron, T.S., Photochemical nucleophile–olefin combination, aromatic substitution (photo-NOCAS) reaction. Part 9: methanol-2,6-dimethyl-1,6-heptadiene and 1,4-dicyanobenzene, *Can. J. Chem.,* 73, 762, 1995.
41. McManus, K.A. and Arnold, D.R., The photochemical nucleophile–olefin combination, aromatic substitution (photo-NOCAS) reaction. Part 10: intramolecular reactions involving alk-4-enols and 1,4-dicyanobenzene, *Can. J. Chem.,* 73, 2158, 1995.
42. Arnold, D.R., Connor, D.A., McManus, K.A., Bakshi, P.K., and Cameron, T.S., The photochemical nucleophile-olefin combination, aromatic substitution (photo-NOCAS) reaction. Part 11: Involving (R)-(+)-α-terpineol and (R)-(+)-limonene, substituting on 1,4-dicyanobenzene, *Can. J. Chem.,* 74, 602, 1996.
43. Arnold, D.R., Chan, M.S.W., and McManus, K.A., Photochemical nucleophile–olefin combination, aromatic substitution (photo-NOCAS) reaction, Part 12. Factors controlling the regiochemistry of the reaction with alcohol as the nucleophile, *Can. J. Chem.,* 74, 2143, 1996.
44. Arnold, D.R., McManus, K.A., and Chan, M.S.W., Photochemical nucleophile–olefin combination, aromatic substitution (photo-NOCAS) reaction, Part 13. The scope and limitations of the reaction with cyanide anions as the nucleophile, *Can. J. Chem.,* 75, 1055, 1997.
45. Chan, M.S.W. and Arnold, D.R., Photochemical nucleophile–olefin combination, aromatic substitution (photo-NOCAS) reaction, Part 15. Investigations involving fluorine anion as the nucleophile and the effect of fluorine substitution on the relative stability of the reaction intermediates, *Can. J. Chem.,* 75, 1810, 1997.

46. Arnold, D.R. and McManus, K.A., Photochemical nucleophile–olefin combination, aromatic substitution (photo-NOCAS) reaction: methanol, β-myrcene and 1,4-dicyanobenzene. Intramolecular cyclization of an ene-diene radical cation, *Can. J. Chem.,* 76, 1238, 1998.
47. De Lijser, H.J.P. and Arnold, D.R., Interconversion and rearrangement of radical cations. Part 2. Photoinduced electron transfer and electrochemical oxidation of 1,4-bis(methylene)cyclohexane, *J. Chem. Soc., Perkin Trans. 2,* 1369, 1997.
48. Mangion, D. and Arnold, D.R., Photochemical nucleophile–olefin combination, aromatic substitution reaction. Its synthetic development and mechanistic exploration, *Acc. Chem. Res.,* 35, 297, 2002.
49. De Lijser, H.J.P. and Arnold, D.R., Radical ions in photochemistry. 44. The photo-NOCAS reaction with acetonitrile as the nucleophile, *J. Org. Chem.,* 62, 8432, 1997.
50. Vanossi, M., Mella, M., and Albini, A., 2 + 2 + 2 Cycloaddition vs. radical ion chemistry in the photoreactions of 1,2,4,5-benzenetetracarbonitrile with alkenes in acetonitrile, *J. Am. Chem. Soc.,* 116, 10070, 1994.
51. Mangion, D. and Arnold, D.R., The photochemistry of 4-halobenzonitriles and 4-haloanisoles with 1,1-diphenylethene in methanol. Homolytic cleavage versus electron transfer pathways, *Can. J. Chem.,* 77, 1655, 1999.
52. Mangion, D., Arnold, D.R., Cameron, T.S., and Robertson, K.N., The electron transfer photochemistry of allenes with cyanoarenes. Photochemical nucleophile–olefin combination, aromatic substitution (photo-NOCAS) and related reactions, *J. Chem. Soc., Perkin Trans. 2,* 48, 2001.
53. Torriani, R., Mella, M., Fasani, E., and Albini, A., On the mechanism of the photochemical reaction between 1,4-dicyanobenzene and 2,3-dimethylbuthene in the presence of nucleophiles, *Tetrahedron,* 53**,** 2573, 1997.
54. Cervera, M. and Marquet, J., Effects of superoxide anion generated from aromatic radical anions produced in nucleophilic aromatic photosubstitution reactions, *Can. J. Chem.,* 76, 966, 1998.
55. Tedesco, A.C., Naal, R.M.Z.G., Carreiro, J.C., and Bonilha, J.B.S., Kinetic studies of the nucleophilic quenching of photoexcited nitroaryl ethers (NArE) by bromide ions in cationic micellar solution, *Tetrahedron,* 50**,** 3071, 1994.
56. Nakagaki, R. and Mutai, K., Photophysical properties and photosubstitution and photoredox reactions of aromatic nitro compounds*, Bull. Chem. Soc. Jpn.,* 69, 261, 1996.
57. Galli, C., Gentili, P., and Guarnieri A., Calculation of the LUMO energy of the substitution product of the aromatic S(RN)1 reaction, G., *Gazz. Chim. Ital.,* 127**,** 159, 1997.
58. Chen, J., Peijnenburg, W.J.G.M., Quan, X., Chen, S., Zhao, Y., and Yang, F., The use of PLS algorithms and quantum chemical parameters derived from PM3 hamiltonian in QSPR studies on direct photolysis quantum yields of substituted aromatic halides, *Chemosphere,* 40**,** 1319, 2000.
59. Córsico, E.F. and Rossi, R.A., Reactions of trimethylstannyl ions with mono-, di and trichloro-substituted aromatic substrates by the $S_{RN}1$ mechanism, *Synlett,* 2, 227, 2000.
60. Chen, Q.-Y. and Li, Z.-T., Photoinduced electron-transfer perfluoroalkylation of aminopyridines with perfluoroalkyl iodides, *J. Chem. Soc., Perkin Trans. 1,* 1443, 1992.
61. Chen, Q.-Y. and Li, Z.-T., Pentafluorophenylation of aromatics with pentafluorophenyl perfluoro- and polyfluoroalkanesulfonates. A photoinduced electron-transfer cation diradical coupling process, *J. Org. Chem.,* 58, 2599, 1992.
62. Chen, Q.-Y. and Li, Z.-T., Photoinduced electron transfer reactions of pentafluoroiodobenzene with aromatic compounds, *J. Chem. Soc., Perkin Trans. 1,* 1705, 1993.
63. Cakmak, O., Bromination of naphthalene. Preparation of 1,3-dibromonaphthalene, *J. Chem. Res. Synop.,* 366, 1999.
64. Mangion, D., Frizzle, M., Arnold, R.D., and Cameron, T.S., The photochemistry of acrylonitrile with methoxylated naphthalenes: introducing the photochemical electrophile–olefin combination, aromatic substitution (Photo-EONAS) reaction, *Synthesis,* 8, 1215, 2001.

65. Arnold., D.R. and Mangion, D., The photochemical aromatic–olefin substitution, nucleophile combination reaction, *Book of Abstracts, 216th ACS National Meeting,* Boston, August 23–27, 1998, American Chemical Society, Washington, 1998.
66. Vanossi, M., Mella, M., and Albini, A., 2 + 2 + 2 Cycloaddition vs. radical ion chemistry in the photoreactions of 1,2,4,5-benzenetetracarbonitrile with alkenes in acetonitrile, *J. Am. Chem. Soc.,* 116, 10070, 1994.
67. Antonioletti, R., D'Auria, M., De Mico, A., Piancatelli, G., and Scettri, A., Photochemical behaviour of 5-bromo-2-furyl ketones. Synthesis of 5-aryl-2-furyl ketones, *Tetrahedron,* 41, 3441, 1985.
68. Antonioletti, R., D'Auria, M., D'Onofrio, F., Piancatelli, G., and Scettri, A., Photochemical synthesis of phenyl-2-thienyl derivatives, *J. Chem. Soc., Perkin Trans. 1,* 1755, 1986.
69. D'Auria, M., De Mico, A., D'Onofrio, F., and Piancatelli, G., Photochemical synthesis of bithienyl derivatives, *J. Chem. Soc., Perkin Trans. 1,* 1777, 1987.
70. D'Auria, M., De Mico, A., D'Onofrio, F., Mendola, D., and Piancatelli, G., Photochemical behavior of halogeno-thiophenes: synthesis of 5-arylthiophene-2-carboxylic esters, *J. Photochem. Photobiol. A: Chem.,* 47, 191, 1989.
71. D'Auria, M., Applications of the photochemical reactions of iodoheterocyclic derivatives with aromatic compounds in the synthesis of new singlet oxygen sensitizers, *J. Photochem. Photobiol. A: Chem.,* 91, 187, 1995.
72. Elisei, F., Latterini, L., Aloisi, G.G., and D'Auria, M, Photoinduced substitution reactions in halothiophene derivatives. Steady state and laser flash photolytic studies, *J. Phys. Chem.,* 99, 5365, 1995.
73. D'Auria, M., De Luca, E., Mauriello, G., Racioppi, R., and Sleiter G., Photochemical substitution of halogenopyrrole derivatives, *J. Chem. Soc., Perkin Trans. 1,* 2369, 1997.
74. Oda, K., Tsujita, H., Ohno, K., and Machida, M., Photochemistry of the nitrogen–thiocarbonyl systems. Part 24. Photoreactions of thiobenzamide with various substituted furans: regioselective β-benzoylation and transformation of furans to other aromatic compounds, *J. Chem. Soc., Perkin Trans. 1,* 2931, 1995.
75. Ivanov, V.L., Lyashkevich, S.Y., and Lemmetyinen, H., The mechanism of photochemical chain substitution of chlorine by sulpho group in 4-chloro-1-hydroxynaphthalene, *J. Photochem. Photobiol. A: Chem.,* 109, 21, 1997.
76. Galli, C. and Gentili, P., Catalysis by ferrous ion in nucleophilic aromatic substitution reactions, *J. Chem. Soc., Perkin Trans. 2,* 1135, 1993.
77. Higuchi, H., Hattori, M., and Ohmiya, S., Direct arylation of 2-pyridones; photostimulated S(RN)1 reaction between caesium phenoxides and chloro-2-pyridones, *Heterocycles,* 52**,** 253, 2000.
78. Mochida, K., Ginyama, H., Takahashi, M., and Kira, M., Photochemical reactions of digermanyl-substituted naphthalenes: the germyl migration to the aromatic ring, *J. Organomet. Chem.,* 553, 163, 1998.
79. Marquet, J., Jiang, Z., Gallardo, I., Batlle, A., and Cayón, E., Reductively activated "polar" nucleophilic aromatic substitution of pentafluoronitrobenzene. The $S_{RN}2$ hypothesis revisited, *Tetrahedron Lett.,* 34, 2801, 1993.
80. Galli, C. and Bunnett, J.F., Evidence further substantiating the $S_{RN}1$ mechanism of aromatic substitution, *J. Am. Chem. Soc.,* 101**,** 6137, 1979.
81. Abe, T. and Ikegami, Y., An anion radical precursor in the nucleophilic substitution of *p*-dinitrobenzene, *Bull. Chem. Soc. Jpn.,* 51, 196, 1978.
82. Denney, D.B. and Denney, D.Z., A reconsideration of the mechanism for the aromatic version of radical nucleophile displacement reactions, *Tetrahedron,* 47, 6577, 1991.
83. Jiang, Z.Q., Marquet, J., Cervera, M., and Gallardo, I., Reductivity activated "polar" nucleophilic aromatic substitution. 4. Thermal and photochemical behavior of polychloro and polyfluoronitrobenzenes in front of soft nucleophiles, *An. Quim. Int. Ed.,* 92**,** 95, 1996.

38

Photodehalogenation of Aryl Halides

Leah Schutt
University of Guelph

Nigel J. Bunce
University of Guelph

38.1 Introduction

The photochemistry of aryl halides (Ar-X) has been studied since the 1960s, and a very large number of citations is available. Previous reviews include Sammes,[1] Grimshaw and de Silva,[2] Lodder,[3] Davidson et al.,[4] Choudhry et al.,[5] and Burrows et al.[6] The examples reviewed in this chapter concern solution phase chemistry, unless noted otherwise.

Photochemical C-X fission in aryl halides may be defined as any photochemical process leading to cleavage of a carbon-to-halogen bond. The emphasis in this review is on mechanisms of C-X bond fission, of which three mechanistic reaction types may be identified.

1. Homolysis $\quad Ar\text{-}X^* \rightarrow Ar^\bullet + X^\bullet$
2. Electron transfer $\quad Ar\text{-}X^* \rightarrow (Ar\text{-}X)^{\bullet -} \rightarrow Ar^\bullet + X^-$
3. Photonucleophilic substitution $\quad Ar\text{-}X^* + Nu:^- \rightarrow Ar\text{-}Nu + X^-$

Aryl halides tend to be chemically unreactive and include persistent environmental pollutants such as dichloro-diphenyl-trichloroethane (DDT), polychlorinated biphenyls (PCBs), dibenzo-*p*-dioxins (PCDDs), dibenzofurans (PCDFs), and polybrominated diphenyl ethers (PBDEs). Many studies of the photochemistry of halogenated aromatic compounds have been stimulated by environmental concerns, the goal often being to understand whether photolysis is an important sink for these compounds in natural waters[7–9] or in the atmosphere.[10] The photochemistry of aryl halides causes problems in this context because many aryl halides have minimal absorption in the region of the tropospheric solar spectrum (>295 nm), and experiments at environmentally irrelevant wavelengths such as 254 nm are

0-8493-1348-1/04/$0.00+$1.50

TABLE 38.1 Energetics (kJ mol^{-1}) of CX Homolysis

Arene System	Triplet Energy	X	D(C_6H_5–X)
Benzene	360	F	520
Naphthalene	255	Cl	350–390
Biphenyl (no *o*-X)	275	Br	335
Biphenyl (one *o*-X)	>285	I	270
Anthracene	180	—	—
Pyrene	200	—	—

often more feasible. In addition, most halogenated aromatic compounds have very low solubility in water, necessitating the use of model solvents such as methanol or aqueous acetonitrile. Both the quantum yield of photoreaction (and hence estimates of environmental persistence) and the reaction products may be solvent dependent. These considerations make it difficult to extrapolate the photochemical behavior observed in the laboratory to natural systems. For this reason, many recent investigations of the photochemistry of aryl halides, in particular those considered to be environmental pollutants, have focused on elucidation of the photodegradative processes that do occur under environmental conditions and identification of systems that can be employed to increase their efficiency.

38.2 Reactions Proceeding Via Homolysis

Homolytic cleavage of the aryl carbon–halogen bond affords aryl free radicals, which can either arylate a suitable aromatic reaction partner or abstract hydrogen from a hydrogen atom donor (reductive dehalogenation), as first reported over 35 years ago. A recent example is the report by Meunier et al.[11] that photolysis of 1,4-dichlorobenzene in the absence of oxygen yielded 4,4′-dichlorobiphenyl and 2,4′,5-trichlorobiphenyl as reaction products. The general reaction mechanism proceeds as follows:

$$\mathrm{Ar - X^{*}} \longrightarrow \mathrm{Ar^{\bullet} + X^{\bullet}}$$

$$\mathrm{Ar^{\bullet} + R - H} \longrightarrow \mathrm{Ar - H + R^{\bullet}}$$

or

$$\mathrm{Ar^{\bullet} + Ar'H} \longrightarrow \mathrm{(ArHAr')^{\bullet}} \xrightarrow{-\mathrm{H}} \mathrm{Ar - Ar'}$$

However, because arylation and dehalogenation may occur by other mechanisms, product studies alone cannot be used to infer that homolysis has occurred.

Homolysis of photoexcited aryl iodides and bromides has been exploited as a means of producing aryl radicals; in some cases, these reactions have synthetic potential for the formation of biaryls, including the use of intramolecular arylation in order to construct polycyclic systems.[2] Reductive dehalogenation has been suggested as a synthetic route to specifically deuterated aromatic compounds by photolysis of aryl halides in solvents containing abstractable deuterium atoms.[12]

The energetics of homolysis is straightforward, requiring the energy of the reactive excited state (usually T_1) to be greater than the CX bond dissociation energy (Table 38.1). Homolysis is thermodynamically unfavorable (and is not seen) for aryl fluorides, in either singlet or triplet π,π^* states. As an example, 1,2,3-trifluorobenzene is unaffected by irradiation at 254 nm for 3 days.[13] 1-Chloropyrene (monomer) and 9,10-dibromoanthracene are unaffected by lengthy photolysis in alkane solvents. If the aromatic nucleus contains more than one type of halogen, the weakest C-X bond is cleaved preferentially. The rate of dechlorination of chlorobenzenes must be very fast, as shown by 1-bromo-3-*p*-chlorophenoxypropane,[4] which loses Cl exclusively upon photoexcitation even though the side chain contains the weaker C-Br bond (i.e., the excitation energy is not transferred to the weaker bond).

The data in Table 38.1 show that homolysis is exothermic for triplet iodo- and bromo-benzenes and probably for chlorobenzenes, although the correct value of the C_6H_5–Cl bond dissociation energy has

been the subject of controversy. In hydrogen-donating solvents, many chlorinated, brominated, and iodinated benzenes exhibit high quantum yields of both intersystem crossing $S_1 \rightarrow T_1$ and dehalogenation, and when $\Phi_{ISC} + \Phi_r$ significantly exceeds 1.0, the reactive excited state can be concluded to be T_1.

Halophenyl ketones have been studied from the point of view of the competition between C-X cleavage and pinacol formation from the ketone functionality. In cyclopentane solution, *m*- and *p*-bromobenzophenones reacted almost exclusively at the carbonyl group; conversely, the corresponding iodobenzophenones and bromoacetophenones gave near-quantitative yields of dehalogenated ketones.[14] These results were explained in terms of the relative ordering of n,π^* and π,π^* triplet excited states. It is suggested that C-X bond cleavage from the lowest π,π^* triplet excited state of halobenzenes involves an endothermic C-X bond stretching until the $^3\pi,\pi^*$ becomes co-energetic with a dissociative state. A follow-up study of the two iodobenzophenones indicated that the quantum inefficiency of deiodination is due to in-cage radical recombination, as shown by severely decreasing quantum yields of dehalogenation with increased solvent viscosity.[15] At some point, interaction between the carbonyl *n* orbital and the CI σ^* is necessary in order to facilitate bond cleavage.[14,15] In π,π^* triplets, it is suggested that the partial positive charge on a *meta* halide close to the negative carbonyl counteracts the normal higher *para* π^* electron density.[14]

In chlorophenols, homolytic C-Cl cleavage is usually a minor pathway compared with heterolysis,[16] but the relative quantum yields depend on the positions and numbers of chlorine atoms on the benzene ring.[6]

Studies have also been conducted on halobenzenes in the gas phase. Quantum yields of homolysis are high.[3,17] Ichimura et al.[17] photolyzed dichlorobenzenes and chlorotoluenes at 193 nm and proposed three different channels for the rupture of the C-Cl bond:

1. A very fast predissociation and/or direct dissociation channel
2. A predissociation channel via vibrationally excited triplet levels
3. A predissociation channel via highly excited vibrational levels of the ground electronic state

In chlorobenzene and dichlorobenzenes, the three pathways have equal probabilities; however, the addition of a methyl group, as in chlorotoluene, greatly increases the flow through the second channel, probably due to enhanced intersystem crossing by the methyl group. Studies with iodo- and bromobenzene suggest that only two dissociation pathways exist for these compounds, due to the presence of the π,π^* electronic system in the phenyl ring in addition to the n,σ^* electronic system in the C-X bond. The first is an instantaneous direct dissociation leading to the formation of photofragments, and the second involves a slower cleavage from the π,π^* triplet state, followed by predissociation via the repulsive n,σ^* state.[18,19] Only two pathways are proposed for *p*- and *o*-bromotoluene: a direct dissociation and a fast predissociation involving fast intersystem crossing.[18,20]

In the presence of hydrogen donors such as ethane,[21] reductive dehalogenation occurs as in solution. The situation is different upon photolysis in air, when little of the starting material has been accounted for. Low yields of phenols were identified, presumably the result of trapping aryl radicals by O_2; the remainder of the starting material is assumed to have been mineralized.[10] The atmospheric chemistry of PCBs, PCDDs, and PCDFs in the gaseous phase has been extensively reviewed by Atkinson.[22]

The regiospecificity of homolysis generally favors relief of steric strain. For example, photolysis of 1,2,3,5-tetrachlorobenzene in hydrogen-donating media gives predominantly 1,3,5-trichlorobenzene and 1,2,4-trichlorobenzene rather than 1,2,3-trichlorobenzene.[5] Halobiphenyls substituted at an *ortho* and another position cleave the *ortho* halogen preferentially,[4] both because loss of an *ortho* chlorine relieves steric strain and because *ortho* substitution raises the energy of the excited state due to partial deconjugation of the biphenyl chromophore, which shifts the absorption spectrum toward the blue. Among simple chlorobiphenyls containing only one to three chlorine substituents, those containing *ortho* chlorines have markedly larger quantum yields of homolysis than those without.[3] This was exemplified in the recent work of Masuzaki et al.,[23] who investigated the photodegradation of mono-, di-, and trichlorobiphenyls in decane at 254 nm. One apparent exception to these generalizations is 2,2′,5,5′-tetrachlorobiphenyl,[24] which is reported to lose both *ortho* and *meta* chlorines with comparable efficiency and which also gave small amounts of chlorobenzenes upon irradiation with a xenon lamp in hexane solution. In the environmental context, the efficiency of photolysis of PCBs is determined both by their intrinsic

photolability (Φ_r) and by the overlap of their absorption spectra with the tropospheric solar spectrum, the *o*-chlorobiphenyls having less spectral overlap but higher quantum yields of homolysis.[9] The photohomolysis of polybrominated biphenyls,[25] polybrominated diphenyl ethers,[26] and polybrominated dibenzofurans[27] has also been described. In the majority of cases, photodegradation in organic solvents by ultraviolet (UV) radiation results in the formation of lower brominated congeners.

Various surfactant solutions have been employed[28,29] to increase the extraction of PCBs from soil matrices and to increase the quantum yield of PCB photodegradation by transferring the PCBs into an alkane-like environment. The problem that remains is that at doses high enough to form micelles the aqueous phase of the soil may be colored due to the solubilization of humic material and hence inhibit the penetration of light into the solution. Chu et al.[29] found sixfold faster degradation of Aroclor 1254 and 2,3,4,5-tetrachlorobiphenyl in 0.5-m*M* Brij 58 micellar solutions than in water alone upon irradiation at 253.7 nm. The major initial product of 2,3,4,5-tetrachlorobiphenyl photodegradation was 3,4,5-trichlorobiphenyl. Two possible pathways were postulated for its formation: (1) by homolysis, forming a biphenyl radical that may abstract a hydrogen from the surfactant hydrocarbon, or (2) by the triplet state of 2,3,4,5-tetrachlorobiphenyl abstracting a hydrogen from the surfactant hydrocarbon. An overall 1,4-shift isomerization reaction was observed, with a high production of 2′,3,4,5-tetrachlorobiphenyl, as a result of the second postulated pathway.

Polychlorinated dibenzo-*p*-dioxins are reported to lose lateral (2, 3, 7, 8) in preference to apical (1, 4, 5, 9) chlorines upon photolysis in solution,[30,31] but in the gas phase photodechlorination occurs preferentially from the *peri* positions, based on relative rates of disappearance of starting material and product studies.[32] In solution, PCDDs give very low yields of dechlorination products under both direct homolysis and amine-assisted photolysis (Section 3.2).[33] Recently, the missing material has been identified as arising through mechanisms involving C-O rather than C-Cl cleavage to afford both polychlorinated hydroxydiphenyl ethers and polychlorinated 2,2′-dihydroxybiphenyls.[34,35]

Under certain conditions, photodegradation of polychlorophenols has been associated with the production of more problematic PCDDs and PCDFs.[36] PCDDs and PCDFs were identified after 5 hours of UV irradiation of pentachlorophenol-containing wastewater using light of wavelength 254 nm. It was noted that complete removal of PCDDs and PCDFs could be achieved by increasing irradiation time or applying high-pressure mercury lamps with higher energy than the low-pressure mercury lamp.

Irradiation of halogenated furans and thiophenes with benzene gives a mixture of arylated and dehalogenated products. It is postulated that excitation of the heterocycle affords a higher excited triplet state (π,σ^*, n,σ^*, or σ,σ^*) localized on the C-X bond and that its reaction with the benzenoid component yields a benzene-complexed halogen atom and a heterocyclic aryl radical that reacts rapidly with the aromatic reagent to give the arylation or dehalogenation products.[37]

38.3 Reactions Proceeding Via Excimers, Exciplexes, and Electron Transfer

These reactions are initiated by the full or partial acquisition of an electron by the aryl halide, affording an excimer, an exciplex, or radical ions, depending upon the electron donor and the solvent. In this review, the term excimer will be used to describe the complexes formed between two arenes, even when they are not identical.

Excimer Reactions

For many aryl halides, a major route of photodehalogenation is via triplet excimer reactions in which the ground state aryl halide absorbs a photon to produce an excited singlet state (S_1). Rapid intersystem crossing affords T_1, usually with high efficiency, due to increased spin-orbit coupling attributed to the "heavy atom effect". The excited triplet interacts with a second ground-state molecule to form a triplet excimer, which leads to dehalogenation products. Deactivation of the triplet monomer by the triplet excimer, returning it to the ground state, is a major cause of quantum inefficiency.[38]

A key mechanistic observation in support of an excimer mechanism is the dependence of the quantum yield of reaction upon the aryl halide concentration: $\Phi_r^{-1}\,\alpha[ArX]^{-1}$. Inferential evidence is provided when an excimer can be detected spectroscopically by fluorescence or flash photolysis.

The photodebromination of 4-bromobiphenyl typifies this mechanism.[39] Biphenyl is the sole product, and the participation of the triplet state is clear in that $\Phi(S_1 \rightarrow T_1) = 0.98$, while $\Phi_r = 0.15$ at high [BpBr]. The involvement of the triplet excimer is shown by the increase of Φ_r with [BpBr]; $\Phi_r^{-1}\,\alpha[BpBr]^{-1}$. The irradiation of 3,4-dibromobiphenyl in acetonitrile afforded 4-bromobiphenyl and 3-bromobiphenyl in a ratio of 7.6 to 1. This reaction also had a linear relationship between Φ_r^{-1} and [3,4-bromobiphenyl]$^{-1}$. AM1 calculations were used to postulate that the products were formed via both excimer and radical anion intermediates.[40] Higher chlorinated biphenyls are also expected to dechlorinate via this mechanism.

Earlier investigations had shown similar increases of Φ_r with concentration in the case of 1-chloronaphthalenes, but a decrease in the case of chlorobenzene,[41] because in the chlorobenzene series the excimer cleaves less efficiently than the monomer ($\Phi_r = 0.54$ in alkanes). Dechlorination via a heteroexcimer is also implicated by studies indicating that benzene "sensitizes" the dechlorination of chlorobenzene.[4]

The reactivity of a heteroexcimer has been exploited as a means of degrading low concentrations of chlorinated pollutants such as polychlorinated biphenyls and polychlorinated benzenes.[42] Copolymers of vinylnaphthalene and styrenesulfonic acid form water-soluble, micellar-like copolymers with a hydrophobic core. When the nonpolar chloro-compounds are dissolved in aqueous solutions containing the water-soluble copolymer, they are scavenged into the core, where they undergo photodehalogenation. In these reactions, essentially all the incident radiation is absorbed by the naphthalene chromophores, which form heteroexcimers with the polychloro-compound. The pattern of dechlorination is characteristic of electron transfer rather than direct homolysis.

The rate of triplet excimer formation appears to be critical in product formation in halogenated benzenes in the presence of oxygen. Recent investigations have revealed a great difference in reactivity upon photolysis of 1,2,4-tribromobenzene, 1,2,3,5-tetrabromobenzene, and pentachlorobenzene in air under natural light.[37] The brominated compounds debrominated readily, but pentachlorobenzene was unreactive. The following kinetic relationship was found for the quantum yield of debromination under direct photolysis:

$$1/\Phi = 1/(\Phi_{ISC}F) + \{(k_q[O_2] + k_{td})/(k_2\Phi_{ISC}F) * (1/[ArX])\}$$

where Φ_{ISC} is the quantum yield of intersystem crossing, which for these compounds is high; F is the efficiency of product formation; k_q is the rate of oxygen quenching of the triplet state (estimated to be 3×10^9 L mol^{-1} s^{-1} for all three compounds); k_{td} is the rate constant for C-X bond cleavage in the triplet excimer; and k_2 is the excimer formation rate constant. In the case of the two brominated benzenes, k_2 is large enough to support dehalogenation, but, in the case of pentachlorobenzene, a smaller value of k_2 leads to total quenching of the triplet by oxygen. In the absence of air, three dechlorination pathways have been deduced for pentachlorobenzene: homolysis from both S_1 and T_1 and fragmentation of a triplet excimer.[43]

The dechlorination of pentachlorobenzene has also been studied in micelles of hexadecyltrimethylammonium bromide in water.[44] The predominant reaction at high [C_6HCl_5] microconcentrations is an excimer-assisted dechlorination, deduced from the relationship $\Phi_r^{-1}\,\alpha[C_6HCl_5]^{-1}$. At low concentrations, a triplet monomer pathway intervenes. Byproducts of the reaction include bromotetrachlorobenzenes, which are postulated to arise through trapping the cationic partner of the excimer by Br^-.

Exciplex Reactions Involving Aliphatic Amines

In these reactions, kinetic evidence for the involvement of the amine is shown by the relationship $\Phi_r^{-1}\,\alpha[\text{amine}]^{-1}$. In cases where the halide has detectable fluorescence, the amine may quench fluorescence according to Stern–Volmer kinetics, and emission from the singlet exciplex is frequently observable in nonpolar solvents.[4] For a predominantly singlet state reaction, concordance is seen between K_{sv} (the Stern–Volmer constant for quenching fluorescence) and K_φ (the parameter intercept/slope from the plot

TABLE 38.2 Photodehalogenation of 9,10-Dihaloanthracenes with Aliphatic Amines

Halogen	Amine	Solvent	K_{SV} (M^{-1})	K_{φ} (M^{-1})
Cl, Br	$EtNH_2$	Heptane	—	—
Br	Et_2NH	Heptane	6.0	5.5
Br	Et_2NH	Benzene	12	14
Br	Et_2NH	Dioxane	8	9
Br	Et_2NH	Methanol	0.55	0.6
Br	Et_3N	Heptane	10	0.9
Br	Et_3N	Benzene	23	—
Br	Et_3N	Dioxane	15	—
Br	Et_3N	Methanol	4.5	—

TABLE 38.3 Amine-Assisted Photoreduction of 4-Chlorobiphenyl

Amine	Solvent	K_{SV} (M^{-1})	K_{φ} (M^{-1})
Et_3N	Cyclohexane	11	44
Et_3N	Methanol	2.7	18
Et_3N	Acetonitrile	23	20[a]
Et_3N	Acetonitrile	20	83
Et_3N	Aq. acetonitrile	11	97
Piperidine	Methanol	0.8	2.2
Piperidine	Acetonitrile	13	61

[a] This value is from Ohashi et al.;[48] all others are from Bunce.[49]

of $\Phi_r^{-1}\alpha[\text{amine}]^{-1}$). This kinetic behavior is observed in the diethylamine-assisted photoreduction of 9,10-dihaloanthracenes to 9-haloanthracenes, which are convenient to study because of the lack of an unassisted reaction, as shown[45,46] by the results of Table 38.2, which shows the excellent agreement between K_{sv} and K_{φ}.

Unlike diethylamine, ethylamine failed to quench fluorescence or to induce dehalogenation, while the tertiary alkylamine (Et_3N) quenched fluorescence but induced dehalogenation inefficiently or not at all. The effect on fluorescence is consistent with the order of oxidation potentials of aliphatic amines; the lack of concordance between K_{sv} and K_{φ} in the case of Et_3N suggests a change of mechanism in this case.

These results parallel those obtained upon photolysis of the parent anthracene with amines: neither reaction nor fluorescence quenching with primary alkylamine; fluorescence quenching and photochemical reaction (reductive addition to give a variety of 9,10-dihydroanthracene derivatives) with dialkylamine with transfer of the NH(D) proton; and fluorescence quenching and a less efficient chemical reaction with bonding of the α-carbon of Et_3N to the arene:[47]

$$^1(\text{ArX}^{\delta-}.\text{Et}_2\text{NCH}_2\text{CH}_3{}^{\delta+}) \rightarrow (\text{ArXH.Et}_2\text{NCH}\cdot\text{CH}_3) \rightarrow \text{ArH.CH(CH}_3)\text{NEt}_2$$

In the case of a triplet-state exciplex mechanism, agreement between K_{sv} and K_{φ} will occur only by coincidence, so that $K_{sv} \neq K_{\varphi}$ is compatible with a triplet-state reaction but not with a singlet-state process. This behavior is exemplified by the photodehalogenation of 4-chlorobiphenyl, which is convenient for study because its quantum yield of reduction in the absence of amines is very low ($\Phi < 0.001$). In acetonitrile, the addition of 0.1 *M* amine increased Φ_r to 0.07 (butylamine), 0.25 (dipropylamine), and 0.49 (triethylamine). Initially,[48] the singlet exciplex mechanism was suggested with Et_3N as the amine ($K_{sv} = 23\ M^{-1}$; $K_{\varphi} = 20\ M^{-1}$), but in later work on the same system K_{φ} was consistently found to be greater than K_{sv} (Table 38.3), suggesting a predominantly triplet-state reaction,[49] compatible with a high value of $\Phi(S_1 \rightarrow T_1)$. Furthermore, quenching of the triplet by tertiary amines has been observed experimentally by flash photolysis.[50] Note, however, that even though $K_{sv} \neq K_{\varphi}$, the two parameters follow the same trend with changes in amine and solvent, indicating parallel rates of electron transfer to both singlet and triplet excited states.

Photodechlorination of 4-chlorobiphenyl/Et_3N systems can be carried out using long-wavelength UV, rather than 254-nm, radiation if anthracene is added as the initial light absorber.[51] Besides biphenyl, photoreduction products are formed. The possibility favored by the authors was endothermic electron transfer between anthracene radical anion and 4-chlorobiphenyl.

$$^1C_{14}H_{10} + Et_3N \rightarrow C_{14}H_{10}^{\bullet -} + Et_3N^{\bullet +}$$

$$C_{14}H_{10}^{\bullet -} + C_{12}H_9Cl \rightarrow C_{14}H_{10} + C_{12}H_9Cl^{\bullet -} \rightarrow C_{12}H_9^{\bullet} + Cl^-$$

However, another possibility is the attack of Et_3N on an anthracene-chlorobiphenyl heteroexcimer.

Polychlorinated biphenyls, bromobiphenyls, and 1-bromonaphthalene, all of which undergo efficient $S_1 \rightarrow T_1$ intersystem crossing, show enhanced photodehalogenation in the presence of tertiary aliphatic amines, a reaction consistent with electron transfer to the triplet excited state. An exception is 2,4,6-trichlorobiphenyl, which showed lower photoefficiency in cyclohexane solution when Et_3N was present, a result attributed to its rather efficient photohomolysis ($\Phi = 0.21$); the major effect of Et_3N is, thus, to quench homolysis without providing an alternative efficient reaction channel. In other cases, curved plots of Φ_r vs. [amine] have been interpreted in terms of competing singlet and triplet quenching by the amine.[49] Dechlorination of the higher polychlorinated biphenyl congeners in Aroclor 1254 in natural sunlight is inefficient due to their low absorptivity and lack of short-wavelength radiation but is accelerated in the presence of diethylamine[52,53] and diethyl phenylenediamine;[54] this reaction has been proposed as a method for the destruction of commercial PCB wastes.

Two possible sequences of events follow formation of the exciplex or radical ion:

(A) Loss of halide followed by hydrogen atom abstraction

$$ArX^{\bullet -} \rightarrow Ar^{\bullet} + X^-;\ Ar^{\bullet} + RH \rightarrow Ar - H + R^{\bullet}$$

(B) Protonation followed by loss of a halogen atom

$$ArX^{\bullet -} + H^+ \rightarrow (ArXH)^{\bullet} \rightarrow Ar - H + X^{\bullet}$$

Deuterated solvents have been used to distinguish these possibilities.[49,55] Mechanism A is predicted to give deuterium incorporation using C_6D_{12}, CD_3OH, etc., while Mechanism B should afford deuterium incorporation with CH_3OD, CH_3CN/D_2O, etc.

Mechanism A is implicated by the formation of deuterated product upon photolysis with Et_3N/CD_3OH, and by the failure in other cases to observe deuterium incorporation when CH_3CN/D_2O was used as the solvent. Mechanism B has been suggested for a number of cases (1-chloronaphthalene, 4-chlorobiphenyl, 1-bromonaphthalene, and 9-chloroanthracene), all of which incorporate deuterium into the dehalogenated product when the starting materials are photolyzed with $CH_3CN/Et_3N/D_2O$ or Et_3N/CH_3OD. For example, when Et_2ND was photolyzed with 9,10-dibromoanthracene in heptane, the product 9-bromoanthracene contained deuterium at the *meso* position, indicating that hydrogen was transferred from the amine as a proton rather than as a neutral hydrogen atom:

$$^1(ArBr^{\delta -}.HNEt_2^{\delta +}) \rightarrow (ArBrH.NEt_2) \rightarrow ArH + Br^{\bullet} + Et_2N^{\bullet}$$

Finally, a substantial fraction of the hydrogen always originates from the C-H bonds of the amine, indicating in-cage hydrogen transfer, as shown by the failure to effect complete deuteration with, for example, Et_3N/CD_3OD or Et_3N/C_6D_{12}.

The amine Et_3N also assists the photodechlorination of 1-chloropyrene in acetonitrile, but in this case reduction is further assisted by cyanide ion.[56] Flash photolysis suggests the following sequence of intermediates:

$$PyCl \rightarrow PyCl^{\bullet -} \rightarrow PyClH^{\bullet} \rightarrow PyCNH^{\bullet} \rightarrow PyH$$

TABLE 38.4 Et_3N-Assisted and Unassisted Reactions of Polychlorobenzenes

Products	Unassisted	Et_3N-Assisted
Pentachlorobenzene		
1,2,3,5-Cl_4	67	25
1,2,4,5-Cl_4	26	66
1,2,3,4-Cl_4	7	8
1,2,3,5-Tetrachlorobenzene		
1,3,5-Cl_3	59	22
1,2,4-Cl_3	40	73
1,2,3-Cl_3	<1	5

Singlet 1-chloropyrene gains an electron from Et_3N followed by in-cage proton transfer. Loss of Cl• from this intermediate is very inefficient; however, chloride is displaced by the attack of CN^-. PyCNH• does not go on to give pyrenecarbonitrile, but instead loses CN• to complete the reduction.

Polychlorobenzenes undergo intersystem crossing with high efficiency, thus making T_1 the likely reactive excited state.[57] In these reactions, plots of $\varphi^{-1}\alpha[Et_3N]^{-1}$ are linear at high $[Et_3N]$ but show little Et_3N dependence at low $[Et_3N]$. This suggests the simultaneous involvement of an amine exciplex mechanism and another reaction (excimer or triplet homolysis) that does not involve the amine. Most importantly, the distribution of dechlorinated products is different for the unassisted and Et_3N-assisted reactions in acetonitrile;[58] hence, the regioselectivity of dechlorination may be used as an indicator of the mechanism (Table 38.4). The intermediacy of the polyhalobenzene anion radical in Et_3N-assisted photolyses has been demonstrated unequivocally by the observation of the "assisted" product spread when the radical anion is generated thermally.[59] Furthermore, the "assisted" product distribution is also obtained in Et_3N-assisted reactions sensitized by acetophenone, thus confirming the triplet as the reactive excited state.

The regioselectivity of Cl^- ejection following electron transfer to a polychlorobenzene cannot be interpreted simply in terms of the maximal relief of steric strain[56] but is rationalized instead by considering the stabilization of the radical anion $C_6H_{6-n}Cl_n^{\bullet -}$ by the chlorine substituents. Loss of chlorine is fastest from the position where least delocalization of the negative charge is possible.

Triethylamine also promotes photoreduction of polyfluorobenzenes in both acetonitrile and alkane solvents.[58] In this case, homolysis cannot be a competing reaction, based on energetic arguments. These reactions appear to be entirely parallel to those with polychlorobenzenes, with electron donation to the polyfluorobenzene followed by fluoride loss, together with an excimer component to the reaction. The latter is independent of Et_3N but has $\Phi_r^{-1}\alpha[ArF]^{-1}$. A different product spread is observed in alkanes compared with acetonitrile, consistent with the relative extents of electron transfer in each solvent. Previous to this work, photodehalogenation of fluoroarenes was almost unknown, although photoaddition and photoreduction to dihydro derivatives had been observed with fluorobenzene and aliphatic amines.[60]

Exciplex Reactions Involving Aromatic Amines

These reactions are often mechanistically less clear cut than those with aliphatic amines because both the amine and the aryl halide can potentially absorb light. The reactions of 9,10-dihaloanthracenes with aniline derivative are unambiguous in this respect, as the use of long-wavelength UV radiation ensures light absorption by the haloarene alone. Photoreduction to the 9-haloanthracene is observed for both X = Cl and X = Br, and the excellent agreement between K_{sv} and K_φ for $PhNH_2$, $PhNHCH_3$, $PhN(CH_3)_2$, and $PhNEt_2$ strongly supports reduction through a singlet exciplex.[61]

Dehalogenation of halobenzenes[62,63] and chlorobiphenyls[64] has been studied under conditions where the radiation was initially absorbed by an *N*,*N*-dialkylaniline. The aryl halide quenched the fluorescence of the aniline, and in the halobenzene series reasonable agreement between K_{sv} and K_φ was observed. In

methanolic solution, the halobenzenes yielded benzene and *o*- (and *p*-)phenyl-*N*,*N*-dimethylaniline. Isotopic substitution of the amine ($PhN(CD_3)_2$) afforded benzene-d_1 (66%, X = Cl; 42%, X = Br; 12%, X = I). The d_1 product is the result of proton transfer from $PhN(CD_3)_2$ within the solvent cage. The photoreaction between *m*-chloronitrobenzene and *N*,*N*-dimethylaniline is also an electron transfer process but in this case it is the nitro group that is reduced rather than the chlorine.[65] More recently, the electron donor photosensitizer *N*,*N*,*N*′,*N*′-tetramethylbenzidine (NTMB) has been used to photosensitize the photodehalogenation of chlorobenzenes, resulting in the departure of a chlorine anion.[66]

Miscellaneous Electron Transfer Processes

Like amines, dienes quench many arene singlet and triplet states, a process attributed to the formation of diene/arene exciplexes; these have a much smaller degree of electron transfer than the corresponding arene-amine exciplexes.[67] Ambiguity arises because dienes are commonly used as triplet quenchers and because simple arenes such as benzenes, naphthalenes, and biphenyls absorb at the same wavelengths as dienes.[62]

9,10-Dichloroanthracene absorbs at longer wavelength than simple dienes. It reacts photochemically with 2,5-dimethyl-2,4-hexadiene by two pathways: in nonpolar solvents (benzene) a photocycloadduct forms by way of a singlet exciplex,[64] whereas in polar solvents reduction to 9-chloroanthracene is observed and a triplex ($C_{14}H_8Cl_2$•2DMH) is implicated.[68] Experiments with added D_2O show that in polar solvent the reduction involved transfer of a proton to the exciplex rather than loss of chloride ion.

The dehalogenation of aryl halides is accelerated by aliphatic sulfides,[69] and an electron transfer mechanism is implicated by the incorporation of deuterium in the reduction product when the reaction is carried out in the presence of D_2O.

Radical Anion Chain Reactions

These reactions are relevant to this review in that they may be photoinduced, but as radical chain processes many of them can be initiated in other ways. Radical chain dehalogenation of aryl halides has been reviewed previously.[70] The chain propagation sequence for the deiodination of aryl iodides with CH_3O^-/CH_3OH is shown in Scheme 1. The species $(ArI)^{\bullet -}$ is very short lived and deiodinates efficiently. Reactivity diminishes in the order ArI > ArBr > ArCl and is enhanced in cases where there is relief of steric strain. Photochemical dehalogenations of aryl halides with AlH_4^- and BH_4^- have been proposed to follow similar radical chain mechanisms. Evidence for electron transfer from BH_4^- to ArCl has been present by Freeman and Ramnath.[71]

$$Ar\bullet + CH_3O^- \rightarrow ArH + CH_2O^{\bullet -}$$

$$CH_2O^{\bullet -} + ArI \rightarrow CH_2{=}O + (ArI)^{\bullet -}$$

$$(ArI)^{\bullet -} \rightarrow Ar\bullet + I^-$$

SCHEME 1

Several aryl halides have been reported to dehalogenate efficiently with the combination 2-propanol/OH^-. The proposed mechanism[72] (Scheme 2) is very similar to Scheme 1, with hydroxide ion playing the key role of deprotonating the product of hydrogen abstraction from 2-propanol.

$$ArX^{\bullet -} \rightarrow Ar\bullet + X^-$$

$$Ar\bullet + (CH_3)_2CHOH \rightarrow ArH + (CH_3)_2C^{\bullet}OH$$

$$(CH_3)_2C^{\bullet}OH + OH^- \rightarrow (CH_3)_2CO^{\bullet -} + H_2O$$

$$(CH_3)_2CO^{\bullet -} + ArX \rightarrow ArX^{\bullet -} + (CH_3)_2C{=}O$$

SCHEME 2

Considerable interest has been shown in this reaction as a possible technology for destruction of commercial PCBs. The photolysis of Aroclor 1254 in alkaline 2-propanol at 254 nm had a dechlorination quantum yield of 35, supporting a free-radical chain mechanism.[73] Studies[74–77] elucidating the photodechlorination pathways of 3,3′,4,4′,5,5′-hexachlorobiphenyl, 3,3′,4,4′-tetrachlorobiphenyl, and related lower chlorinated PCB congeners in alkaline 2-propanol reveal that:

1. The more chlorinated congeners are generally more reactive to photodechlorination.
2. Dechlorination occurs mostly on the more substituted ring.
3. Asymmetrical congeners are more readily dechlorinated than more stable symmetrical ones.
4. Dechlorination occurs preferentially at the position that produces a symmetrical product.
5. The π electronic densities of *para* and *meta* chlorines affect their relative reactivities.

Nucleophilic substitution of halogen by the $S_{RN}1$ mechanism follows a related radical chain pathway (Scheme 3), in which the aryl radical Ar• attacks a nucleophile Nu^- rather than abstracting hydrogen. The solvent should not contain easily abstractable hydrogen atoms in order to depress photodehalogenation. Halo-2-pyridones were also found to undergo nucleophilic substitution via an $S_{RN}1$ mechanism when reacted with cesium phenoxides, yielding hydroxyphenyl-2-pyridones.[78]

$$(ArX)^{\bullet -} \rightarrow Ar^{\bullet} + X^-$$

$$Ar^{\bullet} + Nu^- \rightarrow (ArNu)^{\bullet -}$$

$$(ArNu)^{\bullet -} + ArX \rightarrow Ar - Nu + (ArX)^{\bullet -}$$

SCHEME 3

38.4 Heterolytic Mechanisms

Reactions Involving Carbenes

Investigations conducted to elucidate the dechlorination mechanism of 4-chlorophenol have revealed that elimination of HCl via heterolytic C-Cl bond scission from aqueous 4-chlorophenol in the presence of oxygen produces an initial transient carbene, 4-oxocyclohexa-2,5-dienylidene[11,79,80] that has a triplet character and is stable in aqueous solutions. The addition of O_2 to this intermediate affords a benzoquinone-*O*-oxide, from which loss of an oxygen atom yields the major reaction product *p*-benzoquinone. The involvement of a carbene intermediate has also been indicated for 2-chlorophenol.[81]

The role of singlet oxygen in sensitizing the photolysis of chlorophenols has been recently extensively reviewed by Burrows et al.[6] Inhibition of sensitized photodegradation of 2,4,5-trichlorophenol by adding singlet oxygen quenchers supports the participation of singlet oxygen in this process,[16] while the absence of PCDDs and PCDFs among the products of sensitized transformation of 2,4,5-trichlorophenol favors a singlet oxygen mechanism rather than free radical formation. It is believed that singlet oxygen reacts with chlorophenols to produce a $^1O_2$/quencher exciplex via a charge-transfer-induced intersystem crossing process.

Reactions Proceeding Via Nucleophilic Substitution

Photochemical nucleophilic displacements have been studied extensively, and the early work is documented in the exhaustive review by Cornelisse and Havinga.[82] The most detailed studies have been made of methoxynitroarenes rather than halides, and it is well established that nucleophilic displacement occurs most readily *meta* to NO_2. Of the various halide nucleofuges, only fluoride appears to behave analogously to methoxy. Thus, *m*-fluoronitrobenzene reacts photochemically with OH^- to give *m*-nitrophenol, but the reaction is not observed for *m*-chloro- or *m*-bromonitrobenzenes. With oxidizable "nucleophiles" such as secondary amines, photoreduction of the nitro group takes place in preference to substitution

of halide. However, 1-fluoro-3-nitronaphthalene and other "extended *meta*" fluoronitronaphthalenes undergo replacement of fluorine upon irradiation with OH^-, OCH_3^-, CN^-, and CH_3NH_2.[83]

Photoreactions of nitropolychlorinated dibenzo-*p*-dioxins with sodium ethoxide in anhydrous ethanol undergo S_N2Ar^* substitution reactions, yielding ring-opened products.[84] Irradiation of 2,3,4,7,8-pentachloro-1-nitrodibenzo-*p*-dioxin yielded a tetrachloroethoxynitrodibenzo-*p*-dioxin, presumed to be 2,4,7,8-tetrachloro-3-ethoxy-1-nitrodibenzo-*p*-dioxin, based on the *meta* activation of the nitro group. This reaction was associated with a linear relationship between Φ^{-1} and $[Nu^-]^{-1}$. A secondary thermal reaction was also present, yielding a tetrachlorodiethoxyhydroxynitrodiphenyl ether. Irradiation of 1,3,4,7,8-pentachloro-2-nitrodibenzo-*p*-dioxin under the same conditions produced 1,3,7,8-tetrachloro-4-ethoxy-2-nitrodibenzo-*p*-dioxin as a result of the substitution of chlorine *meta* to the nitro group rather than ring opening. A kinetic study suggested that the excited triplet ArX^* undergoes interaction with the nucleophile to give a σ-complex $[ArXNu]^-$ competitively with radiationless decay to the ground state. The σ-complex may then either afford the substitution product or dissociate to ground state reactants.

Photochemical replacement of a substituent by a nucleophile occurs *ortho* and *para* to electron-donating substituents.[85] These reactions are successful for halides as nucleofuges. An example is the conversion of *p*-chloroanisole to *p*-methoxybenzonitrile upon irradiation with cyanide ion. In the case of the isomeric chlorophenols and chloroanisoles, irradiation with alcohols involves a mixture of substitution (replacement by –Cl or –OR) and dehalogenation.[86] The outcomes of these reactions may be highly solvent dependent, as shown by studies on the replacement of fluoride by CN^- and OH^-, when *o*- and *p*-fluoroanisoles are photolyzed with KCN in water/*t*-butyl alcohol mixtures.[87]

Photosubstitution of hexachlorobenzene and other highly chlorinated aromatics by cyanide systems was recently investigated by Konstantinov et al.[88,89] Photolysis of hexachlorobenzene with sodium cyanide resulted in successive photocyanations occurring with a high quantum yield ($\Phi_{diss} = 0.18$) to give the products pentacyanophenol, 4-chloro-2,3,5,6-tetracyanophenol, and a dichlorotricyanophenol. Quantum yields of substrate disappearance increased with the number of chlorine substituents on a substrate and followed the expected relationship $\Phi^{-1}\alpha[CN^-]^{-1}$. The reaction was proposed to proceed via the S_N2Ar^* mechanism. Sensitization and quenching experiments indicated a triplet reactive excited state to be reactive for all substrates tested.

3-Fluoro- and 3-chlorophenol undergo photomethanolysis to yield resorcinol monomethyl ether when irradiated. They also undergo photoamidation by *N*-methylacetamide, a very weak nucleophile, to yield 3-(*N*-methyl-*N*-acetylamino)-phenol together with a small amount of phenol. Photoamidation of *DL*-2-chlorotyrosine methyl ester and *L*-2-fluorotyrosine methyl ester indicated that fluoro compounds are less reactive than chloro compounds in intramolecular amidation. The reactions proceed via a highly reactive electron-deficient intermediate.[90]

Chlorobenzene is converted to phenol in aqueous solution, in quantum yields comparable with that of dehalogenation.[8] Evidence has been presented that the corresponding photohydrolyses of the monochlorobiphenyls involve homolysis, followed immediately by in-cage electron transfer. The aryl cation is trapped by water but can be diverted back to reactant in the presence of added Cl^-:[91]

$$^3Ar\text{-}Cl \rightarrow (Ar\bullet.Cl\bullet) \rightarrow (Ar^+.Cl^-) \rightarrow \rightarrow ArOH$$

Photohydrolysis can therefore be viewed as a variant of photohomolysis. In an organic solvent such as hexane, the radical pair (Ar•.Cl•) separates and then abstracts hydrogen. Abstractable hydrogens are not present in water, and the high dielectric constant permits electron transfer to occur. An exceptional aspect of the reaction is that both 3- and 4-chlorobiphenyls undergo photoisomerization in parallel with photohydrolysis. This is suggested to proceed by way of valence photoisomerization. Related valence photoisomerizations have been observed occasionally upon photolysis of polychlorobenzenes; for example, photolyses of both 1,2,3- and 1,3,5-trichlorobenzenes in aqueous CH_3CN afford up to 10% of 1,2,4-trichlorobenzene in addition to dechlorination products.[5] Modeling studies[92] suggest that the identity of the halogen and the polarizability of the aryl halide are important factors in determining the photohydrolysis quantum yields of substituted aromatic halides.

38.5 Sensitized Reactions of Aryl Halides

In the context of identifying methods for the degradation of aryl halide environmental pollutants in natural waters, solar photodegradation is attractive in terms of "green chemistry" and the economics of using "free"sunlight.[66] A major problem, however, is that haloaromatics do not absorb strongly above 300 nm, and direct photolysis usually proceeds with very low efficiency. The goal is to find a sensitizer that has strong absorption in the solar region of the spectrum and that can transfer energy efficiently to the ground-state target substrate (ArX) to yield an excited triplet substrate state. Because the same excited state of the substrate is produced in both direct and sensitized photolysis, the photoproducts should be similar:

Sensitized route

$$S + h\nu \rightarrow {}^1S^* \rightarrow {}^3S^*$$

$${}^3S^* + ArX \rightarrow S + {}^3ArX^*$$

Direct route

$$ArX + h\nu \rightarrow {}^1ArX^* \rightarrow {}^3ArX^*$$

$${}^3ArX^* \rightarrow \text{products}$$

Occasionally, the products of direct and sensitized photolysis differ, as in the case of acetone sensitization of the dehalogenation of polychlorobenzenes. For example, upon direct photolysis of 1,2,3,5-tetrachlorobenzene in aqueous CH_3CN, 1,2,4-trichlorobenzene was the major product; acetone sensitization of the same reaction gave predominantly the 1,3,5-isomer. The original hypothesis was that the direct reaction involves S_1 and the acetone-sensitized reaction involves T_1.[5] The suggestion that the direct reaction involves S_1 appears untenable given the high value of $\Phi(S_1 \rightarrow T_1)$; in addition, the formation of 1,2,4-trichlorobenzene in the "direct" reaction is reminiscent of the product spread under electron transfer conditions.[56] One possibility is that the acetone-sensitized reaction indeed involves T_1, but that the direct reaction is actually an excimer-mediated reaction.

Various sensitizing chemicals have been investigated in recent years, including hydroquinone and phenol,[93] phenothiazine,[73] hydrogen peroxide,[31] and 2-methoxyphenol.[66]

38.6 Photoinduced Reactions of Aryl Halides

During induced photolysis, a compound added to the solution generates free radicals, which attack the target molecule, producing various types of radicals. Radicals can be formed by either OH-addition or by direct electron transfer, yielding a wide range of possible products. Investigations of the photoinduced degradation of chlorophenols have identified two main pathways of free radical transformation:[6] (1) degradation to nonaromatic compounds, leading to CO_2 and HCl as final products, and (2) condensation, with the formation of phenolic polymers (humic substances). PCDD, PCDF, and PCB products have also been identified during the recombination of phenolic radicals.

38.7 Decomposition of Aryl Halides by Photochemically Produced Hydroxyl Radicals

These reactions do not involve excitation of the aryl halide but are mentioned here because of interest in degrading chlorinated pollutants. Wastewater treatment involving hydroxyl radical production by photolysis of hydrogen peroxide or ozone is a well-known commercial process. Fe^{3+}, H_2O_2, and UV have been used in combination (the photo-Fenton reaction)[28] to enhance the degradation of Aroclor 1242, a mixture of PCBs. The conventional Fenton reaction produces hydroxyl radicals from H_2O_2 and Fe^{2+}:

$$Fe^{2+} + H_2O_2 \rightarrow Fe^{3+} + OH^{\cdot} + OH^{-}$$

Under UV irradiation, Fe^{3+} reacts with water to produce more hydroxyl radicals and Fe^{2+}, making the reaction catalytic in iron:

$$Fe^{3+} + H_2O + h\nu \rightarrow Fe^{2+} + OH^{\cdot} + H^{+}$$

The maximum observed PCB removal was 88%, following 20-hr irradiation in water containing 1 m*M* Fe^{3+} and 30 mmol H_2O_2 at 66°C. Hydroxyl radicals reacted at nonchlorinated positions to give hydroxypolychlorobiphenyls. Both *ortho*- and *para*-dihydroxy-substituted rings were readily oxidized to quinones and further oxidation led to ring-opened products that undergo hydrodechlorination rapidly, as shown by the high yield (up to 85%) of chloride ion.

Photolysis of ferric ions (and also nitrate ions) has also been used[11] as a hydroxyl radical source for the degradation of 1,4-dichlorobenzene. The major product, 2,5-dichlorophenol, was formed by hydroxylation at one of the unsubstituted ring positions.

Several studies of photoinduced degradation of aryl halides in recent years have involved the use of semiconductors, particularly TiO_2 and ZnO,[94] as photocatalysts to enhance the degradation of aryl halides,[94–101] the objective being photomineralization to CO_2 and HCl. This chemistry depends on the excitation of the semiconductor with light of energy greater than its optical band gap (3.2 eV or 74 kcal mol^{-1} for TiO_2), whereupon electrons are transferred to the conduction band, thereby leaving an equal number of electron vacancies or "holes" in the valence band. The latter can interact with water to form hydroxyl radicals (although the reaction is inefficient due to competing electron-hole recombination):

$$h^{+} + H_2O \rightarrow H^{+} + OH^{-}$$

Uchida et al.[95] found that the degradation of trichlorobenzene was enhanced by the use of TiO_2 supported on nickel-polytetrafluoroethylene compared with normal TiO_2. This behavior was attributed to Ni/PTFE acting as a sink for conduction band electrons, thereby inhibiting electron-hole recombination.

In TiO_2 aqueous suspensions, the electrons generated in the conduction band can reduce dissolved oxygen to the highly reactive superoxide ion $O_2^{\bullet -}$, which Wang and Hong[101] suggest is the dominant reaction partner in the photochemical ring-opening of 2-chlorobiphenyl/TiO_2. The rate of reaction of 2-chlorobiphenyl was found by Huang et al.[100] to be approximately proportional to the concentration of suspended TiO_2, and is argued to be due to the need for the aryl halide to adsorb to the surface of the photocatalyst.

Pandiyan et al.[96] found that the dehalogenation of chlorophenols using TiO_2 systems is faster for monohalogenated phenols than poly-substituted phenols.[98] Patterns of photocatalytic degradation of polychlorinated biphenyls are similar to those seen in direct photolysis, with lesser and *ortho*-chlorinated congeners being preferentially decomposed. In general, photocatalytic degradation rates increase with increasing degree of *ortho* substitution.[99]

Chiarenzelli et al.[98] suggest that the solubility of PCB congeners controls their rate of decomposition by regulating their transfer to the aqueous phase and thus to the TiO_2 surface. The rate and degree of photodegradation of polychlorinated biphenyls is also enhanced by the use of shorter wavelength UV light, which facilitates hydroxylation reactions, again increasing solubility and accessibility to photocatalytic sites. Solubilization has also been explored by adding the anionic surfactant FC-143 to TiO_2 photocatalytic systems.[102] Enhanced quantum yields of reaction were achieved because the hydrophobic PCBs partitioned into the hydrophobic interior of the micelles, which in turn adsorbed preferentially on to the TiO_2 surface where hydroxyl radicals were being produced.

Acknowledgments

We thank the Natural Sciences and Engineering Research Council for financial support to L.S. through a summer scholarship and to N.J.B. through a Research Grant.

References

1. Sammes, P. G., Photochemistry of the C-X group, in *The Chemistry of the Carbon-Halogen Bond*, Part II, S. Patai, Ed., Wiley, New York, 1973, chap. 11.
2. Grimshaw, J. and de Silva, A. P., Photochemistry and photocyclization of aryl halides, *Chem. Soc. Rev.*, 10, 181, 1981.
3. Lodder, G., Recent advances in the photochemistry of the carbon-halogen bond, in *The Chemistry of Functional Groups*, Suppl. D, S. Patai and Z. Rappoport, Eds., Wiley, New York, chap. 29.
4. Davidson, R. S., Goodin, J. W., and Kemp, G., The photochemistry of aryl halides and related compounds, in *Advances in Physical Organic Chemistry*, Vol. 20, Academic Press, London, 1984, 191.
5. Choudhry, G. G., Webster, G. R. B., and Hutzinger, O., Environmental aquatic photochemistry of chlorinated aromatic pollutants, *Toxicol. Environ. Chem.*, 17, 267, 1988.
6. Burrows, H. D., Ernestova, L., Kemp, T. J., Skurlatov, Y. I., Purmal, A. P., and Yermakov, A. N., Kinetics and mechanism of photodegradation of chlorophenols, *Progr. React. Kinet.*, 23, 45–207, 1998.
7. Dulin, D., Drossman, H., and Mill, T., Products and quantum yields for photolysis of chloroaromatics in water, *Environ. Sci. Technol.*, 20, 72, 1986.
8. Choudhry, G. G., Webster, G. R. B., and Hutzinger, O., Environmentally significant photochemistry of chlorinated benzenes and their derivatives in aquatic systems, *Toxicol. Environ. Chem.*, 13, 27, 1986.
9. Pagni, R. M. and Sigman, M. E., The photochemistry of PAHs and PCBs in water and on solids, in *The Handbook of Environmental Photochemistry*, Vol. 2, Part L, *Environmental Photochemistry*, P. Boule, Ed., Springer-Verlag, Berlin, 1999, 139.
10. Bunce, N. J., Landers, J. P., Langshaw, J-A., and Nakai, J. S., An assessment of the importance of direct solar degradation of some simple chlorinated benzenes and biphenyls in the vapour phase, *Environ. Sci. Technol.*, 23, 213, 1989.
11. Meunier, L., Pilichowski, J.-F., and Boule, P., Photochemical behavior of 1,4-dichlorobenzene in aqueous solution. *Can. J. Chem.*, 79, 1179–1186, 2001.
12. Mansour, M., Parlar, H., and Korte, F., Photoinduzierte deuterirung monosubstituierter dichlorobenzole, *Chemosphere*, 9, 59, 1980.
13. Sing, Y.-Q., Yuzuri, T., Suezawa, H., Sakakibara, K., Hirota, M., and Nakada, M., The photolyses of 2,6- and 2,4-difluorohalobenzenes, *Bull. Chem. Soc. Jpn.*, 70, 1875–1878, 1997.
14. Wagner, P. J., Sedon, J., Waite, C., and Gudmundsdottir, A., Photoinduced radical cleavage of acylphenyl halides: different mechanisms for C–I and C–Br bonds, *J. Am. Chem. Soc.*, 116, 10284–10285, 1994.
15. Wagner, P. J. and Waite, C. I., Photoinduced radical cleavage of iodobenzophenones, *J. Phys. Chem.*, 99, 7388–7394, 1995.
16. Skurlatov, Y. I., Ernestova, L. S., Vichutinskaya, E. V., Samsonov, D. P., Semenova, I. V., Rod'Ko, I. Y., Shvidky, V. O., Pervunina, R. I., and Kemp, T. J., Photochemical transformation of polychlorinated phenols, *J. Photochem. Photobiol. A: Chem.*, 107, 207–213, 1997.
17. Ichimura, T., Mori, Y., Shinohara, H., and Nishi, N., Photofragmentation of chlorotoluenes and dichlorobenzenes: substituent effects on the dissociation mechanism and angular distribution of the Cl fragment, *J. Chem. Phys.*, 107, 835–842, 1997.
18. Zhang, H., Zhu, R.-S., Wang, G.-J., Han, K.-L., He, G.-Z., and Lou, N.-Q., Photofragment translational spectroscopy of *p*-bromotoluene at 266 nm, *Chem. Phys. Lett.*, 300, 483–488, 1999.
19. Zhong, D. and Zewail, A. H., Femtosecond real-time probing of reactions. 23. Studies of temporal, velocity, angular and state dynamics from transition states to final products by femtosecond-resolved mass spectrometry, *J. Phys. Chem. A*, 102, 4031–4058, 1998.
20. Zhu, R., Zhang, H., Wang, G.-J., Gu, X., Han, K.-L., He, G.-Z., and Lou, N.-Q., Photodissociation of *o*-bromotoluene at 266 nm, *Chem. Phys. Lett.*, 313, 98–104, 1999.

21. Ichimura, T. and Mori, Y., Photolysis of monochlorobenzene in gas phase, *J. Chem. Phys.*, 58, 288, 1973.
22. Atkinson, R., Atmospheric chemistry of PCBs, PCDDs and PCDFs, *Issues Environ. Sci. Technol.*, 6(Chlorinated Organic Micropollutants), 53–72, 1996.
23. Masuzaki, Y., Matsumura, T., Tsubota, H., Ikeda, Y., Chisaki, Y., Morita, M., and Ito, H., Dechlorination process of chlorobiphenyl by light, *Organohalogen Comp.*, 36, 385–388, 1998.
24. Miao, X.-S., Chu, S.-G., and Xu, X.-B., Photodegradation of 2,2′,5,5′-tetrachlorobiphenyl in hexane. *Bull. Environ. Contam. Toxicol.*, 56, 571–574, 1996.
25. Watanabe, I., Kashimoto, T., and Tatsukawa, R., Confirmation of the presence of the flame retardant decabromobiphenyl ether in river sediment from Osaka, Japan, *Bull. Environ. Contam. Toxicol.*, 36, 839, 1986.
26. Sellström, U., Söderström, G., de Wit, C., and Tysklind, M., Photolytic debromination of decabromodiphenyl ether, DeBDE, *Organohalogen Comp.*, 35, 447–450, 1998.
27. Watanabe, I., Kawano, M., and Tatsukawa, R., Photolytic decomposition of polyhalogenated dibenzofurans in hexane solution by UV and sun light, *Kankyo Kagaku*, 4, 408–409, 1994.
28. Pignatello, J. J. and Chapa, G., Degradation of PCBs by ferric ion, hydrogen peroxide and UV light, *Environ. Toxicol. Chem.*, 13, 423–427, 1994.
29. Chu, W., Jafvert, C. T., Diehl, C. A., Marley, K., and Larson, R. A., Phototransformations of polychlorobiphenyls in Brij 58 micellar solutions. *Environ. Sci. Technol.*, 32, 1989–1993, 1998.
30. Choudhry, G. G. and Hutzinger, O., Photochemical formation and degradation of polychlorinated dibenzofurans and dibenzo-*p*-dioxins, *Residue Rev.*, 84, 113, 1982.
31. Yan, Q., Kapila, S., Sivils, L. D., and Elseewi, A. A., Effects of sensitizers and inhibitors on phototransformation of polychlorinated dibenzo-p-dioxins, PCDDs. *Chemosphere*, 31, 3627–3634, 1995.
32. Sivils, L. D., Kapila, S., Yan, Q., and Zhang, X., Studies on vapor phase phototransformation of polychlorinated dibenzo-*p*-dioxins, PCDDs): effect of environmental parameters, *Organohalogen Comp.,* 24, 167–172, 1995.
33. Konstantinov, A. and Bunce, N. J., Photodechlorination of octachlorodibenzo-*p*-dioxin and octachlorodibenzofuran in alkane solvents in the absence and presence of triethylamine, *J. Photochem. Photobiol. A: Chem.*, 94, 27–35, 1996.
34. Konstantinov, A. D., Johnston, A. M., Cox, B. J., Petrulis, J. R., Orzechowski, M. T., Bunce, N. J., Tashiro, C. H. M., and Chittim, B. G., Photolytic Method for Destruction of Dioxins in Liquid Laboratory Waste and Identification of the Photoproducts from 2,3,7,8-TCDD, *Environ. Sci. Technol.*, 34, 143–148, 2000.
35. Rayne, S., Wan, P., Ikonomou, M. G., and Konstantinov, A. D., Photochemical mass balance of 2,3,7,8-TeCDD in aqueous solution under UV light shows formation of chlorinated dihydroxybiphenyls, phenoxyphenols and dechlorination products, *Environ. Sci. Technol.*, 36, 1995–2002, 2002.
36. Vollmuth, S., Zajc, A., and Niessner, R., Formation of polychlorinated dibenzo-*p*-dioxins and polychlorinated dibenzofurans during the photolysis of pentachlorophenol-containing water, *Environ. Sci. Technol.*, 28, 1145–1149, 1994.
37. D'Auria, M., Photochemical behaviour of halogenoheterocyclic derivatives. The alternative between arylation and dehalogenation reactions, *Heterocycles*, 45, 1775–1780, 1997.
38. Freeman, P. K. and Haugen, C. M., Differential photohydrodehalogenation reactivity of bromobenzenes (1,2,4-tribromobenzene, 1,2,3,5-tetrabromobenzene) and pentachlorobenzene: sunlight-based remediation, *J. Chem. Technol. Biotechnol.*, 72, 45–49, 1998.
39. Freeman, P. K., Jang, J.-S., and Ramnath, N., The photochemistry of polyhaloarenes. 10. The photochemistry of 4-bromobiphenyl, *J. Org. Chem.*, 56, 6072, 1991.
40. Freeman, P. K., Jang, J.-S., and Haugen, C. M., The photochemistry of polyhaloarenes. XIII. The photohydrodehalogenation of 3,4-dibromobiphenyl. *Tetrahedron*, 52, 8397–8406, 1996.

41. Bunce, N. J., Bergsma, J. P., Bergsma, M. D., De Graaf, W., Kumar, Y., and Ravanal, L., Structure and mechanism in the photoreduction of aryl chlorides in alkane solvents, *J. Org. Chem.*, 45, 3708, 1980.
42. Nowakowska, M., Sustar, E., and Guillet, J. E., Studies of the antenna effect in polymer molecules. 23. Photosensitized dechlorination of 2,2′,4,4′,6,6′-hexachlorobiphenyl solubilized in an aqueous solution of poly(sodium styrenesulfonic acid-*co*-2-vinylnaphthalene), *J. Am. Chem. Soc.*, 113, 253, 1991.
43. Freeman, P. K., Ramnath, N., and Richardson, A. D., Photochemistry of polyhalobenzenes. 8. The photodechlorination of pentachlorobenzene, *J. Org. Chem.*, 56, 3643, 1991.
44. Freeman, P. K. and Lee, Y.-S., Photochemistry of polyhaloarenes. 12. The photochemistry of pentachlorobenzene in micellar media, *J. Org. Chem.*, 57, 2846, 1992.
45. Kulis, Y. Y., Poletaeva, I.-Y. and Kuz'min, M. G., Photochemical reactions of halosubstitution by hydrogen in aryl halides by activity of nucleophilic reagents [English transl.], *J. Org. Chem. USSR*, 9, 1242, 1973.
46. Soloveichik, O. M. and Ivanov, V. L., Photochemical elimination in dihalo substituted anthracenes in presence of aliphatic amines [English transl.], *J. Org. Chem. USSR*, 10, 2416, 1974.
47. Yang, N. C. and Libman, J., Chemistry of exciplexes, photochemical addition of secondary amines to anthracene, *J. Am. Chem. Soc.*, 95, 5783, 1973.
48. Ohashi, M., Tsujimoto, K., and Seki, K., Photoreduction of 4-chlorobiphenyl by aliphatic amines, *J. Chem. Soc., Chem. Commun.*, 384, 1973.
49. Bunce, N. J., Photolysis of aryl chlorides with aliphatic amines, *J. Org. Chem.*, 47, 1948, 1982.
50. Beecroft, R. A., Davidson, R. S., and Goodwin, D. C., The amine assisted photo-dehalogenation of halo-aromatic compounds, *Tetrahedron Lett.*, 24, 5673, 1983.
51. Tanaka, Y., Uryu, T., Ohashi, M., Tsujimoto, K., Dechlorination of 4-chlorobiphenyl mediated by aromatic photo-catalysts, *J. Chem. Soc., Chem. Commun.*, 1703, 1987.
52. Lin, Y., Gupta, G., and Baker, J., Photodegradation of Aroclor 1254 using diethylamine and simulated sunlight, *J. Hazard. Mater.*, 45, 259–264, 1996.
53. Lin, Y., Gupta, G., and Baker, J., Photodegradation of polychlorinated biphenyl congeners using simulated sunlight and diethylamine, *Chemosphere*, 31, 3323–3344, 1995.
54. Lin, Y., Gupta, G., and Baker, J., Photodegradation of Aroclor 1254 using simulated sunlight and various sensitizers, *Bull. Environ. Contamin. Toxicol.*, 56, 566–570, 1996.
55. Davidson, R. S. and Goodin, J. W., Mechanistic aspects of the triethylamine assisted photo-induced dehalogenation of halogeno-aromatic compounds, *Tetrahedron Lett.*, 22, 163, 1981.
56. Lemmetyinen, H., Ovaskainen, R., Nieminen, K., and Sychtchikova, I., Photolysis of pyrene and chloropyrene in the presence of triethylamine in acetonitrile: dehalogenation assisted by potassium cyanide, *J. Chem. Soc., Perkin Trans. 2*, 113, 1992.
57. Bunce, N. J., Hayes, P. J. and Lemke, M. E., Photolysis of polychlorinated benzenes in cyclohexane solution, *Can. J. Chem.*, 61, 1103, 1983.
58. Freeman, P. K., Srinivasa, R., Campbell, J.-A., and Deinzer, M. L., The photochemistry of polyhaloarenes. 5. Fragmentation pathways in polychlorobenzene radical anions, *J. Am. Chem. Soc.*, 108, 5531, 1986.
59. Freeman, P. K. and Ramnath, N., Photochemistry of polyhaloarenes 9. Characterization of the radical anion intermediate in the photodehalogenation of polyhalobenzenes, *J. Org. Chem.*, 56, 3646, 1991.
60. Gilbert, A. and Krestonosich, S., Excited state substitution and addition reactions of aryl fluorides with aliphatic amines, *J. Chem. Soc., Perkin Trans. 1*, 1393, 1980.
61. Soloveichik, O. M., Ivanov, V. L., and Kuz'min, M. G., Mechanism of photosubstitution of halogen by hydrogen in dihalo-substituted anthracene by activity of amines [English transl.], *J. Org. Chem. USSR*, 12, 860, 1976.
62. Pac, C., Tosa, T., and Sakurai, H., Photochemical reactions of aromatic compounds. IX. Photochemical reactions of dimethylaniline with halobenzenes, *Bull. Chem. Soc. Jpn.*, 45, 1169, 1972.

63. Grodowski, M. and Latowski, T., A study on a photochemical reaction in the system *N*,*N*-dimethylaniline-bromobenzene, *Tetrahedron*, 30, 767, 1974.
64. Bunce, N. J. and Gallacher, J. C., Photolysis of aryl chlorides with dienes and with aromatic amines, *J. Org. Chem.*, 47, 1955, 1982.
65. Döpp, D. and Heuber, J., *N*-demethylation of *N*,*N*-dimethylaniline by photoexcited 3-nitrochlorobenzene, *Tetrahedron Lett.*, 23, 1553, 1982.
66. Galadi, A., Bitar, H., Chanon, M., and Julliard, M., Photosensitized reductive dechlorination of chloroaromatic pesticides, *Chemosphere*, 30, 1655–1669, 1995.
67. Yang, N. C., Yates, R. L., Masnovi, J., Shold, D. M., and Chiang, W., Chemistry of exciplexes. Photocycloadditions of anthracenes to conjugated polyenes, *Pure Appl. Chem.*, 51, 173, 1979.
68. Smothers, W. K., Schanze, K. S., and Saltiel, J., Concerning the diene-induced photodechlorination of chloroaromatics, *J. Am. Chem. Soc.*, 101, 1895, 1979.
69. Beecroft, R. A., Davidson, R. S., Goodwin, D. C., and Pratt, J. E., Quenching of singlet and triplet excited aromatic hydrocarbons by sulphides: the amine and sulphide enhanced photo-induced degradation of chloro- and cyanoaromatic hydrocarbons, *Tetrahedron*, 40, 4487, 1984.
70. Bunnett, J. F., Radical chain, electron-transfer dehalogenation reactions, *Acc. Chem. Res.*, 25, 2, 1992.
71. Freeman, P. K. and Ramnath, N., Photochemistry of polyhaloarenes. 7. Photodechlorination of pentachlorobenzene in the presence of sodium borohydride, *J. Org. Chem.*, 53, 148, 1988.
72. Nishiwaki, T., Usai, M., Anda, K., and Hida, M., Dechlorination of polychlorinated biphenyls by UV-irradiation. V. Reaction of 2,4,6-trichlorobiphenyl in neutral and alkaline alcoholic solution, *Bull. Chem. Soc. Jpn.*, 52, 821, 1979.
73. Hawari, J., Demeter, A., and Samson, R., Sensitized photolysis of polychlorobiphenyls in alkaline 2-propanol: dechlorination of Aroclor 1254 in soil samples by solar radiation, *Environ. Sci. Technol.*, 26, 2022–2029, 1992.
74. Yao, Y., Kakimoto, K., Ogawa, H. I., Kato, Y., Hanada, Y., Shinohara, R., and Yoshino, E., Photodechlorination pathways of non-*ortho*-substituted PCBs by ultraviolet irradiation in alkaline 2-propanol, *Bull. Environ. Contamin. Toxicol.*, 59, 238–245, 1997.
75. Yao, Y., Kakimoto, K., Ogawa, H. I., Kato, Y., Hanada, Y., Shinohara, R., and Yoshino, E., Reductive dechlorination of non-*ortho*-substituted polychlorinated biphenyls by ultraviolet irradiation in alkaline 2-propanol, *Chemosphere*, 35, 2891–2897, 1997.
76. Yao, K., Kato, Y., Hanada, Y., and Shinohara, R., Study on the photodechlorination pathways of non-*ortho*-substituted PCBs by UV irradiation in alkaline 2-propanol, *Organohalogen Comp.*, 33, 246–249, 1997.
77. Yao, Y., Kato, Y., Kadokami, K., and Shinohara, R., Photochemistry of non-*ortho*-substituted PCBs by UV irradiation in alkaline 2-propanol, *Organohalogen Comp.*, 36, 381–384, 1998.
78. Higuchi, H., Hattori, M., and Ohmiya, S., Direct arylation of 2-pyridones; photostimulated SRN1 reaction between cesium phenoxides and chloro-2-pyridones, *Heterocycles*, 52, 253–260, 2000.
79. Grabner, G., Richard, C., and Koehler, G., Formation and reactivity of 4-oxocyclohexa-2,5-dienylidene in the photolysis of 4-chlorophenol in aqueous solution at ambient temperature, *J. Am. Chem. Soc.*, 116, 11470–114780, 1994.
80. Ouardaoui, A., Steren, C. S., van Willigen, H., and Yang, C., FT-EPR study of the photolysis of 4-chlorophenol, *J. Am. Chem. Soc.*, 117, 6803–6804, 1995.
81. Akai, N., Kudoh, S., Takayanagi, M., and Nakata, M., Photoreaction mechanisms of 2-chlorophenol and its multiple chloro-substituted derivatives studied by low-temperature matrix-isolation infrared spectroscopy and density-functional-theory calculations, *J. Photochem. Photobiol. A: Chem.*, 146, 49–57, 2001.
82. Cornelisse, J. and Havinga, E., Photosubstitution reactions of aromatic compounds, *Chem. Rev.*, 75, 353, 1975.
83. Lammers, J. G. and Cornelisse, J., Photoreactions of aromatic compounds. 37. Photosubstitution reactions of nitronaphthalene derivatives, *Isr. J. Chem.*, 16, 299, 1977.

84. Merica, S. G. and Bunce, N. J., Synthesis of nitropolychlorinated dibenzo-*p*-dioxins (NPCDDs) and their photochemical reaction with nucleophiles, *Can. J. Chem.*, 73, 826–834, 1995.
85. Ivanov, V. L. and Eggert, L., Halogen substitution by sulfite ion in 1-hydroxy-4-chloronaphthalene [English transl.], *J. Org. Chem. USSR*, 19, 2075, 1984.
86. Freeman, P. K. and Ramnath, N., Photochemistry of polyhaloarenes. 7. Photodechlorination of pentachlorobenzene in the presence of sodium borohydride, *J. Org. Chem.*, 53, 148, 1988.
87. Liu, J. H. and Weiss, R. G., Anomalous effects during aromatic photosubstitutions of 2- and 4-fluoroanisoles in solvent mixtures of water and *tert*-butyl alcohol, *J. Org. Chem.*, 50, 3655, 1985.
88. Konstantinov, A., Kingsmill, C. A., Ferguson, G., and Bunce, N. J., Successive photosubstitution of hexachlorobenzene with cyanide ion, *J. Am. Chem. Soc.*, 120, 5464–5468, 1998.
89. Konstantinov, A. D., Johnston, A. N., and Bunce, N. J., Successive photocyanation of highly chlorinated aromatic compounds, *Can. J. Chem.*, 77, 1366–1373, 1999.
90. Zhang, B., Zhang, J., Yang, D.-D. H., and Yang, N-C. C., Photoamidation of *N*-acetyl-2-chlorotyrosine methyl ester and 3-chlorophenol, *J. Org. Chem.*, 61, 3236–3237, 1996.
91. Orvis, J., Weiss, J., and Pagni, R. M., Further studies on the photoisomerization and hydrolysis of chlorobiphenyls in water. Common ion effect in the photohydrolysis of 4-chlorobiphenyl, *J. Org. Chem.*, 56, 1851, 1991.
92. Chen, J., Peijnenburg, W. J. G. M., Quan, X., Chen, S., Zhao, Y., and Yang, F., The use of PLS algorithms and quantum chemical parameters derived from PM3 Hamiltonian in QSPR studies on direct photolysis quantum yields of substituted aromatic halides, *Chemosphere*, 40, 1319–1326, 2000.
93. David-Oudjehani, K. and Boule, P., Photolysis of halophenols in aqueous solution sensitized by hydroquinone or phenol, *New J. Chem.*, 19, 199–206, 1995.
94. Villasenor, J., Reyes, P., and Pecchi, G., Photodegradation of pentachlorophenol on ZnO, *J. Chem. Technol. Biotechnol.*, 72, 105–110, 1998.
95. Uchida, H., Katoh, S., and Watanabe, M., Photocatalytic decomposition of trichlorobenzene using TiO_2 supported on nickel-poly(tetrafluoroethylene) composite plate, *Chem. Lett.*, 261–262, 1995.
96. Pandiyan, T., Martinez, R., Orozco Martinez, J., Burillo Amezcua, G., and Martinez-Carrillo, M.A., Comparison of methods for the photochemical degradation of chlorophenols, *J. Photochem. Photobiol. A: Chem.*, 146, 149–155, 2002.
97. Kuo, C.-Y. and Lo, S.-L., Adsorption of aqueous 4-chlorobiphenyl and treatment with UV-illuminated titanium dioxide, *J. Colloid Interface Sci.*, 196, 199–206, 1997.
98. Chiarenzelli, J., Scrudato, R., Wunderlich, M., Rafferty, D., Jensen, K., Oenga, G., Roberts, R., and Pagano, J., Photodecomposition of PCBs absorbed on sediment and industrial waste: implications for photocatalytic treatment of contaminated solids, *Chemosphere*, 31, 3259–3272, 1995.
99. De Felip, E., Ferri, F., Lupi, C., Trieff, N. M., Volpi, F., and di Domenico, A., Structure-dependent photocatalytic degradation of polychlorobiphenyls in a TiO_2 aqueous system, *Chemosphere*, 33, 2263–2271, 1996.
100. Huang, Q., Hong, C.-S., and Bush, B., Photocatalytic degradation of PCBs in TiO_2 aqueous suspensions, *Chemosphere*, 32, 1869–1881, 1996.
101. Wang, Y. and Hong, C.-S., TiO_2-mediated photomineralization of 2-chlorobophenyl: the role of O_2, *Water Res.*, 34, 2791–2797, 2000.
102. Huang, Q. and Hong, C.-S., TiO_2 photocatalytic degradation of PCBs in soil-water systems containing fluoro surfactant, *Chemosphere*, 41, 871–879, 2000.

39

Photochemistry of Hydroxyarenes

Matthew Lukeman
University of Victoria

Peter Wan
University of Victoria

39.1 Introduction

The excited state properties of hydroxyaromatic compounds (phenols, naphthols, etc.) are of interest to a wide audience in chemistry, including those interested in the environmental decomposition of phenols, chemical physicists interested in the very fast dynamics of excited-state proton transfer (ESPT) and excited-state intramolecular proton transfer (ESIPT), physical chemists interested in photoionization and the photochemical pathways for phenoxyl radical formation, and organic photochemists interested in the mechanisms of phenol and hydroxyarene photochemistry. Due to space limitations, this review is restricted to molecular photochemistry of hydroxyaromatic compounds reported during the last three decades that are of primary interest to organic photochemists. It also includes a brief section on the phenomenon of enhanced acidity of phenols and other hydroxyaromatics because this is central to hydroxyarene photochemistry and forms the basis of much of the mechanistic photochemistry to be discussed later on. Several reviews that offer related coverage to this work have also appeared recently.[1] This review does not cover aspects of electron photoejection from phenols or phenolate ions (and related compounds such as tyrosine) or phenol OH homolysis induced photochemically, as shown in Eq. (39.1), as these are adequately covered elsewhere:[2]

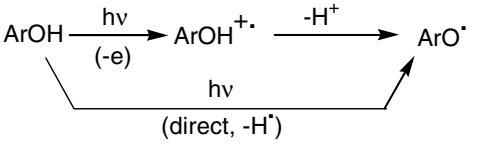

(39.1)

In general, the quantum yields are low (<10%)[2c] and/or arise via two-photon laser excitation. More importantly, to our knowledge, none is known to give rise to well-characterized photoproducts, although the process is important in biological systems.[2d]

0-8493-1348-1/04/$0.00+$1.50

39.2 Enhanced Acidity of Hydroxyaromatic Compounds in the Excited Singlet State

The photoprototopic behavior of phenols and hydroxyarenes in general has been well studied and is based on the enhanced acidity of these types of compounds in S_1 (Scheme 1).[3] For example, the pK_a (S_0)

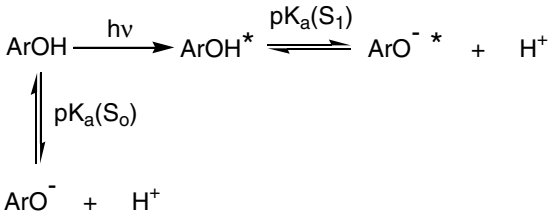

SCHEME 1

of 2-naphthol is 9.5, but its $pK_a(S_1)$ is 2.8, a change in acidity of about 7 orders of magnitude. Even more dramatic is the change in pK_a for 1-naphthol [$pK_a(S_0) = 9.2$; $pK_a(S_1) = 0.4$].[4] The increase in acidity of hydroxyarenes in S_1 is generally believed to be due to the enhanced electron-donating character of the oxygen atom to the benzene π system (more charge transfer character), although other effects such as the symmetry of the lowest singlet also play a role. The enhanced charge transfer character of ArOH* is exemplified by observation of deuterium incorporation of 1-naphthol on photolysis in dilute D_3O^+ where the 5-position is predominately deuterated (Eq. (39.2)), whereas deuterium incorporation in the ground state is observed only on the ring bearing the hydroxyl group:[4,5]

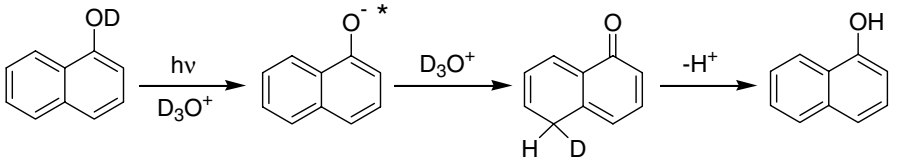

(39.2)

In molecular systems where the phenol or hydroxyarene moiety is in close proximity to a functional group (typically, aromatic ketone or the nitrogen of a heterocycle) that experiences an enhancement in basicity on excitation to S_1, the well-studied phenomenon of excited-state intramolecular proton transfer (ESIPT) is observed.[3] The vast majority of these ESIPT is reversible, some with exceptionally fast rates:[3,6]

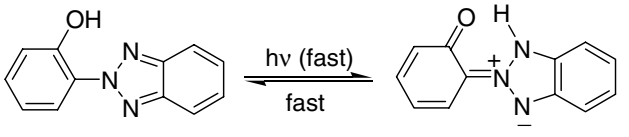

Tinuvin-P

(39.3)

This is a very wide area and is not reviewed in this work except for selected systems that have (or are related to systems that have) net photochemistry and those that are not reversible. These are described in sections to follow.

Simple phenols and naphthols require an aqueous medium for ESPT to take place. The exact role of water in promoting ESPT has been investigated and debated extensively,[5] with the role of water clusters apparently being crucial. Nevertheless, the complete absence of ESPT of simple phenols and naphthols in alcohol (and other organic) solvents is a stark experimental fact. In kinetic terms, the rate of proton dissociation in these solvents cannot compete with other deactivational channels for S_1 of these compounds.

Tolbert and co-workers[5] have carried out extensive studies aimed at enhancing the excited state acidity of naphthols, with the ultimate aim of observing ESPT in organic solvents. Initial work centered on cyano-substituted 1-naphthols **1** and **2**. Both were found to be much more acidic in S_1 and exhibited ESPT in alcohols and DMSO; however, due to the weakness of the fluorescence emission of these naphthols, estimating the $pK_a(S_1)$ was problematic. Fortunately, cyano-substituted 2-naphthols such as **3** and **4** (which have better fluorescence properties) were also stronger acids in S_1. Indeed, the estimated $pK_a(S_1)$ for **4** is –4.5, the most acidic of all the compounds studied to date. Compounds of this type also undergo ESPT in organic solvents such as MeOH, EtOH, DMSO and DMF. These "super photoacids" open up the possibility of carrying out photo-initiated acid-catalyzed reactions in organic solvents.

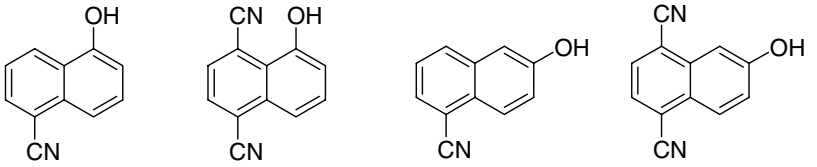

39.3 Photochemistry of Halo and Cyanophenols

The considerable interest in the study of the degradation processes of halophenols is due to their presence as pollutants resulting from pulp and paper processes and from industrial production of herbicides and pesticides.[7] Photochemical methods of breaking down these waste products have received considerable attention, and a detailed mechanistic review of the topic is available.[9] The general mechanisms that govern the photochemical fates of simple (monohalogenated) derivatives are discussed here.

Boule and co-workers[8,11,12] reported very different efficiencies for the phototransformation of 2-chlorophenol (**5**) in neutral (Φ = 0.03) and in alkaline (Φ = 0.32) aqueous media. In alkaline solution, phenolate $\mathbf{5}^-$ gives, upon photolysis, cyclopentadiene carboxylic acids (**6a** and **6b**), which dimerize to **7** in concentrated solution. In neutral solution, this reaction is in competition with the formation of pyrocatechol (**8**) (Scheme 2). Formation of the cyclopentadiene carboxylic acids (**6a** and **6b**) was also observed for 2-fluorophenol and 2-bromophenol. The mechanism shown in Scheme 3 involving a carbene intermediate was proposed as being responsible for the formation of **6**. Although no direct evidence exists for the intermediacy of ketocarbene **9**, more recent studies[10] employing nanosecond laser flash photolysis (LFP) have provided evidence for the presence of ketene **10** and its subsequent conversion to fulvene-6,6-diol (**11**). α-Ketocarbene **9** can quickly undergo a Wolff rearrangement to give **10** and hence is

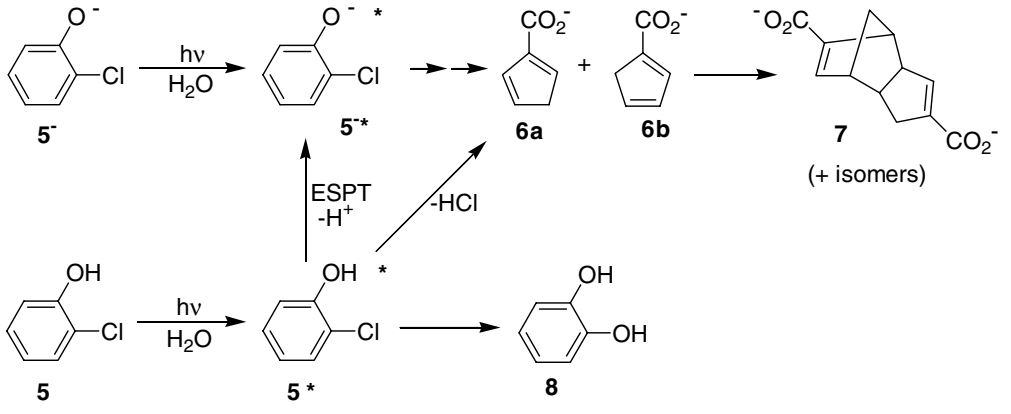

SCHEME 2

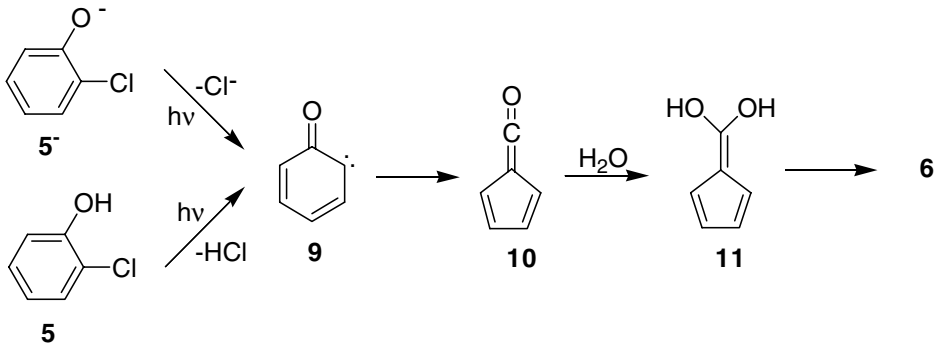

SCHEME 3

too short lived to be detected by nanosecond LFP. Not addressed was whether **5** undergoes direct loss of HCl to give **9**, or whether it undergoes ESPT to solvent to give the excited phenolate prior to dechlorination. Similar transients were observed for LFP of 2-bromophenol and 2-fluorophenol, suggesting that they react via a similar pathway. Although the authors did not propose a mechanism for the formation of **8**, a likely mechanism is loss of Cl^- on photolysis to give an aryl cation that is subsequently trapped by water.

The dominant product (>80% yield) resulting from photolysis of 3-halophenols is resorcinol (**12**), with no dependence on the nature of the halogen:[8,10,13,14]

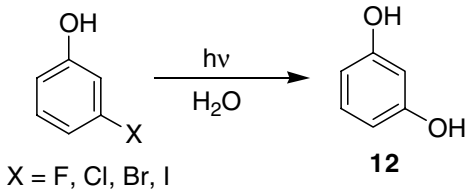

(39.4)

Higher quantum yields were observed on irradiation of the phenolate. The authors[13,14] proposed a mechanism in which a water molecule attacks the ring carbon with concerted loss of Cl^- in an S_N2 fashion, although this mechanism is inconsistent with the higher yields observed on irradiation of the phenolate (the phenolate excited state should be more electron rich than the phenol excited state and thus would be expected to be less reactive toward S_N2 substitutions). Other mechanistic possibilities include ArCl bond heterolysis followed by attack of water on the resultant aryl cation, or initial ESPT to solvent to generate the excited state phenolate, which can then undergo ArCl heterolysis and trapping by solvent. No intermediates were sufficiently long lived to be observed by nanosecond LFP.

4-Chlorophenol (**13**) is perhaps the most studied of the halophenols, as it is a common pollutant found in water that has been treated with chlorine. Early work by Omura and Matsuura[13] revealed that, upon photolysis of concentrated basic solutions, several products are formed, including phenol, hydroquinone (**14**) and the biphenyl based coupling product (**15**). The authors proposed that homolytic cleavage of the ArCl bond is a major pathway from the excited state of **13**, as the formation of aryl radicals would explain the coupling products, although not all observed products could be explained by this pathway. Subsequent studies by Lipczynska–Kochany[14] employing dilute (10^{-4} M) aerated solutions reported that photolysis led to nearly quantitative generation of benzoquinone (**16**). When the solutions were deaerated prior to photolysis, **14** was the major photoproduct recovered, although significant amounts of coupled products were also observed. As the substrate concentration in deaerated solutions was increased, the yield of coupled products also increased, and formation of oligomeric species was detected; in aerated conditions, formation of **16** was still nearly quantitative.

Grabner and co-workers,[15] using nanosecond LFP, were able to observe a transient that they assigned to ketocarbene **17**. This ketocarbene quickly reacts with oxygen, ultimately giving **16** and with H-donating

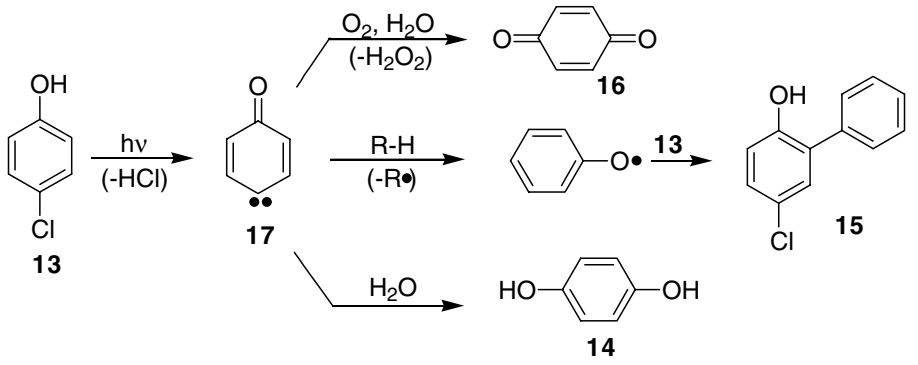

SCHEME 4

solvents giving the phenoxyl radical (Scheme 4). Ketocarbene **17** also undergoes a slow reaction with water, presumably via insertion into an OH bond, to give hydroquinone (**14**). Subsequent studies[16,17] supported the initial formation of **17**. Grabner and co-workers[15] favored a mechanism of reaction involving initial heterolytic loss of chloride followed by deprotonation over a mechanism involving initial ESPT to solvent followed by loss of chloride, as the efficiency of ketocarbene formation is unaffected by pH in the range of 0 to 7 ($pK_a^* \sim 4$ for **13**). Other studies[14,18] indicated that the fluoro, bromo and iodo analogs reacted via the same pathway.

While studying the photochemistry of 2-cyanophenol (**18**), Ferris and Antonucci[19–21] reported that the first formed product of **18** is isonitrile **19**, which then thermally cyclizes to benzoxazole **20** at room temperature:

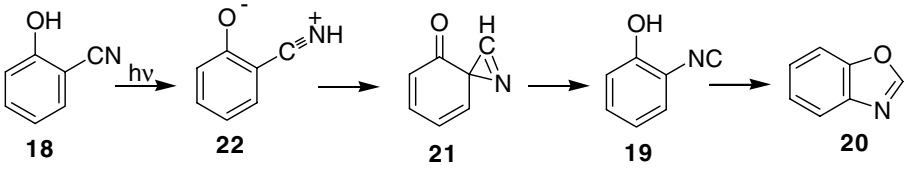

(39.5)

Isonitrile **19** was detected in ultraviolet (UV) and infrared (IR) studies at low temperatures. They speculated[21] that azirine intermediate **21** may precede the formation of **19** and, indeed, LFP studies on **18** performed by Richard and co-workers[22] allowed observation of an intermediate which was assigned to **21** on the basis of the similarity of its UV absorption spectra to that of the cyclohexadienone chromophore. The reaction was not quenchable by piperylene and is presumed to occur via the singlet manifold. The authors did not put forward a mechanism for the formation of **21**, although it may be formed by initial ESIPT from the phenol to the cyano group to give tautomer **22**, which can then rearrange to give **21**. Similar products (substituted benzoxazoles) were observed via presumed initial ESIPT in structurally related *o*-hydroxy substituted aromatic oximes and oxime ethers.[23]

Richard and co-workers[22] observed photoisomerization of 4-cyanophenol (**23**) to 4-hydroxybenzoisonitrile (**24**) in protic solvents:

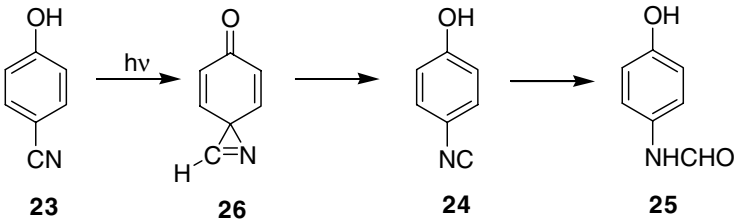

(39.6)

The distal arrangement of the substituents in **24** prevents cyclization to a benzoxazole-type intermediate. While stable in alcohols, this intermediate can undergo hydrolysis (in water) to give hydroxyformanilide (**25**). Further analysis of the reaction revealed that **24** is a secondary photoproduct of the first-formed azirine **26**, in contrast with the thermally induced azirine conversion to isonitrile that is observed for **18**. Triplet quenchers such as oxygen and methyl acrylate quench the reaction efficiently. The authors propose a mechanism for conversion of **23** to **26** that involves a deprotonation–reprotonation sequence preceded by intramolecular electron transfer from the triplet-excited state of **23**.

The interesting photoisomerizations observed for 2- and 4-cyanophenols (**18** and **23**) led Richard and Bonnichon[24] to study the *meta*-isomer **27**. Unlike **18** and **23**, Kekule resonance forms of azirine products stemming from **27** cannot be drawn, suggesting that formation of isonitriles may be an unfavorable pathway for **27**. Photolysis of **27** in deoxygenated aqueous media (pH > 4.0) led to formation of **28** with low yields ($\Phi < 0.001$); for photolyses performed in more acidic media (pH < 4.0), a second photoproduct (**29**) was also formed with quantum yields up to 0.002:

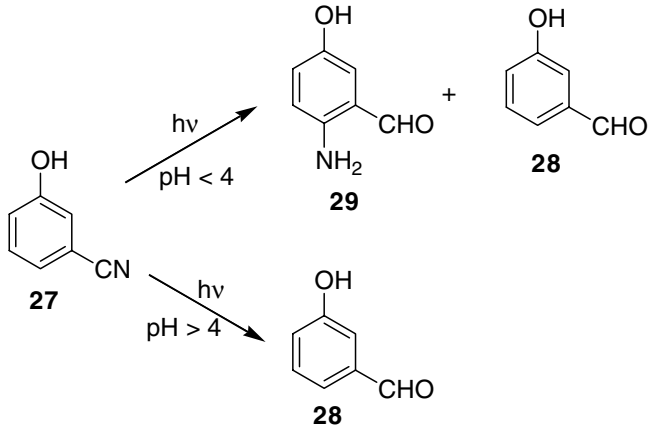

(39.7)

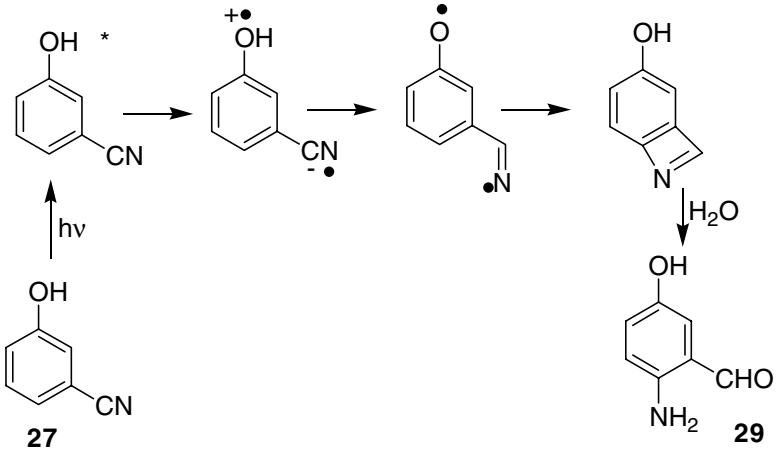

SCHEME 5

Formation of **29** is thought to proceed via the process outlined in Scheme 5. Formation of **28** is poorly understood. The authors[24] proposed a complicated mechanism involving solvated electrons; however, this mechanism is unable to explain the high yields (up to 68%) that were observed. The formation of **28** probably proceeds *via* the triplet state of **27**, as the reaction was efficiently quenched by oxygen and methyl acrylate.

39.4 Photohydration and Photoaddition of Hydroxyarenes

The photohydration of an unsaturated moiety on a phenol ring was first reported by Ferris and Antonucci[20] for *o*-hydroxyphenylacetylene (**30**), which yielded ketone **31**, presumably via initial formation of enol **32**:

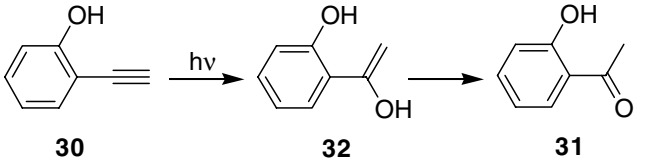

30 **32** **31** (39.8)

Yates and co-workers[25,26] observed a similar reaction for *o*-hydroxystyrene (**33**) (formation of **34**):

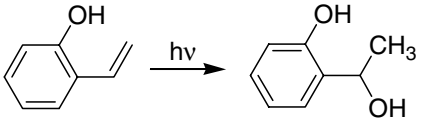

33 **34** (39.9)

Their detailed mechanistic studies revealed that the efficiency of photohydration is independent of the solution pH in the 0 to 7 range. Because the pK_a^* of **30** is expected to lie within this range, it was concluded that the photohydration did not occur via initial protonation of the acetylene by aqueous acid, but instead via initial ESIPT from the phenol to generate quinone methide (**35**) (or **36** from **33**). This quinone methide is trapped by water to give the observed Markovnikov photohydration product. This was the first clear demonstration of ESIPT leading to an irreversible photochemical reaction.

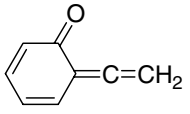

35

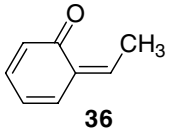

36

Later work by Fischer and Wan[27,28] demonstrated that *meta* (**37** and **38**) and *para* (**39**) hydroxy-substituted styrenes are also active towards photohydration (Φ = 0.22, 0.24 and 0.1, respectively). Evidence for formation of quinone methide intermediates was provided by nanosecond LFP. Both steady-state and time-resolved fluorescence quenching of **37** by water showed a cubic dependence on water concentration. This was attributed to an initial ESIPT process in which a three-water-molecule "bridge" mediates a proton transfer from the phenol to the basic alkene.

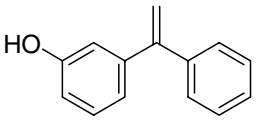

37

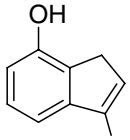

38 Ph

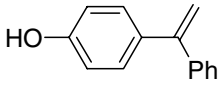

39

ESIPT to an appended vinyl substituent has been proposed to be the integral step in an interesting photochromic system. Uchida and Irie[29] report that vinylnaphthol derivative **40** gives the closed-ring naphthopyran **41** upon photolysis in hexane (λ = 334 nm, Φ = 0.20). Photolysis of **41** (λ = 400 nm) regenerates **40**. The authors propose an initial ESIPT reaction between the phenol OH and appended

vinyl substituent to generate *o*-quinone methide **42**, which can then undergo thermal electrocyclic ring closure to give **41**:

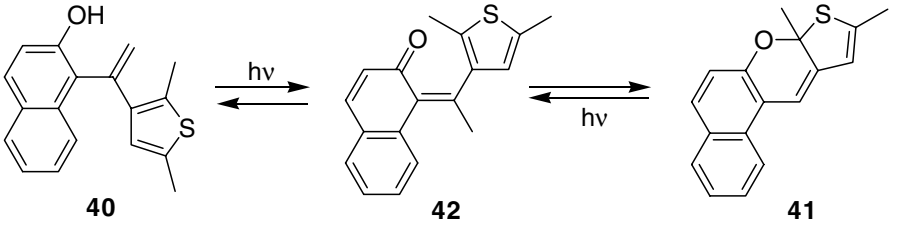

(39.10)

Recently, Lukeman and Wan[30,31] reported that 2-phenylphenol (**43**) undergoes H-D exchange primarily at the 2′-position when it is photolysed in D_2O solution. The exchange reaction was interpreted as arising from initial ESIPT from the phenol to an aromatic ring carbon to generate *o*-quinone methide (**44**), which then undergoes reverse proton transfer to generate deuterium-labeled starting material:

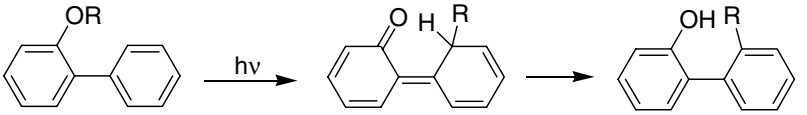

43 R = H
43-*OD* R = D

44

(39.11)

Photolyses of **43**-*OD* in a variety of solvents and in the solid state indicate that the exchange behavior is not water mediated and that the ESIPT process is direct.

Early studies on the photochemistry of *o*-allyl-substituted phenols indicated that photolysis generally gave mixtures of benzofuran and benzopyran cyclization products[32,33] (i.e., **46** and **47** from **45**):

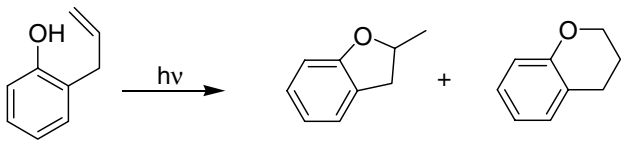

45 **46** **47**

(39.12)

It was proposed that initial ESIPT from the phenol OH to the ground-state alkene gave rise to two possible carbocations, which were then attacked by the phenolate to give the cyclized products; however, it is questionable whether phenols are strong enough acids in S_1 to protonate appended alkenes, as the alkenes are a higher energy chromophore and do not experience enhanced basicity when the phenol is excited. An alternative mechanism has been proposed[34] that involves initial electron transfer between the phenol and alkene, followed by radical ring closure. The work of Shani and co-workers[35] offers support for initial ESIPT. They demonstrated that photocyclization efficiency is reduced when competing hydrogen bond acceptors are available. Recent reports[36,37] showed through product yield and fluorescence quenching studies that the photocyclization of *o*-allyl phenols and naphthols does indeed proceed via ESIPT from S_1 and that a ground-state OH---π interaction is an important prerequisite. The alkene moiety might achieve enhanced basicity through energy transfer from the phenol via an excited-state π-complex.

Phenyl substitution of the alkene in *o*-allylphenols to generate the corresponding cinnamylphenol adds additional mechanistic complexity, as the two chromophores are now of comparable energy. This is evidenced in the photolysis of **48**, as, along with expected ring-closed products **49** and **50**, **51** appears in the product mixture, clearly resulting from *cis/trans* isomerization of the excited styrene chromophore:[38]

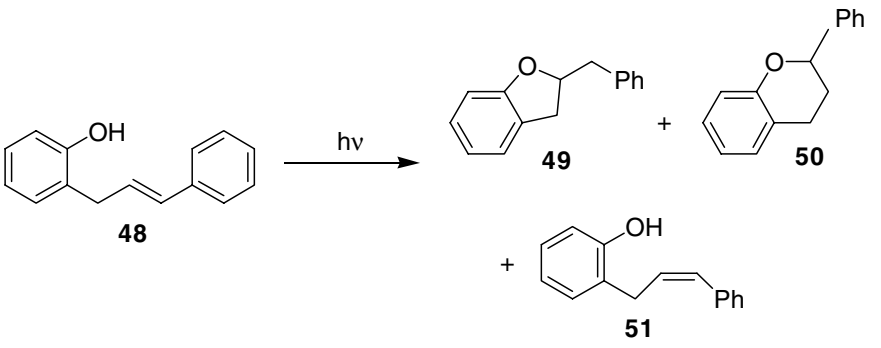

(39.13)

Quenching and sensitization studies indicate that the singlet state of the phenol favors formation of benzofuran **49**, that the styrene singlet state favors the formation of **50**, and that **51** results from the styrene triplet state. The authors invoke an ESIPT mechanism to explain the photocyclization products in this system. Derivitization of the styrenic ring lowers its singlet energy and thus should increase its contribution to the observed photochemistry. Indeed, studies[39] using *trans*-cinnamylphenols substituted with methyl, methoxy, and phenyl groups at the *para* position of the styrenic ring showed that increased proportions of benzopyran and *cis*-isomerized starting material are present in the product mixture. Similar studies in which the phenolic singlet energy is lowered by benzannelation[40] showed that increased proportions of benzopyran products are formed. Although the authors reiterate that ESIPT is responsible for almost all photocyclizations, they do invoke an electron transfer mechanism to explain the very different behavior of a methoxy-substituted derivative.[41]

39.5 Photochemistry of Hydroxyaromatic Ketones

The photogeneration of flavanones **53** and **55** from 2′-hydroxychalcone (**52**) and sorbophenone **54,** respectively, was first reported by Stermitz and co-workers[42]:

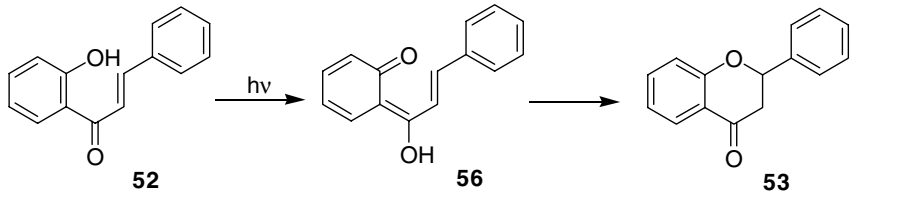

(39.14)

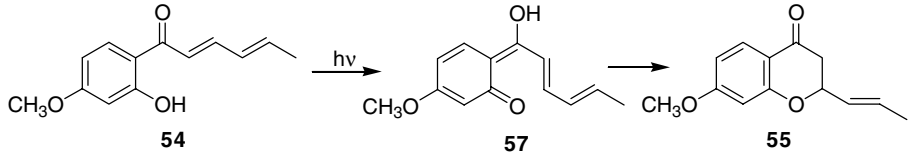

(39.15)

They assumed a mechanism involving ESPT from the phenol to the solvent, followed by attack of the resultant phenolate on the vinyl carbon β to the carbonyl group. Later work by Matsushima and co-workers[43,44] on a number of 2′-hydroxychalcone derivatives demonstrated that triplet quenchers and radical scavengers had no effect on the reaction efficiency, suggesting an ionic singlet-state mechanism. They did notice that the choice of solvent had a dramatic effect; polar aprotic solvents led to the highest efficiencies, polar protic solvents were the least efficient, and nonpolar solvents gave intermediate efficiencies. Such observations led the authors to propose a mechanism involving ESIPT to the carbonyl group to generate an *o*-quinone

methide (**56** or **57**), which can then undergo electrocyclic ring closure. They proposed that isomerization to the *cisoid o*-quinone methide occurred on the excited-state potential energy surface, as the efficiency of reaction had a dependence on light intensity consistent with a one-photon process.

Jurd[45] reported that the slow thermal conversion of 2-hydroxychalcone (**58**) to the flavylium cation (**59**) was markedly accelerated by photolysis:

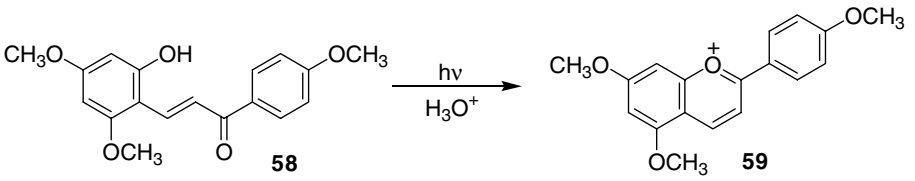

(39.16)

It was assumed that the role of the light was simply to convert the *trans* isomer to the *cis* form and that the cyclization was an acid-catalyzed thermal reaction. The acceleration was realized because the *cis* isomer is in a conformation that is more favorable for cyclization. Later work by Dewar and Sutherland[46] demonstrated that, in neutral ethanol, **60** underwent photocyclization to **61**. They proposed a mechanism involving initial ESPT from the phenol to solvent, followed by attack of the phenolate on the carbonyl to give initially **62** and then **61** (thermal acetal exchange with solvent):

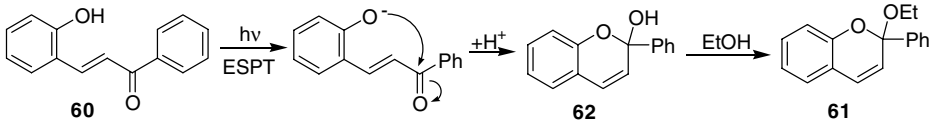

(39.17)

After numerous studies on a variety of 2-hydroxychalcone derivatives, Matsushima and co-workers[47–51] concluded that the reaction is monophotonic and proposed that the reaction proceeds via initial ESIPT from the phenol to the carbonyl group, followed by *cis*/*trans* isomerization (either thermal or adiabatic) to give the *cisoid o*-quinone methide **63**. This intermediate can then undergo electrocyclic ring closure to give the observed products. This interpretation is more realistic than that proposed by Dewar and Sutherland,[46] as few phenols are sufficiently acidic to undergo efficient ESPT to organic solvents.

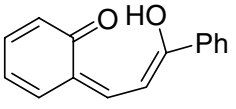

63

Givens and co-workers have reported that the *p*-hydroxyphenacyl chromophore is an effective photocaging group for phosphates (including ATP),[52] amino acids and peptides.[53,54] Photolysis (of **64**) leads to rearrangement of the chromophore to give the non-conjugated acid **65** and heterolytic release of the caged functionality:

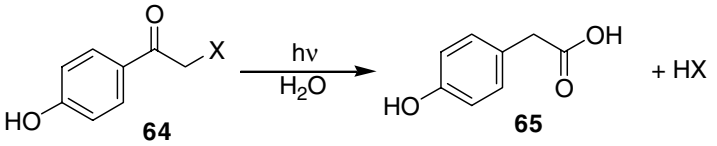

(39.18)

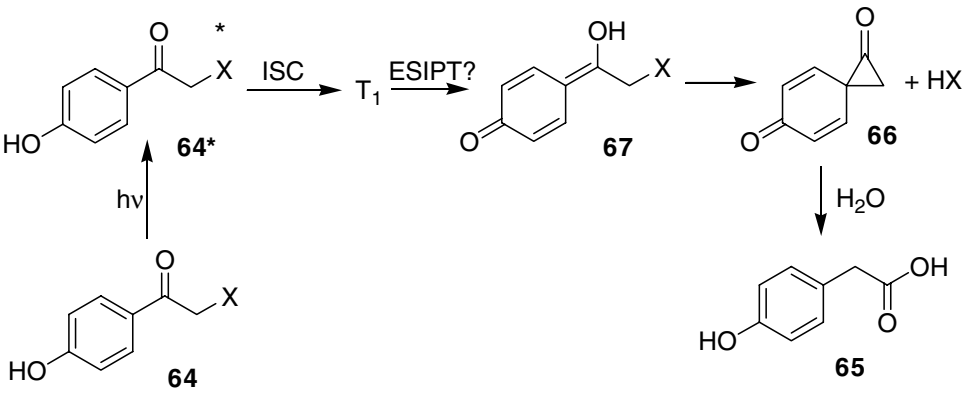

SCHEME 6

The proposed mechanism involves homolytic cleavage of the CX bond from the triplet excited state, followed by rearrangement to cyclopropanone intermediate **66**. Attack on intermediate **66** by water gives **65**. Subsequent studies by Zhang and co-workers[55] resulted in a different mechanism being proposed. Using "radical clock" techniques, they showed that the initial photochemical step is probably not homolytic cleavage. They reported that the reaction is strongly water mediated and proposed ESIPT from the phenol to the carbonyl group as the primary photochemical step, followed by rearrangement to **66** with concerted loss of the caged group. LFP studies allowed identification of tautomer **67**. Furthermore, triplet quenchers had a minimal effect on reaction efficiency, leading the authors to invoke the singlet state as the reactive multiplicity. In later reports, Givens and co-workers[56,57] conceded that the primary photochemical step is probably not CX bond homolysis, but after performing rigorous quenching studies they offered convincing evidence that the reaction proceeds from a short-lived triplet. A mechanistic summary based on what is known to date is provided in Scheme 6.

39.6 Photochemistry of Hydroxyarenes with Benzylic Moieties

Seiler and Wirz[58] reported one of the first systematic investigations into the mechanistic photochemistry of phenols and naphthols containing a benzylic-type moiety. They studied the photohydrolysis of eleven trifluoromethyl-substituted phenols and naphthols. Photolysis of these compounds in aqueous solution gave rise to the corresponding carboxylic acids. The mechanism of reaction (common to all of these compounds) involves S_1, with the initial step (in neutral solution) being deprotonation of the phenol (or naphthol) to form the phenolate (naphtholate) ion, which is believed to remain in S_1. This is followed by heterolytic CF bond cleavage to form quinone-methide-type intermediates (observed for selected compounds using flash photolysis) that are subsequently hydrolyzed by water to the carboxylic acids (Scheme 7). This important paper[58] demonstrated the general photochemical reactivity of hydroxyarenes with labile benzylic substituents and that a variety of quinone-methide-type intermediates are accessible from these compounds; however, these aspects of this reaction were not pursued further by the authors, and the paper remained somewhat unrecognized. Indeed, a recent paper[59] on the photochemistry of 2-hydroxy-4-trifluoromethylbenzoic acid (HTB, a trifluoromethyl-substituted phenol and the active form of Triflusal, a platelet antiaggregant drug) failed to cite the earlier work by Seiler and Wirz, although HTB photolysis resulted in hydrolysis of the trifluoromethyl group, analogous to the results initially reported by Seiler and Wirz.[58]

The photochemistry of phenols with the more accessible benzyl alcohol moiety (compared to trifluoromethyl) was reported on several occasions in the 1970s. Hamai and Kokubun[60] documented the photochromic (and thermochromic) behavior of 2-hydroxytriphenylmethanols **68** and **69**. Exposure of these compounds to UV light in *n*-hexane resulted in highly colored solutions due to the formation of fuchsones (which are *o*-quinone methides):

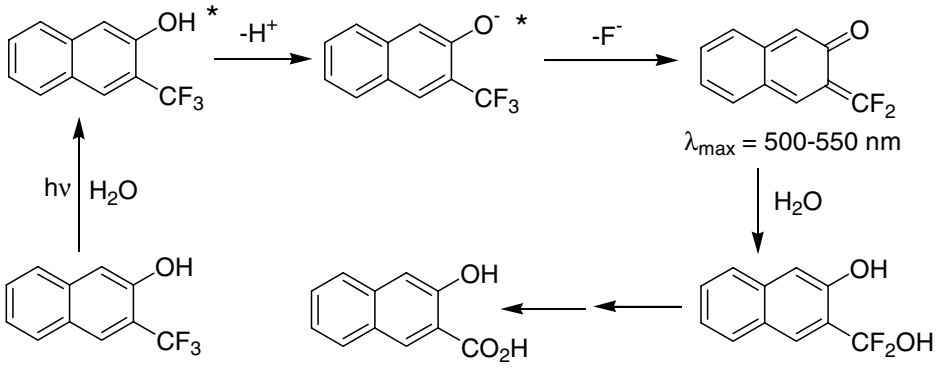

SCHEME 7

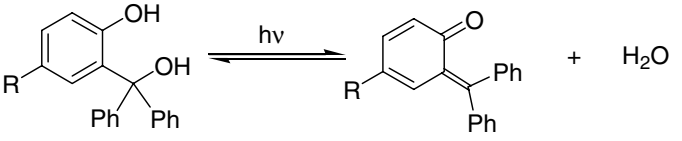

68 R = H
69 R = OCH_3

fuchsones

(39.19)

Addition of water to the organic solvent enhanced the decoloration, an observation that is consistent with the operation of the reverse hydration reaction as responsible for the loss of color.

The mechanism of the photochemical reaction was not investigated. The photochemistry of the closely related *p*-hydroxytriphenylmethanols **70** to **72** has also been studied but only in the solid state. Gomberg[61] first reported that photolysis with sunlight of powdered **70** resulted in the formation of a yellow material only on the top layer of the powder and assigned it to the fuchsone **73**. Lewis et al.[62] have reinvestigated this reaction using additional derivatives **71** and **72**. The x-ray crystal structures of the compounds showed that the phenolic hydrogen is pre-aligned by hydrogen bonding with the triphenylmethyl alcoholic hydroxyl group of an adjacent molecule in a fashion suitable for self-catalyzed dehydration reaction. Indeed, photolysis of these compounds gave highly colored species assignable to **74** and **75**:

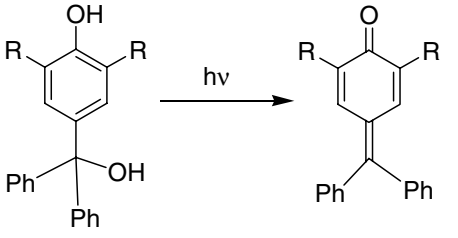

70 R = H
71 R = Br
72 R = CH_3

73 R = H
74 R = Br
75 R = CH_3

(39.20)

The authors suggested that one possible pathway of reaction is deprotonation of the photoexcited phenol, which can then catalyze the loss of water from the triphenylmethyl alcohol moiety.

Systematic investigation into the aqueous photochemistry of phenols substituted with benzylic moieties began in Wan's group with a survey of the photosolvolytic efficiencies (in aqueous MeOH) of a variety

of methoxy-substituted benzyl alcohols.[63] Included along with this group of compounds was *o*-hydroxybenzyl alcohol (**76**), which reacted with one of the highest quantum yields to give methyl ether **78**:

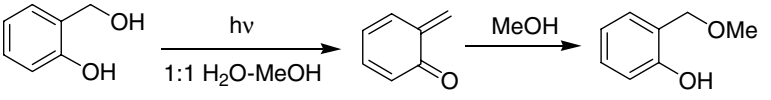

76 **77** **78** (39.21)

It was proposed,[63] at the time, that the propensity to form *o*-quinone methide **77** via a self-catalyzed photoreaction involving ESIPT from the phenol to the benzyl alcohol moiety could account for the enhanced photosolvolytic reactivity. Additional support for the intermediacy of **77** came from photolysis of **76** in basic solution, which gave rise to phenol-formaldehyde-type oligomers.[64] Thus, in the presence of a base, photolysis of the phenolate ion of **76** still gives rise to **77**, but these are now preferentially trapped by the phenolate ion of **76** (via C-alkylation), which is the first step in the formation of phenol-formaldehyde polymers.

These initial studies reporting the high reactivity of *o*-hydroxybenzyl alcohol (**76**) toward *o*-quinone methide (**77**) formation in aqueous solution led to an exploratory investigation of reactivity all the hydroxybenzyl alcohols isomers, including the hydroxybenzhydrols (compounds **79** to **84**):[65]

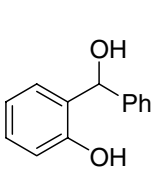

79

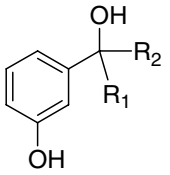

80 $R_1 = R_2 = H$
81 $R_1 = Ph$; $R_2 = H$
82 $R_1 = R_2 = Ph$

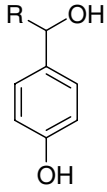

83 R = H
84 R = Ph

The main finding in this work is that all hydroxybenzyl alcohol and hydroxybenzhydrol isomers are photochemically reactive (the *ortho* and *meta* isomers being the most reactive) in aqueous solution, giving rise to the corresponding quinone methides **85** to **87**, some of which are detectable by LFP and/or standard UV-Vis spectrophotometry (e.g., *o*-quinone methide **85**, R = Ph, has λ_{max} = 350 and 450 nm). *o*-Quinone methides **85** are trappable by externally added electron-rich dienophiles such as ethyl vinyl ether (to give chroman adducts in good yields) or can be trappable intramolecularly in an appropriately designed substrate.[66]

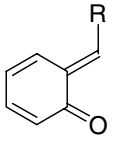

85 R = H or Ph

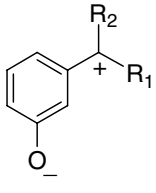

86 R_1, R_2 = H, Ph

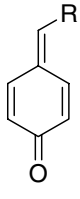

87 R = H or Ph

mechanism of reaction was proposed involving initial deprotonation of the phenol in S_1 followed by dehydroxylation from the excited phenolate ion.[65] Initial studies of efficiency of reaction vs. pH are consistent with this mechanism of reaction, although the *o*-isomer may operate via an ESIPT mechanism in which a discrete phenolate ion is not required, at least in neutral or acidic solution.

Nakantani et al.[67] have since shown that *o*-quinone methides can also be readily photogenerated from Mannich bases of *o*-substituted phenols; for example,

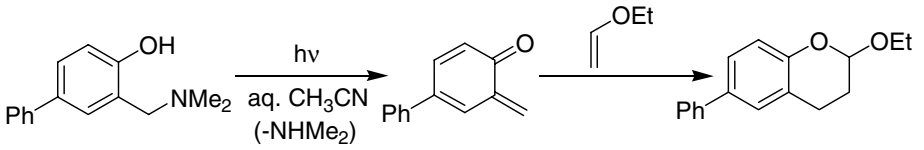

(39.22)

Photolysis of the phenolate ion (at high pH) failed to cause reaction, indicating that an initial ESIPT from phenol to the Mannich base is required to form the ammonium ion species, which then facilitates its departure as a leaving group.

The propensity for hydroxy-substituted benzyl alcohols to react via dehydration on photolysis has now been extended to other chromophores such as fluorenols **88** and **89**[68] and vitamin B_6 (**90**):[69]

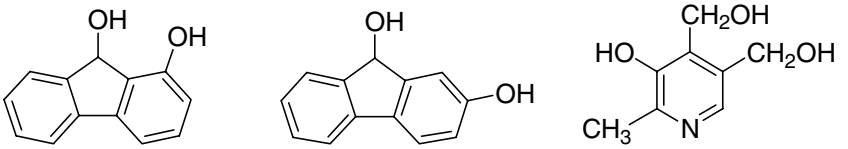

88 **89** **90**

Photolysis of these and related compounds in aqueous solution give rise to the corresponding quinone methide intermediate with good to high yields. Some of these are observable by LFP. The *o*-isomers **88** and **90** give rise to *o*-quinone-methide-type intermediates that are trappable by added ethyl vinyl ether. These papers further demonstrate the general utility of the reaction, which appears not to be restricted to benzenoid systems.

The propensity of hydroxy-substituted biphenyls to undergo photodehydration in a manner like the hydroxybenzyl alcohols above (to give biphenyl-type quinone methides) was discovered during an investigation into the photoisomerization of xanthene (**91**) to 6*H*-dibenzo[*b*,*d*]pyran (**92**):[70]

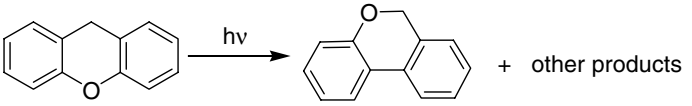

91 **92**

(39.23)

The proposed mechanism of photoisomerization involves initial CO bond homolysis of **91** to form a biradical, which can subsequently transform to the 2-(2′-hydroxyphenyl)benzyl alcohol (**93**), via a spiroketone intermediate.[70] It was proposed that secondary photolysis of **93** leads to **92** via an initial dehydration reaction to form biphenyl quinone methide **94**:

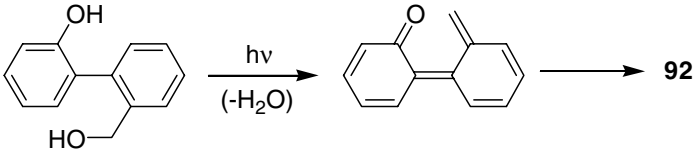

93 **94**

(39.24)

A subsequent study of the photochemistry of **93** and several derivatives[71] confirmed the generality of reaction of these 2,2′-substituted biphenyls to undergo photocyclization via proposed biphenyl quinone methides (e.g., **94**). A particularly novel aspect of this reaction is that the starting alcohols are twisted in the ground state, whereas the pyran products are much more planar. Thus, the photochemical reaction requires a twisting motion to achieve planarity and the enhanced acidity of the phenol moiety, both features apparently available on the S_1 surface. Further studies of this reaction[72] showed that the photocyclization occurs in the solid state and that hydrogen bonding between compounds as observed in the x-ray structure (thereby offering the possibility of intermolecular "acid" catalysis) may be required for reaction.

Isomers of 2-(2′-hydroxyphenyl)benzyl alcohol (**93**) that cannot undergo cyclization in a manner shown by Eq. (39.24) (e.g., **95** and **96**) have been studied. These compounds are also reactive: They give the corresponding methyl ether products (at the benzylic position) when photolysed in 1:1 MeOH–H_2O, and LFP studies have showed formation of long-wavelength transients assignable to biphenyl quinone methides **97** and **98**.[73]

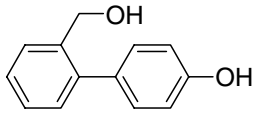

95

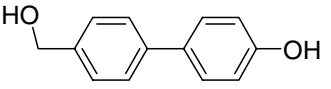

96

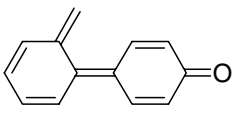

97 (λ_{max} = 570 nm)

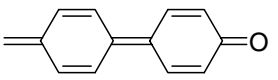

98 (λ_{max} = 525 nm)

Further extension[74] using compounds that are capable of undergoing cyclization (e.g., **99** and **100**; see Eq. (39.25)) showed that the photocyclization occurs even for highly sterically hindered systems such as binaphthyl with respectable quantum yields:

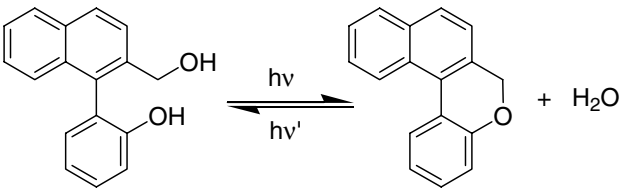

99 **100** (39.25)

In these cases, no transients assignable to biaryl quinone methides were observable by LFP, although Burnham and Schuster[75] have assigned a 560-nm (τ = 5 μs in cyclohexane) transient to the corresponding binaphthyl quinone methide. The photoreversible nature of these reactions (they are photochromic) prompted Burnham and Schuster[75] to investigate the binaphthyl system (Eq. (39.26)) as a possible chiral photochromic optical trigger for liquid crystals:

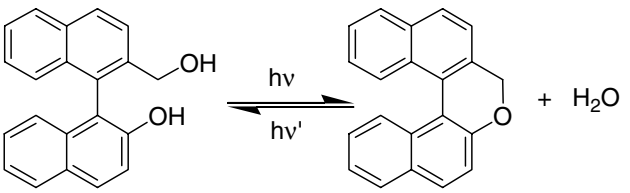

101 **102** (39.26)

Both **101** and **102** are resolvable into their enantiomeric pairs. Photolysis of optically active **101** resulted in optically active **102** without racemization of **101**; however, photolysis of **102** led to its racemization with formation of optically active **101**.

References

1. (a) Wan, P. and Shukla, D., Utility of acid-base behavior of excited states of organic molecules, *Chem. Rev.*, 93, 571, 1993; (b) Wan, P., Barker, B., Diao, L., Fischer, M., Shi, Y., and Yang, C., Quinone methides: relevant intermediates in organic chemistry, *Can. J. Chem.*, 74, 465, 1996; (c) Wan, P., Brousmiche, D., Chen, C.Z., Cole, J., Lukeman, M., and Xu, M., Quinone methide intermediates in organic chemistry, *Pure Appl. Chem.*, 73, 529, 2001; (d) Brousmiche, D., Briggs, A. G. and Wan, P., Photochemistry of hydroxyaromatic compounds, in *Molecular and Supramolecular Photochemistry*, Vol. 6, Ramamurthy, V. and Schanze, K.S., Eds., Marcel Dekker, New York, 2000, chap. 1, 1–32.
2. (a) van Willigen, H., Applications of time-resolved EPR in studies of photochemical reactions, in *Molecular and Supramolecular Photochemistry*, Vol. 6, Ramamurthy, V. and Schanze, K.S., Eds., Marcel Dekker, New York, 2000, chap. 5, 197–247; (b) Bussandri, A. and van Willigen, H., FT-EPR study of the wavelength dependence of the photochemistry of phenols, *J. Phys. Chem. A*, 106, 1524, 2002; (c) Hermann, R., Mahalaxmi, G. R., Jochum, T., Naumov, S., and Brede, O., Balance of the deactivation channels of the first excited singlet state of phenols: effect of alkyl substitution, sterical hindrance and solvent polarity, *J. Phys. Chem. A*, 106, 2379, 2002; (d) Clancy, C. M. R. and Forbes, M. D. E., Time-resolved electron paramagnetic resonance study of photoionization of tyrosine anion in aqueous solution, *Photochem. Photobiol.*, 69, 16, 1999; (e) Mohanty, J., Pal, H., Saini, R. D., Sapre, A. V. and Mittal, J. P., Triplet-state characteristics and photoionization behavior of 2,2′- and 4,4′-biphenyldiol studies at 248 nm laser flash photolysis in aqueous solution, *J. Phys. Chem. A*, 106, 2112, 2002.
3. (a) Ireland, J. F. and Wyatt, P. A. H., Acid-base properties of electronically excited states of organic molecules, *Adv. Phys. Org. Chem.*, 12, 131, 1976; (b) Klöpffer, W., Intramolecular proton transfer in electronically excited molecules, *Adv. Photochem.*, 10, 311, 1977; (c) Arnaut, L. G. and Formosinho, S. J., Excited-state proton transfer reactions. I. Fundamentals and intermolecular reactions, *J. Photochem. Photobiol. A: Chem.*, 75, 1, 1993; (d) Formosinho, S. J. and Arnaut, L. G., Excited-state proton transfer reactions. II. Intramolecular reactions, *J. Photochem. Photobiol. A: Chem.*, 75, 21, 1993; (e) Ormson, S. M. and Brown, R. G., Excited state intramolecular proton transfer. Part 1: ESIPT to nitrogen, *Prog. Reaction Kinetics*, 19, 45, 1994; (f) Le Gourrierec, D., Ormson, S. M., and Brown, R. G., Excited state intramolecular proton transfer. Part 1: ESIPT to oxygen, *Prog. Reaction Kinetics*, 19, 211, 1994.
4. Webb, S. P., Philips, L. A., Yeh, S. W., Tolbert, L. M., and Clark, J. H., Picosecond kinetics of the excited state, proton transfer reactions of 1-naphthol in water, *J. Phys. Chem.*, 90, 5155, 1986.
5. Tolbert, L. M. and Solntsev, K., Excited-state proton transfer: from constrained systems to "super" photoacids to superfast proton transfer, *Acc. Chem. Res.*, 35, 19, 2002.
6. Estévez, C. M., Bach, R. D., Hass, K. C., and Schneider, W. F., Novel structural modification associated with the highly efficient internal conversion of 2-(2′-hydroxyphenyl)benzotriazole ultraviolet stabilizers, *J. Am. Chem. Soc.*, 119, 5445, 1997.
7. Lipczynska-Kochany, E. and Bolton, J. R., Flash-photolysis hplc method applied to the study of photodegradation reactions, *J. Chem. Soc., Chem. Commun.*, 1596, 1990.
8. Boule, P., Guyon, C., and Lemaire, J., Photochemistry and the environment. 4. Photochemical behaviour of monochlorophenols in dilute aqueous solution, *Chemosphere*, 11, 1179, 1982.
9. Burrows, H. D., Ernestova, L. S., Kemp, T. J., Skurlatov, Y. I., Purmal, A. P., and Yermakov, A. N., Kinetics and mechanism of photodegradation of chlorophenols, *Prog. React. Kinet.*, 23, 145, 1998.
10. Boule, P., Richard, C., David-Oudjehani, K., and Grabner, G., Photochemical behaviour of halophenols in aqueous solution, *Proc. Indian Acad. Sci. (Chem. Sci.)*, 109, 509, 1997.

11. Guyon, C., Boule, P., and Lemaire, J., Photochemistry and the environment. 3. Formation of cyclopentadienic acid by irradiation of 2-chlorophenol in basic aqueous-solution, *Tetrahedron Lett.*, **23**, 1581, 1982.
12. Boule, P., Guyon, C. and Lemaire, J., Photochemistry and the environment. 6. Direct phototransformation of chlorophenols and interactions with phenol on UV exposure in aqueous solution, *Toxicol. Environ. Chem.* 7, 97, 1984.
13. Omura, K. and Matsuura, T., Photoinduced reactions-L: photolysis of halogenophenols in aqueous alkali and in aqueous cyanide, *Tetrahedron*, 27, 3101, 1971.
14. Lipczynska-Kochany, E., Direct photolysis of 4-bromophenol and 3-bromophenol as studied by a flash photolysis/HPLC technique, *Chemosphere*, 24, 911, 1992.
15. Grabner, G., Richard, C., and Kohler, G., formation and reactivity of 4-oxocyclohexa-2,5-dienylidene in the photolysis of 4-chlorophenol in aqueous solution at ambient temperature, *J. Am. Chem. Soc.*, 116, 11470, 1994.
16. Durand, A.-P., Brown, R. G., Worral, D., and Wilkinson, F. J., A nanosecond laser flash photolysis study of aqueous 4-chlorophenol, *J. Photochem. Photobiol. A: Chem.*, 96, 35, 1996.
17. Ouardaoui, A., Steren, C., van Willigen, H., and Yang, C., FT-EPR Study of the photolysis of 4-chlorophenol, *J. Am. Chem. Soc.*, 117, 6803, 1995.
18. Durand, A.-P., Brown, R. G., Worral, D., and Wilkinson, F. J., Study of the aqueous photochemistry of 4-fluorophenol, 4-bromophenol and 4-iodophenol by steady state and nanosecond laser flash photolysis, *J. Chem. Soc., Perkin. Trans. 2*, 365, 1998.
19. Ferris, J. P., Antonucci, F. R., and Trimmer, R. W., Mechanism of the photoisomerization of isoxazoles and 2-cyanophenol to oxazoles, *J. Am. Chem. Soc.*, 95, 919, 1973.
20. Ferris, J. P. and Antonucci, F. R., Photochemistry of *ortho*-substituted benzene derivatives and related heterocycles, *J. Am. Chem. Soc.*, 96, 2010, 1974.
21. Ferris, J. P. and Antonucci, F. R., Mechanisms of the photochemical rearrangements of *ortho*-substituted benzene derivatives and related heterocycles, *J. Am. Chem. Soc.*, 96, 2014, 1974.
22. Scavarda, F., Bonnichon, F., Richard, C., and Grabner, G., Photoisomerization of 4-hydroxybenzonitrile into 4-hydroxybenzoisonitrile, *New J. Chem.*, 21, 1119, 1997.
23. Haley, M. F. and Yates, K., The photochemistry of carbon–nitrogen multiple bonds in aqueous solution. 2. *o*-Hydroxy-substituted aromatic oximes and oxime ethers, *J. Org. Chem.*, 52, 1825, 1987.
24. Richard, C. and Bonnichon, F., Phototransformation of 3-hydroxybenzonitrile in water, *J. Photochem. Photobiol. A: Chem.*, 119, 25, 1998.
25. Isaks, M., Yates, K., and Kalanderopoulos, P., Photohydration via intramolecular proton transfer to carbon in electronically excited states, *J. Am. Chem. Soc.*, 106, 2728, 1984.
26. Kalanderopoulos, P. and Yates, K., Intramolecular proton transfer in photohydration reactions, *J. Am. Chem. Soc.*, 108, 6290, 1986.
27. Fischer, M. and Wan, P., *m*-Quinone methides from *m*-hydroxy-1,1-diaryl alkenes via excited-state (formal) intramolecular proton transfer mediated by a water trimer, *J. Am. Chem. Soc.*, 120, 2680, 1998.
28. Fischer, M. and Wan, P., Nonlinear solvent water effects in the excited-state (formal) intramolecular proton transfer (ESIPT) in *m*-hydroxy-1,1-diaryl alkenes: efficient formation of *m*-quinone methides, *J. Am. Chem. Soc.,* 121, 4555, 1999.
29. Uchida, M. and Irie, M., A new photochromic vinylnaphthol derivative, *Chem. Lett.*, 2159, 1991.
30. Lukeman, M. and Wan, P., Excited state intramolecular proton transfer (ESIPT) in 2-phenylphenol: an example of proton transfer to a carbon of an aromatic ring, *J. Chem. Soc., Chem. Commun.*, 1004, 2001.
31. Lukeman, M. and Wan, P., A new type of excited-state intramolecular proton transfer: proton transfer from phenol OH to a carbon atom of an aromatic ring observed for 2-phenylphenol, *J. Am. Chem. Soc.*, 124, 9458, 2002.
32. Horspool, W. M. and Pauson, P. L., Photochemical addition of olefins, *J. Chem. Soc., Chem. Commun.*, 195, 1967.

33. Frater, G. and Schmid, H., Über die Photochemische Cyclisierung von 2-Allylphenolen, *Helv. Chim. Acta*, 50, 255, 1967.
34. Morrison, H., Photochemistry of nonconjugated aryl-olefins, in *Organic Photochemistry*, Vol. 4, Padwa, A., Ed., Marcel Dekker, New York, 1979, 143–189.
35. Geresh, S., Levy, O., Markovits, Y., and Shani, A., On the mechanism of intramolecular photocycloaddition of substituted *o*-allylphenols to cyclic ethers, *Tetrahedron*, 31, 2803, 1975.
36. Chow, Y. L., Zhou, X.-M., Gaitan, T. J., and Wu, Z.-Z., Mechanistic studies of photocyclizations of vicinal allylnaphthols: the duality of excited-state proton-transfer complexes, *J. Am. Chem. Soc.*, 111, 3813, 1989.
37. Bosch-Montalve, M. T., Domingo, L. R., Jiminez, M. C., Miranda, M. A., and Tormos, R., Ground and excited-state intramolecular interactions in phenol-olefin bichromophoric compounds, *J. Chem. Soc., Perkin Trans. 2*, 2175, 1998.
38. Jiminez, M. C., Marquez, F., Miranda, M. A., and Tormos, R., Photochemistry of allylphenol derivatives: role of the phenolic and styrenic excited states in the behavior of bichromophoric cinnamylphenol, *J. Org. Chem.*, 59, 197, 1994.
39. Jiminez, M.C., Miranda, M.A. and Tormos, R., Photocyclization of 2-cinnamylphenols via excited state proton transfer (ESPT) involving the lowest-lying styrenic singlet, *Tetrahedron*, 53, 14729, 1997.
40. Jiminez, M. C., Leal, P., Miranda, M. A., Scaiano, J. C., and Tormos, R., Photocyclization of cinnamylnaphthols, *Tetrahedron*, 54, 4337, 1998.
41. Jiminez, M. C., Leal, P., Miranda, M. A., and Tormos, R., Chemical evidence for intramolecular proton, electron and energy transfer in the photochemistry of *o*-allylphenol derivatives, *J. Org. Chem.*, 60, 3243, 1995.
42. Stermitz, F. R., Adamovics, J. A., and Geigert, J., Synthesis and photoreactions of sorbophenones: a photochemical synthesis of flavone, *Tetrahedron*, 31, 1593, 1975.
43. Matsushima, R. and Hirao, I., Photocyclization of 2′-hydroxychalcones to 4-flavanones, *Bull. Chem. Soc. Jpn.*, 53, 518, 1980.
44. Matsushima, R. and Kageyama, H., Photochemical cyclization of 2′-hydroxychalcones, *J. Chem. Soc., Perkin Trans. 2*, 743, 1985.
45. Jurd, L., Anthocyanidins and related compounds. XV: The effects of sunlight on flavylium salt-chalcone equilibrium in acid solutions, *Tetrahedron*, 25, 2367, 1969.
46. Dewar, D. and Sutherland, R. G., The photolysis of 2-hydroxychalcone and its possible implication in flavonoid biosynthesis, *J. Chem. Soc., Chem. Commun.*, 272, 1970.
47. Matsushima, R., Miyakawa, K., and Nishihata, M., Photochromic properties of 2-hydroxychalcones, *Chem. Lett.*, 1915, 1988.
48. Matsushima, R. and Suzuki, M., Photochromic properties of 2-hydroxychalcones in solution and polymers, *Bull. Chem. Soc. Jpn.*, 65, 39, 1992.
49. Matsushima, R., Mizuno, H., and Kajiura, A., Convenient chemical actinometer with 2-hydroxy-4′-methoxychalcone, *Bull. Chem. Soc. Jpn.*, 67, 1762, 1994.
50. Matsushima, R., Mizuno, H., and Itoh, H., Photochromic properties of 4′-amino-substituted 2-hydroxychalcones, *J. Photochem. Photobiol. A: Chem.*, 89, 251, 1995.
51. Matsushima, R., Suzuki, N., Murakami, T., and Morioka, M., Chemical actinometer with 2-hydroxy-4′-dimethylaminochalcone, *J. Photochem. Photobiol. A: Chem.*, 109, 91, 1997.
52. Givens, R. and Park, C., *p*-Hydroxyphenacyl ATP: a new phototrigger, *Tetrahedron Lett.*, 37, 6259, 1996.
53. Park, C. and Givens, R., New photoactivated protecting groups. 6. *p*-Hydroxyphenacyl: a phototrigger for chemical and biochemical probes, *J. Am. Chem. Soc.*, 119, 2453, 1997.
54. Givens, R., Jung, A., Park, C., Weber, J., and Bartlett, W., New photoactivated protecting groups. 7. *p*-Hydroxyphenacyl: a phototrigger for excitatory amino acids and peptides, *J. Am. Chem. Soc.*, 119, 8369, 1997.

55. Zhang, K., Corrie, J., Munasinghe, R., and Wan, P., Mechanism of photosolvolytic rearrangement of *p*-hydroxyphenacyl esters: evidence for excited-state intramolecular proton transfer as the primary photochemical step, *J. Am. Chem. Soc.*, 121, 5625, 1999.
56. Conrad, R., Givens, R., Hellrung, B., Rajesh, C., Ramseier, M., and Wirz, J., *p*-Hydroxyphenacyl phototriggers: the reactive excited state of phosphate photorelease, *J. Am. Chem. Soc.*, 122, 9346, 2000.
57. Givens, R., Weber, J., Conrad, P., Orosz, G., Donahue, S., and Thayer, S., New phototriggers. 9. *p*-Hydroxyphenacyl as a C-terminal photoremovable protecting group for oligopeptides, *J. Am. Chem. Soc.*, 122, 2687, 2000.
58. Seiler, P. and Wirz, J., Structur and Photochemische Reactivitat: Photohydrolyze von Trifluoromethylsubstituierten Phenolen und Naphtholen, *Helv. Chim. Acta*, 55, 2693, 1972.
59. Boscá, F., Cuquerella, M. C., Marín, M. L., and Miranda, M. A., Photochemistry of 2-hydroxy-4-trifluoromethylbenzoic acid, major metabolite of the photosensitizing antiaggregrant drug Triflusal, *J. Photochem. Photobiol. A: Chem.*, 73, 463, 2001.
60. Hamai, S. and Kokubun, H., Thermal decay of the colored form in photochromism of 2-hydroxy-4-methoxytriphenylmethanol in *n*-hexane, *Bull. Chem. Soc. Jpn*, 47, 2085, 1974.
61. Gomberg, M., On triphenylmethyl. XXIII. Tautomerism of the hydroxy-triphenyl carbinols, *J. Am. Chem. Soc.*, 35, 1035, 1913.
62. Lewis, T. W., Curtin, D. Y., and Paul, I. C., Thermal, photochemical and photonucleated thermal dehydration of *p*-hydroxytriarylmethanols in the solid state. (3,5-Dimethyl-4-hydroxyphenyl) diphenylmethanol and (3,5-dibromo-4-hydroxyphenyl) diphenylmethanol: x-ray crystal structures of (4-hydroxyphenyl)diphenylmethanol and its 3,5-dimethyl derivative, *J. Am. Chem. Soc.*, 101, 5717, 1979.
63. Wan, P. and Chak, B., Structure–reactivity studies and catalytic effects in the photosolvolysis of methoxy-substituted benzyl alcohols, *J. Chem. Soc., Perkin Trans. II*, 1751, 1986.
64. Wan, P. and Hennig, D., Photocondensation of *o*-hydroxybenzyl alcohols in an alkaline medium: synthesis of phenol-formaldehyde resins, *J. Chem. Soc., Chem. Commun.*, 939, 1987.
65. Diao, L., Yang, C., and Wan, P., Quinone methide intermediates from the photolysis of hydroxybenzyl alcohols in aqueous solution, *J. Am. Chem. Soc.*, 117, 5369, 1995.
66. Barker, B., Diao, L., and Wan, P., Intramolecular [4+2] cycloaddition of a photogenerated *o*-quinone methide in aqueous solution, *J. Photochem. Photobiol. A: Chem.*, 104, 91, 1997.
67. Nakatani, K., Higashida, N., and Saito, I., Highly efficient photochemical generation of *o*-quinone methide from Mannich bases of phenol derivatives, *Tetrahedron Lett.*, 38, 5005, 1997.
68. Fischer, M., Shi, Y., Zhao, B.-P., Snieckus, V., and Wan, P., Contrasting behaviour in the photosolvolysis of 1- and 2-hydroxy-9-fluorenols in aqueous solution, *Can. J. Chem.*, 77, 868, 1999.
69. Brousmiche, D. and Wan, P., Photogeneration of quinone methide-type intermediates from pyridoxine and derivatives, *J. Photochem. Photobiol. A: Chem.*, 149, 71, 2002.
70. Huang, C.-G., Shukla, D., and Wan, P., Mechanism of photoisomerization of xanthene to 6*H*-dibenzo[*b,d*]pyran in aqueous solution, *J. Org. Chem.*, 56, 5437, 1991.
71. Huang, C.-G., Beveridge, K. A., and Wan, P., Photocyclization of 2-(2′-hydroxyphenyl)benzyl alcohol and derivatives via *o*-quinone methide type intermediates, *J. Am. Chem. Soc.*, 113, 7676, 1991.
72. Shi, Y., MacKinnon, A., Howard, J.A.K., and Wan, P., Solid state and solution phase photocyclization of a 2-(2′-hydroxyphenyl)benzyl alcohol: twisting motion to planarity occurs efficiently in the crystal, *J. Photochem. Photobiol. A: Chem.*, 113, 271, 1998.
73. Shi, Y. and Wan, P., Charge polarization in photoexcited alkoxy-substituted biphenyls: formation of biphenyl quinone methides, *J. Chem. Soc., Chem. Commun.*, 1217, 1995.
74. Shi, Y. and Wan, P., Photocyclization of a 1,1′-bisnaphthalene: planarization of a highly twisted biaryl system after excited state ArOH dissociation, *J. Chem. Soc., Chem. Commun.*, 273, 1997.
75. Burnham, K. S. and Schuster, G. B., A search for chiral photochromic optical triggers for liquid crystals: photoracemization of 1,1′-binaphthypyran through a transient biaryl quinone methide intermediate, *J. Am. Chem. Soc.*, 120, 12619, 1998.

40

The Photochemical Nucleophile–Olefin Combination, Aromatic Substitution (Photo-NOCAS) Reaction

Dino Mangion
McMaster University

Donald R. Arnold
Dalhousie University

40.1 Introduction

Ever since the pioneering work of Weller,[1] electron transfer photochemistry has received considerable attention, both as a potential synthetic method as well as a convenient technique for generating and studying radical ions in a homogeneous medium.[2] The promotion of an electron from the HOMO to the LUMO of a chemical species enhances both its reducing and oxidizing abilities. This renders electronic excitation a relatively mild and selective way of inducing electron transfer between species that are unreactive toward each other in their ground states.

The change in free energy (ΔG_{PET}) governing the photoinduced electron transfer (PET) process is expressed by means of the Weller equation, Eq. (40.1), an empirical relationship that equates ΔG_{PET} to experimentally measurable terms such as the half-wave redox potentials ($E^{ox}_{1/2}$ and $E^{red}_{1/2}$) of the reactants and the excitation energy ($E_{0,0}$) of the chromophore:

$$\Delta G_{PET} = F\,(E^{ox}_{1/2} - E^{red}_{1/2} - E_{0,0} - e/\varepsilon\alpha) \qquad (40.1)$$

The Coulombic term $e/\varepsilon\alpha$ takes into account the mutual stabilization exerted by the radical ions formed at an encounter distance α. Calculation of ΔG_{PET} is often taken as a preliminary check for assessing the potential of a PET system. Provided that the free energy is exergonic, electron transfer will lead to the formation of the radical cation of the electron donor (D) and the radical anion of the electron acceptor (A) as shown in Scheme 1. These radical ions are typically formed as a contact radical ion pair at an encounter distance of about 7 Å and have the option of either diffusing apart to give free, solvated radical

0-8493-1348-1/04/$0.00+$1.50

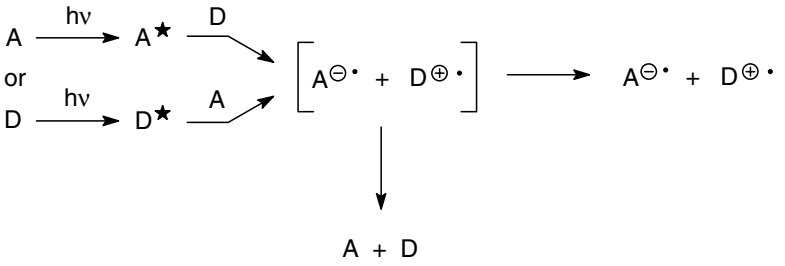

SCHEME 1

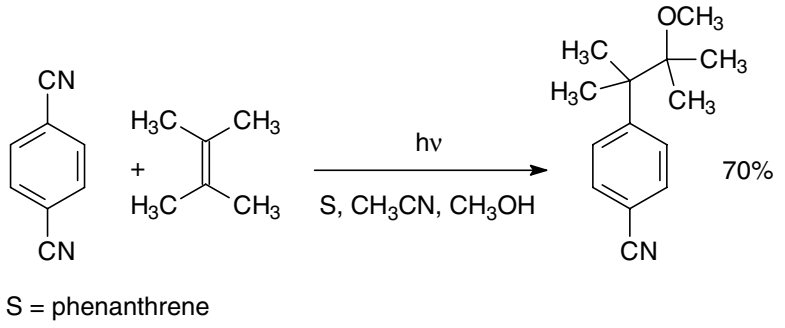

SCHEME 2

ions or reacting with each other within the solvent cage. The course is often dictated by the dielectric constant of the surrounding medium and its ability to solvate the radical ions. In most instances, however, the radical ions undergo back electron transfer (BET), regenerating the ground-state starting materials in what is essentially an energy-wasting process.

40.2 The Photo-NOCAS Reaction: Establishing the Mechanism

One of the photochemical electron transfer reactions developed quite extensively over the past decades, particularly by our research group, is the photochemical nucleophile–olefin combination, aromatic substitution (photo-NOCAS) reaction.[3] We have used this reaction as a framework in which to investigate the behavior of photogenerated radical ions as well as a well-understood reference against which to compare competing PET reactions.

As the name suggests, the photo-NOCAS reaction involves the regioselective combination of three molecules: an aromatic electron acceptor (typically a cyano-substituted arene), an olefin, and a nucleophile. In the paradigm example, 1,4-dicyanobenzene, 2,3-dimethyl-2-butene, and methanol react to give a single, major photo-NOCAS product in 70% yield (Scheme 2).[4] The reaction is co-sensitized by phenanthrene. A pronounced enhancement in both chemical yield and efficiency is often observed in photo-NOCAS reactions upon co-sensitization by aromatic hydrocarbons such as phenanthrene or biphenyl. The co-sensitizer (S) essentially behaves as an electron relay, generating the reactant radical ions ($A^{-\bullet}$ and $D^{+\bullet}$) in separate stages (Scheme 3). This reduces the opportunity for BET and in-cage reactions between the reactant radical ions. The success of the technique relies on the inertness of the co-sensitizer radical cation as well as on reduced rates of BET between the co-sensitizer radical cation and the reactant radical ions as compared to that between the reactant radical ions themselves.[5] Due to its relatively low half-wave reduction potential ($E^{red}_{1/2} = -1.66$ V vs. SCE, CH_3CN) and the large excitation energy for its $S_0 \rightarrow S_1$ transition ($E^{S}_{0,0} = 4.21$ eV, CH_3CN), 1,4-dicyanobenzene will undergo exergonic PET with potential donors having a $E^{ox}_{1/2} < 2.6$ V. This encompasses most alkenes. Because of this,

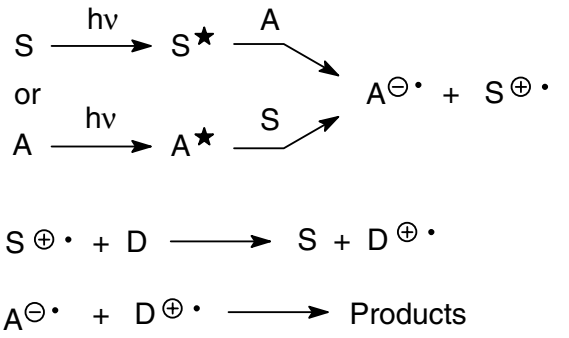

SCHEME 3

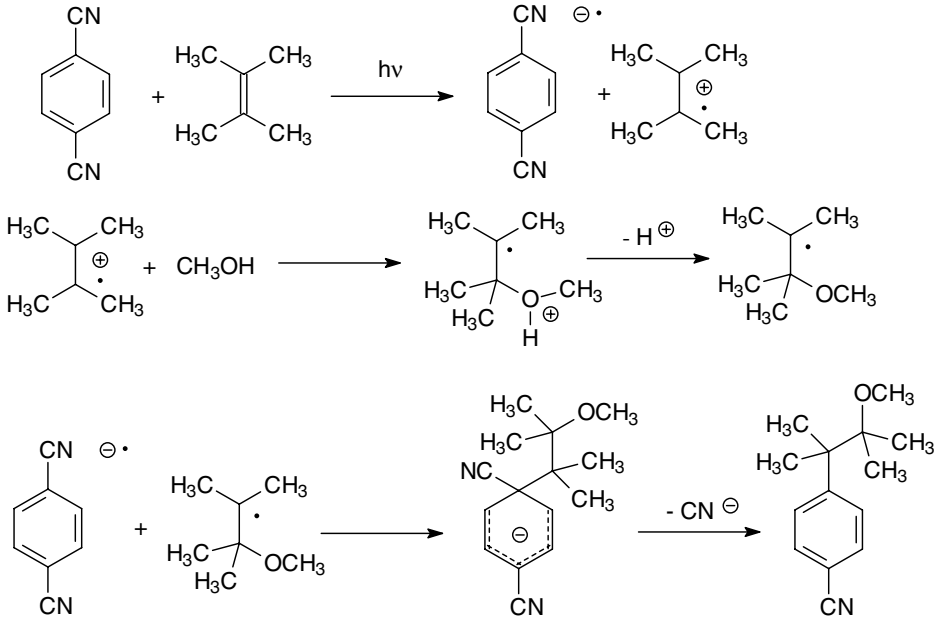

SCHEME 4

1,4-dicyanobenzene has been the electron acceptor of choice in most of the published photo-NOCAS studies, although other cyanoarenes such as 1,2,4,5-tetracyanobenzene ($E^{red}_{1/2}$ = –0.65 V vs. SCE, $E^{S}_{0,0}$ = 3.83 eV, CH_3CN)[6] and methyl 4-cyanobenzoate ($E^{red}_{1/2}$ = –1.76 V vs. SCE, $E^{S}_{0,0}$ = 4.10 eV, CH_3CN)[7] have been used successfully as well.

The basic mechanism involves the generation of the arene radical anion and the olefin radical cation, directly (Scheme 1) or via a co-sensitized route (Scheme 3). The olefin radical cation is attacked by the nucleophile (methanol) to give a distonic radical cation, which subsequently deprotonates to give the corresponding β-alkoxyalkyl radical (combination step, Scheme 4). This radical then adds to an *ipso*-position of the 1,4-dicyanobenzene radical anion. Semi-empirical calculations clearly show that the cyano-substituted positions on the ring are the sites of highest spin density (for several cyano-substituted arenes). The resulting anionic species extrudes cyanide anion in order to rearomatize, generating the photo-NOCAS product (substitution step, Scheme 4).

An early insight into the regiochemistry of the reaction was achieved by studying reactions involving nonsymmetrical olefins such as 2-methylpropene. In this example, a predominance of the product derived

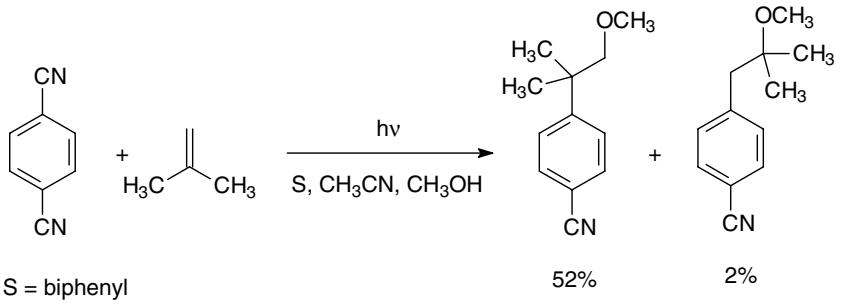

SCHEME 5

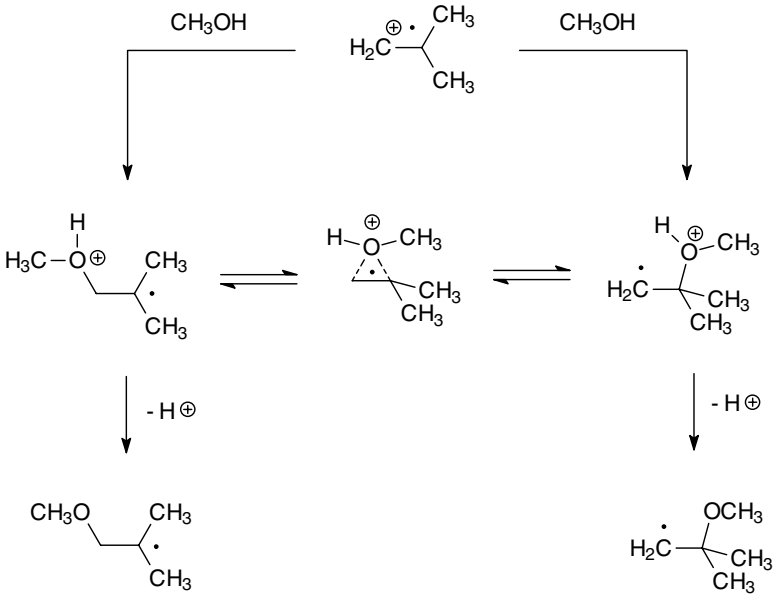

SCHEME 6

from the more highly substituted β-methoxyalkyl radical was observed (Scheme 5).[4a,8] In this case, the predominant radical is also the more energetically stable of the two possible forms. In fact, it has been proposed that, when a protic nucleophile such as methanol is involved, the regiochemistry of the reaction is thermodynamically controlled and determined by the relative stability of the β-methoxyalkyl radicals (or, possibly, of the distonic radical cations).[9] The possibility of equilibration through a non-classical, bridged species has been suggested (Scheme 6). However, empirically derived heats of formation as well as high-level *ab initio* molecular orbital calculations on the intermediate radicals for a series of alkenes and dienes indicate that the more highly substituted radical is not necessarily the more stable species. Whereas in cases such as 2-methylpropene the greater stability of the tertiary β-alkoxyalkyl radical over the primary radical is straightforward, in other olefins, such as 4-methyl-1,3-pentadiene, the rationalization is more complicated. *Ab initio* calculations indicate that the radical bearing the methyl substituents in the β-position is significantly more stable than the alternative isomer having the methyl substituents attached to the allylic system — the extra stability imparted by the methyl groups attached to the methoxy-bearing carbon outweighs that which would result from the methyl groups being part of the allylic system. These theoretical results are in agreement with experimental observation. The dominant photo-NOCAS product in the reaction involving 4-methyl-1,3-pentadiene arises from the less substituted, but more

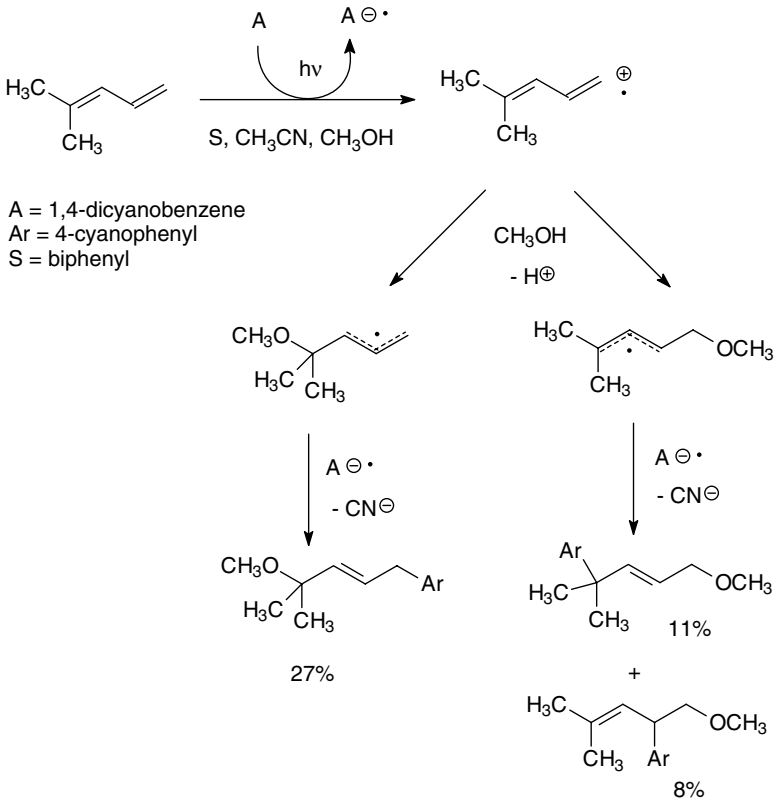

SCHEME 7

stable, β-methoxyallyl radical (Scheme 7).[10] All the alkenes and dienes investigated display a regioselectivity in their photo-NOCAS reactions with methanol that can be rationalized by a thermodynamically controlled mechanism that depends on the relative stability of the intermediate radicals.

The situation changes when non-protic, charged nucleophiles such as cyanide and fluoride anions are involved.[11] In these systems, equilibration between the olefin–nucleophile adducts is not possible; the addition is most likely irreversible, and there is no opportunity for rearrangement through a bridged intermediate. Thus, in contrast with the previous examples, the regioselectivity is now kinetically controlled, with polar and steric factors directing the incoming nucleophile. In the photo-NOCAS reaction involving 2-methyl-2-butene, 1,4-dicyanobenzene, and fluoride anion, the major product arises from the more highly substituted radical (Scheme 8). This might at first appear to be the outcome of thermodynamic control, in which the relative stability of the radicals directs the regiochemistry. However, isodesmic reactions using heats of formation determined by *ab initio* molecular orbital calculations clearly indicate that the more highly substituted β-fluoroalkyl radical derived from trapping by fluoride of the 2-methyl-2-butene radical cation is, in fact, the less stable of the two possible radicals. It is perhaps surprising that the secondary radical is more stable than the tertiary one; however, according to the calculations, the net stabilization gain from an additional methyl group at the fluoro-bearing carbon is greater than that at the radical site. The fact that the reaction actually proceeded via the more highly substituted, and hence less stable, radical intermediate was taken as evidence for a kinetically controlled pathway in which the nucleophile attaches itself predominantly to the less sterically hindered terminus. This is in agreement with the idea that the addition of the nucleophile to the olefin radical cation is irreversible and highly exergonic; the transition state occurs early along the reaction pathway and steric effects control the regioselectivity.

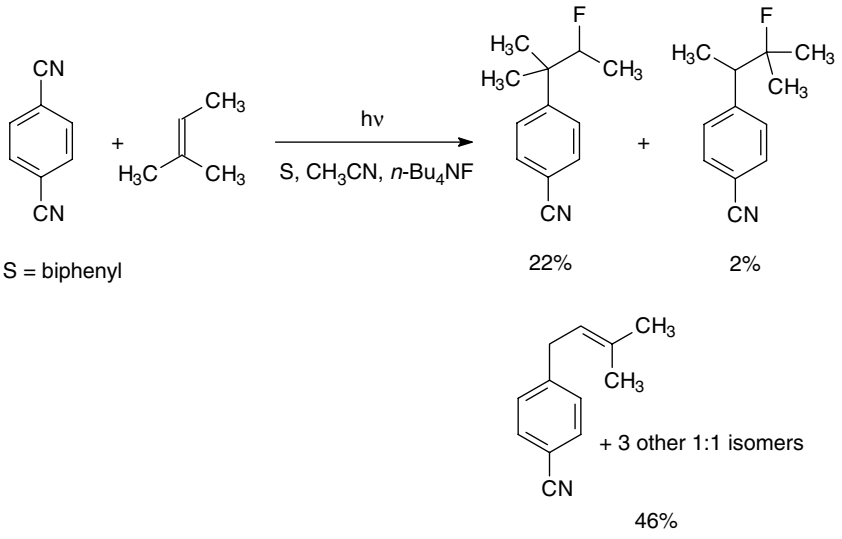

SCHEME 8

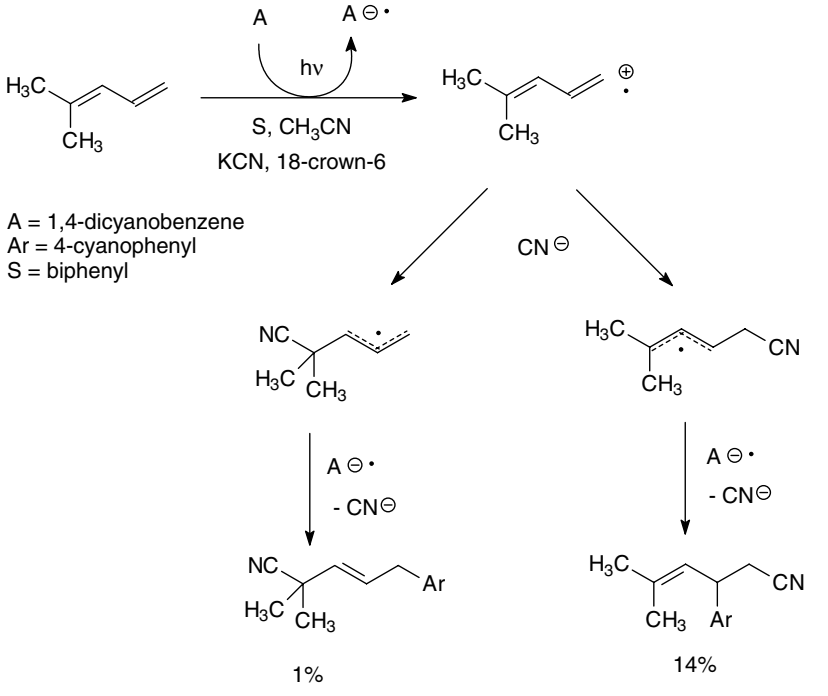

SCHEME 9

Similar trends are observed in photo-NOCAS reactions involving cyanide anion. The reaction of 4-methyl-1,3-pentadiene with cyanide anion can be contrasted directly with its equivalent reaction with methanol (Scheme 7). The regiochemistry is reversed, with cyanide attacking the less sterically hindered terminus to give the less stable intermediate radical (Scheme 9).

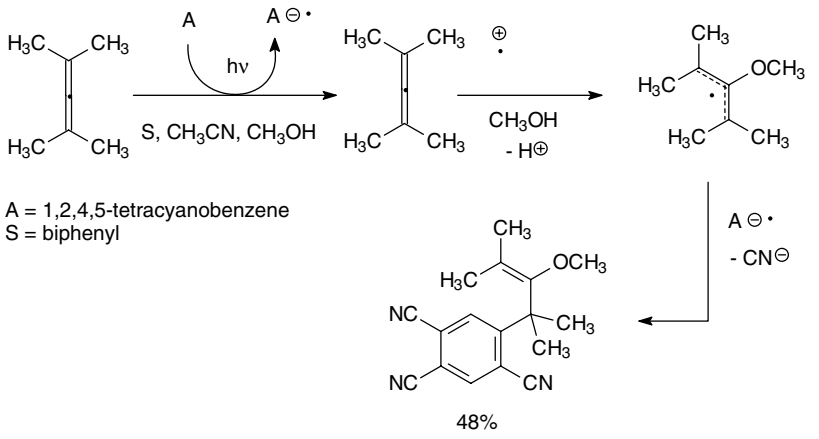

SCHEME 10

The regiochemistry in the reactions involving conjugated dienes has important implications regarding the sequence of events in the photo-NOCAS mechanism, providing us with confirmation that nucleophilic trapping of the olefin radical cation always occurs before association with the arene radical anion. In all the reactions investigated, the nucleophile is exclusively attached to one of the terminal carbons (thereby generating an intermediate allylic radical). The aryl group subsequently adds in a 1,2- or 1,4-fashion, the former placing the aryl group at an internal 2-position. If radical ion coupling occurred before nucleophilic trapping, the aryl group would be attached to a terminal carbon of the diene system. Further verification comes from a study involving allenes. The reaction is again regiospecific, placing the nucleophile exclusively at the central allenyl carbon (Scheme 10). This permits the formation of a relatively stable allylic radical, as opposed to the vinylic radical that would result from addition at a terminal carbon. The absence of any products bearing the aryl group at the central carbon proves that nucleophilic attack always precedes substitution on the arene. In fact, radical ion coupling prior to nucleophilic trapping has only been observed in a few exceptional intramolecular systems.[12]

Olefin radical cations are strongly acidic species. In the absence of a strong nucleophile, deprotonation to give the corresponding allylic radicals will compete with nucleophilic trapping. The formation of olefin–arene substitution products via this deprotonation pathway was observed in the reaction involving 2-methyl-2-butene and fluoride anion shown previously in Scheme 8.[11b] Although these products are negligible in the presence of methanol, the lower nucleophilicity and higher basicity of fluoride anion allow deprotonation to compete successfully with nucleophilic trapping. Deprotonation becomes the sole pathway when the reaction is carried out in pure acetonitrile, in the absence of a formal nucleophile (Scheme 11).[4,13] The allylic radical resulting from deprotonation of the alkene radical cation adds to an *ipso*-position of the arene radical anion from either of its ambident ends to give a mixture of isomeric 1:1 adducts.

In exceptional cases involving highly reactive alkene radical cations, acetonitrile may participate as a nucleophile. One such case is 2-methylpropene, which produces a radical cation exhibiting a localized charge and minimal steric hindrance to the incoming nucleophile.[14] Unlike in the case of methanol, the distonic radical cation resulting from the attack of acetonitrile on the radical cation of 2-methylpropene is incapable of deprotonating (Scheme 12); consequently, coupling with the radical anion of 1,4-dicyanobenzene results in the formation of a zwitterionic species. This species can then cyclize via two possible pathways (A or B) to give the final isoquinoline product. Further insight into the mechanism comes from a study by Albini and co-workers involving 1,2,4,5-tetracyanobenzene and 1-hexene in acetonitrile.[15] Photolysis of this mixture at –40°C led to the formation and isolation of the corresponding non-aromatized isoquinoline precursor, validating pathway B (Scheme 13). These researchers, however, proposed that the reaction proceeds via a termolecular exciplex-mediated pathway that precludes full electron transfer.

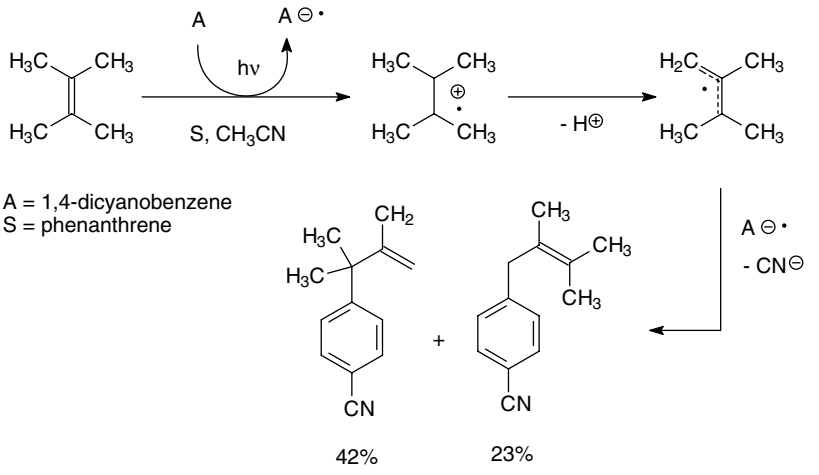

SCHEME 11

40.3 The Photo-NOCAS Reaction: Extending the Scope

The nucleophile–olefin combination step in the photo-NOCAS mechanism was achieved intramolecularly by using alkenols as both the electron donors and nucleophiles.[16] When generated in the absence of added nucleophiles, the alkenol radical cation is trapped intramolecularly by its own hydroxyl terminus. The alk-4-enols investigated had the option to undergo both 1,5-*exo* and 1,6-*endo*-cyclizations. In agreement with rules developed for carbocation/anion and radical cyclizations, the cyclization of the radical cations of the alk-4-enols showed a distinct preference for 1,5-*exo*-cyclization.[17] The alkenol, 6-methyl-5-hepten-2-ol, underwent 1,5-*exo*-cyclization exclusively (Scheme 14). This might be expected from a purely thermodynamic viewpoint due to the relative stabilities of the radicals involved (1,5-*exo*-cyclization gives a tertiary radical; 1,6-*endo*-cyclization would give a secondary radical). However, intermolecular equivalents such as 2-methyl-2-butene and 1-methylcyclohexene do yield products arising from the secondary radical, albeit in a 1:6 ratio. Therefore, comparison of the inter- and intramolecular cases demonstrates an enhancement in regioselectivity beyond that expected from the relative stabilities of the radicals involved. The preference for 1,5-*exo*-cyclization is even more striking in the case of 5-methyl-5-hexen-2-ol (Scheme 15). In this reaction 1,5-*exo*-cyclization is still preferred over 1,6-*endo*-cyclization, despite the fact that 1,5-*exo*-cyclization proceeds via a primary radical as opposed to a tertiary radical in the 1,6-*endo*-cyclization pathway. This is in sharp contrast to the 26:1 preference for a tertiary radical over a primary one, as observed in simple alkene systems such as 2-methylpropene (Scheme 5).

A cyclization step was also introduced into the photo-NOCAS mechanism using nonconjugated dienes as the electron donors.[18] In the reaction of 2,5-dimethyl-1,5-hexadiene, cyclization occurs at the radical cation stage, prior to nucleophilic attack, generating a distonic 1,4-dimethylcyclohexane-1,4-diyl radical cation (Scheme 16). In typical photo-NOCAS fashion, this intermediate is then trapped by methanol to give the corresponding radical, which subsequently substitutes on the arene radical anion. This type of cyclization is dominant at low methanol concentrations and in the presence of co-donors such as biphenyl. Presumably, the co-donor complexes with the initial 1,2-diyl radical cation, thus reducing the availability of its positive charge and decreasing its reactivity towards methanol. Methanol trapping of the 1,2-radical cation is a competing reaction that dominates at high nucleophile concentration. No cyclization occurs at the β-alkoxyalkyl radical stage, however, as 1,4-*exo*-cyclization is thermodynamically unfavorable while 1,5-*endo*-cyclization, usually favored, is now too sterically inhibited. The mechanism becomes more complex when 2,6-dimethyl-1,6-heptadiene is subjected to similar conditions (Scheme 17).[18b] The two pathways rationalized for the hexadiene are active in this reaction as well, but now the formation of the

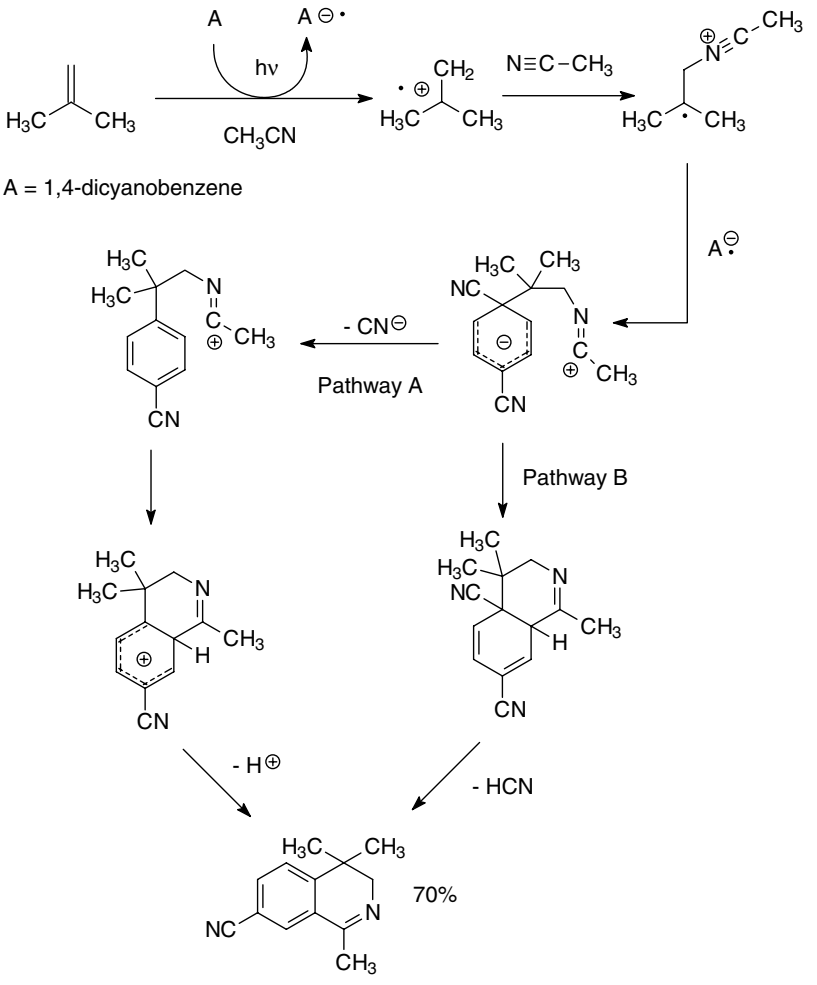

SCHEME 12

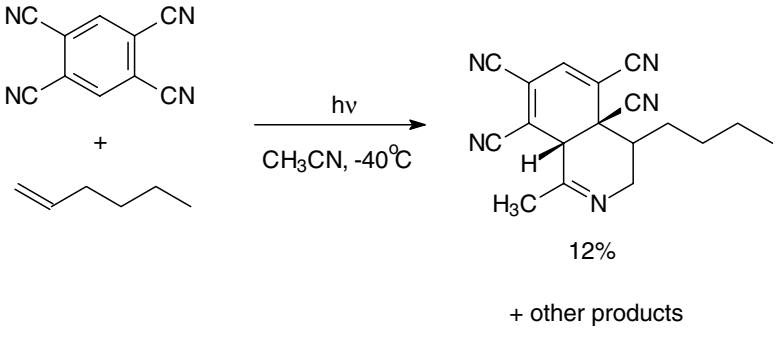

SCHEME 13

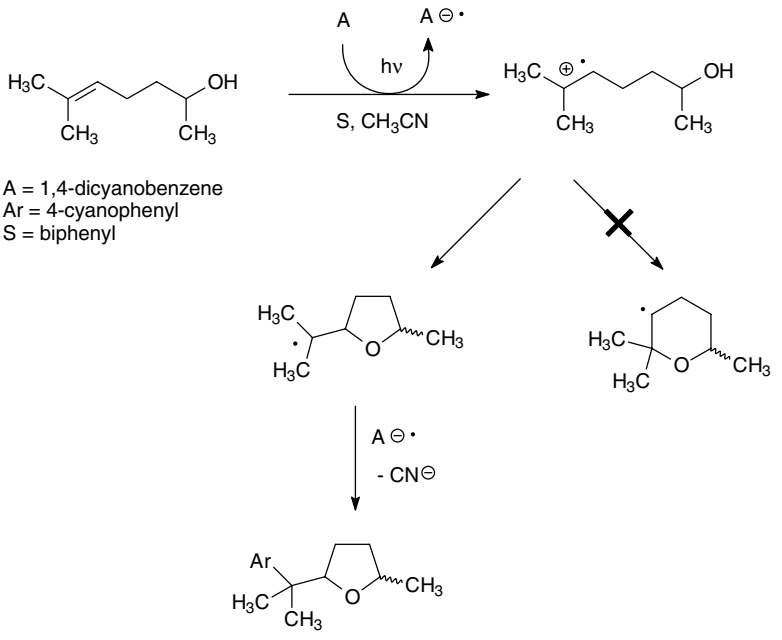

SCHEME 14

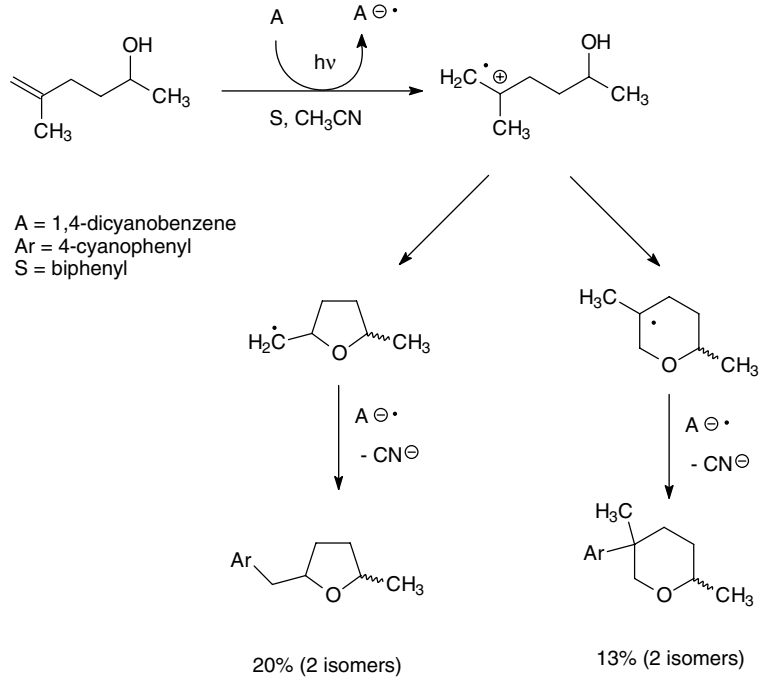

SCHEME 15

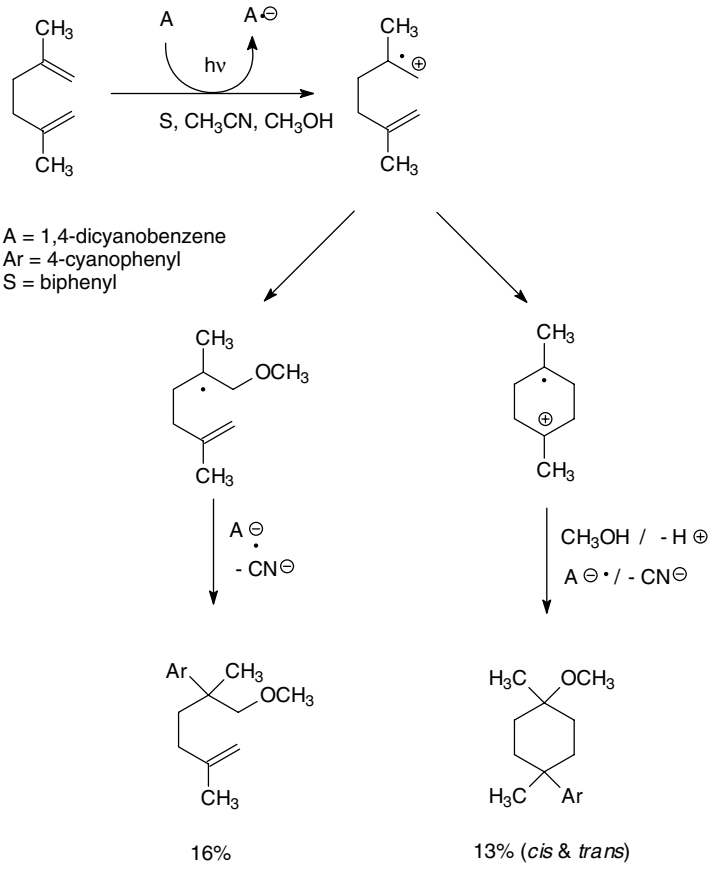

SCHEME 16

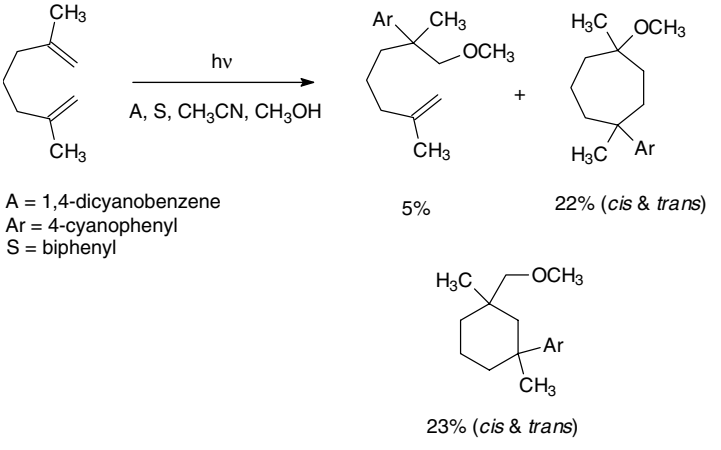

SCHEME 17

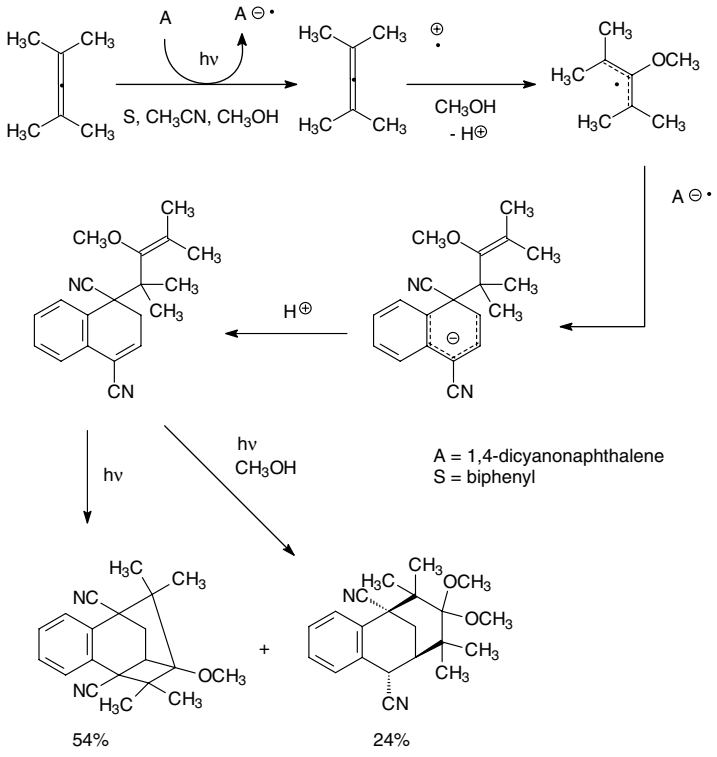

SCHEME 18

β-alkoxyalkyl radical by nucleophilic trapping of the initial 1,2-diyl radical cation provides an additional cyclization route: 1,6-*endo*-cyclization (but not 1,5-*exo*) is a viable pathway. This is in agreement with Beckwith's work on the cyclization of 5-hexenyl radicals.[17c] This work indicated that the preferred mode of cyclization is strongly influenced by the methyl group substitution pattern. Although 1,5-cyclization is typically favored, the directing effects of the 1- and 6-methyl groups in the heptadiene selectively induce a 1,6-*endo*-cyclization. With the basis of the photo-NOCAS mechanism clearly defined, the scope of the reaction was expanded in a series of studies led by the Arnold and Roth research groups.[19] Most of these investigations involve terpenes and related compounds. The radical cations of these substrates underwent a variety of cyclizations, cleavages, and rearrangements, providing a wealth of information on the behavior of radical ions (and their derived radicals and ions) from chemo-, regio-, and stereoselective viewpoints.

40.4 Limitations Due to Competing Pathways

Several potential pathways are available to the olefinic radical cation and the cyanoarene radical anion that will compete with the photo-NOCAS route once certain conditions and structural features in the substrates are altered. It has already been mentioned that deprotonation of the olefinic radical cation and the formation of 1:1 olefin–arene substitution products dominates in the absence of strong nucleophiles.[4a,11b]

The photo-NOCAS reaction is restricted to mononuclear, electron-deficient aromatics as the electron acceptors. Using polynuclear systems such as 1,4-dicyanonaphthalene, for example, leads to the olefin–nucleophile adduct radical adding, rather than substituting, at the *ipso*-position of the arene (Scheme 18). This is most likely due to the reduced rearomatization energy gained in binuclear, as opposed to mononuclear, systems. The photo-NOCAS reaction is limited to aliphatic olefins as electron

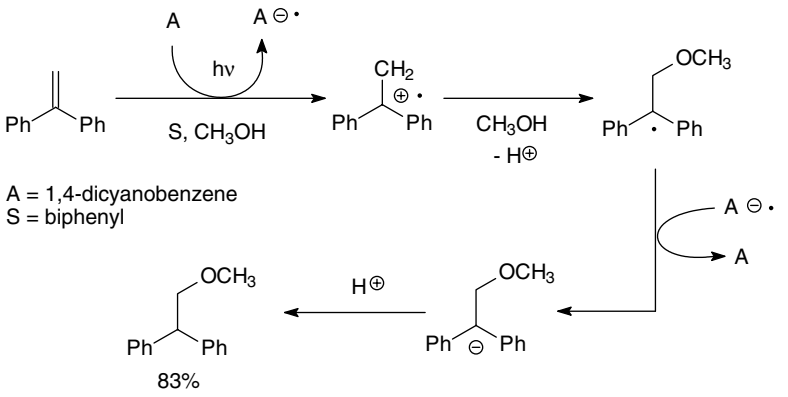

SCHEME 19

donors. The use of aryl alkenes leads to an alternative pathway in which the β-alkoxyalkyl radical is reduced to the corresponding anion by the arene radical anion instead of undergoing a coupling reaction.[20] This anion is subsequently protonated to yield an olefin–nucleophile adduct (Scheme 19). This alteration in mechanism is a consequence of the increased steric bulk offered by the aryl groups at the radical site and the lower reduction potential of the radicals derived from the aryl olefin as compared to the alkyl olefin ones.[21] In this reaction, the cyanoaromatic is not consumed but acts as an electron transfer photosensitizer.

40.5 The Photo-EOCAS Reaction

Some variants of the photo-NOCAS reaction have been developed. The photochemical electrophile–olefin combination, aromatic substitution (photo-EOCAS) reaction is complementary to the photo-NOCAS reaction in the sense that the roles of the olefin and the arene are reversed.[22] In this modification, an electron-deficient olefin (e.g., acrylonitrile) and an electron-rich arene (e.g., 1,2-dimethoxybenzene) are employed (Scheme 20). Photoinduced electron transfer generates the olefin radical *anion* and the arene radical *cation*. In the presence of a proton source (the electrophile) such as methanol, the olefin radical anion is protonated to give an α-cyanoethyl radical (from acrylonitrile). This radical adds to the arene radical cation, presumably at the sites of highest spin density. This generates an adduct cation that subsequently deprotonates and rearomatizes. The regiochemistry observed defines the sequence of events, confirming that electrophilic trapping of the alkene radical anion occurs prior to substitution on the arene, in a fashion similar to the photo-NOCAS reaction. In the absence of an added electrophile, acrylonitrile can function as both the electron acceptor as well as the electrophilic trapping agent.[22d] In this situation, the acrylonitrile radical anion is captured by a neutral acrylonitrile molecule to give a dimeric, distonic radical anion. This species can also be envisaged as a long-bond 1,2-dicyanocyclobutane radical anion (Scheme 21). Substitution on the arene radical cation eventually yields a 1:2 arene–olefin product. The reaction has been demonstrated to occur for a wide variety of electron-rich arenes, including binuclear systems such as naphthalene. [2π+2π]-Cycloadditions start competing once ΔG_{PET} becomes weakly exergonic or endergonic.

40.6 The Photo-ROCAS Reaction

Albini and co-workers have developed another pathway that is formally related to the photo-NOCAS reaction.[23] The photochemical radical–olefin combination, aromatic substitution (photo-ROCAS) reaction involves the regioselective combination of a radical, an olefin, and an arene via a PET pathway

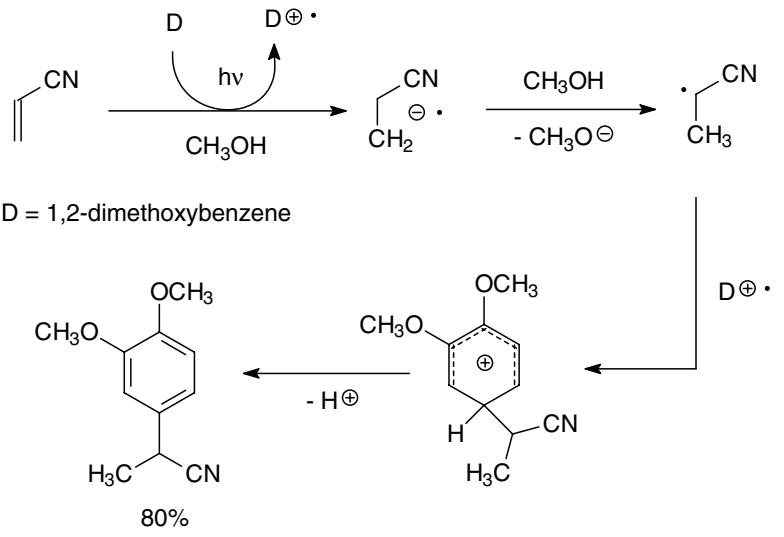

SCHEME 20

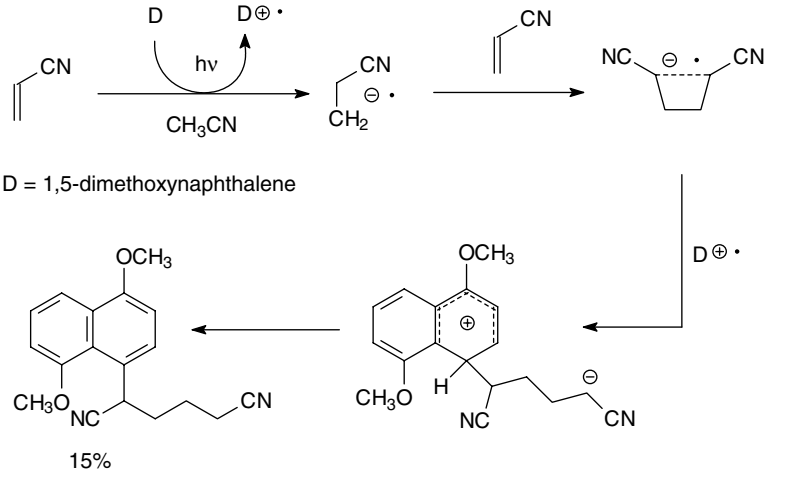

SCHEME 21

(Scheme 22). The initial photoinduced electron transfer process takes place between a cyanoarene, typically 1,2,4,5-tetracyanobenzene in Albini's studies, as electron acceptor and a radical precursor such as a 2,2-dialkyl-1,3-dioxolane as electron donor. The radical cation of the dioxolane formed upon PET is unstable; it undergoes a rapid fragmentation to generate an alkyl radical. This subsequently couples with a ground-state olefin to generate a second adduct radical. This species attacks an *ipso*-position on the arene radical anion, producing an anion that expels cyanide anion, driven by rearomatization. Because the reaction requires the PET to occur between the arene and the radical precursor, only electron-deficient olefins exhibiting higher oxidation potentials than the radical precursors can be used. Nonetheless, the reaction has been found to occur with various electron-deficient olefins. Furthermore, the versatility of the dioxolane radical cation as alkyl radical precursor extends the reaction to a broad selection of radicals.

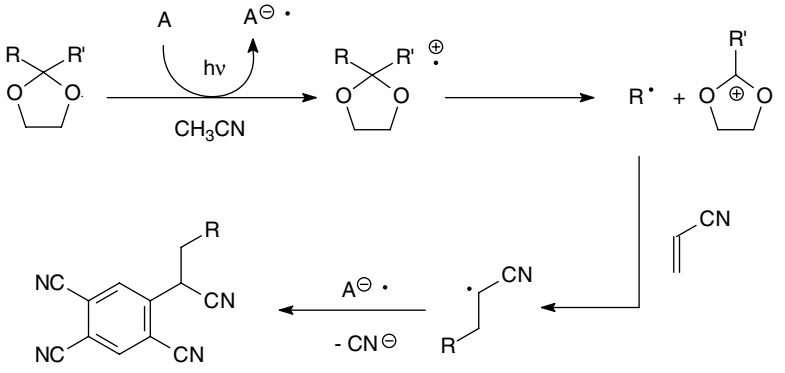

A = 1,2,4,5-tetracyanobenzene

R = $(CH_3)_3C$, R' = CH_3	42%
R = *n*-C_5H_{11}, R' = CH_3	30%
R = CH_3, R' = Ph	80%

SCHEME 22

40.7 Conclusions

The photo-NOCAS reaction has been developed extensively and found to apply to a wide variety of aliphatic olefins. The underlying mechanism has been thoroughly examined and rationalized on the basis of experimental observation in conjunction with detailed, supporting theoretical calculations. Despite minimal optimization from a preparative viewpoint, some of the reactions developed do bear synthetic potential. More importantly, from a more general perspective, the photo-NOCAS reaction serves as a convenient framework in which to investigate how photoinduced radical ions and their derived radicals and ions behave under various competing conditions. The reaction pathway provides the mechanistic chemist with a strict sequence of key steps: photoinduced generation of the radial ions, trapping of the radical cation (nucleophile combination), and trapping of the resultant radical (aromatic substitution). By altering structural features in the substrates and manipulating reaction conditions we have been able to probe and better understand the reactivity and selectivity of radical ions and related transient derivatives.

References

1. Rehm, D. and Weller, A., Kinetics of fluorescence quenching by electron and H-atom transfer, *Isr. J. Chem.*, 21, 259, 1970.
2. (a) Mattes, S. L. and Farid, S., Photochemical electron-transfer reactions of olefins and related compounds, in *Organic Photochemistry*, Vol. 6, Padwa, A., Ed., Marcel Dekker, New York, 1983, chap. 4; (b) Julliard, M. and Chanon, M., Photoelectron-transfer catalysis: its connections with thermal and electrochemical analogues, *Chem. Rev.*, 83, 425, 1983; (c) Kavarnos, G. J. and Turro, N. J., Photosensitization by reversible electron transfer: theories, experimental evidence and examples, *Chem. Rev.*, 86, 401, 1986; (d) Fox, M. A. and Chanon, M., Eds., *Photoinduced Electron Transfer*, Elsevier, Amsterdam, 1988. (e) Pandey, G., Photoinduced electron transfer (PET) in organic synthesis, *Top. Curr. Chem.*, 168, 175, 1993.
3. Mangion, D. and Arnold, D. R., Photochemical nucleophile–olefin combination, aromatic substitution reaction. Its synthetic development and mechanistic exploration, *Acc. Chem. Res.*, 35, 297, 2002.

4. (a) Borg, R. M., Arnold, D. R., and Cameron, T. S., Radical ions in photochemistry. 15. The photosubstitution reaction between dicyanobenzenes and alkyl olefins, *Can. J. Chem.*, 62, 1785, 1984; (b) Torriani, R., Mella, M., Fasani, E., and Albini, A., On the mechanism of the photochemical reaction between 1,4-dicyanobenzene and 2,3-dimethylbutene in the presence of nucleophiles, *Tetrahedron*, 33, 2573, 1997.
5. (a) Gould, I. R., Ege, D., Mattes, S. L., and Farid, S., Return electron-transfer within geminate radical ion pairs. Observation of the Marcus inverted region, *J. Am. Chem. Soc.*, 109, 3794, 1987; (b) Gould, I. R., Ege, D., Moser, J. E., and Farid, S., Efficiencies of photoinduced electron-transfer reactions: role of the Marcus inverted region in return electron transfer within geminate radical-ion pairs, *J. Am. Chem. Soc.*, 112, 4290, 1990; (c) Gould, I. R., Moser, J. E., Armitage, B., and Farid. S., Factors controlling the efficiencies of photoinduced electron-transfer reactions, *Res. Chem. Intermed.*, 21, 793, 1995.
6. Mangion, D., Arnold, D. R., Cameron, T. S., and Robertson, K. N., The electron transfer photochemistry of allenes with cyanoarenes. Photochemical nucleophile–olefin combination, aromatic substitution (photo-NOCAS) and related reactions, *J. Chem. Soc., Perkin Trans. 2*, 48, 2001.
7. McMahon, K. and Arnold, D. R., The photochemical nucleophile–olefin combination, aromatic substitution (photo-NOCAS) reaction. Part 4: Methanol–olefins, methyl 4-cyanobenzoate, *Can. J. Chem*., 71, 450, 1993.
8. Arnold, D. R. and Snow, M. S., The photochemical nucleophile–olefin combination, aromatic substitution reaction. Part 2: Methanol–cyclic olefins, 1,4-dicyanobenzene, *Can. J. Chem.*, 66, 3012, 1988.
9. Arnold, D. R., Chan, M. S. W., and McManus, K. A., Photochemical nucleophile–olefin combination, aromatic substitution (photo-NOCAS) reaction. Part 12: Factors controlling the regiochemistry of the reaction with alcohol as the nucleophile, *Can. J. Chem.*, 74, 2143, 1996.
10. McManus, K. A. and Arnold, D. R., Photochemical nucleophile–olefin combination, aromatic substitution (photo-NOCAS) reaction. Part 7: Methanol, conjugated dienes and 1,4-dicyanobenzene, *Can. J. Chem*., 72, 2291, 1994.
11. (a) Arnold, D. R., McManus, K. A., and Chan, M. S. W., Photochemical nucleophile–olefin combination, aromatic substitution (photo-NOCAS) reaction. Part 13: The scope and limitations of the reaction with cyanide anion as the nucleophile, *Can. J. Chem.*, 75, 1055, 1997; (b) Chan, M. S. W. and Arnold, D. R., Photochemical nucleophile–olefin combination, aromatic substitution (photo-NOCAS) reaction. Part 15: Investigations involving fluoride anion as the nucleophile and the effect of fluorine substitution on the relative stability of the reaction intermediates, *Can. J. Chem.*, 75, 1810, 1997.
12. Mazzocchi, P. H. and Fritz, G., Photolysis of *N*-(2-methyl-2-propenyl)phthalimide in methanol. Evidence supporting radical–radical coupling of a photochemically generated radical ion pair, *J. Am. Chem. Soc.*, 108, 5362, 1986.
13. Arnold, D. R., Wong, A. J., and Cameron, T. S., Radical ions in photochemistry. 12. The photoaddition of olefins to cyano aromatic compounds in polar solvents, *Pure Appl. Chem*., 52, 2609, 1980.
14. de Lijser, H. J. P. and Arnold, D. R., Radical ions in photochemistry. 44. The photo-NOCAS reaction with acetonitrile as the nucleophile, *J. Org. Chem*., 62, 8432, 1997.
15. Vanossi, M., Mella, M., and Albini, A., 2+2+2 Cycloaddition vs. radical ion chemistry in the photoreactions of 1,2,4,5-benzenetetracarbonitrile with alkenes in acetonitrile, *J. Am. Chem. Soc.*, 116, 10070, 1994.
16. (a) McManus, K. A. and Arnold, D. R., The photochemical nucleophile–olefin combination, aromatic substitution (photo-NOCAS) reaction. Part 10: Intramolecular reactions involving alk-4-enols and 1,4-dicyanobenzene, *Can. J. Chem*., 73, 2158, 1995; (b) Weng, H., Scarlata, C., and Roth, H. D., Electron transfer photochemistry of geraniol and (*E*,*E*)-farnesol: a novel "tandem", 1,5-cyclization, intramolecular capture, *J. Am. Chem. Soc.*, 118, 10947, 1996.
17. (a) Baldwin, J. E., Rules for ring closure, *J. Chem. Soc., Chem. Commun*., 734, 1976; (b) Baldwin, J. E., Approach vector analysis: a stereochemical approach to reactivity, *J. Chem. Soc., Chem. Commun*., 738, 1976; (c) Beckwith, A. L. J., Blair, I. A., and Phillipou, G., Substituent effects on

the cyclization of hex-5-enyl radical, *Tetrahedron Lett.*, 38, 2251, 1974; (d) Beckwith, A. L. J. and Schiesser, C. H., Regio- and stereo-selectivity of alkenyl radical ring closure: a theoretical study, *Tetrahedron*, 41, 3925, 1985.

18. (a) Arnold, D. R., McManus, K. A., and Du, X., The photochemical nucleophile–olefin combination, aromatic substitution (photo-NOCAS) reaction. Part 6: Methanol, nonconjugated dienes and 1,4-dicyanobenzene, *Can. J. Chem.*, 72, 415, 1994; (b) Connor, D. A., Arnold, D. R., Bakshi, P. K., and Cameron, T. S., The photochemical nucleophile–olefin combination, aromatic substitution (photo-NOCAS) reaction. Part 9: Methanol–2,6-dimethyl-1,6-heptadiene and 1,4-dicyanobenzene, *Can. J. Chem.*, 73, 762, 1995.
19. (a) Arnold, D. R. and Du, X., The photochemical nucleophile–olefin combination, aromatic substitution (photo-NOCAS) reaction. Part 5: Methanol–monoterpenes (α- and β-pinene, tricyclene and nopol), 1,4-dicyanobenzene, *Can. J. Chem.*, 72, 403, 1994; (b) Arnold, D. R., Connor, D. A., McManus, K. A., Bakshi, P. K., and Cameron, T. S., The photochemical nucleophile–olefin combination, aromatic substitution (photo-NOCAS) reaction. Part 11: Involving (*R*)-(+)-α-terpineol and (R)-(+)-limonene, substituting on 1,4-dicyanobenzene, *Can. J. Chem.*, 74, 602, 1996; (c) Arnold, D. R., Du, X., and de Lijser, H. J. P., The photochemical nucleophile–olefin combination, aromatic substitution (photo-NOCAS) reaction. Part 8: Methanol–2-carene and 1,4-dicyanobenzene, *Can. J. Chem.*, 73, 522, 1995; (d) Weng, H. and Roth, H. D., Electron transfer photochemistry of norbornadiene and quadricyclane: nucleophilic capture of radical cations, free radical rearrangements and hydrogen abstraction, *J. Org. Chem.*, 60, 4136, 1995; (e) Herbertz, T. and Roth, H. D., Electron transfer photochemistry of chrysanthemol: an intramolecular S_N2' reaction of a vinylcyclopropane radical cation, *J. Am. Chem. Soc.*, 118, 10954, 1996; (f) Herbertz, T., Blume, F., and Roth, H. D., Electron transfer photochemistry of a bridged norcaradiene: a mechanistic probe for radical cation nucleophile capture, *J. Am. Chem. Soc.*, 120, 4591, 1998; (g) Arnold, D. R. and McManus, K. A., Photochemical nucleophile–olefin combination, aromatic substitution (photo-NOCAS) reaction: methanol, β-myrcene and 1,4-dicyanobenzene. Intramolecular cyclization of an ene–diene radical cation, *Can. J. Chem.*, 76, 1238, 1998.
20. (a) Neunteufel, R. A. and Arnold, D. R., Radical ions in photochemistry. 1. The 1,1-diphenylethylene cation radical, *J. Am. Chem. Soc.*, 95, 4080, 1973; (b) Shigemitsu, Y. and Arnold, D. R., Radical ions in photochemistry: sensitized (electron-transfer) photochemical reactions of some 1-phenylcycloalkenes in polar, nucleophilic solvents, *J. Chem. Soc., Chem. Commun.*, 407, 1975; (c) Maroulis, A. J., Shigemitsu, Y., and Arnold, D. R., Radical ions in photochemistry. 5. Photosensitized (electron transfer) cyanation of olefins, *J. Am. Chem. Soc.*, 100, 535, 1978; (d) Arnold, D. R., Du, X., and Chen, J., The effect of *meta*- or *para*-cyano substitution on the reactivity of the radical cations of arylalkenes and alkanes, *Can. J. Chem.*, 73, 307, 1995; (e) Mangion, D. and Arnold, D. R., The photochemistry of 4-halobenzonitriles and 4-haloanisoles with 1,1-diphenylethene in methanol: homolytic cleavage versus electron-transfer pathways, *Can. J. Chem.*, 77, 1655, 1999.
21. Wayner, D. D. M., McPhee, D. J., and Griller, D., Oxidation and reduction potentials of transient free radicals, *J. Am. Chem. Soc.*, 110, 132, 1988.
22. (a) McCullough, J. J. and Huang, C. W., Photo-additions of aromatic hydrocarbons–indene and naphthalene with acrylonitrile, *Can. J. Chem.*, 47, 757, 1969; (b) Ohashi, M., Tanaka, Y., and Yamada, S., Photochemical reactions of methoxybenzenes with acrylonitrile, *J. Chem. Soc., Chem. Commun.*, 800, 1976; (c) Ohashi, M., Tanaka, Y., and Yamada, S., The [2+2]-cycloaddition vs. substitution in photochemical reactions of methoxybenzene–acrylonitrile systems, *Tetrahedron Lett.*, 41, 3629, 1977; (d) Mangion, D., Frizzle, M., Arnold D. R., and Cameron T. S., The photochemistry of acrylonitrile with methoxylated naphthalenes: introducing the photochemical electrophile–olefin combination, aromatic substitution (photo-EOCAS) reaction, *Synthesis*, 1215, 2001.
23. (a) Mella, M., Fagnoni, M., and Albini, A., Radicals through photoinduced electron transfer. Addition to olefin and addition to olefin–aromatic substitution reactions, *J. Org. Chem.*, 59, 5614, 1994; (b) Fagnoni, M., Mella, M., and Albini, A., Radical addition to alkenes via electron transfer photosensitization, *J. Am. Chem. Soc.*, 117, 7877, 1995.

41

Intra- and Intermolecular Cycloadditions of Benzene Derivatives

Andrew Gilbert
The University of Reading

41.1 Introduction

As noted by Wender and Dore in the previous edition of this Handbook, "Arene–alkene photocycloadditions are a theoretically intriguing and synthetically unique class of reactions with enormous potential in complex-molecule synthesis."[1] Comprehensive reviews that appeared in the late 1980s and early 1990s have documented the background and mechanistic aspects of intra- and intermolecular photocycloadditions to the benzene ring, including the factors that control selectivites.[1–7] These accounts also outline the numerous examples of the synthetic utility of these processes. By the start of the period of the current review, the photoaddition of ethenes to the benzene ring was already widely acknowledged as a convenient, versatile, and direct access, from simple, readily available starting materials to complex polycyclic systems that are the core architecture of many a synthetic target. The *meta* (1,3-) and *ortho* (1,2-) cycloadditions (Figure 41.1), yielding, respectively, the tricyclo[3.3.0.^{2,8}]oct-3-ene and bicyclo[4.2.0]octa-2,4-diene skeletal, have been well researched and continue to attract appreciable attention. In contrast, the corresponding *para* (1,4-) process remains largely unexplored and exploited mainly because this pathway is seldom observed and also lacks the predictability of the other two modes.

41.2 *meta*-Photocycloaddition

The widely accepted mechanism for the *meta*-photocycloaddition that accounts for essentially all the experimental observations involves initial interaction of the S_0 ethene with the S_1 arene resulting in polarisation of the benzene ring possibly by way of an exciplex intermediate.[1–6] Formation of the *meta* adduct may arise directly from the polarized species or may involve a second intermediate, but evidence for the latter species is lacking. This general mechanism has proved useful not only in providing an understanding of the reactivity and regio- and stereo-selectivities of the process but also in predicting the outcome of the cycloaddition so that it can be applied with confidence as a key step in synthetic sequences. The latter aspect has been particularly well exploited for the intramolecular process, and a number of total syntheses of naturally occurring compounds have thereby been elegantly accomplished

0-8493-1348-1/04/$0.00+$1.50

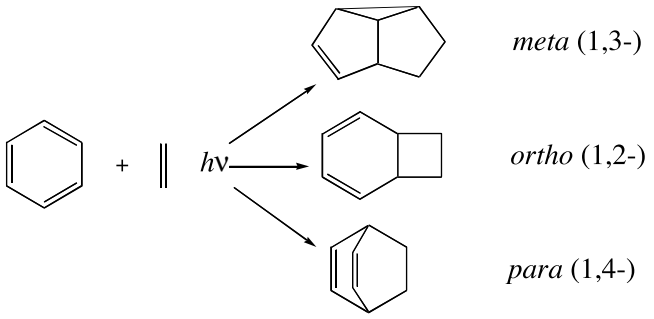

FIGURE 41.1 Modes of photocycloaddition of ethenes to the benzene ring.

in a relatively small number of steps.[2–5] Recent examples of this aspect of the reaction include the use of the intramolecular *meta*-photocycloaddition of **1** to give the angular and linear triquinane adducts **2** and **3**, respectively, the latter of which provides the key framework of (±)-ceratopicanol **4** in five steps with an overall yield of 19%;[8] and the first synthesis of *cis,cis,cis,trans*-[5.5.5.5]-fenestranes **5** from a novel arene–ethene photocycloaddition/radical cyclization sequence from the trichromophore **6** as outlined in Figure 41.2.[9] Furthermore, the angular adduct **7** from the bichromophore **8** has provided the molecular architecture for elaboration to give a formal synthesis of (±)-crinipellin B **9**.[10]

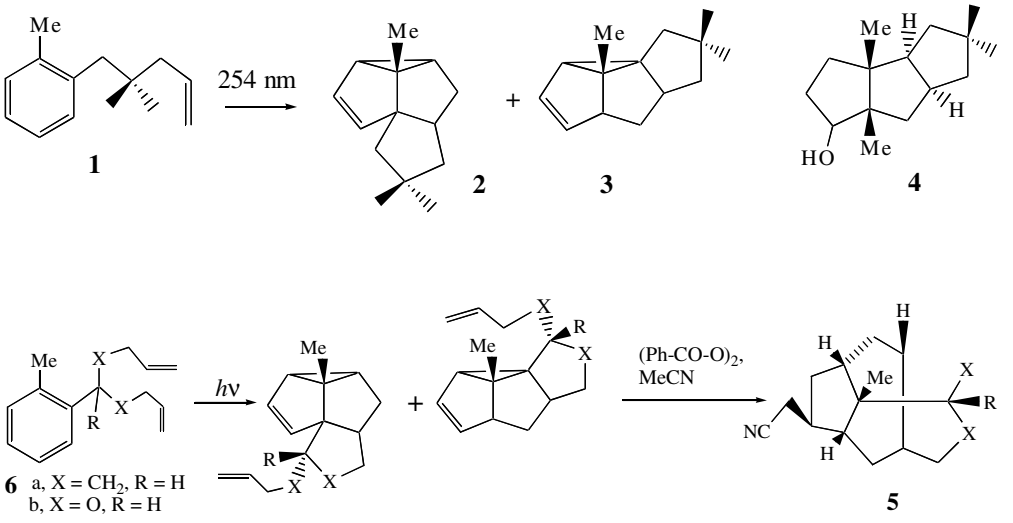

FIGURE 41.2 Synthesis of *cis,cis,cis,trans*[5.5.5.5]fenestranes.

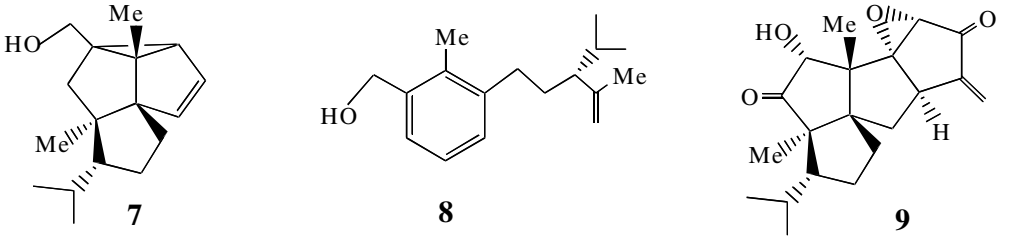

Much recent work on the intramolecular process has been concerned with determining the influence of substituents on the tether between the chromophores and of the presence of heteroatoms in this chain, on the reactivity of the bichromophore and regiochemistry of the addition. Several studies have reported

on the photocycloadditions of 5-phenylpent-1-enes having hydroxy,[11–18] methoxy,[12] trimethylsilyloxy,[17] or trifluoroacetate[18] groups at the 3,[11,13,14,17,18] 4-,[12,14,16,17] or 5-[17] positions and with a methoxy group at the 2′-position to direct the attack to the 1′,3′- sites on the benzene ring. All systems undergo *meta*-photocycloaddition with control by both steric and electronic effects. The major observation is that these reactions occur diastereoselectively with the configuration of the mono-substituent, mainly *endo*, as indicated in the conversion of **10** to **11**, and this is considered to be a result of minimization of steric interactions between the substituent and the methoxy group on the arene. For disubstituted compounds such as **12**, the more sterically demanding group has *exo* stereochemistry in the *meta* adduct. Other results suggest that the stereochemistry may be influenced by hydrogen bonding in the conformation prior to addition[12,15,16] and by solvent polarity for certain bichromophores.[12] Incorporation of rigidity into the tether as in **13** and **14** naturally also restricts the conformation of the bichromophore which leads to addition, and this can markedly affect the reaction selectivity.[19] Thus, while the *cis* isomers of these bichromophores undergo addition of the ethene predominantly at the 1,3- positions of the phenyl group, 2,6- addition occurs in high selectivity for the *trans* isomers.

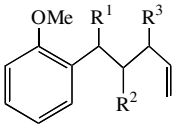

10

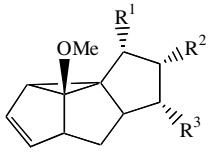

11

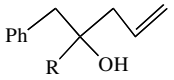

12

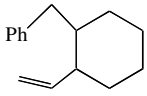

13

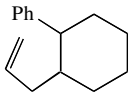

14

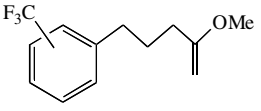

15

It is well known that the pathway discrimination between *meta*- and *ortho*-cycloadditions of ethenes to the benzene ring is dependent upon the electron donor–acceptor relationships between the addends.[6] These relationships can be quantified in terms of the free enthalpy of electron transfer (ΔG^0) given from the Rehm–Weller equation. Not surprisingly, therefore, the reaction mode selectivity of arene–ethene bichromophores is markedly influenced by the position and nature of substituents on the addends and by the presence and position of a heteroatom in the tether between the chromophores. The former effect is illustrated by the photochemistry of 2-methoxy-5-[(trifluoromethyl)phenyl]pent-1-enes **15**, the 3′-isomer of which yields *meta* adducts from 1,3- and 2,6-addition, while the presence of the $-CF_3$ group at the 2′- and 4′- positions results in *ortho*-addition.[20] The latter influence is clearly evident in the differing reaction mode selectivities of 3-benzyloxyprop-1-enes (predominantly *meta*)[21] and 4-phenoxybut-1-enes (both *meta* and *ortho*).[22–26] Furthermore, the 3-benzyloxyprop-1-enes display a marked preference for formation of the linear over the angular isomer following 1,3-addition. This feature in both the oxygen and nitrogen series is rationalized in terms of an unsymmetrical orientation (**16**) in the conformation leading to the adducts, which is considered to result from the smaller bond angle and shorter bond lengths in the $-CH_2-X-CH_2-$ tether compared to the hydrocarbon systems, which generally give approximately equal amounts of the adduct isomers.[27] Bonding between $C_{1'}$ and C_2 then occurs prior to $C_{3'}$ and C_1 in **16**, and closure to give the cyclopropane ring between $C_{2'}$ and $C_{6'}$ is favored by the early attainment of sp^3 hybridization of $C_{1'}$. In support of this proposal, the bichromophore **17** with silicon in the tether preferentially gives the angular isomer **18** because of the longer Si–C bond compared to the C–C bond and this favors $C_{3'}-C_1$ bonding and hence closure between $C_{2'}$ and $C_{4'}$.[28] Diastereofacial differentiation and regiocontrol of the ring closure in the intramolecular process has been achieved with the

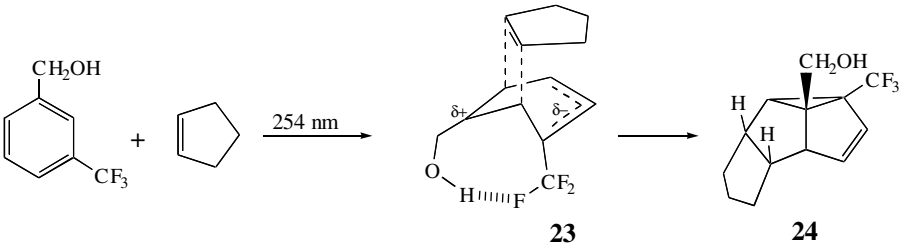

FIGURE 41.3 Control of cyclopropane ring formation by 1,3-substitutents.

bichromophore **19**, which uses the tether as a chiral auxiliary,[29] and regio and enantioselectivities have been induced in the *meta*-photocycloaddition by irradiation of complexes of phenoxyalkenes with β-cyclodextrin.[26] Irradiation of allylphenoxydimethylsilane **20** gives good yields of the 2,6-addition product **21**,[30,31] which can be readily converted into the core skeleton of the alkaloid gelsemine **22**.[31]

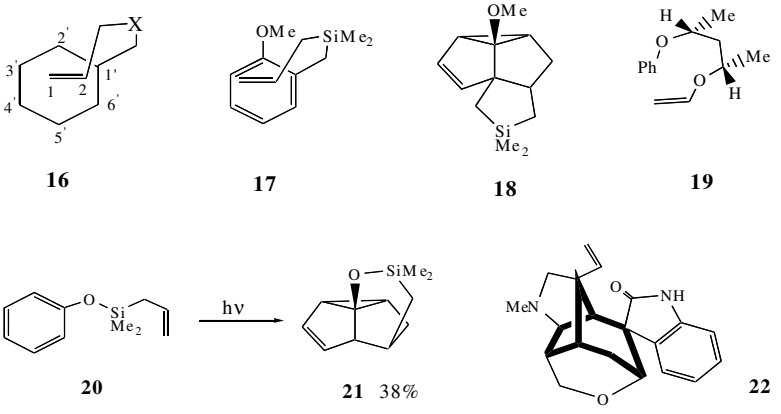

Recent studies of the *meta* process have been mainly concerned with the intramolecular addition and, as outlined above, control over all aspects of the reaction can be achieved including the direction of cyclization to form the cyclopropane ring. In intermolecular reactions of arene–ethene systems, both the reaction mode selectivity and the regiochemistry of the addition can be controlled by the nature of the substituents on the addends.[32] For the *meta* process, the arene substituents may also be used to influence the direction of the formation of the cyclopropane ring in the adduct and so provide specificity in isomer formation. Such specificity has been described for 1,3-additions to 3-trifluormethyl derivatives of phenol, benzyl alcohol, benzyltrimethylsilane, and phenoxytrimethylsilane and is deduced to arise from attractive interactions between the substituents, causing an asymmetric distortion of the C_6 ring in the species (e.g., **23**) immediately prior to addition.[33,34] As outlined in Figure 41.3, cyclization in **23** is favored between C_1 and C_3 to give solely the adduct with the 1,2-disubstitued dihydrosemibullvalene skeleton **24**.

41.3 *ortho*-Photocycloaddition

An excellent review of the *ortho* photocycloaddition of alkenes and alkynes to the benzene ring has recently been published which not only discusses the mechanisms and intermediates of these processes but also presents comprehensive listings of the examples of these reactions which have been reported over the past 40 years or so.[35]

It is common in the intramolecular reaction of arene–ethene nonconjugated bichromophores that, if the molecular architecture allows, the first formed *ortho*-cycloaddition product ring opens thermally to the cyclooctatriene, which then undergoes photochemical electrocyclization to give either or both of the

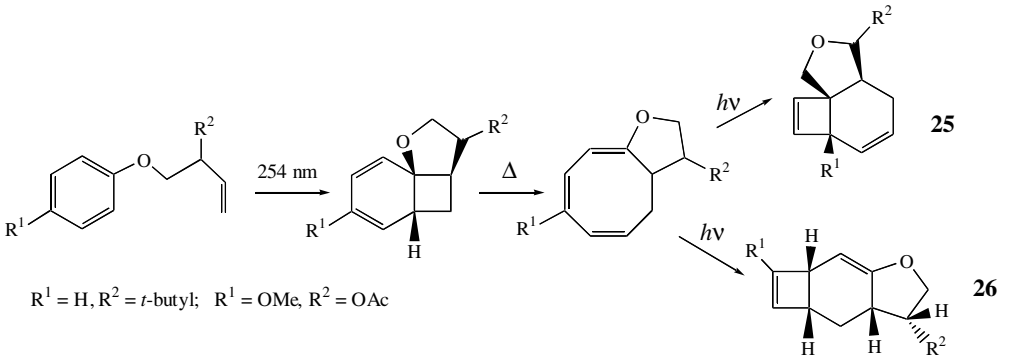

FIGURE 41.4 Intamolecular *ortho* photocycloaddition of 4-phenoxybut-1-enes.

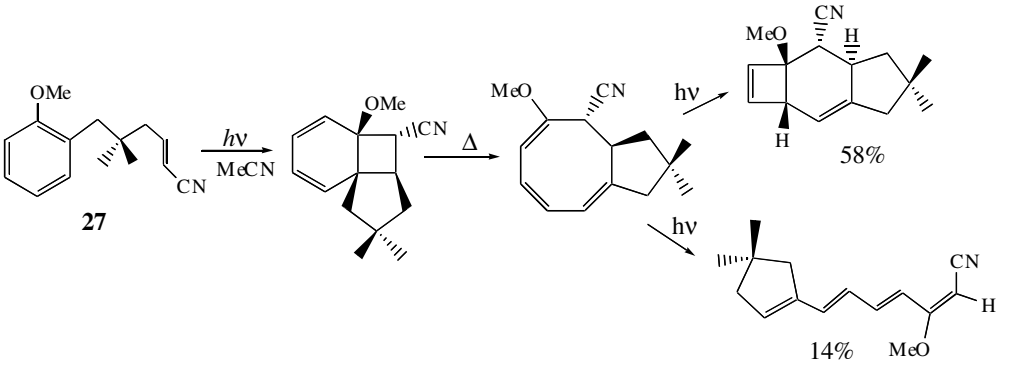

FIGURE 41.5 Intramolecular *ortho* cycloaddition of an electron donor–acceptor bichromophore.

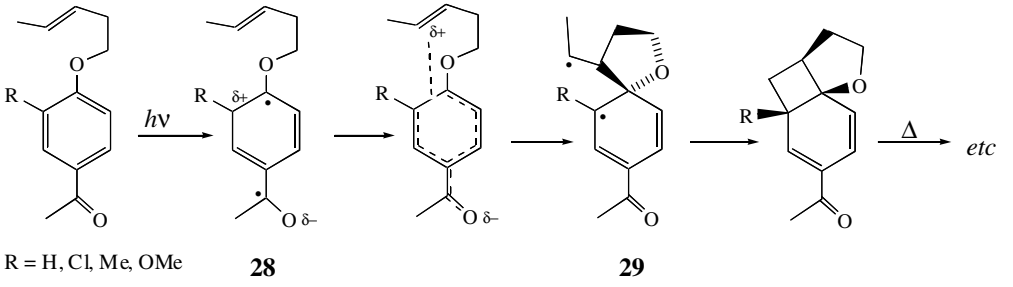

FIGURE 41.6 Mechanism of *ortho* photocycloaddition of alkenylacetophenones.

isomers **25** and **26** as illustrated in Figure 41.4 for the reaction of 4-phenoxybut-1-enes.[25,36] The reaction of these bichromophores may be assumed to arise from the S_1 state of the arene and may also be accompanied by varying amounts of the corresponding *meta*-cycloadducts dependent on the nature and position of substituents. The bichromophore **27,** having an obvious electron donor–acceptor relationship between the addends, undergoes solely *ortho*-cycloaddition (Figure 41.5) from the singlet state as evidenced by the retention of the (*E*) geometry of the ethene unit.[37] However, not surprisingly, the similar reactions reported over the past 15 years for 2- and 4-alkenylacetophenones and related compounds are triplet state processes and are deduced to proceed by charge transfer interaction from the ethene moiety

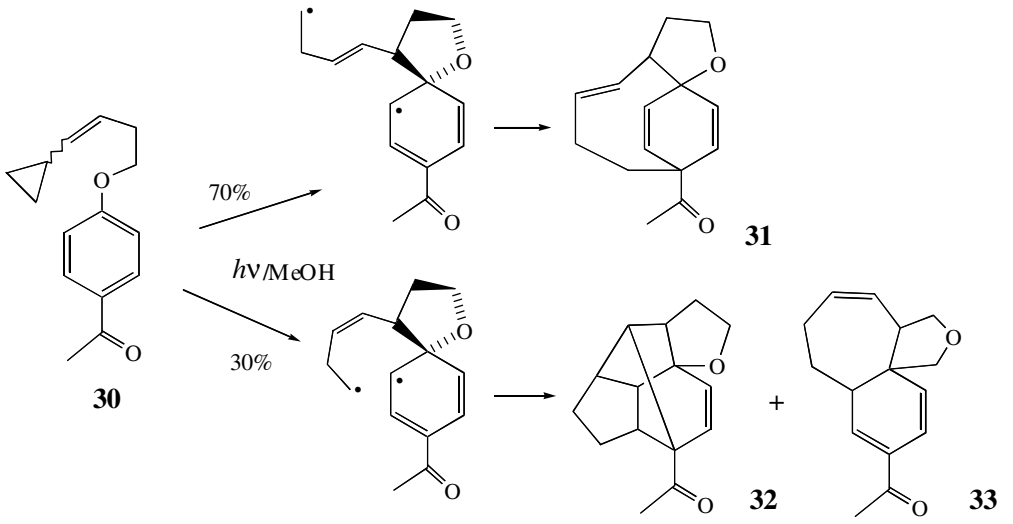

FIGURE 41.7 Evidence for the biradical intermediate **29** using the cyclopropyl compound **30**.

to the T_1 arene and the biradicals **28** and **29** as outlined in Figure 41.6.[38,39] The involvement of the biradical **29** has been proven from a study of the photochemistry of the cyclopropyl-substituted bichromophore **30** which gave none of the *ortho*-cycloaddition-derived products; instead, the three isomers **31**, **32**, and **33** were formed in respective ratios of 5:3:1 by the routes outlined in Figure 41.7.[40] Furthermore, it is deduced that only 30% of the biradicals revert to the starting bichromophore, while 70% undergo rearrangement. In contrast to the 4-phenoxybut-1-enes in Figure 41.4, those having a 2′- or 4′-cyano or 2′-alkoxycarbonyl substituent have been shown by quenching[41] and acetone-sensitization[42] studies to react also from the triplet state, but to yield the same types of product derived exclusively from *ortho*-cycloaddition. Under acid conditions, the photochemistry of 4-phenoxybut-1-enes which are mono- (3′-) or di- (3′,5′-) substituted with hydroxy-,[43–47] methoxy-,[45–47] methoxycarbonyl-,[44,47,48] or cyano-[47] groups provides a convenient access to highly functionalized compounds including cyclobutenes. The reactions proceed by initial intramolecular *ortho*-cycloaddition followed by acid cleavage of the products: typical examples are given in Figures 41.8.[46,47]

Bichromophores of diverse structure undergo intramolecular *ortho*-cycloaddition, and molecular constraints can restrict the ring opening of the initial adduct. Examples of this feature include the formation of **34** by chemo-, regio-, and stereo-selective intramolecular addition of the benzene–thymine bichromophore **35**[49] and the conversion of the chromone **36** in benzene solution to the intramolecular adduct **37**.[50] However, carrying out the latter reaction in methanol or further irradiation of the *ortho* adduct gives the product **38** of a novel rearrangement.

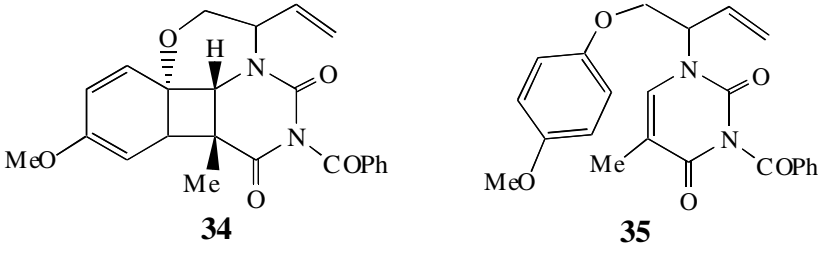

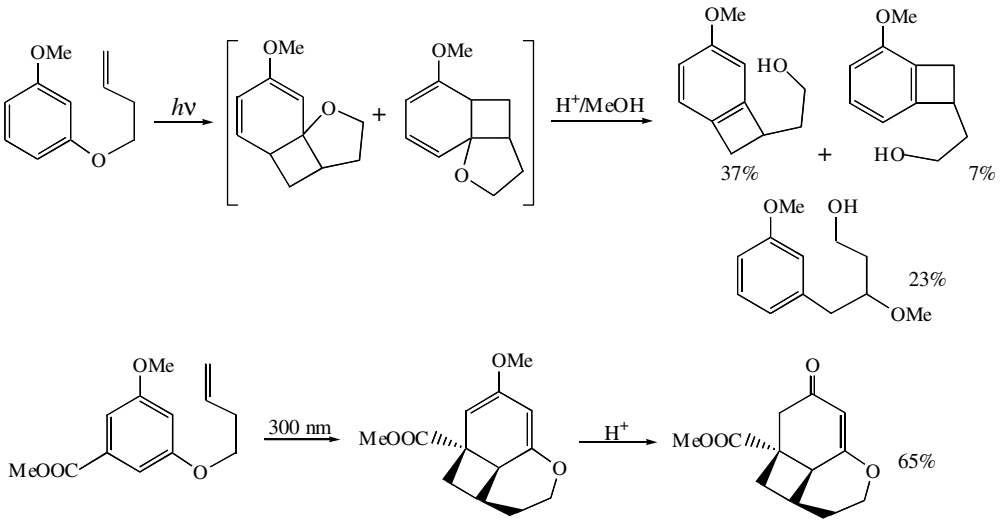

FIGURE 41.8 Intramolecular photocycloaddition of 4-phenoxybut-1-enes under acid conditions.

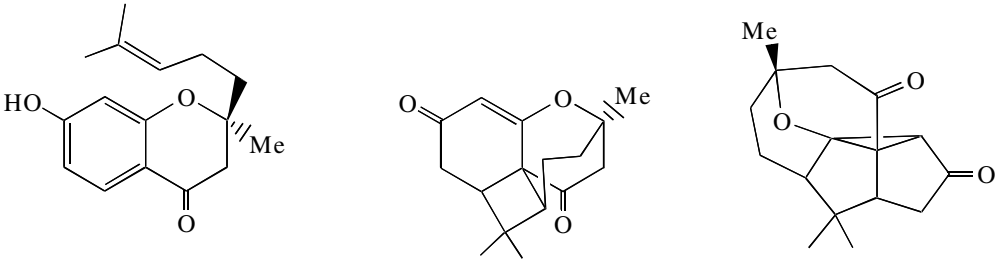

36 **37** **38**

Numerous examples have been reported in the literature of the intermolecular *ortho*-photocycloadditions of ethenes to the benzene ring. Some of these arise by direct or sensitized excitation of a ground-state complex or by way of an exciplex, while others may be assumed to result simply from addition of the S_0 ethene to the S_1 arene.[35] However, a common feature for systems for which the *ortho* adduct is the major product is that an electron donor–acceptor relationship exists between the addends. Depending on the substituents, these bicyclo-octa-2,4-dienes may be thermally stable or, as in intramolecular systems, undergo ring opening to the cyclooctatriene isomer followed by photochemical electrocyclization. In other cases, where the ethene has dienophilic activity, 2:1 adducts are formed. Most of the studies of intermolecular *ortho*-photocycloaddition were reported over 10 years ago,[35] but more recently this process under acid conditions, with 6-chloro-1,3-dimethyluracil and benzene and its simple derivatives, has attracted attention.[51–55] These *ortho* adducts ring open to the cyclooctatriene, which then undergo various photorearrangements. The primary process is illustrated in Figure 41.9 for the addition to mesitylene.[55]

The intra- and intermolecular photoadditions of acetylenes to the benzene ring are solely *ortho* processes, regardless of the electron donor–acceptor relationships of the addends; thus, unfortunately, these systems do not provide an access to semibullvalenes. The bicyclo[4.2.0]octa-2,4,7-trienes formed commonly ring open to the stable cyclo-octatetraenes.[35] These *ortho*-photocycloadditions are generally characterized by low quantum efficiencies (~0.03), and in some cases evidence has been reported that indicates that the reaction may proceed from the photoexcited acetylene. Examples of these processes are given in Figure 41.10.

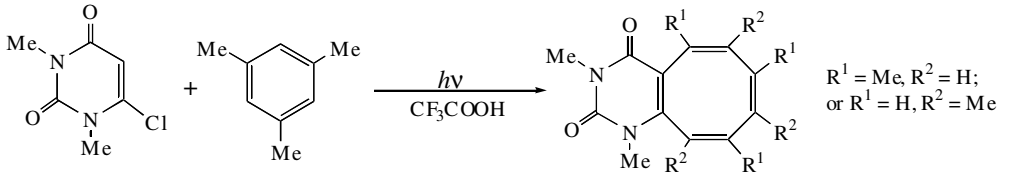

FIGURE 41.9 Photocycloaddition of 6-chloro-1,3-dimethyluracil to mesitylene.

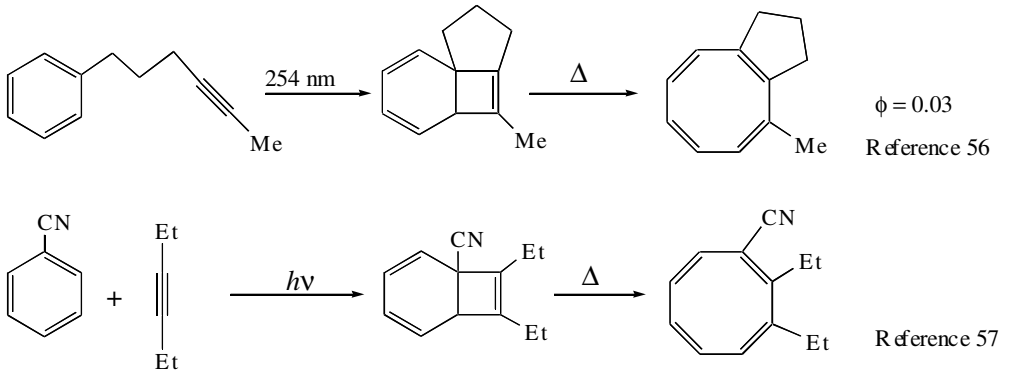

FIGURE 41.10 Intra-and inter-molecular photocycloaddition of acetylenes to the benzene ring.

The cyano group of benzonitrile or acrylonitrile behaves in a similar manner to acetylenes in its addition to benzenes. The addition is particularly favored for benzenes, which are 1,4-substituted with an electron donor and an electron acceptor group. The adducts undergo ring opening and provide a convenient one-step route to azocines **39**.[58]

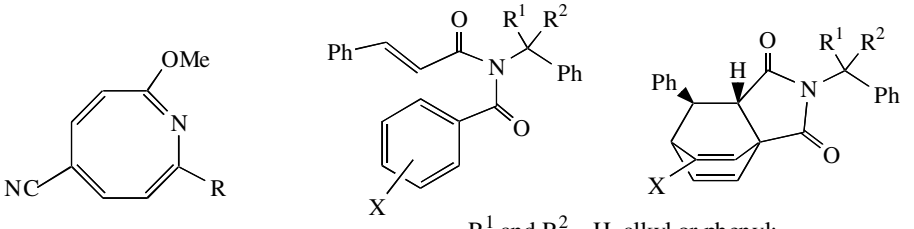

39 R = Ph or -CH=CH_2 **40** **41**

para-Photocycloaddition to the benzene ring is a rare event and is generally a minor process except for 1,2-dienes;[59] however, *N*-benzoyl-*N*-benzylcinnamides **40** and related compounds undergo benzil-sensitized intramolecular cycloaddition in benzene solution to give the bicyclo[2.2.2]octadienes **41**.[60]

References

1. Wender, P. A. and Dore, T. M., Intra and intermolecular cycloadditions of benzene derivatives, in *CRC Handbook of Organic Photochemistry and Photobiology*, Horspool, W. M. and Song, P.-S., Eds., CRC Press, Boca Raton, FL, 1995, 280.
2. Wender, P. A. and von Geldern, T. W., Aromatic compounds: isomerisation and cycloaddition, in *Photochemistry in Organic Synthesis*, Coyle, J. D., Ed., The Royal Society of Chemistry, London, 1986, 226.

3. Wender, P. A., Siggel, L. and Nuss, J. M., Arene–alkene photocycloaddition reactions, in *Organic Photochemistry*, Vol 10, Padwa, A., Ed., Marcel Dekker, New York, 1989, 357.
4. Wender, P. A., Ternansky, R., de Long, M., Singh, S., Olivero, A., and Rice, K., Arene–cycloadditions and organic synthesis, *Pure Appl. Chem*., 62, 1597, 1990.
5. Wender, P. A., Siggel, L., and Nuss, J. M., [3 + 2] and [5 + 2] arene–alkene photocycloadditions, in *Comprehensive Organic Synthesis*, Vol. 5, Trost, B. M., Fleming, I., and Paquette, L. A., Eds., Pergamon Press, Elmsford, NY, 1991, 645.
6. Cornelisse, J., The *meta* photocycloaddition of arenas to alkenes, *Chem. Rev.*, 93, 615, 1993.
7. De Keukeleire, D. and He, S-L., Photochemical strategies for the construction of polycyclic molecules, *Chem. Rev.*, 93, 359, 1993.
8. Baralotto, C., Chanon, M. and Julliard, M., Total synthesis of the tricyclic sesquiterpene (±)-ceratopicanol: an illustration of the holosynthon concept, *J. Org. Chem*., 61, 3576, 1996.
9. Wender, P. A., Dore, T. M., and de Long, M. A., An arene–alkene photocycloaddition–radical cyclization cascade: the first syntheses of *cis*,*cis*,*cis*,*trans*-[5.5.5.5]-fenestranes, *Tetrahedron Lett.*, 37, 7687, 1996.
10. Wender, P. A. and Dore, T. M., A formal synthesis of crinipellin B based on the arene–alkene *meta*-photocycloaddition reaction, *Tetrahedron Lett.*, 39, 8589, 1998.
11. Zhang, C. and Guo, X. C., Intramolecular hydrogen-bond effect in *meta*-cycloaddition of arene to olefin, *Synth. Commun.*, 24, 3157, 1994.
12. Barentsen, H. M., Sieval, A. B., and Cornelisse J., Intramolecular *meta* photocycloaddition of conformationally restrained 5-phenylpent-1-enes. 2. Steric and electronic effects caused by 4-monosubstitution and 4-disubstitution, *Tetrahedron*, 51, 7495, 1995.
13. Zhang, C., Guo, X. C., Shen, X. M., and Xu, Y. F., Diastereoselective intramolecular *meta*-cycloaddition of an arene to an olefin, *Synth. Commun.*, 25, 775, 1995
14. Zhang, C., Guo, X. C., and Shen, X. M., Regioselectivity of photoinduced intramolecular arene–olefin *meta*-cycloaddition, *Chin. Chem. Lett.*, 7, 1, 1996.
15. Shen, X. M., Guo, X. C., Sun, L. D., and Zhang, C., Studies on diastereoselective intramolecular *meta* cycloaddition of arene to olefin (Part I), *Chin. Chem. Lett.*, 9, 131, 1998.
16. Shen, X. M., Sun, L. D., and Zhang, C., Studies on diastereoselective intramolecular *meta* cycloaddition of arene to olefin (Part II), *Chin. Chem. Lett.*, 9, 321, 1998.
17. Timmermans, J. L., Wamelink, M. P., Lodder, G., and Cornelisse, J., Diastereoselective intramolecular *meta* photocycloaddition of side-chain-substituted 5-(2-methoxyphenyl)pent-1-enes, *Eur. J. Org. Chem.*, 2, 463, 1999.
18. Guo, X. C. and Chen, Q. Y., Photo-induced intramolecular arene-olefin *meta*-cycloaddition of 5-phenyl-fluorinated-pent-1-enes, *J. Fluor. Chem*., 97, 149, 1999.
19. Barentsen, H. M., Talman, E. G., Piet, D. P., and Cornelisse, J., Intramolecular *meta* photocycloaddition of conformationally restrained 5-phenylpent-1-enes. 1. Bichromophoric cyclohexane derivatives, *Tetrahedron*, 51, 7469, 1995.
20. De Haan, R., de Zwart, E. W., and Cornelisse, J., Intramolecular photocycloaddition of a vinyl ether to CF_3-substituted 2-methoxy-5-phenylpent-1-enes, *J. Photochem. Photobiol. A: Chem*., 102, 179, 1997.
21. Blakemore, D. C. and Gilbert, A., Intramolecular photocycloaddition of 3-benzyloxyprop-1-enes, *J. Chem. Soc.*, *Perkin Trans. 1*, 2265, 1992.
22. De Keukeleire, D., He, S. L., Blakemore, D. C., and Gilbert, A., Intramolecular photocycloaddition reactions of 4-phenoxybut-1-enes, *J. Photochem. Photobiol. A: Chem.*, 80, 233, 1994.
23. Van der Eycken, E., De Keukeleire, D., and De Bruyn, A., Intramolecular *ortho* and *meta* photocycloadditions of 3-alkyl-4-phenoxybut-1-enes, *Tetrahedron Lett*., 36, 3573, 1995.
24. Van der Eycken, E., De Keukeleire, D., De Bruyn, A., Van der Eycken, J., and Gilbert, A., Stereochemical features of *meta* photocycloadducts derived from 3-alkyl-4-phenoxybut-1-enes, *Recl. Trav. Chim. Pays-Bas*, 114, 480, 1995.

25. Vizvardi, K., Toppet, S., Hoornaert, G. J., De Keukeleire, D., Bako, P., and Van der Eycken, E., Intramolecular *ortho* and *meta* photocycloadditions of 4-phenoxybut-1-enes substituted in the arene residue with carbomethoxy, carbomethoxymethyl and 2-carbomethoxyethyl groups, *J. Photochem. Photobiol. A: Chem*., 133, 135, 2000.
26. Vizvardi, K., Desmet, K., Luyten, I., Sandra, P., Hoornaert, G., and Van der Eycken, E., Asymmetric induction in intramolecular *meta* photocycloaddition: cyclodextrin-mediated solid-phase photochemistry of various phenoxyalkenes, *Org. Lett*., 3, 1173, 2001.
27. Blakemore, D. C. and Gilbert, A., Intramolecular *meta* photocycloaddition of 3-benzylazaprop-1-enes, *Tetrahedron Lett*., 35, 5267, 1994.
28. Amey, D. M., Blakemore, D. C., Drew, M. G. B., Gilbert, A., and Heath, P., Intramolecular *meta* photocycloaddition of 3-benzyl(dimethylsila)prop-1-enes, *J. Photochem. Photobiol. A: Chem.*, 102, 173, 1997.
29. Sugimura, T., Nishiyama, N., Tai, A., and Hakushi, T., Regio-chemically and diastereo-chemically controlled photocycloaddition of an arene and an alkene linked by a chiral auxiliary, *Tetrahedron Asymm.*, 5, 1163, 1994.
30. Bahu, S., Fleming, S. A., Nilsson, B., and Turner, T., Synthesis of 2-silaoxane via 1,3-photocycloaddition, *J. Heterocyclic. Chem*., 38, 1341, 2001.
31. Avent, A. G., Byrne, P. W., and Penkett, C. S., A photochemical approach to the gelsemine skeleton, *Org. Lett*., 1, 2073, 1999.
32. Al Qaradawi, S., Gilbert, A., and Jones, D. T., Factors influencing the reaction-mode selectivity and regiochemistry of intermolecular photocycloaddition reactions of ethenes to polysubstituted benzenes, *Recl. Trav. Chim. Pays-Bas*, 114, 485, 1995.
33. Gilbert, A. and Jones, D. T., Formation of bicyclo[3.2.1]oct-2-en-8-ones and 1-hydroxydihydrosemibullvalenes from the *meta*-photocycloaddition of cyclopentene to phenols, *J. Chem. Soc.*, *Perkin Trans. 2*, 1385, 1996.
34. Amey, D. M., Gilbert, A., and Jones, D. T., Use of arene 1,3-substitutents to control cyclopropane ring formation during *meta* photocycloaddition of ethenes to the benzene ring, *J. Chem. Soc.*, *Perkin Trans. 2*, 213, 1998.
35. Cornelisse, J. and de Haan, R., *ortho*-Photocycloaddition of alkenes and alkynes to the benzene ring, in *Molecular and Supramolecular Photochemistry*, Vol. 8, Ramamurthy, V. and Schanze, K.S., Eds., Marcel-Dekker, New York, 2002, 1.
36. Busson, R., Schraml, J., Saeyens, W., Van der Eycken, E., Herdewijn, P., and De Keukeleire, D., *ortho*-Photocycloaddition of substituted 4-phenoxybut-1-enes. Identification of rearranged photocycloadducts by NMR, *Bull. Soc. Chim. Belg.*, 106, 671, 1997.
37. Nuss, J. M., Chinn, J. P., and Murphy, M. M., Substituent control of excited-state reactivity — the intramolecular *ortho* arene–olefin photocycloaddition, *J. Am. Chem. Soc*., 117, 6801, 1995.
38. Wagner, P. J. and McMahon, K., Chiral auxiliaries promote both diastereoselective cycloaddition and kinetic resolution of products in the *ortho* photocycloaddition of double-bonds to benzene rings, *J. Am. Chem. Soc.*, 116, 10827, 1994.
39. Smart, R. P. and Wagner, P. J., Regioselectivity in intramolecular cycloaddition of double-bonds to triplet acylbenzenes. 2. Effects of substituents *meta* to the tether, *Tetrahedron Lett*., 36, 5131, 1995.
40. Cheng, K. L. and Wagner, P. J., Biradical rearrangements during intramolecular cycloaddition of double-bonds to triplet benzenes, *J. Am. Chem. Soc*., 116, 7945, 1994.
41. Al-Qaradawi, S. Y., Cosstick, K. B., and Gilbert, A., Intramolecular photocycloaddition of 4-phenoxybut-1-enes: a convenient access to the 4-oxatricyclo[7.2.0.$0^{3,7}$]undeca-2,10-diene skeleton, *J. Chem. Soc.*, *Perkin Trans.1*, 1145, 1992.
42. Wagner, P. J. and Smart, R. P., Acetone sensitized intramolecular *ortho* photocyclization of substituted 4-phenoxybut-1-enes and 5-phenoxypent-1-enes, *Tetrahedron Lett*., 36, 5135–5138, 1995.
43. Hoffmann, N. and Pete, J. P., Acid catalyzed intramolecular photochemical reactions of 3-alkenyloxyphenols, *Tetrahedron Lett*., 39, 5027, 1998.

44. Hoffmann, N. and Pete, J. P., Acid catalyzed intramolecular [2+2] photocycloaddition of 3,5-dihydroxybenzoic acid derivatives, *Tetrahedron Lett.*, 37, 2027, 1996.
45. Hoffmann, N. and Pete, J. P., Acid catalyzed intramolecular photochemical reactions of alkenyloxybenzene derivatives, *J. Inf. Rec.*, 24, 133, 1998.
46. Verrat, C., Hoffmann, N., and Pete, J. P., An easy access to benzo[*f*]isoquinoline derivatives using benzocyclobutenes derived from resorcinol, *Synlett*, 1166, 2000.
47. Hoffmann, N. and Pete, J. P., Intramolecular [2+2] photocycloaddition of bichromophoric derivatives of 3,5-dihydroxybenzoic acid and 3,5-dihydroxybenzonitrile, *Synthesis*, 1236, 2001.
48. Hoffmann, N. and Pete, J. P., Intramolecular photochemical reactivity of *o*-alk-3-enylsalicyclic esters, *Tetrahedron Lett.*, 36, 2623, 1995.
49. Saeyens, W., Busson, R., Van der Eycken, J., Herdewijn, P., and De Keukeleire, D., Fully selective intramolecular *ortho* photocycloaddition of 4-(4-methoxyphenoxy)-3-(*N*-3-benzoylthymin-1-yl)but-1-ene: an unprecedented benzene-thymine photocycloaddition, *J. Chem. Soc.*, *Chem. Commun.*, 817, 1997.
50. Kalena, G. P., Pradhan, P., and Banerji, A., Stereo- and regioselectivity of intramolecular 1,2-arene-alkene photocycloaddition in 2-alkenyl-4-chromanones, *Tetrahedron*, 55, 3209, 1999.
51. Ohkura, K., Noguchi, Y., and Seki, K., Photorearrangement of the *ortho*-cycloadduct of 6-chloro-1,3-dimethyluracil to benzene through [pi 4s+pi 2a] photocycloaddition, *Heterocycles*, 46, 141, 1997.
52. Ohkura, K., Seki, K., Hiramatsu, H., Aoe, K., and Terashima, M., Acid-catalyzed photoreaction of 6-chloro-1,3-dimethyluracil to *p*- and *m*-xylene: formation of novel photocycloadducts, 6-methylene-9,11,X-trimethyl-9,11-diazapentacyclo[6.4.0.0(1,3).0(2,5).0(4,8)]dodecane-10,12-diones and 5-methylene-9,11,X-trimethyl-9,11-diazapentacyclo[6.4.0.0(1,3).0(2,6).0(4,8)]dodecane-10,12-diones, *Heterocycles*, 44, 467, 1997.
53. Ohkura, K., Noguchi, Y., and Seki, K. I., Acid-catalyzed photoreaction of 6-chloro-1,3-dimethyluracil in frozen benzene: formation of novel cycloadducts, tetrahydropentaleno[1,2-e]pyrimidine-2,4-dione derivatives, *Chem. Lett.*, 99, 1997.
54. Ohkura, K., Nishijima.K., Sakushima, A., and Seki, K., Photochemistry of 9,10-dihydro-1,3,5,7-tetramethyl-9-methylenecylooctapyrimidine-2,4-dione: synthesis of novel ring systems through electrocyclic reactions, *Heterocycles*, 53, 1247, 2000.
55. Ohkura, K., Nishijima, K., and Seki, K., Acid-catalyzed photoreaction of 6-chloro-1,3-dimethyluracil and mesitylene: formation of photocycloadducts and their characterization, *Chem. Pharm. Bull.*, 49, 384, 2001.
56. Lippke, W., Ferree, W., Jr., and Morrison, H., Organic photochemistry 27. Photochemistry of bichromophoric molecules. Internal photocycloaddition of 6-phenylhex-2-yne, *J. Am. Chem. Soc.*, 96, 2134, 1974.
57. Atkinson, J. G., Ayer, D. E., Büchi, G., and Robb, E. W., Photochemical reactions XII. Addition reactions of olefins and acetylenes with benzonitrile, *J. Am. Chem. Soc.*, 85, 2257, 1963.
58. Al-Jalal, N., Gilbert, A., and Heath, P., Photocycloaddition of ethenes to cyanoanisoles, *Tetrahedron*, 44, 1449, 1988.
59. Berridge, J. C., Forrester, J., Foulger, B. E., and Gilbert, A., The photochemical reactions of benzene with 1,2-, 1,3- and 1,4-dienes, *J. Chem. Soc.*, *Perkin Trans. I*, 2425, 1980.
60. Kishikawa, K., Akimoto, S., Kohmoto, S., Yamamoto, M., and Yamada, K., Intramolecular photo[4+2]cycloaddition of an enone with a benzene ring, *J. Chem. Soc.*, *Perkin Trans. 1*, 77, 1997.

42

Photo-Fries Reaction and Related Processes

Miguel Angel Miranda
Universidad Politecnica de Valencia

Francisco Galindo
Universidad Jaume I de Castellon

42.1 Definition of the Reaction

The photo-Fries rearrangement, analogous to the classical Lewis acid-catalyzed Fries counterpart, was first reported by Anderson and Reese in 1960.[1] The prototype for this reaction is the photochemical transformation of phenyl acetate (**1**) into *o*- and *p*-hydroxyacetophenone (**2** and **3**) (Scheme 1). Since the initial discovery, a number of variations have been devised, and the process has been extended to systems (**4**) such as aryl carbonates, carbamates, sulfonates, and sulfamates, as well as anilides, sulfonanilides, and sulfenanilides. Analogous 1,3-migrations in the corresponding enol derivatives (**7**) have been observed (Scheme 2). In this context, it should be mentioned that the so-called *photo-Claisen rearrangement* is closely related to the photo-Fries rearrangement; it is experienced by aryl ethers (instead of aryl esters) and follows an analogous mechanism.[2] Much of the work on the photo-Fries rearrangement was done during the first decade after the discovery of the reaction and is summarized in several reviews.[3–6] In this chapter, we limit ourselves to the most recent achievements on the rearrangement of aryl esters, paying special attention to the key mechanistic aspects and the most relevant synthetic applications.

42.2 Mechanism

Many reports have appeared during the last few years in connection with the mechanism of the photo-Fries reaction. These contributions have confirmed that the photo-Fries rearrangement is a singlet reaction that occurs through homolytic cleavage of the carbonyl-oxygen single bond to give a caged radical pair. In-cage recombination affords the acyl migration products, while hydrogen abstraction by the aryloxy radical leads to the transformation to phenols, which are the most common byproducts. This is summarized below for phenyl acetate (**1**) (Scheme 3); however, some recent studies point to the fact that in certain esters the rearranged products could arise from upper triplet states.[7] The most convincing arguments in support of this rationalization include: (1) detection of the phenoxyl radical by optical spectroscopy[8] and by spontaneous Raman spectroscopy[9] in the photolysis of phenyl acetate; (2) spin trapping of acetyl or benzoyl radicals in the photolysis of phenyl acetate or phenyl benzoate, respectively, using 2-methyl-2-nitrosopropane;[10] (3) measurement of magnetic isotope effects and external magnetic

0-8493-1348-1/04/$0.00+$1.50

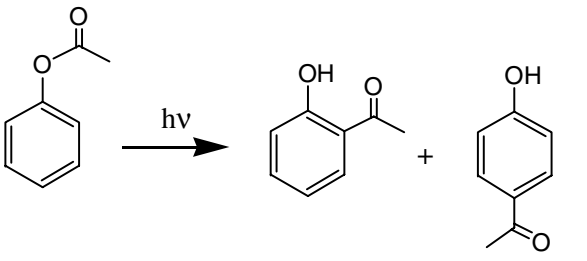

1 **2** (19%) **3** (15 %)

SCHEME 1

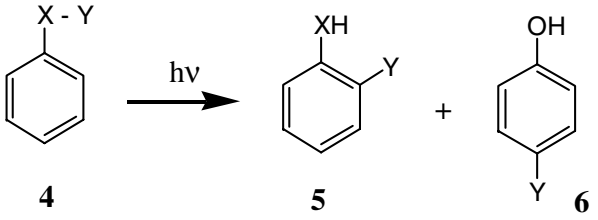

4 **5** **6**

X = O, NH, NR
Y = COR, COOR, CONHR, SO_2R, SO_3H, etc.

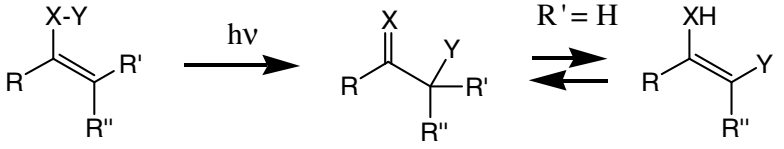

7 **8** **8'**

SCHEME 2

field effects upon the photo-Fries rearrangement of 1-naphthyl acetate and its ^{13}C-carbonyl-labeled analog;[11] (4) measurement of kinetic isotope effects (^{18}O at the phenolic oxygen, ^{14}C at the α-carbon, and ^{14}C at the *ortho*-carbon), as well as magnetic isotope effects (^{13}C at the α-carbon) in the photo-Fries rearrangement of *p*-methoxyphenyl acetate;[12] (5) photolysis of the intermediate *ortho*-cyclohexadienone to yield a ketene as photoproduct by means of the two-laser/two-color technique;[13] (6) formation of identical coupling products by independent generation of the same radicals participating in the intramolecular rearrangement from different sources (intermolecular version of the photo-Fries rearrangement);[14] and (7) calculations made using molecular orbital theory, which point to CO breaking from a dissociative $\pi\sigma^*$ state.[15]

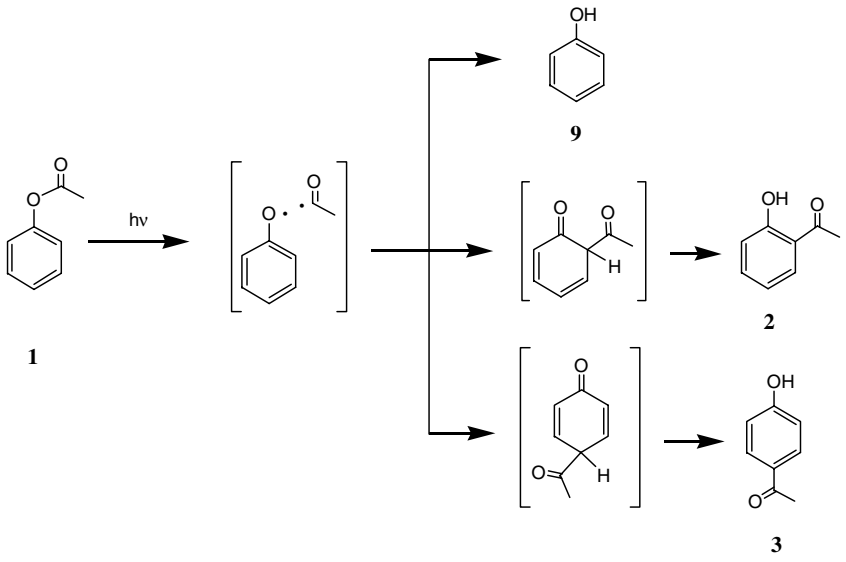

SCHEME 3

42.3 Synthetic Applications

Exploitation of the photo-Fries rearrangement as a general synthetic method depends on the degree of variability in the phenolic and the acyl substructures, as well as the possibility of controlling the outcome of the process through manipulation of the experimental conditions. These aspects have been extensively investigated during recent years.

Variations in the Phenolic Moiety

Soon after its discovery, the photo-Fries reaction was applied to esters of a wide variety of phenols;[3,4] however, the presence of certain electron-withdrawing substituents (for instance acyl groups) in the phenolic ring was found to inhibit the rearrangement, due to the electrophilic nature of such substituents. The fact that the photochemical version of the rearrangement proceeds in neutral media and at room temperature has allowed the polyacylation of phenols, using enol acetates or cyclic acetals as carbonyl blocking groups.[16–19] This is shown below for the conversion of *p*-hydroxyacetophenone (**3**) into the hydroxydiketone (**13**) (Scheme 4).

In addition to the esters of simple phenols, the condensed polynuclear analogs are also prone to undergo the photo-Fries rearrangement. In this context, the studies on naphthyl esters[20–22] can be cited among the most significant work. Likewise, this photoreaction has been employed for the oxygen-to-carbon migration in condensed heterocyclic compounds. Some examples are the ring acylations achieved by photolysis of the acyloxy derivatives of coumarins,[23] benzopyrans,[24] indoles,[25] and dihydrobenzofurans.[26] Thus, the absolute configuration of rutaretin methyl ether (**20**) has been established by transformation into a derivative, whose independent synthesis was achieved from *S*-marmesin, through a sequence that involves photo-Fries rearrangement of the diacetate **14** (Scheme 5).[26] Analogous synthesis of natural products using the photo-Fries reaction as a key step can be found in the recent literature.[27]

Variations in the Acyl Moiety

When the acyl group carries a second functionality (double or triple bond, hydroxyl group, carbonyl group, etc.), interaction of the latter with the *ortho*-hydroxy group, subsequent to the rearrangement step, may be a general principle for the construction of heterocyclic ring systems. This has been applied

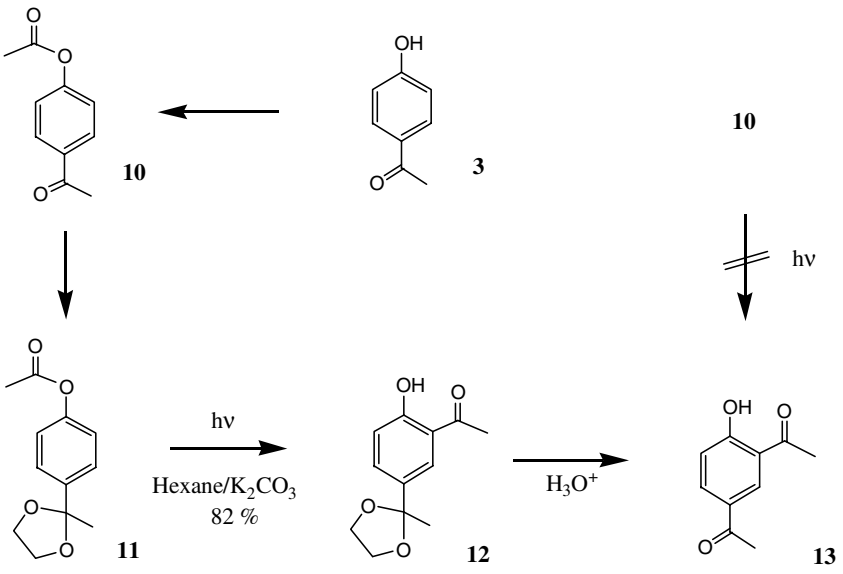

SCHEME 4

to the synthesis of furanones,[28,29] chromones,[30–32] chromenes,[33–35] flavones,[36–38] aurones, xanthones,[39–42] thioxanthones,[43] or acridones.[44]

For instance, photolysis of aryl esters of phenylpropiolic acid (**21**) gives rise to *o*-hydroxyaryl phenylethynyl ketones (**22**). The latter compounds can undergo cyclization in two different ways, depending upon the reaction conditions: When potassium carbonate in acetone is used, flavones (**23**) are formed by a 6-endo-dig process;[45] by contrast, the use of sodium ethoxide in ethanol favors the 5-exo-dig process,[45] to give aurones (**24**) as the major products (Scheme 6).[38] The side-chain functionality can be masked, as in the case of the protected ketoesters (**25**), whose irradiation and subsequent deprotection provide an alternative entry to the flavone system (Scheme 6).[37]

In another application, the total synthesis of bikaverin (**29**) has been achieved using the photo-Fries rearrangement of the protected everninic acid ester (**27**) as a key step for the construction of the benzo[*b*]xanthene skeleton (Scheme 7).[40]

Use of Heterogeneous Media

In view of its paradigmatic nature as a process involving in-cage recombinations vs. diffusion of organic radical pairs, the photo-Fries rearrangement has been chosen as a model reaction to study the influence of heterogeneous media as modifiers of reactivity and selectivity. In an early study, the photo-Fries rearrangement of aryl esters was attempted on the surface of silica gel.[46] Subsequently, cyclodextrins have been employed to carry out the photo-Fries rearrangement of aryl esters in a restricted environment.[47–51] The initial observations[47,48] appeared to indicate cyclodextrin-enhanced *para*-selectivity; however, more recent studies[49–51] report an increase in the *ortho*-product attributable to cyclodextrin complexation. Photo-Fries rearrangements of naphthyl[52] and sulfonate[53] esters have also been studied in the presence of cyclodextrins. Other modifications involve the use of starch, amylose, sodium dodecylsulfate,[54,55] potassium carbonate,[18,56] nafion membranes,[57,58] alkyl alkanoates, or acrylic polymers[59] to create a heterogeneous irradiation system. Recently, the photo-Fries rearrangement has been used to study the morphology of the reaction sites in stretched and unstretched polyethylene films[60] as well as in poly(vinyl acetate).[61]

More conventional liquid–liquid biphasic conditions have been also conveniently employed to increase the efficiency of the photo-Fries reaction. For instance, *p*-methoxyphenyl esters of α,β-unsaturated carboxylic acids (**30**) undergo photochemical rearrangement, followed by basic cyclization to give

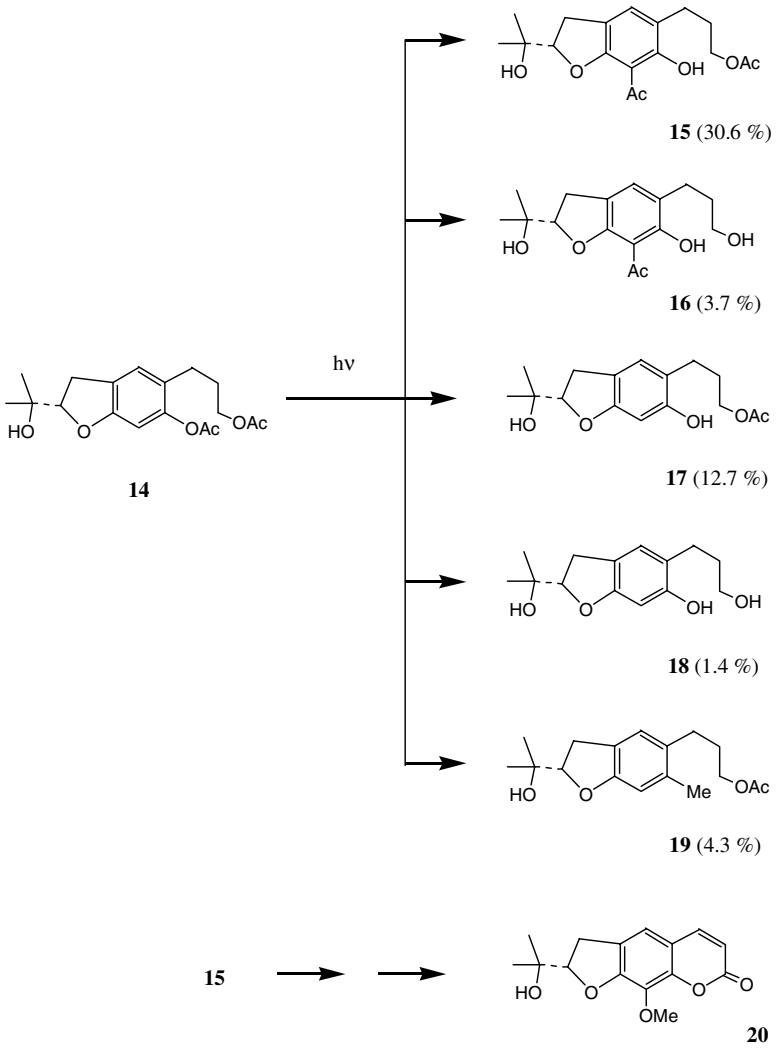

SCHEME 5

4-chromanones (**32**) with moderate overall yields. Using a two-phase system, benzene/aqueous sodium hydroxide, chromanones are obtained directly in nearly quantitative yields. Subsequent reduction/dehydration affords *2H*-chromenes (**33**), interesting because of their antijuvenile hormone activity (Scheme 8).

Inorganic mesoporous materials such as zeolites have also served as hosts for aromatic esters whose irradiation leads to changes in the selectivity of the photoproducts (*ortho* preference) in comparison with the rearrangement in homogeneous media.,[62,63] Finally, the photochemical Fries rearrangement of naphthyl acetate has shown the occurrence of solvent-solute clustering in supercritical carbon dioxide.[64]

42.4 Industrial Applicability

Much attention has been paid to the photo-Fries rearrangement of aromatic polyesters due to the remarkable photostabilization produced by the resulting polymer-bound *o*-hydroxycarbonyl chromophores. This property has been attributed to the high extinction coefficient of the photo-Fries products (internal filter) and to their ability to dissipate the absorbed energy by non-photochemical pathways,

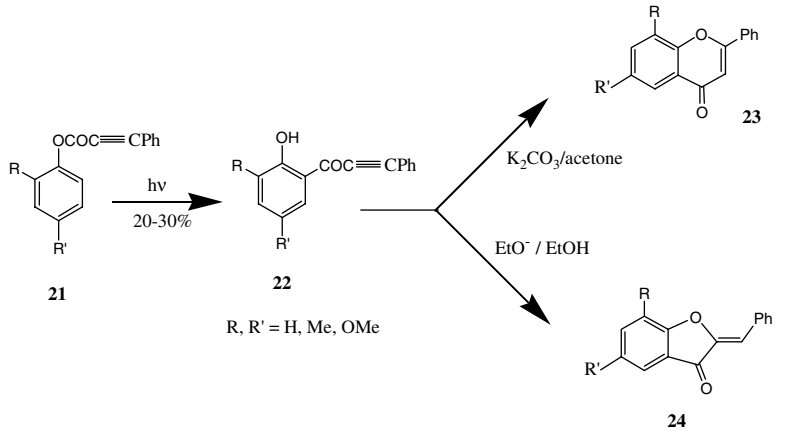

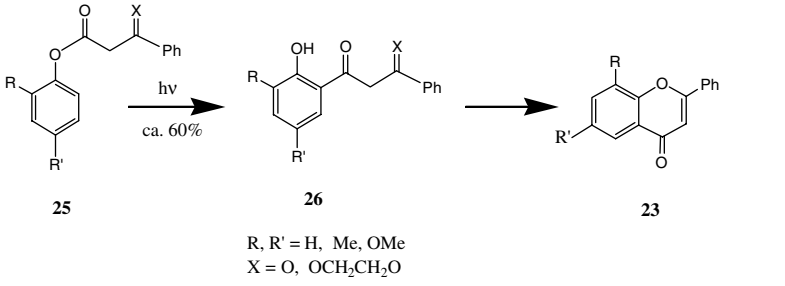

SCHEME 6

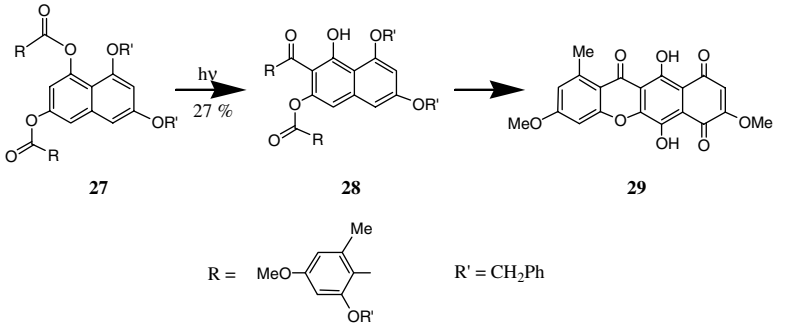

SCHEME 7

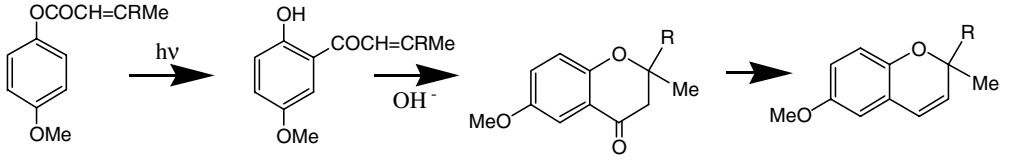

SCHEME 8

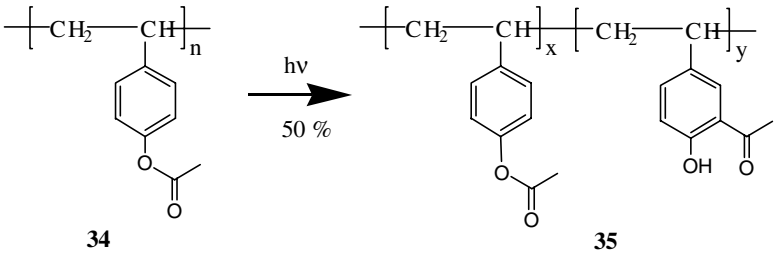

34 **35**

SCHEME 9

such as excited-state proton transfer.[65,66] Polycarbonates,[67–70] poly(arylcinnamates),[68,71,72] polyurethanes,[73–75] fluorene-based polyesters,[76] or 1- and 2-naphthyl methacrylate copolymers[77,78] are among the polymeric materials capable of undergoing this type of photochemical transformation. In some cases, a wavelength-dependent photochemistry of the polymer has been observed,[67,71,72] due to competition between the photo-Fries reaction and other photoprocesses (crosslinking, oxidation, etc.)

Another field of application is the design of polymeric imaging systems.[79] The lithographic potential of a photochemical reaction is based on the possibility of dissolving selectively either the exposed or the unexposed areas of a polymer film. Because all the photo-Fries products are phenols, the irradiated polyester should be easily dissolved in aqueous base, while the unchanged starting material should remain undissolved. The key photochemical step of this sequence is shown above for the conversion of poly(*p*-acetoxystyrene) (**34**) into (**35**) (Scheme 9).[80]

References

1. Anderson, J. C. and Reese, C. B., Photo-induced Fries rearrangement, *Proc. Chem. Soc. London*, 217, 1960.
2. (a) Kharasch, M. S., Stampa, G., and Nudenberg, W., Photochemical *para* rearrangement of phenyl ethers, *Science*, 116, 309, 1952; (b) Carroll, F. A. and Hammond, G. S., Mechanisms of photochemical reactions in solution. 72. Electronic pathways in photodissociation of 3-methyl-1-phenoxybut-2-ene, *J. Am. Chem. Soc.*, 94, 7151, 1972; (c) Adam, W., Fischer H., Hansen, H.-J., Heimgartner, H., Schmid, H., and Waespe, H.-R., CIDNP evidence for divergent behavior of singlet and triplet radical pair encounters in photo-Claisen rearrangement, *Angew. Chem. Int. Ed. Engl.,* 12, 662, 1973; (d) Haga, N. and Takayanagi, H., Mechanisms of the photochemical rearrangement of diphenyl ethers, *J. Org. Chem.*, 61, 735, 1996; (e) Galindo, F., Miranda, M. A., and Tormos, R., Coupling of phenoxy and alkyl radicals derived from the photolysis of phenol/ketone pairs: an intermolecular approach to the photo-Claisen rearrangement, *J. Photochem. Photobiol. A: Chem.*, 117, 17, 1998; (f), DeCosta, D. P., Bennett, A., Pincock, A. L., Pincock, J. A., and Stefanova, R., Photochemistry of aryl *tert*-butyl ethers in methanol: the effect of substituents on an excited state cleavage reaction, *J. Org. Chem.*, 65, 4162, 2000.
3. Stenberg, V. I., Photo-Fries reaction and related arrangements, *Org. Photochem.*, 1, 127, 1967.
4. Bellus, D., Photo-Fries reaction and related photochemical [1,*j*]-shifts (*j* = 3,5,7) of carbonyl and sulfonyl groups, *Adv. Photochem.*, 8, 109, 1971.
5. Martin, R., Uses of the Fries rearrangement for the preparation of hydroxyarylketones: a review, *Org. Prep. Proc. Int.*, 24, 369, 1992.
6. Miranda, M. A. and Galindo, F., The photo-Fries rearrangement, in *Molecular and Supramolecular Photochemistry,* Vol. 9, Ramamurthy, V. and Schanze, K. S., Eds., Marcel Dekker, New York, 2003.
7. Gritsan, N. P., Tsentalovich, Y. P., Yurkovskaya, A. V., and Sagdeev, R., *J. Phys. Chem.,* 100, 4448, 1996.
8. (a) Kalmus, C. E. and Hercules, D. M., Mechanistic study of photo-Fries rearrangement, *Tetrahedron Lett.*, 16, 1575, 1972; (b) Kalmus, C. E. and Hercules, D. M., Mechanistic study of photo-Fries rearrangement of phenyl acetate, *J. Am. Chem. Soc.*, 96, 449, 1974; (c) Arai, T., Tobita, S., and

Shizuka, H., Direct measurements of the rates of 1,3-sigmatropic and 1,5-sigmatropic hydrogen shifts in the photo-Fries rearrangements of phenyl acetate, *Chem. Phys. Lett*., 223, 521, 1994; (d) Arai, T., Tobita, S., and Shizuka, H., Tunneling effects on the 1,3-sigmatropic and 1,5-sigmatropic hydrogen shifts in the ground-state of photo-Fries rearranged intermediates of phenyl acetate studied by laser flash-photolysis, *J. Am. Chem. Soc.*, 117, 3968, 1995.

9. Beck, S. M. and Brus, L. E., Transient intermediates in the photo-Fries isomerization of phenyl acetate via spontaneous Raman spectroscopy, *J. Am. Chem. Soc.,* 104, 1805, 1982.
10. Rosenthal, I., Mosoba, M. M., and Riesz, P., Spin trapping with 2-methyl-2-nitrosopropane: photochemistry of carbonyl-containing compounds. Methyl radical formation from dimethyl sulfoxide, *Can. J. Chem.,* 60, 1468, 1982.
11. Nakagaki, P., Hiramatsu, M., Watanabe, T., Tanimoto, Y., and Nagakura, S., Magnetic isotope and external magnetic field effects upon the photo-Fries rearrangement of 1-naphthyl acetate, *J. Phys. Chem*., 89, 3222, 1985.
12. Shine, H. J. and Subotkowski, W., Kinetic (^{18}O and ^{14}C) and magnetic (^{13}C) isotope effects in the photo-Fries rearrangement of 4-methoxyphenyl acetate, *J. Org. Chem*., 52, 3815, 1987.
13. Jiménez, M. C., Miranda, M. A., Scaiano, J. C., and Tormos, R., Two-photon processes in the photo-Claisen and photo-Fries rearrangements. Direct observation of dienic ketenes generated by photolysis of transient cyclohexa-2,4-dienones, *J. Chem. Soc., Chem. Commun.,* 1487, 1997.
14. Jiménez, M. C., Leal, P., Miranda, M. A., and Tormos, R., Norrish type-I photoreaction in the presence of phenols. An intermolecular photo-Fries rearrangement, *J. Chem. Soc., Chem. Commun*., 2009, 1995.
15. Grimme, S., Theoretical investigation on the photodissociation of carbon oxygen bonds in aromatic-compounds, *Chem. Phys*., 163, 313, 1992.
16. García, H., Miranda, M. A., Roquet-Jalmar, M. F., and Martínez-Utrilla, R., Influence of enol acetylation on the photo-Fries rearrangement of an *ortho*-acylaryl benzoate, *Liebigs Ann. Chem*., 2238, 1982.
17. García, H., Martínez-Utrilla, R., Mirada, M. A., and Roquet-Jalmar, M. F., Intra- and intermolecular photoreactions of *o*-benzoyloxyacetophenone derivatives, *J. Chem. Res*., (S), 350, 1982.
18. García, H., Miranda, M. A., and Primo, J., The photo-Fries rearrangement of acetoxyacetophenones using cyclic acetals as carbonyl blocking groups in the presence of potassium carbonate: an improved procedure for the synthesis of diacylphenols. *J. Chem. Res*., (S), 100, 1986.
19. García, H., Martínez-Utrilla, R., and Miranda, M. A., Cyclic acetals as carbonyl blocking groups in the photo-Fries rearrangement of acyl substituted aryl esters, *Tetrahedron,* 41, 3131, 1985.
20. Crouse, D. J., Hurlbut, S. L., and Wheeler, D. M. S., Photo-Fries rearrangements of 1-naphthyl esters in the synthesis of 2-acylnaphthoquinones*, J. Org. Chem*., 46, 374, 1981.
21. Fariña, F., Martínez-Utrilla, R., and Paredes, M. C., Polycyclic hydroxyquinones. VIII. Preparation of acetylhydroxynaphthazarines by photo-Fries rearrangement: a convenient synthesis of spinochrome A, *Tetrahedron*, 38, 1531, 1982.
22. Greenland, H., Pinhey, J. T., and Sternhell, S. The photochemistry of 2-acetoxynaphthalen-1(2H)-ones, *J. Chem. Soc., Perkin Trans. 1*, 1789, 1986.
23. Kulshrestha, S. K., Dureja, P., and Mukerjee, S. K., Photo-induced reactions. IV. Studies on photo-Fries migration of some coumarins, *Ind. J. Chem*., 23B, 1064, 1984.
24. Miranda, M. A., Primo, J., and Tormos, R., Photochemistry of 7-acetoxybenzopyran derivatives: synthesis of eupatoriochromene and encecalin, *Tetrahedron*, 45, 7593, 1989.
25. Chan, A. C. and Chilliard, P. R., Regioselectivity of the photo-Fries rearrangement in acetoxyindoles, *Tetrahedron Lett.,* 30, 6483, 1989.
26. Ishii, H., Sekiguchi, F., and Ishikawa, T., Studies on the chemical constituents of rutaceous plants. XLI. Absolute configuration of rutaretin methyl ether, *Tetrahedron*, 37, 285, 1981.
27. (a) Marriot, K.-S. C., Anderson, M., and Jackson, Y. A., Synthesis of a 2,3-dimethoxyrotenonoid, *Heterocycles*, 55, 91, 2001; (b) Suau, R., Valpuesta, M., and Torres, G., Photochemical-synthesis of 7,8-dioxygenated isoquinoline alkaloids, *Tetrahedron Lett*., 36, 1315, 1995; (c) Magnus, P. and Lescop, C., Photo-Fries rearrangement for the synthesis of the diazonamide macrocycle, *Tetrahedron*

Lett., 42, 7193, 2001; (d) Okada, K., Suzuki, R., and Yokota, T., Synthesis and root growth-promoting activity of capillarol and its derivatives, *Biosci. Biotechnol. Biochem.*, 63, 257, 1999.
28. Fillol, L., Martínez-Utrilla, R., Miranda, M. A., and Morera, I., Photophysical versus aluminum chloride-catalyzed Fries rearrangement of aryl hydrogen succinates: synthesis of 2(^{3}H)-furanones, *Monatsh. Chem.*, 120, 863, 1989.
29. Martínez-Utrilla, R. and Miranda, M. A., Indirect hydroquinone succinoylation via a photo-Fries rearrangement: application to the synthesis of enol lactones, *Tetrahedron Lett.*, 21, 2281, 1980.
30. Alvaro, M., García, H., Miranda, M. A., and Primo, J., Neighbouring group participation in the photolysis of aryl esters of unsaturated 1,4-dicarboxylic acids, *Recl. Trav. Chim. Pays-Bas*, 105, 233, 1986.
31. Alvaro, M., García, H., Iborra, S., Miranda, M. A., and Primo, J., New photochemical approaches to the synthesis of chromones, *Tetrahedron*, 43, 143, 1987.
32. Miranda, M. A., Primo, J., and Tormos, R., Influence of the stereochemistry on the rate of cyclization of *cis* and *trans o*-hydroxyaryl alkenyl ketones: mechanistic implications, *Tetrahedron*, 43, 2323, 1987.
33. Miranda, M. A., Primo, J., and Tormos, R., A new synthesis of precocene II and precocene III based on the photo-Fries rearrangement of a sesamol ester, *Heterocycles*, 32, 1159, 1991.
34. Miranda, M. A., Primo, J., and Tormos, R., A new synthesis of 4-chromanones, *Heterocycles*, 19, 1819, 1982.
35. Miranda, M. A., Primo, J., and Tormos, R., Studies on the synthesis of precocenes: the photo-Fries rearrangement of esters of α,β-unsaturated carboxylic acids and meta-oxygenated phenols, *Heterocycles*, 27, 673, 1988.
36. García, H., Iborra, S., Miranda, M. A., and Primo, J., Application of the photo-Fries rearrangement of aryl dihydrocinnamates to the synthesis of flavonoids, *Heterocycles*, 23, 1983, 1985.
37. García, H., Iborra, S., Miranda, M. A., and Primo, J., Photolysis of cyclic acetals of aryl benzoyl acetates as the key step in a new synthesis of flavones, *Heterocycles*, 24, 2511, 1986.
38. García, H., Iborra, S., Miranda, M. A., and Primo, J., 6-*Endo*-dig versus 5-*exo*-dig ring closure in *o*-hydroxyaryl phenylethynyl ketones: a new approach to the synthesis of flavones and aurones, *J. Org. Chem.*, 51, 4432, 1986.
39. Lewis, J. R. and Paul J. G., Oxidative coupling. 11. Approaches to the synthesis of bikaverin, *J. Chem. Soc., Perkin Trans. 1*, 770, 1981.
40. Katagiri, N., Nakano, J., and Kato, T., Synthesis of bikaverin, *J. Chem. Soc., Perkin Trans. 1*, 2710, 1981.
41. Díaz-Mondéjar, M. R. and Miranda, M. A., 2′-Acetoxy-2-hydroxy-5-methoxybenzophenone: photochemical synthesis, transacylation and cyclization to 2-methoxyxanthone, *Tetrahedron*, 38, 1523, 1982.
42. Díaz-Mondéjar, M. R. and Miranda, M. A., Photolysis of 2-aryloxy- or 2-arylthio-1,3-benzodioxan-4-ones, *Heterocycles*, 22, 1125, 1984.
43. Belled, C., Miranda, M. A., and Simón-Fuentes, A., Fototransposición de Fries en derivados de tiosalicilato de fenilo: una nueva aproximación a la síntesis de tioxantonas, *An. Quím.*, 85C, 39, 1989.
44. Belled, C., Miranda, M. A., and Simón-Fuentes, A., Fototransposición de Fries de esters fenólicos de los ácidos antranílico y *N*-acetilantranílico: aplicaciones a la síntesis de heterociclos, *An. Quím.*, 86C, 431, 1990.
45. Baldwin, J. E., Rules for ring closure, *J. Chem. Soc., Chem. Commun.*, 734, 1976.
46. Avnir, D., de Mayo, P., and Ono, I., Biphasic photochemistry: the photo-Fries rearrangement on silica gel, *J. Chem. Soc., Chem. Commun.*, 1109, 1978.
47. Ohara, M. and Watanabe, K., Selective photochemical Fries rearrangement of phenyl acetate in the presence of β-cyclodextrin, *Angew. Chem. Int. Ed. Engl.*, 14, 820, 1975.
48. Chênevert, R. and Voyer, N., Photochemical rearrangement of phenyl benzoate in the presence of cyclodextrins and amylose, *Tetrahedron Lett.*, 25, 5007, 1984.

49. Syamala, M. S., Rao, B. N., and Ramamurthy, V., Modification of photochemical reactivity by cyclodextrin complexation: product selectivity in photo-Fries rearrangement, *Tetrahedron*, 44, 7234, 1988.
50. Veglia, A. V., Sánchez, A. M., and de Rossi, R. H., Change of selectivity in the photo-Fries rearrangement of phenyl acetate induced by β-cyclodextrin, *J. Org. Chem.*, 55, 4083, 1990.
51. Veglia, A. V. and de Rossi, R. H., Beta-cyclodextrin effects on the photo-Fries rearrangement of aromatic alkyl esters, *J. Org. Chem.*, 58, 4941, 1993.
52. (a) Xie, R.-Q., Liu, Y.-C., and Lei, X.-G., The photo-Fries rearrangement of alpha-naphthyl acetate in cyclodextrin and micelle, *Res. Chem. Intermed.*, 18, 61, 1992; (b) Banu, H. S., Pitchumani, K., and Srinivasan, C., Effect of cyclodextrin complexation on photo-Fries rearrangement of naphthyl esters, *Tetrahedron,* 55, 9601, 1999.
53. (a) Pitchumani, K., Velusamy, P., Manickam, M. C., Durai, M. C., and Srinivasan, C., Influence of cyclodextrin complexation on photo-Fries rearrangement of sulfonyl derivatives, *Proc. Indian Acad. Sci., Chem. Sci.*, 106, 49, 1994; (b) Pitchumani, K., Manickam, M. C., Durai, M. C., and Srinivasan, C., Modification of photochemical behavior upon cyclodextrin complexation. Photo-Fries rearrangement of sulfonate esters, *Ind. J. Chem., Sect. B*, 32B, 1074, 1993.
54. Singh, A. K. and Sonar, S. N., Photorearrangement of aryl esters in micellar medium, *Synth. Commun.*, 15, 1113, 1985.
55. Suau, R., Torres, G., and Valpuesta, M., The photo-Fries rearrangement of 2,5-disubstituted phenyl acetates, *Tetrahedron Lett.*, 36, 1311, 1995.
56. García, H., Primo, J., and Miranda, M. A., The photo-Fries rearrangement in the presence of potassium carbonate: a convenient synthesis of *ortho*-hydroxyacetophenones, *Synthesis*, 901, 1985.
57. Tung, C.-H. and Xu, X.-H., Selectivity in the photo-Fries reaction of phenyl phenylacetates included in a nafion membrane, *Tetrahedron Lett.*, 40, 127, 1999.
58. (a) Cui, C., Wang, X., and Weiss, R. G., Investigation of the photo-Fries rearrangements of two 2-naphthyl alkanoates by experiment and theory: comparison with the acid-catalyzed reactions, *J. Org. Chem.*, 61, 1962, 1996; (b) Baldvins, J. E., Cui, C., and Weiss, R. G., Investigations of cylindrical reaction cavities from ordered phases of alkyl alkanoates and their influence on some Norrish–Yang and photo-Fries reactions, *Photochem. Photobiol.*, 63, 726, 1996.
59. Hoyle, C. E., Shah, H., and Nelson, G. L., Photochemistry of bisphenol-A based polycarbonate: the effect of the matrix and early detection of photo-Fries product formation, *J. Polym. Sci., Part A: Polym. Chem.*, 30, 1525, 1992.
60. (a) Gu, W. Q., Hill, A. J., Wang, X. C., Cui, C. X., and Weiss, R. G., Photorearrangements of five 1-and 2-naphthyl acylates in three unstretched and stretched polyethylene films. Does reaction selectivity correlate with free volumes measured by positron annihilation lifetime spectroscopy?, *Macromolecules*, 33, 7801, 2000; (b) Gu, W. and Weiss, R. G., Extracting fundamental photochemical and photophysical information from photorearrangements of aryl phenylacylates and aryl benzyl ethers in media comprised of polyolefinic films, *J. Photochem. Photobiol. C: Photochem. Rev.*, 2, 117, 2001.
61. Gu, W. Q., Bi, S. G., and Weiss, R. G., Photo-Fries rearrangements of 1-naphthyl esters in the glassy and melted states of poly(vinyl acetate). Comparisons with reactions in less polar polymers and low-viscosity solvents, *Photochem. Photobiol. Sci.*, 1, 52, 2002.
62. (a) Pitchumani, K., Warrier, M., and Ramamurthy, V., Remarkable product selectivity during photo-Fries and photo-Claisen rearrangements within zeolites, *J. Am. Chem. Soc.*, 118, 9428, 1996; (b) Pitchumani, K., Warrier, M., and Ramamurthy, V., Utility of zeolitic medium in photo-Fries and photo-Claisen rearrangements, *Res. Chem. Intermed.*, 25, 623, 1999; (c) Pitchumani, K., Warrier, M., Cui, C., Weiss, R. G., and Ramamurthy, V., Photo-Fries reaction of naphthyl esters within zeolites, *Tetrahedron Lett.*, 37, 6251, 1996; (d) Balkus, J. K., Khanmamedova, A. K., and Woo, R., Fries rearrangement of acetanilide over zeolite catalysts, *J. Mol. Catal. A: Chem.*, 134, 137, 1998; (e) Gu, W., Warrier, M., Ramamurthy, V., and Weiss, R. G., Photo-Fries reactions of 1-naphthyl esters in cation-exchanged zeolite Y and polyethylene media, *J. Am. Chem. Soc.*, 121, 9467, 1999.

63. (a) Tung, C.-H. and Ying, Y.-M., Photochemistry of phenyl phenylacetates adsorbed on pentasil and faujasite zeolites, *J. Chem. Soc., Perkin. Trans. 2*, 1319, 1997; (b) Tung, C.-H., Wu, L.-Z., Zhang, L.-P., Li, H.-Ru., Yi, X.-Y., Song, K., Xu, M., Yuan, Z.-Y., Guan, J.-Q., Wang, H.-W., Ying, Y.-M., and Xu, X.-H., Microreactor-controlled selectivity in organic photochemical reactions, *Pure Appl. Chem*., 72, 2289, 2000.
64. Andrew, D., Des Islet, B. T., Margaritis, A., and Weedon, A. C., Photo-Fries rearrangement of naphthyl acetate in supercritical carbon-dioxide: chemical evidence for solvent-solute clustering, *J. Am. Chem. Soc*., 117, 6132, 1995.
65. Allen, N. S., Photostabilizing action of *ortho*-hydroxy aromatic compounds: a critical review, *Polym. Photochem*., 3, 167, 1983.
66. Ranby, B. and Rabek, J. F., *Photodegradation, Photo-oxidation and Photostabilization of Polymers,* Wiley, New York, 1975.
67. Rivaton, A., Sallet, D., and Lemaire, J., The photochemistry of bisphenol A polycarbonate reconsidered, *Polym. Photochem*., 3, 463, 1983.
68. Torikai, A., Murata, T., and Fueki, K., Photo-induced reactions of polycarbonate studied by ESR, viscosity and optical absorption measurements, *Polym. Photochem*., 4, 255, 1984.
69. Rivaton, A., Mailhot, B., Soulestin, J., Varghese, H., and Gardette, J. L., Comparison of the photochemical and thermal degradation of bisphenol-A polycarbonate and trimethylcyclohexane-polycarbonate, *Polym. Degrad. Stab.*, 75, 17, 2002.
70. Rivaton, A., Mailhot, B., Soulestin, J., Varghese H., and Gardette, J. L., Influence of the chemical structure of polycarbonates on the contribution of crosslinking and chain scissions to the photothermal ageing, *Eur. Polym. J*., 38, 1349, 2002.
71. David, M., Creed, D., Griffin, A. C., Hoyle, C. E., and Venkataram, K., Photochemical crosslinking of main-chain liquid-crystalline polymers containing cinnamoyl groups, *Makromol. Chem. Rapid Commun*., 10, 391, 1989.
72. David, M., Creed, D., Griffin, A. C., Hoyle, C. E., and Venkataram, K., Chromophore aggregation and concomitant wavelength-dependent photochemistry of a main-chain liquid-crystalline poly(arylcinnamate), *J. Am. Chem. Soc.,* 112, 4049, 1990.
73. Hoyle, C. E. and Kim, K. J., Photolysis of aromatic diisocyanate-based polyurethanes in solution, *J. Polym. Sci., Part A: Polym. Chem*., 24, 1879, 1986.
74. Hoyle, C. E., Chawla, C. P., and Kim K. J., The effect of flexibility on the photodegradation of aromatic diisocyanate-based polyurethanes *J. Polym. Sci., Part A: Polym. Chem*., 26, 1295, 1988.
75. (a) Wilhelm, C., Rivaton, A., and Gardette, J.-L., Infrared analysis of the photochemical behaviour of segmented polyurethanes. 3. Aromatic diisocyanate based polymers, *Polymer,* 39, 1223, 1998; (b) Liaw, D. J., Lin, S. P., and Liaw, B. Y., Photolysis of bisphenol-based polyurethanes in solution, *J. Polym. Sci., Part A: Polym. Chem*., 37, 1331, 1999.
76. Lo, J., Lee, N. S., and Pearce, E. M., Photo-Fries rearrangement of fluorene-based polyacrylates, *J. Appl. Polym. Sci.*, 29, 35, 1984.
77. Holden, D. A., Jordan, K., and Safarzadeh-Amiri, A., Studies of polymer photostabilization using fluorescence spectroscopy: photochemistry of naphthyl methacrylate copolymers, *Macromolecules*, 19, 895, 1986.
78. Wang, Z., Holden, D. A., and McCourt, F. R. W., Generation of nonrandom chromophore distributions by the photo-Fries reaction of 2-naphthyl acetate in poly(methyl methacrylate), *Macromolecules*, 23, 3773, 1990.
79. Tessier, T. G., Frechet, J. M. J., Willson, C. G., and Ito, H., The photo-Fries rearrangement and its use in polymeric imaging systems, *Am. Chem. Soc. Symp. Ser*., 266, 269, 1984.
80. Frechet, J. M. J., Tessier, T. G., Willson, C. G., and Ito, H., Poly[*p*-(formyloxy)styrene]: synthesis and radiation-induced decarbonylation, *Macromolecules*, 18, 317, 1985.

43

Photochemistry of Aryl Diazonium Salts, Triazoles and Tetrazoles

James Grimshaw
Queen's University of Belfast

43.1 Introduction

An observation from 1887 noted that solid benzenediazonium nitrate turns rose-red on exposure to sunlight.[1] This sensitivity to light of diazonium salts was exploited in the textile industry as early as 1890 when a process for printing on silk or cotton was devised involving the photo-decomposition, under stencils, of an applied diazonium salt followed by coupling of the residual material with a phenol.[2] Photodecomposition of diazonium salts with loss of nitrogen, followed by coupling of the residual salt with a phenol, forms the basis of the diazo-copying process, which at one time was used extensively for copying large engineering drawings. Some photolithographic processes also utilize the properties of diazonium salts. The research supporting these technical applications led to investigations into the stability to light of aromatic heterocycles having two adjacent nitrogen atoms.[3] From 1959 on, photochemical reactions, which involve the evolution of nitrogen from triazoles, tetrazoles, and related systems began to be examined in detail.

43.2 Arenediazonium Salts

In aqueous solution, diazonium salts show absorption maxima in the ultraviolet (UV) region; benzenediazonium ion has λ_{max} 261 nm (log ε 4.3) and 300 nm (log ε 3.17).[4] Both absorption bands are shifted toward the visible by electron-donating substituents; 4-dimethylaminobenzenediazonium has λ_{max} 382 nm (log ε 4.6).[5] Photolysis in aqueous solution leads to phenol as the main product, according to Scheme 1. Some replacement of the diazonium group by an atom of chlorine or bromine is also found in solutions containing chloride or bromide ions.[6]

Quantum yields for the photochemical decomposition of aryldiazonium salts in aqueous solution are less than unity. A value of 0.34 has been recorded for decomposition of 4-phenylaminobenzenediazonium

0-8493-1348-1/04/$0.00+$1.50

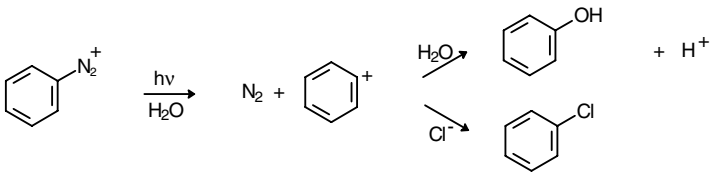

SCHEME 1

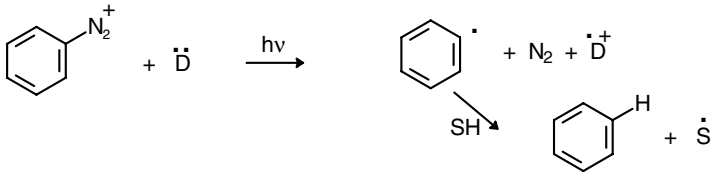

SCHEME 2

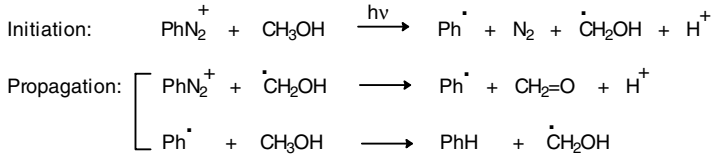

SCHEME 3

on irradiation at 380 nm.[7] Quantum yields of 0.57[8] and 0.97[9] have been noted for the decomposition of 4-dimethylaminobenzenediazonium ions.

The thermal decomposition of aryldiazonium salts also gives phenols, and in a few cases the photochemical processes offer superior yields.[10] Preparation and photodecomposition of diazonium salts in 50% fluoroboric acid has proved useful for the replacement by fluorine in cases where the diazonium salt is exceptionally stable and the usual Schiemann reaction gives poor yields.[11] However the practical problems of avoiding overheating and the eventual screening of light by the reaction product limit the usefulness of these photochemical processes.

The photolysis of benzenediazonium salts in the presence of an electron donor (D) leads to photoelectron transfer according to Scheme 2, followed by carbon–nitrogen bond cleavage to give a phenyl radical. The radical abstracts a hydrogen atom from the solvent (S–H), resulting in overall replacement of the diazonium group by hydrogen. Solvents such as methanol or isopropanol can function as the electron donor but with varying efficiency, depending in the acceptor ability of the diazonium salt.[12] Thus, diazonium salts derived from aminodiphenylamines are decomposed in ethanol to form products derived from the phenyl cation, and photoelectron transfer is not involved.[13] Benzenediazonium salts with less strongly electron-donating substituents (4-methyl or 4-methoxy) afford a mixture of products upon irradiation in methanol because both reaction Schemes 1 and 2 operate. Benzenediazonium salts with electron-withdrawing substituents (4-nitro or 4-chloro) give products only by replacement of the diazonium group by hydrogen.

Quantum yields for the photoelectron transfer process in methanol are generally greater than unity, because the solvent radical takes part in a chain reaction (Scheme 3), the efficiency of which depends on the concentration of the diazonium salt and on the substitution pattern.[14] Quantum yields for decomposition are around 80 for 4-nitrobenzenediazonium (10^{-2} *M*), 5 for 4-chlorobenzenediazonium (10^{-2} *M*), and about 2 for 4-methylbenzenediazonium (5×10^{-3} *M*). Added 2-methyl-2-nitrosopropane acts as a scavenger for phenyl radicals and, under these conditions, the quantum yield for diazonium salt

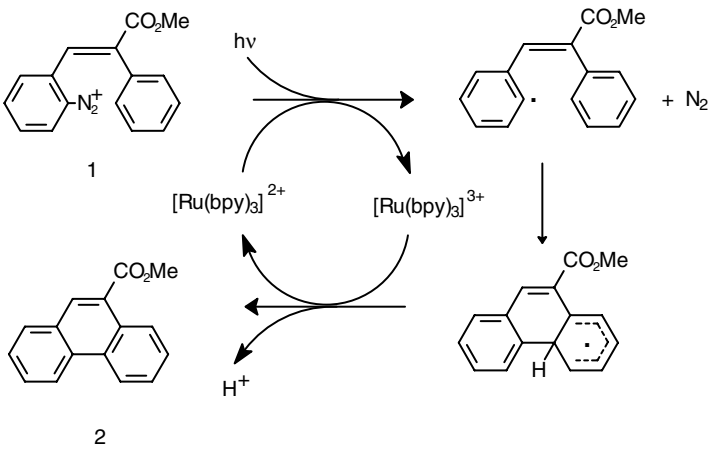

SCHEME 4

decomposition falls. At the same time, the yield of cation-derived product increases at the expense of radical derived materials. This behavior is probably general but few examples seem to have been recorded.

Both the arene cation and the arene radical can be detected using ESR spectroscopy after irradiation of diazonium salts in a glassy matrix at 77 K. The ground state of the phenyl cation bearing an electron donating *para*-substituent is a $(\pi)^5(sp_2)^1$ triplet, and this is easily distinguished from the phenyl radical that may also be formed.[15,16] Phenyl cations in the singlet ground state cannot, of course, be detected by ESR spectroscopy. Irradiation of 4-dimethylaminobenzenediazonium salts at 77 K gives rise to the two reactive intermediates. Warming to 120 K results in gradual decay of the triplet, leaving the radical relatively unaffected. Correlation between the UV and ESR signals allows the absorption at λ_{max} 455 nm to be assigned to the triplet aryl cation.[17]

Other solvents, which lead exclusively to radical derived products from the photolysis of diazonium salts, include formic acid and dimethylformamide. Anions can also act as donors in the photochemical electron transfer process; here, the efficiency increases with decreasing electrochemical oxidation potential of the anion. Tetraphenylboron ion is a good electron donor, while fluoroborate is a poor donor.[18]

Diazonium salts are excellent quenchers of aromatic hydrocarbon triplet states by an electron transfer process. The anthracene radical cation can be detected by UV monitoring as one reaction product after laser flash generation of anthracene triplet in the presence of a diazonium salt.[19] In more concentrated solutions and in the situation where the diazonium and the hydrocarbon are solubilized in aqueous sodium dodecylsulfate micelles, electron transfer occurs from the singlet excited state.[20] A related reaction is electron transfer between the ion pair involving benzenediazonium cation and anthracenesulfonate anion in chloroform, which results in decomposition of the diazonium salt.[21] CIDNP effects during the irradiation of ^{15}N- and ^{13}C-labeled diazonium salts, sensitized by perylene or rubrene, have demonstrated both electron back-transfer within the reaction cage and also escape of both nitrogen and phenyl radicals from the cage.[22,23]

Benzenediazonium salts quench the luminescence of $[Ru(bpy)_3]^{2+}$ by an electron transfer step. The reaction is stoichiometric with no significant back electron transfer from the aryl radical to the resulting Ru(III) complex; however, Ru(III) complexes can be reduced electrochemically to Ru(II). Thus, irradiation of the diazonium salt and $[Ru(bpy)_3]^{2+}$ in the cathode chamber of an electrochemical cell becomes a catalytic process for conversion of the benzenediazonium salt to a phenyl radical.[24]

The photochemical reaction between the diazonium salt **1** and $[Ru(bpy)_3]^{2+}$ produces good yields of the Pschorr-type product **2**, and the process is catalytic; here, the reaction first gives a phenyl radical. This intermediate cyclizes, and then back electron transfer from the cyclized radical to Ru(III) regenerates the catalyst complex (Scheme 4).[25] In contrast, direct photocyclization of **1** in acetonitrile gives poor yields of the phenanthrene. The intermediate in this process now becomes the phenyl cation, and the

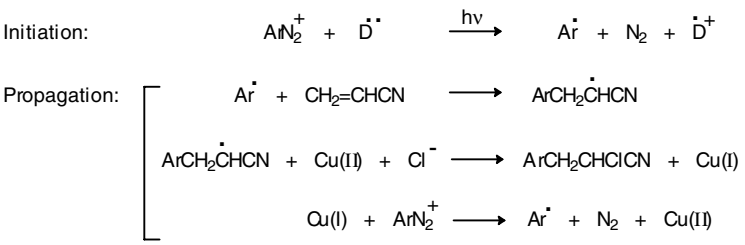

SCHEME 5

principal side product results from reaction of the cation with acetonitrile solvent. Attempts to achieve photocatalysis of five-membered ring cyclizations to form fluorenone, fluorene, and dibenzofuran products result in poor yields due to the unfavorable geometry for the radical cyclization step.[26]

The Meerwein reaction between phenyl radicals, thermally generated from arenediazonium salts, and alkenes in the presence of copper(I) ions can also be initiated photochemically. Irradiation of the diazonium salt in the presence of copper(II) ions leads to photoelectron transfer and the generation of phenyl radicals. Addition of the radical to an alkene bond becomes a chain reaction mediated by copper ions according to Scheme 5. Quantum yields for the evolution of nitrogen are in the region of 700.[27]

Photodecomposition of some *ortho*-substituted aryldiazonium ions leads to unusual reaction products due to hydrogen atom transfer between the *ortho*-substituent and the radical center derived by loss of nitrogen from the diazonium ion. Thus, 2-diethylaminobenzenediazonium salts yield *N*-ethylaniline via the intermediate **3**. Deuterium is not incorporated into the benzene ring from either D_2O or CD_3OD.[28] Decomposition of the diazonium salt **4** leads to a benzocyclobutene as the principal product. The influence of the nitro substituent is important, because the un-nitrated diazonium salt is decomposed to give a phenol in the normal manner.[29]

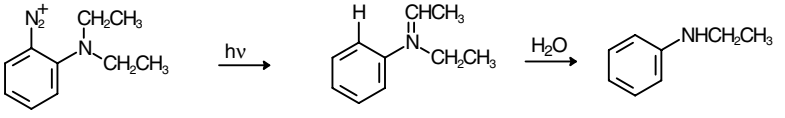

3

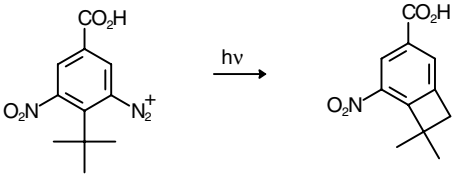

4

Diazonium salts, relatively stable to heat, have been used as photoinitiators in polymerization processes. Both phenyl cations and radicals generated during the illumination stage will initiate polymerization of vinyl ethers and the crosslinking of low-molecular-weight polymers with reactive alkene substituents.[30]

43.3 1,2-Arenediazo-Oxides

The 2-hydroxybenzenediazonium ion is in acid-base equilibrium ($pK_a = 1.14$)[31] with 2-diazocyclohexa-3,5-dien-1-one **5** (the diazo-oxide form). Diazo-oxides show absorption maxima at longer wavelengths than the corresponding diazonium salt form. Thus, 1-diazo-2-oxo-1,2-dihydrobenzene has λ_{max} 395 nm

(log ε 7.0) in water, while in 50% sulfuric acid, where the predominant species is the diazonium ion, λ_{max} 353 nm (log ε 6.3) is found. Photolysis in 50% sulfuric acid leads mainly to products derived from the corresponding phenyl cation analogous to Scheme 1.[32] In nonpolar solvents and in the gas phase, compound **5** is in equilibrium with the 1,2,3-oxadiazole form, and in these solvents the intensity of the UV-absorption band at 395 nm is greatly diminished. The diazo-oxide form predominates in polar solvents.[33] X-ray investigation of 1-oxo-2-diazo-1,2 dihydronaphthalene shows this to be in the diazo-oxide form in the crystalline state.[34] Irradiation of either the diazo-oxide **5** or the oxadiazole form leads to loss of nitrogen and the reaction steps discussed below.

Photolysis of a diazo-oxide is the critical step in the diazo-copying process so that many of these reactions have been studied in detail. Between 1944 and 1958, Süs demonstrated that many 1,2-diazo-oxides are photolysed, with loss of nitrogen and rearrangement to a cyclopentadienecarboxylic acid. Examples include diazo-oxides from benzene **5**, naphthalene **6** (a and b) and further condensed aromatic hydrocarbons,[35–38] pyridine, quinoline **8**, benzotriazole and benzimidazole derivatives.[36,39] Süs ascribed structures to the products in which the alkene bond was not conjugated to the carboxyl group. Modern work with benzene and naphthalene derivatives indicates that the products have the conjugated enecarboxylic acid form. The conversions proceed with high quantum yield for the naphthalene diazo-oxides where $\Phi = 0.72$.[40] In an acidic pH range, some diazonium salts can couple rapidly with the corresponding cyclopentadienecarboxylic acid, leading to products such as **9**.

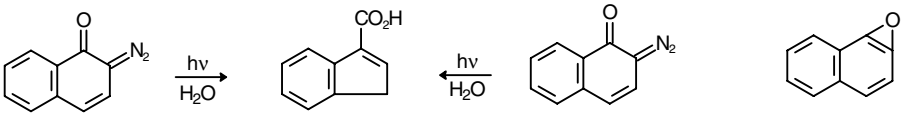

6a 6b 7

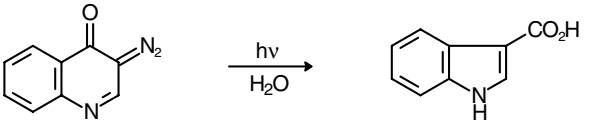

8

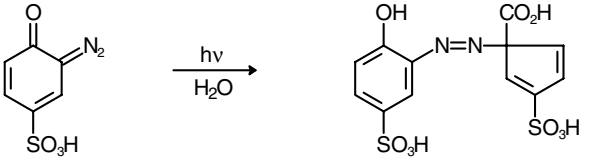

9

Fast-reaction techniques, employing laser flash excitation followed by UV monitoring of the reaction, show that photolysis of diazo-oxides derived from benzene[41] and naphthalene[42] follows the course illustrated in Scheme 6 for the benzene series. In aqueous solution, only the ketene and the ketene hydrate are observed as short-lived intermediates.[43] Rates of the intermediate reactions have been followed over a large pH range and show the expected profiles due to acid-base catalysis. Photolysis within a film of Novolak-resin shows evidence for the short-lived carbene intermediate, and it has been proposed that this species is stabilized as the oxirene form.[44] However, photolysis of the ^{13}C-labeled naphthalene derivatives cannot involve an oxirene intermediate **7** as no scrambling of the ^{13}C label is observed in the products.[45]

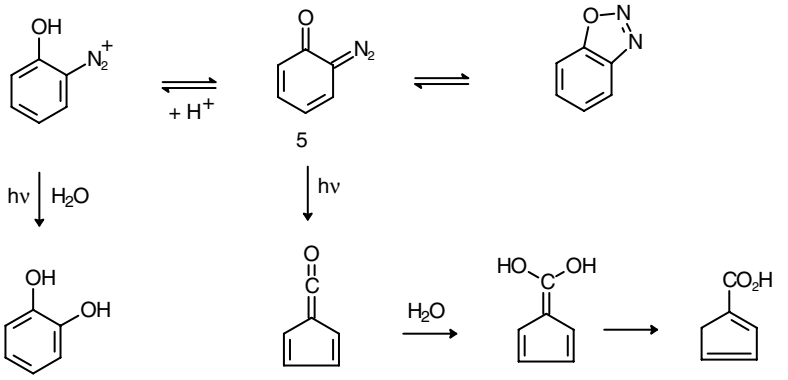

SCHEME 6

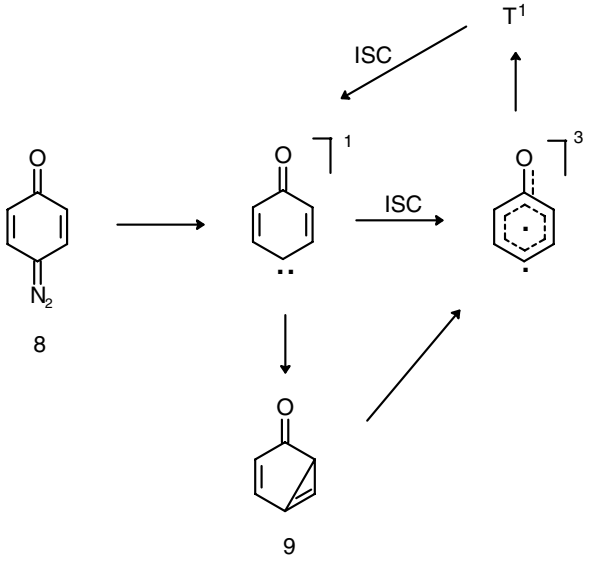

SCHEME 7

43.4 1,4-Aryldiazo-Oxides

The 4-hydroxybenzenediazonium ion is a strong acid that exists in polar and nonpolar solvents as the conjugate base form, 4-diazocyclohexa-2,5-dienone (the 1,4-diazo-oxide) with λ_{max} 342 nm (log ε 4.47) and 448 nm (log ε 1.80).[46] The 1,4-naphthalenediazo-oxides are also well known. Spectroscopic data indicate considerable interaction between the carbonyl and diazo functions in these molecules.[47] Irradiation of 1,4-diazo-oxides follows the course indicated in Scheme 7 for 1,4-benzenediazo-oxide **8**. Loss of nitrogen affords a singlet carbene, which is transformed by ISC into the more stable triplet form. These triplet carbenes have been characterized by spectroscopy in an argon matrix[48] and show an infrared (IR) carbonyl stretching frequency in the range 1550 to 1518 cm^{-1}, indicating considerable delocalization of one electron into the carbonyl function. The triplet has an adsorption maximum in the UV close to that of the parent diazo-oxide. Further irradiation to the T^1 state is followed by ISC and collapse to the short-lived singlet state. The singlet converts either to the triplet or to the bicyclohexadienone **9**. Thus, a photostationary state is established between the triplet and **9**. Isomer **9** can be isolated in an argon matrix

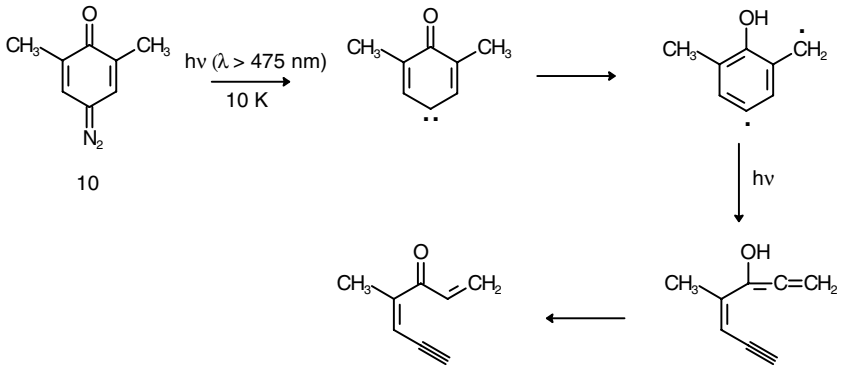

10

SCHEME 8

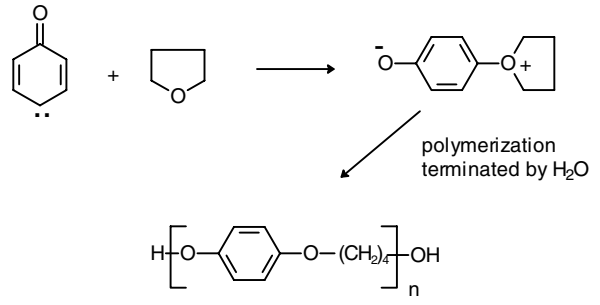

SCHEME 9

and on warming collapses to the triplet carbene.[48,49] Exceptions to this scheme are found with diazo-oxides having a methyl group adjacent to the carbonyl function. Within an argon matrix, the triplet carbene from **10** reacts by hydrogen atom transfer and collapse of the resulting biradical to an open chain structure (Scheme 8).[50]

Preparative scale photochemical reactions of 1,4-diazo-oxides yield products expected from an electrophilic carbene intermediate. The singlet carbene is stabilized in polar solvents.[51] It reacts with primary alcohols as an electrophile, giving the corresponding hydroquinone mono-ether.[52] With isopropanol, and probably other secondary alcohols, hydrogen atom abstraction occurs, giving the phenoxyl radical.[53]

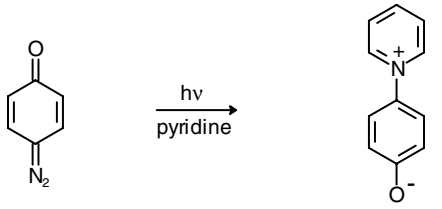

11

The electrophilic behavior of these carbene intermediates is also shown by their reactions with pyridine and with cyclic ethers as electron donors. Pyridine forms betaines of the type **11**, which are strongly colored.[54] In 1956, Süs noted the formation of strongly colored photoproducts with pyridine but assumed these to be C-substituted rather than *N*-substituted pyridines. Reaction with tetrahydrofuran produces a 1:1 copolymer, which probably arises by the mechanism shown in Scheme 9.[55] The photopolymerization

of solid 1,4-benzenediazo-oxide, which yields the polyether **12**, probably also proceeds in a similar manner. Reaction with oxetane is terminated by a Stevens rearrangement of the intermediate ylide to the spiro-compound **13**.[56] Reaction with acetonitrile also forms an ylide **14**.

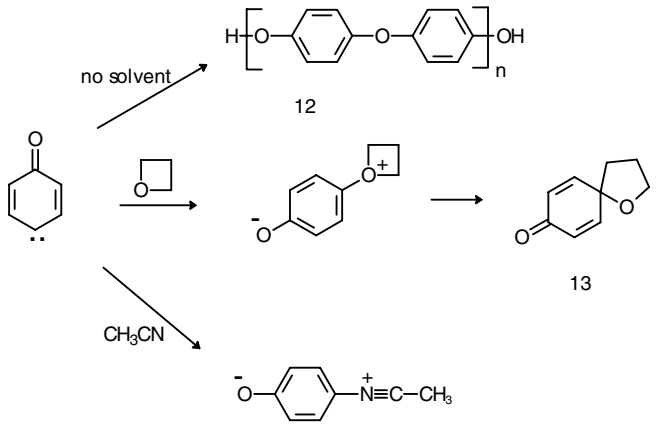

The atom abstracting behavior of the carbene center is shown by reaction with carbon tetrachloride to form the cyclohexadienone **15**.[57] Reactions in alkane solvents also lead to hydrogen atom abstraction, and this step is intermediate in the cross polymerization of piperylene oligomers by irradiation in the presence of 1,4-benzenediazo-oxide.[58]

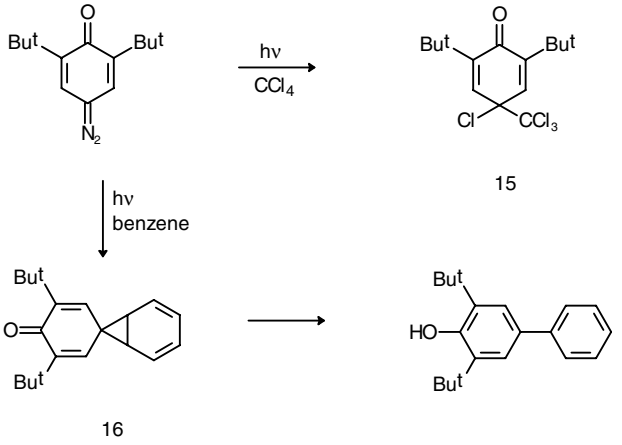

Photodecomposition of 1,4-benzenediazo-oxides in benzene or toluene leads to diphenyl derivatives. Reaction with benzene and with perdeuteriobenzene has been shown to proceed via a tricyclic intermediate **16**.[59] Preparative scale reaction between benzene-1,4-diazo-oxide and toluene led to the isolation of only two products, 4-hydroxy-2′-methyl- and 4-hydroxy-4′-methyl-biphenyl. Presumably the presence of a third isomer was not recognized at the time.

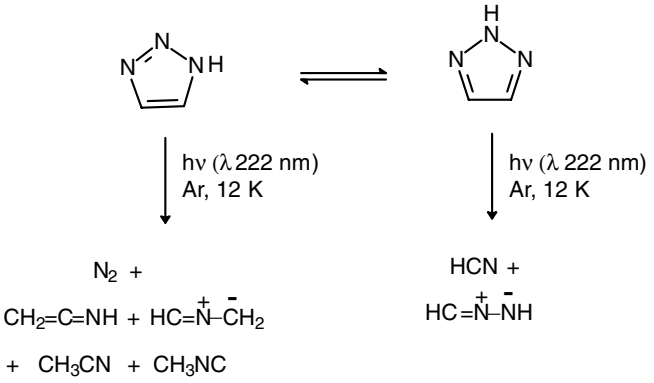

SCHEME 10

43.5 The Diazo Process

Photochemical decomposition of diazonium salts is the key step in a reprographic process once much used with large-scale engineering drawings. Both the Xerox reprographic systems and computer drawing programs have rendered the diazo process much less important than it formally was. Photoresist lacquers used in the manufacture of printed circuit boards employ variations of the diazo process. The earliest process, developed in 1890, used primuline as the source of the diazonium salt.[2] Cloth or paper was coated with primuline and then diazotized *in situ*. Exposure to light through a stencil left a positive image in the undecomposed diazonium compound. This image was developed in an alkaline phenol solution.

Kalle A-G of Wiesbaden developed the first commercially successful process.[60] It is often referred to as the Kögel process (from the author's name attached to the U.S. patent).[61] The Kögel process uses paper coated with both a diazo-oxide and a phenolic component, and the coating is made faintly acidic to slow down coupling of the two components while increasing the shelf life of the material. After exposure to a strong light, a positive image forms by decomposition of the diazo component, and development is achieved by exposing the paper to ammonia vapor when the remaining diazo component couples with the phenol. The usual diazo-oxide employed is a 2-diazo-1-oxo-1,2-dihydronaphthalene bearing a sulfonic acid substituent. Various phenols have been used to give images of different colors. This process has the great advantage that it requires no aqueous solutions; the final prints are dry and are immediately usable.

The Chemische Fabrick L. van der Grinten, of Venlo devised an alternative system,[62] known as a one-component system, that uses paper coated with a stabilized diazonium salt, but no phenol. Coupling is achieved after exposure by developing the paper in an alkaline solution of a phenol. The original diazonium salt used was 4-diethylaminobenzenediazonium associated with a complex anion. Choice of the phenolic component allowed modification of the color of the final image.

43.6 1,2,3-Triazoles

1,2,3-Triazoles with no substituent on nitrogen exist in a rapid tautomeric equilibrium between the *1H* and *2H* forms (Scheme 10). An independent photolysis pathway exists for each tautomer. For the parent

triazole molecule, the first formed intermediates have been characterized at 12 K in an argon matrix. The *1H* isomer loses nitrogen to leave a C_2H_3N residue as several interconverting isomers. The *2H* tautomer loses hydrogen cyanide to leave a 1,3-dipolar residue.[63]

Preparative-scale photolysis of 4- and 5-phenyltriazoles affords products derived from related reactive intermediates.[64] The recombination of intermediates to form unexpected products such as the imidazole 17 is illustrated by the irradiation of 4,5-diphenyl-1,2,3-triazole.

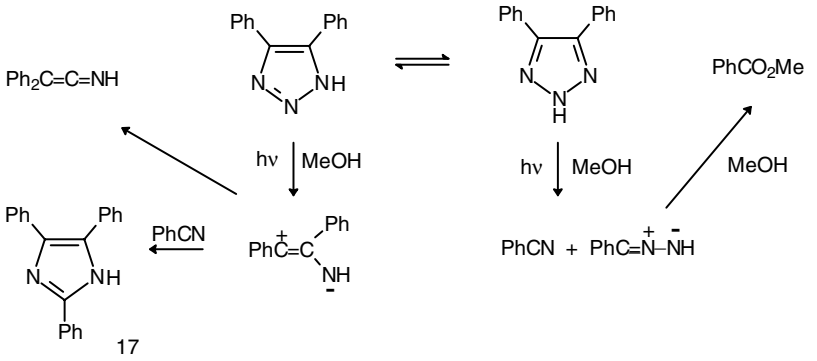

17

1-Phenyl-1,2,3-triazoles **18** do not show this tautomeric equilibrium, and photolysis leads only to the loss of nitrogen. The residual biradical is usually represented as a carbene. It is in equilibrium with an aziridine form, and the reverse equilibrium leads to a mixture of two isomeric carbenes. Two competing reactions then lead to the stable products. First, Wolff rearrangement of the carbene yields a ketene imide. Second, cyclization of the carbene center onto the phenyl group leads to an indole. Two isomeric indoles may be isolated because of rearrangement of the carbene via the aziridine.[65] Ring opening of the aziridine reactive intermediate favors formation of a carbene with an electron-withdrawing group on the carbene carbon center; thus, whereas photolysis of **19** gives two indoles via this carbene rearrangement, reaction of **20** leads to only one indole product. Photolysis of 1,5-diphenyl-1,2,3-triazole gives both 2- and 3-phenylindoles due to interconversion of the carbene intermediates via an aziridine.[66]

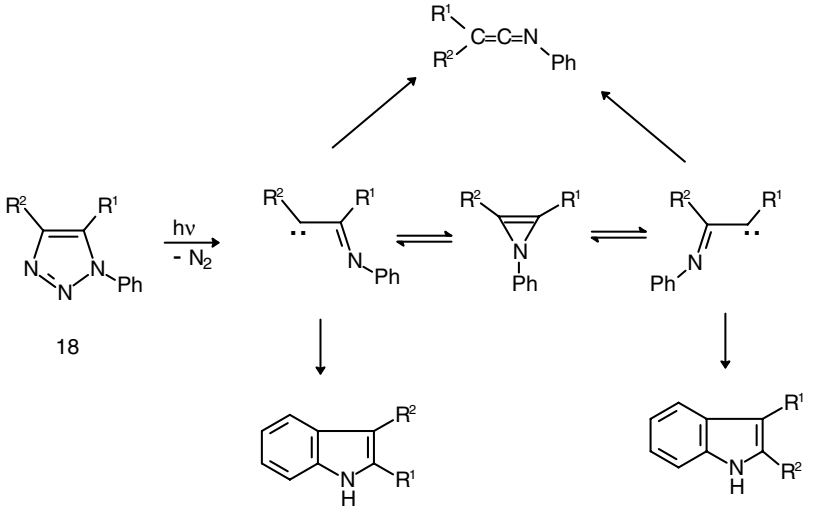

18

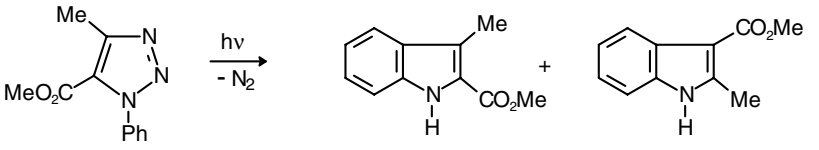

19

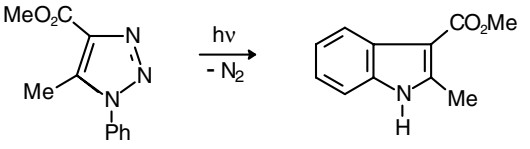

20

The relative rates of Wolff rearrangement and cyclization to the indole depend on the substituent pattern. Fast rearrangement of hydrogen and trimethylsilyl groups in position 5 of the triazole ring is observed so that no indole product can be detected in these reactions. With a phenyl substituent in position 5, both the Wolff rearrangement and cyclization to the indole are observed.[66,67] Photolysis of **21** gives products mainly via the Wolff rearrangement.[68]

Photolysis of 1-tosylamino-1,2,3-triazole anions leads to loss of two molecules of nitrogen and the generation of an alkyne. Strained cycloalkynes, for example **22**, have been generated in this way and trapped as Diels–Alder type adducts.[69]

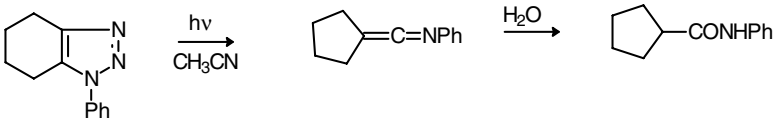

21

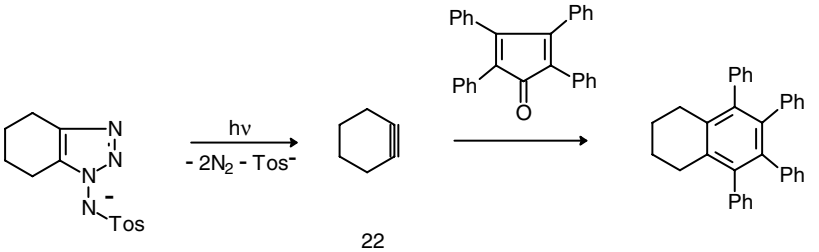

22

43.7 Benzotriazoles

Photolysis of benzotriazoles 23 leads to loss of nitrogen and generation of a 1,3-biradical intermediate. When R = H or alkyl, the intermediate attacks a solvent molecule as shown.[70,71] Photolysis of 1-phenylbenzotriazoles at room temperature takes a different course. An intramolecular radical insertion step leads to a carbazole in good yields.[67,71] Reaction of the dichloro compound **24** gives only one dichlorocarbazole, indicating that the intermediate biradical does not undergo rapid ring closure to give **25** followed by three-membered ring opening. The ESR spectrum of the biradical from 1-phenylbenzotriazole at 77 K is consistent with a triplet ground state, which converts to the singlet and then rapidly cyclizes to carbazole.[72]

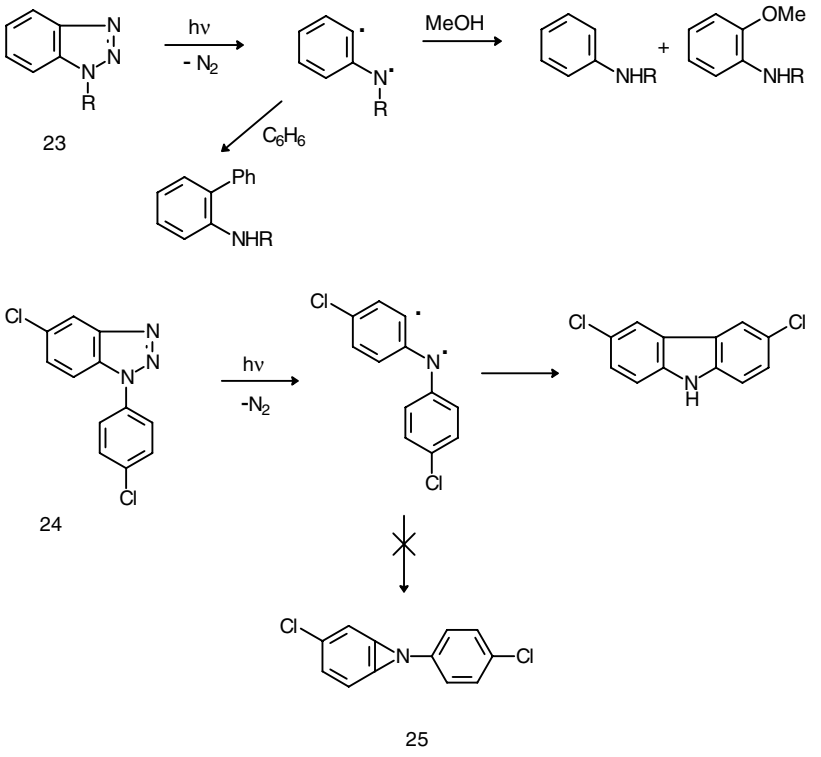

23

24

25

The intermediates from *N*-(1-naphthyl)benzotriazoles cyclize on both the 2- and 8[a]-positions of the naphthalene ring. Where a substituent is already located on the 2-position of the naphthalene ring, this second reaction becomes predominant. Subsequent dark reactions lead to the eight-membered ring carbazole derivative **26**.[73] Cyclization of the biradical intermediate from the benzotriazole **27** occurs principally on the pyridine nitrogen atom.[74]

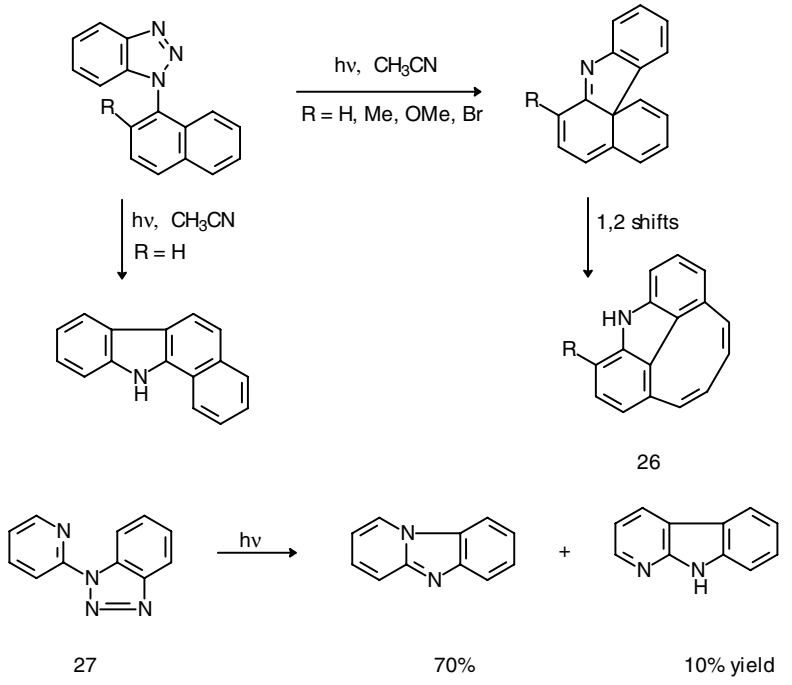

26

27

70%

10% yield

43.8 Tetrazoles

1,5-Disubstituted tetrazoles lose nitrogen on photolysis to generate a biradical intermediate, usually formulated as the nitrene (for example, **28**). Benzimidazoles are formed from 1-phenyltetrazoles by cyclization of the intermediate onto the *N*-phenyl ring.[75,76] Where an *N*-vinyl group is present, cyclization occurs on the vinyl group to form an imidazole. Photoreaction of **29** shows a competition between expulsion of a molecule of nitrogen and electrocyclization to **30**, which generates a new six-membered ring.[77]

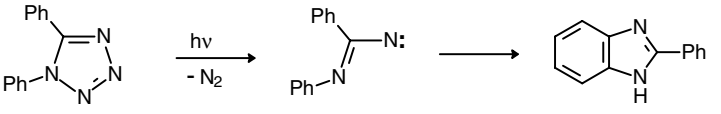

28

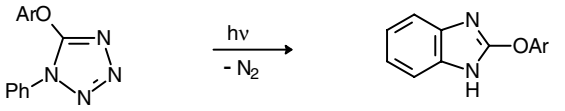

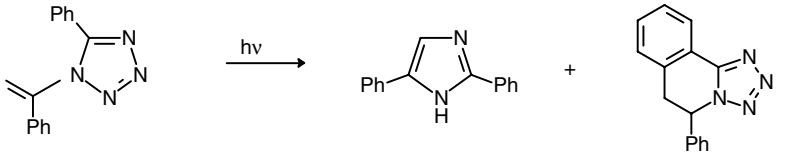

29 30

3,5-Disubstituted tetrazoles are photolysed to nitrilimines with loss of nitrogen. Nitrilimines are short lived at room temperature and can be trapped by 1,3-dipolar addition to an alkene or alkyne.[78] 1,3-Diphenylnitrilimine **31** has been characterized by matrix isolation at 10 K.[79] Prolonged irradiation of the nitrilimine under these conditions leads to conversion to diphenylcarbodiimide and benzonitrile. Intramolecular addition of nitrilimines to an alkene bond in **32** or the alkyne bond in **33** has been used to generate five- and six-membered rings.[80,81]

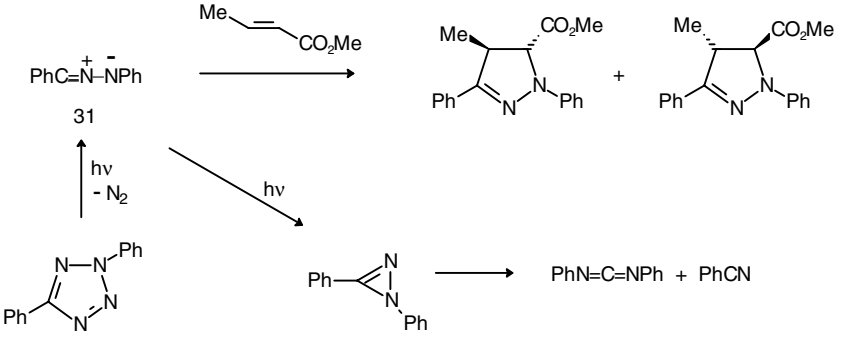

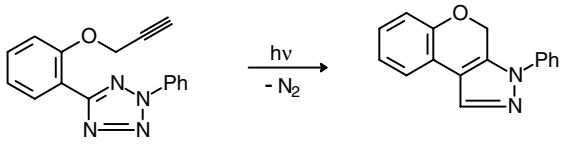

32

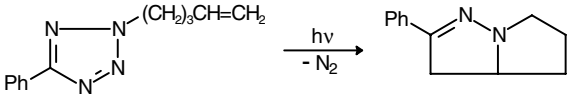

33

Tetrazolo[1,5-*b*]pyridazines **34** also lose nitrogen on photolysis. In these cases, the intermediate biradical rearranges to a diazonitrile. This molecule also loses nitrogen on exposure to light to leave a carbene from which the final stable products are generated. Electrocyclization of the diazonitrile is a competing reaction leading to a 3-*H*-pyrazole **35**:[82]

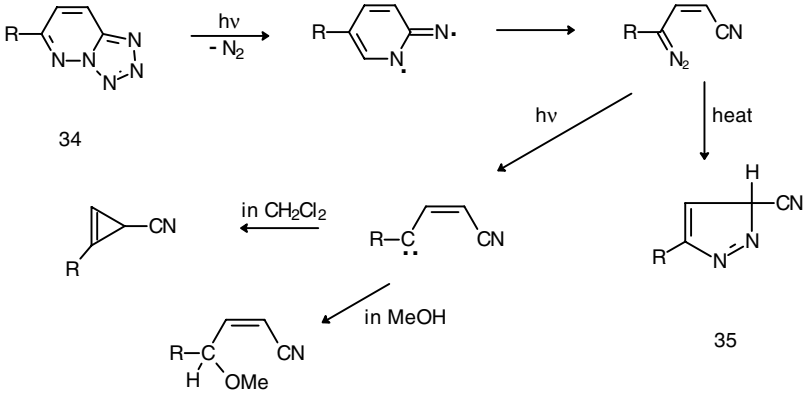

34

35

References

1. Berthelot and Vieille, Sur le nitrate de diazobenzol, *Compt. Rend.*, 92, 1074, 1881.
2. Green, A. G. and Bevan, E. J., Kopirverfarhen mit lichtemfindlicher Farbstoffen, GE 56606, 1890.
3. Kirmse, W. and Horner, L., Photolyse von 1.2.3-thiodiazolen, *Liebigs Ann. Chem.*, 614, 4, 1958.
4. Wohl, A., L'absorption dans l'ultraviolet des sels de diazonium, *Bull. Soc. Chim. Fr.*, 6, 1319, 1939.
5. Schulte-Frohlinde, D. and Blume, H., Quantenausbedeuten des photochemischen Zerfalls von Diazoniumsaltzen in sauren Lösungen, *Z. Physik. Chem., Neue Folge*, 59, 282, 1968.
6. Lewis, E. S., Holliday, R. E., and Hartung, L. D., *J. Am. Chem. Soc.*, 91, 430, 1969.
7. Goodeve, C. F. and Wood, L. J., The photosensitivity of diphenylamine-*p*-diazonium sulphate by the method of photometric curves, *Proc. Roy. Soc. London A*, 166, 342, 1938.
8. Cox, R. J., Bushnell, P., and Evleth, E. M., Photophysical and photochemical properties of sterically hindered aryldiazonium salts, *Tetrahedron Lett.*, 207, 1970.
9. Baril, A, Quantum yields of *p*-diazo-*N*,*N*-dimethylaniline zinc chloride dihydrate at 3660 Å, *J. Chem. Phys.*, 22, 1275, 1954.
10. Orton, K. J. P., Coates, J. E., and Burdett, F., The influence of light on diazo-reactions, *J. Chem. Soc.*, 91, 35, 1907.

11. Kirk, K. L. and Cohen, L. A., Photochemistry of diazonium salts: synthesis of 4-fluoroimidazoles, 4-fluorohistamine and 4-fluorohistidine, *J. Am. Chem. Soc.*, 95, 4619, 1973.
12. Horner, L. and Stöher, H., Über das Verhalten der Diazoniumsaltze gegen UV-Licht, *Chem. Ber.*, 85, 993, 1952.
13. Chen, J., Zhao, C., Wang, R., Cao, S., and Cao, W., Photochemical and thermal decomposition of diphenylamine diazonium salts, *J. Photochem. Photobiol. A: Chem.,* 125, 73, 1999.
14. Becker, H. G. O., Ebisch, R., Israel, G., Kroha, G., Kroha, W., Brede, O., and Mehnert, R., Kinetik und Mechanismus der Photolyse von Aryldiazoniumsalzen in Methanol, *J. Prakt. Chem.*, 319, 98, 1977.
15. Ambroz, H. B. and Kemp, T. J., Substituent factors influencing net stabilization of the triplet level in aryl cations, *J. Chem. Soc., Perkin Trans. 2*, 1420, 1979.
16. Cox, A., Kemp, T. J., Payne, D. R., Symons, M. C. R., and Pinot de Moira, P., Electron spin resonance characterization of ground state triplet aryl cations substituted at the 4-position by dialkylamino group, *J. Am. Chem. Soc.*, 100, 4779, 1978.
17. Ambroz, H. P., Przybytniak, G. K., Stradowski, Cz., and Wolszczak, M., Optical spectroscopy of the aryl cation, the intermediate in the decomposition of arenediazonium salts, *J. Photochem. Photobiol. A: Chem.,* 52, 369, 1990.
18. Becker, H. G. O., Israel, G., Oertel, U., and Vetter, H. U., Photoinduced electron transfer between aryldiazonium cations and anions, *J. Prakt. Chem.*, 327, 399, 1985.
19. Scaiano, J. C. and Nguyen, K. T., Diazonium salts in photochemistry: quenching of triplet photosensitizers, *Can. J. Chem.*, 60, 2286, 1982.
20. Nguyen, K. T. and Scaiano, J. C., Diazonium salts in photochemistry: kinetic studies of the quenching of singlet photosensitizers in anionic micelles, *Chem. Phys. Lett.*, 101, 192, 1983.
21. Tamaoki, N., Takahashi, Y., and Yamaoka, T., Photochemistry of benzenediazonium anthracenesulphonates, *J. Chem. Soc., Chem. Commun.*, 1749, 1994.
22. Becker, H. G. O., Pfeifer, D., and Radeglia, R., CIDNP effects of sensitized photochemical dediazoniation of arene diazonium salts, *Z. Naturforsch. B*, 38, 1591, 1983.
23. Becker, H. G. O., Pfeifer, D., and Urban, K., Evidence for the Marcus inverted region of back-electron transfer in solution by means of chemically induced dynamic nuclear polarization, *J. Chem. Soc., Faraday Trans. 2*, 85, 1765, 1989.
24. Cano-Yelo, H. and Deronzier, A., Photo-oxidation of tris(2,2′-bipyridyl)ruthenium(II) by *p*-substituted benzenediazonium salts in acetonitrile, *J. Chem. Soc., Faraday Trans. 1*, 80, 3011, 1984.
25. Cano-Yelo, H. and Deronzier, A., Photocatalysis of the Pschorr reaction by tris(2,2′-bipyridyl)ruthenium(II) in the phenanthrene series, *J. Chem. Soc., Perkin Trans. 2*, 1093, 1984.
26. Cano-Yelo, H. and Deronzier, A., Photocatalysis of the Pschorr reaction by tris(2,2′-bipyridyl)ruthenium(II) in the fluorenone, fluorene and dibenzofuran series, *J. Photochem.*, 37, 315, 1987.
27. Becker, H. G. O. and Israel, G., Photo-Meerwein-Additionen von Aryldiazoniumsalzen an Olefine, *Z. Phys. Chem. (Leipzig)*, 256, 463, 1975.
28. Böttcher, H., El'cov, A. V., and Ritshchev, N. I., Eigenschaften und photochemisches Verhalten von *o*-Dialkylamino-benzoldiazonium-Saltzen, *J. Prakt. Chem.*, 315, 725, 1973.
29. Knight, M. H., Putkey, T., and Mosher, H. S., Unique formation of a benzocyclobutene derivative: the diazotization of 3-amino-4-*tert*-butyl-5-nitrobenzoic acid, *J. Org. Chem.*, 36, 1483, 1971.
30. Müller, U., Utterodt, A., Mörke, W., Deuber, B., and Herzig, C., New insights about diazonium salts as cationic photoinitiators, *J. Photochem. Photobiol. A: Chem.,* 140, 53, 2001.
31. Kazitsyna, L. A., Klyueva, N. D., and Kazanova, N. N., The basicity of *o*- and *p*-benzoquinone diazides, immediately, *Vestn. Mosk. Univ., Ser. II Chem.*, 22, 68, 1967 (*Chem. Abstr.*, 68, 72897, 1968).
32. de Jonge, J., Alink, R. H. J., and Djikstra, R., Absorption spectrum and photodecomposition of *o*-hydroxybenzenediazonium sulphate, *Rec. Trav. Chim. Pays-Bas*, 69, 1448, 1950.
33. Schweig, A., Baumgartl, A., and Schilz, R., IR and UV matrix photochemistry and solvent effects, *J. Mol. Struct.*, 247, 135, 1991.

34. Seidel, I., Kuban, R.-J., Brandtstädter, H., and Gey, E., Die Kristall- und Molekülstruktur des 1-Oxo-2-diazo-1,2-dihydroxynaphthalenes, *Z. Chem*., 29, 177, 1989.
35. Süs, O., Über die Natur der Belichtungsproduckte von Diazoverbindungen, *Liebigs Ann. Chem.*, 556, 65, 1944.
36. Süs, O., Über die Lichtreaktion der *o*-Chinondiazide, Photosynthese von Cyclopentadienabkömmlingen, *Liebigs Ann. Chem*., 579, 133, 1953.
37. Süs, O., Steppen, H., and Diebrich, R., Photosynthese des Fluorens, des Retenfluorens und des 1,2-Benzofluorens, *Liebigs Ann. Chem*., 617, 20, 1958.
38. Süs, O. and Müller, K., Über die Photosynthese von Cyclopentadien- und Pyrrolabkümmlingen, *Liebigs Ann. Chem*., 593, 91, 1955.
39. Süs, O. Glos, M., Möller, K., and Eberhardt, H. D., Über die Lichtreaktion der *o*-Chinondiazide. *Liebigs Ann. Chem*., 583, 150, 1953.
40. Majer, J. and Dvoracek, I., Photolysis of quinonediazides in alcohol and in water, *Coll. Czech. Chem. Commun*., 44, 756, 1979.
41. Urwyler, B. and Wirz, J., The tautomeric equilibrium between cyclopentadienyl-1-carboxylic acid and fulvene-6,6-diol in aqueous solution, *Angew. Chem. Int. Ed. Engl.*, 29, 790, 1990.
42. Almstead, K., Urwyler, B., and Wirz, J., Flash photolysis of α-diazonaphthoquinones in aqueous solution: determination of rates and equilibria for keto-enol tautomerism of 1-indene-3-carboxylic acid, *J. Am. Chem. Soc*., 116, 954, 1994.
43. Andraos, J., Chiang, Y., Huang, C.-G., Kresge, A. J., and Scaiano, J. C., Flash photolytic generation and study of ketene and carboxylic acid enol intermediates formed by the photolysis of diazonaphthoquinones in aqueous solution, *J. Am. Chem. Soc.*, 115, 10605, 1993.
44. Rosenfeld, A., Mitzner, R., Baumbach, B., and Bendig, J., Laser photolytic and low temperature investigations of naphthoquinone diazides in Novolak films, *J. Photochem. Photobiol. A: Chem.,* 55, 259, 1990.
45. Zeller, K.-P., Die Photolyse von 2-Diazo-[1-^{13}C]naphthalin-1(*2H*)-on und 1-Diazo-[1-^{13}C]naphthalin-2(1H)-on. Ein Beitrag zum Oxiren-Problem, *Chem. Ber.*, 108, 3566, 1975.
46. Anderson, L. C. and Roedel, M. J., The structure of some diazophenols, *J. Am. Chem. Soc.*, 67, 955, 1945.
47. Sander, W., Bucher, G., Komnick, P., Morawietz, J., Bubenitschek, P., Jones, P. G., and Chrapkowski, A., Structure and spectroscopic properties of *p*-benzoquinone diazides, *Chem. Ber.*, 126, 2101, 1993.
48. Bucher, G. and Sander, W., Direct observation of the cyclopropene-vinylcarbene rearrangement. Matrix isolation of bicyclo[3.1.0]hexadien-2-ones, *J. Org. Chem*., 57, 1346, 1992.
49. Sander, W., Bucher, G., Reichel, F., and Cremer, D., *1H*-Bicyclo[3.1.0]hexa-3,5-dien-2-one. A strained 1,3-bridged cyclopropene, *J. Am. Chem. Soc*., 113, 5311, 1991.
50. Sander, W., Wandel, H., Bucher, G., Grafenstein, J., Kraka, E., and Cremer, D., α,3-Didehydro-5-methyl-6-hydroxytoluene. Matrix isolation of a biradical related to the neocarzinostatin chromophore, *J. Am. Chem. Soc*., 120, 8480, 1998.
51. Arnold, B. R., Scaiano, J. C., Bucher, G. F., and Sander, W. W., Laser flash photolysis studies on 4-oxocyclohexa-2,5-dienylidenes, *J. Org. Chem*., 57, 6469, 1992.
52. Süs, O., Möller, K., and Heiss, H., Über Lichtreaktionen der *p*-Chinondiazide und Imino-chinondiazide, *Liebigs Ann. Chem*., 598, 123, 1956.
53. Ouardaoui, A., Steren, C. A., van Willigen, H., and Yang, C., FT-EPR study of the photolysis of 4-chlorophenol, *J. Am. Chem. Soc*., 117, 6803, 1995.
54. Sander, W. and Hintze, F., A new synthetic approach to pyridinium *N*-phenoxide betaine dyes, *Chem. Ber.*, 127, 267, 1994.
55. Stille, J. K., Cassidy, P., and Plummer, L., Photodecomposition of *p*-benzoquinone diazides: copolymerization with tetrahydrofuran, *J. Am. Chem. Soc*., 85, 1318, 1963.
56. Kirmse, W., Lelgemann, R., and Friedrich, K., Carben-Reaktionen mit Oxetan und mit Oxetan/Methanol-Gemischen, *Chem. Ber.*, 124, 1853, 1991.
57. Plekhanova, L. G., Nikiforov, G. A., and Ershov, V. V., *J. Org. Chem. USSR*, 8, 819, 1972.

58. Voratnikov, A. P., Darydov, E. Ya., and Topty, D. Ya., Reaction of cyclohexadienone carbene with piperylene oligomers, *Izv. Akad. Nauk. SSSR, Ser. Khim*., 1275, 1985.
59. Yankelevich, A. Z., Sergeev, A. M., Rykov, S. V., Potapov, V. K. and Nikiforov, G. A., Kinetics and mechanism of the photolysis of 2,6-di-tert-butyl-1,4-benzoquinonediazide in benzene and deuterobenzene, *Izv. Akad. Nauk. SSSR, Ser. Khim.*, 2680, 1986.
60. Kalle and Co. Akt.-Ges., Verfahren zur Herstellung lichempfindlicher Schichten mit Diazoverbindungen, DE 422972, 1924, gives a history of the development.
61. Kögel, G. and Neuenhaus, H., Manufacture of Light Copying Paper, U.S. Patent No. 1444469, 1922.
62. Chemische Fabrick L. van der Grinten, Improvements in the manufacture of diazo-types, GB 294972, 1928.
63. Maier, G., Eckwert, J., Bothur, A. et al., Photochemical fragmentation of unsubstituted tetrazole, 1,2,3-triazole and 1,2,4-triazole: first matrix-spectroscopic identification of nitrilimine HCNNH, *Liebigs Ann. Chem*., 1041, 1996.
64. Selvarajan, R. and Boyer, J. H., Photo- and thermal elimination of nitrogen from 4-phenyl- and 4,5-diphenyl-1,2,3-triazole, *J. Heterocyclic. Chem*., 9, 87, 1972.
65. Mitchell, G. and Rees, C. W., Photolysis of 1-aryl-1,2,3-triazoles; rearrangement via 1H-aziridines, *J. Chem. Soc., Perkin Trans. 1*, 413, 1987.
66. Gilchrist, T. L., Rees, C. W., and Thomas, C., Investigation of the pyrolysis of 1,4- and 1,5-diphenyl-1,2,3-triazoles by use of ^{13}C-labeled compounds, *J. Chem. Soc., Perkin Trans. 1*, 8, 1975.
67. Burgess, E. M., Carithers, R., and McCullagh, L., Photochemical decomposition of *1H*-1,2,3-triazole derivatives, *J. Am. Chem. Soc*., 90, 1923, 1968.
68. Tsujimoto, K., Ohashi, M., and Yonezawa, T., Thermal and photochemical decompositions of 4,5,6,7-tetrahydro-1,2,3-benzotriazole analogues, *Bull. Chem. Soc. Jpn*., 46, 3605, 1973.
69. Willey, F. G., Photolysis of 1-tosylamino-1,2,3-triazole anions: a new synthesis of alkynes, *Angew. Chem. Int. Ed. Engl*., 3, 138, 1964.
70. Boyer, J. H. and Selvarajan, R., Photo-elimination of nitrogen from fused-ring triazoles, *J. Heterocyclic Chem*., 6, 503, 1969.
71. Tsujimoto, K., Ohashi, M., and Yonezawa, T., The photochemical decomposition of benzotriazoles, *Bull. Chem. Soc. Jpn*., 45, 515, 1972.
72. Murai, H., Torres, M., and Strausz, O. P., Electron spin resonance of iminocyclohexadienylidenes: photo induced triplet geometrical isomerization, *J. Am. Chem. Soc.*, 102, 1421, 1980.
73. Mitchell, G. and Rees, C. W., Cyclo-octa[*d,e,f*]carbazole: a new heterocyclic paratropic ring system, *J. Chem. Soc., Perkin Trans. 1*, 403, 1987.
74. Hubert, A. J., A comparison of the thermolysis and photochemistry of benzotriazoles, *J. Chem. Soc., Chem. Commun.*, 328, 1969.
75. Kirmse, W., Reaktionen mit Carbenen und Iminen als Zwischenstufen, *Angew. Chem.*, 71, 537, 1959.
76. Bach, F. L., Karliner, J., and van Lear, G. E., The photochemical and mass spectral properties of 5-phenoxy-1-phenyl-1*H*-tetrazole, *J. Chem. Soc., Chem. Commun.*, 1110, 1969.
77. Casey, M., Moody, C. J., and Rees, C. W., Synthesis of imidazoles from alkenes, *J. Chem. Soc., Perkin Trans. 1*, 1933, 1984.
78. Clovis, J. C., Eckell, A., Huisgen, R., and Sustmann, R., Der Nachweis des freien Diphenylnitrilimins als Zwischenstufe bei Cycloadditionen, *Chem. Ber.*, 100, 60, 1967.
79. Trubro, N. H. and Holm, A., Nitrilimines, *J. Am. Chem. Soc.*, 102, 2093, 1980.
80. Sato, E., Kanaoka, Y., and Padwa, A., Intramolecular photoaddition reactions in the 2-(4-pentenyl)-5-aryl-substituted tetrazole system, *J. Org. Chem.*, 47, 4256, 1982.
81. Meier, H. and Heimgartner, H., Intramolekulare 1,3-dipolare Cycloadditionen von Diarylnitriminen aus 2,5-Diaryltetrazolen, *Helv. Chim. Acta*, 68, 1283, 1985.
82. Tsuchiya, T., Arai, H., and Igeta, H., Photolysis of tetrazolo[1,5-*b*]pyridazines, *Chem. Pharm. Bull*., 21, 2517, 1973.

44

Photochemical Reactivity of Azides

Götz Bucher
Ruhr-Universität Bochum

44.1 Introduction

Photolysis of organic azides leads almost exclusively to the extrusion of molecular nitrogen. The resulting nitrenes, a class of organic 1,1-biradicals, may react from two different spin states (singlet or triplet) and show a very complex chemistry. Nitrenes are the crucial intermediates in azide photochemistry. This chapter provides a survey about the current state of knowledge on nitrene reactivity, focusing on recent results, particularly on the chemistry of singlet aryl nitrenes. For additional information, the reader may consult the corresponding chapter from the first edition of this handbook[1] or one or more of the older reviews and monographs on nitrene chemistry.[2–16]

Direct photolysis of an organic azide will initially yield a singlet nitrene, which in most cases will be an excited state of a ground-state triplet species. In the important case of aryl nitrenes, the singlet nitrene is an open-shell species bearing two unpaired electrons with antiparallel spins in two singly occupied *p*-orbitals. Both the R–N binding electrons and the lone pair on the nitrene nitrogen atom reside in sp hybrid orbitals. Due to this particular electronic configuration of singlet nitrenes, spin reversal to the ground triplet state is not accompanied by a change in orbital momentum as in carbene chemistry. Hence, intersystem crossing (ISC) to the triplet ground state is not aided by spin-orbit coupling, and intermolecular and in particular intramolecular reactions of the singlet nitrene may therefore compete with the relatively inefficient ISC. Efficient formation of ground-state triplet nitrenes may be achieved by conducting the photoreaction at low temperature, as ISC (low Arrhenius pre-exponential factor, no barrier) then becomes more favorable than competing intramolecular reactions (high A-factor, barrier). Alternatively, triplet nitrenes may be formed by sensitized photolysis of azides or by photolysis of azides in the presence of heavy-atom-containing addends such as ethyl iodide.[17]

0-8493-1348-1/04/$0.00+$1.50

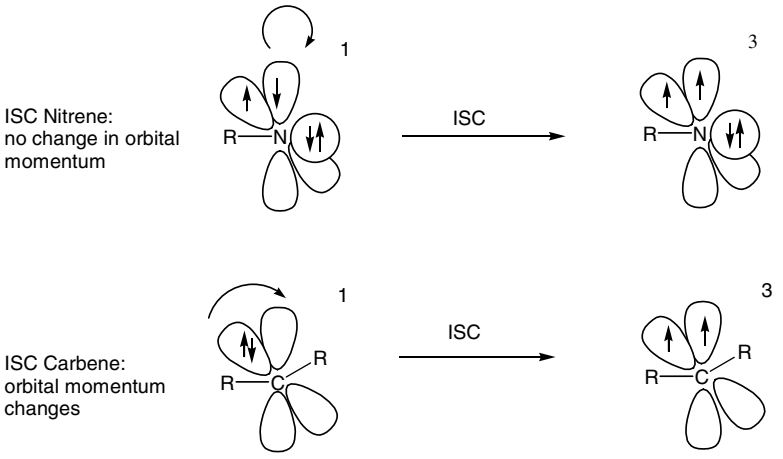

SCHEME 1

Photolysis of aryl azides in acidic media represents a special case. At low pH, singlet aryl nitrenes may be N-protonated, rapidly yielding singlet nitrenium ions. These ionic reactive intermediates undergo reactions different from those of singlet nitrenes.

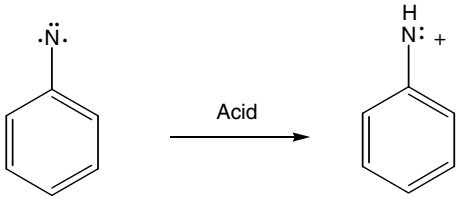

SCHEME 2

44.2 Alkyl Azides

Photolysis of alkyl azides leads to the formation of singlet alkyl nitrenes. According to high-level *ab initio* calculations, singlet methyl nitrene **1** is a minimum on the CH_3N hypersurface, but the barrier for a 1,2-hydrogen shift yielding formimine is very small.[18] Overall, 1,2-migration of adjacent groups is the major reaction pathway for singlet alkyl nitrenes, and the ground-state triplet species are hardly formed at all, even at low temperature. Due to the stability of the carbon-fluorine bond, trifluormethylnitrene **2** represents a remarkable exception to this rule.[19] Triplet alkyl nitrenes may be obtained by inter- or intramolecular sensitization of alkyl azide photolysis. An example for the latter methodology was presented in the photolysis of α-azidoacetophenone **3**.[20] Excitation of **3** leads to the ketone triplet excited state, which can either undergo Norrish type I cleavage, leading to the benzoyl radical, or transfer its excitation energy to the azido functionality with formation of the triplet nitrene **4**. According to product studies, decay of triplet nitrene **4** mainly takes place by hydrogen abstraction and other free-radical reaction pathways.

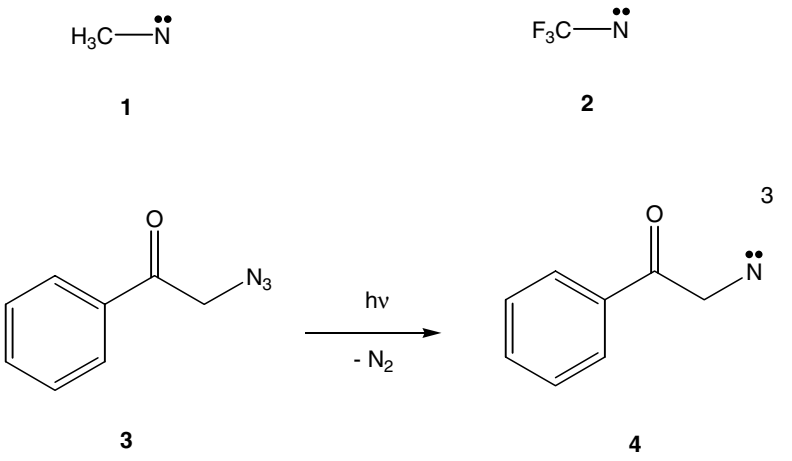

SCHEME 3

44.3 Vinyl Azides

Photolysis of vinyl azides leads to highly reactive singlet vinyl nitrenes, which can either undergo intramolecular cycloaddition to azirines[21–23] or rearrange to ketenimines by a 1,2-shift of the geminal substituent. A recent example of a system showing both reactions is α-azido-β,β-dicyanostyrene. Photolysis of this vinyl azide under conditions of matrix isolation spectroscopy yielded a mixture of an azirine and a ketenimine. Irradiation in chloroform at 0°C, on the other hand, gave exclusively the azirine.[24]

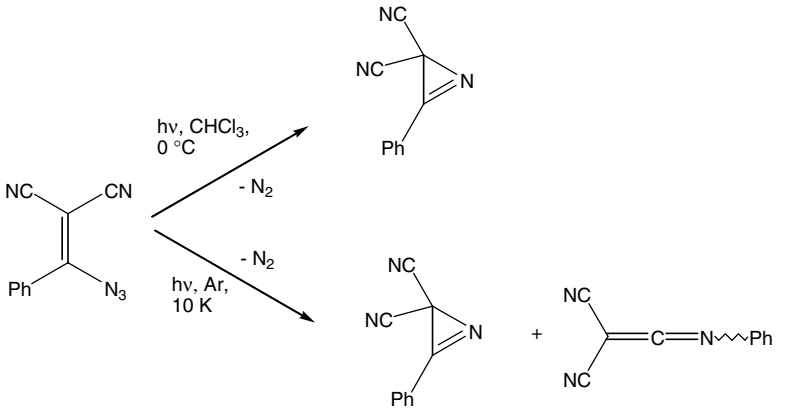

SCHEME 4

Anti-Bredt azirines may be formed upon photolysis of cycloalkenyl azides. In most cases, these strained species will be highly unstable, and evidence for their formation can only be obtained indirectly by product analysis. Photolysis of 3-azido-2-benzyl-2-cyclohexen-1-one **5** in methanolic solution gave a 50% yield of ketal **7**.[25] The formation of **7** can be rationalized in terms of twofold nucleophilic attack of methanol at C6 of azirine **6**. Omitting the benzyl substituent results in the formation of tetrahydroazepinone **9**, which is likely formed by reaction of cyclic ketenimine **8** with methanol.[26]

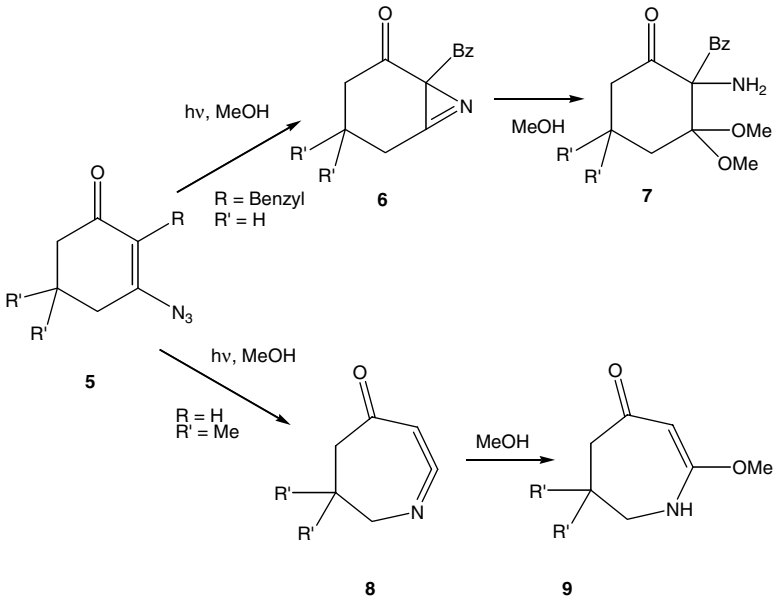

SCHEME 5

44.4 Acyl Azides

Excitation of acyl azides may lead to loss of nitrogen concomitant with rearrangement to an isocyanate. This reaction is called the *Curtius rearrangement* and is frequently observed upon photolysis of acyl azides R-CO-N_3 (R being carbon centered).[27] Singlet nitrenes may be formed in competition with the Curtius rearrangement. The efficiency of the Curtius rearrangement depends strongly on the type of substitution at the carbonyl carbon. Photolysis of amides of azidoformic acid (R = dialkylamino) yields aminoisocyanates efficiently, even under conditions of matrix isolation spectroscopy.[28] Esters of azidoformic acid (R = alkoxy), on the other hand, give singlet acyl nitrenes upon photolysis. The fate of these highly reactive species depends on the experimental conditions. Reactions include ISC to the ground-state triplet[29,30] acyl nitrenes, which further decay by hydrogen abstraction or dimerization to azodicarboxylates. Singlet acyl nitrenes may also undergo stereospecific addition to C=C bonds to yield aziridines,[31] add to aromatic C=C bonds,[32] undergo a 1,3-dipolar cycloaddition to carbon–nitrogen triple bonds in nitriles,[32] or insert into C–H bonds.[33,32] More recent examples of acylnitrene chemistry include addition to fullerene C_{60}[34] or to carbon nanotubes.[35]

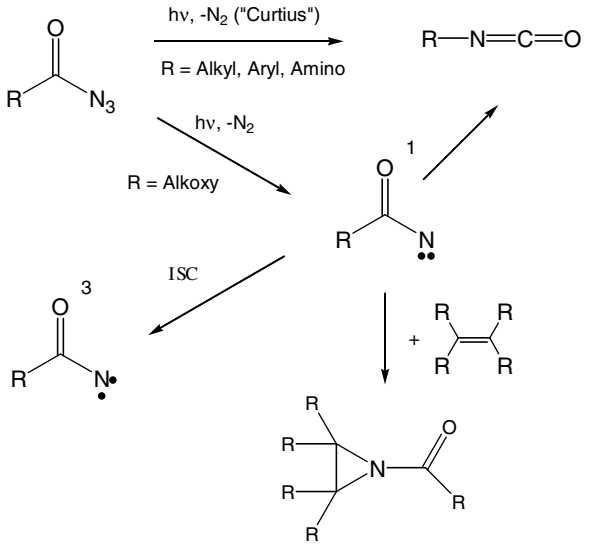

SCHEME 6

44.5 Aryl Azides in Nonacidic Media: The Chemistry of Singlet Aryl Nitrenes

The photolysis of aryl azides primarily leads to the formation of singlet aryl nitrenes, which have an open-shell $\sigma^1\pi^1$ electronic configuration. As described in the introduction to this chapter, this leads to a drastically reduced rate of intersystem crossing due to the lack of spin-orbit coupling. At ambient temperature, singlet aryl nitrenes, therefore, do not predominantly relax to the ground-state triplet nitrenes. Instead, they undergo an intramolecular rearrangement to strained didehydroazepines, which can be trapped by primary[36,37] or secondary amines[38–42] or by intramolecular hydrogen transfer from a hydroxy group.[43]

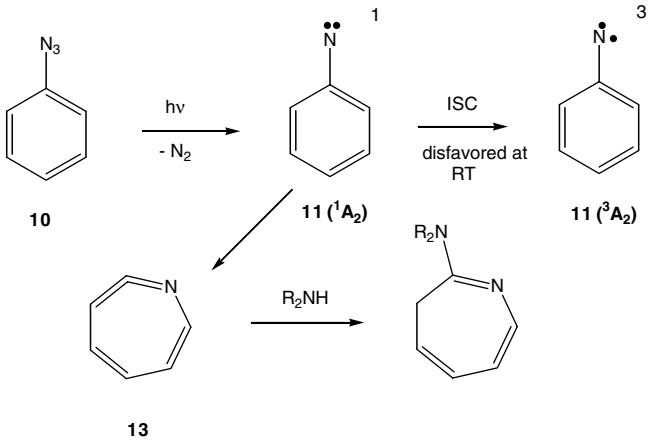

SCHEME 7

The development of highly correlated methods of *ab initio* theory has provided us with insight into the properties of singlet aryl nitrenes. Time-resolved laser flash photolysis (LFP) with picosecond time-

resolution has made it possible to observe singlet aryl nitrenes directly. Matrix isolation spectroscopy has revealed a wealth of spectroscopic data on triplet aryl nitrenes and didehydroazepines. In combination, these methods have given us a detailed and consistent description of the properties of aryl nitrenes, which will be the subject of the following section.

Phenylnitrene **10** can assume different electronic configurations. Of particular relevance are the $^3A_2$ (triplet ground state), $^1A_2$ (open-shell $\sigma^1\pi^1$), and $^1A_1$ (closed-shell σ^2) configurations. The experimentally determined energy gap between the $^3A_2$ ground state and the first singlet excited state is 18.33 ± 0.69 kcal/mol.[44,45] This value is reproduced well by calculations at the CASPT2N/6–311G(2-*d*,*p*) level of theory (ΔE [$^1A_2 - {}^3A_2$] = 18.5 kcal/mol),[46] which also confirm the $^1A_2$-open-shell $\sigma^1\pi^1$ character of the first singlet excited state of phenylnitrene.[47–50] The second singlet excited state bears the $^1A_1$ closed-shell σ^2 character and is calculated to be higher in energy by 18.4 kcal/mol than the $^1A_2$ state. The open-shell $^1A_2$ state can be described as an iminyl-cyclohexadienyl-type diradical, whereas the closed-shell $^1A_1$ state can be compared with a typical singlet carbene.

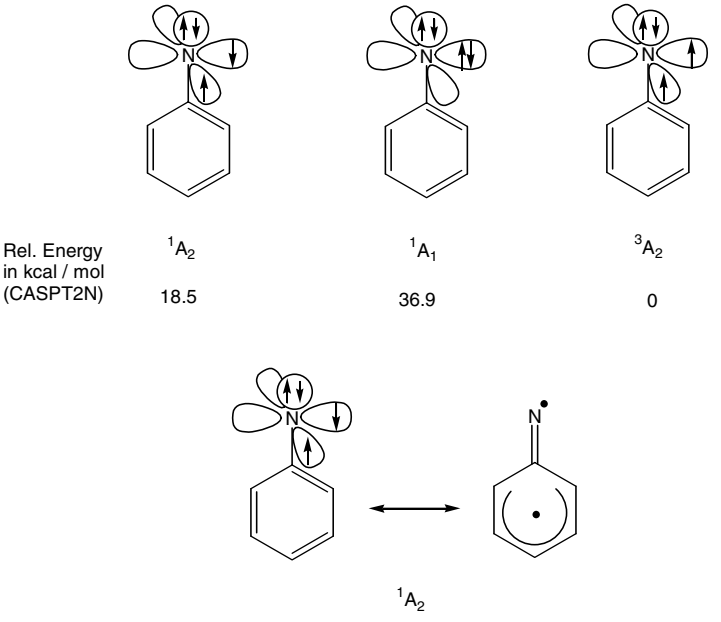

SCHEME 8

Open-shell singlet diradicals such as the $^1A_2$ state of phenylnitrene should show a reactivity differing significantly from the reactivity of typical electrophilic closed-shell intermediates such as singlet phenyl carbene. All intermolecular reactions requiring the presence of empty or doubly occupied *p*-orbitals, such as addition to a C=C double bond or insertion into an O–H bond can be expected to be retarded, while intramolecular reactions, which can be described as formal intramolecular free-radical recombination, should be fast. High level *ab initio* calculations confirm this expectation. Ring-expansion of singlet ($^1A_2$) phenylnitrene **11** to didehydroazepine **13** proceeds via the bicyclic azirine **12** as intermediate. The barrier for formation of azirine **12** is calculated (CASPT2N/6–31G*//CASSCF(8,8)/6–31G*) to be 8.6 kcal/mol.[46] Azirine **12**, which is predicted to be higher in energy than singlet nitrene **11** by 1.6 kcal/mol, then rearranges to didehydroazepine **13** over a barrier of 5.2 kcal/mol. According to the CASPT2N calculations, the reaction **11** → **13** is exothermic by 1.3 kcal/mol, and formation of azirine **12** is calculated to be the rate-determining step of the reaction.[46] On the same level of theory, the transition state connecting singlet phenyl carbene **14** with bicyclic cyclopropene **15** is calculated to be higher in energy than **14** by 11.6 kcal/mol, while the barrier for ring-opening of **15** to cycloheptatetraene **16** is predicted to be very low (2.5 kcal/mol.).[46] These findings convincingly rationalize the experimental observations:[16]

- *Singlet phenylnitrene:* Low barrier for rearrangement in combination with a low ISC rate constant leads to almost exclusive rearrangement to didehydroazepine **13**. In some cases, this rearrangement can be reversible.
- *Singlet phenylcarbene:* High barrier for rearrangement in combination with high ISC rate constant leads to exclusive ISC to the ground-state triplet carbene, if the singlet carbene is not trapped by the solvent, the diazo precursor, or added quenchers.

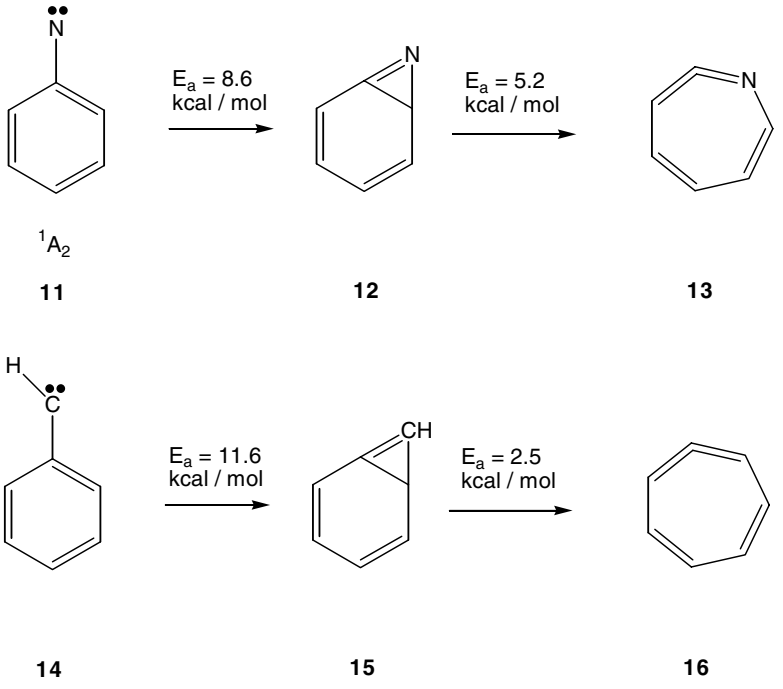

(CASPT2N/6-31G*//CASSCF(8,8)/6-31G*)

SCHEME 9

Picosecond time-resolved laser flash photolysis (ps-LFP) has made it possible to observe singlet phenylnitrene **11** directly and to measure the rate constants for ring expansion to didehydroazepine **13** and for ISC.[51–54] In *n*-pentane solution at 233 K, singlet phenylnitrene **11** has a sharp absorption band at λ_{max} = 350 nm in addition to a very weak band at λ_{max} = 540 nm.[51] Its lifetime at ambient temperature is of the order of ~1 ns, and it decays mainly by rearrangement to didehydroazepine **13.** The rate constant for ISC to triplet phenylnitrene was determined as $k_{ISC} = 3.2 \pm 0.3 \times 10^6\ s^{-1}$, and the activation parameters for rearrangement were found to be E_a = 5.6 ± 0.3 kcal/mol with log (A/s^{-1}) = 13.1 ± 0.3.[51] Triplet phenylnitrene had been characterized earlier by matrix isolation spectroscopy.[55] Irradiation of phenyl azide, matrix-isolated in nitrogen or argon at 12 K, at λ = 334 nm yielded a mixture of mostly triplet nitrene **11** ($^3A_2$) and some didehydroazepine **13**. Visible (λ = 485 nm) irradiation of this mixture resulted in the depletion of the bands due to triplet nitrene **11** and in a growth of the bands assigned to didehydroazepine **13.** Irradiation with λ = 334 nm again shifted the photostationary equilibrium toward nitrene **11.** Due to the relatively low ISC rate constant of singlet phenylnitrene **11** ($^1A_2$), triplet phenylnitrene is not accessible by photolysis of phenyl azide **10** at ambient temperature. It can be obtained by photolysis of carbamates derived from 9-fluorenone oxime, albeit in low yield.[56] In solution, it decays mainly by dimerization, yielding azobenzene, and by hydrogen abstraction.[56]

Replacing one or more of the hydrogen atoms in singlet phenylnitrene **11** with other substituents may drastically alter its reactivity. The following types of substituent effects are encountered:

1. Substituents effects can be related to steric interaction, if the substituents are placed *ortho* to the nitrene center.
2. Significant changes in the reactivity of nitrenes may also occur if the azides are substituted with strong π-donors or π- or σ-acceptors (such as the dimethylamino or nitro substituents, fluorine atoms).
3. Substitution of the aromatic ring with heavy-atom substituents will increase k_{ISC} by enhanced spin-orbit coupling and, therefore, result in a higher yield of triplet nitrenes.
4. Replacing the benzene nucleus of the azide by a larger aromatic system may change nitrene reactivity.
5. The presence of reactive substituents (acyl, nitro, OH, NH_2, certain alkyl groups) *ortho* to the nitrene center may lead to alternative reaction channels.

The presence of substituents *ortho* to the nitrene center has a significant impact on the kinetics of the nitrene → didehydroazepine rearrangement. If only one substituent is present in the 2-position, the nitrene generally attacks the C=C bond pointing away from the substituent.[39] According to high-level *ab initio* calculations (CASPT2N/6–31G*),[57] the barrier for cyclization of singlet 2-methylphenylnitrene **17** away from the methyl group is lower by 2.0 kcal/mol than the barrier for cyclization toward the methyl group. A significant stabilization of the singlet nitrene is achieved only if both *ortho* positions are substituted. Thus, singlet 2-methylphenylnitrene **17** does not live longer than parent singlet phenylnitrene **11** (τ ~ 1 ns in *n*-pentane at 298 K), while singlet 2,6-dimethylphenylnitrene **18** has a lifetime τ = 15 ± 3 ns (*n*-hexane, 298 K).[58] Similar effects are found for *ortho*-chlorine and *ortho*-fluorine substitution.[57,59] 2,6-Fluorine disubstitution leads to a significant rise of the singlet nitrene lifetime. Singlet 2,6-difluorophenylnitrene **19** has a lifetime τ = 240 ± 20 ns in *n*-hexane (298 K), with an experimental barrier E_a = 7.3 ± 0.7 kcal/mol. (log [A/s^{-1}] = 11.5 ± 0.5).[59] A dramatic increase in singlet nitrene lifetime was also reported for *ortho*-phenyl-substituted systems such as singlet 2,6-diphenylphenylnitrene **20**.[60]

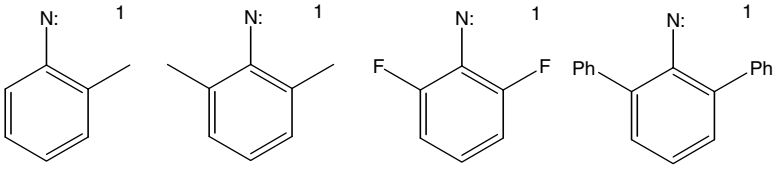

17 **18** **19** **20**

SCHEME 10

Fluorine substitution affects nitrene reactivity not only by sterically shielding the *ortho* carbon atoms but also by increasing the electron-deficient character of the nitrene center. This is particularly obvious from the unusually high reactivity of fluorinated derivatives of singlet phenylnitrene in intermolecular reactions. Matrix-isolated pentafluorophenylnitrene **22** was found not to undergo the ring expansion reaction to the pentafluorodidehydroazepine **24**.[61] Instead, photochemical reaction with carbon monoxide yielding pentafluorophenyl isocyanate **25** was observed.[61] Later, the same nitrene **22** (and 2,6-difluorophenylnitrene **19**) was found to isomerize to the corresponding bridged azirines (**23** in the case of nitrene **22**) upon irradiation in argon matrix.[62] Photolysis of azide **21** in alkane solvents at ambient temperature leads to almost exclusive formation of N–H insertion products such as the *N*-cyclopentylpentafluoroaniline **26**, which is formed upon photolysis of **21** in cyclopentane.[63] Singlet pentafluorophenylnitrene **22** reacts with some Lewis bases, such as pyridine or THF, to give ylides.[17] At ambient temperature, the perfluorodidehydroazepine **24** is also formed and can be trapped.[17,64] The high reactivity of singlet nitrene **22** in intermolecular reactions is also evident from the fact that it is able to add to the

C=C bonds of benzene.[17] Absolute rate constants for the reactions of singlet **22** were determined by LFP.[59,64] In methylene chloride, the ISC rate constant was determined as $k_{ISC} = (1.05 \pm 0.05) \times 10^7$ s^{-1}. The activation parameters for ring-expansion to perfluorodidehydroazepine **24** were determined as E_a = (8.8 ± 0.4) kcal/mol. with log (A/s^{-1}) = 13.8 ± 0.3.[64] The reaction with pyridine is rapid and proceeds via a barrier of only 1.6 ± 0.6 kcal/mol.

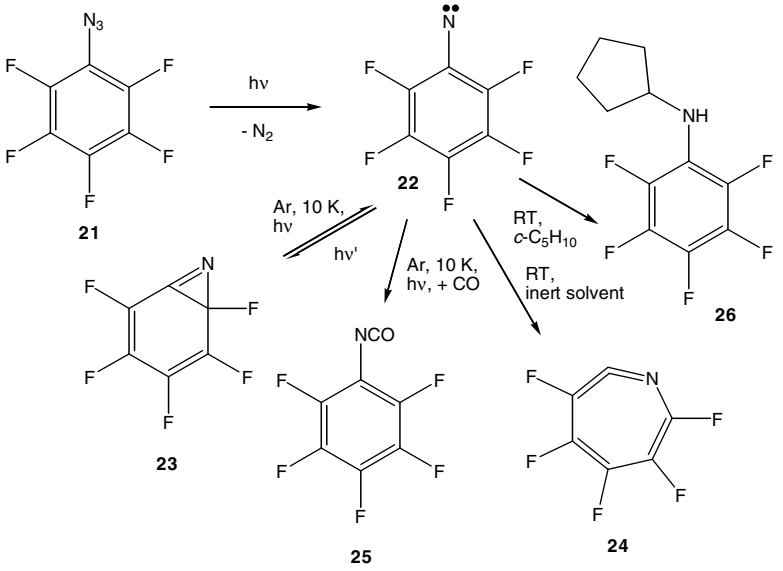

SCHEME 11

Other highly fluorinated derivatives of phenyl azide were investigated as well. Photolysis of perfluoro-4-azidobiphenyl **29** in CH_2Cl_2 at 294 K yielded the corresponding singlet nitrene **30**, which was found to have a relatively long lifetime τ = 254 ± 5 ns. The barrier for ring expansion (E_a = [9.4 + 0.4] kcal/mol) was found to be even higher than in singlet perfluorophenylnitrene **22**.[64] Photolysis of a series of 4-azido-2,3,5,6-tetrafluoro-benzamides (such as **31**) in the presence of pyridine led to pyridine ylides **33**. The growth kinetics of **33** could be resolved by LFP, which allowed for a determination of the rate constants of the reactions of nitrene **32** with further quenchers. Singlet nitrene **32** reacts with dimethylsulfide with a rate constant close to the diffusion-controlled limit ($k_q = 1.27 \times 10^9$ M^{-1} s^{-1}), while reactions with tetramethylethylene ($k_q = 1.62 \times 10^8$ M^{-1} s^{-1}) or diethylamine ($k_q = 2.51 \times 10^8$ M^{-1} s^{-1}) are slightly slower.[65]

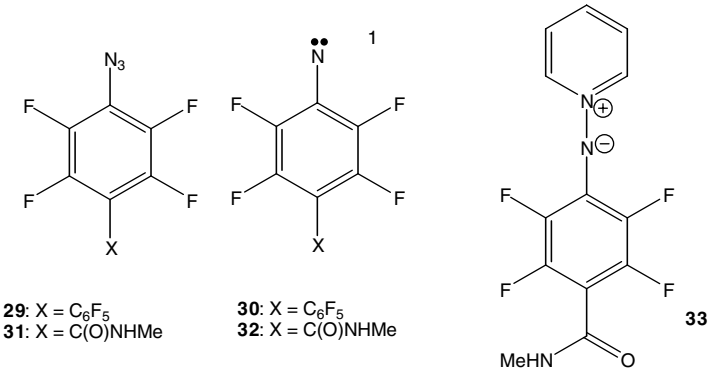

SCHEME 12

TABLE 44.1 Spectroscopic and Kinetic Parameters of Singlet Aryl Nitrenes

Substituents	λ_{max} (nm)	k_{ISC} (x 10^6 s^{-1})	τ_{295K} (ns)	E_a (kcal/mol)	Log A (s^{-1})	Solvent	Ref.
Unsubst.	350	3.2 ± 0.3	~1	5.6 ± 0.3	13.1 ± 0.3	Pentane	51,52
Unsubst.	350	—	~0.6	—	—	CH_2Cl_2	53
4-CH_3	365	5.0 ± 0.2	~1	5.8 ± 0.4	13.2 ± 0.2	Pentane	58
4-CF_3	320	4.6 ± 0.8	1.5	5.6 ± 0.5	12.9 ± 0.5	Pentane	66
4-acetyl	330	8 ± 3	5.0	5.3 ± 0.3	12.5 ± 0.3	Pentane	66
4-CN	—	6 ± 2	8 ± 4	7.2 ± 0.8	13.5 ± 0.6	Pentane	67
4-F	365	3.5 ± 1.4	~0.3	5.3 ± 0.3	13.2 ± 0.3	Pentane	66,59
4-Cl	360	3.9 ± 1.5	~0.6	6.1 ± 0.3	13.3 ± 0.3	Pentane	66
4-Br	361	17 ± 4	~3	4.0 ± 0.2	11.4 ± 0.2	Pentane	66
4-I	328	72 ± 10	—	—	—	Pentane	66
4-OCH_3	—	>500	<1	—	—	Pentane	66
4-NMe_2	460	8300 ± 200	0.12	—	—	Pentane	68
2-CH_3	350	10 ± 1	~1	5.3 ± 0.4	12.8 ± 0.3	Pentane	58
2,6-$(CH_3)_2$	350	15 ± 3	12 ± 1	7.0 ± 0.3	13.0 ± 0.3	Hexane	58
2,6-$(CH_3)_2$	350	30 ± 8	13 ± 1	7.5 ± 0.5	12.9 ± 0.3	Freon-113	58
2,4,6-$(CH_3)_3$	366	29 ± 3	8 ± 1	7.3 ± 0.4	13.4 ± 0.4	Freon-113	58
2-F	342	3.3 ± 0.5	8 ± 1	6.7 ± 0.3	13.0 ± 0.3	Pentane	59
2,6-$(F)_2$	342	2.4 ± 0.3	240 ± 20	7.3 ± 0.7	11.5 ± 0.5	Hexane	59
2,6-$(F)_2$	342	2.7 ± 0.3	260 ± 20	8.0 ± 1.5	12.0 ± 1.2	CCl_4	59
3,5-$(F)_2$	300	3.1 ± 1.5	~3	5.5 ± 0.3	12.8 ± 0.3	Hexane	59
2,3,4,5,6-$(F)_5$	330	3.3 ± 1.5	56 ± 4	7.8 ± 0.6	12.0 ± 1.2	Pentane	59.64
2,3,4,5,6-$(F)_5$	330	10.5 ± 0.5	32 ± 3	8.8 ± 0.4	13.8 ± 0.3	CH_2Cl_2	59,64
2,3,5,6-$(F)_4$ 4-C_6F_5	350	2.2 ± 0.1	254 ± 5	9.4 ± 0.4	13.2 ± 0.2	CH_2Cl_2	64
2,4,6-$(Br)_3$	395	1060 ± 30	0.94 ± 0.03	—	—	CH_2Cl_2	53
2-CN	380	2.8 ± 0.3	~2	5.5 ± 0.3	12.8 ± 0.3	Pentane	67
2,6-$(CN)_2$	405	6.2 ± 0.8	~2.3	6.5 ± 0.4	13.5 ± 0.2	Pentane	67
2,6-$(CN)_2$	405	5.9 ± 1.5	~2.3	6.0 ± 1.1	13.1 ± 1.0	THF	67

The effect of substituents placed *para* to the nitrene center was investigated in a series of matrix isolation, laser flash photolysis, and product studies. Table 44.1 lists a number of rate constants (k_{ISC} for intersystem crossing to the triplet ground-state and k_R for rearrangement to the didehydroazepine). For comparison, the kinetic parameters of several other singlet aryl nitrenes are also given.

If one compares the data for singlet aryl nitrenes substituted at the 4-position, where steric effects are not likely to play an important role, it becomes evident that only strong π-electron donor substituents such as the methoxy and in particular the dimethylamino groups have a significant effect on intramolecular singlet nitrene reactivity. They influence nitrene reactivity via an enormous increase in the intersystem crossing rate constant k_{ISC}. It is noted that, up to now, this effect is not understood.[66] The increase in k_{ISC} is rationalized more easily in the case of heavy-atom-substituted singlet aryl nitrenes, where the effect can be explained in terms of spin-orbit coupling. The increase in k_{ISC} in the series singlet 4-fluoro-, 4-chloro-, 4-bromo-, and 4-iodo-phenylnitrene[66] can be correlated with the known atomic spin-orbit coupling constants for fluorine (269 cm^{-1}), chlorine (587 cm^{-1}), bromine (2460 cm^{-1}), and iodine (5069 cm^{-1}).[69] More important than the spin-orbit coupling constant of the halogen atom, however, seems to be the distance between the halogen atoms and the nitrene center, as k_{ISC} is huge in the case of singlet 2,4,6-tribromophenylnitrene,[53] where the N–Br distance is much shorter than the N–X distance in the 4-substituted derivatives. Electron-acceptor substituents in the *para* position, on the other hand, do not appear to influence intramolecular singlet nitrene reactivity to a large extent. LFP experiments performed on cyano-substituted derivatives of phenyl azide revealed only subtle effects.[67] A nitro group situated in the *para* position, on the other hand, has been reported to lead to a significant increase in intermolecular singlet nitrene reactivity.[70] Singlet 4-nitrophenylnitrene has eluded direct detection so

far,[66] whereas triplet 4-nitrophenylnitrene could be detected by ns-LFP[70] as well as by low-temperature spectroscopy.[71]

The photochemistry of aryl azides incorporating larger aromatic systems has received only limited attention so far. Studies include an early LFP study on 1-azidopyrene **34**.[72] This azide was reported to yield singlet 1-pyrenylnitrene ^{1}**35** (τ = 22 ns in benzene at ambient temperature; pathway A in Scheme 13), which in turn underwent exclusive ISC to triplet 1-pyrenylnitrene ^{3}**35**. In a later study, the short-lived transient was reassigned to azirine **36** (pathway B in Scheme 13).[73] Photolysis of 1-naphthyl azide at 196 K in the presence of diethylamine yielded naphthalene-1,2-diamines, which could only be attributed to a quenching of similar bicyclic azirines.[74,73] This was later confirmed by time-resolved infrared spectroscopy.[42] It is evident from these results, that ring-expansion to didehydroazepines is disfavored for larger aromatic systems. The reaction, however, has been observed upon photolysis of 1- or 2-azidonaphthalene in nitrogen or argon matrices at 12 K.[75]

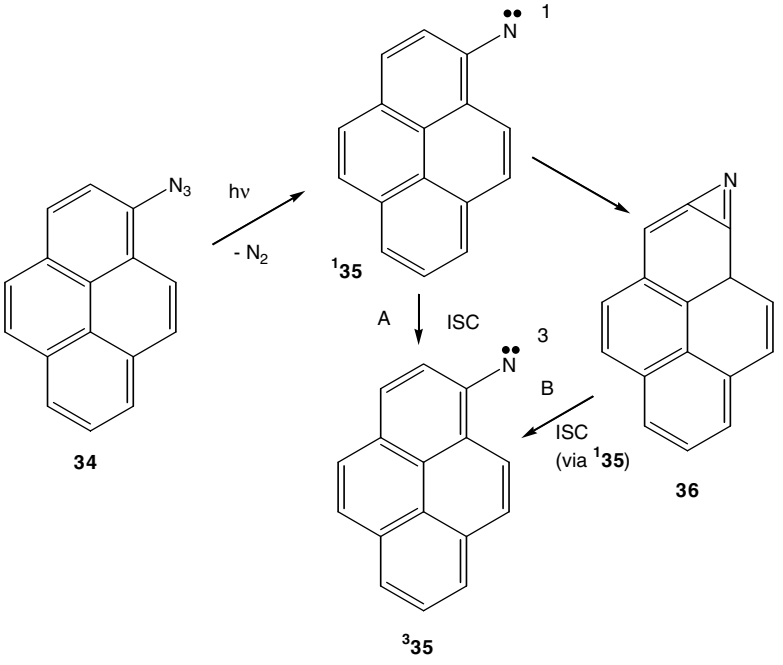

SCHEME 13

If a nitrene bears a substituent in the *ortho* position, a chemical reaction between the nitrene center and this substituent can ensue. A variety of different substituents have been found to undergo reactions with a neighboring nitrene center. Among them are alkyl or aryl groups as well as hydroxy or amino functionalities, acyl or nitro substituents, and nitrogen heterocycles. Hydroxy- or amino-groups are among the simplest substituents to undergo reactions with an *ortho*-nitrene. Broadband photolysis ($\lambda >$ 370 nm) of 2-hydroxy-phenyl azide **37**, matrix-isolated in argon at 10 K, yielded a mixture of the stereoisomeric quinone imines **38** and **39** and one stereoisomer of cumulene **40**.[76] The quinone imines **38/39** and the cumulene **40** could be interconverted photochemically. Neither benzoxazetine **41** nor 2-hydroxy-phenylnitrene itself was observed. Similarly, photolysis of matrix-isolated (Ar, 10 K) 2-aminoazidobenzene gave a mixture of three stereoisomeric quinonediimines. In this case, no cumulenic product was formed as in the photochemistry of **37.** This was explained by unfavorable thermodynamics of the ring-opening reaction.[76]

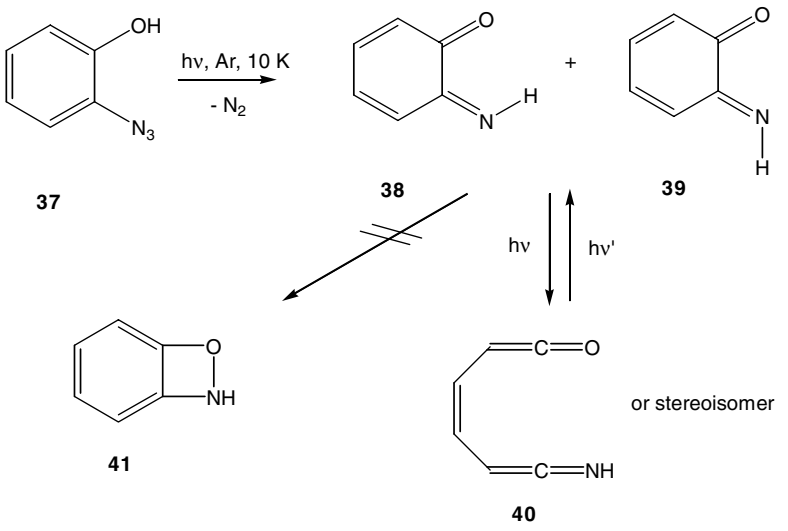

SCHEME 14

A methyl group in the *ortho*-position, while less reactive than a hydroxy or amino functionality, may still react with the adjacent nitrene center. In the parent system *o*-tolylnitrene **43a** (R = H), the photochemical 1,4-hydrogen shift yielding two stereoisomers **45a** and **46a** (R = H) of *o*-iminoquinone methide has been reported to be very inefficient.[77] The reaction gets more favorable if the benzylic hydrogen atoms are activated by electron-donor substituents or by aryl groups. Dialkylamino substituents (R = NR_2) are particularly effective in this respect, but methoxy groups and even halogen atoms still activate the reaction.[78] Benzylic dialkylamino substitution such as in **42c** (R = NEt_2) allows for the monophotonic generation of iminoquinone methides **45c**/**46c** (R = NEt_2) at ambient temperature and their characterization by ns-LFP.[79] The reaction requires a certain amount of flexibility in the side chain. Thus, photolysis of matrix-isolated azidophthalan **47** does not yield an iminoquinone methide, while the reaction is successful for azidotetrahydroisoquinoline **48**.[78] These observations correlate well with the barriers calculated for the 1,4-hydrogen shift.[78] According to the calculations (B3LYP/6–31G(d)), the 1,4-hydrogen shift from the singlet nitrene has a barrier of $\Delta H^{\#}$ = 20.3 kcal/mol for *o*-tolylnitrene **43a** (R = H), which is lowered to $\Delta H^{\#}$ = 9.3 kcal/mol by a dimethylamino group as in **43b** (R = NMe_2). In the case of azide **48**, however, the calculated barrier for 1,4-hydrogen shift is Ea = 20.7 kcal/mol, and for phthalan **47** E_a = 32.2 kcal/mol. Thus, the formation of iminoquinone methides is likely to be a photochemical reaction that occurs either from the vibrationally hot first singlet excited state of the nitrene or from a higher nitrene excited state. The reactive derivatives **42b** (R = NMe_2) and **42c** (R = NEt_2) may represent exceptions to this rule.

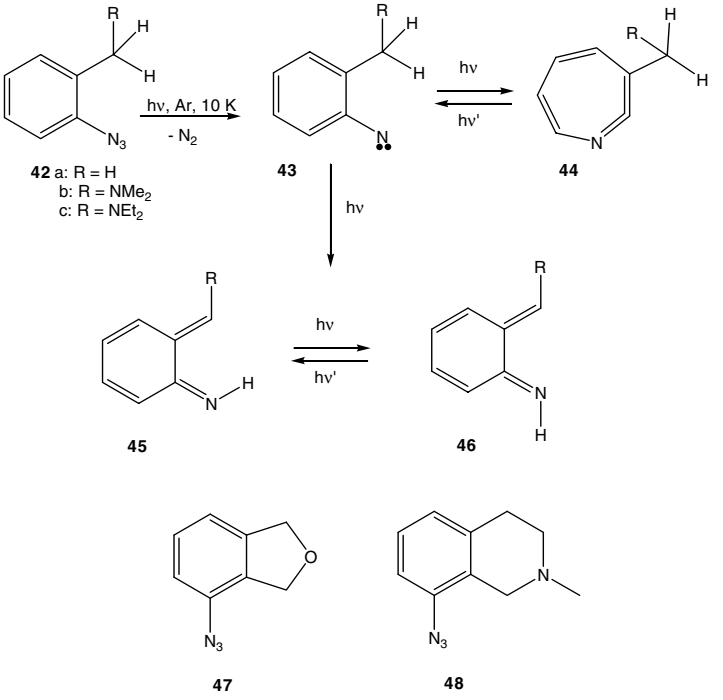

SCHEME 15

Aryl substituents also activate benzylic C–H bonds adjacent to a nitrene center. An interesting study on this topic has dealt with the atropoisomeric 3,5-dimethyl-2-(9-fluorenyl)phenylazides **49** and **52**.[80] The low-temperature photochemistry (77 K) of these rotameric azides proved to be fundamentally different: Photolysis of **49** resulted in the formation of nitrene **50** in addition to azanorcaradiene **51**, while photolysis of **52** gave nitrene **53** in addition to iminoquinone methide **54**. This subsequently underwent intramolecular cycloaddition to yield dihydroindenocridine **55.** Laser flash photolysis showed that the formation of iminoquinone methide **54** from azide **52** occurred in less than 10 ns. Deuteration of the 9-position of the fluorene chromophore resulted in a significantly diminished yield of **55**. LFP of the rotameric azide **49** yielded the rate constant for the formation of azanorcaradiene **51** which was determined as $k = 7.1 \times 10^5\ s^{-1}$.[80]

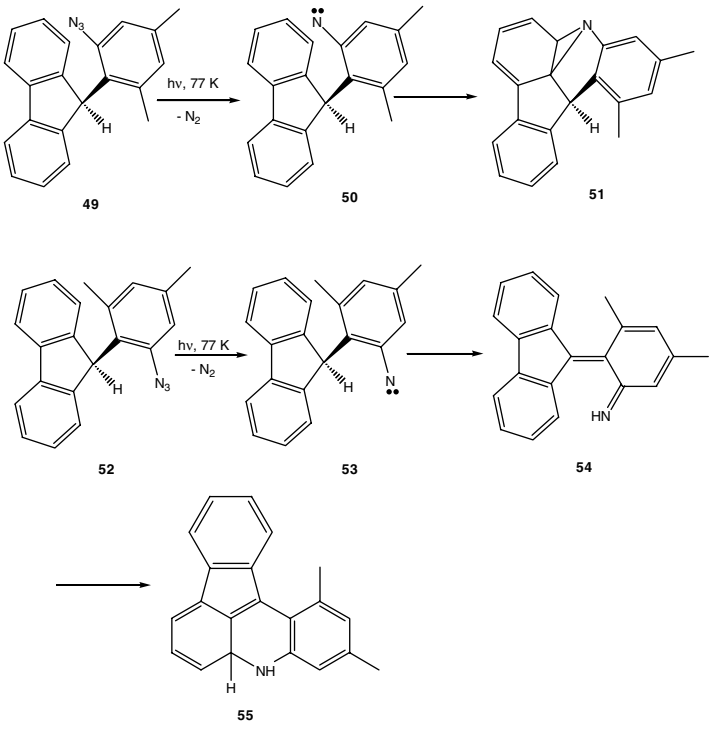

SCHEME 16

Intramolecular hydrogen abstraction from methylene or methyl groups further away from the aromatic nucleus has been reported for 2-(ω-phenylethyl)phenyl azide **56**, which upon photolysis (Ar, 12 K) yields 2-phenylindoline **57** in addition to a didehydroazepine.[81] Similarly, photolysis of 2-(ω-dimethylaminoethyl)phenyl azide **58** (Ar, 10 K) yields the seven-membered ring **59** via the triplet nitrene.[78] The efficiency of intramolecular nitrene hydrogen abstraction reactions strongly depends on both the C–H bond energies and a favorable spatial arrangement of the nitrene center and the reacting C–H bond. If a C–H bond is forced into the vicinity of a nitrene, such as in 2-isopropylphenylazide **60** or 2-dimethylaminophenylazide **62**, efficient H-transfer can occur, even if the reacting C–H bond is not activated. Thus, 2-isopropylphenyl azide **60** has been reported to yield 2-methylindoline **61** under conditions of matrix isolation (photolysis, stepwise reaction via the triplet nitrene)[78] and in solution (thermolysis),[82] while photolysis of matrix-isolated 2-dimethylaminophenyl azide **62** yields 1-methyl-benzimidazoline **63** without evidence of a detectable intermediate.[83]

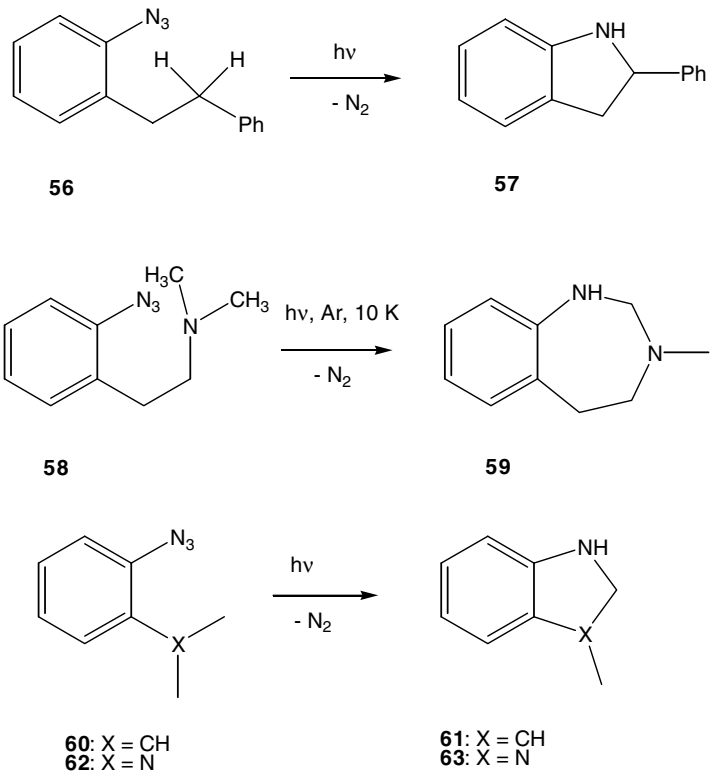

SCHEME 17

The photolysis of 2-azidobiphenyl **64** or similar aryl nitrene precursors yields carbazole **66** by insertion of the singlet nitrene **65** into the *ortho* C–H bond of the neighboring benzene ring.[84] This efficient reaction may be extended to the synthesis of other heterocycles.[85,86]

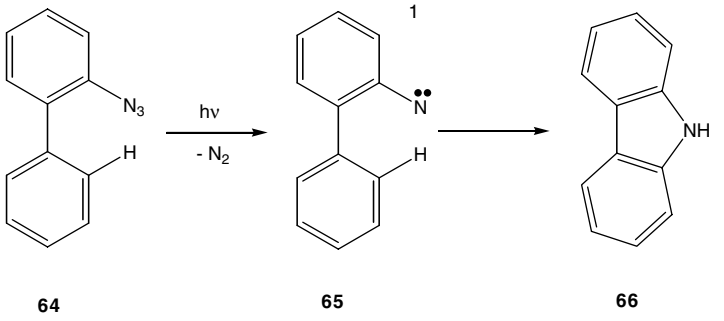

SCHEME 18

Photolysis ($\lambda > 350$ nm) of 2-nitrophenylazide **67,** matrix-isolated in Ar at 10 K, has been reported to lead directly to a mixture of *ortho*-dinitrosobenzene **69** and benzofuroxan **70**.[87] 2-Nitrophenylnitrene **68** was not detected.

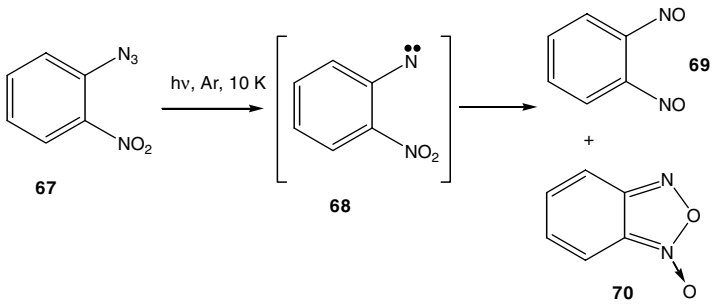

SCHEME 19

Oxygen transfer from an *ortho* substituent to a nitrene was also observed in the photolysis of 2-methoxycarbonylphenylazide **71**.[88] In this system, both the nitrene **72** and the didehydroazepine **73** could be observed. Besides these products of standard azide photochemistry, two stereoisomers of the oximinoketene **74** and the *N*-methoxy-azetidinone **75** were detected. The oxygen transfer can be rationalized to occur via an oxonium ylide **76**, which subsequently ring-opens to ketene **74** that is in photostationary equilibrium with azetidinone **75**.

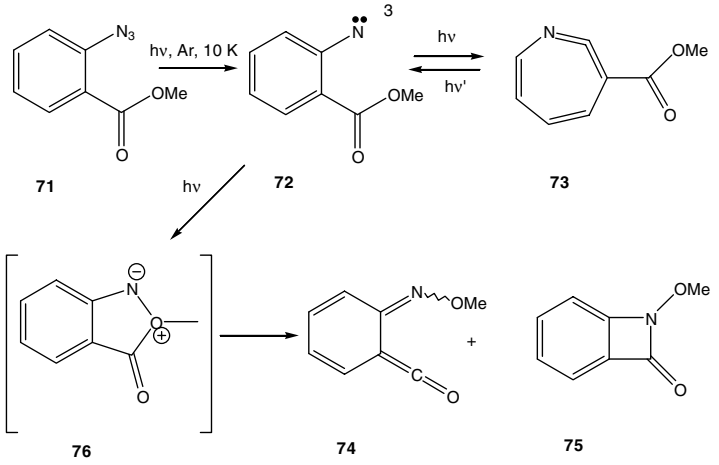

SCHEME 20

Photolysis of matrix-isolated 2-azidobenzoic acid was found to yield mainly ketenimine **78** and benzisoxazolone **79** in addition to some didehydroazepine.[89,90] Depending on the orientation of the carboxy group, the reactions of nitrene **77** split into two channels: Formation of a carbonyl ylide followed by a 1,4-hydrogen shift yields **79**, while H-transfer from the carboxy group to the nitrene center followed by decarboxylation and ring-contraction of the resulting diradical results in the formation of ketenimine **78**.

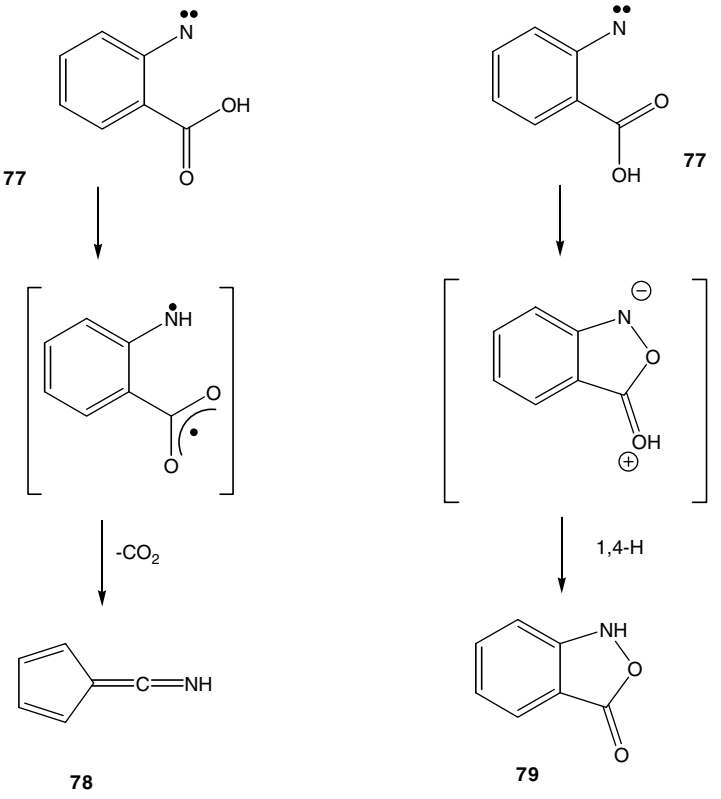

SCHEME 21

The photochemistry of aryl azides substituted with an *ortho*-dimethylpyrazolyl substituent was investigated both by product analysis and by low-temperature spectroscopy.[91–93] Photolysis of azide **80** in ethanol at 295 K led to the formation of the stable heteropentalene **82**, azo compound **83**, and aniline derivative **84**. Addition of diethylamine resulted in trapping of a didehydroazepine, which thus has to be in thermal equilibrium with singlet carbene ^{1}**81**. Low-temperature photolysis (90 K, glassy ethanol) of **80**, on the other hand, resulted in the formation of triplet nitrene ^{3}**81**, which mostly dimerized to the azo dimer **83** upon thawing of the matrix. If ^{3}**81** was subjected to long-wavelength irradiation, high yields of the dihydroquinoxaline **85** were formed by hydrogen abstraction of the pyrazole methyl group followed by radical recombination. Introduction of an additional dimethylamino substituent *para* to the nitrene completely changed the photochemistry of the pyrazolyl-substituted nitrene.[93] Irradiation of azide **86** (ethanol, 295 K) yielded reaction products typical of a triplet nitrene, such as the aniline **87** or azo compound **88**, and no heteropentalene **89**. In the presence of diethylamine as external quencher, no azepine derivative was isolated. Instead, the triaminophenylpyrazole **91** was formed. The formation of **91** can be rationalized only by trapping of an intermediary bicyclic azirine **90** by diethylamine (see bottom part of Scheme 22). A nitro group *para* to the nitrene center was also found to supress didehydroazepine formation, while slightly increasing nitrene reactivity in intermolecular reactions.[94]

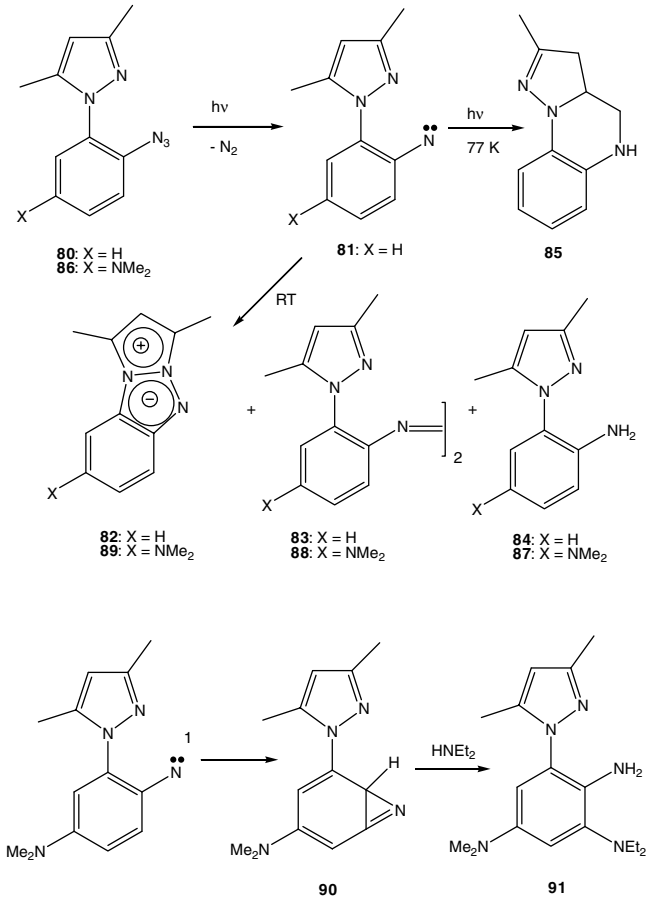

SCHEME 22

44.6 Reactions Typical of Triplet Aryl Nitrenes

Triplet nitrenes generally undergo reactions typical of free radicals or triplet carbenes, such as hydrogen (or heteroatom-) abstraction or dimerization.[56] Dimerization leads to azo dyes and is most frequently observed if an aryl azide is photolyzed at liquid nitrogen temperature and if the glassy matrix is then thawed. Hydrogen abstraction from the solvent is another reaction typical of triplet nitrenes. Both triplet pentafluorophenyl nitrene ^{3}**22** and triplet perfluoro-2-naphthyl nitrene are able to abstract a hydrogen atom from *n*-hexane or *n*-heptane, if the frozen solvent is thawed.[95] For triplet 4-nitrophenylnitrene **92** and triplet 4-nitreno-4′-nitro-*trans*-stilbene, the formation of the corresponding aniline derivatives was shown to occur in a two-step process via an aminyl radical, such as **93**.[71,96]

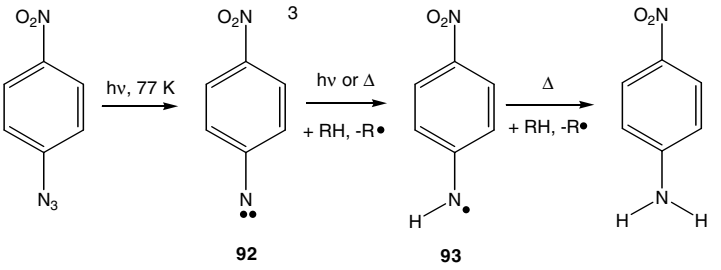

SCHEME 23

Triplet aryl nitrenes can in principle react with triplet oxygen. The reaction proceeds via nitroso *O*-oxides, which then isomerize to nitro compounds, possibly via azadioxiranes. Experimental evidence for this reaction sequence was obtained with a series of *para*-substituted derivatives of phenyl azide.[97] Thus, photolysis of azide **94**, matrix-isolated at 77 K in glassy MTHF saturated with oxygen, yielded triplet nitrene **95**. Warming the glassy matrix to 95 K led to oxidation of triplet nitrene **95** to nitroso *O*-oxide **96**. Irradiation of nitroso *O*-oxide **96** with high-intensity light then resulted in formation of intermediate **97** which decayed thermally at 77 K ($t_{1/2} \sim 4$ minutes) to yield nitro compound **98**.

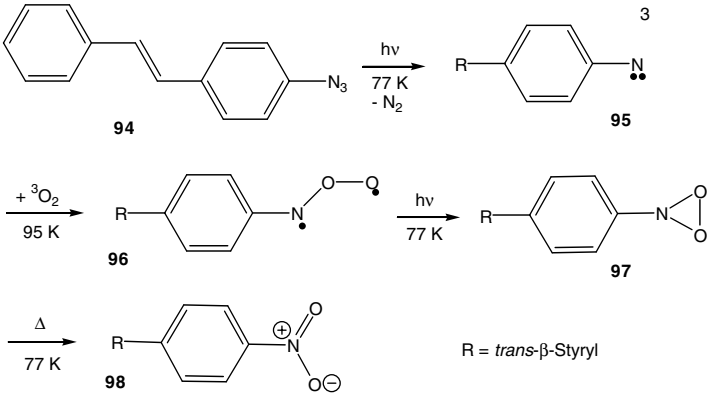

SCHEME 24

Triplet nitrene oxidation appears to work best if it is performed by thawing an organic glass (77 K) containing both the triplet nitrene and triplet oxygen. At ambient temperature, triplet nitrene formation is inefficient for most nitrenes. At temperatures of matrix isolation (10 K), triplet nitrenes are formed efficiently. Under these conditions, however, the reaction with oxygen is obviously hindered by a barrier. To the best of the author's knowledge it has never been observed in a noble gas matrix.

44.7 Heteroaryl Azides

Heteroaromatic azides often show photochemistry that is very similar to the photochemistry of simple homoaromatic azides. Ring expansion to cyclic ketenimines is observed, if the photolysis is performed at ambient temperature, and triplet nitrenes are formed upon low-temperature irradiation. If a nitrogen atom is placed adjacent to the nitrene center, such as in 2-pyridylnitrene **100**, addition generally takes place away from the nitrogen atom. In the case of the photolysis (or pyrolysis) of the 2-azidopyridine **99**, the reaction leads to the cyclic carbodiimide **101**.[98–100] A complication arises from the fact that derivatives of 2-azidopyridine and related heterocycles frequently undergo a thermal isomerization to tetrazolopyridines, which also undergo photochemical dediazotation, albeit with a low quantum yield.[98,99]

As with simple aryl nitrenes, *ortho* halogen-substitution (such as in tetrafluoro-4-pyridylnitrene) suppresses the ring-expansion chemistry.[101]

Ring-expansion is also disfavored if both *ortho* positions are occupied by nitrogen atoms, such as in 2-pyrimidyl nitrene. Laser flash photolysis of 2-azidopyrimidine **102** (CH_2Cl_2, 295 K) allowed for the detection of singlet 2-pyrimidinylnitrene ^{1}**103**, which decayed exclusively by intersystem crossing ($\tau = 13$ ns, $k_{ISC} = (8 \pm 2) \times 10^7\ s^{-1}$) to the triplet nitrene ^{3}**103**.[102] The cyclic carbodiimide **104** was only obtained upon extended irradiation of matrix-isolated (Ar, 14 K) triplet nitrene ^{3}**103**.[102]

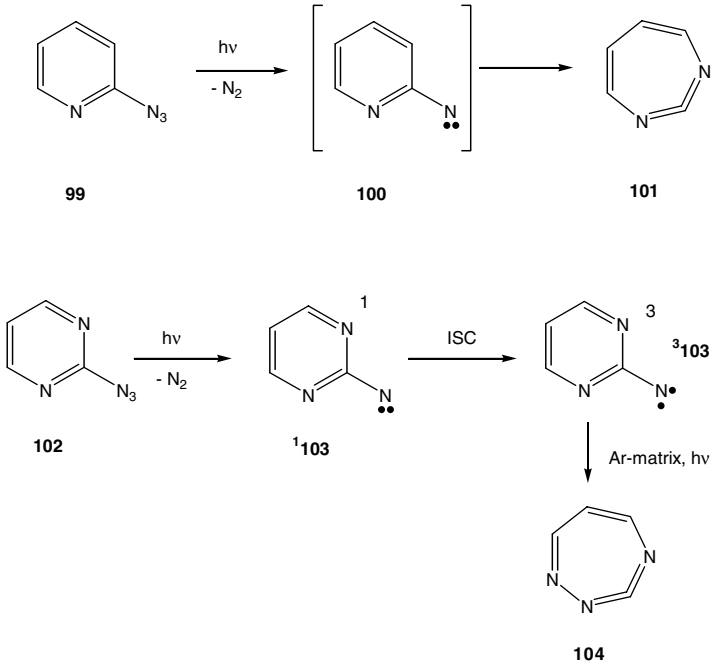

SCHEME 25

In the series of azido-1,3,5-triazines, a similar trend was observed. Photolysis of azidotriazines such as **105** yielded only typical nitrene-derived products, whereas products indicative of dehydrotetrazepine formation were not observed.[103–106] In acetonitrile solution, an interesting cycloaddition of the nitrene **106** to the solvent was observed that led to pyrazolotriazine **107**, which subsequently rearranged further.[107]

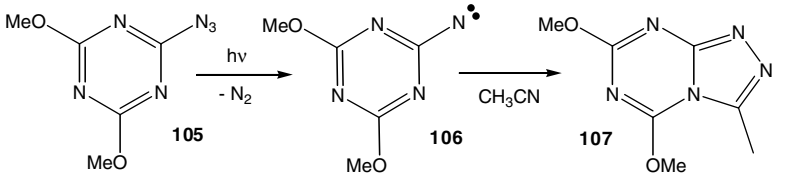

SCHEME 26

The photochemistry of azidotriazines depends on substitution. Photolysis of 2-azido-4,6-dichloro-1,3,5-triazine **108**, matrix-isolated in Ar at 10 K, led to formation of both triplet nitrene **109** and didehydrotetrazepine **110**, which could be interconverted photochemically. Extended photolysis, however, resulted in the formation of an unidentified ring-opened product.[108] Laser flash photolysis experiments indicate that both **109** and **110** are formed at ambient temperature.[109]

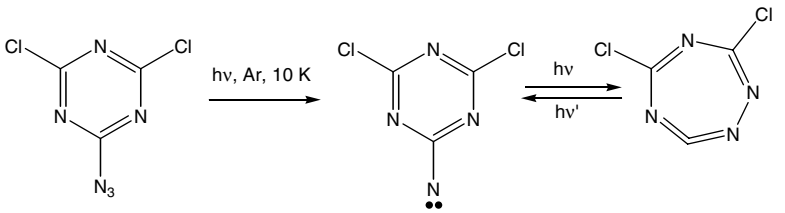

108 **109** **110**

SCHEME 27

44.8 High-Spin Nitrenes

Photolysis of azides that contain more than one azido functionality will in most cases lead to di- or oligonitrenes. These reactive species are formed by stepwise dediazotation reactions. They have recently attracted considerable attention due to the potential use of high-spin intermediates as "organic magnets". Just as in polycarbene chemistry,[110] *para*-phenylene linkage of two nitrene centers generally leads to singlet diradicals,[111,112] while a *meta*-phenylene linkage results in quintet dinitrenes. The different ground-state spin multiplicities can be explained in terms of spin polarization. For simple diradicals, this is demonstrated in the following scheme.

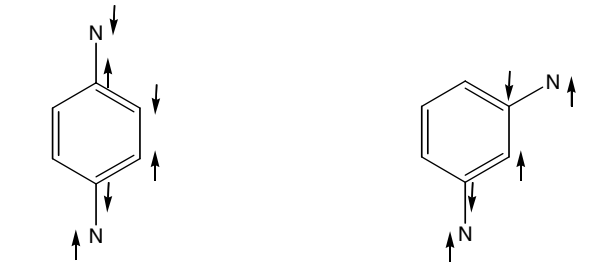

para-Phenylene-bridged:
Low-Spin

meta-Phenylene-bridged:
High-Spin

SCHEME 28

If three nitrene moieties are placed in the 1,3,5-position in an aromatic system, the resulting trisnitrene should have a septet ground state as was indeed observed in several cases.[101] Spin polarization predicts a quartet ground state for the phenylnitrene-4-yl radical. This was confirmed for 2,3,5,6-tetrafluorophenylnitrene-4-yl **113**, which could be prepared by stepwise photodediazotation and photodeiodination of matrix-isolated 4-iodo-2,3,5,6-tetrafluorophenyl azide **111**.[113]

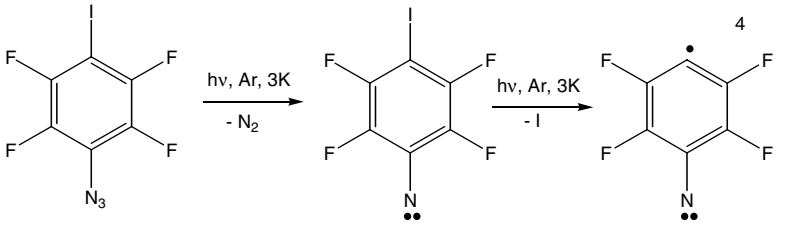

111 **112** **113**

SCHEME 29

44.9 Aryl Azides in Acidic Media: Photogeneration of Nitrenium Ions

Photolysis of aryl azides in acidic media leads to rapid protonation of the initially formed singlet nitrenes with formation of singlet nitrenium ions. Nitrenium ions are nitrogen-centered diradicals that are formally isoelectronic with carbenes. They have been in the focus of research for their role as "ultimate carcinogen" in the metabolism of certain aromatic amines.[114–117] Nitrenium ions can also be made by photolysis of 2,2-benzisoxazolium (anthranilium) salts[118–124] or by irradiation of *N*-aminopyridinium salts.[122,123,125]

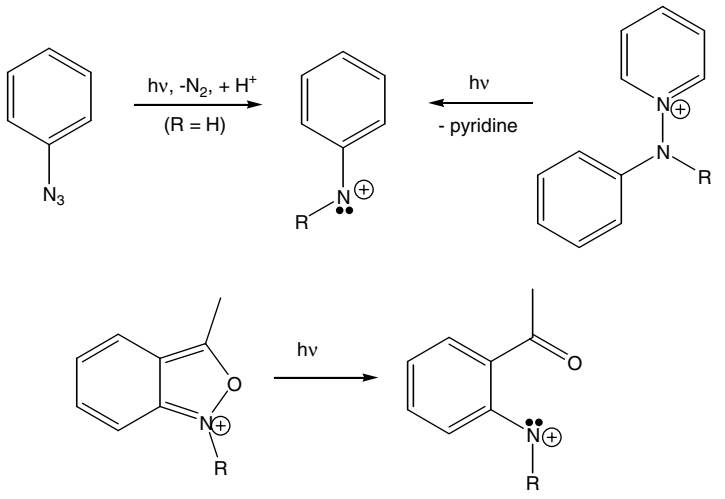

SCHEME 30

The parent nitrenium ion, NH_2^+, was shown both experimentally[126] and by *ab initio* calculations[127,128] to have a triplet ground state. In aryl nitrenium ions, on the other hand, this ordering of states is reversed, and the ground state is a singlet, as was shown in a number of theoretical studies.[129–133] In the phenylnitrenium ion, the singlet state is strongly favored over the triplet state because the benzene ring can act more efficiently as a π-donor if it interacts with an empty nitrogen p-orbital (singlet state) rather than with a half-filled nitrogen p-orbital (as in the triplet state).[132] Due to the very electron-deficient nature of the nitrenium N-atom, this delocalization of positive charge is very important. In fact, the singlet phenylnitrenium ion can be described as an imino-functionalized cyclohexadienyl cation. If the aryl substituent is functionalized with strong π-acceptor substituents (e.g., nitro or a ring nitrogen atom), the nitrenium ion may also have a triplet ground state.[121,134]

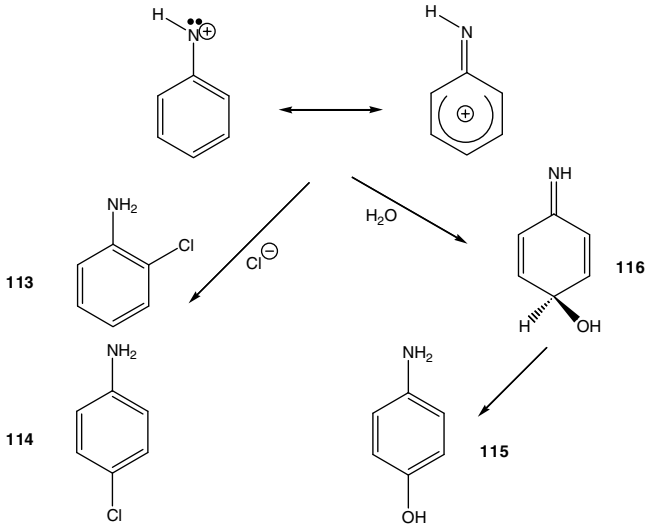

SCHEME 31

The products isolated upon photolysis of phenyl azide **10** in acidic medium agree with this description. At low pH (aq. HCl), *o*- and *p*-chloroaniline **113** and **114** and 4-aminophenol **115** were among the main products.[135] All of these products can be rationalized in terms of cyclohexadienyl-cation-type reactivity of the phenylnitrenium ion. Aminophenol **115** is formed via the iminocyclohexadienol **116**, which was observed by time-resolved spectroscopy.[135]

If aryl azides are irradiated in acidic medium in the presence of arenes, derivatives of diphenylamine are formed.[119] For the diphenylnitrenium ion, σ-complexes with benzene have been detected by laser flash photolysis.[136] In reactions with alkenes, nitrenium ions react more rapidly with electron-deficient olefins. Rate constants for the reaction of diphenylnitrenium with electron-rich olefins such as cyclohexanone trimethylsilyl enol ether are of the order of 1.9×10^9 M^{-1} s^{-1}.[123] In the reaction of 2-fluorenylnitrenium with 2′-deoxyguanosine, reaction at C8 of the guanine base takes place.[137]

Photolysis of azides in acidic media can only yield monosubstituted nitrenium ions. In most cases, the protonation of singlet nitrenes is a highly efficient reaction. Thus, the rate of protonation of singlet 2,4,6-tribromophenylnitrene by perchloric acid in aqueous acetonitrile has been determined as $k_{H+} = (3.5 + 0.1) \times 10^9$ M^{-1} s^{-1}, which is close to the diffusion-controlled limit.[53] In the case of the 4-biphenylyl- and 2-fluorenylnitrenium ions, nitrene protonation in CH_3CN/H_2O also occurred on the picosecond time scale.[135,138] Some nitrenium ions may undergo follow-up deprotonation reactions. The nitrenium ion **117**, which is derived from the strong carcinogen *N*-acetylbenzidine, exists at physiological pHs as a mixture of the reactive **117** and the long-lived conjugate *bis*-imine base **118**.[139]

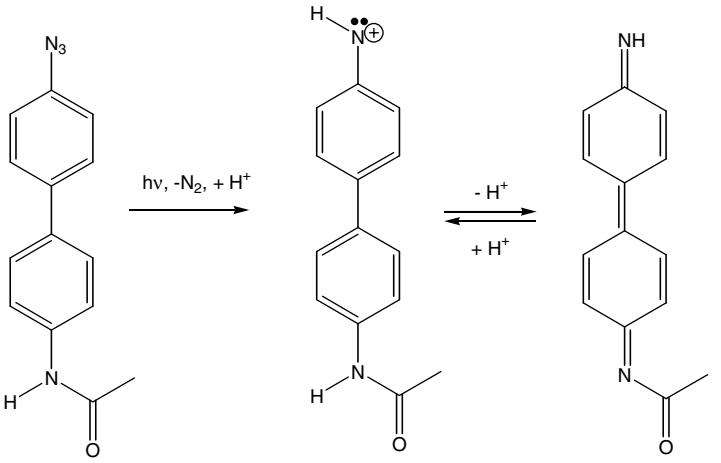

SCHEME 32

Recent advances in time-resolved vibrational spectroscopy (time-resolved infrared [TR-IR] and time-resolved resonance raman spectroscopy) have provided further evidence for the description of aryl nitrenium ions as imino-cyclohexadienyl cations. The C–N stretching frequency in singlet diphenylnitrenium ion (generated by LFP of a *N*-diphenylaminopyridinium salt in acetonitrile) was measured by time-resolved infrared spectroscopy to be $\tilde{\nu}$ = 1392 cm^{-1}, which is significantly higher than the $\tilde{\nu}$ = 1320 cm^{-1} of diphenylamine.[122] In the UV/Vis, the diphenylnitrenium ion shows a λ_{max} = 425 and 660 nm, with a lifetime τ = 1.5 μs.[125]

Similar conclusions were reached for *N*-aryl-*N*-methylnitrenium ions, which were characterized by TR-IR spectroscopy[140] as well as for the 2-fluorenylnitrenium ion and the 4-biphenylylnitrenium ion, which were generated by photolysis of the corresponding azides in water/acetonitrile mixtures and characterized by time-resolved resonance raman spectroscopy.[141,142] Overall, nitrenium ion chemistry constitutes a very active field of research, and further exciting discoveries can be anticipated.

References

1. Tsuchiya, T., Nitrene formation by photoextrusion of nitrogen from azides, in *CRC Handbook of Photochemistry,* Horspool, W. M. and Song, P.-S., Eds., CRC Press, Boca Raton, FL, 1995, chap. 77.
2. Horner, L. and Christmann, A., Nitrenes, *Angew. Chem. Int. Ed. Engl.,* 2, 599, 1963; *Angew. Chem.*, 75, 707, 1963.
3. Abramovitch, R. A. and Davis, B. A., Preparation and properties of imido intermediates (imidogens), *Chem. Rev.*, 64, 149, 1964.
4. Nitrenes, in *Reactive Intermediates in Organic Chemistry*, Lwowski, W., Ed., Interscience Publishers, New York, 1970.
5. L'Abbé, G., Decomposition and addition reactions of organic azides, *Chem. Rev.*, 69, 345, 1969.
6. Lwowski, W., Nitrenes and the decomposition of carbonyl azides, *Angew. Chem. Int. Ed. Engl.,* 6, 897, 1967; *Angew. Chem.*, 79, 922, 1967.
7. Scriven, E. F. and Turnbull, K., Azides: their preparation and synthetic uses, *Chem. Rev.*, 88, 297, 1988.
8. Smalley, R. K. and Suschitzky, H., Reactive intermediates in organic synthesis. Part III: Nitrenes, *Chem. Ind.*, 1338, 1970.
9. Reiser, A. and Wagner, H. M., Photochemistry of the azido group, in *The Chemistry of Functional Groups*, Vol. *The Chemistry of the Azido Group*, Patai, S., Ed., Interscience Publishers, London, 1971, chap. 8.

10. Moor, H. W. and Goldish, D. M., Vinyl, aryl, and acyl azides, in *The Chemistry of Functional Groups,* Suppl. D: *The Chemistry of Halides, Pseudo-Halides, and Azides*, Part 1, Patai, S. and Rappoport, Z., Eds., John Wiley & Sons, New York, 1983, chap. 8.
11. Wentrup, C., Carbenes and nitrenes in heterocyclic chemistry, *Adv Heterocycl. Chem.*, 28, 231, 1981.
12. Reid, S. T., The photochemistry of nitrogen-containing heterocycles, *Adv. Heterocycl. Chem.*, 30, 239, 1982.
13. Iddon, B., Meth-Cohn, O., Scriven, E., Suschitzky, H., and Gallagher, P. T., Developments in arylnitrene chemistry: syntheses and mechanisms, *Angew. Chem. Int. Ed. Engl.,* 18, 900, 1979; *Angew. Chem.*, 91, 965, 1979.
14. Schuster, G. B. and Platz, M., Photochemistry of phenyl azide, *Adv. Phototochem.*, 17, 69, 1992.
15. Smith, P. A. S., Aryl and heteroaryl azides and nitrenes, in *Azides and Nitrenes, Reactivity and Utility*, Scriven, E. F., Ed., Academic Press, Orlando, FL, 1984.
16. Platz, M. S., Comparison of phenylcarbene and phenylnitrene, *Acc. Chem. Res.* 28, 487, 1995.
17. Poe, R., Schnapp, K., Young, M. T., Grayzar, J., and Platz, M. S., Chemistry and kinetics of singlet (pentafluorophenyl)nitrene, *J. Am. Chem. Soc.*, 114, 5054, 1992.
18. Kemnitz, C. R., Ellison, G. B., Karney, W. L., and Borden, W. T., CASSCF and CASPT2 *ab initio* electronic structure calculations find singlet methylnitrene is an energy minimum, *J. Am. Chem. Soc.*, 122, 1098, 2000.
19. Gritsan, N. P., Likhotvorik, I., Zhu, Z., and Platz, M. S., Observation of perfluoromethylnitrene in cryogenic matrixes, *J. Phys. Chem. A*, 105, 3039, 2001.
20. Mandel, S. M., Krause Bauer, J. A., and Gudmundsdóttir, A. D., Photolysis of α-azidoacetophenones: trapping of triplet alkyl nitrenes in solution, *Org. Lett.*, 3, 523, 2001.
21. Fowler, F. F., Synthesis and reactions of 1-azirines, *Adv. Heterocyclic. Chem.*, 13, 45, 1971.
22. Banert, K., Synthesis of new bi-2*H*-azirin-3-yl compounds from diazides, *Tetrahedron Lett.*, 26, 5261, 1985.
23. Ciabattoni, J. and Cabell, M., Jr., 3-Chloro-1-azirines: photochemical formation and thermal isomerization, *J. Am. Chem. Soc.*, 93, 1482, 1971.
24. Finnerty, J., Mitschke, U., and Wentrup, C., Linear Ketenimines. Variable structures of *C*,*C*-dicyanoketenimines and *C*,*C*-bis-sulfonylketenimines, *J. Org. Chem.*, 67, 1084, 2002.
25. Tamura, Y., Yoshimura, Y., Nishimura, T., Kato, S., and Kita, Y., Photolysis and thermolysis of 3-azido-2-cyclohexen-1-ones, *Tetrahedron Lett.*, 5, 351, 1973.
26. Sato, S., Azirines. IV. The photolysis of β-azidovinyl ketones, *Bull. Chem. Soc. Jpn.*, 41, 2524, 1968.
27. Eibler, E. and Sauer, J., A contribution to isocyanate formation in the photolysis of acyl azides, *Tetrahedron Lett.*, 30, 2569, 1974.
28. Lwowski, W., de Mauriac, R. A., Thompson, M., Wilde, R. E. and Chen, S.-Y., Curtius and Lossen rearrangements. III. Photolysis of certain carbamoyl azides, *J. Org. Chem.*, 40, 2608, 1975.
29. Alewood, P. F., Kazmaier, P. M., and Rauk, A., Electronic structure of carbonyl nitrenes: mechanism of insertion and abstraction reactions, *J. Am. Chem. Soc.*, 95, 5466, 1973.
30. Harrison, J. F. and Shalhoub, G., The electronic structure of reactive intermediates: carbonylnitrenes., *J. Am. Chem. Soc.*, 97, 4172, 1975.
31. Kozlowska-Gramsz, E. and Descotes, G., Photochemical addition of alkyl azidoformiates on 2-methylene-tetrahydropyran and 2-methoxy-5,6-dihydro-γ-pyran, *J. Heterocyclic. Chem.*, 20, 671, 1983.
32. Alewood, P. F., Benn, M., and Reinfried, R., Cyclizations of azidoformiates to tetrahydro-1,3-oxazin-2-ones and oxazolidin-2-ones, *Can. J. Chem.*, 52, 4083, 1974.
33. Wright, J. J. and Morton, J. B., Thermolysis and photolysis of 3β-lanostenyl azidocarbonate: functionalization of the 4α-methyl group, *J. Chem. Soc., Chem. Commun.*, 668, 1976.
34. Averdung, J., Mattay, J., Jacobi, D., and Abraham, W., Addition of photochemically generated acylnitrenes to C_{60}. synthesis of fulleroaziridines and thermal rearrangement to fullerooxazoles, *Tetrahedron*, 51, 2543, 1995.

35. Holzinger, M., Vostrowsky, O., Hirsch, A., Hennrich, F., Kappes, M., Weiss, R., and Jellen, F., Sidewall functionalization of carbon nanotubes, *Angew. Chem. Int. Ed. Engl.,* 40, 4016, 2001; *Angew. Chem.*, 113, 4132, 2001.
36. Huisgen, R., Vossius, D., and Appl, M., The thermolysis of phenylazide in primary amines: the consitution of dibenzamil, *Chem. Ber.*, 91, 1, 1958.
37. Huisgen, R. and Appl, M., The mechanism of ring-expansion during the decay of phenylazide in aniline, *Chem. Ber.*, 91, 12, 1958.
38. von E. Doering, W. and Odum, R. A., Ring enlargement in the photolysis of phenyl azide, *Tetrahedron*, 22, 81, 1966.
39. Sundberg, R. J., Suter, S. R., and Brenner, M., Photolysis of *ortho*-substituted aryl azides in diethylamine. formation and autoxidation of 2-diethylamino-1*H*-azepine intermediates, *J. Am. Chem. Soc.*, 94, 513, 1972.
40. DeGraff, B. A., Gillespie, D. W., and Sundberg, R. J., Phenyl nitrene: a flash photolytic investigation of the reaction with secondary amines, *J. Am. Chem. Soc.*, 96, 7491, 1974.
41. Leyva, E., Platz, M. S., Persy, G., and Wirz, J., Photochemistry of phenyl azide: the role of singlet and triplet phenylnitrene as transient intermediates, *J. Am. Chem. Soc.*, 108, 3783, 1986.
42. Li, Y.-Z., Kirby, J. P., George, M. W., Poliakoff, M., and Schuster, G. B., 1,2-Didehydroazepines from the photolysis of substituted aryl azides: analysis of their chemical and physical properties by time-resolved spectroscopic methods, *J. Am. Chem. Soc.*, 110, 8092, 1988.
43. Dunkin, I. R., El Ayeb, A., and Lynch, M. A., A synthetic approach to azepin-4-ones exploiting azide photolysis in low-temperature matrices, *J. Chem. Soc., Chem. Commun.*, 1695, 1994.
44. Travers, M. J., Cowles, D. C., Clifford, E. P., and Ellison, G. B., Photoelectron spectroscopy of the phenylnitrene anion, *J. Am. Chem. Soc.*, 114, 8699, 1992.
45. McDonald, R. N. and Davidson, S. J., Electron photodetachment of the phenylnitrene anion radical: EA, ΔH°_{f}, and the singlet-triplet splitting for phenylnitrene, *J. Am. Chem. Soc.*, 115, 10857, 1993.
46. Karney, W. L. and Borden, W. T., *Ab initio* study of the ring expansion of phenylnitrene and comparison with the ring expansion of phenylcarbene, *J. Am. Chem. Soc.*, 119, 1378, 1997.
47. Kim, S.-J., Hamilton, T. P., and Schaefer, H. F., III., Phenylnitrene: energetics, vibrational frequencies, and molecular structures, *J. Am. Chem. Soc.*, 114, 5349, 1992.
48. Hrovat, D. A., Waali, E. E., and Borden, W. T., *Ab initio* calculations of the singlet-triplet energy difference in phenylnitrene, *J. Am. Chem. Soc.*, 114, 8698, 1992.
49. Liu, R. and Zhou, X., Structures of PhX (X = O and N): importance of polarization functions in the basis set, *Chem. Phys. Lett.*, 207, 185, 1993.
50. Castell, O., García, V. M., Bo, C., and Caballol, R., Relative stability of the $^3A_2$, $^1A_2$, and $^1A_1$ states of phenylnitrene: a difference-dedicated configuration interaction calculation, *J. Comput. Chem.*, 17, 42, 1996.
51. Gritsan, N. P., Zhu, Z., Hadad, C. M., and Platz, M. S., Laser flash photolysis and computational study of singlet phenylnitrene, *J. Am. Chem. Soc.*, 121, 1202, 1999.
52. Gritsan, N. P., Yuzawa, T., and Platz, M. S., Direct observation of singlet phenylnitrene and measurement of its rate of rearrangement, *J. Am. Chem. Soc.*, 119, 5059, 1997.
53. Born, R., Burda, C., Senn, P., and Wirz, J., Transient absorption spectra and reaction kinetics of singlet phenylnitrene and its 2,4,6-tribromo derivative in solution, *J. Am. Chem. Soc.*, 119, 5061, 1997.
54. Schrock, A. K. and Schuster, G. B., Photochemistry of phenyl azide: chemical properties of the transient intermediates, *J. Am. Chem. Soc.*, 106, 5228, 1984.
55. Hayes, J. C. and Sheridan, R. S., Infrared spectrum of triplet phenylnitrene: on the origin of didehydroazepine in low-temperature matrices, *J. Am. Chem. Soc.*, 112, 5879, 1990.
56. Bucher, G., Scaiano, J. C., Sinta, R., Barclay, G., and Cameron, J., Laser flash photolysis of carbamates derived from 9-fluorenone oxime, *J. Am. Chem. Soc.*, 117, 3848, 1995.
57. Karney, W. L. and Borden, W. T., Why does *ortho*-fluorine substitution raise the barrier to ring expansion of phenylnitrene?, *J. Am. Chem. Soc.*, 119, 3347, 1997.

58. Gritsan, N. P., Gudmundsdóttir, A. D., Tigelaar, D., and Platz, M. S., Laser flash photolysis study of methyl derivatives of phenyl azide, *J. Phys. Chem. A*, 103, 3458, 1999.
59. Gritsan, N. P., Gudmundsdóttir, A. D., Tigelaar, D., Zhu, Z., Karney, W. L., Hadad, C. M., and Platz, M. S., A laser flash photolysis and quantum chemical study of the fluorinated derivatives of singlet phenylnitrene, *J. Am. Chem. Soc.*, 123, 1951, 2001.
60. Platz, M. S., Tsao, M.-L., James, T., and Gritsan, N. P., Laser flash photolysis study of ortho biphenylnitrene and related species, in *Int. Symp. on Reactive Intermediates and Unusual Molecules*, Nara, 2001.
61. Dunkin, I. R. and Thomson, P. C. P., Pentafluorophenyl nitrene: a matrix isolated aryl nitrene that does not undergo ring expansion, *J. Chem. Soc., Chem. Commun.*, 1192, 1982.
62. Morawietz, J. and Sander, W., Photochemistry of fluorinated phenyl nitrenes: matrix isolation of fluorinated azirines, *J. Org. Chem.*, 61, 4351, 1996.
63. Young, M. J. T. and Platz, M. S., Mechanistic analysis of the reactions of (pentafluorophenyl)nitrene in alkanes, *J. Org. Chem.*, 56, 6403, 1991.
64. Gritsan, N. P., Zhai, H. B., Yuzawa, T., Karweik, D., Brooke, J., and Platz, M. S., Spectroscopy and kinetics of singlet perfluoro-4-biphenylnitrene and singlet perfluorophenylnitrene, *J. Phys. Chem. A*, 101, 2833, 1997.
65. Marcinek, A., Platz, M. S., Chan, S., Floresca, R., Rajagopalan, K., Golinski, M., and Watt, D., Unusually long lifetimes of the singlet nitrenes derived from 4-azido-2,3,5,6-tetrafluorobenzamides, *J. Phys. Chem.*, 98, 412, 1994.
66. Gritsan, N. P., Tigelaar, D., and Platz, M. S., A laser flash photolysis study of some simple para-substituted derivatives of singlet phenyl nitrene, *J. Phys. Chem. A*, 103, 4465, 1999.
67. Gritsan, N. P., Likhotvorik, I., Tsao, M.-L., Celebi, N., Platz, M. S., Karney, W. L., Kemnitz, C. R., and Borden, W. T., Ring-expansion reaction of cyano-substituted singlet phenyl nitrenes: theoretical predictions and kinetic results from laser flash photolysis and chemical trapping experiments, *J. Am. Chem. Soc.*, 123, 1425, 2001.
68. Kobayashi, T., Ohtani, H., Suzuki, K., and Yamaoka, T., Picosecond and nanosecond laser photolyses of *p*-(dimethylamino)phenyl azide in solution, *J. Phys. Chem.*, 89, 776, 1985.
69. Murov, S. L., Carmichael, I., and Hug, G. L., *Handbook of Photochemistry*, Marcel Dekker, New York, 1993.
70. Liang, T.-Y. and Schuster, G. B., Photochemistry of 3- and 4-nitrophenyl azides: detection and characterization of reactive intermediates, *J. Am. Chem. Soc.*, 109, 7803, 1987.
71. Harder, T., Stößer, R., Wessig, P., and Bendig, J., Low-temperature photochemistry of nitro-substituted aromatic azides; subsequent reactions of intermediates, *J. Photochem. Photobiol. A: Chem.*, 103, 105, 1997.
72. Sumitani, M., Nagakura, S., and Yoshihara, K., The primary process of the photochemical formation of 1-nitrenopyrene, *Bull. Chem. Soc. Jpn.*, 49, 2995, 1976.
73. Schrock, A. K. and Schuster, G. B., Photochemistry of naphthyl and pyrenyl azides: chemical properties of the transient intermediates probed by laser spectroscopy, *J. Am. Chem. Soc.*, 106, 5234, 1984.
74. Leyva, E. and Platz, M. S., The temperature-dependent photochemistry of 1-naphthyl azide, *Tetrahedron Lett.*, 28, 11, 1987.
75. Dunkin, I. R. and Thomson, P. C. P., Infrared evidence for tricyclic azirines and didehydrobenzazepines in the matrix photolysis of azidonaphthalenes, *J. Chem. Soc., Chem. Commun.*, 499, 1980.
76. Tomioka, H., Matsushita, T., Murata, S., and Koseki, S., Photochemistry of phenyl azides bearing 2-hydroxy and 2-amino groups studied by matrix-isolation spectroscopy: generation and characterization of reactive *o*-quinoid compounds, *Liebigs Ann.*, 1971, 1996.
77. Morawietz, J., Sander, W., and Träubel, M., Intramolecular hydrogen transfer in (2-aminophenyl)carbene and 2-tolylnitrene: matrix isolation of 6-methylene-2,4-cyclohexadien-1-imine, *J. Org. Chem.*, 60, 6368, 1995.

78. Bucher, G., Photochemical generation of iminoquinone methides by 1,4-hydrogen migration in derivatives of *o*-tolylnitrene, *Eur. J. Org. Chem.*, 2447, 2001.
79. Bucher, G., A laser flash photolysis study on 2-azido-*N,N*-diethylbenzylamine: the reactivity of iminoquinone methides in solution, *Eur. J. Org. Chem.*, 2463, 2001.
80. Murata, S., Sugawara, T., and Iwamura, H., Reactivities of rotameric *ap*- and *sp*-3,5-dimethyl-2-(9-fluorenyl)phenylnitrenes, *J. Am. Chem. Soc.*, 107, 6317, 1985.
81. Murata, S., Yoshidome, R., Satoh, Y., Kato, N., and Tomioka, H., Reactivities of nitrenes generated by photolysis of 2-(ω-phenylalkyl)phenyl azides, *J. Org. Chem.*, 60, 1428, 1995.
82. Smolinsky, G., Thermal reactions of substituted aryl azides: the nature of the azene intermediate, *J. Am. Chem. Soc.*, 83, 2489, 1961.
83. Bucher, G. and Wolff, J. J., unpublished results.
84. Lindley, J. M., McRobbie, I. M., Meth-Cohn, O., and Suschitzky, H., Competitive cyclisations of singlet and triplet nitrenes. Part 5. Mechanism of cyclisation of 2-nitrenobiphenyls and related systems, *J. Chem. Soc., Perkin Trans. 1*, 2194, 1977.
85. Hyatt, J. A. and Swenton, J. S., A facile synthesis of 9*H*-pyrimido[4,5*b*]indole via photolysis of 4-azido-5-phenylpyrimidine, *J. Heterocyclic. Chem.*, 9, 409, 1972.
86. Lindley, J. M., Meth-Cohn, O., and Suschitzky, H., Competitive cyclisations of singlet and triplet nitrenes. Part 6. The cyclisation of 2-azidophenyl thienyl sulphides, *J. Chem. Soc., Perkin Trans. 1*, 1198, 1978.
87. Murata, S. and Tomioka, H., Photochemistry of *o*-nitrophenylazide in matrices. The first direct spectroscopic observation of *o*-dinitrosobenzene, *Chem. Lett.*, 57, 1992.
88. Tomioka, H., Ichikawa, N., and Komatsu, K., Photochemistry of 2-(methoxycarbonyl)phenyl azide studied by matrix isolation spectroscopy. A new slippery energy surface for phenylnitrene, *J. Am. Chem. Soc.*, 115, 8621, 1993.
89. Tomioka, H., Ichikawa, N., and Komatsu, K., Photochemistry of (2-nitrophenyl)diazomethane studied by a matrix isolation technique: (nitrophenyl)carbene to (carboxylphenyl)nitrene rearrangement by successive reduction of nitro group with carbenic center, *J. Am. Chem. Soc.*, 114, 8045, 1992.
90. Purvis, R., Smalley, R. K., Strachan, W. A., and Suschitzky, H., The photolysis of *o*-azidobenzoic acid derivatives: a practicable synthesis of 2-alkoxy-3-alkoxycarbonyl-3*H*-azepines, *J. Chem. Soc., Perkin Trans. 1*, 191, 1978.
91. Albini, A., Bettinetti, G., and Minoli, G., Dimethylbenzopyrazolotetrazole vs. methylpyrazoloquinoxaline from 3,5-dimethyl-1-(2-nitrenophenyl)pyrazole, *Chem. Lett.*, 331, 1984.
92. Albini, A., Bettinetti, G., and Minoli, G., Reactivity of singlet and triplet arylnitrenes: temperature-dependent photodecomposition of 1-(2-azidophenyl)-3,5-dimethylpyrazole, *J. Am. Chem. Soc.*, 119, 7308, 1997.
93. Albini, A., Bettinetti, G., and Minoli, G., Photodecomposition of some *para*-substituted 2-pyrazolylphenyl azides. substituents affect the phenylnitrene S-T gap more than the barrier to ring expansion, *J. Am. Chem. Soc.*, 121, 3104, 1999.
94. Albini, A., Bettinetti, G., and Minoli, G., The effect of the *p*-nitro group on the chemistry of phenylnitrene. A study via intramolecular trapping, *J. Chem. Soc., Perkin Trans. 2*, 2803, 1999.
95. Kozankiewicz, B., Deperasinska, I., Zhai, H. B., Zhu, Z., and Platz, M. S., Spectroscopic and computational studies of perfluorophenyl and perfluoro-2-naphthyl nitrenes in Shpolskii matrixes, *J. Phys. Chem. A*, 103, 5003, 1999.
96. Dähne, L., Bendig, J., and Stösser, R., About the thermal and photochemical reactivity of triplet aryl nitrenes, *J. Prakt. Chem.*, 334, 707, 1992.
97. Harder, T., Wessig, P., Bendig, J., and Stösser, R., Photochemical reactions of nitroso oxides at low temperatures: the first experimental evidence for dioxaziridines, *J. Am. Chem. Soc.*, 121, 6580, 1999.
98. Wentrup, C. and Winter, H.-W., Isolation of diazacycloheptatetraenes from thermal nitrene-nitrene rearrangements, *J. Am. Chem. Soc.*, 102, 6159, 1980.

99. Evans, R. A. and Wentrup, C., Trifluoromethyl-substituted dehydroazepines and cyanopyrroles from azido-/tetrazolo-pyridines, *J. Chem. Soc., Chem. Commun.*, 1062, 1992.
100. Sawanishi, H. and Tsuchiya, T., Ring expansion of α-azidoazines: formation of the first examples of fully unsaturated monocyclic 1,3,5-triazepines, *J. Chem. Soc., Chem. Commun.*, 723, 1990.
101. Chapyshev, S. V., Kuhn, A., Wong, M. W., and Wentrup, C., Mono-, di-, and trinitrenes in the pyridine series, *J. Am. Chem. Soc.*, 122, 1572, 2000.
102. Cerro-Lopez, M., Gritsan, N. P., Zhu, Z., and Platz, M. S., A matrix isolation spectroscopy and laser-flash photolysis study of 2-pyrimidylnitrene, *J. Phys. Chem. A*, 104, 9681, 2000.
103. Kayama, R., Shizuka, H., Sekiguchi, S., and Matsui, K., Photochemical reactions of azido-1,3,5-triazines with hydrocarbons and ketones, *Bull. Chem. Soc. Jpn.,* 48, 3309, 1975.
104. Goka, T., Hashida, Y., and Matsui, K., Photolyses of azidotriazines in organic nitro compounds, *Bull. Chem. Soc. Jpn.,* 52, 1231, 1979.
105. Tamura, S., Imaizumi, H., Hashida, Y., and Matsui, K., Photochemical reactions of azidotriazines with aromatic substrates, *Bull. Chem. Soc. Jpn.,* 54, 301, 1981.
106. Goka, T., Shizuka, H., and Matsui, K., Photolyses of 2-azido-4-methoxy-6-(1-naphthyl)-1,3,5-triazines: reactions of singlet and triplet 1,3,5-triazinylnitrenes with solvents, *J. Org. Chem.*, 43, 1361, 1978.
107. Yamada, H., Shizuka, H., and Matsui, K., Photolysis of azido-1,3,5-triazine: photocycloaddition of singlet nitrene to nitriles, *J. Org. Chem.*, 40, 1351, 1975.
108. Bucher, G., Siegler, F., and Wolff, J. J., Photochemistry of 2-azido-4,6-dichloro-*s*-triazine: matrix isolation of a strained cyclic carbodiimde containing four nitrogen atoms in a seven-membered ring, *J. Chem. Soc., Chem. Commun.*, 2113, 1999.
109. Bucher, G., Siegler, F., and Wolff, J. J., unpublished results.
110. Sander, W., Bucher, G., and Wierlacher, S., Carbenes in matrixes: spectroscopy, structure, and reactivity, *Chem. Rev.*, 93, 1583, 1993.
111. Flock, M., Pierloot, C., Nguyen, M. T., and Vanquickenborne, L. G., *p*-Phenylbisphosphinidene and its carbene and nitrene analogues: an *ab initio* study, *J. Phys. Chem. A*, 104, 4022, 2000.
112. Nicolaides, A., Enyo, T., Miura, D., and Tomioka, H., *p*-Phenylenecarbenonitrene and its halogen derivatives: how does resonance interaction between a nitrene and a carbene center affect the overall electronic configuration?, *J. Am. Chem. Soc.*, 123, 2628, 2001.
113. Wenk, H.-H. and Sander, W., 2,3,5,6-Tetrafluorophenylnitrene-4-yl: a nitrene radical with a quartet ground state, *Angew. Chem. Int. Ed. Engl.,* 41, 2742, 2002.
114. Novak, M., Xu, L., and Wolf, R. A., Nitrenium ions from food-derived heterocyclic arylamine mutagens, *J. Am. Chem. Soc.*, 120, 1643, 1998.
115. Ramlall, P. and McClelland, R. A., Photochemical generation and lifetimes in water of *p*-aryloxy- and *p*-alkoxyphenylnitrenium ions, *J. Chem. Soc., Perkin Trans. 2*, 225, 1999.
116. Novak, M. and Kazerani, S., Characterization of the 2-(α-carbolinyl)nitrenium ion and its conjugate base produced during the decomposition of the model carcinogen 2-*N*-(pivaloyloxy)-2-amino-α-carboline in aqueous solution, *J. Am. Chem. Soc.*, 122, 3606, 2000.
117. Novak, M., Kahley, M. J., Lin, J., Kennedy, S. A., and James, T. G., Involvement of free nitrenium ions, ion pairs, and preassociation trapping in the reactions of ester derivatives of *N*-arylhydroxylamines and *N*-arylhydroxamic acids in aqueous solutions, *J. Org. Chem.*, 60, 8294, 1995.
118. Haley, N. F., Photochemistry of 2,1-benzisoxazolium (anthranilium) salts, *J. Org. Chem.*, 24, 3929, 1977.
119. Doppler, T., Schmid, H., and Hansen, H.-J., Photolysis of 3-methyl-2,1-benzisoxazol (3-methylanthranil) and 2-azido-acetophenone in the presence of sulfuric acid and of benzene derivatives, *Helv. Chim. Acta*, 62, 304, 1979.
120. Robbins, R. J., Laman, D. M., and Falvey, D. E., Substituent effects on the lifetimes and reactivities of arylnitrenium ions studied by laser flash photolysis and photothermal beam deflection, *J. Am. Chem. Soc.*, 118, 8127, 1996.

121. Srivastava, S. and Falvey, D. E., Reactions of a triplet arylnitrenium ion: laser flash photolysis and product studies of *N-tert*-butyl(2-acetyl-4-nitrophenyl)nitrenium ion, *J. Am. Chem. Soc.*, 117, 10186, 1995.
122. Srivastava, S., Toscano, J. P., Moran, R. J., and Falvey, D. E., Experimental confirmation of the iminocyclohexadienyl cation-like structure of arylnitrenium ions: time-resolved IR studies of diphenylnitrenium ion, *J. Am. Chem. Soc.*, 119, 11552, 1997.
123. Moran, R. J., Cramer, C., and Falvey, D. E., Reactions of diarylnitrenium ions with electron rich alkenes: an experimental and theoretical study, *J. Org. Chem.*, 62, 2742, 1997.
124. Robbins, R. J., Yang, L. L.-N., Anderson, G. B., and Falvey, D. E., Photogenerated arylnitrenium ions: reactions of *N-tert*-butyl (2-acetyl-4-substituted)phenyl nitrenium ions with alcohols and water studied by laser flash photolysis, *J. Am. Chem. Soc.*, 117, 6544, 1995.
125. Moran, R. J. and Falvey, D. E., Photogenerated diarylnitrenium ions: laser flash photolysis and product studies on diphenylnitrenium ion generated from photolysis of 1-(*N,N*-diphenylamino)pyridinium ions, *J. Am. Chem. Soc.*, 118, 8965, 1996.
126. Gibson, S. T., Greene, J. P., and Berkowitz, J., Photoionization of the amidogen radical, *J. Chem. Phys.*, 83, 4319, 1985.
127. Peyerimhoff, S. and Buenker, R. J., *Ab initio* MRD-CI potential surfaces for the low-lying states of the NH_2^+ molecular ion, *Chem. Phys.*, 42, 167, 1979.
128. Cramer, C. J., Dulles, F. J., Storer, J. W., and Worthington, S. E., Full valence complete active space SCF, multireference CI, and density functional calculations of $^1A_1$–$^3B_1$ singlet–triplet gaps for the valence-isoelectronic series BH_2^-, CH_2, NH_2^+, AlH_2^-, SiH_2, PH_2^+, GaH_2^-, GeH_2, and AsH_2^+, *Chem. Phys. Lett.*, 218, 387, 1994.
129. Ford, G. P. and Scribner, J. D., MNDO molecular orbital study of nitrenium ions derived from carcinogenic aromatic amines and amides, *J. Am. Chem. Soc.*, 103, 4281, 1981.
130. Li, Y., Abramovitch, R. A., and Houk, K., Relationship of conformational effects in phenyloxenium and phenylnitrenium cations to intramolecular reactivities: *ab initio* molecular structures, *J. Org. Chem.*, 54, 2911, 1989.
131. Glover, S. A. and Scott, A. P., MNDO properties of heteroatom and phenyl substituted nitrenium ions, *Tetrahedron*, 45, 1763, 1989.
132. Cramer, C. J., Dulles, F. J., and Falvey, D. E., *Ab initio* characterization of phenylnitrenium and phenylcarbene: remarkably different properties for isoelectronic species, *J. Am. Chem. Soc.*, 116, 9787, 1994.
133. Falvey, D. E. and Cramer, C. J., Aryl- and alkylnitrenium ions: singlet-triplet gaps via *ab initio* and semi-empirical calculations, *Tetrahedron Lett.*, 33, 1705, 1992.
134. Sullivan, M. B. and Cramer, C. J., Quantum chemical analysis of heteroarylnitrenium ions and mechanisms for their self-destruction, *J. Am. Chem. Soc.*, 122, 5588, 2000.
135. McClelland, R. A., Kahley, M. J., Davidse, P. A., and Hadzialic, G., Acid-base properties of arylnitrenium ions, *J. Am. Chem. Soc.*, 118, 4794, 1996.
136. McIlroy, S. and Falvey, D. E., Reactions of nitrenium ions with arenes: laser flash photolysis detection of a σ-complex between *N,N*-diphenylnitrenium ion and alkoxybenzenes, *J. Am. Chem. Soc.*, 123, 11329, 2001.
137. McClelland, R. A., Ahmad, A., Dicks, A. P., and Licence, V. E., Spectroscopic characterization of the initial C8 intermediate in the reaction of the 2-fluorenylnitrenium ion with 2′-deoxyguanosine, *J. Am. Chem. Soc.*, 121, 3303, 1999.
138. McClelland, R. A., Davidse, P. A., and Hadzialic, G., Electron deficient strong bases. generation of the 4-biphenylyl- and 2-fluorenylnitrenium, *J. Am. Chem. Soc.* 117, 4173, 1995.
139. Dicks, A. P., Ahmad, A. R., D'Sa, R., and McClelland, R. A., Tautomers and conjugate base of the nitrenium ion derived from *N*-acetylbenzidine, *J. Chem. Soc., Perkin Trans. 2*, 1, 1999.

140. Srivastava, S., Ruane, P. H., Toscano, J. P., Sullivan, M. B., Cramer, C. J., Chiapperino, D., Reed, E. C., and Falvey, D. E., Structures of reactive nitrenium ions: time-resolved laser flash photolysis and computational studies of substituted *N*-methyl-*N*-arylnitrenium ions, *J. Am. Chem. Soc.*, 122, 8271, 2000.
141. Zhu, P., Ong, S. Y., Chan, P. Y., Leung, K. H., and Phillips, D. L., Transient resonance raman and density functional theory investigation of the 2-fluorenylnitrenium ion, *J. Am. Chem. Soc.*, 123, 2645, 2001.
142. Zhu, P., Ong, S. Y., Chan, P. Y., Poon, Y. F., Leung, K. H., and Phillips, D. L., Transient-resonance Raman and density functional theory investigation of 4-biphenylylnitrenium, 2-fluorenylnitrenium, and diphenylnitrenium ions, *Chem.-Eur. J.*, 7, 4928, 2001.

45

Oxidation of Aromatics

Angelo Albini
University of Pavia

Maurizio Fagnoni
University of Pavia

45.1 Introduction

The stability of aromatic compounds limits the application of thermal oxidation methods, which generally require rather drastic conditions; therefore, the mild conditions of photosensitized reactions are particularly appealing for oxidizing these compounds. Depending on structure and conditions, the photoinduced oxidation of aromatic derivatives may takes place via each one of the three main mechanisms of photosensitizations which, as detailed elsewhere, differ in the reagent interacting with the sensitizer in the primary step, as indicated below.

In type I oxygenation, the *substrate* is activated by energy transfer or, more frequently, by hydrogen abstraction. The radical formed in this fashion is trapped by oxygen, and the reaction continues through a radical chain mechanism:[1,2]

$$\text{Sens}^* + \text{Ar–X–H} \rightarrow \text{SensH}^{\bullet} + \text{Ar–X}^{\bullet} \tag{45.1}$$

$$\text{Ar–X}^{\bullet} + \text{O}_2 \rightarrow \text{Ar–X–O}_2^{\bullet} \rightarrow \text{Products} \tag{45.2}$$

In type II oxygenation, *oxygen* is sensitized by electron transfer and the chemical reaction involves singlet oxygen.[2–5]

$$\text{Sens}^* + \text{O}_2 \rightarrow \text{Sens} + {}^1\text{O}_2 \tag{45.3}$$

$${}^1\text{O}_2 + \text{Ar–H} \rightarrow \text{Products} \tag{45.4}$$

In a third mechanism, sometimes referred to as type III photooxidation, the sensitizer interacts with the *substrate* via electron transfer generating the radical cation. In some cases, the radical anion of the sensitizer is oxidized back by oxygen, generating the *superoxide* anion, and the bonding step involves the radical cation and either the superoxide anion or, as is probably more often the case, molecular oxygen:[6,7]

$$\text{Sens}^* + \text{Ar–H} \rightarrow \text{Sens}^{-\bullet} + \text{Ar–H}^{+\bullet} \tag{45.5}$$

$$\text{Sens}^{-\bullet} + \text{O}_2 \rightarrow \text{Sens} + \text{O}_2^{-\bullet} \tag{45.6}$$

$$\text{Ar–H}^{+\bullet} + \text{O}_2^{-\bullet} \text{ or } \text{O}_2 \rightarrow \text{Products} \tag{45.7}$$

0-8493-1348-1/04/$0.00+$1.50

Variations of the last process are reactions in which oxygen traps an exciplex with some degree of charge transfer (and, by extension, a biradical or zwitterionic intermediate of some cycloaddition reaction), or the aromatic is in some way activated by complexation (e.g., on a solid surface). Charge-transfer complexes between an aromatic molecule and molecular oxygen also play a role.

In the following discussion, the reactions are presented according to the substrate undergoing the reaction, an aromatic hydrocarbon, an electron-donating substituted aromatic, a vinylarene, and an aromatic reacting at the side chain ring, and within each class according to the mechanism involved.

45.2 Oxidation of the Ring in Aromatic Hydrocarbons

Singlet Oxygen Reactions

The most important oxidations directly affecting the aromatic ring involve singlet oxygen. As detailed elsewhere in this book, this is a strong dienophile, the reactions of which are facilitated by the small dimensions and minimal steric hindrance. Therefore, $[\pi^4 + \pi^2]$-cycloaddition is expected to occur, with the limitation imposed by the aromaticity loss implied in the process. In fact, singlet oxygen addition takes place with a preparatively useful quantum yield with polynuclear aromatics (*viz.* the same substrates that undergo electrophilic addition in competition with substitution), whereas with simple benzene or naphthalene derivatives the process is slow or insignificant. The rate of reaction increases with the addition of further condensed rings (1,4-dimethylnaphthalene, 1.2×10^4; anthracene, 1.5×10^5; naphthacene, 1.2×10^7; pentacene, 4.2×10^9 mol^{-1} s^{-1} in benzene at 25°C), and both the rate and the regiochemistry of attack are rationalized by the Frontier Molecular Orbital approach.[8–11]

In the benzene series, a strong electron-donating substituent is required for the reaction with singlet oxygen (see next section). Within hydrocarbons, the reaction is significant only when polysubstitution induces some deviation from planarity and thus a loss of aromaticity. Thus, both penta- and hexamethylbenzene undergo $[\pi^4+\pi^2]$-cycloaddition; the first formed *endo*-peroxide (**1**; see Eq. (45.8)) is not isolated and adds a second molecule of singlet oxygen through an ene reaction:[12]

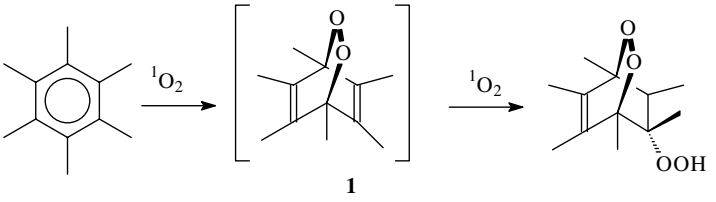

1 (45.8)

Endo-peroxides are isolated from the oxidation of cyclophanes such as compounds **2** and **3** (see E. (45.9)).[13,14] Oxygen addition to the central ring has been suggested to occur also with a benzo[3,4]cyclobuta[1,2-*b*]biphenylene; the final products result from the oxidative cleavage of that ring:[15]

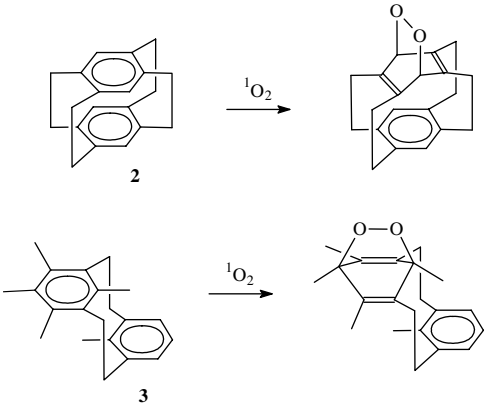

2 **3** (45.9)

1-Methylnaphthalene (but not the 2-substituted isomer) as well as all dimethyl- and polyalkylnaphthalenes undergo dye-sensitized oxidation to give endoperoxides. With asymmetric substrates, the preferred attack is at the more substituted ring or where there is an α substituent; a second (ene) addition follows also with these substrates when possible.[16–19] In a series of chiral 1-(1-naphthyl) alcohols, the corresponding endoperoxides are formed in high yields and with remarkable (8:2 to 9:1) diastereoselectivity. This has been rationalized in terms of steric and electronic control and extends to other 1-(1-X-ethyl) derivatives — for example, with X = Cl, Br, or $SiMe_3$ but not with X = OAc or $OSiMe_3$, nor to 1-*t*-butylnaphthalene. The selectivity is reversed when a methyl group is present in position 2 on the ring.[20–22]

Phenanthrene is not highly reactive with singlet oxygen, and the 1,4-dimethyl derivative adds across the substituted positions.[4] On the other hand, anthracene and most of its derivatives react readily and give the 9,10-endoperoxides (see, for example, **4**):[10,23]

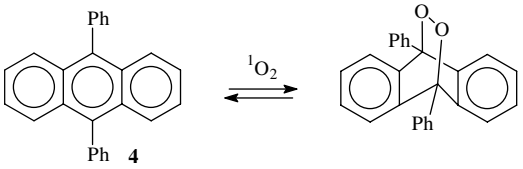

(45.10)

The photoreaction in the presence of oxygen has been long known, although initially it was confused with the likewise easy photodimerization of this compound[24] and only later has been recognized as a self-sensitized process involving singlet oxygen.[25] The ability of anthracene and other polycyclic aromatics to sensitize oxygen has been well documented and may involve both the singlet and triplet state.[26–30] When both the S_1–T_1 and the T_1–S_0 energy gaps are larger than the energy of the $^1\Delta_g$ state of oxygen (22.4 kcal mol^{-1}), two spin-allowed energy transfer steps occur and the limiting quantum yield of sensitization is 2:

$$Ar\text{–}H^{1*} + O_2 \rightarrow Ar\text{–}H^{3*} + {}^1O_2 \tag{45.11}$$

$$Ar\text{–}H^{3*} + O_2 \rightarrow Ar\text{–}H + {}^1O_2 \tag{45.12}$$

Again, the introduction of substituents affects the regiochemistry. Thus, substantial amounts of the 1,4-endoperoxide are formed along with the 9,10-isomer in the case of 1,4-dimethylanthracene,[31,32] and only the former regioisomer is obtained when electron-donating substituents such as alkoxy or dimethylamino are present at positions 1,[33,34] although the reaction remains at the *meso* position with electron-withdrawing substituents, as is the case with heterocoerdianthrones (see below)[35] or with substituents at position 2.[36] Naphthacene and pentacene and some of its derivatives, such as the extensively investigated rubrenes, are likewise oxidized through a self-sensitized process.[37–42] The 11-ring-containing diphenanthro[5,4,3-*abcd*-5′,4′,3′-*jklm*]perylene appears to give the endoperoxide across the central benzene ring, and this reverts back at room temperature.[43] By the use of confocal microscopy it has been possible to detect the formation of an endoperoxide (and then of a *bis*-endoperoxide through a second addition) on a single molecule of the 8-ring-containing terrylene in a *p*-terphenyl host crystal.[44]

Endoperoxides revert thermally to the aromatic molecule and singlet oxygen. This topic has been extensively investigated, and a variety of singlet oxygen sources active at various temperatures has been made available by means of suitable structural variations.[45] Although the topic is not strictly pertinent to this chapter, one should at least mention the water-soluble naphthalene endoperoxides that have been developed for generating singlet oxygen at the physiological temperature.[46–48] The retrocycloaddition also occurs photochemically through a process that at least in some cases has been demonstrated to be adiabatic.[49,50] The oxidation of heterocoerdianthrone (**5**; Eq. (45.13)) is reversible, and the system can be used as a reversible actinometer with oxygen addition in the visible and reversion in the UV range:[51]

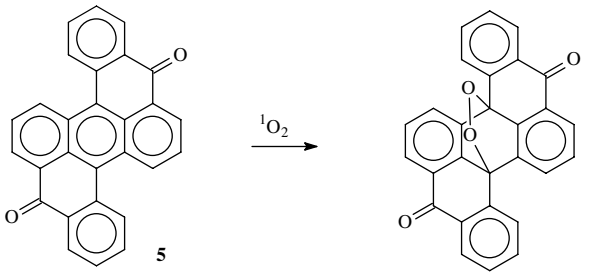

(45.13)

One of the approaches for the degradation of polycyclic aromatic hydrocarbons (PAHs) as pollutants is irradiation of the substrate absorbed onto a solid material, and here singlet oxygen seems to have an important role, besides other mechanisms that will be discussed further in this chapter. In the case of anthracene on a dry surface of silica or alumina, irradiation gives the dimer and the endoperoxide and further products arising from the latter compound;[52] likewise, acenaphthylene gives the dimers along with acenapthenedione and other products suggested to result from the addition of $^1O_2$.[53]

Non-Singlet Oxygen Reactions

Interest is increasing in the oxidation of aromatics through non-singlet oxygen mechanisms. The efficiency of the electron transfer mechanism (type III, above) by using a sensitizer such as 9,10-dicyanoanthracene is generally low due to the scarce reactivity of the aromatic radical cation in comparison to back electron transfer. The use of co-sensitizers such as biphenyl and terphenyls enhances the probability of the reaction and allows the oxidation of biphenyls to benzoic acids, of naphthalene to phthalic anhydride, and of phenanthrene to the same anhydride and biphenyldicarboxylic acid.[54] The same results can be obtained by adding magnesium perchlorate (omission of the salt causes the photohydrolysis of the sensitizer to anthraquinone).[55,56] With the same sensitizer, the oxidation of naphthalene gives different products when using different non-nucleophilic salts.[57] When the trityl cation (which does not form superoxide in the second step of the mechanism) is used as the sensitizer, only anthracene is oxidized to anthraquinone.[58] Perylene (**6**; Eq. (45.14)) is oxidized to two regioisomeric quinones in the presence of (hetero)aromatics containing water-soluble polymers, probably again through an electron transfer mechanism:[59]

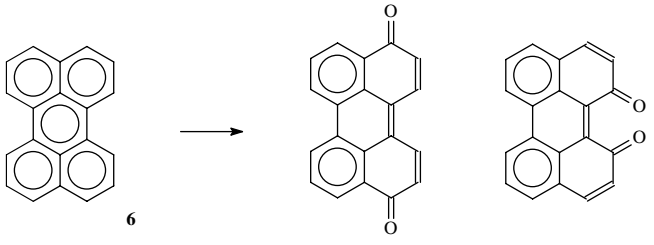

(45.14)

In the absence of added sensitizers, charge-transfer complexes between the aromatic substrate and molecular oxygen, which are revealed by a modification in the UV spectrum,[60,61] may react. A well-documented case is that of hexahelicene, which reacts under acidic conditions because protonation of the superoxide anion avoids reversion to the starting substrate; in acetic acid, a vicinal *trans*-acetoxy alcohol is formed:[62]

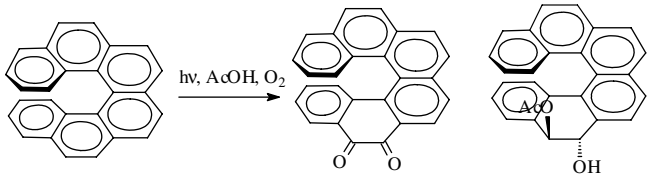

(45.15)

Irradiation of naphthalene in water leads to 2-formylcinnamaldehyde, 2-carboxycinnamaldehyde, and 7-hydroxy-1,4-naphthoquinone, possibly via initial photoionization and production of hydroxyl radicals[63] (with anthracene, a complex mixture is obtained).[64]

Photocatalysis by semiconductor powders, most usually titanium dioxide, has been applied to the oxidation of several aromatics.[65,66] In many such photocatalytic reactions, the key intermediates are hydroxyl radicals formed by oxidation of water. With rather good donors such as aromatic compounds, hole transfer on the excited semiconductor surface is a viable alternative; in this case, the reaction of the radical cation of the substrate or further intermediates arising from it with oxygen or superoxide anion may have a role. Photocatalyzed oxidation of naphthalene yields 2-formylcinnamaldehyde and 1,4-naphthoquinone as the primary products (Eq. (45.16)), similarly to what occurs upon direct irradiation of naphthalene in water:[67]

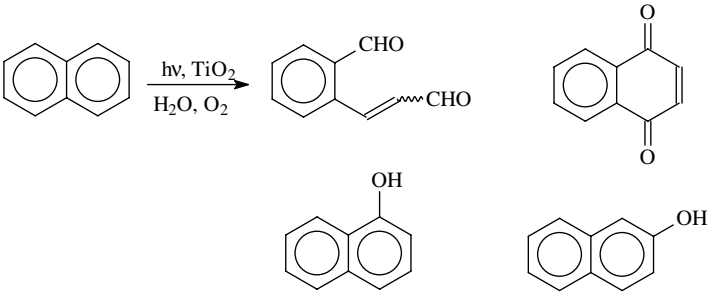

(minor products) (45.16)

Apart from the mechanistic interest, photocatalysis is a promising method for the removal of aromatics from polluted water.

Oxidation processes not involving molecular oxygen have been characterized. Some examples involve oxygen-activated species, besides the superoxide anion mentioned above. Thus, ring hydroxylation occurs by reaction with photogenerated atomic ^3P oxygen in the gas phase,[68] as well as in solution by addition of hydroxyl radicals formed by hydrogen peroxide fragmentation[69] or of hydroperoxyl radicals.[70] Alternatively, excited states of some compounds function as oxygen donors or fragment-producing atomic oxygen or hydroxyl radicals. This applies to excited heterocyclic *N*-oxides, to aromatic sulfoxides,[71,72] and, at least with electron-rich substrates such as methoxynaphthalenes, to nitroaromatics.[73]

Yet another mechanism for oxidation is trapping by oxygen of some intermediate formed in a photochemical reaction of an aromatic. Fitting examples seem to be the formation of cyclopentadienecarboxyaldehyde upon direct irradiation of an oxygen-equilibrated solution of benzene in water, presumably via oxidation of the product of photorearrangement, benzvalene,[74,75] and the formation of epidioxides upon irradiation of naphthylcarboxylimides (**7**; Eq. (45.17)), reasonably via oxygen addition to an intermediate biradical that would otherwise give the [4+4]-intramolecular cycloadduct:[76]

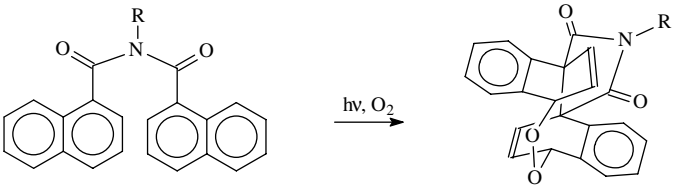

7

besides 2+2 and 4+2 dimers (45.17)

45.3 Oxidation of Vinylarenes

The oxidation of aryl-conjugated olefins occurs smoothly under various conditions and is of both mechanistic and preparative interest. The reaction may be limited to the olefin moiety or involve the aromatic ring. This depends on the structure but primarily on conditions; accordingly, in this section, singlet oxygen and electron transfer photooxygenations are discussed separately. Dye-sensitized singlet oxygen addition occurs easily and often involves the ring. In a typical case, β,β-dimethylstyrene mainly gives di-endoperoxides resulting from [4+2]-cycloaddition to form a dihydrobenzo-1,2-dioxin that rapidly adds a second molecule of singlet oxygen across the cyclohexadiene moiety, with minor amounts of benzaldehyde from the cleavage of the dioxetane and of the hydroperoxide resulting from the ene reaction.[77,78] In contrast, intra-zeolite-sensitized photooxygenation gives the hydroperoxide as by far the main product, whether this is due to an effect of the zeolite on the stability of the initial zwitterionic intermediates or to a conformation of the styrene in the cavity ill-suited to [4+2]-cycloaddition.[79] Likewise, the main product is the di-endoperoxide **8** with *trans*-stilbene (80%; see Eq. (45.18))[80] as well as with vinylnaphthalenes:[81]

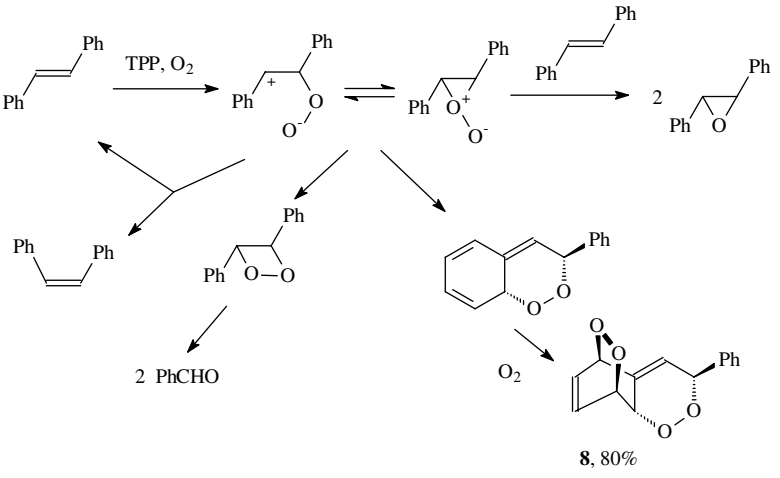

(45.18)

With 1,2-dihydronaphthalenes, competition between the ene reaction giving the 4-hydroperoxide and cycloaddition depends on the substituent;[82] with a chiral 1-phenyl-1,2-dihydronaphthalene-2-carboxylic acid and some related compounds, the *bis*-endoperoxide is the main product and is formed with high diastereoselectivity.[83] With (alkyl)indenes, the result is strongly dependent on conditions. At –78°C, the [4+2]-addition predominates (in this case, leading to rearranged di-epoxyperoxides), while in acetonitrile or methanol the [2+2]-mode predominates and cleaved dicarbonyls are obtained; the ene reaction is one of the processes occurring at room temperature.[84–86]

Alkyl substitution or incorporation of the vinyl moiety into a ring has various effects. The ene reaction is the exclusive process with α,α′-dimethylstilbene[87] and with 1-phenylcyclopentene,[88] while it competes with the [4+2]-cycloaddition in the case of 1-phenylcyclohexene.[88] In the case of 2-phenylnorbornene in methanol, both a methoxyhydroperoxide arising from attack to the double bond and two di-epoxy-endoperoxides arising from initial [4+2]-addition are observed.[89] A [2+2]-addition process, accompanied by formation of 1-(2-hydroxyphenyl)cyclopropancarboxyaldehyde, seemingly via a non-singlet oxygen path, takes place with 1-phenylcyclobutene.[90,91] An electron-donating substituent favors the [4+2]-cycloaddition, which occurs with β-methoxystyrenes and β-methoxyvinylnaphthalenes,[92–95] but 1,2-dioxetanes are formed from 1-silyloxyindenes.[96]

Di-endoperoxides are also formed from the enol ethers and silyl enol ethers of phenylpyruvic acid, phenylacetone, and phenylacetaldehyde; however, carefully controlled photooxygenation gives the mono-endoperoxides, which can be reduced to the *o*-hydroxyphenyl derivatives **9**[97,98] or used as the equivalent of *o*-quinone methides, as in the formation of compounds **10**:[94]

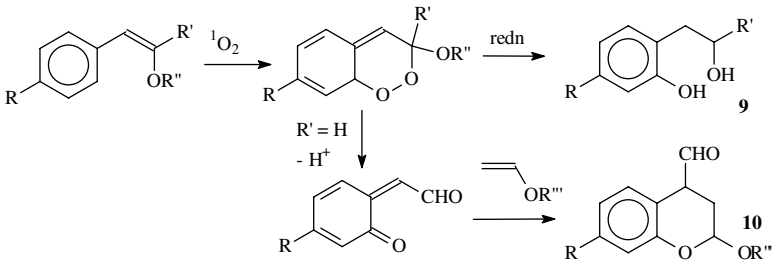

(45.19)

Tautomeric benzoylacetones (**11**) undergo an ene reaction with singlet oxygen via the enolic form, followed by rearrangement and elimination reactions from the initially formed hydroperoxide, which has been characterized at low temperature:[99,100]

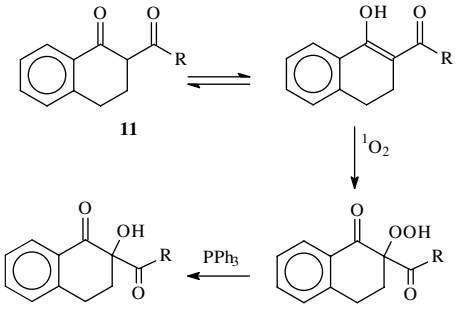

(45.20)

Among derivatives with an electron-donating substituent on the aromatic ring, one should mention the reaction of some estrogens with vinylanisole structure, such as **12**, where the vinyl moiety is oxidatively cleaved:

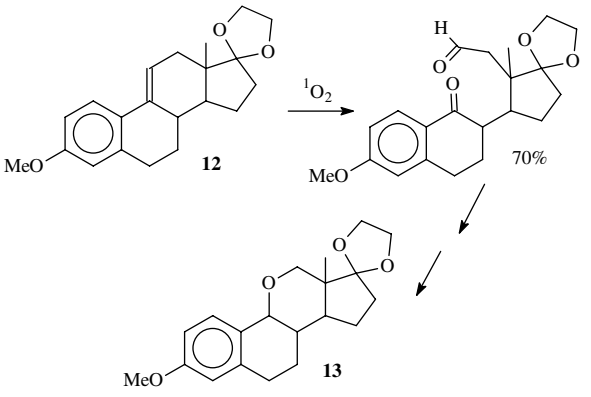

(45.21)

This reaction has been exploited for the synthesis of 11-oxaestrogens (**13**).[101–103]

None of the above singlet oxygen cycloaddition reactions nor, obviously, the ene reaction takes place with 1,1-diphenylethylenes (see below for reactions with allenes), and strongly donating groups may in this case change the course of the reaction with singlet oxygen to electron transfer, as observed with 1,1-*bis*(*p*-dimethylaminophenyl)ethylene (see below).

Conjugated arylbutadienes form the endoperoxides across the diene moiety, just as in the non-arylated derivatives; in particular, both (*E,E*)- and (*Z,Z*)-1-aryl-1,3-pentadienes give the *cis*-endoperoxide.[104] Phenyl- and 1,1-diphenylallenes, on the other hand, undergo both [2+2]-addition, leading to aryl ketones and diketones and [4+2]-addition, leading to arylation or epoxidation of the aromatic ring.[105]

A different mechanism operates upon electron-transfer-sensitized photooxygenation, generally carried out by using electron-accepting sensitizers such as 9,10-dicyanoanthracene, triphenylpyrylium salts, and others.[106–112] The arylalkene radical cation **14** is formed and then reacts either with the superoxide anion or, more likely, with oxygen. Kinetic factors are also important:[113]

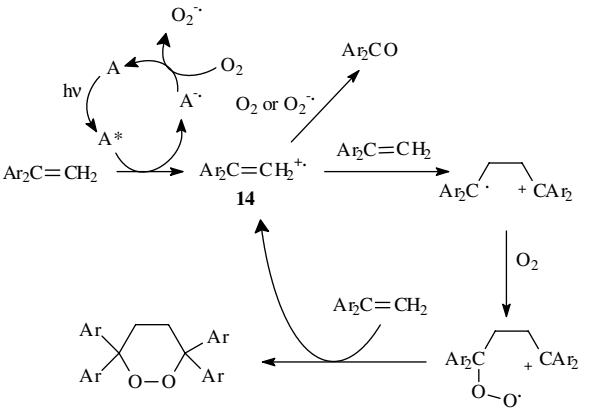

(45.22)

This path is important for good donors, such as polyphenylethylenes, that are cleaved to the corresponding ketones or aldehydes with minor amounts of epoxides (which may in turn be further oxidized to the cleaved carbonyls), reasonably via 1,2-dioxetanes. β-Methoxystyrenes[114] and 2,3-diphenyl-1,4-dioxene as well as 2,3,4,5-tetraphenyl-1,4-dioxin, are similarly oxidized.[115,116] α-Acetoxystyrenes give β-acetoxypropiophenones upon sensitized oxygenation by pyrylium salts.[117] In the case of alkoxyarylmethyleneadamantanes, a stable dioxetane is obtained via a charge-transfer mechanism.[118] Oxidative cleavage of stilbenes is much more efficient when the substrate is included with the (cationic) dye in zeolites.[119] Furthermore, it also occurs upon specific irradiation of the charge-transfer complex that stilbenes form with oxygen in zeolite NaY.[120,121]

An alternative entry to this chemistry is the use of a good electron donor as an indirect sensitizer. Thus, irradiation of α-methylstyrene in the presence of various alkylated 1,4-dimethoxybenzenes gives acetophenone and 1,1-phenylmethyloxirane as the main products, apparently via quenching of the singlet-excited dimethoxybenzenes by oxygen with formation of the superoxide anion and the radical cation of the donor, which then indirectly generates the radical cation of the olefin.[122,123] Another method is titanium dioxide photocatalysis.[124,125] The chemistry of the radical cation can take different paths in the presence of nucleophiles; the photooxidation of 3,3-dimethylindene in methanol gives methoxyhydroperoxides with the opposite regiochemistry depending on whether an electron transfer sensitizer or a singlet oxygen forming dye is used, because activated oxygen and the alcohol react in the opposite order in the two cases.[126]

With sensitizers such as dicyanoanthracene or 10-methylacridinium salts, electron-donating substituted 1,1-diarylethylenes undergo an electron-transfer-initiated chain reaction leading to 1,2-dioxanes via addition of the radical cation to neutral alkene, trapping of the resulting 1,4-distonic radical cation by oxygen, reduction of the 1,6-radical cation, and cyclization (a side path is cleavage to carbonyls as above).[127–131] The reaction has been extended to the intramolecular case with related 1,ω-*bis*(diarylethenyl)alkanes.[132] Noteworthy, 1,2-dioxanes are also formed in the absence of the sensitizer by selective irradiation of the contact charge-transfer band between electron-rich 1,1-diarylethylenes and oxygen.[133] Furthermore, with strongly donating substituents such as the dimethylamino group, the 1,2-dioxane is also formed under singlet oxygen conditions, apparently because electron transfer to singlet oxygen again gives the radical ion pair.[134] On the other hand, 1,2-diphenyl-1,2-diamines, aminoalcohols, and aminoketones undergo electron transfer with singlet oxygen and cleave via the radical cation.[135] Yet, a different oxidative process has been found in the photoreaction of triarylstibines with styrenes, which yields 2-aryl-1-phenylethanols, presumably via attack by styrene on the stibine-oxygen complex and Sb-assisted CC and C–O bond formation.[136]

45.4 Oxidation of Phenols, Aryl Ethers, and Aromatic Amines

A variety of photooxidation paths are available to phenols. These substrates are both good hydrogen donors and good electron donors. Thus, hydrogen abstraction from the OH group or electron transfer followed by deprotonation from the radical cation are possible mechanisms (type I and type III) and both yield phenoxyl radicals, which then add to ground-state oxygen. On the other hand, under dye-sensitized conditions, the reaction follows a type II mechanism via singlet oxygen, but, here again, the interaction with phenol may lead to different paths — concerted addition, ene-type reaction or [4+2]-cycloaddition, or hydrogen abstraction, again giving the phenoxyl radical,[137] in addition to simple physical quenching that yields back the ground state. The conditions leading to the prevalence of the various mechanisms have been discussed in detail.[10] As for the products formed, the main process yielding 4-hydroperoxycyclohexadienones, which may result form whatever of the above paths is operative and indeed are also the products arising from the thermal radical oxidation of the same substrates. The hydroperoxides can be isolated from 4-substituted phenols or are otherwise directly converted to the quinones.[138–142] The sensitized photooxygenation has been considered as a model for enzymatic oxidation.[143] This has been applied to the degradation of biologically important phenols, such as *p*-hydroxyphenylacetic acid,[144] pyruvic acid, and α-tocopherol (**15**):[145,146]

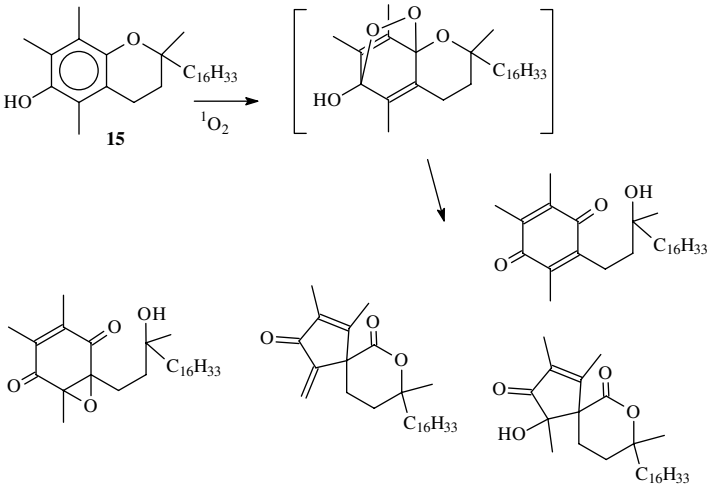

(45.23)

2,5-Dihydroxybenzoic acid is formed from salicylic acid by reaction with singlet oxygen,[147] but the same product is formed also by ZnO photocatalysis, apparently via hole transfer.[148] In several cases, the reaction with singlet oxygen has been used as a mild method of functionalization for synthetic purposes. An example is the hydroperoxidation in 10 of estrone and estradiol as a key step for the conversion into the corresponding 19-norsteroids.[149] Another example is the hydroperoxidation in 6 of anhydrotetracycline (**16**; Eq. (45.24)) for the conversion into tetracycline[150] and the conversion of *N*-(ethoxycarbonyl)norcodeinone dienol acetate to the corresponding 14-hydroxynorcodeinone as the key step for the synthesis of 14-hydroxymorphinans from codeine:[151]

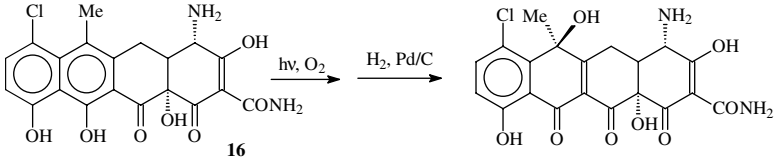

(45.24)

Another important method of oxidation is titanium dioxide photocatalysis, which again involves different reaction paths. These appear to be initiated by hydroxyl radical attack and finally lead to

mineralization of the organic substrate;[152] in this case, the main application is for the purification of polluted water, where phenols and in particular chlorophenols are often present as pollutants. The oxidation can also be carried out with some soluble inorganic complexes.[153]

Naphthols give naphthoquinones or other oxidized products through similar mechanisms.[154–156] Alkoxyphenols, polymethoxylated benzenes,[157–159] and naphthyl ethers[160,161] generally give di-epoxides, epoxyenones, or quinones as well as ring cleavage products that can be rationalized as arising from the rearrangement of the initially formed 1,4-endoperoxides. The electron transfer photosensitized oxidation of 1,2-dimethoxybenzene results in ring cleavage via a dioxetane,[162] and an analogous intermediate is probably involved in the photooxidation of 9,10-dimethoxyphenanthrene.[163]

Tertiary amines are essentially physical quenchers of singlet oxygen; however, chemical reaction, both type I and type II, may have a role and have in fact being observed with some electron-donating substituted dimethylanilines.[164] 2-Naphthylamine undergoes oxidative ring cleavage.[165]

45.5 Side-Chain Oxidation

Side-chain photooxidation occurs under various conditions. A typical mechanism is photosensitized electron transfer with sensitizers such as cyanonaphthalenes, cyanoanthracenes, or pyrylium salts, followed by deprotonation at the benzylic position, in view of the remarkable thermodynamic acidity of alkylbenzenes. The benzyl radicals formed react with molecular oxygen or superoxide anion to yield hydroperoxides that can decompose to aldehydes or ketones. Furthermore, the proton is not the only electrofugal group, and different cations may be cleaved from the benzylic position in the radical cation, such as a stabilized carbocation or a silyl cation (this topic is discussed more extensively elsewhere in this book). Typical examples are the formation of aryl aldehydes or ketones from alkylated benzenes[166–169] and naphthalenes as well as from fluorene and derivatives.[170–172] Similar reactions have been observed with benzyl alcohols and ethers,[173,174] as well as with bibenzyls, arylpinacols, and benzylsilanes.[175–178] As mentioned above, aromatic sensitizers can also activate oxygen and, with good singlet oxygen acceptors such as 1,4-dimethylnaphthalene, both paths — formation of the endoperoxide via [4+2]-cycloaddition and oxidation via benzyl radicals — compete to an extent that depends on the solvent polarity. Benzylic oxidation also takes place under different conditions and with various mechanisms, such as sensitization by quinones[179] or by protonated pteridine or flavin analogs,[180] photocatalysis by semiconductors,[181–183] irradiation in the presence of some inorganic compounds,[184] or simply by irradiation of oxygenated solutions, in this case possibly via an electron transfer complex with oxygen.[185–187] The charge-transfer band has been characterized for the toluene–oxygen complex in barium- and calcium-exchanged zeolite Y, where benzaldehyde is selectively obtained by irradiation in the visible region.[188]

A particular case of the benzyl radical cation fragmentation path with oxygen addition to the benzylic position is the electron-transfer-induced oxygenation of arylated cyclopropanes and three-membered heterocycles. In this case, a carbon–carbon bond is broken in the strained ring; oxygen is added to the distonic radical cation and gives five-membered heterocycles. Thus, cyclopropanes (**17**, Eq. (45.25)) are converted to dioxolanes,[189–191] oxiranes to ozonides,[189,192,193] and aziridines to 1,2,4-dioxazolidines;[189] the oxygenation may occur through a radical chain mechanism:

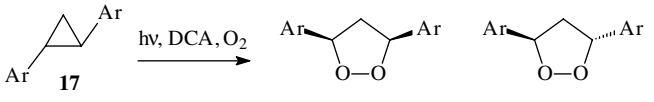

(45.25)

References

1. Livingston, R., Photochemical autoxidation, in *Autoxidation and Antioxidants*, Vol. 1, Lundberg, W. O., Ed., Interscience, New York, 1961, 249.
2. Gollnick, K., Photooxygenation reactions in solution, *Adv. Photochem.*, 6, 1, 1968.
3. Gollnick, K. and Schenk, G. O., Oxygen as dienophile, in *1,4-Cycloaddition Reactions*, Hamer, J., Ed., Academic Press, New York, 1967, 255.
4. Rigaudy, J., Photooxygenation of aromatic derivatives, *Pure Appl. Chem.*, 16, 169, 1968.
5. Frimmer, A. A., *Singlet Oxygen*, CRC Press, Boca Raton, FL, 1985.
6. Fox, M. A., Activation of oxygen by photoinduced electron transfer, in *Photoinduced Electron Transfer*, Vol. D, Fox, M. A. and Chanon, M., Eds., Elsevier, Amsterdam, 1988.
7. Lopez, L., Photoinduced electron transfer oxygenations, *Top. Curr. Chem.*, 156, 119, 1990.
8. Stevens, B., Perez, S. R., and Ors, J. A., $^1O_2$ acceptor properties and reactivities, *J. Am. Chem. Soc.*, 96, 6846, 1974.
9. van den Heuvel, C. J. M., Verhoeven, J. W., and de Boer, T. J., A frontier orbital description of the reaction of singlet oxygen with simple aromatic systems, *Recl. Trav. Chim. Pays-Bas*, 99, 280, 1980.
10. Saito, I. and Matsuura, T., The oxidation of electron-rich aromatic compounds, in *Singlet Oxygen*, Wasserman, H. H. and Murray, R. W., Eds, Academic Press, New York, 1979, 511.
11. Chalvet, O., Daudel, R., Schmid, G. H., and Rigaudy, J., Theoretical treatment of the transitions state: two photochemical reactions, *Tetrahedron*, 26, 365, 1970.
12. van der Heuvel, C. J. M., Hofland, A., Steinberg, H., and de Boer, T. J., The photo-oxidation of hexamethyl- and pentamethylbenzene by singlet oxygen, *Recl. Trav. Chim. Pays-Bas*, 99, 275, 1980.
13. Gray, R. and Boekelheide, V., Synthesis and properties of [2.2.2.2](1,2,4,5)cyclophanes, *J. Am. Chem. Soc.*, 101, 2128, 1979.
14. Sawada, T., Mimura, K., Thiemann, T., Yamato, T., Tashiro, M., and Mataka, S., Stable endoperoxide of 4,5,6,8,16-pentamethyl[2.2]metacyclophane; structural analysis and deoxygenation, *J. Chem. Soc., Perkin Trans. 1,* 1369, 1998.
15. Mestdagh, H. and Vollhart, K. P. C., Photo-oxidation of 2,3,7,8-tetrakis(trimethylsilyl)benzo[3,4]cyclobuta[1,2-*b*]biphenylene in the presence of oxygen. Unusual cleavage of the benzene ring to generate an alkyne unit, *J. Chem. Soc., Chem. Commun.*, 281, 1986.
16. van der Heuvel, C. J. M., Steinberg, H., and de Boer, T. J., The photo-oxidation of mono- and dimethylnaphthalenes by singlet oxygen, *Recl. Trav. Chim. Pays-Bas*, 99, 109, 1980.
17. Wasserman, H. H. and Larsen, D. L., Formation of 1,4-endoperoxides from the dye-sensitized photo-oxygenation of alkylnaphthalenes, *J. Chem. Soc., Chem. Commun.*, 253, 1972.
18. Hart, H. and Oku, A., Octamethylnaphthalene 1,4-endoperoxide, *J. Chem. Soc., Chem. Commun.*, 254, 1972.
19. Pierlot, C., Poprawski, J., Marko, J., and Aubry, J. M., Effects of oxygenated substituents on the [4+2] cycloaddition of singlet oxygen in the photooxygenation of water-soluble naphthyl ethers, *Tetrahedron Lett.*, 41, 5063, 2000.
20. Adam, W., Peters, E. M., Peters, K., Prein, M., and von Schnering, H. G., Diastereoselective photooxygenation of chiral naphthyl alcohols: the hydroxy group directing effect in singlet oxygen [4+2] cycloaddition to arenes, *J. Am. Chem. Soc.*, 117, 6686, 1995.
21. Adam, W. and Prein, M., Substituent effects in the diastereoselective [4+2] cycloaddition of chiral naphthalene derivatives with singlet oxygen, *Tetrahedron Lett.*, 35, 4331, 1994.
22. Adam, W. and Prein, M., π-Facial diastereoselectivity in the [4+2] cycloaddition of singlet oxygen as a mechanistic probe, *Acc. Chem. Res.*, 29, 275, 1996.
23. Rigaudy, J., Baranne-Lafont, J., Defoin, A., and Cuong, N. K., Chemical transformation of anthracene photo-oxides, *Tetrahedron*, 34, 73, 1978.
24. Dufraisse, C. and Le Bras, J., Photooxides of *meso*-diphenylanthracenes: formation, dissociation and properties, *Bull. Soc. Chim. Fr.,* 4, 349, 1937.

25. Corey, E. J. and Taylor, W. C., Peroxidation of organic compounds by externally generated singlet oxygen molecules, *J. Am. Chem. Soc.*, 86, 3881, 1964.
26. Stevens, B., Marsch, K. L., and Barltrop, J. A., Sensitizer yields of O_2 $^1\Delta_g$, *J. Phys. Chem.*, 85, 3079, 1981.
27. Marsch, K. L. and Stevens, B., Dependence of the pyrene-sensitized sensitized O_2 $^1\Delta_g$ yield on pyrene concentration, *J. Phys. Chem.*, 87, 1765, 1983.
28. Wu, C. K. and Trozzolo, A. M., Production of singlet molecular oxygen from the O_2 quenching of the lowest excited state of rubrene, *J. Phys. Chem.*, 83, 1765, 1983.
29. Albini, A. and Spreti, S., The photooxygenation of simple alkenes sensitized by cyanoanthracenes, *Gazz. Chim. Ital.*, 115, 227, 1985.
30. Davidson, R. S. and Pratt, J. E., Excimers and exciplex as sensitizers for photooxidation reactions, *Tetrahedron*, 40, 999, 1984.
31. Rigaudy, J., Guillaume, J., and Maurette, D., Formation of isomeric 1,4- and 9,10-photooxides from 1,4-dimethylanthracene, *Bull. Soc. Chim. Fr.*, 144, 1971.
32. Mellier, M. T., Effect of some substituents on the photooxidation of *meso*-diphenylanthracenes, *Ann. Chim. (Paris) 12*, 10, 666, 1955.
33. Rigaudy, J., Dupont, R., and Cuong, N. K., Photooxidation of 1,4-*bis*-(benzyloxy)anthracenes, *C. R. Hebd. Séances Acad. Sci., Ser. C*, 269, 416, 1969.
34. Rigaudy, J., Defoin, A., and Cuong, N. K., The photo-oxide of 1-dimethylamino-9,10-diphenylanthracene and its transformations, *C. R. Hebd. Séances Acad. Sci., Ser. C*, 271, 1258, 1970.
35. Motoyoshiya, J., Masunaga, T., Harumoto, D., Ishiguro, S., Narita, S., and Hayashi, S., High reactivity of heterocoerdianthrones (HCDs) in photoperoxidation and thermal stability of their endoperoxides: use of HCD as a photosensitizer under sunlight, *Bull. Chem. Soc. Jpn.*, 66, 1166, 1993.
36. Panico, R., Thioethers of *meso*-diphenylanthracenes, *Ann. Chim. (Paris) 12*, 10, 695, 1955.
37. Dufraisse, C. and Horclois, R., Naphthacenes, synthesis and photochemical peculiarities, *Bull. Soc. Chim. Fr. 5*, 3, 1873, 1936.
38. Dufraisse, C. and Horclois, R., Synthesis of naphthacenes with the characteristics of rubrenes, *Bull. Soc. Chim. Fr. 5*, 3, 1894, 1936.
39. Rigaudy, J. and Sparfel, D., Regioselectivity in the photo-oxidation and diene addition with 5, 12-diphenylnaphthacene, *Bull. Soc. Chim. Fr.*, 742, 1977.
40. Sy, A. and Hart, H., Permethylnaphthacene, *J. Org. Chem.*, 44, 7, 1979.
41. Aubry, J. M., Rigaudy, J., and Cuong, N. K., Kinetic studies of self-sensitized photo-oxygenation of a water-soluble rubrene derivative, *Photochem. Photobiol.*, 33, 149, 1981.
42. Aubry, J. M., Rigaudy, J., and Cuong, N. K., A water soluble rubrene derivative: synthesis, properties and $^1O_2$ trapping, *Photochem. Photobiol.*, 33, 149, 1981.
43. Oshima, S., Uchida, A., Horiguchi, S., Suzuki, A., Fujisawa, S., and Oonishi, I., Photooxygenation of diphenanthro[5,4,3-*abcd*-5′,4′,3′-*jklm*]perylene, *Bull. Chem. Soc. Jpn.*, 67, 924, 1994.
44. Christ, T., Kulzer, F., Bordat, P., and Basché, T., Watching the photo-oxidation of a single aromatic hydrocarbon molecule, *Angew. Chem., Int. Ed. Engl.*, 40, 4192, 2001.
45. Turro, N. J., The role of intersystem crossing steps in singlet oxygen chemistry and photo-oxidations, *Tetrahedron*, 41, 2089, 1985.
46. Müller-Breitkreutz, K., Mohr, H., Briviba, K., and Sies, H., Inactivation of viruses by chemically and photochemically generated singlet oxygen, *J. Photochem. Photobiol. B: Biol.*, 30, 63, 1995.
47. Müller, K. and Ziereis, K., Dimethyl 3,3′-(4-methyl-1,3-naphthalene)dipropionate as a singlet oxygen trap in biological systems, *Arch. Pharm.*, 326, 819, 1993.
48. Klotz, L. O., Pellieux, C., Brivida, K., Pierlot, C., Aubry, J. M., and Sies, H., Nitrogen-activated protein kinase (p38-JNK-ERK-) activation pattern induced by extracellular and intracellular singlet oxygen and UVA, *Eur. J. Biochem.*, 260, 917, 1999.
49. Schmidt, R., Drews, W., and Brauer, H. D., Photolysis of the endoperoxide of heterocoerdianthrone. A concerted, adiabatic cycloreversion originating from an upper excited singlet state, *J. Am. Chem. Soc.*, 102, 2791, 1980.

50. Gabriel, R. Schmidt, R., and Brauer, H. D., Wavelength-dependent and adiabatic photochemistry of the 1,4-endoperoxide of 1,4-dimethoxy-9,10-diphenylanthracene, *Z. Phys. Chem. (Munich)*, 141, 41, 1984.
51. Schmidt, R. and Brauer, H. D., Self-sensitized photo-oxidation of aromatic compounds and photocycloreversion of endoperoxides. Application in chemical actinometry, *J. Photochem.*, 25, 489, 1984.
52. Dabestani, R., Ellis, K. J., and Sigman, M. E., Photodecomposition of anthracene on dry surfaces: products and mechanism, *J. Photochem. Photobiol. A: Chem.*, 86, 231, 1995.
53. Barbas, J. T., Dabestani, R., and Sigman, M. E., A mechanistic study of photodecomposition of acenaphthylene on a dry silica surface, *J. Photochem. Photobiol. A: Chem.*, 80, 103, 1994.
54. Tamai, T., Ichinose, N., Tanaka, T., Sasuga, T., Hashida, I., and Mizuno, K., Generation of polyphenylene radical cations and their cosensitization ability in the 9,10-dicyanoanthracene-sensitized photochemical chain reactions of 1,2-*bis*(4-methoxyphenyl)cyclopropane, *J. Org. Chem.*, 63, 3204, 1998.
55. Mizuno, K., Ichinose, N., Tamai, T., and Otsuji, Y., Electron transfer mediated photooxygenation of biphenyl and its derivatives in the presence of $Mg(ClO_4)_2$, *Tetrahedron Lett.*, 5823, 1985.
56. Mizuno, K., Tamai, T., Nakanishi, I., Ichinose, N., and Otsuji, Y., Photooxygenation of cyanoanthracene via their radical anions, *Chem. Lett.*, 2065, 1988.
57. Yamashita, T., Tsurusako, T., Nakamura, N., Yasuda, M., and Shima, K., Electron transfer photosensitized oxygenation of stilbene and naphthalene derivatives in the presence of acetate ion: controlling the reaction of the cation radicals by weak-nucleophilic salts, *Bull. Chem. Soc. Jpn.*, 66, 857, 1993.
58. Futamura, S., Chemical behavior of aromatic radical cations under superoxide-free electron transfer photooxygenation conditions, *Bull. Chem. Soc. Jpn.*, 65, 1779, 1992.
59. Burke, N. A. D., Templin, M., and Guillet, J. E., The mechanism or perylene photo-oxygenation in a water-soluble polymer photocatalyst, *J. Photochem. Photobiol. A: Chem.*, 100, 93, 1996.
60. Tsubomura, T. and Mulliken, R. S., UV absorption caused by the interaction of oxygen with organic molecules, *J. Am. Chem. Soc.,* 82, 5966, 1960.
61. Onodera, K., Furusawa, G., Kojima, M., Tsuchiya, M., Ahihara, S., Akaba, R., Sakuragi, H., and Tokumaru, K., Mechanistic considerations on photoreaction of organic compounds via excitation of contact charge transfer complexes with oxygen, *Tetrahedron*, 41, 2215, 1985.
62. Wilson, R. M., Schnapp, K. A., Memarian, H. R., Wilson, M. L., and Ho, D. M., The photooxidation of hexahelicene in acidic solvents: an example of aromatic hydrocarbons exciplex protonation, *Tetrahedron Lett.*, 34, 7179, 1993.
63. *Via*laton, D., Richard, C., Baglio, D., and Paya-Perez, A. B., Mechanism of the photochemical transformation of naphthalene in water, *J. Photochem. Photobiol. A: Chem.,* 123, 15, 1999.
64. Mallakinn, A., Dixon, D. G., and Greenberg, B. M., Pathway of anthracene modification under simulated solar radiation, *Chemosphere*, 40, 1435, 2000.
65. Fujihira, M., Satoh, Y., and Osa, T., Heterogeneous photocatalytic oxidation of aromatic compounds on titanium dioxide, *Nature*, 293, 206, 1981.
66. Shimamura, Y., Misawa, H., Oguchi, T., Kanno, T., Sakuragi, H., and Tokumaru, K., Titanium dioxide photocatalysed oxidation of aromatic compounds: the role of water and oxygen on aromatic hydroxylation, *Chem. Lett.*, 1691, 1983.
67. Soana, F., Sturini, M., Cermenati, L., and Albini, A., Titanium dioxide photocatalyzed oxygenation of naphthalene and some of its derivatives, *J. Chem. Soc., Perkin Trans. 2*, 699, 2000.
68. Grovenstein, E. and Moser, A. J., Reaction with atomic oxygen with aromatic hydrocarbons, *J. Am. Chem. Soc.*, 92, 3812, 1970.
69. Ogata, Y., Tmizawa, K., and Yamashita, Y., Photoinduced oxidation of benzoic acid with aqueous hydrogen peroxide, *J. Chem. Soc., Perkin Trans. 2*, 616, 1980.
70. Skuratova, S. I., Mordvintsev, P. I., and Fomin, G. V., Photosensitized hydroxylation of aromatic compounds, *Zh. Fiz. Khim.*, 56, 2093, 1982.

71. Lucien, E. and Greer, A., Electrophilic oxidant produced in the photodeoxygenation of 1,2-benzodiphenylene sulfoxide, *J. Org. Chem.*, 66, 4576, 2001.
72. Gregory, D. D., Wan, Z., and Jenks, W. S., Photodeoxygenation of dibenzothiophene sulfoxide: evidence for a unimolecular S–O cleavage product, *J. Am. Chem. Soc.*, 119, 94, 1997.
73. Saito, I., Takami, M., and Matsuura, T., Oxidation of aromatic methoxy compounds via photoexcited aromatic nitro compounds, *Bull. Chem. Soc. Jpn.*, 48, 2865, 1975.
74. Kaplan, L., Wendling, L. A., and Wilsbach, K. E., Photooxidation of aqueous benzene to 1,3-cyclopentadien-1-carboxyaldehyde, *J. Am. Chem. Soc.,* 93, 3819, 1971.
75. Kaplan, L., Wendling, L. A., and Wilsbach, K. E., Role of benzvalene in the formation of cyclopentadiencarboxyaldehyde, *J. Am. Chem. Soc.,* 93, 3821, 1971.
76. Kohmoto, S., Kobayashi, T., Minami, J., Ying, X., Yamaguchi, K., Karatsu, T., Kitamura, A., Kishikawa, K., and Yamamoto, M., Trapping of 1,8-biradical intermediates by molecular oxygen in photocycloaddition of naphthyl-*N*-(naphthylcarbonyl)carboxamides; formation of novel 1,8-epidioxides and evidence of stepwise aromatic cycloaddition, *J. Org. Chem.*, 66, 66, 2001.
77. Matsumoto, M., Dobashi, S., and Kuroda, K., Sensitized photooxygenation of β,β–dimethylstyrenes: synthesis of (±) crotepoxides, *Tetrahedron Lett.*, 3361, 1977.
78. Matsumoto, M. and Kuroda, K., Solvent effect of singlet oxygenation with conjugated dienes, *Synth. Commun.*, 11, 987, 1981.
79. Stratakis, M. and Rabalakos, C., Chemoselective hydroperoxidation of alkenylarenes within thionin-supported zeolite Na-Y, *Tetrahedron Lett.*, 42, 4545, 2001.
80. Kwon, B. M., Foote, C. S., and Khan, S. I., Reaction of singlet oxygen with *trans*-stilbene, *J. Org. Chem.*, 54, 3378, 1989.
81. Matsumoto, M. and Kondo, K., The 1,4 cycloaddition of singlet oxygen and vinylnaphthalenes, *Tetrahedron Lett.*, 18, 3935, 1977.
82. Burns, P.A. and Foote, C. S., Low-temperature photooxygenation of 1,2-dihydronaphthalenes, *J. Org. Chem.*, 41, 908, 1976.
83. Linker, T., Rebien, F. and Toth, G., Highly diastereoselective photooxygenation of chiral 1,2-dihydronaphthalenes: evidence for a common intermediate in the ene reaction and the [4+2] cycloaddition, *J. Chem. Soc., Chem. Commun.*, 1585, 1996.
84. Zhang, J. and Foote, C. S., Photooxidation of substituted indenes at low temperature, *Tetrahedron Lett.*, 6153, 1986.
85. Burns, P. A., Foote, C. S., and Mazur, S., Photooxygenation of indenes in aprotic solvents, *J. Org. Chem.*, 41, 899, 1976.
86. Fenical, W., Kearns, D. R., and Radlick, P., The mechanism of the addition of $^1\Delta_g$ excited oxygen to alkenes: evidence for a 1,2-dioxetane intermediate, *J. Am. Chem. Soc.*, 91, 3396, 1969.
87. Futamura, S., Ohta, H., and Kamiya, Y., Sensitized photooxidation of *cis*-α,α′-dimethylstilbene, *Chem. Lett.,* 697, 1983.
88. Jefford, C. W., Boschung, A. F., and Rimbault, C. G., The reaction of singlet oxygen with 2-phenylcycloalkenes possessing small and common ring, *Tetrahedron Lett.*, 2479, 1976.
89. Jefford, C. W., Boschung, A. F., and Rimbault, C. G., Reaction of singlet and triplet oxygen with 2-phenylnorbornene, *Helv. Chim. Acta*, 59, 2542, 1976.
90. Sakuragi, M. and Sakuragi, H., Photosensitized oxidation of 1-phenylcyclobutene: the role of reactive active species other than singlet oxygen, *Chem. Lett.*, 1017, 1980.
91. Griffin, G. W., Kirschenheuter, G. P., Vaz, C., Umrigar, P., Lakin, D. C., and Christensen, S., The sensitized photo-oxygenation of methyl substituted 1,2-diphenylcyclobutenes, *Tetrahedron*, 41, 2069, 1985.
92. Matsumoto, M. and Kuroda, S., Sensitized photooxygenation of β-methoxystyrene and 1-(β-methoxyvinyl)naphthalene, *Tetrahedron Lett.*, 20, 1607, 1979.
93. Lerdal, D. and Foote, C. S., Directing effect of the methoxy group in additions to β-methoxystyrenes, *Tetrahedron Lett.*, 13, 3227, 1978.

94. Matsumoto, M. and Kuroda, K., *o*-Benzoquinone monoformylmethides by sensitized photooxygenation of *cis*-β–methoxystyrene, *Angew. Chem., Int. Ed. Engl.*, 21, 382, 1982.
95. Matsumoto, M., Kurota, K., and Suzuki, Y., The 1,4-addition of singlet oxygen to 2,6-dimethoxy-1-(2-methoxyethenyl)benzene and 2-methoxy-1-(2-methoxyethenyl)naphthalene. The 1,4-endoperoxide as equivalent of 6-oxo-2,4-cyclohexadienyl acetates, *Tetrahedron Lett.*, 22, 3253, 1981.
96. Einaga, H., Nojima, M., and Abe, M., Photooxygenation ($^1O_2$) of silyl enol ethers derived from indan-1-ones: competitive formation of tricyclic 3-silyloxy-1,2-dioxetane and α-silylperoxy ketone, *J. Chem. Soc., Perkin Trans. 1*, 2507, 1999.
97. Saito, I., Nagata, R., Kotsuki, H., and Matsuura, T., Regiospecificity of the functionalization of substituted benzenes with singlet oxygen, *Tetrahedron Lett.*, 23, 1717, 1982.
98. Kotsuki, H., Saito, I., and Matsuura, T. M., Photosensitized oxygenation of phenylpyruvic acid derivatives as a model for *p*-hydroxyphenylpyruvase dioxygenase, *Tetrahedron Lett.*, 22, 469, 1981.
99. Yoshioka, M., Nishioka, T., and Hasegawa, T., Dye-sensitized photooxygenation of 6-acyl- and 6-carbalkoxybenzocycloalken-5-ones: reaction of singlet oxygen with enolic 1,3-dicarbonyl compounds, *J. Org. Chem.*, 58, 278, 1993.
100. Yoshioka, M., Sakuma, Y., and Saito M., The effect of solvent polarity on the product distribution in the reaction of singlet oxygen with enolic tautomers of 1-(2′,4′,6′-trialkylphenyl)-2-methyl-1,3-diketones, *J. Org. Chem.*, 64, 9247, 1999.
101. Planas, A., Lupon, P., Cascallo, M., and Bonet, J., Product characterization and kinetics of dye-sensitized photo-oxygenation of 9,11-didehydroestrone derivatives, *Helv. Chim. Acta*, 72, 715, 1989.
102. Nowicki, A. W. and Turner, A. B., Photooxidation of an activated styrene, 17β-hydroxy-5-methoxy-de-*A*-oestra-5,7,9,14-tetraene, *J. Chem. Res. (S),* 110, 1981.
103. Planas, A., Sala, N., and Bonet, J. J., Synthesis of 11-oxaestrogens via dye sensitized photo-oxygenation of a 9,11-didehydroestrone derivative, *Helv. Chim. Acta*, 72, 725, 1989.
104. Motoyoshiya, J., Okuda, Y., Matsuoka, I., Hayashi, S., Takaguchi, Y., and Aoyama, H., Tetraphenylporphine-sensitized photooxygenation of *(E,E)* and *(Z,Z)*-1-aryl-1,3-pentadienes generating *cis*-endoperoxides, *J. Org. Chem.*, 64, 493, 1999.
105. Erden, I. and Martinez, T R., Dye-sensitized photooxygenation of arylallenes, *Tetrahedron Lett.*, 32, 1859, 1991.
106. Eriksen, J. and Foote, C. S., Oxidation of phenyl-substituted alkenes sensitized by cyanoanthracenes, *J. Am. Chem. Soc.*, 102, 6083, 1980.
107. Mattes, S. L. and Farid, S., Photo-oxygenation via electron-transfer and its susceptibility to catalysis, *J. Chem. Soc., Chem. Commun.*, 457, 1980.
108. Foote, C. S., Dicyanoanthracene sensitized photo-oxygenation of olefins. Electron transfer and singlet oxygen mechanisms, *Tetrahedron*, 41, 2221, 1985.
109. Konuma, S., Aihara, S., Kuriyama, Y., Misawa, H., Akaba, R., Sakuragi, H., and Tokumaru, K., Structural effects of olefins in the photooxygenation with electron-accepting sensitizers: kinetic approach to reactive intermediates, *Chem. Lett.*, 1897, 1991.
110. Garcia, H., Miranda, M. A., Mojarrad, F., and Sabater, M. J., Involvement of oxirane intermediates in the electron transfer photooxygenation of 1,1- and 1,2-diarylethylenes sensitized by 2,4,6-triphenylpyrilium tetrafluoroborate, *Tetrahedron*, 50, 8773, 1994.
111. D'Auria, M., Photochemical oxidation of *trans*-α,α′-dimethylstilbene in the presence of α-terthienyl, *Tetrahedron Lett.*, 35, 3151, 1994.
112. Delgado, J., Espinòs, A., Jiménez, M. C., Miranda, M. A., and Tormos, R., 2,4,6-Triphenylpyrilyum tetrafluoroborate-photosensitized reactions of *o*-cinnamylphenols and *o*-hydroxystilbenes, *Tetrahedron*, 53, 681, 1997.
113. Tsuchiya, M., Ebbesen, T. W., Nishimura, Y., Sakuragi, H., and Tokumaru, K., Kinetic studies on electron transfer photooxygenation of aromatic olefins. Quenching rate of olefin radical cation by oxygen and superoxide anion, *Chem. Lett.*, 2121, 1987.
114. Steichen, D. S. and Foote, C. S., Indirect sensitized photooxygenation of aryl olefins, *J. Am. Chem. Soc.*, 103, 1855, 1981.

115. Silverman, S. K. and Foote, C. S., Singlet oxygen and electron-transfer mechanisms in the dicyanoanthracene-sensitized photooxidation of 2,3-diphenyl-1,4-dioxene, *J. Am. Chem. Soc.*, 113, 7672, 1991.
116. Lopez, L., Synthesis of *Z*-stilbenediol dibenzoate by sensitized photooxygenation of 2,3,5,6-tetraphenyl-*p*-dioxin, *Tetrahedron Lett.*, 26, 4383, 1985.
117. Algarra, F., Baldovì, M. V., Garcia, H., Miranda, M. A., and Primo, J., Direct photolysis and electron transfer photooxygenation of enol acetates of 3-phenylpropiophenones, *Monatsh. Chem.*, 124, 209, 1993.
118. Lopez, L., Troisi, L., Rashid, S. M. K., and Schaap, A. P., Synthesis of 1,2-dioxetanes via 9,10-dicyanoanthracene sensitized chain electron-transfer photooxygenations, *Tetrahedron Lett.*, 30, 485, 1989.
119. Li, X. and Ramamurthy, V., Electron transfer reactions within zeolites: photooxidation of stilbenes, *Tetrahedron Lett.*, 37, 5235, 1996.
120. Takeya, H., Kuriyama, Y., and Kojima, M., Photooxygenations of stilbenes in zeolite by excitation of their contact charge transfer complexes with oxygen, *Tetrahedron Lett.*, 39, 5967, 1998.
121. Matsubara, C. and Kojima, M., Effect of co-adsorbed water on photodimerization and photooxygenation of 4-methoxystyrene included in NaY, *Tetrahedron Lett.*, 40, 3439, 1999.
122. Mori, T., Takamoto, M., Wada, T., and Inoue, Y., Photoinduced electron-transfer oxidation of olefins with molecular oxygen sensitized by tetrasubstituted dimethoxybenzenes: a non-singlet-oxygen mechanism, *Helv. Chim. Acta*, 84, 2693, 2001.
123. Mori, T., Takamoto, M., Tate, Y., Shinkumura, J., Wada, T., and Inoue, Y., Photoinduced electron transfer oxidation of α-methylstyrene with molecular oxygen sensitized by dimethoxybenzenes: a non-singlet oxygen mechanism, *Tetrahedron Lett.*, 42, 2505, 2001.
124. Fox, M. A. and Chen, C. C., Mechanistic features of the semiconductor photocatalyzed olefin-to-carbonyl oxidative cleavage, *J. Am. Chem. Soc.*, 103, 6757, 1981.
125. Sackett, D. A. and Fox, M. A., Effect of cosolvent additives on the relative rates of photooxidation on semiconductor surfaces, *J. Phys. Org. Chem.*, 1, 103, 1988.
126. Mattes, S. L. and Farid, S., Photooxygenation via electron transfer. 1,1-dimethylindene, *J. Am. Chem. Soc.*, 104, 1454, 1982.
127. Gollnick, K. and Schnatterer, A., Formation of a 1,2-dioxane by electron-transfer photooxygenation of 1,1-di-(*p*-anisyl) ethylene, *Tetrahedron Lett.*, 185, 1984.
128. Gollnick, K. and Schnatterer, A., Formation of 1,2-dioxanes by electron-transfer photooxygenation of 1,1-disubstituted ethylenes, *Tetrahedron Lett.*, 2735, 1984.
129. Gollnick, K., Schnatterer, A., and Utschick, G., Substituent-dependent electron-transfer-induced photooxygenation of 1,1-diarylethylenes, *J. Org. Chem.*, 58, 6049, 1993.
130. Mattes, S. L. and Farid, S., Photochemical electron transfer reactions of 1,1-diarylethylenes, *J. Am. Chem. Soc.* 108, 7356.
131. Fujita, M., Shindo, A., Ishida, A., Majima, T., Takamuku, S., and Fukuzumi, S., Photooxygenation of 1,1-diarylethylenes via addition of oxygen to the 1,4-dimer radical cations, catalyzed by 10-methylacridinium ion, *Bull. Chem. Soc. Jpn.*, 69, 743, 1996.
132. Mizuno, K., Tamai, T., Hashida, I., Otsuji, Y., Kuriyama, Y., and Tokumaru, K., Photooxygenation of 1,ω-*bis*(diarylethenyl)alkanes via photoinduced electron-transfer: formation of 1,4-radical cations and its trapping by molecular dioxygen, *J. Org. Chem.*, 59, 7329, 1994.
133. Kojima, M., Ishida, A., and Takamuku, S., Mechanism of photochemical reaction of contact charge transfer pair between 1,1-diarylethene and oxygen, *Chem. Lett.*, 979, 1993.
134. Gollnick, K. and Held, S., Single-electron transfer from 1,1-*bis*(*p*-dimethylaminophenyl)ethylene to singlet oxygen in a polar aprotic solvent, *J. Photochem. Photobiol. A: Chem.*, 59, 55, 1991.
135. Hauger, C. M., Bergmark, W. R., and Whitten, D. G., Singlet oxygen mediated fragmentation of amino alcohols, 1,2-diamines and amino ketones, *J. Am. Chem. Soc.*, 114, 10293, 1992.
136. Kakusawa, N., Tsuchiya, T., and Kurita, J., Photochemically induced coupling reaction of triarylstibines with olefins, *Tetrahedron Lett.*, 39, 9743, 1998.

137. Matsuura, T., Yoshimura, N., Nishigawa, A., and Saito, I., Participation of singlet oxygen in the hydrogen abstraction from a phenol in the photosensitized oxygenation, *Tetrahedron*, 28, 4933, 1972.
138. Pfoertner, K. and Boese, D., The photosensitized oxidation of monohydric phenols to quinones, *Helv. Chim. Acta*, 53, 1553, 1970.
139. Thomas, M. J. and Foote, C. S., Photosensitized oxygenation of phenols, *Photochem. Photobiol.*, 27, 683, 1978.
140. Saito, I., Yoshimura, N., Arai, T., Omura, K., Nishinaga, A., and Matsuura, T., Addition of singlet oxygen to 4,6-di-*tert*-butylresorcinol and its derivatives, *Tetrahedron*, 28, 5131, 1972.
141. Samsonova, L. V., Taimr, L., and Pospil, J., Oxidation and photooxidation of alkyl-3-(3,5-di-*tert*-butyl-4-hydroxyphenyl)propionates, *Angew. Makromol. Chem.*, 53, 1553, 1970.
142. Tratnyek, P. G. and Hoigné, J., Photo-oxidation of 2,4,6-trimethylphenol in aqueous laboratory solutions and natural waters: kinetics of reaction with singlet oxygen, *J. Photochem. Photobiol. A*, 84, 153, 1994.
143. Matsuura, T., Matsushima, H., Kato, S., and Saito, I., Photosensitized oxygenation of catechol and hydroquinone derivatives: non enzymatic models for the enzymatic cleavage of phenolic rings, *Tetrahedron*, 28, 5119, 1972.
144. Saito, I., Chujio, Y., Shimazu, H., Yamane, M., Matsuura, T., and Cahnmann, H. J., Non-enzymic oxidation of *p*-hydroxyphenylpyruvic acid with singlet oxygen to homogentsic acid: a model for the action of *p*-hydroxyphenylpyruvic hydroxylase, *J. Am. Chem. Soc.,* 97, 5272, 1975.
145. Clough, R. L., Yee, B. C., and Foote, C. S., The unstable primary product of tocopherol photooxygenation, *J. Am. Chem. Soc.*, 97, 5272, 1975.
146. d'Ischia, M., Costantini, C., and Prota, G., Dye-sensitized photooxidation of vitamin E revisited: new 7-oxaspiro[4,5]dec-1-ene-3,6-dione products by oxygenation and ring contraction of α-tocopherol, *J. Am. Chem. Soc.*, 113, 8353, 1991.
147. Kalyanaraman, B., Ramanujam, S., Singh, R. J., Joseph, J., and Feix, J. J., Formation of 2,5-dihydroxybenzoic acid during the reaction between $^1O_2$ and salicylic acid: analysis by ESR oximetry and HPLC with electrochemical detection, *J. Am. Chem. Soc.*, 115, 4007, 1993.
148. Richard, C. and Boule, P., Is the oxidation of salicylic acid to 2,5-dihydroxybenzoic acid a specific reaction of singlet oxygen?, *J. Photochem. Photobiol. A: Chem.*, 84, 151, 1994.
149. Lupon, P., Gomez, J., and Bonet, J. J., The photooxygenation of estrogens: a new synthesis of 19-norsteroids, *Angew. Chem. Int. Ed. Engl.*, 22, 711, 1983.
150. von Wittenau, M. S., Preparation of tetracyclines by phootooxidation of anhydrotetracyclines, *J. Org. Chem.*, 29, 2746, 1964.
151. Schwarts, M. A. and Wallace, R. A., Efficient synthesis of 14-hydroxymorphinans from codeine, *J. Med. Chem.*, 24, 1525, 1981.
152. Mills, A. and Morris, S., Photomineralization of 4-chlorophenol sensitized by titanium dioxide: a study of the initial kinetics of carbon dioxide, *J. Photochem. Photobiol. A: Chem.*, 71, 75, 1993.
153. Sykora, J., Brandsterterovà, E., and Jabconovà, A., Copper α-diimine complexes: a novel catalyst for phenol-to-quinone aerobic photooxidation in condensed media, *Bull. Soc. Chim. Belg.*, 101, 821, 1992.
154. Griffiths, J., Chu, K. Y., and Hawkins, C., Photosensitized oxidation of 1-naphthols, *J. Chem. Soc., Chem. Commun.*, 676, 1976.
155. Bortolus, P., Monti, S., Albini, A., Fasani, E., and Pietra, S., Physical quenching and chemical reaction of singlet molecular oxygen with azo dyes, *J. Org. Chem.*, 54, 534, 1989.
156. Jansen, L. M. G., Wilkes, I. P., Wilkinson, F., and Worrall, D. R., The role of singlet molecular oxygen in the photodegradation of 1-arylazo-2-naphthols in methanol and on cotton, *J. Photochem. Photobiol. A: Chem.*, 125, 99, 1999.
157. Saito, I., Imuta, M., and Matsuura, T., Reactivity of singlet oxygen toward methoxybenzenes, *Tetrahedron*, 28, 5307, 1972.
158. Saito, I. Imuta, M., and Matsuura, T., Arene peroxide intermediates in the photosensitized oxygenation of methoxybenzenes, *Tetrahedron*, 28, 5313, 1972.

159. Dureja, P., Devakumar, C., Walia, S., and Mukerjee, S. K., Evidence of similarity between biooxygenation and photooxygenation: formation of quinone epoxides, *Tetrahedron*, 43, 1129, 1987.
160. Paquette, L. A., Bellamy, F., Böhm, M. C., and Gleiter, R., Directionality of singlet oxygen addition to 1,4-dimethoxynaphthalenes laterally fused to bicyclic systems, *J. Org. Chem.*, 45, 4913, 1980.
161. Fujita, M., Ohshiba, M., Yamasaki, Y., Sugimura, T., and Tai, A., Effective trap of zwitterionic intermediate during oxygenation of electron-rich naphthalenes with singlet oxygen by the intramolecular alcohol, *Chem. Lett.*, 139, 1999.
162. Liang, J. J. and Foote, C. S., Dicyanoanthracene-sensitized photooxygenation of *o*-dimethoxybenzene, *Tetrahedron Lett*., 23, 3039, 1982.
163. Rio, G. and Berthelot, J., Sensitized photooxidation of 9,10-dimethoxyphenanthrene: a dioxetane rapidly dissociating at low temperature, *Bull. Soc. Chim. Fr.*, 822, 1972.
164. Saito, I., Abe, S., Takahashi, Y., and Matsuura, T., Dye-sensitized photooxygenation of dimethylamino-substituted benzenes: cycloaddition of singlet oxygen in competition with type I reaction, *Tetrahedron Lett.*, 4001, 1974.
165. Dubey, R. D., Gandhi, P. B., Ameta, S. C., and Bokadia, M. M., Dye-sensitized photo-oxygenation of β–naphthylamines by singlet oxygen, *Ind. J. Chem.*, 24B, 1186, 1985.
166. Albini, A. and Spreti, S., Photoinduced oxygenation of methylbenzenes, bibenzyls and pinacols in the presence of 1,4-dicyanonaphthalene, *J. Chem. Soc., Perkin Trans. 2,* 1175, 1987.
167. Albini, A. and Spreti, S., Photo-oxidation of methylbenzenes and methylnaphthalenes sensitized by cyanoanthracenes, *Z. Naturforsch.*, 41B, 1286, 1986.
168. Santamaria, J. and Ouchabane, R., 9, 10-Dicyanoanthracene-sensitized photooxygenations. Formation of $O_2^{-\cdot}$ and $^1O_2$, *Tetrahedron*, 42, 5559, 1986.
169. Julliard, M. and Chanon, M., Activation of aromatics towards oxygen by oxidative or reductive photosensitization, *Bull. Soc. Chim. Fr.*, 242, 1992.
170. Santamaria, J. and Jroundi, R., Electron transfer activation: a selective photooxidation method for the preparation of aromatic aldehydes and ketones, *Tetrahedron Lett.*, 32, 4291, 1991.
171. Bokobza, L. and Santamaria, J., Exciplex and radical ion intermediates in electron transfer reactions: solvent effect on the photo-oxygenation of 1,4-dimethylnaphthalene sensitized by 9,10-dicyanoanthracene, *J. Chem. Soc., Perkin Trans. 2*, 269, 1985.
172. Akaba, R., Kamata, M., Itoh, H., Nakao, A. Goto, S., Saito, K., Negishi, A., Sakuragi, H., and Tokumaru, K., Photoinduced electron-transfer oxygenation of arylalkanes: generation and oxygenation pathways of benzylic-types free radicals from the cation radical deprotonation, *Tetrahedron Lett.*, 33, 7011, 1992.
173. Fukuzumi, S., Tanii, K., and Tanaka, T., Protonated pteridine and flavin analogues acting as efficient and substrate-selective photocatalysis in the oxidation of benzylic alcohols derivatives by oxygen, *J. Chem. Soc., Chem. Commun.*, 816, 1989.
174. Pandey, G. and Krishna, A., Photoinduced SET oxidative cleavage of benzylic ethers protecting groups, *Synth. Commun.*, 18, 2309, 1988.
175. Tamai, Mizuno, K., Hashida, I., and Otsuji, Y., Photooxygenation of arylmethylsilanes via photoinduced electron transfer, *Chem. Lett.*, 781, 1992.
176. Tamai, T., Mizuno, K., Hashida, I., and Otsuji, Y., Photoinduced electron-transfer reactions of arylmethyl-substituted 14 group compounds: photoarylmethylation and photooxygenation, *Bull. Chem. Soc. Jpn.*, 66, 3747.
177. Reichel, L. W., Griffin, G. W., Muller, A. J., Das, P. K., and Ege, S. N., Photoinduced electron transfer carbon-carbon bond cleavage reactions: oxidations and isomerizations, *Can. J. Chem.*, 62, 424, 1984.
178. Kato, M., Kakuma, S., Hatakenaka, K., Nakadaira, Y., Yasui, M., and Iwasaki, F., Rearrangement of silanorbornadienes via photoinduced electron-transfer, *Tetrahedron Lett.*, 36, 6293, 1995.
179. Grätzel, C. K., Kira, A., Jirousek, M., and Grätzel, M., Dimer cation formation in microemulsions media: duroquinone-sensitized photooxidation of 2,6-dimethylnaphthalene and tetrathiofulvalene, *J. Phys. Chem.*, 87, 3983, 1983.

180. Fukuzumi, S., Tanii, K., and Tanaka, T., Protonated pteridine and flavin analogues acting as efficient and substrate-selective photocatalysis in the oxidation of benzylic alcohol derivatives by oxygen, *J. Chem. Soc., Chem. Commun.*, 816, 1989.
181. Fujihira, M., Satoh, Y., and Osa, T., Photoelectrochemistry at semiconductor titanium dioxide/insulating hydrocarbon liquid interface, *J. Electroanal. Chem.*, 126, 277, 1981.
182. Fox, M. A., Chen, C. C., and Younathan, J. N. N., Oxidative cleavage of substituted naphthalenes induced by irradiated semiconductor powders, *J. Org. Chem.*, 49, 1969, 1984.
183. Pincock, J. A., Pincock, A. L., and Fox, M. A., Controlled oxidation of benzyl ethers on irradiated semiconductor powders, *Tetrahedron*, 41, 4107, 1985.
184. Barbier, M., Selective photoinduced oxidation of benzylic methylene groups through UV irradiation in the presence of ferric chloride, *Helv. Chim. Acta*, 67, 866, 1984.
185. D'Auria, M., Ferri, T., and Mauriello, G., Photochemical oxidation of alkylbenzenes, *Gazz. Chim. Ital.*, 126, 313, 1996.
186. Sydnes, L. K., Burkow, I. C., and Hanson, S. H., Photooxidation of toluene and xylenes: concurrent formation of products from photooxygenation and photodimerization, *Acta Chem. Scand.*, 39B, 829, 1985.
187. Onodera, K., Sakuragi, H., and Tokumaru, K., Effect of light wavelength on photooxygenation of hexamethylbenzene, *Tetrahedron Lett.*, 2831, 1980.
188. Sun, H., Blatter, F., and Frei, H., Selective oxidation of toluene to benzaldehyde with visible light in barium (2+) and calcium (2+) exchanged zeolite Y, *J. Am. Chem. Soc.*, 116, 7951, 1994.
189. Schaap, A. P., Siddiqui, S., Prasad, G., Palomino, E., and Lopez, L., Cosensitized electron transfer photo-oxygenations. The photochemical preparation of 1,2,4-trioxolanes, 1,2-dioxolanes and 1,2,4-dioxazolidines, *J. Photochem.*, 25, 167, 1984.
190. Ichinose, N., Mizuno, K., Tamai, T., and Otsuji, Y., Photooxygenation of 1-alkyl-2,3-diarylcyclopropanes via PET: stereoselective formation of 4-alkyl-3,5-diaryl-1,2-dioxolanes and their conversion to 1,3-diols, *J. Org. Chem.*, 55, 4079, 1990.
191. Mizuno, K., Kamiyama, N., Ichinose, N., and Otsuji, Y., Photo-oxygenation of 1,2-diarylcyclopropanes via electron transfer, *Tetrahedron*, 41, 2214, 1985.
192. Schaap, A. P., Lopez, L., and Gagnon, S. D., Formation of an ozonide by electron transfer photooxygenation of tetraphenyloxirane: cosensitization by 9,10-dicyanoanthracene and biphenyl, *J. Am. Chem. Soc.*, 105, 663, 1983.
193. Schaap, A. P., Siddiqui, S., Prasad, G., Rahman, A. F. N. M., and Oliver, J. P., Stereoselective formation of *cis*-ozonides by electron transfer photooxygenation of naphthyl-substituted epoxides: stereochemical assignment of the ozonides by x-ray crystallography and chromatographic resolution, *J. Am. Chem. Soc.*, 106, 6087, 1984.

46

The Photochemistry of Substituted Benzenes: Phototranspositions and the Photoadditions of Alcohols

James A. Pincock
Dalhousie University

46.1 Introduction

"The aromatic nucleus, known for its rigidity in the ground state, becomes an extremely flexible and extrovert acrobat when being doped with a light quantum."[1]

Before 1956, benzene **1** and other substituted aromatics were considered to be photochemically unreactive. The historically important discovery in that year of the photoisomerization of benzene to fulvene **2**[2] changed this perception. Soon reports appeared on the photochemical preparation and characterization of other C_6H_6 isomers, *t*-butyl derivatives of prismane **3** (1965),[3,4] benzvalene **4** (1967),[5] and Dewar benzene **5** (1968).[6] Many examples of substituted cases are now also known.

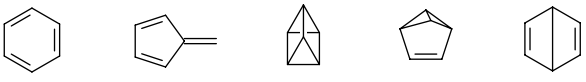

1 **2** **3** **4** **5**

0-8493-1348-1/04/$0.00+$1.50

In an attempt to trap fulvene **2** by the Diels–Alder reaction with maleic anhydride, another new photoreaction was discovered.[7] A cycloadduct was obtained which was suggested to be formed by direct addition to the excited state of benzene. Since then, photoadditions of alkenes to benzene and substituted benzenes have been studied extensively and become a powerful tool for synthetic approaches to complex polycyclic compounds.[8,9]

The photochemical transposition reactions of substituted benzenes were first reported in 1964 by Wilzbach and Kaplan[10] for the xylenes (Eq. (46.1)) and Burgstahler et al.[11] for the di-*t*-butyl benzenes (Eq. (46.2)).

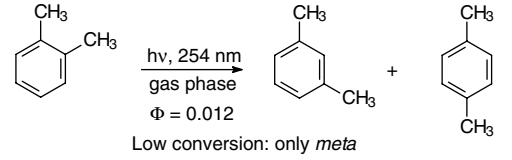

(46.1)

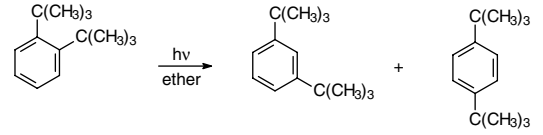

(46.2)

In the latter example, a steady-state composition of 0% *ortho*, 20% *meta*, and 80% *para* was reached starting with each of the three isomers. That these rearrangements proceeded by transposition of the ring carbons and not by alkyl group detachments was demonstrated by photolysis of [1,3,5-$^{14}C_3$]mesitylene (Eq. (46.3); the circles represent the labeled carbons).[12]

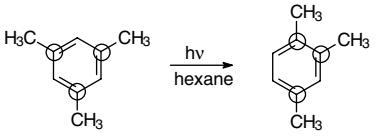

(46.3)

Substituted benzvalenes provide a reasonable intermediate for these transposition reactions, as their photochemical formation (make bonds AC and BD) followed by thermal or secondary photochemical reversal (break bonds AB and CD) leads to the transposition of atoms B and C (Eq. (46.4)).

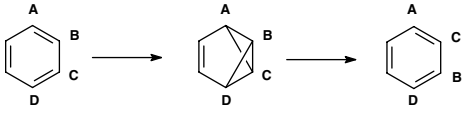

(46.4)

The photochemical preparation of benzvalene[5] was prompted by this proposal. Further strong support for benzvalenes as intermediates in the photochemistry of benzene and substituted benzenes also came from experiments in alcohol solvents under mild acidic conditions.[13,14] The primary products are bicyclo[3.1.0]hexene derivatives resulting from alcohol addition. Moreover, on photolysis of benzene-1,3,5-d_3 and benzene-d_6 in 2,2,2-trifluoroethanol (TFE), the products formed resulted from selective protonation at C_6 with endo stereochemistry (Eq. (46.5)).[15]

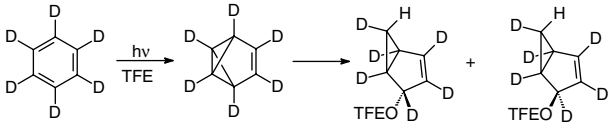

(46.5)

This observation is in agreement with results observed for protonation reactions in the ground state of the highly strained sigma bonds in benzvalene (Eq. (46.6)).[16]

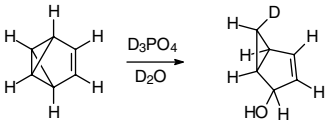

(46.6)

This early work has been reviewed a number of times, including in the previous edition of this Handbook.[17–21]

Our interest in these phototransposition reactions began while studying the photochemistry in methanol of the *meta* isomer, 3-cyanobenzyl acetate (Eq. (46.7)).[22]

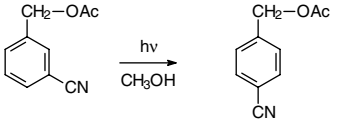

(46.7)

Because the normal carbon–oxygen bond cleavage observed for benzyl esters was very inefficient, another process was detected — namely, the formation of the *para* isomer, 4-cyanobenzyl acetate. A review of the literature revealed that, although phototranspositions had been studied in some detail in the past, virtually nothing was known about the effect that substitutents on the aromatic ring have in determining either the efficiency of conversion or the products formed. We, therefore, began by studying the phototransposition of 4-, 3-, and 2-methylbenzonitrile in acetonitrile to avoid the complication of competing ester photochemistry of Eq. 46.7.[22]

This review focuses on the four papers[23–26] examining phototransposition reactions of substituted benzenes and the photoaddition of 2,2,2-trifluoroethanol to the same compounds published recently from our own research. This parochial approach is a consequence of the fact that, to our knowledge, no other significant results on phototranspositions have been reported since the review in the previous volume of this Handbook.[21]

46.2 Photochemistry of 4-, 3-, and 2-Methylbenzonitrile (6, 7, and 8) in Acetonitrile[23]

Plots for the phototransposition reactions of the methylbenzonitriles **6** (*para*), **7** (*meta*), and **8** (*ortho)* are shown in Figures 46.1, 46.2, and 46.3, respectively. Irradiations were carried out with a Vycor-filtered, 450-W, medium-pressure Hanovia lamp using 200 mg of substrate in 280 mL of acetonitrile at 25°C. The plots are presented with values normalized to 100% for the three isomers but, in fact, the mass balance is very good: above 90% at 50% conversion for both **6** and **7**. Several points can be made about these reactions.

First, the isomers react with very different efficiencies with an order of reactivity of **6** (*para*) > **7** (*meta*) > **8** (*ortho*). Estimates of the relative reactivity of the isomers from low conversion data are **6**:**7**:**8** = 32:4:1; moreover, the reactions do not occur with high efficiency. Quantum yields of disappearance for **6** and **7** were only 0.025 and 0.003, respectively. Second, a photostationary state can be reached starting with either **6** (*para*) or **7** (*meta*) which is the same for both: 7% *para*, 26% *meta*, and 67% *ortho*. The *ortho* isomer reacts too slowly to reach this photostationary state, and the mass balance slowly drops. Third, low conversion data indicate that both 1,2- and 1,3-phototranspositions are occurring in the primary photochemical event. Thus, from Figure 46.1, in the photolysis of **6** (*para*) both the **7** (*meta*) and the **8** (*ortho*) isomers are being formed simultaneously in a ratio of 4.2:1. No delay in the formation of the

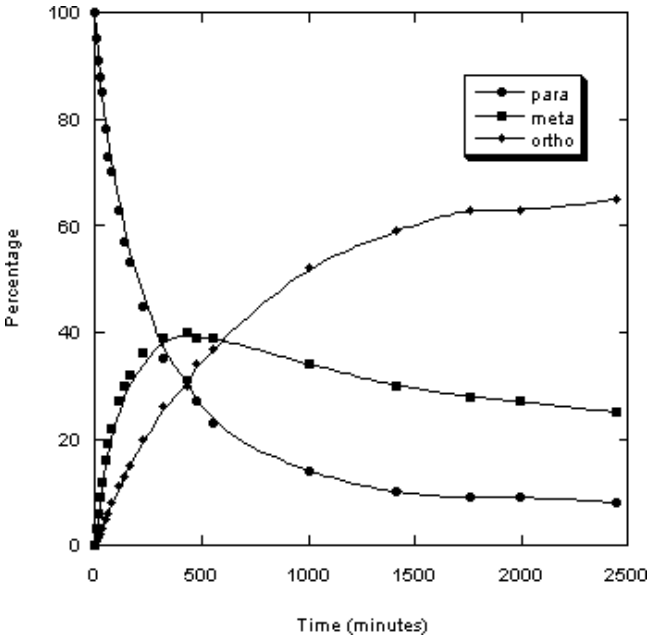

FIGURE 46.1

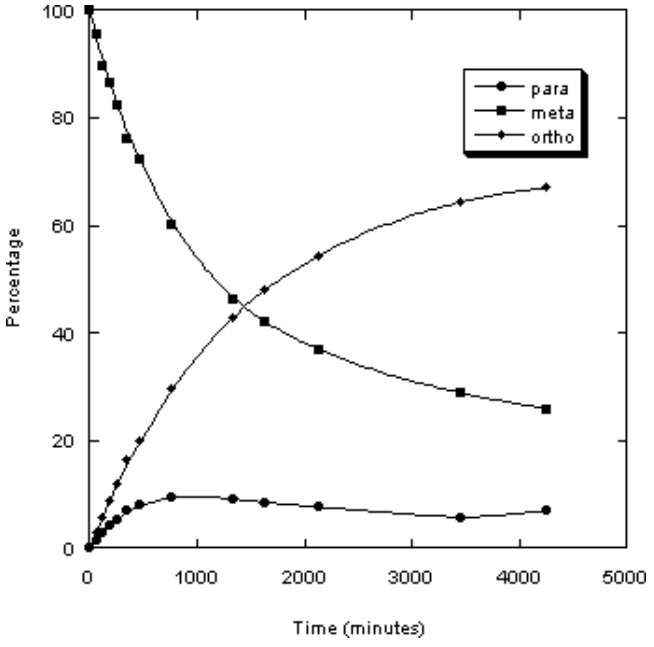

FIGURE 46.2

ortho isomer is observed as would be required if it were formed by secondary photochemistry of the *meta* isomer. Fourth, combining the efficiency data and the initial product ratios with molar absorptivity values for each isomer allows an estimate of the relative efficiencies for all six conversions in the photoequilibration process. These are shown in Scheme 1, scaled to a value of 1 for the least efficient process,

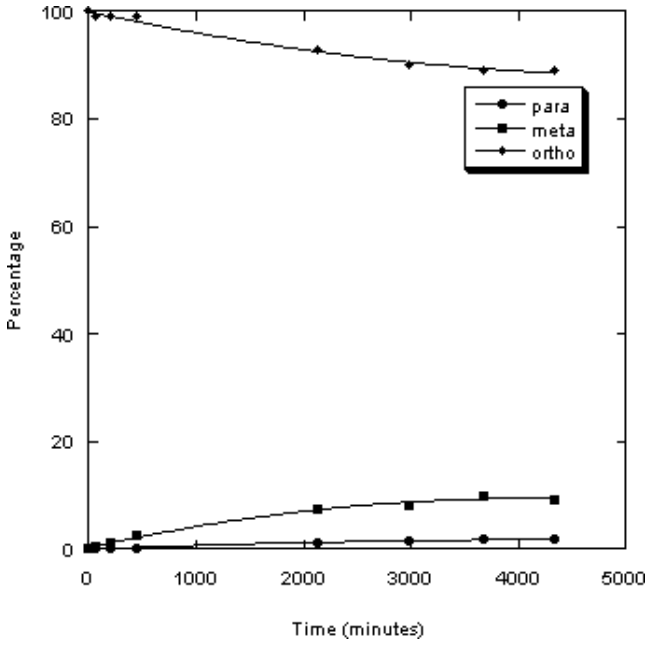

FIGURE 46.3

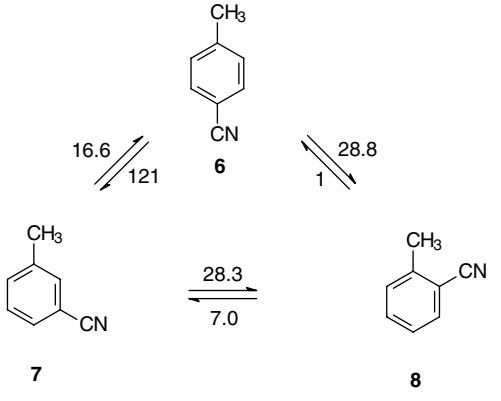

SCHEME 1

conversion of the **8** (*ortho*) to **6** (*para*). By contrast, the most efficient process, conversion of the **6** (*para*) to **7** (*meta*), has a relative efficiency of 121. As expected for a photoequilibration, the most reactive isomer (*para*) reaches the lowest yield (7%) at equilibration. Finally, diene quenching studies indicated that the phototranspositions occur from the excited singlet state, not the triplet state.

In order to determine if a specific carbon was the critical one in the phototransposition reactions of these aromatic nitriles, 2,6-dideutero-4-methylbenzonitrile **6**-d_2 was examined. This substrate has all of the chemically distinct carbons labeled with a substituent so that their positions in the phototransposition can be monitored. As shown in Eq. (46.8), only the cyano-substituted carbon undergoes phototransposition, giving the specifically labeled products **7**-d_2 and **8**-d_2 (as determined by ^{13}C nuclear magnetic resonance [NMR] spectra of reaction mixtures).

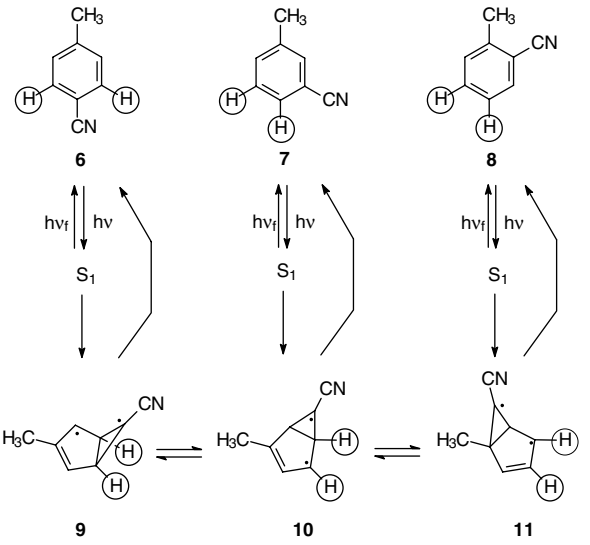

SCHEME 2

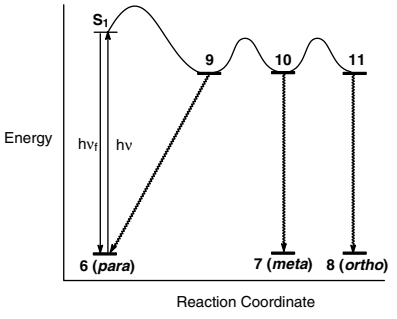

FIGURE 46.4

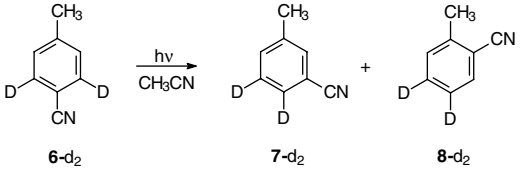

(46.8)

On the basis of these results, we proposed the mechanism outlined in Scheme 2 and the potential energy surface (Figure 46.4). Excitation of the **6** (*para*) isomer, for example, gives S_1, which is a spectroscopic minimum as determined by fluorescence measurements ($\Phi_f = 0.16$, $\tau_s = 9.1$ ns, $E_{0,0} = 101$ kcal/mol). The S_1 state either decays to S_0 or undergoes *meta* bonding to give the biradical **9** (analogous to the "pre-fulvene biradical" proposed for benzene photochemistry). The cyano-substituted carbon then migrates around the periphery of the other five carbons, allowing for the equilibration of the biradicals **9**, **10**, and **11**. By breaking the bridgehead sigma bond, each of these biradicals (presumably ground-state singlets) can return to its corresponding aromatic isomer.

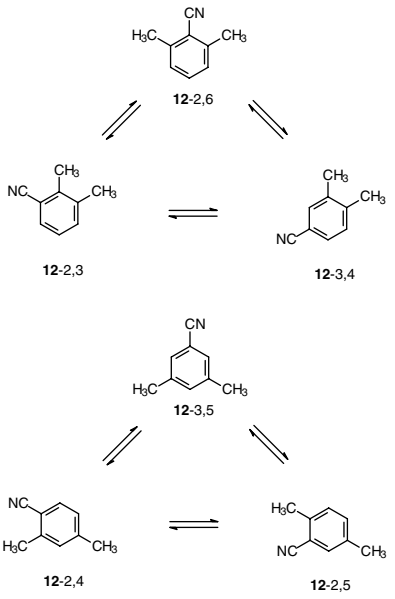

SCHEME 3

Excitation of either of the other isomers puts it on the same surface that equilibrates **9**, **10**, and **11**, although the barrier and thus the efficiency for getting to this surface may be very dependent on the starting isomer. We are in the process of studying the effect of temperature on these phototransposition reactions to see if we can obtain a better understanding of both the barriers on the surface that connects S_1 of each of the isomers to the biradicals and, as well, the surface connecting **9**, **10**, and **11**. We are also attempting high-level MO calculations to see if they would be helpful in understanding these surfaces.

In contrast to the excited-state behavior of benzene- and alkyl-substituted benzenes, where benzvalenes are proposed as the critical intermediates, we have not included them in the mechanism. The observation of both 1,2- and 1,3-phototranspositions in the primary photochemical event requires intermediates like the biradicals proposed.

This proposal is also supported by the photochemistry of the six dimethylbenzonitriles, **12**.[26] These six isomers also photoequilibrate in acetonitrile but in two independent triads. The first triad is comprised of **12**–2,6, **12**–2,3, and **12**–3,4; the second triad is **12**–3,5, **12**–2,5, and **12**–2,4 (Scheme 3). Phototransposition converts the members of one triad to other members of the same triad, although only **12**–3,4 was reactive enough to approach a steady-state ratio. This observation again can be explained if only the cyano-substituted carbon is involved in a transposition reaction with the other five carbons of the ring.

A similar observation has been made for the photochemical transposition reactions in the gas phase of the six isomers of dimethylpyridine.[27] For these compounds, the mechanistic proposal is that the nitrogen atom is the unique one that forms the one-atom bridge in the 6-aza-bicylo[2.1.0]hexenyl biradical and that it migrates around the periphery of the five carbon atoms.

46.3 Photochemistry of Benzonitrile 18 in 2,2,2-Trifluoroethanol[24]

A better understanding of the structure and reactivity of the bicyclic diradical intermediates, **9**, **10**, and **11** proposed in the previous section in Scheme 2 is available from trapping results with TFE, chosen on the basis of literature precedent.[13] We began by repeating and confirming the previous reports, (see Eq. (46.5)[15] on the photochemistry of benzene in TFE (Scheme 4). At low conversion, the major products are **13** and **14**. In agreement with the previous report, by monitoring at low conversions, product **15** was

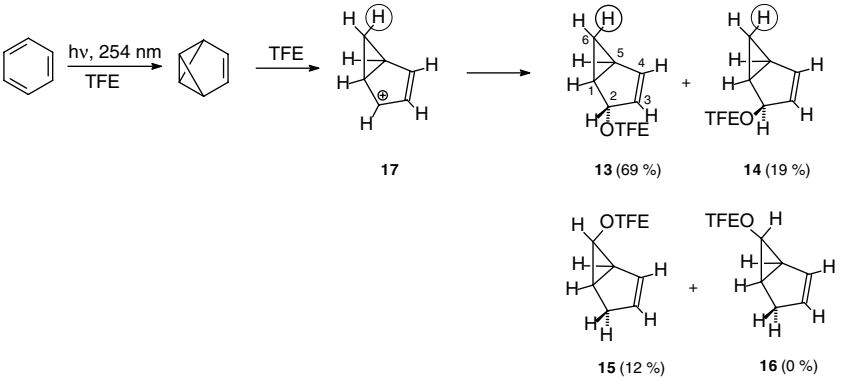

SCHEME 4

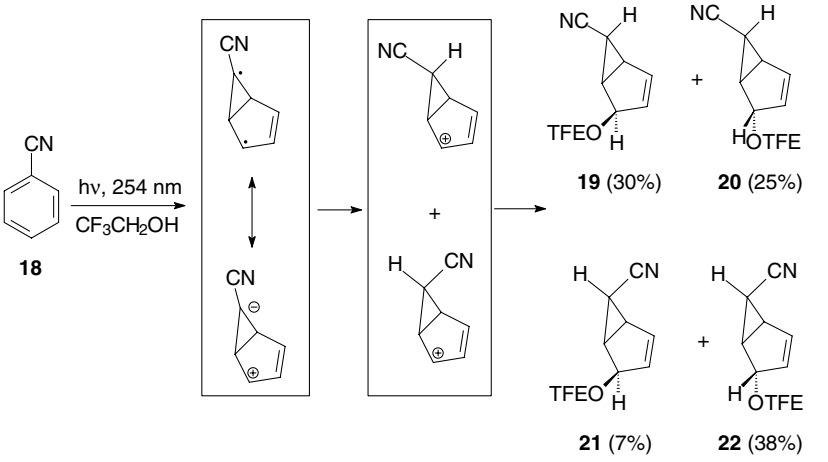

SCHEME 5

found to be a secondary product derived from the photochemistry of **13** and/or **14**. We saw no evidence for formation of the fourth possible isomer **16**. Photolysis of benzene-d_6 in TFE gave the same three products but they now contained only the one proton derived from the solvent. By ^{1}H NMR coupling constants in the cylopropyl ring (~7 Hz when the hydrogen at C6 is *exo* and ~3 Hz when it is *endo*), that proton was clearly at C6 and *endo* in both **13** and **14** (circled in Scheme 4). This result is in agreement with the previously proposed (see Eq. (46.5)) and accepted mechanism, that formation of the alcohol addition products in benzene photochemistry results from *endo* protonation of benzvalene followed by *exo* (major) and *endo* (minor) trapping of the bicyclic allylic cation **17** by TFE.

Photolysis of benzonitrile **18** in TFE gave the four primary photoproducts **19** to **22** as shown in Scheme 5. Because the proton at C6 is solvent derived, the fact that it is observed to be both *endo* (**19** and **20**) and *exo* (**21** and **22**) suggests that a substituted benzvalene is not the critical intermediate. In fact, this observation is in agreement with our mechanistic proposal in Scheme 2, that the important intermediate is analogous to the open singlet "biradicals" **9**, **10**, and **11**. These singlet "biradicals" are expected to have considerable ionic character with negative charge at the cyano-substituted carbon (Scheme 5). Trapping of this zwitterion by TFE protonation at C6, followed by reaction with the nucleophile, gives the observed products.

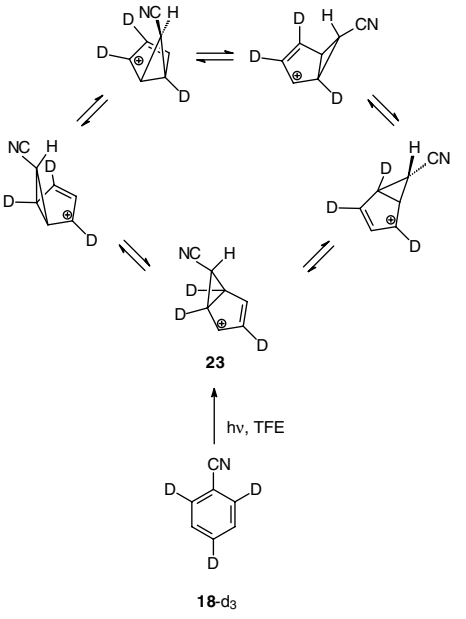

SCHEME 6

Because deuterium substitution had proven to be a useful mechanistic probe for understanding the phototransposition reactions of the methylbenzonitriles, we also examined the deuterated isomer, 2,4,6-trideuteriobenzonitrile, **18**-d_3. Our expectation was that the products would be as in Scheme 5, except specifically deuterated at C1, C3, and C5, if formed from the intermediate **23** (Scheme 6). Indeed, the products had the expected structures, but the deuterium atoms were equally distributed among all five of the carbons C1 to C5 in each of isomeric products **19** to **22** (Scheme 5). This observation can be explained by rapid equilibration of the bicyclo[3.1.0]hexenyl cations by an allowed thermal 1,4-sigmatropic shift. This pathway requires inversion of configuration of the migrating carbon, C6, which keeps the H *endo* (as shown in Scheme 6) leading to **19** and **20** or *exo* leading to **21** and **22**. Therefore, the stereochemistry of the original protonation of the zwitterion determines the stereochemistry of **23** and the final products but not the deuterium distribution. This rearrangement must be very fast to compete with trapping of the cation by TFE. Rapid equilibration of similar cations has been observed previously by NMR. For instance, the heptamethyl derivative has a free energy of activation for rearrangement of only 9 kcal/mol at –89°C.[28]

46.4 Photochemistry of 4-, 3-, and 2-Methylbenzonitrile (6, 7, and 8) in TFE[24]

With an understanding of the photochemistry of benzonitrile in TFE, we next proceeded to the three methyl substituted isomers. The results are shown in Scheme 7. The first point of interest is that no phototranspositions were observed. Instead, reaction with TFE occurred to give a mixture of six addition products that were characterized by ^{1}H and ^{13}C NMR. Second, the same products were obtained from both **6** (*para*) and **7** (*meta*), although in somewhat different ratios. The yields are shown as normalized percentages in Scheme 7, the first number from **6** as substrate and the second from **7**. Again, **8** (*ortho*) was essentially photochemically inert.

These observations are consistent with the previously proposed mechanism for benzonitrile (Schemes 5 and 6). Trapping of the biradical/zwitterion by protonation must be faster than rearrangement because phototranspositions are not observed. The two zwitterions formed, one from 3-methyl and one from

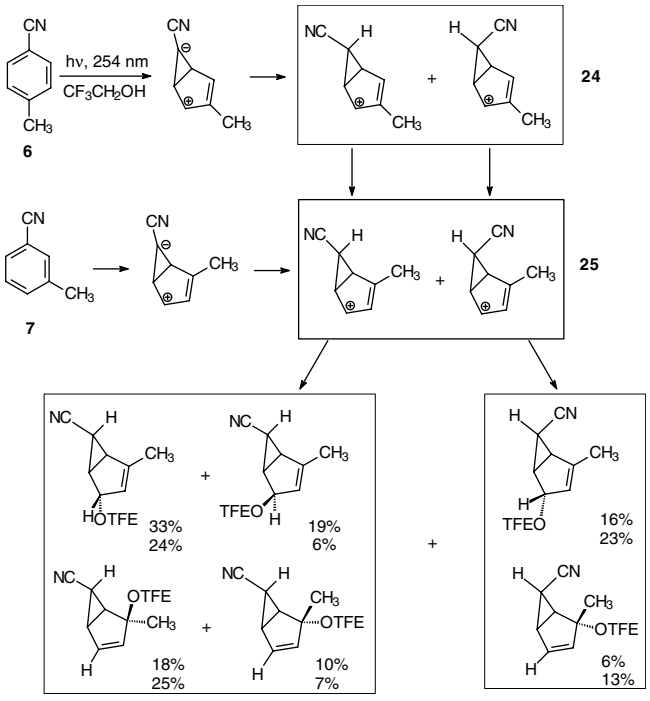

SCHEME 7

4-methylbenzonitrile, will be different but both are protonated either *exo* or *endo* at C6 (Scheme 7). Once formed, the cations will undergo the 1,4-sigmatropic equilibration, but now the five possible cations are not degenerate because of the methyl substitution. The stable ones will have the methyl group at the terminal end of the allylic cation, **25** *exo* and *endo*, rather than **24** *exo* and *endo*. Trapping of **25** by TFE gives the six stereoisomers. The missing isomers are those with both the cyano and TFE groups *endo*.

Photochemical *meta* cycloaddition reactions of benzonitrile and the methylbenzonitriles with alkenes and dienes have been reported previously, and the results are summarized in a recent review.[9] Examples include benzonitrile itself with seven alkenes and dienes (Table 2 in Reference 9) and each of the three isomeric methylbenzonitriles with *E*-1,2-dichloroethene, furan, and cyclopentene (Table 3 in Reference 9). In all cases, cycloadditions were observed to give, along with other products, the dihydrosemibullvalenes expected from the trapping of a bicyclic intermediate analogous to that proposed for the phototranspositions and photoadditions to TFE. However, none of these products resulted from an intermediate that had the cyano group at C6.

This observation indicates that the two reactions are quite different mechanistically. The orientation in cycloadditions of alkenes and dienes apparently proceeds by a polarization of S_1 of the arene by the approach of the alkene or diene. This polarization is determined by substituent stabilization of developing charges. For the phototranspositions and photoadditions of TFE reported here, S_1 of the arene is assumed to undergo a unimolecular deformation to a reactive intermediate before rearrangement or trapping.

46.5 The Phototranspositions in Acetonitrile and the Photoaddition of TFE to Substituted Benzenes: A Survey[25]

Because the reactions described previously are providing fundamental information about how substitutents affect the geometry and reactivity of substituted aromatics, a survey of substituents was undertaken. The results are summarized in Table 46.1 and Figure 46.5.

TABLE 46.1 Summary of Phototranspositions (PTs) in Acetonitrile and Photoadditions (PAs) of TFE of Substituted Benzenes, C_6H_4XY

Compound	X	Y	Isomer	Phototranspositions	Photoadditions
Benzene	H	H	—	Yes, with 1,3,5-d_3[a]	Yes, *endo*[b]
Toluene	CH_3	H	—	—	Yes, *endo*[b]
Anisole	CH_3O	H	—	—	No
Fluorobenzene	F	H	—	—	No
Benzonitrile (**18**)	CN	H	—	—	Yes, *endo* + *exo*[b]
Trifluoromethylbenzene	CF_3	H	—	—	Yes, GC/MS only
Methyl benzoate	CO_2CH_3	H	—	—	No
Xylene	CH_3	CH_3	*ortho*	*meta:para* = 11:1[c]	Yes, *endo*[b]
			meta	*ortho:para* = 6.0:1[c]	No stable products[d]
			para	*meta:ortho* > 25:1[c]	No stable products[d]
				ortho:meta:para = 1:1.4:0.3[d]	
Methylbenzonitrile (**6**, **7**, **8**)	CH_3	CN	*ortho*	*meta:para* = 7.1:1[c]	No[e]
			meta	*ortho:para* = 1.7:1[c]	Yes
			para	*meta:ortho* = 4.2 :1[c]	Yes
				ortho:meta:para = 1:4:32[d]	
Methylanisole	CH_3	OCH_3	*ortho, meta, para*	No	No
Methoxybenzonitrile	OCH_3	CN	*ortho, meta, para*	No	No
Dicyanobenzene	CN	CN	*ortho, meta, para*	No	No
Methyl 4-toluylsulfone	CH_3	SO_2CH_3	*para*	No	No
Trifluoromethyltoluene	CH_3	CF_3	*ortho*	*meta:para* > 10:1[c]	Yes, GC/MS only
			meta	*ortho:para* = 0.25[c]	Yes, GC/MS only
			para	*meta:ortho* > 20:1[c]	No
				ortho:meta:para = 1:0.67: 0.16[d]	
Trifluoromethylbenzonitrile	CF_3	CN	*ortho*	*meta:para* = 1.7:1[c]	No
			meta	*ortho:para* = 0.81:1[c]	No
			para	*meta:ortho* = 7.2:1[c]	No
				ortho:meta:para = 1:2.7:3.1[d]	
				In both acetonitrile and TFE	
Fluorotoluene	CH_3	F	*ortho*	Very slow	No
			meta	*ortho:para* = 5.0:1[c]	No
			para	Very slow	No

[a] Reference 15.
[b] Stereochemisty of the proton at C6 of the bicylo[3.1.0]hexene products; *endo* only implies a benzvalene intermediate.
[c] Product ratio at very low conversion; high values from the *ortho* or *para* starting material suggest that 1,2-transpositions dominate.
[d] Relative reactivity.
[e] Reference 25.

For benzene and monosubtituted benzenes, in the absence of deuterium substitution, only TFE additions can be observed. These additions occur for benzene and alkylbenzenes as well as those that are substituted with electron-withdrawing groups (CN, CF_3) but not electron-donating groups (CH_3O). Unfortunately, the addition products to trifluoromethylbenzene were not characterized because even evaporation of the solvent resulted in non-analyzable (^{1}H NMR) decomposition products (oligomers?). For the disubstituted arenes, electron-withdrawing groups again seemed to favor both phototranspositions and photoadditions of TFE. The trifluoromethyltoluenes **26** (*para*), **27** (*meta*), and **28** (*ortho*) are perhaps the most interesting.

Plots for the phototransposition of these three compounds in acetonitrile are shown in Figures 46.6, 46.7, and 46.8, respectively. In comparison with the three methylbenzonitriles in Figures 46.1 to 46.3, several points are noteworthy. First, the reactions of the trifluoromethyl arenes are faster, with photostationary states being reached in about a tenth of the time. Second, the photostationary state reached is comprised of 9% *para*, 37% *meta*, and 55% *ortho* (i.e., *ortho* is the dominant isomer). The reverse was observed for the methylbenzonitriles (i.e., *para* was the dominant isomer). Finally, examination of product

1. Substrates that isomerize in acetonitrile.

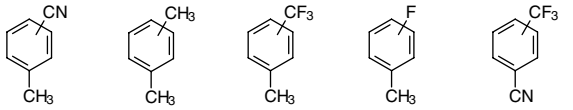

2. Substrates that form addition products with TFE.

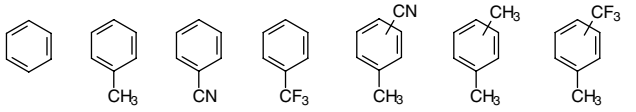

3. Substrates that do not isomerize in acetonitrile

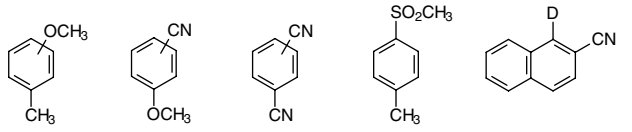

4. Substrates that do not form addition products with TFE.

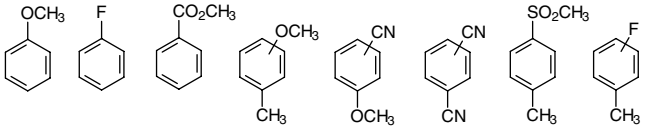

FIGURE 46.5

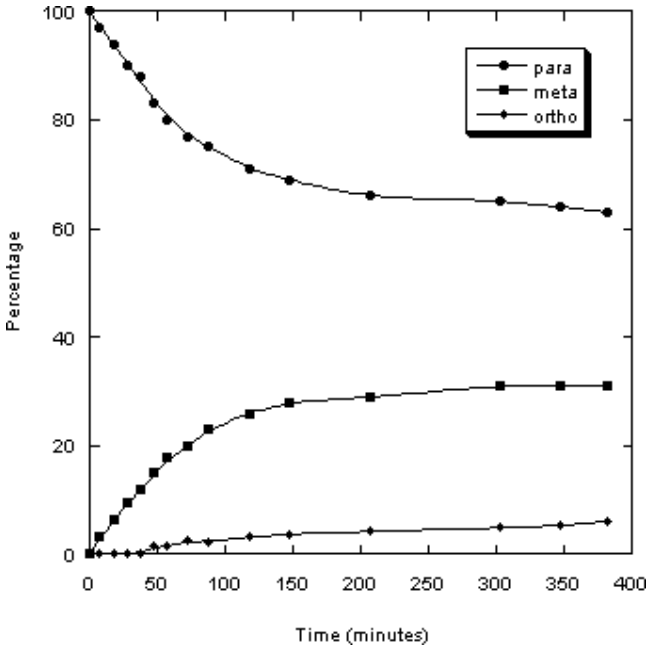

FIGURE 46.6

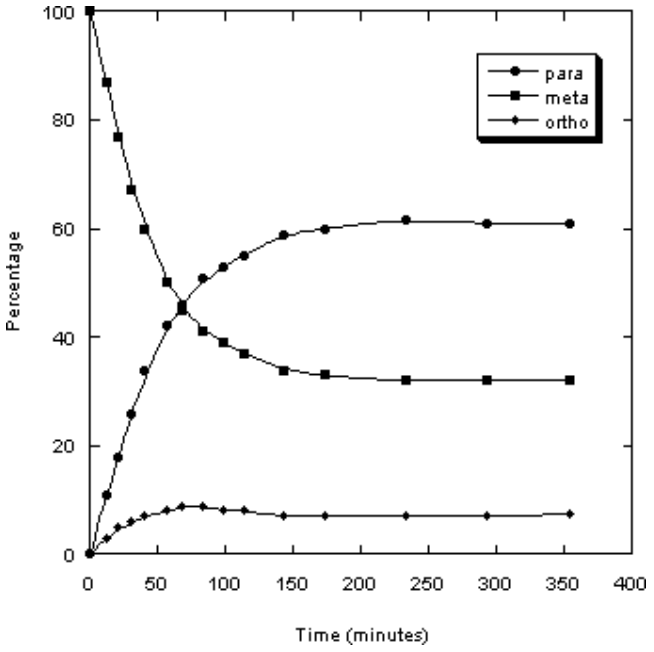

FIGURE 46.7

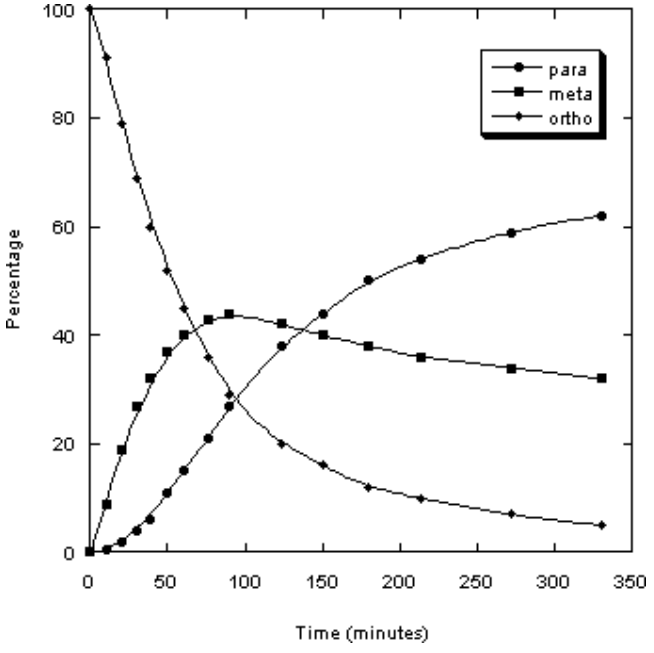

FIGURE 46.8

ratios at very low conversions indicated that 1,2-phototranspositions were much favored over 1,3-. The ratio of *meta*:*para* from *ortho* was greater than 10:1, and the *meta*:*ortho* ratio from *para* was greater than 20:1. These observations suggest that benzvalene intermediates, which allow only 1,2-transpositions, may be more important than for the benzonitriles. The fact that the stable hexa(trifluoromethyl)benzvalene can be

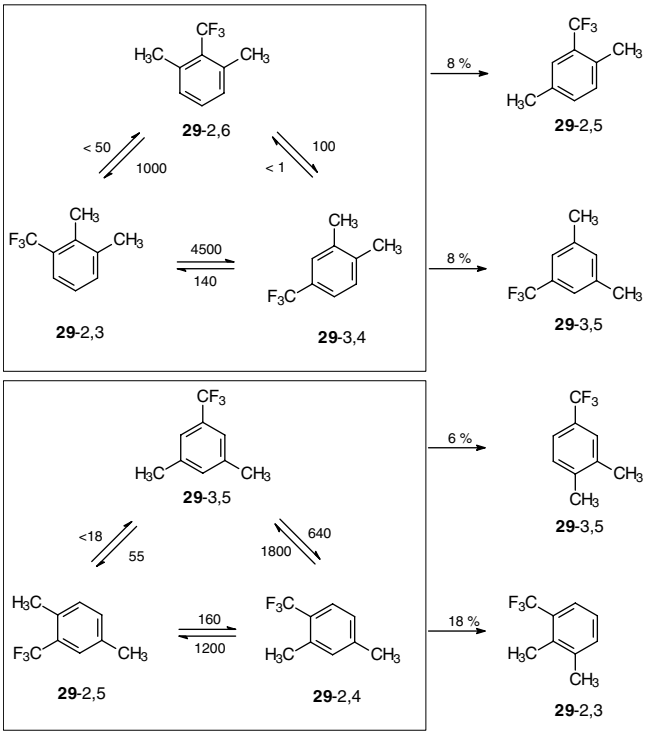

SCHEME 8

isolated from the photochemistry of hexa(trifluoromethyl)benzene indicates that trifluoromethyl groups clearly stabilize these strained σ-bonds.[29] The best probe for benzvalene intermediates would be the stereochemistry (*endo* vs. *exo*) of the protonation in the TFE. Unfortunately, these photoadducts could be observed (by gas chromatography/mass spectrometry [GC/MS]) but not characterized. Another interesting observation in Table 46.1 for the three trifluoromethybenzonitriles is that they undergo phototransposition reactions in both acetonitrile and TFE.

46.6 Photochemistry of the Six Isomers of Dimethylbenzotrifluoride 29 in Acetonitrile[30]

In order to probe which of the substituents was responsible for the phototransposition reactions of trifluoromethyl substituted benzenes, the six isomers of dimethylbenzotrifluoride **29** were synthesized and their photochemistry in acetonitrile examined (Scheme 8). This scheme is analogous to that for the dimethylbenzonitriles in Scheme 3 with the advantage that the reactions are more efficient and go to equilibrium for most substrates. An example is shown in Figure 46.9 for 2,4-dimethylbenzonitrile. These results are summarized in Table 46.2, where the time required for 10% conversion of the substrate is given along with the ratio of the major products from each. The major photochemical process (Figure 46.9, upper three traces) again divides the isomers into the two triads of Scheme 8, demonstrating that the trifluormethyl-substituted carbon is the principle one responsible for phototransposition. Using the relative efficiencies and the product ratio for each isomer allows a relative scale of reactivities for each of the 12 possible conversions to be evaluated (shown with each arrow in Scheme 8), arbitrarily scaled to a value of 4500, the most efficient process, for conversion of **29**–2,3 to **29**–3,4. The values range from <1 to 4500. This large range means that the substrates with the lower reactivity would appear to be photostable unless one was specifically looking for phototranspositions.

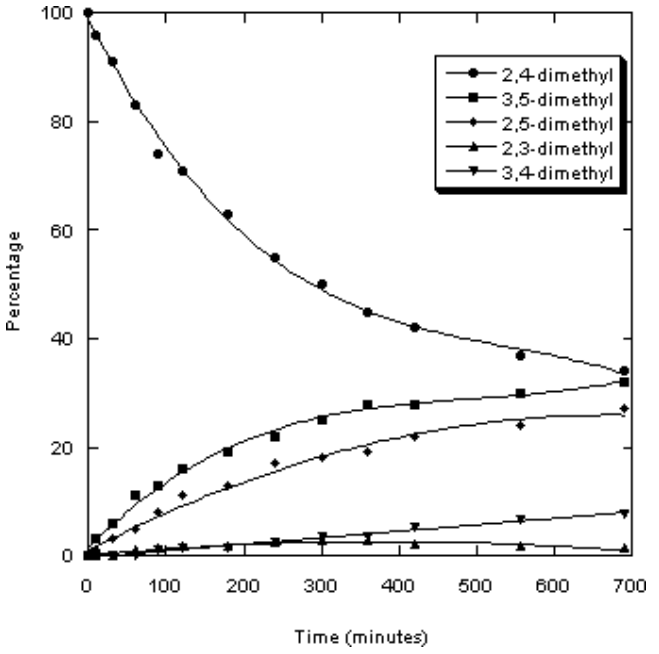

FIGURE 46.9

TABLE 46.2 Photolysis of Dimethylbenzotrifluorides 29 in Acetonitrile

Isomer	Time for 10% Conversion (minutes)	Major Products and Their Ratio at Low Conversion	Leakage
29–2,6	80	**29**–2,3 : **29**–3,4 = 10	**29**–2,5 = 8%
29–2,3	20	**29**–3,4 : **29**–2,6 > 100	—
29–3,4	665	**29**–2,3 : **29**–2,6 > 100	**29**–3,5 = 8%
29–3,5	130	**29**–2,4 : **29**–2,5 = 12	**29**–3,4 = 6%
29–2,4	30	**29**–3,5 : **29**–2,5 = 1.6	**29**–2,4 = 18%
29–2,5	500	**29**–2,4 : **29**–3.5 > 50	—

An important point to make is that some potentially efficient processes will be invisible. For instance, the two least reactive compounds, **29**–3,4 and **29**–2,5, could be interchanging the CF_3-substituted carbon with the neighboring H-substituted carbon with no net structural change. The two steps that may be the most important ones in controlling these reactivities are (1) formation of the bicyclic biradical with the CF_3 group at C6, and (2) migration of that carbon. Overall, the fastest process of the 12 possible ones is that which converts, in a 1,2-transposition step, the sterically crowded **29**–2,3 to **29**–3,4. Conversion of the other sterically congested isomer **29**–2,6 to **29**–2,3 is somewhat slower (1:4), perhaps because the cyclopropyl ring of the intermediate bicyclic biradical will be trisubstituted, as opposed to disubstituted from **29**–2,3; therefore, its efficiency of formation is slower. The slowest process, conversion of **29**–3,4 to **29**–2,6, is the one that makes this most congested isomer. The most reactive compound in the lower triad of Scheme 8 is **29**–2,4, which again will generate a cyclopropyl intermediate that is disubstituted. We conclude that the CF_3 group is necessary to form the reactive biradicals because of the requirement for an electron withdrawing group at C6 and that methyl substitution on the cyclopropyl ring also helps. Relief of steric congestion is also an important factor.

In parallel with the major photochemical events, some of the substrates show leakage from one triad to the other. This is shown in Figure 46.9 (lower two traces), where leakage gives **29**–2,3 which then

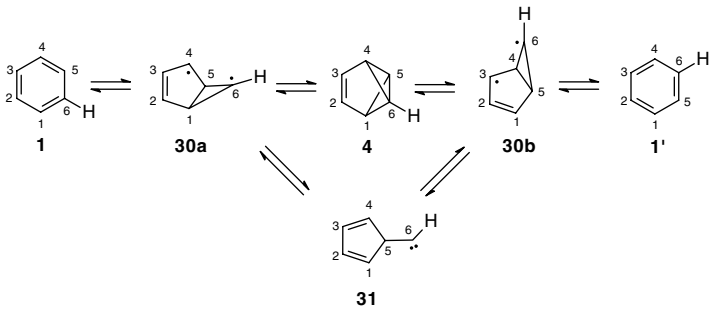

SCHEME 9

undergoes its own phototransposition, mainly to **29**–3,4. These leakage processes, along with the percentage of this pathway, are given in Table 46.2 and shown on the right-hand side of Scheme 8. These processes represent transposition of the methyl-substituted carbons, an example of the first phototransposition ever reported,[10] the isomerization of the xylenes. They provide a minor but significant perturbation in the triads. The relative reactivity of the xylenes in acetonitrile are 1:1.4:0.3 for *ortho*, *meta*, and *para*, respectively.[25] In fact, all of the leakage processes are from the more reactive isomers, three from *meta* dimethyl substrates (**29**–2,5, **29**–3,5 and **29**–2,4) and the fourth from an *ortho* isomer (**29**–3,4).

46.7 Molecular Orbital Calculations

Clearly, computational results could be helpful in understanding the effect that these substituents have on the processes that begin with excitation from S_0 to S_1 followed by conversion of S_1 along the potential energy surface that leads to biradicals, benzvalenes, and other intermediates. Recent high-level calculations for these pathways have been reported for benzene itself and serve as a useful starting point.

Bernardi et al.[31] have reported an MC-SCF study of the S_1 and S_2 surface for benzene. The interest in the S_2 surface is a consequence of the fact that this state leads to Dewar benzene **5**, along with benzvalene **4**. In contrast, S_1 is converted only to benzvalene, which is more relevant to our experimental observations in solution. On the S_1 surface, using a 4–31G basis set, the only minimum found was the initially formed excited state, 110.9 kcal/mol above the ground state, still of D_{6h} symmetry but with slightly longer bond lengths, 1.43 Å vs. 1.39 Å and a C1 to C5 distance of 2.48 Å. A transition state, with a shorter C1 to C5 distance of 2.06 Å leading toward the bicyclic biradical, was found at 133.9 kcal/mol (23.0 kcal/mol above S_1) which proceeds through a conical intersection to the ground state of the biradical where the surface is very flat and has several minima and transition states separated by only a few kcal/mol. The minimum on this flat region, a prebenzvalene diradical **30a** (C1 to C5 distance of 1.60 Å) (Scheme 9), at 125.0 kcal/mol does not have C_s symmetry but is slightly distorted towards benzvalene. The barrier (only 0.12 kcal/mol higher than this minimum) to benzvalene (104.2 kcal/mol) is very small; the barrier to benzene **1**, also small, is only 1.4 kcal/mol. In a second publication from the same groups,[32] dynamics calculations and semiclassical surface-hopping trajectories were used. These methods showed that only a small fraction of the trajectories proceed along the reaction path from S_1 through the conical intersection to the prefulvene biradical. Most trajectories result in return to S_0 of benzene.

Although phototransposition reactions were not discussed in these papers, these computational results suggest a reasonable pathway from S_1 to **30a** over a small barrier (0.12 kcal/mol) to benzvalene **4** and then over a 20.9 kcal/mol barrier to **30b** (Scheme 9). If **30a** returns to benzene, no transposition will occur, but if **30b** does then C5 and C6 are interchanged, leading to transposition if suitable labels are attached to the carbons. In fact, conversion of **4** to **30b** may not be necessary as there is experimental[33] and computational evidence[34] that this conversion of **4** to benzene occurs by concerted pathway of lower energy that does not involve biradicals. For some substituents, conversion of **30a** to **30b** may occur

without the intervention of a benzvalene. Finally, photolysis in TFE would result in rapid trapping of **30a** to give the photoaddition products, thus preventing phototransposition.

In a more recent publication, von R. Schleyer[34] and co-workers examined the ground-state surface for benzene pyrolysis using CCSD calculations to obtain energies. The transition state (100.9 kcal/mol above benzene) for the concerted conversion of benzvalene to benzene is quite asymmetric, the two breaking bonds differing in length by 0.6 Å (2.32 and 1.70 Å), and an E_a of 29.3 kcal/mol was calculated. They also point out that biradical structures such as **30** in Scheme 9 have several possible geometries, **30**-*exo* and **30**-*endo* for the hydrogen at C6, with and without C_s symmetry, all being very close in energy to the transition state. The relative energy of these structures and whether they are minima or not is dependent on the method of calculation.

Another intermediate that has been found on this surface is 2,4-cyclopentadienylcarbene **31**, identified as a key intermediate in the photochemical conversion of benzene **1** to fulvene **2**.[34] Again, several geometries are possible for **31** with the hydrogen at C6 *exo* and *endo*. The *endo* form (107.1 kcal/mol above benzene) is more stable, but a stable form of the *exo* species could not be located as it always collapsed to benzvalene. The structure of the *endo* form is also asymmetric, indicating a hyperconjugative interaction between the carbene center and one of the sigma bonds of the cyclopentadiene ring. This carbene exists in a shallow minimum with low energy barriers to benzene **1** (7.6 kcal/mol), benzvalene **4**, (2.6 kcal/mol), and fulvene **2** (4.6 kcal/mol). In agreement with experiment,[36] collapse to benzvalene is the lowest energy pathway. For the phototransposition reaction, the carbene could also be an intermediate/transition state that connects the two biradical structures (Scheme 9).

For the photoadditions of TFE to benzene and substituted benzenes, cyclopentadienyl carbenes are also possible as intermediates. Protonation will result in the formation of cyclopentadienylmethyl cations. These primary cations would be expected to collapse to the more stable allylic ones (i.e., **17** in Scheme 4), which will be relatively long lived, as the thermal opening to the benzenium ion, although exothermic, is thermally forbidden. In fact, the activation energy for this process has been estimated at 19 kcal/mol at –20°C.[37]

These calculations demonstrate that the potential energy surfaces connecting these intermediates are difficult to evaluate because of the very small energy differences between the various possibilities. Substituents will likely have a significant perturbing effect on their relative stabilities. We are in the process of doing such calculations on substituted (CN, F, OH) cases.

46.8 Summary

The reactions described are clearly giving fundamental information about changes in electron distribution and geometry that occur on excitation of substituted benzenes to S_1. Because electron-withdrawing groups seem to be the most effective at inducing these reactions, we plan to examine other examples. As well, traps other than TFE are being examined with the idea that the addition products might be more easily characterized. Intramolecular traps are also of interest. As the opening sentence of this review states, excited states of aromatics are indeed "extremely flexible and extrovert acrobatics."

References

1. Havinga, E., de Jongh, R. O., and Kronenberg, M. E., Photoreactions of aromatic molecules, *Helv. Chim. Acta*, 50, 2550–2560, 1967.
2. McDonald, B. and Bryce-Smith, D., The photoisomerization of benzene to fulvene, *Proc. Roy. Soc. London*, 287–288, 1957.
3. Katz, T. J. and Acton, N., Synthesis of prismane, *J. Am. Chem. Soc.*, 95, 2738–2739, 1973. (Prismane itself does not seem to have been isolated from the photochemistry of benzene; it has been synthesized by photolysis of an azo precursor.)
4. Wilzbach, K. E. and Kaplan, L., Photoisomerization of tri-*t*-butylbenzenes: prismane and benzvalene isomers, *J. Am. Chem. Soc.*, 87, 4004–4006, 1965.

5. Wilzbach, K. E., Ritscher, J. S., and Kaplan, L., Benzvalene: the tricyclic isomer of benzene, *J. Am. Chem. Soc.*, 89, 1031–1032, 1967.
6. Ward, H. R. and Wishnok, J. S., The vacuum ultraviolet photolysis of liquid benzene. Photoisomerization of benzene to Dewar benzene, J. Am. Chem. Soc., 90, 1085-1086,1968.
7. Angus, H. J. F. and Bryce-Smith, D., Addition of maleic anhydride to benzene, Proc. Roy. Soc. London, 326-327, 1959.
8. Wender, P. A., Siggel, L., and Nuss, J. M., Arene-alkene photocycloaddition reactions, in *Organic Photochemistry*, Vol. 10, Padwa, A., Ed., Marcel Dekker, New York, 1989, 357–473.
9. Cornelisse, J., The meta photocycloaddition of arenes to alkenes, *Chem, Rev.*, 93, 615–669, 1993.
10. Wilzbach, K. E. and Kaplan, L., Photoisomerization of dialkylbenzenes, *J. Am. Chem. Soc.*, 86, 2307–2308, 1964.
11. Burgstahler, A. W., Chien, P.-L., and Abdel-Rahman, M. O., Chemistry of *o*-di-*t*-butylbenzene, *J. Am. Chem. Soc.*, 86, 5291–5290, 1964.
12. Kaplan, L.,Wilzbach, K. E., Brown, W. G., and Yang, S. S., Phototransposition of carbon atoms in the benzene ring, *J. Am. Chem. Soc.*, 87, 675–676,1965.
13. Kaplan, L., Ritscher, J. S., and Wilzbach, K. E., The photochemical 1,3-addition of alcohols to benzenes, *J. Am Chem. Soc.*, 88, 2881–2882, 1966.
14. Farenborst, E. and Bickel, A. F., Photochemical reactions of benzene with acids, *Tetrahedron Lett.*, 5911–5913, 1966.
15. Kaplan, L., Rausch, D. J., and Wilzbach, K. E., Photosolvation of benzene: mechanism of formation of bicyclo[3.1.0]hex-3-en-2-yl and of bicyclo[3.1.0]hex-2-en-6-yl derivatives, *J. Am. Chem. Soc.*, 94, 8638–8640, 1972.
16. Berson, J. A. and Hasty, N. M., Jr., Solvolytic behavior of bicyclo[3.1.0]hex-3-en-2-yl derivatives: some observations on the mechanism of photolysis of benzene in hydroxylic media. *J. Am. Chem. Soc.*, 93, 1549–1551, 1971.
17. Bryce-Smith, D. and Gilbert, A., The organic photochemistry of benzene, Part I, *Tetrahedron*, 32, 1309–1326, 1976.
18. Bryce-Smith, D. and Gilbert, A.,The organic photochemistry of benzene, Part II, *Tetrahedron*, 33, 2459–2490, 1977.
19. Bryce-Smith, D. and Gilbert, A., *Rearrangements of the benzene ring, in Rearrangements in Ground and Excited States*, Vol. 3, deMayo, P., Ed., Academic Press, New York, 1980, 349–379.
20. Kaupp, G., Photochemical rearrangements and fragmentations of benzene derivatives and annelated arenes, *Angew. Chem. Int. Ed. Engl.*, 19, 243–275, 1980.
21. Gilbert, A., Ring isomerization of benzene and naphthalene derivatives, in *Organic Photochemistry and Photobiology*, Horspool, W. M. and Song, P.-S., Eds., CRC Press, Boca Raton, 1995, 229–236.
22. Hilborn, J. W., McKnight, E., Pincock, J. A., and Wedge, P. J., Photochemistry of substituted benzyl acetates and benzyl pivalates: a reinvestigation of substituent effects, *J. Am. Chem. Soc.*, 116, 3337–3346, 1994.
23. MacLeod, P. J., Pincock, A. L., Pincock, J. A., and Thompson, K. A., Photochemical equilibration/isomerization of *p*-, *m*-, and *o*-methylbenzonitrile, *J. Am. Chem. Soc.*, 120, 13354–13361, 1998.
24. Foster, J., Pincock, A. L., Pincock, J. A., and Thompson, K. A., Photochemical addition of 2,2,2-trifluoroethanol to benzonitrile and *p*-, *m*-, and *o*-methylbenzonitrile, *J. Am. Chem. Soc.*, 120, 13354–13361, 1998.
25. Foster, J., Pincock, A. L., Pincock, J. A., Rifai, S., and Thompson, K. A., The photoequilibration of the *ortho*-, *meta*-, and *para*-isomers of substituted benzenes in acetonitrile and the photoaddition of 2,2,2-trifluoroethanol (TFE) to the same isomers: a survey, *Can. J. Chem.*, 78, 1019–1029, 2000.
26. Howell, N., Pincock, J. A., and Stefanova, R., The phototransposition in acetonitrile and the photoaddition of 2,2,2-trifluoroethanol to the six isomers of dimethylbenzonitrile, *J. Org. Chem.*, 65, 6173–6178, 2000.
27. Pavlik, J. W., Kebede, N., Thompson, M., Colin Day, A., and Barltrop, J. A., Vapor-phase photochemistry of dimethylpyridines, *J. Am. Chem. Soc.*, 121, 5666–5673, 1999.

28. Berson, J. A. and Hasty, N. M., Jr., Solvolytic behavior of bicyclo[3.1.0]hex-3-en-2-yl derivatives: some observations on the mechanism of photolysis of benzene in hydroxylic media. *J. Am. Chem. Soc.*, 93, 1549–1551,1971.
29. Barlow, M. G., Haszeldine, R. N., and Hubbard, R., Valence-bond isomer chemistry. Part 1. The valence-bond isomers of hexakis(trifluoromethyl)- and hexakis(pentafluoroethyl)-benzenes, *J. Chem. Soc. (C)*, 1232–1237, 1970.
30. DeCosta, D. P. and Pincock, J. A., The photochemistry of the six isomers of dimethylbenzotrifluoride, *J. Org. Chem.*, submitted.
31. Palmer, I. J., Ragazos, I. N., Bernardi, F., Olivucci, M., and Robb, M. A., An MC-SCF study of the S_1 and S_2 photochemical reactions of benzene, *J. Am. Chem. Soc.*, 115, 673–686, 1993.
32. Smith, B. R., Bearpark, M. J., Robb, M. A., Bernardi, F., and Olivucci, M., "Classical wavepacket" dynamics through a conical intersection: application to the S_1/S_2 photochemistry of benzene, *Chem. Phys. Lett.*, 242, 27–32, 1995.
33. Turro, N. J., Renner, C. A., Katz, T. J., Wiberg, K. B., and Connon, H. A., Kinetics and thermochemistry of the rearrangement of benzvalene to benzene: an energy sufficient but non-chemiluminescent reaction, *Tetrahedron Lett.*, 4133–4136, 1976.
34. Bettinger, H. F., Schreiner, P. R., Schaefer III, H. F., and Schleyer, P. V. R., Rearrangements on the C_6H_6 potential energy surface and the topomerization of benzene, *J. Am. Chem. Soc.*, 120, 5741–5750, 1998.
35. Dreyer, J. and Klessinger, M., The photochemical formation of fulvene from benzene via prefulvene: a theoretical study, *Chem.-Eur. J.*, 2, 335–341, 1996.
36. Burger, U. and Gandillon, G., The ring closure of 5-methylcyclopenta-1,3-dien-5-ylcarbene to methylbenzvalene: an intramolecular 1,4-cheletropic carbene addition, *Tetrahedron Lett.*, 4281–4284, 1979.
37. Vogel, P., Saunders, M., Hasty, Jr., N. M., and Berson, J. A., Bicyclo[3.1.0]hex-3-en-2-yl cation, *J. Am. Chem. Soc.*, 93, 1551–1552, 1971.

47

The Photostimulated $S_{RN}1$ Process: Reaction of Haloarenes with Carbanions

Roberto A. Rossi
Universidad Nacional de Córdoba

Alicia B. Peñéñory
Universidad Nacional de Córdoba

47.1 Introduction

For unactivated aromatic and heteroaromatic substrates, where a polar substitution is not favorable, nucleophilic substitution is feasible through processes that involve electron transfer (ET) steps. In these reactions, an aromatic compound bearing an adequate leaving group is substituted at the *ipso* position by a nucleophile in a unimolecular radical nucleophilic substitution mechanism (or $S_{RN}1$), which is a chain process that involves radicals and radical anions as intermediates.

The process has a considerably wide scope in relation to substrates, nucleophiles, and synthetic possibilities. In addition to halides, other leaving groups are known, such us $(EtO)_2P(O)O$, RS (R = Ar, alkyl), $ArSO_2$, PhSe, RSN_2 (R = *t*-Bu, Ph), N_2BF_4, R_3N^+). For substrates having two leaving groups, disubstitution by the same nucleophiles can be obtained.

Many substituents are compatible with the reaction, such as alkyl groups, OR, OAr, SAr, CF_3, CO_2R, NH_2, NHCOR, NHBoc, SO_2R, CN, COAr, NR_2, F, among others. Even though the reaction is not inhibited by the presence of negatively charged substituents such as carboxylate ions, other charged groups such

0-8493-1348-1/04/$0.00+$1.50

$$(ArX)^{\bullet -} \longrightarrow Ar^{\bullet} + X^{-} \quad (47.1)$$

$$Ar^{\bullet} + Nu^{-} \longrightarrow (ArNu)^{\bullet -} \quad (47.2)$$

$$(ArNu)^{\bullet -} + ArX \longrightarrow ArNu + (ArX)^{\bullet -} \quad (47.3)$$

$$ArX + Nu^{-} \longrightarrow ArNu + X^{-} \quad (1,3)$$

SCHEME 1

as oxyanions hinder the process. In general, substituents such as NO_2 groups are not suitable for $S_{RN}1$ substitution on aromatic substrates.

Some of the most common nucleophiles through which a new CC bond can be formed are carbanions from hydrocarbons, nitriles, ketones, esters, *N*,*N*-dialkyl acetamides and thioamides, and mono- and dianions from β-dicarbonyl compounds. The synthesis of indoles, isocarbostyrils, isoquinolines, benzazepines, binaphthyls, etc. and an important number of natural products has been achieved by ring closure reactions of carbanions with suitable substrates through the $S_{RN}1$ mechanism. Several reviews have been published in relation to aromatic $S_{RN}1$ reactions[1–4] and to the synthetic applications of the process.[5,6]

47.2 Mechanism

The $S_{RN}1$ mechanism is a chain process, for which the main steps are presented in Scheme 1. Overall, Eqs. (47.1) to (47.3) depict a nucleophilic substitution in which radicals and radical anions are intermediates.

This chain process requires an initiation step. Among the methods used for initiation we find the formation of the radical anion of the substrate by the reaction with alkali metals in liquid ammonia or electrochemical initiation at a cathode; however, the most extensively used method is photoinitiation. Other approaches include the use of Fe^{+2}, SmI_2, or Na(Hg). In a few systems, a thermal (spontaneous) initiation is observed.

Once the radical anion of the substrate is formed, it fragments into a radical and the anion of the leaving group (Eq. (47.1)). The aryl radical can react with the nucleophiles to furnish a radical anion (Eq. (47.2)) that, by ET to the substrate, forms the intermediates required to continue the propagation cycle (Eq. (47.3)). The mechanism has termination steps that depend on the substrate, the nucleophile, and experimental conditions. Not many initiation events are needed, but in this case the propagation cycle must be fast and efficient to allow for long chains to build up.

The most common mechanistic evidence used is inhibition by radical traps such as di-*t*-butylnitroxide (DTBN), 2,2,6,6-tetramethyl-1-piperidinyloxy (TEMPO), galvinoxyl, oxygen, etc., as well as by good electron acceptors such as *p*-dinitrobenzene (*p*-DNB). To assess the formation of radicals along the propagation cycle, radical probes have also been used which afford products derived from ring closure, ring opening, and rearrangement of the radicals.

A reaction between a nucleophile and an aryl halide may be rather unreactive at initiation but quite reactive at propagation. The addition of tiny amounts of another nucleophile that is more reactive in the photoinitiated step increases the generation of the reactive intermediates and allows the less reactive nucleophile to start its own propagation.

47.3 Photochemical Initiation

Photoinitiation is one of the most widely used methods and has proven extremely suitable for synthetic purposes. Spontaneous or thermal ET is a possible initiation whenever the substrate is a very good electron acceptor and the nucleophile a very good electron donor.

The enolate ions of aliphatic ketones can react in the dark with iodobenzene and its derivatives in DMSO.[7,8] The occurrence of these spontaneous initiations is facilitated by the electron affinity of the substrates and the ~55°C increment in temperature with respect to liquid ammonia in which no dark reaction takes place. Other substrates that can react in the dark with enolate ions of ketones are halo-substituted pyrimidines,[9,10] pyrazines,[10] pyridazines,[10] and quinoxalines.[11] Although some reactions occur in the dark, photostimulation is recommended to achieve higher yields of substitution in shorter reaction times.

Even though photoinduction is the most commonly used initiation method, not many studies on the mechanism involved have been reported. This step can involve ET within an excited charge-transfer complex (CTC) formed between the nucleophile and the substrate. This type of initiation has been proposed for the reaction of $^{-}CH_2COMe$ ions with iodobenzene and bromobenzene in DMSO,[12] for nitrile carbanions with haloarenes such as 2-bromonaphthalene or *p*-bromobiphenyl in liquid ammonia,[13] and in the reaction of iodobenzene[14] and PhSEt[15] with $(EtO)_2PO^-$ ions in DMSO and DMF, respectively. Acceleration by KI in the substitution of haloarenes with $(EtO)_2PO^-$ ions or with 2-naphthoxide ions has been explained on the same basis.[16,17] Initiation by a CTC has also been suggested for the photoinduced reaction of neophyl iodide with carbanions in DMSO.[18]

Electron transfer from excited nucleophiles is another possibility for initiation, as most of them show absorption at the wavelengths commonly used ($\lambda > 350$ nm). An example of this is the reaction of organic sulfides under laboratory light with Ph_2P^- ions that absorb strongly in the visible region ($\lambda = 475$ nm).[15] Further evidence for this type of initiation is the fluorescence quenching of the diphenylindenyl anion by bromobenzene.[19]

Initiation of the reaction of 1-chloro-2-naphthoxide anion with Na_2SO_3 has been proposed to occur by ET between the excited triplet state of the substrate and its ground state.[20] This reaction can be dye-photoinitiated[21] or initiated by visible light with a Ru complex as sensitizer and a Co complex as the intermediate electron carrier.[22] For the 1-bromo derivative, photohomolytic CBr bond dissociation is proposed.[23]

For a given aryl moiety, a rough correlation exists between the reduction potential and its reactivity in ET reactions.[24–27] The order of reduction potential in liquid ammonia, PhI > PhBr > $PhNMe_3I$ > PhSPh > PhCl > PhF > PhOPh, coincides with the reactivity order determined under photoinitiation. By using competition experiments of pairs of halobenzenes toward $^{-}CH_2COBu$-*t* ions under photoinitiation, the span in reactivity from fluorobenzene to iodobenzene was found to be about 100,000.[28]

Quantum yields of photoinitiated reactions have been used as a qualitative measure of the chain length. The quantum yields for substitution of haloarenes with nitrile-stabilized carbanions range from 7 to 31 in liquid ammonia.[13] Quantum yields from 50 to 20 have been determined for the substitution of halonaphthoxides and iodobenzene by $(EtO)_2PO^-$ ions.[14]

Nevertheless, the photoinduced initiation reaction may have a low quantum yield due to a fast backward ET that annihilates the ion pair before cage separation occurs. This will result in a poorly efficient source of radicals. In the case of nucleophiles reactive at the initiation and propagation pathways, the quantum yields for substitution (Φ_{global}) depend both on the efficiency of initiation and on the turnover in the propagation steps. Thus, the magnitude of the chain length of any $S_{RN}1$ reaction can easily be derived from the overall quantum yield by knowing the quantum yield of initiation. The latter could be obtained provided that the propagation cycle is eliminated or reduced significantly in comparison with the initiation step. The chain length can then be obtained from Eq. (47.4).

$$\text{Chain Length} = \Phi_{propagation} = \Phi_{global} / \Phi_{initiation} \tag{47.4}$$

The quantum yield for substitution of neophyl iodide by $^{-}CH_2COPh$ ion was determined to be 0.127.[18] The quantum yield of initiation, evaluated by suppressing the propagation steps with the presence of DTBN as radical trap, has a value of 10^{-3}. Based on both quantum yields, the chain length or $\Phi_{propagation}$ obtained for the reaction is approximately 127. This is the first report of $\Phi_{propagation}$, which is a direct

measure of the chain length for a $S_{RN}1$ process, demonstrating that overall quantum yields lower than unity cannot be taken as criteria for the absence of a chain reaction.

47.4 Carbanions Derived from Hydrocarbons

A relatively limited set of carbanions derived from hydrocarbons has been used as nucleophiles in $S_{RN}1$ reactions. In the photoinitiated reactions of indenyl, 1- and 2-phenyl-, 2,3- and 1,3-diphenylindenyl anions, products of mono-, di-, and triphenylation are formed. A higher yield of substitution is obtained with the 1,3-diphenylindenyl anion, which affords 1,1,3-triphenylindene as well as 1,2,3-triphenylindene:[19,29]

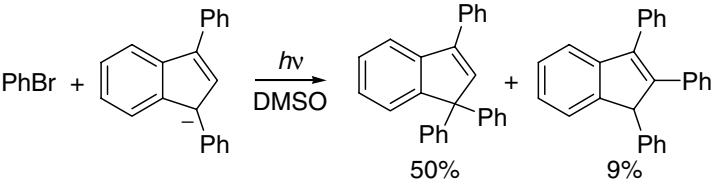

(47.5)

The products from the reaction of Ph_3C^- ion[30] with bromobenzene, iodobenzene, or diphenylsulfoxide and from cyclooctadienyl anion[31] with chlorobenzene, bromobenzene, 9-bromoanthracene, and 1-bromonaphthalene are explained on the basis of a $S_{RN}1$ type of mechanism.

47.5 Enolate Ions from Ketones

The enolate ions of acyclic and cyclic aliphatic ketones are among the most studied carbanions in photostimulated $S_{RN}1$ reactions. Absolute values of rate constants for the reactions of aryl radicals with nucleophiles have been determined electrochemically for a large number of cases. Most of the values are close to the diffusion limit. For instance, the range of rate constants for the coupling of 2-, 3-, and 4-cyanophenyl; 1-naphthyl; 3-pyridyl; and 3- and 4-quinolyl radicals with $^-CH_2COMe$ ions is on the order of 10^9 to 10^{10} M^{-1} s^{-1} in liquid ammonia.[26,32,33]

The solvents and the reaction conditions of choice are usually liquid ammonia or DMSO and irradiation. The enolate ions of acyclic aliphatic ketones such as acetone,[34–37] pinacolone,[37–40] 2-butanone,[41] 3-methyl-2-butanone,[41,42] 3-pentanone,[42,43] 4-heptanone,[43] and 2,4-dimethyl-3-pentanone[10,37,42,43] react through the $S_{RN}1$ mechanism with aryl and heteroaryl halides to afford the α-arylation products under photoinitiation. An example is shown in Eq. (47.6):

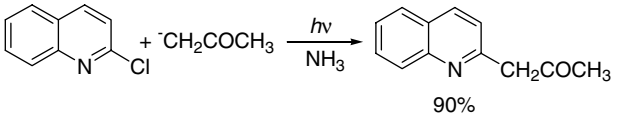

(47.6)

In some cases, α,α-diarylation can also occur but generally in low yields (< 15%).

The yield of substitution is highly dependent on the solvent. For instance, in the reaction of the enolate ion of acetone with 2-chloroquinoline (Eq. (47.6)) with the same reaction time, lower yields are obtained by changing the solvent from liquid ammonia (90%) to THF (82%), DMF (74%), dimethoxyethane (28%), diethyl ether (9%), or benzene (4%).[44] For this reason, the reactions are usually performed in liquid ammonia or DMSO under irradiation.

With unsymmetric dialkyl ketones isomeric enolate ions can be formed. The equilibrium concentration of the two possible enolates and the selectivity of the attacking radical mainly determine the distribution of the two possible arylated products.

For example, phenylation occurred preferentially at the more substituted α-carbon with the anion of 2-butanone (41 to 61%),[7,41] while, with the anion from *i*-propylmethylketone, the 1-phenyl derivative predominates.[41,45] However, the tertiary to primary substitution ratio obtained in the reaction of the same anion with 2-chloroquinoline is approximately 4.8 (Eq. (47.7)).[42] Substituents being located *ortho* to the leaving group of the substrate usually favors the attack at the primary α-carbon of the anion.[46,47]

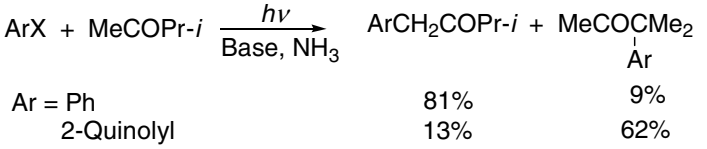

(47.7)

Anions of cyclic ketones can be α-phenylated.[37,43,48] No substitution product is formed with the enolate ion of cyclohex-2-en-1-one.[43]

The $^{-}CH_2COPh$ ion reacts with haloheteroarenes in liquid ammonia under irradiation[9,48] and even in the dark.[10] Low yields are obtained in the reaction of substituted iodoarenes with the anion of 2,4-dimethyl-6-methoxyacetophenone either in DMSO or liquid ammonia.[49] However, besides heteroarylation, phenylation by halobenzenes of $^{-}CH_2COPh$ ion is feasible under photostimulated conditions in DMSO.[50]

The anions of other aromatic ketones such as methyl 2-naphthylketone,[51] 2-acetylfuran,[48,52–54] 2-acetylthiophene,[52,55] 3-acetylthiophene,[55] 2- and 3-acetyl-*N*-methylpyrrole,[56] anthrone,[50] and tetralone[48,54,57] can also be arylated.

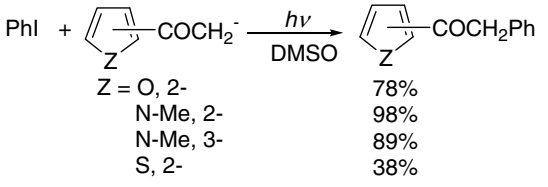

(47.8)

7-Ethyl-4-iodo-7*H*-pyrrolo[3,2-*d*]pyrimidine (6-iodo-9-ethylpurine) reacts under irradiation with the anions of several cyclic and alicyclic ketones to afford substitution products in good yields:[48,53]

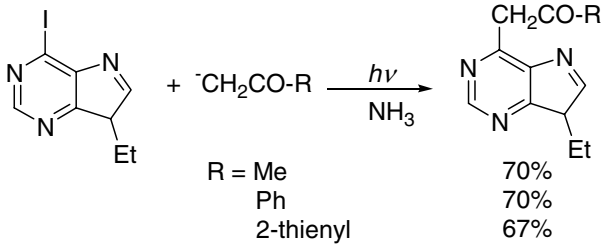

(47.9)

However, 2-iodopurine reacts through an ionic process.[58] 3-Halo (X = Cl, Br, I) 2-aminobenzo[*b*]-thiophene,[59] 3-iodobenzo[*b*]thiophene,[60] and 2-chloro- or 2-bromothiophene are poorly reactive.[61] A slightly higher reactivity is observed with 3-bromothiophene.[61]

β-Hydrogen abstraction is an important side-reaction when the enolate of di-*i*-propyl ketone is allowed to react with halobenzenes.[43] This reaction does not prevent high yields of substitution obtained with this anion upon reacting with heteroaryl halides such as 2-bromopyridine,[37] 2-chloroquinoline,[42] and 2-chloro- and 4-chloropyrimidines[10] under irradiation.

An interesting reaction is the arylation of the enolate ion of (+)-camphor.[62] The excellent yield obtained for the almost exclusive *endo*-arylation at C3 opens up a new stereospecific C3-arylation route of (+)-camphor by this mechanism (Eq. (47.10)).[62]

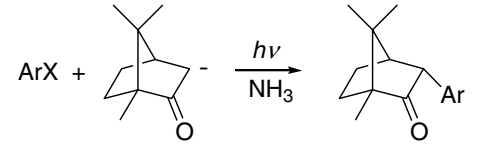

ArX = PhX, Cl, Br	92%, 95%
p-$MeOC_6H_4Cl$	71%
p-PhC_6H_4Br	76%
1-chloronaphthalene	100%

(47.10)

Substrates with Two Leaving Groups

One of the main goals of the $S_{RN}1$ mechanism is the possibility of obtaining disubstituted compounds when the reaction is performed with substrates bearing two leaving groups. These types of compound may react to form monosubstitution and/or disubstitution products depending on the leaving groups, their relative positions in the molecule, and on the nucleophile. In the case of dihalobenzenes, for example, the occurrence of mono- and/or disubstitution is interpreted based on the following mechanistic proposal. The radical anion $\mathbf{1}^{-\bullet}$ of dihalobenzene **1** fragments at the more labile C-halogen bond to furnish a haloaryl radical **2** (Eq. (47.11)), which in turn forms the radical anion of the monosubstituted compound **3** by reaction with the nucleophile. Radical anion **3** can transfer its extra electron to the substrate, and in this case the monosubstitution product **4** with retention of halogen is formed (Eq. (47.12)).

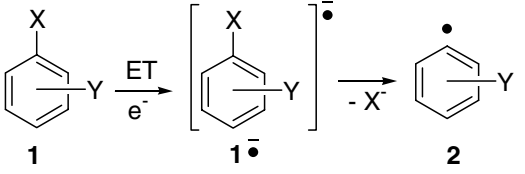

(47.11)

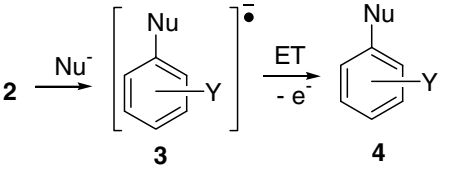

(47.12)

Alternatively, the intramolecular electron transfer to the second CY bond results in fragmentation to form a radical **5**, which by coupling with a second molecule of the nucleophile affords the disubstitution compound **6**:

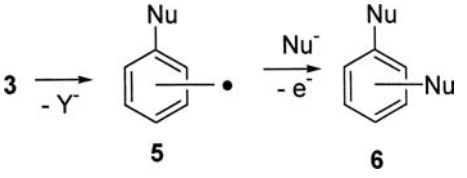

(47.13)

In this case, the monosubstitution product **4** is not an intermediate in the formation of compound **6**. Although the rate of formation of product **4** is bimolecular, depending on the concentration of **1**, and the rate of fragmentation to form radical **5** (that ultimately gives product **6**) is unimolecular, the competition of the two processes is almost independent on the concentration of **1**. The ratio of products **4** to **6** depends on the halogen, its electron affinity in relation to the substrate that acts as another acceptor, and its position on the aromatic ring, as well as on the nature of the nucleophile.

m-Fluoroiodobenzene[35] and 2-fluoro-3-iodopyridine[39] react with retention of fluorine. Synthesis of antiinflammatory drugs, such as fluorobiprophen **7**, can be achieved by reaction of 4-bromo-2-fluorobiphenyl with $^{-}CH_2COMe$ ion followed by methylation and oxidative demethylation:[63]

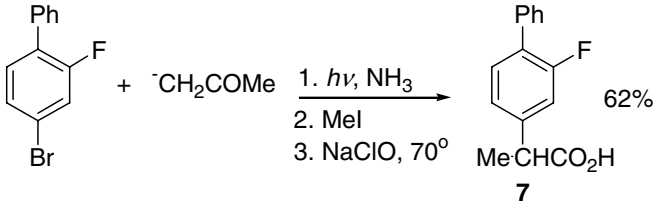

(47.14)

Disubstitution is possible for *p*-dichloro, *p*-dibromo, and *p*-bromoiodo benzenes under irradiation.[64] Disubstitution also occurs by reaction of 2,5- and 2,6-dibromopyridines and 2,3-, 2,6-, and 3,5-dichloropyridines with $^{-}CH_2COBu$-*t* ion:[37,65]

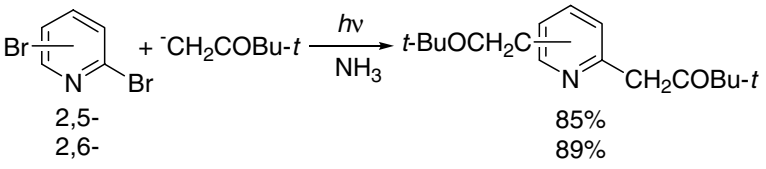

(47.15)

Monosubstitution, resulting from the selective displacement of chlorine from C4, is obtained in the reaction of $^{-}CH_2COBu$-*t* ion with 4,7-dichloroquinoline,[65] and disubstitution is achieved by its reaction with 5,7-dibromo-8-methoxyquinoline:[54]

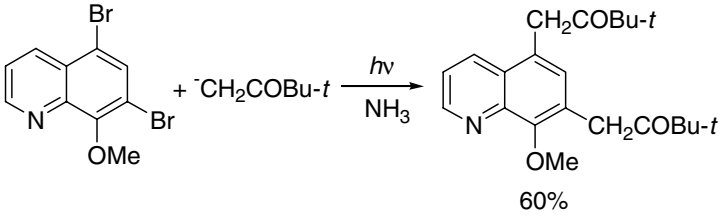

(47.16)

On the other hand, monosubstitution at C7 is the only route to products obtained in good yields in the reactions of 5-chloro-7-iodo or 5,7-dichloro-8-*i*-propoxyquinoline with the anions derived from CH_3COR (R = Me, Et, *t*-Bu, 2-furanyl) (70 to 80% yields).[54] Cyclization of these substituted compounds is possible to obtain furan derivatives (see Section 47.9).

47.6 Carbanions Derived from Esters, Carboxylate Salts, *N,N*-Disubstituted Amides, Thioamides, Imides, and β-Dicarboxylic Compounds

Carbanions Derived from Esters and Carboxylate Salts

α-Arylacetic esters can be obtained through the reaction of haloarenes with $-CH_2CO_2Bu$-*t* ion under light stimulation. For instance, the photostimulated reaction of 2,6-dibromopyridine with the anion derived from phenylacetic acid ethyl ester afforded the disubstitution product in high yields:[65]

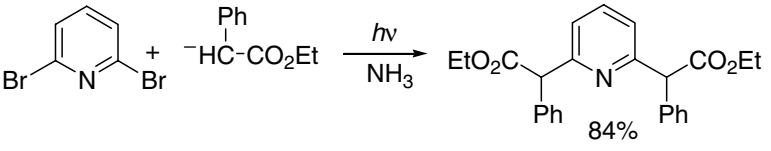

(47.17)

Lower yields of substitution are usually achieved with the anions of tertiary esters bearing β hydrogens.[45,66] A low percentage of substitution is also obtained in the reaction of the secondary anion of *t*-butylpropionate with 2-bromonaphthalene and *p*-bromobiphenyle.[13]

Other carbanions that can be arylated under photoinitiation are the anions of ethyl phenyl acetate,[65,67] methyl diphenyl acetate,[65] and *t*-butyl-3-butenate.[67] Phenylation and heteroarylation of the latter carbanion occur at the terminal site of the π system:[67]

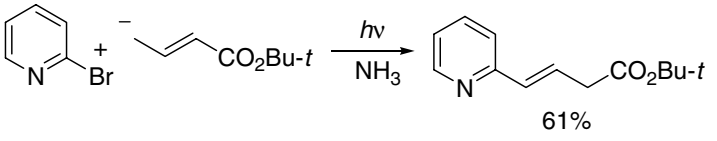

(47.18)

The dianion of phenylacetic acid, when irradiated in the presence of haloarenes, can be arylated at the *p*- or α-carbon depending on the counter ion used:[68]

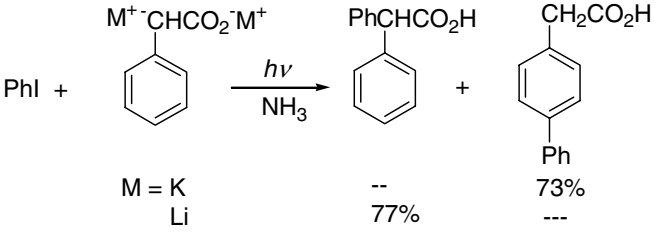

(47.19)

Carbanions Derived from *N,N*-Disubstituted Amide, Thioamide, and Imides Ions

The synthesis of *N,N*-disubstituted-α-arylacetamides can be achieved by reaction of haloarenes with carbanions from *N,N*-disubstituted amides in liquid ammonia under light initiation.[69] The potassium salt of *N*-acetylpiperidine does not react, probably due to its low solubility in liquid ammonia. The anions derived from acetamide and *N*-methyl acetamide are also unreactive.[69]

In the reaction of $^{-}CH_2CONMe_2$ ion with different haloarenes, monoarylation is the main reaction when the nucleophile:substrate ratio is 10 to 15.[63,70] Diarylation becomes more important when the ratio is equal to 2.[70] Yields of about 50% of monosubstitution and 20% of disubstitution are obtained from most substrates when the ratio is equal to 5:[63,70]

$$ArX + {}^{-}CH_2CONMe_2 \xrightarrow[NH_3]{h\nu} ArCH_2CONMe_2 + Ar_2CHCONMe_2 \qquad (47.20)$$

The photoinitiated reaction of haloarenes with the anion $^{-}CH_2CONMe_2$ followed by addition of methyl iodide is an approach to the synthesis of aryl propionic acids. The acids are obtained by hydrolysis.[63] Competition with the benzyne mechanism (i.e., the reaction of the former anion with 4-bromo-2-fluorobiphenyl) and addition to the carbonyl group (when the same anion reacts with *m*-chlorobenzophenone) are responsible for the low yields of substitution from the amide derivatives of fluorobiprophen and ketoprophen, respectively.[63]

Unsymmetrical α,α-diarylated amides can be prepared by reaction of the anions derived from monoarylated products ($Ar^1CH_2CONMe_2$) with haloarenes (Ar = 1-naphthyl, 9-phenanthryl, 9-anthracenyl and Ar^1 = Ph; Ar = Ph and Ar^1 = 9-phenanthryl, 9-anthracenyl):[70]

$$ArX + {}^{-}CHAr^1CONMe_2 \xrightarrow[NH_3]{h\nu} ArAr^1CHCONMe_2 \qquad (47.21)$$

The yields of these unsymmetrical diarylamides depend on the substrate–nucleophile pair used. For the same product and thus for the same radical anion (Ar = Ph and Ar^1 = 9-phenanthryl, or vice versa), the best yield is obtained with the least stabilized anion, where a less significant loss in π energy occurs.[50]

Lactam nucleophiles, such as the anion of 1-methyl-2-pyrrolidinone, react with aryl halides under irradiation.[69] When the reaction of 1-iodonaphthalene with the aforementioned anion is quenched with methyl iodide, the 3-(1-naphthyl)-3-methyl- substituted compound is obtained:[71]

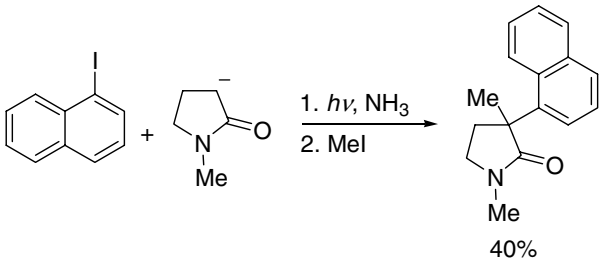

(47.22)

An interesting example of stereoselective coupling of an aromatic radical with a nucleophile is found in the reaction of 1-iodonaphthalene with an imide ion containing a chiral auxiliary. In this reaction, the diastereomeric isomers of the substitution compound are formed:[72]

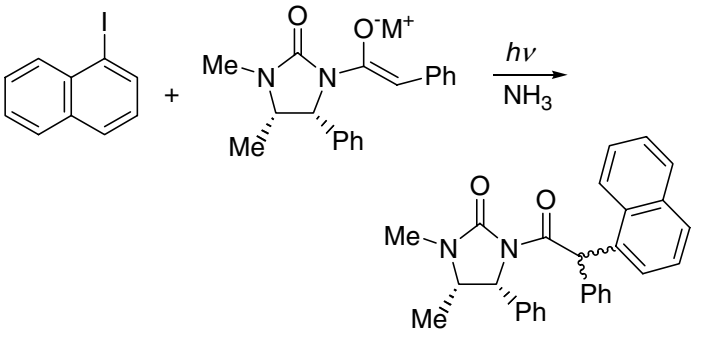

(47.23)

This reaction is highly dependent on the metal counter ion used. All the ions studied — Li, Na, K, Cs, Ti(IV) — are selective, but the highest stereoselectivity is achieved with Li at low temperature (–78°C) and with Ti(IV) (*ca.* 99%).[72] It has recently been reported that the anion derived from *N*-acetylthiomorpholine reacts with aryl iodides in DMSO under irradiation to afford good yields of substitution (60 to 70%).[73]

β-Dicarbonyl and Related Carbanions

1,3-Dianions from β dicarbonyl compounds react quite well at the terminal carbon site, under irradiation.[43,74] Monoanions do not react with 2-bromopyridine,[37] 2-chloroquinoline,[42] or *o*-bromobenzamide but do react with more electrophilic substrates, such as bromobenzonitriles:[75]

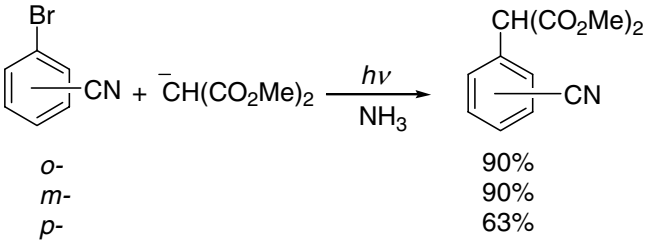

(47.24)

Monosubstitution is achieved in the photoinitiated reaction of different carbanions, such as $^{-}CH(CO_2Et)_2$, $^{-}CH(COMe)_2$, and $^{-}CH(COMe)CO_2Me$ (60 to 83%) with 5-chloro-7-iodo-8-methoxide-quinoline or the 8- *i*-propoxide quinoline.[76]

The reactivity of 2-chloro- trifluoromethyl pyridines depends on the position of the CF_3 substituent. For example, the reaction with $^{-}CH(CO_2Et)_2$ ions fails with the C3- and C4-substituted derivative, while substitution is obtained with the CF_3 group at C5 or C6 with -$CMe(CO_2Et)_2$ ions (100 and 44% yields, respectively):[77]

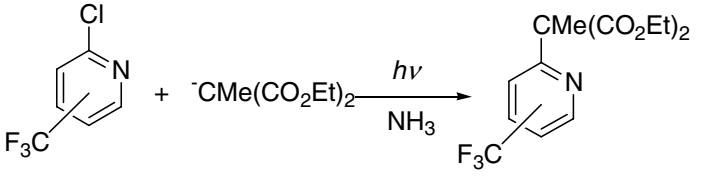

(47.25)

The photoinitiated reactions of 2-bromobenzonitrile and 2-bromo-3-cyano-pyridine with the carbanion of ethyl cyanoacetate afford the substitution product in good yields (90 and 80%, respectively) by an $S_{RN}1$ process.[75] On the other hand, a non-chain radical nucleophilic mechanism is proposed to occur in the almost quantitative substitution of *o*-Cl, *o*-Br, and *p*-$O_2NC_6H_4X$ (F, Cl, Br, I) with this anion in DMSO.[78–80]

47.7 Carbanions Derived from Nitriles

In the coupling reaction of a phenyl radical with carbanions derived from nitriles, the radical anions formed bearing the extra electrons are mainly localized on the CN moiety or at the CCN bond favoring the fragmentation into stabilized benzyl-type radicals. (Scheme 2). For example, in the reaction of $^{-}CH_2CN$ ion with halobenzenes, toluene is the main product observed.[81,82] On the other hand, with 1-chloronaphthalene,[34,83] polycyclic aromatic halides,[83] or substituted haloarenes with a COPh group[83] or halopyridines,[84] the straightforward substitution products $ArCH_2CN$ are formed. With these substrates, the aryl group accommodates the extra electron of the radical anion avoiding fragmentation. For instance, α-arylated nitriles are almost exclusively formed by reaction of $^{-}CHRCN$ ions (R = H, Me, Ph) with

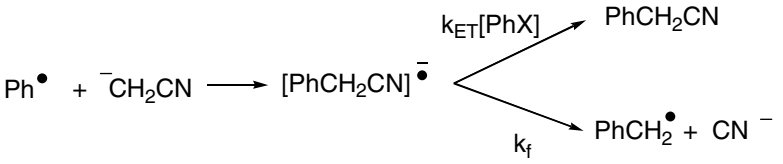

SCHEME 2

stabilized π aromatic compounds, such as naphthyl (Eq. (47.26))[34,83,85] and quinolyl moieties,[86] among others.

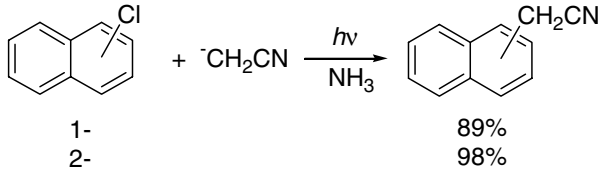

(47.26)

The nitriles obtained by reaction of ⁻CHPhCN ion with heteroaryl halides can lead to the corresponding ketones in excellent yields (77%) by oxidative decyanation under phase-transfer conditions (PTCs):[86]

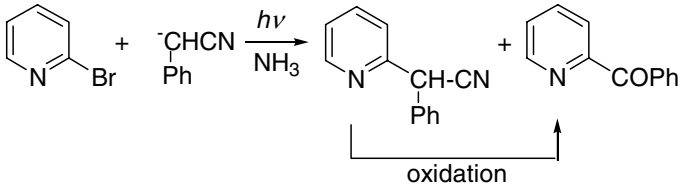

(47.27)

Exclusive substitution at C2 occurs under photostimulation, by reaction of ⁻CHPhCN ion with 2,4-dichloropyrimidine (58% yield).[65] On the other hand, a mixture of monosubstitution, disubstitution, and monosubstitution with reductive dehalogenation occurs in the reaction of this anion and the anion derived from 2-phenyl butyronitrile with 2,6-dibromopyridine.[65] Both anions react with 3-bromoquinoline-1-oxide to afford the corresponding 3-substituted quinoline-1-oxides (82 to 91%) by a thermal-initiated $S_{RN}1$ mechanism.[87]

The carbanion of cyclohexylideneacetonitrile reacts with *p*-bromo and *p*-iodo-anisoles and 1-iodonaphthalene to afford good yields of the isomeric substitution products (60 to 69%) at Cγ together with traces of 2,2-(diaryl)cyclohexylidene acetonitrile:[88]

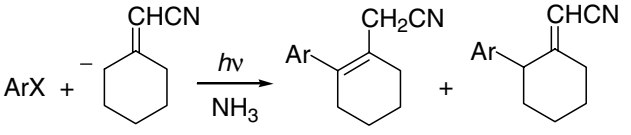

(47.28)

47.8 Other Carbanions

Picolyl anions can be used as nucleophiles in $S_{RN}1$ reactions:[89,90]

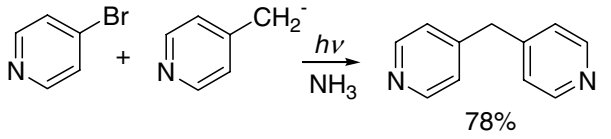

(47.29)

On reaction with bromobenzene and iodobenzene, these ions afford products derived from competition of the benzyne and $S_{RN}1$ mechanisms.[90]

Other carbanions proposed to react by the $S_{RN}1$ process are the anions from 2,4,4-trimethyl-2-oxazoline, 2-benzyl-4,4-dimethyl-2-oxazoline, 2,4-dimethylthiazole, 2-benzyl-4,4-dimethylthiazole, and dimethyl methylphosphonate.[67] Competition with a benzyne process has been determined in some of these reactions. Some examples are illustrated in Eq. (47.30).

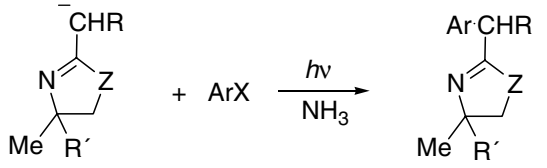

Z = O, R´= Me, R = H, Ph
Z = S, R´= H, R = H; R´= Me, R = Ph

(47.30)

47.9 $S_{RN}1$ and Ring Closure Reactions of Aryl Halides Bearing an *ortho* Substituent

The most studied approaches to ring closure reactions is the $S_{RN}1$ substitution of aromatic substrates that have an appropriate substituent in a position *ortho* to the leaving group. An important example of this approach is the synthesis of substituted indoles by the photoinduced substitution reaction of *o*-haloanilines (bromo, iodo) with carbanions from ketones, followed by spontaneous ring closure in the reaction media:[91–93]

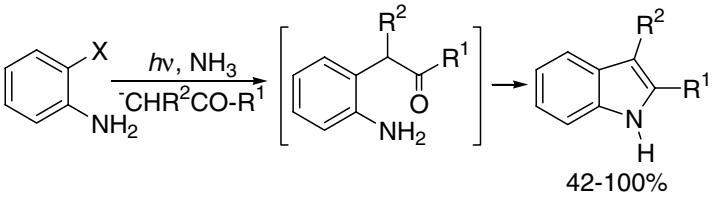

(47.31)

When the reaction is performed with the enolate ion of an aldehyde, 3-substituted indoles are obtained (26 to 49% yield).[91]

Indoles bearing a –CHO or –COMe functionality at the 2-position are synthesized after hydrolysis of the corresponding dimethylacetals obtained from the reaction of *o*-iodoaniline with $^{-}CH_2COCH(OMe)_2$ or $^{-}CH_2COC(OMe)_2Me$ ions in 45 and 55%, respectively.[91]

The synthesis of benzo[*e*] and benzo[*g*]indoles (**8** and **9**) can be performed by reaction of 2-amino-1-bromo or 1-amino-2-bromo-naphthalene with the carbanions $^{-}CH_2COBu$-*t* and $-CH_2COCH(OMe)_2$.[94]

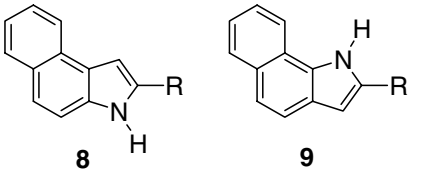

R	**8**	**9**
t-Bu	67%	82%
$CH(OMe)_2$	52%	65%

The enolate anions of aromatic ketones do not react in liquid ammonia with *o*-iodoaniline, but they cyclize to indoles **10** in DMSO under light (acetophenone, 2-naphthyl-methyl ketone) or Fe^{+2} (acetophenone, 2-acetyl-1-methyl-pyrrole and 2-acetylthiophene) initiation:[95]

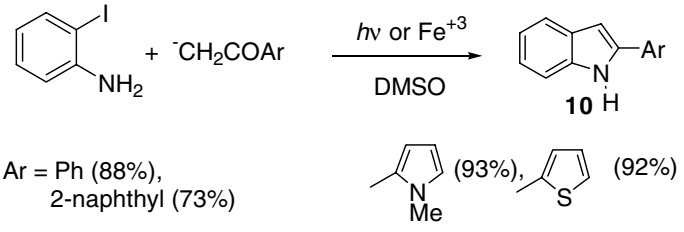

(47.32)

2-*t*-Butylindoles bearing substituents in the phenyl ring (**11**) and tricyclic indoles (**12**) can be synthesized by a combination of S_NAr, reduction of the nitro group and photoinduced $S_{RN}1$ reactions with the pinacolone anion.[96]

R^1 = Me, R^2 = $HO(CH_2)_2S$-, (75%)

R^1 = $HO(CH_2)_2S$-, R^2 = Me, (60%)

R^1= Me·N⟨⟩N–, R^2 = H, (85%)

Y = S (52%)

Y = NH (43%)

Y = NMe (46%)

The photostimulated reaction of *vic* aminohalo pyridines with the anion of $^-CH_2COBu$-*t* or $^-CH_2COMe$ ions leads to azaindoles in high yields (75 to 95%).[39] When the amino group is protected as a pivaloylamino derivative, the substitution compounds obtained by the photoinduced reaction of 2-amino-3-iodo-, 3-amino-4-iodo-, and 4-amino-3-iodopyridines with $^-CH_2COMe$ or $^-CH_2COBu$-*t* ions afford 5-, 6- and 7-azaindoles in almost quantitative yields by cyclization upon deprotection of the amino group and dehydration under acidic conditions:[39]

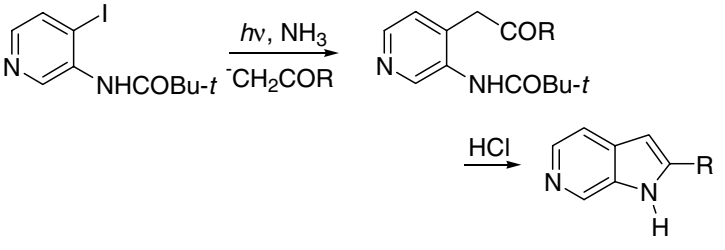

(47.33)

The compounds formed in the $S_{RN}1$ reaction of the enolate of a ketone or aldehyde (MeCOR, R = H, Me, *i*-Pr, *t*-Bu) with *o*-alkoxyhalobenzenes undergo spontaneous cyclodehydration after deblocking of the alkoxy function to afford benzo[*b*]furan **13** derivates quantitatively, as in the reaction with *o*-iodoanisole (Scheme 3).[46] This approach is also used in the synthesis of furo[3,2-*h*]quinolines and furo[3,2-*b*]pyridines, which are quantitatively formed by acidic treatment of the products obtained in the $S_{RN}1$ reaction of 5-chloro-7-iodo-8-*i*-propoxyquinoline and 2-bromo-3-*i*-propoxypyridine, respectively, with the enolate ions of ketones ($^-CH_2COR$, R = Me, Et, *t*-Bu, 2-furanyl, *p*-anisyl):

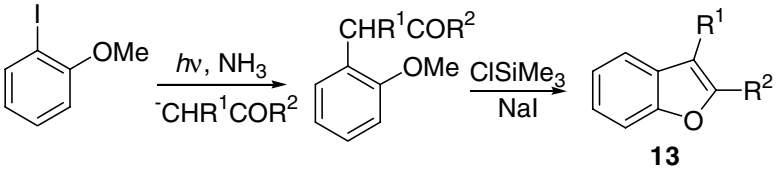

13

SCHEME 3

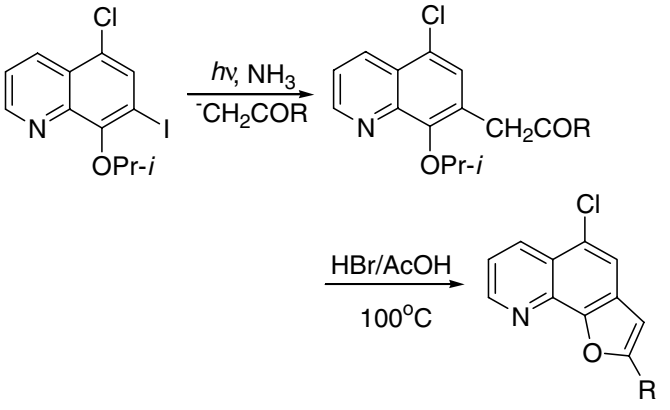

(47.34)

Cyclization at the product is also possible by reaction of 2-methoxide-3-iodopyridine with $^{-}CH_2COBu$-*t* ion.[54]

The $S_{RN}1$ mechanism can be an excellent route to isoquinolines rings and derivatives by reaction of *o*-iodobenzylamines with ketone enolate ions under irradiation.The substitution products formed in their irradiated reactions spontaneously cyclize to give a non-isolable intermediate which affords isoquinolines by Pd/C dehydrogenation (Eq. (47.35a)) or tetrahydroisoquinolines by reduction with $NaBH_4$ in approximately 100% yields (Eq. (47.35b)):[97,98]

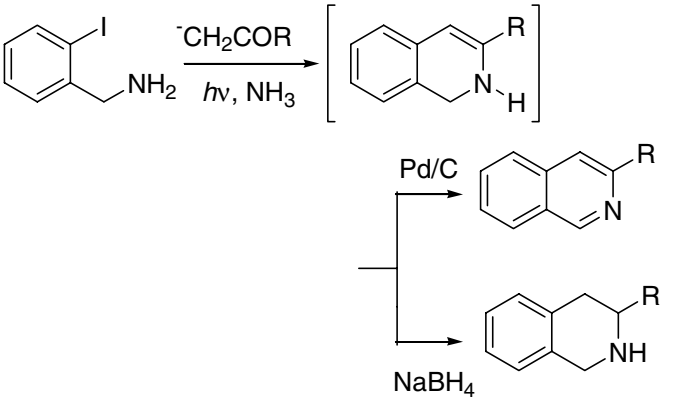

(47.35a)

(47.35b)

11,12-dihydrobenzo[*c*]phenanthridines and phenanthridones are obtained by reaction of tetralone enolate ion with *o*-iodobenzylamines or *o*-iodobenzoic acids, respectively, in moderate to good yields.[57]

Isoquinolones (or isocarbostyrils **14**) are accessible by the reaction of *o*-bromo or *o*-iodobenzamides with carbanions in acceptable yields (60 to 90%):

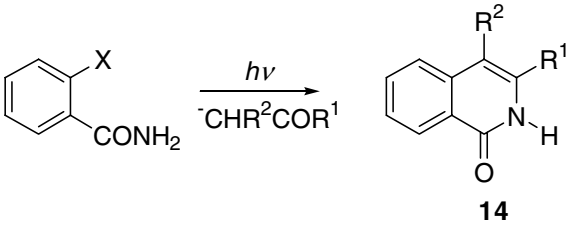

14

R^1 = Me, *i*-Pr, *t*-Bu, CH_2OMe, Et, $(CH_2)_2C_6H_5$, *p*-$MeOC_6H_4$
R^2 = H, $CH_2C_6H_5$, Me

(47.36)

With *N*-methylbenzamides, the yields of substitution products are lower.[99,100] The $S_{RN}1$ reaction between substituted *o*-iodobenzamides and the enolate anion of 2-acetylhomoveratic acid can be used for the synthesis of derivatives of the benzo(*c*)-phenanthridone and berberine alkaloids.[101]

The $S_{RN}1$ reaction of *o*-iodo and *o*-bromo-benzoate salts with $^-CH_2COMe$ ion affords the substitution product (*ca.* 78% yield), which upon acid treatment with toluene *p*-sulphonic acid gives the corresponding isocoumarin **15** (90%) (Scheme 4).[99] Benzazepines **16** can be produced upon ammonium acetate treatment of the substitution compound obtained in the reaction of (*o*-iodophenyl) acetic acid derivatives with enolate ions from ketones ($^-CH_2COR$, R = Me, *i*-Pr, *t*-Bu; 50, 60, and 56%, respectively) (Scheme 5).[47]

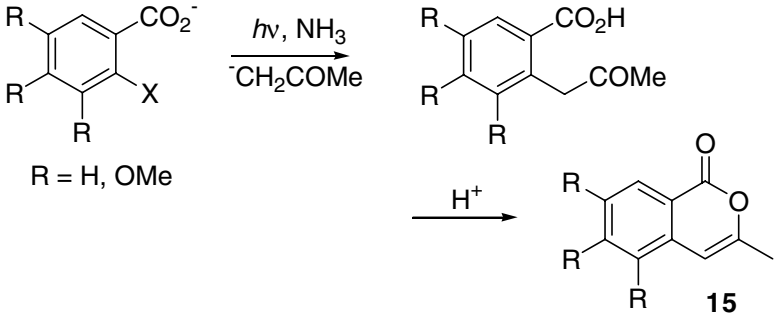

SCHEME 4

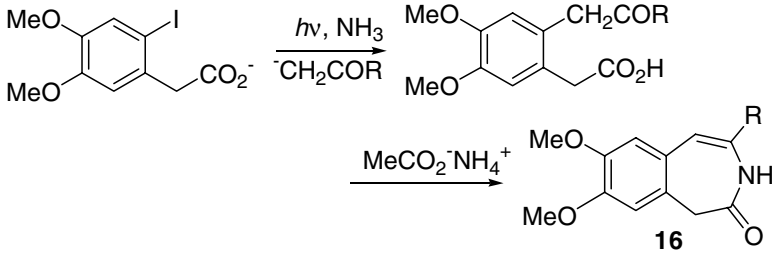

SCHEME 5

The reaction of the enolate ion of methyl 2-naphthylketone with *o*-bromoacetophenone affords 2,2′-binaphthyl under irradiation in liquid ammonia (72%) or in DMSO (82%) Eq. (47.37).[51]

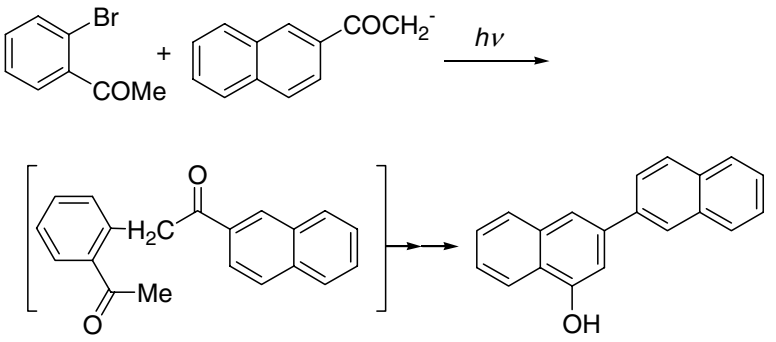

(47.37)

Unsymmetrically substituted binaphthyls (25 to 80%) can also be synthesized by this procedure.[49,51] Naphthylquinolines and naphthylisoquinolines can be formed by reaction of 3-acetyl-2-chloro- and 4-acetyl-3-chloropyridines with the anions from methyl 1- or 2-naphthylketone.[102] Another approach involves reaction of *o*-bromobenzamide with the same nucleophiles.[102]

47.10 Intramolecular $S_{RN}1$ Reactions

The intramolecular $S_{RN}1$ reactions of substrates that have both a nucleophilic center and a leaving group give an interesting example of a ring closure reaction. An example of this is the synthesis of oxindoles by the intramolecular cyclization of *N*-alkyl-*N*-acyl-*o*-haloanilines in the presence of LDA in THF or KNH_2 in liquid ammonia:[103–105]

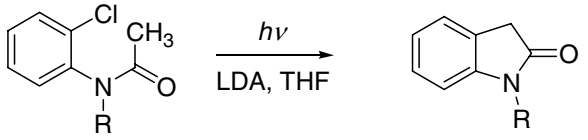

R = Me (81%)
R = $CH_2C_6H_5$ (32%)

(47.38)

N-Methyl-α,β-unsaturated anilides undergo intramolecular arylation exclusively at the α-position to afford 3-alkylideneoxindoles. The best yields of substitution (63 to 90%) are obtained with KNH_2 in liquid ammonia under photoinitiation.[105]

1,4-Dihydro-2*H*-isoquinolin-3-ones can be achieved in fair to good yields by the cyclization of the carbanions from *N*-acyl-*N*-methyl-*o*-chlorobenzylamines under photostimulation:[105]

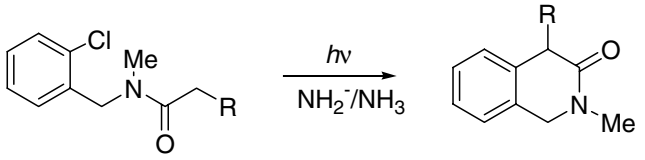

R = H 62%
R = Me 60%
R = Et 54%

(47.39)

The iodoketone **17** cyclizes to the cephalotaxinone (**18**) under metal or light stimulation (45 and 94% yields, respectively):[106–108]

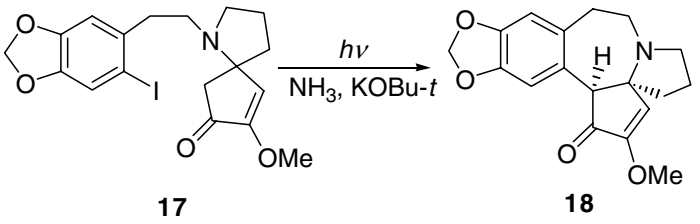

(47.40)

The studies of this system were extended to other analogs in order to determine the ring-size preferences in the cyclizations, the effects of hydrogens β to the carbonyl group, and the regioselectivity with ketones that can give two enolate ions.[45,66,107,108]

The key step in the synthesis of the azaphenanthrene alkaloid eupoulauramine **19** (56% yield) is an intramolecular $S_{RN}1$ reaction, followed by *in situ* stilbene photocyclization and further methylation Eq. (47.41).[109]

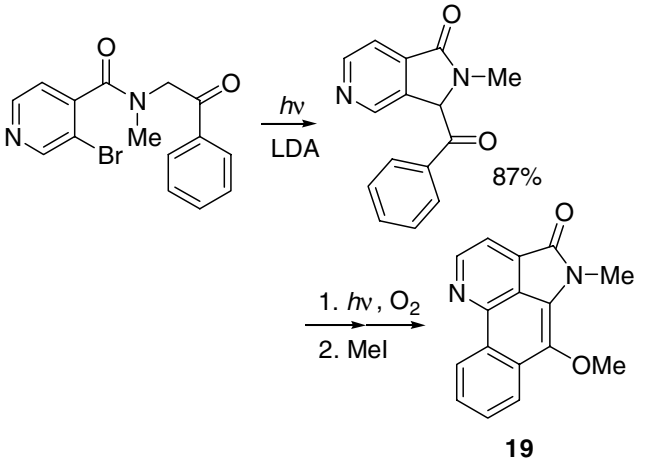

(47.41)

A similar strategy is followed in the synthesis of (±)tortuosamine (54%):[110]

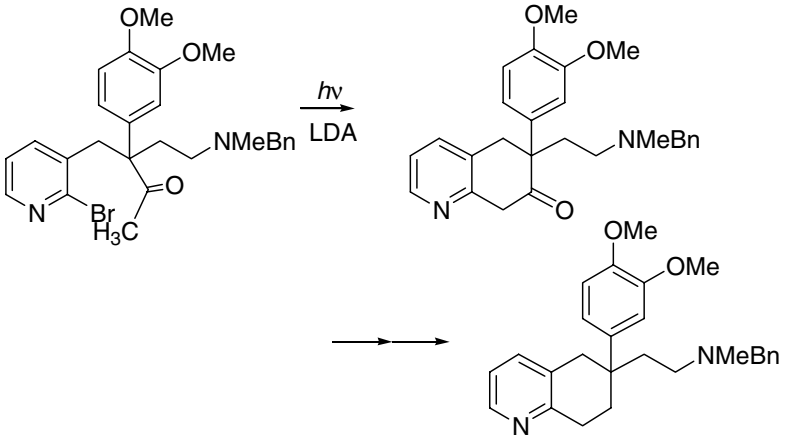

(47.42)

The $S_{RN}1$ mechanism is an excellent alternative to accomplish the following intramolecular cyclization reaction, which constitutes one of the steps in the synthesis of rugulovasine, novel structures within the family of ergot alkaloids:[111,112]

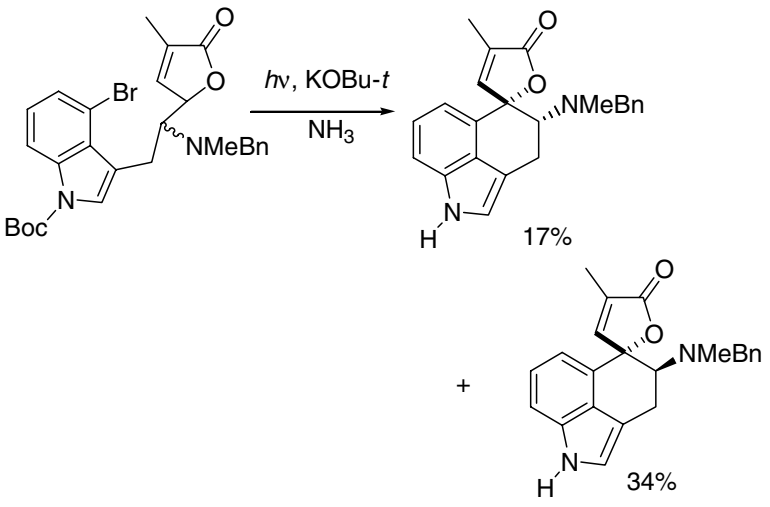

(47.43)

The preparation of *m*-cyclophanes is possible through a combination of inter- and intramolecular $S_{RN}1$ substitutions with substrates bearing the leaving group and nucleophilic center in the same molecule Eq. (47.44).[113,114]

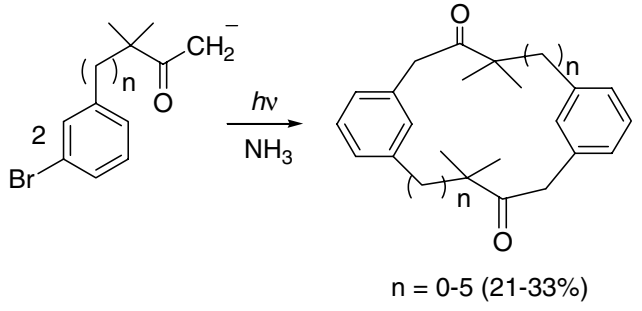

(47.44)

Another approach to the synthesis of *m*- and *p*-cyclophanes is the reaction of *m*- and *p*-dibromobenzene with appropriate dianions, although in low yields.[115,116]

The carbanion derived from 3-(*o*-chlorophenyl)-2-methyl-3*H*-quinazolin-4-one cyclizes in liquid ammonia under irradiation to yield 6*H*-indolo[2,1-*b*]quinazolin-12-one **20** (60%):[117]

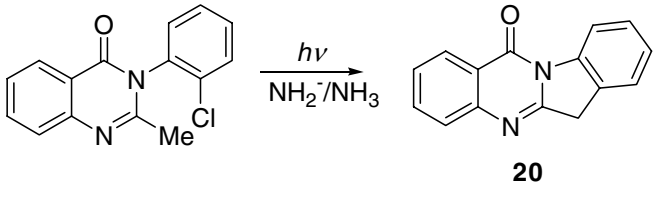

(47.45)

References

1. Rossi, R. A. and de Rossi R. H., in *Aromatic Substitution by the $S_{RN}1$ Mechanism*, American Chemical Society, Washington, D.C., 1983.
2. Norris, R. K., Nucleophilic coupling with aryl radicals, in *Comprehensive Organic Synthesis*, Vol. 4, Trost, B. M., Ed., Pergamon Press, Elmsford, NY, 1991, 451–482.
3. Beugelmans, R., The photostimulated $S_{RN}1$ process: Reaction of haloarenes with enolates, in *CRC Handbook of Organic Photochemistry and Photobiology*, Horspool, W.M., Ed., CRC Press, Boca Raton, FL, 1994, 1200–1217.
4. Rossi, R. A., Pierini A. B., and Peñéñory, A. B., Recent advances in the $S_{RN}1$ reaction of organic halides, in *The Chemistry of Functional Groups*, Suppl. D2, Patai, S. and Rappoport, Z., Eds., Wiley, Chichester, 1995, chap. 24, 1395–1485.
5. Rossi, R. A. and Baumgartner, M. T., Synthesis of heterocycles by the $S_{RN}1$ mechanism, in *Targets in Heterocyclic Systems: Chemistry and Properties*, Vol 3, Attanasi, O. A. and Spinelli, D. Eds., Soc. Chimica Italiana, 1999, 215–243.
6. Rossi, R. A., Pierini, A. B., and Santiago, A. N., Aromatic substitution by the $S_{RN}1$ reaction, in *Organic Reactions*, Paquette, L. A. and Bittman, R. Eds.. John Wiley & Sons, New York, 1999, 1–271.
7. Scamehorn, R. G., Hardacre, J. M., Lukanich, J. M., and Sharpe, L. R., Thermally initiated $S_{RN}1$ reactions of ketone enolates with iodobenzene in dimethyl sulfoxide: relative reactivities of enolate ions with phenyl radical, *J. Org. Chem.*, 49, 4881, 1984.
8. Scamehorn, R. G. and Bunnett, J. F., Dark reactions of halobenzenes with pinacolone enolate ion: evidence for a thermally induced aromatic $S_{RN}1$ reaction, *J. Org. Chem.*, 42, 1449, 1977.
9. Oostvee, E. A. and Plas, H. C. V., Reactions of carbon nucleophiles with 4-phenyl- and 4-*tert*-butyl-5-halogeno pyrimidines: on the occurrence of an $S_{RN}1$ mechanism, *Recl. Trav. Chim. Pays-Bas*, 98, 441, 1979.
10. Carver, D. R., Komin, A. P., Hubbard, J. S., and Wolfe, J. F., $S_{RN}1$ mechanism in heteroaromatic nucleophilic substitution: reactions involving halogenated pyrimidines, pyridazines and pyrazines, *J. Org. Chem.*, 46, 294, 1981.
11. Carver, D. R., Hubbard, J. S., and Wolfe, J. F., $S_{RN}1$ mechanism in heteroaromatic nucleophilic substitution: reactions of 2-chloroquinoxaline and 4-chloroquinazolines with ketones enolates, *J. Org. Chem.*, 47, 1036, 1982.
12. Fox, M. A., Younathan, J., and Fryxell, G. E., Photoinitiation of the $S_{RN}1$ reaction by excitation of charge-transfer complexes, *J. Org. Chem.*, 48, 3109, 1983.
13. Wu, B. Q., Zeng, F. W., Ge, M., Cheng, X., and Wu, G., A new synthetic route to α-aryl propionic acid and a quantitative study of the photo-$S_{RN}1$ reaction of aryl halides with carbanion from alkyl nitrile, *Sci. China*, 34, 777, 1991.
14. Hoz, S. and Bunnett, J. F., A quantitative study of the photostimulated reactions of iodobenzene with diethyl phosphite ion, *J. Am. Chem. Soc.*, 99, 4690, 1977.
15. Cheng, C. and Stock, L. M., Photochemical anion-promoted carbon–sulfur cleavage reactions of diaryl sulfides, aryl alkyl sulfides and related sulfoxides and sulfones, *J. Org. Chem.*, 56, 2436, 1991.
16. Boumekouez, A., About-Jaudet, E., and Collignon, N., A remarkable acceleration effect of iodide ions in the photostimulated phosphonylation of bromoaromatic compounds, *J. Organomet. Chem.*, 440, 297, 1992.
17. Beugelmans, R. and Chbani, M., Photostimulated $S_{RN}1$ reactions on functionalized aryl bromides enhanced by KI: synthetic and mechanistic aspects, *New J. Chem.*, 18, 949, 1994.
18. Argüello, J. E., Peñéñory, A. B., and Rossi, R. A., Quantum yields of the initiation step and chain propagation turnovers in $S_{RN}1$ reactions: photostimulated reaction of 1-iodo-2-methyl-2 phenyl-propane with carbanions in DMSO, *J. Org. Chem.*, 65, 7175, 2000.
19. Tolbert, L. M. and Siddiqui, S., The $S_{RN}1$ photoarylation of indenyl anions, *J. Org. Chem.*, 49, 1744, 1984.

20. Ivanov, V. L., Eggert, L., and Kuzmin, M. G., Kinetics and mechanism of chain photosubstitution of halogen by a sulfo group in halonaphthols, *High Energy Chem.*, 284, 1987.
21. Ivanov, V. L., Aurich, J., Eggert, L., and Kuzmin, M. G., Dye-photoinitiated chain reaction of halogen substitution by a sulfo group in halogenonaphthols, *J. Photochem. Photobiol. A: Chem.*, 50, 275, 1989.
22. Savvina, V. S. and Ivanov, V. L., Reductive quenching of Ru(bipy)3,2*: new method for photoinitiation of the chain reaction of substitution of chlorine by a sulfo group in chloronaphthols, *High Energy Chem.*, 24, 205, 1990.
23. Ivanov, V. L. and Kherbst, A., Chain photochemical substitution of halogen by cyano group in halogenonaphthols [English transl.], *J. Org. Chem. USSR*, 24, 1709, 1988.
24. Andrieux, C. P., Savéant, J. M., and Su, K. B., Kinetics of dissociative ET: direct and mediated electrochemical reductive cleavage of the C-X bond, *J. Phys. Chem.*, 90, 3815, 1986.
25. Amatore, C., Combellas, C., Pinson, J., Oturan, M. A., Robveille, S., Savéant, J. M., and Thiébault, A., Electrochemically induced $S_{RN}1$ aromatic nucleophilic substitution: absolute reactivities of phenyl derivatives in liquid ammonia, *J. Am. Chem. Soc.*, 107, 4846, 1985.
26. Amatore, C., Oturan, M. A., Pinson, J., Savéant, J. M., and Thiébault, A., Nucleophile and aryl radical reactivity in $S_{RN}1$ reactions: absolute and relative electrochemical determination, *J. Am. Chem. Soc.*, 107, 3451, 1985.
27. Andrieux, C. P., Savéant, J. M., and Zann, D., Relationship between reduction potentials and anion radical cleavage rates in aromatic molecules, *New J. Chem.*, 8, 107, 1984.
28. Bunnett, J. F., Aromatic substitution by the $S_{RN}1$ mechanism, *Acc. Chem. Res.*, 11, 413, 1978.
29. Tolbert, L. M. and Siddiqui, S., Reactions following electron transfer origins of selectivity in the reaction of radicals with carbanions, *Tetrahedron*, 38, 1079, 1982.
30. Tolbert, L. M. and Martone, D. P., Carbanion photochemistry. 7. The $S_{RN}1$ vs. Set photoarylation of triphenylmethyl anion, *J. Org. Chem.*, 48, 1185, 1983.
31. Fox, M. A. and Singletary, N. J., Photolysis of the cyclooctadienyl anion, *J. Org. Chem.*, 47, 3412, 1982.
32. Amatore, C., Pinson, J., Savéant, J. M., and Thiébault, A., Electron-transfer-induced reactions. termination steps and efficiency of the chain process in $S_{RN}1$ aromatic substitution, *J. Am. Chem. Soc.*, 103, 6930, 1981.
33. Amatore, C., Oturan, M. A., Pinson, J., Savéant, J. M., and Thiébault, A., Electron-transfer-induced reactions: a novel approach based on electrochemical redox catalysis. Application to aromatic nucleophilic substitutions, *J. Am. Chem. Soc.*, 106, 6318, 1984.
34. Rossi, R. A., Rossi, R. H. D., and López, A. F., Reaction of 1-halonaphthalenes with nucleophiles by the $S_{RN}1$ mechanism of aromatic substitution, *J. Am. Chem. Soc.*, 98, 1252, 1976.
35. Bunnett, J. F. and Sundberg, J. E., On the synthesis of arylacetones by the $S_{RN}1$ arylation of acetone enolate ion, *Chem. Pharm. Bull.*, 23, 2620, 1975.
36. Rossi, R. A. and Bunnett, J. F., Photostimulated aromatic $S_{RN}1$ reactions, *J. Org. Chem.*, 38, 1407, 1973.
37. Komin, A. P. and Wolfe, J. F., The $S_{RN}1$ mechanism in heteroaromatic nucleophilic substitution: photostimulated reactions of halopyridines with ketones enolates, *J. Org. Chem.*, 42, 2481, 1977.
38. Scamehorn, R. G. and Bunnett, J. F., Photostimulated $S_{RN}1$ reactions of halobenzenes with ketone enolate ions in dimethyl sulfoxide solution, *J. Org. Chem.*, 42, 1457, 1977.
39. Estel, L., Marsais, F., and Queguiner, G., Metalation/$S_{RN}1$ coupling in heterocyclic synthesis: a convenient methodology for ring functionalization, *J. Org. Chem.*, 53, 2740, 1988.
40. Dillender, S. C., Greenwood, T. D., Hendi, M. S., and Wolfe, J. F., Reactions of 2-halothiazoles with ketone enolates and nitrile carbanions, *J. Org. Chem.*, 51, 1184, 1986.
41. Rossi, R. A. and Bunnett, J. F., Arylation of several carbanions by the $S_{RN}1$ mechanism, *J. Org. Chem.*, 38, 3020, 1973.

42. Hay, J. V. and Wolfe, J. F., The $S_{RN}1$ mechanism in heteroaromatic nucleophilic substitution: an investigation of the generality of photostimulated reactions of ketones enolates with 2-chloroquinoline, *J. Am. Chem. Soc.*, 97, 3702, 1975.
43. Bunnett, J. F. and Sundberg, J. E., Photostimulated arylation of ketone enolate ions by the $S_{RN}1$ mechanism, *J. Org. Chem.*, 41, 1702, 1976.
44. Moon, M. P. and Wolfe, J. F., Solvent effects in heteroaromatic $S_{RN}1$ reactions, *J. Org. Chem.*, 44, 4081, 1979.
45. Semmelhack, M. F. and Bargar, T. M., Photostimulated nucleophilic aromatic substitution for halides with carbon nucleophiles. Preparative and mechanistic aspects, *J. Am. Chem. Soc.*, 102, 7765, 1980.
46. Beugelmans, R. and Ginsburg, H., New synthesis of benzo[*b*]furan by $S_{RN}1$ reaction of *ortho*-iodoanisole, *J. Chem. Soc.*, *Chem. Commun.*, 508, 1980.
47. Beugelmans, R. and Ginsburg, H., A novel access to β-benzazepines and to 3-benzoxepines via $S_{RN}1$ reactions, *Heterocycles*, 23, 1197, 1985.
48. Nair, V. and Chamberlain, S. D., Novel photoinduced carbon–carbon bond formation in purines, *J. Am. Chem. Soc.*, 107, 2183, 1985.
49. Beugelmans, R., Bois-Choussy, M., and Tang, Q., Synthese par reaction $S_{RN}1$ de phenyl-2 naphtalenes et de binaphtalenes-2,2′ dissymetriques et substitues sur les positions adjacentes a la liaison des cycles. Role des facteurs structuraux, *Tetrahedron*, 45, 4203, 1989.
50. Borosky, G. L., Pierini, A. B., and Rossi, R. A., Differences in reactivity of stabilized carbanions with haloarenes in the initiation and propagation steps of the $S_{RN}1$ mechanism in DMSO, *J. Org. Chem.*, 57, 247, 1992.
51. Beugelmans, R., Bois-Choussy, M., and Tang, Q., A general $S_{RN}1$ based method for total synthesis of unsymmetrically hydroxylated 2,2′-binaphthalenes, *J. Org. Chem.*, 52, 3880, 1987.
52. Baumgartner, M. T., Gallego, M. H., and Pierini, A. B., Synthesis of 2-phenyl-1-(2-thienyl)- and 2-aryl-1-(2-furyl)ethanones by the $S_{RN}1$ mechanism: relative reactivities of enolate ions of ketones, *J. Org. Chem.*, 63, 6394, 1998.
53. Nair, V. and Chamberlain, S. D., Novel photoinduced functionalized C-alkylations in purine systems, *J. Org. Chem.*, 50, 5069, 1985.
54. Beugelmans, R. and Bois-Choussy, M., A convenient access to furo(3.2-*h*) quinolines and to furo[3,2-*b*] pyridine via $S_{RN}1$ reactions, *Heterocycles*, 26, 1863, 1987.
55. Dell'Erba, C., Novi, M., Petrillo, G., and Tavani, C., α-Arylation vs. α-arylhydrazonylation of alkyl aryl ketones with arylazo *tert*-butyl sulfides, *Tetrahedron*, 49, 235, 1993.
56. Baumgartner, M. T., Pierini, A. B., and Rossi, R. A., Reactions of 2-and 3-acetyl-1-methylpyrrole enolate ions with iodoarenes and neopentyl iodides by the $S_{RN}1$ mechanism, *J. Org. Chem.*, 64, 6487, 1999.
57. Beugelmans, R., Chastanet, J., Ginsburg, H., Quinteros-Cortes, L., and Roussi, G., Direct synthesis of benzo[*c*]phenanthridines and benzo[*c*]phenanthridones via $S_{RN}1$ reactions, *J. Org. Chem.*, 50, 4933, 1985.
58. Nair, V., Young, D. A., and DeSilvia, Jr., R., 2-Halogenated purine nucleosides: synthesis and reactivity, *J. Org. Chem.*, 52, 1344, 1987.
59. Beltran, L., Galvez, C., Prats, M., and Salgado, J., Study of the reactivity of ketone enolates with 3-halo-2 amino derivatives of benzo[*b*]thiophene under photostimulated $S_{RN}1$ reaction conditions, *J. Heterocycl. Chem.*, 29, 905, 1992.
60. Prats, M., Galvez, C., and Beltran, L., Study of the reaction of several ketone enolates with 3-iodobenzo[*b*]thiophene under thermally initiated $S_{RN}1$ reaction conditions, *Heterocycles*, 34, 1039, 1992.
61. Bunnett, J. F. and Gloor, B. F., Reactions of halothiophenes with acetone enolate and amide ions, *Heterocycles*, 5, 377, 1976.

62. Wu, B. Q., Zeng, F. W., Zhao, Y., and Wu, G. S., Stereochemistry of the coupling step in photo-$S_{RN}1$ reaction, *Chin. J. Chem.*, 10, 253, 1992.
63. Ferrayoli, C. G., Palacios, S. M., and Alonso, R. A., Alternative synthesis of 2-aryl propanoic acids from enolate and aryl halides, *J. Chem. Soc., Perkin Trans. 1*, 1635, 1995.
64. Alonso, R. A. and Rossi, R. A., $S_{RN}1$ mechanism in bifunctional systems, *J. Org. Chem.*, 45, 4760, 1980.
65. Carver, D. R., Greenwood, T. D., Hubbard, J. S., Komin, A. P., Sachdeva, Y. P., and Wolfe, J. F., $S_{RN}1$ mechanism in heteroaromatic nucleophilic substitution: reaction involving certain dihalogenated π-deficient nitrogen heterocycles, *J. Org. Chem.*, 48, 1180, 1983.
66. Semmelhack, M. F. and Bargar, T. M., Cyclizations of enolates onto aromatic rings via the photo-$S_{RN}1$ reaction: preparative and mechanistic aspects, *J. Org. Chem.*, 42, 1481, 1977.
67. Wong, J. W., Natalie, K. J., Nwokogu, G. C., Pisipati, J. S., Flaherty, P. T., Greenwood, T. D., and Wolfe, J. F., Compatibility of various carbanion nucleophiles with heteroaromatic nucleophilic substitution by the $S_{RN}1$ mechanism, *J. Org. Chem.*, 62, 6152, 1997.
68. Nwokogu, G. C., Wong, J. W., Greenwood, T. D., and Wolfe, J. F., Photostimulated reactions of phenylacetic acid dianions with aryl halides: influence of the metallic cation on the regiochemistry of arylation, *Org. Lett.*, 2, 2643, 2000.
69. Rossi, R. A. and Alonso, R. A., Photostimulated reactions of *N*,*N*-disubstituted amide enolate anions with haloarenes by the $S_{RN}1$ mechanism in liquid ammonia, *J. Org. Chem.*, 45, 1239, 1980.
70. Palacios, S. M., Asis, S. E., and Rossi, R. A., Synthesis of *N*,*N*-dimethyl α-aryl and α,α-diarylacetamides by radical nucleophilic substitution reactions, *Bull. Soc. Chim. Fr.*, 130, 111, 1993.
71. Alonso, R. A., Rodriguez, C. H., and Rossi, R. A., Reactivity of *N*,*N*-dialkylamide enolate ions: arylation of 1-methyl-2-pyrrolidinone enolate ions by the $S_{RN}1$ mechanism, *J. Org. Chem.*, 54, 5983, 1989.
72. Lotz, G. A., Palacios, S. M., and Rossi, R. A., Stereoselective reaction of a chiral assisted amide enolate ion with 1-iodonaphthalene by the $S_{RN}1$ mechanism, *Tetrahedron Lett.*, 35, 7711, 1994.
73. Murguia, M. C. and Rossi, R. A., Reactions of *N*-thioacetylmorpholine anion with iodoarenes and 1-iodoadamantane by the $S_{RN}1$ mechanism, *Tetrahedron Lett.*, 38, 1355, 1997.
74. Wolfe, J. F., Greene, J. C., and Hudlicky, T., Reaction of dialkali salts of benzoylacetone with 2-chloroquinoline: evidence for an $S_{RN}1$ mechanism in heteroaromatic nucleophilic substitution, *J. Org. Chem.*, 37, 3199, 1972.
75. Beugelmans, R., Bois-Choussy, M., and Boudet, B., Studies on $S_{RN}1$ reactions. Part 8. New and direct arylation and hetarylation of β-dicarbonyl compounds by $S_{RN}1$, *Tetrahedron*, 38, 3479, 1982.
76. Beugelmans, R., Bois-Choussy, M., Gayral, P., and Rigothier, M. C., Syntheses par $S_{RN}1$ et evaluation de l'activite amoebicide de nouveaux dérivés quinoléiniques, *Eur. J. Med. Chem.*, 23, 539, 1988.
77. Beugelmans, R. and Chastanet, J., $S_{RN}1$ reactions of chlorotrifluoromethyl pyridines with naphtholate, phenolate, and malonate Anions, *Tetrahedron*, 49, 7883, 1993.
78. Zhang, X. M., Yang, D. L., and Liu, Y. C., Effects of electron acceptors and radical scavengers on nonchain radical nucleophilic substitution reactions, *J. Org. Chem.*, 58, 224, 1993.
79. Zhang, X., Yang, D., Liu, Y., Chen, W., and Cheng, J., Kinetics and mechanism of the reactions of *o*- and *p*-nitrohalobenzenes with the sodium salt of ethyl cyanoacetate carbanion: a non-chain radical nucleophilic substitution mechanism, *Res. Chem. Intermed.*, 11, 281, 1989.
80. Zhang, X., Yang, D., Jia, X., and Liu, Y., Kinetic and mechanistic studies of the non-chain radical nucleophilic substitution reactions, *J. Org. Chem.*, 58, 7350, 1993.
81. Bunnett, J. F. and Gloor, B. F., $S_{RN}1$ phenylation of nitrile carbanions and ensuing reactions: a new route to alkylbenzenes, *J. Org. Chem.*, 38, 4156, 1973.
82. Rossi, R. A., de Rossi, R. H., and Pierini, A. B., Reactions of halobenzenes with cyanomethyl anion in liquid ammonia by the $S_{RN}1$ mechanism, *J. Org. Chem.*, 44, 2662, 1979.
83. Rossi, R. A., de Rossi, R. H., and Lopez, A. F., Photostimulated arylation of cyanomethyl anion by the $S_{RN}1$ mechanism of aromatic substitution, *J. Org. Chem.*, 41, 3371, 1976.
84. Yakubov, A. P., Belen'kii, L. I., and Goldfarb, Y. L., Radical nucleophilic substitution of inactivated heteroaryl bromides, *Izv. Akad. Nauk SSSR Ser. Khim.*, 2812, 1981 (*Chem. Abstr.*, 96, 104049r, 1982).

85. Du, R. and Huang, W., Synthesis of naproxen by photo reaction, *Jinan Daxue Xuebao*, *Ziran Kexue Yu Yixueban*, 12, 46, 1991 (*Chem. Abstr.*, 117, 48037d, 1992).
86. Hermann, C. K. F., Sachdeva, Y. P., and Wolfe, J. F., A new synthesis of aryl hetaryl ketones via $S_{RN}1$ reactions of halogenated heterocycles with potassiophenylacetonitrile followed by phase-transfer catalyzed decyanation [l*a–c*], *J. Heterocyclic. Chem.*, 24, 1061, 1987.
87. Hamana, M., Iwasaki, G., and Saeki, S., Nucleophilic substitution of 4-chloroquinoline 1-oxide and related compounds by means of hydride elimination, *Heterocycles*, 17, 177, 1982.
88. Alonso, R. A., Austin, E., and Rossi, R. A., Photostimulated reaction of carbanions from α, β-unsaturated nitriles with aryl halides by the $S_{RN}1$ mechanism, *J. Org. Chem.*, 53, 6065, 1988.
89. Moon, M. P., Komin, A. P., Wolfe, J. F., and Morris, G. F., Photostimulated reactions of 2-bromopyridine and 2-chloroquinoline with nitrile-stabilized carbanions and certain other nucleophiles, *J. Org. Chem.*, 48, 2392, 1983.
90. Bunnett, J. F. and Gloor, B. F., Mesitylation and phenylation of picolyl anions by the $S_{RN}1$ mechanism, *J. Org. Chem.*, 39, 382, 1974.
91. Beugelmans, R. and Roussi, G., Substitution Nucleophile Aromatique Radicalaire. Nouvelle Synthese du Squelette Indole, *Tetrahedron*, 37, 393, 1981.
92. Beugelmans, R. and Roussi, G., New "one-pot" synthesis of indoles under non-acidic conditions ($S_{RN}1$ reaction), *J. Chem. Soc.*, *Chem. Commun.*, 950, 1979.
93. Bard, R. R. and Bunnett, J. F., Indole synthesis via $S_{RN}1$ reactions, *J. Org. Chem.*, 45, 1546, 1980.
94. Beugelmans, R. and Chbani, M., $S_{RN}1$: synthesis of nitrogen, sulfur and phosphorus heterocyclic compounds linked to naphthalene, *Bull. Soc. Chim. Fr.*, 132, 729, 1995.
95. Baumgartner, M. T., Nazareno, M. A., Murguía, M. C., Pierini, A. B., and Rossi, R. A., Reaction of *o*-iodoaniline with aromatic ketones in DMSO: synthesis of 2-aryl or 2-hetarylindoles, *Synthesis*, 2053, 1999.
96. Beugelmans, R. and Chbani, M., Synthesis of 5- and 6-membered heterocycles by a strategy combining SNAr and $S_{RN}1$ reactions, *Bull. Soc. Chim. Fr.*, 132, 306, 1995.
97. Beugelmans, R., Chastanet, J., and Roussi, G., Nouvelle Synthése du Squelette Dihydro-1,2 Isoquinoléine par Réaction de Substitution Nucleophile Radicalaire en Chaine ($S_{RN}1$), *Tetrahedron Lett.*, 23, 2313, 1982.
98. Beugelmans, R., Chastanet, J., and Roussi, G., Studies on $S_{RN}1$ reactions. 9. A new access to the isoquinolines ring system, *Tetrahedron*, 40, 311, 1984.
99. Beugelmans, R., Ginsburg, H., and Bois-Choussy, M., Studies on $S_{RN}1$ reactions. Part 6. Synthesis of 3-methyl derivatives of the alkaloids thalactamine, doryanine and 6,7-dimethoxy-*N*-methyl-1(2*H*)-isoquinolone, *J. Chem. Soc.*, *Perkin Trans. 1*, 1149, 1982.
100. Beugelmans, R. and Bois-Choussy, M., One-pot synthesis of 1-oxo-1,2-dihydroisoquinolines (isocarbostyrils) via $S_{RN}1$ (Ar) reactions, *Synthesis*, 730, 1981.
101. Beugelmans, R. and Bois-Choussy, M., A common and general access to berberine and benzo[*c*] phenanthridine alkaloids, *Tetrahedron*, 48, 8285, 1992.
102. Beugelmans, R. and Bois-Choussy, M., $S_{RN}1$-based methodology for synthesis of naphthylquinolines and naphthylisoquinolines, *J. Org. Chem.*, 56, 2518, 1991.
103. Wolfe, J. F., Sleevi, M. C., and Goehring, R. R., Photoinduced cyclization of mono- and dianions of *N*-acyl-*o*-chloranilines: a general oxindole synthesis. *J. Am. Chem. Soc.*, 102, 3646, 1980.
104. Wu, G. S., Tao, T., Cao, J. J., and Wei, X. L., Photoinduced $S_{RN}1$ annulation of *N*-alkyl-*N*-acyl-*ortho*-chloroaniline. *Acta Chim. Sinica*, 50, 614, 1992.
105. Goehring, R. R., Sachdeva, Y. P., Pisipati, J. S., Sleevi, M. C., and Wolfe, J. F., Photoinduced cyclizations of mono- and dianions of *N*-acyl-*o*-chloroanilines and *N*-acyl-*o*-chlorobenzylamines as general methods for the synthesis of oxindoles and 1,4-dihydro-3(2*H*)-isoquinolinones, *J. Am. Chem. Soc.*, 107, 435, 1985.
106. Semmelhack, M. F., Stauffer, R., and Rogerson, T. D., Nucleophilic aromatic substitution via a new nickel-catalyzed process and via the $S_{RN}1$ reaction: improved synthesis of cephalotaxinone. *Tetrahedron Lett.*, 4519, 1973.

107. Semmelhack, M. F., Chong, B. P., Stauffer, R. D., Rogerson, T. D., Chong, A., and Jones, L. D., Total synthesis of the cephalotaxus alkaloids: a problem in nucleophilic aromatic substitution, *J. Am. Chem. Soc.*, 97, 2507, 1975.
108. Weinreb, S. M. and Semmelhack, M. F., Synthesis of the cephalotaxus alkaloids, *Acc. Chem. Res.*, 8, 158, 1975.
109. Goehring, R. R., An exceptionally brief synthesis of eupolauramine, *Tetrahedron Lett.*, 33, 6045, 1992.
110. Goehring, R. R., A short synthesis of (±)-tortuosamine, *Tetrahedron Lett.*, 35, 8145, 1994.
111. Martin, S. F. and Liras, S., Novel applications of vinylogous Mannich reactions: total synthesis of rugulovasine A and B, *J. Am. Chem. Soc.*, 113, 10450, 1993.
112. Liras, S., Lynch, C. L., Fryer, A. M., Vu, B. T., and Martin, S. F., Applications of vinylogous Mannich reactions: total synthesis of the ergot alkaloids rugulovasines A and B and setoclavine, *J. Am. Chem. Soc.*, 123, 5918, 2001.
113. Usui, S. and Fukazawa, Y., A facile synthesis of [m.m]-metacyclophadiones, *Tetrahedron Lett.*, 28, 91, 1987.
114. Fukazawa, Y., Takeda, Y., Usui, S., and Kodama, M., Synthesis and conformation of 1,1,10,10-tetramethyl[3.3]metacyclophane, *J. Am. Chem. Soc.*, 110, 7842, 1988.
115. Fukazawa, Y., Usui, S., Tanimoto, K., and Hirai, Y., Conformational analysis by the ring current method: the structure of 2,2,13,13-tetramethyl[4.4]metacyclophane, *J. Am. Chem. Soc.*, 116, 8169, 1994.
116. Fukazawa, Y., Kitayama, H., Yasuhara, K., Yoshimura, K., and Usui, S., Synthesis and conformational analysis of 3,3,12,12-tetramethyl[4.4]paracyclophane-2,13-dione, *J. Org. Chem.*, 60, 1696, 1995.
117. Staskun, B. and Wolfe, J. F., New approach to the Indolo[2,1-*b*]quinazoline ring system by cyclization of 3(*o*-chlorophenyl)-2-methyl-4(3*H*)quinazolinone and its *m*-isomer: synthesis of the antibiotic tryptanthrin, *S. Afr. J. Chem.*, 45, 5, 1992.

48

Photochemical Decarbonylation of Ketones: Recent Advances and Reactions in Crystalline Solids

Miguel A. Garcia-Garibay
University of California
Luis M. Campos
University of California

48.1 Introduction

The photochemical decarbonylation of ketones can be traced back to 1910 when acetone was photolysed in the gas phase to yield ethane and carbon monoxide.[1] A radical process involving α-cleavage (Norrish type I reaction)[2,3] and decarbonylation[4] as two separate steps was proposed a few years later by Norrish and Appleyard (Scheme 1). Each of the two cleavage reactions has been the subject of numerous theoretical and mechanistic studies that have been covered in several reviews.[5–7]

0-8493-1348-1/04/$0.00+$1.50

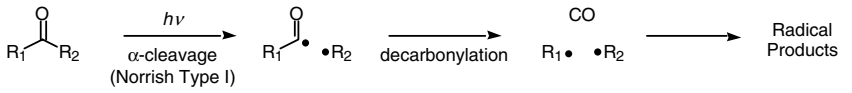

SCHEME 1

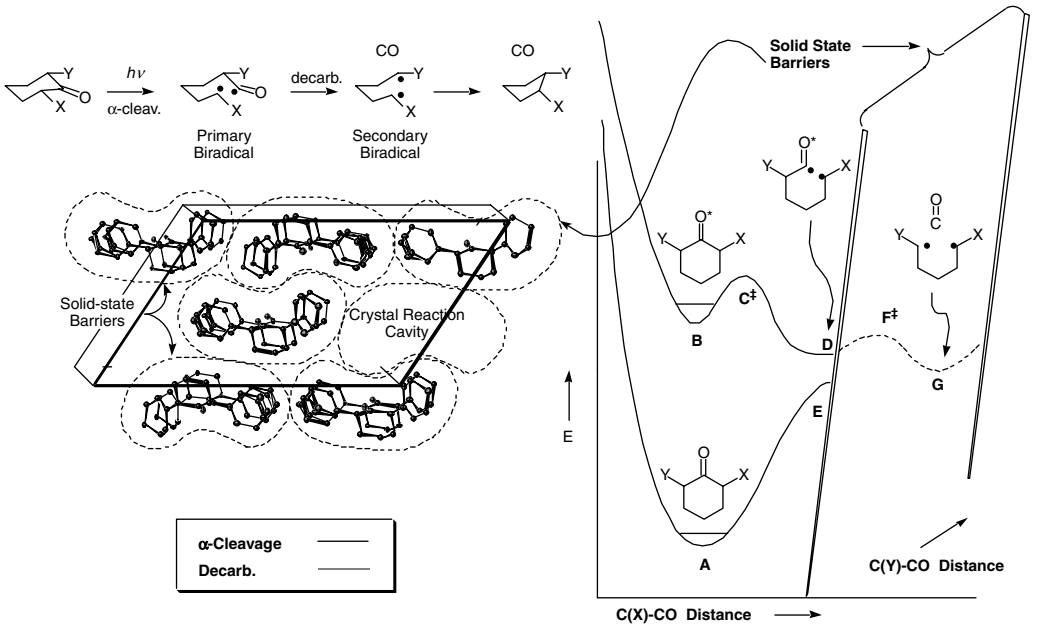

FIGURE 48.1 Hypothetical energy surface for α-cleavage and decarbonylation reactions illustrating the confining effect of a crystalline lattice. Reactions in crystals require low activation energies at points C‡ and F‡ and sufficiently long lifetimes at points B and D in order to increase the probability of efficient decarbonylation.

Current interest in the photodecarbonylation process is primarily maintained by applications that require a simple and reliable method for the preparation of biradicals, radical pairs, and free radicals. At the same time, the relatively well-documented kinetics of the two elementary cleavage reactions and the dynamics of the radical intermediates constitute ideal chemical probes to investigate the structure and dynamics of several micro-heterogeneous media and supramolecular environments. Recent applications range from studies addressing fundamental aspects of chemical dynamics, spin–spin interactions,[8] and computational chemistry[21] to studies addressing self-diffusion in zeolite networks,[9] the dynamics of radicals in polymers,[10] generation of chelotropic NO traps,[11] and long-range electron transfer in DNA,[12] among others. Furthermore, while reactions of radical pairs and biradicals in the gas phase and in solution can be relatively complex, strategies have been developed to control their chemical behavior so that they can be preparatively useful.

Great interest in the decarbonylation process over the last few years has resulted from studies at the two extremes of the kinetic spectrum. On the one end, femtosecond studies in the gas phase have addressed the dynamics of the reaction within time scales that are barely enough for a few molecular vibrations and modest radical–radical separation but not enough for large-amplitude molecular motions. At the other end, studies in crystalline solids focus on reactions where excited molecules and reactive intermediates can only explore a very small fraction of the gas phase energy surface (Figure 48.1; the details of the photochemistry/photophysics are discussed in Section 48.3). When radical pairs and biradicals

are formed in crystals, they are generated under conditions where the two radical centers are forced to coexist within their van der Waals distance for a relatively long period of time (points D and G in Figure 48.1). In Figure 48.1, we represent a hypothetical energy surface determined by the α-cleavage and decarbonylation coordinates. The steric barriers imposed by close neighbors in the crystal lattice or reaction cavity are represented by the dashed-line boundaries. These barriers restrain the separation of the two radical centers and inhibit large atomic displacements in solid-to-solid reactions.

Decarbonylation reactions in crystals must occur by a series of events leading from point A to point G, but many diversions exist along the way. In summary, the reaction begins by electronic excitation from the ground state ketone A to the nπ* excited state surface at point B. While both singlet and triplet surfaces can be dissociative, biradicals initially formed in crystals in the singlet state are likely to be unproductive due to rapid return to the ground state. α-Cleavage is accomplished by passage through transition state $C^{\ddagger}$ when the distance of the C(X)–CO sigma bond is increased to form a constrained acyl–alkyl biradical, D. Whenever the energy of transition state $C^{\ddagger}$ is very high, the α-cleavage reaction is slow and the excited state returns to the ground state (A) by emission of a photon, either fluorescence or phosphorescence, and by thermal deactivation (internal conversion). Once formed, primary acyl–alkyl biradicals (D) may reach the singlet, hot, ground-state surface at E and go back to starting point A in an unproductive cycle of A ⇒ B ⇒ $C^{\ddagger}$ ⇒ D ⇒ E ⇒A. In order to reach target dialkyl biradical G, acyl–alkyl biradical D must lose CO by passing through transition state $F^{\ddagger}$, following the path A ⇒ B ⇒ $C^{\ddagger}$ ⇒ D ⇒ $F^{\ddagger}$ ⇒ G.

Singlet-state nπ* reactions that occur in the gas phase and in solution may not be observed in crystals because the acyl–alkyl radical pair (E) is subject to the perfect "cage effect".[13] Radical–radical recombination in the singlet-state acyl–alkyl biradical (from E ⇒A) may occur within the time scale of a single bond vibration. However, because many decarbonylation reactions have been documented in crystals, conditions may be satisfied for α-cleavage to compete with excited-state decay and for decarbonylation to compete with recombination of the acyl–alkyl radical pair. In this chapter, we review various aspects of the α-cleavage and decarbonylation steps in the reaction, describe recent theoretical advances, and conclude with examples that reflect our current understanding of the reaction in the solid state.[14]

48.2 General Considerations

While α-cleavage and decarbonylation are observed with many simple ketones, the two sequential reactions are only one of many possible outcomes after excitation of the reactive nπ* excited state. Before we analyze several aspects of the two elementary reactions in detail, it may be useful to cover a few general guidelines that help us evaluate the feasibility of the decarbonylation process. In general terms, the efficiency of decarbonylation is directly related to the stability of radical intermediates generated at each of the two steps of the overall reaction. A good correlation between the bond dissociation energies (ΔH^0) and the rates of α-cleavage and decarbonylation indicate a Hammet-type relation between the two reaction free energies and their respective activation barriers.[15] Because reactions occur specifically from nπ* excited states, they are most commonly observed with nonconjugated ketones that have high-energy ππ* excited states. The kinetic requirements for the α-cleavage reaction are relatively straightforward. α-Cleavage in the singlet nπ* state is relatively inefficient as compared with intersystem crossing; however, singlet reactions may be observed in solution with compounds that have very large reaction rate constants (i.e., $k_{\alpha(S)} > 10^8$–10^9 s^{-1}). In contrast, triplet-state reactions are significantly more efficient due to the longer triplet lifetimes (up to 10^{-3} s) and the larger rate constants for the triplet triplet-state α-cleavage. In addition, the longer lifetimes of the primary triplet radical pairs allow them to escape solvent cages, when reactions are carried out in liquid media.[3] Naturally, a successful α-cleavage does not guarantee formation of the second biradical or radical pair. For instance, aryl-alkyl ketones with a low-lying nπ* state may undergo efficient α-cleavage, but formation of a phenyl radical by decarbonylation of benzoyl [Ph-C•(O)] is not observed ($k_{-CO} = 1.5 \times 10^{-7}$).[16] In analogy with α-cleavage, decarbonylation is faster when the bond dissociation energy of the R-CO• bond is lower so that stable alkyl radicals R• are formed.

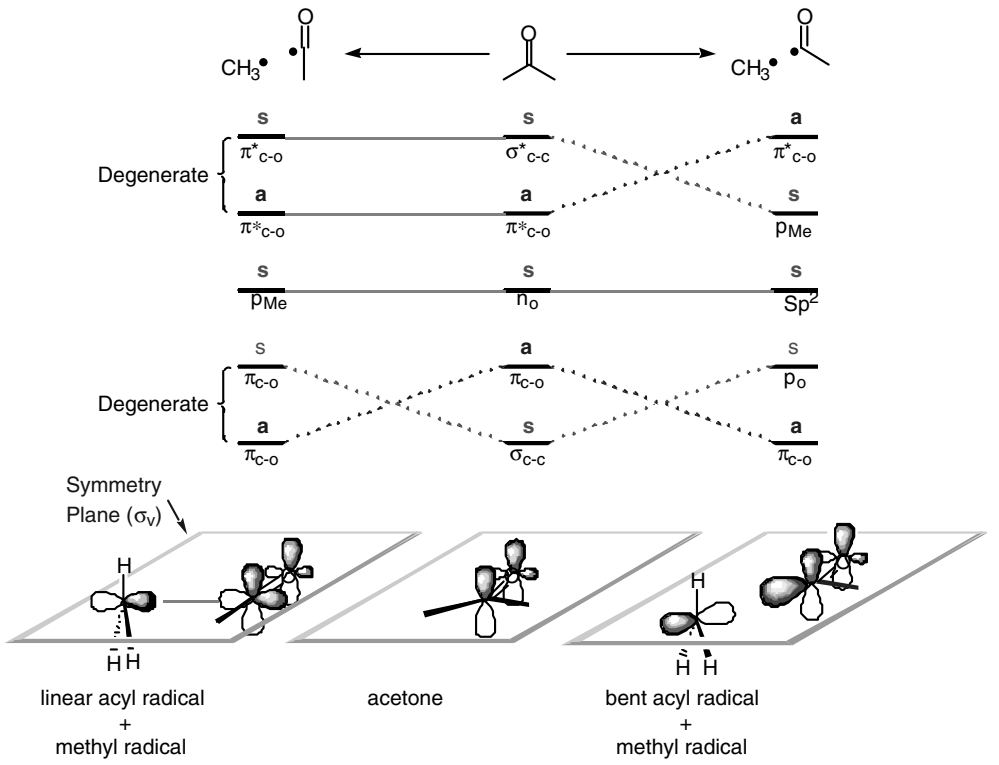

FIGURE 48.2 Orbital correlation diagram illustrating the α-cleavage of acetone. A linear acyl radical (left) is predicted to be photochemically generated from the nπ* excited state of acetone. The orbital symmetry is represented by the letters **a** (asymmetric) and **s** (symmetric), with respect to the σ_v mirror plane.

48.3. Theoretical Aspects

Excited states and radical intermediates generated in gases and in liquids may explore a wide range of molecular structures and reaction paths by taking advantage of molecular translation, rotation, and internal (conformational) motions. In contrast, most molecular degrees of freedom that are present in the gas phase and in solution are transformed into collective lattice vibrations or phonons, when molecules are "trapped" in crystals. Unable to find reaction partners or to explore a variety of nuclear configurations, reactants in solids are restricted to least-motion-reaction pathways along trajectories that are allowed by orbital-symmetry and occur with minimum atomic and molecular motion.[17] Consequently, reaction trajectories in crystals must be very short and have no significant electronic barriers.

The Norrish type I and decarbonylation reactions satisfy these requirements. The orbital symmetry for α-cleavage along the nπ* surface has been studied by several authors.[18] As illustrated in Figure 48.2, the stretching of a C_α-CO bond for the generation of linear (left) or bent acyl (right) and planar methyl radicals is analyzed in terms of a symmetry plane that is conserved along the reaction coordinate. At a first approximation, the path toward the bent acyl radical from the nπ* excited state should be *forbidden*, while the path toward the linear radical should be *allowed*. While symmetry considerations alone suggest that linear acyl radicals should be formed, it has been suggested that they are approximately 26 kcal/mol higher in energy than the bent form.[19] In reality, symmetry constraints are relieved by excited state pyramidalization and partial linearization along the reaction coordinate so that a ground-state, bent, acyl radical is formed with a relatively small energetic cost in the form of a small energy barrier.[20] Experimentally determined energy barriers for α-cleavage in aliphatic nπ* ketones in solution range from close

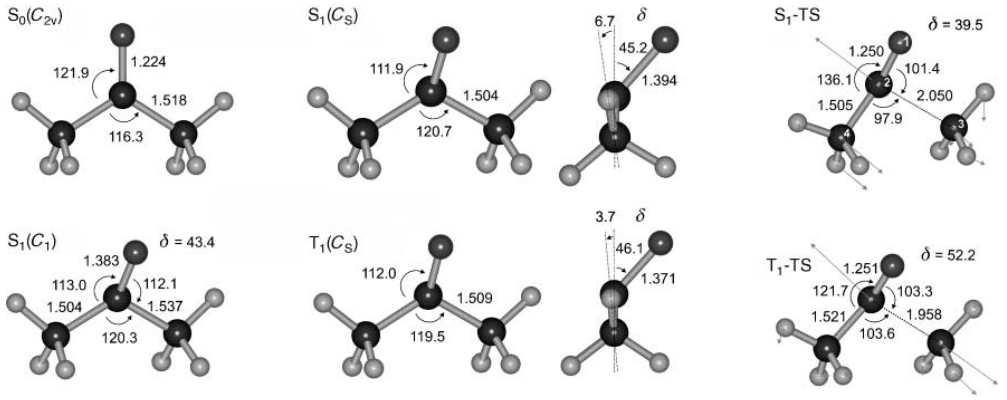

FIGURE 48.3 Optimized structures at the CAS-SCF(10,8)/6–31G* level of theory of acetone in the ground state and S_1 and T_1 excited states (distances in Å and angles in degrees). (Adapted from Reference 21a.)

to 0 to as much as 15 kcal/mol, depending on bond dissociation energies and the spin multiplicity of the excited state.[5a]

Small energy barriers for the dissociation of $n\pi^*$ ketones guarantee reaction rates that are large enough to compete with other decay pathways; however, small barriers alone may not be sufficient to warrant bond dissociation within the confining volume of a crystalline solid. Thus, one should address the following question: Are the inter-radical separation and relative orientation required to form low-energy, ground-state biradicals or radical pairs possible within a crystal? A detailed UB3LYP/6–31G(d) and complete active space/self-consistent field (CAS-SCF) analysis of the ground-state, singlet, and triplet energy surfaces of acetone recently reported by Zewail et al.[21] provides some answers to this question. The optimized structures of stationary points and transition states for the type I cleavage along the S_1 and T_1 surfaces, shown in Figure 48.3, confirm that the ideal plane of symmetry used in Figure 48.2 is not conserved. Prominent structural features of the minimum energy structures of the excited states (S_1 and T_1) include the pyramidalization of the carbonyl group and elongation of the CO bond. The distances of the breaking bond in the transition states along the singlet and triplet surfaces are relatively short (2.050 and 1.958 Å, respectively), and the nuclear displacement vectors in the transition-state imaginary modes describe the separation of the two radical fragments along the axis of the breaking C_α-CO bond.

Calculations suggest that molecular structural changes along the S_1 and T_1 surfaces are relatively small and provide clues for the smaller efficiency of the singlet state α-cleavage reaction. Although both surfaces have nearly the same structure at the transition state (Figure 48.3), generation of the primary radical pair from the S_1 surface involves relaxation via a conical intersection, also allowing for ultra-fast radiationless decay.[22] A three-dimensional surface and a contour plot show a nearly flat region along the minimum energy pathway in the S_1 surface of acetone (Figure 48.4). Additionally, the surfaces reveal a transition state S_1–TS that is 18 kcal/mol above the S_1 minimum (S_1-minimum, located 110 kcal/mol above the S_0 minimum) and a conical intersection (S_0/S_1–CI) after the S_1 transition state. The theoretical structure of acetone at the CI is that of an almost linear acyl radical (CCO angle = 169.7°) and a methyl radical that is 2.874 Å from the acyl radical center. The degeneracy at the conical intersection is removed by nuclear displacements along the direction where a radical pair or a hot acetone molecule is generated. A pathway to return back to the ground state is probably responsible for the relatively low pre-exponential factors ($A = 10^8\ s^{-1}$) observed for the singlet state α-cleavage of simple aliphatic ketones.

Not shown in Figure 48.4, but illustrated in the reaction coordinate in Figure 48.5, intersystem crossing (ISC) leads to the T_1 minimum in the $n\pi^*$ surface which, in the case of acetone, is approximately 80 kcal/mol above the S_0 minimum (Figure 48.5).[23,24] The quantum yield for ISC in solution is 0.90,[25] and it depends on excitation energy when irradiation is carried out in the gas phase. α-Cleavage from the S_1 surface may be efficient when the proper amount of excitation energy is provided in the gas phase. Upon excitation with light greater in energy than the transition state of the S_1 surface [$h\nu \geq E(S_1\text{–TS})$, or ~110

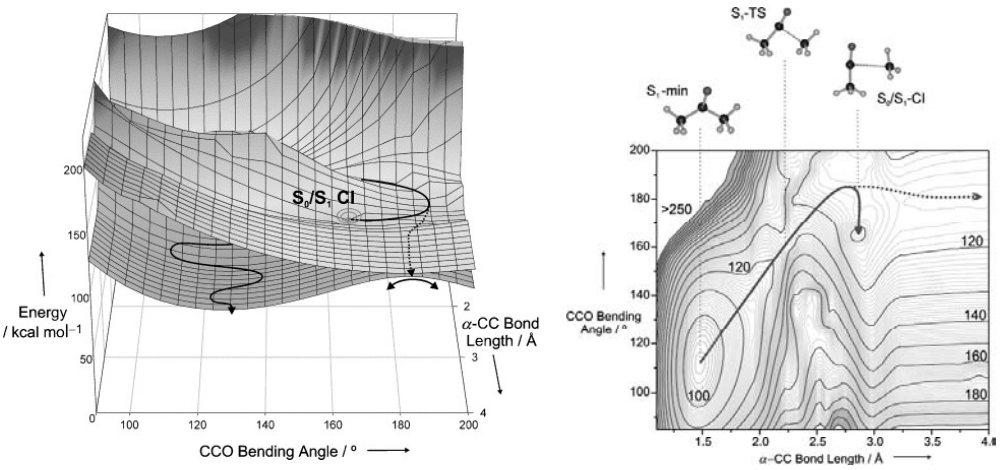

FIGURE 48.4 The three-dimensional graph of the S_1 and S_0 surfaces reveals a conical intersection (CI) where the S_1 relaxes to the S_0 surface. The contour plot shows the minimum energy path in the S_1 surface connecting the S_1-min to the S_0/S_1–CI via the transition state S_1–TS. The dashed arrow in both plots shows a disfavored path for α-cleavage for which another barrier must be surpassed in order to generate the free primary radical pair along the S_1 surface. The calculation was performed at the TD-UB3LYP/6–31G(d)//CASSCF(10,8)/6–31G(d) level of theory. (Adapted from Reference 21a.)

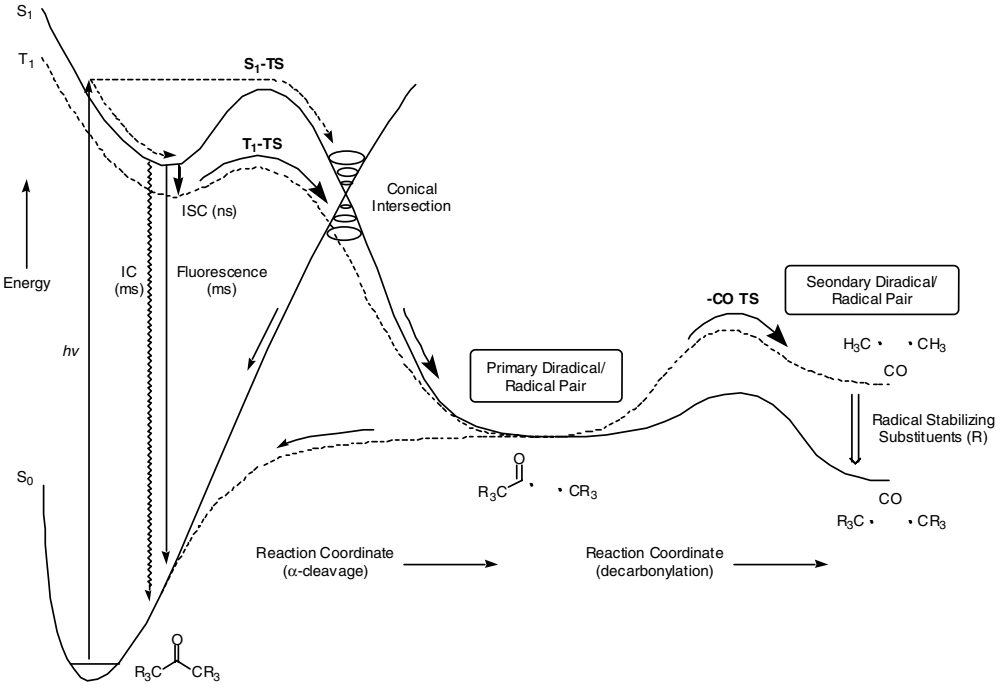

FIGURE 48.5 Reaction coordinate (RC) derived from computational studies of the Norrish type I reaction.[21] The RC shows α-cleavage from both S_1 and T_1 surfaces to yield the acyl–alkyl biradical/radical pair. Subsequent decarbonylation of the acyl radical generates the alkyl–alkyl biradical/radical pair.

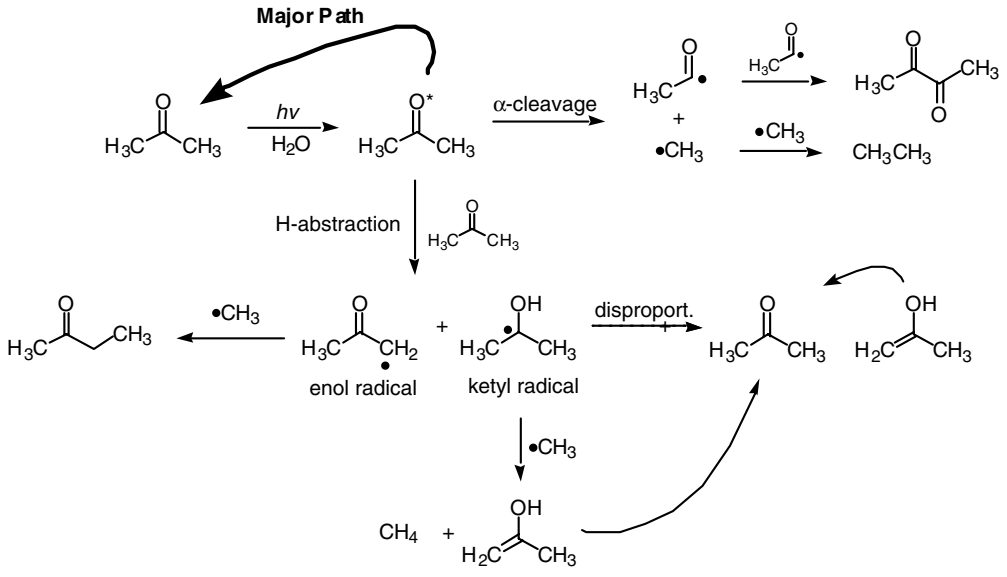

SCHEME 2

kcal/mol in the case of acetone], it may be possible to overcome the S_1 barrier to cleave via the conical intersection or decay to the ground state. However, gas-phase excitation with $h\nu < E(S_1\text{–TS})$ results primarily in intersystem crossing to the T_1 surface.[26] The transition state along the triplet surface (T_1–TS) lies about 13 to 15 kcal/mol above the T_1 minimum, so that α-cleavage along the vibrationally excited T_1 surface is more likely to occur in the gas phase.[27–29]

Finally, decarbonylation of the acetyl radical occurs after overcoming a 17-kcal/mol barrier in an overall endothermic fragmentation in the gas phase. As for α-cleavage, the height of the barrier should decrease significantly by substituting the methyl hydrogens with radical stabilizing substituents that may facilitate decarbonylation reactions in the liquid and solid states.

48.4 α-Cleavage Reactions in the Liquid Phase

While reactions in the gas phase may occur along electronically and vibrationally excited surfaces if high-energy photons are used, reactions in liquids and in solids tend to proceed along the lowest vibrational states as excess excitation energy can be dissipated very rapidly. With a triplet-state barrier of 13 kcal/mol, the rate constant of α-cleavage for acetone in solution is too small to compete with other decay pathways.[30] The lifetime of triplet acetone in inert solvents (e.g., H_2O) is limited by radiationless decay and quenching by adventitious impurities.[31] However, excitation of acetone gives trace amounts of products arising from a bimolecular reaction where the excited carbonyl of one molecule abstracts a hydrogen atom from the methyl group of another molecule in the ground state to form enol- and ketyl-free radicals (Scheme 2). Small yields of α-cleavage reaction also occur in solution and may be observed under some experimental conditions. For example, chemically induced dynamic nuclear polarization (CIDNP) experiments with laser excitation in H_2O reveal polarized signals for ethane and biacetyl along with other minor products (Scheme 2).[32]

The excited state kinetics of simple acetone derivatives in solution are similar. As expected for a weak $n\pi^*$ transition, the rates of fluorescence emission are low and the fluorescence quantum yields small ($\Phi_{Fluor} \leq 0.002$). Singlet lifetimes of a few nanoseconds are primarily limited by intersystem crossing to the triplet state with rate constants of $\sim 10^8\ s^{-1}$ (Table 48.1).[33]

TABLE 48.1 Singlet Excited State Lifetimes, Quantum Yields of ISC and ISC Rate Constants for Several Non-Conjugated Ketones

Ketone	τ_s (ns)	Φ_{ISC}	κ_{ISC} ($\times 10^8$ s^{-1})
Acetone	2.0	0.90	4.5–5.0
2-Pentanone	1.8	0.64	3.1
2-Hexanone	—	0.27	3.7
Cyclopentanone	2.0	—	—
Methyl-*t*-butyl ketone	4.2	<0.78	<1.86–2.47
Di-*t*-butyl ketone	5.6	<0.69	<1.2–1.5
2,2,5,5-Tetramethyl-cyclopentanone	8.7	—	<1.2
Norcamphor	5.2	—	<1.9
2-Adamantanone	8.0	—	<1.25

Source: Adapted from Yang et al.[33]

TABLE 48.2 Quantum Yields of Reaction in the S_1 and T_1 States (at λ = 313 nm) in Hexane

Ketone	Φ^0	Φ_I^S	Φ_{II}^S	Φ_I^T	Φ_{II}^T
Acetone (1)	<0.02	—	—	—	—
2-Pentanone (2)	0.27	—	0.03	—	0.16
2-Hexanone (3)	0.33	—	0.11	—	0.15
t-BuCO(Me) (4)	0.51	0.18	—	0.33	—
t-BuCO(*n*-Pr) (5)	0.59	0.22	0.02	0.35	<0.01
t-BuCO(*n*-Bu) (6)	0.31	0.07	0.07	0.17	<0.01

Source: Adapted from Yang and Feit.[35]

As illustrated in Table 48.2, α-cleavage in solution becomes important for ketones with radical-stabilizing groups in the α-position and, in favorable cases, the solution-phase reaction may proceed from both singlet and triplet states. However, ketones with flexible chains that have γ-hydrogens can also undergo the Norrish type II hydrogen abstraction process[34] in competition with the α-cleavage reaction (Scheme 3).[35]

Shown in Table 48.2 are the quantum yields for the disappearance of several aliphatic ketones (Φ^0) and the quantum yield of products from the Norrish type I and type II reactions in the singlet (Φ_I^S, Φ_{II}^S) and triplet (Φ_I^T, Φ_{II}^T) excited states. As these examples illustrate, saturated ketones with γ-hydrogens (e.g., **2** and **3**) do not undergo α-cleavage reactions in significant yields but undergo type II γ-hydrogen transfer from both singlet and triplet states. Type II reactions give 1,4-ketyl-alkyl biradicals (**3-BR**) that react from the singlet state by cleavage of the C_2-C_3 bond to give an alkene and an enol — which can subsequently tautomerise to the ketone — or by cyclization to form *cis*- and *trans*-cyclobutanol (Scheme 3). Singlet 1,4-biradicals can also revert to the ground-state ketone by a reverse hydrogen transfer. Type I reactions are observed from compounds giving rise to more stable secondary and tertiary radicals. *t*-Butyl-alkyl ketones **4–6** (Table 48.2) undergo efficient α-cleavage from both singlet and triplet states to form free radicals that react by random encounters. Although free acyl radicals from *t*-butylketones **4** to **6** have millisecond lifetimes under typical experimental conditions, no decarbonylation reactions are observed.

48.5 Decarbonylation of Acyl Radicals.

Similar to the rates of α-cleavage reactions, the rates of acyl radical decarbonylation depend very strongly on the stability of the alkyl radicals formed. It was first suggested by Fischer and Paul[15] that the rate

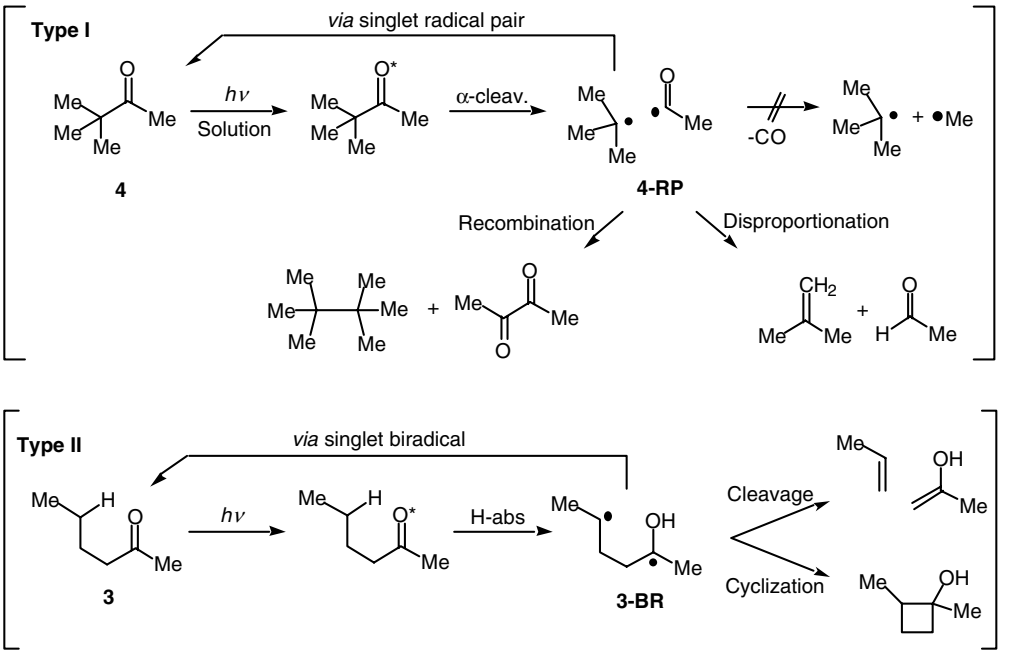

SCHEME 3

constants of decarbonylation (k_{-CO}) are a linear function of the R–CO bond dissociation energy, $DH_{(R–CO)}$. With a compilation of literature values available in 1987, it was shown that the corresponding $DH_{(R–CO)}$ values vary by ~30 kcal/mol and the corresponding rate constants by an astounding 15 orders of magnitude! One of the strongest bonds is that of benzoyl (Ph–CO), which has an estimated value of $DH_{(R–CO)}$ = 26 kcal/mol. On the other hand, α,α-dimethyl-α-phenylacetyl ($PhC(Me)_2$–CO) is less stable than the separated dimethylbenzyl radical and the CO molecule and has an approximate value of $DH_{(R–CO)}$ = –5 kcal/mol. The decarbonylation rate constants at ambient temperature for these two radicals change from an exceedingly slow k_{-CO} Å 10^{-7} s^{-1} for Ph–CO (a lifetime of over 100 days!)[16] to a remarkably fast k_{-CO} Å 10^{8} s^{-1} for $PhC(Me)_2$–CO (a lifetime of 10 ns).[36] These differences are expected if one considers the formation of a highly unstable σ-localized phenyl radical, with formation of a secondary, resonance delocalized, dimethylbenzyl radical.

Table 48.3 provides the activation parameters and ambient temperature rate constants for reactions involving the formation of methyl-, primary-, secondary-, tertiary-, benzylic-, secondary benzylic-, and tertiary benzylic radicals.[4a] As shown in the table, pre-exponential factors are near 10^{13} s^{-1} for alkyl substituents and slightly lower (10^{11}–10^{12} s^{-1}) when the entropically more demanding benzylic radicals are formed. The activation energies in the same set of compounds vary from 17.2 to 4.1 kcal/mol.

It has been suggested that the decarbonylation of acyl radicals may be used as a radical clock to gain information on the rate constants of competing reactions.[39] In the case of ketone photochemistry, the yields of decarbonylation products may be compared with the yields of CO-containing products to obtain information on the rate constants of diffusion, conformational motions, and intersystem crossing, which may determine the rate of reaction of the acyl radical. The rate constant of an ideal radical clock should be independent of polarity, viscosity, and spin multiplicity. Some of these effects have been analyzed in the case of two acyl radicals. Studies with $PhCH_2CO$ and *t*-BuCO suggest that changes in solvent polarity and viscosity result in rate constant changes no greater than a factor of 2 to 3 (Table 48.4).[40] It has also been suggested that rate constants of acyl decarbonylation in radical pairs and biradicals should be independent of their spin multiplicity and similar to those of analogous free radicals.

TABLE 48.3 Thermal Activation Parameters and 296 K Rate Constants for Decarbonylation of Several Acyl Radicals[a]

Acyl Radical	Solvent/Phase	log(A) (s^{-1})	Ea_{RCO} (kcal/mol)	k_{-CO} at 296 (s^{-1})
PhCO	Gas	—	—	1.5×10^{-7}
MeCO	Gas	13.2	17.2	4.0
EtCO	Gas	13.1	14.6	2.1×10^{2}
EtCH(Pr)CO	Toluene	13.0	12.0	1.4×10^{4}
Me_2CHCO	TES[b]	14[b]	13[b]	2.3×10^{4}
t-BuCO	Hexane	13.0[c]	11[c]	8.3×10^{5}
$Me_2C(OH)CO$[d]	MCP[e]	11.6	5.7	5.7×10^{7}
$PhCH_2CO$	Isooctane	12.0	6.9	8.1×10^{6}
PhCH(Me)CO	Isooctane	12.1	6.2	4.2×10^{7}
$PhC(Me)_2CO$	Isooctane	11.2	4.1	1.5×10^{8}

[a] Except when noted, values are those recommended by Chatgilialoglu et al.[4a]
[b] Values in tetraethoxysilane with an assumed pre-exponential factor.[38]
[c] The Ea value was calculated from an assumed pre-exponential of 13.
[d] Rate constant estimated from CIDNP data.[39]
[e] Methyl cyclopentane.

TABLE 48.4 Rate Constants for Decarbonylation of Phenylacetyl and Pivaloyl Radicals at Ambient Temperatures in Different Solvents

Acyl Radical	Solvent	k_{-CO} (s^{-1})
$PhCH_2CO$	Cyclohexane	6.0×10^{6}
	Hexane	5.3×10^{6}
	2-Propanol	3.1×10^{6}
	Ethanol	2.8×10^{6}
	Methanol	2.5×10^{6}
	Acetonitrile	1.7×10^{6}
t-BuCO	Hexane	8.3×10^{5}
	Tetradecane	9.0×10^{5}
	2-Propanol	4.7×10^{5}
	Ethanol	5.0×10^{5}
	Methanol	4.2×10^{5}
	Acetonitrile	8.0×10^{5}

Source: Adapted from Tsentalovich and Fischer.[40]

48.6 Solution Photodecarbonylation of Alkyl-Substituted Ketones

The expected correlation between photodecarbonylation efficiencies and the stability of the radicals formed can be illustrated with symmetric ketones giving rise to primary, secondary, and tertiary radicals in solution (Scheme 4). Results from irradiation of diethylketone (3-pentanone) in the gas and in solution are similar to those obtained with acetone.[30,41] In contrast, with two methyl groups on each α-carbon, the excited state of di-*iso*-propylketone **7** α-cleaves and loses CO to give decarbonylated products in ~51% chemical yield. Finally, as expected from the presence of three radical-stabilizing methyl groups on each α-carbon, di-*t*-butylketone **8** was reported to decarbonylate with a quantum yield of $\Phi = 0.7$ from both singlet ($\Phi 1 = 0.3$) and triplet ($\Phi 3 = 0.4$) states and a yield of CO formation of 90%.[33]

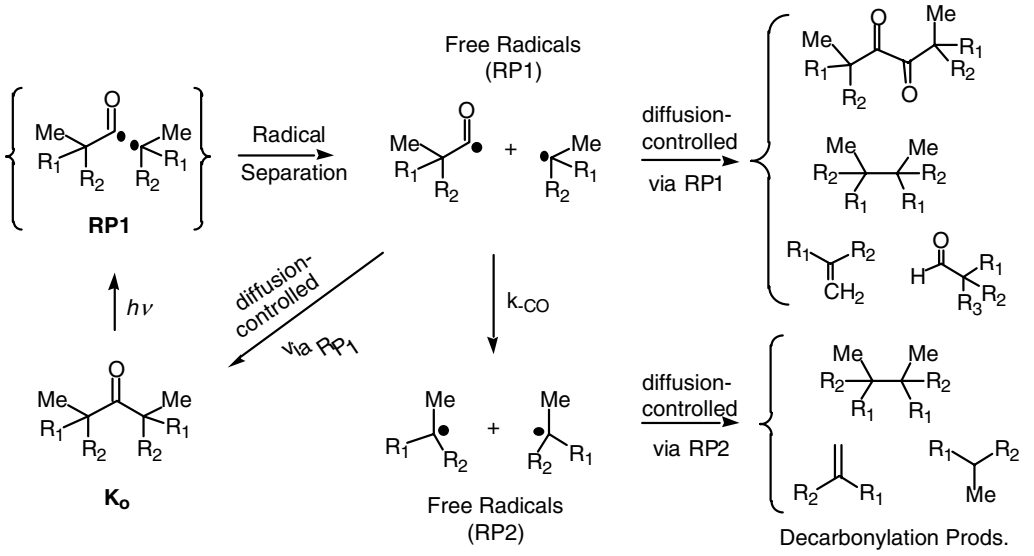

Ketone	R_1 R_2	k_{-CO} (s-1)	% Decarb. Prods. (298 K)
Diethylketone (**2**)	H H	2.1×10^2	< 2%
Di-*i*-propylketone (**7**)	Me H	1.4×10^4	51
Di-*t*-butylketone (**8**)	Me Me	8.3×10^5	>90

SCHEME 4

The high decarbonylation efficiency of di-*t*-butyl ketone **8** implies that the acyl and alkyl fragments of the primary pair can separate and remain separated as free radicals long enough for the pivaloyl radical to lose CO with a time constant of ~1.2 to 1.5 μs.[42,43] In contrast, the decarbonylation efficiency of the cyclic ketone analogs in Scheme 5 is remarkably reduced by the average proximity of the two radical termini, which facilitates faster radical–radical reactions.

It has been shown that triplet biradicals **8**-BR1 (Scheme 5) generated from tetra-alkyl ketones at ambient temperature in nonviscous liquids experience very fast conformational equilibration so that the rate-limiting step for product formation is intersystem crossing to the singlet state **8**-BR1. Studies have shown that rate constants for intersystem crossing for acyl–alkyl biradicals are primarily determined by spin-orbit coupling, which depends on the average distance between the two radical termini. With rates of intersystem crossing for a large range of acyl–alkyl biradicals falling within a range of 10 to 100 ns, the decarbonylation of dimethyl-substituted acyl radicals (expected to have a rate constant similar to that for a free pivaloyl radical in solution, or 1.2–1.5 μs) is very unfavorable.[42,44–46] Solution studies by several authors with α,α,ω,ω-tetramethyl-cycloalkanones with ring sizes between 5 and 26 ($\mathbf{8}_5$ - $\mathbf{8}_{26}$) have shown that intersystem crossing and radical–radical reactions in the tetramethyl acyl–alkyl biradicals **8**-BR1 are indeed faster than decarbonylation (Scheme 5).[42,46] A notable exception is tetramethylcyclooctanone $\mathbf{8}_8$, for which decarbonylation was detected, presumably reflecting the thermodynamically unfavorable end-to-end cyclization of the medium size ring.[42]

The photochemistry of tetramethyl-cycloalkanones with three- and four-membered rings differs substantially from those of the higher analogs (Schemes 6 and 7). The release of ring strain upon α-cleavage in tetramethylcyclobutanone accelerates the reaction to the extent that it occurs faster than intersystem crossing in the singlet-excited state. As illustrated in Scheme 6, irradiation of tetramethylcyclobutanone **12** in methanol solution generates a 1,4-acyl–alkyl biradical **1,4**-BR1.[47] Acyl–alkyl biradicals can decarbonylate to give a 1,3-biradical **1,3**-BR2, which goes on to give cyclopropanone, they can cleave along

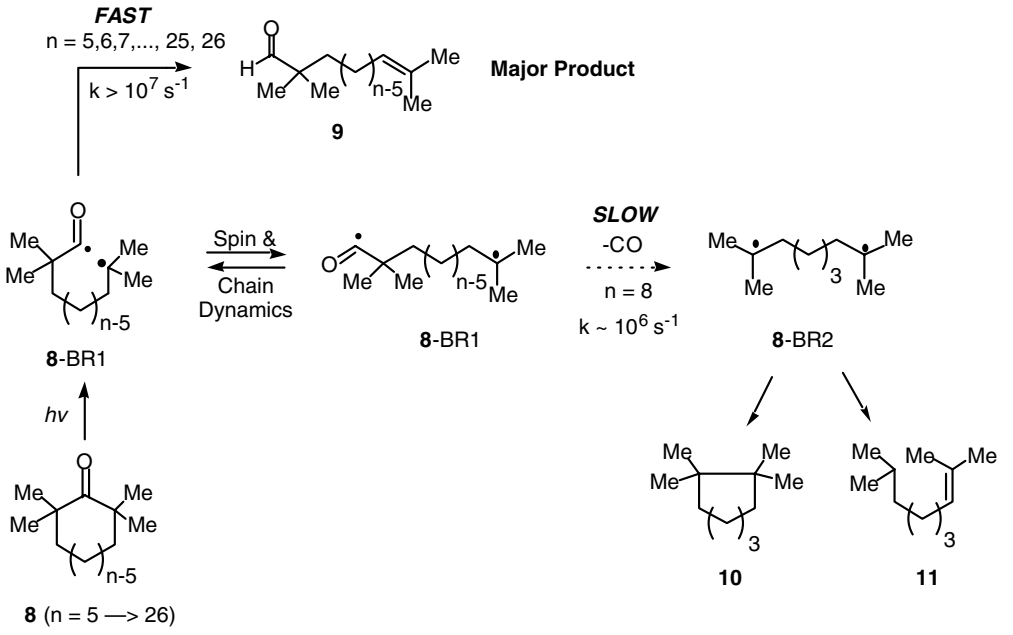

SCHEME 5

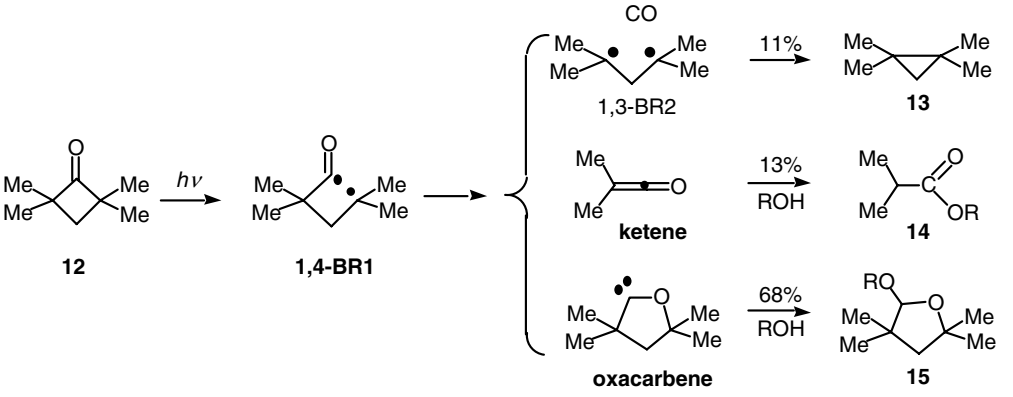

SCHEME 6

the 2,3-bond to generate isobutylene and dimethyl ketene, or they may ring-expand to give an oxacarbene intermediate. Reactions carried out in alcohol result in formation of cyclopropane **13** in 11% yield, isobutyric ester **14** in 13% yield, and cyclic ketal **15** in 68% yield. Compounds **14** and **15** form by reaction of the intermediate dimethylketene and oxacarbene, respectively, with the alcohol solvent.

Studies on the photochemistry of tetramethylcyclopropanone **17** have revealed efficient α-cleavage and decarbonylation reactions to give 2,3-dimethyl-2-butene **19** as the only product (Scheme 7). Interestingly, cyclopropanone **17** is prepared by an efficient decarbonylation of 2,2,4,4-tetramethylcyclobutanedione **16**.[48] Cyclopropanones, in general, are highly reactive compounds that can thermally equilibrate with oxyallyl, the open-shell 1,3-diyl **18**. While cyclopropanones are highly susceptible to nucleophilic attack to form hydrates and hemiketals, oxyallyl was shown to react rapidly with oxygen and furan.

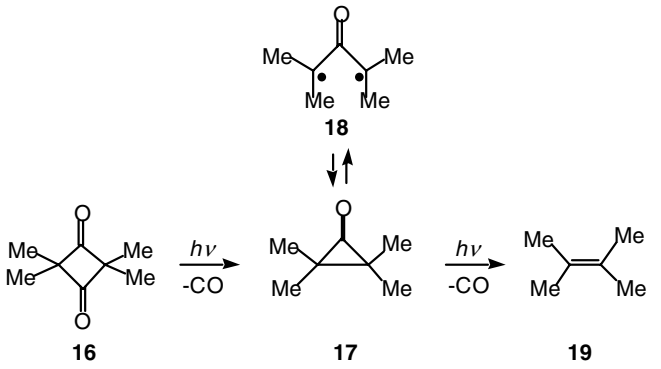

SCHEME 7

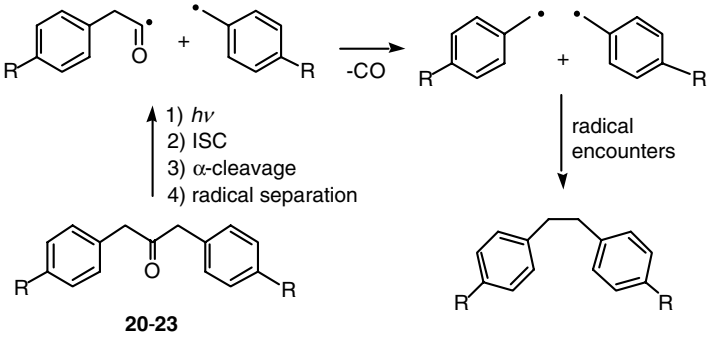

SCHEME 8

TABLE 48.5 Quantum Yields for the Decarbonylation of Ketones 21 to 23 in Benzene at 298 K

Ketone	R	$\Phi_{diarylethane}$
20	H	0.70
21	Me	0.71
22	MeO	0.65
23	CN	<0.02

48.7 Solution Photodecarbonylation of Diaryl-Substituted Ketones

The presence of α- and α′-phenyl groups in 1,3-diphenylpropanones (dibenzyl ketones) results in one of the most efficient and general substrates for photodecarbonylation reactions.[49,50] As a representative set, compounds **20** to **23** (Scheme 8 and Table 48.5) give rise to diphenylethanes as the only observable products in high chemical yield. The reaction is facilitated by high triplet yields, efficient α-cleavage, rapid separation of benzyl and 2-phenylacetyl radicals in solution, and the loss of CO from the phenyl–acetyl fragment with a time constant of ~120 ns (Scheme 8).[36] Combination of the two benzyl radicals gives rise to diphenylethanes with quantum yields higher than 0.65 and chemical yields approaching 100%. An exceptional stability was observed for the 4-cyanophenyl derivative **23**, which was proposed to undergo an intramolecular quenching process.[50]

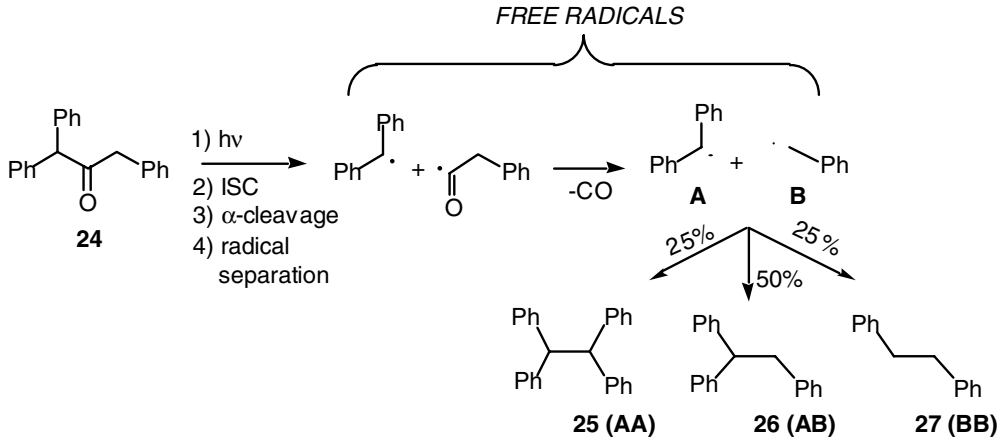

SCHEME 9

As expected from random free-radical recombination, three products are formed in statistical yields when the two benzyl radicals are different (Scheme 9).

As a typical example, excitation of 1,1,3-triphenyl-2-propanone **24** leads to formation of diphenylmethyl (A) and benzyl (B) radicals which re-encounter to yield tetraphenylethane **25** (AA), triphenylethane **26** (AB), and diphenylethane **27** (BB) in statistical 1:2:1 ratios and with a high chemical yield.[51]

With decarbonylation reactions that occur with a time constant of ~25 ns (see Table 48.3), the formation of α-alkyl-benzyl radicals increases the efficiency of the reaction in α,α′-diphenylcycloalkanones, even when the radical centers in the acyl–alkyl biradicals are held relatively close to each other. Thus, unlike the tetramethyl cycloalkanones in Scheme 5, which fail to decarbonylate before intersystem crossing to the singlet state, α,α′-diphenylcycloalkanones **28** undergo a very fast efficient photodecarbonylation reaction in solution. Several studies have been carried out with α,α′-diphenylcycloalkanones **28** with ring sizes that range from 6 (**28**$_6$)[52,53] to 15 (**28**$_{15}$)[54] (Scheme 10). As indicated in Scheme 10, decarbonylation of the triplet acyl–alkyl biradicals (^{3}BR1) at ambient temperature is generally faster than intersystem crossing to the singlet state. While the time constant for intersystem crossing and reaction for dibenzyl biradicals formed is on the order of 200 ns,[55] decarbonylation is expected to occur with a time constant of ~25 ns, assuming a similar value as the PhCH(Me)CO free radical in Table 48.3.

Once formed, the triplet dibenzyl biradicals (^{3}BR2) explore their conformations and intersystem cross to give closed-shell products **29**, **30**, and **31** with rate constants and reaction yields that depend on the length of the alkyl chain. Compounds with small ring sizes (**28**$_6$ to **28**$_8$) react primarily by combination (**29**$_6$ to **29**$_8$) and/or disproportionation (**30**$_6$ to **30**$_8$), and compounds with large ring size react also by attack of one benzyl radical to the *para*-position of the benzyl radical at the other end of the chain. Cyclophanes **31**$_{10}$, **31**$_{11}$, **31**$_{12}$, and **31**$_{15}$ are formed in that manner after a [1,5]-hydrogen shift from the original methylene–cyclohexadiene structure. When reactions are carried out at low temperatures, the rate of decarbonylation of the acyl radical is decreased as compared to the rate of intersystem crossing so that products can form in the singlet acyl–alkyl biradical, including product from attack to the *para*-position of the benzyl radical to form the cyclophane ketones **32**$_{11}$, **32**$_{12}$, and **32**$_{15}$.

48.8 Solution Photodecarbonylation of Ketones with Other α-Substituents

Other radical stabilizing substituents may also facilitate the photodecarbonylation reaction in solution, but very few have been systematically studied. Recent studies with the dodecanones **33a**[56] and **33b**[57] illustrate the enabling effect of α-hydroxyl groups on the decarbonylation reaction (Scheme 11). Although

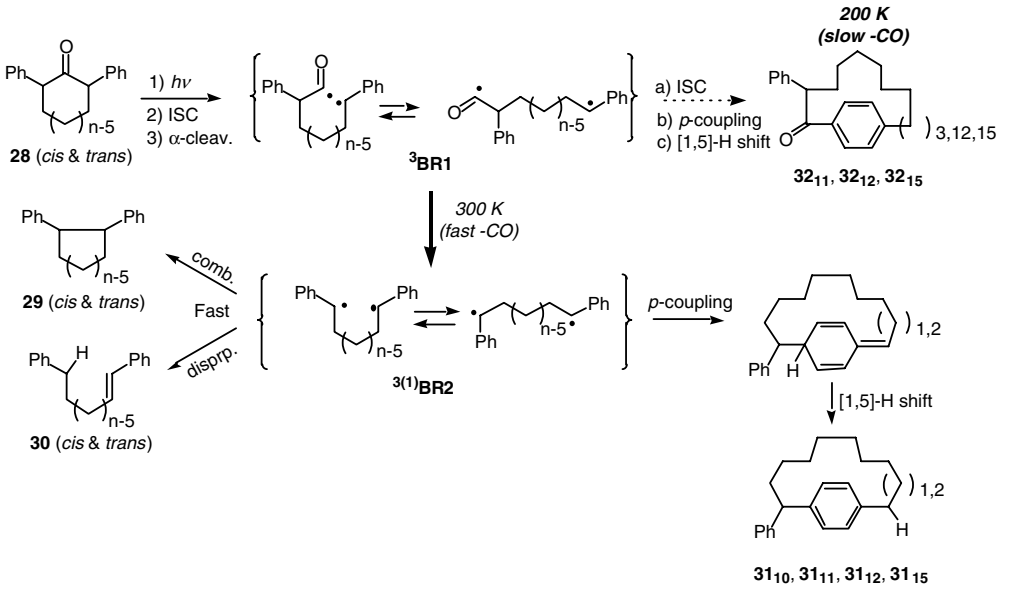

SCHEME 10

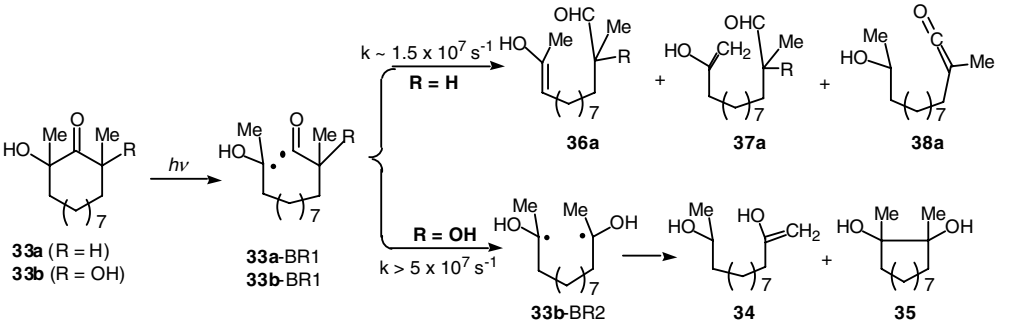

SCHEME 11

efficient α-cleavage from the triplet state of the two ketones generates the primary acyl–ketyl biradicals **33a**-BR1 and **33b**-BR1, only the latter decarbonylates fast enough to generate the secondary diketyl biradical **33b**-BR2 in significant yields. Analysis of time-resolved CIDNP data from **33a** showed that **33a**-BR1 intersystem crosses to the singlet state and reacts by disproportionation to give to **36a–38a** with a rate constant that is ~35 times faster than the rate constant for decarbonylation ($k_{rxn} = 1.5 \times 10^7\ s^{-1}$ and $k_{-CO} = 4.2 \times 10^5\ s^{-1}$). In contrast, with methyl and hydroxy groups in the two α-positions, the rate of decarbonylation of the acyl–ketyl biradical **33b**-BR1 was estimated to be $k_{-co} > 5 \times 10^7\ s^{-1}$, which is 111-fold faster than that of **33a**-BR1. Therefore, in the case of ketone **33b**, products **34** and **35** from biradical **33b**-BR2 are highly favored over products from the short-lived acyl–ketyl biradical **33b**-BR1.

A wide range of radical-stabilizing substituents in the α- and α′-positions may facilitate the photodecarbonylation of ketones in solution and a few examples in Scheme 12 illustrate the enabling effect of vinyl substituents in both cyclic[58] and acyclic compounds.[59]

Remarkably, the photodecarbonylation of ketones **39**, **40**, and **41** proceeds in >90% chemical yield whether occurring via free radical for **39** or biradical intermediates for **40** and **41**. Tetramethyldivinyl

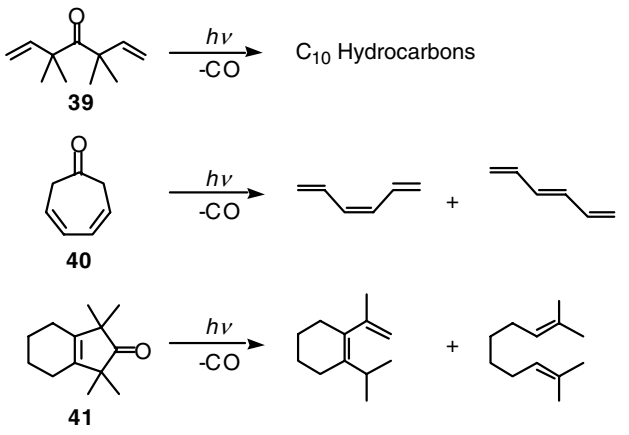

SCHEME 12

acetone **39** was reported to give CO along with a product mixture characterized as C_{10} hydrocarbons, presumably formed by combination of two dimethylvinyl free radicals. Similarly, the efficient formation of decarbonylation products from cyclic ketones **40** and **41** indicates that the loss of CO must occur faster than intersystem crossing and reaction of acyl–alkyl biradical intermediates. The formation of *cis*- and *trans*-hexatrienes from **40** and the formation of a disproportionation product from **41** may be taken as indications of a stepwise radical process rather than concerted elimination of CO by chelotropic reaction.

In another interesting set of examples, the photochemistry of ketones **43** to **46** illustrates the effect of α-hydroxy and α′-ketal groups on the decarbonylation reaction in solution.[60] Compounds **43** to **46** were recently prepared from the optically active α,β-unsaturated compound (–)-**42** and were shown to photodecarbonylate to give products **47** to **50** by enantiospecific radical–radical combination reactions in relatively good chemical yields. The utility of this reaction for a novel strategy for carbohydrate synthesis was nicely demonstrated. The examples in Scheme 13 illustrate reactions leading to the synthesis of D-ribose and D-lyxose, as well as the hexoses, L-talose and L-gulose.

Ketone decarbonylation reactions have been useful for the preparation of highly reactive molecules. A few examples include the preparation of ynols,[61] yneamines,[62] and strained alkynes[63] by *in situ* photolysis of cyclopropenones **51** to **53** (Scheme 14). These high-energy compounds are short-lived transients that must be either detected by fast kinetic methods or kinetically stabilized in cryogenic matrices to facilitate their detection. Phenanthrocyclopropenone **53** was generated *in situ* by photolysis of a *bis*(diazo)ketone or by photodecarboxylation of dicarboxyphenathrene anhydride.[63]

48.9 Photodecarbonylation Reactions in Crystals

The first few examples illustrating the photochemical decarbonylation of pure crystalline ketones were reported by Quinkert and co-workers in 1971 (Scheme 15).[64] It was shown that irradiation of α,α′-diphenyl-indanones **54** to **57** in solution and in crystals proceeded to give decarbonylation products in very high chemical yields, but with remarkably medium-dependent chemo- and stereo-selectivities.[65] Photochemical reactions in crystalline solids were substantially more chemoselective and stereospecific than those carried out in solution. Crystals of *cis*- and *trans*-diphenyl indanones **54** and **55** yielded the corresponding *cis*- and *trans*-diphenylbenzocyclobutanes **58** and **59** in 95% yield, respectively, while crystals of *cis*- and *trans*-α,α′-dimethyl-α,α′-diphenyl-indanones **56** and **57** yielded benzocyclobutanes **60** and **61** as the main products in 90 and 86% yields, respectively. When reactions were carried out in dilute solution, significantly lower selectivities and specificities were observed. Compounds **54** and **55** yielded benzocyclobutanes **58** and **59** in a very similar ratio, suggesting an equilibration process involving

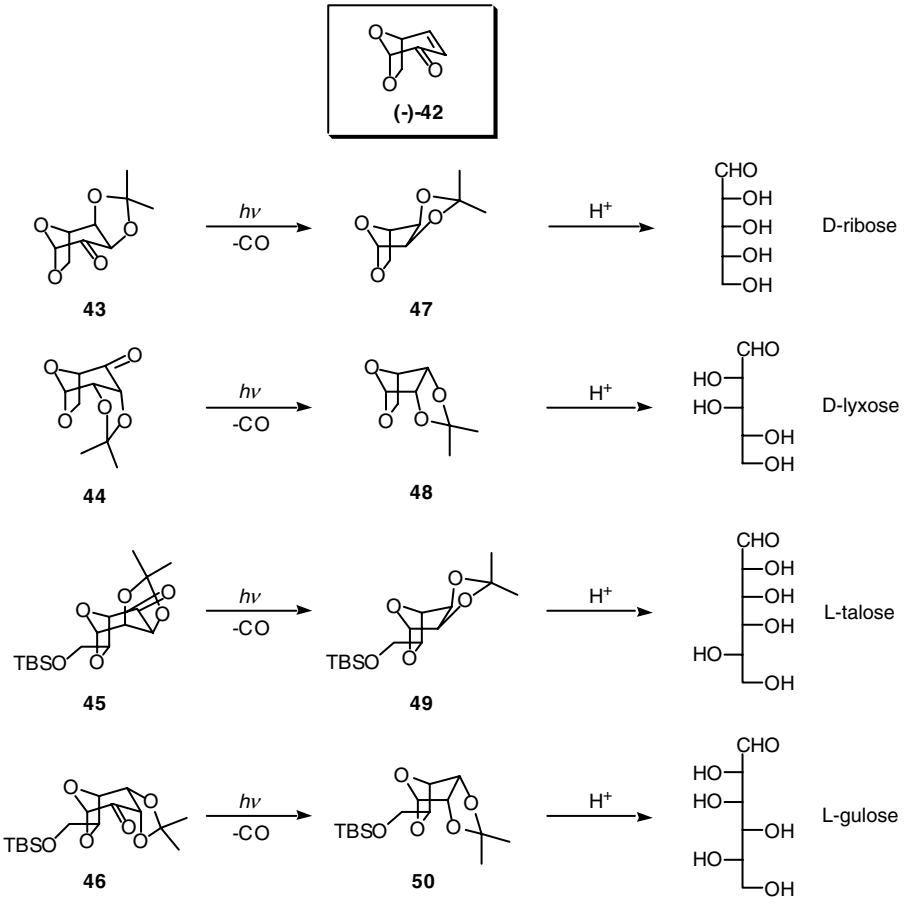

SCHEME 13

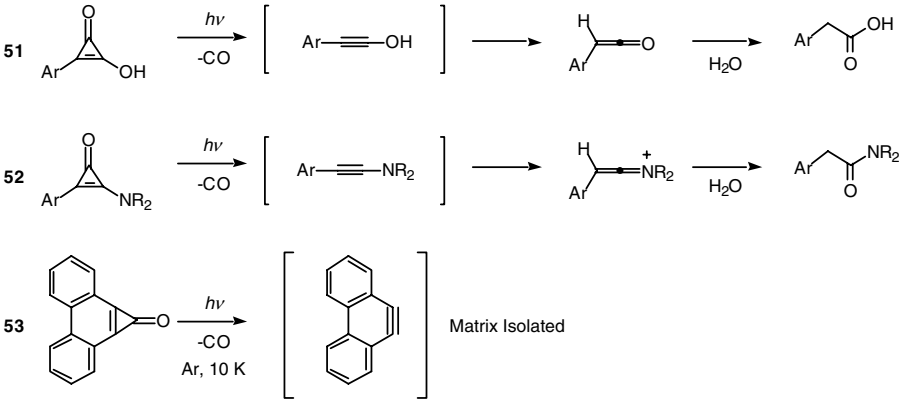

SCHEME 14

common intermediates. In contrast, different product mixtures from the sterically more encumbered **56** and **57** suggested that full equilibration may not take place for the corresponding intermediates. Product mixtures from these ketones included substantial amounts of the vinyl benzene derivative **62** in addition to benzocyclobutanes **60** and **61**.

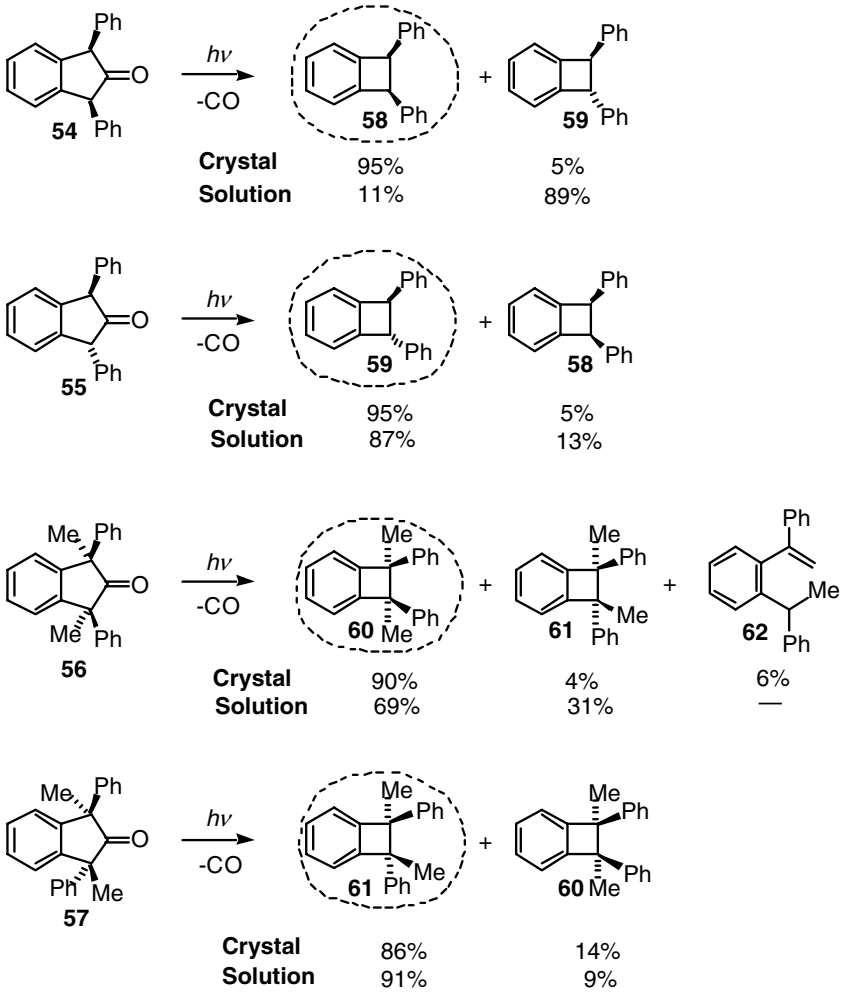

SCHEME 15

The reaction mechanism for the photolysis of 3-indanones in solution has been investigated in some detail. As illustrated in Scheme 16 with 3-indanone **55**, the reaction occurs efficiently in the triplet excited state by stepwise α-cleavage and decarbonylation reactions to give the triplet 1,4-biradical ^{3}**55**-BR2 which corresponds to the triplet excited state (^{3}**63***) of *ortho*-quinodimethanes **63**. Although products (*E,Z*)-**63**, (*E,E*)-**63** and (*Z,Z*)-**63** can be detected by spectroscopic methods, they give rise to benzocyclobutanes **58** and **59** by 8π-electron electrocyclic ring closure.[64] It has been suggested that the vinyl-benzene derivative **62** is formed by [1,5]-hydrogen shift from the analogous *ortho*-quinodimethane from the methyl-substituted 3-indanone **56**. Although it has not been investigated whether an *ortho*-quinodimethane intermediate is also formed in crystals of indanones **54** to **57**, the relative large changes in shape and volume suggest that a 1,4-biradical may close directly to the benzocyclobutane by a least motion pathway.

Twelve years after the pioneering work of Quinkert et al., while the "cage effect" of several diphenyl propanones in several reaction media were being studied,[66] the photodecarbonylation of crystalline 1,3,4-triphenyl-2-pentanone **64** was reported by Turro and co-workers (Scheme 17).[67] It was shown that irradiation of **64** in solution gave a complex mixture of products arising from random free-radical–radical reactions of **64A** and **64B**. In contrast, reactions carried out in crystals to very low conversion values gave

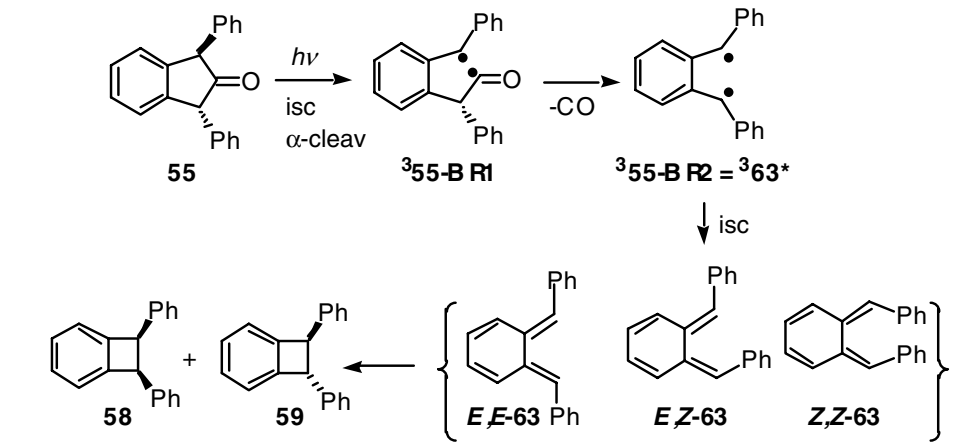

SCHEME 16

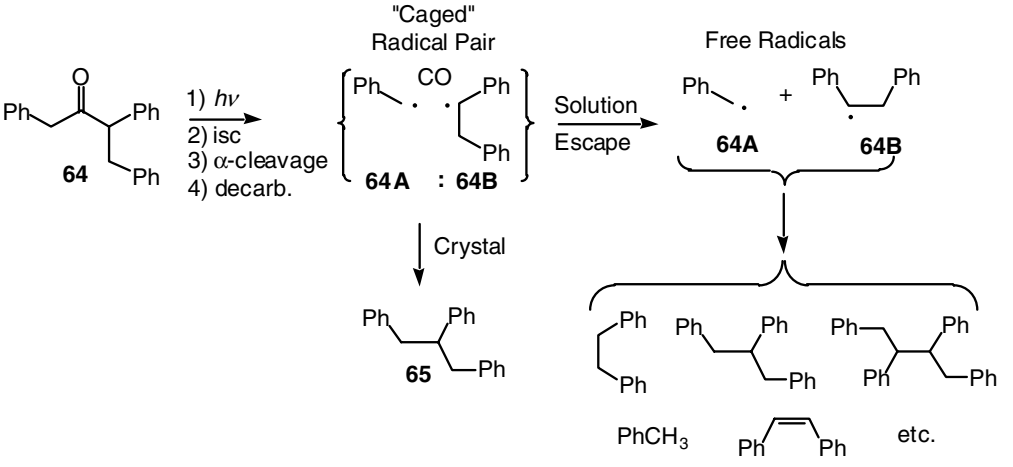

SCHEME 17

1,2,3-triphenylpropane **65** with a remarkable 98% selectivity by radical–radical combination of the caged radical pair {**64A**:**64B**}.

48.10 Photochemical Efficiencies in Crystals of α-Phenyl-Substituted Cyclohexanones

Although the reports by Quinkert and Turro suggested the feasibility of the decarbonylation reaction in crystals and demonstrated a very high chemo- and stereoselectivity, the factors that may facilitate or impede solid-state reactivity remained unexplained. Recognizing that the efficient α-cleavage and rapid acyl-radical decarbonylation of ketones with radical stabilizing α- and α′-phenyl substituents may determine the reactivity of ketones **54** to **57** and **64** (Schemes 15 and 17), Choi et al.[68] carried out the first systematic search for a correlation between the reactivity of solids and the stability of the radicals involved in the reaction (Scheme 18).

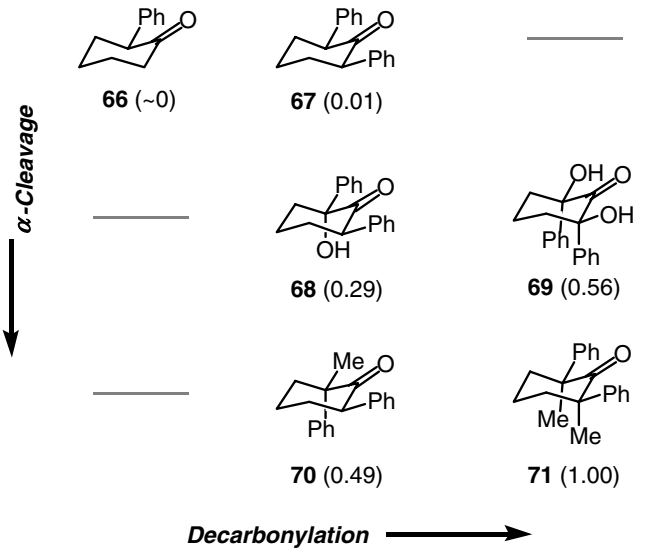

SCHEME 18

The crystalline cyclohexanones **66** to **71**, with various α-substituents, were selected for their study. The *cis*-/*trans*- configurations and axial–equatorial conformations of the substituents shown in Scheme 18 were established by x-ray diffraction. It was also shown that the phenyl groups are oriented in such a way that benzylic delocalization of the putative radical species may occur. Knowing that compounds **66** to **71** react in solution by α-cleavage with similar quantum yields of ketone disappearance (Φ_{-CO} > 0.6),[52,53,59] it was suggested that reactivity differences in the solid state could be assigned both to the ease of α-cleavage from the triplet excited state and the ease of decarbonylation of the acyl–alkyl biradical. To determine this, relative quantum efficiencies were determined in side-by-side irradiations with microcrystalline samples dispersed in KBr matrices using monochromatic ultraviolet light. The extent of reaction was determined by measuring changes in absorbance of the CO band as a function of irradiation time to obtain initial reaction velocities proportional to the intensity of the irradiating light (which was kept constant) and to the quantum yield of reaction.

The results in Figure 48.6 and the relative quantum yields in parentheses in Scheme 18 show a strong correlation between the radical-stabilizing effects of the α-substituents in **66** to **71** and their solid-state reaction efficiencies. A reaction mechanism involving a triplet-state reaction was suggested to explain the photostability of **66** and the 100-fold reactivity difference observed. It was suggested that the rates and efficiencies of triplet-state α-cleavage should be similar for the pair of ketones in each row of Scheme 18. Similar benzyl–acyl biradicals are formed from **66** and **67**, hydroxybenzyl–acyl biradicals from **68** and **69**, and methylbenzyl–acyl biradicals from **70** and **71**. It was also suggested that an increase in relative quantum yields in going from left to right can be correlated with an increase in the yield of decarbonylation.

The lack of reactivity from 2-phenylcylcohexanone **66** may be understood in terms of a cycle given by steps 1, 2, and 3 in Scheme 19. The reaction starts in the triplet excited state with an α-cleavage reaction to give a 1,6-biradical where the acyl and benzyl radical termini are held very closely but are unable to give closed-shell products (step 1).[70] Because decarbonylation of the benzyl–acyl biradical derived from **66** would yield a very unstable primary radical center, it is reasonable to suggest that the reaction is too slow to compete with intersystem crossing to the singlet state (step 2). While the singlet biradical ^{1}BR1 from **66** reacts in solution by disproportionation with a quantum yield for ketone disappearance of 0.6, formation of ^{1}BR-1 in crystals should be ideally set to return the starting material (step 3), thus accounting for lack of product formation in the solid state. In contrast, with phenyl groups at the two α-carbons,

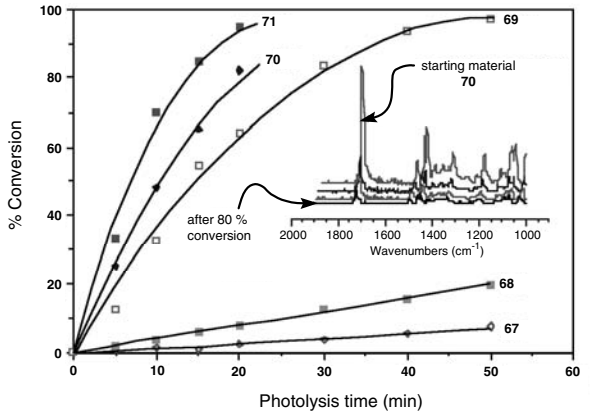

FIGURE 48.6 Normalized conversion vs. irradiation time of microcrystals of cyclohexanones **66** to **71** dispersed in KBr matrices. Inset: Representative FT-IR data from compound **70**.

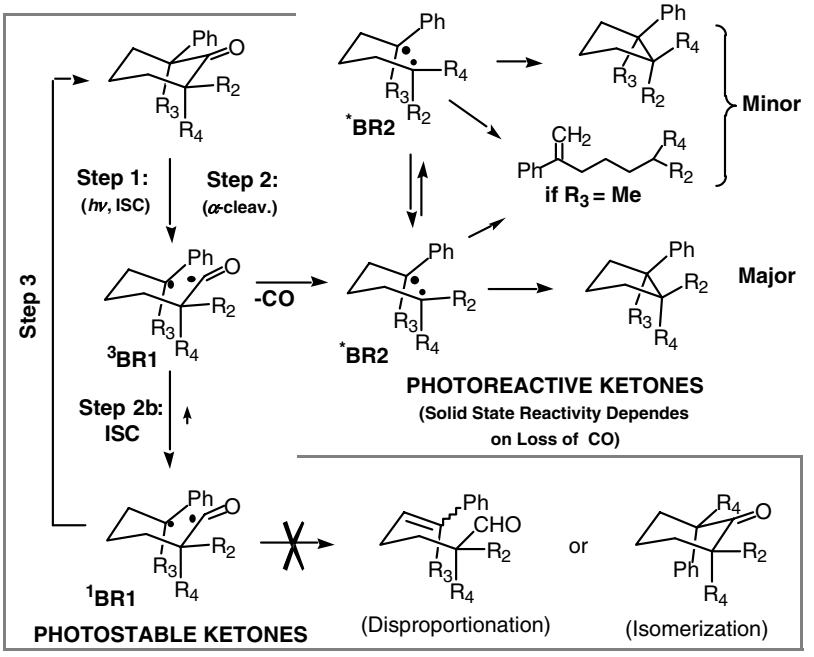

SCHEME 19

decarbonylation of the benzyl–acyl biradicals from *cis*-2,6-diphenylcyclohexanone **67** can give a 1,5-*bis*(benzylic) biradical in competition with steps 2 and 3. While irradiation of **67** in solution yields a conformationally extended biradical that gives mixture of *cis*- and *trans*-diphenylcyclopentane and *cis*- and *trans*-1,5-diphenyl-1-pentene with a high quantum yield ($\Phi \geq 0.6$), irradiations in the solid state give *cis*-diphenylcyclopentane with high selectivity but with a significantly lower efficiency. One may conclude qualitatively that the rate constant for intersystem crossing to the acyl–benzyl biradical **67**-^{1}BR1 is still much greater than the rate of decarbonylation to the *bis*(benzyl) radical pair **67**-^{3}BR2.

The 29- and 49-fold increase in reaction efficiency in going from **67** to **68** and **69** can be assigned to an increase in the efficiency of the α-cleavage reaction. The α-hydroxy and α-methyl substituents in the

latter compounds should lower the bond dissociation energy of the α-bond and reduce the activation energy of the α-cleavage reactions. While reactions of **68** and **69** in solution are less selective than reactions in crystals, both compounds gave mixtures of combination and disproportionation products in the two reaction media. Finally, one may speculate that the rates of α-cleavage of **68** and **70** or **69** and **71** should be very similar to each other and assign the twofold increase in reaction efficiencies observed in going from **68** to **70** and from **69** to **71** to the effects of substituents on the decarbonylation reaction. Ambient temperature rate constants for decarbonylation of analogous free acyl radicals in solution are ~10^8 s^{-1} (Table 48.3), suggesting the approximate order of magnitude for the rate of intersystem crossing in the solid state. It is well known that short biradicals tend to have very short lifetimes due to their fast intersystem crossing rates. The intersystem-crossing limited lifetimes of acyl–alkyl biradicals from the Norrish type I reaction of cyclopentanones are only 10 to 15 ns. Although closer inter-radical distances are expected to result in shorter lifetimes, to our knowledge no data exist for acyl–alkyl biradicals derived from cyclobutanones or cyclopropanones. The distance dependence of biradical lifetimes has also been documented with the triplet α,ω-1,n-diyls[71] where the lifetimes decrease from ~900 ns for 1,5-biradicals and 200 ns for 1,4-biradicals down to 15 to 20 ns for 1,3-biradicals.[69b,72] A dramatic increase in the rate of intersystem crossing as the distance between the two radicals decreases is assigned to an increase in spin-orbit coupling, which mediates the transition between triplet and singlet states. While it is likely that triplet lifetimes in crystals may be short and may lead to acyl–alkyl radical recombination back to the ground state, it is also known that biradical lifetimes tend to increase in highly viscous media when chain dynamics becomes the rate-limiting step.[73] However, given that chain extension (or radical separation) in crystals is not possible, slow radical–radical reactions and singlet–triplet equilibration are unlikely.

48.11 Photodecarbonylation of Crystalline Cyclopentanones

The mechanistic conclusion regarding the effects of substituents drawn from the study of the cyclohexanones in Scheme 18 were supported by analysis of several tetrasubstituted cyclopentanones (**72** to **74**) with α-alkyl and α-phenyl substituents (Scheme 20).[74] It was established that compounds **72** to **74** react cleanly in solution to give the products shown in Scheme 20. Quantum yields of ketone disappearance ranged from $\Phi_{-K} = 0.04$ for **73** to $\Phi_{-K} = 0.9$ for **72**. *trans*-2,5-Dimethyl-2,5-dibenzylcyclopentanone **72** reacted in solution by α-cleavage and disproportionation of the acyl–alkyl biradical **72**-BR1, with no traces of decarbonylation products. A mixture of *cis*- and *trans*-aldehydes **75** was formed in solution by a very efficient α-cleavage reaction followed by a highly favorable disproportionation of singlet **72**-BR1. Given the high photoreactivity of **72**, the results with 2,2-diphenyl-5,5-dimethyl-cyclopentanone **73** are initially surprising. Assuming that excited state α-cleavage of **73** is as efficient as that of **72**, its low photoreactivity ($\Phi_{-K} = 0.04$) is an indication that the acyl–alkyl biradical **73**-BR1 returns to the starting material faster than any competing reaction. The formation of 1,1-diphenylethane **77** and cyclobutane **78** from a 1,1-dipheny-4,4-dimethy-1,4-biradical in a combined 50% yield and a quantum yield of ketone disappearance of 0.04 indicate that decarbonylation occurs with a quantum yield of ~0.02. The high disproportionation efficiencies of **72**-BR1 may reflect the ease of a seven-membered transition state, transfer of a benzylic hydrogen and formation of a very stable double bond as the singlet state of **72** BR1 reacts to form aldehyde **76**. In contrast, the transfer of a secondary hydrogen in a relatively strained transition state appears to disfavor the disproportionation of **73**-BR1 as compared to regeneration of the starting ketone. Not surprisingly, while the solution photochemistry of **72** and **73** were very different, the two ketones failed to react in the solid state. On the contrary, the solution and solid-state reactivity of tetraphenylcyclobutanone **74** was remarkably efficient.[75] While the two phenyl groups on each α-position facilitate the sequential α-cleavage and decarbonylation reactions in the two media, the resulting 1,4-biradical reacted differently in the two reaction media. While reactions in solution yielded cyclobutanone **79** and 1,1-diphenylethane **77** by cyclization and cleavage, reactions in crystals lead exclusively to cyclobutanone **79** in nearly quantitative chemical yields in a very clean solid-to-solid reaction. From a mechanistic standpoint, results in crystals are consistent with the mechanism in Scheme 19. Reactions begin

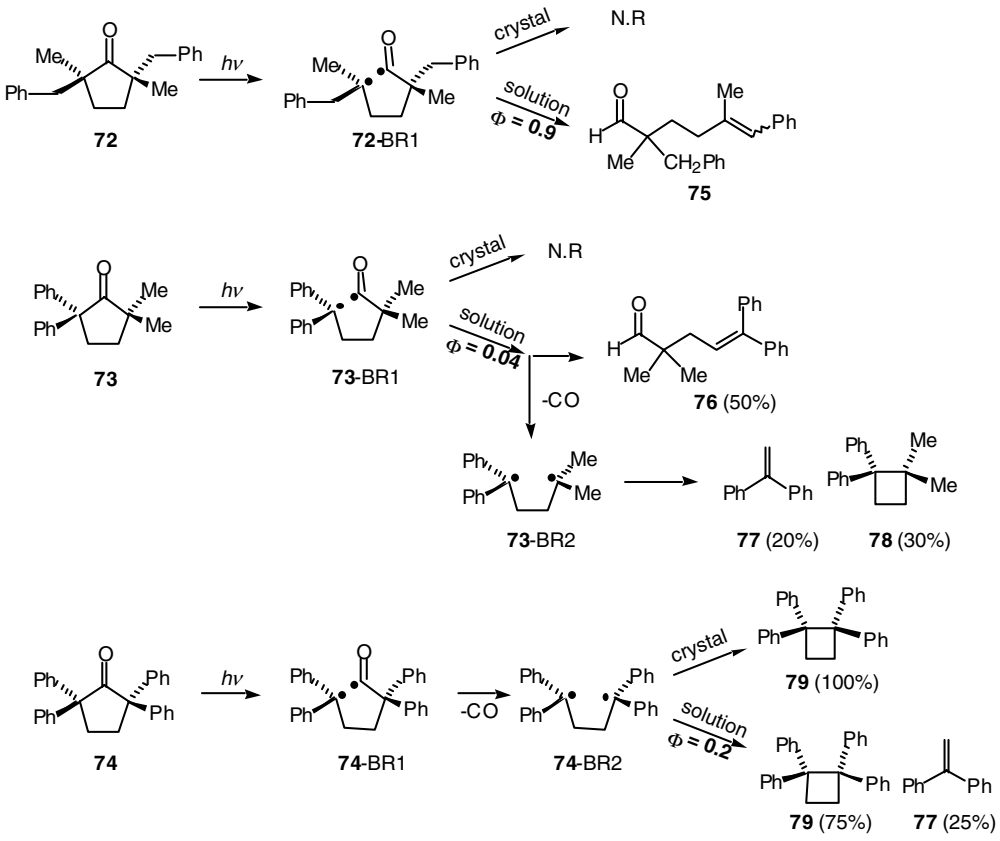

SCHEME 20

by triplet state α-cleavage to generate the acyl–alkyl biradicals ^{3}BR1. Because formation of tertiary alkyl radicals by decarbonylation of ^{3}**72**-BR1 and ^{3}**73**-BR1 is not fast enough to compete with intersystem crossing, the corresponding singlet biradicals return to ground state by reforming the σ-bond that was broken in the initial α-cleavage step. In contrast, decarbonylation of ^{3}**74**-BR1 proceeds very rapidly by formation of CO and a relatively stable diphenylmethyl radical center. The exclusive formation of tetraphenylcyclobutane **79** may reflect the close proximity of the two radical centers or a preference associated with the reaction pathway that requires the smallest change in volume within the close-packed environment of the crystal.

48.12 Conformationally Restricted Benzylic Stabilization in Crystalline 2-Indanones

Although the solid-state reactivity of several 2-indanones was demonstrated by Quinkert et al.[64,65] in the 1970s, one might ask whether intermediate radicals are able to experience benzylic stabilization by conjugation with the central phenyl group. While irradiation of 2-indanones in solution may lead to triplet acyl–alkyl biradicals (^{3}BR1) where bond rotation allows for conjugation of the emerging benzylic radicals with the central double bond, we may not be able to use reactions in crystals to explore such stabilizing interactions if fast rotation within the solid is hindered. This is illustrated in Scheme 21 by initial cleavage of the C1C2 σ-bond to give a C1-alkyl–C2-acyl biradical labeled ^{3}BR1. It may be expected that fast decarbonylation of ^{3}BR1 may require alignment of the breaking C2C3 bond with the π-orbital of the central phenyl ring to form a stable benzylic radical and a molecule of CO. If rotation about the

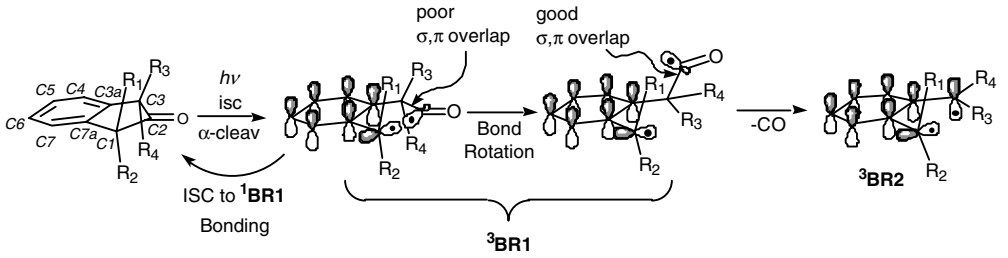

SCHEME 21

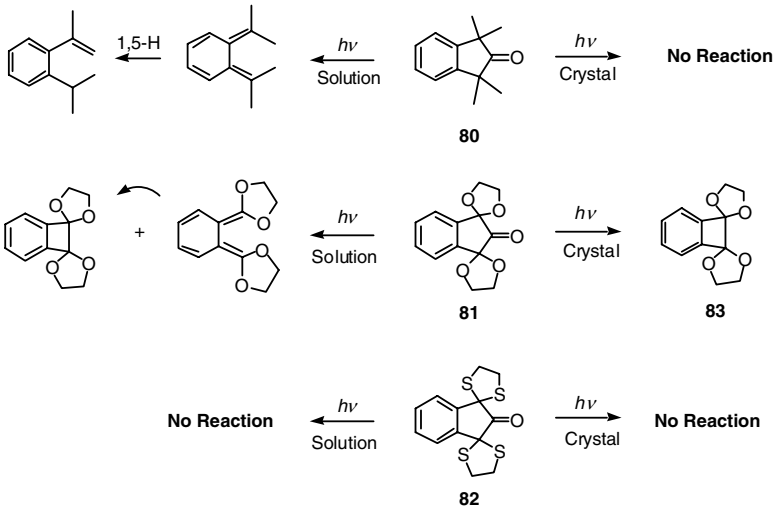

SCHEME 22

C3C3a bond is not possible in crystals, decarbonylation of ^{3}BR1 may be slower than intersystem crossing to ^{1}BR1 which can go back to the starting ketone (Scheme 21).

Because the compounds studied by Quinkert, including 2-indanones **54** and **55**, have α-phenyl-substituents at C1 and C3, one cannot conclude whether the benzocyclopentanone π-system may contribute to the stability of the intermediate biradicals and facilitate the solid-state reaction. In order to answer this question and to test the effect of methyl, oxygen, and sulfur as α-substituents, the solid reactivities of 2-indanone derivatives **80**, **81**, and **82** (Scheme 22) were recently investigated and compared to those of **54** and **55** (Scheme 15); a reasonable answer was rapidly found.[76]

A comparison of the solid-state results obtained with tetramethyl-2-indanone **80** with the 1,3-diphenyl-2-indanones **54** and **55** suggests the 2-indanone chromophore on its own does not facilitate the solid-state reaction. The lack of solid state reactivity of **80** indicates that return of the acyl–alkyl biradical to the ground state is significantly more efficient than decarbonylation. Experiments and calculations[78] indicate that the difference in energy between benzyl radical conformations with parallel and orthogonal p-π-orbital alignment is ~12.5 kcal/mol, with the orthogonal alignment being disfavored (Scheme 23). Assuming the relation between R–CO bond dissociation energies DH_{R-CO} and decarbonylation rate constants (k_{-CO}) proposed by Fisher and Paul,[15] one may expect that different alignments caused by rotation of the Ph–CH_2CO will lead to differences in DH_{R-CO} of ~12 kcal/mol and differences in k_{-CO} of about three orders of magnitude.

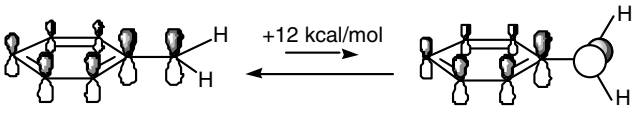

SCHEME 23

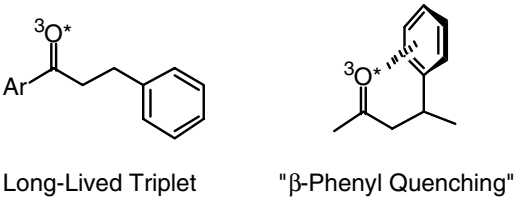

SCHEME 24

Knowing that simple alkyl substituents in **80** are unable to facilitate the solid-state reactivity of 2-indanones, the solid-state reactivity of 1,3-*bis*(ethylenedioxy)-2-indanone **81** can be assigned to the effect of the alkoxy-substituents. The lack of reactivity of the *bis*(thioacetal) **82** is consistent with the well-known intramolecular quenching of excited carbonyls by sulfur.

48.13 Suppression of α-Cleavage by β-Phenyl Quenching in Crystalline Ketones

Although several α,α′-diphenyl-substituted ketones can react cleanly and smoothly in the solid state, it may be expected that additional substituents and structural factors will have a strong effect on the efficiency of the reaction. It is known that ketones with β-phenyl groups are susceptible to conformation-dependent quenching by charge-transfer interactions between the carbonyl $n\pi^*$ excited state and the β-phenyl substituent (Scheme 24).[79–81] Scaiano et al.[82] have shown that β-phenyl quenching can reduce the triplet lifetime of crystalline propiophenones by a factor of 10 to 20 from 8 μs down to 0.7 and 0.4 μs, depending on the proximity of the β-phenyl to the carbonyl and on packing differences between racemic and chiral crystals.

With hopes that mechanistic knowledge gathered from excited state processes in solution and in the solid state may be transfesrable from one crystalline structure to another, the photochemistry of the β-phenyl substituted isomers *cis*-**83** and *trans*-**83** was investigated in solution and in crystals (Scheme 25). With 2-phenyl-2-vinyl and 6-phenyl-6-benzyl substituents, cyclohexanones *cis*-**83** and *trans*-**83** are expected to have very efficient α-cleavage and decarbonylation reactions, unless the β-phenyl group is positioned for intramolecular charge-transfer quenching. In fact, molecular structures obtained by single-crystal x-ray analysis revealed solid-state conformations expected to undergo a very efficient intramolecular quenching (Figure 48.7).

Photochemical experiments carried out in solution led to the efficient formation of *cis*- and *trans*-diphenyl cyclopentanes **84** and cycloheptene **85** in a 10:5:1 ratio after >95% conversion. In contrast, photolysis of *cis*-**83** and *trans*-**83** in the crystalline solid state gave only traces of cyclopentanes *cis*-**84** and *trans*-**84**, respectively, even after 12-hr irradiation.[83] The differences between solution and solid-state photochemical reactivity in the cases of *cis*- and *trans*-**83** were explained by considering the conformations present in the two crystals and the conformational dynamics of the two molecules in solution.

As illustrated in Figure 48.7, compounds *cis*- and *trans*-**83** adopt twist-boat conformations with the benzyl groups in pseudoequatorial positions. An efficient β-phenyl quenching interaction in both crystals is facilitated by the close proximity of the carbonyl oxygen and the edge of the aromatic ring. It was suggested that solution results reflect the presence of reactive (***83** React) and nonreactive conformers (***83** Quench), which are unable to equilibrate within their very short lifetimes (Scheme 25).

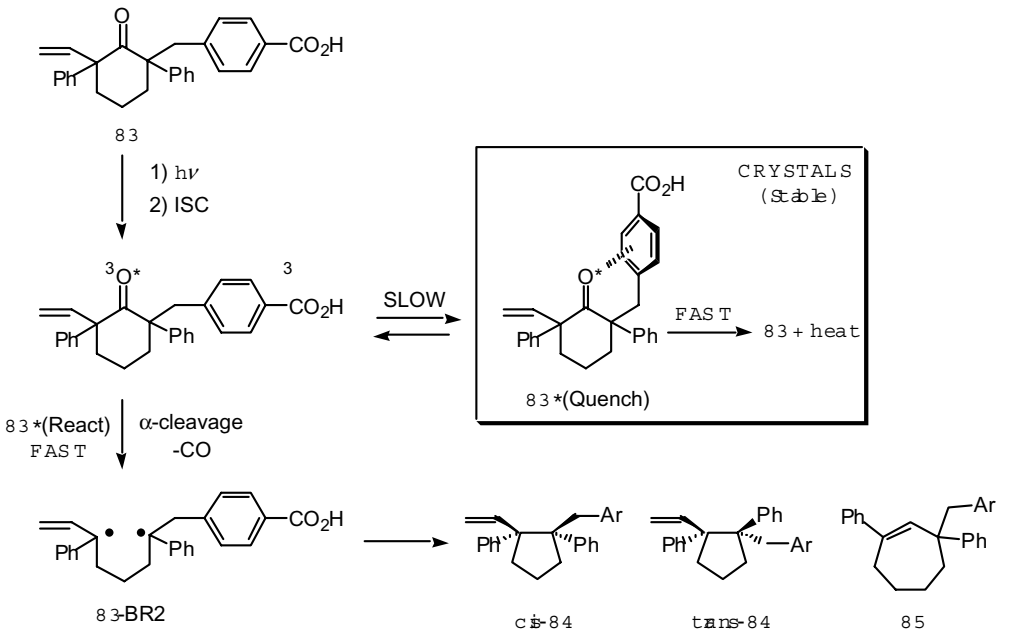

SCHEME 25

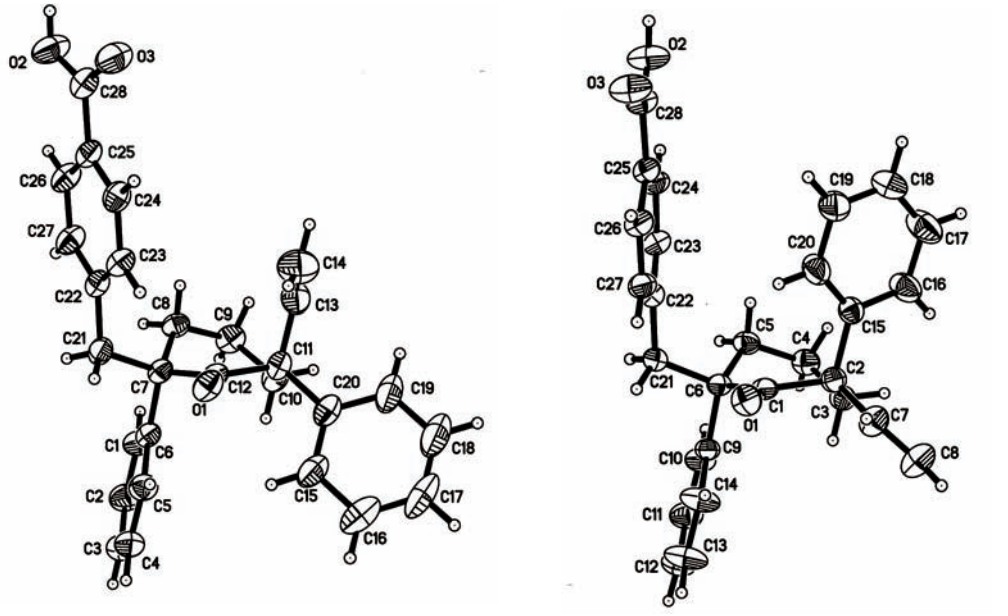

FIGURE 48.7 ORTEP views of compounds *cis*-**83** (left) and *trans*-**83** (right) showing their twist-boat conformations and the disposition of the benzyl group with respect to the ketone carbonyl leading to a very efficient β-phenyl quenching.

Both β-phenyl quenching and α-cleavage for the α,α′-diaryl ketones in solution are known to occur within sub-nanosecond time scales. The results with crystals of *cis*- and *trans*-**83** are consistent with their molecular structures and add confidence to the use of structure–reactivity correlations known from solution to reactions occurring in crystalline solids.

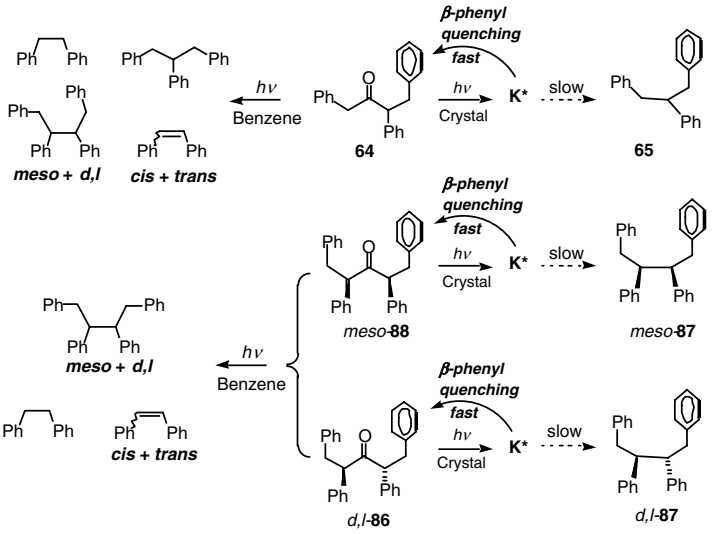

SCHEME 26

Additional examples of β-phenyl quenching in crystals have been recently documented by comparing the relative solid state efficiency of β-phenyl-containing compounds with analogous structures lacking the quenching motif (Scheme 26). Among these is the α-benzyl-1,3-diphenyl acetone **64**, which was reported by Baretz and Turro to react inefficiently. Although photochemical reactions in crystals of triphenylbutanone **64** and *meso*- and *d*,*l*-**86** proceeded in very low yields after long irradiation periods (e.g., less than 5% conversion in 12 hr), reactions in crystals were highly chemoselective and stereospecific. As indicated in Scheme 26, the only products detected in crystals were those formed by decarbonylation and stereospecific radical–radical combination. The *meso*- and *d*,*l*-diastereomers of ketone **86** reacted to give diphenylethanes *meso*-**87** and *d*,*l*-**87**, respectively, as the only solid state products.[84]

48.14 Engineering Reactions in Crystals: Energetic Considerations

The reliable design of reactions in crystalline solids may bring the development of synthetic and materials applications. Our intuition of reactions in crystals is slowly changing as more is known about their possibilities and limitations. As improbable as it may seem, the sequential cleavage of two σ-bonds may become one of the most reliable reactions in the solid state. Although the homolytic cleavage of σ-CC bonds from ground-state ketones would require thermal energies incompatible with the integrity of their low melting solids, the absorption of a UV photons provides a reacting ketone with ~70 to 80 kcal/mol of excitation energy that may be channeled into the two sequential bond-breaking processes required to form two alkyl radicals and a molecule of CO (Scheme 27). However, it may be stressed that the key to reactions in crystals is to have the triplet-state α-cleavage reaction ($T_1 \rightarrow {}^3BR1$) faster than intersystem crossing to the ground state ($T_1 \rightarrow S_0$) and decarbonylation reactions (${}^3BR1 \rightarrow {}^3BR2$) that are faster than acyl–alkyl recombination back to the starting ketone (${}^3BR1 \rightarrow S_0$). Given that a strong correlation exists between the heat of bond-cleavage reactions and their activation energies, it has been suggested that sufficiently fast α-cleavage and decarbonylation should be more likely when they are exothermic.

Taking acetone as a benchmark and knowing that bond dissociation energies are related to the radical stabilization energies of the α-substituents, one can estimate whether the extent of radical stabilization provided by substituents X and X′ is sufficient to make each cleavage step thermochemically favorable (Scheme 27, radical stabilization energies, RSE(X) and RSE(X′)). In the case of acetone, the triplet state

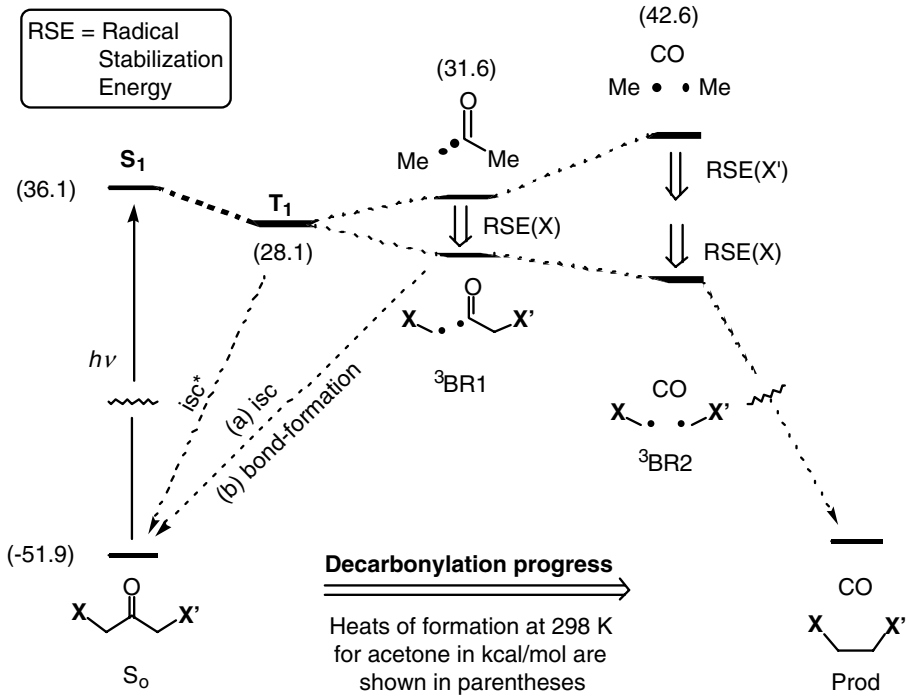

SCHEME 27

has an excitation energy of ~79 kcal/mol.[85] In agreement with the low reaction yields in solution and the energy-dependent results observed in the gas phase, α-cleavage and decarbonylation are endothermic by 3.5 and 11 kcal/mol, respectively.[86] One may predict more efficiently α-cleavage for acetone derivatives with α-bonds that are weaker than 79 kcal/mol and more efficient decarbonylation for acyl radicals with R–CO bonds that are weaker than 11 kcal/mol. However, because the initial α-cleavage occurs at the weakest bond, one may expect that substituents that lower the bond dissociation energy (BDE) of the two α-bonds by >11 kcal/mol are required.

Support for a thermochemical prediction of solid-state reactivity according to the model in Scheme 27 was based on observations with the effects of alkyl and benzyl substituents discussed above along with thermochemical and kinetic data available in the literature. A summary of activation energies, reaction enthalpies, and approximate reaction rate constants for decarbonylation of acyl radicals at ambient temperature is illustrated in Scheme 28. The formation of phenyl, methyl, ethyl, *iso*-propyl, and *t*-butyl radicals from their acyl radical precursors is endothermic. Not surprisingly, the formation of carbonyl compounds by reaction of these radicals with CO gas at medium or high pressures has been used in several synthetic applications. However, with ~12 kcal/mol of resonance stabilization, the formation of benzyl radicals from 2-phenylacetyl is almost thermoneutral, has an activation barrier of only 7 kcal/mol, and occurs in solution with a rate constant of 10^7 s^{-1}. Examples of crystalline ketones giving rise to benzyl radicals have been documented, although their reactions are very inefficient. It may be estimated also from literature values that formation of α-methylbenzyl and α,α-dimethylbenzyl from their acyl radical precursors should be exothermic by ~4 and 8 kcal/mol, respectively. Activation energies and rate constants are 6.2 kcal/mol and 4×10^7 s^{-1}, respectively, for α-methylbenzyl and 4.1 kcal/mol and 1.5×10^8 s^{-1} for α,α-dimethylbenzyl (Scheme 28). Also shown in Scheme 28 is an approximate lower limit for the rate of decarbonylation to compete with radical–radical reactions, estimated from experimental observations in inert media and at ambient temperature.

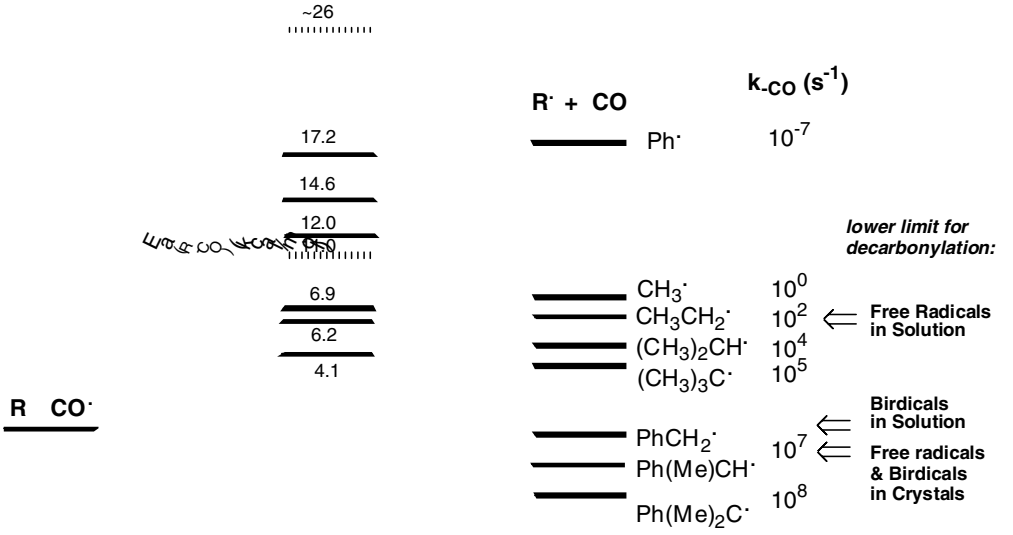

SCHEME 28

A simple test of the thermochemical postulate in Schemes 27 and 28 was recently reported in the literature.[87] From a wide range of potential α-substituents with radical stabilization energies above 11 kcal/mol, ester groups were selected. Based on literature reports,[88] it was expected that an ester carbonyl and two methyl groups would stabilize a carbon radical by >12.3 kcal/mol with respect to the unsubstituted methyl radical. The resulting radical would be stabilized by keto–enol delocalization and by the effect of the methyl substituents. Given that photochemical decarbonylation of ketodiesters had not been previously documented, it was of interest to test if their photochemistry would conform to the prediction. Three crystalline 1,3-acetonedicarboxylates, **88a** to **88c**, were investigated and all three reacted cleanly and smoothly in the solid state (Scheme 29).

As predicted, only decarbonylation products were observed in solution and in crystals. However, while free radicals in solution reacted by combination to give succinates **89a–c** and by disproportionation to give isopropionates **90a–c** and acrylates **91a–c**, reactions in crystals gave rise to the exclusive formation of radical–radical combination products **89a–c** when carried out to low conversion values. Although lower selectivities were observed in reactions carried out to high conversion for low melting crystals of **88b**, irradiation of higher melting ketones **88a** and **88c** proceeded from solid to solid to give the combination product in high chemical yields.

The thermochemical model predicts that reaction efficiencies in crystals will depend on the stability of the radicals formed. To further test this model, a series of highly crystalline adamantyl 1,3-ketodiesters with various methyl substituents were analyzed to compare their reaction efficiencies under conditions that involve the formation primary, secondary, and tertiary enol radicals.[89] After showing that ketodiesters with α-hydrogens crystallize in the keto form, compounds **92a** to **92f** were photolysed in dilute benzene solutions and in crystals (Scheme 30). The results obtained provided a strong support for the thermochemical model. α-Cleavage and decarbonylation reactions involving the formation of primary enol radicals were extremely inefficient in solution and no products were observed in the solid under conditions where melting was rigorously prevented.

Only crystals of **92d**, **92e**, and **92f**, which react through secondary (**R2b**) and tertiary (**R2c**) enol radicals, reacted in the solid state (Scheme 30). Although the relative efficiencies of these compounds were very similar in solution, a plot of conversion vs. irradiation times for reactions in crystals (Figure 48.8) illustrates reaction efficiencies with a ranking **92f** > **92e** > **92d**. Compounds **92a** and **92b** reacted only after some melting had occurred. Compound **92c** was not studied experimentally but was

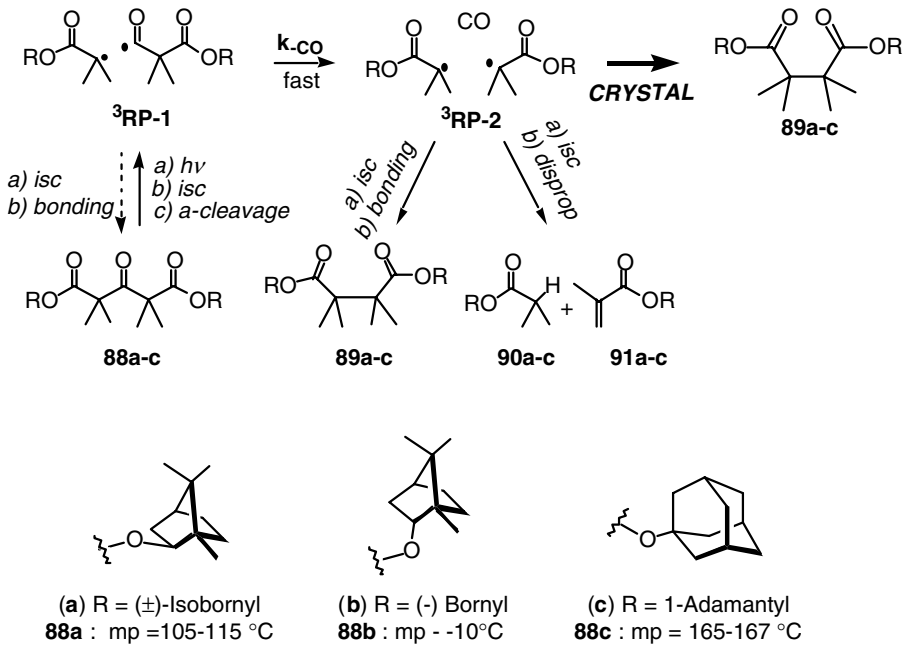

SCHEME 29

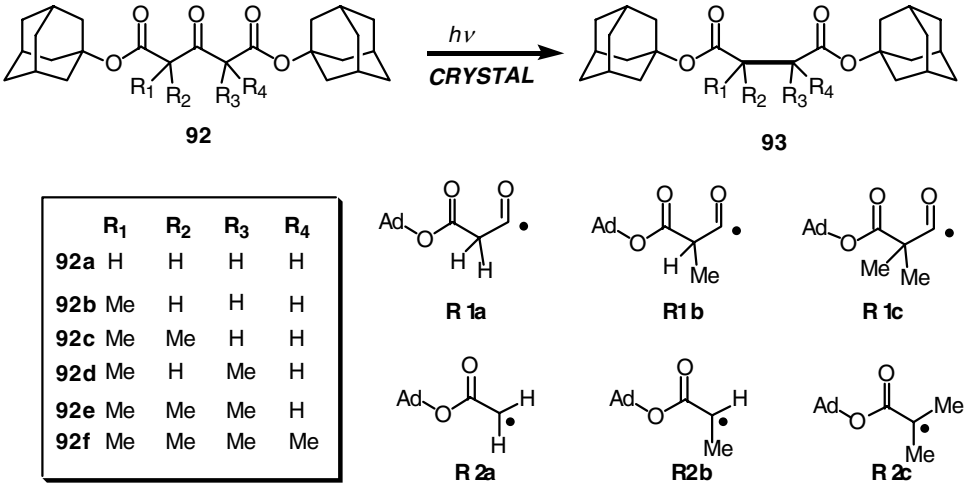

	R_1	R_2	R_3	R_4
92a	H	H	H	H
92b	Me	H	H	H
92c	Me	Me	H	H
92d	Me	H	Me	H
92e	Me	Me	Me	H
92f	Me	Me	Me	Me

SCHEME 30

included in calculations described below. The observed reactivity order reflects the formation of two tertiary enol radicals from **92f**, tertiary and secondary enol radicals from **92e**, and two secondary enol radicals from **92d**. Crystals of **92d** were analyzed as a mixture of *meso*- and *d,l*-isomers and melted after ~10% conversion.

A computational study to confirm the validity of the thermochemical model and to gain more insight into the effect of ester substituents was subsequently published.[90] The heats of formation of acetone and the methyl ester analogs of ketodiesters **92a** to **92f** and their intermediate radicals were calculated at 298 K with the B3LYP/6–31G* density functional method. The heats of formation obtained were used to

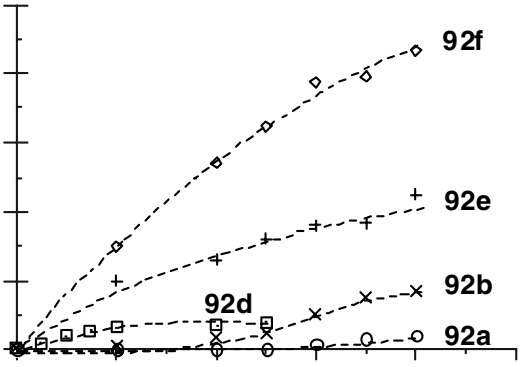

FIGURE 48.8 Yields of decarbonylation of ketones **92a** to **92f** in the solid state as a function of irradiation time. Ketones **92a** and **92b** reacted only after melting with ~2 hr of irradiation. Mixtures of *meso*- and *d,l*-**92d** melted at ambient temperature after reaching about 10% conversion.

TABLE 48.6 Calculated Bond Dissociation Energies (BDE in kcal/mol) for the First and Second Homolytic Dissociations in the Decarbonylation of Acetone and Ketodiesters 92a–f

Reactant	BDE-1	Radicals (BDE-1)	BDE-2	Radicals + CO (BDE-2)
CH_3COCH_3	81.14	CH_3, CH_3CO	9.58	2 CH_3
92a	72.38	R1a, R2a	–1.02	2 **R2a**
92b	67.10	**R1a, R2b**	–1.02	**R2a, R2b**
92c	62.08	**R1a, R2c**	–1.02	**R2a, R2c**
92d	65.90	**R1b, R2b**	–6.49	2 **R2b**
92e	61.64	**R1b, R2c**	–6.49	**R2b, R2c**
92f	55.48	**R1c, R2c**	–9.48	2 **R2c**

determine the BDEs and radical stabilization energies (RSEs) as a function of methyl and ester substituents. The results from those calculations are summarized in Table 48.6 and Figure 48.9. The spectroscopically determined triplet energies of ketodiesters **92a** to **92f** (~82 kcal/mol) were very similar to those of acetone (~79 kcal/mol) and suggest a common starting point to compare the enthalpy changes upon α-cleavage and decarbonylation reactions.[91] The BDE values calculated for α-cleavage and decarbonylation of acetone with the B3LYP/6–31G* method (81.14 and 9.58 kcal/mol, respectively) were in very good agreement with those obtained with higher levels of theory and experimentally (83.5 and 11 kcal/mol, respectively). The formation of a primary enol and an acyl radical from ^{3}**92a** was calculated to be exothermic by ~10 kcal/mol. This reaction is very inefficient in solution and is not observed at all in the solid state. Calculations show that formation of secondary enol and acyl radicals from **92b** and **92d** is exothermic by 15 to 16 kcal/mol. Both compounds react by α-cleavage in solution and in crystals, but only **92d** decarbonylates efficiently. In fact, decarbonylation of acyl radicals from **92a**, **92b**, and **92c** gives primary enol radicals in reactions that are calculated to be exothermic by only 1.02 kcal/mol, and none of these ketones decarbonylates in the solid state. In agreement with the experimental observations, the formation of secondary enol radicals by decarbonylation of acyl radicals from **92d** and **92e** was calculated to be exothermic by 6.5 kcal/mol, and formation of tertiary enol radical from **92f** was calculated to be exothermic by 9.5 kcal/mol.

The need for exothermic α-cleavage and decarbonylation is strongly supported by the results in Figure 48.9, where changes in enthalpy for ketones that react in the solid state are shown with heavy arrows. A comparison of the results from **92b** and **92c** with those obtained from **92d** and **92e** stresses

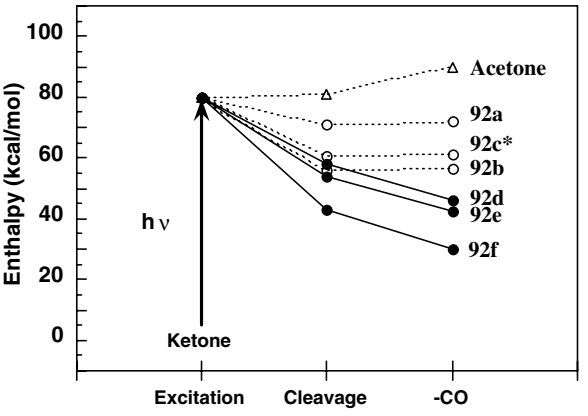

FIGURE 48.9 Calculated heats of reaction (B3LYP/6–31G*) correlating the experimental results of the photochemical decarbonylation of acetone and acetone dicarboxylates **92a** to **92f**. *Compound **92c** has not been studied experimentally.

the notion that efficient α-cleavage in the solid state is not enough for product formation, unless it is followed by a second, irreversible radical–radical reaction.

48.15 Solid-to-Solid Photochemical Reactions

An ideal solid-state photochemical reaction would offer high selectivity and specificity with good quantum and chemical yields; however, while high selectivity and specificity are frequently achieved, there may be limitations on the chemical yields that may be obtained for reactions in crystals. High reaction selectivities in crystals can be generally understood in terms of conformational bias and least-motion pathways for unimolecular reactions and, in terms of the distances and orientation between prospective reactants, in bimolecular reactions. In the case of decarbonylation reactions, several examples of solid-to-solid reactions have been documented in great detail. For instance, photolysis of ketone **70** in solution resulted in a 50:50 mixture of products *cis*-**94** and *trans*-**94**, respectively, in modest chemical yields, while reactions in crystals yielded a *cis*-**94**:*trans*-**94** ratio of 19:1 in nearly quantitative yield.[93] It was shown that reaction selectivity does not change as a function of total conversion when reactions were carried out under optimized conditions (see below). The preferential formation of *cis*-**94** can be readily understood when the structures of the reactant and the two possible products are compared. X-ray structures of ketone **70** and its solid-state photoproduct *cis*-**94** revealed a high degree of structural similarity (Figure 48.10). While formation of *cis*-**94** requires loss of CO and bonding between the two benzylic radicals by a least motion pathway, formation of *trans*-**94** requires bond rotation to form the *trans*-diol in a process that involves a large change in shape and volume.

Although the rigidity of crystalline solids facilitates some reactions while preventing others, rigidity alone is not enough to warrant the high selectivity observed in a structurally homogeneous solid. Experiments carried out with ketone **70** in hydroxylic media spanning more than eight orders of magnitude in viscosity, from methanol to sucrose glasses (caramel), had a modest effect on the selectivity of the reaction which remained close to 1:1 (Figure 48.11). The high selectivity observed in crystals is probably a manifestation of the nearly ideal conformational and environmental homogeneity offered by a crystalline solid.

Experimental factors affecting and controlling the outcome of photochemical reactions in crystals have been recently reviewed.[92] Among them, crystal size, excitation wavelength, and reaction temperature are particularly important. Given that crystalline solids are very strongly absorbing media, irradiations carried out at the tail of the UV-Vis absorption spectrum must be used to facilitate penetration of light

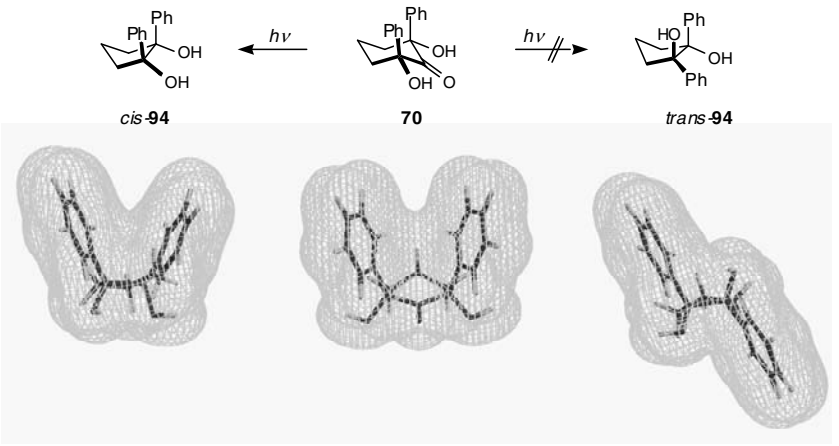

FIGURE 48.10 A comparison of the x-ray structure of ketone **70** with those of its two combination products (*cis*-**94** on the left and *trans*-**94** on the right) helps rationalize the high selectivity observed when reactions are carried out in crystals.

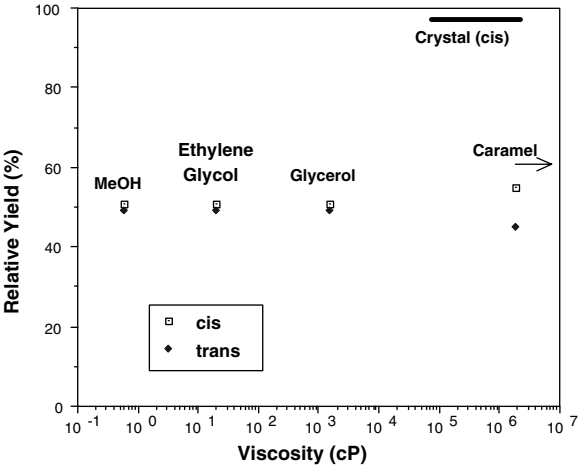

FIGURE 48.11 Effect of viscosity on the selectivity of product formation upon decarbonylation of *cis*-2,6-diphenyl-2,6-dihydroxycyclohexanone **70**. The viscosity of sucrose glasses (caramel) noted in the plot is the value reported value at 100°C.[94]

deep into the bulk of the solid. It is frequently observed that microcrystalline samples retain the selectivity observed in large single crystals while minimizing the problems associated with the limited penetration of light into the large single crystals. Excitation into the lowest energy levels of the excited state limits local heating from internal conversion and helps prevent local melting. Furthermore, light absorption by the photoproduct should be completely avoided. In the case of ketone **70**, irradiation was carried out with monochromatic light at $\lambda = 350$ nm or with a $\lambda > 350$-nm cutoff filter (Figure 48.12).

Decarbonylation reactions such as that of ketone **70** can be easily carried out in a multigram scale with microcrystalline samples and it may be possible to scale up the reaction further. Several decarbonylation reactions have been documented to trap CO gas within the crystal lattice and to proceed by phase-transition mechanisms. It has been suggested that reactions in solids occur heterogeneously with a reaction front determined by exposure to light. When product molecules begin to form, they go into a

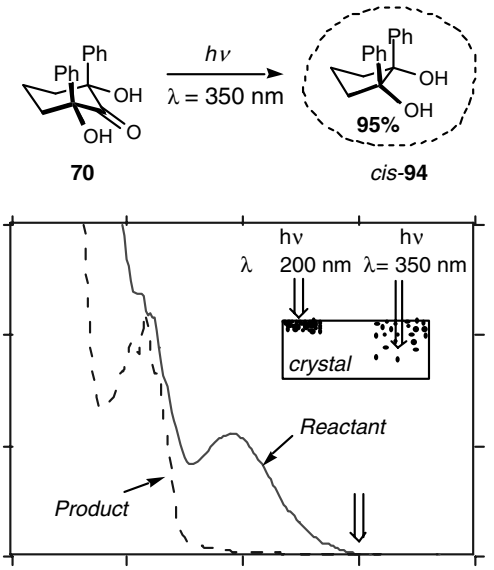

FIGURE 48.12 Ultraviolet absorption spectra of ketone **70** and its solid-state photoproduct **94** illustrating the wavelength selected for excitation in the solid state ($\lambda \geq 350$ nm). Irradiation at this wavelength allows for deeper penetration in the crystal and reduces local heating from excess photon energy.

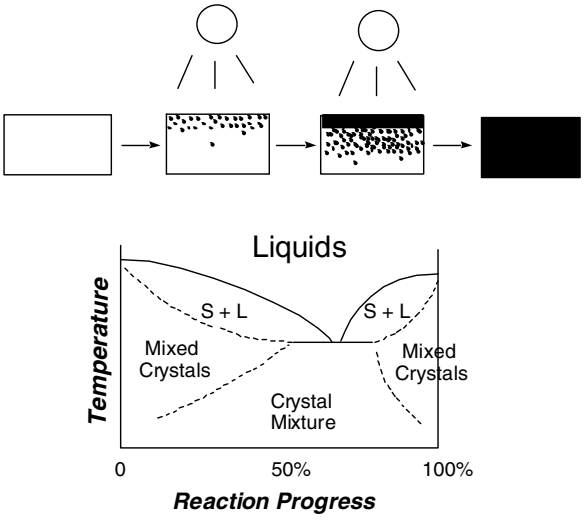

FIGURE 48.13 Schematic representation of the phase diagram for a solid-state reaction that occurs by formation of a solid solution with separation of the product phase. Reactions in crystals must be carried out at temperatures below the eutectic of the two-component phase diagram to ensure that reaction occurs in the solid phase.

solid solution in the crystal lattice of the reactant until the solubility limit is attained (mixed crystals; see Figure 48.13). As the mole fraction of product molecules continues to increase, a new crystal phase may begin to nucleate with a composition that may include both the product and the reactant. The coexistence of two solid phases and two components causes the formation of a eutectic point, which determines the lowest temperature where liquid phases may exist. Several examples of eutectic transitions in reacting crystal have been documented in the literature by differential scanning calorimetry (DSC). It has been

suggested that reactions in crystals will proceed with good environmental control only when they are carried out at temperatures that are below the eutectic transition.

48.16 Conclusions

The photochemically induced Norrish type I cleavage and acyl radical decarbonylation reactions of ketones promise to become a reliable method for the generation of biradicals and radical pairs in crystalline solids. Progress to date has been based on a few simple assumptions, which include the use of mechanistic knowledge from gas phase and solution to formulate the mechanisms and energetics of reactions in crystals. It has been assumed that spin–spin interactions and conformational restrictions in the solid state do not alter the energetics of reactions in crystals by a large measure, so that excitation energies and radical stabilization energies can be used to make predictions regarding the feasibility of α-cleavage and decarbonylation processes. The importance of subtle but predictable effects on the solid-state reactions have begun to emerge, and it is expected that more examples will expose interesting effects unique to reactions in crystals. The successful generation of radical pairs in crystalline ketones gives a promising forecast that should open the doors for many systematic, mechanistic, and synthetic studies, as well as many potential applications in material science.

Acknowledgment

The authors gratefully acknowledge support from the National Science Foundation. Graduate support by the National Science Foundation and the Paul and Daisy Soros Fellowships for New Americans are also acknowledged (LMC).

References

1. Bowen, E. J. and Watts, H. G., The photolysis of acetaldehyde and acetone, *J. Chem. Soc.*, 1607, 1926 (and references therein).
2. Norrish, R. G. W. and Appleyard, M. E. S., Primary photochemical reactions. Part IV. Decomposition of methyl ethyl ketone and methyl butyl ketone, *J. Chem. Soc.*, 874, 1934.
3. (a) Norrish, R. W. G., On the principle of primary recombination in relation to the velocity of thermal reactions in solution, *Trans. Faraday Soc.*, 33, 1521, 1937; (b) Norrish, R. G. W., The primary photochemical production of some free radicals, *Trans. Faraday Soc.*, 30, 103, 1934; (c) Norrish, R. G. W., Crone, H. G., and Saltmarsh, O. D., Primary photochemical reactions. Part V. The spectroscopy and photochemical decomposition of acetone, *J. Chem. Soc.*, 1456, 1934; (d) Bamford, C. H. and Norrish, R. G. W., Primary photochemical reactions. Part VII. Photochemical decomposition of *iso*-valeraldehyde and di-*n*-propyl ketone, *J. Chem. Soc.*, 1504, 1935.
4. (a) Chatgilialoglu, C., Crich, D., Komatsu, M., and Ryu, I., Chemistry of acyl radicals, *Chem. Rev.*, 99, 1991, 1999; (b) Vinogradov, M. G. and Nikishin, G. I., The chemistry of acyl radicals in solution, *Russ. Chem. Rev.*, 40, 916, 1971.
5. (a) Weiss, D., The Norrish type-i reaction in cycloalkanone photochemistry, in *Organic Photochemistry*, Vol. 5, Padwa, A., Ed., Marcel Dekker, New York, 1981, 347; (b) Noyes, Jr., W. A., The contributions of R. G. W. Norrish to photochemistry, in *Photochemistry and Reaction Kinetics*, Ashmore, P. G., Dainton, F. S., and Sugden, T. M., Eds., Cambridge University Press, Cambridge, U.K., 1967, 1; (c) Wagner, P. J. and Hammond, G. S., Properties and reactions of organic molecules in their triplet states, *Adv. Photochem.*, 5, 21, 1968; (d) Schaffner, K., Cyclic ketones: photolytic eliminations and reductions, *Pure Appl. Chem.*, 16, 75, 1968; (e) Dalton, J. C. and Turro, N. J., Photoreactivity of n,π^* excited states of alkyl ketones, *Ann. Rev. Phys. Chem.*, 21, 499, 1970; (f) Horspool, W. M., Photolysis of carbonyl compounds, in *Photochemistry*, 16, 215, 1985; (g) Formosinho, S. J. and Arnaut, L. G., A unified view of ketone photochemistry, in *Advances in Photochemistry*, Volman, D., Hammond, G. S., and Neckers, D., Ed., Wiley-Interscience, New York, 1991, 67.

6. (a) Bohne, C., Norrish type I processes of ketones: selected examples and synthetic applications, in *CRC Handbook of Organic Photochemistry and Photobiology*, Horspool, W. M. and Song, P.-S., Eds., CRC Press, Boca Raton, FL, 1995, 423; (b) Turro, N. J. and Schuster, G., Photochemical reactions as a tool in organic syntheses, *Science*, 187, 303, 1975.
7. Turro, N. J., *Modern Molecular Photochemistry*, University Science Books, Sausalito, CA, 1991.
8. (a) Tsentalovich, Y. P., Forbes, M. D. E., Morozova, O. B., Plotnikov, I. A., McCaffrey, V. P., and Yurkovskaya, A. V., Spin and molecular dynamics in acyl-containing biradicals: time-resolved electron paramagnetic resonance and laser flash photolysis study, *J. Am. Chem. Soc.*, 106, 7121, 2002; (b) Forbes, M. D. E., Ruberu, S. R., and Dukes, K. E., Dynamics of spin-polarized radical pairs at the solid/solution interface, *J. Am. Chem. Soc.*, 116, 7299, 1994; (c) Turro, N. J., Supramolecular organic photochemistry: control of covalent bond formation through noncovalent supramolecular interactions and magnetic effects, *Proc. Nat. Acad. Sci. USA*, 99, 4805, 2002; (d) Turro, N. J., Buchachenko, A. L. and Tarasov, V. F., How spin stereochemistry severely complicates the formation of a carbon–carbon bond between two reactive radicals in a supercage, *Acc. Chem. Res.*, 28, 69, 1995.
9. (a) Turro, N. J., From boiling stones to smart crystals: supramolecular and magnetic isotope control of radical–radical reactions in zeolites, *Acc. Chem. Res.*, 33, 637, 2000 (and references therein); (b) Turro, N. J., Supramolecular photochemistry: a paradigm for the 1990s?, *J. Photochem. Photobiol. A: Chem.*, 100, 53, 1996.
10. Gu, W. and Weiss, R. G., Extracting fundamental photochemical and photophysical information from photorearrangements of aryl phenylacetates and aryl benzyl ethers in media comprised of polyolefinic films, *J. Photochem. Photobiol. C*, 2, 117, 2001.
11. (a) Meineke, P., Rauen, U., Groot, H., Korth, H. G., and Sustmann, R., Cheletropic traps for the fluorescence detection of nitric oxide (nitrogen monoxide) in biological systems, *Chem.-Eur. J.*, 5, 1738, 1999; (b) Paul, T., Hassan, M. A., Korth, H. G., and Sustmann, R., Reaction of phenyl-substituted *o*-quinodimethanes with nitric oxide: are benzocyclobutenes suitable precursors for nitric oxide cheletropic traps?, *J. Org. Chem.*, 61, 6835, 1996.
12. (a) Giese, B. and Biland, A., Recent developments of charge injection and charge transfer in DNA, *J. Chem. Soc., Chem. Commun.*, 667, 2002; (b) Giese, B., Amaudrut, J., Kohler, A. K., Spormann, M., and Wesseley, S., Direct observation of hole transfer by hopping between adenine bases and by tunneling, *Nature*, 412, 318, 2001; (c) Meggers, E., Dussy, A., Schäfer, T., and Giese, B., Electron transfer in DNA from guanine and 8-oxoguanine to a radical cation of the carbohydrate backbone, *Chem.-Eur. J.*, 6, 485, 2000.
13. (a) Noyes, R. M., Kinetics of competitive processes when reactive fragments are produced in pairs, *J. Am. Chem. Soc.*, 77, 2042, 1955; Turro, N. J., Photochemistry of organic molecules in microscopic reactors, *Pure Appl. Chem.*, 58, 1219, 1986; (b) Buchachenko, A. L., Some problems of the kinetics of radical reactions in solid polymers, *Russ. Chem. Rev.*, 51, 203, 1982.
14. Garcia-Garibay, M. A., Chemical reactivity in organized media: statistical entropy and information in crystals and enzymes, *Curr. Opin. Solid State Material Sci.*, 3/4, 399, 1998.
15. Fischer, H. and Paul, H., Rate constants for some prototype radical reactions in liquids by kinetic electron spin resonance, *Acc. Chem. Res.*, 20, 200, 1987.
16. Solly, R. K. and Benson, S. W., Kinetics of the gas-phase unimolecular decomposition of the benzoyl radical, *J. Am. Chem. Soc.*, 93, 2127, 1971.
17. (a) Cohen M. and Schmidt, G. M., Topochemistry. Part I. A survey, *J. Chem. Soc.*, 1996, 1964; (b) Cohen, M. D., The photochemistry of organic solids, *Angew. Chem. Int. Ed. Engl.*, 14, 386, 1975.
18. (a) Bigot, B., Devaquet, A., and Turro, N. J., Natural correlation diagrams: a unifying theoretical basis for analysis of *n*-orbital initiated ketone photochemistry, *J. Am. Chem. Soc.*, 103, 6, 1981; (b) Turro, N. J., Farneth, W. E., and Devaquet, A., Salem diagrams as a device for the elucidation of photochemical reaction mechanisms: application to the cleavage of cyclic alkanones, *J. Am. Chem. Soc.*, 98, 7425, 1976; (c) Salem, L., Theory of photochemical reactions, *Science*, 191, 822, 1976; (d)

Dauben, W. G., Salem, L., and Turro, N. J., A classification of photochemical reactions, *Acc. Chem. Res.*, 8, 41, 1975.

19. Nimlos, M. R., Soderquist, J. A., and Ellison, G. B., Spectroscopy of the acetyl anion $CH_3CO–$ and radical CH_3CO, *J. Am. Chem. Soc.*, 111, 7675, 1989.
20. Michl, J. and Bonacic-Koutecky, V., *Electronic Aspects of Organic Photochemistry*, Wiley-Interscience, New York, 1990, 378–380.
21. (a) Diau, E. W. G., Kötting, C., and Zewail, A. H., Femtochemistry of Norrish type-I reactions. I. Experimental and theoretical studies of acetone and related ketones on the S_1 surface, *ChemPhysChem*, 2, 273, 2001. (b) Other studies by Diau et al. have shown that the photochemical decarbonylation of cyclobutanone and other side reactions occur from the S1 (n,π^*) surface via a conical intersection; see Diau, E. W. G., Kötting, C., and Zewail, A. H., Femtochemistry of Norrish type-I reactions. II. The anomalous predissociation dynamics of cyclobutanone on the S_1 surface, *ChemPhysChem*, 2, 294, 2001. For studies of the higher excited surfaces of ketones, please see (c) Diau, E. W. G., Kötting, C., Sølling, T. I., and Zewail, A. H., Femtochemistry of Norrish type-I Reactions. III. Highly excited ketones: theoretical, *ChemPhysChem*, 3, 57, 2002, and (d) Sølling, T. I., Diau, E. W. G., Kötting, C., De Feyter, S., and Zewail, A. H., Femtochemistry of Norrish type-I reactions. IV. Highly Excited Ketones: experimental, *ChemPhysChem*, 3, 79, 2002.
22. For leading reviews on CIs, please see (a) Robb, M. A., Garavelli, M., Olivucci, M., and Bernardi, F., A computational strategy for organic photochemistry, *Rev. Comp. Chem*, 15, 87, 2000; (b) Klessinger, M., Conical intersections and the mechanism of singlet photoreactions, *Angew. Chem. Int. Ed. Engl.*, 34, 449, 1995.
23. The reported calculated energy values for the T_1 minimum (above the S_0) of acetone are 89.6 kcal/mol (CAS-SCF) and 84. 1 kcal/mol (DFT) (Ref. 21a). The experimentally determined T_1 minimum energy value of acetone is 78.9 kcal/mol (Ref. 24).
24. Carmichael, I. and Hug, G. L., Spectroscopy and intramolecular photophysics of triplet states, in *CRC Handbook of Organic Photochemistry*, Scaiano, J. C., Ed., CRC Press, Boca Raton, FL, 1989, 1, 369.
25. (a) Hansen, D. A. and Lee, E. K. C., Radiative and nonradiative transitions in the first excited singlet state of symmetrical methyl-substituted acetones, *J. Chem. Phys.*, 62, 183, 1975; (b) Breuer, G. M. and Lee, E. K. C., Fluorescence decay times of cyclic ketones, acetone, butanal in the gas phase, *J. Phys. Chem.*, 75, 989, 1971.
26. Fluorescence and internal conversion (IC) in the case of singlet acetone are minimal; see (a) Heicklen, J., The fluorescence and phosphorescence of biacetyl vapor and acetone vapor, *J. Am. Chem. Soc.*, 81, 3863, 1959; (b) Shortridge, Jr., R. G., Rusbult, C. F., and Lee, E. K. C., Fluorescence excitation study of cyclobutanone, cyclopentanone and cyclohexanone in the gas phase, *J. Am. Chem. Soc.*, 93, 1863, 1971.
27. The reported calculated energy values for the T_1–TS (above the S_0 minimum) of acetone are 104.7 kcal/mol (CAS-SCF) and 89.5 kcal/mol (DFT) (Ref. 21a). The experimentally determined energy values for the T_1–TS (above the S_0) of acetone are 91.6 kcal/mol (Ref. 28) and 93.5 kcal/mol (Ref. 29).
28. Copeland, R. A. and Crosley, D. R., Radiative, collisional and dissociative processes in triplet acetone, *Chem. Phys. Lett.*, 115, 362, 1985.
29. Zuckermann, H., Schmitz, B., and Haas, Y., Acetone photophysics in seeded supersonic molecular beams, *J. Phys. Chem.*, 93, 4083, 1989.
30. Encinas, M. V., Lissi, E. A., and Scaiano, J. C., Photochemistry of aliphatic ketones in polar solvents, *J. Phys. Chem.*, 84, 948, 1980.
31. Porter, G., Dogra, S. K., Loufty, R. O., Sugamori, S. E., and Yip, R. W., Triplet state of acetone in solution, *J. Chem. Soc., Faraday Trans. 1*, 69, 1462, 1973.
32. Leushner, R. and Fisher, H., Type-I cleavage of triplet acetone in solution studied by time-resolved CIDNP, *Chem. Phys. Lett.*, 121, 554, 1985.
33. Yang, E. D., Feit, E. D., Hui, M. H., Turro, N. J., and Dalton, J. C., Photochemistry of di-*t*-butyl ketone and structural effects on the rate efficiency of intersystem crossing of aliphatic ketones, *J. Am. Chem. Soc.*, 92, 6974, 1970 (and references therein).

34. For reviews on the Norrish type II reaction, please see: (a) Wagner, P. and Park, B.-S., Photoinduced hydrogen abstraction by carbonyl compounds, in *Organic Photochemistry*, Padwa, A., Ed., Marcel Dekker, New York, 1991, chap. 4, 11; (b) Wagner, P. J., 1,5-Biradicals and five-membered rings generated by δ-hydrogen abstraction in photo-excited ketones, *Acc. Chem. Res.*, 22, 83, 1989.
35. Yang, N. C. and Feit, E. D., The photochemistry of *t*-butyl alkyl ketones in solution, *J. Am. Chem. Soc.*, 90, 504, 1968 (and references therein).
36. (a) Lunazzi, L., Ingold, K. U., and Scaiano, J. C., Absolute rate constants for the decarbonylation of the phenylacetyl radical, *J. Phys. Chem.*, 87, 529, 1983; Turro, N. J., Gould, I. R., and Baretz, B. H., Absolute rate constants for decarbonylation of phenacyl acetyl and related radicals, *J. Phys. Chem.*, 87, 531, 1983.
37. Lipsher, J. and Fisher, H., Absolute rate constants for the self-termination of the isopropyl radical and for the decarbonylation of the 2-methylpropanoyl radical, *J. Phys. Chem.*, 88, 2555, 1984.
38. Salzmann, M., Tsentalovish, Y. P., and Fisher, H., Photolysis of 2,4-dihydroxy-2,4-dimethylcyclopentan-3-one studied by quantitative time-resolved CIDNP and optical spectroscopy, *J. Chem. Soc., Perkin Trans. 2*, 2119, 1994.
39. (a) Griller, D. and Ingold, K. U., Free-Radical Clocks, *Acc. Chem. Res.*, 13, 317, 1980; (b) Newcomb, M., Competition methods and scales for alkyl radical reaction kinetics, *Tetrahedron*, 49, 1151, 1993.
40. Tsentalovich, Y. P. and Fischer, H., Solvent effect on the decarbonylation of acyl radicals studied by laser flash photolysis, *J. Chem. Soc., Perkin Trans. 2*, 729, 1994.
41. Abuin, E. A., Encinas, M. V., and Lissi, E. A., Gas phase photolysis of aliphatic ketones, *J. Photochem.*, 1, 387, 1973.
42. Closs, G. L., Forbes, M. D. E. and Piotrowiak, P., Spin and Reaction Dynamics in Flexible Polymethylene Biradicals As Studied by EPR, NMR and Optical Spectroscopy and Magnetic Field Effects. Measurements and Mechanisms of Scalar Electron Spin-Spin Coupling, *J. Am. Chem. Soc.*, 114, 3285, 1992.
43. Schuh, H., Hamilton, E. J., Paul, H. and Fisher, H., Reaction Rates of *t*-Butyl and Pivaloyl Radicals in Solution, *Helv. Chim. Acta*, 57, 2011, 1974.
44. Weir, D. and Scaiano, J. C., Lifetimes of the Biradicals Produced in the Norrish Type I Reaction of Cycloalkanones, *Chem. Phys. Lett.*, 118, 526, 1985.
45. Dalton, J. C., Dawes, K., Turro, N. J., Weiss, D. S., Barltrop, J. A. and Coyle, J. D., Molecular Photochemistry. XLVIII. Type I and Type II Photochemical Reactions of Some Five- and Six-Membered Cycloalkanones, *J. Am. Chem. Soc.*, 93, 7213, 1971.
46. Forbes, M. D. E. and Schulz, G. R., Low Temperature Disappearance of Spin Correlation in Flexible 1,n-Biradicals (n = 22, 24, 26), *J. Am. Chem. Soc.*, 116, 10174, 1994; Forbes, M. D. E. and Bhagat, K., Quantitative EPR Measurement of Long-Distance Electronic Interactions in Two Geometric Isomers of an Unsaturated Biradical, *J. Am. Chem. Soc.*, 115, 3382, 1993; Forbes, M. D. E., Ball, J. D. and Avdievich, N. I., In Search of Through-Solvent Electronic Coupling in Flexible Biradicals, *J. Am. Chem. Soc.*, 118, 4707, 1996.
47. Morton, D. R., Lee-Ruff, E., Sotham, R. M. and Turro, N. J., Molecular Photochemistry XXVII. Photochemical Ring Expansion of Cyclobutanone, Substituted Cyclobutanones and Related Cyclic Ketones, *J. Am. Chem. Soc.*, 92, 4349, 1970.
48. Turro, N. J., Hammond, W. B. and Leermakers, P. A., Tetramethylcyclopropanone. I. isolation and Characterization, *J. Am. Chem. Soc.*, 87, 2774, 1965.
49. Engel, P. S., Photochemistry of Dibenzyl Ketone, *J. Am. Chem. Soc.*, 92, 6074, 1970.
50. Robbins, W. K. and Eastman, R. H., Photodecarbonylation in Solution. I. Quantum Yields and Quenching Results with Dibenzyl Ketones, *J. Am. Chem. Soc.*, 92, 6076, 1970.
51. Quinkert, G., Opitz, K., Wiersdorf, W. W. and Weinlich, J., Light Induced Decarbonylation of Dissolved Ketones, *Tetrahedron Lett.*, 27, 1863, 1963.
52. Peyman, A., Beckhaus, H.-D. and Ruchardt, C., Intramolecular Reactions of 1,5-Diaryl-1,5-pentadiyl Radicals, *Chem. Ber.*, 121, 1027, 1988.
53. Tarasov, V. F., Klimenko, B. B., Askerov, D. B. and Buchachenko, A. L., Photochemistry of 2,6-Diphenylcyclohexanone, *Izv. Akad. Nauk. SSSR*, 361, 1985.

54. Lei, X., Doubleday, C., Jr. and Turro, N. J., Photochemistry Of Large-Ring 2-Phenylcycloalkanones and 2,N-Diphenylcycloalkanones., *Tetrahedron Lett.*, 27, 4675, 1986.
55. Doubleday, C., Jr., Turro, N. J. and Wang, J. -F., Dynamics of Flexible Triplet Biradicals, *Acc. Chem. Res.*, 22, 199, 1989; Zimmt, M. B., Doubleday, C., Gould, I. R. and Turro, N. J., Nanosecond Flash Photolysis Studies of Intersystem Crossing Rate Constants in Biradicals: Structural Effects Brought About by Spin-Orbit Coupling, *J. Am. Chem. Soc.*, 107, 6724, 1985.
56. Tsentalovich, Y. P., Morozova, O. B., Avdievich, N. I., Ananchenko, G. S., Yurkovskaya, A. V., Ball, J. D. and Forbes, M. D. E., Influence of Molecular Structure on the Rate of Intersystem Crossing in Flexible Biradicals, *J. Phys. Chem. A.*, 101, 8809, 1997; Morozova, O. B., Yurkovskaya, A. V., Tsentalovich, Y. P., Sagdeev, R. Z., Wu, T. and Forbes, M. D. E., Consecutive Biradicals During the Photolysis of 2,12-Dihydroxy-2,12-dimethylcyclododecanone: Low and High-Filed Chemically-Induced Dynamic Nuclear Polarization (CIDNP) Study, *J. Phys. Chem. A*, 102, 3492, 1997.
57. Morozova, O. B., Yurkovskaya, A. V., Tsentalovich, Y. P., Sagdeev, R. Z., Wu, T. and Forbes, M. D. E., Study of Consecutive Biradicals from 2-Hydroxy-2,12-dimethylcyclododecanone by TR-CIDNP, TREPR and Laser Flash Photolysis., *J. Phys. Chem. A*, 101, 8803, 1997.
58. Chapman, O. L., Pasto, D. J., Borden, G. W. and Griswold, A. A., Photochemical Transformations of Conjugated Cycloheptadienes, *J. Am. Chem. Soc.*, 84, 1220, 1962; Starr, J. E. and Eastman, R. H., Structural Features Facilitating the Photodecarbonylation of Cyclic Ketones, *J. Org. Chem.*, 31, 1393, 1966.
59. Engel, P. S., The Photochemistry of an Acyclic Bis-β, γ-Unsaturated Ketone, *J. Am. Chem. Soc.*, 94, 4357, 1972.
60. Kadota, K. and Ogasawara, K., A Carbohydrate Synthesis Employing Photochemical decarbonylation, *Tetrahedron Lett.*, 42, 861, 2001.
61. Kresge, A. J., Flash Photolytic Generation and Study of Reactive Species: From Enols to Ynols, *Acc. Chem. Res.*, 23, 43, 1990.
62. Chiang, Y., Grant, A. S., Kresge, A. J. and Paine, S. W., Flash Photolytic Generation of Primary, Secondary and Tertiary Ynamines in Aqueous Solution and Study of Their Carbon-Protonation Reactions in That Medium, *J. Am. Chem. Soc.*, 118, 4366, 1996.
63. Tomioka, H., Okuno, A., Sugiyama, T. and Murata, S., Synthesis and Photochemistry of 5,7-Bis(diazo)-1,2,3,4-dibenzocyclohepta-1,3-dien-6-one. Generation and Reactions of Phenanthrenodiazacyclopentadiene, Phenanthrenocyclopropenone and 9,10-Phenanthryne, *J. Org. Chem.*, 60, 2344, 1995.
64. Quinkert, G., Tbata, T., Hickmann, E. A. J. and Dobrat, W., Increase in Selectivity of Photoelimination Products on Replacing Liquid Phase by the Crystalline Phase, *Angew. Chem. Int. Ed. Engl.*, 10, 199, 1971.
65. Quinkert, G., Palmowski, J., Lorenz, H. P., Wiersdorff, W. W. and Finke, M., Non-Cheletropic Decarbonylation of 1,3-Diphenyl-Substituted 2-Indanone Derivatives, *Angew. Chem. Int. Ed. Engl.*, 10, 198, 1971.
66. Noyes, R. M., Kinetics of Competitive Processes when Reactive Fragments are Produced in Pairs, *J. Am. Chem. Soc.*, 77, 2042, 1955.
67. Baretz, B. H. and Turro, N. J., Photochemistry of Diastereomeric 2,4-Diphenylpentan-3-ones and Related Ketones in "Super-Cage" Environments Provided by Micelles, Porous Glass and Porous Silica: Temperature and Magnetic Effects, *J. Am. Chem. Soc.*, 105, 1309, 1983.
68. Choi, T., Peterfy, K., Khan, S. I. and Garcia-Garibay, M. A., Molecular Control of Solid State Reactivity and Biradical Formation in Crystalline Ketones, *J. Am. Chem. Soc.*, 118, 12477, 1996.
69. Wagner, P. J. and Stratton, T. J., Kinetically Distinct Triplets in the Photorearrangements of 2-Phenylcyclohexanone to *cis*- and *trans*-6-Phenyl-5-hexenals, *Tetrahedron*, 37, 3317, 1981; Zimmt, M. B., Doubleday, C. and Turro, N. J., Substituent and Solvent Effects on the Lifetimes of Hydrocarbon-Based Biradicals, *Chem. Phys. Lett.*, 134, 549, 1987.
70. Although the rate of α-cleavage and reaction efficiency for similar chromophores in solution are known to be high, they may be systematically lower in the solid state. The α -cleavage reaction in

1,3-diphenyl acetone in solution is known to occur within *ca*. 2 ns: Arbour, C. and Atkinson, G. H., Picosecond Photodissociation of Dibenzyl Ketone, *Chem. Phys. Lett.*, 159, 520, 1989.

71. Johnston, L. J. and Scaiano, J. C., Time-Resolved Studies of Biradical Reactions in Solution, *Chem. Rev.*, 89, 521, 1989.
72. Mizuno, K., Ichinose, N., Otsuji, Y. and Caldwell, R. A., Direct Observation of 1,3-Biradical, *J. Am. Chem. Soc.*, 107, 5797, 1985.
73. Zimmt, M. B., Doubleday, C. and Turro, N. J., On the Rate Determining Step for Decay of Triplet Biradicals: Intersystem Crossing *vs* Chain Dynamics, *J. Am. Chem. Soc.*, 108, 3618, 1986; Doubleday, C., Jr., Turro, N. J. and Wang, J. -F., Dynamics of Flexible Triplet Biradicals, *Acc. Chem. Res.*, 22, 199, 1989; Wang, J., Doubleday, C., Jr. and Turro, N. J., Negative Temperature Dependence in the Decay of Triplet Biradicals, *J. Am. Chem. Soc.*, 111, 3962, 1989.
74. Peterfy, K. and Garcia-Garibay, M. A., Generation and Reactivity of a Triplet 1,4-Biradical Conformationally Trapped in a Crystalline Cyclopentanone, *J. Am. Chem. Soc.*, 120, 4540, 1998.
75. Barton, D. H. R., Charpiot, B., Ingold, K. U., Johnston, L. J., Motherwell, W. B., Scaiano, J. C. and Stanforth, S., Direct Observation and Photochemistry of Biradicals from Photochemical Decarbonylation of α-Perphenylated Cycloalkanones, *J. Am. Chem. Soc.*, 107, 3607, 1985.
76. Ng, D.; Yang, Z.; Garcia-Garibay, M.A., Engineering Reactions in Crystals: *gem*-Dialkoxy Substitution Enables the Photodecarbonylation of Crystalline 2-Indanone, Tetrahedron Lett., 43, 7063, 2002.
77. (a) Nonhebel, D. C. and Walton, J. C., Estimation of bond dissociation energies, including $DH_0(RSCH_2–H)$ from barriers of internal rotation, *J. Chem. Soc.*, *Chem. Commun.*, 731, 1984; (b) Conradi, M. S., Zeides, H., and Livingston, R., Electron spin resonance determination of hindered rotation in benzyl radicals. resonance stabilization energy, *J. Phys. Chem.*, 83, 2160, 1979; (c) Schreiner, K. and Berndt, A., Conformation of sterically hindered benzyl radicals and cations, comparison of ESR and conclusions from space-filling models, *Angew. Chem. Int. Ed. Engl.*, 14, 366, 1975.
78. (a) Nonhebel, D. C. and Walton, J. C., Estimation of bond dissciation energies, including $DH_0(RSCH_2–H)$ from barriers of internal rotation, *J. Chem. Soc.*, *Chem. Commun.*, 731, 1984; (b) Conradi, M. S., Zeides, H., and Livingston, R., Electron spin resonance determination of hindered rotation in benzyl radicals. resonance stabilization energy, *J. Phys. Chem.*, 83, 2160, 1979; (c) Schreiner, K. and Berndt, A., Conformation of sterically hindered benzyl radicals and cations: comparison of ESR and conclusions from space-fillingh models, *Angew. Chem. Int. Ed. Engl.*, 14, 366, 1975. Calculations: (d) Hrovat, D. A. and Borden, W. T., *Ab initio* calculations of the relative resonance stabilization energies of allyl and benzyl radicals, *J. Phys. Chem.*, 98, 10460, 1994; (e) Dorigo, A. E., Li, Y., and Houk, K. N., Theoretical studies of the rotational barriers of benzyl cation, and anion and of singlet and triplet phenylcarbene, *J. Am. Chem. Soc.*, 111, 6942, 1989.
79. (a) Carlson, G. L. B., Quina, F. H., Zarnegar, B. M., and Whitten, D. G., Excited state interactions and decay routes in bichromophoric systems: nonconjugated phenyl ketones, *J. Am. Chem. Soc.*, 97, 347, 1975; (b) Wagner, P. J., Kelso, P. A., Kemppainen, A. E., Haug, A., and Graber, D. R., Deactivation of ketone triplets by β-phenyl substitution, *Mol. Photochem.*, 2, 81, 1970; (c) Netto-Ferreira, J. C., Leigh, W. J., and Scaiano, J. C., Laser flash photolysis study of the photochemistry of ring substituted β-phenylpropiophenones, *J. Am. Chem. Soc.*, 107, 2617, 1985; (d) Boch, R., Bohne, C., Netto-Ferreira, J. C., and Scaiano, J. C., Effect of methyl substitution on the intramolecular triplet deactivation of *p*-Methoxy-b-phenylpropiophenone, *Can. J. Chem.*, 69, 2053, 1991; (e) Leigh, W. J., Banisch, J. H., and Workentin, M. S., Charge-transfer interactions in the intramolecular quenching of carbonyl triplets by β-aryl substituents, *J. Chem. Soc.*, *Chem. Commun.*, 988, 1993.
80. Scaiano, J. C., Perkins, M. J., Sheppard, J. W., Platz, M. S., and Barcus, R. L., Role of β-phenyl rings in the deactivation of aromatic ketone triplets, *J. Photochem.*, 21, 137, 1983.
81. (a) Moorthy, J. N., Peterson, W. S., and Bohne, C., Remarkable discrimination in the triplet lifetimes of the diastereomers of 1,4-*bis*(*p*-methoxyphenyl)-2,3-diphenylbutan-1,4-dione, *J. Am. Chem. Soc.*,

119, 11094, 1997; (b) Moorthy, J. N., Monahan, S. L., Sunoj, R. B., Chandrasekhar, J., and Bohne, C., Modulation of lifetimes and diastereomeric discrimination in triplet-excited substituted butane 1,4-diones through intramolecular charge-transfer quenching, *J. Am. Chem. Soc.*, 121, 3093, 1999.

82. Boch, R., Bohne, C., and Scaiano, J. C., Time-resolved diffuse reflectance studies of β-phenyl ketones in the solid state: conformational and chiral control of triplet lifetime, *J. Org. Chem.*, 61, 1423, 1996.
83. Ng, D., Yang, Z., and Garcia-Garibay, M. A., Engineering reactions in crystals: suppression of photodecarbonylation by intramolecular β-phenyl quenching, *Tetrahedron Lett.*, 42, 9113, 2001.
84. Dang, H., Yang, Z., Ng, D., and Garcia-Garibay, M. A., unpublished results.
85. The excited state energies of triplet ketones are solvent polarity dependent. In the case of acetone, the variation from polar (79.4 kcal/mol) to non-polar solvents (78.9 kcal/mol) is only 0. 5 kcal/mol. Please see Reference 23.
86. (a) McMillen, D. F. and Golden, D. M., Hydrocarbon dissociation energies, *Ann. Rev. Phys. Chem.*, 33, 493, 1982; (b) Brocks, J. J., Beckhaus, H.-D., Beckwith, A. L. J., and Rüchardt, C., Estimation of bond dissociation energies and radical stabilization energies by ESR spectroscopy, *J. Org. Chem.*, 63, 1935, 1998; (c) *CRC Handbook of Chemistry and Physics*, CRC Press, Boca Raton, FL, 1984.
87. Yang, Z. and Garcia-Garibay, M. A., Engineering reactions in crystalline solids: preparation and chemoselective combination of α-carbonyl radical pairs in crystals of dialkyl-1,3-acetonedicarboxylates, *Org. Lett.*, 2, 1963, 2000.
88. (a) Curtiss, L. A., Raghavachari, K., Redfern, P. C., and Pople, J. A., Assessment of gaussian-2 and density functional theories for the computation of enthalpies of formation, *J. Chem. Phys.*, 106, 1063, 1997; (b) Adam, W., Emmert, O., and Heidenfelder, T., The EPR spectral D-parameter of photochemically generated cyclopentane-1,3-diyl triplet diradicals as a qualitative measure of spin delocalization in vinyl-, phenyl-, and carbonyl-substituted radicals, *J. Org. Chem.*, 64, 3417, 1999.
89. Yang, Z., Ng, D., and Garcia-Garibay, M. A., Engineering reactions in crystalline solids: photochemical generation of secondary and tertiary enol radical pairs from the crystalline ketodiesters, *J. Org. Chem.*, 66, 4468, 2001.
90. Campos, L. M., Dang, H., Ng, D., Yang, Z., Martinez, H. L., and Garcia-Garibay, M. A., Engineering reactions in crystalline solids: predicting photochemical decarbonylation from calculated thermochemical parameters, *J. Org. Chem.*, 67, 3749, 2002.
91. Campos, L. M. and Garcia-Garibay, M. A., unpublished results.
92. Keating, A. E. and Garcia-Garibay, M. A., Molecular and supramolecular photochemistry, in *Photochemical Solid-to-Solid Reactions*, Vol. 2, Ramamurthy, V. and Schanze, K., Eds., Marcel Dekker, New York, 1998, 195.
93. Choi, T., Cizmeciyan, D., Khan, S. I., and Garcia-Garibay, M. A., An efficient solid-to-solid reaction via a steady-state phase separation mechanism, *J. Am. Chem. Soc.*, 117, 12893, 1995.
94. *CRC Handbook of Chemistry and Physics*, CRC Press, Boca Raton, FL, 1984.

49

Carbene Formation in the Photochemistry of Cyclic Ketones

S. M. Roberts
University of Liverpool

49.1 Introduction

It is now well established, based largely on early studies by Yates and Turro, that irradiation of cyclobutanones leads to the formation of an oxacarbene as one of the preferred reaction pathways (Scheme 1).[1] The highly reactive oxacarbene can be intercepted by trapping with water or an alcohol to give a lactol or an acetal, respectively (Scheme 1). The same reaction manifold is followed by some cyclopentanones, especially when the five-membered ring is part of a strained structure (Scheme 2).[2] The trapping reagent can be delivered in an intermolecular fashion or intramolecularly; in the latter case, complex polycyclic molecules can be constructed in good yields in a simple way (Scheme 3).[3,4] More rarely the oxacarbene has been trapped by an alkene.[5]

The ring expansion reaction has been used in multistep organic syntheses of natural products and analogs, most notably in the preparation of prostaglandins and prostanoids,[6] thromboxane mimetics,[7] and muscarine[8] (Scheme 4).

49.2 Mechanistic Considerations

The mechanism involved in the conversion of a cyclic ketone into an oxacarbene has been hotly debated over the past 40 years. The involvement of a carbene is beyond question following detailed work by, for example, Sheridan et al.[9] involving low-temperature irradiation of the tricycloalkanone **1** and the tetramethylcyclobutanone **2** in tandem with infrared and ultraviolet spectroscopy. Intermediates derived from the benzobutanedione **3** included the oxacarbene, and these were examined through laser flash photolysis. The oxacarbene was trapped by the usual scavengers — for example, selected alcohols.[10]

49.3 Recent Synthetic Applications

The ring-expansion of cyclobutabenzofuranones has provided a route to benzodioxabicyclo[3.3.0]octanes incorporating a *bis*-furan unit, a structural feature within the molecular skeleton of the aflatoxin family of mycotoxins (Scheme 5).[11]

0-8493-1348-1/04/$0.00+$1.50

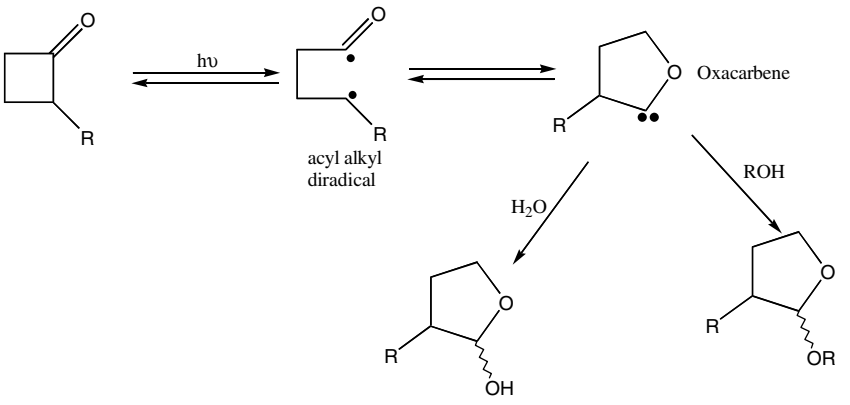

SCHEME 1

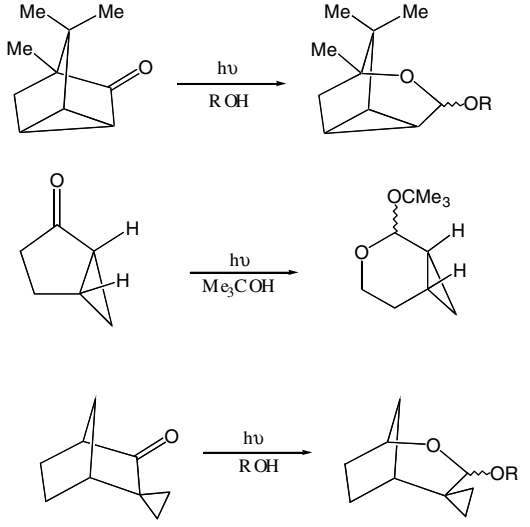

SCHEME 2

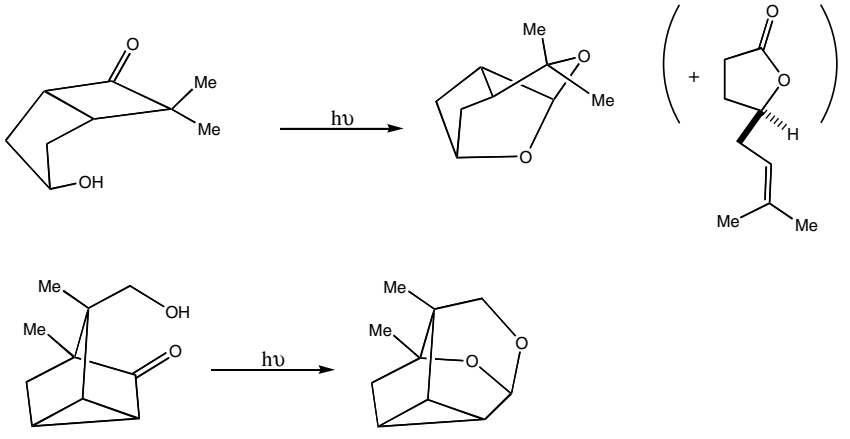

SCHEME 3

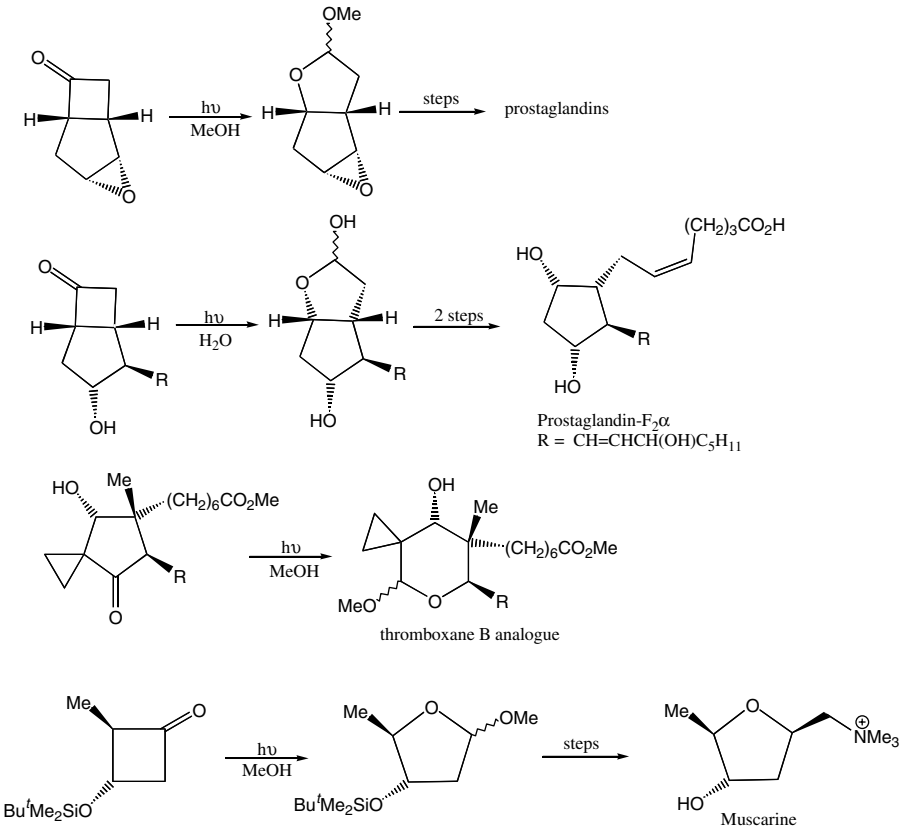

SCHEME 4

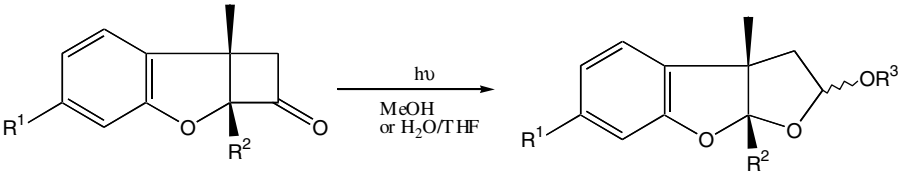

SCHEME 5

For R^1 = Me, H; R^2 = Me, H, $CH_2CH = CH_2$; and R^3 = Me:
Yields 50 to 58%, anomer ratio 1.5:1, β:α
For $R^1 = R^2$ = Me and R^3 = H:
Yield 50%

Lee-Ruff and co-workers[12] have continued their interest in the photochemistry of cyclobutanones. Specifically, they have profitably extended the chemistry of the oxacarbenes by trapping these intermediates with selected amines, to good effect. Thus, the Canadian team photolysed the ketones **4** and **5** in the presence of purines as well as water and alcohols to produce the corresponding nucleoside analogs, lactols, and acetals, respectively (Scheme 6 and Table 49.1).[13,14]

The method has been adapted to prepare 2′,3′-dideoxy-3′-C-hydroxymethyl nucleosides with significant biological activity. Specifically, nucleoside analog **6** was found to inhibit human immunodeficiency virus 1 (HIV-1) replication in acute infection. Complete suppression of the virus was observed at a dose of 100 μ*M*, a level that was shown to be nontoxic to uninfected cells.[15]

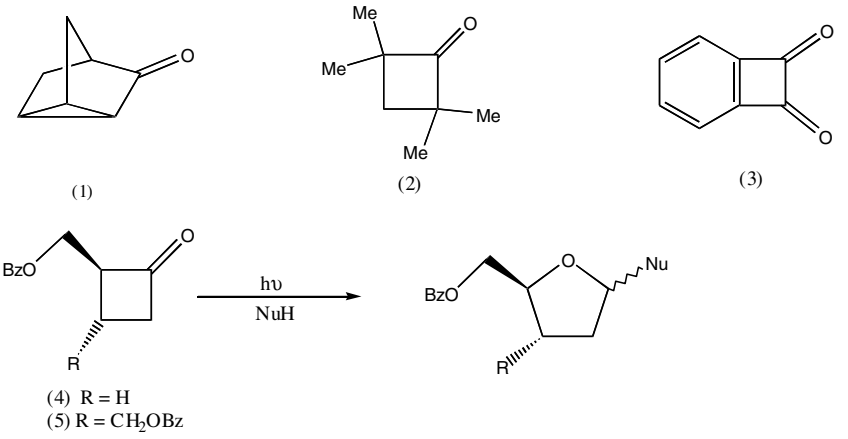

(1) (2) (3)

(4) R = H
(5) R = CH_2OBz

SCHEME 6

TABLE 49.1 Reaction of Oxacarbenes Photochemically Generated from Ketones 4 and 5 with Water, Alcohols, and Selected Purines

Starting Material	Reaction Time (hr)	NuH	Product Yield (%)	Major Anomer	Ref.
4	—	H_2O	55	—	14
4	—	MeOH	77	None	14
4	36	Purine	36	None	14
4	36	6-Chloro- purine	39	None	14
4	36	6-Methoxy-purine	69	None	14
4	36	6-Hexyloxy-purine	45	None	14
5	1–2	H_2O	58	—	13
5	1–2	MeOH	62	β	13
5	1–2	$O^tC_4H_9$	9	—	13
5	36	Succinimide	20	β	13
5	36	Purine	19	β	13
5	36	6-Chloro-purine	41–43	β	13, 15
5	36	6-Methoxy-purine	30	β	15

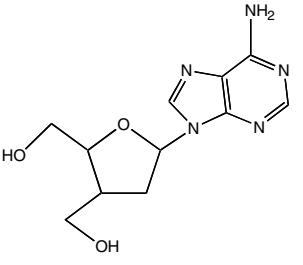

(6)

Finally, photolysis of cyclobutanone **5** in the presence of partially protected sugars and a nucleoside has produced a portfolio of interesting polyoxygenated materials (Scheme 7).[16]

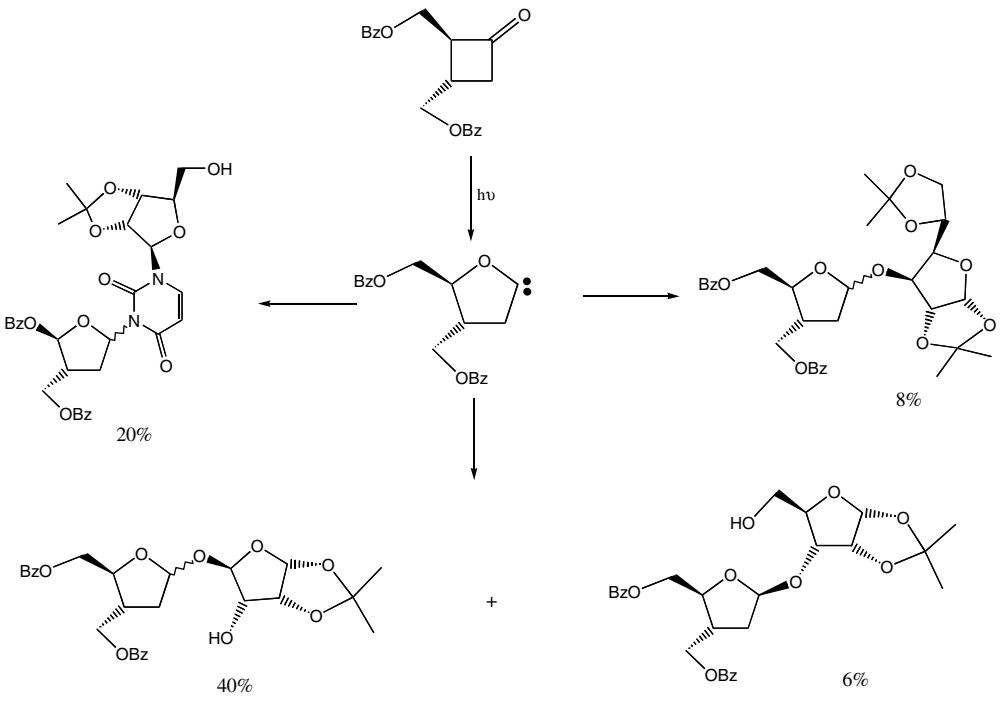

SCHEME 7

References

1. (a) Yates, P. and Kilmurry L., Two photochemical reactions of cyclocamphanone, *Tetrahedron Lett.*, 1739, 1964; (b) Yates, P., The photochemical ring expansion of cyclic ketones, *J. Photochem.*, 5, 91, 1976; (c) Turro, N. J. and Southam, R. M., Molecular photochemistry. IV. Solution photochemistry of cyclobutanone and some derivatives, *Tetrahedron Lett.*, 545, 1967; (d) Morton, D. R. and Turro, N. J., Cyclobutanones: solution phase photochemistry, *Adv. Photchem.*, 9, 197, 1974; (e) Srinivasan, R., Photochemistry of cyclic ketones, *Adv. Photochem.*, 1, 83, 1963.
2. (a) Dauben, W. G., Schutte, L., Schaffer, G. W., and Gagosion, R. B., Photoisomerisation of bicyclo[3.1.0]hexan-2-ones, *J. Am. Chem. Soc.*, 95, 468, 1973; (b) Yates, P. and Loutfy, R. O., Photochemical ring expansion of cyclic ketones via cyclic oxacarbenes, *Acc. Chem. Res.*, 8, 209, 1975.
3. (a) Butt, S., Davies, H. G., Dawson, M. J., Lawrence, G. C., Leaver, J., Roberts, S. M., Turner, M. J., Wakefield, B. J., Wall, W. F., and Winders, J. A., Resolution of 7,7-dimethylbicyclo-[3.2.0]-hept-2-en-6-one using *Mortierella ramanniana* and 3α,20β-hydroxysteroid dehydrogenase: photochemistry of 3-hydroxy-7,7-dimethylbicyclo-[3.2.0]-heptan-6-ones and the synthesis of (+)-eldanolide, *J. Chem. Soc., Perkin Trans. 1*, 903, 1987.
4. Switlak, K., He, D., and Yates, P., Intramolecular trapping of an oxacarbene intermediate in the photochemical ring expansion of a cyclopentanone, *J. Chem. Soc., Perkin Trans. 1*, 2579, 1992.
5. Staab, H. A. and Ipaktschi, J., Photochemische reaktionen des benzocyclobuten-1, 2-dions, *Chem. Ber.*, 101, 1457, 1968.
6. (a) Crossland, N. M., Kelly, D. R., Roberts, S.M., Reynolds, D. P., and Newton R. F., Photosynthetic route to prostanoids: ring expansions of some substituted cyclobutanones to form cyclic acetals or γ-lactols, *J. Chem. Soc., Chem. Commun.*, 681, 1979; (b) Crossland, N. M., Kelly, D. R., Roberts, S. M., Reynolds, D. P., and Newton, R. F., Synthesis of (±)-prostaglandin $F_2\alpha$ involving photolytic conversion of a cyclobutanone to a γ-lactol, *J. Chem. Soc., Chem. Commun.*, 683, 1979; (c) Howard,

C. C., Newton, R. F., Reynolds, D. P., Wadsworth, A. H., Kelly, D. R., and Roberts, S. M., Total synthesis of prostaglandin-$F_2\alpha$ involving stereo-controlled and photo-induced reactions of bicyclo[3.2.0]heptanones, *J. Chem. Soc., Perkin Trans. 1*, 852, 1980.

7. Azadi-Ardakani, M., Loftus, G. C., Mjalli, M. M., Newton, R. F., and Roberts, S. M., Photochemistry of cyclopentanone derivatives in the synthesis of prostaglandin and thromboxane analogues, *J. Chem. Soc., Chem. Commun*., 1709, 1989.
8. Pirrung, M. C. and De Amicis, C. V., Total synthesis of the muscarines, *Tetrahedron Lett*., 29, 159, 1988.
9. (a) Kesselmayer, M. A. and Sheridan, R. S., Direct observation of photochemical cleavage of a cyclopropylalkoxycarbene to an alkyne, *J. Am. Chem. Soc*., 109, 5029, 1987; (b) Matsumura, M., Ammann, J. R., and Sheridan, R. S., Photochemical ring expansion of tetramethylcyclobutanone revisited: angular dependence of electronic absorption of singlet carbenes, *Tetrahedron Lett*., 33, 1843, 1992.
10. Boate, D. R., Johnston, L. J., Kwong, P. C., Lee-Ruff, E., and Scaiano, J. C., First measurements of absolute rate constants for oxacarbene intermediates produced in the photochemistry of benzocyclobutenedione, *J. Am. Chem. Soc*., 112, 8858, 1990.
11. Mittra, A., Biswas, S., and Venkateswaran, R. V., Photolytic ring expansion of cyclobutabenzofuranones: facile route to benzodioxabicyclo[3.3.0]octanes. *J. Org. Chem.*, 58, 7913, 1993.
12. The early work of the Canadian group has been summarized; see Lee-Ruff, E., New synthetic pathways from cyclobutanones, in *Advances in Strain in Organic Chemistry*, Vol. 1, Halton, B., Ed., JAI Press, Greenwich, 1991, 167.
13. Lee-Ruff, E., Wan, W.-Q., and Jiang, J. L., A novel approach toward the synthesis of chiral 2,3-dideoxy nucleosides and their carbocyclic analogues, *J. Org. Chem.*, 59, 2114, 1994; see also Lee-Ruff, E., Jiang, J.-L., and Wan, W.-Q., Process of Preparation of Optically Active Nucleosides from Chiral Cyclobutanones, U.S. Patent No. 5580973, December 1996.
14. Lee-Ruff, E., Xi, F., and Qie, J. H., Enantioselective preparation of 2′,3′-dideoxynucleosides and their analogues from ring-expansion of cyclobutanones. 2. Synthesis of 2′,3′-dideoxyribosides and (1*S*, 3*R*)-l-amino-3-(hydroxymethyl) cyclopentane, *J. Org. Chem*., 61, 1547, 1996.
15. Lee-Ruff, E., Ostrowski, M., Ladha, A., Stynes, D.V., Vernick, I., Jiang, J.-L., Wan, W.-Q., Ding, S.-F., and Joshi, S., Synthesis and HIV-inhibition of 2′,3′-dideoxy-3′-C-hydroxymethylnucleosides, *J. Med. Chem*., 39, 5277, 1996.
16. Angelini, M. P. and Lee-Ruff, E., A novel photochemical synthesis of dedeoxyfuranosyl disaccharides, *Tetrahedron Lett*., 39, 8783, 1998.

50

Photochemistry of Vicinal Polycarbonyl Compounds

Mordecai B. Rubin
Israel Institute of Technology

50.1 Introduction

Organic chemists have been concerned for over 100 years with the question of how many carbonyl groups may be juxtaposed and what will be the properties of the resulting vicinal polycarbonyl compounds. At the present time, the number of vicinal carbonyl groups has reached a maximum of five in compounds such as diphenyl pentaketone (1,5-diphenylpentanepentone, **1**); use of the term *vicinal oligocarbonyl compounds* might be more appropriate but is not accepted usage. Reviews on the chemistry of these compounds appeared in 1975[1] and 2000.[2] Syntheses are quite straightforward; a considerable number of compounds have been prepared and characterized. Their most characteristic chemical property is extremely facile addition of nucleophilic reagents to a central carbonyl group, as illustrated below, which relieves the maximum number of unfavorable dipolar interactions of vicinal carbonyl groups. The chemistry of these compounds has been referred to as the "chemistry of the highly activated carbonyl group." For example, active methylene compounds undergo uncatalyzed addition to the central carbonyl group of vic-triketones to yield the aldol products. Rapid hydration, simply upon exposure to air, is a common problem (Figure 50.1; see Section 50.9).

50.2 Spectra

Absorption

Longest wavelength absorption maxima (n,π^*) for ketones with one to five vicinal carbonyl groups are presented in Table 50.1. The maxima shift steadily to longer wavelengths with increasing numbers of

0-8493-1348-1/04/$0.00+$1.50

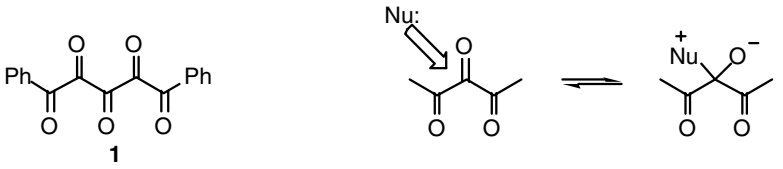

FIGURE 50.1

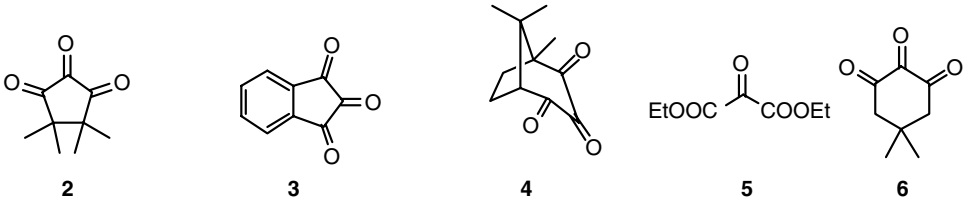

FIGURE 50.2

TABLE 50.1 Long Wavelength Absorption Maxima[a,b] of Ketones $R(CO)_nR$

R	λ_{max} (nm)				
	$n = 1$	$n = 2$	$n = 3$	$n = 4$	$n = 5$
t-Butyl	295	362	457	525	547
Phenyl	337	370	440	510	559

[a] In methylene chloride solution over phosphorus pentoxide.
[b] Typical extinction coefficients were on the order of 100 or less for unconjugated carbonyl groups.
Source: Adapted from Horner and Maurer.[32]

carbonyl groups; many compounds are highly colored. Cyclic compounds absorb at longer wavelengths, as illustrated by three typical examples: tetramethycyclopentane-1,2,3-trione (**2**) at 685 nm, indanetrione (**3**) at 606 nm, and bicyclo[3.2.1]octane-2,3,4-trione (**4**) at 538 nm. Additional n,π^* bands are observed at shorter wavelengths as well as π,π^* bands when aromatic end groups are present. The generalization that the position of the longest wavelength absorption band of α-diketones depends on the torsion angle between the carbonyl groups also seems to apply to polyketones, although systematic investigation has not been performed.

Except for diethyl mesoxalate (**5**, λ_{max} = 347 nm),[3] which behaves very much like a simple ketone (see below for photoreactions), the ultraviolet/visible light (UV-Vis) spectra of tricarbonyl compounds incorporating ketone and ester groups have not been measured. The abundant and synthetically useful α,β-diketoesters have been reported to be yellow substances, but no details are available (Figure 50.2).

Emission

The phosphorescence spectrum of **5**, measured in 1967,[3] exhibited maxima in 1,1-difluorotetrachloroethane at 530 and 537 nm, corresponding to triplet energies of about 54 kcal mol^{-1}. No attention has been paid to date to the photophysics (or photochemistry) of α,β-diketoesters. Emission from acyclic vic-tri- and tetraketones could not be detected with conventional equipment.[4] The phosphorescence maximum of 5,5-dimethylcyclohexane-1,2,3-trione (**6**) was suggested in 1971 to occur at about 615 nm ($\Phi_{phos} < 0.001$) on the basis of results obtained in a study of oxidation of the corresponding 1,3-diketone.[5]

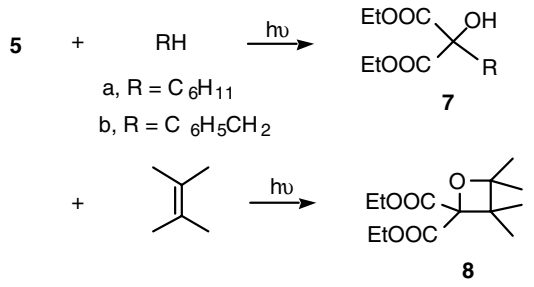

FIGURE 50.3

Indanetrione (**3**) provides an interesting contrast that may be related to the rigid, coplanar structure of this molecule. The first emission studies were reported in 1981.[6,7] Fluorescence was observed ($\Phi_{fl}(CH_2Cl_2)$ Å 650 nm) in a variety of solvents; the authors suggested a specific interaction between the central carbonyl group of **3** and solvents containing C=O or CN groups. The emission was assigned as fluorescence on the basis of the mirror image relationship between absorption and emission, solvent effects, the low value of the extinction coefficients of **3**, the short lifetime (~20 ns for a thin film), and CNDO-CI calculations. Recently, specific interactions between ethers (tetrahydrofuran and 2-methyltetrahydrofuran) and the excited states of **3**, benzo-**3**, and 5-methoxy-**3** have been studied experimentally and theoretically (AM1 calculations).[8]

Phosphorescence of **3** ($\lambda_{em}(CH_3CN)$ = 687 nm, $E_{T=}$ 42 kcal mol^{-1}, lifetime 6.5 μs) was observed using laser excitation.[9] The absorption spectrum of the triplet exhibited maxima at 360 and 570 nm. It was also shown that photoexcited **3** sensitized the formation of singlet oxygen with a quantum yield of 0.65. Rigid binding of indanetrione in a phthalic anhydride matrix was invoked to account for the observation of room-temperature phosphorescence (λ_{em} = 713 nm) in a phthalic anhydride matrix;[10] no other cases of such room-temperature behavior could be detected in matrices or in solution.

50.3 Diethyl Mesoxalate

Diethyl mesoxalate (**5**, λ_{max}(heptane) = 367 (24) and 372 (25)) is the only tricarbonyl compound containing ester group(s) whose photochemical behavior has been investigated. It exhibits normal ketone photochemistry. Photolyses in cyclohexane or toluene solutions at $\lambda > 320$ nm gave moderate yields of the addition products (**7**) expected from H-atom abstraction followed by radical coupling;[11] a number of additional products were not characterized.

Irradiations at 366 nm (unspecified solvent) in the presence of a twofold excess of the following olefins gave oxetanes **8** analogous to the classical Paterno–Buchi reaction of monoketones (Figure 50.3): 1,1-diphenyl ethylene (product yield 64%), α-methylstyrene (76%), norbornene (78% exo, 19% endo isomer), isoprene (90% of product from reaction at the more highly substituted double bond), and 2,3-dimethylbutadiene (42% plus polymer).[3]

50.4 Dialkyl Triketones

The unsymmetrical dialkyl triones **9a** and **9b** were irradiated in refluxing ether solution (~0.2 *M*) with a commercial sunlamp.[12] Photostationary states containing triketones with all permutations of akyl end groups (**9** and **10**) were reached in both cases, together with a yield of about 4% of CO and traces of biacetyl. In the case of **9b**, the photostationary state consisted of an equimolar mixture of all three products (**9b**, **10b**, **10c**); with **9a**, the ratio of **10a**:**9a**:**10b** was 3:1:1. The fact that the same transformations could be effected in the dark under conditions in which acyl free radicals can form (oxygen plus an aldehyde, di-*t*-butyl peroxide plus an aldehyde) prompted the suggestion of a free-radical chain reaction, although quantum yields were not determined. As illustrated below, the photochemical step was suggested to

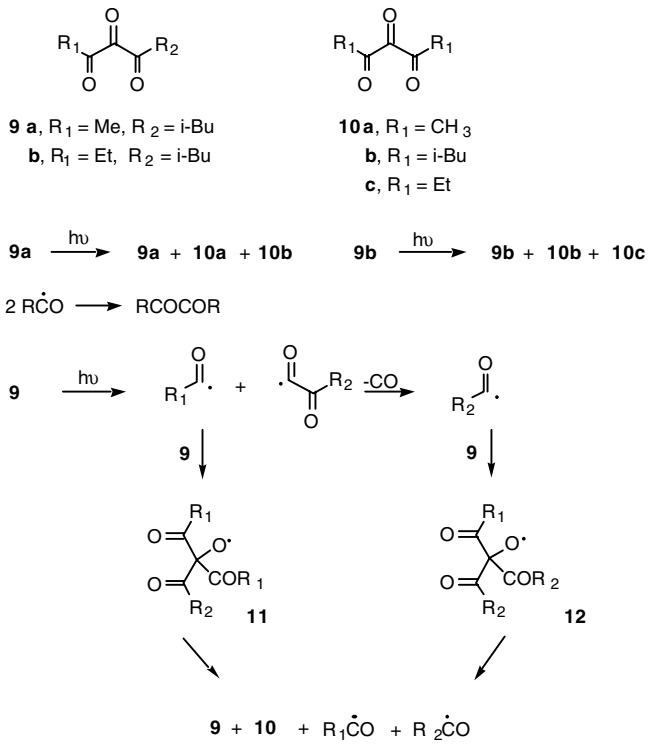

FIGURE 50.4

involve cleavage of an inter-carbonyl bond to give acyl and α-ketoacyl radicals. The small amount of CO observed was attributed to decarbonylation of these radicals. The major process was proposed to be the addition of acyl radicals to the carbon atom of the central carbonyl group of trione, resulting in formation of the oxyradicals **11** or **12**. Fragmentation of these can occur in three ways, leading either to regeneration of the original triketone or formation of a new one plus formation of an acyl radical that continues the chain. The resulting chain reaction finally leads to a photostationary state, the composition of which depends on the alkyl end groups involved, as noted above. Chain termination results in formation of biacetyl that was observed in trace yield. About 15% of a nonvolatile, uncharacterized residue was observed. Tetraketones, which could result from the addition of α-ketoacyl radicals to triones, were not reported (Figure 50.4).

The work described above appeared as a preliminary communication about 40 years ago. A full paper has never appeared nor, to our knowledge, has any subsequent work been performed with these or other dialkyl polyketones. Thus, a variety of interesting synthetic and mechanistic questions remain unanswered.

50.5 Diaryl Triketones

Diaryl triketones do not show the same reactivity as their dialkyl counterparts.[13] This is illustrated by the fact that 19-hr irradiation through Pyrex using the full spectrum of a 1000-W, high-pressure, mercury-vapor lamp was required for 90% disappearance of 250 mg of diphenyl triketone (**13**) in degassed *p*-xylene solution. The major products isolated were *p*,*p*′-dimethylbibenzyl, benzaldehyde, and *p*-methylbenzyl phenyl ketone; in addition, minor amounts of oxidation products such as *p*-methylbenzyl benzoate were identified, as well as traces of benzil. Quantum yields for the disappearance of **13** at 436 nm in degassed or air-saturated *p*-xylene solutions were about 3×10^{-4}; nearly identical values were obtained

in benzene solution, and somewhat higher values were obtained at 313 nm. Analogous chemistry was observed in the reactions of **13** in toluene (bibenzil, benzaldehyde, benzylphenyl ketone), cyclohexane (bicyclohexyl, cyclohexanol, benzaldehyde, phenylcyclohexyl ketone, cyclohexylbenzoate, and traces of benzil), and benzene (biphenyl, benzaldehyde, and phenylbenzoate). The biphenyl obtained from reaction in hexadeuterobenzene was pentadeuterobiphenyl ($C_{12}H_5D_{5)}$, suggesting addition of an intermediate phenyl radical to hexadeuteriobenzene followed by oxidation of the intermediate. *p,p′*-Disubstituted diaryl triketones showed similar behavior, and very sluggish reactivity was also observed with di-*t*-butyl triketone (**14**) in toluene; the products were bibenzyl, trimethylacetaldehyde, and benzyl-*t*-butyl ketone, plus an uncharacterized addition product. Bicyclic trione **4** also reacted very slowly.

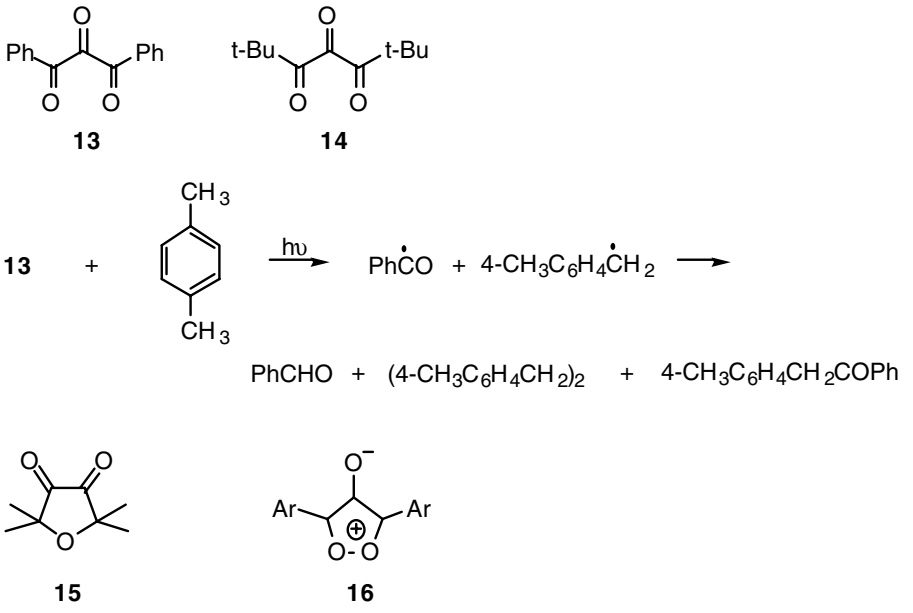

FIGURE 50.5

All the results are consistent with intermediate formation of aroyl or acyl and solvent-derived radicals, as illustrated below for the reaction with *p*-xylene. It was not possible to determine if these are formed via an initial H-atom abstraction by trione from solvent or via an α-cleavage of **13** followed by H-abstraction. The low quantum yields precluded a variety of experiments, such as, for example, examination of deuterium isotope effects on quantum yields. A report that **13** in benzene solution was converted to benzil in Cairo sunlight[14] could not be confirmed in Haifa sunlight.[15]

Irradiation of **13** in the presence of *p*-methoxybenzaldehyde did not afford any *p*-methoxyphenyl phenyl triketone. Similarly, heating a mixture of **13** and *p*-methoxybenzaldehyde in the presence of di-*t*-butyl peroxide had no effect, in contrast to the behavior observed with di-alkyl triones.

A satisfactory explanation for the lack of photochemical reactivity of diaryl triketones has not been forthcoming, but it is clear that radiationless deactivation is the (almost) exclusive process, as confirmed by laser-induced optoacoustic studies.[13] While this sluggishness might be attributed to the low singlet and triplet energies of such molecules, analogous tetraketones, which must have even lower excited state energies, show reasonable photochemical reactivity. Furthermore, α-diketones, such as 2,2,5,5-tetramethyl-tetrahydrofuran-3,4-dione (**15**, λ_{max} = 559 nm), that absorb at longer wavelengths than diphenyl triketone exhibited normal diketone photochemistry with respectable quantum yields.[16] Deactivation of excited diaryl triones could involve cleavage to a pair of radicals that recombine efficiently; we note that

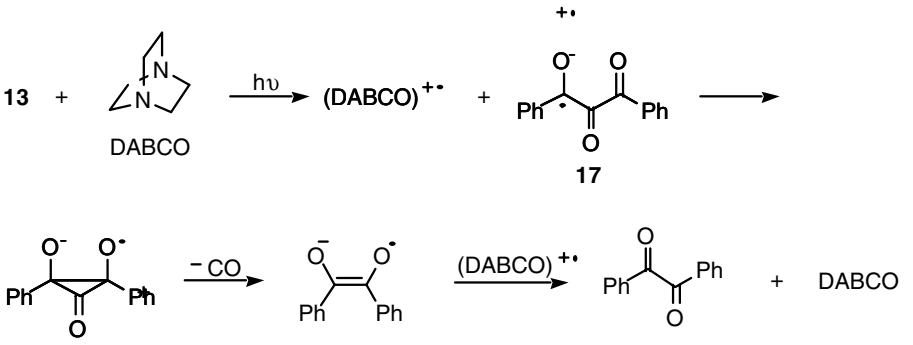

FIGURE 50.6

such radicals could also combine to give ketene **37** (see Section 50.7). An intriguing alternative suggestion that diphenyl triketone is converted by light to the mesoionic form **16**, which undergoes facile thermal reaction to regenerate **13**, could not be supported experimentally. No thermally reversible spectroscopic change was observed on irradiation of **13** in methylcyclohexane using the full spectrum of a mercury vapor lamp through Pyrex at a number of temperatures between +20 and –170°C. X-ray crystallographic evidence that **16** is not important in the electronic ground state of **1** has been provided by Cannon et al.[17]

Very different results were observed when **13** was irradiated in the presence of the electron donor DABCO. The reaction proceeded more efficiently and produced benzil as the only product. Single electron transfer (SET) from DABCO to the trione was assumed to be the reaction of the excited trione, which gives radical anion **17** as the initial photoproduct. Subsequent radical ion chemistry, as illustrated below, was suggested to account for the formation of benzil with regeneration of DABCO. Similarly, irradiation of bicyclic trione **4** in the presence of DABCO afforded the decarbonylation product camphorquinone. The same result could be obtained with **13**, albeit with lower efficiency, using *p,p′*-dimethoxybenzene instead of DABCO as the electron donor.

Irradiation of **13** in benzene solution containing 2,3-dimethyl-2-butene did not give products of olefin cycloaddition or of H-atom abstraction in contrast to the results described in the following section (Figures 50.5 and 50.6).

50.6 Cyclic Triketones

These compounds have been investigated by a number of workers, with particular attention paid to 1,2,3-triketoindane (**3**), the dehydration product of commercially available ninhydrin. Although quantum yields were not determined, the photochemical inertness of **3** in dry acetonitrile is clear from the fact that 250-hr irradiation of a degassed solution with a moderately powerful light source resulted in only 5% conversion![9] The products were the dimeric lactones, which have been shown to be products of the irradiation of benzocyclobutenedione (**21**) under similar conditions;[18] bisketene **20** was shown to be the precursor of these lactones. α-Cleavage of the triplet state of **3** to biradical **18** followed by decarbonylation to **19**, and intersystem crossing to **20** was suggested to occur with triketoindane. Recombination of the initially formed biradical **18** after intersystem crossing could provide a deactivation mechanism accounting for the low quantum yields. Irradiation in the presence of oxygen resulted in exclusive formation of phthalic anhydride, a result reminiscent of α-diketone photochemistry (Figure 50.7).

The results described above were confirmed in the first part of a paper that reported high-intensity ("laser-jet") irradiation of **3**, where about 10% of benzocyclobutenedione (**22**) was obtained.[19] It was suggested that the intermediate bisketene **20** has a very short lifetime and decays rapidly to carbene **21** so it was not possible for it to absorb light under normal irradiation intensities. However, some fraction of the ketene did absorb in the high-intensity experiments and cyclized to **22**, shown to be stable under the conditions of the experiment.

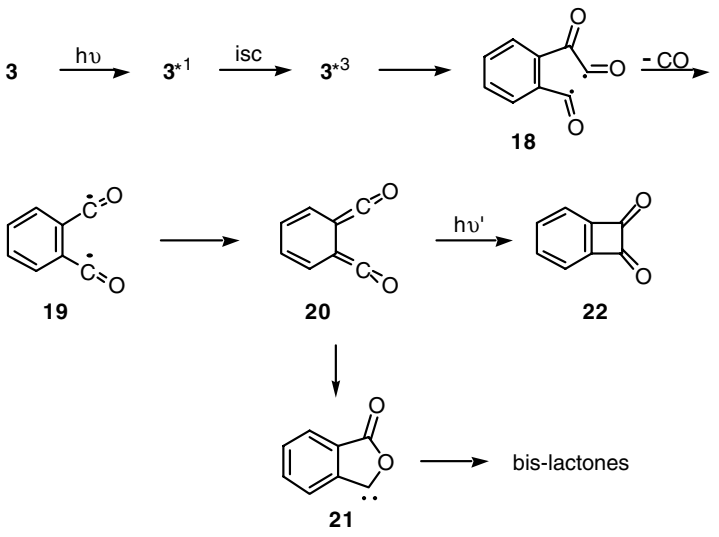

FIGURE 50.7

Very different results were obtained in extensive investigations of the reaction of deaerated solutions of **3** in the presence of olefins using a lamp with emissions centered at 300 nm (Rayonet RPR-3000; excitation to a higher singlet). Quantum yields of about unity were observed for a considerable number of olefins. The exceptions were olefins bearing electron-withdrawing groups, such as maleic anhydride and dimethyl fumarate, that were unreactive. Both hydrogen atom abstractions (path a) to afford allylic hydroxyketones (**23**, **24**) and/or cycloadditions of the Paterno–Buchi type (path b) to give oxetanes (**25**) and dioxenes (**26**) were observed. A general outline of the suggested mechanistic path for these reactions is shown in Figure 50.8. Initial excitation of **3** to a higher singlet state is followed by intersystem crossing to a triplet state of **3** which forms an exciplex with olefins (partial charge transfer), the orientation of which is governed by stereoelectronic factors. This exciplex, common to both types of reaction, then undergoes either (1) H-atom abstraction to ketyl radical **27** and allylic radical **28**, or (2) addition of olefin to **3**, giving the biradical **29**. Allylic radical **28** then couples with the ketyl radical **27** to form product; this may occur at the terminus of the allylic system, giving **23** or **24**. Similarly, two possibilities exist for the biradical **29**: cyclization to oxetane **25** or cyclization to dioxene **26**. The photochemistry is very similar to that observed in reactions of monoketones with olefins, except for the added possibility of dioxene formation; it should be noted that initial reaction occurs at the central carbonyl group of **3**, as expected. Intramolecular H-atom transfer in biradical **29** to give an allylic ether (**30**), a reaction sometimes observed with α-diketones, has not been detected. Formation of the pinacol **31** was observed in the reaction of **3** with cyclohexene. We note that electron transfer followed by proton transfer is equivalent to H-atom transfer.

The results of any particular case depended on the olefin used, with stereoelectronic effects in exciplex formation assumed to play a key role in determining the outcome of reaction. 2,3-Diphenyl-1,4-dioxene, having no allylic hydrogen atoms, gave oxetane exclusively, while 2-neopentylpropene gave exclusively the H-abstraction product (coupling at the primary rather than the neopentyl position was observed in this special case).[20] The reaction with 2,3-dimethyl-2-butene was studied in detail;[21] both radical coupling products were obtained (17.5% yield), but the major products were oxetane (29%) and dioxene (53%). In contrast, 2-methyl-2-butene afforded 82% of the two coupling products and 18% of oxetane.

A flash photolysis study of the quenching of indanetrione triplets by 22 olefins has been reported.[22] Pseudo-first order kinetics were observed for decay of the triplet of **3** at 570 nm, and the second-order rate constants (k_q) for triplet quenching by olefin were obtained; values of k_q ranged from 1.35×10^5 M^{-1}

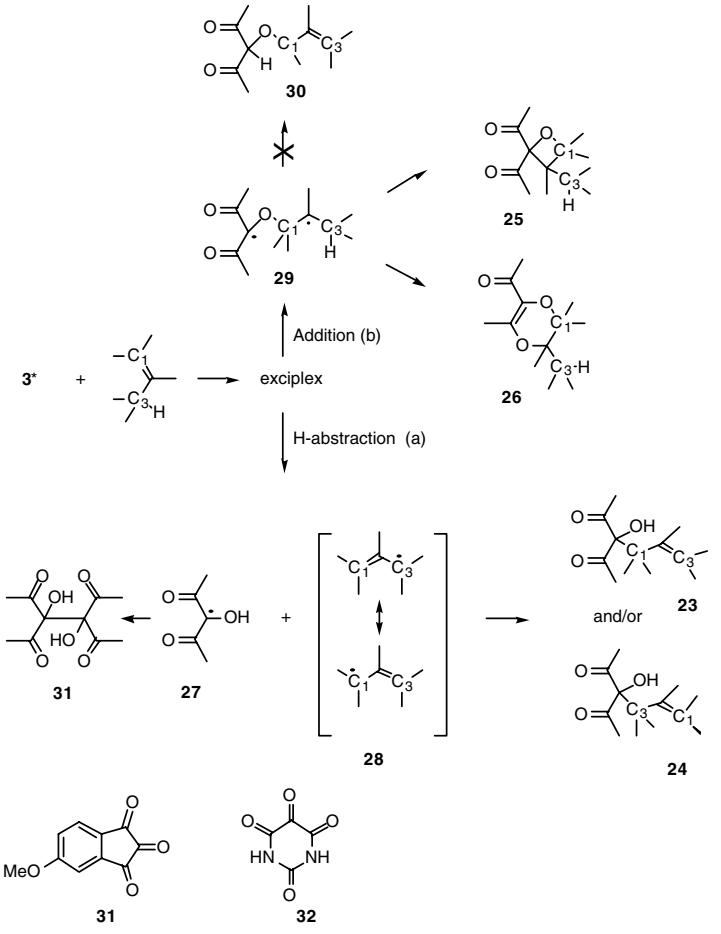

FIGURE 50.8

s^{-1} for 2-methyl-1-butene to 1.8×10^9 M^{-1} s^{-1} for 2.5-dimethyl-1.4-hexadiene. A plot of log k_q vs. ionization potential for seven olefins gave a straight line with a slope of –2.7/eV, supporting the suggestion that a complex with partial charge transfer is involved. The chemistry of these olefins ranged from exclusive H-atom abstraction to predominant cycloaddition, suggesting that the same initial interaction between excited indanetrione and olefin is responsible for all of the observed chemistry. Higher values for ionization potential were reflected in a higher degree of cycloaddition.

Reaction of **3** with *cis*- or *trans*-stilbene using a light source whose emission was centered at 350 nm resulted only in *cis* and *trans* isomerization to give identical mixtures from each pure isomer. Because the triplet energy of **3** is appreciably lower than that of either stilbene isomer, the isomerization cannot involve triplet energy transfer. It must proceed via a reversible interaction between trione and olefin, possibly via a biradical of type **29** in which the stereochemical integrity of the isomers is lost.

Investigation of the photochemical reactions of 5-methoxyindanetrione (**31**) gave results very similar to those obtained with the unsubstituted trione.[22] A plot of k_q values for **3** vs. the values for **31** gave a straight line with a slope close to unity. The authors concluded that the methoxy substituent did not change the reactive excited state of the trione.

The behavior of alloxan (**32**) with olefins in deaerated acetone solution with a light source having maximum emission at 300 nm was very similar to that of indanetrione.[23] Only H-abstraction products were observed with 2,4-hexadiene, 2-neopentylpropene, 2-methyl-2-butene, and 1-methyl-1-cyclopentene. Ethyl-1-propenyl ether yielded H-abstraction products (38%), oxetanes (6%), and dioxenes (56%). Stereoelectronic effects in formation and reaction of a common exciplex with charge transfer character were suggested to account for the results. As observed with **3**, both maleic anhydride and dimethyl fumarate gave no reaction with **31** while *cis*- and *trans*-stilbene were converted to the same mixture of *cis* and *trans* isomers (Figures 50.7 and 50.8).

50.7 Tetraketones

Photochemical reactions of the acyclic tetraketones diphenyl (**33a**), di-*p*-tolyl (**33b**), di-*p*-anisyl (**33c**), di-*p*-bromophenyl (**33d**), dimesityl- (**33e**), and di-*t*-butyltetraketones (**33f**), as well as the cyclophane tetraketone **34**, have been investigated.[24] They provide an interesting contrast to triketone photochemistry. Quantum yields for the disappearance of **33a** in degassed benzene solution at 546 nm were about 0.02; chemical yields of crystalline product(s) were high, approaching quantitative if careful precautions were taken to ensure dryness and absence of oxygen. The flexible acyclic compounds **33a–d** were converted into rigid, tricyclic diketo-orthoester-lactones, as illustrated below. The reaction involves two molecules of tetrone with the loss of one molecule of CO. The exclusive product with **33b–d** was the isomer **35**, which incorporated an α-diketo moiety and an aryl group, with about 10% of isomer **36** having two benzoyl groups in the case of diphenyl tetraketone (**33a**).

The reaction of **33a** was shown, by matrix isolation photolysis at 10 K and other methods, to involve acyloxyketene **37** as an intermediate. It was shown in separate experiments that **37**, synthesized by conventional treatment of the corresponding acid chloride, reacted with tetraketones to form the same adducts **35** and **36** in the same ratio as had been observed in the photochemical reaction of **33a**. The photolysis then involves conversion of excited tetraketone to **37** and CO followed by thermal reaction of **37** with tetraketone presumably via β-lactones. Limited evidence supports the singlet state as the reactive specie. If this is correct, a cyclic mechanism, as illustrated in Figure 50.9, could be involved; a triplet state reaction would require zwitterionic or biradical intermediates, as illustrated.

The exceptions to this behavior were dimesityl (**33e**) and di-*t*-butyl (**33f**) tetraketones and the cyclic tetraketone **34**, all of which have bulky groups flanking the tetraketone moiety and were photochemically inert. Steric effects might be responsible for inhibiting the formation of ketene in these cases; however, a competing photochemical reaction was shown to occur with **33e**. This involved abstraction of a hydrogen atom from an *ortho*-methyl group, a well-known reaction of *o*-methyl-substituted benzophenones and α-(*o*-tolyl)-α,β-diketones. Irradiation of **33e** in benzene solution containing *t*-butyl-OD (shown to react extremely slowly with the tetrone) resulted in significant deuterium incorporation into *o*-methyl groups. This was suggested, as shown in Figure 50.10, to involve initial formation of biradical **40**, which isomerizes to enol **41**, the latter then undergoing deuterium exchange and finally ketonization to the observed product. Similar processes might be involved with **33f**. Ring constraints prohibiting a cyclic mechanism could also apply to cyclophane **34**.

A similar mechanism to form ketenes from triketones without elimination of CO appears unlikely, as it involves a four-membered intermediate.

50.8 Pentaketones

A cyclic mechanism analogous to that suggested for tetraketones could occur with pentaketones. The same acyloxyketenes would form together with ethylenedione (C_2O_2) or 2CO, as illustrated in Figure 50.11. Addition of ketene to ground-state pentaketone could then afford tricyclic compounds such as **42** or **43**. Such experiments have given mixtures of products from which no identifiable pure substance could be isolated,[25] and further experimentation is required.

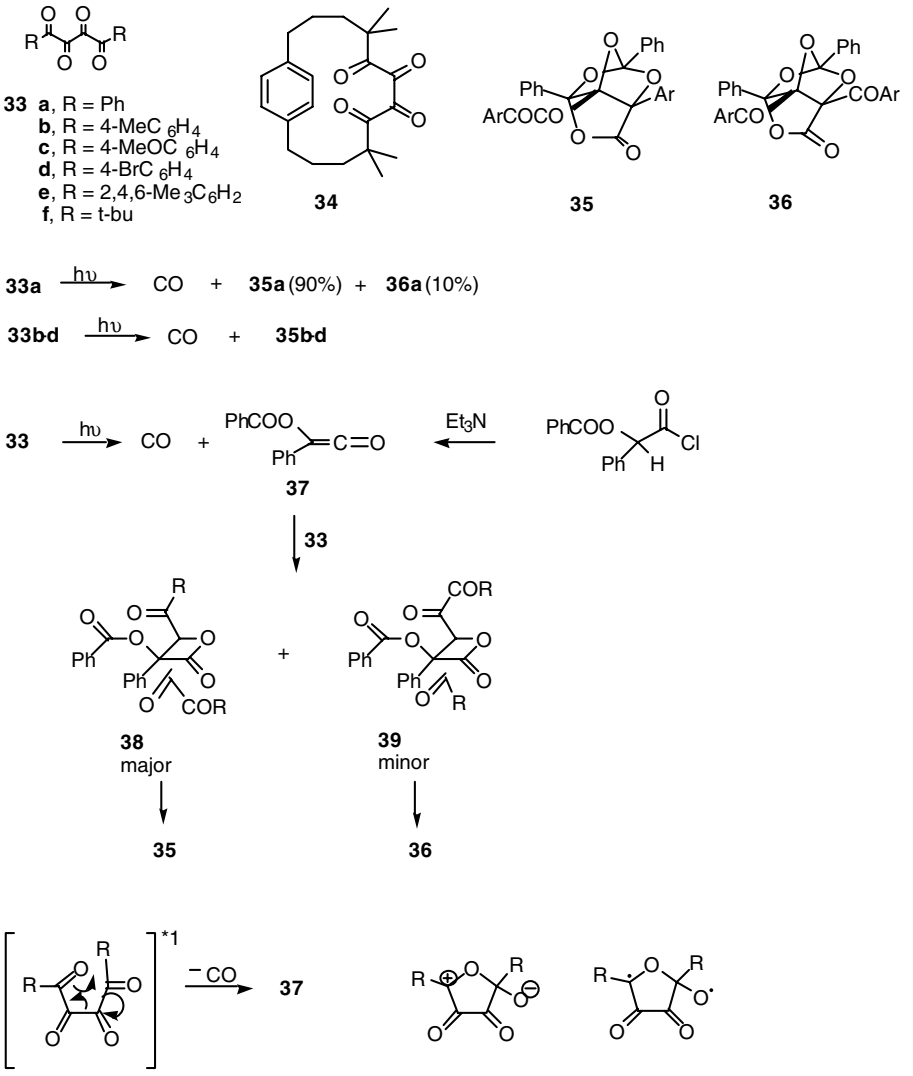

FIGURE 50.9

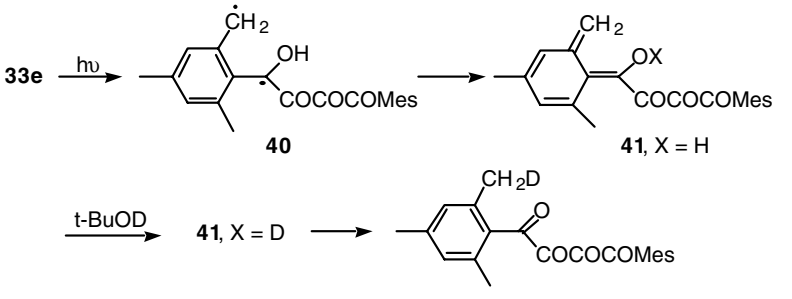

FIGURE 50.10

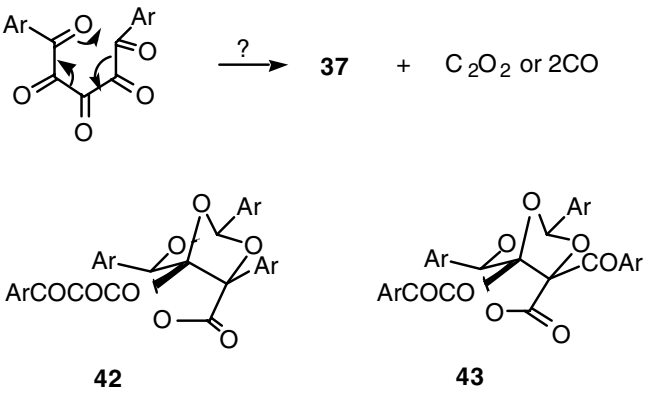

FIGURE 50.11

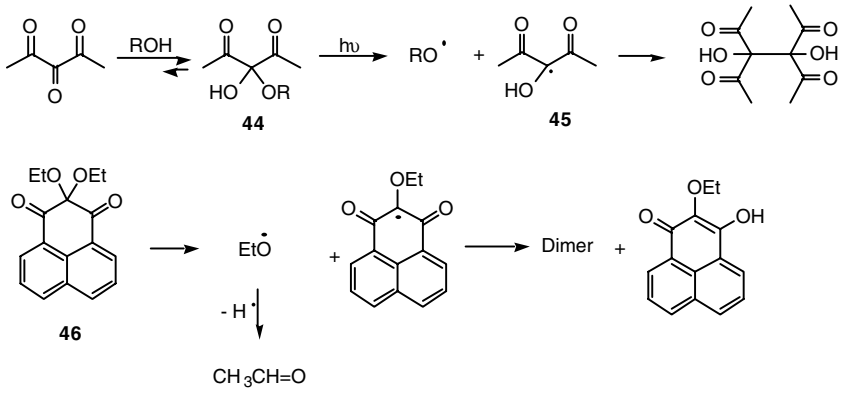

FIGURE 50.12

50.9 Hydrates and Hemiketals: A Trap for the Unwary

The facile reaction of vic-polycarbonyls at their central carbonyl group(s) was noted in the introduction. Normal synthetic procedures usually yield the hydrates **44** which must then be dehydrated to afford the desired polycarbonyl compounds; a variety of procedures are available for this purpose.[1,2] The equilibrium in such reactions is usually far to the right. Hemihydrates as well as di- and higher hydrates have also been observed. Rigorous exclusion of moisture in photochemical reactions is necessary if one wishes to observe the photochemistry of the free polycarbonyl compound. Similar reaction with alcohols (or other protic compounds) afford hemiketals. One ignores these possibilities at one's peril (Figure 50.12).

A number of reports of photopinacolization of tricarbonyls upon irradiation in hydroxylic solvents have appeared with incorrect mechanistic interpretations. The first of these was a 1903 report by Ciamician and Silber,[26] the fathers of organic photochemistry, who irradiated **32** in ethanol solution and obtained the corresponding pinacol, alloxantin. A similar report on the formation of alloxantin from irradiation of **32** hydrate in isopropyl alcohol appeared in 1950. It was assumed that initial H-atom abstraction by **32** results in formation of the ketyl radical which then dimerizes. This conclusion is not correct. These pinacols are, in fact, the products of β-cleavage of the hydrate (or hemiketal) leading to formation of ketyl radicals **45** plus hydroxy or alkoxy radicals; subsequent dimerization of the ketyl radicals affords the pinacol. Support for this point of view was provided by experiments in which

ninhydrin and **32** hydrate were irradiated in *t*-butyl alcohol, a notoriously poor H-atom donor.[27] Products were the pinacol and acetone, the decomposition product of *t*-butoxy radicals. Other workers showed that irradiation of ninhydrin or of **32** hydrate led to a coupled decomposition of water due to the intermediate formation of hydroxyl radicals; some α-cleavage was also observed.[28,29] Abstraction of the H-atom is indeed one of the reactions of excited polycarbonyls, but experiments in an aqueous or alcohol medium are not relevant.

Irradiation of the diethylketal (**46**) of phenalenetrione was shown by Stern–Volmer studies (cyclohexadiene quencher) to involve both singlet and triplet states.[30] Products were the diethyl ether of the corresponding pinacol and a derivative of the dihydrotrione, again a β-cleavage process, accounts nicely for the observed results.

More recently, photolysis of **3** was investigated in alcohol solution using the full spectrum of a mercury lamp.[31] Here, again, the results undoubtedly were due to photochemistry of the corresponding hemiketals.

It is possible to irradiate free polycarbonyls in the presence of hydrate or hemiketal by using light of sufficiently long wavelength so that the hydrate does not absorb, but avoidance of water or other protic solvents in the first place is to be preferred if at all possible.

50.10 Summary

The photochemistry of vic-polycarbonyl compounds can be regarded by optimists as exhibiting a rich range of reactivity or, alternatively, by pessimists as a hodge-podge of differing reactions that depend very much on the specific substances being investigated. For tricarbonyl compounds, we find normal ketone photochemistry with diethyl mesoxalate, α-cleavage and subsequent radical chain reactions with dialkyl triketones, a high degree of inertness with diaryl triketones, and classical carbonyl behavior (with adjustment for the presence of multiple carbonyl groups) for cyclic indanetrione and related compounds. Tetraketones show interesting, albeit photochemically not very efficient, chemistry to give novel structures that would not be predicted in advance. The last remaining type of compound, the acyclic pentaketones, have not yielded the secrets of their excited state reactions as yet. The conclusion that emerges clearly is that there is much room for additional work in this area.

References

1. Rubin, M. B., The chemistry of vicinal polyketones, *Chem. Rev.*, 75, 177, 1975; see also Rubin, M. B., Photochemistry of vicinal polyketones, in *Excited States in Organic Chemistry and Biology*, Pullman, B. and Goldblum, N., Eds., Reidel, Dordrecht, 1977.
2. Rubin M. B. and Gleiter R., The chemistry of vicinal polycarbonyl compounds, *Chem. Rev.*, 100, 1121, 2000.
3. Hara, M., Odaira, Y. and Tutsumi, S., Photoaddition of diethyl oxomalonate to olefins, *Tetrahedron Lett.*, 2981, 1967.
4. Unpublished results from the author's laboratory using an Aminco–Bowman apparatus with a 200-W xenon lamp. Similar failures to detect emission were also observed at the Weizmann Institute of Science, Rehovot, and the ETH, Zurich.
5. Beutel, J., Chemiluminescence in oxidation reactions: the oxidation mechanism of dimedone, *J. Am. Chem. Soc.*, 93, 2615, 1971.
6. Ghosh, S. and Chowdhury, M., Absorption and emission spectra of indantrione, *J. Phys. Chem.*, 85, 1280, 1981.
7. Ghosh, S. and Chowdhury, M., Media effects on the *n,n** transition in indantrione, *J. Phys. Chem.*, 85, 1284, 1981.
8. Roy, J., Ghosh, S., and Bhattacharyya, S. P., Characterization of an unusual specific interaction between aromatic cyclic *cis*-vicinal triketones and cyclic saturated ethers, *J. Mol. Struct (Theochem.)*, 535, 71, 2001.

9. Netto-Ferreira, J. C. and Scaiano, J. C., Photochemistry of 1,2,3-indanetrione, *Photochem. Photobiol.*, 54, 17, 1991.
10. Roy, J., Bhattacharya, S., Mondal, S., and Ghosh, S., Room temperature (n,π^*) phosphorescence of indanetrione (anhydrous ninhydrin) in phthalic anhydride matrix, *Spectrochim. Acta*, *Part A*, 53, 225–231, 1997.
11. Pac, C., Sakurai, H., Shima K., and Ogata, Y., Benzoyl peroxide- and photo-induced reactions of diethyl mesoxalate in cyclohexane and toluene, *Bull. Chem. Soc. Jpn.*, 48, 277, 1975.
12. Urry, W. H., Pai, M. H., and Chen, C. Y., Acyl exchange reactions of vicinal triones, *J. Am. Chem. Soc.*, 86, 5342, 1964.
13. Rubin, M. B., Heller, M., Monisov, R., Gleiter, R., and Doerner, T., Photochemistry of vicinal triketones, *J. Photochem. Photobiol. A: Chem.*, 87, 7, 1995.
14. Schonberg, A. and Mustafa, A., Photochemical reactions in sunlight. Part XII. Reactions with phenanthraquinone, 9-arylxanthene, and diphenyl triketone, *J. Chem Soc.*, 997, 1947.
15. Heller, M., unpublished results, Haifa.
16. Rubin, M. B., Ben-Bassat, J. M., and Weiner, M., Photochemical reaction of 2,2,5,5-tetramethyltetrahydrofuran-3,4-dione: an unusual α-diketone, *Israel J. Chem.*, 16, 326, 1977.
17. Cannon, J. R., Potts, K. T., Raston, C. L., Sierakowski, A. F., and White, A. H., Chemistry and crystal structures of 1,3-bis(4′-bromophenyl) propane-1,2,3-trione, 3,5-diphenyl 1-1,2-dithiolylium-4-olate and 4-hydroxy-3,5-diphenyl-1,2-dithiolium perchlorate, *Aust. J. Chem.*, 31, 297, 1978.
18. Rubin, M. B., Recent photochemistry of α-diketones, *Top. Curr. Chem.*, 129, 1, 1985.
19. Adam, W. and Patterson, W. S., High-intensity laser-jet photochemistry: formation of benzocyclobutenedione from 1,2,3-indantrione via transient targeting, *J. Org. Chem.*, 60, 7769, 1995.
20. Netto-Ferreira, J. C., Silva, M. T., and Puget, F. P., Photochemistry of cyclic vicinal tricarbonyl compounds: [2+2]-photocycloaddition of 1,2,3-indanetrione to electron rich olefins, *J. Photochem. Photobiol. A: Chem.*, 119, 165, 1998.
21. Silva, M. T., Braz-Filho, R., and Netto-Ferreira, J. C., Photochemistry of cyclic vicinal tricarbonyl compounds. Photochemical reaction of 1,2,3-indanetrione with 2,3-dimethyl-2-butene: hydrogen abstraction and photocycloaddition, *J. Braz. Chem. Soc.*, 11, 479, 2000.
22. Netto-Ferreira, J. C., Silva, M. T., and Cardoso da Silva, A. M., Photochemistry of cyclic vicinal tricarbonyl compounds: laser flash photolysis study of the reaction of indane-1,2,3-trione and its 5-methoxy derivative with olefins, *Photochem. Photobiol. Sci.*, 1, 278, 2002.
23. Silva, M. T., Gomes, D. F., Cardoso da Silva, A. M., and Netto-Ferreira, J. C., Photochemistry of cyclic vicinal tricarbonyl compounds: photolysis of alloxan in the presence of olefins containing allylic hydrogen, *J. Photochem. Photobiol. A: Chem.*, 150, 31, 2002.
24. (a) Rubin, M. B., Krochmal, Jr., E. C., and Kaftory, M., Photochemistry of vicinal diaryltetraketones, *Rec. Trav. Chim.*, 98, 85, 1979; (b) Rubin, M. B., Etinger, M., Monosov, R., Wierlacher, S., and Sander, W., Photochemistry of diaryl vicinal tetraketones and chemistry of intermediate (aroyloxy)arylketenes, *J. Org. Chem.*, 63, 480, 1998.
25. Unpublished results, Haifa and Heidelberg.
26. Ciamician, G. and Silber P., Chemische Lichtwirkungen. VI. Mitteilung, *Ber. Dtsch. Chem. Ges.*, 36, 1575, 1903.
27. Matsuura, T., Sugae, R., Nakashima R., and Omura, K., Photo-induced reactions. XVI. Photopinacolizaton of triketoindane derivatives, *Tetrahedron*, 24, 6149, 1968.
28. Otsuji, Y., Wake S., and Imoto, E., Photochemistry of heterocyclic compounds. II. The photochemical decomposition of water catalyzed by alloxan monohydrate and its derivatives, *Tetrahedron*, 26, 4139, 1970.
29. Wake, S., Mawatari, T., Otsuji, Y., and Imoto, E., The mechanism of the photodecomposition of alloxan monohydrate: the effects of solvents, *Bull. Chem. Soc. Jpn.*, 44, 2202, 1971.
30. Otsuji, Y., Wake, S., Maeda, E., and Imoto, E., Photolysis of 2,2-diethoxy-2,3-dihydrophenalene-1,3-dione, *Bull. Chem. Soc. Jpn.*, 47, 189, 1974.

31. Tatsugi, J., Hara, T., and Izawa, Y., Photochemical behavior of indane-1,2,3-trione in degassed alcoholic solutions: formation of 3-substituted phthalides, *Chem. Lett.*, 177, 1977.
32. Horner L. and Maurer, F., Chemische und spektroskopische Eigenshaften vicinaler Di-, Tri-, und Tetraketone, *Liebigs Ann. Chem.*, 736, 145, 1970.

51

Photochemical Routes to Cyclophanes Involving Decarbonylation Reactions and Related Process

Teruo Shinmyozu
Kyushu University

Rika Nogita
Kyushu University

Motoko Akita
Kyushu University

Chultack Lim
Kyushu University

51.1 Photochemical Decarbonylation Reactions for the Synthesis of Cyclophanes

Electronically excited carbonyl compounds undergo various reactions, in which α-cleavage in solution constitutes an important synthetic method.[1] Quinkert et al.[2] first reported the light-induced decarbonylation of ketones in benzene in 1963. Engel[3] and Robbins and Eastman[4a] independently in 1970 found that the decarbonylation of dibenzyl ketone occurs very efficiently from an extremely short-lived quenchable triplet state with a quantum yield (Φ_{CO}) of 0.7 at 313 nm in benzene at 30°C. Robbins and Eastman also reported that the decarbonylation proceeds via a two-step mechanism involving the formation of the phenylacetyl radical.[4b]

[3.3]Cyclophanes ([3.3]CPs) undergo two types of photochemical reactions, irradiation of the $\pi\pi^*$ band of multibridged [3^n]CPs leads to the formation of polycyclic cage compounds via photocycloaddition of the facing benzene rings, followed by rearrangement of the carbocation species generated by protonation of a cyclobutane ring of the cycloadduct (as described in Chapter 23), while irradiation of the n,π^* band of [3.3]CP-2,11-diones **1**[5–7] undergoes decarbonylation to give [2.2]CPs **2** in high yields.[8]

In the course of our study on multilayered [3.3]metacyclophanes, we noticed that the n,π^* bands of the structural units, [3.3]metacyclophane-2,11-diones, appear in the 280- to 330-nm region. We found that photoexcitation of the n,π^* bands of [3.3]cyclophane-2,11-diones **1** in benzene extrudes CO smoothly to give [2.2]CPs **2** in high yields. This method also provides a general synthetic method for [3.2]CP-2-ones **3** by taking advantage of the fact that this reaction proceeds in a stepwise manner via [3.2]CP-2-ones **3**. Thus, this method provides an alternative synthetic route to [2.2]CPs and a simple

0-8493-1348-1/04/$0.00+$1.50

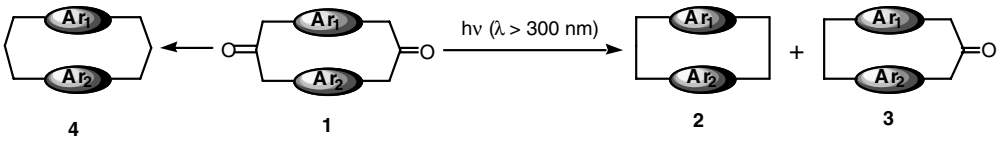

SCHEME 51.1 A new synthetic route to [2.2] and [3.2]cyclophanes **2** and **3** by photochemical decarbonylation of [3,3]cyclophane-2,11-diones **1**.

approach to the synthesis of [3.2]CPs, which are generally inaccessible in a direct manner, from the same starting material **1** for the synthesis of [3.3]CPs **4** (Scheme 1).

The general synthetic methods for [2.2]CPs have been already established.[9] Most of them employ the ring contraction reactions of the 2,11-diheteroatom-substituted [3.3]CPs. Photochemical elimination of sulfur or selenium atoms from [3.3]CP-2,11-disulfide or diselenide and flash vacuum pyrolysis of sulfur dioxide obtained by the oxidation of the corresponding sulfides are the most general methods. 2,11-Diaza[3.3]CPs are converted to the corresponding [2.2]CPs via their nitroso derivatives by reductive elimination of nitrogen.[10] Photoextrusion reactions of CO_2 from cyclic diesters can also be applied to the synthesis of [2.2]paracyclophanes (PCPs)[11,12] and [2.2]heterophanes, as described below.[13]

Recently, Vögtle et al.[14] reported the selective ketone pyrolysis as a new synthetic method for mono- and polycyclic hydrocarbons; that is, flash vacuum pyrolysis (10^{-5} Torr, 610 to 650°C) of [3.3]CP-2,11-diones **1** afforded [2.2]CPs **2** in moderate yields. This ketone pyrolysis is widely applicable to the synthesis of tribridged cyclophanes and of cyclophanes with a large cavity starting from $[3^n]$CP-(one)^n.[15]

Photochemical reaction of [3.3]CP-2,11-dione **1** in benzene gives the corresponding [2.2]CP **2** in satisfactory yield. The isolated yields of products and irradiation times are summarized in Table 51.1. A benzene solution (4.0 mmol/L) of [3.3]MCP-2,11-dione **5** was irradiated with a high-pressure mercury lamp (400-W) as the internal light source at ambient temperature while nitrogen was bubbled into the solution. The reaction was rather slow but [2.2]MCP **6** was obtained in 95% yield after 20-hr irradiation. When irradiation was discontinued after 4 hr, 9% of **6** and 57% of [3.2]MCP-2-one **7** were isolated. This indicated that the reaction proceeded in a stepwise manner. This method was also applicable to the synthesis of [2.2]pyridinophane **9** (56%), but longer irradiation time was required compared with the reaction of **5**. The reaction of [3.3]metaparacyclophane(MPCP)-2,11-dione **11** proceeded smoothly to give [2.2]MPCP **12** (94%). [3.3]PCP-2,11-dione **14** was the most reactive among the [3.3]CP-2,11-diones and afforded [2.2]PCP **15** (97%) after 30-min irradiation. The solvent benzene can be replaced with other solvents such as ethyl acetate. This reaction was successfully applied to the functionalized [2.2]CPs as exemplified by the synthesis of 7,15-di-*t*-butyl-4,12-dimethyl[2.2]MCP **18** and the synthesis of $[2^n]$CPs with large rings; [3.3.3]PCP-2,11,20-trione **20** gave [2.2.2]PCP **21** (39%) after 20-hr irradiation. [3.3.3](1,3,5)CP-2,11,20-trione **22** was inert to irradiation, and the formation of **23** was not observed; whereas, monoketone **24** provided [3.3.2](1,3,5)CP **25** (34%). This suggested the quenching of the photoexcited state of one carbonyl group by neighboring ground-state carbonyl groups in **22**.The reaction conditions can be adjusted to allow the preferential formation of [3.2]CP-2-one **3** from the time-controlled reaction of **1**. As described above, [3.2]MCP-2-one **7** was isolated in 57% after 4-hr irradiation along with [2.2]MCP 6 (9%). Similarly the [3.2]pyridinophane-2-one **10** was obtained in 72% yield after 4-hr irradiation with 16% recovery of **8**. Dione **11** yields [3.2]MPCP-2-one **13** (46%), and dione **14** gives [3.2]PCP-2-one **16** (21%); along with the corresponding [2.2]CPs after 40- and 20-min irradiations, respectively. Furthermore, this method is also applicable to the synthesis of $[2^n]$CPs as host molecules (**20** to **21**) and multilayered [2.2]MCPs (**29** to **30** and **31**).

The advantage of our photochemical method over Vögtle's[14,15] and other conventional methods[9] is the simple and easy experimental procedures, which do not require special apparatus; also, high yields of product are obtained. Thus, [3.3]CP-2,11-diones **1**, which are readily accessible by TosMIC (*p*-tolylsulfonylmethyl isocyanide)[16] coupling,[5–7] serve as common precursors to the synthesis of [3.3]CPs **4** as well as [2.2]- and [3.2]CPs **2** and **3**. The significance of the photodecarbonylation reaction resides in the fact that a series of [3.3]-, [3.2]-, and [2.2]CPs can be prepared from the same starting compound **1**. Therefore,

TABLE 51.1 Yields of [2.2]cyclophanes and [3.2]cyclophane-2-ones Prepared by Irradiation of Diones with a 400-W High-Pressure Hg Lamp

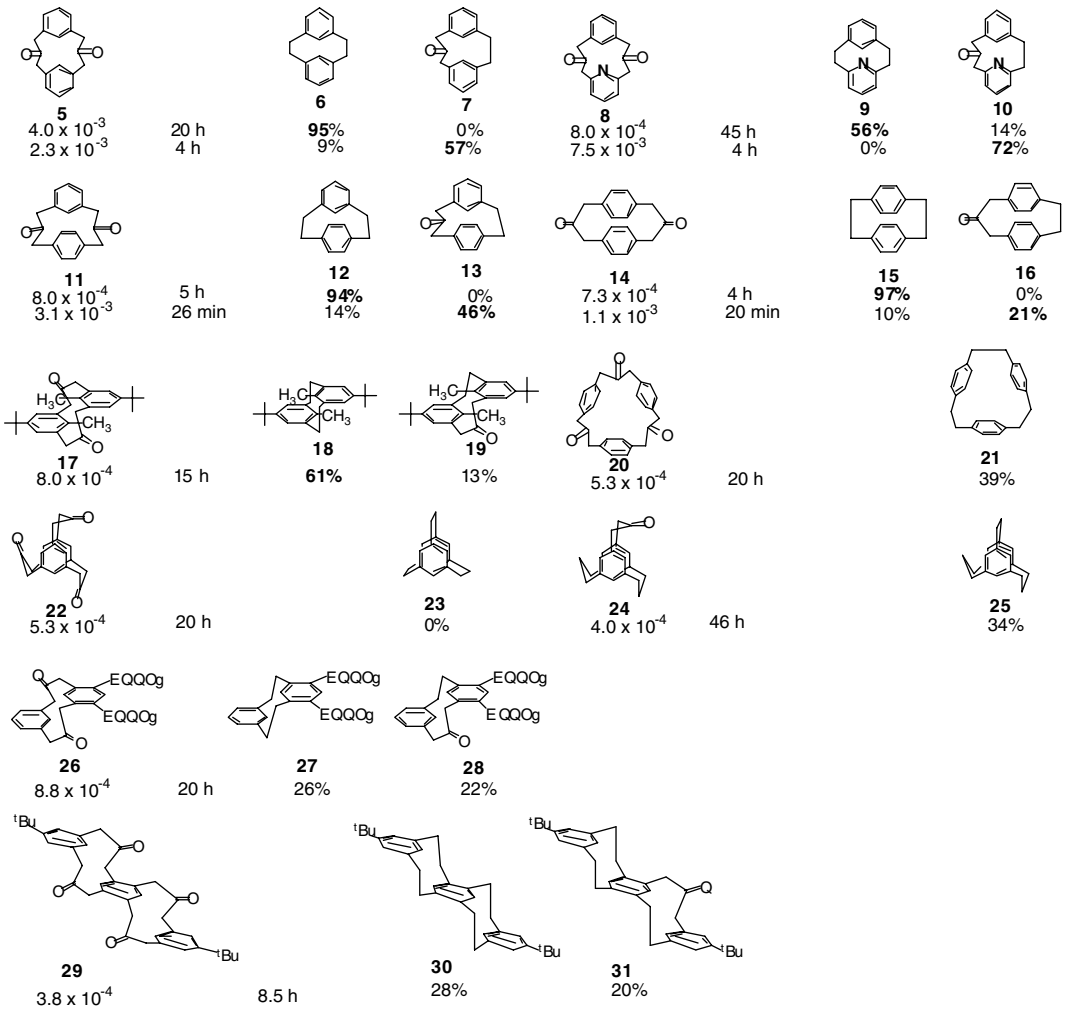

the method may be most conveniently used when a series of [3.3]-, [3.2]-, and [2.2]CPs is required (Scheme 2).

Miranda et al.[17] reported that irradiation (254-nm mercury lamp) of [3.2]PCP-2-one **16** in benzene led to [2.2]PCP **15** as the only product via acyl–alkyl biradical **32** and biradical **33**. A laser-flash photolysis study (266 nm) of **16** in cyclohexane indicated that biradical **33** is detectable at room temperature and does not cleave to *p*-xylylene **35** but cyclizes to [2.2]PCP **15** or dimerizes to [2^4]PCP **34**. Irradiation (laser, 308 nm) of a cyclohexane solution of **15** containing a triplet quencher (cyclooctadiene) showed two absorption maxima, which correspond to *p*-xylylene **35** and the biradical **33**. The cyclophanes [2^3]PCP **21** and [2^4]PCP **34** were formed by irradiation (laser, 248 or 266 nm) of cyclohexane solutions of [2.2]PCP **15**. While the formation of **34** agrees well with the intermediacy of **33**, the detection of [2^3]PCP **21** provided further evidence for the intermediacy of *p*-xylylene **35**, which can couple either its trimeric or tetrameric products.

The exclusive intramolecular coupling following decarbonylation reaction was supported by the exclusive formation of unsymmetrical [2.2] and [3.2]CPs from unsymmetrical starting ketones such as **8** and **11**. This reaction also proceeds in a stepwise manner. Experimental results show that the preferential

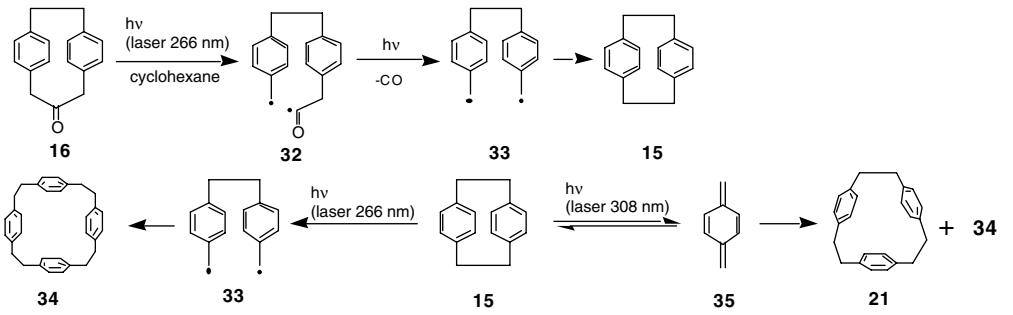

SCHEME 51.2 Photochemical reation of [3.2]paracyclophane-2-one.

formation of [3.2]CP-2-one **3** from the time-controlled reaction of **1** is effective when the reaction is slow, as is the case of the metacyclophane.

51.2 Photochemical Decarboxylation Reactions for the Synthesis of Cyclophanes

This synthetic route permits us to introduce strain by starting from an unstrained molecule that under appropriate conditions decomposes to form an intermediate that can then react by one main pathway. By taking advantage of the high yields and the simplicity of the photoextrusion of esters, Kaplan and Truesdale[11] reported the preparation of [2.2]PCP **15** (Scheme 3). When dilactone **41a**, which was prepared by the reaction of silver salt of 1,4-benzenedi-acetate **36** with 1,4-*bis*(bromomethyl)benzene **40a** in refluxing CH_3CN, was irradiated at room temperature in either MeOH or 1,2-dimethoxyethane, [2.2]PCP **15** was obtained.[11] The yield of **15** approached 70% when 1,2-dimethoxyethane was used as solvent but was somewhat lower in methanol. Hibert and Solladie reported that decarboxylation yields of the dilactones with substituents on the aromatic ring were strongly dependent on the nature of the substituent.[12] The methoxy group **41b** strongly enhanced the decarboxylation process as compared to the carbomethoxy group **41c**. Complete disappearance of the starting dilactone required 12 and 60 min for **41b** (R = OMe) and **41c** (R = CO_2Me), respectively (MeOH, 20°C). In addition, **41c** is first monodecarboxylated and the resultant monolactone is difficult to decarboxylate further. In this case, irradiation in quartz at a higher temperature (58°C) improved the yield of **41c** (85%). Thus, the experimental conditions must be modified depending on the substituent: irradiation through Pyrex at room temperature in the case of electron-donating substituents and through quartz at higher temperatures in the case of electron-withdrawing substituents (Scheme 4). This method could be applied successfully to the synthesis of the benzofused heterophane, *anti*-[2.2](2,6)benzothiazolophane **45**.[13] Irradiation (450-W, high-pressure mercury lamp) of dilactone **44** in MeOH for 6 hr gave the cyclophane **45** (57%). This type of decarboxylation reaction may be useful for the synthesis of a variety of heterophanes and benzenophanes comprised of rather unstable aromatic rings, as large numbers of synthetic methods for preparation of dilactone are available.

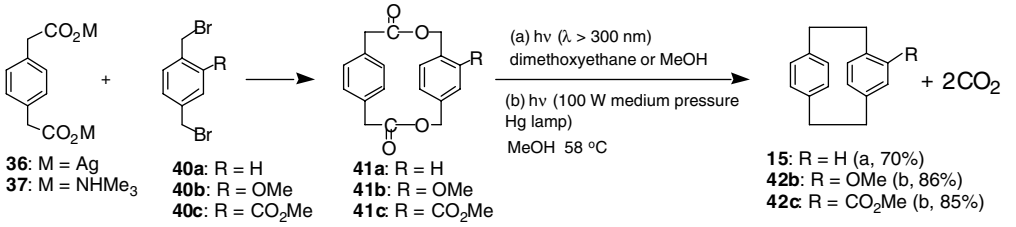

SCHEME 51.3 Synthesis of [2.2]paracyclophanes by photoextgrusion of carbon dioxide from cyclic dilactones.

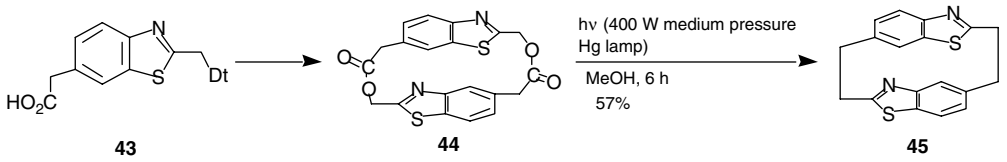

SCHEME 51.4 Synthesis of *anti*-[2.2](2,6)benzothiazolophane by photoextrusion of carbon dioxide from a cyclic lactone.

References

1. Turro, N. J., *Modern Molecular Photochemistry*, University Science Books, Sausalito, CA, 1991.
2. Quinkert, G., Opitz, K., Weirsdorff, W. W., and Weinlich, J., Light induced decarbonylation of dissolved ketones, *Tetrahedron Lett.,* 1863, 1963.
3. Engel, P.S., Photochemistry of dibenzyl ketone, *J. Am. Chem. Soc.,* 92, 6074, 1970.
4. (a) Robbins, W. K. and Eastman, R. H., Photodecarbonylation in solution. I. Quantum yields and quenching results with dibenzyl ketones, *J. Am. Chem. Soc.*, 92, 6076, 1970; (b) Robbins, W. K. and Eastman, R. H., Photodecarbonylation in solution. II. Trapping of intermediates in the photolysis of dibenzyl ketones, *J. Am. Chem. Soc.*, 92, 6077, 1970.
5. (a) Kurosawa, K., Suenaga, M., Inazu, T., and Yoshino, T., A facile synthesis of [3^n]cyclophanes, in which aromatic rings are connected with $–CH_2–CO–CH_2–$ bridges, *Tetrahedron Lett.,* 23, 5335, 1982. (b) Shinmyozu, T., Hirai, Y., and Inazu, T., Synthesis of [3.3]heterophanes containing the pyridine, furan and thiophene rings by the TosMIC method, *J. Org. Chem.,* 51, 1551, 1986.
6. Sasaki, H. and Kitagawa, T., Synthesis of [3^n]cyclophanes and related compounds by alkylation of tosylmethyl isocyanide with *bis*(bromomethyl)benzenes, *Chem. Pharm. Bull.,* 31, 2868, 1983.
7. Breitenbach, J. and Vögtle, F., Macrocyclizations with TosMIC-yielding [3^n]metacyclophanes, *Synthesis,* 41, 1992.
8. (a) Isaji, H., Sako, K., Takemura, H., Tatemitsu, H., and Shinmyozu, T., A new synthetic method of [2.2]cyclophanes from [3.3]cyclophane-2,11-diones via photodecarbonylation, *Tetrahedron Lett.,* 39, 4303, 1998; (b) Isaji, H., Yasutake, M., Takemura, H., Sako, K., Tatemitsu, H., Inazu, T., and Shinmyozu, T., Alternative general synthetic routes of [2.2]cyclophanes and [3.2]cyclophanes from [3.3]cyclophane-2,11-diones by photodecarbonylation and a structural study of [3.2]metacyclophanes, *Eur. J. Org. Chem.,* 2487, 2001; (c) Isaji, H., Photochemical synthesis and structural study of [2·n] cyclophones (n = 3,2) and 15,16-dimethyldihydropyrene derivative. Ph.D. dissertation, Kyushu University, 1999.
9. For a review, see Vögtle, F., *Cyclophan-Chemie,* B.G. Teubner, Stuttgart, 1990.
10. Takemura, H., Shinmyozu, T., and Inazu, T., A new synthetic method of [2.2]cyclophanes, *Tetrahedron Lett.,* 29, 1031, 1988.
11. Kaplan, M. L. and Truesdale, E. A., [2.2]Paracyclophane by photoextrusion of carbon dioxide from a cyclic diester, *Tetrahedron Lett.,* 3665, 1976.
12. Hibert, M. and Solladie, G., Substituent effect during the synthesis of substituted [2.2]paracyclophane by photoextrusion of carbon dioxide from a cyclic diester, *J. Org. Chem.,* 45, 4496, 1980.
13. Mashraqui, S. and Nivalkar, K. R., Synthesis of *anti*-[2.2](2,6)benzothiazolophane: the first example of [2.2]benzo-fused heterophane, *Tetrahedron Lett.,* 38, 4487, 1997.
14. Breitenbach, J., Ott, F., and Vögtle F., Selective ketone pyrolysis: new method for mono- and polycyclic hydrocarbons, *Angew. Chem. Int. Ed. Engl.,* 31, 307, 1992.
15. Ott, F., Breitenbach, J., Nieger, M., and Vögtle, F., Selektive ketonpyrolyse: neue beispiele, *Chem. Ber.,* 126, 97, 1993.

16. Hoogenboom, B. E., Oldenziel, O. H., and van Leusen, A. M., *p*-Tolylsulfonylmethyl isocyanide, *Org. Synth.,* 6(coll.), 987, 1988.
17. Miranda, M. A., Font-Sanchis, E., Perez-Prieto, J., and Scaiano, J. C., The 4,4′-(1,2-ethanediyl)bis-benzyl biradical: its generation, detection and (photo)chemical behavior in solution, *J. Org. Chem.,* 66, 2717, 2001.

52

Norrish Type II Photoelimination of Ketones: Cleavage of 1,4-Biradicals Formed by γ-Hydrogen Abstraction

Peter J. Wagner
Michigan State University

Petr Klán
Masaryk University

0-8493-1348-1/04/$0.00+$1.50

52.1 The Norrish Type II Photoelimination Reaction

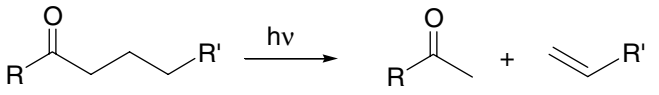

52.2 Mechanism

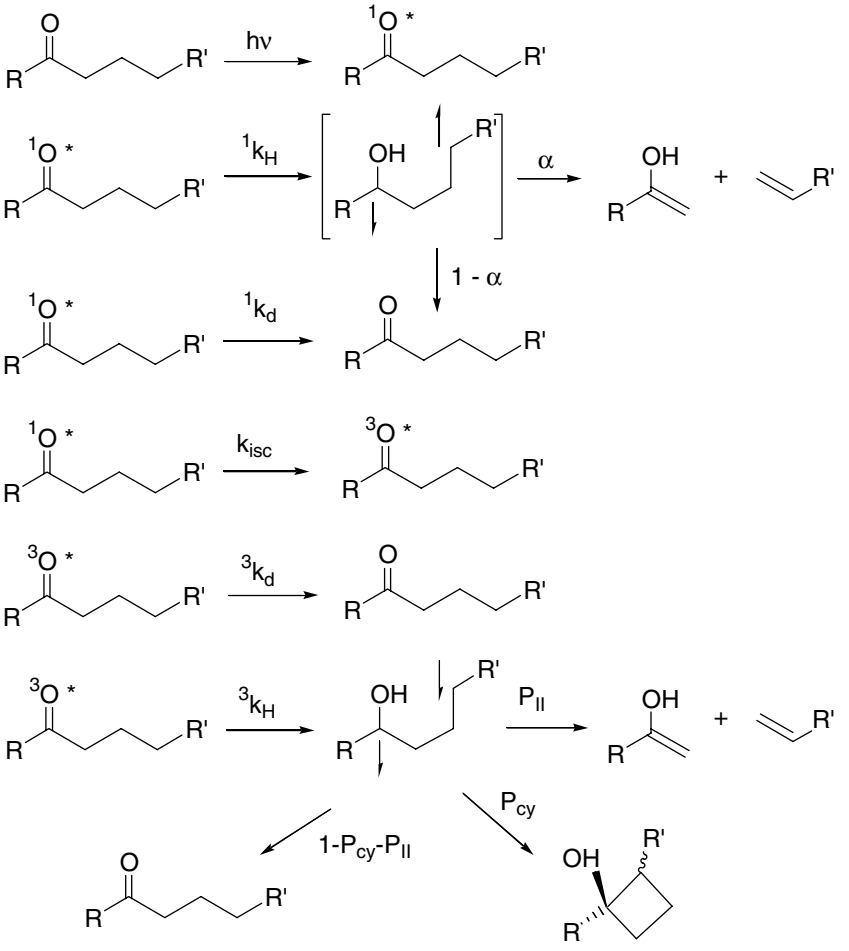

52.3 Byproducts

cyclobutanols (usually)
cyclopentanols (rarely)
γ,δ-unsaturated ketones and cyclohexenones (γ-vinyl)
γ,δ-unsaturated ketones and cycloheptonones (γ-cyclopropyl)
γ,δ-unsaturated ketone (cleavage of δ-substituents)

52.4 History

A wide variety of carbonyl compounds undergo photoinduced intramolecular hydrogen atom abstraction to form biradicals that then undergo two common competing reactions: coupling to produce cyclic alcohols and disproportionation back to a ketone, to various enols, or to alcohols. The overall process closely parallels the well-known bimolecular photoreduction of ketones, the most common products of which are formed by radical coupling. These intramolecular hydrogen abstraction processes have been widely studied and several full reviews are available (including Chapter 58 of this book).[1–5]

The first and still best known example of such intramolecular hydrogen abstraction is the *type II* photoelimination discovered by Norrish,[6] who found that ketones with γ–CH bonds cleave to methyl ketones and alkenes rather than to acyl and alkyl radicals, the earlier discovered *type I* cleavage. Later workers found that both cleavage processes compete in certain ketones and that overall quantum yields are particularly low whenever the type II process occurs. For years, the type II reaction was considered to be concerted; a 1,5-hydrogen transfer together with CC bond cleavage in a six-atom cyclic transition state could lead to the alkene and the enol tautomer of the product ketone. Such a process would now be called a *retro-ene reaction*. In a key experiment, Calvert and Pitts[7] verified by IR that the enol is indeed formed first and then is rapidly converted to ketone. However, Yang and Yang[8] had already discovered competing cyclobutanol formation and suggested that cleavage and cyclization both arise from a common 1,4-biradical intermediate. As realization of this process grew, other workers investigated a large variety of ketones that form different kinds of biradicals and cyclic alcohols. However, the biradicals formed by hydrogen abstraction from positions other than the γ-carbon cannot cleave the way a 1,4-biradical does. Although cleavage and cyclization of 1,4-biradicals are linked mechanistically, the cleavage process is so easy to measure that Norrish type II elimination has been widely studied to gain basic mechanistic information about biradicals and about hydrogen abstraction reactions of excited ketones. This chapter is devoted primarily to this unique cleavage process discovered by and properly named for Norrish. Other sections of this handbook are devoted specifically to cyclic alcohol formation initiated by β-, δ-, and more remote intramolecular hydrogen abstraction, a general process now named after its actual discoverers, Yang and Yang.

Before the concerted vs. two-step question was further elucidated, another basic mechanistic puzzle was raised. One group found that type II cleavage of 2-pentanone was quenched by biacetyl, which was known to quench excited triplets rapidly.[9] Another group found that the reaction of 2-hexanone was not quenched under the same conditions.[10] The two groups obviously differed as to which excited state undergoes the reaction. The apparent conflict was neatly solved by the revelation that each of the two ketones reacts from both states, with 2-hexanone undergoing more unquenchable singlet reaction than 2-pentanone.[11,12]

Before the mid-1960s, most studies were performed on aliphatic ketones. Wan and Pitts then showed that phenyl alkyl ketones also undergo the reaction.[13] Wagner and Hammond[14] then showed that the type II reaction of phenyl ketones is completely triplet derived and suggested that their low quantum yields are caused by disproportionation of Yang's 1,4-biradical intermediate back to ketone. Wagner et al.[15,16] soon discovered that adding Lewis bases markedly increases the quantum yields of triplet type II reactions, often to 100%. This behavior was attributed to suppression of biradical reversion to ketone by hydrogen bonding of the biradical's hydroxy group to the Lewis base; the H-bond must be broken during disproportionation but not during cleavage or cyclization. In 1972, Wagner et al.[17,18] succeeded in trapping the biradicals with mercaptans; they found that the quantum yield for racemization of (+)-4-methyl-1-phenyl-1-hexanone, which could be caused only by disproportionation of the 1,4-biradical, equaled 1 minus the quantum yield for type II products. In so equating racemization at the γ-carbon with what has been called "radiationless decay", they proved what had been thought to be physical decay of the excited state instead was chemical reversion of a biradical intermediate to ketone.[18] At the same time Yang and Elliot[19] showed that the triplet, but not the singlet, component of the photoreactivity of 5-methyl-2-heptanone also produces extensive racemization at the γ-carbon. All of this work firmly established the 1,4-biradical as an intermediate in the triplet reaction but left open how much it is involved

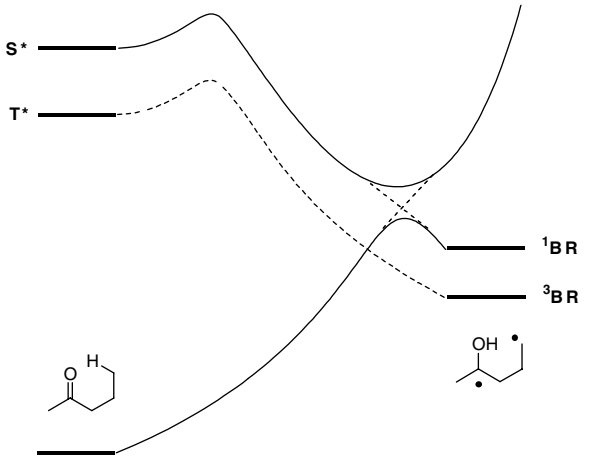

FIGURE 52.1 Potential energy diagram for excited-state hydrogen abstraction.

in the singlet reaction. Some unquenchable cyclization reactions indicated that singlet biradicals are indeed formed, even if they may not account for all the cleavage reaction.[20]

52.5 Quantum Efficiency

As the above description indicates, the Norrish type II reaction involves two consecutive intermediates: first an excited state (that can be singlet or triplet) and then a biradical. Consequently, it is necessary to understand how structure and environment affect the behavior of both species separately. The quantum efficiency for cleavage depends on how many competitive reactions *each* intermediate undergoes, as described by Eq. (52.1) (α is the percentage of singlet reaction that forms biradical; k_H is the rate constant for hydrogen abstraction; τ is the excited state lifetime, the reciprocal of the sum of the rates for all excited state decay processes; P_{II} is the percentage of triplet biradical that cleaves; and Φ_{ISC} is the percentage of excited singlet that crosses to triplet state).

$$\Phi_{II} = \alpha^1 k_H \tau_S + P_{II}\, \Phi_{ISC}{}^3 k_H \tau_T \qquad (52.1)$$

52.6 Excited State Reactivity

Nature of Excited State

Photoexcitation of carbonyls effectively breaks the double bond to form a 1,2-biradical, thus conferring on the more electronegative oxygen atom radical reactivity that closely parallels that of alkoxy radicals. Two multiplicities (singlet and triplet) and two electronic configurations (n,π^* and π,π^*) have been shown to display reactivity.

Singlet vs. Triplet

Aliphatic ketones have n,π^* lowest singlets that undergo intersystem crossing to their n,π^* lowest triplets with rates of $\sim 10^8$ s^{-1}, slow enough that some singlet reaction occurs. The reaction of a given ketone can be partitioned into its singlet or triplet components by the technique of differential quenching with conjugated dienes.[11] All triplet reactions can be quenched, and the singlet reaction is isolated by performing irradiations in dienes or substituted naphthalenes as solvent.[21] Figure 52.1 depicts the well known different potential energy surfaces followed by the two states.[3] The low quantum efficiency always observed for singlet reactions indicates that partial hydrogen abstraction promotes radiationless decay directly back to reactant at the point of a forbidden crossing or conical intersection between ground- and excited-state

TABLE 52.1 Excited-State Behavior of $CH_3COCH_2CH_2R$[1,24–26]

R	$\Phi^{S;II}$	Φ_{ISC}	$\Phi^{T;II}$	^1k_H (10^8 s^{-1})	^3k_H (10^8 s^{-1})
CH_3	0.025	0.81	>0.36	1.0	0.13
CH_3CH_2	0.10	0.37	0.37	8.8	1.0
$(CH_3)_2CH$	0.07	0.18	0.17	20	3.8

surfaces.[22] The characteristic near-zero yields of cyclobutanol from the singlet state, even in alcohol solvents, suggest that some of the singlet reaction may actually occur in a concerted fashion, but triplet reaction occurs exclusively via biradicals that both cleave and cyclize.

The first real-time study of Norrish type II reaction dynamics was reported recently by Zewail and co-workers[23] for a series of methyl alkyl ketones. Their excited singlet states undergo intramolecular hydrogen transfer in 70 to 90 fs to form biradical intermediates with 400- to 700-fs lifetimes. It is interesting to compare this gas-phase study with the data listed in Table 52.1 for the solution photochemistry of simple alkanones; singlet state rate constants for hydrogen abstraction are around 10^9 s^{-1}, values that reflect the equilibrium conformational distribution of the ketones.[1,25]

The rapid (>10^{10} s^{-1}) intersystem crossing in most phenyl ketones usually produces exclusive triplet reactivity. A few intramolecular hydrogen abstraction reactions of aryl ketones have been shown to involve excited singlets at least partially.[27–29] This pattern occurs when the n,π^* singlet reaction is fast enough to compete with intersystem crossing; exclusive singlet reaction can occur if triplet reaction is so slow as to be totally suppressed by trace quenchers or by a rapid competing reaction.

The n,π^* triplet excitation energies of aliphatic ketones have not been measured exactly but generally are considered to be ~78 kcal mol^{-1}; their n,π^* singlet excitation energies are some 10 kcal higher. As Table 52.1 indicates, excited singlets of alkanones undergo hydrogen abstraction some ten times faster than do their lower energy triplet states. For both states, abstraction of even primary hydrogens is exothermic; the higher reactivity of n,π^* singlets relative to triplets most likely reflects greater reaction exothermicity. Even though the triplet excitation energy of phenyl alkyl ketones is only ~72 kcal mol^{-1}; both alkanone and phenyl ketone triplets display similar rate constants for attack on a given type of CH bond;[1,30] benzylic stabilization of the developing hydroxy radical site compensates for the lower energy of the phenyl ketone triplet. The activation energy for triplet state hydrogen abstraction from an unactivated methylene group is only ~3.5 kcal mol^{-1}.[31,32]

Substituent Effects, Conjugative: n,π^* Vs. π,π^*

Aryl ketones can have either n,π^* or π,π^* lowest triplets; the former are far more reactive than the latter. It has been known for some 40 years that *para* electron-donating substituents reduce the hydrogen abstraction reactivity of triplet phenyl ketones by inverting their triplet energy levels such that π,π^* are lowest.[33] Ketones with π,π^* lowest triplets do undergo hydrogen abstraction reactions but display two quite different forms of triplet reactivity. In systems with π,π^* triplets, only a few kcal mol^{-1} below their n,π^* triplets, most of the measured reactivity arises from low concentrations of the n,π^* triplet in thermal equilibrium with the lower π,π^* triplet.[32,34] Equation (52.2) describes observed rate constants for hydrogen abstraction, with the n,π^* state providing most or all of the reactivity when ΔE ($E_{n,\pi} - E_{\pi,\pi}$) < 5 kcal mol^{-1}.

$$k_H^{obs} = \chi_{n,\pi} k_H^{n,\pi} + \chi_{\pi,\pi} k_H^{\pi,\pi} \tag{52.2}$$

$$\chi_{n,\pi} = (1 - \chi_{\pi,\pi}) = e^{-\Delta E/RT}/[1 + e^{-\Delta E/RT}] \tag{52.3}$$

where χ is the percent population of one state.

Table 52.2 compares the effects of ring substituents on rate constants for triplet-state hydrogen abstraction by valerophenone, together with intrinsic $k_{n,\pi}$ values that reflect independently measured substituent effects on rate constants for bimolecular hydrogen abstraction ($\rho = 0.5$)[35] and derived values for the

TABLE 52.2 Rate Constants for Triplet γ-Hydrogen Abstraction by Ring Substituted Valerophenones in Benzene

Substituent	s	k_{obs} (10^7 s^{-1})	n,π^* (%)	k_{n,π^*} (10^7 s^{-1})
m-(NH^+)	—	200	>99	200
p-(NH^+)	—	330	>99	330
o-(N)	—	19	>99	19
m-(N)	—	31	>99	31
p-(N)	—	68	>99	68
H	0	13	99	13
p-OCF_3	0.28	13	95	14
o-CF_3	—	13	>99	13
m-CF_3	0.43	32	>99	32
p-CF_3	0.54	28	>99	28
o-alkyl	—	3.0	25	12
m-alkyl	–0.07	3.9	35	12
p-alkyl	–0.17	1.8	18	10
o-OMe	—	0.30	3	10
m-OMe	0.12	0.02	0.15	15
p-OMe	–0.27	0.06	1	6
p-OAc	0.31	4.4	25	18
o-F	—	14	99	14
m-F	0.34	18	99	18
p-F	0.06	15	99	15
o-Cl	—	3.5	?	—
m-Cl	0.37	16	99	20
p-Cl	0.23	3.0	16	18
o-CO_2Me	—	3.6	?	—
m-CO_2Me	0.37	28	99	28
p-CO_2Me	0.45	12	40	30
o-CN	—	23	99	23
m-CN	0.56	30	99	30
p-CN	0.66	6.8	21	32
m-COR	0.38	14	50	28
p-COR	0.50	2.7	9	30
p-SMe	0	<0.001	<0.01	14
p-SCF_3	0.64	3.0	10	32

Source: Adapted from Wagner and Park.[5]

percentage of n,π^* triplets in equilibrium with π,π^* triplets. The energy gaps between the two triplets are derived from the experimentally measured increases in activation energies for reaction produced by a substituent that causes the π,π^* triplet to be lowest, namely electron donors and conjugative electron-withdrawing groups.[32,36] Only very strong electron donors produce a large enough energy gap that reactivity becomes imperceptible.

The second type of π,π^* reactivity occurs in polynuclear aryl ketones with large $E_{n,\pi} - E_{\pi,\pi}$ values. It is often assumed incorrectly that π,π^* triplets are totally unreactive in hydrogen abstraction. This notion is contradicted by the observed triplet reactivity of some naphthyl ketones, which is only 0.01 to 0.001% that of an n,π^* triplet.[37,38] The original explanation for this large difference still seems reasonable; namely, the distinct spin localization in an n,π^* triplet as opposed to the delocalized spin in a π,π^* triplet.[37] This fact is usually depicted in terms of the n,π^* triplet resembling a 1,2-diradical[39] and thus manifesting the chemical reactivity of an alkoxy radical,[1,40] while the π,π^* triplets have little spin density on oxygen. Despite the intrinsic, if greatly diminished, reactivity of acylnaphthalene triplets, most reported type II cleavages of naphthyl ketones are very low quantum yield reactions from an unquenchable singlet.[27,28]

Substituent Effects: Inductive

As Table 52.2 shows, inductively electron-withdrawing ring substituents (F, CF_3, and N) enhance the reactivity of n,π^* triplets, magnifying the electron deficiency of the carbonyl oxygen. Cyano and carbonyl substituents *ortho* or *meta* have the same type of inductive effect as they are not conjugated to the benzoyl carbonyl in the triplet state. Substituents on the α-carbon of ketones influence excited-state reactivity, although no extensive study has been done. In particular, electron-withdrawing groups seem to increase reactivity. For example, α-fluorination markedly enhances n,π^* reactivity; however, it also promotes a π,π^* lowest triplet.[41] α-Ketohexanoic acid shows enhanced reactivity compared to 2-hexanone.[42] α-Alkoxy ketones also show unusually high reactivity,[43] although much of the increase is due to conformational and bond energy effects, as discussed below.

Solvent Effects

For ketones with n,π^* lowest triplets, there do not appear to be any significant solvent effects on k_H values. However, when the π,π^* triplet is of lower or comparable energy, polar solvents reduce overall reactivity by lowering the excitation energy of the π,π^* triplet and raising that of the n,π^* triplet, thus decreasing $\chi_{n,\pi}$ values.[34] In the case of *p*-methoxyphenyl ketones, quantum yields plummet in methanol.

Zepp and co-workers[44] investigated the photochemistry of valerophenone in aqueous solutions as a function of temperature, pH and wavelength. The results indicated that the rate constant for hydrogen abstraction is significantly lowered in aqueous media due to stabilization of the π,π^* excited state. The study also indicated constant high quantum yields for the photoreactions over the pH range of 9 to 2, but a significant decrease below pH = 2. This decrease was attributed to quenching of the triplet reactivity via protonation of the excited triplet state, behavior previously noted for other ketone reactions.

Nature of Hydrogen Atom

γ–CH Bond Energy Effects

Table 52.3 lists measured rate constants for triplet-state γ-hydrogen abstraction by γ-substituted butyrophenones.[5,45] The relative values should hold for any type of hydrogen abstraction by n,π^* triplets. The 1:30:200 primary/secondary/tertiary per-bond ratio is characteristic of electron-deficient species such as alkoxy radicals. γ-Substituents affect both the bond energies and the electron density of the CH bonds, each of which affects k_H values. The fourth column of Table 52.3 extracts a resonance factor by which conjugation of the γ-substituent with the developing γ-radical site enhances the rate constant. Thus, the positive conjugative effect of a cyano group counteracts its negative inductive effect. This factor was obtained by correcting the observed substituent effect on k_H for inductive deactivation, with a ρ_I value of –4.3 extrapolated from that for δ-substituents (see next section). These results are one example of how the type II reaction can be used to provide information about radical reactions. The table also includes the quantum yields for acetophenone formation, which will be discussed later, as they are determined mainly by biradical behavior and sometimes by excited state behavior. The important fact is that there is very little correlation between quantum efficiency and rate constants for γ-hydrogen abstraction.

Inductive Effects

Table 52.4 lists measured rate constants for triplet state γ-hydrogen abstraction by δ-substituted valerophenones.[5,45] Here, the substituents are not conjugated with the developing γ-radical site so their effects are entirely inductive. They indicate a ρ_I value of –1.85, which demonstrates the highly electron-deficient nature of the carbonyl n,π^* state. It should be noted that I, Br, and RSO substituents enhance reactivity by what has been suggested to be anchimeric assistance.[46]

Geometric Effects

For a bifunctional reaction to occur, two geometric factors must be optimized: the distance between the two reacting groups and their orientation with respect to each other. In the case of hydrogen abstraction,

TABLE 52.3 Rate Constants in Benzene for Triplet γ-Hydrogen Abstraction by γ-Substituted Butyrophenones

γ-Substituent	Φ_{II}	σ_I	k_{obs} (10^7 s^{-1})	Resonance Factor
H	0.35	0.0	0.7	—
Alkyl	0.33	–0.05	14–20	1.0
Dimethyl	0.25	–0.10	50	2.0
Phenyl	0.50	0.10	40	8.4
Vinyl	0.26	0.09	50	8.8
RS	0.27	0.23	64	54
PhS	0.32	0.30	45	60
RSO	0.03	0.52	1.2	13
R_2N	0.025	0.06	80	8
CH_3O	0.23	0.30	62	100
HO	0.31	0.25	40	40
PhO	0.32	0.38	22	60
OC(=O)Me	0.48	0.39	1.2	5
C(=O)OMe	0.50	0.30	1.0	1.6
Chloro	0.11	0.47	1.0	8
N_3	0.006	0.44	0.5	4
Fluoro	0.41	0.52	0.8	10
CN	0.32	0.59	0.4	11
RSO_2	0.20	0.60	0.04	1
NHR_2^+	0.009[a]	0.80	0.01	1
NR_3^+	0.001[a]	0.90	0.001	1

[a] In methanol.
Source: Adapted from Wagner and Park.[5]

the distance between the carbonyl and the CH group and the orientation of the C=O and CH bonds determine reactivity. Whereas in a bimolecular reaction the reactive functional groups of the two molecules are free to rotate into all possible relative orientations and diffuse to van der Waals contact distance, in an intramolecular reaction intervening bonds and structure limit the orientations and proximity available to two separate functional groups. The resulting conformational equilibria and kinetics affect rate constants for hydrogen abstraction and thus determine both rates and regioselectivity. Because these factors affect all intramolecular hydrogen abstractions, their general features are presented fully in Chapter 58, which covers all forms of intramolecular hydrogen abstraction by excited ketones. Only those features unique to or famously clarified by γ-hydrogen abstraction are presented here.

For some time there has been a simplistic belief that the hydrogen atom, being abstracted, should be restricted to lie along the long axis of the carbonyl *n*-orbital. This notion recognizes the directionality of *p* orbitals and the fact that n,π^* radical reactivity is centered on this particular *p* (or sp^2) orbital. However, many examples are known in which efficient hydrogen abstraction takes place, with the developing HO bond making a fairly large angle with respect to the nodal plane of the carbonyl π system.[47–50] It has been pointed out that such reactivity probably demonstrates a $\cos^2$ dependence on this angle,[3] that being the electron density function for a *p* orbital.

Scheffer[51,52] has studied a variety of ketones that undergo γ-hydrogen abstraction in their crystalline states. In analyzing their reactivity, he considered the *ground-state* parameters depicted in Scheme 1, where d is the distance between O and H; θ is the O–H–C angle; Δ is the C=O–H angle; and ω is the dihedral angle that the O–H vector makes with respect to the nodal plane of the carbonyl π system. Such a comparison of triplet reactivity with ground-state geometries is valid because n,π^* excitation is known to be so highly localized on the carbonyl group that geometric changes in the rest of the molecule are negligible, with only a slight lengthening of the carbonyl bonds:[53]

TABLE 52.4 Rate Constants in Benzene for Triplet γ-Hydrogen Abstraction by δ-Substituted Valerophenones

δ-Substituent	σ_I	k_{obs} (10^7 s^{-1})
H	0.0	14
Alkyl	–0.05	18
R_2N	0.06	7.0
Phenyl	0.10	8.4
RS	0.23	4.8
PhS	0.30	4.7
CH_3O	0.30	2.6
C(=O)OMe	0.30	3.8
COOH	0.33	2.6
PhO	0.38	2.1
I	0.39	17
Br	0.44	5.6
Cl	0.47	2.2
CH_2Cl	0.20	5.6
N_3	0.44	1.8
RSO	0.52	12
CN	0.56	1.0
CH_2CN	0.24	4.5
CH_2CH_2CN	0.10	8.0
RSO_2	0.60	1.2
SCN	—	1.4
NHR_2^+	0.80	0.50

Source: Adapted from Wagner and Park[5] and Wagner and Kemppainen.[45]

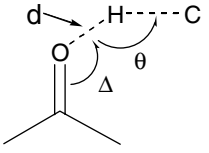

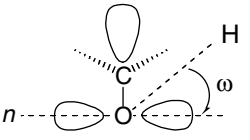

ideal:	Δ = 90-120¡	θ = 180¡	ω = 0¡	d † 2.7
actual:	Δ = 73-110¡	θ = 85-120¡	ω = 20-70¡	d < 3.1

SCHEME 1

Ideal:

$$\Delta = 90–120^\circ,\ \theta = 180^\circ,\ \omega = 0^\circ,\ d \sum 2.7\ \text{Å}$$

Actual:

$$\Delta = 73–110^\circ,\ \theta = 85–120^\circ,\ \omega = 20–70^\circ,\ d < 3.1\ \text{Å}$$

Actually observed values for over two dozen examples in which x-ray crystal structures were obtained for reactive ketones are summarized in the scheme, together with the theoretically ideal values.[54,55] The

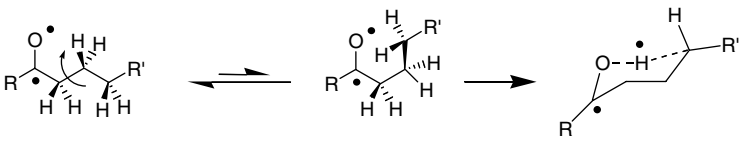

SCHEME 2

most important parameter appears to be d, because whenever two hydrogens at different distances <3.1 Å are available, the closer one is abstracted. Whenever a hydrogen is positioned this close to the carbonyl in the ground state, minimal molecular motion is required for reaction, and minimal motion is all that most crystal lattices allow. The value of θ obviously can vary greatly from the linear arrangement thought to be preferable. Likewise, the value of ω can depart significantly from the "ideal" 0°. Both of these deviations from ideality have long been known from the reactivity of many steroidal ketones.[3,41]

Several experimental observations have suggested zero reactivity when ω = 90°.[56–58] All of these involved rigid polycyclic ketones or crystalline media where the reactants are constrained to maintain their ground-state geometry. This lack of conformational mobility maximizes the possibility that a biradical formed by either α-cleavage or hydrogen abstraction might revert to starting ketone with 100% efficiency and thus present the false impression that hydrogen abstraction did not occur.

Conformational Effects

As discussed in Chapter 58, rate constants for intramolecular hydrogen abstraction reflect conformational effects.[3,59] We assume that interconversion among the various conformers of a given excited state competes with reaction and decay. One or more conformations may have geometries close to that required for reaction and are dubbed *favorable* or *reactive*. Also, *unreactive* geometries are usually observed in which the two functional groups are too far apart for reaction; these must be able to rotate into reactive conformations if they are to react rather than decay to ground state. Molecules that react as solids must have lowest energy conformations that are reactive. Most acyclic ketones exist preferentially in unreactive conformations, such that they may not react in the solid state. The lowest energy conformations of cyclic systems may have either reactive or unreactive geometries.

As Chapter 58 explains, excited states display three types of conformational dynamics. The Norrish type II reaction can be subject to any of these different dynamic boundary conditions.[59] The first dramatic example of ground-state control of triplet reactivity, in which conformational interconversion is slower than reaction of the initial excited-state conformation, was provided by Lewis' study of the Norrish type II reaction of benzoylcyclohexanes.[60] Photoenolization of *ortho*-alkyl ketones was the first reaction recognized to show rotational control of triplet reactivity[61] in which an irreversible bond rotation produces a reactive conformer of the excited state. Conformational equilibrium, in which bond rotations are faster than excited-state decay, is much more common; an early example is the type II reaction of benzoylcyclobutanes.[62]

Normally, the largest α-substituent eclipses the carbonyl group in ketones, with the lowest energy conformation being fully *anti* staggered and unreactive. The α,β–CC bond must become *gauche* for γ-hydrogen abstraction to occur. Extra β-substituents increase the fraction of reactive *gauche* conformers.[47] Because several *gauche* conformers are present, their combined population usually surpasses that of the *anti* conformer such that reaction is quite rapid (Scheme 2); moreover, the energy differences among the conformers are small enough that interconversion is rapid.

When the carbonyl and CH bond are part of a ring or substituents on a ring, the conformational limitations of the ring may either increase or decrease the population of favorable conformations. Lewis demonstrated how incorporation of rings between the carbonyl and the γ-carbon can increase rate constants for γ-hydrogen abstraction.[63] Scheme 3 shows some ketones in which the activation energy for abstraction of a secondary hydrogen remains the 3.5 kcal mol^{-1} that it is required for bimolecular reaction,[32,36] but the entropy of activation becomes less negative as rings freeze intervening CC bond rotations. Each such frozen rotation increases the rate constant by a factor of ~8, which corresponds to

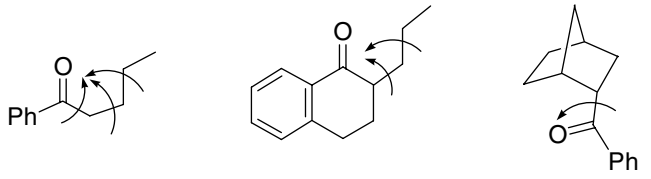

SCHEME 3

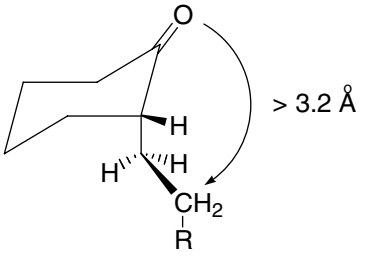

SCHEME 4

4 eu. In all three cases, the major conformation is either a reactive one or of comparable energy, and the rings limit the number of unreactive conformers.

In general, however, *no constant factor exists by which rings change intramolecular reactivity.* They may decrease the population of a reactive conformation, as Alexander and Uliana showed for benzoylcyclobutane;[62] limit reaction to one site, as the selective δ-hydrogen abstractions in Paquette's synthesis of dodecahedrane exemplified;[64] or prevent population of a reactive conformer, as Turro and Weiss reported for cyclohexanones with axial α-alkyl groups (Scheme 4).[65]

Regioselectivity

Acyclic Systems

The predominance of γ-hydrogen abstraction by excited straight-chain ketones is so pronounced that for years it was thought that no ketone containing γ-hydrogens would react at any other position. A few notable exceptions were eventually found; δ-methoxyvalerophenone[66] and γ-benzoylbutyraldehyde[67] undergo both γ- and δ-hydrogen abstraction with comparable rate constants because both possess a highly reactive δ–CH bond and an inductively deactivated γ–CH bond. From these results, it was deduced that the intrinsic γ/δ selectivity in triplet ketones is 20:1.[47] No reaction occurs at any other position.

Houk has published several theoretical studies of intramolecular hydrogen transfer, including one that accurately reproduces the preference for 1,5- vs. 1,6-hydrogen transfers in triplet ketones.[55] Much of the preference is entropic, as expected, but little enthalpy difference exists between the two modes. A chair-like transition state was originally suggested for γ-hydrogen transfers.[47] The calculations predict a strong preference for a linear C–H–O arrangement (θ = 180°), which is more easily accommodated in a seven-atom transition state than in a six-atom one. Thus, relative enthalpies of activation reflect both ring size strain and orbital orientation in the transition state. It must be reiterated that actual ketones react even when θ approaches 90° in the ground state and may adopt a chair-like transition state.

In summary, ketones react preferentially with γ–CH bonds. Reducing their reactivity can allow more remote hydrogen abstractions to compete, but the only way to eliminate γ-hydrogen abstraction is to eliminate γ-hydrogens. This constraint does not apply to similar hydrogen abstraction reactions of thioketones and *N*-alkylimides.[5]

Cyclic Systems

The interposition of even one ring between the carbonyl and any γ–CH bonds imposes conformational restrictions that limit the molecular geometries possible. Consequently, regioselectivity becomes dominated by frozen rotations such that only certain CH bonds are close enough to the carbonyl to react. Such structures can enhance or suppress the reactivity of γ–CH bonds and also enhance the reactivity of more remote sites.

Charge Transfer Followed by Proton Transfer

Bimolecular photoreduction of ketones by good electron donors often proceeds by either electron transfer or charge transfer complexation followed by a proton transfer. Intramolecular hydrogen transfers do not seem to follow this pathway as often. There is good evidence from the behavior of aminoketones that tight overlap of the donor lone pair with the half-empty *n* orbital is necessary for triplet CT reaction. Rate constants for internal quenching in ω-dimethylaminoalkyl phenyl ketones are maximum for β- and γ-amino ketones, in which five- or six-atom rings can be formed by overlap of the nitrogen lone pair with the half-occupied carbonyl *n* orbital.[68] Interestingly, triplet α-dialkylaminoacetophenones do *not* undergo rapid internal charge transfer; they do, however, undergo normal γ-hydrogen abstraction.[29,68] The rapid internal charge transfer in triplet γ-dialkylaminobutyrophenones does not lead to efficient product formation;[68,69] the required orbital overlap seems to enforce a restricted orientation in the exciplex that prevents proton transfer to oxygen such that CT becomes a purely competitive quenching process.

Competing Excited-State Reactions

Bimolecular hydrogen abstraction from solvent rarely competes with the rapid intramolecular process except in solvents with the most labile CH bonds and for the few ketones whose γ–CH bonds are relatively unreactive. Norrish type I α-cleavage is very competitive in the case of triplet α-alkylcycloalkanones, although the relative slowness of excited singlet state α-cleavage provides the opportunity for high chemical yields of singlet state type II cleavage in the presence of triplet quenchers. Occasionally δ-hydrogen abstraction can compete with γ-hydrogen abstraction to yield some cyclopentanols along with the normal type II products, but only in cases where the δ–CH bond is highly reactive and the γ–CH bond is relatively unreactive or when conformational rigidity inhibits proximity of the C=O and γ–CH groups.[47] A trio of such cases was mentioned above.

52.7 Biradical Behavior

Direct Spectroscopic Study of Biradicals

In 1977, Scaiano and Small[70] reported the first flash spectroscopic detection of a triplet 1,4-biradical intermediate produced from γ-methylvalerophenone. They rapidly developed two independent methods to monitor triplet-generated hydroxy-biradicals: (1) direct detection of their transient absorption, or (2) indirect detection by following the growth of the strongly absorbing paraquat radical-cation, which is produced when added paraquat oxidizes the hydroxy radical site.[71,72] Scaiano has thoroughly summarized several basic features of triplet 1,4-biradical lifetimes.[73] They are not very sensitive to substitution on the benzene ring or to steric features at the γ-carbon of the ketone, but they are increased by conjugating substituents such as γ-phenyls.[74] They are lengthened approximately threefold in Lewis-base solvents, having values in the 25- to 50-ns range in hydrocarbons and from 75 to 160 ns in alcohols.[75] They are almost independent of temperature, having activation energies for decay of 0 to 1 kcal mol^{-1}.[71] They are shortened by bimolecular interaction with paramagnetic species such as oxygen[76,77] and nitroxide radicals.[78] The most significant structurally induced change is produced by the internal oxygen atom in the biradicals formed from α-alkoxyacetophenones, which have maximum lifetimes of only a few nanoseconds.[71]

As described above, Zewail recently has reported lifetimes of 400 to 700 fs for the singlet 1,4-biradicals formed from n,π^* singlet alkanones in the gas phase.[23] DFT calculations indicated that although both

cyclization and fragmentation are essentially barrierless, cleavage of the biradical is the dominant reaction channel as a consequence of entropy effects, as conformational requirements for ring closure are more demanding than they are for fragmentation. The measured biradical decay times decreased with increasing numbers of alkyl substituents on the γ-carbon atom. Such behavior reflects relative product energies and thus suggests at least small enthalpic barriers. It also must be noted that the biradical is formed in a geometry better suited for cyclization than for cleavage. It is important to recall that almost no singlet-state cyclization occurs in solution, as the computations would predict.

Multiplicity

Overwhelming evidence has been found for the intermediacy of triplet 1,4-biradicals following internal hydrogen abstraction by triplet ketones, especially phenyl ketones. Some unquenchable cyclization reactions strongly suggest that singlet biradicals can indeed be formed; unfortunately, they appear to be too short lived to be detected by trapping or by nanosecond spectroscopy. This evanescent character of singlet biradicals helped generate one popular view of how triplet biradicals proceed to singlet products.

Based on his study of some 1,4-biradicals formed by γ-hydrogen abstraction in triplet phenyl ketones, Scaiano[79] postulated that biradical lifetimes are determined by rates of intersystem crossing (ISC) to the corresponding singlet biradicals. Moreover, he further suggested that product ratios reflect relative ISC rates for different conformations of the triplet biradicals, the singlet biradical being too short lived to convert into any other product-forming conformation.[79] Scaiano also has provided several dramatic illustrations of how paramagnetic species change the partitioning of 1,4-biradicals, presumably by inducing ISC in conformations that normally decay relatively slowly.

More recently, other workers have suggested an alternative view. From magnetic resonance studies of biradicals, Closs[80] suggested that triplet biradicals cyclize whenever their two ends collide, but with a low probability that reflects the amount of singlet character mixed into the biradical by spin-orbit coupling. Michl[81] has suggested a comparable picture, purely from a theoretical viewpoint, with the added feature that incipient bonding of the two ends of the biradical induces additional spin-orbit coupling through a highly stabilizing covalent interaction. As is discussed in Chapter 58, solvent effects on biradical lifetimes and product quantum yields agree with the notion that ISC and product formation are coupled.

Morita and Kato[82] theoretically examined the intersystem crossing mechanism of a Norrish type II 1,4-biradical in solution. Their calculations revealed that the energy splitting and the spin-orbit coupling element between the singlet and triplet states vary with the molecular geometry and have no apparent correlation to the distance between the radical termini, indicating that a through-bond interaction is dominant.

One thing that is clear is that cleavage of the triplet biradical is not adiabatic. Both Caldwell and Wagner[83] independently showed that only ground-state enes are formed in the type II cleavage of β,γ-diphenylbutyrophenone (Scheme 5). The α-hydroxystyrene (enol) and stilbene products have triplet energies lower than those of the ketone and the biradical, with stilbenes being the lowest. Thus, formation of triplet stilbene would have been preferred over triplet enol and would have yielded a nearly 50:50 mixture of *cis* and *trans* isomers, but the product was almost entirely *trans*, as expected from the thermodynamically preferable biradical conformation, with the β and γ phenyls *anti* to each other.

Biradical Disproportionation Back to Ketone

It cannot be overemphasized that the quantum yields for two-step triplet reactions such as those initiated by hydrogen abstraction often reflect partitioning of the intermediate biradicals more than relative rate constants for triplet reaction. This is especially true for the very rapid intramolecular hydrogen abstractions of n,π^* triplets, such as recorded in Tables 52.1 and 52.3. This fact was first demonstrated by the behavior of 2-hexanone, in which γ-deuteration *increases* the quantum yield of type II cleavage[84] and of γ-substituted butyrophenones, in which quantum yields for some type II cleavages decrease as rate constants for γ-hydrogen abstraction increase, as shown in Table 52.3.[85]

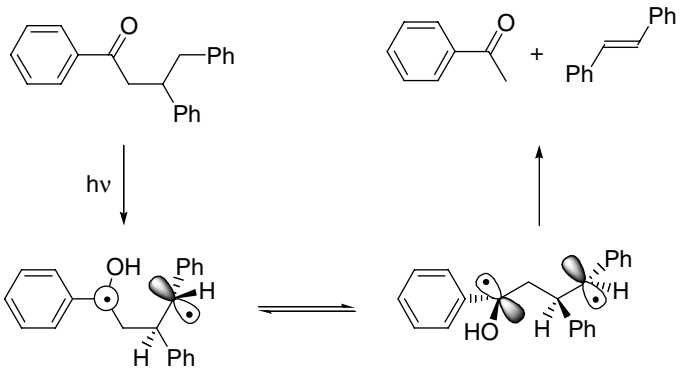

SCHEME 5

It is generally true that almost all the hydroxybiradicals formed by internal hydrogen abstraction partially revert to starting ketone by an internal radical disproportionation reaction in which the carbon-centered radical site abstracts the hydrogen from the hydroxyl group. This process often is the major reaction of the intermediate biradical, so that the overall quantum yield of product formation is low even when hydrogen abstraction by the excited state is 100% efficient. Should the efficiency of hydrogen abstraction be low because of electronic or conformational problems, then biradical disproportionation lowers quantum efficiency even further.

Added Lewis bases inhibit disproportionation back to ketone and thus enhance quantum yields of product formation.[15,16] In many cases, reversion to ketone is totally suppressed and quantum yields approach unity, as discussed above. This phenomenon is attributed to hydrogen bonding by the relatively acidic OH group of the biradical[86] to the Lewis base. Disproportionation requires destruction of this hydrogen bond, whereas, cleavage and cyclization of the biradical do not. The ability of different additives to solvate the biradicals, as determined by the concentration needed to maximize product quantum yields, closely matches their basicities.[16] Alcohols, water, ethers, and pyridines are commonly used for this purpose, but all Lewis bases that are not also strong electron donors work to some extent. Not every ketone reacts with 100% efficiency even in the presence of strong Lewis acids. The equilibrium between solvated and unsolvated biradical obviously varies with biradical structure. Sometimes only a fraction of the biradical is solvated; the rest still reverts to ketone.

Can a biradical undergo only disproportionation so that no product is formed no matter how fast the excited state reacts? A recent example is provided by the behavior of 1,6-cyclodecadione, which is discussed in Chapter 58. In general, cyclic and polycyclic systems with little conformational freedom, such that the two radical sites might not be able to get away from each other, seem the most likely to have this problem.

The only real difference between the reversion to ketone that occurs in both singlet and triplet hydrogen abstractions is the slowness of T-to-S ISC, such that the triplet forms a detectable biradical intermediate. In the singlet process, the molecule can slip onto the pathway for reversion to ground-state ketone directly. This singlet state decay is not suppressed by added Lewis bases,[19,24–26] further evidence that it can proceed without first forming a transient intermediate.

Factors Affecting Biradical Cleavage Efficiency

The cleavage efficiency of triplet-generated 1,4-biradicals varies widely with structure. Fortunately, the short lifetime of these 1,4-biradicals prevents several forms of disproportionation that 1,5-biradicals undergo.[4] Several factors affect the partitioning among cleavage, cyclization, and reversion to starting ketones.[87,88] Four geometries of the 1,4-biradical must be considered: two stretched-out staggered conformations and two coiled *gauche* conformations. Cleavage can occur from either *gauche* or staggered conformations, whereas cyclization and disproportionation require the latter.

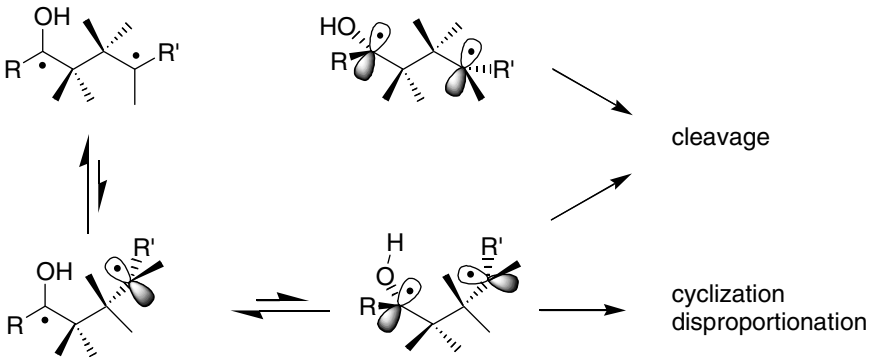

SCHEME 6

TABLE 52.5 Representative Biradical Partitioning Ratios in Benzene

Ketone	Φ_{elim}	Φ_{cycl}	Φ_{disp}	τ (ns)
$PhCOCH_2CH_2CH_2CH_2$	0.33	0.10	0.57	30
$PhCOCH_2CH_2CH_2Ph$	0.47	0.05	0.48	100
$PhCOCH_2OCH_2CH_2$	0.57	0.42	0.01	~2
$PhCOCF_2CH_2CH_2CH_2$	<0.01	0.60	0.40	60
$PhCOCMe_2CH_2CH_2CH_3$	0.04	0.10	0.86	50
PhCO-*c*-C_4H_7	0.01	0.03	0.96	?

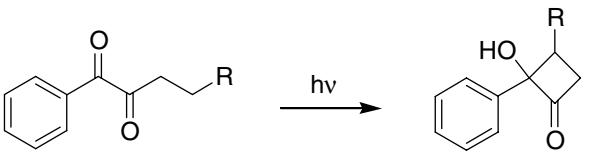

SCHEME 7

Cleavage appears to be governed by the stereoelectronic necessity for overlap of the breaking bond with both half-occupied *p* orbitals (Scheme 6).[85,89] Anything that prevents such molecular alignment retards or suppresses cleavage. In straight-chain ketones, cleavage/cyclization ratios tend to be at least 5:1. However, α-substitution by alkyl groups,[90] fluorines,[91] or rings[92] increases cyclization, primarily by destabilizing the geometry required for cleavage. α–Alkoxy ketones cyclize as much as they cleave;[43] in this case cleavage is not retarded so much as cyclization is enhanced, presumably by the oxygen relieving ring strain.

A distinction is often made between coiled and stretched conformations in order to rationalize cyclization/cleavage ratios. However, disproportionation also requires a coiled conformation; it is not at all clear what affects the competition between cyclization and disproportionation, other than that hydrogen bonding to Lewis bases dramatically inhibits the latter and changes the stereoselectivity of the former. Table 52.5 provides examples of the wide variations among cyclization/disproportionation ratios. Upon irradiation in water, valerophenone undergoes both cleavage and cyclization reactions in quantum yields of 65 and 32%, respectively,[44] which compare to the 33 and 10% yields in hydrocarbon solvents. Cases have been reported in which either cleavage or cyclization is the sole reaction of these 1,4-biradicals, apart from reversion to starting ketone. α-Diketones undergo photocyclization to hydroxycyclobutanones without undergoing any cleavage (Scheme 7).[93,94]

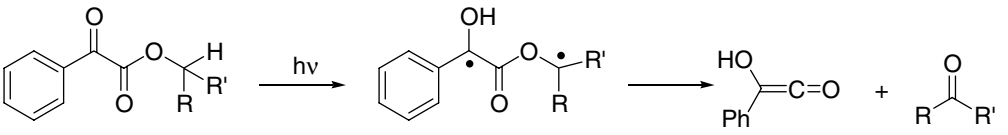

SCHEME 8

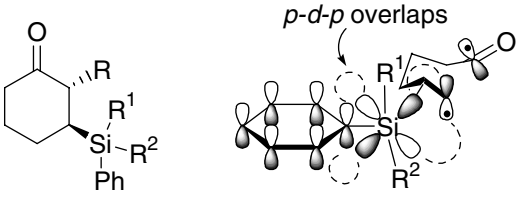

SCHEME 9

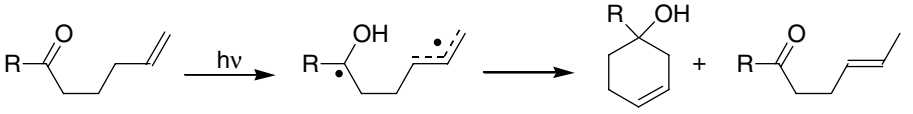

SCHEME 10

The opposite behavior is evident in the Norrish type II photochemistry of arylglyoxylates that Neckers and co-workers have studied (Scheme 8).[95–102] The 1,4-biradical intermediate resulting from triplet-state γ-hydrogen abstraction undergoes, exclusively, the cleavage reaction; no cyclization is observed. The Norrish type II reaction, accompanying a more efficient CO bond cleavage, has been studied also on mixed anhydrides.[103]

Pincock and co-workers have examined the Norrish type II fragmentation of various aromatic esters.[104–106] In contrast to alkyl aryl ketones, esters with lowest π,π* triplets undergo the reaction with a low quantum efficiency, which is induced by intramolecular electron transfer.

Hwu and co-workers[107] reported that the Norrish type I cleavage overwhelms the type II cleavage in the photolysis of α-alkylcycloalkanones bearing a substituted silyl group at the β-position and that the quantum yields are often greater than those of the non-silylated cycloalkanones.[107] The authors reasoned that a silyl group can stabilize a β-carboradical through a *p–d* homoconjugation in the course of the α-cleavage reactions (Scheme 9).

Competing Biradical Reactions

Apart from cyclization to cyclobutanols, type II 1,4-biradicals have been known to undergo radical cleavage from the α and δ carbons, the latter being discussed more fully later. When a vinyl group is attached to the γ-carbon, an allylic rearrangement occurs, producing a 1,6-biradical that can cyclize to a cyclohexenol and disproportionate to a 5-acyl-2-hexene as well as form normal type II products (Scheme 10).

Environmental Effects

Both the rate constants for competing triplet reactions and the partitioning of biradical intermediates may be affected by the environment. The major effects on triplet reactivity involve conformational changes induced by highly ordered media[108] and decreases in the efficiency of radical α-cleavage. The major effects on biradicals involve conformational restrictions that impede or promote coiling and solvation that inhibits disproportionation back to ketone.

Several research groups found high quantum yields and product ratios that suggest a fairly polar environment for ketones irradiated in aqueous surfactant solution.[109] It is now well accepted that the polar end of the ketones and particularly the biradicals reside mostly near the micelle–solvent interface, called the Stern layer, which has Lewis-base character. Although micelles produce negligible effects on triplet rate constants, they can improve type II/type I ratios by their "supercage" effect that enhances the recoupling of radical pairs.[110] That rate constants are not greatly affected reveals that the inside of micelles is flexible enough to allow the alkyl chain of ketones to coil.

The benzoin ethers were a mechanistic puzzle for years, as they were first reported to undergo only α-cleavage to radicals and *no* type II reaction in solution,[111] despite the high rate constants for γ-hydrogen abstraction in simple α-alkoxy ketones.[43] The use of methanol as solvent provides 5 to 10% type II reaction. Cyclization and type II elimination also occur when benzoin ethers, dissolved in micelles[112] or adsorbed on silica, are irradiated.[113] Irradiation of solid complexes of three common benzoin ethers with β-cyclodextrin produces 90% type II reaction.[114] All the "organized" media apparently force the ketone into a more reactive geometry than obtains in solution and, just as important, decrease translational mobility, thus making type I cleavage mostly revertible. Other examples have been observed of ketones that undergo mainly type I cleavage in solution but mostly or entirely type II reaction when complexed with β-cyclodextrin.[115] These high product selectivities are achieved only when the solid complex is irradiated. Aqueous solutions of ketone and cyclodextrin give more type II reaction than occurs in benzene but radical cleavage still competes strongly.

Turro and Wan[116] have looked at the effects of several zeolites on the photochemistry of α,α-dimethylvalerophenone, which undergoes competitive type I and type II reaction in solution.[117] Depending on the cavity size of the zeolite, product ratios vary substantially. Observation of mainly type I cleavage was interpreted as indicating cavities too small to allow the conformational changes required for type II reaction.

Weiss has explored the effects of liquid crystals on the type II reaction.[118] Their effects on short ketones are variable, whereas their effects on long ketones can be dramatic. His study of various *p*-alkylalkanophenones in *n*-butyl stearate reveals key aspects of how guest molecules orient themselves in liquid crystals. In short, when the carbonyl group is in the middle of the ketone molecule, very little γ-hydrogen abstraction occurs, apparently because most of the carbonyls are in the middle of a liquid crystal network and the alkyl chains are fully stretched alongside the stearate molecules. What little reaction does occur arises from random misaligned ketones. When the carbonyl group is at one end of the ketone, much more hydrogen abstraction occurs, presumably because of less rigidity in the stearate framework. Whenever the γ-radical site is part of a long alkyl group that is held in a stretched geometry, α-cleavage dominates cyclization.

Similar results have been found for crystalline *n*-alkanones that exist as layers of fully stretched molecules aligned in parallel. In the case of symmetric alkanones with the carbonyl in the middle, very little type II reaction occurs because the γ-hydrogens are constrained to remain too far from the carbonyl oxygen to be attacked.[119] However, 2-alkanones do undergo type II cleavage efficiently, as the carbonyl groups are now at a nonrigid layer interface.[120]

Whitten and co-workers[121] studied a ketone that is also a surfactant, ω-(*p*-toluyl)pentadecanoic acid. When prepared as a monolayer film in arachidic acid, this ketone undergoes only a trace of type II reaction. In benzene, it cleaves to *p*-methylacetophenone with a normal $\Phi = 0.20$; in an aqueous SDS solution, $\Phi = 0.80$. The enhanced quantum efficiency in the micelle was discussed above; it is interesting that the molecule must be looped so that both carbonyls are in the Stern layer. The lack of γ-hydrogen abstraction in the monolayer is ascribed to the linear rigidity of the monolayer environment. The monolayer would appear to allow even less molecular flexibility than does the liquid crystal.

The photochemistry of polymers containing keto groups has been studied extensively and reviewed by Guillet.[122,123] The type II reaction has been of particular interest inasmuch as it is partially responsible for the photodegradation of polymers. In this regard, temperature effects on the quantum efficiency for cleavage of ethylene-CO copolymers have been associated with glass transitions that reduce conformational mobility and the eventual freezing out of key rotations.[124] At temperatures above the glass transition,

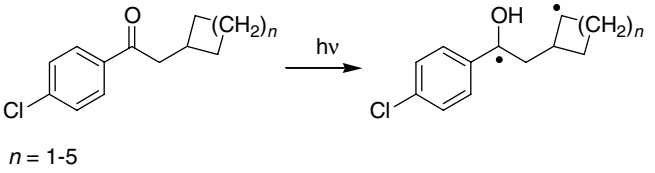

SCHEME 11

TABLE 52.6

Ring Size	d (Å)	ω [°]	Δ [°]	K (10^8 s^{-1})	Cleavage (%)
4	3.1	23	78	0.3	92
5	2.8	31	96	1.2	92
6	2.6	42	90	1.2	38
7	2.7	42	82	5.7	59
8	2.7	48	77	6.7	18

the type II cleavage of both amorphous host polymers and guest ketones proceeds with efficiencies similar to those in solution. Whatever constraints the polymer places on molecular motion are not large enough to prevent the relatively small motions required for γ-hydrogen abstraction and cleavage. Golemba and Guillet[125] have carefully studied the behavior of polyacrylophenones and copolymers of styrene and phenyl vinyl ketone. Guillet has even produced a purposely photodegradable polystyrene copolymer based on type II cleavage of the backbone.

Wamser[126] has studied the photochemistry of cyclohexylacetyl groups bonded by Friedel–Crafts acylation to polystyrene beads, which provides an α-cyclohexyl acetophenone structure. The polymer-bound ketone reacts with almost the same quantum efficiency as the free ketone in pentane, 50%, but is unreactive in ethanol, which does not swell the polymer and allow the molecular motion necessary for reaction.

The crystalline state provides more unique behavior than the example described above. The *Crystal Structure–Solid-State Reactivity Correlation Method*, comprehensively formulated by Weiss and Ramamurthy,[127] has provided many experimental data about the most favorable geometric relationship between the abstracting carbonyl group and the abstracted γ-hydrogen atom. Scheffer[52,128] has studied five α-cycloalkyl-*p*-chloroacetophenones, all of which react both in solution and in the crystal (Scheme 11; Table 52.6). They give comparable product ratios in both phases. With the knowledge that organic molecules normally crystallize in their most stable conformations, examination of solution rate constants for hydrogen abstraction revealed no correlation with the geometric parameters for reaction. The rate constants do correlate well with those for bimolecular attack of various radicals on the different sized cycloalkanes, so the intrinsic reactivities of the different CH bonds appear to determine relative reactivities. Scheffer concluded that Eq. (52.3) applies, with comparable values of χ for all five. He suggests that these ketones react not from their most stable conformations but rather from higher energy ones that provide a more favorable geometry for reaction. The value of θ averages only 114° for the crystals. It is also possible that all these compounds react from their crystal geometries, in which case χ_r values are all close to one. All of the ketones except the cyclobutyl are considerably more reactive than *p*-chlorovalerophenone despite their awkward geometries. The rate enhancements probably represent the normal entropic gain associated with the ring.[63] The high observed k values cannot contain a really low value of χ_r, so any common geometric adjustment in solution must involve a relatively low-energy conformational change.

These results also provide unique insight into biradical behavior. The ketones with the smallest two rings undergo primarily cleavage, the next two examples split nearly 50:50, and the largest ring gives mainly cyclobutanol. In the last case, the 18% elimination gives mainly *cis*-cyclooctene, the *cis*/*trans* ratio

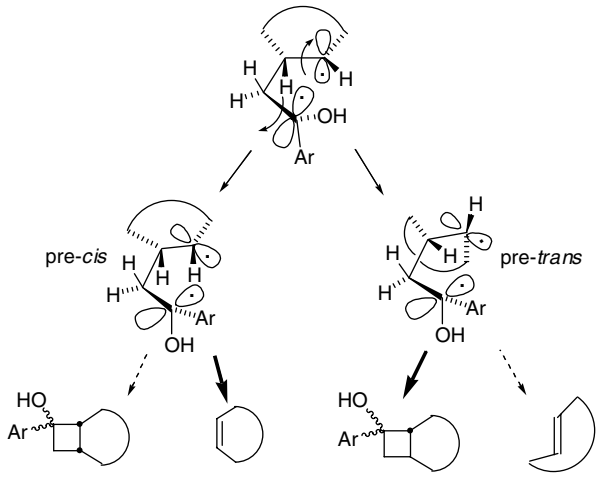

ring size				
4		92 %		
5		92 %		
6	7 %	40 %	53 %	
7	3 %	61 %	36 %	
8	5 %	14 %	77 %	4 %

SCHEME 12

being 9:1 in benzene and 2.5:1 in the crystal. However, over 85% of the cyclization gives the *trans* ring junction. Scheffer[128] provides an intriguing explanation by noting that the *p* orbital on the ring in the biradical must twist 90 ± 45° to become parallel to the *p* orbital at the hydroxy radical site and achieve the geometry required for both cleavage and cyclization. Rotation in the direction that gives *cis* products is favored for the two smallest rings; rotation in the opposite direction, which favors formation of *trans* products, is favored for the largest ring; the two rotations are equally likely for the six- and seven-rings. Because the three largest ketones yield mostly *trans*-fused cyclization products but *cis*-cycloalkene cleavage product, Scheffer concludes that the pre-*cis* biradical undergoes mainly cleavage and the pre-*trans* biradical undergoes mainly cyclization. He further proposes that the phase-independence of the results indicates that these preferences are intrinsic to the molecules' structures. Scheme 12 depicts the proposed biradical geometries and indicates the product ratios as a function of ring size.

Experimental evidence on the relationship between structure and reactivity in Norrish type II photochemistry of spirobenzoyladamantanes in the solid state has been produced.[129] Geometric factors clearly determine partitioning between cleavage, cyclization, and hydrogen transfer reactions of the 1,4-biradical intermediate: Cleavage becomes predominant when the singly occupied orbitals overlap poorly with one another but well with the central CC bond, which, as earlier sections indicate, has been presumed for years based on ketone structure.

Methodology of how compounds are forced to crystallize in a chiral space group[130] has been developed in the concept of the ionic chiral auxiliary: The optically active salt of a ketone with a carboxylic acid functionality was prepared by the reaction with an enantiomerically pure amine.[131–133]

The Norrish type II reaction of various phenyl alkanones in zeolites has been studied by Ramamurthy and his collaborators.[134–136] The size and shape of zeolite reaction cavities control the behavior of triplet ketone as well as the 1,4-biradical intermediate that is consequently monitored as a difference in photoproduct distribution and triplet lifetimes.[137] Norrish type I and type II reactions of 2-pentanone included within cavities of various types of zeolites and the alkali metal cation-exchanged ZSM-5 zeolite have been investigated by experimental and theoretical approaches.[137–139] Ion-exchanged cations had significant effects not only on the adsorption state but also on the photochemical reactions of the ketone. The

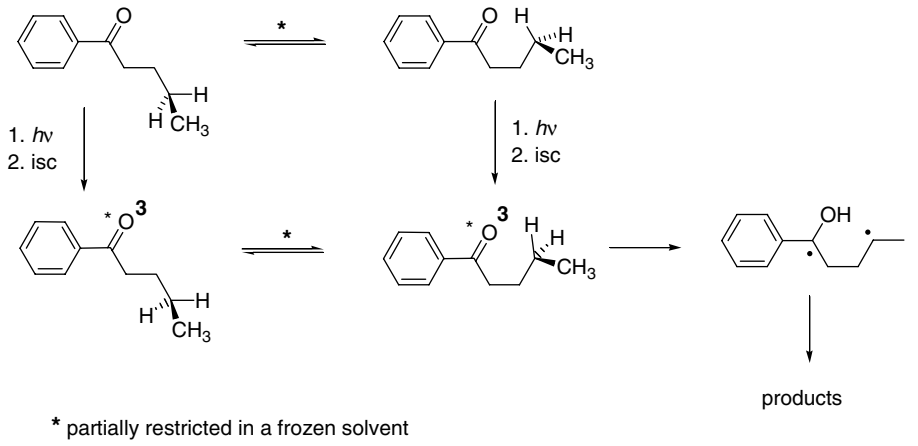

SCHEME 13

observed infrared and phosphorescence spectra of the adsorbed ketones and the *ab initio* molecular orbital calculations of this host–guest system indicate that the ketones interact with two different adsorption sites: the surface OH groups and alkali metal cations.

The Norrish type II reaction of an aryl ketone monolayer-protected colloid was investigated by Workentin and co-workers.[140,141] Photolysis of a mercaptoalkanophenone-modified gold colloid generates free acetophenone in solution and the modified monolayer-protected clusters via the triplet excited state and the 1,4-biradical intermediate. The reaction has been developed as a probe of conformational mobility within the monolayer environment.

Alkyl aryl ketone photolysis has been also studied on a silica-gel surface.[142,143] Molecules in the outermost layer are responsible for the reaction, which has been consequently used for the determination of the solid support surface area.[145] The effect of the alkyl chain length on the type II photoreactivity of alkyl phenyl ketones on the surface was found to be insignificant. Based on the quantum yield measurements of valerophenone and *p*-substituted valerophenone photolysis, a silica-gel surface was reported to be as strong a polar medium as methanol; the surface might cause the inversion of the n,π^* and π,π^* triplet states.

Klán and co-workers investigated the photoreactivity of valerophenone in frozen polar and nonpolar solvents, including water.[144] Results indicated that a portion of the ketone molecules are almost unreactive due to physical restraints of the solid solvent cavity. Free rotation along the CC bonds becomes difficult inside the cavity; thus, large conformational changes are restricted (Scheme 13).

52.8 Synthetic Uses and Other Applications

The Norrish type II reaction is occasionally used in synthetic processes mostly when other procedures leading to a desired product are difficult or costly. Simple type II elimination has been put to use in several ways. Glycosides made from γ-hydroxy ketones undergo photoelimination to give *O*-vinyl glycosides, which can undergo a Claisen rearrangement in certain deoxy sugars (Scheme 14).[145] Properly alkylated bicyclo[4.2.0]-octan-2-ones formed by [2+2]-photocycloaddition of cyclohexenones to alkenes cleave to δ,ε-unsaturated ketones (Scheme 15).[146] Scharf has removed the C17 side chain in steroids by photolysis (Scheme 16).[147] Perhaps the most unusual use of type II elimination was Goodman and Berson's preparation of *m*-xylylene (Scheme 17).[147] Wirz and Kresge[149,150] have brilliantly exploited the type II elimination of various ketones induced by flash photolysis to allow kinetic studies of the transient enols photoproducts.

Synthesis of a new C/D synthon of vitamin D from hydrodeoxycholic acid was performed by employing the type II reaction (Scheme 18).[151]

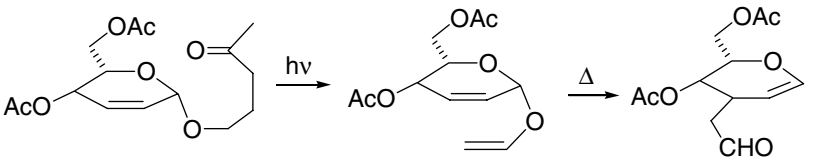

SCHEME 14

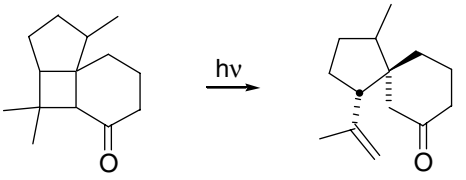

SCHEME 15

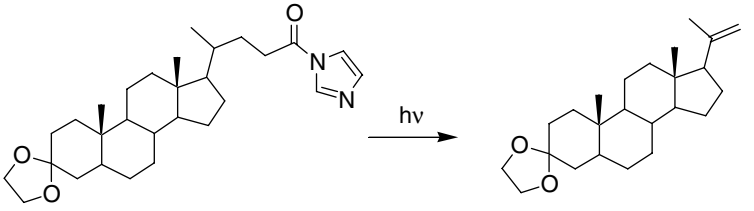

SCHEME 16

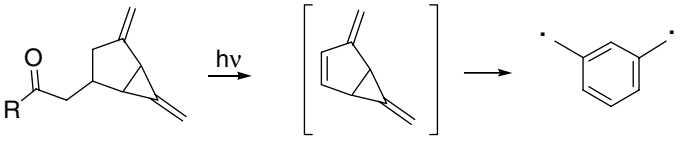

SCHEME 17

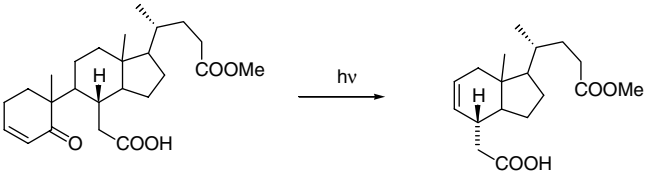

SCHEME 18

Hénin and co-workers[152,153] reported the results from the irradiation of α-disubstituted indanones, tetralones, and propiophenones bearing at least one hydrogen in the γ-position in the presence of catalytic amounts of optically active aminoalcohols. The reaction provided the Norrish type II cleavage compounds with an enantiomeric excess reaching 89% (e.g., Scheme 19). Synthesis of 3-hydroxyindene by a Norrish type II elimination as well as the mechanistic aspects of this reaction were discussed by Jefferson and

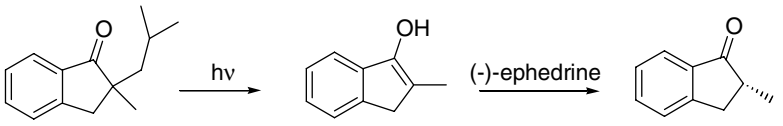

SCHEME 19

co-workers.[154] The syntheses of enediynes[155] or taxane precursors[156] utilizing the Norrish type II reaction provide additional examples.

Alkyl or aryl α-ketoesters of primary or secondary alcohols react upon irradiation in a Norrish type II fashion from the intermediate triplet state into aldehydes.[157] This research was performed in order to study a controlled release of perfumery aldehydes. Lerner, Janda, and their co-workers[158] investigated a catalytic antibody for a multistep Norrish type II photochemical reaction of α-ketoamide substrates. The single product obtained in the antibody-catalyzed reaction was not observed in the uncatalyzed reaction, suggesting that the interplay of conformational control and chemical catalysis were responsible for the high specificity. The antibody described could be a model for the evolution of light-activated enzymes and serve as a foundation for the development of light-dependent antibody catalysts for a range of even more complex photochemical reactions. Inoue and co-workers[159] studied an enantiomeric enrichment occurring by irradiation of a racemic sample of amino acids by circularly polarized light resulting from the preferential excitation/decomposition of one enantiomer over another via the Norrish type II reaction. The enantiomeric excess was found to be dependent on the degree of protonation of the aminocarboxylic acid moiety. The authors discussed the possibility that the origin of biological homochirality may be the result of the absorption of circularly polarized light. The Norrish type II reaction has been also utilized to monitor the production of HCOOH, CO_2, and CO following ultraviolet laser excitation of gas-phase formate esters in time-resolved infrared absorption spectroscopy.[160] Photolysis of *i*-pentanal and *t*-pentanal was investigated by using dye laser photolysis in combination with cavity ring-down spectroscopy.[161]

52.9 The Type II Reaction as a Mechanistic Probe

A good number of compounds have been studied whose triplets undergo both the type II reaction and one or more other processes, either physical or chemical. Because structural effects on rate constants for γ-hydrogen abstraction are well understood, the type II reaction can serve as a clock for measuring rates of the other reactions, with quantum yield measurements allowing triplet lifetimes to be divided into separate rates for the competing reactions.

A very early example is provided by the study of solvent viscosity effects on the rate constants for bimolecular quenching of triplet valerophenone by dienes.[162] Several studies by the Wagner group[163,164] on the competing type II reactions of α,ω-diacylalkanes have provided measures of the rates of internal triplet energy transfer between the two carbonyl groups.

Wagner and Klán[165,166] have determined rate constants for intramolecular triplet energy transfer in various flexible ω-arylalkanophenone systems by comparing type II quantum yields and triplet lifetimes to the known rate constants of the competing γ-hydrogen abstraction reactions (Scheme 20).[165,166] The values of the energy transfer rate constants as a function of *n* provided clear evidence for the importance of through-space interactions.

Rate constants for intramolecular reactions of triplet ketones with double bonds,[167] amino groups,[168] azido groups,[169] and alkylthiyl groups[170] have been established from type II quantum yields and triplet lifetimes of appropriately substituted ketones.

Study of ring-brominated valerophenones revealed high rate constants for radical cleavage of bromine atoms from the benzene rings of the excited triplets,[171] a fact that could lead to new photoactivated chemotherapeutic compounds.[172] Likewise, the study of *p*-(3-buten-4-oxy)-substituted valerophenones revealed large rate constants for [2+2]-cycloaddition of the remote double bond to the benzene ring.[173]

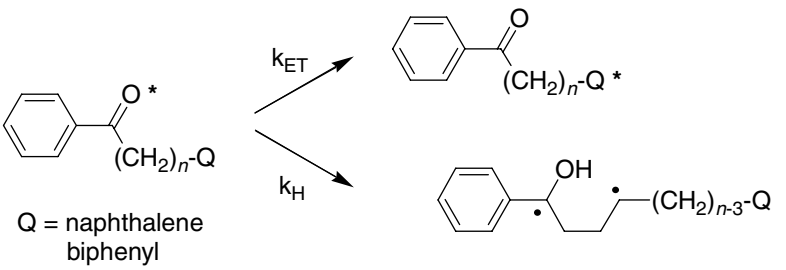

SCHEME 20

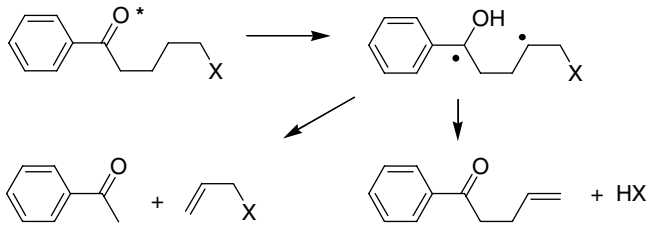

X = Cl, Br, I, SR, S(O)R, SO_2R

SCHEME 21

Other studies have taken advantage of the radical-like behavior of the 1,4-biradical intermediates, such as in their earlier mentioned trapping by thiols. Of special importance was the ability to gauge rate constants for β-cleavage of radicals by the behavior of δ-substituted valerophenones: The acetophenone/4-benzoyl-1-butene ratios reveal ratio of biradical cleavage and radical cleavage rates (Scheme 21).[174]

Most recently, Klán and co-workers[175,176] utilized the type II reaction in studies of temperature-dependent photochemical reactions carried out in a microwave field. Microwave radiation is not a classical energy source but usually serves to accelerate chemical transformations. In an original project of microwave photochemistry, the Norrish type II reaction provided a reliable strategy for the estimation of the microwave superheating effects using the thermally sensitive solvation of the OH group in the Norrish 1,4-biradical intermediate.[177,178]

Photodegradation of various copolymers containing carbonyl group via the Norrish type II reaction has received considerable attention. Originally, the major interest was in preventing photodegradation of polyethylenes. Photolabile copolymers of propylene/carbon monoxide with ethylene/carbon monoxide;[179] methyl methacrylate with acrylophenone, *t*-butyl acrylophenone, or *p*-chloroacrylophenone;[180] styrene with methyl vinyl ketone or phenyl vinyl ketone;[181] or styrene with methylvinyl ketone and ethylene-propylene-diene[182] may serve as representative examples. In addition, crosslinking of poly(3,5-dimethoxyacrylophenone) caused by a hydrogen abstraction reaction between pendent phenylglyoxylate chromophores was reported.[183]

References

1. Wagner, P. J., Type II photoelimination and photocyclization of ketones, *Acc. Chem. Res.*, 4, 168, 1971.
2. Dalton, J. C. and Turro, N. J., Photoreactivity of n,π^* excited states of alkyl ketones, *Ann. Rev. Phys. Chem.*, 21, 499, 1970.
3. Wagner, P. J., Chemistry of excited triplet organic carbonyl compounds, *Topics Curr. Chem.*, 66, 1, 1976.

4. Wagner, P. J., 1,5-Biradicals and five-membered rings generated by δ-hydrogen abstraction in photoexcited ketones, *Acc. Chem. Res.*, 22, 83, 1989.
5. Wagner, P. J. and Park, B.-S., Photoinduced hydrogen atom abstraction by carbonyl compounds, *Org. Photochem.*, 11, 227, 1991.
6. Norrish, R. G. W. and Appleyard, M. E. S., Primary photochemical reactions. Part IV. Decomposition of methyl ethyl ketone and methyl butyl ketone, *J. Chem. Soc.*, 874, 1934.
7. McMillan, G. R., Calvert, J. G., and Pitts, Jr., J. N., Detection and lifetime of enol-acetone in the photolysis of 2-pentanone vapor, *J. Am. Chem. Soc.*, 86, 3602, 1964.
8. Yang, N. C. and Yang, D.-H., Cyclobutanol formation from irradiation of ketones, *J. Am. Chem. Soc.*, 80, 2913, 1958.
9. Ausloos, P. and Rebbert, R. E., Photoelimination of ethylene from 2-pentanone, *J. Am. Chem. Soc.*, 86, 4512, 1964.
10. Michael, J. L. and Noyes, Jr., W. A., Photochemistry of 2-pentanone with biacetyl, *J. Am. Chem. Soc.*, 85, 1027, 1963.
11. Wagner, P. J. and Hammond, G. S., Mechanism of type II photoelimination, *J. Am. Chem. Soc.*, 87, 4009, 1965.
12. Dougherty, T. J., Type II photolysis of 2-octanone, *J. Am. Chem. Soc.*, 87, 4011, 1965.
13. Baum, E. J., Wan, J. K. S., and Pitts, Jr., J. N., Reactivity of excited states. intramolecular hydrogen atom abstraction in substituted butyrophenones, *J. Am. Chem. Soc.*, 88, 2652, 1966.
14. Wagner, P. J. and Hammond, G. S., Quenching of type II photoelimination reaction, *J. Am. Chem. Soc.*, 88, 1245, 1966.
15. Wagner, P. J., Solvent effects on type II photoelimination of phenyl ketones, *J. Am. Chem. Soc.*, 89, 5898, 1967.
16. Wagner, P. J., Kochevar, I. E., and Kemppainen, A. E., Type II photoprocesses of phenyl ketones: procedures for determining meaningful quantum yields and triplet lifetimes, *J. Am. Chem. Soc.*, 94, 7489, 1972.
17. Wagner, P. J. and Zepp, R. G., Trapping by mercaptans of the biradical intermediates in type II photoelimination, *J. Am. Chem. Soc.*, 94, 287, 1972.
18. Wagner, P. J., Kelso, P. A. and Zepp, R. G., Type II photoprocesses of phenyl ketones: evidence for a biradical intermediate, *J. Am. Chem. Soc.*, 94, 7480, 1972.
19. Yang, N. C. and Elliot, S. P., Photochemistry of (S)-(+)-5-methyl-2-heptanone, *J. Am. Chem. Soc.*, 91, 7550, 1969.
20. Yang, N. C., Morduchowitz, A., and Yang, D.-H., On the mechanism of photochemical formation of cyclobutanols, *J. Am. Chem. Soc.* 85, 1017, 1963.
21. Wagner, P. J., 1-Methylnaphthalene-sensitized singlet state reactions of aliphatic ketones, *Mol. Photochem.*, 3, 169, 1971.
22. Salem, L. and Rowland, C., The electronic properties of diradicals, *Angew. Chem. Int. Ed. Engl.*, 11, 92, 1972.
23. De Feyter, S., Diau, E. W. G., and Zewail, A. H., Femtosecond dynamics of Norrish type II reactions: nonconcerted hydrogen-transfer and diradical intermediacy, *Angew. Chem. Int. Ed. Engl.*, 39, 260, 2000.
24. Barltrop, J. A. and Coyle, J. C., Singlet and triplet participation in the photochemistry of simple alkanones, *Tetrahedron Lett.*, 3235, 1968.
25. Wagner, P. J., Differences between singlet and triplet state type II photoelimination of aliphatic ketones, *Tetrahedron Lett.*, 5385, 1968.
26. Yang, N. C., Elliot, S. P., and Kim, B., The mechanism of photochemistry of alkanones with γ-hydrogens, *J. Am. Chem. Soc.*, 91, 7551, 1969.
27. Yang, N. C. and Shani, A., Photochemistry of β-naphthyl alkyl ketones in solution, *J. Chem. Soc., Chem. Commun.*, 815, 1971.
28. Coyle, J. C., A type II photoelimination reaction of 1-naphthyl ketones, *J. Chem. Soc., Perkin Trans. 2*, 233, 1973.

29. Wagner, P. J. and Jellinek, T., Intramolecular quenching of the excited singlets of ω-dialkylamino alkyl ketones: singlet state type II photoelimination of α-dimethylaminoacetophenone, *J. Am. Chem. Soc.*, 93, 7328, 1971.
30. Previtali, C. M. and Scaiano, J. C. The Kinetics of photochemical reactions. Part 1. Application of a modified bond-energy-bond-order method to the atom abstraction reactions of excited carbonyl compounds, *J. Chem. Soc.*, *Perkin Trans. 2*, 1667, 1972.
31. Giering, L., Berger, M., and Steel, C., Rate studies of aromatic triplet carbonyls with hydrocarbons, *J. Am. Chem. Soc.*, 96, 953, 1974.
32. Encina, M. V., Lissi, E. A., Lemp, E., Zanocco, A., and Scaiano, J. C., Temperature dependence of the photochemistry of aryl alkyl ketones, *J. Am. Chem. Soc.*, 105, 1856, 1983.
33. (a) Porter, G. and Suppan, P., Primary photochemical processes in aromatic molecules. XIV. Comparative photochemistry of aromatic carbonyl compounds, *Trans Faraday Soc.*, 62, 3375, 1966. (b) Yang, N. C., McClure, D. S., Murov, S. L., Houser, J. J., and Dusenbery, R., Photoreduction of acetophenone and substituted acetophenones, *J. Am. Chem. Soc.*, 89, 5466, 1967.
34. Wagner, P. J., Kemppainen, A. E., and Schott, H. N., Effect of ring substituents on type II photoreactions of phenyl ketones, *J. Am. Chem. Soc.*, 95, 5604, 1973.
35. Wagner, P. J., Truman, R. J., and Scaiano, J. C., Substituent effects on hydrogen abstraction by phenyl ketone triplets, *J. Am. Chem. Soc.*, 107, 7093, 1985.
36. Berger, M., McAlpine, E., and Steel, C., Substituted acetophenones: importance of activation energies in mixed state models of photoreactivity, *J. Am. Chem. Soc.*, 100, 5147, 1978.
37. Hammond, G. S. and Leermakers, P. A., Photoreduction of 1-naphthaldehyde and 2-acetonaphthone, *J. Am. Chem. Soc.*, 84, 207, 1962.
38. deBoer, C. D., Herkstroeter, W. G., Marchetti, A. P., Schultz, A. P., and Schlessinger, R. H., Norrish type II rearrangement from π,π* triplet states, *J. Am. Chem. Soc.*, 95, 3963, 1973.
39. Zimmerman, H. E., A new approach to mechanistic organic photochemistry, *Adv. Photochem.*, 1, 183, 1963.
40. Walling, C. and Gibian, M. J., Hydrogen abstraction reactions by the triplet states of ketones, *J. Am. Chem. Soc.*, 87, 3361, 1965.
41. Wagner, P. J., Thomas, M. J., and Puchalski, A. E., Photoreactivity of α-fluorinated phenyl alkyl ketones, *J. Am. Chem. Soc.*, 108, 7739, 1986.
42. Evans, T. R. and Leermakers, P. A., The Norrish type II process in α-keto acids: photolysis of α-ketodecanoic acid in benzene, *J. Am. Chem. Soc.*, 90, 1840, 1968.
43. Turro, N. J. and Lewis, F. D., Type II photoelimination and 3-oxetanol formation from αalkoxyacetophenones and related compounds, *J. Am. Chem. Soc.*, 92, 311, 1970.
44. Zepp, R. G., Gumz, M. M., Miller, W. L., and Gao, H., Photoreaction of valerophenone in aqueous solution, *J. Phys. Chem. A*, 102, 5716, 1998.
45. Wagner, P. J. and Kemppainen, A. E., Type II photoprocesses of phenyl ketones: triplet state reactivity as a function of γ- and δ-substitution, *J. Am. Chem. Soc.*, 94, 7495, 1972.
46. Wagner, P. J., Lindstrom, M. J., Sedon, J. H., and Ward, D. R., Photochemistry of δ-halo ketones: anchimeric assistance in triplet-state γ-hydrogen abstraction and β-elimination of halogen atoms from the resulting diradicals, *J. Am. Chem. Soc.*, 103, 3842, 1981.
47. Wagner, P. J., Kelso, P. A., Kemppainen, A. E. and Zepp, R. G., Type II photoprocesses of phenyl ketones: competitive δ-hydrogen abstraction and the geometry of intramolecular hydrogen atom transfers, *J. Am. Chem. Soc.*, 94, 7500, 1972.
48. Chang, H. C., Popovitz-Biro, R., Lahav, M., and Leiserowitz, L., Mapping the molecular pathway during photoaddition of guest acetophenone and *p*-fluoroacetophenone to host deoxycholic acid as studied by *x*-ray diffraction in systems undergoing single-crystal-to-single-crystal transformation, *J. Am. Chem. Soc.*, 109, 3883, 1987.
49. Wagner, P. J., Zhou, B., Hasegawa, T., and Ward, D. L., Diverse photochemistry of sterically congested α-arylacetophenones: ground-state conformational control of reactivity, *J. Am. Chem. Soc.*, 113, 9640, 1991.

50. Ito, Y., Matsuura, T., and Fukuyama, K., Efficiency of solid-state photocyclization of 2,4,6-triisopropylbenzophenones, *Tetrahedron Lett.*, 29, 3087, 1988.
51. Ariel, S., Ramamurthy, V., Scheffer, J. R., and Trotter, J., Norrish type II reaction in the solid state: involvement of a boat-like reactant conformation, *J. Am. Chem. Soc.*, 105, 6959, 1983.
52. Scheffer, J. R., The Influence of the molecular crystalline environment on organic photorearrangements, *Org. Photochem.*, 8, 249, 1987.
53. Chandler, W. D. and Goodman, L., Allowed and forbidden character in π^*-n spectra of cycloalkanones, *J. Mol. Spect.*, 35, 232, 1970.
54. Severance, D., Pandey, B., and Morrison, H., Reaction path analysis of hydrogen abstraction by the formaldehyde triplet state, *J. Am. Chem. Soc.*, 109, 3231, 1987.
55. Dorigo, A. E., McCarrick, M. A., Loncharich, R. J., and Houk, K. N., Transition structures for hydrogen atom transfers to oxygen: comparisons of intermolecular and intramolecular processes and open- and closed-shell systems, *J. Am. Chem. Soc.*, 112, 7508, 1990.
56. Sugiyama, N., Nishio, T., Yamada, K., and Aoyama, H., Photochemical reactions of bridged polycyclic ketones, *Bull. Chem. Soc. Jpn.*, 43, 1879, 1970.
57. Sauers, R. R., Scimone, A., and Shams, H., Synthesis and photochemistry of some new pentacycloundecan-8-ones: probes for hydrogen abstraction in the π-plane, *J. Org. Chem.*, 53, 6084, 1988.
58. Sauers, R. R. and Krogh-Jesperson, K., Analysis of Norrish type II reactions by molecular mechanics methodology, *Tetrahedron Lett.*, 30, 527 , 1989.
59. Wagner, P. J., Conformational flexibility and photochemistry, *Acc. Chem. Res.*, 16, 461, 1983.
60. Lewis, F. D., Johnson, R. W., and Johnson, D. E., Conformational control of photochemical behavior: competitive α-cleavage and γ-hydrogen abstraction of alkyl phenyl ketones, *J. Am. Chem. Soc.*, 96, 6090, 1974.
61. Wagner, P. J. and Chen, C.-P., A rotation-controlled excited state reaction: the photoenolization of *ortho*-alkyl phenyl ketones, *J. Am. Chem. Soc.*, 98, 239, 1976.
62. Alexander, E. C. and Uliana, J. A., Photolysis of cyclobutyl aryl ketones: evidence for the involvement of an excited state conformational equilibrium in their photoconversion to aryl bicyclo[1.1.1]pentanols, *J. Am. Chem. Soc.*, 96, 5644, 1974.
63. Lewis, F. D., Johnson, R. W., and Kory, D. R., Transition state for γ-hydrogen abstraction of alkyl phenyl ketones, *J. Am. Chem. Soc.*, 96, 6100, 1974.
64. Paquette, L. A. and Balogh, D. W., An Expedient Synthesis of 1,16-Dimethyldodecahedrane, *J. Am. Chem. Soc.*, 104, 774, 1982.
65. Turro, N. J. and Weiss, D. S., Stereoelectronic requirements for the type II cleavage of *cis*- and *trans*-4-*t*-butylcyclohexanones, *J. Am. Chem. Soc.*, 90, 2185, 1968.
66. Wagner, P. J. and Zepp, R. G., γvs. δ-Hydrogen abstraction in the photochemistry of δ-alkoxyketones: an overlooked reaction of hydroxybiradicals, *J. Am. Chem. Soc.*, 93, 4958, 1971.
67. Ounsworth, J. and Scheffer, J. R., Intramolecular abstraction of aldehydic hydrogen by ketone triplets: formation of 2-hydroxy-2-phenylcycloalkanones, *J. Chem. Soc., Chem. Commun.*, 232, 1986.
68. Wagner, P. J., Kemppainen, A. E., and Jellinek, T. Type II photoreactions of phenyl ketones: competitive charge transfer in α-, γ-, and δ-dialkylamino ketones, *J. Am. Chem. Soc.*, 94, 7512, 1972.
69. Wagner, P. J. and Ersfeld, D. A., Solvent specific photochemistry involving an intramolecular amino ketone triplet exciplex, *J. Am. Chem. Soc.*, 98, 4515, 1976.
70. Small, Jr., R. D. and Scaiano, J. C., Direct detection of the biradicals generated in the Norrish type II reaction, *Chem. Phys. Lett.*, 50, 431, 1977.
71. Small, Jr., R. D. and Scaiano, J. C., Photochemistry of phenyl alkyl ketones: the lifetime of the intermediate biradicals, *J. Phys. Chem.*, 81, 2126, 1977.
72. Small, R. D. and Scaiano, J. C., One electron reduction of Paraquat dication by photogenerated biradicals, *J. Photochem.*, 6, 453, 1976/77.
73. Scaiano, J. C., Laser flash photolysis studies of the reactions of some 1,4-biradicals, *Acc. Chem. Res.*, 15, 252, 1982.

74. Caldwell, R. A., Majima, T., and Pac, C., Some structural effects on triplet biradical lifetimes: Norrish II and Paterno–Büchi biradicals, *J. Am. Chem. Soc.*, 104, 629, 1982.
75. Small, Jr., R. D. and Scaiano, J. C., Solvent effects on the lifetimes of photogenerated biradicals, *Chem. Phys. Lett.*, 59, 246, 1978.
76. Small, Jr., R. D. and Scaiano, J. C., Interaction of oxygen with transient biradicals photogenerated from γ-methyl valerophenone, *Chem. Phys. Lett.*, 48, 354, 1977.
77. Small, Jr., R. D. and Scaiano, J. C., Differentiation of excited-state and biradical processes: photochemistry of phenyl alkyl ketones in the presence of oxygen, *J. Am. Chem. Soc.*, 100, 4512, 1978.
78. Encinas, M. V. and Scaiano, J. C., Interaction between photogenerated biradicals and free radicals: di-*tert*-butylnitroxide, *J. Photochem.*, 11, 241, 1979.
79. Scaiano, J. C., Does intersystem crossing in triplet biradicals generate singlets with conformational memory?, *Tetrahedron*, 38, 819, 1982.
80. Closs, G. L. and Redwine, O. D., Cyclization and disproportionation kinetics of triplet generated, medium chain length, localized biradicals measured by time-resolved CIDNP, *J. Am. Chem. Soc.* 107, 4543, 1985.
81. Michl, J., Spin-orbit coupling in biradicals. 1. The 2-electrons-in-2-orbitals model revisited, *J. Am. Chem. Soc.*, 118, 3568, 1996.
82. Morita, A. and Kato, S., Theoretical study on the intersystem crossing mechanism of a diradical in Norrish type II reactions in solution, *J. Phys. Chem.*, 97, 3298, 1993.
83. (a) Caldwell, R. A. and Fink, P. M., Norrish II fragmentation of 3,4-dipenylbutyrophenone: loss of spin memory in a 1,4-biradical, *Tetrahedron Lett.*, 2987, 1969. (b) Wagner, P. J. and Kelso, P. A., Photoelimination of stilbene from β,γ-diphenylbutyrophenone, *Tetrahedron Lett.*, 4153, 1969.
84. Coulson, D. R. and Yang, N. C., Deuterium isotope effects in the photochemistry of 2-hexanone, *J. Am. Chem. Soc.,* 88, 4511, 1966.
85. Wagner, P. J. and Kemppainen, A. E., Is there any correlation between quantum yields and triplet-state reactivity in type II photoelimination?, *J. Am. Chem. Soc.*, 90, 5896, 1968.
86. Caldwell, R. A., Dhawan, S. N., and Moore, D. E., pH Dependence of the lifetime of a Norrish II biradical, *J. Am. Chem. Soc.*, 107, 5163, 1985.
87. Scaiano, J. C., Lissi, E. A., and Encina, M. V., Chemistry of the biradicals produced in the Norrish type II reaction, *Rev. Chem. Intermed.*, 2, 139, 1978.
88. Wagner, P. J., Kelso, P. A., Kemppainen, A. E., McGrath, J. M., Schott H. N., and Zepp, R. G., Type II photoprocesses of phenyl ketones: a glimpse at the behavior of 1,4-biradicals, *J. Am. Chem. Soc.*, 94, 7506, 1972.
89. Hoffman, R., Swaminathau, S., Odell, B. G., and Gleiter, R., A potential surface for a nonconcerted reaction. tetramethylene, *J. Am. Chem. Soc.*, 92, 7091, 1970.
90. Lewis, F. D. and Hilliard, T. A., Photochemistry of methyl-substituted butyrophenones, *J. Am. Chem. Soc.*, 94, 3852, 1972.
91. Wagner, P. J. and Thomas, M. J., Enhanced photocyclization of α-fluoroketones, *J. Am. Chem. Soc.*, 98, 241, 1976.
92. Lewis, F. D., Johnson, R. W., and Ruden, R. A., Photochemistry of bicycloalkylphenyl ketones, *J. Am. Chem. Soc.*, 94, 4292, 1972.
93. Urry, W. H. and Trecker, D. J., Photochemical reactions of 1,2-diketones, *J. Am. Chem. Soc.,* 84, 118, 1962.
94. Wagner, P. J. , Zepp, R. G., Liu, K.-C., Thomas, M., Lee, T.-J., and Turro, N. J., Competing photocyclization and photoenolization of phenyl α-diketones, *J. Am. Chem. Soc.*, 98, 8125, 1976.
95. Hu, S. K. and Neckers, D. C., Photochemical reactions of alkoxy-containing alkyl phenylglyoxylates: remote hydrogen abstraction, *J. Chem. Soc.*, *Perkin Trans. 2*, 1751, 1997.
96. Kaneko, Y., Hu, S. K., and Neckers, D. C., Photochemical reactivities of alkyl thiopheneglyoxylates and alkyl furanylglyoxylates, *J. Photochem. Photobiol. A: Chem.*, 114, 173, 1998.
97. Hu, S. K. and Neckers, D. C., Rapid regio- and diastereoselective Paterno–Büchi reaction of alkyl phenylglyoxylates, *J. Org. Chem.*, 62, 564, 1997.

98. Hu, S. K. and Neckers, D. C., Photochemical reactions of mercapto/amino substituted alkyl phenylglyoxylates induced by intramolecular electron transfer, *Tetrahedron*, 53, 2751, 1997.
99. Hu, S. K. and Neckers, D. C., Photochemical reactions of sulfide-containing alkyl phenylglyoxylates, *Tetrahedron*, 53, 7165, 1997.
100. Hu, S. K. and Neckers, D. C., Photochemical reactions of alkenyl phenylglyoxylates, *J. Org. Chem.*, 62, 6820, 1997.
101. Hu, S. K. and Neckers, D. C., Photochemical reactions of halo-/aryl sulfide-substituted alkyl phenylglyoxylate: an assessment of the lifetime of the intermediate 1,4-biradical, *J. Org. Chem.*, 62, 7827, 1997.
102. Hu, S. K., Mejiritski, A., and Neckers, D. C., Photoreactions of polymeric (meth)acryloylethyl phenylglyoxylate-reactivity in solution and film, *Chem. Mater.*, 9, 3171, 1997.
103. Penn, J. H. and Owens, W. H., The photochemistry of mixed anhydrides: a search for selectivity in photochemically initiated bond–cleavage reactions, *J. Am. Chem. Soc.*, 115, 82, 1993.
104. Pincock, J. A., Rifai, S., and Stefanova, R., The photochemistry of the 4-cyanobenzoic acid esters of *trans*- and *cis*-2-phenylcyclohexanol, *Can. J. Chem.*, 79, 63, 2001.
105. Morley, K. and Pincock, J. A., The photochemistry of 2-(1-naphthyl)ethyl benzoates: cycloaddition and intramolecular exciplex formation, *J. Org. Chem.*, 66, 2995, 2001.
106. DeCosta, D. P., Bennett, A. K. and Pincock, J. A., The Norrish type II photofragmentation of esters induced by intramolecular electron transfer, *J. Am. Chem. Soc.*, 121, 3785, 1999.
107. Hwu, J. R., Chen, B. L., Huang, L. W., and Yang, T. H., Influence of beta-silyl groups in cycloalkanones on the Norrish type I and type II cleavages, *J. Chem. Soc., Chem. Commun.*, 299, 1995.
108. Ramamurthy, V., Organic-photochemistry in organized media, *Tetrahedron*, 42, 5753, 1986.
109. Turro, N. J., Liu, K.-C., and Chow, M.-F., Solvent sensitivity of type II photoreaction of ketones as a device to probe solute location in micelles, *Photochem. Photobiol.*, 26, 413, 1977.
110. Turro, N. J. and Weed, G. C., Micellar systems as "supercages" for reactions of geminate radical pairs. magnetic effects, *J. Am. Chem. Soc.*, 105, 1861, 1983.
111. Pappas, S. P. and Chattopadhyay, A., Photochemistry of benzoin ethers: type I cleavage by low energy sensitization, *J. Am. Chem. Soc.*, 95, 6484, 1973.
112. Devanathan, S. and Ramamurthy, V., Intramolecular orientation at the micellar interface: control of Norrish type I and type II reactivity of benzoin alkyl ethers via conformational effects, *J. Phys. Org. Chem.*, 1, 91, 1988.
113. deMayo, P., Nakamura, A., Tsang, P. W. K., and Wong, S. K., Surface photochemistry: deviation of the course of reaction in benzoin ether photolysis by absorption on silica gel, *J. Am. Chem. Soc.*, 104, 6824, 1982.
114. Dasarathu Reddy, G., Ramanathan, K. V., and Ramamurthy, V., Modification of photochemistry by cyclodextrin complexation: competitive Norrish type I and type II reactions of benzoin alkyl ethers, *J. Org. Chem.*, 51, 3085, 1986.
115. Dasarathu Reddy, G. and Ramamurthy, V., Modification of photochemical reactivity by cyclodextrin complexation: alteration of photochemical behavior via restriction of translational and rotational motions. alkyldeoxybenzoins, *J. Org. Chem.*, 52, 5521, 1987.
116. Turro, N. J. and Wan, P., Photochemistry of phenyl alkyl ketones adsorbed on zeolite molecular sieves: observation of pronounced effects on type I/type II photochemistry, *Tetrahedron Lett.*, 25, 3655, 1984.
117. Wagner, P. J. and McGrath, J. M., Competitive types I and II photocleavage of α,α-dimethylvalerophenone, *J. Am. Chem. Soc.*, 94, 3849, 1972.
118. He, Z. and Weiss, R. G., Length and direction-specific solute-solvent interactions as determined from Norrish II reactions of *p*-alkylalkanophenones in ordered phases of *n*-butyl stearate, *J. Am. Chem. Soc.*, 112, 5535, 1990.
119. (a) Slivinskas, J. A. and Guillet, J. E., γ-Radiolysis of ketone polymers. I. Studies of symmetrical aliphatic ketones as model compounds, *J. Polym. Sci., Polym. Chem. Ed.*, 11, 3043, 1973. (b) Treanor, R. L. and Weiss, R. G., Liquid-crystalline solvents as mechanistic probes. 23. Norrish-II reactions

of 2-alkanones and *sym*-alkanones in the isotropic, smectic-B, and crystalline phases of normal-butyl stearate, *Tetrahedron*, 43, 1371, 1987.
120. Weiss, R. G., Chandrasekhar, S., and Vilalt, P. M., Selectivity in the photoproduct ratios from Norrish II reactions of a homologous series of 2-alkanones in their melt and solid-phases. Comparison with other environments, *Coll. Czech. Chem. Commun.*, 58, 142, 1993.
121. Worsham, P. R., Eaker, D. W., and Whitten, D. G., Ketone photoreactivity as a probe of the microenvironment: photochemistry of the surfactant ketone 16-oxo-16-*p*-tolylhexadecanoic acid in monolayers, micelles, and solution, *J. Am. Chem. Soc.*, 100, 7091, 1978.
122. Guillet, J. E., *Polymer Photophysics and Photochemistry*, Cambridge University Press, Cambridge, U.K., 1985, chap. 10.
123. Guillet, J. E., Photochemistry and molecular motion in solid amorphous polymers, *Adv. Photochem.*, 14, 91, 1988.
124. Hartley, G. H. and Guillet, J. E., Photochemistry of ketone polymers. I. Studies of ethylene-carbon monoxide copolymers, *Macromolecules*, 1, 165, 1968.
125. Golemba, F. J. and Guillet, J. E., Photochemistry of ketone polymers. VII. Polymers and copolymers of phenyl vinyl ketone, *Macromolecules*, 5, 212, 1972.
126. Wamser, C. C. and Wagner, W. R., Type II photoelimination from α-cycloalkylacetophenones and a polystyrene-bound analogue, *J. Am. Chem. Soc.*, 103, 7232, 1981.
127. Weiss, R. G., Ramamurthy, V., and Hammond, G. S., Photochemistry in organized and confining media: a model, *Acc. Chem. Res.*, 26, 530, 1993.
128. Ariel, S., Evans, S. V., Garcia-Garibay, M., Harkness, B. R., Omkaram, N., Scheffer, J. R., and Trotter, J., The generation of 1,4-biradicals in rigid media: crystal structure–solid state reactivity correlation, *J. Am. Chem. Soc.*, 110, 5591, 1988.
129. Cheung, E., Netherton, M. R., Scheffer, J. R., and Trotter, J., Competition between cyclization, cleavage, and reverse hydrogen transfer in 1,4-hydroxybiradicals: crystal structure–solid state reactivity correlations, *Org. Lett.*, 2, 77, 2000.
130. Sakamoto, M., Absolute asymmetric synthesis from achiral molecules in the chiral crystalline environment, *Chem.-Eur. J.*, 3, 684, 1997.
131. Jones, R., Scheffer, J. R., Trotter, J., and Yang, J., Crystal to molecular chirality transfer: supramolecular photochemistry of crystalline carboxylate salts, *Tetrahedron Lett.*, 33, 5481, 1992.
132. Koshima, H., Maeda, A., Masuda, N., Matsuura, T., Hirotsu, K., Okada, K., Mizutari, H., Ito, Y., Fu, T. Y., Scheffer, J. R., and Trotter, J., Ionic chiral handle-induced asymmetric-synthesis in a solid-state Norrish type II photoreaction, *Tetrahedron Asymm.*, 5, 1415, 1994.
133. Gamlin, J. N., Jones, R., Leibovitch, M., Patrick, B., Scheffer, J. R., and Trotter, J., The ionic auxiliary concept in solid state organic photochemistry, *Acc. Chem. Res.*, 29, 203, 1996.
134. Ramamurthy, V. and Sanderson, D. R., Relative size of the host and the guest determine the reaction–product selectivity: Norrish type II reaction of alkanones within zeolites, *Tetrahedron Lett.*, 33, 2757, 1992.
135. Ramamurthy, V., Corbin, D. R., and Johnston, L. J., A study of Norrish type II reactions of aryl alkyl ketones included within zeolites, *J. Am. Chem. Soc.*, 114, 3870, 1992.
136. Ramamurthy, V., Lei, X. G., Turro, N. J., Lewis, T. J., and Scheffer, J. R., Photochemistry of macrocyclic ketones within zeolites: competition between Norrish type I and type II reactivity, *Tetrahedron Lett.*, 32, 7675, 1991.
137. Yamashita, H., Nishimura, M., Bessho, H., Takada, S., Nakajima, T., Hada, M., Nakatsuji, H., and Anpo, M., Effect of ion-exchanged alkali metal cations on the photolysis of 2-pentanone included within ZSM-5 zeolite cavities: a study of *ab initio* molecular orbital calculations, *Res. Chem. Intermed.*, 27, 89, 2001.
138. Yamashita, H., Sato, N., Anpo, M., Nakajima, T., Hada, M., and Nakatsuji, H., Photochemistry of alkyl ketones included within the zeolite cavities: the effect of ion-exchanged alkali metal cations and types of zeolites, in *Progress in Zeolite and Microporous Materials*, *Parts A–C*, Chon, H., Ihm, S.-K., and Uh, Y.S. Eds., Elsevier, Amsterdam, 1997, 1141.

139. Nishiguchi, H., Yukawa, K., Yamashita, H., and Anpo, M., The effect of ion-exchanged alkali metal cations on the excited states of xanthone and the photolysis of 2-pentanone included within zeolite cavities, *J. Photochem. Photobiol. A: Chem.*, 92, 85, 1995.
140. Kell, A. J., Stringle, D. L. B., and Workentin, M. S., Norrish type II photochemical reaction of an aryl ketone on a monolayer-protected gold nanocluster: development of a probe of conformational mobility, *Org. Lett.*, 2, 3381, 2000.
141. Kell, A. J. and Workentin, M. S., Aryl ketone photochemistry on monolayer protected clusters: study of the Norrish type II reaction as a probe of conformational mobility and for selective surface modification, *Langmuir*, 17, 7355, 2001.
142. Hasegawa, T., Imada, M., and Yoshioka, M., Photoreaction of 2-benzoylcyclohexanones on a silica-gel surface: deviation from their solution photochemistry, *J. Phys. Org. Chem.*, 6, 494, 1993.
143. Hasegawa, T., Kajiyama, M., and Yamazaki, Y., Surface photochemistry of alkyl aryl ketones: energy transfer and the effect of a silica-gel surface on electronic states of excited molecules, *J. Phys. Org. Chem.*, 13, 437, 2000.
144. Klán, P., Janosek, J., and Kriz, Z., Photochemistry of valerophenone in solid solutions, *J. Photochem. Photobiol. A: Chem.*, 134, 37, 2000.
145. Cottier, L., Remy, G., and Descotes, G., Photochemical synthesis of *o*-vinyl glycosides and their transformation into C-branched sugars, *Synthesis*, 711, 1979.
146. Manh, D. D. K., Ecoto, J., Fetizon, M., Colin, H., and Diez-Masa, J.-C., A new approach to spirosesquiterpenes of the acorane family, *J. Chem. Soc., Chem. Commun.*, 953, 1981.
147. Hilgeis, G. and Scharf, H.-D., Synthese von 5β-Androstan-3,17-dion aus Cholsäure, *Liebigs Ann. Chem.*, 1498, 1985.
148. Goodman, J. L. and Berson, J. A., Formation and intermolecular capture of *m*-quinodimethane, *J. Am. Chem. Soc.*, 106, 1867, 1984.
149. Haspra, P., Sutter, A., and Wirz, J., Acidity of acetophenone enol in aqueous solution, *Angew. Chem., Int. Ed. Engl.*, 18, 617, 1979.
150. Chiang, Y., Kresge, A. J., Tang, Y. S., and Wirz, J., pK_a and keto-enol equilibrium constant of acetone in aqueous solution, *J. Am. Chem. Soc.*, 106, 460, 1984.
151. Gao, L. J., Zhao, T. Z., and Han, G. D., A novel method for the synthesis of a C/D-ring synthon of vitamin D derivatives from hyodeoxycholic acid, *Tetrahedron Lett.*, 40, 131, 1999.
152. Henin, F., Muzart, J., Pete, J. P., Mboungoumpassi, A., and Rau, H., Enantioselective protonation of a simple enol-aminoalcohol-catalyzed ketonization of a photochemically produced 2-methylinden-3-ol, *Angew. Chem., Int. Ed. Engl.*, 30, 416, 1991.
153. Henin, F., Mboungoumpassi, A., Muzart, J., and Pete, J. P., Photoreactivity of alpha-tetrasubstituted arylketones: production and asymmetric tautomerization of arylenols, *Tetrahedron*, 50, 2849, 1994.
154. Jefferson, E. A., Keeffe, J. R., and Kresge, A. J., Characterization of the indan-1-one keto-enol system, *J. Chem. Soc., Perkin Trans. 2*, 2041, 1995.
155. Nuss, J. M. and Murphy, M. M., Highly efficient photochemical-synthesis of the enediyne functionality via a Norrish type II reaction, *Tetrahedron Lett.*, 35, 37, 1994.
156. Le Hocine, M. B., Dokhac, D., Fetizon, M., Guir, F., Guo, Y., and Prange, T., New synthesis of taxane derivatives, *Tetrahedron Lett.*, 33, 1443, 1992.
157. Rochat, S., Minardi, C., de saint Laumer, J. Y., and Herrmann, A., Controlled release of perfumery aldehydes and ketones by Norrish type II photofragmentation of α-keto esters in undegassed solution, *Helv. Chim. Acta*, 83, 1645, 2000.
158. Taylor, M. J., Hoffman, T. Z., Yli-Kauhaluoma, J. T., Lerner, R. A., and Janda, K. D., A light-activated antibody catalyst, *J. Am. Chem. Soc.*, 120, 12783, 1998.
159. Nishino, H., Kosaka, A., Hembury, G. A., Shitomi, H., Onuki, H., and Inoue, Y., Mechanism of pH-dependent photolysis of aliphatic amino acids and enantiomeric enrichment of racemic leucine by circularly polarized light, *Org. Lett.*, 3, 921, 2001.
160. Niu, Y. P., Christophy, E., Pisano, P. J., Zhang, Y., and Hossenlopp, J. M., Formate ester Norrish type II elimination: diode laser probing of gas-phase yields, *J. Am. Chem. Soc.*, 118, 4181, 1996.

161. Zhu, L., Cronin, T., and Narang, A., Wavelength-dependent photolysis of *i*-pentanal and *t*-pentanal from 280 to 330 nm, *J. Phys. Chem. A*, 103, 7248, 1999.
162. Wagner, P. J. and Kochevar, I., How efficient is diffusion-controlled triplet energy transfer?, *J Am. Chem. Soc.*, 90, 2232, 1968.
163. Wagner, P. J. and Nakahira, T., Photochemistry of 1-benzoyl-4-*p*-anisylbutane: reaction from equilibrating upper triplets, *J. Am. Chem. Soc.*, 95, 8474, 1973.
164. Wagner, P. J. and Frerking, H. W., The photochemistry of nonconjugated diketones: internal self-quenching and energy transfer, *Can. J. Chem.*, 73, 2047, 1995.
165. Wagner, P. J. and Klán, P., Intramolecular triplet energy transfer in flexible molecules: electronic, dynamic, and structural aspects, *J. Am. Chem. Soc.*, 121, 9626, 1999.
166. Klán, P. and Wagner, P. J., Intramolecular Triplet energy transfer in bichromophores with long flexible tethers, *J. Am. Chem. Soc.*, 120, 2198, 1998.
167. Morrison, H., Trisdale, V., Wagner, P. J., and Liu, K. C., Intramolecular charge transfer quenching in excited β-vinyl phenyl ketones, *J. Am. Chem. Soc.*, 97, 7189, 1975.
168. Wagner, P. J., Kemppainen, A. E., and Jellinek, T., Type II photoreactions of phenyl ketones: competitive charge transfer in α-, γ-, and δ-dialkylamino ketones, *J. Am. Chem. Soc.*, 94, 7512, 1972.
169. Wagner, P. J. and Scheve, B. J., Competing triplet reactions in azidoketones, *J. Am. Chem. Soc.*, 101, 378, 1979.
170. Wagner, P. J. and Lindstrom, M. J., Intramolecular charge-transfer interactions in triplet keto sulfides, *J. Am. Chem. Soc.*, 109, 3057, 1987.
171. Wagner, P. J., Sedon, J., and Gudmundsdottir, A., Photoinduced radical cleavage of ring brominated phenyl ketones, *J. Am. Chem. Soc.*, 118, 746, 1996.
172. (a) Wender, P. A. and Raok, J., Bromoacetophenone-based photonucleases: photoinduced cleavage of DNA by 4′-bromoacetophenone-pyrrolecarboxamide conjugates, *Org. Lett.*, 1, 2117, 1999. (b) Wender, P. A. and Raok, J., Photocleavage of DNA by 4′-bromoacetophenone analogs, *Arch. Pharmacol. Res.*, 24, 39, 2001.
173. Wagner, P. J. and Nahm, K., Regiospecific intramolecular reaction of an alkene group with the benzene ring of a triplet ketone, *J. Am. Chem. Soc.*, 109, 4404, 1987.
174. Wagner, P. J., Sedon, J. H., and Lindstrom, M. J., Rates of radical β-cleavage in photogenerated diradicals, *J. Am. Chem. Soc.*, 100, 2579, 1978.
175. Klán, P., Literák, J., and Hájek, M., The electrodeless discharge lamp: a prospective tool for photochemistry, *J. Photochem. Photobiol. A: Chem.*, 128, 145, 1999.
176. Literák, J. and Klán, P., The electrodeless discharge lamp: a prospective tool for photochemistry. Part 2. Scope and limitation, *J. Photochem. Photobiol. A: Chem.*, 137, 29, 2000.
177. Klán, P. and Literák, J., Temperature dependent solvent effects in photochemistry of 1- phenylpentan-1-ones, *Coll. Czech. Chem. Commun.*, 64, 2007, 1999.
178. Klán, P., Literák, J., and Relich, S., Molecular photochemical thermometers: investigation of microwave superheating effects by temperature dependent photochemical processes, *J. Photochem. Photobiol. A: Chem.*, 143, 49, 2001.
179. Xu, F. Y. and Chien, J. C. W., Photodegradation of alpha-olefin carbon-monoxide alternating copolymer, *Macromolecules*, 26, 3485, 1993.
180. Bond, S. G. and Ebdon, J. R., Photolysis of vinyl ketone copolymers. 3. Norrish type I versus modified Norrish type II chain scission in some methyl methacrylate–aryl vinyl ketone copolymers, *Polymer*, 35, 4079, 1994.
181. Choi, W. M., Jung, I. D., Ha, C. S., and Cho, W. J., Syntheses and properties of photodegradable polystyrene-containing carbonyl group, *J. Appl. Polym. Sci.*, 67, 1237, 1998.
182. Han, S. W., Choi, W. M., Park, J. G., Ha, C. S., Kwon, S. K., and Cho, W. J., Synthesis and photodegradable properties of methyl vinyl ketone-EPDM-styrene graft terpolymer, *J. Appl. Polym. Sci.*, 67, 1721, 1998.
183. Weir, N. A., Arct, J., and Ceccarelli, A., Photodegradation of poly(3,5-dimethoxyacrylophenone) in the long-wave UV region, *Polym. Degrad. Stabil.*, 48, 333, 1995.

53

Photoinduced Electron Transfer Reactions of Oxiranes and Epoxy Ketones

Eietsu Hasegawa
Niigata University

Masaki Kamata
Niigata University

53.1 Introduction

Much attention has been focused on the photochemistry of three-membered ring compounds due to their interesting reactivities; among these compounds are oxiranes.[1–4] Irradiation of these compounds demonstrates two main types of rearrangements: (1) homolytic CO bond cleavage followed by 1,2-migration of a substituent yielding carbonyl compounds, and (2) heterolytic CC bond cleavage giving carbonyl ylide intermediates (Scheme 1). Several reviews dealing with oxirane photochemistry have already appeared. In this chapter, we will focus on the photoinduced electron transfer (PET) reactivity of oxiranes and epoxy ketones.

Over the last three decades, the PET chemistry of organic molecules has been extensively explored, and considerable advances in the understanding of the PET reaction mechanism as well as the synthetic applications of PET processes have been made.[5–7] Due to large enhancement of the electron-donating and electron-accepting ability of a molecule on irradiation, the photoexcited molecules, compared to their ground-state counterparts, more readily undergo single electron transfer (SET) with other molecules. Rehm and Weller[8,9] demonstrated that the feasibility of this SET process is estimated by Eq. (53.1).

$$\Delta G \text{ (kcal/mol)} = 23.06[E^{ox}_{1/2} - E^{red}_{1/2} + C] - E_{00} \quad (53.1)$$

0-8493-1348-1/04/$0.00+$1.50

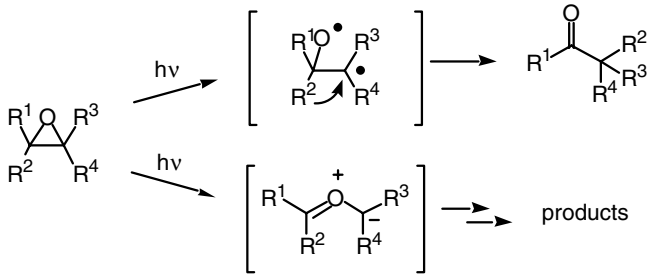

SCHEME 1

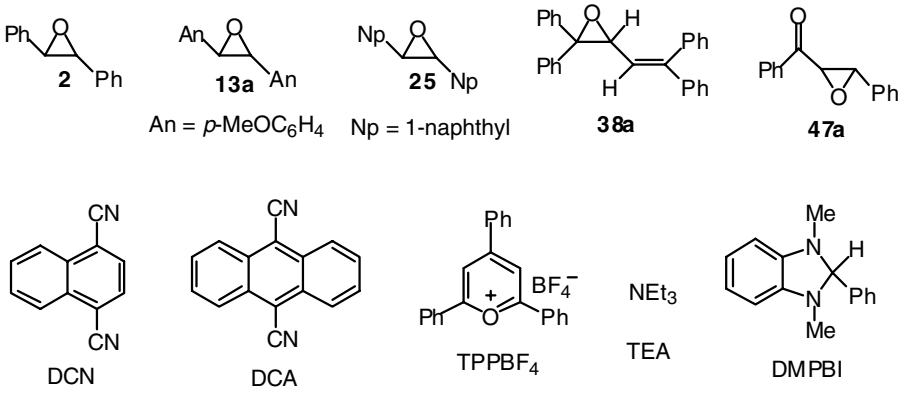

FIGURE 53.1 Representative oxiranes, epoxy ketones, and redox reagents.

The free energy change (ΔG) for the SET process between the donor molecule and the acceptor molecule, one of which is electronically excited, is calculated by using their reduction and oxidation (redox) potentials ($E^{ox}_{1/2}$, $E^{red}_{1/2}$), the excitation energy (E_{00}), and the Coulomb term (C), which depends on the solvent used. The term C is known to be –0.06 eV for a typical polar solvent such as MeCN.

The electron-donating and electron-accepting properties of oxiranes in solution are estimated by their redox potentials which are measured by the electrochemical method.[10,11] Figure 53.1 presents the representative oxiranes, epoxy ketones, and redox reagents (for which the ET reactions will be described later). Their redox properties and the thermodynamic data for their PET processes are listed in Table 53.1. In a general sense, aryl-substituted oxiranes are reasonably good electron donors that undergo PET reaction with several electron-accepting sensitizers such as 1,4-dicyanonaphthalene (DCN), 9,10-dicyanoanthracene (DCA) and 2,4,6-triphenylpyrilium tetrafluoroborate ($TPPBF_4$). On the other hand, PET reduction of oxiranes requires the substitution of certain electron-withdrawing groups such as carbonyls. Thus, the photoexcited triplets of epoxy ketones are recognized as good electron acceptors against certain electron donors such as triethylamine (TEA) and 1,3-dimethyl-2-phenylbenzimidazoline (DMPBI).

53.2 Electron Transfer Reactions involving Radical Cations

Oxirane radical cations undergo the following types of reactions: (1) CC bond cleavage and subsequent formation of carbonyl ylide radical cations which react with dipolarophiles and oxygen, affording tetrahydrofurans and 1,2,4-trioxolanes, respectively; and (2) CO bond cleavage giving the corresponding radical cations which rearrange to carbonyl compounds.

TABLE 53.1 Redox Potentials ($E^{ox}_{1/2}$, $E^{red}_{1/2}$; V vs. SCE) of Oxiranes, Electron Acceptors and Electron Donors, and Free-Energy Changes (ΔG, kcal/mol) for PET Processes Between Oxiranes and Electron Acceptors or Electron Donors in MeCN

Number	Oxirane ($E^{ox}_{1/2}$, $E^{red}_{1/2}$)	Acceptor ($E^{red}_{1/2}$)	Donor ($E^{ox}_{1/2}$)	Excited State	ΔG	Ref.
1[a]	**2** ($E^{ox}_{1/2}$, +1.88)	DCN (–1.67)	—	^{1}DCN*	–6	12
2[b]	**2** ($E^{ox}_{1/2}$, +1.92)	$TPPBF_4$ (–0.37)	—	^{1}[$TPPBF_4$]*	–9	29
3	**13a** ($E^{ox}_{1/2}$, +1.30)	DCA (–0.98)	—	^{1}DCA*	–16	16
4	**25** ($E^{ox}_{1/2}$, +1.50)	DCA (–0.98)	—	^{1}DCA*	–11	19
5	**38a** ($E^{ox}_{1/2}$, +1.72)	DCA (–0.98)	—	^{1}DCA*	–6	24
6	**47a** ($E^{red}_{1/2}$, –1.67)	—	TEA (+0.86)	^{3}[**47a**]*	–14	34
7	**47a** ($E^{red}_{1/2}$, –1.67)	—	DMPBI (+0.29)	^{3}[**47a**]*	–27	48

[a] Redox potentials are reported vs. $Ag/AgNO_3$.

[b] Because the reaction was conducted in CH_2Cl_2,[29] +0.16 eV is used as term *C* in Eq. (53.1).[9]

Abbreviations: DCN, 1,4-dicyanonaphthalene; $TPPBF_4$, 2,4,6-triphenylpyrilium tetrafluoroborate; DCA, 9,10-dicyanoanthracene; DMPBI, 1,3-dimethyl-2-phenylbenzimidazoline.

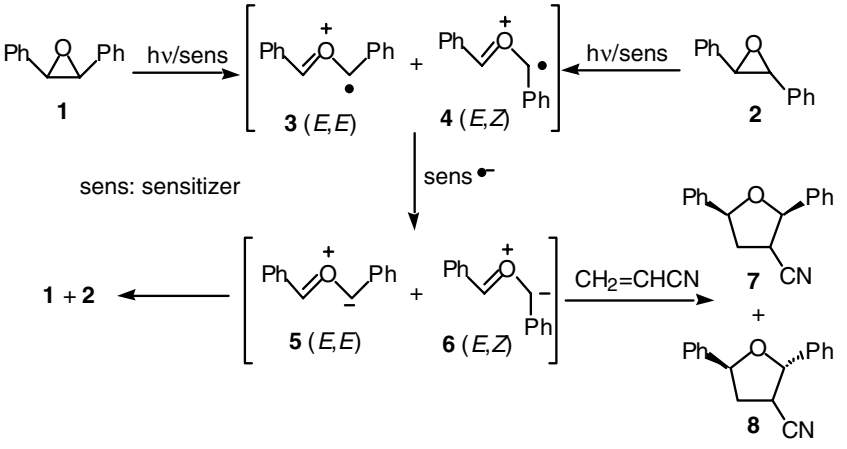

SCHEME 2

Tetrahydrofuran Formation through CC Bond Cleavage

Arnold[12] first discovered that PET reactions of *cis*- and *trans*-2,3-diphenyloxiranes (**1** and **2**) with electron-accepting sensitizers such as DCN, 1,4-dicyanobenzene, dimethyl terephthalate, and methyl 4-cyanobenzoate produce the isomeric tetrahydrofuran derivatives **7** and **8** (Scheme 2). The proposed mechanism involves the CC bond cleavage of the oxirane radical cations to give ylide radical cations **3** and **4**, followed by back electron transfer (BET) to generate carbonyl ylides **5** and **6**. The resulting carbonyl ylides are trapped with dipolarophiles, such as acrylonitrile, maleonitrile, and fumaronitrile, to produce the observed products. In the absence of dipolarophiles, *cis*-/*trans*-isomerization (**1/2** = 0.19–0.28) was observed, which is consistent with the formation of carbonyl ylides **5** and **6**, as well as their radical cations **3** and **4**. This method was successfully applied to the synthesis of various tetrahydrofurans (Scheme 3)[13] and dihydrofurans (Scheme 4).[14]

1,2,4-Trioxolane Formation through CC Bond Cleavage

The PET reactions of oxiranes carried out in the presence of oxygen frequently produce oxygenated products such as 1,2,4-trioxolanes (ozonides). Futamura first reported that DCA-sensitized PET oxygenation of

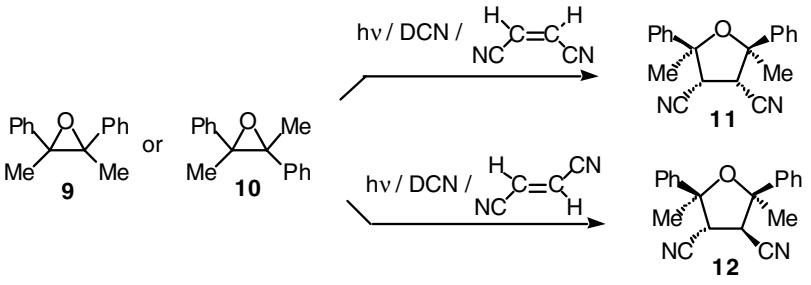

SCHEME 3

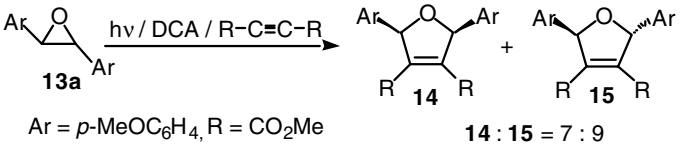

SCHEME 4

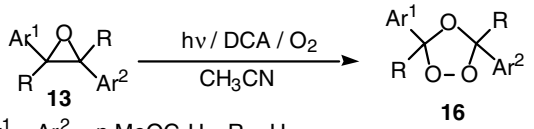

13a: $Ar^1 = Ar^2 = p\text{-}MeOC_6H_4$, R = H
13b: $Ar^1 = Ar^2 = p\text{-}MeOC_6H_4$, R = Et
13c: $Ar^1 = p\text{-}MeOC_6H_4$, Ar^2 = Ph, R = H
13d: $Ar^1 = p\text{-}MeOC_6H_4$, $Ar^2 = p\text{-}MeC_6H_4$, R = H

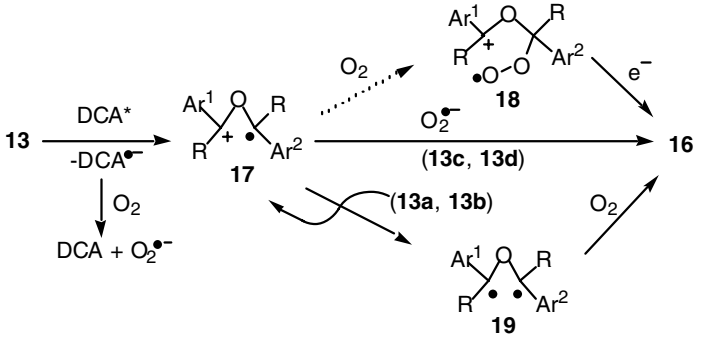

SCHEME 5

1,2-diaryloxiranes **13** possessing an electron-donating aryl group ($p\text{-}MeOC_6H_4$) produces 1,2,4-trioxolanes **16** (Scheme 5).[15,16] In the reactions of **13a** and **13b**, the quantum yields were greater than 1.0, suggesting catalytic generation of the radical cations of **13**; however, the stereochemistry of **16** and the active oxygen species (triplet oxygen, singlet oxygen, or oxygen radical anion) was unclear in the proposed mechanism.

Schaap[17] reported that DCA–biphenyl (BP)-cosensitized PET oxygenation of tetraphenyloxirane **20** produced 1,2,4-trioxolane **21** (Scheme 6). Although **20** does not efficiently quench the fluorescence of

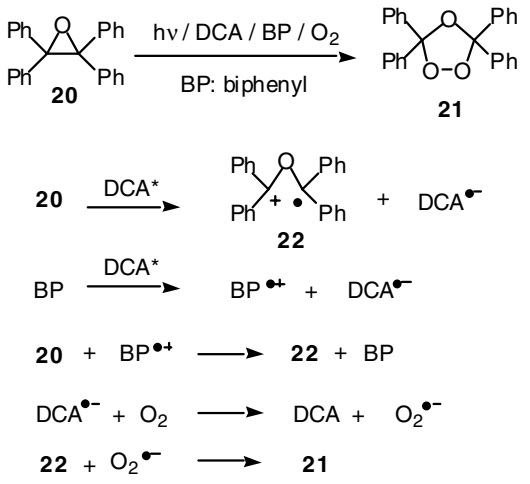

SCHEME 6

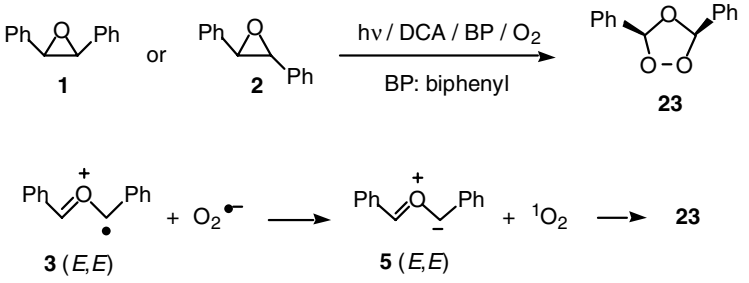

SCHEME 7

DCA, a dramatic rate enhancement of the oxygenation is observed by addition of BP. The rationalization is as follows: BP quenches the fluorescence of DCA to generate a BP radical cation and a DCA radical anion. The lifetime of the BP radical cation is long enough to accept a single electron from **20** to generate radical cation **22**, although this process is endothermic. The resulting **22** reacts with the oxygen radical anion to give **21**. The same method was applied to PET oxygenation of *cis*- and *trans*-1,2-diphenyloxiranes **1** and **2** (Scheme 7).[18] Interestingly, only *cis*-1,2,4-trioxolane **23** was obtained from both **1** and **2**. It was proposed that a more stable carbonyl ylide **5**, generated by BET from the oxygen radical anion to the radical cation **3**, reacts with singlet oxygen to give *cis*-**23**. Addition of BP was not found to be essential to control the stereochemistry of the product.

Oxygenation of 1,2-dinaphthyloxiranes **24** and **25** by PET was conducted without BP, as both **24** and **25** were able to quench the fluorescence of DCA.[19] Thus, *cis*-trioxolane **26** was isolated as the sole stereoisomer (Scheme 8). However, the Schaap mechanisms described above, involving a highly stereoselective formation of *cis*-1,2,4-trioxolanes (Scheme 7 and 8), seem to be inconsistent with the previously described Arnold mechanism (Scheme 2), where two types of radical cations (**3** and **4**) as well as carbonyl ylides (**5** and **6**) are generated by the PET oxidation of **1** and **2**, respectively.

Kamata[20–22] found that *cis*-1,2,4-trioxolanes **29** were stereoselectively produced, while a nonstereoselective [3+2]-cycloaddition (**30** and **31**) with tetracyanoethylene (TCNE) competes with 1,2,4-trioxolane formation on irradiation of the charge transfer (CT) complexes of 2,3-diaryloxiranes (**27** and **28**) with TCNE in the presence of oxygen (Scheme 9). Interesting features of this chemistry are:

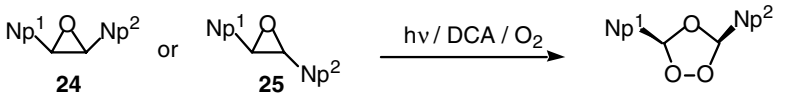

$Np^1 = Np^2$ = 1-naphthyl
$Np^1 = Np^2$ = 2-naphthyl
Np^1 = 1-naphthyl, Np^2 = 2-naphthyl

SCHEME 8

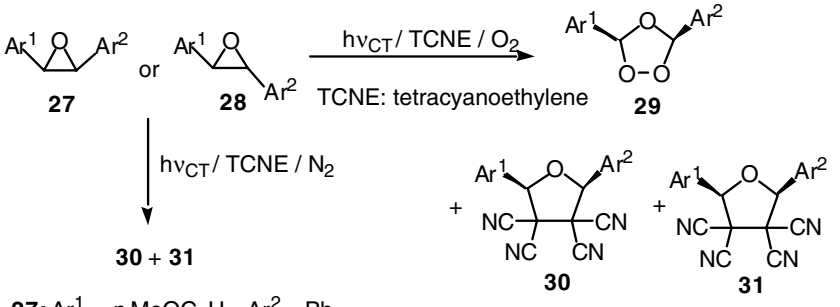

27: Ar^1 = *p*-$MeOC_6H_4$, Ar^2 = Ph
28a: Ar^1 = *p*-$MeOC_6H_4$, Ar^2 = Ph
28b: $Ar^1 = Ar^2$ = *p*-$MeOC_6H_4$
28c: Ar^1 = *p*-$MeOC_6H_4$, Ar^2 = *p*-ClC_6H_4

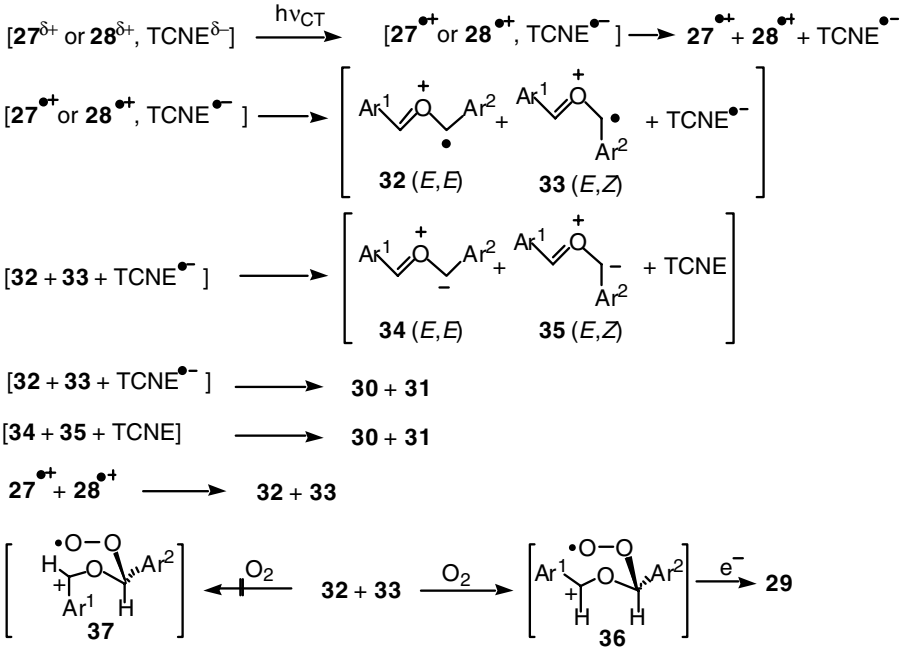

SCHEME 9

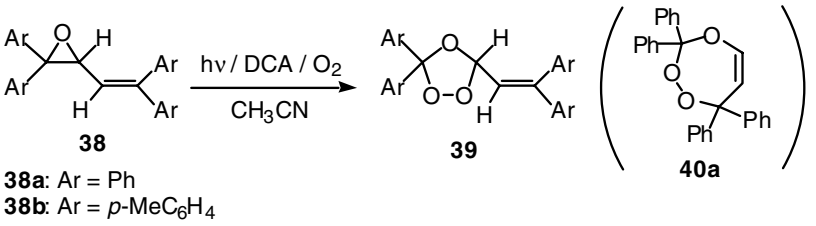

38

38a: Ar = Ph
38b: Ar = *p*-MeC$_6$H$_4$

39

40a

SCHEME 10

1. The amounts of TCNE did not significantly change the yields of oxygenation products **29**, indicating that TCNE is regenerated in the oxygenation cycle.
2. Addition of 1,2,4,5-tetramethoxybenzene (TMB) as a SET quencher completely suppressed the oxygenation but did not affect [3+2]-cycloaddition with TCNE.
3. The solvent polarity could control the reaction pathway, in that **28b** gave **30b** (28%) and **31b** (25%), together with a trace of **29b** in benzene, while **29b** was obtained as the sole product (66%) in acetonitrile.
4. Oxygenation occurred stereoselectively, but [3+2]-cycloaddition did not.

The fact that the same stereoselectivity was observed for photooxygenation products in the reaction with TCNE as that observed under DCA-sensitized conditions (see above) is particularly interesting. Neither an oxygen radical anion nor singlet oxygen is generated in the TCNE cases, implying that singlet oxygen may not always be responsible for the stereoselective oxygenation of oxiranes under DCA-sensitized conditions. In other words, triplet oxygen, as an active species for oxygenation, cannot be ruled out even under DCA-sensitized conditions. Related information was provided by Gollnick and Schnatterer[23] that suggested that triplet oxygen is responsible for the DCA-sensitized PET oxygenation of 1,1-di(*p*-methoxyphenyl)ethylene. It is assumed that the ring cleavage of the radical cations of **27** and **28** occurs nonstereoselectively to form **32** and **33**, both of which, in turn, can be captured by the triplet oxygen to form peroxy radical cations. In these intermediates, the barrier to rotation around the C–O–C$^+$ bond is small, so a second CO bond formation can occur through the least hindered radical **36** (not **37**) to form **29** followed by BET. The nonstereoselective formation of **30** and **31** can be explained either by a concerted [3+2]-cycloaddition of **32** and **33** with the TCNE radical anion or, more likely, by an alternative concerted addition of carbonyl ylides **34** and **35** with TCNE after a BET reaction has occurred within the solvent cage.

Kamata[24] recently reinvestigated DCA-sensitized PET oxygenation of vinyloxirane **38** and found that 1,2,4-trioxolane **39** was a major product without the isolation of the seven-membered 1,2,4-trioxepine **40**, although **40a** was previously reported by Futamura[25] to be the product in the same reaction (Scheme 10).

Recently, extensive efforts have been devoted to the synthesis of cyclic peroxides since the discovery of artemisinin and related antimalarial 1,2,4-trioxanes.[26,27] As described previously, PET oxygenation is a unique but effective method for the preparion of cyclic peroxides, which is also applicable to the synthesis of the peroxide structures from arylated cyclopropanes, aziridines, and olefins.[21,22]

Rearrangement through CO Bond Cleavage

In the absence of dipolarophiles and oxygen, oxirane radical cations sometimes undergo CO bond cleavage to give rearranged carbonyl compounds. Reactions of a ring-opened radical cation with nucleophiles are observed to give the addition products.

Kagan[28] reported that the methanol adduct **43** was obtained on irradiation of a methanol solution of oxirane **41** in the presence of Fe(III) (Scheme 11). The reaction is assumed to proceed through the excitation of a CT complex of **41** with Fe(III) followed by the MeOH-assisted ring-opening of the radical

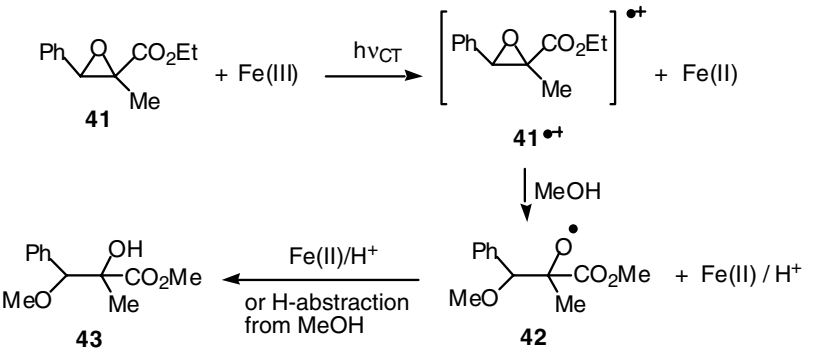

SCHEME 11

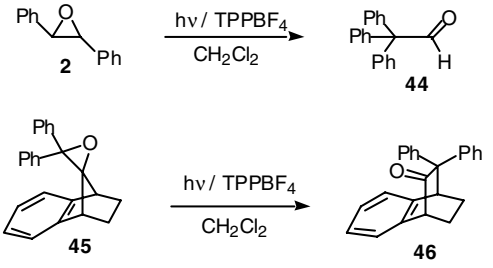

SCHEME 12

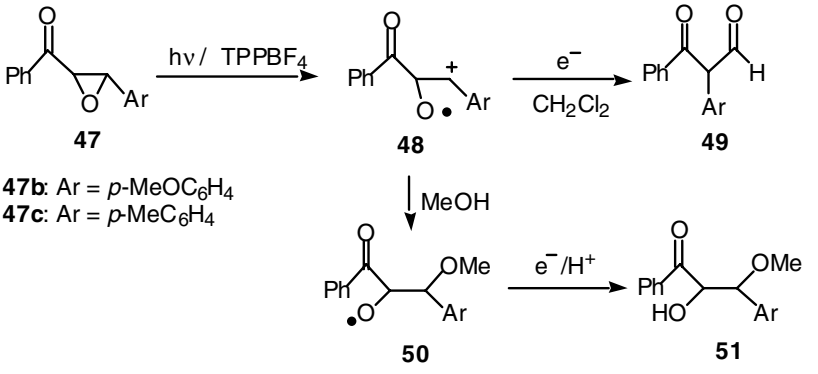

SCHEME 13

cation of **41**. The alkoxy radical **42** is produced and finally converted to **43**. Hasegawa[29] found that 2,4,6-triphenylpyrylium (TPP) salt-sensitized PET reactions of oxiranes **2** and **45** undergo rearrangement to produce carbonyl compounds **44** and **46**, respectively (Scheme 12). Similar rearrangement and methanol addition reaction were also found for the TPP-sensitized PET oxidation of epoxy ketones **47** to afford the products **49** and **51** (Scheme 13).[30] Selective $C_\beta O$ cleavage of the radical cation of **47** gives radical cation **48**, which rearrange to **49** in dichloromethane and is trapped by methanol to produce **51** through the oxy radical **50**.

While these types of reactions are synthetically useful, the understanding of the reaction mechanism is still controversial. Thus, a clear mechanistic distinction between radical cation rearrangements and rearrangements promoted by acid catalysis, presumably generated during ET processes, for the above transformations is often very difficult to make.[31]

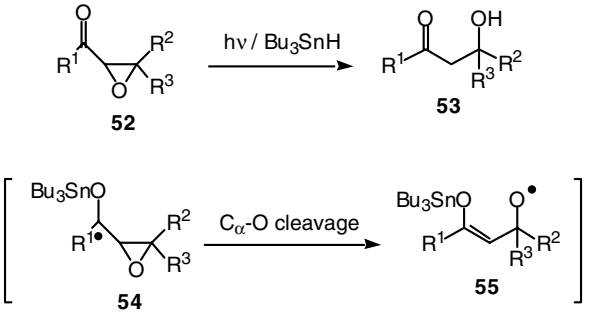

SCHEME 14

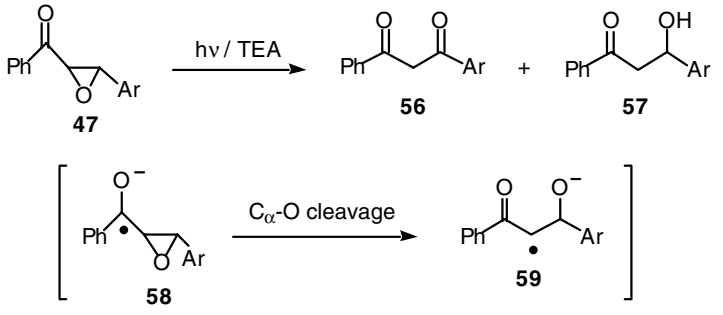

SCHEME 15

53.3 Electron Transfer Reactions Involving Radical Anions

Photoreactions of epoxy ketones have been extensively investigated, and these studies demonstrated that several types of photochemical processes are open to these compounds.[1–4] Thus, it was often difficult to control the regioselectivity of the epoxy ring-opening because the reactivity depends on the substitution and the nature of their excited states.

Photoreactions of Epoxy Ketones with Triethylamine and Other Donors

About 10 years ago, Hasegawa discovered that oxiranyl methyl radicals such as **54** that possess an electron-donating tributylstannyloxy substituent at the radical center undergo selective $C_\alpha O$ bond cleavage to give the oxy radicals **55** in the free-radical reaction of epoxy ketones **52** with tributyltinhydride, which finally produce β-hydroxy ketones **53** in high yields (Scheme 14).[32,33]

This observation suggests that the carbonyl radical anions (ketyl radicals) of epoxy ketones, in which the negative charge builds up at the position adjacent to the epoxy ring, should also cause selective $C_\alpha O$ bond cleavage of these intermediates. As expected, irradiation of some aromatic epoxy ketones **47** with TEA produced β-diketones **56** and β-hydroxy ketones **57** in which the transformation of the ketyl radicals **58** to the ring-opened radical anions **59** was proposed (Scheme 15).[34] The product ratio of **56a** to **57a** obtained from **47a** depends on the reaction conditions as shown in Table 53.2. While both **56a** and **57a** were obtained in MeCN and MeOH, addition of $LiClO_4$ completely suppressed the formation of **57a** together with the formation of acetophenone as well as benzaldehyde (retro-Aldol products). Irradiation of epoxy ketones **60** in the presence of allyltributyltin as an electron donor produced α-allyl-β-hydroxy ketones **61**, which were presumably formed by coupling of the ring-opened radical anions **64** and an allyl radical (Scheme 16).[35] Following a mechanistic study it was demonstrated that the product ratio of β-diketone **62a** and β-hydroxy ketone **63a** was influenced by the amine used (Table 53.3).[36]

TABLE 53.2 Photoreaction of Epoxy Ketone **47a** (Ar = Ph) with Triethylamine (TEA)

Entry	Solvent	$LiClO_4$	Yield of **56a** (%)	Yield of **57a** (%)
1	MeCN	0	60	22
2	MeCN	Added	70	0
3	MeOH	0	49	28

Note: Yields of **56a** and **57a** are reported on the basis of the conversion of **47a**.

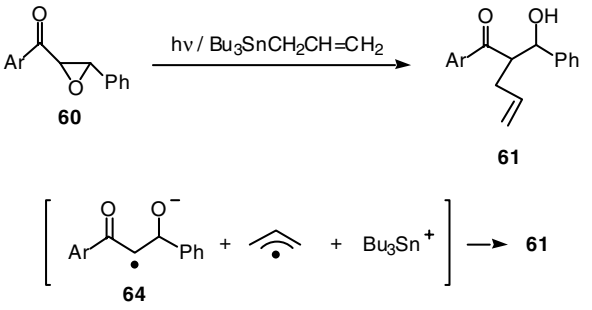

SCHEME 16

TABLE 53.3 Photoreaction of Epoxy Ketone **60a** (Ar = *p*-CNC_6H_4) with Various Amines

Entry	Amine	Solvent	Yield of **62a** (%)	Yield of **63a** (%)
1	TEA	MeCN	40	7
2	TEA	PhH	77	8
3	DABCO	PhH	71	0
4	DEA	PhH	7	42
5	TBA	PhH	12	50

Note: Yields of **62a** and **63a** are reported on the basis of the conversion of **60a**. DABCO, 1,4-diazabicyclo[2.2.2]octane; DEA, *N,N*-diethylaniline; TBA, tribenzylamine.

A reaction mechanism in which interaction between the radical anions derived from epoxy ketones **60** and amine radical cations govern the selective pathway to the observed products **62** and **63** was proposed (Scheme 17).[36]

Such interactions should be more favorable in less polar solvents such as benzene than the more polar solvent MeCN, as this change of solvent shifts the equilibrium of the free radical ions to the radical ion pairs. Hydrogen atom transfer between radical anion **64** and the amine radical cation produces the enolate **65**, which is protonated to become **62.** The efficiency of the hydrogen abstraction by the amine radical cation is qualitatively correlated with the NH bond strength of the corresponding ammonium salt. On the other hand, proton transfer between **64** and the amine radical cation followed by SET gives the anion **67**, which is transformed to **63** by protonation. This first proton transfer step is governed by the proton-donating ability (acidity) of the amine radical cation, which is affected by the α substituents of the amine.

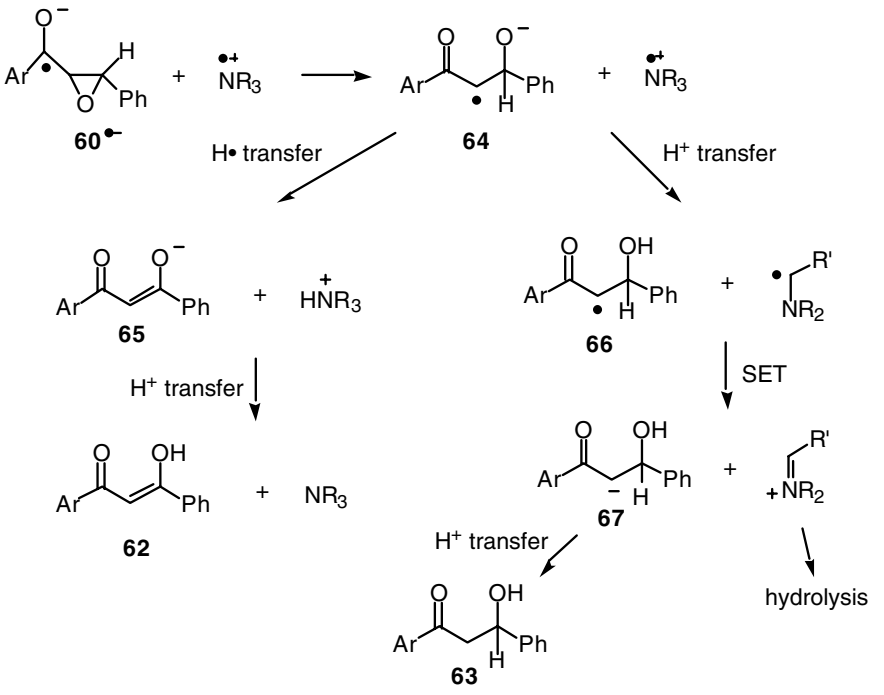

SCHEME 17

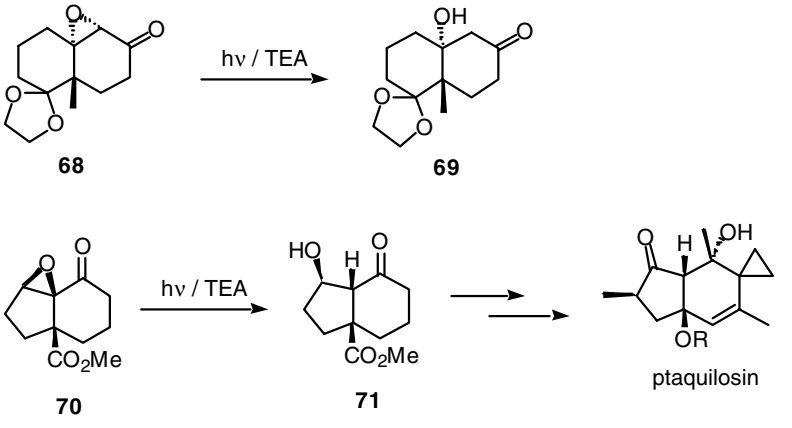

SCHEME 18

The transformation of epoxy ketones to β-hydroxy ketones is recognised as a synthetically important chemical process.;[37] thus, Cossy[38,39] reported photoreactions of several aliphatic and aromatic epoxy ketones with TEA (Scheme 18).

For example, epoxy ketone **68** was irradiated (254 nm) with TEA to give hydroxy ketone **69** (68%) at 56% conversion of **68**. This method was successfully applied to the synthesis of a bioactive compound, ptaquilosin.[40] Mattay[41] examined the photoreaction of epoxy ketone **72** with TEA in expectation of the formation of the cyclized product **77**, which presumably results from the intermediacy of **76** (Scheme 19). However, **77** was not obtained, while enone **73** was isolated in low yield. The rationalization was that

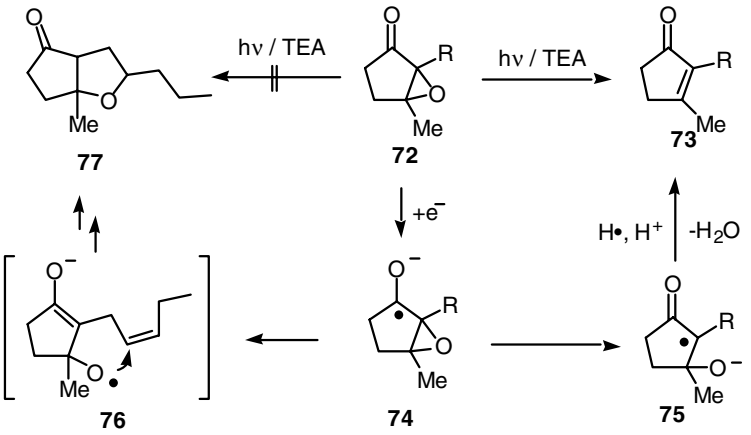

SCHEME 19

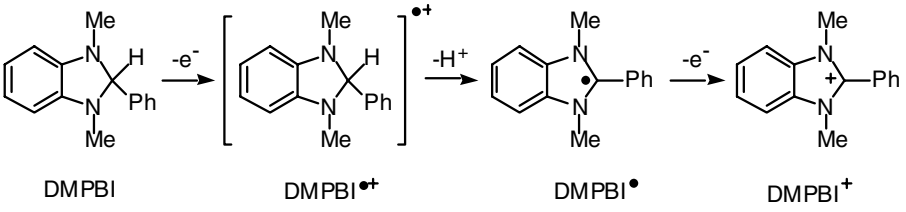

SCHEME 20

ketyl radical **74** chemoselectively rearranges to **75** instead of **76**, which is consistent with Hasegawa's proposal (see Scheme 15).

Photoreactions of Epoxy Ketones with 1,3-Dimethy-2-Phenylbenzimidazoline

In the above experiments, while the yields of β-hydroxy ketones were modest, several problems were encountered. For example, Hasegawa's experimental conditions produced β-diketones as major products.[34,36] Cossy mentioned that prolonged irradiation by quartz-filtered light caused decomposition of the β-hydroxy ketones.[39] Therefore, it was desired to discover the optimal PET conditions to produce β-hydroxy ketones in better yields. On the basis of the proposed mechanism in Scheme 17, the compounds, which act as good electron donors as well as hydrogen donors, could improve the yield of β-hydroxy ketones. As shown in Scheme 20, it was reported that 1,3-dimethy-2-phenylbenzimidazoline (DMPBI)[42,43] is first oxidized to the radical cation ($DMPBI^{+\cdot}$) followed by deprotonation to give an α-amino radical ($DMPBI^{\cdot}$) which is converted to imidazolium ($DMPBI^{+}$).[44–47] Thus, DMPBI was first applied to PET reduction of epoxy ketone **47a** (Scheme 21).[48,49] While the reaction in dry THF did not give the desired result of yielding enone **78** as a major product, the same reaction in wet THF produced **57a** in excellent yield. Following related investigations, it was finally demonstrated that DMPBI-acetic acid is an effective reagent system for photoinduced reductive transformation of α,β-epoxy ketones **52** to β-hydroxy ketones **53** (Scheme 22) (Table 53.4).[50] Irradiation of benzoyl-substituted epoxides **52a**-**d** in THF by Pyrex-filtered light produced the corresponding β-hydroxy ketones **53a**-**d** in good to excellent yields (Table 53.4, entries 1–5). On the other hand, photoreduction of acetyl-substituted epoxide **52e** to **53e** required photosensitized conditions (>360 nm) in DMF using 1,6-*bis*-dimethylaminopyrene as a sensitizer (Table 53.4, entry 5).

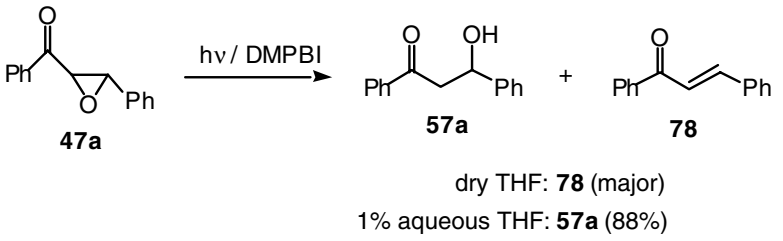

SCHEME 21

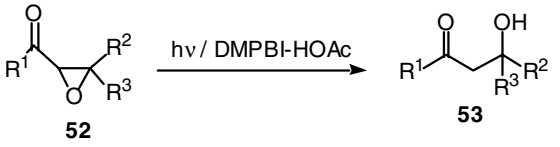

SCHEME 22

TABLE 53.4 Photoreaction of Epoxy Ketones **52** with DMPBI-HOAc

Entry	**52**	R^1	R^2	R^3	Conversion of **52** (%)	Yield of **53** (%)
1	*trans*-**52a**	Ph	H	Ph	100	96
2	*cis*-**52a**	Ph	Ph	H	100	94
3	**52b**	Ph	H	*p*-$MeOC_6H_4$	100	88
4	**52c**	Ph	H	*i*-Pr	100	72
5	**52d**	Ph	H	H	100	69
6	**52e**	Me	H	Ph	70	93

Note: Yield of **53** is reported on the basis of the conversion of **52**.

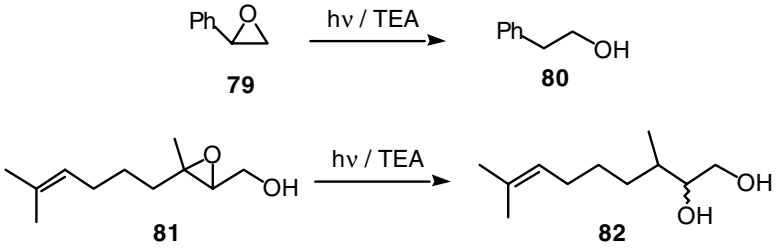

SCHEME 23

Photoreactions of Other Oxiranes with Triethylamine (TEA)

Photoreactions of aryl and alkyl oxiranes such as **79** and **81** with TEA were also reported by Epling[51] to give the corresponding alcohols **80** and **82** (Scheme 23). Other studies by Maruyama[52] using derivatives such as epoxy quinone **83** and by Ishii[53] using epoxy nitrile **86** were also subjected to PET reduction with TEA to produce the various reduction products **84**, **85**, **87**, and **88** (Scheme 24 and Scheme 25).

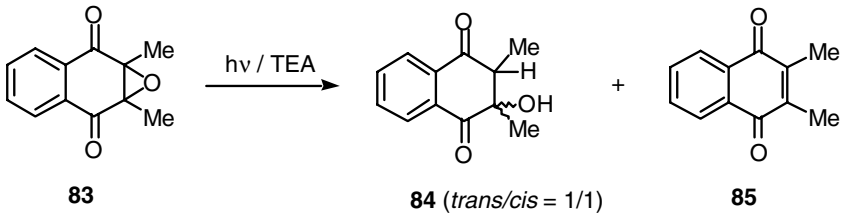

83 **84** (*trans/cis* = 1/1) **85**

SCHEME 24

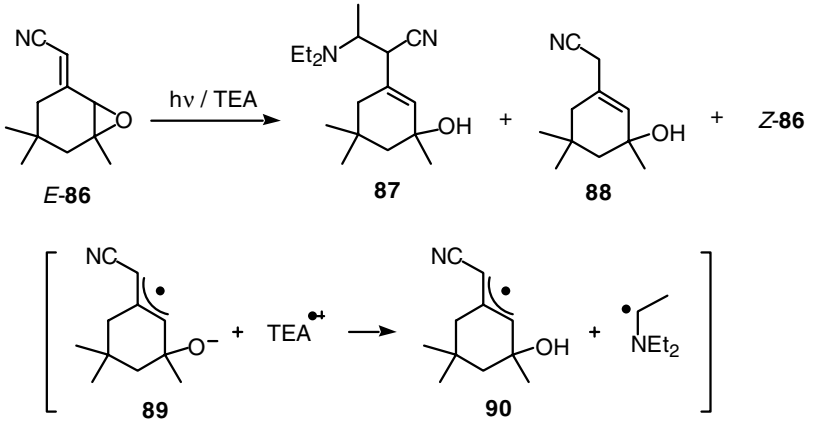

E-**86** **87** **88** **89** **90**

SCHEME 25

53.4 Summary

Photoinduced electron transfer (PET) reactions of oxiranes and epoxy ketones show various chemical pathways, which depend on the substrates and the conditions employed. It is hoped that further investigation on PET reactions of oxiranes and other related compounds will provide a breakthrough in our understanding of the mechanism as well as lead to new synthetically useful methods. To generate radical ions in solution, thermal methods such as reactions promoted by redox reagents as well as electrochemical reactions are perhaps more common to organic chemists. This review, we hope, has demonstrated further that the PET method is a unique but useful way to generate these active species. The reactivity of radical ions is, in general, governed by the nature of the radical ions themselves, as well as the surrounding conditions such as solvents, redox reagents, and incident light. Therefore, the PET method and traditional thermal methods should be complementary in the investigation of ion radical reactions from the mechanistic as well as synthetic viewpoints.

References

1. Padwa, A., Photochemical transformations of small ring carbonyl compounds, in *Organic Photochemistry,* Vol. 1, Chapman, O. L., Ed., Marcel Dekker, New York, 1967, 91.
2. Nastashi, M. and Streith, J., Photochemical rearrangements involving three-membered rings, in *Rearrangements in Ground and Excited States*, Vol. 3, deMayo, P., Ed., Academic Press, New York, 1980, 445.
3. Das, P.K., Absorption spectral data and kinetic behaviors of 1,3-dipolar phototransients, in *Handbook of Organic Photochemistry*, Vol. 2, Scaiano, J. C., Ed., CRC Press, Boca Raton, FL, 1989, 35.

4. Maruyama, K. and Kubo, Y., Photochemistry of oxiranes-photoreactions of epoxynaphthoquinones, in *CRC Handbook of Organic Photochemistry and Photobiology*, Horspool, W. M. and Song, P-S., Eds., CRC Press, Boca Raton, FL, 1995, 375 (and references cited therein).
5. Fox, M. A. and Chanon, M., Eds., *Photoinduced Electron Transfer*, Parts A–D, Elsevier, Amsterdam, 1988.
6. Mariano, P.S., Ed., *Advances in Electron Transfer Chemistry*, Vols. 1–6, JAI Press, Greenwich, 1991–1999.
7. Balzani, V., Ed., *Electron Transfer in Chemistry*, Vols. 1–5, Wiley-VCH, Weinheim, 2001.
8. Rehm, D. and Weller, A., Kinetics of fluorescence quenching by electron and H-atom transfer, *Isr. J. Chem.*, 8, 259, 1970.
9. Weller, A., Photoinduced electron transfer in solution: exciplex and radical ion pair formation free enthalpies and their solvent dependence, *Z. Phys. Chem. Neue Folge*, 133, 93, 1982.
10. Mann, C. K. and Barnes, K. K., *Electrochemical Reactions in Nonaqueous Systems*, Marcel Dekker, New York, 1973.
11. Wayner, D. D. M., Redox properties, in *Handbook of Organic Photochemistry*, Vol. 2, Scaiano, J. C., Ed., CRC Press, Boca Raton, FL, 1989, 363.
12. Albini, A. and Arnold, D. R., The photosensitized (electron transfer) ring opening of aryloxiranes, *Can. J. Chem.*, 56, 2985, 1978.
13. Wong, J. P. K., Fahmi, A., Griffin, G. W., and Bhacca, N. S., Photo- and thermoinduced generation of 1,3-diaryl carbonyl ylides from 2,3-diaryloxiranes: 1,3-dipolar cycloadditions to dipolarophiles, *Tetrahedron*, 37, 3345, 1981.
14. Clawson, P., Lunn, P. M., and Whiting, A., The photochemistry of 2,3-*bis*(*p*-methoxyphenyl)oxirane: trapping of a CC cleaved intermediate in an electron-transfer sensitized process, *J. Chem. Soc., Chem. Commun.*, 134, 1984.
15. Futamura, S., Kusunose, S., Ohta, H., and Kamiya, Y., Formation of ozonides via 9,10-dicyanoanthracene-sensitized photo-oxidation of epoxides, *J. Chem. Soc., Chem. Commun.*, 1223, 1982.
16. Futamura, S., Kusunose, S., Ohta, H., and Kamiya, Y., 9,10-Dicyanoanthracene-sensitized photooxidation of electron-rich stilbene oxides, *J. Chem. Soc., Perkin Trans. 1*, 15, 1984.
17. Schaap, A.P., Lopez, L., and Gagnon, S.D., Formation of an ozonide by electron-transfer photooxygenation of tetraphenyloxirane, *J. Am. Chem. Soc.*, 105, 663, 1983.
18. Schaap, A. P., Siddiqui, S., Gagnon, S. D., and Lopez, L., Stereoselective formation of *cis*-stilbene ozonide from the cosensitized electron-transfer photooxygenation of *cis*- and *trans*-2,3-diphenyloxiranes, *J. Am. Chem. Soc.*, 105, 5149, 1983.
19. Schaap, A.P., Siddiqui, S., Prasad, G., Rahman, A. F. M. M., and Oliver, J. P., Stereoselective formation of *cis* ozonide by electron-transfer photooxygenation of naphthyl-substituted epoxides, *J. Am. Chem. Soc.*, 106, 6087, 1984.
20. Miyashi, T., Kamata, M., and Mukai, T., Stereoselective oxygenation of 2,3-diaryloxiranes by irradiation of electron donor-acceptor complexes of tetracyanoethylene, *J. Chem. Soc., Chem. Commun.*, 1577, 1986.
21. Miyashi, T. and Kamata, M. Organic photoreaction via charge-transfer complexes, *J. Syn. Org. Chem. Jpn.*, 44, 986, 1986.
22. Miyashi, T., Kamata, M., and Mukai, T., Simultaneous capture of two distinct radical ion intermediates generated from the EDA complexes of three-membered compounds with TCNE by photoexcitation and in the dark, *J. Am. Chem. Soc.*, 109, 2780, 1987.
23. Gollnick, K. and Schnatterer, A., Formation of a 1,2-dioxane by electron-transfer photooxygenation of 1,1-di(*p*-anisyl)ethylene, *Tetrahedron Lett.*, 185, 1984.
24. Kamata, M., Komatsu, K., and Akaba, R., Formation of 1,2,4-trioxolanes via 9,10-dicyanoanthracene (DCA)-sensitized photooxygenation of 2,2-diaryl-3-(2,2-diarylvinyl)oxiranes, *Tetrahedron Lett.*, 42, 9203, 2001.
25. Futamura, S. and Kamiya, Y., Formation of 1,2,4-trioxepines via 9,10-dicyanoanthracene (DCA)-sensitized photooxidation of arylvinyloxiranes, *J. Chem. Soc., Chem. Commun.*, 1053, 1988.

26. Meshnick, S. R., Jefford, C. W., Posner, G. H., Avery, M. A., and Peters, W., Second-generation antimalarial endoperoxides, *Parasitol. Today*, 12, 79, 1996 (and references cited therein).
27. Kamata, M., Ohta, M., Komatsu, K., Kim, H.-S., and Wataya, Y., Synthesis, Fe(II)-induced degradation and antimalarial activities of 1,5-diaryl-6,7-dioxabicyclo[3.2.2]nonanes: direct evidence for nucleophilic *O*-1,2-aryl shifts, *Tetrahedron Lett.*, **43**, 2063, 2002.
28. Kagan, J., Juang, P. Y., Firth, B. E., Przybytek, J. T., and Singh, S. P., Catalysis of the ionic-like photoaddition of methanol to epoxides by Fe(III), *Tetrahedron Lett.*, 4289, 1977.
29. Okada, K., Hasegawa, E., and Mukai, T., Photosensitized carbon–oxygen bond cleavage reaction of epoxides by 2,4,6-triphenylpyrylium tetrafluoroborate salt, *Chem. Lett.*, 305, 1983.
30. Hasegawa, E., Ishiyama, K., Kashiwazaki, H., Horaguchi, T., and Shimizu, T., Selective C_β-O bond cleavage of chalcone epoxides induced by pyrylium salt sensitized photoreactions and dark reactions with cerium (IV) salts, *Tetrahedron Lett.*, 31, 4045, 1990.
31. Rathore, R. and Kochi, J. K., Acid catalysis vs. electron-transfer catalysis via organic cations or cation-radicals as the reactive intermediate, *Acta Chem. Scand.*, 52, 114, 1998.
32. Hasegawa, E., Ishiyama, K., Horaguchi, T., and Shimizu, T., Selective C_α-O bond cleavage of α,β-epoxy ketones to aldols induced by free radical processes, *J. Chem. Soc., Chem. Commun.*, 550, 1990.
33. Hasegawa, E., Ishiyama, K., Kato, T., Horaguchi, T., Shimizu, T., Tanaka, S., and Yamashita, Y., Photochemically and thermally induced free radical reactions of α,β-epoxy ketones with tributyltin hydride: selective C_α-O bond cleavage of oxiranylmethyl radicals derived from α,β-epoxy ketones, *J. Org. Chem.*, 57, 5352, 1992.
34. Hasegawa, E., Ishiyama, K., Horaguchi, T., and Shimizu, T., Exploratory study on photoinduced single electron transfer reactions of α,β-epoxy ketones with amines, *J. Org. Chem.*, 56, 1631, 1991.
35. Hasegawa, E., Ishiyama, K., Horaguchi, T., and Shimizu, T., Free radical trapping of α-keto radicals derived from α,β-epoxy ketones via photoinduced single electron transfer process, *Tetrahedron Lett.*, **32**, 2029, 1991.
36. Hasegawa, E., Ishiyama, K., Fujita, T., Kato, T., and Abe, T., Electron transfer reactions of aromatic α,β-epoxy ketones: factors to govern selective conversions to β-diketones and β-hydroxy ketones, *J. Org. Chem.*, 62, 2396, 1997.
37. Lauret, C., Epoxy ketones as versatile building blocks in organic synthesis, *Tetrahedron Asymm.*, 12, 2359, 2001.
38. Cossy, J., Aclinou, P., Bellosta, V., Furet, N., Baranne-Lafont, J., Sparfel, D., and Souchaud, C., Radical anion ring opening reactions via photochemically induced electron transfer, *Tetrahedron Lett.*, 32, 1315, 1991.
39. Cossy, J., Bouzide, A., Ibhi.S., and Aclinou, P., Formation of β-hydroxyketones from α,β-epoxy ketones by photoinduced single electron transfer reactions, *Tetrahedron*, 47, 7775, 1991.
40. Cossy, J., Ibhi, S., Kahn, P. H., and Tacchini, L., A formal synthesis of ptaquilosin, *Tetrahedron Lett.*, 36, 7877, 1995.
41. Kirschberg, T. and Mattay, J., Photoinduced electron transfer reactions of α-cyclopropyl- and α-epoxy ketones, *J. Org. Chem.*, 61, 8885, 1996.
42. Chikashita, H. and Itoh, K., $AlCl_3$-promoted conjugate reduction of α,β-unsaturated carbonyl compounds with 1,3-dimethyl-2-phenyl-benzimidazoline, *Bull. Chem. Soc. Jpn.*, 59, 1747, 1986.
43. Chikashita, H., Ide, H., and Itoh, K., 1,3-dimethyl-2-phenyl-benzimidazoline as a novel and efficient reagent for mild reductive dehalogenation of α-halo carbonyl compounds and acid chlorides, *J. Org. Chem.*, 51, 5400, 1986.
44. Chen, J. and Tanner, D. D., New method for the facile reduction of α-nitro sulphones to nitroalkanes via an electron-transfer-hydrogen atom abstraction mechanism, *J. Org. Chem.*, 53, 3897, 1988.
45. Tanner, D. D. and Chen, J. J., On the mechanism of the reduction of α-halo ketones by 1,3-dimethyl-2-phenyl-benzimidazoline, *J. Org. Chem.*, 54, 3842, 1989.
46. Tanner, D.D., Chen, J. J., Chen, L., and Luelo, C., Fragmentation of substituted acetophenone and halobenzophenone ketyls, *J. Am. Chem. Soc.*, 113, 8074, 1991.

47. Tanner, D. D., Chen, J. J., Luelo, C., and Peters, P. M., Reversible cyclopropyl ring opening of 1-aroyl-2-phenylcyclopropane radical anions, *J. Am. Chem. Soc.*, 114, 713, 1992.
48. Hasegawa, E., Kato, T., Kitazume, T., Yanagi, K., Hasegawa, K., and Horaguchi, T., Photoinduced electron transfer reactions of α,β-epoxy ketones with 2-phenyl-*N*,*N*-dimethylbenzimidazoline (PDMBI): significant water effect on the reaction pathway, *Tetrahedron Lett.*, 37, 7079, 1996.
49. Hasegawa, E., Yoneoka, A., Suzuki, K., Kato, T., Kitazume, T., and Yanagi, K., Reductive transformations of α,β-epoxy ketones and other compounds promoted through photoinduced electron transfer processes with 1,3-dimethyl-2-phenyl-benzimidazoline (DMPBI), *Tetrahedron*, 55, 12957, 1999.
50. Hasegawa, E., Chiba, N., Nakajima, A., Suzuki, K., Yoneoka, A., and Iwaya, K., 1,3-dimethyl-2-phenyl-benzimidazoline (DMPBI)-acetic acid: an effective reagent system for photoinduced reductive transformation of α,β-epoxy ketones to β-hydroxy ketones, *Synthesis*, 1248, 2001.
51. Epling, G. A. and Wang, Q., Regioselective reduction of epoxides by electron transfer: a photochemical approach, *J. Chem. Soc., Chem. Commun.*, 1133, 1992.
52. Maruyama, K., Otsuki, T., Osuka, A., and Suzuki, H., Photochemical reaction of epoxynaphthoquinone with amine, *Chem. Lett.*, 1, 1982.
53. Ishii, K., Kotera, M., and Sakamoto, M., Photoreactions of α,β-unsaturated γ,δ-epoxy nitriles with amines, *J. Chem. Soc., Chem. Commun.*, 2465, 1994.

54

Crystal Structure–Solid-State Reactivity Relationships: Toward a Greater Understanding of Norrish/Yang Type II Photochemistry

John R. Scheffer
University of British Columbia

Carl Scott
University of British Columbia

54.1 Introduction

The Norrish/Yang type II reaction, arguably the most widespread and well-studied transformation in the field of organic photochemistry, remains to this day an important source of strained, small-ring compounds as well as a vehicle for the generation and study of reactive intermediates such as enols and 1,4-biradicals.[1] In this reaction, ketones with geometrically accessible γ-hydrogen atoms undergo six-membered transition state hydrogen atom abstraction from their $n \rightarrow \pi^*$ excited states to afford 1,4-hydroxybiradicals. As shown in Scheme 1, these species have three fates: (1) reverse hydrogen transfer to

0-8493-1348-1/04/$0.00+$1.50

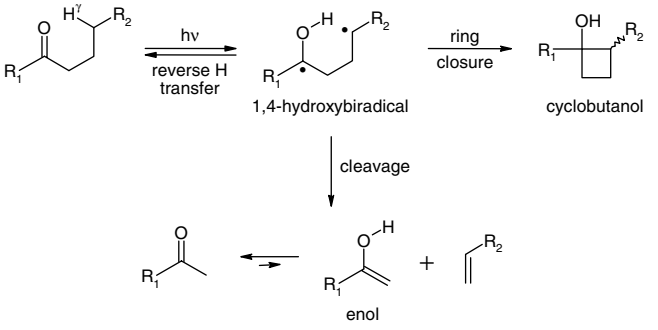

SCHEME 1

regenerate ground-state starting material, (2) cleavage to form an enol and an alkene (Norrish type II cleavage), and (3) ring closure to form a cyclobutanol (Yang photocyclization).[2] In the absence of factors that render it geometrically or energetically unfavorable, cleavage is generally found to be the predominant pathway followed.

Until we began our work in 1983,[3] all studies of the Norrish/Yang type II reaction were conducted in solution or the gas phase. There are, however, several excellent reasons for investigating this reaction in the crystalline state. Chief among these is that it enables correlations to be drawn between the photochemistry observed in this medium and the crystal and molecular structure of the reactant. Put another way, it provides a method by which a three-dimensional "snapshot" of the conformation and environment of the reactant can be obtained — a detailed view of the *preorganized assembly* of reacting molecules in the crystal that is fixed on the photochemical time scale. This differs from the situation in fluid media, where an essentially infinite number of conformers and intermolecular geometries are possible. As an added bonus, if one is fortunate, a so-called "topotactic" solid-state reaction may occur. In such cases, a perfect single crystal of the reactant is continuously and quantitatively transformed into a perfect single crystal of the photoproduct. This permits the entire photochemical transformation to be mapped out crystallographically and allows direct structural correlations between reactant and product to be developed in unprecedented detail. We describe one such topotactic reaction in the pages that follow.

What can we learn about the Norrish/Yang type II reaction by studying it in the crystalline state? In this chapter, we concentrate on the following points: Does γ-hydrogen abstraction actually proceed through a chair-like, six-membered transition state as originally suggested on intuitive grounds by Wagner?[4] Over what distances can abstraction take place, and what is the preferred angular relationship between the carbon–hydrogen bond being broken and the carbon–oxygen double bond of the abstracting carbonyl group? In addressing questions such as these, our goal is to make the Norrish/Yang type II reaction more predictable. By compiling crystallographically determined geometric data for hydrogen abstraction for a large number of structurally diverse type II systems, a database of favorable reaction coordinates can be constructed. A comparison of such data with analogous data for hypothetical type II systems calculated by using molecular mechanics methods then allows predictions to be made concerning the probable success of new Norrish/Yang photoreactions.

A final impetus for investigating the Norrish/Yang photoreaction in the solid state stems from the possibility of using the crystalline medium as a template for asymmetric induction studies. Substances that crystallize in chiral space groups reside in asymmetric environments that are capable of differentiating enantiomeric transition states, and the photochemical conversion of achiral ketones into chiral cyclobutanols offers an ideal vehicle for testing the efficacy of this method of asymmetric synthesis. As we shall see in the following pages, it turns out that it is the asymmetric *conformation* of the reactant in the chiral crystal rather than the asymmetric environment of the surrounding lattice that is responsible for the enantioselectivity of cyclobutanol formation.

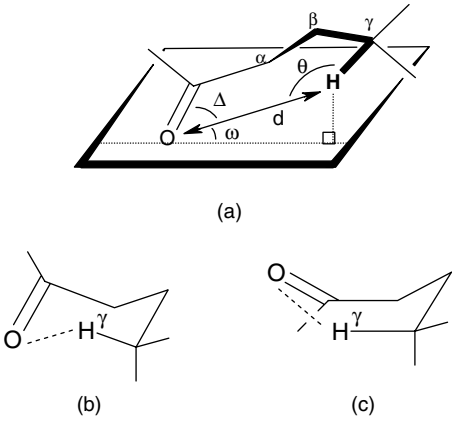

FIGURE 54.1 (a) Definition of geometric parameters *d*, ω, Δ, and θ for γ-hydrogen abstraction. (b) Chair-like hydrogen abstraction geometry. (c) Boat-like hydrogen abstraction geometry.

54.2 The Preferred Geometry of γ-Hydrogen Atom Abstraction

Definition of Geometric Parameters

For discussion purposes, it is useful to define four geometric parameters associated with γ-hydrogen atom abstraction (Figure 54.1a). The first is *d*, the distance between the carbonyl oxygen and the γ-hydrogen atom. It seems reasonable to suggest that the optimum value of *d* should be close to the sum of the van der Waals radii for oxygen and hydrogen, which is 2.72 Å.[5] The second parameter is given the symbol ω and is defined as the angle by which the γ-hydrogen lies outside the mean plane of the carbonyl group. Because hydrogen atom abstraction involves the *n*-orbital on oxygen, which lies in the plane of the carbonyl group, the most favorable angle of ω is expected to be 0°. The third parameter, Δ, is defined as the C=O···H angle, and the best value of this angle should lie between 90° and 120°, depending on the hybridization of the *n*-orbital on oxygen (2p or sp^2). The fourth parameter is θ, the C-H···O angle, which, according to theory, should have an optimum value of 180°.[6] In the discussion that follows, we also characterize the six-atom γ-hydrogen atom abstraction geometry as primarily chair-like (Figure 54.1b) or boat-like (Figure 54.1c).

A Case Study: the *cis*-9-Decalyl Aryl Ketone System

cis-9-Decalyl aryl ketones of general structure 1 (Scheme 2) offer a wealth of possible Norrish/Yang type II reaction pathways. Not only can the *regioselectivity* of hydrogen atom abstraction be probed (H2 vs. H4), but the *enantioselectivity* can be tested as well (H2 vs. H7 and/or H4 vs. H5). Each hydrogen abstraction event can in principle lead to either cleavage or cyclization and, in the latter case, because the resulting cyclobutanol can be formed with two different configurations at the hydroxyl-bearing carbon, *diastereoselectivity* can also be investigated. With these ideas in mind, we synthesized a number of *cis*-9-decalyl aryl ketone derivatives and studied their photochemistry in solution as well as the crystalline state.[7] The compounds investigated and the products formed are outlined in Scheme 2; Table 54.1 summarizes the yields in each case.

Several striking features can be noted in the results presented in Scheme 2 and Table 54.1. First of all, no Norrish type II cleavage products were formed, either in the solid state or solution. Second, small amounts of some unexpected, non-Norrish/Yang photoproducts were isolated and identified. These are the cyclopentanone derivates **8a–f**, formed only in solution, and the novel cyclopropanol derivative **7d**,

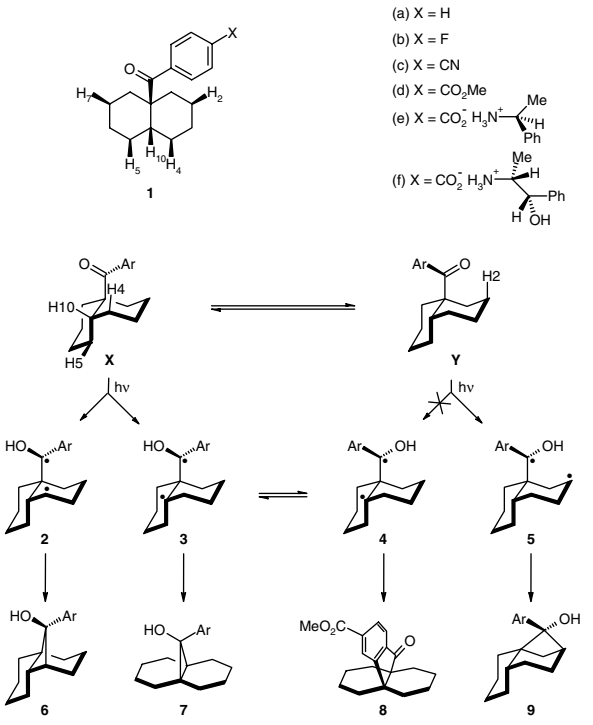

SCHEME 2

TABLE 54.1 Photoproduct Yields by GC in the Photolysis of *cis*-9-Decalyl Aryl Ketones

Ketone	Medium	Temp (°C)	Conversion (%)	6 (%)	7 (%)	8 (%)	9 (%)
1a	CH_3CN	20	100	59	0	2	39
	Crystal	–20	8	0	0	0	100
1b	CH_3CN	20	100	55	0	4	40
	Crystal	–20	9	100	0	0	0
1c	CH_3CN	20	100	39	0	7	50
	Crystal	20	2	100	0	0	0
1d	CH_3CN	20	100	47	0	6	47
	Crystal	–20	100	81	19	0	0
1e[a]	CH_3CN/H_2O	20	100	47	0	6	47
	Crystal	20	17	74[b]	0	0	0
1f[a]	CH_3CN/H_2O	20	100	47	0	6	47
	Crystal	20	10	94[b]	0	0	0

[a] Photoproducts were isolated as the corresponding methyl esters following diazomethane workup.

[b] Yield is reduced due to the presence of several small unidentified GC peaks.

formed exclusively in the solid state. A third notable feature of the experimental results is that cyclobutanol photoproducts **6** and **9** were formed in roughly equal amounts in solution, whereas in the crystalline state only a single cyclobutanol was observed in each case at low conversions. At higher conversions, small amounts of the other photoproducts were observed as a result of crystal breakdown and melting,

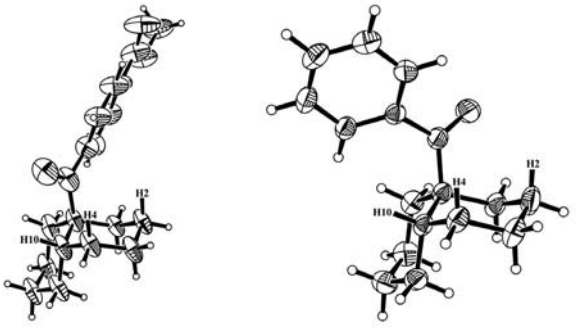

(a) (b)

FIGURE 54.2 ORTEP drawings showing (a) conformer **X** (ketone **1d**) and (b) conformer **Y** (ketone **1a**).

TABLE 54.2 Geometric Parameters for Hydrogen Abstraction in Ketones 1a–f

Ketone	Conformation[a]	Hydrogen	d (Å)	ω (°)	**Δ** (°)	θ (°)
1a	Y	H2	2.65	56	84	113
		H4	3.52	44	44	106
		H10	3.82	8	10	70
1b	X	H2	3.50	46	47	105
		H4	2.67	55	85	111
		H10	2.36	0	85	101
1c	X	H2	3.41	48	51	109
		H4	2.59	40	89	115
		H10	2.42	6	83	99
1d	X	H2	3.47	45	45	107
		H4	2.55	56	85	116
		H10	2.38	1	85	99
1e	X	H2	3.43	45	45	109
		H4	2.62	55	84	115
		H10	2.40	1	84	100
1f[b]	X	H2	3.58	41	41	107
		H2′	3.54	44	44	107
		H4	2.70	56	80	114
		H4′	2.65	55	83	114
		H10	2.40	6	84	101
		H10′	2.38	3	85	101

[a] In the crystalline state.
[b] Two independent molecules in the asymmetric unit.

particularly for the lower melting ketones **1a–d**. Remarkably, only one diastereomer of each cyclobutanol was formed, regardless of the reaction medium or extent of conversion.

As an aid to understanding these results and in order to obtain the hydrogen abstraction geometries (*vide infra*), the crystal and molecular structures of ketones **1a–f** were determined by single crystal x-ray diffraction. This revealed that ketone **1a** crystallizes in a conformation that is quite different from that adopted by ketones **1b–f**, all of which share the same basic conformation. Oak Ridge Thermal Ellipsoid Plot Program (ORTEP) representations of these two conformations are shown in Figure 54.2, and the corresponding line drawings are given in Scheme 2 (conformer **X** for ketones **1b–f** and conformer **Y** for ketone **1a**). Molecular mechanics calculations indicate that structure **X** represents the global minimum energy conformation for this system and that conformer **Y** lies only about 0.1 kcal/mol above the minimum. From the crystal structures of ketones **1a–f**, the values of the hydrogen atom abstraction parameters d, ω, Δ, and θ for each ketone were calculated; the data are presented in Table 54.2.

Crystal Structure–Reactivity Correlations for the *cis*-9-Decalyl Aryl Ketone System

From the experimental results presented above, a clear picture of the structure–reactivity relationships involved in the solid-state photochemistry of the *cis*-9-decalyl aryl ketone system emerges. As depicted in Scheme 2, reaction through conformation **X** leads to photoproducts of type **6** via abstraction of H4 and to photoproducts of type **7** and **8** via abstraction of H10. In contrast, reaction through conformation **Y** leads exclusively to the formation of photoproducts of type **9** via abstraction of H2. These conclusions are borne out by the geometric data presented in Table 54.2. In conformation **X** (ketones **1b–f**), the carbonyl oxygen is much closer to hydrogen atoms H4 and H10 than it is to H2. The average values of *d* (the hydrogen abstraction distances) are 2.63 ± 0.05 Å for H4, 2.39 ± 0.02 Å for H10, and 3.49 ± 0.06 Å for H2. The situation is reversed for ketone **1a**, which crystallizes in conformation **Y**. In this case, the carbonyl oxygen is close to H2 (2.65 Å) and relatively distant from H4 (3.52 Å) and H10 (3.82 Å).

The data in Table 54.2 reveal that the hydrogen atoms with the most favorable values of *d* also have relatively favorable values of the angular parameters ω, Δ, and θ. Consider ketone **1a** (d_{H2} = 2.65 Å; d_{H4} = 3.52 Å). Although the ω angle for H4, at 44°, is slightly closer to the ideal of 0° than it is for H2 (56°), the values of Δ and θ favor abstraction of H2. There is a particularly large difference in the value of Δ, which, at 84° for H2, is much closer to the ideal of 90 to 120° than for H4 (Δ = 44°). Recent work by Griesbeck et al. has highlighted the importance of the Δ angle in hydrogen abstraction reactions.[8] A similar trend is seen in the data for ketones **1b–f**, where abstraction of H4 is favored over abstraction of H2. As above, the values of ω slightly favor abstraction of the more distant hydrogen H2, but the values of θ and particularly Δ favor abstraction of H2.

An interesting aspect of the photochemistry of ketones **1b–f** is that it presents a rare example in which β-hydrogen atom abstraction competes with the normally much more favorable process of γ-hydrogen abstraction.[9] Two main factors conspire to bring this about. First of all, the β-hydrogen H10 is tertiary and therefore more susceptible to abstraction than the secondary γ-hydrogen H4.[10] Second, H10 is particularly well situated for abstraction, with an unusually short abstraction distance, *d*, of 2.39 ± 0.02 Å and a nearly ideal out-of-plane ω angle of 3 ± 2°. Despite this favorable β-hydrogen abstraction geometry, only minor amounts of photoproducts **7** and **8** are formed, a result that may reflect the relative ease of reverse hydrogen atom transfer in hydroxy biradical **3** compared to ring closure, even in hydrogen-bonding solvents such as acetonitrile.[11]

We turn next to a discussion of why the product distribution in solution is so much different from that observed in the crystal (Table 54.1). The simple answer is that, in solution, equilibrium between conformers **X** and **Y** is established and both can react to give a mixture of cyclobutanols **6** and **9**, plus small amounts of cyclopentanone **8** (Scheme 2). In contrast, equilibration between conformers **X** and **Y** is topochemically restricted in the crystalline state and reaction is limited to one or the other.

A subtler question has to do with why cyclopentanones of type **8** are observed only in solution and why cyclopropanol **7d** is formed exclusively in the solid state. We suggest the following scenario (refer to Scheme 2): Ring closure of biradical **3** to form cyclopropanol **7** is slow due to ring strain and in solution conformational isomerization to biradical **4** is faster. This places the aromatic ring in proximity to the radical at C10 and radical coupling of **4** at the *ortho* position followed by tautomerization and oxidation leads to cyclopentanone **8**.[12] In contrast, conformational isomerization of biradical **3** to biradical **4** is topochemically forbidden in the crystalline state, and cyclopentanone **8** is not formed in this medium. Formation of cyclopropanol **7** is slow in the solid state as well, and biradical **3** reverts to starting ketone rather than undergoing ring closure. The one exception to this rule is biradical **3d**, which, for reasons that we do not understand, gives 19% of cyclopropanol **7d** in the crystalline state.

The structure–reactivity relationships developed above also account very nicely for the high diastereoselectivity observed in the formation of cyclobutanols **6** and **9**. This can be understood by reference to Scheme 2, which depicts the structures of conformers **X** and **Y** in the crystalline state. In the case of conformer **X**, abstraction of H4 followed by least motion closure of biradical **2**, *with retention of configuration at the carbonyl carbon*, leads directly to the experimentally observed diastereomer **6**. Formation

of the diastereomer with the opposite configuration at the hydroxyl-bearing carbon atom would require biradical **2** to undergo a large-amplitude rotation of the hydroxybenzyl group, a process that is topochemically forbidden in the crystalline state and is evidently slow in solution as well. A similar analysis applies to the preferential formation of *endo*-arylcyclobutanol **9** rather than its *exo*-aryl diastereomer. Here, abstraction of H2 occurs from conformer **Y** to afford biradical **5**, and closure of this species with retention of configuration at the carbonyl carbon leads naturally and directly to the topochemically allowed cyclobutanol **9**. As above, formation of the unobserved diastereomer requires large-amplitude motions of the hydroxyl and aryl groups, which are prohibited by the rigid, close-packed environment of the crystal. Based on the two examples presented above, plus a number of others that will be discussed later in this review, it seems safe to conclude that 1,4-hydroxy biradical ring closure involving retention of configuration at the carbonyl carbon is a general feature of Yang photocyclization reactions in the crystalline state.

A final point in our discussion of the photochemistry of the *cis*-9-decalyl aryl ketone system concerns the question of the overall geometry of the six-membered transition state hydrogen atom abstraction process: chair-like, boat-like, or other? The unequivocal answer in the present instance is boat-like, a feature that appears to be general to the systems we have investigated in the crystalline state (*vide infra*). Although present in both conformers **X** and **Y**, the boat-like six-atom hydrogen abstraction geometry is most easily visualized in conformer **X** (Scheme 2), where the C4–H4 and C9 to carbonyl carbon bonds form the parallel sides of the boat and C10 and the carbonyl oxygen atom represent the prow and the stern. The normal eclipsing and bowsprit-flagpole interactions present in boat cyclohexane are absent in this particular arrangement.

Summary of Crystallographically Derived γ-Hydrogen Atom Abstraction Geometries for *cis*-9-Decalyl Aryl Ketones and Other Systems

The crystallographically derived geometric data compiled in Table 54.2 for *cis*-9-decalyl aryl ketones **1a–f** represent the results of just one of a number of similar studies on the Norrish/Yang reaction in the crystalline state. In Table 54.3 we summarize the values of *d*, ω, Δ, and θ for a variety of type II systems. These data are taken from our own published work as well as that of other groups working in the field. For comparison purposes, Table 54.3 also includes geometric data for intramolecular hydrogen abstraction reactions taking place through five-membered (β) and seven-membered (δ) transition states. In cases where more than one hydrogen is reasonably situated for abstraction, Table 54.3 reports data only for the hydrogen atom with the smallest value of *d*. This is based on work from our group which demonstrated that a difference in *d* of only 0.27 Å (2.72 vs. 2.99 Å) and comparable values of ω, Δ, and θ leads to exclusive abstraction of the nearer hydrogen in the crystalline state.[13]

Only crystallographically derived geometric parameters are given in Table 54.3 for compounds that actually react in the solid state; some studies report values of *d*, ω, Δ, and θ based on molecular mechanics calculations, but these are not included. In some published reports, only the abstraction distance (*d*) is given, and in others, only *d* and ω are provided. In this review, we have not attempted to calculate the value of missing parameters based on accompanying x-ray coordinates. Finally, we note that entries 1 to 5, 12, and 26 in Table 54.3 report average values for several structurally related compounds. In these cases, standard deviations are supplied along with the number of examples reported.

Discussion of Results Presented in Table 54.3

With 33 entries representing data for 115 separate compounds of widely varying structure, Table 54.3 paints a picture of the geometric requirements for intramolecular hydrogen atom abstraction that is remarkable in its internal consistency. Consider, for example, the parameter *d*, the C=O···H abstraction distance. Ranging from a low of 2.17 Å (entry 20) to a high of 3.15 Å (entry 15), most values of *d* fall within ±0.2 Å of the sum of the van der Waals radii for oxygen and hydrogen (2.72 Å), thus amply justifying our original intuition in this regard. One report of γ-hydrogen atom abstraction occurring over

TABLE 54.3 Values of d, ω, Δ, and θ for Intramolecular Hydrogen Atom Abstraction in the Crystalline State

Entry	Compound	d (Å)	ω (°)	Δ (°)	θ (°)	Boat/Chair	Examples	Comments	Ref.
1	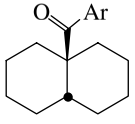	2.63 ± 0.05 (H_γ) 2.39 ± 0.02 (H_β)	53 ± 5 3 ± 2	84 ± 2 84 ± 1	114 ± 2 100 ± 1	Boat N/A	6 6	—	7
2	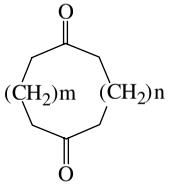	2.73 ± 0.03	52 ± 5	83 ± 4	115 ± 2	Boat	11	$m = n = 2$ to 9 $m = 4$, $n = 6$	14
3	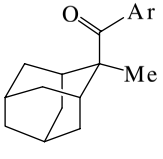	2.63 ± 0.06	58 ± 3	81 ± 4	114 ± 1	Boat	9	Includes some *cis*-4-*t*-butyl cyclohexyl derivatives	15
4	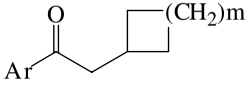	2.74 ± 0.16	43 ± 9	84 ± 8	—	Boat	17	m = 1 to 5 (monocyclic) plus some bicyclic systems	16
5	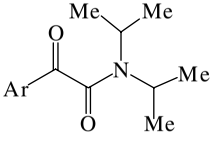	2.72 ± 0.05	—	—	—	—	7	Ar contains appended chiral auxiliary	17

6	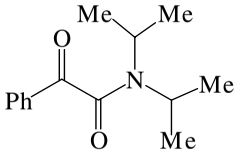	2.78	—	—	—	—	1	—	18
7	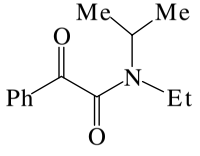	2.74	—	—	—	—	1	Abstraction occurs on isopropyl group	19
8	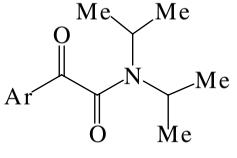	2.65 2.75 2.55	—				3	Ar = *ortho, meta*, and *para*-chlorophenyl	20
9	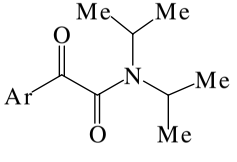	2.72 2.70 2.68	—	—	—	—	3	Ar = 2-methyl, 4-methyl-, and 3,4-dimethylphenyl	21
10	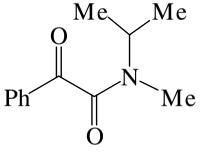	2.56 2.56	—	—	—	—	2	Co-crystallized with an optically pure host	22

TABLE 54.3 Values of d, ω, Δ, and θ for Intramolecular Hydrogen Atom Abstraction in the Crystalline State (continued)

Entry	Compound	d (Å)	ω (°)	Δ (°)	θ (°)	Boat/Chair	Examples	Comments	Ref.
11	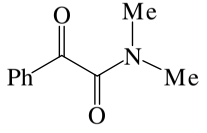	2.79	—	—	—	—	1	Co-crystallized with an optically pure host	23
12	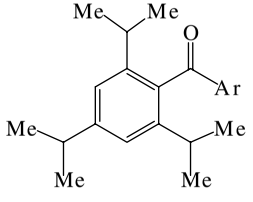	2.83 ± 0.12	—	—	—	—	12	—	24
13	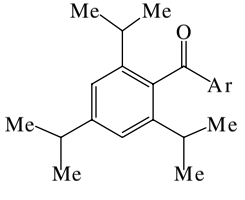	2.74 2.58	58 63	58 69	119 126	—	2	Ar contains chiral auxiliary; both data sets given for one of two independent molecules in asymmetric unit	25
14	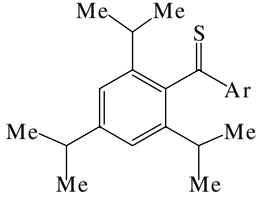	3.06 3.07	51 50	52 52	118 125	—	2	Ar = Ph and anisyl	26

15	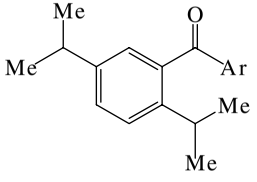	3.15	—	—	—	—	1	Ar contains appended chiral auxiliary	27
16	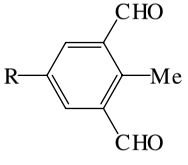	2.58 2.54	17 19	95 101	97 90	—	2	R = Me and *i*-Pr	28
17	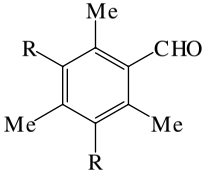	2.55 2.43	—	—	—	—	3	R = H and CN; co-crystallized with an optically pure host	29
18	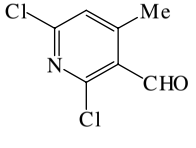	2.60	47	91	100	—	1	—	30
19	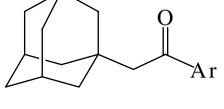	2.70 2.67	46 54	87 83	118 115	—	2	Second set of parameters are for one of two independent molecules in asymmetric unit	31

TABLE 54.3 Values of d, ω, Δ, and θ for Intramolecular Hydrogen Atom Abstraction in the Crystalline State (continued)

Entry	Compound	d (Å)	ω (°)	Δ (°)	θ (°)	Boat/Chair	Examples	Comments	Ref.
20	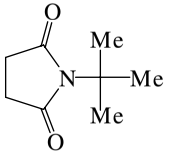	2.17	17.5	100.7	121.4	—	1	—	32
21	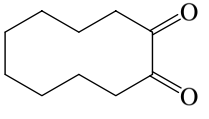	2.67	53	84	118	—	1	Data given for one of two independent molecules in asymmetric unit	33
22	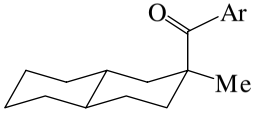	2.66	57	82	115	—	1	Tertiary γ-hydrogen abstracted	34
23	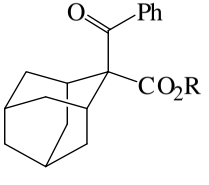	2.50 2.34	—	—	—	—	2	Second value of d is for one of four independent molecules in asymmetric unit	35
24	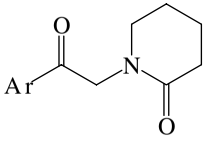	2.82	—	—	—	—	1	Co-crystallized with an optically pure host	36

25	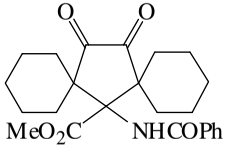	2.46	—	—	—	—	1	Molecule contains four γ-hydrogens with d = 2.46 to 2.60 Å	37
26	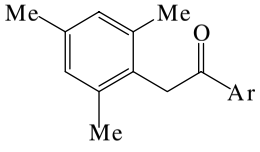	2.80 ± 0.14	57 ± 4	77 ± 12	124 ± 3	N/A	8	—	38
27	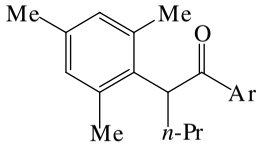	2.72	66	75	115	N/A	1	Abstraction occurs on *ortho*-methyl substituent	39
28	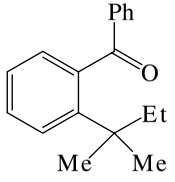	2.63	45	—	—	N/A	1	Abstraction occurs mainly on CH_2 group	40
29	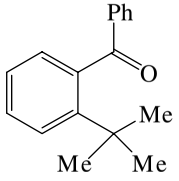	2.2 – 2.4	40	—	—	N/A	1	—	41

TABLE 54.3 Values of d, ω, Δ, and θ for Intramolecular Hydrogen Atom Abstraction in the Crystalline State (continued)

Entry	Compound	d (Å)	ω (°)	Δ (°)	θ (°)	Boat/Chair	Examples	Comments	Ref.
30	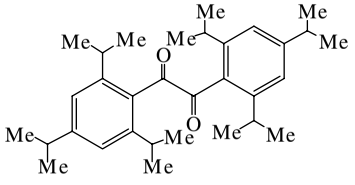	2.86	73	—	—	N/A	1	δ-Hydrogen abstraction favored over γ	42
31	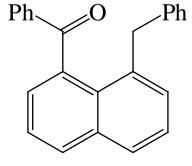	2.36	78	91	121	N/A	1	—	43
32	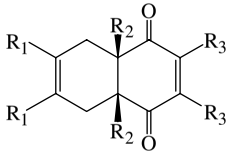	2.5 ± 0.1	4 ± 3	84 ± 2		N/A	7	β-hydrogen abstraction occurs in this system	16
33	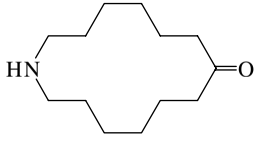	3.09 2.77 2.60	—	—	—	—	2	Last two values of d are for independent molecules in asymmetric unit	44

a distance of 4.45 Å is puzzling,[45] but the authors conclude that this most likely takes place at defect sites in the crystal where different conformers having shorter values of *d* are present.

Turning next to the parameter ω, the prediction that the γ-hydrogen should lie in the same plane as the *n*-orbital on oxygen (ω = 0°) is clearly contradicted by the data in Table 54.3, which includes many ω angles in the 40 to 60° range, with three even higher (66°, entry 27; 73°, entry 30; 78°, entry 31). How can this discrepancy be explained? Wagner has suggested and provided evidence for a $\cos^2\omega$ dependence on the rate of γ-hydrogen atom abstraction.[46] This means that ω can be quite large and still lead to respectable rates of abstraction. For example, when ω = 60°, $\cos^2 60 = 0.25$ and abstraction can occur at 25% of its maximum rate, more than enough for observable solid-state reactivity. In theory, abstraction should cease when ω = 90°, because at this geometry the γ-hydrogen is orthogonal to the abstracting *n*-orbital on oxygen and $\cos^2\omega = 0$. Several examples of such a situation have been noted in the literature.[47] Wagner and co-workers[40] report an interesting case in which abstraction of a methyl hydrogen with *d* = 2.53 Å and ω = 95° competes to the extent of ~15% with abstraction of a methylene hydrogen atom, with *d* = 2.63 Å and ω = 45° (entry 28). One possible explanation for this apparent anomaly is the presence of a small amount of methyl/ethyl disorder in the crystal, which is known to be common.[48] Another interesting hydrogen atom abstraction that occurs with a large value of ω is that shown in entry 31, a seven-membered, transition-state (δ) process. This reaction was first investigated in solution by DeBoer et al.,[49] who showed that it proceeds through a $(\pi,\pi^*)^3$ excited state. This means that it should have a different optimum value of ω, (i.e., 90°). In reasonable agreement with this, the experimentally determined value of ω for the reaction in the crystalline state is 78°.[43]

The data in Table 54.3 are less complete regarding the preference for boat-like or chair-like transition states and for the parameters Δ and θ, but here, too, a few comments are in order. The preference for boat-like abstraction geometries that was noted earlier for the *cis*-9-decalyl aryl ketone system is seen to carry over into entries 2 to 4, and this may prove to be a general feature of type II hydrogen atom abstraction. With respect to the angle Δ (the C=O···H angle), the experimental data are in reasonably good agreement with the hypothetical ideal of 90 to 120° and much closer on average to the former value than the latter. This could be taken as evidence for involvement of a non-bonding orbital on oxygen that is largely 2p-like in character, but more likely it is simply due to the geometric constraints inherent in a six-membered transition state process. This reasoning also applies to the parameter θ (the C–H···O angle), which cannot possibly approach its theoretical ideal of 180° within the confines of a cyclic six-membered transition state. In line with this, typical values of θ lie in the range of 115 ± 10°. On this basis, it might be expected that θ would be somewhat larger for a seven-membered transition state (δ) hydrogen atom abstraction and slightly smaller for the corresponding β (five-membered transition state) process. Entries 1 and 26 to 32 in Table 54.3 do hint in this direction, but the data are really too sketchy to draw any firm conclusions. What the data do indicate is that the values of *d* and ω for β- and δ-hydrogen abstraction are very similar to those for the corresponding six-membered transition state process, and we continue to view these parameters (particularly the former) as being most critical to the success of intramolecular hydrogen atom abstraction.

We close this section with a brief discussion of the significance of the ground state geometric parameters presented in Table 54.3 to reactions that occur in the excited state. Three main factors make the crystal structure–excited state reactivity relationships less than exact. First, n,π^* excitation lengthens CO double bonds by about 0.1 Å;[50] second, x-ray crystallography consistently underestimates CH bond lengths by approximately 0.1 Å due to the low diffraction cross section of hydrogen atoms; and, third, the carbonyl carbon atoms of aliphatic ketones tend to pyramidalize in their n,π^* excited states.[51] This last factor is not a problem for the majority of the data in Table 54.3, which come from conjugated aryl ketones whose n,π^* excited states are not significantly pyramidalized.[52] Furthermore, lengthening the CO double and CH bonds by 0.1 Å at a typical abstraction geometry of Δ = 90° and θ = 115° decreases *d* by only about 0.2 Å. It is safe to conclude, therefore, that, while the abstraction parameters measured by x-ray crystallography do not provide *exact* information on the geometry in the excited state, we have good reason to expect that the structure–reactivity relationships developed above are approximately correct and can be used in a predictive sense. It is a relatively simple matter these days to calculate reasonable estimates of

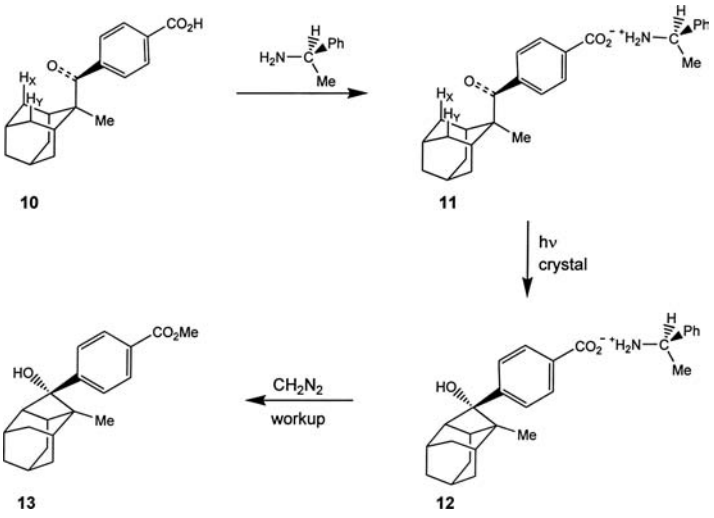

SCHEME 3

d, ω, Δ, and θ for virtually any ketone through the use of molecular mechanics methods and in this way to gauge the probable success or failure of a hypothetical Norrish/Yang type II reaction.

54.3 Asymmetric Induction in the Yang Photocyclization Reaction

As can be seen from Scheme 1, the process of Yang photocyclization produces a chiral cyclobutanol from an achiral ketone — a reaction that is ideal for testing new methods of asymmetric induction in organic photochemistry. Our goal was not the formation of optically pure cyclobutanols for their own sake (although such compounds may prove useful in mechanistic studies of carbocation rearrangements), but rather the development of asymmetric induction techniques applicable to photorearrangement reactions in general. Asymmetric synthesis is nowhere near as well developed for excited-state reactions as for ground-state processes, and this topic remains one of the major relatively unexplored areas of organic photochemistry.[53]

The Concept of the Ionic Chiral Auxiliary

It has been known for some time that chemical reactions conducted in bulk crystalline media can lead to high levels of asymmetric induction provided that the crystals adopt chiral space groups.[54] It was thus natural to extend the solid state work discussed in Section 54.2 of this review to an investigation of asymmetric induction in the Yang photocyclization reaction. To achieve this goal, two conditions must be met. First, the molecules chosen for study must crystallize in conformations that favor hydrogen atom abstraction. This rules out straight-chain aryl alkyl ketones such as valerophenone and its derivatives, which crystallize in extended conformations with inaccessible γ-hydrogen atoms. Second, the reactant molecules must crystallize in chiral space groups. This can be achieved by attaching temporary chiral auxiliaries to the substrates that can be removed once the solid state photoreactions are complete.

These concepts are best illustrated with a specific example. Ketone **10** (Scheme 3) was expected to have a minimum energy conformation in which the ketone oxygen is directed toward the enantiotopic γ-hydrogen atoms Hx and Hy and this was confirmed by molecular mechanics calculations. Because organic molecules generally crystallize in or near their minimum energy conformations, it was anticipated that

ketone **10** would undergo facile γ-hydrogen abstraction in the solid state, a prediction that was amply borne out by experiment (*vide infra*). The *p*-carboxylic acid group in compound **10** was introduced as a site to which the chiral auxiliary could be attached. This could be achieved in two ways — covalently (*via* ester formation with an optically pure alcohol or amide formation with an optically pure amine), or ionically through salt formation with an optically pure amine. For a variety of reasons, including novelty, ease of introduction and removal of the chiral auxiliary and the fact that salts form robust ionic crystals with high melting points (important for studies in the solid state), we chose to work with ionic chiral auxiliaries.

Asymmetric Induction in the Crystalline State

Several salts of general structure **11**, varying only in the nature of the ionic chiral auxiliary, were prepared and irradiated in the crystalline state.[15] The reaction mixtures were worked up with ethereal diazomethane to remove the chiral auxiliaries and form the corresponding methyl esters; this led to the anticipated cyclobutanol **12** (Scheme 3) as the sole photoproduct. Best results were obtained with the 1-phenylethylamine salt, which afforded enantiomeric excesses (*ee*s) of approximately 80% at 100% conversion. Either enantiomer of cyclobutanol **12** could be prepared by using the optical antipodes of 1-phenylethylamine and the critical importance of the crystalline state to the process was shown by the fact that irradiation of salt **11** in acetonitrile or methanol gave racemic **12**.

A remarkable feature of the photorearrangement of salt **11** in the solid state is that it proved to be of the rare single crystal-to-single crystal (topotactic) variety. In such processes, product molecules take the place of reactant molecules in all proportions in the crystal lattice with no change in space group and very little change in unit cell dimensions. This permits the *same crystal* to be analyzed by X-ray diffractometry at the initial, intermediate and final stages of reaction. Such an experiment was carried out for salt **11** and its photoproduct **12** and the results are presented in Scheme 3. Because the absolute configuration of the ionic chiral auxiliary is known, Scheme 3 depicts the absolute steric course of the photorearrangement and we can state with certainty that H_X (**d** = 2.60 Å) is abstracted in preference to H_Y (**d** = 3.59 Å) and that cyclobutanol formation is a least motion process involving "retention of configuration" at the carbonyl carbon. The reader will recall that in our investigation of the *cis*-9-decalyl aryl ketone system discussed earlier, formation of cyclobutanols **6** and **9** (Scheme 2) involved similar ring closures with retention of configuration at the carbonyl carbon.

In fact, one of the major goals of our work with the *cis*-9-decalyl aryl ketone system **1** was to apply the ionic chiral auxiliary approach to the asymmetric synthesis of cyclobutanols **6** and **9**. Like ketone **10**, ketones of general structure **1** are achiral, but unlike **10**, contain *two* pairs of enantiotopic γ-hydrogen atoms (H4/H5 and H2/H7), abstraction of which leads to enantiomeric cyclobutanols of general structure **6** and **9** (see Scheme 2). Hydrolysis of nitrile **1e** provided the corresponding carboxylic acid and reaction of this compound with (*R*)-(+)-1-phenylethylamine gave salt **1e**. X-ray crystallography revealed that this salt crystallizes in conformation **X** (absolute configuration as shown) and in this conformation only γ-hydrogen atom H4 is in position to be abstracted (**d** = 2.62 Å). In accord with this picture, irradiation of crystals of this material to 85% conversion afforded cyclobutanol **6d** in a remarkable 98% *ee*.[7a] The (*R*)-(+)-bornyl amine salt proved to be even better, yielding cyclobutanol **6d** in a particularly clean reaction with >98% *ee* at 78% conversion. Neither of these reactions proved to be topotactic, thus preventing determination of the absolute configuration of cyclobutanol **6d**, but there can be little doubt that it is as shown in Scheme 2.

Our studies on the adamantyl (**10**) and decalyl (**1**) systems are only two of several examples of the successful application of the ionic chiral auxiliary approach to asymmetric induction in the Yang photocyclization reaction. Space does not permit a full exposition of our results in this area. The interested reader may wish to consult references 17, 25, 27, 31, 35, 38 and 44 for additional examples and further details. As a note of interest, reference 44 describes the use of *anionic* chiral auxiliaries in the Yang photocyclization of a cationic counterion in the crystalline state; all of our other studies have been of the reverse type.

Molecular Conformation Determines the Enantioselectivity of Yang Photocyclization

The results presented above highlight the importance of *molecular conformation* in bringing about high levels of asymmetric induction in the Yang photocyclization reaction in the crystalline state *via* the ionic chiral auxiliary approach. In the presence of an ionic chiral auxiliary, the reactive counterions crystallize in chiral conformations in which one of the two γ-hydrogen atoms that were enantiotopic in solution is more favorably oriented for abstraction than the other. It is at this point that the importance of the crystalline state in preventing conformational equilibration becomes apparent. Without this restriction, both enantiotopic hydrogens would become available for abstraction (as they are in solution) and the enantioselectivity would be lost. The role of the ionic chiral auxiliary is therefore one of *preorganizing* the counterions in conformations favorable for the formation of only one enantiomer and the role of the crystalline state is to *immobilize* them in this arrangement. This of course predicts that should the reactant prefer to crystallize in a symmetrical conformation in which both enantiotopic γ-hydrogens are equally accessible (even in the presence of a chiral auxiliary), racemic cyclobutanol will be formed. In this interesting situation, any *ee* that is observed would necessarily be the result of anisotropic *intermolecular* interactions with lattice neighbors in the chiral crystal. We are currently designing symmetrical and conformationally immobile type II systems to test these ideas.

Thus, in comparison to the situation in most conventional, ground state asymmetric induction reactions, where the chiral auxiliary is intimately involved in the enantiodifferentiating step through its stereoelectronic effects or coordinating ability, the role of the ionic chiral auxiliary in solid state cyclobutanol formation is a relatively passive one. For example, the ionic chiral auxiliary does not need to be located close to the site of reaction and all that is required is that its attachment to the reactant *via* salt formation does not give rise to diastereomers. In addition, there is no direct correlation between the size and structure of the ionic chiral auxiliary and the extent of *ee*, nor is it possible to predict which enantiomer of the photoproduct will be favored. This would be akin to making an *a priori* prediction of crystal and molecular structure, a feat that is currently beyond the scope of modern crystal engineering.

Conformational Enantiomerism

Given the presentation of the results so far, one might expect that all ionic chiral auxiliaries would lead to high *ee*s, but such is not the case. For example, in the *cis*-9-decalyl aryl ketone system **1**, use of (1*R*,2*S*)-(−)-norephedrine as the chiral auxiliary (salt **1f**, Scheme 2) led to cyclobutanol **6d** in 30% *ee* at 55% conversion,[7a] and in the 2-benzoyladamantane system **10**, several of the salts investigated led to *ee*s in the 20-30% range.[55] As a matter of fact, for any given prochiral type II photoreactant, finding an ionic chiral auxiliary that gives a high *ee* is entirely a trial and error procedure and low *ee*s are obtained as often as not. How is this possible if the salts crystallize in conformations that permit abstraction of only one of the two enantiotopic γ-hydrogen atoms? We can rule out trivial explanations such as crystal melting in these low *ee* cases, since (a) no melting was detectable upon examination of the crystals following photolysis and (b) the results were not improved by using low temperatures and low conversions, where crystal melting should be minimal.

The origin of the low *ee*s was eventually deduced from the X-ray crystal structures of several of the salts that show this behavior.[56] In these cases it was found that half of the reactant ions crystallize in one enantiomeric conformation while the other half crystallize as its near (but not exact) mirror image. This was shown by computationally inverting one of the conformers, superimposing it on the other and calculating the root mean-square error for the overlap of the heavy atoms of the two species, which proved to very low (0.08 Å in the case of norephedrine salt **1f**). We coined the term *conformational enantiomerism* to describe this heretofore unrecognized mode of crystal packing.[56]

Armed with this knowledge, the reason for the low *ee*s observed in salts that exhibit conformational enantiomerism is straightforward: half of the molecules in the crystal react to give one photoproduct enantiomer while the other half react to form its optical antipode. The reason the *ee* is not zero is that the conformational enantiomers are in fact independent molecules that reside in structurally different

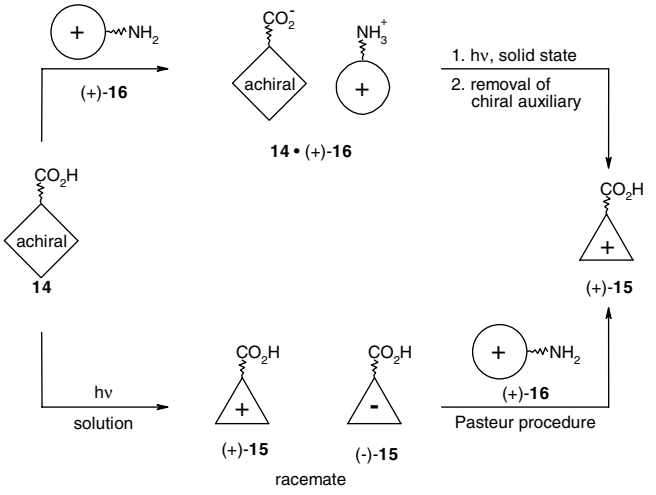

FIGURE 54.3 Comparison of the solid state ionic chiral auxiliary method of asymmetric synthesis with the Pasteur resolution procedure.

environments, thus leading to slightly different reaction rates. Put another way, the conformational enantiomers form diastereomeric salts with the common optically pure amine and should not, therefore, be expected to react at exactly identical rates. Support for this interpretation comes from the crystal structures of salts that give high *ee*s. In these cases, the reactant ions invariably crystallize in a single, homochiral conformation that react to form a single enantiomer of the photoproduct.

Comparison of the Solid State Ionic Chiral Auxiliary Method of Asymmetric Synthesis with the Pasteur Resolution Procedure

Both of the cyclobutanols discussed in this review (compounds **6d** and **13**) could have been prepared in enantiomerically pure form by irradiation of their keto-acid precursors (**1**, X = COOH and **10**) in an isotropic solvent to give a racemic mixture followed by resolution employing the classical Pasteur procedure. This method, which involves treatment of the racemate [(+)-**15**/(−)-**15**] with an optically pure amine [(+)-**16**] followed by fractional crystallization of the resulting diastereomeric salts, is outlined schematically in the bottom half of Figure 54.3. The top half of Figure 54.3 summarizes the solid state ionic chiral auxiliary method of asymmetric synthesis. The difference between this approach and the Pasteur method is one of *timing*: in the chiral auxiliary procedure, crystalline salt formation *precedes* the photochemical reaction, whereas the reverse is true for the Pasteur method. In principle, irradiation of the salt **14**/(+)-**16** can lead to a pair of diastereomeric product salts [(+)-**15**/(+)-**16** and (−)-**15**/(+)-**16**] — a reaction that takes place through diastereomeric transition states. Viewed in this way, the success of the ionic chiral auxiliary approach can be thought of as deriving from a kinetic preference for the transition state of lower energy [(+)-**15**)/(+)-**16** in the example shown in Figure 54.3]. The ionic chiral auxiliary method has an obvious advantage over the Pasteur procedure in terms of yield, since in principle and (as we have seen) in practice, the reactant (**14**) can be completely transformed into one enantiomer of the photoproduct or the other, as desired. By way of contrast, the maximum yield in which a given enantiomer can be obtained using the Pasteur procedure is 50% and in practice is often considerably less.[57]

Synthetic Potential of the Ionic Chiral Auxiliary Approach to Asymmetric Synthesis

The solid state ionic chiral auxiliary method of asymmetric synthesis is not limited to Yang photocyclization and can, in principle, be applied to any chemical reaction — photochemical or thermal — that

occurs in the crystalline state and converts an achiral reactant into a chiral product. Thermal reactions may, of course, present a problem owing to the greater chance of crystal melting, but ionic solids with their high melting points (generally > 160 °C) hold promise in this regard. Current efforts in our laboratory are aimed in this direction. It is to photochemical reactions, however, that the method is most applicable, since temperature control is a simple matter in such reactions and we have extended our studies to a wide variety of excited state processes. The following is a list of photochemical reactions (in addition to Yang photocyclization) to which the ionic chiral auxiliary approach has been applied: the di-π-methane rearrangement,[58,59,61,62] rearrangement of a benzocyclohexadienone,[63] electrocyclic ring closure,[64] *cis*,*trans*-isomerization of cyclopropane derivatives[65,66] and the Paterno-Büchi reaction.[67]

We close with a brief mention of the *scale* on which these reactions can be conducted — an important consideration when it comes to synthetic utility. For practical reasons and because modern methods of analysis do not require large sample sizes, most of our solid-state photolyses have been carried out on a microscale (< 10 mg). In one instance, however, we showed that the method could easily be scaled up to the 500 mg level with an *ee* of 99% and an isolated yield of 91%.[68] This was done by irradiating the salt crystals as a hexane suspension in a conventional immersion well apparatus — a technique that would certainly allow reactions to be conducted on the multi-gram level if desired.

54.4 Summary

The preferred geometry for photochemically-initiated intramolecular hydrogen atom abstraction has been elucidated using the crystal structure-solid state reactivity correlation method. Based on more than a hundred examples taken from our own work and that of others, it has been shown that abstraction is successful when the C=O···H distance, d, is within approximately ± 0.2 Å of the sum of the van der Waals radii for oxygen and hydrogen (2.72 Å), although d values as short as 2.17 Å and as long as 3.15 Å have been recorded. A second important geometric parameter in intramolecular hydrogen atom abstraction is the angle ω, the degree to which the hydrogen lies above or below the mean plane of the carbonyl group. Because hydrogen abstraction involves the n-orbital on oxygen, which lies in the plane of the carbonyl group, the best value of ω is predicted to be 0° and the worst ± 90°. Surprisingly, most successful hydrogen abstraction reactions were found to occur with rather unfavorable ω angles (50 ± 10°) and only when ω approaches 90° does abstraction fail, a result that supports Wagner's proposed $\cos^2\omega$ dependence on the rate of abstraction.[46] Another unexpected experimental finding was that the overall 6-atom geometry for γ-hydrogen abstraction is primarily boat-like rather than chair-like, a result that appears to fly in the face of conventional organic wisdom, but which may be understood when one realizes that two of the six atoms involved (oxygen and hydrogen) are sterically neutral in the sense that they do not possess attached groups that can raise the energy of the boat geometry through eclipsing and bowsprit-flagpole interactions (Figure 54.1c).

In many respects, the present results resemble the pioneering work of the late G. M. J. Schmidt and his co-workers at the Weizmann Institute of Science, who used crystal structure–solid-state reactivity correlations to elucidate the geometric requirements for intermolecular [2+2]-photocycloaddition.[69] In both his case and ours, distance and angular requirements for reaction were established and the structure and stereochemistry of the products were shown to be simply and directly related to the molecular structure existing in the bulk crystal.

With an excellent understanding of the relationship between structure and reactivity in the Norrish/Yang type II reaction, it was logical to use this information to carry out the reaction enantioselectively. In an approach resembling the classical Pasteur procedure for resolving racemic carboxylic acids, this was accomplished by providing the prochiral reactants with a carboxylic acid substituent to which an "ionic chiral auxiliary" was attached through an acid-base reaction with an optically pure amine. The resulting salts were then irradiated in the crystalline state. This approach is based on the fact that salts containing ionic chiral auxiliaries are required to crystallize in chiral space groups, which provide the asymmetric environment necessary for chiral induction. Using this methodology, near-quantitative optical yields could be obtained in a variety of Yang photocyclization reactions, even at very high conversions.

Furthermore, through the use of X-ray crystallography, it could be demonstrated that the high *ee*s observed in these reactions are conformationally rather than topochemically determined; i.e., they are due to the homochiral conformations adopted by the reactive ions in the crystal, which favor the abstraction of one nominally enantiotopic γ-hydrogen atom over the other.

Acknowledgments

JRS wishes to thank the Institute of Advanced Studies, University of Bologna, where this manuscript was written, for financial support in the form of a Senior Guest Fellowship. We also thank the donors of the Petroleum Research Fund, administered by the American Chemical Society, for partial support of this research. Financial support by the Natural Sciences and Engineering Research Council of Canada is also gratefully acknowledged.

References

1. For a general review on the Norrish/Yang type II reaction, see Wagner, P. and Park, B.-S., Photoinduced hydrogen atom abstraction by carbonyl compounds, in *Organic Photochemistry*, Vol. 11, Padwa, A., Ed., Marcel Dekker, New York, 1991, chap. 4.
2. Cyclobutanol formation in type II photochemistry was first reported by Yang, N. C. and Yang, D. H., Photochemical reactions of ketones in solution, *J. Am. Chem. Soc.,* 80, 2913, 1958.
3. Ariel, S., Ramamurthy, V., Scheffer, J. R., and Trotter, J., The Norrish type II reaction in the solid state: involvement of a boatlike reactant conformation, *J. Am. Chem. Soc.,* 105, 6959, 1983.
4. Wagner, P. J., Kelso, P. A., Kemppainen, A. E., and Zepp, R. G., Type II photoprocesses of phenyl ketones: competitive δ-hydrogen abstraction and the geometry of intramolecular hydrogen atom transfers, *J. Am. Chem. Soc.*, 94, 7500, 1972.
5. Bondi, A., Van der Waals volumes and radii, *J. Phys. Chem.,* 68, 441, 1964.
6. Dorigo, A. E. and Houk, K. N., Transition structures for intramolecular hydrogen-atom transfers: the energetic advantage of seven-membered over six-membered transition structures, *J. Am. Chem. Soc.,* 109, 2195, 1987.
7. (a) Cheung, E., Kang, T., Raymond, J. R., Scheffer, J. R., and Trotter, J., An ionic chiral auxiliary-induced regioselective and enantioselective Yang photocyclization reaction in the crystalline state, *Tetrahedron Lett.,* 40, 8729, 1999; (b) Cheung, E., Kang, T., Scheffer, J. R., and Trotter, J., Latent chemical behaviour revealed in the crystalline state: novel photochemistry of a *cis*-9-decalyl aryl ketone, *J. Chem. Soc., Chem. Commun.,* 2309, 2000; (c) Kang, T., Photochemical Asymmetric Synthesis and Novel Photoreactions in the Solid State, Ph.D. thesis, University of British Columbia, 2001.
8. Griesbeck, A. G., Henz, A., Kramer, W., Wamser, P., Peters, K., and Peters, E.-M., Stereo- and spin-selectivity of primary (singlet) and secondary (triplet) Norrish type II reactions, *Tetrahedron Lett.,* 39, 1549, 1998.
9. For another example, see Cormier, R. A., Schreiber, W. L., and Agosta, W. C., Photochemistry of α-methylene ketones: competitive β and γ hydrogen abstraction, *J. Chem. Soc., Chem. Commun.,* 729, 1972.
10. Wagner, P. J. and Kemppainen, A. E., Type II photoprocesses of phenyl ketones: triplet state reactivity as a function of γ and δ substitution, *J. Am. Chem. Soc.,* 94, 7495, 1972.
11. Wagner and co-workers have shown that acetonitrile and other hydrogen-bonding solvents can retard reverse hydrogen atom transfer in the Norrish type II reaction through coordination to the hydroxyl proton of the 1,4-hydroxybiradical intermediate. See Wagner, P. J., Kochevar, I. E., and Kemppainen, A. E., Type II photoprocesses of phenyl ketones: procedures for determining meaningful quantum yields and triplet lifetimes, *J. Am. Chem. Soc.,* 94, 7489, 1972.
12. For an analogous photoreaction involving cyclization to a six-membered ring ketone, see Perkins, M. J., Peynircioglu, N. B., and Smith, B. V., An unusual photochemical rearrangement of a ketone, *J. Chem. Soc., Chem. Commun.,* 222, 1976.

13. Lewis, T. J., Rettig, S. J., Scheffer, J. R., and Trotter, J., Crystallographic determination of the preferred geometry for intramolecular hydrogen atom abstraction in 1,8-cyclohexadecanedione, *Mol. Cryst. Liq. Cryst.*, 219, 17, 1992.
14. Gudmundsdottir, A. D., Lewis, T. J., Randall, L. H., Scheffer, J. R., Rettig, S. J., Trotter, J., and Wu, C.-H., Geometric requirements for hydrogen abstractability and 1,4-biradical reactivity in the Norrish/Yang type II reaction: studies based on the solid state photochemistry and X-ray crystallography of medium-sized ring and macrocyclic diketones, *J. Am. Chem. Soc.*, 118, 6167, 1996.
15. Leibovitch, M., Olovsson, G., Scheffer, J. R., and Trotter, J., An investigation of the Yang photocyclization reaction in the solid state: asymmetric induction studies and crystal structure–reactivity relationships, *J. Am. Chem. Soc.*, 120, 12755, 1998.
16. Scheffer, J. R., Geometric requirements for intramolecular photochemical hydrogen atom abstraction: studies based on a combination of solid state chemistry and x-ray crystallography, in Organic Solid State Chemistry, Desiraju, G. R., Ed., Elsevier, Amsterdam, 1987, 1–45.
17. Natarajan, A., Wang, K., Ramamurthy, V., Scheffer, J. R., and Patrick, B., Control of enantioselectivity in the photochemical conversion of α-oxoamides into β-lactam derivatives, *Org. Lett.*, 4, 1443, 2002.
18. Sekine, A., Hori, K., Ohashi, Y., Yagi, M., and Toda, F., X-ray structural studies of chiral β-lactam formation from an achiral oxo amide using the chiral-crystal environment, *J. Am. Chem. Soc.*, 111, 697, 1989.
19. Toda, F., Miyamoto, H., Koshima, H., and Urbanczyk-Lipkowska, Z., Chiral arrangement of *N*-ethyl-*N*-isopropylphenylglyoxylamide molecule in its own crystal and in an inclusion crystal with a host compound and their photoreactions in the solid state that give optically active β-lactam derivatives: x-ray analytical and CD spectral studies, *J. Org. Chem.*, 62, 9261, 1997.
20. Hashizume, D., Kogo, H., Sekine, A., Ohashi, Y., Miyamoto, H., and Toda, F., Mechanism of asymmetric photocyclization of α-oxoamides, *J. Chem. Soc.*, *Perkin Trans. 2*, 61, 1996.
21. Hashizume, D., Kogo, H. Sekine, A., and Ohashi, Y., Stereochemistry of asymmetric β-lactam formation involving achiral glyoxylamide derivatives, *Acta Cryst.*, C51, 929, 1995.
22. Hashizume, D., Uekusa, H., Ohashi, Y., Matsugawa, R., Miyamoto, H., and Toda, F., Structures and photoreactivities of *N*-isopropyl-*N*-methylphenylglyoxylamide included in two clathrate crystals as a guest, *Bull. Chem. Soc. Jpn.*, 67, 985, 1994.
23. Kaftory, M., Yagi, M., Tanaka, K., and Toda, F., Reactions in the solid state. 4. Enantioselective photochemical reactions in crystalline inclusion compounds, *J. Org. Chem.*, 53, 4391, 1988.
24. (a) Ito, Y., Yasui, S., Yamauchi, J., Ohba, S., and Kano, G., Solid state photocyclization of 2,4,6-triisopropyl-4′-(methoxycarbonyl)benzophenone. Evidence for a narrow reaction cavity and a photoenol diradical intermediate, *J. Phys. Chem. A*, 102, 5415, 1998; (b) Ito, Y., Kano, G., and Nakamura, N., Diastereoselective photocyclization of *N*-(*p*-(2,4,6-triisopropylbenzoyl)benzoyl)-L-phenylalanine methyl ester in the solid state, *J. Org. Chem.*, 63, 5643, 1998; (c) Ito, Y. and Matsuura, T., Efficiency for solid state photocyclization of 2,4,6-triisopropylbenzophenones, *Tetrahedron Lett.*, 29, 3087, 1988.
25. Koshima, H., Maeda, A., Masuda, N., Matsuura, T., Hirotsu, K., Okada, K., Mizutani, H., Ito, Y., Fu, T. Y., Scheffer, J. R., and Trotter, J., Ionic chiral handle-induced synthesis in a solid state Norrish type II photoreaction, *Tetrahedron Asymmetry*, 5, 1415, 1994.
26. Fu, T. Y., Scheffer, J. R., and Trotter, J., Crystal structure–reactivity relationships in the solid state photochemistry of 2,4,6-triisopropylthiobenzophenone: C=O···H versus C=S···H abstraction geometry, *Tetrahedron Lett.*, 37, 2125, 1996.
27. Koshima, H., Matsushige, D., and Miyauchi, M., Enantiospecific single crystal-to-single crystal photocyclization of 2,5-diisopropyl-4′-carboxybenzophenone in the salt crystals with (*S*)- and (*R*)-phenylethylamine, *Cryst. Eng. Comm.*, 33, 1, 2001.
28. Kumar, A. and Venkatesan, K., Photochromism of alkylisophthaldehydes in the solid state: structure–reactivity correlations, *J. Chem. Soc.*, *Perkin Trans. 2*, 829, 1991.

29. Moorthy, J. N., Mal, P., Natarajan, R., and Venugopalan, P., Efficient photocyclization of *o*-alkylbenzaldehydes in the solid state: direct observation of *E*-xylylenols en route to benzocyclobutenols, *J. Org. Chem.*, 66, 7013, 2001.
30. Sarkar, T. K., Ghosh, S. K., Moorthy, J. N., Fang, J.-M., Nandy, S. K., Sathyamurthy, N., and Chakraborty, D., Photochromism and photoreactivity of 2,6-dichloro-4-methyl-3-pyridenecarboxaldehyde in the solid state, *Tetrahedron Lett.*, 41, 6909, 2000.
31. (a) Jones, R., Scheffer, J. R., Trotter, J., and Yang, J., Crystal to molecular chirality transfer: supramolecular photochemistry of crystalline carboxylate salts, *Tetrahedron Lett.*, 33, 5481, 1992; (b) Jones, R., Scheffer, J. R., Trotter, J., and Yang, J., Crystal structures, chiralities and photochemistry of two polymorphs of L-prolinolium α-adamantylacetophenone-*p*-carboxylate, *Acta Cryst.*, B50, 601, 1994.
32. Fu, T.Y., Scheffer, J. R., and Trotter, J., Crystal structure–reactivity correlations in the solid state photochemistry of *N*-(*tert*-butyl)succinimide, *Can. J. Chem.*, 72, 1952, 1994.
33. Olovsson, G., Scheffer, J. R., Trotter, J., and Wu, C.-H., Novel differences between the solid state and solution phase photochemistry of 1,2-cyclodecanedione, *Tetrahedron Lett.*, 38, 6549, 1997.
34. Vishnumurthy, K., Cheung, E., Scheffer, J. R., and Scott, C., Enhanced regioselectivity of Yang photocyclization in the crystalline state, *Org. Lett.*, 4, 1071, 2002.
35. Cheung, E., Netherton, M. R., Scheffer, J. R., Trotter, J., and Zenova, A., Asymmetric induction through the use of remote covalent and ionic chiral auxiliaries in the solid state photochemistry of 2-benzoyladamantane-2-carboxylic acid derivatives, *Tetrahedron Lett.*, 41, 9673, 2000.
36. Hashizume, D., Ohashi, Y., Tanaka, K., and Toda, F., The mechanism of the enantioselective photocyclization of 2-piperidone in the clathrate crystal, *Bull. Chem. Soc. Jpn.*, 67, 2383, 1994.
37. Mohr, S., Reactionen in organischen kristallen. IV. Norrish type II fragmentierung von kristallinen spiro-diketonen und spiro-diketoniminen, *Tetrahedron Lett.*, 21, 593, 1980.
38. Cheung, E., Rademacher, K., Scheffer, J. R., and Trotter, J., An investigation of the solid state photochemistry of α-mesitylacetophenone derivatives: asymmetric induction studies and crystal structure–reactivity relationships, *Tetrahedron*, 56, 6739, 2000.
39. Wagner, P. J., Zhou, B., Hasegawa, T., and Ward, D.,L., Diverse photochemistry of sterically congested α-arylacetophenones: ground state conformational control of reactivity, *J. Am. Chem. Soc.*, 113, 9640, 1991.
40. Wagner, P. J., Pabon, R., Park, B.-S., Zand, A. R., and Ward, D. L., The regioselectivity of internal hydrogen abstraction by triplet *o*-*tert*-amylbenzophenone, *J. Am. Chem. Soc.*, 116, 589, 1994.
41. Wagner, P. J., Giri, B. P., Scaiano, J. C., Ward, D. L., Gabe, E., and Lee, F. L., Photocyclization of *o*-*tert*-butylbenzophenone, *J. Am. Chem. Soc.*, 107, 5483, 1985.
42. Wagner, P. J., Park, B.-S., Sobczak, M., Frey, J., and Rappoport, Z., Photocyclization of 2,4,6,2′,4′,6′-hexaalkylbenzyls, *J. Am. Chem. Soc.*, 117, 7619, 1995.
43. Irngartinger, H., Fettel, P. W., and Siemund, V., Diastereo- and enantioselective δ-H abstraction in the solid state of 1-benzoyl-8-benzylnaphthalene: absolute asymmetric synthesis due to a chiral crystal environment, *Eur. J. Org. Chem.*, 2079, 1998.
44. Cheung, E., Netherton, M. R., Scheffer, J. R., and Trotter, J., In the footsteps of Pasteur: asymmetric induction in the solid state photochemistry of ammonium carboxylate salts, *J. Am. Chem. Soc.*, 121, 2919, 1999.
45. Sakamoto, M., Takahashi, M., Fujita, T., Nishio, T., Iida, I., and Watanabe, S., Solid-state photochemical reaction of *S*-phenyl *N*-(benzoylformyl)thiocarbamates: "absolute" asymmetric synthesis using the chiral crystal environment, *J. Org. Chem.*, 60, 4682, 1995.
46. (a) Wagner, P. J., Chemistry of excited triplet organic carbonyl compounds, *Top. Curr. Chem.*, 66, 1, 1976; (b) Wagner, P. J. and Zhou, B., Efficient solid state photocyclization of sterically congested α-*o*-tolyl ketones despite "poor" geometries for hydrogen abstraction, *Tetrahedron Lett.*, 30, 5389, 1989.
47. (a) Prinzbach, H. and Fessner, W.-D., Novel organic polycycles: an adventure in molecular architecture, in *Organic Synthesis: Modern Trends*, Chizhov, O., Ed., Blackwell, Oxford, 1987, 23–42; (b) Sugiyama, N., Nishio, T., Yamada, K., and Aoyama, H., Photochemical reactions of bridged polycyclic ketones, *Bull. Chem. Soc. Jpn.*, 43, 1879, 1970.

48. Addadi, L., Ariel, S., Lahav, M., Leiserowitz, L., Popovitz-Biro, R., and Tang, C. P., New trends and strategies in organic solid-state chemistry, in *Chemical Physics of Solids and Their Surfaces*, Vol. 8, Roberts, M. W. and Thomas, J. M., Eds., The Royal Society of Chemistry, London, 1980, chap. 7, 202–204.
49. DeBoer, C. D., Herkstroeter, W. G., Marchetti, A. P., Schultz, A. G., and Schlessinger, R. H., Norrish type II rearrangement from π,π^* triplet states, *J. Am. Chem. Soc.*, 95, 3963, 1973.
50. Chandler, W. and Goodman, L., Allowed and forbidden character in $\pi^*\leftarrow$n spectra of cycloalkanones, *J. Mol. Spectrosc.*, 35, 232, 1970.
51. For example, it is well established that formaldehyde adopts a pyramidal geometry in its n,π^* singlet and triplet excited states; see Moule, D. C. and Walsh, A. D., Ultraviolet spectra and excited states of formaldehyde, *Chem. Rev.*, 75, 67, 1975 (and references cited therein). *Ab initio* calculations (by Sauers, R. R. and Edberg, L. A., Modeling of Norrish type II reactions by semiempirical and ab initio methodology, *J. Org. Chem.*, 59, 7061, 1994) on the triplet state geometries of aliphatic aldehydes and ketones support the picture of a partially (22–45°) pyramidalized carbonyl carbon.
52. (a) Hoffman, R. and Swenson, J. R., Ground- and excited-state geometries of benzophenone, *J. Phys. Chem.*, 74, 415, 1970; (b) Wagner, P. J., May, M., and Haug, A., Viscosity-dependent dual phosphorescence of phenyl alkyl ketones, *Chem. Phys. Lett.*, 13, 545, 1972; (c) Birge, R. R., Pringle, W. C., and Leermakers, P. A., Excited-state geometries of the singly substituted methylpropenals. I. Vibrational-electronic analysis of S1(n,π^*), *J. Am. Chem. Soc.*, 93, 6715, 1971; (d) Birge, R. R. and Leermakers, P. A., Excited-state geometries of the singly substituted methylpropenals. II. Bond order reversal and substituent interaction in S1(n,π^*), *J. Am. Chem. Soc.*, 93, 6726, 1971.
53. For reviews dealing with previous work on asymmetric induction in organic photochemical reactions, see (a) Rau, H., Asymmetric photochemistry in solution, *Chem. Rev.*, 83, 535, 1983; (b) Inoue, Y., Asymmetric photochemical reactions in solution, *Chem. Rev.*, 92, 741, 1992; (c) Pete, J. P., Asymmetric photoreactions of conjugated enones and esters, *Adv. Photochem.*, 21, 135, 1996; (d) Everitt, S. R. L. and Inoue, Y., Asymmetric photochemical reactions in solution, in *Molecular and Supramolecular Photochemistry*, Ramamurthy, V. and Schanze, K. S., Eds., Marcel Dekker, New York, 1999, chap. 2.
54. (a) Vaida, M., Popovitz-Biro, R., Leiserowitz, L., and Lahav, M., Probing reaction pathways via asymmetric transformations in chiral and centrosymmetric crystals, in *Photochemistry in Organized and Constrained Media*, Ramamurthy, V., Ed., VCH, New York, 1991, chap. 6; (b) Caswell, L., Garcia-Garibay, M. A., Scheffer, J. R., and Trotter, J., Optical activity can be created from "nothing", *J. Chem. Ed.*, 70, 785, 1993.
55. Leibovitch, M., Olovsson, G., Scheffer, J. R., and Trotter, J., Determination of the absolute steric course of an enantioselective single crystal-to-single crystal photorearrangement, *J. Am. Chem. Soc.*, 119, 1462, 1997.
56. Cheung, E., Kang, T., Netherton, M. R., Scheffer, J. R., and Trotter, J., Conformational enantiomerism in chiral organic salts containing crystallographically independent anion-cation pairs, *J. Am. Chem. Soc.*, 122, 11753, 2000.
57. Eliel, E. L. and Wilen, S. H., *Stereochemistry of Organic Compounds*, Wiley, New York, 1994, chap. 7; (b) Collet, A., Resolution of racemates: did you say "classical"?, *Angew. Chem. Int. Ed. Engl.*, 37, 3239, 1999.
58. Gudmundsdottir, A. D. and Scheffer, J. R., Asymmetric induction in the solid state photochemistry of salts of carboxylic acids with optically active amines, *Tetrahedron Lett.*, 31, 6807, 1990.
59. Gudmundsdottir, A. D. and Scheffer, J. R., Asymmetric induction in the solid state photochemistry of ammonium salts, *Photochem. Photobiol.*, 54, 535, 1991.
60. Gudmundsdottir, A. D., Scheffer, J. R., and Trotter, J., Ionic chiral handle-induced solid state asymmetric synthesis: origin of the asymmetric induction elucidated through absolute configuration correlation studies, *Tetrahedron Lett.*, 35, 1397, 1994.

61. Gudmundsdottir, A. D., Li, W., Scheffer, J. R., Rettig, S., and Trotter, J., Asymmetric induction in the photochemistry of crystalline salts: structure-reactivity correlations, *Mol. Cryst. Liq. Cryst.*, 240, 81, 1994.
62. Janz, K. M. and Scheffer, J. R., The use of ionic chiral sensitizers in the crystalline state: application to the di-π-methane photorearrangement of a benzonorbornadiene derivative, *Tetrahedron Lett.*, 40, 8725, 1999.
63. Cheung, E., Netherton, M. R., Scheffer, J. R., and Trotter, J., Linearly conjugated benzocyclohexadienone photochemistry in the solid state: ionic chiral auxiliary mediated asymmetric induction, *Tetrahedron Lett.*, 40, 8737, 1999.
64. Scheffer, J. R. and Wang, L., Enantioselective photoelectrocyclization of a tropolone derivative in the crystalline state, *J. Phys. Org. Chem.*, 13, 531, 2000.
65. Cheung, E., Chong, K. C. W., Jayaraman, S., Ramamurthy, V., Scheffer, J. R., and Trotter, J., Enantio- and diastereodifferentiating *cis*,*trans*-photoisomerization of 2β,3β-diphenylcyclopropane-1-α-carboxylic acid derivatives in organized media, *Org. Lett.*, 2, 2801, 2000.
66. Chong, K. C. W., Sivaguru, J., Shichi, T., Yoshimi, Y., Ramamurthy, V., and Scheffer, J. R., Use of chirally modified zeolites and crystals in photochemical asymmetric synthesis, *J. Am. Chem. Soc.*, 124, 2858, 2002.
67. Kang, T. and Scheffer, J. R., An unexpected Paterno–Büchi reaction in the crystalline state, *Org. Lett.*, 3, 3361, 2001.
68. Wang, K. and Scheffer, J. R., Enantioselective photochemical synthesis of a β-lactam via the solid state ionic chiral auxiliary method, *Synthesis*, 1253, 2001.
69. Schmidt, G. M. J., Photodimerization in the solid state, *Pure Appl. Chem.*, 27, 647, 1971.

55

Norrish Type II Processes of Ketones: Influence of Environment

Tadashi Hasegawa
Tokyo Gakugei University

55.1 Introduction

Photolysis of a carbonyl compound having γ-hydrogen commonly gives a shorter chain carbonyl compound, an alkene, and a cyclobutanol, which are formed from a 1,4-biradical[1] produced via γ-hydrogen abstraction by the excited carbonyl. The photoreactions derived from the 1,4-biradical are termed the Norrish type II reaction,[2] and those involving intramolecular hydrogen abstraction from γ- and other positions are generically referred to as the type II family.[2b] The chemical behavior of the 1,4-biradical determines the type II reactivity of carbonyl compounds. In this chapter, the influence of environment on the formation and behavior of the 1,4-biradical from simple alkyl aryl ketones will be described. Environmental effects on the type II reaction have been reviewed.[2e,3,4]

55.2 Mechanistic Details of the Type II Reaction

The excited state responsible for hydrogen abstraction by the carbonyl group is the lowest n,π^* state. Ketones with the lowest π,π^* states are far less reactive than ketones with the lowest n,π^* states. The n,π^* transition involves excitation of an electron from a nonbonding orbital localized mainly on oxygen to an antibonding π^* orbital that covers both carbon and oxygen. The yield of intersystem crossing (ISC) from the n,π^* singlet to triplet state in alkyl aryl ketones is generally 100%, so that the type II reaction occurs from the triplet state.[5] The 1,4-biradical (*i*-**BR**) formed initially from the n,π^* triplet state is in a triplet skew form (Scheme 1). The triplet 1,4-biradical has a relatively long lifetime and transforms to the cisoid (*c*-$\mathbf{BR}_1$ or *c*-$\mathbf{BR}_2$) or transoid biradical (*t*-**BR**) via a rotation of the central σ-bond. Intersystem

0-8493-1348-1/04/$0.00+$1.50

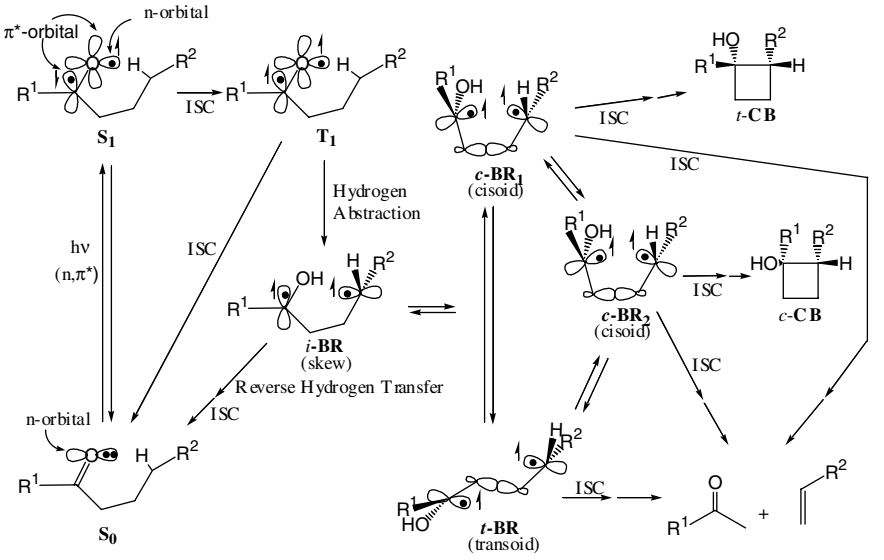

SCHEME 1 A detailed mechanism of the Type II reaction.

crossing changes the triplet to singlet biradicals that have very short lifetimes (sub-nanosecond)[1c] and lead immediately to products. Only elimination occurs from *t*-**BR**, while both cyclization and elimination occur from *c*-**BR**.[6] In cyclobutanol formation, the conformation of the triplet biradicals is maintained because the nascent singlet biradicals have the same conformation as that of the triplet biradicals.[1c] The reaction environment affects both the nature of the lowest excited state of ketones and the formation and behavior of the triplet 1,4-biradicals.

55.3 Environmental Effects on the Electronic States of Alkyl Aryl Ketones

The benzoyl chromophore shows a weak n,π^* band (ε = 5 to 100) in the 300- to 370-nm range and a moderately intense π,π^* band (ε = 1000 to 2000) in the 270- to 290-nm range. The lowest triplet state of phenyl alkyl ketones is n,π^* in hydrocarbon solvents. Introduction of a substituent such as a hydroxy, thiomethoxy, bromo, or phenyl group to the benzoyl phenyl group causes π,π^* states to be lowest.[7,8] The type II photoreactivity of these ketones is quite low ($\phi < 0.001$). The quantum yield for the type II reaction of *p*-methoxyvalerophenone (0.14) in benzene is, however, half of that of valerophenone (0.33), although *p*-methoxy substitution leads to the lowest π,π^* state.[7] The reactivity of ketones having the lowest π,π^* triplets decreases with an increase of the energy gap between the π,π^* and the n,π^* triplets[7] and increases with an increase of reaction temperature.[9] This indicates that the upper n,π^* and lowest π,π^* states are in thermal equilibration, and the reaction of *p*-methoxyvalerophenone occurs from the upper n,π^* triplet state.[7,9] Polar solvents destabilize the n,π^* state by lowering the energy level of the *n* orbital and stabilize the π,π^* state by lowering the level of the π^* orbital.[10] The quantum yield of *p*-methoxyvalerophenone decreases to 0.09 in methanol because of the large contribution of the π,π^* state in the equilibration.[7] The lifetime of valerophenone changes with solvent polarity and is longer in polar solvents than in nonpolar solvents (Table 55.1).[11–15] The lowest excited state of valerophenone in water is the π,π^* state.[11]

A nonreactive solid surface, such as a silica-gel surface, provides an ordered two-dimensional environment for effecting and controlling photochemical processes.[16–20] A silica-gel surface is composed of an interconnected network of polar silanol (Si–OH) and siloxane (Si–O–Si) groups[16] and therefore provides a strong polar reaction medium. Silica gel has a Kosower's *Z* value[21] of 88, intermediate between

TABLE 55.1 Solvent Polarity and Quenching Constants for Valerophenone

Solvent	Z[a]	ε[b]	kqτ / M^{-1}	kq / 10^9 $M^{-1}s^{-1}$	τ / 10^{-9} s	1/τ / 10^{-7} s^{-1}
water (20°C)	94.6	80.2	152[c]	2.9	52	1.9
water (30°C)		76.6	138[c]	3.6	38	2.6
MeOH	83.6	33.0	90[d]	5.5	16	6.3
wet acetonitrile			63[d]	7.2	8.7	12
acetonitrile	71.3	36.64	38[e]	11.0	3.6	28
t-BuOH	71.3	12.47	40[e]	2.3	14.4	6.9
acetone	65.7	21.0	47[e]	11.0	4.2	24
benzene		2.283	40[f]	6.0	6.7	15
cyclooctane		2.116	30[e]	4.2	7.2	14
hexane		1.890	78[e]	11.0	7.2	14

[a] ref. 21
[b] Dean, J. A. *Lange's Handbook of Chemistry,* 15th Ed., McGraw Hill, New York, 1999, 5.105.
[c] ref. 11
[d] ref. 15
[e] ref. 12
[f] ref. 13 and 14

those of water (94.6)[21] and methanol (83.6).[21,22] Indeed, the polar silica-gel surface causes the inversion of the nearby n,π^* and π,π^* triplet states of alkyl aryl ketones.[23]

Zeolites have three-dimensional pore structures in which alkyl aryl ketones are included. The triplet lifetime (τ) of valerophenone included in zeolites is affected by polarity of the zeolite interior: zeolite LiX (τ = 4 to 5 ms), NaX (τ = 0.8), KX (τ = 0.9), PbX (τ = 0.7), and CsX (τ < 0.2).[24] The interior of LiX is more polar than other cation-exchanged X zeolites and changes the lowest triplet state of valerophenone from n,π^* to π,π^*.

55.4 Environmental Effects on the Formation of 1,4-Biradicals

Although the quantum yield for the type II reaction of valerophenone is unity in *t*-BuOH,[5] a small amount (~2%) of phenylcyclopentanol, formed via δ-hydrogen abstraction, has been observed in a highly polar aqueous solution (Scheme 2).[11] Molecular oxygen is a ground-state triplet and dissolves in common organic solvents. The dissolved oxygen quenches the n,π^* triplet state of ketones.[25] The oxygen is also known to trap a 1,4-biradical and causes an increase of the type II product yields.[26]

The type II reaction requires close approach of a γ-hydrogen to carbonyl oxygen and effective overlap of the hydrogen *s*-orbital with the oxygen *n*-orbital responsible for abstraction. Flexible ketone molecules change their conformation freely and achieve conformational equilibrium before γ-hydrogen abstraction.[27] Conformational restriction caused by environment decreases the type II reactivity and may allow appearance of other reactivities.

Valerophenone undergoes the type II reaction in frozen benzene, but a fraction (25 to 30%) of the valerophenone remains unreacted even after prolonged irradiation.[28] This means that 25 to 30% of the valerophenone is in unreactive conformations and the unreactive conformers cannot convert to reactive ones in the frozen solution.

Conformational changes are much more restricted in a crystalline state, so that only γ-hydrogens that meet geometrical requirements can be abstracted. Four parameters have been used for prediction of the occurrence of γ-hydrogen abstraction in the crystalline state (Figure 55.1a). Parameters *d*, Δ, θ, and ω

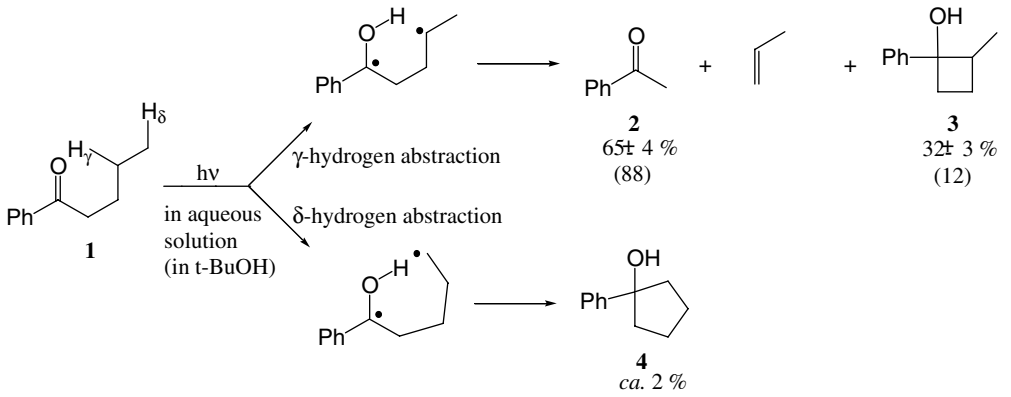

SCHEME 2

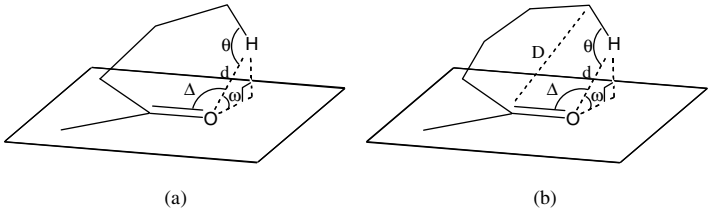

FIGURE 55.1 Definition of geometric parameters for γ-hydrogen abstraction (a) and those for δ-hydrogen atom abstraction (b).

are the distance between the carbonyl oxygen and the γ-hydrogen, the C=O···H angle, the C–H···O angle, and the angle by which the γ-hydrogen atom lies outside the mean plane of the carbonyl group; their respective optimum values are 2.72 Å, 90° to 120° (depending on the hybridization of the orbitals containing the nonbonding electrons on oxygen), 180°, and 0°.[29] An additional parameter *D*, which represents the interatomic distance between the two carbon atoms and is expected to be 3.4 Å (the sum of the van der Waals radii of two carbon atoms), has been proposed for δ-hydrogen abstraction (Figure 55.1b).[30]

Conformational change might be restricted by adsorption of alkyl aryl ketones on a solid surface. Upon irradiation in benzene, 2-benzoylcyclohexanone undergoes the type II elimination to give **6** at an 82% yield (Scheme 3).[31] No cyclization products nor α-cleavage products are formed. On the other hand, the α-cleavage competes with the 1,4-biradical formation on a dry silica-gel surface.[32] A silica-gel surface may act as a possible field, bringing out the latent reactivity of dispersed molecules because of its adsorptivity and high polarity.[33] Although δ-hydrogen abstraction has been also observed on the surface,[34] remote hydrogen abstraction, which requires more conformational flexibility than γ- and δ-hydrogen abstraction, has not been observed so far.[35]

55.5 Environmental Effects on the Behavior of 1,4-Biradicals

Process Regenerating Starting Ketones

Quantum yields for disappearance of the starting material in the type II reaction of simple alkyl aryl ketones having the lowest n,π^* state in hydrocarbon solvents are usually in the range of 0.1 to 0.5.[5,8,30,36–38] The quantum yields show solvent dependency and rise to nearly unity in polar solvents.[5,6,36,38] This effect

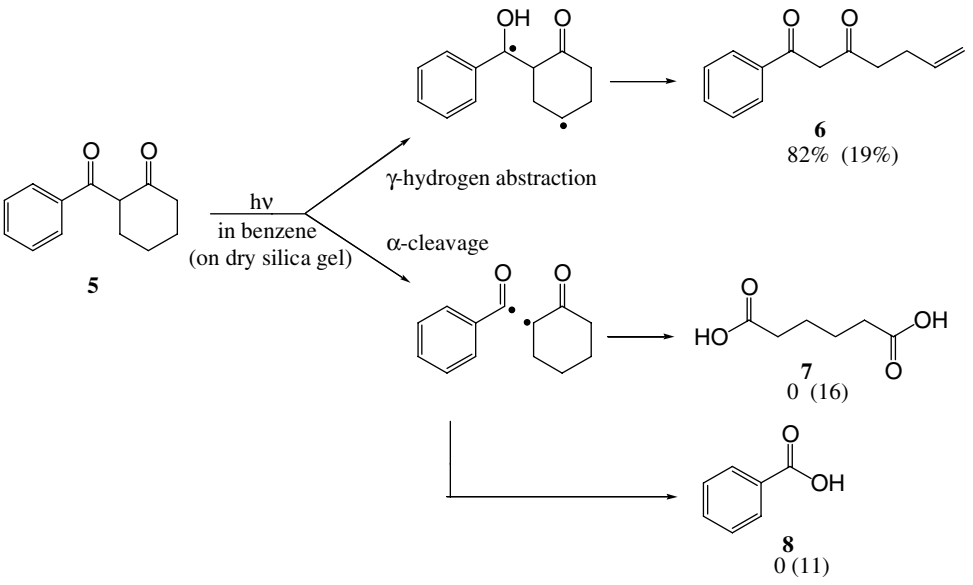

SCHEME 3

is due to suppression of reverse hydrogen transfer, which regenerates the starting ketones from 1,4-biradicals, by hydrogen bonding between the hydroxyl group of the biradical and polar solvents.[2c,5]

In contrast to the behavior in solution, valerophenone shows equal quantum efficiencies in frozen solvents.[34] No significant interaction occurs between a solvent molecule and the OH group of a 1,4-biradical in frozen solvents. The frozen solvents provide passive cavities.[28,39] On the other hand, interfaces of micelles provide active cavities where guest molecules can be oriented through hydrophobic–hydrophilic interactions.[40,41] The quantum yield for the type II reaction of valerophenone in an aqueous hexadecyl tetramethyl ammonium chloride (HTAC) solution is unity.[40] A polar silica-gel surface also provides an active cavity[39] and would enhance the type II quantum efficiency.

Elimination vs. Cyclization

The percentage of cyclization in the type II reaction depends strongly on the structure of ketones and is in the wide range of 5 to 90%, even in simple alkyl aryl ketones.[11,30,37] The percentage increases with α-substitution, although β- and γ-substituents also exert a small influence.[30] Cyclization requires overlap of the orbitals on the ketyl and alkyl radical centers, whereas elimination requires overlap of the orbitals, with orbitals comprising the σ-bond undergoing cleavage. The 1,2-eclipsing interaction in 1,4-biradicals formed from α-substituted ketones is less severe in the transition state for cyclization than that for elimination.[30] Although polar solvents enhance the overall quantum yield of the type II reaction, the solvents decrease the total yield of cyclobutanols because of steric congestion in the solvated biradicals.[5,15] In frozen solvents, the rotation along the CC bonds becomes difficult, and large conformational changes are totally restricted. Transformation from the initially formed 1,4-biradical (*i*-**BR**) to the transoid biradical (*t*-**BR**), from which only elimination occurs, requires larger conformational changes than transformation to the cisoid biradical (*c*-$\mathbf{BR}_1$ or *c*-$\mathbf{BR}_2$). The ratio of type II elimination to cyclization (E/C) becomes lower in frozen solvents than in solution, and the ratio decreases with decreasing temperature (Table 55.2).[28]

The E/C ratio in a crystalline state is often quite different from that in solution. The cyclization predominates greatly over the elimination in the photolysis of **9** (Scheme 4, Table 55.3)[29,42] The x-ray crystallography of **9a–j** shows that all the ketones have the geometrical parameter *d* (see Figure 55.1a) nearly equal to the optimum value of 2.72 Å. The geometric data for the unreactive diketone **9a** are

TABLE 55.2 Temperature Dependency of the Type II Elimination/Cyclization (E/C) Ratio in Valerophenone

	E/C[a]			
Medium	25°	20°	−10°	−30°
t-BuOH	9.00[b]			
t-BuOH-EtOH (9:1)		7.88	6.42	5.93
Acetonitrile	5.67[b]			
Benzene		4.52	5.10	6.28
	5.28[b]			
Cyclohexane		4.62	5.85	6.44
Hexadecane		4.84	5.44	5.68
Water		1.91	2.74	3.62
		2.03[c]		
Silica gel TLC (−125°C)[d]		Only C		
Reverse phase TLC (−125°C)[d]		Only C		

[a] Ref. 28
[b] Ref. 12
[c] Ref. 11
[d] Ref. 17

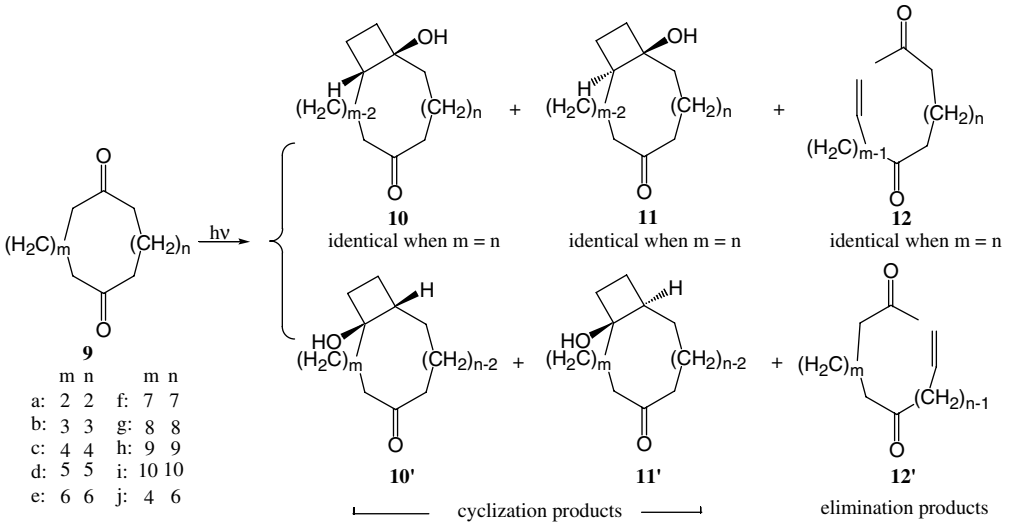

SCHEME 4

virtually indistinguishable from those for reactive diketones **9c** and **9e**.[42] The lack of reactivity of **9a** in the solid state has been attributed to steric strain associated with closure to an eight-membered ring. In α-cyclohexyl-4-chloroacetophenone, the E/C ratio is 0.91 in the solid state, although the ratio is 0.37 in acetonitrile[43] and 0.64 in benzene.[44] The E/C ratios in the solid state must be determined by the geometry of the1,4-biradicals. The spiroketone **13a** undergoes type II elimination exclusively in the crystalline state to give **15**, whereas **13c** and ketone **17**[45] undergo cyclization (Scheme 5).[46] Compound **13b** shows efficient reverse hydrogen transfer in the crystalline state. The x-ray structure analysis of **13a–c** and **17** revealed that compound **13a** has favorable geometry for the elimination reaction.[46]

A silica-gel surface lowers the E/C ratio and allows only cyclization at low temperature (TLC and reverse-phase TLC in Table 55.4).[17] Inclusion of alkyl aryl ketones in zeolites and cyclodextrin (CD) changes the behavior of 1,4-biradicals. The reaction cavities of the zeolites are hard in the sense that they

TABLE 55.3 Product Yields in the Solution Phase and Solid State Photoreaction of **9**

Compound	Hexane					Solid				
	10/%	**11**/%	**12**/%	E/C[a]	t/c[b]	**10**/%	**11**/%	**12**/%	E/C[a]	t/c[b]
9a	No reaction					No reaction				
9b	84	0	16	5.3	0	99	0	1	99	0
9c	65	25	10	9.0	0.38	58	29	13	6.7	0.5
9d	22	35	43	1.3	1.59	89	10	1	99	0.11
9e	17	42	41	1.4	2.47	3	84	13	6.7	28
9f	10	23	67	0.5	2.3	90	4	6	15.7	0.04
9g	10	34	56	0.8	3.4	4	91	5	19.0	22.75
9h	15	27	58	0.7	1.8	98	1	1	99	0.01
9i needles[c]	14	33	53	0.9	2.36	9	91	0	only E	10.11
9i plates[c]						97	3	0	only E	0.03
	10/10'	**11+11'**	**12+12'**			**10/10'**	**11+11'**	**12+12'**		
9j	13/13	35	39	1.6	1.35	100/0	0	0	only E	0

[a] **(10+11)/12**

[b] **11/10**

[c] polymorphic forms

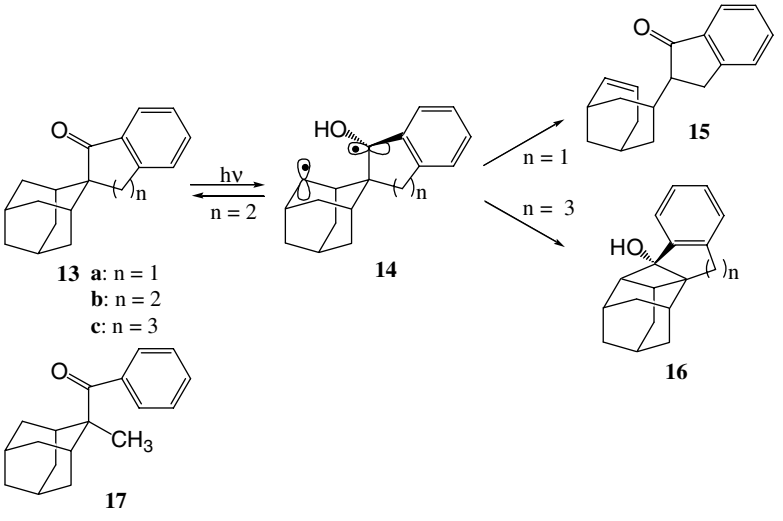

SCHEME 5

are not flexible. The zeolites may be classified on the basis of pore (window) size: (1) zeolites having channel dimensions less than 6.5 Å (e.g., ZSM-5, ZSM-11, ZSM-34, and other offretites), and (2) zeolites having dimensions larger than 7 Å (e.g., X, Y, L, Ω-5, and M-5).[24] Only the type II elimination occurs in photolysis of alkyl aryl ketones in group 1 zeolites, whereas both elimination and cyclization occur in group 2 zeolites (Table 55.4). The preference for elimination in group 1 zeolites is due to suppression of cyclization. Large conformational change are not allowed in the small cavities of group 1 zeolites, although either the alkyl or aryl group must change positions when *i*-**BR**, from which the elimination would occur directly, transforms to *c*-**BR**.[24] An increase of cyclization products has been observed in photolysis of butyrophenone and valerophenone included in CD compared to photolysis in solution. Because addition of more than 1 equivalent of CD does not produce any significant variation in the product distribution, photoreactions occur from 1:1 complexes (Table 55.4).[47] Structures of the β-CD complexes with butyrophenone and valerophenone have been determined from x-ray crystallographic studies to be 2:2 β-CD/guest systems, and the complexes are regarded as reaction nanotubes.[48] Liquid crystals (LCs) are

TABLE 55.4 The E/C and II/I Ratios in the Type II Reaction of Alkyl Phenyl Ketones in Various Media

Medium	Ketone[a]						ref.
	BP	VP	DMBP		DMVP		
	E/C[b]	E/C	E/C	II/I[c]	E/C	II/I	
benzene	6.5	3.8	0.1	1.2	0.1	4.2	47
	8.3	2.7					24
t-BuOH	8.5	5.9	0.2	1.8	0.3	9.0	47
		9.0					12
		4.2					17
	8.0	4.26					50
silica gel TLC		3.7			0.5	0.28	17
reverse phase TLC		3.0			0.5	0.38	17
zeolite ZSM-5	73	only E					24
zeolite ZSM-11	56	only E					24
zeolite Na X	3.0	1.2					24
zeolite Na Y	3.2	1.1					24
β-CD/H_2O							47
1:1[d]	4.0	2.9	0.3	7.32	0.6	16.6	
2:1	3.8	2.9					
3:1	3.8	2.9					
β-CD (solid)							
1:1	3.5	3.1	0.4	5.3	0.6	14.0	47
α-CD/H_2O	4.4	3.8	0.5	7.3	0.8	6.3	47
γ-CD/H_2O		2.7			0.2	19.0	47
liquid crystal CCH-4[e] (smectic) 0.6 mol%[f]	8.6	9.2					50
liquid crystal EB[g] (nematic) 0.6 mol%	9.7	6.1					50
liquid crystal CCH-4 (isot) 40 mol%	7.8	6.0					50
liquid crystal EC[h] (isot) 0.6 mol%	8.5	5.0					50

[a] BP: butyrophenone; VP: valerophenone; DMBP: α,α-dimethylbutyrophenone; DMVP: α,α-dimethylvalerophenone

[b] Ratio of the Type II elimination to the cyclization

[c] Ratio of the Type II reaction to the Type I reaction

[d] Molar ratio of cyclodextrin (CD) to a ketone

[e] *trans,trans*-4'-butyl[1,1'-bicyclohexyl]-4-carbonitrile

[f] concentration of a ketone

[g] CCH-2 (4'-ethyl derivative) / CCH-4 = 2 / 1

[h] CCH-2 / cyclohexane = 6 / 1

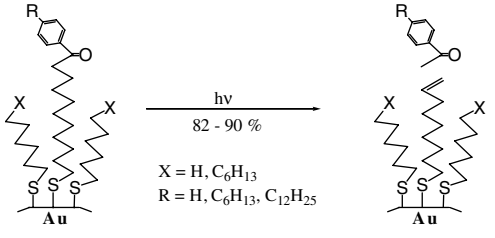

SCHEME 6

considered to be very disturbed solids or ordered liquids.[49] Smectic and nematic LC has commonly been used as solvents for photoreactions of organic compounds. The E/C ratio in the type II reaction of valerophenone is larger in the smectic LC phase than in isotropic solvents (Table 55.4).[50] This might be due to slower interconversion between triplet biradical conformers in the smectic phase.

The type II reaction of *p*-alkylalkanophenones in *n*-butyl stearate has been studied.[51] The E/C ratio in the reaction depends on the length of their two-alkyl chains. The type II elimination occurs exclusively from alkyl aryl ketones on monolayer protected gold clusters (Scheme 6).[52] Although the ketones are not

TABLE 55.5 The t/c Ratio in the Type II Reaction of Alkyl Phenyl Ketones in Various Media

	Ketones[b]					
Medium	VP	HP	OP	DP	TDP	ODP
hexane	5		3.1	2.8	2.7	3.0
MCH[c]	4.0	4.0				
benzene	3.6		2.5	2.4	2.4	2.6
acetone	2					
MeCN	1.40	1.30				
t-BuOH	1.35	1.32	1.1			
MeOH	1.44	1.41	2.0	1.7	1.5	1.8
water	2.4					
HTAC[d]	1.9		1.2			
CCH-4(Sm)[e]	6.3	6.6				
EB (nem)[f]	2.07	1.4				
CCH-4 (iso)[g]	2.00	2.00				
EC (isot)[h]	2.0	2.1				
zeolite Na X			1.0	0.6	0.8	1.2
zeolite Na Y			1.0	0.7	1.2	1.3

[a] ref. 5, 11, 24, 40, and 50

[b] VP: valerophenone; HP: hexanophenone; OP: octanophenone; DP: dodecanophenone; TDP: tetradecanophenone; ODP: octadecanophenone.

[c] methylcyclohexane

[d] 0.05M-hexadectl tetramethyl ammonium chloride (micelle)

[e] 0.6 mol% in *trans,trans*-4'-butyl[1,1'-bicyclohexyl]-4-carbonitrile (smectic liquid crystal)

[f] 0.6 mol% in a mixture of CCH-2 (4'-ethyl derivative) / CCH-4 = 2 / 1 (nematic liquid crystal)

[g] 40 mol% in *trans,trans*-4'-butyl[1,1'-bicyclohexyl]-4-carbonitrile (isotropic liquid)

[h] 0.6 mol % in a mixture of CCH-2 / cyclohexane = 6 / 1 (isotropic liquid)

in extremely rigid environments, but rather dynamic within the monolayer, the environment affects the equilibrium of the biradical conformers. Stringent demands must be made on the biradical to adopt *t*-**BR** over *c*-**BR** in the monolayer protected gold clusters. The type II elimination occurs in polymers of acrylophenones in solution[53a] and in the solid state.[53b] In the solid-state photoreaction of poly(4′-ethoxy-acrylophenone), the O–CH_2CH_3 bond cleavage from the lowest π,π^* state competes with the γ-hydrogen abstraction from the upper n,π^* state.[53b]

Stereochemistry of Cyclobutanols

The triplet biradicals *c*-$\mathbf{BR}_1$ and *c*-$\mathbf{BR}_2$ lead to the stereoisomeric cyclobutanols *t*-**CB** and *c*-**CB**, respectively, via ISC to the singlet biradicals that have very short lifetimes. The ratios of *trans*- to *cis*-cyclobutanol (*t*/*c*) in the type II reaction of alkyl phenyl ketones are in the range from 2 to 5 in nonpolar solvents (Table 55.5).[5,11,24,40,50] The ratios become smaller in polar solvents. The *t*/*c* ratio in the photolysis of valerophenone decreases from 3.6 in benzene to 1.35 in *t*-BuOH.[50] Formation of the *trans*-isomer, where the hydroxy group is *cis* to the γ-alkyl group, is suppressed in polar solvents because of steric interference between a hydrogen bonded solvent molecule and the alkyl group. The *t*/*c* ratio in a HTAC micellar solution is similar to that in polar solvents.[40] The average position of alkyl aryl ketones should be either on the micelle surface or in the Stern layer. The hydrogen bonding is formed between the 1,4-biradical and water on the surface or in the layer. The *t*/*c* ratio is also affected significantly by smectic LC order,

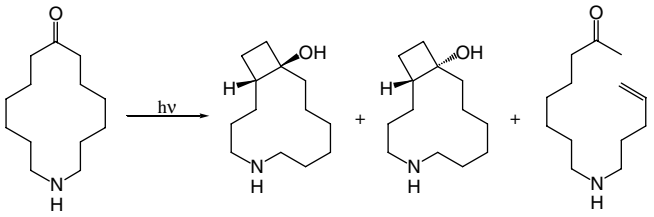

18 ***c*-19** ***t*-19** **20**

SCHEME 7

TABLE 55.6 Product Yields and Enantiomeric Excess (ee) in Photolysis of Chiral Salts Formed between **18** and Acids

acid	conversion / %	yield / %			E/C[a]	ee / %	α[b]
		c-**19**	*t*-**19**	**20**			
free (in benzene)		39	18	44	0.77		
(*S*)-(-)-malic acid	10	5	0	4	0.80	>98	-
	20	9	0	11	1.22	95.3	
	31	13	0	18	1.38	92.9	
	50	20	1	29	1.38	85.5	
	60	24	2	32	1.23	91.3	
(*R*)-(+)-malic acid	11	6	0	5	0.83	>98	+
(*R*)-(-)-2-hydroxy-5,5-dimethyl-4-phenyl-1,3,2-dioxaphosphorinane-2-oxide	6	6	0	trace	0	>98	-
	21	17	0	4	0.24	>98	
	30	23	0	7	0.30	96.0	
	53	35	0	18	0.51	88.7	
	69	45	0	24	0.53	81.9	
(2*R*,3*R*)-(+)-tartaric acid	5	5	0	0	0	42.9	-
	7	7	0	0	0	44.6	
	13	13	0	0	0	44.3	
	24	24	0	0	0	43.8	
(*R*)-(+)-Mosher'sacid	5	5	0	0	0	20.9	+
	9	9	0	trace	0	18.7	
N-Cbz-L-alanine	15	12	1	2	0.15	37.8	-
N-Cbz-L-phenylalanine	22	13	1	8	0.57	2.4	-
N-Cbz-L-valine	15	10	2	3	0.25	30.2	+
(1*S*)-(+)-10-camphorsulfonic acid	4	4	0	trace	0	52.8	-
	12	10	0	2	0.20	44.7	
	24	18	1	5	0.26	35.1	

[a] **20**/(c-**19** + t-**19**)

[b] The sign of rotation of the predominant enantiomer of *c*-**19** at the sodium D-line.

whereas the ratio in the nematic phase is similar to that obtained from the type II reaction in isotropic liquid.[50] The *t*/*c* ratios in the type II reactions of the ketones included in zeolites are dependent on the cavity size of zeolites and cations within the cavities.[24]

Ketones **9a**–**j** undergo stereoselective photocyclization to give cyclobutanols in a solid state.[29,42] The *t*/*c* ratios show an increase and a decrease alternatively with an increase of the ring size of **9** (Table 55.3). Each addition of a methylene group between the two carbonyls in **9** changes the conformation around the γ-carbon. With this conformational change, the γ-hydrogen that is not abstracted alternates between being *syn* or *anti* to the carbonyl oxygen. The γ-hydrogen becomes the bridgehead methine that is either *cis* or *trans* to the hydroxy group in the **CB**.

Selective formation of an optically active cyclobutanol has been achieved in type II cyclization of salts of aminoketone **18** (Scheme 7).[54] While irradiation of the free aminoketone in benzene gives *c*-**19** (ϕ = 0.105), *t*-**19** (0.048), and **20** (0.120), little or none of *t*-**19** is produced when the salts formed between **18** and enantiomerically pure acids are photolysed in the crystalline state (Table 55.6). Enantiomeric excesses obtained for *c*-**19** are fairly good except for the *N*-Cbz-L-phenylalanine salt of **18**. The decrease in enantioselectivity with increasing conversion is due to the breakdown of the ordered crystal lattice as photoproducts replace starting material. The solid-state ionic chiral auxiliary approach may become one of general techniques for asymmetric synthesis in organic photochemistry.

References

1. (a) Wagner, P. J. and Zepp, R. G., Trapping by mercaptans of the biradical intermediates in type II photoelimination, *J. Am. Chem. Soc.*, 94, 287, 1972; (b) Wagner, P. J., Kelso, P. A., and Zepp, R. G., Type II photoprocesses of phenyl ketones: evidence for a biradical intermediate, *J. Am. Chem. Soc.*, 94, 7480, 1972; (c) Scaiano, J. C., Laser flash photolysis studies of the reactions of some 1,4-biradicals, *Acc. Chem. Rec.*, 15, 252, 1982.
2. (a) Wagner, P. J., Type II photoelimination and photocyclization of ketones, *Acc. Chem. Rec.*, 4, 168, 1971; (b) Turro, N. J, *Modern Molecular Photochemistry*, Benjamin/Cummings, Menlo Park, CA, 1978, 386; (c) Wagner, P. J., Photorearrangements via biradicals of simple carbonyl compounds, in *Rearrangements in Ground and Excited States*, Vol. 3, de Mayo, P., Ed., Academic Press, New York, 1980, 381; (d) Wagner, P. J. and Park, B.-S., Photoinduced hydrogen atom abstraction by carbonyl compounds, in *Organic Photochemistry*, Vol. 11, Padwa, A., Ed., Marcel Dekker, New York, 1991, 227; (e) Wagner, P. J., Norrish type II photoelimination of ketones: cleavage of 1,4-biradicals formed by γ-hydrogen abstraction, in *Organic Photochemistry and Photobiology*, Horspool, W. M. and Song, P.-S., Eds., CRC Press, Boca Raton, FL, 1995, 449.
3. Weiss, R. G., Norrish type II processes of ketones: Influence of environment, in *Organic Photochemistry and Photobiology*, Horspool, W. M. and Song, P.-S., Eds., CRC Press, Boca Raton, FL, 1995, 471.
4. Scheffer, J. R., Garcia-Garibay, M., and Nalamasu, O., The influence of the molecular crystalline environment on organic photorearrangements, in *Organic Photochemistry*, Vol. 8, Padwa, A., Ed., Marcel Dekker, New York, 1987, 249.
5. Wagner, P. J., Solvent effects on type II photoelimination of phenyl ketones, *J. Am. Chem. Soc.,* 89, 5898, 1967.
6. Caldwell, R. A., Dhawan, S. N., and Majima, T. J., Lifetime of a conformationally constrained Norrish II biradical: photochemistry of *cis*-1-benzoyl-2-benzydrylcyclohexane, *J. Am. Chem. Soc.*, 106, 6454, 1984.
7. Wagner, P. J., Kemppainen, A. E., and Schott, H. N., Effects of ring substituents on the type II photoreactions of phenyl ketones: how interactions between nearby excited triplets affect chemical reactivity, *J. Am. Chem. Soc.,* 95, 5604, 1973.
8. Wagner, P. J. and Siebert, E. J., Deactivation of triplet phenyl alkyl ketones by conjugatively electron-withdrawing substituents, *J. Am. Chem. Soc.,* 103, 7329, 1981.
9. Encina, M. V., Lissi, E. A., Lemp, E., Zanocco, A., and Scaiano, J. C., Temperature dependence of the photochemistry of aryl alkyl ketones, *J. Am. Chem. Soc.,* 105, 1856, 1983.
10. Jaffe, H. H and Orchin, M., *Theory and Applications of Ultraviolet Spectroscopy*, Wiley, New York, 1962, 186.
11. Zepp, R. G., Gumz, M. M., Miller, W. L., and Gao, H, Photoreaction of valerophenone in aqueous solution, *J. Phys. Chem. A,* 102, 5716, 1998.
12. Wagner, P. J., Solvent effects on type II photoelimination of phenyl ketones, *J. Am. Chem. Soc.,* 89, 5898, 1967.
13. Wagner, P. J. and Kemppainen, A. E., Type II photoprocesses of phenyl ketones: triplet state reactivity as a function of γ and δ substitution, *J. Am. Chem. Soc.,* 94, 7495, 1972.

14. Wagner, P. J. and Frerking, Jr., H., Photochemistry of nonconjugated diketones: internal self-quenching and energy transfer, *Can. J. Chem.,* 73, 2047, 1995.
15. Small Jr., R. D. and Scaiano, J. C., Photochemistry of phenyl alkyl ketones: the lifetime of the intermediate biradicals, *J. Phys. Chem*., 81, 2126, 1977.
16. de Mayo, P., Superficial photochemistry, *Pure Appl. Chem.*, 54, 1623, 1982.
17. Turro, N. J., Photochemistry of ketones adsorbed on porous silica, *Tetrahedron*, 43, 1589, 1987.
18. Kamat, P. V., Photochemistry on nonreactive and reactive (semiconductor) surfaces, *Chem. Rev.*, 93, 267, 1993.
19. Thomas, J. K., Physical aspect of photochemistry and radiation chemistry of molecules adsorbed on SiO_2, γ-Al_2O_3, zeolites and clays, *Chem. Rev.*, 93, 301, 1993.
20. Hasegawa, T. and Yamazaki, Y., Type I and type II photoreactions of carbonyl compounds on a silica-gel surface: possible use of the surface as a new reaction field, *Rec. Develop. Photochem. Photobiol.,* 1, 19, 1997.
21. Kosower, E. M., The effect of solvent on spectra. I. A new empirical measure of solvent polarity: Z value, *J. Am. Chem. Soc.,* 80, 3253, 1958.
22. Weis, L. D., Evans, T. R., and Leermakers, P. A., Electronic spectra and photochemistry of adsorbed organic molecules. VI. Binding effects of silica as a mechanistic probe in systems of photochemical interest, *J. Am. Chem. Soc.,* 90, 6109, 1968.
23. Hasegawa, T., Kajiyama, M., and Yamazaki, Y., Surface photochemistry of alkyl aryl ketones: energy transfer and the effect of a silica-gel surface on electronic states of excited molecules, *J. Phys. Org. Chem.,* 13, 437, 2000.
24. Ramamurthy, V., Corbin, D. R., and Johnston, L. J., A study of Norrish type II reactions of aryl alkyl ketones included within zeolites, *J. Am. Chem. Soc.,*114, 3870, 1992.
25. Birk, J. B., *Photophysics of Aromatic Molecules*, Wiley–Interscience, New York, 1970, 492.
26. (a) Grotewold, J., Previtali, C. M., Soria, D., and Scaiano, J. C., Effect of oxygen on the photochemistry of 4-methyl-1-phenylpentan-1-one, *J. Chem. Soc., Chem. Commun.,* 207, 1973; (b) Small Jr., R. D. and Scaiano, J. C., Differentiation of excited-state and biradical processes: photochemistry of phenyl alkyl ketones in the presence of oxygen, *J. Am. Chem. Soc.,* 100, 4512, 1978
27. Wagner, P. J., Conformational flexibility and photochemistry, *Acc. Chem. Rec.,* 16, 461, 1983.
28. Klan, P., Janosek, J., and Kriz, Z., Photochemistry of valerophenone in solid solutions, *J. Photochem. Photobiol. A: Chem.,* 134, 37, 2000.
29. Ihmels, H. and Scheffer, J. R., The Norrish type II reaction in the crystalline state: toward a better understanding of the geometric requirements for γ-hydrogen atom abstraction, *Tetrahedron*, 55, 885, 1999.
30. Cheung, E., Rademacher, K., Scheffer, J. R., and Trotter, J., An investigation of the solid-state photochemistry of a-mesitylacetophenone derivatives: asymmetric induction studies and crystal structure–reactivity relationships, *Tetrahedron*, 56, 6739, 2000.
31. (a) McIntosh, C. L., Concerning the irradiation of enol benzoates, *Can. J. Chem.,* 45, 2267, 1967; (b) Hasegawa, T., Nishimura, M., and Yoshioka, M., Stern–Volmer quenching kinetics in photoreaction system with strong internal filtering: type II photoreaction of 2-benzoylcyclohesanone, *J. Phys. Org. Chem.,* 3, 230, 1990.
32. Hasegawa, T., Imada, M., and Yoshioka, M., Photoreaction of 2-benzoylcyclohexanones on a silica gel surface: deviation from their solution photochemistry, *J. Phys. Org. Chem.,* 6, 494, 1993.
33. Hasegawa, T., Imase, Y., Imada, M., Kumakura, K., and Yoshioka, M., Surface photoreactions of 2-benzoylcyclopentanones: silica gel surface as a possible field bringing out the latent reactivity of dispersed molecules, *J. Phys. Org. Chem.,* 9, 677, 1996.
34. Hasegawa, T., Moribe, J., and Yoshioka, M., The photocyclization of *N*,*N*-dialkyl β-oxo amides adsorbed on silica gel, *Bull. Chem. Soc. Jpn.,* 61, 1437, 1988.
35. (a) Hasegawa, T., Yamazaki, Y., and Yoshioka, M., Novel biradical cyclization via remote-hydrogen transfer in photochemistry of 2-dialkylaminoethyl 3-benzoylacrylates, *Bull. Chem. Soc. Jpn.,* 66,

3128, 1993; (b) Hasegawa, T., Yamazaki, Y., and Yoshioka, M., Photoisomerisation of 3-benzoylacrylates on a silica gel surface: effect of reaction environment on selectivity, *J. Phys. Org. Chem.,* 8, 31, 1995.

36. Lewis, F. D. and Turro, N. J., Molecular photochemistry. XVIII. Type II photoelimination and 3-oxetanol formation from α-alkoxyacetophenones and related compounds, *J. Am. Chem. Soc.,* 92, 311, 1970.
37. Wagner, P. J., Thomas, M. J., and Harris, E., Effects of methyl substitution on the photoreactivity of phenyl ketones: the inapplicability of Hammett σ values in correlations of excitation energies, *J. Am. Chem. Soc.,* 98, 7675, 1976.
38. Wagner, P. J., Polar solvent enhancement of the quantum efficiency of the type II photoelimination, *Tetrahedron Lett.,* 1753, 1967.
39. Weiss, R. G., Ramamurthy, V., and Hammond, G. S., Photochemistry in organized and confining media: a model, *Acc. Chem. Res.,* 26, 530, 1993.
40. Turro, N. J., Liu, K.-C., and Chow, M.-F., Solvent sensitivity of type II photoreactions of ketones as a device to probe solute location in micelles, *Photochem. Photobiol.*, 26, 413, 1977.
41. Winkle, J. P., Worsham, P. R., Schanze, K. S., and Whitten, D. G., Photoreactivity of surfactant ketones as a probe of the microenvironment of organic media, *J. Am. Chem. Soc.,* 105, 3951, 1983.
42. Gudmundsdottir, A. D., Lewis, T. H., Rand, L. H., Scheffer, J. R., Rettig, S. V., Trotter, R., and Wu, C.-H., Geometric requirements for hydrogen abstractability in the Norrish/Yang type II reaction: studies based on the solid state photochemistry and x-ray crystallography of medium-sized and macrocyclic diketones, *J. Am. Chem. Soc.,* 118, 6167, 1996.
43. Ariel, S., Ramamurthy, V., Scheffer, J. R., and Trotter, J., Norrish type II reaction in the solid state: involvement of a boat like reactant conformation, *J. Am. Chem. Soc.,* 105, 6959, 1983.
44. Ariel, S., Evans, S. V., Garcia-Garibay, M., Harkness, B. R., Omkaram, N., Scheffer, J. R., and Trotter, J., The generation of 1,4-biradicals in rigid media: crystal structure–solid state reactivity correlation, *J. Am. Chem. Soc.,* 110, 5591, 1988.
45. Leibovitch, M., Olovsson, G., Scheffer, J. R., and Trotter, J., An investigation of the Yang photocyclization reaction in the solid state: asymmetric induction studies and crystal structure-reactivity relationship, *J. Am. Chem. Soc.,* 120, 12755, 1998.
46. Cheung, E., Netherton, M. R., Scheffer, J. R., and Trotter, J., Competition between cyclization, cleavage and reverse hydrogen transfer in 1,4-hydrogenbiradicals: crystal structure–solid state reactivity correlations, *Org. Lett.,* 2, 77, 2000.
47. Singh, S., Govindarajan, U., Tung, C-H., Turro, N. J., and Ramamurthy, V., Modification of chemical reactivity by cyclodextrins: observation of moderate effects on Norrish type I and type II photobehavior, *J. Org. Chem.,* 51, 941, 1986.
48. Brett, T. J. and Stezowski, J. J., Structural studies of supramolecular β-cyclodextrin complexes with butyrophenone and valerophenone: an explanation for photochemical reaction modification, *J. Chem. Soc., Chem. Commun.,* 857, 2000.
49. Weiss, R. G., Thermotropic liquid crystals as reaction media for mechanistic investigations, *Tetrahedron*, 44, 3413, 1988.
50. Woekentin, M. S., Leigh, W. J., and Jeffrey, K. R., Organic reactions in liquid crystalline solvents. 10. Studies of the ordering and mobilities of simple alkanophenones in CCH-*n* liquid crystals by ^{2}H NMR spectroscopy and Norrish II photoreactivity, *J. Am. Chem. Soc.,* 112, 7329, 1990.
51. He, Z. and Weiss, R. G., Length- and direction-specific solute–solvent interactions as determined from Norrish II reactions of *p*-alkylalkanophenones in ordered phases of *n*-butyl stearate, *J. Am. Chem. Soc.,* 112, 5535, 1990.
52. (a) Kell, A. J., Stringle, D. L. B., and Workentin, M. S., Norrish type II photochemical reaction of an aryl ketone on a monolayer-protected gold nanocluster: development of a probe of conformational mobility, *Org. Lett.*, 2, 3381, 2000; (b) Kell, A. J. and Workentin, M. S., Aryl ketone photochemistry on monolayer protected clusters: study of the Norrish type II reaction as a probe of conformational mobility and for selective surface modification, *Langmuir,* 17, 7355, 2001.

53. (a) Weir, N. A. and Delaney-Luu, M., Photophysics and photochemistry of poly(4′-ethoxyacrylophenone), *J. Photochem. Photobiol. A: Chem.,* 136, 189, 2000; (b) Weir, N. A. and Delaney-Luu, M., The photochemistry of poly(4′-ethoxyacrylophenone) in the solid state, *Eur. Polymer J.,* 37, 1339, 2001.
54. Cheung, E., Netherton, M. R., Scheffer, J. R., and Trotter, J., In the footsteps of Pasteur: asymmetric induction in the solid-state photochemistry of ammonium carboxylate salts, *J. Am. Chem. Soc.,* 121, 2919, 1999.

56

Photochemical Reactions of α-Halocyclic Ketones and Related Systems

C. Akira Horiuchi
Rikkyo (St. Paul's) University

Shun-Jun Ji
Suzhou University

56.1 Introduction

Organic photochemical synthesis has developed to an important and pervasive field within current organic chemistry. In photochemical reactions and photobiological reactions, electron transfer, transfer of excited energy, and photoinduced intramolecular and intermolecular isomerizations are important and fundamental.[1] Photolysis, photosynthesis, photopolymerization, and photochemical isomerization arise by excited atoms and molecules under irradiation by light. These reactions are different from reactions carried out thermally, under pressure, or by catalysis.

We have been investigating an iodination method using iodine–copper(II) acetate and iodine–ammonium cerium(IV) nitrate (CAN) to synthesize iodoletones.[2] These iodoketones are more active than chloro- and bromoketones, and it was found that they are unstable and sensitive to light. From the viewpoint of green chemistry,[3] we have tried to transform these iodo compounds into useful products by photochemical methods.

After many years of investigation of the photochemistry of alkyl halides RX (X = Cl, Br, I),[4] it was found that the photochemical reaction of alkyl iodides in nonpolar solvent leads to radical products;[5] in polar solvent, to carbocationic products (Scheme 1).[6] Photoinduced alcoholysis and photodehalogenation of α-halo ketones (X = Cl, Br) in alcohols have been investigated by Tomioka et al.[7] In their interesting work on photosolvolysis of α-halo ketones, they proposed that the homolysis of CX bonds produces a

0-8493-1348-1/04/$0.00+$1.50

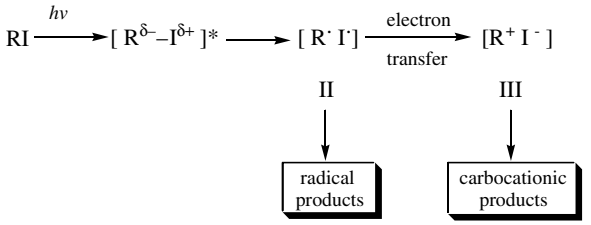

SCHEME 1

radical pair, which may undergo radical reaction or electron transfer to afford an ion pair. This pair would then undergo carbocationic reactions. A little information is found in the literature concerning the photochemical reactions of α-halocycloalkanones. Orito et al.[8] reported that the photolysis of α-bromocamphor in methanol provides a dimerized α-camphorylcamphor derivative. However, the photochemical reactions of α-iodo cyclic ketones have not been reported until now.

The purpose of this study is to transform these iodo compounds into useful products using photochemistry with a high-pressure mercury lamp ($\lambda > 300$ nm). The subjects of the study are classified into five areas:

1. Irradiation of α-iodocycloalkanones in some alcohols afforded the corresponding ω,ω-dialkoxy esters by photochemical cleavage of the C(X)–C=O bond at room temperature.[9]
2. α-Iodo- and α,α′-diiodocycloalkanone were irradiated in alcohol under the presence of air to give the corresponding α-hydroxy- and α,α′-dihydroxyketones in good yields.
3. Irradiation of α-iodoketones (steroidal α-iodoketones, α-iodoketones, and α,α′-diiodoketones) in hexane under a nitrogen atmosphere at room temperature yields the corresponding α,β-unsaturated ketones.[10]
4. Cycloalkanones and 1-tetralone were irradiated in alcohol to give the corresponding pinacol-type compounds in good yields.[11]
5. Camphorquinone was irradiated under oxygen with a high-pressure mercury lamp to give camphoric anhydride in good yields.[12]

ω,ω-Dialkoxy ester derivatives are important intermediates in organic synthesis.[13] Some syntheses of ω,ω-dialkoxy ester involve regiospecific oxidative ring cleavage of cycloalkenes with ozone in various alcohols;[14] ring-opening oxygenation on treatment with lead(IV) acetate,[15] sodium periodate,[16] perbenzoic acid,[17] iron(III) salt,[18] and oxovanadium(V)[19] in alcohol under oxygen; and electrochemical oxidative cleavage of α-substituted cycloalkanones and cycloalkanone enol acetates.[20] Our co-workers reported that the reaction of α-alkylcycloalkanones with iodine–cerium(IV) salts[21] and cerium(IV) salts[22] in alcohol yields the corresponding oxo ester and ω,ω-dialkoxy ester. Most of these processes suffer from disadvantages by using toxic reagents and heavy metals; consequently, development from the viewpoint of green chemistry is needed.

The photochemistry of organic halides RX (X = Cl, Br, I) has been intensively investigated for many years, as it became clear that cationic, as well as free-radical, intermediates play an important role in the solution-phase photochemistry of these halides.[4] Competing ionic and radical photobehavior has been observed for haloalkenes and cycloalkyl halides.[6,23]

In this chapter, we report that the irradiation, under a high-pressure mercury lamp, of α-iodocycloalkanones **1** to **7** in alcohols containing a small amount of water gave the corresponding ω,ω-dialkoxy esters **1c–10c** by cleavage of a CC bond. Moreover, it was found that photochemical ring opening can take place, and 2-hydroxycycloalkanones and formyl esters are intermediates.

It is known that α-hydroxyketones are important as intermediates for organic synthesis. In order to increase the yield of an α-hydroxyketone we carried out a detailed investigation of the reaction conditions. The reaction of α-iodo- and α,α′-diiodoketone using photoirradiation in alcohols, hexane, and acetone, etc. in the presence of air afforded the corresponding α-hydroxy- and α,α′-dihydroxy ketones in good yield.

α,β-Unsaturated ketones are also important intermediates in many addition reactions involving the addition of nucleophiles at the β-position under the influence of the inductive polarization of a carbonyl group. They are usually prepared by one of the following methods in steroidal systems: dehydrobromination of α-bromoketones by the treatment of nitrogenous bases and by lithium salts,[24] dehydrogenation of a steroidal ketone using DDQ (dichlorodicyano quinone) in boiling benzene,[25] or dehydrogenation of 3-oxo steroids using selenium dioxide in *t*-butyl alcohol.[26] However, in the case of a steroidal α,β-unsaturated ketone, it is known that these reactions tend to give abnormal products (i.e., α′, β′-unsaturated ketones).[27] It is difficult to separate these isomers because they have similar properties.

We observed that the irradiation of α-iodoketones in hexane under a nitrogen atmosphere with a high-pressure mercury lamp ($\lambda > 300$ nm) at room temperature yields the corresponding α,β-unsaturated ketones, accompanied by some deiodination products. Moreover, it was shown that the reaction was dependent upon the media used, and such changes resulted in different photoproduct distribution.

During the course of our studies, we found that cyclic ketones undergo a novel self-coupling reaction brought about by irradiation using a high-pressure mercury lamp. This yields the corresponding pinacol-type compound in good yields. Moreover, we determined that camphorquinone undergoes a novel unsensitized photooxidation in polar solvents such as alcohol under oxygen to give camphoric anhydride in 85% yield.

56.2 Photocleavage of Carbon–Carbon bonds of α-Iodocycloalkanones Giving ω,ω-Dialkoxy Esters in Alcohol

The photochemical reaction of α-iodocycloalkanones **1** to **7** in methanol, brought about by irradiation with a high-pressure mercury lamp at room temperature, afforded predominantly photocleavage products, methyl ω,ω-dimethoxyalkanoates **1c** to **10c**, in good yields. These reactions did not occur under the same conditions in the absence of light. Similarly, the reaction of α-iodocyclododecanone **6** in ethanol, 1-propanol, and 2-propanol yielded the corresponding ω,ω-dialkoxyalkanoates. These results are summarized in Scheme 2 and Table 56.1.

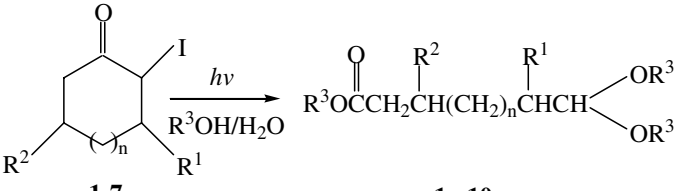

1-7 **1c-10c**

		n	R^1	R^2	R^3
1	**1c**	1	H	H	Me
2	**2c**	1	H	Me	Me
3	**3c**	1	Me	H	Me
4	**4c**	2	H	H	Me
5	**5c**	3	H	H	Me
6	**6c**	7	H	H	Me
6	**7c**	7	H	H	Et
6	**8c**	7	H	H	Pr^n
6	**9c**	7	H	H	Pr^i
7	**10c**	10	H	H	Me

SCHEME 2

TABLE 56.1 Irradiaton of α-Iodocycloalkanone in Alcohols at Room Temperature

Entry	Substrates[a]	Solvents	Methods[b]	Time/h	Product/%[c]
1	**1**	MeOH	400 W	18	**1c** (65)
2	**2**	MeOH	400 W	14	**2c** (72)
3	**3**	MeOH	400 W	14	**3c** (70)
4	**4**	MeOH	400 W	15	**4c** (80)[d]
5	**5**	MeOH	400 W	18	**5c** (75)[d]
6	**6**	MeOH	100 W	12	**6c** (87)[d]
7	**6**	MeOH	400 W	10	**6c** (88)
8	**6**	EtOH	100 W	16	**7c** (77)[d]
9	**6**	EtOH	400 W	16	**7c** (80)
10	**6**	Pr^n OH	100 W	18	**8c** (69)
11	**6**	Pr^n OH	400 W	16	**8c** (70)
12	**6**	Pr^i OH	100 W	20	**9c** (n) **6a** (18) **9b** (64)
13	**6**	Pr^i OH	400 W	20	**9c** (n) **6a** (15) **9b** (65)
14	**7**	MeOH	100 W	20	**10c** (73)[d]
15	**7**	MeOH	400 W	20	**10c** (75)

[a] Substrate (15.7 mmol/l) in hydrous alcohol (0.02%) was employed.
[b] Reactions were carried out with high-pressure mercury lamp as irradiation source under a nitrogen atmosphere.
[c] Isolated yields. n = no obtained.
[d] Traces of methyl 6-formylhexanoate (**4b**), methyl 7-formylheptanoate (**5b**),[25a] methyl 11-formylundecanate (**6b**), ethyl 11-formylundecanoate (**7b**), and 14-formyltetradecanoate (**10b**) were obtained, respectively.

On the basis of these results, it was found that the photochemical cleavage of the carbon–carbon bond occurred between the C1 and C2 positions of α-iodocycloalkanones to give finally ω,ω-dialkoxy esters **1c** to **10c** in 65 to 88% yields. Also, it was found that in methanol the yield of the ring-opened product, methyl 12,12-dimethoxydodecanoate **6c**,[13,19a] was higher and the reaction proceeded faster than in other alcohols (entries 6 to 11). However, isopropyl 12,12-diisopropoxydodecanoate **9c** was not obtained from the reaction in 2-propanol, and isopropyl 11-formylundecanoate **9b** and 2-hydroxycyclododecanone **6a** [19] were formed in 65 and 15% yields (entries 12, 13), respectively. It seems that acetalization of **9b** with 2-propanol is difficult due to the bulkier alkoxy group. The ^{1}H nuclear magnetic resonance (NMR) spectra exhibited the presence of a formyl group δ 9.76 (t, J = 1.83 Hz, CHO). It is particularly noteworthy that this photoreaction provides a new synthetic method for ω,ω-dialkoxy esters that is more convenient and cleaner than many methods reported heretofore.[13–21] Therefore, the new photocleavage products, **7c, 8c**, and **9b** were obtained from α-iodocyclododecanone in ethanol, 1-propanol, and 2-propanol containing a small amount of water.

In order to investigate the reaction pathway of photocleavage for α-iodocycloalkanones in alcohol, irradiation of **6** was carried out. The results are summarized in Tables 56.2 and 56.3. It was found that the relative ratios of the photochemical products depend on the reaction conditions. Irradiation of **6** for 3 hr in MeOH–H_2O (0.02%) with a 100-W, high-pressure mercury lamp gave **6a**, methyl 11-formylundecanoate **6b**,[13,28] and **6c** in 33, 38, and 7% yields, respectively. (Table 56.2, entry 1). On irradiation of **6** for 12 hr, products **6a** and **6b** were minor, and the major photoproduct **6c** was obtained in 87% yield (Table 56.2, entry 4). When a 400-W, high-pressure mercury lamp or a commercial fluorescent lamp was used, the same behavior was observed for **6** (Table 56.2, entries 5 to 9). From these results, it was found that in the cases of a high-pressure mercury lamp and a commercial fluorescent lamp as irradiation sources, the photocleavage product methyl 12,12-dimethoxydodecanoate **6c** was obtained preferentially.

From the above results, it seems that **6a** and **6b** are intermediates for **6c**. Formation of **6a** may be due to the presence of a small amount of water in methanol. In order to clarify this hypothesis, irradiation of **6** was carried out in absolute methanol and hydrated methanol. As can be seen from Table 56.3, the irradiation of **6** in absolute methanol gave the photoalcoholysis product 2-methoxycyclododecanone **6d** (65%), accompanied by the reduction product cyclododecanone **6e** (17%) and the elimination product

TABLE 56.2 Distributions of Photochemical Products of α-Iodocyclododecanone(**6**) at Room Temperature[a]

Entry	Methods[b]	Time/h	Products/%[c]		
			6a	**6b**	**6c**
1	100 W	3	33	38	7
2	100 W	6	25	28	36
3	100 W	9	8	15	60
4	100 W	12	t	5	87
5	400 W	3	23	27	40
6	400 W	6	10	16	60
7	400 W	10	t	3	88
8	F.L[d]	480	23	34	25
9	F.L[d]	960	5	3	78

[a] A deoxygenated solution (15.7 mmol/l) of α-iodocyclododecanone (**6**) in methanol (H_2O, 0.02%) was irradiated until complete comsumption of subtrate **6** which was apparent by TLC.
[b] The high-pressure mercury lamp in a water-cooled quartz immersion well as irradiation source.
[c] Isolated yields after purification by column chromatography on silica gel. A trace of **6e** and **6f** was also obtained.
[d] Reactions were carried out with a commercial fluorescent lamp. t = trace.

TABLE 56.3 Irradiation of α-Iodocyclododecanone (**6**) in Methanol at Room Temperature[a]

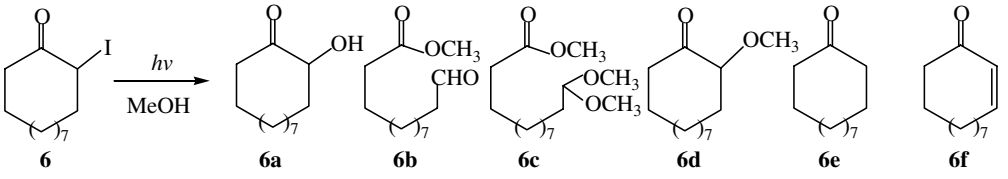

6 **6a** **6b** **6c** **6d** **6e** **6f**

Entry	MeOH (H_2O%)	Method	Time/h	Products/%[c]					
				6a	**6b**	**6c**	**6d**	**6e**	**6f**
1	MeOH (0)	100 W[b,e]	12	t	t	t	65	17	8
2	MeOH (0)	F.L W[d,e]	480	t	t	t	78	6	3
3	MeOH (0.01)	100 W	18	17	9	41	—	13	3
4	MeOH (0.02)	100 W	12	5	3	84	—	t	t
5	MeOH (0.04)	100 W	12	t	3	85	—	t	t
6	MeOH (1.68)	100 W[f]	10	t	t	86	—	t	t
7	MeOH (1.68)	F.L[f,d]	480	3	3	84	—	t	t

[a] A deoxygenated solution (15.7 mmol/l) of α-iodocyclododecanone (**6**) in methanol were irradiated until complete consumption of substrate **6** which was apparent by TLC.
[b] The high-pressure mercury lamp in a water-cooled quartz immersion well as irradiation source.
[c] Isolated yields after purification by column chromatography on silica gel.
[d] Reactions were carried out with a commercial fluorescent lamp.
[e] Methanol was dried completely by stored over 4A molecular sieves.
[f] The 2 ml water was added in methano (150 ml). t = trace.

2-cyclododecen-1-one **6f** (8%)[29] (Table 56.3, entry 1). However, in methanol containing 0.6 or 1.2 molar equivalents of water, the ring-opening product **6c** was obtained in 84 and 85% yields, respectively (Table 56.3, entries 4 and 5), while with methanol containing water (0.01%), the reduction product **6e** and the elimination product **6f** were obtained (Table 56.3, entry 3). From these results, the influence of water on the photochemical reaction of α-iodocycloalkanones is clear.

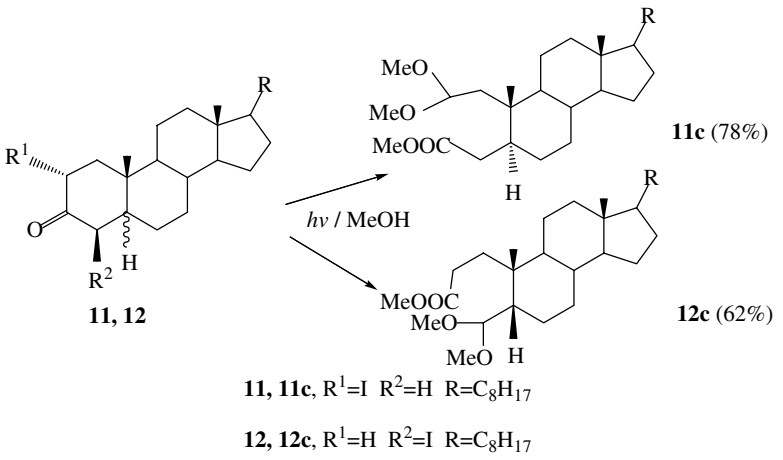

SCHEME 3

2α-Iodo-5α-cholestan-3-one (**11**) and 4β-iodo-5β-isomer (**12**) were also irradiated with a high-pressure mercury lamp under the same conditions, and the results are shown in Scheme 3. From these results, it was determined that the reaction of **11** and **12** gave methyl 2,2-dimethoxy-2,3-seco-5α-cholestan-3-oate (**11c,** 78%) and methyl 4,4-dimethoxy-3,4-seco-5β-cholestan-3-oate (**12c,** 62%),[4,30] respectively. These results show that the photocleavage reaction is also operative with steroidal α-iodoketones. Moreover, the photocleavage reaction is preferred to the oxidative ring cleavage reaction.[4]

Kropp and his co-workers[6] reported competing ionic and radical photobehavior for a number of alkyl halides. Photolysis of α-halo ketones (ROCCX) is understood to proceed via competing homolysis of CC and CX bonds as the primary processes.[4] Tomioka et al.[7] also proposed that irradiation of α-halo ketones in alcohols brings about competition between ionic and radical reaction paths with the formation of photoalcoholysis and photoreduction products. During the course of our studies, it was found that irradiation of α-iodocycloalkanones in the nonpolar solvents (e.g., hexane) afforded mainly the elimination product, an α,β-unsaturated cyclic ketone, accompanied by a small amount of photoreduction product.[10] Therefore, it is considered that this photochemical behavior can be explained as shown in Figure 56.1 on the basis of the results mentioned above.

As can be seen from Figure 56.1, irradiation of α-iodocycloalkanones generates the radical pair (I) via a process involving light-induced homolytic cleavage of the CI bond.[6,22] In polar solvents, electron transfer competes efficiently to produce an ion pair (II) and then photosubstituted product **6a** is formed preferentially. This product is formed by nucleophilic trapping of the ion pair (II). Under the present irradiation conditions, the ring opening of **6a** by cleavage of the C1C2 bond gives secondary photoproduct, the formyl ester, which probably arises from the biradical pair (III) by electron transfer and intermolecular addition of alcohol. It seems that these formyl compounds undergo ready acetalization to afford stable products.

Suginome et al.[31] reported that the irradiation of α-hydroxy cyclic ketones with mercury(II) oxide and iodine in benzene gives CC bond cleavage products. On the basis of our results, it is considered that this reaction proceeds through photocleavage of the C(OH)–C=O bond of **6a** after displacement of iodide by hydroxide ion, followed by acetalization (Scheme 4). Although the reason has not yet been clarified, it seems that α-iodo groups of cycloalkanones are essential for the cleavage reaction of the CC bond.[32] Thus, in the case of **6a** in methanol containing iodine and HI, the methyl ω,ω-dimethoxy ester was obtained. This fact apparently supports the validity of **6a** as intermediate (Figure 56.2).

In order to investigate the photochemical behavior of iodo-substituted aromatic compounds, 2-iodo-1-tetralone **17** was chosen as a model. The irradiation of **17** in methanol gave 1-naphthanol **17g** and 1-tetralone **17e**. These results are summarized in Table 56.4. From these results, it was found that the photochemical behavior is quite different compared to α-iodocycloalkanones. Moreover, the photochemical products are not affected by the polarity of the solvents used. It seems that **17** undergoes aromatization

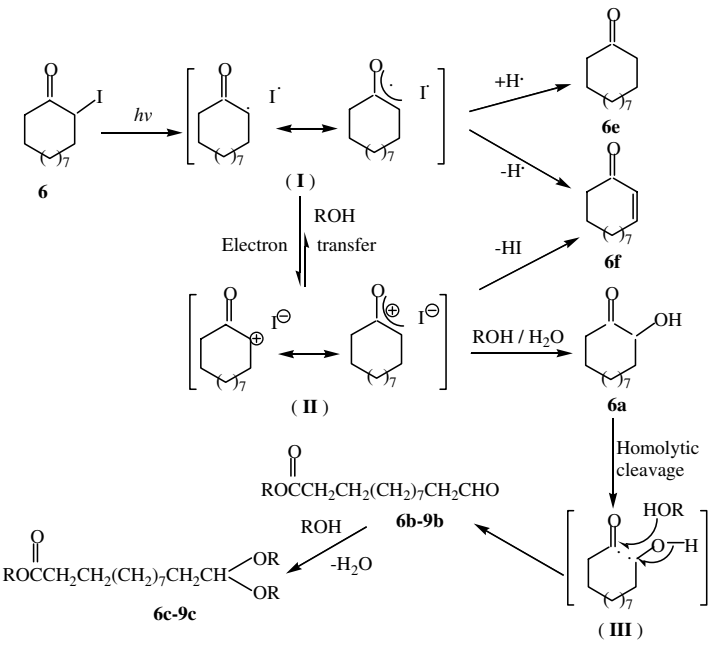

FIGURE 56.1 Photochemical cleavage behavior of α-iodocyclododecanone.

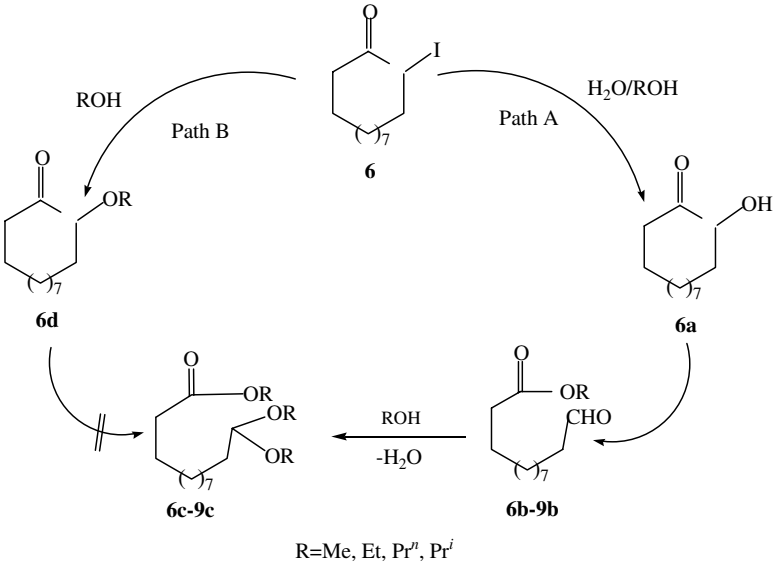

SCHEME 4 Photochemical process of α-iodocycloalkanones.

rather than CC bond cleavage. In the presence of 1 molar equivalent of triethylamine, the formation of the aromatized product **17g** is greatly enhanced (Table 56.4, entry 3).[7f]

For comparison, the reactivity of the α-iodo cyclic ketone was compared with that of the corresponding chloro and bromo derivatives, and the results are summarized in Table 56.5. On the basis of these results, it was found that irradiation of 2-chloro- (**13**) or 2-bromocyclohexanone (**14**)[33] afforded mainly acetalization

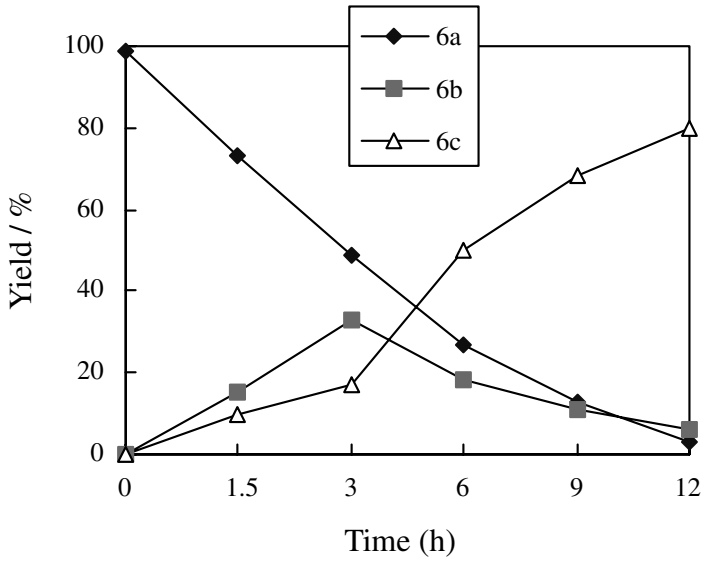

FIGURE 56.2 Yields of **6b** and **6c** during irradiation of **6a** in degassed methanol.

TABLE 56.4 Irradiation of 3,4-Dihydro-2-iodo-1(2H)-naphthalenone (**17**) in Solvents at Room Temperature

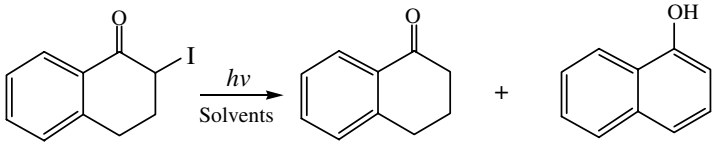

17 **17e** **17g**

			Product/%[b]	
Entry	Solvents[a]	Time/h	**17e**	**17g**
1	Hexane[c]	1.0	46	53
2	Hexane[d]	1.2	45	52
3	Hexane[e]	10.0	25	71
4	Cyclohexane[c]	1.0	52	47
5	Acetonitrile[c]	3.5	51	47
6	Ethyl ether[c]	2.0	57	42
7	Methanol[c]	5.0	43	56
8	Methanol[f]	5.0	46	53

[a] Substrate (2.355 mmol) in solvents (150 ml) under nitrogen atmosphere with 100 W high-pressure mercury lamp was irradiated.

[b] Determined by GC. Isolated product **17g** was identified by the NMR spectra and HRMS.

[c] Dried by 4A molecular sieves.

[d] Hexane:H_2O=10:1 (*v/v*).

[e] 1 molar equiv. triethylamine was employed.

[f] Methanol containing a small amount of water (0.02%)

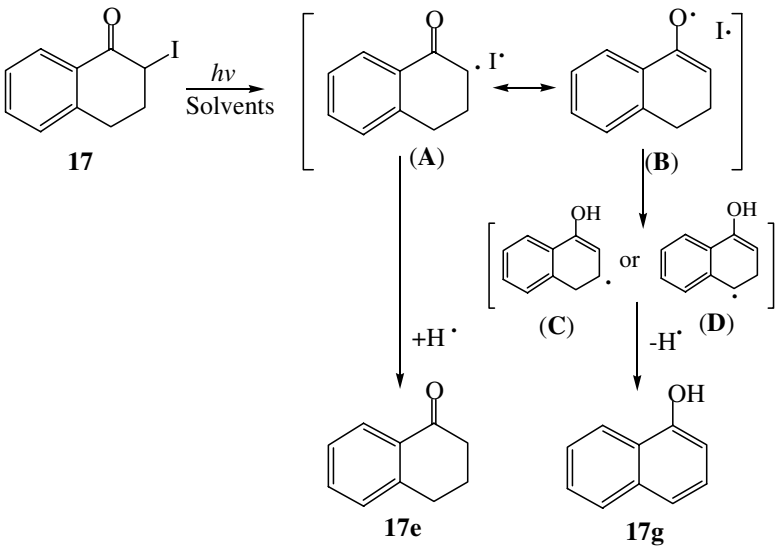

FIGURE 56.3 Probable photochemical behavior of 3,4-dihydro-2-iodo-1(2H)-naphthalenone.

TABLE 56.5 Photochemical Reaction of α-Halocycloalkanone at Room Temperature

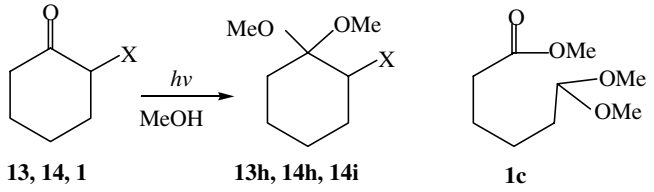

Entry	Substrate[a]	Method	Time/h	Product/%[b]
1	**13** (X=Cl)	100 W	20	**13h** (X=Cl) (90)
2	**13** (X=Cl)	400 W	18	**13h** (X=Cl) (86)
3	**14** (X=Br)	100 W	20	**14h** (X=Br) (85) **14i** (7)
4	**14** (X=Br)	400 W	18	**14h** (X=Br) (82) **14i** (8)
5	**1** (X=I)	100 W	20	**14i** (X=OMe) (13) **1c** (68)
6	**1** (X=1)	400 W	18	**14i** (X=OMe) (15) **1c** (65)

[a] Substrate (2.355 mmol) in methanol (150 ml) under a nitrogen atmosphere with 100 W high-pressure mercury lamp was irradiated.
[b] Isolated yields.

products 2-chloro- (**13h**) or 2-bromo-1,1-dimethoxycyclohexane (**14h**)[2d] in 90 and 85% yields, respectively. It is suggested that the difference in the reactivity of the iodo compound, compared with the bromo and chloro derivatives, is due to the weaker CI bond and the ease with which this undergoes photochemical reaction.

In conclusion, we have encountered a novel photochemical cleavage reaction of α-iodocycloalkanones in alcohols using a high-pressure mercury lamp and a commercial fluorescent lamp. This reactivity results in an efficient and direct synthesis of ω,ω-dialkoxyalkanoic esters. It is noteworthy that the present photocleavage reaction affords a new synthetic method that is more convenient and cleaner than methods used previously.

56.3 Synthesis of α-Hydroxy- and α,α′-Dihydroxyketone from α-Iodo- and α,α′-Diiodoketone Using Photoirradiation[34]

α-Hydroxy ketones are usually prepared by one of the following methods: α-hydroxylated by treatment of their enolate forms with a molybdenum peroxide reagent in THF-hexane at –70°C,[35] transformation of enamine derivatives of ketones to α-hydroxy derivatives by molecular oxygen,[36] and α-hydroxylation of silyl enol ethers with *m*-chloroperbenzoic acid[37] or with other oxidizing agents.[38]

Considerable interest has been expressed in the development of direct methods for the synthesis of α-hydroxy ketones using nontoxic hypervalent iodine reagents and which involve the following methods: reaction of a ketone with iodobenzene diacetate in the presence of potassium hydroxide in methanol and then hydrolysis of the dimethylacetals;[39] oxidation of the enol silyl ether of acetophenone using the system iodosobenzene/boron trifluoride etherate/water in methylene chloride at –40°C;[40] and reaction of ketones with [*bis*(trifluoroacetoxy)]iodobenzene and trifluoroacetic acid in acetonitrile–water under acidic conditions.[41]

We have found that the photocleavage of the CC bond of α-iodocycloalkanones in alcohol gives ω,ω-dialkoxy esters via the intermediacy of α-hydroxy ketones. In order to increase the yield of the α-hydroxyketone, we carried out a detailed study of the reaction conditions employed. The reaction of α-iodo- and α,α′-diiodoketone using photoirradiation in, for example, alcohols, hexane, and acetone in the presence of air afforded the corresponding α-hydroxy- and α,α′-dihydroxy ketone in good yield.

The irradiation of α-iodoketones (**1**, **4**, **5**, **6**) in a solvent at room temperature under an atmosphere of air with a 400-W mercury lamp for 2 to 20 hr gave the corresponding α-hydroxy ketones (**1a, 4a** to **6a**) in good yields. These results are summarized in Table 56.6, which shows that the α-hydroxy ketones are formed preferentially when triethylamine is added. Moreover, this reaction affords hydroxydiosphenol present in buchu oil obtained from the leaves of *Barosma betulina* Bartl. (mountain buchu) (Table 56.7).

It is interesting that, in the case of α,α′-diiodoketones, α,α′-dihydroxyketones were obtained in good yields. The reaction of α,α′-diiodoketones (**23** to **26**) in acetone afforded the corresponding α,α′-dihydroxyketones (**23a′** to **26a′**) in good yield. These results are summarized in Table 56.8. On the basis of these results, it is interesting that, for the first time, we have succeeded in developing a novel and convenient synthesis of α,α′-dihydroxyketones.

56.4 Synthesis of α,β-Unsaturated Ketones from α-Iodoketones Using Photoirradiation

The photochemical reaction of steroidal α-iodo ketones **11**, **12**, **27**, **28**, and **29** in hexane under a high-pressure mercury lamp gave the corresponding steroidal α,β-unsaturated ketones **11f**, **12f**, **27f**, **28f**, and **29f** under a nitrogen atmosphere at room temperature. These results are summarized in Table 56.9, where it is seen that 5α-steroidal α-iodo ketone derivatives **11**, **28**, and **29** gave α,β-unsaturated ketones **11f**, **28f**, and **29f** in higher yield than the 4β-iodo-5β-isomer (**12**) under the same conditions (Table 56.9, entries 3, 5, 7, and 8). It is considered that the difference is due to the stereochemical structure of the 5α- and the 5β- isomers.[42] In the presence of a 1 molar equivalent of triethylamine[6c] in hexane, a marked increase of 5α-cholest-1-en-3-one (**11f**) for 2α-iodo-5α-cholestan-3-one (**11**) could be observed (Table 56.9, entries 1 and 2). In the absence of light, the reaction did not occur.

Extension of the reaction to α-iodocycloalkanones (**1** to **6**) also demonstrated that these compounds reacted to give α,β-unsaturated ketones (**1f** to **6f**). These results are summarized in Table 56.10, where it can be seen that the medium-sized ring α-iodocycloalkanones (**1** to **5**) gave the α,β-unsaturated ketones (**1f** to **5f**) in higher yield (72 to 80%) than the macrocyclic α-iodoketone (**6**). Similarly, the irradiation of α-iodo acyclic ketones (**19** and **30**) and α,α′-diiodoketones (**24** and **26**) gave the corresponding α,β-unsaturated ketones (**19f** and **30f**) and α,β,α′,β′-dienone derivatives (**24f′** and **26f′**) (Table 56.11). Thus, we have demonstrated that this method is applicable to the synthesis of α,β-unsaturated ketones from α-iodocycloalkanones, α-iodo acyclic ketones, and α,α′-diiodoketones.

TABLE 56.6 Synthesis of α-Hydroxyketone from α-Iodocycloalkanone (**1,4-6**) using Photoirradiation

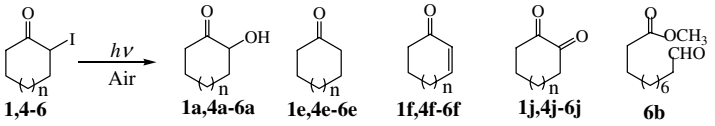

1,4-6 **1a,4a-6a** **1e,4e-6e** **1f,4f-6f** **1j,4j-6j** **6b**

						Product (%)[a]				
Entry	Substrate	Solvent	n	Reagent (eq)	Time/h	**a**	**b**	**e**	**f**	**j**
1	**1**	An	1	Et_3N(1)	10	49	—	4	<1	10
2	**4**	An	2	Et_3N(1)	10	56	—	<1	<1	41
3	**5**	An	3	Et_3N(1)	10	60	—	<1	<1	35
4	**5′**	An	5	Et_3N(1)	10	70	—	<1	<1	24
5	**6**	An	7	—	10	5	42	50	<1	3
6	**6**	*n*-Hex	7	—	10	5	41	<1	6	8
7	**6**	CH_3CN	7	—	10	3	59	<1	3	17
8	**6**	An	7	Et_3N(1)	10	>95	—	<1	<1	<1
9	**6**	*n*-Hex	7	Et_3N(1)	15	68	—	<1	2	3
10	**6**	CH_3CN	7	Et_3N(1)	17	77	—	7	<1	<1
11	**6**	An	7	Et_3N(0.5)	10	67	22	<1	<1	<1
12	**6**	An	7	Et_3N(5)	10	>95	—	3	<1	1
13	**6**	An	7	$(i\text{-Pr})_2NH$(1)	10	>95	—	4	<1	<1
14	**6**	An	7	$(i\text{-Pr})_3NH$(1)	10	>95	—	2	<1	<1
15	**6**	An	7	NH_3(1)	20	90	—	5	<1	4
16	**17**	An	—	Et_3N(1)	12	70	—	5	15	<1
17	**18**	An	—	Et_3N(1)	10	70	—	<1	<1	<1
18	**19**	An	—	Et_3N(1)	10	76	—	<1	<1	<1
19	**20**	An	—	Et_3N(1)	10	86	—	<1	<1	<1

Reaction conditions: Substrate (0.1 mmol) in solvent (10 ml) was irradiated by High Pressure Mercury Lamp (400 W) under air.

[a] Yields were determined by GLC.

α-Iodocyclododecanone (**6**) was chosen as a model compound to study the effect of solvents on the photochemical reaction of α-iodoketones, as we have sought to decrease the formation of the reduced ketones. It was thought that the α-iodoketone is reduced by hydrogen iodide. In order to justify this explanation, we carried out a reaction in the presence of an amine to remove HI from the reaction mixture. The reaction of **6** in hexane containing triethylamine (1 molar equivalent) at room temperature under a nitrogen atmosphere with a 400-W high-pressure mercury lamp for 2 hr gave 2-cyclododecen-1-one (**6f**) and cyclododecanone (**6e**) in 70 and 30% yields, respectively. These results are summarized in Table 56.12, and it is obvious that the presence of triethylamine and pyridine increased the yield of α,β-unsaturated ketone (**6f**) (Table 56.12, entries 1 and 2). Entry 4 in Table 56.12 shows that the use of hexane containing hydrogen iodide increases the yield of the reduced product. These observations support the proposal that HI is involved in the formation of the reduced ketone.

Irradiation of alkyl iodides in solution is a powerful and convenient method for the generation of carbocations via a process thought to involve light-induced homolytic cleavage of the carbon–iodine bond followed by electron transfer within the initially formed caged radical pair.[7f,43] Kropp et al.[6] reported that irradiation of 1-iodooctane in a variety of solvents affords mainly 1-octene accompanied by small amounts of octane and substituted octane. It appeared that α-iodoketone would be a more reactive substrate than the alkyl iodide. The reaction containing benzophenone (Table 56.12, entry 3) preferentially gave ketone **6e** due to hydrogen abstraction and protonation. In the case of benzene or acetonitrile, it was found that ketone **6e** is increased (Table 56.12, entries 11 and 12).

TABLE 56.7 Synthesis of α-Hydroxyketone from 3-Iodo-3,6-dialkylcyclohexane-1,2-dione (**21,22**) using Photoirradiation

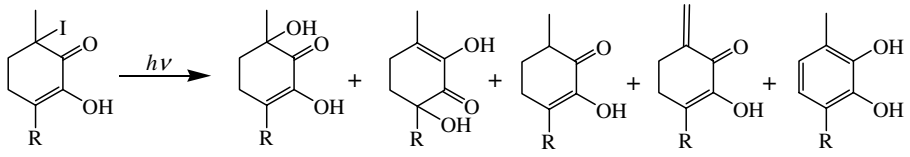

21:R=Me **21a**:R=Me **22a'**:R=*i*-Pr **21e**:R=Me **21f**:R=Me **21g**:R=Me
22:R=*i*-Pr **22a**:R=*i*-Pr **22e**:R=*i*-Pr **22f**:R=*i*-Pr **22g**:R=*i*-Pr

Entry[a]	Substrate	Solvent	Time/h	Product (%)[d]				
				a	**a′**	**e**	**f**	**g**
1	**21**	MeOH	4	6		6	<1	65
2[b]	**21**	2-PrOH	4	11		—	36	50
3[b]	**21**	n-Hex	4	12		—	42	5
4[d]	**21**	n-Hex	4	56		—	—	—
5	**22**	MeOH	2	<1	<1	18	15	61
6[b]	**22**	2-PrOH	2	<1	<1	—	32	63
7[b]	**22**	n-Hex	2	—	—	—	45	20
8[c]	**22**	2-PrOH	2	34	16	—	16	19
9[c]	**22**	n-Hex	2	41	18	—	14	—

[a] Reaction conditions: Substrate (15.7 mmol) in solvent (10 ml) was irradiated by high pressure mercury lamp (400 W) under argon.
[b] In the presence of triethylamine (15.7 mmol).
[c] Under air.
[d] Yields were determined from GLC using n-dodecane as internal standard.

TABLE 56.8 Synthesis of α,α′-Dihydroxyketone from α,α′-Diiodoalkanone (**23**-**26**) using Photoirradiation

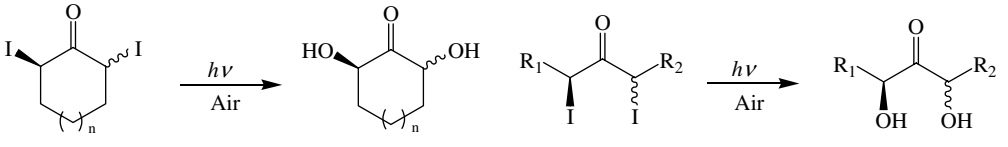

23,24 **23'a,24'a** **25,26** **25'a,26'a**
23,23'a: n=7
24,24'a: n=2
25,25'a:R_1=n-C_2H_5 R_2=n-C_2H_5
26,26'a:R_1=n-C_3H_7 R_2=n-C_3H_7

Entry[a]	Substrate	Time/h	Product (%)[b]
1	**23**(*cis*/*trans* = 100/0)	6	**23′a**(82,*cis*/*trans* = 87/13)
2	**24**(*cis*/*trans* = 8/92)	5	**24′a**(54,*cis*/*trans* = 90/10)
3	**25**(*cis*/*trans* = 90/10)	6	**25′a**(58,*cis*/*trans* = 50/50)
4	**26**(*cis*/*trans* = 75/25)	6	**26′a**(65,*cis*/*trans* = 50/50)

Reaction conditions:
[a] Substrate (0.1 mmol) in acetone (10 ml) in the presence of triethylamine (0.2 mmol) was irradiated by High Pressure Mercury Lamp (400 W) under air atmosphere.
[b] Isolated yields.

In the case of hexane containing a small amount of water, the irradiation of **6** gave **6e**, **6f**, and an unexpected substitution product, 2-hydroxycyclododecanone (**6a**) (Table 56.12, entries 5 to 10).[6] When **6** was irradiated under a commercial fluorescent lamp, the yields of photochemical products **6a**, **6e**, and **6f** were almost invariable (Table 56.12, entry 10). Apparently, the photoproduct distribution is due to

TABLE 56.9 Irradiation of Steroidal α-Iodo Ketones in Hexane[a] with a High-Pressure Mercury Lamp

Entry	Substrates	Method	Time (h)	Products (%)[b]	
1	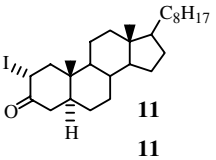 **11**	100 W[c)]	1.0	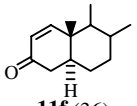 **11f** (36)	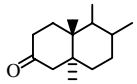 **11e** (55)
2	**11**	100 W[c,e)]	3.0	**11f** (65)	**11e** (25)
3	**11**	400 W[d)]	0.3	**11f** (68)	**11e** (29)
4	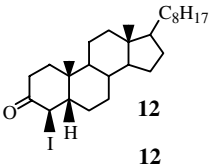 **12**	100 W[c)]	1.0	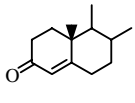 **12f** (32)	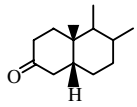 **12e** (50)
5	**12**	400 W[d)]	0.3	**12f** (48)	**12e** (40)
6	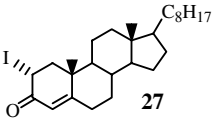 **27**	100 W[c)]	4.0	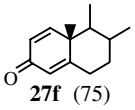 **27f** (75)	**12f** (14)
7	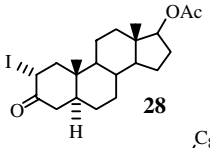 **28**	100 W[c)]	4.0	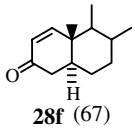 **28f** (67)	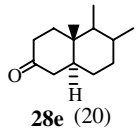 **28e** (20)
8	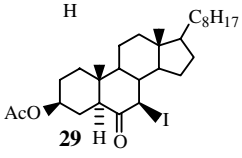 **29**	100 W[c)]	6.0	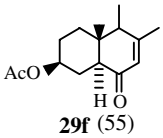 **29f** (55)	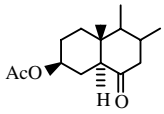 **29e** (30)

[a] Irradiation was carried out under a nitrogen atmosphere at room temperature.
[b] Isolated yield.
[c] Steroidal α-iodo ketone (0.26 mmol) in hexane (233 ml) was employed.
[d] Steroidal α-iodo ketone (0.39 mmol) in hexane (350 ml) was employed.
[e] Contained 1 molar equiv. of triethylamine.

competition of both substitution and elimination reactions. Similarly, irradiation of **6** in hexane containing a small amount of water for 576 hr under a commercial fluorescent lamp as the irradiated light source gave predominantly **6a** in 50% yield. Therefore, it seems that dried hexane is an excellent solvent for the photosynthesis of α,β-unsaturated ketones from α-iodocycloalkanones.

In nonpolar solvents, electron transfers become unfavorable, and the escape of intermediates from the solvent cage leads to radical products.[5] In polar solvents, electron transfer competes efficiently with escape from the solvent cage to produce an ion pair and ultimately products derived from carbocations.[6] During the course of our studies, it was found that irradiation of α-iodoketones in hexane mainly afforded the elimination product α,β-unsaturated ketones. In the presence of a small amount of water in hexane, an α-substituted product was also obtained; therefore, the general photochemical behavior of α-iodoketones can be explained in Figure 56.1 on the basis of the results described above.

Figure 56.1 shows that irradiation of α-iodoketones involves light-induced homolytic cleavage of the CI bond proceeding to the radical pair (I) in solvents. When hexane is used, α,β-unsaturated ketone **6f** and reduced product **6e** are obtained by elimination and reduction. These processes involve free radicals.[5] However, in the presence of a small amount of water in hexane, the radical pair (I) can undergo subsequent electron transfer to afford the ion pair (II); ultimately, the substituted product 2-hydroxycyclododecanone is formed.[6]

TABLE 56.10 Irradiation of α-Iodo Ketones (**1-6**) in Hexane

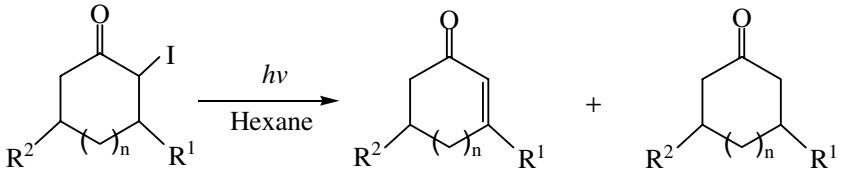

1-6 **1f-6f** **1e-6e**

Entry	Substrates[a]	Method	Time (h)	Products/%[b]
1	**1** (n=1 R^1=R^2=H)	400 W	1.5	**1f** 72(60) **1e** 25
2	**2** (n=1 R^1=HR^2=Me)	400 W	3.0	**2f** 76(64) **2e** 24
3	**3** (n=1 R^1=HR^2=H)	400 W	3.0	**3f** 80(66) **3e** 20
4	**4** (n=2 R^1=R^2=H)	400 W	1.0	**4f** 80(65) **4e** 20
5	**5** (n=3 R^1=R^2=H)	400 W	1.0	**5f** 78(70) **5e** 21
6	**6** (n=7 R^1=R^2=H)	100 W	1.5	**6f** 50(34) **6e** 41
7	**6** (n=7 R^1=R^2=H)	400 W	1.5	**7f** 55(37) **6e** 30

[a] Irradiation solution containing 7.85 mmol/l of substrate under a nitrogen atmosphere that was achieved by bubbling nitrogen gas through the hexane for 20 min prior at room temperature.

[b] Determined by GLC analysis using *n*-dodecane as an internal hydrocarbon standard. All products were characterized by IR. NMR and HRMS.

Isolated yield in parentheses.

TABLE 56.11 Irradiation of α-Iodo Ketones (**19, 24, 26, 30**) in Hexane

Entry	Substrates[a]	Method	Time (h)	Products/%[b]
1	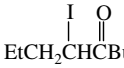 **19**	400 W	1.0	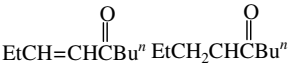 **19f** 68 (58) **19e** 26
2	 **24**	400 W	1.0	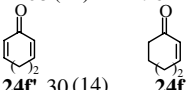 **24f'** 30 (14) **24f** 56
3	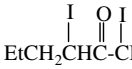 **26**	400 W	1.0	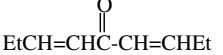 **26f'** 45 (32)
4	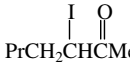 **30**	400 W	1.0	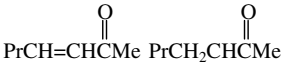 **30f** 65 (53) **30e** 32

[a] Irradiation solution contianing 7.85 mmol/l of substrate under a nitrogen atmosphere that was achieved by bubbling nitrogen gas through the hexane for 20 min prior at room temperature.

[b] Determined by GLC analysis using *n*-dodecane as an internal hydrocarbon standard. All products were characterized by IR. NMR and HRMS.

Isolated yield in parentheses.

In conclusion, this method is very clean, simple, and convenient for the synthesis of α,β-unsaturated ketones. It is particularly noteworthy that this reaction affords a new synthetic method for the synthesis of steroidal α,β-unsaturated ketones. The reaction is more convenient than the methods described previously.

TABLE 56.12 Photochemical Behavior of α-Iodocyclododecanone (**6**)[a]

				Products/%[b], Yield (Isolated)		
Entry	Solvents	Method	Time (h)	**6a**[j]	**6e**	**6f**
1	Hexane	400 W[c,f]	2.0	—	(30)	67 (53)
2	Hexane	400 W[c,g]	2.0	—	(30)	70 (55)
3	Hexane	400 W[c,h]	0.3	—	(82)	15 (7)
4	Hexane	100 W[c,k]	1.5	—	(64)	28 (22)
5	Hexane	400 W[d]	1.5	(trace)	(50)	40 (33)
6	Hexane	100 W[d]	1.5	(5)	(47)	41 (32)
7	Hexane	F.L[d,i]	576	(34)	(43)	14 (7)
8	Hexane-H_2O	400 W[e]	2.0	(12)	(34)	35 (26)
9	Hexane-H_2O	100 W[e]	2.0	(35)	(35)	25 (17)
10	Hexane-H_2O	F.L[e,i]	576	(50)	(41)	3 (trace)
11	PhH	400 W[c]	1.0	—	(65)	32 (28)
12	MeCN	400 W[c]	1.0	—	(57)	35 (27)

[a] Unless otherwise stated, photochemical reactions were carried out under a nitrogen atmosphere with a high pressure mercury lamp. Substrate (α-iodocyclododecanone) (2.75 mmol) in hexane (350 ml) was employed.
[b] GLC yield and isolated yield in the parentheses.
[c] Dried solvents.
[d] No dried.
[e] Hexane: H_2O = 10:1 (v/v) was employed.
[f] Contained 1 molar equiv. of pyridine.
[g] Contained 1 molar equiv. of triethylamine.
[h] Contained 1 molar equiv. of benzophenone.
[i] Reactions were carried out under a fluorescent lamp using a 200 ml triangular reaction vessel contianing 1.57 mmol of α-iodocyclododecanone.
[j] 2-Hydroxycyclododecanone(**11c**) was obtained.
[k] Contained 0.1 molar equiv. of 57% hydroiodic acid.

56.5 A Novel Self-Coupling Reaction of Cyclic Ketones Under High-Pressure Mercury Lamp

Pinacol type 1,2-diols can be synthesized by reduction of ketones and aldehydes with active metals (sodium, magnesium, or aluminum),[44] Mg–MgI_2,[45] SmI_2,[46] Ce–I_2,[47] Yb,[48] and a reagent prepared from $TiCl_4$ and Mg amalgam.[49] Again, some of these methods use toxic reagents and heavy metals. However, it is known that the dimerization of ketones to 1,2-diols can be accomplished by photochemical methods. These are usually the irradiation of aromatic aldehydes and dialkyl ketones in the presence of a hydrogen donor such as 2-propanol, toluene or amines.[50]

The pinacol-type 1,2-diols of cycloalkanone are usually prepared by one of the following methods: reduction of ketone in THF with [Mg–Hg]/$TiCl_4$,[51] reaction of magnesium atoms with cycloheptanone,[52] pinacolization of cyclohexanone using samarium(II) bromide,[53] and reductive coupling of carbonyl compounds to pinacols using low-valent cerium;[47] however, these methods are not applicable to cyclododecanone. Nickon and Zurer[54] reported that reductive coupling of cyclododecanone with $TiCl_4$ and Zn in THF and pyridine gave 1,1-bicyclododecanol (16%).

We have observed that the irradiation of cycloalkanones (cyclohexanone **1e**, cycloheptanone **4e**, cyclooctanone **5e**, cyclodecanone **5′e**, cyclododecanone **6e**, 2-methylcyclohexanone **31e**, 2-phenylcyclohexanone **32e**, α-tetralone **17e**, 5α-cholestan-3-one **11e**, and 5β-cholestan-3-one **12e**) in methanol under a nitrogen atmosphere with a high-pressure mercury lamp ($\lambda > 300$nm) at room temperature yields the corresponding pinacol 1,2-diols. The irradiation of cyclododecanone **6e** in methanol at room temperature under nitrogen atmosphere with a 400-W mercury lamp for 4 hr gave 1,1-bicyclododecanol **6l** (84%) and cyclododecanol **6k** (8%). These results are summarized in Table 56.13, where it can be seen that the

TABLE 56.13 Photochemical Coupling Reaction of Cycloalkanone at Room Temperature

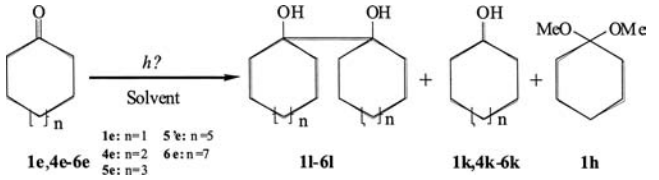

1e,4e-6e **1l-6l** **1k,4k-6k** **1h**

Substrates[a]	Solvents	Method	Time (h)	Products[b] (Yields, %)[c]
Cyclohexanone (**1e**)	MeOH	400 W	4	No Reaction
	MeOH	100 W	18	**1h** (92)
	MeOH[d]	100 W	22	**1h** (73)
	i-PrOH	100 W	20	**1k** (62)
Cycloheptanone (**4e**)	MeOH	400 W	4	**4l** (71), **4k** (15)
Cyclooctanone (**5e**)	MeOH	400 W	8	**5l** (76)
Cyclodecanone (**5′e**)	MeOH	400 W	12	**5′k** (65)
Cyclododecanone (**6e**)	MeOH	100 W	4	**6l** (84), **6k** (8)
	MeOH	400 W	3	**6l** (85), **6k** (9)
	EtOH	100 W	8	**6l** (79), **6k** (10)
	EtOH	400 W	6	**6l** (82), **6k** (10)
	Hexane	400 W	4	No Reaction
	Hex-H_2O	400 W	4	**6l** (81), **6k** (8)
	Cyclohex-H_2O	400 W	10	**6l** (79), **6k** (8)
2-Methylcyclohexanone (**31e**)	MeOH	100 W	18	Dimethyl Acetal (**31h**) (76)
2-Phenylcyclohexanone (**32e**)	MeOH	100 W	30	Dimethyl Acetal (**32h**) (33)
4-Methylcyclohexanone (**33e**)	MeOH	100 W	18	Dimethyl Acetal (**33h**) (91)
5?-Cholestan-3-one (**11e**)	MeOH	400 W	12	Dimethyl Acetal (**11h**) (87)
5?-Cholestan-3-one (**12e**)	MeOH	400 W	10	Dimethyl Acetal (**12h**) (85)

[a] Substrate (3.23 mmol) in alcohol (200 ml) was employed.
[b] All products displayed satisfactory spectral data (IR, ^{1}H-NMR, ^{13}C-NMR, and MS).
[c] Isolated yield.
[d] MeOH: H_2O = 20:1.

method is applicable to some cycloalkanones. There are limitations, however, and cyclohexanone **1e**, 2-methylcyclohexanone **31e**, 2-phenylcyclohexanone **32e**, 4-methylcyclohexanone **33e**, 5α-cholestan-3-one **11e**, and 5β-cholestan-3-one **12e** do not form the corresponding pinacols. Instead, the dimethyl acetals **31h**, **32h**, **33h**, **11h**, and **12h** are formed in 92, 76, 33, 87, and 85% yields, respectively. Also, cyclodecanone (**5′e**) affords cyclodecanol in 65% yield. Moreover, when 2-propanol is used as the solvent, **1e** is transformed to cyclohexanol **1k** but not to the diisopropyl acetal. The reaction of benzaldehyde **34** in methanol at room temperature under the same conditions gave pinacol **34m** (31%) and phenyl-1,2-ethanediol **34n** (69%). These results are summarized in Table 56.14.

The photoreduction of benzophenone in methanol and ethanol gives benzopinacol and a cross-coupled product.[55] Moreover, Weiner reported that photoreduction of benzophenone in 2-propanol yields a pinacol-type compound and the mixed pinacol $(C_6H_5)_2C(OH)C(OH)(CH_3)_2$.[56] These reactions occur by the free ketyl radicals.

The reaction of benzaldehyde **34** in methanol gave the cross-coupling diol, phenyl-1,2-ethanediol **34m** (69%) and pinacol **34a** (31%); however, due to the bulkiness of the alkoxyl group (methanol, ethanol, 1-propanol and 2-propanol), it is difficult to form the cross-coupled product.

In conclusion, the present method, while not widely applicable, has a notable characteristic that was not observed previously.[4,11] This reaction affords a new simple synthetic method for the pinacols of cycloheptanone, cyclooctanone, and cyclododecanone. It is particularly noteworthy that this reaction is a new, clean method.

TABLE 56.14 Photochemical Coupling Reaction of Benzaldehyde at Room Temperature

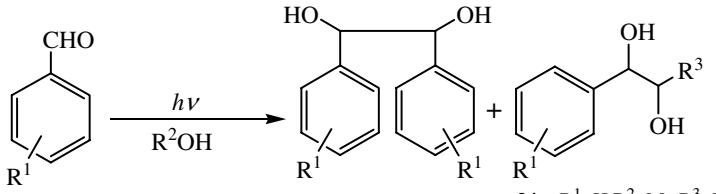

34:R^1=H
35:R^1=*p*-OMe
36:R^1=*o*-OMe

34a:R^1=H,R^2=Me
35a:R^1=*p*-OMe,R^2=Me

34m:R^1=H,R^2=Me,R^3=H
34n:R^1=H,R^2=Et,R^3=Me
34o:R^1=H,R^2=Pr,R^3=Et
34p:R^1=H,R^2=i-Pr,R^3=Me_2
35m:R^1=*p*-OMe,R^2=Me,R^3=H
36m:R^1=*o*-OMe,R^2=Me,R^3=H

Substrate	Solvent	Method	Time (h)	Products[a] (Yields, %)[b]
34	MeOH	100 W	3	**34a** (31) (dl/meso = 50/50) **34m** (69)
	MeOH	400 W	2	**34a** (32) (dl/meso = 48/52) **34m** (68)
	EtOH	100 W	3	**34a** (49) (dl/meso = 55/45) **34n** (51) (dl/meso = 55/45)
	PrOH	100 W	10	**34a** (58) (dl/meso = 52/48) **34o** (42) (dl/meso = 50/50)
	i-PrOH	100 W	15	**34a** (69) (dl/meso = 56/44) **34p** (31)
	H_2O	400 W	10	**34a** (39) (dl/meso = 50/50)
35	MeOH	400W	2	**35a** (15) (dl/meso = 54/46) **35m** (85)
36	MeOH	400W	10	**36m** (85)
 **17e**	MeOH	100 W	18	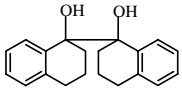 **17ea** (17) 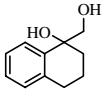 **17em** (80)
17e	i-PrOH	100 W	12	**17ea** (67) 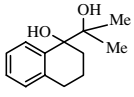 **17ep** (29)

[a] All products displayed satisfactory spectral data (IR, ^{1}H-NMR, ^{13}C-NMR, and MS).
[b] Almost quantitative yields of the pinacol and the cross-coupling diols were obtained. The composition of the reaction mixture was determined from the peak area ratio of the NMR spectrum.

56.6 Synthesis of Camphoric Anhydride Via Unsensitized Photooxidation of Camphorquinone

The photochemical reactions of carbonyl compounds has been thoroughly investigated and the behavior is well established.[57] Some ketones show different photochemical behavior on a silica gel surface from that in solution as reported by Hasegawa et al.[58] Scheffer et al.[59] reported that the irradiation of an

TABLE 56.15 Irradiation of Camphorquinone (**37**) Under an Oxygen Atmosphere at Room Temperature[a]

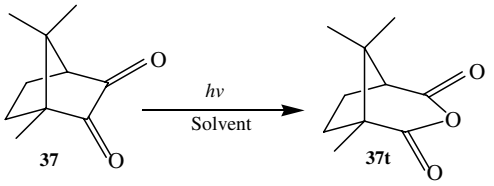

Entry	Condition	Method[b] (W)	Time (h)	Yields[c] (%)
1	MeOH/Ar	100	12	N.R.
2	MeOH/Air	100	12	45
3	MeOH/O_2	100	12	85
4	MeOH/O_2	400	10	82
5	EtOH/O_2	100	12	80
6	Hex./O_2[d]	100	14	N.R.
7	Hex.$^{-H_2O}$/O_2	100	14	78
8	CH_2Cl_2/O_2	100	14	N.R.

[a] Camphorquinone (3.14 mmol) in solvent (200 ml) was employed.
[b] Reaction was carried out with a high-pressure mercury lamp in a water-cooled quartz immersion well as the irradiation source.
[c] Isolated yields after purification by column chromatography on silica gel and was identified by satisfactory spectral data (IR, NMR, and HRMS). N.R. = did not react.
[d] n-Hexane was dried completely by storing over 4A molecular sieves.

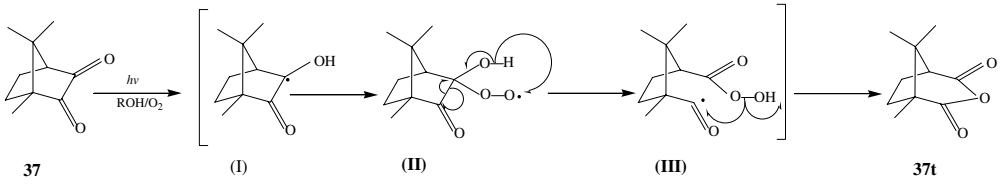

SCHEME 5 Reaction mechanism of camphorquinone (37).

α-diketone brought about a novel photorearrangement in the crystalline state that is different from the Norrish/Yang type II photocyclization process observed in solution. We have observed that direct irradiation of camphorquinone under oxygen with a high-pressure mercury lamp afforded the camphoric anhydride in good yield in a novel reaction. The unsensitized photooxidation of (1*R*)-(−)-camphorquinone gave (+)-*cis*-camphoric anhydride in 85% yield. These results are summarized in Table 56.15. The photoreaction is very simple, clean, and convenient for the synthesis of camphoric anhydride. In the case of methanol and ethanol as solvents, irradiation of camphorquinone **37** gave the camphoric anhydride **37t**[31] in 80 to 85% yields, respectively (Table 56.15, entries 1–4, 7); however, the product **37t** was not obtained under an atmosphere of argon (entry 1). When hexane was used as the solvent under oxygen, the product **37t** was not formed (entry 5). These results indicate that solvent-polarity is important for the success or failure of the unsensitized photooxidation of camphorquinone.

Suginome et al.[31] reported that the irradiation of α-hydroxy cyclic ketones with mercury(II) oxide and iodine in benzene gives camphoric anhydride.[31] On the basis of our results, it is considered that anhydride **37t** can be formed through an intermediate (III) that is formed through the cleavage of a CC bond in radical (II). This is followed by migration of hydrogen. The polar solvent is important role for the generation of radical (I) (Scheme 5). The reactivity of the cyclic diketone was compared with that of the

TABLE 56.16 Irradiation of Cyclic Diketones in Methanol at Room Temperature[a]

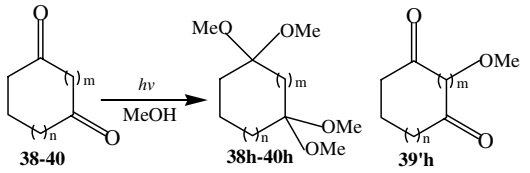

38-40 **38h-40h** **39'h**

Entry	Substrate	Method (W)	Time (h)	Product	Yield[b] (%)
1	**38** (m=0, n=2)	100	18	**38h**	(0)
2	**39** (m=1, n=1)	100	18	**39′h**	(33)
3	**39** (m=1, n=1)	400	16	**39′h**	(53)
4	**40** (m=2, n=0)	100	18	**40h**	(85)
5	**40** (m=2, n=0)	400	16	**40h**	(87)

[a] Substrate (3.14 mmol) in methanol (200 ml) was employed under an oxygen atmosphere.
[b] Isolated yield and all products were identified by satisfactory spectral data (IR, NMR, and HRMS).

cyclohexanedione derivatives, and the results are summarized in Table 56.16. These results show that the photochemical behavior, under identical conditions, is quite different compared with camphorquinone (**37**). The influence of stereochemistry could be important in this case. In conclusion, we have observed that camphorquinone undergoes a novel unsensitized photooxidation, which provides a more efficient, simple, and clean method for the synthesis of camphoric anhydride than the method used heretofore.

References

1. Mataga, N., New Developments of photomolecular sciences, *Chem. Chemical Indust. Jpn.*, 50, 705, 1997.
2. (a) Horiuchi, C. A. and Satoh, J. Y., Novel α-iodination of ketones using iodine/copper(II) acetate, *Synthesis,* 312, 1981; (b) Horiuchi, C.A. and Satoh, J. Y., Novel regioselective iodination of estradiol, estriol and estrone using iodine–copper(II) acetate, *J. Chem. Soc., Chem. Commun*., 671, 1982; (c) Horiuchi, C. A. and Satoh, J. Y., A convenient procedure for iodination of electron-rich aromatic compounds using iodine–copper(II) acetate, *Bull. Chem. Soc. Jpn.,* 57, 2691, 1984; (d) Horiuchi, C. A. and Satoh, J. Y., A new synthesis of α-iodo carboxylic acid using iodine–copper salt, *Chem. Lett.,* 1509, 1984; (e) Horiuchi, C. A., Haga, A., and Satoh, J. Y., Novel regioselective iodination of estradiol 17β-acetate, *Bull. Chem Soc. Jpn.,* 59, 2459, 1986. (f) Horiuchi, C. A. and Satoh, J. Y., Syntheses of steroidal *trans*-iodo acetates, *Bull. Chem Soc. Jpn.,* 60, 426, 1987. (g) Horiuchi, C. A. and Kiji, S., A new α-iodination of ketones using iodine–cerium(IV) ammonium nitrate, *Chem. Lett*., 31, 1988; (h) Horiuchi, C. A., Nishio, Y., Gong, D., Fujisaki, T., and Kiji, S., A new alkoxy-iodination and nitratoiodination of olefins using iodine–cerium(IV) ammonium nitrate, *Chem. Lett.,* 607, 1991; (i) Horiuchi, C. A., Ochiai, K., and Fukunishi, H., A new alkoxyiodination and nitrateiodination of α,β-unsaturated ketones and ester using iodine–cerium(IV) ammonium nitrate, *Chem. Lett.,* 185, 1994; (j) Horiuchi, C. A. and Takahashi, E., A new α,α′-diiodination of ketones using iodine–cerium(IV) ammonium nitrate, *Bull. Chem. Soc. Jpn*., 67, 271, 1994; (k) Horiuchi, C. A., Hosokawa, H., Kanamori, M., Muramatsu, Y., Ochiai, K., and Takahashi, E., Regio- and stereo-controlled alkoxyiodination of 1,3-diene using iodine–cerium(IV) ammonium nitrate, *Chem. Lett.,* 13, 1995; (l) A new α-iodination of ketones using iodine–ammonium cerium(IV) nitrate in alcohol or acetic acid, Horiuchi, C. A. and Kiji, S., *Bull. Chem. Soc. Jpn*., 70, 421, 1997.
3. (a) Clark, J. H., Green chemistry: challenges and opportunities, *Green Chem.,* 1, 1999; (b) Sato, K. and Noyori, R., A "green" route to adipic acid practical oxidation using hydrogen peroxide, *Chem. Chemical Indust. Jpn.*, 52, 1166, 1999.
4. Wagniere, G. H., *The Chemistry of the Carbon-Halogen Bond*, Wiley, New York, 1973.

5. (a) Dannenberg, J. J. and Dill, K., Photolysis of phenylbromopropanes in hexane. Free radical reaction involving a kinetic phenyl migration, *Tetrahedron Lett.*, 1972, 1571; (b) Bakale, D. K. and Gillis, H. A., Free radical chain reaction in the radiolysis and photolysis of isobutyl bromide, *J. Phys. Chem.*, 74, 2074, 1970.
6. (a) Kropp, P. J., Jones, T. H., and Poindexter, G. S, Photochemistry of alkyl halides. I. Ionic versus radical behavior, *J. Am. Chem. Soc.*, 95, 5420, 1973; (b) Poindexter, G. S. and Kropp, P. J., Photochemistry of alkyl halides. II. Support for an electron transfer process., *J. Am. Chem. Soc.*, 96, 7142,1974; (c) Kropp, P. J., Poindexter, G. S., Pienta, N. J., and Hamilton, D. C., Photochemistry of alkyl halides. 4. 1-Norbonyl, 1-nornornylmethyl, 1- and 2-adamantyl and 1-octyl bromides and iodides, *J. Am. Chem. Soc.,* 98, 8135, 1976; (d) Kropp, P. J., Worsham, P. R., Davidson, R., and Jones, T. H., Photochemistry of alkyl halides. 8. Formation of bridgehead alkene., *J. Am. Chem. Soc.,* 104, 3972,1982; (e) Kropp, P. J., McNeely, S. A., and Davis, R. D., Photochemistry of alkyl halides 10. Vinyl halides and vinylidene dihalides, *J. Am. Chem. Soc.*, 105, 6907, 1983; (f) Kropp, P. J., Sawyer, J. A., and Snyder, J. J., Photochemistry of alkyl halides. 11. Competing reaction via carbene and carbocationic intermediates, *J. Org. Chem.*, 49, 1583, 1984.
7. (a) Tomioka, H., Izawa, Y., and Ogata, Y., The photochemical reactions of substituted acetones with triethylphosphite, *Tetrahedron*, 24, 5739, 1968; (b) Izawa, Y., Tomioka, H., Kutsuna, M., and Toyama, Y., Photochemical ethoxycarbonylmethylation of anisole with ethyl chloroacetate in the presence of zinc chloride, *Bull. Chem. Soc. Jpn.*, 52, 3465, 1979; (c) Izawa, Y., Tomioka, H., Natsume, M., Beppu, S., and Tsujii, H., Photoinduced alcoholysis of the trichloroacetyl group, *J. Org. Chem.*, 45, 4835,1980; (d) Izawa, Y., Ishiguro, K., and Tomioka, H., Photoinduced alcoholysis of trihaloacetyl group, *Bull. Chem. Soc. Jpn.*, 56, 951, 1983; (e) Izawa, Y., Ishiguro, K., and Tomioka, H., Photoinduced alcoholysis of α,α,α-tribromoacetophenone to benzoyl formate, *Bull. Chem. Soc. Jpn.*, 56, 1490, 1983; (f) Izawa, Y., Takeuchi, M., and Tomioka, H., Photo-dehalogenation of vicinal dihalides to olefins, *Chem. Lett.*, 1297, 1983; (g) Izawa, Y., Watoh, Y., and Tomioka, H., Effect of structure on photoalcoholysis of aromatic α-halo ketones, *Chem. Lett.*, 33, 1984.
8. Orito, K., Yorita, K., Miyazwa, M., and Suginome, H., Photolysis of α-haloketone: synthesis of three α-camphorylcamphors from 3-bromocamphor, *Synlett*, 37, 1994.
9. Ji, S. -J. and Horiuchi, C. A., Photo-cleavage of carbon-carbon bond of α-iodocycloalkanones giving ω,ω-dialkoxyalkanoic ester in alcohol, *Bull. Chem. Soc. Jpn.*, 73, 1645, 2000.
10. Ji, S. -J., Takahashi, E., Takahashi, T. T., and Horiuchi, C. A., Synthesis of α,β-unsaturated ketone from α-iodoketone using photoirradiation, *Tetrahedron Lett.*, 40, 9263, 1999.
11. Ji, S. -J., Matsushita, M., Takahashi, T. T., and Horiuchi, C. A., Novel self-coupling reaction of cyclic ketones under a high-pressure mercury lamp, *Tetrahedron Lett.*, 40, 6791, 1999.
12. Ji, S.-J., Lu, J., Lang, J.-P. and Horiuchi, C. A., Synthesis of camphoric anhydride via unsensitized photo-oxidation of camphorquinone, *Synth. Commun.,* 32, 1659, 2002.
13. Gil, S., Lazaro, M. A., Mestres, R. and Parra, M., Sex pheromone of *Chilo suppressalis*: efficient syntheses of (Z)-11-hexadecenal, (Z)-13-octadecenal, and (Z)-9-hexadecenal, *Synth. Commun.*, 26, 2329, 1996.
14. (a) Schreiber, S. L., Claus, R. E., and Reagan, J., Ozonolytic cleavage of cycloalkenes to terminally differentiated products, *Tetrahedron Lett.,* 23, 3867, 1982; (b) Tolstikov, G. A., Miftakhov, M. S., Valeev, F. A., Akhmetvaleev, R. R., Khalilov, L. M., and Panasenko, A. A., Prostanoids. XII. Synthesis of key synthons and some α-homoanalogs of 11-deoxyprostaglandin E1, *Zh. Org. Khim.*, 21, 72, 1985.
15. (a) Baer, E., Oxidative cleavage of α-keto acids and α-keto alcohols by means of lead tetraacetate, *J. Am. Chem. Soc.*, 62, 1597, 1940; (b) Baer, E., Oxidative cleavage of cyclic α-keto alcohols by means of lead tetraacetate, *J. Am. Chem. Soc.*, 64, 1416, 1942.
16. (a) Clutterbuck, P. W. and Reuter, F., Reaction of periodic acid with α-ketols, α-diketones and α-ketone aldehydes, *J. Chem. Soc., B*, 1467, 1935; (b) Buse, C. T., Kleschick, W. A., Pirrung, M. C., Sohn, J. E., and Lampe, J., Acyclic stereoselection. 7. Stereoselective synthesis of 2-alkyl-3-hydroxy carbonyl compounds by aldol condensation, *J. Org. Chem.*, 45, 1066, 1980.

17. Knof, L., 3β-Hydroxy-5-oxo-5,6-secocholestan-6-oic acid and conversion products, *Justus Liebigs Ann. Chem.,* 656, 183, 1962.
18. Ito, S. and Matsumoto, M., Ferric salt catalyzed oxygenation of cycloalkanones to oxo esters by molecular oxygen, *J. Org. Chem.*, 48, 1133, 1983.
19. Hirao, T., Mori, M., and Ohshiro, Y., Oxovanadium(V)-induced ring-opening oxygenation of cyclic ketones in alcohol, *Bull. Chem. Soc. Jpn.*, 62, 2399, 1989.
20. (a)Torii, S., Inokuchi, T., and Oi, R., Electrooxidative cleavage of carbon–carbon linkages. I. Preparation of acyclic oxoalkanoates from 2-hydroxy- and 2-acetoxy-1-cycloalkanones and cycloalkanone enol acetates, *J. Org. Chem.*, 47, 47, 1982. (b) Tsuji, T., Acid-catalyzed oxidation of oxiranes with dimethyl sulfoxide giving α-hydroxy ketones, *Bull. Chem. Soc. Jpn.*, 62, 645, 1989.
21. He, L., Kanamori, M., and Horiuchi, C. A., Oxidation of 2-alkylcycloalkanone derivatives with iodine–cerium(IV) salts in alcohol, *J. Chem. Res. (S)*, 122, 1999.
22. He, L. and Horiuchi, C. A., Oxidation of 2-substituted cycloalkanones with cerium(IV) sulfate, *Bull. Chem. Soc. Jpn.*, 72, 2515, 1999.
23. (a) Suzuki, T., Sonoda, T., Kobayashi, S., and Taniguchi, H., Photochemistry of vinyl bromides: a novel 1,2-aryl group migration, *J. Chem. Soc.*, *Chem. Commun.*, 180, 1976; (b) Kitamura, T., Kobayashi, S., and Taniguchi, H., Photolysis of vinyl bromides in the presence of tetrabutylammonium azide. Trapping of a vinyl cation with azide ion, *Tetrahedron Lett.*, 1619, 1979; (c) Sket, B. and Zupan, M., Photochemistry of 2-halo-1,1-diphenylethylenes: the photo–Fritsch–Buttenberg–Wiechell rearrangement, *J. Chem. Soc.*, *Perkin Trans. 1*, 752, 1979; (d) Appleton, D. C., Brocklehurst, B., McKenna, J., McKenna, J. M., Thackeray, S., and Walley, A. R., The mechanism of photolysis of benzyl halides and benzyl acetate in alcohols, *J. Chem. Soc.*, *Perkin Trans. 2*, 87, 1980.
24. (a) Jones, R. N., Ramsay, D. A., Herling, F., and Dobriner, K., The Infrared spectra of α-brominated keto steroids, *J. Am. Chem. Soc.*, 74, 2828, 1952; (b) Kuehne, M. E., A spectroscopic route to the dehydroabietic acid configuration, *J. Am. Chem. Soc.*, 83, 1492, 1961; (c) Warnhoff, E. W., α-Halo ketones. II. Rearrangement, reduction, elimination and displacement in the reaction of pyridines with 2α-bromocholestan-3-one, *J. Org. Chem.*, 27, 4587, 1962; (d) Lourdusamy, M., Labrie, F., and Singh, S. M., Synthesis of atamestane (SH 489): an aromatase inhibitor, *Synth. Commun.*, 25, 3655, 1995.
25. (a) Braude, E. A., Brook, A. G., and Linsted, R. P., Hydrogen transfer. IV. The use of quinones of high potential as dehydrogenation reagents, *J. Chem. Soc.*, 3569, 1954; (b) Burn, D., Kirk, D. N., and Petrow, V., A new reagent for the preparation of δ1,4- and δ1,4,6-steroidal ketones, *Proc. Chem. Soc.*, 14, 1960.
26. Jerussi, R. A. and Speyer, D., Selenium dioxide oxidation of 5α-androstane-3,17-dione. Stereochemistry of dehydrogenation, *J. Org. Chem.*, 31, 3199, 1966.
27. (a) Kirk, D. N. and Hartshorn, M. P., *Steroid Reaction Mechanisms*; Elsevier, Amsterdam, 1968, 109–110; (b) Djerassi, C. and Scholz, C. R., The bromination of 3-ketosteroids in acetic acid and the effect of trace substances in the solvent, *J. Am. Chem. Soc.*, 69, 2404, 1947. (c) Fuchs, B. and Loewenthal, H. J. E., Contraction of ring A in 5α-cholestane derivatives, *Tetrahedron*, 199, 1960.
28. (a) Hiuchi, F., Nakamura, N., Saitoh, M., Komagome, K., Hiramatsu, H., Takimoto, N., Akao, N., Kondo, K., and Tsuda, Y., Studies on crude drugs effective on visceral larva migrans. XVIII. Synthesis and nematocidal activity of aralkyl- and aralkenylamides related to piperamide on second-stage larvae of *Toxocara canis*, *Chem. Pharm. Bull.*, 45, 685, 1997. (b) Claus, R. E. and Schleiber, S. L., Ozonolytic cleavage of cyclohexene to terminally differentiated products: methyl 6-oxohexanoates, 6,6-dimethoxyhexanal, methyl 6,6-dimethoxyhexanoate, *Org. Synth.*, *Collect. Vol.*, VII, 168, 1960.
29. Sharpless, K. B., Lauer, R. F., and Teranishi, A. Y., Electrophilic and nucleophilic organoselenium reagents: new routes to α,β-unsaturated carbonyl compounds, *J. Am. Chem. Soc.*, 95, 6137, 1973.
30. (a) Alvarez, E., Betancor, C., Freire, R., Martin, A., and Suarez, E., Reaction of 5α- and 5β-3-keto steroids with potassium superoxide, *Tetrahedron Lett.*, 22, 4335, 1981; (b) Masters, J. J., Jung, D. K., Danishefsky, S. J., Snyder, L. B., Park, T. K., Isaacs, R. C. A., Alaimo, C. A., and Young, W. B.,

A novel intramolecular, Heck reaction: synthesis of a cholesterol-baccatin III hybrid, *Angew. Chem. Int. Ed. Engl.*, 34, 452, 1995.

31. (a) Suginome, H., Yamada, Y., and Orito, K., The formation of cyclic anhydrides via regioselective β-scission of alkoxyl radicals generated from 5- and 6-membered α-hydroxy cyclic ketones, *J. Chem. Soc., Perkin Trans. 1*, 1239, 1990; (b) Suginome, H., Satoh, G., Yamamoto, Y., and Orito, K., Photoinduced molecular transformations. 106. Intramolecular addition vs. β-scission of oxyl radicals generated from A-homo-5α–cholest-1-en-4α- and -4β-ol hypoiodites and 4-methyl-A-homo-5α-cholest-1-en-4α- and -4β-ol hypoiodites, *J. Chem. Soc., Perkin Trans. 1*, 1033, 1990; (c) Kalita, D. J., Borah, R., and Sarma, J. C., A new selective catalytic acetalization method promoted by microwave irradiation, *Tetrahedron Lett.*, 39, 4573, 1998.
32. Yang, D. T. C., Cao, Y. H., Evans, T. T., and Kabalka, G. W., The ultrasound associated oxidation of α-substituted carbonyl compounds to carboxylic acids, *Synth. Commun.*, 26, 4275, 1996.
33. Morrison, H. and de Cardenas, L., Organic photochemistry. 70. Stereoelectronic control in the photolytic cleavage of α-chloro ketones, *J. Org. Chem.*, 52, 2590, 1987.
34. Unpublished data by Takeda, A., Ji, S.-J., Takahashi, T. T., and Horiuchi, C. A.
35. (a) Vedejs, E., Method for direct hydroxylation of enolates: transition metal peroxide reactions, *J. Am. Chem. Soc.*, 96, 5944, 1974; (b) Vedejs, E. and Telschow, J. E., Synthesis of cyanohydrins from cyanides: transition metal peroxide reactions, *J. Org. Chem.*, 41, 740, 1976; (c) Vedejs, E. and Larsen, S., Hydroxylation of enolates with oxodiperoxymolybdenum(pyridine)hexamethylphosphoric triamide, MoO_5PyHMPA(MoOPH): 3-Hydroxy-1, 7,7-trimethylbicyclo[2.2.1]heptan-2-one, *Org. Synth., Collect. Vol.*, VII, 277, 1990; (d) Gamboni, R. and Tamm, C., Structure and diastereoselectivity of α-hydroxylation of chiral ester enolates by molybdenum peroxo complex, *Tetrahedron Lett.*, 27, 3999, 1986.
36. Cuvigny, T., Valette, G., Larcheveque, M., and Normant, H., Regioselective transformation of ketones into primary or secondary α-ketols, *J. Organomet. Chem.*, 155, 147, 1978.
37. (a) Rubottom, G. M., Vazquez, M. A., and Pelegrina, D. R., Peracid oxidation of trimethylsilyl enol ethers: facile α-hydoxylation procedure, *Tetrahedron Lett.*, 4319, 1974; (b) Horiguchi, Y., Nakamura, E., and Kuwajima, I., Double hydroxylation of enol silyl ethers: a single-step synthesis of α,α′-dihydoxy ketones, *Tetrahedron Lett.*, 30, 3323, 1989.
38. (a) Takai, T., Yamada, T., Rhode, O., and Mukaiyama, T., Oxygenation of silyl enol ethers and silyl ketene acetals with molecular oxygen and aldehyde catalyzed by nickel(II) complex: a convenient method for the preparation of α-hydroxy carbonyl compounds, *Chem. Lett.*, 281, 1991; (b) Davis, F. A. and Sheppard, A. C., Oxidation of silyl enol ethers using 2-sulfonyloxaziridines: synthesis of α-siloxy epoxides and α-hydroxy carbonyl compounds, *J. Org. Chem.*, 52, 954, 1987.
39. Moriarty, R. M., Hu, H., and Gupta, S. C., Direct α-hydroxylation of ketones using iodosobenzene, *Tetrahedron Lett.*, 22, 1283, 1981,
40. Moriarty, R. M., Duncan, M. P., and Prakash, O., Hypervalent iodine oxidation of silyl enol ethers: a direct route to α-hydroxy ketones, *J. Chem. Soc., Perkin Trans. 1*, 1781, 1987.
41. Moriarty, R. M., Berglund, B. A., and Penmasta, R., Direct α-hydroxylation of ketones under acidic conditions using [*bis*(trifluoroacetoxy)]iodobenzene, *Tetrahedron Lett.*, 33, 6065, 1992.
42. (a) Joly, R., Warnant, J., Nomine, G., and Bertin, D., Dehydrobromination of 2,4-dibromo-3-oxo steroids in the presence of lithium carbonate. I. *Bull. Soc. Chim. France*, 366, 1958; (b) Schmitz, F. J. and Johnson, W. S., Proton magnetic resonance (NMR) spectra of 1α-deuterio-2-acetoxy-3-cholestanones: mechanism of dehydrohalogenation of α-halo ketones, *Tetrahedron Lett.*, 647, 1962.
43. (a) Banks, J. T., Garcia, H., Miranda, M. A., Perez-Prieto, J., and Scaiano, J. C., Laser flash, laser drop and preparative photochemistry of 1,5-diiodo-1,5-diphenylpentane: detection of a hypervalent iodine radical intermediate, *J. Am. Chem. Soc.*, 117, 5049, 1995; (b) Perez-Prieto, J., Miranda, M. A., Garcia, H., Konya, K., and Scaiano, J. C., Lamp versus laser photolysis of a bichromophoric dichloroalkane: chemical evidence for the two-photon generation of the 1,5-diphenylpentanediyl biradical, *J. Org. Chem.*, 61, 3773, 1996; (c) Miranda, M. A., Perez-Prieto, J., Font-Sanchis, E.,

Konya, K., and Scaiano, J. C., Laser flash, laser-drop and lamp photolysis of 1,3-dichloro-1,3-diphenylpropane. One- versus two-photon reaction pathways, *J. Org. Chem.*, 62, 5713, 1997.
44. March, J., *Advanced Organic Chemistry*, John Wiley & Sons, New York, 1991, 1225.
45. Griffin, G. W. and Hager, R. B., Pinacol reduction of 1,2-dibenzoylethane: formation of a strained cyclic pinacol, *J. Org. Chem.*, 28, 599, 1963.
46. Namy, J. L., Souppe, J., and Kagan, H. B., Efficient formation of pinacols from aldehydes or ketones mediated by samarium diiodide, *Tetrahedron Lett.*, 24, 765, 1983.
47. Imamoto, T., Kusumoto, T., Hatanaka, Y., and Yokoyama, M., Reductive coupling of carbonyl compounds to pinacols by using low-valent cerium, *Tetrahedron Lett.*, 23, 1353, 1982.
48. Hou, Z., Takamine, K., Fujiwara, Y., and Taniguchi, H., Ytterbium metal mediated synthesis of symmetrical and unsymmetrical pinacols from carbonyl compounds, *Chem. Lett.*, 2061, 1987.
49. (a) Corey, E. J., Danheiser, R. L., and Chandrasekaran, S., New reagents for the intermolecular and intramolecular pinacolic coupling of ketones and aldehydes, *J. Org. Chem.*, 41, 260, 1976; (b) Pons, J. M., Zahra, J. P., and Santelli, M., Reductive coupling of α,β-enones. I. Reduction of methyl vinyl ketone and mesityl oxide, *Tetrahedron Lett.*, 22, 3965, 1981; (c) Cohen, S., Palora, A., and Parsons, G. H., Jr., Photoreduction by amines, *Chem. Rev.*, 73, 141, 1973.
50. Mundy, B. P., Srinivasa, R., Kim, Y., and Dolph, T., Studies on the pinacol coupling reaction, *J. Org. Chem.*, 47, 1657, 1982.
51. Wescott, L. D., Jr., Williford, C., Parks F., Dowling, M., Sublett, S., and Klabunde, K. J., Reaction of magnesium atoms with cyclic ketones, *J. Am. Chem. Soc.*, 98, 7853, 1976.
52. Lebrun, A., Namy, J.-L., and Kagan, H. B., Samarium dibromide, an efficient reagent for pinacol coupling reactions, *Tetrahedron Lett.*, 34, 2311, 1993.
53. Nickon, A. and Zurer, P. St. J., Isolation of a diazoalkane intermediate in the photic Bamford–Stevens reaction, *J. Org. Chem.*, 46, 4685, 1981.
54. Mauser, H. and Bihl, V., Formation of mixed pinacols in the photoreduction of benzophenone, *Z. Naturforsch.*, B22, 1077, 1967.
55. Weiner, S. A., Behavior of photochemically generated ketyl radicals: modified mechanism for benzophenone photoreduction, *J. Am. Chem. Soc.*, 93, 425, 1971.
56. (a) Weiss, D. S., *Organic Photochemistry*, Vol. 11, Padwa, A., Ed., Marcel Dekker, New York, 1981, 347; (b) Wagner, P. J. and Park, B.-S., *Organic Photochemistry*, Vol. 11, Padwa, A., Ed., Marcel Dekker, New York, 1991, 227; (c) DeMayo, P., Nakamura, A., Tsang, P. W. I., and Wong, S. K., Surface photochemistry: deviation of the course of reaction in benzoin ether photolysis by adsorption on silica gel, *J. Am. Chem. Soc.*, 104, 6824, 1982; (d) Aoyama, H., Miyazaki, K., Sakamoto, M., and Omote, Y., Photochemical reactions of *N*,*N*-dialkyl-α-oxo amides adsorbed on silica gel and alumina, *Chem. Lett.*, 1583, 1983.
57. Hasegawa, T., Moribe, J., and Yoshioka, M., The photocyclization of *N*,*N*-dialkyl-β-oxo amides adsorbed on silica gel, *Bull. Chem. Soc. Jpn.*, 61, 1437, 1988.
58. (a) Olovsson, G., Scheffer, J. R., Trotter, J., and Wu, C. -H., Novel differences between the solid state and solution phase, *Tetrahedron Lett.*, 38, 6549, 1997; (b) Urry, W. H., Trecker, D. J., and Winey, D. A., Photochemistry of 1,2-diketones: 1,2-cyclodecanedione and 2,3-pentanedione, *Tetrahedron Lett.*, 609, 1962.
59. (a) Ross, J., Gebhardt, A. I., and Gerecht, J. F., The autoxidation of methyl oleate, *J. Am. Chem. Soc.*, 71, 282, 1949; (b) Lundberg, W. O., *Autoxidation and Antioxidants*, Interscience, New York, 1961; (c) Schenck, G. O. and Krauch, C. H., The benzophenone-photosensitized autoxidation of secondary alcohols and ethers: preparation of α-hydroperoxides, *Chem. Ber.*, 96, 517, 1963; (d) Urry, W. H. and Trecker, D. J., Photochemical reactions of 1,2-diketones, *J. Am. Chem. Soc.*, 84, 118, 1962.

57

Regioselective Photochemical Synthesis of Carbo- and Heterocyclic Compounds: The Norrish/Yang Reaction

Pablo Wessig
Humboldt University Berlin

57.1 Introduction

Photochemical reactions of the carbonyl group are among the most extensively investigated areas of organic photochemistry. In this chapter, the regioselective route to a variety of carbocyclic and heterocyclic compounds by means of the Norrish/Yang reaction are discussed. The main emphasis is on preparative applications. First, the history of this reaction is briefly outlined. In 1934, Norrish and Appleyard observed, upon irradiation of aliphatic ketones, a cleavage reaction providing products whose alkyl chain was cleaved between the α- and the β-carbon atom with respect to the carbonyl group.[1] Today, this cleavage reaction is referred to as *Norrish type II cleavage*. As a result of the limited analytical capabilities almost 70 years ago, Norrish and Appleyard did not identify any cyclization products that are formed in competition with the cleavage process. Yang and Yang were the first to recognize, in 1958, the formation of cyclobutanes as well as the Norrish type II cleavage products.[2] This discovery was the basis of a very versatile and valuable ring-closure reaction that is referred to as the *Norrish/Yang reaction* (Scheme 1).

0-8493-1348-1/04/$0.00+$1.50

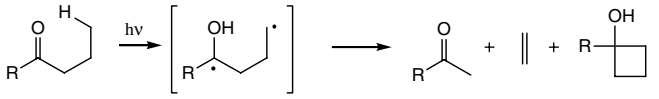

SCHEME 1

Mechanistic details of the Norrish/Yang reaction have been reviewed in many excellent articles[3] and are duplicated in this chapter only as necessary for the understanding of a specific reaction outcome. Nevertheless, two fundamental facts should be mentioned here. The initial step of the Norrish/Yang reaction is a n,π^* excitation of the carbonyl group followed by an intramolecular hydrogen migration from an sp^3-carbon atom to the oxygen atom of the carbonyl group to provide a biradical. In this context, the spin multiplicity of the excited carbonyl group is of great significance for the outcome of the reaction. From a preparative point of view, phenomena of regio- and stereoselectivity are of particular importance and therefore receive special attention. The aim is to show that, in spite of the apparently low structural flexibility of the original Yang reaction (formation of cyclobutanes), it is possible to influence regio- and stereoselectivity and thus gain access to a variety of cyclic products. It should be noted that the Yang reaction itself will be discussed only briefly in this chapter, and the reader is referred to other articles in this volume.

57.2 Cyclopropanes

The precondition for the synthesis of cyclopropanes as products of a Norrish/Yang reaction is the formation of 1,3-biradicals and consequently a hydrogen abstraction from the β-position with respect to the carbonyl group. (Unless otherwise stated, the terms α-, β-, etc. always refer to sites adjacent to the carbonyl carbon atom.) The geometrical parameters of the corresponding five-membered transition state, especially the O–H–C bond angle, differ substantially from the ideal parameters reported by Scheffer et al.[4] Therefore, it is not surprising that only few syntheses of cyclopropanes via the Norrish/Yang reaction are known.[5,6] In most of these cases, it was either proven or it is very likely that the initial step is a photoelectron transfer (PET). In addition, the hydrogen atom is transferred not homolytically but by a proton shift that occurs after PET. These conditions limit the preparative value because the electron-rich functional groups responsible for the PET cause a great sensitivity of the cyclopropanes to oxidative ring opening.

A recently developed method utilizes a leaving group attached to a carbon adjacent to one of the radical centers that is formed following the hydrogen transfer process. This is shown in **1**, where the leaving group X is attached to the carbon atom adjacent to the carbonyl group. Once the initial biradical is formed, an elimination of the acid HX occurs at the stage of biradicals **2**, which proceeds fast enough to compete with the "classic" Norrish/Yang processes (cleavage, cyclization). As a result, the left half of biradicals **2** (hydroxy radical) is converted into an enolate radical (oxoallyl radical), and the spin density is shifted to the adjacent atom. In fact, 1,4-biradical **2** is transformed into 1,3-biradical **3**. This approach has been named the *spin center shift* of biradicals.[7] After intersystem crossing (ISC), biradicals **3** cyclize to acyl-cyclopropanes **4**. (Scheme 2, Table 57.1)

The method tolerates a wide range of functional groups. Although the lifetimes of biradicals **3** have not yet been measured, the experimental results strongly suggest that the lifetimes are very short (<25 ns). This can be concluded especially from irradiation of the cyclopropyl-substituted compound **1f**, which cyclized in good yields to *bis*-cyclopropylketone **4f** without any detectable opening of the cyclopropyl ring. In general, cyclopropylcarbinyl radicals undergo very fast ring opening to butenyl radicals ($k = 4.0 \times 10^7\ s^{-1}$) and this reaction is often used to determine radical lifetimes (the *radical clock*).[8]

The cyclopropane synthesis is also suited for the preparation of highly strained bicyclic hydrocarbons such as [2.1.0]bicyclopentanes **6** and spiropentanes **8**.[7,9] The formation of spiropentane **8** is particularly remarkable in that it is the result of a homolytic hydrogen abstraction from a cyclopropane ring, which is very rarely observed. (Scheme 3).

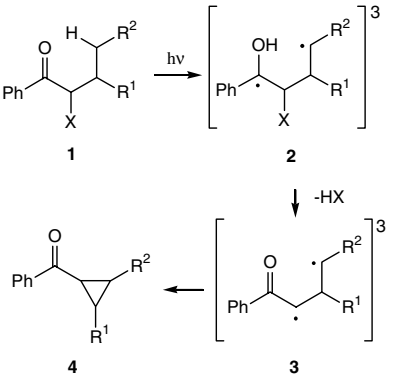

1 **2** **3** **4**

SCHEME 2

TABLE 57.1 Yields of Cyclopropanes **4**

4	R^1	R^2	X[a]	Yield (%)
a	H	H	OMs	87
b	Me	H	OMs	90
c	COOMe	H	ONO_2	59
d	H	OBn	OMs	46
e	H	Ph	OMs	78
f	H	C_3H_5[b]	OTs	68
g	H	C_2H_3[c]	OTs	80

[a] Ms, methanesulfonyl; Ts, 4-tolulenesulfonyl.
[b] Cyclopropyl.
[c] Vinyl.

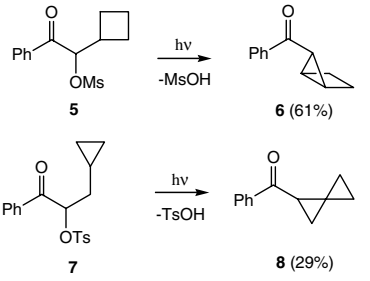

5 **6** (61%) **7** **8** (29%)

SCHEME 3

57.3 Four-Membered Rings

Cyclobutanes

The synthesis of cyclobutanes is the classical area of application of the Norrish/Yang reaction. It has been discussed comprehensively elsewhere.[3a,b,10] Here, only two special aspects are addressed. The main drawback of Yang cyclization from a practical point of view is the Norrish type II cleavage, which almost always competes with the cyclization and is often the only observed process. Nevertheless, the cleavage can be suppressed if the overlap of both radical p_z orbitals with the breaking C–C bond is disturbed by

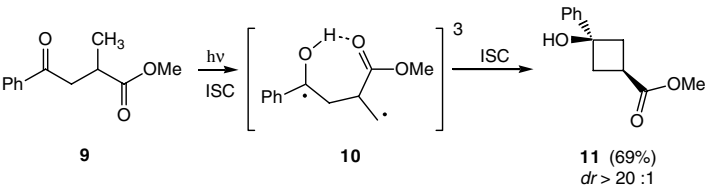

SCHEME 4

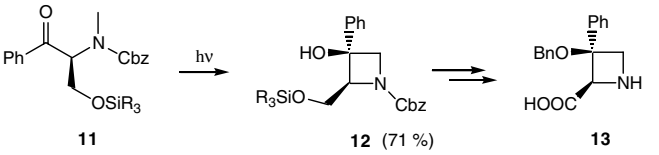

SCHEME 5

steric or electronic factors. This is exemplified in the irradiation of oxoester **9**. On irradiation of α-methyl-γ-oxoester **9**, cyclobutane **11** is formed in good yield as only one diastereomer. The explanation for the low extent of Norrish type II cleavage is that biradical **10** is conformationally fixed by a hydrogen bond, thus preventing the overlap of the benzylic radical with the breaking bond and causing the exclusive formation of the *cis*-configured product (Scheme 4).[11]

Azetidines and Oxetanes

Another approach to repress the cleavage is to replace the β-carbon atom by a nitrogen atom. The mesomerism between the γ-radical center and the nitrogen lone pair forces a conformation unfavorable for Norrish type II cleavage. This concept was used in the stereoselective synthesis of the highly functionalized azetidine **12**, which was subsequently converted into azetidine carboxylic acid **13**, an unnatural α-amino acid. Interestingly, no Norrish type II cleavage was observed, and, due to an intramolecular hydrogen bond, only one diastereomer was obtained (Scheme 5).[12]

β-Lactams play an important role both as versatile building blocks and as compounds, often exhibiting interesting biological activity such as antibiotic activity. In the course of Sheehan's penicillin synthesis, the construction of the β-lactam ring was the most striking and challenging task.[13] In this regard, it is noteworthy that β-lactams can also be prepared using the Norrish/Yang reaction. Thus, upon irradiation of α-ketoamides **14**, the excited carbonyl group abstracts a hydrogen atom from one of the nitrogen-bound alkyl groups forming 1,4-biradicals, which cyclize to β-lactams **19** (Scheme 6). It was shown that the observed range of products depends remarkably on the substituents and the solvent used during photolysis. A thorough discussion of the complex reaction course would go beyond the scope of this chapter; therefore, only the most important facts are mentioned. α-Ketoamides **14** first form biradicals **15**, which should exist, at least partially, in the singlet state.

In contrast to the examples presented thus far, the appearance of zwitterionic intermediate **18** was proven unambiguously. This intermediate may be formed either directly from the singlet biradical **15** or by recombination of Norrish type II products **16** and **17**. The zwitterion may then cyclize to β-lactams **19**. It seems that this ring closure is limited to radical stabilizing substituents (Ph) when performed in solution, whereas less stabilizing substituents preferentially afford oxazolidin-4-ones.[14a] Interestingly, the product ratio can be altered substantially in favor of β-lactams **19**, if amides **14** are irradiated as inclusion complexes with desoxycholic acid or cyclodextrin (Scheme 6, Table 57.2).[14b,c] Very recently, this ring closure approach was applied by Griesbeck and Heckroth[14d] to derivatives of amino acids. In this way, enantiomerically pure β-lactams were synthesized.

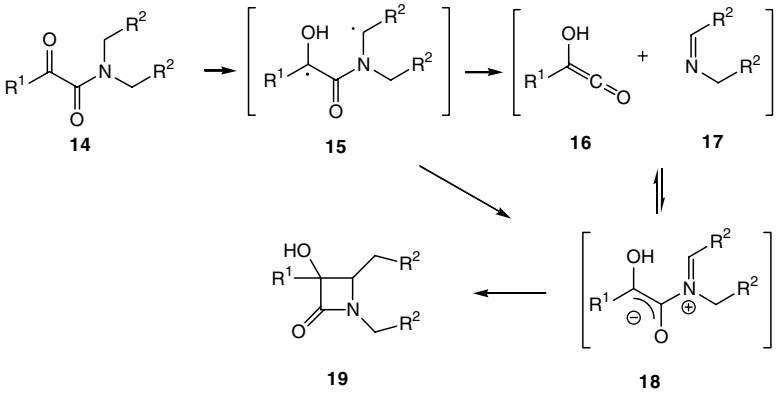

SCHEME 6

TABLE 57.2 β-Lactams by Photocyclization of α-Ketoamides **14**

R^1	R^2	Yield of 19 (%)
Me	CH_2Ph	94
Ph	CH_2Ph	100
Me	H	42[a]
Me	Me	74[a]
Me	$(CH_2)_3$	52[a]

[a] Inclusion complex with desoxycholic acid.

The photochemical preparation of oxetanes is the domain of the Paternò–Büchi reaction, but only a few examples have been published where these heterocycles were prepared in the course of a Norrish/Yang reaction. This is presumably due to the remarkable tendency of the corresponding 1,4-biradicals to undergo Norrish type II cleavage. Lewis and Turro[15] explored the photochemical behavior of α-alkoxyacetophenones as early as 1970 and found that oxetanes are generally formed as minor products only.

57.4 Five-Membered Rings

Cyclopentanes and Indanes

Usually, the regioselectivity of the Norrish/Yang reaction may be described by a simple rule. If sp^3–CH bonds are present in the γ-position with respect to the carbonyl group 1,4-biradicals are formed that undergo Norrish type II cleavage or cyclization to four-membered rings. This reaction path may be circumvented by decreasing the CH bond energy in the δ-position or by blocking the γ-position with quaternary carbon atoms or heteroatoms or by spin center shift. The first approach is not very convenient, because it rarely succeeds in suppressing the γ-hydrogen abstraction completely. On the other hand, blocking the γ-position has been used several times. In Scheme 7, three different types of molecular framework are depicted that fulfill this concept; thus, cyclopentane **21**[16] and indenes **23**[17] and **25**[18] were prepared from the corresponding *t*-butyl-substituted ketones **20** and **22** and phenacyl ketone **24**, respectively (Scheme 7).

The idea of spin center shift, which was successfully applied to the preparation of cyclopropanes (see Section 57.2) can be extended to five-membered rings. Accordingly, *o*-alkyl-substituted aryl ketones **26** bearing a leaving group in the α-position undergo γ-hydrogen abstraction, giving 1,4-biradicals **27**, which quantitatively eliminate HX, providing 1,5-biradicals **28**. After ISC, the 1,5-biradicals cyclize to indanones

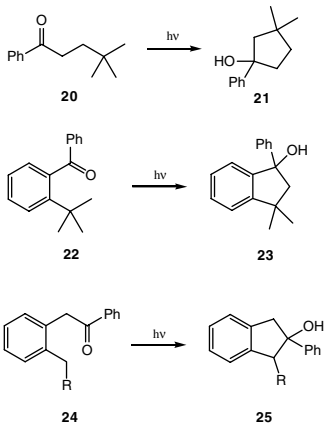

SCHEME 7

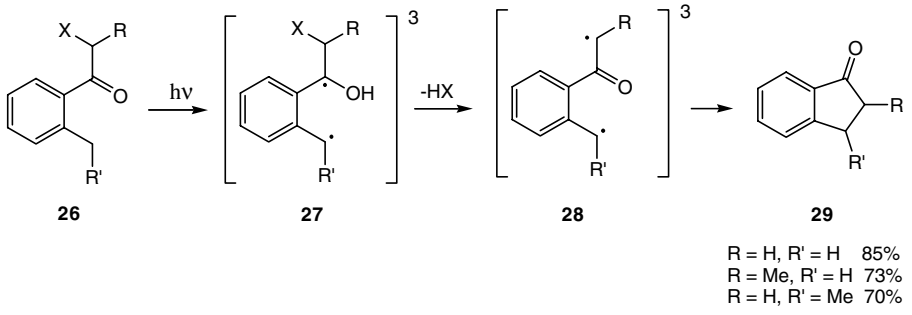

SCHEME 8

29 in good yields (Scheme 8).[19] This elimination process reaction was originally developed for photochemically removable protective groups[20] and has not been used in the preparation of such compounds. This is all the more surprising given that the indanone moiety is regularly found in natural products (e.g., in the cytotoxic pterosines).[21]

Pyrrolidines and Indoles

In 1981, Henning and co-workers[22a] developed a synthesis of pyrrolidines from β-aminopropiophenones. It should be noted that the introduction of an electron-withdrawing group at the nitrogen atom retarded the formation of cyclopropanes. In due course, Henning investigated thoroughly the influence of various substituents and developed a diastereoselective route to substituted prolines.[22b,c] Based on this work, enantiomerically pure prolines were prepared. Thus, *N*-substituted glycine amide **30** bearing a C_2-symmetric chiral auxiliary gave, on irradiation, proline amide **31** in high yields and in a fully diastereoselective manner.[23] Besides the chiral auxiliary controlled asymmetric synthesis, utilization of the chiral pool of natural products is widespread and was also applied to the photochemical synthesis of prolines. Starting from aspartic acid **32**, glycine esters **33** were prepared and cyclized stereoselectively to pyrrolidines **34**, which are recognizably L- and D-prolines (Scheme 9).[24] Remarkably, the three protective groups in **34b** are orthogonal to each other and could be removed independently, which makes this pyrrolidine derivative a very attractive building block for peptide synthesis.

The necessity of protecting the nitrogen atom by an electron-withdrawing group to avoid PET can also be carried out by the introduction of a carbonyl group in the β position, affording β-ketoamides **35**. On irradiation, they provided an access to γ-lactams **36** (Scheme 10, Table 57.3).[25]

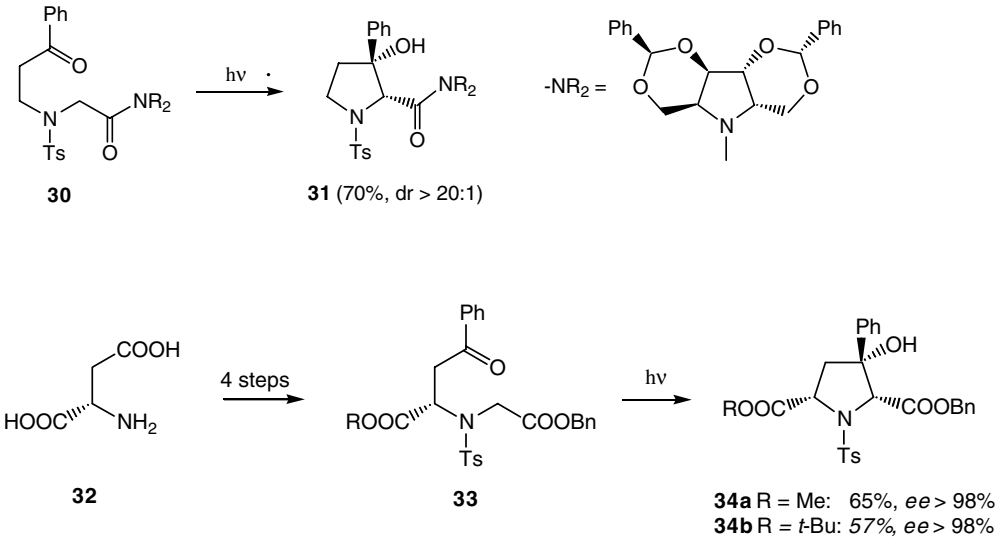

SCHEME 9

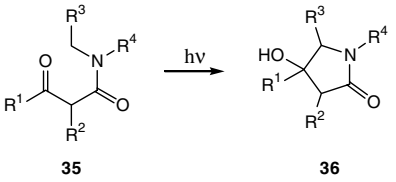

SCHEME 10

TABLE 57.3 Yields of γ-Lactams **36**

Entry	R^1	R^2	R^3	R^4	Yield (%)	Ref.
a	COOMe	H		$-(CH_2)_3-$	44	25a
b	Ph	H	Ph	CH_2Ph	83	25c
c	Ph	Et	Me	Et	66	25d
d	Ph	*i*Bu	Ph	CH_2Ph	86	25e

The reaction possesses considerable flexibility with respect to the substituents R^1 to R^4, as shown with the examples summarized in Table 57.3. Notably, δ-hydrogen transfer proceeds even in those cases where γ-hydrogen atoms are present (**35c,d**).

A special case exists if the two carbon atoms between the carbonyl group and the nitrogen atom are members of an aromatic ring. Due to the strong electron-donating character of the nitrogen atom, the lowest excited state of these compounds is π,π* in character; consequently, barely any Norrish/Yang reactivity is observed. But, the introduction of electron acceptor groups also introduces pitfalls. Taking into account that the nitrogen atom is part of the chromophore, it is not surprising that the photochemical behavior of compounds **37** (R^2 = Tosyl) is mainly characterized by a homolytic cleavage of the N-S bond. Such reactions were described previously for *N*-tosyl-β-amino-α,β-unsaturated ketones.[26] Only the trifluoromethanesulfonyl group (Tf) facilitates formation of 2,3-dihydro indoles **38**.[27] Another interesting approach to suppressing the electron-donating character of the nitrogen atom exists if this atom is a part of a quaternary ammonium salt, as in **39**, which cyclizes upon irradiation to give indoline **40** (Scheme 11).[28]

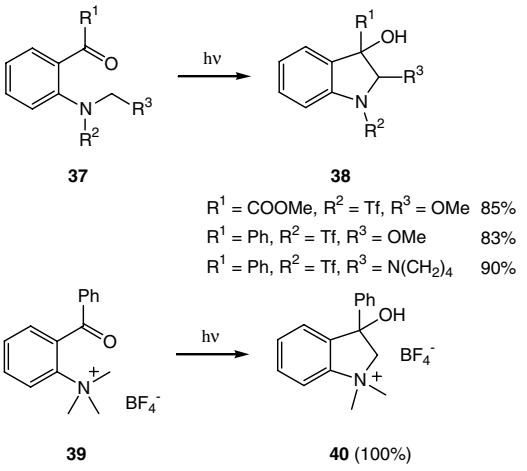

SCHEME 11

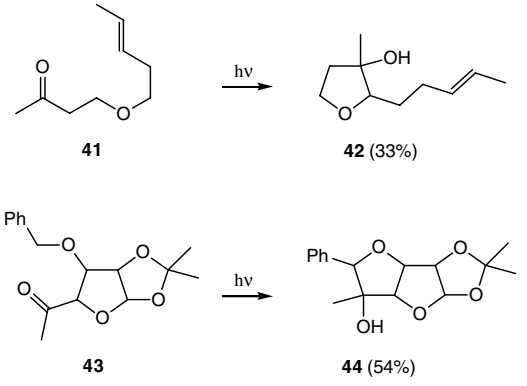

SCHEME 12

Furans and Benzofurans

Taking into consideration the widespread occurrence of molecules containing the tetrahydrofuran substructure, it is amazing that we have only a few examples of synthesis of these heterocycles by means of the Norrish/Yang reaction.[29] Interestingly, aliphatic ketones were used as exemplified by the photocyclization of ketones **41**[29b] and **43**[29c] (Scheme 12). Despite the moderate yields, these examples illustrate the huge potential of the Norrish/Yang reaction for natural product syntheses.

The replacement of the two sp^3 carbon atoms between the oxygen atom and the carbonyl group ring furnishes *o*-alkoxy-alkyl-aryl ketones **45**, the photochemical behavior of which have been intensively studied. The variability of substituents, both at the two side chains and at the aromatic core, tolerated by the photocyclization is remarkable. Furthermore, in many cases only one diastereomer of benzofurans **46** is obtained upon irradiation of **45** (Scheme 13, Table 57.4).[30]

57.5 Six-Membered Rings

Naphthalenes

Synthesis of six-membered rings by means of the Norrish/Yang reaction is rather rare;[31] nevertheless, with the appropriate choice of molecular framework these rings may be prepared in good yields. The

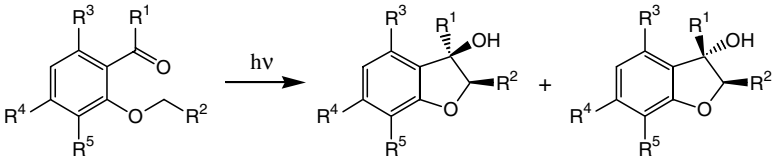

45 **46a** **46b**

SCHEME 13

TABLE 57.4 Yields of Benzofurans **46**

R^1	R^2	R^3	R^4	R^5	Yield (%)[a]	Ref.
Ph	H	H	H	CO-Ph	77	30a
Ph	Ph	H	H	CO-Ph	100	30a
Me	Ph	H	H	CO-Me	17	30a
Me	OMe	MOM[b]	OMe	H	47	30b
Me	OMe	MOM[b]	H	H	77	30b
Me	H	OMe	H	H	55	30b
$(CH_2)_2OH$	OMe	MOM[b]	H	H	30	30b
Ph	Ph	H	$O(C_{11}H_{25})$	H	67	30c
COOMe	$PhCH_2$	H	H	H	89	30d
H	COOEt	H	H	H	46	30e
Me	COOEt	H	H	H	86	30e

[a] Yield of **46a** + **46b**.
[b] MOM = $MeOCH_2$.

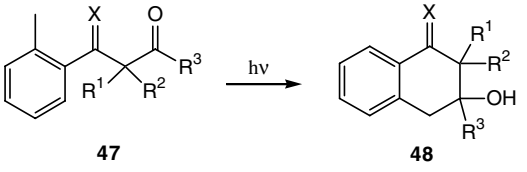

47 **48**

SCHEME 14

essential prerequisite is to block both the γ- and δ-position with respect to the excited carbonyl group. In addition, a restriction of the molecular flexibility is necessary in order to obtain six-membered rings.

Blocking of the γ- and δ-positions may be achieved either by an aromatic ring or an amide group (see Section 57.4). The former approach is taken by compounds **47**. The preparative applicability of compounds bearing two sp^3-carbon atoms between the carbonyl group and the aromatic ring (**47a**) is limited, because the quantum yield of product formation is very low (**Φ** = 0.0012 in MeOH for **47a**). The low reactivity is attributed to a rapid internal CT quenching as a result of an efficient interaction between the β-aryl and the carbonyl group in the excited state.[31c] The behavior of diketones **47b–d** is surprising because they bear two carbonyl groups, and one would expect, taking into account both enthalpic and entropic considerations, that we should observe a preference for the carbonyl group adjacent to the aromatic ring to react, affording benzocyclobutenes. Indeed, these products were isolated if irradiation is performed in hexane, whereas the utilization of methanol as solvent furnished benzocyclobutenes in trace amounts only. The unusual outcome of the reaction was explained either by a hydrogen shift from a primarily formed hydroxy benzyl radical to the aliphatic carbonyl group[31d] or by a radical attack of the *o*-benzyl radical onto the aliphatic carbonyl group forming an alkoxy radical[31e] (Scheme 14, Table 57.5).

TABLE 57.5 Yields of Naphthalenes **48**

Entry	R^1	R^2	R^3	X	Yield (%)	Ref.
a	H	Me	Ph	CH_2	60–90	31c
b	H	H	Me	O	35	31d
c	Me	Me	Prop	O	85	31e
d	Me	Me	Me	O	88	31e

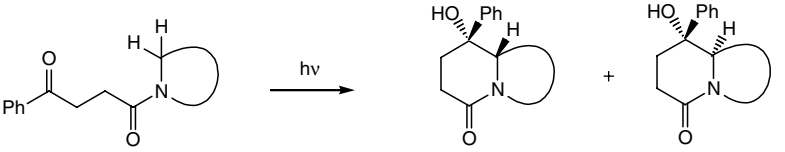

49 **50a** **50b**

SCHEME 15

δ-Lactams

The second approach (i.e., the introduction of an amide group) was successfully used for the synthesis of γ-lactams (see Section 57.4). An extension of the concept to γ-keto amides provides not only a method attractive from a synthetic point of view but also a molecular system that has potential for a better understanding of the Norrish/Yang reaction. Thus, γ-keto amides **49** cyclize on irradiation to δ-lactams **50** in good yields.[32] It should be noted that the reaction outcome strongly depends on the solvent used. The irradiation in dichloromethane gives δ-lactams **50**, while the only products formed in diethyl ether were pinacols.[33] Earlier work describing the formation of cyclopropanes from **49**[34] was shown to be in error.[33]

The δ-lactams have two newly formed stereogenic centers, thus two diastereomers may be formed. The ratio of these diastereomers depends on the ring size of the cyclic secondary amine in **49**, on the substituents, and on the solvent. It has been shown that small rings and substituents at the carbon atom adjacent to the nitrogen atom increase the diastereoselectivity in favor of **50a** (Scheme 15, Table 57.6); this preference could be substantiated by consideration of different triplet biradical conformers.[32]

β-Ketoamides such as **49** not only are versatile reactants for the synthesis of δ-lactams but also are valuable for studying the mechanism of the Norrish/Yang reaction. If β-ketoamides with two different residues at the nitrogen atom of the secondary amine are used, the question of regioselectivity arises. In this connection, the photochemical behavior of sarcosine derivative **51** is very instructive. In the ground state, **51** consists of the two rotamers **51-A** and **51-B** in ratios of 2:1 to 4:1, depending on the solvent. Bearing in mind the relatively high barrier for the rotation around the amide bond (18 to 20 kcal/mol[33]), one would expect the product ratio of **52**:**53** to reflect the ground-state ratio. Surprisingly, the irradiation of **51** in aprotic solvents provides only the product **52**; however, if **51** is irradiated in protic solvents, a product ratio of 2.8:1 for **52**:**53** is observed, which is very close to the rotamer ratio of the ground state. Obviously, the product ratio in aprotic solvents is dominated by an exclusive back hydrogen transfer of the biradical **BR**2. The frequently observed phenomenon that the regioselectivity of the Norrish/Yang reaction is decided by neither relative rates of hydrogen transfer nor ground-state conformational equilibria but solely by back hydrogen transfer was originally recognized by Sauers and Huang,[31a] and its importance must not be underestimated (Scheme 16).

The stereochemical situation is more complicated if a chirality center is already present in the reactant. In such cases, two features must be considered: the simple diastereoselectivity and the asymmetric induction. Commencing with aspartic acid, the enantiomerically pure benzoylalanine amides **54** were prepared in a fashion similar to that described for **33** (see Section 57.4) and irradiated to give the ornithine lactams **55** (Scheme 17);[35] similar results were later also recorded by Griesbeck, who employed differently substituted compounds.[36]

TABLE 57.6 Yields of δ-Lactams **50**

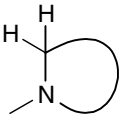	**50a** (%)	**50b** (%)	*de*(**50a**)
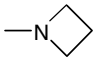	52	0	>99
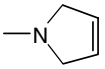	67	23	49
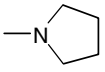	54	9	71
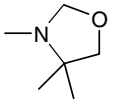	55	0	>99
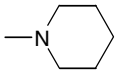	33	8	61
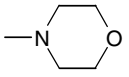	34	8	61
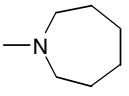	48	6	78

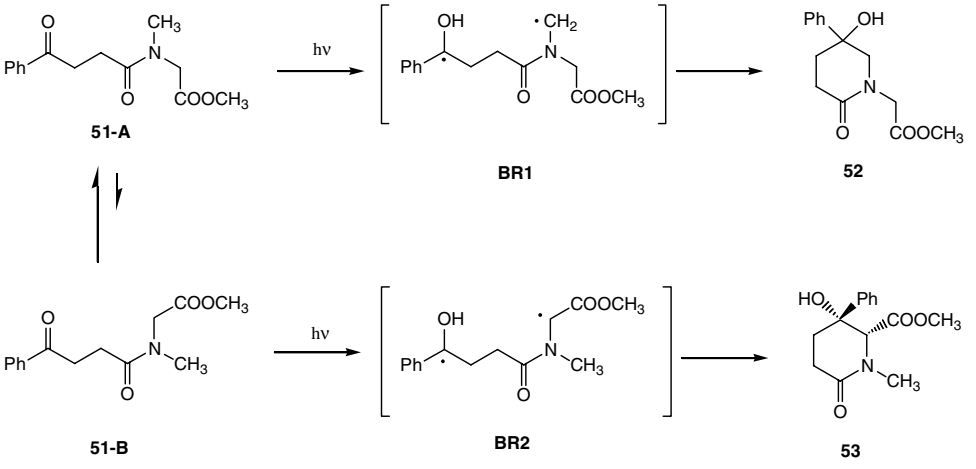

SCHEME 16

Despite the fact that the asymmetric induction from the chirality center C3 on C6 proceeds with high selectivity (>99%), the simple diastereoselectivity with respect to the C5–C6 bond is only moderate. For this reason, it is not very promising to complicate the system by the introduction of additional chiral centers. In view of that proposal, the photochemical behavior of dipeptides **57** is surprising. Prepared from *N*-protected benzoylalanines **56** by peptide coupling with proline esters, they cyclize photochemically in good yields to "bicyclic β-turn dipeptides" **58**, which are potential peptide mimetics. The high

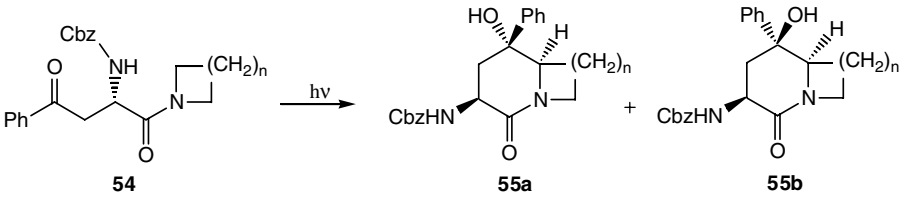

SCHEME 17

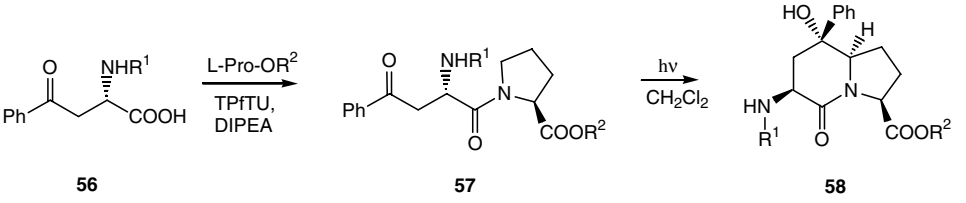

SCHEME 18

stereoselectivity can be explained by a synergistic effect of the two chiral centers at the triplet biradicals stage (Scheme 18; TPfTU, *O*-pentafluorphenyl-*N*,*N*,*N*,*N*-tetramethyluronium tetrafluoroborate).[37]

Oxazines

The idea of a spin center shift was already discussed twice in this chapter as a means of broadening the synthetic scope of the Norrish/Yang reaction. A third example applies to the preparation of six-membered rings. Thus, by treating of β-ketoamides **35** (Section 57.4) with hypervalent iodine(III) reagents, α-methanesulfonyloxy-β-ketoamides **59** are obtained in excellent yields. On irradiation, 1,5-biradicals **60** are formed, which are converted into biradicals **61** by elimination of methanesulfonic acid. In the methods described previously for preparation of cyclopropanes and indanones, the enolate radical moiety reacts as a carbon radical. Such reactivity is in agreement with the higher spin density at the carbon atom. Surprisingly, the enolate radical moiety of biradicals **61** reacts solely as oxygen radicals **61-A**, giving the oxazinones **62**. This result could be explained considering the relative energy of different biradical conformers (Scheme 19, Table 57.7).[38]

Chromenes

In 1985, Meador and Wagner[39] described the photocyclization of α-(*o*-benzyloxyphenyl)acetophenone **63**, which may formally be derived from ketones **45** by insertion of a methylene group between the keto group and the aromatic ring. The 3-hydroxychromene **64** was obtained in 80% yield as a 1.6/1 mixture of the two diastereomers (Scheme 20). It is instructive to draw attention to the fact that, despite the huge importance of oxygen-containing heterocycles in biological context, considerably fewer examples of syntheses of these ring systems by means of the Norrish/Yang reaction have been observed compared with those of nitrogen-containing heterocycles. As revealed in the preceding sections, the hydrogen abstraction from a definite position often demands the blocking of two positions in the chain between

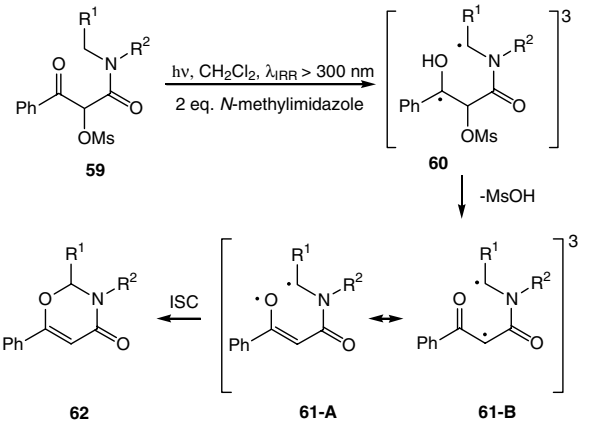

SCHEME 19

TABLE 57.7 Yields of Oxazinones **62**

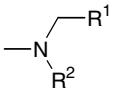	Yield (%)
-NMe_2	44
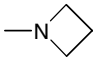	58
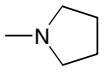	42
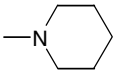	57
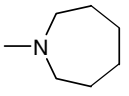	64
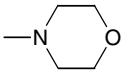	42

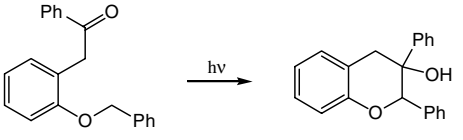

SCHEME 20

the excited carbonyl group and the position from which abstraction should take place. In many cases, this was accomplished by introduction of an amide bond. Surprisingly, secondary amides (R′ = H in **A**, Scheme 21) have not been used. The simple reason for this is that secondary amides exclusively adopt the *trans* conformation, thus the alkyl group (RCH_2 in **A**) is unreachable by the carbonyl oxygen. Tertiary amides consist of an equilibrium mixture of rotamers that can be converted into each other (see

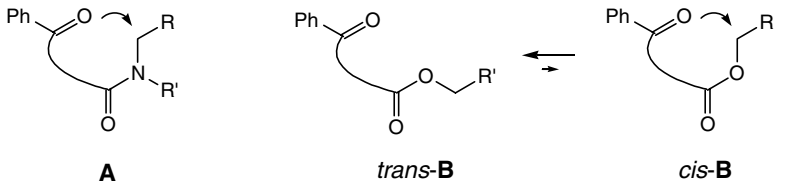

SCHEME 21

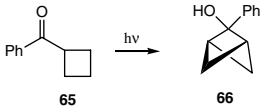

SCHEME 22

Scheme 16). Esters almost entirely adopt the *trans* conformation (*trans*-**B**); therefore, it is not surprising that no hydrogen abstraction can occur. The energy difference between *trans*-**B** and *cis*-**B** amounts to more than 8 kcal/mol; consequently, the *cis* conformer is not populated at room temperature.[40] It should be noted that, if the chain between the excited carbonyl group and the ester group is long enough, a hydrogen abstraction from the alkoxy group could be observed; however, macrocyclizations are not a topic for this chapter.

57.6 Bi- and Tricyclic Compounds

This last section deals with such applications of the Norrish/Yang reaction furnishing bi- and tricyclic compounds. It seems to be justifiable to dedicate a separate section to this topic because often the regioselectivity rules may be circumvented if the conformational flexibility of the molecules is reduced. In fact, a rigid molecular framework is an alternative to the hitherto presented concept of blocking positions with heteroatoms or quaternary carbon atoms. Naturally, it is not possible to structure the reactions according to ring size and type of ring; furthermore, vastly different examples are known. In this section, then, only some representative examples are discussed, and the selection does not claim to be complete.

Presumably, the most popular example of a transannular hydrogen abstraction giving a bicyclic molecule is Padwa's bicyclo[1.1.1]pentane synthesis, published in 1967.[41] By virtue of the considerable ring strain of bicyclo[1.1.1]pentanes, the formation of **66** from **65** demonstrates impressively the synthetic scope of the Norrish/Yang reaction (Scheme 22).

Two other examples for the synthesis of bicyclic compounds whose skeleta bear only carbon atoms are shown in Schemes 23 and 24, each of which is instructive in its own way. Upon irradiation of cyclohexane derivative **67**, one tends to expect a hydrogen abstraction from the allylic position, but bicyclo[3.3.1]heptane **69** was obtained by cyclization of the less stable biradical **68-A**.[42] The reason for this unusual reaction course is the exclusive back hydrogen transfer of the more stable biradical **68-B** (Scheme 23).

Bicyclo[2.2.1]heptane **73** is not directly formed in the course of a Norrish/Yang reaction, but the primarily formed 1,4-biradical is trapped intramolecularly by a vinyl group in a kind of 1,5-*exo*-cyclization of a hexenyl radical, well known from monoradical chemistry.[43] Compared with the concept of acid elimination from hydroxy radicals bearing a leaving group at the adjacent carbon atom (see preceding sections), the cyclization of **71** to **72** can also be regarded as a spin center shift. Unfortunately, cyclization of alkenyl radicals in most cases proceeds too slowly[44] to compete with the "normal" reactions of the Norrish/Yang biradicals, thus this concept seems not to be commonly applicable (Scheme 24; byproducts not shown).

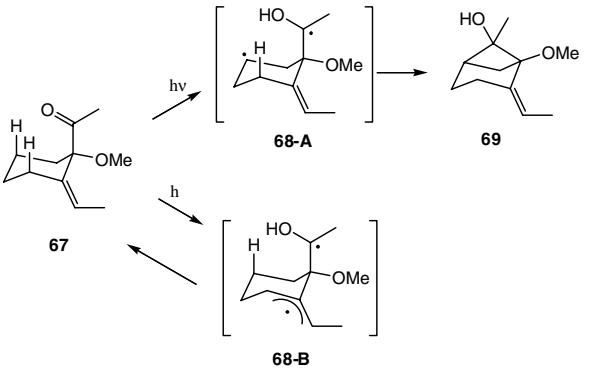

SCHEME 23

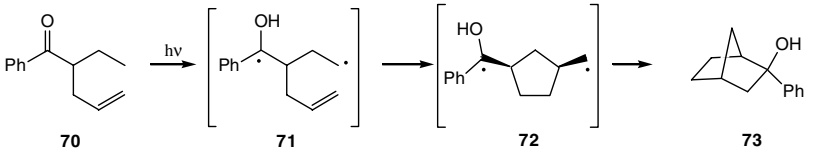

SCHEME 24

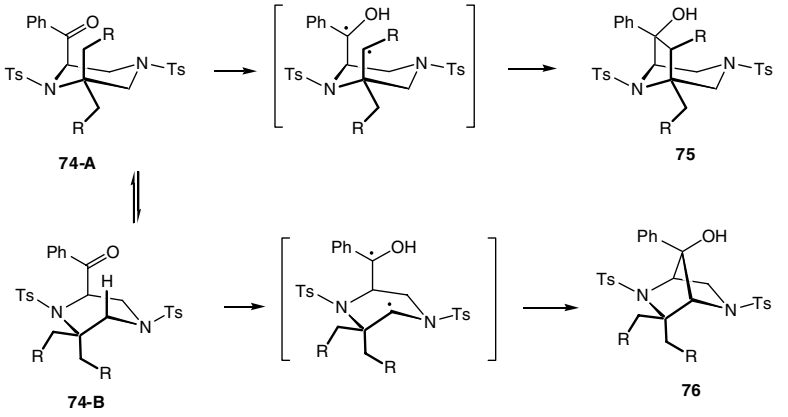

SCHEME 25

Different CH bond energies as well as different ring conformers of the reactant may be responsible for the photochemical reaction course of 1,4-ditosylpiperazines **74**. From the chair-like conformer **74-A**, the 3,8-diazabicyclo[3.2.1]octanes **75** are formed by a hydrogen abstraction from one of the alkyl groups affixed to the 6-position of the piperazine ring in yields between 3 and 6%, whereas 2,5-diazabicyclo[2.2.1]heptanes **76** are formed from conformer **74-B** in yields between 15 and 29% (Scheme 25).[45]

Undoubtedly, the regioselective attack at non-activated CH bonds by an excited carbonyl group is one of the most remarkable features of the Norrish/Yang reaction. This will be demonstrated with the transannular cyclization of bicyclic diketones **78**, which can be easily prepared from cyclic ketones **77**, according to Stetter et al.[46] The α,α′ fusion to **78** proceeds fully diastereoselectively and furnishes, fortunately, the diastereomer that fulfills the structural requirements for the subsequent photochemical step. Upon irradiation, the selectively excited benzoyl group abstracts a hydrogen atom from the formal

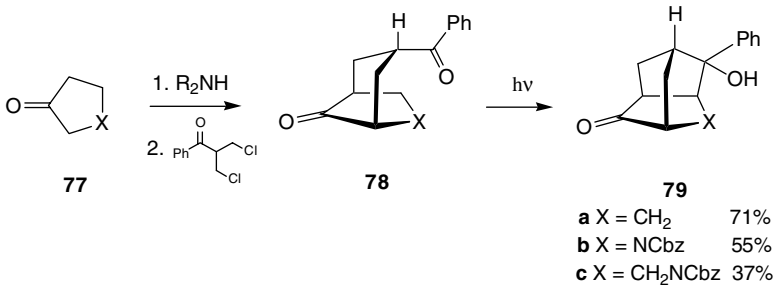

SCHEME 26

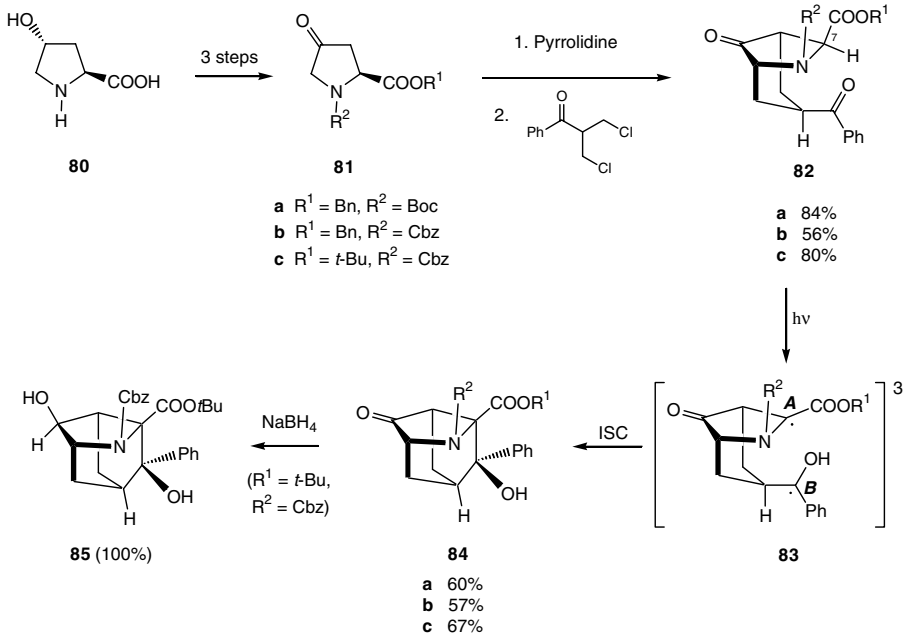

SCHEME 27

δ-position, because the γ-position is unreachable due to the rigid molecular framework. Whereas noradamantane **79a** was obtained as a mixture of diastereomers, heterocyclic compounds **79b** and **79c** were, despite lower yields, formed fully diastereoselectively with respect to the newly formed C–C bond. This result was substantiated by the directing effect of intramolecular hydrogen bonds at the triplet biradical stage (Scheme 26).[47]

The strategy outlined in Scheme 26 was extended to enantiomerically pure tricyclic α-amino acids. The synthesis commences with the natural amino acid *trans*-4-hydroxyproline **80**, which was converted in a straightforward manner in three steps into the 4-oxo-prolines **81**. Application of Stetter's α,α′ fusion afforded bicyclic diketones **82**. Interestingly, in the photochemical key step, the chirality center at C7 is destroyed by the hydrogen abstraction. But, naturally, the radical center **A** can only be attacked by radical center **B** from the underside of the pyrrolidine ring; therefore, no racemization can take place. In the final step, the keto group is stereoselectively reduced, affording the highly functionalized compound **85**. It should be noted that in the course of the discussed reaction sequence, five new chiral centers were selectively set up originating from one chiral center in **81** (Scheme 27).[48] Tricyclic compound **85** may be

regarded as a "chimerical" amino acid because it bears the substructures of a whole lot of natural and unnatural amino acids. Its preparation impressively reveals the synthetic scope of the Norrish/Yang reaction in the construction of complex molecules.

References

1. Norrish, R. G. W. and Appleyard, M. E. S., Primary photochemical reactions. IV. Decomposition of methyl ethyl ketone and methyl butyl ketone, *J. Chem. Soc.*, 874, 1934.
2. Yang, N. C. and Yang, D.-D. H., Photochemical reactions of ketones in solution, *J. Am. Chem. Soc.*, 80, 2913, 1958.
3. (a) Wagner, P. J., Type II photoelimination and photocyclization of ketones, *Acc. Chem. Res.*, 4, 168, 1971; (b) Wagner, P. J., Chemistry of excited triplet organic carbonyl compounds, *Topics Curr. Chem.*, 66, 1, 1976; (c) Wagner, P. J., 1,5-Biradicals and five-membered rings generated by δ-hydrogen abstraction in photoexcited ketones, *Acc. Chem. Res.*, 22, 83, 1989; (d) Wagner, P. J. and Park, B.-S., Photoinduced hydrogen atom abstraction by carbonyl compounds, in *Organic Photochemistry*, Padwa, A., Ed., Marcel Dekker, New York, 1991, 227; (e) Wagner, P. J., Norrish type II photoelimination of ketones: Cleavage of 1,4-biradicals formed by γ-hydrogen abstraction, in *CRC Handbook of Organic Photochemistry and Photobiology*, Horspool, W. M. and Song, P.-S., Eds., CRC Press, Boca Raton, FL, 1995, 449.
4. (a) Ariel, S., Ramamurthy, V., Scheffer, J. R., and Trotter, J., Norrish type II reaction in the solid state: involvement of a boatlike reactant conformation, *J. Am. Chem. Soc.*, 105, 6959, 1983; (b) Scheffer, J. R., Garcia-Garibay, M., and Nalamasu, O., Influence of the molecular crystalline environment on organic photorearrangements, *Org. Photochem.*, 8, 249, 1987.
5. (a) Roth, H. J., ElRaie, M. H., and Schrauth, T., Photocyclization of 3-amino ketones to 2-amino-1-cyclopropanols and their isomerization, *Arch. Pharm.*, 307, 584, 1974; (b) Abdul-Baki, A., Rotter, F., Schrauth, T., and Roth, H. J., Experiments on the photochemical synthesis of ephedrine-type compounds. III. Photocyclization of 3-(alkylamino) propiophenones to 2-(alkylamino)cyclopropan-1-ols and their isomerization, *Arch. Pharm.* 311, 341, 1978; (c) Roth, H. J. and George, H., Photoreactions of anilino-benzyl-alkyl-aryl ketones. II. Photochemical reactions of anilino-benzyl ketones, *Arch. Pharm.*, 303, 725, 1970; (d) Weigel, W., Schiller, S., and Henning, H.-G., Stereoselective photocyclization to 2-aminocyclopropanols by photolysis of β-aminoketones and oxidative ring opening to enaminones, *Tetrahedron*, 53, 7855, 1997.
6. (a) Zimmerman, H., Nuss, J., and Tantillo, A., Photochemistry. 152. Cyclopropanols and the di-π-methane rearrangement: mechanistic and exploratory organic photochemistry, *J. Org. Chem.*, 53, 3792, 1988; (b) Yoshioka, M., Miyazoe, S., and Hasegawa, T., Photochemical reaction of 3-hydroxy-1-(o-methylaryl)alkan-1-ones: formation of cyclopropane-1,2-diols and benzocyclobutenols through β- and γ-hydrogen abstractions, *J. Chem. Soc., Perkin Trans. 1*, 22, 2781, 1993.
7. Wessig, P. and Mühling, O., A new photochemical route to cyclopropanes, *Angew. Chem. Int. Ed. Engl.*, 40, 1064, 2001.
8. Newcomb, M., Choi, S. Y., and Horner, J. H., Adjusting the top end of the alkyl radical rinetic scale: laser flash photolysis calibrations of fast radical clocks and rate constants for reactions of benzeneselenol, *J. Org. Chem.*, 64, 1225, 1999.
9. Wessig, P. and Mühling, O., unpublished results.
10. (a) Horspool, W. M., Photolysis of carbonyl compounds, *Photochemistry*, 32, 49, 2001; (b) Horspool, W. M., Photolysis of carbonyl compounds, *Photochemistry*, 29, 71, 1998; (c) Horspool, W. M., Photolysis of carbonyl compounds, *Photochemistry*, 27, 63, 1996; (d) Horspool, W. M., Photolysis of carbonyl compounds, *Photochemistry*, 25, 67, 1994.
11. Lindemann, U., Wulff-Molder, D., and Wessig, P., Diastereoselective synthesis of 3-hydroxy-3-phenyl cyclobutanoic derivatives by photocyclization, *J. Photochem. Photobiol. A: Chem.*, 73, 119, 1998.
12. Wessig, P. and Schwarz, J., Enantioselective preparation of (2*R*)- and (2*S*)-azetidin-2-carboxylic acids, *Helv. Chim. Acta*, 81, 1803, 1998.

13. Sheehan, J. C., *The Enchanted Ring: The Untold Story of Penicillin*, MIT Press, Cambridge, MA, 1982.
14. (a) Aoyama, H., Sakamoto, M., Kuwabara, K., Yoshida, K., and Omote, Y., Photochemical reactions of α-oxo amides. Norrish type II reactions via zwitterionic intermediates, *J. Am. Chem. Soc.*, 105, 1958, 1983; (b) Aoyama, H., Miyazaki, K., Sakamoto, M., and Omote, Y., Photochemical reaction of inclusion molecular complexes of *N*,*N*-dialkylpyruvamides with desoxycholic acid: host-controlled reaction of guest compounds in the solid state, *J. Chem. Soc. Chem. Commun.*, 333, 1983; (c) Aoyama, H., Miyazaki, K., Sakamoto, M., and Omote, Y., Solid state photoreaction of *N*,*N*-dialkylpyruvamides: inclusion complexes with deoxycholic acid or cyclodextrin, *Tetrahedron* 43, 1513, 1987; (d) Griesbeck, A. G. and Heckroth, H., Reversible diastereoselective photocyclization of phenylglyoxylamides of ω-amino acid methyl esters to 3-hydroxy β-lactams, *Synlett*, 131, 2002.
15. Lewis, F. D. and Turro, N. J., Molecular photochemistry. XVIII. Type II photoelimination and 3-oxetanol formation from α-alkoxyacetophenones and related compounds, *J. Am. Chem. Soc.*, 92, 311, 1970.
16. Wagner, P. J., Kelso, P. A., Kemppainen, A. E., and Zepp, R. G., Type II photoprocesses of phenyl ketones: competitive δ-hydrogen abstraction and the geometry of intramolecular hydrogen atom transfers, *J. Am. Chem. Soc.*, 94, 7500, 1972.
17. (a) Wagner, P. J., Meador, M. A., Giri, B. P., and Scaiano, J. C., Photoreactivities of *o*-alkoxy- and *o-tert*-butylphenyl ketones: a dramatic example of conformational inversion of selectivity, *J. Am. Chem. Soc.*, 107, 1087, 1985. (b) Wagner, P. J., Giri, B. P., Scaiano, J. C., Ward, D. L., Gabe, E., and Lee, F. L., Photocyclization of *o-tert*-butylbenzophenone, *J. Am. Chem. Soc.*, 107, 5483, 1985.
18. Zand, A., Park, B.-S., and Wagner, P.J., Conformational control of product ratios from triplet 1,5-biradicals, *J. Org. Chem.*, 62, 2326, 1997.
19. Wessig, P. and Müller, G., unpublished results.
20. (a) Bergmark, W. R., Barnes, C., Clark, J., Paparian, S., and Marynowski, S., Photoenolization with α-chloro substituents, *J. Org. Chem.*, 50, 5612, 1985; (b) Klán, P., Zabadal, M., and Heger, D., 2,5-Dimethylphenacyl as a new photoreleasable protecting group for carboxylic acids, *Org. Lett.*, 2, 1569, 2000.
21. (a) Yoshihira, K., Fukuoka, M., Kuroyanagi, M., and Natori, S., Further characterization of 1-indanone derivatives from bracken, *Pteridium aquilinum* var. *latiusculum*, *Chem. Pharm. Bull.*, 20, 426, 1972; (b) Fukuoka, M., Kuroyanagi, M., Toyama, M., Yoshihira, K., and Natori, S., Pterosins J, K, and L and six acylated pterosins from bracken, *Pteridium aquilinum* var. *latiusculum*, *Chem. Pharm. Bull.*, 20, 2282, 1972.
22. (a) Henning, H.-G., Dietzsch, T., and Fuhrmann, J., Photochemistry of amino ketones. IV. Synthesis of 3-aryl-3-pyrrolidinols via photocyclization of β-aminopropiophenones, *J. Prakt. Chem.*, 323, 435, 1981; (b) Haber, H., Buchholz, H., Sukale, R., and Henning, H.-G., Photochemistry of aminoketones. VIII. Diastereoselective synthesis of 3-hydroxyprolines, *J. Prakt. Chem.*, 327, 51, 1985; (c) Walther, K., Kranz, U., and Henning, H.-G., Photochemistry of amino ketones. X. Preparation and diastereoselective photocyclization of *N*-(β-benzoylethyl)-*N*-tosylglycinamides, *J. Prakt. Chem.*, 329, 859, 1987.
23. Wessig, P., Wettstein, P., Giese, B., Neuburger, M., and Zehnder, M., Asymmetric synthesis of 3-hydroxyprolines by photocyclization of *N*-(2-benzoylethyl)-glycinamides, *Helv. Chim. Acta*, 77, 829, 1994.
24. Steiner, A., Wessig, P., and Polborn, K., Asymmetric synthesis of 3-hydroxyprolines by photocyclization of C(1′)-substituted *N*-(2-benzoylethyl)glycine esters, *Helv. Chim. Acta*, 79, 1843, 1996.
25. (a) Gramain, J. C., Remuson, R., Vallee-Goyet, D., Guilhem, J., and Lavaud, C., Total synthesis and determination of structure of the pyrrolizidine alkaloid curassanecine, *J. Nat. Prod.*, 54, 1062, 1991; (b) Gramain, J. C., Remuson, R., and Vallee, D., Intramolecular photoreduction of α-keto esters: total synthesis of (±)-isoretronecanol, *J. Org. Chem.*, 50, 710, 1985; (c) Hasegawa, T., Moribe, J., and Yoshioka, M., The photocyclization of *N*,*N*-dialkyl-β-oxo amides adsorbed on silica gel, *Bull. Chem. Soc. Jpn.*, 61, 1437, 1988; (d) Hasegawa, T., Arata, Y., Mizuno, K., Masuda, K., and Yoshihara, N., Photochemical reaction of α-alkyl-β-oxo amides: competitive γ- and δ-hydrogen abstraction

by excited ketone carbonyl groups, *J. Chem. Soc., Perkin Trans. 1*, 541, 1986; (e) Hasegawa, T., Arata, Y., and Mizuno, K., γ- vs. δ-Hydrogen abstraction in the photochemistry of α-alkyl-β-oxoamides, *J. Chem. Soc., Chem. Commun.*, 395, 1983.

26. (a) Henning, H.-G., Amin, M., and Wessig, P., Photochemische Acylgruppenwanderung in *N*-Tosyl-β-aminovinyl-phenylketonen, *J. Prakt. Chem.*, 42, 335, 1993; (b) Wessig, P., Amin, M., Henning, H.-G., Schulz, B., and Reck, G., Über den Einfluss der *N*-Substituenten auf das Photoverhalten von Enaminoketonen, *J. Prakt. Chem.*, 336, 169, 1994.
27. Seiler, M., Schumacher, A., Lindemann, U., Barbosa, F., and Giese, B., Diastereoselective photocyclization to dihydroindolinols, *Synlett*, 1588, 1999.
28. Wagner, P. J. and Cao, Q., Photocyclization of benzoyl-*N*-alkylanilinium ions, *Tetrahedron Lett.*, 32, 3915, 1991.
29. (a) Roy, S. C. and Adhikari, S., Stereoselective total synthesis of (±)-paulownin and (±)-isogmelinol through a radical annulation route, *Tetrahedron*, 49, 8415, 1993; (b) Carless, H. A. J., Swan, D. I., and Haywood, D. J., Stereoselective synthesis of tetrahydrofuran-3-ols by photochemical δ-hydrogen abstraction of β-allyloxy-carbonyl compounds, *Tetrahedron*, 49, 1665, 1993; (c) Araki, Y., Arai, Y., Endo, T., and Ishido, Y., Stereoselective photochemical cyclization of 3-*O*-benzyl-6-deoxy-1,2-*O*-isopropylidene-α-D-xylo-hexofuranos-5-ulose derivatives, *Chem. Lett.*, 1, 1989; (d) Cottier, L. and Descotes, G., Stereoselective synthesis of kinetic and thermodynamic isomers of alkoxy spiroketals and trioxa-*bis*-spiroketals, *Tetrahedron*, 41, 409, 1985; (e) Cottier, L., Descotes, G., Grenier, M. F., and Metras, F., Photochemical synthesis and structural study of alkoxyspiroacetals and trioxabis-spiroacetals, *Tetrahedron*, 37, 2515, 1981.
30. (a) Wagner, P. J., Meador, M. A., and Park, B.-S., The photocyclization of o-alkoxy phenyl ketones, *J. Am. Chem. Soc.* 112, 5199, 1990; Kraus, G.A., Thomas, P.J. and Schwinden, M.D., An approach to aflatoxins using type II photocyclization reactions, *Tetrahedron Lett.* 31, 1819, 1990; (b) Lappin, G.R. and Zanucci, J. S., Photolysis of 2-(benzyloxy)-4-(dodecyloxy)benzophenone and 2-isopropoxy-4-methoxybenzophenone, *J. Org. Chem.* 36, 1808, 1971; (c) Pappas, S.P. and Zehr, R.D. Jr., Heavy-atom effects on the stereochemistry of photoabstraction-cyclization in a carbonyl system, *J. Am. Chem. Soc.* 93, 7112, 1971; (d) Horaguchi, T., Tsukada, C., Hasegawa, E., Shimizu, T., Suzuki, T. and Tanemura, K., Photocyclization reactions. Part 2. Synthesis of dihydrobenzofuranols using photocyclization of ethyl 2-formylphenoxyacetates and ethyl 2-acetylphenoxyacetates, *J. Heterocyclic Chem.,* 28, 1273, 1991.
31. (a) Sauers, R. R. and Huang, S.-Y., Analysis of Norrish type II reactions by molecular mechanics methodology: cyclodecanone, *Tetrahedron Lett.*, 31, 5709, 1990; (b) Azzouzi, A., Dufour, M., Gramain, J.-C., and Remuson, R., Photocyclization of keto lactams: a new synthesis of functionalized 1-azabicyclo(x.y.0)alkanes, *Heterocycles*, 27, 133, 1988; (c) Zhou, B. and Wagner, P. J., Long-range triplet hydrogen abstraction: photochemical formation of 2-tetralols from β-arylpropiophenones, *J. Am. Chem. Soc.*, 111, 6796, 1989; (d) Hornback, J. M., Poundstone, M. L., Vadlamani, B., Graham, S. M., Gabay, J., and Patton, S. T., Photochemical cyclization of o-methylphenyl 1,3-diketones, *J. Org. Chem.*, 53, 5597, 1988; (e) Yoshioka, M., Nishizawa, K., Arai, M., and Hasegawa, T., Photochemical reaction of 1-(*o*-methylphenyl)-2,2-dimethyl 1,3-diketones, *J. Chem. Soc.*, *Perkin Trans. 1*, 541, 1991.
32. Lindemann, U., Reck, G., Wulff-Molder, D., and Wessig, P., Photocyclization of 4-oxo-4-phenylbutanoyl amines to δ-lactams, *Tetrahedron*, 54, 2529, 1998.
33. Lindemann, U., Neuburger, M., Neuburger-Zehnder, M., Wulff-Molder, D., and Wessig, P., Photoinduced diastereoselective pinacolization of 4-oxo-4-phenyl-butanoic amines to 4,5-dihydroxy-4,5-diphenyl-octanediamides, *J. Chem. Soc.*, *Perkin Trans. 2*, 2029, 1999.
34. Henning, H.-G., Berlinghoff, R., Mahlow, A., Köppel, H., and Schleinitz, K.-D., *N*,*N*-dialkylamides of 2-hydroxy-2-phenylcyclopropane-1-carboxylic acid: photochemical synthesis and determination of the structure, *J. Prakt. Chem.*, 323, 914, 1981.
35. Lindemann, U., Wulff-Molder, D., and Wessig, P., Synthesis of ornithine lactams via stereoselective photocyclization of 2-amino-4-oxo-4-phenyl-butanoyl amines, *Tetrahedron Asymm.*, 9, 4459, 1998.

36. Griesbeck, A. G., Heckroth, H., and Schmickler, H., Regio- and stereoselective 1,6-photocyclization of aspartic acid-derived chiral γ-ketoamides, *Tetrahedron Lett.*, 40, 3137, 1999.
37. Wessig, P., An efficient synthesis of bicyclic b-turn dipeptides via a photochemical key step, *Tetrahedron Lett.*, 40, 5987, 1999.
38. Wessig, P., Schwarz, J., Lindemann, U., and Holthausen, M. C., Photochemical synthesis of 3,4-dihydro-2H-1,3-oxazin-4-ones, *Synthesis*, 1258, 2001.
39. Meador, M. A. and Wagner, P. J., Photocyclization of α-(*o*-benzyloxyphenyl)acetophenone: triplet state ε-hydrogen abstraction, *J. Org. Chem.*, 50, 419–420, 1985.
40. Wiberg, K. B. and Laidig, K. E., Barriers to rotation adjacent to double bonds. 3. The carbon–oxygen barrier in formic acid, methyl formate, acetic acid, and methyl acetate. The origin of ester and amide resonance, *J. Am. Chem. Soc.*, 109, 5935, 1987.
41. Padwa, A. and Alexander, E., Photochemical formation of a substituted bicyclo[1.1.1]pentane, *Izv. Akad. Nauk SSSR, Ser. Khim.*, 89, 6376–6377, 1967.
42. Blondeel, G., De Bruyn, A., and De Keukeleire, D., Unusual course of a type II photoreaction, *Tetrahedron Lett.*, 25, 2055, 1984.
43. Wagner, P. J., Liu, K., and Noguchi, Y., Monoradical rearrangements of the 1,4-biradicals involved in Norrish type II photoreactions, *J. Am. Chem. Soc.*, 103, 3837, 1981.
44. Newcomb, M., Renaud, P., and Sibi, M. P., Eds., *Radicals in Organic Synthesis*, Vol. 1, Wiley-VCH, Weinheim, 2001, 329.
45. Wessig, P., Legart, F., Hoffmann, B., and Henning, H.-G., Synthese und transannulare Photocyclisierung von 2-Benzoyl-1,4-*bis*(tosyl)piperazinen, *Liebigs Ann. Chem.*, 979, 1991.
46. Stetter, H., Rämsch, K.-D., and Elfert, K., Compounds with urotropine structure. LIV. 2,2-*Bis*(chloromethyl)acetophenone as a new α,α′-fusion reagent, *Liebigs Ann. Chem.*, 1322, 1974.
47. Wessig, P., Schwarz, J., Wulff-Molder, D., and Reck, G., Photochemical preparation of tricyclic hydroxyketones by transannular cyclization of bridged 4-benzoylcyclohexanones, *Monatshefte Chem.*, 128, 849, 1997.
48. Wessig, P., Stereoselective synthesis of novel chimerical amino acids via a photochemical key step, *Synlett*, 1465, 1999.

58

Yang Photocyclization: Coupling of Biradicals Formed by Intramolecular Hydrogen Abstraction of Ketones

Peter J. Wagner
Michigan State University

0-8493-1348-1/04/$0.00+$1.50

58.1 The Yang Photocyclization Reaction

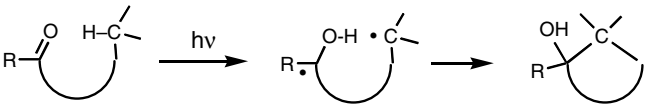

58.2 Mechanism

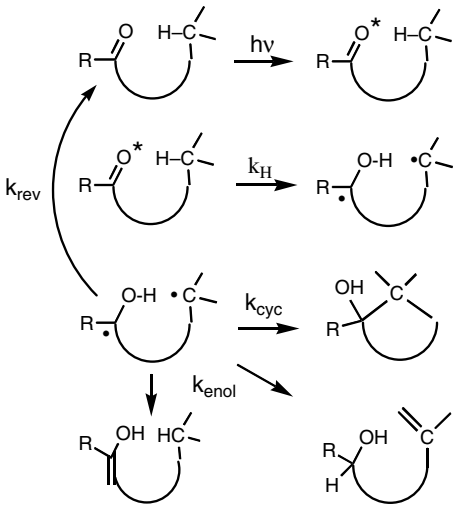

58.3 Byproducts

enol of reactant
reduction of carbonyl to alcohol, oxidation of CC bond to double bond

58.4 History

A wide variety of carbonyl compounds undergo photoinduced intramolecular hydrogen atom abstraction to form 1-hydroxy-1,*x*-biradicals, which then undergo two common competing reactions: (1) coupling to produce cyclic alcohols and (2) disproportionation back to ketone or to various enols. The overall process closely parallels the well-known bimolecular photoreduction of ketones, the most common products of which are formed by radical coupling. These intramolecular hydrogen abstraction processes have been widely studied, and several reviews are available.[1–6]

The first and still best known example of such intramolecular hydrogen abstraction is the type II photoelimination discovered by Norrish,[7] who found that ketones with γ–CH bonds cleave to methyl ketones and alkenes. Later, the Yangs found that cyclobutanols accompany cleavage and suggested that both processes arise from a common 1,4-biradical intermediate formed by γ-hydrogen abstraction of the excited ketone,[8] although at the time type II cleavage was generally considered to be a concerted reaction. At about the same time, Barnard and Yang[9] reported that irradiation transforms cyclodecanone to bicyclo[4.4.0]decan-1-ol, the cyclization product of a 1,6-biradical formed by ε-hydrogen abstraction. As realization of this intramolecular hydrogen abstraction process grew, other workers, for both synthetic and mechanistic purposes, investigated a variety of carbonyl compounds that form different kinds of biradicals and cyclic alcohols, with δ-hydrogen abstraction drawing the most attention. In the meantime,

it had become clear that Norrish type II cleavage proceeds via the intermediacy of 1,4-biradicals, as Yang had suggested, and that their cleavage and cyclization are linked mechanistically (see Chapter 52).[10] Consequently, it became common to also refer to the more general cyclization reaction as Norrish, although Norrish himself studied only the cleavage reactions. Because only 1,4-biradicals can cleave to give Norrish type II products, it seems most proper to name cyclic alcohol formation initiated by any mode of intramolecular hydrogen abstraction after its actual discoverers, as Breslow did in 1969.[11]

58.5 Quantum Efficiency

As the above description indicates, the mechanism for Yang photocyclization reactions involves at least two consecutive intermediates: first an excited state and then a biradical. (As with most excited carbonyl reactions, both singlet and triplet states can react.) The quantum efficiency for cyclization, as described by Eq. (8.1), depends on how many competitive reactions *each* intermediate undergoes:

$$\Phi\mathrm{II} = \alpha^1 k_\mathrm{H}\tau_\mathrm{S} + P_\mathrm{cyc}\Phi_\mathrm{ISC}{}^3 k_\mathrm{H}\tau_\mathrm{T} \tag{58.1}$$

where α is the percentage of singlet reaction that forms biradical; k_H is the rate constant for hydrogen abstraction; τ is the excited state lifetime; P_cyc is the percentage of triplet biradical that cyclizes; and Φ_ISC is the percentage of excited singlet that crosses to triplet state. Consequently, it is necessary to understand how structure and environment affect the behavior of each species separately.

It cannot be overemphasized that the quantum yields for two-step reactions such as those initiated by hydrogen abstraction often reflect partitioning of the intermediate biradicals more than relative rate constants for triplet reaction. This is especially true for the very rapid intramolecular hydrogen abstractions of n,π^* triplets. This fact was first demonstrated by the behavior of 2-hexanone, for which γ-deuteration *increases* the quantum yield of type II cleavage,[12] and of γ-substituted butyrophenones, for which quantum yields for type II cleavage decrease as rate constants for γ-hydrogen abstraction increase.[13]

58.6 Excited-State Reactivity

Most of the characteristics that allow excited carbonyl compounds to abstract hydrogen atoms have been determined by studies of bimolecular photoreductions and Norrish type II elimination reactions (see Chapter 52). The following sections provide abbreviated descriptions of various aspects that are more fully covered in Chapter 52.

Nature of Excited State

The lowest excited states of most ketones are n,π^* in nature; the C=O double bond is effectively broken into a 1,2-biradical, thus conferring on the electron-deficient oxygen atom radical reactivity that closely parallels that of alkoxy radicals.[1,14] Both singlet and triplet n,π^* states thus are highly reactive in abstracting hydrogen atoms.

Singlet vs. Triplet

Aliphatic ketones have n,π^* lowest singlets that undergo intersystem crossing (ISC) to their n,π^* lowest triplets slowly enough that both singlet and triplet reaction products can be formed. The singlet reactions generally occur in low quantum efficiency due to partial radiationless decay directly back to reactant at the point of a forbidden crossing between ground and excited singlet surfaces along the hydrogen abstraction reaction coordinate.[15] Triplet reaction occurs exclusively via biradicals. The rapid ($>10^{10}\,\mathrm{s}^{-1}$) intersystem crossing in most phenyl ketones usually produces exclusive triplet reactivity. A few intramolecular hydrogen abstraction reactions of aryl ketones have been shown to involve excited singlets at least partially.[16,17] This pattern occurs when the n,π^* singlet reaction is fast enough to compete with intersystem crossing. Exclusive singlet reactions can occur if the triplet reaction is so slow that it is totally suppressed by added quenchers.

Substituent Effects: n,π^* vs. π,π^*

Aryl ketones can have either n,π^* or π,π^* lowest triplets; the former being far more reactive than the latter. Ketones with π,π^* lowest triplets do undergo hydrogen abstraction reactions and display two quite different forms of reactivity. In systems with π,π^* triplets, only a few kcal/mol below their n,π^* triplets, most of the measured reactivity arises from low concentrations of the n,π^* triplet in thermal equilibrium with the lower π,π^* triplet.[18–20] Equation (58.2) describes observed rate constants for hydrogen abstraction, with the n,π^* state providing most or all of the reactivity when ΔE ($E_{n,\pi} - E_{\pi,\pi}$) < 4 kcal/mol:

$$k_{\text{obs}}^{\text{H}} = \chi_{n,\pi} k_{\text{H}}^{n,\pi} + \chi_{\pi,\pi} k_{\text{H}}^{\pi,\pi} \tag{58.2}$$

$$\chi_{n,\pi} = \left(1 - \chi_{\pi,\pi}\right) = e^{-\Delta E/\text{RT}} \Big/ \left[1 + e^{-\Delta E/\text{RT}}\right] \tag{58.3}$$

Table 52.2 (Chapter 52) lists rate constants for triplet-state γ-hydrogen abstraction in ring-substituted valerophenones. These values reflect variations only in excited-state reactivity, as the CH bond being attacked is fixed; therefore, their *relative* values should hold for more remote hydrogen abstractions as well and thus provide a guide to predicting relative reactivities of aryl ketone triplets. Electron-donating groups (RO, alkyl, Cl, RS), as well as conjugatively electron-withdrawing groups (CN, RCO) *para* to the carbonyl, decrease reactivity by promoting π,π^* lowest triplets.

The second type of π,π^* reactivity occurs in polynuclear aryl ketones with large $E_{n,\pi} - E_{\pi,\pi}$ values. The observed triplet reactivity of some naphthyl ketones is only 0.01 to 0.001% that of an n,π^* triplet.[21,22] This large rate difference reflects the distinct spin localization on the carbonyl oxygen in an n,π^* triplet as opposed to the delocalized spin in a π,π^* triplet.

Substituent Effects: Inductive

Inductively, electron-withdrawing ring substituents (F, CF_3, N, N^+) enhance the reactivity of n,π^* triplets, magnifying the electron deficiency of the carbonyl oxygen (groups on the α-carbon of ketones increase excited state reactivity). Cyano and carbonyl substituents *ortho* or *meta* have the same effect, as they are not conjugated to the benzoyl carbonyl in the triplet state. Electron-withdrawing groups on the α-carbon of ketones likewise increase reactivity.

Solvent Effects

For ketones with n,π^* lowest triplets, significant intrinsic solvent effects on k_{H} values are not apparent, although solvation of other functionalities in the molecule can affect conformational kinetics. Also, when the π,π^* triplet is of lower or comparable energy, polar solvents reduce overall reactivity by lowering the excitation energy of the π,π^* triplet and raising that of the n,π^* triplet, thus decreasing $\chi_{n,\pi}$ values.[18,19]

Energetics

Generally speaking, hydrogen abstraction rate constants for singlet n,π^* states are an order of magnitude greater than for the corresponding triplet states. The higher reactivity of n,π^* singlets relative to triplets most likely reflects the greater exothermicity of the singlet reaction. Abstraction of even primary hydrogens is exothermic; both aliphatic and phenyl ketone triplets display similar rate constants for attack on a given type of CH bond.[1,23]

Nature of Hydrogen Atom

C–H bond Energy Effects

Tables 52.3 and 52.4 (Chapter 52) list how different substituents on or near the γ-carbon affect the rate constants for triplet-state γ-hydrogen abstraction. γ-Substituents affect intrinsic CH bond energies and the electron density of the CH bonds, both of which affect k_{H} values. Substituents one or two carbons away create inductive effects that generally lower reactivity, as most substituents (aside from alkyl groups)

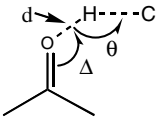

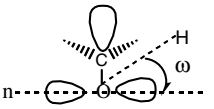

ideal: Δ = 90-120°	θ = 180°	ω = 0°	d ≤ 2.7
actual: Δ = 73-110°	θ = 85-120°	ω = 20-70°	d < 3.1

SCHEME 1

are inductively electron withdrawing. The relative effects of comparably situated substituents should hold for any type of hydrogen abstraction by n,π^* triplets.

Geometric Effects

CH and CO Double-Bond Orientation

For a bifunctional reaction to occur, two geometric factors must be optimized: the distance between the two reacting groups and their orientation with respect to each other. In the case of hydrogen abstraction, the distance between the carbonyl and the CH group and the orientation of the CO double bond and CH bonds determine reactivity. Whereas the reactive functional groups of the two molecules in a bimolecular reaction are free to diffuse to the van der Waals contact distance and to rotate into all possible relative orientations, in an intramolecular reaction intervening bonds and structure limit the orientations and proximity available to two separate functional groups. The resulting conformational equilibria and kinetics affect rate constants for hydrogen abstraction and thus determine both reaction rates and regioselectivity.

What are the orientational features required for hydrogen abstraction by ketone n,π^* states? Scheffer[24,25] has studied a variety of ketones that undergo γ-hydrogen abstraction in their crystalline states. In analyzing their reactivity, Scheffer considered the four ground-state parameters depicted in Scheme 1 to be the most important in determining reactivity: *d*, the distance between O and H; θ, the O–H–C angle; Δ, the C=O–H angle; and ω, the dihedral angle that the O–H vector makes with respect to the nodal plane of the carbonyl π system. Such a comparison of triplet reactivity with ground-state geometries is valid because n,π^* excitation is known to be so highly localized on the carbonyl group that geometric changes in the rest of the molecule are negligible and further are suppressed by the crystal lattice.

Scheffer suggested the theoretically "ideal" values for these parameters noted in Scheme 1, and theoretical approaches to answering these orientational questions have confirmed the "ideal" values of Scheme 1.[26,27] The values actually observed in over two dozen examples in which x-ray crystal structures were obtained for reactive ketones are summarized in the scheme. The most important parameter appears to be *d*; whenever two hydrogens at different distances <3.1 Å are available, the closer one is abstracted. Whenever a hydrogen is positioned this close to the carbonyl in the ground state, minimal molecular motion is required for reaction, and minimal motion is all that most crystal lattices allow. The value of θ obviously can vary greatly from the linear arrangement thought to be preferable. Likewise, the value of ω can depart significantly from the "ideal" 0°. Both of these deviations from ideality have long been known from the reactivity of many steroidal ketones.[3,28] The meaning of Δ is the least clear, as n,π^* excitation lengthens carbonyl bonds.[29]

For some time, it has been commonly believed that the hydrogen atom being abstracted must lie along the long axis of the carbonyl *n*-orbital. This notion recognizes the directionality of *p* orbitals and the fact that n,π^* radical reactivity is centered on this particular *p* (or sp^2) orbital; however, to augment Scheffer's evidence, several examples are described later in this chapter in which efficient hydrogen abstraction takes place, with the developing HO bond making a fairly large angle with respect to the nodal plane of the carbonyl π system.[28,30–32] It has been pointed out that such reactivity probably demonstrates a $\cos^2$ dependence on this angle,[3] that being the electron density function for a *p* orbital. Several experimental

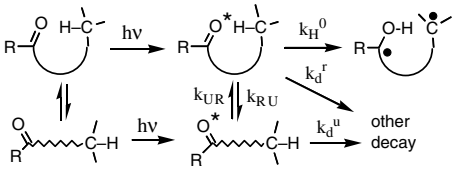

SCHEME 2

observations suggest zero reactivity when ω = 90°.[33,34] All of these involved rigid polycyclic ketones or crystalline media, where the reactants are constrained to maintain their ground-state geometry. This lack of conformational mobility maximizes the possibility that a biradical formed by either α-cleavage or hydrogen abstraction might revert to starting ketone with 100% efficiency. This very problem affects cyclodecanone in solution. Yang[8] originally found that it provides only the product of ε-hydrogen abstraction in benzene. However, Sauers and Huang[35] have since found that products of both γ- and ε-hydrogen abstraction are formed in *t*-butyl alcohol, despite the fact that the ε-hydrogen lies at an angle ω of 90°, whereas ω is only 56° for the γ-hydrogen.

It appears that hydrogen abstraction becomes slow as ω approaches 90°, but, without systematic measurements of rate constants as a function of ω, no generalization is possible. One example has been reported for some sterically congested ketones whose triplets undergo δ-hydrogen abstraction. For hydrogens held at nearly identical distances from the oxygen, those with ω = 20–30° react three to four times faster that those with ω = 65–70°, the difference being predicted by a $\cos^2$ relationship.[35] More such measurements are needed for compounds that cannot undergo revertible competing photoreactions. In particular, more ways to measure rate constants for solid-state reactions need to be developed.

Conformational Effects

Rate constants for intramolecular hydrogen abstraction reflect conformational effects,[3,36] as depicted in Scheme 2. It is assumed that interconversion among the various conformers of a given excited state competes with reaction and decay. One or more conformations may have geometries close to that required for reaction and are dubbed *favorable* or *reactive*. Also, *unreactive* geometries are usually present in which the two functional groups are too far apart for reaction; these must be able to rotate into reactive conformations if they are to react rather than decay to ground state or undergo a competing reaction such as α-cleavage. Molecules that react as solids must have lowest energy conformations that are reactive. Many acyclic ketones exist primarily in unreactive conformations, such that they do not react in the solid state. The lowest energy conformations of cyclic systems may have either reactive or unreactive geometries.

Molecules can be classified both structurally and dynamically in terms of their intramolecular reactivity. The three structural classes are (1) those with a reactive geometry as the most stable or only conformation, (2) those with a reactive geometry that interconverts with other more stable but unreactive conformations, and (3) those with no reactive conformations populated. Dynamically, the three classes of excited states are (1) those in which interconversion among conformers is much faster than decay reactions of the individual conformers, such that conformational equilibrium is established before reaction; (2) those in which conformational interconversions are all slower than decay, such that ground-state conformational preferences control photoreactivity; and (3) those in which unreactive conformers undergo irreversible rotation into a reactive conformer, which reacts faster than it can rotate back into the unreactive geometry. In this third case, reaction of the excited state is subject to rotational control, the intramolecular equivalent of intermolecular diffusion control.

Intramolecular hydrogen abstraction can be subject to any of these different dynamic boundary conditions.[39] The first dramatic example of ground-state control of triplet reactivity was provided by Lewis' study[37] of the Norrish type II reaction of benzoylcyclohexanes. Photoenolization of *ortho*-alkyl ketones was the first reaction recognized to show rotational control of triplet reactivity.[38] Conformational equilibrium is much more common; an early example is the type II reaction of benzoylcyclobutanes.[39] Scheme 3 defines observed k_H values for each of the three cases. For systems in which the excited state

Conformationalequilibrium $$\left[1/\tau = \Sigma\chi_u/k_d^u + \Sigma\chi_r/\left(k_H^o + k_d^r\right)\right] \quad (58.4a)$$

$$\left[k_H^{obs} = \Sigma\chi_r k_H\right] \quad (58.4b)$$

Ground-state control $$\left[k_H^{obs} = k_H^o\right] \quad (58.5)$$

Rotational control $$\left[k_H^{obs} = \chi_u k_{ur} + \chi_r k_H^o\right] \quad (58.6)$$

SCHEME 3

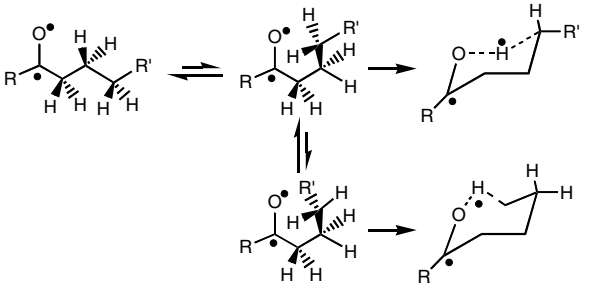

SCHEME 4

establishes conformational equilibrium before decay, only one excited state lifetime exists and is determined by the weighted decay rates of all conformers. If more than one conformer is reactive, then the observed rate constant for reaction is the sum of possibly different rate constants k_r weighted by their individual equilibrium populations χ_r ($\Sigma\chi_r + \Sigma\chi_u = 1$). When ground-state or rotational control obtains, different excited states have different lifetimes whether they undergo the same or different reactions.

Several general comments can be made about different classes of structure. In acyclic ketones, the regioselectivity of hydrogen abstraction reflects different rate constants for cyclic transition states of different sizes, which are closely related to χ_r values. Normally, the largest α-substituent eclipses the carbonyl in ketones, with the lowest energy conformation being fully staggered. No internal hydrogen abstraction is possible except in higher energy conformers that contain some *gauche* conformations. The α,β-CC bond must become *gauche* for γ-hydrogen abstraction to occur, as must the β,γ-CC bond for δ-hydrogen abstraction, as Scheme 4 depicts. Needless to say, more remote hydrogen abstractions require even more twists between carbonyl and the target CH bond which can be provided by rings and *cis* double bonds.

When the carbonyl and CH bond are part of a ring or substituents on a ring, the conformational limitations of the ring may either increase or decrease the population χ_r of favorable conformations. Lewis demonstrated how incorporation of rings between the carbonyl and the γ-carbon can increase rate constants for γ-hydrogen abstraction.[40] Scheme 5 shows some ketones in which the activation energy for abstraction of a secondary hydrogen remains the 3.5 kcal/mol for bimolecular reaction,[41] but the entropy of activation becomes less negative as rings freeze intervening CC bond rotations. Each such frozen rotation increases the rate constant by a factor of ~8, which corresponds to 4 EU. In all three cases, the major conformation is either reactive or of comparable energy, and the rings limit the number of unreactive conformers.

In general, however, no constant factor exists by which rings change intramolecular reactivity**.** They may decrease population of a reactive conformation, as Alexander and Uliana[39] showed for benzoylcyclobutane;[39]

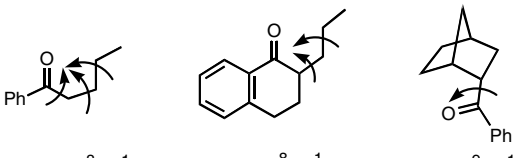

SCHEME 5

limit reaction to one site, as exemplified by the selective δ-hydrogen abstractions in the synthesis of dodecahedrane by Paquette and Balogh;[42] or prevent population of a reactive conformer, as Turro and Weiss[43] reported for cyclohexanones with axial α-alkyl groups.

Regioselectivity

Competing intramolecular reaction rates are determined by differences in the energy required for the molecule to rotate and/or twist into different geometries that bring the excited carbonyl and a remote CH bond into the proper distance and orientation for reaction. Regioselectivities are determined by such energy and rate differences.

Acyclic Systems

The predominance of γ-hydrogen abstraction by excited straight-chain ketones is so pronounced that for years it was thought that no ketone containing γ-hydrogens would react at any other position. A few notable exceptions were eventually found; δ-methoxyvalerophenone[44] and γ-benzoylbutyraldehyde[45] undergo both γ- and δ-hydrogen abstraction with comparable rate constants, because both possess a highly reactive δ–CH bond and an inductively deactivated γ–CH bond. From these results, it was deduced that the intrinsic γ/δ selectivity in triplet ketones is 20:1, the same as that already established for alkoxy radicals.[28]

Houk has published several theoretical studies of intramolecular hydrogen transfer that accurately reproduce the preference for 1,5- vs. 1,6-hydrogen transfers in triplet ketones.[27] Much of the preference is entropic, as expected, but little enthalpy difference exists between the two modes. A chair-like transition state was originally suggested for γ-hydrogen transfers.[28] The calculations predict a strong preference for a linear C–H–O arrangement ($\theta = 180^\circ$), which is more easily accommodated in a seven-atom transition state than in a six-atom one. Thus, relative enthalpies of activation reflect both ring size strain and orbital orientation in the transition state. It must be reiterated that actual ketones react even when θ approaches 90° in the ground state and may adopt a chair-like transition state.

In summary, ketones react preferentially at γ–CH bonds but, as Schemes 4 and 5 show, only if the nearby bonds are free to rotate. Substituents that reduce γ–CH bond lability can allow more remote hydrogen abstraction to compete, but the only way to eliminate γ-hydrogen abstraction is to eliminate γ-hydrogens. Reaction occurs at more remote positions only if the overall structure of a compound allows remote carbons to rotate within a few angstroms of the carbonyl.

Cyclic Systems

The interposition of even one ring between the carbonyl and potentially reactive CH bonds imposes conformational restrictions that limit the molecular geometries possible. Consequently, regioselectivity becomes dominated by frozen rotations such that only certain CH bonds get close enough to the carbonyl to react.

Charge Transfer Followed by Proton Transfer

Bimolecular photoreduction of ketones by good electron donors often proceeds by either electron transfer or charge transfer complexation, followed by a proton transfer. Intramolecular hydrogen transfers sometimes follow this pathway as well. There is good evidence from the behavior of aminoketones that tight

overlap of the donor lone pair with the half-empty *n* orbital is necessary for triplet CT reaction. Rate constants for internal quenching in ω-dimethylaminoalkyl phenyl ketones are maximum for β- and γ-amino ketones, in which five- or six-atom rings can be formed by overlap of the nitrogen lone pair with the half-occupied carbonyl *n* orbital.[46] How the separation between amino and carbonyl groups affects the efficiency of biradical formation is described in several sections that follow.

Competing Reactions

Obviously the most efficient photocylizations occur when rate constants for internal hydrogen abstraction are faster than those for bimolecular hydrogen abstraction from solvent and those for α-cleavage. Thus, the more remote hydrogen abstractions generally work best at low ketone concentrations and in solvents such as benzene and acetonitrile that are very poor substrates for hydrogen atom abstraction. One would not want to attempt photocyclizations by irradiating ketones in strongly electron-donating solvents such as amines and certain alkenes. When irradiated in solution, ketones with significant α-substitution often undergo competing type I cleavage to radicals. Fortunately, various groups have shown that such compounds primarily form the products of intramolecular hydrogen abstraction in the solid state as well as in other confining environments such as micelles, zeolites, and cyclodextrins. When the two radicals formed by α-cleavage cannot diffuse apart, they rapidly recouple to regenerate the ground state of reactant; in contrast, the biradicals produced by hydrogen abstraction are born in a geometry appropriate for cyclization.

Chapter 52 describes the competition between cyclization and cleavage unique to the 1,4-biradicals formed by γ-hydrogen abstraction. Examples of this competition are included later in this chapter.

58.7 Biradical Behavior

Chapter 52 presents a thorough description of the general properties and behavior of the hydroxybiradicals formed by n,π^* hydrogen abstraction as well as the history of their detection. This chapter focuses on how biradicals of different sizes differ in behavior and how these differences affect our general understanding of biradical behavior.

Overwhelming evidence has been found for the intermediacy of triplet biradicals following internal hydrogen abstraction by triplet ketones, especially phenyl ketones. Some unquenchable cyclization reactions indicate that singlet biradicals can indeed be formed in dialkyl ketones.

In most cases, the biradicals formed by intramolecular hydrogen abstraction can both cyclize and disproportionate. In the case of Norrish type II 1,4-biradicals, reversion to starting ketone is the sole result of disproportionation, but biradicals with more connecting atoms between the two radical sites can disproportionate to various enol structures, as is described below. It appears that singlet 1,4-biradicals undergo little if any cyclization or disproportionation. It is not known to what extent larger singlet biradicals partition between cyclization and disproportionation.

Direct Study of Triplet Biradicals

In 1977, Small and Scaiano[47] reported the first flash spectroscopic detection of a triplet 1,4-biradical intermediate from γ-methylvalerophenone. Scaiano[48] has thoroughly summarized several basic features of triplet 1,4-biradical lifetimes (described in Chapter 52). They are lengthened approximately threefold in Lewis base solvents, having values in the 25- to 50-nsec range in hydrocarbons and 75- to 160-nsec range in alcohols.[49] They are almost independent of temperature, having activation energies for decay of 0 to 1 kcal/mol.[50] They are not very sensitive to substitution on the benzene ring or to steric features at the γ-carbon of the ketone, but they are increased by conjugating substituents such as γ-phenyls.[50] They are shortened by bimolecular interaction with paramagnetic species such as oxygen[51] and nitroxide radicals.[52] These general features have been observed for some 1,5-biradicals as well, as shown in Table 58.1. Thus, they may hold for even longer biradicals.

TABLE 58.1 Lifetimes and Product-Forming Efficiencies of Some Hydroxy-Biradicals

Biradical	E_a, kcal	τ, ns		$\Phi_{H\text{-abs}}$	
		CH_3OH	Alkane	Polar	Hydrocarbon
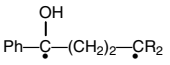	0	100–200	30–70	1	0.3
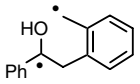	1	30	25	1	1
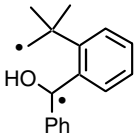	0	43	≤4	1	0.05
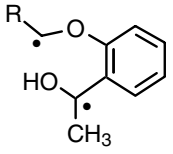	?	5	1	0.20	0.023

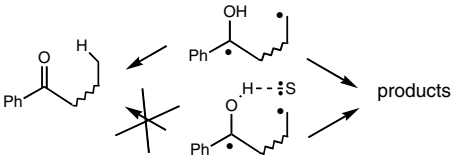

A biradical's lifetime is the reciprocal of its overall rate of decay by both product formation and reversion to ketone. Because the biradicals are formed as triplets in the majority of cases, they must convert to singlets in order to form ground-state products and ketone. Thus, biradical decay involves both physical and chemical changes. These two processes can occur in two ways: one after the other or concurrently. For many decades, it generally has been believed that T ∅ S intersystem crossing of triplet biradicals precedes product formation.

$$\tau = 1/(k_{cyc} + k_{rev}) \tag{58.7}$$

Based entirely on his study of 1,4-biradicals formed by γ-hydrogen abstraction in triplet phenyl ketones, Scaiano postulated that biradical lifetimes are determined by rates of irreversible ISC to the corresponding singlet biradicals. Moreover, he further suggested that product ratios reflect relative ISC rates for different conformations of the triplet biradicals, the singlet biradical being too short-lived to convert into any other product-forming conformation.[53] This view is supported by the temperature independence of some of the biradical lifetimes, ISC not having any enthalpic barrier, but assumes that conformational interconversions are fast enough that conformational equilibrium is established before ISC occurs. Such kinetics are likely in the case for acyclic systems but not for cyclic ones.

It must be emphasized that 1,4-biradicals are unique in being able to form a product from almost any conformation, because they alone can cleave to form two double bonds. Although it is possible that little if any conformational change can occur after ISC in such short, relatively constrained biradicals, larger

biradicals that cannot undergo any chemical reaction in stretched conformations must rotate into cyclic geometries before any products can be formed.

More recently, other workers have suggested an alternative view. From magnetic resonance studies of biradicals, Closs and Redwine[54] suggested that triplet biradicals cyclize whenever their two ends collide, but with a low probability that reflects the amount of singlet character mixed into the biradical by spin-orbit coupling. Michl[55] has suggested a comparable picture, purely from a theoretical viewpoint, with the added feature that incipient bonding of the two ends of the biradical induces additional spin-orbit coupling through a highly stabilizing covalent interaction.

The behavior of the biradicals shown in Table 58.1 suggests that attainment of product-forming geometries does indeed induce ISC so that product ratios reflect normal (small) barriers to bond rotation and product formation.[4] As Table 58.1 shows, the solvent effect on the lifetimes of several biradicals parallels the solvent effect on product quantum yields, indicating that rates of biradical decay are linked to product formation. (The lifetimes of biradicals that do not contain a hydroxy group are not affected by protic solvents.[56]) Inasmuch as hydrogen bonding of the biradical to solvent prevents the disproportionation that regenerates starting ketone, it must lower the rate of biradical decay and thus lengthen biradical lifetime.

Thus, two apparently contradictory experimental facts regarding triplet biradical lifetimes can be identified: Zero or near-zero temperature effects suggest a physical rather than chemical rate-determining step for decay, whereas the solvent effects suggest that the rate-determining step involves product formation. These can be reconciled with the premise that the triplet state rises only slightly in energy along product-forming reaction coordinates before it interconverts with the singlet state, in accord with the Closs and Michl proposals.

Biradical Cyclization

Inasmuch as this chapter covers the cyclization of hydroxy-biradicals, it is important to remember that excited-state hydrogen abstraction forms a biradical with its two radical sites initially very close to each other. Unless some of the connecting bonds rotate very rapidly, disproportionation back to ketone would be all that happens. One would think that rather simple conformational changes are all that is required for cyclization to take place. In order to predict cyclization quantum efficiency, the challenge is to understand the kinetics of those bond rotations as well as other conformational changes that lead to competing disproportionations and cleavage (only 1,4-biradicals).

Because cyclization is of great synthetic interest, the factors that determine stereoselectivity are of major importance. It is only in the past decade that significant interest has developed in understanding the stereoselectivity of biradical cyclizations. Interestingly, renewed interest in the stereoselectivity of bimolecular radical coupling has also developed. The photoreduction of acetophenone to pinacol forms both diastereomers in comparable yields, with the coupling of two prochiral 1-phenyl-1-hydroxyethyl radicals being stereorandom. In the case of biradicals with two prochiral radical sites, selectivity can be determined by nonbonded interactions that occur during cyclization or by pre-existing nonbonded interactions built into the molecule.[57] Therefore, the question that must be addressed is how and to what extent the intervening structure may affect diastereoselectivity in biradical cyclization. Both the relative energy of isomeric conformers and their relative interconversion rates must play a role.

Biradical Disproportionation

It is generally true that almost all the hydroxy-biradicals formed by internal hydrogen abstraction partially revert to starting ketone by an internal radical disproportionation reaction in which the carbon-centered radical site abstracts the hydrogen from the hydroxyl group. This process often is the major reaction of the intermediate biradical, so that the overall quantum yield of product formation is low even when hydrogen abstraction by the excited state is 100% efficient. Should the efficiency of hydrogen abstraction

be low because of electronic or conformational problems, then biradical disproportionation lowers quantum efficiency even further.

Added Lewis bases inhibit disproportionation back to ketone and thus enhance quantum yields of product formation.[58] In many cases, reversion to ketone is totally suppressed and quantum yields approach unity. This phenomenon is attributed to hydrogen bonding by the relatively acidic OH group[59] of the biradical to the Lewis base. Disproportionation entails breaking this hydrogen bond, whereas all other reactions of the biradical do not. The ability of different additives to solvate the biradicals, as determined by the concentration needed to maximize product quantum yields, closely matches their basicities.[58b] Alcohols, water, ethers, and pyridines are commonly used for this purpose, but all Lewis bases that are not also strong electron donors work to some extent. Not every ketone reacts with 100% efficiency even in the presence of strong Lewis acids. The equilibrium between solvated and unsolvated biradicals obviously varies with biradical structure. Sometimes only a fraction of the biradical is solvated; the rest still reverts to ketone.

Occasionally, intramolecular hydrogen bonding of the hydroxyl group to a Lewis base substituent in the biradical can be quite effective in suppressing reversion to ketone. In any event, it is important to remember that disproportionation back to ketone is a chemical reaction of these triplet hydroxy-biradicals and must be taken into account when analyzing structural and kinetic factors that determine product ratios. It usually is the major cause of low quantum yields for product formation. In fact, in some cases disproportionation and reversion to starting ketone is the only biradical reaction.

These biradicals can also disproportionate by attack of one radical site on a CH bond next to the other radical site. As mentioned above, such behavior is limited to biradicals with three or more atoms connecting the two radical sites, as shorter biradicals are unable to twist into the necessary geometry for such a hydrogen transfer.

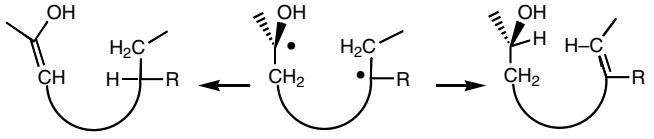

58.8 Environmental Effects

Both the rate constants for competing triplet reactions and the partitioning of biradical intermediates may be affected by the environment. The major effects on triplet reactivity involve conformational changes induced by highly ordered media and decreases in the efficiency of radical α-cleavage. The major effects on biradicals involve conformational restrictions that impede or promote coiling and solvation that affects disproportionation back to ketone. Quite thorough studies have been conducted on systems that undergo γ-hydrogen abstraction (described in Chapter 52). Only a few such studies have been applied to more remote hydrogen abstraction reactions.

58.9 Formation and Behavior of Biradicals of Different Sizes

1,3-Biradicals: β-Hydrogen Abstraction

Even though β-hydrogen atom abstraction could proceed through a five-atom transition state, which normally is not a bad thing, it rarely occurs, probably because the necessary alignment of atoms discussed above is not possible. The rapid internal charge transfer that occurs in certain triplet β-dialkylamino ketones is followed by β-proton transfer to oxygen, and the resulting 1,3-biradicals cyclize to cyclopropanols.[60] Why can a β-hydrogen be transferred to the carbonyl oxygen as a proton, but not as a neutral atom? Presumably, the charge-transfer exciplex geometry draws the donor entity fairly close to the carbonyl to maximize overlap of the donor and acceptor orbitals, in so doing dragging a β-proton within striking distance of the oxygen.

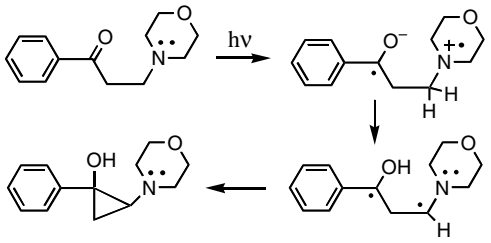

There are some confusing aspects of this reaction. Protic solvents lower the quantum yield of cyclization, for reasons that are not fully understood, while ether and hydrocarbon solvents promote different cyclization diastereoselectivity. Hydrogen bonding to the amino nitrogen decreases its basicity and electron-donating potential. The hydroxy-biradicals most likely hydrogen-bond to ether solvents, a fact known to alter stereoselectivity.[58] Equally interesting is the strong deactivating effect of α-methyl groups; the quantum yield drops from 0.59 to <0.02 when two α-methyls are present on β-dimethylaminopropiophenone. Steric interactions probably impede proton transfer rather than electron transfer.

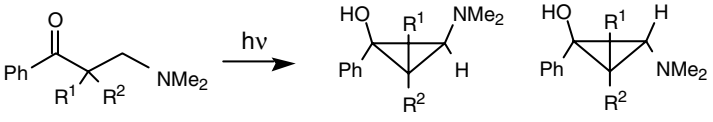

$R^1 = R^2 = H$	Benzene	>95%	<5%
$R^1 = R^2 = H$	Dioxane	50%	50%
$R^1 = Me$; $R^2 = H$	Either	<5%	>95%

Henning and co-workers[61] have found that in other β-alkylamino ketones proton transfer takes place partially or exclusively from a δ-carbon to generate a 1,5-biradical that cyclizes to a pyrrolidine. More about these reactions is provided in the 1,5-biradical section. Differing regioselectivities are thought to be due to differing geometries of the intermediate exciplexes.

More recently this form of cyclopropanol formation was found to occur with β-(*p*-aminophenyl)propiophenones, in which the aniline electron donor promotes a β-proton transfer and 1,3-biradical formation.[62] This study was particularly interesting in that phosphorescence of the intermediate exciplex was detected. Various structural modifications led to interesting diastereoselectivity in the products.

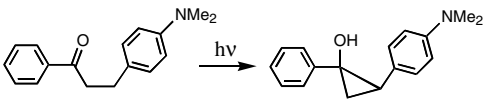

One of the few examples of apparently straightforward β-hydrogen abstraction is afforded by the reaction below, in which Yang photoenolization competes depending on the size of R.[63] The larger R groups cause the ketone to adopt a conformation with the β–CH bond neatly aligned for abstraction, which is not the case for small R's. This behavior presents strong evidence for the proximity of a CH to the carbonyl oxygen being the major factor driving H-abstraction.

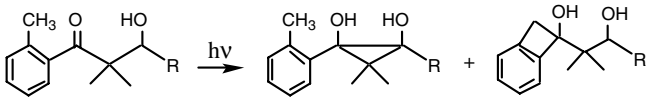

R = ^{i}Pr, ^{t}Bu, Ph, *o*-tolyl R = Et, Me, H

Another instance of direct β-hydrogen abstraction is provided by the behavior of α-methylene ketones, which form both cyclopropanols and methylenecyclobutanols.[64] The reaction appears to occur only from excited singlet states.

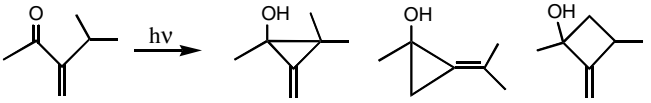

1,4-Biradicals: γ-Hydrogen Abstraction

Chapter 52 covers this topic thoroughly, but, because that chapter focuses on type II cleavage products, cyclobutanol formation is covered mainly as a competing byproduct. Here, the cleavage and disproportionation that compete with cyclization are byproducts. The cyclization efficiency of triplet-generated 1,4-biradicals varies widely with structure. Fortunately, the short length of 1,4-biradicals prevents several forms of disproportionation that 1,5-biradicals undergo. Several factors affect the partitioning among cleavage, cyclization, and reversion to starting ketones.[65,66] Four geometries of the 1,4-biradical must be considered: two stretched-out, staggered conformations and two coiled *gauche* conformations. Cleavage can occur from either *gauche* or staggered conformations, whereas cyclization and disproportionation require the latter.

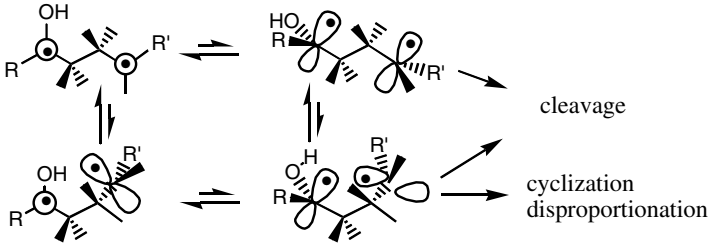

Cleavage appears to be governed by the stereoelectronic necessity for overlap of the breaking bond with both half-occupied *p* orbitals.[66,67] Anything that prevents reasonably parallel alignment of the two half-occupied *p* orbitals and the central CC bond retards or suppresses cleavage. In straight-chain ketones, cleavage/cyclization ratios tend to be at least 5:1. However, α-substitution by alkyl groups,[68] fluorines,[69] or rings[70] increases cyclization, primarily by destabilizing the geometry required for cleavage. α-Alkoxy ketones cyclize more than they cleave;[71] in this case, cleavage is not retarded so much as cyclization is enhanced, presumably by the oxygen relieving ring strain.

Because various bonds in biradicals are free to rotate in solution and thus to allow population of several different conformers, some of which can cyclize and some not, cleavage/cyclization ratios tend to be higher in solution than they are in more rigid environments. Biradicals formed from crystalline ketones tend to maintain shapes very similar to those of the ground-state ketones, which means that the two ends of the biradical remain close enough to cyclize but may not be properly aligned for cleavage. Thus, irradiation of solid ketones presents the best chance of getting good yields of cyclobutanols following γ-hydrogen abstraction.

3-Benzoylpropanal is unique in that it yields only a 2-hydroxycyclobutanone at low conversions but mostly acetophenone at high conversions when irradiated with wavelengths of ~300 nm.[45] The problem is that the cyclization product undergoes photo-induced α-cleavage back to the 1,5-biradical, only a small fraction of which cleaves to the enol, with most reverting to ketoaldehyde, which then repeats the cycle. Fortunately, irradiation at wavelengths greater than 354 nm provides high yields of cyclobutanone, which does not absorb light above 330 nm. This case is a rare example of Yang photocyclization products undergoing secondary photochemistry, a common phenomenon in many photoreactions.

TABLE 58.2 Solvent Effects on Some 1,4-Biradical Partitioning Ratios

Ketone	Benzene ϕ_{elim}	Benzene $\phi_{cyc\ (Z/E)}$	Alcohol ϕ_{elim}	Alcohol $\phi_{cyc\ (Z/E)}$	Ref.
$PhCOCH_2CH_2CH_3$	0.36	0.04	~0.90	~0.10	66
$PhCOCHMeCH_2CH_3$	0.28	0.12 (>20)	—	—	68
$PhCOCMe_2CH_2CH_3$[a]	0.007	0.057	—	—	68a
$PhCOCH_2CHMeCH_3$	0.26	0.045	—	—	68a
$PhCOCH_2CMe_2CH_3$	0.19	0.01	—	—	66
$PhCOCH_2CH_2CH_2CH_3$	0.30	0.06 (3:1)	0.88	0.12 (2:1)	66
$PhCOCH_2CH_2CH_2$-*n*-alkyl	0.24	0.06 (3:1)	0.82	0.12	66
$PhCOCH_2CH_2CH_2CMe_3$	0.22	0.086 (2:1)	0.83	0.17 (1:1)	66
$PhCOCHMeCH_2CH_2CH_3$	0.17	0.12 (3:1)	—	—	68a
$PhCOCMe_2CH_2CH_2CH_3$[a]	0.04	0.08 (4:3)	~0.10	~0.20 (4:5)	68b
$PhCOCH_2CH_2CHMe_2$	0.26	0.04	—	—	66
$PhCOCF_2CH_2CH_2CH_3$	<0.01	0.60	—	—	69
$PhCOCH_2CH_2CH_2Ph$	0.47	0.05	—	—	68
$PhCOCH_2CH_2CH_2OMe$	0.21	0.11 (7:1)	—	—	66
$PhCOCH_2(CH_2)_3OMe$[b]	0.33	0.10 (>20)	0.47	0.8 (4:1)	66
$PhCOCH_2(CH_2)_3CO_2Me$	0.58	0.17	—	—	66
$PhCOCH_2$–O–CH_2CH_3	0.35	0.62 (11:1)	—	—	71
$PhCOCH_2CH_2CH$=O	<0.05	0.30	<0.05	0.40	45
PhCOc–C_4H_7	0.01	0.03	—	—	83
PhCOc–C_5H_9	0.40[c]	None	—	—	82
PhCOc–C_6H_{11}	0.008	0.005	—	—	84

[a] Competing α-cleavage.
[b] Competing δ-H-abstraction.
[c] 0.22 in Reference 70.

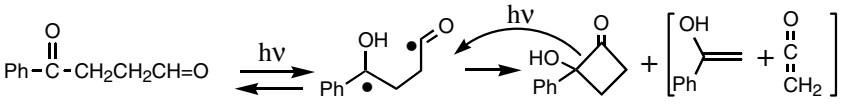

Acyclic Ketones

A distinction is often made between coiled and stretched conformations in order to rationalize cyclization/cleavage ratios; however, disproportionation also requires a coiled conformation, and it is not at all clear what affects the competition between cyclization and disproportionation, other than that hydrogen bonding to Lewis bases dramatically inhibits the latter and changes the stereoselectivity of the former. The bond rotations needed to initiate both cyclization and disproportionation must be different, but they likely are quite small and thus not very different. Examples of the wide variations among cyclization/disproportionation ratios are provided in Table 58.2. Inasmuch as conformer populations determine product ratios, cyclobutanol yields are determined primarily by how well cyclization competes with disproportionation.

Table 58.2 also indicates diastereomer ratios for the cyclobutanols formed from some of the ketones. One particularly interesting case involves α-methylbutyrophenone (αMeBP) and valerophenone (VP) forming the same 2-methyl-1-phenylcyclobutanol but with much different stereoselectivity. αMeBP forms a single isomer with the methyl and phenyl groups *trans*, whereas VP forms a 3:1 ratio favoring that isomer. VP exemplifies stereoselectivity induced by nonbonded interactions created as the two radical sites approach each other, whereas αMeBP exemplifies stereoselectivity induced by pre-existing nonbonded interactions in the biradical. In the former case, selectivity appears to mirror relative product energies; in the latter, it mirrors relative biradical conformational preferences. Scheme 6 illustrates both types of selectivity.

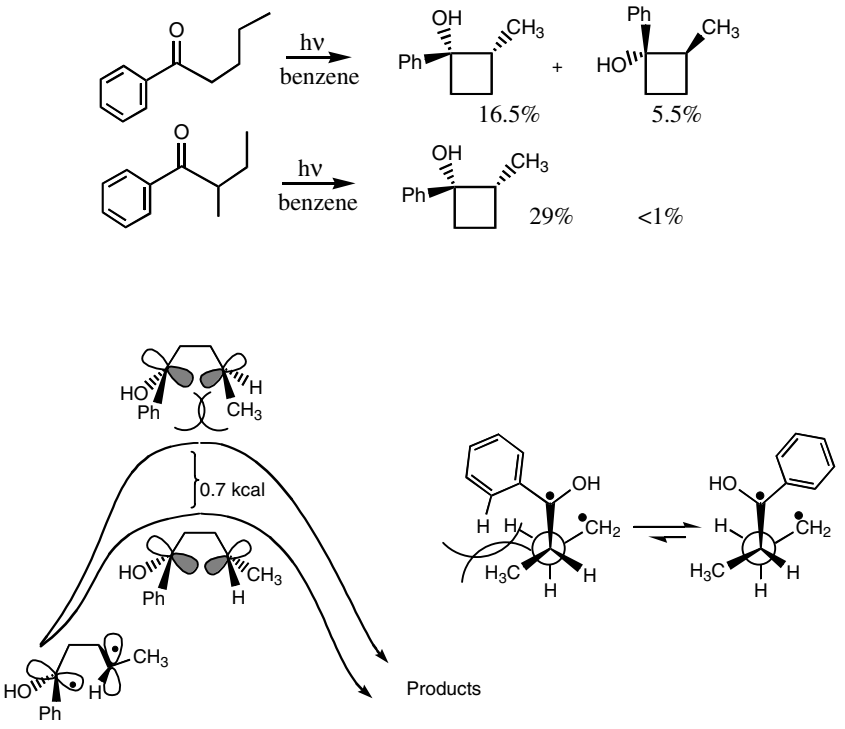

SCHEME 6 Left: nonbonded interactions created during cyclization of valerophenone. Right: pre-existing nonbonded interactions in α-methylbutyrophenone.

A more recent study[72] displayed intriguing variations in both cleavage/cyclization ratios and *cis*/*trans* stereoselectivity. The γ-dimethyl-γ-benzoyl ester, true to form, undergoes significant cyclization, but with the phenyl and carboxyethyl groups *cis*; the α-keto ester, however, undergoes just a little cyclization, but the phenyl and carboxyethyl groups stay *anti*, as in α-methylbutyrophenone.[72] The low cyclization/cleavage ratio undoubtedly reflects the low radical coupling proclivity of tertiary radical sites.

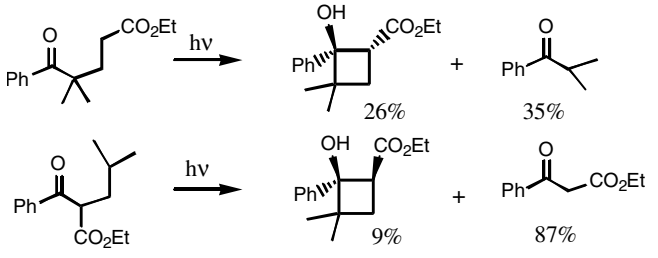

Because polar solvents usually improve quantum efficiency and thus actual rates, they also can affect the diastereoselectivity of cyclization, presumably because hydrogen bonding to solvent enlarges the steric bulk of the OH groups. In many cases, *cis*/*trans* ratios become 50:50, and no stereoselectivity is observed.

Ketones Containing Heteroatoms

γ-Methoxybutyrophenone and δ-methoxyvalerophenone both show very high selectivity in forming mainly the cyclobutanol, with the phenyl and methoxy groups *trans*. This behavior most likely represents an early example of intramolecular hydrogen bonding holding the biradical in a geometry with the OH and OMe necessarily *syn*. Ethers being quite weak bases, internal hydrogen bonding is apparently not

sufficient to prevent a large percentage of reversion to ketone. In contrast, ketones with carboxyl groups at their γ and δ positions display unusually high quantum yields for product formation, presumably because the internal hydrogen bonding to carbonyl oxygens is strong enough that the majority of biradicals are protected from reversion to reactant.

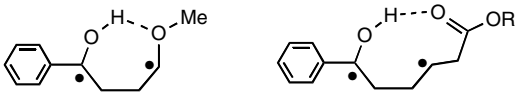

γ-Thioalkoxybutyrophenones undergo Norrish type II cleavage and also form about 10% cyclobutanols, both in very low quantum yield due to rapid internal charge transfer quenching of the triplet ketones.[73]

The behavior of α-alkoxy ketones has been of great interest for years, first because of their unusually high cyclization yields, next because of their very short biradical lifetimes, and more recently for their synthetic potential in making oxetane rings, for which case one attempt to model the oxetane of the D ring of Taxol is shown in the following.[74] Unfortunately, no one has figured out how to induce stereoselectivity in this particular biradical cyclization, although more successful examples in other biradical systems are described later.

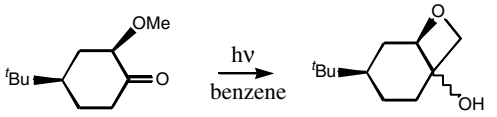

cis/trans = 3

α-Ethoxyacetophenone produces an oxetane not only in high yield but with over 90% diastereoselectivity. It and other α-alkoxy ketones also have the unique feature of reacting in lower quantum efficiency in alcohol than in hydrocarbon solvents, the opposite of most ketones. Both effects might be due to internal hydrogen bonding by the hydroxyl group to the ether carbon in the β position. However, the very short lifetime of the intermediate biradical indicates that cyclization happens much faster than in biradicals not containing heteroatoms; thus, rapid kinetics of product formation may induce both regio- and stereoselectivities.

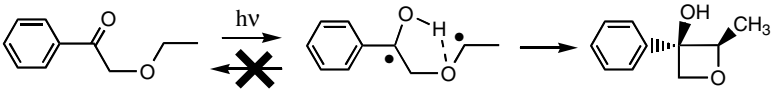

α-Thioalkoxy ketones undergo γ-hydrogen abstraction in competition with radical cleavage of the α-CS bond. The 1,4-biradical cleaves but does not cyclize.

Nonenolizable 1,3-diketones photocyclize to hydroxycyclobutanones, which requires that the two carbonyls be aligned in opposite directions so that the γ–C–H bonds are within reactive distance of the excited carbonyl.[75] As shown below, phenyl ketones cyclize, whereas aliphatic ketones undergo only type I α-cleavage instead.

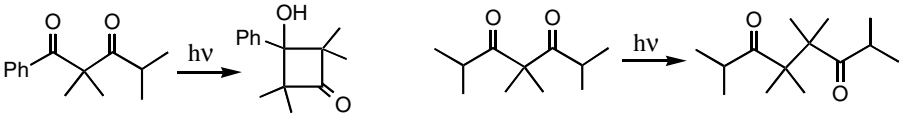

Unlike β-aminopropiophenones, triplet α-dialkylaminoacetophenones do not undergo rapid internal charge transfer; they do, however, undergo singlet state γ-hydrogen abstraction that leads only to cleavage.[17,76]

Gold[77] later discovered that α-(*N*-alkylamido)acetophenones undergo γ-hydrogen abstraction to produce azetidinols, revealing the fact that acylation of nitrogen makes electron transfer less competitive by weakening the electron donating ability of nitrogen. Below are three recent examples.

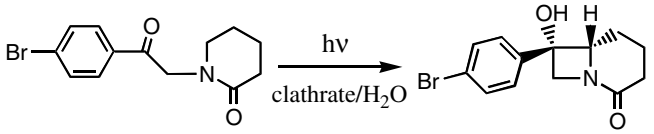

Irradiation of an *N*-phenacyl-δ-lactam in water containing a chiral clathrate produced a single diastereomer of the bicyclic lactam in >90% enantiomeric excess.[78]

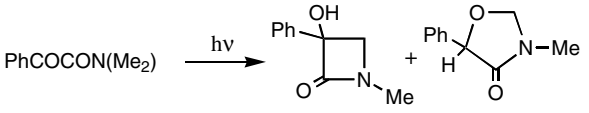

Irradiation of a phenylglyoxylamide as a solid inclusion complex formed a β-lactam as well as a oxazolidinone rearrangement product.[79]

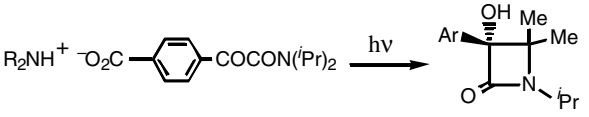

Irradiation of a *para*-substituted phenylglyoxylamide as a suspension of crystals in hexane also formed a β-lactam in >91% yield and 99% enantiomeric excess, the selectivity induced by a chiral ammonium cation paired with the carboxylate anion.[80]

The rapid internal charge transfer in triplet γ-dialkylaminobutyrophenones does not lead to efficient product formation;[46,81] the required orbital overlap seems to enforce a restricted orientation in the exciplex that prevents proton transfer to oxygen, such that CT becomes a purely competitive quenching process. However, simple γ-hydrogen abstraction does compete and forms a 1,4-biradical that cleaves but undergoes very little cyclization.

Acylcycloalkanes and Cycloalkanones

Table 58.2 includes the behavior of the three 4- to 6-carbon cycloalkyl phenyl ketones, all of which undergo γ-hydrogen abstraction with quite different results.[82] Early evidence for the ability of light to convert a reactant into a higher energy isomer was provided by the very low quantum yield photocyclization of benzoylcyclobutane to a bicyclo[1.1.1]-pentanol.[83] That it undergoes more cyclization than cleavage is similar to the behavior of the α,α-dialkyl acyclic ketones. The rate constant for γ-hydrogen abstraction is very low, presumably because of a low population of reactive conformers. Partitioning of the biradical apparently is determined by the poor alignment of its SOMOs for cleavage and by a barrier to twisting the cyclobutadiyl ring enough for radical coupling, leaving disproportionation as the fastest reaction.

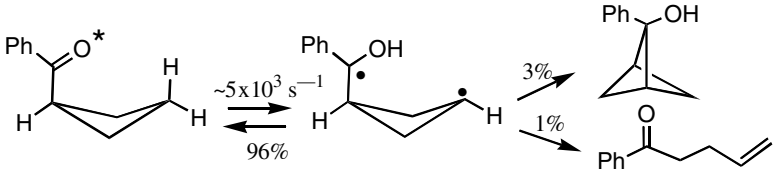

Benzoylcyclopentane undergoes much faster triplet hydrogen abstraction, but the 1,4-biradical does not cyclize, instead cleaving with 22 to 40% efficiency.[82] The k_H value is 1/50th that of valerophenone, indicating the modest barrier required for transannular bond stretches. The 5-benzoyl-1-pentene product undergoes Norrish type II cleavage and also forms a cyclic alcohol, as will be discussed below. An α-methyl group enhances k_H sixfold, most likely by increasing population of the conformer with the benzoyl group in a pseudo-axial position. More important, the 1,4-biradical undergoes only a few percent cleavage and cyclizes with 19% efficiency,[70] paralleling the effect already discussed for acyclic ketones.

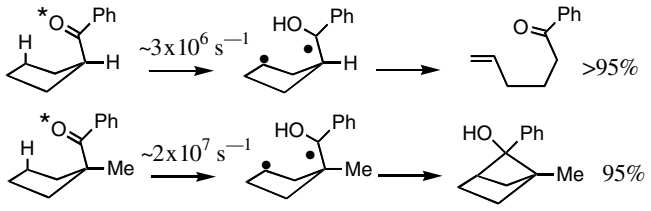

The behavior of benzoylcyclohexane took a while to figure out, as quantum yields for products are extremely low. Lewis and co-workers[84] discovered that the compound has two kinetically distinct triplet conformers, both of which give products. The axial conformer reacts ten times faster than valerophenone, indicating an ideal geometry for reaction as discussed above. The equatorial conformer cannot react directly but undergoes an irreversible chair inversion as the rate determining step to form the highly reactive conformer. The stereochemistry of the cyclobutanol ring was not ascertained, but more recent work indicates that the phenyl is *endo* to the six-ring.

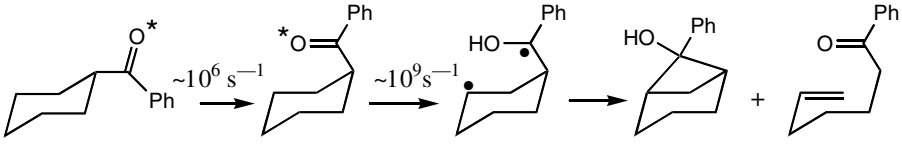

Lewis solved this conformational problem by adding a methyl group to the carbon bearing the benzoyl group, which enhances population of the chair conformer with the benzoyl axial and thus within abstraction range of an axial γ-hydrogen.[84] Its triplet abstracts a hydrogen much faster than it can undergo α-cleavage. The other conformer cannot abstract a hydrogen but, because of the α-methyl, undergoes type I cleavage faster than chair inversion. Quenching studies showed that the two types of reaction occur from kinetically distinct triplets, providing one of the first clear examples of ground-state control of reactivity. The bicyclic alcohol is formed predominately with the phenyl ring *endo*, because H-abstraction occurs with the phenyl twisted away from the α-methyl, where it stays until the biradical cyclizes. As usual, the α-methyl decreases the amount of type II cleavage by the biradical.

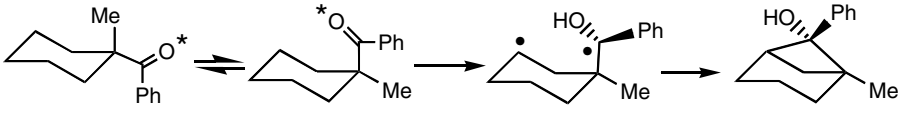

A similar study of 4-methyl-4-benzoyl-*N*-methylpiperidine provided comparable results and the important conclusion that no charge-transfer quenching of the triplet ketone occurs as it does with acyclic γ-amino ketones, proving that the charge transfer does not occur through bonds but requires close through space contact.[85]

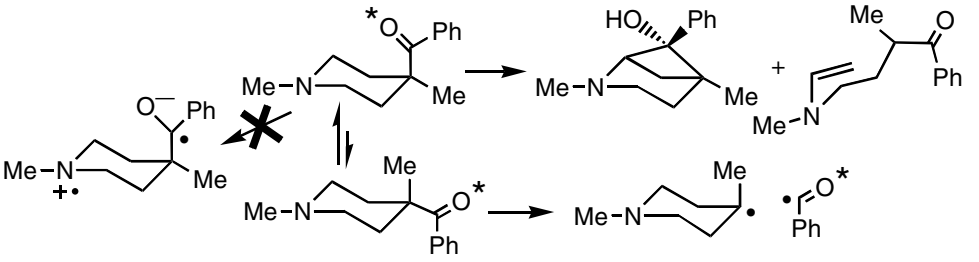

Several studies have explored environmental effects on the stereoselectivity of this photocyclization. One particularly nice example is provided by the solid-state photocyclization shown below, in which the counter-ion of the benzoate is a chiral ammonium ion, which results in formation of a single enantiomer of the bicyclic alcohol, presumably by inducing a tilt of the benzoyl group that leads to preferable abstraction from one of the two γ carbons.[86]

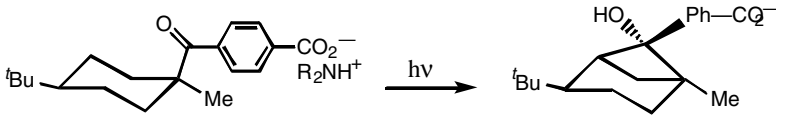

A recent study of benzoyldecalins revealed how the regioselectivity of photocyclization is enhanced in the crystalline state compared to solution.[87] Irradiation of **A** (X = CO_2Me) in CH_3CN results in 42% each of **B** and **C**, with only 6% total of the opposite two diastereomers. Irradiation of crystals produces more **B** than **C** — 2:1 for racemic **A** and 4.6:1 for optically pure **A**. The differences appear to represent conformer populations, there being but one in the crystal but three of similar energies in solution. In the crystal, the benzoyl group is aligned so as to favor abstraction of the tertiary bridgehead hydrogen, whereas the three lowest energy conformers in solution are all aligned differently and thus allow abstraction of both methylene and methine hydrogens. Interestingly, when X is COOH, the **B**:**C** selectivity is reversed to favor **C** both in solution and crystal, probably due to the effect of dimer formation on conformation.

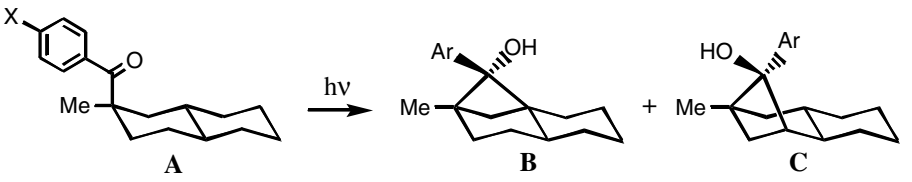

An earlier study of 9-benzoyl-*cis*-decalins produced some unexpected results.[88] Irradiation in acetonitrile solution produces **W**, **Y**, and **Z** in yields of 47, 6, and 47%, respectively. With both pictured conformers of the ketone about equally populated, hydrogens at carbons 4, 10, and 2 are abstracted, and biradical **T** is free to rotate into **U**, which cannot be formed by direct H-abstraction. Compound **Y** was not anticipated, but its formation by radical addition *ortho* to a benzylic radical site would represent a

well-precedented mechanism. The crystalline ketone exists only in the leftmost geometry, with the carbonyl oxygen pointed over the shared CC bond such that only hydrogens on carbons 4 and 10 are close enough for abstraction. Thus, irradiation forms only biradicals **S** and **T**, which form **W** and **X** in 84 and 19% yields, respectively. With an ammonium carboxylate ionic chiral auxiliary attached *para* to the benzene ring, **W** is formed in 99% yield and 91% EE from the crystalline ketone.[89]

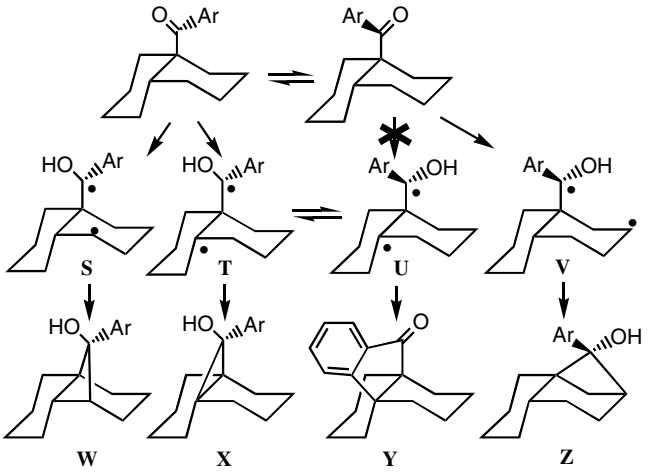

An early example of regioselectivity was provided by the behavior of an acetyl-2-methylenecyclohexane, which photocyclizes primarily via what would appear to be the less readily formed biradical. Only traces of product were found from the allylic biradical, which should be formed at least as fast or faster than the one leading to the observed product.[90]

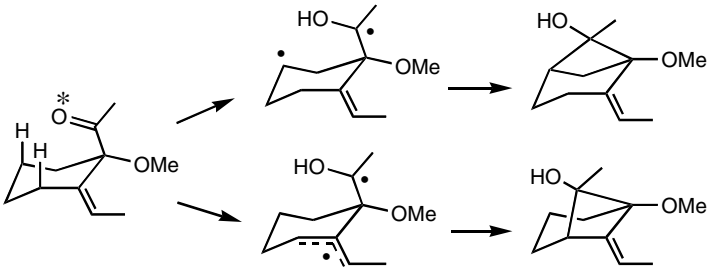

Several studies of benzoylbicycloalkanes indicate that the *endo*-isomers undergo very rapid triplet-state γ-hydrogen abstraction, with k_H values of 9×10^7, 7×10^9, 3×10^8, and 1×10^{10} s^{-1} for **1**, **2**, **3**, and **4**, respectively.[70] It is noteworthy that the *exo* 2-methyl groups on **1** and **3** slows hydrogen abstraction by two orders of magnitude, presumably because of eclipsing interactions between the methyl and phenyl groups in the transition state for hydrogen abstraction. However, these same eclipsing interactions in the 1,4-biradicals enhance product quantum yields by destabilizing the rotamer, with the OH aimed at the distance radical site and thus minimizing disproportionation. They also must destabilize the geometry required for type II cleavage, because tricyclic alcohols are the only products. In contrast, the 1,4-biradicals from ketones **2** and **4** without methyl groups do not cyclize and cleave with very low efficiency, presumably

because the phenyl group is now free to extend outward and stabilize the geometry required for disproportionation but not cyclization. Interestingly, the biradical geometries required for both cleavage and cyclization are so similar with and without the methyl group that the cyclization/cleavage ratios may be determined by product energies.

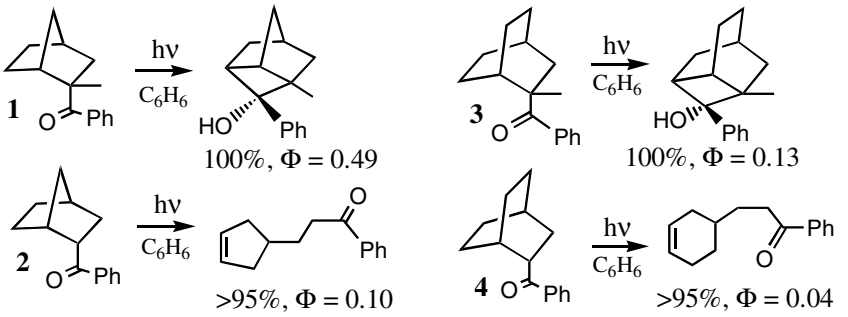

The isomers of **1** and **2** with the benzoyl group *exo* do not photocyclize. Their triplets coincidentally react with the same 1×10^7 s^{-1} rate constant for two different reactions: (1) *exo*-**1** undergoes only type I α-cleavage, the 10^7 rate constant being the same as that for other *t*-alkyl phenyl ketones; and (2) *exo*-**2** does abstract a methylene hydrogen, thus accounting for its low rate compared to *endo*-**2**, while the biradical so produced undergoes only type II cleavage.

Scheffer[25,91] has conducted a thorough study of five α-cycloalkylacetophenones that provide unique insight into biradical behavior. All of them react both in solution and in the crystal and give comparable product ratios in both phases. With the knowledge that organic molecules normally crystallize in their most stable conformations, examination of solution rate constants for hydrogen abstraction revealed no correlation with the geometric parameters for reaction. The rate constants do correlate well with those for bimolecular attack of various radicals on the different sized cycloalkanes, so the intrinsic reactivities of the different C–H bonds appear to determine relative reactivities. Scheffer concluded that Eq. (58.4) applies, with comparable values of χ for all five α-cycloalkylacetophenones. He suggests that these ketones react not from their most stable conformations but rather from higher energy ones that provide a more favorable geometry for reaction. The value of θ averages only 114° for the crystals. It is also possible that these compounds all react from their crystal geometries, in which case χ_r values are all close to one. All of the ketones except the cyclobutyl are considerably more reactive than *p*-chlorovalerophenone despite their awkward geometries. The rate enhancements probably represent the normal entropic gain associated with the ring.[40] The high observed k_H values cannot contain a really low value of χ_r, so any common geometric adjustment in solution must involve a relatively low energy conformational change.

The two ketones with the smallest rings undergo primarily cleavage, the next two split nearly 50:50, and the largest ring gives mainly cyclobutanol. In the last case, over 85% of the cyclization gives the *trans* ring junction. Scheffer provides an intriguing explanation by noting that the *p* orbital on the ring in the biradical must twist 90 ± 45° to become parallel to the *p* orbital at the hydroxy radical site and achieve the geometry required for both cleavage and cyclization. Rotation in the direction that gives *cis* products is favored for the two smallest rings; rotation in the opposite direction, which favors formation of *trans* products, is favored for the largest ring; the two rotations are equally likely for the six- and seven-rings. Because the three largest ketones yield mostly *trans*-fused cyclization products but *cis*-cycloalkene cleavage product, Scheffer concluded that the pre-*cis* biradical undergoes mainly cleavage, and the pre-*trans*

biradical undergoes mainly cyclization. He further proposed that the phase independence of the results indicates that these preferences are intrinsic to the structure of the molecules.

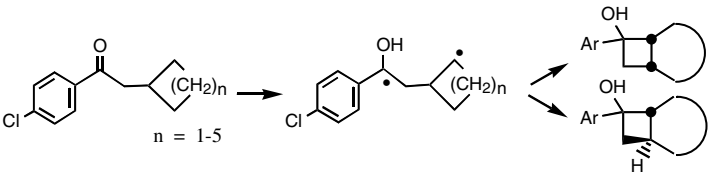

n	*d* (Å)	ω	Δ	k_H (10^8 s^{-1})	% Cleavage	% Cyclization (*t*/*c*)
1	3.1	23	78	0.3	92	8
2	2.8	31	96	1.2	92	8
3	2.6	42	90	1.2	40	60 (7.5:1)
4	2.7	42	82	5.7	61	41 (12:1)
5	2.7	48	77	6.7	18	82 (15.4:1)

Study of adamantylacetophenones has revealed several types of selectivity. In a chiral (methyladamantyl)acetophenone, hydrogen abstraction takes place only across the ring from the bridgehead methyl group, and the biradical cyclizes to opposite diastereomers in benzene and the solid state.[92] Under topological control in the rigid crystal, the biradical maintains its initial pre-*cis* geometry and cyclizes to a single isomer in 82% EE. In solution, the biradical is free to rotate into a less crowded geometry and forms a racemic epimer as major product. Attachment of a chiral auxiliary via a carboxylate group provides very high EE but no diastereoselectivity in the alcohol products of a skeletally achiral compound irradiated in solution.[93]

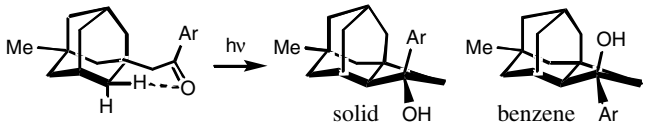

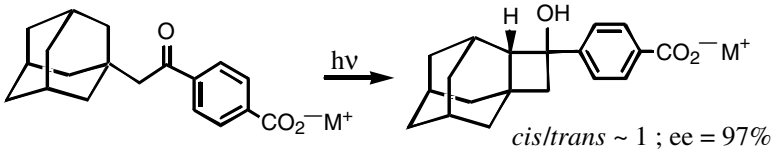

Lewis and Hirsch[94] studied four α-cycloalkoxyacetophenones, in which the ring is even farther away from the carbonyl and the γ-hydrogen is tertiary.[94] Table 58.3 lists the results, which consist of oxaspiro[3,*n*]alkanol and cycloalkanone formation, via normal cyclization and cleavage of the 1,4-biradicals. Simple isopropoxyacetophenone is included for the sake of comparison to acyclic compounds. As with other α-alkoxy ketones, overall quantum yields are quite high and cyclization yields are reasonable, except for the cyclopropyloxy ketone. Hydrogen abstraction rate constants are very high and decrease as expected as the rings get smaller.

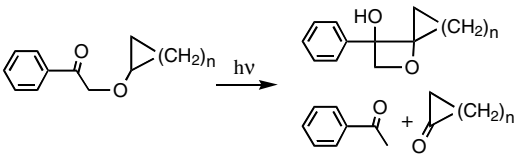

TABLE 58.3 Product Quantum Yields from α-Cycloalkoxy Ketones

Ketone	Φ_{cyc}	Φ_{elim}	k_H (10^9 s^{-1})
Isopropoxy	0.40	0.59	8.2
$n = 4$	0.20	0.38	8.9
$n = 3$	0.28	0.33	6.9
$n = 2$	0.42	0.40	3.3
$n = 1$	0.06	0.02	0.24

Cycloalkanones themselves undergo photoinduced α-cleavage to produce biradicals that disproportionate in various ways. Both singlet and triplet excited states of simple α-alkylcycloalkanones undergo γ-hydrogen abstraction, but the 1,4-biradicals mainly cleave to cycloalkanone and alkene. Yields are very low due to very rapid competing α-cleavage of the ring; consequently, cyclobutanol formation occurs at best in small amounts.

Yoshioka and co-workers[95] have studied several 1,3-diketones that undergo γ-hydrogen abstraction to yield primarily hydroxycyclobutanones. The behavior of three benzocyclohexenones reveals how the competition between cyclization and cleavage of the 1,4-biradicals varies with ring size. As shown in Structure 33, the percentage of cyclization decreases as ring size increases from 6 to 8, while the yield of type I α-cleavage increases from 0 to 50%.

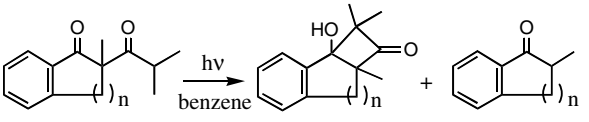

n		
2	65%	1%
3	47%	4%
4	7%	10%

The larger cycloalkanones can undergo cross-ring hydrogen abstraction, the first example of which was provided by cyclodecanone, which is now known to undergo both γ- and ε-hydrogen abstraction, such that both bicyclo[6.2.0]- and bicyclo[4.4.0]decanols are formed.[35] The fact that only the 1,4-biradical reverts to ketone in benzene must be a subtle conformational effect, although it is not clear why the two biradicals would differ enough in geometry that only one would disproportionate. It cannot be due to differences in cyclization rates: Cyclization to six-membered rings should be thermodynamically favored over cyclization to an eight/four bicycle, but both biradicals manage to cyclize when solvated by alcohol, with three times as much cyclobutanol as hydroxydecalin being formed. The nearly 3:1 preference strongly suggests that γ- is faster than ε-hydrogen abstraction in this molecule, but not by as large a ratio as would occur in an acyclic ketone.

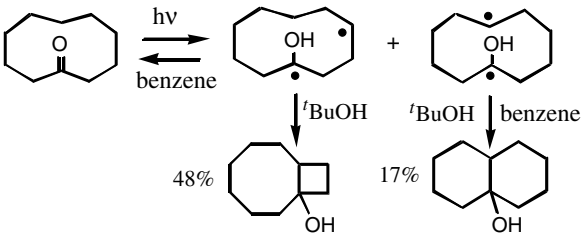

Scheffer's group has extended investigation of the conformational aspects of cycloalkanone photochemistry to a group of macrocyclic diketones. An early study is shown in Structure 35.[96] Four symmetric cyclic diketones photocyclize with the same sort of phase dependent stereoselectivity noted for monoketones. Cyclohexadecane-1,9-dione and cycloeicosane-1,11-dione undergo photocyclization in the crystal primarily to *cis*-cyclobutanols. In contrast, cyclooctadecane-1,10-dione and cyclodocosane-1,12-dione produce mainly *trans*-cyclobutanols in the crystal. Each compound has two pairs of symmetry-related γ-carbons, one of which has a γ-hydrogen closest to the carbonyl (~2.7 Å). Each additional methylene between the two carbonyls causes the ring puckering to alternate such that, on the carbon attacked, the hydrogen that is *not* abstracted is alternately *syn* or *anti* to the carbonyl oxygen. This hydrogen becomes the bridgehead methine that is either *cis* or *trans* to the hydroxy group in the cyclobutanols. The few percent type II elimination in the crystal increases to 45 to 50% in solution, and the *trans*/cis cyclobutanol ratio is 2.5–3:1 for all four diketones; obviously, topological control is not present in solution. The stereoselectivity shown by these diketones is temperature dependent because of solid-state phase transitions.

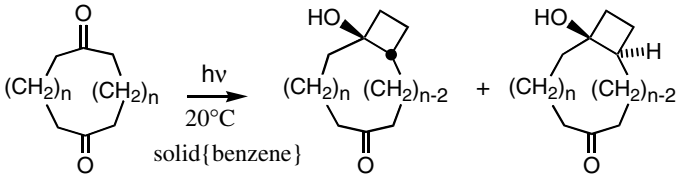

n = 5 or 7	85%	{12%}	13%	{43%}
n = 6 or 8	3%	{13%}	88%	{37%}

Two other symmetric cyclic diones show unique behavior. Cyclodecane-1,6-dione is photoinert, both as a solid and in solution.[97] Evidence indicates that it undergoes excited-state γ-hydrogen abstraction, but the biradical does nothing except revert to ground-state reactant, presumably for the same reasons as the 1,4-biradical from cyclodecanone. Unlike the monoketone, the dione has no ε-hydrogens to abstract.

A much bigger symmetric macrocycle, crystalline 1,14-cyclohexacosanedione exists as both plates and needles. When irradiated as crystals, the former yields only a *cis*-cyclobutanol, while the latter form gives the *trans*-cyclobutanol with >90% selectivity; neither undergoes type II elimination. In solution, type II cleavage accounts for half the products, the other half are cyclobutanols in a 2.3:1 *trans/cis* ratio. These results provide another example of how crystal lattices enforce conformationally driven stereoselectivity, which can vary with the exact crystal morphology.[98] A full paper has been published that provides details for a wide range of symmetric and unsymmetric cycloalkanediones.[99]

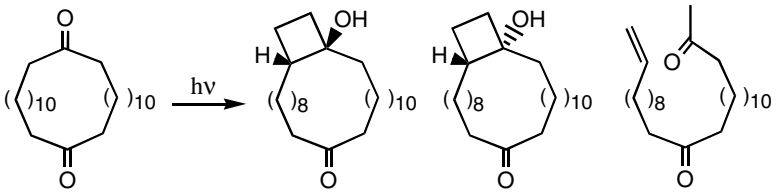

o-Alkylphenyl Ketones: Yang Photoenolization

In 1961, Yang and Rivas[100] discovered that some *o*-tolyl and *o*-benzylphenyl ketones undergo γ-hydrogen abstraction to form *o*-xylylenes that are trapped by dienophiles to form benzocyclohexenols. In CH_3OD, the benzylic carbon of the starting ketone is deuterated, additional evidence that a dienol intermediate (an *o*-xylylenol) is involved.

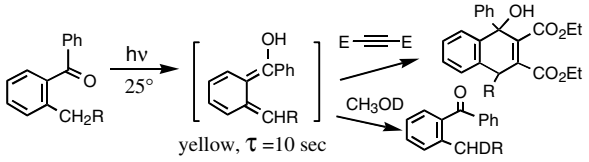

Over the intervening decades, various details of this enigmatic reaction have been clarified, as shown in Scheme 7. First came the realization that the initially formed triplet biradical is an excited state of the product xylylenol and its decay to ground state requires bond rotations, which partially answered the puzzle as to why Diels–Alder adducts are generated stereospecifically from a single dienol isomer (labeled E in Scheme 7).[101] Wagner and Chen[38] then found that the two rotamers of *o*-alkylacetophenones have kinetically distinct triplets, with rotation to the reactive geometry being the pathway for decay of the unreactive rotamer. Laser flash kinetics soon identified the two isomeric xylylenols in Scheme 7 and found that the *Z*-isomer undergoes very rapid reversion to starting ketone via a 1,5-sigmatropic hydrogen transfer, leaving only the *E*-isomer to form new products.[102]

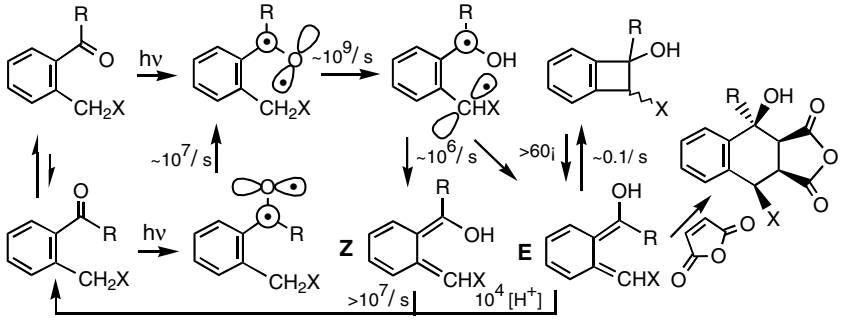

SCHEME 7 Intermediates and alcohol products formed from *o*-alkylphenyl ketones.

Meanwhile, and most relevant to this chapter, Matsuura and Kitaura[103] reported the formation of benzocyclobutenols from 2,4,6-trialkylphenyl ketones. Matsuura et al.[104] studied these photocyclizations quite extensively, including the photocyclization by crystalline 2,4,6-triisopropylbenzophenone, which occurs cleanly despite a 76° value for ω.[30] Until recently, only two examples had been reported of benzocyclobutenol formation from simple *ortho*-alkyl ketones.[101,105]

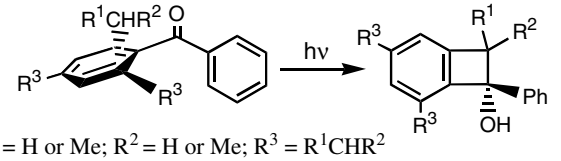

R^1 = H or Me; R^2 = H or Me; $R^3 = R^1CHR^2$

Carré and co-workers[106] studied a group of benzocycloalkenones that form tricylic benzocyclobutenols. As might be expected, transannular γ-hydrogen abstraction competed with *o*-methyl abstraction only for ring sizes of 10 or more carbons, and again ω was nowhere near 0°. The *cis* geometry of the [4,*n*+1]bicycles formed is explained below.

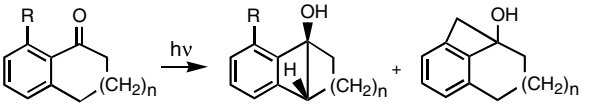

R = H ; n = 4 - 6 R = Me ; n = 3 - 6
R = Me ; n = 5 - 9

Eventually it was found that many *o*-alkylphenyl ketones not only undergo photocyclization to benzocyclobutenols but do so stereoselectively; a few early examples are shown in Structure 40.[107] Acids quench the photocyclization, indicating that the *o*-xylylenols are the precursors to the cyclobutenols and form them by thermal electrocyclization. The reason for their not having been discovered earlier is their thermal instability above 60 to 80°C.

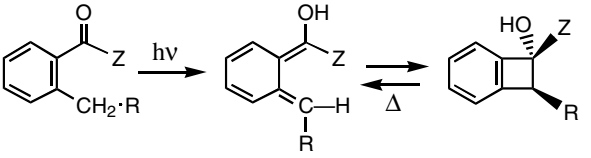

Z = CH_3 : R = OCH_3 or $OCH_2CH{=}CH_2$
Z = Ph : R = H, CH_3 or Ph

The stereochemistry for the electrocyclization of one of these *o*-xylylenols is explained by Scheme 8; the lowest energy conformer of the triplet biradical is the one that decays to two xylylenols, one with the OH pointed out forming the cyclobutenol by conrotatory motion, and any Diels–Alder cycloaddition occurs by disrotatory motion.[108] More specific examples are described in Reference 108.

Thus, this form of γ-hydrogen abstraction does produce cyclic alcohols, but it does not do so in two simple steps, as the initial biradical converts to ground-state *o*-xylylenols, which then undergo thermal pericyclic reactions. As noted earlier, the thermal equilibrium between *o*-xylylenol and benzocyclobutenol generally favors the latter. Because heating regenerates *o*-xylylenol, doing so in the presence of a dienophile can produce Diels–Alder adducts quite cleanly, thus giving these cyclobutenols significant synthetic potential. *ortho*-Benzylbenzophenone displays unique behavior in that the equilibrium between its

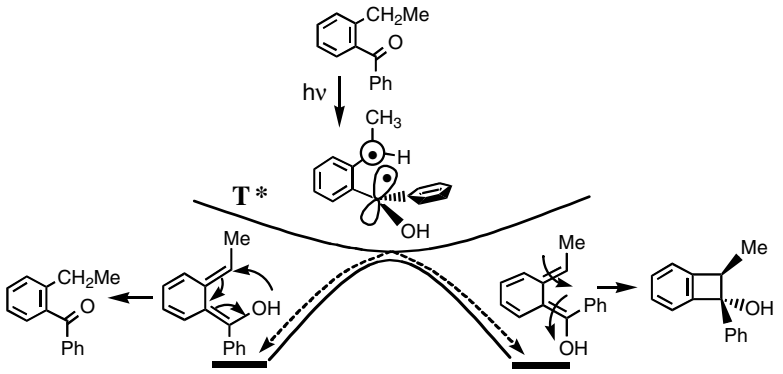

SCHEME 8

o-xylylenol and cyclobutenol photoproducts keeps small amounts of the xylylenol populated at room temperature, so that addition of dienophiles produces Diels–Alder products.[109]

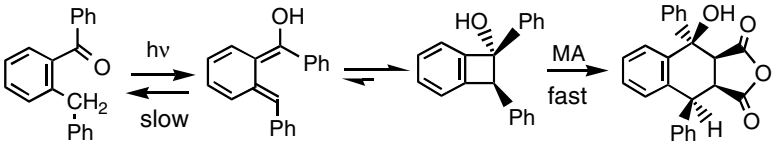

α-Diketones

In the early 1960s, Urry and Trecker[110] discovered that aliphatic α-diketones undergo photoinduced cyclization to α-hydroxycyclobutanones. Most interestingly, they do not form any acylcyclobutanols and, unlike α-ketoesters, do not undergo any type II cleavage. One of the carbonyl groups abstracts a hydrogen only from the alkyl group attached to the other carbonyl.

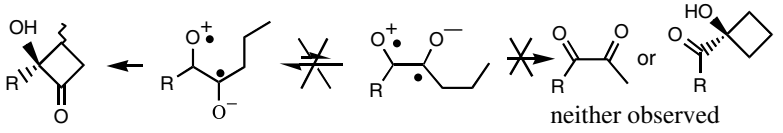

This regioselectivity originally was ascribed to the preferred geometry of the excited triplet being *anti*. The *syn* geometry could not possibly produce the observed products, but it is not obvious why an alkyl group next to either carbonyl could not be aligned in a reactive position; however, it is the unusual nature of the n,π^* excited state that causes the observed regioselectivity, with through-bond coupling splitting the *n* orbitals such that radical-like reactivity appears to be greatest on the inner lobe of the oxygen *n* orbitals. The structurally symmetric 1,8-diphenyloctan-4,5-dione provided an impressive early example of this selectivity, with simple methylene γ-hydrogen abstraction being preferred over benzylic.[111] Interestingly, some 10% of a 3-phenyl-2-hydroxycyclopentanone was also formed. Given the creed of the times, only γ-hydrogen abstractions were considered possible, so it was suggested that the **X**-ed out forbidden γ-hydrogen transfer had occurred; however, current knowledge recognizes this as an early demonstration of the ~20 γ/δ rate ratio, as abstraction of a secondary benzylic hydrogen is only three

times faster than abstraction of an unactivated methylene hydrogen. This new interpretation is consistent with the nonreactivity of the outer lobe of the *n* orbital.

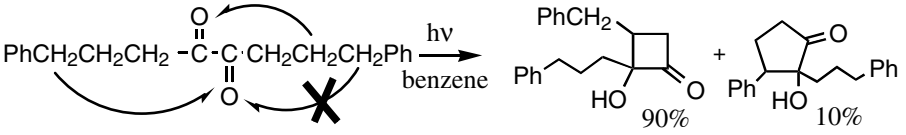

One cyclic α-dione has been studied — 1,2-cyclodecanedione. As in the nonconjugated diketones described previously, one of its carbonyls abstracts a γ-hydrogen, but from across the other carbonyl, like acyclic diketones.[112] When irradiated as crystals, it forms only the *cis*-cyclobutanol product. In benzene, both isomers are formed in a 7:1 *cis*/*trans* ratio; a cleavage product, 2-ketocyclooctanecarboxaldehyde, is also formed, either by direct cleavage of the reactant's O=C–C=O bond or by α-cleavage of a product's HOC–C=O bond, followed by disproportionation of the resulting biradical in either case. It does not appear as though as much attention has been given to the stereochemistry of the products formed from most other α-diketones.

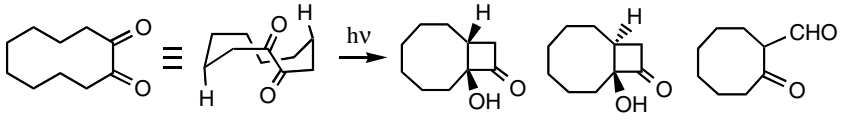

Rate constants for hydrogen abstraction by α-diketone triplets are only 0.1% as large as those for comparable monoketones, although relative rates toward primary, secondary, etc. hydrogens are similar for both mono- and diketones.[113,114] The low rate constants for triplet reaction allow phosphorescence to compete, something that almost never occurs for monoketones. Phenyl alkyl diketones undergo another competing reaction: enolization of the β-carbonyl in diketones with α-hydrogens. The mechanism is not known but could involve β-hydrogen abstraction. It definitely affects the efficiency of cyclization. However, slight amounts of acid catalyze the enols back to diketone and should maximize cyclobutanol formation, as long as irradiation is done at wavelengths long enough to be absorbed only by the diketone.

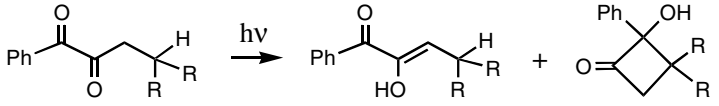

Table 58.4 lists kinetic parameters for a group of phenyl alkyl diketones.[114] When R is neopentyl there are no γ-hydrogens (just three γ-methyls) but nine δ-hydrogens, none of which is abstracted by either carbonyl group. The analogous monoketone, γ-dimethylvalerophenone, undergoes triplet δ-hydrogen abstraction with a rate constant ~4×10^5 s^{-1}. That indicates a rate ~1×10^3 s^{-1} for the diketone, less than 1% the rate of enolization, which explains the lack of photocyclization of this compound.

The electronic asymmetry of the phenyl alkyl diketones prompts, as a possible explanation for the regioselectivity that they show, the idea that reactivity is localized on the benzoyl carbonyl, but the regioselective behavior of the symmetric aliphatic diketones refutes that notion. Moreover, no distal γ-hydrogens are present on the phenyl diketones for the β-carbonyl to abstract.

TABLE 58.4 Kinetic Parameters for 1-Phenyl-1,2-Diones PhCOCOR in Benzene

R	Φ_{CB}[a]	Φ_{-K}[b]	$k\gamma_{-H}$ (10^5 s^{-1})	k_{enol} (10^5 s^{-1})
CH_2CH_3	0.04 (0.06)	0.50 (0.61)	0.10	1.6
$CH_2CH_2CH_3$	0.52 (0.71)	0.73 (0.87)	3.9	1.6
$CH_2CH(CH_3)_2$	0.81 (0.88)	0.88 (0.93)	13.0	1.7
$CH_2C(CH_3)_3$	0	0.62 (0.94)	—	2.3
$CH(CH_2CH_3)_2$	0.015	0.53	5.0	260
$C(CH_3)_3$	0.28 (0.75)	—	36	0
$CH_2CH_2CH_3$[c]	0.56 (0.78)	0.81 (0.95)	3.3	0.9

[a] Cyclobutanone formation (values) in wet CH_3CN.
[b] Diketone disappearance.
[c] *p*-Methoxy.

Another reaction of aryl α-diketones originally was thought to involve γ-hydrogen abstraction from an *ortho*-alkyl group, although the product is a hydroxyindanone.[111,115] The quantum yield in methanol for the *o*-tolyl compound was 83%, but only a few percent when the *ortho*-alkyl group was bulky. At the time this reaction was discovered, it was still generally assumed that internal hydrogen abstraction occurred only from γ-carbons. Thus, several hypotheses were advanced for rearrangement following abstraction from an *ortho*-carbon. One is shown in Structure 46 and is plausible but no longer considered too likely. The fact that no benzylic deuteration occurred when the reaction was run in methanol-*O*-d did provide a warning that a dienol may not have been formed. Likewise, an 83% quantum yield for a Yang enolization seems unlikely given that half the *o*-xylylenols usually revert to starting ketone. More details, together with some stereochemistry, appear later in the section on δ-hydrogen abstraction.

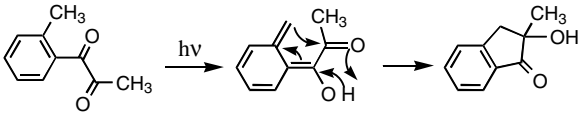

1,5-Biradicals: δ-Hydrogen Abstraction

As noted above, efficient δ-hydrogen abstraction requires the absence of reactive γ-hydrogens, where the definition of "reactive" involves both CH bond strength and proximity to the carbonyl. Several classes of compounds fulfill these requirements, and many papers have been published describing a wide variety of reactants. Paquette's synthesis of dodecahedrane is the model for overall geometry being more important than intrinsic reactivities, excited cyclopentanone units undergoing hydrogen abstraction only at δ-carbons and faster than the very rapid type I α-cleavage of cyclopentanones.[42]

Acyclic Ketones

Two ketones were mentioned above that undergo both γ- and δ-H-abstraction because their structure enhance δ-reactivity and lower γ-reactivity. 4-Benzoylbutanal forms both an α-hydroxycyclopentanone and acetophenone in a 2:1 ratio.[45]

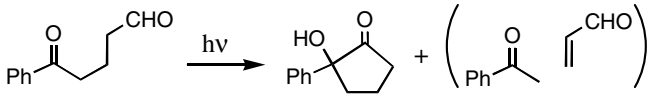

δ-Methoxyvalerophenone behaves similarly; quantum yields are shown below.[44] Product yields from the 1,4-biradical are much greater than cyclopentanol yields, although the rate constants for hydrogen abstraction are each ~2.6×10^7 s^{-1}.

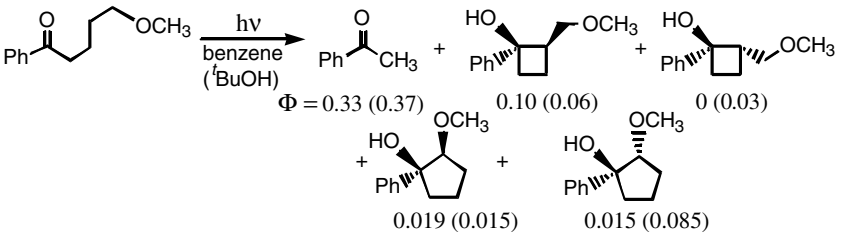

Quantum yields for cyclization of hydroxy biradicals formed from acyclic ketones in general are low because of rapid reversion to ketone, especially so for 1,5-biradicals, the cause for which is explained below and in Scheme 9. It is noteworthy that the alcohol solvent enhances formation of the cyclic alcohols with the OH and methoxymethyl groups *trans* to each other and lowers yields of the *cis*-isomers. It also should be noted that no 1,8-hydrogen transfer competes with the δ-hydrogen abstraction, even though the methoxy group possesses highly reactive CH bonds except for their distance from the carbonyl.

δ-Thioalkoxyvalerophenones form cyclobutanols but no measurable cyclopentanols for two reasons: (1) internal charge transfer quenching by the sulfide causes 78% of the triplet decay; and (2) the δ-alkylthiyl group activates δ–CH bonds and deactivates γ–CH bonds less than does a δ-alkoxy group, so that no more than 5% of the triplets undergo δ hydrogen abstraction and only 10% of them cyclize (as is the case for the δ-methoxy compound).[73]

The simplest example of δ-hydrogen abstraction is provided by γ-dimethylvalerophenone, which has no γ-hydrogens. It forms a 3,3-dimethylcyclopentanol in high yield but low quantum efficiency (0.04 in benzene). Its measured triplet lifetime of only 500 nsec indicates a rate constant for δ-hydrogen abstraction only 1/30th the rate constant for γ-hydrogen abstraction by triplet β-dimethylbutyrophenone.[28]

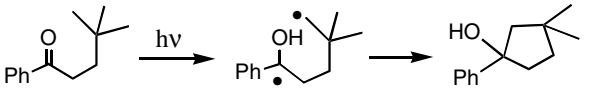

Photocyclization of 5,5-dimethyl-3-hexen-2-one provides an aliphatic example, with the added twist that the α,β-unsaturated ketone undergoes photoinduced *cis*/*trans* equilibration, which allows the *cis*-isomer to undergo δ-hydrogen abstraction.[116]

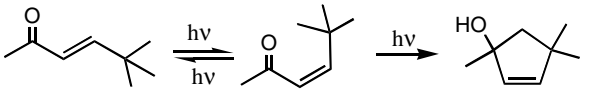

β-Alkoxy Ketones

Photocyclization of β-alkoxy ketones provided the earliest examples of δ-hydrogen abstraction in acyclic ketones.[117] Some of the compounds studied had readily abstractable γ-hydrogens but no oxetanes or type II cleavage products were formed. Instead, oxacyclopentanols and α,β-unsaturated ketones were formed. Originally it was thought that only δ and no γ-hydrogen abstraction occurred. Later it was suggested that γ-hydrogen abstraction must have occurred but that the 1,4-biradical eliminated methanol rather than cyclize.[44]

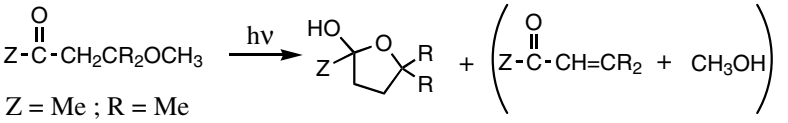

Irradiation of β-ethoxypropiophenone produces oxacyclopentanols in good yield and reveals the surprising fact that most of the biradical reversion to ketone involves a 1,4-hydrogen transfer to produce the enol of starting ketone.[118] It is this second path for reversion of the biradical to ketone, which is twice as fast as the one that transfers an OH hydrogen, which causes the low quantum yields for cyclization in many other 1,5-biradicals. In this case, as with α-alkoxy ketones, cyclization quantum yields are quite high and indicate again that biradical reactions are affected by energies of the products being formed; in this case an oxygen eliminates eclipsing interactions in the developing oxacyclopentanols. Scheme 9 shows how the 1,5-biradical partitions between reversion and cyclization. As usual, an alcohol solvent, by solvating the biradical OH group, lowers the yields of cyclization and reverses the *trans*/*cis* ratio of the diastereomeric products. α-Deuteration of the ketone raises the cyclization yields because of a primary isotope effect on the rate of enolization. The rate constant for triplet δ-hydrogen abstraction is 1.4×10^7 s^{-1}, much smaller than the $\sim 5 \times 10^9$ for the equivalent α-ethoxy ketone.

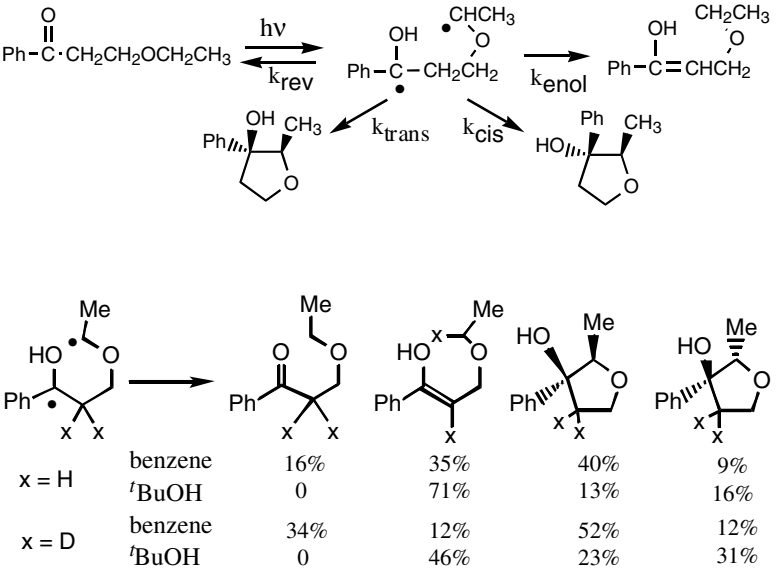

SCHEME 9

Following are a few examples of photoinduced δ-hydrogen abstraction in β–alkoxy ketones as a synthetic method. Descotes has studied the photoreactions of ketones tethered to sugars as 4-hydroxy-2-butanone glycosides.[119] In Structure 53, one isomer is formed as a single diastereomer, likely due to hydrogen bonding of the biradical OH to the axial acetate group. In Structure 54, a simple synthesis of a pheremone is displayed.[120] Descotes also has reviewed many aspects of sugar photochemistry.[121]

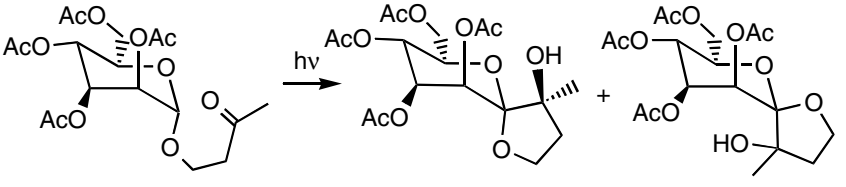

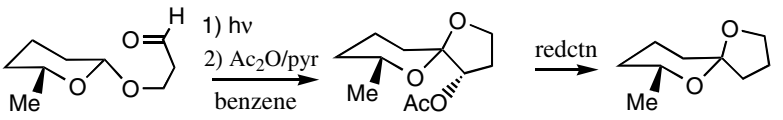

Kraus and Schwinden[122] utilized protecting groups, especially methoxymethyl (MOM), which allowed the pentose xylose to undergo photoinduced δ-hydrogen abstraction, which produces a cyclic acetal. Acid catalysis converts the acetal carbon to an aldehyde, such that the overall process produces two epimeric hexoses, gulose and idose. The same paper provides a short review of other sugar photochemistry.

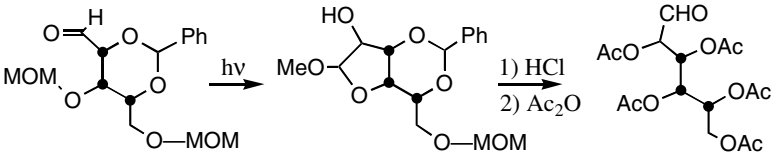

Kraus and Chen[123] have reported the completely stereospecific synthesis of racemic paulownin based on δ-hydrogen abstraction by a β-alkoxy ketone. It is particularly interesting that only one of four possible diastereomers is formed during cyclization of the 1,5-biradical intermediate, the one that would arise if coupling occurs only on the same face of the initial five-membered ring as hydrogen abstraction took place and with the substituents at the δ-radical site maintaining the same relative configuration they had before hydrogen abstraction. Further such examples follow.

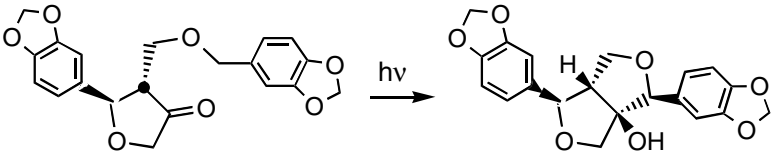

Carless and co-workers[124] tested the ability of β-allyloxy ketones to maintain the original geometry of the allyl double bond upon formation of the 1,5-biradical. In the examples below, the biradicals cyclize faster than the allyl radicals can interconvert between their *cis* and *trans* geometries. Both diastereomers of the oxacyclopentanols are formed in this case, unlike the Kraus example.[123]

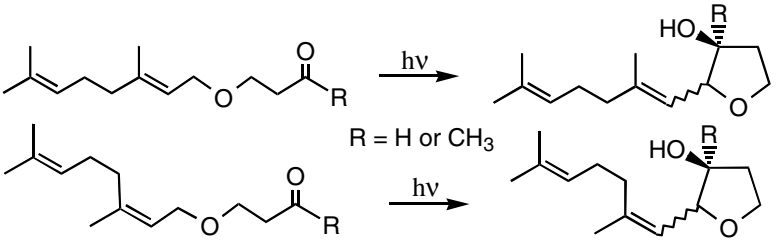

β-Amido Ketones

As mentioned above, *N*-acylation of amino ketones suppresses the basicity of the nitrogen lone pair and thus its electron-donor potential. That being the case, β-amido ketones operate much like β-alkoxy

ketones, in that δ-hydrogen abstraction is possible and γ-hydrogens may be absent. The nitrogen atom in *N*-alkyl-acylacetamides is also in a β position with respect to the ketone carbonyl. Thus, irradiation of *N*-alkyl-2-acylacetamides produces γ-lactams, as shown below.[125]

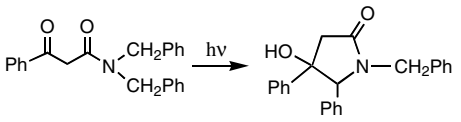

Henning's group was the first to show that δ-hydrogen abstraction by photoexcited *N*-(2-acylethyl)-*N*-tosyl aminoacid derivatives produces substituted prolines with high diastereoselectivity.[125] Since then, a large number of remotely acylated *N*-tosyl aminoacid derivatives have been studied, primarily by the groups of Wessig and Giese. Below are three reactions that exemplify different modes of hydrogen abstraction.[127] The first shows a proline synthesis from a *N*-alkyl alanine ester with the β–benzoyl group part of the aminoacid itself. Both diastereomers are formed and the S configuration of the alanine is maintained, because hydrogen abstraction takes place from an *N*-alkyl group.

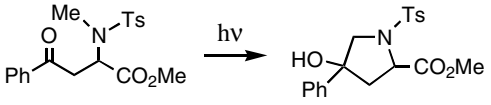

In the next reaction, the acylethyl group is attached to the nitrogen and the δ-hydrogen abstracted is on the stereocenter of the amino acid. CH bonds α to a carboxyl group normally are not highly reactive, but in this case they are modestly activated by the amide nitrogen. The OH and carbobenzyloxy groups are *cis* in the racemic major products, due to internal hydrogen bonding in the biradical.

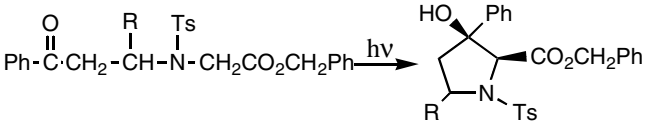

The third reactant, a γ-benzoyl-β-(*N*-alkylamido)butanoate ester, is a one-carbon homolog of the first reactant; its reaction exemplifies the greater reactivity of γ relative to δ-hydrogens. Triplet γ-benzoylbutanoate esters undergo γ-hydrogen abstraction with rate constants of only 1×10^7 s^{-1}, so the k_H values for CH bonds next to amide nitrogens must be considerably lower than those for δ-hydrogens in β-alkoxy ketones, which are also in the 1×10^7 range.

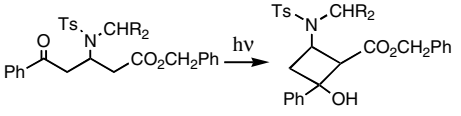

With a pyrrolidine chiral auxiliary, the *N*-(2-benzoylethyl)-*N*-tosylglycinamide below undergoes δ-hydrogen abstraction to enantioselectively form two proline diastereomers, the one with OH *cis* to the carboxamide group favored 4:1.[128] The major product has the S configuration shown as the pyrrolidine structure induces the hydrogen abstraction to occur mainly from the top face (as drawn) of the molecule, from which the biradical cyclizes. With even larger groups on the pyrrolidine, the EE for product formation actually rises to 100%.

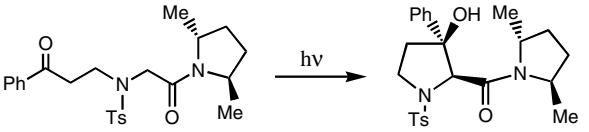

With *N*-(2-acylethyl)-*N*-tosyl-alanine esters, the proline products retain the configuration of the α-carbon of the alanine to various degrees depending upon conditions, as shown in Scheme 10.[129] With added benzophenone, which sensitizes triplet reaction of the ketoester, a triplet biradical is formed and there is little stereoselectivity. With air replaced by argon, both singlet and triplet states react and selectivity is higher. Addition of 1-*M* naphthalene greatly enhances both enantio- and diastereoselectivity. The naphthalene sensitizes excited singlet formation and quenches all triplet reaction so that only singlet biradicals are formed.[130] The selectivity trends illustrate the varying speeds with which singlet and triplet biradical coupling competes with conformational changes. Thus, the triplet biradicals clearly approach conformational equilibrium before cyclizing in this quite flexible molecule, whereas only a little bond rotation occurs before singlet biradicals cyclize. When R = phenyl, as in the above examples, only triplet reaction occurs.

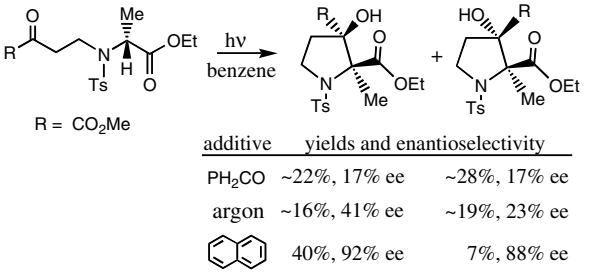

SCHEME 10

Giese has summarized the different approaches to achieving enantioselective photocyclization of remotely acylated aminoacids as follows: With triplet ketone reactions, asymmetric induction via chiral auxiliaries is needed to coax the long-lived biradicals into appropriate geometries, as triplet biradicals tend to live long enough to assume several conformations before cyclizing; with singlet ketone reactions, molecular chirality such as that of alanine can induce the triplet carbonyl into an appropriate geometry for hydrogen abstraction from which the singlet biradical can cyclize quite rapidly.[131]

Henning and co-workers[132] earlier studied the photocyclization of some cyclic amides, such as the tosylated piperazines shown below. With no alkyl groups on the piperazine ring, only γ-hydrogen abstraction and type II elimination occur, just as with acylcyclohexanes. With an alkyl group on the γ-carbon, two things happen: In the chair conformation, δ-hydrogen abstraction from that alkyl group generates a bicyclo[3.2.1]octanol product; in a twist-boat conformation, cross-ring abstraction of a δ-hydrogen occurs to yield a bicyclo[2.2.1]heptanol product.

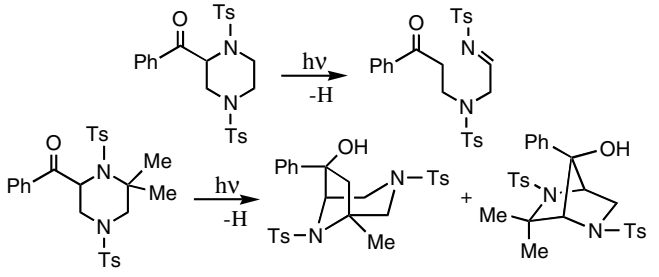

o-t-Alkylphenyl Ketones

Triplet *o-t*-butylbenzophenone does not undergo bimolecular photoreduction but instead undergoes rapid intramolecular δ-hydrogen abstraction to form an indanol both in solution and as crystals.[133] The quantum yield for cyclization is only 5% in hydrocarbon solvents, a value that leaps to 100% in alcohol solvents. It is not clear why the unsolvated 1,5-biradical undergoes disproportionation so much more than cyclization, but its 4-ns lifetime (Table 58.1) indicates that it disproportionates back to ground-state ketone some ten times faster than do 1,4-biradicals. This ketone provides the best evidence that rates of hydrogen abstraction in solution are determined by the distance, not the number of connecting atoms, between a hydrogen and the carbonyl. Hydrogens on two of its methyl groups are within 2.5 Å of the oxygen, and its k_H of 10^9 s^{-1} is close to the value for γ-hydrogen abstraction by triplet *o*-methylbenzophenone. The temperature dependence of its triplet lifetime revealed an E_a value of 2.5 kcal/mole and an A value of 10.6.

The high rate constant and the low activation energy for abstraction of a plain methyl hydrogen raised the question of whether hydrogen abstraction in these molecules involves tunneling. Measurement of the activation parameters for 2,4-di(*t*-butyl-h_9) and di(*t*-butyl-d_9) benzophenones revealed identical $\Delta S^{\ddagger}$ values for the two and a 1.1-kcal/mol higher $\Delta H^{\ddagger}$ for the deuterated ketone.[134] This behavior is exactly what is predicted for primary isotope effects driven by zero point energy differences and rules out tunneling as a mechanism for hydrogen transfer in these compounds.

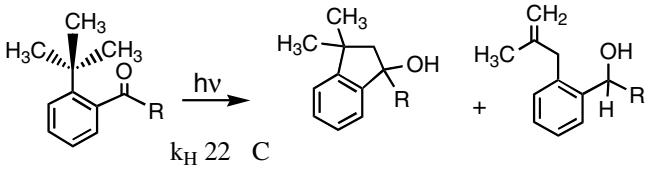

	k_H 22 C		
R = Ph	1×10^9 s^1	99%	< 1%
R = CH_3	~2×10^8 s^1	5%	95%

For analogous acetophenones, the major product is not an indanol but an *ortho*-alkenylbenzyl alcohol, which is formed by internal rearrangement.[135] It is believed that the 1,5-biradical formed by δ-hydrogen abstraction forms a spiro-triene, possibly as a triplet, which can reopen to a rearranged biradical that disproportionates so as to yield an alcohol rather than a ketone. The reason for this reverse form of disproportionation has yet to be found, but that the rearranged biradical disproportionates rather than cyclizes is normal for the interaction of two tertiary radicals. However, the different behavior of the benzophenone- and acetophenone-derived biradicals is readily explained by the different geometries of the two ketones. The coplanar alignment of the acetyl group and benzene ring in the triplet state is transferred to the biradical, maintaining benzylic π-conjugation; the bond rotation required for biradical cyclization is slow, as it weakens benzylic conjugation. In contrast, the *t*-butylphenyl ring is twisted over 70° out of coplanarity with the carbonyl, such that the 1,5-biradical is formed in a geometry ideal for coupling of its two radical sites, which explains its efficient cyclization in crystals. Thus, what little rearrangement may compete could not be detected.

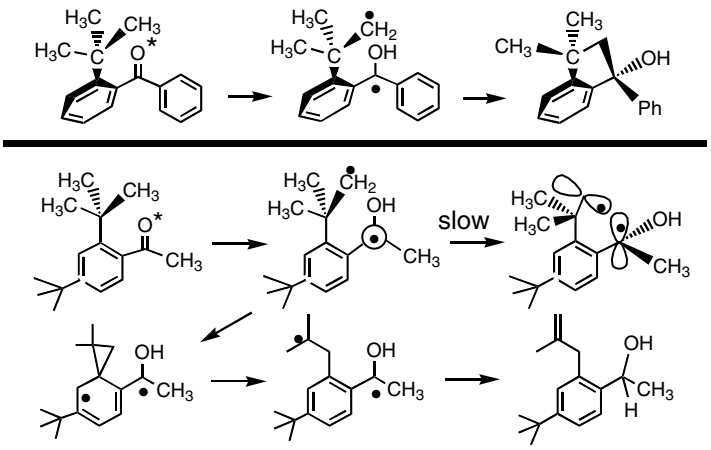

Irradiation of *o-t*-amylbenzophenone produces indanols with varying regio- and diastereoselectivity depending on conditions.[136] The former is of particular interest because one hydrogen on the methylene and one on a methyl group, both 2.5 Å from the oxygen, have dihedral angles ω of 45° and 90°, respectively, in relation to the carbonyl. That 30% or more of the products are formed by abstraction of an intrinsically less reactive primary hydrogen at a theoretically terrible angle supports the view described previously that distance is more important than alignment. The shift in regioselectivity as solvents get more polar probably reflects differences between the ease with which biradicals **BR**1 and **BR**2 can disproportionate back to ground-state reactant. This question requires more study, especially because total product quantum yields are only 0.034 in hydrocarbon solvents and 0.43 in methanol.

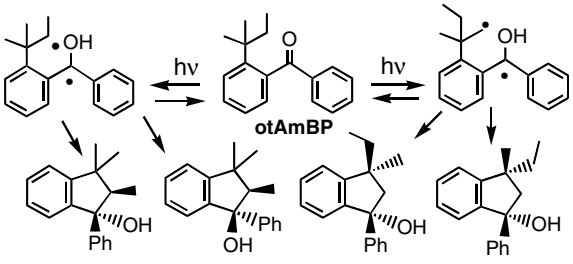

benzene, 20¡C	20%	20%	30%	30%
toluene, -78¡	10	10	40	40
dioxane, 20¡	27	20	21	32
acetonitrile, 20¡	27	25	23	25
MeOH, -78 to 70¡	35	28	13	24
MeOH, 77¡K	12	48	7	33
crystal, 20¡	26	54	8	21

Some recent, yet to be published work revealed that **otAmBP** forms a small amount of a rearranged benzhydrol similar to that formed by *o-t*-butylacetophenone. Even more is formed by irradiation of 2′-(2,3-dimethyl-2-butyl)benzophenone, which undergoes δ-hydrogen abstraction from both a methyl and the isopropyl group to yield three indanols in a total quantum yield of 0.07 in benzene and 0.36 in methanol.[137] It is noteworthy that a single hexenylbenzhydrol isomer is formed. The rearranged biradical disproportionates at the methyl group in preference to the isopropyl group, the opposite of bimolecular radical behavior but understandable in an intramolecular process where the large isopropyl group is pointed away from the body of the biradical structure in order to minimize steric interactions.

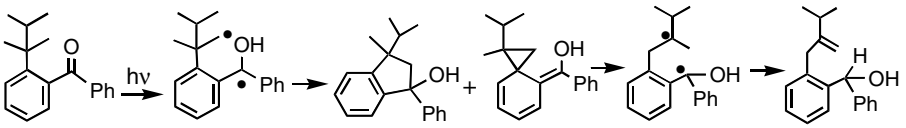

The carbonyls on naphthoquinones and anthraquinones also can abstract hydrogens from *ortho* substituents. One such example is a 1,2-di-*t*-butylanthraquinone, which undergoes the same photocyclization as the similarly substituted benzophenones and acetophenones as well as some butyl rearrangement.[138] Interestingly, the ratio of cyclization to rearrangement and disproportionation is 2:1, with neither reaction of the biradical intermediate dominating, unlike the simple monoketone cases.

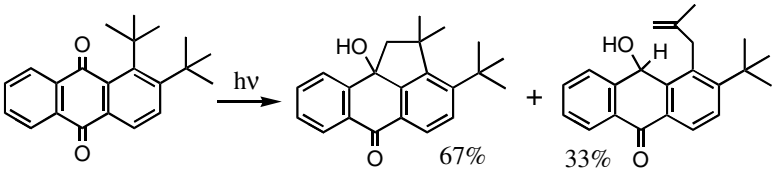

o-Alkoxyphenyl Ketones

Studies of the photocyclization of various *o*-alkoxyphenyl ketones provided some of the earliest examples of δ-hydrogen abstraction.[139–141] More recent studies of these compounds have dealt with structure–reactivity relationships, stereoselectivity, and biradical behavior. Horaguchi[142] has reviewed the synthetic potential of the reaction. Although the formation of benzofuranols following δ-hydrogen abstraction seems straightforward enough, the low reactivity of the triplet is what attracted mechanistic interest. One factor fueling this interest was the report that photoexcited 2,4-dimethoxy-6-t-butylbenzophenone cyclizes by abstracting a hydrogen only from the *t*-butyl group,[143] even though methoxy methyl hydrogens are intrinsically far more labile than simple methyl hydrogens.

Wagner and co-workers[144] studied the photokinetics of a variety of *o*-alkoxyphenyl ketones. Table 58.5 lists the data for some of the ketones studied. Cyclization quantum yields for the five benzophenones are all normal, but the value for the acetophenone is quite low. Ketones **2**, **3**, **4**, and **6** cyclize with high diastereoselectivity in benzene, which as shown below is diminished in polar solvents. The dihydrobenzofuranol products readily undergo acid-catalyzed dehydration to benzofurans.

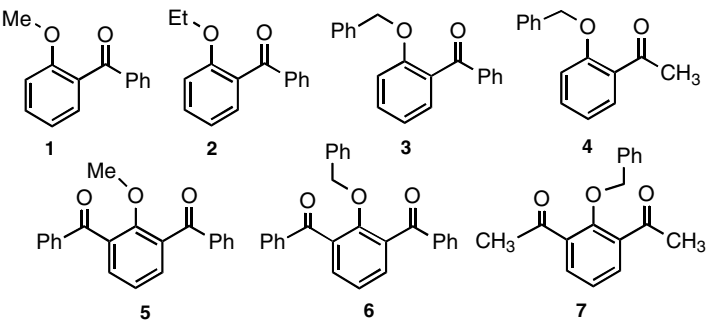

TABLE 58.5 Photokinetics of *o*-Alkoxyphenyl Ketones in Benzene

Ketone	Φ_{cyc}	(*Z*/*E*)	k_H (10^6 s^{-1})	$1/\tau$ (10^6 s^{-1})	E_a (kcal)	log A
1	0.30	—	0.6	0.9	4.2	9.2
2	0.62	11:1	5.3	5.3	—	—
3	0.94	8:1	19.0	19.0	2.8	9.2
4	0.023[a]	1:0[b]	2.0	2.2	3.7	9.0
5	0.77	—	8.0	8.0	—	—
6	1.0	1:0	150.0	150.0	—	—
7	0.17	—	25.0	25.0	—	—

[a] 0.20 with 1-*M* pyridine.
[b] 1.6:1 with 1-*M* pyridine.

TABLE 58.6 Dihydrobenzofuranol Yields from *o*-Alkoxybenzophenones

	% Yield (*Z*/*E*)		
R in *o*-OCH_2R	Benzene	Acetonitrile	Methanol
H	80	68	7
Me	94 (12/1)	81 (2.4/1)	40 (1/1)
Et	84 (1/0)	77 (3.5/1)	33 (1/1)
*i*Pr	82 (15/1)	71 (2.6/1)	35 (1/1.7)
Ph	84 (14/1)	81 (1.7/1)	75 (1/1.3)
Vinyl	90 (1/0)	70 (1.3/1)	69 (2/1)
CN	97 (1.2/1)	84 (1/1.6)	28 (1/3)
CF_3[a]	95 (1/2)	—	—
o-O*i*Pr[b]	74	69	80

[a] From Reference 146.
[b] *o*-Isopropoxybenzophenone.

Rate constants k_H for δ-hydrogen abstraction are extremely low for ketones **1** and **2**. The *o*-benzyloxy **3** reacts faster, but **4** with partial π,π^* character is only 1/10 as fast as **3**. The key results are the **6/3**, **5/1**, and **7/4** rate constant ratios of 8:1, 13:1, and 12:1, respectively. Compounds **5**, **6**, and **7** were studied to address the suspicion that the low rate constants for the simple *o*-alkoxy ketones are due to the alkyl part of the alkoxy groups being pointed away from the *o*-carbonyl in their most populated equilibrium conformations. Ketones **5** to **7** obviously have their methyl and benzyl groups pointed toward one of the benzoyl groups, and their high k_H values confirm the idea that k_H values reflect conformational populations, in accord with Eq. (58.4).

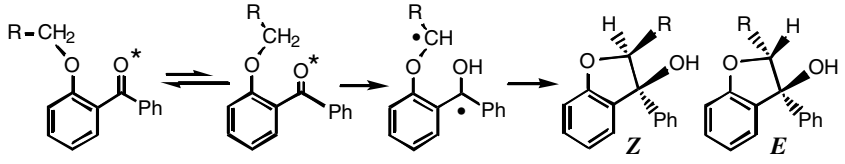

The early findings that polar solvents lower the yields and the diastereoselectivity of cyclization prompted a thorough study by Horaguchi and co-workers.[145] They varied both solvents and the groups attached to the δ-carbon. Tables 58.6 and 58.7 list their results together, with those of Kim and Park.[146]

The results in Table 58.6 are quite informative. In benzene, yields approach 100%, and, with two exceptions, over 90% of the benzofuranols consist of the isomer with R and phenyl *trans*. Diastereoselectivity this high

likely involves biradical conformational preferences more than steric interactions between the two radical sites as they couple. The change to acetonitrile lowers yields only slightly but drastically lowers diastereoselectivity, possibly due to trace water solvating the biradicals. Methanol just about eliminates diastereoselectivity, as it does for many hydroxy-biradicals. Its major effect, however, is to lower yields significantly, probably because low k_H values allow bimolecular hydrogen abstraction from solvent to dominate, except for the benzyloxy and allyloxy ketones, where the δ-hydrogens are activated. The most intriguing result is the inversion of diastereoselectivity by strong electron-withdrawing groups. Park has suggested that a captodative effect alters the electrostatics of the biradical such that the partially positive OH and the partially negative CN or CF_3 interact enough to force the phenyl and R groups *cis* during cyclization.

Table 58.6 includes data for *o*-isopropoxybenzophenone, which cyclizes in lower yield than the others, despite the fact that triplet δ-hydrogen abstraction in it is sufficiently faster than in many of the others that its cyclization yield is not lowered in methanol. It turns out that it undergoes a competing reaction that was reported in 1971[139] and is described below.

Horaguchi's team also studied some α-substituted (2-benzoylphenoxy)acetate esters, which have a moderately electron-withdrawing carboxy group on the δ-carbon. Table 58.7 shows the same kind of data for these compounds as did Table 58.6 for the others. Interestingly, product yields and *Z/E* ratios in both benzene and acetonitrile are much the same as for the other ketones in which R is not electron-withdrawing. Apparently, the alkyl substituent also on the δ-carbon negates any electron withdrawal and activates the δ-hydrogen sufficiently that yields are high even in methanol. However, for the two largest R groups, diastereoselectivity is inverted from their acetonitrile values, with only the phenyl-substituted compound maintaining high *Z/E* selectivity. One would have thought that in aprotic solvents hydrogen bonding would hold the OH and carboxy groups together sufficiently that they would end up *cis* and that methanol would solvate the hydroxy group sufficiently to allow the R and phenyl groups to be *trans*. As shown below, in polar solvents an additional product was found in 6 to 8% yield for R = Et. The process whereby such byproducts are produced is discussed below.

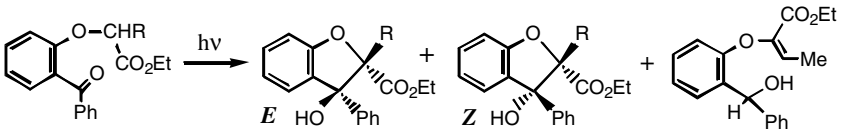

TABLE 58.7 Photocyclization of Ethyl α-(*o*-Benzoylphenoxy)Carboxylates

	% Yield (*Z*/*E*)		
α-R in *o*-OCHR-CO_2Et	Benzene	Acetonitrile	Methanol
H	74 (15/1)	75 (1.5/1)	0
Me	93 (30/1)	72 (4/1)	68 (1/1.4)
Et	84 (50/1)	74 (5/1)	61 (1/5)
*i*Pr	70 (1/0)	75 (6/1)	48 (1/4)
Ph	74 (1/0)	75 (18/1)	72 (8/1)

As mentioned, Pappas[141] was one of the first investigators of *o*-alkoxyphenyl ketone photochemistry. He studied exclusively *o*-alkoxyphenylglyoxylate esters, which cyclize only by δ-hydrogen abstraction, and acquired some interesting early results about solvent effects that have since been found to affect many other ketones. The k_H values were found to be $\sim 3 \times 107 s^{-1}$, faster than for γ-hydrogen abstraction in phenylglyoxylates. In later work it was found that lowering the temperature to 0° doubles the *trans*/*cis* ratio and that brominated solvents raise it even more.[147] Both would seem to indicate forced cyclization of the initially formed biradical geometry.

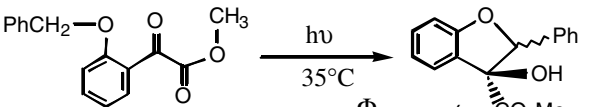

	Φ_{cyc}	*t/c*
benzene	0.89	6.7
CH_3CN	0.56	1.9
^tBuOH	0.47	1.0

As already mentioned, some byproducts are formed from these *o*-alkoxyphenyl ketones, one of which resembles the rearrangement that the *o*-*t*-alkylphenyl ketones undergo. The scheme below depicts these byproducts for *o*-ethoxy ketones; the benzophenone undergoes only cyclization, whereas the acetophenone rearranges to a hemiketal and to a vinyloxybenzyl alcohol.

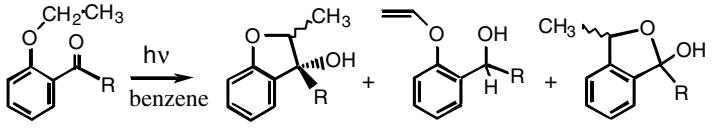

R = Ph	100% (11:1 *Z*/*E*)	0	0
R = CH_3	12% (all *Z*)	19%	69%

The O-C switch presumably occurs for the same reason that a similar switch does in the *o*-*t*-alkylacetophenones, namely that the coplanarity of the carbonyl and benzene ring in excited acetophenone is transferred to the 1,5-biradical, slowing its cyclization and favoring spiro-enol formation, subsequent opening of the epoxy group, and either direct coupling to the hemiketal or disproportionation followed by addition of the alcohol to the ketone.

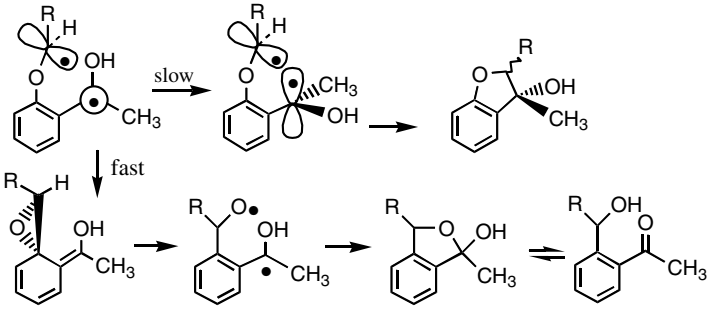

The rearrangement to vinyloxybenzhydrol involves disproportionation of the original 1,5-biradical to a compound with a vinyl ether and an alcohol *ortho* to each other, thus providing a perfect geometry for acid-catalyzed addition of the alcohol to the vinyl ether. The following shows the mechanism developed by Wagner and Laidig[148] that explains the earlier observed formation of a dioxane from *o*-isopropoxybenzophenone. When the ketone is irradiated in benzene, a 2:1 ratio of benzofuranol and *o*-propenoxybenzhydrol is formed. Addition of just a trace of acid causes the vinyl and hydroxy groups of the latter to disappear. When the ketone was made from acetone-d_6, the benzylic hydrogen in both vinyl ether and dioxane was replaced by deuterium.

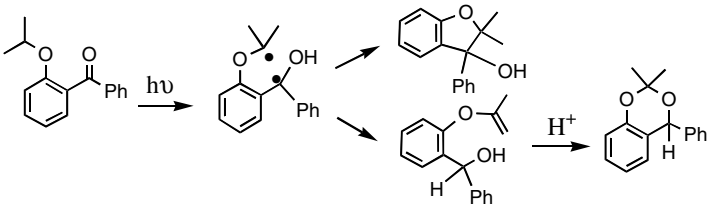

Horaguchi's group[149] provided another example of competition between cyclization and an internal redox process in some *ortho*-substituted benzocyclohexenones. These compounds have the electronic nature of comparable acetophenones, with rings of different sizes providing variable amounts of flexibility to the carbonyl group. Vinyl ether formation occurs only in the six- and seven-membered rings, which remain fairly rigid compared to larger rings, which allow enough twisting of the phenyl–C(OH) bond for the biradical to cyclize rapidly.

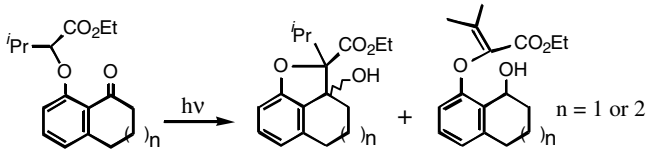

A similar study of simple 8-alkoxytetralones highlighted the effect of coplanarity in that a rearranged 8-hydroxyalkyltetralone is formed in 5 to 12 times the amount of a benzofuranol, depending on the size of R.[150] The corresponding *o*-alkoxybenzosuberones undergo only cyclization, just like simple *o*-alkoxybenzophenones.

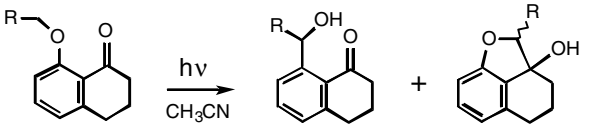

R = H	36%	34%
Me	62%	5%
Et	43%	8%
^{i}Pr	69%	11%
^{t}Bu	71%	9%

As described previously, β-alkoxyketones form 1,4-biradicals with lifetimes of only a few nanoseconds, values which are now generally understood as reflecting high through bond spin-orbit coupling. An obvious question arises as to what effect the extra atom might have on lifetimes of 1,5-oxabiradicals. Because triplet hydrogen abstraction rate constants are slower than the decay rate of most biradicals, the cyclopropylcarbinyl radical clock was employed to provide 1,5-biradical lifetimes.[151] The following scheme shows the products formed from *o*-cyclopropylmethoxy ketones.

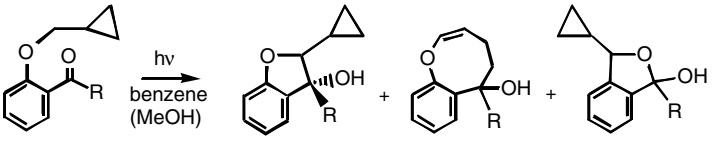

R = Ph	Φ = 0.26	92% (8:1 *Z*/*E*)	8%	
R = CH_3	Φ = 0.02	7% (all *Z*)	13%	80%
		(35% (1:2 *Z*/*E*)	15%	50%

As with other *o*-alkoxyphenyl ketones, the benzophenone forms mainly a benzofuranol, while the acetophenone forms mainly a hemiketal, its yield being lessened by methanol in favor of the benzofuranol. (This change of solvents could possibly be a general way of minimizing unwanted byproduct.) Both ketones gave small amounts of a benzocyclooctadienol, the cyclization product of the 1,8-biradical formed by opening of the cyclopropyl ring of the original 1,5-biradical. From the product ratios, quantum yields, and known rate constants for cyclopropylethyl radical ring opening, the rate constants shown below could be estimated for the various reactions of the 1,5-biradical (the hemiketal comes from the spiroepoxide), which add up to much the same decay rates as measured for the 1,4-oxabiradicals. Their values may be smaller if the oxygen stabilizes the δ-radical site enough to slow opening of the cyclopropyl ring.

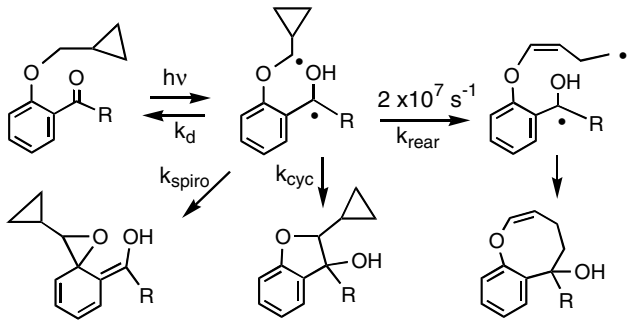

R	k_{spiro}	k_{cyc}	k_d	$1/\tau_{BR}$
Ph	$< 1 \times 10^7$	2.5×10^8	7.5×10^8	$10 \times 10^8\ s^{-1}$
CH_3	1.2×10^8	1×10^7	$4—40 \times 10^7$	$2—5 \times 10^8\ s^{-1}$

Descotes et al.[152] reported an approach to the synthesis of crombénine that involves δ-hydrogen abstraction from an acetal to generate the required spiroketal structure. Unfortunately the required 2,4-dioxy substituents lower the yield from 87% when R = H to 20 and 0% when R = OAc and OMe. Because *p*-methoxy groups deactivate triplet phenyl alkyl ketones by causing the lowest triplet to become π,π*, electronic and conformational effects apparently combine to lower k_H values so much that they barely compete with phosphorescence. Moreover, the bulk of the cyclic ether very likely worsens the conformational problem common to *o*-alkoxyphenyl ketones.

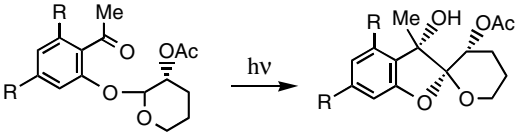

Kraus et al.[153] have reported several uses of intramolecular hydrogen abstraction for synthetic purposes. One example used *o*-alkoxyphenyl alkyl ketones to prepare an aflatoxin precursor. In the process the substituent problem encountered by Descotes was partially solved. Elaboration of the dihydrobenzofuranol photoproduct to aflatoxin required the presence of a methoxy group *para* to the acyl group in the original ketone reactant. The result was no reaction for 4-methoxy-2-alkoxyphenyl alkyl ketones. However, 2,6-dialkoxyphenyl ketones undergo photocyclization even with a *p*-methoxy group. It turns out that, with both *ortho* positions occupied, the acyl group twists out of conjugation with the benzene ring to avoid nonbonded interactions, providing a much better geometry for δ-hydrogen abstraction and likely increasing the population of *n*,π* triplets.

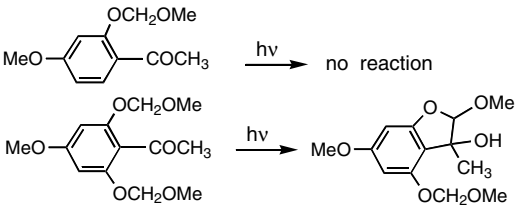

o-Amino phenyl ketones have excited states with mainly charge transfer character and are not reactive as hydrogen atom abstractors, providing rather messy mixtures of photoproducts that include very small yields of indoles.[154] Although acyclic amidoketone excited states readily undergo hydrogen abstraction, as described above, Hasegawa and co-workers[154] reported that irradiation of *N*-(*o*-benzoylphenyl)-*N*-methylacetamide causes only deacylation in polar solvents and dealkylation in nonpolar solvents. Though acylation lowers the electron-donating potential of amines, the lowest excited states of *ortho*-amidophenyl ketones retain charge transfer character.

Two examples of *o*-acyl-*N*-alkylanilines being activated by conversion to anilinium salts have been reported.[155] *o*-Benzoyl trimethylanilinium tetrafluoroborate, as either crystals or in acetonitrile solution, undergoes quantitative photocyclization to an *N*,*N*-dimethylindolium salt. The reactant *o*-benzoyl anilinium cation has the same structure as *o*-*t*-butylbenzophenone and undergoes δ-hydrogen abstraction followed by cyclization of the resulting 1,5-biradical. In acetonitrile, the quantum yield is 0.56; k_H is 1/30 as large as k_H for the *t*-butyl ketone, as would be anticipated for hydrogen abstraction from carbons bonded to positively charged atoms (see Chapter 52). The temperature dependence of the triplet decay of the *o*-trimethylammonium benzophenone revealed the same 2.36 kcal/mol activation energy already measured for *o*-*t*-butylbenzophenone, but a 7.6 EU more negative entropy of activation.[134] Thus, the entire factor of 30 difference in their rate constants for δ-hydrogen abstraction is entropic or at least nonenthalpic.

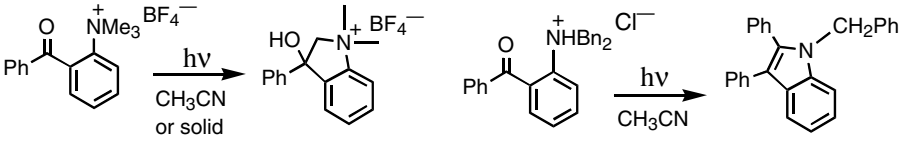

The hydrochloride salt of *o*-benzoyl-*N*,*N*-dibenzylaniline also photocyclizes and then dehydrates to an indole, although with low quantum efficiency; the free base exists in equilibrium with its conjugate acid and acts as both a quencher and an internal filter.

Giese's group has now activated *o*-acylanilines by converting them to triflamides, which undergo photocyclization to indolinols in high yield. The reaction shows high, solvent-mediated stereoselectivity, with R mainly *cis* to the OH when R = CO_2Me and *trans* when R = phenyl.[156]

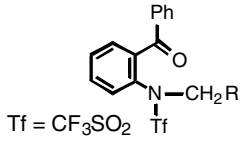

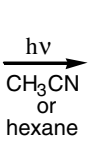

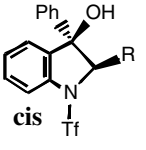

	cis/trans	
R	hexane	CH_3CN
Ph	4 : 96	11 : 89
CO_2Me	92 : 8	52 : 48

Alkoxy-substituted naphtho- and anthraquinones undergo δ-hydrogen abstraction to form a variety of products. Kraus et al.[157] have studied some naphthoquinones, and Blankespoor et al.[158] have studied some anthraquinones. The addition of a methyl next to the alkoxy group has the beneficial effect of

increasing the population of the conformer with the benzyl group tilted toward the carbonyl, thus increasing k_H and the quantum yield for cyclization.

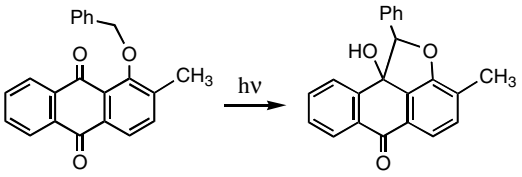

α-(*o*-Alkylphenyl) Ketones

Reactivity

Prompted by the behavior of *N*-(*o*-tolyl)phthalimide, Meador and Wagner[159] found that α-(*o*-tolyl)acetophenone photocyclizes to 2-phenyl-2-indanol quantitatively and with a quantum yield of 1.0. Follow-up studies by Wagner et al.[160,161] have revealed an interesting array of structure–reactivity relationships as substituents add to the steric congestion of the molecules. These α-aryl ketones provide unique examples of kinetic competition between conformational change and product formation as well as potential for indanol synthesis. Table 58.8 lists rate constants for triplet δ-hydrogen abstraction from representative α-aryl ketones and quantum yields for both cyclization and Norrish type I α-cleavage when it competes with hydrogen abstraction. Rate constants for triplet α-cleavage are 0.2, 2, and 12 × 10^7 s^{-1}, respectively, for α-phenyl acetophenone, propiophenone, and isobutyrophenone. Thus, cleavage competes with cyclization in the α-aryl propiophenones and totally dominates in α-dialkyl ketones.

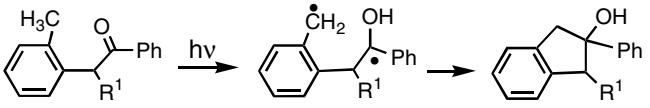

TABLE 58.8 Photokinetics of ArCHR¹R²COPh in Benzene

Ar	R^1	R^2	Φ_{cyc}	$\Phi_{\alpha\text{-cl}}$	k_H (10^8 s^{-1})
o-Tolyl	H	H	1.0	0	1.6
o-Tolyl	CH_3	H	0.05	0.28	0.025
o-Tolyl	CH_3	CH_3	0	0.38	—
Mesityl	H	H	0.44 (0.54)[a]	0	6.0
Mesityl	CH_3	H	0.24 (0.71)[a]	0.02	1.6
Mesityl	CH_3	CH_3	0	0.31	—
o-Ethylphenyl	H	H	0.80	0	8.0
o-Isopropylphenyl	H	H	0.42	0	7.5
o-Benzylphenyl	H	H	0.36 (0.45)[a]	0	1.7
Tip[b]	H	H	0.23 (0.016)[a]	0	8.5
Tip[c]	D[c]	H	0.38 (0.027)[a]	0	—

[a] Maximum in polar solvent.
[b] 2,4,6-Tri-isopropylphenyl.
[c] Tip, CD_2COPh.

That hydrogen abstraction rate constants range from 1.6–8.5 × 10^8 s^{-1} indicates a molecular geometry, with the δ–CH bonds quite close to the carbonyl. Structure 86 illustrates why the mesityl acetophenone reacts 3.5 times faster than the *o*-tolyl. The α-aryl groups are oriented perpendicular to the CH_2–CO bond and eclipse the carbonyl group. For hydrogen abstraction to take place, the ring must rotate a little to get a methyl close to the carbonyl, but the opposite rotation is favored for an *o*-tolyl group. In the mesityl ketones, rotation in either sense delivers a methyl to the carbonyl.

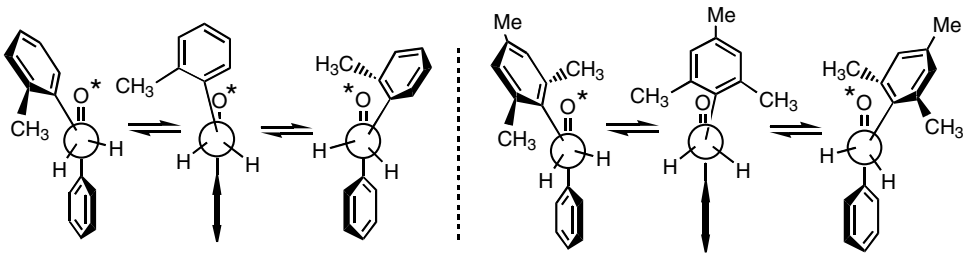

Flash kinetic measurements of biradical decay rates revealed average lifetimes of 20 nsec in toluene and 30 nsec in methanol when the α-aryl group of the ketone has *o*-methyl groups, 40 nsec in toluene, and 45 nsec in methanol when the α-aryl group has *o*-isopropyl groups. How lifetimes and quantum yields are increased by Lewis-base solvents was discussed earlier. That lifetimes vary with substituents on the *ortho*-carbon, with tertiary radical sites coupling more slowly than primary radical sites, adds evidence that ease of product formation contributes to biradical lifetimes.

Acetophenones react with much larger rate constants compared to propiophenones with the same α-aryl group — a 64:1 ratio for *o*-tolyl and 3.8:1 for mesityl. Scheme 11 illustrates the reason, which is due to the different geometry of α-disubstituted ketones. The α-alkyl group nearly eclipses the carbonyl, forcing the α-aryl ring to twist off to the side. In the mesityl case, one of the *ortho* methyls is close to the oxygen at the time of photoexcitation, but at a dihedral angle ω of some 66°, the cosine of which would predict a fivefold lowering of k_H, almost as observed. In the *o*-tolyl case, the methyl group can be tilted toward the oxygen in much the same position as a mesityl methyl, but more often it is tilted away from the carbonyl. The low k_H thus is due to a combination of an unfavorable conformational equilibrium and an imperfect CH alignment relative to the carbonyl in the lowly populated reactive conformer.

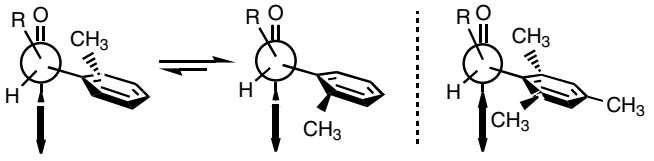

SCHEME 11 Preferred geometries of some α-arylpropiophenones.

Two other reactions besides α-cleavage compete with cyclization, but only from the most sterically crowded compounds. A 1,3-shift of α-mesityl groups forms enol ethers in low chemical and quantum yields (1 to 2%).[162] This reaction may be initiated by charge transfer from mesityl to excited carbonyl.

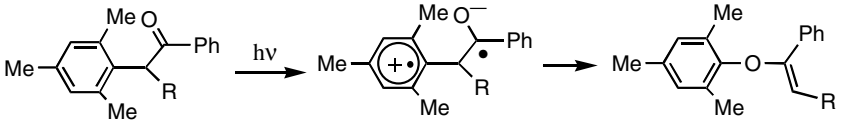

Another example of 1,5-biradicals disproportionating to enols is provided by *o*-(2,4,6-triisopropylphenyl)acetophenone, which forms an enol that is long lived due to its steric congestion.[163] Table 58.8 indicates that the cyclization yield of the compound is larger for the α-deuterated form, thanks to a primary isotope effect on the biradical disproportionation. However, Lewis-base solvents greatly diminish cyclization yields, probably because the solvated OH group presents a steric barrier to cyclization.

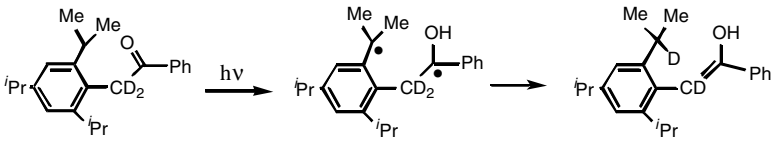

Stereoselectivity

When the biradicals from most α-aryl ketones cyclize, the carbon holding the phenyl and hydroxy groups becomes a stereocenter. An additional α-substituent and/or an *ortho* CH_2R group on the α-aryl ring provide extra stereocenters and introduce the possibility of two to four diastereomeric indanol products. Table 58.9 lists the stereoselectivity of cyclization for several ketones as well as the quantum yields for any competing α-cleavage. One column lists the *trans*/*cis* ratios for the *ortho* R relative to the phenyl; the other lists *trans*/*cis* ratios for α-methyl relative to the phenyl. Two of the ketones have both methyls so two *trans*/*cis* ratios are listed.

TABLE 58.9 Photo-Behavior of Ar CHR–COPh in Benzene at 22°C[a]

Ar	R	Φ_{cyc}	*trans/cis*[b]	*trans/cis*[c]	$\Phi_{\alpha\text{-cl}}$	k_H (10^8 s^{-1})
o-Tolyl	CH_3	0.05 (0.02)	—	15/1	0.28	0.025
Mesityl	CH_3	0.24 (0.71)	—	9/1	0.02	3.0
o-Ethylphenyl	H	0.80	95/5 (2/1)	—	—	8.0
o-Ethylphenyl	CH_3	0.07	5/1 (3/2)	6/0	0.08	41
2,4,6-Triethylphenyl	H	0.52	97/3 (5/1)	—	—	4.0
2,4,6-Triethylphenyl	CH_3	0.24	28/0	11/9 (17/1)	—	7.7
o-Benzylphenyl	H	0.40 (0.45)	11/9 (1.2/1)	—	—	16.5
o-Benzylphenyl	CH_3	0.05	11/9	—	0.06	8.3

[a] Values in methanol in parentheses.
[b] *ortho*-CH_2–R vs. Ph.
[c] α-Me vs. Ph.

In all but one case the α-methyl group ends up predominately *trans* to the phenyl, the exception being one of the two diastereomeric products from the triethylphenylpropiophenone. As described earlier, the α-methyl of these α-arylpropiophenones is oriented *anti* to the benzoyl phenyl and stays so in the triplet and the initially formed 1,5-biradical. Thus, its predominantly *trans* position relative to the phenyl in the indanols is a result of a not easily changed pre-existing conformational preference.

For the four ketones with *ortho*-ethyl groups, at ambient temperatures the ethyl-derived methyl group also is predominantly *trans* to the phenyl in the indanol products, but the predominance fades in methanol as solvent and disappears at low temperatures and for the solid state. In contrast, the indanol products from the α-(*o*-benzylphenyl) ketones are formed with almost no diastereoselectivity in any solvent.

The photocyclization of α-(*o*-ethylphenyl)acetophenone in benzene or as a solid occurs with 90 to 100% diastereomeric excess, favoring the isomer with the methyl and phenyl groups *trans*.[164] Analysis indicates that conformational preferences in the 1,5-biradical determine this selectivity. Hydrogen abstraction creates the biradical **BR**1 in a geometry from which simple disrotatory rotation of the two radical sites produces the major product. the same rotation forms the isomeric product in a higher energy conformer, **BR**2. A **BR**1-to-**BR**2 conversion cannot occur in the solid, so only *trans*-indanol is formed. What is most interesting is that **BR**1 is lower in energy because its OH group hydrogen-bonds to the benzene ring which prevents the normal reversion to ketone that causes low quantum yields in many Yang photocyclizations and Norrish type II eliminations, thus allowing these biradicals to cyclize in high quantum yields. Stereoselectivity drops to 5:1 in dioxane and 2:1 in methanol, mainly because solvation of the OH destabilizes **BR**1 and allows a larger population of **BR**2.

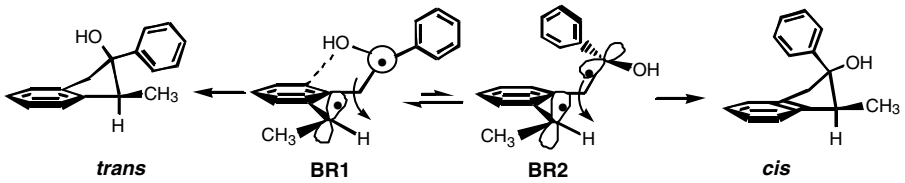

The lack of stereoselectivity in the photocyclization of α-(*o*-benzylphenyl) ketones most likely is due to the fact that δ-hydrogen abstraction creates a benzhydryl radical site that does not allow both phenyl groups to be fully conjugated with the half-occupied *p* orbital. Although conformers exist that are analogous to the **BR**2 above, they remain less populated than **BR**1e and **BR**1z, which are roughly equally populated and maintain the hydrogen bonding that stabilizes **BR**1. It is the fact that their individual least-motion pathways to cyclize require rotations in the opposite sense (**BR**1z disrotatory like **BR**1 and **BR**1e conrotatory) that removes stereoselectivity.

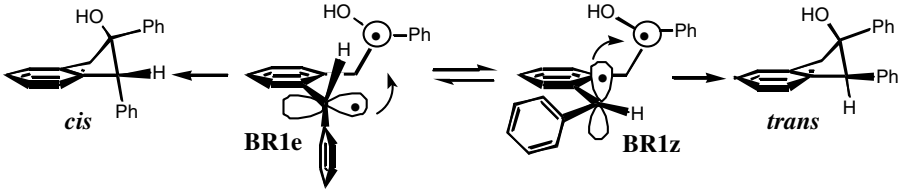

Although most of the indanols formed from these α-aryl ketones are chiral, they are all produced racemic by simple irradiation. However, Scheffer et al.[165] have shown that his method for inducing enantioselectivity with ionic chiral auxiliaries works well for *para*-carboxylated α-mesitylacetophenone in the solid state, which produces one enantiomer in 90% EE. The twisting of the mesityl ring required to bring an *o*-methyl group close enough to the carbonyl, as described above, normally can occur both clockwise and counterclockwise, thus allowing either *o*-methyl group to be attacked by the excited carbonyl. The twisting motion amounts to a form of helical chirality and in the presence of an outside chiral force one methyl is favored.

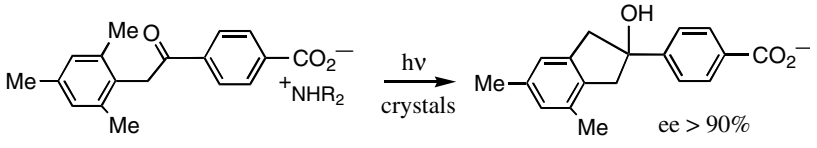

Wagner et al.[166] have studied temperature effects on the cyclization diastereoselectivity of the ketones shown in Table 58.9. The ketones were irradiated in toluene at various temperatures from –78°C to 110°C, and the product isomer ratios provided linear Arrhenius plots. A graphical table of the results includes the differential activation parameters for formation of *cis*- and *trans*-isomers of each indanol. The results are analyzed in Table 58.10.

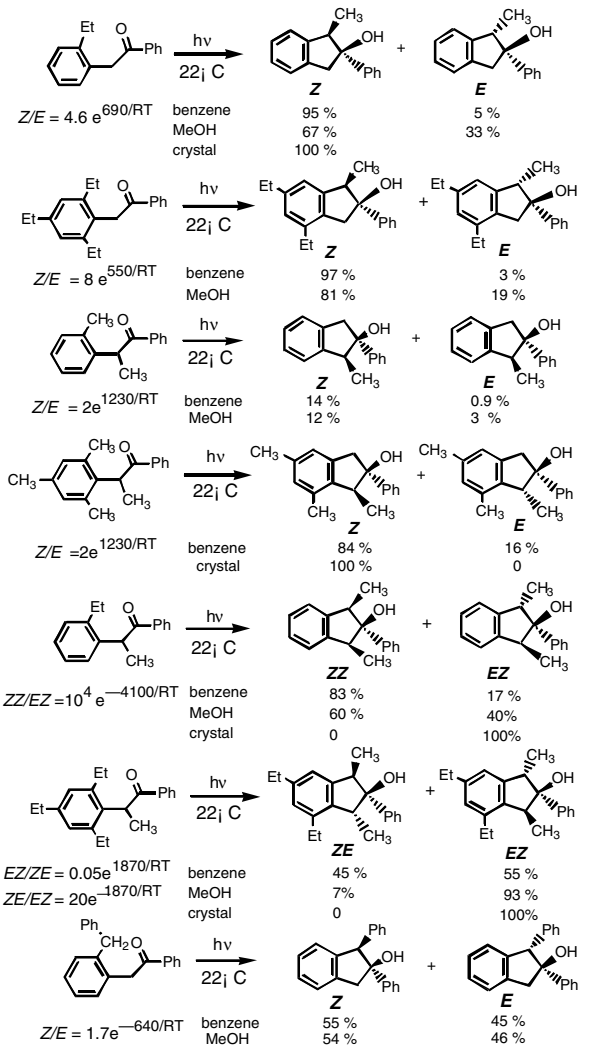

TABLE 58.10 Range of Indanol Diastereoselectivities from ArCHRCOPh

			Toluene[a]	
Ar	R	Ratio	–72°C	110°C
o-Tolyl	CH_3	*Z*/*E*	48/1 (49%)	10/1 (22%)
Mesityl	CH_3	Z/E	26/1 (100%)	9/2 (100%)
o-Ethylphenyl	H	Z/E	26/1 (96%)	11/1 (96%)
Triethylphenyl	H	Z/E	32/1 (100%)	36/1 (100%)
o-Ethylphenyl	CH_3	ZZ/EZ	1/10 (100%)	6/1 (48%)[b]
Triethylphenyl	CH_3	ZE/EZ	1/6 (100%)	3/2 (100%)
o-Benzylphenyl	H	Z/E	2/3 (100%)	3/2 (100%)

[a] Chemical yields in parentheses.
[b] Highest temperature was 22°C.

The two *o*-ethylphenyl acetophenones display very similar behavior: similar small $\Delta\Delta E_a$ values and non-zero A factors indicating nonenthalpic effects favoring formation of the *Z* product from **BR**1. Because the half-occupied *p* orbitals of **BR**1 and **BR**2 are aligned differently, **BR**1 apparently enjoys more spin-orbit coupling, converts from triplet to singlet more efficiently, and thus cyclizes more. In solution, the biradicals displays conformational equilibrium in their cyclization selectivity.

The two *o*-methylphenyl propiophenones show nearly identical temperature effects. (The low yields for the *o*-tolyl compound reflect the large amount of competing cleavage.) They each have both enthalpic and entropic preferences for keeping the α-methyl *anti* to the phenyl group. The latter again probably reflects different spin-orbit coupling in the biradical conformers that cyclize. The cyclization selectivity reflects primarily ground-state control, as the initial **BR**2-like geometry has a difficult time converting to a **BR**1-like geometry, which can form the *E*-isomer.

The *o*-ethylphenyl propiophenones do not mimic any of the above four ketones. They both could yield four diastereomers, but each forms only two. The simple *o*-ethylphenyl compound forms one isomer (*ZZ*) that keeps both methyls *trans* to the phenyl and that is favored at room temperature, but at low temperatures and as crystals it forms only the *ZE*-isomer, in which the ethyl-derived methyl is *cis* to the phenyl. Under the conditions favoring the *ZE* product, ground-state control determines selectivity, but at higher temperatures in solution rotational control takes over with regard to the ethyl-derived methyl. The large $\Delta\Delta E_a$ and A values can only represent a bond rotation, not a conformational equilibrium or a spin-orbit coupling difference. As described previously, the geometry of the ketone is such that hydrogen abstraction produces **BR**2ze; in order for it to convert to a **BR**1-like geometry (**BR**1zz), two bond rotations are required to keep the α-methyl and phenyl groups apart. At temperatures above 20°C, the rise in *ZZ*/*ZE* ratios slows and Norrish type I cleavage lowers cyclization yields.

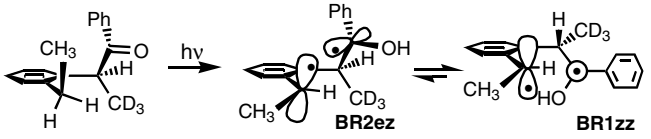

The triethylphenyl propiophenone also forms only two indanol isomers, each of which has one of the two methyls *cis* to the phenyl. Again, the *EZ*-isomer is favored under conditions that retard rapid bond rotations. The favored ground-state geometry produces a biradical with a **BR**2ez shape, but with the extra *ortho*-ethyl group it cannot rotate to a **BR**1zz geometry and has a difficult time rotating to a **BR**1ze geometry. That the $\Delta\Delta E_a$ and A factors favor opposite isomers is intriguing. The 20-fold entropic preference for the *ZE*-isomer could again be a spin-orbit effect. The 1.9-kcal $\Delta\Delta E_a$ could represent conformational equilibrium between either biradical or ground-state conformers.

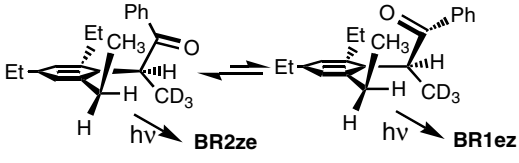

Finally, α-(*o*-benzylphenyl)acetophenone not only shows little diastereoselectivity but also starts to favor the *E*-indanol as the temperature decreases. Its *Z*/*E* ratio ranges from 1.2:1 to 1:1.2 over the temperature range. Nonetheless, its A factor still favors cyclization to the *Z*-indanol, again most likely due to different *p* orbital orientations.

Park et al.[167] recently added an interesting twist to known photoreactivity by studying the behavior of acylcyclopropanes such as 1-benzoyl-1-(*o*-ethylphenyl)cyclopropane. It does not undergo any Norrish

type I cleavage as α-dialkyl ketones do, but its cyclopropane ring takes the place of two methyls in affecting biradical geometries. It undergoes normal photocyclization to an indanol, and the intermediate biradical obviously does not undergo a cyclopropyl ring opening which might have produced a benzoyltetralin. What is most interesting is that the *Z*/*E* indanol ratio ranges from 1:19 to 1:2.5 from –72° to 90°C in toluene and goes as low as 1:99 in methanol at 25°C. As in the *o*-ethylphenyl propiophenones, the initially formed biradical cyclizes to the *E*-indanol but faces a large barrier to rotation into a *Z*-forming geometry.

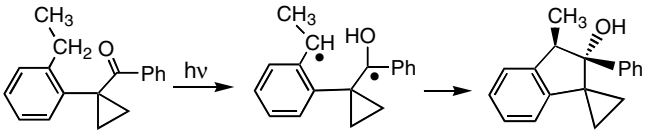

Park's group[168] has also studied the effect of zeolites on diastereoselectivity. When the model (*o*-ethylphenyl)acetophenone was irradiated in X and Y zeolites, *Z*/*E* indanol ratios were much lower than in solution.

Excited States Other Than Simple n,π* Triplets

An early and unique example of δ-hydrogen abstraction was provided by 8-benzyl-1-benzoylnaphthalene (BBN), which undergoes photocyclization despite having a π,π* lowest triplet.[22] (Most naphthyl ketone reactions involve excited singlet states.) Its ground-state geometry is almost perfect for hydrogen abstraction and resembles that of α-(*o*-benzylphenyl) acetophenone. Its measured triplet hydrogen abstraction rate constant of 7×10^3 s^{-1} is 0.001% as large as k_H for the *n*,π* triplet of the *o*-benzylphenylacetophenone. This ratio provides a rare measure of the intrinsic reactivity of π,π* ketone triplets in hydrogen atom abstraction. Measurements of the temperature dependence of the BBN triplet lifetime revealed an E_a of 4.7 kcal/mol and a log A of 7.25. These numbers indicate that the low reactivity is mostly entropic in origin.

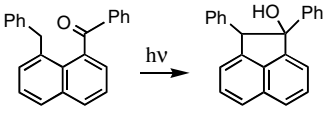

Turro and co-workers[169] discovered that the excited singlet states of *o*-tolyl acetones, but not their triplets, undergo cyclization to indanols, another example of *n*,π* singlet hydrogen abstraction in aliphatic ketones competing with intersystem crossing while triplet hydrogen abstraction is slower than α-cleavage. Quantum yields are very low as described above for singlet-state hydrogen abstraction in general.

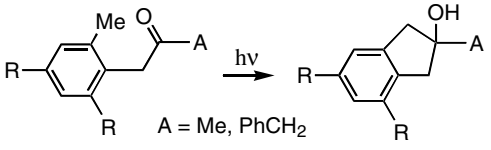

There have been few studies of stereoselectivity in the cyclization of singlet biradicals formed by intramolecular hydrogen abstraction. Zand and Wagner[170] have studied α-(*o*-ethylphenyl)acetone, which photocyclizes to a mixture of both the *cis*- and *trans*-1,2-dimethyl-2-indanols, suggesting that singlet biradicals do undergo some bond rotations before cyclizing. Interestingly, over a 182°C range, the cyclization yield increases with temperature at the expense of cleavage, as singlet hydrogen abstraction becomes faster relative to ISC.

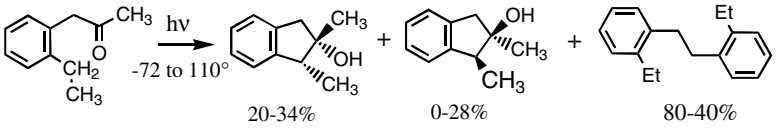

Benzils may be considered 2-aryl-2-keto-1-arylethanones (i.e., slightly modified α-arylacetophenones. The photochemistry of several symmetric 2,4,6,2′,4′,6′-hexaalkyl benzils has been studied in depth[171] in order to ascertain whether the rather puzzling photocyclization of *o*-alkylphenyl diketones to hydroxyindanones is initiated by γ- or δ-hydrogen abstraction, as discussed above. The hexa-methyl, -ethyl, and -isopropyl benzils all photocyclize cleanly to 2-hydroxyindanones in modest quantum yields, the hexaethyl benzil even showing some diastereoselectivity, especially as a solid, where only the pictured *Z*-isomer was formed. It now seems certain that the reaction proceeds only through a 1,5-biradical intermediate, as rearrangement of a benzocyclobutenol in a crystal seems doubtful. More important, in excited diketones one carbonyl abstracts hydrogen only from the moiety attached to the other carbonyl.

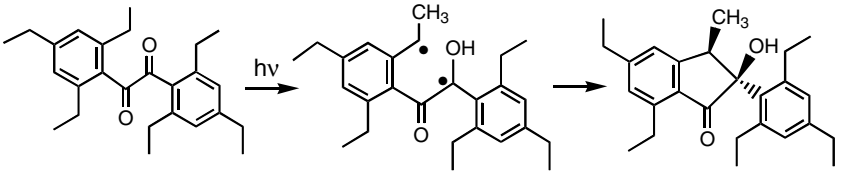

Returning to the methyl *o*-alkylphenyl diketones, Hamer et al.[115] reported that two chiral diketones form hydroxyindanones in methanol with retention of configuration and with modest diastereoselectivity, but in quantum yields of only 1–5%.[115] Remarkably, the stereochemistry parallels that of the α-(*o*-alkylphenyl)acetophenones, with OH preferentially *cis* to an ethyl group but showing only slight selectivity when R is phenyl. This fact further supports the idea that a 1,5-biradical is the precursor to the products.

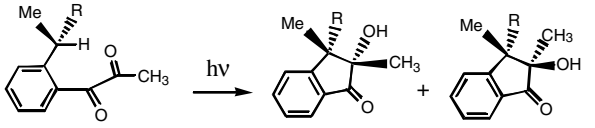

1,6-Iradicals: ε-Hydrogen Abstraction

A few systematic studies of ε-hydrogen abstraction, which generally requires the absence of both γ- and δ-hydrogen atoms, have been performed. Carless and Fekarurhobo[172] provided one of the earliest examples in γ-allyloxy ketones and aldehydes, which photocyclize to roughly equal amounts of diastereomeric tetrahydropyranols. The ε-allylic radical site can disproportionate at each end to generate both starting ketone and a vinyl ether.

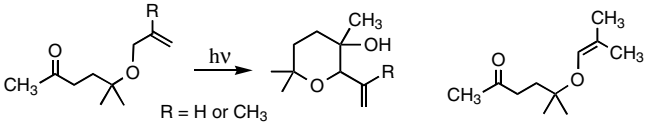

Meador and Wagner[173] found that α-(*o*-benzyloxyphenyl)acetophenone photocyclizes to a dihydrobenzopyran. Park and Wagner[174] have studied a few more examples, as listed in Table 58.11, with an average $k_H \sim 4 \times 10^7\ s^{-1}$, significantly faster than k_H for δ-hydrogen abstraction in *o*-alkoxy phenyl ketones. The difference is due to the very favorable orientation of the α-phenyl ring relative to the carbonyl, as in the α-(*o*-alkylphenyl) ketones. Quantum yields are low, in the 3 to 18% range, but type I α-cleavage accounts for only 25% of the products. The pyranol isomer with R and phenyl *cis* is favored, a sharp departure from normal diastereoselectivity, but that is reversed in the products from 1-benzoyl-1-(*o*-alkoxyphenyl)cyclopropanes.[174]

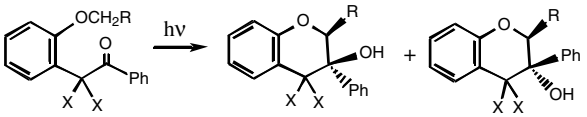

R = Et, Ph *Z* isomer *E* isomer

TABLE 58.11 Products from Ketones (*o*-ROPh)CX_2COPh in Benzene

		% Cyclization Products		% α-Cleavage Products	
ortho-RO	*X*	*Z*-Isomer[a]	*E*-Isomer	Ar_2Ethane	Benzoyl[b]
EtO	H	21.4	53.5	18.2	6.8
$PhCH_2O$	H	35.7	64.3	0	0
iPrO	H	71.0	—	21.0	8.0
EtO	CH_2[c]	>99	<1	—	—
$PhCH_2O$	CH_2[c]	>99	<1	—	—

[a] R and OH *cis*.
[b] Benzil and benzaldehyde.
[c] Half of cyclopropyl CH_2CH_2.

Another class of compounds that undergo ε-hydrogen abstraction is the β-(*o*-tolylphenyl) propiophenones.[175] As Table 58.12 shows, quantum yields and rate constants are much smaller than in the *o*-alkoxyphenyl acetophenones, the former because CT quenching of triplet carbonyls by β-aryl groups is very rapid; the latter because of conformational issues.

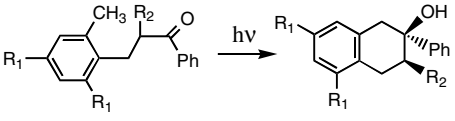

TABLE 58.12 Photochemistry of β-(*o*-Tolyl)Propiophenones

R_1	R_2	Φ (C_6H_6)	Φ (MeOH)	k_H ($10^7 s^{-1}$)
H	H	<0.0001	—	<0.003
CH_3	H	0.0002	0.0003	0.01
H	CH_3	0.0003	0.0012	0.026
CH_3	CH_3	0.002	0.012	0.18

Giese et al.[176] have reported a case in which an *N*-benzoylethyl dipeptide undergoes ε-hydrogen abstraction in preference to δ-hydrogen abstraction. The ε/δ ratio was 8:1 for R = H and 20:1 for R =

benzyl, suggesting a steric reason for the selectivity. The diastereoselectivity of cyclization also depended on the size of R.

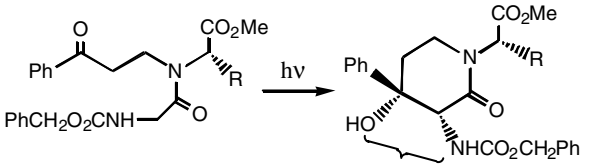

8/1, R = Bn ; 1:1, R = H *cis/trans*

Wessig et al.[177] have explored the effect of amine ring size on the diastereoselectivity of photocyclization of 3-benzoylpropanoamides.

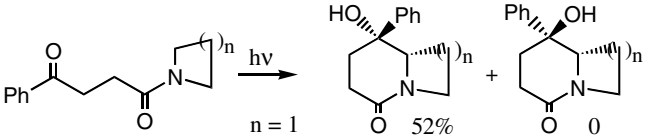

n = 1	52%	0
n = 2	54%	0
n = 3	33%	6%
n = 4	48%	8%

Following a similar theme, Wessig[178] has also synthesized an indolizinone by stereoselective photocyclization of an *N*-protected β-benzoylalanyl proline ester. The product was formed in 60% yield and simulates a β-turn dipeptide.

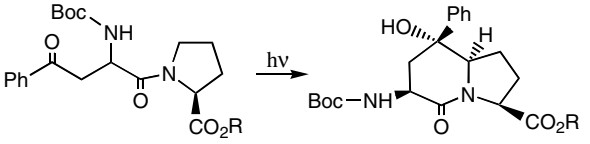

1,7-Biradicals: ζ-Hydrogen Abstraction

Carless and Mwesigye-Kibende[179] provided a rare example with the photocyclization of some β-(*o*-alkylphenyl)propiophenones. With R^2 = Ph or allyl and R^1 = H, the isomeric benzoxipenols were formed in a 2:1 ratio, in rather low quantum yields.

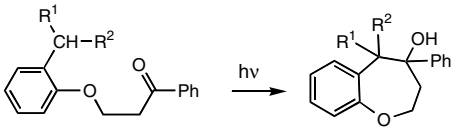

Hasegawa and Yamazaki[180] have reported ζ-hydrogen abstraction in some 2-(alkylamino)ethyl phenylglyoxylates, initiated by electron transfer. No products of γ- or δ-hydrogen abstraction were formed.

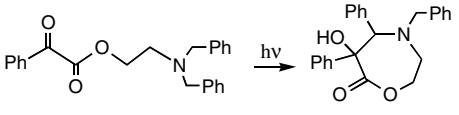

In Descotes' synthetic efforts toward making crombénine that were described above, the desired δ-hydrogen abstraction did not occur unless a bulky OR substituent was present to block the ζ-hydrogen abstraction that otherwise was the major reaction and that led to a bicyclic ether.[152]

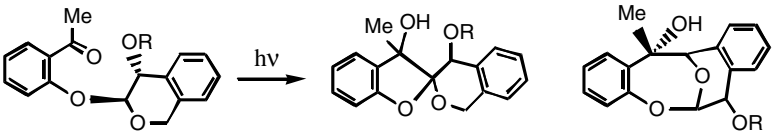

R = H	0	41%
Ac	10%	24%
$Me_2(^tBu)Si$	70%	14%

1,8-Biradicals: η-Hydrogen Abstraction

Kraus and Wu[181] has achieved the synthesis of an eight-atom lactone via η-hydrogen abstraction by a cyclopropyl phenylglyoxylate. The *cis* geometry of the cyclopropyl ring places the ethoxy group closer to the carbonyl than the ester γ-carbon.

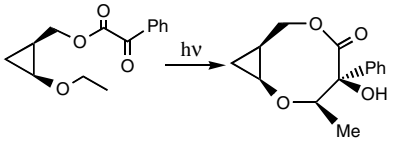

Yoshioka and co-workers[182] have studied the photochemistry of a variety of 2-aminoethyl benzoylacetates, which cyclize to η-lactones, likely by electron transfer followed by proton transfer to generate a 1,8-biradical. It is noteworthy that no δ-hydrogen abstraction occurs.

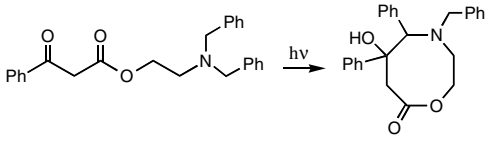

In a similar study, some β-thioalkoxyethyl α-benzoylacetate esters also were shown to undergo photocyclization to lactones.[183] A charge-transfer process again is thought to initiate the reaction, with a proton on the more remote α-carbon being the one transferred to oxygen. The CT nature of the reaction is upheld by the fact that the sulfone version of the compound does not react. Triplet quenching by 2,5-dimethyl-2,5-hexadiene indicates a 2.7×10^7 s^{-1} rate of triplet decay in acetonitrile, an order of magnitude faster than the analogous reaction of the phenylglyoxylate esters. Both the ethyl and benzyl sulfides cyclized in good yield, but for R = Ph only the lactone isomer with the two phenyls *cis* was formed, whereas for R = Me both isomers were formed equally. There is no explanation for such disparate stereoselectivity.

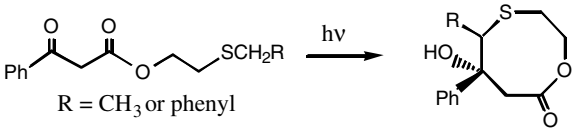

R	%yield	*c/t*
Me	55	1:1
Ph	65	1: 0

Very Remote Hydrogen Abstraction

Breslow[185] and Winnick et al.[184] really opened the field of remote intramolecular hydrogen abstraction with their study of *n*-alkyl *p*-benzoylbenzoates, with the alkyl group containing from 14 to 20 carbons.[11] The ketones photocyclize by hydrogen abstraction from methylene groups between C9 and C17, showing preference for ones between C11 and C15. Quantum yields ranged from 4 to 17%. Values of k_H are in the 0.1 to 5.4×10^5 s^{-1} range, increasing by roughly 1×10^5 with each additional methylene beyond C9.[184]

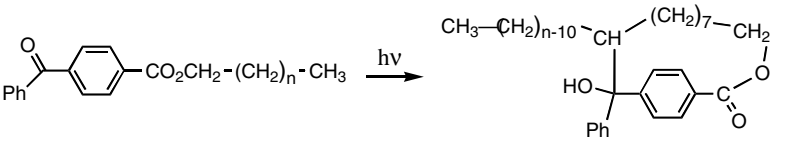

Breslow[185] showed that chaining benzophenone to the A ring of a steroid could lead to regioselective hydrogen abstraction depending on chain length. For example, when $n = 2$, cholestanol undergoes hydrogen abstraction on its α-face from both C7 (shown) and C12 that results in cyclic alcohols; when $n = 1$, hydrogen abstraction is from C14 and the biradical disproportionates instead of cyclizing, as tertiary radical sites tend to do. The ability of Yang hydroxybiradicals to disproportionate to unsaturated alcohols and the promise of high stereoselectivity of cyclization within chiral molecules have been rediscovered in the past decade.

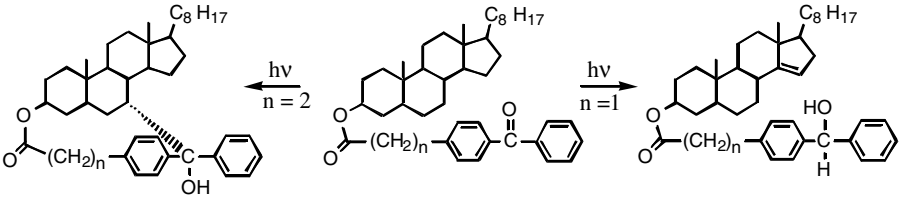

Recent elaborations of the early Winnik work with dipeptides has tethered remote alkyl groups to benzophenone and induced regioselective hydrogen abstraction[186] and hydrogen abstraction from the polymethylene part of a benzophenone embedded in a cyclophane.[187]

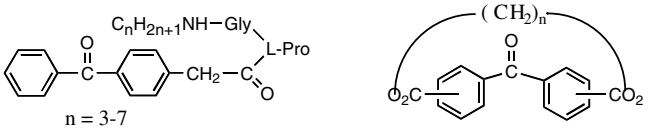

Attaching a 2-alkoxyethyl carboxylate group *ortho* rather than *para* on benzophenone provides an example of θ-hydrogen abstraction and cyclization of the 1,9-biradical to a lactone.[188]

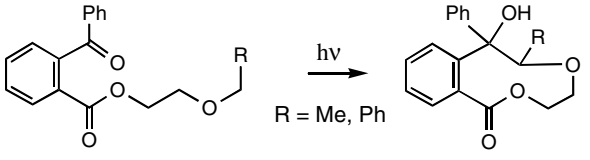

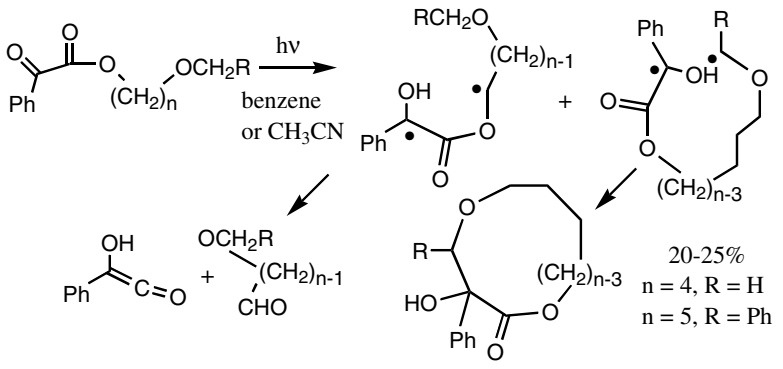

SCHEME 12

Chapter 52 describes the Norrish type II cleavage of alkyl phenylglyoxylate esters; the 1,4-biradicals formed by γ-hydrogen abstraction cleave to yield an aldehyde and a ketene but do not cyclize. Neckers and Hu[189] performed much of this work and have since found that some ω-alkoxyalkyl esters undergo remote hydrogen abstraction to produce macrocyclic lactones. Scheme 12 shows what happens in a group of eight compounds with *n* ranging from 2 to 6 and R being methyl, ethyl, or phenyl.

All eight ketoesters undergo type II cleavage, but only the two ketoesters indicated form cyclic lactones in modest yields, stereochemistry not determined. No compounds with $n < 4$ cyclize, including two ω-ethoxy and one ω-benzyloxy, nor do ω-methoxy esters with $n = 5$ and 6. Thus, no δ-hydrogen abstraction occurs in the ketoesters with $n = 2$, unlike the case for δ-alkoxyketones. Moreover, *t*-butyl phenylglyoxylate is photoinert, unlike the β-*t*-butylpropiophenone described above. The conformational requirements for remote hydrogen abstraction are not stringent, but factors promoting coiling of the alkyl group are needed to allow remote hydrogen abstraction to compete with the type II reaction. It has not been established whether the scantiness of cyclization is due to slow triplet hydrogen abstraction or rapid biradical disproportionation. The measured triplet lifetimes indicated overall rates of reaction in the range of 2 to 5×10^6 s^{-1}, values that likely represent mainly γ-hydrogen abstraction.[190] The fact that rates for abstraction of methyl and benzyl hydrogens are within a factor of two of each other indicates that the rate-determining step involves conformational change.

Analogous ω-thioethoxy ketoesters also undergo photocyclization.[191] Unlike the case for the ω-alkoxy ketoesters, nine of the ten sulfide-containing compounds studied, with *n* ranging from 2 to 11, formed cyclic lactones. In this case, remote hydrogen transfer is due to prior charge transfer from sulfur to triplet carbonyl, with subsequent proton transfer coming exclusively from the carbon on the far side of the sulfur atom. The fact that β-thiophenoxyethyl phenylglyoxylate undergoes no photocyclization emphasizes the lack of δ-hydrogen atom abstraction as well as the nonavailability of a proton on the near side of the positive sulfur in the charge transfer complex.[192]

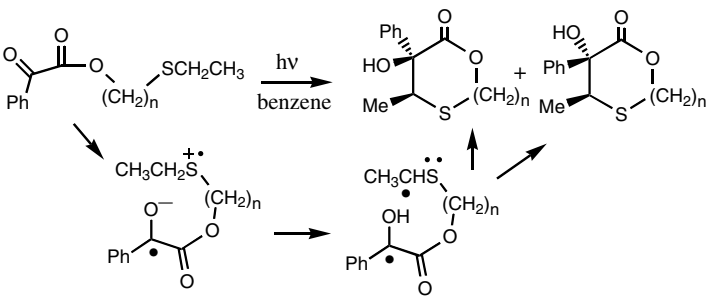

TABLE 58.13 Product Yields from $PhCOCO_2(CH_2)_nSCH_2CH_3$ in Benzene

n	2	3	4	5	6	7	8	9	10	11
Φ_{cyc}	—	0.32	—	0.16	—	0.10	—	0.08	—	0.06
% Yield[a]	100	96	89	71	53	43	32	30	25	0
t/*c*	1.2:1	3.6:1	2.9:1	3.5:1	2.5:1	—	—	—	—	—
% Other[b]	—	—	—	19	30	30	24	30	50	63

[a] Of lactone.
[b] Of type II cleavage and bimolecular photoreduction.
Source: Adapted from Hu and Neckers.[191]

As Table 58.13 indicates, both chemical and quantum yields decrease as n gets larger. For $n = 2$ and 3, cyclization was quantitative, but as n increases products resulting from bimolecular and internal γ-hydrogen abstraction compete more. The total range of triplet ketone decay rates increase from 1.5×10^6 to 3.2×10^7 s^{-1} as n increases, but it is not clear why competing triplet reactions get faster as n increases. Not surprisingly, the diastereomeric (*t*/*c*) ratio is small, varies slightly with n, and favors the phenyl being *trans* to the methyl. The flexibility of the relatively long chains connecting the two radical sites apparently allows stereochemistry to be dominated by nonbonded interactions in the transition state for cyclization. The low quantum yields for cyclization are partially due to the competing reactions of the triplet ketoester as well as nonradiative decay associated with the charge transfer interaction. The extent of any biradical reversion to ketone cannot be deduced from the data.

Some (ω-dialkylamino)alkyl benzoylacetate esters undergo remote hydrogen abstraction probably initiated by electron transfer to form 1,8, 1,9, or 1,10 biradicals and their azalactone cyclization products.[193] Contrary to most other such reactions, a hydrogen gets transferred from an internal methylene next to nitrogen to produce aminolactones.

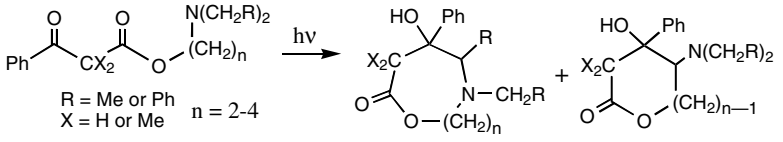

Kraus et al.[194] have reported examples of triplet phenylglyoxylate esters undergoing 1,12- and 1,13-hydrogen transfers leading to macrocyclic lactones. In this case, even a *cis*-hexenyl group and an *ortho*-substituted phenyl group do not prevent competition from simple γ-hydrogen abstraction, as β-lactones are also formed.

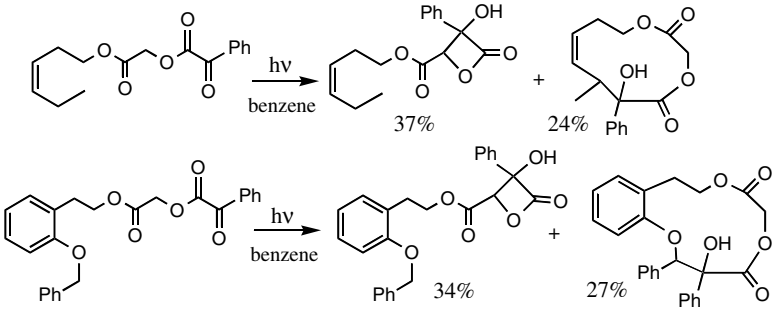

Hydrogen Abstraction Followed by Biradical Rearrangements

The most obvious case involves abstraction of an allylic hydrogen, such that the biradical can react at either end of its allyl radical site. Thus, γ-vinylbutyrophenone forms more cyclohexenol than 2-allylcyclobutanol.[4,82] In contrast, *o*-allyloxyphenyl ketones photocyclize without any allylic rearrangement,[140,145] and several β-allyloxy ketones[195] behave similarly. It is not clear why 1,5-biradicals behave differently than 1,4-biradicals in this regard. If any group attached to the γ-carbon undergoes a radical rearrangement, then the lifetime of the 1,4-biradical is shortened due to that rearrangement competing with its normal cyclization, disproportionation, and cleavage reactions.

An early example involved a 1,4-biradical that underwent a hexenyl-radical cyclization to a 1,5-biradical that cyclized to a hydroxynorbornane.[196]

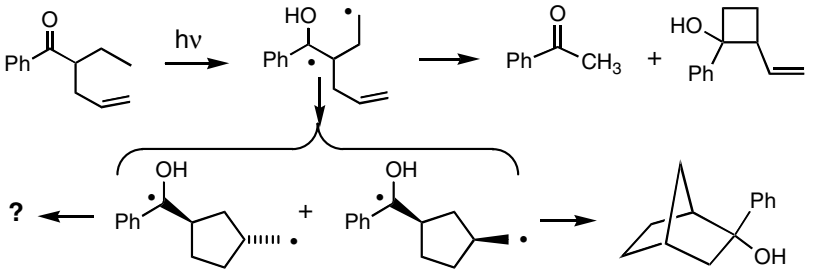

A later example presented a 1,4-biradical undergoing a cyclopropyl-carbinyl ring opening to a 1,7-biradical that both cyclizes to a cycloheptenol and disproportionates to a 1-benzoyl-3-hexene.[197]

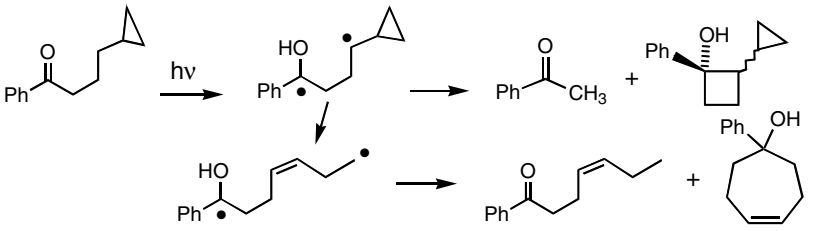

A different example involving cyclopropyl ring-opening is provided by a benzoylcyclopropane which cyclizes normally and ring-opens as a type II cleavage to generate a 5,6-unsaturated ketone.[198]

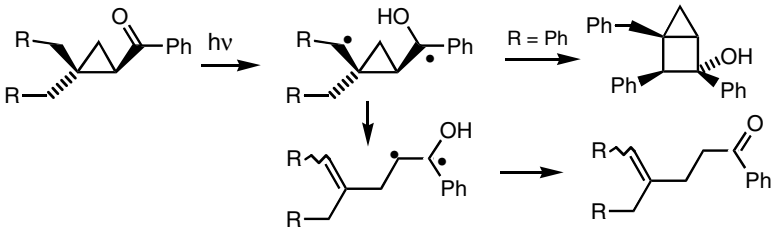

Kraus and Wu[181] put cyclopropyl ring-opening to use as a synthetic method to make ε-lactones without requiring a 1,8-hydrogen transfer. With R = phenyl, only ring-opening occurs, but with R = methyl, both type II cleavages also occur, probably because of some singlet γ-hydrogen abstraction. Without the phenyl group on the cyclopropane ring, only type II cleavage to cyclohexanone occurs.

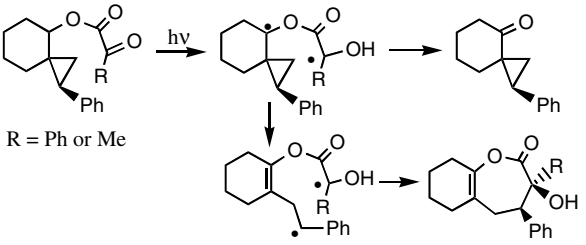

A rather unique example is provided by a δ-hydrogen abstraction of an acetal hydrogen; the 1,5-biradical so formed both cyclizes and undergoes β-elimination at the dioxy radical site to produce a 1,3-biradical that cyclizes to a cyclopropylmethyl formate ester.[199]

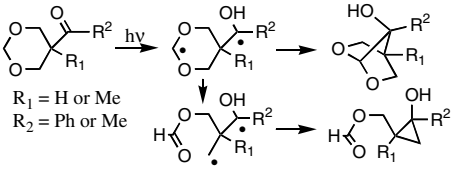

As described earlier, *o*-alkylphenyl ketones undergo γ-hydrogen abstraction, and the *o*-xylylenols so formed are highly reactive towards dienophiles. Quite a few tricyclic structures have been synthesized by such photoinduced intramolecular Diels–Alder reactions. Below is an example provided by Kraus and Wu.[200]

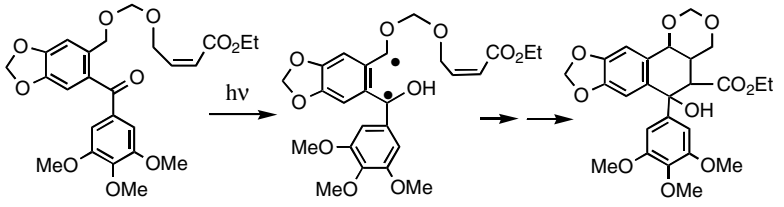

Finally, Hasegawa and co-workers[201] have reported an interesting method to separate two carbonyl groups via photocyclization of a 2-alkyl-1,3-diketone, with the 2-acylcyclobutanol product readily undergoing a retro-Aldol reaction. Note that the carbonyl with the lower triplet excitation energy is the one that reacts.

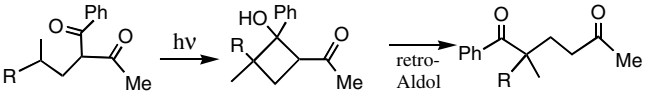

References

1. Wagner, P. J., Type II photoelimination and photocyclisation of ketones, *Acc. Chem. Res.*, 4, 168, 1971.
2. Wagner, P. and Park, B.-S., Photoinduced hydrogen atom abstraction by carbonyl compounds, *Org. Photochem.*, 11, 227, 1991.
3. Dalton, J. C. and Turro, N. J., Photoreactivity of *n*,π* excited states of alkyl ketones, *Ann. Rev. Phys. Chem.*, 21, 499, 1970.

4. Wagner, P. J., Chemistry of excited triplet organic carbonyl compounds, *Top. Curr. Chem.*, 66, 1, 1976.
5. Wagner, P. J., 1,5-Biradicals and five-membered rings generated by δ-hydrogen abstraction in photoexcited ketones, *Acc. Chem. Res.*, 22, 83, 1989.
6. Hasegawa, T., Yamazuki, Y., and Yoshioka, M., Photocyclisation via remote hydrogen transfer to ketone carbonyl oxygen, *Trends Photochem. Photobiol.*, 4, 27–41, 1997.
7. Norrish, R. G. W. and Appleyard, M. E. S., Primary photochemical reactions. Part IV. Decomposition of methyl ethyl ketone and methyl butyl ketone, *J. Chem. Soc.*, 874, 1934.
8. Yang, N. C. and Yang, D.-H., Cyclobutanol formation from irradiation of ketones, *J. Am. Chem. Soc.*, 80, 2913, 1958.
9. Barnard, M. and Yang, N. C., Proximity effect in photochemical reactions, *Proc. Chem. Soc.*, *London*, 302, 1958.
10. Wagner, P. J., Type II photoelimination and photocyclisation of ketones, *Accts. Chem. Res.*, 4, 168, 1971.
11. Breslow, R. and Winnik, M., A., Remote Oxidation of unactivated methylene groups, *J. Am. Chem. Soc.*, 91, 3083, 1969.
12. Coulson, D. R. and Yang, N. C., Deuterium isotope effects in the photochemistry of 2-hexanone, *J. Am. Chem. Soc.*, 88, 4511, 1966.
13. Wagner, P. J. and Kemppainen, A. E., Is there any correlation between quantum yields and triplet-state reactivity in type II photoelimination?, *J. Am. Chem. Soc.*, 90, 5896, 1968.
14. Walling, C. and Gibian, M. J., Hydrogen abstraction reactions by the triplet states of ketones, *J. Am. Chem. Soc.*, 87, 3361, 1965.
15. Salem, L. and Rowland, C., The electronic properties of diradicals, *Angew. Chem. Int. Ed. Engl.*, 11, 92, 1972.
16. (a) Yang, N. C. and Shani, A., Photochemistry of β-naphthyl alkyl ketones in solution, *J. Chem. Soc.*, *Chem. Commun.*, 815 1971; (b) Coyle, J. C., A type 2 photoelimination reaction of 1-naphthyl ketones, *J. Chem. Soc.*, *Perkin Trans. 2*, 233, 1973.
17. Wagner, P. J. and Jellinek, T., Intramolecular quenching of the excited singlets of ω-dialkylamino alkyl ketones: singlet state type II photoelimination of α-dimethylaminoacetophenone, *J. Am. Chem. Soc.*, 93, 7328, 1971.
18. Wagner, P. J., Kemppainen, A. E., and Schott, H. N., Effect of ring substituents on type II photoreactions of phenyl ketones, *J. Am. Chem. Soc.*, 95, 5604, 1973.
19. Encina, M. V., Lissi, E. A., Lemp, E., Zanocco, A., and Scaiano, J. C., Temperature dependence of the photochemistry of aryl alkyl ketones, *J. Am. Chem. Soc.*, 105, 1856, 1983.
20. Berger, M., McAlpine, E., and Steel, C., Substituted acetophenones. Importance of activation energies in mixed state models of photoreactivity, *J. Am. Chem. Soc.*, 100, 5147, 1978.
21. Hammond, G. S. and Leermakers, P. A., Photoreduction of 1-naphthaldehyde and 2-acetonaphthone, *J. Am. Chem. Soc.*, 84, 207, 1962.
22. De Boer, C. D., Herkstroeter, W. G., Marchetti, A. P., Schultz, A. P., and Schlessinger, R. H., Norrish type II rearrangement from π,π^* triplet states, *J. Am. Chem. Soc.*, 95, 3963, 1973.
23. Previtali, C. M. and Scaiano, J. C., The kinetics of photochemical reactions. Part 1. Application of a modified bond-energy–bond-order method to the atom abstraction reactions of excited carbonyl compounds, *J. Chem. Soc.*, *Perkin Trans. 2*, 1667, 1972.
24. Ariel, S., Ramamurthy, V., Scheffer, J. R., and Trotter, J., Norrish type II reaction in the solid state: involvement of a boatlike reactant conformation, *J. Am. Chem. Soc.*, 105, 6959, 1983.
25. Scheffer, J. R., The influence of the molecular crystalline environment on organic photorearrangements, *Org. Photochem.*, 8, 249, 1987.
26. Severance, D., Pandey, B., and Morrison, H., Reaction path analysis of hydrogen abstraction by the formaldehyde triplet state, *J. Am. Chem. Soc.*, 109, 3231, 1987.
27. Dorigo, A. E., McCarrick, M. A., Loncharich, R. J., and Houk, K. N., Transition structures for hydrogen atom transfers to oxygen: comparisons of intermolecular and intramolecular processes and open- and closed-shell systems, *J. Am. Chem. Soc.*, 112, 7508, 1990.

28. Wagner, P. J., Kelso, P. A., Kemppainen, A. E., and Zepp, R. G., Type II photoprocesses of phenyl ketones: competitive δ-hydrogen abstraction and the geometry of intramolecular hydrogen atom transfers, *J. Am. Chem. Soc.*, 94, 7500, 1972.
29. Chandler, W. D. and Goodman, L., Allowed and forbidden character in $\pi^* \leftarrow n$ spectra of cycloalkanones, *J. Mol. Spectr.*, 35, 232, 1970.
30. Ito, Y., Matsuura, T., and Fukuyama, K., Efficiency for solid-state photocyclisation of 2,4,6-triisopropylbenzophenones, *Tetrahedron Lett.*, 29, 3087, 1988.
31. Chang, H. C., Popovitz-Biro, R., Lahav, M., and Leiserowitz, L., Mapping the molecular pathway during photoaddition of guest acetophenone and *p*-fluoroacetopheone to host deoxycholic acid as studied by x-ray diffraction in systems undergoing single-crystal-to-single-crystal transformation, *J. Am. Chem. Soc.*, 109, 3883, 1987.
32. Wagner, P. J., Zhou, B., Hasegawa, T., and Ward, D. L., Diverse photochemistry of sterically congested α-arylacetophenones: ground-state conformational control of reactivity, *J. Am. Chem. Soc.*, 113, 9640, 1991.
33. Sugiyama, N., Nishio, T., Yamada, K., and Aoyama, H., Photochemical reactions of bridged polycyclic ketones, *Bull. Chem. Soc. Jpn.*, 43, 1879, 1970
34. (a) Sauers, R. R., Scimone, A., and Shams, H., Synthesis and Photochemistry of Some New Pentacycloundecan-8-ones: probes for hydrogen abstraction in the π-plane, *J. Org. Chem.*, 53, 6084 1988; (b) Sauers, R. R. and Krogh-Jesperson, K., Analysis of Norrish type II reactions by molecular mechanics methodology, *Tetrahedron Lett.*, 30, 527, 1989.
35. Sauers, R. R. and Huang, S.-Y., Analysis of Norrish type II reactions by molecular mechanics methodology: cyclodecanone, *Tetrahedron Lett.*, 31, 5709, 1990.
36. Wagner, P. J., Conformational flexibility and photochemistry, *Acc. Chem. Res.*, 16, 461, 1983.
37. Lewis, F. D., Johnson, R. W., and Johnson, D. E., Conformational control of photochemical behavior: competitive α cleavage and γ-hydrogen abstraction of alkyl phenyl ketones, *J. Am. Chem. Soc.*, 96, 6090, 1974.
38. Wagner, P. J. and Chen, C.-P., A rotation-controlled excited state reaction: the photoenolization of *ortho*-alkyl phenyl ketones, *J. Am. Chem. Soc.*, 98, 239, 1976.
39. Alexander, E. C. and Uliana, J. A., Photolysis of cyclobutyl aryl ketones: evidence for the involvement of an excited state conformational equilibrium in their photoconversion to aryl bicyclo[1.1.1]pentanols, *J. Am. Chem. Soc.*, 96, 5644, 1974.
40. Lewis, F. D., Johnson, R. W., and Kory, D. R., Transition state for γ-hydrogen abstraction of alkyl phenyl ketones, *J. Am. Chem. Soc.*, 96, 6100, 1974.
41. Giering, L., Berger, M., and Steel, C., Rate studies of aromatic triplet carbonyls with hydrocarbons, *J. Am. Chem. Soc.*, 96, 953, 1974.
42. Paquette, L. A. and Balogh, D. W., An expedient synthesis of 1,16-dimethyldodecahedrane, *J. Am. Chem. Soc.*, 104, 774, 1982..
43. Turro, N. J. and Weiss, D. S., Stereoelectronic requirements for the type II cleavage of *cis*- and *trans*-4-*t*-butylcyclohexanones, *J. Am. Chem. Soc.*, 90, 2185, 1968.
44. Wagner, P. J. and Zepp, R. G., γ vs. δ-Hydrogen abstraction in the photochemistry of β-alkoxyketones: an overlooked reaction of hydroxybiradicals, *J. Am. Chem. Soc.*, 93, 4958, 1971.
45. Ounsworth, J. and Scheffer, J. R., Intramolecular abstraction of aldehydic hydrogen by ketone triplets: formation of 2-hydroxy-2-phenylcycloalkanones, *J. Chem. Soc.*, *Chem. Commun.*, 232, 1986.
46. Wagner, P. J., Kemppainen, A. E., and Jellinek, T., Type II photoreactions of phenyl ketones: competitive charge transfer in α-, γ- and δ-dialkylamino ketones, *J. Am. Chem. Soc.*, 94, 7512, 1972.
47. Small, Jr., R. D. and Scaiano, J. C., Direct detection of the biradicals generated in the Norrish type II reaction, *Chem. Phys. Lett.*, 50, 431, 1977.
48. Scaiano, J. C., Laser flash photolysis studies of the reactions of some 1,4-biradicals, *Acc. Chem. Res.*, 15, 252, 1982.

49. Small, Jr., R. D. and Scaiano, J. C., Solvent effects on the lifetimes of photogenerated biradicals, *Chem. Phys. Lett.*, 59, 246, 1978.
50. Caldwell, R. A., Majima, T., and Pac, C., Some structural effects on triplet biradical lifetimes: Norrish II and Paternò–Büchi biradicals, *J. Am. Chem. Soc.*, 104, 629 1982.
51. (a) Small, Jr., R. D. and Scaiano, J. C., Interaction of oxygen with transient biradicals photogenerated from γ-methyl valerophenone, *Chem. Phys. Lett.*, 48, 354, 1977; (b) Small, Jr., R. D. and Scaiano, J. C., Differentiation of excited-state and biradical processes: photochemistry of phenyl alkyl ketones in the presence of oxygen, *J. Am. Chem. Soc.*, 100, 4512, 1978.
52. Encinas, M. V. and Scaiano, J. C., Interaction between photogenerated biradicals and free radicals: di-*tert*-butylnitroxide, *J. Photochem.*, 11, 241, 1979.
53. Scaiano, J. C., Does intersystem crossing in triplet biradicals generate singlets with conformational memory?, *Tetrahedron*, 38, 819, 1982.
54. Closs, G. and Redwine, O. D., Cyclisation and disproportionation kinetics of triplet generated, medium chain length, localized biradicals measured by time-resolved CIDNP, *J. Am. Chem. Soc.*, 107, 4543, 1985.
55. Michl, J., Spin-orbit coupling in biradicals. 1. The 2-electrons-in-2-orbitals model revisited, *J. Am. Chem. Soc.*, 118, 3568, 1996.
56. Caldwell, R. A., Intersystem crossing in organic photochemical intermediates, *Pure Appl. Chem.*, 56, 1167, 1984.
57. (a) Wagner, P. J. and Park, B.-S., High diastereoselectivity in the cyclisation of 1,5-biradicals: what causes such sizeable steric barriers to biradical coupling?, *Tetrahedron Lett.*, 32, 165, 1991; (b) Wagner, P. J., Meador, M. A., Zhou, B., and Park, B.-S., Photocyclisation of α-o-tolylacetophenones: triplet and 1,5-biradical reactivity, *J. Am. Chem. Soc.*, 113, 9630, 1991.
58. (a) Wagner, P. J., Solvent effects on type II photoelimination of phenyl ketones, *J. Am. Chem. Soc.*, 89, 5898, 1967; (b) Wagner, P. J., Kochevar, I. E., and Kemppainen, A. E., Type II photoprocesses of phenyl ketones: procedures for determining meaningful quantum yields and triplet lifetimes, *J. Am. Chem. Soc.*, 94, 7489, 1972.
59. Caldwell, R. A., Dhawan, S. N., and Moore, D. E., pH Dependence of the lifetime of a Norrish II biradical, *J. Am. Chem. Soc.*, 107, 5163, 1985.
60. (a) Roth, H. J. and El Raie, M. H., Photocyclisation of 3-aminoketones into 2-aminocyclopropanols, *Tetrahedron Lett.*, 2445 1970; (b) Abdul-Baki, A., Rotter, F., Schrauth, T., and Roth, H. J., Photochemical synthesis of ephedrine-type compounds. III: Photocyclisation of 3-(alkyl-amino) propiophenones to 2-(alkylamino)cyclopropan-1-ols and their isomerization, *Arch. Pharm.*, 311, 341, 1978.
61. Henning, H. G., Sukale, R., Buchholz, H., and Haber, H., Photochemistry of aminoketones. VIII. Diastereoselective synthesis of 3-hydroxyprolines, *J. Prakt. Chem.*, 327, 51, 1985.
62. Weigel, W. and Wagner, P. J., Photocyclisation to cyclopropanols and exciplex emission of β-arylpropiophenones, *J. Am. Chem. Soc.*, 118, 12858,1996.
63. Yoshioka, M., Miyazoe, S., and Hasegawa, T., Photochemical reaction of 3-hydroxy-1-(*o*-methylaryl)alkan-1-ones: formation of cyclopropane-1,2-diols and benzoylcyclobutenols through β- and γ-hydrogen abstractions, *J. Chem. Soc., Perkin Trans. 1*, 2781, 1993
64. (a) Cormier, R. A., Schreiber, W. L., and Agosta, W. C., Photochemical rearrangements of α-methylene ketones. *J. Am. Chem. Soc.*, 95, 4873, 1973; (b) Cormier, R. A. and Agosta, W. C., Singlet biradical intermediates in the photochemistry of α-methylene ketones, *J. Am. Chem. Soc.*, 96, 618, 1974.
65. Scaiano, J. C., Lissi, E. A., and Encina, M. V., Chemistry of the biradicals produced in the Norrish type II reaction, *Rev. Chem. Intermed.*, 2, 139, 1978.
66. Wagner, P. J., Kelso, P. A., Kemppainen, A. E., McGrath, J. M., Schott, H. N., and Zepp, R. G., Type II photoprocesses of phenyl ketones: a glimpse at the behavior of 1,4 biradicals, *J. Am. Chem. Soc.*, 94, 7506, 1972.

67. Hoffman, R., Swaminathau, S., Odell, B. G., and Gleiter, R., A potential surface for a nonconcerted reaction: tetramethylene, *J. Am. Chem. Soc.*, 92, 7091, 1970.
68. (a) Lewis, F. D. and Hilliard, T. A., Photochemistry of methyl-substituted butyrophenones, *J. Am. Chem. Soc.* 94, 3852, 1972; (b) Wagner, P. J. and McGrath, J. M., Competitive types I and II photocleavage of α,α-dimethylvalerophenone, *J. Am. Chem. Soc.*, 94, 3849, 1972.
69. Wagner, P. J. and Thomas, M. J., Enhanced photocyclisation of α-fluoroketones, *J. Am. Chem. Soc*, 98, 241, 1976.
70. Lewis, F. D., Johnson, R. W., and Ruden, R. A., Photochemistry of bicycloalkylphenyl ketones, *J. Am. Chem. Soc.*, 94, 4292, 1972.
71. Turro, N. J. and Lewis, F. D., Type II photoelimination and 3-oxetanol formation from α-alkoxy-acetophenones and related compounds, *J. Am. Chem. Soc.*, 92, 311, 1970.
72. Hasegawa, T., Arata, Y., and Kageyama, A., The Norrish type II photoreaction of benzoylvalerates: stereochemical control in 1,4-biradical cyclisation, *Tetrahedron Lett.*, 24, 1995, 1983.
73. Wagner, P. J. and Lindstrom, M. J., Intramolecular charge-transfer interactions in triplet keto sulfides., *J. Am. Chem. Soc.*, 109, 3057, 1987.
74. Wender, P. A. and Rawlins. D. B., Toward the synthesis of the taxol C,D ring system: photolysis of α-methoxy ketones, *Tetrahedron*, 48, 7033, 1992.
75. Yoshioka, M., Suzuki, T., and Oka, M., Photochemical reaction of phenyl-substituted 1,3-diketones, *Bull. Chem. Soc. Jpn.*, 57, 1604, 1984.
76. Padwa, A., Eisenhardt, W. A., Gruber, R., and Pashayan, D., Evidence for electron transfer in the photochemistry of π,π* triplet states, *J. Am. Chem. Soc.*, 91, 1857, 1969.
77. Gold, E. H., Photolysis of α-*N*-alkylamidoacetophenones, a direct route to 3-azetidinols, *J. Am. Chem. Soc.*, 93, 2793, 1971.
78. Toda, F., Selective photochemical reaction in lactam manufacture, *Jpn. Kokai Tokkyo Koho*, JP 06,135,857 *Chem. Abstr.*, 121, 255656, 1994.
79. Toda, F., Miyamoto, H., and Kanemoto, K., Formation of mixing of chiral host-achiral guest inclusion complexes in which the guest mols are arranged in a chiral form: production of optically active photocyclisation compounds by irradiation of the inclusion complexes, *J. Chem. Soc.*, *Chem. Commun.*, 1719, 1995.
80. Natarajan, A., Wang, K., Ramamurthy, V., Scheffer, J. R., and Patrick, B., Control of enantioselectivity in the photochemical conversion of α-oxoamides into β-lactam derivatives, *Org. Lett.*, 4, 1443, 2002.
81. Wagner, P. J. and Ersfeld, D. A., Solvent specific photochemistry involving an intramolecular amino ketone triplet exciplex, *J. Am. Chem. Soc.*, 98, 4515, 1976.
82. Padwa, A. and Eastman, D., Photochemical transformations of small ring carbonyl compounds. XX. Transannular hydrogen abstraction in small ring carbocyclic systems, *J. Am. Chem. Soc.*, 91, 462, 1969.
83. Padwa, A. and Alexander, E., Photochemical formation of a substituted bicyclo[1.1.1]pentane., *J. Am. Chem. Soc.*, 89, 6376, 1967.
84. Lewis, F. D. and Johnson, R. W., Conformational control of photochemical behavior: cyclohexyl phenyl ketone, *Tetrahedron Lett.* 2557, 1973; Lewis, F. D., Johnson, R. W., and Johnson, D. E., Conformational control of photochemical behavior: competitive α-cleavage and γ-hydrogen abstraction of alkyl phenyl ketones., *J. Am. Chem. Soc.*, 96, 6090, 1974.
85. Wagner, P. J. and Scheve, B. J., Absence of intramolecular charge-transfer quenching in photoexcited 4-benzoylpiperidines, *J. Am. Chem. Soc.*, 99, 1858, 1977.
86. Leibovich, M., Olovsson, G., Sundarababu, G., Ramamurthy, V., Scheffer, J. R., and Trotter, J., Asymmetric induction in photochemical reactions conducted in zeolites and in the crystalline state, *J. Am. Chem. Soc.*, 118, 1219, 1996.
87. Vishnumurthy, K., Cheung, E., Scheffer, J. R., and Scott, C., Enhanced regioselectivity of Yang photocyclisation in the crystalline state, *Org. Lett.*, 4, 1071, 2002.

88. Cheung, E., Kang, T., Scheffer, J. R., and Trotter, J., Latent chemical behavior revealed in the crystalline state: novel photochemistry of a *cis*-9-decalyl aryl ketone, *J. Chem. Soc.*, *Chem. Commun.*, 2309, 2000.
89. Cheung, E., Kang, T., Raymond, J. R., Scheffer, J. R., and Trotter, J., An ionic chiral auxiliary-induced regioselective and enantioselective Yang photocyclisation reaction in the crystalline state, *Tetrahedron Lett.*, 40, 8729, 1999.
90. DeKeukeleire, D., Blondeel, G., and deBruyn, A., Unusual course of a type II photoreaction, *Tetrahedron Lett.*, 25, 2055, 1984.
91. Ariel, S., Evans, S. V., Garcia-Garibay, M., Harkness, B. R., Omkaram, N., Scheffer, J. R., and Trotter, J., The generation of 1,4-biradicals in rigid media: crystal structure–solid state reactivity correlation, *J. Am. Chem. Soc.*, 110, 5591 1988.
92. (a) Evans, S. V., Garcia-Garibay, M., Omkaram, N., Scheffer, J. R., and Trotter, J., Use of chiral single crystals to convert achiral reactants to chiral products in high optical yield: application to the di-π-methane and Norrish type II photorearrangements, *J. Am. Chem. Soc.*, 108, 5648, 1986; (b) Evans, S. V., Omkaram, N., Scheffer, J. R., and Trotter, J., Reactivity differences between dimorphs in a crystalline state Norrish type II reaction, *Tetrahedron Lett.*, 27, 1419, 1986.
93. Jones, R., Scheffer, J. R., Trotter, J., and Yang, J., Crystal to molecular chirality transfer: supramolecular photochemistry of crystalline carboxylate salts, *Tetrahedron Lett.*, 33, 5481, 1992.
94. Lewis, F. D. and Hirsch, R. H., Photochemistry of α-cycloalkoxyacetophenones, *Mol. Photochem.*, 2, 259, 1970.
95. Yoshioka, M., Saitoh, M., Arai, H., Ichikawa, K., and Hasegawa, T., Type I and type II photochemical reaction of α-isobutyryl-α-methyl-2,3-benzocycloalk-2-en-1-ones, *Tetrahedron*, 43, 5237, 1987
96. Lewis, T. J., Rettig, S. J., Scheffer, J. R., Trotter, J., and Wireko, F., Conformation–reactivity correlations in the solid state photochemistry of macrocyclic diketones, *J. Am. Chem. Soc.*, 112, 3679, 1990.
97. Lewis, T., Rettig, S. G., Sauers, R. R., Scheffer, J. R., Trotter, J., and Wu, C.-H., On the conformational analysis of photoreactivity of 1,6-cyclodecanedione *Mol. Cryst. Liq. Cryst. Sci. Technol.*, *Sect A*, 277, 649, 1996 (*Chem. Abstr.*, 123, 295241, 1996).
98. Lewis, T. J., Rettig, S. J., Scheffer, J. R., and Trotter, J., The chemical consequences of conformational polymorphism: the phase-transition dependent photochemistry of crystalline 1,14-cyclohexacosanedione, *J. Am. Chem. Soc.*, 113, 8180, 1991.
99. Gudmundsdottir, A. D., Lewis, T. J., Randall, L. H., Scheffer, J. R., Rettig, S. J., Trotter, J., and Wu, C. H., Geometric requirements for hydrogen abstractability and 1,4-biradical reactivity in the Norrish/Yang type II reactions: studies based on the solid state photochemistry and x-ray crystallography of medium-sized ring and macrocyclic diketones, *J. Am. Chem. Soc.*, 118, 6167, 1996.
100. Yang, N. C. and Rivas, C., Photochemical primary process, the photochemical enolization of *o*-substituted benzophenones, *J. Am. Chem. Soc.*, 83, 2213, 1961.
101. Sammes, P. G., Photoenolization, *Tetrahedron*, 32, 405, 1976.
102. (a) Haag, R., Wirz, J., and Wagner, P. J., The photoenolization of 2-methylacetophenone and related compounds, *Helv. Chim. Acta*, 60, 2595, 1977; (b) Das, P. K., Encinas, M. V., Small, Jr., R. D., and Scaiano, J. C., Photoenolization of *o*-alkyl-substituted carbonyl compounds: use of electron transfer processes to characterize transient intermediates, *J. Am. Chem. Soc.*, 101, 6965, 1979.
103. (a) Matsuura, T. and Kitaura, Y., Photo-induced reactions. XI. Photochemical reaction of hindered aromatic ketones, *Tetrahedron Lett.*, 3309, 1967; (b) Kitaura, Y. and Matsuura, T., Steric and substituent effects on photoreactions of 2,4,6-trialkylphenyl ketones, *Tetrahedron*, 27, 1597, 1971.
104. (a) Ito, Y., Kawatsuki, N., Giri, B. P., Yoshida, M., and Matsuura, T., Photochemistry of *meta*-substituted and *para*-substituted aromatic polycarbonyl compounds, *J. Org. Chem.*, 50, 2893, 1985; (b) Nakayama, T., Hidaka, T., Kuramoto, T., Hamanoue, K., Teranishi, H., Ito, Y., and Matsuura, T., Photocyclobutenolization of 2,4,6-triisopropylbenzophenone and its derivatives studied by pico- and nanosecond spectroscopy, *Chem. Lett.*, 1953, 1984; (c) Ito, Y. and Matsuura, T., Photo-induced reactions. 143. Spin inversion in the 1,4-diradical derived from 2,4,6-triisopropylbenzophenone: importance of lone-pair orbital rotation, *J. Am. Chem. Soc.*, 105, 5237, 1983.

105. Wilson, R. M. and Hannemann, K., Conventional and laser-jet photochemistry of 2-methylbenzophenone, *J. Am. Chem. Soc.*, 109, 4741, 1987.
106. Carré, M. C., Viriot-Vilaume, M.-L., and Caub `e Re, P., *J. Chem. Soc.*, *Perkin Trans. 1*, 1395, 2542, 1979.
107. Wagner, P. J., Subrahmanyam, D., and Park, B.-S., Mechanism for the photocyclisation of *o*-alkyl ketones to cyclobutenols, *J. Am. Chem. Soc.*, 113, 709, 1991.
108. Wagner, P. J., Sobczak, M., and Park, B.-S., How many *o*-xylylenols can a triplet *o*-alkylphenyl ketone form?, *J. Am. Chem. Soc.*, 120, 2488, 1998.
109. Sobczak, M. and Wagner, P. J., The photochemistry of *o*-benzylbenzophenone: a pericyclic cornucopia, *Tetrahedron Lett.*, 39, 2523,1998.
110. Urry, W. H. and Trecker, D. J., Photochemical reactions of 1,2-diketones, *J. Am. Chem. Soc.*, 84, 118, 1962.
111. Burkoth, T. and Ullman, E., New photochemical reactions of α-diketones, *Tetrahedron Lett.*, 145, 1970.
112. Olovsson, G., Scheffer, J. R., Trotter, J., and Wu, C.-H., Novel differences between the solid state and solution phase photochemistry of 1,2-cyclodecanedione, *Tetrahedron Lett.*, 38, 6549, 1997.
113. Turro, N. J. and Lee, T., Intramolecular photoreduction of alkyl α-diketones, *J. Am. Chem. Soc.*, 91, 5651, 1969.
114. Wagner, P. J., Zepp, R. G., Liu, K.-C., Thomas, M., Lee, T.-J., and Turro, N. J., Competing photocyclisation and photoenolization of phenyl α-diketones., *J. Am. Chem. Soc.*, 98, 8125, 1976.
115. (a) Bishop, R. and Hamer, N. K., 2-Hydroxycyclopentenone derivatives from photocyclisation of αβ-unsaturated 1,2-diketones: a suggested triplet biradical intermediate, *J. Chem. Soc. C*, 1193, 1970; (b) Hamer, N. K. and Samuel, C. J., Photocyclisation of 1-*o*-alkylphenylpropane-1,2-diones: stereochemistry, *J. Chem. Soc.*, *Perkin Trans. 2*, 1316, 1973.
116. Jorgenson, M. J. and Yang, N. C., A novel photochemical reaction: conversion of α,β-unsaturated ketones to acetonylcyclopropanes, *J. Am. Chem. Soc.*, 85, 1698, 1973.
117. (a) Coyle, D. J., Peterson, R. V., and Heicklen, J., The photolysis and pyrolysis of 4-methyl-4-methoxy-2-pentanone, *J. Am. Chem. Soc.*, 86, 3850, 1964; (b) Yates, P. and Pal, J. M., δ- Versus γ-hydrogen abstraction in the photocyclisation of β-alkoxy-ketones. *J. Chem. Soc. D*, 553, 1970; (c) Stephenson, L. M. and Parlett, R. V., The photochemistry of 4-methyl-4-alkoxy-2-pentanone, *J. Org. Chem.*, 36, 1093, 1971.
118. Wagner, P. J. and Chiu, C., Preferential 1,4- vs. 1,6-hydrogen transfer in a 1,5-biradical. Photochemistry of β-ethoxypropiophenone, *J. Am. Chem. Soc.*, 1051, 7134, 1979.
119. Descotes, G., Acetal photoreactivity in the heterocyclic and glycoside series, *Bull. Soc. Chim. Belg.*, 91, 974, 1982.
120. Koziuk, T., Cottier, L., and Descotes, G., Photochemical syntheses of dioxa-1,6-spiro[4.5]decane pheromones of *Paravespula vulgaris* L, *Tetrahedron*, 37, 1875, 1981.
121. Descotes, G. Synthetic saccharide photochemistry, *Top. Curr. Chem.*, 154, 39, 1990.
122. Kraus, G. A. and Schwinden, M. D., Type II photocyclisations of carbohydrates, *J. Photochem. Photobiol. A: Chem.*, 62, 241, 1991.
123. Kraus, G. A. and Chen, L., A total synthesis of racemic paulownin using a type II photocyclisation reaction, *J. Am. Chem. Soc.*, 112, 3464, 1990.
124. Carless, H. A. J., Swan, D. L., and Haywood, D. J., Stereoselective synthesis of tetrahydrofuran-3-ols by photochemical δ-hydrogen abstraction of β-allyloxy-carbonyl compounds, *Tetrahedron*, 49, 1665, 1993.
125. Hasegawa, T., Moribe, J., and Yoshioka, M., The photocyclisation of *N*,*N*-dialkyl-2-oxo amides absorbed on silica gel, *Bull. Chem. Soc. Jpn.*, 61, 1437, 1988.
126. Walther, K., Kranz, U., and Henning, H.-G., Photochemistry of amino ketones. X. Preparation and diastereoselective photocyclisation of *N*-(β-benzoylethyl)-*N*-tosylglycinamides, *J. Prakt. Chem.*, 329, 859, 1987.

127. Steiner, A., Wessig, P., and Polborn, K., Asymmetric synthesis of 3-hydroxyprolines by photocyclisation of C(1′)-substituted *N*-(2-benzoylethyl)glycine esters, *Helv. Chim. Acta*, 79, 1843, 1996.
128. Wessig, P., Wettstein, Ph., Giese, B., Neuburger, M., and Zehnder, M., Stereoselective photocyclisation of chiral *N*-(2-benzoylethyl)glycinamides, *Helv. Chim. Acta*, 77, 829, 1994.
129. Giese, B., Wettsein, Ph., Stähelin, C., Barbosa, F., Neuburger, M., Zehnder, M., and Wessig, P., Memory effect of chirality in photochemistry, *Angew. Chem. Int. Ed. Engl.*, 38, 2586, 1999.
130. Wagner, P. J., 1-Methylnaphthalene-sensitized singlet state reactions of aliphatic ketones, *Mol. Photochem.*, 3, 169, 1971.
131. Giese, B., Barbosa, F., Stahelin, C., Sauer, S., Wettstein, Ph., and Wyss, C., Stereoselective C,C-bond formation: cyclisations of biradicals, *Pure Appl. Chem.*, 72, 1623, 2000.
132. Wessig, P., Legart, F., Hoffmann, B., and Henning, H.-G., Photochemistry of amino ketones. 14. Synthesis and transannular photocyclisation of 2-benzoyl-1,4-*bis*(tosyl)piperazines, *Liebigs Ann. Chem.*, 10, 979, 1991.
133. Wagner, P. J., Giri, B. P., Scaiano, J. C., Ward, D. L., Gabe, E., and Lee, F. L., Photocyclisation of *o*-*tert*-butylbenzophenone., *J. Am. Chem. Soc.*, 107, 5483, 1985.
134. Wagner, P. J., Cao, Q., and Pabon, R., Activation parameters for triplet δ-hydrogen abstraction by *o*-*tert*-butylbenzophenones: no tunneling but an entropy-controlled inductive effect in the isoelectronic anilinium ion, *J. Am. Chem. Soc.*, 114, 346, 1992.
135. Wagner, P. J., Giri, B. P., Pabon, R., and Singh, S. B., Divergent photochemistry of 2,4-di-*tert*-butylacetophenone and -benzophenone, *J. Am. Chem. Soc.*, 109, 8104, 1987.
136. Wagner, P. J., Pabon, R., Park, B.-S., Zand, A., and Ward, D. L., Regioselectivity in the photocyclisation of *o*-*tert*-amylbenzophenone, *J. Am. Chem. Soc.*, 116, 589, 1994.
137. Zand, A. R., Effect of Temperature on the Behavior of Biradical Intermediates: Conformational Control of Product Ratios in Photocyclization Reactions, Ph.D. thesis, Michigan State University, 1996.
138. Miki, S., Matsuo, K., Yoshida, M., and Yoshida, Z., Novel anthraquinone derivatives undergoing photochemical valence isomerization, *Tetrahedron Lett.*, 29, 2211, 1988.
139. Lappin, G. R. and Zannucci, J. S., Photolysis of 2-(benzyloxy)-4-(dodecyloxy)benzophenone and 2-isopropoxy-4-methoxybenzophenone, *J. Org. Chem.*, 36, 1808, 1971.
140. Sullivan, F. R. and Jones, L. B., Photoreactions of 2-alloxyacetophenone, *J. Chem. Soc., Chem. Commun.*, 312, 1974.
141. Pappas, S. P., Alexander, Jr., J. E., and Zehr, R. D., Photochemistry of *o*-benzyloxyphenylglyoxylates: a case of favored intramolecular hydrogen transfer via a seven-membered cyclic transition state, *J. Am. Chem. Soc.*, 92, 6927, 1970.
142. Horaguchi, T., Synthesis of benzofurans using photocyclisation reactions of aromatic carbonyl compounds, *Trends Heterocyclic Chem.*, 6, 1–19, 1997.
143. O'Connell, E. J., 2-Hydroxy-4,6-di-*t*-butylbenzophenone photoreactivity, *J. Am. Chem. Soc.*, 90, 6550, 1968.
144. Wagner, P. J., Meador, M. A., and Park, B.-S., The photocyclisation of *o*-alkoxy phenyl ketones, *J. Am. Chem. Soc.*, 112, 5199, 1990.
145. Sharshira, E., Essam, M., Okamura, M., Hasegawa, E., and Horaguchi, T., Photochemical reactions. 6. Solvent and substituent effects in the synthesis of dihydrobenzofuranols using photocyclisations of 2-alkoxybenzophenones and ethyl 2-benzoylphenoxyacetates, *J. Heterocyclic Chem.*, 34, 861, 1997.
146. Kim, T. Y. and Park, B. S., Unusually low diastereoselectivity in the photocyclisation of *ortho*-(2,2,2-trifluoroethoxy)benzophenone, *Bull. Korean Chem. Soc.*, 18, 141, 1997 (*Chem. Abstr.*, 126, 277351, 1997).
147. Pappas, S. P. and Zehr, Jr., R. D., Heavy-atom effects on the stereochemistry of photoabstraction–cyclisation in a carbonyl system, *J. Am. Chem. Soc.*, 93, 7112, 1971.
148. Wagner, P. J. and Laidig, G., Enol ether formation by disproportionation of the biradical intermediate in the photocyclisation of *o*-isopropoxybenzophenone, *Tetrahedron Lett.*, 32, 895, 1991.

149. Sharshira, E. M., Iwanami, H., Okamura, M., Hasegawa, E., and Horaguchi, T., Photocyclisation reactions. Part 3. Synthesis of naphtho[1,8-*b*,*c*]furans and cyclohepta[*c*,*d*]benzofurans using photocyclisation of 8-alkoxy-1,2,3,4-tetrahydro-1-naphthalenones and 4-alkoxy-6,7,8,9-tetrahydro-5H-benzocyclohepten-5-ones, *J. Heterocyclic Chem.*, 33, 17, 1996.
150. Horaguchi, T., Iwanami, H., Tanaka, T., Hasegawa, E., and Shimizu, T., Conformational effects in photocyclisation of six- and seven-membered ring alkoxy ketones, *J. Chem. Soc.*, *Chem. Commun.*, 44, 1991.
151. Wagner, P. J. and Jang, J.-S., Lifetimes of 1,5-biradicals formed from triplet *o*-alkoxy ketones, *J. Am. Chem. Soc.*, 115, 7914,1993.
152. Cottet, F., Cottier, L., and Descotes, G., Photocyclisations of aromatic ketoacetals as an approach to the synthesis of crombénine, *Can. J. Chem.*, 68, 1251, 1990.
153. Kraus, G. A., Thomas, P. J., and Schwinden, M. D., An approach to aflatoxins using type II photocyclisation reactions, *Tetrahedron Lett.*, 31, 1819, 1990.
154. Hasegawa, T., Kosaku, S., Ueno, J., and Oguchi, S., Photolysis of *o*-[*N*-(alkylacyl)amino]benzophenones, *Bull. Chem. Soc. Jpn.*, 55, 3659,.1982,
155. Wagner, P. J. and Cao, Q., Photocyclisation of *ortho*-benzoyl *N*-alkylanilinium ions, *Tetrahedron Lett.*, 32, 3915, 1991.
156. Seiler, M., Schumacher, A., Lindemann, U., Barbosa, F., and Giese, B., Diastereoselective photocyclisations to dihydroindolinols, *Synlett*, 1588, 1999.
157. Kraus, G., A., Shi, J., and Reynolds, D., A reinvestigation of the photochemistry of 2-alkoxy-1,2-naphthoquinones, *Synth. Commun.*, 20, 1837, 1990.
158. Blankespoor, R. L., Smart, R. P., Batts, E. D., Kiste, A. A., Lew, R. E., and Van der Viet, M. E., Photochemistry of 1-alkoxy- and 1-(benzyloxy)-9,10-anthraquinones in methanol: a facile process for the preparation of aldehydes and ketones, *J. Org. Chem.*, 60, 6852, 1995.
159. Meador, M. A. and Wagner, P. J., 2-Indanol formation from photocyclisation of α-arylacetophenones, *J. Am. Chem. Soc.*, 105, 4484, 1983.
160. Wagner, P. J., Meador, M. A., Zhou, B., and Park, B.-S., Photocyclisation of α-(*o*-tolyl)acetophenones: triplet and 1,5-biradical reactivity, *J. Am. Chem. Soc.*, 113, 9630, 1991.
161. Wagner, P. J., Zhou, B., Hasegawa, T., and Ward, D. L., Diverse photochemistry of sterically congested α-arylacetophenones: ground-state conformational control of reactivity, *J. Am. Chem. Soc.*, 113, 9640, 1991.
162. Wagner, P. J. and Zhou, B., Effects of steric congestion on photochemistry: enol ether formation from α-mesityl ketones, *J. Am. Chem. Soc.*, 110, 611, 1988.
163. Wagner, P. J. and Meador, M. A., Photoenolization of α-(2,4,6-triisopropylphenyl)acetophenone., *J. Am. Chem. Soc.*, 106, 3684, 1984.
164. Wagner, P. J. and Park, B.-S., High diastereoselectivity in the cyclisation of 1,5-biradicals: what causes such sizeable steric barriers to biradical coupling?, *Tetrahedron Lett.*, 32, 165, 1991.
165. Cheung, E., Rademacher, K., Scheffer, J. R., and Trotter, J., Asymmetric induction in the solid state photochemistry of an α-mesitylacetophenone derivative through the use of ionic chiral auxiliaries, *Tetrahedron Lett.*, 40, 8733, 1999.
166. (a) Wagner, P. J., Zand, A., and Park, B.-S., Entropy vs. enthalpy control of 1,5-biradical cyclisation in the photochemistry of α-(*o*-alkyl-phenyl)acetophenones, *J. Am. Chem. Soc.*, 118, 12856, 1996; (b) Zand, A., Park, B.-S., and Wagner, P. J., Conformational control of product ratios from triplet 1,5-biradicals, *J. Org. Chem.*, 62, 2326, 1997.
167. Chang, D. J., Nahm, K., and Park, B. S., Reversed diastereoselectivity in the Yang photocyclisation upon introducing a cyclopropyl group at the alpha position of carbonyls, *Tetrahedron Lett.*, 43, 249, 2002.
168. Noh, T., Choi, K., Kwon, H., Chang, D. J., and Park, B. S., Photocyclisation of α-(*o*-ethylphenyl)acetophenone in zeolites, *Bull. Korean Chem. Soc.*, 20, 539, 1999 (*Chem. Abstr.*, 131, 144395, 1999).

169. Noh, T., Lei, X. G., and Turro, N. J., Photochemistry of α-(o-tolyl)acetone and some derivatives: triplet α-cleavage and singlet δ-hydrogen abstraction, *J. Am. Chem. Soc.*, 115, 3105, 1993.
170. Zand, A. R. and Wagner, P. J., unpublished work.
171. Wagner, P. J., Park, B. S., Sobczak, M., Frey, J., and Rappoport, Z., Photocyclisation of 2,4,6,2′,4′,6′-hexaalkylbenzils, *J. Am. Chem. Soc.*, 117, 7619, 1995.
172. Carless, H., A., J. and Fekarurhobo, G., K., Photochemical ε-hydrogen abstraction as a route to tetrahydropyran-3-ols, *Tetrahedron Lett.*, 25, 5943, 1984.
173. Meador, M., A. and Wagner, P. J., Photocyclisation of α-(o-benzyloxyphenyl) acetophenone: triplet state ε-hydrogen abstraction, *J. Org. Chem.*, 50, 419, 1985.
174. Park, B. S. and Wagner, P. J., Photoinduced ε-hydrogen abstraction reactions of α-(o-alkoxyphenyl)acetophenones and their benzoylcyclopropane derivatives, in press.
175. Zhou, B. and Wagner, P. J., Long-range triplet hydrogen abstraction: photochemical formation of 2-tetralols from β-arylpropiophenones, *J. Am. Chem. Soc.*, 111, 6796, 1989.
176. Wyss, C., Batra, R., Lehmann, C., Sauer, S., and Giese, B., Selective photocyclisation of glycine in dipeptides, *Angew. Chem. Int. Ed. Engl.*, 35, 2529, 1996.
177. Lindemann, U., Reck, G., Wulff-Molder, D., and Wessig, P., Photocyclisation of 4-oxo-4-phenylbutanoyl amines to δ-lactams, *Tetrahedron*, 54, 2529, 1998.
178. Wessig, P., An efficient synthesis of bicyclic beta-turn dipeptides via a photochemical key step, *Tetrahedron Lett.*, 40, 5987, 1999.
179. Carless, H. A. J. and Mwesigye-Kibende, S., Intramolecular hydrogen abstraction in ketone photochemistry: the first examples of zeta-hydrogen abstraction, *J. Chem. Soc.*, *Chem. Commun.*, 1673, 1987.
180. Hasegawa, T. and Yamazaki, Y., Regioselectivity in photocyclisation of 2-(*N*,*N*-dialkylamino)- and 2-*N*-alkylanilino)ethyl benzoylformates via remote proton transfer, *Tetrahedron*, 54, 12223, 1998.
181. Kraus, G. A. and Wu, Y., 1,5- and 1,9-Hydrogen atom abstractions: photochemical strategies for radical cyclisations, *J. Am Chem. Soc.*, 114, 8705, 1992.
182. Hasegawa, T., Miyata, K., Ogawa, T., Yoshihara, N., and Yoshioka, M., Remote photocyclisation of (dibenzylamino)ethyl benzoylacetate. Intramolecular hydrogen abstraction through a ten-membered cyclic transition state, *J. Chem. Soc.*, *Chem. Commun.*, 363, 1985.
183. Yamazaki, Y., Miyagawa, T., and Hasegawa, T., Photocyclisation of (alkylthio)ethyl benzoyl acetates via remote proton transfer following charge transfer interaction between excited ketone carbonyl and thioether chromophore, *J. Chem. Soc.*, *Perkin Trans.1*, 2971, 1997.
184. Winnik, M. A., Lee, C. K., Basu, S., and Saunders, D., S., Conformational analysis of hydrocarbon chains in solution. carbon tetrachloride, *J. Am. Chem. Soc.*, 96, 6182, 1974.
185. Breslow, R., Biomimetic control of chemical selectivity, *Acc. Chem. Res.*, 13, 170, 1980.
186. Tamiaki, H., Kiyomori, A., and Maruyama, K., Intramolecular photochemistry in β-turned dipeptide bridged molecules, *Bull. Chem. Soc. Jpn.*, 66, 1768, 1993.
187. Wang, G., Winnik, M. A., Schaefer, H. J., and Schmidt, W., Intramolecular photochemical hydrogen abstraction rate and its temperature dependence in doubly anchored alkane chains, *Chin. Sci. Bull.*, 38, 615, 1993 (*Chem. Abstr.*, 119, 159622, 1993).
188. Hasegawa, T., Takashima, K., Aoyama, H., and Yoshioka, M., Photochemical reactions of 4-oxo carboxylic esters: remote hydrogen abstraction and *cis-trans* isomerization, *Bull. Chem. Soc. Jpn.*, 65, 3498, 1992.
189. Hu, S. and Neckers, D. C., Photochemical reactions of alkoxy-containing alkyl phenylglyoxylates: remote hydrogen abstraction, *J. Chem. Soc.*, *Perkin Trans. 2*, 1751, 1997.
190. Hu, S. and Neckers, D. C., Photochemical reactions of alkyl phenylglyoxylates, *J. Org. Chem.*, 61, 6407, 1996.
191. Hu, S. and Neckers, D. C., Photocyclisation reactions of sulfide-containing-alkyl phenyl glyoxylates, *Tetrahedron*, 53, 7165, 1997.
192. Hu, S. and Neckers, D. C., Photochemical reactions of halo-/aryl sulfide-substituted alkyl phenylglyoxylates: an assessment of the lifetime of the intermediate biradical, *J. Org. Chem.*, 62, 7827, 1997.

193. Hasegawa, T., Ogawa, T., Miyata, K., Karakizawa, A., Komiyama, M., Nishizawa, K., and Yoshioka, M., Photocyclisation of (ω-dialkylamino)alkyl β-oxoesters via remote hydrogen transfer, *J. Chem. Soc.*, *Perkin Trans. 1*, 901, 1990.
194. Kraus, G. A., Zhang, W., and Wu, Y., 1,12-Hydrogen atom abstraction reactions of α-keto esters, *J. Chem. Soc.*, *Chem. Commun.*, 2439, 1996.
195. Carless, H. A. J. and Haywood, D. J., Photochemical cyclisation of β-allyloxy carbonyl compounds: synthesis of 2-alkenyl-3-hydroxytetrahydrofurans, *J. Chem. Soc.*, *Chem. Commun.*, 657 1980.
196. Wagner, P. J. and Liu, K.-C., Photorearrangement of α-allylbutyrophenone to 2-phenyl-2-norbornanol: determination of 1,4-diradical lifetimes, *J. Am. Chem. Soc.*, 96, 5952, 1974.
197. Wagner, P. J., Liu, K.-C., and Noguchi, Y., Monoradical rearrangements of the 1,4-biradicals involved in Norrish type II photoreactions, *J. Am. Chem. Soc.*, 103, 3837, 1981.
198. Caldwell, R. A. and Gupta, S. C., Absence of conformational dependence of Norrish II biradical lifetimes, *J. Am. Chem. Soc.*, 111, 740, 1989.
199. Timpe, H.-J., Rakhmankulov, D. L., Zlotzkij, S. S., and Akhmetkhanova, F. M., Preparation of cyclopropanols via photoinduced δ-hydrogen abstraction in 5-acyl 1,3-dioxanes, *J. Photochem. Photobiol. A: Chem.*, 74, 31, 1993.
200. Kraus, G. A. and Wu, Y., Hydrogen atom abstraction reactions in organic synthesis: a formal total synthesis of podophyllotoxin, *J. Org. Chem.*, 57, 2922, 1993.
201. Hasegawa, T., Ohkanda, J., and Kobayashi, M., Unusual substituent effect by the α-acetyl group on the type II photoreaction of valerophenones: strong wavelength dependence of quantum yields, *J. Photochem. Photobiol. A: Chem.*, 64, 299, 1992.

59

Oxetane Formation: Stereocontrol

Axel G. Griesbeck
University of Cologne

Samir Bondock
University of Cologne

59.1 Introduction

The combination of two prostereogenic substrate molecules, the carbonyl and the alkene component, in the course of a Paternò–Büchi reaction leads to a photoadduct with three new stereogenic centers. Control of the relative and absolute configuration of these stereogenic centers is a challenge for synthetic chemistry in that many interesting products could in principle be derived from oxetane precursors. A detailed knowledge of the photophysical properties of the electronically excited compound (which in most cases is the carbonyl addend) is necessary to understand (and predict) the stereochemical result of such a [2+2]-cycloaddition reaction. Therefore, the configuration of the excited state, its lifetime, and IC as well as intersystem crossing (ISC) properties should be known. For clean transformations, the carbonyl group should be the only absorbing chromophore in the reaction mixture (i.e., the product should not absorb at the wavelength used), the solvent should not interfere with the cycloaddition step by competing reactions (e.g., hydrogen abstraction), and the polarity influence of the reaction medium on biradical or photoinduced electron transfer (PET) steps ought to be carefully investigated.

0-8493-1348-1/04/$0.00+$1.50

59.2 The Carbonyl Part

Parallel and Perpendicular Approach

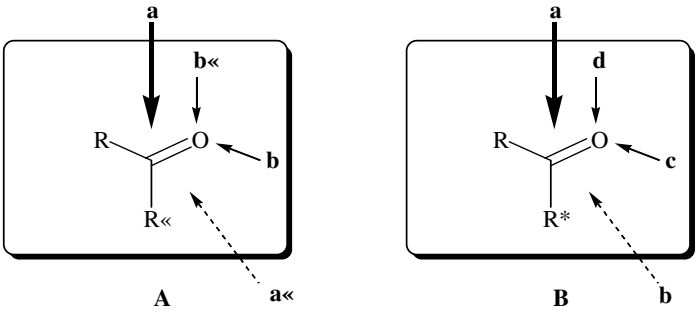

enantiotopic faces a,a«and b,b« *diastereotopic* faces a,b and c,d

Considering the simple model for the spatial distribution of electron density in the n,π^* state, a non-prostereogenic n,π^* excited carbonyl compound (**A**) has two pairs of enantiotopic faces for interaction with an alkene addend. Analogous to the ground-state nucleophilic addition reaction, and considering the *Umpolung* effect, electron-deficient alkenes should preferentially interact with the nucleophilic π^* orbital. Such an orientation has been named the *parallel approach*. On the other hand, electron-rich alkenes should preferentially interact with the electrophilic *n*-orbital perpendicular to the π-plane; consequently, such an orientation has been named the *perpendicular approach*. Analyses of the product stereochemistry cannot uncover these primary orientation phenomena. A study of Stern–Volmer kinetics of several 2-norbornanones with the electron-rich *cis*-diethoxyethylene (*c*-DEE) and the electron-poor *trans*-dicyanoethylene (*t*-DCE) as quenchers did corroborate this model.[1] In these cases, the carbonyl compounds are chiral (**B**) and exhibit two pairs of diastereotopic faces for interaction with the alkene addends. The 2-norbornanone skeleton could be attacked by *t*-DCE via a parallel approach from the *exo*- or *endo*-face. From the fluorescence quenching data in Table 59.1, it can be seen that *exo*-blocked compound **2** is quenched with a five-times-lower rate constant than parent compound **1**. The quenching by *c*-DEE, however, is not affected by groups blocking the π-plane of the carbonyl group. If the two diastereotopic faces of the perpendicular *n* plane are additionally blocked by methyl groups (e.g., in compound **3**) the rate constant for *c*-DEE quenching drops by a factor of >50, whereas the rate constant for *t*-DCE is now not affected.

In an additional paper it was shown by Turro and Farrington[2] that the *t*-DCE addition is a highly stereoselective process, indicating an exclusive interaction with the first excited singlet state of the carbonyl compound. An increase in steric hindrance toward the approach from the *exo*-side reduced the rate of fluorescence quenching; however, the efficiency of oxetane formation was increased. Therefore, it was interpreted that for sterically more hindered ketones a possible exciplex intermediate is much more effectively transformed into the photoproduct. This may be due to a puckering effect of the n,π^* excited carbonyl group, which leads to enhanced efficiency of photoproduct formation from the exciplex intermediate.

Non-Prostereogenic Carbonyls

Ketones with homotopic faces have been widely used to determine the stereoselectivity in Paternò–Büchi reactions with *E*- and *Z*-isomers of electron-rich and electron-poor olefins. The photocycloaddition of

TABLE 59.1 Fluorescence Quenching of 2-Norbornanone Singlets by *trans*-DCE and *cis*-DEE[1]

	$k_q^r \times 10^{-9}$ [M^{-1} sec^{-1}]	
	NC, CN	EtO, OEt
1	5.1	1.2
2	1.0	1.5
3	0.48	<0.03

acetone **4** to *cis*- or *trans*-2-butene **5** leads to a mixture of diastereomeric oxetanes **6** and **7** in a constant ratio of 64:36 (±2%) independent of the substrate configuration.[3] No isomerization of the alkene substrates could be detected at low to medium conversion. The photocycloaddition of acetone **4** to *cis*- and *trans*-1-methoxy-1-butene **8** and **9** has been studied in order to show the divergent stereoselectivity of singlet and triplet excited carbonyl states.[4] By use of piperylene as triplet quencher and investigation of the concentration (quencher as well as substrate) dependency of the stereoselectivity of the Paternò–Büchi reaction, a consistent mechanism was established. At high concentrations of the alkene or the triplet quencher maximum diastereomeric ratio, values of 82:18 and 27:73 were found for the oxetanes from **8** and **9**, respectively. Therefore, it was concluded that the stereochemistry of the initial butene is retained in oxetanes **10** and **11** (regioisomers ignored) when singlet excited acetone attacks the alkene, whereas a scrambling effect is obtained for the triplet case indicating a long-lived triplet biradical intermediate.

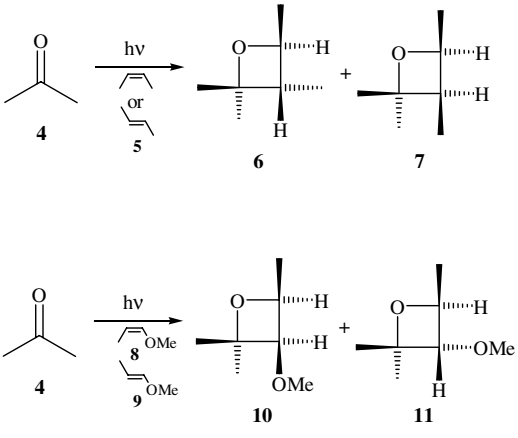

In some cases, however, a high degree of stereoselectivity could be obtained even with "pure" triplet excited carbonyl compounds. In these cases (e.g., the photocycloaddition of benzophenone to several methyl vinyl sulfides **12**), the intermediary triplet 1,4-biradical preferentially undergoes one of two possible cyclization modes after intersystem crossing.[5] The nonstereospecific (using Zimmerman's definition)[6] nature of this reaction has been demonstrated by the use of stereoisomeric substrates that lead to oxetanes **13** in identical diastereomeric ratios. Another possibility for obtaining stereoisomerically pure oxetanes is the use of alkenes that simultaneously serve as quenchers for the carbonyl triplets (e.g., dienes). The photocycloaddition of acetone **4** and 2-methyl-2,4-hexadiene **14** represents such a process leading to the two regioisomeric oxetanes **15** and **16** where the substrate configuration is retained in **16**.[7]

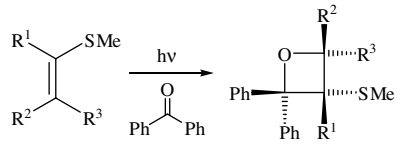

12 **13**

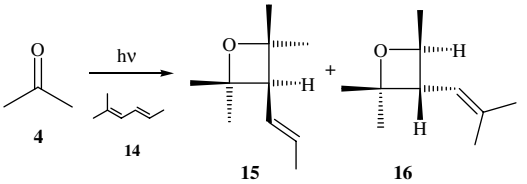

4 **14** **15** **16**

Prostereogenic Carbonyls: Product Stereoselectivity

Simple (non-induced) diastereoselectivity in general describes a selection process where two stereogenic elements (or more) are generated in a chemical process without stereogenic elements present already in the starting materials, whereas induced diastereoselectivity describes a selection process where stereogenic elements are generated in a chemical process from substrates with at least one stereogenic element already present. Thus, in the case of Paternò–Büchi reactions, the combination of two prostereogenic substrate molecules leads to a photoadduct with a maximum of three new stereogenic centers with a characteristic simple diastereoselectivity.

Simple Diastereoselectivity

In contrast to the results with acetone (*vide infra*), the photoaddition of acetaldehyde **17** with the 2-butenes **5** is highly stereoselective (or stereospecific[6]).[8] Aromatic carbonyl compounds such as benzaldehyde **18** show low stereoselectivities independent of their concentrations (in contrast to aliphatic ketones) due to fast intersystem crossing into the triplet manifold of the carbonyl substrate. If, however, the configuration of the triplet excited state switches from n,π^* to π,π^*, the product stereoselectivity rises again. In these cases (e.g., 2-naphthaldehyde **19**), the carbonyl singlet is the reactive state in photocycloaddition reactions involving the carbonyl group. Obviously, the quantum yields for such a process are low (about 5% of triplet reactivity) because of efficient deactivation via the triplet π,π^* states. Jones et al.[9] have published another concentration study where they describe the photocycloaddition of aliphatic aldehydes to medium ring cycloalkenes. The variation in photoadduct distribution is due to stereospecific addition of the aldehyde singlet (dominant at high alkene concentrations) accompanied by a more stereorandom triplet pathway at lower concentrations of the cycloalkenes.[9]

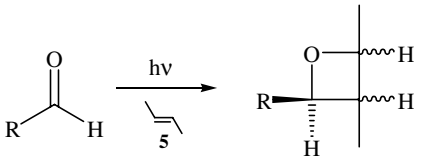

17 (R = Me)
18 (R = Ph)
19 (R = Naphth)

Selectivity ratio (E/Z):
95 : 5
62 : 38
94 : 6

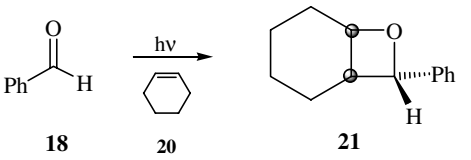

18 **20** **21**

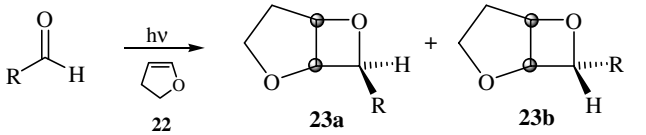

22 **23a** **23b**

18 (R = Ph)
24 (R = Mes)
25 (R = Naphth)

12 : 88
< 2 : 98
>98: 2

In the case of Paternò–Büchi reaction of cycloalkenes with prostereogenic aromatic carbonyl compounds (which show rapid ISC to the triplet excited carbonyl), less clear results were obtained. The reaction of cyclohexene **20** with benzaldehyde **18** was reported in the literature,[10] and the spectral data of the main product **21** (35%) was described as "consistent with the unusual assignment of *endo*-stereochemistry."[11] A detailed study of the photocycloaddition of (triplet) benzaldehyde with several cycloalkenes revealed that *endo* stereoselectivity is an inherent property for these processes.[12] The addition of **18** to 2,3-dihydrofuran **22** was especially significant; only one regioisomer, **23** (analogous to the reaction with acetone),[13] is formed in a diastereomeric ratio of 88:12. Increasing steric demand of the carbonyl addend leads to an increase in diastereoselectivity; for example, for mesityl aldehyde **24** only the *endo*-diastereomer **23b** could be detected.[14] Substituent effects have also been described for methyl-substituted cycloalkenes that were in accord with the postulated principle for control of stereoselectivity in triplet reactions.[15] This selectivity effect could be explained by the assumption of certain 1,4-biradical conformers that fulfill the prerequisites (Salem rules)[16] for rapid intersystem crossing to form the 1,4-singlet biradicals. These can interconvert without spin barrier into the products and thus exhibit a "conformational memory". In contrast to the triplet pathway, singlet excited carbonyl compounds such as 1- or 2-naphthaldehydes **25** do add with high *exo* stereoselectivity to 2,3-dihydrofuran.[17] Both singlet- *and* triplet excited carbonyl compounds underwent photocycloaddition to furan **26** with high *exo* selectivity to give adducts **27**. Additionally, only one regioisomer is formed in these reactions, which show high efficiency and proceed with excellent yields.[18] The oxetanes formed in these reactions are acid-labile compounds and can be converted into the corresponding aldol products. Schreiber and Satake[19] used this property for the synthesis of several key compounds as substrates for the synthesis of natural products by the "photo–Aldol reaction".[19] Besides the addition of aldehydes to furan, ketones and esters as well as substituted furans have been used as starting materials.[20,21] In most cases, the locoselectivity (for furans with unsymmetric substitution pattern) is moderate,[22] but the regioselectivity (exclusive formation of the acetal product) and the stereoselectivity stay high (>500:1 in some cases).[23] The same degree of regio- and

stereoselectivity has been observed for other heterocyclic substrates, such as thiophenes, oxazoles, pyrazoles, and many more.[24] A somewhat lower degree in stereoselectivity was reported for the photocycloaddition of carbonyl compounds to 1,3-cyclopentadiene (with propanal, *exo*/*endo* = 80:20)[25] and 1,3-cyclohexadiene (with acetaldehyde, *exo*/*endo* = 88:12).[26] Another group of highly efficient carbonyl addends are α-keto esters such as alkyl pyruvates, alkyl glyoxylates, and esters of phenylglyoxylic acid. Photocycloaddition with electron-rich cycloalkenes such as dioxoles and furans have been reported to proceed highly regio- and diastereoselectively. The Paternò–Büchi reaction of 2,2-diisopropyl-1,3-dioxole **28** with ethyl pyruvate **29** leads to an 80:20 mixture of diastereomeric oxetanes **30**.[27] Zamojski and Kozluk[28] have reported a highly selective reaction of triplet excited *n*-butyl glyoxylate **31** with furan **26**. Similar to the reactions with aromatic aldehydes,[18] only the *exo*-photoproduct **32** is formed.

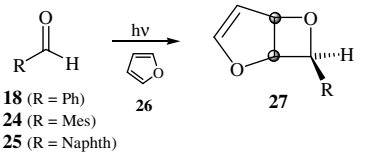

18 (R = Ph)
24 (R = Mes)
25 (R = Naphth)

26 **27**

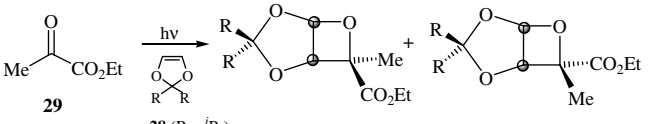

29 **28** (R = ^{i}Pr) **30** (80:20)

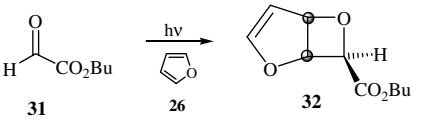

31 **26** **32**

The simple diastereoselectivity of the photocycloaddition of electronically excited carbonyl compounds with electron rich olefins was studied as a function of the substituent size – at identical starting conditions ignoring the electronic state involved in the reaction mechanism.[29] The [2+2]-photocycloaddition of 2,3-dihydrofuran (**22**) with different aldehydes in the nonpolar solvent benzene resulted in oxetanes **23** with highly regioselectivity and surprising simple diastereoselectivities: the addition to acetaldehyde resulted in 45:55 mixture of *endo* and *exo* diastereoisomer, with increasing the size of the α-carbonyl substituent (Me, Et, *i*-Bu, *t*-Bu), the simple diastereoselectivity increased with preferential formation of the *endo* stereoisomer.

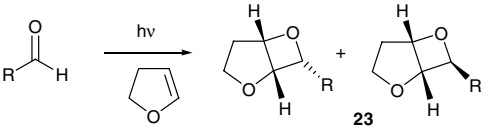

22 **23**

R =	d.r. (endo : exo)
Me	45 : 55
Et	58 : 42
^{i}Bu	67 : 33
^{t}Bu	91 : 9

The benzaldehyde addition, which was most intensively investigated, gave a 88:12 mixture of *endo*- and *exo*-diastereoisomers. Thus, the thermodynamically less-stable stereoisomers (>1.5 kcal/mol, from *ab initio* calculation) were formed preferentially. To further enlarge the phenyl substituent, *o*-tolyl and mesitaldehyde, as well as 2,4-di-*t*-butyl-6-methylbenzaldehyde, were applied, and the diastereoselectivity did actually further increase.

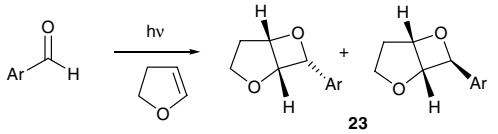

22 **23**

Ar =	d.r. (endo : exo)
Ph	88 : 12
o-Tol	92 : 8
Mes	>98 : 2
2,4-di-*t*-Bu-Ph	>98 : 2

In contrast to the diastereoselectivity of the 2,3-dihydrofuran photocycloaddition, the photocycloaddition of furan **26** with aromatic as well as aliphatic aldehydes proceeded with unusually high *exo*-diastereoselectivity to give the bicyclic oxetanes **27** in good yield.[29] The diastereoselectivity of reaction of furan with acetaldehyde, propionaldehyde, and benzaldehyde (*exo*/*endo*) were 19:1, 82:1, and 212:1, respectively. The exchange of the hydrogen in benzaldehyde by a methoxy group completely inverted the diastereoselectivity in the photocycloaddition with furan. Further modification of the α-substituent in the benzoyl substrates disclosed a distinct dependence of the *exo*/*endo* ratio on the size of this substituent. The photocycloaddition of acetophenone with furan gave only one product, whereas a 77:23 mixture of diastereoisomers resulted from the addition of benzoyl cyanide. Increasing the size of the aryl group from phenyl to mesityl in aroyl cyanides led to an increase in *exo*-diastereoselectivity from 3.7:1 up to 16:1.

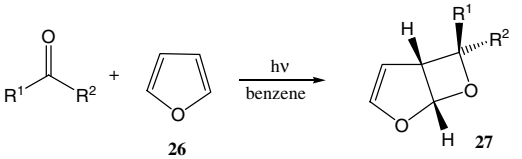

26 **27**

R^1 =	R^2 =	d.r. (*exo*-R^1 : *endo*-R^1)
Ph	H	212 : 1
Ph	Me	>49 : 1
Ph	CN	3.7 : 1
Ph	CO_2Me	1 : 9
Ph	OMe	1 : 19
Ph	CO_2R	<1 : 49
Mes	CN	16 : 1
^{t}Bu	CO_2Me	<1 :49

Steric hindrance can also reach a critical value during bond formation and might favor the formation of thermodynamically more stable product. In a report by Park and co-workers,[30] the photocycloaddition of benzaldehyde **18** to 2,2-diethoxy-3,4-dihydro-2*H*-pyran **33** is described to give preferentially the *exo*-phenyl product **34**.[30]

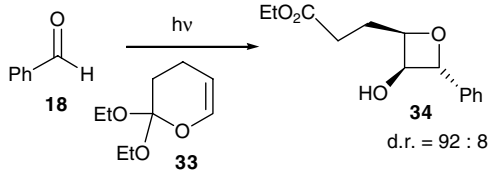

18 **33** **34**

d.r. = 92 : 8

Bach and Schröder[31] investigated the photocycloaddition of electron-rich *N*-acyl enamines **35** with benzaldehyde.[31] The 3-amidooxetanes **36** were formed with excellent regioselectivity (analogous to reactions with enol ethers, *vide supra*) and good diastereoselectivity.

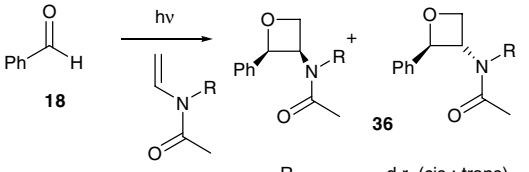

R =	d.r. (cis : trans)
H	79 : 21
Bn	89 : 11
Pr	90 : 10

Silylenol ethers **37** were also investigated by Bach and Jödicke[32] in the last decade. A series of photocycloaddition reactions of benzaldehyde with these substrates showed a trend in stereoselectivity which at first sight was in contradiction to the rules described above; that is, the thermodynamically more stable *trans*-diastereoisomers **38** (with respect to the substituent at C2 and C3) were formed preferentially and the *trans*/*cis* ratio increases with increasing size of the C3 substituent. This peculiar stereoselectivity might be attributed to a memory effect from the approach geometry between the triplet excited benzaldehyde and the alkene.

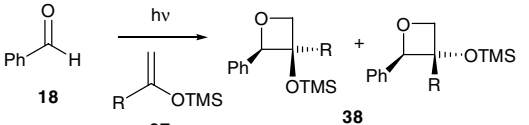

R =	d.r. (cis : trans)
Me	70 : 30
Et	83 : 17
^{i}Pr	88 : 12
^{t}Bu	91 : 9
Ph	92 : 8

Abe and co-workers[33] have also observed a comparable stereochemical effect in the Paternò–Büchi reaction of 4-cycanobenzaldehyde with thiosilylketene acetals **39**.[33]

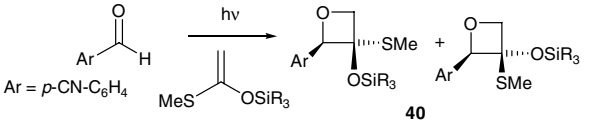

SiR_3 =	d.r. (cis : trans)
$Si^{t}BuMe_2$	20 : 80
$SiMe_3$	18 : 82

Recently, Bach and Schröder[34] reported the photocycloaddition of α-alkyl-substituted enecarbamates **41** to benzaldehyde affording 3-aminooxetanes **42** in moderate to good yields (46 to 71%). The α-phenyl-substituted enecarbamate did not lead to a photocycloaddition product presumably due to rapid energy transfer (triplet sensitization) from the electronically excited aldehyde. An increase in steric bulk of the alkyl substituent R shifted the diastereomeric ratio *cis*/*trans* in the direction of the thermodynamically more stable *cis* product.

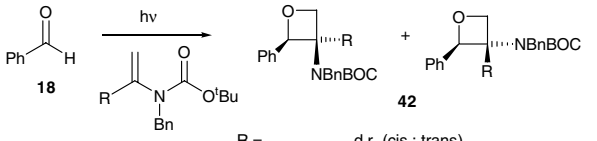

R =	d.r. (cis : trans)
Me	29 : 71
Et	34 : 66
^{i}Pr	54 : 46
Cyclohex	57 : 43
H	87 : 13

Induced Diastereoselectivity

The first report concerning an "asymmetric" Paternò–Büchi reaction with a chiral carbonyl component was made in 1979 by Gotthardt and Lenz.[35] The photocycloaddition of the enantiomerically pure menthyl ester of phenylglyoxylic acid **43** with 2,3-dimethyl-2-butene **44** gave the oxetane **45** with a diastereomeric excess of only 37%. The corresponding chiral glyoxylates gave, with furan, even lower diastereomeric excesses of 5 ± 2%.[36] The unique behavior of chiral phenyl glyoxylates was later demonstrated by Scharf and co-workers.[37] Despite the fact that in all cases the stereogenic centers are localized in the alcohol part of the α-keto ester and therefore remarkably far away from the reactive (triplet excited) carbonyl group, the (induced) diastereoselectivities were exceedingly high (>96% in many cases) with 8-phenylmenthol as chiral auxiliary.[37] The same group has studied the temperature dependence of the auxiliary-induced diastereoselectivity.[38] As substrates for the photoaddition of phenyl glyoxylates several electron-rich cycloalkenes were used that had already been studied with α-keto esters.[39] Besides normal isoselectivity effects, in most cases an *inversion* of the induced diastereoselectivity was found at certain temperatures. Consequently, this effect was named the *isoinversion principle* and has been demonstrated to be a general phenomenon for many two-step reactions.[40] The inherent (non-induced) diastereoselectivity for these photoadditions (e.g., oxetane **47** from the dioxole **28** and 8-phenylmenthyl phenyl glyoxylate **46**) was >96%, with the phenyl group being directed into the *endo*-position. The applications of Cram-like model compounds such as isopropylidene glyceraldehyde[41] or acyclic α-chiral ketones[42] did not, however, lead to high stereoselectivities.

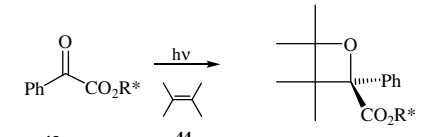

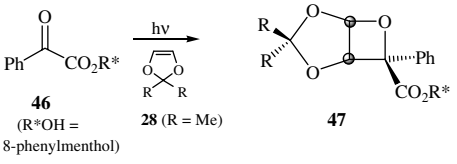

Effect of Temperature on Diastereoselectivity

Recently, Adam and Stegmann[43] reinvestigated the Paternò–Büchi reaction of *cis*- as well as *trans*-cyclooctene (**48**) with electronically excited benzophenone (**49**). They reported an unprecedented temperature-dependent diastereoselectivity, where the more stable substrate diastereoisomer (*cis*-cyclooctene) leads, with increasing reaction temperature, to increasing amounts of the less stable product diastereoisomer **50** (*trans*-oxetane). Adam rationalized the unprecedented experimental facts for the

[2+2]-photocycloaddition of the diastereoisomeric cyclooctenes with benzophenone in terms of a consistent mechanism:[44] (1) The *cis*-**48** displays a remarkable temperature dependence in that the *trans*-2-oxetane is favored with increasing temperature; (2) for *trans*-**48** the *trans* geometry is preserved in *trans*-cycloadduct over a broad temperature range of 180°C; (3) the extent of *trans* to *cis* isomerization in the cycloaddition with the *trans*-cyclooctene increases with temperature.

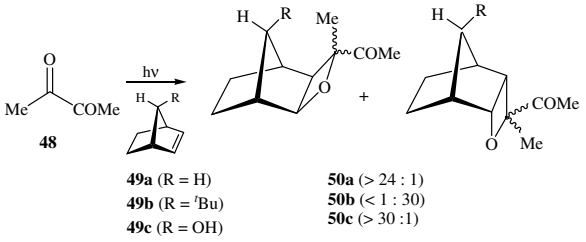

49a (R = H)
49b (R = ^{t}Bu)
49c (R = OH)

50a (> 24 : 1)
50b (< 1 : 30)
50c (> 30 :1)

59.3 The Alkene Part

Inherent Diastereoselectivity

A huge number of acyclic and cyclic alkenes and alkadienes have been used as addends for Paternò–Büchi reactions with carbonyl compounds, and many of them are mentioned in other chapters. Dioxoles[45] and 2,3-dihydrooxazoles[46] have been found to be remarkably effective addends. These alkenes are highly electron-rich compounds with low ionization potentials and also serve as potent electron-donor substrates. This property makes the application of electron-rich alkenes sometimes critical because PET reactions can interfere with the normal photocycloadditions via triplet 1,4-biradicals. The use of nonpolar solvents is therefore recommended; however, an analysis of the energetics (Rehm–Weller relationship) should always be included.[45] Intensive investigations of the diastereofacial selectivity of ketone photocycloaddition to norbornene and norbornadiene have been reported. The biacetyl (**51**) addition to norbornene **52a** is highly (>24:1) *exo* selective, whereas the *syn*-7-*t*-butyl derivative (**52b**) showed inverted (<1:30) *exo* selectivity.[48] Introduction of a hydroxy group at the 7-*syn*-position of norbornene (**52c**) reinverts the diastereoselectivity; in this case, the *exo*-adduct **53c** is formed, with the diastereomeric excess > 97%. The latter effect could be due to hydrogen bonding, which pre-complexes the excited carbonyl species. A similar photoreaction has been reported for norbornadiene.[49] As was shown by Gorman et al.,[50] ketone triplets do not add to but interconvert norbornadiene into the quadricyclane isomer that serves as the substrate for the subsequent Paternò–Büchi reaction.

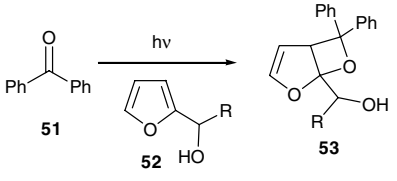

R = Et, ^{i}Pr

Effect of Hydrogen Bonding on Diastereoselectivity of Paternò–Büchi Reaction

The Paternò–Büchi reaction of 2-furylmethanol derivatives **54** with benzophenone was recently investigated by D'Auria and co-workers.[51] The regio- and stereoselectivity of the reaction was exceedingly high

and rationalized by assuming a decisive hydroxy bonding interaction favoring the approach of the electronically excited carbonyl group toward one of the diastereotopic faces of the furan ring and formation of only one diastereoisomeric oxetane **55**. When the OH group was masked by means of a methyl ether, the reactivity dropped remarkably.

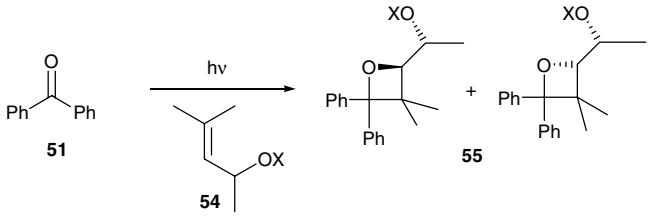

X =	solvent	d.r. (threo : erythro)
H	C_6D_6	90 : 10
H	C_6D_6/CD_3COD (1:1)	69 : 31
$SiMe_2{}^tBu$	C_6D_6	52 :48

Hydrogen bonding is also a possible reason for the diastereoselectivity of the [2+2]-photocycloaddition of benzophenone in the case of acyclic chiral allylic alcohols **56**. These substrates afforded only one regioisomer of the diastereomeric *threo*, *erythro* oxetanes **57** with a preference for the *threo* isomer.[52] The diastereoselectivity was remarkably reduced in the presence of a protic solvent (methanol as a competitive intermolecular hydrogen bonding substrate) and totally disappeared in case of the silylated substrate **56**.[53]

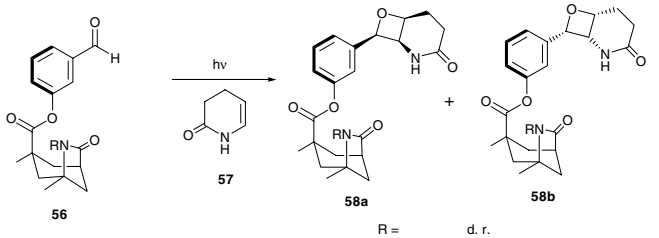

R =	d. r.
H	83 : 17
Me	50 : 50

Bach and co-workers investigated the effect of *ground-state* hydrogen bonding interactions in a complex between a rigid chiral host **58** that assists the control of enantiofacial- and diastereofacial selectivity.[54] Irradiation of this chiral host with 3,4-dihydro-1*H*-pyridino-2-one **59** in benzene gave the oxetane **60** with high selectivity, with attack of the electronically excited aldehyde occurring exclusively on one of the enantiotopic faces of the alkene. The *N*-methylated chiral host that is no longer hydrogen-bond active gave no significant diastereomeric excess.

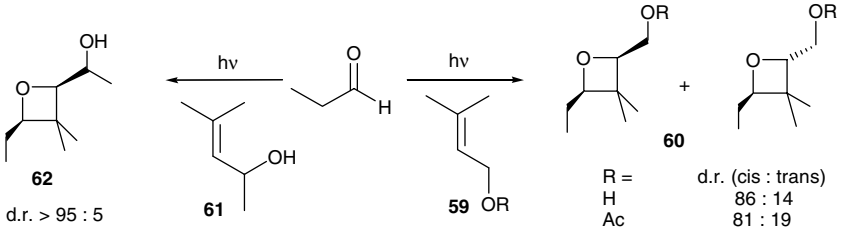

R =	d.r. (cis : trans)
H	86 : 14
Ac	81 : 19

Recently, Griesbeck and Bondock[55] compared the effect of hydrogen bonding in the first excited singlet vs. the first excited triplet state of aliphatic aldehydes in the photocycloaddition to allylic alcohols and acetates (**61**). The simple diastereoselectivity was nearly the same, but the presence of hydrogen bonding interactions increases the rate of the Paternò–Büchi reaction. Moreover, the effect of hydrogen bonding for simple diastereoselectivity was completely different than that for the induced diastereoselectivity. This was confirmed by comparison with the mesitylol (**63**)-photocycloaddition to aliphatic aldehydes.

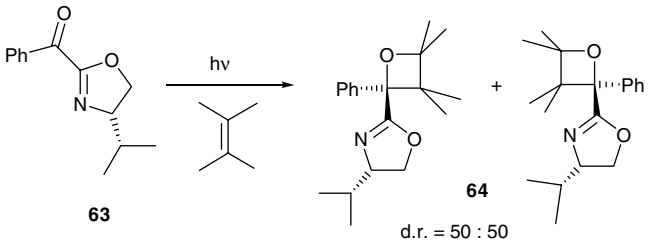

Induced Diastereoselectivity

Asymmetric Induction Via Chiral Carbonyl Compounds

Numerous applications were developed by the Scharf group[37–40,45,46] using chiral α-keto esters in [2+2]-photocycloadditions to electron-rich cycloalkenes that have already been mentioned in the text. An optically active acetal was used as substrate in the synthesis of prostaglandins. The induced (*anti*) diastereoselectivity was high (>90%); the inherent diastereoselectivity was not reported.[56] An interesting solvent dependency of the face selectivity was reported for 3,4,6-tri-*O*-acetyl-D-glucal as carbohydrate substrate.[57] Oppenländer and Schönholzer studied the diastereoface differentiation in the Paternò–Büchi reaction using the 4-(*S*)isopropyl-2-benzoyl-2-oxazoline **65** (prepared from condensation of phenylglyoxylic acid with (*S*)-valinol) as a chiral auxiliary.[58] The [2+2]-photocycloaddition gave a mixture of diastereoisomeric *l*- and *u*- (*like* and *unlike*) oxetanes **66** in equal amounts.

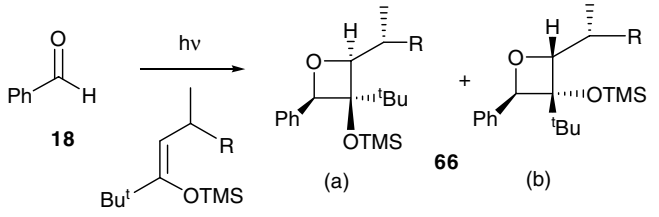

R =	d. r.
Et	61 : 39
^{i}Pr	70 : 30
Ph	71 : 29
^{t}Bu	95 : 5

Asymmetric Induction Via Chiral Alkenes

The induced diastereoselectivity in a Paternò–Büchi reaction resulting from a stereogenic center in the alkene part was recently described by Bach and co-workers[59] in the photocycloaddition of chiral silylenol ethers **67** with benzaldehyde **18**. The substituents, R, at the stereogenic center were varied in order to evaluate the influence of steric bulk and possible electronic effects. In accord with the 1,3-allylic strain model, the facial diastereoselectivity was at a maximum with large (R = *t*-Bu, $SiMe_2Ph$) and polar (R = OMe) substituents at the γ-position of silyl enol ether (diastereomeric ratio of oxetanes **68** > 95:5).

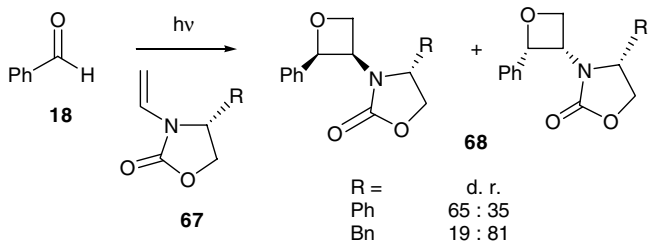

Several efforts were also made by the same group to achieve chiral auxiliary control in *N*-acyl enamines **69**, but only moderate diastereoselectivities for the 3-amido oxetanes **70** were reported.[60]

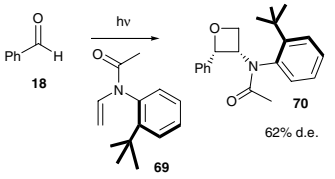

The photocycloaddition of an axial chiral *N*-acyl enamine **71** with benzaldehyde resulted in oxetane (**72**) formation with moderate diastereomeric excess.[61]

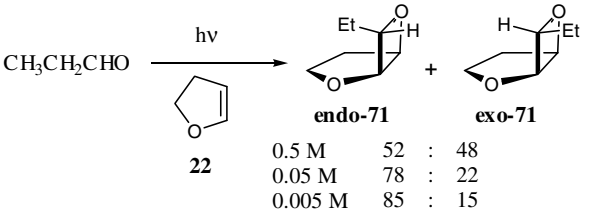

The stereogenic center in a dihydropyrrole derivative was used as the key directing element in the synthesis of natural product (+)-preussin via a [2+2]-photocycloaddition with benzaldehyde.[62]

Effect of Concentration on the Stereoselectivity of the Paternò–Büchi Reaction

The difference between the simple diastereoselectivities in photocycloaddition reactions following the singlet vs. the triplet route were studied by determination of the concentration dependence of the Paternò–Büchi reaction.[63] Carbonyl substrates that have both reactive singlet and triplet states exhibit one characteristic substrate concentration where a 1:1 ratio of singlet and triplet reactivity, (i.e., *spin selectivity*) could be detected. The shape of these concentration/diastereoselectivity correlations reflects the different kinetic contributions to this complex reaction scenario. The mixtures of diastereoisomers formed in the singlet and triplet pathway, respectively, are termed C and D.

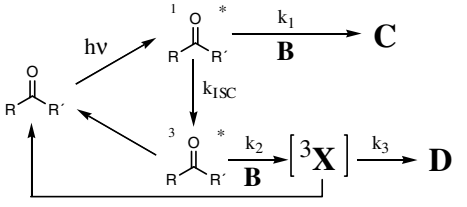

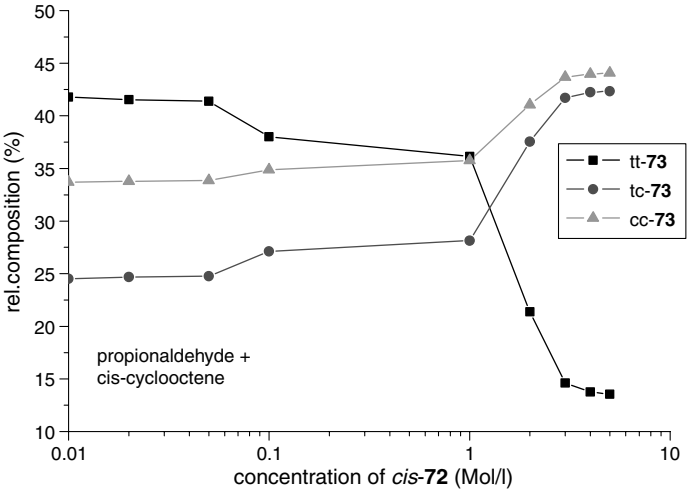

FIGURE 59.1

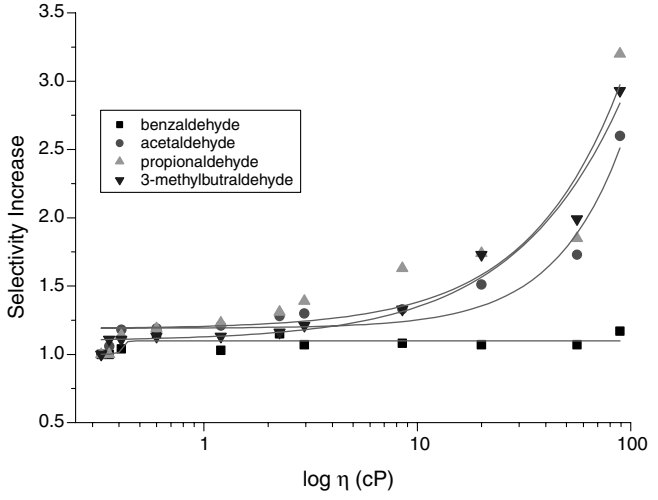

FIGURE 59.2 Viscosity dependence (normalized) of the Paternò-Büchi reaction of 2,3-dihydrofuran with aldehydes (1M) at 293 K.

The selectivity (C/D) is controlled by the geometry of the conical intersection for the singlet reaction and by the optimal ISC geometry of the 2-oxatetramethylene biradical (^{3}X) for the triplet reaction. The situation is described for the propionaldehyde/2,3-dihydrofuran photocycloaddition reaction. At low concentrations (0.005 *M*, triplet conditions), the diastereoselectivity approaches a maximum *endo*/*exo* value of 85:15. At high concentrations (0.5 *M*, singlet conditions), the diastereoselectivity decreased to 52:48.

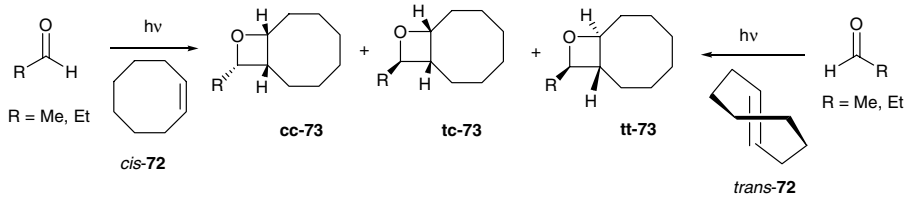

The concentration dependence of the photocycloaddition of *cis*- and *trans*-cyclooctene **48** with aliphatic aldehydes was studied in order to test the spin selectivity with respect to the *cis*/*trans* oxetane ratio and/or the *endo*/*exo* selectivity relevant for the *cis*-photoadduct.[64] The results depicted in Figure 59.2 indicate a moderate but still significant spin correlation effect in the Paternò–Büchi reaction of cyclooctene with aliphatic aldehydes. The *exo*-diastereoisomers **tc**-**74** were formed with similar probability as the *endo*-diastereoisomers **cc**-**74** in the singlet carbonyl manifold, whereas the triplet excited aldehydes preferred the formation of the *endo*-diastereoisomer and *trans*-fused products **tt-74**.

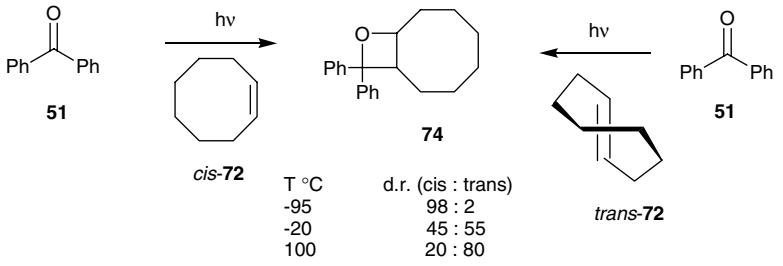

Effect of Temperature and Solvent Viscosity on the Stereoselectivity of the Paternò–Büchi Reaction

As an extension of the work on the temperature dependence of the induced diastereoselectivity in α-keto ester photocycloadditions by Scharf et al.,[38,40] the temperature dependence of spin-selective reactions (singlet vs. triplet photocycloaddition) was determined and a characteristic nonlinear behavior was detected.[65] Prior to these experiments, solvent viscosity effects were studied in order to separate these influences from temperature effects. The photocycloaddition of benzaldehyde **18** with 2,3-dihydrofuran **22** was investigated as a typical triplet reaction with concentration-independent diastereoselectivity. Variation of the solvent viscosity over a large effective range (η = 0.3 to 1500 cp) resulted in a weak but significant increase in *endo* selectivity from 82 to 91% (see Figure 59.2).

More pronounced effects were detected for reactions of aliphatic aldehydes with **22**. In all cases, the diastereoselectivity increased with increasing solvent viscosity. In the context of the mechanistic model above, an increase in solvent viscosity favors the triplet channel due to a reduction in the diffusion rate limit (about 4 orders of magnitude in the experimental range). The temperature dependence of the *endo*/*exo* selectivity with aliphatic aldehydes RCHO (R = Et, Me, *i*-Bu) showed characteristic nonlinear curves with inversion points from which activation parameters for the singlet as well as the triplet photocycloaddition were determined.

References

1. Turro, N. J. and Farrington, G. L., Quenching of the fluorescence of 2-norbornanone and derivatives by electron-rich and electron-poor ethylenes, *J. Am. Chem. Soc.*, 102, 6051, 1980.
2. Turro, N. J. and Farrington, G. L., Photoinduced oxetane formation between 2-norbornanone and derivatives with electron-poor ethylenes, *J. Am. Chem. Soc.*, 102, 6056, 1980.
3. Carless, H. A. J., Photocycloaddition of acetone to acyclic olefins, *Tetrahedron Lett.*, 3173, 1973.
4. Turro, N. J. and Wriede, P. A., The photocycloaddition of acetone to 1-methoxy-1-butene: a comparison of singlet and triplet mechanisms and singlet and triplet biradical intermediates, *J. Am. Chem. Soc.*, 92, 320, 1970.
5. Morris, T. H., Smith, E. H., and Walsh, R., Oxetane synthesis: methyl vinyl sulphides as new traps of excited benzophenone in a stereoselective and regiospecific Paternò–Büchi reaction, *J. Chem. Soc., Chem. Commun.*, 964, 1987.

6. Zimmerman, H. E., Singer, L., and Thyagarajan, B. S., Overlap control of carbanionoid reactions. I. Stereoselectivity in alkaline epoxidation, *J. Am. Chem. Soc.*, 81, 108, 1959, footnote 16.
7. Hautala, R. R., Dawes, K., and Turro, N. J., Stereoselectivity and regioselectivity of the photocycloaddition of 2-methyl-2,4-hexadiene and acetone, *Tetrahedron Lett.*, 1229, 1972.
8. Yang, N. C., Kimura, M., and Eisenhardt, W., Paternò–Büchi reaction of aromatic aldehydes with 2-butenes and their implication on the rate of intersystem crossing of aromatic aldehydes, *J. Am. Chem. Soc.*, 95, 5058, 1973.
9. Jones II, G., Khalil, Z. H., Phan, X. T., Chen, T.-J., and Welankiwar, S., Divergent stereoselectivity in the photoaddition of alkanals and medium ring cycloalkenes, *Tetrahedron Lett.*, 22, 3823, 1981.
10. Bradshaw, J. S., Ultraviolet irradiation of carbonyl compounds in cyclohexene and 1-hexene, *J. Org. Chem.*, 31, 237, 1966.
11. Jones II, G., Synthetic applications of the Paternò–Büchi reaction, in *Organic Photochemistry*, Vol. 5, Padwa, A., Ed., Marcel Dekker, New York, 1981, 1.
12. Griesbeck, A. G. and Stadtmüller, S., Photocycloaddition of benzaldehyde to cyclic olefins: electronic control of endo stereoselectivity, *J. Am. Chem. Soc.*, 112, 1281, 1990.
13. Carless, H. A. J. and Haywood, D. J., Photochemical synthesis of 2,6-dioxabicyclo[3.2.0]heptanes, *J. Chem. Soc., Chem. Commun.*, 1067, 1980.
14. Griesbeck, A. G. and Stadtmüller, S., Regio- and stereoselective photocycloaddition reactions of aromatic aldehydes to furan and 2,3-dihydrofuran, *Chem. Ber.*, 123, 357, 1990.
15. Griesbeck, A. G. and Stadtmüller, S., Electronic control of stereoselectivity in photocycloaddition reactions. 4. Effects of methyl substituents at the donor olefin, *J. Am. Chem. Soc.*, 113, 6923, 1991.
16. Salem, L. and Rowland, C., The electronic properties of biradicals, *Angew. Chem. Int. Ed. Engl.*, 11, 92, 1972.
17. Griesbeck, A. G., Mauder, H., Peters, K., Peters, E.-M., and von Schnering, H. G., Photocycloadditions with α- and β-naphthaldehyde: complete inversion of diastereoselectivity as a consequence of differently configurated electronic states, *Chem. Ber.*, 124, 407, 1991.
18. (a) Schenck, G. O., Hartmann, W., and Steinmetz, R., Four-membered ring synthesis by the photosensitized cycloaddition of dimethyl maleic anhydride to olefins, *Chem. Ber.*, 96, 498, 1963; (b) Toki, S., Shima, K., and Sakurai, H., Organic photochemical reactions. I. The synthesis of substituted oxetanes by the photoaddition of aldehydes to furans, *Bull. Chem. Soc. Jpn.*, 38, 760, 1965; (c) Shima, K. and Sakurai, H., Photoaddition reactions of various carbonyl compounds to furan, *Bull. Chem. Soc. Jpn.*, 39, 1806, 1966.
19. (a) Schreiber, S. L. and Satake, K., Application of the furan–carbonyl photocycloaddition reaction to the synthesis of the *bis*(tetrahydrofuran) moiety of asteltoxin, *J. Am. Chem. Soc.*, 105, 6723, 1983; (b) Schreiber, S. L., Hoveyda, A. H., and Wu, H.-J., A photochemical route to the formation of threo aldols, *J. Am. Chem. Soc.*, 105, 660, 1983; (c) Schreiber, S. L. and Satake, K., Total synthesis of (±)-asteltoxin, *J. Am. Chem. Soc.*, 106, 4186, 1984; (d) Schreiber, S. L., [2+2]-Photocycloadditions in the synthesis of chiral molecules, *Science*, 227, 857, 1985.
20. Feigenbaum, A., Pete, J.-P., and Poquet-Dhimane, A.-L., Stereoselective synthesis of unsaturated oxetanes, *Heterocycles*, 27, 125, 1988.
21. Cantrell, T. S., Allen, A. C., and Ziffer, H., Photochemical 2+2 cycloaddition of arenecarboxylic acid esters to furans and 1,3-dienes: 2+2 cycloreversion of oxetanes to dienol esters and ketones, *J. Org. Chem.*, 54, 140, 1989.
22. Exceptions due to steric and electronic reasons are known; see (a) Carless, H. A. J. and Halfhide, A. F. E., Highly regioselective [2+2]-photocycloaddition of aromatic aldehydes to acylfurans, *J. Chem. Soc., Perkin Trans. 1*, 1081, 1992; (b) Schreiber, S. L., Desmaele, D., and Porco, Jr., J. A., On the use of unsymmetrically substituted furans in the furan-carbonyl photocycloaddition reaction: synthesis of a kadsurenone–ginkgolide hybrid, *Tetrahedron Lett.*, 29, 6689, 1988.
23. Jarosz, S. and Zamojski, A., Asymmetric photocycloaddition between furan and optically active ketones, *Tetrahedron*, 38, 1453, 1982.

24. (a) Rivas, C. and Bolivar, R. A., Synthesis of oxetanes by photoaddition of carbonyl compounds to pyrrole derivatives, *J. Heterocyclic Chem.*, 13, 1037, 1976; (b) Julian, D. R. and Tringham, G. D., Photoaddition of ketones to indoles: synthesis of oxeto[2,3-*b*]indoles, *J. Chem. Soc., Chem. Commun.*, 13, 1973; (c) Rivas, C., Pacheco, D., Vargas, F., and Ascanio, J., Synthesis of oxetanes by photoaddition of carbonyl compounds to thiophene derivatives, *J. Heterocyclic Chem.*, 18, 1065, 1981; (d) Nakano, T., Rodriquez, W., de Roche, S. Z., Larrauri, J. M., Rivas, C., and Pérez, C., Photoaddition of ketones to imidazoles, thiazoles, isothiazoles and isoxazoles: synthesis of their oxetanes, *J. Heterocyclic Chem.*, 17, 1777, 1980.
25. Shima, K., Kubota, T., and Sakurai, H., Organic photochemical reactions. XXIV. Photocycloaddition of propanal to 1,3-cyclohexadiene, *Bull. Chem. Soc. Jpn.*, 49, 2567, 1976.
26. Hoye, T. R. and Richardson, W. S., A short, oxetane-based synthesis of (±)-sarracenin, *J. Org. Chem.*, 54, 688, 1989.
27. Mattay, J. and Buchkremer, K., Thermal and photochemical oxetane formation with α-ketoesters, *Heterocycles*, 27, 2153, 1988.
28. Zamojski, A. and Kozluk, T., Synthesis of 3-substituted furans, *J. Org. Chem.*, 42, 1089, 1977.
29. Griesbeck, A. G., Buhr, S., Fiege, M., Schmickler, H., and Lex, J., Stereoselectivity of triplet photocycloadditions: diene-carbonyl reaction and solvent effects, *J. Org. Chem.*, 63, 3847, 1998.
30. Park, S. K., Lee, S. J., Baek, K., and Yu, C. M., Diastereoselective routes in the Paternò–Büchi reaction of cyclic enol ortho ester with aldehydes, *Bull. Korean. Chem. Soc.*, 19, 35, 1998.
31. Bach, T. and Schröder, J., Photocycloaddition of *N*-acyl enamines to aldehydes and its application to the synthesis of diastereomerically pure 1,2-amino alcohols, *J. Org. Chem.*, 64, 1265, 1999.
32. Bach, T. and Jödicke, K., Diastereomerically pure 3-(silyloxy)oxetanes by a selective Paternò–Büchi reaction, *Chem. Ber.*, 126, 2457, 1993.
33. Abe, M., Fujimoto, K., and Nojima, M., Notable sulfur atom effects on the regio- and stereoselective formation of oxetanes in Paternò–Büchi photocycloaddition of aromatic aldehydes with silyl *O*,*S*-ketene acetals, *J. Am. Chem. Soc.*, 122, 4005, 2000.
34. Bach, T. and Schröder, J., The Paternò–Büchi reaction of α-alkyl-substituted ene carbamates and benzaldehyde, *Synthesis*, 1117, 2001.
35. Gotthardt, H. and Lenz, W., Unusually high asymmetric induction in the photochemical formation of oxetanes, *Angew. Chem. Int. Ed. Engl.*, 18, 868, 1979.
36. Jarosz, S. and Zamojski, A., Asymmetric photocycloaddition between furan and chiral alkyl glyoxylates, *Tetrahedron*, 38, 1447, 1982.
37. Nehrings, A., Scharf, H.-D., and Runsink, J., Chiral induction during photochemical reactions. 3. Photochemical preparation of an L-erythrose unit and its insertion during the synthesis of methyl-2,3-*O*-isopropylidene-β-L-apio-L-furanoside, *Angew. Chem. Int. Ed. Engl.*, 25, 877, 1985.
38. Buschmann, H., Scharf, H.-D., Hoffmann, N., Plath, M., and Runsink, J., Chiral induction in photochemical reactions. 10. The principle of isoinversion: a model of stereoselection developed from the diastereoselectivity of the Paternò–Büchi reaction, *J. Am. Chem. Soc.*, 111, 5367, 1989.
39. (a) Koch, H., Runsink, J., and Scharf, H.-D., Investigation of chiral induction in photochemical oxetane formation, *Tetrahedron Lett.*, 24, 3217, 1983; (b) Koch, H., Scharf, H.-D., Runsink, J., and Leismann, H., Regio- and diastereoselectivity in the oxetane formation of chiral phenylglyoxylates with electron rich olefins, *Chem. Ber.*, 118, 1485, 1985; (c) Pelzer, R., Jütten, P., and Scharf, H.-D., Chiral induction in photochemical reactions. IX. Isoselectivity in the asymmetric Paternò–Büchi reaction using carbohydrates as chiral auxiliaries, *Chem. Ber.*, 122, 487, 1989.
40. Buschmann, H., Scharf, H.-D., Hoffmann, N., and Esser, P., The isoinversion principle: a general selection model in chemistry, *Angew. Chem. Int. Ed. Engl.*, 30, 477, 1991.
41. Schreiber, S. L. and Satake, K., Studies of the furan–carbonyl photocycloaddition reaction: the determination of the absolute stereostructure of asteltoxin, *Tetrahedron Lett.*, 27, 2575, 1986.
42. Jarosz, S. and Zamojski, A., Asymmetric photocycloaddition between furan and optically active ketones, *Tetrahedron*, 38, 1453, 1982.

43. Adam, W. and Stegmann, V. R., Unusual temperature dependence in the *cis*/*trans*-oxetane formation discloses competitive *syn* versus *anti* attack for the Paternò–Büchi reaction of triplet excited ketones with *cis*- and *trans*-cyclooctenes: conformational control of diastereoselectivity in the cyclization and cleavage of preoxetane biradicals, *J. Am. Chem. Soc.*, 124, 3600, 2002.
44. Adam, W., Stegmann, V. R., and Weinkoetz, S., Unusual temperature-dependent diastereoselectivity in the [2+2]-photocycloaddition (Paternò–Büchi reaction) of benzophenone to *cis*- and *trans*-cyclooctene through conformational control, *J. Am. Chem. Soc.*, 123, 2452, 2001.
45. Meier, L. and Scharf, H.-D., A new synthesis of 4,5-unsubstituted 1,3-dioxoles, *Synthesis*, 517, 1987.
46. Weuthen, M., Scharf, H.-D., and Runsink, J., 3-Acetyl-2,3-dihydro-2,2-dimethyloxazole; synthesis, properties and its application as olefinic partner in the Paternò–Büchi reaction, *Chem. Ber.*, 120, 1023, 1987.
47. Mattay, J., Radical ions and photochemical charge-transfer phenomena. Part 17. Charge transfer and radical ions in photochemistry, *Angew. Chem.*, 99, 849, 1987.
48. Sauers, R. R., Valenti, P. C., and Tavss, E., The importance of steric effects on the photocycloadditions of biacetyl to norbornenes, *Tetrahedron Lett.*, 3129, 1975.
49. Kubota, T., Shima, K., and Sakurai, H., The photocycloaddition of benzophenone to norbornadiene, *Tetrahedron Lett.*, 343, 1972.
50. (a) Barwise, A. J. G., Gorman, A. A., Leyland, R. L., Parekh, C. T., and Smith, P. G., The inter- and intramolecular addition of aromatic ketone triplets to quadricyclane, *Tetrahedron*, 36, 397, 1980; (b) Gorman, A. A. and Leyland, R. L., The reaction of benzophenone triplets with norbornadiene and quadricyclane, *Tetrahedron Lett.*, 5345, 1972; (c) Gorman, A. A., Leyland, R. L., Rodgers, M. A. J., and Smith, P. G., Concerning the mechanism of interactions of triplet benzophenone with norbornadienes and quadricyclanes, *Tetrahedron Lett.*, 5085, 1973.
51. D´Auria, M., Racioppi, R., and Romaniello, G., The Paternò–Büchi reaction of 2-furylmethanols, *Eur. J. Org. Chem.*, 3265, 2000.
52. Adam, W., Peters, K., Peters, E. M., and Stegmann, V. R., Hydroxy-directed regio- and diastereoselective [2+2]-photocycloaddition (Paternò–Büchi reaction) of benzophenone to chiral allylic alcohols, *J. Am. Chem. Soc.*, 122, 2958, 2000.
53. Adam, W. and Stegmann, V. R., Hydroxy-group directivity in the regioselective and diastereoselective [2+2]-photocycloaddition (Paternò–Büchi reaction) of aromatic carbonyl compounds to chiral and achiral substrates: the preparation of oxetanes with up to three stereogenic centers as synthetic building blocks, *Synthesis*, 1203, 2001.
54. Bach, T., Bergmann, H., and Harms, K., High facial diastereoselectivity in the photocycloaddition of a chiral aromatic aldehyde and an enamide induced by intermolecular hydrogen bonding, *J. Am. Chem. Soc.*, 121, 10650, 1999.
55. Griesbeck, A. G. and Bondock, S., Paternò–Büchi reaction of allylic alcohols and acetates with aldehydes: hydrogen bond interaction in the excited singlet and triplet states?, *J. Am. Chem. Soc.*, 123, 6191, 2001.
56. Morton, D. R. and Morge, R. A., Total synthesis of 3-oxa-4,5,6-trinor-3,7-inter-*m*-phenylene prostaglandins. 1. Photochemical approach, *J. Org. Chem.*, 43, 2093, 1978.
57. Araki, Y., Senna, K., Matsuura, K., and Ishido, Y., Supplementary aspects in the photochemical addition of acetone to 3,4,6-tri-*O*-acetyl-D-glucal, *Carbohydr. Res.*, 60, 389, 1978.
58. Oppenländer, T. and Schönholzer, P., Synthesis, reactivity and application as chiral auxiliaries of the novel (3R)- and (3S)-4,5-dihydro-3-hydroxy-4,4,5,5-tetramethyl-3-phenylfuran-2(3H)-ones in the Paternò–Büchi reaction, *Helv. Chim. Acta*, 72, 1792, 1989.
59. Bach, T., Jödicke, K., and Wibbeling, B., Reversal of the facial diastereoselectivity in the Paternò–Büchi reaction of silyl enol ethers carrying a chiral substituent in α-position, *Tetrahedron*, 52, 10861, 1996.
60. Bach, T., Schröder, J., Brandl, T., Hecht, J., and Harms, K., Facial diastereoselectivity in the photocycloaddition of chiral *N*-acyl enamines to benzaldehyde, *Tetrahedron*, 54, 4507, 1998.

61. Bach, T., Schröder, J., and Harms, K., Diastereoselective photocycloaddition of an axial chiral enamide, *Tetrahedron Lett*., 40, 9003, 1999.
62. Bach, T., Brummerhop, H., and Harms, K., The synthesis of (+)-preussin and related pyrrolidinols by diastereoselective Paternò–Büchi reactions of chiral 2-substituted 2,3-dihydropyrrroles, *Chem.-Eur. J.*, 6, 3838, 2000.
63. Griesbeck, A. G., Fiege, M., Bondock, S., and Gudipati, M. S., Spin-directed stereoselectivity of carbonyl-alkene photocycloadditions, *Org. Lett.*, 2, 3623, 2000.
64. Griesbeck, A. G. and Bondock, S., Spin-imposed stereoselection in the photocycloaddition of (*Z*) and (*E*)-cyclooctene to aliphatic aldehydes, *Photochem. Photobiol. Sci*., 1, 81, 2002.
65. Griesbeck, A. G., Bondock, S., and Gudipati, M. S., Temperature and viscosity dependence of the spin-directed stereoselectivity of the carbonyl-alkene photocycloaddition, *Angew. Chem. Int. Ed.* Engl., 40, 4684, 2001.

60

Oxetane Formation: Intermolecular Additions

Axel G. Griesbeck
University of Cologne

Samir Bondock
University of Cologne

60.1 Introduction and Definition of the Reaction

The first intermolecular photocycloaddition of an aromatic carbonyl compound (benzaldehyde) to an alkene (2-methyl-2-butene) was reported by Paternò and Chieffi: "*In una prima esperienza abbiamo esposto un miscuglio equimolecolare di amilene (gr. 43) e di aldeide benzoica (gr. 67) in un tubo chiuso, dal 5 dicembre 1907 al 20 marzo 1908, cioè per circa tre mesi e mezzo della stagione invernale*".[1] When this prolonged experiment (104 days!) was repeated by Büchi and co-workers in the mid-1950s, they confirmed the oxetane structure of the main product.[2] The regioselectivity of this specific transformation, however, was not correctly established until a publication by Yang et al.,[3] and still today no exact analysis of the stereoselectivity has been reported. Several special features about this reaction are worthwhile for discussion; for example, the influence of the *state properties* of the electronically excited species (which normally is the carbonyl compound) and of the alkene properties on rate, efficiency, and selectivity of the oxetane formation. Furthermore, a detailed discussion of diastereo- and enantioselective modifications and of intramolecular variants is given in Chapter 59. This chapter describes applications of intermolecular Paternò–Büchi reactions. After discussion of the features of the carbonyl addends, the olefinic counterparts are discussed. A number of extensive reviews about special features of this reaction type have appeared in the last 15 years and are recommended for those seeking further information.[4]

60.2 Mechanism of the Paternò–Büchi Reaction

Theoretical Models

Considering orbital interactions between alkenes and n,π^* excited carbonyls, Turro et al.[5] have classified two possible primary trajectories: (1) the nucleophilic attack of the alkene toward the carbonyl half-filled *n* orbital, characterized as the *perpendicular approach*, and (2) the nucleophilic attack of the carbonyl by its half-filled π^* orbital toward the empty π^* orbital of the alkene, characterized as the *parallel approach*. First-order orbital correlation diagrams are in line with this model and predict the formation of a carbon–carbon bonded 1,4-biradical for the parallel approach and a carbon–oxygen bonded biradical

0-8493-1348-1/04/$0.00+$1.50

for the perpendicular approach.[6] Which approach dominates is controlled by the relative positions of the alkene HOMO and LUMO. For interaction between electron-rich alkenes with carbonyl compounds, the perpendicular approach is favored; for electron-deficient alkenes, the parallel approach. Several *ab initio* calculations have been published.[7] A recent MC-SCF study resulted in the prediction that intersystem crossing (ISC) from triplet to singlet leads to the same biradical ground-state pathways that are entered via singlet photochemistry.[8] Following this line of argument, the product-determining molecular geometry is expected to be similar either from the first excited singlet or triplet state of the carbonyl reactant.

Experimental Results

The biradical model has been in vogue for at least three decades to describe chemo- and regioselectivity phenomena. At least for triplet 1,4-biradicals (2-oxatetramethylenes or preoxetanes), this assumption has been confirmed by experimental facts. Trapping experiments (triplet oxygen and sulfur dioxide),[9] as well as the application of radical clocks,[10] have demonstrated that short-lived (1- to 10-ns) triplet 1,4-biradicals are formed when triplet excited carbonyl compounds interact with alkenes. Spectroscopic evidence for these species came from laser flash photolysis of electron-rich olefins with benzophenone.[11] In this case, also, the radical anion of the ketone was detected, demonstrating that electron transfer processes can interfere with the formation of oxetanes. The existence of an exciplex as precursor of the 1,4-biradicals as well as of the radical ion pair was deduced from a comparison of oxetane formation with the fluorescence quenching of singlet excited ketones by electron-rich and electron-deficient alkenes.[12] A series of experiments on substrate diastereoselectivity have been undertaken to differentiate between reactive states (n,π^* vs. π,π^*) and multiplicities (singlet vs. triplet). Simple rules have been deduced that could be used as first approximations; for example, triplet n,π^* carbonyls show much less stereoselectivity than singlet n,π^* carbonyls.[13] More details are given in the preceding chapter, which covers stereoselectivity in oxetane formation.

60.3 Substrates for the Paternò–Büchi Reaction

Carbonyl Compounds

Aromatic Ketones and Aldehydes

An impressive number of Paternò–Büchi reactions have substituted benzophenones or benzaldehydes. Some of these reactions are discussed in context with their olefinic reaction partners. A special group of aromatic carbonyl reagents are heteroaromatic substrates such as acyl derivatives of furan and thiophene which could in principle undergo [2+2]-cycloaddition toward the C=O group as well as toward one of the ring C=C groups. The reaction periselectivity is controlled by the heteroatom and the substitution pattern, which influences the nature of the lowest excited triplet state.[14] Cantrell[15] has published a series of experiments with 2- and 3-substituted benzoyl-, acetyl-, and formylthiophenes and furans. The aldehydes **1** and **3** (X = S, O) gave, with high selectivity, the oxetanes **2** and **4**, with 2,3-dimethyl-2-butene as the alkene addend. Similar results were reported for 2-benzoylfuran and 2-benzoylthiophene **5** (X = S, O), whereas the corresponding 2-acetyl substrates **6** gave mixtures of [2+2]- and [4+2]-photoproducts **7** to **9**.[16]

Vargas and Rivas[17] reported the photocycloaddition of acetylselenophene **10** to tetrasubstituted alkenes, resulting in two [2+2]-photoadducts, one of them, **11**, involves the C=C bond of the monoalkene and the β,γ-double bond of the selenophene. The second product, **12**, is a Paternò–Büchi photoadduct involving the carbonyl group of the selenophene and the C=C bond of the monoalkene. In contrast to 2-acetylthiophenone, which also yields a [4+2]-cycloaddition product, no such adducts were found with 2-acetylselenophene. This was rationalized by the difference in size of the heteroatom, which might disfavor a Diels–Alder approach for the selenium compound in contrast to the corresponding sulfur and oxygen heterocycles.

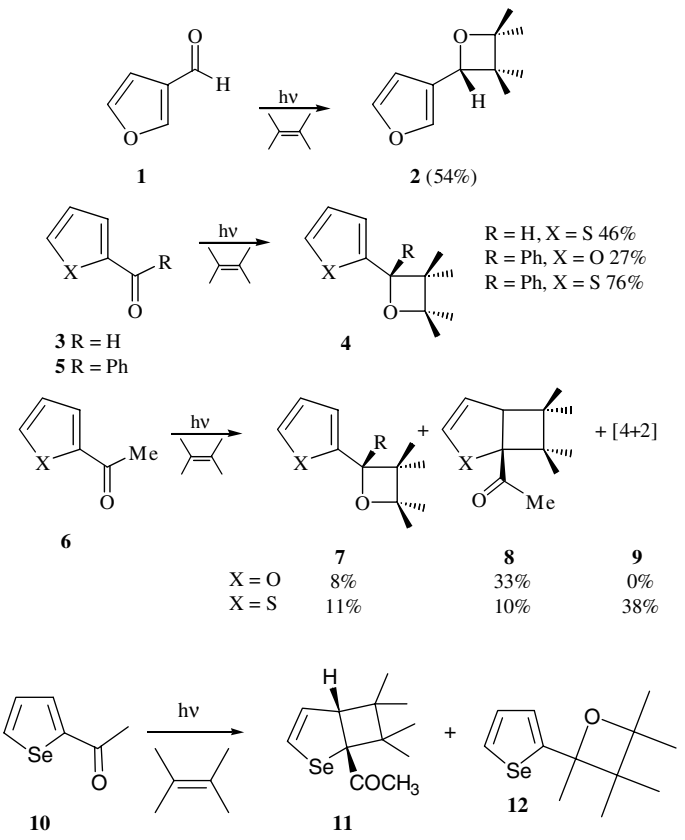

Photoinduced [2+2]-cycloadditions of [1]H-1-acetylindole-2,3-dione **13** with alkenes gave spirooxetanes **14** in moderate to high yields, displaying the typical triplet n,π^* reactivity of acetylisatin.[18] The regioselectivity and diastereoselectivity of these reactions depend on the reaction mechanism; reactions involving alkenes with high oxidation potential exclude single electron transfer (SET) processes, thus the regioselectivity can be rationalized by considering frontier molecular orbital interactions of the two addends and the diastereoselectivity by applying the Salem–Rowland rules for triplet-to-singlet biradical intersystem crossing (*vide infra*).

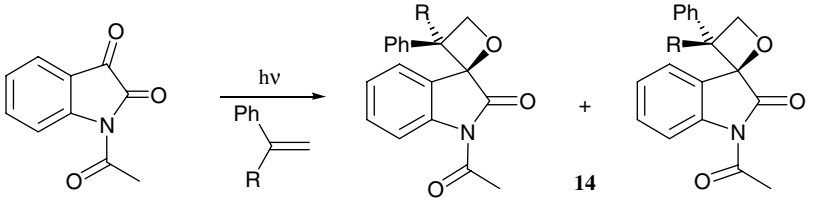

R =	solvent	syn : anti	yield (%)
H	benzene	1.42 : 1	96
H	acetonitrile	2.57 : 1	98
Me	benzene	1.00 : 1	96
Me	acetonitrile	2.19 : 1	96

As an extension of this work, photoinduced [2+2]-cycloadditions of 1-acetylisatin **13** with cyclic enol ethers (furan, benzofuran, 2-phenylfuran, 8-methoxypsoralen) and acyclic enol ethers (*n*-butyl vinyl ether and vinyl acetate) were investigated which afforded the spirooxetanes in high yields (82 to 96%)

and with high regio- and diastereoselectivity.[19] Treatment of the furan-derived oxetane **15** with acid resulted in oxetane ring opening and yielded the 3-(furan-3-yl)indole derivative **16**.

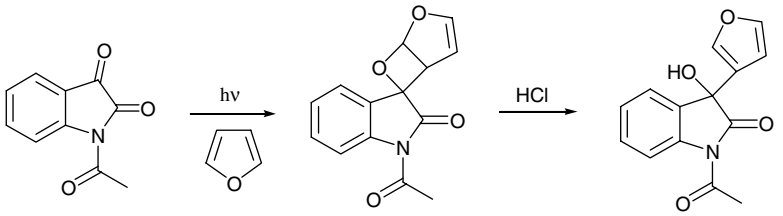

13 **15** **16**

Carboxylic Acid Derivatives and Nitriles

Coyle[20] has summarized the photochemistry of carboxylic acid derivatives. For arene carboxylic acid esters it has been shown that [2+2]-cycloaddition competes with hydrogen abstraction by the excited ester from an allylic position of the alkene. The addition of methyl benzoate **17** to 2-methyl-2-butene gave a 1:1 mixture of the Paternò–Büchi adduct **18** and the coupling product **19**.[21] Less electron-rich alkenes (e.g., cyclopentene) did add preferentially toward the benzene ring of **17** in an *ortho*- and *meta*-cycloaddition manner. Furans could also be added photochemically to methyl benzoate and other arenecarboxylic acid esters. The resulting bicyclic oxetanes could be transformed into a series of synthetically valuable products.[22] [2+2]-Cycloadducts and/or their cleavage or rearrangement products have also been described for photoreactions of alkenes with diethyl oxalate,[23] benzoic acid,[24] and carbamates.[25]

The site selectivity of alkene addition to benzonitrile **20** has been studied with a series of cyclic and acyclic olefins. Again, two reaction modes could be observed: [2+2]-cycloaddition to the nitrile group leading to 2-azabutadienes, deriving from the primarily formed azetines, (e.g., **21** from 2,3-dimethyl-2-butene),[26] and *ortho*-cycloaddition to the benzene ring (e.g., **22** from 2,3-dihydrofuran).[27]

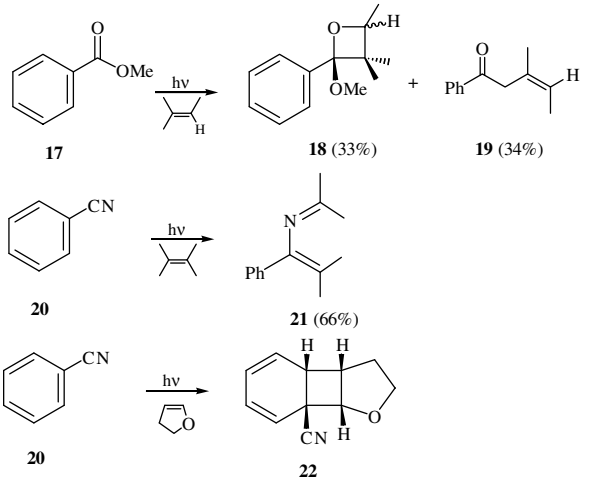

17 **18** (33%) **19** (34%)

20 **21** (66%)

20 **22**

Recently, Hu and Neckers[28] reported that triplet excited states of alkyl phenyl glyoxylates react rapidly and with high chemical yields with electron-rich alkenes forming oxetanes **24** with high regio- and stereoselectivity. The intramolecular γ-hydrogen abstraction (Norrish type II) cannot compete with intermolecular reactions in most cases. When less electron-rich alkenes were used, the Norrish type II reaction became competitive.

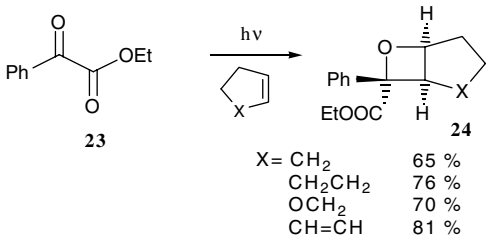

Buhr et al.[29] described the photocycloaddition of methyl and ethyl trimethyl pyruvates (**25**) with diisopropyl-1,3-dioxole. In contrast to the reaction with ethyl pyruvate, the bicyclic oxetane **26** was formed with very high (>98%) diastereoisomeric excess. An x-ray analysis revealed the unusual *endo-t*-butyl configuration. Semi-empirical calculation indicated that this clearly is the kinetic product formed by a biradical combination reaction, which might be controlled by favorable spin-orbit coupling geometries.

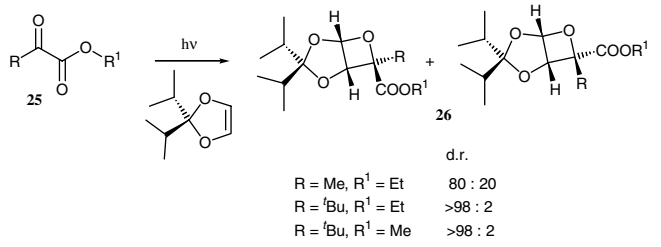

α-Ketocarbonyl Compounds, Acyl Cyanides

α-Diketones undergo primary photochemical addition to olefins to form [4+2]- and [2+2]-cycloadducts in competition to hydrogen abstraction, α-cleavage, and enol formation. The product ratios (**28**:**29**:**30**:**31**) of the biacetyl (**27**)/2,3-dimethyl-2-butene photoreaction strongly depend on the solvent polarity and reaction temperature, indicating an exciplex intermediate with pronounced charge separation and possibly free radical ions from a photoelectron transfer (PET) step.[30] Similar product ratios were reported for the methyl pyruvate/2,3-dimethyl-2-butene photoreaction. In this case, however, a state selectivity effect is responsible for the formation of the different ether and alcohol products.[31] Obviously, the existence of allylic hydrogens favors the formation of unsaturated acyclic products via hydrogen migration steps at the triplet biradical level. More electron-rich alkenes without (or with unfavorable) allylic hydrogens do give oxetanes with excited α-dicarbonyl compounds. Furan, indene,[32] as well as isopropenyl ethyl ether,[33] were converted to the corresponding [2+2]-cycloadducts (e.g., **32**) with biacetyl **27** and methyl pyruvate, respectively. Chiral phenyl pyruvates have been investigated intensively as carbonyl addends with medium to remarkably high diastereoselectivities (*vide infra*). Benzoyl cyanide **33** gives mixtures of cycloaddition and coupling products with 2,3-dimethyl-2-butene,[34] whereas the addition of **33** and a series of other acyl cyanides to furan is chemoselective and leads to bicyclic oxetanes **34** with variable *endo*/*exo* ratios.[35]

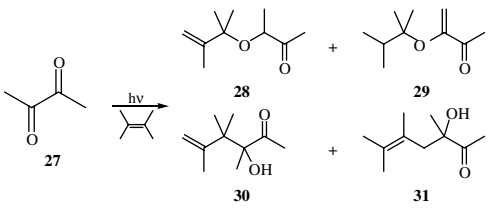

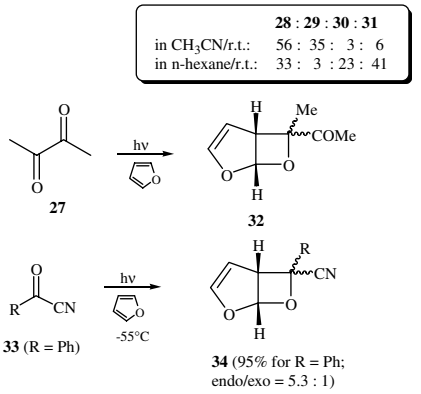

Symmetric $^3n,\pi^*$ excited 1,2-diarylethanediones (**35**) undergo highly regio- and stereoselective head-to-head additions to various captodative-substituted alkenes (2-aminopropenenitriles **36**), forming oxetanes **37** in moderate to good yield.[36]

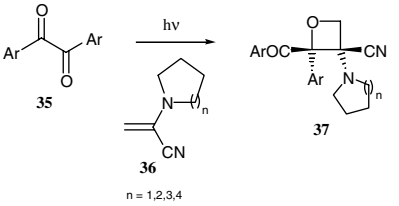

Also, unsymmetric 1,2-diarylethanediones **38** undergo addition, resulting in the formation of cycloadducts **39**.[37] Only one regioisomer of the *a priori* conceivable regioisomers has been detected for each case. The connectivity and the preferred configuration of the products are rationalized in terms of the geometry of the more stable (including captodative stabilization) 1,4-biradical intermediate. In all cases, the cyclic amino substituent in the major diastereoisomer is oriented *cis* to the aryl moiety of the participating aroyl group, whereas the nonparticipating aroyl group is *cis* to the nitrile function.

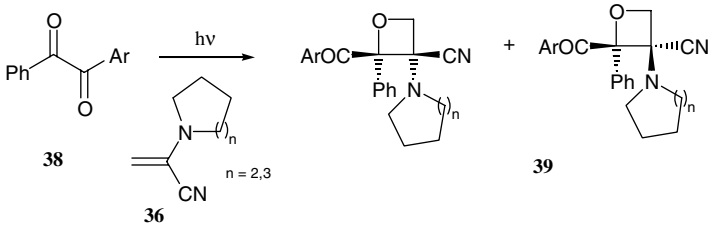

Whereas 2-naphthyl-substituted diones form oxetanes, 1,1′-naphthyl- and 1-(1-naphthyl)-2-phenyl ethanedione are unreactive, an effect that probably reflects the $\pi\pi^*$ nature of the lowest excited triplet state of these diones.

Enones and Ynones

A striking difference exists between the photochemical reactivity of α,β-unsaturated enones and the corresponding ynones. Whereas many cyclic enones undergo [2+2]-cycloaddition to alkenes at the CC double bond of the enone (probably from the triplet π,π^* state) to yield cyclobutanes, acyclic enones easily deactivate without radiation by rotation about the central CC single bond. Ynones, on the other hand, behave much more like alkyl-substituted carbonyl compounds and add to (sterically less encumbered) alkenes to yield oxetanes.[38,39] The *regioselectivity* of the Paternò–Büchi reaction is similar to that

of aliphatic or aromatic carbonyl compounds with a preference for primary attack at the less substituted carbon atom (e.g., **41** and **42** from the reaction of but-3-yne-2-one **40** with isobutylene). A serious drawback is the low *chemoselectivity*. For most substrates, a (formal) [3+2]-cycloaddition is the major reaction path that constitutes a possible rearrangement at the preoxetane biradical level.[40] A detailed kinetic and spectroscopic investigation of the reaction showed that the [2+2]-adducts **43** are formed from the singlet biradical precursors, whereas the [3+2]-adducts **44** derive from the corresponding triplet biradicals.[41]

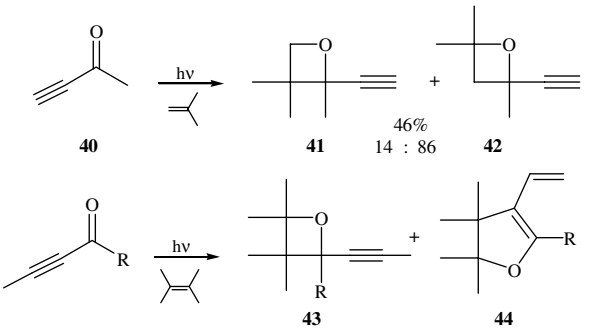

Catalani and co-workers[42] reported the first examples of exclusive oxetane formation upon olefin photoaddition to the cyclohexen-1,4-dione 4-oxoisophorone **45**, leading to two novel 2-substitited 1-oxaspiro[3.5]non-5-en-7-ones **46** and **47**, respectively. They demonstrated that the chemoselectivity of the olefin–enone photochemistry could be directed to exclusive oxetane formation when sufficient steric hindrance inhibits cyclobutane formation.

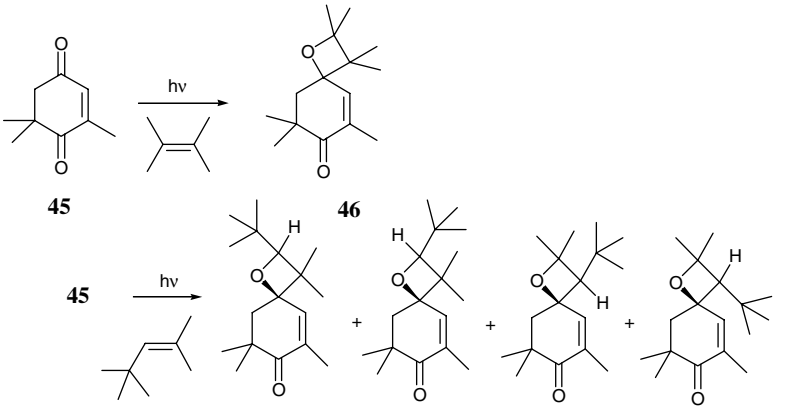

47 (9.8 : 5.1 : 3.6 : 81.5)

Quinones

The photoaddition of 1,4-benzoquinone **48** to electron-donor-substituted alkenes is an efficient process that leads to spirooxetanes (e.g., **49a**) in high yield.[43] The use of quinones as carbonyl compounds is advantageous because of their long-wavelength-shifted n,π^* transitions (430 to 480 nm). Most reactive are strained alkenes, such as norbornene or norbornadiene, for which rearrangement products are also formed.[44] Due to their convenient absorption behavior, benzoquinones have been used to study trapping reactions of intermediates. Wilson and Musser[45] reported the first oxygen trapping experiments using the 1,4-benzoquinone **48**/*t*-butylethene system. Whereas a triplet 1,4-biradical was assigned as the most probable intermediate at that time, later work on intramolecular trapping reaction favored the assumption of radical ion pairs.[46] An efficient lactonization reaction to form **51** during irradiation of pent-4-enoic acid

50 and **48** accounts for an olefin radical cation that undergoes electrophilic addition toward the carboxyl group. Another type of rearrangement has been detected in the photoreaction of tetramethylallene and **48**.[47] 5-Hydroxy-indan-2-ones **52** are formed in high yields, probably via unstable spirooxetanes **49b** as intermediates.

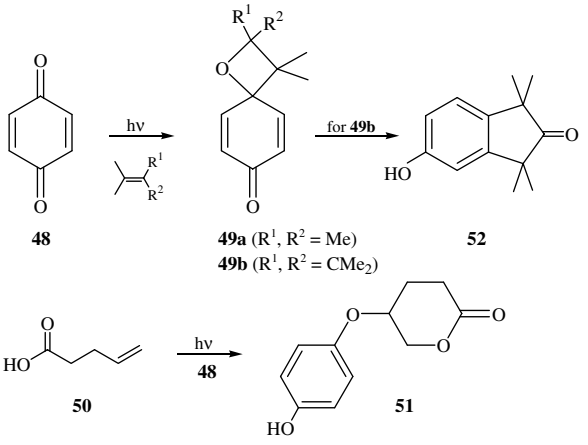

Kochi and co-workers[48] reported the photochemical addition of various stilbenes to chloroanil **53**, which is controlled by the charge-transfer (CT) activation of the precursor electron-donor/acceptor (EDA) complex. The [2+2]-cycloaddition products **54** were established by an x-ray structure of the *trans*-oxetane formed selectively in high yields. Time-resolved (fs/ps) spectroscopy revealed that the (singlet) ion-radical pair is the primary reaction intermediate and established the electron-transfer pathway for this Paternò–Büchi transformation. The alternative pathway via direct electronic activation of the carbonyl component led to the same oxetane regioisomers in identical ratios. Thus, a common electron-transfer mechanism applies that involves quenching of the excited quinone acceptor by the stilbene donor to afford a triplet ion-radical intermediate, which appears on a nanosecond/microsecond time scale. The spin multiplicities of the critical ion-pair intermediates in the two photoactivation paths determine the time scale of the reaction sequences and also the efficiency of the relatively slow ion-pair collapse ($k_c \cong 10^8\ s^{-1}$) to the 1,4-biradical that ultimately leads to the oxetane product **54**.

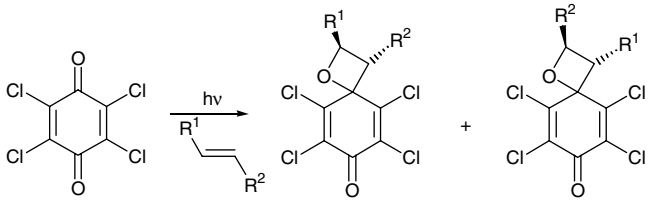

Olefin Compounds

Alkenes, Alkyl-, and Aryl-Substituted

Arnold and co-workers reported a series of reactions between benzophenones and monoalkenes. In most cases, the oxetanes were the major products and could be isolated in good yields.[49] Benzaldehyde **55**, which has a triplet n,π^* as the reactive state,[50] is less chemoselective and, with cyclohexene and the oxetane **56**, gave the hydrogen abstraction and radical coupling products **57** and **58**.[51] Clear evidence for a long-lived

intermediate came from investigations of the stereoselectivity of the Paternò–Büchi reaction with *cis*- and *trans*-2-butene as substrates. When acetone[52] or benzaldehyde[53] was used as carbonyl addends, complete stereorandomization was observed. Acetaldehyde and 2-naphthaldehyde showed stereoselective addition reactions, which accounts for the singlet n,π^* as the reactive state.[43]

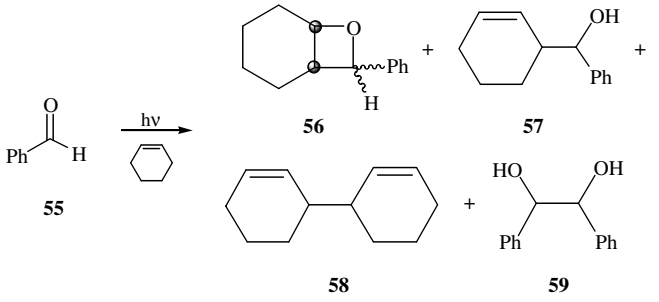

Fleming and Gao[54] reported that the photocycloaddition of the trimethylsilyl ether of phenylpropenol with benzaldehyde proceeds with high stereoselectivity to give the *trans*-oxetane **60** in 20% yield. In competition to the Paternò–Büchi reaction, *cis*/*trans* isomerization leads to *cis* and *trans* isomers of the substrate in a 1.6:1 ratio.

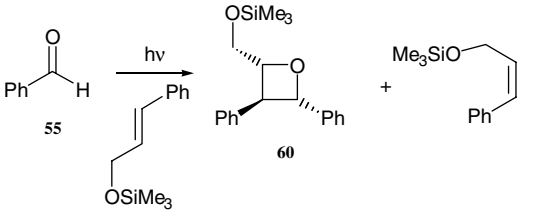

Alkenes, Electron-Donor-Substituted

The regioselectivity of the Paternò–Büchi reaction with acyclic enol ethers is substantially higher than with the corresponding unsymmetrically alkyl-substituted olefins. This effect was used for the synthesis of a variety of 3-alkoxyoxetanes and a series of derivatives.[55] The diastereoisomeric *cis*- and *trans*-1-methoxy-1-butenes were used as substrates for the investigation of the spin state influence on reactivity and regio- and stereoselectivity.[56] The use of trimethylsilyloxyethene **62** as an electron-rich alkene is advantageous, and several 1,3-anhydroapiitol derivatives such as **63** could be synthesized via photocycloaddition with 1,3-diacetoxy-2-propanone **61**.[57] Branched erythrono-1,4-lactones are accessible from the oxetane **66** that was derived thermally from diethyl mesoxalate **64** and 2,2-diisopropyl-1,3-dioxole **65**.[58] An impressive improvement in the regioselectivity of oxetane formation was discovered with 2,3-dihydrofuran **67** as the alkene addend. For the acetone/2,3-dihydrofuran cycloadduct **68**, a >200:1 ratio of the two possible regioisomers was found.[59] Acyclic thioenol ethers also have been investigated in their photocycloaddition behavior with benzophenone. In contrast to acyclic enol ethers, these substrates exhibit high regioselectivity, with almost exclusive formation of the 3-alkylthio oxetanes.[60]

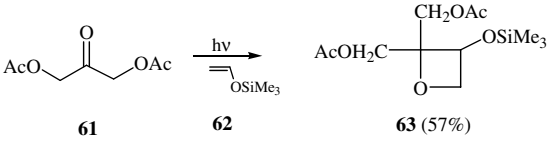

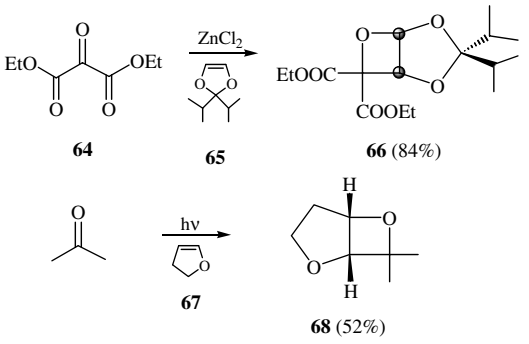

Photocycloaddition reactions of aromatic aldehydes with cyclic ketene silylacetates have been investigated by Abe and co-workers.[61] Regio- and diastereoselective formation of the bicyclic 2-alkoxyoxetanes **69** was observed in high yields. Hydrolysis of these acid-labile cycloadducts with neutral water efficiently gave aldol-type adducts **70** with high *threo* selectivity.

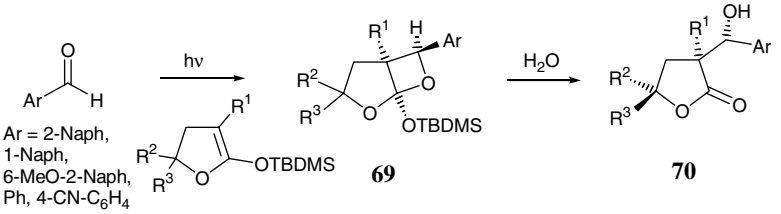

R^1	R^2	R^3
Me	H	H
Me	Me	Me
H	H	H
Me	Me	H
Me	Ph	H

The Paternò–Büchi photocycloaddition of silyl O,X-ketene acetals (with X = O, S, Se) and aromatic aldehydes was intensively investigated by Abe and co-workers in the last decade.[62] The regioselectivity of the reaction (**69** vs. **70**) is highly affected by the heteroatom.[63,64] The regioselectivity is rationalized by: (1) the relative stability of the 1,4-biradicals, and (2) the relative nucleophilicity of sp^2-carbons in the respective O,X-ketene acetal.

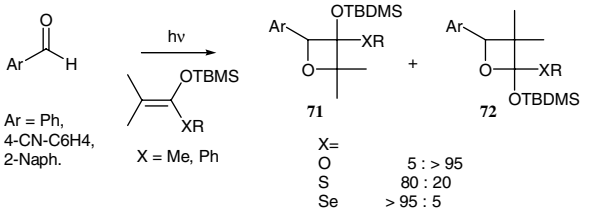

Thopate et al.[65] described the photocycloaddition of L-ascorbic acid derivatives **73** with 4-chlorobenzaldehyde and benzylmethyl ketone, which led to preferential attack on the less hindered α-face of the enone to give the oxetanes **74** and **75**, respectively, with approximately 2:1 regioselectivity (33% diastereomeric excess each). When the substrate was changed to benzophenone, the regioselectivity was reversed, even though the facial selectivity remained the same (35% diastereomeric excess). This was proposed to be the result of a mechanistic switchover, from a 1,4-biradical process for benzophenone to a photoinduced electron transfer process for the other substrates.

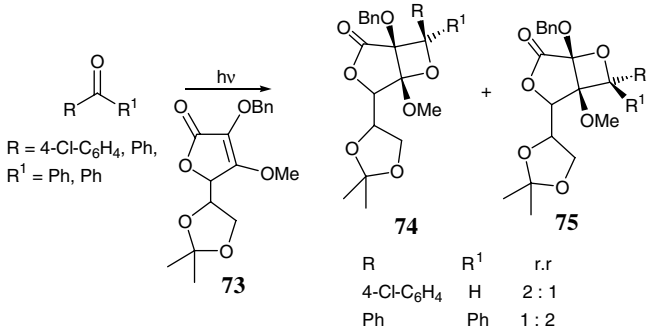

Alkynes

Oxetenes (oxetes) have been postulated as primary photoadducts between carbonyl compounds and alkyl- and aryl-substituted alkynes and alkylthioacetylenes.[66] The first evidence for an unstable intermediate with a lifetime of several hours at –35°C was reported for the benzaldehyde **55**/2-butyne-photoproduct **76**.[67] On further irradiation in the presence of excess benzaldehyde, a *bis*-oxetane **77** was formed. At elevated temperatures, rapid ring opening to α,β-unsaturated ketones occurs; these are the major products for photocycloaddition of alkynes with carbonyl addends at room temperature. The parent oxetene has been prepared from 3-hydroxyoxetane.[68]

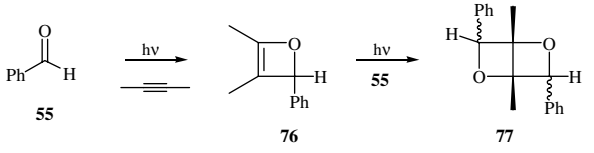

Allenes and Ketenimines

The photocycloaddition of a variety of carbonyl compounds with methyl-substituted allenes has been reported to proceed with high quantum yields (0.59 for acetophenone/tetramethylallene)[69] to give 1:1 and 1:2 adducts.[70] The 2-alkylideneoxetanes are useful precursors for cyclobutanones (e.g., **79a**,**b** from the benzophenone/tetramethylallene-cycloadduct **78**).[71] Upon prolonged irradiation in the presence of excess ketone, the monoadducts are converted into 1,5- and 1,6-dioxaspiro[3.3]heptanes (e.g., **80a**,**b**).[53] The regioisomeric 2- and 3-iminooxetanes could be prepared by photolysis of ketenimines in the presence of aliphatic or aromatic ketones.[72]

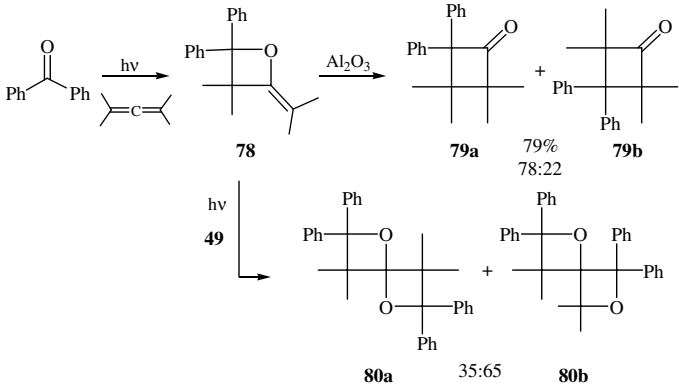

The photocycloaddition of aliphatic aldehydes to 1,1-dimethylallene was investigated by Howell et al.[73] The major products, the 2-alkylidene oxetanes **81** and **82**, were obtained in a ratio of 2:1. This low degree

of regioselectivity was rationalized by both steric and electronic factors. On the other hand, the allene **83** with an enol ether structure reacted with isovaleraldehyde with a high degree of regioselectivity to give the 2-methylene oxetane **84**.

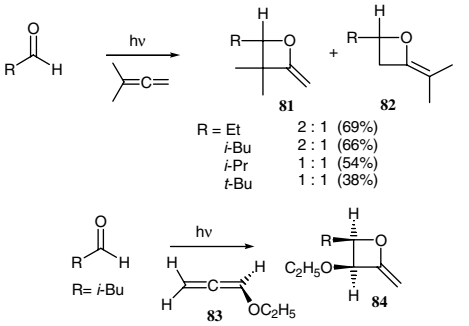

Dienes and Enynes

Because of their low triplet energies (55 to 60 kcal/mol), 1,3-dienes are often used as quenchers for excited triplet states of carbonyl compounds. Besides physical quenching, however, cycloaddition leading to oxetanes can also occur as a side reaction, as demonstrated for benzophenone.[74] Chemical yields are low because of competing diene dimerization and hydrogen abstraction reactions. The corresponding photoreactions with aliphatic ketones[75] or aldehydes[76] are much more effective in the sense that oxetanes are formed with high quantum yields and good chemical yields by a mechanism involving the singlet excited carbonyl addend. Carless and Maitra[77] have shown that the photocycloaddition of acetaldehyde **85** to the diastereomeric *E*- and *Z*-penta-1,3-dienes is highly regio- and stereoselective (e.g., oxetanes **86a–d** are obtained from the *Z* isomer) which also accounts for a singlet mechanism.[77] A locoselective reaction has been reported for the benzophenone cycloaddition to a 1,3-enyne with exclusive addition to the CC double bond.[78]

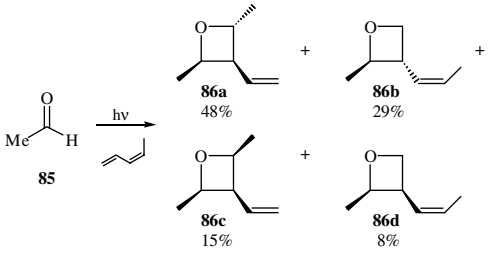

Furans

The photocycloaddition of benzophenone to furan **87a** was originally described by Schenck et al.[79] In addition to the 1:1 adduct **88**, two regioisomeric 2:1 adducts **89a**,**b** were also isolated[80] and the structure of **89a** was revised.[81] All prostereogenic carbonyl addends when photochemically added to furan showed regioselectivities >99:1 in favor of the bicyclic acetal product. This is also the case for 2-substituted furans; however, mixtures of acetal- and ketal-type oxetanes (e.g., for **87b**) were obtained.[82] The use of furans with steric-demanding substituents (e.g., **87c**)[66a,83] or an acetyl substituent (e.g., **87d**)[66b] at the 2-position greatly improves the regioselectivity. A huge number of carbonyl compounds have been investigated in the last 10 years by, for example, Zamojski[84] and especially by Schreiber,[85] who used furan–carbonyl adducts as intermediates in total synthesis of natural products. Acid-catalyzed rearrangement of these adducts is a useful method for the synthesis of 3-substituted furans.[86]

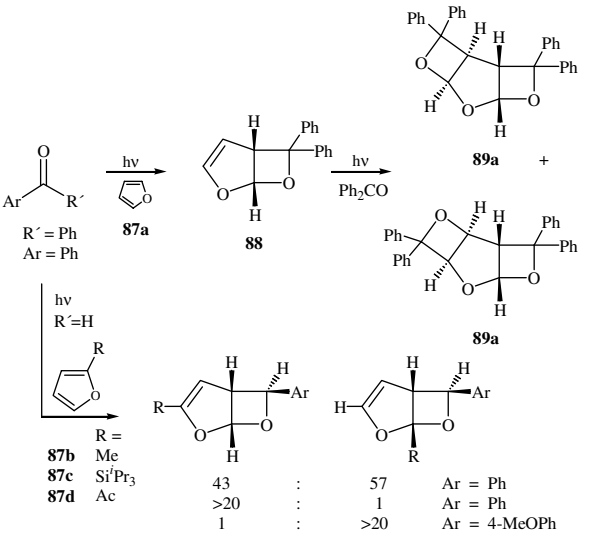

The photocycloaddition of methyl arylglyoxylates **90** with cyclo-1,3-dienes was investigated by Hu and Neckers.[87] These reactions proceed with high regioselectivity, whereas the diastereoselectivity strongly depends on the nature of the aryl substituent. Oxetanes **91** (shown with furan as the diene component) were formed with high *endo*-aryl selectivity with bulky aryl groups, while insignificant stereoselectivity was observed with glyoxylates containing sterically less demanding aryl groups. This observation was rationalized by the stability of the intermediate triplet 1,4-biradical geometries during the ISC process. The rates of the competing *ortho*-hydrogen abstraction (for *ortho*-methylated aryl groups) varied significantly among the substrates.

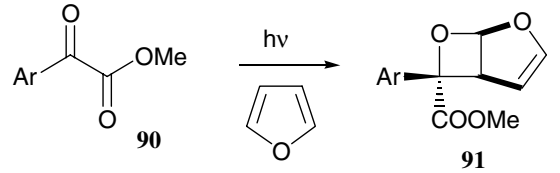

D'Auria and co-workers[88] investigated the photocycloaddition of 5-methyl-2-furyl-phenylmethanol **92** with benzophenone, which resulted in two adducts **93** and **94** in a 1:1 ratio; the addition to 4,4′-dimethoxybenzophenone, benzaldehyde, or 4-methoxybenzaldehyde gave only the adducts **93**.

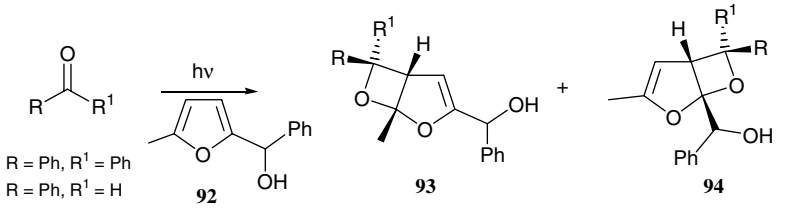

The photocycloaddition of carbonyl compounds with 2-siloxyfurans **95** has been investigated in detail by Abe and co-workers.[89] The stereoselective formations of *exo*-oxetanes **96** and **97** were observed in high yields. The regioselectivity was found to be largely dependent upon the nature of the carbonyl component,

the substituents at the furan ring, and the excited state of the carbonyls (singlet vs. triplet). Aldehydes resulted in bicyclic oxetanes **96** and **97**, respectively, with low regioselectivity independent of the nature of the excited states and the substituents at the furan. Triplet excited ketones gave, regioselectively, the *exo*-oxetanes, except for 4-methyl-2-siloxyfuran.

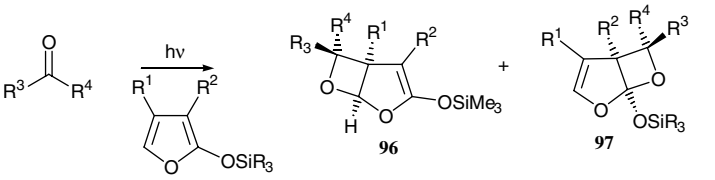

95 **96** **97**

d.r.	SiR_3	R^1	R^2	R^3	R^4
61 : 39	TIPS	H	H	Me	H
54 : 46	TIPS	H	H	Ph	H
40 : 60	TBDMS	Me	H	Ph	H

Other Heteroaromatic Substrates

Methyl-substituted thiophenes afford oxetanes with high regioselectivity when reacted with excited benzophenone.[90] Pyrroles, imidazoles, and indoles behave similarly when substituted at the nitrogen atom with electron-acceptor groups.[91] Pyrroles, when alkyl-substituted at the nitrogen atom, however, gave rearranged pyrroles, probably via an oxetane intermediate.[92] The photocycloaddition of 2,4,5-trimethyloxazole **98** to carbonyl compounds afforded the bicyclic oxetanes **99** with high regio and excellent (*exo*) diastereoselectivity.[93] Hydrolytic ring opening of bicyclic oxetane yielded *erythro* α-acetamido-β-hydroxy ketones **100**.

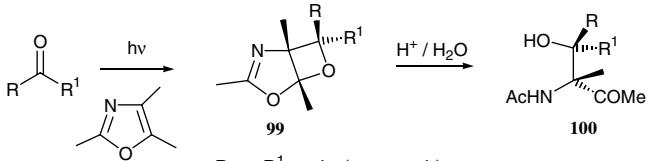

98 **99** **100**

R	R^1	d.r. (*exo* : *endo*)
Ph	H	>99 : 1
Et	H	>99 : 1
t-Bu	H	>99 : 1
Ph	COOMe	74 : 26

Strained Hydrocarbons

The photocycloaddition of triplet benzophenone to norbornene was originally reported by Scharf and Korte.[94] The photoproduct **101** that is formed in high *exo*-selectivity could be thermally cleaved to the δ,ε-unsaturated ketone **102**, an application of the carbonyl–olefin metathesis (COM) concept.[95] The 1,4-biradical formed in the interaction of norbornene with *o*-dibenzoyl-benzene was trapped in an intramolecular fashion by the second carbonyl moiety.[96] A highly regioselective reaction of triplet benzophenone was reported with 5-methylenenorborn-2-ene, with preferential attack toward the *exo* CC double bond.[97] A number of publications have discussed the photocycloaddition reactions of triplet carbonyl compounds to norbornadiene and quadricyclane, as well as the competition between the Paternò–Büchi reaction and the sensitized norbornadiene/quadricyclane interconversion.[98] Oxetane formation has also been reported for the photoreaction of biacetyl and *para*-quinones with benzvalene.[99]

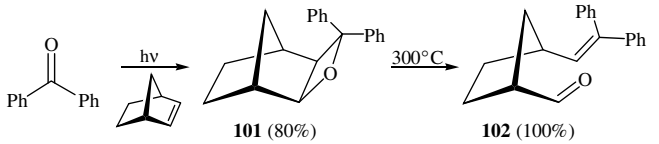

101 (80%) **102** (100%)

The irradiation of methyl phenylglyoxylate, benzil, benzophenone, and 1,4-benzoquinone in the presence of homobenzvalene **103** gave, as products of the Paternò–Büchi reaction, oxetane derivatives that contain the tricyclo[4.1.0.0^{2,7}]heptane subunit as well as ring-opened products.[100] In the case of benzophenone, the cycloaddition competes with the isomerization of **103** to cycloheptatriene. Exclusive isomerization was observed with acetophenone and acetone. Carbonyl compounds with triplet energies lower than 69 kcal/mol prefer the cycloaddition path. Cyclopent-2-en-1-one is an exception to this rule; in spite of its triplet energy of 74 kcal/mol, [2+2]-cycloadducts were formed rather efficiently.

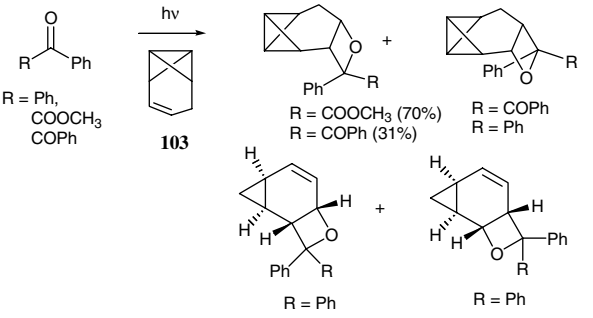

Alkenes, Electron Acceptor-Substituted

In contrast to photocycloaddition reactions of carbonyl compounds to electron-rich alkenes (which proceed with a low degree of stereoselectivity in the case of triplet excited carbonyls), reactions with electron-deficient alkenes, such as cyanoalkenes, are highly stereoselective, although rather inefficient.[101] Kinetic analysis showed that these reactions involve the interaction with the singlet excited carbonyl via a parallel approach.[102] An important side reaction is that the photosensitized geometrical isomerization of the alkene CC double bond (e.g., *cis*-1,2-dicyanoethylene) and acetone gives the *cis*-oxetane and *trans*-1,2-dicyanoethylene. 2-Norbornanone was used as a model reagent for investigation of the influence of steric hindrance on the face selectivity of oxetane formation with electron-donor- and electron-acceptor-substituted alkenes.[103] Chung and co-workers[104] have reported that the photocycloaddition of methacrylonitrile to 5-substitiuted adamant-2-ones **104** produces two geometrically isomeric oxetanes **105** and **106**, respectively, with the oxetane-ring oxygen and the substituent at C5 in *anti* or *syn* positions. This selectivity is discussed for the *syn*-face attack in terms of transition-state hyperconjugation.

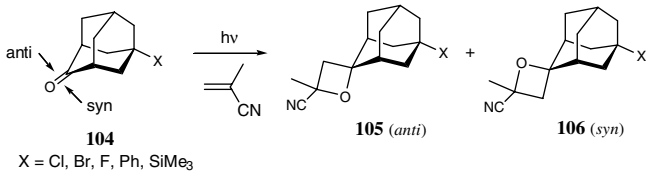

Exocyclic Alkenes

The photochemistry of ketones in the presence of exocyclic olefins has not yet been systematically studied. Chung and Ho[105] reported the photochemistry of acetone in the presence of several exocyclic olefins. Surprisingly, homoalkylation occurred, resulting in a series of 4-cycloalkylbutan-2-ones (with quantum yields of 0.14 ± 0.01) rather than the expected Paternò–Büchi reaction. With perdeuterated acetone, the photocycloaddition path increased due to the primary kinetic isotope effect (as shown for products **108** and **109**, respectively, from 2-methyleneadamantane **107**). Similar effects were obtained for methylenecycloalkanes **110** with preferential formation of the photo-Conia products **111**. Increasing ring size in **110** as well as H/D exchange favored the formation of the Paternò–Büchi products **112**.

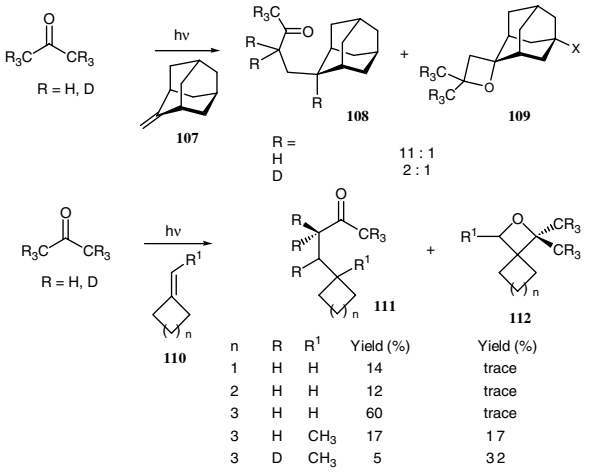

n	R	R^1	Yield (%)	Yield (%)
1	H	H	14	trace
2	H	H	12	trace
3	H	H	60	trace
3	H	CH_3	17	17
3	D	CH_3	5	32

References

1. Paternò, E. and Chieffi, G., Sintesi in chimica organica per mezzo della luce. Nota II. Composti degli idrocarburi non saturi con aldeidi e chetoni, *Gazz. Chim. Ital.*, 341, 1909.
2. Büchi, G., Inman, C. G., and Lipinsky, E. S., Light-catalyzed organic reactions. I. The reaction of carbonyl compounds with 2-methyl-2-butene in the presence of ultraviolet light, *J. Am. Chem. Soc.*, 76, 4327, 1954.
3. Yang, N. C., Nussim, M., Jorgenson, M. J., and Murov, S., Photochemical reactions of carbonyl compounds in solution: the Paternò-Büchi reaction, *Tetrahedron Lett.*, 3657, 1964.
4. (a) Inoue, Y., Asymmetric photochemical reactions in solution, *Chem. Rev.*, 92, 741, 1992; (b) Porco, J. A., Jr. and Schreiber, S. L., The Paternò–Büchi reaction, in *Comprehensive Organic Synthesis*, Vol. 5, Trost, B. M., Fleming, I., and Paquette, L. A., Eds., Pergamon Press, Oxford, 1991, 5; (c) Demuth, M. and Mikhail, G., New developments in the field of photochemical synthesis, *Synthesis*, 145, 1989; (d) Carless, H. A. J., Carbonyl compounds: cycloaddition, in *Photochemistry in Organic Chemistry*, Coyle, J. D., Ed., Special Publication 57, The Royal Society of Chemistry, London, 1986, 95; (e) Carless, H. A. J., Photochemical synthesis of oxetanes, *Synthetic Organic Photochemistry*, Horspool, W. M., Ed., Plenum Press, New York, 1984, 425; (f) Jones II, G., Synthetic applications of the Paternò–Büchi reaction, *Org. Photochem.*, 5, 1, 1981.
5. Turro, N. J., Dalton, J. C., Dawes, K., Farrington, G., Hautala, R., Morton, D., Niemczyk, M., and Schore, N., Molecular photochemistry of alkanones in solution: α-cleavage, hydrogen abstraction, cycloaddition and sensitisation reactions, *Acc. Chem. Res.*, 5, 92, 1972.
6. Dauben, W. G., Salem, L., and Turro, N. J., A classification of photochemical reactions, *Acc. Chem. Res.*, 8, 41, 1975.
7. (a) Salem, L., Surface crossings and surface touchings in photochemistry, *J. Am. Chem. Soc.*, 96, 3486, 1974; (b) Bigot, B., Devaquet, A., and Turro, N. J., Natural correlation diagrams: a unifying theoretical basis for analysis of *n* orbital initiated ketone photoreactions, *J. Am. Chem. Soc.*, 103, 6, 1981.
8. Palmer, I. J., Ragazos, I. N., Bernardi, F., Olivucci, M., and Robb, M. A., An MC-SCF study of the (photochemical) Paternò–Büchi reaction. *J. Am. Chem. Soc.*, 116, 2121, 1994.
9. Wilson, R. M., The trapping of biradicals and related photochemical intermediates, *Org. Photochem.*, 7, 339, 1985.
10. Shimizu, N., Ishikawa, M., Ishikura, K., and Nishida, S., Photocycloaddition of aromatic carbonyl compounds to vinylcyclopropene and its derivatives, *J. Am. Chem. Soc.*, 96, 6456, 1974.
11. Freilich, S. C. and Peters, K. S., Observation of the 1,4-biradical in the Paternò–Büchi reaction, *J. Am. Chem. Soc.*, 103, 6255, 1981.

12. (a) Barltrop, J. A. and Carless, H. A. J., Photocycloaddition of aliphatic ketones to α,β-unsaturated nitriles, *J. Am. Chem. Soc.*, 94, 1951, 1972; (b) Dalton, J. C., Wriede, P. A., and Turro, N. J., Photocycloaddition of acetone to 1,2-dicyanoethylene, *J. Am. Chem. Soc.*, 92, 1318, 1970.
13. Turro, N. J. and Wriede, P. A., The photocycloaddition of acetone to 1-methoxy-1-butene: a comparison of singlet and triplet mechanisms and biradical intermediates, *J. Am. Chem. Soc.*, 92, 320, 1970.
14. (a) Arnold, D. R. and Clarke, B. M., The effect of an adjacent methyl group on the excited state reactivity of 2-benzoylthiophene, *Can. J. Chem.*, 53, 1, 1975; (b) Arnold, D. R. and Hadjiantoniou, C.P., The effect of an adjacent methyl group on the excited state reactivity of 3-benzoylthiophene, *Can. J. Chem.*, 56, 1970, 1978.
15. Cantrell, T. S., Reactivity of photochemically excited 3-acylthiophenes, 3-acylfurans and the formyl-thiophenes and -furans, *J. Org. Chem.*, 42, 3774, 1977.
16. Cantrell, T. S., Photochemical reactions of 2-acylthiophenes, -furans and -pyrroles with alkenes, *J. Org. Chem.*, 39, 2242, 1974.
17. Vargas, F. and Rivas, C., Photocycloaddition of acetylselenophene to double bond containing substrates, *J. Photochem. Photobiol. A: Chem*., 138, 1–5, 2001.
18. Xue, J., Zhang, Y., Wu, T., Kunfun, H., and Hua, X. J., Photoinduced [2+2]-cycloadditions (the Paternò–Büchi reaction) of ^{1}H-1-acetylindole-2,3-dione with alkenes, *J. Chem. Soc.*, *Perkin Trans. 1*, 183, 2001.
19. Zhang, Y., Xue, J., Gao, Y., Fun, H. K., and Xu, J. H., Photoinduced [2+2]-cycloadditions (the Paternò–Büchi reaction) of 1-acetylisatin with enol ethers: regioselectivity, diastereoselectivity and acid catalysed transformations of the spirooxetane products, *J. Chem. Soc.*, *Perkin. Trans. 1*, 345, 2002.
20. Coyle, J. D., Photochemistry of carboxylic acid derivatives, *Chem. Rev.*, 78, 97, 1978.
21. Cantrell, T. S. and Allen, A. C., Photochemical reactions of arenecarboxylic acid esters with electron-rich alkenes: 2+2 cycloaddition, hydrogen abstraction and cycloreversion, *J. Org. Chem.*, 54, 135, 1989.
22. Cantrell, T. S., Allen, A. C., and Ziffer, H., Photochemical 2+2 cycloaddition of arenecarboxylic acid esters to furans and 1,3-dienes. 2+2 cycloreversion of oxetanes to dienol esters and ketones, *J. Org. Chem.*, 54, 140, 1989.
23. Tominaga, T., Odaira, Y., and Tsutsumi, S., Photochemical synthesis of oxetanes from diethyl oxalate, *Bull. Chem. Soc.*, *Jpn.*, 40, 2451, 1967.
24. Cantrell, T. S., Photochemical reactions of benzoic acid: cycloaddition, hydrogen abstraction and reverse type II elimination, *J. Am. Chem. Soc.*, 95, 2714, 1973.
25. Tominaga, T. and Tsutsumi, S., Photocycloaddition of carbamates to 1,1-diphenylethylene, *Tetrahedron Lett.*, 3175, 1969.
26. Cantrell, T. S., Photochemical cycloadditions of benzonitrile to alkenes, factors controlling the site of the addition, *J. Org. Chem.*, 42, 4238, 1977.
27. Mattay, J., Runsink, J., Heckendorn, R., and Winkler, T., Photoreactions of benzonitrile with cyclic enol ethers, *Tetrahedron*, 43, 5781, 1987.
28. Hu, S. and Neckers, D. C., Rapid regio- and diastereoselective Paternò–Büchi reaction of alkyl phenylglyoxylates, *J. Org. Chem.*, 62, 564, 1997.
29. Buhr, S., Griesbeck, A. G., Lex, J., Mattay, J., and Schroer, J., Stereochemistry in the Paternó–Büchi reaction of 2,2-diisopropyl-1,3-dioxol with methyl trimethyl pyruvate, *Tetrahedron Lett.*, 37, 1195, 1996.
30. Turro, N. J., Shima, K., Chung, C.-J., Tanielian, C., and Kanfer, S., Photoreactions of biacetyl and tetramethylethylene: solvent and temperature effects, *Tetrahedron Lett.*, 2775, 1980.
31. Shima, K., Sawada, T., and Yoshinaga, H., Photoaddition of singlet and triplet methyl pyruvate with 2,3-dimethyl-2-butene, *Bull. Chem. Soc. Jpn.*, 51, 608, 1978.
32. Ryang, H.-S., Shima, K., and Sakurai, H., Photoaddition reaction of biacetyl, *J. Org. Chem.*, 38, 2860, 1973.

33. Shima, K., Kawamura, T., and Tanabe, K., The photoaddition of methyl pyruvate to methyl-substituted olefins, *Bull. Chem. Soc. Jpn.*, 47, 2347, 1974.
34. Cantrell, T. S., Photochemical reactions of benzoyl cyanide and benzoyl halides with alkenes, *J. Chem. Soc., Chem. Commun.*, 637, 1975.
35. Zagar, C. and Scharf, H.-D., The Paternò–Büchi reaction of achiral and chiral acyl cyanides with furan, *Chem. Ber.*, 124, 967, 1991.
36. Döpp, D., Memarian, H. R., Fischer, M. A., Van Eij, A. M. O., and Varma, C. A. G. O., Paternò–Büchi reaction of 2-morpholinoarylonitrile with benzil, *Chem. Ber.*, 125, 983, 1992.
37. Döpp, D. and Fischer, M. A., [2+2]-Photocycloaddition of 2-amino propenenitriles to diaryl ethanediones: a product study, *Rec. Trav. Chim. Pays-Bas*, 114, 498, 1995.
38. Jorgenson, M. J., Photoaddition of acetylenic ketones to olefines, *Tetrahedron Lett.*, 5811, 1966.
39. Kwiatkowski, G. T. and Selley, D. B., The photochemistry of conjugated acetylenic olefins and carbonyl derivatives, *Tetrahedron Lett.*, 3471, 1968.
40. Hussain, S. and Agosta, W. C., Photochemical [3+2]-cycloaddition of α,β-acetylenic ketones with simple olefins, *Tetrahedron*, 37, 3301, 1981.
41. Saba, S., Wolff, S., Schröder, C., Margaretha, P., and Agosta, W. C., Studies on the photochemical reactions of α,β-acetylenic ketones with tetramethylethylene, *J. Am. Chem. Soc.*, 105, 6902, 1983.
42. Catalani, L. H., Rezende, D. B. and Campos, I. A., Olefin photoaddition to 4-oxoisophorone, *J. Chem. Res. (S)*, 111, 2000.
43. Bryce-Smith, D., Gilbert, A., and Johnson, M. G., Formation of spiro-oxetanes by photoaddition of olefins to *p*-benzoquinone, *J. Chem. Soc. (C)*, 383, 1967.
44. Bunce, N. J. and Hadley, M., Mechanism of oxetane formation in the photocycloaddition of *p*-benzoquinone to alkenes, *Can. J. Chem.*, 53, 3240, 1975.
45. Wilson, R. M. and Musser, A. K., Photocyclizations involving quinone-olefin charge-transfer exciplexes, *J. Am. Chem. Soc.*, 102, 1720, 1980.
46. Fehnel, E. A. and Brokaw, F. C., Photocycloaddition reactions of norbornadiene and quadricyclane with *p*-benzoquinone, *J. Org. Chem.*, 45, 578, 1980.
47. Ishibe, N., Hashimoto, K., and Yamaguchi, Y., Photochemical addition of allenes to *p*-quinones, *J. Chem. Soc., Perkin Trans. 1*, 318, 1975.
48. Sun, D., Hubig, S. M., and Kochi, J. K., Oxetanes from [2+2]-cycloaddition of stilbenes to quinone via photoinduced electron transfer, *J. Org. Chem.*, 64, 2250, 1999.
49. Arnold, D. R., Hinman, R. L., and Glick, A. H., Chemical properties of the carbonyl n,π^* state. The photochemical preparation of oxetanes, *Tetrahedron Lett.*, 1425, 1964.
50. Yang, N. C., Loeschen, R., and Mitchell, D., On the mechanism of the Paternò–Büchi reaction, *J. Am. Chem. Soc.*, 89, 5465, 1967.
51. Bradshaw, J. S., Ultraviolet irradiation of carbonyl compounds in cyclohexene and 1-hexene, *J. Org. Chem.*, 31, 237, 1966.
52. Carless, H. A. J., Photocycloaddition of acetone to acyclic olefins, *Tetrahedron Lett.*, 3173, 1973.
53. Yang, N. C., Kimura, M., and Eisenhardt, W., Paternò–Büchi reactions of aromatic aldehydes with 2-butenes and their implication on the rate of intersystem crossing of aromatic aldehydes, *J. Am. Chem. Soc.*, 95, 5058, 1973.
54. Fleming, S. A. and Gao, J. J., Stereocontrol of Paternò–Büchi photocycloadditions, *Tetrahedron Lett.*, 38, 5407, 1997.
55. (a) Schroeter, S. H. and Orlando, C. M., The photocycloaddition of various ketones and aldehydes to vinyl ethers and ketene diethyl acetal, *J. Org. Chem.*, 34, 1181, 1969; (b) Schroeter, S. H., The synthesis of 3-hydroxyaldehydes, 3-hydroxy acetals and 3-hydroxy ethers from 2-alkoxyoxetanes, *J. Org. Chem.*, 34, 1188, 1969.
56. (a) Turro, N. J. and Wriede, P. A., The photocycloaddition of acetone to 1-methoxy-1-butene: a comparison of singlet and triplet mechanisms and biradical intermediates, *J. Am. Chem. Soc.*, 90, 6863, 1968; (b) Turro, N. J. and Wriede, P. A., The photocycloaddition of acetone to 1-methoxy-

1-butene: a comparison of singlet and triplet mechanisms and biradical intermediates, *J. Am. Chem. Soc.*, 92, 320, 1970.
57. Araki, Y., Nagasawa, J.-I. and Ishido, Y., Photochemical cycloaddition of 1,3-diacetoxy-2-propanone to (trimethylsilyloxy)ethylene, *Carbohydrate Res.*, 91, 77, 1981.
58. Mattay, J. and Buchkremer, K., Thermal and photochemical oxetane formation. A contribution to the synthesis of branched-chain aldonolactones, *Helv. Chim. Acta*, 71, 981, 1988.
59. Carless, H. A. J. and Haywood, D. J., Photochemical synthesis of 2,6-dioxabicyclo-[3.2.0]heptanes, *J. Chem. Soc.*, *Chem. Commun.*, 1067, 1980.
60. Morris, T. H., Smith, E. H., and Walsh, R., Oxetane synthesis: methyl vinyl sulphides as new traps of excited benzophenone in a stereoselective and regiospecific Paternò–Büchi reaction, *J. Chem. Soc.*, *Chem. Commun.*, 964, 1987.
61. Abe, M., Ikeda, M., and Nojima, M., A stereoselective tandem [2+2]-photocycloaddition-hydrolysis route to aldol-type adducts, *J. Chem. Soc.*, *Perkin Trans. 1*, 3261, 1998.
62. Abe, M., Tachibana, K., Fujimoto, K., and Nojima, M., Regioselective formation of 3-selanyl-3-siloxyoxetanes in the Paternò–Büchi reaction of silyl O, Se-ketene acetals (O, Se-SKA), *Synthesis*, 1243, 2001.
63. Abe, M., Shirodai, Y., and Nojima, M., Regioselective formation of 2-alkoxy oxetanes in the photoreaction of aromatic carbonyl compounds with β,β-dimethyl ketene silyl acetals: notable solvent and silyl group effects, *J. Chem. Soc., Perkin Trans. 1* , 3253, 1998.
64. Abe, M., Fujimoto, K., and Nojima, M., Notable sulfur atom effects on the regio- and stereoselective formation of oxetanes in Paternò–Büchi photocycloaddition of aromatic aldehydes with silyl O, S-ketene acetals, *J. Am. Chem. Soc.*, 122, 4005, 2000.
65. Thopate, S. R., Kulkarni, M. G., and Puranik, V. G., Chemistry of L-ascorbic acid. 2. The Paterno-Buchi reaction of L-ascorbic acid, *Angew. Chem. Int. Ed. Engl.*, 37, 1110, 1998.
66. (a) Büchi, G., Kofron, J. T., Koller, E., and Rosenthal, D., Light catalyzed organic reactions. V. The addition of aromatic carbonyl compounds to a disubstituted acetylene, *J. Am. Chem. Soc.*, 78, 876, 1956; (b) Miyamoto, T., Shigemitsu, Y., and Odaira, Y., Photoaddition of carboxylate esters to diphenylacetylene, *J. Chem. Soc.*, *Chem. Commun.*, 1410, 1969; (c) Bradshaw, J. S., Knudsen, R. D., and Parish, W. W., Irradiation of benzaldehyde in 1-hexyne, *J. Org. Chem.*, 40, 529, 1975; (d) Mosterd, A., Matser, H. J., and Bos, H. J. T., Photoaddition of non-cisoid 1,2-diketones and phenylglyoxal to alkylthioacetylenes; preparation of 3-alkylthiofurans, *Tetrahedron Lett.*, 4179, 1974.
67. Friedrich, L. E. and Bower, J. D., Detection of an oxetene intermediate in the photoreaction of benzaldehyde with 2-butyne, *J. Am. Chem. Soc.*, 95, 6869, 1973.
68. Friedrich, L. E. and Lam, P. Y.-S., Syntheses and reactions of 3-phenyloxete and the parent unsubstituted oxete, *J. Org. Chem.*, 46, 306, 1981.
69. Gotthardt, H., Steinmetz, R., and Hammond, G. S., Cycloaddition of carbonyl compounds to allenes, *J. Org. Chem.*, 33, 2774, 1968.
70. Arnold, D. R. and Glick, A. H., The photocycloaddition of carbonyl compounds to allenes, *J. Chem. Soc.*, *Chem. Commun.*, 813, 1966.
71. Gotthardt, H. and Hammond, G. S., Some interesting rearrangements in the 2-isopropylidene oxetane series, *Chem. Ber.*, 107, 3922, 1974.
72. (a) Singer, L. A., Davis, G. A., and Knutsen, R. L., Photocycloaddition of acetone to ketenimines: *syn-anti* exchange barriers in β-imino oxetanes, *J. Am. Chem. Soc.*, 94, 1188, 1972; (b) Singer, L. A. and Davis, G. A., Photokinetic studies on benzophenone: photocycloaddition to ketenimines and self-quenching of the benzophenone triplet, *J. Am. Chem. Soc.*, 95, 8638, 1973; (c) Howell, A. R., Fan, R., and Truong, A., Preparation of 2-alkylidene oxetanes: an investigation of the Paternò–Büchi reaction between aliphatic aldehydes and allenes, *Tetrahedron Lett.*, 37, 8651, 1996.
73. Howell, A. R., Fan, R., and Truong, A., Preparation of 2-alkylidene oxetanes: an investigation of the Paternò–Büchi reaction between aliphatic aldehydes and allenes, *Tetrahedron Lett.*, 37, 8651, 1996.

74. Barltrop, J. A. and Carless, H. A. J., Organic photochemistry. XI. The photocycloaddition of benzophenone to conjugated dienes, *J. Am. Chem. Soc.*, 93, 4794, 1971.
75. (a) Hautala, R. R., Dawes, K., and Turro, N. J., Stereoselectivity and regioselectivity in the photocycloaddition of 2-methyl-2,4-hexadiene and acetone, *Tetrahedron Lett.*, 1229, 1972; (b) Barltrop, J. A. and Carless, H. A. J., Organic photochemistry. XIV. Photocycloaddition of alkyl ketones to conjugated dienes, *J. Am. Chem. Soc.*, 94, 8761, 1972.
76. (a) Kubota, T., Shima, K., Toki, S., and Sakurai, H., The photoaddition of propionaldehyde to cyclohexa-1,3-diene. oxetane formation by a singlet mechanism, *J. Chem. Soc.*, *Chem. Commun.*, 1462, 1969; (b) Shima, K., Kubota, T., and Sakurai, H., Organic photochemical reactions XXIV. Photocycloaddition of propanal to 1,3-cyclohexadiene, *Bull. Chem. Soc. Jpn.*, 49, 2567, 1976.
77. Carless, H. A. J. and Maitra, A. K., Photocycloaddition of acetaldehyde to (*E*)- and (*Z*)-penta-1,3-diene, *Tetrahedron Lett.*, 1411, 1977.
78. Carless, H. A. J., Photocycloaddition of benzophenone to a conjugated enyne, *Tetrahedron Lett.*, 2265, 1972.
79. Schenck, G. O., Hartmann, W., and Steinmetz, R., Four-membered ring synthesis by the photosensitized cycloaddition of dimethyl maleic anhydride to olefins, *Chem. Ber.*, 96, 498, 1963.
80. Ogata, M., Watanabe, H., and Kano, H., Photochemical cycloaddition of benzophenone to furans, *Tetrahedron Lett.*, 533, 1967.
81. (a) Toki, S. and Sakurai, H., On the structure of the 2:1 adduct of benzophenone with furan, *Tetrahedron Lett.*, 4119, 1967; (b) Evanega, G. R. and Whipple, E. B., The photochemical addition of benzophenone to furan, *Tetrahedron Lett.*, 2163, 1967.
82. (a) Toki, S., Shima, K., and Sakurai, H., Organic photochemical reactions. I. The synthesis of substituted oxetanes by the photoaddition of aldehydes to furans, *Bull. Chem. Soc. Jpn.*, 38, 760, 1965; (b) Sekretár, S., Rudá, J., and Stibrányi, L., Photochemical reactions of 2-substituted furans with some carbonyl compounds, *Coll. Czech. Chem. Commun.*, 49, 71, 1984.
83. (a) Schreiber, S. L., Desmaele, D., and Porco, Jr., J. A., On the use of unsymmetrically substituted furans in the furan-carbonyl photocycloaddition reaction: synthesis of a kadsurenone-ginkgolide hybrid, *Tetrahedron Lett.*, 29, 6689, 1988; (b) Carless, H. A. J. and Halfhide, A. F. E., Highly regioselective [2+2]-photocycloaddition of aromatic aldehydes to acetylfurans, *J. Chem. Soc.*, *Perkin Trans. 1*, 1081, 1992.
84. (a) Jarosz, S. and Zamojski, A., Asymmetric photocycloaddition between furan and optically active ketones, *Tetrahedron*, 38, 1453, 1982; (b) Kozluk, T. and Zamojski, A., The synthesis of 3-deoxy-D,L-streptose, *Tetrahedron*, 39, 805, 1983.
85. (a) Schreiber, S. L. and Satake, K., Application of the furan–carbonyl photocycloaddition reaction to the synthesis of the *bis*(tetrahydrofuran) moiety of asteltoxin, *J. Am. Chem. Soc.*, 105, 6723, 1983; (b) Schreiber, S. L. and Satake, K., Total synthesis of (±)-asteltoxin, *J. Am. Chem. Soc.*, 106, 4186, 1984; (c) Schreiber, S. L. and Satake, K., Studies of the furan–carbonyl photocycloaddition reaction: the determination of the absolute stereostructure of asteltoxin, *Tetrahedron Lett.*, 27, 2575, 1986.
86. (a) Kitamura, T., Kawakami, Y., Imegawa, T., and Kawanishi, M., One-pot synthesis of 3-substituted furan: a synthesis of perillaketone, *Synth. Commun.*, 7, 521, 1977; (b) Jarosz, S. and Zamojski, A., Rearrangement of 6-substituted 2,7-dioxabicyclo[3.2.0]hept-3-enes to furans, *J. Org. Chem.*, 44, 3720, 1979.
87. Hu, S. and Neckers, D.C., Photocycloaddition and ortho-hydrogen abstraction reactions of methyl arylglyoxylates: structure dependent reactivities, *J. Chem. Soc.*, *Perkin Trans. 2*, 1771, 1999
88. D'Auria, M., Emanuele, L., Poggi, G., Racioppi, R., and Romanielli, G., On the stereoselectivity of the Paternò–Büchi reaction between carbonyl compounds and 2-furylmethanol derivatives: the case of aliphatic aldehydes and ketones, *Tetrahedron*, 58, 5045, 2002.
89. Abe, M., Torii, E., and Nojima, M., Paternò–Büchi photocycloaddition of 2-siloxyfurans and carbonyl compounds: notable substituent and carbonyl (aldehyde vs. ketone and singlet- vs. triplet excited state) effects on the regioselectivity (double-bond selection) in the formation of bicyclic *exo*-oxetanes, *J. Org. Chem.*, 65, 3426, 2000.

90. Rivas, C., Pacheco, D., Vargas, F., and Ascanio, J., Synthesis of oxetanes by photoaddition of carbonyl compounds to thiophene derivatives, *J. Heterocyclic Chem.*, 18, 1065, 1981.
91. (a) Rivas, C. and Bolivar, R. A., Synthesis of oxetanes by photoaddition of carbonyl compounds to pyrrole derivatives, *J. Heterocyclic Chem.*, 13, 1037, 1976; (b) Nakano, T., Rodriquez, W., de Roche, S. Z., Larrauri, J. M., and Rivas, C., Pérez, Photoaddition of ketones to imidazoles, thiazoles, isothiazoles and isoxazoles: synthesis of their oxetanes, *J. Heterocyclic Chem.*, 17, 1777, 1980; (c) Julian, D. R. and Tringham, G. D., Photoaddition of ketones to indoles: synthesis of oxeto[2,3-*b*] indoles, *J. Chem. Soc.*, *Chem. Commun.*, 13, 1973.
92. (a) Matsuura, T., Banba, A., and Ogura, K., Photoinduced reactions. XLV Photoaddition of ketones to methylimidazoles, *Tetrahedron*, 27, 1211, 1971; (b) Jones II, G., Gilow, H. M., and Low, J., Regioselective photoaddition of pyrroles and aliphatic carbonyl compounds: a new synthesis of 3(4)-substituted pyrroles, *J. Org. Chem.*, 44, 2949, 1979.
93. Griesbeck, A. G., Fiege, M., and Lex, J., Oxazole–carbonyl photocycloaddition: selectivity pattern and synthetic route to erythro α-amino-β-hydroxy ketones, *J. Chem. Soc.*, *Chem. Commun*., 589, 2000.
94. Scharf, D. and Korte, F., Photosensitized cyclodimerization of norbornene, *Tetrahedron Lett.*, 821, 1963.
95. Jones II, G., Schwartz, S. B., and Marton, M. T., Regiospecific thermal cleavage of some oxetane photoadducts: carbonyl-olefin metathesis in sequential photochemical and thermal steps, *J. Chem. Soc.*, *Chem. Commun.*, 374, 1973.
96. Shigemitsu, Y., Yamamoto, S., Miyamoto, T., and Odaira, Y., A novel photocycloaddition of dibenzoylbenzene to olefins, *Tetrahedron Lett.*, 2819, 1975.
97. Gorman, A. A., Leyland, R. L., Parekh, C. T., and Rodgers, M. A. J., The reaction of triplet benzophenone with 5-methylenenorborn-2-ene: regiospecific oxetane formation, *Tetrahedron Lett.*, 1391, 1976.
98. (a) Barwise, A. J. G., Gorman, A. A., Leyland, R. L., Parekh, C. T., and Smith, P. G., The inter- and intramolecular addition of aromatic ketone triplets to quadricyclane, *Tetrahedron*, 36, 397, 1980; (b) Gorman, A. A., Leyland, R. L., Rodgers, M. A. J., and Smith, P. G., Concerning the mechanism of interactions of triplet benzophenone with norbornadienes and quadricyclanes, *Tetrahedron Lett.*, 5085, 1973; (c) Kubota, T., Shima, K., and Sakurai, H., The photocycloaddition of benzophenone to norbornadiene, *Chem. Lett.*, 343, 1972.
99. Christl, M. and Braun, M., Photocycloadditions of benzvalene, *Angew. Chem. Int. Ed. Engl.*, 28, 601, 1989.
100. Christl, M. and Braun, M., [2+2]-Photocycloadditions of homobenzvalene., *Liebigs Ann.*, 1135, 1997.
101. (a) Beereboom, J. J. and von Wittenau, M. S., The photochemical conversion of fumaronitrile and acetone to oxetanes, *J. Org. Chem.*, 30, 1231, 1965; (b) Turro, N. J., Wriede, P. A., Dalton, J. C., Arnold, D., and Glick, A., Photocycloaddition of alkyl ketones to electron-deficient double bonds, *J. Am. Chem. Soc.*, 89, 3950, 1967.
102. (a) Turro, N. J., Wriede, P. A., and Dalton, J. C., Evidence for a singlet-state complex in the photocycloaddition of acetone to *trans*-1,2-dicyanoethylene, *J. Am. Chem. Soc.*, 90, 3274, 1968; (b) Dalton, J. C., Wriede, P. A., and Turro, N. J., Photocycloaddition of acetone to 1,2-dicyanoethylene, *J. Am. Chem. Soc.*, 92, 1318, 1970.
103. (a) Turro, N. J. and Farrington, G. L., Quenching of the fluorescence of 2-norbornanone and derivatives by electron-rich and electron-poor ethylenes, *J. Am. Chem. Soc.*, 102, 6051, 1980; (b) Turro, N. J. and Farrington, G. L., Photoinduced oxetane formation between 2-norbornanone and derivatives with electron-poor ethylenes, *J. Am. Chem. Soc.*, 102, 6056, 1980.
104. Chung, W. S., Liu, Y. D., and Wang, N. J., Face selectivity in the Paternò–Büchi reaction of methacrylonitrile to 5-substituted adamantan-2-ones, *J. Chem. Soc., Perkin Trans. 2*, 581, 1995.
105. Chung, W. S. and Ho, C. C., Photochemistry of acetone in the presence of exocyclic olefins: an unexpected competition between the Photo–Conia and Paternò–Büchi reactions, *J. Chem. Soc.*, *Chem. Commun*., 317, 1997.

61

Enantioselective Photocycloaddition Reactions in Solution

Benjamin Grosch
Technische Universität München

Thorsten Bach
Technische Universität München

61.1 Introduction

By definition, enantioselective reactions are transformations in which a prochiral substrate is converted into a chiral product such that one of the two enantiomers is formed in significant excess. The degree of enantioselectivity is given by the enantiomeric excess (*ee*). Schematically, such a transformation is depicted in Scheme 1, with the triangle (substrate S) representing a prochiral unit and the two tetrahedrons (products P and *ent*-P) representing two enantiomeric chiral products.

In photocycloaddition reactions, the degree of enantioselectivity depends on the effectiveness with which the enantiotopic faces of a prochiral olefin can be distinguished (enantioface-differentiation). The conventional way to achieve this goal is to covalently attach a chiral auxiliary (see Section 61.2) to the prochiral substrate. The consecutive reaction is diastereoselective, and the auxiliary has to be removed afterwards. The degree of diastereoselectivity in the selectivity-determining step is measured by the diastereomeric excess (DE), which is defined by analogy to the enantiomeric excess, and the *ee* corresponds to the DE after removal of the auxiliary. The auxiliary-based process consequently consists of three steps, two of which are, in principle, superfluous as they are not concerned with the reaction under scrutiny.

In recent years, efforts have been made to achieve enantioselective photocycloaddition reactions in the true sense (i.e., going from S directly to either P or *ent*-P with high *ee*). The main goal of this account is to summarize these developments. The subject has been divided into three sections according to the method used for the enantioface-differentiation: asymmetric induction by chiral complexing agent (Section 61.3), asymmetric photosensitization (Section 61.4), and asymmetric induction by circularly polarized light (Section 61.5). Results published before mid-2002 were taken into consideration. Reviews related to this area have been previously published by Rau[1] and by Inoue et al.[2,3] Finally, it should be mentioned that this account deals exclusively with solution-phase photochemistry. Reviews summarizing recent achievements in enantioselective solid-state photochemistry can be found elsewhere in this book.

0-8493-1348-1/04/$0.00+$1.50

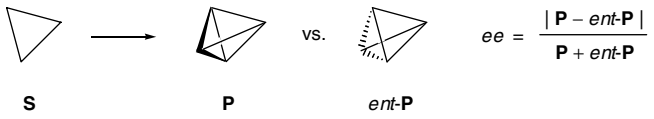

SCHEME 1

TABLE 61.1 Survey on Topical Reviews Concerned with the Most Important Diastereoselective Photocycloaddition Reactions

Reaction	References	
	General, Mechanistically Orientated	Focus on Induced Diastereoselectivity
Intermolecular [2+2]-photocycloaddition	7–18	2, 3, 7–9, 11–13, 15, 17, 18, 19
Intramolecular [2+2]-photocycloaddition	8–18, 20, 21	2, 3, 8, 9, 11–13, 15, 17–21
Paternò–Büchi reaction	7, 16, 17, 19, 22, 23	2, 3, 7, 17, 19, 22, 23
[4+4]-photocycloaddition	8, 16, 24, 25	9, 24
[4+2]-photocycloaddition	16, 26	2, 3, 9, 26
Arene *meta*-photocycloaddition	16, 26, 27–29	2, 26, 27
Arene *ortho*-photocycloaddition	16, 26–28, 30	26, 27

61.2 Asymmetric Induction by Chiral Auxiliary

Diastereoselective photocycloaddition reactions, especially intra- and intermolecular [2+2]-photocycloaddition and Paternò–Büchi reactions, are established tools in organic synthesis. Their use and applicability have been proven in the framework of natural product syntheses and in the preparation of many other compounds. In this context, auxiliaries well established in conventional chemistry[4–6] have been employed to prepare enantiomerically pure substrates for further elaboration. The tremendous amount of work that has been done in the area of auxiliary-induced photocycloaddition reactions is by far beyond the scope of this review. More detailed information on a specific auxiliary-induced photochemical reaction can be found in individual chapters of this book which in turn deal with the corresponding transformation in a broader context. In addition, we have compiled topical reviews on photocycloaddition reactions (Table 61.1). These reviews have been roughly divided according to their focus and their relevance to auxiliary-induced diastereoselective reactions.

Despite what has been said in the previous section, three more recent developments are mentioned here, as they have not been extensively reviewed in the above-mentioned articles. This treatment is not comprehensive but rather tries to give the reader a flavor of the modern trends in the area.

Piva et al.[31,32] have established removable chiral tethers that attach an alkene to an enone and render the intramolecular [2+2]-photocycloaddition between these groups highly diastereoselective. Chiral α- and β-hydroxy acids such as (*S*)-lactic acid, (*S*)-phenyllactic acid, or (*S*)-mandelic acid proved to be highly effective auxiliaries. Butenyl lactate **1** was converted regioselectively to the straight adduct **2**. The diastereoselectivity reached 94% DE at –40°C, albeit with a reduction in yield. At –20°C, 92% DE and 78% yield were obtained (Scheme 2).

After separation of the diastereoisomers, cleavage of the tether afforded the cyclobutane lactones in good yield and in enantiomerically pure form. This strategy has been applied in a synthetic approach to (–)-italicene and (+)-isoitalicene.[33]

Mariano and co-workers[34] have employed chiral eniminium salts as surrogates for enones to control the stereoselectivity of the enone-olefin [2+2]-photocycloaddition. Eniminium salts have only π,π^* excited states and intersystem crossing to triplet excited states is therefore slow. As a consequence, the photocyclization should occur from the singlet state via a concerted mechanistic pathway. The chiral iminium salt **3**, accessible by condensation of the corresponding ketone with an enantiomerically pure *trans*-2,5-disubstituted pyrrolidine, cyclized in good yield. After removal of the chiral auxiliary, the tricyclic ketone **4** was obtained in enantiomeric excesses of up to 82% *ee* (Scheme 3).

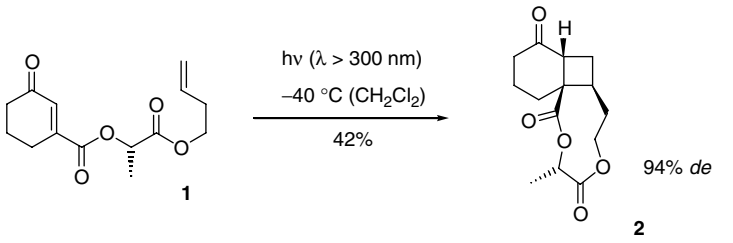

SCHEME 2

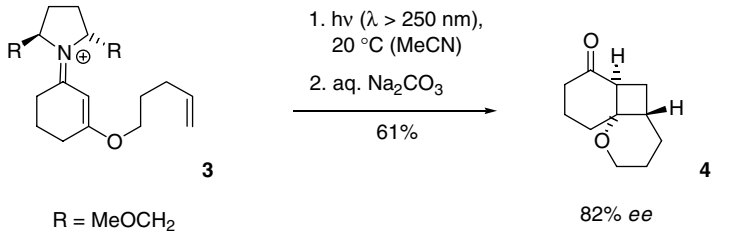

SCHEME 3

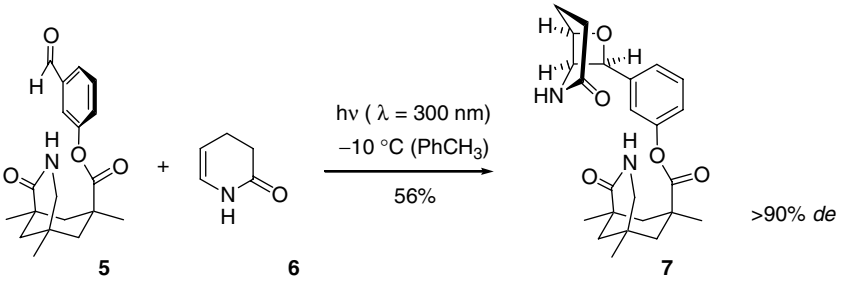

SCHEME 4

A highly diastereoselective Paternò–Büchi reaction by a new approach was reported by Bach et al.[35,36] The chiral auxiliary bound to *m*-hydroxybenzaldehyde **5** offers a binding site to which the reaction partner can be attached by two hydrogen bonds. In the complex, the two enantiotopic faces of the alkene **6** become diastereotopic and can be differentiated. The dihydropyridone **6** approaches the aldehyde from one face only (Scheme 4). Because the reaction within the complex is presumably faster than the reaction with unbound dihydropyridone, the face selection is enhanced by this rate acceleration. In toluene at –10°C, lactam **5** was converted with high diastereoselectivity to diastereoisomer **7** (>90% DE). The oxetano[2,3-*b*]piperidone fragment could be cleaved from the auxiliary by transesterification (NaOMe in MeOH).

61.3 Asymmetric Induction by Chiral Complexing Agent

Chiral complexing agents transfer the chiral information to a non-covalently bound substrate molecule as it undergoes photochemical conversion. In the enantiodifferentiating process, a complex equilibrium is set up between both species in their ground state, in contrast to enantiodifferentiating sensitized photochemical reactions (Section 61.4), where the excited states of both species are involved. Hydrogen or electron-donor/acceptor complexes with the ground-state substrate or the photochemically produced

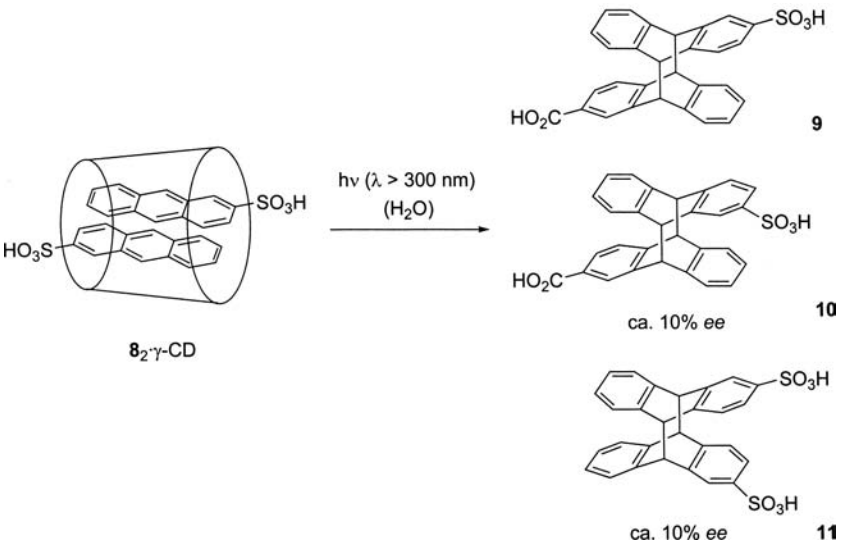

SCHEME 5

reactive intermediate have been employed to differentiate diastereotopic transition states. Ideally, the association constant of the chiral complexing agent with the photoproduct is significantly lower than that with the starting material. Then, after chiral induction and dissociation of the product, the host is available for the next chirality transfer. In this case of catalytic turnover, only substoichiometric amounts of the chiral complexing agent are necessary. For high enantioselectivity at a substoichiometric level, another prerequisite must be met. The photochemical reaction must be significantly accelerated in the complex with the chiral host, because unbound starting material is converted unspecifically and dilutes the enantiomeric excess of the product. The acceleration can be accomplished through electronic or steric effects. Even if chiral amplification is not achieved through catalytic use, a photostable chiral complexing agent used in stoichiometric or excessive amounts can be recovered and reused. Generally, the complexing agent should be readily separable from the reaction mixture without an additional and possibly damaging cleavage step, as in the case of a covalently bound auxiliary.

In the last decade, three main approaches have been employed to direct a photocycloaddition reaction enantioselectively by chiral complexing agents: host–guest complexes using chiral cyclodextrins as host molecules, catalysis by transition metal complexes with a chiral ligand sphere, and host–guest complexes using a rationally designed host compound. A variety of photoreactions such as photopinacolization, photocyclization, photorearrangement, photodeconjugation, and photoisomerization have been examined in the presence of chiral complexing agents. The results obtained have been reviewed thoroughly by Inoue[3] and by Everitt and Inoue.[2] Several photocycloaddition reactions have been conducted in complexes with cyclodextrins, and the results have been reviewed.[37–39] Studies have essentially focused on how the rate, regioselectivity, and diastereoselectivity of photoreactions are influenced by the cyclodextrin complexation of the starting material. The photodimerization of anthracene derivatives[40,41] and the [2+2]-cycloaddition of adamantan-2-ones[42] have been tested to examine the possibility of enantiocontrol of photocycloaddition reactions by cyclodextrin complexes.

An aqueous solution of 2-anthracenesulfonate **8** was irradiated in the presence of γ-cyclodextrin. The cyclodextrin accelerated the photodimerization to dimers **9**, **10**, and **11** by almost one order of magnitude (Scheme 5). Even at dilute concentrations, a sandwich complex of two anthracene molecules in the host cavity (8.5 Å) is formed which accelerates the cycloaddition reaction. In the presence of γ-cyclodextrin, the relative yields of the three isomers did not significantly change, suggesting that the guest molecules are nonspecifically trapped in the cavity.

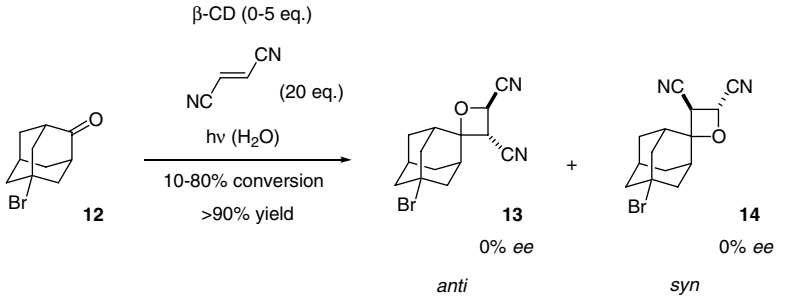

SCHEME 6

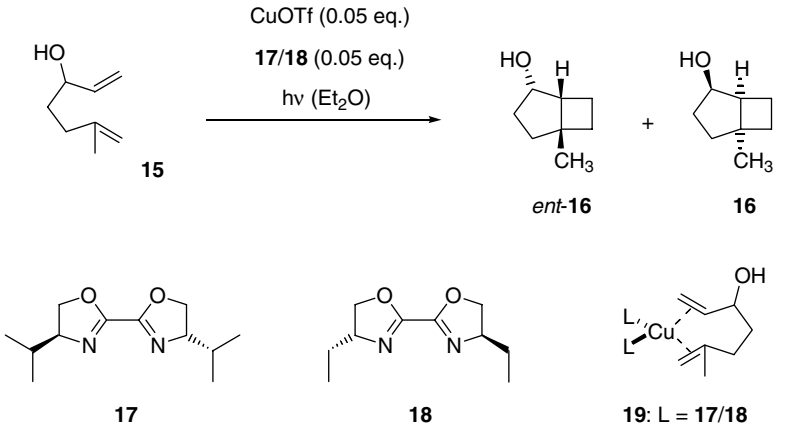

SCHEME 7

In the presence of γ-cyclodextrin, the dimers **10** and **11** were obtained with about 10% *ee*.[40] The absolute configuration of the predominating enantiomer was not identified, but CD-spectra indicated that the two anthracenes prefer *R*-helicity in the complex. From the two *R*-helical complexes that lead to the enantiomers of **10**, one seems to be sterically favored over the other because of fewer interactions between the substituents and the cyclodextrin.

The presence of β-cyclodextrin led to no significant enantiomeric excess in the [2+2]-photocycloaddition of fumaronitrile to 5-bromoadamantan-2-one (**12**) in D_2O (Scheme 6).[42] The facial diastereoselectivity, however, changed from *anti*/*syn* of 59/41 with no cyclodextrin to 20/80 in the presence of five equivalents of β-cyclodextrin upon irradiation in water.

Asymmetric copper(I)-catalyzed intramolecular [2+2]-photocycloaddition reactions were examined by Mattay et al.[43] In a synthetic approach to (+)- and (–)-grandisol, racemic dienol **15** was irradiated in the presence of CuOTf and a chiral ligand to yield mainly cyclobutanes **16** and *ent*-**16** as a mixture of enantiomers. Other 1,6-dienes were also employed. The effectiveness of a number of chiral, nitrogen-containing bidentate ligands were tested, the most successful of which, (4*S*,4′*S*)-4,4′-diisopropyl-2,2′-bisoxazoline **17** and (4*R*,4′*R*)-4,4′-diethyl-2,2′-bisoxazoline **18**, ensured a minor enantiomeric excess of <5% *ee* (Scheme 7). As the coordination of the diene to the chiral Cu(I)-complex **19** was proved by CD analysis, the authors suggest a lower reactivity of the chiral complex compared to the copper ion coordinated to solvent molecules as the reason for the low enantioselectivities observed.

A major step toward synthetically useful enantioselectivities induced by chiral complexing agents was achieved by the introduction of rationally designed hosts. These chiral hosts serve as stoichiometric complexing agents, which differentiate the enantiotopic faces of the starting material by binding to it in

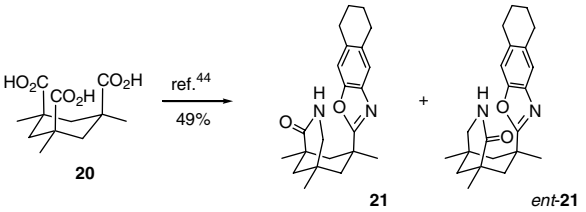

SCHEME 8

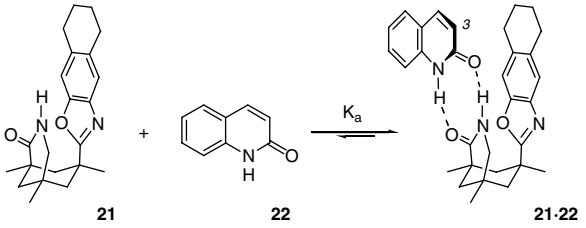

SCHEME 9

a defined orientation via hydrogen bonds. The conformational flexibility is constrained by a rigid backbone that offers an easily accessible binding site and at the same time exhibits an effective sterically demanding shield. The best results were obtained by chiral lactams **21** and *ent*-**21**, in which the hydrogen acceptor and hydrogen donor site define a plane parallel to the flat tetrahydronaphthyl residue. This shield is photochemically stable in contrast to further extended aromatics. The required spatial alignment is provided by Kemp's triacid **20**, from which racemic host *rac*-**21** is accessible in 49% overall yield (Scheme 8). The optical resolution to chiral benzoxazoles **21** and *ent*-**21** is readily achieved via the *N*-(–)-menthyloxycarbonyl derivative by column chromatographic separation.[44]

The effectiveness of these chiral host compounds has been shown in highly enantioselective [2+2]- and [4+4]-cycloadditions of prochiral lactams. Prochiral lactams such as 2-quinolone derivatives are expected to coordinate to lactam **21** with its NH-group as the hydrogen donor and the carbonyl group as the hydrogen acceptor, as depicted in Scheme 9. In this complex, any intra- or intermolecular attack at the quinolone double bond can occur exclusively from the *Re*-face relative to carbon atom C3. The other face of the molecule is shielded by the bulky tetrahydronaphthalene unit. Following ^{1}H nuclear magnetic resonance (^{1}H-NMR) titration experiments, the association constant of 2-quinolone **22** and host **21** in toluene was determined as $K_a \cong 500\ M^{-1}$ at 30°C, and a 1:1 complex stoichiometry was proved.[45] Because the complex formation was found to be exothermic, an enhanced association was expected at lower temperatures.

Upon irradiation with $\lambda > 300$ nm, the 4-alkenyloxy-2-quinolones **23** and **25** cyclized in an intramolecular [2+2]-photocycloaddition diastereoselectively to the crossed and straight cycloadducts **24** and **26**, respectively. In the presence of 2.6 equivalents of host compound **21** or *ent*-**21**, high enantioselectivities were achieved in a nonpolar solvent at low temperatures.[45,46] At –60°C in toluene, **24** and **26** were obtained with >90% *ee* (Scheme 10). Higher temperatures (84% *ee* at –15°C, 39% *ee* at 30°C) and more polar solvents (4% *ee* at 30°C in acetonitrile) significantly reduced the enantioselectivity under otherwise identical conditions.

The absolute configuration of photoproducts **24** and **26** was proved by single crystal x-ray crystallography and is in accordance with the *Si*-face attack with respect to C3, as the *Re*-face is shielded in the complex with chiral host *ent*-**21**. The observed enantioselectivities can be satisfactorily rationalized by a simple model that postulates perfect face differentiation of the complexed guest and no face differentiation if the starting material is not coordinated to the host. Therefore, the achievable enantioselectivities are

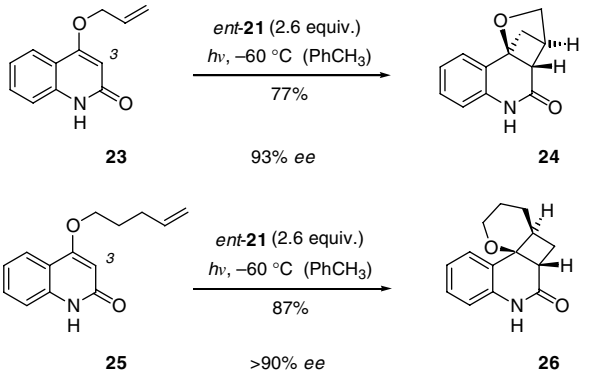

23 **24** **25** **26**

SCHEME 10

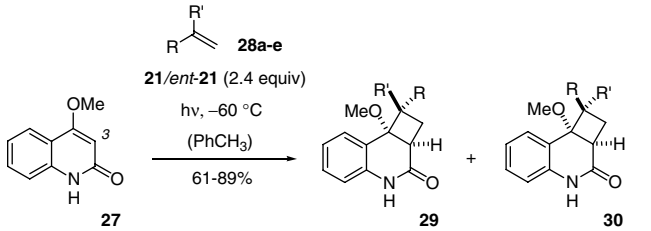

27 **29** **30**

			dr (**29**/**30**)	*ee*
28a	R = $CH_2CH_2CH_2OH$	R' = H	>95/5	81% (**29a**)
28b	R = CH_2OAc	R' = H	>95/5	92% (**29b**)
28c	R = COOMe	R' = H	90/10	82% (**29c**)
28d	R = OAc	R' = H	63/27	93% (**29d**), 98% (**30d**)
28e	R = CH_2CH_3	R' = CH_2CH_3	-	92% (**29e**)

SCHEME 11

determined by the association equilibrium. The host is photostable under the irradiation conditions ($\lambda \geq 300$ nm) and was recovered after each irradiation by column chromatography in >95% yield.

The scope of this approach was widened by the observation of excellent enantioselectivities in intermolecular [2+2]-photocycloaddition reactions with various alkenes.[45,47] 4-Methoxy-2-quinolone **27** was converted with high chemo- and regioselectivity to cyclobutanes **29** and **30** in the presence of an excess of alkene. With 4-penten-1-ol **28a**, allyl acetate **28b**, methyl acrylate **28c**, and vinyl acetate **28d**, the *exo*-diastereomers **29a–d** were formed with high simple diastereoselectivity and high yields (80 to 89%). Under optimized irradiation conditions (2.4 eq. of host **21** or *ent*-**21**, –60°C), high enantiomeric excesses were achieved in all instances, as depicted in Scheme 11; these enantiomeric excesses are unprecedented for an intermolecular photochemical reaction. As in the intermolecular case, host **21** induced *Re*-attack at carbon C3, and host *ent*-**21** induced a *Si*-attack.

The applicability of the developed complexing agent was further demonstrated by differentiating the faces of 2-pyridones. In this context, the [4+4]-photocycloaddition of 2-pyridone (pyridine-2(1H)-one, **31**) with cyclopentadiene was examined.[48] Irradiation of 2-pyridone at –50°C in the presence of host *ent*-**21** and cyclopentadiene led to a 3:2 mixture of *exo* and *endo* products **32** and **33**. Both diastereoisomers were obtained in high enantiomeric excess, *exo*-cycloadduct **32** with 84% *ee* and *endo*-cycloadduct **33** with 87% *ee* (Scheme 12). The absolute configuration of the predominating enantiomer was elucidated by single x-ray crystallography. As expected, the photoexcited 2-pyridone was attacked by cyclopentadiene from the *Si*-face relative to the prostereogenic carbon atom C3, because the *Re*-face is shielded following complexation with host *ent*-**21**.

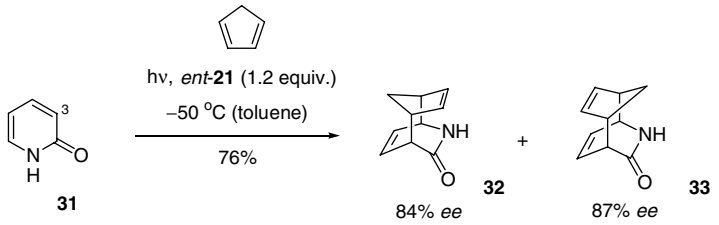

31 **32** 84% *ee* **33** 87% *ee*

SCHEME 12

The asymmetric induction achieved in the reactions examined suggests that host compounds **21** and *ent*-**21** are highly versatile and effective complexing agents when employed in enantioselective photocycloaddition reactions of prochiral, flat lactams. The complexing agents are restricted to lactams or amides as guest compounds. High enantioselectivities are achieved if the reaction center is in the vicinity of the binding site and the photoreaction is conducted at low temperatures in nonpolar solvents.

61.4 Asymmetric Photosensitization

Photosensitized enantiodifferentiating reactions are synthetically attractive and mechanistically interesting photochemical processes. The chiral information of the sensitizer is transferred to the substrate by short-lived interactions in the excited state (i.e., during the lifetime of an exciplex of a reaction intermediate and the chiral sensitizer that is involved in the reaction mechanism); hence, the chirality is multiplied, and only catalytic amounts of the optically active sensitizer are required. The stabilization energy of an exciplex compared to the locally excited state and its lifetime are often found to be strongly dependent on both electronic and steric properties of its components. Chiral induction can be achieved by different stabilization energies or lifetimes of the exciplex between the sensitizer and the intermediates that lead to the enantiomeric photoproducts. The absence of other reaction pathways without intimate contact to the sensitizer and of racemization processes in the further course of the reaction mechanism is an additional requirement to ensure effective chirality transfer.

Since the first report on the asymmetric photosensitization (7.7% *ee*) of the isomerization of *trans*-1,2-diphenylcyclopropane by Hammond and Cole,[49] attention has been focused on enantiodifferentiating photosensitized isomerization reactions.[1–3] The observed asymmetric induction was limited, until Inoue et al. achieved remarkable enantiomeric excesses of up to 64% *ee* in the photoisomerization of *Z*-cyclooctene to the optically active *E*-cyclooctene, sensitized by chiral benzenepolycarboxylates at –89°C. Valuable insights into the mechanism (e.g., the entropy influence) were gained from the temperature and pressure dependence of the observed enantioselectivities.[50–52]

In contrast, until very recently only a few studies of asymmetric photocycloadditions by chiral sensitizers have been reported. Kim and Schuster[53,54] achieved enantiomeric excesses of up to 23% *ee* in the sensitized [4+2]-cycloaddition of *trans*-β-methylstyrene **34** with cyclohexa-1,3-diene (**35**), which represents the first reported enantioselective photocycloaddition reaction. This reaction is called the *triplex Diels–Alder reaction*, as it was shown to occur by formation of a ternary complex of the singlet excited sensitizer, (–)-1,1′-*bis*(2,4-dicyanonaphthalene) **36**, with the diene and the dienophile. The Diels–Alder product **38** is formed in up to 11% chemical yield (Scheme 13); other products are the dimers of cyclohexa-1,3-diene (83%) and [2+2]-cycloadducts of **34** and **35** (5%).[55]

In the presence of enantiomerically enriched sensitizer **36** (77% *ee*), the observed enantiomeric excesses increased from 1% *ee* at room temperature to 15% *ee* at –65°C.[53] With the enantiomerically enriched anthracene derivative **37** (91% *ee*), the enantioselectivity was enhanced to 23% *ee* at –65°C, favoring the opposite enantiomer. Based on fluorescence quenching experiments and the concentration dependence of the observed enantioselectivities, the authors suggest the formation of diastereomeric exciplexes by complexation of the different prochiral faces of the styrene to the chiral surface of the sensitizer. The

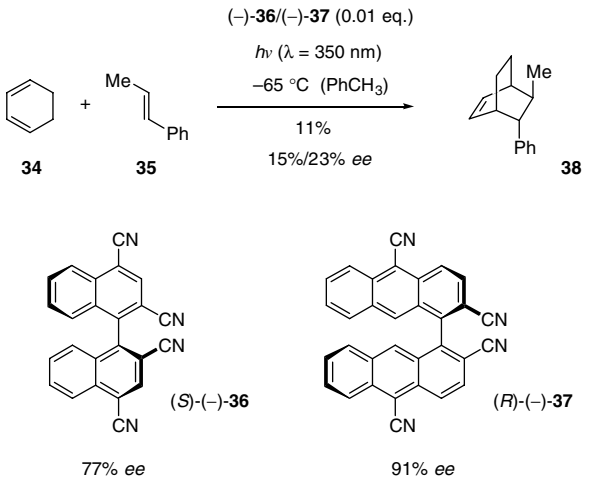

SCHEME 13

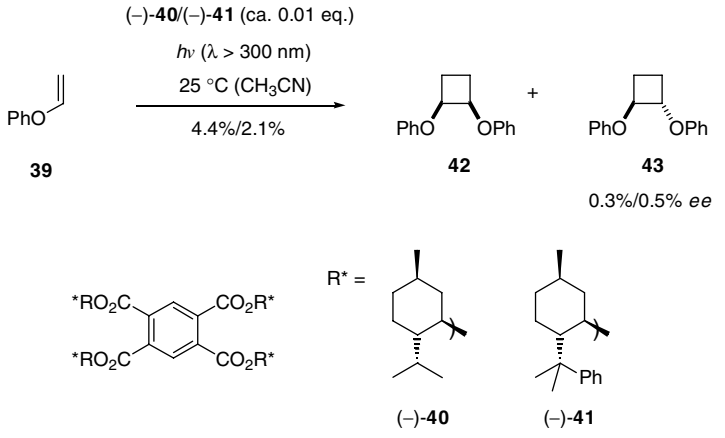

SCHEME 14

enantiomeric excess results from differential lifetimes of these exciplexes and therefore unequal capture by the cyclohexa-1,3-diene.[54]

For the sake of completeness, the synthesis of chiral 1,1′-binaphthalene derivatives as sensitizers for the photochemical dimerization of cyclohexa-1,3-diene by Vondenhof and Mattay should be mentioned.[56] However, only the racemic sensitizers were employed in the photoreactions, and their potential in asymmetric induction was not examined.

Inoue et al.[57] have performed the enantiodifferentiating [2+2]-photocyclodimerization of phenyl vinyl ether **39** in the presence of optically active menthyl or 8-phenylmenthyl arene(poly)carboxylate sensitizers (**40** and **41**). The reaction yielded the corresponding dimers **42** and **43** in a ratio of about 3:2 (Scheme 14). The highest enantioselectivity for dimer **43** (0.5% *ee*) was obtained with the sterically congested 8-phenylmenthyl ester (–)-**41**, albeit in low yields. The less congested menthyl ester (–)-**40** gave a lower optical yield (0.3% *ee*) but a slightly higher chemical yield. The asymmetric induction was not improved by irradiation at lower temperatures. The dimerization of 4-methoxystyrene gave better yields of up to 60%, but the enantioselectivities remained low (≤0.2% *ee*).

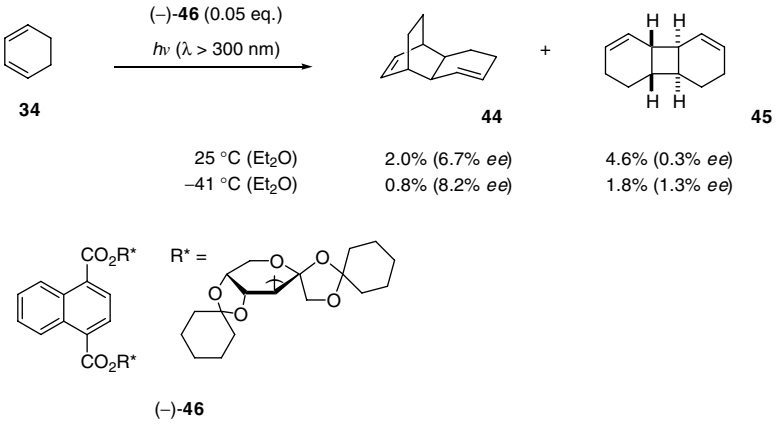

SCHEME 15

With similar chiral sensitizers enantiomeric excesses of up to 8.2% *ee* were observed in the photosensitized cyclodimerization of cyclohexa-1,3-diene **34** to the *exo*-[4+2]-cyclodimer **44** and the *anti*-[2+2]-cyclodimer **45**.[58] The *endo*-[4+2]-adduct and *syn*-[2+2]-adduct were obtained as minor components. Polymenthyl benzenepolycarboxylates similar to **40** yielded dimers **44** and **45** in low yield and with enantioselectivities of up to 2.5% *ee* at room temperature and 4.0% *ee* at –41°C. Protected saccharides as chiral substituents of the photosensitizer **46** enhanced the asymmetric induction in dimethyl ether up to 8.2% *ee*, but only in the case of the [4+2]-dimer **44** (Scheme 15).

This effect is attributed to the increased microenvironmental polarity around the sensitizer chromophore that stabilizes the exciplex or contact ion pair in nonpolar solvents. As a result of this effect, the stereochemical interaction between the sensitizer and the substrate is more intimate. Because significant enantioselectivities were only observed for dimer **44**, an independent cyclodimerization pathway to **44** via an exciplex or contact ion pair of cyclohexadiene and the chiral sensitizer was suggested. Dimer **45** gave much lower *ee* values even at low temperatures, but the product chirality was inverted within the tested temperature range in favor of enantiomer *ent*-**45**. Similar temperature switching of product chirality has been reported in the enantiodifferentiating photoisomerization of cycloalkenes and in the polar addition of alcohols to 1,1-diphenylalkenes.[59] This effect has been rationalized by a non-zero differential activation entropy of the same sign as the differential activation enthalpy.

The asymmetric induction of chiral saccharide substituents was more effective in the cyclodimerization of cyclohexene **47**.[60] *Trans–anti-trans* dimer **48** was obtained in low enantioselectivity (2.1% *ee*) at 25°C, but in much higher enantioselectivity (68% *ee*) at –78°C in pentane with the chiral sensitizer (–)-**50** (Scheme 16); this represents the highest *ee* value reported for an enantiodifferentiating-photosensitized cyclodimerization.

Cis/*trans* cyclodimer **49** is produced with almost no enantioface differentiation. The authors of the original publication suggest that dimer **48** is produced through the concerted $[2\pi_s + 2\pi_a]$-cycloaddition of *Z*-cyclohexene to *E*-cyclohexene that is initially formed by an asymmetric photosensitization process retaining its chiral information. Dimer **49**, however, arises from a nonconcerted process from *E*-cyclohexene with concurrent loss of its optical activity.

61.5 Asymmetric Induction by Circularly Polarized Light

Asymmetric photoreactions by circularly polarized light (CPL) are induced through the preferential excitation of one enantiomer. The chiral information is introduced by a physical source of chirality that renders this approach most effective in terms of chiral amplification. Asymmetric photodestruction causes a racemic mixture to be enantiomerically enriched when one enantiomer is consumed more rapidly by CPL. Photoderacemization creates an enantiomerically enriched reaction mixture when one enantiomer

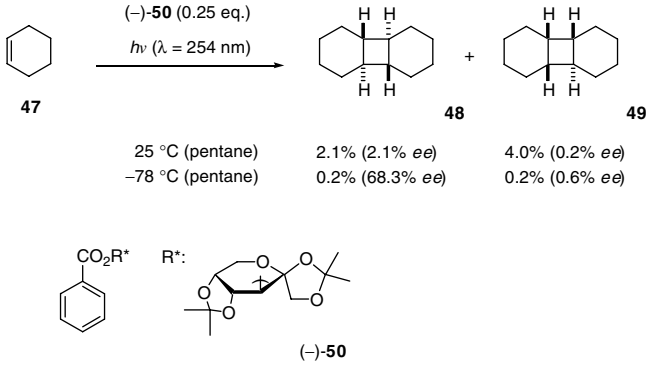

SCHEME 16

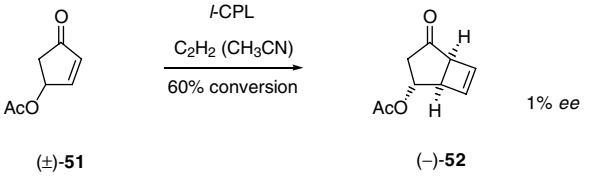

SCHEME 17

is interconverted to the other more effectively. Another possible way is the asymmetric fixation of thermally equilibrating enantiomers. The critical parameter in these processes is the anisotropy factor *g*, defined as the relative difference of the molar extinction coefficients of an optically pure compound toward *l*- or *r*-CPL at a given wavelength: $g = (\varepsilon_1 - \varepsilon_2)/\varepsilon = \Delta\varepsilon/\varepsilon$). The *g* factor for most compounds is very low ($<10^{-2}$). Only some carbonyl compounds with a partially forbidden n,π^* transition show high *g* factors of up to 0.30.[3] Because *g* is wavelength dependent, a highly monochromatic light source is a prerequisite for effective asymmetric induction by CPL to avoid a reduction of *g* by averaging over several wavelengths.

Enantioselective photoreactions induced by CPL have received considerable interest, particularly in regard to answering the question of how enantiomerically enriched material in the universe has been generated.[61,62] From a synthetic point of view, however, this method has seen limited success. In the few asymmetric fixation reactions examined (in most cases, photocyclizations), only low enantiomeric excesses were achieved.[2,3,63] A single example of an asymmetric photocycloaddition has been reported.[64,65] By preferential excitation of the (–)-antipode of racemic cyclopentanone (±)-**51** by *l*-CPL (351- to 363-nm laser) in the presence of acetylene, enantiomerically enriched (1% *ee*) (–)-**52** was obtained (Scheme 17). The unreacted starting material **51** was optically enriched in the (+)-enantiomer. This method provided product of sufficient optical purity to examine the chiroptical data.

61.6 Conclusion

Major improvements directed towards enantioselective generally applicable photocycloaddition reactions have recently been made. With regard to chemoselectivity and stereoselectivity, the use of chiral complexing agents is currently most promising. In several cases, high chemical yields and enantioselectivities (up to 98% *ee*) have been reported. In terms of synthetic efficiency, the use of chiral sensitizers is most appealing. In this field, significant progress toward a catalytic process is likely in the near future. The achieved enantioselectivies are not yet satisfactory. The use of CPL will most likely not be widely applicable in photocycloaddition reactions, as the *ee* values are very small. It is safe to say that the topic of enantioselective photochemical reactions will remain, for many years to come, one of the most challenging and most intriguing subjects in organic photochemistry.

References

1. Rau, H., Asymmetric photochemistry in solution, *Chem. Rev.*, 83, 535, 1983.
2. Everitt, S. R. L. and Inoue, Y., Asymmetric photochemical reactions in solution, in *Molecular and Supramolecular Photochemistry: Organic Molecular Photochemistry*, Vol. 3, Ramamurthy, V. and Schanze, K. S., Eds., Marcel Dekker, New York, 1999, 71.
3. Inoue, Y., Asymmetric photochemical reactions in solution, *Chem. Rev.*, 92, 741, 1992.
4. Rück-Braun, K. and Kunz, H., *Chiral Auxiliaries in Cycloadditions*, Wiley-VCH, Weinheim, 1999.
5. Roos, G., *Compendium of Chiral Auxiliary Applications*, Academic Press, San Diego, 2002.
6. Seyden-Penne, J., *Chiral Auxiliaries and Ligands in Asymmetric Synthesis*, Wiley, New York, 1995.
7. Bach, T., Stereoselective intermolecular [2+2]-photocycloaddition reactions and their application in synthesis, *Synthesis*, 683, 1998.
8. Horspool, W. M., Enone cycloadditions and rearrangements: photoreactions of dienones and quinones, *Photochemistry*, 32, 74, 2001.
9. Pete, J.-P., Asymmetric photoreactions of conjugated enones and esters, *Adv. Photochem.*, 21, 135, 1996.
10. Horspool, W. M., Photochemistry of alkenes, alkynes and related compounds, *Photochemistry*, 30, 117, 1999.
11. Fleming, S. A., Bradford, C. L., and Gao, J. J., Regioselective and stereoselective [2+2] photocycloadditions, in *Molecular and Supramolecular Photochemistry: Organic Photochemistry*, Vol. 1, Ramamurthy, V. and Schanze, K. S., Eds., Marcel Dekker, New York, 1997, 187.
12. Mattay, J., Conrads, R., and Hoffmann, R., Formation of C–C bonds by light-induced [2+2] cycloadditions, in *Houben-Weyl*, 4th ed., Vol. E21c, Helmchen, G., Hoffman, R. W., Mulzer, J., and Schaumann, E., Eds., Thieme, Stuttgart, 1995, 3085.
13. Winkler, J. D., Bowen, C. M., and Liotta, F., [2+2] Photocycloaddition/fragmentation strategies for the synthesis of natural and unnatural products, *Chem. Rev.*, 95, 2003, 1995.
14. Schuster, D. I., Lem, G., and Kaprinidis, N. A., New insights into an old mechanism: [2+2] photocycloaddition of enones to alkenes, *Chem. Rev.*, 93, 3, 1993.
15. Crimmins, M. T. and Reinhold, T. L., Enone olefin [2+2] photochemical cycloadditions, *Org. React.*, 44, 297, 1993.
16. Müller, F. and Mattay, J., Photocycloadditions: control by energy and electron transfer, *Chem. Rev.*, 93, 99, 1993.
17. Demuth, M. and Mikhail, G., New developments in the field of photochemical syntheses, *Synthesis*, 145, 1989.
18. Crimmins, M. T., Photochemical cycloadditions, in *Comprehensive Organic Synthesis*, Vol. 5, Trost, B., Ed., Pergamon Press, Oxford, 1991, 123.
19. Griesbeck, A. G. and Fiege, M., Stereoselectivity of photocycloadditions and photocyclizations, in *Molecular and Supramolecular Photochemistry*, Vol. 6, Ramamurthy, V. and Schanze, K. S., Eds., Marcel Dekker, New York, 2000, 33.
20. Becker, D. and Haddad, N., Applications of intramolecular [2+2]-photocycloadditions in organic synthesis, *Org. Photochem.*, 10, 1, 1989.
21. Crimmins, M. T., Synthetic applications of intramolecular enone-olefin photocycloadditions, *Chem. Rev.*, 88, 1453, 1988.
22. Mattay, J., Conrads, R., and Hoffmann, R., Oxetanes via [2+2] cycloadditions to carbonyl compounds (Paternò–Büchi reaction), in *Houben-Weyl*, 4th ed., Vol. E21c, Helmchen, G., Hoffman, R. W., Mulzer, J., and Schaumann, E., Eds., Thieme, Stuttgart, 1995, 3133.
23. Porco, J. A. and Schreiber, S. L., The Paternò–Büchi reaction, in *Comprehensive Organic Synthesis*, Vol. 5, Trost, B., Ed., Pergamon Press, Oxford, 1991, 151.
24. Sieburth, S. McN., The inter- and intramolecular [4+4] photocycloaddition of 2-pyridones and its application to natural product synthesis, *Adv. Cycloaddit.*, 5, 85, 1999.
25. West, F. G., Photocyclization and photocycloaddition reactions of 4- and 2-pyrones, *Adv. Cycloaddit.*, 4, 1, 1997.

26. Keukeleire, D. De and He, S.-L., Photochemical strategies for the construction of polycyclic molecules, *Chem. Rev.*, 93, 359, 1993.
27. Wender, P. A., Siggel, L., and Nuss, J. M., Arene-alkene photocycloaddition reactions, *Org. Photochem.*, 10, 357, 1989.
28. Mattay, J., Selectivities in photocycloadditions of arenes to olefins, *J. Photochem.*, 37, 167, 1987.
29. Cornelisse, J., The meta photocycloaddition of arenes to alkenes, *Chem. Rev.*, 93, 615, 1993.
30. Wagner, P. J., Photoinduced *ortho* [2+2] cycloaddition of double bonds to triplet benzenes, *Acc. Chem. Res.*, 34, 1, 2001.
31. Faure, S., Piva-le-Blanc, S., Piva, O., and Pete, J.-P., Hydroxyacids as efficient chiral spacers for asymmetric intramolecular [2+2] photocycloadditions, *Tetrahedron Lett.*, 38, 1045, 1997.
32. Faure, S., Piva-Le-Blanc, S., Bertrand, C., Pete, J.-P., Faure, R., and Piva, O., Asymmetric intramolecular [2+2] photocycloadditions: α- und β-hydroxy acids as chiral tether groups, *J. Org. Chem.*, 67, 1061, 2002.
33. Faure, S. and Piva, O., Application of chiral tethers to intramolecular [2+2] photocycloadditions: synthetic approach to (–)-italicene and (+)-isoitalicene, *Tetrahedron Lett.*, 42, 255, 2001.
34. Chen, C., Chang, V., Cai, X., Duesler, E., and Mariano, P. S., A general strategy for absolute stereochemical control in enone-olefin [2+2] photocycloaddition reactions, *J. Am. Chem. Soc.*, 123, 6433, 2001.
35. Bach, T., Bergmann, H., and Harms, K., High facial diastereoselectivity in the photocycloaddition of a chiral aromatic aldehyde and an enamide induced by intermolecular hydrogen bonding, *J. Am. Chem. Soc.*, 121, 10650, 1999.
36. Bach, T., Bergmann, H., Brummerhop, H., Lewis, W., and Harms, K., The [2+2]-photocycloaddition of aromatic aldehydes and ketones to 3,4-dihydro-2-pyridones: regioselectivity, diastereoselectivity and reductive ring opening of the product oxetanes, *Chem.-Eur. J.*, 7, 4512, 2001.
37. Bortolus, P. and Monti, S., Photochemistry in cyclodextrin cavities, *Adv. Photochem.*, 21, 1, 1996.
38. Bortolus, P., Grabner, G., Köhler, G., and Monti, S., Photochemistry of cyclodextrin host–guest complexes, *Coord. Chem. Rev.*, 123, 261, 1993.
39. Ramamurthy, V., Organic photochemistry in organized media, *Tetrahedron*, 42, 5753, 1986.
40. Tamaki, T., Kokubu, T., and Ichimura, K., Regio- and stereoselective photoisomerization of anthracene derivatives included by cyclodextrins, *Tetrahedron*, 43, 1485, 1987.
41. Tamaki, T., Kawanishi, Y., Seki, T., and Sakuragi, M., Triplet sensitization of anthracene photodimerization in γ-cyclodextrin, *J. Photochem. Photobiol. A: Chem.*, 65, 313, 1992.
42. Chung, W.-S., Turro, N. J., Silver, J., and Noble, W. J. le, Modification of face selectivity by inclusion in cyclodextrins, *J. Am. Chem. Soc.*, 112, 1202, 1990.
43. Langer, K. and Mattay, J., Stereoselective intramolecular copper(I)-catalyzed [2+2]-photocycloaddition: enantioselective synthesis of (+)- and (–)-grandisol, *J. Org. Chem.*, 60, 7256, 1995.
44. Bach, T., Bergmann, H., Grosch, B., Harms, K., and Herdtweck, E., Synthesis of enantiomerically pure 1,5,7-trimethyl-3-azabicyclo[3.3.1]nonan-2-ones as chiral host compounds for enantioselective photochemical reactions in solution, *Synthesis*, 1395, 2001.
45. Bach, T., Bergmann, H., Grosch, B., and Harms, K., Highly enantioselective intra- and intermolecular [2+2]-photocycloaddition reactions of 2-quinolones mediated by a chiral lactam host: host–guest interactions, product configuration and the origin of the stereoselectivity in solution, *J. Am. Chem. Soc.*, 124, 7983, 2002.
46. Bach, T., Bergmann, H., and Harms, K., Enantioselective intramolecular [2+2]-photocycloaddition reactions in solution, *Angew. Chem. Int. Ed. Engl.*, 39, 2302, 2000.
47. Bach, T. and Bergmann, H., Enantioselective intermolecular [2+2]-photocycloaddition reaction of alkenes and a 2-quinolone in solution, *J. Am. Chem. Soc.*, 122, 11525, 2000.
48. Bach, T., Bergmann, H., and Harms, K., Enantioselective photochemical reactions of 2-pyridones in solution, *Org. Lett.*, 3, 601, 2001.
49. Hammond, G. S. and Cole, R. S., Asymmetric induction during energy transfer, *J. Am. Chem. Soc.*, 87, 3256, 1965.

50. Inoue, Y., Matsushima, E., and Wada, T., Pressure and temperature control of product chirality in asymmetric photochemistry: enantiodifferentiating photoisomerization of cyclooctene sensitized by chiral benzenecarboxylates, *J. Am. Chem. Soc.*, 120, 10687, 1998.
51. Inoue, Y., Wada, T., Asaoka, S., Sato, H., and Pete, J.-P., Photochirogenesis: multidimensional control of asymmetric photochemistry, *J. Chem. Soc.*, *Chem. Commun.*, 251, 2000.
52. Kaneda, M., Asaoka, S., Ikeda, H., Mori, T., Wada, T., and Inoue, Y., Discontinuous pressure effect upon enantiodifferentiating photoisomerization of cyclooctene, *J. Chem. Soc.*, *Chem. Commun.*, 1272, 2002.
53. Kim, J.-I. and Schuster, G. B., Enantioselective catalysis of the triplex Diels–Alder reaction: addition of *trans*-β-methylstyrene to 1,3-cyclohexadiene photosensitized with (–)-1,1′-*bis*(2,4-dicycanonaphthalene), *J. Am. Chem. Soc.*, 112, 9635, 1990.
54. Kim, J.-I. and Schuster, G. B., Enantioselective catalysis of the triplex Diels–Alder reaction: a study of scope and mechanism, *J. Am. Chem. Soc.*, 114, 9309, 1992.
55. Akbulut, N., Hartsough, D., Kim, J.-I., and Schuster, G. B., The triplex Diels–Alder reaction of 1,3-dienes with enol, alkene and acetylenic dienophiles: scope and utility, *J. Am. Chem. Soc.*, 54, 2549, 1989.
56. Vondenhof, M. and Mattay, J., Sulfonic acid esters derived from 1,1′-binaphthalene as new axially chiral photosensitizers, *Tetrahedron Lett.*, 31, 985, 1990.
57. Inoue, Y., Okano, T., Yamasaki, N., and Tai, A., Enantiodifferentiating photocyclodimerization of phenyl vinyl ethers and 4-methoxystyrene sensitized by chiral aromatic esters, *J. Photochem. Photobiol. A: Chem.*, 66, 61, 1992.
58. Asaoka, S., Ooi, M., Jiang, P., Wada, T., and Inoue, Y., Enantiodifferentiating photocyclodimerization of cyclohexa-1,3-diene sensitized by chiral arenecarboxylates, *J. Chem. Soc., Perkin Trans. 2*, 77, 2000.
59. Inoue, Y., Sugahara, N., and Wada, T., Vital role of entropy in photochirogenesis, *Pure Appl. Chem.*, 73, 475, 2001.
60. Asaoka, S., Horiguchi, H., Wada, T. and Inoue, Y., Enantiodifferentiating photocyclodimerization of cyclohexene sensitized by chiral benzenecarboxylates, *J. Chem. Soc., Perkin Trans. 2*, 737, 2000.
61. Feringa, B. L. and Delden, R. A. van, Absolute asymmetric synthesis: the origin, control and amplification of chirality, *Angew. Chem. Int. Ed. Engl.*, 38, 3418, 1999.
62. Bonner, W. A., Origin of chiral homogeneity in nature, *Top. Stereochem.*, 18, 1, 1988.
63. Buchardt, O., Photochemistry with circularly polarized light, *Angew. Chem. Int. Ed. Engl.*, 13, 179, 1974.
64. Cavazza, M. and Zandomeneghi, M., Photocycloaddition of acetylene and 1-hexyne to 4-acetoxycyclopent-2-en-1-ones. Intermolecular asymmetric photosyntheses induced by circularly polarized light, *Gazz. Chim. Ital.*, 117, 17, 1987.
65. Zandomeneghi, M. and Cavazza, M., Enantiomeric enrichment of *cis*-bicyclo[3.2.0]hept-3,6-dien-2-one with circularly polarized light via the photointerconversion of the enantiomers, *J. Am. Chem. Soc.*, 106, 7261, 1984.

62

Photochemical Oxetane Formation: Addition to Heterocycles

Manabu Abe
Osaka University

62.1 Introduction

Photochemical [2+2]-cycloaddition of alkenes with carbonyls, the so-called Paternò-Büchi reaction, is one of the important photochemical processes to give oxetanes (Scheme 1); Paternò and Chieffi first reported the oxetane formation in 1909, almost 100 years ago.[1] The predicted structure of the oxetane was confirmed by further research carried out by Büchi et al.[2] Since their discovery, the importance of the photochemical process has been recognized and many examples have appeared in the literature. The generally accepted mechanism for the formation of oxetane rings (**OX**) is a stepwise cycloaddition via intermediate 2-oxa-1,4-diradicals (**1,4-DR**), that can be generated by the attack of the n,π^*-carbonyl oxygen at the sp^2 carbon of the alkene (Scheme 1).[3–15]

Among the photochemical cycloadditions, the reactions with heterocyclic alkenes have attracted considerable attention from both the synthetic[16–35] and biological[36–39] points of view, and a number of reviews have been published in literatures;[26,31,40–42] however, a systematic description of the mechanism that explains the observed inherent selectivities (*regioselectivity* and *stereoselectivity*) in the photochemical reactions has not been described elsewhere. This chapter concentrates on an explanation of the current understanding of this addition reaction that leads to the observed selectivities. For this purpose, the Paternò–Büchi reaction of furan derivatives is considered as a good example to illustrate the general mechanism (Scheme 2). The mechanism of the photoaddition within this system used to explain the observed selectivities should be applicable to other cases. A good mechanistic understanding will be beneficial in the design of reactions for the preparation of synthetically and/or biologically important oxetanes.

0-8493-1348-1/04/$0.00+$1.50

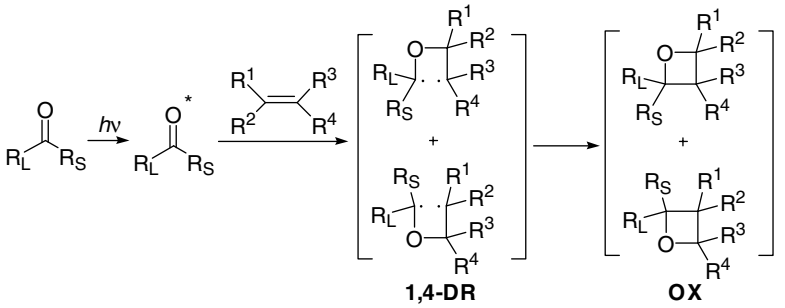

SCHEME 1

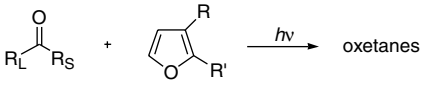

SCHEME 2

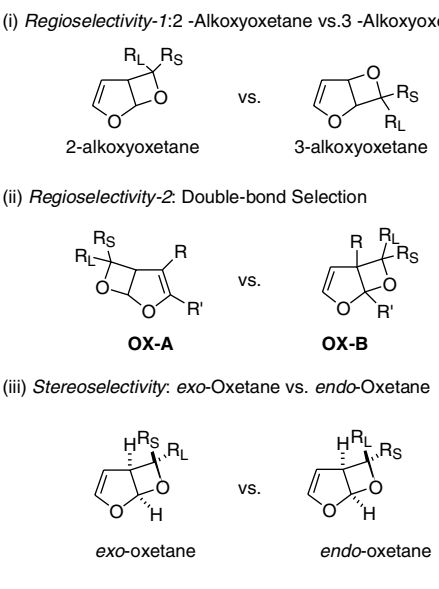

SCHEME 3

62.1 Selectivities Observed in the Paternò–Büchi Reaction of Furans

In principle, the three inherent selectivities in the reactions with furan derivatives (Scheme 3) are (i) regioselectivity (2-alkoxyoxetane vs. 3-alkoxyoxetane); (ii) double-bond selection (R, R′ ≠ H) (**OX-A** vs. **OX-B**); and (iii) stereoselectivity ($R_L \neq R_S$) (*exo*-oxetane vs. *endo*-oxetane). In the following sections, the origins for the selectivities observed in the experiments are rationalized.

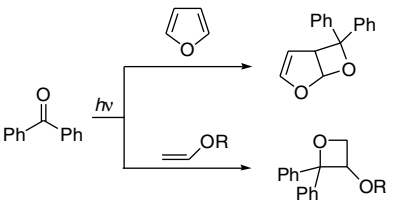

SCHEME 4

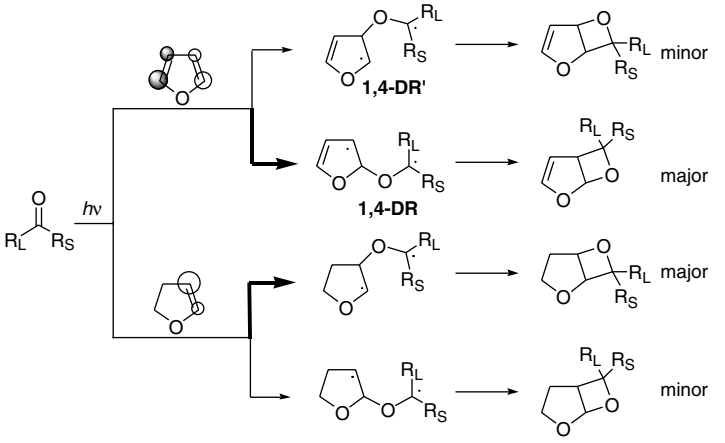

SCHEME 5

62.3 Regioselectivity-1: Formation of 2-Alkoxyoxetanes vs. 3-Alkoxyoxetanes

Schenck first reported the exclusive formation of 2-alkoxyoxetane in the reaction of furan with benzophenone (Scheme 4).[43] The generality of such regioselectivity (> 98: 2) was confirmed by Shima and coworkers in the photoreaction of furan with a variety of carbonyl compounds including aliphatic ketones and aldehydes.[44] At first glance, the almost exclusive formation of the 2-alkoxyoxetanes seems to be unusual, since the preferred formation of 3-alkoxyoxetanes is known in the reaction of carbonyl compounds with acyclic and cyclic vinyl ethers (Scheme 4).[45–50] This mechanistic dilemma can be readily rationalized when we consider the character of the n,π^* excited-state carbonyls and the intermediate 1,4-diradicals. First, as suggested by Hammond,[51] the excited state of carbonyls has electrophilic radical character at the oxygen. Thus, the carbonyl oxygen will attack the alkenes preferably at the site of higher frontier electron density. As can be easily imagined from the orbital coefficients of their HOMOs (Scheme 5), the oxygen will attack preferably at the β-position of the vinyl ethers and at the 2-position of furan.[52] The orbital interaction is one of the reasonable explanations for the contrasting regioselectivity observed in the experiments of vinyl ethers. Secondary, the almost quantitative regioselectivity for the furan reaction can be also explained by considering the relative stability of the intermediate 1,4-diradicals (**1,4-DRs**).[2, 3, 15] Namely, the diradical (**1,4-DR**), which afford 2-alkoxyoxetane, is relatively stabilized in terms of the allylic delocalization of the spin, compared with the regioisomeric diradical (**1,4-DR′**).

62.4 Regioselectvity-2: Double-bond Selection

When unsymmetrically substituted furans such as 2-methylfuran and 3-methylfuran are used for the photochemical reactions another regioselectivity is apparent: i.e., double-bond selection (**OX-A** vs. **OX-B**). The

TABLE 62.1 Regioselectivity-2: Double-Bond Selection

	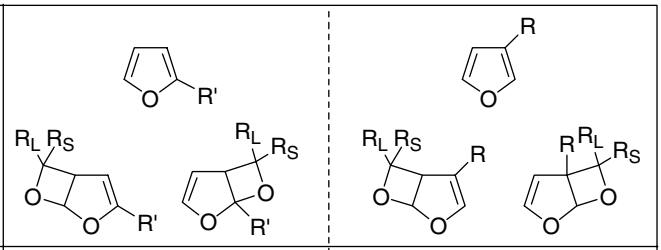	
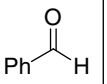	44 : 56 (R' = Me, ref. 53)	52 : 48 (R = CH_2OH, ref. 56)
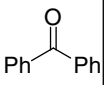	< 2 : 98 (R' = Me, ref. 54) < 2 : 98 (R' = CH_2OH, ref. 55)	< 2 : 98 (R = Me, ref. 54)

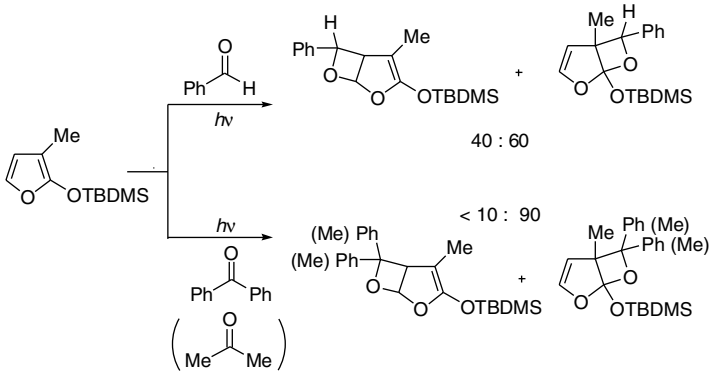

SCHEME 6

experimental data are summarized in Table 62.1. In contrast to the product mixture of the two isomeric oxetanes from the reaction with benzaldehyde (E_T = 71 kcal/mol, E_T = excited-triplet energy), the benzophenone (E_T = 69 kcal/mol) invariably adds to the double bond having the alkyl substituent at the C2 or the C3 position on the furan ring.[53–56] A similar trend is reported for the 2-siloxyfuran derivatives in the synthetic approach to γ-butyrolactones (Scheme 6).[57]

In this example the aldehyde adds to both double bonds in a regio-random fashion to give the two isomeric oxetanes. However, the sterically congested oxetanes are selectively formed in the reaction with ketones, i.e., benzophenone and acetone (E_T = 79 kcal/mol). Apparently, the selectivity is not due to the energetic difference of the excited carbonyls. What is the origin for the dramatic difference in the selectivity? Informatively, in the reaction with acetone, the regioselectivity is reported to be largely dependent upon the concentration of the furan derivative (Scheme 7). Namely, in contrast to the regioselective formation of the oxetane at the lower concentration of the 2-siloxyfuran (0.01 M), the two isomeric oxetanes are observed at higher concentration of the furan (0.2 M). The results clearly suggest that the triplet state (low concentration of the furan) gives higher selectivity and the low selectivity arises from the singlet state (high concentration of the furan).

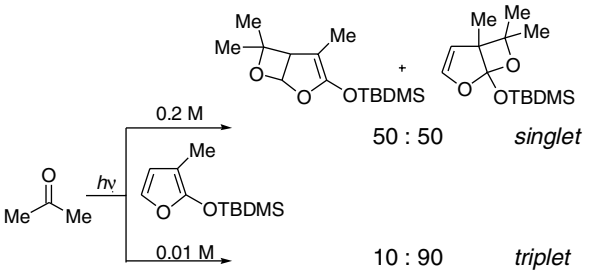

SCHEME 7

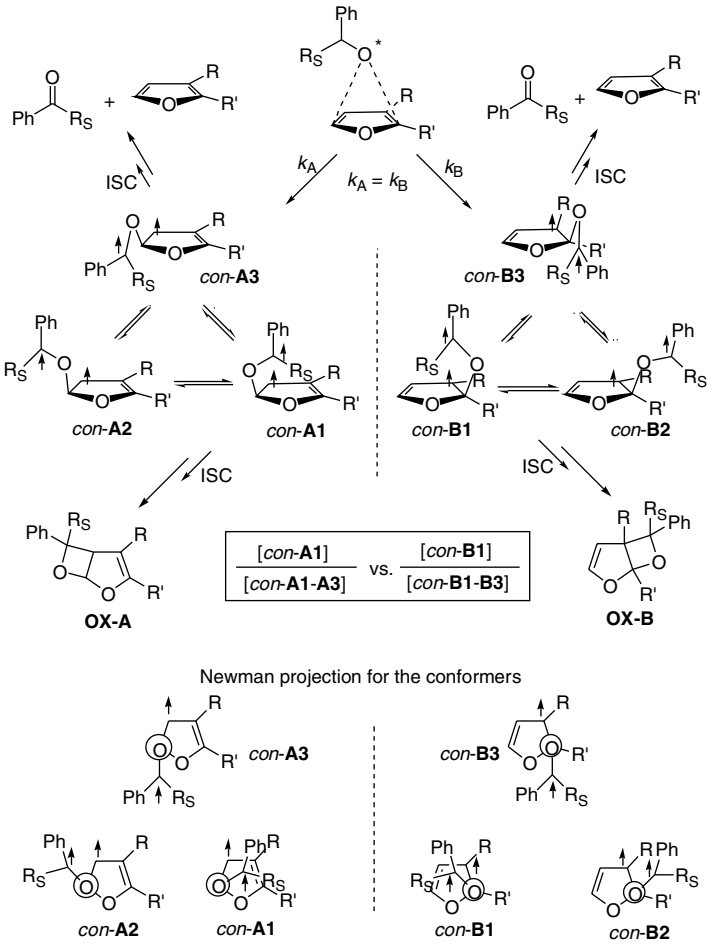

SCHEME 8

As judged by the reported experimental results mentioned above, the intermediate triplet 1,4-diradicals play an important role in the control of selectivity. A reasonable explanation is depicted in Scheme 8 (R, R′ ≠ H). In this scheme I propose that the high-energy excited carbonyls will attack both double bonds equally to give the regioisomeric triplet diradicals, i.e., $k_A = k_B$. There are three possible conformers in each diradical, i.e., productive conformers *con*-**A1,** *con*-**A2,** *con*-**B-1** and *con*-**B2** and non-productive conformers *con*-**A3** and *con*-**B3** that go back to the starting materials. The product ratio of **OX-A**/**OX-B**

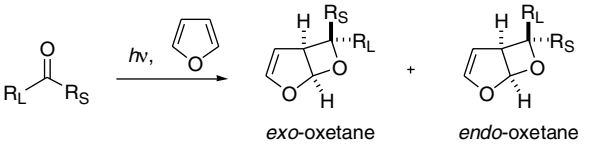

SCHEME 9

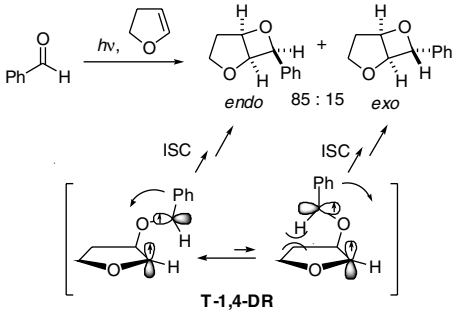

SCHEME 10

should be reflected by the population of the productive conformers in the possible triplet 1,4-diradicals. When R_S = Ph, the population of the productive conformer *con*-**B1** in *con*-**B1-B3** is higher than the conformer *con*-**A1** in *con*-**A1-A3**. This arises as a result of the steric repulsion between R_S and R, R′ in the conformers *con*-**B2** and *con*-**B3**. Such a non-bonded interaction is negligible for the **type A** conformers. Thus, the regioselectivity in the reaction with triplet-excited ketones is not only determined at the first stage of the reaction (k_A vs. k_B), but also the population of the productive conformers of the triplet diradicals, i.e., [*con*-**A1**]/[*con*-**A1-A3**] vs. [*con*-**B1**]/[*con*-**B1-B3**]. In the case of the aldehyde (R_S = H), such a steric repulsion is quite small and the population of the productive conformers would be the same for the each type of the diradicals, i.e., **OX-A/OX-B** = k_A/k_B.

62.5 Stereoselectivity: Formation of *exo*-Oxetanes vs. *endo*-Oxetanes

When unsymmetrical carbonyls ($R_L \neq R_S$) are used for the photochemical cycloaddition with furans, the inherent stereoselectivity should be considered, i.e., *exo*-oxetanes vs. *endo*-oxetanes (Scheme 9). Shima initially investigated the photocycloaddition reaction in 1965[53] and an NMR study by Whipple and Evanega[58] later provided evidence for the preference of the *exo*-selective cycloaddition. The *exo*-selective formation of the bicyclic oxetanes and their chemical transformations are now accepted as powerful tools for preparing the synthetically and biologically important materials.[16–35]

The mechanistic rationalization of the highly *exo*-selective formation of oxetanes has been exemplified by Griesbeck et al.[59] The idea was originally used for rationalization of the *endo*-selectivity in the reaction with 2,three-dimensionalihydrofuran derivatives (Scheme 10).[60–67] Namely, the stereochemical outcome is proposed to come from the relative stability of the intermediary triplet 1,4 diradicals (**T-1,4-DR**), whose conformations are suitable for the spin-orbit coupling (SOC) induced intersystem crossing (ISC) process. The "Conformational Memory Effects (Griesbeck Model)" in the stereoselectivity can be applicable to the stereochemical outcome for the reaction with furan (Scheme 11).

Among the possible conformations (**T-1,4-DR-A,B**) of the intermediary triplet 1,4-diradicals, the conformer (**T-1,4-DR-B**), that is expected to lead to the *exo*-isomer, has the most appropriate orientation of the two singly occupied p-orbitals for the SOC-induced ISC process, as judged by the perpendicularity and the distance between the spins.[68]

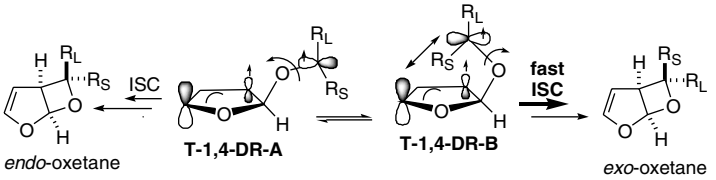

SCHEME 11

Griesbeck's proposal excellently explains the preferred formation of the *exo*-isomers reported so far in the experiments and predicts the stereochemistry for the related reactions.[69, 70]

62.6 Summary

In this chapter, I have summarized the important role of the triplet diradicals in the regio- and stereoselectivity for the Paternò-Büchi oxetane formations that have been reported so far. Since triplet diradical species are quite common intermediates in a variety of photochemical processes, the concept would be helpful to understand the selectivities and design the reactions for a synthetic purpose.

References

1. Paternò, E. and Chieffi, G., Sintesi in Chemica Organica per Mezzo Della Luce. Composti Degli Idrocarburi non Saturi con Aldeidi e Chetoni, *Gazz. Chim. Ital.*, 39, 341, 1909.
2. Büchi, G., Inman, C. G., and Lipinsky, E. S., The Reaction of carbonyl compounds with 2-methyl-2-butene in the presence of ultraviolet light, *J. Am. Chem. Soc.*, 76, 4327, 1954.
3. Arnold, D. R., Hinman, R. L., and Glick, A. H., Chemical properties of the carbonyl n,π^* state: the photochemical preparation of oxetanes, *Tetrahedron Lett.*, 1425, 1964.
4. Yang, N. C., Loeschen, R., and Mitchell, D., On the mechanism of the Paternò–Büchi reaction, *J. Am. Chem. Soc.*, 89, 5465, 1967.
5. Toki, S. and Sakurai, H., Kinetic studies of the photoreaction of benzophenone with furan, *Bull. Chem. Soc. Jpn.,* 40, 2885, 1967.
6. Freilich, S. C. and Peters, K. S., Observation of the 1,4-biradical in the Paternò–Büchi reaction, *J. Am. Chem. Soc.*, 103, 6255, 1981.
7. Caldwell, R. A., Majima, T., and Pac, C., Some structural effects on triplet biradical lifetimes. Norrish II and Paternò–Büchi biradicals, *J. Am. Chem. Soc.*, 104, 1982, 629.
8. Wilson, R. M., Wunderly, S. W., Walsh, T. F., Musser, A. K., Outcalt, R., Geiser, F., Gee, S. K., Brabender, W., Yerino, Jr., L., Conrad, T. T., and Tharp, G. A., Laser photochemistry: trapping of quinone-olefin preoxetane intermediates with molecular oxygen and chemistry of the resulting 1,2,4-trioxanes, *J. Am. Chem. Soc.*, 104, 4429, 1982.
9. Freilich, S. C. and Peters, K. S., Picosecond dynamics of the Paternò–Büchi reaction, *J. Am. Chem. Soc.*, 107, 3819, 1985.
10. Adam, W., Kliem, U., and Lucchini, V., Preparative UV-Vis laser photochemistry: molecular oxygen trapping of the Paternò–Büchi triplet diradicals derived from 1,4-dioxene, *Tetrahedron Lett.*, 27, 2953, 1986.
11. Adam, W., Kliem U., Mosandl, T., Peters, E.-M., Peters, K., and von Schnering, H. G., Preparative visible-laser photochemistry: Qinghaosu-type 1,2,4-trioxanes by molecular oxygen trapping of Paternò–Büchi triplet 1,4-diradicals derived from 3,4-dihydro-4,4-dimethyl-2*H*-pyran-2-one and quinones, *J. Org. Chem.*, 53, 4986, 1988.
12. Pelzer, R., Jutten, P., and Scharf, H.-D., Isoselectivitat bei der Asymmetrischen Paternò-Büchi-Reaktion unter Verwendung von Kohlenhydraten als Chirale Auxiliare, *Chem. Ber.*, 122, 487, 1989.

13. Pelzer, R., Scharf, H.-D., Buschmann, H., and Runsink, J., Derivate der (+)-Menthyl-glyoxylate in der Paternò-Büchi-Reaktion. Einfluss von Substituenten im Glyoxysaurerest auf die Diastereoselektivitat, *Chem. Ber.*, 122, 1187, 1989.
14. Buschmann, H., Scharf, H.-D., Hoffmann, N., Plath, M. W., and Runsink, J., Chiral induction in photochemical reactions. The principle of isoinversion: a model of stereoselection developed from the diastereoselectivity of the Paternò–Büchi reaction, *J. Am. Chem. Soc.*, 111, 5367, 1989.
15. Arnold, D.R., The photocycloaddition of carbonyl compounds to unsaturated systems: the synthesis of oxetanes, *Adv. Photochem.*, 6, 301, 1968.
16. Jarosz, S. and Zamojski, A., Asymmetric photocycloaddition between furan and chiral alkyl glyoxylates, *Tetrahedron*, 38, 1447, 1982.
17. Jarosz, S. and Zamojski, A. Asymmetric photocycloaddition between furan and optically active ketones, *Tetrahedron*, 38, 1453, 1982.
18. Schreiber, S. L., Hoveyda, A. H., and Wu, H.-J., A photochemical route to the formation of threo aldols, *J. Am. Chem. Soc.*, 105, 660, 1983.
19. Schreiber, S. L. and Satake, K., Application of the furan-carbonyl photocycloaddition reaction to the synthesis of the *bis*(tetrahydrofuran) moiety of asteltoxin, *J. Am. Chem. Soc.,* 105, 6723, 1983.
20. Schreiber, S. L. and Satake, K., Total synthesis of (±)-asteltoxin, *J. Am. Chem. Soc.*, 106, 4186, 1984.
21. Schreiber, S. L. and Hoveyda, A. H., Synthetic studies of the furan–carbonyl photocycloaddition reaction: a total synthesis of (±)-avenaciolide, *J. Am. Chem. Soc.,* 106, 7200, 1984.
22. Schreiber, S. L., Desmaele, D., and Porco, Jr., J. A., On the use of unsymmetrically substituted furans in the furan-carbonyl photocycloaddition reaction: synthesis of a kadsurenone-ginkgolide hybrid, *Tetrahedron Lett.*, 29, 6689, 1988.
23. Schreiber, S. L. and Porco, J. A., Jr., Studies of the furan-carbonyl photocycloaddition reaction: vinylic substitution reactions, *J. Org. Chem.*, 54, 4721, 1989.
24. Hambalek, R. and Just, G., Trisubstituted oxetanes from 2,7-dioxa-bicyclo-[3.2.0]-hept-3-enes, *Tetrahedron Lett.*, 31, 4693, 1990.
25. Hambalek, R. and Just, G., A short synthesis of (±)-oxetanocin, *Tetrahedron Lett.*, 31, 5445, 1990.
26. Porco, Jr., J. A. and Schreiber, S. L., The Paternò–Büchi reaction, in *Comprehensive Organic Synthesis*, Vol. 5, Trost, B. M., Ed., Pergamon Press, Oxford, 1991, 151.
27. Cantrell, T. S. and Allen, A. C., Photochemical reactions of arenecarboxylic acid esters with electron-rich alkenes: 2+2 cycloaddition, hydrogen abstraction, and cycloreversion, *J. Org. Chem.*, 54, 135, 1989.
28. Cantrell, T. S., Allen, A. C., and Ziffer, H., Photochemical 2+2 cycloaddition of arenecarboxylic acid esters to furans and 1,3-dienes: 2+2 cycloreversion of oxetanes to dienol esters and ketones, *J. Org. Chem.*, 54, 140, 1989.
29. Bach, T., Regioselective carbohydroxylation of enol ethers by a photocycloaddition–hydrogenation sequence, *Tetrahedron Lett.*, 35, 1855, 1994.
30. Bach, T., The β-silicon effects as a control element for the regioselective ring opening of oxetanes, *Tetrahedron*, 50, 12319, 1994.
31. Bach, T., Regioselective ring opening of oxetanes by hydrogenolysis: a convenient method for the carbohydroxylation of enol ethers, *Liebigs Ann.*, 1045, 1995.
32. Bach, T., The Paternò–Büchi reaction of 3-heteroatom-substituted alkenes as a stereoselective entry to polyfunctional cyclic and acyclic molecules, *Liebigs Ann./Recueil*, 1627, 1997.
33. Bach, T., Unprecedented facial diastereoselectivity in the Paternò–Büchi reaction of a chiral dihydropyrrole: a short total synthesis of (±)-preussin, *Angew. Chem. Int. Edn. Engl.,* 37, 3400, 1998.
34. Bach, T., The Paternò–Büchi Reaction of *N*-acyl enamines and aldehydes: development of a new synthetic method and its application to total synthesis and molecular recognition studies, *Synlett*, 1699, 2000.
35. Abe, M. and Nojima, M., The Paternò–Büchi photocycloaddition reactions of silyl ketene acetals: controlling factors on the regio- and stereoselectivity in the oxetane formation, *J. Synth. Org. Chem. Jpn.*, 59, 855, 2001.

36. Prakash, G. and Falvey, D. E., Model studies of the (6–4) photoproduct DNA photolyase: synthesis and photosensitized splitting of a thymine-5,6-oxetane, *J. Am. Chem. Soc.*, 117, 11375, 1995.
37. Joseph, A., Prakash, G., and Falvey, D. E., Model studies of the (6–4) photoproduct photolyase enzyme: laser flash photolysis experiments confirm radical ion intermediates in the sensitized repair of thymine oxetane Adducts, *J. Am. Chem. Soc.*, 122, 11219, 2000.
38. Joseph, A. and Falvey, D. E., Photolysis of thymine oxetanes products triplet excited carbonyl compounds with high efficiency, *J. Am. Chem. Soc.*, 123, 3145, 2001.
39. Nakatani, K., Yoshida, T., and Saito, I., Photochemistry of benzophenone immobilized in a major groove of DNA: formation thermally reversible interstrand cross-link, *J. Am. Chem. Soc.*, 124, 2118, 2002.
40. Sakurai, H., Shima, K., and Toki, S., Photo-cycloaddition reaction of carbonyl compounds to olefins, *Nippon Kagaku Zasshi*, 89, 537, 1968.
41. Carless, H. A. J., Photochemical synthesis of oxetanes, in *Synthetic Organic Photochemistry*, Horspool, W. M., Ed., Plenum Press, New York, 1984, 425.
42. Rivas, C., Oxetane formation: addition to heterocycles, in *Organic Photochemistry and Photobiology*, Horspool, W. M. and Song, P.-S., Eds., CRC Press, Boca Raton, 1994, 536.
43. Schenck, G.O., Hartmann, W., and Steinmetz, R., Vierringsynthesen durch Photosensibilisierte Cycloaddition von Dimethylmaleinsäureanhydrid an Olefine, *Chem. Ber.*, 96, 498, 1963.
44. Shima, K. and Sakurai, H., Organic photochemical reactions. IV. Photoaddition reactions of various carbonyl compounds to furan, *Bull. Chem. Soc. Jpn.*, 39, 1806, 1965,
45. Turro, N. J. and Wiede, P. A., The photocycloaddition of acetone to 1-methoxy-1-butene: a comparison of singlet and triplet mechanisms and biradical intermediates, *J. Am. Chem. Soc.*, 90, 6863, 1968.
46. Schroeter, S. H. and Orlando, C. M., The photocycloaddition of various ketones and aldehydes to vinyl ethers and ketene diethyl acetal, *J. Org. Chem.,* 34, 1181, 1969.
47. Shima, K. and Sakurai, H., Photocycloaddition of propionaldehyde to ethyl vinyl ether, *Bull. Chem. Soc. Jpn.*, 42, 849, 1969.
48. Schroeter, S. H., The directing effect of alkoxy-groups in the photocycloaddition of carbonyl compounds to olefins, *J. Chem. Soc., Chem. Commun.*, 12, 1969.
49. Schore, N. E. and Turro, N. J., Mechanism of the interaction of n,π^* excited alkanones with electron-rich ethylenes, *J. Am. Chem. Soc.,* 97, 2482, 1975.
50. Carless, H. A. J. and Haywood, D. J., Photochemical cycloaddition of 2,6-dioxabicyclo[3.2.0]heptanes, *J. Chem. Soc., Chem. Commun.,* 1067, 1980.
51. (a) Moore, W. M., Hammond, G. S., and Foss, R. P., Mechanisms of photoreactions in solutions. I. Reduction of benzophenone by benzhydrol, *J. Am. Chem. Soc.*, 83, 2789, 1961; (b) Hammond, G. S., Baker, W. P., and Moore, W. M., Mechanisms of photoreactions in solution. II. Reduction of benzophenone by toluene and cumene, *J. Am. Chem. Soc.*, 83, 2795, 1961.
52. (a) Turro, N. J., Dalton, J. C., Dawes, K., Farrington, G., Hautala, R., Morton, D., Niemczyk, M., and Schore, N., Molecular photochemistry of alkanones in solution: α-cleavage, hydrogen abstraction, cycloaddition, and sensitization reactions, *Acc. Chem. Res.*, 5, 92, 1972; (b) Sengupta, D., Chandra, A. K., and Nguyen, M. T., Regioselectivity of oxetane formation in the photocycloaddition of lowest $^3(n,\pi^*)$ state of carbonyl compounds: interpretation using local softness, *J. Org. Chem.*, 62, 6404, 1997.
53. Toki, S., Shima, K., and Sakurai, H., Organic photochemical reactions. I. The synthesis of substituted oxetanes by the photoaddition of aldehydes to furans, *Bull. Chem. Soc. Jpn.*, 38, 760, 1965.
54. Rivas, C. and Payo, E., Synthesis of oxetanes by photoaddition of benzophenone to furans, *J. Org. Chem.*, 32, 2918, 1967.
55. Nakano, T., Rivas, C., and Perez, C., Configuration and stereochemistry of photoproducts by application of the nuclear overhauser effect: adducts of benzophenone with methyl-substituted furans and 2,5-dimethylthiophene, and of methyl-substituted maleic anhydrides with thiophene and its methyl derivatives, and benzo[*b*]thiophene, *J. Chem. Soc., Perkin Trans. 1*, 2322, 1973.

56. Carless, H. A. J. and Halfhide, A. F. E., Highly regioselective [2+2]-photocycloaddition of aromatic aldehydes to acetylfurans, *J. Chem. Soc., Perkin Trans. 1*, 1081, 1992.
57. Abe, M., Torii, E., and Nojima, M., Paternò–Büchi photocyclization of 2-siloxyfurans and carbonyl compounds: notable substituent and carbonyl (aldehyde vs. ketone and singlet- vs. triplet-excited state) effects on the regioselectivity (double-bond selection) in the formation of bicyclic *exo*-oxetanes, *J. Org. Chem.*, 65, 3426, 2000.
58. Whipple, E. B. and Evanega, G. R., The assignment of configuration to the photoaddition product of unsymmetrical carbonyls to furan using pseudocontact shifts, *Tetrahedron*, 24, 1299, 1968.
59. Griesbeck, A. G., Buhr, S., Fiege, M., Schmickler, H., and Lex, J., Stereoselectivity of triplet photocycloadditions: diene-carbonyl reactions and solvent effects, *J. Org. Chem.*, 63, 3847, 1998.
60. Griesbeck, A. G. and Stadtmüller, S., Regio- und Stereoselektive Photocycloadditionen Aromatischer Aldehyde an Furan und 2,three-dimensionalihydrofuran, *Chem. Ber.*, 123, 357, 1990.
61. Griesbeck, A. G. and Stadtmüller, S., Photocycloaddition of benzaldehyde to cyclic olefins: electronic control of endo selectivity, *J. Am. Chem. Soc.*, 112, 1281, 1990.
62. Griesbeck, A. G., Mauder, H., Peters, K., Peters, E.-M., and von Schnering, H.G., Photocycloadditionen mit α- und β-Naphthaldehyd: Vollständige Umkehr der Diastereoselektivitat als Konsequenz Unterschiedlich Konfigurierter Electronischer Zustände, *Chem. Ber.*, 124, 407, 1991.
63. Griesbeck, A. G. and Stadtmüller, S., Electronic control of stereoselectivity in photocycloaddition reactions. 4. Effects of methyl substituents at the donor olefin, *J. Am Chem. Soc.*, 113, 6923, 1991.
64. Griesbeck, A. G., Mauder, H., and Stadtmüller, S., Intersystem crossing in triplet 1,4-biradicals: conformational memory effects on the stereoselectivity of photocycloaddition reactions, *Acc. Chem. Res.*, 27, 70, 1994.
65. Griesbeck, A. G., Fiege, M., Bondock, S., and Gudipati, M. S., Spin-directed stereoselectivity of carbonyl-alkene photocycloadditions, *Org. Lett.*, 2, 3623, 2000.
66. Kutateladze, A. G., Conformational analysis of singlet–triplet state mixing in Paternò-Büchi diradicals, *J. Am. Chem. Soc.*, 123, 9279, 2001.
67. Griesbeck, A. G., Bondock, S., and Gudipati, M. S., Temperature and viscosity dependence of the spin-directed stereoselectivity of the carbonyl-alkene photocycloaddition, *Angew. Chem. Int. Ed. Engl.,* 40, 4684, 2001.
68. (a) Carlacci, L., Doubleday, Jr., C., Furlani, T. R., King, H. F., and McIver, J. W., Jr., Spin-Orbit Coupling in biradicals: *ab initio* MCSCF calculations on trimethylene and the methyl–methyl radical pair, *J. Am. Chem. Soc.*, 109, 5323, 1987; (b) Adam, W., Grabowski, S., and Wilson, R. M., Localized cyclic triplet diradicals: lifetime determination by trapping with oxygen, *Acc. Chem. Res.*, 23, 165, 1990; (c) Caldwell, R. A., Laser flash photolysis studies of intersystem crossing in biradicals and alkene triplets, in *Kinetics and Spectroscopy of Carbenes and Biradicals*, Platz, M. S., Ed., Plenum Press, New York, 1990, 77.
69. Hu, S. and Neckers, D. C., Photocycloaddition and *ortho*-hydrogen abstraction reactions of methyl arylglyoxylates: structure dependent reactivities, *J. Chem. Soc., Perkin Trans. 2*, 1771, 1999.
70. Zhang, Y., Xue, J., Gao, Y., Fun, H.-K., and Xu, J.-H., Photoinduced [2+2] cycloadditions (the Paternò–Böchi reaction) of 1-acetylisatin with enol ethers: regioselectivity, diastereoselectivity and acid catalyzed transformations of the spirooxetane products, *J. Chem. Soc., Perkin Trans. 1*, 345, 2002.

63

Mechanistic Studies on the Photochemistry and Phototoxicity of Diuretic Drugs

Franklin Vargas
Instituto Venezolano de Investigaciones Científicas

Carlos Rivas
Instituto Venezolano de Investigaciones Científicas

63.1 Introduction

The number and variety of phototoxic compounds are large. Furthermore, for most phototoxic xenobiotics, a correlation between structure and photoreactivity is not easily found. It is obvious that, in general, a relationship must exist between photochemical behavior and phototoxicity. This chapter discusses the role of type II reactions involving the photoactivated drug in its triplet state transferring energy to molecular oxygen to generate singlet oxygen, superoxide anion, or hydroxyl radical, causing oxidation or peroxidation of membrane lipids. In the last 10 years, we have examined the photolysis of diuretic drugs under mild conditions, similar to those encountered in biological systems — namely, neutral, oxygenated media or under argon atmosphere and irradiation carried out with visible light. These investigations were performed keeping two main goals in mind: (1) to establish the nature of the different photoproducts, and (2) to obtain evidence of the role of oxygen in these photoprocesses and in the *in vitro* phototoxicity.

63.2 Photochemistry of Diuretic Drugs

Thiazide Derivatives

The photosensitized reactions due to thiazide, chlorothiazide, and hydrochlorothiazide were described in the 1950s, soon after their introduction in the field of medicine for the treatment of hypertension. Many of these substances in different systems have been shown to induce *in vitro* phototoxicity, just as phenothiazines and tetracycline do, but few derived from oral administered sulfonamides have been studied from the standpoint of their phototoxic properties (Figure 63.1).

0-8493-1348-1/04/$0.00+$1.50

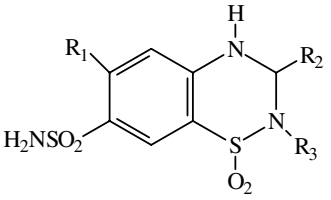

Penflutizide (**1**) : R_1= CF_3; R_2 = $(CH_2)_4CH_3$; R_3 = H
Hydrochlorothiazide (**2**) : R_1= Cl; R_2= R_3 = H
MethylChlorothiazide (**3**) : R_1= Cl; R_2= CH_2Cl; R_3= CH_3
Benzylhydrochlorothiazide (**4**) : R_1= Cl; R_2= CH_2Ph; R_3= H
Trichloromethiazide (**5**) : R_1= Cl; R_2= $CHCl_2$; R_3= H

FIGURE 63.1 Structure of some photosensitizer thiazide.

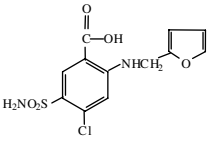

Furosemide (6)

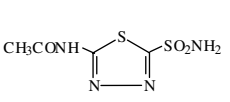

Acetazolamide (7)

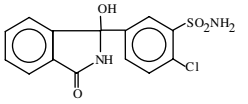

Chlorthalidone (8)

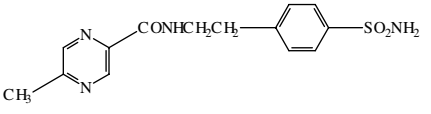

Glipizide (9)

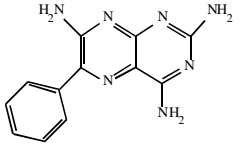

Triamterene (10)

FIGURE 63.2 Structure of some photosensitizer diuretics.

Diuretic Agents Photosensitizer (Sulfonamides): Furosemide, Acetazolamide, Chlorthalidone, Glipizide, and Triamterene

Furosemide and chlorthalidone are considered potent diuretics, as they are capable of bringing about the elimination of more than 15% of the filtered load of salt and water. This property is primarily due to their action on the upward branch of the Henle handle of the kidney. Although powerful, this action has a short duration (4 to 6 hours). Although it is not a benzothiadiazine, furosemide is structurally similar to hydrochlorothiazide. Many adverse effects on the skin have been reported for this substance, such as exfoliative dermatitis, among others. Cases have been reported on adverse effects caused by carbutamide, the first sulfonylurea derivative to show photosensitization among the various sulfonamides used as antidiabetic agents. Afterwards, tolbutamide, chlorpropamide, and, more recently, glipizide and glibenclamide were reported to cause reactions of skin photosensitization in patients under antidiabetic treatment (Figure 63.2).

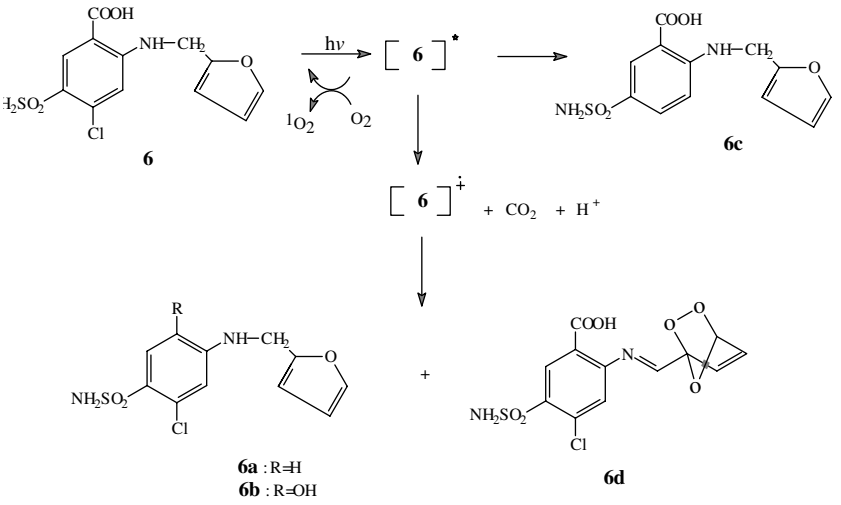

FIGURE 63.3 Mechanism of photodegradation of furosemide.

The phototoxic diuretic drug furosemide **6**, a 5-(aminosulfonyl)-4-chloro-2-[(2-furanylmethyl)-amino] benzoic acid, is photolabile under aerobic and anaerobic conditions. Previous studies have established that furosemide causes adverse photosensitizing effects *in vivo* and has a high *in vitro* photosensitizing capability. In this context, it is capable of initiating both energy transfer and free radical reactions.[1–4] Irradiation of a methanol solution of **6** produces under an oxygen atmosphere photoproducts such as **6a**, **6b**, **6c**, as well as singlet oxygen, while under an argon atmosphere only the photoproducts **6a** and **6c** have been isolated. Furthermore, a peroxidic, unstable photoproduct has also been detected during photolysis under an oxygen atmosphere. In another investigation, a photocycloaddition process of singlet oxygen to the furan group of furosemide (compound **6d**) was detected by Zanocco et al.[5]

The mechanism of this reaction under aerobic conditions proceeds presumably via decarboxylation of **6** (Figure 63.3), forming in this way a free-radical intermediate, as has already been proposed for carboxylic acids. One process leads to the hydrogen abstraction product **6a**. The formation of **6a** and **6c** does not require oxygen, as was demonstrated by its detection under argon atmosphere. A second process is photodechlorination of **6**, generating photoproduct **6c**, which was detected under anaerobic conditions.

Furosemide was screened *in vitro* at different concentrations for UV-Vis-induced phototoxic effects in a photohemolysis test, in the presence and absence of different radical scavengers, singlet oxygen, and hydroxyl radical quenchers. Furthermore, furosemide photosensitized the peroxidation of linoleic acid.[6] Data obtained in these studies show that the furosemide photodynamic action can be related, at least partially, to the ability of the drug to produce biologically significant quantities of singlet oxygen in polar and nonpolar media. Several authors have proposed that the adverse photosensitivity effects of furosemide can be related to photoproducts arising from direct photolysis or to those coming from type I photoreactions.

Acetazolamide (5-acetamido-1,3,4-thiadiazole-2-sulfonamide, **7**) is a drug commonly used as a diuretic. Cutaneous adverse reactions mediated by light have been described after oral intake of acetazolamide.[7] Phototoxic properties of this drug and related similar diuretics were determined *in vitro* by means of a photohemolysis test.[6,8–10] The photosensitivity *in vitro* of these drugs was inhibited by antioxidants and under nitrogen atmosphere.[11] These findings indicate an oxygen dependence of the phototoxic action of this drug *in vitro*.[12]

The phototoxic diuretic drug acetazolamide **7** is photolabile under aerobic and anaerobic conditions in methanolic solution as well as in buffered aqueous medium (pH = 7.2). The quantum yield under aerobic conditions was $\Phi = 0.24$, and the reaction led to the formation of photoproducts **7a** (yield 75%) and **7b** (yield 25%) (Figure 63.4). The results indicate that O_2 is directly involved in the photolysis of acetazolamide. The study of the influence of oxygen radicals on the decomposition of acetazolamide (irradiations in the presence of singlet oxygen quenchers) indicate that $^1O_2$ may lead to degradation of **7** by oxygenation.

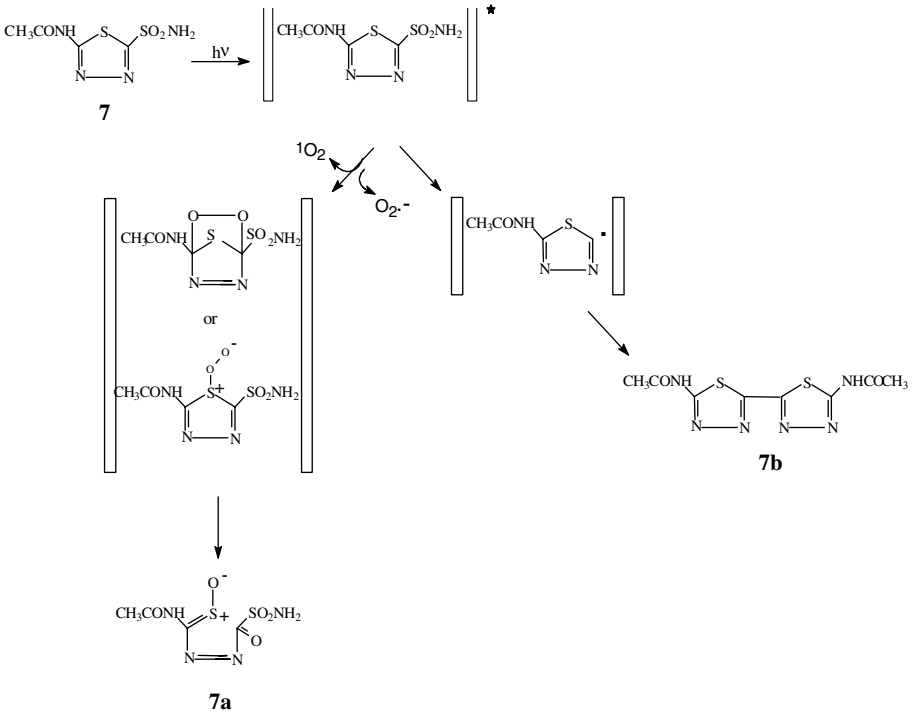

FIGURE 63.4 Mechanism of photodegradation of acetazolamide.

Although the oxygenated product **7b** may also be formed by reactions with molecular oxygen (O_2 or $O_2^{\cdot-}$), this reaction pathway was discarded as a consequence of the results obtained from the addition of singlet oxygen quenchers and superoxide dismutase (SOD) as superoxide scavenger during irradiation. Being aware of the fact that the photodegradation process was also efficient under an oxygen atmosphere and is essential to produce photoproduct **7a** is necessary to understand the mechanism of the oxygen-dependent photobiological effects of **7**.

With the determination of $^1O_2$ and $O_2^{\cdot-}$ in the photolysis of **7** and its participation in the photodegradation of acetazolamide, we can look forward to a better understanding of the role of singlet oxygen generated in photoreactions of this type of drugs in biological systems. Another photochemical process that appears to compete with the latter is the formation of the free-radical intermediate from the cleavage of the sulfonamide group in the thiadiazole ring. This intermediate produces a dimerization to yield compound **7b** and does not require oxygen.

The phototoxic diuretic drug chlorthalidone **8** is photolabile under aerobic conditions and UV-B (290- to 320-nm) light. Irradiation under an oxygen atmosphere of a phosphate-buffered saline solution of **8** produces photoproducts **8a** to **8c** and singlet oxygen (Figure 63.5). Its photolability under UV-B (290- to 320-nm) irradiation was followed by a progressive decrease in its main absorption bands at 220 and 280 nm.[13,14] The isolation of the photoproducts suggests that the photodegradation occurs via the intermediacy of radicals and with oxygen participation.

Glipizide **9** induced phototoxicity in cell cultures when irradiated with broadband UV. The phototoxic antidiabetes drug glipizide, a benzenesulfonamide derivative, is photolabile under aerobic conditions and UV-B (290- to 320-nm) light. The photolysis of **9** was followed by monitoring the disappearance of the 280-nm band and the appearance of a new band at 230 nm. Irradiation of a phosphate-buffered solution of **9** under an oxygen atmosphere produces four photoproducts as well as singlet oxygen. Incubation of this pre-irradiated drug with the cell cultures revealed no phototoxic effects.[15] The photochemistry of **9** involves cleavage of the sulfon–amine and the sulfonamine–R bonds.[11,16,17]

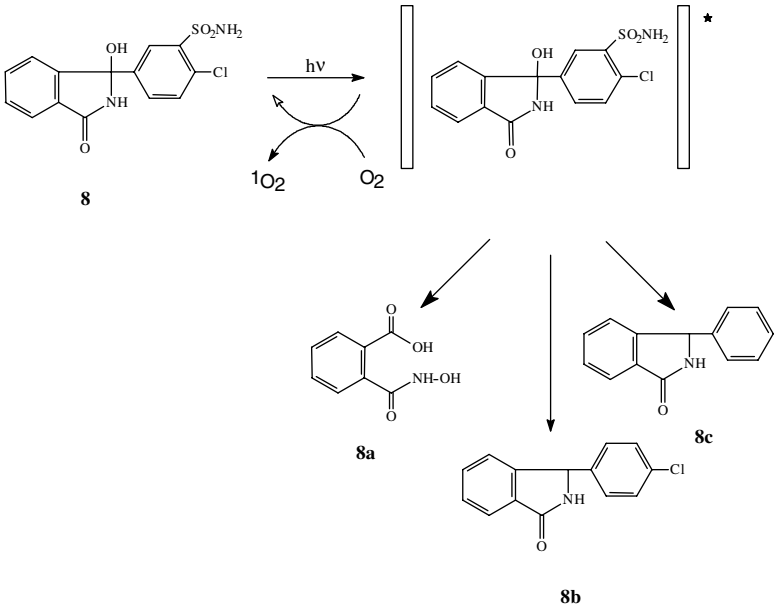

FIGURE 63.5 Mechanism of photodegradation of chlorthalidone.

Triamterene (2,4,7-triamino-6-phenylpteridine, **10**) is a drug commonly used as a potassium-sparing diuretic that inhibits sodium resorption and potassium secretion in the distal tubule in the treatment of antiarrhythmic activity. Cutaneous adverse reactions mediated by light, developing photosensitive non-scarring skin eruptions, and the onset of subacute cutaneous lupus erythematosus after intake of triamterene have been reported.[18] As an isolated clinical case, a diagnosis of photodermatitis from triamterene has been demonstrated.[19] Clinical manifestations in association with hydrochlorothiazide **11** photosensitivity include lichen planus, erythema, and acute eczema, as well as phototoxicity *in vitro*.[20,21] Photodecomposition studies of triamterene **10** in methanol, phosphate-buffered saline solution, and human serum in the presence of oxygen were followed by UV spectrophotometry and high-performance liquid chromatographic (HPLC) analysis using a sensitive HPLC method. Photodegradation was observed only under irradiation with UV-B (290- to 320-nm) light to produce the photoproduct **10a** (Figure 63.6). No photodecomposition was detected under UV-A irradiation, yet singlet oxygen ($^1O_2$) was generated.[22] The UV spectra showed a progressive decrease (under UV-B irradiation) in the main absorption bands at 235 and 375 nm, also a high quantum yield for its fluorescence was measured ($\Phi_{Fl} = 0.54$).

Hydrochlorothiazide, as shown in Figure 63.6, is completely dechlorinated upon irradiation with a medium-pressure mercury arc lamp through a glass filter in deaerated aqueous or alcohol solution with a quantum yield of 0.18.[14]

Amiloride **12**, another potent diuretic drug, shows a similar behavior under irradiation in the UV-A–Vis region, producing dechlorination products, and the photoreaction is pH dependent.[23] Presumably, the strong absorption at 360 nm in the UV-A is responsible for its phototoxic properties (Figure 63.7).[24]

63.3 Reactive Oxygen Species (ROS) Generation and Phototoxicity

Clinical photosensitization has been recognized to result from a number of pharmacological agents. The mechanism of type II reactions involves the photoactivated drug in its triplet excited state photosensitizing molecular oxygen to generate singlet oxygen that causes oxidation or peroxidation of membrane lipids, or strand breaks. Oxidation of purine or pyrimidine bases has been discussed.

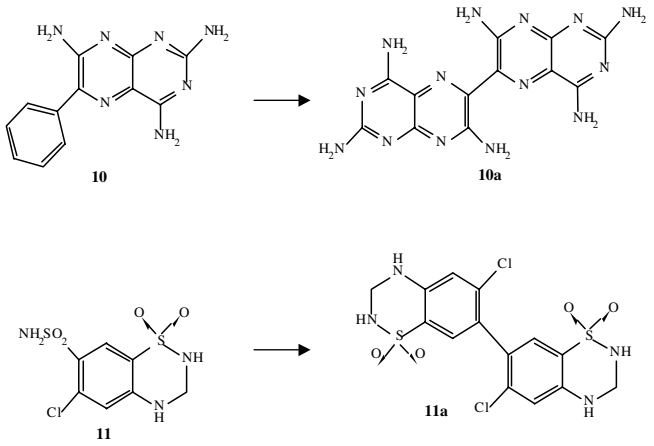

FIGURE 63.6 Photodegradation of triamterene (**10**) and hydrochlorothiazide (**11**).

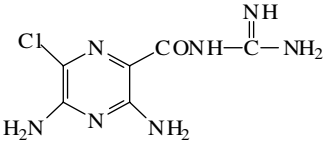

FIGURE 63.7 Structure of amiloride (**12**).

In the case of reactions when oxygen is present, the triplet state of these drugs (photosensitizer) sensitizes molecular oxygen, producing $^1O_2$, which then reacts with the biological substrate. This has been verified by trapping tests with 2,5-dimethylfuran, furfural, and 1,3-cyclohexadiene-1,4-diethanoate, as well as testing for the oxidation of histidine.[13,22,25]

Lipid peroxidative potency of thiazide diuretics has been demonstrated using squalene as the substrate, and participation of $^1O_2$ in the lipid peroxidation is possible.[26] Irradiation by UV-A of squalene in the presence of penflutizide **1**, hydrochlorothiazide **2**, methylchlorothiazide **3**, benzylhydrochlorothiazide **4**, or trichloromethiazide **5** induced *in vitro* peroxidation, as measured by production of the hydroperoxides and thiobarbituric acid-reactive substances. An especially high intensity has been observed in the penflutizide-sensitized photohemolysis with the production of ever-increasing amounts of hydroperoxides in lipids of red blood cell membranes. This fact strongly supports the idea that lipids are one of the subcellular targets of the phototoxicity.

We have extensively examined the family of diuretic-related drugs such as furosemide, acetazolamide, triamterene, and chlorthalidonem, which can induce phototoxicity through the generation of singlet oxygen. This family of diuretic drugs is capable of producing singlet oxygen through photosensitization via a type II mechanism. This process was detected by trapping the oxygen with 2,5-dimethylfuran during photolysis of these drugs in oxygenated media. The formation of $^1O_2$ was also confirmed by trapping with furfuryl alcohol (determined by HPLC) and by the histidine test. An alternative method for measuring the amount of singlet oxygen photogenerated in aqueous solution was necessary because of ambiguity about the specificity of the simple traps, such as 2,5-dimethylfuran, furfuryl alcohol, and histidine. This method is the specific chemical trapping of $^1O_2$ with 1,3-cyclohexadiene-1,4-diethanoate. The measurements with this compound were determined in water using the phosphorescence method; quantum yields with values of 0.047 and 0.078 were determined for singlet oxygen formation by furosemide photosensitization in acetonitrile and benzene, respectively. This method is much more reliable than the indirect trapping methods with, for example, diphenylisobenzofuran. [27]

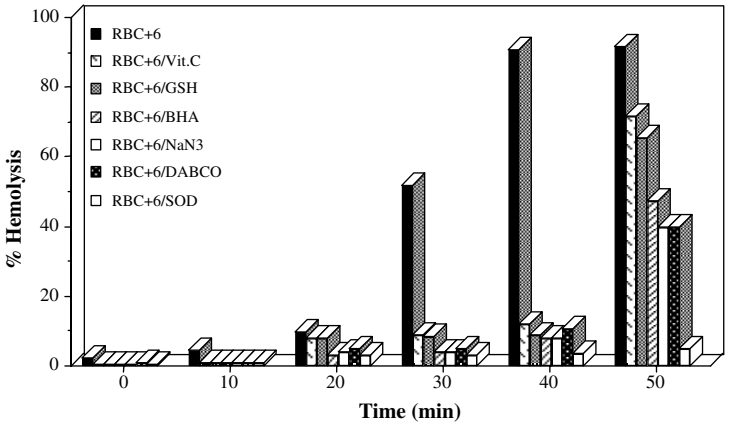

FIGURE 63.8 Photohemolysis of RBC sensitized by Furosemide (**6**) in the absence and presence of radical scavengers and singlet oxygen quenchers.

Sulfonamides and diuretics such as furosemide and chlorthalidone were the first chemotherapeutics reported to exert unwanted side effects.[28–29] Patients sensitized to diuretics after their use run the risk of generalized eruptions. One of the side effects reported in patients taking thiazide diuretics is photosensitivity. Brown and Deng,[30] as well as Darken and McBurney[18] and De Fernandez et al.,[19] have reported patients who developed lupus-like lesions (erythematous scaling papules, patches and plaques on the upper extremities, multiple flesh-colored urticarial plaques on the trunk) during treatment with diuretics and up to one year after beginning the therapy. Phototoxic compounds with different molecular structures can also produce singlet oxygen by energy transfer. The variety and number of phototoxic compounds are large. Furthermore, for most phototoxic xenobiotics, a relationship between structure and photoreactivity *in vivo* cannot be determined.[8,11,21,31–33]

Furosemide was screened *in vitro* at different concentrations for UV-Vis-induced phototoxic effects in a photohemolysis test in the presence and absence of different radical scavengers and singlet oxygen and hydroxyl radical quenchers. Furosemide-photosensitized peroxidation of linoleic acid was monitored by the UV detection of dienic hydroperoxides. The mechanism of phototoxicity for this drug probably involves reactions of singlet oxygen and superoxide ion with cellular components rather than reactions of a free radical intermediate or stable photoproducts (Figure 63.8).

Acetazolamide **7** and chlorthalidone **8** photosensitize the oxidation of either 2,5-dimethylfuran (an efficient trap for $^1O_2$ independently of the pH of the system) or histidine. This result demonstrates that compounds **7** and **8** possess type II photodynamic activity and are themselves susceptible to photosensitized oxidation. This observation is consistent with the fact that the photodegradation of this drug under aerobic conditions is affected by the addition of singlet oxygen and oxygen superoxide quenchers such as vitamin C and sodium azide and also of superoxide dismutase.[12,13] Drugs **7** and **8** were screened *in vitro* at different concentrations for UV-Vis-induced phototoxic effects in a photohemolysis test in the presence and absence of different radical scavengers, singlet oxygen traps, and hydroxyl radical quenchers. Both drugs showed a positive photohemolytic effect on human erythrocytes.

Acetazolamide and chlorthalidone have also been shown to photosensitize the reduction of nitro blue tetrazolium in phosphate-buffered saline solution. The reaction is more efficient under deoxygenated conditions and in the presence of superoxide dismutase. These results indicate that direct electron transfer occurs from either the excited state of **7** or **8** to the substrate, especially oxygen. No doubt, superoxide ion could be involved as an intermediate when oxygen is present. On the basis of these results, a photochemical reaction mechanism of acetazolamide and nitro blue tetrazolium is postulated as shown in Figure 63.9.

Red blood cell lysis, photosensitized by glipizide **9**, and the products of its aerobic photolysis were demonstrated. The photohemolysis rate was lower for **9** than for its photoproducts. Inhibition of this

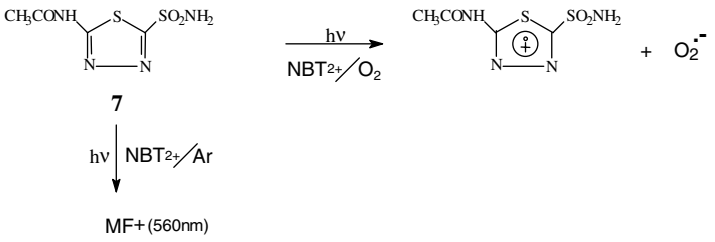

FIGURE 63.9 Photosensitized reduction of nitro blue tetrazolium (NBT) by acetazolamide.

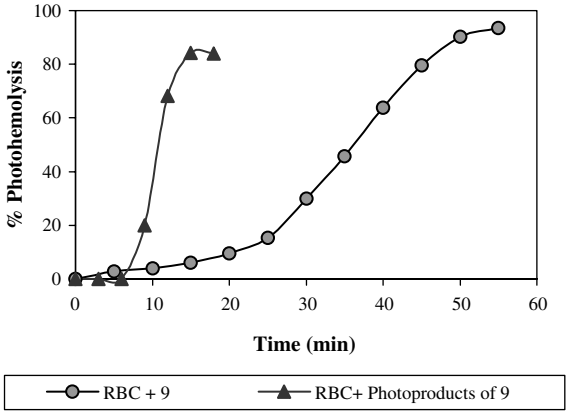

FIGURE 63.10 Photohemolysis of RBC sensitized by glipizide (**9**).

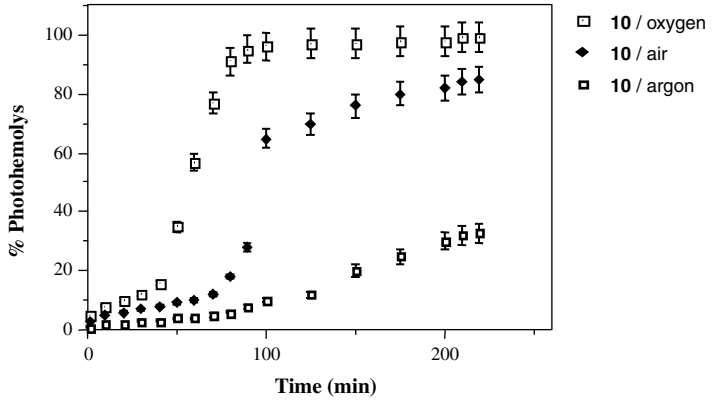

FIGURE 63.11 Photohemolysis of RBC sensitized with **Triamterene** (**10**) in the presence of oxygen, air, and argon ([**Triamterene**] = 50 mg · mL^{-1}; [**RBC**] = 3.3 × 106 cells · mL^{-1}])

process upon addition of 1,4-diazabicyclo[2.2.2]octane, glutathione, vitamin C, sodium azide, superoxide dismutase, and α-tocopherol confirmed the possibility of singlet oxygen, superoxide ion, or free-radical participation. The degree of phototoxicity induced by glipizide could depend on the balance between the generation of singlet oxygen, radical oxygen, and free-radical species and the effectiveness of the defense systems against toxic radicals.[17] Figure 63.10 shows the photohemolysis of red blood cells sensitized with **9** (2.5×10^{-4} *M*) in the presence of oxygen.

The UV-A-excited (320 to 400 nm) triamterene molecule transferred its energy to molecular oxygen, with subsequent formation of $^1O_2$; however, photodegradation was not observed. Triamterene itself shows a photohemolytic effect and photoinduced lipid peroxidation.

In the presence of oxygen, triamterene was able to induce photohemolysis of human erythrocytes. The same process was observed under an inert atmosphere, although at a significantly lower rate. The photoreactivity of triamterene *in vitro* is amply demonstrated by its capability to photosensitize the hemolysis of erythrocytes, lipid peroxidation, and decreasing cell viability of lymphocytes and neutrophils (polymorphonuclear cells).[22] The mechanisms of phototoxicity for this drug most probably involve reactions of a free-radical intermediate and/or of singlet oxygen with cellular components.

To determine the mechanism of triamterene-induced photohemolysis, the above studies were repeated in the presence of singlet oxygen quenchers sodium azide and 1,4-diazabicyclo[2.2.2]octane and the radical scavengers butylated hydroxyanisole and reduced glutathione. The photohemolytic effect was efficiently inhibited by the singlet oxygen quenchers; in contrast, the radical scavengers used produced no significant inhibition of this process.

63.4 Conclusions

The studies of phototoxicity carried out in this work may help explain the damage produced in proteins and organs. Radical-mediated damage to protein may be initiated by electron leakage and photoinduced oxidation of lipids and amino acids. As a consequence, protein oxidation can also be oxygen dependentm and it is often functionally inactive.[34] These observations may contribute to elucidate the observed accumulation and damaging activity of oxidized proteins during aging and in pathologies such as diabetes, atherosclerosis, and neurodegenerative diseases such as Alzheimer's disease.[35] The results obtained may also be very useful from the medical standpoint in elucidation of the biological action of many pharmaceutical products *in vitro* and *in vivo*.

References

1. Magnus, I. A., *Dermatological Photobiology*, Blackwells, London, 1976, 213–216.
2. Moore, D. E., Photosensitization by drugs, *J. Pharm. Sci.*, 66, 1282, 1977.
3. Moore, D. E. and Burt, C. D., Photosensitization by drugs in surfactant solutions, *Photochem. Photobiol.*, 34, 431, 1981.
4. Kochevar, I. E., Mechanism of drug photosensitization, *Photochem. Photobiol.*, 45, 891, 1987.
5. Zanocco, A. L., Günther G. S., Lemp, E. M., de la Fuente, J. R., and Pizarro, N. U., Kinetics and mechanism of the photosensitized oxidation of furosemide, *Photochem. Photobiol.*, 68, 487, 1998.
6. Vargas, F., Martinez, I., Sequera, J., Mendez, H., Rojas, Y., Fraile, G., Velazquez, M., and Medina, R., Photodegradation and phototoxicity studies of furosemide: involvement of singlet oxygen in the photoinduced hemolysis and lipid peroxidation, *J. Photochem. Photobiol.*, 42, 219, 1998.
7. Farrington, D., A simple microbiological method for demonstrating phototoxic compounds, *J. Invest. Dermatol.*, 44, 259, 1965.
8. Selvaag, E., Evaluation of phototoxic properties of oral antidiabetics and diuretics, *Arzneimittels Forsch.*, 47, 1031, 1997.
9. Selvaag, E., Bergner T., and Przybilla, B., Photosensitivity due to thiazides *in vitro* is inhibited by antioxydants and a nitrogen atmosphere, *Proc. of the Fifth Congress of the European Society for Photobiology*, V-12/O3, Marburg, Germany, 1993, 219.
10. Pathak, M. A. and Brunello, C., Drug phototoxicity and the role of type II photoreactions involving reactive oxygen species: abstracts for the 1993 annual meeting of the society for investigative dermatology, *J. Invest. Dermatol.*, 100, 599, 1993.
11. Selvaag, E., Anholt, H., Moan, J., and Thune, P., Inhibiting effects of antioxidants on drug-induced phototoxicity in cell cultures. Investigation with sulphonamide-derived oral antidiabetics and diuretics, *J. Photochem. Photobiol. B: Biol.*, 38, 88, 1997.
12. Vargas, F., Méndez, H., and Rojas, J., Photolysis and photosensitized degradation of the diuretic drug acetazolamide, *J. Photochem. Photobiol. A: Chem.*, 118, 19, 1998.

13. Vargas, F. and Méndez, H., Study of the photochemical and *in vitro* phototoxicity of chlorthalidone, *Die Pharmazie*, 54, 920, 1999.
14. Moore, D. E., Photochemistry of diuretic drugs in solution, in *Drugs: Photochemistry and Photostability*, Albini, A. and Fasani, E., Eds., The Royal Society of Chemistry, London, 1998, 100–115.
15. Selvaag, E. and Thune, P., Photodegradation products of sulphonamide-derived oral antidiabetics and diuretics are not phototoxic *in vitro*, *Photodermatol. Photoimmunol. Photomed.*, 12, 79, 1996.
16. Brown, C. W. and Deng, J. S., Thiazide diuretics induce cutaneous lupus-like adverse reaction, *J. Toxicol. Clin. Toxicol.*, 33, 729, 1995.
17. Vargas, F., Méndez, H., Tropper, E., Velásquez, M., and Fraile, G., Studies on the *in vitro* phototoxicity of the antidiabetics drug glipizide, *In Vitro Molec. Toxicol.*, 13, 17, 2000.
18. Darken, M. and McBurney, E., Subacute cutaneous lupus erythematosus-like drug eruption due to combination diuretic hydrochloro-thiazide and triamterene, *J. Am. Acad. Dermatol.*, 18, 38, 1988.
19. De Fernández, C. L., Bernaola, G., Fernández, E., Leanizbarrutia, I., and Muñoz, D., Photodermatitis from triamterene, *Contact Dermatitis*, 17, 114, 1987.
20. Moore D. E. and Mallesch J. L., Photochemical interaction between triamterene and hydrochlorothiazide, *Int.J. Pharm.*, 76, 187, 1991.
21. Vargas, F. and Fuentes, A., Evidence of formation and participation of singlet oxygen in the *in vitro* phototoxicity of the combined diuretic triamterene and hydrochlorothiazide, *Die Pharmazie*, 52, 328, 1997.
22. Vargas, F., Fuentes, A., Sequera, J., Méndez, H., Fraile, G., Velásquez, M., and Medina, R., *In vitro* approach to investigate the phototoxicity of the diuretic drug triamterene., *Toxicol. In Vitro*, 12, 661, 1998.
23. Hamoudi, H. I., Heelis P. F., Jones, R. A., Navaratnam, S., Parsons, B. J., Phillips, G. O., Vandenburg, M. J., and Currie, W. J., A laser flash photolysis and pulse radiolysis study of amiloride in aqueous and alcoholic solution, *Photochem. Photobiol.*, 40, 35, 1984.
24. Mirossay, L., Mirossay, A., Kocisova, E., Radvakova, I., Miskovsky, P., and Mojzis, J., Hypericin-induced phototoxicity of human leukemic cell line HL-60 is potentiated by omeprazole, an inhibitor of H^+K^+–ATPase, and 5′-(*N*,*N*-dimethyl)-amiloride, an inhibitor of Na^+/H^+ exchanger, *Physiol. Res.*, 48, 135, 1999.
25. Vargas, F., Méndez, H., Sequera, J., Rojas, J., Fraile, G., and Velásques, M., Phototoxicity induced by $^1O_2$ generation during the photodegradation of some diuretic drugs, *Toxic Substance Mechanism J.*, 18, 53, 1999.
26. Matsuo, I., Fujita, H., Hayakawa, K., and Ohkido, M., Lipid peroxidative potency of photosensitized thiazide diuretics, *J. Invest. Dermatol.*, 87, 637, 1986.
27. Scaiano, J. C., Redmond, R. W., Mehta, B., and Arnanson, J. T., Efficiency of the photoprocesses leading to singlet oxygen generation by α-terthienyl: optical absorption, optoacoustic calorimetry and infrared luminescence studies, *Photochem. Photobiol.*, 52, 655, 1990.
28. Harber, L. C. and Bickers, D. R., *Photosensitivity Disease*, Deckers, B. C., Ed., W.B. Saunders and Co., Philadelphia, PA, 1981.
29. Albini, A. and Fasani, E., *Drugs: Photochemistry and Photostability*, Albini, A. and Fasani, E., Eds., The Royal Society of Chemistry, London, 1998.
30. Brown, C. W. and Deng, J. S., Thiazide diuretics induce cutaneous lupus-like adverse reaction, *J. Toxicol. Clin. Toxicol.*, 33, 729, 1995.
31. Epstein, J. H. and Wintroub, B. U., Photosensitization due to drugs, *Drugs*, 30, 42, 1985.
32. Beijersbergen van Henegouwen, G. M. J., (Systemic) phototoxicity of drugs and other xenobiotics, *J. Photochem. Photobiol. B: Biol.*, 10, 183, 1991.
33. Costanzo, L. L., De Guidi, G., Condorelli, G., Cambria, A., and Fama, M., Molecular mechanism of naproxen photosensitization in red blood cells, *J. Photochem. Photobiol. B: Biol.*, 3, 223, 1989.
34. Dean, R. T., Fu, S., Stoker, R., and Davies, J. D., Biochemistry and pathology of radical-mediated protein oxidation, *Biochem. J.*, 324, 1, 1997.
35. Cohen, G., Oxidative stress in the nervous system, in *Oxidative Stress*, Sies, H., Ed., Academic Press, London, 1985, 383.

64

Photodecarboxylation of Acids and Lactones: Antiinflammatory Drugs

Francisco Boscá
Universidad Politécnica de Valencia

María Luisa Marín
Universidad Politécnica de Valencia

Miguel Angel Miranda
Universidad Politécnica de Valencia

64.1 Mechanisms and Applications of the Photodecarboxylation of Carboxylic Acid and Lactones

The decarboxylation of carboxylic acids is a photochemical process of significance in several areas of study; thus, photodecarboxylation reactions are used in synthetic chemistry to generate radical intermediates or in agriculture to produce pesticides. In the case of pharmaceuticals, this process is responsible for a decreased stability of some compounds and seems to be directly or indirectly involved in adverse photosensitizing side effects.

In the presence of light, organic compounds containing a carboxylic group can extrude carbon dioxide. This process can occur either from the free acid or from the dissociated carboxylate form. In general, photodecarboxylation of non-dissociated acids involves direct homolytic cleavage of the C–C bond α to the carboxyl group. By contrast, in the carboxylates formal heterolytic and/or homolytic mechanisms can participate. Photoionization or photoinduced electron transfer (PET) reactions can also be involved (see Scheme 1).[1,2]

Most of the studies on photodecarboxylation of simple aliphatic carboxylic acids and lactones (such as formic, acetic, or pyruvic acids; β-propiolactone; or δ-valerolactone) were summarized by Calvert and Pitts in 1966,[3] and different aspects of the photodecarboxylation of organic compounds were analyzed in the 1970s;[4,5] however, a full review of photodecarboxylation reactions did not appear until 1992.[1] A chapter in the first edition of this *Handbook of Organic Photochemistry and Photobiology* summarized the literature existing up to 1992 on the loss of carbon dioxide from photoexcited aliphatic and aromatic acids and lactones.[2] For this reason, although some earlier work will be cited here, the literature coverage will in general be limited to the work published during the last decade.

0-8493-1348-1/04/$0.00+$1.50

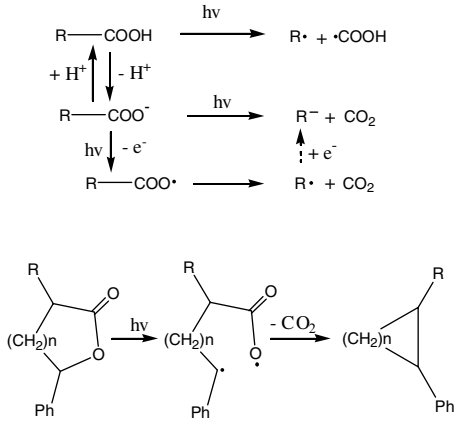

SCHEME 1

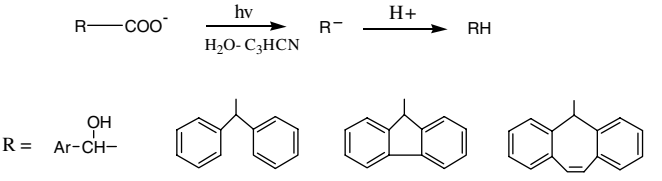

SCHEME 2

The photodecarboxylation mechanism of simple arylacetic acids is not completely understood due to the relatively low quantum yields of reaction ($\Phi < 0.06$). The formation of benzylic radicals (which show a transient absorption spectrum, with λ_{max} ~315 nm) has been taken as evidence for the homolytic cleavage of the undissociated acid. By contrast, photolysis of carboxylate forms gives rise to carbanion intermediates (λ_{max} ~350 nm) via heterolytic cleavage (Scheme 1). However, the possibility of initial electron photoejection and subsequent homolytic decarboxylation (eventually followed by recombination of the electron with the benzyl radical) cannot be ruled out, as the hydrated electron has been observed as a transient species.[6,7]

Within the cavities of cation-exchanged Y faujasites (where the carboxylate ion is the predominating species), benzyl radicals are formed and generation of benzyl anions is highly dependent on the hydration state of the zeolite.[8] Other studies in basic faujasites have shown some diastereoselectivity in the formation of 2,3-diphenylbutanes by photodecarboxylation of 2-phenylpropionic acid.[9,10]

Photodecarboxylation of the dissociated form of α-hydroxy-substituted arylacetic acids and related substrates occurs from the singlet excited state (S_1) and leads to the corresponding benzyl alcohols with high quantum yields (Φ = 0.2 to 0.7) via a heterolytic mechanism (Scheme 2).[1] Photodecarboxylation of some diarylacetic acids (Scheme 2) also proceeds from S_1 via heterolytic mechanism. It is remarkable that these compounds show dramatic differences in their relative photodecarboxylation efficiency (Φ = 0.04 to 0.6). The reaction is enhanced when a cyclic delocalized carbanion with $4n$ electrons is formed.[1] By contrast, photodecarboxylation of *m*- and *p*-nitrophenylacetic acids in aqueous solutions occurs via a heterolytic mechanism from T_1.[11] The photodecarboxylation of pyruvic and benzoylformic acids takes place with high quantum yields ($\Phi > 0.6$) in aqueous solutions, to give acetaldehyde and benzaldehyde, respectively as the primary photoproducts.[1,12,13] On the other hand, 2-, 3-, and 4-pyridinylacetic acids undergo photodecarboxylation in aqueous solutions via a heterolytic mechanism from their zwitterionic forms.[14]

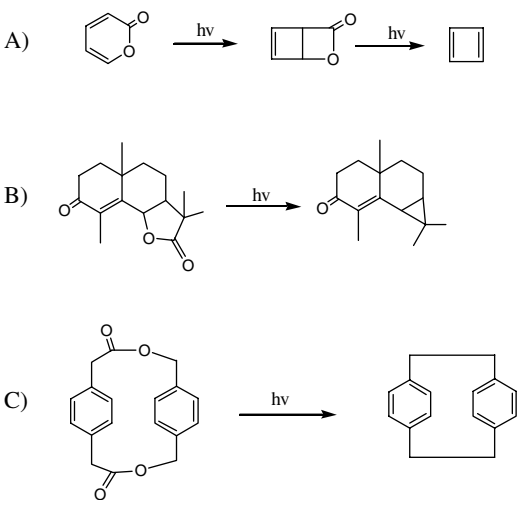

SCHEME 3

The photodecarboxylation of lactones usually involves homolysis of the OC bond β to the carbonyl group, to generate a biradical after loss of CO_2 (see Scheme 1).[1,2] This process has been used to make strained ring systems (such as cyclopropanes, cyclobutenes, and cyclophanes) via intramolecular CC coupling of the biradicals formed. Some applications of this reaction are shown in Scheme 3. Thus, upon irradiation of α-pyrone, cyclobutadiene is formed by a two-step decarboxylative process (Scheme 3A).[15] Likewise, the natural product aubergenone has been synthesized from α-santonin using the photodecarboxylation of a γ-lactone to a cyclopropane as the key step (Scheme 3B).[16] Photolysis of lactones has also been used for the preparation of cyclophanes (Scheme 3C).[17,18]

In general, photodecarboxylation of lactones arises upon cleavage of an ester bond from an excited chromophore.[1,2] However, when a naphthalene is the main light-absorbing moiety, the decarboxylation requires absorption of two photons (one to produce the T_1 triplet excited state and another one to promote the T_1 to a higher energy triplet state).[19]

64.2 Photodecarboxylation of the Antiinflammatory 2-Arylpropionic Acids and Analogous Compounds

During the last decade, a large number of photochemical studies have appeared regarding the photoreactivity of non-steroidal antiinflammatory 2-arylpropionic acids. These studies have been aimed at establishing the molecular bases of their phototoxic properties[20–39] and have contributed significantly to insight into the general photodecarboxylation mechanisms of arylalkanoic acids, which are classified into two different groups, depending on the ability of the aryl ring to act as an electron-acceptor moiety (ketoprofen, suprofen, tiaprofenic acid, tolmetin, and benoxaprofen) or as an electron-donor moiety (naproxen, carprofen) (Figure 64.1).

The most important common features in the photodecarboxylation of ketoprofen, suprofen, tiaprofenic acid, tolmetin, and benoxaprofen in neutral aqueous solutions are the following: (1) All of them produce carbanion intermediates, which upon protonation give rise to the decarboxylated photoproducts (Scheme 4), and (2) the photodecarboxylation quantum yields are much higher from the carboxylate forms than from the non-dissociated acids.[20–35] However, there are also some differences. Thus, while photodecarboxylation of benoxaprofen is produced from its singlet excited state, in the case of the benzophenone derivatives (ketoprofen, suprofen, tiaprofenic acid, tolmetin), the process seems to take place from the triplet excited states.[20,21,35] Clear evidence for the participation of these states has been provided by laser flash photolysis studies.[21,35] Thus, picosecond laser excitation of ketoprofen in aqueous

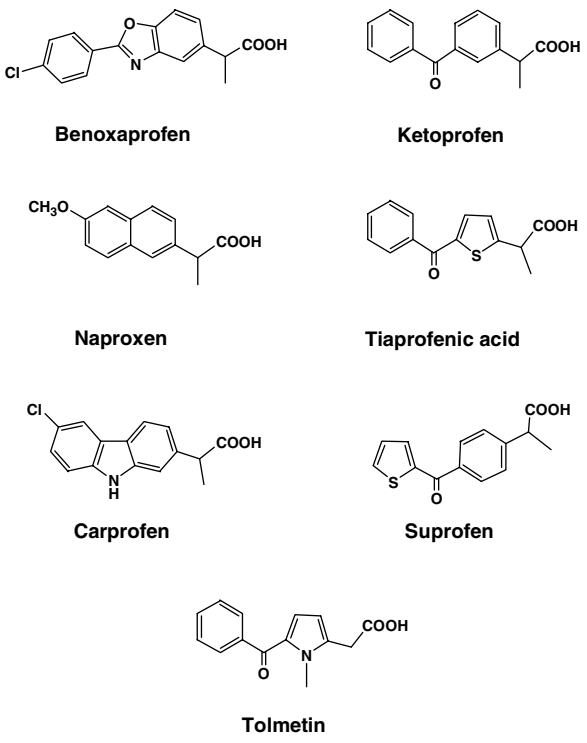

FIGURE 64.1

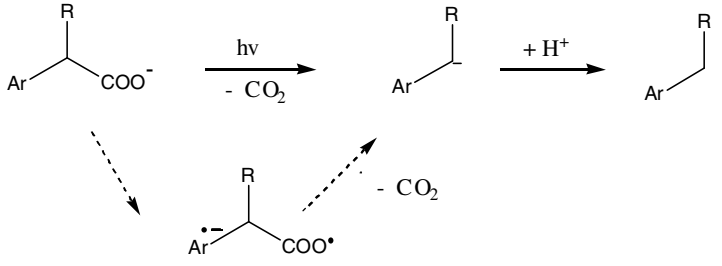

SCHEME 4 Photodecarboxylation process for benoxaprofen, ketoprofen, tiaprofen acid, suprofen and tolmetin.

solutions gives rise to its triplet excited state (λ_{max} ~525 nm, with a lifetime of ~250 ps) and subsequently to the decarboxylated ground-state carbanion (lifetime of 200 ns, λ_{max} at 330 and 600 nm). Photolysis of the carboxylate form of ketoprofen in methanol also generates the carbanion; however, a typical benzophenone-type photochemistry (ketone photoreduction) rather than decarboxylation is observed for the non-dissociated acid.[21] Nanosecond laser excitation of tolmetin in aqueous solution does not allow observation of the initial triplet excited state; instead, the triplet decarboxylated carbanion (lifetime of 6.6 μs, λ_{max} of 640 nm) that results is detected.[35] Laser flash photolysis of aqueous solution of suprofen and tiaprofenic acid in the nanosecond time scale leads to observation of the triplet excited states (transient absorption spectra with two bands at λ_{max} ~360 and 600 nm, lifetimes of 1.2 and 0.8 μs, respectively).[30,34] The decarboxylated carbanions of these drugs are also observed (λ_{max} of 380 and 600 nm for the triplet excited-state carbanions, and 380 nm for ground-state carbanions). Suprofen and tiaprofenic acid undergo photodecarboxylation less efficiently than the other benzophenone derivatives due to the activation energy of 10 kcal mol^{-1} associated with promotion of these drugs from T_1 (π,π^*) to the "reactive" T_2 (n,π^*).[30,31,34] In the cases of tolmetin and ketoprofen (typical T_1 [n,π^*]), the process

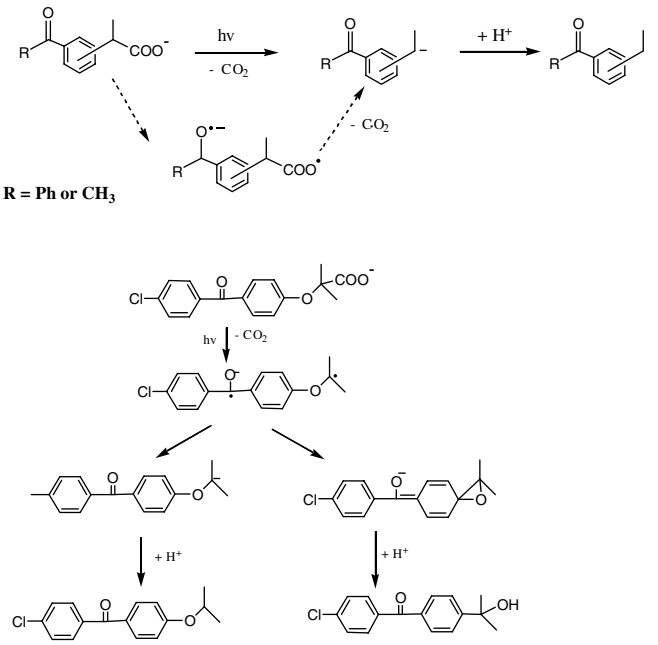

SCHEME 5

is not activated.[25,27,35] Photolysis of several other aroyl-substituted phenylacetic acids in aqueous solutions has also been reported to produce the typical photodecarboxylated compounds (see Scheme 5).[40] All the above results suggest that photodecarboxylation can be initiated by electron transfer from the carboxylate to the electron-deficient ring system. Very clear evidence for the involvement of such electron transfer reaction has been found in the photolysis of fenofibric acid in aqueous solution, where two compounds are formed by photodecarboxylation through the intermediacy of a common biradical anion generated by intramolecular electron transfer (see Scheme 5).[41,42]

On the other hand, 2-arylpropionic acids with electron-rich aryl rings, such as naproxen, its demethyl analog 6-methoxy-2-naphthylacetic, carprofen, or its dechlorinated photoproduct, have a very low photodecarboxylation efficiency, both from the free acids and the carboxylate forms.[21,36–39] In the case of the naphthalene derivatives, decarboxylation is enhanced in the presence of oxygen and appears to proceed by photoionization of their singlet excited states (Scheme 6).

In this context, laser flash photolysis studies have provided clear evidence for the generation of naphthalene radical cations (λ_{max} of 380 and 600 nm). Addition of increasing amounts of CCl_4 in the photolysis of 6-methoxy-2-naphthylacetic acid results in fluorescence quenching, together with enhanced generation of the radical cation and a higher efficiency of the photodecarboxylation process.[39]

64.3 Photosensitized Decarboxylation

Photodecarboxylation of organic carboxylic acids in solution can be achieved via photoinduced electron transfer using electron acceptors such as aza aromatic compounds, dyes, or polycyanoaromatics as photosensitizers.[1,2,43–50] This methodology induces photodecarboxylation through generation of radical intermediates which can be useful in organic synthesis.[1,2]

Recent advances in laser spectroscopy (femtosecond time scale) have made it possible to determine the rate constants for decarboxylation (k_{dc}) and back-electron transfer (k_{bet}) in the photolysis of electron donor/acceptor salts such as methylviologen/benzilates ($MV^{2+}/Ar_2C(OH)CO_2^-$) and methylviologen/arylacetates ($MV^{2+}/ArCH_2CO_2^-$) (Scheme 7). The k_{dc} values are much higher for the benzilates ($2–8 \times 10^{11}$ s^{-1}) than for the arylacetates ($1–2 \times 10^9$ s^{-1}).[44,45] Decarboxylation of these donors is thus almost a barrier-free

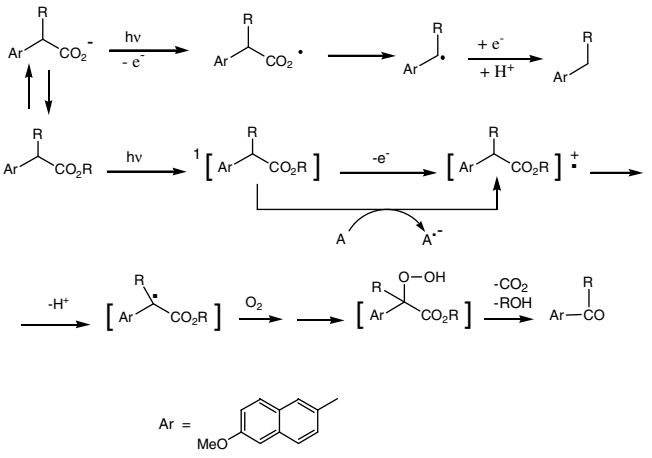

R = CH_3, H and A = CCl_4, O_2 or other electron acceptors

SCHEME 6

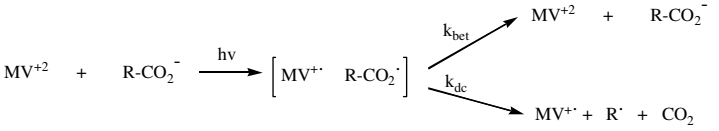

R	$k_{bet}(s^{-1})$	$k_{dc}(s^{-1})$
$Ar_2C(OH)$-	2-8 x 10^{11}	2-8 x 10^{11}
$ArCH_2$-	0.1-2 x 10^{11}	1-2 x 10^9

SCHEME 7

unimolecular reaction; its real time monitoring allows direct observation of the transition state for CC bond scission.

In general, the PET decarboxylation of carboxylic acids exhibits low product selectivity, due to the subsequent radical coupling in solution; however, the PET reaction between potassium propionate and the methyl ester of *N*-methyltrimellitic acid imide is highly regioselective to the *para*-addition product. This contrasts with other intramolecular and intermolecular PET reactions of quinolinic acid imides, which do not show a high degree of regioselectivity (Scheme 8).[46]

A possible way to induce selectivity in the photodecarboxylation process could be through photosensitized reactions in the solid state. In fact, when a two-component molecular crystal of phenanthridine and 3-indoleacetic acid is irradiated at low temperature (–70°C), 3-methylindole is formed in high yield as the sole product; by contrast, when the same reaction is carried out in acetonitrile solution, four products are obtained.[47] Furthermore, irradiation of two-component molecular crystals of arylalkyl carboxylic acids with stoichiometric amounts of electron acceptor causes decarboxylative condensation between the two components with important selectivities.[48–51] Thus, irradiation of (*S*)-naproxen in a chiral crystal with 1,2,4,5-tetracyanobenzene produces a decarboxylated condensation product retaining the initial chirality.[48] Photolysis of an enantiomorphous bimolecular crystal of acridine with the R or S enantiomer of 2-phenylpropionic acid causes stereoselective condensation to give three optically active products.[49] An absolute asymmetric synthesis has also been achieved by the enantioselective decarboxylative condensation of a chiral molecular crystal formed from achiral diphenylacetic acid and acridine (Scheme 9).[50]

PET of Quinolinic acid imides

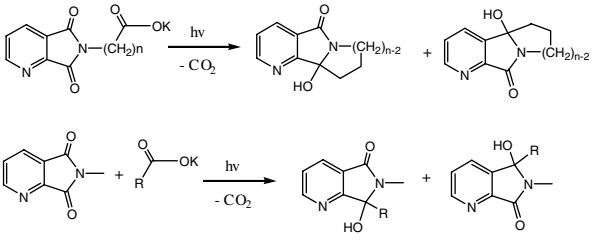

PET of *N*-methyltrimellitic acid imide

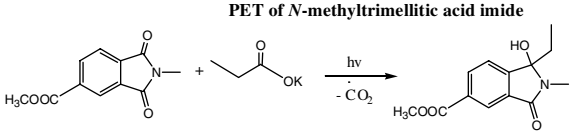

SCHEME 8

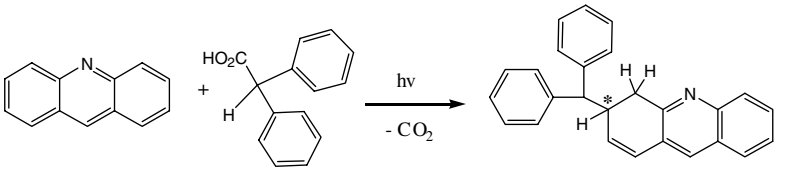

SCHEME 9

64.4 Summarizing Remarks

During the last decade, the major contributions to the field of photodecarboxylations have been associated with two areas: (1) the mechanistic studies to gain insight into the molecular basis of the photosensitizing side effects of non-steroidal antiinflammatory drugs, and (2) the application of electron transfer photosensitizers to achieve selective photodecarboxylation. The extensive use of time-resolved techniques (mainly laser flash photolysis), both in homogeneous solutions and in heterogeneous organized systems, has allowed us to establish the nature of the involved excited states and transient intermediates (benzylic radicals vs. anions) in the different media. Moreover, the possibility of obtaining high product yields and selectivities (including stereoselectivities) by the adequate selection of reaction conditions and photosensitizers opens the door for using photodecarboxylation as a reasonable alternative in organic synthesis.

References

1. Budac, D. and Wan, P., Photodecarboxylation: mechanism and synthetic utility, *J. Photochem. Photobiol. A: Chem.*, 67, 135, 1992.
2. Wan, P. and Budac, D., Photodecarboxylation of acids and lactones, in *CRC Handbook of Organic Photochemistry and Photobiology*, Horspool, W. M., and Song, P.-S., Eds., CRC Press, Boca Raton, 1995.
3. Calvert, J. G. and Pitts, Jr., J. N., *Photochemistry*, Wiley, New York, 1966.
4. Coyle, J. D., Photochemistry of carboxylic acid derivatives, *Chem. Rev.*, 78, 97, 1978.
5. Fox, M. A., The photoexcited states of organic anions, *Chem. Rev.*, 79, 253, 1979.

6. . Epling, G. A. and Lopes, A., Fragmentation pathways in the photolysis of phenylacetic acid, *J. Am. Chem. Soc.*, 99, 2700, 1977.
7. Meiggs, T. O., Grossweiner, L. I., and Miller, S. I., Extinction coefficient and recombination rate of benzyl radicals. I. Photolysis of sodium phenylacetate, *J. Am. Chem. Soc.*, 94, 7981, 1972.
8. Cozens, F. L., Ortiz, W., and Schepp, N. P., Direct observation of the benzyl radical and the benzyl anion within cation-exchanged zeolites: a nanosecond laser study, *J. Am. Chem. Soc.*, 120, 13543, 1998.
9. Lalitha, A., Pitchumani, K., and Srinivasan, C., Induced diastereoselectivity in photodecarboxylation of 2-phenylpropionic acid in faujasite zeolites, *Tetrahedron*, 57, 4455, 2001.
10. Jimenez, M. C., Miranda, M. A., and Tormos, R., Photodecarboxylation of 2-phenylpropionic acid in solution and included within β-cyclodextrin, *Tetrahedron*, 51, 2953, 1995.
11. Craig, B. B., Weiss, R. G., and Atherton, S. J., Picosecond and nanosecond laser photolyses of *p*-nitrophenyl acetate in aqueous media: a photoadiabatic decarboxylation process?, *J. Phys. Chem.*, 91, 5906, 1987.
12. Leermakers, P. A. and Vesley, G. F., The photochemistry of α-keto acids and α-keto esters. I. Photolysis of pyruvic acid and benzoylformic acid, *J. Am. Chem. Soc.*, 85, 3776, 1963.
13. Hall, G. E., Muckerman, J. T., Preses, J. M., Weston, Jr., R. E., and Flynn, G. W., Time-resolved FTIR studies of the photodissociation of pyruvic acid at 193 nm, *Chem. Phys. Lett.*, 193, 77, 1992.
14. Stermitz, F. R. and Huang, W. H., Photochemistry of *N*-heterocycles. VII. Thermal and photodecarboxylation of 2-, 3- and 4-pyridylacetic acid, *J. Am. Chem. Soc.*, 93, 3427, 1971.
15. Cram, D. J., Tanner, M. E., and Thomas, R., A cyclobutadiene that is stable at room temperature, *Angew. Chem., Int. Ed. Engl.*, 30, 1024, 1991.
16. Murai, A., Abiko, A., Ono, M., and Masamune, T., Studies on the phytoalexins. XXXI. Synthetic studies of rishitin and related compounds. XI. Synthesis of aubergenone, a sesquiterpenoid phytoalexin from diseased eggplants, *Bull. Chem. Soc. Jpn.*, 55, 1191, 1982.
17. Hibert, M. and Solladie, G., Substituent effect during the synthesis of substituted [2.2]-paracyclophane by photoextrusion of carbon dioxide from a cyclic diester, *J. Org. Chem.*, 45, 4496, 1980.
18. Kaplan, M. L. and Truesdale, E. A., [2.2]Paracyclophane by photoextrusion of carbon dioxide from a cyclic diester, *Tetrahedron Lett.*, 3665, 1976.
19. Xu, M. and Wan, P., Efficient photodecarboxylation of aroyl-substituted phenylacetic acids in aqueous solution: a general photochemical reaction, *J. Chem. Soc., Chem. Commun.*, 2147, 2000.
20. Bosca, F. and Miranda, M. A., Photosensitizing drugs containing the benzophenone chromophore, *J. Photochem. Photobiol. B: Biol.*, 43, 1, 1998.
21. F. Boscá, Marin, M. L., and Miranda, M. A., Photoreactivity of the nonsteroidal anti-inflammatory 2-arylpropionic acids with photosensitizing side effects, *Photochem. Photobiol.*, 74, 637, 2001.
22. Navaratnam, S., Parsons, B. J., and Hughes, J. L., Laser-flash photolysis studies of benoxaprofen and its analogues 1. Yields of triplet states and singlet oxygen in acetonitrile solutions, *J. Photochem. Photobiol. A: Chem.*, 73, 97, 1993.
23. De la Peña, D., Marti, C., Nonell, S., Martinez L. A., and Miranda M. A., Time-resolved near infrared studies on singlet oxygen production by the photosensitizing 2-arylpropionic acids, *Photochem. Photobiol.*, 65, 828, 1998.
24. Lhiaubet, V., Gutierrez, F., Penaud-Berruyer, F., Amouyal, E., Daudey, J. P., Poteau, R., Chouini-Lalanne, N., and Paillous, N., Spectroscopic and theoretical studies of the excited states of fenofibric acid and ketoprofen in relation with their photosensitizing properties, *New J. Chem.*, 24, 403, 2000.
25. Monti S., Sortino, S., De Guidi, G., and Marconi, G., Photochemistry of 2-(3-benzoylphenyl)propionic acid (ketoprofen). Part I. A picosecond and nanosecond time resolved study in aqueous solution, *J. Chem. Soc., Faraday Trans.*, 93, 2269, 1997.
26. Borsarelli, C. D., Braslavsky, S., Sortino, S., Marconi, G., and Monti, S., Photodecarboxylation of ketoprofen in aqueous solutions: a time-resolved laser-induced optoacoustic study, *Photochem. Photobiol.*, 72, 163, 2000.

27. Martinez, L. J. and Scaiano, J. C., Transient intermediates in the laser flash photolysis of ketoprofen in aqueous solution: unusual photochemistry for the benzophenone chromophore, *J. Am. Chem. Soc.*, 119, 11066, 1997.
28. Cosa, G., Martinez, L. J., and Scaiano J. C., Influence of solvent polarity and base concentration on the photochemistry of ketoprofen-independent singlet and triplet pathways, *Phys. Chem. Chem. Phys.*, 1, 3533, 1999.
29. Bosca, F., Miranda, M. A., Carganico, G., and Mauleon, D., Photochemical and photobiological properties of ketoprofen associated with the benzophenone chromophore, *Photochem. Photobiol.*, 60, 96, 1994.
30. Encinas, S., Miranda, M. A., Marconi, G., and Monti, S., Triplet photoreactivity of the diaryl ketone tiaprofenic acid and its decarboxylated photoproduct: photobiological implications, *Photochem. Photobiol.*, 67, 420, 1998.
31. Encinas, S., Miranda, M. A., Marconi, G., and Monti, S., Transient species in the photochemistry of tiaprofenic acid and its decarboxylated photoproduct, *Photochem. Photobiol.*, 68, 633, 1998.
32. Miranda, M. A., Castell, J. V., Hernandez, D., Gomez-Lechon, M. J., Bosca, F., Morera I. M., and Sarabia, Z., Drug-photosensitized protein modification: identification of the reactive sites and elucidation of the reaction mechanism with tiaprofenic acid/albumin as a model, *Chem. Res. Toxicol.*, 11, 172, 1998.
33. Miranda, M. A., Lahoz, A., Martinez-Manez, R., Bosca, F., Castell, J. V., and Perez-Prieto, J., Enantioselective discrimination in the intramolecular quenching of an excited aromatic ketone by a ground-state phenol, *J. Am. Chem. Soc.*, 121, 11569, 1999.
34. Sortino, S., De Guidi, G., Marconi, G., and Monti, S., Triplet photochemistry of suprofen in aqueous environment and in the β-cyclodextrin inclusion complex, *Photochem. Photobiol.*, 67, 603, 1998.
35. Sortino, S. and Scaiano, J. C., Laser flash photolysis of tolmetin: a photoadiabatic decarboxylation with a triplet carbanion as the key intermediate in the photodecomposition, *Photochem. Photobiol.*, 69, 167, 1999.
36. Martinez, L. J. and Scaiano, J. C., Characterization of the transient intermediates generated from the photoexcitation of nabumetone: a comparison with naproxen, *Photochem. Photobiol.*, 68, 646, 1998.
37. Bosca, F., Encinas, S., Heelis, P., and Miranda, M. A., Photophysical and photochemical characterization of a photosensitizing drug: a combined steady state photolysis and laser flash photolysis study on carprofen, *Chem. Res. Toxicol.*, 10, 820, 1997.
38. Encinas, S., Bosca, F., and Miranda, M. A., Phototoxicity associated with diclofenac: a photophysical, photochemical and photobiological study on the drug and its photoproducts, *Chem. Res. Toxicol.*, 11, 946, 1998.
39. Bosca, F., Canudas, N., Marin, M. L., and Miranda, M. A., A photophysical and photochemical study on 6-methoxy-2-naphthylacetic acid, the major metabolite of the phototoxic nonsteroidal anti-inflammatory drug nabumetone, *Photochem. Photobiol.*, 71, 173, 2000.
40. Xu, M. and Wan, P., Efficient photodecarboxylation of aroyl-substituted phenylacetic acids in aqueous solution: a general photochemical reaction, *J. Chem. Soc., Chem. Commun.*, 2147, 2000.
41. Miranda, M. A., Boscá, F., Vargas, F., and Canudas., N., Unusual [1,2] Wittig rearrangement of a carbanion generated in neutral aqueous medium by photodecarboxylation of a phenoxyacetic acid analogue, *J. Photochem. Photobiol. A: Chem.*, 78, 149, 1994.
42. Cosa, G., Purohit, S., Scaiano, J. C., Bosca, F., and Miranda, M. A., A laser flash photolysis study of fenofibric acid in aqueous buffered media: unexpected triplet state inversion in a derivative of 4-alkoxybenzophenone, *Photochem. Photobiol.*, 75, 193, 2002.
43. Habibi, M. H. and Farhadi., S., Photodecarboxylation of arylacetic acids induced by light-sensitive Hg_2F_2, *Tetrahedron Lett.* 40, 2821, 1999.
44. Bockman, T. M., Hubig, S. M., and Kochi, J. K., Direct observation of carbon-carbon bond cleavage in ultrafast decarboxylations, *J. Am. Chem. Soc.*, 118, 4502, 1996.

45. Bockman, T. M., Hubig, S. M., and Kochi, J. K., Direct observation of ultrafast decarboxylation of acyloxy radicals via photoinduced electron transfer in carboxylate ion pairs, *J. Org. Chem.*, 62, 2210, 1997.
46. Griesbeck, A. G., Gudipati, M. S., Hirt, J., Lex, J., Oelgemoeller, M., Schmickler, H., and Schouren, F., Photoinduced electron-transfer reactions with quinolinic and trimellitic acid imides: experiments and spin density calculations, *J. Org. Chem.*, 65, 7151, 2000.
47. Koshima, H., Ding, K., and Matsuura T., Stoichiometrically sensitized decarboxylation occurring in a molecular crystal composed of phenanthridine and 3-indoleacetic acid, *J. Chem. Soc.*, *Chem. Commun.* 2053–2054. 1994.
48. Koshima, H., Ding, K., Chisaka, Y., Matsuura, T., Miyahara, I., and Hirotsu, K., Stoichiometrically sensitized decarboxylation occurring in the two-component molecular crystals of aza aromatic compounds and aralkyl carboxylic acids, *J. Am. Chem. Soc.*, 119, 10317, 1997.
49. Koshima, H., Nakagawa, T., and Matsuura, T., Enantioselective photoreaction occurring in a chiral bimolecular crystal formed from acridine and *R*-(–)- or *S*-(+)-2-phenylpropionic acid, *Tetrahedron Lett.*, 38, 6063, 1997.
50. Koshima, H., Ding, K., Chisaka, Y., and Matsuura. T., Generation of chirality in a two-component molecular crystal of acridine and diphenylacetic acid and its absolute asymmetric photodecarboxylating condensation, *J. Am. Chem. Soc.*, 118, 12059, 1996.
51. Koshima, H., Ding, K., Chisaka, Y., Matsuura, T., Ohashi, Y., and Mukasa, M., Solid-state photodecarboxylation induced by exciting the CT bands of the complexes of arylacetic acids and 1,2,4,5-tetracyanobenzene, *J. Org. Chem.*, 61, 2352, 1996.

65

Induced Diastereoselectivity in Photodecarboxylation Reactions

K. Pitchumani
Madurai Kamaraj University

D. Madhavan
Madurai Kamaraj University

65.1 Introduction

Decarboxylation, particularly by the thermal route, plays a major role in a number of biological processes such as the thiamine-mediated decarboxylation of pyruvic acid to acetaldehyde and CO_2 and the pyridoxal-phosphate-mediated decarboxylation of amino acids[1] that involves radical intermediates. Most of the earlier studies on photodecarboxylation were carried out in the gas phase and are accompanied by a large number of competing reaction channels. This factor coupled with the high energy absorption of a carboxylic group (less than 250 nm) has resulted in the photochemistry of the carboxylic group receiving less attention than aldehyde and ketones. Only recently has the reaction attracted wide academic interest and synthetic utility, and excellent reviews have appeared on this topic.[2,3]

Photodecarboxylation is used to prepare radical intermediates in synthetic organic chemistry.[4] In the fields of agriculture and pharmaceuticals photodecarboxylation also plays a major role,[5–9] as many drugs, pesticides, and herbicides possessing a carboxylic group extrude CO_2 upon exposure to sunlight, leaving behind toxic components. Photodecarboxylation also has relevance in the study of techniques for solar energy conversion (photovoltaic cells), photoelectrosynthesis, and the photo-Kolbe reaction.

65.2 Mechanism

The mode of bond cleavage in carboxyl groups depends on the conditions of photolysis, and often other processes such as photodecarbonylation, intramolecular hydrogen transfer,[10] or electron transfer[11] compete with photodecarboxylation. The first two are observed in alkyl carboxylic acids and the last in aryl

0-8493-1348-1/04/$0.00+$1.50

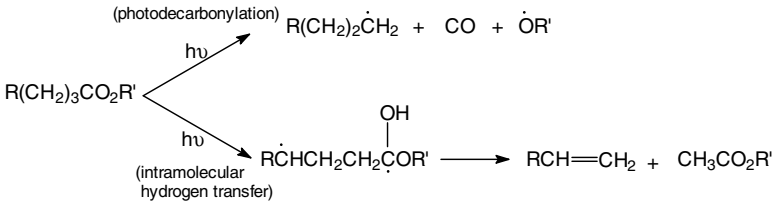

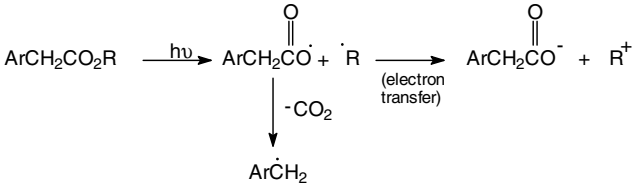

SCHEME 1

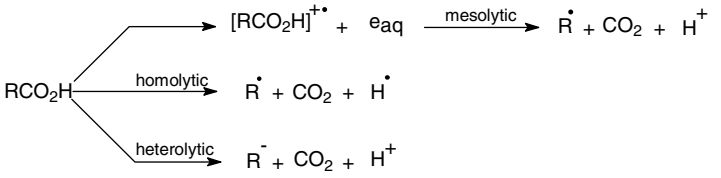

SCHEME 2

esters (Scheme 1). Photodecarboxylation results when the CC bond α to the carbonyl group is cleaved with loss of either a proton or a hydrogen atom from the carboxyl group. Subsequent cleavage of the α-CC bond may occur via homolytic, mesolytic, or heterolytic pathways (Scheme 2).[2]

In homolytic cleavage, the OC bond in anhydrides and esters, β to the carbonyl, is cleaved first to form an acyloxy radical, which then undergoes decarboxylation via homolytic cleavage of the α-CC bond. For example, phenylacetic acid in methanol undergoes homolytic cleavage as evidenced by the identification of benzyl radicals in laser flash photolysis and formation of bibenzyl and a polyacid.[12] Homolytic photodecarboxylation is also induced by electron transfer which occurs in some aryl alkyl carboxylates in aqueous solution.[13,14] Other carboxylic compounds, such as acyl peroxides, anhydrides, and esters, also undergo photodecarboxylation via a homolytic route.[15] The first step is the homolytic cleavage of the OO bond (in peroxides) or the OC bond (in anhydrides and esters) β to the carbonyl group to form an acyloxy radical, which decarboxylates via homolytic cleavage of the α-CC bond in the second step and thus is a biphotonic process. Ibuprofen undergoes photodecarboxylation via homolytic cleavage in methanol.[8] Laser flash photolysis[12] and deuterium exchange studies[16] reveal that the photodecarboxylation of phenylacetic acid follows predominantly homolytic cleavage in solvents such as methanol.

In heterolytic cleavage, an ion pair is formed by the complete transfer of both the bonding electrons to one of the fragments. Photodecarboxylation of sodium phenylacetate in a 1% $(CH_3)_2CDOH/H_2O$

mixture or in methanol involves heterolytic cleavage on irradiation.[14] Similarly, sodium *p*-nitrophenylacetate, diphenylacetic acid, and heteroaryl acetic acids such as pyridylacetic acid undergo photodecarboxylation heterolytically.[17]

Mesolytic cleavage involves an initial photoionization leading to the formation of a radical ion, which cleaves further to give a radical and an ionic fragment.[18] 1-Naphthylacetic acid, naproxen, ketoprofen, pyruvic acid etc. are some of the well-known examples that undergo photodecarboxylation via mesolytic cleavage. Naphthylacetic acid[19–21] undergoes photodecarboxylation via mesolytic cleavage to give naphthaldehyde in aqueous medium. The ionization of the aryl portion prior to decarboxylation to form the naphthylmethyl radical has been proposed. Among the non-steroidal antiinflammatory drugs (NSAIDs), naproxen[8] and benoxaprofen[22] are found to undergo photodecarboxylation through mesolytic cleavage in a similar manner. Pyruvic acid is found to undergo photodecarboxylation via mesolytic cleavage in the presence of electron acceptors such as naphthalene.[23] Similarly, ketoprofen undergoes photodecarboxylation in the presence of methyl viologen again by a mesolytic process.[7]

Photolysis of aroyl-substituted phenylacetic acid and *p*-acetylphenylacetic acid in aqueous solution leads to efficient decarboxylation through the formation of the arylmethyl carbanion.[24] *ortho*-Acetyl- or *ortho*-benzoyl-substituted phenylacetic acids undergo efficient photodecarboxylation in benzene solution whereas the *meta*- and *para*-isomers do not undergo this process.[25] Several α-hydroxyarylacetic acids,[26,27] such as mandelic acid and benzilic acid, photodecarboxylate readily via α-hydroxyarylmethyl carbanions to give arylmethanols in high quantum yields. The photodecarboxylation of chromone-2-carboxylic acid[28] (containing a heterocyclic ring) in deaerated ethanol produces 2-(1′-hydroxyethyl)chromone by recombination of ketyl and 1-hydroxyethyl radicals formed with the release of CO_2.

The photoinduced electron transfer (PET) reactivity of phthalimidoacetic acid and the corresponding acetates has been studied in their photodecarboxylation reactions.[29] A variety of medium- and large-ring compounds are synthesised from ω-phthalimidoalkanoates using a triplet sensitized photodecarboxylation reaction initiated by intramolecular photoelectron transfer.[30] Photodecarboxylation of *N*-phthaloyl[31–33] and *N*-benzoyl esters of α-amino acids[34] has also been reported.

65.3 Photodecarboxylation of NSAIDs

The photochemistry of 2-arylpropionic acid[35] has received considerable attention in recent years as this is the basic skeleton of NSAIDs such as naproxen, ketoprofen, tiaprotenic acid, caprofen, and suprofen (Scheme 3a, NSAIDs with a 2-PPA skeleton; Scheme 3b, NSAIDs without a 2-PPA skeleton). They are the most frequently prescribed therapeutic agents for the alleviation of minor aches and pains and for the treatment of rheumatic fever, rheumatoid arthritis, and osteoarthritis.[36]

These NSAIDs are photolabile and are known to exhibit phototoxicity, causing a number of side effects such as dizziness, drowsiness, nausea, and gastrointestinal tract irritation. Many of them can also induce skin photosensitivity in some patients. In addition, ketoprofen, one of the commonly prescribed NSAIDs, produces photohemolytic activity toward red blood cells and is also capable of causing photocleavage of DNA.[37,38] The photosensitization of NSAIDs can be traced to their photochemistry and, upon excitation, decarboxylation is the major reaction pathway.[39] The aryl methyl radical can then react with molecular oxygen to yield a peroxide radical. It can also undergo coupling and other related radical reactions.

Photodecarboxylation of 2-(3-benzoyl)phenylpropionate, the ketoprofen anion, was studied[40] in water by time-resolved, laser-induced optoacoustic spectroscopy (LIOAS). The various transient species involved in the title reaction were identified and their lifetimes measured. The intrinsic photoreactivity of the 2-benzoylthiophene chromophore of the photosensitizing drug, tiaprofenic acid, was also studied.[41] The observed photoprocesses account readily for the biological photosensitization reactions such as membrane damage and protein modification. The transient photochemistry in photodecarboxylation of rufloxacin (a fluoroquinolone antibacterial drug),[42] fenofibric acid (used in the treatment of hyperlipidemia),[43] and tolmetin[44] has also been reported.

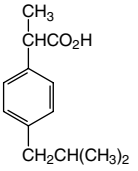

Ibuprofen

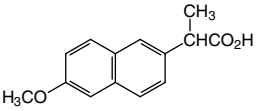

Naproxen

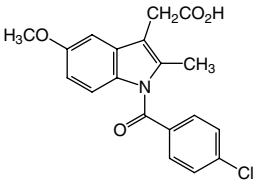

Indomethacin

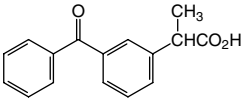

Ketoprofen

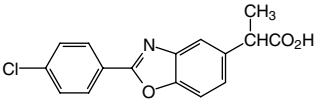

Benoxaprofen

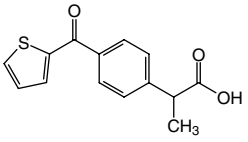

Tiaprofenic acid

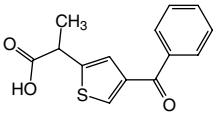

Suprofen

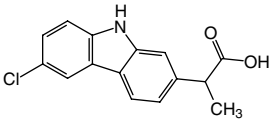

Caprofen

SCHEME 3A

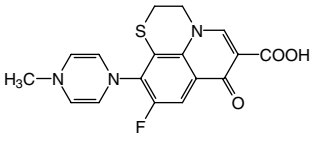

Rufloxacin

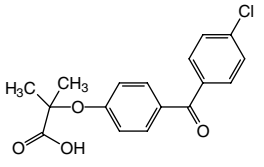

Fenofibric acid

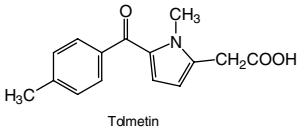

Tolmetin

SCHEME 3B

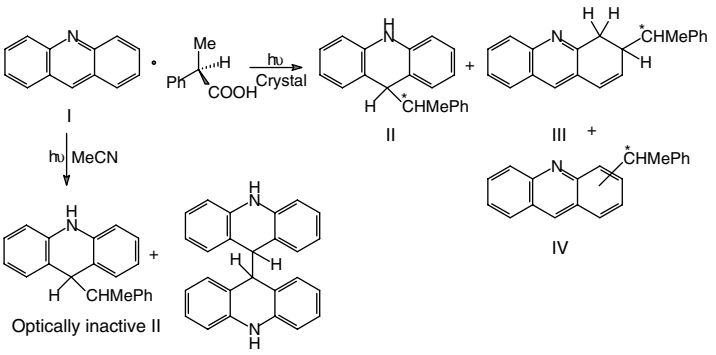

SCHEME 4

65.4. Photodecarboxylation in Confined Spaces and Induced Diastereoselectivity

The mesoporous silica FSM-16 has been found to catalyze oxidative photodecarboxylation of α-hydroxy acids and phenylacetic acid derivatives[27] to yield the corresponding carbonyl compounds. It also promotes the oxidative photodecarboxylation of *N*-acyl-protected α-amino acids to afford the corresponding imides.[45]

Photodecarboxylation in the presence of photocatalysts such as TiO_2 has also been studied.[46] For example, the photodegradation of (4-chloro-2-methylphenoxy)acetic acid, a herbicide, in an aqueous solution of TiO_2 involves elimination of carbon dioxide from the initially formed radical species on the catalyst surface.[46] The templating of carboxylic acids with polyethylene films has been found to enhance the photodecarboxylation at the expense of the photo-Fries rearrangement in simple aryl esters such as phenyl and 1-naphthyl esters.[47]

Irradiation of a chiral bimolecular crystals formed from acridine with diphenylacetic acid[48] and R/S-2-phenylpropionic acid (2-PPA)[49] results in enantioselective photodecarboxylation, which is followed by stereoselective condensation between the ·CHMePh radical and the hydroacridine radical species (Scheme 4, enantioselective photodecarboxylation in a chiral bimolecular crystal). The radical coupling occurs in the crystal lattice to give the optically active products II to IV. On the other hand, photolysis in solution phase results in the formation of the optically inactive II and biacridine IV.

Solid-state irradiation of two component molecular crystals of thienylacetic acids with aza aromatic compounds (acridine and phenanthridine)[50] results in photodecarboxylation and gives decarboxylated and condensation products. Two-component molecular crystals of the above azo aromatic compounds with 3-indolepropionic acid and 1-naphthylacetic acid, upon solid-state irradiation,[51] give radical intermediates via electron transfer and ultimately afford decarboxylated compounds in near quantitative yield. Irradiation of crystalline charge-transfer complexes of 3-indoleacetic acid and 2-naphthylacetic acid with 1,2,4,5-tetracyanobenzene[52] gives methylnaphthalene (decarboxylation) and naphthyl(2,4,5-tricyano)methane (dehydrocyanating condensation) in the solid state.

Photodecarboxylation of NSAIDs Inside Cyclodextrin

Photolysis of 2-phenylpropionic acid in solution (acetonitrile/methanol/benzene) under a nitrogen atmosphere produces ethylbenzene **2**, the *meso*- (**3**) and *dl*- (**4**) forms of 2,3-diphenylbutane, 1-(2-ethylphenyl)-1-phenylethane **6**, 1-(4-ethylphenyl)-1-phenylethane **7**, and acetophenone **5**, involving homolytic cleavage of the CC bond α to the carboxyl group affording 1-phenylethyl radical (PER) as the key intermediate. In solution, the radical is not stereoselective and can be converted to a mixture of *meso*- and *dl*-diphenylbutane. Acetophenone is the major product in the presence of oxygen (Scheme 5, photolysis of 2-PPA in solution).[35]

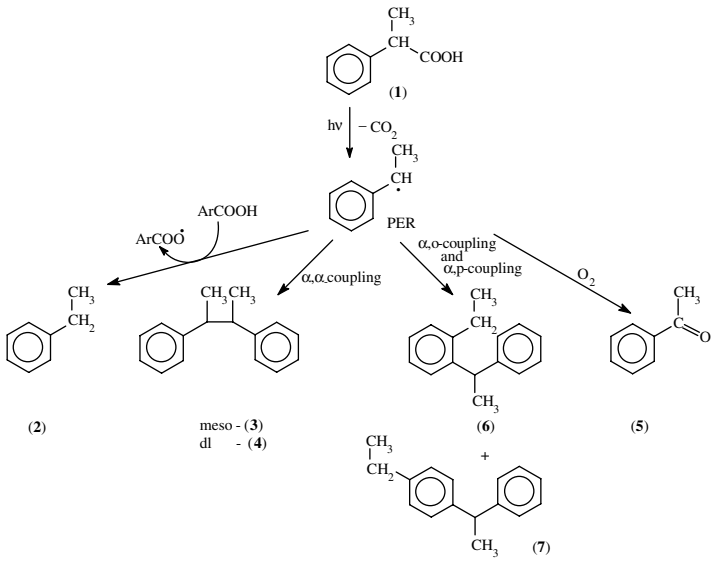

SCHEME 5

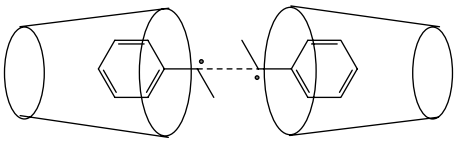

FIGURE 65.1

Upon complexation with β-cyclodextrin, a marked stereoselectivity is observed in favor of the *meso*-isomer **3**.[35] This stereochemical control in photodecarboxylation of 2-phenylpropionic acid is attributed to the chiral nature of cyclodextrin, which imposes translational and rotational constraints on the photochemically generated 1-phenylethyl radical. It is also reported that the lifetime of the phenylethyl radical within β-cyclodextrin is extremely long (up to several days).[53] Also, identical *meso* selectivities are achieved starting from optically active R or S enantiomers of 2-phenylpropionic acid. All these observations are rationalized by proposing that the more preferred geometrical arrangement for the approach of two phenyl ethyl radical–CD units has antiperiplanar methyl groups (Figure 65.1), and this is the precursor for the *meso*-diastereomer. CD complexation is also reported to cause considerable changes in the photochemistry of NSAIDs. For example, with ketoprofen and naproxen, the photohemolysis is inhibited by addition of β-cyclodextrin.[54] The photodecarboxylation of suprofen in the carboxylate form was studied in aqueous medium and as its β-CD complex.[55] The precursor state is the lowest (π,π^*) triplet, and in the β-CD inclusion complex an additional photoreaction involving the macrocycle as reactive species is also observed. Photolysis of naproxen in the presence of β-CD produces photodecarboxylated products with ethyl, 1-hydroxyethyl (major), and acetyl side chains (Scheme 6). Interestingly, β-CD causes a more rapid disappearance of the drug, rather than offering protection against photodegradation. The reduced photohemolytic activity in β-CD is attributed to the sequestering and stabilization of the radical intermediates by complexation.[54] The protective effect of CD is attributed to a reduction in the quantum yield of decarboxylation in CD-included drug molecules, with a resulting decrease in the amount of radical products.[56] It is also likely that cyclodextrin complexation might reduce the amount of singlet oxygen produced in the system by protecting the excited drug molecule from endogenous oxygen. Suppression of photodecarboxylation by cyclodextrin complexation is also observed in the case of ketoprofen[57] and tolmetin.[58] In their studies on tolmetin, Scaiano and Monti have suggested

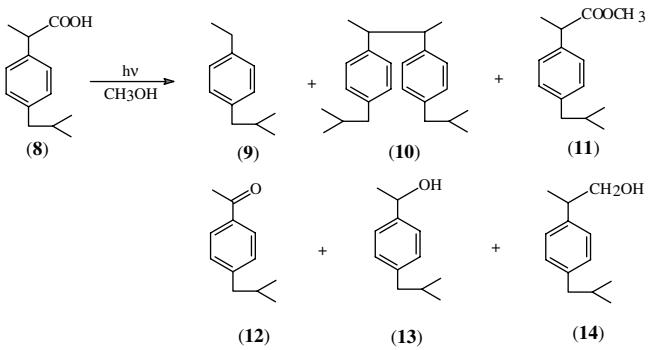

SCHEME 6

that the observed reduction in biodamage cannot be entirely attributed to a decrease in NSAID photoconversion in the presence of cyclodextrin. The inhibition in phototoxicity may be due in part to cyclodextrin complexation of toxic photoproducts (rendering them inactive) and also to the possibility of cyclodextrin trapping of radical species formed during tolmetin photolysis. A decrease in photodecarboxylation and suppressed benoxaprofen-photosensitized hemolysis is also reported[59] upon CD complexation. However, recent studies on the role of CDs as phototoxicity inhibitors in drug formulation with naproxen as model systems[39] in the presence of alcohols or protein (bovine serum albumin, BSA) have cautioned that cyclodextrin complexation of drugs will be significantly weaker *in vivo* than *in vitro*. As the reduction in phototoxicity cannot be attributed solely to the ability of cyclodextrin to complex the drugs or their photoproducts, additional work both on model systems and *in vivo* seems desirable.

Diastereoselective Photodecarboxylation of 2-Phenylpropionic Acid in Zeolite Medium

2-Phenylpropionic acid loaded into various cation-exchanged Y zeolites[60] (Si/Al ratio 2.43) was irradiated as a hexane slurry, and in all the cation-exchanged zeolites a remarkable diastereoselectivity can be observed. The *dl*-2,3-diphenylbutane is the major product, with a small amount of the meso-isomer. Ethylbenzene is also formed as one of the products, and the amount of ethylbenzene increases with an increase in cation size. A decrease in cage free volume with an increase in the cation size prevents the loading of two molecules/cage that facilitates the unimolecular reaction pathway, namely, hydrogen abstraction to yield ethylbenzene. The formation of ethylbenzene may be due to the abstraction of proton by the α-methylbenzyl anion, which is likely to be formed along with α-methylbenzyl radicals. The *ortho*- or the *para*-coupled products of the α-methylbenzyl radical are not formed in the zeolite-mediated reactions.

The data in Table 65.1 show an interesting dependence of reactivity (unimolecular/bimolecular) on the loading level. With LiY, NaY, and KY, about two molecules can be accommodated inside the super cage, whereas in RbY and CsY the loading level decreases to 1.5 and 1.3, respectively. The mobility of the α-methylbenzyl radical inside the cages of LiY and NaY is also greater compared to RbY and CsY. This higher mobility inside the smaller LiY and NaY zeolites coupled with the higher loading level leads to a faster α,α-coupling with another radical as is evident by the higher percentage conversions in LiY and NaY in relation to RbY and CsY. Correspondingly, in the case of larger cations, the lower loading level and decreased mobility of the α-methylbenzyl radical promotes, in addition to coupling, significant unimolecular hydrogen abstraction to give ethylbenzene and oxidation to acetophenone.

In an oxygen atmosphere, acetophenone is the only product due to the reaction of oxygen with the α-methylbenzyl radical;[35] however, in the photolysis of 2-PPA in a zeolite slurry and as a solid complex under an oxygen atmosphere, only a minor amount of acetophenone is obtained along with considerable

TABLE 65.1 Products Distribution in Photolysis of 2-PPA (1) Inside Zeolites[a]

Medium	Loading Level of 2-PPA[b] (1)	% Conversion	Ethylbenzene (2)	2,3-Diphenylbutane *meso-dl-* (3, 4)		Acetophenone (5)	X[c]	*dl*/*meso* Ratio
CH_3CN	—	63	16	45	34	—	5.0	0.76
CH_3CN[d]	—	76	13	41	40	—	6.0	0.98
CH_3OH[d]	—	37	8.0	42	40	—	10	0.95
β-CD[d]	—	49	—	66	34	—	—	0.52
LiY	1.82	55	3.0	2.0	95	—	—	48
NaY	1.92	51	2.0	1.0	97	—	—	97
KY	2.02	45	5.0	3.0	92	—	—	31
RbY	1.56	39	43	5.0	52	—	—	10
CsY	1.30	36	43	5.0	52	—	—	10
NaY[e]	1.92	33	1.0	2.0	78	19	—	39
NaY[f]	1.92	47	2.0	2.0	52	44	—	26

[a] Irradiated as hexane slurry in nitrogen atm. for 6 h; analyzed by gas chromatography; error limit ±5%.
[b] Loading level refers to the number of 2-PPA molecules/cage.
[c] X includes *ortho*- (**6**) and *para*- (**7**) coupled products of α-methylbenzyl radical.
[d] Literature data[35] (irradiated in water under argon atmosphere).
[e] Irradiated as hexane slurry in oxygen atmosphere.
[f] Irradiated as solid complex in oxygen atmosphere for 25 h.

amounts of the *dl*-isomer **4**. This observation is presumably due to the preassociation of the 2-PPA molecules inside the cage in such a way that the radicals are not completely free. The *dl*/*meso* ratio is very high compared to that obtained in the irradiation of 2,4-diphenylpentan-3-one (~2.0),[61] where the same α-methylbenzyl radical is identified as the intermediate.

The predominant formation of the *dl* form of 2,3-diphenylbutane over the *meso*-isomer is explained on the basis of steric and electronic factors. Binding to the walls of the zeolite cage takes place through the more polar carboxyl groups, and this pushes the hydrocarbon part into the interior of the zeolite cavity. This factor, along with the higher electrostatic field present in LiY and NaY zeolites, results in hydrophobic association between the phenyl rings of adjacent 2-PPA molecules (Figure 65.2). Thus, the preferred geometrical arrangement in zeolite cages is one in which the methyl groups are *anti*- to each other (Figure 65.2a,b). As the *syn*- arrangement of methyl groups will have considerable steric hindrance (Figure 65.2c), it may not be energetically favored. Dimeric association, which is commonly encountered in carboxylic acids, may not be significant here due to (1) the spatial constraints imposed by the cavity on the formation of the eight-membered ring in the dimer, and (2) the intrinsic polarity of the inner walls of the zeolite, which attracts the carboxyl group toward them (more pronounced in a hydrocarbon solvent, as in the present study). With RbY and CsY zeolites, a combination of lower loading and decreased electrostatic field results in a weaker preassociation (hydrophobic interaction) between the adjacent aryl rings which leads to a decrease in diastereoselective induction.

It is relevant to note here that the chemistry of benzylic radicals from the steady-state photolysis of dibenzyl ketones inside cavities of pentasil zeolites have been reported.[61,62] From a study on the lifetime of simple benzyl radicals generated inside the zeolite cages in the photolysis of phenylacetic acid using nanosecond diffuse reflectance spectroscopy, it has been concluded that the benzyl radicals decay rapidly by a coupling reaction with a second benzyl radical, and the mobility decreases within the series from LiY to CsY.[63]

Turro et al.[61,62] have reported the generation of benzyl radicals and α-methylbenzyl radicals (from diastereomeric dibenzyl ketone and 2,4-diphenylpentan-3-one, respectively) inside the cages of cation-exchanged faujasites X and Y. In the case of LiY and NaY, which show greater diastereoselectivity, the *dl*-isomer of 2,3-diphenylbutane is the major product (the *dl*/*meso* ratio for LiY is ~1.8 and for NaY is ~1.9; the ratio decreases in the case of KY) compared to that of LiX and NaX. The magnitude of diastereoselectivity is a function of the substrate configuration inside the zeolite cavity, and the observed zeolite-induced diastereoselection is more significant compared to other organized media such as micelles and

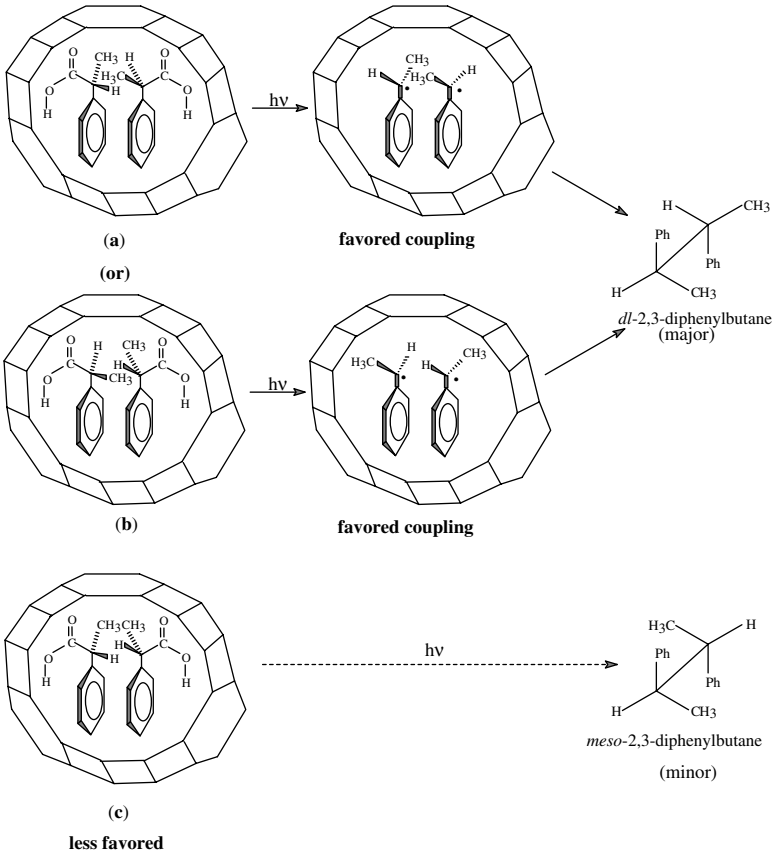

FIGURE 65.2 Packing of 2-PPA molecules inside the faujasite cage and the preferred modes of coupling of α-methylbenzyl radicals.

porous glass.[61,62] It is also interesting to note that the zeolites have preferentially retained the *dl*-isomer of both 2,3-diphenylbutane and 2,4-diphenylpentan-3-one.[61] Cozens et al.,[63] using nanosecond photolysis, have reported the direct observation of benzyl radicals inside cation-exchanged zeolites.

When the results are compared with the photolysis of 2,4-diphenylbutan-3-one (which also involves the generation and subsequent coupling of a similar α-methylbenzyl radical) the induced diastereoselectivity is very high, which may be attributed to preassociation of the 2-PPA molecules in a preferred geometrical arrangement inside the zeolite cavities (Figure 65.2). The results are also remarkable in that the dramatic diastereoselectivity is achieved from a racemic mixture of 2-PPA. A closer look at Figure 65.2 points out an interesting observation. Preassociation of a *d*-isomer with another *d*-isomer (Figure 65.2a) is sterically favored, while with an *l*-isomer it leads to considerable repulsion (Figure 65.2c). Similarly an *l*-isomer associates only with another *l*-isomer (Figure 65.2b), and this enatioselection is largely responsible for the observed zeolite-induced diastereoselectivity in decarboxylation.

It is interesting to note that, while the *meso*-2,3-diphenylbutane **3** is the predominant product in β-cyclodextrin[35] (with a hydrophobic cavity), the corresponding *dl*-isomer (**4**) is the exclusive product in zeolite cages. This striking reversal of diasteroselectivity, in comparison to β-CD, is attributed to (1) the polar environment inside the zeolite cage, wherein more efficient binding by the carboxyl moiety may be visualized, and (2) the larger cage size in the zeolite, which ensures packing of approximately two 2-PPA molecules, thereby facilitating preassociation. Thus, it is obvious that the photodecarboxylation of 2-PPA is controlled not only by the confining spaces inside the zeolite cages/cyclodextrin cavities but also by their polarities.

TABLE 65.2 Product Distribution (in%) from the Photolysis of Ibuprofen (8) Inside Zeolites[a]

Medium	Loading Level	% Conversion	(9)[d]	(10)	(12)	(13)	(11) + (14)
CH_3CN[b]	—	49	10	—	65	25	—
CH_3OH[b,c]	—	48	2.0	10	17	17	54
LiY	1.29	Nil	—	—	—	—	—
NaY	1.32	2.7	—	—	50	50	—
CsY	1.04	1.8	—	—	23	77	—

[a] Irradiated as a hexane slurry in nitrogen atmosphere for 6 h.
[b] Irradiated in nitrogen atmosphere for 6 h.
[c] Reported in the literature.[6]
[d] For structures of products **9** to **14**, see Scheme 6.

In a typical experiment, activated zeolite is added to a solution of the substrate in hexane and stirred overnight. The solid complex is filtered, washed with hexane to remove the substrate present on the surface, and then made into a slurry with about 5 ml of hexane. This slurry is stirred and irradiated using a 400-W, medium-pressure mercury vapor lamp. After completion of irradiation, the hexane portion is filtered. The zeolite framework is broken with ~4-*M* Hcl, and the acidic solution is extracted with diethyl ether. After drying over anhydrous sodium sulfate, the ether is removed. The hexane and the ether portions are combined and analyzed by gas chromatography using an OV-1 (10% phenylmethylsilicone) column and a flame ionization detector. A bulk solution of 2-phenylpropionic acid is irradiated, and the *dl*- and *meso*-isomers of 2,3-diphenylbutane are separated by column chromatography and identified by their characteristic nuclear magnetic resonance (NMR) spectra.[64] The NMR resonances for the *dl*-isomers are $\delta = 1.26$ (*m*, 6, $2CH_3$–), 3.14 (*m*, 2, 2CH–), and 7.27 (*m*, 10, $2C_6H_5$); for the *meso*-isomers, $\delta = 1.05$ (*m*, 6, $2CH_3$–), 2.80 (*m*, 2, 2CH–), and 7.25 (*m*, 10, $2C_6H_5$).

Photolysis of Ibuprofen and the Methyl Ester of Naproxen

Castell et al.[6] have demonstrated that the photolytic degradation of ibuprofen (2-[4-isobutylphenyl]propionic acid, **8**) in methanol results in photodecarboxylation followed by secondary reactions (Scheme 6, photodecarboxylation of ibuprofen), giving products of hydrogen abstraction, dimerization, incorporation of methanol, or reaction with oxygen (**9** to **14**). With a view to achieving induced diastereoselectivity, ibuprofen entrapped in various cation-exchanged zeolites has been irradiated, and the results of the photolyses are shown in Table 65.2. In all the cation-exchanged faujasites, a decreased photoreactivity (~2 to 3% photoconversion) is observed, indicating that the zeolite microenvironment offers better protection to this drug against the action of light. Due to an increase in the size of the arylalkanoic acid, even when a high concentration of the guest is employed, only a loading level of about one molecule per super cage is observed in all the three zeolites. This rules out the formation of a dimer. Though the irradiation is carried out under a nitrogen atmosphere, only the oxygenated products **12** and **13** are formed in small amounts. The presence of trace amounts of zeolite-bound oxygen may contribute to their formation.

Significant results obtained in photodecarboxylation of 2-phenylpropionic acid have prompted a study of naproxen. The molecular mechanism of photosensitization of naproxen (2-[6-methoxy-2-naphthyl]propionic acid, **15**) in red blood cells has been reported.[8] In aqueous buffered solutions, photodegradation of naproxen leads to decarboxylated products with ethyl (**16**), 1-hydroxyethyl (**17**), and/or acetyl (**18**) side chains (Scheme 7, photodecarboxylation of naproxen).[54,65] When the methyl ester of naproxen complexed with LiY, NaY, and CsY zeolites is irradiated as hexane slurries under a nitrogen atmosphere for 6 h, no photoproducts are formed, and the methyl ester is photostable under the conditions employed, indicating that the zeolite environment also offers better protection to naproxen against the action of light.

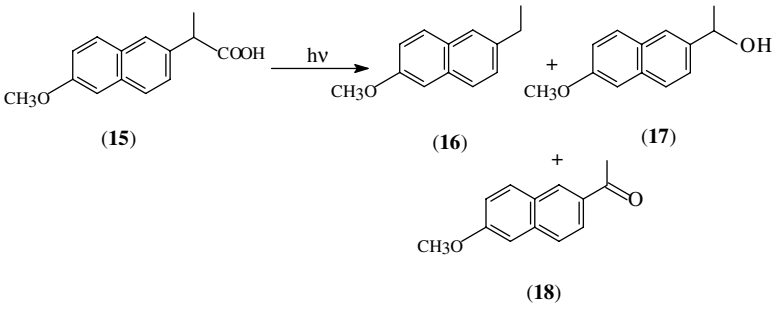

(**15**) (**16**) (**17**) (**18**)

SCHEME 7

64.5 Conclusion

Photodecarboxylation reactions have great relevance in synthesis, mechanistic studies, and a wide range of biological applications, especially in the area of drugs such as NSAIDs. Considerable attention has been paid in recent years to utilize the confined spaces of a host matrix to control the photochemistry of these drugs with a view to improve their photostability. In many instances, a very significant diastereoselective induction is observed in these reactions, unlike the corresponding solution-phase processes. Detailed studies in cyclodextrins as host matrices have been carried out, and inorganic hosts such as zeolite can also offer a wide scope of application in this area. Further exploration in these domains will provide valuable insight and exciting prospects in a variety of areas such as drug stability, skin photosensitivity, and chiral applications in photoprocesses, as well as mechanistic insights into these processes.

References

1. Fersht, A., *Enzyme Structure and Mechanism*, Freeman, Reading, U.K., 1977.
2. Budac, D. and Wan., P., Photodecarboxylation: mechanism and synthetic utility, *J. Photochem. Photobiol. A: Chem.*, 67, 135, 1992.
3. Budac, D. and Wan., P., Photodecarboxylation of acids and lactones, in *CRC Handbook of Organic Photochemistry and Photobiology*, Horspool, W. M. and Song, P. S., Eds., CRC Press, Boca Raton, 1995, 384.
4. Barton, D. H. R., Blundell, P., and Jaszberenyi, J. C., Quantum yields in the photochemically induced radical chemistry of acyl derivatives of thiohydroxamic acids, *J. Am. Chem. Soc.*, 113, 6937, 1991.
5. Navaratnam, S., Hughes, J. L., Parsons, B. J., and Philips, G. O., Laser flash and steady-state photolysis of benoxaprofen in aqueous solution, *Photochem. Photobiol.*, 41, 375, 1985.
6. Castell, J. V., Gomez-L, M. J., Miranda, M. A., and Morera, I. M., Photolytic degradation of ibuprofen: toxicity of the isolated photoproducts on fibroblasts and erythrocytes, *Photochem. Photobiol.*, 46, 991, 1987.
7. Costanzo, L. L., De Guidi, G., Condorelli, G., Cambria, A., and Fama, M., molecular mechanism of drug photosensitization. II. Photohemolysis sensitized by ketoprofen, *Photochem. Photobiol.*, 50, 359, 1989.
8. Costanzo, L. L., De Guidi, G., and Condorelli, G., Molecular mechanism of naproxen photosensitization in red blood cells, *J. Photochem. Photobiol. B: Biol.*, 3, 223, 1989.
9. Holmsted, R. L. and Fullmer, D. G., Photodecarboxylation of cyanohydrin esters: models for pyrethroid photodecomposition, *J. Agric. Food Chem.*, 25, 56, 1977.
10. Borrell, P. and Norrish, R. G. W., Photochemistry of butyric acid and some related compounds, *Proc. Roy. Soc. London, Ser. A*, 262, 19, 1961.

11. DeCosta, D. P. and Pincock, J. A., Intramolecular electron transfer in the photochemistry of substituted 1-naphthylmethyl esters of benzoic acids, *Can. J. Chem.*, 70, 1879, 1992.
12. Meiggs, T. O. and Miller, S. I., Photolysis of phenylacetic acid and methyl-phenylacetate in methanol, *J. Am. Chem. Soc.*, 94, 1989, 1972.
13. Grossweiner, L. I. and Joschek, H. I., Optical generation of hydrated electrons from aromatic compounds, *Adv. Chem. Ser.*, 50, 279, 1965.
14. Meiggs, T. O., Grossweiner, L. I., and Miller, S. I., Extinction coefficient and recombination rate of benzyl radicals. I. Photolysis of sodium phenylacetate, *J. Am. Chem. Soc.*, 94, 7981, 1972.
15. Coyle, J. D., Photochemistry of carboxylic acid derivatives, *Chem. Rev.*, 78, 97, 1978.
16. Epling, G. A. and Lopes, A., Fragmentation pathways in the photolysis of phenylacetic acid, *J. Am. Chem. Soc.*, 99, 2700, 1977.
17. Stermitz, F. R. and Huang, W. H., Thermal and photodecarboxylation of 2-, 3-, and 4-pyridylacetic acid, *J. Am. Chem. Soc.*, 93, 3427, 1971.
18. Maslak, P. and Narvaez, J. N., Mesolytic cleavage of carbon-carbon bonds: a comparison of homolytic and heterolytic processes with similar substrates, *Angew. Chem. Int. Ed. Engl.*, 29, 283, 1990.
19. Crosby, D. G. and Tang, C. S., Photodecomposition of 1-naphthaleneacetic acid, *J. Agric. Food. Chem.*, 17, 1291, 1969.
20. Watkins, D. A. M., The effect of ultra-violet light on 1-naphthaleneacetic acid, *Phytochemistry*, 8, 979, 1969.
21. Bosca, F., Canudas, N., Marin, M. L., and Miranda, M. A., A photophysical and photochemical study of 6-methoxy-2-naphthylacetic acid, the major metabolite of phototoxic nonsteroidal anti-inflammatory drug nambetone, *Photochem. Photobiol.*, 71, 173, 2000.
22. Reszka, K. and Ghignell, C. F., Spectroscopic studies of cutaneous photosensitizing agents. IV. The photolysis of benoxaprofen, an anti-inflammatory drug with phototoxic properties, *Photochem. Photobiol.*, 38, 281, 1983.
23. Davidson, R. S. and Goodwin, D., The role of electron transfer process in the photoinduced decarboxylation reaction of α-oxocarboxylic acid, *J. Chem. Soc., Perkin Trans. 2*, 1559, 1982.
24. Xu, M. and Wan, P., Efficient photodecarboxylation of aroyl-substituted phenylacetic acids in aqueous solution: a general photochemical reaction, *J. Chem. Soc., Chem. Commun.,* 2147, 2000.
25. Sobczak, M. and Wagner, P. J., Light-induced decarboxylation of (*o*-acyl-phenylacetic acids, *Org. Lett.*, 4, 379, 2002.
26. Peter, W. and Xu, X., Enhanced photodecarboxylation efficiency of α-hydroxy substituted arylacetic acids in aqueous solution, *Tetrahedron Lett.*, 31, 2809, 1990.
27. Itoh, A., Kodama, T., Inagaki, S., and Masaki, Y., Oxidative photo-decarboxylation of α-hydroxy-carboxylic acids and phenylacetic acid derivatives with FSM-16, *Org. Lett.*, 2, 331, 2000.
28. Kawata, H., Kumagi, T., Morita, T., and Niizuma, S., Photodecarboxylation of chromone-2-carboxylic acid in aerated and deaerated ethanol solution, *J. Photochem. Photobiol. A: Chem.,* 138, 281, 2001.
29. Michael, O., Griesbeck, A. G., Lex, J., and Haeuseler, A., Structure, CV and IR spectroscopic evidence for preorientation in PET-active phthalimido carboxylic acids, *Org. Lett.*, 3, 1593, 2001.
30. Griesbeck, A. G., Henz, A., Kramer, W., Lex, J., and Nerowski, F., Synthesis of medium- and large-ring compounds initiated by photochemical decarboxylation of ω-phthalimidoalkanoates, *Helv. Chim. Acta*, 80, 912, 1997.
31. Griesbeck, A. G., Mauder, H., Mueller, I., Peters, E., Peters, K., and von Schnering, H. G., Photochemistry of *N*-phthaloyl derivatives of methionine, *Tetrahedron Lett.*, 34, 453, 1993.
32. Griesbeck, A. G., Mauder, H., and Mueller, I., Photochemistry of *N*-phthaloyl α-amino acid esters: a new approach to β,γ-unsaturated α-amino acid, dihydrobenzazepinedione and pyrrolizidinone derivative, *Chem. Ber.*, 125, 2467, 1992.
33. Sato, Y., Nakai, H., Mizoguchi, T., Kawanishi, M., Hatanaka, Y., and Kanaoka, Y., Photodecarboxylation of *N*-phthaloyl-α-amino acids, *Chem. Pharm. Bull.*, 30, 1263, 1982.

34. Nakai, H., Sato, Y., Mizoguchi, T., and Kanaoka, Y., Preparation of *N*-benzoylamines by photodecarboxylation of *N*-benzoyl-α-amino acids, *Synthesis,* 141, 1982.
35. Jimenez, M. C., Miranda, M. A., and Tormos, R., Photodecarboxylation of 2-phenylpropionic acid in solution and included within β-cyclodextrin, *Tetrahedron*, 51, 2953, 1995.
36. Delgado, J. A. and Remers, W. A., Eds., *Wilson and Gisvold's Textbook of Organic Medicinal and Pharmaceutical Chemistry*, 10th ed., Lippincott-Raven, New York, 1998.
37. De Guidi, G., Condorelli, G., Giuffrida, S., Puglisi, G., and Giammona, G., Effect of β-cyclodextrin complexation on the photohameolitic activity induced by ketoprofen and naproxen sensitization, *J. Incl. Phenom. Mol. Recogn. Chem.,* 15, 43, 1993.
38. Artuso, T., Bernadou, J., Meunier, B., Piette, J., and Paillous, N., Mechanism of DNA cleavage mediated by photoexcited nonsteroidal anti-inflammatory drugs, *Photochem. Photobiol.*, 54, 205, 1991.
39. Partyka, M., Au, B. H., and Evans, C. H., Cyclodextrins as phototoxicity inhibitors in drug formulations: studies on model systems involving naproxen and β-cyclodextrin, *J. Photochem. Photobiol. A: Chem.,* 140, 67, 2001.
40. Borsarelli, C. D., Braslavsky, S. E., Sortino, S., Marconi, G., and Monti, S., Photodecarboxylation of ketoprofen in aqueous solution: a time-resolved laser induced optoacoustic study, *Photochem. Photobiol.*, 72, 163, 2000.
41. Encinas, S., Miranda, M. A., Marconi, G., and Monti, S., Triplet photoreactivity of the diaryl ketone tiaprofenic acid and its decarboxylated photoproduct: photobiological implications, *Photochem. Photobiol.,* 67, 420, 1998.
42. Sortino, S., Marconi, G., Giuffrida, S., De Guidi, G. and Monti, S., Photophysical properties of rufloxacin in neutral aqueous solution, *Photochem. Photobiol.*, 70, 731, 1999.
43. Bosca, F. and Miranda, M. A., A laser flash photolysis study on fenofibric acid, *Photochem. Photobiol.*, 70, 731, 1999.
44. Sortino, S. and Scaiano, J. C., Laser flash photolysis of tolmetin: a photoadiabatic decarboxylation with a triplet carbanion as the key intermediate in the photodecomposition, *Photochem. Photobiol.*, 69, 167, 1999.
45. Itoh, A., Kodama, T., Inagaki, S., and Masaki, Y., New synthetic method of Imides through oxidative photodecarboxylation reaction of *N*-protected α-amino acids with FSM-16, *Chem. Lett.*, 542, 2000.
46. Topalov, A., Abramovic, B., Gabor, D. M., Csanadi, J., and Arcson, O., Photocatalytic oxidation of the herbicide (4-chloro-2-methylphenoxy)acetic acid (MCPA) over TiO_2, *J. Photochem. Photobiol. A: Chem.*, 140, 249, 2001.
47. Gu, W., Abdallah, D. J., and Weiss, R. G., Conformational control of photoinduced decarboxylation of simple aryl esters: enhancement by templating effects in polyethylene films, *J. Photochem. Photobiol. A: Chem.,* 139, 79, 2001.
48. Koshima, H., Ding, K., Chisaka, Y., and Matsuura, T., Generation of chirality in a two-component molecular crystal of acridine and diphenylacetic acid and its absolute asymmetric photodecarboxylation condensation, *J. Am. Chem. Soc.*, 118, 12059, 1996.
49. Koshima, H., Nakagawa, T., and Matsuura, T., Enantioselective photoreaction occurring in a chiral bimolecular crystal formed from acridine and R-(–)- or S-(+)-2-phenylpropionic acid, *Tetrahedron Lett.,* 38, 6063, 1997.
50. Koshima, H., Matsushige, D., Miyauchi, M., and Fujita, J., Solid-state photoreaction in two-component molecular crystals of thienylaceticacids and aza aromatic compounds, *Tetrahedron*, 56, 6845, 2000.
51. Koshima, H., Ding, K., Chisaka, Y., Matsuura, T., Miyahara, I., and Hirotsu, K., Stoichiometrically sensitized decarboxylation occurring in the two-component molecular crystals of aza aromatic compounds and aralkyl carboxylic acids, *J. Am. Chem. Soc.*, 119, 10317, 1997.
52. Koshima, H., Ding, K., Chisaka, Y., Matsuura, T., Ohashi, Y., and Mukasa, M., Solid-state photodecarboxylation induced by exciting the CT bands of the complexes of arylacetic acids and 1,2,4,5-tetracyanobenzene, *J. Org. Chem.*, 61, 2352, 1996.

53. Rao, V. P., Zimmt, M. B., and Turro, N. J., Photoproduction of remarkably stable benzylic radicals in cyclodextrin inclusion complexes, *J. Photochem. Photobiol. A: Chem.,* 60, 355, 1991.
54. Jimenez, M. C., Miranda, M. A., and Tormos, R., Photochemistry of naproxen in the presence of β-cyclodextrin, *J. Photochem. Photobiol. A: Chem.*, 104, 119, 1997.
55. Sortino, D., De Guidi, G., Marconi, G., and Monti, S., Triplet photochemistry of suprofen in aqueous environment and in the β-cyclodextrin inclusion complex, *Photochem. Photobiol.*, 67, 603, 1998.
56. McAuley, I., Krogh., E., and Wan, P., Carbanion intermediates in the photodecarboxylation of benzannelated acetic acid in aqueous solution, *J. Am. Chem. Soc.*, 110, 600, 1988.
57. Monti, S., Sortino, S., De Guidi, G., and Marconi, G., Supramolecular photochemistry of 2-(3-benzoylphenyl)propionic acid (ketoprofen): a study in the β-cyclodextrin cavity, *New J. Chem.*, 22, 599, 1998.
58. Sortino, S., Scaiano, J. C., De Guidi, G., and Monti, S., Effect of β-cyclodextrin complexation on the photochemical and photosensitizing properties of tolmetin: a steady-state and time-resolved study, *Photochem. Photobiol.*, 70, 549, 1999.
59. Hoshino, T., Ishida, K., Irie, T., Hirayama, F., Uekama, K., and Yamasaki, M., Reduction of photohemolytic activity of benoxaprofen by β-cyclodextrin complexation, *J. Incl. Phenom.*, 6, 415, 1988.
60. Lalitha, A., Pitchumani, K., and Srinivasan, C., Induced diastereoselectivity in photodecarboxylation of 2-phenylpropionic acid in faujasite zeolites, *Tetrahedron*, 57, 4455, 2001.
61. Ghatlia, N. D. and Turro, N. J., Diastereoselective induction in radical coupling reactions: photolysis of 2,4-diphenylpentan-3-ones adsorbed on faujasite zeolite, *J. Photochem. Photobiol. A: Chem.*, 57, 7, 1991.
62. Baretz, B. H. and Turro, N. J., Photochemistry of diastereomeric 2,4-diphenylpentan-3-ones and related ketones in "super cage" environments provided by micelles, porous glass and porous silica: temperature and magnetic field effects, *J. Am. Chem. Soc.*, 105, 1309, 1983.
63. Cozens, F. L., Ortiz, W., and Schepp, N. P., Direct observation of the benzyl radical and the benzyl anion within cation-exchanged zeolites: a nanosecond laser study, *J. Am. Chem. Soc.,* 120, 13543, 1998.
64. Yamasaki, R. B., Tarle, M., and Casanova, J., Electrochemistry. 5. Products and stereochemistry of the electroreduction of 1-bromo-1-phenylethane and (±)-1-deuterio-1-bromo-1-phenylethane, *J. Org. Chem.*, 44, 4519, 1979.
65. Bosca, F., Miranda, M. A., Vano, L., and Vargas, F., New photodegradation pathways for naproxen, a phototoxic non-steroidal anti-inflammatory drug, *J. Photochem. Photobiol. A: Chem.*, 54, 131, 1990.

66

The Photochemistry of Esters of Carboxylic Acids

James A. Pincock
Dalhousie University

66.1 Introduction

This topic was reviewed in 1995 in Chapter 32 of the first volume of the *CRC Handbook of Organic Photochemistry and Photobiology* and in several earlier reviews on carboxylic acid esters[1] and photodecarboxylation.[2] Reviews on phosphate[3] and sulfonate ester[4] photochemistry have also appeared. In addition, a recent review on the photochemistry of arylmethyl esters[5] and on benzylic cleavage reactions in general[6] provides useful background. Two excellent reviews[7,8] of photolabile protecting groups in general have appeared very recently, parts of which discuss the ester photochemistry covered below. Finally, the *Chemical Society Reports* continues to be a valuable resource. This chapter covers material more recent than 1995 and up to mid-2002 and, rather than being exhaustive, focuses on a few recent, well-referenced papers.

Aliphatic esters have only a weak n,π^* transition (λ_{max} 212 nm; $\varepsilon = 48\ M^{-1}\ cm^{-1}$ for ethyl acetate);[1] therefore, their photochemistry cannot be examined by the usual solution techniques that use Hg or Hg/Xe light sources. Consequently, essentially all of the photochemistry reported in any detail is that of substrates with other chromophores (almost exclusively aromatic rings) that allow reactivity of the ester functional group. A considerable amount of this research has been aimed at "phototriggers" or photolabile protecting groups, which allow spatial and temporal control of the release of the carboxylic acid functional group, often as a probe of biological pathways. The review that follows is divided into seven sections: arylmethyl esters, phenacyl esters, benzoin esters, *ortho*-nitrobenzyl esters, orthogonal deprotection of diesters, radical anions of esters generated by single electron transfer (SET), and miscellaneous.

0-8493-1348-1/04/$0.00+$1.50

66.2 Arylmethyl Esters

Benzylic Esters

Since the pioneering study by Zimmerman and co-workers on substituted 4-methoxy, 3-methoxy and 3,5-dimethoxybenzyl acetate in aqueous dioxane,[9] the photochemistry of arylmethyl esters has attracted considerable attention:

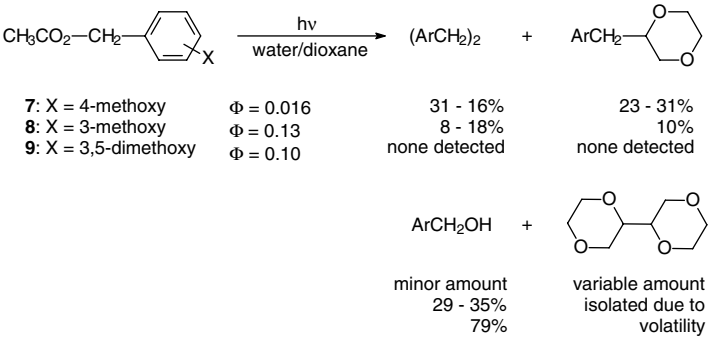

(66.1)

Of particular interest has been the pathway for formation of ion-derived products and the observation of high yields of these from the 3-methoxy and 3,5-dimethoxy substrates (originally called the *meta* effect but now recognized as *ortho*/*meta*). A generalized mechanism is shown in Scheme 1. This scheme

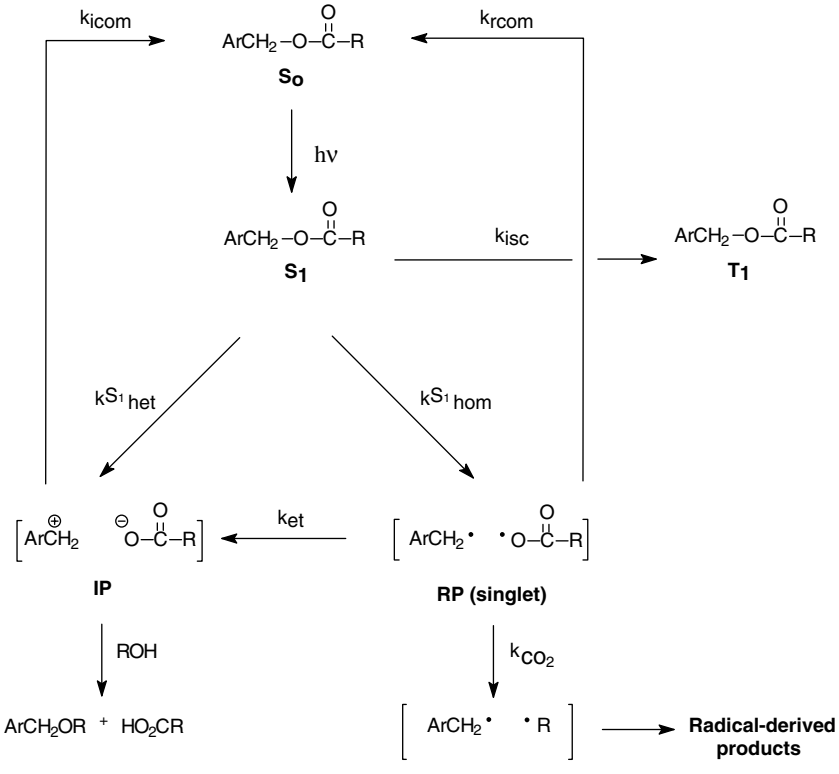

SCHEME 1

would be even more complicated if the triplet state was also reactive, but sensitization and quenching studies for 1-naphthylmethyl esters[10] and quenching studies for arylmethyl esters[11] indicate that it is not. In this scheme, no distinction has been made between the possible forms of radical (in cage, separated) and ion (contact, solvent separated, separated) pairs. Esters have the added advantage for mechanistic studies that radical pair intermediates have a built-in radical clock, the decarboxylation of the acyloxy radical (k_{CO2}). Rate constants for this process vary from around 10^6 s^{-1} for aromatic cases ($ArCO_2\cdot$)[12] to 10^9 s^{-1} for aliphatic cases ($RCO_2\cdot$)[13] and up to 10^{12} s^{-1} for cases that lead to highly stabilized radicals ($Ph_2C(OH)CO_2\cdot$)[14] after decarboxylation.

A considerable body of experimental work, mainly from our own laboratory and including product yields, quantum yields, and fluorescence studies indicates that the major pathway in ester photochemistry is homolytic cleavage (k_{hom}) from S_1 to give singlet radical pairs. We examined nine structurally different sets of substituted arylmethylesters: **1**,[13,15] **2**,[16] **3**,[16] **4**,[17] **5**,[15] **6**,[11,18] **7**,[19] **8**,[20] and **9**[21] (73 compounds in all). Decarboxylation of the acyloxy radical then competes with electron transfer (k_{et}) for formation of ion pairs. The rates of electron transfer for both substituted 1-naphthylmethyl **2** and benzyl substrates **6** follow Marcus' theory in both the normal and inverted region when correlated with the oxidation potential of the arylmethyl radical.[22,23] The *meta*-methoxy compounds give high yields of ion-derived products because the oxidation potentials of their arylmethyl radicals place them near the maximum on the Marcus plot; therefore, k_{et} is competitive with k_{CO2}. This work has been reviewed in the previous volume of this Handbook and in other places.[5,6]

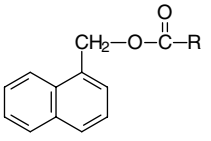

1: R = methyl, ethyl, 2-propyl, *t*-butyl, 3-propenyl, cyanomethyl, methoxymethyl

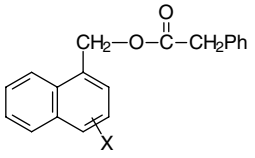

2: X = 4-cyano, 4-carbomethoxy, 4-methoxy, 4-ethoxy, 3-methoxy, 4-methyl, hydrogen, 4-fluoro, 4,8-dimethoxy, 4,5-dimethoxy, 4,7-dimethoxy

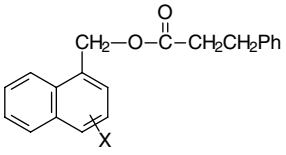

3: X = 4-methoxy, 3-methoxy, hydrogen

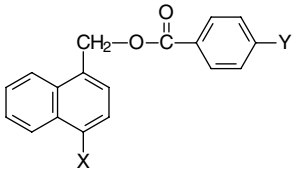

4: X = hydrogen, Y = hydrogen, cyano, methoxy
X = methoxy, Y = hydrogen, cyano
X = cyano, Y = hydrogen, methoxy

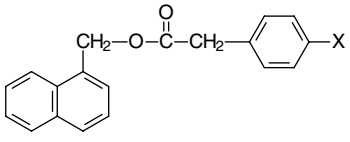

5: X = 4-cyano, 3-cyano, 4-trifluoromethyl, 3-trifluoromethyl, hydrogen, 4-fluoro, 3-fluoro, 4-methyl, 3-methyl, 4-methoxy, 3-methoxy

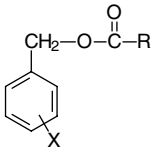

6: R = methyl, *t*-butyl
X = 4-cyano, 4-trifluoromethyl, hydrogen, 4-methyl, 3-methyl, 4-methoxy, 3-methoxy, 3,4-dimethoxy, 3,5-dimethoxy, 3,4,5-trimethoxy

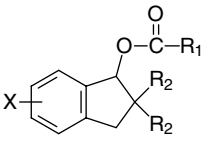

7: R_1 = methyl, R_2 = hydrogen, X = hydrogen
R_1 = *t*-butyl, R_2 = hydrogen, X = hydrogen
R_1 = methyl, *t*-butyl, R_2 = methyl, X = hydrogen,
5-methoxy, 6-methoxy

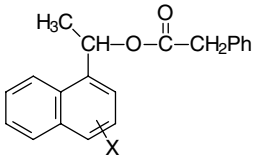

8: X = 4-cyano, hydrogen, 4-methoxy,
4,7-dimethoxy

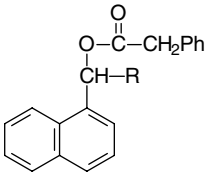

9: R = CH_2Br, CH_2-(SO)-CH_3, CH_2-(SO)-C_6H_5

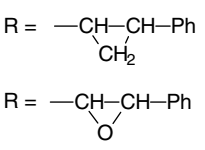

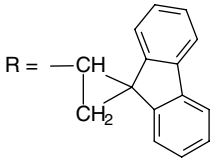

In contrast to this conclusion, high-level MO calculations by Zimmerman[24,25] suggest that ion pairs are formed directly from S_1 (k_{het}) and that this process is accelerated by *meta*-methoxy substitution. The heterolytic σ-bond cleavage proceeds directly from S_1 through a conical intersection to the ion pair. In agreement with the initial SHMO calculations,[9] the 3-methoxybenzyl cation in the excited state is more stable than the 4-methoxy one at these higher levels of theory.

The observation that the chromophore in **6** (X = 3,5-dimethoxy) results in particularly high reactivity for σ-bond cleavage has resulted in it being advocated as a particularly useful one for photolabile protecting groups. In fact, this substrate gives a much higher yield of ion-derived product (56%) than predicted (32%) from the Marcus plot established by the remaining isomers in set **6**.[18] However, as shown in Scheme 2, the photo-Claisen type product **10** is formed as a primary photoproduct on irradiation in methanol.[26] Its half-life in methanol is only 2.7 minutes, with a 40% return to starting material and 60% to the solvolysis product **11**. The quantum yield for the formation of **10** is 0.061; therefore, the efficiency of formation of **11** via **10** is 0.036, and $(0.036/0.22) \times 100 = 16\%$ of the photosolvolysis product is formed by a pathway that does not involve direct formation of ion pairs from **6**. Therefore, at least for this substrate, the high yield of ion-derived products is a result of two pathways. A similar observation was made for diethylphosphate and triethylamine as leaving groups.

Allyl Esters

A recent report[27] on the photochemistry of the 3-(1-naphthyl)propenyl acetate derivatives **12** (Scheme 3; yields normalized to 100%) is clearly related to the arylmethyl ester reactivity. Along with rearranged acetate and *E* to *Z* isomerization, photosolvolysis in methanol results in the ethers **13**. Two observations are surprising: First, no ethers resulting from trapping of the allylic cation at the terminal end were reported, and, second, no products derived from allylic radical intermediates were observed.

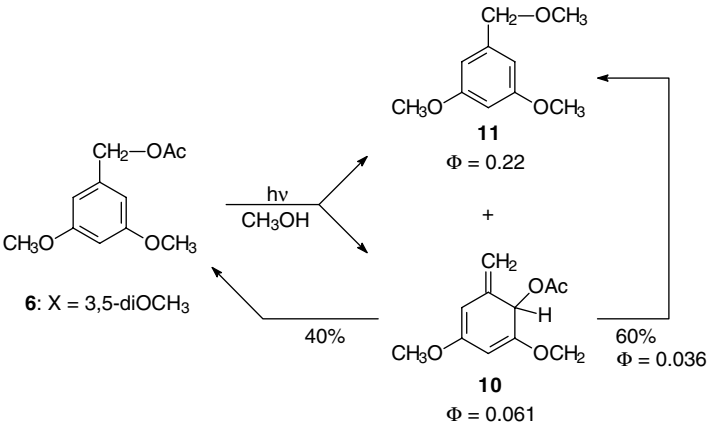

SCHEME 2

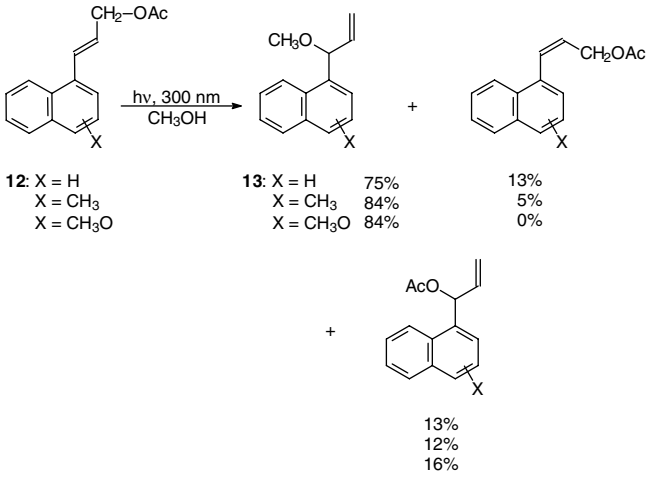

SCHEME 3

Coumarinyl Esters

Coumarin derivatives **14** are a special class of arylmethyl compounds that are unusual in that the photochemistry yields products that are exclusively ion pair derived, Scheme 4.[28] The quantum yields for product formation increase and the fluorescence quantum yields decrease systematically as the leaving group ability of the carboxylate anion increases (lower pK_a of the corresponding acid). This suggests that ion pairs are formed directly from S_1, but the intervention of precursor radical pairs was not ruled out.

66.3 Phenacyl Esters

Considerable effort has been made recently to develop photochemically removable protecting groups based on phenylacyl (i.e., $PhCOCH_2$–) chromophores, particularly as "phototriggers" for the study of physiological pathways. The focuses of this research have been to develop systems that allow the phototrigger to be activated efficiently at longer wavelengths (>300 nm) to avoid competitive absorption by the usual biomolecules (proteins), to improve solubility and thermal ground-state stability in aqueous media, to yield byproducts that do not absorb at long wavelengths and that are also physiologically benign, and

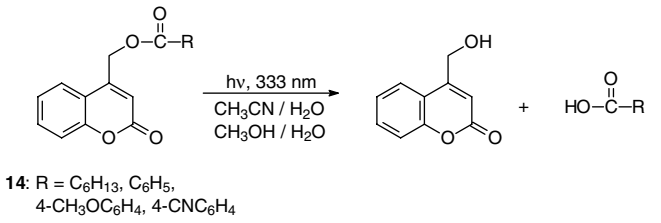

SCHEME 4

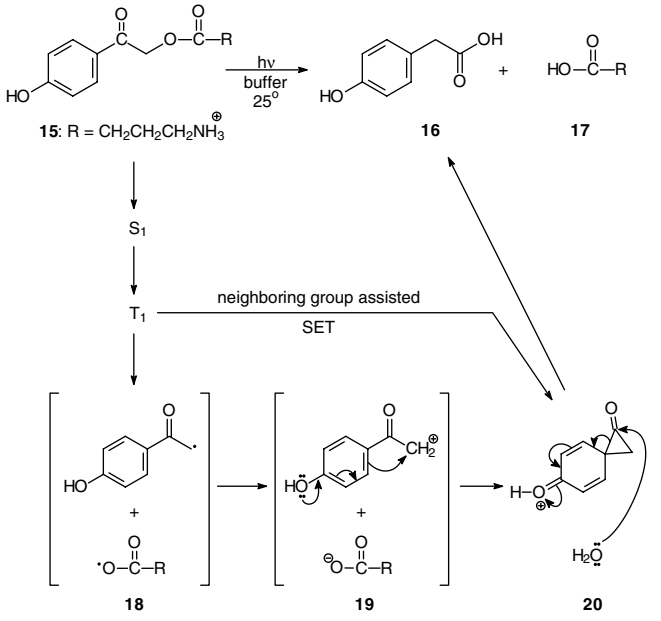

SCHEME 5

to give rapid photorelease (shorter than microseconds). The use of these new chromophores/functional groups will probably supercede the more traditional σ-nitrobenzyl derivatives, which have disadvantages because of the relatively slow deprotection rate (a ground-state process following the excited-state process) and the undesirable reactivity with biomolecules of the aromatic nitroso compounds generated. A recent manuscript describing the photorelease of a cage protein kinase is an excellent example.[29]

para-Hydroxyphenacyl

The example[30] shown in Scheme 5 is based on the preliminary research on phosphate release by the Givens group.[31] The yield of amino acid **17** on irradiation at $\lambda > 300$ nm is quantitative, and the disappearance of the precursor **15** has $\Phi = 0.35$. By Stern–Volmer quenching results, the rate constant for release from the excited triplet state of **15** was 7×10^7 s^{-1}. The ester **15** does not hydrolyze in buffered aqueous media over a period of 24 hours at room temperature. The mechanism originally proposed involves homolytic cleavage of the excited triplet state to give a radical pair **18** followed by rapid electron transfer to give the ion pair **19**. Rapid cyclization gives the spiroketone **20**, which is then hydrolyzed to the acid **16**. Because acyloxy radicals decarboxylate so rapidly (~10^9 s^{-1}, for this case), a mechanism involving radical pairs is problematic because it cannot correctly explain a high yield for the carboxylic acid released. An alternate proposal was, therefore, that the excited triplet state proceeded directly to the

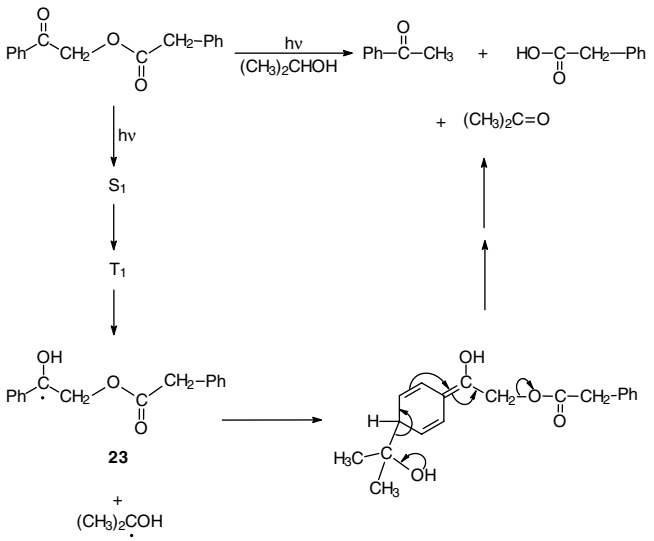

SCHEME 6

spiroketone and the carboxylate anion by electron transfer from the π^* aromatic orbital to the σ^* orbital of the reacting σ bond (neighboring group assisted SET). In either case, the role of the *p*-hydroxy group is critical. Givens and co-workers[32] have more recently extended this approach for the photorelease of small peptides (ala-ala and bradykinin) and to a longer wavelength chromophore by introduction of 3-methoxy (λ_{max} = 350 nm) and 3,5-dimethoxy (λ_{max} = 370 nm) substituents.[33]

Because the phenolic –OH group is critical for the photoactivity of these compounds, a mechanism involving excited-state proton transfer has been suggested.[34] Particularly important in this regard is the observation that, on irradiation in 1:1 D_2O–CD_3CN at 300 nm, carboxylic acids were formed in >90% yield for all members of the set of esters **21**, even though the rate of decarboxylation of the potential acyloxy radicals generated would vary over more than two orders of magnitude (~10^9 s^{-1} to ~10^{12} s^{-1}). Therefore, radical pairs are highly improbable. Also, the *p*-methoxy compound **22** gave no observable reaction under the same conditions. In this water/acetonitrile medium, the reactions only occur efficiently between pH 2 and 10. On the basis of these observations and the properties of the transients observed by laser flash photolysis (LFP), a mechanism involving excited-state proton transfer (either intramolecular [ESIPT] or intermolecular [ESPT]) in the excited singlet state was proposed. The conflict between this mechanism and the triplet-state mechanism proposed above seems to have been resolved in favor of the latter by LFP results.[35]

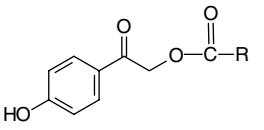

21: R = CH_3, CH_2Ph, $C(CH_3)_3$, $C(OH)Ph_2$

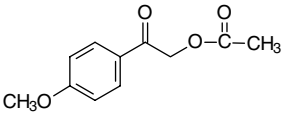

22

H-Atom Transfer

An important observation by Banerjee and Falvey[36] related to the mechanism of phenacyl photochemistry is that, in the presence of H-atom donors, the excited triplet state of the ketone chromophore is quenched to give ketyl radicals **23** clearly observed by LFP. As shown in Scheme 6, carboxylic acids are photoreleased but, again, originally as carboxylate anions, not acyloxy radicals.

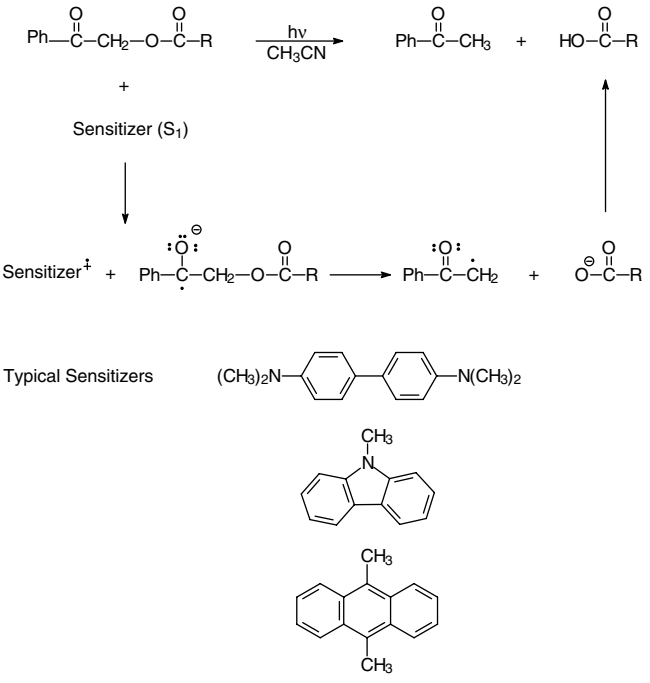

SCHEME 8

their low solubility in aqueous media and hydrolytic instability. The 3,5-dimethoxy derivatives **29** (Scheme 9) have been of particular interest because, on photolysis in 1:1 water/acetonitrile, they release carboxylic acids (along with the furan **30**) in high yield with little indication of radical derived byproducts.[45] The fact that the potential acyl radicals from these substrates span several orders of magnitude in their rate of decarboxylation indicates that the product acids must be released as carboxylates. Initial suggestions that this observation was a consequence of activation of the carbon–oxygen bond to heterolytic cleavage by the *meta*-methoxy groups seem to be incorrect. A mechanism involving intramolecular charge/electron transfer in the excited singlet state is more reasonable as it takes into account the easily oxidized electron-rich aromatic ring. Rearrangement and fragmentation of this intermediate gives the carboxylate anion and **31** (detected by LFP), which is nicely stabilized as a carbocation by the methoxy groups.

Rock and Chan have reported[46]that the low water solubility of benzoin derivatives can be overcome by replacement of the methoxy groups in **29** by $-OCH_2CO_2H$ groups (**32**). Photolysis in aqueous media releases acetic acid and gives the expected furan (30% yield) along with **33** resulting from trapping of a carbocation intermediate. Products resulting from nucleophilic trapping of benzoin-ester-derived carbocations had not been reported previously. The biradical **34** in Scheme 10 has been proposed as the critical intermediate. Finally, an important recent result in benzoin photochemistry has been reported for phosphate (not carboxylate) release.[47] The LFP evidence indicates that benzoin phosphate does react from its excited triplet state. The triplet state then partitions between two pathways — cyclization to the usual benzofuran and adiabatic heterolytic cleavage of the carbon–oxygen bond of the phosphate — to give the excited triplet state of the α-keto carbocation. This species is long lived and does not react with solvent before intersystem crossing to the singlet state. This surprising result, which may be more general than previously thought, should be considered in future mechanistic proposals.

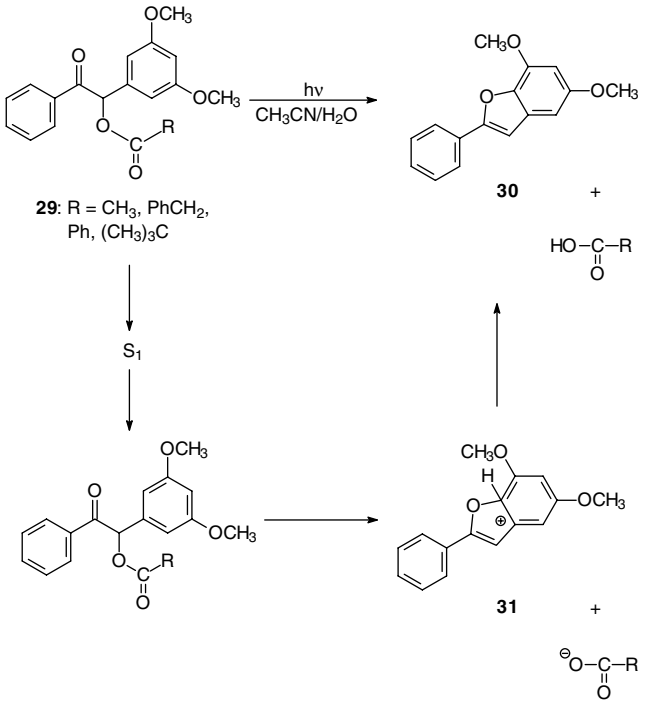

SCHEME 9

66.5 *ortho*-Nitrobenzyl Esters, Orthogonal Deprotection of Diesters

For photodeprotection, the wavelength of incident light required is often critically important in order to avoid competitive absorption by other chromophores. o*rtho*-Nitrobenzyl chromophores, particularly when methoxy substituted, allow long-wavelength/low-energy (up to 420 nm) excitation. An interesting "chromatic" orthogonal protocol for the selective deprotection of dicarboxylic acids has been developed (Scheme 11) that takes advantage of both σ-nitrobenzyl and benzoin photochemistry.[48]

Irradiation of the bichromophoric molecule **35** ($n = 5$) in CH_3CN at 254 nm resulted in deprotection of the benzoin carboxylate to give **36** (92% yield). In contrast, irradiation at 420 nm gave *ortho*-nitrobenzyl deprotection, (**37**; 70% yield). The latter reaction occurred some two orders of magnitude more slowly. Remarkably, this same chromatic orthogonality was maintained as the linker between the two chromophores was decreased from $n = 5$ to $n = 0$. The surprising feature of this observation is that normally bichromophoric molecules rapidly transfer excitation energy to the lowest energy chromophore. Perhaps, as discussed above (Section 66.4), the higher energy benzoin excited state undergoes very rapid electron/charge transfer from the excited singlet state that is faster than the exergonic energy transfer to the *ortho*-nitrobenzyl chromophore.

66.6 Radical Anions of Esters

As discussed above (Section 66.3), phenacyl ester radical anions fragment readily to phenacyl radicals and carboxylate anions. The radical anions of benzoate esters also fragment to carboxylate anions and alkyl radicals, and this process is faster if the alkyl radical is stabilized (3°, benzylic).[49] This concept has been applied successfully to the deoxygenation of carbohydrate alcohols by photoinduced electron transfer (PET) sensitization.[50,51] For instance, irradiation of **38** in water/2-propanol, using a substituted

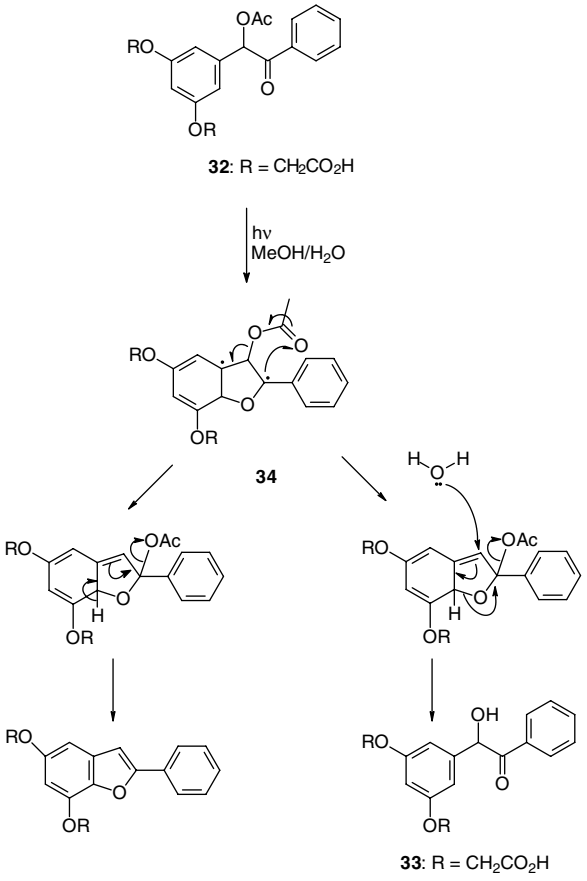

SCHEME 10

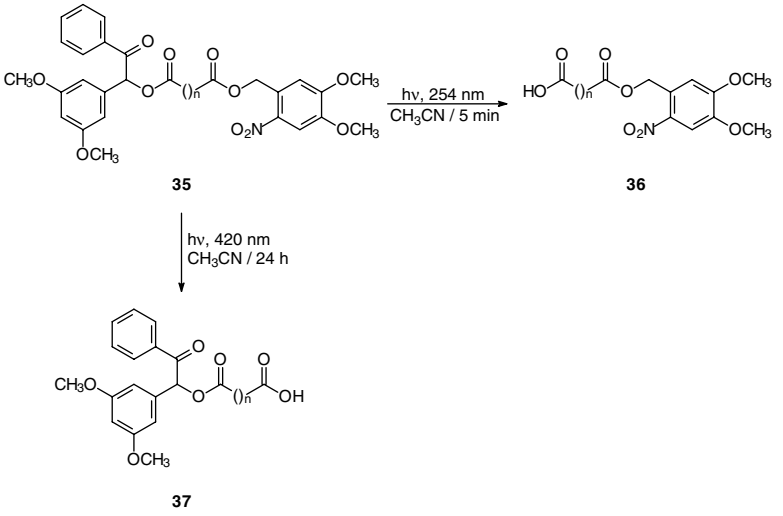

SCHEME 11

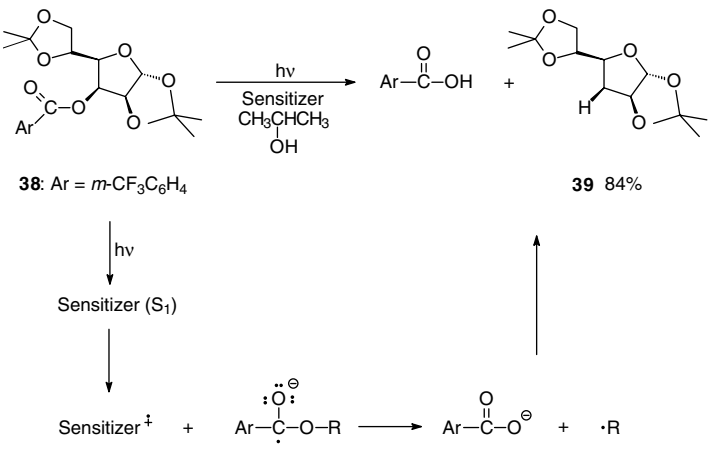

SCHEME 12

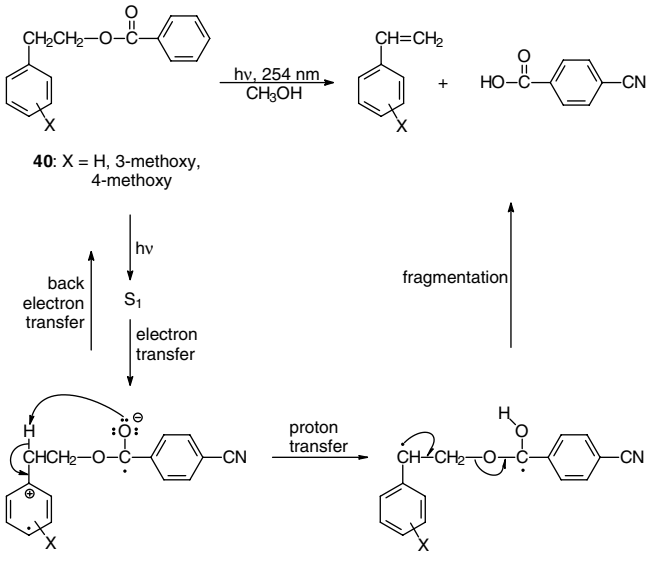

SCHEME 13

carbazole as a sensitizer, gave the deoxygenated derivative **39** (84% yield).[51] The proposed mechanism is outlined in Scheme 12.

Intramolecular Electron Transfer and Norrish Type II Fragmentation

Normally esters do not undergo the classic Norrish type II reaction of aromatic ketones because their lowest energy exited state is not of the n,π^* configuration required for efficient intramolecular H-atom transfer. The reactions are known but with quantum yields less than 0.01. Recently, we have observed that the process can be 5 to 50 times more efficient if induced by intramolecular electron transfer (Scheme 13).[52]

Irradiation of esters **40** in methanol gives the styrenes and 4-cyanobenzoic acid. The mechanism proposed involves excitation to S_1 and efficient intramolecular electron transfer (as indicated by redox

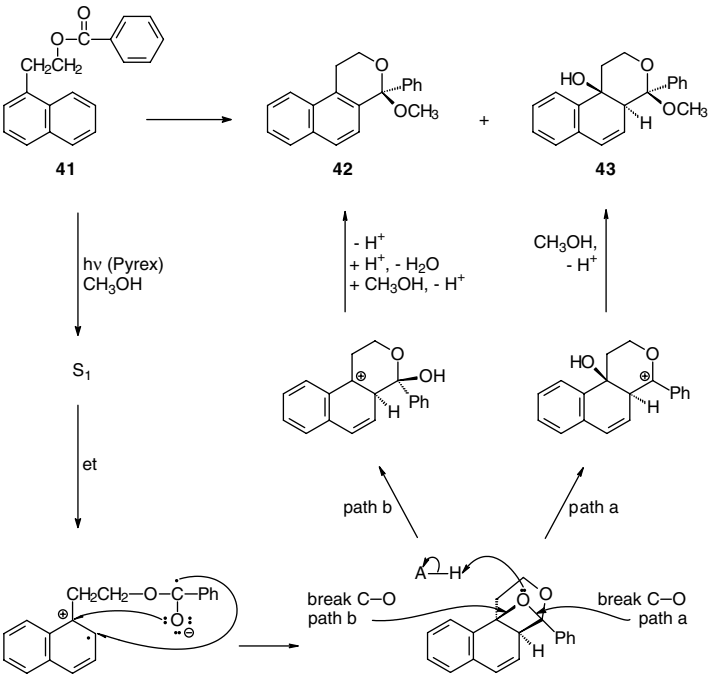

SCHEME 14

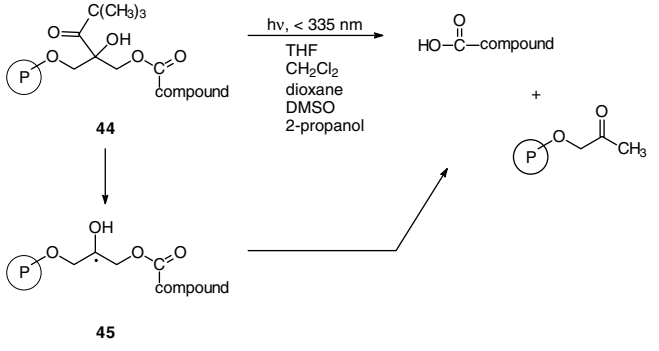

SCHEME 15

potentials and fluorescence spectra), followed by proton transfer in the intramolecular radical ion pair. The driving force for proton transfer is the enhanced acidity of the arylmethyl hydrogen in the radical cation and the enhanced basicity of the carbonyl radical anion. The result is formation of the 1,4-biradical required for fragmentation. Thus, the usual H-atom transfer of the Norrish type II process occurs by sequential electron and proton transfer. The styrenes formed are not isolated in high yield because they are rapidly degraded by secondary photochemistry.

In an attempt to study these reaction at longer wavelengths, particularly for fluorescence experiments, substrates with naphthalene chromophores **41** were examined, (Scheme 14).[53] Again, intramolecular electron transfer was clearly demonstrated by fluorescence, but the products formed, **42** and **43**, resulted from an unusual [2π+2π]-cycloaddition of the ester carbonyl to the aromatic π system of the naphthalene ring. Intermolecular cycloadditions of ester carbonyls to aromatic rings are known, but only for furan.[54,55]

66.7 Miscellaneous

Deprotection of esters induced by Norrish type I has been suggested as a possible photochemical method of fragmenting a linker in solid-phase peptide synthesis (Scheme 15).[56] The linker with this chromophore cleaved more efficiently than an *ortho*-nitrobenzyl one by a factor of three to four, and, moreover, high-level conversions occurred with greater efficiency. The mechanism proposed is via Norrish type I α-cleavage of **44** at the carbonyl group of the *t*-butyl ketone. Decarbonylation gives the C2 glyceryl radical **45**, which fragments to the carboxylic acid (presumably avoiding intervention of an acyloxy radical). PTOC (pyridine-2-thioneoxycarbonyl) esters (e.g., **46**; Eq. (66.2)) are only mentioned here because, although they are not alcohol-derived esters of carboxylic acids, they have been important in both the generation and the study of reactivity of acyloxy radicals.[57,58] Rapid decarboxylation then gives the alkyl radical.

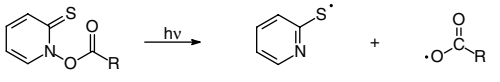

46 (66.2)

References

1. Givens, R. S. and Levi, N., The photochemistry of organic acids, esters, anhydrides, lactones and imides, in *The Chemistry of Functional Groups,* Suppl. B, *The Chemistry of Acid Derivatives*, Patai, S., Ed., Wiley, New York, 1979, 641–753.
2. Budac, D. and Wan, P., Photodecarboxylation: mechanism and synthetic utility, *J. Photochem. Photobiol. A: Chem.*, 67, 135–166, 1992.
3. Givens, R. S. and Kueper III, L. W., Photochemistry of phosphate esters, *Chem. Revs.*, 93, 55–66, 1993.
4. Horspool, W. M., Photochemistry and radiation chemistry, in *The Chemistry of Sulfonic Acids, Esters and Their Derivatives*, Patai, S. and Rappaport, Z., Eds., John Wiley & Sons, New York, 1991, 501.
5. Pincock, J. A., Photochemistry of arylmethyl esters in nucleophilic solvents: radical pair and ion pair intermediates, *Acc. Chem. Res.*, 30, 43-49, 1997.
6. Fleming, S. A. and Pincock, J. A., Photochemical cleavage reactions of benzyl-heteroatom sigma bonds, in *Organic Molecular Photochemistry*, Vol. 3, Ramamurthy, V. and Schanze, K. S., Eds., Marcel Dekker, New York, 1999, 211–281.
7. Bochet, C. G., Photolabile protecting groups and linkers, *J. Chem. Soc., Perkin Trans. 1*, 125–142, 2002.
8. Pelliccioli, A. P. and Wirz, J., Photoremovable protecting groups: reaction mechanisms and applications, *Photochem. Photobiol. Sci.*, 1, 441–458, 2002.
9. Zimmerman, H. E. and Sandel, V. R., Mechanistic organic photochemistry. II. Solvolytic photochemical reactions, *J. Am. Chem. Soc.*, 85, 915–921, 1963.
10. Givens, R. S., Matuszewski, B., and Neywick, C. V., Photodecarboxylation of esters. Photolysis of α- and β-naphthalenemethyl derivatives, *J. Am. Chem. Soc.*, 96, 5547–5552, 1974.
11. Hilborn, J. W., MacKnight, E., Pincock, J. A., and Wedge, P. J., Photochemistry of substituted benzyl acetates and benzyl pivalates: a reinvestigation of substituent effects, *J. Am. Chem. Soc.*, 116, 3337–3346, 1994.
12. Chateauneuf, J., Lusztyk, J. and Ingold, K. U., Spectroscopic and kinetic characteristics of aroyloxyl radicals. 1. The 4-methoxybenzoyloxyl radical, *J. Am. Chem. Soc.*, 110, 2877–2885, 1988.
13. Hilborn, J. W. and Pincock, J. A., Rates of decarboxylation of acyloxy radicals formed in the photocleavage of substituted 1-naphthylmethyl alkanoates, *J. Am. Chem. Soc.*, 113, 2683–2686, 1991.

14. Bockman, T. M., Hubig, S. M., and Kochi, J. K., Direct observation of ultrafast decarboxylation of acyloxy radicals via photoinduced electron transfer in carboxylate ion pairs, *J. Org. Chem.*, 62, 2210–2221, 1997.
15. Hilborn, J. W. and Pincock, J. A., Photolysis of the 1-naphthylmethyl ester of substituted phenylacetic acids: intramolecular charge transfer and rates of decarboxylation of arylacyloxy radicals, *Can. J. Chem.*, 70, 992–999, 1992.
16. DeCosta, D. P. and Pincock, J. A., Photochemistry of substituted 1-naphthylmethyl esters of phenylacetic and 3-phenylpropionic acid: radical pairs, ion pairs and Marcus electron transfer, *J. Am. Chem. Soc.*, 115, 2180–2190,1993.
17. DeCosta, D. P. and Pincock, J. A., Intramolecular electron transfer in the photochemistry of substituted 1-naphthylmethyl esters of benzoic acids, *Can. J. Chem.*, 70, 1879–1885, 1992.
18. Pincock, J. A. and Wedge, P. J., The photochemistry of methoxy-substituted benzyl acetates and benzyl pivalates: homolytic *vs* heterolytic cleavage, *J. Org. Chem.*, 59, 5587–5595, 1994.
19. Pincock, J. A. and Wedge, P. J., The photochemistry of conformationally rigid benzylic esters: 2,2-dimethyl-1-indanyl acetates and pivalates, *J. Org. Chem.*, 60, 4067–4076, 1995.
20. Kim, J. M. and Pincock, J. A., Internal return in the photochemistry of ring-substituted 1-(1-naphthyl)ethyl esters of phenylacetic acid, *Can. J. Chem.*, 73, 885–895, 1995.
21. Nevill, S. M. and Pincock, J. A., The design of radical clocks to probe the reactivity of the intermediates in arylmethyl ester photochemistry, *Can. J. Chem.*, 75, 232–247, 1997.
22. Wayner, D. D. M., McPhee, D. J., and Griller, D., Oxidation and reduction potentials of transient free radicals, *J. Am. Chem. Soc.*, 110, 132–137, 1988.
23. Milne, P. H., Wayner, D. D. M., DeCosta, D. P., and Pincock, J. A., Substituent and charge distribution effects on the redox potentials of radicals: thermodynamics for homolytic versus heterolytic cleavage in the 1-naphthylmethyl system, *Can. J. Chem.*, 70, 121–127, 1992.
24. Zimmerman, H. E., The meta effect in organic photochemistry: mechanistic and exploratory organic chemistry, *J. Am. Chem. Soc.*, 117, 8988–8991, 1995.
25. Zimmerman, H. E., *meta-ortho* Effect in organic photochemistry: mechanistic and exploratory organic photochemistry, *J. Phys. Chem. A*, 102, 5616–5621, 1998.
26. DeCosta, D. P., Howell, N., Pincock, A. L., Pincock, J. A., and Rifai, S., 1,3-Dimethoxy-5-methylene-1,3-cyclohexadiene compounds with leaving groups at C6: generation, solvolytic reactivity and their importance in the photochemistry of 3,5-dimethoxybenzyl derivatives, *J. Org. Chem.*, 65, 4698-4705, 2000.
27. Rao, G. V., Reddy, M. J. R., Srinivas, K., Reddy, M. J. R., Bushan, K. M., and Rao, V. J., Ionic photodissociation in arylallyl acetates, *Photochem. Photobiol.*, 76, 29–34, 2002.
28. Schade. B., Hagen, V., Schmidt, R., Herbrich, R., Krause, E., Eckardt, T., and Bendig, J., Deactivation behaviour and excited-state properties of (coumarin-4-yl)methyl derivatives. 1. Photocleavage of (7-methoxycoumarin-4-yl)methyl-caged acids with fluorescence enhancement, *J. Org. Chem.*, 64, 9109–9117, 1999.
29. Zou, K., Cheley, S., Givens, R. S., and Bayley, H., Catalytic subunit of protein kinase A caged at the activating phosphothreonine, *J. Am. Chem. Soc.*, 124, 8220–8229, 2002.
30. Givens, R. S., Jung, A., Park, C.-H., Weber, J., and Bartlett, W., New photoactivated protecting groups. 7. *p*-Hydroxyphenacyl: a phototrigger for excitatory amino acids and peptides, *J. Am. Chem. Soc.*, 119, 8369–8370, 1997.
31. Park, C.-H. and Givens, R. S., New photoactivated protecting groups. 6. *p*-Hydroxyphenacyl: a phototrigger for chemical and biochemical probes, *J. Am. Chem. Soc.*, 119, 2453–2463, 1997.
32. Givens, R. S., Weber, J. F. W., Conrad II, P. G., Orosz, G., Donahue, S. L., and Thayer, S. A, New phototriggers. 9. *p*-Hydroxyphenacyl as a C-terminal photoremovable protecting group for oligopeptides, *J. Am. Chem. Soc.*, 122, 2687–2697, 2000.
33. Conrad II, P. G., Givens, R. S., Weber, J. F. W., and Kandler, K., New phototriggers: extending the *p*-hydroxyphenacyl π,π^* absorption range, *Org. Lett.*, 2, 1545–1547, 2000.

34. Zhang, K., Corrie, J. E. T., Munasinghe, R. N., and Wan, P., Mechanism of photosolvolytic rearrangement of *p*-hydroxyphenacyl esters: evidence for excited-state intramolecular proton transfer as the primary photochemical step, *J. Am. Chem. Soc.*, 121, 5625–5632, 1999.
35. Conrad II, P. G., Givens, R. S., Hellrung, B., Rajesh, C. S., Ramseier, M., and Wirz, J., *p*-Hydroxyphenacyl phototriggers: the reactive excited state of phosphate photorelease, *J. Am. Chem. Soc.*, 122, 9346–9347, 2000.
36. Banerjee, A. and Falvey, D. E., Direct photolysis of phenacyl protecting groups studied by laser flash photolysis: an excited state hydrogen atom abstraction pathway leads to formation of carboxylic acids and acetophenone, *J. Am. Chem. Soc.*, 120, 2965–2966, 1998.
37. Klán, P., Zabadal, M., and Heger, D., 2,5-Dimethylphenacyl as a new photoreleasable protecting group for carboxylic acids, *Org. Lett.*, 2, 1569–1571, 2000.
38. Pelliccioli, A. P., Klán, P., Zabadal, M., and Wirz, J., Photorelease of HCl from *o*-methylphenacyl chloride proceeds through the *Z*-xylylenol, *J. Am. Chem. Soc.*, 123, 7931–7932, 2001.
39. Zabadal. M., Pelliccioli, A. P., Klán, P., and Wirz, J., 2,5-Dimethylphenacyl esters: a photoremovable protecting group for carboxylic acids, *J. Phys. Chem. A*, 105, 10329–10333, 2001.
40. Banerjee, A. and Falvey, D. E., Protecting groups that can be removed through photochemical electron transfer: mechanistic and product studies on photosensitized release of carboxylates from phenacyl esters, *J. Org. Chem.*, 62, 6245–6251, 1997.
41. Banerjee, A., Lee, K., Qing, Y., Fang, A. G., and Falvey, D. E., Protecting group release through photoinduced electron transfer: wavelength control through sensitized irradiation, *Tetrahedron Lett.*, 39, 4635–4638, 1998.
42. Banerjee, A., Lee, K., and Falvey, D. E., Photoreleasable protecting groups based on electron transfer chemistry: donor sensitized release of phenacyl groups from alcohols, phosphates and diacids, *Tetrahedron*, 55, 12699–12710, 1999.
43. Lee, K. and Falvey, D. E., Photochemically removable protecting groups based on covalently linked electron donor–acceptor systems, *J. Am. Chem. Soc.*, 122, 9361–9366, 2000.
44. Ruzicka, R., Zabadal, M., and Klán, P., Photolysis of phenacyl esters in a two-phase system, *Synth. Commun.*, 32, 2581–2590, 2002.
45. She, Y., Corrie, J. E. T., and Wan, P., Mechanism of 3′,5′-dimethoxybenzoin ester photochemistry: heterolytic cleavage intramolecularly assisted by the dimethoxybenzene ring is the primary photochemical step, *J. Org. Chem.*, 62, 8278, 1997.
46. Rock, R. S. and Chan, S. I., Preparation of a water-soluble "cage" based on 3′,5′-dimethoxybenzoin, *J. Am. Chem. Soc.*, 120, 10766–10767, 1998.
47. Rajesh, C. S., Givens, R. S. and Wirz, J., Kinetics and mechanism of phosphate photorelease from benzoin diethyl phosphate: evidence for adiabatic fission to an α-keto cation in the triplet state, *J. Am. Chem. Soc.*, 122, 611-618, 2000.
48. Blanc, A and Bochet, C. G., Wavelength-controlled orthogonal photolysis of protecting groups, *J. Org. Chem.*, 67, 5567–5577, 2002.
49. Masnovi, J., Radical anions of esters of carboxylic acids: effects of structure and solvent on unimolecular fragmentations, *J. Am. Chem. Soc.*, 111, 9081–9089, 1989.
50. Saito, I., Ikehira, H., Kasatani, R, Watanabe, M., and Matsuura, T., Selective deoxygenation of secondary alcohols by photosensitized electron-transfer reactions: a general procedure for deoxygenation of ribonucleosides, *J. Am. Chem. Soc.*, 108, 3115–3117, 1986.
51. Prudhomme, D. R., Wang, Z., and Rizzo, C. J., An improved photosensitizer for the photoinduced electron-transfer deoxygenation of benzoates and *m*-(trifluoromethyl)benzoates, *J. Org. Chem.*, 62, 8257–8260, 1997.
52. DeCosta, D. P., Bennett, A. K., and Pincock, J. A., The Norrish type II photofragmentation of esters induced by intramolecular electron transfer, *J. Am. Chem. Soc.*, 121, 3785–3786, 1999.
53. Morley, K. and Pincock, J. A., The photochemistry of 2-(1-naphthyl)ethyl benzoates: cycloaddition and intramolecular exciplex formation, *J. Org. Chem.*, 66, 2995–3003, 2001.

54. Cantrell, T. S. and Allen, A. C., Photochemical reactions of arenecarboxylic acid esters with electron-rich alkenes: 2+2 cycloaddition, hydrogen abstraction and cycloreversion, *J. Org. Chem.*, 54, 135–139, 1989.
55. Cantrell, T. S., Allen, A. C., and Ziffer, H., Photochemical 2+2 cycloaddition of arenecarboxylic acid esters to furans and 1,3-dienes: 2+2 cycloreversion of oxetanes to dienol esters and ketones, *J. Org. Chem.*, 54, 140–145, 1989.
56. Peukert S. and Giese, B., The pivaloylglycol anchor group: a new platform for a photolabile linker in solid-phase synthesis, *J. Org. Chem.*, 63, 9045–9051, 1998.
57. Aveline, B. M., Kochevar, I. E., and Redmond, R. W., Photochemistry of *N*-hydroxypyridine-2-thione derivatives: involvement of the 2-pyridylthiyl radical in the radical chain reaction mechanism, *J. Am. Chem. Soc.*, 117, 9699–9708, 1995.
58. Choi, S.-Y., Toy, P. H., and Newcomb, M., Picosecond radical kinetics: fast ring openings of secondary and tertiary *trans*-2-phenylcyclopropylcarbinyl radicals, *J. Org. Chem.*, 63, 8609–8613, 1998.

67

The Photochemistry of Barton Esters

Peter I. Dalko
Centre National de la Recherche Scientifique

67.1 Introduction

The third part of the 20th century witnessed a spectacular advancement in free-radical chemistry. This progress had a major impact on organic synthesis. Among the number of methods developed, one of the mildest and most flexible ways of generating "disciplined radicals" is by using thiohydroxamates, usually known as Barton esters.[1] Due to the remarkably simple experimental conditions required for both the preparation and the subsequent radical reaction and, also, to the environmentally friendly "green" aspect of this chemistry,[2] this class of compounds has received considerable interest.[3,4] The broad potential of this chemistry has been described in a number of excellent reviews, books, and chapter of books, and it ultimately found application in the synthesis of biologically relevant compounds.

67.2 Structure and Reactivity

According to the classical definition, Barton esters are mixed anhydrides of carboxylic acids with thiohydroxamic acid such as I (Scheme 1).[5] This class of compound was originally developed to allow the transformation of carboxylic acids to a convenient source of radicals for synthetic application. Even now, they are one of the most important entries to *C*-radicals. Over time, the scope of the reaction was broadened, allowing the generation of heteroatom-centered radicals, particularly oxyl-, aminyl-, and iminyl radicals of synthetic interest. For these transformations, carbonates and carbamates (II), acetates (IV), and ethers (V) were developed (Scheme 1). Finally, oxalates (III) were used for deoxygenation of secondary and tertiary alcohols. The radical fragmentation reaction of these compounds can be carried out either by irradiation or by thermal activation. Both methods are discussed here briefly.

PTOC Esters

Among the most popular chromophores that usually offer the mildest and highest yielding radical-forming reaction is the *N*-hydroxypyridine-2(1*H*)-thione **1** (Scheme 2). It is interesting to notice the

0-8493-1348-1/04/$0.00+$1.50

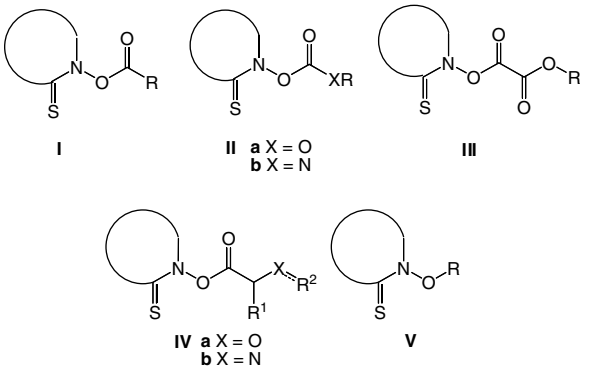

SCHEME 1

SCHEME 2

structural similarity between **1** and the *N*-hydroxy-2-pyridone **2** developed earlier by the Taylor group for photolytic generation of oxyl radicals.[6]

The free acid **1** (R = H; *N*-HPT; Scheme 2) undergoes homolytic fragmentation under ultraviolet (UV) irradiation[7] and produces ·OH radicals in aqueous media[8] as well as in organic solvents,[9] with concomitant formation of the 2-pyridylthiyl (PyS·) radical.[10] The fragmentation is pH dependent. In neutral aqueous media, photoionization occurs, generating highly reactive solvated electrons (e^-_{aq}) in a relatively efficient process ($\Phi_{e^-} = 0.1$ using $\lambda_{exc} = 308$ nm).[11] In addition to ·OH and e_{aq}^-, *N*-HPT generates two distinct thiyl radicals, an excited triplet state and an *N*-oxide radical, under various conditions. The primary homolytic process of the *N*-HPT fragmentation displays similar photochemical behavior under nonaqueous media conditions (i.e., NO bond scission generating ·OH and PyS· radicals and triplet-state formation). This fragmentation has low selectivity due to the simultaneous generation of several highly reactive species. This fact spoils the potential use of this compound as a simple photolytic source of hydroxyl radicals.

In contrast, esters derived from **1** (R = acyl; pyridine-2-thioneoxycarbonyl [PTOC] esters)[12] have been the focus of considerable attention (Scheme 3). These compounds are usually stable at room temperature or below when shielded from light and can be eventually heated up to 60 to 80°C with no special precautions taken. Compounds derived from **1** undergo radical chain reactions above ~80°C by irradiation at room temperature or even below, with a convenient light source or by ultrasound. The absorption spectra of **1** recorded between 250 and 450 nm displays two absorption bands with maxima around 300 and 375 nm in benzene (Table 67.1).[14] These bands are blue shifted in acetonitrile ($\Delta\lambda = 8$ nm). The wavelength absorbance extends into the visible range, giving the compounds a characteristic light yellow color. These broad absorption bands allow irradiation under a variety of conditions, including irradiation in the visible spectrum by using a simple tungsten tube, discharge lamp, sunlight, halogen (xenon) spotlight, or laser beam. A radical initiator is not required for this process, as Barton esters can ensure both the initiation and propagation steps.

Generation of radicals by irradiation has been proven to occur via an initial photoexcitation of the thiocarbonyl group, resulting ultimately in cleavage of the NO bond (Scheme 3, Table 67.1).[13,14] The initial homolysis gives an acyloxyl radical and the 2-pyridinethiyl radical, the latter having a long wavelength absorbance (λ_{max}, ~500 nm). No long-lived excited states are produced during preparation of the radical species.[13] The UV spectrum of the reaction is characterized by a marked negative band with a

maximum at 375 nm due to ground-state depletion resulting from the photoinduced decomposition of the starting material by NO bond cleavage and by a secondary bleaching process corresponding to the reaction of PyS$^{\bullet}$ with the ground state of the starting ester.[14] Irrespective of the R group, the quantum yield of photoinduced NO bond cleavage Φ_{NO} was found to be around 0.5.[14]

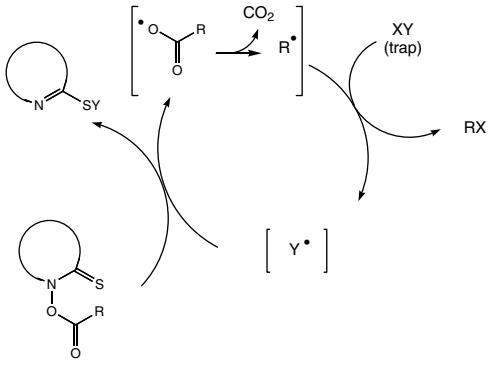

SCHEME 3

TABLE 67.1

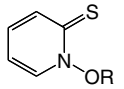

1

		λ (nm) [ε ($M^{-1}cm^{-1}$)]			
		benzene		acetonitrile	
a R = Bn-	**1a**	296 [13 300]	374 [5 200]	288	366
b R = Ph_2CH-	**1b**	296 [13 850]	374 [5 300]	288	366
c R = Me_3C-	**1c**	296 [13 500]	374 [5 100]	288	366
d R = Ph-	**1d**	296 [13 800]	374 [5 100]	288 [12 750]	366 [5 700]

The generated alkylacyloxyl radicals are unstable under the reaction conditions and undergo decarboxylation, giving rise to the corresponding alkyl radicals almost instantly (i.e., in less than 1 ns) (Scheme 3).[15–18] In contrast, the decarboxylation of arylcarbonyloxyl or vinylic acyl radicals is reasonably slow below 100°C,[17] and the intermediate carboxyl radicals can be trapped at room temperature by electron-rich olefins such as vinyl ethers[7b,18] or alkynes.[19] In the absence of added trap, such radicals eventually afford acid anhydrides. When decarboxylation occurs, excess of good trap XY can immediately react with the carbon radical R$^{\bullet}$, resulting in formation of the trapped product RX and the chain carrier radical Y$^{\bullet}$. The radical chain sequence is perpetuated by the addition of radical Y$^{\bullet}$ to the sulfur center of the starting thione, thus reforming the acyloxyl radical. The chain length varies sensitively with the reaction conditions and typically is 10 to 30, although it can be as high as 60 (as observed in halogenation reactions) or 600 (as seen in phosphonylation reactions under photolytic conditions).[3g] The efficiency depends on the concentration and reactivity ratios of the Barton ester and of the trap XY.

The driving forces for the reaction are the formation of a strong C=O bond at the expense of the weak thiocarbonyl bond and the aromatization of the heterocycle. Compounds having non-aromatizable cycles undergo thermal rearrangement reluctantly, although the UV photolysis remains efficient in generating radicals.[20] The fragmentation reaction also makes the reaction favored from an entropy point of view, and the loss of CO_2 renders the entire process irreversible. The chain propagation is assured by the affinity of the thione toward sulfur-centered or, alternatively, tin- or silicon-centered radicals and the weakness of the NO bond.

In the absence of external traps, Barton esters undergo decarboxylative rearrangement in which the formed carbon-centered radicals add to their precursor, affording alkyl 2-pyridyl sulfides (Scheme 4).[21a] Competitive

studies have determined rate constants of 2×10^6 (50°C) and 4.6×10^5 (30°C) M^{-1} s^{-1} for the addition of primary and tertiary carbon radicals to their precursor, respectively. This is the simplest and most characteristic reaction of this type of chemistry. Even in more complex reactions and independently of the nature of the radical trap used, this rearrangement occurs as a competing background reaction. The rearrangement becomes dominant when the trapping reaction (by an olefin, for example) is otherwise too slow.

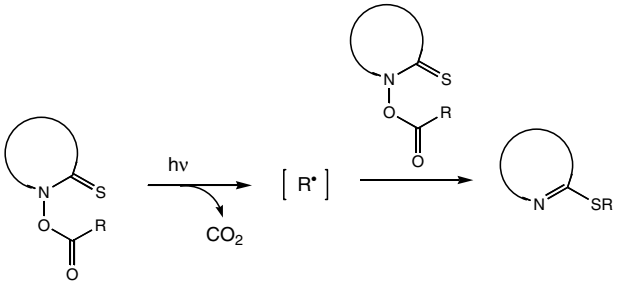

SCHEME 4

In some cases, the reaction affords a non-negligible amount of dipyridyl-disulfide and dialkyl dimers, particularly when the photolysis is run at the lower temperature of 80°C. One explanation can be the recombination of the thiopyridyl radicals and the stabilized (alkyl) radicals, respectively, suggesting that this process competes or even supplants the chain pathway at low temperature.[22,23a] Evidence was found, however, that bisulfide formation is rather the consequence of chain reactions of the type depicted in Scheme 5, in which the PyS· reacts with its precursor and leads to further production of R·.[14] Arguably, this process is even more dominant where the steady-state concentration of the radicals are lower and the concentration of the starting ester is higher. Yet, increasing the temperature (to 110°C) is sufficient to simplify the reaction course to the normal radical chain process.[22]

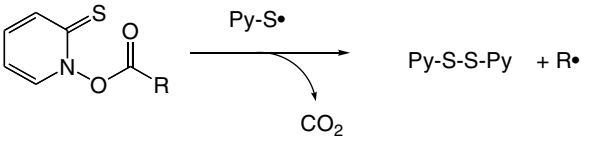

SCHEME 5

Related Thiohydroxamate Systems

In the wake of efficient free-radical chemistry by means of PTOC esters, a number of related hydroxamate systems have been devised and tested (Scheme 6).[18a,20–24,61] The influence of the substitution pattern of the thiopyridone moiety (**3** to **6**) as well as the nature of the heterocycle (**7** to **9**) and the effect (absence) of the aromatizable cycle (**10** and **11**) have been addressed.[18a,20,23,61] Related compounds having no thiohydroxamate backbone, such as compound **12** and the seleno-derivative **13**, have also been prepared.[21,23a]

Similar to esters derived from *N*-hydroxypyridine–2(1*H*)-thione **1**, the *O*-esters of 4-methyl and 4-phenyl *N*-hydroxythiazoline-2-thiones (**7a** and **7b**) undergo smooth thermal decarboxylative rearrangement in refluxing toluene but require UV photolysis at ~320 nm (medium mercury pressure) for the photochemical reaction.[18a,61]

In contrast, the 2-substituted *N*-acyloxyquinazoline-4-thione derivatives **8a–c** are highly light-sensitive products and rearrange easily. Varying the substituents on the aromatic side chain of **8**, however, changes only ε, but does not shift λ_{max}, which is around 356 nm.[23a] The reactivity and light sensitivity of these compounds are also reflected in their half-lives. The half-life of the photolytic rearrangement (tungsten light, 300 W) of **8a** is 14 s, the shortest ever observed in this type of Barton chemistry. For comparison,

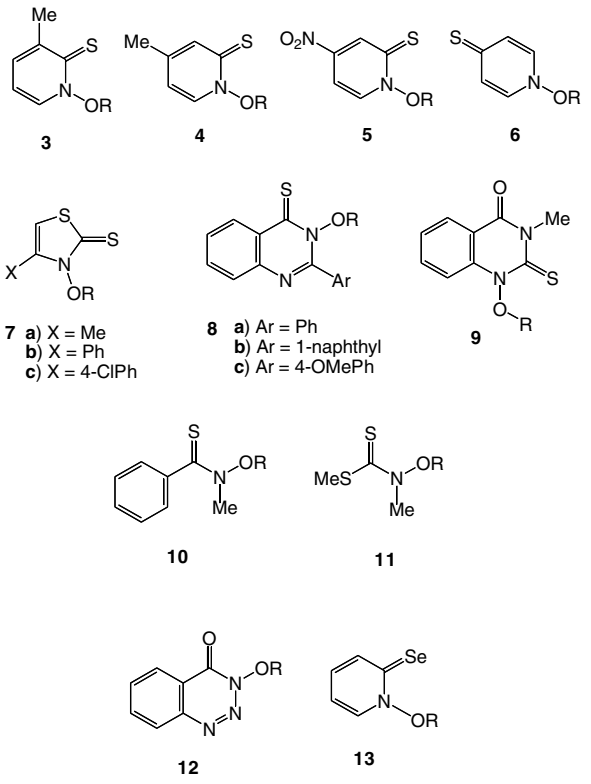

SCHEME 6

the half-life of compound **12** is 19 s under similar conditions, which is one magnitude shorter than half-lives usually observed for thiopyridone derivatives such as **1** (200 s). Although compounds **3** to **7** can be stored at –25°C in a dark vial without decomposition, **8** is too unstable at this temperature and rearranges within a few hours to the corresponding thioether.

The thione function of the Barton ester **1** can be replaced by other elements such as Se (**13**) without significant alteration of the reactivity (Scheme 6).[21] Although the starting esters are more air sensitive than the analogous *N*-hydroxypyridine 2-thione derivatives (**1**), the method has some advantages; for example, the adducts of the free-radical fragmentation reactions of *N*-hydroxypyridine-2-selenone derivatives **13** (i.e., alkylpyridylselenides) can usually be more easily modeled and transformed to other chemical functions than thioethers.

Recently, solid-supported reagents were proposed.[24] This technique may allow easier separation of the radical end product and also open the way for automated parallel synthesis of products arising from CC, CN, and CO bond-forming radical chain reactions.

Preparation of Barton Esters

In addition to the general usefulness of this class of compounds, the popularity of this chemistry is largely due to the facile preparation of the starting materials (Scheme 7). The most straightforward method of preparation of Barton esters of types I to IV is acylation by activation of the corresponding carboxylic acid (paths A and B). Accordingly, the hydroxamic acid sodium salt can be *O*-acylated with the acyl chlorides or, alternatively, the free hydroxamic acid can be condensed with primary carboxylic acids in the presence of *N,N′*-dicyclohexylcarbodiimide and dimethylaminopyridine (DMAP).[25] Likewise, condensation of the free thiohydroxamic acid or the corresponding sodium salt with the mixed anhydride formed from the acid and isobutyl chloroformate in the presence of *N*-methylmorpholine has proven to

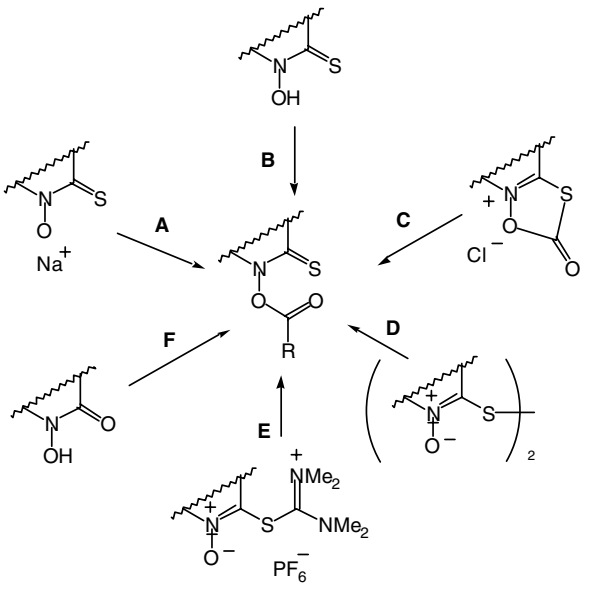

SCHEME 7

be the most useful method in the activation of amino acids.[26] In some cases, this activation fails, but addition of phosphonic acid anhydride (PPAA) to a solution of thiohydroxamic acid, acetic acid, and pyridine or DABCO® may overcome this difficulty.[27] A conceptually different approach is when the thiohydroxamic acid is activated and condensed with the carboxylic acid. Cyclic carbonate salt (path C), which is prepared from 2-mercaptopyridine-*N*-oxide with phosgene, was used to prepare *O*-acyl thiohydroxamates. Also, the use of disulfide in the presence of tributylphosphine is a particularly mild activation methodology that can be used in connection with easily epimerizable substrates (path D).[28] The use of HOTT (*S*-(1-oxido-2-pyridinyl)-1,1,3,3-tetramethyl thiouronium hexafluorophosphate) salt is a recent alternative. The activated ester is a stable crystalline solid, which allows esterification even with hindered carboxylic acids (path E).[29] A third type of approach consists of transforming the *O*-acyl hydroxamates to *O*-acyl thiohydroxamates by Lawesson's reagent, although this method is reputedly low yielding (path F).[30]

The preparation of *N*-alkoxy derivatives (i.e., type V) is somewhat more difficult. They can be prepared by treatment of the sodium salt of 2-mercaptopyridine-N-oxide with 1 molar equivalent of the suitable alkyl halide in DMF at 80°C.[80] By using this coupling reaction, alkylation occurs at sulfur rather than at oxygen, and the reaction affords pyridyl sulfides as the major product. In such cases, the Mitsonobu method using diethyl azodicarboxylate and triphenylphosphine may provide a solution (Scheme 8).[31]

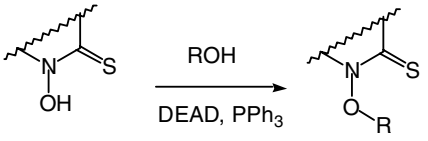

SCHEME 8

67.3 Elementary Reactions

Formation of C-Centered Radicals

Barton esters were used in a number of standard and also in more complex free-radical transformations including substitution, fragmentation/elimination, and addition reactions. Some representative examples are collected in the following sections.

Free-Radical Substitution Reactions

Reductive Decarboxylation

The photolysis or thermolysis of *O*-acyl-thiohydroxamates in the presence of appropriate H-donors gives rise to reductive decarboxylation via a free-radical mechanism. Hydrogen donors can be tin hydrides such as Bu_3SnH or Ph_3SnH, silicon hydrides such as $(TMS)_3SiH$, or more generally thiols such as Me_3CSH or PhSH. The general usefulness of the reaction has been validated in a number of syntheses.[32] The scope of the reaction is illustrated in Scheme 9, which shows the reduction of a key intermediate in the synthesis of the (±)-kopsidasine.[33]

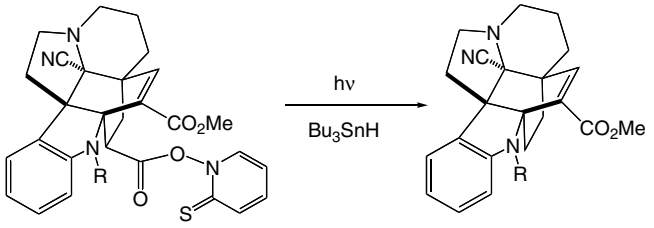

SCHEME 9

Decarboxylative Halogenation

The free-radical halogenation reaction using Barton chemistry has proved to be particularly mild and selective.[34–36] The radical chain is relatively long in the case of bromination (up to 60) by using $CBrCl_3$. Halogen donors can be CBrCl3, CCl4, CH3I, or CHI3. Scheme 10 shows decarboxylative halogenation on the aziridine cycle in the synthesis of the antitumor agent FR-900482;[35] it is worth pointing out the chemoselectivity of the transformation and the absence of the intramolecular alkylation reaction in the presence of activated indole.

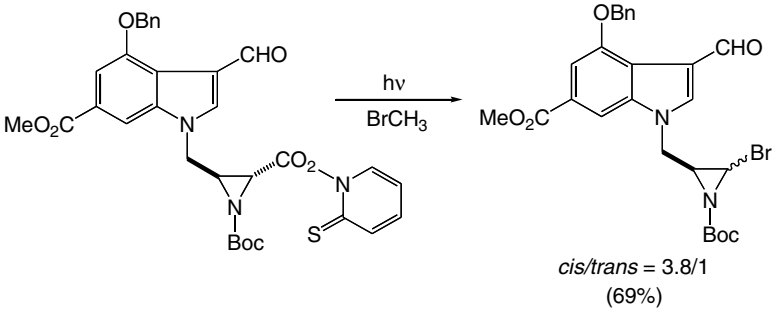

SCHEME 10

Aryl carboxylic acids can be halogenated conveniently under free-radical conditions.[34a–c,36] This transformation offers an alternative to the Hunsdiecker reaction. Under the classical conditions, the substrate undergoes a parasite electrophilic (Friedel–Crafts) halogenation reaction, which is translated in decreased yields. The radical variant of this transformation allows the use of very strong electrophiles and can be performed in the absence of heavy metals. The reaction is performed at high temperatures (~100 to 130°C) in order to favor the unimolecular decarboxylation step of the intermediate acyloxyl radical. Even under such drastic conditions, the sluggish decarboxylation may hamper the efficiency of the radical chain process, causing a buildup of ester concentration. The addition of external initiator such as AIBN may circumvent this difficulty by increasing the number of radical chains in operation (Scheme 11).

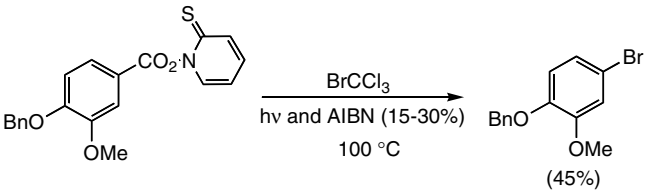

SCHEME 11

Deoxygenation of Tertiary Alcohols

A conceptually different fragmentation reaction is the homolytic fragmentation of mixed oxalate esters such as III.[37] This reaction offers an alternative to the more frequently used Barton–McCombie deoxygenation reaction.[38] The fragmentation requires thermal activation. Reactions produced by using tertiary alcohols as substrates are usually performed in refluxing benzene and are heated in PhCl (132°C) for deoxygenation of secondary alcohols. Deoxygenation of tertiary alcohols is of interest when the Barton–McCombie reaction offers only limited utility due to competing Tsugaev olefination reactions. The intermediate transient free radical can be reduced in the presence of hindered H-donors, such as 1,1-dimethylethane-thiol or, better, 1,1-diethylpropane-thiol, or alternatively can be captured by simple Michael acceptors (Scheme 12).[38] The corresponding alkyl halide can be obtained when the reaction is carried out in refluxing carbon tetrachloride.[39]

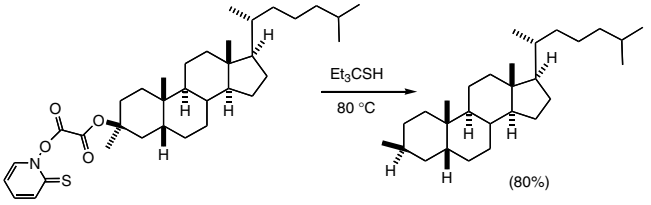

SCHEME 12

Free-Radical nor-Hydroxylation and Peroxide Formation

Basically, two standard methods are used to obtain nor-hydroxy or hydroperoxy compounds by free-radical decarboxylative fragmentation of Barton esters, either under photochemical or thermal conditions. The trapping of the intermediate radicals by triplet oxygen (bubbling) is a simple reaction both from a mechanistic and preparative standpoint (Scheme 13).[41] The reaction gives rise, in the presence of *t*-butyl-mercaptan, to the corresponding hydroperoxides. The kinetic basis of this reaction is the fact that the capture of the molecular oxygen is some ten thousand times faster than the competitive hydrogen atom abstraction from a thiol. The hydroperoxide can be isolated or alternatively can be transformed either into alcohol by using reductive work-up[41] or can be transformed into a ketone in the presence of TsCl and pyridine (Scheme 13).

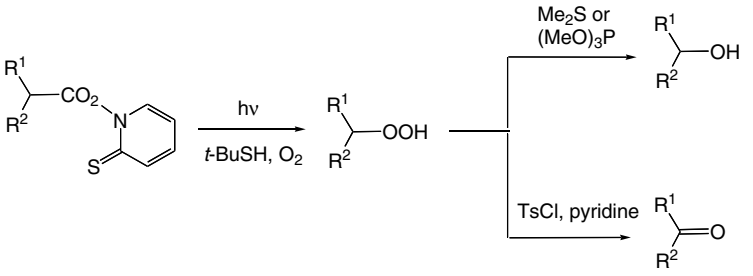

SCHEME 13

The nor-hydroxylation reaction by using *tris*(phenylthio)antimony was developed later.[42] In this reaction, the organoantimony reagent traps the intermediate free radical. The formed organoantimony derivative is air sensitive and undergoes oxygen insertion into the C-Sb bond in the presence of air. The corresponding alcohol is obtained after aqueous hydrolysis. Scheme 14 is represents the synthesis of a carbocyclic analog of glucose.[43]

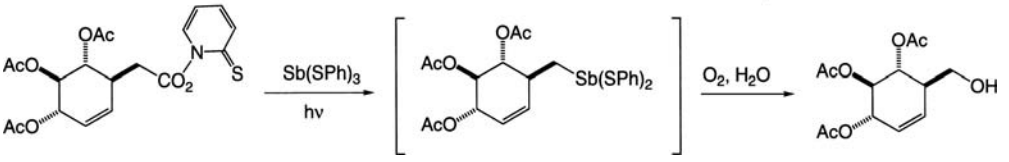

SCHEME 14

Decarboxylative Phosphonylation

Analogous to the free-radical hydroxylation using *tris*(phenylthio)antimony, the trapping of radicals derived from *O*-acyl-thiohydroxamates with *tris*(phenylthio)phosphorous proceeds via a free-radical chain process (Scheme 15).[44] The formation of the thiophosphonate end product is the result of a consecutive rearrangement of a pentavalent intermediate under the reaction condition and hydrolysis under aqueous work-up.

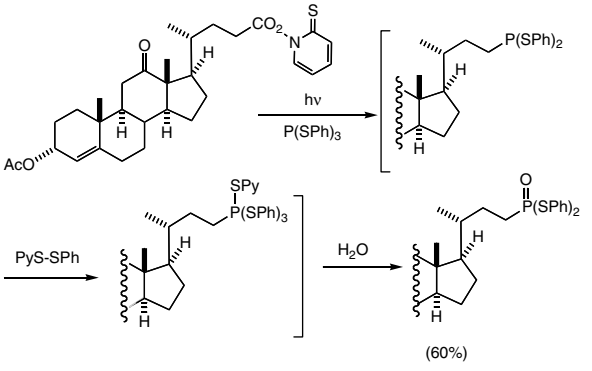

SCHEME 15

A conceptually different and even more elegant method was to convert carboxylic acids into phosphonates by the use of elemental white phosphorous (P_4) as a trap.[45] The reaction can be initiated by light in a CH_2Cl_2/CS_2 binary mixture or in the dark by traces of oxygen by using tetrahydrofurane (THF) as solvent. Oxidation of the intermediary products provides a convenient synthesis of phosphonic acids.[43]

Substitution on Selenium, Tellurium, and Boron

Aryl-tellurides undergo radical fragmentation reactions in the presence of methyl radical generated by photochemical decarboxylation of *O*-acetyl thiohydroxamate.[46] The driving force of this reaction is the formation of the relatively strong methyl-tellurium bond at the expense of the R-tellurium bond. Conventional radical traps can react with the formed alkyl radical. Scheme 16 shows an application of this reaction in the synthesis of *showdomycin*.[46a]

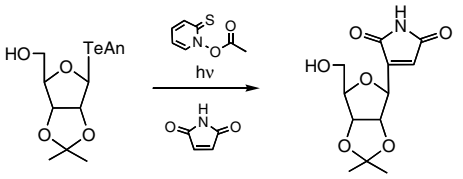

SCHEME 16

Another application concerns the preparation of selenides and tellurides from diaryl diselenides[40] or ditellurides.[47] While selenide formation is carried out in refluxing toluene by using a large excess of diselenides, diaryl ditellurides give the best results by utilizing visible irradiation at 35°C. Aryl, benzyl, methyl, and dicyanogen selenides can be prepared in this way.

The substitution reaction can also be carried out under intramolecular conditions.[48] Scheme 17 illustrates synthesis of the selenopenam. When a solution of the acid chloride in benzene was slowly added to a water-cooled, irradiated (250-W tungsten lamp) suspension of the sodium salt of *N*-hydroxypyridynethione in benzene, the selenopenam analog was isolated in 38% yields as a 7:3 mixture of diastereoisomers.[48a]

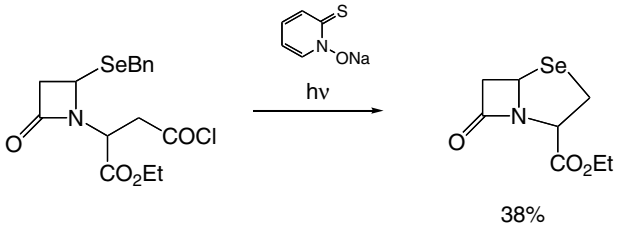

SCHEME 17

The use of PTOC esters under photochemical conditions offers a logical solution to the lack of reactivity and to the chain propagation problems, usually encountered in free-radical fragmentation of organoboranes (Scheme 18).[49] In the postulated mechanism of the reaction, the formed arylcarbonyloxyl radical[49b]

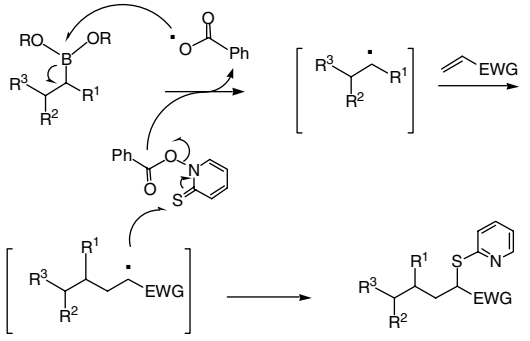

SCHEME 18

or eventually alkoxy radical[49c] reacts with the boronic ester, resulting in selective fragmentation of the weak B-alkyl bond (Scheme 18). Best results were obtained by using catechol boronates, with $(RO)_2$ = catechol. Under these conditions, the alkylation reaction can be extended to a seemingly unrestricted array of Michael acceptors.

Free-Radical Fragmentation/Elimination Reactions

Homolytic vs. Heterolytic Fragmentation Problem of the Transient Radical

When a radical is generated in a position adjacent to a homolytically easily fragmenting function (such as a thioether, nitro-group, halogen, epoxide, or other strained cycles), the radical intermediate can be stabilized by fragmentation and may evolve toward the formation of olefins.[50] In some cases, the dissociation of the radical intermediate occurs by a heterolytic path, giving rise to radical ionic intermediates. This radical/polar crossover sequence occurs in the fragmentation of β-phosphatoxyalkyl radicals. Because of the biochemical relevance of this reaction and because of the synthetic/mechanistic potential of this transformation, the study of β-phosphatoxyalkyl radicals has moved into the spotlight. The intermediate radical may evolve toward either the elimination or phosphate-migration product.[51] Dissociation occurs with the formation of a radical-cation intermediate that can be intercepted by conveniently chosen nucleophiles. Scheme 19 illustrates a short application in the synthesis of substituted tetrahydrofurans.[52]

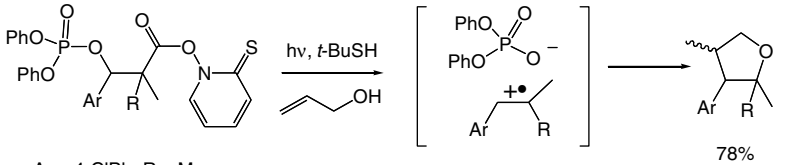

Ar = 4-ClPh; R = Me

SCHEME 19

Photoinduced Nucleic Acid Cleavage

Hydroxyl radicals are known to cleave DNA in a variety of ways, including direct hydrogen atom abstraction from the backbone and nucleobase modification. One of the main H-abstraction pathways occurs by generating nucleotide C4′ radicals. This transformation is implicated in the cleavage of DNA by antitumor antibiotics such as bleomycin, a process that is blamed for related DNA degradation reactions under anaerobic conditions. In these reactions, the C4′ radicals formed are thought to undergo initial heterolysis, producing enol-ether radical cations and phosphate anions.[53] Evidence of heterolysis of C4′ radicals has been reported by the Giese group.[54,55] As was discussed earlier, the heterolysis produces a contact ion pair (CIP) that can collapse back to a radical or solvate to give a solvent-separated ion pair (SSIP) evolving toward the diffusively free species.[56]

Such "artificial" photonucleases can be generated by UV excitation of *N*-hydroxypyridinethiones (*N*-HTP) **1** and **6** (R = H) and *N*-aroyloxypyridine-2-thiones (**1**, R = $ArCO_2$), which can photocleave DNA through release of hydroxyl or aryloyloxyl radicals, repectively.[7,10,11,14,57–59] Some more complex structures based on Barton esters were also prepared. Recent efforts are focused on combining these highly efficient DNA-cleaving families with an intercalative moiety (Scheme 20).[60]

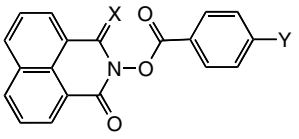

X = S, O
Y = H, F, Cl, CH_3, OCH_3,

SCHEME 20

Free-Radical Addition Reactions

Alkylation Reactions

Carbon-centered radicals generated from **1** add preferentially to electron-deficient olefins in a regioselective manner.[61,62] The reaction follows the classical trend observed for free-radical reactions (Scheme 21). A characteristic feature of this reaction is the incorporation of a thiopyridyl unit in to the β-position. This bonus reaction may open the way for further functionalization of the molecule. Eventually, the thiopyridyl moiety can be removed by using Zn/acetic acid,[63] $NiCl_2/NaBH_4$ or Raney Ni,[64] Na_2Te reduction,[63f] catalytic hydrogenation over Pd/C, or by reductive cleavage of the corresponding pyridyl sulfone in the presence of SmI_2.[49a] Activated terminal alkenes (e.g., β-unsubstituted Michael acceptors) afford moderate to good yields in intermolecular alkylation reactions. A great variety of activating groups, such as ketones, esters, amides, phosphonates, sulfones, nitriles, and nitro compounds were tested and shown to afford high yields for alkylation.[65] The following example was taken from the stereoselective synthesis of indolizidine 167B (Scheme 21).[63a]

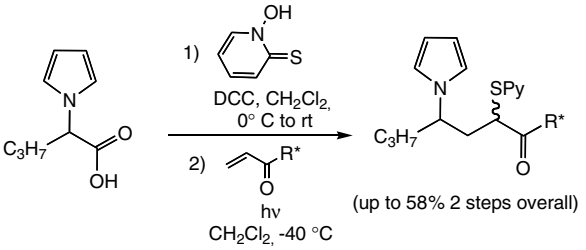

SCHEME 21

In contrast, β-substituted olefins generally reacted too slowly to afford synthetically useful yields of the alkylated product. In these reactions, the main reaction path is the rearrangement of the Barton ester affording thiopyridyl ethers. The use of the strongly electron-withdrawing nitro-group as the activating group or *bis*-activation as in maleates, fumarates, and quinones may allow such alkylation.[61,66] An elegant example of this type of alkylation reaction is presented in the synthesis of avarol and its structural analog avarone (Scheme 22).[67] The transformation involves photochemical activation at 350 nm of the thiohydroxamic ester and *in situ* trapping of the generated carbon radicals by benzoquinone. The reaction affords the hydroquinone, which is further oxidized with the excess of benzoquinone.[68]

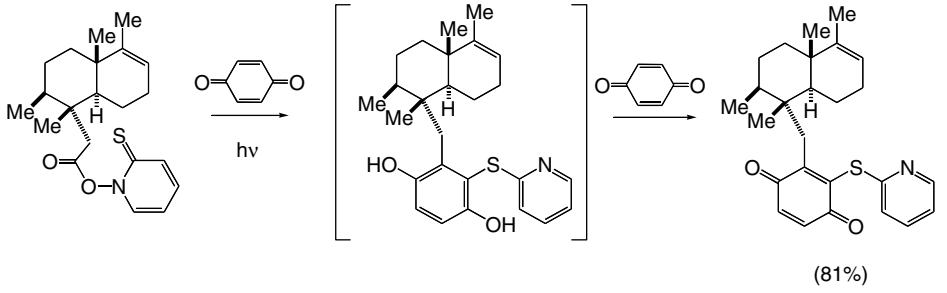

SCHEME 22

The free-radical alkylation is not restricted to the use of classical Michael acceptors. Vinylphosphonium salts are also good radicophiles, allowing the formation of the corresponding pyridyl-sulfide after basic hydrolysis (Scheme 23).[3d]

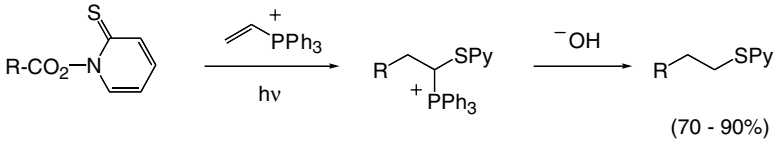

SCHEME 23

Likewise, protonated heteroaromatic bases are also good acceptors. Addition of alkyl radicals derived from Barton esters to pyridinium salts leads to the mixture of 2- and 4-substituted pyridines, in which the 2-isomer form predominates.[69]

Related free-radical alkylation reactions include the trapping of isocyanides[70] and the decarboxylative cyanation reaction.[71] Both methods allow entry to the preparation of labeled carboxylic acids.

Remarkably, only a small number of intramolecular reactions utilize Barton esters;[41a,61,72] likewise, the use of the Barton chemistry in making CC bonds in tandem or domino reactions is far less exploited compared to the tin-hydride-mediated free-radical sequences.[73] The following example is taken from the biomimetic conversion of isoflavone to the rotenoid, where the reaction affords the 6-*endo* product (Scheme 24).[72a]

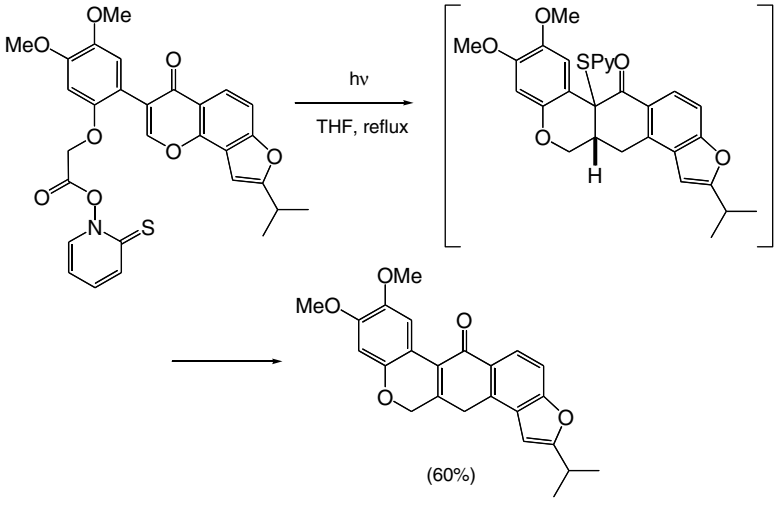

SCHEME 24

Sulfonation

A large excess of sulfur dioxide (i.e., a mixture of sulfur dioxide and dichloromethane at –10°C) can overcome the problem of the competing rearrangement, which is the result of the sluggish addition of the carbon-centered radical to the SO double bond.[74] The reaction allows entry to the preparation of sulfones.

Amination and Nitrosation

Free radicals generated under photochemical conditions from thiohydroxamates add readily to the NN double bond of diaziridines and in particular to the 3-bromo or 3-trifluoromethyl-3-phenyldiazirine to produce diaziridinyl radicals (Scheme 25);[75] these intermediates undergo dimerization and fragmentation to yield the corresponding imines, which can be hydrolyzed to the corresponding amines. Barton esters can also be used for the direct preparation of nitroso compounds.[76] From a synthetic standpoint, the yields are moderate and the method is limited to primary and secondary carboxylic acids, which form dimers as an end product. Tertiary nitroso compounds do not dimerize and further react with the radical present under the reaction conditions.

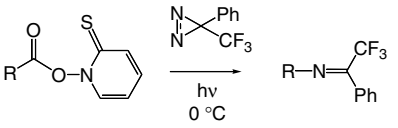

SCHEME 25

Generation of Heteroatom-Centered Radicals

Hydroxyl radicals can be generated by photolysis of thiohydroxamic acid **1** (Scheme 2, R=H) and its derivatives (Barton esters of type **I**).[9] Likewise, the photo- or thermolysis of mixed carbonates (IIa), carbamates (IIb),[77] and α-substituted acetates (IV)[78] may give rise to *O*- and *N*-centered radicals, respectively.[7b;65e,g;77b;79] Analogously, pyridinethione *O*-ethers, such as V have also been shown to give alkoxy radicals.[80,81] Although the original *N*-(alkenoxy)pyridine-2(1*H*)-thiones and in particular the *N*-benzyloxy derivatives are usually rather unstable, modified derivatives were proposed.[82] These *N*-(alkoxy)thiazolethiones (**7**, Scheme 6) are less sensitive to visible light than the corresponding pyridinethiones and require irradiation at $\lambda \leq \sum$ 350 nm. When *N*-cyclopentoxy- or carbohydrate-derived thiazole-2(3*H*)-thiones are photolysed in the presence of a hydrogen donor, the product of the reaction is the corresponding substituted aldehyde formed via highly regioselective radical fragmentation.[82] Primary oxyl radicals are more stable toward fragmentation.[31b] Usually, electron-donating substituents can improve the stability of oxygen and, in a larger sense, heteroatom-centered radicals, while electron-withdrawing substituents do not.[83] In the presence of a suitable intramolecular trap, the formed oxyl radical undergoes fast cyclization, forming tetrahydrofurans and tetrahydropyrans, respectively, often with remarkably high regio- and stereoselectivity.[84] The key 6-*exo trig* cyclization in the synthesis of (+)-*allo* muscarine illustrates the synthetic potential of this transformation (Scheme 26).[85] The cyclization reaction can be run also in water by using *N*-alkoxy-(*p*-chlorophenyl)thiazole-thione **7c** as an activator (see Scheme 6) and irradiation at 350 nm.[86]

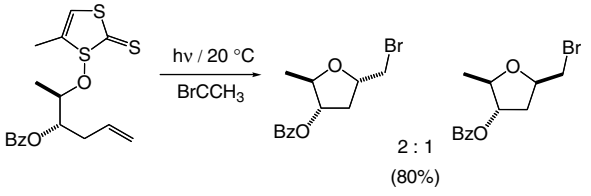

SCHEME 26

67.4 Kinetic Measurements: Radical Clocks

The PTOC method in kinetic studies was originally developed to avoid the inherent boundary and precursor instability encountered at the upper limit of the tin-hydride method. This technique relies on the generation and simultaneous competitive trapping of the radicals by convenient radical traps, such as thiols or tin-hydrides, and on the analysis of the product distribution. PTOC esters are excellent radical sources for LFP studies because they have a strong long-wavelength absorbance at λ_{max} of about 360 nm and are efficiently cleaved either by 355-nm light from a Nd:YAG laser[13,72,87] or at 308 nm by using XeCl excimer laser over a large temperature range (–40 to 50°C). For the LFP studies, a dilute solution of the starting ester in a static cell or, more frequently, in a flow-cell assembly is used. It should be noted that complete chain collapse resulting from highly dilute solution of PTOC esters could be accommodated by extended photolysis, because Barton esters are not only chain carriers but also radical initiators. It is technically advantageous that the 2-pyridinethiyl radical formed during the course of the homolytic fragmentation reaction has a long-wavelength absorbance with λ_{max} at 490 nm but does not absorb strongly between ~3l0 and 350 nm.

67.5 Alternative Reactions

Hypervalent iodine compounds, especially (diacetoxyiodo)arenes, have been used for the generation of C-centered radicals through thermal or photochemical fragmentation of carboxylic acids.[88] The reaction works well to generate carbon-centered radicals by β-cleavage of alcohols. The reaction, which is usually known as the Suàrez reaction, was extended to oxygen- and nitrogen-centered radicals. The radicals were employed in oxidative addition, substitution, β-fragmentation, Hofmann–Löffler–Freytag reactions, and reductive addition reactions were used successfully for functional group transformation, formation of new skeletons, and synthesis of natural products.[89] Depending on the reaction conditions, the intermediate radical can be oxidized to the corresponding carbocation. Scheme 27 shows this transformation in the synthesis of gibberellins.[90]

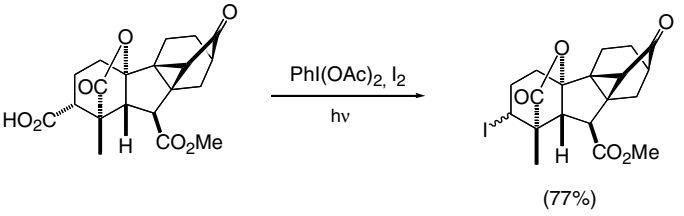

SCHEME 27

Acknowledgment

I wish to thank Professors David Crich and Emmanuil A. Theodorakis for their help in correcting this manuscript.

References and Notes

1. Barton, D. H. R., Crich, D., and Motherwell, W. B., New and improved methods for the radical decarboxylation of acids, *J. Chem. Soc., Chem. Commun.,* 939, 1983.
2. The generation of free radicals can be realized in the absence of metals.
3. For reviews see: (a) Barton, D. H. R. and Motherwell, W. B., Some recent progress in natural product chemistry, *Heterocycles*, 21, 1, 1984; (b) Barton, D. H. R. and Zard, S. Z., Invention of new reactions useful in the chemistry of natural products, *Pure Appl. Chem.*, 58, 675, 1986; (c) Barton, D. H. R. and Zard, S. Z., A novel radical decarboxylation, *Janssen Chim. Acta*, 4, 3, 1986; (d) Crich, D., *O*-acyl Thiohydroxamates: new and versatile sources of alkyl radicals for use in organic synthesis, *Aldrichim. Acta*, 20, 35, 1987; (e) Crich, D. and Quintero, L., Radical chemistry associated with the thiocarbonyl group, *Chem. Rev.*, 89, 1413, 1989; (f) Barton, D. H. R., The invention of chemical reactions, *Aldrichim. Acta*, 23, 3, 1990; (g) Barton, D. H. R., The invention of chemical reactions: the last 5 years, *Tetrahedron*, 48, 2529, 1992; (h) Barton, D. H. R., The invention of chemical reactions of relevance to the chemistry of natural products, *Pure Appl. Chem.*, 66, 1943, 1994; (i) Baguley, P. A. and Walton, J. C., Flight from the tyranny of tin: the quest for practical radical sources free from metal encoumbrances, *Angew. Chem. Int. Ed. Engl.*, 37, 3072, 1998.
4. See also in (a) Motherwell, W. B. and Imboden, C., Decarboxylation via *O*-acyl thiohydroxamates; in *Radicals in Organic Synthesis*; Renaud, P. and Sibi, M., Eds., VCH, Weinheim, 2001; (b) Barton, D. H. R. and Parekh, S. I., *Half a Century of Free-Radical Chemistry*, Cambridge University Press, Cambridge, U.K., 1993; (c) Crich, D. and Motherwell, W. B., *Free Radical Chain Reactions in Organic Synthesis*, Academic Press, London, 1992.
5. For a general review on the chemistry of thiohydroxamate containing compounds, see: Chimiak, A., Przychodzen, W., and Rachon, J., The thiohydroxamate system, *Heteroatom Chem.*, 13, 169, 2002.

6. (a) Taylor, E. C., Kienzle, F. and McKillop, A., Thallium in organic synthesis. XII. Improved syntheses of the 1-acyloxy-2(1*H*)-pyridone class of active esters, *J. Org. Chem.*, 35, 1672, 1970; (b) Taylor, E. C., Altland, H. W., Kienzle, F., and McKillop, A., Thallium in organic synthesis. XLI. Synthesis of 1-substituted 2(1*H*)-pyridones: new synthesis of unsymmetrical biphenyls via photochemical nitrogen–oxygen bond cleavage of 1-aroyloxy-2(1*H*)-pyridones, *J. Org. Chem*. 41, 24, 1976.
7. (a) Boivin, J., Crepon, E., and Zard, S. Z., *N*-Hydroxy-2-Pyridinethione: a mild and convenient source of hydroxyl radicals, *Tetrahedron Lett.*, 31, 6869, 1990; (b) Barton, D. H. R., Jaszberényi, J. Cs., and Morrell, A. I., The generation and reactivity of oxygen centered radicals from the photolysis of derivatives of *N*-hydroxy-2-thiopyridone, *Tetrahedron Lett.*, 32, 311, 1991; (c) Hess, K. M. and Dix, T. A., Evaluation of *N*-hydroxy-2-thiopyridone as a nonmetal dependent source of the hydroxyl radical (HO·) in aqueous systems, *Anal. Biochem.*, 206, 309, 1992.
8. Reszka, K. J. and Chignell, C. F., Photochemistry of 2-mercaptopyridines. 3. EPR study of photoproduction of hydroxyl radicals by *N*-hydroxypyridine-2-thione using 5,5-dimethyl-1-pyrroline *N*-oxide in aqueous-solutions *Photochem. Photobiol.*, 61, 269, 1995.
9. (a) Boivin, J., Crepon, E., and Zard, S. Z., Generation of hydroxyl radicals from 1-hydroxypyridine-2(1*H*)-thione and their application to organic synthesis, *Bull. Soc. Chim. Fr.*, 129, 145, 1992; (b) Willie, U., Radical oxygenations with inorganic radicals: can hydroxyl radicals (HO) act as donors of oxygen atoms? *Tetrahedron Lett.,* 43, 1239, 2002.
10. Aveline, B. M., Kochevar, E. E., and Redmond, R. W., Photochemistry of the nonspecific hydroxyl radical generator *N*-hydroxypyridine-2(1*H*)-thione, *J. Am. Chem. Soc.*, 118, 10113, 1996.
11. Aveline, B. M., Kochevar, E. E., and Redmond, R. W., *N*-hydroxypyridine-2(1*H*)-thione: not a selective generator of hydroxyl radicals in aqueous solution, *J. Am. Chem. Soc.*, 118, 289, 1996.
12. The acronym PTOC is derived from pyridine-2-thioneoxycarbonyl.
13. Bohne, C., Boch, R., and Scaiano, J. C., Exploratory studies of the photochemistry of *N*-hydroxypyridine-2-thione esters: generation of excited radicals by laser flash photolysis and in a conventional fluorescence spectrometer, *J. Org. Chem.*, 55, 5414, 1990.
14. Aveline, B. M., Kochevar, E. E., and Redmond, R. W., Photochemistry of *N*-hydroxypyridine-2 thione derivatives: involvement of the 2-pyridylthiylradical in the radical-chain reaction mechanism, *J. Am. Chem. Soc.*, 117, 9699, 1995.
15. Bockman, T. M., Hubig, S. M., and Kochi, J. K., Direct observation of ultrafast decarboxylation of acyloxy radicals via photoinduced electron transfer in carboxylate ion pairs, *J. Org. Chem.*, 62, 2210, 1997.
16. $k = 10^9\ M^{-1}\ s^{-1}$; see Newcomb, M. and Park, S. U., *N*-hydroxypyridine-2-thione esters as radical precursors in kinetic studies: measurements of rate constants for hydrogen-atom-abstraction reactions, *J. Am. Chem. Soc.*, 108, 4132, 1986.
17. (a) Barton, D. H. R. and Ramesh, M., Generation and fate of nondecarboxylating acyloxy radicals derived from the photolysis of acyl derivatives of *N*-hydroxy-2-thiopyridone, *Tetrahedron Lett.*, 31, 949, 1990. The rate constant of this decarboxylative process is approximately $k = 10^6\ s^{-1}$ at 25°C; (b) see Chateauneuf, J., Lusztyk, J., and Ingold, K. U., Spectroscopic and kinetic characteristics of aroyloxyl radicals. 2. Benzoyloxyl and ring-substituted aroyloxyl radicals, *J. Am. Chem. Soc.*, 110, 2886, 1988.
18. (a) Barton, D. H. R., Crich, D., and Potier, P., On the mechanism of the decarboxylative rearrangement of thiohydroxamic esters, *Tetrahedron Lett.,* 26, 5943, 1985; (b) Barton, D. H. R. and Ramesh, M., Generation and fate of non-decarboxylating acyloxy radicals derived from the photolysis of acyl derivatives of *N*-hydroxy-2-thiopyridone, *Tetrahedron Lett.*, 31, 949, 1990.
19. (a) Wille, U., Self-terminating, oxidative radical cyclizations: a novel reaction of acyloxyl radicals, *J. Am. Chem. Soc.*, 124, 14, 2002; (b) Wille, U. and Jargstorff, C., Self-terminating, oxidative radical cyclizations of medium-sized cycloalkynones with inorganic and organic oxygen-centered radicals of type XO·: the reaction pathway depends on the nature of X, *J. Chem. Soc.*, *Perkin Trans. 1*, 1036, 2002.

20. Kim, S., Lim, C. J., Song, S. E., and Kang, H. Y., Decarboxylative acylation approach of thiohydroxamate esters, *J. Chem. Soc.*, *Chem. Commun.*, 1410, 2001.
21. (a) Barton, D. H. R., Crich, D., Herve, Y., Potier, P., and Thierry, J., The free radical chemistry of carboxylic esters of 2-selenopyridine-*N*-oxide: a convenient Synthesis of (L)-vinylglycine, *Tetrahedron*, 41, 4347, 1985; (b) Barton, D. H. R. and Tachdjian, C., The invention of radical reactions. 26. New thiohydroxamic and seleno-hydroxamic acids: radical chemistry of their *O*-acyl derivatives, *Tetrahedron*, 48, 7091, 1992.
22. Barton, D. H. R., Bridon, D., Fernandez-Picot, I., and Zard, S. Z., The invention of radical reactions. 15. Some mechanistic aspects of the decarboxylative rearrangement of thiohydroxamic esters, *Tetrahedron*, 43, 2733, 1987.
23. (a) Barton, D. H. R., Blundell, P., and Jaszberényi, J. Cs., The invention of radical reactions. *Tetrahedron*, 48, 7121, 1992. (b) For application of these substituted analogs, see Rao, U. N. and Biehl, E., Preparation of benzo[4,5]thieno[2,3-*b*]pyridines and naphtho[*b*-4,5]thieno[2,3-*b*]pyridines via the reaction of Barton esters and benzynes, *J. Org. Chem.*, 67, 3409, 2002.
24. (a) For Wang resin-bonded *N*-hydroxy thiazole-2(3)-thione, see De Luca, L., Giacomelli, G., Porcu, G., and Taddei, M., A new supported reagent for the photochemical generation of radicals in solution, *Org. Lett.*, 3, 855–857, 2001; (b) for Wang resin-bonded *N*-hydroxy pyridine-2(3)-thione derivatives, see Attardi, M. E. and Taddei, M., The Barton radical decarboxylation on solid phase: a versatile synthesis of peptides containing modified amino acids, *Tetrahedron Lett.*, 42, 3519, 2001.
25. Barton, D. H. R., Crich, D., and Motherwell, W. B., The invention of new radical chain reactions. 8. Radical chemistry of thiohydroxamic esters: a new method for the generation of carbon radicals from carboxylic acids, *Tetrahedron*, 41, 3901, 1985.
26. (a) Barton, D. H. R., Hervé, Y., Potier, P., and Thierry, J., Reductive radical decarboxylation of amino acids and peptides, *J Chem. Soc.*, *Chem. Commun.*, 1298, 1984; (b) Barton, D. H. R., Herve, Y., Potier, P., and Thierry, J., Manipulation of the carboxyl groups of alpha-amino-acids and peptides using radical chemistry based on esters of *N*-hydroxy-2-thiopyridone., *Tetrahedron*, 44, 5479, 1988.
27. Hartung, J. and Schwarz, M., The use of propane phosphonic acid anhydride (PPAA) in the synthesis of *N*-acyloxythiazole-2(3*H*)-thiones, *Synlett*, 371, 2000.
28. Barton, D. H. R. and Samadi, M., The invention of radical reactions. 25. A convenient method for the synthesis of the acyl derivatives of *N*-hydroxypyridine-2-thione, *Tetrahedron*, 48, 7083, 1992.
29. Garner, P., Anderson, J. T. and Dey, S., *S*-(1-oxido-2-pyridinyl)-1,1,3,3-tetramethylthiouronium hexafluorophosphate: a new reagent for preparing hindered barton esters, *J. Org. Chem.*, 63, 5732, 1998.
30. Prabhakar, S., Lobo, A. M., and Santos, A., A, Convenient method for the synthesis of *N*-hydroxy thiobenzamides (*C*-arylthiohydroxamic acids), *Synthesis*, 829, 1984.
31. (a) Kim, S., Lim, C. J., Song, S. E., and Kang, H. Y., A new convenient method for the generation of alkoxy radicals from *N*-alkoxydithiocarbamates, *Synlett*, 688, 2001; (b) Hartung, J., Gottwald, T., and Kneuer, R., Cyclopentyl and carbohydrate derivatives of *N*-hydroxy-4-methyl-thiazole-2(3*H*)-thione: synthesis by Mitsunobu reaction and highly selective photochemical conversion into aldehydes, *Synlett*, 749, 2001.
32. For selected examples, see (a) Braeckman, J. C., Daloze, D., Kaisin, M., and Moussiaux, B., Ichthyotoxic sesterpenoids from the neo guinean sponge *Carteriospongia foliascens*, *Tetrahedron*, 41, 4603, 1985; (b) Campopiano, O., Little, R. D., and Petersen, J. L., Evidence for hydrogen-atom abstraction and loss of diylophil stereochemistry in an intramolecular 1,3-diyl trapping reaction, *J. Am. Chem. Soc.*, 107, 3721, 1985; (c) Otterbach, A. and Musso, H., Asteranes. 18. Diasterane (tricyclo[3.1.1.$1^{2,4}$]octane), *Angew. Chem. Int. Ed. Engl.*, 26, 554, 1987; (d) Winkler, J. D. and Sridar, V., Stereochemical control of transannular radical cyclizations: a new approach to the synthesis of linearly fused cyclopentanoids, *J. Am. Chem. Soc.*, 108, 1708, 1986; (e) Winkler, J. D., Hey, J. P., and Williard, P. G., Inside outside stereoisomerism. 1. The synthesis of *trans*-bicyclo[5.3.1]undecan-11-one, *J. Am. Chem. Soc.*, 108, 6425, 1986; (f) Winkler, J. D., Heuegar, K. F., and Williard, P. G., Inside outside stereoisomerism. 2. Synthesis of the carbocyclic ring-system of the ingenane diterpenes via the intramolecular dioxolenone photocycloaddition, *J. Am. Chem. Soc.*, 109, 2850, 1987;

(g) Hell, Z. and Töke, L., Efficient method for removal of a carboxylic acid moiety from sterically crowded cyclopropanedicarboxylic acid derivatives, *Synth. Commun.*, 26, 2127, 1996.

33. Magnus, P., Payne, A. H., and Hobson, L., Synthesis of the *Kopsia* alkaloids (±)-11,12-demethoxylahadinine B, (±)-kopsidasine and (±)-kopsidasine-*N*-oxide, *Tetrahedron Lett.*, 41, 2077, 2000.
34. (a) Barton, D. H. R., Lacher, B., and Zard, S. Z., Radical decarboxylative bromination of aromatic-acids, *Tetrahedron Lett.*, 26, 5939, 1985; (b) Vogel, E., Schieb, T., Schulz, Wh., Schmidt, K., Schmickler, H., and Lex, J., Bridged [14]annulenes with a phenanthrene-perimeter: anti-1,6-7,12-bismethano[14]annulene, *Angew, Chem. Int. Ed. Engl.*, 25, 723, 1986; (c) Zhu, J., KIunder, A. J. H., and Zwanenburg, B., Generation and characterization of tricyclodecatrienone, a norbornene annulated cyclopentadienone, *Tetrahedron Lett.*, 34, 3335, 1993; (d) Fleet, G. W. J., Son, J. C., Peach, J. M., and Hamor, T. A., Synthesis and X-ray crystal structure of a stable α-chlorooxethane, *Tetrahedron Lett.*, 29, 1449, 1988.
35. Ziegler, R. E. and Belema, M., Chiral aziridinyl radicals: an application to the synthesis of the core nucleus of FR-900482, *J. Org. Chem.*, 62, 1083, 1997.
36. Barton, D. H. R., Lacher, B., and Zard, S. Z., The invention of radical reactions. Part XVI. Radical decarboxylative bromination and iodination of aromatic acids, *Tetrahedron*, 43, 4321, 1987.
37. (a) Barton, D. H. R. and Crich, D., A new method for the radical deoxygenation of tertiary alcohols, *J. Chem. Soc.*, *Chem. Commun.*, 774, 1984; (b) Barton, D. H. R. and Crich, D., The invention of new radical chain reactions. Part 11. A new method for the generation of tertiary radicals from tertiary alcohols, *J. Chem. Soc.*, *Perkin Trans. 1*, 1603, 1986.
38. Barton, D. H. R. and McCombie, S. W., A new method for the deoxygenation of secondary alcohols, *J. Chem. Soc.*, *Perkin Trans. 1*, 1575, 1975.
39. Crich, D. and Fortt, S. M., A new method for the synthesis of *tert*-alkyl chlorides from *tert*-alcohols, *Synthesis*, 35, 1987.
40. Barton, D. H. R., Bridon, D., Herve, Y., Potier, P., Thierry, J., and Zard, S. Z., Concise syntheses of *L*-selenomethionine and of *L*-selenocystine using radical chain-reactions, *Tetrahedron*, 42, 4983, 1986.
41. (a) Bloodworth, A. J., Crich, D., and Melvin, T., Chemistry of the (*z*)-cyclo-oct-4-enyl radical including the preparation of $^{18}O_2$-labelled (*z*)-cyclo-oct-4-enyl hydroperoxide, *J. Chem. Soc., Perkins Trans. 1,* 2957, 1990; (b) Barton, D. H. R., Gero, S. D., Holliday, P., Quiclet-Sire, B., and Zard, S. Z., A practical decarboxylative hydroxylation of carboxylic acids, *Tetrahedron*, 54, 6751 1998.
42. (a) Barton, D. H. R., Bridon, D., and Zard, S. Z. The invention of radical reactions. Part XVIII. Decarboxylative radical addition to arsenic, antimony, and bismuth phenylsulphides: a novel synthesis of nor-alcohols from carboxylic acids, *Tetrahedron*, 45, 2615, 1989; (b) Barton, D. H. R., Bridon, D., and Zard, S. Z., A convenient high yielding synthesis of nor-alcohols from carboxylic-acids, *J. Chem. Soc.*, *Chem. Commun.*, 1066, 1985; (c) Barton, D. H. R., Ozbalik, N., and Schmitt, M., Radical chemistry based on (+)-*cis*-pinonic acid, *Tetrahedron Lett.*, 30, 3263, 1989; (d) Cardoso, A. S., Srinivasan, N., Lobo, A. M., and Prabhakar, S., A new synthesis of (–)-debromoflustramine B, (+)-*ent*-debromoflustramine B and (+)-debromoflustramide B, *Tetrahedron Lett.*, 42, 6663, 2001.
43. Barton, D. H. R., Dalko, P. and Gero, S. D., Synthesis of branched-chain cyclitols using a palladium(0)-catalyzed allylic coupling reaction, *Tetrahedron Lett.*, 32, 2471, 1991.
44. Barton, D. H. R., Bridon, D., and Zard, S. Z., Radical decarboxylative phosphorylation of carboxylic acids, *Tetrahedron Lett.*, 27, 4309, 1986.
45. (a) Barton, D. H. R. and Zhu, J., Elemental white phosphorus as a radical trap: a new and general route to phosphonic acids, *J. Am. Chem. Soc.*, 115, 2071, 1993; (b) Barton, D. H. R. and Fmbse, R. A. V., The invention of radical reactions. Part 39. The reaction of white phosphorus with carbon-centered radicals: an improved procedure for the synthesis of phosphonic acids and further mechanistic insights, *Tetrahedron*, 54, 12475, 1998.
46. (a) Barton, D. H. R. and Ramesh, M., Tandem nucleophilic and radical chemistry in the replacement of the hydroxyl group by a carbon–carbon bond: a concise synthesis of showdomycin, *J. Am.*

Chem. Soc., 112, 891, 1990; (b) Barton, D. H. R., Dalko, P. I. and Géro, S. D., Preparation of six membered carbocycles by aryl-tellurium mediated free-radical cyclisation, *Tetrahedron Lett.*, 36, 4713, 1991.

47. Barton, D. H. R., Bridon, D., and Zard, S. Z., New decarboxylative chalcogenation of aliphatic and alicyclic carboxylic acids, *Tetrahedron Lett.*, 25, 5777, 1984.
48. (a) Carland, M. W., Martin, R. L., and Schiesser, C. H., Nucleophilic and radical chemistry of benzylselenides: preparation of novel selenocephems and selenopenams, *Tetrahedron Lett.*, 42, 4737, 2001; (b) Fong, M. C. and Schiesser, C. H., Homolytic substitution by iminyl radical at selenium: A free-radical route to 1,2-benzoselenazoles, *Tetrahedron Lett.,* 34, 4347, 1993.
49. (a) Ollivier, C. and Renaud P., Organoboranes as a source of radicals, *Chem. Rev.*, 101, 3415, 2001; (b) Cadot, C., Cossy, J., and Dalko, P. I., Radical carbon-carbon coupling reactions via organoboranes, *J. Chem. Soc.*, *Chem. Commun.*, 1017, 2000; (c) Ollivier, C. and Renaud, P., A convenient and general tin-free procedure for radical conjugate addition, *Angew. Chem. Int. Ed. Engl.*, 39, 925–928, 2000.
50. (a) Kim S. and Cheong, J. H., Relative beta-elimination rates of heteroatoms from alkyl and aminyl radicals, *J. Chem. Soc.*, *Chem. Commun.*, 1143, 1998; (b) Bales, B. C., Horner, J. H., Huang, X., Newcomb, M., Crich, D., and Greenberg, M. M., Product studies and laser flash photolysis on alkyl radicals containing two different leaving groups are consonant with the formation of an olefin cation radical, *J. Am. Chem. Soc.* 123, 3623, 2001; (c) Masterson, D. S. and Porter, N. A., Diastereo selective free radical halogenation, azidation, and rearrangement of -silyl Barton esters, *Org. Lett.,* 4, 4253, 2002.
51. See, for example, Newcomb, M., Horner, J. H., Whitted, P. O., Crich, D., Huang, X., Yao, Q., and Zipse, H., β-Phosphatoxyalkyl radical reactions: competing phosphate migration and phosphoric acid elimination from a radical cation–phosphate anion pair formed by heterolytic fragmentation, *J. Am. Chem. Soc.* 121, 10685, 1999 (and references cited).
52. (a) Crich, D., Huang, X., and Newcomb, M., Inter- and intramolecular pathways for the formation of tetrahydrofurans from beta-(phosphatoxy)alkyl radicals: evidence for a dissociative mechanism, *J. Org. Chem.* 65, 523, 2000; (b) Newcomb, M., Miranda, N., Sannigrahi, M., Huang, X., and Crich, D., Direct measurement of enol ether radical cation reaction kinetics, *J. Am. Chem. Soc.,* 123, 6445, 2001.
53. Beckwith, A. L. J., Crich, D., Duggan, P. J., and Yao, Q. W., Chemistry of beta-(acyloxy)alkyl and beta-(phosphatoxy)alkyl radicals and related species: radical and radical ionic migrations and fragmentations of carbon–oxygen bonds, *Chem. Rev.*, 97, 3273, 1997.
54. Meggers, E., Dussy, A., Schäfer, Th., and Giese, B., Electron transfer in DNA from guanine and 8-oxoguanine to a radical cation of the carbohydrate backbone, *Chem.-Eur. J.*, 6, 485, 2000.
55. Giese, B., Long distance charge transport in DNA: The hopping mechanism, *Acc. Chem. Res.*, 33, 631, 2000.
56. Newcomb, M., Miranda, N., Huang, X., and Crich, D., Laser flash photolysis kinetic studies of α-methoxy-β-phosphatoxyalkyl radical heterolysis reactions: a method for alkoxyalkyl radical cation detection, *J. Am. Chem. Soc.*, 122, 6128, 2000.
57. (a) Epe, B., Ballmaier, D., Adam, W., Grimm, G. N., and Saha-Moller, C. R., Photolysis of *N*-hydroxypyridinethiones: a new source of hydroxyl radicals for the direct damage of cell-free and cellular DNA, *Nucl. Acids Res.*, 24, 1625, 1996; (b) Theodorakis, E. A. and Wilcoxen, K. M., *N*-aroyloxy-2-thiopyridones as efficient oxygen-radical generators: novel time-controlled DNA photocleaving reagents, *J. Chem. Soc.*, *Chem. Commun.*, 1927, 1996; (c) Theodorakis, E. A., Xiang, X., and Blom, P., Photochemical cleavage of duplex DNA by *N*-benzoyloxy-2-thiopyridone linked to 9-aminoacridine, *J. Chem. Soc.*, *Chem. Commun.*, 1463, 1997.
58. Theodorakis, E. A., Xin, X. A., Lee, M. D., and Gibson, T., On the mechanism of photo-induced nucleic acid cleavage using *N*-aroyloxy-2-thiopyridones, *Tetrahedron Lett.*, 39, 3383, 1998.
59. Adam, W., Ballmaier, D., Epe, B., Grimm, Gn., and Saha-Moller, C. R., *N*-hydroxypyridinethiones as photochemical hydroxyl radical sources for oxidative DNA-damage, *Angew. Chem. Int. Ed. Engl.*, 34, 2156, 1995.

60. Qian, X., Yao, W., Chen, G., Huang X., and Mao, P., *N*-aroyloxynaphthalimides as novel highly efficient DNA photocleavers: substituent effects, *Tetrahedron Lett.*, 42, 6175, 2001.
61. Barton, D. H. R., Crich, D., and Kretzschrnar, G., The invention of new radical chain reactions. Part 9. Further radical chemistry of thiohydroxamic esters: formation of carbon–carbon bonds, *J. Chem. Soc.*, *Perkin Trans. 1*, 39, 1986.
62. See also: Barton, D. H. R., Chern, C.-Y., and Jaszberenyi, J. Cs., The invention of radical reactions. XXXIII. Homologation reactions of carboxylic acids by radical chain chemistry, *Aust. J. Chem.*, 48, 407, 1995.
63. Boivin, J., Lallemand, J.-Y., Schmitt, A., and Zard, S. Z., Reduction of activated thiopyridyl compounds by zinc metal, *Tetrahedron Lett.* 40, 7243, 1995.
64. Barton, D. H. R., Gateau-Olesker, A., Gero, S. D., Lacher, B., Tachdjian, C., and Zard, S. Z., Radical decarboxylative alkylation of tartaric acid, *Tetrahedron*, 49, 4589, 1993.
65. For some selected examples, see (a) Corovo, M. C. and Pereira, M. A., A radical approach towards indolizidine 167B, *Tetrahedron Lett.*, 43, 455, 2002; (b) Avenoza, A., Busto, J. H., Cativiela, C., and Peregrina, J. M., Synthesis of 7-azabicyclo[2.2.1]heptane derivatives via bridgehead radicals, *Tetrahedron*, 58, 1193, 2002; (c) Barton, D. H. R., Herve, Y., Potier, P., and Thierry, J., Synthesis of novel α-amino acids and derivatives using radical chemistry: synthesis of *l*- and *d*-α-amino-adipic acids, *l*-α-aminopimelic acid and appropriate unsaturated derivatives, *Tetrahedron*, 43, 4297, 1987; (d) Barton, D. H. R., Togo, H., and Zard, S. Z., The invention of new radical chain-reactions. 10. High-yield radical addition reactions of α-β-unsaturated nitroolefins: an expedient construction of the 25-hydroxy-vitamin-D_3 side-chain from bile-acids, *Tetrahedron*, 41, 5507, 1985; (e) Barton, D. H. R., Togo, H., and Zard, S. Z., Radical addition to vinyl sulfones and vinyl phosphonium salts, *Tetrahedron Lett.*, 26, 6349, 1985; (f) Barton, D. H. R., Boivin, J., Sarma, J., da Silva, E., and Zard, S. Z., Some further novel transformations of geminal (pyridine-2-thiyl) phenylsulfones, *Tetrahedron Lett.*, 30, 4237, 1989; (g) Barton, D. H. R., Boivin, J., Crepon, E., Sarma, J., Togo, H., and Zard, S. Z., Decarboxylative radical addition to vinylsulphones and vinylphosphonium bromide: some further novel transformations of geminal (pyridine-2-thiyl) phenylsulphones, *Tetrahedron*, 47, 7091, 1991; (h) Barton, D. H. R., Lacher, B., and Zard, S. Z., The invention of new radical chain-reactions. 13. Generation and reactivity of perfluoroalkyl radicals from thiohydroxamic esters, *Tetrahedron*, 42, 2325, 1986; (i) Barton, D. H. R. and Liu, W., Two carbon homologation of carboxylic acids using acrylamide as a radical trap, *Tetrahedron Lett.*, 38, 2431, 1997; (j) Barton, D. H. R. and Liu, W., The invention of radical reactions. XXXVIII. Homologation of carboxylic acids with acrylamide and synthetic studies of 3-deoxy-*d*-arabino-2-heptulosonic acid (DAH) and its 4-epimer, *Tetrahedron*, 53, 12067, 1997; (k) Barton, D. H. R., Gero, S. D., Quiclet-Sire, B., and Samadi, M., Stereoselectivity in radical reactions of 2′-deoxynucleosides: a synthesis of an isostere of 3′-azido-3′-deoxythymidine-5′-monophosphate (AZT-5′-monophosphate), *Tetrahedron Lett.*, 30, 4969, 1989; (l) Barton, D. H. R., Gero, S, D., Quiclet-Sire, B., and Samadi, M., Stereospecificity in the synthesis of C-5 modified nucleosides using radical chemistry: furanosidic chain lengthening through C-4, *J. Chem. Soc.*, *Chem. Commun.*,1372, 1988; (m) Barton, D. H. R., Gero, Sd., Quiclet-Sire, B., and Samadi, M., Radical addition to vinyl phosphonates: a new synthesis of isosteric phosphonates and phosphonate analogs of alpha-amino-acids, *J. Chem. Soc.*, *Chem. Commun.*, 1000, 1989; (n) Barton, D. H. R., Gero, S. D., Quiclet-Sire, B., and Samadi, M., Expedient synthesis of natural (s)-sinefungin and of its C-6′ epimer, *J. Chem. Soc.*, *Perkin. Trans. 1*, 981, 1991; (o) Barton, D. H. R., Cleophax, J., Gateau-Olesker, A., Gero, S. D., and Tachdjian, C., Synthesis of 3α-alkoxy-4β-substituted-2-azetidinones from L(+)-tartaric acid, *Tetrahedron*, 49, 8381, 1993; (p) Barton, D. H. R., Gero, S. D., Quiclet-Sire, B., and Samadi, M., Stereocontrolled radical reactions in carbohydrate and nucleoside chemistry, *Tetrahedron Asymm.*, 5, 2123, 1994; (q) Barton, D. H. R., Gero, S. D., Negron, G., Quiclet-Sire, B., Samadi, M., and Voncent, C., Total synthesis of the thymidine analogue of sinefungin, *Nucleosides Nucleotides*, 14, 1619 1995; (r) Anaya, J., Barton, D. H. R., Caballero, M. C., Gero, S. D., Grande, M., Laso, N. M., and Hernando, J. I. M., The use of radical decarboxylation in the preparation of 1-methylcarbapenem antibiotic precursors from

D-glucosamine, *Tetrahedron Asymm.*, 5, 2137, 1994; (s) Barton, D. H. R., Chern, C.-Y., and Jaszberenyi, J. Cs., Homologation of carboxylic acids by improved methods based on radical chain chemistry of acyl derivatives of *N*-hydroxy-2-thiopyridone, *Tetrahedron Lett.,* 33, 5013, 1992; (t) Barton, D. H. R., Chern, C.-Y., and Jaszberenyi, J. Cs., Two carbon homologation of carboxylic acids via carbon radicals generated from the acyl derivatives of *N*-hydroxy-2-thiopyridone: synthesis of C_{n+2} α-keto-acids from C_n acids. (The "three carbon" problem), *Tetrahedron Lett.,* 33, 5017, 1992.

66. For related 1,2-disubstituted alkenes, see also Barton, D. H. R., Chern, C.-Y., and Jaszberényi, J. Cs., Synthesis of substituted malonic-acids from carbon radicals generated from carboxylic-acids, *Tetrahedron Lett.*, 33, 7299, 1992.
67. Ling, T., Xiang, A. X., and Theodorakis, E. A., Enantioselective total synthesis of avarol and avarone, *Angew. Chem. Int. Ed. Engl.*, 38, 3089, 1999.
68. See also Ling, T., Poupon, E., Rueden, E. J., and Theodorakis E. A., Unified synthesis of quinone sesquiterpenes based on a radical decarboxylation and quinone addition reaction, *J. Am. Chem. Soc.*, 124, 2002.
69. (a) Barton, D. H. R., Garcia, B., Togo, H., and Zard, S. Z., Radical decarboxylative addition onto protonated heteroaromatic (and related) compounds, *Tetrahedron Lett.*, 27, 1327, 1986; (b) Castagnino, F., Corsano, S., Barton, D. H. R., and Zard, S. Z., Decarboxylative radical addition onto protonated heteroaromatic systems including purine bases, *Tetrahedron Lett.*, 27, 6337, 1986.
70. Barton, D. H. R., Ozbalik, N., and Lacher, B., The invention of radical reactions. XVIII. A convenient solution to the 1-carbon problem ($R\text{-}CO_2H \rightarrow R\text{-}^{13}CO_2H$), *Tetrahedron*, 44, 3501, 1988.
71. (a) Barton, D. H. R., Jaszberenyi, J. Cs., and Theodorakis, E. A., Radical nitrile transfer with methanesulfonyl cyanide or *para*-toluenesulfonyl cyanide to carbon radicals generated from the acyl derivatives of *N*-hydroxy-2-thiopyridone, *Tetrahedron Lett.*, 32, 3321, 1991; (b) Barton, D. H. R., Jaszberenyi, J. Cs., and Theodorakis, E. A., The invention of radical reactions. 23. New reactions: nitrile and thiocyanate transfer to carbon radicals from sulfonyl cyanides and sulfonyl isothiocyanates, *Tetrahedron*, 48, 2613, 1992.
72. Some selected examples include: (a) Ahrnad-Junan, S. A., Walkington, A. J., and Whiting, D. A., The mechanism of biological C–C bond formation to methoxy groups: biomimetic cyclisation via alkyloxyl radicals, *J. Chem. Soc., Chem. Commun.*, 1613, 1989; (b) Ziegler, F. F. and Wang, Y., Carbon–carbon bond forming reactions with oxiranyl radicals, *Tetrahedron Lett.*, 37, 6299, 1996; (c) Barton, D. H. R., da Silva, F., and Zard, S. Z., *J. Chem. Soc., Chem. Commun.*, 285, 1998; (d) Barton, D. H. R., Guilhem, J., Hervé, Y., Potier, P., and Thierry, J., Synthesis of 2S, 3aS, 7aS- and of 2S, 3aR, 7aR-Perhydroindole-2-carboxylic acid derivatives from L-aspartic acid, *Tetrahedron Lett.,* 28, 1413, 1987.
73. (a) Ferjančič, Z., Čekovič, Z., and Saičič, R., Free radical domino reactions in the synthesis of small ring compounds: multiple annulation of cyclopropane-containing polycycles, *C. R. Acad. Sci. Paris*, *Chimie/Chemistry*, 4, 599–610, 2001; (b) Curran, D. P. and Shen, W., Tandem transannular radical cyclizations. Total synthesis of (±)-modhephene and (±)-*epi*-modhephene, *Tetrahedron,* 49, 755, 1993; (c) Boivin, J., Crépon (née da Silva), E., and Zard, S. Z., Further observations on the thermal stability of *N*-hydroxy-2-thiopyridone esters: improved decarboxylative radical additions to olefins, *Tetrahedron Lett.,* 32, 199, 1991.
74. (a) Barton, D. H. R., Lacher, B., Misterkiewicz, B., and Zard, S.Z., The invention of radical reactions. XVII. A decarboxylative sulphonylation of carboxylic acids, *Tetrahedron*, 44, 1153, 1988. Trapping of alkyl radicals from *O*-acyl thiohydroxamates with sulfur followed by borohydride reduction also provides a convenient synthesis of thiols; (b) see Barton, D. H. R., Castagnino, F., and Jaszberényi, J. Cs., The reaction of carbon radicals with sulfur: a convenient synthesis of thiols from carboxylic acids, *Tetrahedron Lett.*, 35, 6057, 1994.
75. (a) Barton, D. H. R., Jaszberényi, J. Cs., and Theodorakis, E. A., Nitrogen transfer to carbon radicals, *J. Am. Chem. Soc.*, 114, 5904, 1992; (b) Barton, D. H. R., Jaszberenyi, J. Cs., Theodorakis, E. A., and Reibenspies, J. H., The invention of radical reactions. 30. Diazirines as carbon radical traps:

mechanistic aspects and synthetic applications of a novel and efficient amination process, *J. Am. Chem. Soc.*, 115, 8050, 1993.

76. (a) Girard, P., Guillot, N., Motherwell, W. B., and Potier, P., Observations on the reaction of *O*-acylthiohydroxamates with thionitrite esters: a novel free radical chain reaction for decarboxylative amination, *J. Chem. Soc.*, *Chem. Commun.*, 2385, 1995; (b) Girard, P., Guillot, N., Motherwell, W. B., Hay-Motherwell R. S., and Potier, P., The reaction of thionitrites with Barton esters: a convenient free radical chain reaction for decarboxylative nitrosation, *Tetrahedron*, 55, 3573, 1999.
77. (a) Newcomb, M., Park, S. U., Kaplan, J., and Marquardt, D. J., Facile generation of dialkylaminyl radicals from *N*-hydroxypyridine-2-thione carbamates: application in kinetic studies of small ring cycloalkylaminyl radical ring openings, *Tetrahedron Lett.*, 26, 5651, 1985; (b) Newcomb, M. and Deeb, T. B., *N*-hydroxypyridine-2-thione carbamates as aminyl and aminium radical precursors: cyclizations for synthesis of the pyrrolidine nucleus, *J. Am. Chem. Soc.*, 109, 3163, 1987; (c) Newcomb, M., Deeb, T. M., and Marquardt, D. J., *N*-hydroxypyridine-2-thione carbamates. IV. A comparison of 5-*exo* cyclizations of an aminyl radical and an aminium cation radical, *Tetrahedron,* 46, 2317, 1990; (d) Newcomb, M., Marquardt, D. J., and Deeb, T. M., *N*-hydroxy-pyridine-2-thione carbamates. V. Syntheses of alkaloid skeletons by aminium cation radical cyclizations, *Tetrahedron,* 46, 2329, 1990; (e) Newcomb, M., Marquardt, D. J., and Kumar, M. U., *N*-hydroxypyridine-2-thione carbamates. VI. Functionalization of carbon radicals formed by aminium cation radical cyclizations, *Tetrahedron,* 46, 2345, 1990; (f) Newcomb, M. and Ha, C., Lewis acid activated and catalyzed cyclizations of aminyl radicals from *N*-hydroxypyridine-2-thione carbamates, *Tetrahedron Lett.,* 32, 6493, 1991.
78. Boivin, J., Fouquet E., Schiano A. M., and Zard S. Z., Iminyl radicals. 3. Further synthetically useful sources of iminyl radicals, *Tetrahedron*, 50, 1769, 1994.
79. Newcomb, M. and Kumar, M. U., *N*-hydroxypyridine-2-thione carbamates. VII. Intermolecular addition and addition-cyclization reactions of aminium cation radicals, *Tetrahedron Lett.*, 31, 1675, 1990.
80. Beckwith, A. L. J. and Hay, B. P., Generation of alkoxy radicals from *N*-alkoxypyridinethiones, *J. Am. Chem. Soc.*, 110, 4415, 1988.
81. For recent reviews, see (a) Hartung, J., Gottwald, T., and Spehar, K., Selectivity in the chemistry of oxygen-centered radicals: the formation of carbon-oxygen bonds, *Synthesis*, 1469, 2002; (b) Hartung, J., Stereoselective construction of the tetrahydrofuran nucleus by alkoxyl radical cyclizations, *Eur. J. Org. Chem.*, 619, 2001.
82. Hartung, J., A new generation of alkoxyl radical precursors: preparation and properties of *N*-(alkoxy)-4-arylthiazole-2(3H)-thiones, *Eur. J. Org. Chem.*, 1275, 2002.
83. Cheng, J. P., Liu, B., Zhao, Y., Wen, Z., and Sun, Y., Homolytic cleavage energies of R–H bonds centered on carbon atoms of high electronegativity: first general observations of *O*-type variation on C–H BDEs and the implication for the governing factors leading to the distinct *O*/*S* patterns of radical substituent effects, *J. Am. Chem. Soc.*, 122, 9987, 2000.
84. Hartung, J., Kneuer, R., Kopf, T. M., and Schmidt, P., A radical version of the bromine cyclization of alkenols, *Acad. Sci. Paris*, *Chimie/Chemistry*, 649, 2001.
85. Hartung, J. and Kneuer, R., Ring closure reactions of disubstituted 4-penten-1-oxyl radicals: towards a stereoselective synthesis of *allo*-muscarine, *Eur. J. Org. Chem.*, 1677, 2000.
86. Hartung, J., Kneuer, R., and Spehar, K., Photoreactions of *N*-alkoxy-4-(*p*-chlorophenyl)thiazole-2(3*H*)-thiones with *L*-cysteine derivatives in aqueous solutions, *J. Chem. Soc.*, *Chem. Commun.*, 799, 2001.
87. Ha, C., Horner, J. H., Newcomb, M., Varick, T. R., Arnold, B. R., and Lusztyk, J., Kinetic studies of the cyclization of the 6,6-diphenyl-5-hexenyl radical: a test of the accuracy of rate constants for reactions of hydrogen transfer agents, *J. Org. Chem.*, 58, 1194, 1993.
88. For a recent review on this topic, see Togo, H. and Katohgi, M., Synthetic uses of organohypervalent iodine compounds through radical pathways, *Synlett*, 565, 2001.

89. For a recent application of this reaction, see (a) Boto, A., Hernandez R., and Suarez, E., Oxidative decarboxylation of alpha-amino acids: a mild and efficient method for the generation of *N*-acyliminium ions, *Tetrahedron Lett.*, 40, 5945, 1999; (b) Francisco, C. G., Herrera, A. J., and Suárez, E., Intramolecular hydrogen abstraction reaction promoted by alkoxy radicals in carbohydrates. synthesis of chiral 2,7-dioxabicyclo[2.2.1]heptane and 6,8-dioxabicyclo[3.2.1]octane ring systems, *J. Org. Chem.*, 67, 7439, 2002.
90. King, G. R., Mander, L. N., Monck, N. J. T., Morris, J. C., and Zhang, H., A new and efficient strategy for the total synthesis of polycyclic diterpenoids: the preparation of gibberellins (±)-GA_{103} and (±)-GA_{73}, *J. Am. Chem. Soc.*, 119, 3828, 1997.

68

Photochemically Induced Tautomerism of Salicylic Acid and Its Related Derivatives

Minjoong Yoon
Chungnam National University

68.1 Introduction

Salicylic acid (SA) and its derivatives such as methyl salicylate (MSA) have strong hydrogen bonds between the phenolic hydroxy groups and the nearby carbonyl proton-accepting groups, which become, respectively, more acidic and more basic in the excited state. Consequently, in aprotic solution, this gives rise to a dual emission with a large Stokes shift, as observed initially by Weller,[1,2] which has been attributed to an excited-state intramolecular proton transfer (ESIPT), as shown in Scheme 1. The proton transfer is driven by a pK change of –6 in the phenolic oxygen and a pK change of +8 in the carbonyl oxygen of the carbonyl group upon excitation.[3]

The dual emission has been attributed to double-well potentials arising from the proton transfer in the excited state as well as in the ground state, as shown in Figure 68.1. The primary form (I) in the ground state is more stable than the tautomeric form (T), whereas the tautomeric form in the excited state (T*) is more stable than the excited primary form (I*). According to Weller, the initially excited phenol form (P*) is in equilibrium during its lifetime, with the proton-transferred tautomer form T* resulting from ESIPT. The anomalous large Stokes-shifted fluorescence (blue fluorescence) is assigned to the formation of the tautomer T*, while the ultraviolet (UV) component of the fluorescence was attributed to the fluorescence of the phenol form (II*).

0-8493-1348-1/04/$0.00+$1.50

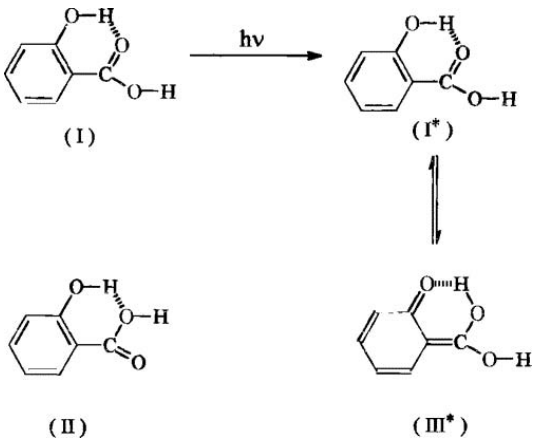

SCHEME 1

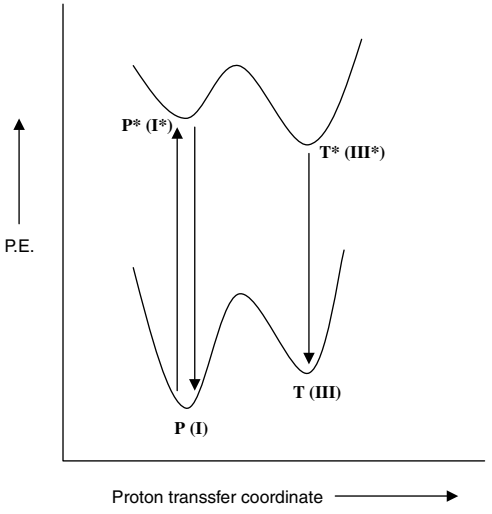

FIGURE 68.1 Schematic diagram of asymmetric double well potentials proposed by Weller for the ground and excited state of salicylic acid.

The excited-state equilibrium is sometime broken, depending on the substituents (R and R′) or the environment of the media employed. For example further work on methyl salicylate[3,4] has demonstrated the different excitation spectrum for the two emission species, indicating that the excited species are not in equilibrium but originate from different ground-state species. In this case, there are two different conformers (open form or closed form) depending on the hydrogen bonding strength due to intermolecular hydrogen bonding with solvent molecules. These findings have been confirmed in the spectroscopic study of several derivatives of salicylic acid in a supersonic jet.[5,6] This has been explained in terms of a single minimum distorted potential energy surface along the tautomerization coordinate, as confirmed by the Zewail group by real-time measurements of the proton-transfer reaction.[7] The time for the process was reported to be 60 fs.

Earlier investigations have shown that in certain derivatives, such as aminosalicylates[8–14] and salicylideneanilines,[15–18] a twisted intramolecular charge transfer (TICT) state is formed and is followed by the ESIPT. These compounds show multiple fluorescence.

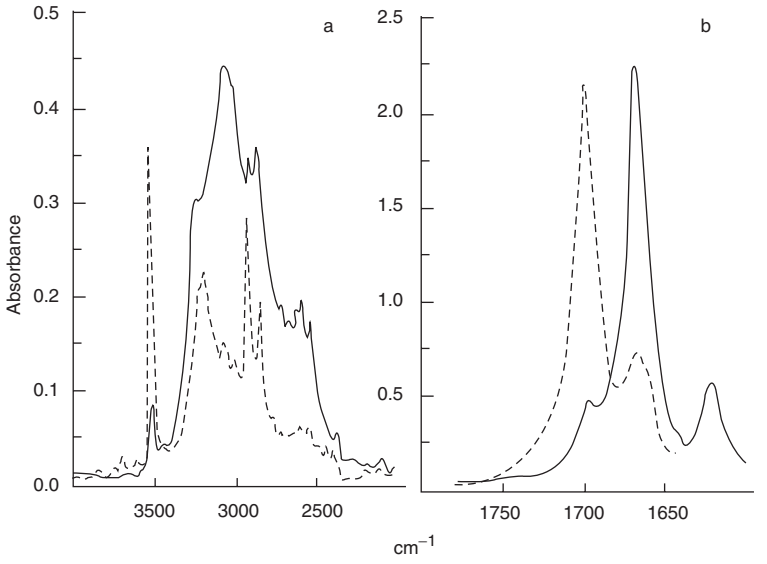

FIGURE 68.2 IR spectra of SA solutions in CCl_4 (10^{-2}mol/l(———), 5×10^{-5} mol/l (•••••••) in ν OH (a) and ν C=O (b) regions.

The excited-state dynamics of these complex molecules have also been studied by ultrafast time-resolved spectroscopy[19,20] to elucidate the mechanistic details. The potential energy (PE) function of the first excited singlet state of the ESIPT process in salicylic acid has been calculated by *ab initio* MO calculations using the 6–31G** basis set at the restricted Hartree–Fock and configuration interaction single excitation (CIS) levels, as well as the semi-empirical method AM1.[21,22]

68.2 Fluorescence Spectroscopic Evidences of Excited-State Intramolecular Proton Transfer of Salicylic Acid and Methyl Salicylate

In Solution

Weller[1,2] observed the dual emission in the fluorescence spectrum of SA and MSA in methylcyclohexane (10^{-4} mol/L), characterized by a strong emission with a maximum at 450 nm and a shoulder at 350 to 370 nm. The features of the emission spectrum of salicylic acid and its derivatives in solution are sensitive to the concentration of the solute and the solvent composition. This effect could be due to self-dimerization[23,24] or the existence of intermolecular hydrogen bonds formed by the carboxylic acid influencing the intramolecular hydrogen bond, C=O···HO in salicylic acid providing ESIPT.

The self-dimerization of salicylic acid in nonpolar aprotic solvents is also the cause of its dual emission.[23] Similar emission has been found for heterodimers formed by salicylic acid with other carboxylic acids such as 2,6-dihydroxybenzoic acid.[25] In this case, a weakening of the intramolecular hydrogen bond is caused by the intermolecular hydrogen bond with another acid, followed by an increase of the UV component with a decrease of the blue emission from the ESIPT. The concentration dependence of intra- and intermolecular hydrogen bonds of SA and its related compounds has been proved by NMR and IR studies in CCl_4 or in solvents such as hexane.[25–27] The typical example of dimerization has been confirmed by observation of the relative change of intensities of the two bands for the C=O stretch at 1697 and 1660 cm^{-1} (23) with concentration variation (see Figure 68.2). From this study, it was shown that the two bands at 1697 and 1660 cm^{-1} originate from the monomer and the dimer, respectively. Simultaneously similar changes in the OH stretching bands at 3200 to 3540 cm^{-1} were also observed. Usually, the

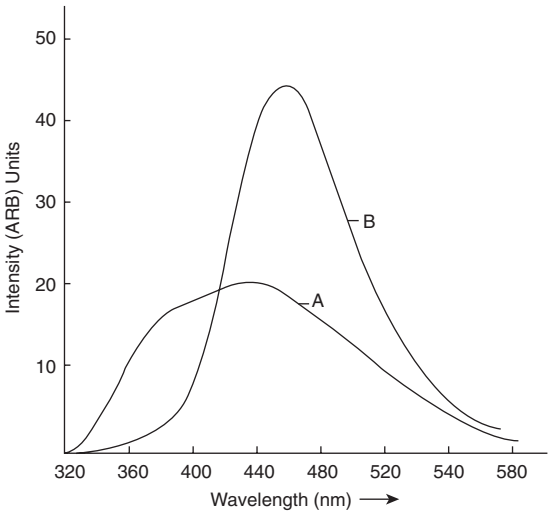

FIGURE 68.3 Emission spectra of SA (10^{-3}M) in hydrocarbon at 290K in the presence of Et_2O (A) 0.0M and (B) 0.9M.

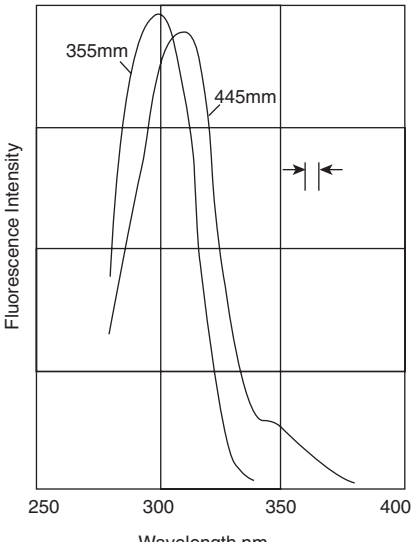

FIGURE 68.4 Fluorescence excitation spectra of MSA, 10^{-4}mol/l in methanol, corrected for equal photon intensity; emission wavelengths and excitation slit width indicated.

dimerization of SA and its derivatives in nonpolar solvents at room temperature is negligible when the total concentration is less than 10^{-6} mol/L. The early observations of dual emission of SA and MSA (1, 2) have been performed at higher concentrations in nonpolar solvents ($>10^{-5}$ mol/L). Under such conditions, the relative intensity ratio of the UV emission to the blue emission increases as the concentration increases (Figure 68.3). The excitation spectrum of the visible emission of SA or MSA at 445 is shifted by ~10 nm to the blue of the UV excitation maximum (355 nm) either in cyclohexane or in methanol (Figure 68.4). These indicate that the ESIPT is inhibited by self-dimerization or intermolecular hydrogen bond in the ground state, as described above. However, at very dilute concentrations less than

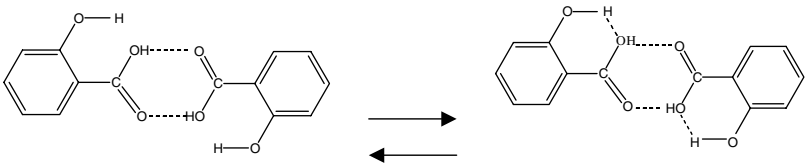

(D) (T)

SCHEME 2

TABLE 68.1 Shift of the Emission Band of Solid Salicylic Acid at 10 K with the Excitation Wavelength

λ_{exc} (nm)	λ_{em} (nm)	Shift (cm^{-1})
351	390	2849
355	397	2980
360	400	2777
370	410	2636
375	415	2570

10^{-6} mol/L, the hexane solution of SA shows a fluorescence emission maximum in the blue region (410 to 450 nm) with no pronounced maximum in the UV region (380 nm). The excitation spectra of both the blue and UV emissions are identical, indicating that the species from which the blue emission originates is the same as that of the small UV emission. The blue emission, peaking at 450 nm, exhibits a large Stokes shift (9000 cm^{-1}) and appears to be associated with the monomer rotamer form I (Scheme 1) undergoing ESIPT, in accordance with other works.[1–3,24–26] In other words, in the diluted nonpolar solution, the rotamer (Scheme 1, I) is stabilized by the intramolecular hydrogen bond, and it is relatively dominant in the ground state. Thus, the initially excited rotamer P* emits UV fluorescence, and consequently it is in equilibrium during its lifetime with the proton-transferred form T*, which emits the blue fluorescence.

When the intramolecular hydrogen bond is weakened by intermolecular hydrogen bonding with solvent or by esterification of the carboxylic acid, another rotamer (Scheme 1, II) in which the ESIPT is not accessible, becomes dominant. Further work on methylsalicylate[26–27] has shown two different excitation spectra in aprotic nonpolar solvent. The existence of two different excitation spectra implies that two different ground species, such as rotamers I and II (Scheme 1), are also involved. The relative population of rotamer I/rotamer II is expected to increase as the strength of intramolecular hydrogen bonding increases.

On the other hand, with the intermolecular hydrogen bonding formed by self-dimerization in the concentrated solutions, a double proton transfer is known to take place converting dimer D to tautomer T, as shown in Scheme 2; this is confirmed by observing the cryogenic effects (10 to 293 K) on the steady-state and time-resolved fluorescence spectroscopic techniques.[23]

The fluorescence emission obtained by excitation at energies lower than the 0–0 band of the dimer absorption (351 to 380 nm) exhibits a maximum around 390 nm, which shifts toward the red with increasing wavelength (see Table 68.1), indicating that the red-edge effect results from different distorted forms of dimers. However, with higher energy excitation (343 to 265 nm), the tautomeric blue emission (430 nm) is also observed as well as the dimeric UV emission (Figure 68.5).[23] The tautomeric emission bands at 428 and 455 nm are shifted by 5125 and 6,512 cm^{-1}, respectively, from the 0–0 band of the dimer at 28,490 cm^{-1}. These shifts are well in accord with the jet-cooled studies[5,6] and correspond to the C=O and OH stretch assigned for the tautomer of the SA monomer (see below). The excitation spectral feature

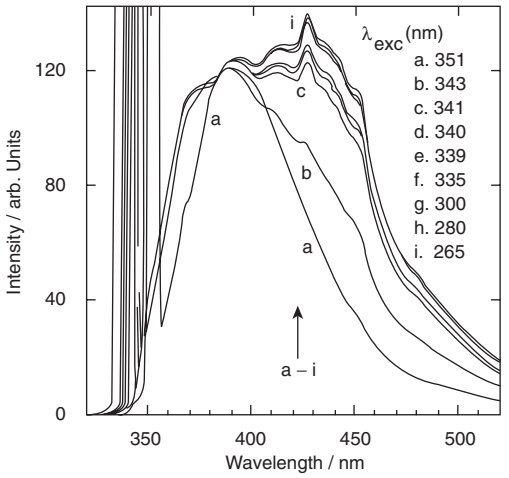

FIGURE 68.5 Emission spectra of solid SA at 10K with different excitation wavelengths shorter than the (0-0) band as indicated in the figure. The truncated sharp peak in each spectrum is the scattered excitation light.

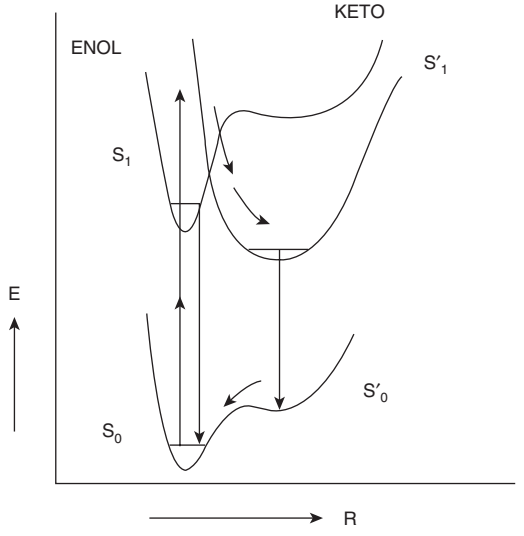

FIGURE 68.6 Schematic diagram of the double potential minimum for the proton transfer reaction in the SA dimer Enol and keto represent the D and T forms of the SA dimer respectively.

of the UV emission and the blue emission show differences at 10 K, but both excitation spectra become identical at higher temperatures, indicating the loss of the identity of the two potentials in the excited state at higher energies (Figure 68.6). The barrier height (1050 cm^{-1}) is calculated by the energy difference between the two-excitation spectra peaks and is sensitive to the temperature variation.

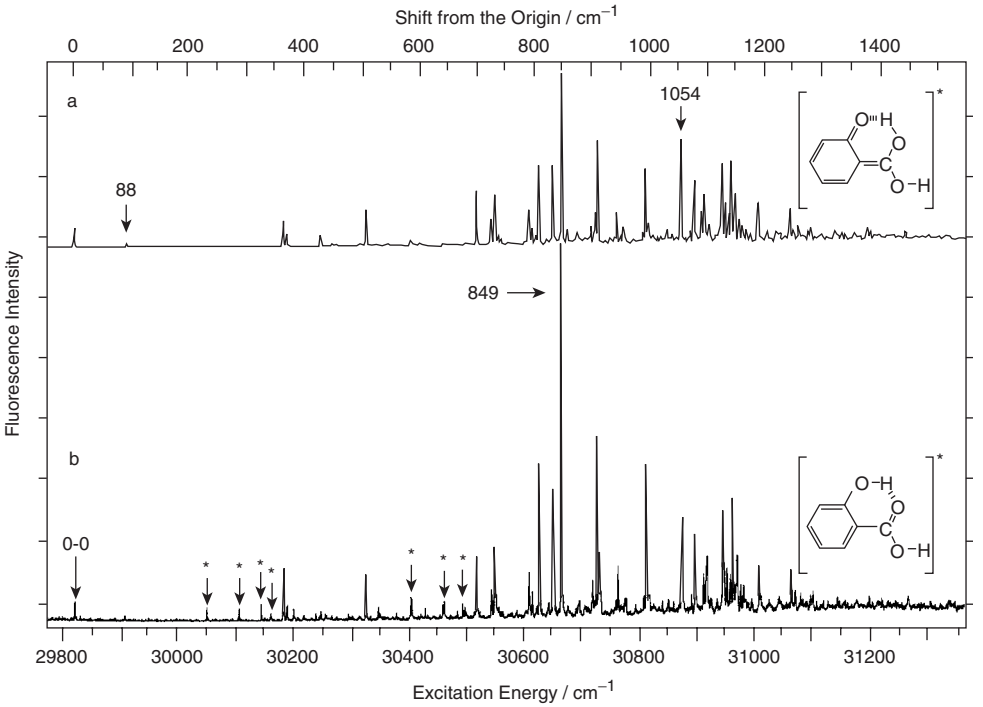

FIGURE 68.7 The fluorescence excitation spectra of the rotamer I on monitoring (a) BLUE fluorescence, (b) UV fluorescence. Asterisk (*) indicates the bands due to the SA dimer. The spectra are normalized at the origin.

In a Supersonic Jet

Figure 68.7 shows the fluorescence excitation spectra of rotamer I of SA in a supersonic jet obtained by adjusting the reservoir temperature between 35 and 100°C. The fluorescence excitation spectra were measured by monitoring separately the UV (340 to 370 nm; Figure 68.7a) and the blue (380–480 nm; Figure 68.7b) emissions.[6] The same supersonic jet excitation spectra were also measured for MSA by monitoring the light emitted above 420 nm.[5] The frequencies of the main vibronic bands for the SA and MSA are summarized in Table 68.2. The excitation spectrum of SA shows the first weak feature at 29,820 cm^{-1}, which is assigned to the 0–0 transition, while those of MSA shows the origins at 30,052, cm^{-1}. Due to the methoxy group, MSA has additional bands, and the density of vibrational states is significantly higher, but the general shape of the spectrum is similar to that of SA. This indicates that rotamer I, having a strong OH···O=C hydrogen bond, is dominant enough to exhibit the ESIPT in the S_1 state.

The excitation spectrum monitored by the UV emission shows several very weak bands that appear in the 0- to 1000-cm^{-1} region (Figure 68.8) and are due to the dimer, as shown in Scheme 3.[5,6] This is contrast to the fluorescence excitation spectrum monitored by the blue emission. The frequencies of the main vibronic bands for the dimer are summarized in Table 68.3. The 364 and 511 cm^{-1} modes correspond to the doubly degenerate, in-plane breathing modes of benzene and are commonly found in benzene derivatives such as MSA, phenol, and benzoic acid dimer.[30–32] These two modes may originate from the OH in-plane bending mode. The 704-cm^{-1} mode of SA is not observed from MSA, which shows the 569 or 595 cm^{-1} bands instead, indicating that these modes involve the motion of the –COOH group or –COOMe, respectively. It is noted that the transitions in the 800- to 1100-cm^{-1} region are the most intense for both SA and MSA. The intensities for SA are lower than for MSA, especially the 849 cm^{-1} band, which is about 2.2 times more intense in the UV than in the blue fluorescence excitation spectra. These differences in the relative intensities may be due to different Franck–Condon factors or to a large

TABLE 68.2 Observed Vibrational Frequencies[a] and Assignments for SA-d_0[b] and SA-d_1 (Rotamer I)

Frequency/cm^{-1}	Ultraviolet Intensity[c]	Blue Intensity[d]	Assignments (SA-d_0)	Frequency (SA-d_1)	MS Assignments[e] and Frequencies
0	36	36	0–0 (29,820 cm^{-1})	0–0 (29,840 cm^{-1})	0–0 (30,052.3 cm^{-1})
88	12	9	ν_1	84	ν_1 (176)
364	85	45	ν_2	363	ν_2 (347)
370	30	27	ν_3	—	$\nu_2 + 6$
431	17	20	ν_4	432	ν_4 (424)
511	81	66	ν_5	489	$\nu_1 + \nu_2$ (521)
704	106	91	ν_6	674 or 688	ν_5 (569)
727	52	47	$2\nu_2$	720	$2\nu_2$ (694)
734	117	80	$\nu_2 + \nu_3$	724	ν_7 (739)
795	81	64	$\nu_5 + \nu_1$, $\nu_2 + \nu_4$	787	$\nu_8 + \nu_1$, $\nu_2 + \nu_4$ (770)
800	40	35	$\nu_3 + \nu_4$	795	$\nu_2 + \nu_4 + 6$ (776)
811	262	134	$2\nu_2 + \nu_1$, ν_7	804	ν_8 (810)
835	215	133	$2\nu_3 + \nu_1$, ν_8	825	—
849[f]	623	283	ν_9	844	$2\nu_4$ (847)
589	25	29	$2\nu_4$	—	—
900	65	39	$\nu_7 + \nu_1$	—	—
906	68	58	ν_{10}	899	ν_9 (904)
910	301	167	ν_{11}	882	$\nu_9 + 6$ (908)
914	114	95	ν_{12}	—	$\nu_2 + \nu_5$ (913)
930	5	16	$\nu_8 + \nu_1$	—	—
944	90	60	$\nu_9 + \nu_1$, ν_2	932	ν_{11} (908)
956	36	31	ν_{13}	—	—
958	36	20	ν_{14}	—	—
989	3	26	ν_{15}	—	$\nu_1 + \nu_8$ (987)
994	20	131	$\nu_{10} + \nu_1$	—	—
998	43	44	$\nu_{11} + \nu_1$	—	ν_{12} (999)
1030	39	30	$\nu_{12} + \nu_1$	1023	$\nu_1 + 2\nu_4$ (1022)
1054	171	173	ν_{16}	1028	—
1072	43	30	$\nu_2 + \nu_6$	1053	—
1079	142	108	$\nu_6 + \nu_3$	—	$\nu_1 + \nu_9$ (1080)
1092	77	59	ν_{17}	—	—
1098	106	85	$3\nu_2$	—	ν_{13} (1094)
1104	36	34	ν_{18}	—	—
1125	178	136	ν_{19}	1116	—
1132	86	73	ν_{20}	—	—
1138	76	57	$\nu_{14} + \nu_1$	—	—
1140	199	130	ν_{21}	—	$2\nu_5$, $\nu_2 + \nu_3 + \nu_4$ (1140)
1150	107	91	$\nu_4 + \nu_2$	1145	—
1156	59	44	ν_{22}	—	$\nu_5 + \nu_6$ (1164)
1162	4.5	33	$\nu_7 + 4\nu_1$	—	—
1175	30	24	$2\nu_{23}$	—	—
1185	63	69	$3\nu_2 + \nu_1$	1185	—
1205	34	28	ν_{24}	1198	—
1244	81	60	$\nu_7 + \nu_4$	—	—
1251	50	30	$\nu_7 + 5\nu_1$	—	—
1261	45	34	$\nu_8 + \nu_4$	—	—
1281	48	28	$\nu_9 + \nu_4$	—	$\nu_3 + \nu_9$ (1280)
1379	37	31	$\nu_{12} + \nu_3 + \nu_1$	—	$4\nu_1 + 2\nu_2$ (1396)
1449	40	27	ν_{25}	—	—

[a] Frequency shift from the 0–0, estimated accuracy ±3cm^{-1}.

[b] Intensity are normalized at the origin.

[c] On monitoring UV fluorescence (340–370 nm).

[d] On monitoring blue fluorescence (380–480 nm).

[e] Assignments of MS are taken from Heimbrook et al.[11] The numbers in parentheses indicate the frequency shifts from 0–0 of MS.

[f] Most intense transition.

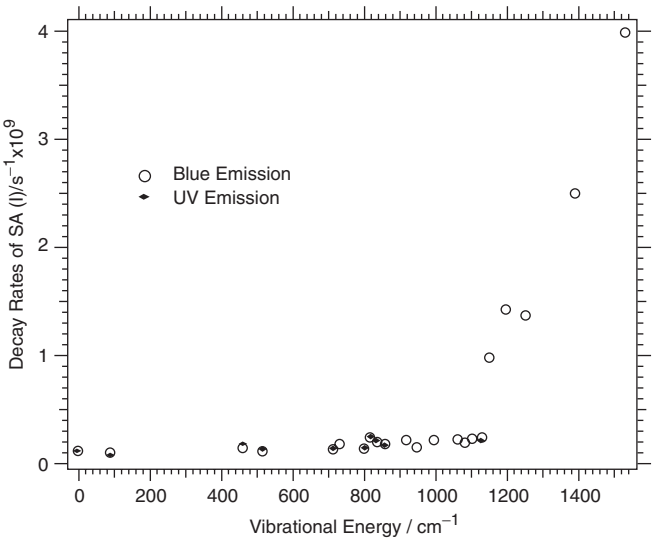

FIGURE 68.8 Fluorescence decay rates as a function of energy of the rotamer I on monitoring BLUE (♦) and UV (○) fluorescence.

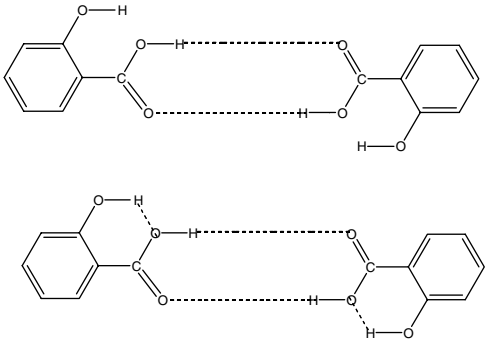

SCHEME 3

vibronic-state dependence of fluorescence quantum yields. However, the lack of vibronic-state dependence of the lifetime, the quantum yields for both molecules, and the differences in relative intensities are attributed to different molecular structures of the dimer of rotamer I, in which a double proton transfer takes place, as shown in Scheme 3, supporting the interpretation of the fluorescence spectroscopic results obtained from solution (*vide infra*).

Studies of SA and MSA in the gas phase[6] and in free jet systems[7] also support the existence of a different rotamer II in addition to rotamer I. In vapor at room temperature, rotamer II of MSA is estimated to be 1/70 the concentration of rotamer I.[6] The UV emission usually originates from both rotamers I and II, but the blue emission does not involve rotamer II, as this rotamer has no ESIPT. In solution, the UV emission of MSA excited at 33,131 cm^{-1} (UV region) is observed, in addition to the blue emission in a supersonic jet, indicating the presence of two rotamers. The intensity ratio of these two emissions (I_{UV}/I_{blue}) depends on the temperature, giving rise to the enthalpy change associated with the ground-state conversion of the two rotamers, 10.5 kJ/mol.[6] Rotamer II of SA probably is similar to that of MSA; the fluorescence excitation spectrum of rotamer II of SA up to 1300 cm^{-1} above the origin could be observed

TABLE 68.3 Salicylic Acid (SA) Dimer Spectrum

Shift from SA Dimer Origin[a]	Benzoic Acid Dimer S_0, (S_1)[b,c]	Intensity	Assignments of Dimer[d]
–229	—	5.6	Origin SA (I) 29,820 cm^{-1}
–141	—	1.8	+88 SA (I)
0	—	190	Origin (dimmer) 30,049 cm^{-1}
57	57 (57)	197	ν_1 (HB twist)
95	(70)	143	ν_2 (HB op bend)
101	117 (110)	36	ν_3 (C–COOH tor)
111	—	92	$2\nu_1$
112	168 (209)	51	$2\nu_1$
151	—	195	$\nu_1 + \nu_2$, ν_4 (HB str)
158	—	32	$\nu_1 + \nu_3$
169	—	52	$3\nu_1$
189	—	108	$2\nu_2$
195	—	37	$\nu_2 + \nu_3$
206	—	83	$\nu_2 + 2\nu_1$
246	—	109	$\nu_2 + \nu_4$, $\nu_1 + 2\nu_2$
252	—	39	$\nu_1 + \nu_2 + \nu_3$
263	—	48	$\nu_2 + 3\nu_1$, $\nu_4 + 2\nu_1$
274	223 (221)	66	ν_5 (C–COOH op bend)
283	—	45	$3\nu_2$
289	—	19	$\nu_3 + 2\nu_2$
298	258 (248)	180	ν_6 (COOH ip bend)
300	—	66	$2\nu_4$, $3\nu_3$
329	—	132	$\nu_5 + \nu_1$
340	—	41	$\nu_4 + 2\nu_2$
354	388	223	$\nu_6 + \nu_1$, ν_7 (skeletal defor)
355	—	223	$\nu_7 + 1$
366	—	46	$\nu_5 + \nu_2$
378	—	176	$\nu_5 + \nu_3$
383	—	62	$4\nu_2$
393	—	59	$\nu_6 + \nu_2$
395	—	43	$\nu_2 + 2\nu_4$
404	—	70	$\nu_1 + \nu_2 + \nu_3 + \nu_4$, $4\nu_3$
409	—	203	$\nu_7 + \nu_1$
411	—	217	$\nu_7 + \nu_1 + 2$
422	—	55	$\nu_5 + \nu_1 + \nu_2$
437	422	105	ν_8 (skeletal defor)
446	—	180	$\nu_6 + \nu_4$
450	—	171	$\nu_6 + \nu_1 + \nu_2$, $\nu_6 + \nu_4 + 4$
460	—	52	$4\nu_3 + \nu_1$
466	—	104	$\nu_7 + 2\nu_1$
477	—	109	$\nu_5 + 2\nu_3$, $5\nu_2$
492	—	50	$2\nu_2 + 2\nu_4$, $\nu_8 + \nu_1$
501	616	140	ν_9 (skeletal defor)
503	—	119	$\nu_9 + 2$
505	—	95	$\nu_7 + \nu_1 + \nu_2$, $\nu_4 + \nu_7$, $5\nu_3$
507	—	105	$\nu_7 + \nu_4 + 2$, $\nu_6 + \nu_1 + 2\nu_2$
516	—	35	$4\nu_3 + 2\nu_1$
540	—	115	$\nu_6 + \nu_4 + \nu_2$, ν_{10} (skeletal defor)
556	—	87	$\nu_9 + \nu_1$
572	—	59	—
574	—	54	—
596	—	198	$2\nu_6$, $\nu_9 + \nu_2$, $\nu_6 + 2\nu_4$
620	—	130	(ν_8 of monomer)
649	—	187	ν_{11}
660	—	96	$2\nu_5 + 2\nu_1$
671	—	90	ν_{12}

TABLE 68.3 Salicylic Acid (SA) Dimer Spectrum (continued)

Shift from SA Dimer Origin[a]	Benzoic Acid Dimer S_0, (S_1)[b,c]	Intensity	Assignments of Dimer[d]
679	—	87	$\nu_6 + \nu_5 + \nu_3$
691	—	72	$2\nu_6 + \nu_2$
707	—	109	$2\nu_7$, $\nu_{11} + \nu_1$
716	—	106	$2\nu_5 + 3\nu_1$
726	—	75	$\nu_{12} + \nu_1$
742	—	93	—
762	—	94	$2\nu_7 + \nu_1$, $\nu_{11} + 2\nu_1$
771	—	84	$2\nu_5 + 4\nu_1$
799	—	83	$\nu_{12} + 2\nu_1$
813	—	49	$2\nu_5 + 3\nu_1 + \nu_2$
825	—	112	ν_{12} of monomer
889	—	91	ν_{13}
911	—	75	($\nu_{12} + \nu_1$ of monomer)
943	—	91	$\nu_{13} + \nu_1$
956	—	79	($3\nu_2 + \nu_1$ of monomer)
999	—	61	$\nu_{13} + \nu_3$

[a] Estimated accuracy ±3 cm^{-1}.
[b] Jashi (1991).[24]
[c] The values in parentheses are for the S_1 state.
[d] HB = hydrogen, tor = torsion, ip = in-plane, op = out-of-plane, defor = deformation.
Note: Experimental conditions of the sample holder were 90°C (~0.8 Torr), He = 800 Torr, and emission monitored at 340 to 380 nm.

by monitoring the UV emission (320 to 360 nm; Figure 68.9).[6] The vibrational shifts and intensities for rotamer II are listed in Table 68.4. The spectrum is considerably weaker than that for rotamer I. This is due to a larger contribution from the n,π^* transition because the open form lacks the internal hydrogen bond as suggested for MSA.[5] The original band corresponding to the 0–0 vibrational transition is observed at 32,101 cm^{-1} (~2280 cm^{-1} above the origin of rotamer I). For comparison, the origin of the rotamer II spectrum of MSA is 32,303 cm^{-1}. The phenolic OH and COOH vibrational modes appear at 240, 363, 403, and 521 cm^{-1} above the origin, a finding that is similar to the corresponding bands of rotamer I at 364, 431, and 531 cm^{-1}. The fluorescence excitation of SA dimer measured in a supersonic jet provides the vibrational assignment of a ground state (see Table 68.3).

68.3 Excited-State Dynamics of ESIPT of Salicylic Acid and Methyl Salicylate

Ultrafast studies of the excited-state proton transfer dynamics of molecules have been performed both in solution[32–34] and in a gas matrix.[35] About three decades ago, Smith and Kaufmann[19] performed the picosecond studies of ESIPT of MSA in nonpolar solvent such as methylcyclohexane at different temperatures. They found that the fluorescence decay time of the blue (450-nm) emission of MSA is about 280 ps at room temperature. They also measured the rise time of the blue emission and estimated the ESIPT rate as $>10^{11}$ s^{-1}.

The lifetime is independent of temperature between 40 and 160 K; however, above 160 K the lifetime becomes shorter, with the relative quantum yield decreasing as the temperature increases (see Table 68.5). These data make it possible to calculate the temperature-dependent nonradiative rates, which yield an activation energy of 3.7 kcal/mol, implying the existence of the excited zwitterions as well as the tautomer form. Nevertheless, interpretation of these experiments is complicated by thermal and solvent effects, thus a proper description of the formation of the blue emission has not been unambiguously established. In order to eliminate these problems, supersonic jet excitation spectroscopy was found to provide new information regarding the spectra of the isolated molecule and dynamics at different excess vibrational

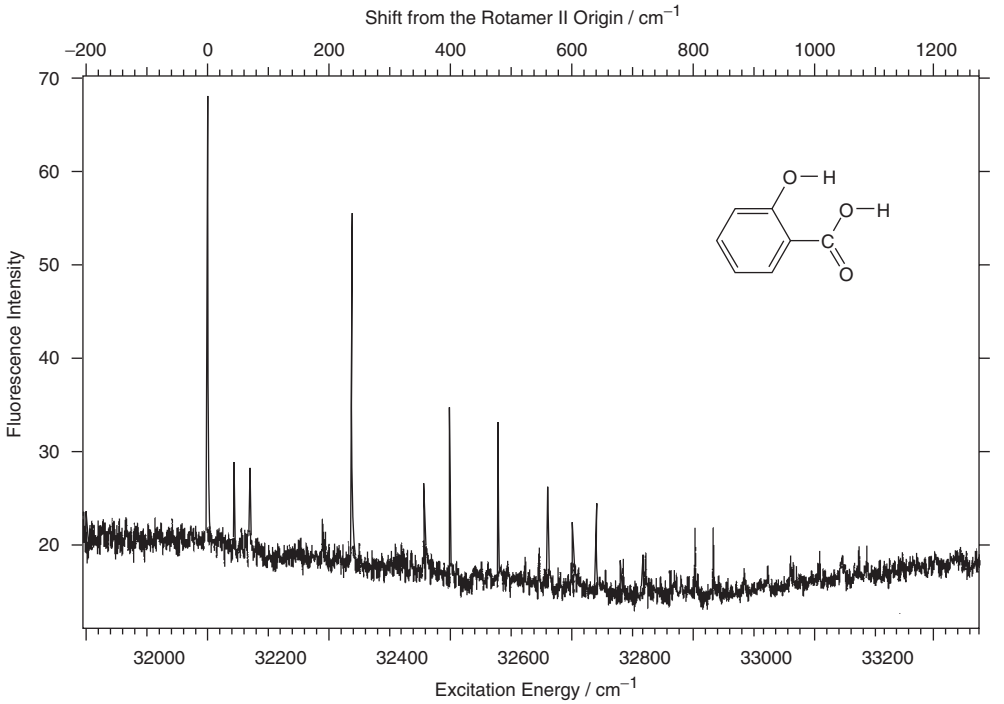

FIGURE 68.9 Fluorescence excitation spectrum of rotamer II on monitoring UV fluorescence.

energies.[7] Felker et al.[7] have observed a dispersed fluorescence of jet-cooled MSA excited at 332.75 nm. This fluorescence shows long progressions from the excitation original to 3220 cm^{-1}, with frequency intervals of 180 cm^{-1} that correspond to a ground-state, out-of-plane bending motion of the ring, including the intramolecular hydrogen bond. The fluorescence decay rate of MSA as a function of the excess vibrational energy is shown in Figure 68.8. As the excitation energy increases, the decay rate is observed to decrease markedly (from 12 ns to 160 ps), with a threshold at ~1300 cm^{-1}. This is in good agreement with the presence of the nonradiative process in solution with the activation energy (3.7 kcal/mol) as described above. The nonradiative process involves low-frequency torsions and bends as supported by the prominence of the 180-cm^{-1} progression leading to formation of zwitterions in the excited state.

The fluorescence spectrum and fluorescence lifetime of SA are strongly dependent on the solvent conditions, as shown in Table 68.6, because of the presence of several forms of the molecule in different solvent conditions; furthermore, SA has a much greater tendency to form dimers than MSA. Thus, it is difficult and complicated to analyze the dynamics of SA in solution at room temperature.

Bisht et al.[6] observed cryogenic effects (10 to 293 K) on time-resolved fluorescence spectroscopy, confirming the ESIPT in the dimeric state of crystalline SA. The time-resolved fluorescence decay curves for solid SA at 10 K observed at 410 nm with different excitation wavelengths are shown in Figure 68.9, and the analyzed data are summarized in Table 68.6. The emission decays are bi-exponential and are resolved into two lifetime components: the first one shows a shorter and constant lifetime (3.0 ns), and the other one shows longer and variable lifetimes (7.95 to 4.7 ns), depending on the excitation wavelength. The relative amplitude also changes and is greater for the longer component in the long-wavelength region. This red-edge effect (REE) at 10 K is due to various distortions of sites/oligomers. The decays of both the UV and blue emissions show single exponential behavior as the temperature increases above 160 K. These results indicate that a ground- and an excited-state double proton transfer, as well as the simultaneous intramolecular fast proton transfer, take place.[23]

TABLE 68.4 Frequency Shift, Intensity, and Assignments of Rotamer II of Salicylic Acid

Shift[a]	Intensity	Assignments
–226	13.5	?
0	36	Origin (32,098 cm^{-1})
44	14	ν_1
69	14.2	ν_2
203	12.8	ν_3
240	24.8	ν_4
358	11.5	ν_5, $\nu_1 + \nu_2 + \nu_4$
363	14.6	ν_4
403	18.2	$\nu_5 + \nu_1$
481	14.7	$2\nu_4$
521	7.8	$\nu_6 + 2\nu_1 + \nu_2$, ν_7
546	9.2	ν_8
561	11.2	$\nu_7 + \nu_1$
584	7.6	$\nu_7 + \nu_2$
598	7.8	$\nu_8 + \nu_1$
603	12.9	$\nu_4 + \nu_6$
643	13.8	$\nu_4 + \nu_5 + \nu_1$
683	13.1	$\nu_4 + \nu_5 + 2\nu_1$
720	13.6	$3\nu_4$, $\nu_7 + \nu_3 + 2\nu_5$
801	18	—
806	16	$2\nu_5 + 2\nu_1$
809	14	—
832	21	$2\nu_4 + \nu_5$
842	15.5	$2\nu_4 + \nu_6$
861	16.6	—
882	18.2	$2\nu_4 + \nu_5 + \nu_1$
920	27.3	$\nu_6 + \nu_7 + \nu_1$

[a] Relative to the origin (cm^{-1}).

TABLE 68.5

			Relative Quantum[a]	
Temperature (K)	τ (ps)	$k_{nr}(T)$ (s^{-1})	450 nm	340 nm
160	8300	—	—	—
184	5020	7.87×10^7	—	—
197	4650	9.46×10^7	—	—
212	2250	3.24×10^8	—	—
213	2092	3.58×10^8	—	—
233	1189	7.21×10^8	—	—
253	803	1.12×10^9	—	—
273	470	2.01×10^9	2.02	1.15
296	280	3.45×10^9	1.00	1.0
303	239	4.06×10^9	0.88	1.20
313	218	4.47×10^9	0.63	1.20
323	176	5.56×10^9	0.48	1.13
333	150	6.55×10^9	0.35	1.03
343	124	7.94×10^9	—	—
353	113	8.73×10^9	—	—

[a] Normalized so that at this wavelength the quantum yield is unity at 296 K.

TABLE 68.6

	λ_{max} (nm)		
	Absorption	Fluorescence	Lifetime (ns)
Salicylic acid (MeOH 10^{-2} *M* + H^+)	304	350 + 438	0.38
Salicylic acid (MeOH 10^{-3} *M* + OH^-)	302	398	~3.4
Salicylic acid (6N KOH 10^{-2} *M*)	304	400	~3.5
Salicylic acid (conc. H_2SO_4)	305	410	0.33
Salicylic acid (MCH 10^{-3} *M*)	313	415	0.62
Methyl salicylate (MeOH 10^{-4} *M*)	308	350 + 450	0.28

Yoshihara's group[6] has also measured the lifetimes of SA rotamers in a supersonic free jet expansion. The fluorescence decays of rotamer II were too fast to measure with their experimental time resolution (<1 ns); however, the excitation energy dependence of decay rates of rotamer I fluorescence could be observed. At low energy, the fluorescence decay was measured to be single exponential with a lifetime of 9.6 ns (12.0 ns for MSA). On the other hand, at higher energies above ~1100 cm^{-1}, the decay curves show bi-exponential behavior with lifetimes decreasing to ~4.3 ns due to an efficient intramolecular nonradiative decay process, as observed in solution, which may be attributed to the proton transfer. The 9.6-ns component is nonlinearly dependent on SA concentration and is attributed to the dimer.

68.4 Substituent Effects on the ESIPT in Salicylic Acid and Its Derivatives

ESIPT in 5-Methyl- and 5-Methoxysalicylic Acid

Modification of the excited-state acidity of the phenolic OH of SA and MSA has been observed to exhibit the possibility of modulating the ESIPT process and the excited-state equilibrium between enol and keto forms.[36] The proton-donating ability of the phenolic OH is known to be reduced by introducing an electron-donating group such as a CH_3 or an alkoxy in the 5-position (*para*) to the OH of MSA. The effect of an ethoxy substituent in the 5-position of MSA was first investigated by Weller[37] 40 years ago and studied further in by Acuna et al.[38] for the 5-methoxy derivative in the gas phase and in solution. The fluorescence of the 5-methoxy MSA exhibits a strong maximum at 400 nm and a shoulder at 490 nm. Both emissions have the same excitation spectrum, indicating that they originate from the same ground-state species. The 400-nm emission observed in 5-MSA deviates from the usual UV emission of other SA derivatives (~380 nm). This may be attributed to the emission from the initially excited rotamer I (Scheme 1) in its enol form, while the 490-nm shoulder originates from the ESIPT process, indicating a keto-enol equilibrium mechanism involved in the excited state.

Lahrmani and Zehnacker-Rentien[36] have investigated the influence of methyl and methoxy substitution in a position *para* to the phenolic OH group on the intramolecular proton-transfer properties of the electronically excited of SA (ESIPT), both in different solvents and in the isolated gas-phase condition provided by supersonic cooling. The absorption spectra and the emission of 5-MeSA and 5-MeOSA in cyclohexane at a concentration of ~$2–3 \times 10^{-5}$ *M* are shown in Figure 68.10. The substitution with methyl- and methoxy groups in the 5-position induces a bathochromic shift of the absorption with respect to the non-substituted SA (310 nm). The fluorescence of 5-MeSA is weak and consists of two bands with two distinct maxima in the UV at 380 nm and in the blue at 450 nm. On the other hand, the fluorescence from 5-MeOSA exhibits a strong band at 400 nm and a shoulder at about 430 nm. The relative intensity of the UV/blue emission of 5-MeSA increases with concentration but is independent of concentration in 5-MeOSA. The excitation spectrum of 5-MeSA for the UV emission is red-shifted by ~10 nm from that of the blue emission; however, those two emissions for 5-MeOSA show identical excitation spectra (Figure 68.11). These results indicate that MeSA and MeOSA behave differently. The increase of UV emission with increased concentration of 5-MeSA and the emission wavelength-dependent excitation

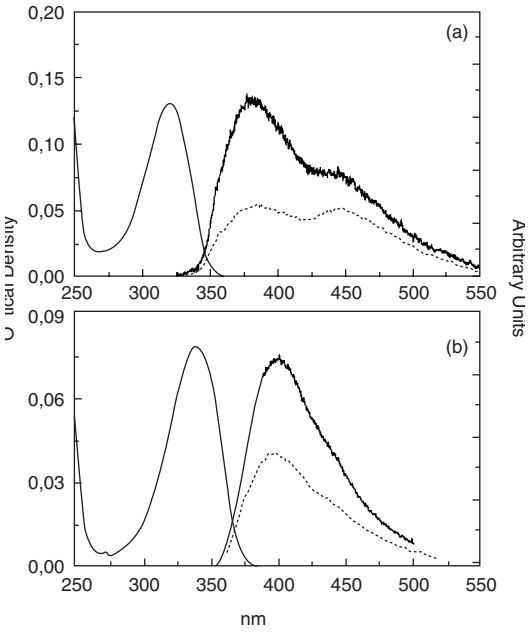

FIGURE 68.10 Absorption and emission spectra of 5-MeSA and 5-MeOSA in cyclohexane solutions: (a) 5-MeSA, $c = 3 \times 10^{-5}$ M (continuous line), $c = 0.9 \times 10^{-5}$ M (dotted line); (b) 5-MeOSA, $c = 2.13 \times 10^{-5}$ M (continuous line), $c = 0.5 \times 10^{-5}$ M (dotted line).

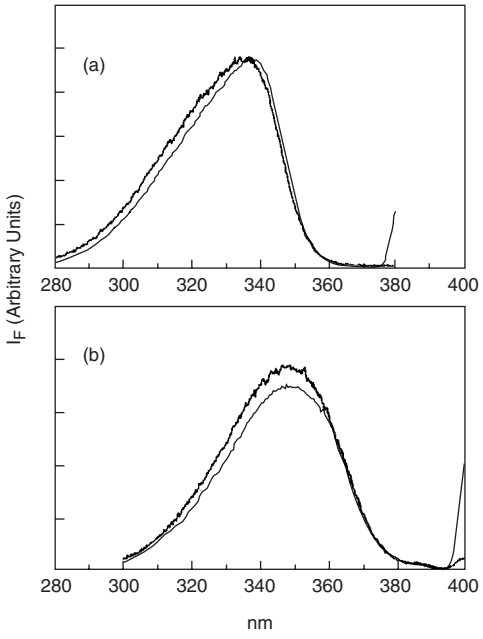

FIGURE 68.11 Excitation spectra of 5-MeSA and 5-MeOSA in cyclohexane solutions: (a) 5-MeSA, — bold line λ_{obs} = 450 nm, — light line λ_{obs} = 380 nm; (b) 5-MeOSA, — bold line λ_{obs} = 450 nm; — light line λ_{obs} = 400 nm.

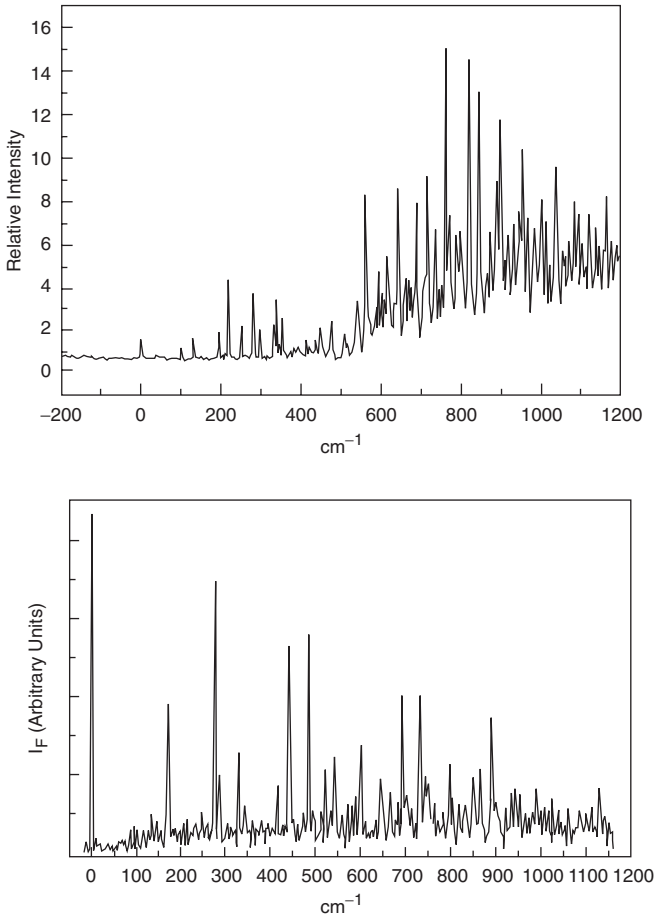

FIGURE 68.12 (a) Fluorescence excitation spectrum of jet-cooled 5-MeSA (T = 80°C, WG 420 Schott filter). The 0-0 transition is at 29,040 cm^{-1} (b) Fluorescence excitation spectrum of jet-cooled 5-MeOSA (T = 80°C) observed at 400 nm through a low-resolution monochromator ($\Delta\lambda$ = 20 nm). The 0-0 transition is at 28,615 cm^{-1}.

spectrum can be related to the equilibrium between the monomer and the dimer as observed for SA;[23] however, no evidence for a dimeric form can be found in the case of 5-MeOSA. Nevertheless, it is very difficult to characterize unambiguously the excited-state properties of SA derivatives in solution as described above. This is because several species including monomers in different conformations (rotamers I and II) and the dimer coexist in the SA derivatives depending on the solvent and the concentration. In order to isolate molecules and elucidate the photophysical properties selectively, a supersonic jet experiment is helpful.

The fluorescence excitation spectra of jet-cooled 5-MeSA and 5-MeOSA heated at 80°C, obtained by monitoring the light emitted at 400 nm and longer wavelengths, are shown in Figure 68.12. The first weak features at 29,040 cm^{-1} and 28,615 cm^{-1} are assigned to the 0–0 transition. The frequencies of the main vibrational bands are listed in Table 68.7. The density of vibrational bands is significantly larger in 5-MeSA then in SA (Figure 68.12A), but the general shape of the spectrum looks similar to that of SA. Thus, it can be assigned to the S_0–S_1 transition of the rotamer involving the strong OH···O=C hydrogen bond. The fluorescence excitation spectrum of jet-cooled 5-MeOSA shows a red shift of ~1200 cm^{-1} relative to that of SA. The spectrum at the origin of 5-MeOSA is stronger that that of SA or MSA, indicating that the Franck–Condon distribution of 5-MeOSA is different from that of SA or MSA. Thus,

TABLE 68.7 Observed Vibrational Frequencies for 5-MeSA and 5-MeOSA (cm^{-1})

5-MeSA 0–0 (29,040 cm^{-1})	5-MeOSA 0–0 (28,615 cm^{-1})		SA 0–0 (29 480 cm^{-1})	MS 0–0 (30 052 cm^{-1})
S_1	S_1	S_0	S_1	S_1
100	171	170	88	176
127	—	—	—	—
194	—	—	—	—
217	—	—	—	—
246	—	—	—	—
279	272	—	—	—
296	283	285	—	—
335	330	332	—	347
353	—	—	364	—
—	—	—	370	—
446	440	430	431	—
—	—	444	—	—
475	482	480	—	—
505	520	504	511	521
556	537	—	—	—
—	542	564	—	569
—	601	599	—	—
—	645	657	—	—
—	694	717	704	694
—	734	780	727	739
—	798	—	734	770
—	—	—	795	776
—	847	—	811	—
—	863	—	835	—
—	890	936	849	—

the excited-state potential surface is deeply modified and the intramolecular proton transfer in the isolated molecule is inhibited in 5-MeOSA, while the ESIPT takes place in the isolated 5-MeSA, as confirmed by the difference in the low-resolution dispersed fluorescence spectra of jet-cooled 5-MeSA (Figure 68.13A) and 5-MeOSA (Figure 68.13B). In nonpolar solvent, no ESIPT process takes place in 5-MeOSA, in agreement with the conclusions of the isolated jet-cooled, gas-phase results. Nevertheless, the presence of diethyl ether or of a stronger proton acceptor such as triethylamine promotes the ESIPT reaction in 5-MeOSA. These results show that intermolecular hydrogen bonding of the solvent to the carboxylic OH does not break the intramolecular hydrogen bond but rather reinforces it, thus allowing the ESIPT reaction to occur by increasing the electron density on the C=O group. This effect can be interpreted in terms of the charge transfer within the intermolecular hydrogen bond from the electron-rich ligand to the carboxylic group, which in turn results in a strengthening of the intramolecular hydrogen bond. Consequently, such ESIPT has also been demonstrated to enhance the intramolecular charge transfer in the *N*,*N*-dialkyammonium substitution of SA.[13,14]

ESIPT in *p*-Aminosalicylic Acid and Its Derivatives

Molecular structures of *p*-aminosalicylic acid and its derivatives are shown in Scheme 4, which shows the molecular structures of 2-methoxy-4-aminobenzoic methyl ester (MABAE, I), 2-methoxy-4-dimethylaminobenzoic acid methyl ester (MDABAE, II), *p*-aminosalicylic acid (PASA, III), *p*-aminosalicylic acid methyl ester (PASE, IV), *p*-dimethyl-aminosalicylic acid (PDASA, V) and *p*-dimethylaminosalicylic acid methyl ester (PDASE, VI). In these molecules, the hydroxy group, when hydrogen bonded to the ester or acid carbonyl group, permits an ESIPT fluorescence. Simultaneously, the *p*-amino group permits the so-called twisted intramolecular charge transfer (TICT) fluorescence to be observed when activated

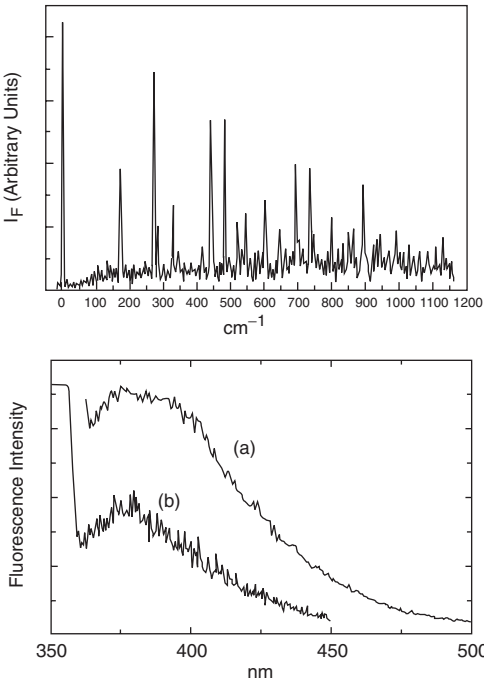

FIGURE 68.13 (a) Low-resolution dispersed fluorescence spectra ($\Delta\lambda$ = 20 nm) of jet-cooled 5-MeSA: (a) ν_{exc} = 0-0 + 217 cm^{-1}; (b) ν_{exc} = 0-0 + 556 cm^{-1} (b) Low-resolution ($\Delta\lambda$ = 20 nm) dispersed fluorescence from jet-cooled 5-MeOSA excited (a) on the 0-0 transition at 28 615 cm^{-1} and (b) the first vibronic level at 170 cm^{-1}.

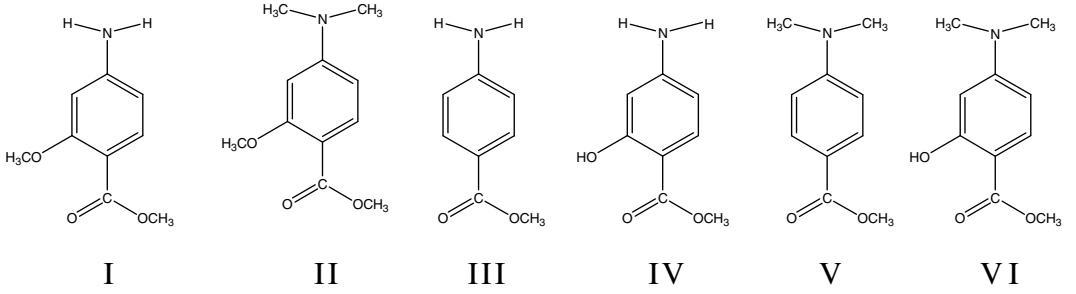

SCHEME 4

in a suitable dielectric media. Kasha et al.[9,10] have observed the ESIPT, which is competitive with the excited-state ICT. However, they proposed that the absence of double alkyl substitution of the amino group and α-hydroxy group *ortho* to the ester carbonyl, as shown in structure I, does not exhibit either ESIPT or the excited-state ICT. These molecules are observed to exhibit only normal $S_1 \rightarrow S_0$ fluorescence emission at 332 nm, as shown in Figure 68.14.

On the other hand, structure II exhibits the usual dual fluorescence as well as TICT emission at 350 and 423 nm, but no ESIPT is observed. This is due to the lack of a hydroxy group *ortho* to the ester carbonyl. The bulky *p*-amino-substituted molecule is known to exhibit TICT. Structures III and IV show the dual emissions similar to that of structure II. Kasha et al.[9,10] interpreted this dual emission as the normal and ESIPT emission, as it does not include bulky *p*-amino-substituents.

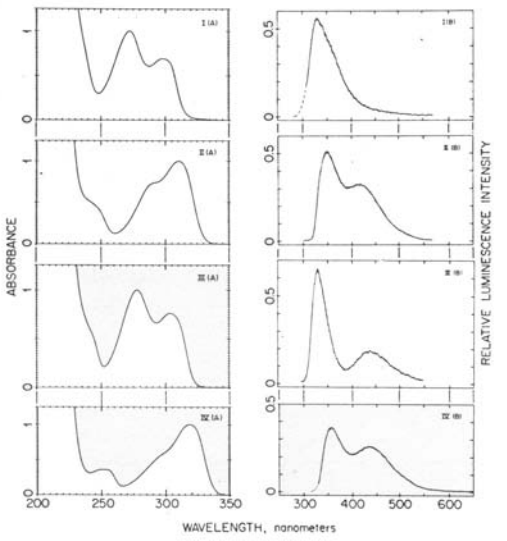

FIGURE 68.14 The absorption and fluorescence emission spectra of compounds I, II, III and IV in methylene chloride at 298K C ≈ 2×10^{-5} M. Excitation wavelength: I (B) = 297, II (B) = 287, III (B) = 277 and IV (B) = 318nm

Structures V and VI exhibit intramolecular proton transfer originating from the OH group and a TICT state emission as a result of the dimethylamino substituent. The second emission band is broadened, indicating the existence of the two emission components originating from the ESIPT and TICT, which are relaxed from the emission originating from the initial excited state. The intensities of these two emissions are competitively changed depending on the polarity of the solvent used. As the polarity increases, the TICT emission is stronger than the ESIPT emission. Such competitive relaxation channels involved in normal emission (i.e., TICT and ESIPT reactions) have been investigated by Gomin and Kasha[9,10] based on the observation of multiple fluorescences from various selected aminosalicylates. As a prototype, *p*-dimethylaminomethylsalicylate (PDASE) exhibits ESIPT emission in nonpolar solvents, while multiple emissions from normal TICT states are observed in polar, aprotic solvents. According to the steady-state fluorescence measurements of the PDASE in different solvent conditions, the excited-state processes were assigned as the normal emission ($S_1 \rightarrow S_0$). The TICT emission (S_1[TICT] $\rightarrow S_0$[FC]) and the ESIPT emission (S_1'[ESIPT] $\rightarrow S_0$[FC]) are shown in Figure 68.15; however, these two emissions overlap more closely at longer wavelengths (F_2) than the normal emission band (F_1), and it is difficult to resolve them into the two bands by steady-state fluorescence techniques. Thus, in order to confirm this assignment, Gormin[11] has measured the picosecond transient absorption spectra of PDASE, PASE, and MDABAE in methylene chloride and cyclohexane at 50-ps time delay. The transient absorption spectra of MDABAE (panel A), PASE (panel B), and PDASE (panel C) are shown in Figure 68.16. Because MDABAE has the phenolic OH replaced by methoxy, no ESIPT is expected; however, a broad transient absorption is exhibited at ~470 nm for MDABAE in methylene chloride. In cyclohexane, this transient is not observed, indicating that the transient observed in methylene chloride originates from the TICT because of the bulky amino group as observed for the *p*-dimethylaminobenzoate.[39] In contrast to MDABAE, PASE is known to be a molecule capable of exhibiting ESIPT-type and not TICT-type behavior as a result of the poor electron-donating ability of the amino group to induce TICT. Consequently, the comparative dynamics between ESIPT and TICT are dependent on the substituent and solvents used. Thus, the Kasha and Gormin groups proposed that the ESIPT can be tuned by changing the charge-transfer functional groups.

Chou et al.[12] have also observed dual emission bands from *p-N,N*-diethylamino salicylic acid (PEAS) that appear in ratios dependent upon the excitation wavelength, consistent with the results of Shabestary

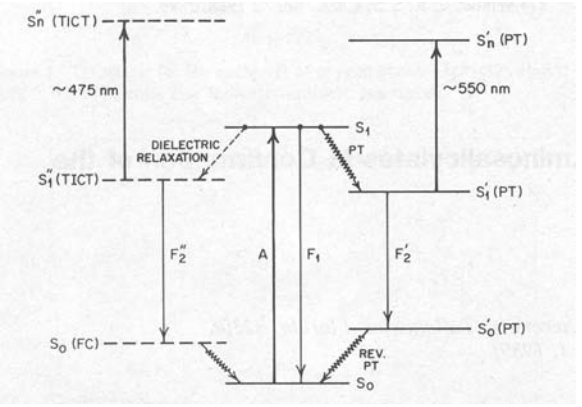

FIGURE 68.15 Energy level diagram indicating the origins of the three competitive fluorescence transitions and two possible transient absorption transitions. The dashed level (S_1") represents a 90 twist between the planes of the donor and acceptor protons of structures II and III.

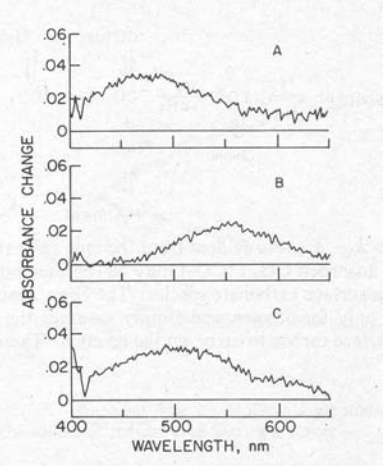

FIGURE 68.16 Room temperature picosecond transient absorption spectra of structure I (panel A), structure II (panel B) and structure III (panel C), in methylene chloride solution at a 50-ps time delay. The concentrations used are 0.722, 0.317 and 0.902 mM for A, B and C, respectively.

and El-Bayoumi;[8] however, they found that these two emission bands also showed significant concentration dependence in heptane (Figure 68.17). In combination with the concentration-dependent absorption spectra (Figure 68.18), they concluded that no emission results from the amino-*N*-charge-transfer state. Instead, the normal Stokes-shifted emission is assigned to the emission from a dimer (Figure 68.19c) overlapping the normal emission of conformer b or b′.

These controversial results were obtained using a limited number of aprotic solvents such as methylene chloride or cyclohexane. Such a limited solvent system does not provide full information of the complex excited-state reactions including TICT and ESIPT. When one considers the ICT and ESIPT together, specific solvent effects such as hydrogen bonding should be considered in addition to the polarization effects. Thus, Yoon's group has attempted to explore the hydrogen bonding effects more systematically on the excited-state process of PASA and its derivatives by observing the steady-state and time-resolved fluorescence properties in various protic and aprotic solvents[13] as well as aqueous cyclodextrin solutions.[14] The concentration effects on the fluorescence spectral properties were also observed. The fluorescence

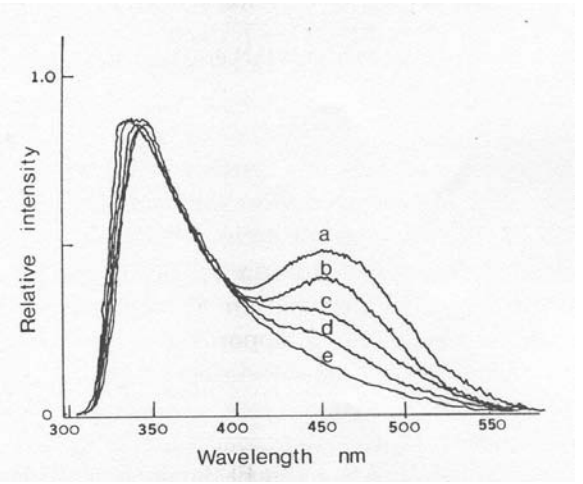

FIGURE 68.17 Room temperature fluorescence of PEAS in *n*-heptane at various concentrations : (a) 5.0×10^{-7}M, (b) 5.0×10^{-6}M, (c) 2.0×10^{-5}M, (d) 1.0×10^{-4}M and (e) 1.27×10^{-3}M. The spectra have been normalized at 340nm.

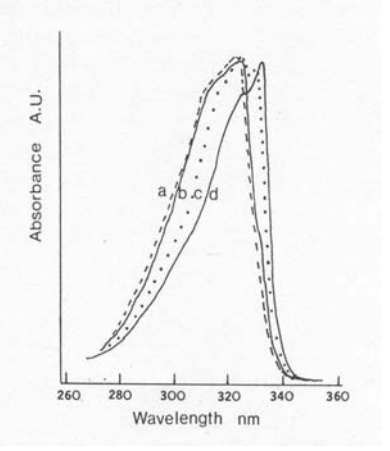

FIGURE 68.18 Room-temperature absorption spectra of PEAS in n-heptane at various concentrations: (a) 5.0×10^{-7}M, (b) 2.0×10^{-5}M, (c) 1.0×10^{-4}M and (d) 1.27×10^{-3}M. Since the spectra have been normalized the absorbance is in arbitrary units.

emission spectra of PASA (1.0×10^{-5} *M*) in various aprotic solvents are shown in Figure 68.20. Upon increased solvent polarity, the large Stokes-shifted emission at 440 nm is quenched and broadened. This is accompanied by an increase in the normal emission band at 330 nm; however, no absorption spectral change is observed as the solvent polarity increases. These results indicate that the normal excited state is relaxed into two different excited states, which are related to solvent polarity. This is consistent with the fact that the large Stokes-shifted band is resolved into 430 nm and 470 nm by band analysis (Figure 68.21). Table 68.8 shows the fluorescence lifetimes of PASA in various aprotic solvents. In non-polar aprotic solvents, the decay profile of the 430-nm emission is single exponential and its decay time is within ~300 ps. This is attributed to the ESIPT state of PASA, in agreement with result obtained by Kasha et al.[9,10] However, as the solvent polarity increases, the decay of the large Stokes-shifted emission at ~430 nm exhibits a bi-exponential behavior with two lifetime components, ~300 ps and ~150 ps. Furthermore, the relative amplitude of the 150-ps component is observed to increase with increasing

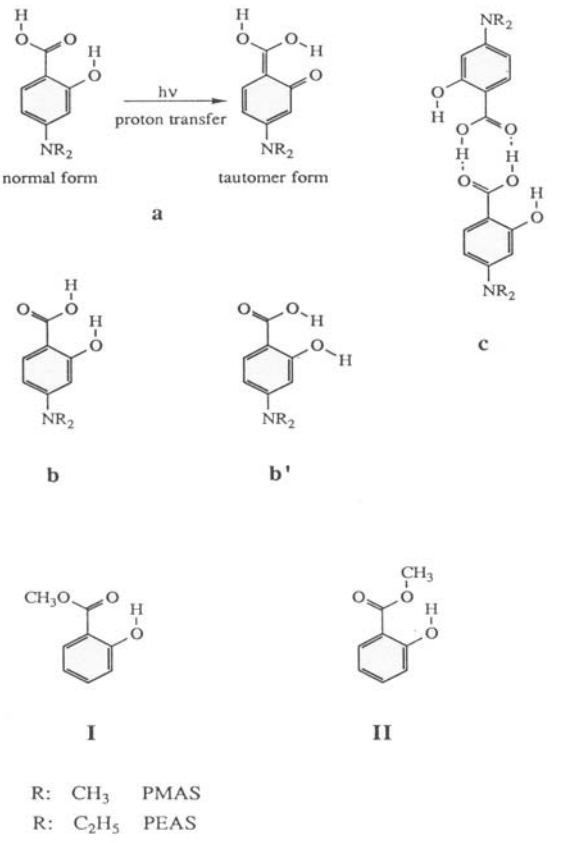

FIGURE 68.19 Various structures of *p-N,N*-dialkylaminosalicylic acids and methyl salicylate.

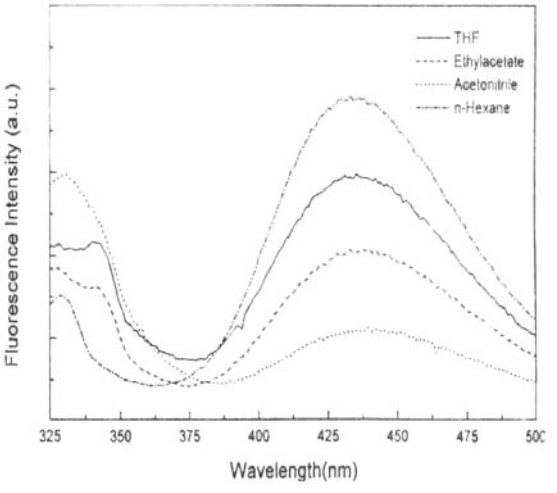

FIGURE 68.20 Fluorescence emission spectra of 1.0×10^{-5} M aminosalicylic acid in various aprotic solvents. The excitation wavelength is 300 nm.

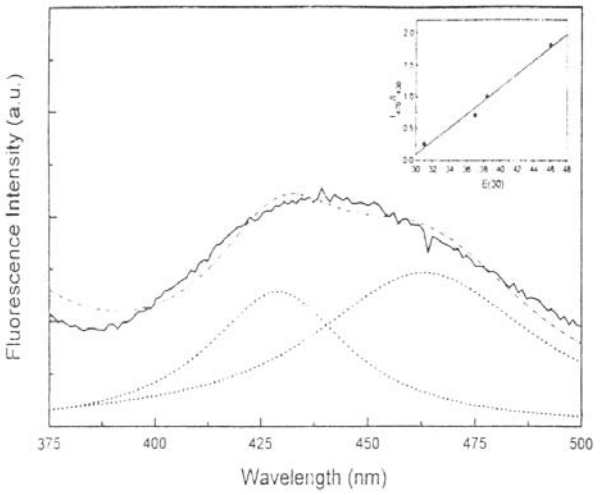

FIGURE 68.21 The band analysis of the Stokes-shifted emission of AS. The excitation wavelength is 300 nm. The inset is relative area ratio of the 470 nm emission band to the 430 nm emission band.

TABLE 68.8 Fluorescence Lifetimes of AS in Various Aprotic Solutions

	Wavelength	
Solvent	430 nm	465 nm
THF	330 ps (1)	330ps (1)
Ethyl acetate	270 ps (0.85)	280 ps (0.73)
	160 ps (0.15)	150 ps (0.27)
	Rise time: 40 ps	Rise time: 40 ps
Acetonitrile	270 ps (0.09)	270 ps (0.02)
	150 ps (0.91)	150 ps (0.98)
	Rise time: 40ps	Rise time: 40 ps

solvent polarity, while that of the 300-ps component decreases. These results contrast with the kinetics observed for PASA by Kasha et al.,[9,10] who suggested the existence of the ESIPT state only in aprotic polar solvents. It is also noteworthy that a rise component (~40 ps) is observed in polar solvents in contrast to its absence in nonpolar solvents. The rise time is too large to be the rate of ESIPT and its origin, we believe, is due to the forward conformational relaxation of the excited PASA followed by the polar solvent reorganization to facilitate the formation of the ICT state. Thus, the 150-ps component should be originated from the excited ICT state.

Previous work revealed that the hydrogen bonding plays an important role in the excited ICT of PDASA;[40–42] thus, the excited-state ICT in PASA could also be coupled with the inter- and intramolecular hydrogen bonding. In order to clarify this possibility, the influence of concentration effects on the fluorescence decay kinetics of PASA in ethanol were investigated by Kim and Yoon.[13] In dilute concentrations (0.005 m*M*), the decay of the large Stokes-shifted emission is bi-exponential (1.2 ns and 420 ps); however, in concentrated solutions (0.1 m*M*), an additional lifetime component of ~200 ps was observed in addition to the two components observed in the dilute solutions. In conclusion, this new lifetime component is solvent polarity dependent, and the ESPT is a prerequisite to form the ICT state even in the case of the PASA. In other words, the ICT is feasible when a closed conformer is formed by intramolecular hydrogen bonding which makes ESIPT feasible.

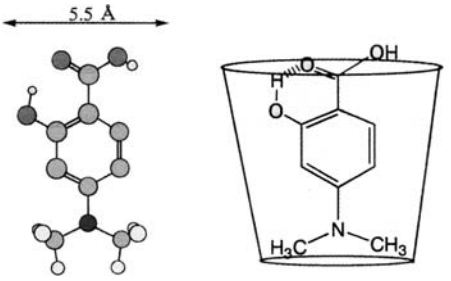

SCHEME 5

Yoon's group has also attempted to explore systematically the effect of hydrogen bonding on the excited-state processes of PDASA by observing the steady-state and time-resolved fluorescence spectral properties in aqueous cyclodextrin (CD) solutions. CD forms a hydrophobic and restrictive cavity with hydrophilic external walls in aqueous solution, providing two different microenvironments with an incorporated guest molecule. Thus, CD is an ideal system for controlling the relative microenvironment of each functional group of PDASA. This helps to distinguish the hydrogen bonding and polarity dependence of the electron-donating group from the inter- or intramolecular hydrogen bonding effect of the carboxylic acid. Actually, many scientists have employed the CD system to control the ICT process of various ICT molecules.[43–46] According to the absorption and fluorescence studies of FDASA in the aqueous β-CD solutions, the optimized structure of PDASA and the proposed pattern of inclusion complex with β-CD has been proposed, as shown in Scheme 5.

A single emission at 400 nm is observed for 0.05-m*M* PDASA in aqueous solution. This originates mostly from excited-state intermolecular hydrogen bonding. Upon addition of β-CD, the 400 nm emission band is diminished, accompanied by broadening of the bandwidth along with an appearance of a new band at 350 nm (Figure 68.22). These spectral changes were further confirmed by band analysis using the Gaussian distribution function (Figure 68.23). Even in CD-free aqueous solution, the emission band of PDASA was found to be composed of two different bands at 390 and 420 nm, indicating that two different conformers exist even in aqueous solution (one a closed-form conformer due to intramolecular hydrogen bonding between the OH and COOH group, and the other an open conformer formed by intermolecular hydrogen bonding). As the concentration of CD increases, two additional emission bands appear at 350 and 460 nm, indicating the presence of two corresponding excited species in addition to the open and closed conformers formed by the CD complex formation. These two emission are considered as originating from the ESIPT and ICT process, respectively. Consistent with these steady-state spectroscopic results, the picosecond time-resolved fluorescence study unraveled three decay components corresponding to two different proton transfer processes (5.6 ns, 160 ps) and the excited ICT (1.5 ns) (see Table 68.9).[14] It is noteworthy that the relative amplitude of the 1.5-ns component, attributable to the ICT state, is enhanced in parallel with an increase in the 160-ps ESIPT component. These results are interpreted in terms of the proton transfer with charge-coupling processes. Based on these experimental and theoretical observations, the excited-state potential surface for the reaction of PDASA in CD has been proposed as shown in Figure 68.24.

ESIPT in Salicylideneanilines and Related Compounds

The salicylideneaniline (SAN) molecule and related molecules are highly useful model compounds for the investigation of the role of structural flexibility in light-induced structural transformations. This photochromic transformation is connected with adiabatic ESIPT OH→NH in the S_1 state of the structure (E, Scheme 6), which is the origin of the fluorescence anomalous Stokes shift.[16–18,47] The anomalous Stokes-shifted fluorescence and absorption spectral maxima of SAN observed under several conditions are listed in Table 68.9. The anomalous Stokes-shifted emission was found to be observed only in rigid matrices, especially in a glassy solvent at 77 K, as well as in crystals.[17] This implies that the necessary step

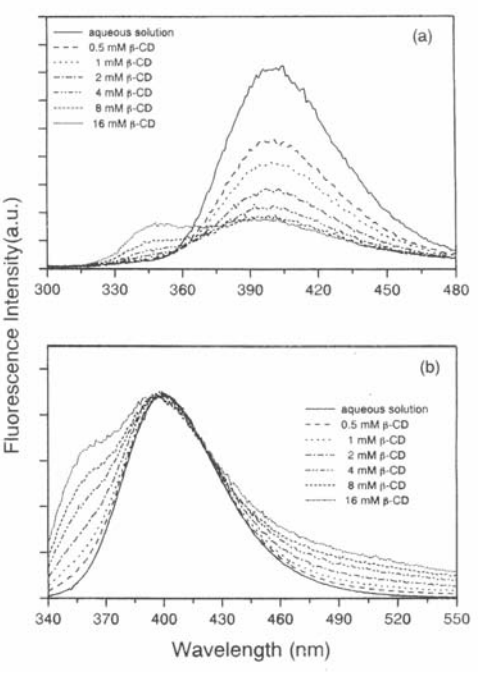

FIGURE 68.22 (a) Fluorescence emission spectra of DMAS (5.0×10^{-5} M) in aqueous buffer solution (pH = 1.7) containing different concentrations of β-CD: the excitation wavelength was 280 nm; (b) the excitation wavelength was 320 nm and all the spectra were normalized at 400 nm.

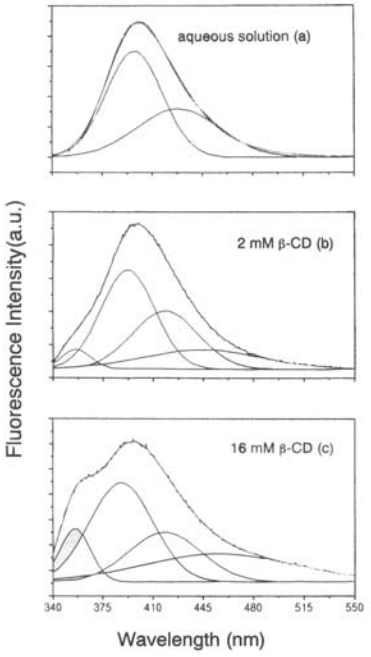

FIGURE 68.23 Band analysis of fluorescence emission of DMAS: (a) aqueous buffer solution (pH = 1.7); (b) 2 mM β-CD; (c) 12 mM β-CD. The excitation wavelength was 280 nm.

TABLE 68.9 Fluorescence Lifetimes (τ_i) and Relative Amplitudes (a_i) for DMAS in β-CD Aqueous Solutions (pH 1.7) and Aprotic Solvents[a]

Solvent	Wavelength (nm)	τ_1 (ns)	a_1	τ_2 (ps)	a_2	τ_3 (ps)	a_3	τ_4 (ns)	a_4
Water	365	4.6	0.64	60	0.36	—	—	—	—
	400	5.3	0.99	—	—	160	0.01	—	—
	440	5.5	0.95	—	—	155	0.05	—	—
β-CD (2 m*M*)	365	4.2	0.18	50	0.65	170	0.15	—	—
	400	5.5	0.60	—	—	160	0.26	1.5	0.14
	440	5.6	0.47	—	—	155	0.32	1.5	0.20
β-CD (16 m*M*)	365	4.2	0.12	50	0.70	220	0.18	—	—
	400	5.6	0.24	—	—	155	0.49	1.5	0.26
	440	5.6	0.14	—	—	160	0.51	1.5	0.35
Hecane[b]	440	—	—	—	—	398	0.94	1	0.06
	510	—	—	—	—	390	0.91	1	0.09
Acetonitrile[b]	440	—	—	—	—	110	0.35	2	0.65
	510	—	—	—	—	150	0.14	1.7	0.86

[a] Excitation wavelength is 300 nm. Measurement error limits are <10% of the values.
[b] Emission at wavelength 360 nm could not be measured because of its low quantum yield.

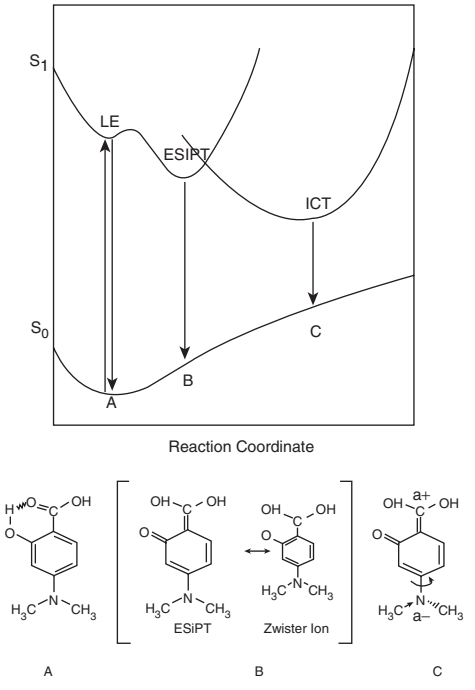

FIGURE 68.24 Proposed potential energy surface diagram for the proton-transfer-coupled intramolecular charge transfer of DMAS/ß-CD system.

for the phototautomerism may be connected with NH···O bond and disruption due to the ring A twist around the CC double bond (K_{tr}) in the ground-state structure (NH, Scheme 6). In other words, the ring A rotation may inhibit the reverse general ground state NH→HO proton transfer and secure the metastability of the colored NH structure formed by the ESIPT, leading to the adiabatic formation of the intermediate S_1-zwitterionic NH structure (K_z^*). The ESIPT is followed by adiabatic disruption of the intramolecular hydrogen bond NH–O with the formation of a colored, metastable, ground-state keto structure having *trans* configuration with respect to the CC double bond (K_{tr}).

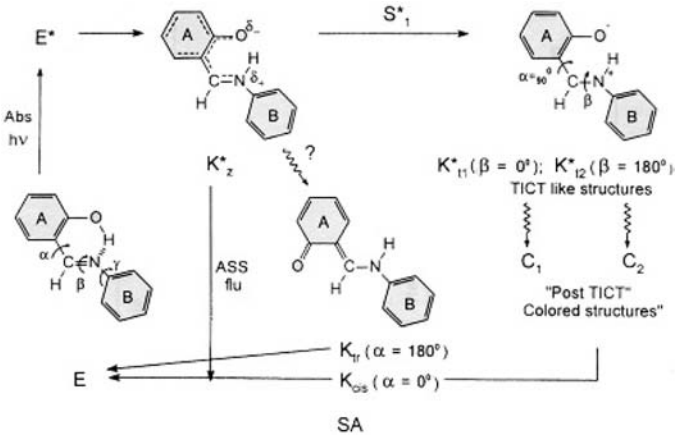

SCHEME 6

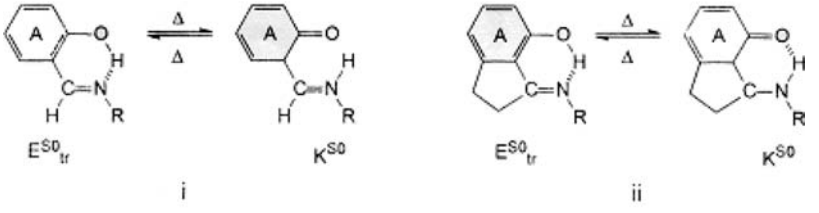

SCHEME 7

In earlier papers,[17,18] rather different interpretations of the anomalous Stokes-shifted emission have been presented. Luminescence spectral[48] and quantum chemical[17,47] methods applied to model compounds such as salicylidene methylimine (i_a in Scheme 7) revealed that the longest wavelength transition in the SA molecule responsible for photochromism is localized mainly on the A–C=N– moiety of the SAN molecules, as in i_a. Intramolecular charge transfer (ICT) from *o*-hydroxy (OH) into the azomethine (C=N) group is also proposed to be involved in the ESIPT by the participation of the N-ph π-electron system.[48] It is certain that the twist in ring A plays a crucial role in ESIPT and the photochromic phenomenon. Thus, in order to elucidate the role of ring A rotation in the ESIPT more directly, Knyazhansky et al.[47] have recently performed comparative studies of the derivatives (i and ii, Scheme 7) by using PNMR, x-ray crystallography, and fluorescence techniques, as well as quantum chemical calculations. A comparison of the spectroscopic characteristics obtained from these derivatives is listed in Table 68.9. Quantum chemical studies by semiempirical and *ab initio* methods were carried out to obtain the necessary information of the structural mechanism and the energetics of the photoinduced processes. The semiempirical calculations were carried out by PM3 using the Mopac program;[50,51] the *ab initio* calculations used the restricted Hartree–Fock method in the STO-3–21G basis set (for detailed results of these calculations, see references 47 and 52).

The simplified scheme (Figure 68.25) for the photoinduced processes in salicylideneaniline molecules is based on spectroscopic work and quantum chemical calculations, together with well-known kinetic data for the excited state of molecule i. The primary photoinduced process, a fast ESIPT, takes place in the S_1 state, leading to the formation of the planar NH structure (I*), which is responsible for the anomalously large Stokes-shifted (ASS) fluorescence displayed only in rigid media. Two processes then compete with the ASS fluorescence; adiabatic ring A twisting occurs only in liquids and leads to the TICT state [(I*), $\tau = 90°$] in the *Z*-structure of the NH form. This structure makes a considerable contribution

TABLE 68.10 Comparative Structural, Spectral, and Fluorescent Characteristics of the Initial (E,K) and Photo-Colored (C) Forms of the Studied and Model Structures (Isopentane)

Compound	Isomer Structure	PMR Proton Signal (δ_{OH})[a] (ppm)	Absorption (λ_{max}) (nm) Temperature (K)		Fluorescence Emission (λ_{max}) (nm) Temperature (K)		Fluorescence Excitation (λ_{max}) (nm) Temperature (K)		Stokes Shift $\Delta\nu$ (cm^{-1}) Temperature (K)	
			293	77[b]	293	77[b]	293	77	293	77
i_a	E	13.38	317	320 (vw)	—	500 (vw)	—	320	—	11,250
	K	—	—	390 (st)	465 (vw)	465 (st)	390	395	4136	3800
	C	—	—	450–460 (vw)	—	535 (wk)	—	450	—	3530
i_b	E	13.61	317	320 (st)	—	506 (st)	—	320	—	11,490
	K	—	—	390 (wk)	465	465 (st)	390	400	4136	3500
	C	—	—	460,490,520 (st)	—	540 (st)	—	460–520	—	3220
ii_b	E	11.55	311	313 (wk)	510	510 (wk)	311	310	12,550	12650
	K	—	—	400 (st)	465	468 (st)	390	390	4136	4270
	C	—	—	—	—	—	—	—	—	—
ii_c	E	—	310	—	500	500 (wk)	310	310	12,260	12,260
	K	—	—	390 (st)	460	460 (st)	400	400	3260	3260
	C	—	—	—	—	—	—	—	—	—
SA	E	13.24	340	342 (st)	—	512 (st)	—	340	—	9880
	K	—	—	430 (vw)	—	520 (vw)	—	430	—	4025
	C	—	—	480,520 (vs)	—	560 (wk)	—	520	—	1370

[a] In toluene at T = 293 K.

[b] Relative absorption band intensity: vw, very weak; wk, weak; st, strong; vs, very strong.

Note: E, enol; K, keto; C, photo-colored structures (irradiation in E-bond for 10 min).

to the ASS fluorescence quenching. The process is completely reversible via the ground state but is inhibited in rigid media (viscosity barrier) in the S_1 state. In both liquid and rigid media, in spite of a viscosity barrier in the latter, the concerted diabatic process — including *Z,E*-isomerization about the C=N bond and ring A 70° rotation around the CC double bond — may be the origin of the feebly fluorescent colored form (i_{col}). This is assumed to have a nonplanar structure as the result of steric interaction between the *N*-aryl and keto A rings solely in the *E*-isomer with respect to the C=N bond.

The photochromic reaction may be an additional efficient channel of ASS fluorescence quenching. In liquid solvents, bleaching occurs in the ground state ($t = 10^{-7}$). In rigid media, the bleaching is drastically delayed ($t = 10$ s in poly[methyl methacrylate] at T = 290 K and depends on temperature and viscosity)[22] and was found to be virtually absent in the glassy solvent at liquid-nitrogen temperature due to the viscosity barrier in the ground state. The scheme is proposed to be qualitatively valid for crystals also.

68.5 Applications

The ESIPT of aminosalicylate derivatives is the primary process for the photochromic phenomenon. The development of useful photochromic systems is very promising for high-resolution imaging systems and for the storage of information in computers. The theoretical spatial resolution of a photochromic imaging or storage system is of the order of molecular dimensions, as the photochemical process itself takes place at the molecular level. The very high spatial resolution of photochromic systems implies a very low sensitivity, so these systems are most useful in conditions of high light intensity (flash or laser light). Thus, a potential application of such photochromic materials could be the protection of eyesight against light pulses of extremely high intensity, such as flashes from nuclear explosions. The photochromic material must respond instantly and must recover very quickly. It has also been suggested to make Plexiglas by dispersing the photochromic material into the polymer. The Plexiglas can act as a rapidly reversible photochromic material through triplet–triplet absorptions in the visible region. The photochromic material can be used to protect the polymer material by femto- or picosecond dissipation of the UV energy absorbed so that oxidation of polymer is inhibited.

Acknowledgment

This is supported financially by the Korea Research Foundation and the Korea Science and Engineering Foundation.

References

1. Weller, A., Fluorescence of salicylic acid and related compounds, *Naturwiss.*, 42, 175, 1955.
2. Weller, A., Intramolecular proton transfer in excited states, *Z. Elektrochem.*, 60, 1144, 1956.
3. Kovi, P. J., Miller C. L., and Schulman S. G., Biprotonic versus intramolecular phototautomerism of salicylic acid and some of its methylated derivatives in the lowest excited singlet state, *Anal. Chim. Acta*, 61, 7, 1972.
4. Kloepffer, W. and Naundorf, G., Fluorescence of methyl salicylate in hydrogen bonding solvents, *J. Lumin.*, 8, 457, 1974.
5. Helmbrook, L., Kenny, J. E., Kohlen, B. E., and Scott, G. W., Lowest excited singlet state and hydrogen-bonded metal salicylate, *J. Phys. Chem.*, 87, 280, 1983.
6. Bisht, P.B., Petek, H., Yoshihara, K., and Nagashima, U., Excited state enol-keto tautomerization in salicylic acid: a supersonic free jet study, *J. Chem. Phys.*, 103, 5290, 1995.
7. Felker, P. M., Lambert, William R., and Zewail, A. H., Picosecond excitation of jet-cooled hydrogen-bonded systems: dispersed fluorescence and time-resolved studies of methyl salicylate, *J. Chem. Phys.*, 77, 1603, 1982.
8. Shabestanyl, N. and El Bayaumi, M. A., A unique excitation wavelength dependence of excited-state proton transfer in *para-N,N*-dimethylaminosalicylic acid, *Chem. Phys. Lett.*, 106, 107, 1984.

9. Gormin, D. and Kasha, M., Triple fluorescence in aminosalicylates modulation of normal proton-transfer and twisted intramolecular charge-transfer (TICT) fluorescence by physical and chemical perturbations, *Chem. Phys. Lett.*, 153, 574, 1988.
10. Heldt, J., Gormin, D., and Kasha, M., A comparative picosecond spectroscopic study of the competitive triple fluorescence of aminosalicylates and benzanilides, *Chem. Phys.*, 136, 321, 1989.
11. Gormin, D., Picosecond transient absorptions spectra of aminosalicylates in confirmation of the triple excitation mechanism, *J. Phys. Chem.*, 93, 5979, 1989.
12. Chou, P-T., Martinez, M. L., and Cooper, W. C., Multiple fluorescences in *para-N,N*-diethylaminosalicylic acid, *Chem. Phys, Lett.*, 198, 188, 1992.
13. Kim, Y. and Yoon, M., Intramolecular hydrogen bonding effect on the excited state intramolecular-charge transfer of *p*-aminosalicylic acid, *Bull. Korean Chem. Soc.*, 19, 980, 1998.
14. Kim, Y., Yoon, M., and Kim, D., Excited-state intramolecular proton transfer coupled-charge transfer of *N,N*-dimethylaminosalicylic acid in aqueous β-cyclodextrin solutions, *J. Photochem. Photobiol. A: Chem*., 138, 167, 2001.
15. Eadjentis, E., in Durr, H. and Bouas-Laurent, H., Eds., *Photochromism, Molecules and Systems,* Elsevier, Amsterdam, 1990, 685.
16. Cohen, M. D. and Flavian, S., The luminescence properties of *N*-salicylideneaniline and related anils in solution, *J. Chem. Soc. B*, 317, 1967.
17. Cohen, E. R. and Birnbaum, G., Influence of the potential function on the determination of multipole moments from pressure-induced far-infrared spectra, *J. Chem. Phys*., 66, 2443, 1977.
18. Barbara, P. F., Rentzepis, P. M., and Brus, L. E., Photochemical kinetics of salicylideneaniline, *J. Am. Chem. Soc.*, 102, 2786, 1980.
19. Smith, K. K. and Kaufmann, K. J., Picosecond studies of intramolecular proton transfer, *J. Phys. Chem.*, 82, 2286, 1978.
20. Nagaoka, S. I., Hirota, N., Sumitanis, M., and Yoshiland, K., Investigation of the dynamic processes of the excited states of *o*-hydroxybenzaldehyde and its derivatives: effects of structural change and solvent, *J. Am. Chem. Soc.*, 106, 6913, 1984.
21. Sobolewski, A. L. and Domcke, W., *Ab initio* study of exited-state intramolecular proton dislocation in salicylic acid, *Chem. Phys.*, 232, 257, 1998.
22. Knyazhansky, M. I., Metelitsa, A. V., Bushkov, A. J., and Aldoshin, S. M., Role of structural flexibility in fluorescence and photochromism of the salicylidene aniline: the aldehyde ring rotation, *J. Photochem. Photobiol. A: Chem.*, 97, 121, 1996.
23. Bisht P. B., Tripathi, H. B., and Pant, D. D., Cryogenic studies, site selectivity and discrete fluorescence in salicylic acid dimer, *J. Photochem. Photobiol. A: Chem.*, 90, 103, 1995.
24. Jashi, H. C., Hydrogen effect on the dual emission of salicylic acid, *Chem. Phys. Lett.*, 28, 172, 1991.
25. Denisov, G. S, Golubev, N. S., Schreiler, V. M., Shajakhmedov, Sh. S., and Shrukhina, A. V., Effect of intermolecular hydrogen bonding and proton transfer on fluorescence of salicylic acid, *J. Mol. Struct.*, 436, 153, 1997.
26. Golubev, N. S. and Denisov, G. S., Study of mutual influence of hydrogen bonds in complicated complexes by low-temperature ^{1}H NMR spectroscopy, *J. Mol. Struct.*, 270, 263, 1992.
27. Sandros, K., Fluorescence and triplet yields of benzene and toluene in cyclohexane solutions: temperature and deuteration effects, *Acta Chem. Scand.*, 25, 3651, 1971.
28. Kloepffer, W. and Kaufmann, G., Absorption and fluorescence spectra of methyl salicylate in the vapor phase, *J. Lumin.*, 20, 283, 1979.
29. Heimbrook, L. A., Kenny, J. E., Kohler, B. E., and Scott, G. W., Dual fluorescence excitation spectra of methyl salicylate in a free jet, *J. Chem. Phys.*, 75, 5201, 1981.
30. Abe, H., Mikami, N., Ito, M., and Udagawa, Y., Vibrational energy redistribution in jet-cooled hydrogen-bonded phenols, *Chem. Phys. Lett.*, 93, 217, 1982.
31. Volovsek, V., Colombo, L., and Furic, K., Vibrational spectrum and normal coordinate calculations of the salicylic acid molecule, *J. Raman Spectrosc.*, 14, 347, 1983.

32. Hetherington, W. M., III, Micheels, R. H., and Eisenthal, K. B., Picosecond dynamics of double proton transfer in 7-azaindole dimers, *Chem. Phys. Lett.*, 66, 230, 1979.
33. Ford, D., Thistlethwaite, P. J., and Woolff, G. J., The fluorescence behavior of methyl and phenyl salicylate, *Chem. Phys. Lett.*, 69, 246, 1980.
34. Barbara, P. F., Rentzepis, P. M., and Brus, L. E., Photochemical kinetics of salicylideneaniline, *J. Am. Chem. Soc.*, 102, 2786, 1980.
35. Lopez–Delgado, R. and Lazare, S., Fluorescence properties of methyl salicylate in vapor, liquid and solution, *J. Phys. Chem.*, 85, 763, 1981.
36. Lahrmani, F. and Zehnacker-Rentien, A., Effect of salicylic acid on the photon reduced proton transfer in salicylic acid, *J. Phys. Chem. A,* 101, 6141, 1997.
37. Weller, A., Fast reactions of excited molecules, *Progr. React. Kinet.*, 1, 187, 1961.
38. Acuna, A. U., Amat-Guerri, F., Catalan, J., and Gonzalez-Tablas, F., Dual fluorescence and ground state equilibriums in methyl salicylate, methyl 3-chlorosalicylate and methyl 3-*tert*-butylsalicylate, *J. Phys. Chem.*, 84, 629, 1980.
39. Rettig, W., Charge separation in excited states of decoupled systems: TICT compounds and implications regarding the development of new laser dyes and the primary processes of vision and photosynthesis, *Angew. Chem. Int. Ed. Engl.*, 25, 971, 1986.
40. Kim, Y., Chem, H. W., Yoon, M., Song, N. W., and Kim, D., SiO_2 colloidal effects on the twisted intramolecular charge transfer of *p*-*N*,*N*-dimethylaminobenzoic acid in acetonitrile, *Chem. Phys. Lett*., 264, 673, 1997.
41. Kim, Y., Cho, D.W., Yoon, M., and Kim, D., Observation of hydrogen-bonding effects on twisted intramolecular charge transfer of *p*-(*N*,*N*-diethylaminobenzoic acid in aqueous cyclodextrin solutions, *J. Phys. Chem.*, 100, 15670, 1996.
42. Kim, Y., Lee, B. I., and Yoon, M., Excited-state intramolecular charge transfer of *p*-*N*,*N*-dimethylaminobenzoic acid in Y zeolites: hydrogen bonding effects, *Chem. Phys. Lett.*, 286, 466, 1988.
43. Nag, A. and Bhattacharyya, K., Twisted intramolecular charge-transfer emission of dimethylaminobenzonitrile in α-cyclodextrin cavities, *Chem. Phys. Lett.*, 151, 474, 1998.
44. Al-Hassan, K., Klein, Uwe, K. A., and Suwaiyan, A., Normal and twisted intramolecular charge-transfer fluorescence of 4-dimethylaminobenzonitrile in α-cyclodextrin cavities, *Chem. Phys. Lett.*, 212, 581, 1993.
45. Kundu, S. and Chattopadhyay, N., Dual luminescence of dimethylaminobenzaldehyde in aqueous cyclodextrin: non-polar and TICT emissions, *J. Photochem. Photobiol. A: Chem*., 88, 105, 1995.
46. Cho, D. W., Kim, Y. H., Kang, S. G., Yoon, M., and Kim, D., Cyclodextrin effects on intramolecular charge transfer of 2-biphenylcarboxylic acid: a pre-twisted molecule, *J. Chem. Soc., Faraday Trans.*, 92, 29, 1986.
47. Kletskii, M. E., Millov, A. A., Metelitsa, A. V., and Knyazhansky, M. I., Role of structural flexibility in the fluorescence and photochromism of salicylidene aniline: the general scheme of the photo-transformations, *J. Photochem. Photobiol. A: Chem.*, 110, 267, 1997.
48. Formosinho, S. J. and Arnaut, L. G., Excited-state proton transfer reactions II. Intramolecular reactions, *J. Photochem. Photobiol. A: Chem.*, 75, 21, 1994.
49. Kownacki, K., Mordzinski, A., Wilbrandt, R., and Grabowska, A., Laser-induced absorption and fluorescence studies of photochromic Schiff bases, *Chem. Phys. Lett.*, 227, 270, 1994.
50. Stewart, J. J. P., Optimization of parameters for semiempirical methods. I. Method, *J. Comput. Chem.*, 10, 209, 1989.
51. Stewart, J. J. P., *Mopac 7.0: A Semiempirical Molecular Orbital Program*, Kb455, Quantum Chemistry Program Exchange (QCPE). Indiana University, Bloomington, IN, 1989.
52. Knyazhansky, M. I., Metalitsa, A. V., and Kletskii, M. E., The structural transformations and photo-induced processes in salicylidene alkylimines, *J. Mol. Struct.*, 526, 65, 2000.

69

Photoremovable Protecting Groups

Richard S. Givens
University of Kansas

Peter G. Conrad, II
University of Kansas

Abraham L. Yousef
University of Kansas

Jong-Ill Lee
University of Kansas

69.1 Introduction

Photoremovable protecting groups are enjoying a resurgence of interest since their introduction by Kaplan[1a] and Epstein[1b] in the late 1970s. A review of published work since 1993[2] is timely and will provide information about several new groups that have been recently developed. The scope of this review is, therefore, limited to recent developments in the field and will cover only the applications with major functional groups that have been "protected" by a photoremovable chromophore. The review is not intended to be comprehensive but focuses instead on a series of well-chosen examples of chromophores that were deployed as protecting groups with a select group of representative functional groups. Because the focus of this review is the application of photoremovable protecting groups, emphasis is placed on synthesis of the protected functionality and on the procedures employed for deprotection, including the protection and photodeprotection yields, the deprotection reaction rates, and the quantum efficiencies, when available. An attempt has been made to list the advantages and disadvantages of each photoremovable protecting group as well as a brief discussion of the mechanism for the photodeprotection.

0-8493-1348-1/04/$0.00+$1.50

When the literature is insufficient for providing a comprehensive treatment of applications of a photoprotecting group, then only a brief discussion is provided. An exhaustive list of applications for any of the chromophores is not included; these may be found by consulting other reviews or the original literature on a topic. Several good reviews on photoremovable protecting groups have appeared since this topic was reviewed in 1993 (e.g., Adams and Tsien[3] and Corrie and Trentham[4]). Notable among the more recent reviews are those by Wirz,[5] Bochet,[6] and Givens.[7] A volume of *Methods in Enzymology* devoted entirely to the chemistry and applications of photoremovable protecting groups, also termed "caged" compounds, that are employed in biochemistry and other biological studies has also appeared.

In general, photolysis reactions present a noteworthy and often ideal alternative to all other methods for introducing reagents or substrates into reactions or biological media. The ability to control the spatial, temporal, and concentration variables by using light to photochemically release a substrate provides the researcher with the ability to design more precisely the experimental applications in synthesis, physiology, and molecular biology. Among the many possible examples is the recently reported inhibition–reactivation of protein kinase A by photolysis of the dormant enzyme.[8–10] In this demonstration, it is necessary that the deprotection process be initiated by photolysis of the dominant chromophore of the protecting group. Covalent blocking of the functional groups at the active site of an enzyme essentially suspends its mode of action and virtually shuts down the catalytic cycle. It is this feature that has attracted biochemists to the use of protecting groups for the investigation of biological mechanisms.

In synthesis, the protecting group serves as a mask that renders a functional group inert to subsequent synthetic reaction conditions,[11] except, of course, conditions that are required for the removal of the protecting group. Construction of combinatorial platforms with photoremovable linkers is just one example of the applications in synthesis. Photorelease is sometimes termed a *traceless reagent process* because no reagents other than light are needed. The advantage of a process that requires no further separation of spent reagents is attractive.

There are several limitations to the use of commonly employed protecting groups in synthesis and for mechanistic studies of biological processes. The reactions for incorporating and subsequently removing protecting groups often involve acid or base that may be too harsh and interfere with the normal processes or otherwise be incompatible with the chemistry or biology under investigation. In mechanistic biochemistry, it is often the case that the typical hydrolysis deprotection reaction is far too slow to serve as a means of investigating the initial rates of reaction for rapid biochemical processes.

An ideal remedy to these limitations is a protecting group that could be removed under neutral buffered aqueous conditions, thus avoiding any alterations to the substrate or to the natural biological environment.[12] The release should occur on a time scale fast enough for kinetic analysis of any subsequent rapid biological processes. Such a group may be a photoremovable protecting group.

69.2 Historical Review

In 1962, Barltrop et al.[13] were among the first to report a photochemical deprotection reaction of a biologically significant substrate; here, glycine was released from *N*-benzyloxycarbonyl glycine:

(69.1)

This seminal discovery prompted the development of several additional photoremovable protecting groups. The success of many researchers in biology, particularly Kaplan,[1a] led to the description of the photoactivatable group as a "cage" to describe its deactivating influence on the biological substrate to which it is covalently attached.[14–17] Ideally, the cage detaches only through the action of light.

It is important that the photoremovable protecting group also possess several other desirable properties. The properties were originally compiled by several researchers in the field, including Sheehan and Umezawa[12] and Lester and Nerbonne,[18] who provide a series of benchmarks for evaluating the efficacy of a photoremovable group in a given circumstance or for evaluating the potential of a new cage chromophore. A more useful adaptation of the Lester rules and Sheehan criteria includes the following:

1. The substrate, caged substrate, and photoproducts have good aqueous solubility for biological studies. For synthetic applications, this requirement is relaxed.
2. The photochemical release must be efficient (e.g., $\Phi > 0.10$).
3. The departure of the substrate from the protecting group should be a primary photochemical process (i.e., occurring directly from the excited state of the cage chromophore).
4. All photoproducts should be stable to the photolysis environment.
5. Excitation wavelengths should be longer than 300 nm and must not be absorbed by the media, photoproducts, or substrate.
6. The chromophore should have a reasonable absorptivity (a) to capture the incident light efficiently.
7. The caged compounds, as well as the photoproduct from the cage portion, should be inert or at least benign with respect to the media, other reagents, and products.
8. A general, high-yielding synthetic procedure for attachment of the cage to the substrate must be available.
9. In the synthesis of a caged substrate, the separation of caged and uncaged derivatives must be quantitative. This is also necessary for the deprotection process for synthetic applications.

While these are the desirable guidelines for an ideal photoremovable protecting group, a potential cage that lacks one or two of these properties may still be very useful; however, the absence of several of these features may militate against the use of that group as a photoremovable protecting group for a specific application.

Some representative examples of photoremovable protecting groups that qualify as meeting the Lester and Sheehan criteria include α-substituted acetophenones, benzoins, benzyl groups, cinnamate esters, coumaryl groups, and, the most popular of them all, the *o*-nitrobenzyl esters and their analogs.

o-Nitrobenzyl

It was also Barltrop et al.[19] who first reported the use of an *o*-nitrobenzyl group to release benzoic acid (see Eq. (69.2)). The poor yield stemmed from the subsequent conversion of 2-nitrosobenzaldehyde (**3**), the initial photoproduct, into azobenzene-2,2′-dicarboxylic acid (**4**),[20] which then competed for the incident light. Yields were dramatically improved with the use of α-substituted nitrobenzyl esters (75 to 95% conversion), as seen from **5** in Eq. (69.3). The resulting photoproduct from *o*-nitrobenzyl ester **5** was a less reactive nitroso benzophenone derivative.

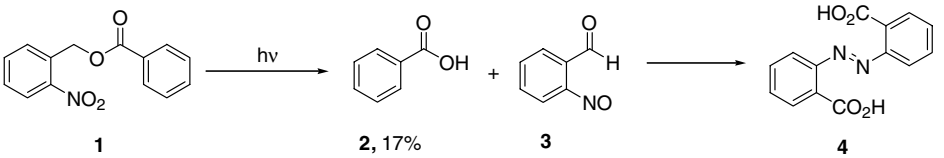

1 **2**, 17% **3** **4**

(69.2)

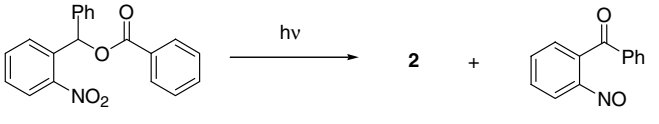

5 **6**

(69.3)

The report of the release of ATP by this method appeared in a 1978 rate study reported by Kaplan and co-workers.[1a] Inorganic phosphate ($\mathbf{P}_i$) and ATP were released from their 1-(2-nitrophenyl)ethyl (NPE) and 2-nitrobenzyl (NB) esters, respectively:

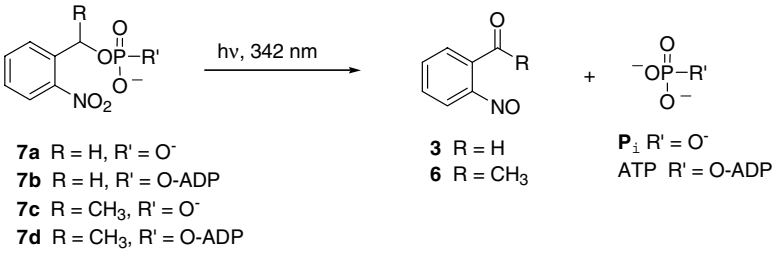

7a R = H, R' = O^-
7b R = H, R' = O-ADP
7c R = CH_3, R' = O^-
7d R = CH_3, R' = O-ADP

3 R = H
6 R = CH_3

$\mathbf{P}_i$ R' = O^-
ATP R' = O-ADP

(69.4)

The results of the release of $\mathbf{P}_i$ from NPE and NB showed very similar quantum efficiencies of 0.58 and 0.50, respectively; however, the release of ATP from the two cages gave very different rates of conversion. NPE released 80% of the caged ATP in less than 60 s compared with 25% for release from the NB caged ATP. These results further indicated that the α-substituted nitrobenzyl esters were better suited as phototriggers.

Kaplan's investigation also explored the potential use of photoprotecting groups in a physiological environment. Na^+,K^+-ATPase, the enzyme responsible for sodium/potassium transport through cell walls, served as the model for exploring the effect of the caged ATP (NPE-ATP) on the Na^+:K^+ transport associated with enzymatic activity. The enzyme acquires ATP as the energy source through hydrolysis of the terminal γ-phosphate. The hydrolytic activity of the enzyme can be monitored by the detection of $\mathbf{P}_i$ generated from the free ATP consumed by the enzyme. In the absence of photolysis, NPE-ATP was shown to be resistant to hydrolysis by the enzyme. Upon photolysis, the liberated ATP triggered the response of the enzyme and $\mathbf{P}_i$ release was observed.

The successful introduction of *o*-nitrobenzyl caged ATP into physiological media instigated interest in expanding the applications of caged release to a wide variety of biochemical systems. The list includes the mechanism of release of $\mathbf{P}_i$ in skeletal muscle,[21] the function of cAMP in the relaxation of distal muscle,[22] the ATP-induced mechanism of actomyosin in muscle contraction,[23] and the activation of antitumor antibiotics to highly reactive pyrrolic-type intermediates responsible for DNA crosslinking reactions.[24]

Benzoin

Sheehan and Wilson[25] were the first to explore the photochemical rearrangement of certain benzoin derivatives to yield 2-phenylbenzofuran (**9**). These rearrangements occurred with concurrent loss of groups attached α to the carbonyl just as in the case of the α-chloroacetophenones. They suggested that benzoins, especially the 3′,5′-dimethoxybenzoin chromophore, could serve as a photoremovable protecting group for carboxylic acids. In 1984, Givens et al.[26] showed that phosphates were quantitatively expelled from the ungarnished benzoin cage, as shown in Eq. (69.5), thus extending the range of applications and the nature of the parent chromophore. The only major product accompanying the released phosphate

TABLE 69.1 Quantum Efficiencies for Benzoin Phosphate Esters **8a–c**

Phosphate Ester	Solvent	pH	Φ_{dis}	Φ_{furan}	$\Phi_{phosphate}$
8a	C_6H_6	nd	0.28	0.26	nd
8b	H_2O/CH_3CN	2.0	0.37	0.20	0.12
8b	H_2O/CH_3CN	7.0	nd	0.07	0.013
8c	H_2O/CH_3CN	2.0	0.38	0.14	0.15
8c	H_2O/CH_3CN	7.0	nd	0.08	0.01

Note: All reactions were run in 60% aqueous acetonitrile, except **8a**, as indicated; phosphate esters were irradiated at 350 nm and monitored via ^{31}P NMR; nd = not determined.

Source: Adapted from Givens et al.[27]

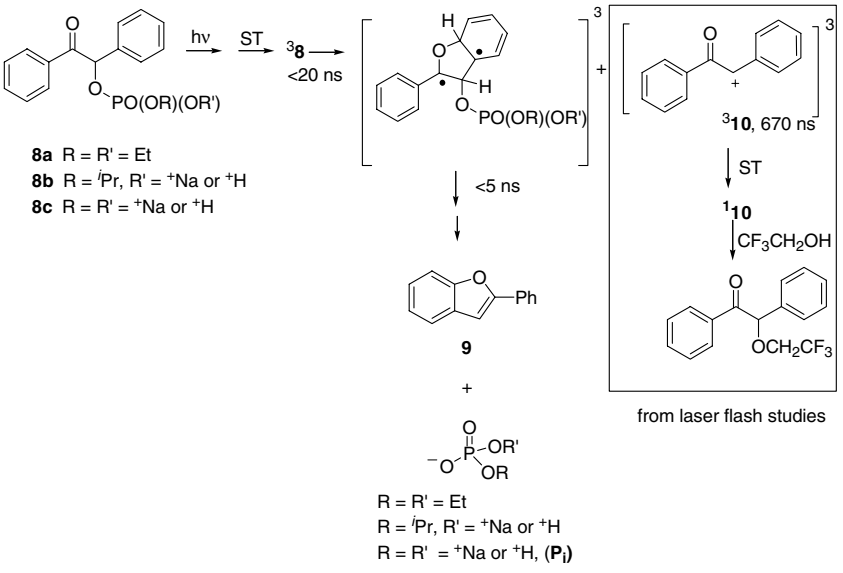

(69.5)

was 2-phenylbenzofuran **9**. These reactions were quenched with naphthalene, piperylene, or, for aqueous studies, sodium 2-naphthalenesulfonate, all well-known triplet quenchers; this established the short-lived triplet (3 to 14 ns) as the reactive excited state for benzoin. Further information was revealed from Stern–Volmer quenching analyses which provided the rate of release of phosphate from the benzoin-caged ester. Extremely fast rates ($k_r > 10^8\ s^{-1}$) were measured along with good efficiencies for the reaction, ranging from 28 to 38% (Table 69.1).[27,28] Phosphorescence spectra supported the multiplicity assignments and also established the triplet energy at 73 ± 1 kcal/mol.

The efficiencies for the disappearance of the caged phosphates (Φ_{dis}), as well as the appearance of 2-phenylbenzofuran (Φ_{furan}) and phosphate ($\Phi_{phosphate}$), were determined to be pH dependent with higher efficiencies reported under acidic conditions. The greater efficiency at lower pH suggests that the protonated phosphate is a more favorable leaving group than its conjugate base. This study was extended to nucleotide release from the benzoin cage through the synthesis and photolysis of benzoin cAMP. The efficient release of cAMP as the exclusive product with quantum efficiencies on the same order of magnitude as the model phosphate esters first demonstrated the application of benzoin as a cage for

TABLE 69.2 Quantum Efficiencies for Photolysis of Benzoin Adenosine Cyclic 3′,5′-Monophosphate[a]

Aqueous Buffer	pH	Φ_{dis}	Φ_{furan}	Φ_{cAMP}
Tris (D_2O)	7.3	0.39	0.19	0.34
Tris (H_2O)	7.3	0.37	0.17	0.34
Phosphate (D_2O)	8.4	nd	0.17	nd
Phosphate (H_2O)	8.4	nd	0.17	nd
Perchloric (D_2O)	1.6	0.40	0.16	0.36

[a] Irradiations were carried out in 1:1 buffer: 1,4-dioxane at 350 nm. Quantum efficiencies (**Φ**) were measured using ^{31}P NMR, except where indicated (nd).

Source: Adapted from Givens et al.[28]

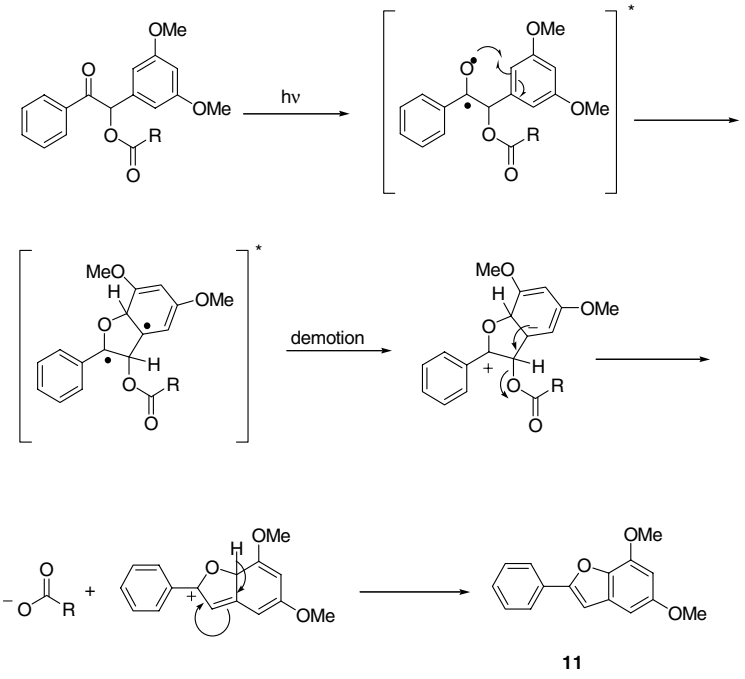

SCHEME 1 Benzoin photorelease mechanism.

nucleotides (Table 69.2). ^{31}P spectra of released cAMP demonstrated that cAMP was the only phosphate present after release. As Table 69.2 indicates, the quantum efficiencies remained relatively constant throughout the pH range examined.

It has been determined that carboxylate derivatives are released more readily when there are electron-donating substituents at the *meta* positions of the benzyl ring.[29] The absorption spectra of the benzoin esters along with the observations that cyclization was enhanced by *meta* electron donating groups led observers to believe that reaction was taking place through an n,π^* singlet state (see Scheme 1). It was suggested that the excitation of the phenacyl group led to a short-lived 1,3-biradical, followed by demotion to the ground state. The zwitterionic intermediate led directly to the loss of the leaving group. Aromatization through loss of a proton gave the benzofuran **11** as the principal photoproduct. The inability to quench the reactions with high concentrations of piperylene suggested that the reaction originated from the singlet excited state or, alternatively, from a very short-lived, unquenchable triplet.

Based on these observations Corrie and Trentham[4] re-examined the photochemistry of several substituted benzoin phosphates. They found that the 3′,5′-dimethoxybenzoin cage was best suited among those investigated for the release of $\mathbf{P}_i$. The formation of 3′,5′-dimethoxy-2-phenylbenzofuran (**11**) occurred at a rate that exceeded 10^5 s^{-1} and a quantum efficiency of 0.78. While the rate of product formation was lower than that reported by Givens and Matuszewski,[26] the efficiency for the substituted benzofuran analog was much higher. For the benzoin series, the primary photoproduct **11** is also a strongly absorbing chromophore and thus competes for incident light and forms photodimers along with several other unidentified products upon further irradiation. Yet another limitation of this system is the presence of a chiral center alpha to the carbonyl, which engenders isolation and purification problems in the synthesis of benzoin-protected chiral substrates.

More recently, Rajesh et al.[30] examined the earliest events in the photolysis of benzoin diethyl phosphate (**8a**). With nanosecond resolution, the LFP excitation of **8a** in trifluoroethanol gave an immediate, permanent 300-nm absorption identified as the benzofuran photoproduct (Eq. (69.5)). A second transient absorption at 570 nm was also observed which decayed with a first-order rate constant of $\sim 2 \times 10^6$ s^{-1} in degassed acetonitrile or trifluoroethanol that was assigned to the triplet α-ketocation **10.** The intermediate could be trapped by trifluoroethanol, yielding trifluoroethyl benzoin ether. Evidence for the intermediacy of the α-ketocation triplet came from experiments with added halide ion or azide in which electron transfer quenching of the transient was observed. Oxygen and naphthalene quenching experiments demonstrated that ^{3}**10** was formed adiabatically on the triplet manifold from ^{3}**8a**. Temperature-dependent studies indicated an activation energy for decay of ^{3}**10** of 8.6 kcal/mol to the singlet, which then reacted with trifluoroethanol to form the trifluoroethyl ether. Stern–Volmer analysis of the naphthalene quenching gave a triplet lifetime for ^{3}**8a** of $\tau^3 = 18$ ns.

The formation of 2-phenylbenzofuran during the nanosecond laser flash experiment was corroborated by a picosecond study of **8a**. A rise time of 2 to 4 ps was determined for the 340 nm transient. A rich fluorescence emission obtained in the nanosecond study was shown to arise from ^{1}**9** generated during the nanosecond laser excitation pulse. Naphthalene also quenched the formation of **9** at the same rate as the formation of ^{3}**10**, establishing that the two primary photoproducts came from the same triplet (i.e., ^{3}**8a**). Thus, for the unsubstituted benzoin phosphates, reaction proceeds exclusively through the triplet manifold

Phenacyl

In a similar study, Sheehan and Umezawa[12] employed a stripped-down version of the benzoin chromophore, the *p*-methoxyphenacyl group, for the release of benzoic acid, several amino acid derivatives, and peptides, as shown in Eq. (69.6) and Table 69.3.

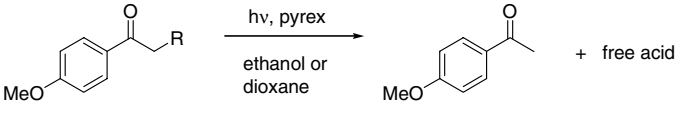

12 **13** (69.6)

In this case, the photoproduct was the *p*-methoxyacetophenone (**13**), a reduction product. The proposed mechanism (Scheme 2) was a simple homolysis of the carbon-oxygen bond. Ethanol serves as a hydrogen atom donor during this process, and in the presence of 1-*M* benzophenone or naphthalene the reaction was completely quenched, indicating a triplet reaction pathway. Benzophenone and naphthalene are known quenchers of acetophenones and have triplet energies of 68 and 62 kcal/mol, respectively.

Epstein and Garrossian[31] reported the release of ethyl and phenyl phosphate esters from the corresponding *p*-methoxyphenacyl phosphates in 1,4-dioxane. The released phosphates were recovered in high yields (Et, 86%; Ph, 74%) along with **13** (91–84%) as the only observed photoproducts. The absence of any rearranged ester products contrasted with reports by Anderson and Reese[34] for substituted α-chloroacetophenones (*vide infra*). The rationale for the discrepancy advanced by Epstein was an altered

TABLE 69.3 Percent Yield for the Release of Various Acids[a] from the Corresponding 4-Methoxyphenacyl Esters (12)

R	Solvent	Irradiation Time (hr)	Yield of ROOH (%)
PhCOO	Dioxane	17	81
PhCOO	Ethanol	6	96
Boc-L-Ala	Dioxane	17	82
Boc-L-Ala	Ethanol	6	93
Boc-Gly	Ethanol	6	94
Boc-L-Phe	Dioxane	17	89
Z-D, L-Ala	Dioxane	6	84
Phthaloyl-Gly	Dioxane	17	80
Tri-Gly	Dioxane	17	58
Z-L-Trp	Ethanol	4	33
Z-Gly-Gly	Ethanol	5.5	77
Z-L-Asp(OBZ)-L-Ser	Dioxane	9	49

[a] All reactions were carried out below room temperature at $(5 \times 10^{-3}$–$10^{-2})$ *M* using a Pyrex filter. Irradiations were complete in 6 hr in ethanol and 11–17 hr in dioxane. Yields were determined from product isolation following photolysis.

Source: Adapted from Sheehan and Umezawa.[12]

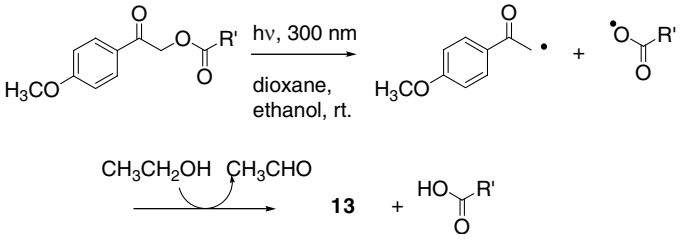

SCHEME 2 Sheehan et al. mechanism

mechanism due to a change in solvent. The solvent 1,4-dioxane may not be sufficiently polar to support the formation of the zwitterionic precursor to the Favorskii-like rearrangement that was proposed by Anderson and Reese. This was required for the rearrangement to the spirodienedione intermediate. Reinvestigation of the photolytic cleavage using polar solvents would have been an interesting test of this hypothesis.

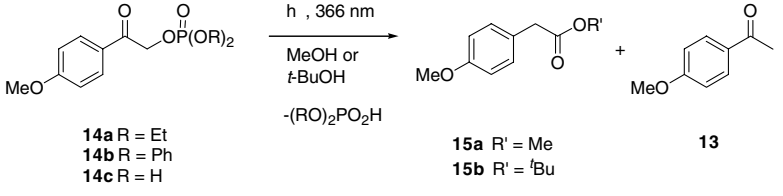

(69.7)

Givens et al.[28] examined the photorelease of phosphate esters using *t*-butyl alcohol and methanol as solvents, the former being a poor hydrogen atom donor and both exhibiting increased polarity compared with 1,4-dioxane. The results correlated well with those of Anderson and Reese in that the major photoproduct was the rearranged ester, not the photoreduction product (Eq. (69.7)). The amount of **13** was decreased to 21% in methanol and 14% in *t*-butyl alcohol. Further investigation of the solvent dependency for the release of phosphates revealed a solvent isotope effect with deuterated vs. protiated methanol as the solvent (Table 69.4). The formation of *p*-methoxyacetophenone was suppressed by a factor of five when

TABLE 69.4 Quantum Efficiencies and Solvent Isotope Effects (k_H/k_D) for Photolysis of 4-Methoxyphenacyl Diethyl Phosphate (**14a**)[a]

Solvent	Φ_{14a}	Φ_{15}	k_H/k_D[15]	Φ_{13}	k_H/k_D[13]
C_6H_6, *t*-BuOH (3:1)	0.036	0.026	—	0.074	—
CH_3OH	0.42	0.20	—	0.07	—
CD_3OD	—	0.14	1.4	0.013	5.4
CH_3OD	—	0.11	1.8	0.053	1.3

[a] Irradiations were performed in the indicated solvent at 300 nm. k_H/k_D is a relative efficiency for H vs. D abstraction. Error limits are ±10%.

Source: Adapted from Givens et al.[28]

TABLE 69.5 Photolysis of α-Chloroacetophenones: Yields Obtained for Photoproducts **17** to **20** Under Varying Conditions[a]

		Methanol		$Acetone_{(aq)}$			$Acetonitrile_{(aq)}$		
16	Ar	**17**	**19**	**17**	**18**	**20**	**17**	**18**	**20**
a	Phenyl	60	00	37	24	29	14	47	18
b	4-Methyl phenyl	62	06	24	47	23	14	70	11
c	4-Methoxy phenyl	35	34	16	43	14	09	54	08
d	4-Chloro phenyl	60	00	10	14	31	06	35	18

[a] Photolysis of 2% degassed solution of **16a–d** in methanol, 95:5 acetone/water, or 95:5 acetonitrile/water using 300-nm lamps was carried out in the presence of propylene oxide as a halogen scavenger. Irradiations were 4 hr and yields are isolated products.

Source: Adapted from Dhavale et al.[32]

photolysis was carried out in CD_3OD compared with either CH_3OD or CH_3OH, suggesting that a rate-determining hydrogen abstraction occurs in the photoreduction process. Sheehan first suggested this mechanistic pathway (*vide supra*).

Indeed, Dhavale et al.[32] have shown that the ratio of rearrangement to reduction for substituted α-chloroacetophenones is solvent dependent [Eq. (69.5) and Table 69.5]. Dhavale's group reported that irradiation of substituted α-choroacetophenones in methanol resulted in more photoreduction, whereas in aqueous acetonitrile rearrangement to the phenylacetate esters became the major pathway. For a given solvent, the ratio of rearrangement to reduction increased with the electron-donating power of the substituent.

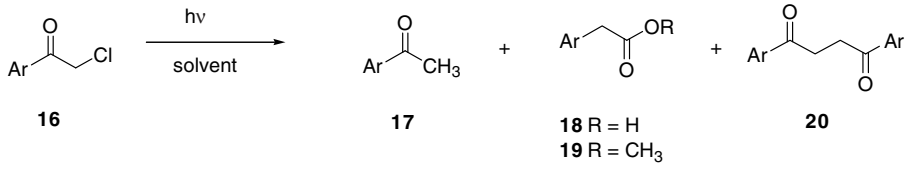

(69.8)

Scheme 3 outlines Dhavale's proposed mechanism for the chloride loss and subsequent rearrangement, beginning with carbon–chlorine bond homolysis. An electron transfer from the α-ketoradical to the chlorine atom leads to the ion pair **21**. The ion pair is more susceptible to Favorskii-like rearrangement in polar solvents; therefore, the rearranged phenylacetic acid is favored in polar, protic solvents. Hydrogen abstraction, resulting in the formation of **17**, prevails in those solvents that are good hydrogen atom donors.

Sonawane et al.[33] investigated the photorearrangement of several *para*-substituted propiophenones as a convenient entry for substituted α-arylpropionic acids, as shown in Eq. (69.9):

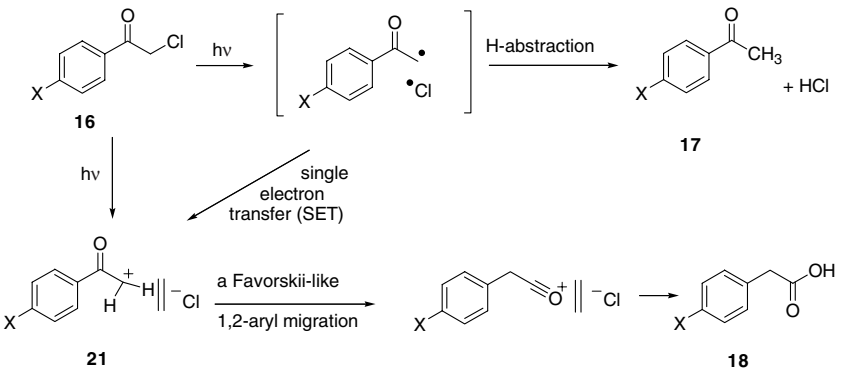

16 **17** **21** **18**

SCHEME 3 The mechanism suggested by Dhavale et al.[32]

TABLE 69.6 Product Distribution from Photolysis of **22a–i** in Aqueous Acetone or Aqueous Methanol[a]

Substrate		Acetone$_{(aq)}$			Methanol$_{(aq)}$		
22	**X**	**23**	**24**	**25**	**23**	**24**	**26**
a	H	58	25	—	39	30	—
b	CH_3	84	5	—	76	8	—
c	C_2H_5	82	6	—	74	9	—
d	*n*-C_3H_7	84	5	—	77	9	—
e	*i*-C_4H_9	74	10	—	65	15	—
f	*t*-C_4H_9	78	7	—	69	8	—
g	Cl	45	25	20	30	51	30
h	Ph	40	25	35	18	26	35
i	OCH_3	32	10	50	80	12	70

[a] Irradiations were carried out in 95:5 solvent/water solutions employing a Hanovia 200-W, medium-pressure mercury vapor lamp with a Pyrex filter until the complete disappearance of starting material. The photoreaction was monitored and yields were determined with GLC and ^{1}H NMR.

Source: Adapted from Sonawane et al.[33]

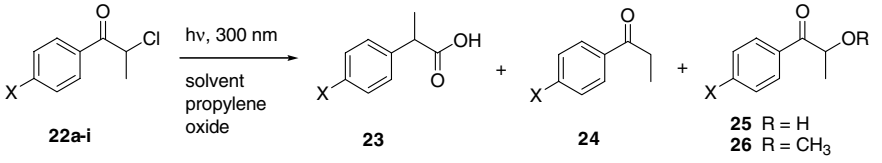

22a-i **23** **24** **25** R = H **26** R = CH_3

(69.9)

In almost every case, *para*-substitution promoted rearrangement (Table 69.6). Phenyl- and chloro-substitutions in the *para* position were the only cited examples where rearrangement did not dominate in methanol. These cases also showed significant reduced and hydrolyzed products.

TABLE 69.7 Product Formation from Photolysis of Substituted Phenacyl Chlorides[a]

Aryl Substitution, X	% Ethyl Aryl Acetate	% Acetophenone
p-OH (**27**)	32	26
p-OMe (**16c**)	32	30
o-OH	—	3
o-OMe	32	16
p-Me (**16b**)	4	58
H	—	53
p-CO_2Me	—	48
p-Cl (**16d**)	—	55
o-Cl	—	45
m-OMe	—	15

[a] Photolyses were carried out in 1% alcoholic solutions using a 500-W Hanovia mercury arc lamp. Reactions were carried out for 1 to 2 hr. Products were isolated via vapor phase chromatography.

Source: Adapted from Anderson and Reese.[34]

While not purported to be a photoremovable protecting group, the study by Anderson and Reese[34] on substituted phenacyl chlorides did reveal an interesting photochemical rearrangement for certain members of the series, particularly the report that the Favorskii-like rearrangement of *p*-hydroxyphenacyl chloride (**27**) in 1% aqueous ethanol gave two major photoproducts: *p*-hydroxyacetophenone (**28**) and ethyl *p*-hydroxyphenyl acetate (**29**), as shown in Eq. (69.10). The authors proposed a spiro intermediate **30**.

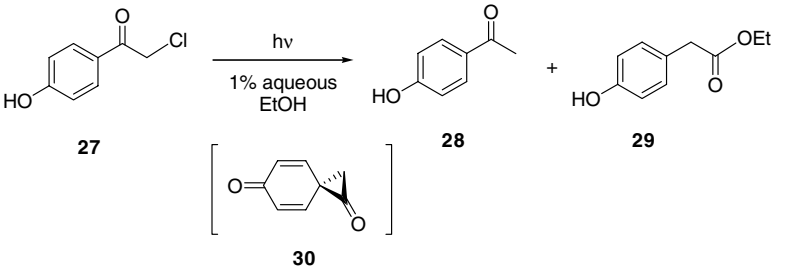

(69.10)

Further examination of the proposed aryl participation hypothesis led to the observation that electron-donating groups in the *ortho* or *para* positions were necessary for the rearrangement to occur (Table 69.7).

The results of Anderson and Reese coupled with the efficacy of the benzoin chromophore for cleavage of α substituents attracted our interest in developing the *p*-hydroxyphenacyl group as a photoremovable protecting group. We further rationalized that the introduction of a phenolic hydroxy group would enhance the aqueous solubility. The absence of the attendant α phenyl substituents on benzoin alleviated the stereogenic center problem present with benzoin derivatives. Furthermore, Anderson and Reese reported a Favorskii-like rearrangement of the chromophore, e.g., *p*-hydroxyphenacyl to *p*-hydroxyphenylacetate for **27** → **29** and for **16b,c**, suggesting a significant hypsochromic shift in the chromophore. Thus the promise of *p*-hydroxyphenacyl as a possible phototrigger was too enticing to pass up.

In 1995, we began a comprehensive exploration of a variety of *p*-substituted phenacyl phosphates for their efficacy toward releasing phosphate.[2,28] Among the substituents examined, the *p*-acetamido, methyl *p*-carbamoyl, and *n*-butyl *p*-carbamoyl groups proved untenable because they gave a plethora of products, most of which resulted from coupling or reduction of an intermediate phenacyl radical [Eq. (69.11)][35,36]

TABLE 69.8 Disappearance and Product Efficiencies for Ammonium Salts of ***p***-Substituted Phenacyl Phosphate in pH 7.2 Tris Buffer at 300 nm

p-Substituent	Φ_{dis}	Φ_{34}	$\Phi_{32,13}$	Φ_{other}
31a NH_2	<0.05	0.0	<0.05	Not available
31b CH_3CONH	0.38	0.0	0.11	Dimers
31c CH_3OCONH	0.34	0.0	Not determined	Two unknowns
14c CH_3O[a]	0.42	0.20	0.07	Not available
33 HO[b]	0.38	0.12	0.0	0.0
33 HO[c]	0.37	0.31	0.0	0.0

[a] Solvent was MeOH and diethyl phosphate was the leaving group.
[b] The diammonium salt of the mono ester; 10% CH_3CN was added to the solvent.
[c] The ATP derivative.

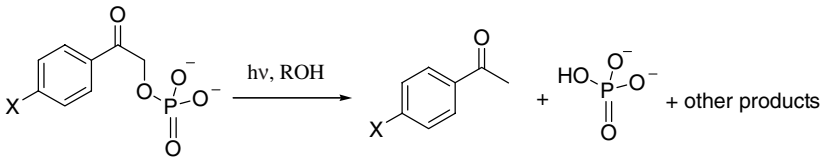

31a-c, 14c **32a-c, 13**

a) X = NH_2, **b**) X = $NHCOCH_3$, **c**) X = $NHCO_2CH_3$, **14c**) X = OCH_3

(69.11)

Table 69.8 gives the disappearance efficiencies for several *p*-substituted phenacyl phosphates from which it is evident that release of phosphate does occur very efficiently for the acetamido and carbamoyl derivatives; however, the large array of products of the phototrigger discouraged our further interest in these three electron-donating groups.

The methoxy substituent (**14c**) showed a much cleaner behavior, yielding only two products from the chromophore, *p*-methoxyacetophenone and the rearrangement product *p*-methoxyphenylacetic acid. The *p*-hydroxyphenacyl phosphate (**33**) gave the rearranged *p*-hydroxyphenylacetic acid when photolyzed in mixed aqueous organic solvents (Eq. (69.12)); in fact, of all of the groups examined, only *p*-hydroxy and *p*-methoxy produced any rearranged phenylacetic acids.

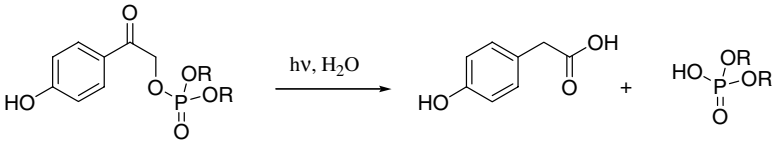

33, R = Et **34**

(69.12)

The initial discovery that diethyl *p*-hydroxyphenacyl phosphate exclusively followed a rearrangement pathway was followed by an extension of our study to *p*-hydroxyphenacyl ATP (**35**). Irradiation of **35** at 350 nm released ATP and *p*-hydroxyphenylacetic acid with a quantum efficiency of 0.37 ± 0.01 and a rate constant for ATP appearance of $5.5 \pm 1.0 \times 10^8$ s^{-1} [Eq. (69.13)].

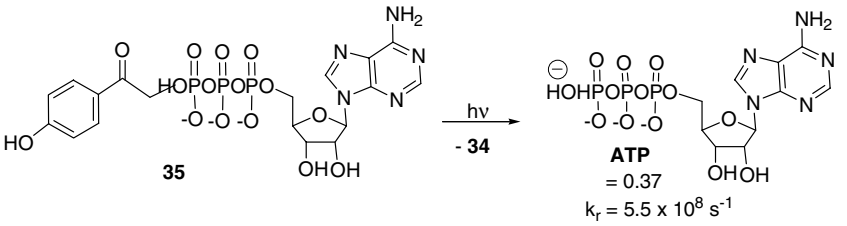

(69.13)

While the mechanism of this process is unknown, the *p*-hydroxyphenacyl photorelease likely involves an initial triplet state deprotonation of the phenolic hydrogen. In one scenario, the initially generated triplet intermediate partitions between loss of a proton and C-O bond cleavage, as pictured in Scheme 4. The exact course of the reaction depends greatly on the leaving group, solvent, and substituents attached to the chromophore. Here, the triplet phenol undergoes the equivalent of a homolytic cleavage of the bond to the substrate. In this scenario, it was envisaged that initial homolysis of the C-Y bond might be followed by a rapid single-electron transfer process; that is, the triplet phenol is essentially converted to its conjugate base (Y^-) before other competing processes for the radical pair can intervene. In this sequence, a spirodienedione is eventually generated by electrocyclic closure of the intermediate zwitterion or possibly the diradical.

The conjugate base formed by the proton loss undergoes bond reorganization to the putative spirodienedione **30** accompanied by release of ATP. Further hydration of the spirodienedione and bond reorganization lead to the phenylacetic acid that is suggested for both pathways.

A second mechanistic scenario involves proton loss concomitant with direct neighboring group assistance for the release of the substrate and formation of the spirodienedione. The subsequent proposed nucleophilic hydrolysis of the spirodienedione follows as above. Current evidence from subsequent solvent and substituent studies favor the latter mechanism (*vide infra*).

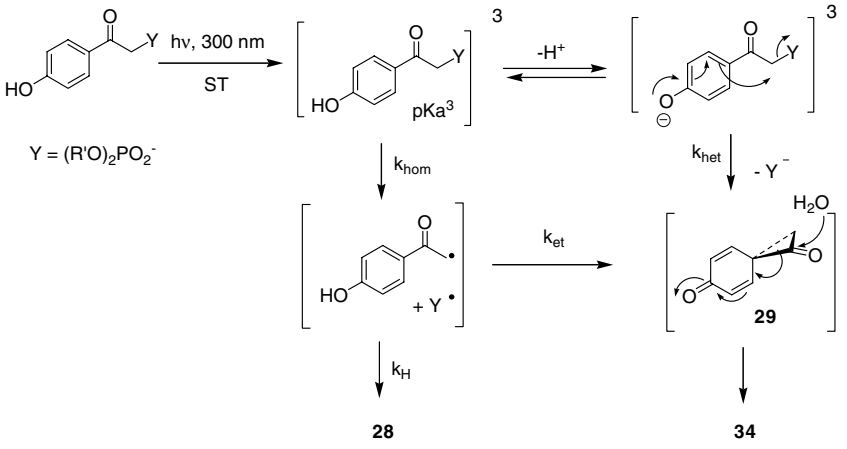

SCHEME 4 Proposed triplet state mechanisms for photorelease of substrates from the *p*-hydroxyphenacyl protecting group.

The onset of the triplet-state phosphorescence emission of several *p*-hydroxyphenacyl esters indicated triplet energies of 68.9 to 70.6 kcal/mol. The phosphorescence emissions were quenched by sodium 2-naphthalenesulfonate or potassium sorbate. Quenching studies confirmed the reactivity of the triplet state and further provided a lifetime of 5.5 ns for the triplet with a release rate of $1.82 \times 10^8\ s^{-1}$ in later studies (*vide infra*).

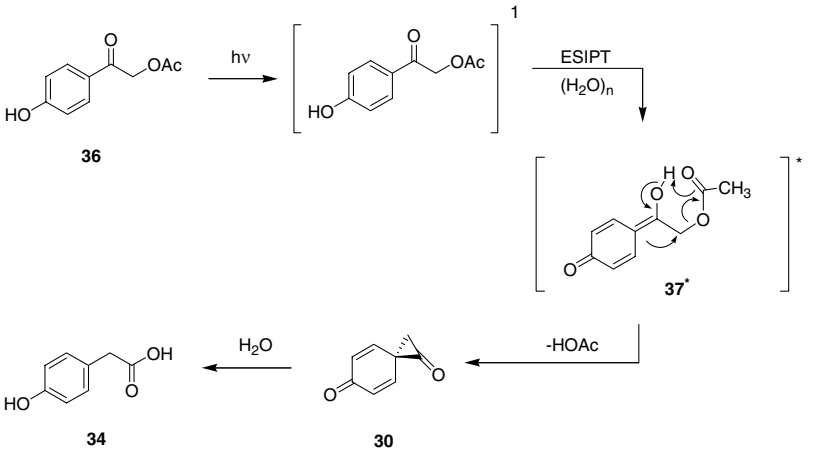

SCHEME 5 ESIPT singlet state photorelease mechanism of *p*-hydroxyphenacyl acetate.[37]

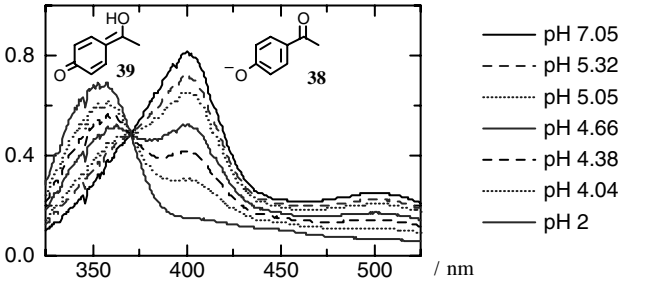

FIGURE 69.1 Transient absorption spectra obtained by LFP of *p*-hydroxyacetophenone in water (10% CH_3CN) with various buffers. (From Conrad II, P. G. et al., *J. Am. Chem. Soc.*, 122, 9346–9347, 2000. With permission.)

The original proposal that the triplet state was the reactive state was challenged by Zhang et al.[37] An excited singlet state or possibly a tautomeric ground state (e.g., **37***) was proposed as the reaction intermediate. In their studies, quenching by triplet quentchers was not observed during photolysis of *p*-hydroxyphenacylacetate (**36**), suggesting that the release of acetate occurred through an excited singlet state possibly involving an intramolecular proton transfer. They postulated that the excitedsinglet state intramolecular proton transfer (ESIPT) mechanism would form the quinone methide **37*** that could either continue on to the spirodienedione (**30**) or decay to ground state and subsequently undergo release of acetate to form **34**. Such a mechanism has precedence in the earlier work of Wan[37,38a] and Yates.[38b]

Laser flash photolysis (LFP) studies by Givens and Wirz[38] with diethyl pHP phosphate (Eq. (69.12)) confirmed the intermediacy of the phenacyl triplet state. Energy transfer quenching to naphthalene gave a rate of formation of the naphthalene triplet of $7.8 \times 10^9\ M^{-1}\ s^{-1}$. The presence of dioxygen increased the decay rate of the pHP phosphate triplet ($k_q \approx 3 \times 10^9\ M^{-1}\ s^{-1}$). It was estimated from this study that pHP intersystem crosses with a rate constant of $3.1 \times 10^{11}\ s^{-1}$ in aqueous acetonitrile. Quenching studies of the photochemical release of substrates from a series of pHP derivatives employing potassium sorbate gave excellent linear Stern–Volmer quenching results with lifetimes of 10^{-8} to 10^{-9} s for their pHP triplet states. These combined results firmly established the triplet as the reactive excited state.

LFP studies on the parent chromophore proved revealing. The *p*-hydroxyacetophenone triplet undergoes a facile adiabatic proton tautomerization conerting the phenol **28** into its conjugate base **38**. Evidence

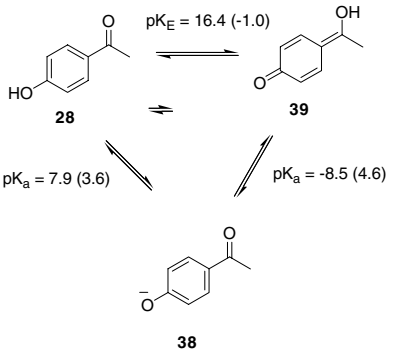

SCHEME 6 Tautomerization of *p*-hydroxyacetophenone in the ground state and triplet excited state (in parentheses). (From Conrad II, P.G. et al., *J. Am. Chem. Soc.,* 122, 9346-9347, 2000. With permission.)

for this unusual adiabatic proton transfer to solvent from the triplet *p*-hydroxyacetophenone came from analysis of the transient triplet absorption spectra of **28** as a function of the pH (Figure 69.1).

These results were further supported by DFT calculations that provided the tpK$_E$ values for the equilibrium **28** $\rightleftharpoons$ **39** in their ground and triplet excited states. A pK$_a$[3] for **28**[3] of 3.6 was derived from these data and the triplet state pK$_a$[3] of **39** (4.6) and the known ground state pK$_a$ of **28** (7.9) (Scheme 6). These studies revealed an increase in acidity over four pK$_a$ units relative to the ground state. The proton tautomer 39 is a non-productive intermediate because it is thermodynamically incapable of cleaving the ester C–O bond.

Incorporating the rapid deprotonation that results from the large adiabatic decrease in pK$_a$ of **28** as a feature of the *p*-hydroxyphenacyl mechanism suggests that the conjugate base **38** is an attractive precursor to the rate-limiting release of the substrate. Because the triplet is formed with a ST rate constant of 3.1 $\times 10^{11}$ s^{-1}, it is unlikely that there is any singlet state contribution to the deprotonation step. Rather, this appears to be exclusively a triplet process occurring on the excited triplet surface; that is, the two protonated species and the unprotonated ion undergo adiabatic proton tautomerizations (Scheme 6). The electron-rich aromatic ring increases the potential for intramolecular neighboring group attack at the α-carbon, leading to the release of the substrate and rearrangement of the chromophore. Thus, it becomes prudent to carefully explore the change in the pK$_a$ of the phenolic protons transitioning between the ground and excited triplet states as a key element in understanding the role played by aryl participation in the release step.

Coumaryl and Arylmethyl

Zimmerman's early studies[40] on the photosolvolysis of benzyl acetates in 50% aqueous dioxane set the stage for a variety of studies that employ *m*,*m*′-dimethoxybenzyl as a photoremovable protecting group. In general, the photofragmentation reactions of benzyl acetates are quite rapid, with rate constants of 10^8 s^{-1} or higher and are primarily singlet-state processes. According to Zimmerman, *meta* activation of the excited singlet state of benzyl acetates occurs through the approach of the excited- and ground-state energy surfaces, funneling the excited state toward heterolysis of the benzyl–ester bond. Substituents, including electron donors, in the *para* position lead primarily to homolytic fission and radical derived products.

Direct heterolytic fission of the substrate-photoprotecting group bond is the required course for photorelease of most biologically important substrates. This process avoids the generation of destructive radicals that could result in reactions such as decarboxylation, radical dimerization, or redox processes. Thus, the effect of *m*-substitution on the photochemistry of benzyl, naphthyl, and other aromatic chromophores has become the object of many studies in search of alternatives to the *o*-nitrobenzyl class of protecting group.

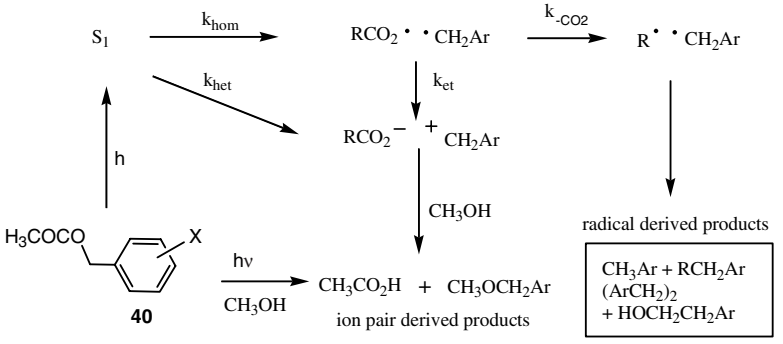

SCHEME 7 Mechanistic scheme for arylmethyl ester photolysis in methanol.[43]

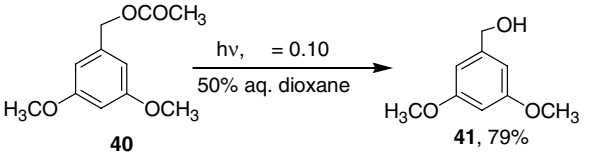

(69.14)

Recent studies by both Zimmerman[41] and DeCosta and Pincock[42,43] on the nature of the *meta* effect have raised concerns about whether heterolytic or homolytic cleavage should be considered the primary photochemical process. According to Pincock, the mechanistic pathway for all substituted arylmethyl substrates begins with homolysis of theC–O ester bond to the substrate followed by a competition between electron transfer to an ion pair or typical ground-state radical reactions (Scheme 7).[43] For those arylmethyl derivatives substituted with a *meta* electron-donating group, such as methoxy, the electron transfer occurs more rapidly than competing radical processes due to favorable redox properties of the radical pair.

Normally, the details of the steps leading to the ion pair would not play a significant role in the outcome of the photorelease process except in those circumstances where the radical pair precursors have rapid, favorable divergent pathways available. Such could be the case for carboxylate esters, such as C-protected amino acid, peptides, and protein derivatives, where decarboxylation of the initially generated carboxy radical may compete with electron transfer to the ion pair. This deleterious process can become significant, leading to destruction of a portion of the released substrate. By either of these mechanisms, however, the product-determining process for *meta*- and especially the di-*meta*-substituted arylmethyl chromophores leads principally to an ion pair, an intermediate arylmethyl carbocation, and the conjugate base of the leaving group.

The coumaryl chromophore is essentially another arylmethyl analog, which has the attractive feature of high yields of fluorescence emission, sometimes a useful property for following the course of substrate-chromophore processes. One of the earliest studies using coumarin as a chromophore was the photorelease of diethyl phosphate from coumarylmethyl diethyl phosphate.[26] The resulting coumarylmethyl cation covalently attaches to a wide variety of nucleophiles, as shown in Eq. (69.15):

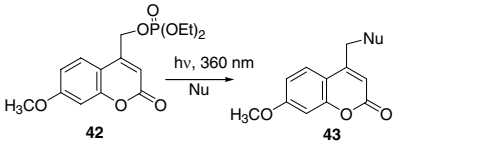

(69.15)

Furuta et al.[43] have reported the application of the coumaryl chromophore as a phototrigger for the release of cAMP (Eq. (69.16)); as shown in Table 69.9, the methoxy and hydroxy methylcoumarins gave the best conversions.

TABLE 69.9 Percent Conversion of Coumarylmethyl cAMP After a 10-s Irradiation at 334 to 365 nm

Caged cAMP	R = Acetyl	R = Propionyl	R = Hydroxy	R = Methoxy
Conversion (%)	23	9	64	60

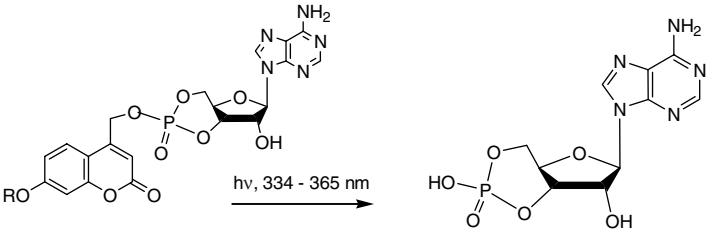

44

(69.16)

The historical and mechanistic background for the most common photoprotecting groups were presented above. Examples that employ photoremovable protecting groups are given to illustrate the range and variety of the applications in chemistry and biology. As noted earlier, these are a very limited set of examples of the numerous published applications in biology and, to a lesser extent, in chemistry. Further information can be obtained from the reviews listed in References 1 through 7.

69.3 Carboxylic Acids

o-Nitrobenzyl

Because *o*-nitrobenzyl derivatives have been the most widely applied photoremovable protecting groups, modifications of this chromophore have received considerable attention. A recent study[45] employing 2,2′-dinitrobenzhydryl (DNB) for *N*-methyl-D-aspartate (NMDA) probed the NMDA receptor, which is one of the general classes of known glutamate receptors. The carboxyl group of NMDA was esterified with DNB, a stronger UV absorber (λ_{max} 350 nm: $\varepsilon = 1.69 \times 10^4\ M^{-1}\ cm^{-1}$) than typical *o*-nitrobenzyl analogs. The poor aqueous solubility of DNB-NMDA, however, required addition of 20% DMSO to attain complete dissolution. A single 308-nm laser pulse was sufficient to release NMDA within 4.2 μs, with a quantum efficiency of 0.18, as shown in Eq. (69.17).

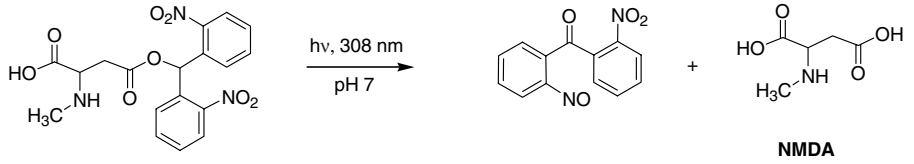

β-O-DNB-NMDA **NMDA**

(69.17)

The time constant for the release of NMDA is pH dependent, occurring within 3.8 μs at pH 3.8 and 13.8 μs at pH 10.6, consistent with the rate of decay of the aci-nitro intermediate. The relatively rapid release rate from DNB suggests that this protecting group could be useful for further studies of the NMDA receptor.

The versatility of the *o*-nitrobenzyl group has also been demonstrated in solid-phase synthesis. The phosphate group of the nucleotide tethered to a carboxylic acid through an alkyl chain provides a convenient link to the *o*-nitrobenzyl group, which is attached to a solid support. Synthetic manipulation of the oligonucleotide can be carried out under standard conditions and then release of the synthesized

TABLE 69.10 Isolated Yields of Completely Deprotected Oligonucleotides

	Protection (%)	Deprotection (%) 45	Deprotection (%) 45′
a	96	70	77
b	89	91	80
c	97	92	71
d	90	69	70

oligonucleotide from the support is conducted photochemically.[46] The carboxylate and substituted *o*-nitrobenzyl alcohol were coupled in 89 to 97% yields followed by the controlled pore glass (CPG) loading. Standard oligonucleotide synthesis was then carried out at the 3′-terminus of **45a–d** and **45′a–d** to obtain **45′a-d** (Eq. (69.18).

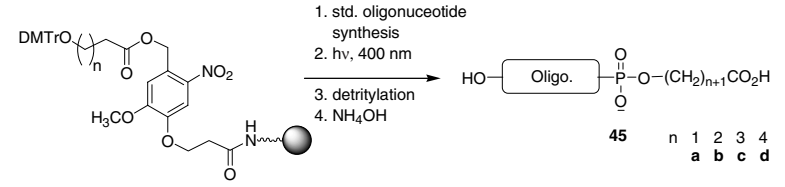

DMTr = 4,4'-dimethoxytrityl

45a-d (n = 1-4) Oligo = T_{20}
45'a-d (n = 1-4) Oligo = TAC GCA ATC CTA GAT CTA AT

(69.18)

Upon completion of the synthesis, the oligonucleotides were severed from the CPG solid support photochemically using a 400-nm light source. The efficiency of the release process was as high as 92%, as shown in Table 69.10. This protocol is useful for elaborating the 3′-terminus of oligopeptides using mild, traceless reagent conditions at room temperature and neutral pH.

Coumaryl

The photochemical and photophysical behavior of 4-(hydroxymethyl)-7-methoxycoumarin (MCM) caged acids was studied under physiological conditions by Bendig et al.[47] (Eq. (69.19)).

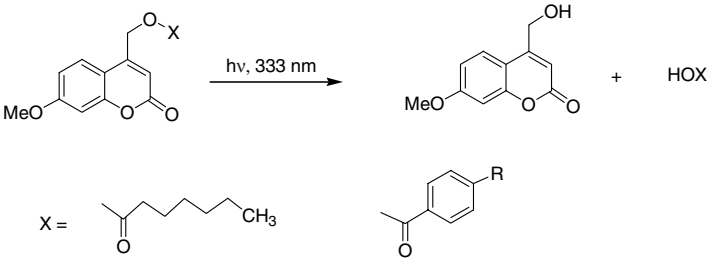

46a

46b: R = OCH_3
46c: R = H
46d: R = CN

(69.19)

Photocleavage of the excited singlet state of MCM caged compounds is thought to proceed via a photo-S_N1 mechanism (solvent-assisted photoheterolysis). Evidence favoring this mechanism was found from irradiation of MCM caged derivatives in ^{18}O-labeled water, which exclusively incorporated the ^{18}O-label in the MCM–^{18}OH product (see Scheme 8). The deprotection process of the MCM derivatives was

TABLE 69.11 Data for 4-(Hydroxymethyl)-7-Methoxycoumarin (MCM) Caged Acids

Acid	Protection (% Yield)	Deprotection (Φ)
46a	82.6	0.0043
46b	90.0	0.0045
46c	98.0	0.0052
46d	83.8	0.0064

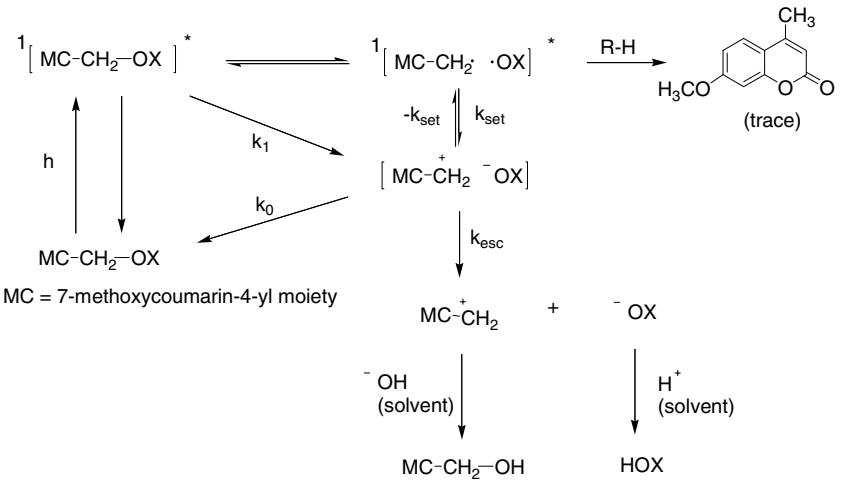

SCHEME 8 Reaction pathways for photolytic cleavage of MCM esters.

dependent on the leaving group and the solvent polarity. The quantum efficiencies for the reactions of **46a–d** were low, in the range of 0.0043 to 0.0064 as listed in Table 69.11. MCM–OH is a highly fluorescent product that can be conveniently monitored during the course of the reaction. Furthermore, MCM caged compounds are very stable to the hydrolysis.

Phenacyl

The rapid release (~10^8 s^{-1}) of substrates from the *p*-hydroxyphenacyl (pHP) group enables fast biological processes to be studied. *p*-Hydroxyphenylacetic acid (**34**) is generated with a quantum efficiency (Φ_{rea}) of ~0.18. In contrast, the presence of added electron-donating substituents on the aromatic ring of the pHP group makes the rearrangement a minor pathway for **47′a–b** and completely suppress it for **47″a–b** (Scheme 9).[48] The quantum efficiencies for the disappearance of the various pHP esters, the appearance of (**34**), and corresponding pHP-protected substrates are given in Table 69.12 .

A complication that could arise in such systems is the potential for decarboxylation of the released carboxylate ion. However, no decarboxylation products were observed within the detection limits of ^{1}H-NMR and HPLC.

With the production of a biologically benign photoproduct, the pHP protecting group has proven to be an efficient tool for investigations of fast biological processes. For example, Givens et al.[49] applied the pHP phototrigger to the investigation of the bradykinin BK2 receptor. It is known that bradykinin acts as an active pain-transducer when released during tissue damage. A major difficulty in studying the detailed physiological mechanism of the action of bradykinin is a concomitant rapid enzymatic degradation of the nonapeptide immediately after its release from its precursor protein. Therefore, the photorelease from pHP bradykinin (**48**), which protects bradykinin from degradation of the agonist prior

TABLE 69.12 Quantum Yields of pHP Esters for Irradiation at 300 nm[a]

	Ester	Solvent (Water/AcCN)	Φ_{dis}	Φ_{app}	Φ_{rea}
47a	pHP GABA	Water	0.21	0.21	0.19
47b	pHP glutamate	Water	0.14	0.14	0.08
47c	pHP cyclopropylacetate	6:4	~0.2[b]	—	—
47d	pHP phenylacetate	6:4	0.18	0.17	0.14
47e	pHP pivalate	6:4	~0.18[b]	—	—
47f	pHP oleate	7:3	0.24	0.23	0.17
48	pHP bradykinin	Water	0.21	0.22	0.19

[a] An NMR tube was charged with ~10 mg (~40 μmol) of the appropriate photoprotected acid and 10 mol% of 1,2,3-benzenetricarboxylic acid as an internal standard in 2 mL of solvent. The quantum efficiencies were determined at less than 20% conversion of the starting ester.

[b] By comparison with **47d**.

Abbreviations: dis = disappearance, app = appearance of acid, rea = rearrangement to phenylacetic acid.

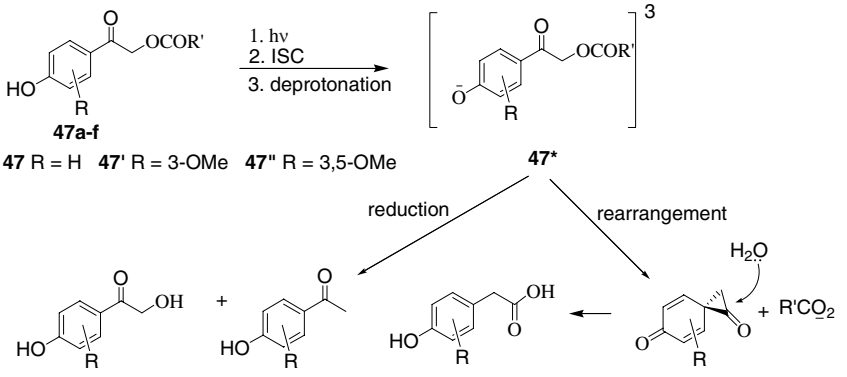

SCHEME 9 Photoreaction for the pHP esters.

to release, facilitates the investigation of its action during the transduction process by allowing precise temporal and spatial release of bradykinin to activate the bradykinin BK2 receptor (Eq. (69.20).

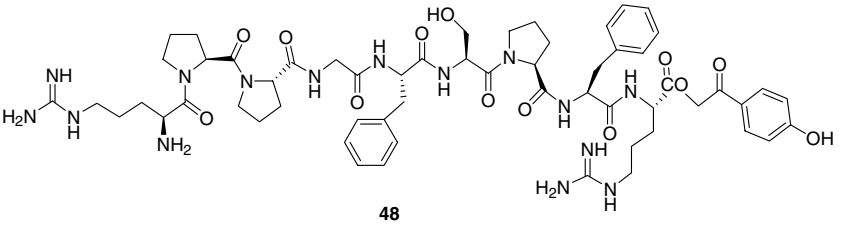

(69.20)

pHP Bradykinin **48** was obtained in an overall yield of 84% by derivatizing the partially protected brdykinin, obtained by cleavage of the C-terminus from the resin after sold-phase Merrifield synthesis.[49]

Reaction of the C-termnus with *p*-hydroxyphenacyl bromide followed by treatment with 1% TFA gave pHP bradykinin 48, free of the other protecting groups employed during the solid phase synthesis.[49]

A single 337-nm flash (<1 ns) released sufficient bradykinin to excite the BK2 receptors on single rat sensory neurons, which dramatically increased the intracellular calcium concentration measured with Indo-1, a Ca^{2+}-chelating fluorescent indicator. The quantum efficiency of bradykinin appearance was idependently determined to be 0.22, as shown in Table 69.12.

Benzoin

There are a number of examples of benzoin and substituted benzoin esters that have been employed as photoremovable protecting groups for carboxylic acids. Among these, the application of benzoin as a traceless linker for solid-phase synthesis of oligopeptides and introduction of Fmoc-protected amino acids by Balasubramanian[50] is instructive. As an example, the release of Fmoc-Ala shown in Eq. 69.21 occurs upon photolysis at 350. Balasubramanian found that the maximum yield was obtained after a 2-h photolysis as determined by HPLC (Eq. (69.21).

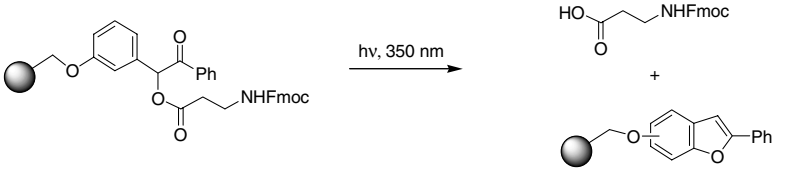

(69.21)

In order to avoide premature photolysis of the benzoin linker by adventitious room light during the course of the synthesis, the dithiane-protected 3-alkoxybenzoin (**49a**) has been suggested as a "UV-inactive" linker. The dithiane-protected 3-alkoxybenzoin (**49a**) released less than 3% of the product after irradiation at 350 nm. The photosensitivity is restored by hydrolysis of the dithiane prior to photocleavage, as illustrated in Eq. (69.22). Photolysis of the deprotected linker resulted in a 75% yield of the product.

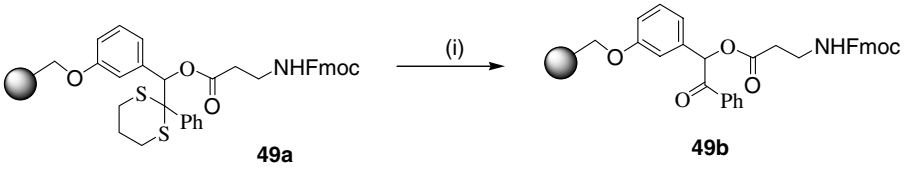

49a **49b**

(i) (a) bis[(trifluoroacetoxy)iodo]benzene, (b) mercury (II) perchlorate, or (c) periodic acid (4 eq.), THF:water (10:1) (for a and c), THF (for b), ambient temperature, 18 h. >95% conversion

(69.22)

Other

A series of 2,5-dimethylphenacyl (DMP) esters were photolyzed in benzene or methanol (Eq. (69.23)).

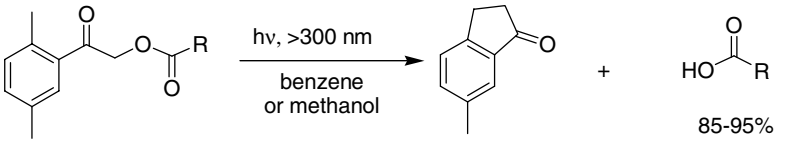

50 **51**

(69.23)

TABLE 69.13 Data for 2,5-Dimethylphenacyl Esters

R	Protection (%Yield)	Photolysis Condition (nm)	Deprotection (% Yield)[a]
CH_3	84	Benzene, >280	85[b]
C_6H_5	95	Benzene, >280	86
C_6H_5	95	Methanol, >254	92
$C_6H_5CH_2$	84	Benzene, >280	91
n-Pentadecyl	69	Benzene, >280	95
N-(*t*-butoxycarbonyl)-L-phenylalanine	51	Benzene, >280	90

[a] Isolated yield of the crude acids (>95% purity).
[b] Determined by gas chromatography.

TABLE 69.14 Quantum Yields[a] of DMP Esters

X	Protection (% Yield)	Photolysis Condition	Deprotection (Φ)
–OCOPh	95	Benzene	0.23
		Methanol	0.09
$-OCOCH_2Ph$	84	Benzene	0.18
		Methanol	0.11
$-OCOCH_3$	84	Benzene	0.25
		Methanol	0.14

[a] Quantum yield for ester release; valerophenone was used as an actinometer; irradiated at λ >300 nm. Error margins are approximately 10%.

The formation of the corresponding carboxylic acids occurred with almost quantitative isolated yields, as shown in Table 69.13.[51] In contrast with the structurally related *p*-hydroxyphenacyl esters, the release mechanism from **50** occurs through an efficient intramolecular γ-hydrogen abstraction via the (n,π^*) excited ketone.

Recently, Wirz's group[51] conducted LFP of 2,5-dimethylphenacyl (DMP) esters in benzene or cyclohexane (Eq. (69.24)).

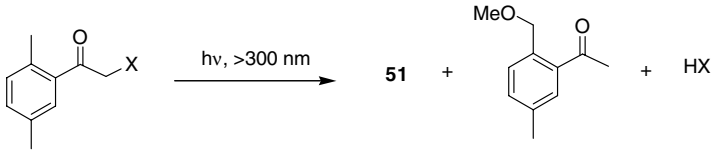

(69.24)

Recently, Wirz and Klan[52] reported LFP studies on several of the DMP esters in benzene and methanol (Eq. (69.24)). Quantum efficiencies (Φ) in benzene are 0.18 to 0.25, while those in methanol fell to 0.09 to 0.14. Thus, this photoprotecting group appears to be better suited to applications in nonpolar media such as benzene rather than methanol (Table 69.14).

A novel design of "orthogonal" protecting groups, i.e., the removal of protecting groups selectively from a multi-protected substrate, has been reported by Bochet[53] in which the irradiation wavelengths

serve as the "orthogonal reagents". A mixed diester of pimelic acid was capped with a dimethoxybenzoin group at one end and an *o*-nitrobenzyl group at the other terminus. Despite the possibility that intramolecular energy transfer or equilibration could occur between the two chromophores, selective photolysis led to the sequential removal of each with high chemical yield, as shown in Eq. (69.25). Upon photolysis of **52** at 254 nm for 5 minutes, 92% of **53b** was released, whereas irradiation at 420 nm for 24 hours released 70% of **53a**, as determined by ^{1}H NMR.

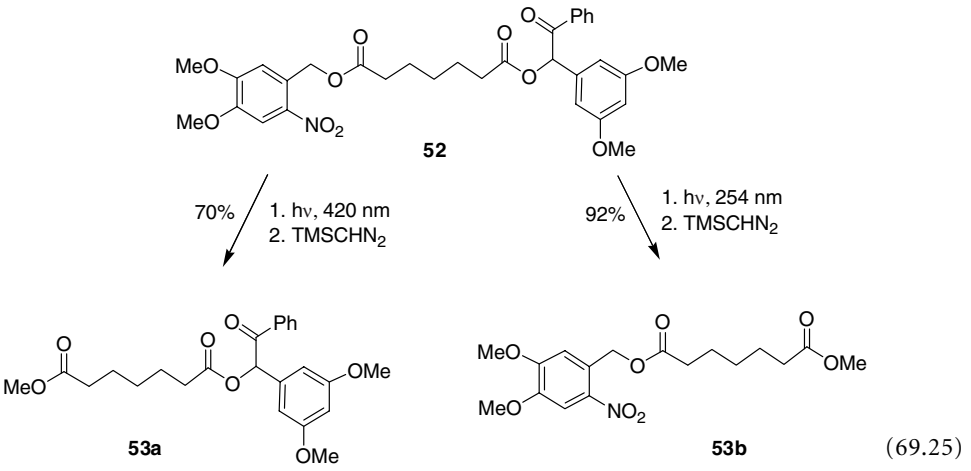

(69.25)

69.4 Phosphates and Phosphites

o-Nitrobenzyl

The most notable example of *o*-nitrobenzyl (ONB) caged phosphates remains that reported by Trentham and co-workers[54] on the synthesis and photochemistry of caged ATP in the late 1980s. Caged ATP, P^3-1-(2-nitrophenyl)ethyladenosine 5′-triphosphate (**54**), was synthesized in nearly quantitative yield in three steps starting with commercially available *o*-nitroacetophenone. Reaction with hydrazine to give the corresponding hydrazone, followed by oxidation with MnO_2 provided the aryldiazoethane precursor that was used to alkylate ATP. The photolysis of caged ATP furnished ATP with an efficiency of 0.63, as illustrated in Eq. (69.26):

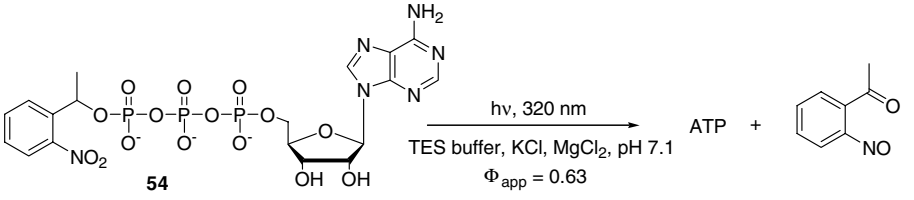

(69.26)

The rate of release of ATP was found to be dependent on the pH and the relative concentration of magnesium ion in solution. Pelliccioli and Wirz[5] have shown that the rate-determining step is the decay of the hemiacetal (or hemiketal) intermediate between pH 4 and 8. In this region, the slow hydrolysis of the hemiacetal limits the mechanistic value of the *o*-nitrobenzyl protecting group to studies of relatively slow reactions (e.g., $k_r < 10^3\ s^{-1}$).

The nitroso byproduct has also proved problematic for spectroscopic analyses of ONB reactions due to its reactivity with some substrates and with proteins. This problem was circumvented by conducting the photolysis in the presence of dithiothreitol, a hydrophilic thiol and an excellent nucleophile that readily sequesters the nitroso byproduct.

TABLE 69.15 Results of Photolysis of cAMP and cGMP Coumaryl Esters

Coumaryl Derivative	Solvent	Φ_{dis} [a]	λ_{max} (nm)
55a	80:20 HEPES-KCl buffer/MeOH	0.21 (0.25)	402
55b	HEPES-KCl buffer, pH 7.2	0.12 (0.16)	326
55c	HEPES-KCl buffer, pH 7.4	0.10 (0.14)	346

[a] For the cAMP ester; quantum efficiency for the cGMP derivative is in parentheses.

Coumaryl

Coumarylmethyl esters have been used as photoprotecting groups by several groups (e.g., Furuta et al.[55,56] and Hagen et al.[57]) for deprotection of cAMP and cGMP. To overcome the limited aqueous solubility of these derivatives, Hagen has modified the coumaryl chromophore with carboxyl and amino substituents.[57] Three new variants of the coumaryl system were synthesized and their photochemistry explored — (7-diethylaminocoumarin-4-yl)methyl (DEACM), (7-carboxymethoxycoumarin-4-yl)methyl (CMCM), and (6,7-*bis*[carboxymethoxy]coumarin-4-yl)methyl (BCMCM) as esters of cAMP and cGMP. Photolysis resulted in liberation of the free cyclic phosphate along with the hydrolyzed chromophores, i.e., **56a-c** (Eq. (69.27).

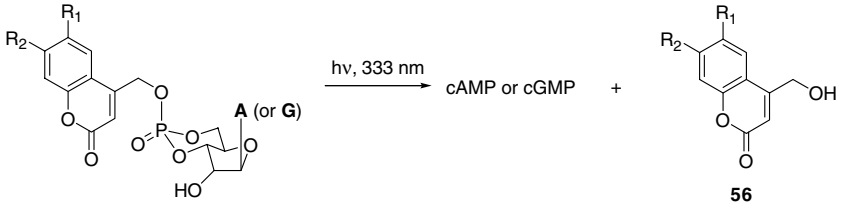

55a R_1 = H, R_2 = Et_2N
55b R_1 = H, R_2 = OCH_2CO_2H
55c R_1 = R_2 = OCH_2CO_2H

(69.27)

The caged coumaryl compounds were synthesized in 11 to 34% yield, clearly a limitation with this photoremovable protecting group. The addition of the carboxymethoxy groups in **55b** and **55c** dramatically enhanced the water solubility of these analogs as compared with the ester **55a**, and their photorelease occurred with good quantum efficiencies as seen in Table 69.15. On the other hand, the less water-soluble **55a** had the best quantum efficiency, and its absorption maximum was the most red shifted in the series.

Phenacyl

In light of its inherent advantages over other chromophores, the *p*-hydroxyphenacyl group has received recent attention as a promising photoprotecting group for phosphates. Recent reports on *p*-hydroxyphenacyl esters of phosphate, diethyl phosphate, and ATP by Givens et al.[36] and on GTP by Du et al.[58] indicate that these phosphate esters undergo efficient photorelease of the phosphoric acid moiety along with the rearranged *p*-hydroxyphenylacetic acid as the sole photoproducts of the reaction (Eq. (69.28).

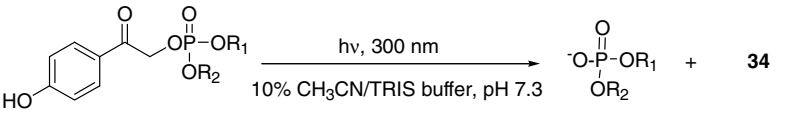

57a $R_1 = R_2 = Et$
57b $R_1 = R_2 = NH_4^+$
57c $R_1 = GDP$, $R_2 = NH_4^+$
35 $R_1 = ADP$, $R_2 = NH_4^+$

(69.28)

TABLE 69.16 Data for pHP Caged Phosphates

Caged Phosphate[a]	Protection (% Yield)	Deprotection (% Yield)	Φ_{dis}
57a	87	Not determined	0.77
57b	96	Quant	0.38
35	42	Quant	0.37 (0.30)[b]
57c	20	Not determined	Not determined

[a] Results shown for **57c** are from Du et al.;[58] derivative **57c** was photolyzed at 308 nm.
[b] The value in parentheses for **35** is the quantum efficiency for the appearance of ATP.

Derivative **57a** was synthesized by reacting the phosphate directly with *p*-hydroxyacetophenone bromide. Derivative **57b** was synthesized from hydrogenolysis of the pHP dibenzyl phosphate ester. For **35** and **57c**, the pHP monophosphate (**57b**) was first protected as the corresponding ketal that was then coupled with ADP or GDP, respectively. The caged ATP and GTP analogs were then obtained by hydrolysis of the ketal. Yields and quantum efficiencies for the disappearance of the pHP phosphate esters are given in Table 69.16.

pHP caged ATP was recently used as a probe in the study of $Na,^+$ K^+-ATPase, an enzyme involved in the intracellular transport of sodium and potassium ions.[59] Membrane samples possessing the ion-channel proteins were bathed in caged ATP which was activated by UV laser flash photolysis. $Na,^+$ K^+ channel transport was observed as a result of the activation of the enzyme by the released ATP. Direct spectroscopic evidence of the release of ATP was obtained by time-resolved Fourier transform infrared (FTIR) spectroscopy (Figure 69.2). The changes in the characteristic absorptions of the prominent functional groups of the reactant and product include the disappearance of the γ-PO_2^- ester band of the caged ATP at 1270 cm^{-1} and the appearance of the free γ-PO_3^{-2} band of the released ATP at 1129 cm^{-1}.

Benzoin

In 1994, Pirrung and Shuey[60] reported the protection of phosphates using the dimethoxybenzoin. Resolved *(R)*3′,5′-dimethoxybenzoin (optically active) was converted to the phosphoramidite by treatment with diisopropylaminocyanoethoxychlorophosphine. Subsequent reaction with the appropriate primary or secondary alcohol followed by oxidation led to the series of phosphate esters **58a-e** in moderate to high yields:

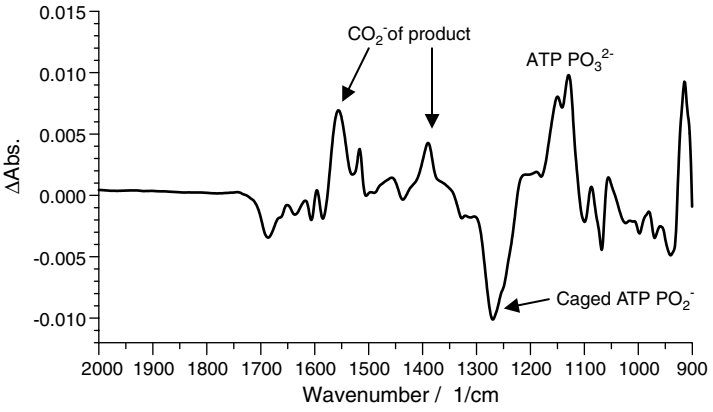

FIGURE 69.2 Time-resolved FTIR difference spectrum for the photolysis of pHP caged ATP. The absorbance was measured 10 ms to 11 s after the photolysis flash and subtracted from the absorbance prior to photolysis. (We thank Professors Klaus Fendler and Andreas Barth for the TR-FTIR results with pHP ATP.)

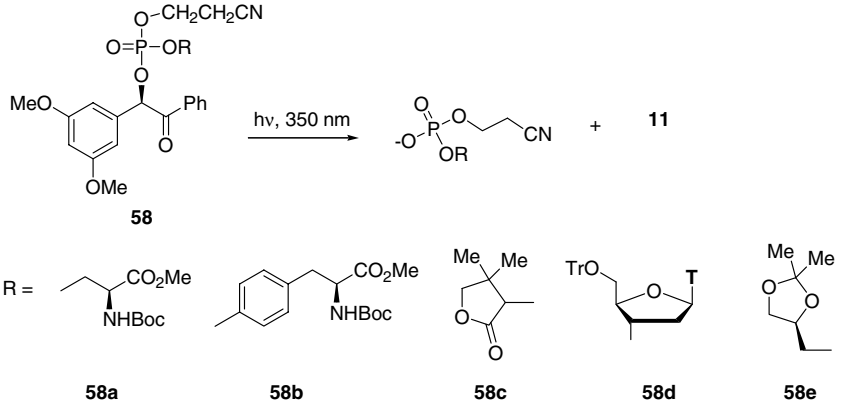

(69.29)

Photolysis of **58a-e** shown in Eq. (69.29) led to release of the phosphate derivative along with the benzofuran byproduct **11**. The overall sequence from the phosphoramidites to phosphate esters **58a–e** was accomplished in moderate yields, and the unprotected phosphates were obtained in good yields upon photolysis, as seen from Table 69.17.

TABLE 69.17 Yields for the Photolysis of DMB Phosphoramidites

R	Protection (% Yield)	Deprotection (% Yield)
58a	45	85
58b	82	86
58c[a]	58	85
58d	60	83
58e	55	87

[a] The (*R*) enantiomer.

69.5 Sulfates and Other Acids

Sulfonic acids have largely remained unexplored in terms of a functional group that is released from a photoremovable protecting group. One recent example has been reported by Bendig et al.,[46] in which methanesulfonic acid was protected as the corresponding methoxycoumarin derivative. (7-Methoxycoumarin-4-yl)methylmethanesulfonate **59** was synthesized from reaction of methanesulfonic acid with 4-(diazomethyl)-7-methoxycoumarin in refluxing chloroform. Photolysis at 333 nm resulted in the release of methanesulfonic acid, as shown in Eq. (69.30).

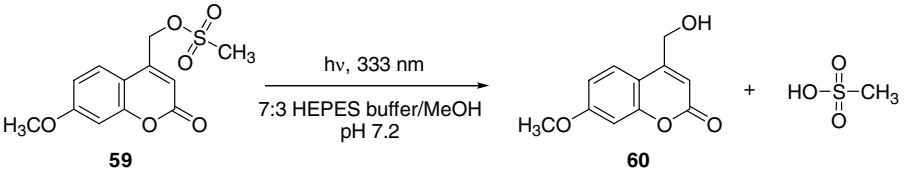

59 **60**

HEPES = *N*-(2-hydroxyethyl)piperazine-*N*'-(2-ethanesulfonic acid)

(69.30)

While the protection yield for **59** was low (26%), the quantum efficiency of 0.081 is reasonable when compared with other leaving groups that were reported in this study. The chemical yield of the deprotection was not provided; however, the photoproduct **60** was recovered in ≥95% yield, suggesting a high yield of the released sulfonic acid.

69.6 Alcohols, Thiols, and *N*-Oxides

o-Nitrobenzyl

Among the most common photoprotecting groups used for alcohols are the *o*-nitrobenzyl derivatives. Recently, Iwamura[61] reported the synthesis and photochemistry of caged carbohydrates protected with an *o*-nitrobenzyl group at one or more positions within the molecule. Equation (69.31) illustrates a typical example in which photolysis of the caged glucopyranoside **61** at 350 nm in methanol led to the release of the free methylglycoside **62** in 60% yield, along with the nitroso byproduct **3**.

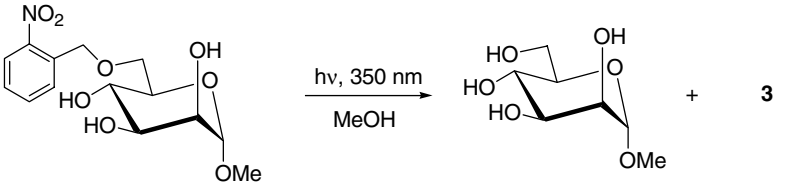

61 **62** **3**

(69.31)

Derivative **61** was synthesized in 71% yield by reductive bond cleavage of the corresponding 4,6-*O*-*o*-nitrobenzylidene acetal of methyl 3,4-acetyl-β-glucoside with triethylsilane and boron trifluoride etherate, followed by deacetylation of the 3,4-diacetates with sodium methoxide in methanol.

o-Nitrobenzyl chemistry was also extended to the release of thiols as demonstrated by Smith et al.,[62] who demonstrated that a cysteine congener was protected as the corresponding thioether **63** in 89% yield. Photocleavage occurred at 366 nm to give the liberated Boc-protected thiol **64** in 44% yield in the presence of semicarbazide hydrochloride, a carbonyl scavenger (Eq. 69.32).

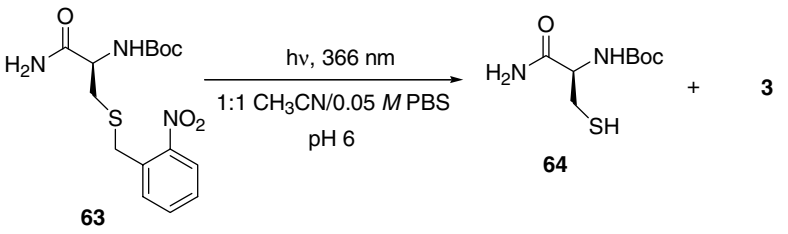

(69.32)

Finally, the addition of ascorbic acid as an antioxidant to the reaction mixture gave a quantitative yield of **64**. No thiol was recovered when the photolysis was carried out in the absence of ascorbic acid, despite experimental evidence of the disappearance of **63**.

While the *o*-nitrobenzyl system is well accepted as a photoremovable protecting group, it nevertheless suffers the limitation of toxicity to the biological entity and a highly reactive nitroso functional group formed as the byproduct. As was seen in the case of the cysteine cogener **63**, the photodeprotection may require a scavenging or reducing agent if thiols are to be generated in such a strategy.

In the late 1990s, Pfleiderer and co-workers[63] developed a new, β-substituted variant of the *o*-nitrobenzyl chromophore, 2-(*o*-nitrophenyl)ethoxycarbonate. The 5′-*O*-2-(*o*-nitrophenyl)ethoxycarbonyl thymidines were obtained from 2-(*o*-nitrophenyl)ethanol carbonates by reaction with diphosgene under basic conditions, followed by treatment with thymidine in anhydrous methylene chloride at reduced temperature. The synthetic yields ranged from 41 to 81%.

Photolysis of a 0.1-m*M* solution of the photoprotected thymidine **65** in a 1:1 methanol/water mixture at 365 nm resulted in the release of thymidine (**66**), carbon dioxide, and the photolabile *o*-nitrostyrene derivative **67** (Eq. (69.33).The photorelease is believed to occur through a β-elimination mechanism[64,65] from the aci-nitro intermediate **67′** shown in Scheme 10.

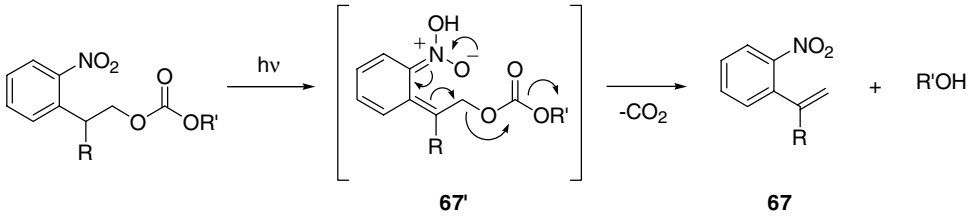

SCHEME 10 β-Elimination mechanism proposed for 2-(*o*-nitrophenyl)ethoxycarbonyl thymidines.

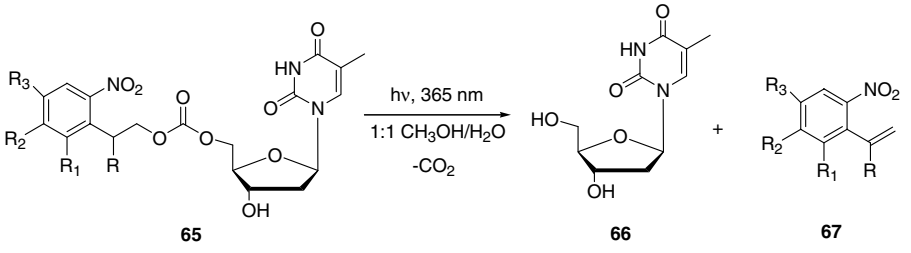

65a R = CH_3, R_1, R_2,R_3 = H
65b R = *o*-nitrophenyl, R_1, R_2,R_3 = H
65c R = H, R_1 = I, R_2,R_3 = H
65d R = H, R_1 = Br, R_2,R_3 = H
65e R = H, R_1 = Cl, R_2,R_3 = H
65f R = H, R_1, R_3 = Cl, R_2 = H
65g R = H, R_1 = F, R_2,R_3 = H
65h R = R_1 = H, R_2,R_3 = OCH_3

(69.33)

TABLE 69.18 Yields for 2-(*o*-Nitrophenyl)-ethoxycarbonyl Thymidine Derivatives

Derivative	Protection (% Yield)	Φ	Deprotection[a] (% Yield)
65a	71	0.35	76
65b	70	0.20	nd
65c	68	0.10	nd
65d	73	0.076	nd
65e	80	0.070	80
65f	81	0.072	nd
65g	70	0.037	nd
65h	41	0.0013	nd

[a] Based on the recovery of thymidine; Buhler, S., Giegrich, H., and Pfleiderer, W., *Nucleosides & Nucleotides,* 18, 1281-1283, 1999.

nd = not determined

Some advantages of this nitrobenzyl variant include the lack of the nitroso byproduct and release rates that are relatively fast compared with the parent *o*-nitrobenzyloxycarbonyl derivative. For example, the release of thymidine from **65b** is reported to be twice as fast as that for the α-substituted derivative; however, the nitrostyrenes (i.e., **67**) are photolabile and thus can compete with the starting material for incident light.

The quantum efficiencies for the release of thymidine varied depending on the substituents on **65**. Substitutions at the benzylic carbon appeared to give the highest release efficiencies, whereas the chloro derivatives gave slightly better conversions, as seen in Table 69.18.

The high quantum efficiency and respectable protection and deprotection yields obtained for the methyl-substituted 2-(*o*-nitrophenyl)ethoxycarbonyl photoprotecting group prompted Pirrung et al.[66] to use this protecting group for the solid-phase synthesis of oligodeoxynucleotides.

Thiopixyl and Coumaryl

Coleman and Boyd[67] introduced the 9-phenylthioxanthyl or S-pixyl photoprotecting group for the fourt principal nucleosides, thymidine and three other benzoyl protected nucleoside bases. The chromophore was synthesized in three steps, starting with thioxanthone, through Grignard addition of phenylmagnesium bromide, followed by dehydration with trimethylsilyl chloride and dimethylsulfoxide to give the 9-chloro-9-phenylthioxanthene. Treatment with the corresponding alcohol in a dry solution of pyridine and dimethylaminopyridine (DMAP) afforded the photoremovable protected hydroxy derivatives **68** in good yields (Table 69.19). Irradiation of **68** in aqueous acetonitrile resulted in the release of the nucleoside or alcohol along with **69** (Eq. (69.34)).

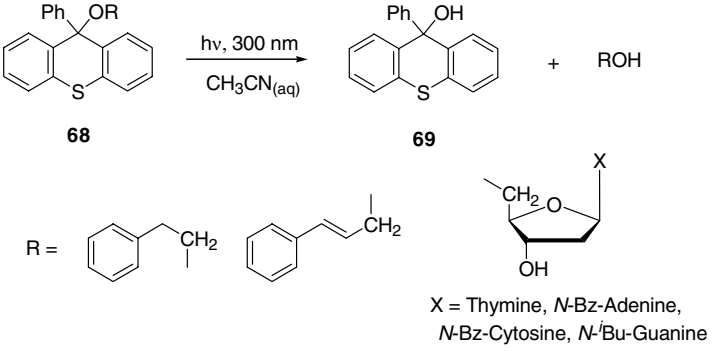

(69.34)

TABLE 69.19 Synthesis and Deprotection Yields for Various Derivatives of **68**

R	Protection[a] (% Yield)	Deprotection[b] (% Yield)
CH_2-benzyl	80	93
CH_2-(E)styryl	94	95
Thymidine	79	97
N-Bz-adenosine	86	96
N-Bz-cytidine	82	75
N-^{i}Bu-guanosine	92	89

[a] Based on isolated yields after column chromatography.
[b] Substrate concentrations were approximately 0.1 m*M*; yields were determined by HPLC.

Mechanistically, this photorelease reaction occurs via photosolvolysis of the aryl ether carbon–oxygen bond. The resulting resonance stabilized S-pixyl carbocation reacts with water to form **69**. Control experiments showed that the photoprotected alcohols are stable under thermal conditions; that is, refluxing in aqueous acetonitrile resulted in no detectable decomposition. Each of the caged products was obtained as a solid, a convenience for laboratory purification and manipulation. The best deprotection yields were obtained with solvent mixtures containing the maximum concentration of water permissible, limited only by the solubility of the protected alcohol. Concentrations of water ranged from 40 to 60%, depending on the type of alcohol used. In most cases, excellent deprotection yields were obtained.

A factor that limits the versatility of the S-pixyl group is the wavelength range required for photolysis. The range of excitation wavelengths from 200 to 300 nm overlaps with a number of functional groups that could compete with the incident light. For example, the pyrimidine base cytosine has substantial absorptivity at 300 nm. As a result, extended irradiation times were required to effect deprotection of the *N*-Bz-cytidine analog and a lower yield was obtained, as seen from Table 69.19.

Coumaryl photoprotecting groups have also been used for the protection of alcohols. A recent study by Lin and Lawrence[69] described the synthesis and photorelease of caged diols using a coumaryl acetal derivative **70** (Eq. (69.35)).

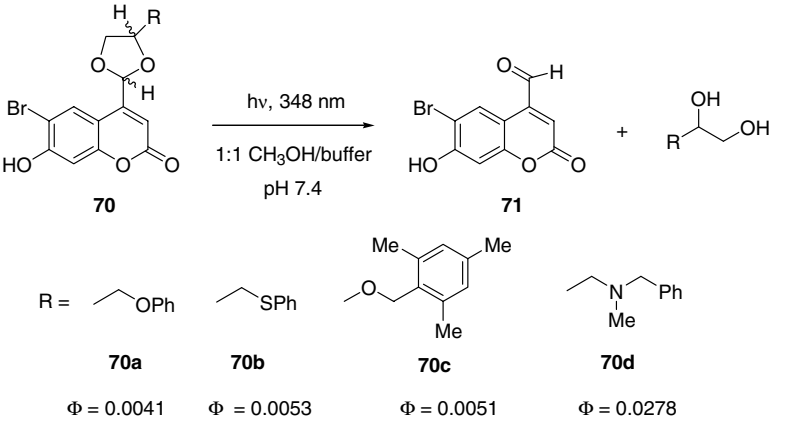

(69.35)

Acetal **70** was prepared in a two-step sequence starting with oxidation of 6-bromo-7-hydroxy-4-hydroxymethylcoumarin with manganese dioxide, followed by addition of the corresponding diol in

anhydrous toluene. Protection yields ranged from 94% for **70a** to 15% for **70d**. Photolysis of **70** at 348 nm in a methanol/aqueous buffer solution afforded the free diol accompanied by the aldehyde photoproduct **71**. The specific deprotection yields were not provided but in all cases were reported to exceed 75%.

The photorelease mechanism is not well understood but is speculated to proceed through an intramolecular ion pair[69] generated from photoheterolysis of the carbon oxygen bond, as shown in Scheme 11. Attack of a water molecule at the electrophilic carbon generates a hemiacetal that eliminates the alkoxy group to afford the diol and byproduct **71**.

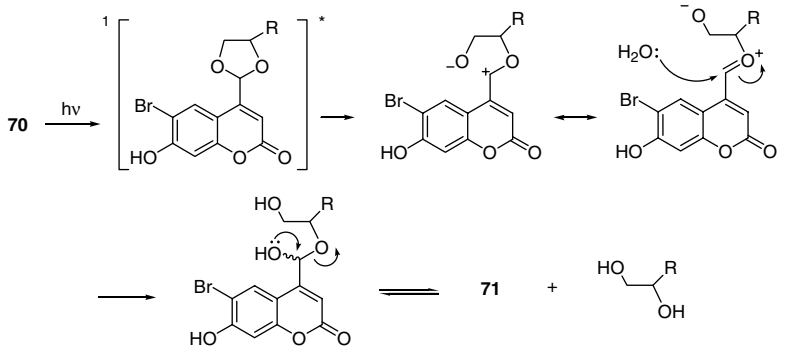

SCHEME 11 Mechanism proposed for the photorelease of caged diols from **70**.

This particular coumaryl variant offers a unique advantage in essentially being able to protect both hydroxyl groups of a diol using only one equivalent of the protecting group. In addition, the derivatives in this study were shown to be stable to hydrolysis in aqueous solvents at neutral or basic pH. For example, incubation of compounds **70a–d** in a 1:1 methanol/buffer solution (pH 7.4) resulted in no detectable degradation after a period of two weeks. Despite these advantages, the range of applications of the coumarin group is limited thus far to 1,2- and 1,4-diols (1,3-diols were found to be inert to photolysis). Like the *o*-nitrobenzyl group, the coumaryl group also has the disadvantage of producing a highly absorbing photoproduct. In addition, further studies need to be carried out in order to elucidate the mechanism of the photocleavage.

Benzoin

In 1995, Pirrung and Bradley[70] reported the use of dimethoxybenzoin (DMB) carbonate to protect various alcohols, including the 5′-hydroxyl group of nucleosides. The DMB carbonate was synthesized in three steps, starting with methylation of carbonyldiimidazole with methyl triflate followed by addition of 2-(3,5-dimethoxyphenyl)-2-hydroxy-1-phenylethanone to form a relatively stable activated acylating agent. Treatment with an alcohol under basic conditions in nitromethane furnished the protected alcohol **72** in yields that ranged from 42 to 95%.

Irradiation of **72** at 350 nm resulted in release of the alcohol and formation of dimethoxybenzofuran **11** (Eq. (69.36)). A wide variety of alcohols, including a thiol, were explored in this protection/deprotection scheme. Excellent deprotection yields were obtained, as high as 98% for the protected thymidine derivative. The mechanism as discussed earlier is postulated to proceed through intramolecular cyclization followed by demotion to form a zwitterionic intermediate. Expulsion of the alcohol occurs either concomitantly with the release of carbon dioxide or by a stepwise decarboxylation of the initially released carbonate **73**. In most cases, excellent deprotection yields were obtained.

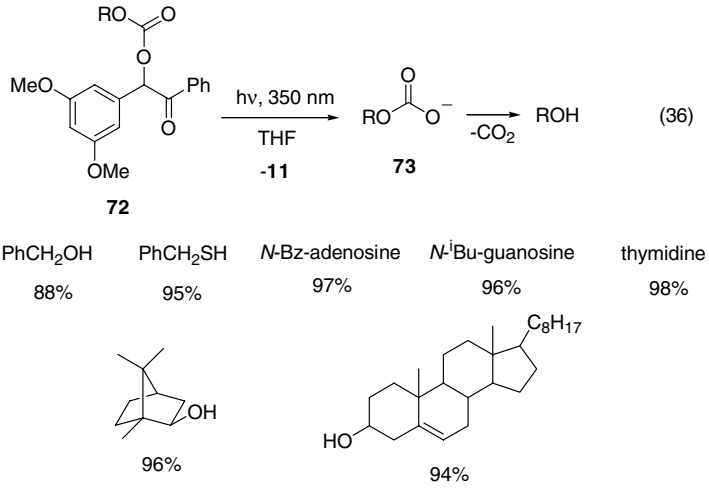

(69.36)

Attractive features of the DMB photoprotecting group are that the benzofuran photoproduct **11** is inert and exhibits strong fluorescence at 396 nm, allowing the deprotection conversions to be monitored spectroscopically. In the same study, the DMB group was successfully used to synthesize two trinucleotides bearing adjacent thymidine residues, demonstrating its potential in solid-phase DNA synthesis. Compared with nitrobenzyl photoprotecting groups, the rate of release of substrate is much faster for the DMB group[70] ($k_{release} \sim 10^8$–10^9 s^{-1}). The main disadvantages of the DMB group are the competition for incident light by the photoproducts and poor solubility in aqueous media.

Other

The anthraquinon-2-ylmethoxycarbonyl (Aqmoc) photoprotecting group is a relatively recent addition to the chromophores used as photoremovable groups. In a recent application for alcohols, Furuta et al.[71] reported that the caged derivative could be synthesized in two steps from anthraquinonylmethanol by treatment with 4-nitrophenylchloroformate in DMAP followed by coupling to the desired alcohol with DMAP to provide **74** in good yields (Table 69.20). Photolysis of **74** in 50% aqueous tetrahydrofurane (THF) at 350 nm resulted in the release of the alcohol (Eq. (69.37)).

TABLE 69.20 Yields and Quantum Efficiencies[a] for Aqmoc Derivatives

Aqmoc Derivative	Protection (% Yield)	Φ	Deprotection (% Yield)
74a	76	0.1	68
74b	86	Not determined	91[b]

[a] For the disappearance of starting material.
[b] Determined by HPLC.

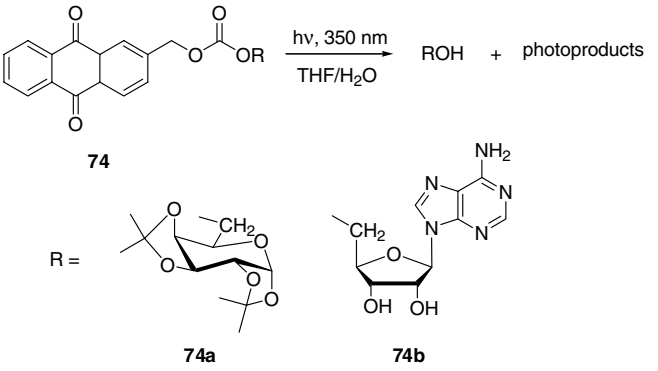

(69.37)

The photoproducts from the anthraquinone moiety were not fully characterized; however, in the case of **74a**, an anthraquinon-2-ylmethanol tetrahydrofuranyl ether was isolated, probably the result of hydrogen atom abstraction from the solvent. Also, a small amount of *bis*(1,2,3,4-di-*O*-isopropylidene-D-galacto-pyranosyl) carbonate was obtained after photolysis of **74a**, likely the result of attack of the released alcohol on the starting material.

Little is known about the photorelease mechanism of the Aqmoc group. Stern–Volmer analysis showed that the triplet excited state is the reactive excited state that leads to release of the alcohol. The rate constant determined for **74a** (4.6×10^6 s^{-1}) is consistent with rapid release of the carbonate followed by a slower, rate-limiting loss of carbon dioxide to give the free alcohol. Additional studies are needed to confirm this mechanism.

Recently, it was shown that nitro-substituted aryl carbamates could be used as photolabile protecting groups for alcohols.[72] *N*-Methyl-*N*-(*o*-nitrophenyl)carbamate **75** (Eq. (69.38)) was synthesized in two steps, beginning with acylation of *N*-methyl-2-nitroaniline with phosgene followed by nucleophilic addition of the alcohol, either as an alkoxide or in the presence of DMAP and triethylamine. An alternative synthetic route involved the generation of the corresponding chloroformate from the alcohol and phosgene followed by nucleophilic addition of the nitroaniline. The carbamate derivatives **75a-d** were synthesized in yields ranging from 58 to 94%.

Photolysis of carbamate **75** at various wavelengths led to deprotection of the alcohol, which was accompanied by formation of nitrosoaniline **76** as a byproduct. Deprotection yields for all derivatives were not provided; however, the reported yields for **75c** and **75d** were 100% and 91%, respectively. Such high yields are a definite advantage in terms of both synthetic and biological applications. Another attractive feature is the solubility in ethanol and water, solvents suitable for biological studies. Despite these advantages, two main limitations are worthy of note. First, the carbamate cages are susceptible to hydrolysis, particularly in basic media,[73] thus limiting their use to aqueous solvents with relatively neutral pH. Second, longer irradiation wavelengths were found to result in decreased deprotection yields; for example, when **75c** was irradiated at 312 nm, a quantitative deprotection yield was obtained. The yield dropped to 76% when the photolysis was carried out at 365 nm.

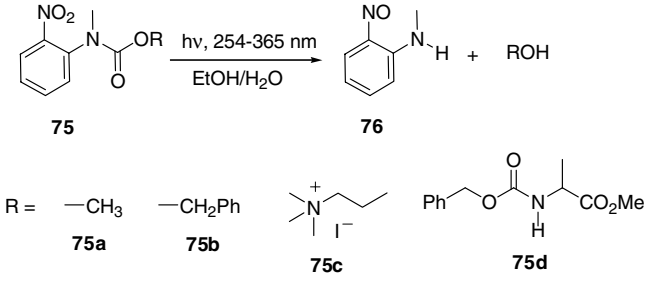

(69.38)

TABLE 69.21 Caged Silyl Derivatives and Their Corresponding Deprotection Yields in Methanol

Silyl Ether	Protection (% Yield)	Deprotection (% Yield)
77a	82	94[a]
77b	80	89
77c	77	90
77d	79	92
77e	81	86[a]
77f	85	90

[a] Based on the yield of the byproduct **78**.

Silyl photoprotecting groups have recently been developed for primary and secondary alcohols.[74] The silyl cage, (2-hydroxy-3-naphthylvinyl)-diisopropylsilyl ether **77,** was synthesized in nine steps starting with the commercially available naphthalene-2,3-diol. Irradiation at 350 nm in methanol triggered the release of the alcohol, accompanied by the formation of a cyclic silyl byproduct **78** (Eq. (69.39). This byproduct is likely formed via intramolecular attack of the naphthol oxygen at silicon following a trans,cis-isomerization of the starting material. Synthetic and photochemical yields are listed in Table 69.21.

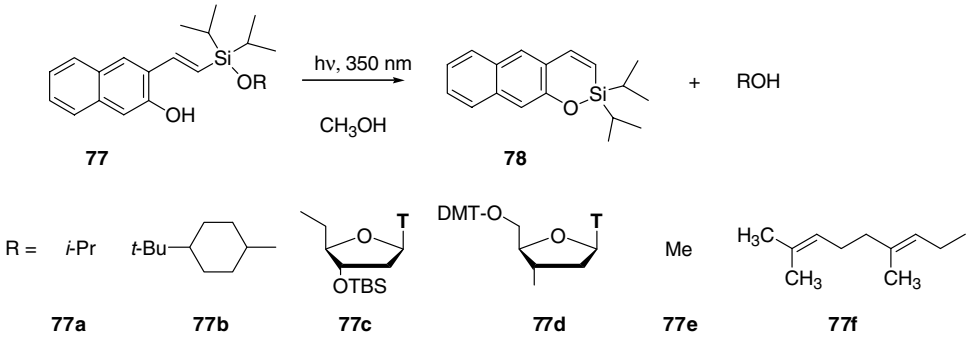

(69.39)

Byproduct **78** exhibits its strongest absorption in the region below 310 nm and, therefore, does not significantly compete with **77** for incident light. The yields from Table 69.21 are sufficiently high to enable the practical use of the silyl photoprotecting group in synthetic applications; however, the silyl cages lack the water solubility necessary for application in aqueous media. Like triisopropylsilyl ethers, the cages are also susceptible to cleavage in the presence of acidic media or solutions containing fluoride such as 1-*N* HCl or TBAF.[75]

The importance of nitric oxide (NO) in bioregulatory processes and other physiological functions prompted the development of photoprotecting groups specifically designed for its release. A most recent example is the synthesis and photochemistry of a series of naphthylmethyl and naphthylallyl diazeniumdiolates.[76] These derivatives, represented by **79** in Eq. (69.40), were prepared from reaction of 1-(*N*,*N*-diethylamino)-diazen-1-ium-1,3-diolate (**81**) with the corresponding alkyl bromide. Photolysis produced a mixture of products that resulted from two different reaction pathways. Path *a* is a nonproductive pathway that leads to the formation of nitrosamine **80** and oxime byproducts. Path *b* leads to diazeniumdiolate **81,** which collapses to give free NO, along with diethylamine and other photoproducts. The extent to which the reaction follows one pathway over another is dependent on the substituents present on the naphthyl ring. As Table 69.22 shows, the best deprotection yields were obtained with a methoxy group at the 5 and 8 positions of the ring.

TABLE 69.22 NO Cages and Their Corresponding Deprotection Yields and Quantum Efficiencies

NO cage	Protection (% Yield)	Φ	Deprotection[a,b] (% Yield)
79a	90	0.007	1
79b	25	Not determined	1
79c	30	0.12	25
79d	36	0.12	40
79e	5	0.66	95

[a] Based on the disappearance of starting material (using HPLC) and the amount of NO measured; thermal decomposition of **81** was found to produce 1.5 equivalents of NO.

[b] For **79a–c**, a wavelength of 300 nm was used; for **79d,e**, the wavelength was 350 nm.

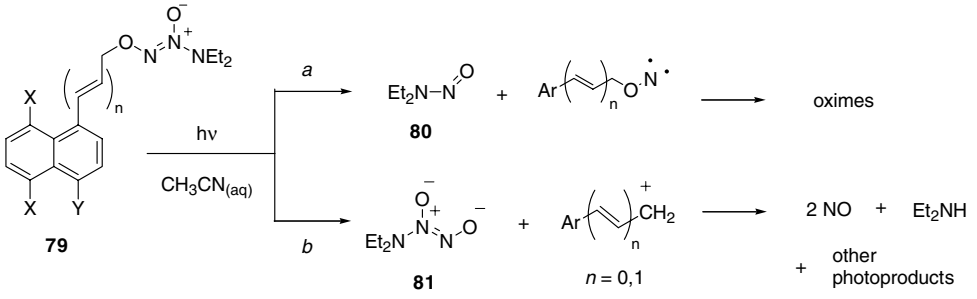

79a *n* = 0, X = Y = H
79b *n* = 0, X = H, Y = Me
79c *n* = 1, X = Y = H
79d *n* = 0, X = OMe, Y = H
79e *n* = 1, X = OMe, Y = H

(69.40)

The likely mechanism proceeds through photosolvolysis of the carbon–oxygen bond, resulting in a resonance-stabilized carbocation. Subsequent release of NO occurs from the diazeniumdiolate **81**. Acidic conditions that protonated the amine greatly enhanced the rate of NO release. Derivative **79e** undergoes clean deprotection and exhibits an excellent quantum efficiency, making it the most attractive of the NO cages studied thus far. Some additional advantages are its absorption beyond 300 nm (λ_{max} = 336 nm) and its stability in acidic and basic solutions at room temperature for up to 24 hr. Unfortunately, it suffers from a low protection yield of only 5%, and its solubility is limited to 20 μ*M* in 95% aqueous acetonitrile. Despite these shortcomings, its development may pave the way for similar methoxy-substituted naphthylallyl derivatives with increased solubility in aqueous media and higher protection yields.

A unique photoprotecting group for alcohols and thiols was reported in the mid 1990s.[77] Benzoylbenzoate ester **82** (Eq. (69.41)) was synthesized in one step from DCC coupling of the corresponding alcohol or thiol to 2-benzoylbenzoic acid. Photolysis at ~300 nm in the presence of cyclohexylamine, an electron donor, afforded 3-phenylphthalide **84** along with the free alcohol or thiol.

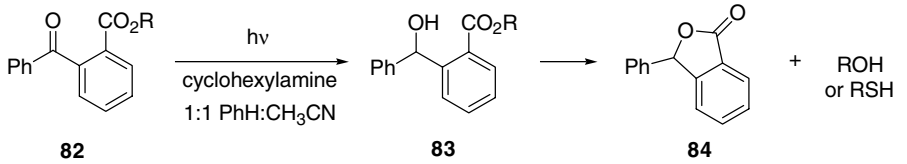

R = n-$C_{12}H_{25}$-, c-$C_{12}H_{23}$-, cholesteryl-, geranyl-, 2',3'-isopropylidene uridinyl-, n-$C_{12}H_{25}$ (thioester) (69.41)

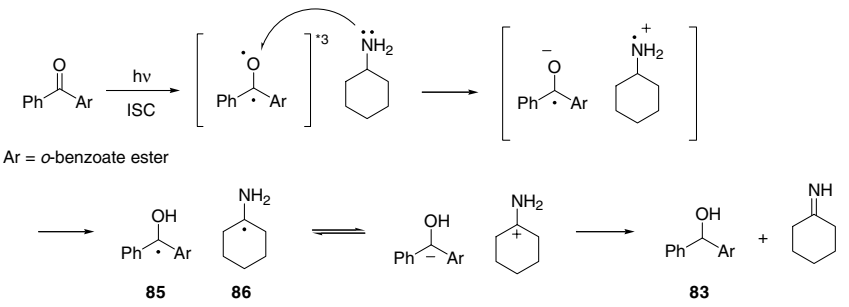

SCHEME 12 Proposed photoreduction mechanism of benzoylbenzoate esters.[65]

TABLE 69.23 Data for Benzoylbenzoate Esters

R	Protection (% Yield)	Deprotection[a] (% Yield)
n-$C_{12}H_{25}$-	76	95
c-$C_{12}H_{23}$-	50	85
Cholesteryl-	67	100
Geranyl-	63	90[b]
2′,3′-isopropylidene uridinyl	79	90[c]
n-$C_{12}H_{25}$ (thioester)	76	60

[a] Yield of the recovered alcohol (thiol) was determined with NMR.
[b] *sec*-Butylamine was used as the electron donor; the solvent was 1:1 benzene/isopropanol.
[c] *sec*-Butylamine was the electron donor; photolysis was carried out with a uranium filter.

The mechanism outlined in Scheme 12[78] involves electron transfer from the amine to the ketone in the excited state followed by intermolecular proton transfer to generate radical pair **85**–**86**; a second electron transfer and proton exchange lead to the reduced alcohol **83**, which lactonizes to form **84** concurrently with release of the alcohol. In general, the benzoylbenzoate photoprotecting group worked well for the particular substrates studied. Synthesis yields for the benzoylbenzoate cages were respectable, and the deprotection occurred in most cases with good recoveries of the alcohol (Table 69.23). Problems were encountered in the photolysis of the caged thiol that led to the formation of side products and thus a lower overall deprotection yield.

While the benzoylbenzoate cages exhibit good deprotection yields for alcohols, their application is limited to organic solvents. The presence of an electron donor (i.e., aliphatic amine) is also required, a necessity that may complicate the reaction mixture in the presence of other sensitive functional groups. Finally, the release process must be inherently a slow one due to the ground state lactonization process involved.

69.7 Phenols and Other Weak Acids

o-Nitrobenzyl

The photolabile *o*-nitrobenzyl derivative was utilized to protect the phenolic OH group of serotonin.[79] The serotonin type-3 receptor is the only ligand-gated ion channel in the 5-HT receptor family.[80,81] The protection of the phenolic hydroxy group of serotonin required four steps, as shown in Scheme 13. The substrate was released upon excitation with 337-nm laser pulses. The signal decay from pulsed laser

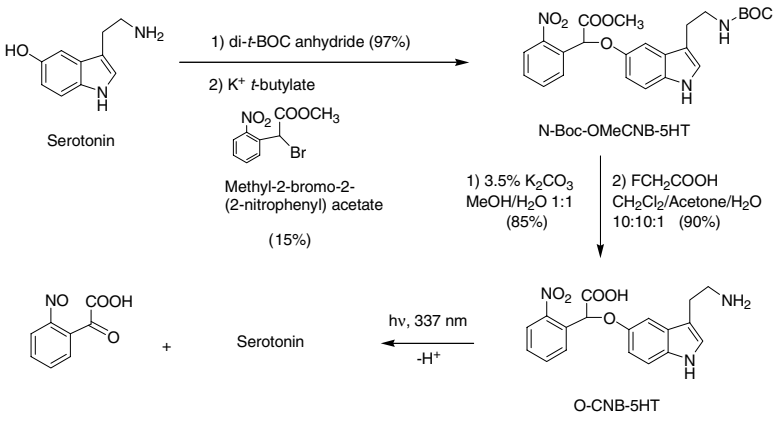

SCHEME 13 Protection and photochemical deprotection of serotonin.

studies gave a time constant of 16 μs, and the quantum yield was determined to be 0.03. The rate of decay of the intermediate was observed to be pH dependent. The caged serotonin showed good solubility in buffered aqueous media (in excess of 2 m*M*); however, the authors suggested that the caged compound was subject to hydrolysis in the dark on standing.

This photoremovable protecting group has been employed as a photocleavable linker to reagents bound to Au surfaces.[82] 4-Hydroxy-stilbene was linked to 6-bromohexyl-3-nitro-4-bromomethylbenzoate in 51% yield, then thiolated by trimethylsilylthioxy dehalogenation in THF, followed by desilylation *in situ*. The self-assembled monolayers of long-chain alkyl thiolate on bulk polycrystalline gold were constructed. Upon irradiation at 350 nm, the *Z,E*-photoisomerization attained a photostationary state within 25 min, while the dissociation took about 60 min; however, sensitization with 1,4-dibromonaphthalene (E_T = 58.1 kcal/mol) produced a cleaner photoisomerization. The unidirectional isomerization, from cis to trans, by both direct irradiation and sensitization was followed by the release of a bound chain from the metal surface.

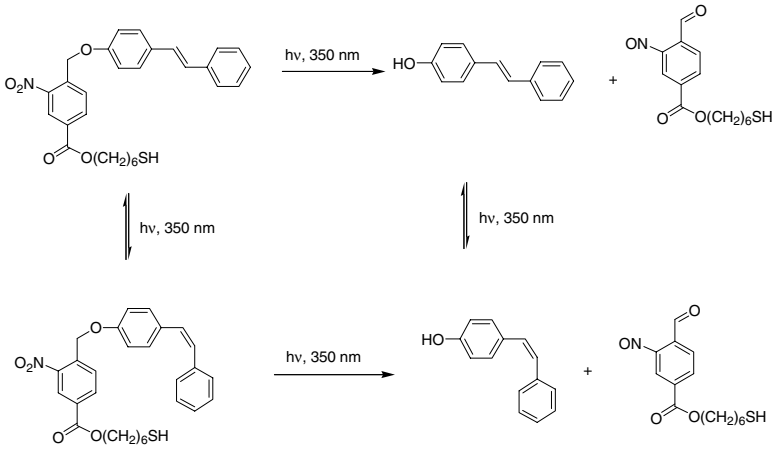

SCHEME 14

Benzoin

The ubiquinol oxidizing enzyme is a redox active enzyme that requires a fast two-electron reduction of ubiquinone. 3′,5′-Dimethoxybenzoin (DMB) caged ubiquinol[83] was synthesized to study the detailed enzymatic mechanism of the fast electron-transfer process in redox active enzymes. The monosilylated ubiquinol was coupled to the protecting group to form the *o*-nitrophenylcarbonate ester of 3′,5′-dimethoxyphenyl(phenyldithiane) in 55% yield. Upon photolysis, DMB caged ubiquinol generated ubiquinone with a rate greater than 10^6 s^{-1}(Eq. (69.42)).

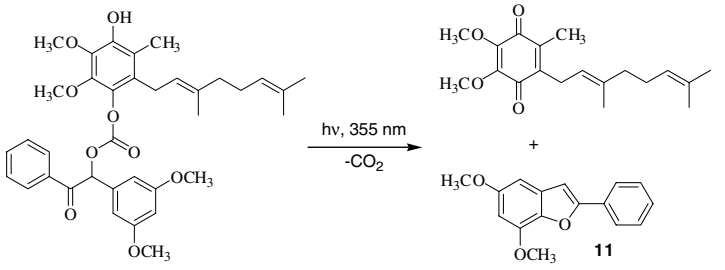

(69.42)

Pirrung and Bradley[70] also applied DMB (3′,5′-dimethoxybenzoin) to protect the phenolic group, demonstrating that 4-methoxyphenol was released upon irradiation at 350 nm in 90% yield (Eq. (69.43)).

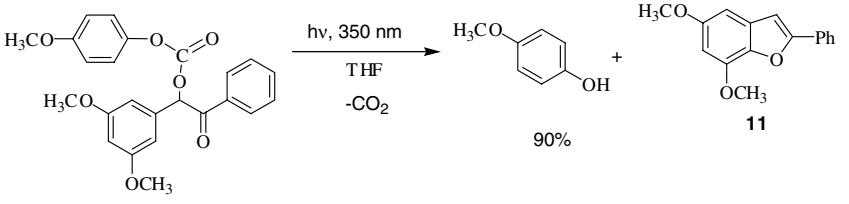

(69.43)

69.8 Amines

o-Nitrobenzyl

There are few variations for effective amine photoremovable protecting groups. The *o*-nitrobenzyl group remains the most popular group and among the many examples the studies by Cameron and Frechet are noteworthy.[84] In general, *o*-Nitrobenzylcarbamates of aliphatic amines upon photolysis release the amine in good yield. For example, cyclohexyl amine is released from its *o*-nitrobenzyl carbamate **87** as the corresponding free carbamate upon irradiation in THF at 254 nm (Eq. (69.44)).

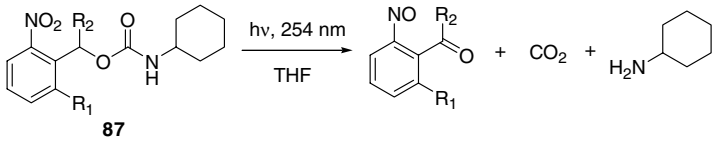

(69.44)

Subsequent loss of carbon dioxide frees the amine. Quantum efficiencies varied depending on the substituents present at the ortho and benzylic positions (Table 69.24). The best efficiencies were obtained with two *o*-nitro groups on the aryl ring, likely increasing the probability for the hydrogen atom abstraction by one of the nitro groups.

TABLE 69.24 Protection Yields[a] and Quantum Efficiencies for Various Substituted *o*-Nitrobenzyl Carbamates

R_1	R_2	Protection (% Yield)	Φ
H	H	71	0.13
NO_2	H	78	0.62
H	Me	71	0.11
NO_2	Me	71	0.35
H	*o*-Nitrophenyl	79	0.26
NO_2	2,6-Dinitrophenyl	52	0.28

[a] Deprotection yields were not provided.

A problem that is not entirely avoidable is the formation of imine byproducts via reaction of the released amine with the aldehydic group in the photoproduct. This occurrence could be suppressed with alkyl or aryl substitution at the benzylic position, leading to the formation of a less reactive ketone in comparison with the nitroso aldehyde formed with no substitution at the benzylic position. Imine byproduct formation is also less likely to occur in relatively nonpolar solvent systems, such as THF, which ultimately limits the application of the *o*-nitrobenzyl carbamate photoprotecting group to nonaqueous systems in this regard.

Benzoin Derivatives

In the mid-1990s, Pirrung and Huang[85] extended the use of the benzoin photoprotecting group to the release of amines by synthesizing *m*,*m*′-dimethoxybenzoin (DMB) carbamates. The DMB derivatives were synthesized by coupling the corresponding amine with benzoin carbonyl chloride that had been elaborated by reaction of carbonyldiimidazole with the methyl triflate of **88** followed by nucleophilic addition of DMB. Irradiation in benzene or THF at 350 nm produced the free amine, carbon dioxide, and the benzofuran byproduct (Eq. (69.45)).

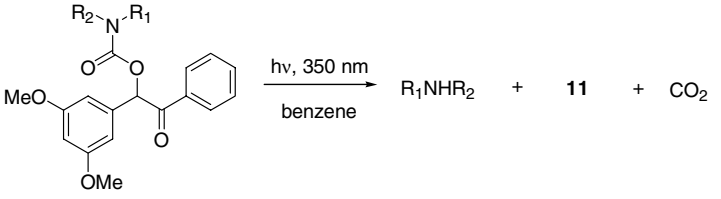

88

(69.45)

Five different amines were protected and recovered in moderate to good yields as shown in Table 69.25. The DMB carbamates appeared to work well for a variety of amines in the presence of other functional groups, such as alcohols or esters; however, the reaction is limited to secondary amines, as primary amines were found to undergo intramolecular cyclization leading to byproducts that are inert to photolysis.

Arylsulfonamides

Corrie and Papageorgious[86] have reported the synthesis and photochemistry of various methoxy-substituted arylsulfonamides. Similar derivatives had been previously found to undergo single electron transfer reactions in the excited state, leading to cleavage of the sulfur–nitrogen bond.[87,88] It was reasoned that such a process could be used for the rapid release of neurologically active amines.

The arylsulfonamide derivatives were synthesized in several steps, starting from 1,5-dimethoxynaphthalene. Photolysis of **89** in phosphate buffer (pH 7.0) in the presence of ascorbate resulted in release of

TABLE 69.25 Protection and Deprotection Yields for DMB Carbamates

Amine	Protection (% Yield)	Deprotection (% Yield)
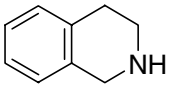	85	89[a]
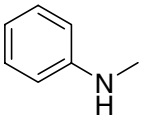	76	79
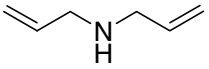	90	56
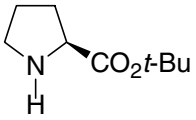	90	73
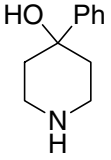	88	97[a]

[a] The amine was recovered as the corresponding hydrochloride salt.

TABLE 69.26 Synthesis and Photochemistry Yields of Arylsulfonamides

R_1	R_2	Protection (% Yield)	Deprotection[a] (% Yield)
$(CH_2)_3OPO_3^{-2}$	CO_2^-	71	35
$(CH_2)_3OPO_3^{-3}$	$CH_2CO_2^-$	61	22[b]
Me	CO_2Me	59	53

[a] Yields were determined using quantitative amino acid analysis; irradiations were only carried out to approximately 50% conversion of the starting material in the presence of 10-m*M* ascorbate.
[b] Photolyzed in buffer solution only.

the free amine in low to moderate yields, accompanied by the reduced arylsulfonyl byproduct **90** (Eq. (69.46) and Table 69.26).

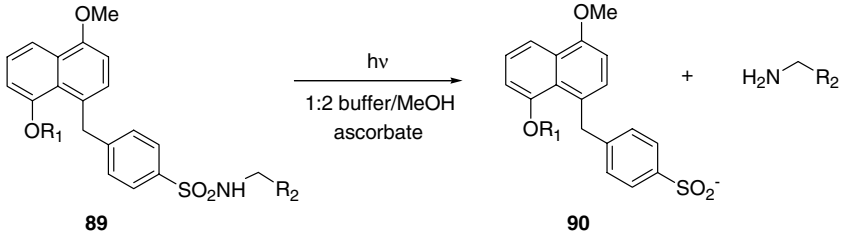

89 **90**

(69.46)

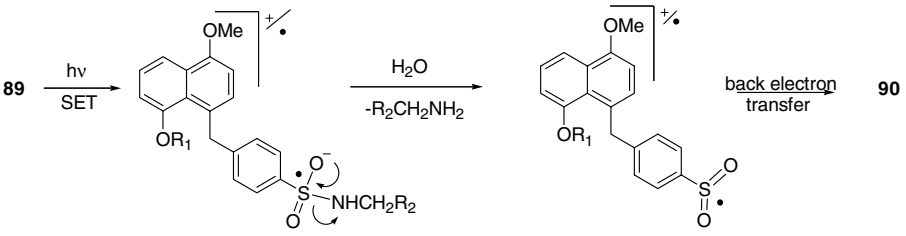

SCHEME 15 Proposed mechanism for amino acid release from arylsulfonamides.

The mechanism is thought to involve an excited state intramolecular single eletron trnasfer from the electron-rich naphthalene sulfur (Scheme 15); release of the amine then occurs via assistance from the neighboring oxygen, leading to a radical cation that is subsequently reduced to **90** by ascorbate.

It was speculated that, in the case of the glycine and β-alanine substrates, a competitive electron transfer was occurring from the carboxylate group to the radical cation of **90**. Such a process would yield a carboxyl radical that would undergo subsequent decarboxylation, leading to a mixture of side products and thus a lower yield of the free amino acid. Spectroscopic evidence using LFP combined with FTIR spectroscopy supported this hypothesis. Low yields were still encountered even in the presence of increased amounts of ascorbate, suggesting that the electron transfer was taking place within a solvent cage.

Despite this shortcoming, the arylsulfonamide group may still hold promise as a photoremovable protecting group for amines lacking a carboxylate moiety. Further studies would need to be carried out to fully establish its capabilities in this regard.

69.9 Conclusion

A wide variety of photoremovable protecting groups have been added to the veteran *o*-nitrobenzyl series. Each new group has been developed to address the shortcomings of the *o*-nitrobenzyl group or to add features such as faster rates for release, extension of the absorption range into the near UV-visible region, improved solubility, higher efficiencies, improved conversions and yields, and more benign photoproducts from the protecting group. Extensions and applications of this chemistry to two photon excitation processes, to traceless reagents in the combinatorial and photolithography, as orthogonal reagents in synthesis, and to time-resolved spectroscopic techniques wil make even more demands on the design, synthesis, and development of new photoremovable protecting groups.

Even now, however, no single photoremovable protecting group fulfills all nine criteria Sheehan and Lester had suggested (outlined at the beginning of this chapter). Nevertheless, important progress has been achieved as evidenced by the growing number of applications reported for many of these photoremovable groups, especially in biological studies. Applications in synthesis, combinatorial chemistry, micro arrays, and photolithography are also forthcoming. These fields have benefited and will continue to draw the interest of science community as improvements of existing systems and discovery of new photoactive protecting groups are developed. This field of photoremovable protecting groups is still in its infancy.

Acknowledgments

We acknowledge the support of the Department of Energy, University of Kansas and the National Science Foundation.

References and Notes

1. (a) Kaplan, J. H., Forbush, B. I., and Hoffman, J. F., Rapid photolytic release of adenosine 5′-triphosphate from a protected analogue: utilization by the Na:K pump of human red blood cell ghosts, *Biochemistry*, 17, 1929–1935, 1978. (b) Engels, J. and Schlaeger, E.-J., Synthesis, structure, and reactivity of adenosine cyclic 3′,5′-phosphate benzyl triesters, *J. Med. Chem.*, 20, 907-911, 1977.
2. Givens, R. S. and Kueper III, L. W., Photochemistry of phosphate esters, *Chem. Rev.*, 93, 55–66, 1993.
3. Adams, S. R. and Tsien, R. Y., Controlling cell chemistry with caged compounds, *Ann. Rev. Physiol.*, 18, 755–784, 2000.
4. Corrie, J. E. T. and Trentham, D. R., Synthetic, mechanistic and photochemical studies of phosphate esters of substituted benzoins, *J. Chem. Soc., Perkin Trans. 1*, 2409–2417, 1992.
5. Pelliccioli, A. P. and Wirz, J., Photoremovable-protecting groups: reaction mechanism and applications, *Photochem. Photobiol. Sci.*, 1, 441–458, 2002.
6. Bochet, C. G., Photolabile protecting groups and linkers, *J. Chem. Soc., Perkin Trans. 1*, 125–142, 2002.
7. Givens, R. S. and Lee, J.-I., The *p*-hydroxyphenacyl photoremovable protecting group, *J. Photosci.*, 2002, in press.
8. Zou, K., Miller, W. T., Givens, R. S., and Bayley, H., Caged thiophosphotryosine peptides, *Angew. Chem. Int. Ed. Engl.*, 40, 3049–3051, 2001.
9. Zou, K., Cheley, S., Givens, R. S., and Bayley, H., Catalytic subunit of protein kinase caged at the activating phosphothreonine, *J. Am. Chem. Soc.*, 124, 8220–8229, 2002.
10. Arabaci, G., Guo, X.-C., Beebe, K. D., Coggeshall, K. M., and Pei, D., α-Haloacetophenone derivatives as photoreversible covalent inhibitors of protein tyrosine phosphates, *J. Am. Chem. Soc.*, 121, 5085–5086, 1999.
11. Corey, E. J. and Cheng, X.-M., *The Logic of Chemical Synthesis*, John Wiley & Sons, New York, 1995, 78–79.
12. Sheehan, J. C. and Umezawa, K., Phenacyl photosensitive blocking groups, *J. Org. Chem.*, 38, 3771–3774, 1973.
13. Barltrop, J. A. and Schofield, P., Photosensitive protecting groups, *Tetrahedron Lett.*, 697–699, 1962.
14. Givens, R. S., Weber, J. F. W., Jung, A. H., and Park, C.-H., New photoprotecting groups: desyl and *p*-hydroxyphenacyl phosphate and carboxylate esters, in *Methods in Enzymology*, Vol. 291, Marriott, G., Ed., Academic Press, New York, 1998, 1–29.
15. Baldwin, J. E., McConnaughie, A. W., Moloney, M. G., Pratt, A. J., and Shim, S. B., New photolabile phosphate protecting groups, *Tetrahedron*, 46, 6879–6884, 1990.
16. Wang, B. and Zheng, A., A photosensitive protecting group for amines based on coumarin chemistry, *Chem. Pharm. Bull.*, 45, 715–718, 1997.
17. Koenigs, P. M., Faust, B. C., and Porter, N. A., Photochemistry of enzyme-bound cinnamoyl derivatives, *J. Am. Chem. Soc.*, 115, 9371–9379, 1993.
18. Lester, H. A. and Nerbonne, J. M., Physiological and pharmacological manipulations with light flashes, *Ann. Rev. Biophys. Bioeng.*, 11, 151–175, 1982.
19. Barltrop, J. A., Plant, P. J., and Schofield, P., Photosensitive protective groups, *J. Chem. Soc., Chem. Commun.*, 822–823, 1966.
20. Ried, V. W. and Wilk, M., The photochemistry of unsaturated nitrocompounds. II. Relations among polarizability, reduction potential and photochemical behavior of some nitro compounds, *Justus Liebigs Ann. Chem.*, 590, 91–110, 1954.
21. Walker, J. W., Lu, Z., and Moss, R. L., Effects of Ca^{+2} on the kinetics of phosphate release in skeletal muscle, *J. Biol. Chem.*, 267, 2459–2466, 1992.
22. Willenbucher, R. F., Xie, Y. N., Eysselein, V. E., and Snape, Jr., W. J., Mechanisms of cAMP-mediated relaxation of distal circular muscle in rabbit colon, *Am. J. Physiol.*, 262, G159–G164, 1992.
23. Ostap, E. M. and Thomas, D. D., Rotational dynamics of spin-labeled F-actin during activation of myosin S1 ATPase using caged ATP, *Biophys. J.*, 59, 1235–1241, 1991.

24. Tepe, J. J. and Williams, R. M., DNA crosslinking by a phototriggered dehydromonocrotaline progenitor., *J. Am. Chem. Soc.*, 121, 2951–2955, 1999.
25. Sheehan, J. C. and Wilson, R. M., Photolysis of desyl compounds: a new photolytic cyclization, *J. Am. Chem. Soc.*, 86, 5277–5281, 1964.
26. Givens, R. S. and Matuszewski, B., Photochemistry of phosphate esters: an efficient method for the generation of electrophiles, *J. Am. Chem. Soc.*, 106, 6860–6861, 1984.
27. Givens, R. S., Athey, P. S., Kueper, L. W. I., Matuszewski, B., and Xue, J.-Y., Photochemistry of α-keto phosphate esters: photorelease of a caged cAMP, *J. Am. Chem. Soc.*, 114, 8708–8710, 1992.
28. Givens, R. S., Athey, P. S., Matuszewski, B., Kueper, L. W., Xue, J., and Fisher, T., Photochemistry of phosphate esters: α-keto phosphates as a photoprotecting group for caged phosphate, *J. Am. Chem. Soc.*, 115, 6001–6012, 1993.
29. Sheehan, J. C., Wilson, R. M., and Oxford, A. W., The photolysis of methoxy-substituted benzoin esters, *J. Am. Chem. Soc.*, 93, 7222–7228, 1971.
30. Rajesh, C. S. Givens, R. S., and Wirz, J., Kinetics and mechanism of phosphate photorelease from benzoin diethyl phosphate: evidence for adiabatic fission to an α-keto cation in the triplet state, *J. Am. Chem. Soc.*, 122, 611–618, 2000.
31. Epstein, W. W. and Garrossian, M., *p*-Methoxyphenacyl esters as photodeblockable-protecting groups for phosphates, *J. Chem. Soc., Chem. Commun.,* 532–533, 1987.
32. Dhavale, D. D., Mali, V. P., Sudrik, S. G., and Sonawane, H. R., Media controlled photo-Favorskii type rearrangement of α-chloro acetophenones: synthesis of phenylacetic acids, *Tetrahedron*, 53, 16789–16794, 1997.
33. Sonawane, H. R., Bellur, N. S., Kulkarni, D. G., and Ayyangar, N. R., Photochemical rearrangement of α-chloropropiophenones to α-arylpropanoic acids: studies on chirality transfer and synthesis of (S)-(+)-ibuprofen and (S)-(+)-ketoprofen, *Tetrahedron*, 50, 1243–1260, 1994.
34. Anderson, J. C. and Reese, C. B., A photo-induced rearrangement involving aryl participation, *Tetrahedron Lett.*, 1–4, 1962.
35. Givens, R. S. and Park, C.-H., Hydroxyphenacyl ATP: a new phototrigger, *Tetrahedron Lett.*, 37, 6259–6262, 1996.
36. Park, C.-H. and Givens, R. S., New photoactivated protecting groups. 6. *p*-Hydroxyphenacyl: a phototrigger for chemical and biochemical probes *J. Am. Chem. Soc.*, 119, 2453–2463, 1997.
37. Zhang, K., Corrie, J. E. T., Munasinghe, R. N., and Wan, P., Mechanism of photosolvolytic rearrangement of *p*-hydroxyphenacyl esters: evidence for excited-state intramolecular proton transfer as the primary photochemical step, *J. Am. Chem. Soc.*, 121, 5625–5632, 1999.
38. (a) Fischer, M. and Wan, P., *m*-Quinone methides from *m*-hydroxy-1,1-diaryl alkenes via excited-state (formal)intramolecular proton transfer mediated by a witer timer, *J. Am. Chem. Soc.,* 120, 2680-2681, 1998. (b) Kalanderopoulos, P. and Yates, P., Intramolecular proton transfer in photohydration reactions, *J. Am. Chem. Soc.,* 108, 6290-6295, 1986.
39. Conrad II, P. G., Givens, R. S., Hellrung, B., Rajesh, C. S., Ramseiir, M., and Wirz, J., *p*-Hydroxyphenacyl phototriggers: the reactive excited state of phosphate photorelease, *J. Am. Chem. Soc.*, 122, 9346–9347, 2000.
40. Zimmerman, H. E. and Sandel, V. R., Mechanistic organic photochemistry. II. Solvolytic photochemical reactions, *J. Am. Chem. Soc.,* 85, 915–922, 1963.
41. Zimmerman, H. E., *Meta-ortho* effect in organic photochemistry: mechanistic and exploratory organic photochemistry, *J. Phys. Chem. A,* 102, 5616-5621, 1998. (See also, Zimmerman, H. E., *Meta-ortho* effect in organic photochemistry: mechanistic and exploratory organic photochemistry. [Erratum to document cited in CA129:81353] *J. Phys. Chem. A,* 102, 7725, 1998.)
42. DeCosta, D. P. and Pincock, J. A., Photochemistry of substituted 1-naphthylmethyl esters of phenylacetic and 3-phenylpropanoic acid: radical pairs, ion pairs and Marcus electron transfer, *J. Am. Chem. Soc.*, 115, 2180–2190, 1993.
43. Pincock, J. A., Photochemistry of arylmethyl esters in nucleophilic solvents: radical pair and ion pair intermediates, *Acc. Chem. Res.*, 30, 43–49, 1997.

44. Furuta, T., Momotaka, A., Sugimoto, M., Hatayajma, M., Torigai, H., and Iwamura, M., Acyloxycoumarinylmethyl-caged cAMP: the photolabile and membrane-permeable derivative of cAMP that effectively stimulates pigment-dispersion response of melanophores, *Biochem. Biophys. Res. Commun.*, 228, 193–198, 1996.
45. Gee, K. R., Niu, L., Schaper, K., Jayaraman, V., and Hess, G. P., Synthesis and photochemistry of a photolabile precursor of *N*-methyl-D-aspartate (NMDA) that is photolyzed in the microsecond time region and is suitable for chemical kinetic investigations of the NMDA receptor, *Biochemistry*, 38, 3140–3147, 1999.
46. Yoo, D. J. and Greenberg, M., Synthesis of oligonucleotides containing 3′-alkyl carboxylic acids using universal, photolabile solid phase synthesis supports, *J. Org. Chem.*, 60, 3358–3364, 1995.
47. Schade, B., Hagen, V., Schmidt, R., Herbrich, R., Krause, E., Eckardt, T., and Bendig, J., Deactivation behavior and excited-state properties of (coumarin-4-yl)methyl derivatives. 1. Photocleavage of (7-methoxycoumarin-4-yl)methyl caged acids with fluorescence enhancement, *J. Org. Chem.*, 64, 9109–9117, 1999.
48. Conrad II, P. G., Givens, R. S., Weber, J. F. W., and Kandler, K., New phototriggers: extending the *p*-hydroxyphenacyl π-π^* absorption range, *Org. Lett.*, 2, 1545–1547, 2000.
49. Givens, R. S., Weber, J. F. W., Conrad II, P. G., Orosz, G., Donahue, S. L., and Thayer, S. A., New phototriggers. 9. *p*-Cydroxyphenacyl as a C-terminal photoremovable protecting group for oligopeptides, *J. Am. Chem. Soc.*, 122, 2687–2697, 2000.
50. Routledge, A., Abell, C., and Balasubramanian, S., The use of a dithiane protected benzoin photolabile safety catch linker for solid-phase synthesis, *Tetrahedron Lett.*, 38, 1227–1230, 1997.
51. Klan, P., Zabadal, M., and Heger, D., 2,5-Dimethylphenacyl as a new photoreleasable-protecting group for carboxylic acids, *Org. Lett.*, 2, 1569–1571, 2000.
52. Zabadal, M., Pelliccioli, A. P., Klan, P., and Wirz, J., 2,5-Dimethylphenacyl esters: a photoremovable protecting group for carboxylic acids, *J. Phys. Chem. A*, 105, 10329–10333, 2001.
53. Bochet, C. G., Orthogonal photolysis of protecting groups, *Angew. Chem., Int. Ed. Engl.,* 40, 2071–2073, 2001.
54. Walker, J. W., Reid, G. P., McCray, J. A., and Trentham, D. R., Photolabile 1-(2-nitrophenyl)ethyl phosphate esters of adenine nucleotide analogues: synthesis and mechanism of photolysis, *J. Am. Chem. Soc.*, 110, 7170–7177, 1988.
55. Furuta, T., Torigai, M., Sugimoto, M., and Iwamura, M., Photochemical properties of new photolabile cAMP derivatives in a physiological saline solution, *J. Org. Chem.*, 60, 3953–3956, 1995.
56. Furuta, T. and Iwamura, M., New caged groups: 7-substituted coumarinylmethyl phosphate esters, in *Methods in Enzymology*, Vol. 291, Marriott, G., Ed., Academic Press, New York, 1998, 50–63.
57. Hagen, V., Bendig, J., Frings, S., Eckardt, T., Helm, S., Reuter, D., and Kaupp, U. B., Highly efficient and ultrafast phototriggers for cAMP and cGMP by using long-wavelength UV/VIS activation, *Angew. Chem., Int. Ed. Engl.,* 40, 1046–1048, 2001.
58. Du, X., Frei, H., and Kim, S.-H., The mechanism of GTP hydrolysis by Ras probed by Fourier transform infrared spectroscopy, *J. Biol. Chem.*, 275, 8492–8500, 2000.
59. Geibel, S., Barth, A., Amslinger, S., Jung, A. H., Burzik, C., Clarke, R. J., Givens, R. S., and Fendler, K., P^3-[2-(4-hydroxyphenyl)-2-oxo]ethyl ATP for the rapid activation of the Na^+, K^+-ATPase, *Biophys. J.*, 79, 1346–1357, 2000.
60. Pirrung, M. C. and Shuey, S. W., Photoremovable-protecting groups for phosphorylation of chiral alcohols: asymmetric synthesis of phosphotriesters of (-)-3′,5′-dimethoxybenzoin, *J. Org. Chem.*, 59, 3890–3897, 1994.
61. Watanabe, S., Sueyoshi, T., Ichihara, M., Uehara, C., and Iwamura, M., Reductive ring opening of *o*-nitrobenzylidene acetals of monosaccharides: synthesis and photolysis of some photolabile sugars, *Org. Lett.*, 3, 255–257, 2001.
62. Smith, A. B., Savinov, S. N., Manjappara, U. V., and Chaiken, I. M., Peptide–small molecule hybrids via orthogonal deprotection-chemoselective conjugation to cysteine-anchored scaffolds: a model study, *Org. Lett.*, 4, 4041–4044, 2002.

63. Hasan, A., Stengele, K.-P., Giegrich, H., Cornwell, P., Isham, K. R., Sachleben, R. A., Pfleiderer, W., and Foote, R. S., Photolabile protecting groups for nucleosides: synthesis and photodeprotection rates, *Tetrahedron*, 53, 4247–4264, 1997.
64. Giegrich, H., Eisele-Buhler, S., Hermann, C., Kvasyuk, E., Charubala, R., and Pfleiderer, W., New photolabile protecting groups in nucleoside and nucleotide chemistry: synthesis, cleavage mechanisms and applications, *Nucleosides Nucleotides*, 17, 1987–1996, 1998.
65. Walbert, S., Pfleiderer, W., and Steiner, U. E., Photolabile protecting groups for nucleosides: mechanistic studies of the 2-(2-nitrophenyl)ethyl group, *Helv. Chim. Acta*, 84, 1601–1611, 2001.
66. Pirrung, M. C., Wang, L., and Montague-Smith, M. P., 3′-Nitrophenylpropyloxycarbonyl (NPPOC) protecting groups for high-fidelity automated 5′ → 3′ photochemical DNA synthesis, *Org. Lett.*, 3, 1105–1108, 2001.
67. Coleman, M. P. and Boyd, M. K., The S-pixyl group: an efficient photocleavable-protecting group for the 5′ hydroxy function of deoxyribonucleosides, *Tetrahedron Lett.*, 40, 7911–7915, 1999.
68. Lin, W. and Lawrence, D. S., A strategy for the construction of caged diols using a photolabile protecting group, *J. Org. Chem.*, 67, 2723–2726, 2002.
69. Intermolecular ion pairs have been observed in the photolysis of caged methoxycoumarin derivatives; see Reference 46.
70. Pirrung, M. C. and Bradley, J.-C., Dimethoxybenzoin carbonates: photochemically removable alcohol protecting groups suitable for phosphoramidite-based DNA synthesis, *J. Org. Chem.*, 60, 1116–1117, 1995.
71. Furuta, T., Hirayama, Y., and Iwamura, M., Anthraquinon-2-ylmethoxycarbonyl (Aqmoc): a new photochemically removable-protecting group for alcohols, *Org. Lett.*, 3, 1809–1812, 2001.
72. Loudwig, S. and Goeldner, M., *N*-methyl-*N*-(*o*-nitrophenyl)carbamates as photolabile alcohol protecting groups, *Tetrahedron Lett.*, 42, 7957–7959, 2001.
73. The carbamate cage is inert to strong non-nucleophilic bases such as LDA.
74. Pirrung, M. C., Fallon, L., Zhu, J., and Lee, Y. R. Photochemically removable silyl protecting groups, *J. Am. Chem. Soc.*, 123, 3638–3643, 2001.
75. Pirrung, M. C. and Lee, Y. R., Photochemically removable silyl protecting groups, *J. Org. Chem.*, 58, 6961–6963, 1993.
76. Bushan, K. M., Xu, H., Ruane, P. H., D'Sa, R. A., Pavlos, C. M., Smith, J. A., Celius, T. C., and Toscano, J. P., Controlled photochemical release of nitric oxide from O^2-naphthylmethyl- and O^2-naphthylallyl-substituted diazeniumdiolates, *J. Am. Chem. Soc.*, 124, 12640–12641, 2002.
77. Jones, P. B., Pollastri, M. P., and Porter, N. A., 2-Benzoylbenzoic acid: a photolabile mask for alcohols and thiols, *J. Org. Chem.*, 61, 9455–9461, 1996.
78. Based on the photoreduction mechanism proposed for benzophenone in the presence of amines, Cohen, S. G. and Chao, H. M., Photoreduction of aromatic ketones by amines: studies of quantum yields and mechanism, *J. Am. Chem. Soc.*, 90, 165–173, 1968.
79. Breitinger, H. A., Wieboldt, R., Ramesh, D., Carpenter, B., and Hess, G., Synthesis and characterization of photolabile derivatives of serotonin for chemical kinetic investigations of the serotonin 5-HT_3 receptor, *Biochemistry*, 39, 5500–5508, 2000.
80. Derkach, V., Surprenant, A., and North, R. A., 5-HT_3 receptors are membrane ion channels, *Nature*, 339, 706–709, 1989.
81. Tyers, M. B., 5-HT_3 receptors, *Ann. N.Y. Acad. Sci.*, 600, 194–205, 1990.
82. Hu, J., Zhang, J., Liu, F., Kittredge, K., Whitesell, J. K., and Fox, M. A., Competitive photochemical reactivity in a self-assembled monolayer on a colloidal gold cluster, *J. Am. Chem. Soc.*, 123, 1464–1470, 2001.
83. Stowell, M. H. B., Wang, G., Day, M. W., and Chan, S. I., Design, synthesis and photochemical properties of a photoreleasable ubiquinol-2: a novel compound for studying rapid electron-transfer kinetics in ubiquinol-oxidizing enzymes, *J. Am. Chem. Soc.*, 120, 1657–1664, 1998.
84. Cameron, J. F. and Frechet, J. M. J., Photogeneration of organic bases from *o*-nitrobenzyl derived carbamates, *J. Am. Chem. Soc.*, 113, 4303–4313, 1991.

85. Pirrung, M. C. and Huang, C.-Y., Photochemical deprotection of 3′,5′-dimethoxybenzoin (DMB) carbamates derived from secondary amines, *Tetrahedron Lett.*, 36, 5883–5884, 1995.
86. Corrie, J. E. T. and Papageorgiou, G., Synthesis and evaluation of photolabile sulfonamides as potential reagents for rapid photorelease of neuroactive amines, *J. Chem. Soc., Perkin Trans. 1,* 1583–1591, 1996.
87. Hamada, T., Nishida, A., and Yonemitsu, O., Selective removal of electron-accepting *p*-toluene and naphthalenesulfonyl protecting groups for amino function *via* photoinduced donor–acceptor ion pairs with electron donating aromatics, *J. Am. Chem. Soc.*, 108, 140–145, 1986.
88. Hamada, T., Nishida, A., and Yonemitsu, O., A new amino protecting group readily removable with near ultraviolet light as an application of electron-transfer photochemistry, *Tetrahedron Lett.*, 30, 4241–4244, 1989.

70

Photodeconjugation of Enones and Carboxylic Acid Derivatives

Olivier Piva
Centre National de la Recherche Scientifique–Université Claude Bernard Lyon I

70.1 Introduction

Photodeconjugation of carboxylic acid derivatives **1** (Scheme 1) and α,β-unsaturated carbonyl compounds (enones or alkenals **2**) is a general process that has been studied for a long time[1–3] and reviewed.[4–6] Since the first reports devoted to mechanistic studies[7–17] and the observation of photodienol species, reports on synthetic developments have appeared more recently. In this context, β,γ-unsaturated carboxylic acid derivatives represent the starting materials of choice for the synthesis of butyrolactones and other five-membered-ring frameworks of numerous natural products. Their synthesis has attracted the attention of a growing number of chemists, and photoirradiation of α,β-unsaturated carboxylic acid derivatives is nowadays a very convenient method that excludes the use of strong bases required for similar isomerizations performed in the ground state.[18] Finally, an asymmetric version has also been successfully designed, in particular from α,β-unsaturated esters under either enantioselective or diastereoselective approaches, and has been applied to the synthesis of natural products.

70.2 Photophysical Properties of Enones and α,β-Unsaturated Carboxylic Derivatives

Enones and α,β-unsaturated acid derivatives possess two absorption bands in the ultraviolet (UV) spectrum corresponding to n,π^* and π,π^* transitions. For enones, two distinct absorptions can be observed: typically a very strong band around 210 to 240 nm, corresponding to the π,π^* absorption, and a weaker band at 300 to 320 nm, corresponding to the n,π^* transition. For acid derivatives (esters and lactones), a very strong band has been attributed to the π,π^* absorption, which usually masks the n,π^* absorption band.

0-8493-1348-1/04/$0.00+$1.50

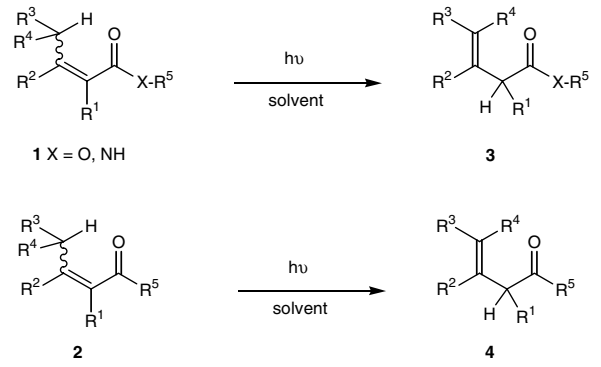

SCHEME 1

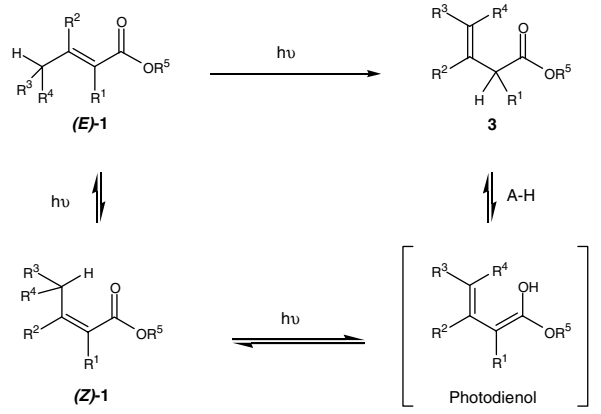

SCHEME 2

70.3 General Mechanism of Deconjugation

Under irradiation, aliphatic and medium ring size enones or acid derivatives undergo a rapid *E/Z* isomerization of the CC double bond leading to a photostationary mixture of geometric isomers. This process can be performed in the presence of triplet sensitizers such as acetone. With longer irradiation times, new compounds have appeared that have been identified as β,γ-unsaturated isomers. The position of the maximum absorption of these new structures is typically at a shorter wavelength compared to the starting molecules; therefore, the reaction can be carried out to complete conversion without significant chemical alteration. The representative mechanism of deconjugation is depicted for esters (X = O) in Scheme 2.

The formation of deconjugated isomers **3** results from a two-step procedure starting from the unsaturated isomer (*Z*)-**1**. This isomer is the only one capable, for steric reasons, of undergoing a concerted and antarafacial [1,5]-sigmatropic hydrogen migration following the Woodward–Hoffman rules. This affords a photodienol intermediate, via the singlet-excited state. The six-membered cyclic transition state imposes, at least for low conversions, a unique stereochemistry to the newly formed 1,2-double bond. This photodienol can finally revert to the starting material according to a thermal suprafacial [1,5]-sigmatropic migration or can furnish after tautomerism the β,γ-unsaturated isomer. The process has been applied to a wide range of α,β-unsaturated substrates such as aliphatic enones **2a**,[19–34] medium ring size unsaturated ketones **2c–d**,[35–37] alkenals **2b**,[38–40] conjugated esters **1a**,[7,9–15,41–49] alkylidene lactones **1b**,[51–52] and acids **1c** [1,10,53–54] (Scheme 3).

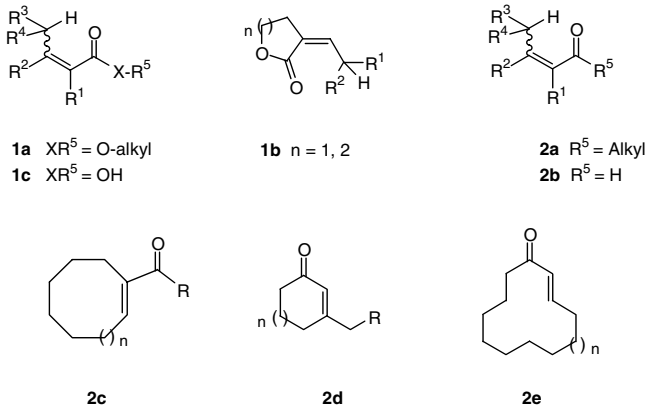

SCHEME 3

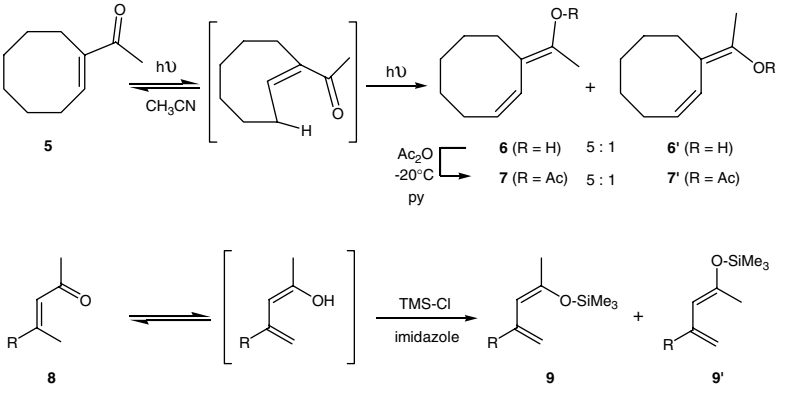

SCHEME 4

Evidence of a dienolic intermediate has been confirmed by infrared (IR) spectroscopy during the irradiation of acetyl cyclooctene in acetonitrile.[55,56] Irradiation of crotonal in the gas phase (either at 254 and 313 nm) also allows the detection of a dienol intermediate.[39] Nuclear magnetic resonance (NMR) spectroscopy can also be a useful method to characterize these species formed from acetyl cyclooctene[55] or also from mesityl oxide.[57–58] Similarly, UV spectroscopy can also be of interest for this purpose.[58]

Moreover, dienols derived from enones have been trapped by acetic anhydride as enol acetates **7**[55] or as dienol silyl ethers **9**[59] (Scheme 4). Noteworthy, a careful NMR study shows the unique stereochemistry of C1C2 double bond, at least for low conversion, which confirms that a cyclic transition state is involved. At higher conversion, the *E*-siloxydiene **9′** can finally be detected, resulting from a triplet-sensitized isomerization of the CC double bond.

Lifetimes of dienols depend strongly on their substitution pattern. For enones, this value has been estimated to be in the order of 1 s at room temperature.[5] Usually, the lifetime is longer for enones than for those obtained from carboxylic acid derivatives.

The formation of β,γ-unsaturated isomers from photodienols is also strongly dependent on the nature of the solvent and/or the presence of additives, which could catalyze the phototropic step. By using nonpolar solvents, such as methylene chloride or hexane, irradiation is usually unsuccessful. By contrast, introduction to the medium of a small amount of an acid[60–61] or a base such as imidazole and dimethylimidazole[45–46,48] or diethylamine[62] greatly enhances the rate of the reaction and also the yields

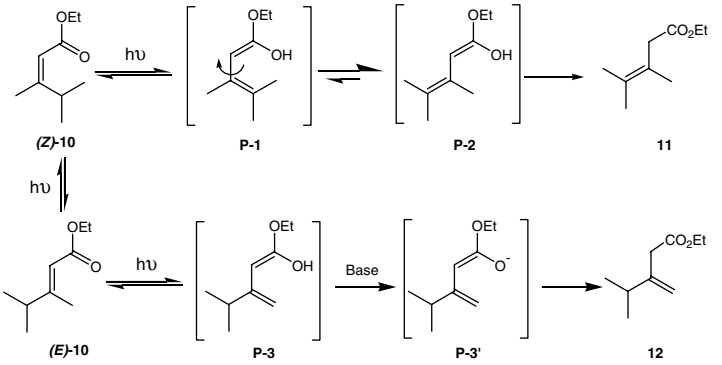

SCHEME 5

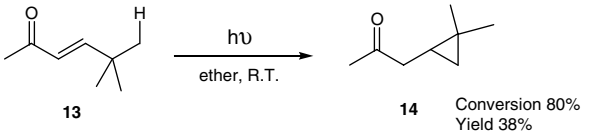

SCHEME 6

of products. In polar solvents such as methanol, the reaction is also efficient; however, exchange of the dienolic proton can occur and can affect the rate of the process. For example, when O-deuterated methanol is used, irradiation of substrates yields products with incorporation of deuterium at the α or γ-position, while the starting material was only partly deuterated at the γ position.[12,21,25]

Obviously, the reaction of deconjugation is also highly sensitive to the substitution of the substrates, especially on the γ-position. With substrates without substituents at this site, the reaction is not synthetically efficient, and starting materials are recovered almost quantitatively even after prolonged irradiation.[23]

If different alkyl substituents are present on the γ-position, two regioisomers are usually obtained after irradiation. The regioselectivity depends strongly on the presence of additives which could favor the re-ketonization of one of the two dienol species.[45–46] Thus, in methanol, irradiation of ester **10** gives predominantly deconjugated ester **11** via the formation of photodienol that can exist in two conformations **P-1** and **P-2**. The latter is far less favorable for a reverse thermal [1,5]-hydrogen shift and can rapidly undergo re-ketonization to **11**. In contrast, when the reaction is performed in the presence of *N*-methylimidazole, the regioselectivity is totally reversed, and compound **12** is isolated in good yield. The base can interact with the less hindered photoenol **P-3** to afford the dienolate **P-3′**, thus preventing the much easier reverse [1,5]-hydrogen shift (Scheme 5).

With substrates (esters or ketones) without hydrogen on the γ-position, the expected isomerization is not possible, and a rearrangement can take place to give cyclopropane derivatives (Scheme 6).[12,20]

Another limitation for the deconjugation process is linked to the size of the cycloalkenones and 1-acylcycloalkenes.[63] For example, unsubstituted 2-cyclopentenone ($n = 1$) and 2-cyclohexenone ($n = 2$) affords cyclobutane dimers or rearranged products on irradiation. The homologous substrates ($n = 3$, 4) undergo isomerization to the highly strained *trans*-2-cycloheptenone and cyclooctanone (Scheme 7).

With 3-alkyl-2-cyclohexenones[64–67] and related fused ring systems,[68–79] the irradiation affords deconjugated compounds only when the reaction is performed in the presence of small amounts of a weak acid like acetic acid. This occurs irrespective of the solvent. The course of the process is depicted in Scheme 8. The isomerization is not a concerted process but occurs by a fast protonation of the highly

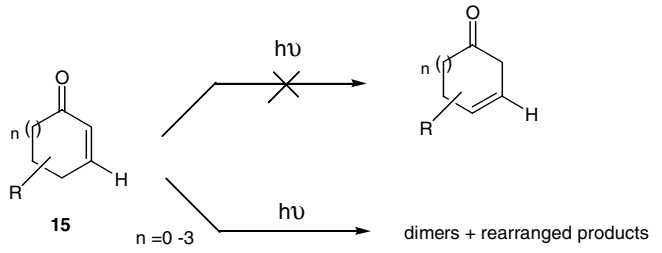

15

SCHEME 7

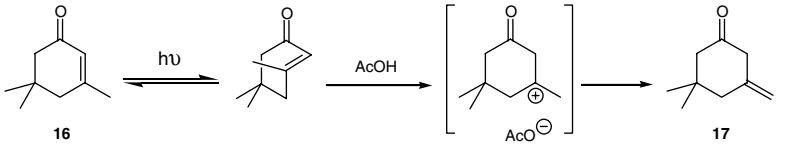

16 **17**

SCHEME 8

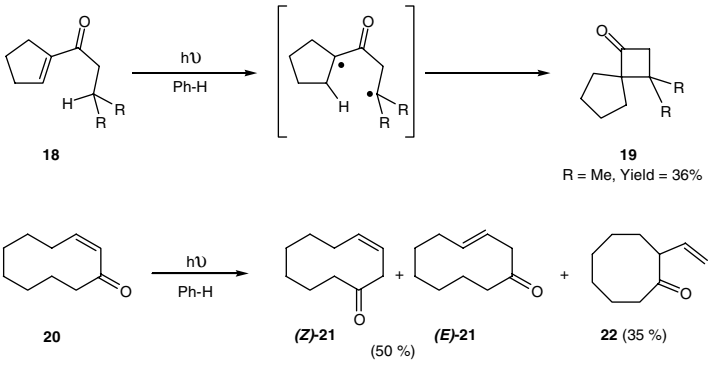

18 **19**
R = Me, Yield = 36%

20 ***(Z)*-21** ***(E)*-21** **22** (35 %)

SCHEME 9

strained twisted enone in the triplet excited state.[80–84] The tertiary carbocation can then eliminate a proton to reform the starting enone or to yield the deconjugated isomer **17**.[67]

Instead of the deconjugated product, acetylcyclopentenes lead, under photochemical activation, to spiranic ketones.[85] In this case, the γ-abstraction is not effective for steric reasons. Instead, a competitive intramolecular hydrogen abstraction gives a new biradical, which collapses to the spiranic cyclobutanone **19** (Scheme 9). With larger membered ring alkenones, the isomerization proceeds like the acyclic substrates.[35–37,86] Interestingly, when the reaction is carried out for a longer time, a rearrangement of the deconjugated isomers by α-cleavage can be observed.[36] Thus starting from (*Z*)-2-cyclodecenone **20**, *E* and *Z* isomers **21** are isolated in 50% yield along with 2-vinylcyclooctane **22** in moderate yield (Scheme 9).

The reaction can also be carried out in conjugated dienoic acids and esters or dienones. For example, after irradiation in ether, sorbic acid leads to 3,4-hexadienoic acid.[60] The process is much more efficient if the reaction is performed in the presence of formic acid (Scheme 10). Similar substrates have been irradiated in the presence of hindered amines such as tetramethylpiperidine or Bronsted acids to give, quantitatively, the corresponding allenic derivatives **24**.[87]

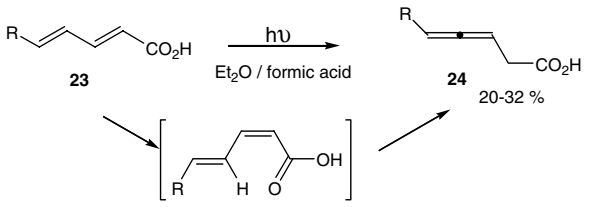

SCHEME 10

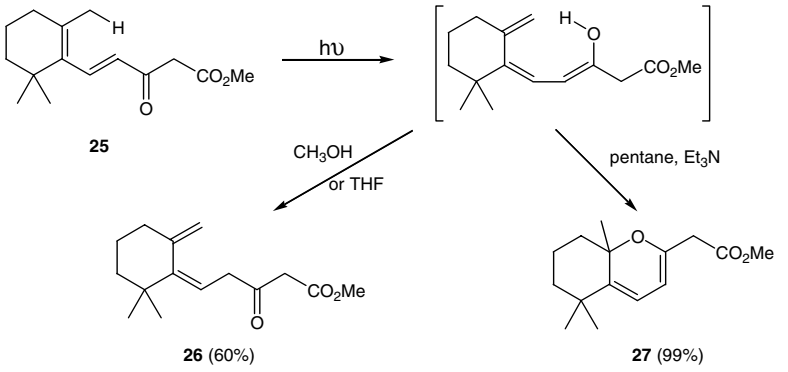

SCHEME 11

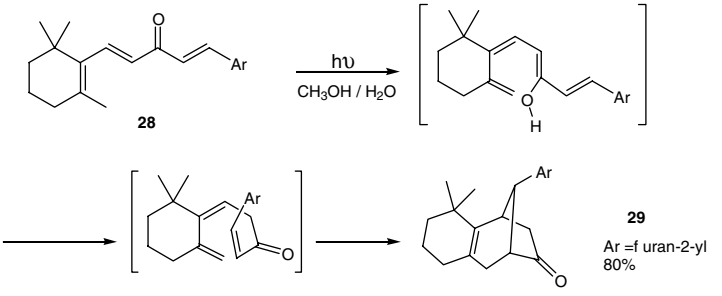

SCHEME 12

With nonlinear substrates such as β-ketoester **25**, the deconjugation can take place according to a [1,7]-hydrogen shift and formation of a putative phototrienol. Depending on the nature of the medium, this intermediate gives the 3-keto-5,6,7,8-dienoate **26** in methanol or a pyran derivative **27** by thermal cyclization initiated by the presence of a tertiary amine[88–89] (Scheme 11). α- and β-ionones derivatives and α-damascone have been converted advantageously by irradiation in acetonitrile into the deconjugated isomers.[3,90–94] With more functionalized substrates such as **28**, the deconjugation[95] performed in aqueous methanol can also be combined with a Diels–Alder reaction to yield tricyclic adducts **29** (Scheme 12).

70.4 Synthetic Applications

The photodeconjugation process has been successfully applied to the synthesis of various natural or bioactive compounds.[96–104] In only a few steps, the aggregation pheromone of San Jose scale (**28**, a pest in North American orchards) has been prepared. This reaction also yields regio- and stereoisomers[99]

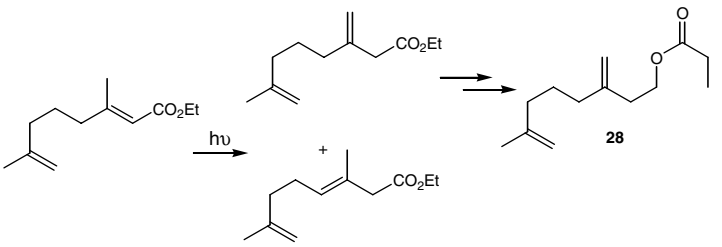

SCHEME 13

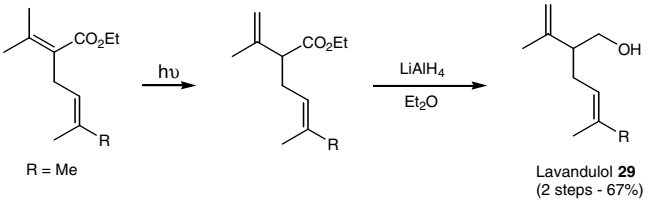

SCHEME 14

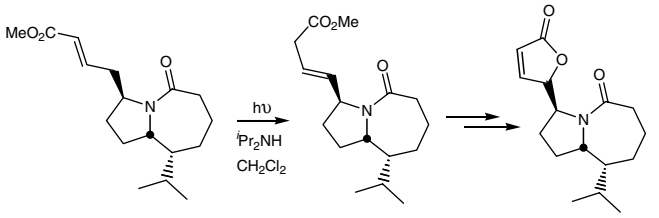

SCHEME 15

(Scheme 13). Recently, a similar process was used to prepare *rac*-lavandulol **29**[101] (Scheme 14) and also to confirm the structure of bisanhydrofarnesol (named also peplusol), a terpene isolated from *Euphorbia* sp.[102]

As already pointed out in the introduction, β,γ-unsaturated esters are suitable substrates to prepare related butyrolactones. For example, irradiation of ethyl esters followed by treatment with TMS-I allows a short access to this class of compounds.[62] Hydroxybutyrolactones can also be synthesized by osmylation of deconjugated esters. This strategy has been developed to prepare α-fluorobutyrolactones[103] or to achieve a synthetic approach to *Stemona* alkaloids[104] (Scheme 15).

70.5 Asymmetric Photodeconjugation

Principle

When the starting ester is substituted by a R^2 group different from a hydrogen atom, the photodienol produced can be considered as a prochiral species. The selective protonation[105] of one of the two *Si* or *Re* faces can then be expected under appropriate conditions to furnish a mixture enriched in one of the two stereoisomers. Two approaches toward this goal have been considered for esters, as depicted on Scheme 16:

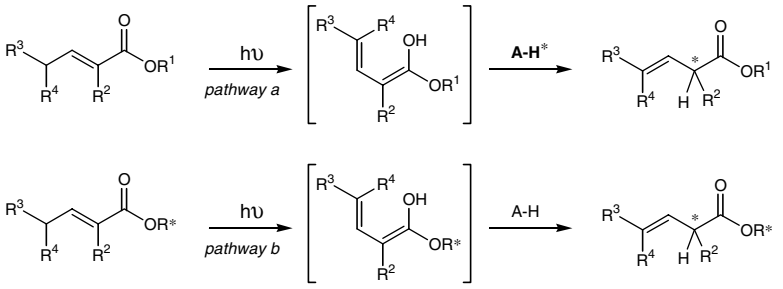

SCHEME 16

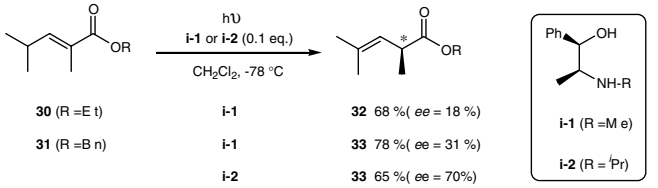

SCHEME 17

- Enantioselective protonation of the prochiral photodienol performed by use of an external chiral source of protons AH* (pathway a)
- A diastereoselective reaction for which the asymmetric information is already present on the substrate (e.g., R*O) and which can direct the formation of the new CH bond during the protonation step (pathway b)

Enantioselective Photodeconjugation of α,β-Unsaturated Esters and Lactones

The primary results in this field have been obtained starting from achiral ethyl and benzyl unsaturated esters **30** and **31**. When irradiation of these substrates is performed at low temperature in the presence of (–)-ephedrine **i-1**, a common amino-alcohol, the deconjugated isomers **32** and **33** are isolated in good yields and with enantioselectivities up to 31% (Scheme 17).[106–109] These selectivities, although low, have demonstrated the potential of this strategy. Furthermore, only catalytic amounts (10%) of the protonating agent AH* are sufficient to deliver the highest value of enantioselectivity for a given inductor. A general study of the enantioselective reaction has been undertaken first to improve the selectivities but also to try to understand the recognition step. The nature of the solvent, the effect of the temperature and the substitution of the amino-alcohol on the efficiency of the process have been investigated in detail.[110–111] The nature of the solvent is crucial. When the irradiation of ester **31** (R = benzyl) is performed in the presence of ephedrine and in a solvent with donor groups (Et_2O or CH_3CN), the selectivities are either considerably reduced or nil, probably due to competition in the protonation step between the chiral inductor, present only in catalytic amounts (0.1 equivalent) and the solvent itself which can also promote the ketoenolization step without chiral induction. Thus, the media of choice for asymmetric photodeconjugation are alkanes (*n*-pentane, *n*-hexane), arenes (benzene, toluene), or chlorinated solvents (CH_2Cl_2). As with many procedures, the temperature effect is also of considerable interest. While the enantiomeric excess (EE) for **33** reaches only less than 10% at 25°C, a decrease in the temperature to –40°C results in an increase in the enantioselectivities of up to 37%.

Photodeconjugations of **31** performed in the presence of a chiral alcohol or a chiral amine or a 1:1 mixture of both these protonating agents in methylene chloride are successful but afford the isomer **33**

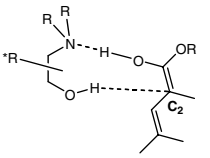

SCHEME 18

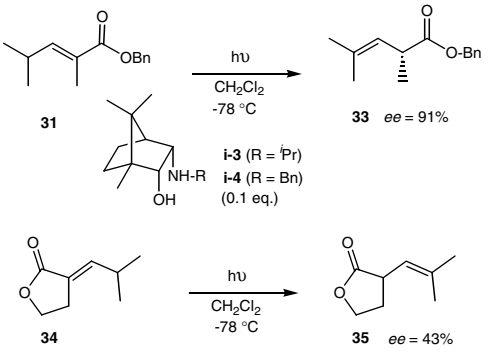

SCHEME 19

in miserable EE, in comparison with the previous result obtained with ephedrine. The hypothesis in which both the amino and the hydroxy groups are essential for a convenient level of induction has been assumed and a very simple model has been designed (Scheme 18). The amino group is considered to abstract the most acidic hydrogen atom (in other words, the hydrogen of the OH group of the photodienolic intermediate), whereas the hydroxy group of the amino-alcohol allows the protonation of carbon C2. In order to improve the selectivities, new aminoalcohols have been synthesized. Among them, the *N*-isopropylephedrine derivative **i-2** furnishes **33** with EEs up to 70% (Scheme 17).[112]

According to the hypothesis on the synergism of both hydroxy and amino group for the enantioselective protonation, the use of more rigid cyclic aminoalcohols has been also investigated. Results observed with endo,endo-aminobornanols **i-3** and **i-4** are really impressive for **33** with EEs up to 91%[113] (Scheme 19). Using these aminoalcohols as chiral protonating agents, the enantioselective photodeconjugation of other substrates has been undertaken (e.g., enones[114] and α-alkylidene lactones[113]). In these cases, the selectivities are much lower: 52 and 43%, respectively.

Diastereoselective Photodeconjugations

While the concept of enantioselective photodeconjugation is of great interest, the process is efficient in relatively few cases and cannot be applied to the total synthesis of natural products. The diastereoselective reaction has been also examined in parallel to the enantioselective one. High levels of induction (up to 88%) were first achieved using Helmchen's derivatives as chiral alkoxy moieties (Scheme 20, entry a);[115,116] unfortunately, these chiral alcohols are expensive or require numerous steps to be prepared.

Two other less expensive and commercially available compounds were then considered for this diastereoselective process. L-Lactic acid and its ethyl ester have been successfully tested, giving diastereoselective excesses of up to 86% at room temperature (Scheme 20, entries b and c).[117] Sugars also represent a valuable source of chiral inductors. Among them, D-glucose, one of the most abundant carbohydrates, has been chosen. Its diacetonide derivative (DAG) has been attached to various α,β-unsaturated acid chains, and irradiation of the corresponding esters has been performed in the presence of different protonating agents. The most efficient is *N*,*N*-dimethylaminoethanol **38**, introduced in stoichiometric

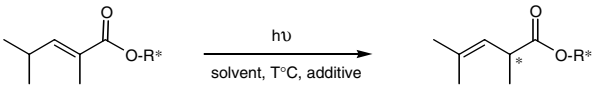

36 **37**

Entry	R*-OH	solvent	additive	T°C	*de*	Config.
a	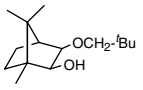	hexane	$^{i}Pr_2NH$	-40 °C	88%	(*R*)
b	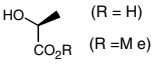 (R = H)	^{t}Butanol	-	20 °C	86%	(*S*)
c	(R =M e)				68%	(*S*)
d	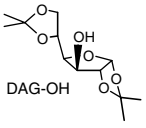	n-hexane	 **38**	-50 °C	96%	(*R*)
e	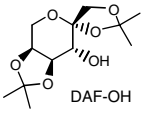	n-hexane	 **38**	-40 °C	95%	(*S*)
f		CH_2Cl_2	 **38**	-40 °C	88%	(*R*)

SCHEME 20

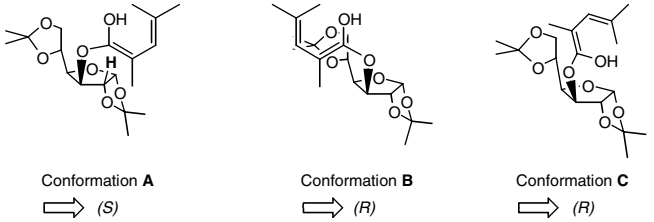

SCHEME 21

or in catalytic amounts. At low temperature (–50°C), selectivities higher than 97% have been obtained regardless of the nature of R^1 or R^2 (Scheme 20, entry d).[118]

An empirical model to link the shape of the chiral moiety to the configuration of the new chiral center (on C2) has been proposed. The 5,6-isopropylidene group of the sugar moiety could have a shielding effect towards the approach of the bidentate protonating agent (Scheme 21). In conformation **A,** leading to the minor diastereoisomer, steric hindrance could occur between the hydrogen on C2 of the sugar and the α-substituent of the dienol. In contrast, no interactions between the acid chain and the rest of the sugar group are present in conformation **B**. Furthermore, a hydrogen bond between the hydrogen of the dienol and one oxygen of the sugar moiety could stabilize and even block this conformation. Due to the shielding effect of the 5,6-isopropylidene group, the bidentate molecule **38** could protonate the less hindered face, giving selectively the deconjugated ester with the (R)-configuration. Conformation **C**, recently proposed, can be of equal importance.[119]

This effect was demonstrated by considering the irradiation of an epimeric ester bearing the diacetonide allo-furanose group.[120] In this case, the selectivity decreased to 52%, which can be attributed to the absence of the shielding effect described above.

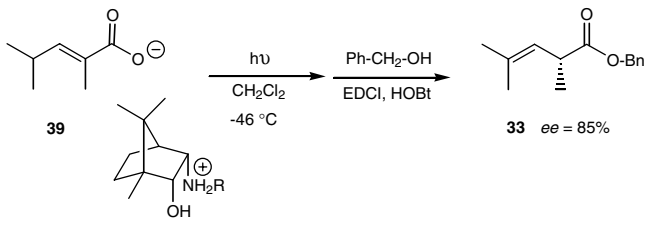

39 **33** *ee* = 85%

SCHEME 22

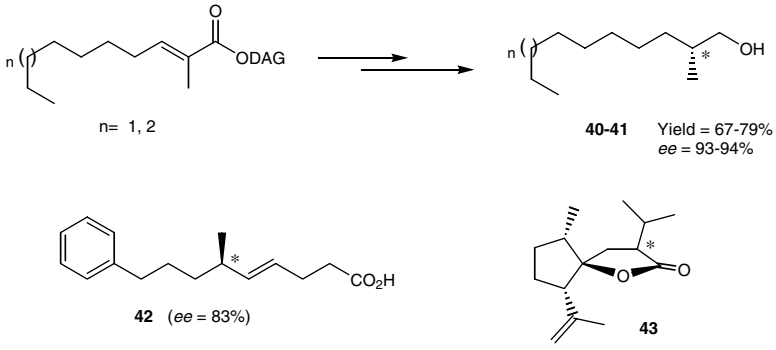

n= 1, 2 **40-41** Yield = 67-79%, *ee* = 93-94%

42 (*ee* = 83%) **43**

SCHEME 23

A major drawback of the use of the chiral pool in asymmetric synthesis is the difficulty and the cost of having to handle the chiral auxiliary in both enantiomeric forms. By this method, the configuration of the new chiral center created during the process could be controlled and chosen, but L-glucose is not readily available; therefore, a search for new chiral entities has been carried out. For example, diacetone L-fructopyranose, prepared in few steps from L-sorbose, can be advantageously used for this purpose, and selectivities are of the same level (Scheme 20, entry e) as those measured with DAG derivatives.[119] Similarly, (R)-pantolactone, which possesses only one stereogenic center, has been attached to various unsaturated acid chains according to two different activation procedures: DCC activation delivers the expected substrates with the same configuration, while the enantiomer can be prepared by condensation under Mitsunobu conditions. Irradiation affords in this case selectivities up to 88% (Scheme 20, entry f).[121]

Finally, it should be pointed out that enantiopure ammonium ene carboxylates derived from aminobornanol **i-4** have been subjected to irradiation in dichloromethane to furnish, after acidification and esterification, the deconjugated ester **33** with EEs up to 85%.[122] Obviously, in that case, aminobornanol **i-4** was used in stoichiometric amounts (Scheme 22).

70.6 Recent Applications to the Synthesis of Natural Products

Finally, this new asymmetric reaction (and more particularly the diastereoselective version) has been applied to the synthesis of natural products. First, rapid access to 2-methyldecanol and undecanol **40** and **41**, two insect pheromones, has been performed. The β,γ-unsaturated esters have been hydrogenated over catalytic amounts of PtO_2 and then reduced without epimerization to the chiral 2-methylalkanols.[123] According to a similar approach, the side chain of Zaragozic acid C **42** has been prepared in high EE,[124] while access to curcumanolide A **43** and its analogs has been developed (Scheme 23).[125]

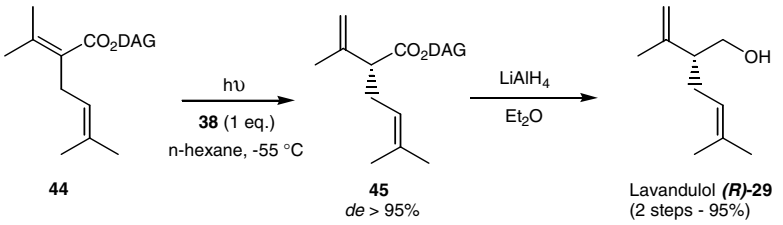

SCHEME 24

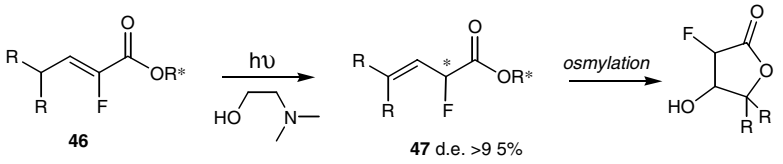

SCHEME 25

The diastereoselective synthesis of (R)-(–)-lavandulol **29**, a constituent of lavender oil, has been also accomplished.[101] The crucial step is the photoisomerization of **44** to **45** that allows both the creation of the chiral center and the generation of the double bond in the required position (Scheme 24).

Because the synthesis of chiral fluoro compounds is of great interest, due to their biological properties, the asymmetric photodeconjugation of α-fluoro-α,β-unsaturated esters **46** has been explored.[126] Despite the high acidity of the hydrogen on the C2 atom, the diastereoselective isomerization to the β,γ-unsaturated isomers is effective with levels of induction for **47** similar to those for non-fluorinated substrates (Scheme 25).

In conclusion, photodeconjugation of enones or carboxylic acid derivatives is a mild process by which to prepare β,γ-unsaturated carbonyl and carboxylic derivatives in good yields. These substrates represent interesting frameworks useful for the synthesis of natural products. The asymmetric version of the process also allows the formation of new chiral centers under very mild conditions and with high selectivities.

References

1. Lutz, R. E., Bailey, P. S., Dien, C. K., and Rinker, J. W., The *cis*- and *trans*-β-aroyl-α- and β-methylacrylic acids and β-aroyl-α-methylenepropionic acids, *J. Am. Chem. Soc.*, 75, 5039, 1953.
2. Levina, R. Y., Kostin, V. N., and Gembitskii, P. A., Photochemical isomerization of vinylketones into allylketones, *Zhur. Obshch. Khim.*, 29, 2456, 1959.
3. Mousseron-Canet, M., Mousseron, M., and Legendre, P., Isomérisation photochimique dans la série de l'α-ionone, *Bull. Soc. Chim. Fr.*, 1509, 1961.
4. Sammes, P. G., Photoenolization, *Tetrahedron*, 32, 405, 1976.
5. Weedon, A. C., Photochemical reactions involving enols, in *The Chemistry of Enols*, Rappoport, Z., Ed., John Wiley & Sons, New York, 1990, chap. 9.
6. Pete, J. P., Photodeconjugation of unsaturated enones and acid derivatives, in *CRC Handbook of Photochemistry and Photobiology*, Horspool, W. M. and Song, P.-S., Eds., CRC Press, Boca Raton, 1994, chap. 49.
7. Jorgenson, M. J., Photochemical hydrogen abstraction in unsaturated esters. *J. Chem. Soc., Chem. Commun.*, 137, 1965.
8. Kropp, P. J. and Krauss, H. J., Photochemistry of cycloalkenes. IV. Comparison with crotonic acid, *J. Org. Chem.*, 32, 3222, 1967.

9. Rando, R. R. and Doering, W. E., β,γ-Unsaturated acids and esters by photochemical isomerization of α,β-congeners, *J. Org. Chem.*, 33, 1671, 1968.
10. Jorgenson, M. J. and Gundel, L., On the mechanism of the photochemical reaction of conjugated esters: the importance of geometrically isomeric excited states, *Tetrahedron Lett.*, 4991, 1968.
11. Barltrop, J. A. and Wills, J., The mechanism of the photoisomerisation of α,β-unsaturated esters, *Tetrahedron Lett.*, 32, 4987, 1968.
12. Jorgenson, M. J., A large deuterium solvent isotope effect on a photochemical reaction, *J. Am. Chem. Soc.*, 91, 198, 1969.
13. Jorgenson, M. J., Photochemistry of α,β-unsaturated esters. VII. The photolytic behavior of vinylcyclopropanecarboxylates, *J. Am. Chem. Soc.*, 91, 6432, 1969.
14. Jorgenson, M. J. and Patumtevapibal, S., Ring size and conformational effects on photodeconjugation of cycloalkylidene esters, *Tetrahedron Lett.*, 489, 1970.
15. Rhoads, S. J., Chattopadhyay, J. K., and Waali, E., Double bond isomerizations in unsaturated esters and enol ethers. I. Equilibrium studies in cyclic and acyclic systems, *J. Org. Chem.*, 35, 3352, 1970.
16. Borrell, P. and Holmes, J. D., Photochemical *cis-trans* isomerization of 2-carbomethoxy-2-butene, *J. Photochem.*, 1, 433, 1972/73.
17. Morrison, H. and Rodriguez, O., Organic photochemistry. XXIX. *Z-E* photoisomerization of 3-methyl-3-penten-2-one: evidence for non-radiative decay, *J. Photochem.*, 3, 471, 1974/75.
18. Kende, A. S. and Toder, B. H., Stereochemistry of deconjugative alkylation of ester dienolates: stereospecific total synthesis of the litsenolides, *J. Org. Chem.*, 47, 167, 1982.
19. Crandall, J. K. and Mayer, C. F., Photochemistry of some carbonyl conjugated 1,5-hexadienes, *J. Org. Chem.*, 35, 3049, 1970.
20. Jorgenson, M. J. and Yang, N. C., A novel photochemical reaction: conversion of α,β-unsaturated ketones to acetonylcyclopropanes, *J. Am. Chem. Soc.*, 85, 1698, 1963.
21. Yang, N. C. and Jorgenson, M. J., Photochemical isomerization of simple α,β-unsaturated ketones, *Tetrahedron Lett.*, 1203, 1964.
22. Schneider, R. A. and Meinwald, J., Photochemical reaction of α,β-unsaturated carbonyl compounds with olefins, *J. Am. Chem. Soc.*, 89, 2023, 1967.
23. Bonnet, F. and Lemaire, J., Transitions non radiatives de l'oxyde de mésityle, *Bull. Soc. Chim. Fr.*, 1973, 1185.
24. Cookson, R. C. and Rogers, N. R., Photochemistry of 2-(cycloalk-1-enyl) cycloalkanones: new photochemical reaction of β,γ-unsaturated ketones, *J. Chem. Soc., Perkin Trans. 1*, 1037, 1974.
25. Tada, K. and Miura, K., The photo-enolization of β-disubstituted α,β-unsaturated ketones, *Bull. Soc. Chim. Jpn.*, 49, 713, 1976.
26. Deflandre, A., Lheureux, A., Rioual, A., and Lemaire, J., Comportement photochimique de cétones α,β-insaturées sous excitation directe, *Can. J. Chem.*, 54, 2127, 1976.
27. Arnould, J. C., Enger, A., Feigenbaum, A., and Pete, J. P., Photolyse de cétones conjuguées hétérosubstituées linéaires, *Tetrahedron*, 35, 2501, 1979.
28. Wan, C. S. K. and Weedon, A. C., The photochemical enolization of an aliphatic α,β-unsaturated ketone, *J. Chem. Soc., Chem. Commun.*, 1235, 1981.
29. Crowley, K. J., Schneider, R. A., and Meinwald, J., Photoisomerization of phorone, *J. Chem. Soc. C*, 571, 1966.
30. Friedrich, L. E. and Schuster, G. B., Irradiation of α,β-unsaturated ketones: search for intermediate oxabicyclobutanes, *J. Am. Chem., Soc.*, 94, 1193, 1972.
31. Kawai, M. and Naya, K., Photochemistry of fukinone and pulegone, *Chem. Lett.*, 389, 1972.
32. Henderson, Jr., W. A. and Ullman, E. F., Photochemistry of 2-benzyl- and 2-benzhydryl-3-benzoylchromones, *J. Am. Chem. Soc.,* 87, 5424, 1965.
33. Eng, S. L., Ricard, R., Wan, C. S. K., and Weedon, A. C., Photochemical deconjugation of α,β-unsaturated ketones, *J. Chem. Soc., Chem. Commun.*, 236, 1983.
34. (a) Ricard, R., Sauvage, P., Wan, C. S. K., Weedon, A. C., and Wong, D. F., Photochemical enolization of β-alkyl-α,β-unsaturated ketones, *J. Org. Chem.*, 51, 62, 1986; (b) Duhaime, R. M. and Weedon,

A. C., Direct measurement of the rates of reketonization of dienolates produced by photochemical enolization of β-alkyl α,β-unsaturated ketones in aqueous basic solution, *J. Am. Chem. Soc.*, 109, 2479, 1987.

35. Nozaki, H., Mori, T., and Noyori, R., Preparation and photochemical isomerization of 2-cyclodecenones, *Tetrahedron*, 22, 1207, 1966.
36. Carlson, R. G. and Bateman, J. H., The photochemical rearrangement of *cis*-2-cyclodecenone, *Tetrahedron Lett.*, 4151, 1967.
37. Marchesini, A., Pagani, G., and Pagnoni, U. M., The stereochemical fate of the biradical intermediate in the photolysis of cyclododecen-2-one, *Tetrahedron Lett.*, 1041, 1973.
38. McDowell, C. A. and Sifniades, S., Isomerization as a primary process in the photolysis of crotonaldehyde, *J. Am. Chem. Soc.*, 84, 4606, 1962.
39. Coomber, J. W. and Pitts, Jr., J. N., Molecular structure and photochemical reactivity. XIV. The vapor phase photochemistry of *trans*-crotonaldehyde, *J. Am. Chem. Soc.*, 91, 4955, 1969.
40. Hatanaka, A. and Ohgi, T., Leaf alcohol. XIX. Photochemical isomerization of leaf aldehyde, *Agric. Biol. Chem.*, 36, 1263, 1972.
41. Sundberg, R. J., Lin, L. S., and Smith, F. X., Photochemical deconjugation as a synthetic route to 1,2,3,6-tetrahydropyridine-4-acetic acid esters from $\Delta^{4,\alpha}$-piperidine-4-acetic acid esters, *J. Org. Chem.*, 38, 2558, 1973.
42. Majeti, S. and Gibson, T. W., Photochemistry of esters: contrast in reactivity between acyclic and cyclic conjugated esters, *Tetrahedron Lett.*, 4889, 1973.
43. Gibson, T. W., Majeti, S., and Barnett, B. L., Photochemistry of esters. II. Effects of ring size on the photochemical behavior of α,β-unsaturated esters, *Tetrahedron Lett.*, 4801, 1976.
44. Leitich, J., Partale, H., and Polansky, O. E., Über die Photochemie cyclischer Acylale von Alkyliden-, Alkenyliden- und Benzylidenmalonsaüren, *Chem. Ber.*, 112, 3293, 1979.
45. Skinner, I. A. and Weedon, A. C., Photoenolization of α,β-unsaturated esters; effect of base upon product distribution and reaction rate in photochemical deconjugation, *Tetrahedron Lett.*, 4299, 1983.
46. Weedon, A. C., Base catalysis as an alternative explanation for an apparent deuterium solvent isotope effect in the photochemical reactions of α,β-unsaturated esters. *Can. J. Chem.*, 62, 1933, 1984.
47. Duhaime, R., Lombardo, D., Skinner, I. A., and Weedon, A. C., Conversion of α,β-unsaturated esters to their β,γ-unsaturated isomers by photochemical deconjugation, *J. Org. Chem.,* 50, 873, 1985.
48. Freeman, P. K. and Siggel, L., The kinetics of photochemical deconjugation reactions of methyl geranate, *Tetrahedron*, 44, 5065, 1988.
49. Buchi, G. and Feairheller, S. H., Photochemical reactions. XIV. Additions to ethyl propiolate, *J. Org. Chem.*, 34, 609, 1969.
50. Geraghty, N. W. A. and Hannan, J. J., Functionalisation of cycloalkanes: the photomediated reaction of cycloalkanes with alkynes, *Tetrahedron Lett.*, 42, 3211, 2001.
51. Ohga, K. and Matsuo, T., A study on the photochemistry of α,β-unsaturated γ-lactones. II. Photoisomerization of 3-ethylidene-4,5-dihydro-2(3H)-furanone, *Bull. Soc. Chim. Jpn.*, 46, 2181, 1973.
52. Henin, F., Mortezaei, R., and Pete, J. P., A convenient synthesis of α-vinyllactones: the photodeconjugation of α,β-unsaturated γ or δ-lactones, *Synthesis*, 1019, 1983.
53. Itoh, M., Tokuda, M., Hataya, M., and Suzuki, A., Photochemical reaction of α,β-unsaturated acids and esters, *Hokkaido Daigaku Kogakubu Kenkyu Kokoku*, 60, 37, 1971.
54. Biot, J. M., de Keukeleire, D., and Verzele, M., Photoisomerization in α,β-unsaturated carboxylic acids, *Bull. Soc. Chim. Belg.*, 86, 973, 1977.
55. Noyori, R., Inoue, H., and Kato, M., Photolysis of 1-acetylcyclooctene: direct observation of dienol intermediate in photochemical deconjugation of α,β-unsaturated ketone, *J. Am. Chem. Soc.,* 92, 6699, 1970.

56. Noyori, R., Inoue, H., and Kato, M., Direct observation of dienol intermediates in photochemical deconjugation of an α,β-unsaturated ketone: photoisomerization of 1-acetylcyclooctene, *Bull. Soc. Chem. Jpn*, 49, 3673, 1976.
57. Duhaime, R. M. and Weedon, A. C., Direct observation of a photochemically produced dienol: evidence for a non-catalyzed reketonization pathway unavailable to simple enols, *J. Am. Chem. Soc.,* 107, 6723, 1985.
58. Duhaime, R. M. and Weedon, A. C., Direct observation of dienols produced by photochemical enolisation of α,β-unsaturated ketones: rates and activation parameters for dienol reketonisation via a 1,5-hydrogen shift, *Can. J. Chem*., 65, 1867, 1987.
59. Wan, C. S. K., Weedon, A. C., and Wong, D. F., Stereoselective and regioselective thermal and photochemical preparation of siloxy dienes, *J. Org. Chem*., 51, 3335, 1986.
60. Crowley, K. J., Photochemical formation of allenes in solution, *J. Am. Chem. Soc*., 85, 1210, 1963.
61. Lewis, F. D. and Oxman, J. D., Lewis acid enhancement of photochemical *trans-cis* isomerization of α,β-unsaturated esters*, J. Am. Chem. Soc.,* 103, 7345, 1981.
62. Piva, O., Direct conversion of β,γ-unsaturated esters into lactones induced by TMS-I, *Tetrahedron*, 50, 13687, 1994.
63. Lam, E. Y. Y., Valentine, D., and Hammond, G. S., Mechanisms of photochemical reactions in solution. XLIV. Photodimerization of cyclohexenone, *J. Am. Chem. Soc.,* 89, 3482, 1967.
64. Dauben, W. G., Shaffer, G. W., and Wietmeyer, N. D., Alkyl-substitution effects in the photochemistry of 2-cyclohexenones, *J. Org. Chem*., 33, 4061, 1968.
65. Shiloff, J. D. and Hunter, N. R., Solvent effects on the photocycloaddition and photoenolisation reactions of isophorone, *Can. J. Chem.,* 57, 3301, 1979.
66. Gioia, B., Ballabio, M., Beccali, E. M., Cecchi, R., and Marchesini, A., Photochemical behaviour of bicyclo[5.3.1]undec-1(10)-en-9-one, *J. Chem. Soc., Perkin Trans. 1*, 560, 1981.
67. Rudolph, A. and Weedon, A. C., Acid catalysis of the photochemical deconjugation reaction of 3-alkyl-2-cyclohexenones, *J. Am. Chem. Soc*., 111, 8756, 1989.
68. Wehrli, H., Wenger, R., Schaffner, K., and Jeger, O., Zur photochemischen Isomerisierung von 10α-Testosteron, *Helv. Chim. Acta*, 46, 678, 1963.
69. Furutachi, N., Wakadaira, Y., and Nakanishi, K., Photoirradiation of steroid 5-en-7-one systems and a mutual exchange of C_4 and C_6 in 3β-acetoxycholest-5-en-7-one, *J. Am. Chem. Soc*., 91, 1028, 1969.
70. Kuwata, S. and Schaffner, K., Spezifisch π→π* — induzierte Keton-Photoreraktionen: Die doppelbindungsverschiebung von *O*-Acetyl-10α-testosteron. Protonisierung der Doppelbindung seines Δ^5 Isomeren, *Helv. Chim. Acta*, 52, 173, 1969.
71. Bellus, D., Kearns, D. R., and Schaffner, K., Zur Photochemie von α,β-ungesättigten cyclischen Ketonen: Spezifische Reactionen der n,π* and π,π*-Triplettzustände von *O*-Acetyl-testosteron und 10-Methyl-$\Delta^{1,9}$-octalon-2, *Helv. Chim. Acta*, 52, 971, 1969.
72. Schuster, D. I. and Brizzolara, D. F., The mechanism of photoisomerization of cyclohexenones. 10-hydroxymethyl-$\Delta^{1,9}$-2-octalone: the question of hydrogen abstraction from benzene by ketone triplets, *J. Am. Chem. Soc*., 92, 4357, 1970.
73. Jeger, O. and Schaffner, K., On photochemical transformations of steroids, *Pure Appl. Chem*., 21, 247, 1970.
74. Gloor, J., Schaffner, K., and Jeger, O., Spezifisch π→π* — induzierte Photoisomerisierungen von 10-Dimethoxymethyl-$\Delta^{1,9}$-octal-2-one. Ein Photochemischer Zugang zu [4.4.3]-12-oxapropellan-Derivaten, *Helv. Chim. Acta*, 54, 1864, 1971.
75. Margaretha, P. and Schaffner, K., Zur Photochemie von $\Delta^{1,9}$-10-methyl-2-octalon, *Helv. Chim. Acta*, 56, 2884, 1973.
76. Gloor, J. and Schaffner, K., Spezifisch π→π* — induzierte Reactionen von γ-Dimethoxy-methyl-cyclohexen-2-onen: 1,3-Umlagerung und Wasserstoffabstraktion durch das α-Kohlenstoffatom, *Helv. Chim. Acta*, 57, 1815, 1974.

77. Nobs, F., Burger, U., and Schaffner, K., Specifically (π,π^*)-induced cyclohexenone reactions. 4a-(*Z*-1-propenyl)-bicyclo[4.4.0]dec-1-(8a)-en-2-one and 4a-(*Z*-1-propenyl bicyclo[4.4.0]deca-1 (8a) 7-dien-2-one, *Helv. Chim. Acta*, 60, 1607, 1977.
78. Williams, J. R., Mattei, P. L., Abdel-Magid, A., and Blount, J. F., Photochemistry of estr-4-en-3-ones: 17β-hydroxy-4-estren-3-one, 17β-acetoxy-4,9-estradien-3-one, 17β-hydroxy-4,9,11-estratrien-3-one and norgestrel. Photochemistry of 5α-estran-3-ones, *J. Org. Chem*., 51, 769, 1986.
79. Wintgens, V., Guérin, B., Lenholm, H., Brisson, J. R., and Scaiano, J. C., Photochemistry of the inclusion complex of (R)-$\Delta^{1,9}$-10-methyl-2-octalone with α-cyclodextrin, *J. Photochem. Photobiol. A: Chem.,* 44, 367, 1988.
80. Bonneau, R. and Fornier De Violet, P., Evidence for the strained *trans*-acetyl-1-cyclohexene and a transient species assigned to the orthogonal triplet state*, C. R. Acad. Soc. Ser. C*, 284, 631, 1977.
81. Goldfarb, T. D., Kinetic studies of transient photochemical isomers of 2-cycloheptenone, 1-acetyl-cyclohexene and 2-cyclohexenone, *J. Photochem*., 8, 39, 1978.
82. Bonneau, R., Transient species in photochemistry of enones: the orthogonal triplet state revealed by laser photolysis, *J. Am. Chem. Soc*., 102, 3816, 1980.
83. Pienta, N. J., Photoreactivity of α,β-unsaturated carbonyl compounds. 2. Fast transients from irradiation of 2-cyclohexenones and amines, *J. Am. Chem. Soc*., 106, 2704, 1984.
84. Schuster, D. I., Dum, D. A., Heibel, G. E., Brown, P. B., Rao, J. M., Woning, J., and Bonneau, R., Enone photochemistry: dynamic properties of triplet excited states of cyclic conjugated enones as revealed by transient absorption spectroscopy, *J. Am. Chem. Soc.,* 113, 6245, 1991.
85. Smith, A. B. and Agosta, W. C., Photochemical reactions of 1-cyclopentenyl and 1-cyclohexenyl ketones, *J. Am. Chem. Soc*., 95, 1961, 1973.
86. Gleiter, R., Sander, W., Irngartinger, H., and Lenz, A., A simple path to tricyclo[5.3.0.0^{2,8}]decane and its derivatives, *Tetrahedron Lett*., 23, 2647, 1982.
87. Lewis, F. D., Howard, D. K., Barancyk, S. V., and Oxman, J. D., Lewis acid catalysis of photochemical reactions 5. Selective isomerization of conjugated butenoic and dienoic esters, *J. Am. Chem. Soc.,* 108, 3016, 1986.
88. White, J. D. and Skeean, R. W., Photochemistry of enolate anions: anion-directed photochemical cyclization of a dienone, *J. Am. Chem. Soc.,* 100, 6296, 1978.
89. White, J. D., Skeean, R. W., and Trammell, G. L., Lewis acid and photochemically mediated cyclization of olefinic β-keto esters, *J. Org. Chem.,* 50, 1939, 1985.
90. De Mayo, P., Stothers, J. B., and Yip, R. W., Irradiation of β-ionone, *Can. J. Chem*., 39, 2135, 1961.
91. Van Wageningen, A. and de Boer, Th., Irradiation of *trans*-α-ionone, *Recl. Trav. Chim. Pays-Bas*, 89, 797, 1970.
92. Visser, C. P. and Cerfontain, H., Photochemistry of dienones. Part IX. Photochemistry of (*E*)- and (*Z*)-α-ionone, *Recl. Trav. Chim. Pays-Bas*, 100, 153, 1981.
93. Visser, C. P., van der Wel, H., and Cerfontain, H., Photochemistry of dienones. Part 11. Photochemistry of the pivaloyl analogues of the pivaloyl analogues of *(E)*-α and *(E)*-β-ionone, *Recl. Trav. Chim. Pays-Bas*, 102, 302, 1983.
94. Visser, C. P. and Cerfontain, H., Photochemistry of dienones. Part 12. Photochemistry of (*E*)-α and (*Z*)-α-ionone, *Recl. Trav. Chim. Pays-Bas*, 100, 307, 1983.
95. Ishar, M. P. S., Singh, R., Kumar, K., Singh, G., Velmurugan, D., Pandi, A. S., Raj, S. S. S., and Fun, H. K., Photochemistry of arylidene-β-ionones: a highly efficient route to novel tricyclic ketones through intramolecular, exoselective photochemical [4+2]-cycloadditions, occurring only in an aqueous–organic solvent, *J. Org. Chem.*, 67, 2234, 2002.
96. Hatanaka, A. and Ohgi, T., Leaf alcohol: photochemical isomerization of leaf aldehyde, *Agric. Biol. Chem.*, 36, 1263, 1972.
97. Stevens, R. V. and Pruit, J. R., On the annulation of Δ^2-tetrahydropyridines: an expeditious total synthesis of the protoberberine alkaloid karachine, *J. Chem. Soc., Chem. Commun*., 1425, 1983.
98. Ferrier, R. J. and Tyler, P. C., Synthesis and photolysis of some carbohydrate 1,6-dienes, *Carbohydr. Res.*, 136, 249, 1985.

99. Lombardo, D. A. and Weedon, A. C., Photoenolization of conjugated esters: synthesis of a San Jose scale pheromone by partially regio-controlled photochemical deconjugation, *Tetrahedron Lett.*, 27, 5555, 1986.
100. Freeman, P. K., Siggel, L., Chamberlain, P. H., and Clapp, G. E., The photochemistry of methyl geranate, a model chromophore for insect juvenile hormone analogs, *Tetrahedron*, 44, 5051, 1988.
101. Piva, O., Enantio- and diasteroselective protonation of photodienols: total synthesis of (R)-(–)-lavandulol, *J. Org. Chem.* 60, 7879, 1995.
102. Faure, S., Connolly, J. D., Fakunle, C. O., and Piva, O., Structure and synthesis of anhydrobisfarnesol from *Euphorbia lateriflora* and asymmetric synthesis of (R)-sesquilavandulol, *Tetrahedron*, 56, 9647, 2000.
103. Piva, O., A short access to α-fluoro β,γ-unsaturated esters, *Synlett*, 729, 1994.
104. Hinman, M. M. and Heathcock, C. H., A synthetic approach to the *Stemona* alkaloids, *J. Org. Chem.*, 66, 7751, 2001.
105. (a) Fehr, C., Enantioselective protonation of enolates and enols, *Angew. Chem. Int. Ed. Engl.,* 35, 2566, 1996; (b) Eames, J. and Weerasooriya, N., Recent advances into enantioselective protonation of prostereogenic enol derivatives, *Tetrahedron Asymm.*, 12, 1, 2001.
106. Mortezaei, R., Henin, F., Muzart, J., and Pete, J. P., Enantioselective photodeconjugation of α,β-unsaturated esters in the presence of catalytic amounts of a chiral-inducing entity, *Tetrahedron Lett.*, 26, 6079, 1985.
107. Mortezaei, R., Piva, O., Henin, F., Muzart, J., and Pete, J. P., Evaluation of the steric interactions responsible for the enantioselective photodeconjugation of α,β-unsaturated esters, *Tetrahedron Lett.*, 27, 2997, 1986.
108. Piva, O., Henin, F., Muzart, J., and Pete, J. P., Enantioselective photodeconjugation of α,β-unsaturated esters: effect of the nature of the chiral agent, *Tetrahedron Lett.*, 27, 3001, 1986.
109. Pete, J. P., Henin, F., Mortezaei, R., Muzart, J., and Piva, O., Enantioselective photodeconjugation of conjugated esters and lactones, *Pure Appl. Chem.*, 58, 1257, 1986.
110. Henin, F., Mortezaei, R., Pete, J. P., and Piva, O., Photodéconjugaison énantiosélective d'esters et de lactones conjuguées en présence d'éphédrine, *Tetrahedron*, 45, 6171, 1989.
111. Piva, O., Mortezaei, R., Henin, F., Muzart, J., and Pete, J. P., Highly enantioselective photodeconjugation of α,β-unsaturated esters: origin of the chiral discrimination, *J. Am. Chem. Soc.,* 112, 9263, 1990.
112. Piva, O., Henin, F., Muzart, J., and Pete, J. P., A very enantioselective photodeconjugation of α,β-unsaturated esters, *Tetrahedron Lett.*, 28, 4825, 1987.
113. Piva, O. and Pete, J. P., Highly enantioselective protonation of dienols: an unusual substituent effect on the induced chirality, *Tetrahedron Lett.*, 31, 5157, 1990.
114. Henin, F., Muzart, J., Pete, J. P., and Piva, O., Enantioselective photodeconjugation of α-substituted α,β-unsaturated ketones, *New J. Chem.*, 15, 611, 1991.
115. Mortezaei, R., Awandi, D., Henin, F., Muzart, J., and Pete, J. P., Diastereoselective photodeconjugation of α,β-unsaturated esters, *J. Am. Chem. Soc.*, 110, 4824, 1988.
116. Awandi, D., Henin, F., Muzart, J., and Pete, J. P., Reversal of diastereoselectivity in protonation of chiral photodienols, *Tetrahedron Asymm.*, 2, 1101, 1991.
117. Charlton, J. L., Pham, V. C., and Pete, J. P., Lactate as chiral auxiliary in asymmetric photodeconjugation of unsaturated esters, *Tetrahedron Lett.*, 33, 6073, 1992.
118. Piva, O. and Pete, J. P., Diacetone D-glucose: efficient chiral building block for asymmetric photodeconjugation, *Tetrahedron Asymm.*, 3, 759, 1992.
119. Bach, T. and Höfer, F., Photochemical deconjugation of chiral 3-methyl-2-butenoates derived from carbohydrate-based alcohols: the influence of the sugar backbone on the facial diastereoselectivity, *J. Org. Chem.,* 66, 3427, 2001.
120. Piva, O. unpublished results (see also Reference 119).
121. Bargiggia, F. and Piva, O., Diastereoselective photodeconjugation of chiral α,β-unsaturated esters, *Tetrahedron Asymm.*, 12, 1389, 2001.

122. Hénin, F., Létinois, S., and Muzart, J., Asymmetric photodeconjugation of ammonium ene-carboxylates: temperature effects and evidence for the α-carbon of the dienolic species as a latent trigonal centre, *Tetrahedron Asymm.*, 11, 2037, 2000.
123. Piva, O. and Caramelle, D., Asymmetric protonation of photodienols: enantioselective synthesis of (R)-2-methylalkanols, *Tetrahedron Asymm.*, 6, 831, 1995.
124. Comesse, S. and Piva, O., Diastereoselective protonation of dienols: a formal approach to zaragozic acid C side chain, *Tetrahedron Asymm.*, 10, 1061, 1999.
125. Adams, J. and Piva, O., unpublished results.
126. Bargiggia, F., Dos Santos, S., and Piva, O., Asymmetric photodeconjugation: highly stereoselective synthesis of α-fluoro carboxylic derivatives, *Synthesis*, 427, 2002.

71

[2+2]-Photocycloaddition Reactions of Cyclopentenones with Alkenes

Jean-Pierre Pete
Université de Reims Champagne Ardenne

71.1 Introduction

The photocycloaddition reaction of cyclic enones with alkenes has previously been reviewed,[1,2] especially in the preceding edition of this Handbook.[3] The multistep mechanism of the reaction was established on the basis of spectroscopic and kinetic data and from the selective intermediate trapping. However, new experiments were needed not only to extend the value of the mechanistic conclusions to a larger variety of substituted cyclopentenones but also to give a better understanding of intramolecular photocycloaddition processes. These new investigations, using the selective trapping of intermediates, have allowed determination of the relative deactivation rates for 1,4-biradical intermediates. Furthermore, a verification of the validity of the "rule of five" in intramolecular processes has been possible. Simultaneously, attempts to develop asymmetric [2+2]-photocycloadditions have been described in connection with synthetic applications. The high efficiency and high selectivity usually observed in the [2+2]-photocycloaddition of cyclopentenone derivatives with alkenes have led synthetic chemists to use this reaction for the building of complex structures and polyfunctional molecules. Thus, the purpose of this chapter is to summarize the recent findings on the chemo- or stereoselectivity of the cycloaddition process of cyclopentenones and related systems (furanones, maleic anhydrides, and maleimides) with alkenes or alkynes. A review of some recent synthetic applications of the reaction is also presented.

71.2 Mechanistic Aspects

As previously established, the mechanism of the [2+2]-photocycloaddition of cyclopentenones with alkenes can be summarized as shown in Scheme 1. The interaction of the alkene with the enone, excited

0-8493-1348-1/04/$0.00+$1.50

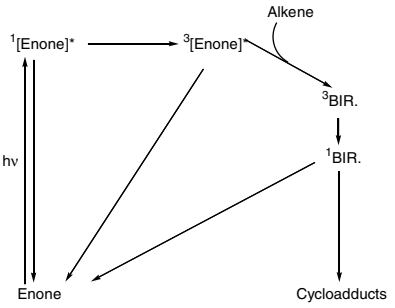

SCHEME 1

in its triplet state, is believed to form one or more of the possible 1,4-biradical intermediates. These biradicals can either cyclize and lead to the final cyclobutane products or revert to the ground-state starting materials.[4] The composition of the final reaction mixture reflects the respective rates of cleavage and cyclization of the 1,4-biradical intermediates.

In order to gain better knowledge of the influence of substituents on these respective rates and the regioselectivity of the reaction, new experiments involving selective chemical trapping of the 1,4-biradicals by hydrogen selenide have been carried out. Previous studies have now been extended to the cycloaddition of 2-cyclopentenones to polar alkenes and of substituted cyclopentenones with 2-methylpropene. The results confirm that the regiochemistry of the cycloaddition process is dominated by the relative rates of closure to the cycloadducts or reversion to the starting materials of the 1,4-biradical intermediates.[5,6] Furthermore, a detailed analysis of the photocycloaddition of 3-phenylcyclopentenone with 1-phenylpropene indicated that only 5% of the 1,4-biradicals convert to adducts.[7]

In contrast to intermolecular processes, intramolecular photocycloadditions are usually highly regio- and stereoselective. To explain this selectivity in the case of ω-heptadienic systems (according to the "rule of five"), 1,4-biradicals in which a cyclopentane ring has been formed are believed to be produced preferentially. In order to test the validity of this rule in the case of intramolecular [2+2]-photocycloaddition of 3-(ω-pentenyl)cyclopent-2-enone, a selective trapping of the 1,4-biradical intermediates was attempted. When the irradiation was performed in toluene using a Pyrex-filtered light with a medium-pressure mercury lamp, a single cycloadduct was isolated. When the same irradiation was carried out in the presence of SeH_2, the cycloadduct could not be observed, and a mixture of two diastereoisomeric spiroketones was isolated in a ratio that did not depend on the concentration of hydrogen selenide. These results were considered as proof that only two biradical intermediates (resulting from a 5-exotrig addition of the enone in its triplet state) were produced during the reaction. As shown in Scheme 2 and for steric reasons, only biradical **A** could cyclize to the corresponding cyclobutane.[8]

If the "rule of five" applies to the intramolecular photocycloaddition of β-substituted cyclic enones having a ω-pentenyl residue, the question of which bond is formed first and the problem of the efficiency of the cyclization step remains open as soon as the tether between the ethylenic bonds becomes longer.[9,10] As already determined for cyclohexenone derivatives, the efficiency of the cycloaddition of cyclopentenones drops rapidly with the length of the tether, except if some steric restrictions can favor the reactive conformation (Scheme 3);[11] similar results were obtained for the intramolecular [2+2]-photocycloaddition of furanones.

The fate of the reaction can also depend on the nature and the position of the substituents on the cyclopentenone unit. Furthermore, the efficiency of the cycloaddition process is usually very similar for cyclopentenone and the corresponding cyclohexenone derivatives (Scheme 4).[12]

When polar substituents are introduced on the linker, intramolecular hydrogen abstraction processes can be competitive and rearranged products can be obtained, as illustrated in Scheme 5.[13,14]

When the unsaturated side chain is located on the β-carbon of the enone, the diastereoisomeric ratio of the adducts does not depend on the stereochemistry of the alkene if a cyclopentane ring has been

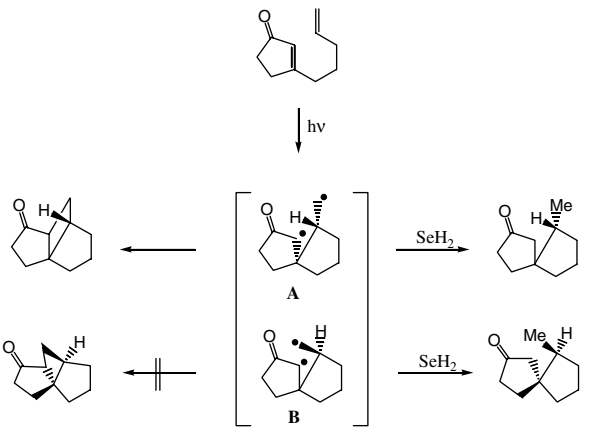

SCHEME 2

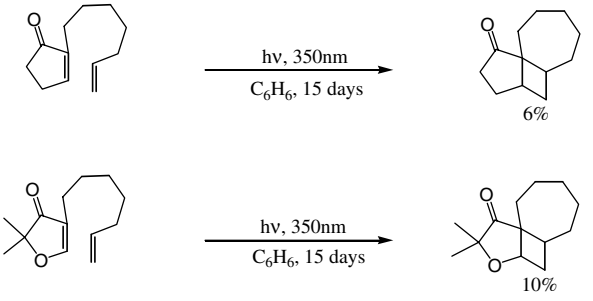

SCHEME 3

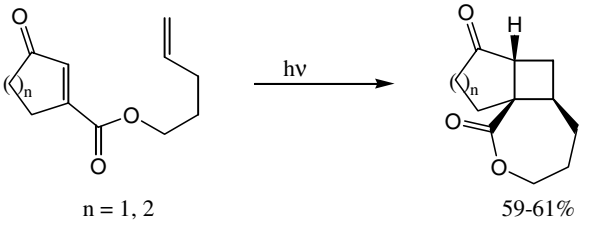

SCHEME 4

formed in the intermediate; however, as shown in Scheme 6, more complex results can be observed from α-substituted enones.[15]

When *cis*- and *trans*-2-(hex-4-enyl)cyclopent-2-enones were irradiated separately, a different ratio between the stereoisomeric adducts was obtained. This observation was taken as evidence that biradicals **A** and **B**, resulting from the initial formation of either a cyclopentane or a cycloheptane ring on the alkene unit, respectively, were required to explain the results. When a large *t*-butyl substituent was present, only the less hindered stereoisomer could be observed.

The stereoselectivity of intramolecular cycloadditions is due primarily to the steric restrictions appearing during the cyclization step. In the presence of stereogenic centers in the starting molecules, the stereochemistry of the newly created asymmetric carbons can be influenced and the reaction can even

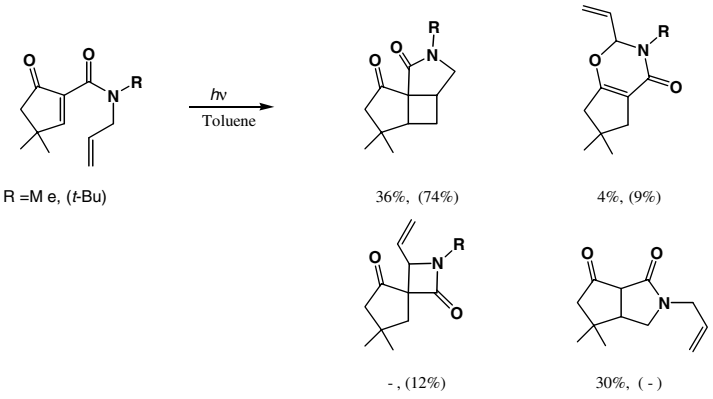

SCHEME 5

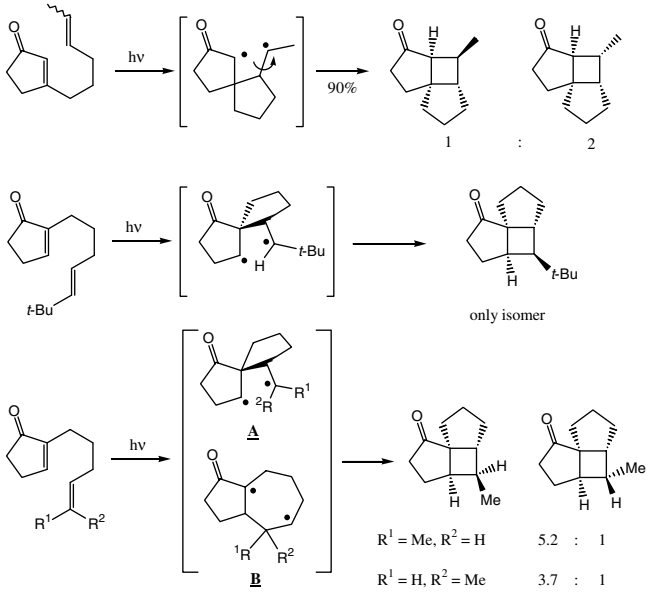

SCHEME 6

become highly stereoselective when several stereogenic centers are present on the tether. Interestingly, the stereochemistry of the major adduct can be explained on the basis of transition states having the tether either in a chair or a boat conformation and the substituents in an equatorial position. When the relative configurations of 1,3-stereogenic centers on the tether are either *anti* or *syn*, transition states **ET-A** or **ET-B** involving the formation of a six-membered ring are preferred (Scheme 7).[16]

Although steric hindrance is usually the determining factor that controls the stereoselectivity, hydrogen bonding can also be important. Among large substituents that prefer to occupy an equatorial position in the chair transition state, **ET-1** trialkylsilyl ethers can induce a high selectivity. Interestingly, when hydroxyl groups rather than their corresponding silyl ethers are present on the tether, a reversal of the diastereoselectivity can be observed in nonpolar solvents. This effect could be explained by an inversion of the chair conformation of the linker in transition state **ET-2** due to an intramolecular hydrogen bond (Scheme 8).[17] In alcohol, intermolecular hydrogen bonding can become competitive, and hydroxyl groups again behave as large substituents favoring transition state **ET-1**.

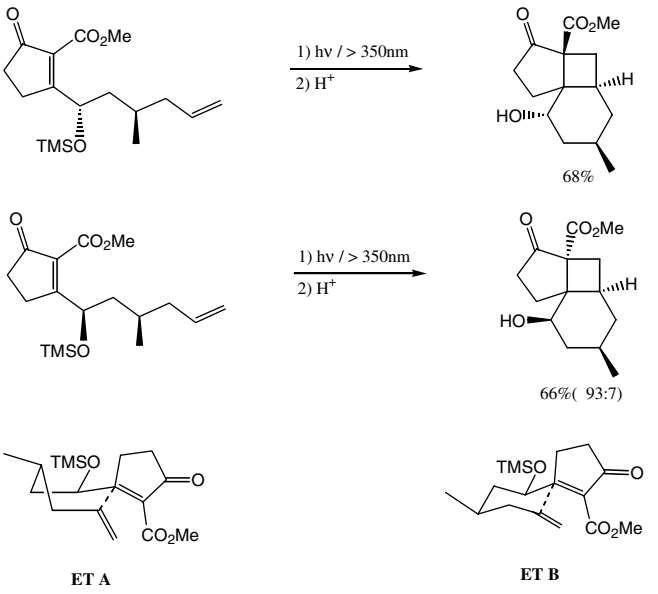

SCHEME 7

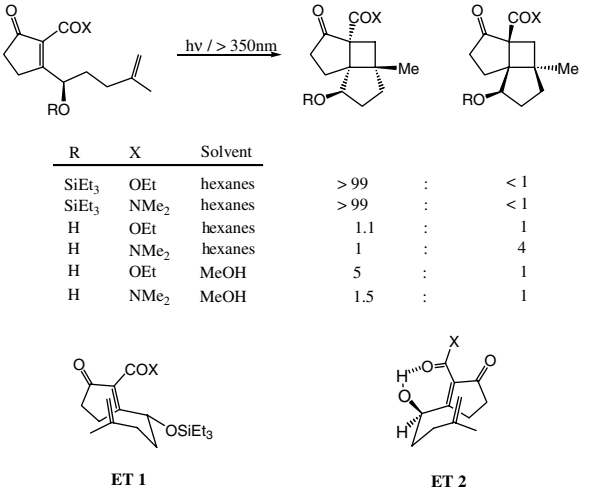

R	X	Solvent			
$SiEt_3$	OEt	hexanes	> 99	:	< 1
$SiEt_3$	NMe_2	hexanes	> 99	:	< 1
H	OEt	hexanes	1.1	:	1
H	NMe_2	hexanes	1	:	4
H	OEt	MeOH	5	:	1
H	NMe_2	MeOH	1.5	:	1

SCHEME 8

In order to support this rationalization, a computation of the possible transition states by molecular mechanics was carried out. The low deformation of a cyclopentenone unit in its $^3(\pi,\pi^*)$ excited state[18] allows an approach of the reacting double bonds in almost parallel planes. Among the possible conformations available in the transition states, six-membered chair and boat conformations placing the substituents in equatorial position were favored. The calculated energy difference between the competitive transition states was found to be close to the experimental value derived from the observed product ratio.[19,20] Similar conclusions, based on MM2 calculations, were obtained with cyclopentenones linked to a 3-furylpropanyl substituent (Scheme 9).[21]

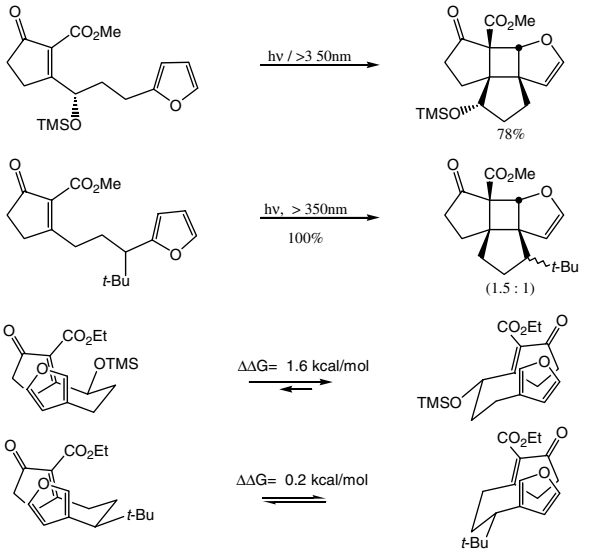

SCHEME 9

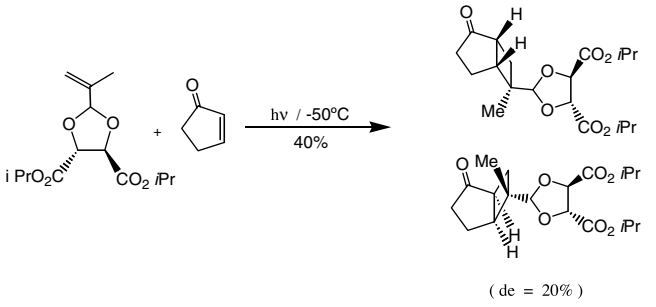

SCHEME 10

From the high diastereoselectivities usually observed in the [2+2]-photocycloaddition of chiral cyclopentenones, it was tempting to examine the effect of removable chiral auxiliaries. The development of enantioselective synthetic schemes requires chiral auxiliaries that can be easily introduced and easily removed. Among the possible functional groups that could be envisaged, ketals and esters were particularly attractive. By utilizing chiral ketals derived from cyclopentenone and a tartaric ester having a C2 axis of symmetry, an important asymmetric induction could be observed.[22] With aliphatic enones ketals, the stereoselectivity dropped considerably, and mixtures of regioisomers were observed (Scheme 10).[23]

5-Menthyloxy-2[5*H*]-furanone, with one face of the ethylenic bond selectively hindered by the alkoxy group, is another interesting chiral unsaturated ketal known to allow ground-state additions of nucleophiles or radicals with a total facial selectivity.[24] Excited cyclopentenones and cyclohexenones, which can relax to a low and twisted π,π^* triplet state, possess a biradical character. They should behave as radicals and add stereospecifically from the less hindered side of 5-menthyloxyfuranone. However, no regioselectivity and no stereoselectivity could be detected when cyclopentenone was selectively excited in the presence of 5-menthyloxyfuranone (Scheme 11). An initial energy transfer followed by cycloaddition of the triplet-excited furanone to cyclopentenone in its ground state accounted for these disappointing results.[25]

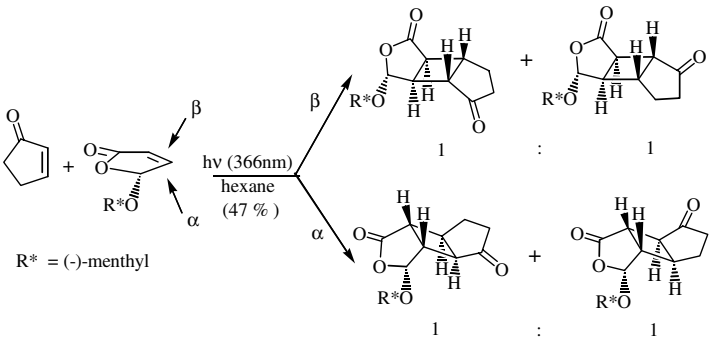

SCHEME 11

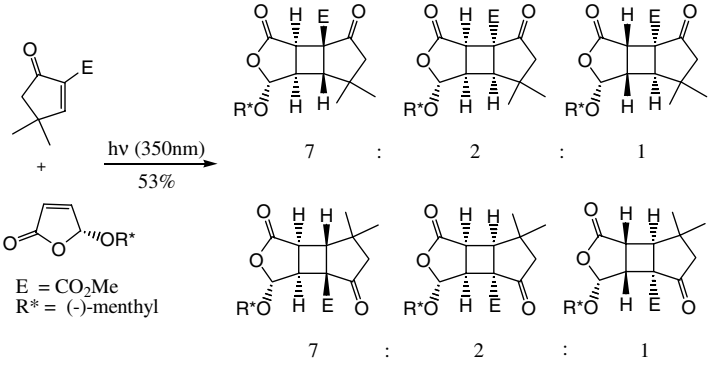

SCHEME 12

Although the facial selectivity increased with more flexible or more electron-deficient cyclic enones, a mixture of regioisomers and *syn*/*anti* stereoisomers was obtained that precluded synthetic applications (Scheme 12).

The use of removable chiral tethers between the reacting double bonds could be an interesting solution for the synthesis of enantiomerically pure cycloadducts. Derivatives of inexpensive chiral hydroxy acids such as lactic and β-hydroxy acids allow high asymmetric inductions with cyclohexenone derivatives.[26] Unfortunately, the diastereoselectivities obtained during the photochemical step with the corresponding cyclopentenones were considerably lower (Scheme 13).[27]

71.3 Synthetic Applications

All of these photoadducts obtained are polycyclic, and even polyfunctional molecules that have an α-cyclobutyl keto group. They can be used as very versatile starting materials for the synthesis of complex molecules. The [2+2]-photocycloaddition reaction constitutes a method of choice for creating a four-membered ring in polycyclic molecules. The photoreaction of a cyclopentenone unit with an alkene has recently been used in the synthesis of two natural products containing a cyclobutane unit — namely, sulcatine G[28] and (±)-kelsoene (Scheme 14).[29]

Ring opening or rearrangement with ring expansion of the cyclobutanes, present in the primary photoadducts, is still very attractive for organic chemists. For example, the intramolecular [2+2]-photocycloaddition of a cyclopentenone with a cyclobutene unit can be followed by consecutive thermal rearrangements to lead stereoselectively to 5–8–5 ring systems (Scheme 15).[30]

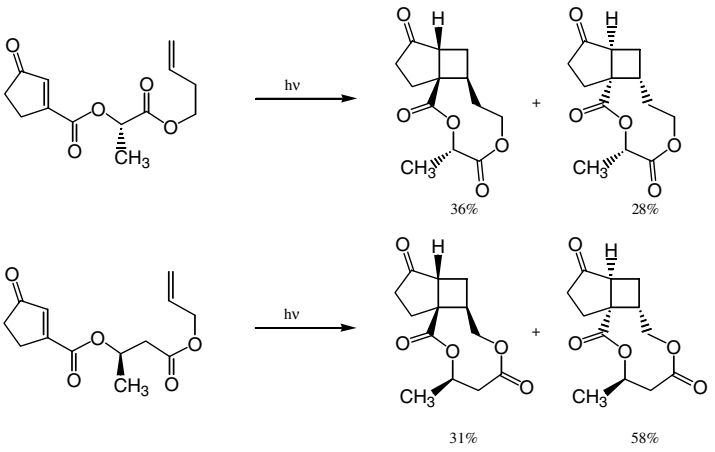

SCHEME 13

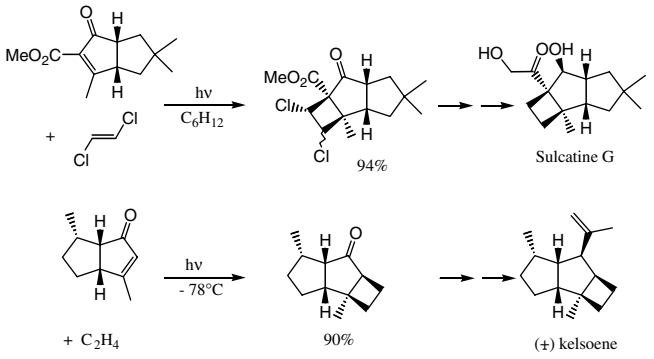

SCHEME 14

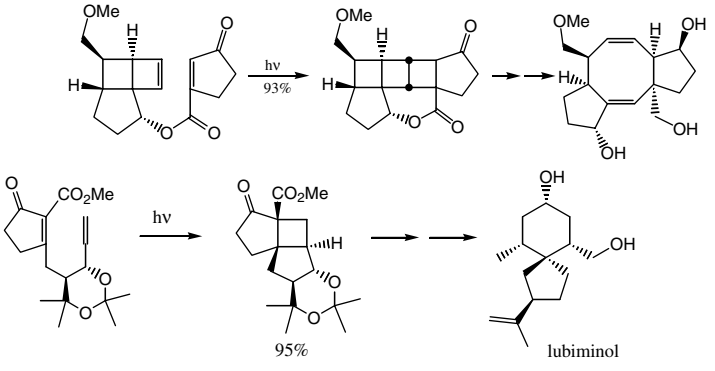

SCHEME 15

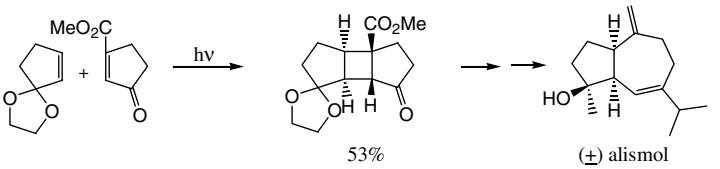

SCHEME 16

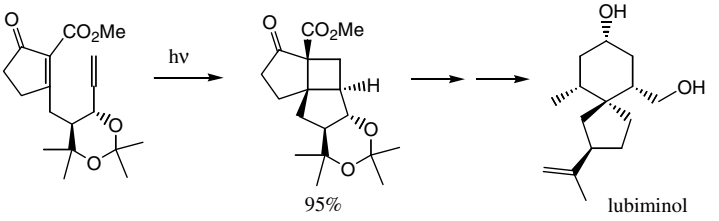

SCHEME 17

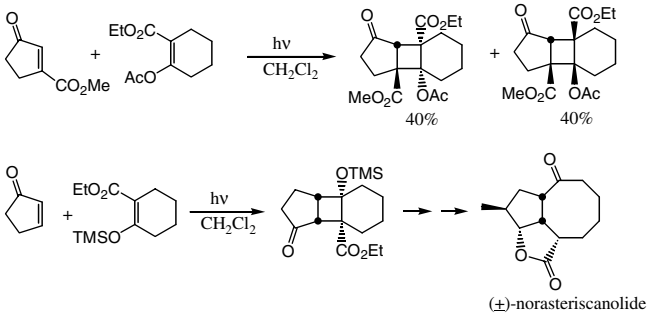

SCHEME 18

By using a free-radical fragmentation of α-cyclobutylmethyl radicals, a variety of polycyclic structures can be obtained. When applied to the initial photocycloadduct of a 3-cyclopentenone carboxylic acid with a substituted cyclopentene, a 5–7 ring system can be obtained. This approach was used for a total synthesis of (±)-alismol (Scheme 16).[31]

Similarly, radical opening of an α-cyclobutylmethyl radical can be followed by an efficient rearrangement involving a carbonyl group. This technique was used to transform the tetracyclic adduct obtained through an intramolecular photocycloaddition into a spiranic skeleton and to (±)-lubiminol (Scheme 17).[19]

When enol esters derived from β-diketones are used in the photocycloaddition reaction with an alkene (de Mayo's reaction), a hydrolysis of the ester group of the cyclobutyl intermediate allows opening of the cyclobutane ring by a retro-Aldolization process and the formation of medium-ring cyclic compounds. Similarly, hydrolysis of the cycloadduct obtained by irradiation of 3-carbomethoxycyclopentenone in the presence of a β-ketoester allowed facile access to (±)-norasteriscanolide (Scheme 18).[32]

The creation of up to four new asymmetric centers during the photochemical addition step allows very fast access to complex structures. This is illustrated by the synthesis of bilobalide (Scheme 19).[21]

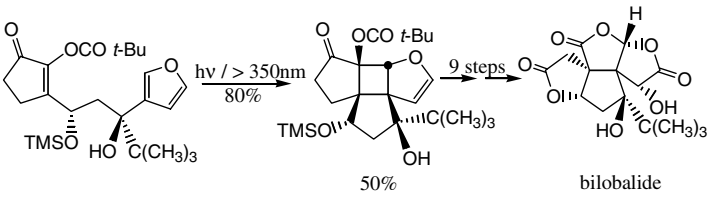

SCHEME 19

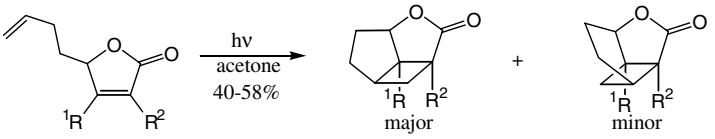

SCHEME 20

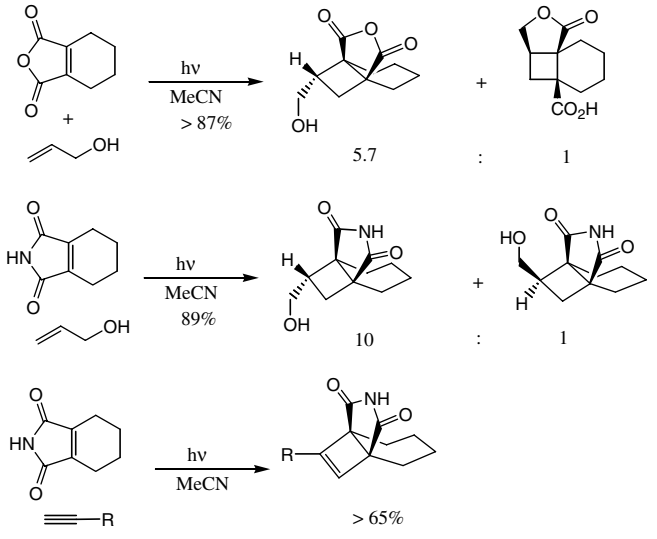

SCHEME 21

71.4 Related Photocycloadditions: Furanones, Maleic Anhydride, and Maleimides

Furanones, maleic anhydride, maleimides, and cyclopentenones behave similarly when irradiated in the presence of alkenes. [2+2]-Photocycloaddition reactions of furanones, especially γ-substituted furanones with alkenes, can be highly diastereoselective. A detailed analysis of the cycloaddition of ethylene with substituted furanones gave a deep insight into the origin of the diastereoselectivity. Based on product ratio dependence on temperature and the substituents, it was proposed that a pyramidalization of the β-carbon of furanones in their relaxed $^3(\pi,\pi^*)$ excited state and a homo-anomeric effect determined the observed selectivity.[33] Cycloadducts can also be obtained in good yields from furanones by intermolecular or intramolecular processes (Scheme 20).[34]

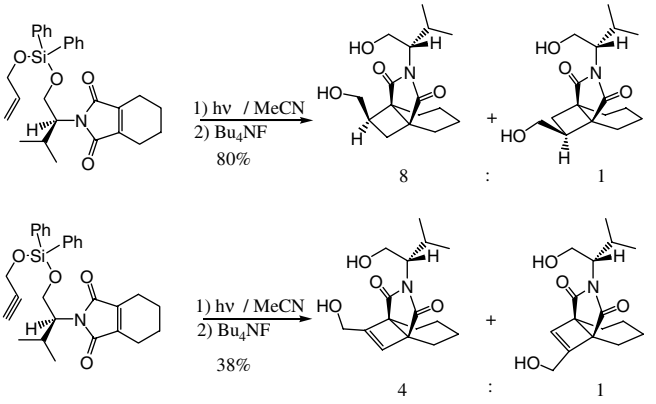

SCHEME 22

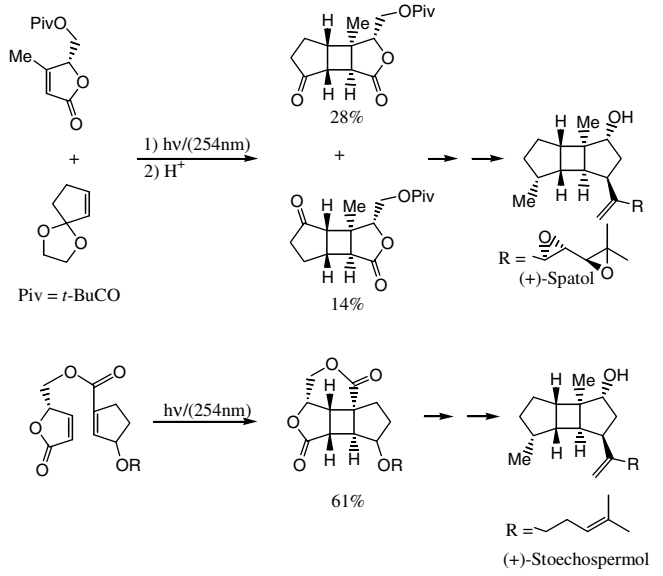

SCHEME 23

Recently, it was reported that the [2+2]-photocycloaddition of 3,4,5,6-tetrahydrophthalic anhydride and the related imide occurred efficiently and stereoselectively with a variety of alkenes and alkyn-3-ols (Scheme 21).[35,36]

Furthermore, the method was extended to an intramolecular [2+2]-photocycloaddition of imides linked to an allylic alcohol or a propargyl alcohol by a chiral tether (Scheme 22).[37] Interestingly, when L-valinol was used as a chiral auxiliary, a high diastereoselectivity was also observed for the cycloaddition of the unsaturated anhydride with an alkenyl or an alkynyl unit.

The high facial stereoselectivity observed for the [2+2]-photocycloadditions of alkenes with chiral butenolides and the polyfunctional nature of the cycloadducts have led to interesting new applications in the field of natural products. The total synthesis of (+)-stoechospermol[38] and (+)-spatol (Scheme 23),[39] as well as new syntheses of (+)-grandisol,[40,41] including photochemical cycloaddition as a key step, have been recently reported (Scheme 23).

71.5 Conclusion

The mechanism of the [2+2]-photocycloaddition of cyclopentenones with alkenes is now well established. A similar mechanism seems to be involved in the corresponding photocycloaddition of maleic anhydrides, maleimides, and furanones; therefore, interest in this reaction resides primarily in the formation of strained and polyfunctional cycloadducts. The high versatility of the cyclobutanes can be used for access to a great variety of polycyclic structures and to the skeleton of many natural products. Some progress remains to be made to improve the diastereoselectivity, especially in the presence of a removable chiral auxiliary. The search for new chiral auxiliaries has to deal with creation of polyfunctional starting materials. Unfortunately, and despite the generality of the photocycloaddition reaction, hydrogen abstraction or electron transfer processes and other rearrangements might become competitive.

References

1. Crimmins, M. T., Synthetic applications of intramolecular enone-olefin photocycloadditions, *Chem. Rev.*, 88, 1453–1473, 1988.
2. Crimmins, M. T. and Reinhold, T. C., Enone olefin (2+2)-photochemical cycloadditions, in *Organic Reactions*, Vol. 44, Paquette, L. A., Ed., John Wiley & Sons, New-York, 1993, 296–588.
3. Weedon, A. C., Photocycloaddition reactions of cyclopentenones with alkenes, in *CRC Handbook of Organic Photochemistry and Photobiology,* Horspool, W. M. and Song P-S., Eds., CRC Press, Boca Raton, FL, 1995, 634–651.
4. Schuster, D. I., Lem G., and Kaprinidis, N. A., New insights into an old mechanism: (2+2)-photocycloaddition of enones to alkenes, *Chem. Rev.*, 93, 3–22, 1993.
5. Andrew, D., Hastings, D. J., and Weedon, A. C., The mechanism of the photochemical cycloaddition reaction between 2-cyclopentenone and polar alkenes: trapping of triplet 1,4-biradical intermediates with hydrogen selenide, *J. Am. Chem. Soc.*, 116, 10870–10882, 1994.
6. Andrew, D. and Weedon A. C., Determination of the relative rates of formation, fates and structures of triplet 1,4-biradicals generated in the photochemical cycloaddition reactions of 2-cyclopentenones with 2-methylpropene, *J. Am. Chem. Soc.*, 117, 5647–5663, 1995.
7. Daniel Kelly, J. F., Kelly, J. M., and McMurry, T. B. H., Photochemistry of substituted cyclic enones. Part 12. Photocycloaddition of 3-phenylcyclopentenone and 3-phenylcyclohexenone to (*E*)- and (*Z*)-1-phenylpropene, *J. Chem.Soc., Perkin Trans. 2*, 1933–1941, 1999.
8. Maradyn, D. J. and Weedon, A. C., Trapping of triplet 1,4-biradicals with hydrogen selenide in the intramolecular photochemical cycloaddition reaction of 3-(4′-pentenyl)cycloalk-2-enones: verification of the rule of five, *J. Am. Chem. Soc.*, 117, 5359–5360, 1995.
9. Mattay, J., Intramolecular photocycloadditions to enones: influence of the chain length, in *CRC Handbook of Organic Photochemistry and Photobiology*, Horspool, W. M. and Song P.-S., Eds., CRC Press, Boca Raton, FL, 1995, 618–633.
10. Gebel, R. F. and Margaretha, P., Photoisomerization of 2-(hept-6-enyl)cyclopent-2-enones to tricyclo[7.3.0.$0^{1,7}$] dodecan-12-ones, *J. Chem. Res. (S)*, 1, 1997 (*J. Chem. Res. (M)*, 163–170, 1996).
11. Piva-Le Blanc, S., Pete J. P., and Piva, O., Conformational effects and cyclodimer formation in intramolecular (2+2)-photocycloadditions, *J. Chem. Soc., Chem. Commun.*, 235–236, 1998.
12. Le Blanc, S., Pete, J. P., and Piva, O., Intramolecular (2+2)-photocycloaddition of oxoesters and oxoamides, *Tetrahedron Lett.*, 34, 635–638, 1993.
13. Meyer, C., Piva, O., and Pete, J. P., Competition betweeen intramolecular [2+2]-photocycloaddition and hydrogen-abstraction reactions from 2-carboxamidocyclopent-2-enones, *Tetrahedron Lett.*, 37, 5885–5888, 1996.
14. Meyer, C., Piva, O., and Pete, J. P., [2+2]-photocycloadditions and photorearrangements of 2-carboxamidocyclopent-2-enones, *Tetrahedron*, 56, 4479–4489, 2000.
15. Becker, D. and Klimovich, N., Regio- and stereochemistry in (2+2)-intramolecular photocycloaddition of substituted olefins to cyclopentenones, *Tetrahedron Lett.*, 35, 261–264, 1994.

16. Crimmins, M. T. and Watson, P. S., Stereoselective intramolecular enone-olefin photocycloadditions of 1,7-dienes: model studies on the synthesis of lycopodium alkaloids, *Tetrahedron Lett.*, 34, 199–202, 1993.
17. Crimmins, M. T. and Choy, A. L., Solvent effects on diastereoselective intramolecular (2+2)-photocycloadditions: reversal of the selectivity through intramolecular hydrogen bonding, *J. Am. Chem. Soc.*, 119, 10237–10238, 1997.
18. Broeker, J. L., Eksterowicz, J. E., Belk, A. J., and Houk, K., N., On the regioselectivity of photocycloadditions of triplet cyclohexenones to alkenes, *J. Am. Chem. Soc*, 117, 1847–1848, 1995.
19. Crimmins, M. T., Wang, Z., and McKerlie, L. A., Rearrangement of cyclobutyl carbinyl radicals: total synthesis of the spirovetivane phytoalexin (±)-lubiminol, *Tetrahedron Lett.*, 37, 8703–8706, 1996.
20. Pete, J. P., Asymmetric photoreactions of conjugated enones and esters, in *Advances in Photochemistry*, Vol. 21, Neckers, D. C., Volman, D. H., and Von Bünau, G., Ed., John Wiley & Sons, 1996, 135–216.
21. Crimmins, M. T., Jung, D. K., and Gray, J. L., Synthetic studies on the ginkolides: total synthesis of (±)-bisobalide, *J. Am. Chem. Soc.*, 115, 3146–3155, 1993.
22. Lange, G. L. and Decicco, C. P., Asymmetric induction in mixed photoadditions employing α,β-unsaturated homochiral ketals, *Tetrahedron Lett.*, 29, 2613–2614, 1988.
23. Bonvalet, C., Bouquant, J., Feigenbaum, A., Pete, J. P., and Scholler, D., Photocycloaddition of cyclopentenone to propenal acetals, *Bull. Soc. Chim. Fr.*, 131, 687–692, 1994.
24. Bertrand, S., Hoffmann, N., and Pete, J. P., Highly efficient and stereoselective radicalar addition of tertiary amines with electron deficient alkenes: application to the enantioselective synthesis of necine bases, *Eur. J. Org. Chem.*, 2227–2238, 2000.
25. Bertrand, S., Hoffmann, N., and Pete J. P., Photochemical (2+2)-cycloaddition of cyclic enones to (5R)-5-menthyloxy-2[5H]-furanone, *Tetrahedron*, 54, 4873–4888, 1998.
26. Faure, S., Piva-Le Blanc, S., Piva, O., and Pete, J. P., Hydroxyacids as efficient chiral spacers for asymmetric intramolecular (2+2)-photocycloadditions, *Tetrahedron Lett.*, 38, 1045–1048, 1997.
27. Faure, S., Piva-Le Blanc, S., Bertrand, C., Pete, J. P., Faure, R., and Piva O., Asymmetric intramolecular (2+2)-photocycloadditions: α and β-hydroxy acids as chiral tether groups, *J. Org. Chem.*, 67, 1061–1070, 2002.
28. Mehta, G. and Sreenivas, K., Total synthesis of the novel tricyclic sesquiterpene sulcatine G, *J. Chem. Soc., Chem. Commun.*,1892–1893, 2001.
29. Piers, E. and Orellana, A., Total synthesis of (±)-kelsoene, *Synthesis*, 2138–2142, 2001.
30. Lo, P. C. K. and Snapper, M. L., Intramolecular (2+2)-photoaddition/thermal fragmentation approach toward 5–8–5 ring systems, *Org. Lett.*, 3, 2819, 2001.
31. Lange, G. L. and Gottardo, C., Synthesis of the guaiane (±)-alismol using a free radical fragmentation/elimination sequence, *Tetrahedron Lett.*, 35, 8513–8516, 1994.
32. Lange, G. L. and Organ, M. G., Use of cyclic β-ketoester derivatives in photocycloadditions: synthesis of (±)-norasteriscanolide, *J. Org. Chem*, 61, 5358–5361, 1996.
33. Hoffmann, N., Buschmann, H., Raabe, G., and Scharf, H. D., Chiral induction in photochemical reactions. 15. Detection of stereoelectronic effects by temperature dependent measurements of the diastereoselectivity in the photosensitized [2+2]-cycloaddition, *Tetrahedron*, 50, 11167–11186, 1994.
34. Busqué, F., De March, P., Figueredo, M., Font, J., Margaretha, P., and Raya, J., Regioselectivity of the intramolecular photocycloaddition of α,β-butenolides to a terminal alkene, *Synthesis*, 1143–1148, 2001.
35. Booker-Milburn, K. I., Cowell, J. K., Sharpe, A., and Jiménez, F. D., Tetrahydrophthalic anhydride and imide: remarkably efficient partners in photochemical [2+2]-cycloaddition reactions with alkenols and alkynols, *J. Chem. Soc., Chem. Commun.*, 249–251, 1996.
36. Booker-Milburn, K. I., Cowell, J. K., Jiménez, F. D., Sharpe, A., and White, A. J., Stereoselective intermolecular (2+2)-photocycloaddition reactions of tetrahydrophthalic anhydrides and derivatives with alkenols and alkynols, *Tetrahedron*, 55, 5875–5888, 1999.

37. Booker-Milburn, K. I., Gulten, S., and Sharpe, A., Diastereoselective intramolecular photochemical (2+2)-cycloaddition reactions of tethered L-(+)-valinol derived tetrahydrophthalimides, *J. Chem. Soc., Chem. Commun.*, 1385–1386, 1997.
38. Tanaka, M., Tomioka, K., and Koga, K., Enantioselective total synthesis of (+)-stoechospermol via stereoselective intramolecular (2+2)-photocycloaddition of chiral butenolide, *Tetrahedron*, 50, 12829–12842, 1994.
39. Tanaka, M., Tomioka, K., and Koga, K., Total synthesis of natural (+)-spatol: confirmation of the absolute stereostructure, *Tetrahedron*, 50, 12843–12852, 1994.
40. Alibés, R., Bourdelande, J. L., and Font, J., Highly efficient approach to (+)-grandisol via a diastereoselective [2+2]-photocycloaddition to 2(5H)-furanones, *Tetrahedron Lett.*, 34, 7455–7458, 1993.
41. De March, P., Figueredo, M., Font, J., Margaretha, P., and Raya, J., Highly efficient, enantioselective synthesis of (+)-grandisol from a C2-symmetric *bis*(α,β-butenolide), *Org. Lett.*, 2, 163–165, 2000.

72

Mechanistic Issues in [2+2]-Photocycloadditions of Cyclic Enones to Alkenes

David I. Schuster
New York University

72.1 Introduction

Following Eaton's original discovery of the photocyclodimerization of 2-cyclopentenone (CP)[1] and of photocycloaddition of this enone to cyclopentene (Eq. (72.1)),[2] Corey and co-workers reported [2+2]-photocycloadditions of 2-cyclohexenone (CH) to a variety of alkenes,[3] and established many of the characteristic features of this reaction.

0-8493-1348-1/04/$0.00+$1.50

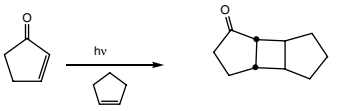

(72.1)

The potential of this type of reaction, as a key step in the synthesis of natural products, was first shown by Corey in his landmark synthesis of caryophyllene (Eq. (72.2)).[4]

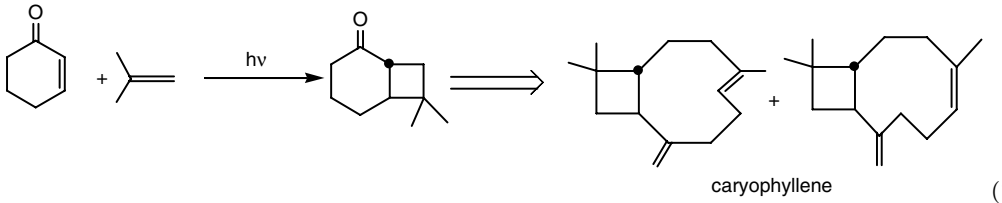

(72.2)

Subsequently, inter- as well as intramolecular [2+2]-photocycloadditions have become part of the standard repertoire of synthetic organic chemists, and this process is now probably the most widely used photochemical reaction in synthetic organic chemistry.[5] Numerous reviews on the synthetic utility[5] and mechanism of this reaction[6] have been published. The salient features of this process, as well as new theoretical calculations that bear directly on the mechanism, are presented in this chapter.

Photodimerization of cyclic enones in solution to give mixtures of *cis-anti* head-to-head (HH) and head-to-tail (HT) [2+2]-photodimers occurs via the lowest energy enone triplet excited state, as established using triplet sensitization and quenching techniques.[7–11] In 1969, Wagner and Bucheck[10,11] suggested that the inefficiency in photodimerization of CP and CH was principally associated with reversion of initially formed dimeric intermediates, possibly 1,4-biradicals, to two enone ground-state molecules and that the extent of this biradical reversion was probably different for the biradicals leading to HH as opposed to HT dimers. If this were the case, there would be no direct relationship between quantum efficiencies of dimer formation and triplet state reactivities (i.e., the rate of attack of the triplet enone on a corresponding ground-state molecule). Even at this early date, the lack of a correlation between quantum yields and excited-state reactivity in nonconcerted reactions involving triplet-excited states was well established.[10] de Mayo came to similar conclusions at the same time regarding photoaddition of CP to alkenes where CP triplet states were postulated to be reaction intermediates.[12]

Based upon earlier spectroscopic studies of steroid enones[13] and calculations of energies of relaxed n,π^* and π,π^* states,[14] de Mayo concluded that the lowest energy enone triplet state of cyclic enones and the one responsible for photoaddition reactions, was probably the $^3(\pi,\pi^*)$ state.[15] This conclusion was later confirmed by studies using transient absorption spectroscopy and time-resolved photoacoustic calorimetry carried out by Schuster and co-workers.[16,17] However, in the case of very rigid cyclic enones, where conformational relaxation is difficult or impossible, the lowest n,π^* and π,π^* triplet states are very close in energy.[5a,16,18] Estimates by de Mayo[12,15] of the rate constants k_d and k_r, corresponding to radiationless decay of the enone triplet and triplet reaction with alkenes, respectively, were made on the basis of quenching kinetics. As in Wagner's photodimerization study,[11] piperylene and acenaphthylene were used as triplet quenchers, and it was assumed that quenching of enone triplets occurred at the diffusion-controlled rate. Schuster and co-workers[16] later measured triplet lifetimes of a number of cyclic enones in solution using flash photolysis and demonstrated that alkenes directly quench these triplets, allowing direct determination of the reaction rate constants.[19,20] Trends in these values will be discussed later, but it should be noted that these rate constants are about an order of magnitude smaller than de Mayo's estimates[12,15] because of the overly generous value assumed by de Mayo for the rate constant for triplet–triplet energy transfer.

72.2 General Characteristics of [2+2]-Photocycloadditions of Cyclic Enones to Alkenes

Stereochemistry of Ring Fusion of Cycloadducts

Corey established in 1964 that *trans*- as well as *cis*-fused cycloadducts are formed on photoaddition of CH to simple alkenes, the former often being the major products.[3] This is illustrated in Eq. (72.3) for photoaddition of CH to 1,1-dimethoxyethene.

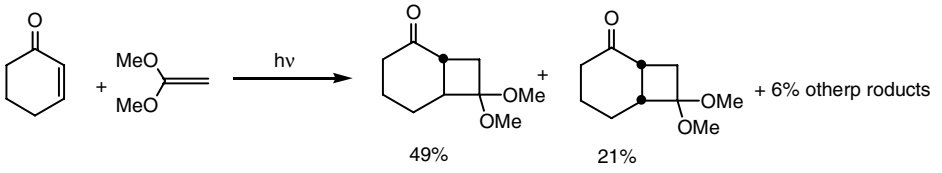

(72.3)

This observation is not confined to simple monocyclic systems. Thus, photoaddition of testosterone acetate **1** to cyclopentene gives both *cis*- and *trans*-fused photoadducts (**2** and **3**) in an initial ratio of 2:1 (Eq. (72.4)).[21]

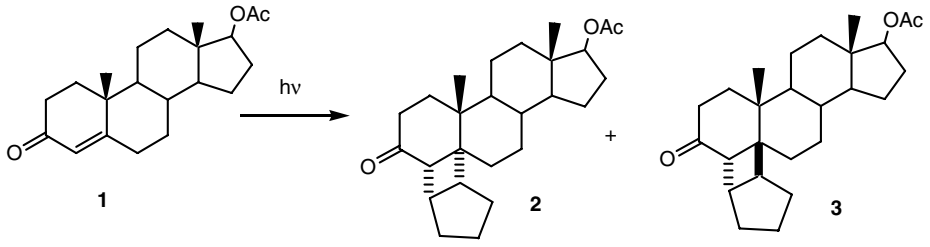

(72.4)

A gradual change in favor of the *cis*-adduct **2** as the reaction proceeds is due to secondary phototransformations that preferentially consume **3**.[22] This stereoselectivity in the [2+2]-addition must have a kinetic rather than thermodynamic basis, as x-ray crystal structures show that the cyclohexanone in the *cis*-fused adduct **2** is in a boat conformation and the cyclobutane ring is relatively flat, while in *trans*-fused structure **3** a relatively undistorted half-chair cyclohexanone ring is linked diequatorially to a severely twisted cyclobutane.[21] Thus, there is no question that *cis*-fused adduct **2** is thermodynamically much more stable than the *trans*-fused adduct **3**. The difference in energies of the stereoisomeric adducts derived from CH and 2,3-dimethyl-2-butene, according to MM2 calculations, is ~3.0 kcal/mol in favor of the *cis*-adduct but increases to 7.4 kcal/mol for CH–cyclopentene adducts analogous to **2** and **3**.[21] In some cases (e.g., photoaddition of CH to 2-methylpropene), formation of [2+2]-cycloaddition products is accompanied by products attributable to disproportionation of 1,4-biradical intermediates:[3]

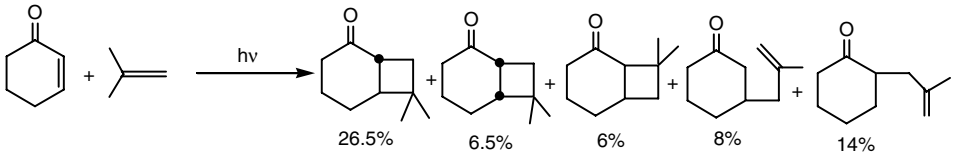

(72.5)

Stereochemistry of the Alkene Component in Enone Photocycloadditions

Intermolecular Photocycloadditions

Corey[3] reported that an identical mixture of cycloadducts was obtained from photoaddition of CH to either *Z*- or *E*-2-butene, indicating that the stereochemistry of the alkene component is lost in the course of the reaction. Recovery of the alkene component at various reaction times indicated that <1% isomerization of the starting material had occurred. Thus, stereomutation must occur at some intermediate reaction stage, indicating that the two new sigma bonds in the cycloadduct must be formed sequentially. The generally accepted mechanistic interpretation, which has received ample experimental and theoretical validation, is that the addition process involves rotationally equilibrated triplet 1,4-biradicals as precyclization intermediates. It was not clear in Corey's study whether initial bonding occurred at the α- or β-carbon of the enone, or both, a question that was unresolved for some time. The reported lack of isomerization of the starting alkene indicated that reversion of the 1,4-biradicals to starting materials by fragmentation is not competitive with cyclization, which is surprising in light of more recent findings (see below).

Cargill and co-workers[23] found that bicyclo[4.3.0]non-1(6)-en-2-one (BNEN, **4**) gives the same four products on photoaddition to either *Z*- or *E*-2-butene, again indicating that the stereochemical integrity of the alkene component is lost during the reaction:

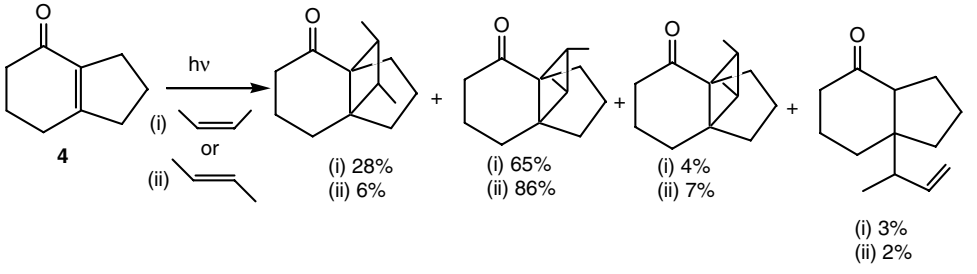

(72.6)

A similar study involving photoaddition of CP to *Z*- and *E*-1,2-dichloroethene was reported by Dilling et al.[24] In both of these cases, the possibility of biradical reversion to starting materials resulting in *Z,E*-isomerization of the alkene was not explicitly considered or investigated. McCullough et al.[25] found that, at 2% conversion in the photoaddition of 3-phenyl-CH to *Z*-2-butene, recovered alkene contained 9% of the *E* alkene, consistent with biradical reversion to ground-state starting materials and demonstrating that this process is in most cases a major source of inefficiency in these photoreactions.

Biradical reversion appears to be a much more important process in enone additions to electron-deficient alkenes. Thus, Schuster and co-workers[26] found that, in the reaction of 3-methylcyclohexenone (3-MCH) with *Z*- and *E*-1,2-dicyanoethene (maleo- and fumaronitrile), isomerization of the alkenes accompanies formation of cycloadducts. Based upon quantum yields for all processes and the rate constants for quenching of the enone triplet by these alkenes, Schuster et al.[26] concluded that alkene isomerization occurred by reversion of 1,4-biradical intermediates (i.e., a Schenck-type mechanism)[27] rather than by triplet–triplet energy transfer from the enone to the alkenes, although the latter was a distinct possibility due to the relatively low triplet energies of these particular alkenes.[28] The full significance of biradical reversion as a critical factor in affecting the course of enone photocycloadditions is discussed below.

Intramolecular Photocycloadditions

Stereochemical scrambling in intramolecular photocycloadditions of cyclohexenones with tethered alkene moieties has also been extensively investigated. Becker and Haddad[29] found that the isomeric β-linked 1-acyl-1,6-heptadienes **5** and **6** (R = CH_3) give a 1:1 mixture of stereoisomeric cycloadducts **7** and **8,** but the dienes do not isomerize during the irradiation process:[29]

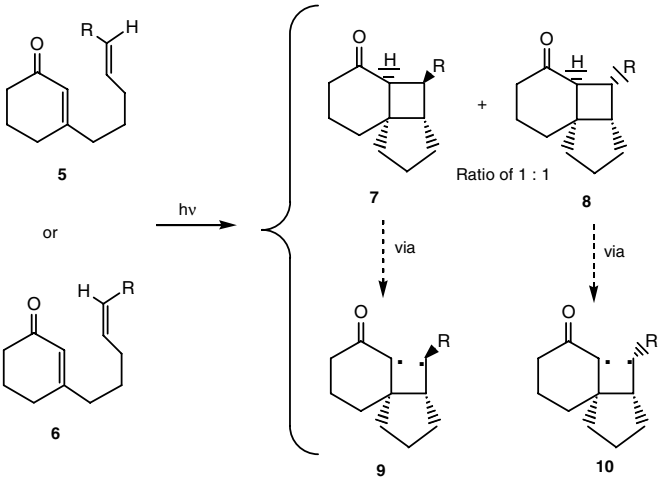

(72.7)

Similar results were also obtained with **5** (R = isopropyl) and with a *cis*-dideuterio analog, demonstrating that steric effects did not play an important role. The results indicate that initial bonding occurs between C2 (the β-carbon of the enone) and C6 of the heptadiene moiety in accord with the notorious "rule of five"[30] to give triplet 1,4-biradicals **9** and **10**, whose lifetimes are sufficiently long to allow complete rotational equilibration prior to ring closure. Curiously, 1,4-biradicals **9** and **10** do not appear to revert to starting materials accompanied by isomerization (see Eq. (72.5)).

In contrast, Agosta found that the acylhexadienes **11** undergo scrambling of the label (D or CH_3) on the CC double bond in the side chain competitive with formation of photoproducts:[31]

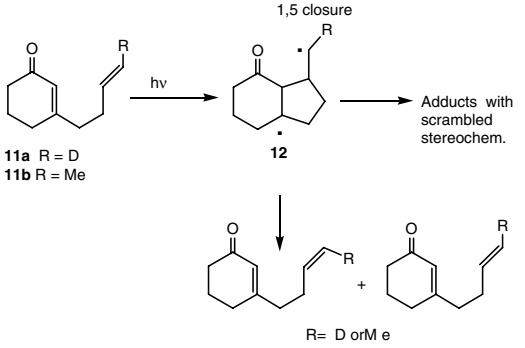

(72.8)

Similar results were found for an acyclic analog. For **11**, reaction almost surely occurs via 1,4-biradicals **12** formed by initial 1,5-bonding to the α-carbon of the enone. Inversion and rotation at the radical center then occurs prior to fragmentation or cyclization. Based upon quantum yields, the ratios of the rate of biradical reversion to product formation (k_r/k_p) are 0.75 for **11a** and 1.81 for **11b**. It is obvious that the competition between the various pathways for biradical formation and decay depends critically on the substitution pattern in these systems.

Becker and Haddad[29] later investigated the photoreactions of the α-linked cyclohexenones **13** to **17**, where once again *Z,E*-isomerization of the starting materials was not observed:

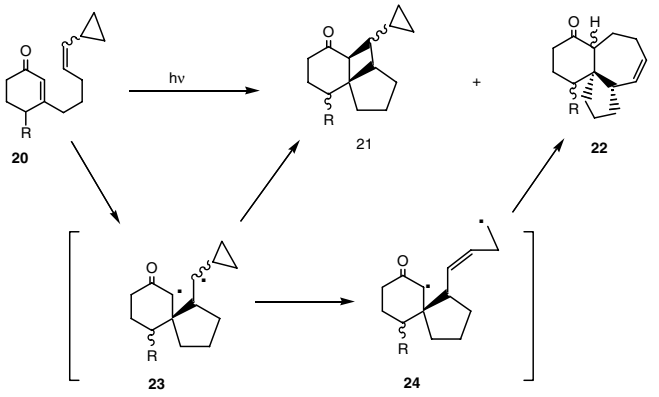

SCHEME 1

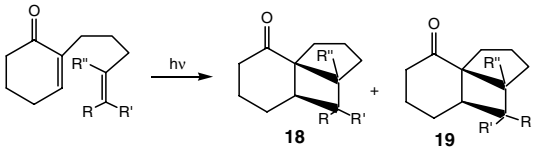

13 R = Me, R' = R'' = H
14 R' = Me, R = R'' = H
15 R = *i*-Pr, R = R''= H
16 R' = *i*-Pr, R= R''= H
17 R = R'' = D, R' = H

Ratio of **18 : 19** = 35 : 1 for **13**
Ratio of **18 : 19** = 5.8 : 1 for **14**
Ratio of **18 : 19** = 3.8 : 1 for **15**
Ratio of **18 : 19** = 1.4 : 1 for **16**
Ratioo f **18 : 19** = 2 : 1 for **17**

(72.9)

While mixtures of stereoisomeric cycloadducts were formed in each case, no simple pattern of reactivity emerges. Both **13** and **14** preferentially afford diastereomer **18**, but the ratio of **18** to **19** is quite different in each case, indicating that the reaction is more complicated than with the analogous β-linked dienones. With the isomeric *n*-propyl-substituted dienones **15** and **16**, cycloaddition again gave **18** in preference to **19**, but to different extents than above. Even with the dideuteriodienone **17**, diastereoselectivity is observed on ring closure. These results clearly require the participation of several competing reaction pathways.

To further probe the nature and properties of the biradicals generated on photoexcitation of **13** to **17**, Becker et al.[32] studied the analogous dienones **20** (as a *Z/E* mixture) with a cyclopropyl substituent on the CC double bond in the β-linked side chain. The ring opening of cyclopropylcarbinyl to 3-butenyl radicals, for which a rate constant of 1×10^8 s^{-1} has been determined,[33] is considered to be a reliable radical clock for estimation of biradical lifetimes. Photoexcitation of **20** gave rearranged products **22** in competition with normal intramolecular [2+2]- cycloadducts **21** in a ratio of 45:55, as shown in Scheme 1, indicating that (1) bonding in this system occurs exclusively between the β-carbon of the enone and the alkene carbon β to cyclopropyl to give **23**, and (2) ring opening of **23** to give biradical **24** (which closes to **22**) occurs at about the same rate as ring closure of **23** to **21**. From this, the lifetime of biradical **23** can be estimated to be on the order of 10 ns. In a related study, photoaddition of CP to vinylcyclopropane gave HH and HT cycloadducts, as well as products derived from ring opening of the intermediate biradicals, whose lifetimes were estimated to be ~50 ns.[34] Because ring opening of phenyl-substituted cyclopropylcarbinyl radicals is estimated to be much faster than the parent system by about three orders of magnitude, the analogous phenyl-substituted compound **25** was prepared and irradiated.[35]

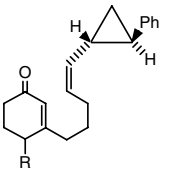

25 *Z,E*

Indeed, as anticipated, only rearrangement products analogous to **22** were isolated, with no detectable amounts of the [2+2]-adducts analogous to **21**.[35] Similar studies of the α-linked compounds analogous to **20** and **25** showed that in this case the first bond forms at both the α (major) and β (minor) carbons of the enone, followed by competitive cyclization and ring-opening reactions.[35]

Regiochemistry in Enone-Alkene [2+2]-Photocycloadditions

One of the most significant findings in Corey's pioneering study[3] was that photocycloadditions of cyclohexenones to unsymmetrical alkenes were invariably regioselective. Thus, the reaction of CH and 2-methylpropene (Eq. (72.3)) and 1,1-dimethoxyethene (Eq. (72.1)) showed a clear preference for formation of HT vs. HH adducts. Corey[3] observed similar selectivity for photoaddition of CH to allene, vinyl acetate, methyl vinyl ether, and benzyl vinyl ether, as was found also by Cantrell et al.[36] for the reaction of 3-MCH with 1,1-dimethoxyethene (DME) and by Lenz[37] for photoaddition of a steroid enone to 1,1-dialkoxyethene and 2-methylpropene. In contrast, HH adducts were preferentially formed between CH and acrylonitrile, although the structures of the adducts (including stereochemistry) were not firmly established.[3] Although photoaddition of 3-MCH to acrylonitrile also gave mainly two HH adducts[36] (the structure of a third adduct was not firmly established), Rao et al.[38] found that the major photoadduct from 4,4-dimethylcyclohexenone (DMCH) and acrylonitrile had a HT structure, while Weedon and coworkers[39] established that the ratio of HH to HT adducts formed from 2-cyclopentenone and acrylonitrile was 40:60. Thus, the original suggestion[3] that the regioselectivity in [2+2]-photocycloadditions of cyclic enone and alkenes is generally reversed using electron-deficient in place of electron-rich alkenes appears is clearly incorrect.

Strong evidence that regioselectivity in [2+2]-photocycloadditions does not follow a simple pattern comes from a study by Lange et al.[40] on addition of enones **26a** and **26b** to a series of methyl 1-cycloalkene-1-carboxylates:

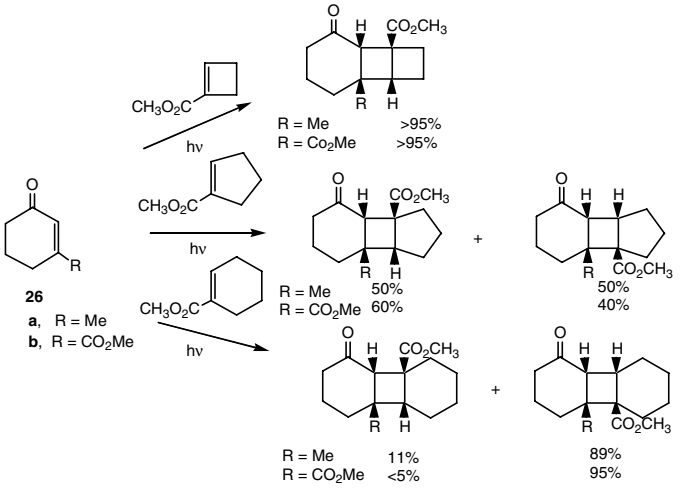

(72.10)

While additions to the cyclobutenyl ester gave exclusively HH adducts in line with Corey's generalization, increasing proportions of HT adducts were obtained as the ring size of the alkene was increased, resulting eventually in a reversal of regioselectivity. Thus, the HH to HT adduct ratio was 1:1 for **26a** and 60:40 for **26b** with the cyclopentenyl ester, but turned around to 1:9 and <1:20 for reactions of **26a** and **26b**, respectively, with the analogous cyclohexenyl ester. It is obvious that the regiochemistry associated with enone–alkene photocycloadditions is clearly much more complex than originally envisioned.[3] The mechanistic rationalization of these findings is deferred until Section 72.3.

Reactivity of Alkenes Toward Photoexcited Enones

In 1964, Corey and co-workers[3] determined "relative reactivities" for competitive additions of photoexcited CH to alkenes by measuring the ratio of adducts derived from 1:1 alkene mixtures. The so-called "relative rate factors," correcting for statistical factors, were 4.66 for 1,1-dimethxyethene, 1.57 for methoxyethene, 1.00 for cyclopentene (reference compound), 0.40 for isobutene, and 0.234 for allene; acrylonitrile was much less reactive than any of the other alkenes listed. Based upon these data, Corey concluded that photoexcited CH was a moderately electrophilic species toward alkenes.

These data were accepted for a long time as proper measures of alkene reactivity in photocycloadditions and were critical elements in the formulation of Corey's famous "exciplex mechanism" to explain enone photocycloadditions.[5b–d] However, as is now well known, product ratios in photochemical processes reflect relative quantum efficiencies for disappearance of starting materials and/or formation of products and rarely reflect relative rates of reaction of the photoexcited state, particularly when it is a triplet state.[6,10–12,41,42]

The lack of a relationship between product quantum yields and the rate constants of a single reaction step in a multistep reaction pathway was demonstrated dramatically many years ago by Wagner[42] for Norrish type II reactions of aromatic ketones. In this reaction, quantum efficiencies are determined by the competition between reversion of 1,4-biradical intermediates to starting material and product formation and do not correlate at all with the rate constants for formation of the biradicals from ketone triplet states.[42] Because 1,4-biradicals clearly play a crucial role in enone photocycloaddition to alkenes, it would be surprising if relative yields of enone–alkene photoadducts directly reflect the rates of the initial interaction of alkenes with enone triplet excited states.[5a,6,15,19,20,43] In fact, such a correlation does not exist.

Rate constants for interaction of triplet excited states of cyclic enones with alkenes were first reported by Schuster et al.[16,19,20] using transient absorption spectroscopy (nanosecond flash photolysis). The rate constants k_q were obtained from the relationship $(\tau_T)^{-1} = (\tau_0)^{-1} + k_q$ (alkene), where τ_0 is the limiting triplet lifetime of the enone at a given concentration in the absence of alkene. The decay of enone triplet absorption at 280 nm could be conveniently followed upon excitation of the enones (cyclopentenone [CP], 3-methylcyclohexenone [3-MCH], testosterone acetate [TA], and BNEN [**4**] were all studied]) in acetonitrile and cyclohexane at 355 nm using the third harmonic of a Nd:YAG laser. In all cases, triplet decays were clearly first order. Quantum efficiencies for capture of enone triplets by alkenes (Φ_{tc}) are given by $k_q\tau_T$ (alkene) using the experimentally determined values of k_q and τ_T.

No correlation exists between the rate constants k_q for interaction of the enone triplets with the alkenes and the overall quantum efficiency for formation of products.[16,19,20] In general, electron-rich alkenes give higher quantum yields for adduct formation, while the highest rate constants for triplet quenching are found with electron-deficient alkenes, such as acrylonitrile and fumaronitrile. Efficiencies of triplet capture (Φ_{tc}) at the alkene concentrations (typically 0. 5 *M*) at which quantum yields for product formation (Φ_{add}) were measured are invariably higher than Φ_{add}. This is definitive evidence for formation of intermediates that revert to starting materials in competition with progress to adducts. Furthermore, no correlation exists between k_q and the ionization potentials of the alkenes, as would be expected if quenching involved formation of a donor–acceptor complex, with the alkene as electron donor and the electronically excited enone as electron acceptor. Also, no significant difference has been observed between

rate constants measured in polar (acetonitrile) and nonpolar (cyclohexane) solvents, arguing against charge polarization in the transition state for the initial electronic interaction between enone triplets and alkenes.

Two different mechanisms for quenching of enone triplets could be operating with electron-deficient alkenes, triplet energy transfer, and a Schenck-like addition mechanism involving intermediate 1,4-biradicals.[26] It was shown that quenching of 3-MCH by 1,2-dicyanoethenes involves a Schenck mechanism,[27] while interaction of higher energy triplets of the rigid enone BNEN with the same alkenes involves triplet–triplet energy transfer.[18] Inhibition of triplet energy transfer from 3-MCH and similar conformationally flexible enones by the Dexter exchange mechanism can be attributed to poor π overlap between the twisted chromophore of the enone triplets and the alkenes.[44] No such inhibition would occur with conformationally constrained enones such as BNEN.

72.3 Mechanistic Proposals

The Corey–de Mayo Exciplex Mechanism

On the basis of the regiochemistry and the relative rate factors observed in his studies of alkene additions to photoexcited CH (see above), Corey[3] proposed in 1964 that the first step of the [2+2]- photocycloaddition of enones to alkenes involved interaction of a polarized enone triplet excited state with the ground-state alkene to give an "oriented π-complex" (illustrated in structure **27**) for the case of addition of CH to methoxyethene.

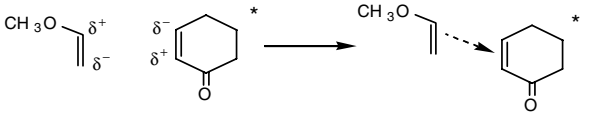

27

Assuming (incorrectly as it subsequently turned out) that the reactive excited state of the enone was an $^3(n,\pi^*)$ state, the electron polarization from extended Huckel calculations was predicted to be as shown, with higher electron density at C_β than at C_α.[45] In this donor–acceptor π-complex, the alkene ground state was proposed to act as the electron donor and the enone-excited state as the electron acceptor, the two moieties being held together by coulombic attraction. Corey noted[3] that it was likely that the π-complex model could not be extended to enone photodimerization or to reactions of enones with alkenes possessing strong electron-withdrawing substituents such as CN or COOR. Steric factors remained to be assessed. The alternative hypothesis (namely, that the regiospecificity in these reactions might be governed by preferences in formation of 1,4-biradicals) was rejected, because it did not explain the observed selectivity in photoaddition of CH to DME nor the relative rate factors. However, biradical intermediates on the reaction pathway were invoked to rationalize the occasional formation of disproportionation products (see Eq. (72.3)), as well as the loss of stereochemistry observed on photoaddition of CH to the isomeric 2-butenes.

de Mayo later suggested that Corey's proposed π-complexes might decay to ground-state reactants competitive with formation of products.[9,12,42] He noted that quantum yields for adduct formation from CP and a variety of alkenes were never greater than 0.50, even in neat alkene. de Mayo initially concluded that the intermediate undergoing reversion to ground-state reactants was the exciplex, rather than a biradical derived from the exciplex, because little if any alkene isomerization occurred ($\Phi < 0.033$) on irradiation of CP in the presence of 3-hexene.[46] He also suggested that adducts might arise, at least in part, directly from the exciplex, bypassing the biradical; however, de Mayo recognized that variations with temperature of the quantum yield for photoadditions could most easily be explained in terms of changes in the partitioning of the 1,4-biradical intermediate.[47]

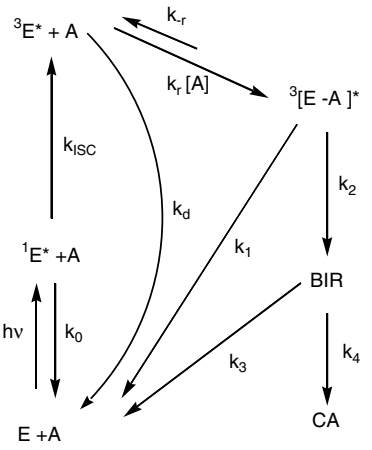

E= enone, A = alkene, BIR = 1,4-biradical, CA = cycloadducts

SCHEME 2

Loutfy and de Mayo[48] maintained that a triplet exciplex is formed first, and irreversibly, from the enone triplet and the alkene ground state and that the exciplex collapses to one or more triplet 1,4-biradicals, which either cyclize or revert to ground-state starting materials. Insufficient evidence was available to indicate whether the first bond in the adduct is formed α or β to the carbonyl group on the enone. However, their kinetic data[48] in no way *requires* formation of an exciplex precursor to biradicals in these reactions. For the analogous process of oxetane formation from benzophenone and alkenes, Caldwell et al.[49] concluded that some kind of complex, most likely a π-complex, was an *obligatory* precursor to triplet 1,4-biradicals, based on secondary kinetic isotope effects associated with initial quenching of the ketone triplet, formation of oxetanes, and *cis-trans* isomerization of the alkenes. The Corey-de Mayo exciplex mechanism is shown in Scheme 2.[48]

Identification of the Reactive Enone Intermediate

As noted previously, it was concluded earlier from spectroscopic data that the lowest energy triplet state of cyclic enones and cyclohexenones, in particular, is a $^3(\pi,\pi^*)$ state, not a $^3(n,\pi^*)$ state.[13] Evidence that the $^3(\pi,\pi^*)$ state is the reactive excited state in [2+2]-photocycloadditions derives from the nanosecond flash photolysis studies of Schuster and co-workers referred to earlier,[16,19,20] as well as studies on 4,4-dimethylcyclohexenone (DMCH) **28**. The latter gives the rearranged lumiketone **29** and cycloadducts **30** and **31** upon irradiation in the presence of 2,3-dimethyl-2-butene:[37,50,51]

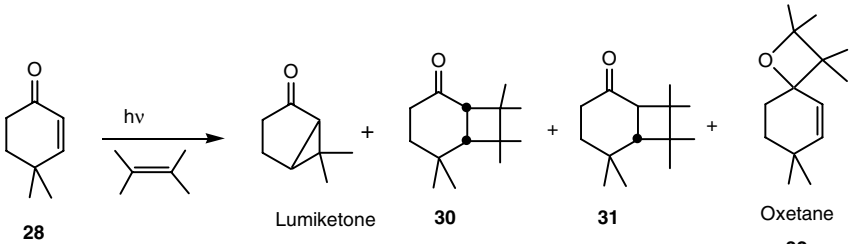

(72.11)

Kinetic studies demonstrated that adducts **30** and **31** and lumiketone **29** arise from the same enone excited state. Abundant data indicates that the photorearrangement arises from the enone $^3(\pi,\pi^*)$ state.[52] When DMCH is irradiated in neat alkene, oxetane **32** is formed in addition to the other products. The

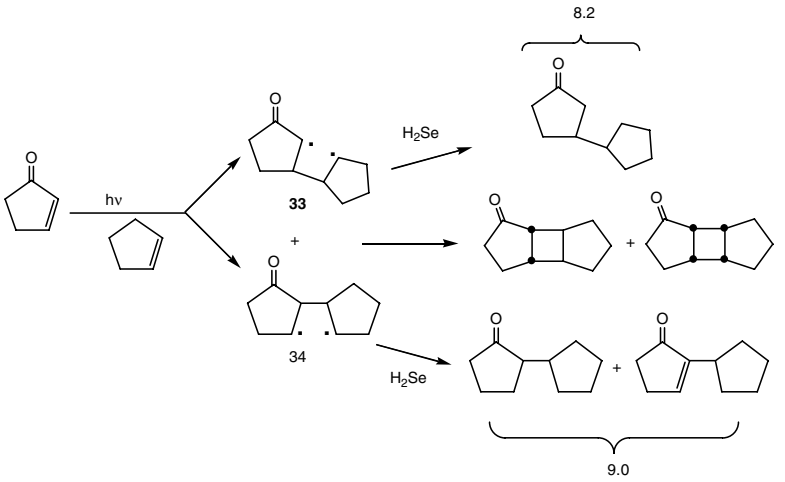

SCHEME 3

Stern–Volmer slope for quenching by naphthalene of oxetane formation, a reaction attributed to $^3(n,\pi^*)$ states,[41] is indeed different from that for quenching **29**, **30**, and **31**. This leaves no doubt that in this system and, by extension, in other cyclohexenones the reactive excited state is the enone $^3(\pi,\pi^*)$ state. There is convincing evidence from transient absorption spectroscopy[16] and photoacoustic calorimetry[17] that relaxed $^3(\pi,\pi^*)$ states of simple cyclohexenones are highly twisted. This twisting is indeed crucial in the photorearrangement pathway[52] and may well be an important factor in formation of both *cis*- and *trans*-fused products in the cycloaddition pathway. The suggestion that ground-state *trans*-cyclohexenones might be on the pathway for formation of [2+2]-cycloadducts as well as rearrangement products has been frequently considered[52–59] but remains controversial to this day. In any event, these experimental studies establish that at least for conformationally flexible cyclic enones, the reactive excited state in [2+2]-cycloaddition to alkenes is definitely a $^3(\pi,\pi^*)$ state. Theoretical studies to be described later strongly support this conclusion.

Bauslaugh's Biradical Proposal: Trapping and Detection of Biradical Intermediates in Enone [2+2]-Photocycloadditions

In 1970, Bauslaugh[60] proposed that the regiochemistry in [2+2]-photocycloadditions of enones could be explained without invoking exciplexes, by considering the most likely conformations of various possible HH and HT 1,4-biradicals and whether they were more likely to either cyclize or to undergo fragmentation to regenerate starting materials.. This proposal received strong experimental support from studies by Weedon and co-workers,[39,61] who succeeded in trapping intermediate 1,4-biradicals in [2+2]-photocycloaddition reactions using hydrogen selenide. Thus, while photocycloaddition of CP to cyclopentene in benzene gives a mixture of *cis-syn-cis* and *cis-anti-cis* adducts (Eq. (72.1)), no cycloadducts were formed in the presence of 0.3-*M* H_2Se (see Scheme 3). Rather, a series of new products were observed, attributable to H-transfer from H_2Se to the putative 1,4-biradical intermediates, followed by reduction and disproportionation of the resulting monoradicals. From the product ratio, it was concluded that the HH and HT 1,4- biradicals **33** and **34** are formed in a 1:1 ratio; that is, there is no significant difference in reactivity of the α and β carbons of the CP triplet toward cyclopentene.

An even more revealing finding involves [2+2]-photoaddition of CP to ethyl vinyl ether (EVE),[39,61] which gives a 3:1 mixture of HT and HH cycloadducts **35** and **36**, in accord with Corey's original findings.[3] Adduct formation is again totally suppressed by H_2Se, yielding instead a mixture of four new products **37** to **40** directly attributable to trapping of the HT and HH 1,4-biradicals **41** and **42** (see Scheme 4). From the product yields, it can be concluded that HH and HT biradicals **41** are again formed in a 1:1

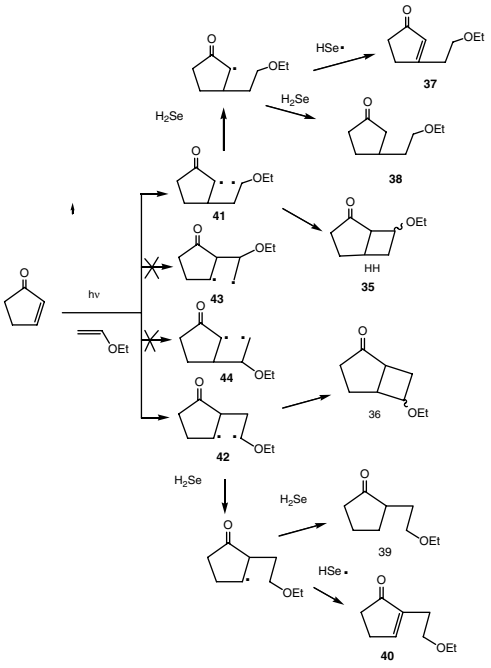

SCHEME 4

ratio. Furthermore, only the more substituted biradicals are formed (i.e., no products derived from biradicals **43** and **44** containing a primary radical center were observed). The observed 3:1 HT/HH regioselectivity in adduct formation, therefore, must originate from differences in cyclization vs. fragmentation to starting materials of the HH and HT 1,4-biradicals. It was suggested that the fact that the HT biradical shows a much greater preference to undergo cyclization vs. scission, while the HH biradical shows a greater tendency for scission as opposed to cyclization, may relate to differing populations of extended vs. closed conformations of these isomeric biradicals. Recent theoretical studies that validate this hypothesis are discussed later.

Further biradical trapping studies using H_2Se demonstrate the generality of the conclusion that the regiochemistry of enone photocycloaddition reactions is entirely determined by the fates of the various 1,4-biradical intermediates (i.e., fragmentation to regenerate ground-state enone and alkene *vs.* cyclization to cyclobutane adducts) and not by the relative rates of formation of these biradicals. For CP, such studies have been successively carried out for photoadditions to allene, 2-methylpropene, 1,1-difluoroethene, and methyl acrylate.[62] In general, comparable amounts of HH and HT biradicals are formed (see Scheme 4) by bonding between the α and β carbons of the enone and the less substituted alkene carbon, generating the more stable biradical intermediate. Thus, for photoaddition of CP and 3-methyl-CP to 2-methylpropene,[62a] the biradicals of type **45**, which are precursors to HH cycloadducts and arise from reaction at the β position of the enone, are formed in 64.5 and 70.5% relative yields. However, they overwhelmingly undergo fragmentation to enone and alkene (95.5 and 88%, respectively) as opposed to cyclization. The corresponding 1,4-biradicals **46** which are precursors to the HT adducts are formed to a much lesser extent by reaction at the α position of the enone, but fragment to a significantly lesser extent (79 and 68%, respectively). The overall result is that more of the HT than the HH product is formed, even though the rate of formation of the biradical precursors is precisely the reverse; that is, HH (**45**) > HT (**46**). Perhaps the most extreme illustration of this curious phenomenon is the photoaddition of 2-methyl-CP to 2-methylpropene,[62a] in which biradical **47** is formed in 90.4% yield but undergoes fragmentation to starting materials to the extent of 97%! As a consequence, only 3% of the isolated products in this reaction are derived from **47**. Furthermore, the presence of the methyl group at C3 (β)

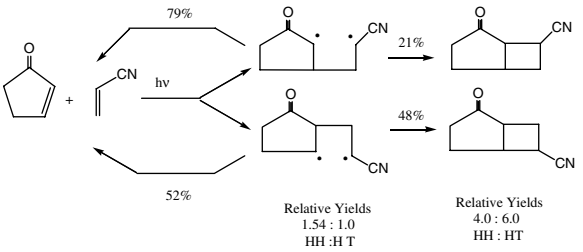

SCHEME 5

on CP has little affect on either the formation of the biradicals or on their tendency to undergo ring closure, while a methyl group at C2 (α) clearly inhibits ring closure. Weedon[62a] interprets these findings to mean that the radical center at C3 in the 1,4-biradical adopts a pyramidalized sp^3 configuration, directing the methyl group on the ring away from the side-chain isobutyl radical in the ring closure step, while the radical center at C2 remains sp^2, so that the methyl is now in the way of the approaching isobutyl radical.

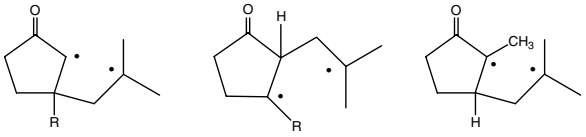

45 R = H, CH_3 **46** R = H, CH_3 **47**

For photoaddition of CP to acrylonitrile (AN), Weedon[62d] found that the ratio of HT to HH diastereomeric cycloadducts was 60:40, reversed from the ratio of 24:76 for addition of AN to 2-cyclohexenone. The latter is in agreement with Corey's original finding.[3] Thus, as in Lange's study discussed earlier,[40] enone ring size clearly affects overall regioselectivity, which directly conflicts with the exciplex hypothesis. While biradical trapping experiments were not successful in the first of these reactions, it was possible to generate the intermediate HH and HT CP/AN biradicals by an alternative route from diketone precursors and determine the cyclization/fragmentation ratio for each of them. From these data, it was possible to construct the reaction scheme shown in Scheme 5,* in which it can be seen that the HH biradical is preferentially formed, but that this biradical again shows a greater propensity to undergo fragmentation than the HT biradical, accounting for the higher yields of HT than of HH adducts.

Finally, analogous radical trapping studies were reported on photoaddition of CH to cyclopentene and ethoxyethene.[63] Once again, a discrepancy is observed between the rates of formation of the various biradical intermediates and the relative yields of the adducts. For CH and cyclopentene, HH and HT biradicals were formed to similar extents, just as was found for CP. For the CH and ethoxyethene reaction, the ratio of HH to HT adducts was 19:81, while the yields of the biradical precursors was 55:45, again demonstrating that overall regiochemistry is determined by the differing extent to which the precursor biradicals undergo cyclization vs. fragmentation. The fact that the reaction pattern is the same as with the CP photoaddition reactions[39,61,62] indicates that the factors operating in both systems are similar.

Weedon's data clearly demonstrate that not only is it not necessary to invoke exciplexes or oriented π-complexes in order to explain the regioselectivity in [2+2]-photocycloaddition of cyclopentenones and cyclohexenones to alkenes, but also that expectations based on the exciplex mechanism are contrary to experimental observations. It is clear that regioselectivity is entirely due to differences in behavior of the intermediate triplet 1,4-biradicals, not to their rates of formation, as was originally hypothesized.[3]

*Reprinted from Krug, P. et al., *Tetrahedron Lett.*, 34, 7221, 1993. With permission.)

Lifetimes and Energies of 1,4-Biradical Intermediates in Enone–Alkene Photocycloadditions

As already discussed, one approach to determination of lifetimes of triplet 1,4-biradicals is by using a radical clock, most commonly the ring opening of cyclopropylcarbinyl to 3-butenyl radicals.[33] Thus, in the work of Becker and co-workers[32] on dienones analogous to **5** with a cyclopropyl substituent on the CC double bond in the side chain, the biradical lifetimes were estimated to be on the order of 50 ns. Photoaddition of CP to vinylcyclopropane (see Eq. (72.12)) gave cycloadducts as well as products derived from the ring opening of the intermediate HH and HT biradicals, whose average lifetimes were also estimated to be ~50 ns.[34]

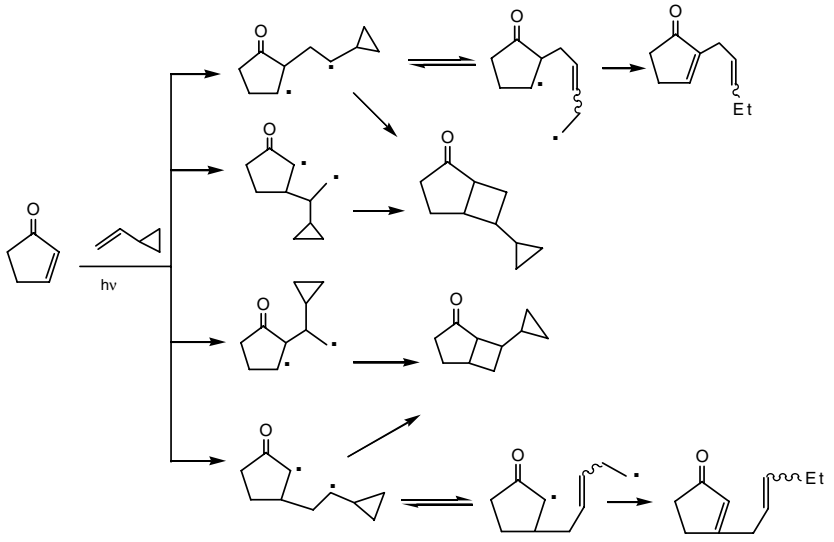

(72.12)

However, in the photoaddition of cyclopentenone to 1,6-heptadiene, the initial 1,4-biradicals were observed, consistent with the lower rate of rearrangement of 1-hexenyl to cyclopentylmethyl radicals, $<10^5$ s^{-1}.[64] The initially formed triplet 1,4-biradicals in the cycloaddition reactions must therefore have lifetimes substantially less than 10 μs, consistent with the results on the cyclopropyl-substituted systems. A similar observation was made in intramolecular photoadditions of cyclohexenones possessing a tethered diene moiety.[29]

Caldwell et al.[65] succeeded in directly detecting triplet 1,4-biradicals in enone cycloadditions using nanosecond flash photolysis. Excitation of CP in acetonitrile gives complex transient decay profiles at 280 nm that can be resolved into two first-order decays, one dependent on the concentration of the enone and a second that is not. The former is concluded to be the CP triplet,[6,11,12,53,65] whose limiting lifetime in acetonitrile is 380 ± 75 ns. The much smaller CP triplet lifetime of 30 ns reported earlier by Bonneau[55] is consistent with the concentration-independent lifetime of 37 ns for the second transient in the laser flash studies,[65] which is now attributed to the (weighted) average lifetime of the HH and HT triplet 1,4-biradicals formed by CP self-quenching:

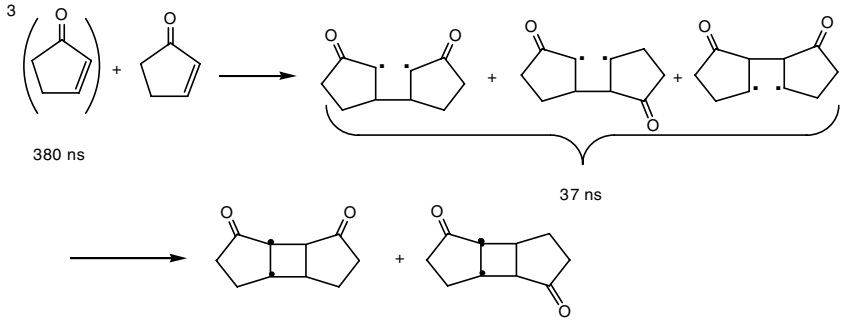

(72.13)

Note that two stereogenic centers are generated on formation of the first CC bond, so that each of the three 1,4-biradicals in Eq. (72.9) is actually a mixture of two diastereomers; thus, as many as six 1,4-biradicals can be formed in this reaction. Using time-resolved photoacoustic calorimetry (PAC) at moderate CP concentrations, a short-lived transient species was detected whose lifetime was in perfect agreement with that derived from the flash photolysis study and is identified with the dimeric biradicals shown in equation 9.[65] From the PAC data the energy of the biradicals (relative to a pair of ground-state CP molecules) was determined to be 47.4 ± 1.7 kcal/mol, in excellent agreement with values of 44 and 51 kcal/mol for the HH and HT biradicals estimated using the Benson group additivity technique.[66] These are the only such data reported for enone-derived triplet 1,4-biradicals.

More recently, the PAC technique has been used to measure lifetimes and energies of triplet 1,4-biradicals derived from a number of model enones and alkenes.[67] The biradical lifetimes vary from 20 to 600 ns. The shortest lifetimes are for biradicals derived from 3-MCH and cyanoalkenes, while the longest is for 3-MCH and 2,3-dimethyl-2-butene. A typical value is 59 ± 5 ns for the biradical(s) derived from testosterone acetate and cyclopentene. Again, these represent average lifetimes of the biradicals formed in the reaction, some of which may not even yield products to a significant extent, as discussed above. The average energies of these biradicals range from 36 to 60 kcal/mol, relative to the ground states of the reactants. These values are again in good agreement with estimates based upon Benson's additivity rules.[66] It is clear that the triplet 1,4-biradicals derived from enone triplets and alkenes have lifetimes allowing for complete conformational equilibration. On this basis, it is not at all obvious why certain cyclohexenone photoadditions (e.g., to *Z*- and *E*-2-butene) are apparently not accompanied by at least partial isomerization of the recovered alkene[3] and why there is no loss of alkene stereochemistry in recovered starting material in the intramolecular photocycloadditions reported by Becker.[29]

The Bauslaugh–Schuster–Weedon Mechanism for Enone–Alkene Photocycloadditions

The Corey–de Mayo exciplex mechanism[3,15,48] for photocycloaddition of enones to alkenes has provided a stimulus for workers in this field and undoubtedly has had heuristic value in accounting for experimental observations in a vast number of reactions.[5] Nonetheless, the experimental findings discussed above make it clear that this mechanism for enone [2+2]-photocycloadditions has been discredited and should be abandoned.

There is a single isolated case in which spectroscopic evidence for formation of a triplet exciplex in an enone photocycloaddition has been reported, involving the photoreaction between 4,4-dimethyl-2-cyclohexenone (DMCH, **28**) and 1,1-diphenylethene (DPE).[68a] Laser flash photolysis (LFP) of DMCH in cyclohexane yields the expected enone triplet (λ_{max} = 280 nm), with a lifetime of 24 ns, as previously reported,[16] and the DPE triplet was similarly characterized (λ_{max} = 335 nm, τ = 34 ns). Photolysis of DMCH in the presence of DPE leads to quenching of DMCH triplets at a rate constant in line with those previously reported and formation of a new transient whose spectrum is essentially identical to that of ^{3}DPE*, but which decays with a lifetime of 50 ns. Oxygen quenching studies indicate that the 50-ns transient is a source of the $^1O_2$ formed in this reaction, which is greater than if the enone triplet was the only sensitizer of $^1O_2$ formation. Azulene quenching studies show that the yield of azulene triplets in the presence of DPE is also considerably higher than that attributable to DMCH triplets under these conditions, as DPE triplets are themselves not quenched by azulene. On the basis of these findings, Caldwell et al.[68a] originally argued that the 50 ns transient is a triplet exciplex resulting from interaction of DPE with ^{3}DMCH*, and that it is formed prior to or in competition with triplet 1,4-biradicals. Based upon new laser flash photolysis experiments, Caldwell now concludes[68b] that the temporal data and quenching studies are best fit by a composite of triplet state transients including the triplet state of DPE and a triplet 1,4-biradical and perhaps other species. The earlier interpretation[68a] that the transient was a ^{3}DMCH*-DPE exciplex is now concluded to be "unnecessary and unlikely".

Thus, the role of exciplexes as intermediates in [2+2]-photocycloadditions of enones to alkenes in general remains highly doubtful. The mechanism for [2+2]-photocycloaddition shown in Scheme 6,[6a]

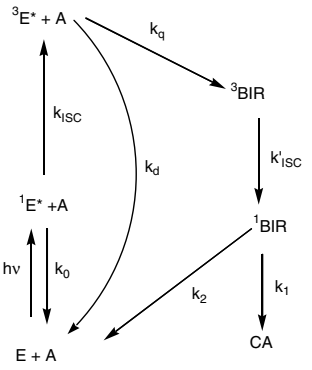

E = enone, A= alkene,B IR = 1,4-biradical, CA = cycloadducts

SCHEME 6

essentially an elaboration of that postulated by Bauslaugh,[60] is sufficient to rationalize all the data obtained to date concerning this process. In this mechanism, the only intermediates invoked in the addition process are the enone triplet excited states and triplet and singlet adduct 1,4-biradicals. Further specification of the nature and behavior of the intermediate biradicals comes from the theoretical studies discussed in the next section.

72.4 Theoretical Studies of [2+2]-Photocycloadditions of Enones to Alkenes

Several theoretical descriptions of this reaction have appeared in the past few years.[69,70] The following discussion is based on the very thorough treatment published by Wilsey et al.[70] in which the potential energy surfaces of the ground-state (S_0), triplet excited state (both $^3[\pi,\pi^*]$ and $^3[n,\pi^*]$), and singlet excited state ($^1[n,\pi^*]$) potential surfaces for the addition of acrolein (CH_2=CH–CH=O) to ethene to give formylcyclobutane were calculated by *ab initio* techniques. Calculations were performed using CASSCF (complete active space SCF) procedures and the standard 6–31G* basis set available in Gaussian 94. This approach was used specifically because it allows for balanced representation of several electronic states simultaneously. Dynamic correlation effects, which should not affect arguments regarding biradicaloid structures, were neglected in these calculations. The geometry and energy of the optimized 1,4-biradical intermediates formed on attack at the α- and β-carbons of acrolein and transition structures leading to these biradicals on each of the potential surfaces, as well as transition structures for reaction of each of these biradicals, were determined. The transition structures on the excited-state surface determine the nature of the initially formed biradical intermediate, while those on the ground-state surface control the competition between cyclization (i.e., product formation) and cleavage (reversion to starting materials).

A number of general observations were made.[70] The initial part of the reaction involves attack by the alkene on the triplet state of *s-cis*- or *s-trans*-acrolein at either the α- or β- carbon, leading to a large set of *anti* and *gauche* conformations of the triplet biradical intermediate, which then undergo intersystem crossing to the ground-state potential surface. The second part of the reaction is controlled by the topology on the ground-state surface. Not unexpectedly and in accord with Bauslaugh's original hypothesis,[60] the *anti* biradicals have a tendency to dissociate to regenerate starting materials, whereas the *gauche* biradicals favor cyclobutane formation. At the geometry of the ground-state reactants, the lowest energy excited state is the $^3(n,\pi^*)$ state, with both $^3(\pi,\pi^*)$ and $^1(n,\pi^*)$ lying 4 to 5 kcal/mol higher in energy. As soon as the geometries are allowed to relax, the $^3(\pi,\pi^*)$ state becomes the lowest energy excited state, and the reaction with the alkene follows from this state. Specifically, the $^3(\pi,\pi^*)$ minimum is 60 kcal/mol above the minimum on the ground-state surface and is 9.2 kcal/mol below the planar $^3(n,\pi^*)$ state. Furthermore, the barriers for addition of the $^3(n,\pi^*)$ state to ethylene at both the α- and β-carbons are significantly

higher than found for the $^3(\pi,\pi^*)$ state, α-attack being particularly disfavored as it involves decoupling of electrons. Therefore, reaction from the $^3(n,\pi^*)$ surface, if it occurs at all, should occur only by β-attack. This is expected only in rigid enone systems that cannot undergo conformational relaxation. Thus, as already concluded on the basis of experimental data,[50–53] we need only be concerned with reaction via the $^3(\pi,\pi^*)$ state for enones with some degree of conformational flexibility, such as cyclohexenones and probably also cyclopentenones.

The lowest energy *anti* and *gauche* transition structures for α-attack on the $^3(\pi,\pi^*)$ state both lie about 20 kcal/mol above the reactant minimum, with no preference between them. The three most stable biradicals that result after conformational relaxation are shown in structures **48**, **49**, and **50**.* The energies of the transition structures for β-attack on the $^3(\pi,\pi^*)$ state are 3 to 4 kcal/mol lower than for α-attack, leading to biradicals **51**, **52** and **53**,* which themselves are some 10 kcal/mol than the biradicals formed by α-attack. Interestingly, these biradical minima are almost degenerate with the corresponding minima on the ground-state surface, but spin-orbit coupling at these topologies is negligible. Nonetheless, the fact that the excited- and ground-state surfaces are parallel to each other over a wide range of geometries provides a high probability of intersystem crossing to the ground-state surface.

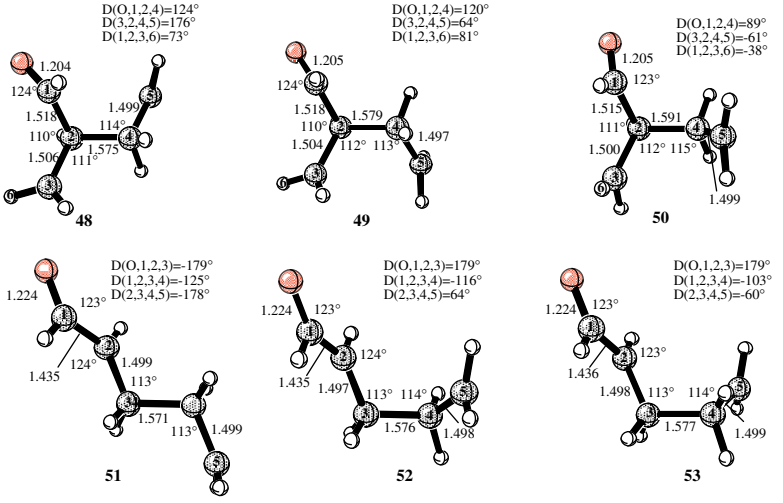

The barriers for dissociation (cleavage) on the ground-state surface are only 0.3 and 0.7 kcal/mol for the α-biradicals in the two *gauche* conformations **49** and **50** and disappear entirely for the corresponding *anti* biradical **48**. The barriers for ring closure of **48** and **49** are comparable (0.3 and 0.8 kcal/mol), suggesting a slight preference for ring closure from **48** over **49**. The barrier for interconversion of the *anti* and *gauche* biradicals on the ground-state surface is approximately 3.4 kcal/mol and is slightly higher on the excited-state surface. Nonetheless, the barrier is such that *anti/gauche* interconversion could occur before intersystem crossing to the ground-state surface. For the β-biradicals, the energies of the transition structures for dissociation on the ground-state surface are slightly higher (1.8 to 2.7 kcal/mol), while the competing barriers for ring closure (from **52** and **53**) are only 0.1 and 0.7 kcal/mol. The barriers for conformational equilibration are similar to those for the α-biradicals. Thus, once again, the *gauche* β-biradicals prefer to cyclize, while the *anti* biradicals prefer to fragment. It is noted that the barriers for dissociation of the α-biradicals are about 1 kcal/mol lower than for the analogous tetramethylene biradical,[71] indicating that fragmentation competes more effectively with ring closure for the α–biradicals even in the *gauche* minima; however, for the corresponding β-biradicals, the dissociation transition structures are higher in energy than for tetramethylene biradicals,[71] indicating a higher tendency of the former to undergo cyclization.

*Reprinted from Wilsey, S. et al., *J. Am. Chem. Soc.*, 122, 5866, 2000. With permission.

In summary, the calculations indicate that for ethylene the *anti* biradical formed by β-attack on the enone $^3(\pi,\pi^*)$ state should form most rapidly but will mainly undergo dissociation. The *gauche* biradicals will form more slowly but have a better chance of undergoing ring closure. Similar behavior is expected with electron-deficient alkenes. For electron-rich alkenes, Houk and co-workers[69a,70] propose that attack occurs preferentially at the more electrophilic α-carbon of the enone $^3(\pi,\pi^*)$ state, affording both *anti* and *gauche* biradicals to a similar extent, but that these α-biradicals will mainly dissociate. In this scenario, cyclobutane formation will occur slowly from the gauche α-biradicals, leading to HT products. However, Weedon's studies[39,61–63] indicate that even with electron-rich alkenes, such as ethoxyethene, reaction at the β-carbon of the enone competes effectively with reaction at the α–carbon, for both CP and CH, demonstrating that both β- and α-biradicals play a significant role in these systems. That is, the difference in electrophilicity at the two carbons of the enone $^3(\pi,\pi^*)$ state appears in reality to be quite small.

In most significant respects, these calculations provide a very strong theoretical framework for the mechanism presented in Scheme 3, providing values for the energies of the transition structures for formation of the biradicals on the excited-state surface and for the competitive dissociation/cyclization pathways of the various biradicals on the ground-state surface, data that would be difficult to obtain experimentally. They also clearly demonstrate the great importance of molecular topology on both the ground state and excited-state surfaces in determining the course of these reactions.

72.5 Conclusions and Future Directions in Research on Enone Photocycloadditions

The mechanistic questions regarding this reaction, after intensive research for almost 40 years, are essentially resolved in favor of the triplet biradical mechanism shown in Scheme 3. It is unlikely that further research on the reaction mechanism will be profitable, although further insight into the properties (energies, lifetimes, and geometry) of the intermediate biradicals may yet evolve. One possible benefit of this revised mechanism is that more attention may be paid to photoadditions of cyclohexenones to electron-deficient alkenes, now that the mechanistic bias against such reactions has been removed. While these are sometimes accompanied by unwanted side reactions, such as polymer formation in the case of AN,[19,32] such reactions oftentimes proceed quite cleanly.[36] Just as [2+2]-photoaddition of enones to electron-rich alkenes have been profitably used by synthetic chemists,[5] there is no reason why analogous reactions using electron-poor alkenes should not also find synthetic utility.

One example of this is the photochemical [2+2]-addition of cyclic enones to C_{60}, which in many ways behaves as an electron deficient alkene. Thus, C_{60} is readily attacked by nucleophiles and free radicals but not by electrophiles.[72] Schuster and co-workers[73] have shown that ultraviolet irradiation of a large variety of cyclic enones in the presence of C_{60} leads to both *cis*- and *trans*-fused [2+2]-cycloadducts in good yields by a reaction that involves attack of enone triplet excited states on ground-state fullerene. Photoaddition does not occur if the fullerene is selectively excited at longer wavelengths (532 nm). The reaction, which is an effective route for functionalisation of fullerenes, appears to occur by the general triplet biradical mechanism outlined in Scheme 6. More recently, Vassilikogiannakis and Orfanopoulos[74] reported that acyclic enones also undergo reversible [2+2]-photoaddition to C_{60} upon ultraviolet irradiation. This reaction is unusual in that acyclic enones rarely undergo photoaddition to alkenes, because *Z,E*-isomerization of the enone excited state is typically the dominant process upon photoexcitation of the enone.[6] The observed regio- and stereoselectivity of the addition reaction[74] could be explained in terms of the relative stability of the 1,4-biradical intermediates that are presumably involved. It is additionally interesting to note that these photocycloadditions occur despite the fact that the triplet excited state of C_{60} is of much lower energy than that of the enones. Thus, addition of the enone triplet to the fullerene is faster than intermolecular triplet–triplet energy transfer. Possible explanations for this observation have been discussed by Schuster et al.[73]

The possibility of altering the course of enone [2+2]-photocycloadditions by modification of reaction conditions needs to be investigated. One approach would be to carry out such reactions in nonhomog-

enous media.[75] For example, photodimerization of coumarin in cyclodextrins[76] as well as of CP and CH in dry zeolites[77] give product distributions that are quite different from those in fluid solution. The factors that control the stereochemistry of the 6/4-ring fusion in [2+2]-photoadditions of CH systems still remain to be completely elucidated. Nonetheless, approaches to achieving stereochemical control in enone-alkene [2+2]-photocycloadditions have been reported[78] that will further enhance the synthetic utility of these reactions.

Acknowledgment

The author gratefully acknowledges continued support of the photochemical and photophysical research in his laboratory by the National Science Foundation

References

1. (a) Eaton, P. E., The tricyclo[5.3..O.O^{2,6}]decane system. The photodimers of cyclopentenone, *J. Am. Chem. Soc.,* 84, 2344, 1962; (b) Eaton, P. E. and Hurt, W. S., Photodimerization of cyclopentenone: singlet or triplet?, *J. Am. Chem. Soc*., 88, 5038, 1966.
2. Eaton, P. E., On the mechanism of the photodimerization of cyclopentenone, *J. Am. Chem. Soc.,* 84, 2454, 1962.
3. Corey, E. J., Bass, J. D., LeMahieu, R., and Mitra, R. B., A study of the photochemical reactions of 2-cyclohexenones with substituted olefins, *J. Am. Chem. Soc.*, 86, 5570, 1964.
4. Corey, E. J, Mitra, R. B., and Uda, H., Total synthesis of the *d,l*-caryophyllene and *d,l*-isocaryophyllene, *J. Am. Chem. Soc.,* 86, 485, 1964.
5. (a) Weedon, A. C., Enone photochemical cycloaddition in organic synthesis, in *Synthetic Organic Chemistry*, Horspool, W. M., Ed., Plenum Press, New York, 1984, chap. 2; (b) Baldwin, S. W., Synthetic organic aspects of 2+2 cycloadditions of α,β-unsaturated carbonyl compounds, in *Organic Photochemistry*, Vol. 5, Padwa, A., Ed., Marcel Dekker, New York, 1981, 123–225; (c) Carless, H. A. J., Enone and dienone rearrangements, in *Photochemistry in Organic Synthesis*, Coyle, J. D., Ed., Royal Society of Chemistry, London, 1986, 95–117; (d) Oppolzer, W., Intramolecular [2+2] photoaddition/fragmentation sequence in organic chemistry, *Acc. Chem. Res.,* 15, 135, 1982; (e) Wender, P. A., Alkene cycloaddition, in *Photochemistry in Organic Synthesis*, Coyle, J. D., Ed., Royal Society of Chemistry, London, 1986, 163.
6. (a) Schuster, D. I., Lem, G., Kaprinidis, N. A., New insights into an old mechanism: [2+2] photocycloaddition of enones to alkenes, *Chem. Rev.*, 93. 3, 1993; (b) Schuster, D. I., The photochemistry of enones, in *The Chemistry of Enones*, Patai, S. and Rappoport, Z., Eds., John Wiley & Sons, Chichester, U.K., 1989, chap. 15.
7. (a) Lam, E. Y. Y., Valentine, D., and Hammond, G. S., Mechanisms of photochemical reactions in solution. XLIV. Photodimerization of cyclohexenone, *J. Am. Chem. Soc.*, 89, 3482, 1967; (b) Ruhlen, J. L. and Leermakers, P. A., Photochemistry of cyclopentenone in various media, *J. Am. Chem. Soc.*, 89, 4944, 1967.
8. Chapman, O. L., Koch, T. H., Klein, F., Nelson, P. J., and Brown, E. L., Two Triplet mechanisms in photochemical addition of 2-cyclohexenones to 1,1-dimethoxyethylene, *J. Am. Chem. Soc.*, 90, 1657, 1968.
9. (a) de Mayo, P., Pete, J.-P., and Tchir, M., Cyclopentenone photocycloaddition: a reaction from a higher triplet state, *J. Am. Chem. Soc.* 89, 5712, 1967; (b) de Mayo, P., Pete, J.-P., and Tchir, M., Photochemical synthesis. 22. On photochemical cycloaddition: cyclopentenone, *Can. J. Chem.*, 46, 2535, 1968.
10. Wagner, P. J. and Bucheck, D. J., Inefficiency and reversibility in the photodimerizations of 2-cyclopentenone, *Can. J. Chem.*, 47, 713, 1969.
11. Wagner, P. J. and Bucheck, D. J., A comparison of the photodimerizations of 2-cyclopentenone and of 2-cyclohexenone in acetonitrile, *J. Am. Chem. Soc.*, 91, 5090, 1969.

12. De Mayo, P, Nicholson, A. A., and Tchir, M. F. Evidence for reversible intermediate formation in cyclopentenone cycloaddition, *Can. J. Chem.*, 47, 711, 1969.
13. (a) Kearns, D. R., Marsh, G., and Schaffner, K., Excited singlet and triplet states of a cyclic conjugated enone, *J. Chem. Phys.*, 49, 3316,1968; (b) Marsh, G., Kearns, D. R., and Schaffner, K., Spectroskopische Untersuchung Einiger α,β-Ungesättigter Cyclischer Ketone, *Helv. Chim. Acta*, 51, 1890, 1968; (c) Marsh, G., Kearns, D. R., and Schaffner, K., Investigations of singlet-triplet transitions by phosphorescence excitation spectroscopy. IX. Conjugated enones, *J. Am. Chem. Soc.*, 93, 3129, 1971.
14. Devaquet, A., Potential energy sheets for the n,π^* and π,π^* triplet states of α,β-unsaturated ketones, *J. Am. Chem. Soc.*, 94, 5160, 1972.
15. de Mayo, P., Enone Photoannelation, *Acc. Chem. Res.*, 4, 41, 1971.
16. Schuster, D. I., Dunn, D. A., Heibel, G. E., Brown, P. B., Rao, J. M., Woning, J., and Bonneau, R., Enone photochemistry: dynamic properties of triplet excited states of cyclic conjugated enones as revealed by transient absorption spectroscopy, *J. Am. Chem. Soc.*, 113, 6245, 1991 (and earlier papers cited).
17. Schuster, D. I., Heibel, G. E., Caldwell, R. A., and Tang, W., Determination of triplet excitation energies of cyclic enones by time-resolved photoacoustic calorimetry, *Photochem. Photobiol.*, 52, 645, 1990.
18. Schuster, D. I., Woning, J., Kaprinidis, N. A., Pan, Y., Cai, B., Barra, M., and Rhodes, C. A., Photochemical and photophysical studies of bicyclo[4.3.0]non-1(6)-en-2-one, *J. Am. Chem. Soc.*, 114, 7029, 1992.
19. Schuster, D. I., Heibel, G. E., Brown, P. B., Turro, N. J., and Kumar, C. V., Are triplet exciplexes involved in [2+2]-photocycloaddition of cyclic enones to alkenes?, *J. Am. Chem. Soc.*, 110, 8261, 1988.
20. (a) Heibel, G. E., Energetics and Reactivity of Excited States of Cyclic α,β-Unsaturated Ketones, Ph.D. dissertation, New York University, 1990; (b) Brown, P. B., Photocycloaddition Reactions of Alkenes and 2-Cyclohexenone: A Mechanistic Study, Ph.D. dissertation, New York University, 1988.
21. Schuster, D. I., Kaprinidis, N. A., Wink, D. J., and Dewan, J. C., Stereochemistry of [2+2] photocycloaddition of cyclic enones to alkenes: structural, and mechanistic considerations in formation of *trans*-fused cycloadducts, *J. Org. Chem.*, 56, 561, 1991.
22. Kaprinidis, N. A., Woning, J., Schuster, D. I., and Ghatlia, N. D., Photochemistry of steroidal enones: formation of an exceptionally stable ketene by an α-cleavage reaction, *J. Org. Chem.*, 57, 755, 1992.
23. Peet, N. P, Cargill, R. L., and Bushey, D. F., Synthesis and acid-catalyzed rearrangements of tricyclo[4.3.2.0]undecanones, *J. Org. Chem.*, 38, 1218, 1973.
24. Dilling, W. L., Tabor, T. E., Boer, F. P., and North, P. P., Organic photochemistry. IX. The photocycloaddition of 2-cyclopentenone to *cis*- and *trans*-dichloroethylene: evidence for initial attack at carbon-3 and rotational equilibration of biradical intermediates, *J. Am. Chem. Soc.*, 92, 1399, 1970.
25. McCullough, J. J., Ramachandran, B. R., Snyder, F. F., and Taylor, G. N., Kinetics of photochemical addition of 3-phenyl-2-cyclohexenone to tetramethylethylene, *J. Am. Chem. Soc.*, 97, 6767, 1975.
26. Schuster, D. I., Heibel, G. E., and Woning, J., The mechanism of interaction of triplet 3-methylcyclohex-2-en-1-one with maleo- and fumaronitrile: evidence for direct formation of triplet 1,4-biradicals in [2+2] photocycloadditions without the intermediacy of exciplexes, *Angew. Chem. Int. Ed. Engl.*, 30, 1345, 1991.
27. (a) Schenck, G. O. and Steinmetz, R., Neuratige durch Benzsophenon Photosensibilisierte Additionene von Maleinsäureanhydrid an Benzol und Andere Aromaten, *Tetrahedron Lett.*, 1, 1960; (b) Gollnick, K. and Schenck, G. O., Mechanism and stereoselectivity of photosensitized oxygen transfer reactions, *Pure Appl. Chem.*, 9, 507, 1964.
28. (a) Wong, P. C., Triplet energies of fumaronitrile and maleonitrile, *Can. J. Chem.*, 60, 339, 1982; (b) Lavilla, J. A. and Goodman, J. L., The energetics and kinetics of relaxed alkene triplet states as determined by pulsed time-resolved photoacoustic calorimetry, *Chem. Phys. Lett.*, 141, 149, 1987.

29. (a) Becker, D. and Haddad, Y. S., Topological and steric effects in mechanism of intramolecular [2+2] photocycloadditions, *Tetrahedron Lett.*, 30, 4429, 1989; (b) Becker, D., Nagler, M., Sahali, Y., and Haddad, N., Regiochemistry and stereochemistry of intramolecular [2+2] photocycloaddition of carbon–carbon double bonds to cyclohexenones, *J. Org. Chem.*, 56, 4537, 1991.
30. (a) Srinivasan, R. and Carlough, K. H., Mercury ($^3P_1$) photosensitized internal cycloaddition reactions in 1,4-, 1,5- and 1,6-dienes, *J. Am. Chem. Soc.*, 89, 4932, 1967; (b) Liu, R. S. H. and Hammond, G. S., Photosensitized internal additions of dienes to olefins, *J. Am. Chem. Soc.*, 89, 4936, 1967; (c) Gleiter, R. and Sander, W., Light-induced [2+2] cycloaddition reactions of non-conjugated dienes: the effect of through-bond interaction, *Angew. Chem. Int. Ed. Engl.*, 24, 566, 1985; (d) Fischer, E. and Gleiter, R., Regiochemistry of the intramolecular [2+2]-photocycloaddition of cyclohexenone to vinyl ethers, *Angew. Chem. Int. Ed. Engl.*, 28, 925, 1989,
31. Schroder, C., Wolff, S., and Agosta, W. C., Biradical reversion in the intramolecular photochemistry of carbonyl-substituted 1,5-hexadienes, *J. Am. Chem. Soc.*, 109, 5491, 1987.
32. Becker, D., Haddad, N., and Sahali, Y., Trapping of 1,4-diradical intermediate in intramolecular [2+2] photocycloaddition, *Tetrahedron Lett.*, 30, 2661, 1989.
33. Mathew, L. and Warkentin, J., The cyclopropylmethyl free radical clock: calibration for the 30–89°C range, *J. Am. Chem. Soc.*, 108, 7981, 1986.
34. Rudolph, A. and Weedon, A. C., Radical clocks as probes of 1,4-biradical intermediates in the photochemical cycloaddition reactions of 2-cyclopentenone with alkenes, *Can. J. Chem.*, 68, 1590, 1990.
35. (a) Becker, D., Galili, N., and Haddad, N., Highly efficient trapping of short-lived 1,4-diradicals: the order of first bond formation in the intramolecular photocycloaddition of 3-(4′pentenyl)-cyclohex-2-enones, *Tetrahedron Lett.*, 37, 8941, 1996; (b) Haddad, N. and Galili, N., The order of first bond formation in the intramolecular photocycloaddition of 2-(4′pentenyl)-cyclohex-2-ennes, *Tetrahedron Lett.*, 38, 6083, 1997.
36. Cantrell, T. S., Haller, W. S., and Williams, J. C., Photocycloaddition reactions of some 3-substituted cyclohexenones, *J. Org. Chem.*, 34, 509, 1969.
37. (a) Lenz, G. R., Photocycloaddition reactions of conjugated enones, *Rev. Chem. Intermed.*, 4, 369, 1981; (b) Lenz, G. R., The isolation and characterization of a steroidal *trans*-fused cyclobutanone from an enone [2+2] photoadduct, *J. Chem. Soc.*, *Chem. Commun.*, 803, 1982; (c) Lenz, G. R., The photocycloaddition of an 5α-androst-1-en-3-one to olefins, *J. Chem. Soc.*, *Perkin Trans. 1*, 2397, 1984.
38. Swapna, G. V. T., Lakshmi, A. B., Rao, J. M., and Kunwar, A. C., Mechanistic implications of photoannelation reaction of 4,4-dimethylcyclohex-2-en-1-one and acrylonitrile; regio- and stereochemistry of the major photoadduct by ^{1}H and ^{13}C NMR spectroscopy, *Tetrahedron*, 45, 1777, 1989.
39. Andrew, D., Hastings, D. J., Oldroyd, D. L., Rudolph, A., Weedon, A. C., Wong, D. F., and Zhang, B., Triplet 1,4-biradical intermediates in the reactions of enones and *N*-acylindoles with alkenes, *Pure Appl. Chem.*, 64, 1327, 1992.
40. Lange, G. L., Organ, M. G., and Lee, M., Reversal of regioselectivity with increasing ring size of alkene component in [2+2] photoadditions, *Tetrahedron Lett.*, 31, 4689, 1990.
41. Turro, N. J., *Modern Molecular Photochemistry*, Benjamin/Cummings, Menlo Park, CA, 1978; (b) Cowan, D. O. and Drisko, R. L., *Elements of Organic Photochemistry*, Plenum Press, New York, 1976.
42. Wagner, P. J., Type II photoelimination and photocyclization of ketones, *Acc. Chem. Res.*, 4, 168, 1971.
43. Cargill, R. L., Morton, G. H., and Bordner, J., Stereochemistry of photochemical cycloadditions: 4-*tert*-butylcyclohex-2-en-1-one and ethylene, *J. Org. Chem.*, 45, 3930, 1980.
44. Scaiano, J. C., Leigh, W. J., Meador, M. A., and Wagner, P. J., Sterically hindered triplet energy transfer, *J. Am. Chem. Soc.*, 107, 5806, 1985.
45. (a) Hoffmann, R., An extended Hückel theory, *J. Chem. Phys.*, 39, 1397, 1963; (b) Hoffmann, R., Extended Hückel theory. IV. Carbonium ions, *J. Chem. Phys.*, 40, 2480, 1964; (c) Zimmerman, H. E. and Swenton, J. S., Mechanistic organic photochemistry. VIII. Identification of the n,π^* triplet excited states in the rearrangement of 4,4-diphenyl-cyclohexadienone, *J. Am. Chem. Soc.*, 86, 1436. 1964.

46. de Mayo. P., Nicholson, A. A., and Tchir, M. F., Photochemical synthesis. 22. On photochemical cycloaddition: cyclopentenone, *Can J. Chem.*, 48, 225, 1970.
47. (a) Montgomery, L. K., Schueler, K., and Bartlett, P. D., Cycloaddition. II. Evidence of a biradical intermediate in the thermal addition of 1,1-dichloro-2,2-difluoroethylene to the geometrical isomers of 2,4-hexadiene, *J. Am. Chem. Soc.*, 86, 622, 1964; (b) Bartlett, P. D. and Wallbillich, G. E. H., Cycloaddition. XI. Evidence for reversible biradical formation in the addition of 1,1-dichloro-2,2-difluoroethylene to the stereoisomers of 1,4-dichloro-1,3-butadiene, *J. Am. Chem. Soc.*, 91, 409, 1969; (c) Bartlett, P. D. and Porter, N. A., The stereochemical course of cyclic azo decompositions, *J. Am. Chem. Soc.*, 90, 5317, 1968; (d) Wagner, P. J. and Schott, H. N., Polar substituent effects in the reactions of 1,4-biradicals, *J. Am. Chem. Soc.*, 91, 5383, 1969.
48. Loutfy, R. D. and de Mayo, P., On the mechanism of enone photoannelation: activation energies and the role of exciplexes, *J. Am. Chem. Soc.*, 99, 3559, 1977.
49. Caldwell, R. A., Sovocool, G. W., and Gajewski, R., Primary interaction between diaryl ketone triplets and simple alkenes: isotope effects, *J. Am. Chem. Soc.*, 95, 2549, 1973.
50. Schuster, D. I., Greenberg, M. M., Nuñez, I. M., and Tucker, P. C., Identification of the reactive electronic excited state in the photocycloaddition of alkenes to cyclic enones, *J. Org. Chem.*, 48, 2615, 1983.
51. Tucker, P. C., The Photochemistry of 3-Cyclohexenones: The [2+2] Photocycloaddition of 2-Cyclohexenones to Alkenes, Ph.D. dissertation, New York University, 1988.
52. Schuster, D. I., Photochemical rearrangements of enones, in *Rearrangements in Ground and Excited States*, Vol. 3, De Mayo, P., Ed., Academic Press, New York, 1980, Essay 17.
53. Schuster, D. I., Brown, P. B., Capponi, L. J., Rhodes, C. A., Scaiano, J. C., Tucker, P. C., and Weir, D., Mechanistic alternatives in photocycloaddition of cyclohexenones to alkenes, *J. Am. Chem. Soc.*, 109, 2533, 1987.
54. (a) Bonneau, R. and Fornier de Violet, P., Mise en Évidence d'un Isomère trans tendu de l'Acetyl-1-cyclohèxene et d'une Forme Métastable Attribueé a un État Triplet Orthogonal, *C. R. Acad. Sci. Paris*, *Ser. C.*, 284, 631, 1977; (b) Goldfarb, T. J., Kinetic studies of transient photochemical isomers of 2-cycloheptenone, 1-acetylcyclohexene and 2-cyclohexenone, *J. Photochem.*, 8, 29, 1978.
55. Bonneau, R., Transient Species in photochemistry of enones: the orthogonal triplet state revealed by laser photolysis, *J. Am. Chem. Soc.*, 102, 3816, 1980.
56. Eaton, P. E., Photochemical reactions of simple acyclic enones, *Acc. Chem. Res.*, 1, 50, 1968.
56. Bowman, R. M., Calvo, C., McCullough, J. J., Rasmussen, P. W., and Snyder, F. F., Photoaddition of 2-cyclohexenone derivatives to cyclopentene: an investigation of stereochemistry, *J. Org. Chem.*, 37, 2084, 1972.
57. Verbeek, J., van Lenthe, J. H., Timmermans, P. J. J. A., Mackor, A., and Budzelaar, P. H. M., On the existence of *trans*-cyclohexene, *J. Org. Chem.*, 52, 2955, 1987.
58. (a) Dunkelblum, E., Hart, H., and Jeffares, M., Stereochemistry of the photoinduced addition of methanol to Pummerer's ketone, a 2-cyclohexenone, *J. Org. Chem.*, 43, 3409, 1978; (b) Mintas, M., Schuster, D. I., and Williard, P. G., Stereochemistry and mechanism of [4+2] photocycloaddition of Pummerer's ketone to furan, *J. Am. Chem. Soc.*, 110, 2305, 1988; (c) Mintas, M., Schuster, D. I., and Williard, P. G., Stereochemistry and mechanism of the [2+2] and [4+2] photocycloaddition of alkenes and dienes to Pummerer's ketone, *Tetrahedron*, 44, 6001, 1988.
59. Rudolph, A. and Weedon, A. C., Acid catalysis of the photochemical deconjugation reaction of 3-alkyl-2-cyclohexenones, *J. Am. Chem. Soc.*, 111, 8756, 1989.
60. Bauslaugh, P. G., Photochemical cycloaddition reactions of enones to alkenes: synthetic applications, *Synthesis*, 287, 1970.
61. Hastings, D. J. and Weedon, A. C., Origin of the regioselectivity in the photochemical cycloaddition reactions of cyclic enones with alkenes. chemical trapping: evidence for structures, mechanism of formation and fates of 1,4-biradical intermediates, *J. Am. Chem. Soc.*, 113, 8525. 1991.

62. (a) Andrew, D. and Weedon, A. C., Determination of the relative rates of formation, fates and structures of triplet 1,4-biradicals generated in the photochemical cycloaddition reactions of 2-cyclopentenones with 2-methylpropene, *J. Am. Chem. Soc.*, 117, 5647, 1995: (b) Andrew, D., Hastings, D. J., and Weedon, A. C., The mechanism of the photochemical cycloaddition reaction between 2-cyclopentenone and polar alkenes: trapping of triplet 1,4-biradical intermediates with hydrogen selenide, *J. Am. Chem. Soc.*, 116, 10870, 1994; (c) Maradyn, D. J., Sydnes, L. K., and Weedon, A. C., Origin of the regiochemistry in the photochemical cycloaddition reaction of 20cyclopentenone with allene: trapping of triplet 1,4-biradical intermediates with hydrogen selenide, *Tetrahedron Lett.*, 34, 2413, 1993; (d) Krug, P., Rudolph, A., and Weedon, A. C., Independent generation of triplet 1,4-biradical intermediates implicated in the photochemical cycloaddition reaction between 2-cyclopentenone and acrylonitrile, *Tetrahedron Lett.*, 34, 7221, 1993.
63. Maradyn, D. J. and Weedon, A. C., The photochemical cycloaddition of 2-cyclohexenone with alkenes: trapping of triplet 1,4-biradical intermediates with hydrogen selenide, *Tetrahedron Lett.*, 44, 8107, 1994.
64. Lusztyk, J., Maillard, B., Deyard, S., Lindsay, D. A., and Ingold, K. U., Kinetics for the reaction of a secondary alkyl radical with tri-*n*-butylgermanium hydride and calibration of a secondary alkyl radical clock reaction, *J. Org. Chem.*, 52, 3509, 1987.
65. Caldwell, R. A., Tang, W., Schuster, D. I., and Heibel, G. E., Nanosecond kinetic absorption and calorimetric studies of cyclopentenone: the triplet, self quenching and the predimerization biradicals, *Photochem. Photobiol.*, 53, 159, 1991.
66. Benson, S. W., *Thermochemical Kinetics*, 2nd ed., Wiley, New York, 1976.
67. Kaprinidis, N. A., Lem, G., Courtney, S. H., and Schuster, D. I., Determination of the energies and lifetimes of triplet 1,4-biradicals derived in [2+2] photocycloaddition reactions of enones with alkenes using photoacoustic calorimetry, *J. Am. Chem. Soc.*, 115, 3324, 1993.
68. (a) Caldwell, R. A., Hrncir, D. C., Muñoz, Jr., T., and Unett, D. J., Photocycloaddition of 4,4-dimethylcyclohexenone to 1,1-diphenylethylene: evidence for a triplet exciplex intermediate, *J. Am. Chem. Soc.*, 118, 8741, 1996; (b) Caldwell, R. A., Constien, R., and Kriel, B. G., Photoannulation of 4,4-dimethylcyclohex-2-en-1-one to 1,1-diphenylethylene, *J. Phys. Chem. A,* 107, 3277, 2003.
69. (a) Broeker, J. L., Eksterowicz, J. E., Belk, A. J., and Houk, K. N., On the regioselectivity of photocycloadditions of triplet cyclohexenones to alkenes, *J. Am. Chem. Soc.*, 117, 1847, 1995; (b) Bertrand, C,. Bouquant, J., Pete, J. P., and Humbel, S., Theoretical description of [2+2] photocycloadditions: enone and ethylene as a model of the reactivity of cycloenones, *J. Mol. Struct.*, 538, 165, 2001; (c) Garcia-Expósito, E., Bearpark, M. J., Ortuño, R. M., Robb, M. A., and Branchadell, V., Theoretical study of the photochemical [2+2]-cycloadditions of cyclic and acyclic α,β-unsaturated carbonyl compounds to ethylene, *J. Org. Chem.*, 67, 6070, 2002.
70. Wilsey, S., Gonzalez, L., Robb, M. A., and Houk, K. N., Ground- and excited-state surfaces for the [2+2]-photocycloaddition of α,β-enones to alkenes, *J. Am. Chem. Soc.*, 122, 5866, 2000.
71. Doubleday, C., Jr., Tetramethylene, *J. Am. Chem. Soc.*, 115, 11968, 1993.
72. Wilson, S. R., Schuster, D. I., Nuber, B., Meier, M. S., Magginig, M., Prato, M., and Taylor, R., Organic chemistry of fullerenes, in *Fullerenes: Chemistry, Physics and Technology*, Kadish, K. M. and Ruoff, R. S., Eds., Wiley Interscience, New York, 2000, chap. 3.
73. (a) Schuster, D. I., Cao, J., Kaprinidis, N., Wu, Y., Jensen, A. W., Lu, Q., Wang, H., and Wilson, S. R., [2+2] Photocycloaddition of cyclic enones to C_{60}, *J. Am. Chem. Soc.*, 118, 5639, 1996 (and earlier references cited therein); (b) Jensen, A. W., Khong, A., Saunders, M., Wilson, S. R., and Schuster, D. I., Photocycloaddition of cyclic 1,3-diones to C_{60}, *J. Am. Chem. Soc.*, 119, 7303, 1997.
74. Vassilikogiannakis, G. and Orfanopoulos, M., Regio- and stereoselectivity of the [2+2] photocycloaddition of acyclic enones to C_{60}, *J. Org. Chem.*, 64, 3392, 1999.
75. Fox, M. A., Ed., *Organic Transformations in Nonhomogeneous Media*, ACS Symp. Series 278, American Chemical Society, Washington, D.C., 1985.

76. Moorthy, J. M., Venkatesan, K., and Weiss, R. G., Photodimerizations of coumarins in solid cyclodextrin inclusion complexes, *J. Org. Chem.*, 57, 3292, 1992.
77. Lem, G., Kaprinidis, N. A., Schuster, D. I., Ghatlia, N. D., and Turro, N. J., Regioselective photodimerization of enones in zeolites, *J. Am. Chem. Soc.*, 115, 7009, 1993.
78. (a) Chen, C., Chang, V., Cai, X., Duesler, E., and Mariano, P. S., A general strategy for absolute stereochemical control of enone–olefin [2+2] photocycloaddition reactions, *J. Am. Chem. Soc.*, 123, 6433, 2001; (b) Shepard, M. S. and Carreira, E. M., Asymmetric photocycloadditions with an optically active allenylsilane: trimethylsilyl as a removable stereocontrolling group for the enantioselective synthesis of *exo*-methylenecyclobutanes, *J. Am. Chem. Soc.*, 119, 2597, 1997.

73

[2+2]-Photocycloadditions in the Solid State

Yoriko Sonoda
National Institute of Advanced Industrial Science and Technology

73.1 Introduction[1,2]

[2+2]-Photocycloaddition is one of the best known reactions in solid-state organic photochemistry. The reactions, in general, occur more selectively and efficiently than in homogeneous solution due to tight and regular molecular arrangements in crystals. It is often observed that the photoproducts in the solid state are entirely different from those in solution.

During the 1960s and 1970s, Schmidt and co-workers studied the solid-state [2+2]-cycloadditions of cinnamic acids thoroughly and systematically.[1–4] From the crystallographic investigations, topochemical rules, which connect the configuration of the product and crystal structure of the reactant, were revealed. It is well known that for topochemical [2+2]-photocycloaddition, the distances between the potentially reactive double bonds should be less than ~4.2 Å.[3,4] Following the pioneering work of Schmidt et al., several groups have investigated structure–reactivity correlations in the solid state, and the main factors required for the cycloaddition to occur in the solid state are now understood fairly well. However, the principal problem — namely, complete control of molecular arrangements in the crystal lattice— has not been overcome fully. Although several kinds of steering groups are known to make olefinic compounds photoreactive in the solid state, our understanding of the various forces that control the crystal packing is highly fragmentary. One of the major problems is lack of complete understanding of the intra- and intermolecular interactions leading to the observed crystal packing.

For aligning the reactive double bonds, three distinct strategies have been employed and are discussed in this chapter: intramolecular substitution, formation of mixed crystal using donor–acceptor charge transfer (CT) type of intermolecular interactions, and, more recently, inclusion within host structures. Recent developments in this field are mainly concerned with absolute asymmetric synthesis of organic compounds using [2+2]-photocycloaddition in the solid state. Optically active products can be obtained in the absence of any external chiral source using chiral crystals of achiral molecules, mixed crystals of two different kinds of achiral molecules, and inclusion crystals of achiral guest molecules in chiral host crystals.

0-8493-1348-1/04/$0.00+$1.50

73.2 Crystal Photolysis

One-Component Crystals[3–5]

It is known that chlorine substitution is very effective in inducing photoreactivity in the solid state.[3,4] Recently, fluorine substitution, as well, has been proven to be useful for constructing photoreactive crystals. The effect of fluorine substitution on the crystal structure and the solid-state photochemical behavior of benzylidenepiperitone has been examined.[6] No F···F contacts are less than the sum of the van der Waals radii (2.94 Å); however, C–H···F interactions are observed in the crystal structure of **1.** The fact that the unsubstituted parent compound does not photodimerize in the crystalline state whereas the fluorine-substituted **1** does illustrates the importance of fluorine substitution.

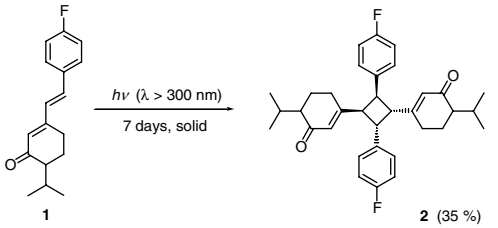

1 **2** (35 %)

The effects of fluorine substitution on crystal packing and topological photodimerization have also been investigated for styrylcoumarins.[7,8] Styrylcoumarin **3** yields the centrosymmetric (α-mode, *anti*-head-to-tail [HT]) photodimer **5** when irradiated in the solid state; however, the inclusion of a fluorine substituent dramatically alters the packing mode and steers molecules **4a** and **4b** to form stereospecific photodimers **6a** and **6b** (β-mode, *syn*-head-to-head [HH]) by reaction at the styrenic double bonds.

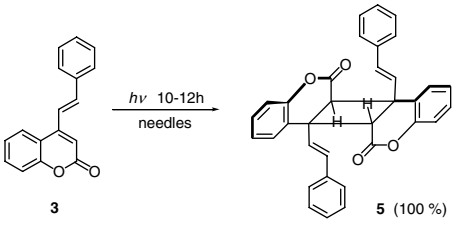

3 **5** (100 %)

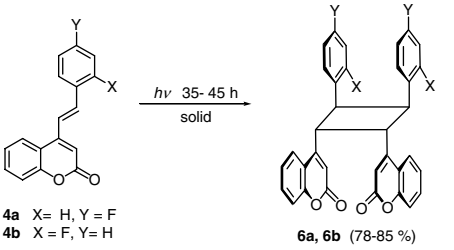

4a X= H, Y = F
4b X = F, Y= H

6a, 6b (78-85 %)

The face-to-face stacking interaction between the phenyl and the perfluorophenyl groups is shown to be a general supramolecular synthon. The solid-state packing structure and reactivity of several monoolefins and diolefins substituted with phenyl and perfluorophenyl groups has been investigated.[9] Compounds **7** and **9** undergo photoinduced [2+2]-cycloaddition reactions in the solid state to give dimer **8** and polymer **10**, respectively. Although compound **11** is completely photostable, the co-crystal of **9** and **11** is photoreactive to give a cyclobutane-containing polymer. The stereochemistry of the photoproduct and/or x-ray structural analysis of the olefinic precursors reveals the stacked interaction between phenyl and perfluorophenyl groups in the photoactive crystals.

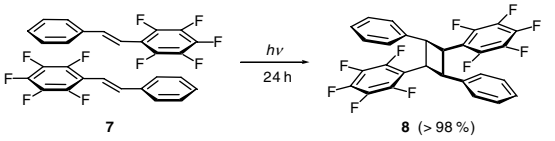

7 **8** (> 98 %)

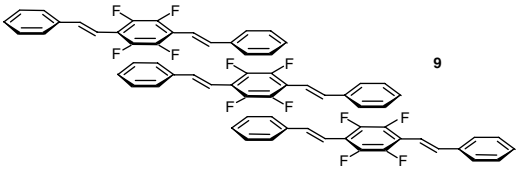

9

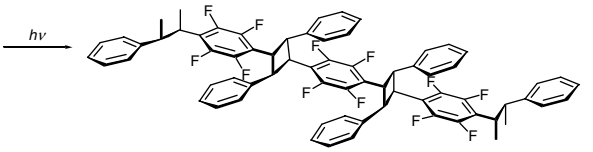

10 (proposed structure)

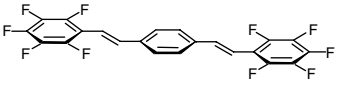

11

The strong hydrogen bonds of C=O···H–O in carboxylic acids are often used to control molecular arrangements in the solid state.[10,11] For the U-shaped diacid **12**, efficient stereo- and regiocontrolled photodimerization through preorganization enforced by C=O···H–O hydrogen bonds in the solid state has been reported.[12] Irradiation of **12** gives dimer **13** quantitatively. Thus, it is demonstrated that hydrogen bonding can be used to enforce a particular and desirable stereo- and regiochemical outcome in a solid-state transformation that otherwise might not follow this reaction course. The parallel alignment of the acid groups on a single molecule ensures that proximity between the alkene moieties of different acids can be achieved.

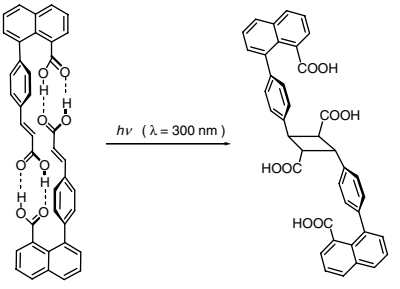

12 **13** (~100 %)

The relative orientation of olefins within metal complexes provides an alternative approach to induce stereoselectivity in the cycloadditions of olefins in the solid state. Irradiation of $SnCl_4$ complexes of cyclopentenones **14a–c** in the solid state leads to stereoselective photodimerization to give *anti*-HT cyclodimers **15a–c** in high yields.[13]

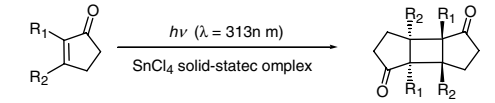

14a $R_1 = H$, $R_2 = H$
14b $R_1 = H$, $R_2 = CH_3$
14c $R_1 = CH_3$, $R_2 = H$

15a (75 %)
15b (60 %)
15c (85 %)

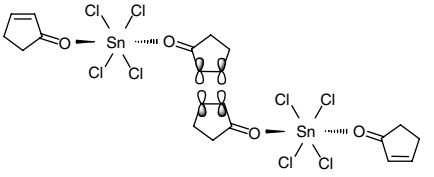

$SnCl_4$ Solid-State Complex of **14a**

The photodimerizatiom of 3-cyanocinnamic acid **16** is temperature dependent.[14] The crystals of **16** and **17** are isostructural, both being β-structures with the short axes ~4 Å. In spite of the close similarity in the crystal structures, however, only **17** undergoes a topochemical [2+2]-photodimerization at ambient temperature to give dimer **18b**. Compound **16** is found to be photostable; however, while **16** is unreactive at room temperature, it becomes photoreactive when heated at 130°C and forms dimer **18a**. The seeming difference in the topochemical [2+2]-photoreactivity of **16** and **17** is explained by differing degrees of molecular motion in the crystals.

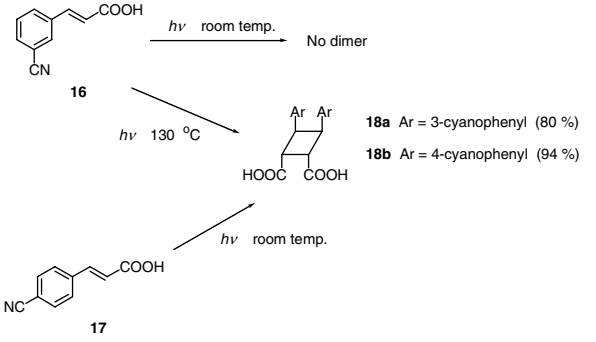

16

17

18a Ar = 3-cyanophenyl (80 %)
18b Ar = 4-cyanophenyl (94 %)

The solid-state photodimerization of 1-thiocoumarin **19**, on the other hand, is shown to be wavelength dependent.[15] Irradiation of **19** with λ > 390-nm light leads to the exclusive formation of HH *cis-syn-cis* dimer **20**, whereas irradiation with shorter wavelengths (λ > 340 nm) results in the formation of a mixture of all four *cis*-fused tricyclic dimers **20** to **23**. The selective formation of HH-*cis-cisoid-cis* dimer in the solid-state irradiation of substituted coumarins occurs quite frequently. The topochemical reactions occur within minimum atomic movements if the reactive double bonds are within the correct distance and aligned in a parallel fashion. The conversion of **19** to **20** on irradiation with λ > 390-nm light proceeds accordingly, the prealignment favoring dimer **20** to the exclusion of others. In contrast, the wavelength dependence observed during irradiation with λ > 340-nm light is most unusual. The novel wavelength effect in the solid-state photochemistry is explained by assuming that the excitation at 340 nm populates two excited states. If one of them has a much longer lifetime, this would allow exciton migration to defect sites, leading to the non-topochemical behavior.

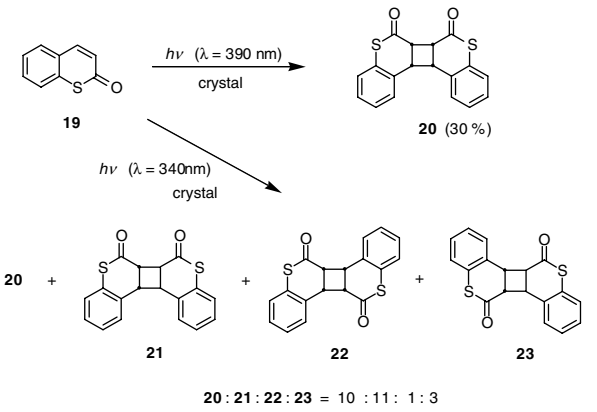

Styrylpyrilium salt **24** shows reversible [2+2]-photodimerization in the solid state when irradiated with λ > 570-nm light.[16] The system of **24** and its dimer **25** not only undergoes single-crystal-to-single-crystal photodimerization but also returns thermally to pure crystals of the monomer. With light of wavelengths around its absorption maximum (λ = 420 nm), a heterogeneous reaction is observed and the original monomer crystals break up completely on further irradiation.

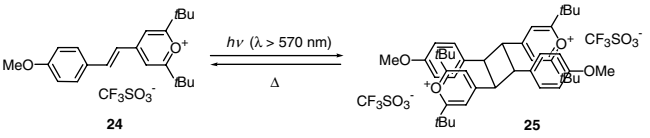

Styrylpyrazine amphiphile **26** shows reversible photodimerization in aqueous dispersion.[17] Compound **26** undergoes quantitative photodimerization with λ > 300-nm light, and the reverse reaction from **27** occurs with 254-nm light. The corresponding stilbene analog **28** undergoes similar photodimerization to give **29**, but the reaction is not photochemically reversible.

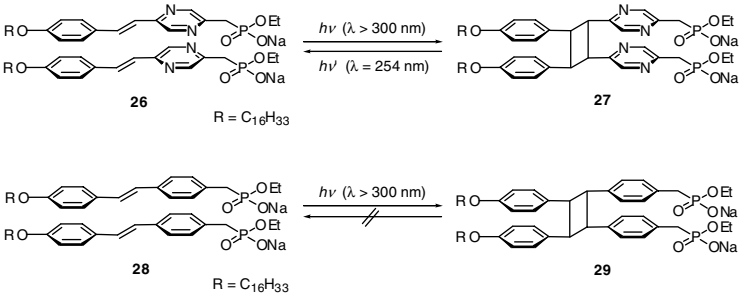

Asymmetric [2+2]-cycloadditions for one-component crystals have been reported. Ethyl ester **30a** forms chiral crystals of β-type packing. Irradiation of the single crystals of **30a** affords the optically active dimer **31** with an enantiomeric excess (EE) of >90%.[18,19] In contrast, methyl ester **30b** yields the highly crystalline polymer **32** through a typical [2+2]-topochemical photopolymerization.

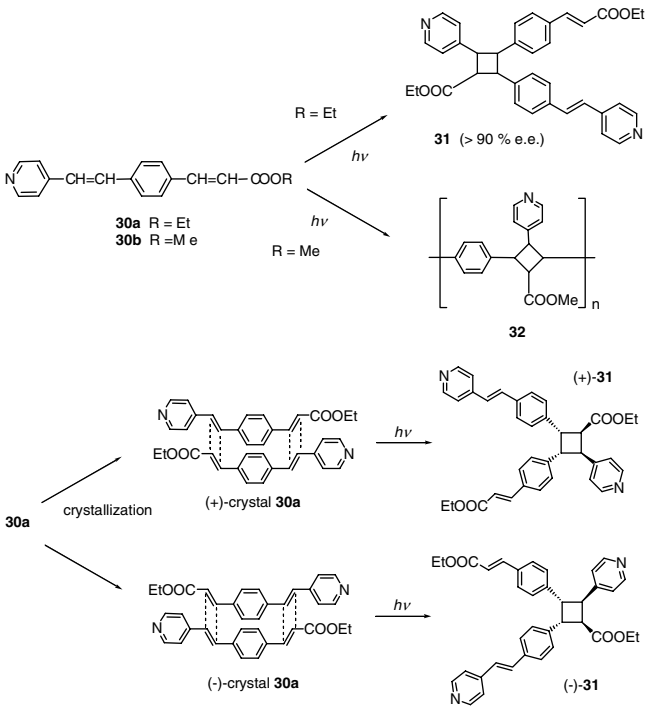

The signs of optical rotations are arbitrary.

Mixed Crystals[4,5,20]

The 1:1 molecular CT complex of 3,5-dinitrocinnamic acid **33a** with 2,5-dimethoxycinnamic acid **33d** is irradiated for 5 days in the solid state to give the unsymmetrical dimer **34** in 60% yield.[21] Similarly, the 1:1 mixed crystals of **33a** and **33c** yields the corresponding truxinic acid. The complex of **33b** and **33c** and that of **33b** and **33d** are completely photostable.

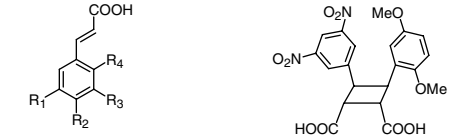

33a $R_1 = R_3 = NO_2$, $R_2 = R_4 = H$
33b $R_2 = R_4 = NO_2$, $R_1 = R_3 = H$
33c $R_2 = R_3 = OMe$, $R_1 = R_4 = H$
33d $R_1 = R_4 = OMe$, $R_2 = R_3 = H$

34

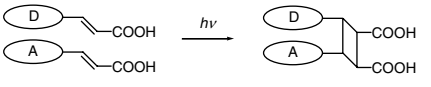

Irradiation of the 1:1 complex crystals of 4-methoxy-6-methyl-2-pyrone **35** and maleimide **36** gives **37** in 54% yield as a sole product, which is entirely different from the solution products **39** and **40**.[22] The peri-, site-, and stereospecific photoreaction in the solid state is considered to be brought about by two sets of the hydrogen bonding and CT stacking between **35** and **36** in the complex.

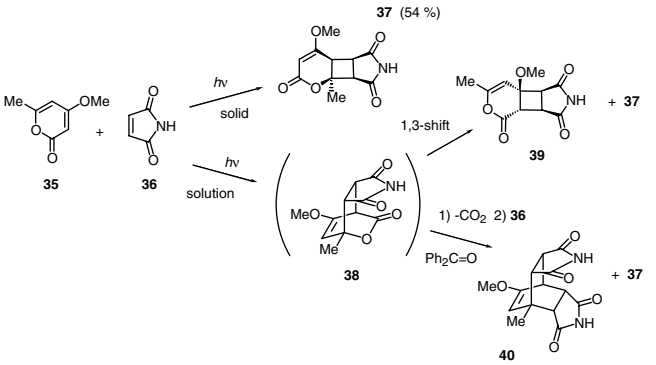

Selective excitation of the CT complex between acenaphthylene **41** and tetracyanoethylene **42** in the crystalline state exclusively affords the 1:1 [2+2]-cycloadduct **43**, in contrast to the excitation in solution.[23,24] On irradiation of the complex of **41** and **42** with light of wavelength $\lambda > 500$ nm, where neither **41** nor **42** is excited, **43** is obtained in 80% yield. Irradiation of an equimolar mixture of **41** and **42** in solution with $\lambda > 500$ nm light induces no reaction.

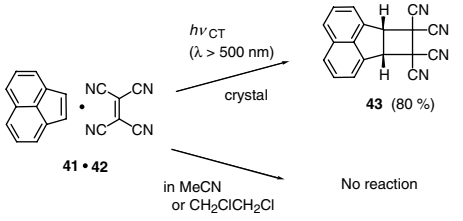

A crystalline salt of tryptamine **44** and *trans*-3-nitrocinnamic acid **45** undergoes cross photocycloaddition to give **46** in 39% yield.[25] In contrast, irradiation of the solid mixture of **44** and **45** fails to give the product.

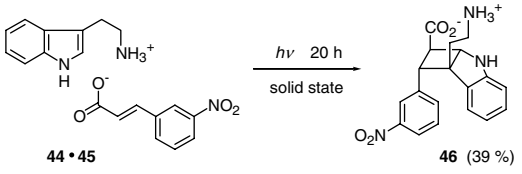

Photodimerization of *trans*-cinnamic acid **47** is controlled by the formation of a double salt with diamines.[26,27] It is known that **47** gives α-truxillic acid **49** efficiently on irradiation. The double salt crystals of **47** and *cis*-1,2-cyclohexanediamine **48**, on the other hand, yield β-truxinic acid **50** predominantly.

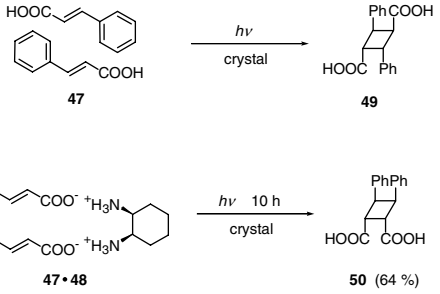

One of the earliest examples for the formation of an optically active heterophotodimer from mixed crystals of achiral molecules is the photoreaction of the single crystals of *trans, trans*-1-(2,6-dichlorophenyl)-4-phenyl-1,3-butadiene **51**, and its thiophene analog **52**.[28,29] Irradiation of crystalline samples of **51** or of **52** yield achiral cyclobutane dimers **53** and **54**, respectively. When a (polycrystalline) sample of mixed crystals of **51** and **52** is irradiated, the reaction affords the enantiomeric heterodimers **55a** and **55b** in addition to the homodimers **53** and **54**. The formation of **53** and **54** can be minimized by using small amounts of the thiophene monomer **52**, which absorbs at slightly longer wavelengths than does the phenyl monomer **51** and by irradiating through appropriate cutoff filters so that only **52** absorbs light. The dilution of **52** in a large excess of **51** minimizes the formation of **54**, and the lack of excitation of **51** prevents the formation of **53**. With the use of a 400-nm cutoff filter, irradiation of large, single, mixed crystals containing 15% **52** and 85% **51** leads to high yields of the optically active heterodimers. The optical yield of the reaction is reported to be ~70%.[29]

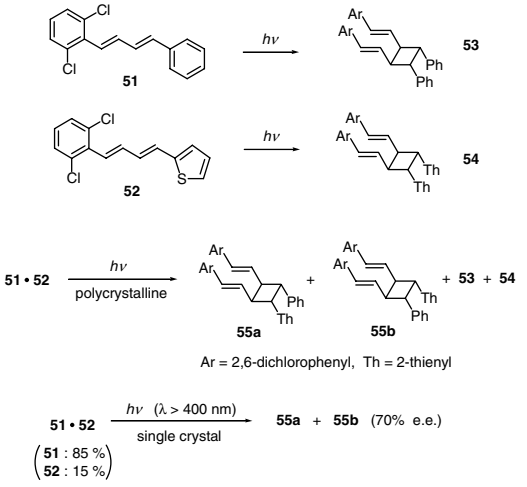

Absolute asymmetric synthesis has been performed by controlled reduction in crystal symmetry.[30] The principle is based on selective induction of a guest molecule into a centrosymmetric host structure, thus reducing the symmetry of the mixed crystals. Crystallization of the *trans*-cinnamamide host **56** in the presence of the *trans*-cinnamic acid guest **47** results in the formation of mixed crystals composed of two enantiomorphous halves each containing 0.5 to 1.0% of the acid. Irradiation of each half separately yields the optically active dimers **57a** and **57b** in excess with an enantiomeric yield in the range of 40 to 60%. This varies from one single crystal to another.

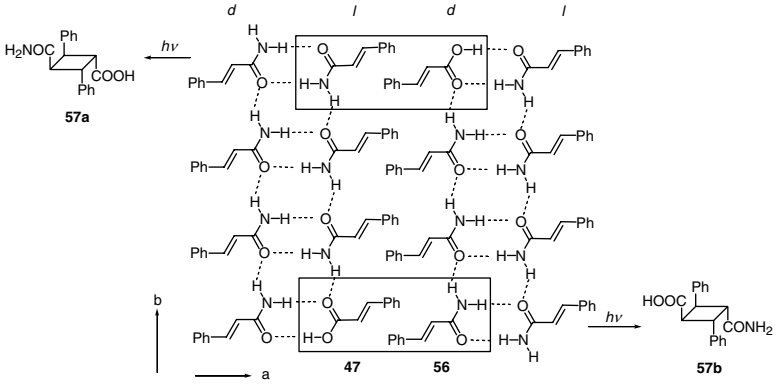

Charge transfer excitation of the solid-state molecular complex of **58** with *o*-divinylbenzene **59** yields [2+2]-cycloadducts **60** via single-crystal-to-single-crystal transformation.[31] The apparent reactivity of the complex crystals is much higher than that in solution. Due to the asymmetric structure of the complex crystals of **58** and **59**, the optically active product (71% EE at 15°C and 95% EE at –70°C) is obtained from the achiral components without any external chiral source.

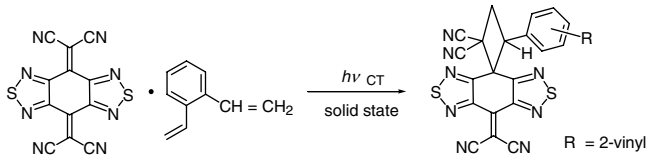

58 **59** **60**

Inclusion (Host–Guest) Crystals[5,32–35]

The [2+2]-cycloaddition reactions in inclusion crystals, or host–guest crystals, have been thoroughly reviewed.[5] Coumarin **61a**, thiocoumarin **61b**, and cyclohex-2-enone **62** efficiently undergo single-crystal-to-single-crystal enantioselective photodimerization in inclusion complexes with chiral host compounds (R,R)-(–)-*trans* **63a**, (R,R)-(–)-*trans* **63b**, and (–)-**64**, respectively.[36] The products are (–)-*anti*-HH **65a** (100% EE), (+)-*anti*-HH **65b** (100% EE), and (–)-*syn-trans* **66** (48% EE) dimers. An example for enantioselective intramolecular [2+2]-photocycloadditions in inclusion crystals is the reaction of guest **67** in chiral host **68**.[37] Irradiation of the powdered inclusion crystals in water suspension affords the optically active photocyclization product **69** with 100% EE in 90% yield.

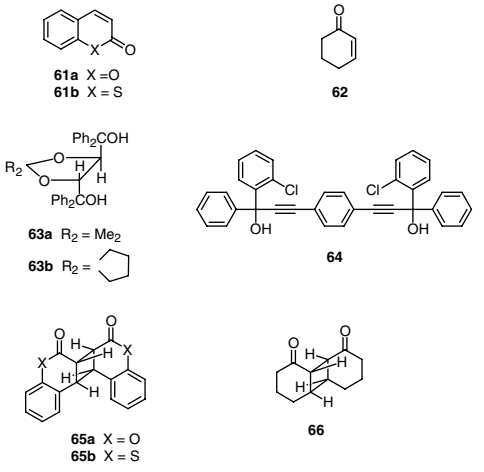

61a X = O
61b X = S

62

63a R_2 = Me_2

63b R_2 =

64

65a X = O
65b X = S

66

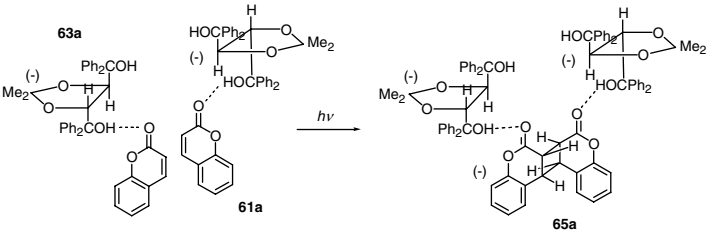

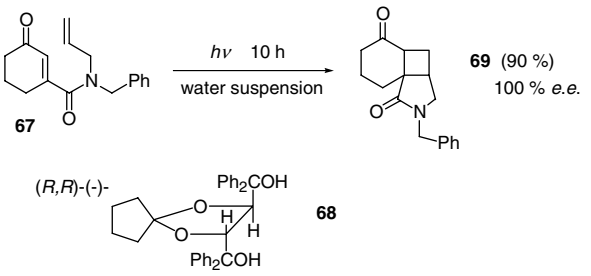

TABLE 73.1 Irradiation of Coumarins 70a and 70b as Solid Complexes with CDs

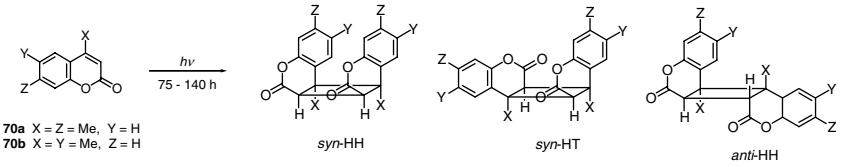

Coumarin	Host CD	Dimer type	Yield (5)	Inferred complex (H:G)
70a	β	anti-HH	94	2:2
	γ	syn-HH	57	1:2
		syn-HT	28	
70b	β	syn-HH	48	2:2
	γ	syn-HH	74	1:2

73.3 Inclusion Complexes in the Solid State

Host compounds such as cyclodextrins (CDs) and zeolites have attracted considerable attention recently because they are expected to be useful as artificial reaction cavities to control photoreactions in the solid state. In spite of many examples of the photoreactions in these media being identified, however, much chemistry still remains to be done.

Cyclodextrin Hosts[35,38]

The [2+2]-photodimerizations of coumarin and its derivatives proceed selectively in solid inclusion complexes with CDs.[39] The yield and distribution of the photodimers are very different from those in the neat coumarin solids. For the 4,7-dimethyl (**70a**) and the 4,6-dimethyl (**70b**) derivatives, for example, photodimers are obtained by irradiation of the CD complexes as shown in Table 73.1, whereas no dimer is formed from neat solid coumarins. Depending on the substitution pattern of the coumarin molecules and the type of CD employed, complexes whose host/guest ratios are 1:1, 1:2, and 2:2 are identified. The stereochemistry of the dimers depends on the cavity size of the CD and the relative orientations of coumarins within a complex. The photodimerization of acenaphthylene **41** is accelerated by the formation of 1:2 inclusion compound between γ-CD and **41** to give *cis* (**71a**) and *trans* (**71b**) dimers (*cis* : *trans* = 99:1).[40] In contrast, the dimerization is inhibited by β-CD due to the formation of 1:1 inclusion complex.

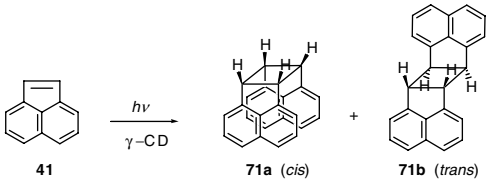

TABLE 73.2 Product Ratio from Photodimerization of 14a in Zeolites and in Solution

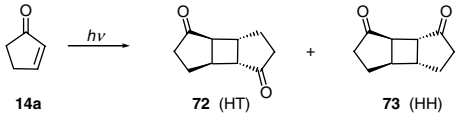

14a **72** (HT) **73** (HH)

Medium	Ratio 72/73	Medium	Ratio 72/73	Medium	Ratio 72/73
LiX	0.93 ± 0.006	LiY	1.36 ± 0.01	Benzene	3.64 ± 0.07
KX	0.80 ± 0.03	KY	0.68 ± 0.04	Methanol	1.66 ± 0.02
CsX	0.50	CsY	0.79 ± 0.02		

Zeolites[41–43]

One of the most well-known examples of controlled photoreactions in zeolites may be the cation-controlled photodimerization of acenaphthylene **41** in faujasites reported by Ramamurthy and co-workers.[44,45] Irradiation of **41** in organic solvents yields both *cis* (**71a**) and *trans* (**71b**) dimers. It is believed that the singlet excited state gives predominantly the *cis* dimer, whereas the triplet excited state gives the *cis* and *trans* dimers in comparable amounts. Irradiation of dry solid inclusion complexes of **41** in various cation (Li, Na, K, Rb, Cs, and Tl) exchanged Y zeolites gives the *cis* and *trans* dimers. The ratio of *cis* to *trans* dimer depends on the types of cation present in the zeolite supercage (and the number of guest molecules per supercage). In the case of lower atomic weight cations such as Li and Na, the dimerization occurs via the singlet excited state resulting in the preferential formation of the *cis* dimer. For higher atomic weight cations, on the other hand, the reaction occurs via the triplet state, which is in agreement with the formation of the *trans* and *cis* dimers in the cages of K, Rb, and CsY. In the dry RbY zeolite solid, the major part of the dimer is rationalized to come from the reaction between acenaphthylene molecules in different cages.[45] On irradiation of **41** in the zeolite (RbY)–solvent (hexane) slurry, on the other hand, the dimerization is expected to occur preferentially from doubly occupied cages, leading to a higher yield of the *cis* dimer with respect to that in dry RbY.

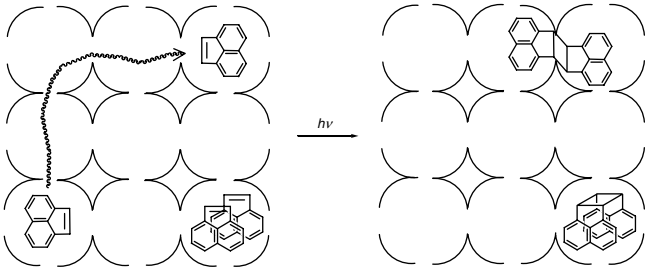

The effects of zeolites on photodimerization of cyclopentenone **14a** and cyclohexenone have been investigated (Table 73.2).[46] Little control over the regiochemistry of such reactions is attainable when they are carried out in isotropic solvents. A relatively high degree of regioselectivity in the dimerization can be achieved in zeolites due to cavity-size effects in the supercages of X- and Y-type faujasites as well as the complexing ability of the cation within the zeolite with included guests. An increase in the formation of the HH (**73**) relative to the HT (**72**) dimer occurs in both X- and Y-type faujasites, as the size of the cation increases and the available space in the zeolite cavity decreases.

Intramolecular [2+2]-photocycloaddition of enone **74** is affected by zeolites.[47,48] On irradiation of **74** adsorbed in cation-exchanged X and Y zeolites, the products from closure of the 1,6-biradical, **77** to **79**, are more efficiently formed when compared to the results in solution. The regio- and stereochemical outcomes of the photocycloadditions in zeolites are interpreted by the binding of the guest molecules with the cations in the zeolite supercages. It is possible that the carbonyl group and the olefinic bond of the guest molecules electronically interact with the cation within the cages, resulting in a configuration favoring the formation of **77** to **79**.

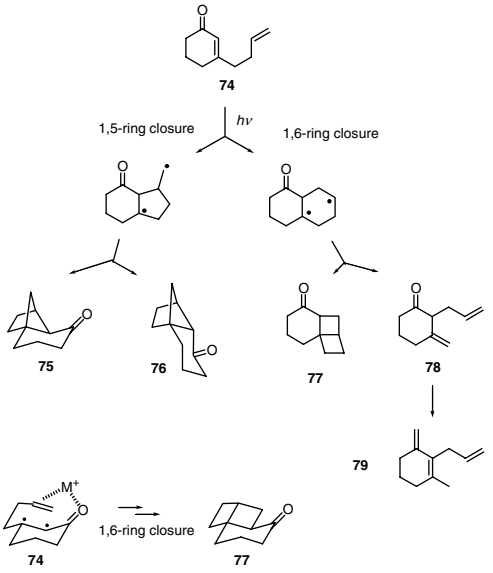

73.4 Industrial Applicability[49]

The most industrial applications of solid-state [2+2]-photocycloadditions are in the field of polymer layers via crosslinking (photoresists) or by photopolymerization of doubly unsaturated crystalline alkenes. One of the recent examples for such a polymerization is the photoreaction of cyano-substituted diphenylhexatriene **80** in the solid state.[50] Compound **80** undergoes intermolecular photocycloaddition at the 1,2-positions of the trienes to give oligomers **82** in addition to the *syn*-HH dimer **81**.

The photochemical reversible reaction ([2+2]-photocycloaddition and the reverse reaction) of oriented chromophores in aggregates with alternate irradiation at two independent wavelengths has attracted much attention due to the potential application to photomemory, to on–off photoswitching systems, and to its availability in controlling the release of entrapped reagents in vesicles.[16,17] If the reacting monomers are colored their photochromism may be used technically in various ways.

Photochemical valence isomerization between norbornadiene **83** and quadricyclane **84**, which includes [2+2]-cycloaddition, has long been of interest because of its potential use in solar energy conversion and storage. Photoenergy can be stored as strain energy (~20 kcal/mol) in a molecule of **84**; however, the problem is that the photoreaction of **83** does not ordinarily occur on irradiation with sunlight due to

inefficient absorption of visible light by the compound. To extend the absorption to longer wavelengths, suitable chromophores are often introduced into **83**. It has recently been reported, for example, that trifluoromethyl-substituted derivatives **85a–c** not only absorb visible light efficiently but also produce stable derivatives of **84**.[51] The key to this behavior may lie in the CT character of **85a–c**. Solar energy storage has been realized in several cases; however, no large-scale applications have yet been reported.

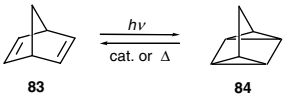

83 **84**

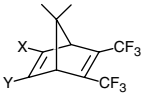

85a X = Y = 4-methoxyphenyl
85b X = 4-dimethylaminophenyl, Y = 4-methoxyphenyl
85c X = Y = 2-benzofuryl

References

1. Ramamurthy, V., Ed., *Photochemistry in Organized and Constrained Media*, VCH, New York, 1991.
2. Ramamurthy, V., Organic photochemistry in organized media, *Tetrahedron*, 42, 5753–5839, 1986.
3. Ramamurthy, V. and Venkatesan, K., Photochemical reactions of organic crystals, *Chem. Rev.*, 87, 433–481, 1987.
4. Venkatesan, K. and Ramamurthy, V., Bimolecular photoreactions in crystals, in *Photochemistry in Organized and Constrained Media*, Ramamurthy, V., Ed., VCH, New York, 1991, 133–184.
5. Tanaka, K. and Toda, F., Solvent-free organic synthesis, *Chem. Rev.*, 100, 1025–1074, 2000.
6. Kumar, V. A. and Venkatesan, K., Studies in crystal engineering: topochemical photodimerization of (±)-*p*-fluorobenzylidenepiperitone, *J. Chem. Soc., Perkin Trans. 2,* 2429–2433, 1993.
7. Vishnumurthy, K., Guru Row, T. N., and Venkatesan, K., Studies in crystal engineering: effect of fluorine substitution in crystal packing and topological photodimerization of styryl coumarins in the solid state, *J. Chem. Soc., Perkin Trans. 2,* 1475–1478, 1996.
8. Vishnumurthy, K., Guru Row, T. N., and Venkatesan, K., Studies in crystal engineering: crystal packing, topological photodimerization and structure–reactivity correlations in fluoro-substituted styrylcoumarins, *J. Chem. Soc., Perkin Trans. 2,* 615–619, 1997.
9. Coates, G. W., Dunn, A. R., Henling, L. M., Ziller, J. W., Lobkovsky, E. B., and Grubbs, R. H., Phenyl-perfluorophenyl stacking interactions: topochemical [2+2]-photodimerization and photopolymerization of olefinic compounds, *J. Am. Chem. Soc.,* 120, 3641–3649, 1998.
10. Desiraju, G. R., Designer crystals: intermolecular interactions, network structures and supramolecular synthons, *J. Chem. Soc., Chem. Commun.*, 1475–1482, 1997.
11. Meléndez, R. E. and Hamilton, A. D., Hydrogen-bonded ribbons, tapes and sheets as motifs for crystal engineering, *Top. Curr. Chem.*, 198, 97–129, 1998.
12. Feldman, K. S. and Campbell, R. F., Efficient stereo- and regiocontrolled alkene photodimerization through hydrogen bond enforced preorganization in the solid state, *J. Org. Chem.,* 60, 1924–1925, 1995.
13. Rao, V. P. and Fech, J., Stereoselective photodimerization of $SnCl_4$ complexes of cyclic α,β-unsaturated ketones in the solid state, *J. Photochem. Photobiol. A: Chem.,* 67, 51–56, 1992.
14. Dhurjati, M. S. K., Sarma, J. A. R. P., and Desiraju, G. R., Unusual [2+2]-topochemical cycloadditions of 3-cyano- and 4-cyano-cinnamic acids: temperature dependent solid state photochemical reactions, *J. Chem. Soc., Chem. Commun.*, 1702–1703, 1991.
15. Klaus, C.P., Thiemann, C., Kopf, J., and Margaretha, P., Solid-state photocyclodimerization of 1-thiocoumarin (= 2*H*-1-benzothiopyran-2-one), *Helv. Chim. Acta*, 78, 1079–1082, 1995.
16. Novak, K., Enkelmann, V., Wegner, G., and Wagener, K. B., Crystallographic study of a single crystal to single crystal photodimerization and its thermal reverse reaction, *Angew. Chem. Int. Ed. Engl.*, 32, 1614–1616, 1993.

17. Park, J.-M., Zhang, W., Nakatsuji, Y., Majima, T., and Ikeda, I., The fast photochemical [2+2]-cycloaddition and reverse reaction of a styrylpyrazine amphiphile in aqueous dispersion, *Chem. Lett.*, 1309–1310, 1999.
18. Hasegawa, M., Chung, C.-M., Muro, N., and Maekawa, Y., Asymmetric synthesis through the topochemical reaction in a chiral crystal of a prochiral diolefin molecule having a "cisoid" molecular structure and amplification of asymmetry by a seeding procedure, *J. Am. Chem. Soc.*, 112, 5676–5677, 1990.
19. Chung, C.-M. and Hasegawa, M., "Kaleidoscopic" photoreaction behavior of alkyl 4-[2-(4-pyridyl)ethenyl]cinnamate crystals: a crystalline linear high polymer from the methyl ester, an "absolute" asymmetric reaction of the ethyl ester, and two types of dimer formation from the propyl ester, *J. Am. Chem. Soc.*, 113, 7311–7316, 1991.
20. Ito, Y., Solid-state photoreactions in two-component crystals, *Synthesis*, 1, 1998.
21. Sharma, C.V. K., Panneerselvam, K., Shimoni, L., Katz, H., Carrell, H. L., and Desiraju, G. R., 3-(3′,5′-Dinitrophenyl)-4-(2′,5′-dimethoxyphenyl)cyclobutane-1, 2-dicarboxylic acid: engineered topochemical synthesis and molecular and supramolecular properties, *Chem. Mater.*, 6, 1282–1292, 1994.
22. Obata, T., Shimo, T., Yoshimoto, S., Somekawa, K., and Kawaminami, M., Peri-, site- and stereo-controlled photocycloaddition of 4-methoxy-6-methyl-2-pyrone with maleimide induced by the hydrogen bond and CT stacking in the solid state, *Chem. Lett.*, 181–182, 1999.
23. Haga, N., Nakajima, H., Takayanagi, H., and Tokumaru, K., Exclusive production of a cycloadduct from selective excitation of the charge-transfer complex between acenaphthylene and tetracyanoethylene in the crystalline state in contrast to failure of reaction in solution, *J. Chem. Soc., Chem. Commun.*, 1171–1172, 1997.
24. Haga, N., Nakajima, H., Takayanagi, H., and Tokumaru, K., Photoinduced electron transfer between acenaphthylene and tetracyanoethylene: effect of irradiation mode on reactivity of the charge-transfer complex and the resulted radical ion pair in solution and crystalline state, *J. Org. Chem.*, 63, 5372–5384, 1998.
25. Ito, Y. and Fujita, H., Unusual [2+2]-photocycloaddition between tryptamine and 3-nitrocinnamic acid in the solid state, *Chem. Lett.*, 288–289, 2000.
26. Ito, Y., Borecka, B., Trotter, J., and Scheffer, J. R., Control of solid-state photodimerization of *trans*-cinnamic acid by double salt formation with diamines, *Tetrahedron Lett.*, 36, 6083–6086, 1995.
27. Ito, Y., Borecka, B., Olovsson, G., Trotter, J., and Scheffer, J. R., Control of the solid-state photodimerization of some derivatives and analogs of *trans*-cinnamic acid by ethylenediamine, *Tetrahedron Lett.*, 36, 6087–6090, 1995.
28. Elgavi, A., Green, B. S., and Schmidt, G. M. J., Reactions in chiral crystals. Optically active heterophotodimer formation from chiral single crystals, *J. Am. Chem. Soc.*, 95, 2058–2059, 1973.
29. Green, B. S., Lahav, M., and Rabinovich, D., Asymmetric synthesis via reactions in chiral crystals, *Acc. Chem. Res.,* 12, 191–197, 1979.
30. Vaida, M., Shimon, L. J. W., van Mil, J., Ernst-Cabrera, K., Addadi, L., Leiserowitz, L., and Lahav, M., Absolute asymmetric photochemistry using centrosymmetric single crystals: the host/guest system (*E*)-cinnamamide/(*E*)-cinnamic acid, *J. Am. Chem. Soc.*, 111, 1029–1034, 1989.
31. Suzuki, T., Fukushima, T., Yamashita, Y., and Miyashi, T., An absolute asymmetric synthesis of the [2+2]-cycloadduct via single crystal-to-single crystal transformation by charge-transfer excitation of solid-state molecular complexes composed of arylolefins and *bis*[1,2,5]thiadiazolotetracyanoquinodimethane, *J. Am. Chem. Soc.*, 116, 2793–2803, 1994.
32. Toda, F., Solid state organic chemistry: efficient reactions, remarkable yields, and stereoselectivity, *Acc. Chem. Res.*, 28, 480–486, 1995.
33. Pete, J.-P., Asymmetric photoreactions of conjugated enones and esters, *Adv. Photochem.*, 21, 135–216, 1996.
34. Sakamoto, M., Absolute asymmetric synthesis from achiral molecules in the chiral crystalline environment, *Chem. Eur. J.*, 3, 684–689, 1997.

35. Ramamurthy, V., Photoprocesses of host–guest complexes in the solid state, in *Photochemistry in Organized and Constrained Media*, Ramamurthy, V., Ed., VCH, New York, 1991, 303–358.
36. Tanaka, K., Mochizuki, E., Yasui, N., Kai, Y., Miyahara, I., Hirotsu, K., and Toda, F., Single-crystal-to-single-crystal enantioselective [2+2]-photodimerization of coumarin, thiocoumarin and cyclohex-2-enone in the inclusion complexes with chiral host compounds, *Tetrahedron,* 56, 6853–6865, 2000.
37. Toda, F., Miyamoto, H., and Kikuchi, S., Enantioselective intramolecular [2+2]-photocycloaddition reaction of *N*-allyl-3-oxo-1-cyclohexenecarboxamides in inclusion crystals with chiral host compounds, *J. Chem. Soc., Chem. Commun.*, 621–622, 1995.
38. Bortolus, P. and Monti, S., Photochemistry in cyclodextrin cavities, *Adv. Photochem.*, 21, 1–133, 1996.
39. Moorthy, J. N., Venkatesan, K., and Weiss, R. G., Photodimerization of coumarins in solid cyclodextrin inclusion complexes, *J. Org. Chem.,* 57, 3292–3297, 1992.
40. Tong, Z. and Zhen, Z., Microenvironmental effects of cyclodextrins. II. Effects of cyclodextrins on photodimerization of acenaphthylene, *Youji Huaxue,* 44–46, 1986 (*Chem. Abstr.,* 105, 152330g, 1986).
41. Ramamurthy, V., Eaton, D. F., and Caspar, J. V., Photochemical and photophysical studies of organic molecules included within zeolites, *Acc. Chem. Res.*, 25, 299–307, 1992.
42. Scaiano, J. C. and García, H., Intrazeolite photochemistry: toward supramolecular control of molecular photochemistry, *Acc. Chem. Res.*, 32, 783–793, 1999.
43. Ramamurthy, V., Photoprocesses of organic molecules included in zeolites, in *Photochemistry in Organized and Constrained Media*, Ramamurthy, V., Ed., VCH, New York, 1991, 429–494.
44. Ramamurthy, V., Corbin, D. R., Kumar, C. V., and Turro, N. J., Modification of photochemical reactivity by zeolites: cation controlled photodimerisation of acenaphthylene within faujasites, *Tetrahedron Lett.*, 31, 47–50, 1990.
45. Ramamurthy, V., Corbin, D. R., Turro, N. J., Zhang, Z., and Garcia-Garibay, M. A., A comparison between zeolite–solvent slurry and dry solid photolyses, *J. Org. Chem.*, 56, 255–261, 1991.
46. Lem, G., Kaprinidis, N. A., and Schuster, D. I., Regioselective photodimerization of enones in zeolites, *J. Am. Chem. Soc.,* 115, 7009–7010, 1993.
47. Noh, T., Choi, K., and Park, J., The effects of media on the intramolecular photocycloaddition of 3-(3-butenyl)cyclohex-2-enone, *Bull. Korean Chem. Soc.*, 19, 501–503, 1998.
48. Noh, T., Kwon, H., Choi, K., and Choi, K., Intramolecular photocycloaddition of 3-(3-butenyl)cyclohex-2-enone and 3-(2-propenoxy)cyclohex-2-enone in zeolites, *Bull. Korean Chem. Soc.*, 20, 76–80, 1999.
49. Kaupp, G., Cyclobutane synthesis in the solid phase, in *CRC Handbook of Organic Photochemistry and Photobiology*, Horspool, W. M. and Song, P.-S., Eds., CRC Press, Boca Raton, FL, 1995, 50–63.
50. Sonoda, Y., Miyazawa, A., Hayashi, S., and Sakuragi, M., Intermolecular [2+2]-photocycloaddition of formyl- and cyano-substituted diphenylhexatrienes in the solid state, *Chem. Lett.,* 410–411, 2001.
51. Nagai, T., Takahashi, I., and Shimada, M., Trifluoromethyl-substituted norbornadiene, useful solar energy material, *Chem. Lett.,* 897–898, 1999.

74

Photochemistry of Homoquinones

Ken Kokubo
Osaka University

Takumi Oshima
Osaka University

74.1 Introduction

Homoquinone is a compound that is formally constructed by the fusion of a cyclopropane ring to the electron-deficient CC double bond of a quinone. The methylene homologation certainly exerts significant electronic and structural effects on the highly conjugated planar quinone. The two carbonyl groups are slightly warped toward opposite sides of the fused cyclopropane ring.[1] Such modification results in a considerable hypsochromic (or blue) shift of the longest wavelength absorption compared to the parent quinone (Figure 74.1).[2]

Due to the conjunction of a functional quinone and the cyclopropane ring, homoquinones attract much attention from the synthetic, mechanistic, and theoretical points of view; however, only a few scattered studies have addressed the photochemical and thermal reactions of these quinone derivatives mainly because of somewhat restricted synthetic methods (*vide infra*). Therefore, the photochemical behavior of these fascinating compounds has been studied to gain further insight into quinone photochemistry.[3]

In this chapter, we focus on the photoreactions of homoquinones. First, the [2+2]-photoaddition of the enedione linkage with alkenes and alkynes is described in order to elucidate the factors controlling the regio- and stereochemistry of the photoadducts. The next topic is the photoinduced hydrogen abstraction of the carbonyl function and/or the cleavage of the incorporated cyclopropane ring. Finally, the photoinduced electron transfer (PET) reactions with typical donor components such as amines and arene derivatives are discussed. This is of importance because the attachment of two carbonyl groups on the central π-bond bestows greater ability to accept electrons on these species as compared with the α,β-unsaturated ketones.

74.2 Synthesis of Homoquinones

The classical synthetic method for homoquinones is based on the 1,3-dipolar cycloaddition of diazoalkanes to 1,4-quinones.[4] This reaction consists of the addition of diazoalkanes to the quinonoid CC double

0-8493-1348-1/04/$0.00+$1.50

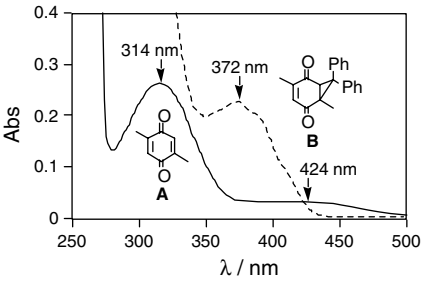

FIGURE 74.1 Absorption spectra of 2,5-dimethyl-1,4-benzoquinone **A** (solid line) and the corresponding diphenylhomoquinone **B** (dotted line) in acetonitrile (1 mM).

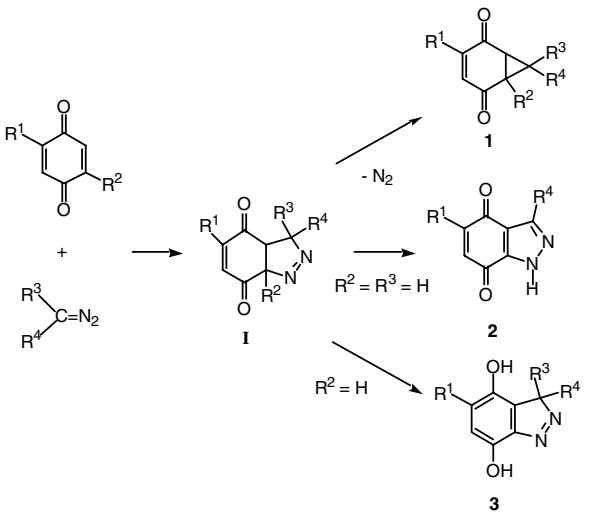

SCHEME 1

bond to give primarily the pyrazolines **I** (Scheme 1). Depending on the substitution pattern of the quinone and the diazoalkane used, the pyrazolines can undergo several transformations, such as loss of nitrogen, isomerization of the azo-containing ring, and *bis*-enolization of the fused quinone function. Homoquinones **1** are usually formed by loss of nitrogen from the pyrazolines when secondary diazoalkanes, bearing no mobile hydrogen on the diazo-carbon atom, are added to the substituted quinonoid ethylene linkage.[5] Otherwise, the pyrazolines derived from diazoalkanes, such as diazomethane, are transformed into pyrazoles **2** *via* isomerization as well as oxidation in preference to the nitrogen release.[6] Moreover, the pyrazolines from such quinones as 1,4-benzoquinone and 1,4-naphthoquinone tend to preferentially suffer the *bis*-enolization to 3*H*-indazole **3**.[5a,7] Another limitation of this method is deactivation of the quinonoid CC double bond by the steric or the electronic factors of the substituents as well as the bulk of the diazoalkanes. These factors change the site of reaction to the less hindered quinonoid CO double bond to afford oxiranes or poly(hydroquinone benzhydryl ether)s as found in the reactions of diazomethane with chloranil[8] and of diphenyldiazomethane with 2,3-dichloro-5,6-dicyanobenzoquinone (DDQ).[9]

Homoquinones are also prepared by a variety of methods that involve the free-radical reactions of propellanes with benzoquinones,[10] the Michael addition of sulfoxonium methylide[11] and ethyl cyanoacetate anion[12] to naphthoquinone and of sulfonium methylides to benzoquinones,[13] the photooxygenation of norcaradienes,[14] the reaction of diethoxyphthalans with quinones,[15] and the Diels–Alder reactions of siloxy- and alkoxy-substituted furans with cyclopropenes.[16]

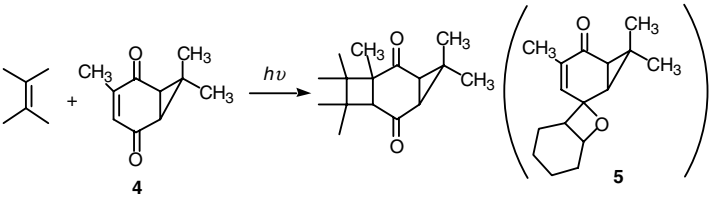

SCHEME 2

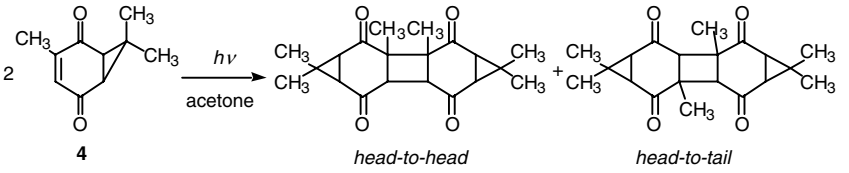

SCHEME 3

74.3 [2+2]-Photocycloaddition Reaction

Intermolecular Reaction

Some homoquinones are known to have a biological activity[17] and are exemplified by the terpenoid Eucarvone[18] and 3-carene-2,5-dione[19] which were isolated from natural resources.[20] In 1968, Still et al.[21] reported the first [2+2]-photocycloaddition of the homoquinone, 3-carene-2,5-dione **4**, with various alkenes and alkynes. They obtained the cyclobutane (and cyclobutene) adducts exclusively in moderate to excellent yields. Low yields of the spirooxetane **5** were obtained with cyclohexene resulting from addition to the carbonyl group (Scheme 2).[21] However, the regio- and stereochemical assignment was not established in great detail, and some products were obtained as a mixture of stereoisomers. Furthermore, using acetone as a photosensitizer, the [2+2]-photodimerization of **4** could be brought about to yield two major stereoisomers of the *head-to-head* (HH) adduct and one minor isomer of *head-to-tail* (HT) orientation (Scheme 3).[22]

About 30 years later, the Kokubo et al.[23] conducted the [2+2]-photocycloadditions of variously *p*-substituted (R,[1] R[2]) diphenylhomoquinones **6a–f** with various alkenes or alkynes. Detailed assignment of the structures for all the regio- and stereoisomers obtained allowed detailed considerations of the stereochemical features of the photoadditions. Irradiation of the homoquinones **6a–e** with ethyl vinyl ether proceeded regio- and stereoselectively to give the *endo*-**7a–e** in preference to the *exo*-isomer **7e** in good total yields (Scheme 4).[23a]

In case of *p*-dibromo-substituted **6f**, the dihydro-*o*-benzoquinone monomethide **9f**, involving ring opening of the cyclopropane moiety, was only obtained as a secondary product by way of a subsequent acid-catalyzed skeletal rearrangement. (Initially, formed (but not detected) **7f** gave **9f** during the irradiation time; the acid-catalyzed rearrangement was confirmed by the independent experiment of the conversion of **7c** to **9c**). Similar products were formed on irradiation of *m*-substituted homoquinones **6g–i** which gave, preferentially, the *endo*-**7g–i** analogous to the reaction of *p*-substituted **6a–e**, although the primary adduct from **6j** underwent the skeletal transformation to **10j** (Scheme 5).

The regiochemistry of the [2+2]-additions of *p*- and *m*-substituted **6** was only affected by the substituents at the CC double bond of homobenzoquinones and not by the cyclopropane substituents, although the *endo* selectivity was appreciably reduced by the methoxy substituent. As a result, it is concluded that the spin density and the steric nature of the excited triplet state as well as the relative stability of the HH 1,4-biradical play a crucial role in the stereochemical course of these reactions.

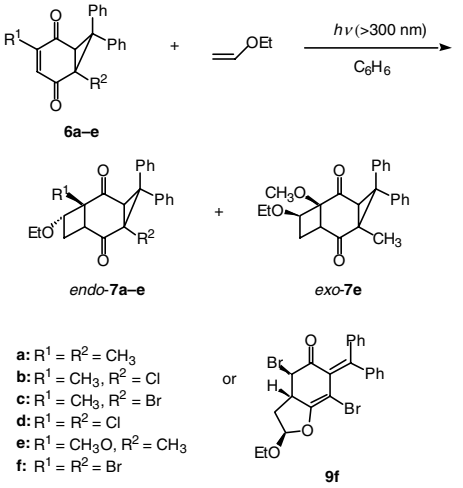

SCHEME 4

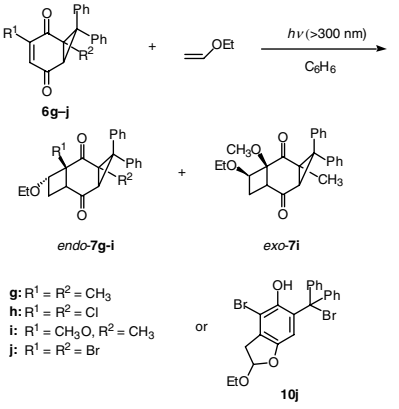

SCHEME 5

In the next study, further details of these [2+2]-photoreactions were investigated for *p*-dimethyl-substituted **6a** as a common substrate with various alkenes **11a–h** in order to explore the factors that control the regiochemistry and the *exo*/*endo*-selectivity (Scheme 6).[23b] The relative configuration of all the tricyclic-ring skeletons was identified as *cis-transoid-cis*, showing the exclusive *anti* approach of the alkenes with respect to the cyclopropane ring of homoquinone **6a**. This is probably the result of steric hindrance of the *endo* phenyl group. The sum of the yields of *endo*- and *exo*-**7** exceeded that of the regioisomeric *endo*- and *exo*-**8**. It is also noted that the major HH addition mode preferentially provides *endo*-**7** for the alkenes **11a–d** with smaller substituents but *exo*-**7** for alkenes **11e–h** with aromatic and/or bulky substituents. Similar substituent effects on the *exo*/*endo* selectivity were also observed for the minor HT addition mode giving **8**, although the effects were not so appreciable. The preferred regiochemistry was rationalized in terms of the more stable 1,4-biradical intermediates as described above. In fact, a trapping experiment using PhSeH in the reaction of **6a** with ethyl vinyl ether **11b** proved the involvement of the two regioisomeric triplet 1,4-biradical intermediates as indicated by the isolation of **12** (34%) and **13** (9%) (Scheme 7).

The observed reversal of *exo*/*endo* selectivity on changing alkene substituents was interpreted as follows. According to Griesbeck's concept proposed for the Paternò–Büchi reaction, it is necessary to orient the

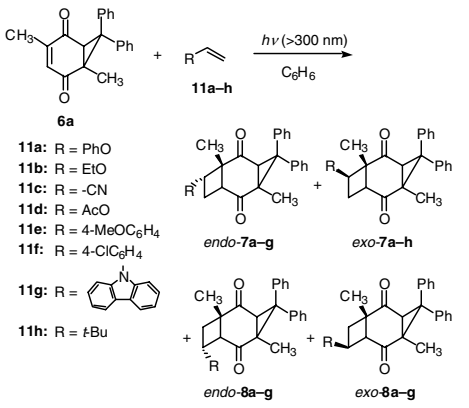

SCHEME 6

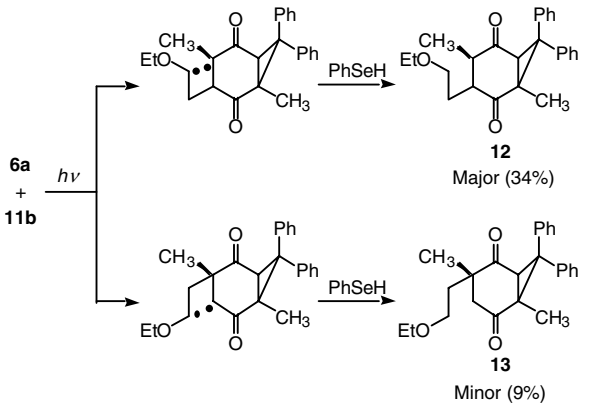

SCHEME 7

two singly occupied orbitals of the triplet 1,4-biradicals perpendicular to each other in order to maximize spin-orbit coupling (SOC), as represented for the conformers **II** and **III** responsible for the major HH addition (Scheme 8). Thus, in the case of the smaller substituent R, the fast cyclization in the spin-inverted singlet 1,4-biradical affords *endo* adducts preferentially. The stereochemical *exo*/*endo* reversal for the bulky **11e–h** can be rationalized by the occurrence of some CC bond rotation around the substituted radical chain of the singlet 1,4-biradical prior to the ring-closure. As a result of the increased population of the sterically less hindered conformer **VI**, the larger substituent R prefers the formation of the *exo* adducts.

Intramolecular Reaction

Intramolecular photocycloaddition of alkenes to α,β-conjugated enones was first reported by Ciamician and Silber.[24] Since then, the reaction has received much attention in view of its utility for the synthesis of polycyclic systems incorporating a cyclobutane ring.[25] The intramolecular [2+2]-photocycloaddition has been examined for homobenzoquinones bearing alkenyl side chains. Although 3-butenyl-substituted homobenzoquinone **6k** (n = 2) was quantitatively recovered even when irradiated for 1 hr, chain-elongated 4-pentenyl-substituted **6l** (n = 3) successfully achieved an intramolecular reaction to give tetracyclic dione **14l** in good yield, obeying the "rule of five" (Scheme 9).[26] This compound has a unique tetracyclic dione structure containing three-, four-, five-, and six-membered rings. All the rings are *cis*-fused, and the three- and four-membered rings adopt the *anti* structure.

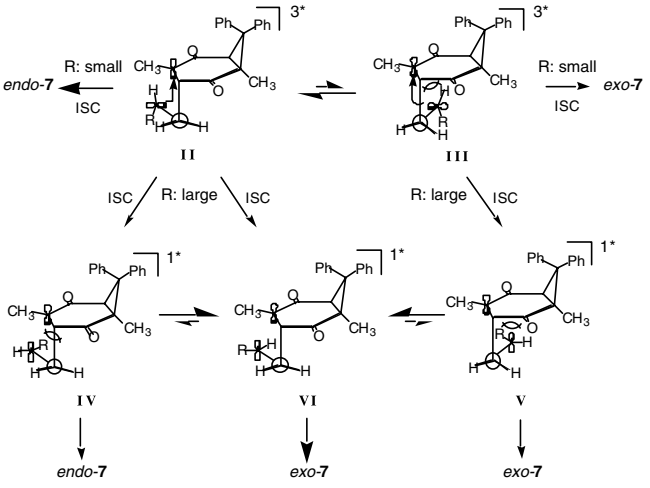

SCHEME 8

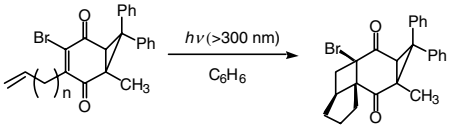

SCHEME 9

74.4 Hydrogen Abstraction Reaction

Intermolecular Reaction

The photoinduced inter- and intramolecular hydrogen abstraction is a matter of interest in the field of ketone photochemistry from both synthetic and mechanistic points of view.[27] In general, the radical species generated by hydrogen abstraction lead to recombination, rearrangement, or disproportionation. Thus, the hydrogen abstraction of homoquinones is of interest in regard to the site selectivity of carbonyl functions as well as possible cleavage of the cyclopropane ring.

Maruyama and Tanioka[28] found that the photoreaction of homonaphthoquinones **15**, in the presence of xanthene as a hydrogen donor, gave the stereoisomeric 1:1 adducts (**16** and **17**) and ring-expanded cycloheptadione **18** together with 9,9′-bixanthenyl (Scheme 10).

The exclusive addition of the xanthene moiety to the sterically less hindered carbonyl group was observed in **15b**, in accordance with the lower reactivity of dimethyl-substituted **15c**. The CIDNP experiment revealed that **16** and **17** are recombination products via an initially formed triplet radical pair. The proposed mechanism is shown in Scheme 11. The hydrogen abstraction of the excited triplet state of **15** from xanthene generates ketyl and xanthenyl radicals. A possible product derived from outer cyclopropane bond cleavage was not obtained because of the lower stability of a primary radical compared with the conjugated radical formed by inner cyclopropane bond cleavage.

In contrast, irradiation of diethoxycarbonyl-substituted **15d** afforded the cyclopropane bond-cleaved **19** and **20** even in the absence of xanthene (Scheme 12). The photoisomerized **19** may be formed through subsequent 1,4-hydrogen atom migration. The presence of xanthene resulted in a higher yield (45%) of **20** but no appreciable change in the yield of **19**. The results indicate that compound **20** is a reduction

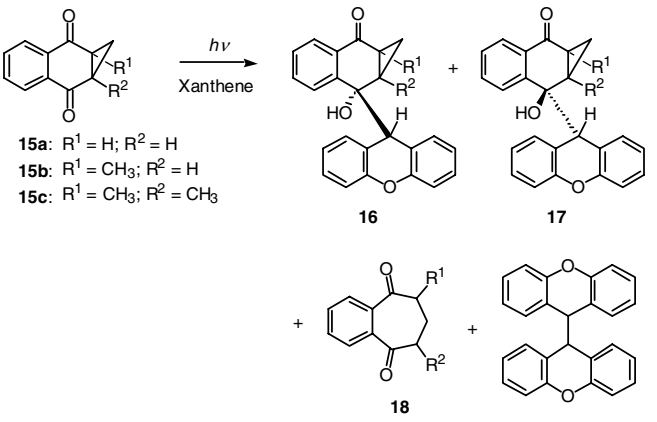

SCHEME 10

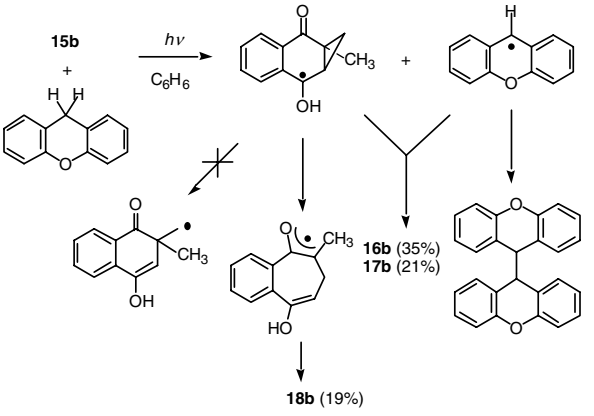

SCHEME 11

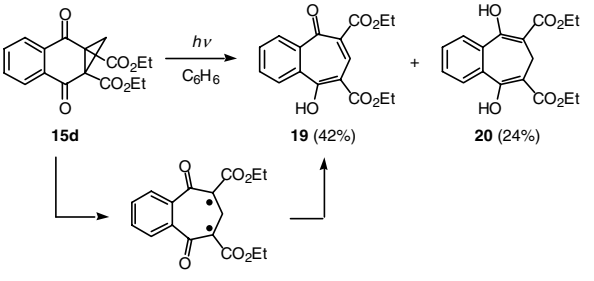

SCHEME 12

product arising from the intermolecular hydrogen abstraction by the photoexcited **15d** from another molecule of **15d** or xanthene. The preferred rupture of the inner bond of **15d** is probably due to the spin delocalization over the ethoxycarbonyl functions within the 1,3-biradical.

Contrary to the reaction of **15a–d**, diaryl-substituted **21a** and **21b** showed no reaction in the presence of xanthene even under completely deaerated conditions; however, oxygen introduction brought about a drastic change in the photochemical behavior to give 2-methylnaphthoquinone and the corresponding

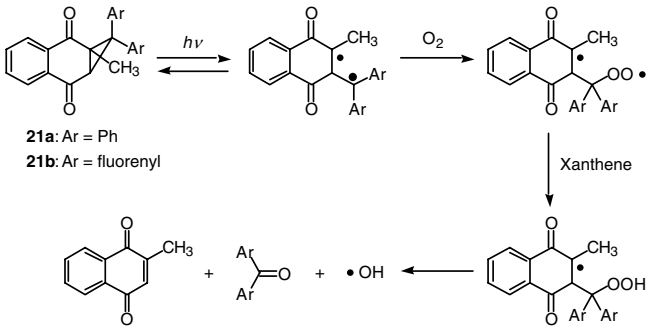

SCHEME 13

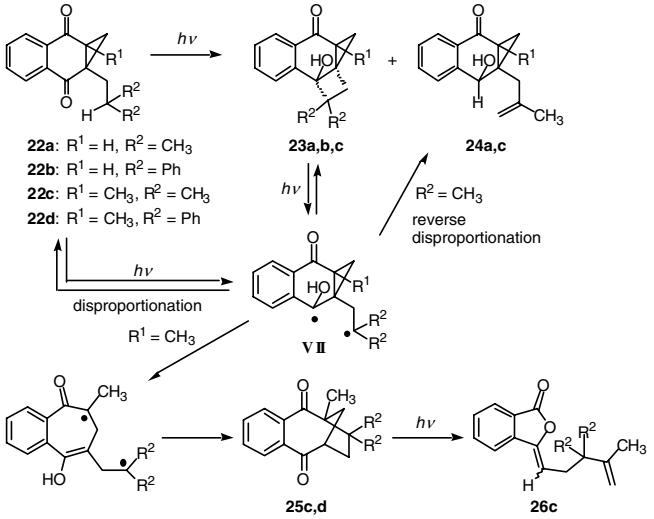

SCHEME 14

diaryl ketones together with 9,9′-bixanthenyl (Scheme 13). The mechanism involving a carbene intermediate was ruled out because the absence of xanthene afforded no photoproduct and the reaction in benzene/methanol solution gave no methanol adduct attributable to carbene insertion. As a result, the diaryl-substituted biradicals can add an oxygen molecule but cannot abstract a hydrogen atom from xanthene.

Intramolecular Reaction

The intramolecular photoinduced hydrogen abstraction of carbonyl compounds, known as the Norrish type II reaction, is one of the most important primary photochemical processes, usually giving the corresponding cyclic alcohols via hydrogen abstraction of the excited triplet carbonyl oxygen followed by radical recombination.

Osuka et al.[29] described the type II photoreaction of various homonaphthoquinones **22a–d** with abstractable γ-hydrogens. The photochemical behavior of these substrates is very dependent on the cyclopropane substituents (R^1 and R^2). Irradiation of **22a** (R^1 = H, R^2 = CH_3) gave the usual cyclobutanol **23a** along with the unsubstituted alcohol **24a** (Scheme 14). The compound **24** may be derived by hydrogen transfer from a δ-carbon to the less reactive ketyl radical center of the primary biradical **VII**. It was confirmed that a photoequilibrium takes place between **22** and **23** via **VII** as a common intermediate.

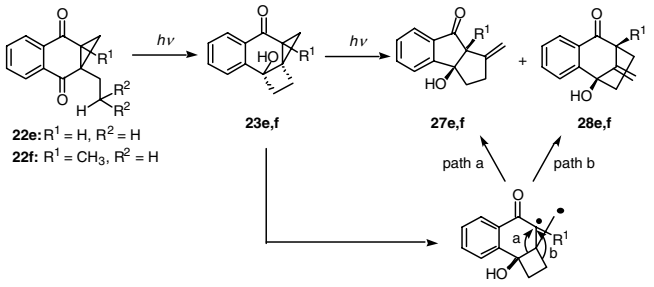

SCHEME 15

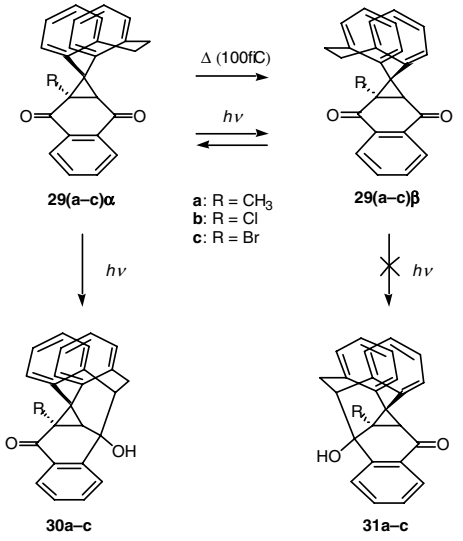

SCHEME 16

This allows slow leakage to **24** via a very rare reverse disproportionation. Replacement of the CH_3 on R^2 by Ph also attained photoequilibration, as indicated by the constant ratio of **22b** to cyclobutanol **23b** on extended irradiation.

In contrast, irradiation of **22c** ($R^1 = CH_3$, $R^2 = CH_3$) produced bicyclic diketone **25c** and alkylidene phthalide **26c** together with cyclobutanol **23c** and the unsaturated alcohol **24c**. Compound **26** is the result of secondary photoisomerization of **25**. The formation of **25** can be explained by a cyclopropylcarbinyl rearrangement of ketyl radical **VII** followed by 1,5-biradical-recombination. Such an inner cyclopropane bond fission may be favored by the better stabilization by R^1 (= CH_3) of the new radical center. As found in **22d**, replacement of $R^2 = CH_3$ by a Ph group simplified the reaction outcome to provide only **25**.

Interestingly, in the case of R^2 = H, further irradiation of the cyclobutanol products **23e** and **23f** led to β,γ-unsaturated bicyclic ketones **27** and **28** via cleavage of an outer cyclopropane ring bond followed by a dual 1,2-alkyl migration (Scheme 15).

The conformationally restricted 1,7-hydrogen abstraction was observed for homonaphthoquinones **29a–c** with a spiro-linked dibenzocycloheptene[30] (Scheme 16). This homoquinones have two isolable conformational isomers **29α** and **29β** at room temperature, and when heated the less stable **29α** isomerizes almost completely to 29**β** via a conformational inversion of the twist-boat cycloheptene ring.

The irradiation of the less stable isomer **29α** brought about a conformationally specific 1,7-hydrogen abstraction to give the tetracyclic alcohol **30**; the stable **29β** did not lead to the corresponding **31** but did

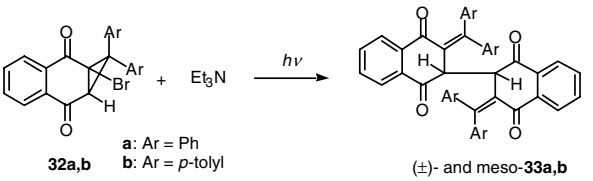

SCHEME 17

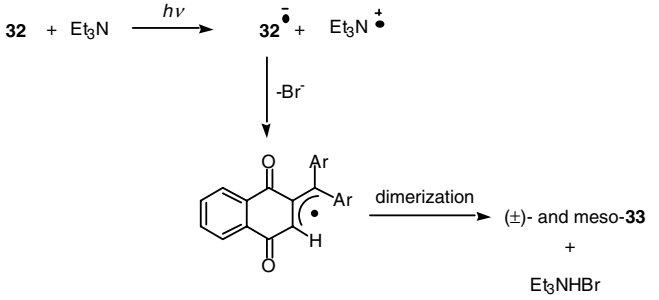

SCHEME 18

yield identical **30** via a reversible photoisomerization between **29α** and **29β**. Thus, the hydrogen abstraction in this system requires proper spatial orientation of the relevant hydrogen atom toward the excited carbonyl oxygen as proposed by Scheffer et al.[31]

74.5 Photoinduced Electron Transfer Reaction

Intermolecular Reaction

Because of the fusion of the quinone function, homoquinone is expected still to be capable of behaving as an electron acceptor; however, the electron-accepting capabilities of homoquinone are considerably reduced as compared with the parent quinone. The photoirradiation of bromo-substituted diarylhomonaphthoquinones **32a,b** in the presence of triethylamine (Et_3N) in acetonitrile gave dimeric products **33a,b** as a mixture of (±)- and *meso*-isomers (1:1) (Scheme 17);[32] the reaction did not occur when the labile bromine was substituted by chlorine or methyl groups.

The fluorescence of compound **32** was quenched by Et_3N. Stern–Volmer plots of the fluorescence quenching in acetonitrile were linear with amine concentration, suggesting electron transfer to the excited singlet state of **32**. The value of the quenching rate constant k_q obtained was 2.90×10^9 dm^3/mol/s. The free-energy changes (ΔG), calculated according to the Rehm–Weller equation for the system of **32a** and various amines used, are all negative.[33] This means electron transfer from amines to excited **32a** should be spontaneous. No new emission attributable to exciplex fluorescence was observed in the quenching experiments. No essential differences in the absorption spectra were found in a mixture of **32** and amines at various concentrations. From these results, it is proposed that the photoreaction proceeds through the mechanism outlined in Scheme 18.

The first step is photoexcitation of **32** followed by a single electron transfer (SET) from the amine to the excited **32**. The generated radical anion then undergoes ring opening with loss of bromide to generate the allyl radical. In contrast, the possible radical anions with poor or less labile chloro or methyl substituents would undergo back-electron transfer to the amine radical cation. The allyl radical collapses to give the dimer **33**. The hydrogen bromide salt of the Et_3N was quantitatively obtained as a byproduct.

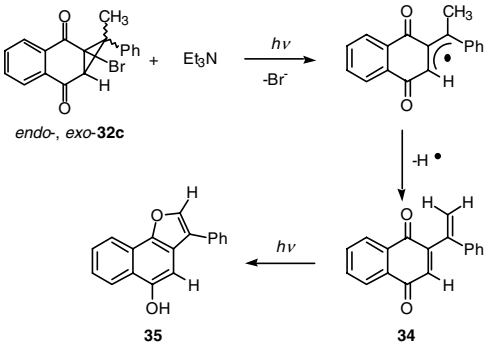

SCHEME 19

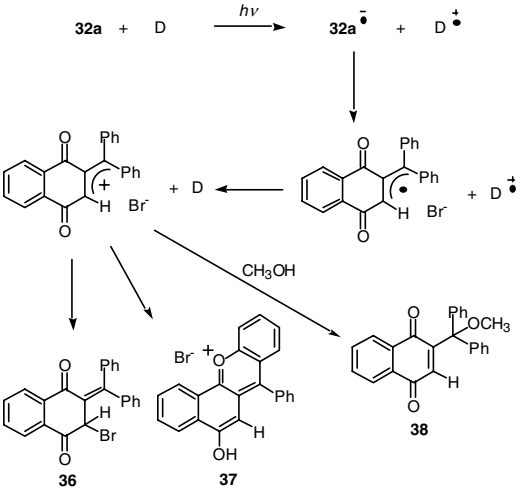

SCHEME 20

A similar irradiation of methylphenylhomonaphthoquinone (*endo*- and *exo*-**32c**) afforded the naphthofuran derivative **35** instead of the expected dimer (Scheme 19). It was reported that the direct irradiation of the analogous 2-(α-phenylvinyl)-1,4-benzoquinone **34** resulted in the quantitative formation of the corresponding benzofuran derivative.[34]

On the other hand, irradiation of **32a** with an equimolar amount of arene donors, such as naphthalene, dimethoxybenzene, or triphenylamine, afforded 2-bromo-3-diphenylmethylene-2,3-dihydronaphthoquinone **36** and xanthylium salt **37** instead of the corresponding dimer (Scheme 20).

The photoreaction in methanol gave the methanol adduct **38** along with **37**. The path involving back-electron transfer from the allyl radical intermediate to the radical cation of the arene donor rationalized the major change in product distribution. For the amine donors, proton abstraction by a second molecule of amine occurred exclusively rather than the back-electron transfer, and the formed radical collapsed to the dimer. It is of interest that the similar photoreaction of **32a** in the presence of xanthene as the donor gave both the dimer **33** and the ring-opened **36** together with xanthylium salt **37** and 9,9′-bixanthenyl. This result indicates that xanthene occupies a borderline position in this photoreaction due to its increased proton-donating ability relative to other arene donors.

The reactivity of homobenzoquinones was quite different from that of homonaphthoquinones. The irradiation of bromo-substituted homobenzoquinone **6c** in the presence of Et_3N as an electron donor

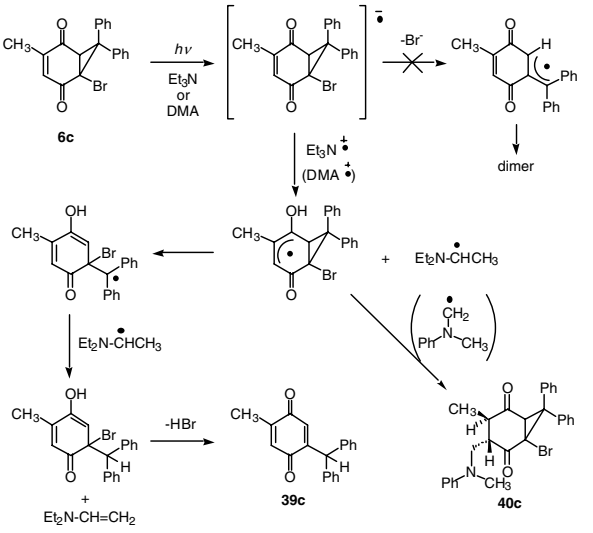

SCHEME 21

resulted in debromination and cyclopropane ring cleavage to give **39c** instead of the corresponding dimer (Scheme 21).[35]

Other secondary and tertiary amines or diethylaniline could be used in place of Et_3N; however, in the case of dimethylaniline (DMA) as an electron donor, the aniline adduct **40c** was obtained as a major product along with **39c**. These reactions failed to occur in the absence of amine or in the dark. Replacement of amine by 2-propanol as the hydrogen donor also resulted in the quantitative recovery of **6c**. Stern–Volmer plots of the fluorescence quenching of **6c** by Et_3N were linear with amine concentration, indicating electron transfer to the excited singlet state of **6c**. Free-energy changes (ΔG) calculated according to the Rehm–Weller equation for the system of **6c** and various amines used are all negative.

These observations indicate that the radical anion of homobenzoquinone arising from the photoinduced electron transfer from the amine to the excited **6c** afforded the allyl radical intermediate via fast proton transfer from the radical cation of the amine (Scheme 21). The successive cleavage of cyclopropane ring and elimination of hydrogen bromide gave diphenylmethyl-substituted quinone **39c**, while the fast radical coupling gave **40c** in the case of DMA. This different mode of reaction can be attributed to the bulkiness and hydrogen-donating ability of the respective amino radicals. Further interest lies in the marked difference in the products between the photoreaction of the homobenzoquinone and that of the homonaphthoquinone described above. The radical anion derived from homobenzoquinone exhibits preferred proton acceptability. The fused-benzene nuclei of the radical anion of homonaphthoquinone may allow the accumulation of spin density on the adjacent ketyl carbon atom, just as in a π-conjugative benzyl radical, by which the outer cyclopropane ring opening is favored to give rise to the corresponding allyl radical.

Irradiation of dimethyl-substituted homobenzoquinone **6a** in the presence of Et_3N or diethylamine gave dihydrogenated **41a** without cyclopropane ring cleavage (Scheme 22). In the case of DMA, only the aniline adduct **40a** was produced as well as in the reaction of **6c**. The stereoselective formation of **40** and **41** is rationalized by the stability of their half-chair conformations.[36] In conclusion, irradiation of homoquinones in the presence of donors resulted in a photoinduced electron transfer that is responsible for the subsequent dimerization, donor amine addition, and hydrogenation, depending on the nature of the homoquinone and the donor.

Intramolecular Reaction

Homoquinones also undergo intramolecular photoinduced electron transfer reactions when the electron-donating substituent is attached to the geminal diaryl group. Semiempirical calculations revealed that

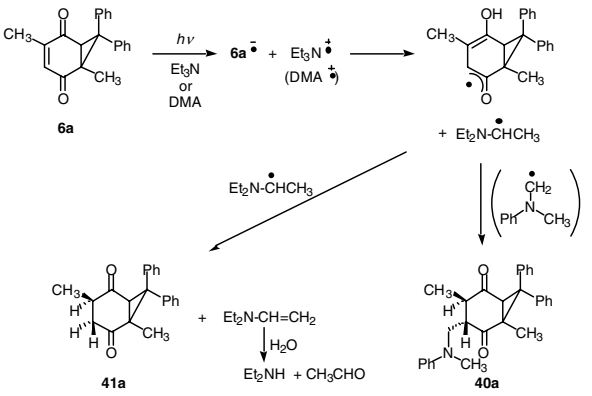

SCHEME 22

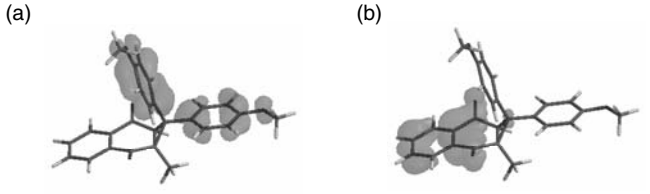

FIGURE 74.2 HOMO (a) and LUMO (b) of Dianisylhomonaphthoquinone **42a** calculated at MOPAC PM3 level.

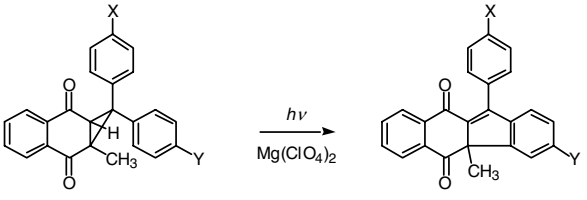

42a: X = Y = OCH_3
endo-**42b:** X = OCH_3, Y = H
exo-**42b:** X = H, Y = OCH_3
42c: X = Y = CH_3
42d: X = Y = H

43a: X = Y = OCH_3
43b: X = OCH_3, Y = H

SCHEME 23

the HOMO of *bis*(*p*-anisyl)homonaphthoquinone **42a** is located on the diaryl ring and the LUMO is on the quinone moiety (Figure 74.2). Indeed, the irradiation of **42a** gave the cyclopropane ring-expanded indenonaphthoquinone derivative **43a** quantitatively under the influence of $Mg(ClO_4)_2$ (Scheme 23).[37]

Similar treatment of *p*-anisylphenylhomonaphthoquinones (*endo*- and *exo*-**42b**) provided the identical **43b** accompanied by the *endo-exo* photoisomerization of the starting homoquinone **42b**; however, these reactions did not occur in the absence of $Mg(ClO_4)_2$. Due to the poor donor ability of aryl groups, *bis*(*p*-tolyl)- and diphenyl-homonaphthoquinones **42c** and **42d** remained intact on such irradiation. It was proposed that these photoreactions proceed by way of the mechanism outlined for **42a** in Scheme 24. The photoinduced intramolecular electron transfer furnishes the radical ion **VIII** capable of undergoing ring opening into the zwitterion **IX**; the zwitterion **IX** degrades to **43a** via cyclization involving the loss of two hydrogen atoms (Scheme 24).

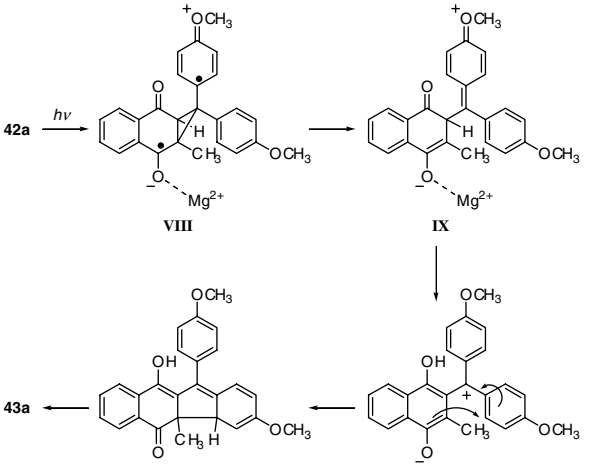

SCHEME 24

The role of added magnesium perchlorate is probably suppression of the intramolecular back-electron transfer as well as stabilization of **VIII** and **IX**. Such effects of metal ions added to enhance PET reactions are well known.[38]

74.6 Conclusions

A survey of the literature reveals some characteristic photochemical features of homoquinones: (1) [2+2]-photocycloaddition with alkenes and alkynes, (2) hydrogen abstraction and/or ring opening of incorporated cyclopropane, and (3) photoinduced electron transfer reactions, as described below. The photocycloaddition with alkenes and alkynes took place exclusively at the ethylene linkage of homobenzoquinones to afford cyclobutanes (or cyclobutene derivatives) regio- and *exo*/*endo* stereoselectively, depending on the identity of both the homobenzoquinones as well as the alkenes.

Photoinduced intermolecular hydrogen abstraction of homonaphthoquinone occurred in the presence of hydrogen sources such as xanthene to furnish dimerization of initially formed ketyl radicals as well as the ring opening of an inner cyclopropane bond. However, diaryl-substituted homologs did not show such a hydrogen abstraction but instead showed oxygen uptake at the biradical formed by cleavage of an outer bond of the cyclopropane moiety. Contrary to the foregoing, homonaphthoquinones bearing γ-hydrogens afforded cyclobutanols and unsaturated keto alcohols via Norrish type II biradicals. Further reactivity of these occurred when the substrates have additional spin-stabilizing alkyl substituents that can influence the inner cyclopropane ring-cleavage process. The conformationally specific 1,7-hydrogen abstraction was observed for the homonaphthoquinones with spatially restricted orientation of relevant hydrogen toward the carbonyl group.

Irradiation of bromo-substituted homonaphthoquinone with donor amines and arene compounds resulted in photoinduced electron transfer to bring about dimerization of the intermediate allyl radical or intramolecular cyclization to xanthylium salt via cyclopropane ring-opening associated with bromide release or bromide recombination, respectively. However, similar reactions of homobenzoquinone brought about hydrogenated cyclopropane ring opening and amination of the homoquinone CC double bond. Moreover, intramolecular electron transfer was found for homonaphthoquinones with anisyl substituents to yield indenonaphthoquinone derivatives.

References and Notes

1. Oshima, T., Fukushima, K., and Kawamoto, T., 2-Bromo-2,3-diphenylmethano-2,3-dihydronaphthoquinone, *Acta Cryst*., C55, 608, 1999.
2. The longest wavelength band of diphenylhomoquinone (λ_{max} = 372nm, ε = 210 in acetonitrile, pale yellow), which is derived from the reaction of diphenyldiazomethane and 2,5-dimethyl-1,4-benzoquinone, is largely shifted about 60 nm to the shorter wavelength compared to the corresponding quinone (λ_{max} = 424 nm, ε = 32, yellow).
3. Maruyama, K. and Osuka, A., Recent advances of the photochemistry of quinones, in *The Chemistry of the Quinonoid Compounds*, Vol. 2, Patai, S. and Rappoport, Z., Eds., Wiley, Chichester, 1988, chap. 13.
4. Regitz, M. and Heydt, H., Diazoalkanes, in *1,3-Dipolar Cycloaddition Chemistry*, Vol. 1, Padwa, A., Ed., Wiley, New York, 1984, 449.
5. (a) Eistert, B., Fink, H., Schulz, T., and Riedinger, J., Weitere versuche mit Naphthochinon-(1.4) und dessen halogen-, alkyl- und phenyl-derivaten, *Liebigs Ann. Chem*., 750, 1, 1971; (b) Oshima, T. and Nagai, T., Products and kinetic substituent effects in the reactions of diaryldiazomethanes with 2,5-dichloro-*p*-benzoquinone, *Bull. Chem. Soc. Jpn*., 55, 551, 1982.
6. Eistert, B., Pfleger, K., Arackal, T. J., and Holzer, G., Reactions of quinones and α-dicarbonyl compounds with diazoalkanes. XXII. Reactions of 2,3-dichloro-p-benzoquinone with diazoalkanes, *Chem. Ber.*, 108, 693, 1975.
7. Oshima, T. and Nagai, T., Addition of diphenyldiazomethane to unsubstituted and chloro-substituted 1,4-benzoquinones: effects of chloro substituents on the addition modes, *Bull. Chem. Soc. Jpn*., 61, 2507, 1988.
8. Eistert, B. and Bock, G., Reactions of α-dicarbonyl compounds and quinones with diazoalkanes. II. The reaction of some substituted *p*-benzoquinones with diazomethane to *p*-epoxymethylcyclohexadienones, *Chem. Ber*., 92, 1247, 1959.
9. Oshima, T., Nishioka, R., Ueno, S., and Nagai, T., A novel synthetic method for crown ethers by a redox reaction utilizing the intermediate from diphenyldiazomethane and 2,3-dichloro-5,6-dicyanobenzoquinone, *J. Org. Chem*., 47, 2114, 1982.
10. (a) Majersky, K.-M., Majersky, Z., Rakvin, B., and Veksli, Z., Free-radical reactions of a [3.1.1]propellane, 2,4-methano-2,4-didehydroadamantane, *J. Org. Chem*., 54, 545, 1989; (b) Wiberg, K. B. and Waddle, S. T., Reactions of [1.1.1]propellane, *J. Am. Chem. Soc*., 112, 2194, 1990.
11. Tamura, Y., Miyamoto, T., Nishimura, T., and Kita, Y., Pyrolysis of dimethylsulfoxonium (3-oxo-1-cyclohexen-1-yl)methylides, *Tetrahedron Lett*., 2351, 1973.
12. Boyle, P. H., O'Mahony, M. J., and Cardin, C. J., Reaction of 2-methyl-1,4-naphthoquinone and its 3-substituted derivatives with active methylene group anions and with diazo compounds, *J. Chem. Soc., Perkin Trans. 1*, 593, 1984.
13. (a) Bien, S., Kapon, M., Gronowitz, S., and Hörnfeldt, A.-B., Cyclopropanation of some Michael acceptors with thiophenium *bis*(methoxycarbonyl)methylides, *Acta Chem. Scand*., B42, 166, 1988; (b) Keith, D. D., Stipitatic acid: synthesis via cyclopropanated quinones, *Tetrahedron Lett*., 26, 5907, 1985.
14. (a) Adam, W., Balci, M., and Rivera, J., A convenient synthesis of homobenzoquinones, *Synthesis*, 807, 1979; (b) Asano, T., Yagihara, M., and Kitahara, Y., Photooxygenation of 7-substituted cycloheptatrienes, *Heterocycles*, 15, 985, 1981; (c) Klärner, F.-G., Schmidt, E. K. G., and Rahman, M. A., The effect of an annelated cyclobutene or cyclobutadiene ring on the norcaradiene–cycloheptatriene equilibrium, *Angew. Chem. Int. Ed. Engl*., 21, 138, 1982; (d) Saraçoglu, N., Menzek, A., Sayan, S., Salzner, U., and Balci, M., Pyramidalized double bonds containing endoperoxide linkages: photooxygenation of dimethyl *cis*-3,8-dihydroheptalene-3,8-dicarboxylate, *J. Org. Chem*., 64, 6670, 1999.

15. Contreras, L., MacLean, D. B., Faggiani, R., and Lock, C. J. L., Reactions of phthalans with dienophiles. III. Formation of homoquinones by reaction of 1,1-diethoxyphthalans with quinones, *Can. J. Chem*., 59, 1247, 1981.
16. (a) Seiz, V. G. and Gemmern, R. V., Zur [4+2]-Cycloaddition trimethylsilyloxy-substituierter Furane an Tetrachlorcyclopropen, ein neuer Weg zu Cycloheptadiendionen, *Chemiker-Zeitung*, 111, 209, 1987; (b) Collis, G. E., Jayatilaka, D., and Wege, D., Cyclopropa-fused quinones: the generation and trapping of bicyclo[4.1.0]hepta-1(6),3-diene-2,5-dione and 1*H*-cyclopropa[*b*]naphthalene-2,7-dione, *Aust. J. Chem*., 50, 505, 1997.
17. (a) Hashimoto, K., Yanagisawa, T., Okui, Y., Ikeya, Y., Maruno, M., and Fujita, T., Studies on anti-allergic components in the roots of *Asiasarum sieboldi*, *Planta Med.*, 60, 124, 1994; (b) Giannetti, B. M., Steffan, B., Steglich, W., Quack, W., and Anke, T., Antibiotics from basidiomycetes. Part 23. Merulidial, an isolactarane derivative from *Merulius tremellosus*, *Tetrahedron*, 42, 3579, 1986.
18. Corey, E. J. and Burke, H. J., Formation of carene [bicyclo(4.1.0)heptene] derivatives from *Eucarvone*, *J. Am. Chem. Soc.*, 78, 174, 1956.
19. (a) Burns, W. D. P., Carson, M. S., Cocker, W., and Shannon, P. V. R., The chemistry of terpenes. Part VIII. Some volatile neutral products of the oxidation of (+)-car-3-ene with permanganate, *J. Chem. Soc.*, *C*, 3073, 1968; (b) Suga, T., Shishibori, T., and Matsuura, T., The oxidation of (+)-3-carene and the related compounds with *t*-butyl chromate, *Bull. Chem. Soc. Jpn.*, 45, 1873, 1972.
20. (a) Endo, J. and Nakamura, T., Studies in *Asiasarum* (Aristolochiaceae). I. Three new compounds in *Asiasarum heteropoides*, *Yakugaku Zasshi*, 98, 789, 1978 (*Chem. Abstr.,* 89,135657, 1978); (b) Hashimoto, K., Katsuhara, T., Itoh, H., Ikeya, Y., Okada, M., and Mitsuhashi, H., Monoterpenes from *Asiasari radix* from *Asiasarum* sp., *Phytochemistry,* 29, 3571, 1990.
21. Still, I. W. J., Kwan, M.-H., and Palmer, G. E., Photo-addition of alkenes and alkynes to 3-carene-2,5-dione, *Can. J. Chem.,* 46, 3731, 1968.
22. Still, I. W. J., Macdonald, C. J., and Oh, Y.-N., Acetone-sensitized photodimerization of 3-carene-2,5-dione, *Can. J. Chem.,* 48, 1526, 1970.
23. (a) Kokubo, K., Nakajima, Y., Iijima, K., Yamaguchi, H., Kawamoto, T., and Oshima, T., Regio- and endo-selective [2+2]-photocycloadditions of homobenzoquinones with ethyl vinyl ether, *J. Org. Chem.,* 65, 3371, 2000; (b) Kokubo, K., Yamaguchi, H., Kawamoto, T., and Oshima, T., Substituent effects on the stereochemistry in [2+2]-photocycloaddition reaction of homobenzoquinone with variously substituted alkenes and alkynes, *J. Am. Chem. Soc.,* 124, 8912, 2002.
24. Ciamician, G. and Silber, P., Chemical action of light (XIII), *Ber. Dtsch. Chem. Ges*., 41, 1928, 1908.
25. For reviews, see (a) Becker, D. and Haddad, N., Applications of intramolecular [2+2]-photocycloadditions in organic synthesis, in *Organic Photochemistry*, Vol. 10, Padwa, A., Ed., Marcel Dekker, New York, 1989, chap. 1; (b) Mattay, J., Intramolecular photocycloadditions to enones: influence of the chain length, in *Organic Photochemistry and Photobiology*, Horspool, W. M. and Song, S.-P., Eds., CRC Press, Boca Raton, FL, 1995, chap. 51.
26. For example, see (a) Conrads, R., Mattay, J., and Hoffmann, R., *Stereoselective Synthesis*, Vol. E21, Helmchen, G., Ed., Georg Thieme, Stuttgart, 1996, 3119; (b) Crimmins, M. T., Photochemical cycloadditions, *Comprehensive Organic Synthesis,* Vol. 5, Trost, B. M., Ed., Pergamon, Oxford, 1991, chap. 2.3.
27. Wagner, P. and Park, B.-S., Photoinduced hydrogen atom abstraction by carbonyl compounds, in *Organic Photochemistry*, Vol. 11, Padwa, A., Ed., Marcel Dekker, New York, 1991, chap. 4.
28. (a) Maruyama, K. and Tanioka, S., Photochemical reduction of 2,3-dihydro-2,3-methano-1,4-naphthoquinones with xanthene, *Bull. Chem. Soc. Jpn.*, 49, 2647, 1976; (b) Maruyama, K. and Tanioka, S., Photochemical reaction of 2,3-dihydro-2,3-methano-1,4-naphthoquinone derivatives: three different types of reaction, *J. Org. Chem.,* 43, 310, 1978.
29. (a) Osuka, A., Chiba, M. H., Shimizu, H., Suzuki, H., and Maruyama, K., Type II photoreaction of 1a,2a-dihydro-2*H*-cyclopropa[*b*]naphthalene-1,3-dione, *J. Chem. Soc., Chem. Commun.*, 919, 1980; (b) Osuka, A., Shimizu, H., Suzuki, H., and Maruyama, K., Monoradical rearrangement of

1,4-biradicals involved in Norrish type II photoreaction of methanonaphthoquinones, *Chem. Lett.,* 329, 1982; (c) Osuka, A., Shimizu, H., Chiba, M. H., Suzuki, H., and Maruyama, K., Type II photoreaction of 1a,7a-dihydro-1*H*-cyclopropa[*b*]naphthalene-2,7-diones: photochemical generation of type II biradicals from cyclobutanols, *J. Chem. Soc., Perkin Trans. 1*, 2037, 1983.

30. Kokubo, K., Kawahara, K., Takatani, T., Moriwaki, H., Kawamoto, T., and Oshima, T., Conformational specificity in photoinduced intramolecular 1,7-hydrogen abstraction of spiro-linked dibenzocycloheptene ring *Org. Lett.*, 2, 559, 2000.
31. (a) Scheffer, J. R. and Dzakpasu, A. A., Organic photochemistry in the solid state: the distance and geometric requirements for intramolecular hydrogen abstraction reactions. Structure–reactivity relationships based on x-ray crystallographic data, *J. Am. Chem. Soc.,* 100, 2163, 1978; (b) Ariel, S., Askari, S., Scheffer, J. R., and Trotter, J., Latent photochemical hydrogen abstraction reactions realized in crystalline media, *J. Org. Chem.*, 54, 4324, 1989; (c) Gudmundsdottir, A. D., Lewis, T. J., Randall, L. H., Scheffer, J. R., Rettig, S. J., Trotter, J., and Wu, C.-H., Geometric requirements for hydrogen abstractability and 1,4-biradical reactivity in the Norrish/Yang type II reaction: studies based on the solid state photochemistry and x-ray crystallography of medium-sized ring and macrocyclic diketones, *J. Am. Chem. Soc.*, 118, 6167, 1996.
32. (a) Moriwaki, H., Oshima, T., and Nagai, T., Photoinduced reductive cleavage of diarylcyclopropanes fused with bromonaphthoquinone in the presence of amines, *J. Chem. Soc., Chem. Commun.*, 255, 1994; (b) Moriwaki, H., Oshima, T., and Nagai, T., Photoisomerization of bromonaphthoquinone-fused diphenylcyclopropane into xanthylium salt in the presence of arene donors, *J. Chem. Soc., Chem. Commun.*, 1681, 1994; (c) Moriwaki, H., Oshima, T., and Nagai, T., Photoinduced electron-transfer reactions of homonaphthoquinones with amine and arene donors, *J. Chem. Soc., Perkin Trans. 1*, 2517, 1995.
33. Rehm, D. and Weller, A., Kinetics of fluorescence quenching by electron and hydrogen-atom transfer, *Isr. J. Chem.*, 8, 259, 1970.
34. Iwamoto, H., Takuwa, A., Hamada, K., and Fujiwara, R., Intra- and intermolecular photocyclization of vinylbenzo-1,4-quinones, *J. Chem. Soc., Perkin Trans. 1*, 575, 1999.
35. Moriwaki, H., Matsumoto, T., Nagai, T., and Oshima, T., Photoreaction of homobenzoquinones with amine donors, *J. Chem. Soc., Perkin Trans. 1*, 1461, 1996.
36. Moriwaki, H., Kawamoto, T., and Oshima, T., Half-chair conformation of *trans*-1,4-dimethyl-7,7-diphenylbicyclo[4.1.0]hepta-2,5-dione, *Acta Cryst.*, C52, 2269, 1996.
37. Moriwaki, H., Fukushima, K., Nagai, T., and Oshima, T., Conversion of donor-substituted homonaphthoquinones to indenonaphthoquinones via intramolecular photoinduced electron-transfer, *J. Chem. Soc., Chem. Commun.*, 495, 1996.
38. (a) Fukuzumi, S., Okamoto, T., and Otera, J., Addition of organosilanes with aromatic carbonyl compounds via photoinduced electron transfer in the presence of magnesium perchlorate, *J. Am. Chem. Soc.,* 116, 5503, 1994; (b) Mizuno, K., Ichinose, N., Tamai, T., and Otsuji, Y., Electron-transfer mediated photooxygenation of biphenyl and its derivatives in the presence of magnesium perchlorate, *Tetrahedron Lett.,* 26, 5823, 1985.

75

The Quantitative Cavity Concept in Crystal Lattice Organic Photochemistry: Mechanistic and Exploratory Organic Photochemistry

Howard E. Zimmerman
University of Wisconsin

75.1 Introduction

Solid-state organic photochemistry had its beginnings over a century ago. For the most part, it has been an empirical science. Where theory has been applied, the tendency has been to apply a method either to a single reaction or to a type of reaction, such as a [2+2]-cycloaddition involving little molecular motion. In view of the present author's interest in molecular rearrangements and reactions involving considerable molecular reorganization, the approach taken in our group has been to search for methodology that is quantitative and also can be tested on a variety reactions.

One of the most important beginnings in the field of solid-state photochemistry was the concept of the reaction cavity proposed by Cohen and Schmidt.[1] Another suggestion by the same authors was that reactions take place with least motion. Both suggestions were qualitative. The first is quite valid, while the least motion idea has proven not to be general. This chapter aims at presenting the methods of most use in our research on solid-state photochemistry.

0-8493-1348-1/04/$0.00+$1.50

75.2 Methodology and Examples

There are a number of approaches to understanding the course of solid-state reactions which are reasonably complex. Thus, the treatment of molecular rearrangements poses more difficulty than other types (e.g., [2+2]-cycloadditions). Most of the methods require having x-ray structures of the reactant. A simple approach involves inspection of the x-ray coordinates of the reactant and determining if some functional group is hindered by the surrounding shell of neighbors.

A second approach[2] (note Scheme 1) relies on a "mini-crystal lattice" composed of the reactant molecule and the nearest layers of neighboring molecules. If one envisions the central molecule being absent, one has a cavity. The atoms nearest the center of the cavity and their x-ray coordinates then define a quantitative cavity of the type suggested qualitatively by Schmidt and Cohen. One then can consider all the reasonable reaction mechanisms leading to the experimentally observed photoproducts and the first intermediates in each of the mechanisms can be generated theoretically using quantum mechanics. Then, one needs to see how well each intermediate fits into the cavity. In effect, one replaces the originally extracted reactant molecule with a molecule of the first intermediate. In doing this, one keeps corresponding atoms of reactant and first intermediate as geometrically close as possible. The "fit" of each intermediate in the cavity is then determined by the amount of van der Waals overlap with the surrounding neighbors or by using molecular mechanics to obtain the energy of the aggregate.

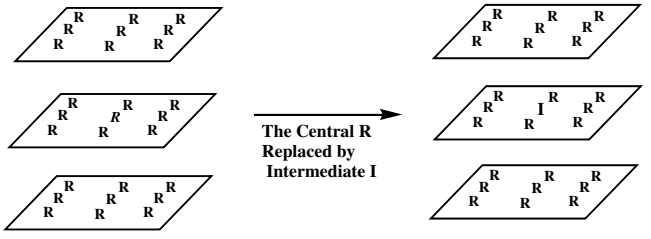

SCHEME 1 The mini-crystal lattice and injection of a reaction intermediate I replacing the central reactant molecule.

A third approach[3] is aimed at avoiding use of molecular mechanics to treat reaction intermediates, which are triplets or other open shell species. The method takes the mini-crystal lattice consisting of the reacting species surrounded by a shell of neighbors. The atoms of this shell that are closest to the imbedded central molecule are retained, while all remaining atoms of the surrounding molecules are computationally annihilated. To circumvent the problem of having "dangling" free valences at the residual atoms of the neighbors, the hydrogen atoms are computationally converted to heliums, and the carbons, oxygens, and nitrogens are converted to neons. This then provides an "inert gas shell" that defines the reaction cavity. While the inert gas atoms of this shell are kept fixed, the entirety is geometry optimized using quantum mechanics, which may range from AM1 to Hartree-Fock to CASSCF. The inert gas atoms take virtually no computation time and thus one can quite easily determine the energies of a variety of alternative reacting species in the shell. The method then circumvents the matter of treating an open shell species with a molecular mechanics calculation. After all, molecular mechanics completely ignores the electronic contributions to the total energy.

A fourth approach[4] utilizes ONIOM, a computational method devised by Morokuma.[5] The method was intended to dissect a large molecule into portions. One portion is subject to quantum mechanical computation. Further portions are treated by molecular mechanics. In dissecting a molecule by breaking bonds, the Morokuma method "caps" the dangling valences with light atoms as hydrogens.

In applying ONIOM to a mini-crystal lattice consisting of a reacting molecule imbedded in an aggregate of reactant neighbors, it is not necessary to break bonds. The reacting molecule can be treated with *ab initio* quantum mechanics. Then, a next layer of neighbors can be treated by molecular mechanics with geometry optimization. Our treatment, however, adds an outer layer of reactant molecules that is held rigid. The aim is to permit and simulate relaxation of the first layer of molecules while keeping the outer layer fixed.

75.3 Some Examples

In one study we compared solution and solid-state photochemistry for a series of reactions.[2,6] Scheme 2 outlines the solution photochemistry of pentenol **1,** which underwent a long-range phenyl migration giving ketone **6.** In contrast, in a crystal lattice, the same reactant cyclized to tetrahydropyran (**4**) and tetrahydrofuran derivatives (**5**), respectively. In this study we considered three reactivity factors as possibly involved:

1. Least motion had been considered as an important controlling factor
2. Overlap of the reacting species with the neighboring molecules (i.e., the cavity)
3. The energy of the imbedded species in the surrounding cavity.

We note in Scheme 2 that the formation of the ketone **6** involves more molecular reorganization, considerably more motion, more of an increase in molecular volume, and more overlap with the neighboring crystal lattice than the formation of products **4** and **5**. In considering these reactions, we focus on the requirements in the molecule reaching the first intermediates — **2a** affording product **4**, **2b** affording **5**, and **3** leading to product **6**.

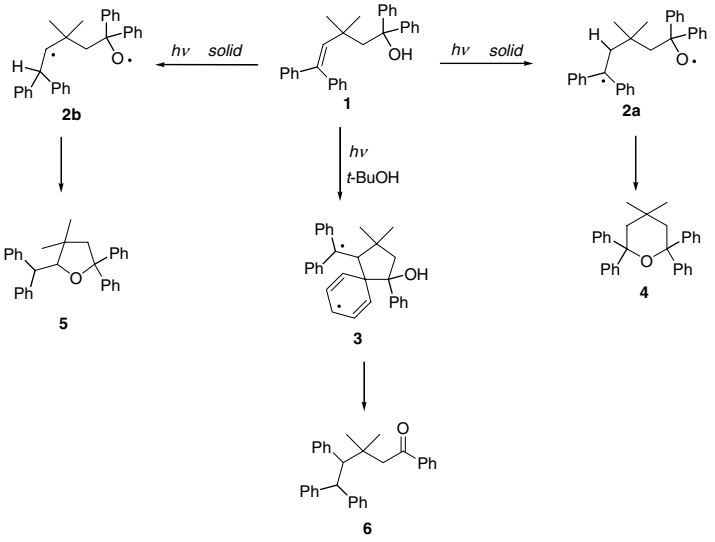

SCHEME 2 Contrasting solution and solid-state reactivity.

Reference to Table 75.1 confirms the intuitive conclusions above. Thus, for this case, each of the three factors considered seems to play a role. However, this turns out not to be generally the case for all of these factors.

One of the most reliable parameters in this early study was overlap of the reacting species with the neighbors. For example, in the rearrangement depicted in Equation 75.1, the overlap with the surrounding neighbors of the cavity of the *cis*-cyanophenyl enone **7** was 27.8 Å^3 while the overlap for migration of the C-4 phenyl group was 5.6 Å^3.[7,8]

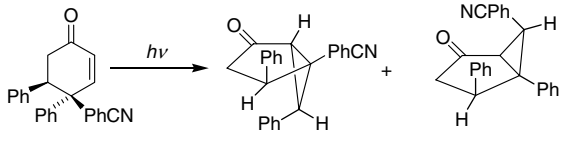

7 **8** **9**

Solution Ratios:	*1.0*	*1.0*
Crystal Ratios:	*1.0*	*0.0*

(75.1)

TABLE 75.1 Reactivity Indices for Formation of First Intermediates (**3, 4, 5**) from Pentenol **1**

Photoproduct	RMS Motion (Å)[a]	Δ Volume (%)	Δ Overlap (%)[b]
Pentanone **6**	1.00	18	5
Tetrahydropyran **4**	0.20	8	2
Tetrahydrofuran **5**	0.20	8	1

Note: The first intermediates were maximally superimposed on reactants.
[a] Sum of non-hydrogen root-mean-square (RMS) atomic displacements.
[b] Relative decrease in lattice volume due to van der Waals overlap.

A particularly intriguing example was found when crystallization of 4-phenyl-4-*p*-cyanophenyl **10** was found to afford two different modifications (i.e., dimorphs). These gave differing reactivity, as might have been anticipated from the differing crystal lattices. But more interesting results ensued.

Thus, a series of critical results arose from this observation.[9] The solution photolysis of this reactant (i.e., **10**) is an example of the well-known Type B Rearrangement[10] and affords a preferential cyanophenyl migration in a 15:1 ratio as depicted in Equation 75.2.[10c]

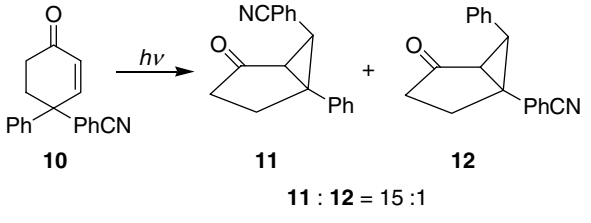

(75.2)

This result is not surprising in view of the greater electron delocalization[11] (2.5 kcal/mole) in the initial triplet bridged diradical **13,** which has the *p*-cyano group on the migrating aryl group, compared with species **14,** which has only a migrating phenyl group (see Figure 75.1).

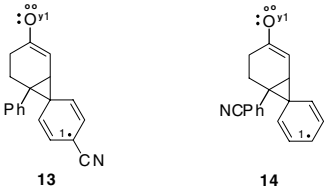

FIGURE 75.1 Alternative Triplet Biradical Intermediates. Solid dots represent π-system electrons, *y*s are p_y-orbital electrons, and circles are the collinear sp-hybrid electrons.

What was intriguing was the observation that one of the two dimorphs (termed "Crystal B"), in the crystalline state, underwent a preferential phenyl migration, in complete contrast with the solution preference for cyanophenyl migration. A second remarkable observation was that this regioselectivity was constant to 16% conversion, at which point the regioselectivity switched to a constant 1:1 ratio of phenyl vs. cyanophenyl migration. This result proved especially important and is considered below in the context of reactions proceeding in stages.

The usual treatment of imbedding each of the two alternative half-migrated triplet biradicals in the mini-crystal lattice of reactant — afforded only a prediction of a preferred cyanophenyl migration. However, careful study of the x-ray structure of the reactant provided a clue. The crystal had *C*2/*c* symmetry; being centrosymmetric, the enone molecules were ordered in pairs of enantiomers. However, the crystal that initially was thought to be slightly disordered, actually had each molecule surrounded by five neighbors, and one neighbor was the "wrong" enantiomer. This occurred systematically throughout the crystal. This might be termed "orderly disorder."

We developed a computer program called "Pairs."[3b] This considered each atom of a single molecule and its distance to all other atoms of surrounding molecules. The sorted pairs of atoms thus indicated which neighboring atoms were closest to a given reactant molecule. Interestingly, it was the nearest molecule of the five neighbors that was the "wrong" enantiomer. When our treatment replaced this nearest reactant molecule with its enantiomer, then a mini-crystal was produced in which the phenyl-half-migrated species was lower in energy despite the extra delocalization with *p*-cyanophenyl migrating and in contrast to the solution regioselectivity.

75.4 The Inert Gas Model

Up to this point we had been using molecular mechanics to assess energy effects. While this is quite reasonable for estimating reactant/neighbor van der Waals interactions, and while our molecular mechanics assessment of the relative energies of a variety of reaction intermediates were successful in predicting the lowest energy reaction path, nevertheless, there was an inherent problem. Many of these reaction intermediates were excited-state species and thus had electronic features not accounted for by molecular mechanics. For example, there is no account taken of the species' multiplicities. This fact was noted by one referee of one our manuscripts. The point was that, while one cannot argue with success, nevertheless one ideally should be using quantum mechanical and not molecular mechanical treatments to deal with excited states.

This led the present author to consider ways of dealing quantum mechanically with very large aggregates of molecules. The main impediment to a quantum mechanical computation is the size of a typical mini-crystal lattice. Even with AM1, such a large molecular system cannot be handled practically.

Our approach was to use Pairs,[3b] the program we had developed and which is described above, to determine which atoms of the neighbors were reasonably close to the reaction intermediate in the mini-crystal lattice. Then, all of the more distant atoms were computationally annihilated. However, this step leaves "dangling" free valencies originating from the remaining atoms not annihilated and yet surrounding the reacting species. The next step was to computationally convert each of the residual atoms to inert gas atoms, thus limiting the dangling free valence problem. Hydrogens are converted to heliums, and carbons, oxygens, and nitrogens are converted to argons. This does make these surrounding atoms somewhat larger than the originals, and a method was developed to expand this shell of inert gas atoms from the center (i.e., where the reacting species resides) to compensate for the slightly greater proximity before expansion. However, this gave only minor differences in the final computations. The final step of the procedure involved keeping the inert gas shell rigid and carrying out a quantum mechanical computation on the entirety, with the reacting species being permitted to undergo geometry optimization. While this could involve using just a semi-empirical computation such as AM1, it proved quite efficient to use Gaussian 98.[11] Thus, the presence of the inert gas atoms did not appreciably increase the computation times. This approach then provides an irregularly shaped, yet rigid cavity of the type considered qualitatively by Cohen and Schmidt. Thus, in a number of our publications we have termed this approach as the "quantitative cavity."

We found that this method properly predicts the reactivity of a number of solid-state reactions.[3] For example, note Equation 75.3 and the reactivity of the bicyclo[3.1.0]hexenones **15a** and **15b,** which were in agreement with the Inert Gas model.

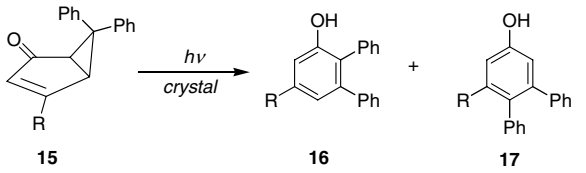

15 **16** **17**

Reactant	*Product Ratios*	
15a R = H	*3.0*	*2.0*
15b R = Me	*0.0*	*1.0*

(75.3)

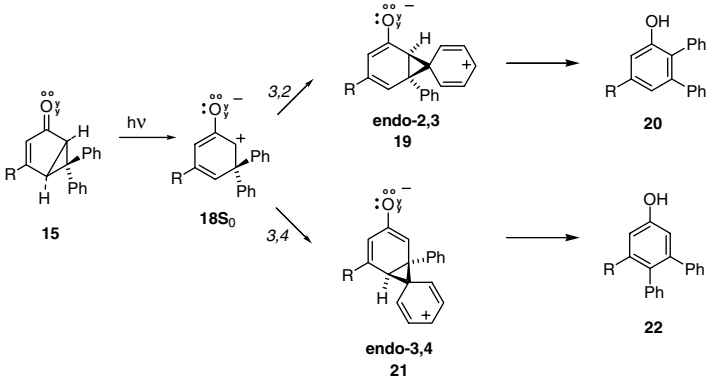

SCHEME 3 The mechanism of the last steps of the bicyclic Type B rearrangement.

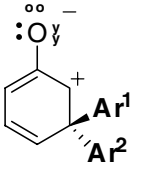

23

FIGURE 75.2 The Type A Zwitterion (i.e., **18S$_o$** with the aryl groups shown as different due to substitution or to cavity asymmetry).

Scheme 3 shows both possible pathways available to zwitterion **18S$_o$**, migration to C2 and to C4. In solution photochemistry, migration to C2 is preferred. However, this is seen not to be the case in the solid-state photochemistry.

Furthermore, there is one additional item of particular interest. While Equation 75.3 and Scheme 3 describe the photochemistry of the 5,5-diphenyl reactant **15a**, the photochemistry of counterparts in which one of the two phenyl groups bears a *p*-cyano or *p*-methoxy substituent was also studied. In the solution photochemistry, it is seen that the two faces of zwitterion **18S$_o$** are equivalent. This is not the

case in the crystal lattice photochemistry (see Figure 75.2) where the cavity makes the two faces of the zwitterion **23** non-equivalent.

Most interestingly, it is the *endo* aryl group in the substituted **15** that undergoes the migration. Indeed, the computations confirm that this is the energetically preferred reaction course in the cavity. In the case of the unsubstituted reactant **15** itself, without labeling, there is no way to tell which of the two phenyl groups does the migration. But here, the computational results agree that it is the *endo* group that, again, does the migration.

75.5 The ONIOM QM/MM Approach

Despite the success of the inert gas cavity method, it seemed important to see if computations could include the neighboring molecules more realistically and yet still use quantum mechanics for the reacting species. The ONIOM-QM/MM method of Morokuma[5] provided a practical method. The method permits quantum mechanical computations on part of a large molecular system, along with molecular mechanical computations on the rest of the molecule. Our aim was to use *ab initio* quantum mechanics for the reacting species and molecular mechanics on the rest of the mini-crystal lattice. This proved highly successful.[4] Thus, Gaussian 98[11] was reserved for the reacting species. The results, as in the Inert Gas model, were usefully predictive for the reaction course in general. However, they proved most useful in the case of host–guest reactivity (*vide infra*). One further result derived from this study, namely the finding that least motion, often termed the "topochemical principle," does not correlate well with the molecular rearrangements studied.

75.6 Host–Guest Reactivity

In the case of the two dimorphs with differing reactivity[9] (*vida supra*) we had the interesting possibility that, in general, one might obtain varying reactivity by just looking at the chemistry of dimorphs. However, these are rather difficult to obtain. The requirement is that the thermodynamic stability of the two modifications does not differ very appreciably and that the modifications do not interconvert so rapidly that the individual isomeric crystals cannot be studied.

However, host–guest complexes are known, and each such inclusion compound will have a different crystal morphology. Thus, with an infinite number of host–guest complexes possible for a given reactant, one can anticipate each host–guest pair to exhibitits own unique reactivity. Some hosts, which have proven useful to us, are given in Figure 75.3.[4] The chiral host **A** is Taddol,[12a,b] also termed the Seebach-Toda host. Each host has a differing shaped cavity and leads to differing reactivity. Thus, Taddol forms both1:1 and 2:1 inclusion compounds with 4-phenyl-4-*p*-cyanophenylcyclohexenone. The 1:1 inclusion compound (**10R+A,** 1:1) is seen in Scheme 4 to afford **11a**, one enantiomer of the cyanophenyl migrated Type-B enone rearrangement product. With host B, the otherenantiomer, **11b**, of the *p*-cyanophenyl migration product results. The 2:1 inclusion compound of reactant with Taddol (**10S+A**, 1:2) leads to both phenyl and *p*-cyanophenyl migration (i.e., products **10b** and **12a**), but with only one enantiomer of each being formed. With the chiral hosts, formation of chiral product is not unexpected. Most remarkably, with host **C**, phenyl migration results and the product is racemic.

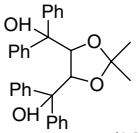

A (24)

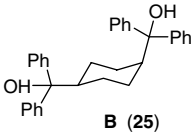

B (25)

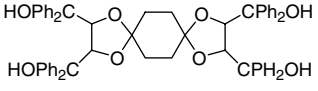

C (26)

FIGURE 75.3 Three host molecules of interest.

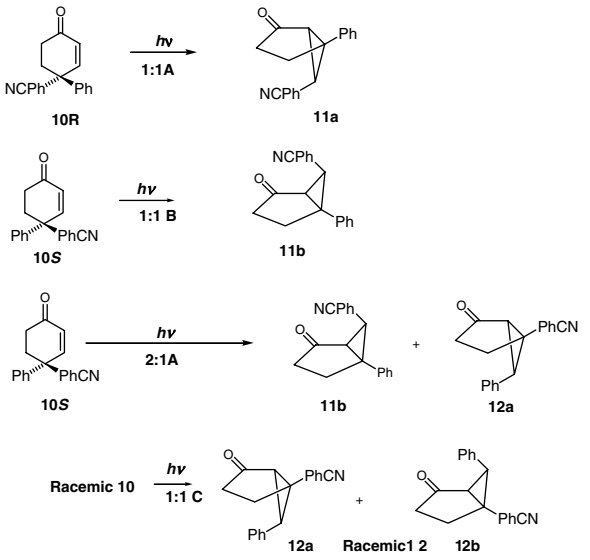

SCHEME 4 Reactivity using inclusion compounds with varying hosts — **A**, **B,** and **C**.

TABLE 75.2 ONIOM Energies of Mini-Crystal Lattices with Alternative Migration Intermediates for Host-Guest Complexes of Phenyl-*p*-Cyanophenylcyclohexenone

Inclusion Compound	Phenyl Migration Intermediate **14**[a]	Cyanophenyl Migration Intermediate **13**[a]	*f* Energy[b]	Experiment
Seebach-Toda **10R** 1:1	−855.4092	−855.4249	9.9	CNPh migr
Cyclohexyldiol **25**	−855.5556	−855.5523	−2.1	Phenyl migr

Note: ONIOM(ROHF/6–31G*:MM3) host-guest complexes.

[a] Energies in Hartrees (627.5 kcal/mole).

[b] kcal/mole.

Treatment of the host–cavity energetics in these cases required some new software programming. For conversion of x-ray coordinates to our mini-crystal lattices having single molecules imbedded, we wrote a program termed Smartpack. For cases of the host–guest type, modification was required and we called this program Icepack. With this programming we could again use ONIOM Gaussian 98 *ab initio* computations. The results for some of the photochemistry described above is summarized in Table 75.2. For the two cases cited in Table 75.2, as well as the other examples studied, the energetics proved in agreement with experiment. Some further interesting results were uncovered in this study of inclusion compounds. One was that in using ONIOM, the boundary between the outer layer of molecules and the intermediate layer just outside the reactant could be adjusted to afford fewer or more molecules in the layer immediately surrounding the reactant. The intermediate layer was permitted to geometry optimize while the outermost layer was kept fixed and rigid. This is equivalent to permitting a varied number of molecules immediately surrounding the reactant to be susceptible to relaxation. Interestingly, beyond one layer of surrounding neighbors there is very little effect on the energy of a reacting species. Thus, long-range stress effects seem minor.

75.7 The General Concept of Stages

It has often been erroneously assumed that solid-state photochemistry cannot be taken to high conversion because as product is formed, the crystal is pictured as disintegrating. However, in many solid-state photolyses, the crystal maintains its integrity.

Nevertheless, for a number of reactions, a rather interesting and important phenomenon was uncovered. The first case was that of the dimorphs of 4-phenyl-4-*p*-cyanophenylcyclohexenone **10**. In the case of "Crystal B," which initially exhibited only phenyl migration, sharply at 16% conversion, the regioselectivity changed to a 1:1 ratio of phenyl to cyanophenyl migration. Thus, there were two "stages," one up to 16% conversion and the other beyond that point.[7]

This result led us to consider whether more generally there were succeeding stages of reactions of crystal lattices. Indeed, this turned out to be a general phenomenon.[13,14] Thus, material that in the past had been discarded (i.e., material formed in Stage 2), often provides photoproducts not otherwise obtainable. One example is given in Scheme 5, which describes the photochemistry of 2-methyl-4,4-diphenylcyclohex-2-enone **27** in solution and in two stages of crystal-lattice reactivity. In solution, only the typical Type B enone photoproduct **28** is formed. In Stage 1 of the reaction, two photoproducts,(**28** and **29**) result. In contrast, in Stage 2 of the reaction, only photoproduct **28** is formed. Thus, the use of crystal-lattice photochemistry permits one to obtain a photoproduct (i.e., **29**) not otherwise accessible. Additionally, if one wishes to obtain photoproduct **29** in solid-state photochemistry, one needs to not permit the reaction to proceed to Stage 2.

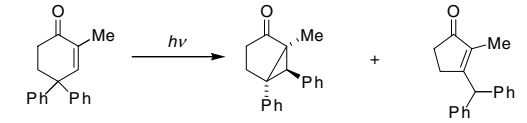

27 **28** **29**

Solution:	1.0	0
Solid-state stage 1 (to10%):	1.0	1.0
Solid-state stage 2 (above 10%):	1.0	0

SCHEME 5 Photochemistry of 2-methyl-4,4-diphenylcyclohex-2-enone **27.**

75.8 Solid-State Kinetics

Curiously, despite the fact that crystal-lattice photochemistry has a long history, the matter of a kinetic treatment had not been investigated. Our treatment of the photochemistry of "Crystal B" of the dimorphs of 4-phenyl-4-*p*-cyanophenylcyclohexenone **10** provides one example.[9] In Equation 75.4 we take ***C*** to represent the extent of conversion of the photolysis. ***Ph*1** represents the amount of phenyl migration product in Stage 1; ***Ph*2**, the amount of phenyl migration in Stage 2; and ***CN*2,** the amount of cyanophenyl migration in Stage 2. The sum of ***Ph*1, *Ph*2,** and ***CN*2** (note: no cyano product ***CN1*** is formed in Stage 1) gives the total conversion ***C*** as indicated in this equation. The ratio of the two photoproducts, from phenyl migration and from cyanophenyl migration, is then given by **R** in Equation 75.5. Properly combining Equations 75.4 and 75.5 obtains Equation 75.6, which indicates a linearity between the ratio of photoproducts and the ratio plus unity divided by the conversion. Thus, the plot of ***R*** versus (***R***+1)/***C*** in Figure 75.4 is linear. In plotting data points after the end of Stage 1, the slope gives *Ph*1, the amount

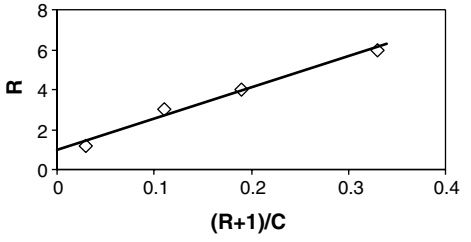

FIGURE 75.4 Plot of phenyl to cyanophenyl migration ratio *R* vs, (*R*+1)/*C*.

of phenyl migration in Stage 1 (i.e., 0.16), and the intercept affords the ratio of the two regioisomers in Stage 2 (i.e., unity). The actual slope and intercept as measured are close to these expected values.

$$\boldsymbol{C} = \boldsymbol{Ph1} + \boldsymbol{Ph2} + \boldsymbol{CN2} \text{ [Three product components giving conversion]} \tag{75.4}$$

$$\boldsymbol{R} = (\boldsymbol{Ph1} + \boldsymbol{Ph2})/\boldsymbol{CN2} \text{ [Ratio of phenyl to cyanophenyl products]} \tag{75.5}$$

$$R = Ph1(R + 1)/C + (Ph2/CN2) \tag{75.6}$$

75.9 Conclusion

Crystal lattice photochemistry, a field with a very long history, has proven to be of practical value in affording photoproducts not obtainable otherwise. However, a comprehensive quantitative treatment had been lacking. This chapter outlined some of our attempts to put this chemistry on a more quantitative basis.

Acknowledgment

Our research in crystal lattice photochemistry has been supported by the National Science Foundation. This support is gratefully acknowledged, in particular because of NSF's interest in supporting basic science.

References

1. (a) Cohen, M.D., The Photochemistry of Organic Solids, *Angew. Chem. Int. Ed. Engl.*, 14, 386–393, 1975; (b) Cohen, M.D. and Schmidt, G.M. J., Topochemistry. I. A Survey, *J. Chem. Soc.*, 1996–2000, 1964.
2. (a) Zimmerman, H.E. and Zuraw, M.J., Confinement Control in Solid State Photochemistry; Photochemistry in a Box, *J. Am. Chem. Soc.*, 111, 2358–2361, 1989; (b) Zimmerman, H.E. and Zuraw, M.J., Photochemistry in a Box; Photochemical Reactions of Molecules Entrapped in Crystal Lattices; Mechanistic and Exploratory Organic Photochemistry, *J. Am. Chem. Soc.*, 111, 7974–7989, 1989.
3. (a) Zimmerman, H.E. and Sebek, P., Photochemistry in a Crystalline Cage. Control of the Type-B Bicyclic Reaction Course; Mechanistic and Exploratory Photochemistry, *J. Am. Chem. Soc.*, 119, 3677–3690, 1997; (b) Zimmerman, H.E., Sebek, P., and Zhu, Z., *Ab Initio* Computations of Reacting Species in Crystal Lattices; Mechanistic and Exploratory Organic Photochemistry, *J. Am. Chem. Soc.*, 120, 8549ñ8550, 1998.
4. Zimmerman, H.E., Alabugin, I.V., and Smolenskaya, V.N., Experimental and Theoretical Host-Guest Photochemistry; Control of Reactivity with Host Variation and Theoretical Treatment with a Stress Shaped Reaction Cavity; Mechanistic and Exploratory Organic Photochemistry, *Tetrahedron*, Symposium-in-Print, 6821–6831, 2000.
5. (a) Maseras, F. and Morokuma, K., IMOMM: A New Integrated *ab initio* + Molecular Mechanics Geometry Optimization Scheme of Equilibrium Structures and Transition States, *J. Comput. Chem.*, 16, 1170–1179, 1995; (b) Matsubara, T., Sieber.S., and Morokuma, K., A Test of the New Integrated MO + MM (IMOMM) Method for the Conformational Energy of Ethane and n-Butane, *Int. J. Quantum Chem.*, 60, 1101–1109, 1996.
6. Zimmerman, H.E. and Nuss, J.M., A Photochemical Long Range Pinacol Rearrangement; Mechanistic and Exploratory Organic Photochemistry, *J. Org. Chem.*, 51, 4604–4617, 1986.
7. Zimmerman, H.E. and Zhu, Z., A General Predictor for Photoreactivity in Crystal Lattices: Molecular Mechanics in Crystalline Media and Lock and Key Control; Reaction Examples, *J. Am. Chem. Soc.*, 116, 9757–9758, 1994.

8. Zimmerman, H.E. and Zhu, Z., General Theoretical Treatments of Solid-State Photochemical Rearrangements; And, A Variety of Contrasting Crystal Versus Solution Photochemistry, *J. Am. Chem. Soc.*, 117, 5245–5262, 1995.
9. Zimmerman, H.E., Alabugin, I.V., Chen, W., and Zhu, Z., Dramatic Effects of Crystal Morphology on Solid State Reaction Course; Control by Crystal Disorder; Mechanistic and Exploratory Organic Photochemistry, *J. Am. Chem. Soc.*, 121, 11930–11931, 1999.
10. (a) Zimmerman, H.E. and Wilson, J.W., Mechanistic and Exploratory Organic Photochemistry, IX. Phenyl Migration in the Irradiation of 4.4-Diphenylcyclohexenone, *J. Am. Chem. Soc.*, 86, 4036–4042, 1964; (b) Zimmerman, H.E. and Hancock, K.G., Electronic Details of the Photochemical Phenyl Migration in 4,4-Diphenylcyclohexenone. Mechanistic Organic Photochemistry. XXXI, *J. Am. Chem. Soc.*, 90, 3749–3760, 1968; (c) Zimmerman, H.E., Rieke, R.D., and Scheffer, J.R., Photochemical Migratory Aptitudes in Cyclohexenones. Mechanistic and Exploratory Organic Photochemistry. XXIII., *J. Am. Chem. Soc.*, 89, 2033–2047, 1967.
11. Gaussian 98, Revision A.6. Frisch, M.J., Trucks, G.W., Schlegel, H.B., Scuseria, G.E., Robb, M.A., Cheeseman, J.R., Zakrzewski, V.G., Montgomery, Jr., J.A., Stratmann, R.E., Burant, J.C., Millam, J.M., Daniels, A.D., Kudin, K.N., Strain, M.C., Farkas, O., Tomasi, J; Barone, V., Cossi, M., Cammi, R; Mennucci, B., Pomelli, C; Adamo, C., Clifford, C; Ochterski, J., Petersson, G.A., Ayala, P.Y., Cui, Q., Morokuma, K., Malick, D.K., Rabuck, A.D., Raghavachari, K., Foresman, J.B., Cioslowski, J., Ortiz, J.V., Stefanov, B.B., Liu, G., Liashenko, A., Piskorz, P., Komaromi, I., Gomperts, R., Martin, R.L., Fox, D.J., Keith, T., Al-Laham, M.A., Peng, C.Y., Nanayakkara, A., Gonzalez, C; Challacombe, M., Gill, P.M. W., Johnson, B., Chen, W., Wong, M.W., Andres, J.L., Gonzalez, C., Head-Gordon, M., Replogle, E.S., and Pople, J.A., Gaussian, Inc., Pittsburgh PA, 1998.
12. (a) Beck, A.K., Bastani, B., Plattner, D.A., Petter, W., Seebach, D., Braunschweiger, H., Gysi, P,. and Vecchia, L.L., Large-Scale Preparation of $\alpha,\alpha,\alpha,\alpha$-Tetraaryl-1,3-dioxolane-4,5-methanols (taddole) — Versatile Auxiliaries for the epc Synthesis and its Solid-state Structure, *Chimia*, 45, 238–244, 1991; (b) Seebach, D., Beck, A.K., Imwinkelried, R., Roggo, S., and Wonnacott, A., Chiral Alkoxytitanium(V) Complexes for Enantioselective Nucleophilic Additions to Aldehydes and as Lewis-Acids in Diels-Alder Reactions, *Helv. Chim. Acta,* 70, 954–974, 1987; (c) Toda, F. and Tanaka, K., Design of a New Chiral Host Compound, *trans*-4,5-bis(hydroxydiphenylmethyl)-2,2-dimethyl-1,3-dioxacyclopentane — An Effective Optical Resolution of Bicyclic Enones through Host-Guest Complex-Formation, *Tetrahedron Lett.*, 29, 551–554, 1988.
13. Zimmerman, H.E. and Nesterov, E.E., Crystal Lattice Photochemistry Often Proceeds in Discrete Stages; Mechanistic and Exploratory Organic Photochemistry, *Org. Lett.*, 2, 1169–1171, 2000.
14. Zimmerman, H.E. and Nesterov, E.E., Quantitative Cavities and Reactivity in Stages of Crystal Lattices; Mechanistic and Exploratory Organic Photochemistry, *J. Am. Chem. Soc.*, 124, 2818–2830, 2002.

76

Photorearrangement Reactions of Cyclohex-2-enones

Paul Margaretha
University of Hamburg

76.1 Introduction

Despite the fact that synthetically relevant reactions of cyclohex-2-enones are more often bimolecular ones, for example, wherein the excited enone undergoes cycloaddition to an alkene, (monomolecular) photorearrangements of cyclohex-2-enones have been extensively investigated in recent decades and appropriately reviewed ten years ago.[1] This chapter presents and discusses both novel preparative results as well as alternative mechanistic interpretations to apparently well-known reactions.

76.2 Photorearrangement of 4,4-Dialkylcyclohex-2-enones

The light-induced rearrangement of 4,4-dialkylcyclohex-2-enones **1** with concommitant formation of 6,6-dialkylbicyclo[3.1.0]hexan-2-ones ("lumiketones" **2**) and cyclopent-2-enones **3** has been quite thoroughly investigated by the author of this corresponding review in 1995.[1] Nevertheless, the question of the mechanism (Scheme 1) of this rearrangement remained unanswered as both a concerted as well as a stepwise mechanism had been proposed. In any event, the lifetime of the eventual propane-1,3-diyl-biradical **4** has to be short, as (1) in some cases the reaction proceeds with retention of configuration at the dialkyl-substituted C-atom, and (2) no products derived from a cyclopropylcarbinyl-radical-ring opening were detected in the corresponding photorearrangement of 4,4-dicyclopropylcyclohex-2-enone (**5**).[2]

Detailed investigations of a series of 4,4-dimethylcyclohex-2-enones bearing further substituents on C(5) or C(6) were undertaken.[3] It was found that on irradiation with light of $\lambda = 350$ nm in acetonitrile, cyclohexenones **6** rearranged to mixtures of bicyclohexanones **7** and cyclopentenones **8** with similar quantum yields ($\Phi_{\text{-}\mathbf{6}} \cong 0.004$–$0.024$) as well as product ratios (**7**/**8** = 2:1–1:2), indicating the rearrangement to be relatively insensitive to these additional substituents. The cyclohexenones with just one alkyl group

0-8493-1348-1/04/$0.00+$1.50

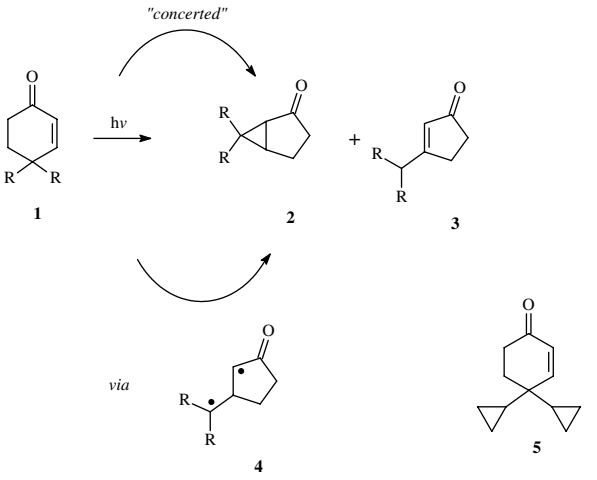

SCHEME 1

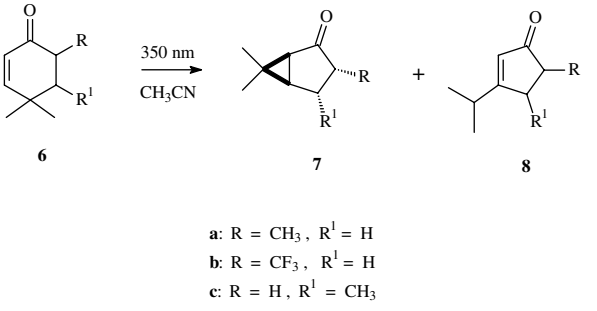

a: R = CH_3, R^1 = H
b: R = CF_3, R^1 = H
c: R = H, R^1 = CH_3

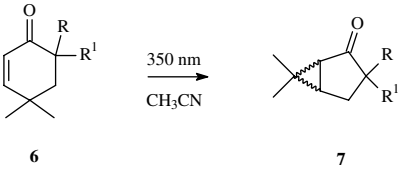

d: R = F, R^1 = H (1:1 mixture of diastereomers)
e: R = F, R^1 = CH_3 (2:1 mixture of diastereomers)

SCHEME 2

at either C(5) or C(6) (i.e., **6a**, **6b,** and **6c**) rearrange selectively to the diastereoisomer **7** with the alkyl group and the three-membered ring in *trans*-configuration (Scheme 2), while the 6-fluorocyclohexenones **6d** and **6e** afford mixtures of diastereomeric bicyclohexanones.

According to the authors,[3] the conversion of triplet cyclohexenone is best described as an intramolecular homolytic substitution (S_H2 reaction) with attack of the radical center C(3) on C(5), the leaving group (i.e., the dialkyl-substituted C(4)) then being *trans* to the alkyl group at C(5) or C(6) (Scheme 3). The propane-1,3-diyl triplet intermediate **4** is then expected not to relax thermally on the triplet surface, but rather undergo very rapid intersystem crossing.

A somewhat different situation arises for 4,4-dialkylcyclohex-2-enones bearing an additional CH-substituent on C(3). Thus, 4a-methyl-4,4a,5,6,7,8-hexahydro-2(3*H*)-naphthalenone (**9**) affords selectively the

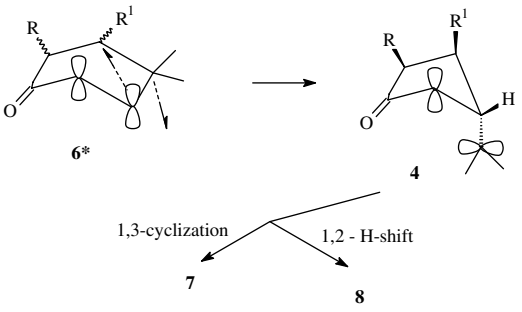

SCHEME 3

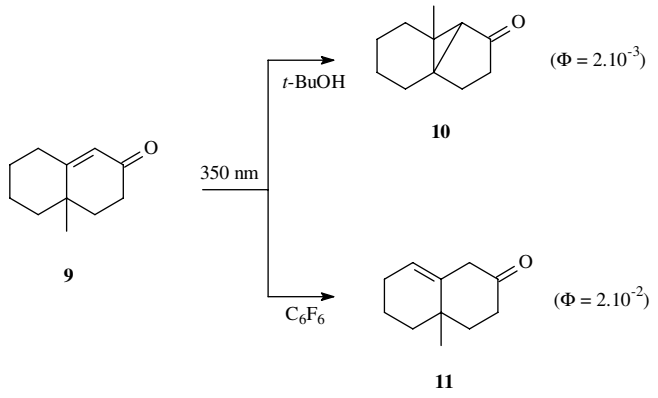

SCHEME 4

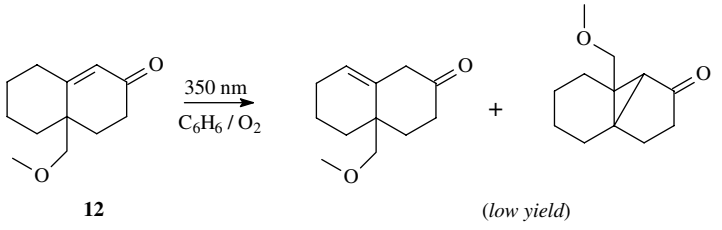

SCHEME 5

"lumiketone" **10** on irradiation in *t*-butanol; while in hydrocarbon solvents (C_6H_6, C_6F_6), deconjugation to the β,γ-unsaturated ketone **11** becomes the predominant process (Scheme 4).[4]

Interestingly, the corresponding 4a-methoxymethylnaphthalenone **12** only undergoes very slow rearrangement and deconjugation (Scheme 5) in deaerated hydrocarbon solutions, but both processes are accelerated by the presence of air. An explanation for this peculiar finding was not given.[5]

76.3 Photorearrangement of 4,6-Methano-Bridged Cyclohex-2-enones

It has already been reported more than 40 years ago that verbenone (**13**) undergoes isomerization to chrysanthenone (**14**) on irradiation in cyclohexane.6 More detailed studies revealed that (1) the reaction

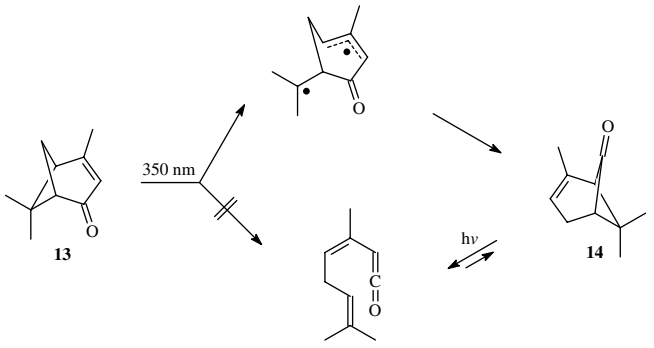

13 **14**

SCHEME 6

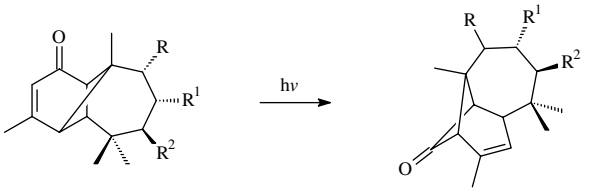

15	all R = H	**18**
16	R, R^2 = OAc	**19**
17	all R = OAc	**20**

SCHEME 7

proceeds with a reasonable degree of stereoselectivity, (i.e.,with only a small degree of racemization, and (2) (−)-chrysanthenone obtained from (−)-verbenone (Scheme 6) on irradiation ($\lambda = 350$ nm) undergoes subsequent photoreactions when using light of shorter wavelength.[7] It was therefore assumed that this rearrangement occurs via a formal 1,3-shift of the dialkylated C-atom rather than via α-cleavage to an (achiral) ketene intermediate followed by electrocyclic ring closure, albeit this latter intermediate might be of importance in the consecutive photoreactions of **14**.

This same type of rearrangement has also been observed for a series of tricyclic sesquiterpenes. Thus, in the field of longipin-2-en-1-ones, both the parent vulgarone B (**15**) as well as the acetoxy derivatives **16** and **17** photorearrange (Scheme 7) to vulgarone A (**18**) and the corresponding acetoxy derivatives **19** and **20**, respectively.[8,9]

76.4 Photorearrangement of 4,4-Diarylcyclohex-2-enones

Cyclohex-2-enones bearing at least one aryl group (in addition to an alkyl group) on C(4) undergo photorearrangements different from that presented in Section 76.1. The so-called "di-π-methane rearrangement" mode — typical of molecules containing a 3-phenylprop-1-ene substructure which isomerizes to a phenylcyclopropane moiety — now becomes predominant, as illustrated for the photoisomerization of 4,4-diphenylcyclohex-2-enone (**21**) to a mixture of diastereomeric 5,6-diphenylbicyclo[3.1.0]hexan-2-ones **22** (Scheme 8).[10]

Further investigations were run on the chiral cyclohexenone **23** showing that the formal 1,2-phenyl migration to **24** occurred without any loss of optical purity.[11] A bridged intermediate was proposed to explain the selective formation of the *endo*-bicyclic derivative **24** to the exclusion of any *exo*-derivative (Scheme 9).

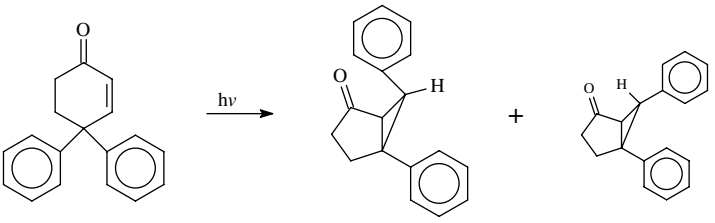

21 (major) **22** (minor)

SCHEME 8

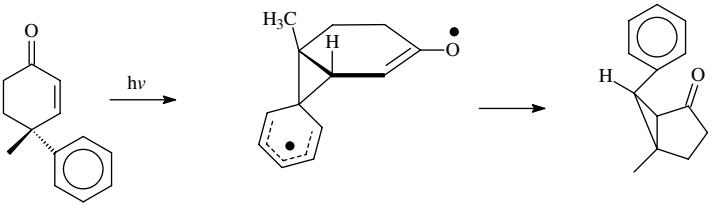

23 **24**

SCHEME 9

Zimmerman has recently reviewed his research work of the past two decades focusing on the photorearrangement of 4,4-diarylcyclohex-2-enones in the crystalline state.[12] A comparison of the different criteria of crystal lattice reactivity was provided in a study of 5-substituted 4,4-diarylcyclohex-2-enones.[13] As shown for **25** and **26**, the product distributions in the crystal lattice chemistry differ from those in solution photochemistry (Scheme 10). It becomes evident from the synthetic viewpoint that one can obtain, using solid-state irradiation, photoproducts that are unobtainable as appreciable products in solution. A highly interesting result started with the observation that 4-phenyl-4-cyanophenylcyclohexenone **27** crystallizes in two modifications. The first of the two dimorphs, the one with $P2_1/c$ symmetry, afforded only the cyanophenyl-migrated bicyclic ketone **28**, while the other one, with *C2/c* symmetry, underwent only phenyl migration to give product **29** (Scheme 11). In this latter example, the preference for phenyl migration was observed only during the first 16% conversion ("Stage 1"). Beyond this point ("Stage 2"), a consistent 1:1 regioselectivity resulted.[14]

76.5 Photorearrangement of 2*H*,6*H*-Thiin-3-ones to Thietan-3-ones

In contrast to the rather inefficient triplet state photorearrangement of (4,4-dialkyl)-cyclohex-2-enones to bicyclo[3.1.0]hexan-2-ones, 5-thiacyclohex-2-enones **30, 31,** and **32** undergo a highly efficient (Φ = 0.8) ring contraction from the first excited singlet state, affording 2-alkenylthietan-3-ones **33, 34**, and **35,** respectively (Scheme 12).[15] This rearrangement also seems to be typical for bicyclic compounds **36** through **39** containing this same ring system. Depending on the substitution pattern and on the wavelength chosen, the bicyclic thietanones (**40, 41**) are stable,[16] or (**42, 43**) undergo further light-induced conversions (e.g., a 1,3-acyl shift) to the final products (**44, 45**) as shown in Scheme 13.[17,18] The proposed mechanism for these ring contractions involves a sulfuranyl-alkyl biradical **46** as intermediate.[15,19] Evidence for such an intermediate (Scheme 14) comes from the fact that the efficiency of ring contraction

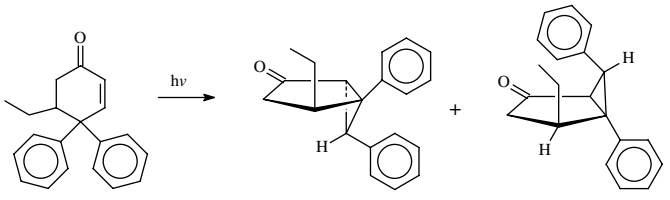

25

a) benzene 33 : 66

b) solid-state 100 : 0

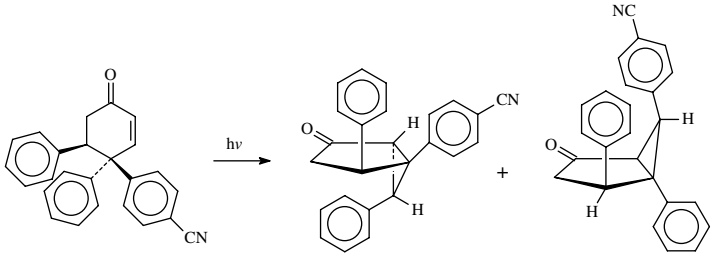

26

a) benzene 50 : 50

b) solid-state 100 : 0

SCHEME 10

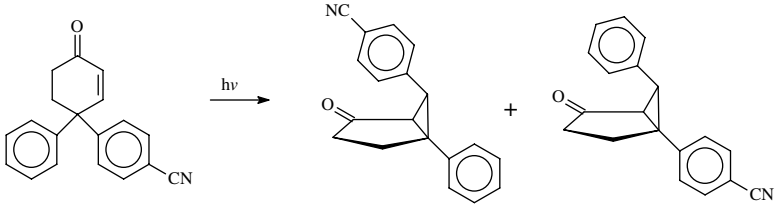

27 **28** **29**

in solution: 15 : 1

SCHEME 11

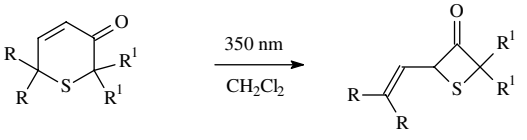

30	$R = H$, $R^1 = CH_3$	**33**
31	$R = CH_3$, $R^1 = H$	**34**
32	$R = R^1 = CH_3$	**35**

SCHEME 12

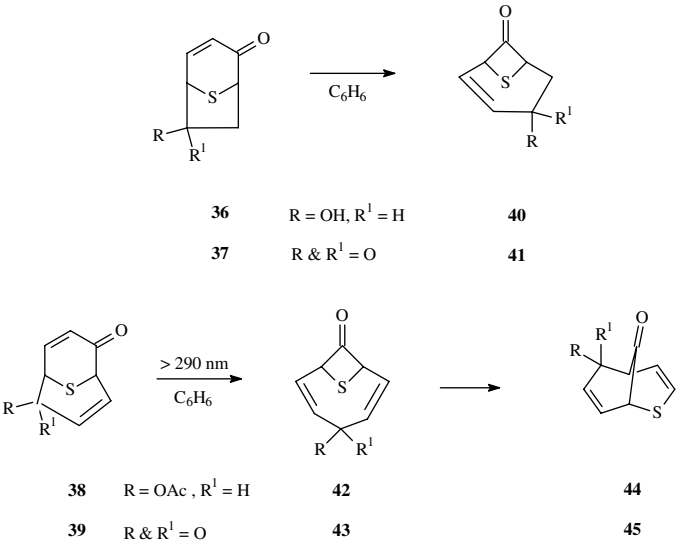

36 R = OH, R^1 = H **40**

37 R & R^1 = O **41**

38 R = OAc , R^1 = H **42** **44**

39 R & R^1 = O **43** **45**

SCHEME 13

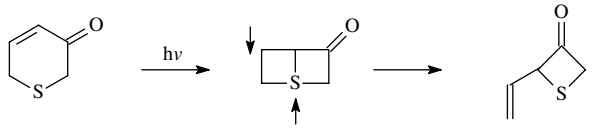

46

SCHEME 14

for compounds **33, 34,** and **35** is not sensitive to the stability of the — formally — displaced radical group (H_2C vs. $(CH_3)_2C$), which excludes a possible C–S bond cleavage step as the rate-determining one.

In contrast, the corresponding sulfoxides do undergo such a bond rupture between the *allylic C*-atom and the neighboring S-atom as a first chemical step after photoexcitation.[20] As shown in Scheme 15, 2*H*,6*H*-thiin-3-one-1-oxides **47** photoisomerize to 3*H*,7*H*-1,2-oxathiepin-4-ones **48**, which undergo a further thermal ring contraction to thietanone-1-oxides **49** via a 2,3-sigmatropic rearrangement.

Interestingly, ethyl 2,2-dimethyl-5-oxo-5,6-dihydro-2*H*-pyridine-1-carboxylate (**50**), an aza-derivative of thiinone **34**, behaves in a totally different way.[21] On irradiation in benzene, it undergoes slow photodecomposition, while in the same solvent in the presence of 2,3-dimethylbut-2-ene, pyrrolidinone **51** is formed as the major (50%) photocycloadduct. Although the authors[21] proposed a rearrangement sequence of the intermediate biradical **52** formed by addition of the alkene to triplet excited **50**, an alternative path (Scheme 16), including first photoisomerization of **50** to oxabicyclobutane **53** and then to the ring-contracted carbene **54**, which then would be trapped by the alkene, cannot be excluded.

It is unfortunate that no irradiations of **50** were run in methanol, as this would have allowed trapping of the postulated carbene intermediate **54**. The photoisomerization of *s-trans*-1,3-dienes to bicyclobutanes in general and that of 3-methylenecyclohexene to tricyclo[3.2.0.$0^{1,6}$]heptane (the all-carbon analogue of **53**) in particular are well-established reactions.[22]

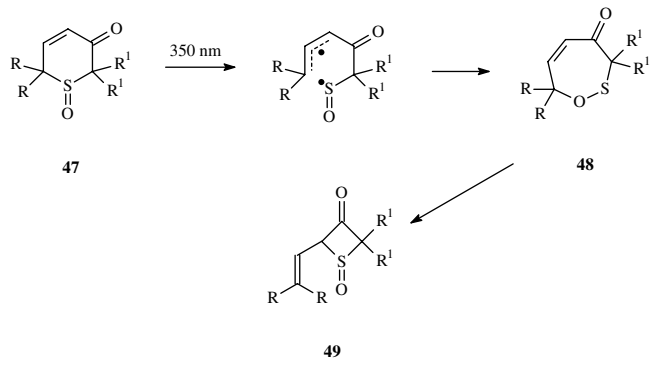

SCHEME 15

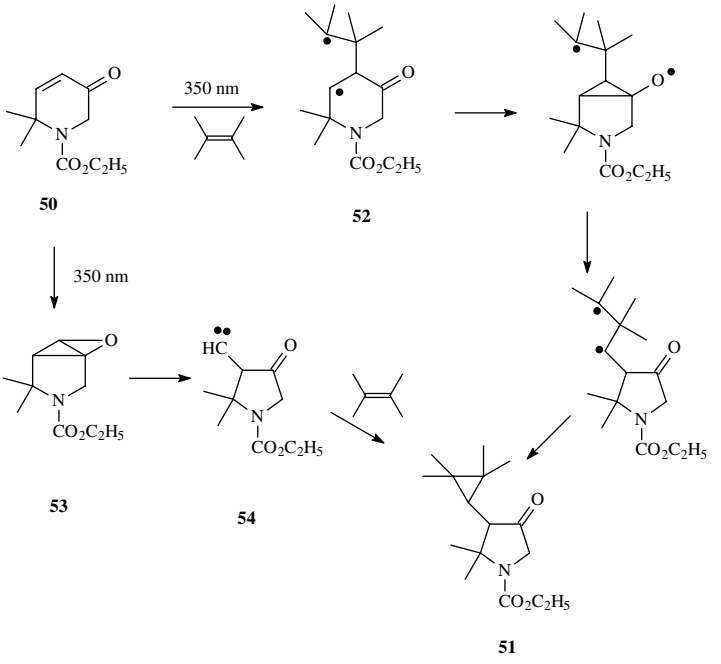

SCHEME 16

76.6 *Z-E*-Photoisomerization of Cyclohexenones

Cyclooct-2-enone and cyclohept-2-enone undergo $Z \rightarrow E$ isomerization on irradiation. While *E*-cycloocten-2-one can be characterized spectroscopically at room temperature, *E*-cyclohep-2-enone is stable only at temperatures around –180°C, but can be trapped with dienes in a dark reaction at –78°C.[23–26] The photoisomerization of these medium-ring cycloalkenones appears to occur much faster than intermolecular processes, e.g., cycloaddition to alkenes or energy transfer to triplet quenchers. Another seven-membered ring enone, 2,3-benzocyclohepta-2,6-dienone (**55**) was found to afford *trans*-fused [4+2]

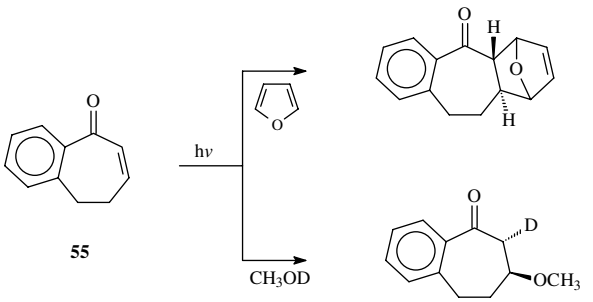

SCHEME 17

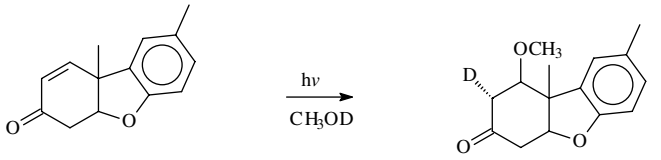

SCHEME 18

cycloadducts on irradiation in furan, and, on irradiation in methanol, a 6-MeO adduct wherein the MeO group and the (new) H-atom are *trans* to each other (Scheme 17). The authors[27, 28] inferred from these results that the primary process was *Z-E* isomerization of the C–C double bond in the seven-membered ring, and that the *E*-enone was then trapped by either furan or MeOH.[27,28]

As for six-membered enones, cyclohex-2-enone on irradiation in furan afforded both [4+2] and [2+2] cycloadducts.[29] Although the configuration of these products is unknown, a mechanism involving attack of an enone triplet on a ground-state diene molecule was proposed. Triplet biradicals have also been proposed as intermediates in the photocycloaddition of *Pummerer*'s ketone (**56**) with furan. [30,31] This dihydrodibenzofuranone also gives a methanol adduct (Scheme 18), wherein the MeO group and the new H-atom are again *trans* to each other. The authors proposed a reactive excited molecule or an intermediate in which the C–C double bond is twisted by nearly 90 on which then MeOH undergoes a regio- and stereospecific *cis*-addition.[32]

Irradiation of 2,2-dimethyl-2,3-dihydro-4*H*-thiin-4-one (**57**) — a "4-thiacyclohex-2-enone" — in neat furan afforded three cycloadducts **58**, **59**, and **60**, in a 5:4:1 ratio, whose formation is quenched by appropriate triplet quenchers. Irradiation of **57** in methanol afforded a 3:2 mixture of adducts **61** and **62**; and in CD_3OD, a similar mixture of $\mathbf{D_4}$**–61** and $\mathbf{D_4}$**–62**. Finally, irradiation of **57** in furan:MeOH (1:1) gives only cycloadducts **58**, **59**, and **60** to the exclusion of adducts **61** and **62** (Scheme 19). Compound **57** was chosen for these studies because the longer C–S bonds (as compared to C–C bonds) should make such dihydrothiinones ideal model compounds for the investigation of photochemically generated, highly twisted monocyclic cyclohexenones.[33]

These latter results, combined with the older ones reported, were interpreted as follows.[33] Excitation of **57,** followed by intersystem crossing, gives triplet enone **63**, which reacts with furan to give two diastereomeric biradicals, **64** and **65**, the precursors of **58** and **60**, and **59**, respectively. In the absence of furan, **63** affords *E*-enone **64,** which either re-isomerizes to **57** or is trapped by methanol to give **61** and **62.** In contrast to (carbocyclic) cyclohexenones, two regioisomers are formed from **57** as both the carbonyl group and the S-atom stabilize an adjacent carbanionic center (Scheme 20).

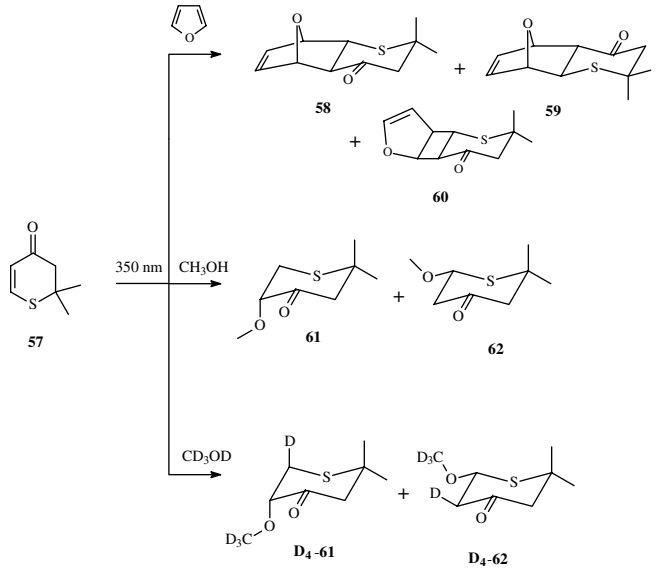

SCHEME 19

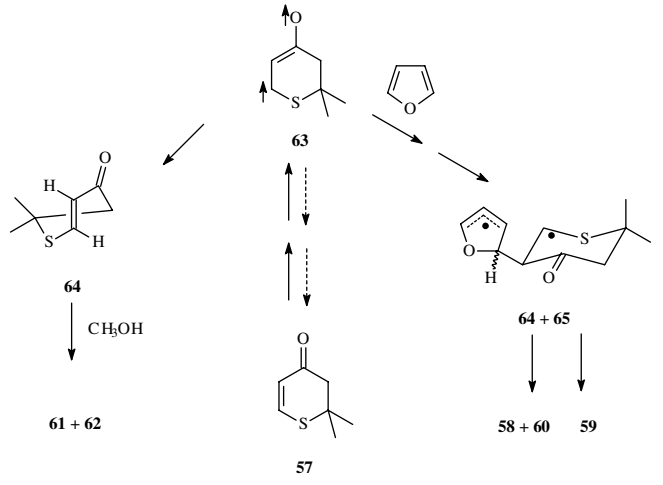

SCHEME 20

References

1. Schuster, D.I., Photorearrangement Reactions of Cyclohexenones, in *CRC Handbook of Organic Photochemistry and Photobiology*, Horspool, W.M. and Song, P.-S., Eds., CRC Press, Boca Raton, FL, 1995, 579–592.
2. Hahn, R.C. and Jones, G.W., Photochemistry of 4,4-Dicyclopropylcyclohexenone, *J. Am. Chem. Soc.*, 93, 4232, 1971.
3. Cruciani, G. and Margaretha, P., Photorearrangement of 4,4-Dimethylcyclohex-2-enones, *Helv. Chim. Acta*, 73, 890, 1990.
4. Margaretha, P. and Schaffner, K., Zur Photochemie von $\Delta^{1,9}$-10-Methyl-2-Octalon, *Helv. Chim. Acta*, 56, 2884, 1973.

5. Lai, A.K. and Liao, C.C., Photochemical Rearrangements of 6-Methoxymethylbicycloalk-1-en-3-ones, *J. Chin. Chem. Soc.*, 39, 423, 1992.
6. Hurst, J.J. and Whitham, G.H., Photochemistry of Verbenone, *J. Chem. Soc.*, 2864, 1960.
7. Erman, W.F., Photochemical Transformations of Unsaturated Bicyclic Ketones, *J. Am. Chem. Soc.*, 89, 3828, 1967.
8. Uchio, Y., Isolation of Vulgarone A and B, Two Novel Sesquiterpene Ketones, *Tetrahedron*, 34, 2893, 1978.
9. Melendez-Rodriguez, M, Cerda-Garcias-Rojas, C.M., Catalan, C.A.N., and Joseph- Nathan, P, Mechanistic Studies of the Photochemical Rearrangement of 1-Oxolongipin-2-ene Derivatives, *Tetrahedron*, 58, 2338, 2002.
10. Zimmerman, H.E. and Wilson, J.W., Phenyl Migration in the Irradiation of 4,4-Diphenylcyclohexenone, *J. Am. Chem. Soc.*, 86, 4036, 1964.
11. Schuster, D.I., Brown, R.H., and Resnick, B.M., Stereospecific Triplet-State Photorearrangements of Chiral Cyclohex-2-enones, *J. Am. Chem. Soc.*, 100, 4504, 1978.
12. Zimmerman, H.E. and Nesterov, E.E., Crystal Lattice Organic Photochemistry, *Acc. Chem. Res.*, 35, 77, 2002.
13. Zimmerman, H.E. and Zhu, Z., Solid-State Photochemical Rearrangements, *J. Am. Chem. Soc.*, 117, 5245, 1995.
14. Zimmerman, H.E., Alabugin, I.V., Chen, W., and Zhu, Z., Dramatic Effects of Crystal Morphology on Solid-State Reaction Course, *J. Am. Chem. Soc.*, 121 11930, 1999.
15. Er, E. and Margaretha, P., Photoisomerization of 2*H*,6*H*-Thiin-3-ones, *Helv. Chim. Acta,* 75, 2265, 1992.
16. Tsuruta, H., Ogasawara, M., and Mukai, T., Photochemical Conversion of 8-Thiabicyclo[3.2.1]oct-3-en-2-ones, *Chem. Lett.*, 887, 1974.
17. Mellor, J. M. and Webb, C.F., Photorearrangement of 9-Thiabicyclo[3.3.1]nona-3,7-dien-2,6-diones, *J. Chem. Soc., Perkin Trans. 1,* 211, 1972.
18. Miyashi, T., Suto, N., Yamaki, T., and Mukai, T., Photochemistry of Bicyclic 4-Thia-unsaturated Ketones, *Tetrahedron Lett.,* 22, 4421, 1981.
19. Margaretha, P., *Organic Sulfuranyl Radicals in S-Centered Radicals*, Alfassi, Z.B., Ed., J. Wiley & Sons, Chichester, 1999, 277–288.
20. Kowalewski, R. and Margaretha, P., Photoisomerization of 2*H*,6*H*-Thiin-3-one-1-Oxides, *Helv. Chim. Acta,* 76, 1251, 1993.
21. Jeandon, C., Constien, R., Sinnwell, V., and Margaretha, P., Photoaddition of Ethyl 2,2-Dimethyl-5-oxo-5,6-dihydro-2H-pyridine-1-carboxylate to 2,3-Dimethylbut-2-ene, *Helv. Chim. Acta,* 81, 303, 1998.
22. Dauben, W.G. and Spitzer, W.A., Photochemistry of 4,4-Dimethyl-1-methylecyclohexene, *J. Am. Chem. Soc.,* 90, 802, 1968.
23. Eaton, P.E. and Lin, K., *trans*-2-Cyclooctenone, *J. Am. Chem. Soc.,* 86, 2087, 1964.
24. Eaton, P.E. and Lin, K., *trans*-2-Cycloheptenone, *J. Am. Chem. Soc.,* 87, 2052, 1965.
25. Corey, E.J., Tada, M., LaMahieu, R., and Libit, L., *trans*-2-Cycloheptenone, *J. Am. Chem. Soc.,* 87, 2051, 1965.
26. Eaton, P.E., Photochemical Reactions of Enones, *Acc. Chem. Res.,* 1, 50, 1968.
27. Dunkelblum, E. and Hart, H., Photochemical Addition of Methanol to Cycloheptenones, *J. Am. Chem. Soc.,* 99, 644, 1977.
28. Hart, H. and Dunkelblum, E., Stereochemistry of the Photoinduced Addition of Methanol to Seven- and Eight-Membered 2-Cycloalkenones, *J. Am. Chem. Soc.,* 100, 5141, 1978.
29. Cantrell, T.S., Photocycloaddition of Cyclohexenones to Conjugated Dienes, *J. Org. Chem.,* 39, 3063, 1974.
30. Mintas, M., Schuster, D.I., and Willard, P.G., Photocycloaddition of Pummerer's Ketone to Furan, *J. Am. Chem. Soc.,* 110, 2305, 1988.

31. Mintas, M., Schuster, D.I., and Willard, P.G., Photocycloaddition of Alkenes and Dienes to Pummerer's Ketone, *Tetrahedron,* 44, 6001, 1988.
32. Dunkelblum, E., Hart, H., and Jeffares, M., Photoinduced Addition of Methanol to Pummerer's Ketone, *J. Org. Chem.,* 43, 3409, 1978.
33. Kowalewski, R. and Margaretha, P., Light-Induced Cycloaddition of Furan and Addition of Methanol to a 4-Thiacyclohex-2-enone, *Helv. Chim. Acta,* 75, 1925, 1992.

77

New Results on the Triplet Reactivity of β,γ-Unsaturated Carbonyl Compounds

Diego Armesto
Universidad Complutense of Madrid

Maria J. Ortiz
Universidad Complutense of Madrid

Antonia R. Agarrabeitia
Universidad Complutense of Madrid

77.1 Introduction

The photochemistry of carbonyl compounds has been one of the main areas of research in organic photochemistry for many years.[1] Among all the different types of carbonyl compounds, β,γ-unsaturated ketones have been the subject of extensive studies.[2] The results obtained from these efforts, conducted over a 30-year period, show that, in general, direct irradiation of β,γ-unsaturated ketones yields products resulting from 1,3-acyl migration, while triplet-sensitized reactions of these compounds affords cyclopropyl ketones by oxa-di-π-methane (ODPM) rearrangement pathways.[2] Alternative reaction routes, such as decarbonylation, ketene formation, epimerization, [2+2]-intramolecular cycloadditions, Norrish Type I and Norrish Type II reactions, *cis-trans* isomerizations, and reductions of the C–C double bond, have also been described in some instances, depending on some particular structural features present in the β,γ-unsaturated ketone.[2a] However, the photoreactivity of these compounds is dominated by the two main processes mentioned above.

The ODPM rearrangement has proven to have important synthetic applications.[2e-g] This is due to the fact that most of these reactions are very general; they usually take place with high chemical and quantum yields and also, in many instances, a high degree of stereoselectivity or even enantioselectivity has been observed. As a result, this rearrangement has been used as the key step in the synthesis of natural products and complicated molecules that are difficult to obtain by alternative reaction paths.[2e-g] Despite the large number of examples reported in the literature of cyclic and polycyclic β,γ-unsaturated ketones that undergo the ODPM reaction, there are only a few examples of acyclic ketones that undergo this reaction.[2g] The reasons for the lack of ODPM reactivity in some acyclic compounds are difficult to understand. For example it is surprising that ketones **1** and **2** have been reported to be reactive in the ODPM mode by Cerfontain et al.,[3] whereas the closely related compounds **3**[3] and **4**[4] do not undergo the rearrangement.

0-8493-1348-1/04/$0.00+$1.50

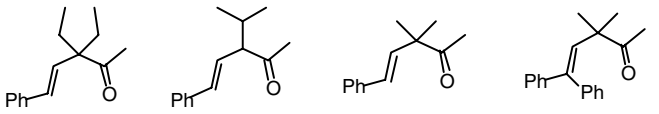

1 **2** **3** **4**

β,γ-Unsaturated aldehydes are a family of carbonyl compounds that have been considered ODPM unreactive for many years. This conclusion was based on literature precedents that indicated that the normal photochemical reactivity of such compounds, both on direct and sensitized irradiation, was decarbonylation to the corresponding alkene.[2c,2f,5] Thus, compounds **5**,[6] **6**,[7] **7**,[8] and **8**[8] are representative examples of a series of steroidal and cyclic β,γ-unsaturated aldehydes, studied by Schaffner et al. about 20 years ago, that undergo decarbonylation on irradiation. Dürr et al.[9] have studied the photochemistry of some aryl-substituted-2-cyclopentene-1-carbaldehydes **9**. In this instance, *cis*-stilbene-type electrocyclic cyclization and decarbonylation were the only reactions observed. Other authors have also reported the decarbonylation of the acyclic β,γ-unsaturated aldehydes **10**[4] and **11**[10] on direct irradiation.

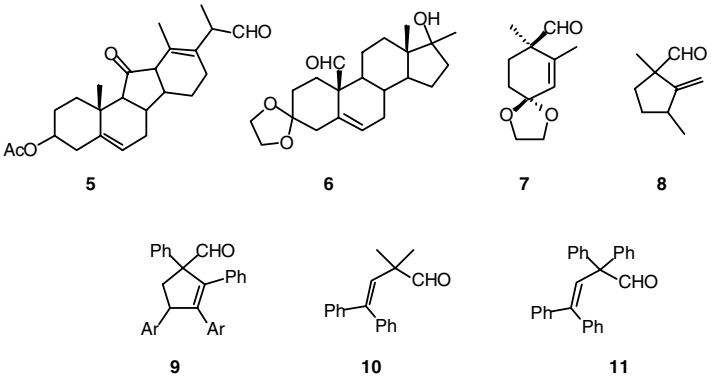

5 **6** **7** **8**

9 **10** **11**

However, two examples of aldehydes that did not follow this general rule were described in the early studies. The first example of an ODPM reaction in a β,γ-unsaturated aldehyde was observed by Schaffner et al.[11] in the direct and triplet-sensitized irradiation of the steroidal aldehyde **12** that gives the alkene **13** resulting from decarbonylation, and two other compounds, **14** and **15**, derived from the ODPM rearrangement and the 1,3-formyl migration, respectively (Scheme 1).

Many years later, Zimmerman and Cassel[12] reported the ODPM triplet reactivity of the aldehyde **16**, which contains two isopropyl groups at C2 and quantitatively yields the cyclopropyl aldehyde **17** (Scheme 2). Therefore, β,γ-unsaturated aldehydes were considered to be unreactive in the ODPM mode, apart from the two exceptions mentioned above.[2c,2f,5]

These ideas on the photo-behavior of β,γ-unsaturated aldehydes have changed due to the results emanating from recent studies carried out in our laboratory demonstrating that suitably substituted aldehydes do undergo the ODPM reaction with high chemical efficiency and a high degree of diastereoselectivity, in some cases. Furthermore, a comparative study on the photoreactivity of β,γ-unsaturated aldehydes and the corresponding methyl ketones show that aldehydes undergo the ODPM rearrangement even more efficiently than the corresponding methyl ketones, contrary to common belief. Finally, alternative reaction modes, such as 1,3-formyl migration and decarbonylation, that take place via the T_1 ($\pi\pi^*$) excited state and are, therefore, not typical Norrish Type I processes, have also been uncovered in some cases. The following sections summarize these novel results.

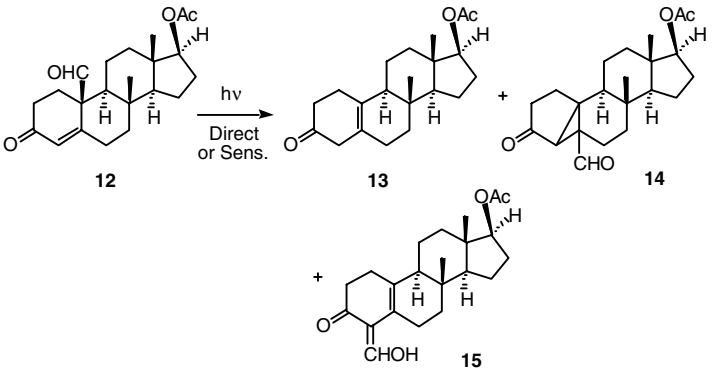

SCHEME 1

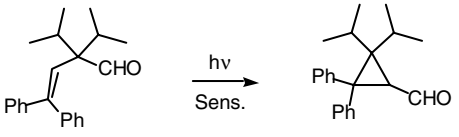

SCHEME 2

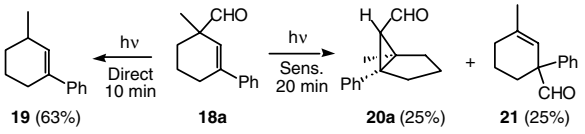

SCHEME 3

77.2 The Oxa-di-π-methane Rearrangement of β,γ-Unsaturated Aldehydes

Our interest in the photochemistry of β,γ-unsaturated aldehydes was serendipitous. At one point in our studies on the 1-aza-di-π-methane (1-ADPM) rearrangement, we were interested in its application to the synthesis of bicyclo[n.1.0]alkanes.[13] An extension of such a study was aimed at identifying ring contraction processes. To this end, the aldehyde **18a** that could be transformed into different imine derivatives, was selected as the target molecule. Because the photochemistry of the aldehyde **18a** was not described, it was of importance to establish the photochemical behavior of this compound to compare its reactivity with that of the corresponding nitrogen derivatives. Thus, direct irradiation of **18a**, for 10 min, afforded a mixture of starting material (20%) and the alkene **19** (63%), resulting from decarbonylation of aldehyde **18a** (Scheme 3).[14] This result was not a surprise because, as mentioned, it has been established that decarbonylation is the main photochemical reactivity of β,γ-unsaturated aldehydes. However, acetophenone-sensitized irradiation of **18a**, for 20 min, brought about different reactions, affording starting material (11%), the ODPM product **20a** (25%), and the 1,3-migration product **21** (25%) (Scheme 3). The ODPM rearrangement of **18a** is diastereoselective, affording the bicyclic aldehyde **20a** as the *endo*-isomer exclusively.[14]

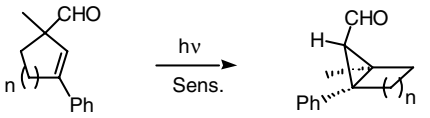

18b: n = 1 5 min **20b:** n = 1 (90%)
18c: n = 3 10 min **20c:** n = 3 (25%)

SCHEME 4

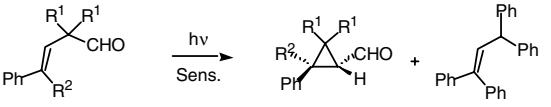

22: R^1 = Me; R^2 = H 15 min **23** (90%) ------
10: R^1 = Me; R^2 = Ph 2 h **24** (57%) ------
11: $R^1 = R^2$ = Ph 10 min **25** (82%) **26** (8%)

SCHEME 5

The formation of 1,3-migration products under sensitized conditions involving the T_2 excited state has been reported for several β,γ-unsaturated ketones.[15] However, it is extremely rare to observe such a reaction with analogous aldehydes, and the formation of the ODPM product **20a** is even more surprising. At this point it was difficult to explain the photoreactivity observed in the irradiation of **18a**, although it was thought to be due to the influence of some unknown structural factors present in this aldehyde. Therefore, the study was extended to aldehydes **18b** and **18c** to determine whether this unexpected reactivity could also occur in other related aldehydes. Acetophenone-sensitized irradiation of **18b** afforded the ODPM product **20b** in 90% isolated yield. Similarly, irradiation of **18c** under the same conditions gave the cyclopropyl aldehyde **20c** in 25% yield. In these two instances, the corresponding 1,3-formyl migration products were not formed (Scheme 4).[14b]

To clarify whether or not the unexpected ODPM reactivity of aldehydes **18** was due to some structural factors present in these compounds, we decided to study the photoreactivity the β,γ-unsaturated aldehyde **22**, which presents a substitution pattern that promotes the 1-ADPM rearrangement very efficiently.[16] Triplet-sensitized irradiation of **22**, for 15 min, afforded the cyclopropyl aldehyde **23**, resulting from an ODPM rearrangement, as the *trans*-diastereoisomer, in 90% isolated yield (Scheme 5). This result clearly demonstrated that the ODPM reactivity of β,γ-unsaturated aldehydes is not restricted to cyclic derivatives, such as **18**, or to molecules with special structural features as in the two cases previously reported, but can be extended to acyclic compounds. Furthermore, the efficient ODPM rearrangement of compounds **18a–c** and **22** suggested that the main factor that controls the ODPM reactivity of these aldehydes is the stabilizing influence of phenyl groups on the bridging 1,4-biradical reaction intermediates. To test this hypothesis, the study was extended to aldehydes **10** and **11**. As mentioned, previous reports demonstrate that these two compounds undergo decarbonylation on direct irradiation.[4,10] However, triplet-sensitized irradiation of **10**, for 2 h, afforded the cyclopropyl aldehyde **24** in 57% yield. Similarly, irradiation of **11**, for 10 min, under the same conditions yielded the ODPM product **25** in 82% yield and the alkene **26** (8%), resulting from decarbonylation (Scheme 5).[14b]

These results demonstrate that β,γ-unsaturated aldehydes with phenyl substitution at the γ-position of the β,γ-unsaturated aldehyde skeleton do undergo efficient ODPM rearrangement, according to our postulates. This influence of substitution was further demonstrated in the irradiation of aldehydes **27** and **28**, in which the biradical intermediates are also stabilized by conjugation with phenyl rings. These compounds undergo the ODPM rearrangement, yielding the corresponding cyclopropyl aldehydes **29** (83%) and **30** (96%), respectively, after short irradiation times (Scheme 6).[14b]

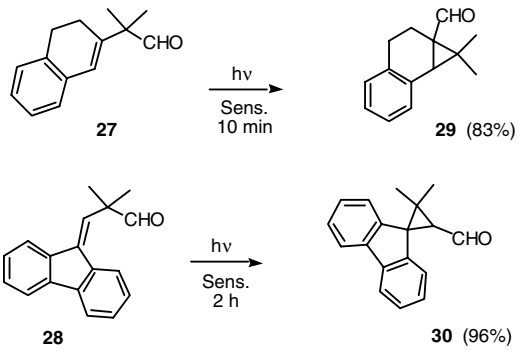

SCHEME 6

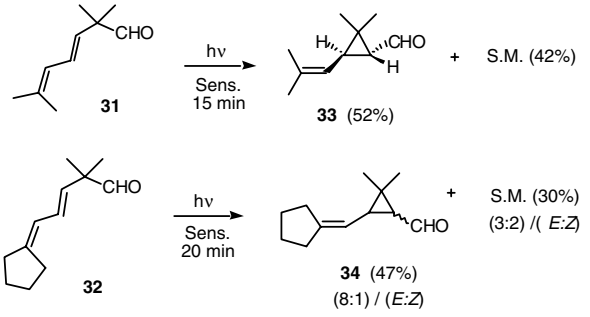

SCHEME 7

The next question to be answered was whether or not substituents other than phenyl at that position could also promote the reaction. Therefore, the study was extended to aldehydes **31** and **32**, with differently substituted vinyl units at the γ-position. Previously we have observed efficient 1-ADPM rearrangement of the corresponding oxime acetates, showing that the substitution pattern present in **31** and **32** was suitable for promoting DPM reactivity.[17] Triplet-sensitized irradiation of **31**, for 15 min, afforded the ODPM product **33** (52%) as the *trans*-isomer exclusively and starting material (42%), as shown in Scheme 7. Similarly, irradiation of **32**, for 20 min, under the same conditions used for **31**, yielded starting material (30%) as a 3:2 mixture of *E,Z*-isomers and the cyclopropane derivative **34** (47%) as a 8:1 mixture of *E,Z*-isomers (Scheme 7).[14b]

The rearrangements of aldehydes **31** and **32** demonstrated that the ODPM reactivity of β,γ-unsaturated aldehydes is not restricted to phenyl-substituted compounds, but can also be extended to systems in which the intermediate biradicals are stabilized by conjugation with a vinyl group. Furthermore, the efficient synthesis of compounds **33** and **34** is of importance because it opens a novel photochemical route to chrysanthemic acid and other cyclopropyl components present in pyrethrins and pyrethroids.[18] In fact, aldehyde **33** can be transformed to *trans*-chrysanthemic acid by simple oxidation. This new synthetic route to ecologically benign insecticides competes with the one previously described by us using the 1-ADPM rearrangement of β,γ-unsaturated oxime acetates.[17]

In the absence of phenyl or vinyl substituents at the γ-position of the β,γ-unsaturated aldehyde, the rearrangement can also take place, although very inefficiently. Thus, acetone-sensitized irradiation of aldehyde **35**, with diphenyl substitution at C2, for 30 min, gives the ODPM aldehyde **24** in 8% yield, the corresponding alkene **36** (14%) resulting from decarbonylation, and starting material (70%). However, irradiation of aldehyde **37**, in which there are no phenyl or vinyl groups to stabilize the biradical intermediates, under the same conditions used for **35** yielded the diene **38,** resulting from the dimerization of the radical **39** formed by decarbonylation of **37**.[14b]

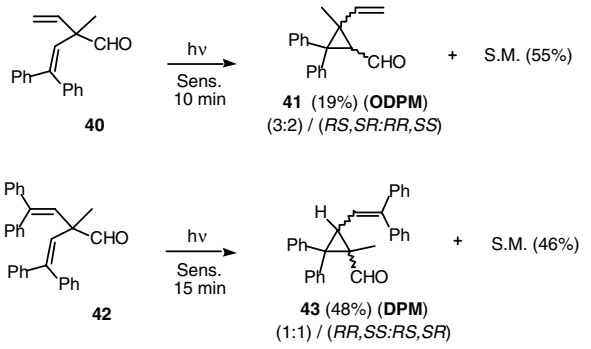

SCHEME 8

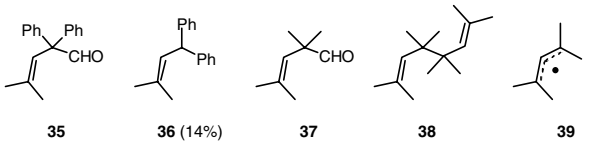

The possible competition between the ODPM and the DPM processes was also studied. Triplet-sensitized irradiation of **40**, for 10 min, afforded recovered starting material (55%) and the cyclopropyl aldehyde **41** (19%), as a 3:2 mixture of *RS,SR:RR,SS* isomers, resulting from an ODPM rearrangement, exclusively, showing that in this instance the ODPM rearrangement dominates over the DPM process (Scheme 8). However, irradiation of aldehyde **42** under the same conditions used for **40**, for 15 min, yielded starting material (46%) and the cyclopropane **43** (48%), resulting from a DPM rearrangement, as a 1:1 mixture of *RR,SS:RS,SR* isomers (Scheme 8). The regioselectivity observed in the rearrangements of **40** and **42** can be justified by taking into account the relative stabilities of the 1,4-bridged biradicals for the two possible rearrangement paths.[14b]

The above results have changed the ideas that most photochemists had for many years about the photoreactivity of β,γ-unsaturated aldehydes. From the previous work on the study of a series of compounds of this type, a general consensus surrounding their lack of ODPM reactivity was originated. Most of the compounds studied previously undergo decarbonylation, with only two exceptions. The decarbonylation takes place via either the S_1 ($n\pi^*$) or T_2 ($n\pi^*$) excited states. However, based on studies with analogous ketones, the ODPM rearrangement of β,γ-unsaturated aldehydes almost surely occurs via the T_1 ($\pi\pi^*$) excited state. The lack of ODPM reactivity of the aldehydes previously studied is probably due to the absence of the adequate substitution pattern that would allow efficient transfer of the triplet energy from the sensitizer to the alkene moiety. Therefore, the T_1 ($\pi\pi^*$) excited state, necessary for the ODPM rearrangement, would not be generated.

Based on our results, we proposed that β,γ-unsaturated aldehydes do indeed undergo efficient triplet ODPM rearrangement when the following criteria are met. First, the triplet energy of the sensitizer must be efficiently transferred to the C–C double bond in order to generate a T_1 ($\pi\pi^*$) excited state of the substrate. Second, the biradical intermediates in the non-concerted ODPM pathway must be stabilized by conjugation with phenyl or vinyl groups. β,γ-Unsaturated aldehydes that do not meet these two requirements, as in most of the cases previously probed, undergo exclusive photodecarbonylation.[14b]

77.3 Reactions of β,γ-Unsaturated Carbonyl Compounds Reminiscent of Norrish Type I Processes

Trying to confirm the above postulates, we have recently investigated the photoreactivity of aldehyde **44** that presents a substitution pattern that should favor the ODPM rearrangement, according to our

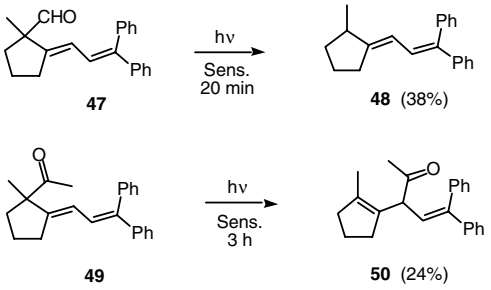

SCHEME 9

hypothesis. Compound **44** was selected because the related aldehyde **8**, previously studied by Schaffner et al., undergoes decarbonylation on irradiation, exclusively.[8] If our postulates on the ODPM rearrangement of aldehydes are correct, it would be possible to overcome the lack of ODPM reactivity by modifying the substitution in **8** in such a way to ensure efficient triplet energy transfer to the C-C double bond and stabilization of the biradical intermediates. The conjugation of the C-C double bond with a phenyl ring and the replacement of the methyl at C3 present in **8** by a hydrogen, should favor the ODPM rearrangement of **44**. Unfortunately, all synthetic attempts yielded an inseparable mixture of **44** and its endocyclic double bond isomer **45**. Nevertheless, a 1:1 mixture of **44** and **45** was irradiated using acetophenone as sensitizer. Despite the complexity of the photomixture, ^{1}H NMR analysis suggested that the bicyclic aldehyde **46**, the product of ODPM rearrangement of the aldehyde **44**, was present in the crude photolysate.[19]

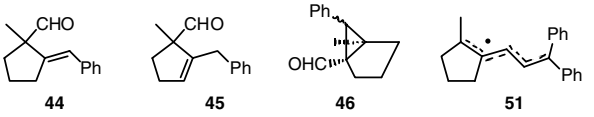

44 **45** **46** **51**

To avoid synthetic problems, we prepared aldehyde **47**, a substrate in which isomerization of the C-C double bond to the endocyclic position is less likely due to the extended conjugation of the alkene moiety. Compound **47** was obtained as a pure substance and also presents a substitution pattern that, according to the above postulates, should favor the ODPM rearrangement. However, irradiation of **47**, using *m*-methoxyacetophenone as sensitizer, led to formation of the diene **48** (38%), as a result of photodecarbonylation (Scheme 9). No ODPM product was formed in this process.[19] Irradiation of the corresponding methyl ketone **49**, under the same conditions as used for **47**, afforded the product of 1,3-acyl migration **50** in 24% yield (Scheme 9). Again, no ODPM product was formed in this instance.[19] The formation of **48** and **50** is reminiscent of Norrish Type I processes. However, in these cases, homolytic bond fission does not occur in the carbonyl nπ^* excited state, as is the case in normal Norrish Type I reactions.[20]

As far as we are aware, these observations show for the first time that the well-known Norrish Type I reactions of β,γ-unsaturated carbonyl compounds can take place by excitation of the alkene moiety rather than the carbonyl group. The reason for this unusual reactivity may be that the T_1 ($\pi\pi^*$) excited states of **47** and **49** have sufficient energy to promote the homolytic bond fission between the carbonyl and the α-carbon due to the stability of the resulting pentadienyl radical **51**. As a consequence, the photodecarbonylation path competes favorably with the ODPM rearrangement.

These observations have forced us to modify some of the conclusions of our previous studies. Specifically, the results indicate that, although substituents should be present to stabilize the intermediate biradicals in order to detect ODPM photoreactivity in β,γ-unsaturated aldehydes, they should not enhance alternative reactions, such as allylic homolytic cleavage. Additional examples of this unusual reactivity are collected in the following section. However, further studies will be necessary to confirm this hypothesis and to determine the scope of these new reactions.

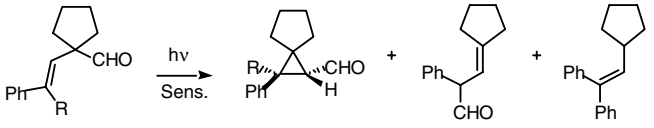

SCHEME 10

77.4 A Comparative Study on the ODPM Rearrangements of β,γ-Unsaturated Aldehydes and Methyl Ketones

An interesting observation made in our preliminary study is that β,γ-unsaturated aldehyde **10** undergoes photoinduced ODPM rearrangement while the analogous methyl ketone **4** does not react in this manner.[14b] This result suggests that other aldehydes with substitution patterns similar to those found in ODPM unreactive ketones might participate in this photorearrangement process. Previous studies have shown that methyl ketone **52a** is not reactive in the ODPM mode.[3a] The corresponding aldehyde **53a**, which has the same substitution pattern as **52a**, according to our postulates should undergo the ODPM rearrangement. To test this proposal, we have carried out a study on the photoreactivity of aldehydes **53a** and **53b**. Triplet-sensitized irradiation of **53a**, for 1 h, leads to generation of the spirocyclic derivative **54a** (36%), as the *trans*-diastereoisomer, and the aldehyde **55** (13%), resulting from 1,3-formyl migration (Scheme 10). Irradiation of the diphenyl analog **53b**, for 2 h, under the same conditions used for **53a**, gives rise to the ODPM product **54b** (24%), the alkene **56** (5%), and recovered starting material (53%) (Scheme 10).[19]

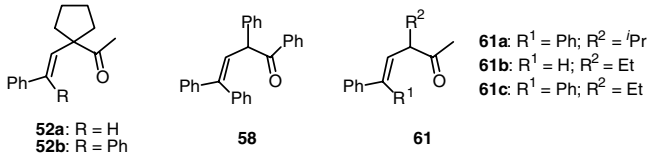

The formation of **56** is a further example of the novel reaction similar to a Norrish Type I process that takes place via the T_1 ($\pi\pi^*$) excited state. This decarbonylation reaction might be due to the stabilization of the radical resulting from homolytic fission of the bond between the formyl group and the α-carbon, similar to the reaction observed for compound **47**. In contrast, the methyl ketone derivative **52b** does not undergo the ODPM rearrangement on triplet-sensitized irradiation for 17 h; rather it yields recovered starting material (71%) and a complex mixture of products.[19] These additional examples add further support to the proposal that β,γ-unsaturated aldehydes are more prone to undergo the ODPM rearrangement than the corresponding methyl ketones.

In an attempt to establish the limits for ODPM reactivity of β,γ-unsaturated aldehydes, we have extended our studies to aldehydes **57a,b,c,d**, which are monosubstituted at C2. The large number of studies carried out in the di-π-methane area have established that disubstitution at the central carbon of acyclic 1,4-unsaturated substrates is an important structural requirement for efficient rearrangement. In fact, compounds **2**[3] and **58**[21] are the only acyclic β,γ-unsaturated ketones monosubstituted at C2 that undergo the ODPM rearrangement.

Triplet-sensitized irradiation of **57a,b,c,d** leads to formation of the corresponding cyclopropanecarbaldehydes **59ab,c,d** in *ca.* 20% yield (Scheme 11). The ODPM rearrangement of aldehydes **57** is stereoselective, yielding only one diastereoisomer of **59**. The diphenyl-substituted aldehydes **57b** and **57d** yielded, in addition to the ODPM products, the corresponding alkenes **60a** and **60b**, resulting from photodecarbonylation. The formation of these alkenes is probably due to stabilization of the radical, formed by allylic cleavage, by diphenyl-conjugation, as in the cases of aldehydes **47** and **53b**.[19]

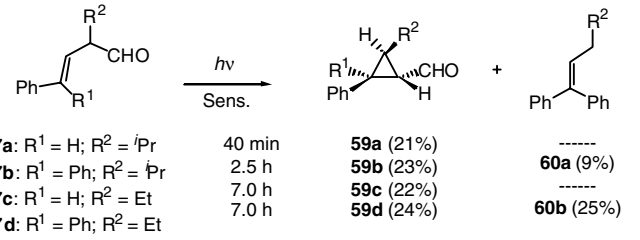

SCHEME 11

The ODPM reactivity of aldehydes **57** is surprising because, as mentioned before, the only two ODPM reactive acyclic β,γ-unsaturated mono-C2 substituted ketones are compounds **2**[3] and **58**,[21] each containing bulky substituents at C2. However, the observations made with **57c** and **57d**, each having ethyl groups at C2, clearly demonstrates that the bulk of the C2 substituent is not an important feature in determining the ODPM reactivity of β,γ-unsaturated aldehydes. However, it should be noted that, the isopropyl-substituted aldehydes **57a** and **57b** do react more efficiently, in qualitative terms, than **57c** and **57d**.

Compounds **61a,b,c** were synthesized in an effort to determine if the aldehydes **57** are more reactive toward the ODPM than the corresponding methyl ketones. Prolonged irradiation of **61a** and **61c**, under the same conditions used for **57**, afforded a complex mixture of highly polar materials (*ca.* 20%) along with recovered starting material (*ca.* 80%). Compound (*E*)-**61b** does not undergo the ODPM rearrangement. Irradiation of this ketone affords the corresponding diastereoisomer (*Z*)-**61b** in 50% yield and 25% of recovered starting material, exclusively.[19] These results confirm the postulate that β,γ-unsaturated aldehydes are better substrates for ODPM rearrangement. In this regard, there are questions that still remain to be answered. For example, it is surprising that ketone **2** has been reported to be ODPM reactive[3] while ketones **61a,b,c** do not undergo this rearrangement reaction.

In summary, the results of our current studies contrast with firmly established, but apparently incorrect, ideas about the photochemical reactivity of β,γ-unsaturated aldehydes and corresponding methyl ketones. Thus, from previous studies on photoreactivity of β,γ-unsaturated aldehydes a general consensus surrounding their lack of ODPM reactivity was originated. Most of the compounds studied previously underwent decarbonylation, with only two exceptions. The decarbonylation takes place via either the S_1 ($n\pi^*$) or T_2 ($n\pi^*$) excited states. The lack of ODPM reactivity of the aldehydes previously studied is probably due to the absence of the adequate substitution pattern that would allow efficient transfer of the triplet energy from the sensitizer to the alkene moiety. Therefore, the T_1 ($\pi\pi^*$) excited state, necessary for the ODPM rearrangement, would not be generated. However, our studies show that suitably substituted β,γ-unsaturated aldehydes do undergo the ODPM rearrangement with high chemical efficiency. The results obtained by us indicate that the ODPM rearrangement of β,γ-unsaturated aldehydes occurs when the triplet energy from the sensitizer is efficiently transferred to the alkene moiety generating a T_1 ($\pi\pi^*$) excited state and, furthermore, when the biradical intermediates are stabilized by phenyl or vinyl substitution. However, we have observed the first examples of reactions, similar to the well-known Norrish Type I process, which take place in the triplet excited state of β,γ-unsaturated carbonyl compounds by excitation of the C-C double bond instead of the carbonyl group. This situation occurs when the radical resulting from allylic homolytic bond cleavage is highly stabilized. In addition, a comparison of the photochemical reactivity of β,γ-unsaturated aldehydes and corresponding methyl ketones has shown that the ketones do not undergo the ODPM rearrangement while the corresponding aldehydes are reactive by this pathway. Finally, ODPM rearrangement of aldehydes monosubstituted at C2 is surprising because there are only two precedents of acyclic ketones with this type of substitution that undergo this photoreaction. Furthermore, the photoreactions of these substances are stereoselective, yielding only one of the possible diastereoisomeric cyclopropanecarbaldehyde products. When combined, the results of our studies broaden the synthetic potential of the ODPM rearrangement.

References

1. For example, see: (a) Calvert, G.J. and Pitts, J.N., *Photochemistry*, John Wiley & Sons, New York, 1966; (b) Turro, N.J., *Modern Molecular Photochemistry*, Benjamin Cummings Publishing, Menlo Park, CA, 1978; (c) Gilbert, A. and Baggott, J., *Essentials of Molecular Photochemistry*, Blackwell Scientific , Oxford, 1991; (d) Horspool, W.M. and Armesto, D., *Organic Photochemistry*, Ellis Horwood and PTR Prentice Hall, Chichester, England, 1992; (e) *CRC Handbook of Organic Photochemistry and Photobiology*, Horspool, W.M. and Song, P.-S., Eds., CRC Press, Boca Raton, FL, , 1995.
2. For example, see: (a) Hixson, S.S., Mariano, P.S., and Zimmerman, H.E., The di-π-methane and oxa-di-π-methane rearrangements, *Chem. Rev.*, 73, 531–551, 1973; (b) Dauben, G.W., Lodder, G., and Ipaktschi, J., Photochemistry of β,γ-unsaturated ketones, *Top. Curr. Chem.*, 54, 73–114, 1975; (c) Houk, K.N., The photochemistry and spectroscopy of β,γ-unsaturated carbonyl compounds, *Chem. Rev.*, 76, 1–74, 1976; (d) Schuster, D.I., Photochemical rearrangements of β,γ-enones, in *Rearrangements in Ground and Excited States*, Vol. 3, de Mayo P., Ed., Academic Press, New York, 1980, 167–279; (e) Demuth, M., Oxa-di-π-methane photoisomerizations, in *Comprehensive Organic Synthesis*, Vol. 5, Trost, B.M., Fleming.I., and Paquette, L.A., Eds., Pergamon Press, Oxford, 1991, 215–237; (f) Demuth, M., The Oxa-di-π-methane rearrangement, in *Organic Photochemistry*, Vol. 11, Padwa, A., Ed., Marcel Dekker, New York, 1991, 37–109; (g) Zimmerman, H.E. and Armesto, D., Synthetic aspects of the di-π-methane rearrangement, *Chem. Rev.*, 96, 3065–3112, 1996; (h) Armesto, D., Ortiz, M.J. and Agarrabeitia, A.R., Recent advances in di-π-methane photochemistry. A new look at a classical reaction, in *Photochemistry of Organic Molecules in Isotropic and Anisotropic Media*, Ramamurthy, V. and Schanze, K.S., Eds., Marcel Dekker, New York, 2003, 1–41.
3. (a) van der Weerdt, A.J.A. and Cerfontain H., Photochemistry of β,γ-unsaturated ketones. The effect of substituents at the α-C and the carbonyl group on the occurrence of the oxa-di-π-methane rearrangement, *Recl. Trav. Chim. Pays-Bas*, 96, 247–248, 1977; (b) van der Weerdt, A.J.A. and Cerfontain H., Photochemistry of β,γ-unsaturated ketones. V. The direct irradiation of some γ-phenyl β,γ-enones, *Tetrahedron*, 37, 2120–2130, 1981.
4. Pratt, A.C., Photochemistry of β,γ-unsaturated carbonyl compounds. 3,3-Dimethyl-5,5-diphenyl-pent-4-en-2-one and 2,2-dimethyl-4,4-diphenylbut-3-enal, *J. Chem. Soc., Perkin Trans. 1*, 2496–2499, 1973.
5. Tsuji, T. and Nishida, S. Preparation of cyclopropyl derivatives, in *The Chemistry of Functional Groups, The Chemistry of the Cyclopropyl Group, Part 1*, Patai, S. and Rappoport, Z., Eds., John Wiley & Sons, New York, 1987, chap. 7, 347.
6. Baggiolini, von E., Berscheid, H.G., Bozzato, G., Cavalieri, E., Schaffner, K., and Jeger, O., Die photofragmentierung von O-acetyljervin, *Helv. Chim. Acta*, 54, 429–449, 1971.
7. Hill, J., Iriarte, J., Schaffner, K., and Jeger, O., UV.-Bestrahlung von gesättigten und β,γ-ungesättigten, homoallylisch konjugierten steroidaldehyden, *Helv. Chim. Acta*, 49, 292–311, 1966.
8. Baggiolini, E., Hamlow, H.P., and Schaffner, K., Photochemical reactions. LIX. On the mechanism of the photodecarbonylation of β,γ-unsaturated aldehydes, *J. Am. Chem. Soc.*, 92, 4906–4921, 1970.
9. Dürr, H., Herbst, P., Heitkämper, P., and Leismann, H., Photochemie β,γ-unsättigter aldehyde. Mechanismus der photofragmentierung phenylsubstituierter cyclopentenecarbaldehyde, *Chem. Ber.*, 107, 1835–1855, 1974.
10. Adam, W., Berkessel, A., Hildenbrand, K., Peters, E.-M., Peters, K., and von Schnering, H.G., The photochemistry of bis(2,2-diphenylvinyl) ether: A search for the 3-oxa-di-π-methane rearrangement, *J. Org. Chem.*, 50, 4899–4909, 1985.
11. Pfenninger, E., Poel, D.E., Berse, C., Wehrli, H., Schaffner, K., and Jeger, O., Zur photochemie von α,β-ungesättigten γ-aldehydoketonen I. Die UV.-bestrahlung von 3,19-dioxo-17β-acetoxy-Δ^4-andostren, *Helv. Chim. Acta*, 51, 772–803, 1968.

12. Zimmerman, H.E. and Cassel, J.M., Unusual rearrangements in di-π-methane systems: Mechanistic and exploratory organic photochemistry, *J. Org. Chem.*, 54, 3800–3816, 1989.
13. Armesto, D. and Ramos, A., Photochemical synthesis of oxime acetates derivatives of 1-carbaldehydobicyclo[n.1.0]alkanes by the aza-di-π-methane rearrangement, *Tetrahedron*, 49, 7159–7168, 1993.
14. (a) Armesto, D., Ortiz, M.J. and Romano, S., The oxa-di-π-methane rearrangement of β,γ-unsaturated aldehydes, *Tetrahedron Lett.*, 36, 965–968, 1995; (b) Armesto, D., Ortiz, M.J., Romano, S., Agarrabeitia, A.R., Gallego, M.G., and Ramos, A., Unexpected oxa-di-π-methane rearrangement of β,γ-unsaturated aldehydes, *J. Org. Chem.*, 61, 1459–1466, 1996.
15. (a) Dalton, J.C., Shen, M., and Snyder, J.J., Mechanistic photochemistry of β,γ-unsaturated ketones. An alternative excited state assignment for the 1,3-acyl shift reaction of alkyl β,γ-enones, *J. Am. Chem. Soc.*, 98, 5023–5025, 1976; (b) Schaffner, K., 1-Acyl-2-cyclopentenes and 5-acylbicyclo[2.1.0]pentanes: photochemical and thermal isomerizations, *Tetrahedron*, 32, 641–653, 1976; (c) Schuster, D.I. and Calcaterra, L.T., Photochemistry of ketones in solution. 66. Experimental evidence for the intermediacy of singlet (S_1) and triplet (T_2) n,π* states in the [1,3]-sigmatropic acyl shift of photoexcited 3-methyl-3-(1-cyclopentenyl)butan-2-one, *J. Am. Chem. Soc.*, 104, 6397–6405, 1982.
16. (a) Armesto, D., Agarrabeitia, A.R., Horspool, W.M., and Gallego, M.G., Unexpected influence of mono-phenyl substitution on the photochemistry of β,γ-unsaturated oxime acetates, *J. Chem. Soc., Chem. Commun.*, 934–936, 1990; (b) Armesto, D., Horspool, W.M., Gallego, M.G., and Agarrabeitia, A.R., Steric and electronic effects on the photochemical reactivity of oxime acetates of β,γ-unsaturated aldehydes, *J. Chem. Soc., Perkin Trans. 1*, 163–169, 1992.
17. Armesto, D., Gallego, M.G., Horspool, W.M., and Agarrabeitia, A.R., A new photochemical synthesis of cyclopropanecarboxylic acids present in pyrethroids by the aza-di-π-methane rearrangement, *Tetrahedron*, 51, 9223–9240, 1995.
18. Naumann, K., *Synthetic Pyrethroid Insecticides*, Springer-Verlag, Berlin, 1990, Vols. 4 and 5.
19. Armesto, D., Ortiz, M.J., Agarrabeitia A.R., and Aparicio-Lara S., Diastereoselective synthesis of cyclopropanecarbaldehydes, *Synthesis*, 1149–1158, 2001.
20. Braslavsky, S.E. and Houk, K.N., Glossary of terms used in photochemistry, *Pure Appl. Chem.*, 60, 1055–1106, 1988.
21. Tenney, L.P., Boykin Jr.D.W., and Lutz R.E., Novel photocyclization of a highly phenylated β,γ-unsaturated ketone to a cyclopropyl ketone, involving benzoyl group migration, *J. Am. Chem. Soc.*, 88, 1835–1836, 1966.

78

Photochemical Rearrangements in β,γ-Unsaturated Enones: The Oxa-di-π-methane Rearrangement

Vishwakarma Singh
Indian Institute of Technology, Bombay

78.1 Introduction and Background

Photochemical reactions of compounds containing a β,γ-enone chromophore have generated intense interest for more than two decades[1–4] and even more so in recent years.[5–7] Several excellent reviews dealing with various aspects of β,γ-enone photochemistry have appeared.[1–7] A good historical background on the photoreactions of β,γ-enones is described by Schuster.[4] In principle, β,γ-enones can undergo photoreactions that are characteristic of carbonyl and olefinic chromophores, such as photoreduction, epimerization and *cis,trans*-isomerization, [2+2]-cycloaddition, etc. They also undergo two unique reactions as

0-8493-1348-1/04/$0.00+$1.50

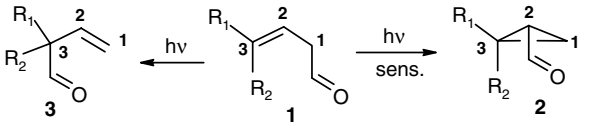

SCHEME 1

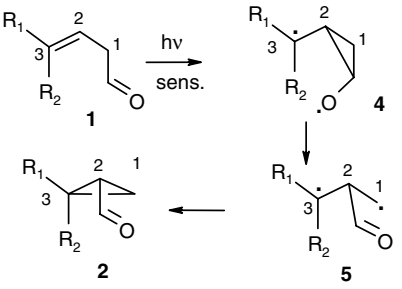

SCHEME 2

a result of interaction between the alkene and carbonyl chromophore. In general, it has been observed that sensitized irradiation of β,γ-enones induces a 1,2-acyl migration that results in the formation of cyclopropyl conjugated ketones of type **2**, a reaction also known as oxa-di-π-methane rearrangement because of its analogy to the di-π-methane (Zimmerman) rearrangement. The direct irradiation of β,γ-enones leads to formation of enones of type **3** as a result of 1,3-acyl migration (Scheme 1).[4]

Of these photochemical reactions, the oxa-di-π-methane rearrangement (**1** → **2**) has been extensively studied from both mechanistic and synthetic perspectives. This reaction is highly general for constrained β,γ-enones and proved to be an excellent tool for organic synthesis.

78.2 Mechanism and Correlation of Excited State and Reactivity

The mechanism of the oxa-di-π-methane reaction and 1,3-acyl shift has been studied in great detail, and the correlation of excited-state reactivity has been established.[4–7] In general, the oxa-di-π-methane reaction occurs from the lowest triplet excited state (T_1, ππ*), while 1,3-acyl shift occurs either from the excited singlet (S_1, nπ*) state or the higher triplet (T_2, nπ*) state.[4,7–10] To induce the oxa-di-π-methane reaction (or 1,2-acyl shift) in β,γ-enones, direct excitation to a singlet state should be avoided and a careful choice of sensitizer having an E_T value close to the E_T of the enone should be made so as to selectively populate the lowest triplet excited state. The oxa-di-π-methane reaction path involves two biradical intermediates of type **4** and **5,** as first suggested by Givens and Oettle.[8] The biradical **4** is formed as a result of initial bonding between the carbonyl carbon and β-carbon of the C–C double bond, which undergoes cleavage of the cyclopropane ring to regenerate the CO group and gives the short-lived biradical **5** that rapidly closes to give the cyclopropyl ketone **2** (Scheme 2).[8–13] Although the existence of the biradicals **4** and **5** and the multiplicity of the surfaces on which these are formed have not been demonstrated directly, experimental results [stereochemistry of the reaction CIDNP (chemically induced dynamic nuclear polarization), radical trapping experiments, and quantum yield measurements] support their existence.[4–7] The detailed mechanism of these reactions, however, depends on the structure of the chromophore and the presence of other functionalities in a subtle fashion.[4,5] Recently, the mechanism of ODPM and 1,3-acyl shift based on theoretical calculation and other studies, in terms of potential energy surface and decay funnels, has been described.[14]

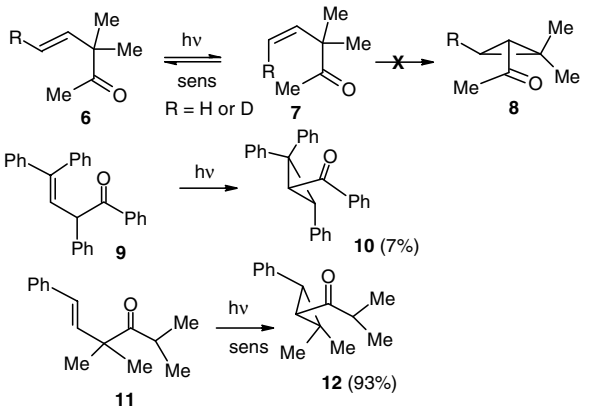

SCHEME 3

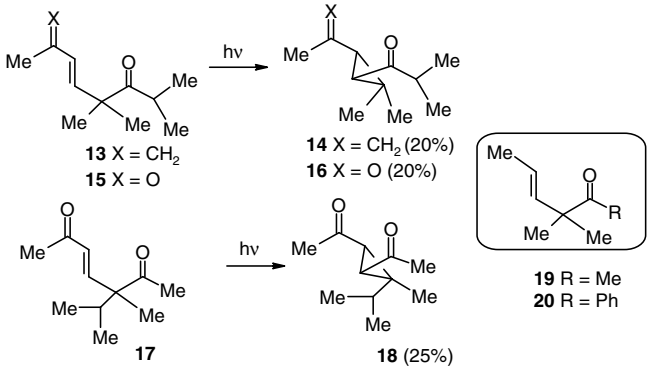

SCHEME 4

78.3 Oxa-di-π-methane Reactions in Acyclic β,γ-Enones

Acyclic compounds having a β,γ-enone chromophore do not undergo oxa-di-π-methane rearrangement efficiently, except in those cases where the C–C double bond is further conjugated to a phenyl or vinyl group and with a substituted central carbon. This is mainly because other channels of deactivation of the triplet excited state, such as *cis,trans-* isomerization, become more important than the oxa-di-π-methane pathway. This type of energy dissipation is also known as the free rotor effect in β,γ-enones, which is analogous to similar formulations for the lack of di-π-methane reactivity in acyclic 1,4-dienes in unconstrained systems.[1] Thus, the simple β,γ-enones with an unsubstituted C–C double bond such as **6** undergo *cis,trans*-isomerization without formation of ODPM product **8**.[15] The ketone **9,** having phenyl substituents on the central, γ-, and carbonyl carbons, gave the ODPM product **10** in low yield upon direct irradiation,[16] and the ketone **11** was found to give the cyclopropyl ketone **12** efficiently (93%) (Scheme 3) as a result of ODPM reaction.[17] Moreover, the ketone **13**, in which the β,γ-ene moiety is conjugated with a vinyl group, underwent smooth ODPM reaction upon sensitized irradiation to give **14**.[18] Interestingly, the direct irradiation of **15** and **17** led to ODPM reaction (albeit in low yield) to furnish the cyclopropyl compounds **16** and **18,** respectively (Scheme 4).[18] From these results and photochemical reactions of other acyclic β,γ-enones,[19–23] it appears that the conjugation of the alkene moiety with vinyl, phenyl, or oxo groups and disubstitution or substitution by bulky groups are important

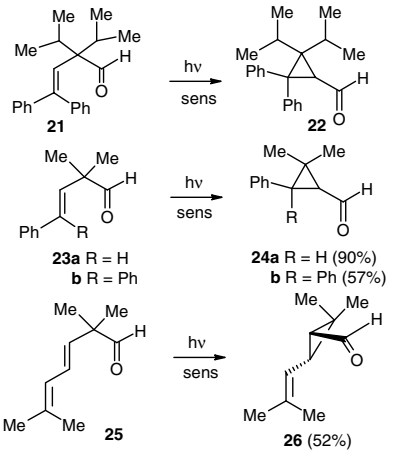

SCHEME 5

structural features that control ODPM reaction in acyclic β,γ-enones. However, the ketones **19** and **20** did not undergo oxa-di-π-methane reaction.[23]

Earlier attempts to bring about an oxa-di-π-methane reaction of β,γ-unsaturated aldehydes were unsuccessful.[24–26] Zimmerman and Cassel reported ODPM reaction of the aldehyde **21** (Scheme 5) to give the highly crowded cyclopropyl compound **22** in moderate yield.[27] Recently, Armesto and co-workers[28,29] reported efficient oxa-di-π-methane reactivity in the aldehydes **23** on sensitized irradiation to give the corresponding products **24**. Interestingly, the diene-aldehyde **25** undergoes a stereoselective oxa-di-π-methane reaction to give the *trans*-cyclopropane aldehyde **26** upon *m*-methoxyacetophenone-sensitized irradiation, in reasonably good yield (Scheme 5).[29]

78.4 Oxa-di-π-methane Reaction in Semicyclic β,γ-Enones

β,γ-Enones in which one (or both) of the chromophores form part of a ring, undergo oxa-di-π-methane reactions with better efficiency compared to their acyclic counterparts and are less dependent on substitution pattern. Excitation of a series of ketones of type **27,** in which the double bond is present in a five-membered ring, led to the oxa-di-π-methane products **28**.[29,30] It has been shown that the degree of flexibility of the C–C double bond (effect of ring size) affects the efficiency of the oxa-di-π-methane reaction. Thus, the ketones **29** and **30,** having a C–C double bond in the four- and five-membered rings, respectively, gave ODPM products upon sensitized irradiation in acetone, but the ketones **33**, **34**, and **35** were unreactive (Scheme 6).[31] Interestingly, the enone **36** underwent ODPM reaction to give **37** upon direct irradiation, apparently via $S_2(\pi\pi^*)$.[32] Further, ketones of type **38,**[33] **39,**[18] and **40,**[34] wherein the β,γ C–C double bond is further conjugated, also gave ODPM products **41**, **42**, and **43**, respectively (Scheme 7). The efficiency and yield of the ODPM product in photoreaction of **39** and **40** are wavelength dependent.

Studies on photochemical reaction of β,γ-enones in which both the chromophores are present in different rings provided an in-depth understanding of the stereochemical and mechanistic features of oxa-di-π-methane rearrangements.[9,10] Sensitized irradiation of the optically active enone **44** gave ODPM product **47** in optically pure form.[9] Irradiation of **45** also gave the ODPM product **48** (Scheme 8).[10] Similarly, sensitized photoreaction of the enone **46,** in which five-membered ring is part of the indane ring system, also gave the corresponding ODPM product **49**.[32] Recently, an interesting ionic heavy-atom effect on the photochemical reaction of **44** was observed by Scheffer and co-workers.[35] While the direct irradiation of **44** primarily affords the 1,3-acyl shift product, irradiation of the heavy-atom salts of **44** in the crystalline state gives the ODPM product.[35]

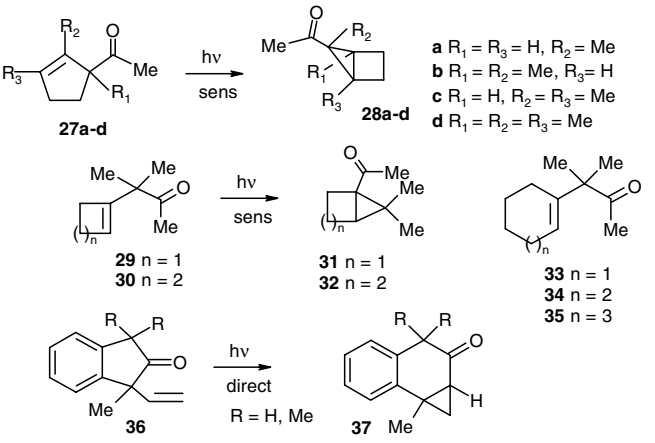

SCHEME 6

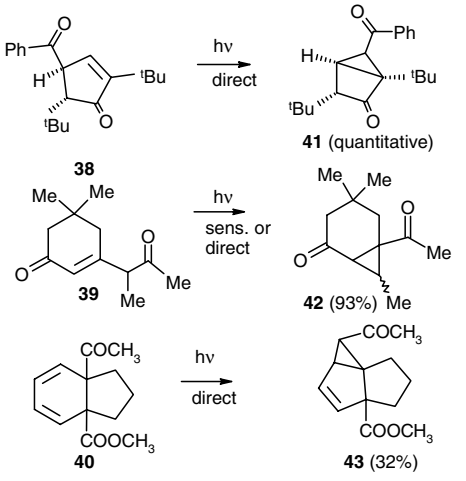

SCHEME 7

Some of the aldehydes that were reactive toward oxa-di-π-methane reaction are given in Scheme 9. Direct irradiation of the steroidal aldehyde **50** was reported to give the ODPM product **51** in 30% yield, along with two other products.[36] Armesto recently reported the photoreaction of a number of aldehydes, including **52** and **54** that rearranged to the corresponding ODPM products **53** and **55**, respectively, on sensitized irradiation.[28,29]

78.5 Oxa-di-π-methane Reactions in Monocyclic and Ring-Fused Bicyclic β,γ-Enones

The ketones **56**, **57**, and **58** are some of the monocyclic β,γ-enones whose photochemical reactions upon sensitized irradiation have been examined. Irradiation of the dienone **56** in ether is reported to give the bicyclic ketone **59** via oxa-di-π-methane reaction.[37] Recently, the photoreaction of cyclohexadienone **56** and its derivatives having chiral auxiliaries was examined in alkali ion exchanged Y zeolites.[38] Thus, irradiation of **56** in dry (−)-ephedrine-modified zeolite gave the ODPM product in 30% *ee*. Significant

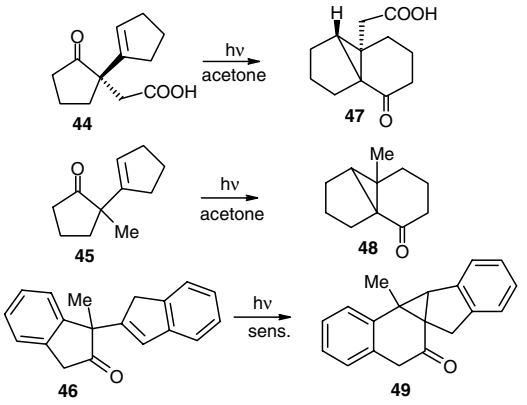

SCHEME 8

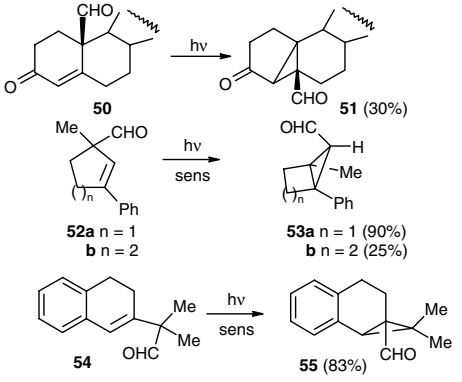

SCHEME 9

enantioselectivity (in the case of achiral) and diastereoselectivity (in the case of chiral) in cyclohexadienones was observed.[38] These studies indicated that photoreaction in modified zeolites may induce asymmetric induction. The cycloheptadienone **57a**, having methyl groups, also gives the ODPM product **60** upon sensitized irradiation, but the unsubstituted analogue **57b** undergoes conrotatory pericyclic reaction and does not give the ODPM product.[39] The enones **58a** and**58b**, in which the β,γ-C=C double bond is exocyclic, also do not undergo oxa-di-π-methane reaction; instead *cis*,*trans*-isomerization is observed (Scheme 10).[40]

A variety of fused bicyclic compounds having a β,γ-enone chromophore have been reported to undergo oxa-di-π-methane reaction upon irradiation.[41–44] Interestingly, both the direct as well as sensitized irradiation of enone **61a** gives the oxa-di-π-methane reaction product **64a**, while the dimethyl analogue **61b** gives ODPM product **64b** only upon sensitized irradiation.[41] It appears that **61a** undergoes efficient intersystem crossing to produce the triplet state, which is responsible for the oxa-di-π-methane reaction.[41] The presence of methyl groups in **61b** induces α-cleavage upon direct irradiation and hence leads to a 1,3-acyl shift. Similarly, the enone **63a** gives the ODPM product **66a** as a major product upon direct irradiation,[44] while the optically pure ketones **62** undergo the oxa-di-π-methane reaction upon sensitized irradiation to give **65** as a mixture of diastereomers.[42] Photochemical reaction of **63b** and **63c** were examined in solution and solid state, respectively.[45] Irradiation of **63b** in solution at 350 nm gave the ODPM product **66b** in excellent yield (87%). Irradiation of the quaternary ammonium salts of type **63c**

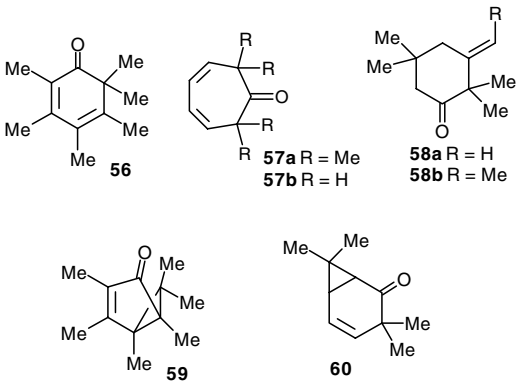

SCHEME 10

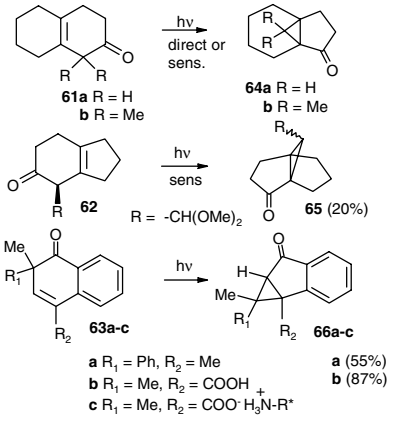

SCHEME 11

containing chirality furnished ODPM products in an enantioselective manner. The best ee (81%) was obtained with the salt derived from α-methylbenzylamine (Scheme 11).[45] These studies may form a basis for developing methods for asymmetric induction in photoreaction of β,γ-enones.

Photochemical reaction of several steroidal β,γ-enones have been examined.[46–49] Thus, the ketones **67** and **70** underwent oxa-di-π-methane reaction on sensitized irradiation,[46,49] while **68** and **69** gave ODPM products upon direct irradiation (Scheme 12).[47,48] The modified steroidal ketone **70** gave the ODPM product **74** on direct irradiation as well.[49] It appears that the dihedral angle between the carbonyl and vinyl groups in the enones controls the efficiency of population of the triplet excited state on direct irradiation and, hence 1,3-acyl shift vs. 1,2-acyl shift (oxa-di-π-methane) selectivity.[50]

78.6 Oxa-di-π-methane Reactions in Spirocyclic β,γ-Enones

Photoreaction of a series of spirocyclic compounds having β,γ,δ,ε-unsaturated carbonyl groups have been studied (Scheme 13).[51–53] The spirodienones of type **75** exhibited interesting photochemical reactions depending on the wavelength of irradiation. While direct irradiation at 350nm gave the oxa-di-π-methane product **76** in a regio- and stereoselective fashion, sensitized irradiation in acetone gave **77** due to vinylogous ODPM reaction, in addition to **76**.[51,52] The ratios of various products formed in acetone-sensitized irradiation was found to be dependent on substitution. It is suggested that the compound **76**

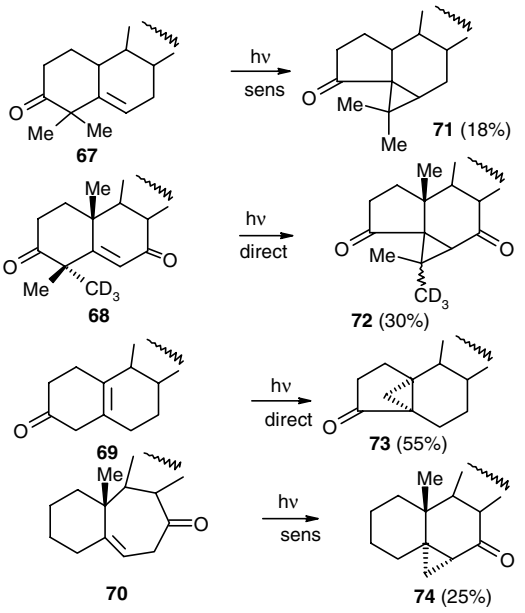

SCHEME 12

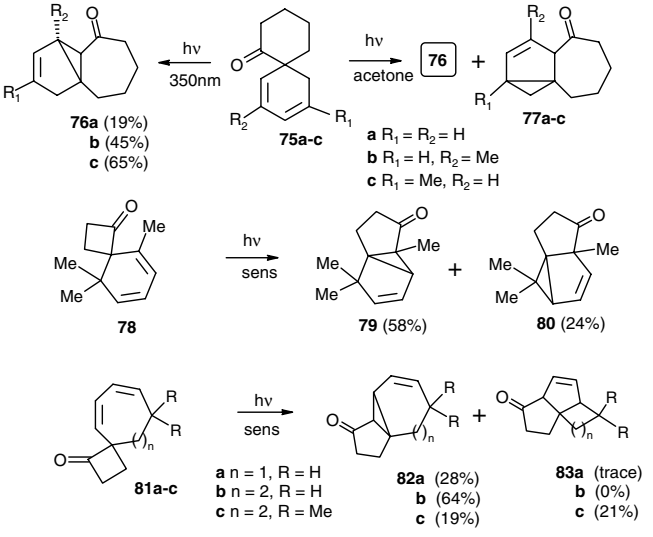

SCHEME 13

arises during direct irradiation from $T_2(\pi\pi^*)$, which is populated via intersystem crossing, while the vinylogous ODPM product **77** formed from $T_1(\pi\pi^*)$.[52] Enantioselective oxa-di-π-methane reaction in compounds of type **75** (R_1 = H, R_2 = COOMe) has also been observed.[51] Sensitized irradiation of the spiro dienone **78** gave significant amounts of **80** as a result of vinylogous ODPM reaction, in addition to **79**. Similarly, irradiation of the compound **81c** also gave **82** and **83**. The enones **81a** and **81b** without methyl groups gave primarily the ODPM products **82a** and **82b** (Scheme 13), respectively.[53] Here also, the effect of substitution on the formation of vinylogous ODPM products was noted.[53]

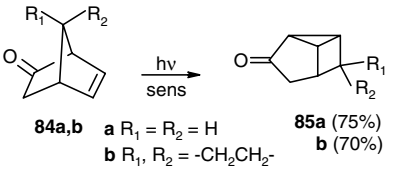

84a,b **a** $R_1 = R_2 = H$ **85a** (75%)
b R_1, $R_2 = -CH_2CH_2-$ **b** (70%)

SCHEME 14

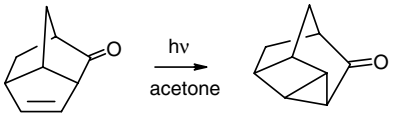

86 **87** (25%)

SCHEME 15

78.7 Oxa-di-π-methane Reactions in Cyclic Bridged β,γ-Enones

Compounds containing a β,γ-enone chromophore in a conformationally rigid carbocyclic framework undergo oxa-di-π-methane rearrangement more efficiently than other structural types. Bridged compounds in which both the alkene and the carbonyl chromophores are part of constrained ring systems constitute the largest class of β,γ-enones that have been studied and found to undergo oxa-di-π-methane reaction and constitute a very important synthetic methodology. Oxa-di-π-methane reactions in bridged cyclic systems generally give very good yields of the rearranged products in a highly regio- and stereoselective fashion, and also efficiently generate novel carbocyclic structures that are otherwise not readily accessible through ground-state chemical reactions. Photochemical studies on bridged ketones, especially the oxa-di-π-methane reaction, have been most fruitful in terms of the theoretical and mechanistic understanding of this rearrangement and have also provided a unique methodology for organic synthesis. There are a number of examples wherein oxa-di-π-methane reaction in a bridged cyclic system has been employed as a key step in the total synthesis of natural products (*vide infra*).

Bicyclo[2.2.1]heptenones

Among bridged bicyclic β,γ-enones, photoreactions of only a few systems with a bicyclo[2.2.1]heptane framework have been studied.[54–56] Thus, sensitized irradiation of **84a** and **84b** gave the corresponding ODPM products **85a** and **85b** in major amounts, respectively (Scheme 14).[54] Recently, ODPM reaction in **84a** induced by an external heavy cationic effect in zeolite was also observed.[56] Acetone-sensitized irradiation of the tricyclic system **86** was reported to give 2,8-didehydro-9-noradamantanone **87** in moderate yield (Scheme 15).[57]

Bicyclo[3.2.1]octenones and Congeners

In context with mechanistic studies on the photoreaction of β,γ-enones, especially to resolve the singlet–triplet dichotomy, Givens and co-workers examined the photoreaction of **88a,b,c** upon sensitized and direct irradiations.[58] While direct irradiation led to the characteristic 1,3-acyl shift, acetone-sensitized irradiation of **88a,b,c** gave ODPM products **89a,b,c** (Scheme 16) along with 1,3-acyl shift products. The formation of the 1,3-shift product during sensitized irradiation presumably results either from direct absorption of light or singlet sensitization.[58] The chromophoric systems **90a** and **90b**, in which the CO group is present in the longer bridge, also gave ODPM products **91a** and **90b**, respectively, upon sensitized irradiation in acetone.[59] However, many systems closely related to **90** gave 1,3-acyl shift products during irradiation in acetone.

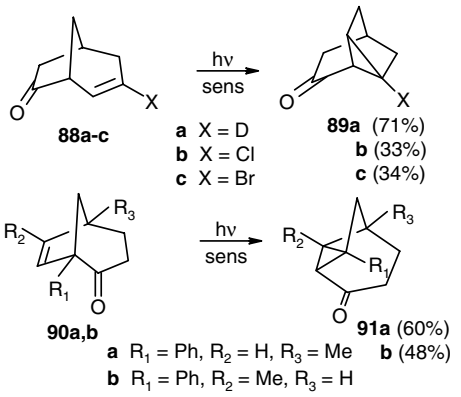

SCHEME 16

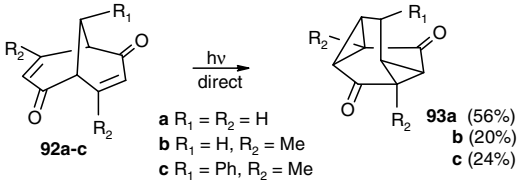

SCHEME 17

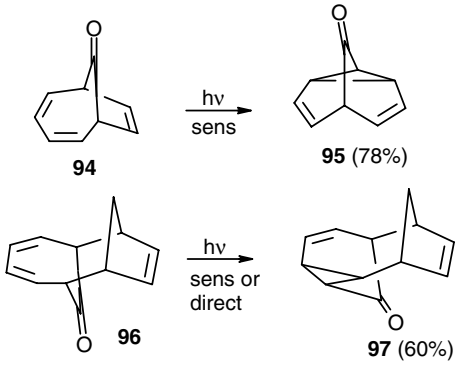

SCHEME 18

Interestingly, the dienediones **92** underwent double oxa-di-π-methane rearrangements upon direct irradiation to give triasteranedione **93** in moderate yields (Scheme 17).[60] The trienone **94** with a bicyclo[4.2.1]nonane ring system gave **95,** wherein the β,γ-C–C double bond of the diene moiety participated in the oxa-di-π-methane reaction.[61] Similarly, the trienone **96** also furnished the oxa-di-π-methane product **97** (Scheme 18).[62]

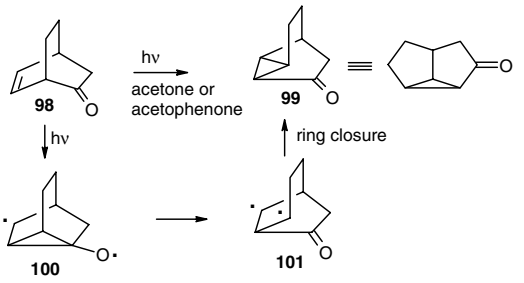

SCHEME 19

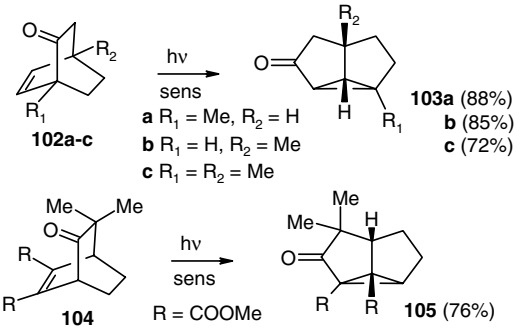

SCHEME 20

Bicyclo[2.2.2]octenones

Photochemical reactions of this class of compounds have been extensively studied. Bicyclo[2.2.2]octenones constitute an important class of β,γ-enones that stimulated intense interest in their photochemical reactions and a large amount of work has been reported. The oxa-di-π-methane rearrangement is one of the most general and versatile reactions of this class of β,γ-enones. Givens and co-workers reported the transformation of bicyclo[2.2.2]oct-5-en-2-one **98** into tricyclo[3.3.0^{2,8}]octan-3-one **99** upon sensitized irradiation in acetone.[63] Demuth and co-workers later examined the photoreaction of (+)- and (−)-**98** on sensitized irradiation in acetophenone, which gave the corresponding ODPM products in excellent yield (~85%) and demonstrated the stereoselectivity in the oxa-di-π-methane reaction.[64] The reaction proceeds through biradicals **100** and **101** (Scheme 19).[63,64] Photochemical reactions of a variety of bicyclo[2.2.2]octenones were studied and found to undergo efficient oxa-di-π-methane reaction. Thus, acetophenone-sensitized irradiation of **102**[64,65] and **104**[66] gave the tricyclooctanones **103** and **105**, respectively (Scheme 20). Other functionalized analogues of **104** have also been shown to undergo oxa-di-π-methane reaction upon sensitized irradiation.[67] Furthermore, the photoreaction of **106** and **107**, which contain ester and hydroxyl groups at the α′ position, also gave ODPM products **108** and **109,** respectively, upon acetophenone-sensitized irradiation (Scheme 21).[68,69] Liao[70] and Paquette[71] reported oxa-di-π-methane rearrangement of bicyclo[2.2.2]octenones **110** and **111,** leading to the tricyclic compounds **112** and **113,** respectively, upon acetone-sensitized irradiation (Scheme 21).

Bicyclo[2.2.2]octenones with α-methoxy groups undergo a remarkable photoreaction. Rogers and Parker investigated the photochemistry of **114** and its isomer **117,** and other related ketones, upon sensitized as well as direct irradiation.[72–74] Sensitized (acetone or acetophenone in benzene) irradiation of the enone **114**, with a methoxy group at the α-position, was found to give the dione **116** in major quantity; the expected ODPM product was obtained only in minor amounts (Scheme 22).[72] It was

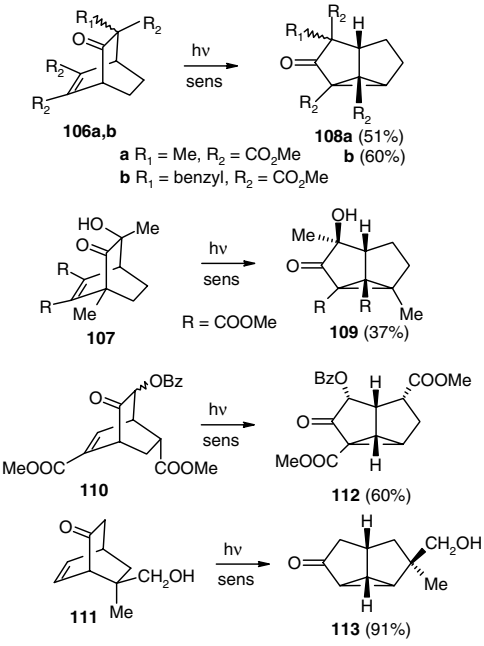

SCHEME 21

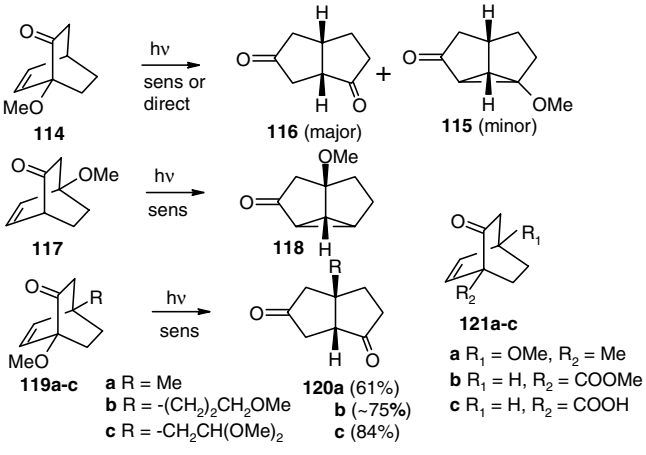

SCHEME 22

suggested that the final product **116** is formed via oxa-di-π-methane reaction followed by cleavage of the cyclopropane ring, loss of a methyl radical, and capture of a hydrogen radical.[72] Sensitized irradiation of **117**, on the other hand, gave the ODPM product **118,** accompanied by a small amount of the 1,3-shift product. It was suggested that the ODPM reaction in **117** originates from the excited singlet state.[74] The photochemical transformation of **114** provided a unique methodology for the synthesis of bicyclo[3.3.0]oct-2,5-dione of type **116** that are not readily available, and also enhanced the synthetic potential of the oxa-di-π-methane reaction. Demuth and co-workers also studied the photoreaction of more elaborate bicyclooctenones with α-methoxy groups and reported transformation of **119a,b,c** into **120a,b,c,** respectively, upon acetophenone-sensitized irradiation.[65,75] While a large number of substrates

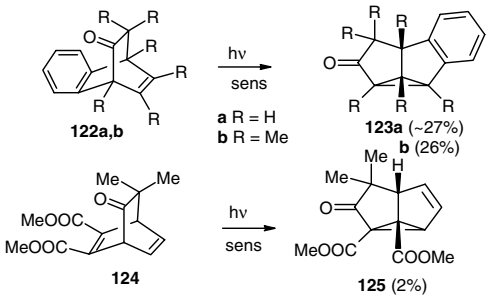

SCHEME 23

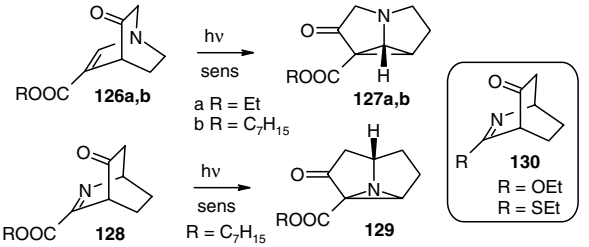

SCHEME 24

containing a β,γ-enone group in a bicyclo[2.2.2]octane system underwent oxa-di-π-methane rearrangement upon sensitized irradiation, it seems that minor structural changes in the chromophoric system affects this photorearrangement in a very subtle fashion because the compounds of type **121** did not undergo the ODPM reaction (Scheme 22).[65]

The photoreaction of other bicyclo[2.2.2]octenones, and their congeners with more than one β,γ-C–C double bond, have the possibility of dual deactivation pathways; for example, ODPM and di-π-methane reaction upon excitation have been examined.[8,68,76–79] The benzobicyclo[2.2.2]octenones **122a**[8] and **122b**[76] are some of the earlier examples that were found to follow the ODPM reaction pathway upon acetone-sensitized irradiation that involved the non-benzenoid C–C double bond to give the products **123a** and **123b**, respectively, albeit in low yield (Scheme 23). The bicyclo[2.2.2]octadienone **124,** however, yielded a very small amount of ODPM product. The major product was due to di-π-methane reaction.[77]

Most recently, oxa-di-π-methane rearrangement in aza-bicyclo[2.2.2]oct-2-en-5-one was explored; this provides a novel route to pyrrozolidine alkaloids.[78] Thus, sensitized irradiation of **126** and **128** furnished azabicyclo[3.3.0]octanones **127** and **129,** respectively (Scheme 24). However, the derivatives **130** did not undergo the oxa-di-π-methane reaction.[78]

Oxa-di-π-methane Rearrangements in Polycyclic-Bridged β,γ-Enones

A variety of compounds containing a β,γ-enone chromophore in a complex molecular framework have been synthesized and their photochemical reactions have been examined. In the majority of the chromophoric systems, the β,γ-enone group is part of a bicyclo[2.2.2]octane framework in which the oxa-di-π-methane reaction is most general and efficient. Mehta and Srikrishna[79] reported an oxa-di-π-methane reaction in the tricyclic compound **131** and its halo analogue that, upon sensitized irradiation, gave **132**. It is interesting to note that $[\pi^{2s}+\pi^{2s}]$-cycloaddition was not observed. Similarly, the β,γ-enone **133** underwent the ODPM reaction to give the compound **134** with a cyclopropane annulated bicyclo[3.3.0]octane framework, in excellent yield (Scheme 25).[80]

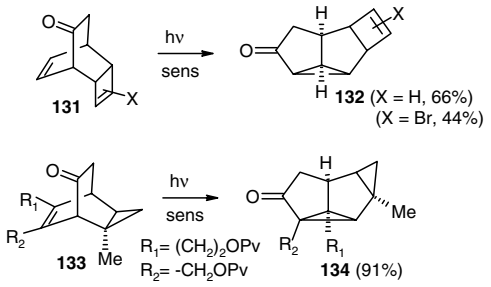

SCHEME 25

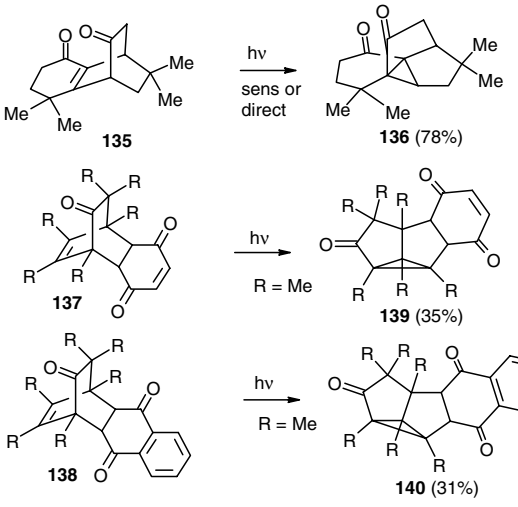

SCHEME 26

The functionally more complex ene-dione **135** also gave an oxa-di-π-methane reaction product **136** upon direct as well as sensitized irradiation. It is suggested that the ODPM occurs from the lowest triplet state (T_1) during direct irradiation.[81] Hart and co-workers[82] examined the photoreaction of the tri- and tetracyclic compounds **137** and **138** in various solvents. Irradiation of **137** in acetone, as well as in acetonitrile, dichloromethane, and cyclohexane, gave the ODPM product **139** in addition to a cage compound as a result of intramolecular [$\pi^{2s}+\pi^{2s}$]-addition. Irradiation of **138** gave the ODPM product exclusively (Scheme 26).

Schmid and Kanagawa reported the photoreaction of the β,γ, γ′, δ′unsaturated ketone **141** and analogues.[83] Thus, the dienone **141** was found to undergo the oxa-di-π-methane (1,2-shift) reaction upon sensitized irradiation in acetone to give **142,** in addition to **143** arising as a result of 1,4-shift. The ratio of **142**:**143** depends on irradiation time. Interestingly, the enedione **144** underwent a very efficient ODPM reaction to yield the tetracyclic product **145** in excellent yield (Scheme 27).[83] Apparently, the photochemistry of the β,γ-enone takes preference over the reaction of the carbonyl group. Schultz and co-workers reported the oxa-di-π-methane rearrangement of ketoesters **148** and their analogues. The ketoesters **148a** and **148c** underwent acetophenone-sensitized irradiation to give **149a** and **149c,** while **148b** gave the corresponding ODPM product upon acetone sensitization, in high yields.[84]

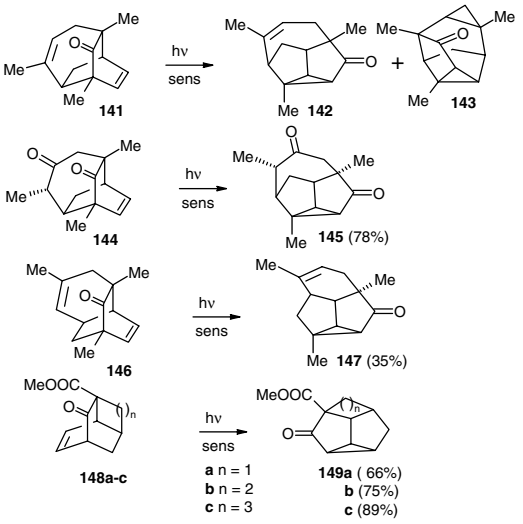

SCHEME 27

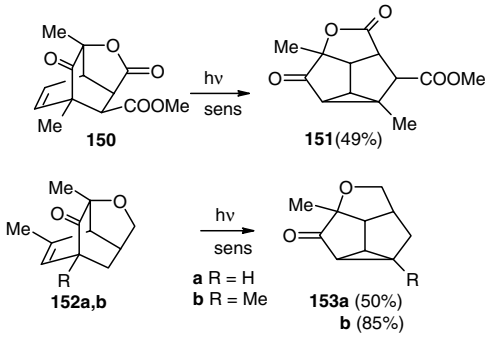

SCHEME 28

Bicyclic[2.2.2]octenones annellated with an oxygen heterocyclic ring also underwent the oxa-di-π-methane reaction upon sensitized irradiation. The tricyclic compounds **150**[66] and **152**[85] gave oxa-di-π-methane products **151** and **153,** respectively, upon sensitized irradiation in acetone (Scheme 28).

Another class of bicyclooctenones whose photoreaction was examined is shown in Scheme 29. Acetone-sensitized irradiation of the tricyclic enones **154a**[86] and **154b**[87] furnished the tetracyclic products **155a** and **155b** in excellent yield and provide a novel method for the synthesis of angular triquinanes. Similarly, the tricyclic compounds **156** and **158** underwent the oxa-di-π-methane reaction upon irradiation in acetone to give the tetracyclic compound **157** containing the [3.3.3]propellane framework and the compound **159,** respectively (Scheme 29).[88,89] The compounds of type **160a–e** containing the δ-keto-β,γ-enone chromophore were also reported to give ODPM products upon direct as well as sensitized irradiation, and the products arise through excited states other than the lowest triplet (Scheme 30).[90,91] It may be noted that the oxa-di-π-methane reaction of these and the other compounds described above provide an efficient preparative route to a variety of carbocyclic systems that are not readily accessible otherwise.

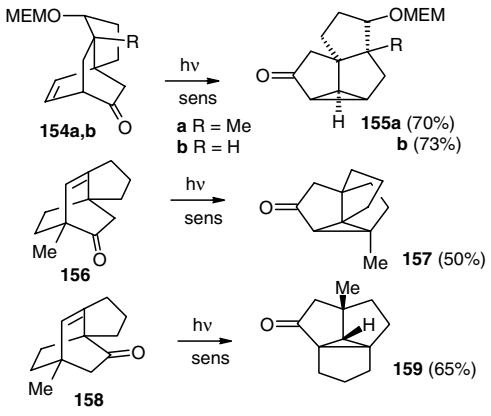

SCHEME 29

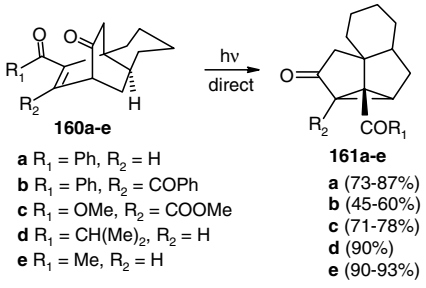

SCHEME 30

Oxa-di-π-methane Reactions in Polycyclic-Bridged β,γ-Enones Leading to the Linear Triquinane Framework

The recent interest in the chemistry of polyquinane natural products[92,93] has stimulated intense activity in the development of novel, efficient, and stereoselective methodologies for the construction of triquinanes, and the oxa-di-π-methane reaction has played a very important role in this endeavor. A number of tricyclic systems containing a β,γ-enone chromophore were designed, and their photochemical reactions upon triplet-sensitized irradiation were investigated and provided excellent routes to triquinanes. The tricyclo[5.2.2.0.^{2,6}]undecanes of type **162**, incorporating an α′–hydroxy-β,γ-enone, are transformed to the tetracyclic compounds **163** on sensitized irradiation[94,95] and are some of the earlier examples of oxa-di-π-methane reaction in such compounds. Other interesting examples include ODPM reactivity in compounds **164**, **165**, and **166,** which gave the tetracyclic compounds **167**, **168**, and **169**, respectively, in good yields (Scheme 31).[95–97] It is interesting to note that no intramolecular cycloaddition was observed during the irradiation of compounds **162**, **165**, and **166**.

Other examples of oxa-di-π-methane rearrangements of the tricyclo[5.2.2.0^{2,6}]undecane framework containing various substituents and functional groups are presented in the Scheme 32. The tricyclic compound **170** underwent an efficient ODPM reaction to give **171** upon acetone-sensitized irradiation (300 nm).[86] A number of other chromophoric systems having substituents and functional groups were prepared and their oxa-di-π-methane reaction was examined. Thus, compounds **172a,b,c**, **174**, **175**, and **178** all underwent oxa-di-π-methane reaction upon sensitized irradiation in acetone to give the corresponding photoproducts (Scheme 32).[98] It is interesting to note that the tricyclic ene-dione **178** gave the

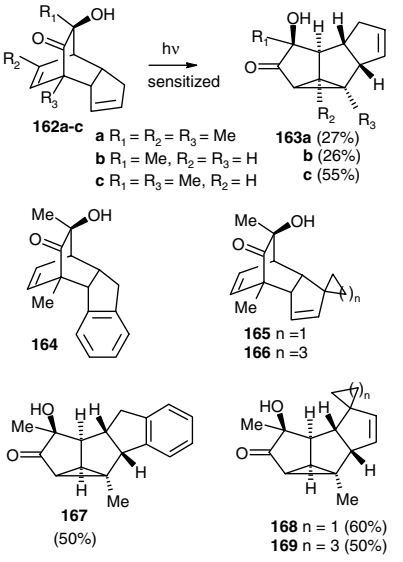

SCHEME 31

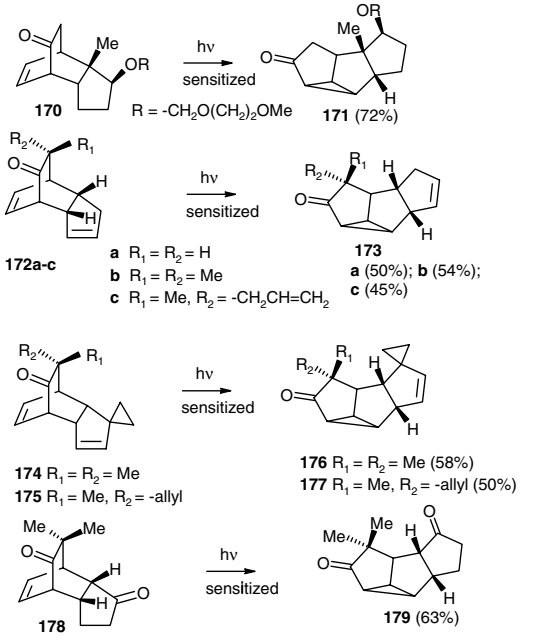

SCHEME 32

ODPM product selectively, even in the presence of the highly reactive carbonyl chromophore present in the five-membered ring.

The *cis:anti:cis*-orientation of the tricyclic framework in the ODPM products depicted above is obviously a result of the *endo*-stereochemistry of the ring annulated to the bicyclo[2.2.2]octenone framework. It should be mentioned that the generation of *cis:anti:cis*-tricyclic framework in a single stereoselective

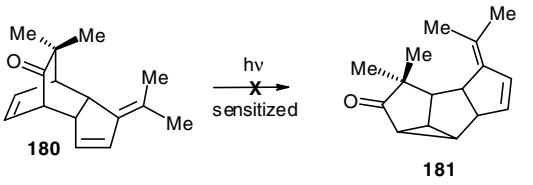

SCHEME 33

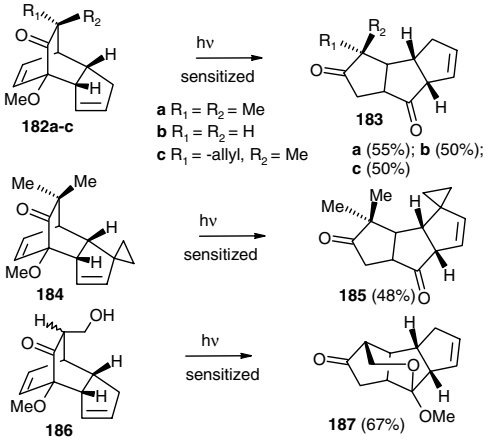

SCHEME 34

photochemical step has made oxa-di-π-methane reactions a potentially useful tool in the synthesis of polyquinane natural products.

Although a number of tricyclic compounds of the type mentioned above were ODPM reactive, sensitized irradiation of the trienone **180** did not give the ODPM product **181** (Scheme 33).[98] This is presumably due to the quenching effect of the *exo*-cyclic-1,3-diene moiety present in the annulated five-membered ring. The trienone **180**, however, undergoes a 1,3-acyl shift on direct irradiation.[98] These observations further confirm the general understanding regarding reactivity vs. excited states of β,γ-enones.

It is evident that the oxa-di-π-methane reaction of the *endo*-tricyclo[5.2.2.0^{2,6}]undecanes depicted above provides tetracyclic compounds containing a linearly fused *cis:anti:cis*-triquinane framework present in many natural products. However, the transformation of ODPM products to the tricyclopentanoid ring requires selective cleavage of the peripheral cyclopropane bond and thus poses various problems of regioselectivity.[97,98] To circumvent this difficulty, another class of *endo*-tricyclo[5.2.2.0^{2,6}]undecanes, with an α-methoxy group in addition to the β,γ-enone chromophore, was synthesized and their photochemical reactions investigated.[99–103] Sensitized irradiation of **182**, **184,** and their congeners were found to furnish the triquinane diones **183** and **185,** respectively, in reasonably good yields, thus providing a direct route to functionalized linear *cis:anti:cis* triquinanes (Scheme 34).[99,100] The photoreaction proceeds through initial oxa-di-π-methane rearrangement, followed by cleavage of the cyclopropane ring, loss of a methyl radical, and hydrogen abstraction.[74,100] Interestingly, tricyclic compounds **186** having hydroxyl methyl group at the α′ position gave the tetracyclic product **187** after sensitized irradiation in acetone (Scheme 34).[100] While the alcohol **188** underwent ODPM reaction to give the highly functionalized tricyclopentanoid **189**, the dienedione **190** gave a complex mixture of products, including the cage compound **191**, arising through intramolecular [$\pi^{2s}+\pi^{2s}$]-cycloaddition, the usual ODPM product **192,** and tricyclic enetrione **193** (Scheme 35).[101]

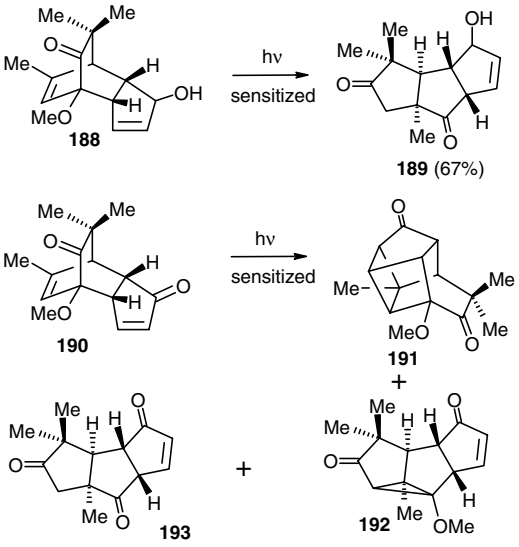

SCHEME 35

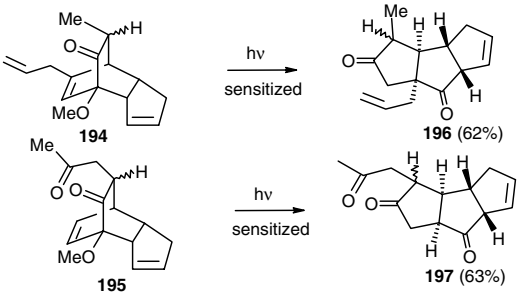

SCHEME 36

In addition to the above examples, more heavily substituted *endo*-tricyclic compounds **194** and **195** also underwent oxa-di-π-methane reaction to give **196** and **197**, respectively, on sensitized irradiation in acetone (Scheme 36).[102] These intermediates were converted into higher polyquinanes.[102] The dominance of the oxa-di-π–methane reaction in **195,** even in the presence of the additional carbonyl chromophore, is noteworthy. Bicyclo[2.2.2]octenones annulated with other higher rings have also been reported to show oxa-di-π-methane reactivity.[98,104]

The aforementioned examples of *endo*-annulated bicyclo[2.2.2]octenones led to photoproducts containing a linear *cis:anti:cis*-triquinane framework. The stereochemical feature of the photoproducts in these examples is a direct consequence of stereoselectivity in the ODPM reaction and the orientation of the annulated ring. It is interesting to note that the sensitized irradiation of compound **198** with an *exo*-annulated five-membered ring gave the tetracyclic compound **199** containing a folded *cis:syn:cis*-triquinane ring system (Scheme 37).[105]

Oxa-di-π-methane Reactions in Miscellaneous Carbocyclic β,γ-Enones

The compound **200** with a bicyclo[3.2.2]nonadienone ring system underwent oxa-di-π-methane reaction involving the C–C double bond in the ethano-bridge. This gives the product **201** selectively upon

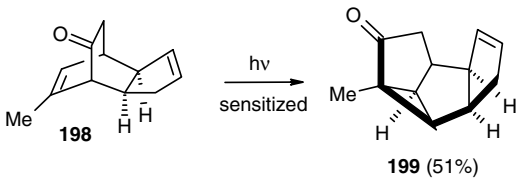

SCHEME 37

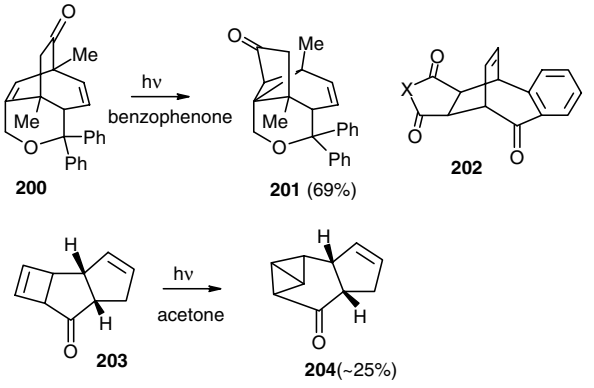

SCHEME 38

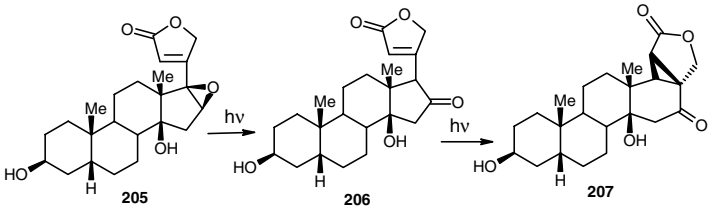

SCHEME 39

benzophenone-sensitized irradiation.[106] Other closely related compounds did not give ODPM products. Other benzo annulated compounds of type **202** did not undergo the ODPM reaction; instead, a di-π-methane reaction was observed upon sensitized irradiation.[107] Murata and co-workers reported oxa-di-π-methane reactions in the tricyclic compound **203** that gave the highly strained ring system **204** (Scheme 38).[108]

The steroidal epoxy compound **205** was reported to undergo rearrangement to the ketone **206,** which subsequently underwent an oxa-di-π-methane reaction to give the cyclopropyl compound **207** along with its stereoisomer and other compounds (Scheme 39).[109]

Recently, Sulikowski reported the oxa-di-π-methane rearrangement of **208a** with a bicyclo[4.4.1]undecane framework and a cross-conjugated dienone moiety in one of the bridges. This rearranges to **209a** upon direct irradiation in benzene. This reaction provides an interesting avenue to convert the bicyclo[4.4.1]undecane ring into a bicyclo[5.3.1]undecane ring system of taxanes. However, the analogue with a methoxy group at the bridgehead did not react by this path and instead undergoes a 1,3-acyl shift (Scheme 40).[110]

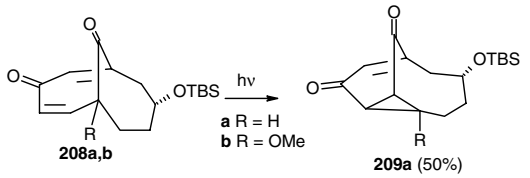

SCHEME 40

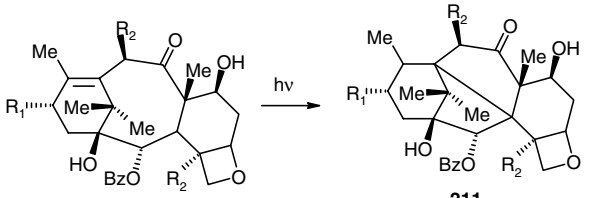

R_1 = -COCH(OH)CH(Ph)NHCOC$_6$H$_5$
R_2 = OCOCH$_3$

SCHEME 41

Taxol has been reported to undergo a highly interesting photochemical reaction that is dependent on the irradiation wavelength, the solvent, and also remote functional groups. Irradiation of taxol **210** at 280 nm in CCl_4 gave a pentacyclic isomer **211** in 55% yield (Scheme 41).[111] Similar results were also obtained in solvents such benzene and toluene, although the yield of the photoproduct was low. However, irradiation in acetone did not yield the pentacyclic isomer **211**. Remarkably, this photoreaction involves intramolecular energy transfer. The photoreaction proceeds through initial oxa-di-π-methane reaction via excitation of CO [$T_1(\pi\pi^*)$] group at C9, followed by migration of a hydrogen atom from C3 and subsequent bond formation between C3 and C11.[111]

Oxa-di-π-methane Reactions in the Synthesis of Natural Products

It may be evident from the foregoing examples that the oxa-di-π-methane rearrangement is a highly general reaction of β,γ-enones. A variety of substrates, especially those with constrained ring systems, undergo efficient ODPM reactions leading to different molecular frameworks in a stereo- and regioselective fashion. These systems are not readily accessible otherwise. However, its true synthetic potential was realized only recently. As a consequence, many types of chromophoric systems containing a β,γ-enone chromophore were synthesized and the oxa-di-π-methane reaction was employed in the synthesis of compounds of both natural and unnatural origin.[92,93,112] Some examples of the synthesis of natural products in which the ODPM reaction was employed as a key element are presented below. In such synthetic approaches, the assembly of the appropriate chromophoric system is also one of the important aspects and in many cases new methods were developed.

Demuth and co-workers reported the synthesis of a number of natural products containing a cyclopentane ring, such as boschnialactone, allodolicholactone, iridomyrmecin, and isoiridomyrmecin, employing a common intermediate **212** obtained by the oxa-di-π-methane rearrangement. Thus, cleavage of the cyclopropane ring with sodium–ammonia gave the diastereomers **213** and **214**. The intermediate **213** was converted to boschnialactone **215,** and the diastereomer **214** was elaborated to the allodolicholactone **216**. This latter compound was converted into iridomyrmecin and isoiridomyrmecin (Scheme 42).[65] The authors have also employed the ODPM reaction in an enantiospecific synthesis of loganin aglucone

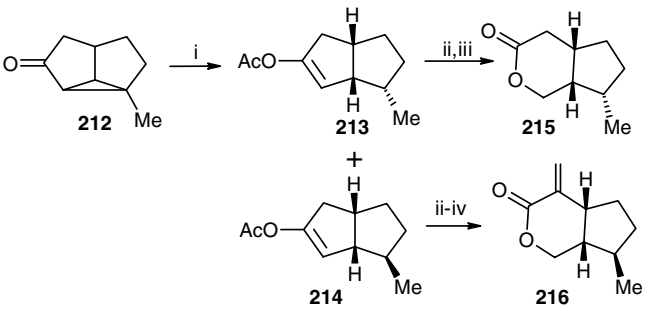

Reagents/conditions: (i) Na, NH_3, ^{t}BuOH, Ac_2O, 60%; (ii) OsO_4, $NaIO_4$; (iii) $NaBH_4$, H_3O^+, 84%; (iv) $CH_2{=}N(Me)_2I$, LDA, MeI, DBN

SCHEME 42

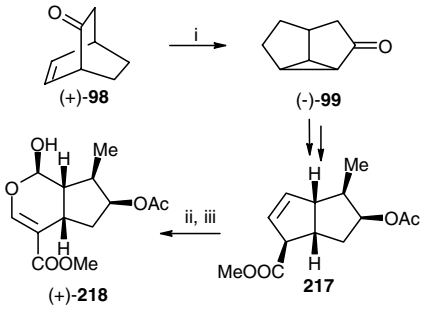

Reagents/conditions: (i) hν, acetophenone, 84%; (ii) OsO_4, $Na_2S_2O_5$; (iii) $NaIO_4$ (50% for both steps)

SCHEME 43

acetate **218,** as shown in Scheme 43. Kon and Isoe have developed an alternate strategy for the synthesis of loganin from the same precursor **212**. [113]

Liao and co-workers carried out the synthesis of (±)-forsythide aglucone dimethyl ester **220** (Scheme 44). Cycloaddition of masked *o*-benzoquinone with DMAD was used to prepare the desired bicyclo[2.2.2]octenone **110**, which upon sensitized irradiation gave the diquinane intermediate **112**. Cleavage of the cyclopropane ring and functional group manipulation led to the dihydroxydiester **219,** which upon oxidative cleavage gave **220.**[70] In another synthesis of forsythide, the diquinane intermediate **98** was employed as a precursor.[114]

Studies on the synthesis of cedranoids, a class of sesquiterpenes that contains a bicyclo[3.2.1]octane ring system as well as diquinane ring, by Yates et al. constitute some of the earlier examples of the use of the oxa-di-π-methane reaction as a key step in this synthetic strategy.[66,67,115,116] Thus, the bicyclic compound **221** was prepared from 2,6,6-trimethylcyclohex-2-en-1,4-dione. Treatment with sodium methoxide furnished the bicyclic chromophoric system **222**, which contains the 12 carbons of a sesquiterpene and the diquinane framework in latent form. Sensitized irradiation of **222** in acetophenone provided the compound **223** in excellent yield. Cleavage of the cyclopropane ring and selective functional group manipulation, followed by the introduction of a two-carbon unit, gave the intermediate **224**. Cyclization gave the compound **225** containing the tricyclic framework of cedranoids. This was elaborated to cedranoid sesquiterpenes, biotols **226** (Scheme 45).[67,115]

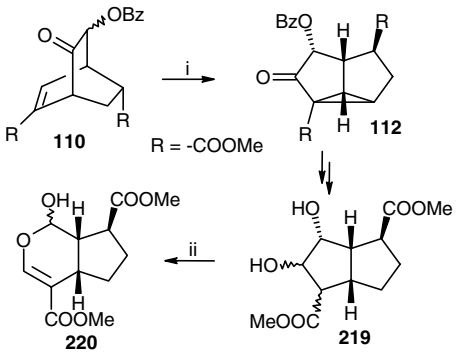

Reagents/conditions: (i) hν, acetone, 60%;
(ii) $Pb(OAc)_4$, K_2CO_3, 82%

SCHEME 44

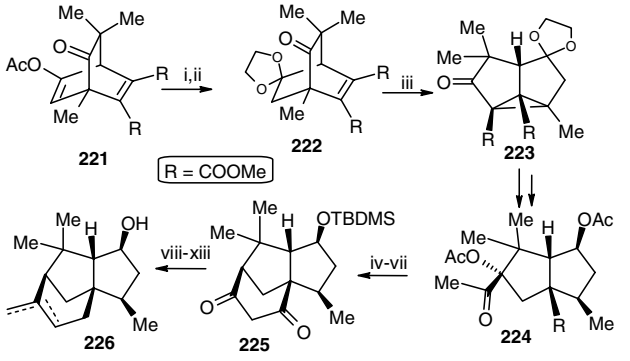

Reagents/conditions: (i) NaOMe,83%; (ii) $HOCH_2CH_2OH$, H^+,92%;
(iii) hν, $PhCOCH_3$, 94%; (iv) $^nBu_3SnH$, AIBN, 91%; (v) K_2CO_3, 100%;
(vi) TBDMSOTf, lutidine, 85%; (vii) KO^tBu, 96%; (viii) LAH; (ix) CrO_3: Py;
(x) H_2, Pd-C, 74%(viii-x); (xi) MeLi, 95%; (xii) $SOCl_2$, Py, 81%; (xiii) HF,

SCHEME 45

Demuth and Hinsken reported the first synthesis of enantiomerically pure (−)-silphiperfol-6-en-5-one **228** from the optically pure tricyclic compound (+)-**154a** whose irradiation in acetone at 300 nm gave the ODPM product (−)-**155a**. This product contains most of the structural and functional features of **228**. Cleavage of the cyclopropane ring, introduction of a methyl group, and deoxygenation of the CO group furnished the triquinane intermediate **227** that was elaborated into the natural product **228** (Scheme 46).[117]

Uyehara and co-workers also employed the oxa-di-π-methane rearrangement to develop a common strategy for the formal syntheses of (±)-isocomene and (±)-modhephene.[118] The required bicycloocten-ones **229** and **232** were prepared from a common bicyclo[3.2.1]octenone precursor in several steps. The oxa-di-π-methane reaction of **229** gave the diquinane **230** in excellent yield. Cleavage of the cyclopropane ring and further manipulation led to the triquinane **231** containing the framework of isocomene. The keto-alcohol **231** was then elaborated to a known intermediate for isocomene. Similarly, photoreaction of the bicyclic octenone **232** gave the ODPM product **233** that was manipulated to give the intermediate **234** for modhephene (Scheme 47).[118]

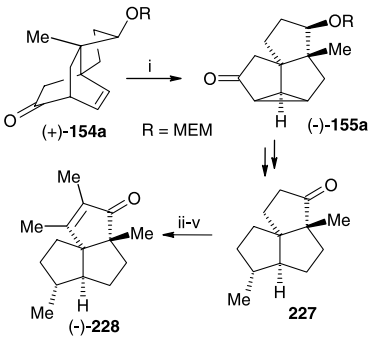

Reagents/conditions: (i) hν, acetone, 70%; (ii) LDA, TMSCl; (iii) DDQ, N,O-bis(trimethylsilyl)-2,2,2,-trifluoroacetamide, r.t., 70% yield for steps (ii, iii); (iv) Me_2CuLi, MeI, HMPA; v, DDQ, N,O-bis(trimethylsilyl)-2,2,2-trifluoroacetamide, 45°C, 52% yield for steps (iv, v)

SCHEME 46

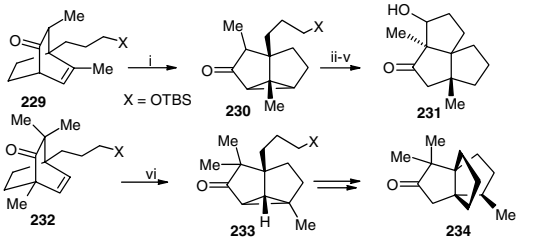

Reagents/conditions:(i) hν, acetone, 83%; (ii) Li, NH_3, 75%; (iii) TBAF, 99%; (iv) CrO_3:Py; (v) KOH, MeOH, 83%; (vi) hν, 91%

SCHEME 47

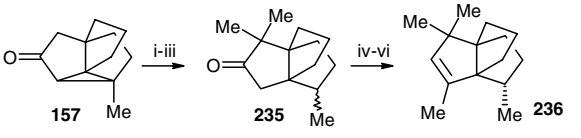

Reagents/conditions: (i) KO^{t}Bu, MeI, 65%; (ii) Li, NH_3, (iii) PCC, 75%; (iv) LHMDS, MeI, 60%; (v) LAH, ether, 68%; (vi) $POCl_3$,Py, DBU 38%

SCHEME 48

Mehta's approach to modhephene also relied on the oxa-di-π-methane reaction. In this approach, the tricyclic compound **157** with the propellane framework of modhephene was directly generated by the ODPM reaction of the tricyclic system **156** (*vide supra*). The intermediate **157** was then elaborated into (±)-modhephene **236** (Scheme 48).[89] Thus, alkylation, reductive cleavage of the cyclopropane ring, followed by oxidation, gave the intermediate **235.** Alkylation followed by reduction of the carbonyl group gave a mixture of alcohols that was separated and the desired stereoisomer was treated with $POCl_3$ to give the natural product modhephene **236.**

Paquette and co-workers employed the oxa-di-π-methane product **134** for the synthesis of the antibiotic pentalenolactone P methyl ester, a highly functionalized sesquiterpene lactone. The oxa-di-π-methane reaction of **133** into **134** sets most of the stereochemical requirements of the target in a highly

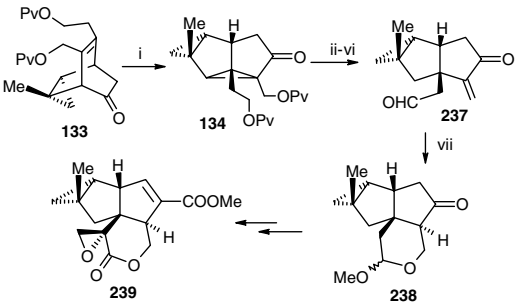

Reagents/conditions: (i) hν, acetone, 91%; (ii) NaOH, H_2O, EtOH, 80%; (iii) Li, NH_3; (iv) Ac_2O, DMAP; (v) Na_2CO_3, MeOH, H_2O, 62% yield for steps (iii-v); (vi) Swern oxidation; (vii) NaOMe, MeOH, 62% yield for steps (vi, vii)

SCHEME 49

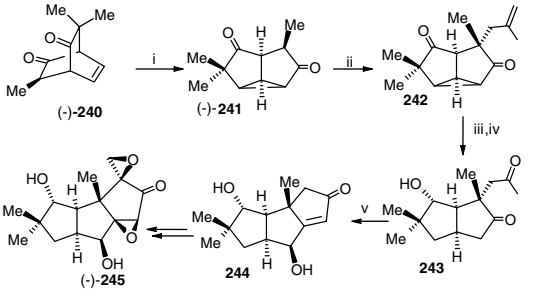

Reagents/conditions: (i) hν, acetone, 74%; (ii) methylallyl chloride, KBr, ^{t}BuOH, ^{t}BuOK, toluene, 95%; (iii) Li, NH_3; (iv) OsO_4, $NaIO_4$, 43% yield for steps (iii and iv); (v) ^{t}BuOK, ^{t}BuOH, toluene, p-TsOH, reflux, ozone, 36%

SCHEME 50

selective fashion. Thus, **134** was converted to the enone aldehyde **237**. Reaction of **237** with methanolic sodium methoxide furnished the intermediate **238** having the tricyclic framework of pentalenolactone. Further manipulation gave the *dl*-pentalenolactone P methyl ester **239** (Scheme 49).[119]

Synthesis of (−)-coriolin **245**, a triquinane antibiotic, by Demuth and co-workers is one of the earliest examples wherein the oxa-di-π-methane reaction of the optically pure bicyclo[2.2.2]octenone **240** was a key step.[120] The requisite chromophoric system (−)-**240** was synthesized from hydroquinone and maleic anhydride in several steps, including resolution. Sensitized irradiation of **240** gave the diquinane intermediate **241** containing 11 of the carbons of coriolin. Introduction of an allyl chain, followed by reductive cleavage of the cyclopropane ring and oxidative degradation, furnished the intermediate **243** that was ready for annelation to create the third cyclopentane ring. Aldol condensation in **243** gave the tricyclic compound **244,** which was elaborated to coriolin (Scheme 50).[120]

It can be seen from the above examples that most of the syntheses involve diquinane intermediates that are generated by the oxa-di-π-methane reaction. The third ring is usually created through annelation. *endo*-Tricyclo[5.2.2.$0^{2,6}$]undecane skeleta of the type represented by **172** and **182** (*vide supra*) have been used as an approach to the synthesis of tricyclopentanoid natural products. It was envisaged that the oxa-di-π-methane reaction of such systems would lead directly to carbocyclic frameworks containing a *cis:anti:cis*-fused triquinane ring system in a single step. It was further postulated that such a methodology would provide an efficient and stereoselective route to polyquinane natural products. Syntheses of

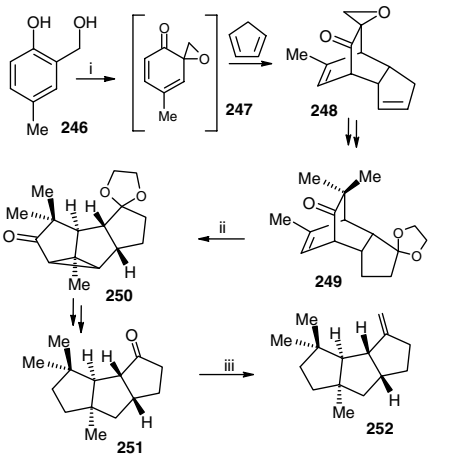

Reagents/conditions; (i) aq. $NaIO_4$, MeCN-H_2O, 85%; (ii) hν, acetone, 64%; (iii) $PPh_3{=}CH_2$, toluene, Δ, 72%

SCHEME 51

capnellene, coriolin, and hirsutene were achieved employing the oxa-di-π-methane reaction of strategically designed tricyclic chromophoric systems.

Capnellene **252**, a sesquiterpene isolated from marine soft coral *Capnella imbricata*, has been a popular target for synthesis due to its role in biosynthesis and defense mechanisms. It also served as a test case for cyclopentane construction.[92,93] Photochemical oxa-di-π-methane reaction provided a novel, stereoselective, and efficient route to (±)-capnellene, as shown in Scheme 51. The *endo*-tricyclic chromophoric system **249** was synthesized from *p*-cresol. Controlled hydroxymethylation of *p*-cresol gave **246**, which upon oxidation with sodium metaperiodate generated the spiroepoxycyclohexa-2,4-dienone **247** that was intercepted with cyclopentadiene to give the *endo*-adduct **248**. Manipulation of the oxirane ring and the annulated five-membered ring furnished the intermediate **249** containing 14 carbons, including the angular and geminal methyl groups and the tricyclic framework of capnellene in latent fashion. Sensitized irradiation of **249** provided the tetracyclic compound **250** in a stereoselective fashion and in very good yield. Cleavage of the peripheral cyclopropane bond, Barton deoxygenation of the carbonyl group, followed by hydrolysis of the ketal group, yielded the ketone **251**. Methylenation by a Wittig reagent furnished (±)-capnellene (Scheme 51).[121,122]

A synthesis of coriolin was devised starting from the aromatic precursor **253**. This was readily transformed into epoxyketone **254** containing a β,γ-enone chromophore. Deoxygenation of the oxirane ring and functionalization of the five-membered ring furnished the crucial tricyclic compound **255** with the major structural and functional features of coriolin. Sensitized irradiation gave the intermediate **256** in good yield. This was then elaborated to the triquinane **257**, a known precursor to coriolin (Scheme 52).[123,124] In yet another formal synthesis of coriolin, the triquinane intermediate **263** was synthesized in a stereoselective fashion via oxa-di-π-methane reaction of the unusual chromophoric system **261** with a five-membered ring attached to one of the bridgeheads. The required chromophoric system was obtained via *in situ* generation of **259** and intramolecular Diels-Alder reaction, followed by manipulation of the resulting adduct (Scheme 53).[125] More recently, a synthesis of hirsutene was also developed as shown in Scheme 54. The tricyclic chromophoric system **265** was prepared by oxidation of salicyl alcohol, followed by manipulation of the resulting adduct and introduction of a methyl group at the ring junction. Oxa-di-π-methane reaction of **265** occurred efficiently and led to the key intermediate **266** that can be readily elaborated to (±)-hirsutene. [126]

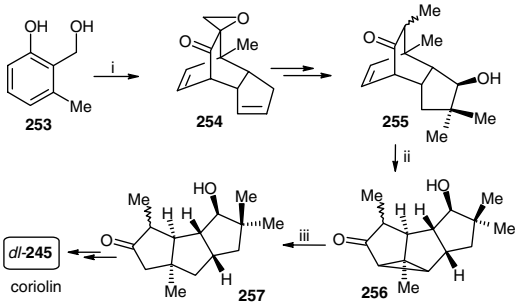

Reagents/conditions; (i) $NaIO_4$, cyclopentadiene, MeCN-H_2O, 45%; (ii) hν, acetone, 65%; (iii) $n(Bu)_3SnH$, toluene, Δ, 61%

SCHEME 52

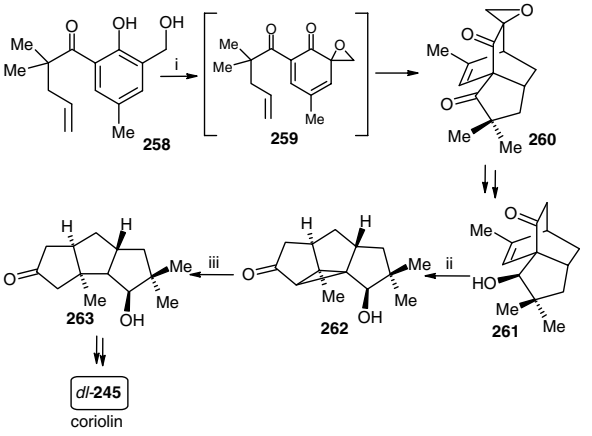

Reagents/conditions; (i) $NaIO_4$, MeCN-H_2O,71%; (ii) hν, acetone, 78%; (iii) $n(Bu)_3SnH$, toluene, Δ, 70%

SCHEME 53

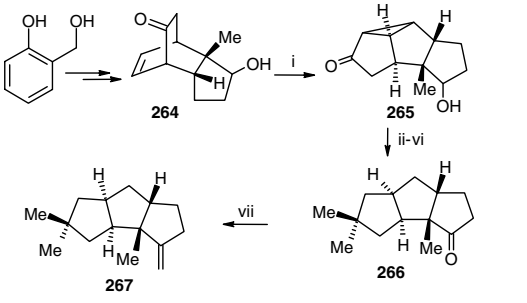

Reagents/conditions; (i) hν, acetone, 70%; (ii) $n(Bu)_3SnH$, toluene, Δ, 65%; (iii) $Ph_3P{=}CH_2$, 80%; (iv) CH_2I_2, Et_2Zn, 46%; (v) H_2, PtO_2, AcOH,74 %; (vi) PCC. CH_2Cl_2, 71 %; (vii) $Ph_3P{=}CH_2$, 44%

SCHEME 54

78.8 Conclusions

The photochemical reactions of β,γ-enones, especially the oxa-di-π-methane rearrangement or 1,2-acyl shift that began with curiosity about the spectroscopic properties, has evolved into a sub-area of organic photochemistry. Studies on β,γ-enones led to an enhanced understanding of interactions between the alkene and carbonyl chromophores and provided a sound mechanistic picture of the photochemical processes and relationship between excited states and reactivity (despite the debate on singlet–triplet dichotomy). It may be seen from the foregoing discussion that a vast number of compounds with varying structural and functional features undergo the oxa-di-π-methane reaction. Further, oxa-di-π-methane rearrangements appear to be highly general and versatile reactions, especially in rigid systems wherein there exists the possibility of homoconjugation or interaction between the two chromophores. The oxa-di-π-methane reaction has far-reaching significance from a synthetic viewpoint because it provides reaction paths to numerous structural types in a highly stereo- and regioselective manner. The ODPM reaction has been extremely rewarding for the synthesis of cyclopentanoidal natural products. It appears that the design and availability of the requisite chromophoric system may prove to be a limitation — and not the oxa-di-π-methane reaction itself. In the future, it is likely that the oxa-di-π-methane reaction will play a much greater role in organic synthesis.

Acknowledgments

The author thanks DST, CSIR New Delhi, and BRNS Bombay for their continued support. The author is also grateful to his students, whose dedicated efforts led to the results, some of which have been reported herein. Thanks also to Professor A. Srikrishna for his kindness and support in our endeavor.

References

1. Hixson, S.S., Mariano, P.S., and Zimmerman, H.E., The di-π-methane and oxa-di-π-methane Rearrangements, *Chem. Rev.*, 73, 531, 1973.
2. Dauben, W.G., Lodder, G., and Ipakstchi, J., Photochemistry of β-γ-unsaturated ketones, *Top. Curr. Chem.*, 54, 73, 1975.
3. Houk, K.N., The photochemistry and spectroscopy of β,γ-unsaturated carbonyl compounds, *Chem. Rev.*, 76, 1, 1976.
4. Schuster, D.I., in *Rearrangement in Ground and Excited States*, de Mayo, P., Ed., Academic Press, New York, 1980, Vol. 3, 167 and references cited therein.
5. Schaffner, K. and Demuth, M. in *Modern Synthetic Methods*, Scheffold, R., Ed., Springer Verlag, Berlin 1986, Vol 4, 61.
6. Zimmerman, H.E., The di-π-methane rearrangement, *Org. Photochem.*, 11, 1, 1991.
7. Zimmerman, H.E. and Armesto, D., Synthetic aspects of the di-π-methane rearrangement, *Chem. Rev.*, 96, 3065, 1996 and references cited therein.
8. Givens, R.S. and Oettle, W.F., Photorearrangement of a γ-butyrolactone; generation of intermediates in photochemical reactions, *J. Chem. Soc. D.*, 1164, 1969.
9. Coffin, R.L., Givens, R.S., and Carlson, R.G., Stereospecificity in triplet state photorearrangements. The oxa-di-π-methane photorearrangement. Mechanistic studies in photochemistry, *J. Am. Chem. Soc.*, 96, 7554, 1974.
10. Coffin, R.L., Cox, W.W., Carlson, R.G., and Givens, R.S., Photochemical studies on the mechanism of the oxa-di-π-methane rearrangement. An example of a stereospecific rearrangement, *J. Am. Chem. Soc.*, 101, 3261, 1979.
11. Dauben, W.G., Lodder, G., and Robbins, J.D., The "methane carbon" stereochemistry of the acyclic oxa-di-π-methane photo rearrangement, *J. Am. Chem. Soc.*, 98, 3030, 1976.
12. Henne, A., Siew, N.P.Y., and Schaffner, K., S1 vs T2 photoreactivity of β,γ-unsaturated ketones. Temperature dependant photo-CIDNP of 2-cyclopentenyl methyl ketones, *J. Am. Chem. Soc.*, 101, 3671, 1979.

13. Calcaterra, L.T. and Schuster, D.I., Observation of an unprecedented heavy-atom effect on the rate of 1n,π in a β,γ-unsaturated ketone, *J. Am. Chem. Soc.*,103, 2460, 1981.
14. Wilsey, S., Bearpark, M.J., Bernardi, F., Olivucci, M., and Robb, M.A., Mechanism of the oxa-di-π-methane and [1,3]-acyl sigmatropic rearrangements of β,γ-enones: A theoretical study, *J. Am. Chem. Soc.*, 118, 176, 1996.
15. Engel, P.S. and Schexnayder, M.A., Effect of ring size on the photochemical behaviour of β,γ-unsaturated ketones, *J. Am. Chem. Soc.*, 94, 9252, 1972.
16. Tenny, L.P., Boykin Jr., D.W., and Lutz, R.E., Novel photocyclization of a highly phenylated β,γ-unsaturated ketone to a cyclopropyl ketone, involving benzoyl group migration, *J. Am. Chem. Soc.*, 88, 1835, 1966.
17. Dauben, W.G., Kellogg, M.S., Seeman, J.I. and Spitzer, W.A., Photochemical rearrangement of an acyclic β,γ-unsaturated ketone to a conjugated cyclopropyl ketone. An oxa-di–π-methane rearrangement, *J. Am. Chem. Soc.*, 92, 1786, 1970.
18. Eichenberger, von H., Tsutsumi, K., de Weck, G., and Wolf, H.R., Photochemische reaktionen Zur photochemie konjugierter δ-keto-enone und β,γ,δ,ε–ungesattigter ketone, *Helv. Chim. Acta*, 63, 1499, 1980.
19. Van der Weerdt, A.J.A. and Cerfontain, H., Photochemistry of β,γ-unsaturated ketones. V. The direct irradiation of some γ-phenyl β,γ-enones, *Tetrahedron*, 37, 2121, 1981.
20. Cowan, D.O. and Baum, A.A., Intramolecular triplet-energy transfer, *J. Am. Chem. Soc.*, 93, 1153, 1971.
21. Schexnayder, M.A. and Engel, P.S., Systematic structural modifications in the photochemistry of β,γ-unsaturated ketones. II. Acyclic olefins and acetylenes, *J. Am. Chem. Soc.*, 97, 4825, 1975.
22. Hancock, K.G., Wylie, P.L., and Lau, J.T., Photochemistry of α-hydroxy-β,γ-unsaturated ketones: a photochemical synthesis of 1,4-diketones, *J. Am. Chem. Soc.*, 99, 1149, 1977.
23. Van der Weerdt, A.J.A. and Cerfontain, H., Photochemistry of acyclic β,γ-unsaturated ketones. 4. The effect of α-methyl substitution with some hex-4-en-2-ones and 1-phenylpent-3-en-1-ones, *J. Chem. Soc., Perkin Trans. 2*, 592, 1980.
24. Pratt, A.C., Photochemistry of β,γ-unsaturated carbonyl compounds. 3,3-Dimethyl-5,5-diphenylpent-4-en-2-one and 2,2-dimethyl-4,4-diphenylbut-3-enal, *J. Chem. Soc, Perkin Trans. 1*, 2496, 1973.
25. Baggiolini, E., Hamlow, H.P., and Schaffner, K., Photochemical reactions. LIX. Mechanism of the photodecarbonylation of β,γ-unsaturated aldehydes, *J. Am. Chem. Soc.*, 92, 4906, 1970.
26. Durr, H., Heitkamper, P., and Herbst, P., Eine neue synthese von cyclopentenaldehyden und ihre photofragmentierung, *Tetrahedron Lett.*, 1599, 1970.
27. Zimmerman, H.E. and Cassel, J.M., Unusual rearrangements in di-π-methane systems: mechanistic and exploratory organic photochemistry, *J. Org. Chem.*, 54, 3800, 1989.
28. Armesto, D., Ortiz, M.J., and Romano, S., The oxa-di-π-methane rearrangement of β,γ-unsaturated aldehydes, *Tetrahedron Lett.*, 36, 965, 1995.
29. Armesto, D., Ortiz, M.J., Romano, S., Agarrabeitia, A.R., Gallego, M.G., and Ramos, A., Unexpected oxa-di-π-methane rearrangement of β,γ-unsaturated aldehydes, *J. Org. Chem.*, 61, 1459, 1996.
30. Gonzenbach, H.-U., Tegmo-Larsson, I.-M., Grosclaude, J.-P., and Schaffner, K., The photochemistry of 2-cyclopentenyl methyl ketones, *Helv. Chim. Acta*, 60, 1091, 1977.
31. Engel, P.S. and Schexnayder, M.A., Systematic structural modifications in the photochemistry of β,γ-unsaturated ketones. I. Cyclic olefins *J. Am. Chem. Soc.*, 97, 145, 1975 and references therein.
32. Koppes, M.J.C.M. and Cerfontain, H., Photochemistry of β,γ-enones. 11. Photochemical reactivities of cyclic-α-phenyl β,γ-enones. Singlet 1,3-acyl shift, decarbonylation and unquenchable oxa-di-π-methane reactions upon direct irradiation., *Recl. Trav. Chim. Pays-Bas*, 107, 549, 1988.
33. Plank, D.A. and Floyd, J.C., Photorearrangement of a 4-benzoylcyclopentenone, *Tetrahedron Lett.*, 4811, 1971.
34. Oren, J., Schleifer, L., Weinman, S., and Fuchs, B., Unusual photorearrangements of homoconjugated diacylcyclohexa-2,4-dienes, *J. Chem. Soc., Chem. Commun.*, 315, 1988.

35. Borecka, B., Gudmundsdottir, A.D., Olovsson, G., Ramamurthy, V., Scheffer, J.R., and Trotter, J., An ionic heavy atom effect in the solid state photochemistry of a β,γ-unsaturated ketone, *J. Am. Chem. Soc.*, 116, 10322, 1994.
36. Pfenninger, E., Poel, D.E., Berse, C., Wehrli, H., Schaffner, K., and Jeger, O., Photochemische reaktionen. Zur photochemie von α,β-ungesattigten γ-aldehydoketonen I. Die UV – Bestrahlung von 3,19-dioxo-17β-acetoxy-Δ^4-androsten, *Helv. Chim. Acta*, 51, 772, 1968.
37. Hart, H., Collins, P.M., and Waring, A.J., Preparation, chemistry and photochemistry of hexaalkyl-2,4-cyclohexadienones, *J. Am. Chem. Soc.*, 88, 1005, 1966.
38. Sundararajan, U. and Ramamurthy, V., Enhanced enantio- and diastereoselectivities via confinement: photorearrangement of 2,4-cyclohexadienones included in zeolites, *Org. Lett.,* 4, 87, 2002.
39. Paquette, L.A., Eizember, R.F., and Cox, O., Photochemical transformations of selected 3-cycloheptenone derivatives, *J. Am. Chem. Soc.*, 90, 5153, 1968.
40. Hancock, K.G. and Grider, R.O., A free rotor effect in β,γ-unsaturated ketone photochemistry. The diverging singlet and triplet reactions of 3-ethylidene-2,2,5,5-tetramethylcyclohexanone *Tetrahedron Lett.*, 1367, 1972.
41. Engel, P.S., Schexnayder, M.A., Ziffer, H., and Seeman, J.I., The effect of α-methyl groups on the photochemistry of 3,4,5,6,7,8-hexahydronaphthalene-2(1*H*)-one, *J. Am. Chem. Soc.*, 96, 924, 1974.
42. Winter, B. and Schaffner, K., Photochemistry of a cyclohex-3-enone. Evidence for a stepwise pathway in an oxa-di-π-methane rearrangement, *J. Am. Chem. Soc.*, 98, 2022, 1976.
43. Sato, H., Nakanishi, K., Hayashi, J., and Nakadaira, Y., Structural aspects of photosensitized β,γ-enone isomerizations, *Tetrahedron*, 29, 275, 1973.
44. Greenland, H., Kozyrod, R.P., and Pinhey, J. T., The photochemistry of 2,2-dimethyl- and 2-aryl-2-methylnaphthalen-1(2H)-ones. Substitution requirement for the oxa-di-π-methane rearrangement, *J. Chem. Soc., Perkin Trans. 1*, 2011, 1986.
45. Cheung, E., Netherton, M.R., Scheffer, J.R., and Trotter, J., Linearly conjugated benzocyclohexadienone photochemistry in the solid state: ionic chiral auxiliary mediated asymmetric induction, *Tetrahedron Lett.,* 40, 8737, 1999.
46. Kojima, K., Sakai, K., and Tanabe, K., The photosensitized rearrangement of β,γ-unsaturated ketosteroids, *Tetrahedron Lett.*, 1925, 1969.
47. Domb, S. and Schaffner, K., Photochemical reactions. 58[1]. On the mechanism of the rearrangement of the triplet excited α,β-unsaturated δ-diketone 3,7-dioxo-4,4-dimethyl-17β-acetoxy-Δ^5-androstene, *Helv. Chim. Acta*, 53, 677, 1970.
48. Williams, J.R. and Ziffer, H., Photochemical rearrangement of β,γ-unsaturated cyclic ketones, *Tetrahedron*, 24, 6725, 1968.
49. Suginome, H., Ohtsuka, T., Yamamoto, Y., Orito, K., Jaime, C., and Osawa, E., Photoinduced molecular transformations. 109. Conformational dependence of the stereochemistry of photochemical 1,3-acylshift of β,γ-unsaturated cyclic ketones: conformation specific photorearrangements of steroidal β,γ-unsaturated cyclic ketones, 7a-homocholest-5-en-7a-one and 4a-homo-5α-cholest-1-en-4-one, *J. Chem. Soc., Perkin Trans. 1*, 1247, 1990.
50. Williams, J.R. and Sarkisian, G.M., [1,3] vs [1,2] Sigmatropic photorearrangements in cyclic β,γ-unsaturated ketones. Conversion of bicyclo[5.4.0]undec-1(7)en-3-one into 6-methylenespiro[4,5]decan-1-one, *J. Chem. Soc., Chem. Commun.,* 1564, 1971.
51. Oren, J., Vardi, M., Viskin, R., Abramson, S., and Fuchs, B., Homoconjugated ketones with extended unsaturation: wavelength selective, diastereoselective and enantiospecific photochemical transformations of methyl 7-oxospiro[5.5]undeca-1,3-and 2,4-diene-2-carboxylate, *Helv. Chim. Acta,* 76, 1182, 1993.
52. Oren, J. and Fuchs, B., Irradiation-induced transformations of homoconjugated dienones. Highly selective photorearrangements in the spiro[5.5]undeca-1,3-dien-7-one system, *J. Am. Chem. Soc.,* 108, 4881, 1986.

53. Lyle, T.A., Mereyala, H.B., Pascuel, A., and Frei, B., Photochemical reactions. Photochemistry of homoconjugated cyclobutanones. II. Decisive effect of *gem*-dimethyl substitution on the course of oxa-di-π-methane rearrangement, *Helv. Chim. Acta*, 67, 774, 1984 and references therein.
54. Ipakstchi, J., Photochemie β,γ-ungesattigter ketone. IV. Photoisomerisierung von bicyclo[2.2.1]hepten-(5)-on-(2)-derivaten, *Chem. Ber.*, 105, 1840, 1972.
55. Schexnayder, M.A. and Engel, P.S., Triplet photosensitization of 2-norbornenone and other β,γ-unsaturated ketones, *Tetrahedron Lett.*, 1153, 1975.
56. Sadeghpoor, R., Ghandi, M., Najafi, H.M., and Farzaneh, F., The oxa-di-π-methane rearrangement of β,γ-unsaturated ketones induced by the external heavy atom cation effect within a zeolite, *J. Chem. Soc., Chem. Commun.,* 329, 1998.
57. Sindler-Kulyk, M., Majerski, Z., Pavlovic, D., and Mlinaric-Majerski, K., Synthesis of 2,8-didehydro-9-noradamantanone, *Tetrahedron Lett.,* 30, 3577, 1989.
58. Givens, R.S., Chae, W.K., and Matuszewski, B., Singlet-triplet reactivity of a β,γ-unsaturated ketone: mechanistic studies in photochemistry, *J. Am. Chem. Soc.,* 104, 2456, 1982.
59. Uyehara, T., Furuta, T., Akamatsu, M., Kato, T., and Yamamoto, Y., Construction of fused ring skeletons based on photochemical rearrangement of bicyclo[3.2.1]oct-6-en-2-ones and application to a total synthesis of (±)- $\Delta^{9,12}$-capnellene, *J. Org. Chem.,* 54, 5411, 1989.
60. Knott, P.A. and Mellor, J.M., Photochemical rearrangements of bicyclo[3.2.1]nona-3,7-diene-2,6-dione, *J. Chem. Soc., Perkin Trans. 1*, 1030, 1972.
61. Kurabayashi, K. and Mukai, T., Photochemical and thermal behavior of bicyclo[4.2.1]nona-2,4,7-trien-9-one, *Tetrahedron Lett.*, 1049, 1972.
62. Houk, K.N. and Northington, D.J., Solvent dependence in the photochemical dimerization and $[\pi^{2a}+\sigma^{2a}]$ rearrangement of a bridged 3,5-cycloheptadienone, *J. Am. Chem. Soc.*, 94, 1387, 1972.
63. Givens, R.S., Oettle, W.F., Coffin, R.L., and Carlson, R.G., Mechanistic studies in organic photochemistry. III. The photochemistry of bicyclo[2.2.2]octenone and benzobicyclo[2.2.2]octadienone, *J. Am. Chem. Soc.,* 93, 3957, 1971.
64. Demuth, M., Raghvan, P.R., Carter, C., Nakano, K., and Schaffner, K., Photochemical high yield preparation of tricyclo[3.3.0.$0^{2,8}$]octan-3-ones. Potential synthons for polycyclopentanoid terpenes and prostacyclin analogs, *Helv. Chim. Acta,* 63, 2434, 1980.
65. Demuth, M. and Schaffner, K., Tricyclo[3.3.0.$0^{2,8}$]octan-3-ones: photochemically prepared building blocks for enantiospecific total syntheses of cyclopentanoid natural products, *Angew. Chem. Int. Ed. Engl.,* 21, 820, 1982.
66. Yates, P. and Stevens, K.E., Bicyclopentanoid sesquiterpenes. The synthesis of cedranoid sesquiterpenes via the photorearrangement of bicyclo[2.2.2]octenones, *Tetrahedron*, 37, 4401, 1981.
67. Yates, P., Burnell, D.J., Freer, V.J., and Sawyer, J.F., Synthesis of cedranoid sesquiterpenes. III. Functionalization at carbon 4, *Can. J. Chem*., 65, 69, 1987.
68. Schultz, A.G., Dittami, J.P., Lavieri, F.P., Salowey, C., Sundararaman, P., and Szymula, M.B., The synthesis and selected chemistry of 6-alkyl-6-carbalkoxy- and 6-alkyl-6-(aminocarbonyl)-2,4-cyclohexadien-1-ones and cyclohexadienone ketals, *J. Org. Chem.*, 49, 4429, 1984.
69. Becker, H.-D. and Ruge, B., Photochemical reactions of bicyclo[2.2.2]octadienones, *J. Org. Chem.,* 45, 2189, 1980.
70. Liao, C.-C. and Wei, C.-P., Synthetic applications of masked o-benzoquinones. A novel total synthesis of (±) forsythide aglucone dimethyl ester, *Tetrahedron Lett.,* 30, 2255, 1989.
71. Paquette, L.A., Ra, C.S., and Silvestri, T.W., Free radical cyclization approach to a functionalized [3]peristylane, *Tetrahedron,* 45, 3099, 1989.
72. Parker, S.D. and Rogers, N.A.J., Photochemistry of β,γ-enones: 1-methoxybicyclo[2.2.2]oct-5-en-2-one, *Tetrahedron Lett.,* 4389, 1976.
73. Eckersley, T.J., Parker, S.D., and Rogers, N.A. J., Photochemistry of 1-methoxybicyclo[2.2.2] oct-5-en-3-one: a singlet state oxa-di-π-methane rearrangement, *Tetrahedron Lett.,* 4393, 1976.

74. Eckersley, T.J. and Rogers, N.A.J., Photochemical studies on bicyclic β,γ-unsaturated ketones. II. Oxa-di-π-methane rearrangements originating from some state other than $T_1(\pi\text{-}\pi^*)$, *Tetrahedron*, 40, 3759, 1984.
75. Demuth, M., Wietfeld, B., Pandey, B., and Schaffner, K., Photochemistry of 1-methoxybicyclo[2.2.2]octenones; photolytic cyclopropane cleavage of the initially formed tricyclo[3.3.0.$0^{2,8}$]octan-3-ones, *Angew. Chem. Int. Ed. Engl.*, 24, 763, 1985.
76. Hart, H. and Murray, Jr., R.K., The photosensitized rearrangement of benzobicyclo[2.2.2] octadienones, *Tetrahedron Lett.,* 379, 1969.
77. Yates, P. and Stevens, K.E., Synthesis of cedranoid sesquiterpenes. II. Functionalization at carbon 12, *Can. J. Chem.,* 60, 825, 1982.
78. McClure, C.K., Link, J.S., and Kiessling, A., The oxa-di-π-methane photochemical rearrangement of quinuclidinones, 1- and 2-aza-3-carboxybicyclo[2.2.2]oct-2-ene-5-ones: Application to the synthesis of pyrrolizidine alkaloids, Abstract no. ORGN 480, 221st ACS Meeting, San Diego, CA, 2001.
79. Mehta, G. and Srikrishna, A., Photochemistry of Tricyclo[4.2.2.$0^{2,5}$]deca-3,7-dien-9-one: A Source of Many Interesting Polycycles, *Tetrahedron Lett.,* 3187, 1979.
80. Paquette, L.A., Kang, H.-J., and Ra, C.S., Stereocontrolled access to the most highly condensed pentalenolactone antibiotic. From cycloheptatriene to pentalenolactone P methyl ester, *J. Am. Chem. Soc.,* 114, 7387, 1992.
81. Kilger, R., Korner, W., and Margaretha, P., Photochemistry of 8,8,9,9-tetramethyl-1,3,4,6,7,8-hexahydro-1,4-ethanonaphthalene-2,5-dione, a δ-oxo-β,γ-unsaturated ketone, *Helv. Chim. Acta,* 67, 1493, 1985.
82. Hart, H. and Takagi, K., Benzo- and naphthoquinone adducts of hexamethyl-2,4-cyclohexadienone. Synthesis, enolization and rearrangements, *J. Org. Chem.,* 45, 34, 1980.
83. Hayakawa, K., Schmid, H., and Frater, G., Photochemie von tricyclischen β,γ–γ′,δ′ ungesattigten ketonen, *Helv. Chim. Acta*, 60, 561, 1977.
84. Schultz, A.G., Lavieri, F.P., and Snead, T.E., 2,4-Cyclohexadien-1-ones in organic synthesis. Intramolecular Diels-Alder reactivity and the oxa-di-π-methane photorearrangement of the Diels-Alder adducts, *J. Org. Chem*., 50, 3086, 1985.
85. Singh, V., Alam, S.Q., and Porinchu, M., Intramolecular Diels-Alder reaction of cyclohexa-2,4-dienones: synthesis and photochemical reactions of oxa-homobrendanes, *Tetrahedron*, 51, 13423, 1995.
86. Demuth, M. and Hinsken, W., Extension of the tricyclooctanone concept. A general principle for the synthesis of linearly and angularly annelated triquinanes, *Angew. Chem. Int. Ed. Engl*., 24, 973, 1985.
87. Hwang, J.-T. and Liao, C.-C., Synthesis of angularly and linearly fused triquinanes via the common intramolecular Diels-Alder adduct of a masked o-benzoquinone, *Tetrahedron Lett*., 32, 6583, 1991.
88. Mehta, G. and Subrahmanyam, D., A total synthesis of (±) modhephene, *J. Chem. Soc., Chem. Commun*., 768, 1985.
89. Mehta, G. and Subrahmanyam, D., Photochemical oxa-di-π-methane rearrangement approach to [3.3.3]propellanes. Total synthesis of sesquiterpene hydrocarbon (±)-modhephene, *J. Chem. Soc., Perkin Trans. 1*, 395, 1991.
90. Maiti, B.C., Singh, R., and Lahiri, S., Photoreactivity in δ-keto-β,γ-enones: oxa-di-π-methane rearrangements from states other than $T1(\pi,\pi^*)$, *J. Photochem. Photobiol. A: Chem.*, 91, 27, 1995.
91. Maiti, B.C. and Lahiri, S., Tetracyclo[6.4.0.0.$^{3,5}0^{4,8}$]dodecan-6-ones: A novel construction of tricyclo[7.2.1.$0^{1,6}$]dodecan-10-one skeleton by acid catalysed cyclopropyl bond cleavage, *Tetrahedron*, 53, 13053, 1997.
92. Paquette, L.A. and Doherty, A.M., *Polyquinane Chemistry*, Springer-Verlag, New York, 1987.
93. Mehta, G. and Srikrishna, A., Synthesis of polyquinane natural products: An update, *Chem. Rev.*, 97, 671, 1997.
94. Hirao, K., Unno, S., Miura, H., and Yonemitsu, O., Singlet and triplet excited state photochemistry of tricyclo[5.2.2.$0^{2,6}$]undeca-3,10-dien-9-one derivatives, *Chem. Pharm. Bull.*, 25, 3354, 1977.

95. Singh, V.K., Deota, P.T., and Raju, B.N. S., Diels-Alder cycloaddition: synthesis and oxa-di-π-rearrangement of tricyclo[5.2.2.0 ^{2,6}]undecadienone, *Synth. Commun*., 17, 115, 1987.
96. Singh, V. and Raju, B.N.S., $\Pi^{4s}+\Pi^{2s}$ cycloaddition: synthesis and oxa-di-π-methane rearrangement of annulated bicyclo[2.2.2]octenones, *Synth. Commun*., 18, 1513, 1988.
97. Singh, V.K., Deota, P.T., and Bedekar, A.V., Studies in the synthesis of polycyclopentanoids: synthesis, oxa-di-π-methane rearrangement of annulated bicyclo[2.2.2]octenones and cyclopropane ring cleavage of tetracyclo[6.3.0.0.^{2,4}0^{3,7}]undecenones, *J. Chem. Soc., Perkin Trans. 1*, 903, 1992.
98. Singh, V. and Porinchu, M., Sigmatropic 1,2- and 1,3-acyl shifts in excited states: a novel, general protocol for the synthesis of tricyclopentanoids and protoilludanes, *Tetrahedron*, 52, 7087, 1996.
99. Singh, V. and Thomas, B., o-Vanillyl alcohol as a synthetic equivalent of 2-methoxycyclohexa-2,4-dienones: a novel synthesis of linearly fused *cis:anti:cis* tricyclopentanoids, *J. Chem. Soc., Chem. Commun*., 1211, 1992.
100. Singh, V. and Thomas, B., Aromatics to triquinanes: synthesis and photoreaction of tricyclo[5.2.2.0^{2,6}]undecanes having an α-methoxy-β,γ-unsaturated carbonyl chromophore: a novel efficient and general route to linearly fused *cis:anti:cis* tricyclopentanoids, *J. Org. Chem.*, 62, 5310, 1997.
101. Singh, V. and Prathap, S., Photochemical reactions of α-methoxy-β,γ-enones: Isolation of 1,2-acylshift intermediate and synthesis of versatile precursors to oxygenated capnellanes, *Synlett*, 542, 1994.
102. Singh, V. and Prathap, S., Photochemical reactions in organic synthesis: a novel and efficient route to angular and linear tetraquinanes, *Tetrahedron,* 52, 14287, 1996.
103. Singh, V., Thomas, B., and Vedantham, P., Aromatics to triquinanes. Synthesis of 1,4,4,11-tetramethyltricyclo[6.3.0.0^{2,6}]undeca-3,7,10-trione: a potential precursor for coriolin and congeners, *Tetrahedron*, 54, 6539, 1998.
104. Singh, V., Sharma, U., Prasanna, V., and Porinchu, M., Pericyclic reaction of cyclohexa-2,4-dienones with cyclohexa-1,3-diene and cycloheptatriene: the role of cyclohexadienones as π^4 and π^2 component, Cope rearrangement and photoreaction of the adducts, *Tetrahedron*, 51, 6015, 1995.
105. Singh, V. and Jagadish, B., Synthesis of *exo*-annulated bicyclo[2.2.2]octenone and its oxa-di-π-methane rearrangement to *cis:syn:cis* triquinane, *Indian J. Chem*., 35B, 401,1996.
106. Nitta, M. and Sugiyama, H., Photocycloaddition of benzophenone with 6-methylenetricyclo[3.2.1.0^{2,7}]oct-3-en-8-one and related compounds. Di-π-methane photorearrangement of the primary photocycloadducts, *Bull. Chem. Soc. Jpn.*, 55, 1127, 1982.
107. Hassner, A., Middlemiss, D., Murray-Rust, J., and Murray-Rust, P., Photochemistry of ethenobenzocycloheptenones. A di-π-methane rearrangement of β,γ-unsaturated aryl ketones, *Tetrahedron*, 38, 2539, 1982.
108. Sugihara, Y., Sugimura, T., and Murata, I., Valence isomer of 4-methoxyazulene. Synthesis of 6-methoxytetracyclo[5.3.0.0.^{2,4}0^{3,5}]deca-6,8,10-triene, *J. Am. Chem. Soc*., 103, 6738, 1981.
109. Ishii, K., Hashimoto, T., Sakamoto, M., Taira, Z., and Asakawa, Y., Photochemical rearrangement of 16β,17β-epoxydigitoxigenin 3-acetate. The formation of cyclopropyl ketones, *Chem. Lett*., 609, 1988.
110. Corbett, R.M., Lee, C.-S., Sulikowski, M.M., Reibenspies, J., and Sulikowski, G.A., Application of the oxa-di-π-methane photoisomerisation in the rearrangement of carbocycles possessing bridgehead unsaturation, *Tetrahedron*, 53, 11099, 1997.
111. Chen, S-H., Farina, V., Huang, S., Gao, Q., Golik, J., and Doyle, T.W., Studies on the photochemistry of taxol, *Tetrahedron,* 50, 8633, 1994.
112. Singh, V., Spiroepoxycyclohexa-2,4-dienones in organic synthesis, *Acc. Chem. Res.*, 32, 324, 1999.
113. Kon, K. and Isoe, S., Tricyclo[3.3.0.0^{2,8}]octanones as building blocks in natural product synthesis. II. A new synthesis of loganin, *Helv. Chim. Acta*, 66, 755, 1983.
114. Takemoto, T. and Isoe, S., Tricyclo[3.3.0.0^{2,8}]octanones as building blocks in natural product synthesis. Synthesis of (±) forsythide aglycone dimethyl ester, *Chem. Lett*. 1931, 1982.

115. Yates, P., Grewal, R.S., Hayes, P.C., and Sawyer, J.F., Synthesis of cedranoids sesquiterpenes. V. The biotols, *Can. J. Chem*., 66, 2805, 1988.
116. Grewal, R.S., Hayes, P.C., Sawyer, J.F., and Yates, P., Total synthesis of (±)-α-biotol, (±)-β-biotol and (±)-4-epi-α-biotol, *J. Chem. Soc., Chem. Commun*., 1290, 1987.
117. Demuth, M. and Hinsken, W., First total synthesis of enantiomerically pure (–)-silphiperfol-6-en-5-one, *Helv. Chim. Acta*, 71, 569, 1988.
118. Uyehara, T., Murayama, T., Sakai, K., Onda, K., Ueno, M., and Sato, T., Rearrangement approaches to cyclic skeletons. XIII. Total synthesis of triquinane sesquiterpenes, (±)-modhephene and (±)-isocomene, on the basis of formal substitution at both bridgeheads of a bicyclo[2.2.2]oct-5-en-2-one, *Bull. Chem. Soc. Jpn.,* 71, 231, 1998.
119. Paquette, L.A., Kang, H-J., and Ra, C.S., Stereocontrolled access to the most highly condensed pentalenolactone antibiotic. From cycloheptatriene to pentalenolactone P methyl ester, *J. Am. Chem. Soc*., 114, 7387, 1992.
120. Demuth, M., Ritterskamp, P., Weigt, E., and Schaffner, K., Total synthesis of (–)-coriolin, *J. Am. Chem. Soc*., 108, 4149, 1986.
121. Singh, V., Prathap, S., and Porinchu, M., A novel stereospecific total synthesis of (±)-$\Delta^{9(12)}$-capnellene from *p*-cresol, *Tetrahedron Lett*., 38, 2911, 1997.
122. Singh, V., Prathap, S., and Porinchu, M., Aromatics to triquinanes: *p*-cresol to (±)-$\Delta^{9(12)}$-capnellene, *J. Org. Chem*., 63, 4011,1998.
123. Singh, V. and Samanta, B., Generation of molecular complexity from aromatics: a formal total synthesis of coriolin from 6-methylsaligenin, *Tetrahedron Lett*., 40, 383, 1999.
124. Singh, V., Samanta, B., and Kane, V.V., Molecular complexity from aromatics: synthesis and photoreaction of *endo*-tricyclo[5.2.2.$0^{2,6}$]undecanes. Formal total syntheses of (±)- coriolin, *Tetrahedron*, 56, 7785, 2000.
125. Singh, V. and Alam, S.Q., Intramolecular Diels-Alder reaction in 1-oxaspiro-[2,5]octa-5,7-dien-4-one and sigmatropic shifts in excited states: novel route to sterpuranes and linear triquinanes: formal total synthesis of (±)- coriolin, *J. Chem. Soc., Chem. Commun*., 2519, 1999.
126. Singh, V., Vedantham, P., and Sahu, P.K., A novel stereoselective total synthesis of (±)-hirsutene from saligenin, *Tetrahedron Lett.,* 43, 519, 2002.

79

1,3-Acyl Migrations in β,γ-Unsaturated Ketones

Vishwakarma Singh
Indian Institute of Technology Bombay

79.1 Introduction and Background

The photochemical reactions of β,γ-unsaturated enones have stimulated intense interest due to their spectroscopic properties, interesting mechanistic implications,[1–4] and application in organic synthesis.[5–7] The interest in β,γ-enone photochemistry was initiated due to the spectroscopic properties of these enones, which indicated interaction between the two chromophores,[1–4] which was further enhanced significantly after a novel observation by Buchi and Burgess,[8] who noted that irradiation of the bicyclic compound **1a** leads to the formation of **1b** (Scheme 1).

Subsequent to the aforementioned photoisomerization, which was later rationalized as a 1,3-acyl sigmatropic shift,[9] photochemical reactions of various types of β,γ-enones were examined. It was observed that β,γ-unsaturated enones undergo two unique reactions (*viz.* 1,3-acyl sigmatropic shift and oxa-di-π-methane (ODPM) reaction or 1,2-acyl shift), which are characteristic of their excited states. The direct irradiation of β,γ-enones such as **2**, in general leads to the formation of another enone **3** as a result of migration of the carbonyl group to the γ-carbon and formation of a new π-bond between the α– and β–carbons (Scheme 2). Sensitized irradiation, on the other hand, causes a 1,2-acyl shift (or oxa-di-π-methane reaction), leading to a cyclopropyl ketone of type **4**.

0-8493-1348-1/04/$0.00+$1.50

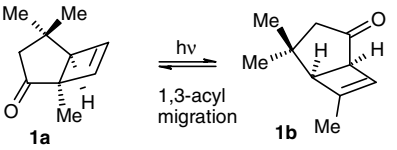

SCHEME 1

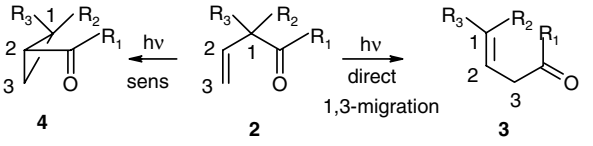

SCHEME 2

1,3-Migration of the carbonyl group appears to be a characteristic reaction of β,γ-unsaturated ketones upon direct excitation, although it may be accompanied by photoreactions of ketones such as Norrish Type I and Type II, and other photoreactions such as oxetane formation, *cis,trans*-isomerizations, etc., depending on the structure of the chromophoric system.[3,4]

79.2 Mechanism and the Correlation between Excited State and Reactivity

The mechanism of photoreactions has been studied in great detail and the correlation between excited state and reactivity has been established.[3–5] Excellent discussions on the mechanism of both the 1,3-migration and the oxa-di-π-methane reaction have been presented by Schuster and co-workers[4] and by Houk.[3] In general, it is agreed that the 1,3-migration can occur either from the lowest excited singlet (S_1, $n\pi^*$) state or the higher triplet (T_2, $n\pi^*$) state, whereas the lowest triplet excited state (T_1, $\pi\pi^*$) is responsible for the oxa-di-π-methane reaction in β,γ-unsaturated ketones.[3,4,10–12] The 1,3-migration in β,γ-enones can occur competitively from both the S_1 ($n\pi^*$) and T_2($n\pi^*$) states; the latter may be generated from S_1 via intersystem crossing, albeit inefficiently. 1,3-Acyl shifts can be induced via α-cleavage (Norrish Type I reaction) and lead to the formation of biradicaloids of type **5** that gives the final product via radical combination or may proceed via a quasi-concerted pathway through biradicals of type **6** (Scheme 3). In general, acyclic ketones follow the dissociation-recombination pathway,[13–15] while cyclic ketones follow the quasi-concerted pathway.[4,16–18]

The existence of the biradicals and the multiplicity of the surfaces on which these are formed have not been demonstrated directly; however, experimental results (stereochemistry of the reaction, CIDNP [chemically induced dynamic nuclear polarization], radical trapping experiments, and quantum yield measurements) support their existence.[4,10,15–18] Recently, the mechanism of 1,3-migration and oxa-di-π-methane reactions in terms of potential energy surface and decay funnels has been described; this also supports the aforementioned mechanistic implications.[18] The detailed mechanism, however, depends, in a very subtle way, on the structure of the chromophoric system and the presence of the functional groups.

1,3-Migration and oxa-di-π-methane rearrangements are the two fascinating aspects of β,γ-enone photochemistry and studies on both were done in parallel. Oxa-di-π-methane reactions, however, received somewhat more attention, perhaps due to their synthetic applications and, as such, have been discussed in several reviews.[1–6] Most of the studies on 1,3-shifts were made in conjunction with the ODPM reaction with a view to resolve the singlet—triplet dichotomy. Nevertheless, the literature on the 1,3-migration is fairly vast and only some representative examples from various classes of β,γ-enones and the emerging synthetic applications are presented here.

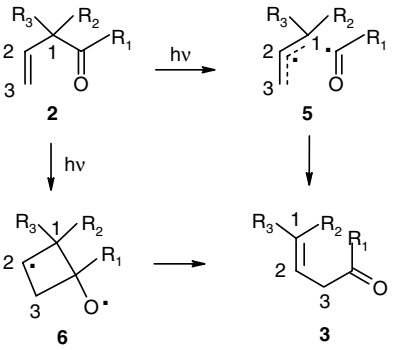

SCHEME 3

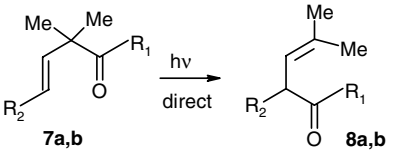

SCHEME 4

79.3 1,3-Acyl Migrations in Acyclic β,γ-Unsaturated Ketones

The direct irradiation of acyclic ketones can, in principle, lead to a number of photoreactions, such as *cis,trans*-isomerization, Norrish Type II and Type I reactions, oxetane formation, and 1,3-shifts. The deactivation pathway is dependant on the substituents in the chromophoric systems. Substitution at the α-carbon exerts a fair amount of control on the occurrence of 1,3-migration. Simple acyclic β,γ-enones with mono-substitution at the β-carbon undergo *cis,trans*-isomerization, α-cleavage, and decarbonylation to give radical combination products.[3,4,13,17,19] Similarly, sensitized irradiation of phenyl allyl ketone with a phenyl group at the γ-carbon also led to *cis,trans*-isomerization.[20] In their pioneering studies on photochemistry of β,γ-enones, Dauben and co-workers reported that the ketone **7a** with a gem dimethyl group and a phenyl group at the α- and γ-carbons, respectively, undergoes a 1,3-acyl shift on direct irradiation to give the product **8a**. It was observed that further irradiation of **8a** gives products as a result of decarbonylation and radical combination.[21] Similarly, the direct irradiation of the ketone **7b** containing an α,α-dimethyl group also led to the formation of 1,3-acyl shift product **8b** (Scheme 4) in addition to other products.[13] Other related ketones with substitutents at the α–carbon were also found to undergo a 1,3-acyl shift upon direct irradiation.[22,23]

Engel and Schexnayder examined the photoreaction of a highly interesting set of acyclic β,γ-enones **9** through **12** upon direct and sensitized irradiation.[13] While the direct irradiation of dienone **9a** and acetylenic enone **9b** gave 1,3-shift products **13a** and **13b**, respectively, along with C_{10} hydrocarbons, the acetylenic ketone **10** gave the allenic ketone **14** in addition to biacetyl and hydrocarbons. The photoreaction of the ketone **11** gave a mixture of products containing **15** and products due to γ-hydrogen abstraction, oxetane formation, and biacetyl and hydrocarbons. Interestingly, the direct irradiation of ketone **12** gave only oxetane **16** as a result of intramolecular photocycloaddition (Scheme 5). It was suggested that at least some of the 1,3-shift products arise from the combination of free radicals.[13]

Photochemical reactions of β,γ-enones of type **17** with α,α-disubstitution and a substituent at the β-carbon were examined. While the irradiation of **17a** in solution gave the isomerized enone **18a** and

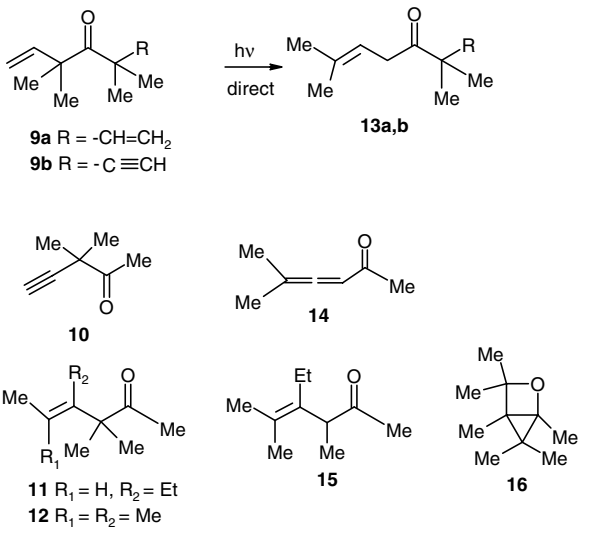

SCHEME 5

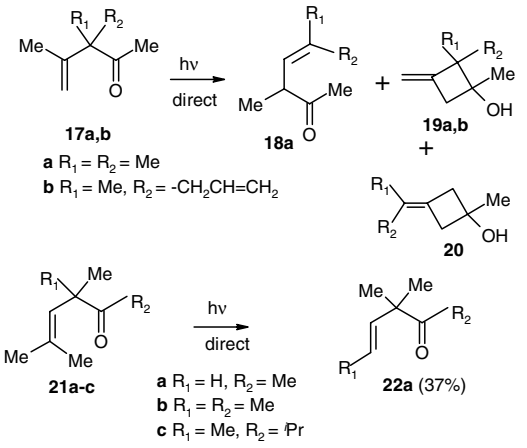

SCHEME 6

cyclobutanols **19a**, **20** arising from a 1,3-acyl shift and hydrogen abstraction, respectively,[24] photoreaction of **17b** gave only cyclobutanols **19b**.[22] Cerfontain and co-workers[25–27] examined the photoreactions of a series of β,γ-enones having various substituents at the α-, β-, and γ-carbons. Direct irradiation of **21a** gave 1,3-acyl shift product **22a** in addition to other products arising via α-cleavage, decarbonylation, and radical combination. However, the ketones **21b,c** did not give products due to a 1,3-acyl shift; instead, decarbonylation occurred and hydrocarbons were obtained via radical combination (Scheme 6).[25] Photoreaction of β,γ-enones containing a phenyl group at γ-carbon and alkyl groups at the α-carbon, such as **23,** were also investigated. The direct irradiation of ketone **23a** underwent a 1,3-acyl shift to give products of type **24a** (Scheme 7) as well as products due to *cis,trans*-isomerization. Irradiation of the enones **23b** gave products as a result of *cis,trans*-isomersization, decarbonylation, and radical combination, in addition to the 1,3-shift product.[26] The enone **23c,** on the other hand, underwent *cis,trans*-isomerization and gave some benzaldehyde.[26] The direct irradiation of ketone **25** gave a complex mixture of products, including the 1,3-acyl shift product **26**.[27]

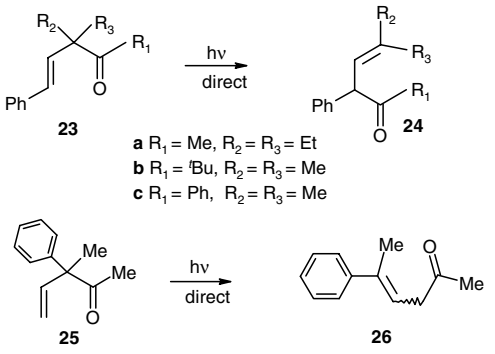

SCHEME 7

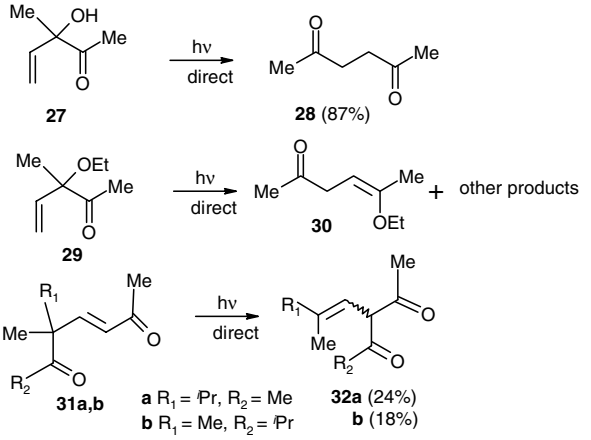

SCHEME 8

Hancock and co-workers investigated the photoreaction of β,γ-enones with α-hydroxy and alkoxy substituents.[28,29] While the direct irradiation of α-hydroxyenone **27** led to the formation of 1,4-dione **28** via an efficient 1,3-acyl shift followed by tautomerization,[28] photoreaction of **29** gave a complex mixture of products arising from various other reactions in addition to the 1,3-acyl shift product **30** (Scheme 8).[29] Eichenberger and co-workers reported 1,3-acyl shift in ketones **31a** and **31b** on photoreaction from a ($^1\pi\pi^*$) state to give **32a** and **32b**, respectively, in addition to an oxa-di-π-methane rearrangement.[30]

79.4 1,3-Acyl Migration in Semicyclic β,γ-Unsaurated Ketones

It is evident from the foregoing examples that photoreaction of acyclic β,γ-enones is quite diverse and highly dependent on the structure of the chromophoric system and substituents present. However, this is not surprising because the remarkable reactions of β,γ-enones (*viz.* 1,3-acyl migration and oxa-di-π-methane reactions) are presumably due to the interaction between the alkene and carbonyl chromophores. The interaction between the chromophores will depend on the structure and conformation of the molecule. To gain a better understanding, the photoreaction of a number of β,γ-enones containing the chromophores in various structural surroundings were examined. Photoreactions of those β,γ-enones in which one of the chromophores is present in a cyclic ring and the other in an acyclic chain, and the enones with the alkene and carbonyl chromophores in two different cycles, are presented below.

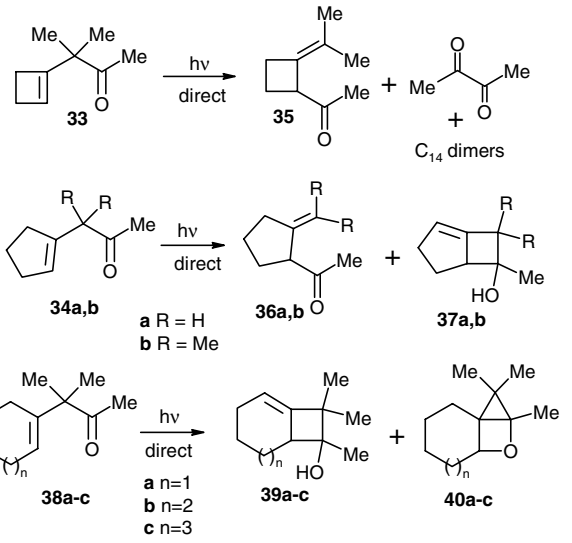

SCHEME 9

Engel and Schexnayder studied the photoreaction of β,γ-enones in which the alkene chromophore is present in rings of various sizes, and observed very interesting behavior on direct as well as sensitized irradiation.[31] Thus, direct irradiation of the enone **33,** having alkene chromophore in a four-membered ring, gave the 1,3-acyl shift product **35** along with biacetyl and hydrocarbons. The formation of biacetyl and other hydrocarbons in this photoreaction parallels that of acyclic β,γ-enones. The irradiation of **34a** and **34b** yielded the 1,3-acyl shift products **36a** and **36b**, along with the cyclobutanols **37a** and **37b** as a result of γ-hydrogen abstraction (Scheme 9). On the other hand, direct photolysis of the enones **38a,b,c**, in which the alkene chromophore is present in six-, seven-, and eight-membered rings, does not lead to a 1,3-acyl shift; instead, products due to γ-hydrogen abstraction and intramolecular cycloaddition are obtained (Scheme 9). Formation of the products and the different behaviors of these ketones on excitation has been explained in terms of the ionization potential and electron richness of the alkenes.[31]

Schaffner and co-workers examined the photoreactions of several cyclopentenyl methyl ketones of type **41** and **43,** and suggested the intramolecular nature of the 1,3-acyl shift.[16,32–34] The direct irradiation ($n\pi^*$) of optically active ketone (*R*)-**41a** at >300 nm led to the 1,3-acyl shift product (*S*)-**42a** in addition to other products.[32] Photolysis of a mixture of ketones **41b** and **41c** with CD_3 groups did not give hexadeuterated compounds, which indicated the intramolecular nature of the 1,3-acyl migration. These mechanistic implications were further supported by subsequent studies on the photoreaction of ketones **43** and their labeled analogues.[33] While the direct irradiation of **43a** gave a photostationary mixture of **44a** and **43a**, the phenyl ketones **43b** and **43c** disappeared to give the corresponding 1,3-shift products **44b** and **44c**, respectively (Scheme 10). These and other studies on the photoreaction of enantiomerically enriched cyclopent-2-enyl methyl ketones, measurements of quantum yields, fluorescence lifetimes, and kinetic studies suggested the concerted nature of the 1,3-acyl shift.[16,33,34]

Cerfontain and co-workers have examined the photoreaction of ketones **45** and **48** upon direct and sensitized irradiation. The enones **45a** and **45b** were found to undergo a reversible 1,3-shift on direct irradiation. A photostationary state is reached in the case of **45a** (45a:46a = 1:4). The dienal **47** was detected during the irradiation of the cyclohexenyl ketone **45b** in addition to the 1,3-acyl shift product **46b**. Interestingly, the ketone **48a** with a phenyl group at the α-carbon did not undergo any photoreaction, while its higher analogue **48b** gave the 1,3-acyl shift product **49** and the dienal **50** (Scheme 11).[35] Cerfontain and Koppes[36] have examined the photochemical reactivity of a number of ketones of type **51** and **56**. Interestingly, the direct irradiation of indanone **51a** gives products due to decarbonylation, the

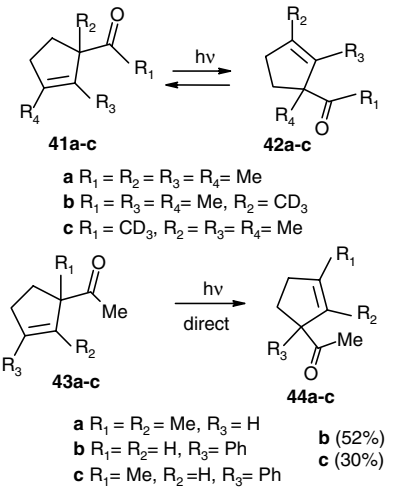

SCHEME 10

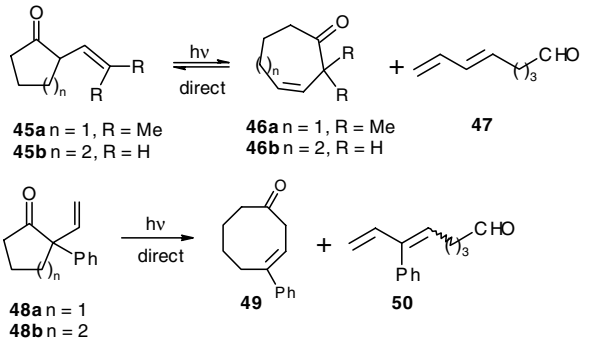

SCHEME 11

1,3-acyl shift product, as well as a product from an oxa-di-π-methane reaction, while the analogue **51b** with a gem-dimethyl group at the α′–position affords only the oxa-di-π-methane product **55** (Scheme 12). On the other hand, the homologous ketone **56** underwent a reversible 1,3-acyl shift to yield **57,** along with products due to ketene elimination.[36]

The direct irradiation of ketone **58** containing an α-hydroxy group also gave similar results and produced the ring-expanded ketone **59** and the aldehyde **60**.[37] In view of these results, it is of interest to note that irradiation of ketone **61,** in which the positions of the carbonyl group and the β,γ–olefinic group are exchanged, gives a complex mixture of products containing cyclohexenone, biacetyl, cyclohexanone, and acetaldehyde in addition to the 1,3-acyl shift product **62**.[38] The cyclooctanedione **59** and the 1,4-dione **62** are formed via 1,3-acyl migration followed by tautomerization (Scheme 13).

(+)-4-Acetyl-2-carene **63** was shown to undergo a 1,3-acyl migration on direct irradiation to give the product **64** along with the cyclobutanol **65** arising from Norrish Type II cyclization of **64**. Longer irradiation led to the formation of cyclobutanol **66** derived from **63** (Scheme 14). The reaction occurred from the excited singlet state because the presence of piperylene had no effect on the product distribution.[39]

Chae and co-workers studied the photoreaction of optically active ketones **67a,b,c,d** under both direct as well as sensitized conditions. Only the naphthylketone **67a** underwent a 1,3-acyl shift upon direct

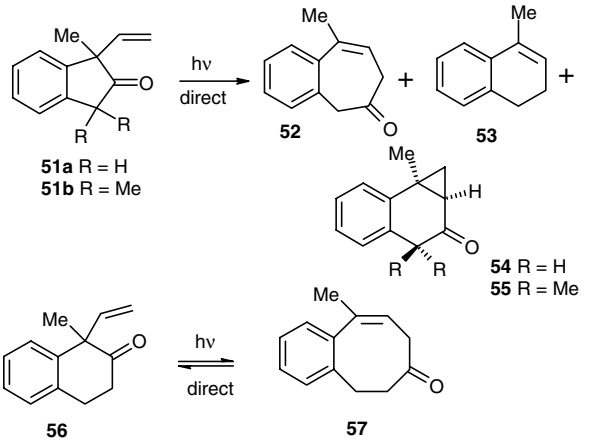

SCHEME 12

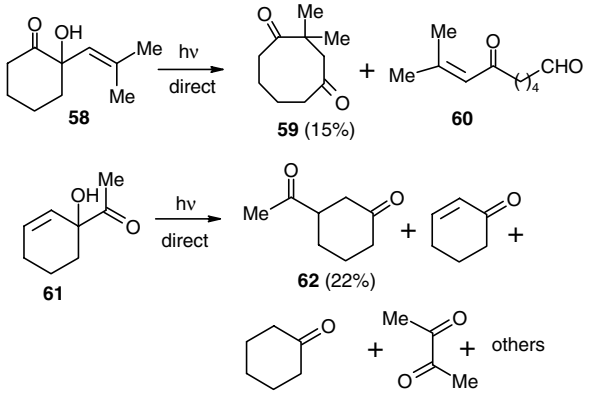

SCHEME 13

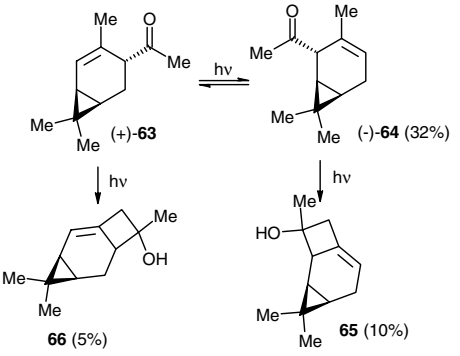

SCHEME 14

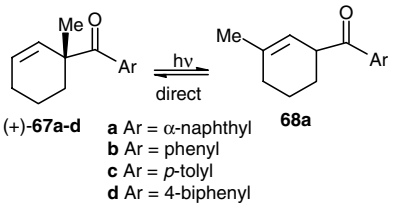

SCHEME 15

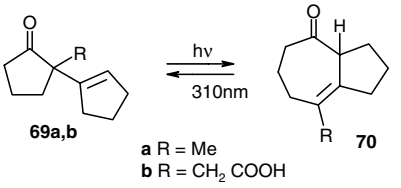

SCHEME 16

irradiation, whereas the other ketones **67b,c,d** underwent racemization with good quantum efficiency (>0.75) and no 1,3-acyl shift product was obtained. It was noted that the formation of the 1,3-acyl shift product **68a** was not quenched by *trans*-piperylene, while racemization was quenched. Sensitized irradiation of **67a,b,c,d** showed racemization, but neither 1,3-migration nor oxa-di-π-methane reactions were observed. It was concluded that the 1,3-acyl shift in **67a** arises from the excited singlet state and that intersystem crossing is very efficient for **67b,c,d** (Scheme 15).[40]

Studies on β,γ-unsaturated ketones of type **69,** in which both the chromophores are present in different rings that are connected through a single bond, played a key role in understanding the mechanism and stereochemistry of both the 1,3-acyl migration and the oxa-di-π-methane reaction. Direct irradiation of **69a** and **69b** gave a single product **70,** and a photostationary state was reached after 33 h. Irradiation of (*R*)-(−)-**69b** gave the (*S*)-(+)-**70b** with the same optical purity as **69b** at low conversions. At higher photochemical conversion, the optical purity of both **69b** and **70b** decreased, which indicated stereochemical equilbration. To probe the origin of this reaction, direct irradiation of **70b** was also studied. Thus, irradiation of **70b** proceeded with loss of stereochemical integrity, even at low photochemical conversion, and gave **69b**. However, **70b** was not racemized to a large extent, suggesting that the transformation **70b** → **69b** occurs with racemization. On the basis of these and other results, it was concluded that the ring-expansion reaction **69** to **70** may be described as [1,3]-suprafacial migration whereas the reverse reaction **70** to **69** is a biradical process with equilibration (Scheme 16).[41] Cerfontain and coworkers have studied the photoreaction of a number of similar ketones **69c,d,e,** which were also found to undergo a 1,3-acyl shift upon direct irradiation; however, the ketones **71** and **72** (Scheme 17) with a vinyl substituent at the α-carbon were unreactive, presumably because of rapid radiationless decay from the excited singlet state.[42]

79.5 1,3-Acyl Migration in Monocyclic and Ring-Fused Bicyclic β,γ-Ketones

Paquette and co-workers examined the photoreactions of cycloheptenones **73** and **74,** and cycloheptadienone **77b** (Scheme 18). The direct irradiation of **73** and **74** gave the corresponding 1,3-acyl shift products **75** and **76,** respectively.[43] In the case of **73**, a photostationary state was reached after 4 h (**75**:**73** = 4). Interestingly, tetramethyl cycloheptadiene **77a** did not undergo a 1,3-acyl shift on direct irradiation;

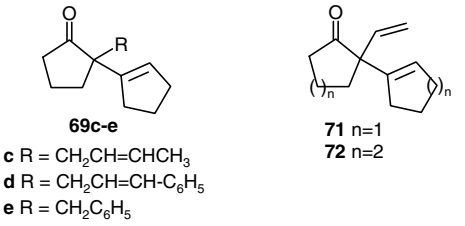

69c-e
c R = $CH_2CH{=}CHCH_3$
d R = $CH_2CH{=}CH\text{-}C_6H_5$
e R = $CH_2C_6H_5$

71 n=1
72 n=2

SCHEME 17

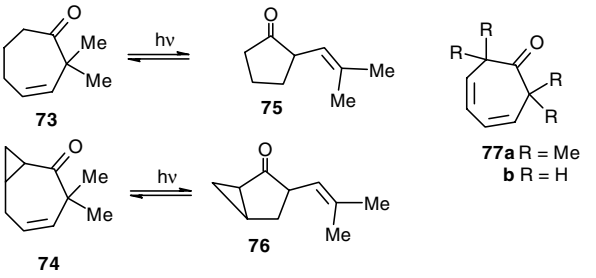

73 **75** **77a** R = Me, **b** R = H

74 **76**

SCHEME 18

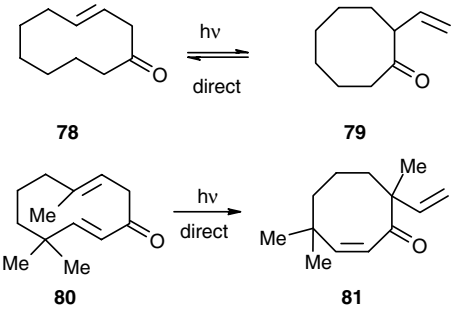

78 **79**

80 **81**

SCHEME 19

instead, an oxa-di-π-methane rearrangement was observed.[43] The parent cycloheptadienone **77b**, however, underwent decarbonylation.[44] Similar behavior is also exhibited by 3-cyclooctenone on direct irradiation, which gives products due to 1,3-acyl shifts and intramolecular disproportionation.[45]

The behavior of cyclodecenones is slightly different, as compound **78** was found to undergo a reversible 1,3-migration on direct irradiation to give **79**.[46] The cyclodecenone derivative **80,** with an additional double bond, undergoes a 1,3-acyl shift to give **81**, in addition to products due to *cis,trans*-isomerization (Scheme 19).[47]

Studies of the photoreactions of bicyclic ketones **82** and **83** provided interesting results. While the six-membered ketone **82a** did not undergo a 1,3-migration on direct irradiation but instead underwent an oxa-di-π-methane process, the homologous ketone **82b** underwent 1,3-migration on direct irradiation and gave **84b**.[48] The ketone **82c,** with a methyl substituent at the α-carbon, undergoes a 1,3-acyl shift to give **84c** in addition to oxa-di-π-methane reaction products upon direct irradiation. Whereas, **82d** with a gem-dimethyl group undergoes a selective 1,3-acyl migration to give **84d**.[49] The ketone **83** also underwent

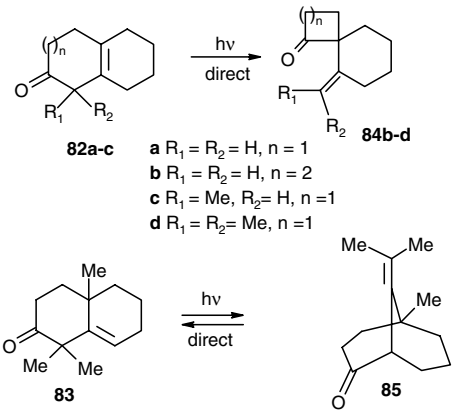

SCHEME 20

1,3-acyl migration to give **85** (Scheme 20).[50] Other related ketones exhibited similar behavior upon direct irradiation.[51]

Photochemical reactions of several steroids containing β,γ-enone chromophores have been investigated and found to undergo 1,3-acyl migration on direct irradiation.[51–57] The direct irradiation of **86** has been reported to give the compound **87** as the major product, along with a samll amount of the decarbonylated product **88**.[52] Similar results were obtained on direct irradiation of **89**.[53] The direct irradiation of homologated stereoid **91** led to 1,3-acyl migration and gave two products, **92** and **93**.[54] Suginome and co-workers have examined the photoreaction of several modified steroids.[55,56] Thus direct irradiation of **94** in *t*-butanol gave the ring-contracted products **95** as a result of a 1,3-acyl shift, along with an oxa-di-π-methane product.[55] The stereochemistry of the products was found to be conformation dependent (Scheme 21).[55,56] Other steroids, such as 3,19-dioxo-17β-acetoxy-Δ^4-androstene and its derivative, have also been reported to undergo 1,3-migration in addition to other photoreactions.[57]

79.6 1,3-Acyl Migrations in Spirocyclic β,γ-Unsaturated Ketones

Photochemical reactions of a number of spirocylic compounds, such as **96**, **97**, and **98** (Scheme 22), upon triplet excitation have been investigated.[58,59] The direct excitation of ketones of type **96** led to an electrocyclic reaction and α-cleavage instead of 1,3-acyl migration.[58]

79.7 1,3-Acyl Migrations in Bridged β,γ-Unsaturated Ketones

Bicyclo[2.2.1]heptenones and Bicyclo[3.2.1]octenones

The photochemistry of bridged carbocyclic systems containing a β,γ-unsaturated carbonyl group has stimulated great interest and provided a good probe to unravel various aspects of the photochemical reactions of β,γ-enones. This is presumably due to enhanced interaction between the carbonyl and alkene chromophores, and also to molecular rigidity. The photochemical reaction of bicyclo[2.2.1]heptenone **99** was examined in great detail by several groups (Scheme 23).[60–63] Schenk and co-workers[60] observed photofragmentation to ketene and cyclopentadiene in a variety of solvents, while Schuster[61] found that **99** undergoes a 1,3-acyl migration faster than ketene elimination. Cyclopentadiene and ketene are formed to a large extent from the 1,3-acyl shift product **100**, and that reaction proceeds through the biradical **104**. Ipakscthi reported that the 1,3-acyl shift product **100** is also formed in addition to the oxa-di-π-methane reaction product **103** during sensitized irradiation of **99**.[62] Schexnayder and co-workers also noted the formation of **100** during sensitized irradiation of **99** and that the former is converted into the

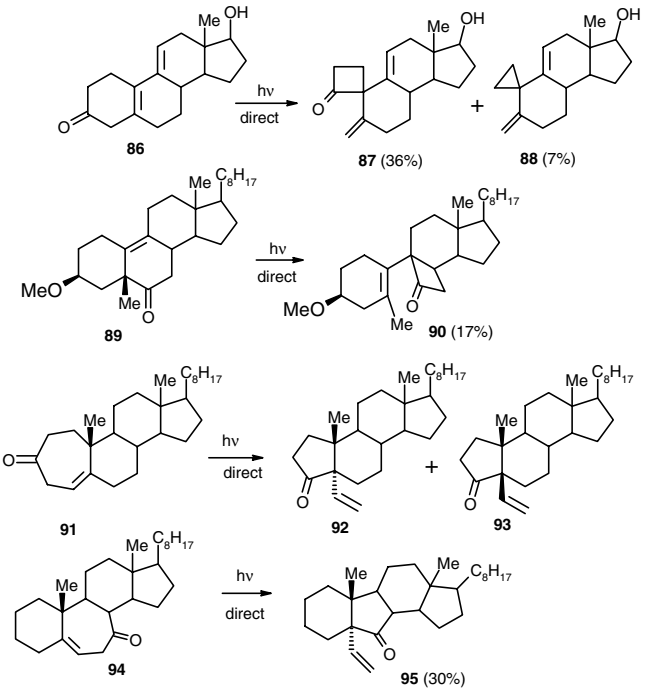

SCHEME 21

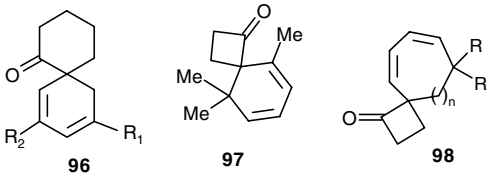

SCHEME 22

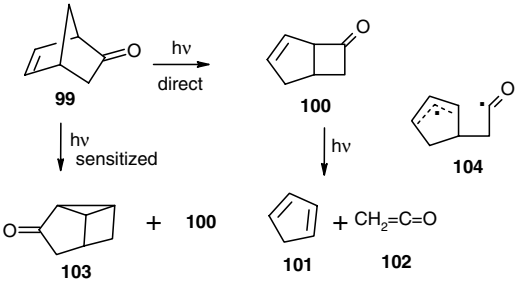

SCHEME 23

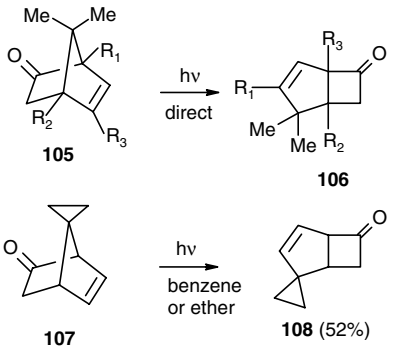

SCHEME 24

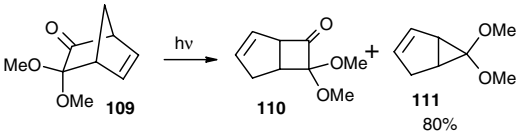

SCHEME 25

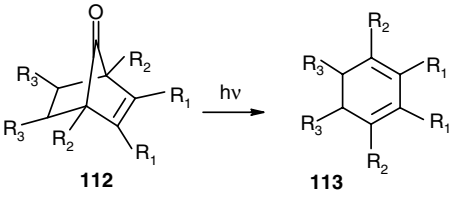

SCHEME 26

ODPM product on sensitized irradiation in acetone.[63] Similar results were obtained on direct irradiation of bicyclo[2.2.1]heptenones **105** and **107**, which gave the 1,3-acyl migration products **106** and **108**, respectively, in addition to the corresponding cyclopentadienes (Scheme 24).[64,65] Direct irradiation of ketone **107** in methanol, however, gave a complex mixture of products.[65]

Similarly, photolysis of 3,3-dimethoxy-5-norbornen-2-one **109** in various solvents (dioxane, acetonitrile, and acetone) gave the 1,3-acyl shift product **110** in minor amounts and the decarbonylated product **111** as the major product (Scheme 25). Irradiation of **109** in methanol gave a complex mixture of products arising through an oxa-carbene formed from the biradical generated after initial α-cleavage.[66] It was also observed that the decarbonylated product **111** was obtained at the expense of the initially formed 1,3-acyl shift product **110**.

Irradiation of 7-norbornenones of type **112**, wherein the carbonyl group is sited at the methano bridge, does not lead to a 1,3-acyl shift; instead, they undergo decarbonylation to give the corresponding cyclohexadienes (Scheme 26) in addition to 1,3,5-hexatrienes that arise as a result of photochemical electrocyclic ring opening of the initial product.[67] Other compounds of type **112**, readily available by Diels-Alder reaction of cyclopentadienone with dienophiles, undergo a facile decarbonylation upon irradiation.[68]

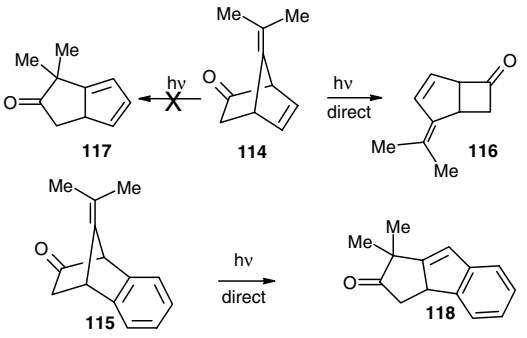

SCHEME 27

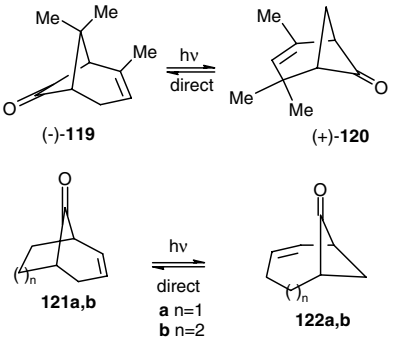

SCHEME 28

The photochemistry of the bis-(β,γ-unsaturated) ketone **114** and the benzo analogue **115** is interesting. The direct irradiation of **114** leads to the formation of a 1,3-acyl shift product **116** selectively. The alternative possibility, **117**, which could arise via participation of the alkene moiety in the methano bridge was not formed. However, irradiation of **115** gave the product **118** (Scheme 27).[65]

Photochemical reaction of chrysanthenone **119**, a photoisomer of verbenone, has been examined in detail.[69,70] Irradiation of (−)-**119** in cyclohexane led to a reversible 1,3-acyl migration to give (+)-**120** in addition to other products formed as a result of decarbonylation. Other higher homologues such as **121a** and **121b** were also found to undergo reversible 1,3-acyl migration to give **122a** and **122b**, respectively (Scheme 28), in addition to other products.[69,70]

In pioneering studies, Givens and co-workers examined the photochemical reactions of optically active bicyclo[3.2.1]oct-2-en-7-one **123a** and deuterated and halogenated analogues in order to resolve the singlet–triplet reactivity of β,γ-unsaturated ketones and the mechanism of the 1,3-acyl migration and oxa-di-π–methane reaction.[71] The direct irradiation of all the enones led to 1,3-acyl shifts, while the sensitized irradiation gave products due to both the oxa-di-π-methane reaction as well as 1,3-acyl migration. Irradiation of (+)-**123a** at 300 nm in ether gave (−)-**124a** (Scheme 29). Other ketones **123b,c,d** also gave the corresponding 1,3-shift products **124b,c,d** on direct irradiation. No oxa-di-π-methane products were detected on direct irradiation. It was further observed that introduction of halogens at the double bond (as in **123c** and **123d**) or at the bridgehead (**124c** and **124d**) reduces the efficiency of the 1,3-acyl migration. However, this heavy-atom effect does not lead to more efficient intersystem crossing to give triplet ketone because no oxa-di-π-methane reaction was observed.

Ueyhara and co-workers[72] have studied the photoreaction of a number of bicyclo[3.2.1]octenone systems, wherein the position of the chromophores is switched; that is, the alkene chromophore is in the

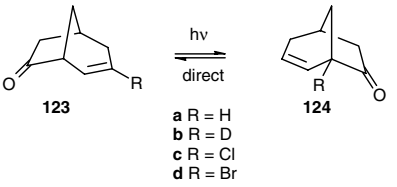

SCHEME 29

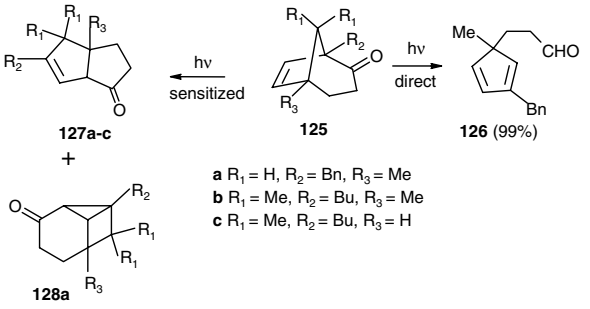

SCHEME 30

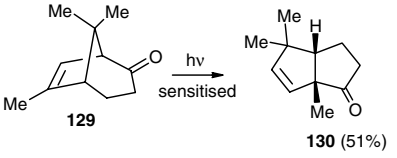

SCHEME 31

ethano bridge and the carbonyl group is in the 3-carbon bridge. Direct irradiation of the enone **125a** with a benzyl substituent at the bridgehead did not give a 1,3-acyl shift product; instead, the cyclopentadiene derivative **126** was obtained. The sensitized irradiation of **125a**, however, furnished the 1,3-acyl shift product **127a** (32%) and the oxa-di-π-methane product **128a** (18%). The ketone **125b,** on the other hand, underwent 1,3-acyl migration both upon direct and sensitized irradiation to give **127b** in good yields (50 to 60%) (Scheme 30). The analogue **125c** also behaved similarly and gave the 1,3-acyl shift product **127c** in addition to a small amount of another product. It is interesting to note that the 1,3-acyl shift in such systems provides a novel route to *cis*-bicyclo[3.3.0]octenones, which are generally obtained via oxa-di-π-methane reaction in bicyclo[2.2.2]octenones. The authors have successfully employed the 1,3-acyl shift in **129** to prepare the diquinane intermediate **130** (Scheme 31),[72] which was employed for a formal synthesis of capnellene, a triquinane natural product isolated from *capnella imbricate*.[73,74] The ketoester **131** also undergoes efficient 1,3-acyl migration on direct irradiation in benzene to give the diquinane **132** (Scheme 32) in excellent yield. This is a known precursor for the synthesis of (±)-8-epiloganin aglucones and (±)- mussaenoside.[75]

Uyehara and co-workers have also reported efficient photochemical 1,3-sigmatropic acyl shifts in a variety of bicyclo[3.2.2]nonenones of type **133** and **135** that provided an excellent synthetic entry into the *cis*-hydrindanone ring system (Scheme 33)[76] and also employed 1,3-migration in total syntheses of pinguisone, deoxypinguisone and ptilocaulin.[77,78]

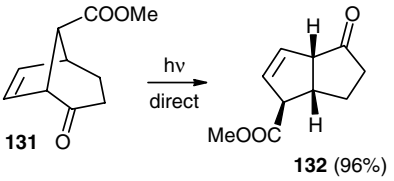

SCHEME 32

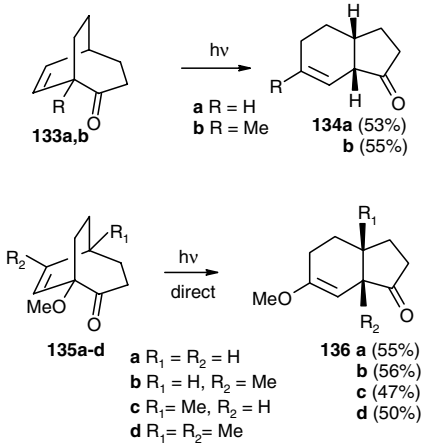

SCHEME 33

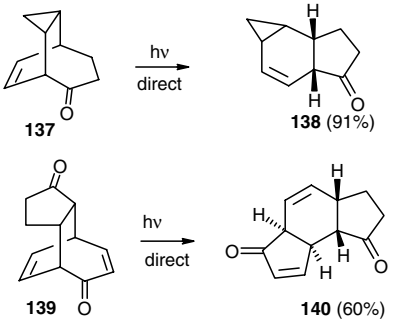

SCHEME 34

Annulated bicyclo[3.2.2]nonanes with β,γ-enone chromophores have also been reported to undergo an efficient 1,3-acyl shift. Thus, irradiation of **137** in benzene/methanol gave the tricyclic compound **138** in excellent yield (Scheme 34).[79] The more complex system **139** also underwent 1,3-acyl migration on irradiation in $CDCl_3$ through quartz to give the *cis:anti:cis* tricyclic compound **140**. However, the diendione **139** was inert on irradiation through Pyrex.[80] Other, more functionalized systems with a β,γ-enone chromophore in the bicyclo[3.3.1]nonane ring system have also been found to undergo 1,3-acyl migrations.[81]

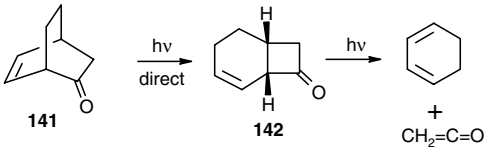

141 **142**

SCHEME 35

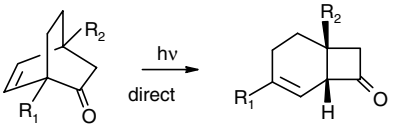

143 **144**

a R_1 = H, R_2 = Me
b R_1 = Me, R_2 = H
c, R_1 = OMe, R_2 = H
d, R_1 = H, R_2 = OMe

SCHEME 36

1,3-Acyl Migrations in Bicyclo[2.2.2]octenones and Their Congeners

Studies on the photochemical reactions of bicyclo[2.2.2]octanes with β,γ-enone groups provided greater insight into the excited-state reactivity correlation as well as the mechanism of both the 1,3-acyl migration and the oxa-di-π-methane reactions. The photochemical reaction of the parent bicyclo[2.2.2]octenone **141** and its benzoannulated analogue reported by Givens and co-workers is a seminal example.[82,83] The direct irradiation of **141** in ether gave the enone **142**, with a bicyclo[4.2.0]octane framework, as the sole product. The reaction was irreversible. Further irradiation of **142** led to ketene elimination and formation of cyclohexadiene (Scheme 35). In sharp contrast, the sensitized irradiation brought about an oxa-di-π-methane reaction exclusively.[82] Based on these studies, the authors suggested a concerted symmetry allowed process.[82, 10]

Subsequently, Demuth and co-workers examined the photoreaction of the bicyclo[2.2.2]octenones **143a**,**b** on sensitized as well as direct irradiation. Direct irradiation of **143a** and **143b** exclusively gave the 1,3-acyl shift products **144a** and **144b,** respectively (Scheme 36).[84,85] However, the formation of 1,3-acyl shift products along with oxa-di-π-methane products were also observed during acetone-sensitized irradiation of **143a**,**143b**, and congeners.[84,85] Rogers and co-workers examined the photoreaction of the bicyclo[2.2.2]octenones **143c** and **143d** with methoxy substitutents on direct and sensitized irradiation. Direct irradiation of **143c** and **143d** in benzene, ether, methanol, or pentane led to the formation of the 1,3-acyl shift product **144c** and **144d**, respectively. It was noted that **143c** and **143d** also gave products due to ketene elimination. The bicyclic compound **144d** was also formed in small amounts during sensitized irradiation of **143d**.[86,87] From these studies it was suggested that a 1,3-acyl shift is initiated through α-cleavage and proceeds through a biradicaloid intermediate that subsequently undergoes ring closure to give the final product.[86–88]

Yamauchi et al. have recently examined the photoreaction of a large number of functionally more complex bicyclo[2.2.2]octenones (**145** and **147**) that contain methoxy substituents at both α– and α′-positions. However, these enones were found to undergo decarbonylation on direct irradiation in benzene to give bicyclo[4.1.0]hept-2-enes **146** and **148**, respectively (Scheme 37).[89] The decarbonylated products are thought to arise via cyclobutanone derivatives that are initially formed as a result of 1,3-acyl migration. In some cases, the 1,3-acyl shift product was isolated, and these were found to give the decarbonylated products after prolonged irradiation. However, irradiation of cyano-substituted bicyclooctenone **145d** gave a complex mixture of products. Similarly, formyl-substituted **145e** underwent deformylation along

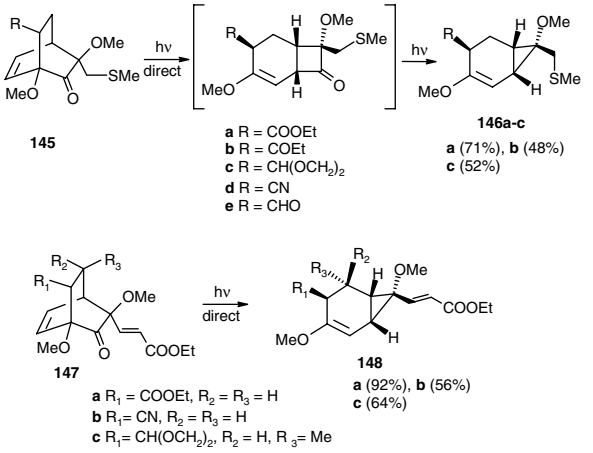

SCHEME 37

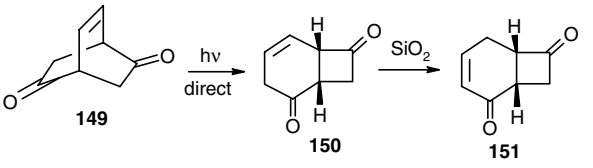

SCHEME 38

with decarbonylation.[89] The photoreactions of **145a,b,c** and **147a,b,c** provide a new and stereoselective route to trinorcarenes, which are otherwise not readily accessible. In this context, it can be mentioned that many other highly substituted bicyclic octenones have been reported to undergo ketene elimination on direct irradiation.[90,91]

Dekkers and Schippers have examined the photoreactivity of the bicyclo[2.2.2]oct-2-ene-5,7-dione **149** with circularly polarized light to determine its chiroptical properties and to develop a method for enantiomeric enrichment through photodestruction.[92] Irradiation of **149** with 313-nm light in pentane was found to give the 1,3-acyl shift product **150** along with phenol, which is formed from **149** via ketene elimination and aromatization. The product **150** could not be isolated because it rearranged to the conjugated enone **151** during chromatography (Scheme 38). [92]

The aforementioned results indicate that 1,3-migration is a general reaction during direct irradiation of rigid bicyclo[2.2.2]octenones, although it is dependent on structure and the other functional groups present in the chromophoric system. In addition to the examples presented above, photoreaction of a variety of other annulated bicyclo[2.2.2]octenones has been studied and found to undergo 1,3-acyl migration on direct irradiation, and some of these examples are presented below. The photochemistry of benzobicyclo[2.2.2]octadienone **152a** was investigated by Givens and co-workers[82,83] and Ipaktschi.[93] Ipaktschi reported that direct irradiation of **152a** gives naphthalene and ketene. Givens and co-workers irradiated an ether solution of **152a** in a Pyrex vessel and two products were detected at 50% disappearence of **152a**. The major product was naphthalene **154a**, as reported by Ipakstchi, and the minor product was found to be **153,** the result of 1,3-acyl migration (Scheme 39).[82] The analogues of **152** with methyl substituents also behaved in a similar fashion.[90,91,94] Thus, the hexamethylated compound **152b** gave tetramethyl naphthalene **154b** as a major product on direct irradiation in ether.[90]

The photochemical reaction of other annulated derivatives, such as **155a**, **155b**, and their diasteroisomers **156a** and **156b**, was studied and found to undergo 1,3-acyl migration.[79,95] Agosta and Takakis

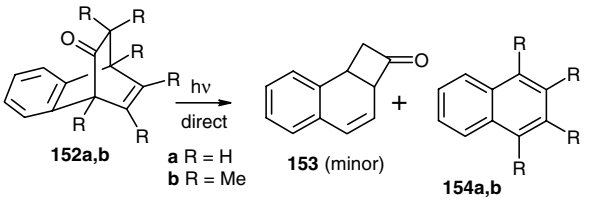

SCHEME 39

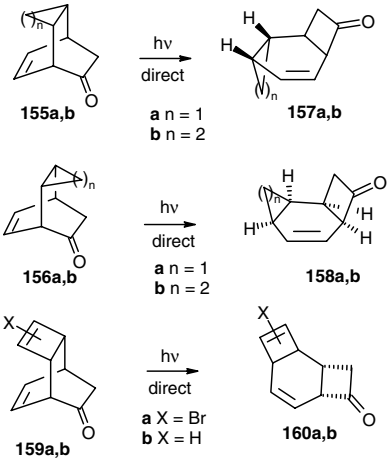

SCHEME 40

obtained the 1,3-acyl shift product **157a** (60%, at 10% conversion), in addition to other products, by irradiation of **155a** in benzene containing methanol. Prinzbach also investigated the photoreaction of **155a**, the higher homologue **155b** and their diastereomers **156a** and **156b**. These enones also behaved in a similar fashion and underwent 1,3-acyl migration and ketene elimination. The ketone **155b** gave the *cis*:*anti*:*cis* tricyclic compound **157b** (75% yield at 55% conversion), whereas the stereoisomers **156a** and **156b** furnished the corresponding 1,3-acyl shift product **158a** (~75% yield, at ~80% conversion) and **158b** (30 to 40%, at 80% conversion), respectively (Scheme 40).[95] Mehta and Srikrishna have examined the photochemistry of the tricyclic compounds **159a** and **159b** that are available through cycloaddition of cyclooctatetraene and its dibromoderivative with acrylonitrile. Direct irradiation of **159a** in benzene gave the 1,3-acyl shift product **160a** in 40% yield, along with other products arising via decarbonylation and ketene elimination. Similar irradiation of **159b** gave the 1,3-acyl shift product **160b** in low yield (20%), while cyclooctatetraene was as the major product.[96]

Photochemical reaction of complex tricyclic compounds **161**, **162**, **167**, **168**, and their congeners containing a β,γ-enone chromophore follow a similar course on direct excitation. Thus, irradiation of **161** in ether leads to 1,3-acyl migration to give **163**, which subsequently undergoes decarbonylation to yield the cyclopropyl compound **164**. Interestingly, the ene-dione **162** underwent selective photoreaction characteristic of β,γ-enones and furnished **165** and **166** on direct excitation in ether as a result of 1,3-shift followed by decarbonylation (Scheme 41). The tricyclic compounds **167**, **168,** and their derivatives were also found to behave similarily.[97]

Yates and Stevens[98] studied the photoreaction of heteroannulated bicyclo[2.2.2]octenone **169** under direct and sensitized conditions. Irradiation of **169** in ether gave a mixture of **170** and the decarbonylated product **171,** from which the 1,3-acyl shift product **170** was isolated by crystallization (Scheme 42).

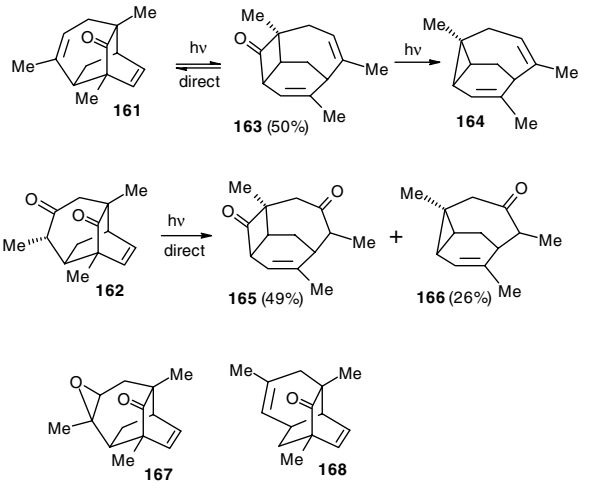

SCHEME 41

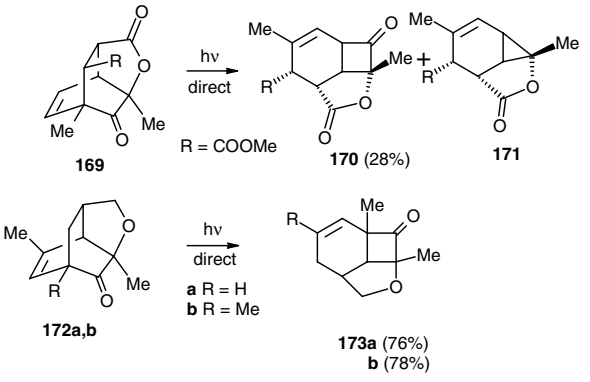

SCHEME 42

Further irradiation of a mixture of **170** and **171** gave **171**, thus indicating that the product **171** is formed from the 1,3-acyl shift product by decarbonylation.[98] Similarly, irradiation of **172a** and **172b** in benzene for short duration gave the 1,3-acyl shift products **173a** and **173b** in good yields (Scheme 42). It was observed that longer periods of irradiation led to decarbonylation.[99]

The photochemical reactivity of a variety of tricyclic systems such as **174**, **175**, **178**, and **179** containing a β,γ-unsaturated carbonyl group in an *endo*-tricyclo[5.2.2.0^{2,6}] undecane framework has been studied.[100–102] Irradiation of **174** and **175** in benzene furnished the 1,3-acyl migration products **176** and **177**, respectively (Scheme 43), along with unreacted starting material. Interestingly, the dione **178,** with the highly reactive α,β-epoxyketo chromophore, also underwent a 1,3-acyl shift on irradiation in benzene to give the 1,3-acyl migration product **181** with reasonably good efficiency. It should be mentioned that the trienone **179**, unreactive on triplet sensitized irradiation, smoothly undergoes a 1,3-acyl shift to give the corresponding tricyclic compound **182** on irradiation in benzene. This observation further strengthens the general view that 1,3-acyl migration occurs from excited singlet state. Furthermore, the dienone **180**, with an eight membered ring, also gave the tricyclic compound **183** as a result of 1,3-acyl migration (Scheme 44). It should be noted that, in general, these compounds are labile and they decompose during storage even at low temperature.[100,101]

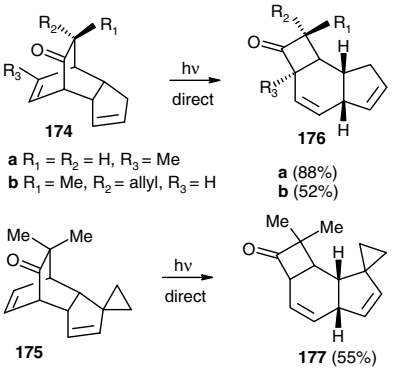

SCHEME 43

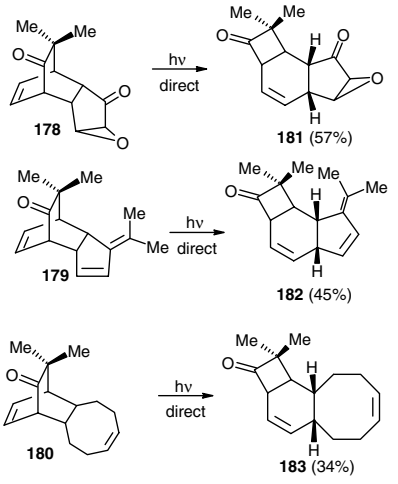

SCHEME 44

The direct irradiation of tricyclic compounds such as **184** and **185**, with methoxy groups at the α-carbon, however, led to decarbonylation. Thus, irradiation of a benzene solution of **184** and **185** in a Pyrex immersion well with a mercury vapor lamp (400 W) gave the tricyclic products **186** and **187**, respectively, containing a cyclopropane ring fused to a *cis*-hydrindane ring system (Scheme 45). The photoreaction proceeds through an initial 1,3-acyl shift to give the corresponding cyclobutanone which subsequently undergoes decarbonylation to give the final product.[102] It appears that the presence of methoxy groups at the bridgehead is partly responsible for the tendency of such β,γ-enones to decarbonylate because other simple bicyclic compounds with a methoxy substituent at the bridgehead also exhibit similar behavior.[86,89]

The photoreaction of tricyclic undecadienones **188** and **189** with hydroxyl groups at the α′-carbon have also been investigated.[103–107] While the triplet excitation of these ketones led to an efficient oxa-di-π-methane rearrangement, the direct irradiation gave complex results. Thus, the irradiation of tricyclic hydroxyketone **188** in ethyl acetate gave a very small amount of the highly unstable 1,3-acyl shift product **190,** which was isolated as the hydrogenated product **191** (7%).[103] The direct excitation of **189a** and **189b** in benzene for 2h furnished an inseparable mixture of dienones **192a**, **193a** (66%) and **192b**, **193b** (60%), respectively (Scheme 46).[104]

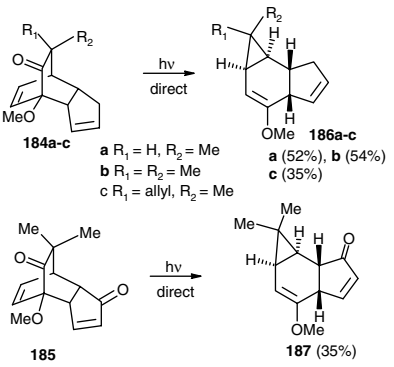

184a-c **a** R_1 = H, R_2 = Me; **b** R_1 = R_2 = Me; c R_1 = allyl, R_2 = Me

186a-c **a** (52%), **b** (54%) **c** (35%)

185

187 (35%)

SCHEME 45

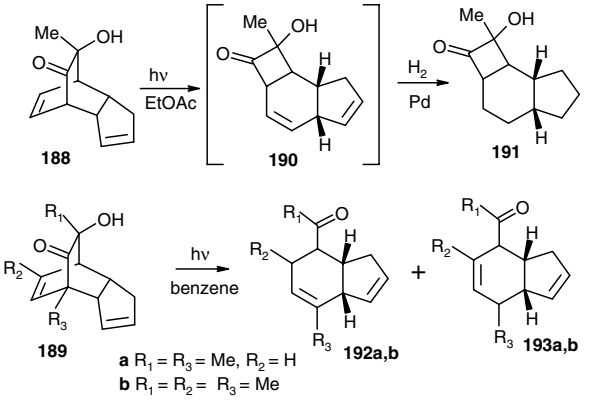

188 **190** **191**

189 **a** R_1 = R_3 = Me, R_2 = H; **b** R_1 = R_2 = R_3 = Me

192a,b **193a,b**

SCHEME 46

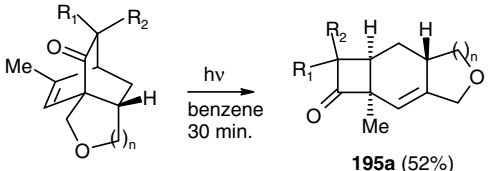

194a,b **a** n = 1, R_1 = R_2 = H; **b** n = 3, R_1 = R_2 = Me

195a (52%) **b** (40%)

SCHEME 47

Another class of tricyclic compounds with a β,γ-enone chromophore in the bicyclo[2.2.2]octane framework that undergo a reasonably efficient 1,3-acyl migration on direct irradiation is shown in Scheme 47. The direct excitation of the *endo*-tricyclic chromophoric systems **194a** and **194b**, readily available from *p*-cresol, in benzene for short duration gave the linearly fused tricyclic compounds **195a** and **195b** containing a cyclobutanone ring in reasonably good yield along with some unreacted starting material. It was noted that irradiation for longer periods leads to decarbonylation and ketene elimination at the expense of the 1,3-acyl shift products.[108–110]

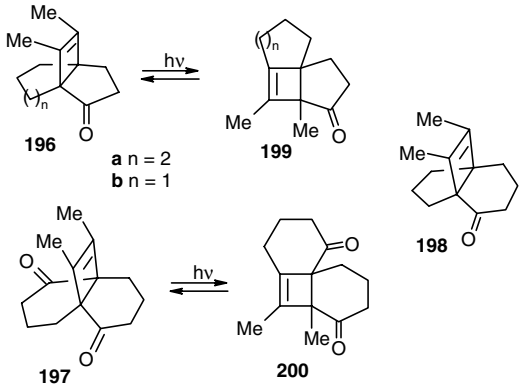

SCHEME 48

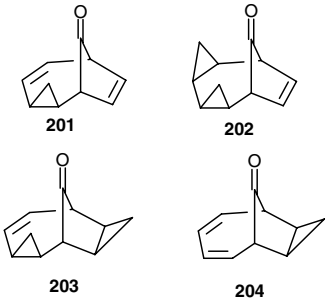

SCHEME 49

79.8 1,3-Acyl Migrations in Miscellaneous β,γ-Unsaturated Ketones

Cargill and co-workers examined the photoreactions of a number of interesting tricyclic compounds, such as **196 197,** and **198,** with a propellane framework. They observed reactions such as the 1,3-acyl shift, photoreduction and [1,3]-hydrogen migration upon direct irradiation.[111–113] Thus, the enones **196** and **197** underwent a reversible 1,3-acyl shift (Scheme 48).[111,112] However, the related enone **198** did not undergo 1,3-shift; instead, other reactions such as photoreduction and 1,3-hydrogen shift were observed.[113] The difference in the behavior of **196**, **197,** and **198** was explained in terms of the ε_{max} of the ketones.[113]

Agosta and Takakis investigated photochemical reactions of ketones **201** through **204** (Scheme 49). However, while irradiation of the **201**, **202,** and **204** gave products due to decarbonylation and rearrangement of cyclopropropyl groups, the enone **203** was found to be unreactive under a variety of conditions. This unreactivity of **203** was explained in terms of a reversible 1,3-acyl shift.[114] Sasaki and associates have examined the photoreactions of compounds **205** and reported 1,3-acyl migration on direct irradiation to give the corresponding photoproducts **206** (Scheme 50).[115]

A highly interesting 1,3-acyl migration in the protoadamantane derivative **207** was observed on both sensitized and direct irradiation, to give **208** (Scheme 51).[116] Recently, photoreaction of 4-methylene-2-protoadamantanone **209** was examined under both direct and sensitized irradiation. However, irradiation

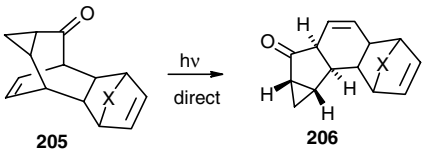

205 **206**

SCHEME 50

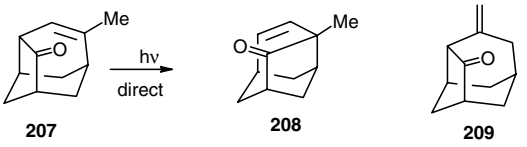

207 **208** **209**

SCHEME 51

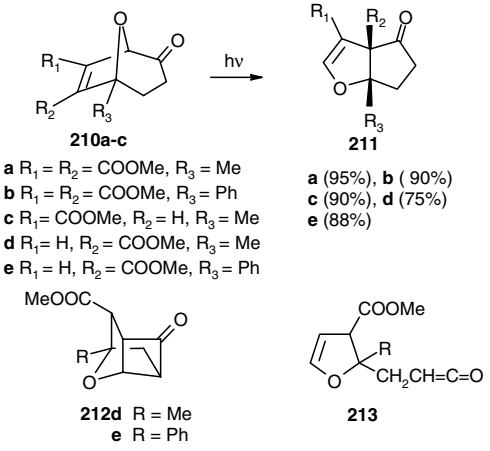

210a-c

a $R_1 = R_2 = COOMe$, $R_3 = Me$
b $R_1 = R_2 = COOMe$, $R_3 = Ph$
c $R_1 = COOMe$, $R_2 = H$, $R_3 = Me$
d $R_1 = H$, $R_2 = COOMe$, $R_3 = Me$
e $R_1 = H$, $R_2 = COOMe$, $R_3 = Ph$

211

a (95%), **b** (90%)
c (90%), **d** (75%)
e (88%)

212d R = Me
e R = Ph

213

SCHEME 52

of **209** in benzene gave tarry material due to rapid photodecomposition, while sensitized irradiation in acetone led to addition of the anacetonyl radical at the γ-carbon.[117] Padwa and co-workers reported a remarkably efficient 1,3-acyl migration in 8-oxa-bicyclo[3.2.1]oct-6-en-2-ones **210** (Scheme 52) on both direct as well as sensitized irradiation.[118] While irradiation of **210a,b,c** in benzene led to a clean 1,3-acyl migration and afforded the bicyclic products **211a,b,c** in excellent yields, the direct excitation of the isomeric compounds **210d** and **210e** was found to give the tricyclic compounds **212** (Scheme 52). Subsequent studies showed that the tricyclic compounds **212** are not the primary photoproducts but are formed via photoreaction of the initially generated 1,3-acyl shift products **210d** and **210e** and that short irradiation led to only 1,3-acyl migration. The formation of the tricyclic compound **212** containing a cyclobutanone ring occurs via cycloaddition in the ketene intermediate **213**, which is formed by hydrogen abstraction in the biradical generated after initial Norrish Type I cleavage.[118]

Recently, Link and Keissling studied the photobehavior of aza-bicyclo[2.2.2]octenones **214** and reported 1,3-acyl migration upon direct irradiation, which gave the lactam **215** (Scheme 53).[119]

From the foregoing examples, it appears that 1,3-acyl migration is a general photoreaction that occurs mostly on direct excitation of rigid β,γ-unsaturated ketones although other reactions such as decarbonylation

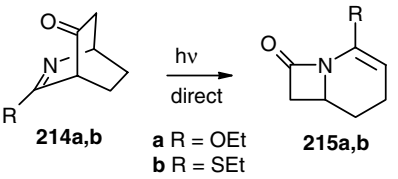

214a,b **a** R = OEt **b** R = SEt **215a,b**

SCHEME 53

and ketene elimination may also compete. The structure of the chromophoric system and the presence of other functional groups also influence the photoreaction in a subtle fashion. The direct excitation of β,γ-unsaturated aldehydes generally does not lead to 1,3-acyl migration; instead, another photoreaction such as deformylation is observed. Recently, however, Armesto and co-workers reported a few examples of 1,3-acyl migration on sensitized irradiation of β,γ-unsaturated aldehydes.[120]

79.9 Applications of 1,3-Acyl Migrations toward Synthesis of Natural Products

It may be evident from the above that 1,3-acyl migration in rigid β,γ-unsaturated ketones have immense potential as a methodology because it provides the opportunity to create a variety of molecular frameworks in stereoselective fashion via appropriate design of the starting chromophoric system. Except for a few, most of the earlier studies on 1,3-acyl migration in β,γ-enones deal with elucidation of the mechanism and establish the structure-reactivity-excited state relationship. The potential of the 1,3-acyl shift in organic synthesis was realized only recently. In contrast to the oxa-di-π-methane reaction of β,γ-unsaturated ketones, there are only a few examples of applications of 1,3-acyl migration toward synthesis of natural products. Some of these are presented below.

Uyehara and co-workers[77,121] developed a synthesis of (±)-pinguisone **216** and (±)-deoxypinguisone **217** containing an unusual terpene skeleton, employing 1,3-acyl migration in a bicyclo[3.2.2]nonane framework. Thus, the 1,3-acyl shift in the bicyclic precursor **218**, on direct irradiation in tetrahydrofuran, gave the ketoenol ether **219** in good yield (59%). It may be noted that the *cis*-hydrindane framework and three contiguous stereocenters of the target molecules are generated in the photochemical reaction (**218** → **219**). The photoproduct **219** was then elaborated into **220** and **221,** which were subsequently transformed into pinguisone **216** and deoxypinguisone **217,** respectively (Scheme 54).[77,121] Similarly, the synthesis of (±)-ptilocaulin **225**, a cytotoxic cyclic guanidine isolated from the Caribbean sponge *Ptilocaulis* aff. P. *Spiculifer*[122] was also carried out via photochemical 1,3-acyl shift in the bicyclo[3.2.2]nonenone framework.[78,123] The bicyclic precursor **222** was synthesized from tropone. Irradiation of **222** in benzene yielded the intermediate **223** in excellent yield (65%). This has most of the structural, functional, and stereochemical features of ptilocaulin. Transformation of the photoproduct **223** into enone **224** followed by treatment with guanidine gave ptilocaulin (Scheme 55). The same research group has also employed the 1,3-acyl migration protocol with the bicyclo[3.2.1]octenone **129** (Scheme 31) (*vide infra*) to prepare a diquinane precursor for the synthesis of (±)-$\Delta^{9(12)}$-capnellene, a triquinane natural product.[72] Chang and co-workers have also utilized the 1,3-acyl shift as a key reaction for the synthesis of *the* diquinane precursor **132** (Scheme 32) *vide infra*, which is readily converted into a known intermediate for the synthesis of (±)-mussaenoside and (±)-8-epiloganin aglucones.[75]

The photochemical 1,3-acyl shift in the *endo*-tricyclo[5.2.2.$0^{2,6}$]undecane ring system provides a stereoselective route to protoilludanes,[100,101] a unique class of sesquiterpene containing a cyclobutane ring angularly fused to a *cis*-hydraindane ring in their molecular framework.[124] We developed a route to the tricyclic chromophoric systems **228** and **230a,b,c,** and examined their photoreaction upon direct irradiation as a route to protoilludene. Thus, oxidation of hydroxymethylphenol **226** in the presence of cyclopentadiene gave the *endo*-ketoepoxide **227**, which was transformed into **228** and **230** by manipulation

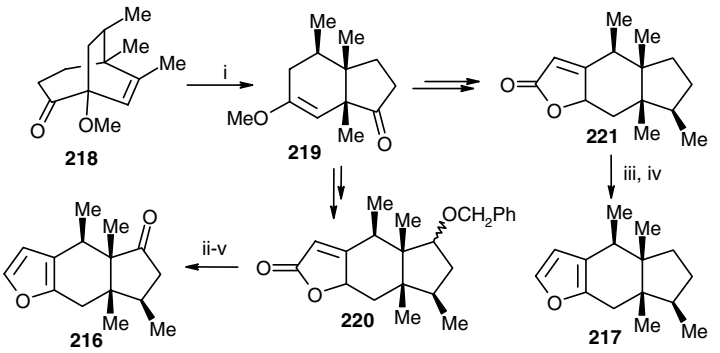

Reagents/conditions: i, hν, THF; ii, BBr_3, CH_2Cl_2; iii, DIBAH; iv, 1M H_2SO_4; v, Ac_2O, DMSO.

SCHEME 54

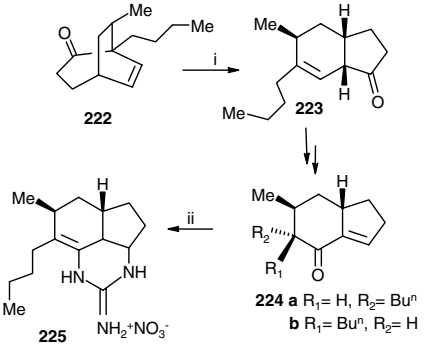

Reagents/conditions: i, hν, THF; ii, guanidine

SCHEME 55

of the oxirane and cyclopentene ring. Irradiation of dienone **228** in benzene in a Pyrex immersion well gave the compound **229** (33%) with the tricyclic framework of protoilludanes, along with some unreacted starting material. Interestingly, the tricyclic ene-dione **230a** with an additional carbonyl group in the five-membered ring, smoothly underwent 1,3-acyl migration to give the corresponding product **231a** (30%). The α,α-dimethyl substituted ene-dione **230b** also underwent 1,3-acyl migration but formation of a very small amount of aldehyde, the result of α-cleavage in the five-membered ring, was observed. The enone **230c** underwent a more efficient 1,3-acyl migration on similar irradiation to give the tricyclic compound **231c** (44%) (Scheme 56), which is a potential precursor to protoilludene.[125]

In continuation of our interest in designing new methodology based on the chemistry of cyclohexadienone and photoreaction of β,γ-enones,[126–128] we developed a new stereoselective route to sterpuranes, another class of sesquiterpenes containing a tricyclic framework wherein the cyclobutane ring is fused with a hydrindane unit in a linear fashion. In this context, the tricyclic β,γ-enones of type **235** were synthesized and their photochemistry was examined upon direct as well as sensitized irradiation.[126] The desired tricyclic compound **235**, containing a β,γ-enone chromophore, was prepared from hydroxymethylphenol **232.** Oxidation of **232** with sodium metaperiodate generated the cyclohexadienone **233**, which

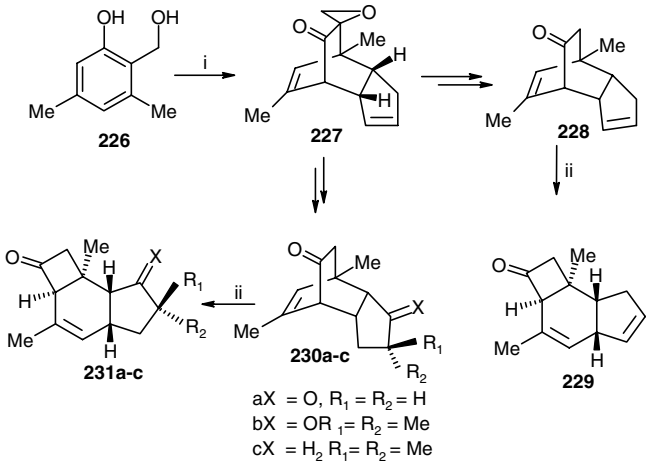

Reagents/conditions: i, $NaIO_4$, aq.CH_3CN, cyclopentadiene;
ii hν, benzene

SCHEME 56

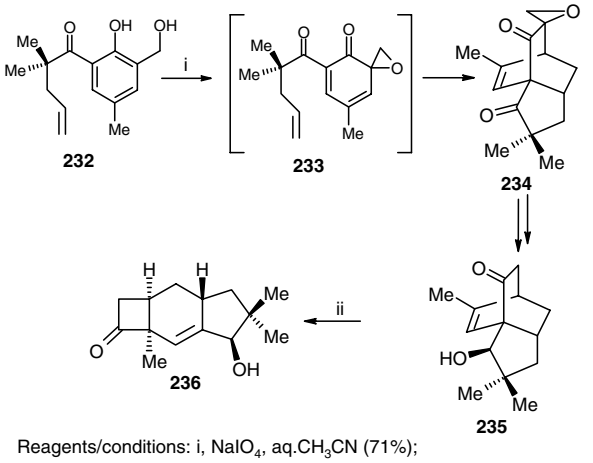

Reagents/conditions: i, $NaIO_4$, aq.CH_3CN (71%);
ii hν, benzene (55%)

SCHEME 57

underwent intramolecular cycloaddition to give the adduct **234,** which upon further manipulation provided the chromophoric system **235**. Irradiation of **235** in benzene gave the compound **236** as a result of 1,3-acyl migration (Scheme 57).[126] This methodology provides a novel and stereoselective route to sterpuranes. Interestingly, sensitized irradiation of **235** led to a triquinane intermediate that can be used in the synthesis of coriolin, a triquinane natural product.[126] In addition to these examples of 1,3-acyl migration in β,γ-enones that clearly indicate the synthetic potential of this reaction, the decarbonylation reaction, which is occasionally observed upon direct irradiation, can also be developed as a synthetic method.[128]

79.10 Conclusion

The 1,3-acyl migration is another characteristic and fascinating facet of the photochemistry of β,γ-unsaturated ketones. The reaction is fairly general for rigid β,γ-enones, and a wide variety of substrates undergo 1,3-acyl shift although sometimes it may be accompanied by decarbonylation and ketene elimination. Although the structure of the chromophoric system and the presence of functional groups control the nature of the excited states and their mode of deactivation in a subtle fashion, in general, the rearrangement is observed either from the excited singlet (S_1, $n\pi^*$) or triplet (T_2, $n\pi^*$) states. It is evident from the foregoing examples that 1,3-acyl migration, especially in rigid systems, has immense potential as a versatile synthetic methodology because it provides opportunities to create a diverse array of molecular structures with high stereoselectivity. It provides methods for ring contraction, ring expansion, annulation, etc., depending on the structure of the chromophoric systems. Further, it can be noted that the structures generated via 1,3-acyl migration are difficult to obtain via ground-state chemical reactions. Although the synthetic applications of 1,3-acyl migration have been explored only to a limited extent thus far, the examples presented herein clearly indicate its potential as a stereoselective method and its strategic role in synthesis design.

Acknowledgments

The author thanks DST, CSIR New Delhi, and BRNS Bombay for continued support. The author is also grateful to his students, whose dedicated efforts led to the results, some of which have been reported herein. Thanks also to Professor A. Srikrishna for his kindness and support in our endeavor.

References

1. Hixson, S.S., Mariano, P.S., and Zimmerman, H.E., The di-π-methane and oxa-di-π-methane Rearrangements, *Chem. Rev.*, 73, 531, 1973.
2. Dauben, W.G., Lodder, G., and Ipakstchi, J., Photochemistry of β-γ-unsaturated ketones, *Top. Curr. Chem.*, 54, 73, 1975.
3. Houk, K.N., The photochemistry and spectroscopy of β,γ-unsaturated carbonyl compounds, *Chem. Rev.*, 76, 1, 1976.
4. Schuster, D.I., in *Rearrangement in Ground and Excited States*, de Mayo, P., Ed., Academic Press, New York, 1980, Vol. 3, 167 and references cited therein.
5. Schaffner, K. and Demuth, M., in *Modern Synthetic Methods*, Scheffold, R., Ed., Springer Verlag, Berlin, 1986, Vol. 4, 61.
6. Zimmerman, H.E. and Armesto, D., Synthetic aspects of the di-π-methane rearrangement, *Chem. Rev.*, 96, 3065, 1996 and references cited therein.
7. Singh, V. and Thomas, B., Recent methodology in the synthesis of polyquinanes, *Tetrahedron*, 54, 3647, 1998,
8. Buchi, G. and Burgess, E.M., Photochemical reactions. IX. Isomerisation of eucarvone, *J. Am. Chem. Soc.*, 82, 4333, 1960.
9. Woodward, R.B. and Hoffmann, R., *The Conservation of Orbital Symmetry*, chap. 7, Academic Press, New York, 1972.
10. Demuth, M., The oxa-di-π-methane rearrangement, *Org. Photochem.*, 11, 37, 1991.
11. Henne, A., Siew, N.P.Y., and Schaffner, K., S1 vs T2 photoreactivity of β,γ-unsaturated ketones. Temperature dependant photo-CIDNP of 2-cyclopentenyl methyl ketones, *J. Am. Chem. Soc.*, 101, 3671, 1979.
12. Dalton, J.C., Shen, M., and Snyder, J.J., Mechanistic photochemistry of β,γ-unsaturated ketones. An alternative excited state assignment for the 1,3-acyl shift reaction of alkyl β,γ-enones, *J. Am. Chem. Soc.*, 98, 5023, 1976.

13. Schexnayder, M.A. and Engel, P.S., Systematic structural modifications in the photochemistry of β,γ-unsaturated ketones. II. Acyclic olefins and acetylenes, *J. Am. Chem. Soc.*, 97, 4825, 1975.
14. Van der Weerdt, A.J.A., Cerfontain, H., van der Ploeg, J.P.M., and den Hollander, J.A., Photochemistry of acyclic β,γ-unsaturated ketones. Determination of the electronically excited state responsible for α-cleavage by chemically induced dynamic nuclear polarization, *J. Chem. Soc., Perkin Trans. 2*, 155, 1978
15. Sadler, D.E., Wendler, J., Olbrich, G., and Schaffner, K., Photochemical reaction mechanisms of β,γ-unsaturated ketones. The 1,3-acetyl shift in cyclopent-2-enyl methyl ketones, *J. Am. Chem. Soc.*, 106, 2064, 1984.
16. Reimann, B., Sadler, D.E., and Schaffner, K., Gas phase photochemistry of a β,γ-unsaturated ketone. Concerted and radical mechanisms of the 1,3-acetyl shift in 1,2-dimethylcyclopent-2-enyl methyl ketone, *J. Am. Chem. Soc.*, 108, 5527, 1986.
17. Hess, L.D., Jacobson, J.L., Schaffner, K., and Pitts Jr., J.N., Structure and reactivity in the vapour phase photolysis of ketones. V. Aliphatic cyclopropyl and olefinic ketones, *J. Am. Chem. Soc.*, 89, 3684, 1967.
18. Wilsey, S., Bearpark, M.J., Bernardi, F., Olivucci, M., and Robb, M.A., Mechanism of the oxa-di-π-methane and [1,3]-acyl sigmatropic rearrangements of β,γ-enones: a theoretical study, *J. Am. Chem. Soc.*, 118, 176, 1996.
19. Morrison, H., The photolysis of *trans*-4-hexen-2-one: a novel *trans-cis* isomerization, *Tetrahedron Lett.*, 3653, 1964.
20. Cowan, D.O. and Baum, A.A., Intramolecular triplet-energy transfer, *J. Am. Chem. Soc.*, 93, 1153, 1971.
21. Dauben, W.G., Kellogg, M.S., Seeman, J.I., and Spitzer, W.A., Photochemical rearrangement of an acyclic β,γ-unsaturated ketone to a conjugated cyclopropyl ketone. An oxa-di-π-methane rearrangement, *J. Am. Chem. Soc.*, 92, 1786, 1970.
22. Conia, J.M. and Bortolussi, M., Thermolyse et photolyse de cetones non saturees. XX. Thermolyse et photolyse comparees de l'isopropenyl-3-methyl-3-hexen-5-one-2 et de chacun des produits de transposition formes, *Bull. Soc. Chim. Fr.*, 3402, 1972.
23. Pratt, A.C., Photochemistry of β,γ-unsaturated carbonyl compounds. 3,3-dimethyl-5,5-diphenylpent-4-en-2-one and 2,2-dimethyl-4,4-diphenylbut-3-enal, *J. Chem. Soc., Perkin Trans. 1*, 2496, 1973.
24. Kiefer, E.F. and Carlson, D.A., Photochemistry of β,γ-unsaturated carbonyl compounds. 2,3,3-Trimethyl-1-penten-4-one, *Tetrahedron Lett.*, 1617, 1967.
25. Van der Weerdt, A.J.A. and Cerfontain, H., Photochemistry of acyclic β,γ-unsaturated ketones: the effect of α-methyl substitution, *J. Chem. Soc., Perkin Trans. 2*, 1357, 1977.
26. Van der Weerdt, A.J.A. and Cerfontain, H., Photochemistry of β,γ-unsaturated ketones. V. The direct irradiation of some γ-phenyl β,γ-enones, *Tetrahedron*, 37, 2121, 1981.
27. Koppes, M.J.C. M., Beentjes, P.C. J., and Cerfontain, H., Photochemical reactivity of α-phenyl β,γ-enones. Singlet 1,3-acyl shift, triplet aromatic di-π-methane (DPM) rearrangement and triplet aryl-carbonyl bridging, *Recl. Trav. Chim. Pays-Bas*, 107, 313, 1988.
28. Hancock, K.G., Lau, J.T., and Wylie, P.L., Photochemical synthesis of 1,4-diketones *via* the 1,3-acyl shift of α-hydroxy-β,γ-unsaturated ketones, *Tetrahedron Lett.*, 4149, 1974.
29. Hancock, K.G. and Wylie, P.L., Photochemistry of 3-ethoxy-3-methylpent-4-en-2-one, an α-alkoxy β,γ-unsaturated ketone, *J. Org. Chem.*, 42, 1850, 1977.
30. Eichenberger, von H., Tsutsumi, K., de Weck, G., and Wolf, H.R., Photochemische reaktionen Zur photochemie konjugierter δ-keto-enone und β,γ,δ,ε– ungesattigter ketone, *Helv. Chim. Acta*, 63, 1499, 1980.
31. Engel, P.S. and Schexnayder, M.A., Systematic structural modifications in the photochemistry of β,γ-unsaturated ketones. I. Cyclic olefins *J. Am. Chem. Soc.*, 97, 145, 1975 and references therein.

32. Baggiolini, E., Schaffner, K., and Jeger, O., Acetyl migrations in a photoexcited β,γ-unsaturated methyl ketone: 1,3-shift in the excited singlet state and 1,2-shift in the triplet state, *J. Chem. Soc., Chem. Commun.*, 1103, 1969.
33. Gonzenbach, H.-U., Tegmo-Larsson, I.-M., Grosclaude, J.-P., and Schaffner, K., The Photochemistry of 2-cyclopentenyl methyl ketones, *Helv. Chim. Acta*, 60, 1091, 1977.
34. Schaffner, K., 1-Acyl-2-cyclopentenes and 5-acylbicyclo[2.1.0]pentanes: photochemical and thermal isomerizations, *Tetrahedron.*, 32, 641, 1976.
35. Koppes, M.J.C.M. and Cerfontain, H., Photochemical isomerizations of 2-vinyl-2-phenylcyclohexanone; ketene, alkenal and 1,3-acyl shift product formation from the excited singlet state, *Recl. Trav. Chim. Pays-Bas*, 107, 412, 1988.
36. Koppes, M.J.C. M. and Cerfontain, H., Photochemical reactivities of cyclic-α-phenyl-β,γ-enones. Singlet 1,3-acyl shift, decarbonylation and unquenchable oxa-di-π-methane reactions upon direct irradiation, *Recl. Trav. Chim. Pays-Bas*, 107, 549, 1988.
37. Carlson, R.G. and Prabhu, A.V., Synthetic organic photochemistry. VI. The photochemical ring expansion of an α-hydroxy-β,γ-unsaturated ketone, *J. Org. Chem.* 39, 1753, 1974.
38. Hancock, K.G., Wylie, P.L., and Lau, J.T., Photochemistry of α-hydroxy-β,γ-unsaturated ketones. A photochemical Synthesis of 1,4-diketones, *J. Am. Chem. Soc.*, 99, 1149, 1977.
39. Sonawane, H.R., Naik, V.G., Nanjundiah, B.S., and Purihit, P.C., Photochemistry of organic multichromophoric molecules and reaction selectivity. I. Reactions of (+)-4α-acetyl-2-carene, *Tetahedron Lett.*, 3025, 1983.
40. Chae, W.K., Chae, M.Y., Park, M.K., Lee, C.H., and You, E.H., Singlet- triplet reactivity of 1-methyl-2-cyclohexenyl aryl ketones: racemization vs 1,3-acylshift in the excited states, *Bull. Korean Chem. Soc.*, 11, 241, 1990.
41. Coffin, R.L., Cox, W.W., Carlson, R.G., and Givens, R.S., Photochemical studies on the mechanism of the oxa-di-π-methane rearrangement. An example of a stereospecific rearrangement, *J. Am. Chem. Soc.*, 101, 3261, 1979.
42. Van Der Veen, R.H. and Cefontain, H., Photochemistry of β,γ-enones. VIII. On the remarkable photostability of some β,γ.β′,γ′-dienones and the 1,3-acyl shift photoreactivity of two β,γ.γ′,δ′-dienones, *Tetrahedron*, 41, 585, 1985.
43. Paquette, L.A., Eizember, R.F., and Cox, O., Photochemical transformations of selected 3-cycloheptenone derivatives, *J. Am. Chem. Soc.*, 90, 5153, 1968.
44. Schuster, D.I., Sckolnick, B.R., and Lee, F.-T.H., The role of singlet and triplet excited states in the photochemistry of 3,5-cycloheptadienone, *J. Am. Chem. Soc.*, 90, 1300, 1968.
45. Crandall, J.K., Arrington, J.P., and Hen, J., The photochemistry of 3-cyclooctenone, *J. Am. Chem. Soc.*, 89, 6208, 1967.
46. Carlson, R.G. and Bateman, J.H., The photochemical rearrangement of *cis*-2-cyclodecenone, *Tetrahedron Lett.*, 4151, 1967.
47. Miyashita, M. and Yoshikoshi, A., Intramolecular photocyclization of 1,5,5-trimethyl-8-methylene-6,10-cyclodecadiene, *J. Chem. Soc., Chem. Commun.*, 1091, 1971.
48. Williams, J.R. and Sarkisian, G.M., [1,3] vs [1,2] Sigmatropic photorearrangements in cyclic β,γ-unsaturated ketones. Conversion of bicyclo[5.4.0]undec-1(7)-en-3-one into 6-methylenespiro[4,5]decan-1-one, *J. Chem. Soc., Chem. Commun.,* 1564, 1971.
49. Engel, P.S., Schexnayder, M.A., Ziffer, H., and Seeman, J.I., The effect of α-methyl groups on the photochemistry of 3,4,5,6,7,8-hexahydronaphthalene-2(1*H*)-one, *J. Am. Chem. Soc.*, 96, 924, 1974.
50. Paquette, L.A. and Meehan, G.V., Photorearrangement of β,γ-unsaturated ketones. Application to the synthesis of bridged bicyclic ketones, *J. Org. Chem.*, 34, 450, 1969.
51. Sato, H., Furutachi, N., and Nakanishi, K., Factors involved in photoinduced n,π* singlet isomerizations of cyclic β,γ-unsaturated ketones, *J. Am. Chem. Soc.*, 94, 2150, 1972.
52. Williams, J.R., Salama, H., and Leber, J.D., Photochemistry 17β-hydroxyestra-5(10), 9(11)dien-3-one. Synthesis of AB spirosteroids, *J. Org. Chem.*, 42, 102, 1977.

53. Chambers, R.J. and Marples, B.A., Photoisomerisation of β,γ-unsaturated oxo-steroids, *Tetrahedron Lett.*, 3751, 1971.
54. Seeman, J.I. and Ziffer, H., The role of α-cleavage in the photochemistry of a homo-4A-cholestene-3-one. Structure revision of photoproducts, *Tetrahedron Lett.*, 4409, 1973.
55. Suginome, H., Ohtsuka, T., Yamamoto, Y., Orito, K., Jaime, C., and Osawa, E., Photoinduced molecular transformations. 109. Conformational dependence of the stereochemistry of photochemical 1,3-acyl shift of β,γ-unsaturated cyclic ketones: conformation specific photorearrangements of steroidal β,γ-unsaturated cyclic ketones, 7a-homocholest-5-en-7a-one and 4a-homo-5α-cholest-1-en-4-one, *J. Chem. Soc., Perkin Trans. 1*, 1247, 1990.
56. Suginome, H., Takemura, M., Shimoyama, N., and Orito, K., Photoinduced molecular transformations. 126. Photo double ring contraction of a 4a-homo-5α-cholest-3-en-1-one, a steroidal β,γ-unsaturated cyclic ketone, involving photochemical 1,3-acyl migration, *J. Chem. Soc., Perkin Trans. 1*, 2721, 1991.
57. Pfenninger, von E., Poel, D.E., Berse, C., Wehrli, H., Schaffner, K., and Jeger, O., Photochemische reaktionen. Zur photochemie von α,β-ungesattigten γ-aldehydoketonen I. Die UV –Bestrahlung von 3,19-dioxo-17β-acetoxy-Δ^4-androsten, *Helv. Chim. Acta*, 51, 772, 1968.
58. Oren, J. and Fuchs, B., Irradiation-induced transformations of homoconjugated dienones. Highly selective photorearrangements in the spiro[5.5]undeca-1,3-dien-7-one system, *J. Am. Chem. Soc.,* 108, 4881, 1986.
59. Lyle, T.A., Mereyala, H.B., Pascual, A., and Frei, B., Photochemical reactions. Photochemistry of homoconjugated cyclobutanones. II. Decisive effect of *gem*-dimethyl substitution on the course of oxa-di-π-methane rearrangement, *Helv. Chim. Acta*, 67, 774, 1984 and references therein.
60. Schenk, G.O. and Steinmetz, R., Photofragmentierung von dehydronorcampher in cyclopentadien und keten und photosensibilisierte synthese de pentacyclo[5.2.1.0.^{2,6}0.^{3,9}0^{4,8}]decans, *Chem. Ber.*, 96, 520, 1963.
61. Schuster, D.I., Axelrod, M., and Auerbach, J., The photochemical isomerization and fragmentation of dehydronorcamphor, *Tetrahedron Lett.*, 1911, 1963.
62. Ipaktschi, J., Photochemie β,γ-ungesattigter ketone. II. Photosensibilisierte umlagerung von bicyclo[2.2.1]hepten-5-on-2, *Tetrahedron Lett.*, 2153, 1969.
63. Schexnayder, M.A. and Engel, P.S., Triplet photosensitization of 2-norbornenone and other β,γ-unsaturated ketones, *Tetrahedron Lett.*, 1153, 1975.
64. Bays, D.E. and Cookson, R.C., Absorption spectra of ketones. X. Photochemical rearrangement of bicyclo[2.2.1]hepten-2-ones to bicyclo[3.2.0]hept-2-en-7-ones and their ultraviolet and circular dichroic spectra, *J. Chem. Soc. B.*, 226, 1967.
65. Ipaktschi, J., Photochemie β,γ-ungesattigter ketone. IV. Photoisomerisierung von bicyclo[2.2.1]hepten-(5)-on-(2)-derivaten, *Chem. Ber.*, 105, 1840, 1972.
66. Scharf, H.-D. and Kusters, W., Die photochemie des 6.6-dimethoxy-bicyclo[2.2.1]hepten-(2)-ons-(5), *Chem. Ber.*, 104, 3016, 1971.
67. Schuster, D.I., Lee, F.-T. H, Padwa, A., and Gassman, P.G., The photolysis of 7-ketonorbornene, *J. Org. Chem.*, 30, 2262, 1965.
68. Fuchs, B. and Scharf, G., Photochemical fragmentation of 7-Oxonorbornen-2,3-dicarboxylic anhydride and 1,2-dihydrophthalic anhydride, *J. Chem. Soc., Chem. Commun.*, 226, 1974.
69. Erman, W.F., Photochemical transformations of unsaturated bicyclic ketones. Verbenone and its photodynamic products of ultraviolet irradiation, *J. Am. Chem. Soc.*, 89, 3828, 1967.
70. Erman, W.F. and Kretschmar, H.C., Photochemistry of β,γ-unsaturated bicyclic ketones. A novel synthesis of bridged cyclobutanones, *J. Am. Chem. Soc.*, 89, 3842, 1967.
71. Givens, R.S., Chae, W.K., and Matuszewski, B., Singlet-triplet reactivity of a β,γ-unsaturated ketone: mechanistic studies in photochemistry, *J. Am. Chem. Soc.,* 104, 2456, 1982.
72. Uyehara, T., Furuta, T., Akamatsu, M., Kato, T., and Yamamoto, Y., Construction of fused ring skeletons based on photochemical rearrangement of bicyclo[3.2.1]oct-6-en-2-ones and application to a total synthesis of (±)- $\Delta^{9,12}$-capnellene, *J. Org. Chem.,* 54, 5411, 1989.

73. Paquette, L.A. and Doherty, A.M., *Polyquinane Chemistry*, Springer-Verlag, New York, 1987.
74. Mehta, G. and Srikrishna, A., Synthesis of polyquinane natural products: an update, *Chem. Rev.*, 97, 671, 1997.
75. Hsu, L.-F., Chang, C.-P., Li, M.-C., and Chang, N.-C., Bicyclo[3.2.1]octenones as building blocks in natural products synthesis. 1. Formal synthesis of (±)-mussaenoside and (±)-8-epiloganin aglucones, *J. Org. Chem*., 58, 4756, 1993.
76. Uyehara, T., Kabasawa, Y., Furuta, T., and Kato, T., Rearrangement approaches to cyclic skeletons. III. Practical route to *cis*-bicyclo[4.3.0]non-4-en-7-ones based on photochemical [1,3]-acyl migration of bicyclo[3.2.2]non-6-en-2-ones, *Bull. Chem. Soc. Jpn.*, 59, 539,1986.
77. Uyehara, T., Kabasawa, Y., Kato, T., and Furuta, T., Photochemical rearrangement approach to the total synthesis of (±)-pinguisone and (±)-deoxopinguisone, *Tetrahedron Lett*., 26, 2343,1985.
78. Uyehara, T., Furuta, T., Kabasawa, Y., Yamada, J., and Kato, T., Total synthesis of (±)-ptilocaulin starting from tropolone, *J. Chem. Soc., Chem. Commun*., 539,1986.
79. Takakis, I.M. and Agosta, W.C., Photochemistry of two homologous β,γ-unsaturated β′,γ′ cyclopropyl ketones, *Tetrahedron Lett*., 531, 1978.
80. Li, Z.-H., Mori, A., Kato, N., and Takeshita, H., Synthetic photochemistry. LVII. Facile photochemical construction of hexahydro-*as*- indacene skeleton, a carbon framework of ikarugamycin, from high pressure Diels-Alder adducts of tropones-cyclopentenone, *Bull. Chem. Soc. Jpn.*, 64, 2778, 1991.
81. Knott, P.A. and Mellor, J.M., Photochemical rearrangement of bicyclo[3.3.1]nona-3,7-diene-2,6-diones, *J. Chem. Soc., Perkin Trans. 1*, 1030, 1972.
82. Givens, R.S., Oettle, W.F., Coffin, R.L., and Carlson, R.G., Mechanistic studies in organic photochemistry. III. The photochemistry of bicyclo[2.2.2]octenone and benzobicyclo[2.2.2]octadienone, *J. Am. Chem. Soc.,* 93, 3957, 1971.
83. Givens, R.S. and Oettle, W.F., Mechanistic studies in organic photochemistry. IV. The mechanism of the photorearrangement of bicyclo[2.2.2]octadienones to tricyclo[3.3.0.0 ^{2,8}]octen-3-ones, *J. Am. Chem. Soc.,* 93, 3963, 1971.
84. Demuth, M., Raghavan, P.R., Carter, C., Nakano, K., and Schaffner, K., Photochemical high yield preparation of tricyclo[3.3.0.0^{2,8}]octan-3-ones. Potential synthons for polycyclopentanoid terpenes and prostacyclin analogs, *Helv. Chim. Acta,* 63, 2434, 1980.
85. Demuth, M., Wietfeld, B., Pandey, B., and Schaffner, K., Photochemistry of 1-methoxybicyclo[2.2.2]octenones; photolytic cyclopropane cleavage of the initially formed tricyclo[3.3.0.0^{2,8}]octan-3-ones, *Angew. Chem. Int. Ed. Engl.*, 24, 763, 1985.
86. Parker, S.D. and Rogers, N.A.J., Photochemistry of β,γ-enones: 1-methoxybicyclo[2.2.2]oct-5-en-2-one, *Tetrahedron Lett.,* 4389, 1976.
87. Eckersley, T., Parker, S.D., and Rogers, N.A. J., Photochemistry of 1-methoxybicyclo [2.2.2]oct-5-en-3-one: a singlet oxa-di-π-methane rearrangement, *Tetrahedron Lett.,* 4393, 1976.
88. Eckersley, T.J., Parker, S.D., and Rogers, N.A. J., Substituent and structural effects on the photochemistry of bicyclic β,γ-unsaturated ketones, *Tetrahedron,* 40, 3749, 1984.
89. Katayama, S., Hiramatsu, H., Aoe, K., and Yamauchi.M., Synthesis of bicyclo[4.1.0]hept-2-enes(trinorcarenes) by photochemical reaction of bicyclo[2.2.2]oct-5-en-2-ones, *J. Chem. Soc., Perkin Trans. 1*, 561, 1997.
90. Murray, Jr., R.K. and Hart, H., Contrast between thermal and photochemical reverse Diels-Alder reactions involving ketenes, *Tetrahedron Lett*., 4995, 1968.
91. Hart, H., Murray, Jr., R.K. and Appleyard, G.D., Direct and sensitized photoisomerizations of a diazabicyclo[2.2.2]octenone, *Tetrahedron Lett*., 4785, 1969.
92. Schippers, P.H. and Dekkers, H.P. J.M., Asymmetric photodestruction of bicyclo[2.2.2] oct-2-ene-5,7-dione: absolute configuration and ^{1}n-π* excited state geometry, *J. Chem. Soc., Perkin Trans. 2,* 1429, 1982.
93. Ipaktschi, J., Photochemische reaktionen des benzobicyclo[2.2.2]octa-5,7-dien-2-on, *Tetrahedron Lett*., 215, 1969.

94. Hart, H. and Murray, R.K., The photosensitized rearrangement of benzobicyclo[2.2.2]octadienones, *Tetrahedron Lett.*, 379, 1969.
95. Prinzbach, H., Schal, H.-P., and Hunkler, D., Bis-[2.X]-σ-homobenzenes, *Tetrahedron Lett.*, 2195, 1978.
96. Mehta, G. and Srikrishna, A., Photochemistry of tricyclo[4.2.2.$0^{2,5}$]deca-3,7-dien-9-one: a source of many interesting polycycles, *Tetrahedron Lett.,* 3187, 1979.
97. Hayakawa, K., Schmid, H., and Frater, G., Photochemie von tricyclischen β,γ–γ′,δ′ ungesattigten ketonen, *Helv. Chim. Acta*, 60, 561, 1977.
98. Yates, P. and Stevens, K.E., Bicyclopentanoid sesquiterpenes. The synthesis of cedranoid sesquiterpenes via the photorearrangement of bicyclo[2.2.2]octenones, *Tetrahedron*, 37, 4401, 1981.
99. Singh, V., Alam, S.Q., and Porinchu, M., Intramolecular Diels-Alder reaction of cyclohexa-2,4-dienones: synthesis and photochemical reactions of oxa-homobrendanes, *Tetrahedron*, 51, 13423, 1995.
100. Singh, V. and Porinchu, M., Sigmatropic 1,3-acyl shift in excited state: a novel, stereoselective route to protoilludanoids, *J. Chem. Soc., Chem. Commun.*, 134, 1993.
101. Singh, V. and Porinchu, M., Sigmatropic 1,2- and 1,3-acyl shifts in excited states: a novel, general protocol for the synthesis of tricyclopentanoids and protoilludanes, *Tetrahedron*, 52, 7087, 1996.
102. Singh, V., Thomas, B., and Sharma, U., Photodecarbonylation: a novel photoreaction of rigid β,γ-enones, *Tetrahedron Lett.*, 3421, 1995.
103. Hirao, K., Unno, S., Miura, H., and Yonemitsu, O., Singlet and triplet excited state photochemistry of tricyclo[5.2.2.$0^{2,6}$]undeca-3,10-dien-9-one derivatives, *Chem. Pharm. Bull.*, 25, 3354, 1977.
104. Singh, V. and Thomas, B., Studies on photoreaction of *endo*-tricyclo[5.2.2.$0^{2,6}$] undecadienones in excited singlet state, *J. Indian. Chem. Soc.,* 75, 640, 1998.
105. Singh, V.K., Deota, P.T., and Raju, B.N. S., Diels-Alder cycloaddition: synthesis and oxa-di-π-rearrangement of tricyclo[5.2.2.0 ^{2,6}]undecadienone, *Synth. Commun.*, 17, 115, 1987.
106. Singh, V. and Raju, B.N.S., $\Pi^{4s}+\Pi^{2s}$ cycloaddition: synthesis and oxa-di-π-methane rearrangement of annulated bicyclo[2.2.2]octenones, *Synth. Commun.*, 18, 1513, 1988.
107. Singh, V.K., Deota, P.T., and Bedekar, A.V., Studies in the synthesis of polycyclopentanoids: synthesis, oxa-di-π-methane rearrangement of annulated bicyclo[2.2.2]octenones and cyclopropane ring cleavage of tetracyclo[6.3.0.0.$^{2,4}0^{3,7}$] undecenones, *J. Chem. Soc., Perkin Trans. 1*, 903, 1992.
108. Singh, V. and Alam, S.Q., Structural diversity through intramolecular cycloaddition and modulation of chemical reactivity in excited state. Synthesis and photoreactions of 3-oxa-tricyclo[5.2.2.$0^{1,5}$]undecenones; novel stereoselective route to oxa-triquinanes and oxa-sterpuranes, *Bioorg. Med. Chem. Lett.*, 2517, 2000.
109. Singh, V., Alam, S.Q., and Praveena, G.D., Synthesis and photoreactions of 3-oxa-tricyclo[5.2.2.$0^{1,5}$] undecenones: a novel, stereoselective route to oxa-triquinanes and oxa-sterpuranes, *Tetrahedron*, 58, 9729, 2002.
110. Singh, V., Vedantham, P., Kane, V.V., and Polborn, K., Novel entry into oxepane-diquinane and oxepane–sterpurane hybrids: synthesis and photochemistry of 3-oxatricyclo [7.2.2.$0^{1,7}$]tridecenones, *Tetrahedron Lett.* 44, 475, 2003.
111. Cargill, R.L. and Sears, A.B., The tricyclo[5.3.0.$0^{3,4}$]dec-1-ene system, *Tetrahedron Lett.*, 3555, 1972, and references cited therein.
112. Peet, N.P. and Cargill, R.L., Photochemical and acid catalysed rearrangements of tricyclo[4.4.2.0]dodecanones, *J. Org. Chem.*, 38, 4281, 1973.
113. Peet, N.P., Cargill, R.L., and Crawford, J.W., Photochemistry of β,γ-unsaturated ketones. 10,11-Dimethyltricyclo[4.3.2.0]undec-10-en-2-one, *J. Org. Chem.*, 38, 1222, 1973.
114. Takakis, I.M. and Agosta, W.C., Photochemical reactions of six β,γ-cyclopropyl ketones derived from bicyclo[4.2.1]nona-2,4,7-trien-9-one, *J. Org. Chem.*, 44, 1294, 1979.
115. Sasaki, T., Kanematsu, K., and Naoya, O., Molecular design by cycloaddition. 29. Photolyses of tricyclo[4.2.2.$0^{3,5}$]deca-7-en-2-one systems, *Chem. Lett.*, 7, 743, 1976.

116. Murray, Jr., R.K. and Babiak, K.A., Synthesis of 8,9-dehydro-2-adamantanone by the oxa-di-π-methane photorearrangement of 2-protoadamantenone, *Tetrahedron Lett.*, 319, 1974.
117. Mlinaric-Majerski, K., Pavlovic, D., and Sindler-Kulyk, M., Synthesis and photochemistry of 4-methylene-2-protoadamantanone, *J. Org. Chem.*, 58, 252, 1993.
118. Padwa, A., Zhi, L., and Fryxel, G.E., Studies dealing with the excited state behaviour of substituted 8-oxabicyclo[3.2.1]oct-6-en-2-ones, *J. Org. Chem.*, 56, 1077, 1991.
119. McClure, C.K., Link, J.S., and Kiessling, A., The Oxa-di-π-methane Photochemical Rearrangement of Quinuclidinones, 1- and 2-Aza-3-carboxybicyclo[2.2.2]oct-2-ene-5-ones: application to the Synthesis of Pyrrolizidine Alkaloids, Abstract No. ORGN 480, 221st ACS Meeting, San Diego, CA, 2001.
120. Armesto, D., Ortiz, M.J., Romano, S., Agarrabeitia, A.R., Gallego, M.G., and Ramos, A., Unexpected oxa-di-π-methane rearrangement of β,γ-unsaturated aldehydes, *J. Org. Chem.*, 61, 1459, 1996.
121. Uyehara, T., Kabasawa, Y., and Kato, T., Rearrangement approaches to cyclic skeletons. IV. The total synthesis of (±)-pinguisone and (±)-deoxypinguisone based on photochemical [1,3]-acyl migration of a bicyclo[3.2.2]non-6-en-2-one, *Bull. Chem. Soc. Jpn.*, 59, 2521,1986.
122. Harbour, G.C., Tymiak, A.A., Rinehart, Jr., K.L., Shaw, P.D., Hughes, Jr., R.G., Mizsak, S.A., Coats, J.H., Zurenko, G.E., Li, L.H., and Kuentzel, S.L., Ptilocaulin and isoptilocaulin, antimicrobial and cytotoxic cyclic guanidines from the Caribbean sponge *Ptilocaulis* aff.*P. spiculifer (Lamarck, 1814), J. Am. Chem. Soc.*, 103, 5604, 1981.
123. Uyehara, T., Furuta, T., Kabasawa, Y., Yamada, J., Kato, T., and Yamamoto, Y., Rearrangement approaches to cyclic skeletons. 6. Total synthesis of (±)-ptilocaulin on the basis of formal bridgehead substitution and photochemical [1,3] acyl migration of a bicyclo[3.2.2]non-6-en-2-one system, *J. Org. Chem.*, 53, 3669,1988.
124. Ayer, W.A. and Browne, L.M., Terpenoid metabolites of mushrooms and related basidomycetes, *Tetrahedron*, 37, 2199, 1981.
125. Singh, V. and Sharma U., Synthesis and photoreaction of tricyclo[5.2.2.$0^{2,6}$]undecanes in excited singlet (^{1}S) state: a novel and stereospecific route to protoilludanoids, *J. Chem. Soc., Perkin Trans. 1*, 305, 1998.
126. Singh, V. and Alam, S.Q., Intramolecular Diels-Alder reaction in 1-oxaspiro-[2.5]octa-5,7-dien-4-one and sigmatropic shifts in excited states: novel route to sterpuranes and linear triquinanes: Formal total synthesis of (±)- coriolin, *J. Chem. Soc., Chem. Commun.*, 2519, 1999.
127. Singh, V., Spiroepoxycyclohexa-2,4-dienones in organic synthesis, *Acc. Chem. Res.*, 32, 324, 1999.
128. Singh, V. and Samanta, B., Synthesis of tricyclo[7.2.2.$0^{2,8}$]tridecanes and photoreaction in the excited singlet state: a novel entry to the DCB carbon framework of phorbol, *Tetrahedron Lett.*, 40, 1807, 1999.

80

Photochemical Rearrangements of 6/6- and 6/5-Fused Cross-Conjugated Cyclohexadienones

Gonzalo Blay
Universitat de València

80.1 Introduction

Interest in the photochemical reactivity of cross-conjugated cyclohexadienones began in the 19th century with reports of the light-induced reactions of the naturally occurring sesquiterpene α-santonin.[1] However, the complexity of the structures involved, combined with the variety of products obtained under different irradiation conditions, prevented accurate characterization of this reaction until the mid-1950s, when the pioneering studies by Barton,[2-4] Jeger,[5] van Tamelen,[6] and their groups allowed the elucidation of the structures of the photoproducts of santonin and related steroid dienones.[7,8]

The fascinating, deep-seated rearrangements exhibited by these systems and the recognition of the potential synthetic value of these types of reactions led to the investigation of the photochemistry of a variety of compounds containing the cross-conjugated cyclohexadienone system.[9-11] The photochemistry of 6/6- and 6/5-fused cyclohexadienones, which forms the subject of this chapter, received particular attention between the 1960s and 1980s, with the pioneering works of Kropp and the extensive study carried out by Caine on bicyclic cyclohexadienones being particularly outstanding.[12] In recent years, the number of explorative and mechanistic studies on this reaction has fallen, although the synthetic potential of the process is clear, given the large number of syntheses published that still use this reaction as a key step.

80.2 Mechanism

The photoreactions of cyclic enones and dienones have played a special role in the development of synthetic and mechanistic photochemistry. These compounds undergo many complex structural rearrangements that appear to be unrelated on superficial inspection of product structures. However, after

0-8493-1348-1/04/$0.00+$1.50

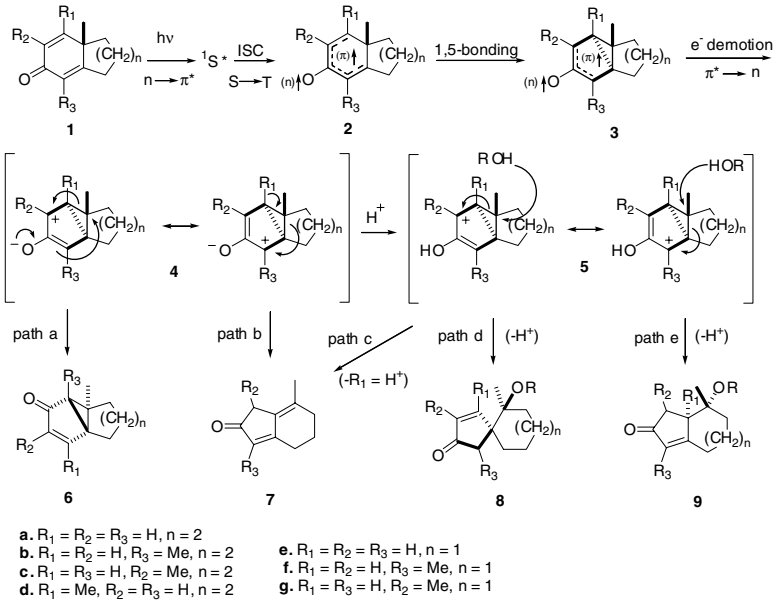

SCHEME 1

extensive studies involving monocyclic 4,4-disubstituted-2,5-cyclohexadienones, Zimmerman and Schuster proposed a generally accepted mechanism that accounts for the photochemical behavior of most cross-conjugated cyclohexadienones — as illustrated in Scheme 1.[13]

In general, it is accepted that photorearrangements of cyclohexadienones proceed via triplet n,π* excited states **2**,[14] which are populated by intersystem crossing from the initial n,π* singlet excited states ^{1}S* obtained by absorption of light at around 300 nm in the ultraviolet region. These n,π* excited states can also be obtained when shorter wavelength light is used (λ ~ 240 nm), in which case the transitions occur by intersystem-crossing and internal conversion of the higher-energy π,π* excited states produced by the initial irradiation. The n,π* excited state of the dienone evolves with the formation of a covalent bond between C1 and C5 (1,5-bonding or β–β bonding) to give a still electronically excited-state n,π* intermediate **3**, which after a π*,n electron-demotion process to the ground state gives a mesoionic zwitterionic intermediate **4**.[15] The intermediate **4** is the key to understanding the rearrangement of cross-conjugated dienones. In nonnucleophilic solvents, intermediate **4** rearranges to bicyclo[3,1,0]hex-2-ones **6** (lumiketones), a process designated a [1,4]-sigmatropic shift, the equivalent to the type A rearrangement of monocyclic dienones (path a).

However, in protic nucleophilic solvents, irradiation of cross-conjugated dienones is commonly found to induce rearrangement to spiro compounds **8** and/or cyclopentenones **9**. These rearrangements can be viewed as resulting from protonation of the oxygen of intermediate **4** to give a carbocation ion **5**, which can subsequently evolve through the following pathways: (1) nucleophilic attack of the solvent from the β-side of the molecule with concomitant cleavage of the external bond of the cyclopropane ring to give spiro compounds **8** (path d); (2) nucleophilic attack of the solvent from the α-side of the molecule with concomitant cleavage of the internal bond of the cyclopropane ring to give cyclopentenones **9** (path e); or (3) less commonly, proton loss from C1 (R_1 = H, n = 1) with concomitant cleavage of the internal bond of the cyclopropane ring to give the linearly conjugated dienones **7** (path c). Direct collapse of zwitterion **4** (n = 1) to compounds **7** may also occur in aprotic media (path b).

It has been pointed out that bicyclohexenones such as **6** may arise directly from the starting dienones through photochemically allowed [σ2a+σ2a] cycloaddition processes.[16] However, evidence for the participation of zwitterionic species **4** is available from alternate synthesis methods,[17] isolation[18] and chemical trapping.[19]

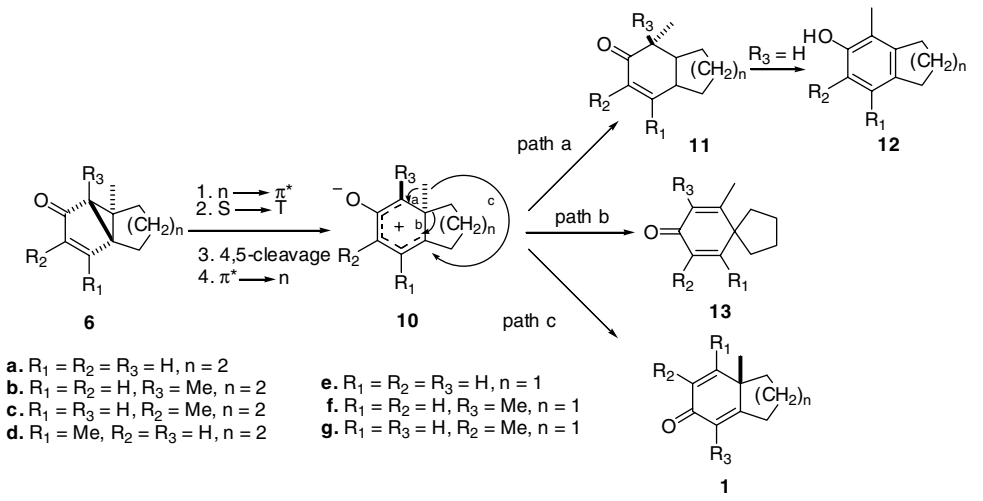

SCHEME 2

Lumiketones are prone to undergo secondary or even tertiary and quaternary photolysis, leading to further rearrangements, a situation that adds considerable complexity to cyclohexadienone photochemistry. In general, the products can be rationalized starting with the postulate that an excited state is produced from **6** that can lead to a zwitterionic intermediate **10** (Scheme 2). Such an intermediate can rearrange in three possible ways: (1) a [1,2]-methyl shift to give the linearly conjugated cyclohexadienone **11** (path a) or its phenolic tautomer **12** (in cases where $R_3 = H$); (2) a [1,2]-methylene migration to give the spiranic cross-conjugated cyclohexadienone **13** (path b); or (3) a [1,2]-methyl shift to give the initial cross-conjugated cyclohexadienone **1** (reverse reaction). These rearrangements are influenced by the nature of the substituents and, in particular, by the size of ring B and its substitution pattern.

80.3 Scope and Limitations

The Effects of Solvent and Wavelengths

Bicyclo[3,1,0]hex-2-en-3-ones related to **6** (lumiketones) are normally prepared by irradiation of dilute solutions of dienones in dioxane or toluene. Best results are obtained with a low-pressure mercury lamp that emits most of its radiation at 253.7 nm. Control of the irradiation time and of the wavelength are important to avoid further rearrangement of the lumiketones to dienones and phenolic products, which are formed on irradiation with light of wavelength greater than 300 nm.[20]

Hydroxycyclopentenones related to **8** and **9** are obtained by irradiation of dilute aqueous acetic acid solutions of dienones with a medium- or high-pressure mercury lamp in a quartz reactor or screened by a Pyrex filter. Acetoxy or alkoxy ketones are obtained under these conditions using acetic acid or alcohols (or alcoholic acetic acid), respectively, as the solvent.[12] However, deviations from this general trend are possible, depending on the nature of the substituents in or around the chromophore.

The Effects of Substituents

The mechanism shown in Schemes 1 and 2 explains the formation of most of the products obtained upon irradiation of cross-conjugated dienones. However, the presence of substituents on the chromophore or in remote positions, or indeed the size of ring B, can have an influence on the outcome of these transformations.

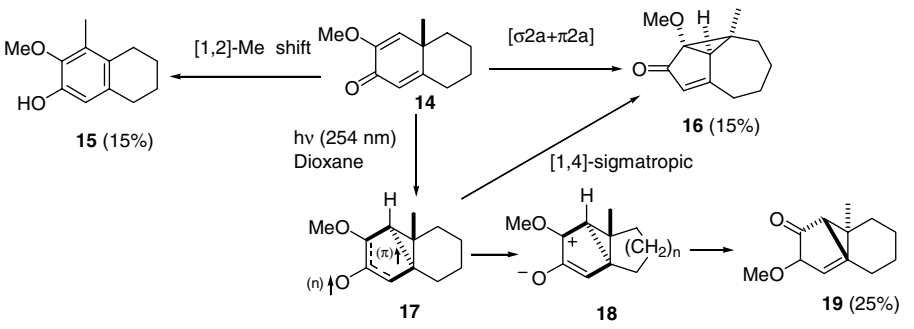

SCHEME 3

Influence of Substituents on the Dienone Chromophore

Aprotic Solvents

Irradiation at 253.7 nm of unsubstituted or methyl-substituted 6/6-fused bicyclic **1a,b,c,d** and steroid cross-conjugated cyclohexadienones in inert solvents (such as dioxane) leads to a rearrangement that gives rise to the corresponding lumiketones **6a,b,c,d** in good yields.[9] Changes in the position of a methyl group on the chromophore do not have a noticeable effect on the course of the reaction. Lumiketones **6e,f,g** are also the main photoproducts obtained by irradiation of 6/5-fused bicyclic cyclohexadienones **1e,f,g**. In addition to these lumiketones, linearly conjugated dienones **7e** and **7f** were produced upon irradiation of **1e** and **1f**, respectively.[21] Under similar conditions, B-*nor*-1-dehydrotestosterone acetate, which contains a 6/5-fused cyclohexadienone ring, gave the corresponding linearly conjugated dienone as the only product.[22] The exclusive formation of this compound must result from the added strain due to the *trans* fusion of the C ring to the five-membered ring in the steroidal system.

The presence of a methoxy group at C4 in the dienone does not appear to influence the course of the reaction in dioxane. Indeed, irradiation of 4-methoxy-2,4-cholestadien-3-one in dioxane was found to give the corresponding lumiproduct exclusively.[23] However, irradiation of 2-methoxydienone **14** in dioxane at 253.7 nm gave rise to phenol **15** and the tricyclic enone **16**, in addition to the lumiproduct **19** (Scheme 3). Both of these compounds are primary photoproducts that are not obtained by photolysis of lumiproduct **19**.[24]

Phenol **15** is probably produced by a simple photochemically induced 1,2-methyl shift. The unusual enone **16** can be considered to arise by either a symmetry-allowed [1,4]-sigmatropic rearrangement in the excited triplet cyclopropane intermediate **17** (related to **3**) or directly from dienone **14** by a photoinduced [σ2a+π2a] cycloaddition process involving the 5,10-σ and the 1,2-π bond of the dienone with inversion at C10. The exact manner in which the methoxy group influences these rearrangements is not clear. The presence of this group may increase the lifetime of the triplet species **17** to such an extent that it allows time for rearrangement prior to electron demotion to a zwitterionic species **18** (related to **4**), which leads to the lumiproduct **19**, or it may cause selective excitation of the 1,2-π bond of the dienone.

The presence of electron-withdrawing groups on the chromophore in 6/6-fused cyclohexadienones suppresses rearrangement to the lumiproducts in aprotic solvents. Irradiation of the 2-formyl derivative of the bicyclic cyclohexadienone **1a** (compound **46** in Scheme 9) gave a mixture of products in low yields along with a polymeric material,[25] while a related 2-formyl steroidal dienone was stable to light at 253.7 nm but gave a complex mixture when irradiated with a broad-spectrum lamp.[26] The 4-formyl derivative of dienone **1a** (R_3 = formyl) does not give rearranged products.[25]

In contrast, irradiation of a dienone **20**, which bears a carboxy group at C2, in dioxane gave the azulene dienone **23** and enone **24** in 67% and 16% yields, respectively, while under similar conditions the 4-carboxydienone **25** yielded the spirodienone **28** in 60% yield (Scheme 4).[25] The ability of the carboxy group to internally protonate the carbonyl group at C3 in the zwitterionic intermediates **21** and **26** is likely to be the major factor driving the rearrangement to azulene or spiro compounds rather than to

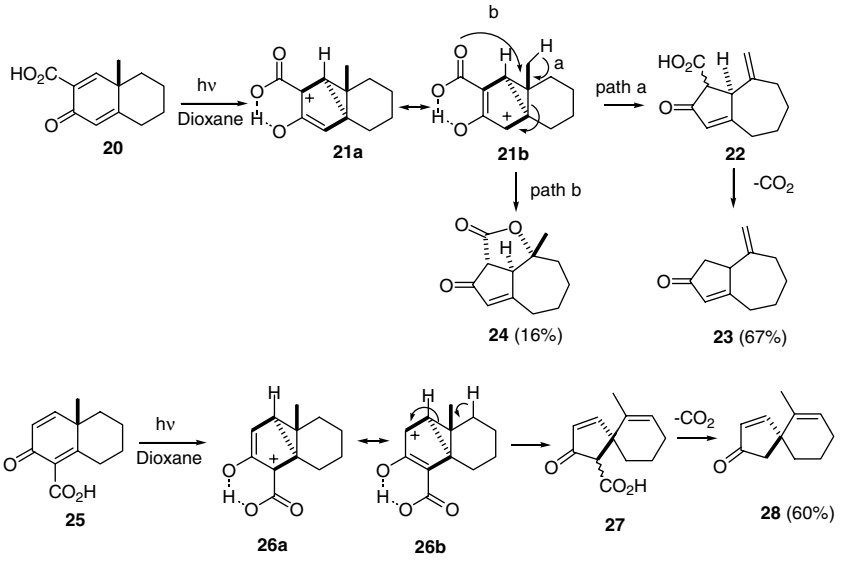

SCHEME 4

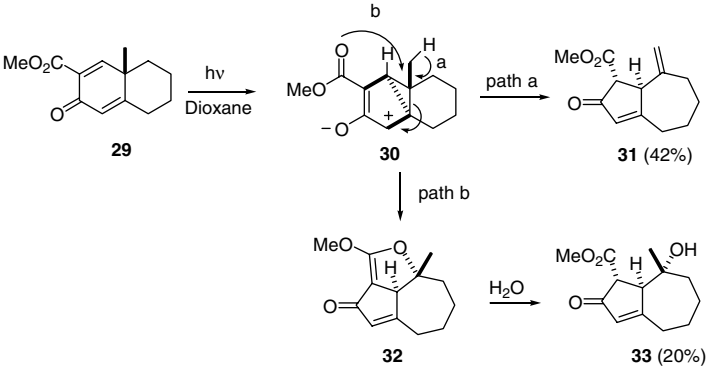

SCHEME 5

lumiketones. Cleavage of the 5,10-bond of the cyclopropane ring (path a), which is favored in the more stable conjugate structure **21b**, would lead to the β-keto acid **22**. Compound **22** would then decarboxylate to give the major product **23**. On the other hand, direct intramolecular attack of the C2 carboxylate at C7 (path b) would form compound **24**.

Spirodienone **28** arose through decarboxylation of the corresponding β-keto acid **27**, which was obtained by proton loss from C9 and concomitant cleavage of the 1,10-bond — a process that would be favored in the chelated conjugated cyclopropyl intermediate **26b** (Scheme 4).

Similarly, irradiation of the 2-carbomethoxydienone **29** in toluene or dioxane afforded azulene dienone **31** (33 to 42%) and hydroxyenone **33** (19 to 20%) as primary photoproducts (Scheme 5).[27] Suppression of lumiproducts is explained by considering intramolecular attack of the ester group. Intramolecular deprotonation of the C10 methyl group by the carbomethoxy group (path a) in the zwitterionic intermediate **30** would account for the major product, while attack by the carboxylate group on the electron deficient C10 position (path b) would generate **32**, the subsequent hydrolysis of which would afford alcohol **33**.

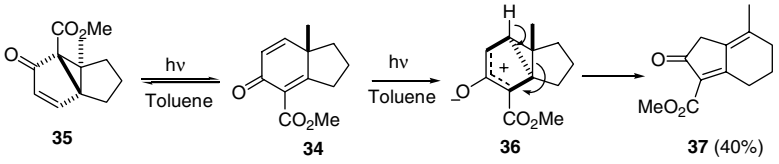

SCHEME 6

The 4-carbomethoxy derivative of dienone **1a** (R_3 = carbomethoxy), in a similar way to the 4-formyl derivative (R_3 = formyl), fails to yield photorearranged products. This lack of reactivity is attributed to a photochemical deconjugation of the 4,5-double bond to the 5,6-position and enolization of the C4 carbonyl group.[25] However, the corresponding 4-carbomethoxy 6/5-fused dienone **34**, in which double bond deconjugation is less favorable for steric reasons, rearranges in toluene to give the 5/6-fused dienone **37** (Scheme 6), which would be formed following a path similar to path b in Scheme 1. In this process, the corresponding lumiketone **35** is formed reversibly and can be isolated if irradiation is interrupted in midcourse.[27] The divergent behavior of compound **34** suggests that the location of the carbomethoxy group in relation to the migrating bond does influence the ease of the [1,4]-sigmatropic rearrangement (path a in Scheme 1): When the ester group occupies the position at which the new bond is formed, rearrangement to lumiproducts is observed. When the ester occupies an alternative position, as is the case with compound **29**, the [1,4]-shift is rendered less favorable and other processes dominate in its absence.[27]

Protic Solvents

In protic solvents, 6/6-fused cyclohexadienones undergo photorearrangement to 5/7-fused or spiro enones through protonated mesoionic species such **5** (Scheme 1). The mode of cleavage is controlled by the electronic influence of the substituents. For example, on irradiation in aqueous acetic acid, the 4-methyldienone **1b** yielded exclusively the 5/7-fused hydroxyketone **9b** (R = H)[28,29] while the 2-methyl compound **1c** yielded exclusively the spiro hydroxy ketone **8c** (R = H).[20] Under similar conditions, the unsubstituted dienone **1a** yielded an approximately 1:1 mixture of **8a** (R = H) and **9a** (R = H).[30] In each case, the hydroxy ketones were accompanied by varying amounts of phenols that arise as secondary photoproducts from the related lumiketones **6**. Thus, the presence of an electron-releasing group at C2 or C4 increases the stability of the resonance form with a positive charge at that position and cleavage via path d or path e, respectively, takes place (Scheme 1). When ring A is unsubstituted, both resonance forms are approximately equal in energy and, in this case, products derived from both possible cleavage pathways are isolated.

According to this mechanism, it is anticipated that methoxy and methyl substituents must exert a similar influence on the course of the photochemical rearrangement in protic solvents. Indeed, the 4-methoxydienone **38** yielded exclusively the 5/7-fused compound **39** on irradiation in acetic acid,[31] while under similar conditions, the 2-methoxydienone **40** gave the spiro enone **41** in high yield (Scheme 7).[32] The use of aqueous acetic acid in these cases led to a decrease in the amounts of rearranged products due to a light-catalyzed hydrolysis of the enol ether function.

The 4-methyl substituted 6/5-fused dienone **1f** showed similar behavior to the parent 6/6-fused dienone, and gave the 5/6-fused hydroxy ketone **8b** (R = H) in 59% yield upon irradiation in aqueous acetic acid and the related ethoxy ketone **8b** (R = Et) upon irradiation in ethanol. However, the unsubstituted dienone **1e** and the 2-methyl derivative **1g** underwent additional photochemical rearrangements when irradiated in protic solvents. Thus, irradiation of **1e** in methanolic acetic acid yielded the tricyclic methoxy ketone **42**, the 5/6-fused ketone **9e** (R = Me) and the dienone **7e** in *ca.* 3:3:2 ratio. Under similar conditions, photolysis of **1g** gave **43** and **9g** (as a *ca.* 9:1 mixture of C2 epimers) in a 5:8 ratio (Scheme 8). Compounds such as **9e**, **9g**, and **7e** are rationalized as resulting from cleavage of the internal bond of the cyclopropane ring in the mesoionic intermediate **4e** or **4g** (Scheme 1), while the tricyclic ketones **42** and **43** would be formed through a pathway similar to that for ketone **16** (Scheme 3).[33]

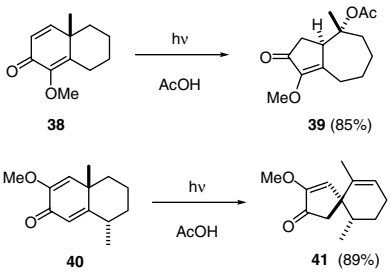

SCHEME 7

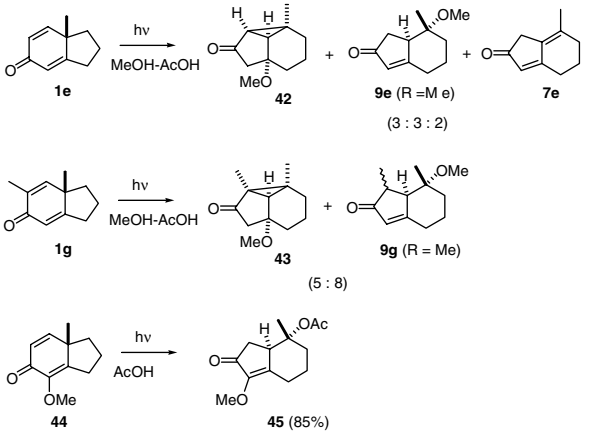

SCHEME 8

The photochemical rearrangement of 2-methoxy 6/5-fused dienones in protic solvents has not been reported. However, irradiation of the 4-methoxy 6/5-fused dienone **44** in acetic acid gave the 5/6-acetoxy ketone **45** in 85% yield and showed behavior similar to the corresponding 6/6-systems.[31]

6/6-Fused dienones bearing an electron-withdrawing substituent at C2 rearrange to azulene derivatives upon irradiation in protic solvents. In this case, the presence of an electron-withdrawing group would favor build-up of more positive charge at C4 than at C2 in the protonated mesoionic intermediate related to **5,** and this would then undergo solvolytic attack at C10 with cleavage of the internal 5,10-bond of the cyclopropane ring to give the 5/7-fused compounds. For example, irradiation of 2-formyl 6/6-fused dienone **46** in aqueous acetic acid leads to 5/7-fused hydroxymethylene compounds that can be deformylated to the corresponding ring A unsubstituted 5/7-fused systems **49**.[25,34] Dienone **29** was converted into **33** in high yield upon irradiation in aqueous acetic acid. Under similar conditions, the 2-carboxydienone **20** gave the 5/7-fused hydroxy ketone **9a** (R = H) in 65% yield, along with small quantities of other products (<7%). Compound **9a** would be formed after decarboxylation of the β-keto acid **50** resulting from the initial photorearrangement of **20**. In aqueous dioxane, **20** gave compound **9a** (R = H) in 60% yield and lactone **24** in 12% yield, while in anhydrous methanol the methyl ether **9a** (R = Me) was obtained as the major product in 48% yield along with dienone **23** (13%) and lactone **24** (14%).[25] Irradiation of dienone **25**, which contains a carboxyl group at C4, gave the lactone **52** in 40% yield. This compound would be formed after solvolytic attack at C10 in the protonated mesoionic intermediate related to **5**, with subsequent cleavage of the external bond of the cyclopropane ring to produce a γ-hydroxy-β-keto acid **51** that could lactonize to **52** (Scheme 9).

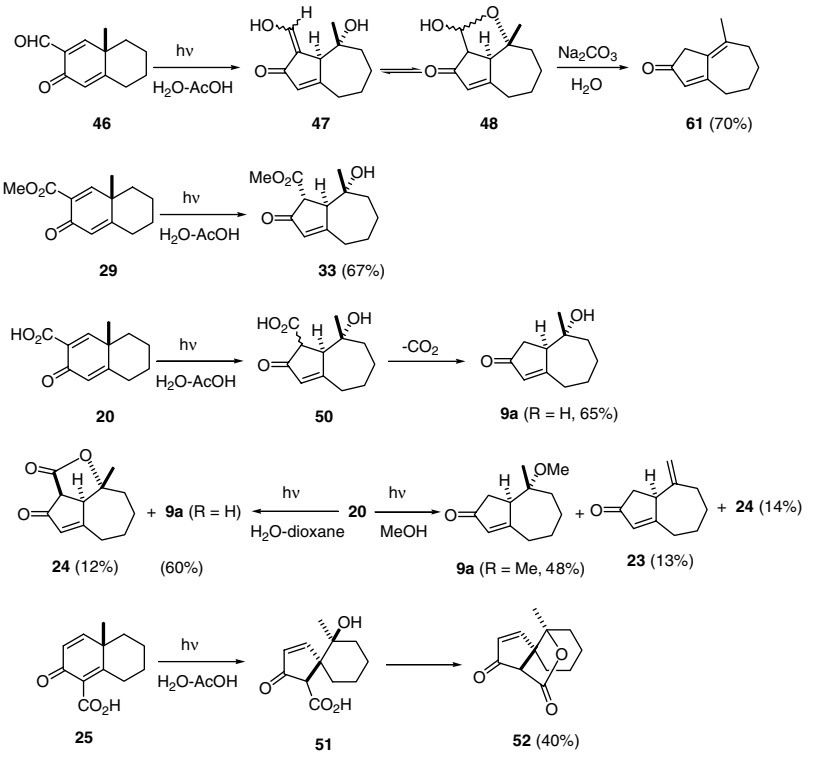

SCHEME 9

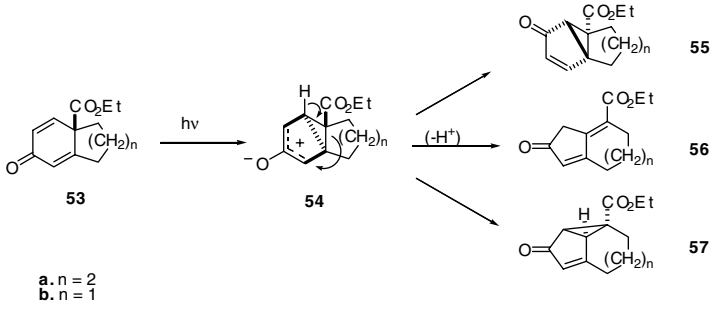

SCHEME 10

The irradiation of 4-formyl and 4-carbomethoxydienones in protic solvents fails to react, as they also failed in aprotic solvents.

Other Ring A Substituent Effects

The presence of electron-withdrawing groups at the angular position of bicyclic dienones strongly influences the photochemical reactivity and modes of rearrangement. The lumiketone **55a** is the main photoproduct resulting from the irradiation of the 6/6-fused dienone **53a** in either dioxane or aqueous acetic acid. Compound **55a** is obtained along with small amounts of the linearly conjugated dienone **56a**, the tricyclic ester **57a,** and other minor products (Scheme 10).[12,35]

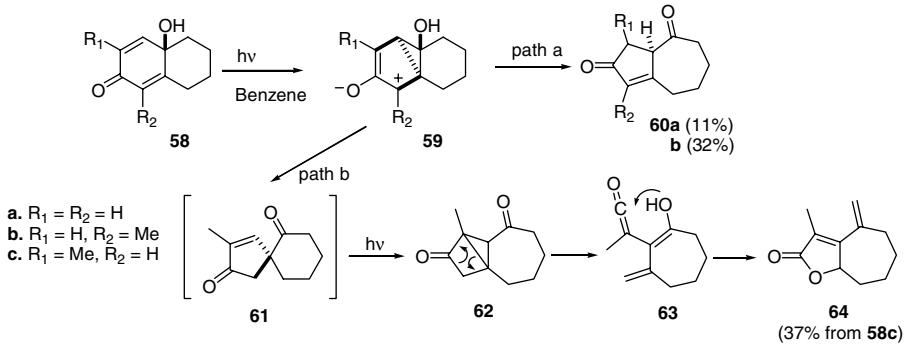

SCHEME 11

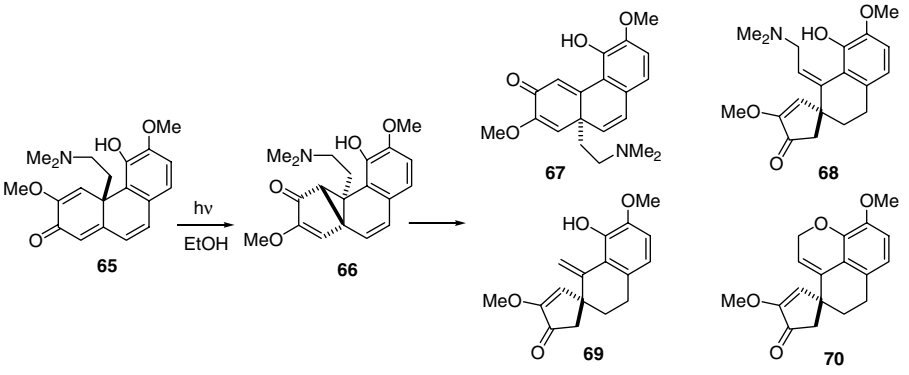

SCHEME 12

It appears that the ester group in the zwitterionic intermediate **54a** stabilizes the cyclopropane ring toward solvolytic cleavage, although the [1,4]-sigmatropic rearrangement to the lumiketone still occurs. Dienone **56a** could arise through collapse of **54a** with loss of a proton. The tricyclic compound **57a**, which has the same carbon skeleton as ketone **16**, is obtained possibly by a similar pathway (Scheme 3). On the other hand, the 6/5-fused dienone **53b** gave exclusively dienone **56b** under similar conditions,[12] providing further evidence of the propensity of the 6/5-fused dienones to yield 5/6-fused systems.

The presence of a hydroxyl group at the angular position prevents photorearrangement to the lumiketone products. Thus, photolysis of the bicyclo-dienones **58a** and **58b** in benzene gave azulene diketones **60a** and **60b**, respectively, as the chief isolable products (Scheme 11), albeit in low yields (11% and 32%, respectively). These compounds are formed by collapse of the zwitterionic cyclopropanol intermediate **59** with cleavage of the 5,10-bond (path a). Under the same conditions, compound **58c** gave butenolide **64** as the sole isolable product in 37% yield. It is considered that this product is formed via the spirodiketone **61**, which in turn is produced from cleavage of the 1,10-bond in **59** (path b).[36] Spirodiketone products have been isolated from irradiation mixtures of steroidal and diterpenoid hydroxydienones with structures related to **58** and, moreover, it has been shown that these compounds can undergo photoconversion to the butenolides.[36,37] This photoconversion is rationalized in terms of cyclization of a ketoketene formed by isomerization of the spiroketone (Scheme 11).

Irradiation of the tricyclic dienone **65**, which bears an *N*,*N*-dimethylethylene moiety at the angular position, in EtOH produced four amorphous products in low yield (Scheme 12). It is suggested that these products arise from the decomposition of the non-isolated lumiketone **66** by any of the following

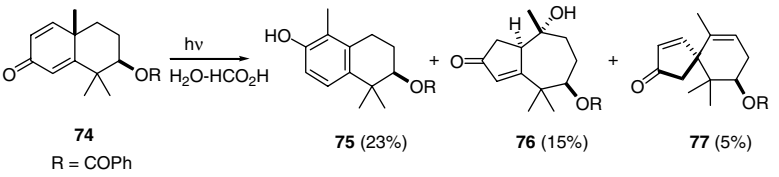

SCHEME 13

pathways: (1) migration of the side chain from the C4b to C8a with concomitant dienone formation would lead to compound **67**; (2) the genesis of the second photoproduct **68** would involve stereospecific loss of one of the two C11 hydrogens of lumiketone **65** with formation of a 4b,11-double bond and cleavage of the 4b,5-bond; or (3) compounds **69** and **70** would be formed by a mechanism related to that discussed above, where the 4b,11-double bond would be formed through loss of the dimethylaminomethyl moiety or dimethylamine from species **68**, respectively.[38]

The presence of other rings fused to the cyclohexadienone chromophore may lead to failure of the photochemical rearrangement, probably as a consequence of steric factors preventing β,β'-bonding in the excited states. This is the case with dienones **71**,[38] **72**[39] and **73**.[40]

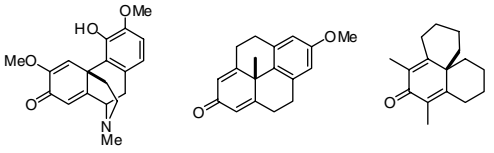

Effects of Ring B Substituents

Substituents on ring B may impose steric and conformational restrictions onto the rearrangement of fused dienones. Irradiation of the 6-disubstituted dienone **74** in aqueous acetic acid gave principally the *o*-cresol-type product **75** and the 5/7-fused ketone **76**, along with small amounts of the spiroketone **77** (Scheme 13). The unfavorable ratio of **77**/**76**, in comparison to that obtained upon irradiation of **1a**, is attributed to the fact that the 6β-methyl substituent strongly hinders the approach of solvent at C10 from the top side of the mesoionic cyclopropyl intermediate derived from **74**. However, spiroketone formation still occurs to some extent, but with accompanying loss of a proton at C9 replacing the usual attack of solvent. Phenol **75** is probably formed by rearrangement of the lumiproduct derived from **74** following a pathway similar to that described in Scheme 2.[41]

The photochemical behavior of tricyclic dienones **78** and **80** is strongly dependent on the relative disposition between the cyclopropane ring and the bridge methyl group (Scheme 14). For example, dienone **78a**, in which the two aforementioned elements are in a *trans* disposition, has been found to be stable upon direct irradiation in aprotic[42] or protic[43] media. The failure of **78a** to undergo rearrangement has been attributed to the fact that the zwitterionic intermediate that should be formed is expected to be highly strained because the two adjacent cyclopropane rings on the six-membered ring would have a *cis* relationship to each other. Interestingly, compound **78b**, which contains a carboxyl group at C2, was converted into tricyclic dienone **79** upon irradiation in dioxane. In this case, the carboxyl group may sufficiently influence the energy and electronic distribution of the photoexcited species to allow the formation of a cyclopropyl intermediate analogous to **21** (Scheme 4), although it is also possible that a different reaction pathway may be taken in this case.[43]

In contrast to **78a**, its C10 epimer **80a**, which has a *cis* relationship between the methyl and the cyclopropane ring, rearranges in the normal way to give the lumiketone **81a** or the 5/7-fused hydroxy ketone **82a** upon irradiation in dioxane[44] or aqueous acetic acid, respectively.[45] The related dienone **80b** reacted similarly to **80a** in dioxane but it was prone to undergo thermal cleavage of the cyclopropane

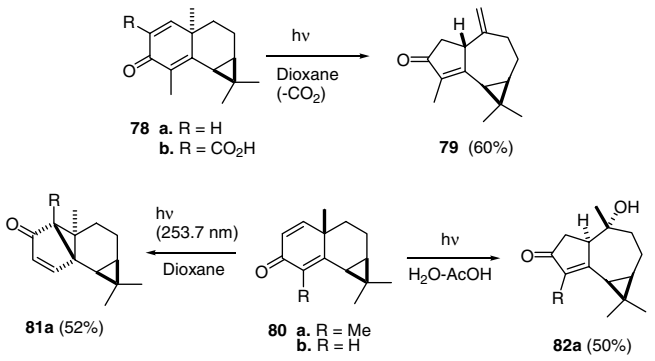

SCHEME 14

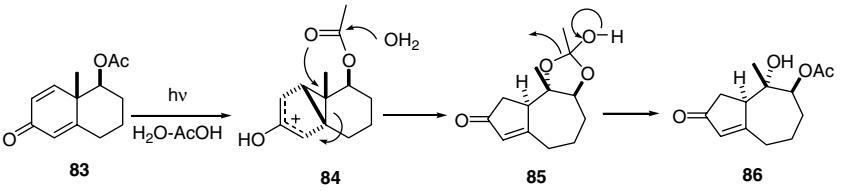

SCHEME 15

ring in aqueous acetic acid. However, it was transformed into the acetyl derivative of **82b** in 71% yield upon irradiation in glacial acetic acid.[44]

Several bicyclic 6/6- and 6/5-fused dienones containing oxy substituents (ether or ester groups) at the contiguous atom to the bridge carbon have been prepared and irradiated. The 6/6-fused 9-acetoxydienone **83** underwent photorearrangement to give largely the 5/7-fused enone **86** upon irradiation in aqueous acetic acid (Scheme 15). The exclusive formation of **86** is attributed to participation of the acetoxy group in the selective cleavage of the internal bond of the cyclopropane ring in the corresponding cationic intermediate **84**.[46]

Irradiation of the 6/5-fused dienone **87a**, which bears a β-TBDPS group at C8, in glacial acetic acid furnished the 5/6-acetoxy ketone **88a** as the major product, along with three tricyclic ketones **89a**, **90a**, and **91a** (Scheme 16). Spirocyclic products were not obtained. Compounds **88a** and **91a** are probably formed by similar pathways as compounds **9e** and **42** (Scheme 8). Tricyclic acetoxy ketones **89a** and **90a** are probably derived from trapping of the cyclopropyl carbocation intermediate. It appears that, in this case, the β-substituent reduces the rate of cleavage of the cyclopropane ring in the protonated intermediate (analogous to **5**) to such an extent that the trapping process can occur. The effect may be steric or electronic. Clearly, the bulky β-substituent could reduce the rate of solvent attack, but it is also feasible that the electron-withdrawing effect of the silyl ether may destabilize the transition state for opening of the cyclopropane ring by increasing the positive charge at C9. The photochemical behavior of the epimeric ketone **87b** in acetic acid was similar to that of **87a**, except that the tricyclic cyclopropyl ketone related to **91a** was not detected (Scheme 16). It seems that the strong interaction between the α-methyl and the α-TBDPS groups, which does not occur when the OTBDPS group is in the β-position, could prevent the [1,4]-sigmatropic rearrangement from occurring. The phenolic hemiacetal acetate **92**, produced by thermal cleavage of the 1,9-bond, is also isolated in 15% yield. However, both compounds differ in their photochemical behavior in water:THF solutions containing acetic acid. Under these conditions, thermal cleavage was the main process for compound **87b**, with a small amount of compound **88b** being the only photoproduct detected. However, under similar conditions, photolysis of **87a** proceeded smoothly to give

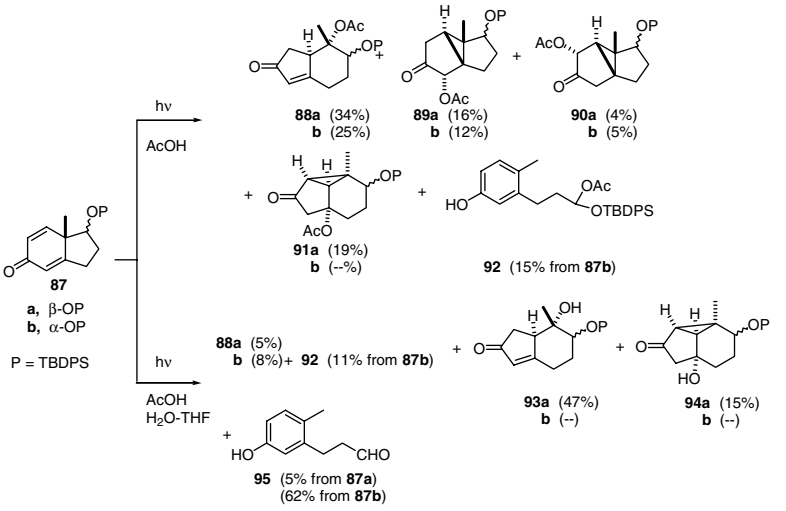

SCHEME 16

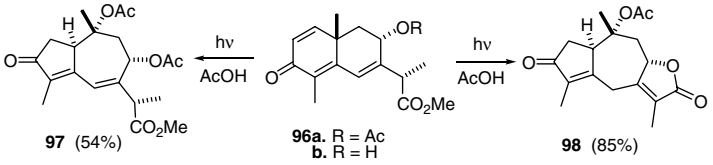

SCHEME 17

88a, **93a**, **94a**, and **95**.[47] Thus, the configuration of the δ-oxy substituent at C8 can profoundly affect the rates of the competing photochemical and thermal processes in these systems.

Extended π Systems

Irradiation of trienone **96a**, which bears an additional double bond conjugated with the 4,5-double bond of the dienone, in glacial acetic acid yielded exclusively the azulene linearly conjugated dienone **97** in 54% yield (Scheme 17). Under similar conditions, trienone **96b** yielded lactone **98** in 85% yield.[48] Thus, it seems that the 6,7-double bond does not interfere in the photochemical rearrangement.

In contrast, the extension of the π-system at both ends of the dienone moiety changes its photochemistry dramatically.[49] Irradiation of **99** in methanol or isopropyl alcohol gave a major photoproduct **104** that incorporated a molecule of solvent and a molecule of molecular oxygen, along with a small amount of triphenylnaphthol **108**. Compound **104** was formed by reaction of oxygen with the intermediate **103**, which can be obtained under conditions of total exclusion of oxygen. In non-nucleophilic solvents such as acetonitrile, the triphenylnaphthol **108** is obtained exclusively (Scheme 18).

The mechanism for the formation of **103** is seen to be analogous to that proposed for the "type A" 2,5-cyclohexadienone rearrangement. The initial δ–δ bonding step here is the counterpart of the β–β bonding in monocyclic dienones. However, unlike monocyclic zwitterionic intermediates, zwitterion **102** captures solvent faster than it rearranges. This solvent capture gives intermediate **103**, which, after reaction with oxygen, yields product **104**. The minor product **108** derives from the bicyclic rearrangement: in the absence of nucleophilic solvents, zwitterion **102** undergoes a sigmatropic rearrangement to triphenyl quinone methide **105**, a process that is analogous to the "type A" rearrangement characteristic of monocyclic 2,5-cyclohexadienones. The secondary photoexcitation of **105** and intersystem crossing leads to

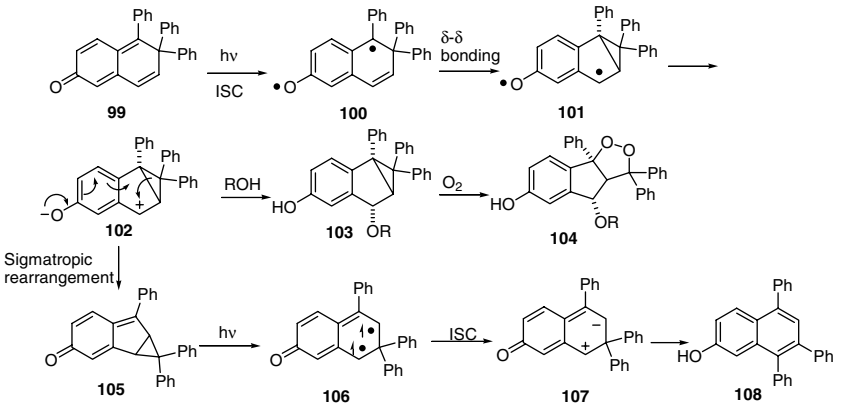

SCHEME 18

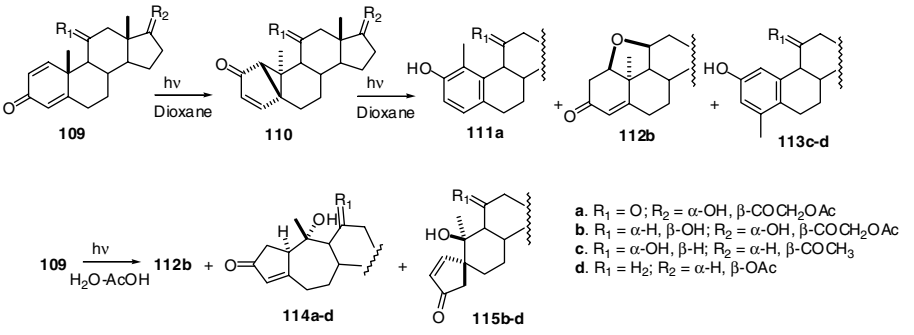

SCHEME 19

the ground-state zwitterionic species **107**, which, after phenyl migration, gives **108.** This process is the counterpart of the "type B" rearrangement that is common in the photochemistry of bicyclo[3,1,0]hexen-2-ones.

Remote Substituent Effects

The photochemistry of several steroid cross-conjugated cyclohexadienones substituted at C11 has been studied.[50] Photolysis of the prednisone acetate **109a**, prednisolone acetate **109b**, and 11α-hydroxypregna-1,4-diene-3,20-dione **109c** in dioxane afforded the expected lumiproducts. Apparently, the presence of a substituent at this position does not affect the photochemistry of these compounds in neutral conditions, but it does affect the photolysis of the corresponding lumiproducts. Irradiation of **110a** and **110b** in dioxane gave the *o*-methylphenol **111a** and the 1,11-oxy steroid **112b**, respectively. In contrast, the α-hydroxy compound **110c** gave a *m*-methyl-phenol **113c** as does the C11 unsubstituted steroid lumiproduct **110d**.

In aqueous acetic acid, irradiation of compounds **109** gave the expected bicyclo[5,3,0]-systems **114** and spiro steroids **115**, although variable product ratios and yields were obtained. In addition, the 11β-hydroxysteroid **109b** gave the 1,11-oxy steroid **112b** as the major product (Scheme 19). Compounds **111**, **112**, and **113** are photoproducts derived from the corresponding lumi-intermediates formed through zwitterionic intermediate **116**, which can rearrange in a number of ways (Scheme 20): (a) 1,2-migration of the angular methyl group leading to phenol **111** or (b) rearrangement through spiro structure **117**, which can collapse to the spiro cross-conjugated dienone **118** or undergo further 1,2-bond migration to

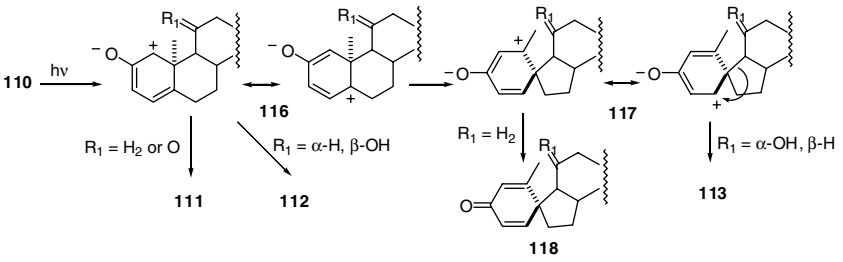

SCHEME 20

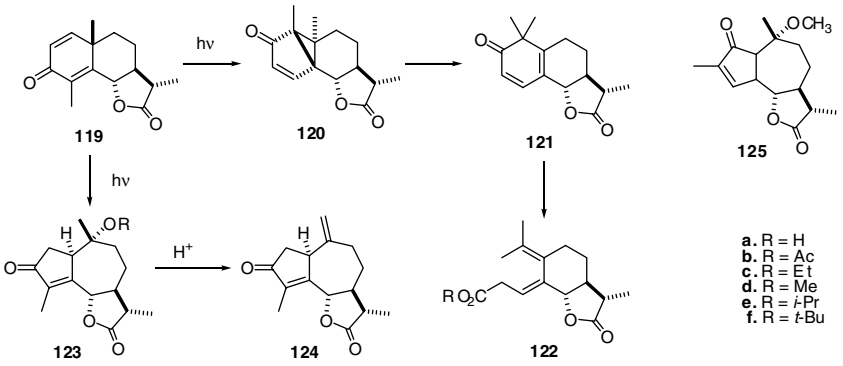

SCHEME 21

give 4-methylphenol **113**. When a C11 ketone is present the latter process does not occur – probably because cleavage of the 9,10-bond and migration of C9 to C5 would involve the formation of a partial positive charge adjacent to the electron deficient C11 carbonyl carbon. On the other hand, nucleophilic attack by the β-OH group on the C1 carbocation **116** would lead to the formation of the 1,11-oxy steroid-type compounds **112**. In the 11α-hydroxy steroids, the OH group is too far away from C1 and, therefore, these kinds of products are not obtained.

The ratio of **114:115** is also dependent on the substitution at C11. For example, a ratio of *ca.* 50:50 is obtained from the C11 unsubstituted dienone **109d** and also from the 11β-hydroxy compound **109b**. However, when the 11α-hydroxyl group is present, the yield of **114c** is four times that of **115c**, while the C11 keto compound **109a** yields only **114a**. The increased amount of **114** is attributed to hydrogen bonding between the C11 oxygen and the solvent in the corresponding carbocation intermediates related to **5**. Hydrogen bonding in **109a** and **109c** would favor solvent attack from the α-side giving rise to compounds **114a** and **114c**, whereas the C18 methyl group would block the formation of hydrogen bonds on the β-side in compound **109b**.

80.4 Photochemistry of Santonin

Santonin (**119**) undergoes a number of interesting rearrangements that are solvent dependent (Scheme 21). There are three main products resulting from irradiation of santonin: lumisantonin (**120**), photosantonic acid derivatives **122**, and isophotosantonic lactone derivatives **123**. Lumisantonin is best obtained by the photolysis of **119** in dioxane,[5] while photosantonic acid derivatives **122** and isophotosantonic lactone derivatives **123** are produced when irradiation of santonin is carried out in protic media of the type R–OH or R–COOH.[51] Photosantonic acid (**122a**)[6] can be prepared by irradiation of santonin

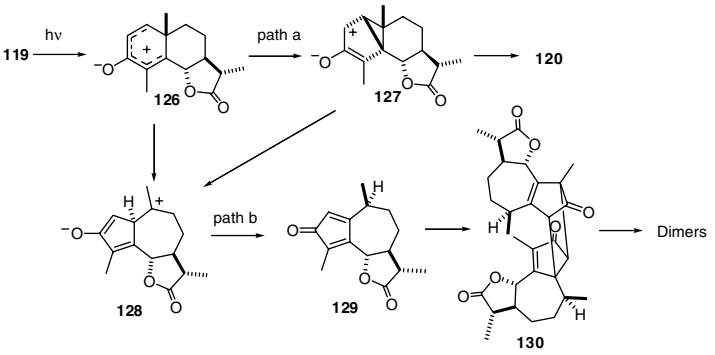

SCHEME 22

in aqueous solution containing one equivalent of potassium hydroxide,[1,3] while isophotosantonic lactone (**123a**) and *O*-acetyl isophotosantonic lactone (**123b**) are the major products of irradiation in aqueous and glacial acetic acid, respectively. Photosantonic acid (**122a**) is also obtained as an additional product under these conditions.

Irradiation of santonin in alcoholic solutions[51] gives addition products of type **123c,d,e,f** as well as the main product, lumisantonin (**120**) and the corresponding esters **122c** (photosantonin)[3-5] and **122d** and**122e**. The amount of **123** diminishes with the bulkiness of the solvent and also depends on the acidity of the medium up to a limiting value above which *exo* anhydro-isophotosantonic lactone **124** is also formed.[51]

The formation of compounds **120** and **123** can be explained in terms of the mechanism outlined in Scheme 1. Thus, lumisantonin (**120**) is obtained through path a from the zwitterionic intermediate related to **4**, while the isophotosantonic intermediates **123** are produced by attack of the solvent on the cationic intermediate related to **5** (path e). Elimination of the OR group occurs on increasing the acidity of the reaction medium and this must be responsible for the formation of compound **124**. The presence of the *trans* γ-lactone in this case prevents spiran formation because the resulting spiro intermediate would require the highly strained *trans* fusion of two five-membered rings.

On the other hand, photosantonic acid derivatives **122** arise from subsequent photolysis of lumisantonin (**120**) and may indicate the participation of the intermediate with a linear dienone structure (i.e., **121**), which is called mazdasantonin. Mazdasantonin has been obtained by irradiation of lumisantonin (**120**) in aprotic media such as ether or benzene and this compound is rapidly transformed into photosantonic acid when the irradiation is continued in the presence of water.[52]

Another, less common, photoproduct of santonin is neoisosantonic lactone methyl ether (**125**) and this has been obtained in 73% yield upon irradiating santonin in $CHCl_3$/MeOH in the presence of maleic anhydride.[53]

The irradiation of santonin in the solid state leads mainly to cyclopentadienone **129**, which spontaneously dimerizes to give compound **130** as well as small amounts of other dimers and lumisantonin (**120**) (Scheme 22). The formation of **129** can be understood in terms of the migration of a hydrogen atom from C1 in the zwitterionic intermediate **128** (path b). The selective transformation of **119** into **130**, which predominates over lumisantonin formation (path a), is interpreted by considering that path b requires less atomic movement in the geometry of santonin and, therefore, is preferred in the solid state.[54]

80.5 Synthetic Applications

The photochemical rearrangement of fused cross-conjugated dienones is a powerful synthetic tool. Due to the high stereoselectivity of this reaction and to the structures of the resulting products, which can be

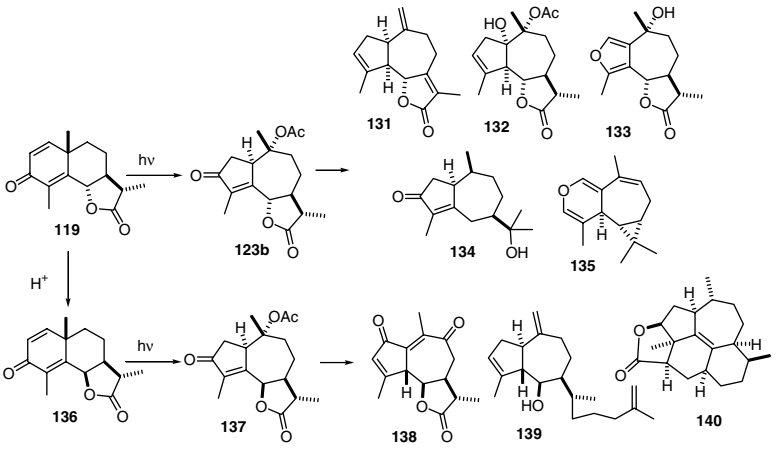

SCHEME 23

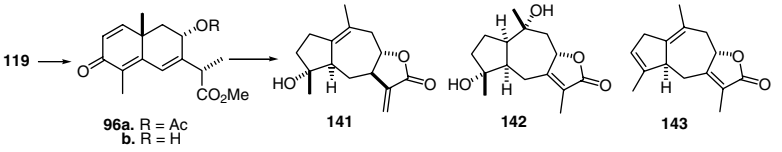

SCHEME 24

controlled by varying solvents, irradiation wavelength, and substituents, these reactions have been used in a large number of total syntheses of natural products.

The original photochemical rearrangements of α-santonin (**119**) or 6-*epi*-α-santonin (**136**) in protic media to give the corresponding isophotosantonic lactone derivatives have been extensively applied to the synthesis of terpenes, especially 6,12-guaianolides. Recent examples (Scheme 23) include the synthesis of *ent*-isodehydrocostus lactone (**131**),[55] 8-deoxy-11,13-dihydrorupiculin B (**132**),[56] 3-oxaguaianolides **133**,[57] (+)-hydrocolorenone (**134**)[58] and oxoisodehydroleucodin (**138**),[59] as well as the synthesis of the *ent*-seco-aromadendrane plagiochilline N (**135**),[60] the diterpene (+)-pachidictyol A (**139**)[61] and the synthesis of a tetracyclic precursor of 3α-hydroxy-15-rippertene **140**.[62]

Furthermore, santonin has been readily transformed into 8-oxyfunctionalized trienones **96a** and **96b**, which after photochemical rearrangement and lactonization provided a convenient method for the preparation of, among others, the 8,12-guaianolides 8-*epi*-pseudoivalin (**141**), (+)-zedolactone A (**142**), and podoandin (**143**) (Scheme 24).[48]

Other molecules possessing a 5/7-fused ring system have been synthesized by pathways involving the photochemical conversion of 6/6-fused dienones. Among these, it is worth mentioning the synthesis of the aromadendrane-type sesquitepenes cyclocolorenone,[43] (−)-4-epiglobulol and (+)-4-epiaromadendrane[45] from compounds **78** and **80**. The rearrangement of a highly functionalized tricyclic cyclohexadienone **144** in TFA/pentane is the key step in a general synthetic route to daphnanes and (+)-resiniferatoxin (Scheme 25).[63]

The rearrangement of 6/5-fused dienones has also been applied to the synthesis of natural products. The 6β-isopropyl derivative of acetoxy ketone **45**, obtained upon irradiation of the 6β-isopropyl derivative of dienone **44**, was used in the synthesis of oplopanone.[31] On the other hand, expansion of the A ring in the 5/6-fused methoxy ketone resulting from irradiation of the 6β-isopropyl derivative of **1e**, allowed the synthesis of the cadinane sesquiterpene 3-oxo-α-cadinol and α-cadinol.[64]

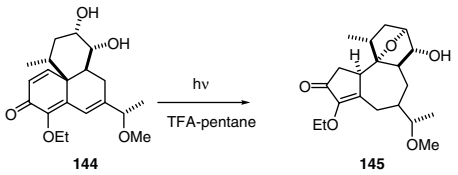

SCHEME 25

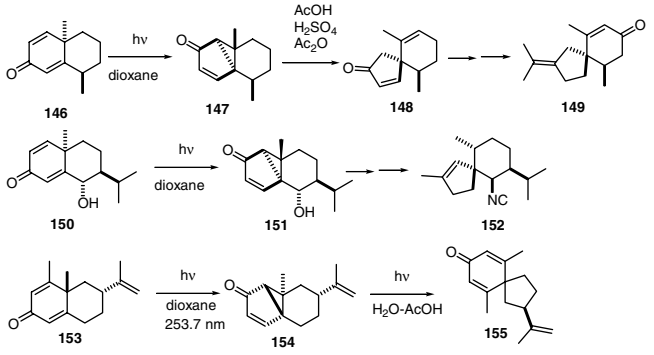

SCHEME 26

Lumiproducts obtained by irradiation of cyclohexadienones in neutral media can be transformed in several ways into useful synthetic intermediates (Scheme 26). For example acid treatment of lumiproducts such as **147** gives spirocyclic compounds. This strategy has been used in the synthesis of spirovetivane sesquiterpenes such as (±)-β-vetivone (**149**).[65]

The lumiproduct **151** was converted in several steps, including reductive cleavage of the cyclopropane ring with Li/$EtNH_2$, into a 5/6-spirocyclic system that was subsequently transformed into (−)-axisonitrile-3 (**152**).[66]

Irradiation of lumiproducts in aqueous acetic acid with UV light above 300 nm brings about photorearrangement to spirocyclic dienones. This type of transformation was used for the conversion of the nootkatane sesquiterpenes 3,4-dehydronootkatone (**153**) into the spirovetivane anhydro-β-rotunol (**155**) and in the synthesis of β-vetivone and 4-*epi*-β-vetivone from dehydro-β-vetivone.[67]

References

1. Simonsen, J., Barton, D.H.R., *The Terpenes, Vol. 3*, Cambridge University Press, New York, 1952, 292.
2. Barton, D.H.R., de Mayo, P., and Shafiq, M., Photochemical transformations. I. Some preliminary investigations, *J. Chem. Soc.*, 929, 1957.
3. (a) Barton, D.H.R., de Mayo, P., and Shafiq, M., Photochemical transformations. II. The constitution of luminosantonin, *J. Chem. Soc.*, 140, 1958; (b) Barton, D.H.R. and Gilham, P.T., Photochemical transformations. IX. The stereochemistry of luminosantonin, *J. Chem. Soc.*, 4596, 1960.
4. Barton, D.H.R., de Mayo, P., and Shafiq, M., Photochemical transformations. V. The constitution of photosantonic acid and derivatives, *J. Chem. Soc.*, 3314, 1958.
5. Arigoni, D., Bosshard, H., Bruderer, H., Büchi, G., Jeger, O., and Krebaum, L.J., Photochemical reactions. 2. Reciprocal relations and transformations in irradiation products of the santonins, *Helv. Chim. Acta,* 40, 1732, 1957.

6. Van Tamelen, E.E., Levin, S.H., Brenner, G., Wolinsky, J., and Aldrich, P.E., The structure of photosantonic acid, *J. Am. Chem. Soc.*, 81, 1666, 1959.
7. Barton, D.H.R. and Taylor, W.C., Photochemical transformations. IV. The photochemistry of prednisone acetate, *J. Chem. Soc.*, 2500, 1958.
8. Dutler, H., Bosshard, H., and Jeger, O., Photochemical reactions. Light-catalyzed dienone-phenol rearrangement, *Helv. Chim. Acta*, 40, 494, 1957.
9. Kropp, P.J., Photochemical rearrangement of cyclohexadienones and related compounds, *Org. Photochem.*, 1, 1, 1967.
10. Schaffner, K. and Demuth, M., Photochemical rearrangements of conjugated cyclic dienones, in *Rearrangements in Ground and Excited States*, Vol. 3, de Mayo, P. Ed., Academic Press, New York, 1980, 281.
11. Schultz, A.G., New photochemistry of 2,5-cyclohexadien-1-ones and related compounds, *Pure Appl. Chem.*, 60, 981, 1988.
12. This topic has been excellently reviewed in the previous edition of this handbook. Caine, D., Photochemical rearrangements of 6/6-and 6/5-fused cross-conjugated cyclohexadienones, in *Handbook of Organic Photochemistry*, Horspool, W.M. Ed., C.R.C. Press, Boca Raton, FL, 1995, 701.
13. Zimmerman, H.E. and Schuster, D.I., A new approach to mechanistic organic photochemistry. IV. Photochemical rearrangements of 4,4-diphenylcyclohexadienone, *J. Am. Chem. Soc.*, 84, 4527, 1962.
14. Zimmerman, H.E. and Swenton, J.S., Mechanistic organic photochemistry. XXI. Electronic details of the 2,5-cyclohexadienone rearrangement, *J. Am. Chem. Soc.*, 89, 906, 1967.
15. Schuster, D.I., Mechanisms of photochemical transformations of cross-conjugated cyclohexadienones, *Acct. Chem. Res.,* 11, 65, 1978.
16. Coxon, J.M. and Halton, B., *Organic Photochemistry*, Cambridge University Press, New York, 1974, 92.
17. Zimmerman, H.E., Crumrine, D.S., Döpp, D., and Huyffer P.S., Photochemistry without light and the stereochemistry of the type A dienone rearrangement. Organic Photochemistry. XXXVIII, *J. Am. Chem. Soc.*, 91, 434, 1969.
18. (a) Schuster, D.I. and Abraitys, V.Y., Isolation of a bicyclo[3.1.0]hexan-3-one on photolysis of a cyclohexan-2,5-dione. Direct evidence for a zwitterion intermediate, *J. Chem. Soc., Chem. Commun.*, 419, 1969; (b) Schuster, D.I. and Liu, K.-C., Experimental proof for the intermediacy of zwitterions in the pathway leading to lumiketones upon irradiation of 2,5-cyclohexadiones, *Tetrahedron*, 37, 3329, 1981.
19. (a) Samuel, C.J., The type A zwitterion in cyclohexadienone photochemistry: Chemical trapping and stereochemistry, *J. Chem. Soc., Perkin Trans. II*, 736, 1981; (b) Schultz, A.G., Myong, S.O., and Puig, S., Intramolecular azide cycloaddition to a photochemically generated zwitterion, *Tetrahedron Lett.*, 25, 1011, 1984.
20. Kropp, P.J., The photochemical properties of a 2-methyl-1,4-dien-3-one, *J. Am. Chem. Soc.*, 86, 4053, 1964.
21. Caine, D., Alejande, A.M., Ming, K., and Powers, W.J., III, Photochemical rearrangements of bicyclic 6/5-fused cross-conjugated cyclohexadienones and related compounds, *J. Org. Chem.*, 37, 706, 1972.
22. Bozzato, G., Throndsen, H.P., Schaffner, K., and Jeger, O., The photochemical isomerization of B-*nor*-1-dehydrotestosterone acetate in dioxane solution, *J. Am. Chem. Soc.*, 86, 2073, 1964.
23. Pète, J.P. and Wolfhugel, J.L., Photochemical transformations of enones: influence of the environment on the reactivity of α-methoxy cyclohexenones, *Tetrahedron Lett.*, 4637, 1973.
24. Caine, D., Deutsch, H., Chao, S.T., Van Derveer, D.G., and Bertrand, J.A., Photochemical conversion of methoxy-substituted 6/6-fused cross-conjugated cyclohexadienones into isomeric tricyclodecenones, *J. Org. Chem.*, 43, 1114, 1978.

25. Caine, D., Brake, P.F., DeBardelen, J.F., Jr., and Dawson, J.B., The influence of electron-withdrawing substituents on the photochemical behavior of bicyclic 6/6-fused cross-conjugated cyclohexadienones, *J. Org. Chem.*, 38, 967, 1973.
26. Altenburger, E., Schaffner, K., and Wehrli, H., Photochemical reactions. 25. The irradiation with UV light of *o*-acetyl-1-dehydro-2-formyl-testosterone, *Helv. Chim. Acta*, 46, 2753, 1963.
27. Broka, C.A., Photorearrangements of carbomethoxy-substituted cyclohexadienones in neutral media, *J. Org. Chem.,* 53, 575, 1988.
28. Kropp, P.J., Photochemical rearrangements of cross-conjugated cyclohexadienones. V. A model for the santonin series*, J. Org. Chem*., 29, 3110, 1964.
29. Caine, D. and Dawson, J.B., The synthesis of a model perhydroazulene derivative, *J. Org. Chem.*, 29, 3108, 1964.
30. Kropp, P.J. and Erman, W.F., Photochemical rearrangements of cross-conjugated cyclohexadienones. II. Unsubstituted 1,4-dien-3-ones, *J. Am. Chem. Soc.*, 85, 2456, 1963.
31. (a) Caine, D. and Tuller, F.N., Photochemical rearrangements of 6/5-fused cross-conjugated cyclohexadienones. Application to the total synthesis of dl-oplopanone, *J. Am. Chem. Soc.,* 93, 6311, 1971; (b) Caine, D. and Tuller, F.N., The total synthesis of dl-oplopanone, *J. Org. Chem*., 38, 3663, 1973.
32. Caine, D., Boucugnani, A.A., Chao, S.T., Dawson, J.B., and Ingwalson, P.F., Stereospecific synthesis of 6,*c*-10-dimethyl(*r*-5-*C*[1])spiro[4.5]dec-6-en-2-one and its conversion into (±)-α-vetispirene, *J. Org. Chem*., 41, 1539, 1976.
33. Caine, D., Gupton, J.T., III, Ming, K., and Powers, W.J., III, Photochemical rearrangements of 6/5-fused cross-conjugated cyclohexadienones in protic solvents, *J. Chem. Soc., Chem. Commun.*, 469, 1973.
34. Shiozaki, M., Mori, K., Matsui, M., and Hiroka, T., Photochemical synthesis of compounds with grayanotoxin skeleton, *Tetrahedron Lett*., 657, 1972.
35. Kropp, P.J., The photochemical behavior of 3-keto-9-carboethoxy-$\Delta^{1,4}$-hexahydronaphthalene, *Tetrahedron Lett*., 3647,1964.
36. Burkinshaw, G.F., Davis, B.R., and Woodgate, P.D., The photochemistry of some 4-hydroxycyclohexa-2,5-dienones, *J. Chem. Soc. (C)*, 1607,1970.
37. Ganter, C.G., Warszawski, R., Wehrli, H., Schaffner, K., and Jeger, O., Photochemical reactions. 19. The irradiation with UV light of 3-oxo-10β-hydroxy-17β-acetoxy-$\Delta^{1,4}$-estradiene, *Helv. Chim. Acta*, 46, 320, 1963.
38. Bashir, M., Freyer, A.J., Shamma, M., Rahman, A-U., and Sariyar, G., The photolysis of salutaridinemethine, *J. Nat. Prod.,* 48, 654, 1985.
39. Zimmerman, H.E. and Jones, G., II, The photochemistry of a cyclohexadienone structurally incapable of rearrangement. Exploratory and mechanistic organic photochemistry. XLVII, *J. Am. Chem. Soc.,* 92, 2753, 1970.
40. Mock, W.L. and Rumon, K.A., Photoreduction of 2,4-dimethyl-3-oxo-3,5,6,7,8,8a-hexahydro-1,8a-butanonaphthalene, a nonphotorearranging cross-conjugated cyclohexadienone, *J. Org. Chem.,* 37, 400, 1972.
41. Kropp, P.J., Photochemical rearrangements of cross-conjugated cyclohexadienones. III. An example of steric control, *J. Am. Chem. Soc*., 85, 3779, 1963.
42. Kropp, P.J. and Krauss, H.J., Photochemical rearrangement of a γ,δ-cyclopropyl-α,β-unsaturated ketone, *J. Org. Chem*., 32, 4118, 1967.
43. Caine, D. and Ingwalson, P.F., The influence of substituents on the photochemical behavior of cross-conjugated cyclohexadienones. A facile total synthesis of (−)-cyclocolorenone, *J. Org. Chem.*, 37, 3751, 1972.
44. Caine, D., Deutsch, H., and Gupton, J.T., III, Photochemical rearrangements of cross-conjugated cyclohexadienones related to epimaalienone, *J. Org. Chem*., 43, 343, 1978.

45. Caine, D. and Gupton, J.T., III, Photochemical rearrangements of cross-conjugated cyclohexadienones. Application to the synthesis of (−)-4-epiglobulol and (+)-4-epiaromadendrene, *J. Org. Chem.*, 40, 809, 1975.
46. Caine, D., Kotian, P.L., and McGuiness, M.D., Synthesis and photochemical rearrangements of bicyclic cross-conjugated cyclohexadienones containing δ-oxy substituents, *J. Org. Chem.*, 56, 6307, 1991.
47. Caine, D. and Kotian, P.L., Synthesis and photochemical rearrangement of (1*R*, 7a*S*)-1-(*tert*-butyldiphenylsiloxy)-7a-methyl-5(7a*H*)-indanone, *J. Org. Chem.*, 57, 6587, 1992.
48. (a) Blay, G., Bargues, V., Cardona, L., Collado, A.M., García, B., Muñoz, M.C., and Pedro, J.R., Stereoselective synthesis of 4α-hydroxy-8,12-guaianolides from santonin, *J. Org. Chem.*, 65, 2138, 2000; (b) Blay, G., Bargues, V., Cardona, L., García, B., and Pedro, J.R., Stereoselective synthesis of 7,11-guaien-8,12-olides from santonin. Synthesis of podoandin and (+)-zedolactone A, *J. Org. Chem.*, 65, 6703, 2000.
49. Zimmerman, H.E. and Lamers, P.H., Photochemistry of some extended π-systems: type A and aryl rearrangements of systems with extended conjugation related to cyclohexadienones and cyclohexenones. Mechanistic and exploratory organic photochemistry, *J. Org. Chem.*, 54, 5788, 1989.
50. (a) Williams, J.R., Moore, R.H., Li, R., and Blount, J.F., Structure and photochemistry of lumiprednisone and lumiprednisone acetate, *J. Am. Chem. Soc.*, 101, 5019, 1979; (b) Williams, J.R., Moore, R.H., Li, R., and Weeks, C.M., Photochemistry of 11α- and 11β-hydroxy steroidal 1,4-dien-3-ones and 11α- and 11β-hydroxy steroidal bicyclo[3,1,0]hex-3-en-2-ones in neutral and acidic media, *J. Org. Chem.*, 45, 2324, 1980.
51. Schaffner-Sabba, K., α-Santonin: photochemistry in protic solvents and pyrolysis, *Helv. Chim. Acta*, 52, 1237, 1969.
52. (a) Chapman, O.L. and Englert, L.F., A mechanistically significant intermediate in the lumisantonin to photosantonic acid conversion, *J. Am. Chem. Soc.*, 85, 3028, 1963; (b) Fisch, M.H. and Richards, J.H., The mechanism of the photochemical rearrangement of lumisantonin, *J. Am. Chem. Soc.*, 90, 1547, 1968.
53. Ayalp, A., Özden, T., and Özden, S., ^{13}C NMR spectra of santonin photoproducts: characterization of a novel product, *Spectroscopy Lett.*, 25, 559, 1992.
54. Matsuura, T., Sata, Y., Ogura, K., and Mori, M., Photoinduced reactions. XXIII. A novel photorearrangement of santonin in the solid state, *Tetrahedron Lett.*, 4627, 1968.
55. Delair, P., Kann, N., and Greene A.E., Synthesis (in *ent*-form) of a novel jalcaguaianolide from *Ferula arrigoni* bocchieri, *J. Chem. Soc., Perkin Trans. 1*, 1651, 1994.
56. Bargues, V., Blay, G., Cardona, L., García, B., and Pedro, J.R., Regio- and stereoselective oxyfunctionalization at C1 and C5 in sesquiterpene guaianolides, *Tetrahedron*, 54, 1845, 1998.
57. Blay, G., Cardona, L., García, B., Lahoz, L., Monje, B., and Pedro, J.R., Synthesis of 3-oxaguaianolides from santonin, *Tetrahedron*, 56, 6331, 2000.
58. Blay, G., Bargues, V., Cardona, L., García, B., and Pedro, J.R., Ultrasound assisted reductive cleavage of eudesmane and guaiane γ-enonelactones. Synthesis of 1α,7α,10αH-guaian-4,11-dien-3-one and hydrocolorenone from santonin, *Tetrahedron*, 57, 9719, 2001.
59. Greene, A.E. and Edgar, M.T., Synthesis of oxoisodehydroleucodin: a novel guaianolide from *Montanoa imbricata*, *J. Org. Chem.,* 54, 1468, 1989.
60. Blay, G., Cardona, L., García, B., Lahoz, L., and Pedro, J.R., Synthesis of plagiochiline N from santonin, *J. Org. Chem.*, 66, 7700, 2001.
61. Greene, A.E., Highly stereoselective total syntheses of (+)-pachydictyol A and (−)-dictyolene, novel marine diterpenes from brown seaweeds of the family dictyotaceae, *J. Am. Chem. Soc.*, 102, 5337, 1980.
62. Metz, P., Bertels, S., and Fröhlich, R., An enantioselective approach to 3α-hydroxy-15-rippertene. Construction of the tetracyclic ring system, *J. Am. Chem. Soc.,* 115, 12595, 1993.

63. Jackson, S.R., Johnson, M.G., Mikami, M., Shiokawa, S., and Carreira, E.M., Rearrangement of a tricyclic 2,5-cyclohexadienone: towards a general synthetic route to the daphnanes and (+)-resiniferatoxin, *Angew. Chem. Int. Ed. Engl.,* 40, 2694, 2001.
64. Caine, D. and Frobese, A.S., The photochemical total synthesis of (±)-3-oxo-α-cadinol and (±)-α-cadinol, *Tetrahedron Lett*., 3107, 1977.
65. Marshall, J.A. and Johnson, P.C., The structure and synthesis of β-vetivone, *J. Org. Chem.*, 35, 192, 1970.
66. Caine, D. and Deutsch, H., Total synthesis of (−)-axisonitrile-3. An application of the reductive ring opening of vinylcyclopropanes, *J. Am. Chem. Soc*., 100, 8030, 1978.
67. Caine, D., Chu, C.-Y., and Graham S.L., Photochemical pathways for the interconversion of nootkatane and spirovetivane sesquiterpenes, *J. Org. Chem.*, 45, 3790, 1980.

81

Photocycloaddition/ Trapping Reactions of Cross-Conjugated Cyclic Dienones: Capture of Oxyallyl Intermediates

Albert R. Matlin
Oberlin College

81.1 Introduction

Cross-conjugated cyclic dienones with 6-, 7-, and 8-membered rings exhibit a rich and diverse photochemistry. The deep-seated photochemical rearrangements found in these systems have attracted numerous mechanistic studies. Cyclohexadienones have received the most attention and provide the general framework for the mechanistic understanding of the photochemistry for this class of compounds.[1] The key intermediate in these systems is an oxyallyl transient that is formed by ring closure across the β, β′-carbons in the dienone systems: **A** → **B**.

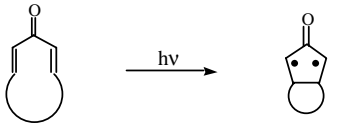

A **B**

More recently, the synthetic potential of the oxyallyl intermediates has been explored in intra- and intermolecular trapping studies. This chapter focuses on studies directed at capturing oxyallyl intermediates generated by the irradiation of cyclic dienones.

0-8493-1348-1/04/$0.00+$1.50

81.2 Oxyallyl Intermediates

Oxyallyl intermediates have been invoked in the mechanisms for a wide range of reactions, including the photoisomerizations of cross-conjugated dienones,[2] stereomutation, and cycloaddition reactions of cyclopropanones,[3,4] reductive-elimination reactions of α, α′-dibromoketones,[5,6] and the Favorskii reaction.[7] Despite all this attention (and speculation), there has not been any definitive kinetic[8] or spectroscopic observation of an oxyallyl intermediate.[9] Historically, oxyallyl systems have been described as zwitterions. However, molecular orbital calculations consistently indicate that the parent system **1** is a ground-state triplet lying 1 to 2 kcal/mol below the lowest singlet state.[10-12] The singlet–triplet separation is delicately balanced and calculations indicate that the ordering can be reversed to give a singlet ground state by either alkyl substitution[11] (e.g., **2**) or by incorporation of the oxyallyl into a cyclic system (e.g., **3**).[13,14] The potential energy surface shows that the singlet state of **1** lives in a flat, shallow minimum with only a 0.3-kcal/mol barrier to closure to cyclopropanone.[15] This small barrier should give rise to a very short lifetimes for acyclic oxyallyls and suggests that bimolecular trapping reactions will not be fast enough to compete with closure to the more stable cyclopropanone isomer. In contrast, cyclopentyl oxyallyl **3** is calculated to be more stable than the covalent cyclopropanone isomer, bicyclo[2.1.0]pentan-5-one. This is consistent with the observations that cyclic oxyallyl systems can be captured in bimolecular reactions. In addition, calculations show that the CO bond lengths in **1**, **2**, and **3** are relatively short, indicating considerable double-bond character with the unpaired electron spin density residing largely on the α-carbons. While there is some contribution from zwitterionic resonance structures, which slightly polarize the π-system, the lowest energy oxyallyl singlet state is best described as a biradical, and not a zwitterion.

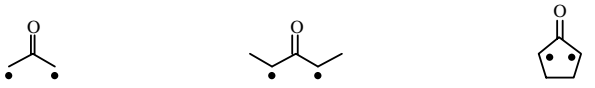

1 **2** **3**

81.3 Photocycloadditions of 2,5-Cyclohexadienones

The literature on the photochemical reactions of 2,5-cyclohexadien-1-ones is extensive and has been reviewed several times.[1,2,16,17] The chemistry of these systems is dominated by the Type A rearrangement to form bicyclo[3.10]hex-3-en-2-ones. The basic understanding of the mechanism can be attributed to the work of Zimmerman and Schuster and is outlined in Scheme 1.[1] Dienone **4** is photoexcited to an n,π* singlet state **4-S*,** which rapidly undergoes intersystem crossing to the n, π* triplet **4-T**. Bond formation across the β, β-positions produces the bicyclic triplet **5-T**, which demotes to the ground-state oxyallyl species **5-S**. The transient oxyallyl zwitterion suffers a thermal [1,4]-sigmatropic rearrangement

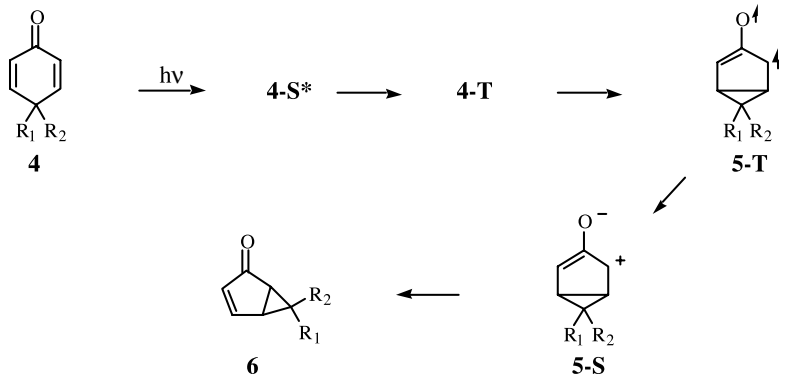

SCHEME 1

to give the observed bicyclohexenone **6**. Schuster demonstrated that alcohols and chloride ion could trap oxyallyl intermediate **5-S** in suitably designed systems where the apparent rate of the sigmatropic rearrangement to **6** was retarded (e.g., **4**, $R_1 = CH_3$, $R_2 = CCl_3$). These experiments were interpreted as support for the zwitterionic nature of oxyallyl intermediate **5-S**.

Swenton has shown that irradiation of 4,4-dimethyl-2,5-cyclohexadienone **4** ($R_1 = R_2 = CH_3$) in the gas phase produces the Type A rearrangement product bicyclic enone **6** ($R_1 = R_2 = CH_3$).[18] Swenton argued that a zwitterion would be energetically unreasonable in the gas phase and interpreted this result as supportive of a biradical oxyallyl transient. On the other hand, the solution trapping studies with alcohols and halides appear more consistent with ionic intermediates. It is possible that these discordant results may be a function of solvation. Lim et al. addressed this question by carrying out a combined *ab initio*/Monte Carlo study of the solvent effects for the ring opening of cyclopropanones to oxyallyls.[15] The relatively small solvent effects computed were interpreted to "confirm the principally biradical rather than zwitterionic nature of oxyallyls." The disconnection between these studies points to the chameleon nature of oxyallyl systems in which the relative energy of closely lying electronic states (triplet, open shell singlet, closed shell singlet) changes with substitution and reaction conditions (e.g., solvent). Attacking nucleophiles may also perturb the electron distribution in the oxyallyl, causing increasing contributions from the zwitterionic structure as the reaction proceeds. The net effect is that oxyallyl intermediates may behave operationally as zwitterions under nucleophilic conditions.

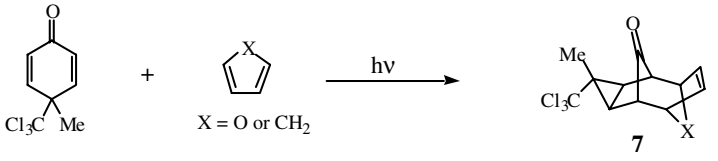

7

Samuel provided the first example that the oxyallyl intermediate in the Type A rearrangement could be trapped intermolecularly with a diene in a [3+4]-cycloaddition.[19] Samuel found that the apparent lifetime of simple 4,4-dialkyl substituted cyclohexadienones was too short to permit intermolecular capture. However, irradiation of Schuster's 4-methyl-4-trichloromethyl-2.5-cyclohexadienone **1** ($R_1 = CH_3$, $R_2 = CCl_3$) in the presence of either furan or cyclopentadiene produced 1:1 adducts **7** (X = O or CH_2). This type of [4+3]-cycloaddition reaction has long been considered as evidence for an oxyallyl transient and is compatible with either a biradical or zwitterionic species.[20]

Schultz carried out extensive studies exploiting the rich photochemistry of 2,5-cyclohexadienones to generate complex multi-cyclic systems amenable to further synthetic elaboration. These studies have explored the intramolecular photocycloadditions of 2,5-cyclohexadienone with alkene and diene traps appended to the 4-position of the ring.[21] This work has been previously reviewed.[17] This chapter focuses on the ability to capture the transient oxyallyl species.

Irradiation of dienone **8** containing a furan tethered to the 4-position produced cycloadduct **11** when R = CH_2OAc and phenol **12** when R = CO_2Me (Scheme 2).[21] The reactions proceed by initial Type A photorearrangement to enone **9**. Secondary photolysis of **9** produces a Type B photorearrangement (**8** → **11**) via the delocalized Type B oxyallyl **10**. The vinylogous oxyallyl **10** (R = CH_2OAc) lives long enough to be trapped intramolecularly by the furan ring. There was no evidence that the furan was able to trap the initial Type A oxyallyl derived from **8**. In principle, this behavior may be due to a short lifetime for the Type A oxyallyl or geometric constraints to the intramolecular [4+3]-cycloaddition with the Type A oxyallyl. As noted above, electron-withdrawing substituents at C4 are known to slow the rate of rearrangement of Type A oxyallyls intermediates and permit trapping of the Type A oxyallyl. Because only Type B photochemistry was observed with **8**, it seems likely that geometric factors are inhibiting the intramolecular trapping of the Type A oxyallyl. Interestingly, the substituents at C4 in **8** have the opposite effect on the partitioning of the Type B delocalized oxyallyl intermediate **10**. In this case, the electron-withdrawing carbomethoxy substituent raises the barrier for rearrangement (**10** → **12**), thereby increasing the lifetime of **10**.

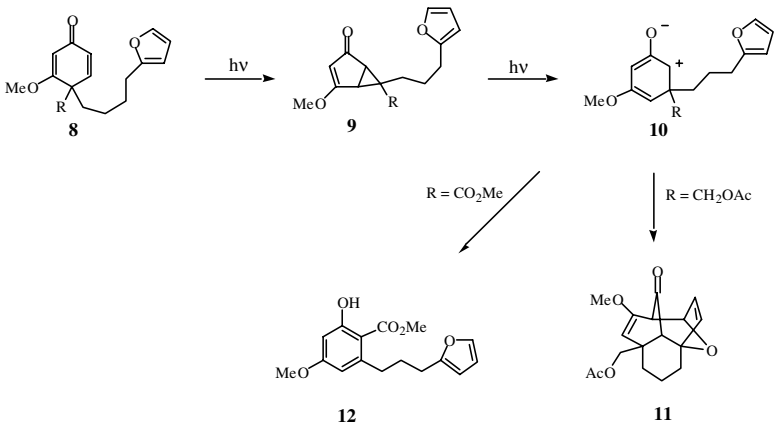

SCHEME 2

Schultz also found that C-3 methoxy substitution decreases the quantum efficiency for the Type A photorearrangement of **8** to **9**. The electron-donating methoxy group causes mixing of the π,π* triplet state with the n,π* triplet that is believed to be associated with the Type A photoreaction.[22] The change in the nature of the reacting triplet state makes it possible to trap the photoexcited state with alkenes prior to formation of the Type A oxyallyl. Irradiation of **13** produces a "conventional" intramolecular [2+2]-photocycloaddition[23] adduct **14** with no leakage into the Type A reaction manifold. The triplet state of **15** could also be captured in an intermolecular reaction with cyclopentene. Irradiation of **15** and cyclopentene at 25C produced ~20% of **16** (Type A photoproduct) and 62% [2+2]-cycloadducts **17**.[24] When the irradiation was conducted at −80C, [2+2]-adducts were observed in high chemical yield (96%) with less than 4% of Type A products detected. While the efficiencies of both reaction paths were reduced at low temperature, the Type A reaction was affected to a greater extent.

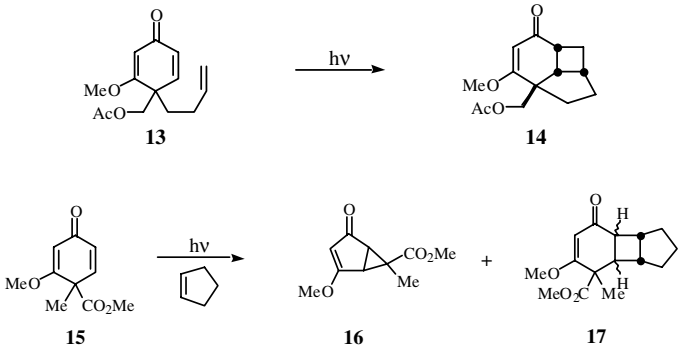

81.4 Photocycloaddition and Photocyclizations of Pyran-4-ones

Pyran-4-ones are structurally analogous to 2,5-cyclohexadienones and exhibit similar Type A photoreactivity. Barltrop reported a mechanistic study of this reaction, which is summarized in Scheme 3.[25] Irradiation of 3,5-dimethylpyran-4-one (**18**) forms the transient oxyallyl **19**. In the absence of trapping agent, **18** rearranges to 6-oxabicyclo[3.1.0]hexenone (**20**) (Type A rearrangement) that, under continued irradiation, suffers secondary photorearrangement to a 2-pyranone. Oxyallyl **19** can be trapped with alcohols and furan (in trifluoroethanol) to give, respectively, cyclopentenone **21** and the [4+3]-cycloadduct **22.** Irradiation of **18** in neat furan gave rise to [2+2]-photocycloaddition between one of the furan double bonds and the pyranone. Under these conditions, the furan was able to capture the excited state **18*** prior to the intramolecular rearrangement to oxyallyl **19**.

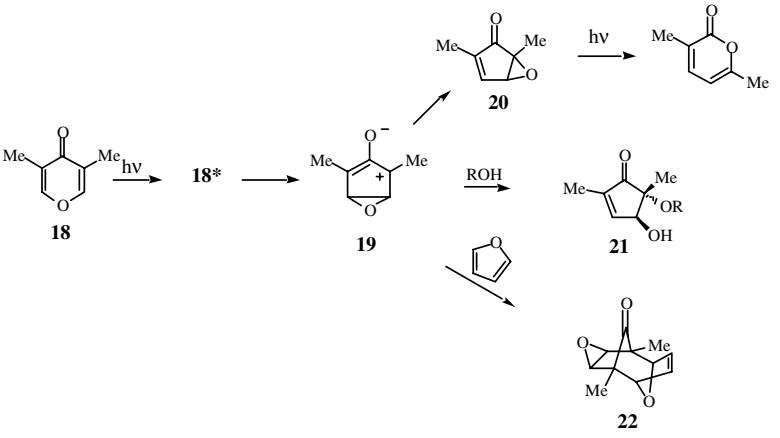

SCHEME 3

TABLE 81.1 Irradiation of 2-(Hydroxyalkyl)pyran-4-ones **23**

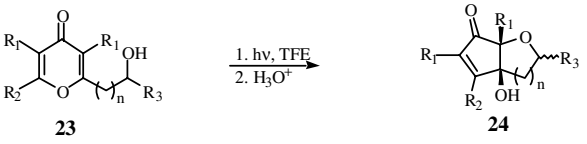

Entry	R_1	R_2	R_3	n	24 (yield, %)
a	Me	Me	H	1	75
b	Me	Me	Me	1	84
c	Me	Me	Ph	1	92
d	H	Me	Me	1	75
e	Me	Me	H	2	99
f	Me	Me	*i*-Pr	2	61
g	H	H	H	2	43

Source: Reprinted in part with permission from Ref. 26. Copyright 1990, American Chemical Society.

The West group made an extensive study of the intramolecular capture of the putative zwitterionic OA intermediate to produce highly functionalized multi-cyclic systems. Irradiation of pyranone **23** containing an alcohol tethered to the 2-position of the ring furnished bicyclic cyclopentenone ethers **24** in good to excellent yield (Table 81.1).[26] Polar solvents were needed to promote "effective partitioning through the zwitterionic pathway." Initial experiments employed methanol as solvent but this typically resulted in competing intermolecular capture by solvent. Use of the less nucleophilic trifluoroethanol (TFE) as solvent completely suppressed this side reaction.

In contrast to Schultz's studies with 2,5-cyclohexadienones, West demonstrated that the Type A oxyallyl intermediate in pyran-4-one systems could be captured by alkenes and furans. Irradiation of pyran-4-ones with alkenes tethered to the 2-position **25** gave diquinanes **26**, **27**, and **28** via the endocyclic addition of the oxyallyl to the alkene (Scheme 4, Table 81.2).[27] The mode of cyclization could be switched to exocyclic by placement of electron-donating substituents on the interior of the alkene (**29**) to give hydrindanes **30.**

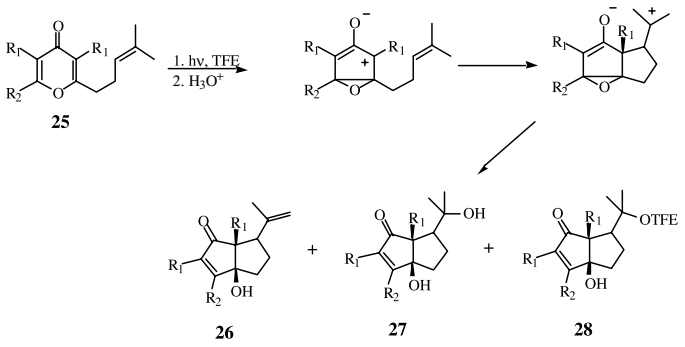

SCHEME 4

TABLE 81.2 Irradiation of 2-Alkenylpyran-4-ones **25**

Entry	R_1	R_2	R_3	Products (yield, %)
a	Me	Me	Me	27a (69)
b	Me	Me	H	26b (18), 27b (22), 28b (9)
c	H	Me	H	26c (5), 27c (17), 28c (5)
d	H	H	OMe	27d (75)
e	$-(CH_2)_4-$		H	26e (22), 27e (14), 28e (5)

Source: Reprinted in part with permission from Ref. 27. Copyright 1993, American Chemical Society.

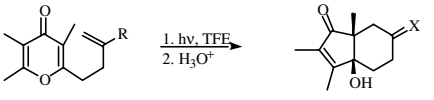

a: R = OCH_3, X = O, (61%)
b: R = CH_2SiMe_3, X = CH_2, (69%)

Irradiation of pyran-4-ones with furans tethered to the 3-position **31** produced [4+3]-cycloadducts **32** and **33** (Table 81.3).[28] The loss of the usual *endo*-selectivity in the cycloaddition was attributed to steric constraints in the compact intramolecular transition states. The reaction proved to be inefficient in nonpolar solvents such as CH_2Cl_2 and required the use of TFE for optimum results.

The ability to trap oxyallyl intermediates with alkenes and furans intramolecularly in the pyran-4-one systems but not in the 2,5-cyclohexadienone systems discussed above is most likely due to geometric factors relating to the length and point of attachment of the tether.

West also demonstrated that oxyallyls derived from pyran-4-ones can participate in electrophilic aromatic substitution reactions. Irradiation of pyran-4-ones **34** with aryl groups appended in the 2-position produced tricyclic tetrahydrobenz[e]indenone **35** in fair to moderate yield (Table 81.4).[29] Capture of the oxyallyl intermediate by solvent and Type A rearrangement to pyran-2-ones competed with the desired intramolecular EAS reaction. Interestingly, the yield of **35** was concentration dependent (higher yields with dilution). It is not clear how concentration affects the bifurcation of the oxyallyl intermediate between intramolecular trapping and rearrangement.

TABLE 81.3 Irradiation of Furan-Tethered Pyranones **31**

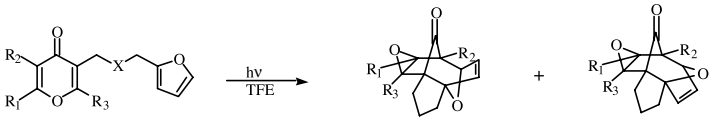

31 **32** **33**

Entry	R_1	R_2	R_3	X	32 (yield, %)	33 (yield, %)
a	Me	Me	Me	O	30	20
b	Me	Me	Me	CH_2	17	52
c	H	Me	H	O	—	10
d	Et	Me	Et	CH_2	—	27
e	Et	Et	Et	O	19	10

Source: Reprinted in part with permission from ref 28. Copyright 1993, American Chemical Society.

TABLE 81.4 Irradiation of 2-Arylethylpyran-4-ones **34**

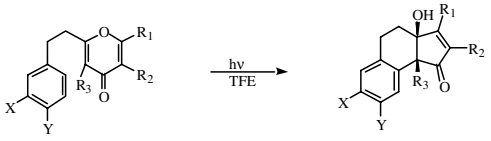

34 **35**

Entry	R_1	R_2	R_3	X	Y	35 (yield, %)
a	Me	Me	Me	H	H	32
b	Me	Me	Me	OMe	H	68
c	Me	Me	Me	OCH_2O		75
d	Me	Me	H	OCH_2O		57
e	Me	H	Me	OCH_2O		11

Source: Reprinted in part with permission from Ref. 29. Copyright 1993, American Chemical Society.

81.5 Photocycloadditions of 2,7-Cyclooctadienone

Initial studies by Crandall[30] and Noyori[31] on the photochemistry of 2,7-cyclooctadienone **36** were consistent with formation of a bicyclic[3.3.0]oxyallyl intermediate **37** that could be trapped with alcohols (**39**) or furan (**38**) (Scheme 5). In addition, Crandall showed that irradiation of **36** at −78C, followed by addition of furan in the dark, also produced cycloadduct **38**. Low-temperature ^{13}C NMR studies by Matlin and Jin identified *cis*,*trans*-2,7-cyclooctadienone **40** as the storable reactive intermediate.[32] The intensity of the NMR signals for **40** decreases at temperatures above −30C. Thermal conrotatory cyclization of **40** produces *cis*-fused bicyclic oxyallyl **37**, which can be trapped. DFT calculations place the strained *cis*,*trans*-cyclooctadienone **40** 15 kcal/mol above the *cis*,*cis*-isomer **36**.[33] The singlet biradical **37** is calculated to be only 12 kcal/mol higher in energy than **40**, which is qualitatively consistent with the behavior observed in the low-temperature NMR studies. The computational studies also support the biradical description of oxyallyl **37** in the absence of solvent. Crandall and Haseltine have reported that electron deficient π-systems such as dimethylacetylene dicarboxylate and 1,2-dichloroethylene do not give any 1:1 adducts

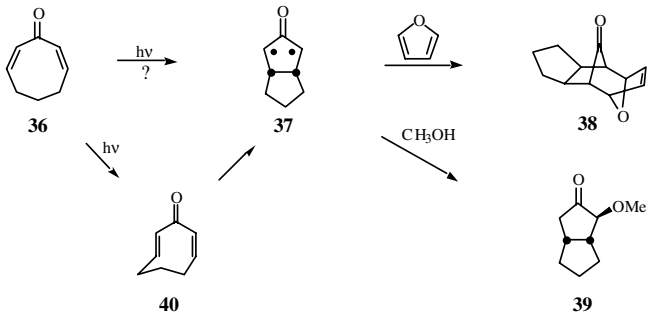

36 **37** **38** **40** **39**

SCHEME 5

TABLE 81.5 Photoproducts from the Irradiation of 36 with Vinyl Ethers

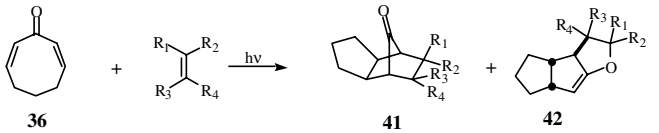

36 **41** **42**

Entry	R_1	R_2	R_3	R_4	41 (yield, %)	42 (yield, %)
a	OEt	H	H	H	19	51
b	OMe	Me	H	H	34	39
c	OEt	OEt	H	H	24	39
d	OMe	OMe	Me	Me	14	30
e	OMe	OMe	OMe	OMe	45	23

Source: Reprinted with permission from Ref. 33. Copyright 1999, American Chemical Society.

with **37**.[30,34] This behavior contrasts the reactivity seen with isoelectronic trimethylenemethane reactive intermediates, which give 1:1 adducts in high yields with electron-deficient π-systems.[35]

The Matlin group has shown that irradiation of cyclooctadienone **36** in the presence of vinyl ethers produces 7-norbornanones **41** and oxa-triquinanes **42** (Table 81.5).[33] The reaction is envisioned as proceeding via the step-wise cycloaddition to oxyallyl **37**. The electron-rich vinyl ether stabilizes the incipient cationic center in **43**, which then undergoes internal O- and C-alkylation of the enolate moiety to give **41** and **42**. The product distribution and yields did not show any significant variation with the polarity of the solvent (hexanes, benzene, CH_2Cl_2, or neat vinyl ether). It is interesting to note that no enone-alkene [2+2]-adduct was observed, even when ethyl vinyl ether was used as solvent. This is in contrast to the behavior of pyran-4-one, where irradiation in neat furan produced [2+2]-adducts. The photoexcited state lifetime of **36** is limited by rapid *cis*,*trans*-isomerization to **40**, which does not permit intermolecular capture to be competitive.

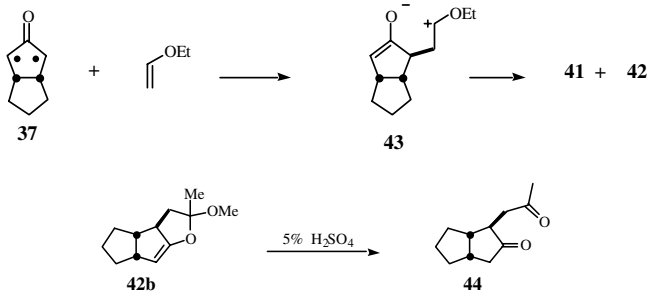

37 **43** **42b** **44**

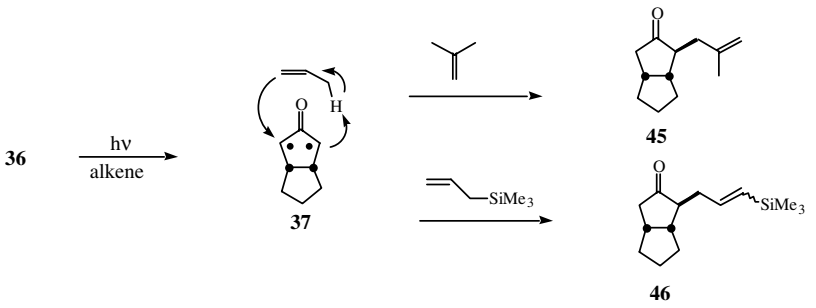

SCHEME 6

The vinyl ether acetal functionality in the oxa-triquinanes can be readily hydrolyzed to dicarbonyl containing diquinanes, for example, **42b** → **44**.

In contrast to the vinyl ethers, simple alkenes such as isobutylene and allyltrimethylsilane trap oxyallyl **37** in a concerted ene-reaction to ketoalkenes **45** and **46** in yields of 15 to 25% (Scheme 6).[33] The *E*- and *Z*- silylketones **46** are formed in about equal amounts. Noyori has reported a similar ene-reaction for oxyallyl-iron complexes with isobutylene.[36]

Isoprene and 2,3-dimethyl-1,3-butadiene were also found to trap oxyallyl **37** in a [3+4]-cycloaddition to give bridged adducts **47** in ~50% yield.[33] These reactions are interesting in that most examples of [4+3]-cycloadditions with putative oxyallyl intermediates have used cyclic dienes.

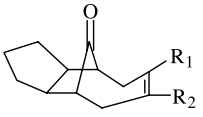

47

Irradiation of **36** in the presence of 2,3-dimethyl-2-butene gives the anomalous and novel 1:1 tricyclic adduct **48** in 33% yield.[37]

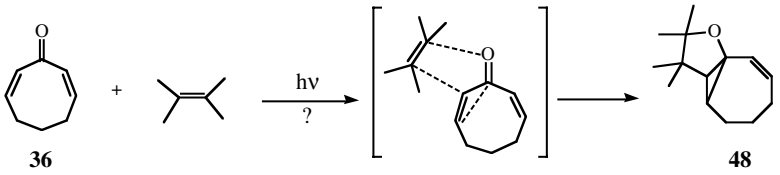

36 **48**

The tricyclic product is formally a [2+2+2]-cycloaddition where the alkene is adding to the carbonyl-oxygen and α-carbon in dienone **3** concomitant with σ-bond formation between the carbonyl-carbon and the β-enone carbon. This mode of reactivity, 1,3-addition of an alkene to an enone, is unprecedented, and a specific mechanistic explanation for this process is currently lacking. Oxyallyl **37** and *cis trans*-dienone **40** do not appear to be involved in this process, and the reactive intermediate being trapped must appear earlier in the reaction cascade. It is unclear whether this intermediate is an excited state of **36** or possibly an oxabicyclobutane **49**. In either case, it is curious why this reaction is seen with 2,3-dimethyl-2-butene and not with any of the other alkene traps.

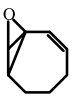

49

81.6 2,6-Cycloheptadienone

The photochemistry of 2,6-cycloheptadienone does not appear to be as rich as its higher and lower homologuess and has not been widely studied. Noyori reported that irradiation of cycloheptadienone **50** in methanol results in conjugate addition to the enone producing enone ether **51**.[38] Irradiation of **50** in acidic media, such as acetic acid or *t*-butanol with a trace of sulfuric acid, results in formation of bicyclic adducts **52**.

50

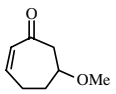

51

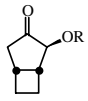

52 a: R = OAc
b: R = *t*-Bu

While these products are similar to the trapped products seen in the reactions with cyclooctadienone, it seems unlikely that a true oxyallyl intermediate is being captured. Noyori has presented a mechanism where the excited dienone **50*** is protonated under the acidic conditions (Scheme 7). Cation **53** then undergoes a Nazarov-type cyclization to the bicyclic cation **54,** which is captured by ROH. In unpublished work, Matlin and Hall have found that irradiation of **50** in the presence of ethyl vinyl ether does not give any 1:1 adducts. The apparent reluctance of the seven-membered ring dienone to form a trappable oxyallyl intermediate is surprising in light of the results with the higher and lower homologs.

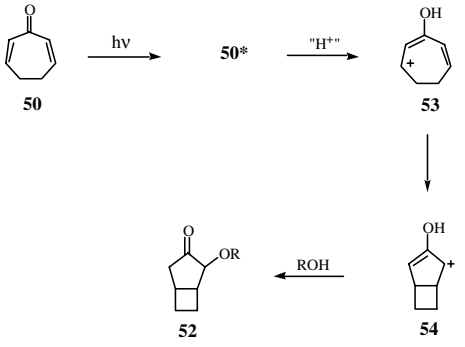

SCHEME 7

References

1. Schuster, D.I., Mechanisms of photochemical transformations of cross-conjugated cyclohexadienones, *Acc. Chem. Res.,* 11, 65–73, 1978.
2. Schuster, D.I., The photochemistry of enones, in *The Chemistry of Enones*, S. Patai and Z. Rappoport, Eds., John Wiley & Sons, 1989, 664–673.
3. Turro, N.J., Cyclopropanones, *Acc. Chem. Res.,* 2, 25–32, 1969.
4. Cordes, M.H.J. and Berson, J.A., Medium effects on the rates of stereomutation of a pair of diastereomeric cyclopropanones. Ground state stabilization in nucleophilic solvents induces deviation from solvent polarity controlled behavior, *J. Am. Chem. Soc.*, 118, 6241–6251, 1996.
5. Black, C., Lario, P., Masters, A.P., Sorenson, T.S., and Sun, R., A new synthesis of *in situ* cyclopropanones and the observation of a thermal cyclopropanone-dienol rearrangement, *Can. J. Chem.,* 71, 1910–1918, 1993.
6. Noyori, R., Organic syntheses via the polybromo ketone-iron carbonyl reaction, *Acc. Chem. Res.,* 12, 61–73, 1979.

7. Hunter, D.H., Strothers, J.B., and Warnoff, E.W., in *Rearrangements in the Ground and Excited States*, Vol. 1, P. D. Mayo, Ed., Academic Press, New York, 1980, 391–470.
8. Edelson, S.S. and Turro, N.J., Cyclopropanones. XVII. Kinetics of the cycloaddition reaction of cyclopropanones with 1,3-Dienes, *J. Am. Chem. Soc.,* 92, 2770–2773, 1970.
9. Fisch, M.H., The photochemistry of santonin: zwitterionic intermediates, *J. Chem. Soc., Chem. Commun.,* 1472–1473, 1969.
10. Hoffmann, R.J., Trimethylene and the addition of methylene to ethylene, *J. Am. Chem. Soc.,* 90, 1475–1485, 1968.
11. Coolidge, M., Yamashita, K., Morokuma, K., and Borden, W.T., *Ab initio* MCSCF and CI calculations of the singlet-triplet energy differences in oxyallyl and dimethyloxyallyl, *J. Am. Chem. Soc.*, 112, 1751–1754, 1990.
12. Hess, B.A. and Smentek, L., On the relative stabilities of singlet and triplet oxyallyl and cyclopropanones: a density functional study, *Eur. J. Org. Chem.*, 3363–3367, 1999.
13. Ichimura, A.S., Lahti, P.M., and Matlin, A.R., *Ab initio* computational study of methano-and ethano-bridged derivatives of oxyallyl, *J. Am. Chem. Soc.,* 112, 2868–2875, 1990.
14. Powell, H.K. and Borden, W.T., CASSCF and CASPT2N calculations predict singlet cyclopentan-2-one-1,3-diyl is stable toward closure to bicyclo[2.1.0]pentan-5-one, *J. Org. Chem.*, 60, 2654–2655, 1995.
15. Lim, D., Hrovat, D.A., Borden, W.T., and Jorgensen, W.L., Solvent effects on the ring opening of cyclopropanones to oxyallyls: a combined ab initio and Monte Carlo study, *J. Am. Chem. Soc.,* 116, 3494–3499, 1994.
16. Schultz, A.G., Cyclohexadienone photochemistry: trapping reactions, in *CRC Handbook of Organic Photochemistry and Photobiology*, W.M. Horspool and P.-S. Song, Eds., CRC Press, Boca Raton, FL, 1995. 716-727.
17. Schultz, A.G., Photorearrangement reactions of cross-conjugated cyclohexadienones, in *CRC Handbook of Organic Photochemistry and Photobiology*, W.M. Horspool and P.-S. Song, Eds., CRC Press, Boca Raton, FL, 1995, 685-700.
18. Swenton, J.S., Saurborn, E., Srinivasan, R., and Sontag, F.I., A criterion for zwitterionic intermediates in the photochemistry of 2,5-cyclohexadienones, *J. Am. Chem. Soc.*, 90, 2990–2991, 1968.
19. Samuel, C.J., Type A zwitterion in cyclohexadienone photochemistry: chemical trapping and stereochemistry, *J. Chem. Soc., Perkin II*, 736–740, 1981.
20. Leitich, J. and Heise, I., The addition of 2-oxido-2-cyclopenten-1-ylium to some olefins and dienes in 2,2,2-trifluoroethanol, *Eur. J. Org. Chem.*, 2702–2718, 2001.
21. Schultz, A.G., New photochemistry of 2,5-cyclohexandien-1-ones and related compounds, *Pure Appl. Chem.,* 60, 981–988, 1988.
22. Schultz, A.G., Plummer, M., Taveras, A.G., and Kullnig, R.K., Intramolecular 2+2 photocycloadditions of 4-(3'-Alkenyl)- and 4-(3'-pentynyl)-2,5-cyclohexadien-1-ones, *J. Am. Chem. Soc.,* 110, 5547–5555, 1988.
23. Matlin, A.R., George, C.F., Wolff, S., and Agosta, W.C., Regiochemical control in intramolecular photochemical reactions of 1,6-heptadienones: carbonyl-substituted 1-(4-alkenyl)-1-cyclopentenes, *J. Am. Chem. Soc.,* 108, 3385–3394, 1986.
24. Schultz, A.G. and Taveras, A.G., The first intermolecular 2+2 photocycloadditions of 2,5-cyclohexadien-1-ones to alkenes, *Tetrahedron Lett.,* 29, 6881–6884, 1988.
25. Barltrop, J.A., Day, A.C., and Samuel, C.J., Heterocyclic photochemistry. 2. 4-pyranones. a mechanistic study, *J. Am. Chem. Soc.,* 101, 7521–7528, 1979.
26. West, F.G., Fisher, P.V., and Willoughby, C.A., Photochemistry of pyran-4-ones: intramolecular trapping of zwitterionic intermediate with pendant hydroxyl groups, *J. Org. Chem.,* 55, 5936–5938, 1990.
27. West, F.G., Fisher, P.V., and Arif, A.M., Intramolecular alkene trapping of pyran-4-one derived zwitterions: a novel synthesis of diquinanes and hydrindanes, *J. Am. Chem. Soc.,* 115, 1595–1597, 1993.

28. West, F.G., Hartke-Karger, C., Koch, D.J., Kuehn, C.E., and Arif, A.M., Intramolecular [4+3]-cycloadditions of photochemically generated oxyallyl zwitterions: a route to functionalized cyclooctanoid skeletons, *J. Org. Chem.,* 58, 6795–6803, 1993.
29. West, F.G. and Willoughby, D.W., Intramolecular arene trapping of pyran-4-one derived zwitterions: a two-step synthesis of tetrahydrobenz[e]inden-1-ones, *J. Org. Chem.,* 58, 3796–3797, 1993.
30. Crandall, J.K. and Haseltine, R.P., The photochemistry of 2,7-cyclooctadienone, *J. Am. Chem. Soc.,* 90, 6251–6252, 1968.
31. Noyori, R. and Kato, M., Photochemical reactions of 2,7-cyclooctadienone in protic solvents, *Tetrahedron Lett.,* 5075–5077, 1968.
32. Matlin, A.R. and Jin, K., Photochemically induced reactions of cis,cis-cyclooctadienone, *Tetrahedron Lett.,* 30, 637–640, 1989.
33. Matlin, A.R., Lahti, P.M., Appella, D., Straumanis, A., Lin, S.C., Patel, H.R., Jin, K., Schrieber, K.P., Pauls, J., and Raulerson, P., Photoinduced cycloaddition and ene reactions of 2,7-cyclooctadienone: experimental and computational studies of a cyclopentyl oxyallyl intermediate, *J. Am. Chem. Soc.,* 121, 2164–2173, 1999.
34. Haseltine, R.P., The Photochemistry of 2,7-Cyclooctadienone, Ph.D. thesis, University of Indiana, 1970.
35. Berson, J.A., The chemistry of trimethylenemethanes, a new class of biradical reactive intermediates, *Acc. Chem. Res.*, 11, 446–453, 1978.
36. Noyori, R., Shimizu, F., and Hayakawa, Y., Iron carbonyl promoted reactions of α,α'-dibromo ketones and isobutylene. An ene reaction involving allylic cations, *Tetrahedron Lett.*, 2091–2094, 1978.
37. Matlin, A.R., Lin, S.C., Patel, H.R., and Chai, M., First example of an enone-alkene [2 + 2 + 2] photocycloaddition: 1,3-photocycloaddition of tetramethylethylene across 2,7-cyclooctadienone, *Org. Lett.*, 1, 303–305, 1999.
38. Nozaki, H., Kurita, M., and Noyori, R., Photochemical reactions of 2,6-cycloheptadienones, *Tetrahedron Lett.*, 33, 3635–3638, 1968.

82

Photocycloaddition Reactions of 2-Pyrones

Tetsuro Shimo
Kagoshima University

Kenichi Somekawa
Kagoshima University

82.1 Introduction

The photochemistry of 2-pyrones, which are simple 2, 4-pentadien-5-olides and have an α, β: γ, δ-unsaturated carbonyl system, is interesting because of the wide range of unique carbon-carbon bond-forming processes they undergo. Diels-Alder reactions of 2-pyrones with many kinds of dienophiles have been widely studied for about 70 years and are known to give [4+2]-cycloadducts stereoselectively, together with bis-adducts and benzene derivatives.[1] The use of Diels-Alder cycloadditions of 2-pyrones was applied to the synthesis of many useful compounds, such as barrelene,[2] colchicine,[3] etc. This chapter discusses the some selective cycloaddition reactions of photochemically excited 2-pyrones with various alkenes, together with the photochemistry of 2-pyrone itself. It is well known that the 2-pyrone ring itself undergoes a wide range of photochemical reactions, such as an electrocyclic ring-opening reaction of **1** to give **3** by way of ketene formation **2**,[4] valence isomerization[5] of **4** to give **5** and dimerization[6] of **1** to give **7**, **8**, and **9** (Schemes 1, 2, and 3). The valence isomerization reaction of 2-pyrone **4** provided a path to the synthesis of cyclobutadiene **6**,[7] which was also synthesized in the hemicarcerand as a host compound.[8] Photodimers **7** and **8** afford a cyclooctatetraene derivative **10** by way of thermolytic extrusion of carbon dioxide.[6] The cross photocycloadditions of the heterocyclic 2, 4-cyclohexadienones with various ethylenes are peri-, site-, regio-, and stereoselective, depending on the substituents of 2- pyrones and ethylenes and also the reaction conditions. These phenomena are theoretically interesting and are explained later by the MO method.

82.2 Intermolecular Photocycloadditions of 2-Pyrones

Intermolecular photocycloaddition reactions of 2-pyrones with alkenes have been much less extensively studied than those of coumarins. A typical reaction of coumarin **11** with an alkene is the formation of **12**[9] (Scheme 4). The photocycloaddition reaction of dehydroacetic acid **13** with cyclohexene was first reported by Takeshita et al.[10] in 1973 (Scheme 5). Irradiation of a mixture of **13** and cyclohexene leads to the formation of a diastereomeric mixture of [2+2]-cycloadducts **14**, together with the usual dimer of the 2-pyrone.

Photocycloaddition reactions of the 2-pyrones **15** with alkenes are expected to lead to the [4+2]-cycloadduct **16**, the 5, 6-[2+2]-cycloadduct 17 (formed by addition to the C5-C6 double bond), and/or

0-8493-1348-1/04/$0.00+$1.50

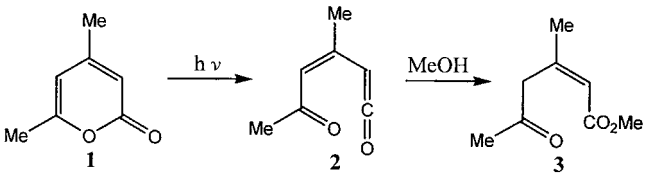

SCHEME 1

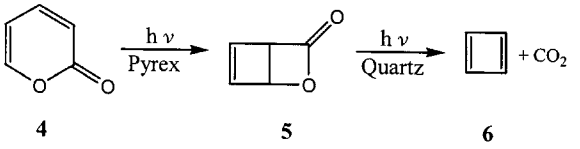

SCHEME 2

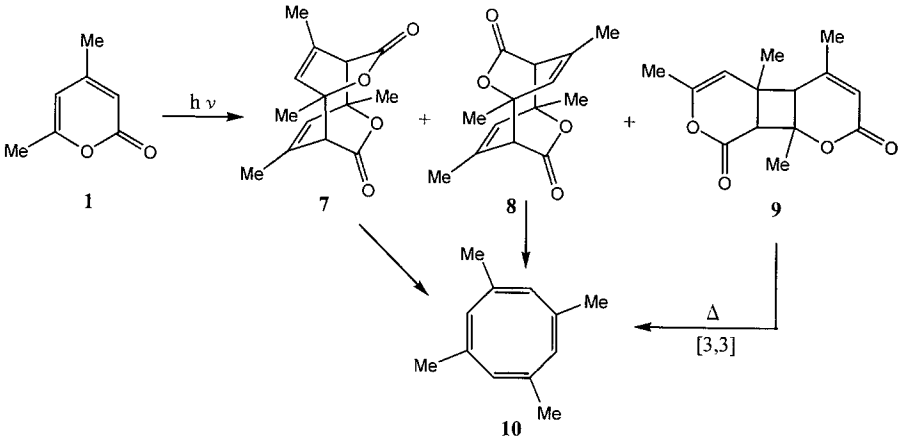

SCHEME 3

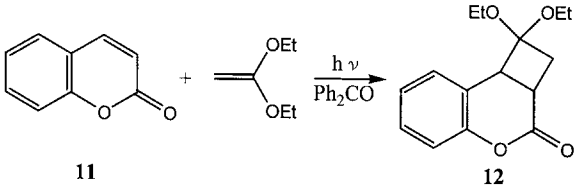

SCHEME 4

the [2+2]-cycloadduct **18** (formed by addition to the C3-C4 double bond) as illustrated in Scheme 6. The photochemical reaction of methyl 2-pyrone-5-carboxylate **15a** (with an electron-withdrawing substituent) with acrylonitrile **19e** in the presence of benzophenone gives a mixture of [4+2]-cycloadducts **16ae** (endo-CN/exo-CN; ratio = 1.4) as major products together with a [2+2]-cycloadduct **17ae**[11] (Scheme 7). On the other hand, photosensitized reaction of 4, 6-dimethyl-2-pyrone **15c** (with electron-donating groups) with **19e** affords a mixture of [2+2]-cycloadducts **17ce** (endo-CN/exo-CN; ratio = 1.0) as major products and a cyclobutanecarboxylic acid **20**. This secondary product is formed by hydrolysis

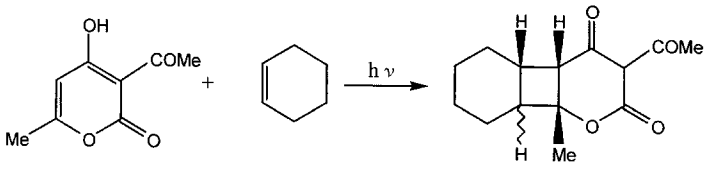

13 **14**

SCHEME 5

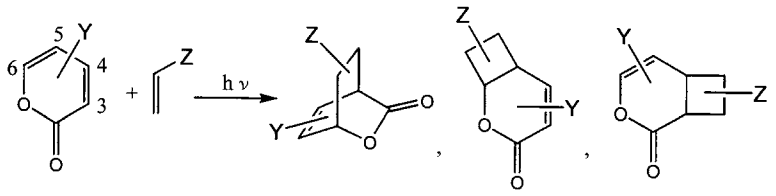

15 **16** **17** **18**

SCHEME 6

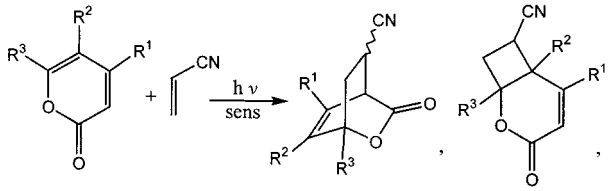

19e

	R^1	R^2	R^3				
15a	H	CO_2Me	H	**16ae**	29%	**17ae**	9%
15b	Me	CO_2Et	Me	**16be**	16%	**17be**	61%
15c	Me	H	Me			**17ce**	39%
15d	OMe	H	Me			**17de**	46%

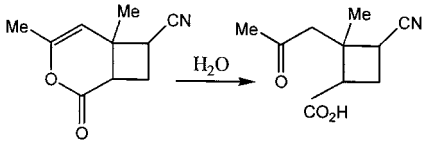

18 **20**

(3%)

SCHEME 7

of the [2+2]-cycloadduct **18**.[12] The reaction of **15b** with **19e** gives a mixture of [4+2]-cycloadducts **16be** (endo-CN/exo-CN; ratio = 1.0), together with a mixture of [2+2]-cycloadducts **17be** (endo-CN:exo-CN ratio = 1.0) (major products), while the reaction of **15d** with **19e** yields a mixture of **17de** (endo-CN:exo-CN ratio = 2.0).[13] These photocycloaddition reactions take place only under irradiation in the presence of triplet sensitizers (ET > 56 kcal/mol). Similar photoreactions of 2-pyrones **15a** and **15c** with methacrylonitrile or 2-chloroacrylonitrile also afford compounds of type **16**, **17**, and/or **18**.[14]

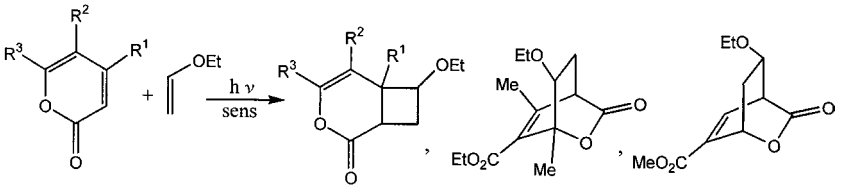

19f **21**(9%) **22**

	R^1	R^2	R^3		
15a	H	CO_2Me	H		
15b	Me	CO_2Et	Me	**18bf**	76%
15c	Me	H	Me	**18cf**	68%
15d	OMe	H	Me	**18df**	21%

94% (thermal)

SCHEME 8

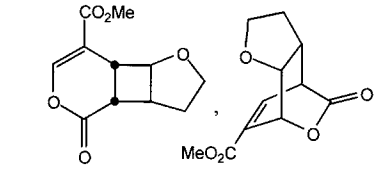

23 **24**

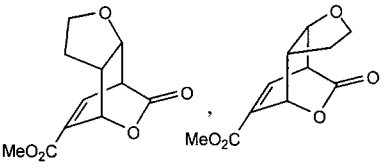

25 **26**

SCHEME 9

2-Pyrone **15a** readily reacts thermally with ethyl vinyl ether **19f** at room temperature to give the [4+2]-cycloadduct **22** as the sole product. The photoreaction of ethyl 4, 6-dimethyl-2-pyrone-5-carboxylate **15b** with **19f** affords a mixture of [2+2]-cycloadducts **18bf** (endo-OEt:exo-OEt ratio = 0.65) as major products, together with a [4+2]-cycloadduct **21**[13] whose orientation is different from the product **22** obtained from the thermal reaction of **15a** with **19f** (Scheme 8).[11] 2-Pyrone **15c** reacts photochemically with **19f** to give a mixture of **18cf** (endo-OEt:exo-OEt;ratio = 0.79),[12] and the reaction of **15d** with **19f** gives 18df (endo-OEt:exo-OEt ratio = 1.0).[13] Photoreaction of 15a with 2,3-dihydrofuran affords the [2+2]-cycloadduct **23** and the [4+2]-cycloadduct **24**[15] in 24% and 12% yields, respectively (Scheme 9). Product **24** showed different orientation to that observed in the thermal [4+2]-cycloadducts **25** and **26**. From these results the details of the reaction modes within the various photocycloaddition reactions of 2-pyrones with alkenes are summarized as shown in Scheme 10. 2-Pyrone **15a**, having an electron-withdrawing group, reacts with acrylonitrile **19e** at the C3-C6 atoms of the diene system and at the C5-C6 double bond in **15a** to give the [4+2]-cycloadduct and the [2+2]-cycloadduct, respectively. Diels-Alder reaction occurs preferentially in the reaction of **15a** with ethyl vinyl ether **19f**. 2-Pyrone **15c** (with electron-donating groups) reacts with **19e** mainly at the C5-C6 double bond in **15c** to give a [2+2]-cycloadduct. On the other hand, **15c** reacts with **19f** at the C3-C4 double bond in **15c** to afford another type of [2+2]-cycloadduct. The reaction mechanism containing peri-, site-, and regioselectivities will be described later making use of MO analysis.

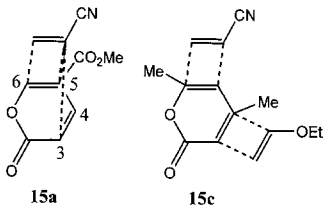

SCHEME 10

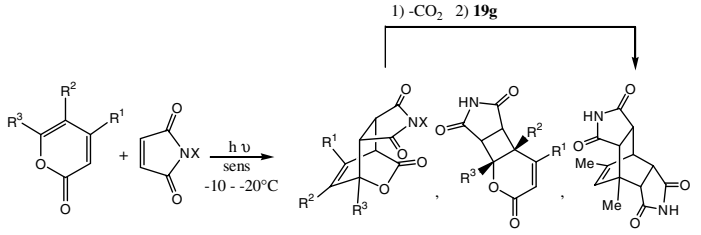

	R^1	R^2	R^3					
15a	H	CO_2Me	H	**19g**	X = H	**16ag'** 50%		
15b	Me	CO_2Et	Me	**19g'**	X = p-$NO_2C_6H_4$	**16bg** 59%	**17bg** 19%	
15c	Me	H	Me			**16cg** 78%	**17cg** 12%	
						(π	**17cg** 10%	**27** 43%)

SCHEME 11

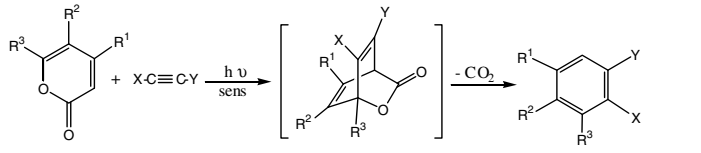

	R^1	R^2	R^3	X	Y
15a	H	CO_2Me	H	CO_2Me	CO_2Me
15d	OMe	H	Me	Ph	H

	R^1	R^2	R^3	X	Y
28	H	CO_2Me	H	CO_2Me	CO_2Me
29	H	CO_2Me	H	H	Ph
30	OMe	H	Me	CO_2Me	CO_2Me

SCHEME 12

Photosensitized reaction of **15c** with maleimide **19g** at low temperature (–10 to –20°C) affords the exo-[4+2]-adduct **16cg** as a major product, together with the [2+2]-adduct **17cg** (Scheme 11).[16] The same reaction was carried out at room temperature to afford the bis-adduct **27**, which was formed via decarboxylation of **16cg** followed by addition of another molecule of **19g**, in addition to the formation of **17cg**. The low-temperature photoreactions of 2-pyrones **15a**, **15b** with **19g** or 19g′ also gives [4+2]-adducts **16ag′**, **16bg**, and [2+2]-adduct **17bg**. Similar photoreactions of 2-pyrones **15b**, **15c** with maleic anhydride afford exo-[4+2]-adducts (major products) and/or [2+2]-adducts. Photosensitized reaction of **15a** with dimethyl acetylenedicarboxylate affords 1, 2, 4-tris(methoxycarbonyl)benzene **28** in 50% yield by way of decarboxylation of the [4+2]-adduct, which was difficult to isolate even from the reaction mixture obtained from the low-temperature irradiation (Scheme 12).[11,13] Similar reactions of **15a** with

TABLE 82.1 Reaction Results between 2-Pyrones (**15**)[a] and Alkenes (**19**)[b]

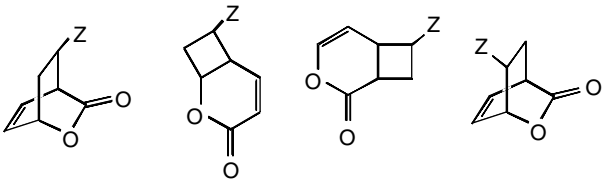

Pyrone/Alkene	19g	19e	19f
15a	**16ag** (50%)[c]	**16ae** (29%)	**22** (94%)[d]
		17ae (9%)	
15b	**16bg** (59%)[e]	**16be** (16%)	**18bf** (76%)
		17be (61%)	**21** (9%)
15c	**16cg** (78%)[e]	**17ce** (39%)	**18cf** (68%)
	17cg (12%)	**18cew** (3%)[f]	

[a] See Scheme 7.
[b] See Schemes 7, 8, and 11.
[c] x = p-NO_2-C_6H_4
[d] thermal reaction
[e] x = H
[f] w means hydration

phenylacetylene and that of **15d** with dimethyl acetylenedicarboxylate give benzene derivatives **29** and **30** in 2% and 35% yields, respectively.

The photochemical reaction that takes place between 2-pyrones and selected alkenes are summarized in Table 82.1 according to the types of cycloadducts. In the sensitized photoreactions of 2-pyrones with several alkenes, there are four kinds of primary products, **16**, **17**, **18**, and **21**. Products **16** is one of the peri- and regioselective [4+2]-cycloadducts, **17** and **18** are site- and regioselective [2+2]-cycloadducts, and **21** is also another regioselective [4+2]-cycloadduct. The product distribution is proposed to depend mainly on the electronic properties of the two substrates. Namely, the decrease in the electron-withdrawing property of the substrates on the two substrates, **15** and **19** (left to right and high to low in Table 82.1), changes the product-distribution as follows: **16** → **16** + **17** → **17** + **18** → **18** + **21** (minor) → **18**.

The peri-, site-, and regioselectivities in the photocycloadditions of the triplet 2-pyrones with alkenes are confirmed to be mainly controlled by the interaction between frontier molecular orbitals (FMOs), calculated using PM3-CI level (Figure 82.1 and Table 82.2).[17,18] The regioselective [4+2]-cycloadducts **16** and site-selective [2+2]-cycloadducts **17** across the C5-C6 double bonds of the 2-pyrones with electron-poor alkenes are deduced to be formed by the preferred HSOMO-LUMO interactions and via more stable biradicals by C6-Cβ bonding (Scheme 13). On the other hand, the other kinds of regioselective [4+2]-adduct **21** and the [2+2]-adducts **18** across the C3-C4 double bonds of the 2-pyrones with electron-rich alkenes are inferred to arise from LSOMO-HOMO interactions and via biradicals by C3-Cβ bondings. Selectivities between **16** and **17**, and **18** and **21** are also proposed to be influenced by the SOMOs of the biradicals.

82.3 Intramolecular Photocycloadditions of 2-Pyrones

Intramolecular [2+2]-photocycloadditions of cyclic α,β-unsaturated enones with remote double bonds have been extensively used to synthesize a variety of interesting compounds, including natural products. An analysis of the mechanism of the additions has also been carried out. 2-Pyrones having pendant enes and dienes undergo synthetically useful photocycloaddition processes to give tricyclic lactones and lactone-bridged cyclooctadienes by [2+2]-and [4+4]-cycloadditions, respectively. The photochemical reactions

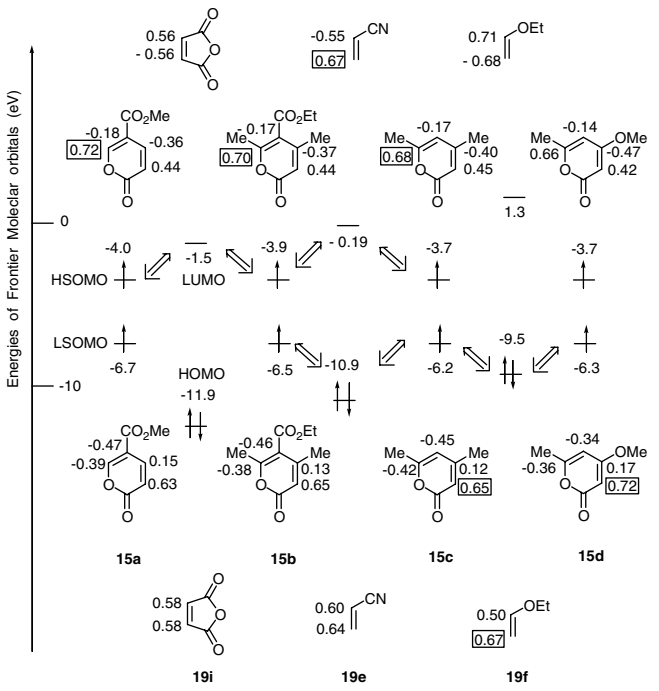

FIGURE 82.1 Estimated energies and coefficients of triplet 2-pyrones and ground-state alkenes calculated by means of PM3-CI methods.

TABLE 82.2 Estimated Frontier Orbital Interactions between **15** and **19** by the PM3-CI Calculation (γ^2/eV)

		19i		19e		19f	
	bonding	6-β[a]	3-β[b]	6-β	3-β	6-β	3-β
$(CiCr)^2/\Delta\varepsilon$	15a	0.064	0.026	0.060	0.039	0.048	0.064
	15b	0.064	0.027	0.060	0.039	0.047	0.063
	15c	0.068	0.025	0.060	0.057	0.047	0.056
	15d	0.064	0.031	0.057	0.046	0.044	0.027

[a] HSOMO(**15**)-LUMO(**19**) interaction
[b] LSOMO(**15**)-HOMO(**19**) interaction

of 4-(ω-alkenyloxy)-2-pyrone **31b** afford intramolecular [2+2]-cycloadduct **32b** in quantitative yield (Scheme 14).

Similar photoreactions of **31c**- through **31h** give **32c** through **32h**, in 70%, 31%, 26%, 70%, 48%, and 32% yields, respectively.[19,20] On the other hand, 2-pyrone **31a** was found to be completely photostable. The intramolecular [2+2]-cycloadditions of **31b** through **31h** proceed by way of triplet excited states of **31** with high site-, regio-, and stereoselectivities. The reaction mechanism is analyzed using MO calculations, and the reasonable biradical intermediates to give **32e** and **32f** through **32h** are considered to be **33** and **34**, respectively. 6-(ω-Alkenyl)-2-pyrones **35b** and **35c** also afford intramolecular [2+2]-cycloadducts **36b** and **36c** in 55% and 33% yields, respectively (Scheme 15),[21] while 2-pyrone **35a** was completely photostable. From these results, photochemical reactions of 4-(ω-alkenyloxy)-2-pyrones **31** and 6-(ω-alkenyl)-2-pyrones **35** provide a simple route to synthesize oxatricyclic lactones, depending on the number of methylene groups between the 2-pyrone ring and the olefinic moiety.

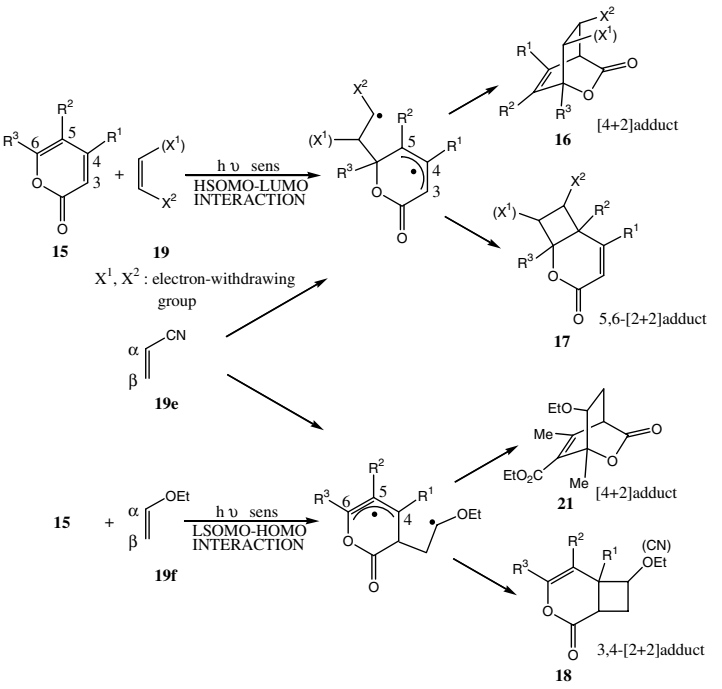

SCHEME 13

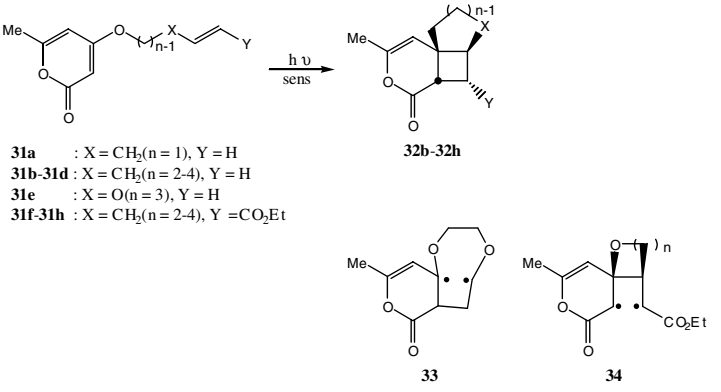

SCHEME 14

Photoreactions of 2-pyrones **37a** and **37b** bearing acyclic ω-dienes do not afford cycloadducts, instead undergo geometric isomerism (Scheme 16).[22] Different reactivity is seen with 2-pyrones bearing cyclic ω-dienes where [4+4]-cycloadducts, which are fused bicyclic cyclooctanoids with lactone bridges, together with [2+2]-cycloadducts are formed. Irradiation of 2-pyrones **38** connected to a pendant furan by a three-carbon tether gives a mixture of [4+4]-and [2+2]-cycloadducts **39**, **40**, and **41** (Scheme 17).[23] The yields and product distribution are greatly affected by hydrophobic effects of solvents as shown in Scheme 17. Similar photoreactions of 2-pyrones **42** connected to a pendant furan by a three-carbon tether afford a mixture of endo- and exo-[4+4]-adducts **43** and **44** in good yield when OR′ = carboxylate or sulfonate (Scheme 18).[24] In some cases, small amounts of cyclooctatriene **45** resulting from decarboxylation

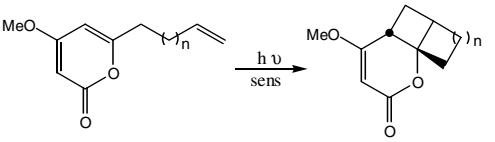

35a : n = 1
35b : n = 2
35c : n = 3

36b, **36c**

SCHEME 15

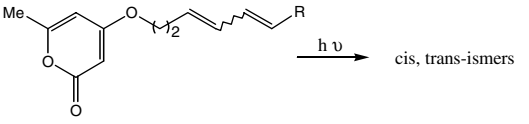

37a : R = Me
37b : R = Ph

SCHEME 16

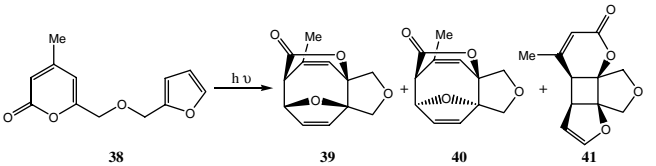

38 **39** **40** **41**

solvent	yield(%)	ratio **39** : **40** : **41**
PhMe	15	1 :1 : 1
aq. LiCl	86	3.9 : 2.1 : 1.0
$Et_2O/LiClO_4$	56	1.0 : 5.7 : trace

SCHEME 17

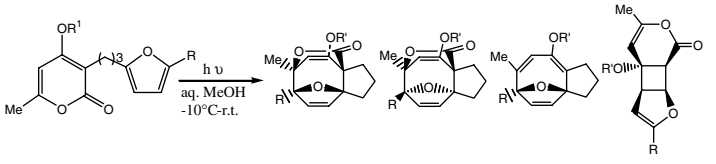

42 **43** **44** **45** **46**

	R	R'	**43** (%)	**44** (%)	**45** (%)	**46** (%)
42a	H	H	12	11	5	15
42b	Me	H	7	19	-	10
42c	H	Ac	22	46	7	6
42d	H	Tf	17	74	-	-

SCHEME 18

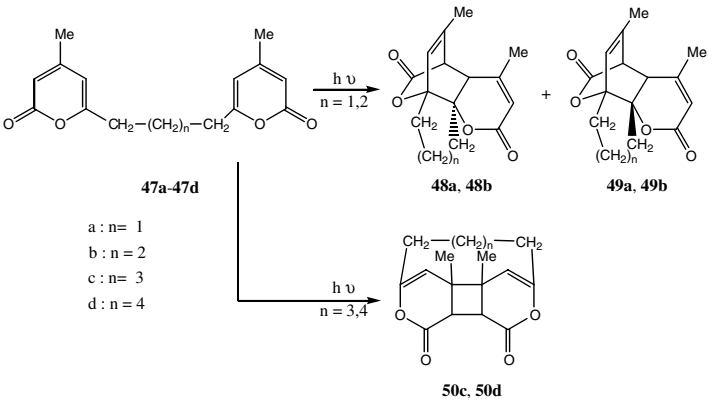

SCHEME 19

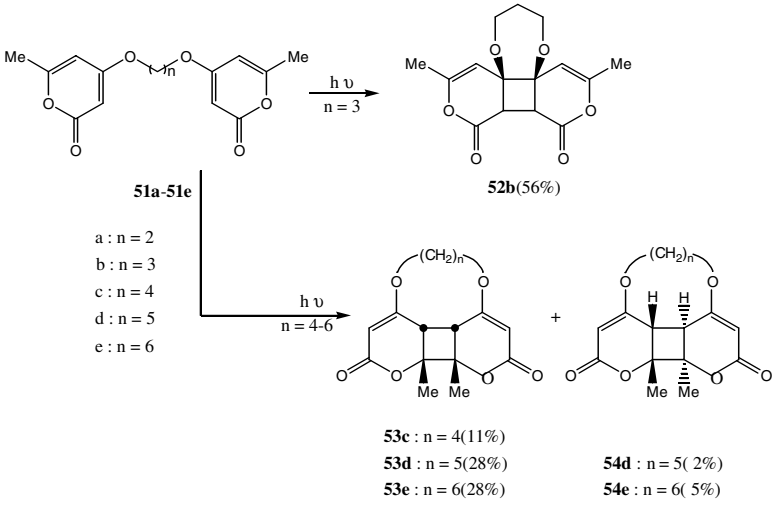

SCHEME 20

of one or both diastereomers are isolated. Sensitized photoreactions of bis-2-pyrones **47a** (n = 1), **47b** (n = 2) give [4+2]-cycloadducts **48a**, **49a** and **48b**, **49b** (Scheme 19).[25] On the other hand, **47c** (n = 3) and **47d** (n = 4) afford only [2+2]-cycloadducts, **50c** and **50d**. The [4+2]- and [2+2]-cycloadducts distribution depends on the number of methylene units in the chain. Photoreactions of 2-pyrones **51b** (n = 3) and **51e** (n = 6) give three kinds of site-selective [2+2]-cycloadducts **52b**, **53c** through **53e**, and **54d** and **54e** (Scheme 20).[26] The selectivity also depends on the methylene chain length. The reaction mechanism is explained from the results calculated by the PM3-CI method.

82.4 Solid-State Photocycloadditions of 2-Pyrones

While photochemical [2+2]-cycloadditions in solution have been utilized to synthesize many kinds of important compounds, the reactions encountered are not so regio- or stereoselective. On the other hand, solid-state photoreactions are strictly controlled by their crystal structures and can, therefore, be highly selective. The use of single- and two-component organic crystals has recently been shown to provide an environment for controlling the selectivity of photochemical reactions because of the tight and regular

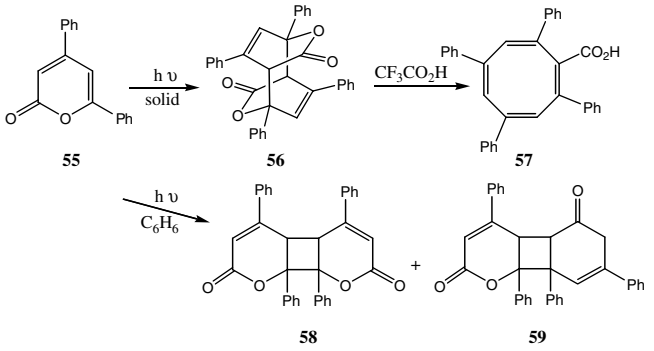

SCHEME 21

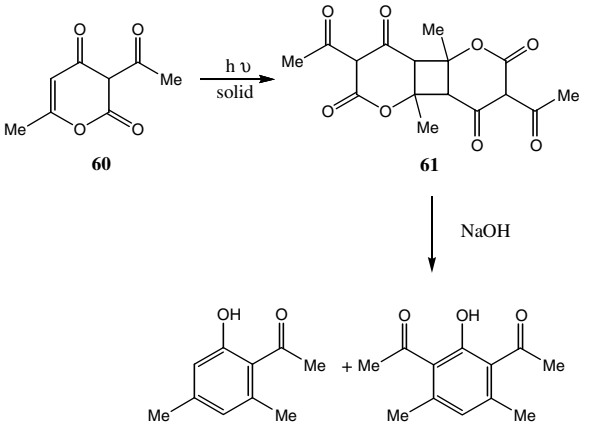

SCHEME 22

arrangement of the molecules within the crystals[27] using a non-covalent interaction such as a hydrogen bond, charge transfer interaction, or π-π stacking. Much attention has been devoted to the photodimerisation reactions[27] in the crystals, including asymmetric synthesis in host-guest inclusion complexes, but only limited investigation of [2+2]-cycloaddition between two different organic molecules has been reported.[28]

Photolysis of 2-pyrone **55** in the solid state affords the [4+4]-dimer **56** in 100% yield, based on recovered **55** (Scheme 21).[29] Photolysis in benzene gives two kinds of [2+2]-dimers **58** and **59** in 20% and 60% yields, respectively. The treatment of **56** with trifluoroacetic acid gives the cyclooctatetraene carboxylic acid **57** in 50% yield.

2-Pyrone 60 is irradiated for a week in the solid state to give [2+2]-dimer **61** in 4% yield (Scheme 22).[30] Hydrolysis of **61** affords the substituted phenols illustrated. Irradiation of a suspension of crystalline **62** in water gives two types of [2+2]-dimers **63** and **64** in 18% and 21% yields, respectively (Scheme 23).[31]

The x-ray crystallographic analysis shows that the distances between the reacting double bonds to yield **63** and **64** are ca. 4.2Å and 4.0Å, respectively,. The solid-state photoreaction of 2-pyrone-5-carboxylate **15** with maleimides **19** yields the endo-[4+2]-cycloadducts **65**. This is in contrast to the sensitized photoreaction that leads exclusively to the exo-[4+2]-cycloadducts **66** (Scheme 24).[32] Solid-state photoirradiations of 1:1 complex crystals formed between the 2-pyrone **15d** and 4-(ω-arylalkyloxy)- 2-pyrones **66a** through **66e** and maleimide **19g** gives [2+2]-cycloadducts **67dg** and **67a** through **67e** with exclusive stereoselectivity (Scheme 25).[33,34]

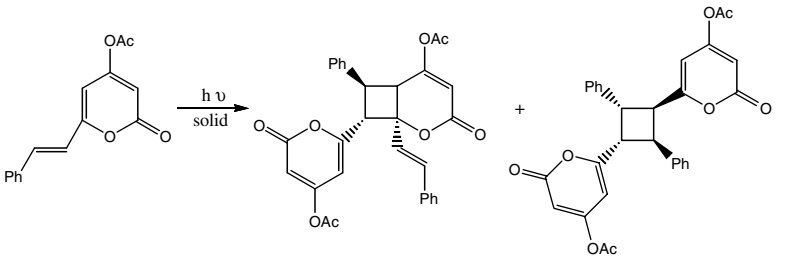

62 **63** **64**

SCHEME 23

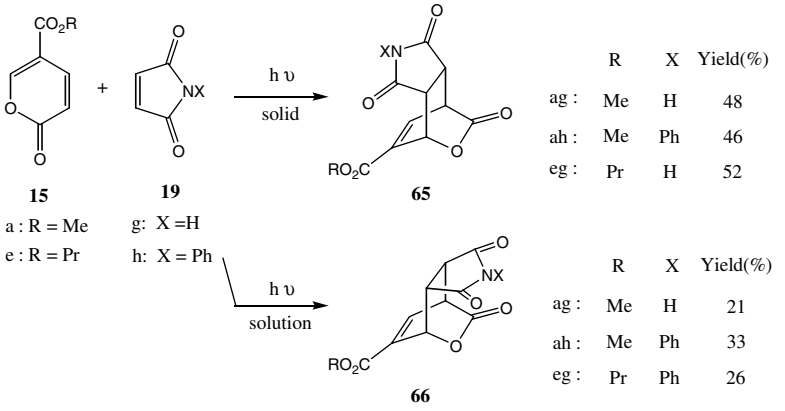

	R	X	Yield(%)
ag :	Me	H	48
ah :	Me	Ph	46
eg :	Pr	H	52

15 **19** **65**

a : R = Me
e : R = Pr

g: X =H
h: X = Ph

	R	X	Yield(%)
ag :	Me	H	21
ah :	Me	Ph	33
eg :	Pr	Ph	26

66

SCHEME 24

These highly stereoselective cycloadditions also occur on photoirradiation of grind up mixtures of crystals of 2-pyrones with maleimide. On the other hand, the photoreactions in solution afford another type of [2+2]-cycloadduct **68** or bis-adducts **69** as major products. The latter products are formed through decarboxylation of the [4+2]-cycloadducts, followed by addition of another molecule of **19g**.

The high reaction selectivity for **67** in the solid-state photoreactions is confirmed by x-ray crystallographic analyses (Figure 82.2 and Figure 82.3), powder x-ray diffraction analyses and MO method (Figure 82.4)* of the complex crystals, which are composed of two sets of a 1:1 complex between 2-pyrone (**15d** or **66**) and **19g**, arising from an CH-π interaction between **19g** and aromatic rings of **66** and/or π-π stacking between the aromatic rings together with four kinds of hydrogen bonding between the ground state 2-pyrone moieties and **19g**. The high stereoselective photocycloaddition reactions are possible because the two reacting double bonds are nearly parallel and separated by less than 4.0 Å. The photoreaction mechanism is quantitatively analyzed to proceed via some interactions such as four kinds of hydrogen bonding and electrostatic interactions of the singlet excited state of 2-pyrone with the ground state of maleimide, by MO transition state calculation using the Win MOPAC AM1 method (Figure 82.5).**[35]

*Figures 82.2, 82.3, and 82.4 were reprinted from *Tetrahedron*, 57, T. Obata, T. Shimo, M. Yasutake, T. Shinmyozu, M. Kawaminami, R. Yoshida, and K. Somekawa, Remarkable interaction effects of molecular packing on site- and stereoselectivity in photocycloaddition of 2-pyrones with maleimide in the solid state, pp. 1533, 1534 ,and 1537, 2001, with permission from Elsevier Science.

**Figure 82.5 was reprinted from *Tetrahedron*, 58, T. Shimo, T. Uezono, T. Obata, M. Yasutake, T. Shinmyozu, and K. Somekawa, x-ray and MO analysis of highly stereoselective solid-state photocycloadditions of 2-pyrones with maleimide, p. 6114, 2002, with permission from Elsevier Science.

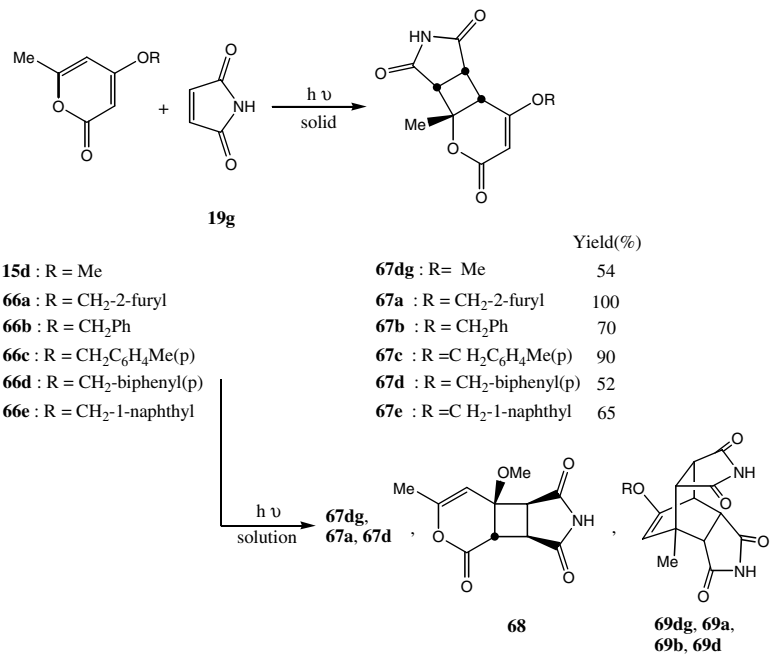

SCHEME 25

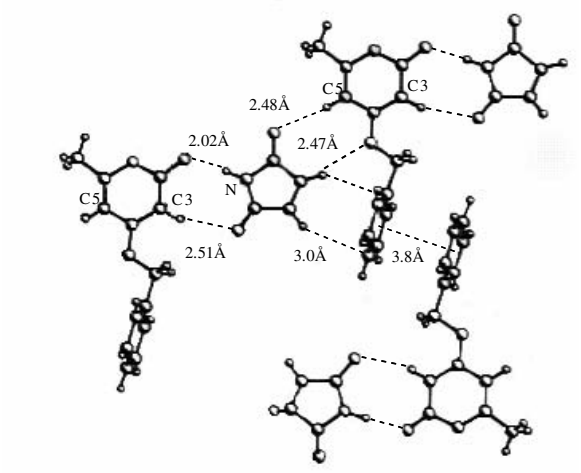

FIGURE 82.2 Molecular packing diagram by hydrogen bondings, CH-π and π-π interactions in the 1:1 complex crystal of **66b** with **19g**. (From Obata, T., Shimo, T., Yasutake, M., Shinmyozu, T., Kawaminami, M., Yoshida, R., and Somekawa, K., *Tetrahedron*, 57, 1533, 2001. With permission from Elsevier Science.)

82.5 Synthetic Applications

The formation of cycloadducts by photochemical [2+2]-, [4+2]-, and [4+4]-cycloaddition reactions of 2-pyrones shows considerable potential. The addition reactions can provide adducts that can undergo ring transformations to natural products, among other compounds of interest. Cyclobutanes can often be used to enhance the reactivity of the heterocyclic rings in the adducts. This path usually uses the

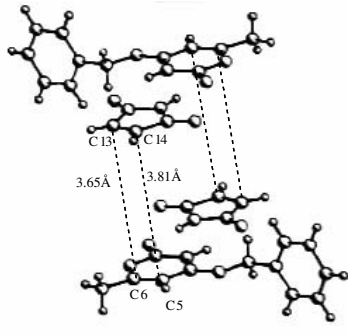

FIGURE 82.3 Molecular packing diagram of the 1:1 complex crystal of **66b** with **19g**. (From Obata, T., Shimo, T., Yasutake, M., Shinmyozu, T., Kawaminami, M., Yoshida, R., and Somekawa, K., *Tetrahedron*, 57, 1533, 2001. With permission from Elsevier Science.)

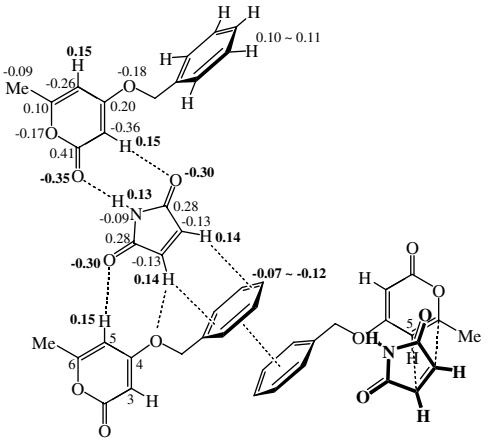

FIGURE 82.4 Calculated atomic charges of the two ground states of **66b** and **19g** and their interactions. (From Obata, T., Shimo, T., Yasutake, M., Shinmyozu, T., Kawaminami, M., Yoshida, R., and Somekawa, K., *Tetrahedron*, 57, 1533, 2001. With permission from Elsevier Science.)

conversion of the cyclobutane into a cyclobutene. This technique is seen in the reaction of [2+2]-cycloadducts derived from 2-pyridones and coumarin with chloroethylenes.[36] The [2+2]-cycloadducts **70** formed by reaction of 2-pyrones and chloroethylenes provide a route to prepare ethenyl-2-pyrone **72** and ethynyl-2-pyrone **73** via the ring-opening of cyclobutenes **71** by triethylamine (Scheme 26).[37] Another [2+2]-cycloadducts **74** can be transformed into the pyrano[4,3-b]pyran-2,5-diones **75** in the presence of DBU via cyclobutene formation and S_N2' displacement (Scheme 27).[38]

The [4+2]-cycloadducts of 2-pyrones, which are cyclohexadiene equivalents by decarboxylation, are attractive starting materials for the preparation of polyfunctionalized bicyclo[2.2.2]octenes. For example, photochemically obtained [4+2]-cycloadducts **16** between 4,6-dimethyl-2-pyrone and cyclic olefins react with second olefins, such as acrylonitrile or p-benzophenone, to give cross-adducts, **76**, **76′**, **77**, with the concurrent decarboxylation (Scheme 28).[16, 39] Irradiation of the cross-adducts **77** gives cage compounds **78**.

The intramolecular photo [4+4]-cycloaddition of a pendant furan to a 2-pyrone has been applied to the development of a route leading to 5-8-5-tricyclic cyclooctanoid natural products. For example, irradiation of 2-pyrone **79** affords two kinds of [4+4]-cycloadducts **80**, **81**, whose structure is a skeleton of fusicoccane and ophiobolane (Scheme 29).[24]

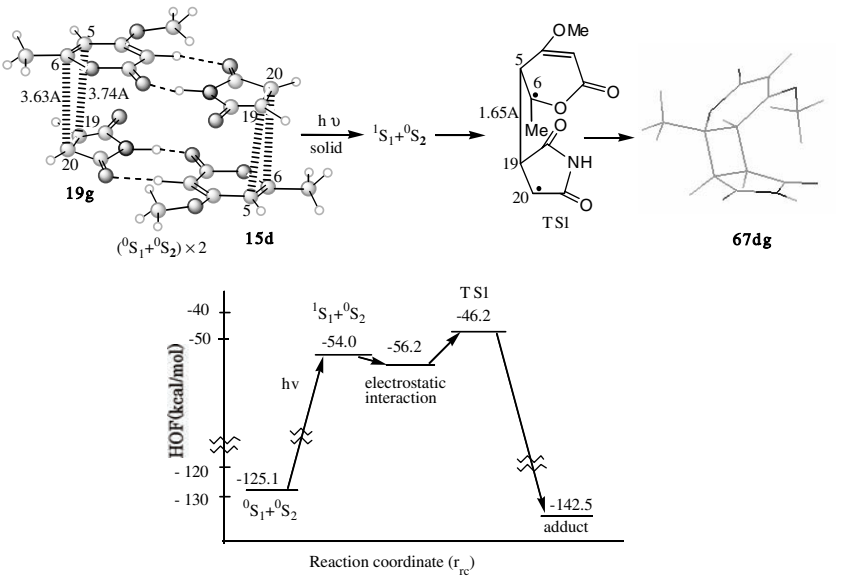

FIGURE 82.5 Heat of formation (HOF) of the photoreaction of **15d** with **19g** calculated by MOPAC AM1.

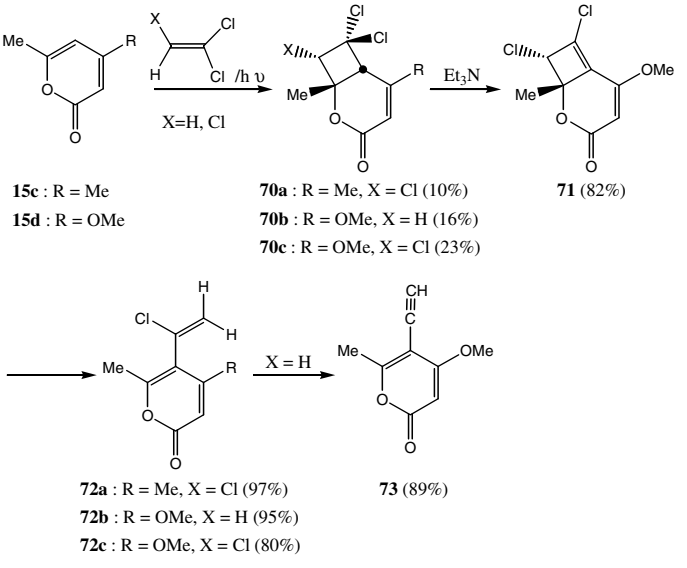

15c : R = Me
15d : R = OMe

70a : R = Me, X = Cl (10%)
70b : R = OMe, X = H (16%)
70c : R = OMe, X = Cl (23%)

71 (82%)

72a : R = Me, X = Cl (97%)
72b : R = OMe, X = H (95%)
72c : R = OMe, X = Cl (80%)

73 (89%)

SCHEME 26

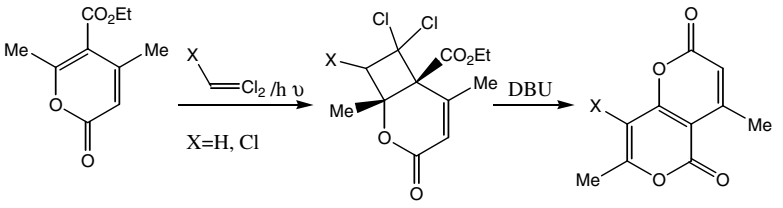

15b

74a : X = H (20%)
74b : X = Cl (13%)

75a : X = H (54%)
75b : X = Cl (23%)

SCHEME 27

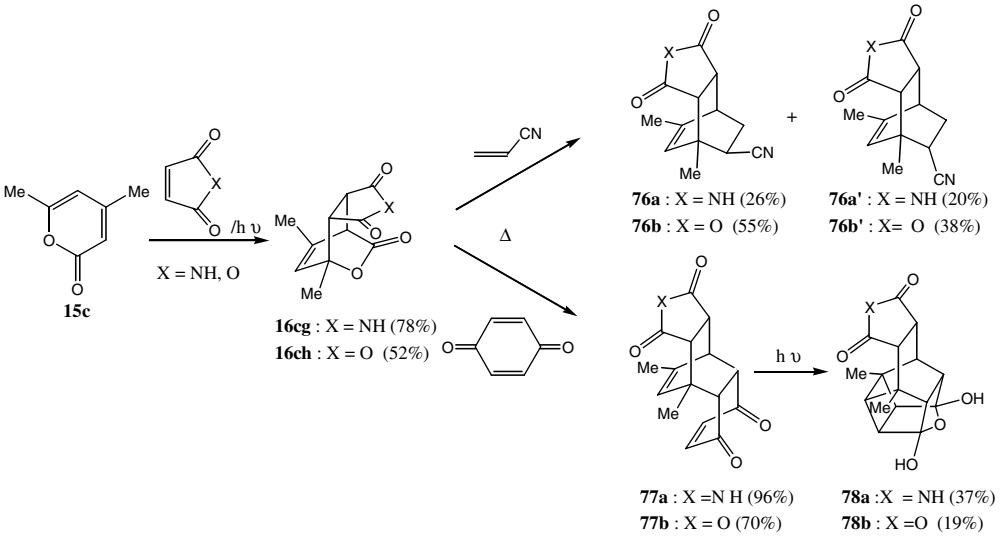

16cg : X = NH (78%)
16ch : X = O (52%)

76a : X = NH (26%)
76b : X = O (55%)

76a' : X = NH (20%)
76b' : X= O (38%)

77a : X =N H (96%)
77b : X = O (70%)

78a :X = NH (37%)
78b : X =O (19%)

SCHEME 28

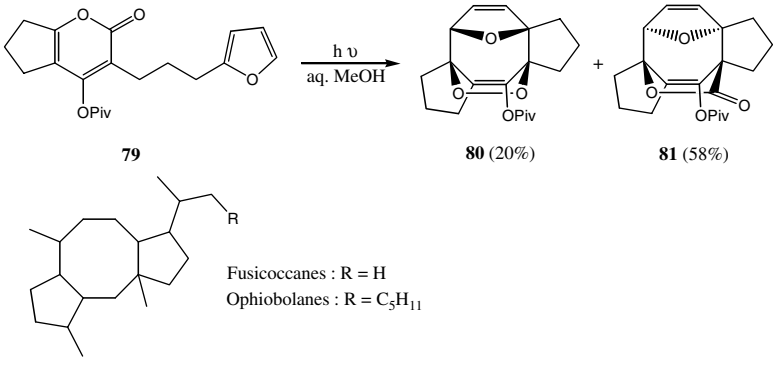

79

80 (20%)

81 (58%)

Fusicoccanes : R = H
Ophiobolanes : R = C_5H_{11}

SCHEME 29

Acknowledgments

The authors thank Drs. O. Tsuge and T. Obata (Kagoshima Prefectural Institute of Industrial Technology) for their numerous fruitful discussions and comments.

References

1. Shusherina, N.P., Diene synthesis with 2-pyrones and 2-pyridones, *Russ. Chem. Rev.,* 43, 851, 1974; Afarinkia, K., Vinader, V., Nelson, T.D. and Posner, G.H., Diels-Alder cycloadditions of 2-pyrones and 2-pyridones, *Tetrahedron,* 48, 9111, 1992.
2. Zimmerman, H.E., Grunewald, G.L., Paufler, R.M. and Sherwin, M.A., Synthesis and physical properties of barrelene, a unique Möbius-like model, *J. Am. Chem. Soc.,* 91, 2330, 1969.
3. Schreiber, von J., Leimgruber, W., Pesaro, M., Schudel, P., Threlfall, T. and Eschenmoser, A., 65. Synthese des colchicins, *Helv. Chim. Acta,* 44, 540, 1961.
4. de Mayo, P. Ultraviolet photochemistry of simple unsaturated systems, in *Advances in Organic Chemistry,* 2, Raphael, R.A., Taylor, E.C. and Wynberg, H., Eds., Interscience, New York, 1960, 394; for further electrocyclic ring-opening of 2-pyrones see Pirkle, W.H. and McKendry, L.H., Photochemical reactions of 2-pyrone and thermal reactions of the 2-pyrone photoproducts, *J. Am. Chem. Soc.,* 91, 1179, 1969; Chapman, O.L., McIntosh, C.L. and Pacansky, J., Photochemistry of α-pyrone in argon at 8°K, *J. Am. Chem. Soc.,* 95, 244, 1973.
5. Corey, E.J. and Streith, J., Internal photoaddition reactions of 2-pyrone and N-methyl-2-pyridone: A new synthetic approach to cyclobutadiene, *J. Am. Chem. Soc.,* 86, 950, 1964.
6. de Mayo, P. and Yip, R.W., The photo-dimerisation of 2, 4-dimethylcoumalin: The synthesis of 1, 3, 5, 7-tetramethylcyclo-octatetraene, *Proc. Chem. Soc.,* 84, 1964; for further photodimerisations of 2-pyrones see Pirkle, W.H. and McKendry, L.H., The multiplicity of the reactive 2-pyrone excited states, *Tetrahedron Lett.,* 5279, 1968.
7. Chapman, O.L., McIntosh, C.L. and Pacansky, J., Cyclobutadiene, *J. Am. Chem. Soc.,* 95, 614, 1973.
8. Cram, D.J., Tanner, M.E. and Thomas, R., The taming of cyclobutadiene, *Angew. Chem. Int. Ed. Engl.,* 30, 1024, 1991.
9. Hanifin, J. W. and Cohen, E., Some photochemical cycloadditions of coumarin, *Tetrahedron Lett.,* 1419, 1966; for further photocycloaddition reactions of coumarins see Pfoertner, K.-H., 84. Photoreaktionen von 3-substituierten cumarinen, *Helv. Chim. Acta,* 59, 834, 1976; Haywood, D.J., Hunt, R.G., Potter, C., J. and Reid, S.T., Photochemical transformations. Part 10. Photocycloaddition reactions of 4-hydroxycoumarin with cycloalkenes, *J. Chem. Soc., Perkin Trans. 1,* 2458, 1977; Naito, T., Nakayama, N. and Kaneko, C., A general synthetic method of 1, 2-dihydrocyclobuta[c]-coumarin and its 1-substituted derivatives, *Chem. Lett.,* 423, 1981; Nonoyama, S., Yonezawa, N., Saigo, K., Hasegawa, M. and Iitaka, Y., Synthesis of dichlorocyclobuta[b]benzofuran-2a-carboxylic derivatives and 3-(trichloroethenyl)coumarin through cross photocycloadduct of coumarin and tetrachloroethylene, *Bull. Chem. Soc. Jpn.,* 60, 349, 1987; Yasuda, M., Kishi, T., Goto, C., Satoda, H., Nakabayashi, K., Minami, T. and Shima, K., Efficient cross-photocycloadditions of 3-vinylcoumarins to olefins, *Tetrahedron Lett.,* 33, 6465, 1992; Kobayashi, K., Suzuki, M. and Suginome, H., Photoinduced molecular transformations. Part 143. (2+2) Photoaddition of 3-hydroxy-1-benzopyran-2-one, 3-benzyloxycarbonyloxy-1-benzopyran-2-one and their 8-methoxy derivatives, with alkenes and formation of 1, 2-disubstituted 1, 2-dihydrofuro[2,3-c][1]benzopyran-4-ones by way of β-scission of cyclobutanoxyl radical generated from the resulting [2+2]-photoadducts, *J. Chem. Soc., Perkin Trans. 1,* 2837, 1993.
10. Takeshita, H., Kikuchi, R. and Shoji, Y., Synthetic photochemistry. II. The cycloaddition reaction of dehydroacetic acid with olefins, *Bull. Chem. Soc. Jpn.,* 46, 690, 1973.
11. Shimo, T., Somekawa, K., Sato, M. and Kumamoto, S., Thermal and photoaddition reactions of methyl 2-pyrone-5-carboxylate with unsaturated compounds, *Nippon Kagaku Kaishi,* 1927, 1984; *Chem. Abstr.,* 102, 149041w, 1985.

12. Shimo, T., Somekawa, K. and Kumamoto, S., Photochemical cycloadditions of 4, 6-dimethyl-2-pyrone to a few substituted ethylenes, *Nippon Kagaku Kaishi,* 394, 1983; Chem. Abstr., 99, 53539h, 1983.
13. Somekawa, K., Shimo, T., Yoshimura, H. and Suishu, T., Photo-cycloaddition reactions of 2-pyrones, *Bull. Chem. Soc. Jpn.,* 63, 3456, 1990.
14. Shimo, T., Yamasaki, S., Date, K., Uemura, H. and Somekawa, K., Site-selective photocycloadditions of 2-pyrones with electron-poor olefins and the derivation from the cycloadducts, *J. Heterocyclic Chem.,* 30, 419, 1993.
15. Shimo, T., Iwakiri, T. and Somekawa, K., Peri-selective photocycloadditions of methyl 2-pyrone-5-carboxylate with unsaturated cyclic ethers, *J. Heterocyclic Chem.,* 29, 199, 1992.
16. Shimo, T., Yoshimura, H., Uemura, H., Somekawa, K. and Tsuge, O., Isolation of photo-Diels-Alder mono-adducts of 4, 6-dimethyl-2-pyrone and formation of cross-adducts, *Heterocycles,* 24, 3031, 1986.
17. Somekawa, K., Shimo, T. and Suishu, T., MO Analysis of photocycloaddition reactions of 2-pyrones, *Bull. Chem. Soc. Jpn.,* 65, 354, 1992.
18. Suishu, T., Obata, T., Shimo, T. and Somekawa, K., Species specificity and regio-selectivities in the photocycloadditions of cyclic conjugated enones and heterocyclic conjugated dienones and their frontier MO analysis, *Nippon Kagaku Kaishi,* 167, 2000; Chem. Abstr., 132, 293339m, 2000.
19. Shimo, T., Yasuda, M., Tajima, J. and Somekawa, K., Intramolecular photoreactions of 4-(ω-alkenyloxy)-6-methyl-2-pyrones, *J. Heterocyclic Chem.,* 28, 745, 1991.
20. Shimo, T., Tajima, J., Suishu, T. and Somekawa, K., Intramolecular photochemical reactions of 4-(ω-alkenyloxy)-6-methyl-2-pyrones having an alkoxycarbonyl group at the olefinic carbon chain, *J. Org. Chem.,* 56, 7150, 1991.
21. Shimo, T., Matsuzaki, S. and Somekawa, K., Intramolecular photoreactions of 6-(ω-alkenyl)-4-methoxy- 2-pyrones, *J. Heterocyclic Chem.,* 31, 387, 1994.
22. Shimo, T., Ueda, S. and Somekawa, K., Photochemical behavior of 4-(ω-enyl)- and 4-(ω-dienyl)-2- pyrones, *J. Heterocyclic Chem.,* 32, 341, 1995.
23. West, F.G., Chase, C., E. and Arif, A.M., Intramolecular [4+4]-photocycloadditions of 2-pyrones: An efficient approach to cyclooctanoid construction, *J. Org. Chem.,* 58, 3794, 1993.
24. Chase, C.E., Bender, J. A. and West, F.G., Efficient construction of bi- and tricyclic cyclooctanoid systems via crossed [4+4]-photocycloadditions of pyrone-2-ones, *Synlett,* 1173, 1996.
25. van Meerbeck, M., Toppet, S. and de Schryver, F.C., Intramolecular photocycloaddition of 6, 6′-polymethylene-bis-(4-methyl-2-pyrone), *Tetrahedron Lett.,* 2247, 1972.
26. Shimo, T., Ueda, S., Suishu, T. and Somekawa, K., Intramolecular photocycloadditions of 6, 6′-dimethyl- 4, 4′-polymethylenedioxy-di-2-pyrones, *J. Heterocyclic Chem.,* 32, 727, 1995.
27. Ramamurthy, V. and Venkatesan, K., Photochemical reactions of organic crystals, *Chem. Rev.,* 87, 433, 1987; Ito, Y., Solid-state photoreactions in two-component crystals, *Synthesis,* 1, 1998.
28. Meng, J.-B., Zhu, Z.-L., Wang, R.-J., Yao, Z.-K., Ito, Y., Ihara, H. and Matsuura T., Selectivity in the solid-state photoreaction of 6-cyanouracils with aromatic hydrocarbons, *Chem. Lett.,* 1247, 1990; Suzuki, T., Fukushima, T., Yamashita, Y. and Miyashi, T., An absolute asymmetric synthesis of the [2+2]-cycloadduct via single crystal-to-single crystal transformation by charge-transfer excitation of solid-state molecular complexes composed of arylolefins and bis[1,2,5]thiadiazolotetracyanoquinodimethane, *J. Am. Chem. Soc.,* 116, 2793, 1994.
29. Rieke, R.D. and Copenhafer, R.A., Solid state organic photochemistry II. Photolysis of 4, 6-diphenyl-α-pyrone, *Tetrahedron Lett.,* 879, 1971.
30. Sugiyama, N., Sato, T., Kataoka, H. and Kashima, C., The photoreaction of dehydroacetic acid, *Bull. Chem. Soc. Jpn.,* 44, 555, 1971.
31. Ortmann, I., Werner, S., Krüger, C., Mohr, S. and Schaffner, K., Intermolecular π electron interactions made visible. Correlation of ground- and excited-state interactions with specific photoreactivities of isomorphously crystallized isoelectronic compounds, *J. Am. Chem. Soc.,* 114, 5048, 1992 and references cited therein.

32. Obata, T., Shimo, T., Suishu, T. and Somekawa, K., Stereoselective photo [4+2]-cycloadditions of 2-pyrone-5-carboxylate with maleimides in the solid state and in solution, *J. Heterocyclic Chem.,* 35, 1361, 1998.
33. Obata, T., Shimo, T., Yoshimoto, S., Somekawa, K. and Kawaminami, M., Peri-, site- and stereo-controlled photocycloaddition of 4-methoxy-6-methyl-2-pyrone with maleimide induced by the hydrogen bond and CT stacking in the solid state, *Chem. Lett.,* 181, 1999.
34. Obata, T., Shimo, T., Yasutake, M., Shinmyozu, T., Kawaminami, M., Yoshida, R. and Somekawa, K., Remarkable interaction effects of molecular packing on site- and stereoselectivity in photocycloaddition of 2-pyrones with maleimide in the solid state, *Tetrahedron,* 57, 1531, 2001.
35. Shimo, T., Uezono, T., Obata, T., Yasutake, M., Shinmyozu, T. and Somekawa, K., x-ray and MO analysis of highly stereoselective solid-state photocycloadditions of 2-pyrones with maleimide, *Tetrahedron,* 58, 6111, 2002.
36. Somekawa, K., Imai, R., Furukido, R. and Kumamoto, S., Photoadducts of 2-pyridones with chloroethylenes and their derivatives, *Bull. Chem. Soc. Jpn.,* 54, 1112, 1981; Yonezawa, N., Nonoyama, S., Saigo, K. and Hasegawa, M., Synthesis of dichlorocyclobuta[b]benzofuran-2a- carboxylic derivatives and 3-(trichlorovinyl)coumarin through the cross photocycloadduct of coumarin and tetrachloroethylene, *J. Org. Chem.,* 50, 3026, 1985.
37. Shimo, T., Somekawa, K., Wakikawa, Y., Uemura, H., Tsuge, O., Imada, K. and Tanabe, K., Photoadducts of 4,6-dimethyl- and 4-methoxy-6-methyl-2-pyrones with chloroethylenes and their dehydrochlorination, *Bull. Chem. Soc. Jpn.,* 60, 621, 1987.
38. Shimo, T., Date, K. and Somekawa, K., Novel transformations of two kinds of chlorinated photo [2+2]-cycloadducts of 2-pyrone-5-carboxylate, *J. Heterocyclic Chem.,* 29, 387, 1992.
39. Shimo, T., Matsuo, K., Somekawa, K. and Tsuge, O., Diels-Alder reactions of cyclohexadienes derived from decarboxylation of photo [4+2]-cycloadducts between 4,6-dimethyl-2-pyrone and cyclic olefins, *J. Heterocyclic Chem.,* 28, 549, 1991.

83

Photochemical Rearrangement and Trapping Reactions of 4-Pyrones

Frederick G. West
University of Alberta

The previous edition of this Handbook included a thorough discussion of the literature of phototransposition and photo-ring contraction chemistry of 4-pyrones and their 4-hydroxypyrylium conjugate acids through 1990.[1] This chapter briefly reiterates the historical background of this area and the original mechanistic work, and then focuses on the synthetic studies that have appeared in the time period since the previous edition went to press.

83.1 Background

The earliest report of a photochemical transformation involving 4-pyrones was made by Paterno,[2] who observed an apparent dimerization involving 2,6-dimethylpyran-4-one **1a** (Scheme 1). However, the structure of the dimer was not elucidated until 1958, when Yates and Jorgenson demonstrated it to be the cage system **2a** resulting from successive inter- and intramolecular head-to-tail [2+2]-photocycloadditions.[3] This was followed by several examples of alternative, non-dimeric photoproducts, which included dimethylfurfural **4a**[4] and 2-pyrones **5b,c,d**.[5,6] It was suggested that both of these products could arise from an intermediate epoxycyclopentenone **3** via acid-catalyzed rearrangement or secondary photochemical processes, respectively. (See the Section 83.2 for a more detailed discussion.) In one instance, it was possible to isolate the putative intermediate **3e** during the photorearrangement of **1e** to **5e**.[7] Finally, solvent adducts **6** were isolated following irradiation of 4-pyrones in hydroxylic solvents.[7,8] The more nucleophilic methanol gave greater yields of adducts **6'** than did trifluoroethanol. These studies lent

0-8493-1348-1/04/$0.00+$1.50

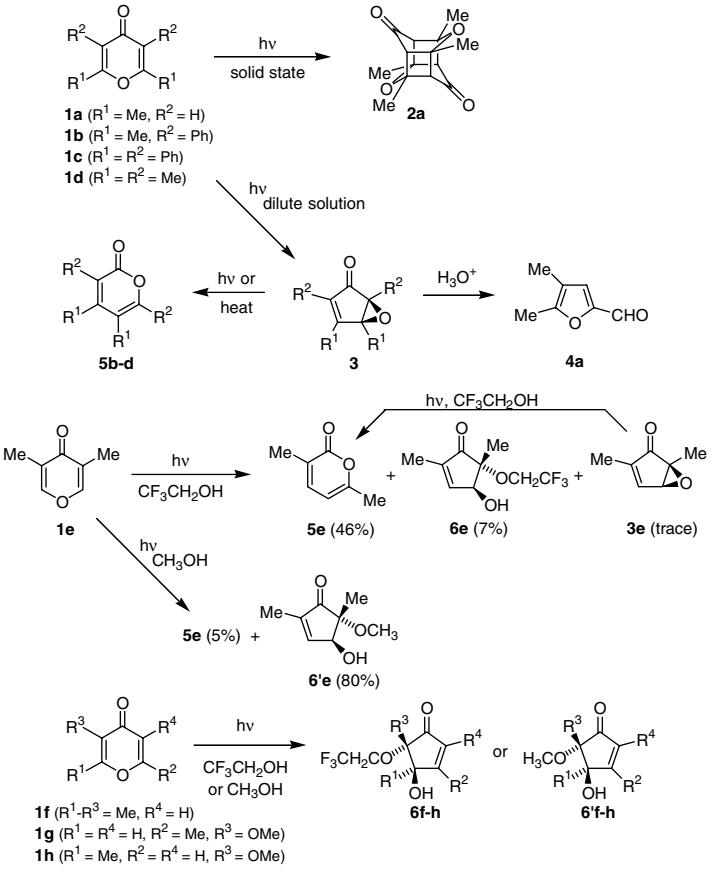

SCHEME 1

support to the notion of a photochemical ring contraction mechanism via oxyallyl zwitterion intermediates, analogous to that elucidated for related 2,5-cyclohexadien-4-ones.[9]

83.2 Mechanism

Formation and Rearrangement of Epoxycyclopentenone Intermediates

4-Pyrones bear an obvious structural similarity to cross-conjugated cyclohexadienones, but the presence of a ring oxygen in conjugation with the ketone is expected to perturb the ordering of the pyrone excited states relative to the all-carbon analogue. 4-Pyrones display an intense absorption between 250 and 260 nm, characteristic of a $\pi \rightarrow \pi^*$ transition, and direct irradiation at this wavelength leads to rearrangement products such as **3**, **4**, and **5** and trapping products **6**.[10] In contrast, cyclohexadienones are believed to undergo Type A rearrangement via a lower-energy $n\pi^*$ excited state. It is suggested that the $S_1(\pi\pi^*)$ state that is populated by direct irradiation of 4-pyrones near 250 nm participates in a symmetry-allowed electrocyclization process to form the bicyclic zwitterion **7** (Scheme 2).[5–7] This key intermediate can then undergo a variety of processes that lead to the observed primary photoproducts. Also notable is the consistent requirement for polar media in the photochemical rearrangement processes of 4-pyrones, again in contrast to cyclohexadienones and indicative of excitation to a low-lying $\pi\pi^*$ state. In the absence of effective trapping agents, zwitterion **7** can rearrange to epoxycyclopentenone **3** via an oxoniabenzvalene intermediate arising from attack by the proximal epoxide lone pair on one of the termini of the allyl

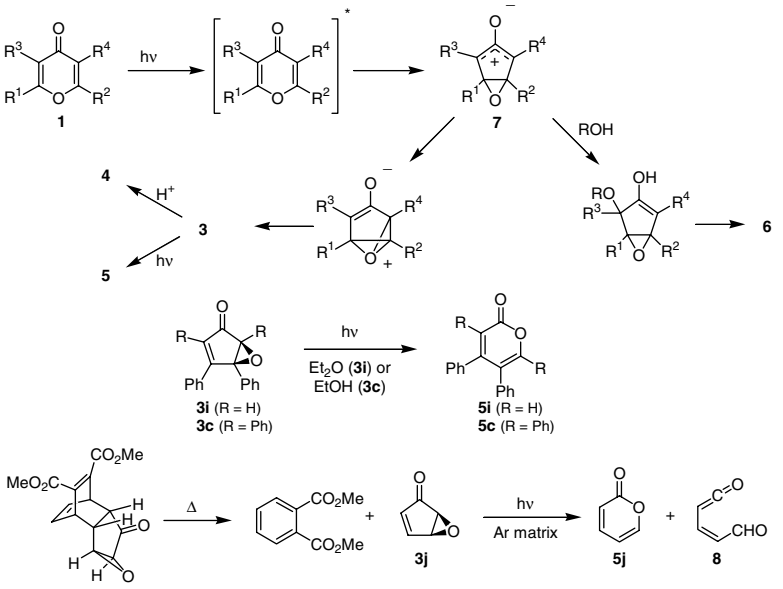

SCHEME 2

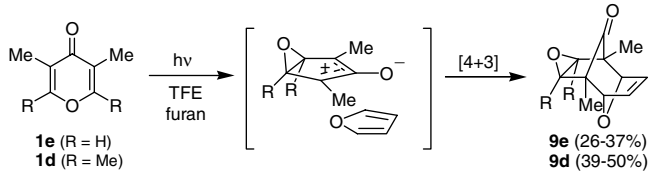

SCHEME 3

cation. Evidence for the intermediacy of **3** in the formation of **4** and **5** includes the isolation of **3e** from the reaction mixture during the photochemical conversion of **1e** to **5e**, as noted above.[7] In addition, Padwa and Hartman independently synthesized epoxide **3i** and showed that it formed 2-pyrone **5i** when irradiated through a Pyrex filter.[11] Likewise, Dunston and Yates found that the tetraphenyl derivative **3c** was converted to **5c** upon irradiation with sunlight or a UV lamp.[12] More recently, the parent epoxycyclopentenone **3j** was generated by vacuum pyrolysis and shown to undergo photolytic conversion in an argon matrix to 2-pyrone **5j** and formyl vinylketene **8**, the latter presumably resulting from photochemical electrocyclic opening of **5j**.[13]

Evidence for Oxyallyl Zwitterion Intermediates

There is considerable evidence for the formation of the bicyclic oxyallyl zwitterion prior to the epoxycyclopentenone. Pavlik and Barltrop showed that irradiation in trifluoroethanol (TFE) or methanol furnished solvent adducts as primary photoproducts,[8] and Barltrop and co-workers excluded the possible formation of the TFE adduct **6e** from epoxycyclopentenone **3e**.[7] Barltrop demonstrated that irradiation of 3,5-dimethyl-4-pyrone **1e** in furan/trifluoroethanol mixtures furnished the [4+3]-cycloadduct **9e** as one of the major photoproducts (Scheme 3).[14] A similar result was reported by West and co-workers using tetramethylpyrone **1d**.[15] Interestingly, in both cases, a single diastereomer was observed, corresponding to approach of furan from the face opposite the epoxide oxygen and reaction via an *endo*

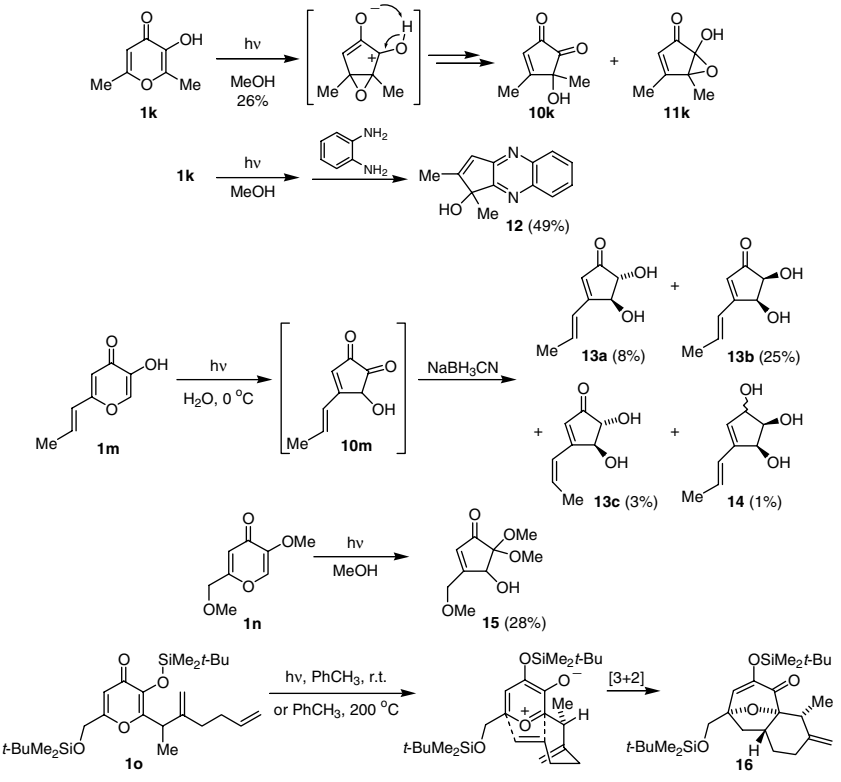

SCHEME 4

transition state allowing secondary orbital overlap between the middle carbon of the allyl system and the inner carbons of the furan 1,3-dene system. Finally, two cases involving photo-ring contraction of 3-hydroxy-4-pyrones were reported, in both cases providing cyclopentenediones that almost certainly result from the intermediate zwitterions (see Section 83.3 for details).[16]

83.3 Synthetic Studies

3-Hydroxy-4-Pyrone Ring-Contractions

As noted above, the photochemical ring contraction of 3-hydroxy-4-pyrones occurs readily, leading to unusual cyclopentenedione products.[16] These compounds are quite unstable and are subject to various self-condensation processes, but *in situ* derivatization has been an effective approach to improving the overall yields. For example, Shiozaki and Hiraoka found that irradiation of 2,6-dimethyl-3-hydroxy-4-pyrone **1k** in methanol produced a mixture of dione **10k** and epoxyhemiketal **11k** in 26% yield after work-up and crystallization (Scheme 4).[16a] However, treatment of the crude reaction mixture with *o*-phenylenediamine gave quinoxaline **12** in 49% yield. Barton and Hulshof irradiated 5-hydroxy-2-(*E*)-propenyl-4-pyrone **1m** in water at 0°C, with addition of sodium cyanoborohydride during the first 15 minutes, obtaining a mixture consisting of the natural product terrein **13a**, isoterrein **13b**, the (*Z*) isomer **13c**, and over-reduction product **14** in a combined 37% yield.[16b] Compounds **13a** and **13b** are presumed to arise from hydride reduction of intermediate dione **10m**, while **13c** was shown to form from terrein during irradiation. Irradiation of a dilute aqueous solution of **1m** in the presence of sodium borohydride provided **13b** in 35% yield. Photo-ring contraction of the kojic acid derivative **1n** was also investigated, furnishing dimethyl ketal **15** in 28% yield. It should be noted that 3-silyloxy-4-pyrone derivatives are

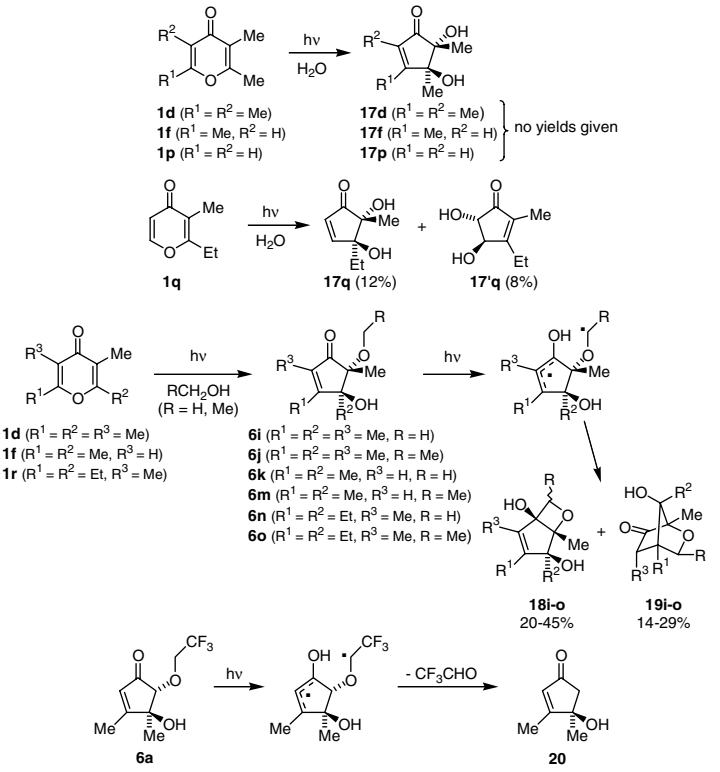

SCHEME 5

also subject to alternative photochemical transformations involving silatropic rearrangement to generate transient 3-oxidopyrylium ylides. These transient intermediates can undergo formal [5+2]-cycloaddition processes, as exemplified by Wender and McDonald's conversion of **1o** to tricyclic adduct **16**.[17] However, thermal isomerization appears to be the favored method for effecting this rearrangement.[18]

Solvent Trapping

As mentioned in the introduction, Pavlik showed that irradiation of substituted 4-pyrones in protic solvents provided 5-alkoxy-4-hydroxycyclopent-2-en-1-ones or 4,5-dihydroxycyclopent-2-en-1-ones via nucleophilic attack of the oxyallyl zwitterion by solvent.[8,19] Aside from providing good support for the intermediacy of an epoxy-fused oxyallyl species, this trapping process offers a convenient method for the preparation of highly oxidized cyclopentanoids. Several unsymmetrically substituted 4-pyrones were irradiated in water and a consistent preference for attack at the more substituted terminus of the oxyallyl intermediate was seen, presumably due to greater charge density at that site. Moreover, *trans* products **17** arising from attack by solvent *anti* to the epoxide oxygen dominated over the relatively minor amounts of *cis* dioxygenated products (Scheme 5). In a more recent study, West and co-workers observed that alcohol adducts of simple polyalkyl 4-pyrones were subject to secondary photochemistry under the conditions of their formation.[20] When γ-hydrogens were present on the 5-alkoxy side-chain (e.g., **6n** and **6o**), their abstraction by the excited enone carbonyl was seen, with subsequent recombination to form either fused bicyclic oxetanes **18** or oxabicycloheptanones **19** in a process analogous to that previously reported by Agosta and Smith.[21] Keil and Pavlik have also observed secondary photoprocesses involving the trifluoroethanol adduct **6a** of 2,6-dimethyl-4-pyrone, in that case undergoing Norrish Type II cleavage to provide 4-hydroxy-3,4-dimethylcyclopent-2-en-1-one **20**.[8b]

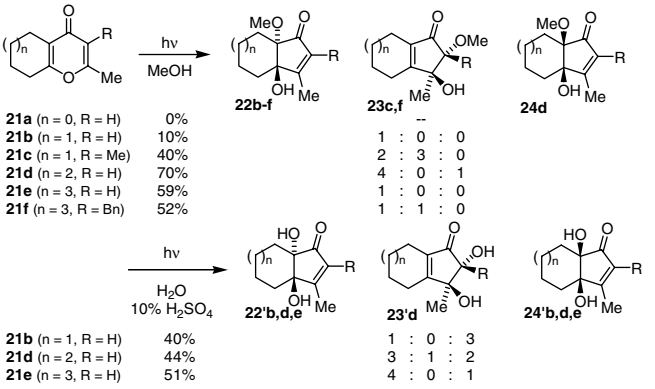

SCHEME 6

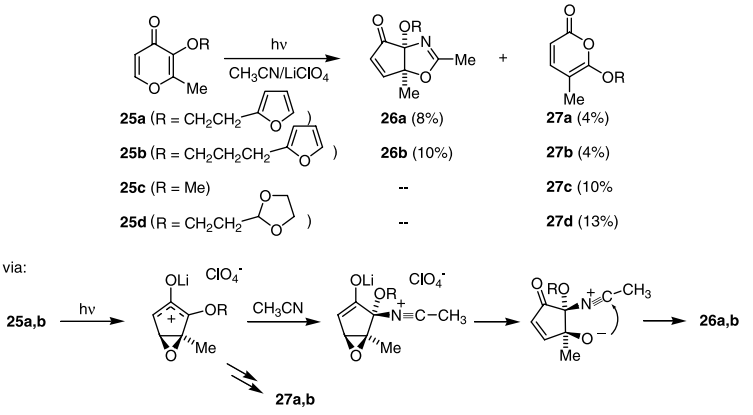

SCHEME 7

The observation of good regio- and diastereoselectivity in the solvent trapping studies prompted West and co-workers to investigate the use of this process in conjunction with Hünig's one-step route to fused bicyclic 4-pyrones from cycloalkanone enamines.[22] A series of substrates **21**a–n was prepared and irradiated in methanol or water to furnish adducts **22**, **23**, and **24** (Scheme 6).[23] Certain generalizations can be made from this study: (1) higher alcohols such as ethanol gave much lower yields that cannot be considered synthetically useful; (2) annulation of the pyrone ring onto a cyclopentane resulted in an unreactive substrate, presumably due to prohibitive ring strain in the ring-contraction transition state; (3) substrates lacking a substituent at C5 (R = H) generally displayed good regioselectivity in favor of attack at the more substituted bridgehead position; (4) small but significant amounts of the *cis*-products were seen in some cases, especially with water;[24] and (5) catalytic sulfuric acid was helpful in a number of cases, especially those involving trapping with water. The beneficial effect of acid suggests the possible involvement of 4-hydroxypyrylium cations, which have been shown to undergo photochemical ring contraction to hydroxyallyl cations comparable to those of the neutral 4-pyrones.[6,25] Notably, secondary photoproducts analogous to **18** and **19** were not seen, although one case did undergo apparent Norrish Type II cleavage.

West and Koch also reported an example of solvent capture of zwitterions derived from 4-pyrones **25a** and **25b** by acetonitrile in the presence of lithium perchlorate (Scheme 7).[26] A Ritter-type process was invoked to explain the isolation of bicyclic oxazolines **26**, together with 2-pyrones **27**. It is important to

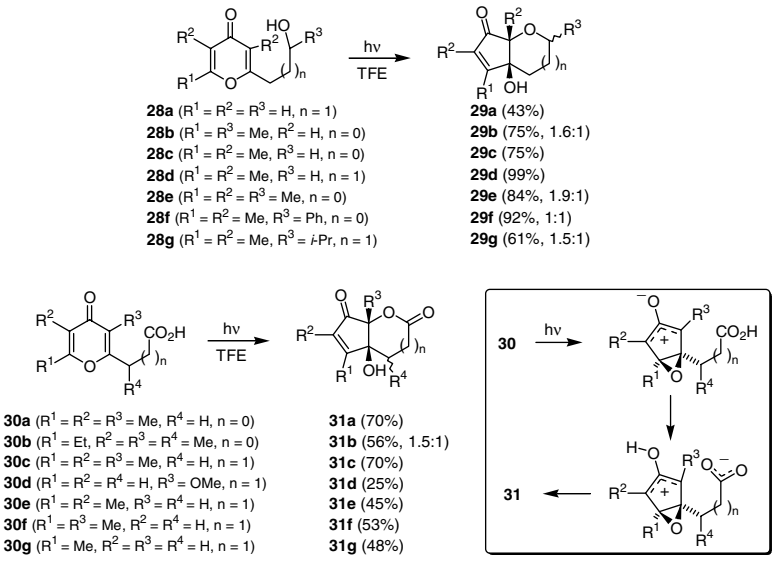

SCHEME 8

note that oxazolines **26** derive from apparent *syn* attack by acetonitrile. It was suggested that the poor mass recovery in these cases might be due to decomposition or oligomerization of the corresponding *anti*-adducts, which cannot undergo cyclization to the *trans*-fused oxazolines due to excessive ring strain. Similar substrates **25c** and **25d** lacking remote furan rings failed to provide any of the oxazoline products, furnishing only low yields of the ring-transposed 2-pyrones **27c** and **27d**.

Intramolecular Trapping by Oxygen Nucleophiles

West and co-workers prepared a series of substituted 4-pyrones containing pendant hydroxyl groups in order to explore the intramolecular version of the solvent trapping process.[27] The ready availability of the simple polyalkyl 4-pyrones and their straightforward deprotonation and functionalization at the 2-alkyl position permitted the synthesis of a variety of photosubstrates **28a–g** (Scheme 8). In all cases except the monosubstituted 4-pyrone **28a**, the desired bicyclic cyclopentenone ethers **29** were formed in good to excellent yield. The isolation of relatively little solvent adduct at the expense of cyclization product **29** when substrates **28c,e,f** were irradiated in methanol illustrated the efficiency of the intramolecular trapping process. The authors noted the significant complexity increase seen in the conversion of planar heterocycles **28** to fused bicyclic products **29**. However, little or no diastereoselectivity was observed in those cases involving secondary alcohols. A related study employed carboxyl groups as internal traps.[28] In these cases, 4-pyrones **30a–g** with pendant carboxylic acids attached via the 2-position were prepared via either carboxylation of simple polyalkylpyrone anions or by ozonolysis of ω-alkenyl-4-pyrones with oxidative work-up. Irradiation in trifluoroethanol furnished bicyclic lactones **31a–g** in generally good yields. The authors suggested the possibility of a proton transfer prior to cyclization to form hydroxyallyl cation-carboxylate zwitterion **32**.

Intramolecular Trapping by Carbon Nucleophiles

The examples above were simple intramolecular analogies of the well precedented solvent trapping reactions of 4-pyrones. West and co-workers also sought to accomplish carbon-carbon bond-forming processes that had no intermolecular counterpart. To this end, they prepared a series of 4-pyrones **33a–j** with pendant alkenes to examine the feasibility of a cation-olefin cyclization process involving the oxyallyl intermediate (Scheme 9).[29] Irradiation of pyrones **33** yielded fused bicyclic products **34**, **35**, and **36** in

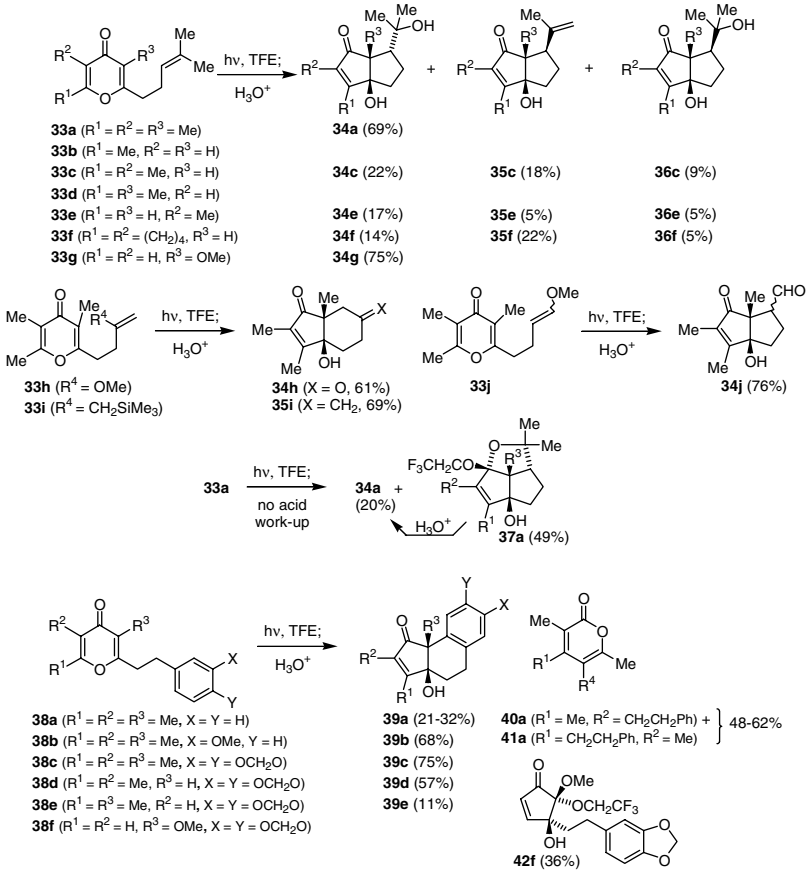

SCHEME 9

good to excellent yield, with the exception of **33b** and **33d**, which were inert to the conditions. The origin of this apparent requirement for a non-hydrogen substituent at the remote C5 position was not discerned by the authors. Interestingly, 4-pyrones **33a–g** with simple trisubstituted alkene traps underwent an unexpected additional cyclization involving the carbonyl oxygen to form tricyclic mixed ketals as exemplified by **37a** that were isolable when acidic work-up was omitted. In a related study, the photochemical behavior of arylethyl 4-pyrones **38a–f** was investigated.[30] Electrophilic aromatic substitution onto electron-rich arenes by the oxyallyl species proved to be efficient, yielding tricyclic adducts **39b,c,d.** However, in the case of monosubstituted arene **38a**, competing phototransposition to 2-pyrones **40a** and **41a** predominated. In analogy to the unreactive alkenyl pyrones **33b** and **33d**, substrate **38e** gave only small amounts of **39e** with most of the starting material unconsumed after extended irradiation, again illustrating the surprising requirement for substitution at C5 in the case of carbon π nucleophiles.[31] Maltol derivative **38f** gave only mixed ketal solvent trapping product **42f**, in analogy to the diene-substituted examples discussed below (Scheme 10).

Trapping by [4+3]-Cycloaddition

Trapping of the oxyallyl intermediate with furan in a [4+3]-cycloaddition was known but was found to be an inefficient process with solvent trapping, phototransposition, and [2+2]-photocycloaddition processes all competing with the desired pathway.[14,15] West and co-workers examined the intramolecular version to ascertain whether tethering a 1,3-diene to the 4-pyrone could enhance the [4+3]-process at the expense of the other pathways (Scheme 10).[15] The need to attach the diene trap via C3 complicated

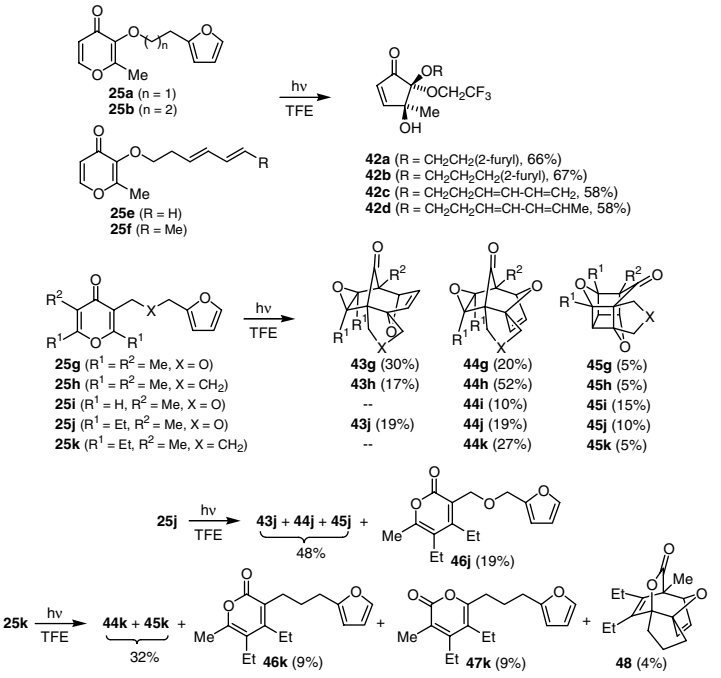

SCHEME 10

the synthetic plans, as this position is much less easily functionalized in the case of polyalkyl 4-pyrones. Ether-linked substrates **25a,b,e,f** could be readily prepared from the naturally occurring maltol but irradiation in trifluoroethanol furnished only the solvent trapping products 42a–d, albeit in good yield. Simple nucleophilic capture of the zwitterion in preference to cycloaddition was attributed to the polarizing effect of the C3 oxygen substituent. Attachment via a carbon linker was also possible and substrates **25g–k** all yielded [4+3]-adducts **43** and/or **44** in moderate yield, with an apparent preference for the *exo*-cycloadduct **44**. The failure to observe the high *endo* selectivity observed with intermolecular trapping of **1d** and **1e** (see Scheme 3) was explained in terms of unfavorable non-bonded interactions between side-chain atoms and the alkyl substituent at C2 (R^2). In all cases, small amounts of the cage products **45g–k** resulting from two successive [2+2]-photocycloadditions of the 4-pyrone and furan systems were also isolated. Notably, 2,6-diethyl substituted substrates **25j** and **25k** also yielded significant amounts of the corresponding 2-pyrone ring-transposition products **46** and **47** and, in the case of **47k**, a small amount of photochemical [4+4]-cycloadduct **48**, a *ternary* photoproduct, was obtained. The observation of an intramolecular crossed [4+4]-photocycloaddition involving a 2-pyrone tethered to a furan spurred the development of this reaction as an approach to functionalized cyclooctadienes.[32]

Stereocontrol in Oxyallyl Zwitterion Formation

West and co-workers also showed that the photocyclization products from intramolecular nucleophilic trapping of oxyallyl zwitterions can be further processed to medium-sized rings using a photocyclization/Grob fragmentation process (e.g., **49**→**50**, Scheme 11).[33] However, because that methodology in not photochemically based, it will not be discussed in detail. Most recently, efforts have focused on methods for controlling the configuration of the ring-contracted oxyallyl species. Fused bicyclic 4-pyrones in which the adjacent ring contains a stereogenic center are potentially subject to conformational control of the ring-contraction process. In the aqueous trapping of substrate **51**, a 2:1 ratio of products derived from diastereomeric zwitterions **52a** and **52b** was seen.[23b] Intramolecular trapping of substrates **53a** and **53b**

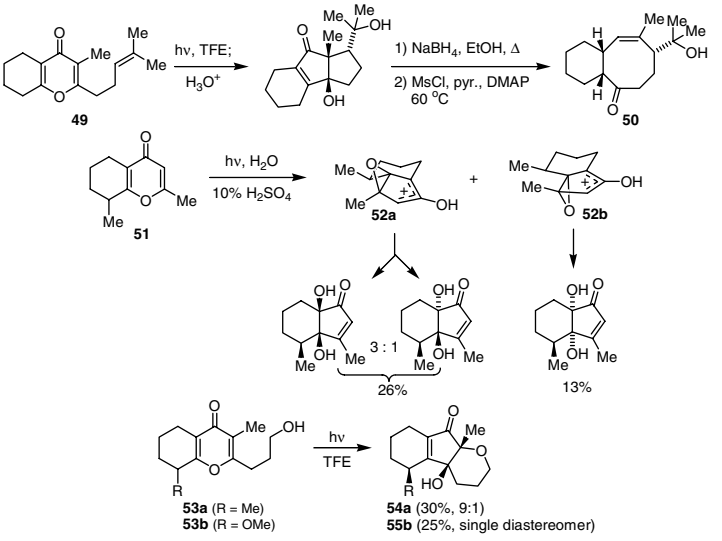

SCHEME 11

showed excellent diastereoselectivity but moderate yields of cyclized products **54**.[34] The relative configuration of the major products in these cases were inferred in analogy to the solvent trapping products of **51**, which were validated by x-ray crystallography.

References

1. Pavlik, J.W., Phototransposition and photo-ring contraction reactions of 4-pyrones and 4-hydroxypyrilium cations, in *CRC Handbook of Organic Photochemistry and Photobiology*, Horspool, W.M. and Song, P.S., Eds., CRC Press, Boca Raton, FL, 1995, 237.
2. Paterno, E., Synthesis in organic chemistry by means of light. VII. Various experiments, *Gazz. Chim. Ital.*, 44, 151, 1914.
3. (a) Yates, P. and Jorgenson, M.J., The photodimer of 2,6-dimethyl-4-pyrone, *J. Am. Chem. Soc.*, 80, 6150, 1958; (b) Yates, P. and Jorgenson, M.J., Photodimeric cage compounds. I. The structure of the photodimer of 2,6-dimethyl-4-pyrone, *J. Am. Chem. Soc.*, 85, 2956, 1963.
4. Yates, P. and Still, I.W. J., Photorearrangement of a 4-pyrone to a furan derivative, *J. Am. Chem. Soc.*, 85, 1208, 1963.
5. Ishibe, N., Odani, M., and Sunami, M., Photochemical rearrangement of 4H-pyran-4-ones to 2H-pyran-2-ones, *J. Chem. Soc., Chem. Commun.*, 1034, 1971; (b) Ishibe, N., Odani, M., and Sunami, M., Photoisomerization of 4H-pyran-4-ones to 2H-pyran-2-ones, *J. Am. Chem. Soc.*, **95**, 463, 1971.
6. Pavlik, J.W. and Kwong, J., Photochemical rearrangements of neutral and protonated 4-pyrones, *J. Am. Chem. Soc.*, 95, 7914, 1973.
7. Barltrop, J.A., Day, A.C., and Samuel, C.J., 4-pyrone photochemistry. The intermediacy of a cyclopentadienone epoxide, *J. Chem. Soc., Chem. Commun.*, 598, 1977.
8. (a) Pavlik, J.W. and Pauliukonis, L.T., Photoisomerization of 4-pyrones. Nucleophilic trapping of reactive intermediates, *Tetrahedron Lett.,* 1939, 1976; (b) Keil, E.B. and Pavlik, J.W., Photochemistry of 2,6-dimethylpyrone in trifluoroethanol, *J. Heterocyclic. Chem.,* 13, 1149, 1976; (c) Barltrop, J.A., Day, A.C., and Samuel, C.J., Evidence for a zwitterionic 2,6-bonded intermediate in 4-pyrone photochemistry. Following the time evolution of an excited state, *J. Chem. Soc., Chem. Commun.,* 822, 1976.
9. Schultz, A.G., Photorearrangement reactions of cross-conjugated cyclohexadienones, in *CRC Handbook of Organic Photochemistry and Photobiology*, Horspool, W.M. and Song, P.-S., Eds., CRC Press, Boca Raton, FL, 1995, 685; (b) Zimmerman, H.E. and Lynch, D.C., Rapidly rearranging

excited states of bichromophoric molecules. Mechanistic and exploratory organic photochemistry, *J. Am. Chem. Soc.,* **107,** 7745, 1985; (c) Schuster, D.I., Mechanisms of photochemical transformations of cross-conjugated cyclohexadienones, *Acc. Chem. Res.,* 11, 65, 1978.

10. Ishibe, N., Sugimoto, H., and Gallivan, J.B., Electronic absorption and emission spectra of 4-pyrones, 4-thiopyrones and 4-pyridones, *J. Chem. Soc., Faraday Trans. 2*, 71, 1812, 1975.
11. Padwa, A. and Hartman, R., Photochemical transformations of small ring carbonyl compounds. VIII. Photorearrangements in the cyclopentenone oxide series, *J. Am. Chem. Soc.,* 88, 1518, 1966.
12. Dunston, J.W. and Yates, P., Pyrylium 3-oxide and 4,5-epoxy-2-cyclopentenone valence tautomerism, *Tetrahedron Lett.,* 505, 1964.
13. Chapman, O.L. and Hess, T.C., Cyclopentadienone epoxide: synthesis and photochemistry, *J. Org. Chem.,* 44, 962, 1979.
14. Barltrop, J. A., Day, A.C. and Samuel, C.J., Heterocyclic photochemistry. 4-Pyrones. A mechanistic study, *J. Am. Chem. Soc.,* 101, 7521, 1979.
15. West, F.G., Harke-Karger, C., Koch, D.J., Kuehn, C.E. and Arif, A.M., Intramolecular [4+3]-cycloadditions of photochemically generated oxyallyl zwitterions: a route to functionalized cyclooctanoid skeletons, *J. Org. Chem.,* 58, 6795, 1993.
16. (a) Shiozaki, M. and Hiraoka, T., Photochemistry of β-hydroxy-γ-pyrone. A new synthesis of 3-methylcyclopent-2-en-2-ol-1-one from maltol, *Tetrahedron Lett.,* 4655, 1972; (b) Barton, D.H.R. and Hulshof, L.A., Photochemical transformations. 35. A simple synthesis of racemic terrein, *J. Chem. Soc., Perkin Trans. 1*, 1103, 1977.
17. Wender P.A. and McDonald, F.E., Studies on tumor promoters. 9. A second-generation synthesis of phorbol, *J. Am. Chem. Soc.,* 112, 4956, 1990.
18. (a) Wender, P.A. and Mascarenas, J.L. Studies on tumor promoters. 11. A new [5+2] cycloaddition method and its application to the synthesis of BC ring precursors of phorboids, *J. Org. Chem.,* 56, 6267, 1991; (b) Wender, P.A. and Mascarenas, J.L., Preparation and cycloadditions of a 4-methoxy-3-oxidopyrylium ylide — a reagent for the synthesis of highly substituted 7-membered rings and tetrahydrofurans, *Tetrahedron Lett.,* 33, 2115, 1992; (c) Ohmori, N., Yoshimura, M., and Ohkata, K., Asymmetric induction in intramolecular [5+2] cycloaddition of 2-(4-alkenyl)-5-benzoyloxy (or 5-silyloxy)-4-pyrones involving migration of the pyrone O-5 group to O-4, *Heterocycles,* 45, 2097, 1997.
19. (a) Pavlik, J.W., Snead, T.E., and Tata, J.R., Photochemistry of 4-pyrones in water. Formation of dihydroxycyclopentenones and furan-derivatives, *J. Heterocyclic. Chem.,* 18, 1481, 1981; (b) Pavlik, J.W., Kirincich, S.J., and Pires, R.M., Regiochemistry and stereochemistry of the photo-ring contraction of 4-pyrones, *J. Heterocyclic. Chem.,* 28, 537, 1991; (c) Pavlik, J.W., Keil, E.B., and Sullivan, E.L., Photochemistry of tetramethyl-4-pyrone in alcohol solvents, *J. Heterocyclic. Chem.,* 29, 1829, 1992.
20. Fleming, M., Basta, R., Fisher, P.V., Mitchell, S., and West, F.G., Synthesis of bridged bicyclic ethers and fused oxetanes from pyran-4-ones via tandem solvent trapping and Norrish type II cyclization, *J. Org. Chem.,* 64, 1626, 1999.
21. (a) Smith, A.B., III and Agosta, W.C., A new photochemical reaction of cyclopentenones, *J. Chem. Soc., Chem. Commun.,* 343, 1971; (b) Agosta, W.C. and Smith, A.B., III, Photochemical reactions of simple cyclopentenones, *J. Am. Chem. Soc.,* 93, 5513, 1971.
22. Hünig, S., Benzing, E., and Hübner, K., Reaktionen mit diketen zu γ-pyronen, *Chem. Ber.,* 94, 486, 1961.
23. (a) West, F.G., Fisher, P.V., Gunawardena, G.U., and Mitchell, S., Photochemical ring-contraction of fused bicyclic 4-pyrones: a novel 2-step cyclopentannulation approach, *Tetrahedron Lett.,* 34, 4583, 1993; (b) Fleming, M., Fisher, P.V., Gunawardena, G.U., Jin, Y., Zhang, C., Zhang, W., Arif, A., and West, F.G., Solvent trapping of photochemically generated pyran-4-one-derived oxyallyls: a convenient cyclopentannulation method, *Synthesis*, 1268, 2001.
24. While it is possible that the *cis*-glycols observed in these cases derive from attack by water *syn* to the epoxide moiety, it was shown that in the case of *trans*-hydrindenone **20n**, equilibration with

cis isomer **21n** occurred under the reaction conditions, presumably via an acid-catalyzed retro-aldol/aldol mechanism.[23b]

25. (a) Pavlik, J.W. and Clennan, E.L., Photochemical rearrangements of pyrylium cations, *J. Am. Chem. Soc.,* 95, 1697, 1973; (b) Barltrop, J., Carder, J., Day, A.C., Harding, J.R., and Samuel, C., Ring permutations in the photochemistry of hydroxypyrylium cations, *J. Chem. Soc., Chem. Commun.,* 729, 1975; (c) Barltrop, J.A., Day, A.C., and Samuel, C.J., Hydroxypyrylium photochemistry, *J. Chem. Soc., Chem. Commun.*, 823, 1976; (d) Pavlik, J.W. and Spada, A., Photo-ring contraction reactions of 4-hydroxypyrylium cations, *Tetrahedron Lett.*, 4441, 1979; (e) Barltrop, J.A., Barrett, J.C., Carder, R.W., Day, A.C., Harding, J.R., Long, W.E., and Samuel, C.J., Heterocyclic photochemistry. I. Phototranspositions in hydroxypyrylium cations. Permutation pattern analysis and mechanistic studies, *J. Am. Chem. Soc.,* 101, 7510, 1979; (f) Pavlik, J.W., Patten, A.D., Bolin, D.R., Bradford, K.C. ,and Clennan, E.L., Photoisomerization of 4-hydroxypyrylium cations in concentrated sulfuric acid, *J. Org. Chem.,* 49, 4523, 1984; (g) Pavlik, J. W., Spada, A.P., and Snead, T.E., Photochemistry of 4-hydroxypyrylium cations in aqueous sulfuric acid, *J. Org. Chem.,* 50, 3046, 1985.
26. West, F.G. and Koch, D.J., Novel bicyclic oxazolines via nitrile capture of photochemically generated oxyallyl zwitterions, *J. Chem. Soc., Chem. Commun.,* 1681, 1993.
27. West, F.G., Fisher, P.V., and Willoughby, C.A., The photochemistry of pyran-4-ones: intramolecular trapping of the zwitterionic intermediate with pendant hydroxyl groups, *J. Org. Chem.,* 55, 5936, 1990.
28. West, F.G., Amann, C.M., and Fisher, P.V., Intramolecular carboxylic acid trapping of pyran-4-one derived zwitterions: a novel synthesis of fused bicyclic lactones, *Tetrahedron Lett.,* 35, 9653, 1994.
29. West, F.G., Fisher, P.V., and Arif, A.M., Intramolecular alkene trapping of pyran-4-one-derived zwitterions: a novel synthesis of diquinanes and hydrindans, *J. Am. Chem. Soc.,* 115, 1595, 1993.
30. West, F.G. and Willoughby, D.W., Intramolecular arene trapping of pyran-4-one derived zwitterions: a two-step synthesis of tetrahydrobenz[*e*]inden-1-ones, *J. Org. Chem.,* 58, 3796, 1993.
31. Note that successful intramolecular trapping *was* observed when C5 was unsubstituted in the case of hydroxyl-containing and carboxyl-containing substrates **28a,b** and **30f,g** (see Scheme 8).
32. (a) West, F.G., Chase, C. E., and Arif, A.M., Intramolecular photochemical [4+4]-cycloadditions of 2-pyrones: an efficient approach to substituted cyclooctanoids, *J. Org. Chem.,* 58, 3794, 1993; (b) Chase, C.E., Bender, J.A., and West, F.G., Efficient construction of bi- and tricyclic cyclooctanoid systems via crossed [4+4]-photocycloadditions of pyran-2-ones, *Synlett,* 1173, 1996.
33. Amann, C.M., Fisher, P.V., Pugh, M.L., and West, F.G., Medium-sized carbocycles and ethers from 4-pyrones: a photocyclization-fragmentation approach, *J. Org. Chem.,* 63, 2806, 1998.
34. Fleming, M., Nucleophilic Trapping of Cross-Conjugated Dienone Derived Cyclic Oxyallyls and Their Potential Torquoselective Formation, Ph.D. dissertation, University of Utah, 2000.

84

Photoinduced Electron-Transfer Processes of Phthalimides

Michael Oelgemöller
Bayer CropScience K.K.

Axel G. Griesbeck
University of Cologne

84.1 Introduction and General Features

In terms of synthetic applications, the phthalimide system has attracted much attention over the past three decades, as noticeable by a number of summarizing reviews.[1] Although the photochemistry of phthalimide derivatives is similar to that of carbonyl compounds, it covers additional reactivity features due to the remarkably high oxidizing power of the excited singlet and triplet states. Thus, the presence of energetically feasible electron donor groups leads to the generation of radical ions that can undergo nonproductive (back) electron transfer, direct radical ion combination, or mesolytic extrusion of a suitable leaving group (e.g., a proton, silyl cation, or carbon dioxide), respectively. The competition between these processes can be controlled by varying the redox potentials, the stability of the radical cations, and the leaving group ability.

The photophysical[2] and electrochemical[3] properties of phthalimides are well documented. In acetonitrile, *N*-alkylphthalimides show relatively unstructured UV absorption spectra with absorption maxima around 235 nm (π,π^*) and 290 nm (n,π^*), respectively.[2a] In ethanol or acetonitrile at room temperature, they exhibit weak fluorescence with low quantum yields ($\Phi_f < 1 \times 10^{-3}$).[2b] In the absence of oxygen in

0-8493-1348-1/04/$0.00+$1.50

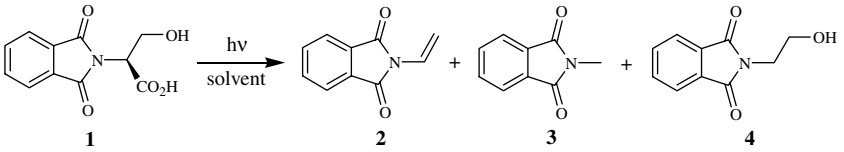

SCHEME 1

TABLE 84.1 Solvent-Dependent Photolysis of **1**: Product Composition (Normalized to 100%)[6b]

Solvent	Conversion (%)	2 (%)	3 (%)	4 (%)
Acetone	60	74	—	26
MeCN	100	83	8	9
Benzene	100	76	12	12
MeOH	100	—	38	62
Water	100	—	—	100

alcohol, *N*-alkylphthalimides show broad structureless phosphorescence centered around 450 nm with quantum yields between Φ_p = 0.4–0.7 and triplet lifetimes of τ_p = 0.7–1.04 s (at –196°C).[2a-c]

N-Methylphthalimide is reversibly reduced to the corresponding radical anion at *ca.* −1.35 V in DMF,[3a,b] and at *ca.* −1.5 V in acetonitrile (vs. SCE),[3b] respectively, but the presence of a hydrogen donor site in the side chain has a dramatic effect on the redox properties.[4] Based on the available photophysical and electrochemical data, it is possible to estimate the feasibility of a photoinduced electron transfer (PET) for various phthalimide/donor pairs. The limiting maximum oxidation potential of the electron donor thus depends on the nature of the electronically excited state of the phthalimide electron acceptor[2a] and can be estimated from the Rehm-Weller equation.[5] Thus, if the first excited singlet state is involved (E_{00} = 3.8 eV), the limiting oxidizing power for an isoenergetic electron transfer is *ca.* 2.4 V (vs. SCE). If the first excited triplet state is involved (E_{00} = 3.1 eV), the limiting oxidizing power decreases to *ca.* 1.7 V (vs. SCE). In cases where the spectroscopically nondetectable second triplet state is populated (E_{00} = 3.6 eV), the oxidizing power increases by about 500 mV.

84.2 PET Involving Oxygen as Electron Donor

Due to the decreasing oxidation potential of the oxygen atom in the groups –OH > –OCH_2R > –OCH_2TMS, PET reactions involving oxygen-bearing substituents are energetically limited to derivatives activated by α-trialkylsilyl methoxy groups. Nevertheless, the product spectra of photoreactions involving hydroxy-and dialkylether-substituted *N*-alkylphthalimides show similarities to that of the corresponding sulfur- or nitrogen-activated analogues and therefore reactions of these derivatives will be described here.

Hydroxy- and Dialkylether-Substituted *N*-Alkylphthalimides

Photochemical transformations of the hydroxy-substituted amino acids serine **1** and threonine have been described, and mechanistic outlines based on an electron or a hydrogen transfer key-step have been discussed.[6] The broad spectrum of photoproducts obtained from the C-unprotected serine derivative **1** originated from both reactive sites of the molecule: the carboxyl and the hydroxy group (Scheme 1; Table 84.1). Product **4** derived from primary α-photodecarboxylation, and further β-elimination led to the olefinic compound **2**. *N*-Methylphthalimide **3** was formed via initial extrusion of formaldehyde followed by rapid α-photodecarboxylation (*vide infra*). When this α-photodecarboxylation site was blocked, as for the corresponding methyl ester, solely retro-Aldol cleavage occurred. Although azomethine

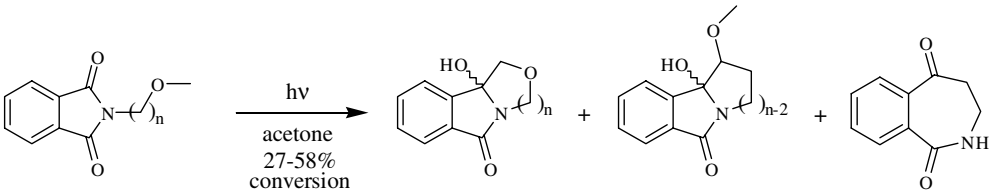

5 (n = 1-3) **6** (12%, n = 1) **7** (34%, n = 3) **8** (33%, n = 2)

SCHEME 2

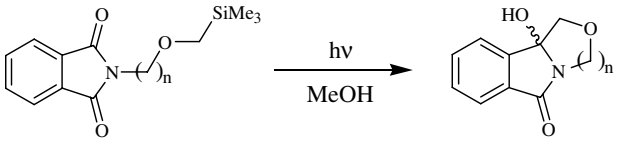

9 (n = 2-5, 8) **10** (78-99%)

SCHEME 3

ylides have been postulated as intermediates, trapping experiments with several dipolarophiles were less efficient.[6c]

Due to the high oxidation potential of dialkylethers (>2.5 V vs. SCE),[7] *N*-methoxyalkylphthalimides **5** react preferentially via homolytic C-H abstraction rather than via a PET mechanism. Whereas the carbon-hydrogen bond cleavage always occurs from the activated positions α to the ether oxygen,[8] the regioselectivity of this process (methyl vs. methylene) critically depends on the position of the oxygen atom separating the chromophore and the ether linker (Scheme 2). Hydrogen transfer occurred exclusively from the terminal methyl δ-position (resulting in product **6**) if the ether oxygen was located in the γ-position (δ and γ with respect to the carbonyl function of the phthalimide) and from the δ-methylene position (yielding the branched derivatives **7**) for substrates with the ether oxygen in the ε-position of the side chain. In the case of *N*-methoxyethylphthalimide (**5**, n = 2), which carries the ether oxygen in the δ-position, the primary photolysis product underwent immediate ring expansion and secondary Norrish Type II cleavage to give the unsubstituted benzazepinedione **8** in 33% yield.[8a]

ω-Trialkylsilylmethoxy-Substituted *N*-Alkylphthalimides

PET reactions of α-trialkylsilyl (TMS) methoxy-substituted phthalimides **9** have been developed by Yoon and Mariano (Scheme 3).[9] The introduction of the α-TMS group lowers the oxidation potential of the ether oxygen by about 500 mV[7] and, consequently, electron transfer from the heteroatom to the electronically excited phthalimide becomes energetically feasible. The incorporation of the trialkylsilyl-leaving group additionally enhances the efficiency and regioselectivity of the entire photocyclization and improves the yields and conversion rates in comparison with *N*-alkoxyalkylphthalimides **5**.[10]

The synthetic scope was further expanded to the preparation of structurally complex heterocycles and to photoaddition reactions.[11] However, limitations appeared when other potent electron donors were incorporated in the side chains, as evident for polyheteroatom-linked substrates.[12] In these cases, photoproducts arising from competing PET were also formed. Furthermore, the product composition from substrates **9** was sensitive to the solvent conditions; for example, larger amounts of silylated compounds were obtained in acetone. Even in methanol, the yields decreased significantly with increasing length of the carbon chain and simple desilylation or dimerization products were found, respectively.[10] An improvement in yield and selectivity was achieved when the terminal trimethylsilyl-group was replaced by the tributylstannyl group.[13]

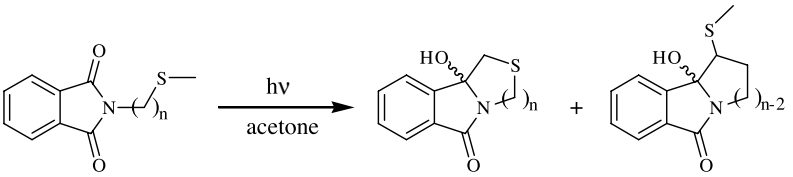

11 (n = 1-6, 8-10, 12) **12** (1-86%) **13** (3-85%)

SCHEME 4

TABLE 84.2 Photolysis of **11**: Product Composition (Isolated Yields)[15]

n	Conversion (%)	12 (%)	13 (%)	8 (%)
1	3 (in benzene)	1	—	—
2	94	47	—	6
3	100	86	—	—
4	100	—	85	—
5	100	79	6	—
6	100	60	5	—
8	89	49	3	—
9	85	29	—	—
10	90	26	4	—
12	59	25	5	—

84.3 PET Involving Sulfur as Electron Donor

Alkylthio-Substituted *N*-Alkylphthalimides

Due to the favorable low oxidation potentials of the thioether fragment (Me_2S: $E_{Ox.}$ = 1.25 V in MeCN vs. SCE),[14] alkylthio-substituted *N*-alkylphthalimides are excellent substrates for *intramolecular* PET reactions. From the acyclic phthalimide derivatives **11**,[15] the corresponding unbranched azathiacyclols **12** were formed as major products (Scheme 4; Table 84.2). The only exception was the butylene-linked substrate, which exclusively gave the branched product **13** by means of ε-CH_2 activation. Similar to its oxygen-analogue (*vide supra*), the corresponding branched cyclization product of *N*-methylthioethylphthalimide (n = 2) underwent further ring enlargement and secondary Norrish Type II cleavage to give the unsubstituted benzazepinedione **8** in 6% yield. The yields and conversion rates depended on the spacer length and vary between 25 and 86%. Solely the simplest substrate *N*-methylthiomethylphthalimide (n = 1) gave a surprisingly low yield when irradiated in benzene. Upon irradiation in acetone, cleavage of the methylthio group was found to be the dominant pathway.[15b]

Using the phthalimide/methylthioether pair, a variety of photochemical transformations resulting in medium- and macrocyclic sulfur-containing amines,[15] lactams, lactones, and crown ether analogues, respectively, with a maximum ring-size of 38 atoms have been described.[16] In most of these examples, irradiations were performed under sensitized conditions using acetone as solvent and triplet sensitizer. Cyclization is (most likely) initiated via an *intermolecular* PET involving triplet-excited acetone. In contrast to that, an *intramolecular* PET from the thioether fragment to the electronically excited chromophore has been established for direct excitation of the chromophore.[17] In both cases, the thioether fragment is oxidized to the sulfur-centered radical cation, which shows rapid mesolytic proton transfer from one of its α-CH-positions.

The undesired incorporation of the thioether group into the product ring system could be circumvented using the 1,3-dithiolanyl group as the electron donor substituent.[18a] Upon photolysis of these

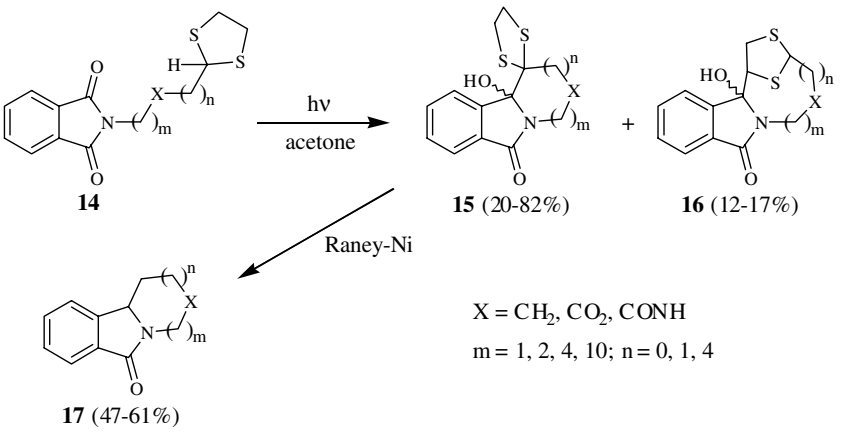

14 **15** (20-82%) **16** (12-17%) **17** (47-61%)

SCHEME 5

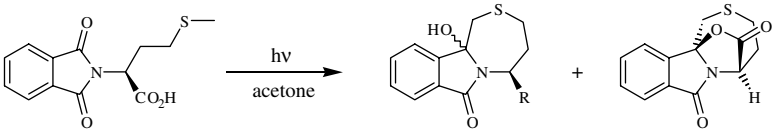

18 **19a** (15%, R = H) **19b** (5%, R = CO_2H) **20** (72%)

SCHEME 6

substrates (**14**), activation of the methine CH group dominated and the spiro-annelated thioacetals **15** were obtained as major products in moderate to good yields (Scheme 5). The corresponding sulfur-free compounds **17** were available by subsequent treatment with Raney nickel. An interesting application of this concept was described for the synthesis of aporhoeadane analogues.[18b,c]

Griesbeck and co-workers[19] further investigated PET reactions of sulfur-containing proteinogenic and non-proteinogenic amino acids and discovered an unusual solvent dependence of the product composition. Even more remarkable was the photochemical behavior of phthaloyl *L*-methionine **18**: irradiation in acetone gave the tetracyclic lactone **20** in 72% yield (Scheme 6).[19c] In this particular case, PET oxidation at sulfur proceeds faster than α-decarboxylation (*vide infra*).

The PET-induced macrocyclization of ester-linked substrates **21** was influenced by the terminal methylthioalkyl-group, and photolysis of the methylthiomethyl ester derivatives (m = 1) resulted in deprotection as an additional reaction mode (Scheme 7).[16b] Among the starting materials, only compounds derived from β-alanine or γ-aminobutyric acid gave the corresponding macrocycles **22**, whereas shorter as well as longer tethers disfavored the radical combination step and preferentially yielded the free *N*-phthaloyl amino acids **23**. Elongation of the methylthioalkyl moiety restored the cyclization efficiency and already the methylthioethyl esters (m = 2) gave the corresponding macrocycles in good yields. In some cases, however, products from hydrolysis or regioisomeric cyclization (**24**) were obtained.[16b,c]

ω-Trialkylsilylmethylthio-Substituted and Related *N*-Alkylphthalimides

Upon irradiation in methanol, ω-trialkylsilyl methylthio-substituted *N*-alkylphthalimides **25** gave the corresponding desilylated photocyclization products **26** with high regioselectivities.[9,20] Although the yields were moderate to high, the conversions were relatively low (30 to 37%), except for the largest ring system

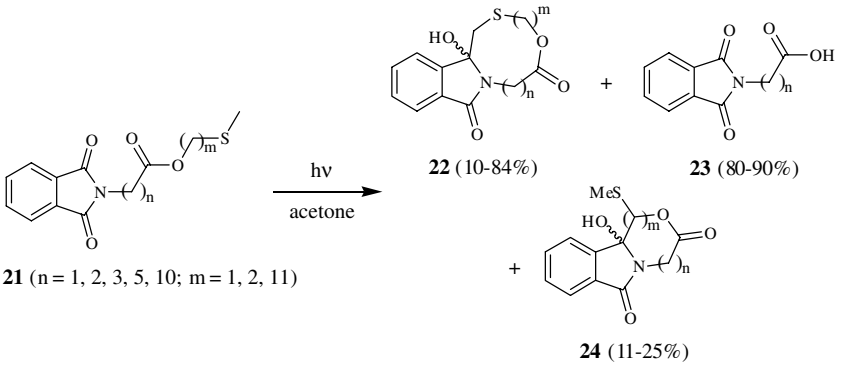

SCHEME 7

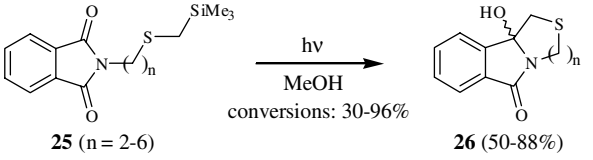

SCHEME 8

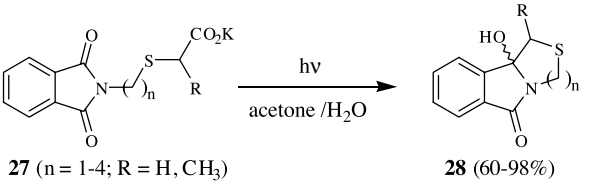

SCHEME 9

(Scheme 8). From the thioethyl-linked substrate, the benzazepinedione **8** was additionally observed as a minor product in 6% yield. In sharp contrast, silylated cyclization products were exclusively or mainly obtained when substrates **25** were irradiated in acetone, which accounts for solvent participation in the desilylation step. Conversely, the conversion rates significantly increased in acetone.

A more powerful directing and activating group for PET reactions is the carboxylate group in the α-position with respect to the thioether.[21] Thus, phthalimidoalkylsulfanyl acetates **27** were regioselectively transformed into the corresponding tricyclic ring systems **28** with high quantum yields (Φ *ca.* 0.1)[17a] and in excellent chemical yields of 60 to 98% (Scheme 9). The cyclization efficiency was drastically reduced for the free acids or for substrates with the carboxylate group in the β-position, and cyclization occurred with much lower quantum yields (Φ < 0.03).[17a]

Both α-silylthiomethoxy- (**25**) and α-carboxymethyl- (**27**) substituted derivatives showed similar photocyclization behavior when compared with α-stannylthiomethoxy-substrates where the trialkylstannyl cation serves as the leaving group.[13,22]

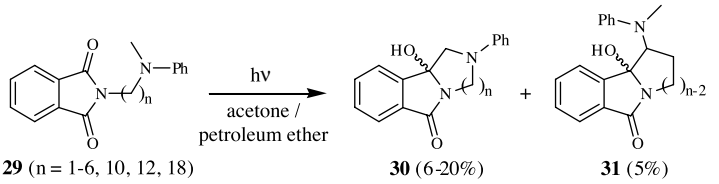

SCHEME 10

TABLE 84.3 Photolysis of **29**: Product Composition (Isolated Yields)[24a]

n	Conversion (%)	30 (%)	31 (%)
1	17	13	—
2	39	12	—
3	37	20	—
4	27	6	5
5	34	15	—
6	49	15	—
10	84	8	—
12	78	9	—
18	86	9	—

84.4 PET Involving Nitrogen as Electron Donor

Alkylamino-Substituted *N*-Alkylphthalimides

Due to the low oxidation potentials of tertiary amines (R_3N: $E_{Ox.}$ = 0.7–1.3 V vs. SCE),[14] photoinduced electron transfer reactions of aminoalkyl-substituted phthalimides are highly exergonic. On the other hand, amines are also potent hydrogen donors and, consequently, photoreductions are commonly observed side reactions, especially in *intermolecular* reactions.[11b,23]

Irradiation of the tertiary *N*-methyl, *N*-phenyl amines **29** gave the corresponding cyclization products **30** in yields of 6 to 20% (Scheme 10; Table 84.3). The regioselectivity of the mesolytic CH-activation step was pronounced, except for the case where n = 4.[24] This observation goes parallel with the thioether case (*vide supra*). The conversions were low for the precursors to medium-sized ring systems; higher conversions and yields up to 39% were obtained for dibenzylated amines.[24c]

The regioselectivity of the cyclization step was further studied with unsymmetrically substituted phthalimides and pyridinecarboximides resulting in divergent selectivity patterns.[24b] As an interesting application of the *intramolecular* photocyclization, the synthesis of tetracyclic protoberine (Scheme 11) and yohimbane skeletons was reported.[25] In both cases, PET cyclization of compounds (as **32**) was followed by Brønsted-acid catalyzed retro-Mannich reaction[25c] to give the corresponding isoquinoline derivatives **34**.

ω-Trialkylsilylmethylamino-Substituted and Related *N*-Alkylphthalimides

The synthetic disadvantages of aminoalkyl-substituted substrates (i.e., low conversion rates, regioselectivity problems) could be overcome by introduction of the α-trialkylsilyl group as a more efficient leaving group. Irradiation of the α-silylamide-linked phthalimides **35** in methanol (Scheme 12) led to efficient (Φ *ca.* 0.1 to 0.2) and high yielding production of the corresponding cyclization products **36** with conversions >80%.[26] Compared with these improvements, limitations came from the substitution pattern at nitrogen; for example,

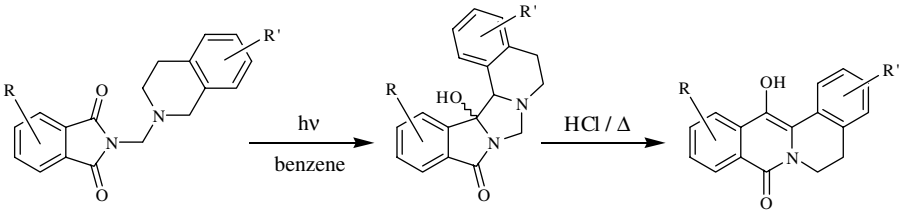

32 **33** (25-85%) **34** (28-59%)

SCHEME 11

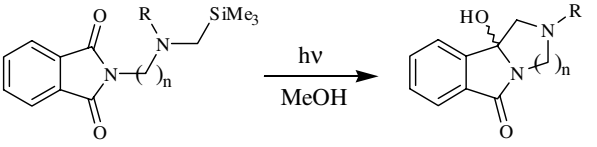

35 (n = 2-6; R = Ms, Ac) **36** (59-92%)

SCHEME 12

silylamines with n = 2 and R = Me gave larger amounts of photoreduction and C-H abstraction products and additionally showed a significant drop in the quantum yield (Φ = 0.05).[26a] When suitable amino substituents were applied, macrocyclic polyamides were efficiently synthesized following this method.[12]

The efficiencies of cyclization conducted via desilylation, decarboxylation, as well as deprotonation of various aminoethyl- and amidoethyl-linked phthalimides have been compared by Mariano and co-workers.[26b] In particular, the quantum yields for the PET-induced cyclization increased in the series H, TMS, or CO_2 as the terminal leaving group, respectively.

84.5 PET Involving the Carboxylate Group as Electron Donor

Intramolecular Decarboxylative Cyclization Reactions

N-Phthaloyl-activated α-amino acids give clean and efficient α-photodecarboxylation (PDC) when irradiated in organic solvents.[27] Griesbeck and Henz[27b] adopted this process as a straightforward route to α-monodeuterated amines by irradiation in the presence of D_2O. The α-decarboxylation is initiated by hydrogen atom abstraction and proceeds via azomethine ylide intermediates, which could be trapped by cycloaddition with suitable dipolarophiles and which were additionally observed by laser flash photolysis studies.[27c] "Remote" ω-carboxyl groups could be activated for elimination by converting them into the corresponding potassium salts and irradiation in aqueous solvents.[28] An illustrative example of this concept is the photodecarboxylation of the potassium salt of *N*-phthaloyl glutamic acid **37**: irradiation in a water/acetone mixture gave the cyclization product **39** in 89% yield (Scheme 13). In contrast, *N*-phthalimido γ-butyric acid **38** was obtained in 86% yield as the sole product when the free acid of **37** was irradiated in acetone.

Although the oxidation potentials of carboxylates are relatively high compared to other electron donor groups (e.g., acetate: $E_{Ox.}$ = 1.54 V in MeCN, 2.65 V in H_2O vs. SCE),[29] the decarboxylative cyclization proceeds very efficiently and many functional groups are tolerated. As the key step in the reaction, rapid *intramolecular* photoinduced electron transfer proceeds via the $^3\pi,\pi^*$ state or the higher excited $^3n,\pi^*$ triplet state in the nanosecond time regime.[17]

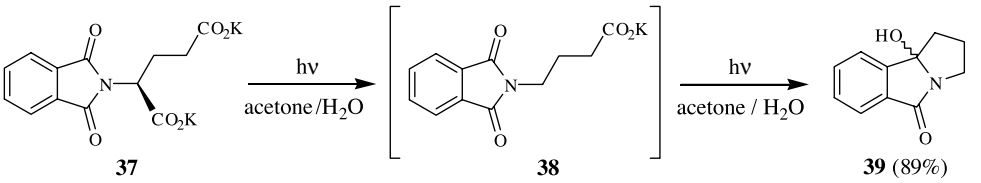

37 **38** **39** (89%)

SCHEME 13

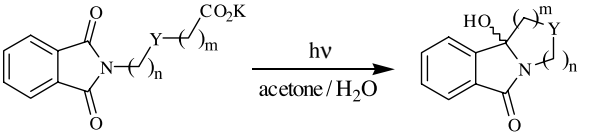

Y = CH_2, CO_2, O_2C, O, CONH, S, C≡C

SCHEME 14

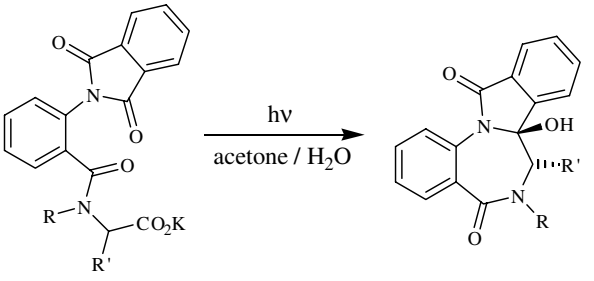

40 **41** (54-83%)

SCHEME 15

Using the decarboxylative photocyclization, the synthesis of medium- and macrocyclic amines, lactones, polyethers, lactams, as well as cycloalkynes were accessible in ring sizes up to 26 (Scheme 14)[30] and even in multigram quantities.[31] The regioselectivity of the radical cyclization step was studied for unsymmetrically substituted pyridinecarboximides and trimellitic acid imides, respectively, where the site of the C-C-bond formation is controlled by the maximum spin density of the radical anion intermediates.[32]

An interesting application (Scheme 15) was the diastereoselective synthesis of [1,4]benzodiazepines and pyrrolo[1,4]benzodiazepines (**41**).[33] The photolysis of chiral, α-amino-acid-derived substrates proceeded with high diastereoselectivity and the *trans*-diastereoisomers were formed exclusively. Additionally, for two substrates derived from proline and a proline analogue, remarkably high memory of chirality effects were determined with *ee* values of 86% and >98%, respectively.

Exchange of the terminal amino acid in substrates **40** by β-, γ- or δ-amino acids led to a significant decrease in the cyclization efficiency, and other processes such as photoinduced decomposition became relevant.[33c] On replacement of the *ortho*-phenylene linker by the conformationally more flexible ethylene linker, memory of chirality vanished and a mixture of stereoisomeric products was obtained.[33d]

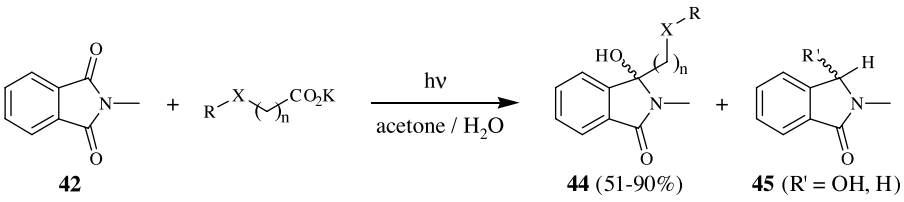

42 **44** (51-90%) **45** (R' = OH, H)

SCHEME 16

TABLE 84.4 Photolysis of **42** in the Presence of **43**: Product Composition (Isolated Yields)[34c]

X	n	R	**44** (%)	**45** (%)
S	1	Me	90	—
S	1	Ph	57	—
S	2	Me	—	—
O	1	Me	57	—
O	1	2,4-Cl_2Ph	76	—
O	2	Me	51	—
O	1	H	57	<5 (OH)
NMe	1	Me	—	21 (H)
NMe	2	Me	—	57 (H)

Intermolecular Decarboxylative Addition Reactions

The photodecarboxylation also took place in its *intermolecular* mode and efficient photochemical additions of carboxylates, α-keto carboxylates, and heteroatom-substituted carboxylates to phthalimides were reported.[34] The photoaddition proceeded with high chemoselectivity solely at the imide carbonyl group when *N*-phthaloyl amino acid esters were used as starting materials and products arising from *intramolecular* hydrogen abstractions were not observed. The influence of additional heteroatoms in the alkylcarboxylate was a function of the respective electron donor capacity[14] and either strongly increased or decreased the addition efficiency. α-Thioalkyl and α-oxoalkyl-substituted carboxylates **43** led to the corresponding addition products **44** in moderate to good yields of 57 to 90%. In contrast, the β-thioalkyl-substituted carboxylate was inert under the reaction conditions, whereas the corresponding β-oxoalkyl carboxylate reacted efficiently to give the addition product in 51% yield (Scheme 16; Table 84.4). From a comparison of the sulfur- and the oxygen-substituted carboxylates, it was concluded that oxidation of the heteroatom plays the dominant role for thioethers. In the case of the β-thioalkyl substrate and in contrast to the *intramolecular* version (*vide supra*), the sulfur atom acts as a hole trap (fast nonproductive back electron transfer)[14,35] and prevents oxidation of the carboxylate. The alkylamino-substituted carboxylates underwent photoreduction exclusively to give products **45**. For the trimethylamine equivalent (**43**, R = Me, X = NMe, n = 1), radical combination with the solvent acetone was additionally observed.[34c]

The products from the irradiation of phthalimides in the presence of α-keto carboxylates **46** included alkylation, acylation, and ring expansion, respectively, depending on the substitution pattern of the α-keto carboxylate (Scheme 17).[34b] Glyoxylate as well as secondary and tertiary α-keto carboxylates gave the corresponding reduction or alkylation products **47** in yields of 52 to 86%, whereas pyruvate and α-keto-leucine gave dihydroisoquinolinyl esters **49** as ring-expansion products in yields of 40 to 53%. In the latter case, the acylated product **48** was additionally found in 43% yield.

The course of the reaction is controlled by the stability of the acyl radical intermediates.[36] When less reactive acyl radicals are generated, C–C-bond formation could successfully compete with decarbonylation, whereas, in the case of more reactive acyl radicals, decarbonylation preceded C–C-bond formation.

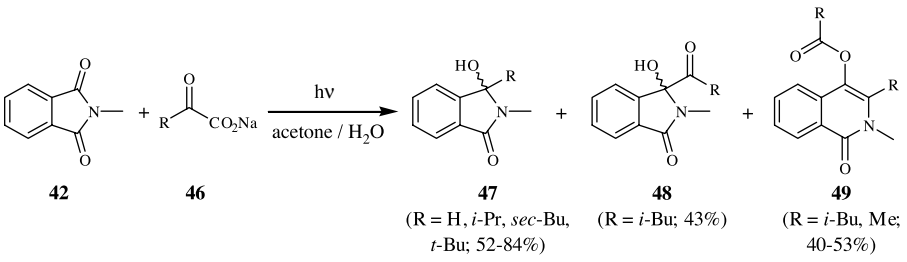

SCHEME 17

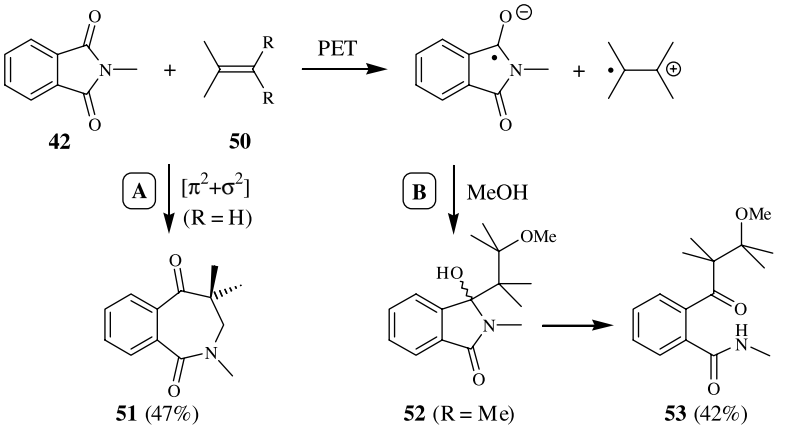

SCHEME 18

The unusual ring-expansion products **49** most reasonably originate from the monoacylated compounds **48** via rearrangement to the corresponding isomeric isoquinolines.

84.6 PET Involving Electron-Rich Alkenes and Arenes

Electron-Rich Alkenes

The progress of *intra-* and *intermolecular* photoreactions of phthalimides and alkenes **50** is essentially dictated by the thermodynamics of the electron-transfer step.[37] In cases where this electron transfer is endergonic with ΔG_{ET} >5 kcal/mol, $[\pi^2+\sigma^2]$-addition reactions to benzazepinediones **51** take place (Scheme 18; path A). If the electron transfer becomes more and more exergonic, electron transfer starts to dominate. In the presence of suitable nucleophiles (e.g., when alcohols were used as solvents), the intermediate radical ionic pair that is formed is trapped in an *anti*-Markovnikov fashion (Scheme 18; path B). The efficiency of this trapping reaction depends on the polarity as well as the nucleophilicity of the solvent.[38] In the absence of nucleophiles or suitable trapping agents, back electron transfer, regenerating the starting materials, efficiently competes with proton transfer and radical combination.[37] In cases where the electron transfer is only slightly endergonic, both pathways can compete and mixtures of the $[\pi^2+\sigma^2]$-addition and PET products are obtained.

An interesting variation of these PET reactions is the photochemical phthalimidation of inactivated double bonds using the phthalimide anion as trapping agent (Scheme 19).[39a] The reaction can be controlled by variation of the anion concentration: at higher NaOH concentration, $[\pi^2+\sigma^2]$-addition was

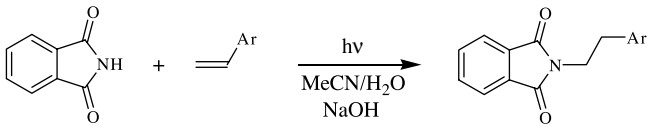

54 **55** (30-90%)

SCHEME 19

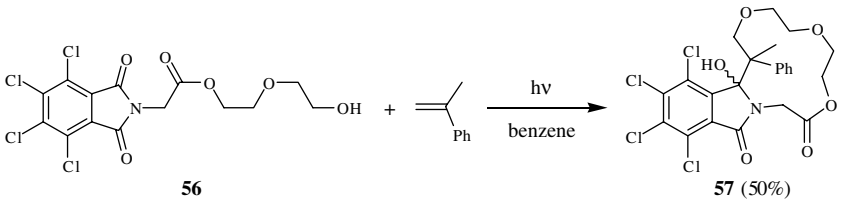

56 **57** (50%)

SCHEME 20

the sole process observed,[39b,c] whereas efficient phthalimidation to give **55** occurred at low NaOH concentrations, respectively. In the latter case, the phthalimide anion itself acts as a nucleophile and traps the olefin radical cation intermediate.

Various examples of similar *intramolecular* photocyclizations have been reported.[40] Recently, Xue and co-workers[41] described macrocyclization reactions using tetrachlorophthalimides with remote hydroxyalkyl substituents (**56**) in the presence of alkenes. During photolysis in benzene, the alkene radical cation intermediate was trapped by the terminal hydroxy function, followed by an *intramolecular* radical–radical combination to give macrocyclic lactones (e.g., **57** in 50% yield [Scheme 20]).

Electron-Rich Arenes

Toluene derivatives add to electronically excited phthalimides to give the corresponding addition products in poor to moderate yields of 5 to 35%.[23,42] A primary hydrogen abstraction from the benzylic position or, alternatively, electron transfer pathways were postulated. The efficiency via the electron-transfer route could be significantly enhanced for cyano-substituted phthalimides **58** as the electron-transfer step became more exergonic. Most remarkably, substitution of the cyano group was observed beside addition to the carbonyl-position when diphenylmethane (**59**; R′ = Ph) was used as the toluene derivative (Scheme 21).[42] The latter process was rationalized on the basis of an *in-cage* vs. *out-of-cage* scenario.

PET cyclizations of substituted *N*-arylalkylphthalimides have been studied, and the efficiency of the cyclization (yields between 11 and 47%) strongly depended on the linking carbon chain separating the electron acceptor and electron donor.[43] Griesbeck and co-workers[6b,44] recently applied this PET reaction to aromatic amino acid derivatives as an efficient route to benzazepinediones **63**. The PET reactivity was pronounced for the DOPA derivatives **62** and cyclization occurred with high yields (Scheme 22). Most remarkably, even the free acid underwent exclusive photocyclization in acetone and no α-decarboxylation was observed (*vide supra*).[27]

Another solvent dependent *intermolecular* addition reaction involving phenylcyclopropane (**64**) as the electron donor was recently reported.[45] Irradiation of *N*-methylphthalimide **42** in acetonitrile in the presence of **64** afforded a 1:1 mixture of isomeric *spiro*-tetrahydrofuranyl lactams **65** in 22% yield. An *intramolecular* version of this PET reaction has also been described.[45c] When the photolysis was performed in methanol, solvent-incorporated addition to produce **66** took place (Scheme 23).

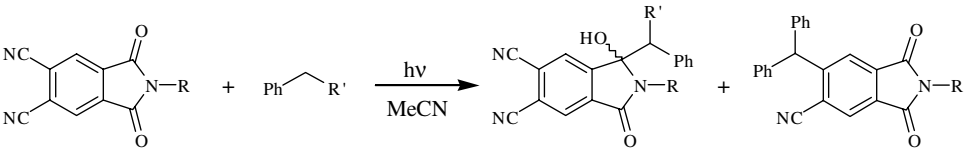

58 (R = H, CH_3) **59** (R' = H, Ph) **60** (14-50%) **61** (R' = Ph; 70-79%)

SCHEME 21

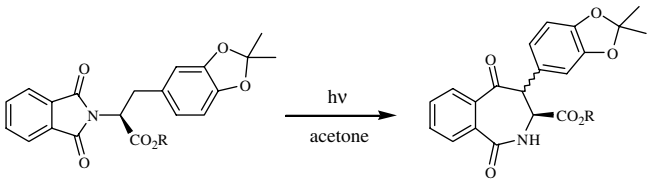

62 (R = H, Me) **63** (58-65%)

SCHEME 22

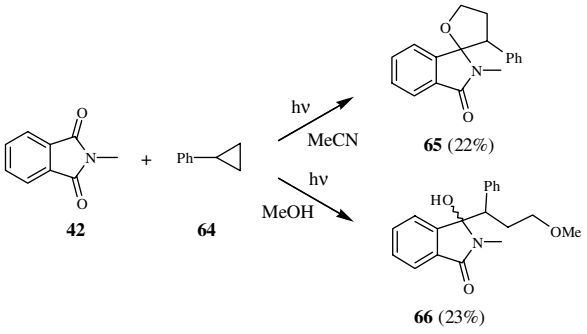

42 **64** **65** (22%) **66** (23%)

SCHEME 23

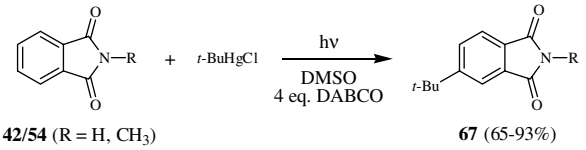

42/54 (R = H, CH_3) **67** (65-93%)

SCHEME 24

84.7 Miscellaneous Reactions

A base-promoted *t*-butylation of the aromatic ring of phthalimides involving a thermal electron-transfer step was developed by Russell and co-workers.[46a] This radical chain reaction is initiated by photochemical cleavage of alkylmercury halides, leading to *t*-butyl radicals that add to the aromatic ring in a highly regioselective fashion (Scheme 24). The yields of the corresponding alkylated phthalimides **67** were

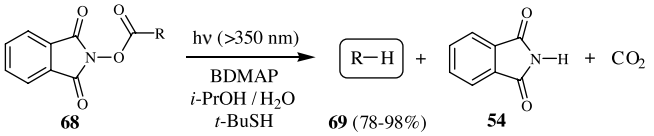

68 **69** (78-98%) **54**

SCHEME 25

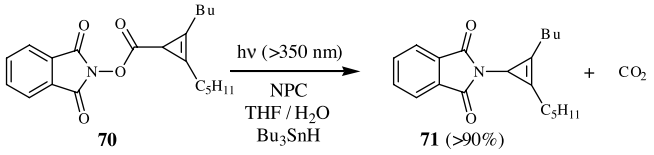

70 **71** (>90%)

SCHEME 26

generally high. A similar reaction has been described for 1-iodoadamantane and the phthalimide anion.[46b] In this case, however, the regioselectivity decreased and, additionally, a larger amount of adamantane was isolated.

Okada and Oda[47] described an efficient method for PET-induced decarboxylation of non-activated carboxylic acids. When irradiated as the corresponding *N*-acyloxyphthalimide derivatives **68** in the presence of 1,6-bis(dimethylamino)pyrene (BDMAP) as sensitizer and *t*-BuSH as hydrogen donor, the corresponding alkanes **69** were obtained in high to excellent yields of 78 to 98% (Scheme 25). The reaction could also be performed with visible light when a $Ru(bpy)_3Cl_2$/1-benzyl-1,4-dihydronicotinamide (BNAH) combination was used.[47b]

An unusual and high yielding formation of *N*-(2-cyclopropenyl)phthalimides **71** via this photosensitized decarboxylation method was reported (Scheme 26).[48] The intermediacy of cyclopropenyl radicals was confirmed by a trapping reaction with 5,5-dimethyl-1-pyrroline-*N*-oxide and also by ESR spectroscopy.[48b] Most reasonably, the carboxyl radical of this cyclopropenyl radical intermediate undergoes rapid decarboxylation followed by initial trapping by the phthalimidyl radical within the solvent cage.

References

1. (a) Kanaoka, Y., Organic photochemistry of imides, *J. Synth. Org. Chem.*, 33, 949, 1975; (b) Kanaoka, Y., Photoreactions of cyclic imides. Examples of synthetic organic photochemistry, *Acc. Chem. Res.*, 11, 407, 1978; (c) Coyle, J.D., Phthalimide and its derivatives, in *Synthetic Organic Photochemistry*, Horspool, W.M., Ed., Plenum Press, New York, 1984, 259; (d) Mazzocchi, P.H., The photochemistry of imides, in *Organic Photochemistry*, Vol. 5, Padwa, A., Ed., Marcel Dekker, New York, 1981, 421; (e) Griesbeck, A.G. and Mauder, H., Electron transfer processes in phthalimide systems, in *CRC Handbook of Organic Photochemistry and Photobiology*, Horspool, W.M. and Song, P.S., Eds., CRC Press, Boca Raton, FL, 1995, 513; (f) Oelgemöller, M. and Griesbeck, A.G., Photoinduced electron transfer chemistry of phthalimides: an efficient tool for C-C bond formation, *J. Photochem. Photobiol. C: Photochem. Rev.*, 3, 109, 2002.
2. (a) Wintgens, V., Valat, P., Kossanyi, J., Biczok, L., Demeter, A., and Bérces, T., Spectroscopic properties of aromatic dicarboximides, *J. Chem. Soc., Faraday Trans.*, 90, 411, 1994; (b) Griesbeck, A.G. and Görner, H., Laser flash photolysis study of *N*-alkyl phthalimides, *J. Photochem. Photobiol. A: Chem.*, 129, 111, 1999; (c) Hayashi, H., Nagakura, S., Kubo, Y., and Maruyama, K., Mechanistic studies of photochemical reactions of *N*-ethylphthalimide with olefins, *Chem. Phys. Lett.*, 72, 291, 1980; (d) Coyle, J.D., Harriman, A., and Newport, G.L., Reversible photorearrangement of *N*-substituted

phthalimides: a flash photolysis study, *J. Chem. Soc., Perkin Trans. 2*, 799, 1979; (e) Filho, P.B., Toscano, V.G., and Politi, M.J., Solvent induced changes in the photophysical properties of *N*-alkylphthalimides, *J. Photochem. Photobiol. A: Chem.*, 43, 51, 1988; *J. Photochem. Photobiol. A: Chem.*, 45, 265, 1988.

3. (a) Leedy, D.W. and Muck, D.L., Cathodic reduction of phthalimide systems in nonaqueous solutions, *J. Am. Chem. Soc.*, 93, 4264, 1971; (b) Farnia, G., Romanin, A., Capobianco, G., and Torzo, F., Electrochemical reduction mechanism of phthalimide and some of its *N*-derivatives in DMF, *J. Electroanal. Chem.*, 33, 31, 1971; (c) Capobianco, G., Farnia, G., and Torzo, F., Electrochemical reduction mechanism of phthalylglycine in DMF, *Ric. Sci.*, 38, 842, 1968.
4. (a) Oelgemöller, M., Griesbeck, A.G., Lex, J., Haeuseler, A., Schmittel, M., Niki, M., Hesek, D., and Inoue, Y., Structural, CV and IR spectroscopic evidences of preorientation in PET-active phthalimido carboxylic acids, *Org. Lett.*, 3, 1593, 2001; (b) Oelgemöller, M., Haeuseler, A., Schmittel, M., Griesbeck, A.G., Lex, J., and Inoue, Y., Hydrogen bonding in phthalimido carboxylic acids: voltammetric study and correlation with photochemical reactivity, *J. Chem. Soc., Perkin Trans. 2*, 676, 2002.
5. Rehm, D. and Weller, A., Kinetics of fluorescence quenching by electron and H-atom transfer, *Isr. J. Chem.*, 8, 259, 1970.
6. (a) Yoon, U.C., Kim, D.U., Lee, C.W., Choi, Y.S., Lee, Y.-J., Ammon, H.L., and Mariano, P.S., Novel and efficient azomethine ylide forming photoreactions of *N*-(silylmethyl)phthalimides and related acid and alcohol derivatives, *J. Am. Chem. Soc.*, 117, 2698, 1995; (b) Griesbeck, A.G., Henz, A., Hirt, J., Ptatschek, V., Engel, T., Löffler, D., and Schneider, F.W., Photochemistry of *N*-phthaloyl derivatives of electron-donor-substituted amino acids, *Tetrahedron*, 50, 701, 1994; (c) Yoon, U.C., Lee, C.W., Oh, S.W., and Mariano, P.S., Exploratory studies probing the intermediacy of azomethine ylides in the photochemistry of *N*-phthaloyl derivatives of α-amino acids and β-amino alcohols, *Tetrahedron*, 55, 11997, 1999.
7. Gutenberger, G., Meggers, E., and Steckhan, E., The generation of hydroxymethyl radicals. Photoinduced electron transfer as opposed to electrochemical electron transfer, in *Novel Trends in Electroorganic Synthesis*, Torii, S., Ed., Springer, Tokyo, 1998, 367.
8. (a) Sato, Y., Nakai, H., Wada, M., Ogiwara, H., Mizoguchi, T., Migita, Y., Hatanaka, Y., and Kanaoka, Y., Photocyclization of *N*-alkoxyalkylphthalimides with favored δ-hydrogen abstraction, *Chem. Pharm. Bull.*, 30, 1639, 1982; (b) Kanaoka, Y., Migita, Y., Sato, Y., and Nakai, H., Photochemistry of the phthalimide system. III. Photocyclization with favored δ-hydrogen abstraction, *Tetrahedron Lett.*, 51, 1973.
9. Yoon, U.C. and Mariano, P.S., The synthetic potential of phthalimide SET photochemistry, *Acc. Chem. Res.*, 34, 523, 2001.
10. (a) Yoon, U.C., Oh, J.H., Lee, S.J., Kim, D.U., Lee, J.G., Kang, K.T., and Mariano, P.S., Photocyclization reactions of *N*-(trimethylsilylmethoxyalkyl)-phthalimides. Efficient and regioselective route to heterocycles, *Bull. Korean Chem. Soc.*, 13, 166, 1992; (b) Yoon, U.C., Cho, S.J., Oh, J.H., Lee, J.G., Kang, K.T., and Mariano, P.S., Photocyclization reactions of phthalimide-α-silyl-n-electron donor systems via singlet single electron transfer and triplet hydrogen abstraction and silyl group abstraction pathways, *Bull. Korean Chem. Soc.*, 12, 241, 1991.
11. (a) Yoon, U.C., Oh, S.W., and Lee, C.W., Efficient and regioselective photocyclization reactions of *N*-[(ω-trimethylsilylmethoxy)polyoxalkyl]phthalimides to azacrown ethers, *Heterocycles*, 41, 2665, 1995; (b) Yoon, U.C., Kim, H.J., and Mariano, P.S., Electron transfer-induced photochemical reactions in imide-$RXCH_2TMS$ systems. Photoaddition of α-trimethylsilyl substituted heteroatom-containing compounds to phthalimides, *Heterocycles*, 29, 1041, 1989.
12. Yoon, U.C., Oh, S.W., Lee, J.H., Park, J.H., Kang, K.T., and Mariano, P.S., Applications of phthalimide photochemistry to macrocyclic polyether, polythioether and polyamide synthesis, *J. Org. Chem.*, 66, 939, 2001.
13. Yoon, U.C., Jin, Y.X., Oh, S.W., Cho, D.W., Park, K. H., and Mariano, P.S., Comparison of photomacrocyclization reactions of trimethylsilyl- and tributylstannyl-terminated phthalimido- and maleimido-polyethers, *J. Photochem. Photobiol. A: Chem.*, 150, 77, 2002.

14. Pienta, N.J., Amines, thiols and thioethers: heteroatomic electron donors, in *Photoinduced Electron Transfer*, Fox, M.A. and Chanon, M., Eds., Elsevier, Amsterdam, 1988, 421.
15. (a) Hatanaka, Y., Sato, Y., Nakai, H., Wada, M., Mizoguchi, T., and Kanaoka, Y., Regioselective remote photocyclization: examples of a photochemical macrocyclic synthesis with sulfide-containing phthalimides, *Liebigs Ann. Chem.*, 1113, 1992; (b) Sato, Y., Nakai, H., Wada, M., Mizoguchi, T., Hatanaka, Y., Migata, Y., and Kanaoka, Y., Thiazacycloalkanols by photocyclization of S-substituted *N*-(thioalkyl) phthalimides, *Liebigs Ann. Chem.*, 1099, 1985.
16. (a) Sato, Y., Nakai, H., Wada, M., Mizoguchi, T., Hatanaka, Y., and Kanaoka, Y., Application of remote photocyclization with a pair system of phthalimide and methylthio groups. A photochemical synthesis of cyclic peptide models, *Chem. Pharm. Bull.*, 40, 3174, 1992; (b) Griesbeck, A.G., Oelgemöller, M., and Lex, J., Photochemistry of MTM- and MTE-esters of ω-phthalimido carboxylic acids: macrocyclization versus deprotection, *J. Org. Chem.*, 65, 9028, 2000; (c) Wada, M., Nakai, H., Aoe, K., Kotera, K., Sato, Y., Hatanaka, Y., and Kanaoka, Y., Application of the remote photocyclization with a pair system of phthalimide and methylthio groups. A photochemical synthesis of macrolide models, *Tetrahedron*, 39, 1273, 1983; (d) Wada, M., Nakai, H., Sato, Y., Hatanaka, Y., and Kanaoka, Y., Application of the remote photocyclization with a pair system of phthalimide and methylthio groups. A photochemical synthesis of crown ether analogs, *Chem. Pharm. Bull.*, 31, 429, 1983.
17. (a) Görner, H., Oelgemöller, M., and Griesbeck, A.G., Photodecarboxylation study of carboxy-substituted *N*-alkylphthalimides in aqueous solution: time resolved UV-Vis spectroscopy and conductometry, *J. Phys. Chem. A*, 106, 1458, 2002; (b) Görner, H., Griesbeck, A.G., Heinrich, T., Kramer, W., and Oelgemöller, M., Time-resolved spectroscopy of sulfur- and carboxy-substituted *N*-alkylphthalimides, *Chem.-Eur. J.*, 7, 1530, 2001.
18. (a) Wada, M., Nakai, H., Sato, Y., and Kanaoka, Y., A removable functional group in a photochemical macrocyclic synthesis. Remote photocyclization with a pair system of phthalimide and 1,3-dithiolanyl groups, *Chem. Pharm. Bull.*, 30, 3414, 1982; (b) Kessar, S. V., Singh, T., and Vohra, R., An interesting application of the photocyclization in aporhoeadane alkaloid synthesis, *Tetrahedron Lett.*, 28, 5323, 1987; (c) alternative approach: Mazzocchi, P.H., King, C.R., and Ammon, H.L., A photochemical approach to the fully functionalized ring system of chilinene, a key alkaloid of the berberine family, *Tetrahedron Lett.*, 28, 2473, 1987.
19. (a) Griesbeck, A.G., Hirt, J., Kramer, W., and Dallakian, P., Photochemistry of phthaloylcysteine, its methyl ester and C-unprotected S-alkyl derivatives, *Tetrahedron*, 54, 3169, 1998; (b) Griesbeck, A.G., Hirt, J., Peters, K., Peters, E.-M., and von Schnering, H.G., Photochemistry of *N*-phthaloylcysteine derivatives: multiplicity-directed regioselective CH activation, *Chem.-Eur. J.*, 2, 1388, 1996; (c) Griesbeck, A.G., Mauder, H., and Müller, I., Photochemistry of *N*-phthaloyl derivatives of methionine, *Tetrahedron Lett.*, 34, 453, 1993.
20. Yoon, U.C., Lee, S.J., Lee, K.J., Cho, S.J., Lee, C.W., and Mariano, P.S., Exploratory study of photocyclization reactions of *N*-(trimethylsilylmethylthioalkyl) phthalimides, *Bull. Korean Chem. Soc.*, 15, 154, 1994.
21. Griesbeck, A.G., Oelgemöller, M., Lex, J., Haeuseler, A., and Schmittel, M., Synthesis of sulfur-containing tricyclic ring systems by means of photoinduced decarboxylative cyclizations, *Eur. J. Org. Chem.*, 1831, 2001.
22. (a) Ikeno, T., Harada, M., Arai, N., and Narasaka, K., Generation of α-alkylthio radicals by photoinduced one-electron oxidation of α-stannyl sulfides and their use for carbon-carbon bond formation, *Chem. Lett.*, 169, 1997; (b) Mikami, T., Harada, M., and Narasaka, K., Photochemical generation of radical species from α-stannyl ethers and their reaction with conjugated enones, *Chem. Lett.*, 425, 1999.
23. Kanaoka, Y., Sakai, K., Murata, R., and Hatanaka, Y., Photoaddition reactions of *N*-methylphthalimide with toluenes and amines, *Heterocycles*, 3, 719, 1975.
24. (a) Machida, M., Takechi, H. and Kanaoka, Y., Photocyclization of ω-anilinoalkylphthalimides: a photochemical macrocyclic synthesis, *Chem. Pharm. Bull.*, 30, 1579, 1982; (b) Coyle, J.D., Smart,

L.E., Challiner, J.F., and Haws, E.J., Photocyclization of *N*-(dialkylaminoalkyl) aromatic 1,2-dicarboximides. X-ray molecular structure of a stereoisomer of 4-benzyl-2-hydroxy-3-phenyl-4,6-diazatricyclo[6.4.0.$0^{2,6}$]dodeca-1(12),8,10-trien-7-one, *J. Chem. Soc., Perkin Trans. 1*, 121, 1985; (c) Coyle, J.D. and Newport, G.L., Fused imidazolidines, hexahydropyrazines and hexahydro-1,4-diazepines, *Synthesis*, 381, 1979.

25. (a) Coyle, J.D., Bryant, L.R.B., Cragg, J.E., Challiner, J.F., and Haws, E.J., A photochemical route to the protoberberine skeleton, *J. Chem. Soc., Perkin Trans. 1*, 1177, 1985; (b) Coyle, J.D. and Patel, P., A photochemical route to the yohimbane skeleton, *J. Chem. Research (S)*, 102, 1985; (c) Close, M., Coyle, J.D., Haws, E.J., and Perry, C.J., The reaction of ω-hydroxylactams obtained from the photocyclisation of dicarboximide Mannich base: a route to substituted imidazoles, *J. Chem. Research (S)*, 115, 1997; *J. Chem. Research (M)*, 701, 1997.
26. (a) Yoon, U.C., Kim, J.W., Ryu, J.Y., Cho, S.J., Oh, S.W., and Mariano, P.S., Single electron transfer-induced photocyclization reactions of *N*-[(*N*-trimethylsilylmethyl)aminoalkyl]phthalimides, *J. Photochem. Photobiol. A: Chem.*, 106, 145, 1997; (b) Su, Z., Mariano, P.S., Faley, D.E., Yoon, U.C., and Oh, S.W., Dynamics of anilinium radical α-heterolytic fragmentation processes. Elecrofugal group, substituent and medium effects on desilylation, decarboxylation and retro-Aldol cleavage pathways, *J. Am. Chem. Soc.*, 120, 10676, 1998.
27. (a) Sato, Y., Nakai, H., Mizoguchi, T., Kawanishi, M., Hatanaka, Y., and Kanaoka, Y., Photodecarboxylation of *N*-phthaloyl-α-amino acids, *Chem. Pharm. Bull.*, 30, 1262, 1982; (b) Griesbeck, A.G. and Henz, A., Synthesis of α-[^{2}H]-amines via photodecarboxylation of *N*-phthaloyl α-amino acids, *Synlett*, 931, 1994; (c) Takahashi, Y., Miyashi, T., Yoon, U.C., Oh, S.W., Mancheno, M., Su, Z., Falvey, D.F., and Mariano, P.S., Mechanistic studies of the azomethine ylide-forming photoreactions of *N*-(silylmethyl)phthalimides and *N*-phthaloylglycine, *J. Am. Chem. Soc.*, 121, 3926, 1999.
28. (a) Griesbeck, A.G., Kramer, W., and Oelgemöller, M., Synthetic applications of photoinduced electron transfer decarboxylation reactions, *Synlett*, 1169, 1999; (b) Griesbeck, A.G., Henz, A., Peters, K., Peters, E.-M., and von Schnering, H.G., Photo electron transfer induced macrocyclization of *N*-phthaloyl-ω-amino-carboxylic acids, *Angew. Chem. Int. Ed. Engl.*, 34, 474, 1995.
29. Eberson, L., in *Electron Transfer Reactions in Organic Chemistry (Reactivity and Structure-Concepts in Organic Chemistry)*, Vol. 25, Hafner, K., Ed., Springer-Verlag, Berlin, 1987.
30. (a) Griesbeck, A.G., Henz, A., Kramer, W., Lex, J., Nerowski, F., Oelgemöller, M., Peters, K., and Peters, E.-M., Synthesis of medium- and large-ring compounds initiated by photochemical decarboxylation of ω-phthalimidoalkanoates, *Helv. Chim. Acta*, 80, 912, 1997; (b) Griesbeck, A.G., Nerowski, F., and Lex, J., Decarboxylative photocyclization: synthesis of benzopyrrolizidines and macrocyclic lactones, *J. Org. Chem.*, 64, 5213, 1999; (c) Bartoschek, A., Griesbeck, A.G., and Oelgemöller, M., Photoinduced electron transfer reactions of phthalimides, *J. Inf. Rec.*, 25, 119, 2000; (d) Yoo, D.J., Kim, E.Y., Oelgemöller, M., and Shim, S.C., Synthesis of a macroheterocyclic compound through photodecarboxylation of potassium ω-phthalimidoalkynoate, *Heterocycles*, 54, 1049, 2001.
31. Griesbeck, A.G., Kramer, W., and Oelgemöller, M., Photoinduced decarboxylation reactions. Radical chemistry in water, *Green Chem.*, 1, 205, 1999.
32. Griesbeck, A.G., Gudipati, M.S., Hirt, J., Lex, J., Oelgemöller, M., Schmickler, H., and Schouren, F., Photoinduced electron-transfer reactions with quinolinic and trimellitic acid imides: experimental and spin density calculations, *J. Org. Chem.*, 65, 7151, 2000.
33. (a) Griesbeck, A.G., Kramer, W., and Lex, J., Diastereo- and enantioselective synthesis of pyrrolo[1,4]benzodiazepines through decarboxylative photocyclization, *Angew. Chem. Int. Ed. Engl.*, 40, 577, 2001; (b) Griesbeck, A.G., Kramer, W., and Lex, J., Stereoselective synthesis of 1,4-benzodiazepins via photoinduced decarboxylation of *N*-phthaloylanthranilic acid amides, *Synthesis*, 1159, 2001; (c) Griesbeck, A.G., Kramer, W., Heinrich, T., and Lex, J., Photocyclization of *N*,*N*-phthaloylanthranilic amides coupled to ω-amino acids with increasing chain lengths, *Photochem. Photobiol. Sci.*, 1, 237, 2002; (d) Griesbeck, A.G., Kramer, W., Bartoschek, A., and Schmickler, H., Photocyclization of 2-azabicyclo[3.3.0]octane-3-carboxylate derivatives: induced and noninduced diastereoselectivity, *Org. Lett.*, 3, 537, 2001.

34. (a) Griesbeck, A.G. and Oelgemöller, M., Photodecarboxylative addition of carboxylates and α-keto carboxylates to phthalimides, *Synlett*, 492, 1999; (b) Griesbeck, A.G., Oelgemöller, M., and Lex, J., Photodecarboxylative additions of α-keto carboxylates to phthalimides: alkylation, acylation and ring expansion, *Synlett*, 1455, 2000; (c) Griesbeck, A.G., and Oelgemöller, M., Decarboxylative photoadditions of heteroatom-substituted carboxylates to phthalimides, *Synlett*, 71, 2000.
35. Fox, M.A., Photoinduced electron transfer in organic systems: control of back electron transfer, *Adv. Photochem.*, 13, 237, 1986.
36. (a) Chatgilialoglu, C., Crich, D., Komatsu, M., and Ryu, I., Chemistry of acyl radicals, *Chem. Rev.*, 99, 1991, 1999; (b) Caronna, T. and Minisci, F., The chemistry of acyl radicals, *Rev. React. Species Chem.*, 1, 263, 1976.
37. (a) Mazzocchi, P.H., Minamikawa, S., and Wilson, P., Competitive photochemical $\sigma^2+\pi^2$ addition and electron transfer in the *N*-methylphthalimide-alkene system, *J. Org. Chem.*, 50, 2681, 1985; (b) Mazzocchi, P.H. and Klinger, L., Photoreduction of *N*-methylphthalimide with 2,3-dimethyl-2-butene. Evidence for reaction through an electron transfer generated ion pair, *J. Am. Chem. Soc.*, 106, 7567, 1984; (c) Maruyama, K. and Kubo, Y., Photochemistry of phthalimides with olefins. Solvent-incorporated addition vs. cycloaddition to imide C(=O)-N bond accompanying ring enlargement, *J. Org. Chem.*, 50, 1426, 1985.
38. (a) Mazzocchi, P.H., Shook, D., and Liu, L., The importance of alcohol nucleophilicity in the trapping of the photochemically generated radical ion pair from *N*-methylphthalimide and α-methylstyrene, *Heterocycles*, 26, 1165, 1987; (b) Maruyama, K. and Kubo, Y., Photo-induced solvent-incorporated addition of *N*-methylphthalimide to olefins. Reactions promoted by way of initial one electron transfer, *Chem. Lett.*, 851, 1978.
39. (a) Suau, R., García-Segura, R., Sánchez, C., and Pedraza, A.M., Photophthalimidation of unactivated double bonds. Synthesis of protected phenethylamines, *Tetrahedron Lett.*, 29, 1071, 1988; (b) Suau, R. and García-Segura, R., Photochemical addition of alkenes and alcohols to sodium phthalimide, *Tetrahedron Lett.*, 29, 1071, 1988; (c) Suau, R., Sánchez-Sánchez, C., García-Segura, R., and Pérez-Inestrosa, E., Photocycloaddition of phthalimide anion to alkenes — a highly efficient, convergent method for [2]benzazepine synthesis, *Eur. J. Org. Chem.*, 1903, 2002.
40. (a) Maruyama, K., Ogawa, T., Kubo, Y., and Araki, T., Photochemistry of *N*-alk-4-enyl- and *N*-alk-5-enyl-phthalimides: two different types of cyclization reaction, *J. Chem. Soc., Perkin Trans. 1*, 2025, 1985; (b) Machida, M., Oda, K., and Kanaoka, Y., Photocyclization of *N*-[ω-(cycloalken-1-yl)alkyl]- and *N*-[ω-(inden-3-yl)alkyl]phthalimides, *Tetrahedron*, 41, 4995, 1985; (c) Mazzocchi, P.H. and Fritz, G., Photolysis of *N*-(2-methyl-2-propenyl)phthalimide in methanol. Evidence supporting radical-radical coupling of a photochemically generated radical ion pair, *J. Am. Chem. Soc.*, 108, 5362, 1986; (d) Maruyama, K. and Kubo, Y., Photochemistry of *N*-(2-alkenyl)phthalimides. Photoinduced cyclization and elimination reactions, *J. Org. Chem.*, 46, 3612, 1981.
41. Xue, J., Zhu, L., Fun, H.-K., and Xu, J.-H., Synthesis of medium and large ring heterocycles by photoinduced intermolecular and intramolecular electron transfer reactions of tetrachlorophthalimides with alkenes, *Tetrahedron Lett.*, 41, 8553, 2000.
42. Freccero, M., Fasani, E., and Albini, A., Photochemical reaction of phthalimides and dicyanophthalimides with benzylic donors, *J. Org. Chem.*, 58, 1740, 1993.
43. Kanaoka, Y. and Migita, Y., Photocyclization of *N*-aralkylphthalimides: an example of possible synthetic control in a heterocyclic series, *Tetrahedron Lett.*, 3693, 1974.
44. Griesbeck, A.G., Photochemical activation of amino acids: from the synthesis of enantiomerically pure β,γ-unsaturated amino acids to macrocyclic ring systems, *Liebigs Ann.*, 1951, 1996.
45. (a) Somich, C., Mazzocchi, P.H., Edwards, M., Morgan, T., and Ammon, H.L., Photoinitiated electron-transfer reactions of aromatic imides with phenylcyclopropanes. Formation of radical ion pairs cycloadducts. Mechanism of the reaction, *J. Org. Chem.*, 55, 2624, 1990; (b) Mazzocchi, P.H., Somich, C., Edwards, M., Morgan, T., and Ammon, H.L., Electron transfer photochemistry of aromatic imides and phenylcyclopropane. Radical anion-radical cation cycloaddition, *J. Am. Chem.*

Soc., 108, 6828, 1986; (c) Weidner-Wells, M.A., Oda, K., and Mazzocchi, P.H., The intramolecular electron transfer reactions of *N*-alkylcyclopropyl phthalimides, *Tetrahedron*, 53, 3475, 1997.

46. (a) Russell, G.A., Chen, P., Kim, B.H., and Rajaratnam, R., Homolytic base-promoted aromatic alkylations by alkylmercury halides, *J. Am. Chem. Soc.*, 119, 8795, 1997; (b) Maquieira, M.B., Peñéñory, A.B., and Rossi, R.A., Regiochemistry of the photostimulated reaction of the phthalimide anion with 1-iodoadamantane and *tert*-butylmercury chloride by the $S_{RN}1$ mechanism, *J. Org. Chem.*, 67, 1012, 2002.
47. (a) Okada, K., Ogamoto, K., and Oda, M., A new and practical method of decarboxylation: photosensitized decarboxylation of *N*-acyloxyphthalimides via electron transfer mechanism, *J. Am. Chem. Soc.*, 110, 8736, 1988; (b) Okada, K., Okamoto, K., Morita, N., Okubo, K., and Oda, M., Photosensitized decarboxylative Michael addition through *N*-(acyloxy)phthalimides via an electron-transfer mechanism, *J. Am. Chem. Soc.*, 113, 9401, 1991; (c) Okada, K., Okubo, K., Morita, N., and Oda, M., Reductive decarboxylation of *N*-(acyloxy)phthalimides via redox-initiated radical chain mechanism, *Tetrahedron Lett.*, 33, 7377, 1992.
48. (a) Cano, M., Fabriàs, G., Camps, F., and Joglar, J., Unexpected formation of *N*-(2-cyclopropenyl)phthalimides in the photosensitized decarboxylation of *N*-(2-cyclopropenylcarbonyloxy)phthalimides, *Tetrahedron Lett.*, 39, 1079, 1998; (b) Cano, M., Quintana, J., Juliá, L., Camps, F., and Joglar, J., Trapping of cyclopropenyl radicals by 5,5-dimethyl-1-pyrroline-*N*-oxide, *J. Org. Chem.*, 64, 5096, 1999.

85

The Photochemistry of Silicon-Substituted Phthalimides

Ung Chan Yoon
Pusan National University

Patrick S. Mariano
University of New Mexico, Albuquerque

85.1 Overview

SET Photochemistry of Organosilanes

Silicon-containing organic compounds serve as key reagents in numerous, synthetically useful chemical reactions.[1] Perhaps the most common role played by these substances is as equivalents of allylic and enolate anions. For example, activation of allylsilanes using potent silophiles leads to the formation of silylate anions, which react with electrophilic reagents to yield products resulting from nucleophilic addition and substitution. In addition, when partnered with strong electrophiles, allylsilanes and enolsilanes undergo addition reactions proceeding via the intermediacy of β-silicon stabilized carbenium ions that readily transfer their silyl groups to even weakly silophilic substances.

A variety of photochemical and electrochemical investigations over the past two decades have uncovered another interesting feature of organosilanes. Substances in this family that possess silyl-substitution at sites adjacent to electron donor centers undergo ready oxidation to generate silicon stabilized cation radical intermediates (Scheme 1). Comprehensive theoretical and electrochemical studiesby Yoshida and co-workers[2,3] have shown that stabilization by trialkylsilyl groups in these reactive intermediates is a consequence of hyperconjugative interactions. Specifically, the effect results from overlap of the relatively (compared to C–C bonded analogues) high energy, doubly occupied $\sigma_{C\text{-}Si}$ orbitals with half-filled heteroatom n- or alkene π-orbitals in the cation radicals. Moreover, the odd electron and positive charge delocalization, resulting from this interaction, weakens the $\sigma_{C\text{-}Si}$ bond and makes the silicon center more electropositive. Consequently, these short-lived intermediates participate in fast desilylation reactions to produce neutral, carbon-centered free radical intermediates.

0-8493-1348-1/04/$0.00+$1.50

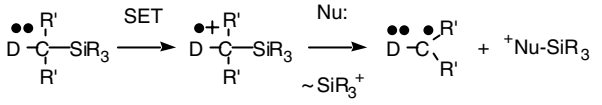

SCHEME 1

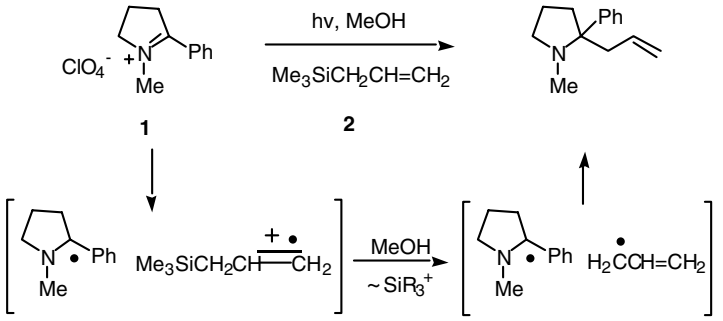

SCHEME 2

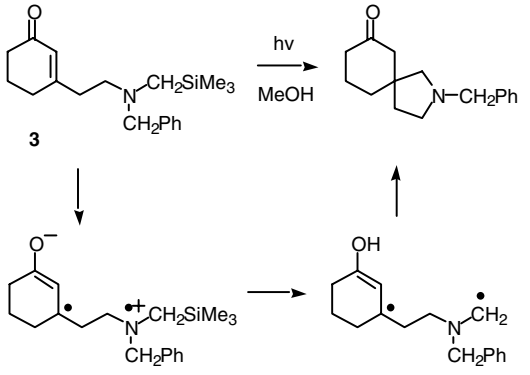

SCHEME 3

The redox properties of organosilanes have a profound impact on the nature of SET-promoted photochemical reactions. Owing to their low oxidation potentials, substances in this family serve as excellent electron donors to excited states of a variety of acceptors, including iminium salts, conjugated ketones, and cyanoarenes. In addition, the large rates of desilylation of cation radicals, formed in this manner, often drive efficient and selective formation of radicals that undergo C–C bond formation with either acceptor-derived radicals or neutral unsaturated substrates. Early examples of this reactivity profile are found in the direct irradiation-induced photoaddition of allyltrimethylsilane **2** to 1-methyl-2-phenylpyrrolinium perchlorate (**1**) (Scheme 2)[4,5] and the SET-sensitized photocyclization of the silylamino-tethered cyclohexenone **3** (Scheme 3).[6,7] When viewed from the perspective of SET photochemistry, α-silyl substituted electron donors are chemical equivalents of carbon-centered free radical intermediates. This conceptual connection enables the design of new excited state reactions, in which C–C bond formation occurs by radical coupling and addition pathways.

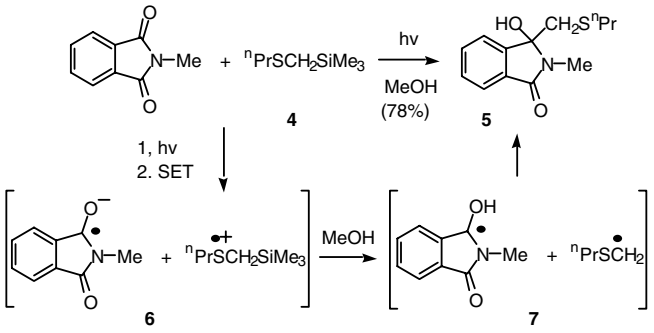

SCHEME 4

Phthalimide SET Photochemistry

The SET photochemistry of a wide variety of electron acceptors has been explored since the early recognition that SET pathways play prominent roles in excited-state reactions of organic substances. Included in this group are cyanoarenes, arylketones, and iminium and related *N*-heteroaromatic salts.[8] Owing to their large positive excited-state reduction potentials ($E^*(-)$ *ca.* 1.6–2.1 V),[9] phthalimides participate as electron acceptors in photoinduced SET processes with donors having ground-state oxidation potentials lower than *ca.* 2 V.

Early pioneering studies by Kanaoka[12–15] and Coyle[16,17] provided the first examples of intramolecular SET photochemical reactions of thioether and amine-tethered phthalimides. More recently, Griesbeck and co-workers[18–20] have fully probed the SET photochemistry of ω-carboxylate-linked phthalimides and have highlighted the synthetic potential of processes driven by sequential SET decarboxylation routes. Investigations in our laboratories have concentrated on developing the preparative potential of inter- and intramolecular reactions of phthalimides with silicon-substituted electron donors. A summary of observations made during the course of these efforts is given below using a format in which mechanistic analysis is interwoven with synthetic methodology development.

85.2 Photoadditons and Photocyclizations of Phthalimides with α-Silyl-ether, -Thioether, -Amine, and -Amide Substrates

Studies of SET-induced excited-state reactions of phthalimides with α-trialkylsilyl substituted ethers, thioethers, and amines have shown that cation radical desilylation is the foundation of interesting photochemical reactions that proceed by pathways involving the generation and coupling of radical intermediates. In an early effort, we observed that simple, α-silyl-substituted ethers, thioethers, amines, and amides undergo efficient photoadditions to phthalimide and its *N*-methyl derivative.[21] One example in this series of closely related reactions is the photoaddition of silylmethylpropylthioether **4** to *N*-methylphthalimide, which produces the product **5** (Scheme 4). In the mechanistic route for this process, thermodynamically/kinetically driven SET from **4** to the excited phthalimide leads to formation of the ion radical pair **6**. Solvent (MeOH)-promoted desilylation of the cation radical and protonation of the phthalimide anion radical then provides radical pair **7**, the direct precursor of adduct **5**.

Photocyclization reactions of phthalimides containing *N*-tethered α-silyl donors proceed with high chemical efficiencies to generate a variety of novel heterocyclic products. For example, irradiation of MeOH solutions of the phthalimido silyl ethers **8** leads to formation of the amidol-containing, oxygen heterocycles **9** in excellent yields (Scheme 5).[22] Analogous photocyclization reactions are observed with the phthalimido thioethers **10**.[23] Although dehydration of the primary photoproducts (**11** → **12**) occurs with varying ease in these systems, the overall yields of the reactions remain high even when the size of the ring that is formed in the ultimate diradical cyclization steps is large.

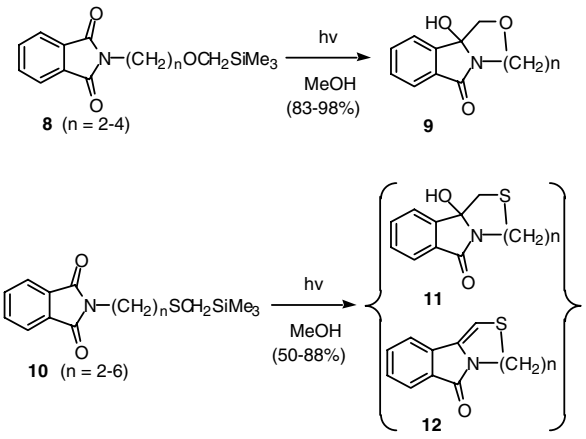

SCHEME 5

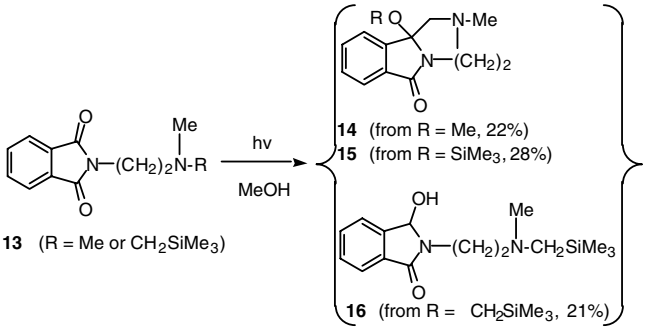

SCHEME 6

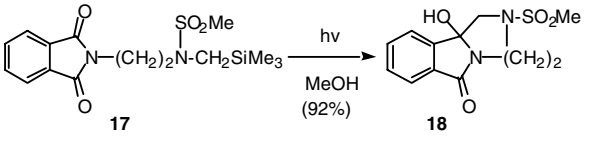

SCHEME 7

A parallel investigation of the photochemistry of α-silyl-amine and α-silyl-amide linked phthalimides has provided a more in-depth understanding of the factors that govern both the chemical and quantum yields of SET-promoted photocyclization reactions.[24,25] We observed that irradiation of a MeOH solution of the silylamino-phthalimides **13** leads to nonselective formation of a mixture of products, including the fused diazines **14** and **15**, and amidol **16** (Scheme 6). In stark contrast, the tricyclic sulfonamide **18** is formed in high yield when the silylamido-phthalimide **17** is irradiated in MeOH (Scheme 7). These divergent results suggest that the preparative utility of photocyclization reactions, operating by sequential SET desilylation pathways, could be enhanced using substrates that contain α-silylamide rather than α-silylamine donor sites. Support for this proposal is found in photoinduced cyclization of the acetamide

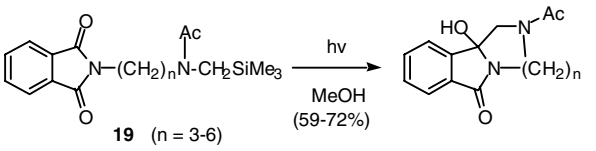

SCHEME 8

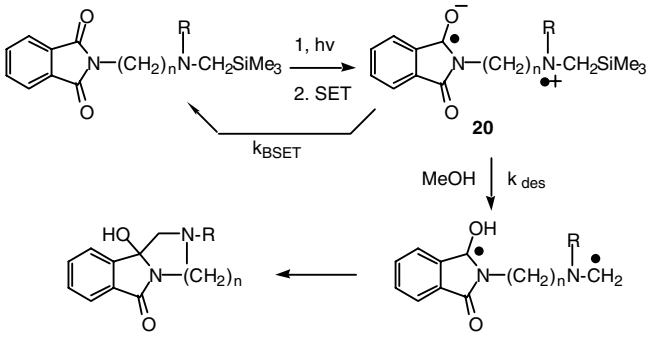

SCHEME 9

derivatives **19** shown in Scheme 8. Quantitative studies showed that the quantum yields of photocyclization reactions of the linked phthalimides **13** and **17** are also greatly dependent on the nitrogen substituent with the amide substrate **17** reacting with a greater efficiency ($\phi = 0.12$) than the amine analogue **13** ($\phi = 0.04$).

When first viewed, the results presented above appear counterintuitive and they lead one to question why the SET-promoted photoreactions are more efficient when they involve poorer electron donors (oxidation potentials of amines are often *ca.* 0.5 V lower than that of the corresponding amides). The answer to this question comes from an analysis of the key factors involved in determining the chemical and quantum efficiencies of excited-state reactions that proceed via pathways in which initial SET is followed by secondary reaction of charged radical intermediates. In the case at hand, SET from both α-silylamide and α-silylamine donors to the singlet excited state of the phthalimide chromophores in **13** and **17**, respectively, should both be highly exothermic. As a result, both intramolecular SET processes should occur at rates ($>1 \times 10^{10}$ s^{-1})[26] that are highly competitive with other pathways responsible for decay of the excited phthalimide. In this respect, Coyle and co-workers[11] have suggested that the n-π* singlet excited state of phthalimides is quenched by SET from pendant amino groups, and that this quenching process is on the pathway for cyclization reaction of these substrates. The intermediate zwitterionic biradicals **20** (Scheme 9) formed by excited-state SET in silylamino and silylamido phthalimides can react by several different routes. For example, exothermic back-SET, with rates that are essentially independent of the nitrogen substituent, would generate the ground-state starting materials. Competitive with this decay mode is methanol-induced α-desilylation. Our earlier laser flash photolysis studies[27,28] demonstrated convincingly that the rates of aminium radical fragmentation are highly dependent on the nitrogen substituent. Specifically, methanol-induced desilylation of silylamine cation radicals is two orders of magnitude slower than the analogous reaction of α-silylamide cation radicals. In more general terms, the rates of ion radical reactions are inversely proportional to the stability of these short-lived intermediates, as judged by the redox potentials of neutral precursors. In summary, the larger rate constants for desilylation of zwitterionic biradicals derived by photoinduced, intramolecular SET in α-silylamido-phthalimides translates into a larger rate constant ratio, $k_{des}/(k_{des} + k_{BSET})$. Consequently, larger quantum efficiencies are observed for diradical and product formation.

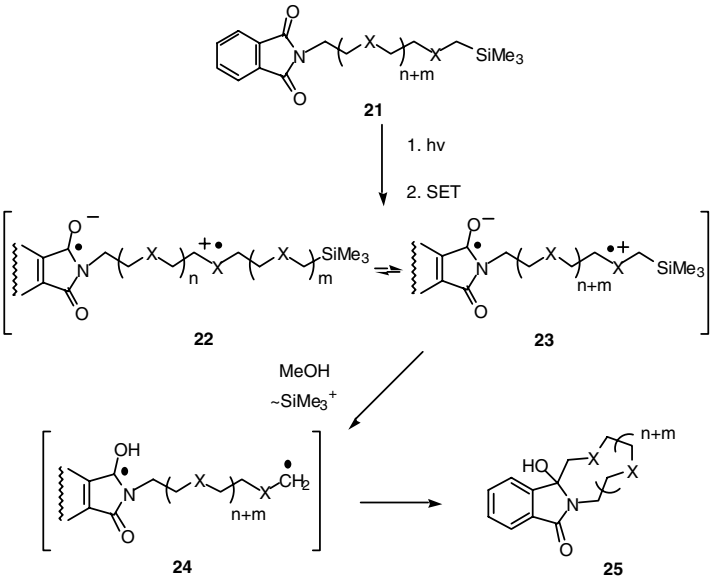

SCHEME 10

85.3 The Use of Phthalimide Photochemistry in Macrocyclec Polyamide, Polyether, and Polythioether Synthesis

The chemical yields of photoaddition and photocyclization reactions of systems comprised of phthalimides and α-silyl heteroatom donors are in the range normally deemed acceptable for synthetic applications. Based on this conclusion, we have designed strategies for the preparation of families of macrocyclic substances that rely on the use of this excited-state chemistry as the principal ring-building methodology. As depicted in Scheme 10, irradiation of phthalimides **21**, which have *N*-linked, silylmethyl terminated, polyheteroatom chains, should result in regioselective production of macrocyclic poly-amides, -ethers, and thioethers **25**. Accordingly, photoinduced SET in these substrates would yield a mixture of rapidly interconverting zwitterionic biradicals **22** + **23**, whose relative abundance would be governed by the relative energies of the cation radicals (as judged by the oxidation potential at each heteroatom center). Importantly, the rates of secondary α-deprotonation and α-desilylation adjacent to each of the rapidly interconverting cation radical sites will not depend on their relative populations. Rather, the relative rates of these processes, and thus the relative yields of 1,n-biradicals, will be determined by the rates of the competing fragmentation reactions. Since desilylation of the terminal cation radical **23** should be the most rapid process,[27,28] selective generation of the diradical precursors (**24**) of the macrocyclic products **25** should be observed.

The phthalimides, that serve as starting materials for these photomacrocylization reactions are readily prepared by *N*-alkylation of potassium phthalimide with polyamide, polyether, and polythioether-linked mesylates or halides. As seen by viewing the processes included in Schemes 11 through 16, irradiation of the phthalimido-silylpolyamides, -ethers and -thioethers in MeOH solution does indeed result in modestly to highly efficient production of the corresponding macrocyclic products.[29,30]

Although less well studied, SET-promoted ground- and excited-state reactions driven by α-destannylation of intermediate cation radicals are also known. One example is found in the photoaddition of allylstannane **26** to the pyrrolinium salt **28** (Scheme 17), which produces the pyrrolidine adduct **29**.[31] The quantum yield for the SET-promored addition of 26 to 28 is *ca.* tenfold greater than that for photoaddition of the corresponding allylsilane **27**. The enhanced efficiency is a result of the larger rate of destannation vs. desilylation of the intermediate π-cation radical.

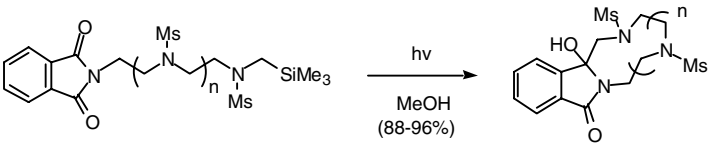

SCHEME 11

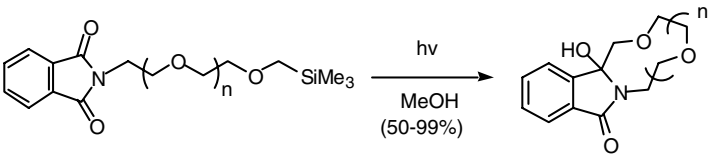

SCHEME 12

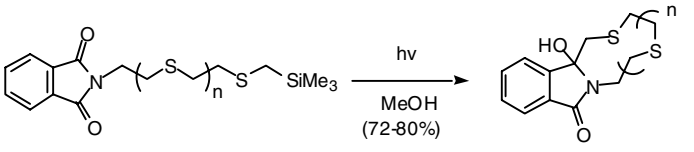

SCHEME 13

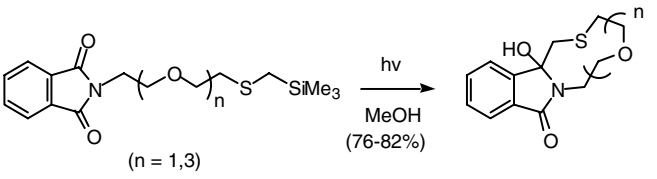

SCHEME 14

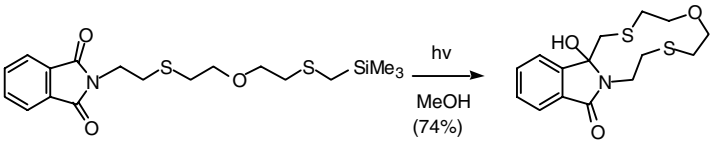

SCHEME 15

Trialkylstannyl substitution has a similar effect on the chemical efficiencies of photocyclization reactions of phthalimido-linked polyethers and related maleimides. As seen by viewing the data compiled in Table 85.1, the yields for formation of the macrocyclic polyethers **32a–f** are generally higher when the tin-substituted substrates **30a–f**, rather than silicon-substituted substrates **31a–f**, are irradiated.[32] This is especially true in the case of the larger ring forming reactions.

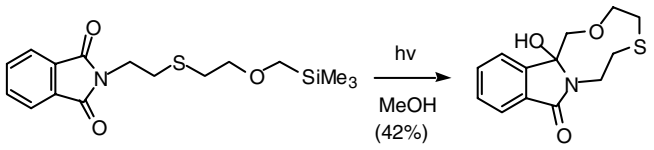

SCHEME 16

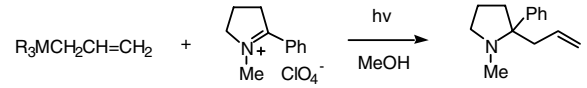

26 (MR_3 = $SiMe_3$)
27 (MR_3 = $SnBu_3$)

28 **29**

SCHEME 17

TABLE 85.1 Chemical Efficiencies of Photomacrocyclization Reactions of the Tin- and Silicon- Substituted Phthalimides 30a–f and 31a–f

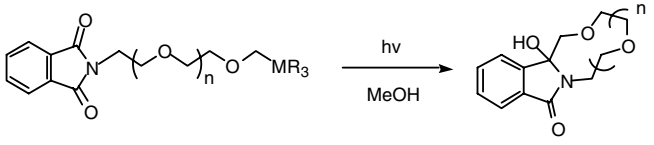

30a-f (n = 0-5, MR_3 = $SnBu_3$)
31a-f (n = 0-5, MR_3 = $SiMe_3$)

32a-f

Substrates	% Yields	Substrates	% Yields
30a	98	31a	98
30b	98	31b	99
30c	95	31c	60
30d	68	31d	64
30e	88	31e	50
30f	72	31f	53

85.4 Photoreactions of ω-Phthalimido-Alkylsilanes

Hydrogen atom abstraction dominates the excited-state reactivity profiles of *N*-alkylphthalimides. This is exemplified by the photochemistry of *N*-ethylphthalimide **32**, where irradiation leads to formation of the benzazepinedione **33** (Scheme 18).[13] Here, initial γ-hydrogen abstraction is followed by biradical coupling and ensuing amidol ring opening. However, the yield of this process (*ca*. 5%), as well as those of related *N*-alkylphthalimide photocyclizations, are not preparatively acceptable.

In contrast, *N*-silylethylphthalimide **34** efficiently (68%) produces benzazepinedione **33** (Scheme 19) when irradiated in MeCN solution.[33] Introduction of the trimethylsilyl substituent transforms a minor photoreaction into one that has synthetic value. Insight into the factors responsible for the yield enhancement was gained from the results of experiments in which photoreaction solvent was varied. Irradiation of **34** in 35% D_2O-MeCN leads to exclusive production of the mono-*N*-deuteriated product $\mathbf{33d_1}$ while photoreaction of **34** in 1% D_2O-MeCN yields the N,C-dideuteriated benzazepinedione $\mathbf{33d_2}$ (Scheme 20). In addition, ^{1}H NMR monitoring of the photoreaction of **34** in CD_3CN shows that the α-silyl product

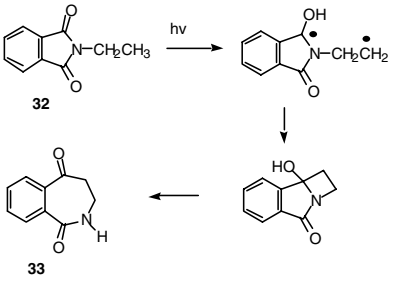

SCHEME 18

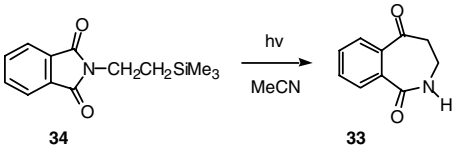

SCHEME 19

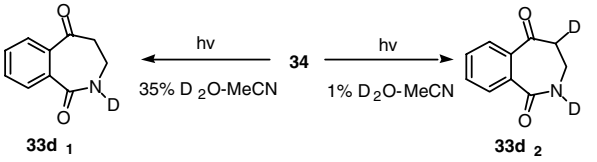

SCHEME 20

37 is produced initially and that this substance is converted to **33** or **33d**$_2$ when treated with H_2O or D_2O, respectively (Scheme 20).

The results suggest that two pathways (Scheme 21) are responsible for the photochemical transformation of silylethylphthalimide **34** to benzazepinedione **33**. In low water content solvents (e.g., 1% D_2O-MeCN), the reaction is initiated by γ-hydrogen atom transfer, which yields sequentially the silicon-containing tricyclic amidol **36** and silyl-benzazepinedione **37**. In contrast, desilylation must precede C–C bond formation in the reaction of **34** in the highly polar silophilic solvent systems 35% D_2O-MeCN. In this case, intramolecular SET from the σ-$_{C-Si}$ bond ($E_{p/2}$ = 2.5 V vs. SCE)[34] to the singlet excited phthalimide leads to the solvent-stabilized, but transient[34,35] zwitterionic biradical **38**. Desilylation of **38** then generates the precursor of the non-silicon-containing benzazepinedione **33**.

Another example that demonstrates the level of control offered by solvent variation is found in the photochemistry of the silylpropyl-phthalimide **42**. Kanaoka has reported that irradiation of the *N*-propyl substrate **39** leads to low-yield (29%) formation of methyl-benzazepinedione **40**, along with the unsaturated amidol **41** (18%) (Scheme 22).[13] Similarly, irradiation of the silicon analog **42** in MeCN gives rise to a mixture of products, including benzazepinedione **43** (28%), amidol **44** (18%), and benzopyrrolizidinone **45** (21%) (Scheme 23).[33] The major products generated in both photoreactions arise by initial γ-hydrogen atom abstraction. The biradical formed in this way cyclizes or disproportionates to produce the respective benzazepidione and unsaturated amidol products.

In contrast, irradiation of the silylpropylphthalimide **42** in 35% H_2O-MeCN results in nearly quantitative (96%) formation of the benzopyrrolizidinone **45** (Scheme 24). In addition, the quantum efficiency

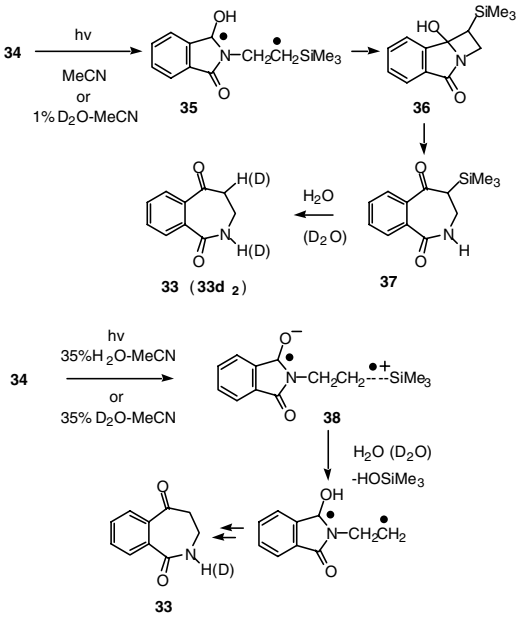

SCHEME 21

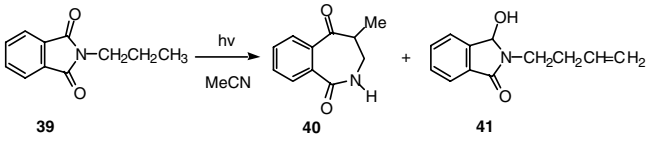

SCHEME 22

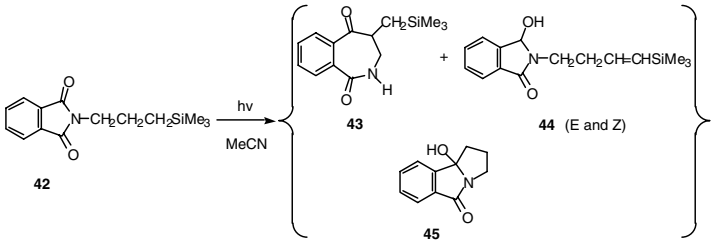

SCHEME 23

for photoreaction of **42** in the aqueous solvent system is *ca.* 20-fold greater than for the process in MeCN. As in the case of **34**, a change to an aqueous solvent system produces a dramatic change in the excited-state reactivity of the silylpropylphthalimide. The "water effect" also profoundly impacts the photochemistry of a number of silicon-substituted maleimides.[36]

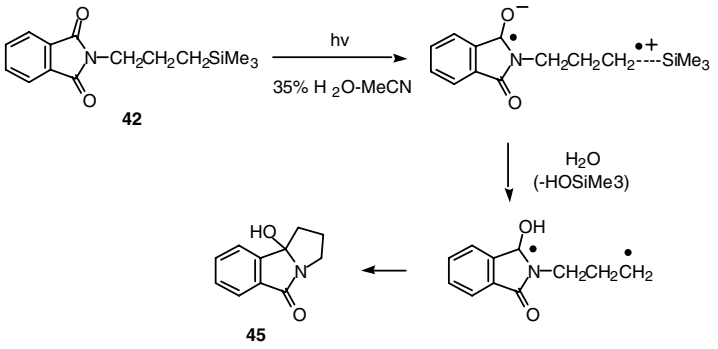

42 **45**

SCHEME 24

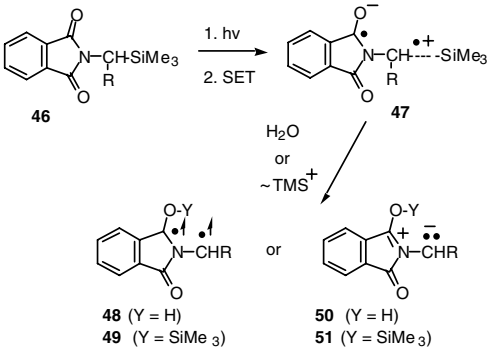

46 **47** **48** (Y = H) **49** (Y = SiMe 3) **50** (Y = H) **51** (Y = SiMe 3)

SCHEME 25

85.5 Azomethine Ylide Forming Photoreactions of *N*-Trimethylsilylphthalimides and Related Conjugated Imides

The studies described above show that the unique redox properties of alkylsilanes and conjugated imide excited states serve to drive synthetically interesting photoreactions. The efforts have also uncovered interesting excited-state reactions of *N*-silylalkyl-phthalimides, in which 1,ω-biradicals are produced as reactive intermediates by SET and subsequent desilylation of σ_{C-Si} cation radicals. A consideration of how this reactivity pattern might be applied to silylmethyl-phthalimides **46** results in the prediction that 1,3-biradicals or azomethine ylides would be formed as reactive intermediates (Scheme 25). In this case, the zwitterionic biradicals **47** generated by SET in the triplet or singlet excited states of **46** could undergo nucleophile-induced desilylation to form 1,3-biradicals **48** (if triplets) or azomethine ylides **50** (if singlets). Alternatively, the oxyanion center in **47** could serve as an internal nucleophile for desilylation at the σ_{C-Si} cation radical site. This process, being both energetically and entropically favored, would result in production of the silicon containing biradical or dipolar intermediates, **49** or **51**.

Observations made in studies with the parent silylmethylphthalimide **52** confirm the operation of a unique excited-state process involving sequential SET-silyl transfer.[37,38] We found that irradiation of **52** in D_2O-MeCN results in efficient production of *N*-(d_1-methyl)phthalimide **54**, while excited-state reaction of this phthalimide in acetone gives rise to the adduct **55** (Scheme 26). The intermediate in these

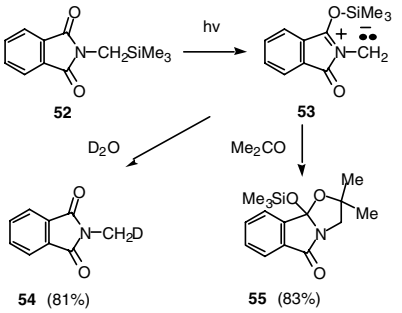

SCHEME 26

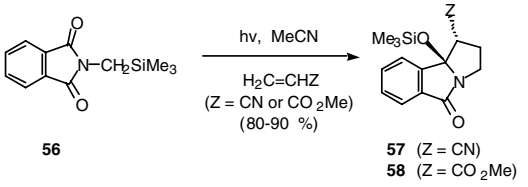

SCHEME 27

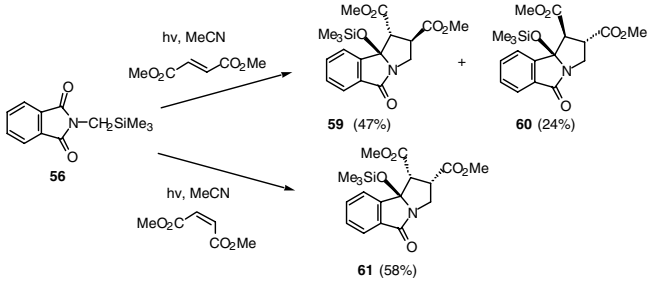

SCHEME 28

processes is the azomethine ylide **53**, which reacts by C-deuteriation with D_2O or dipolar cycloaddition with acetone to form **54** and **55**, respectively. Laser flash photolysis techniques were used to gain evidence for the intermediacy of azomethine ylides in these processes.[39]

Preparative photochemical experiments have provided supporting evidence for this proposal.[37,38] Irradiation of **56** in MeCN solutions containing 90 mM acrylonitrile or methyl acrylate leads to efficient (80 to 90%) formation of the respective benzopyrrolizidines **57** and **58** (Scheme 27). The ylide trapping reactions are *endo*-selective and stereospecific (preferential production of **59** + **60** and **61** from photoreactions of **56** with dimethyl fumarate and dimethyl maleate, respectively [Scheme 28]).

This novel and preparatively useful azomethine ylide-forming photoreaction is not restricted to phthalimide substrates.[40] Other conjugated imides that contain *N*-silylmethyl substitution are transformed to their corresponding azomethine ylides by photoinduced C-to-O silyl migration reaction.

Observations made in these studies suggest that the novel C-to-O silyl migration reaction of conjugated imides is a general excited-state process. It is reasonable to propose that these reactions occur in imides that have low-energy π-π^* singlet or triplet excited states. As suggested above, the driving force for silyl

migration could reside in both the respective redox potentials of the conjugated imide acceptor and σ_{C-Si} donor sites and the entropic favorability of silyl transfer in the intermediate zwitterionic biradicals.

Acknowledgments

The authors express their deep appreciation to their enthusiastic, hard-working, and productive coworkers whose studies in the area of amine electron-transfer photochemistry established the basis for the results presented in this review. Also, the generous financial support given to the PSM research group by the National Institutes of Health and the National Science Foundation and to the UCY research group by the Korea Science and Engineering Foundation (Basic Research Program 2001-1-12300-006-3, International Cooperative Research Program, and CBM of POSTECH) is acknowledged.

References

1. Colvin, E., *Silicon in Organic Synthesis*, Butterworth, London, 1981.
2. Yoshida, J., Maekawa, T., Murata, T., Matsunaya, S., and Isoe, S., Electrochemical Oxidation of Organosilicon Compounds. The Origin of β-Silicon Effect in Electron Transfer Reactions of Silicon Substituted Heteroatom Compounds. Electrochemical and Theoretical Studies, *J. Am. Chem. Soc.*, 112, 1962–1970, 1990.
3. Yoshida, J., Matsunaga, S., Murata, T., and Isoe, S., Electrochemical Oxidation of Organosilicon Compounds. New One Carbon Homologation Reagents Utilizing Electrochemical Oxidation of Organosilicon Compounds, *Tetrahedron*, 47, 615–624, 1991.
4. Ohga, K and Mariano, P.S., Electron Transfer Initiated Photoaddition of Allysilanes to 1-Methyl-2-phenylpyrrolinium Perchlorate, *J. Am Chem. Soc.*, 104, 617–619, 1982.
5. Ohga, K, Yoon, U.C., and Mariano, P.S., Electron Transfer Initiated Photoaddition of Allysilanes to 1-Methyl-2-phenylpyrrolinium Perchlorate, *J. Org. Chem.*, 49, 213–219, 1984.
6. Yoon, U.C. and Mariano, P.S., Mechanistic and Synthetic Aspects of Amine-Enone Single Electron-Transfer Photochemistry, *Acc. Chem. Res.*, 25, 233–240, 1992.
7. Xu, W., Zhang, X.M., and Mariano, P.S., Single Electron-Transfer Promoted Photocyclization Reactions of (Aminoalkyl)cyclohexenones. Mechanistic and Synthetic Features of Processes Involving the Generation and Reactions of Amine Cation and alpha-Amino Radicals, *J. Am. Chem. Soc.*, 113, 8869–8878. 1991.
8. Mariano, P.S. and Stavinoha, J., Synthetic Aspects of Photochemical Electron Transfer Reactions in *Synthetic Organic Photochemistry*, Horspool, W.M., Ed., Plenum, New York, 1984, 259–284.
9. The excited state reduction potentials are calculated by use of the relationships $E^{S1}(-) = E^{S1} + E_{1/2}(-)$ and $E^{T1}(-) = E^{T1} + E_{1/2}(-)$, where $E_{1/2}(-)$ is the ground state reduction potential (−1.4 V vs. SCE, ref. 10) of *N*-methylphthalimide, and E^{S1} and E^{T1} are the excited singlet (79.5 kcal/mol, ref. 11) and triplet (68.5 kcal/mol, ref. 8c) state energies of *N*-methylphthalimide.Leedy, D.W. and Muck, D.L., Cathodic Reduction of Phthalimide Systems in Nonaqueous Solutions, *J. Am. Chem. Soc.*, 93, 4264–4275, 1971.
10. Coyle, J.D., Newport, G.L., and Harriman, A.J., Nitrogen Substituted Phthalimides. Fluorescence, Phosphorescence, and Mechanism of Photocyclization, *J. Chem. Soc., Perkin Trans. 2*, 133–137, 1978.
11. Kanaoka, Y., Photoreactions of Cyclic Imides. Examples of Synthetic Organic Photochemistry, *Acc. Chem. Res.*, 11, 407–413, 1978.
12. Kanaoka, Y., Migita, Y., Koyama, K., Sato, Y., Nakai, H., and Mizoguchi, T., Photocyclization of *N*-Alkylphthalimides to Benzazepinone Lactams. Unusual Two-Fold Norrish Type II Reactions, *Tetrahedron Lett.*, 1193–1196, 1973.
13. Kanaoka, Y., Koyama, K., Flippen, J.L., Karle, I.L., and Witkop, B., Photocyclization of *N*-Alicyclic Phthalimides. Synthesis of Multicyclic Benzazepine Systems,*J. Am. Chem. Soc.*, 96, 4719–4721, 1974.
14. Machida, M., Takechi, H., and Kanaoka, Y., Photochemical Synthesis of Multicyclic Fused Imidazolidines, Hydropyrazines, and Hydro-1,4-diazepines, *Synthesis*, 1078–1080, 1982.

15. For a recent comprehensive review, see Coyle, J.D., Phthalimide and Its Derivatives. in *Synthetic Organic Photochemistry*, Horspool, W.M., Ed., Plenum, New York, 1984, 259–284.
16. Coyle, J.D. and Newport, G.L., Fused Imidazolidines, Hexahydropyrazines, and Hexahydro-1,4-Diazepines, *Synthesis*, 381–382. 1979.
17. Griesbeck, A.G., Henz, A., Hirt, J., Ptatschek, V., Engel, T., Loffler, D., and Schneider, F.W., Photochemistry of *N*-Phthaloyl Derivatives of Electron-Donor-Substituted Amino Acids, *Tetrahedron*, 50, 701–714, 1994.
18. Griesbeck, A.G., Henz, A., Peters, K., Peters, E.M., and von Schnering, H.G., Photo-Electron Transfer Induced Macrocyclization of *N*-Phthaloyl-Omega-Aminocarboxylic Acids, *Angew. Chem. Int. Ed. Engl.*, 34, 474–476, 1995.
19. For other recent reviews of phthalimide photochemistry, see Griesbeck, A.G., *Chimia*, 52, 272–283, 1998; Griesbeck, A.G., Photochemical Activation of Amino Acids. From the Synthesis of Enantiomerically Pure β,γ-Unsaturated Amino Acids to Macrocyclic Ring Systems, *Liebigs Ann.*, 1951–1958, 1996.
20. Yoon, U.C., Kim, H.J., and Mariano, P.S., Electron Transfer Induced Photochemical Reactions in Imide Systems. Photoaddition of α-Trimethylsilyl Substituted Heteroatom Containing Compounds to Phthalimides. *Heterocycles*, 29, 1041–1064. 1989.
21. Yoon, U.C., Lee, S.J., Lee, K.J., Cho, S.J., Lee, C.W., and Mariano, P.S., Exploratory Study of Photocyclization Reactions of *N*-(Trimethylsilylmethylthioalkyl)phthalimides, *Bull. Korean Chem. Soc.*, 15, 154–161, 1994.
22. Yoon, U.C., Cho, S.J., Oh, J.H., Lee, J.G., Kang, K.T., and Mariano, P.S., Photocyclization Reactions of Phthalimide $RXCH_2TMS$ Systems via Singlet Single Electron Transfer and Triplet Hydrogen Abstraction and Silyl Group Abstraction Pathways, *Bull. Korean Chem. Soc.*, 12, 241–243, 1991.
23. Yoon, U.C., Oh, J.H., Lee, S.J., Kim, D.U., Lee, J.G., Kang, K.T., and Mariano, P.S., Photocyclization Reactions of *N*-(Trimethylsilylmethoxyalkyl)phthalimides Efficient and Regioselective Route to Heterocycles, *Bull. Korean Chem. Soc.*, 13, 166–172, 1992.
24. Yoon, U.C., Kim, J.W., Ryu, J.Y., Cho, S.J., Oh, S.W., and Mariano, P.S., Single Electron Transfer-Induced Photocyclization Reactions of *N*-[(*N*-Trimethylsilylmethyl)aminoalkyl]phthalimides, *J. Photochem. Photobiol. A: Chem.,* 106, 145–154, 1997.
25. Rehm, D. and Weller, A. Kinetics of Fluorescence Quenching by Electron and H-Atom Transfer. *Isr. J. Chem.*, 8, 259–271, 1970.
26. Zhang, X.M., Yeh, S.R., Hong, S., Freccero, M., Albini, A., Falvey, D.F., and Mariano, P.S., Dynamics of α-CH Deprotonation and α-Desilylation Reactions of Tertiary Amine Cation Radicals. *J. Am. Chem. Soc.*, 116, 4211–4220, 1994.
27. Su, Z., Falvey, D.F., Yoon, U.C., Oh, S.W., and Mariano, P.S., Dynamics of Anilinium Radical α-Heterolytic Fragmentation Processes. Electrofugal Group, Substituent, and Medium Effects on Desilylation, Decarboxylation, and Retro-Aldol Cleavage Pathways, *J. Am. Chem. Soc.*, 120, 10676–10686, 1998.
28. Yoon, U.C., Oh, S.W.. and Lee, C.W., Efficient and Regioselective Photocyclization Reactions of *N*-[(ω-Trimethylsilymethoxy)polyoxalkyl]phthalimides to Azacrown Ethers, *Heterocycles*, 41, 2665–2682, 1995.
29. Yoon, U.C., Oh, S.W., Lee, J.H., Park, J.H., Kang, K.T., and Mariano, P.S., Applications of Phthalimide Photochemistry to Macrocyclic Polyether, Polythioether, and Polyamide Synthesis, *J. Org. Chem.*, 66, 939–943, 2001.
30. Borg, R.M. and Mariano, P.S., Allylstannane Photoadditions to Iminium salts. Efficiencies of Destannylation vs. Desilylation Reactions, *Tetrahedron Lett*, 27, 2821–2824, 1986.
31. Yoon, U.C., Jin, Y.X., Oh, S.W., Cho, D.W., Park, K.H., and Mariano, P.S., Comparison of Photomacrocyclization Reactions of Trimethylsilyl and Tributylstannyl-Terminated Phthalimido and Maleimido-Polyethers., *J. Photochem. Photobiol. A: Chem.*, 150, 77–84, 2002.
32. Lee, Y.J., Ling, R., Mariano, P.S., Yoon, U.C., Kim, D.U., and Oh, S.W., Exploratory Studies of H-Atom Abstraction and Silyl-Transfer Photoreactions of Silylalkyl Ketones and (Silylalkyl)phthalimides, *J. Org. Chem.*, 61, 3304–3314, 1996.

33. Klinger, R.J. and Kochi, J.K., Heterogeneous Rates of Electron Transfer. Application of Cyclic Voltammetric Techniques to Irreversible Electrochemical Processes, *J. Am. Chem. Soc.*, 102, 4790–4798, 1980.
34. Hanafey, M.K., Scott, R.L., Ridgway, T.H., and Reilley, C.N., Analysis of Electrochemical Mechanisms by Finite-Difference Simulation and Simplex Fitting of Double Potential Step Current, Charge, and Absorbance Responses, *Anal. Chem.*, 50, 116–137, 1978.
35. Yoon, U.C., Oh, S.W., Lee, S.M., Cho, S.J., Gamlin, J., and Mariano, P.S., A Solvent Effect that Influences the Preparative Utility of *N*-(Silylalkyl)phthalimide and *N*-(Silylalkyl)maleimide Photochemistry, *J. Org. Chem*., 64, 4411–4418, 1999.
36. Yoon, U.C., Kim, D.U., Lee, C.W., Choi, Y.S., Lee, Y.-J., Ammon, H.L., and Mariano, P.S., Novel and Efficient Azomethine Ylide Forming Photoreactions of *N*-(Silylmethyl)phthalimides and Related Acid and Alcohol Derivatives, *J. Am. Chem. Soc*., 117, 2698–2710, 1995.
37. Yoon, U.C., Kim, D.U., Kim, J. C., Lee, J. G., Mariano, P.S., Lee, Y.J., and Ammon, H.L., The Operation of H-Atom and TMS-Group Transfer Processes in the Photochemistry of Silylamidoalkyl-Ketones and Silylalkyl-Ketones and Silylalkyl-Phthalimides, *Tetrahedron Lett*., 34, 5855–5858, 1993.
38. Takahashi, Y., Miyashi, T., Yoon, U.C., Oh, S.W., Mancheno, M., Su, Z., Falvey, D.F., and Mariano, P.S., Mechanistic Studies of the Azomethine Ylide-Forming Photoreactions of *N*-(Silylmethyl)phthalimides and *N*-Phthaloylglycine, *J. Am. Chem. Soc*., 121, 3926–3932, 1999.
39. Yoon, U.C., Cho, S.J., Lee, Y.J., Mancheno, M.J. and Mariano, P.S., Investigations of Novel Azomethine Ylide Forming Photoreactions of Silylmethylimides, *J. Org. Chem*., 60, 2353–2360, 1995.

86

Fulgides and Related Systems

Yasushi Yokoyama
Yokohama National University

Mahmut Kose
Zonguldak Karaelmas University

86.1 Fulgides

Fulgides were first synthesized, named, and found to exhibit photochromism by Stobbe more than 100 years ago.[1] At that time, fulgides like **1** were shown to undergo thermally reversible cyclization with some irreversible side reactions. In 1981, Heller et al. synthesized a furylfulgide **2**, the colored form of which (**2C**) did not revert to the starting **2E** by a thermal pathway. In addition, **2E** showed few side reactions (hydrogen migration and oxidation to generate an aromatic ring became impossible) as well as exhibiting high conversion to **2C**.[2–4] This was the first reported example of a thermally irreversible photochromic compound. The important modifications to the basic structure to produce **2** were the replacement of all the hydrogen atoms attached to the carbon atoms involved in the ring closing by methyl groups and the employment of the heteroaromatic furan instead of a phenyl substituent.

0-8493-1348-1/04/$0.00+$1.50

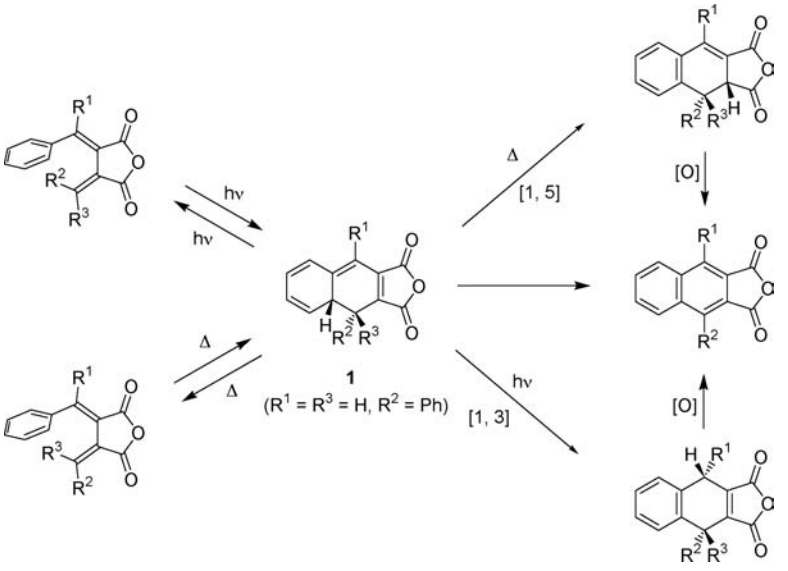

Since then, fulgides have been regarded as prime candidates for application as photon-mode rewritable recording media.[5]

Recently, the structures of fulgides have been modified to give them more sophisticated properties. This work is aimed at using fulgides as photo-switches for particular functions,[6] such as changes in the character of liquid crystalline phases, changes in fluorescent properties or changes in the nature of supramolecular systems. This chapter describes various aspects of recent developments in the chemistry of fulgides. However, it is not meant to be encyclopedic and some degree of selection will be used. Readers who wish to know more about the area should refer to the reviews and books on the subject.[5–10]

86.2 Fulgides Modified on the Acid Anhydride Moiety

Fulgides have at least one aromatic ring on the bismethylenesuccinic anhydride. Although a number of fulgides have been synthesized with different aromatic rings[11] changes to the succinic anhydride moiety have been limited, and the only other functionality used has been the succinimde group.[12] However, recent studies of fulgides have been extended to the structural modification of the anhydride moiety, resulting in many unique fulgides.

Dicyanomethylene-Condensed Fulgides

The absorption maxima of the C-forms of fulgides lie in the visible region as a result of the electronic push–pull effect of the aromatic ring and the anhydride moiety. If the electron-withdrawing properties of the anhydride moiety are enhanced, the resultant compounds could absorb in the near-IR or the IR region of the spectrum. Heller et al. have carried out such modifications extensively. Some of these results are reported here.

Condensation of malononitrile with **2Z** in the presence of diethylamine gave a (Z)-α-dicyanomethylene derivative **3Z**. Similarly, **2E** gave the corresponding (E)-β-dicyanomethylene derivatives **4E**.[13] While the replacement of either of the carbonyl groups (α or β) by the powerful electron withdrawing dicyanomethylene group causes a large red shift in the absorption maxima of the C-forms, **3C** (λ_{max} = 610 nm in toluene) has an absorption maximum that is more red-shifted than **4C** (λ_{max} = 601 nm in toluene) because of the linear conjugation within **3C** rather than the cross-conjugation of **4C**. These conversions were applied to several furyl- and thienylfulgides.

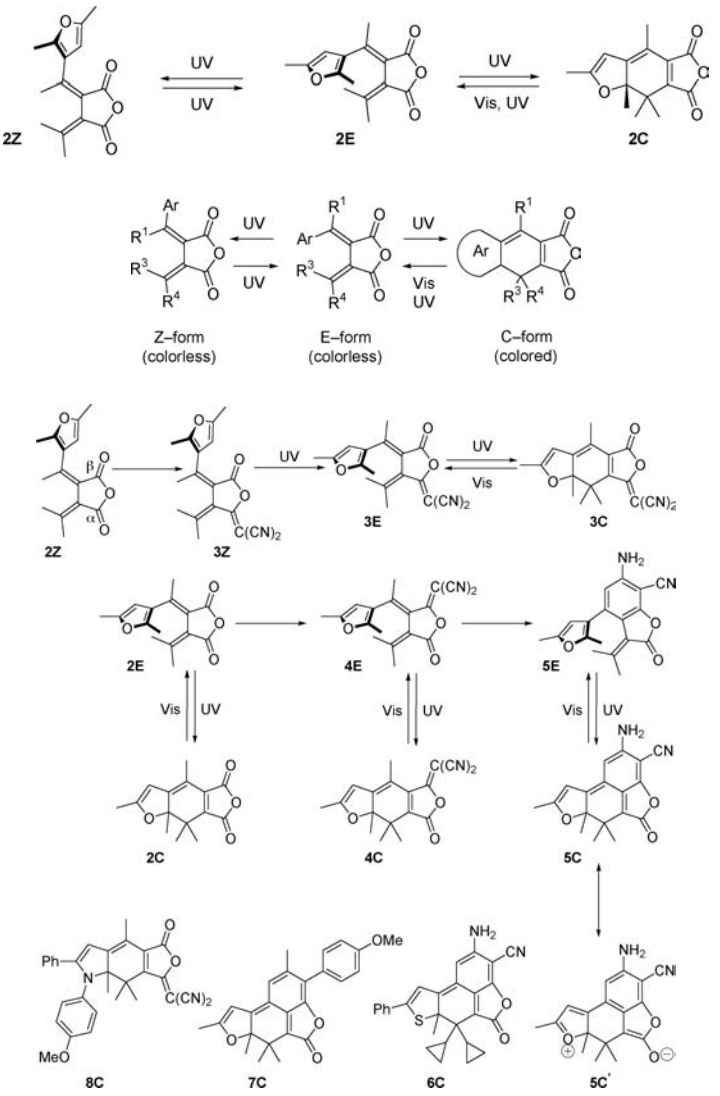

When the cross-conjugated (*E*)-β-dicyanomethylene derivative **4E** was treated with diisopropylamine, a new infrared-absorbing photochromic lactone **5E** was obtained. Although the central benzene ring of **5C**, formed by photocyclization, loses its aromaticity, it could be recovered by an intramolecular charge transfer from the lone pair of the oxygen atom to the lactone carbonyl oxygen atom (**5C'**). As a consequence, **5C** has a broad absorption band in the infrared region in toluene. The longest absorption maximum (λ_{max} = 776 nm in toluene) was recorded for **6C**, whose spectrum (photostationary state (pss) of 366-nm irradiation in toluene) together with that of **6E** is shown in Figure 86.1.

As an important extension, Heller, Köse, and co-workers developed a general method for the preparation of this type of photochromic lactone.[14] Condensation of a ketone, possessing a methylene adjacent to the carbonyl group, with an (*E*)-fulgide by KOBu^t in toluene afforded the phenyl lactone in low yield. Although the skeleton of the product is the same as **5E**, the substituents on the phenyl ring are not limited to amino and cyano groups. For example, condensation of 4-methoxybenzyl methyl ketone with **2E** afforded **7** with a beautiful green color similar to Caledon Jade Green dye upon UV irradiation (λ_{max} = 622 nm in toluene). Fan et al.[15] reported that the absorption maximum of **8C** in acetonitrile was 820 nm. Similar compounds were also reported by Hosmane et al.[16,17]

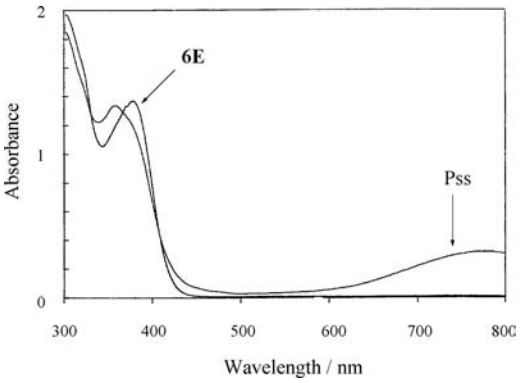

FIGURE 86.1 Absorption spectra of **6E** and the photostationary state (pss: **6C** has λ_{max} at 776 nm) of 366-nm light irradiation. (Kindly provided by Professor Harry G. Heller, University of Wales, Cardiff, U.K.)

Fulgenates and Fulgenolides

Several diesters (fulgenates) corresponding to the indolylfulgide **9**, exemplified by **10**, were synthesized and the photochromic properties were examined by Yokoyama et al.[18] Although the quantum yields of photoreactions were generally low for the esters of simple alcohols, the cyclic diesters of diols such as **11** with short alkyl chains showed as good photochromic properties as the parent fulgide **9**.[19] The absorption of both colored and colorless forms of fulgenates moved towards shorter wavelengths compared to the parent fulgide **9** (**9C**; 585 nm, **10C**; 437 nm, **11C**; 447 nm, in toluene).

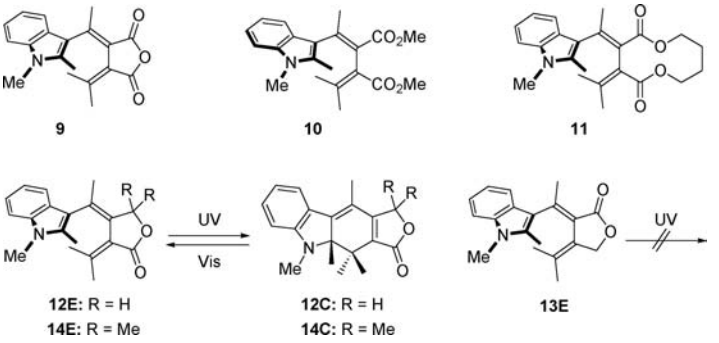

Reduction of one of the carbonyl groups of **9** to an sp^3 alkyl carbon atom yields the regioisomers of lactones (fulgenolides) **12** and **13**. They were synthesized regioselectively by Yokoyama[20] and only **12**, possessing the carbonyl group close to the isopropylidene group showed excellent photochromic properties. Again the absorption maximum was at wavelengths shorter than that of the parent fulgide **9** (**12C**; 462 nm in toluene). The dimethyl-fulgenolide **14** (**14C**; 464 nm in toluene) also showed good photochromic properties.[20]

(*R*)-Binaphthol-Condensed Fulgides

Since 2,2′-dihydroxy-1,1′-dinaphthyl (binaphthol) is known to be chiral with regard to the C_2 axis, compounds with a binaphthyl as a partial structure are chiral. If the compound also has intrinsic chirality in addition to the binaphthol, the resultant molecule will form a pair of diastereomers. Because the *E*-form of fulgides has helical chirality with regard to the hexatriene moiety that undergoes ring closing because of steric factors, introduction of binaphthol should generate diastereomers. Such fulgides **15** and **16** were synthesized by Yokoyama et al. to elucidate the relationship of the two chiral factors.[21] The binaphthol was attached like an ortho ester to the lower carbonyl group as shown.

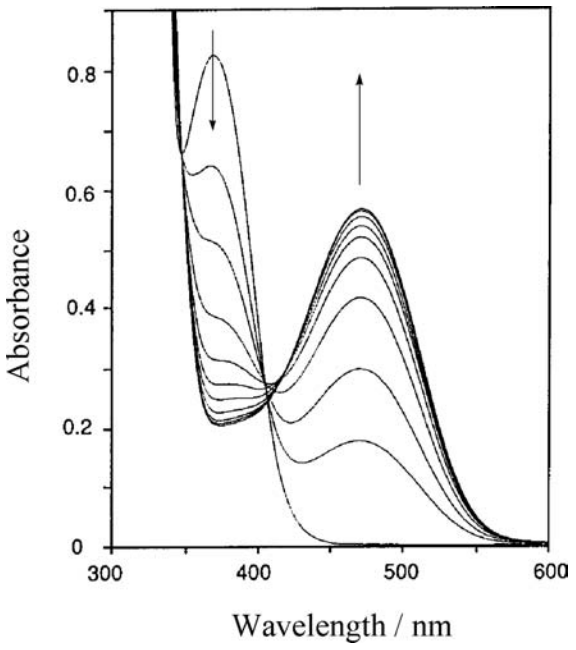

FIGURE 86.2 Absorption spectral change of **15E** upon irradiatioin of 366-nm light.

In the event, the rigid chirality of binaphthol controlled the flexible helical chirality of the hexatriene moiety. When the (*R*)-enantiomer of binaphthol was employed, the helical array of the hexatriene adopted the right-handed screw (*P*-helicity) because of the steric repulsion between one of the naphthalene rings and the *Z*-methyl group of the isopropylidene moiety. This was reflected in the ratio of the diastereomer of the C-forms (96/4 for **15C** (λ_{max} = 471 nm) and 98/2 for **16C** (λ_{max} = 456 nm)) upon 366-nm light irradiation in toluene. This diastereoselective photocyclization concept was also applied to a benzofuryl-fulgide **17** by Yokoyama et al.[22] The absorption spectra of **15E** and the pss of 366-nm light irradiation are shown in Figure 86.2.

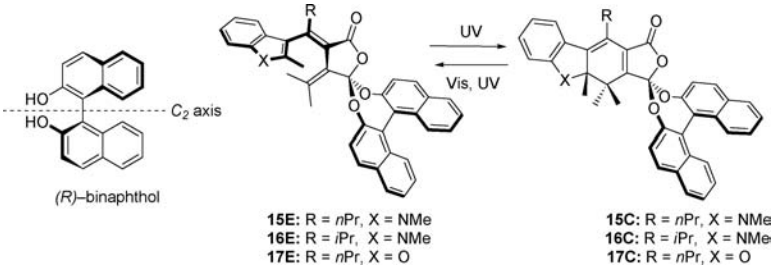

Similarly, but differently, condensation of a chiral diol **18** to the indolylfulgide **9** yielded an ortho-ester type compound **19**, where condensation occurred to the upper carbonyl.[23] The diastereoselectivity of the photocyclization of **19** (λ_{max} of **19C** in toluene = 490 nm) was 95% *de*.

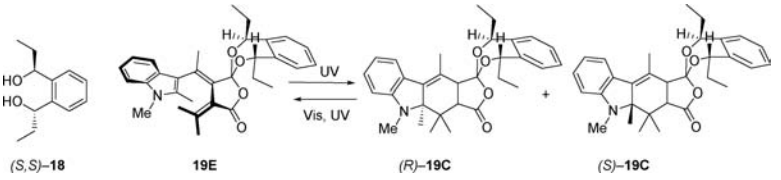

Fulgides with Thioanhydride Moiety

Heller et al.[24] reported that the fulgides **20**, in which the ether oxygen of the anhydride moiety was replaced by sulfur, showed the significant red-shift of the absorption maximum of the C-forms by 40 nm (R = Me) to 60 nm (R = Ph).

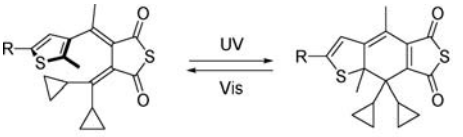

20E (R = CH_3 or Ph) **20C** (R = CH_3 or Ph)

86.3 Fulgides and Liquid Crystals

The photochemical reaction of photochromic compounds changes the structure of the compound. This feature has been used to control the properties of liquid crystals. Thus, the irradiation of photochromic compounds doped in liquid crystals changes the ordering ability of the liquid crystalline material. These changes have been examined for a number of photochromic compounds such as azobenzenes. Fulgides have also been used for this purpose. The earliest examples were reported by Ringssorf et al.[25] for polymer liquid crystals **21** and **22**, and by Gleeson et al.[26] for the control of properties of nematic liquid crystals by a thienylfulgide **23** and some derivatives. Schuster et al.[27] reported that the pitch of a cholesteric liquid crystal was changed a little by the photochromic reaction of the added indolylfulgide **9**. Yokoyama et al.[28,29] reported that doping of the binaphthol-condensed indolylfulgides **15** and **16** induced the cholesteric liquid crystalline phase from a nematic liquid crystalline phase and the cholesteric pitch was changed drastically by their photochromic reactions. It was also shown that the optically resolved indolylfulgide **24** functioned as a chiral photochromic dopant, although the effect was small.[29]

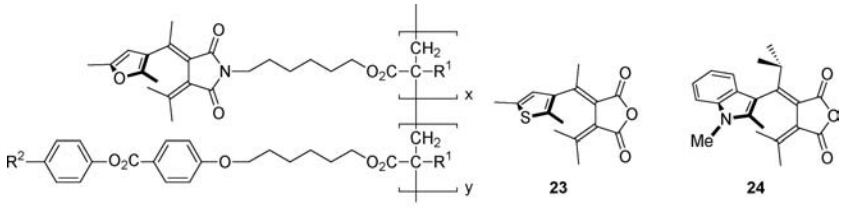

22: R^1 = H, R^2 = CN
22: R^1 = Me, R^2 = OMe

23 **24**

86.4 Control of Fluorescent Properties

The first fulgide found to exhibit fluorescence at room temperature, although in the weak/strong manner, was reported by Port et al.[30] as the derivative **25** that possesses a light-absorbing antenna and a fluorescent dye at either end of a thienylfulgide core. A binaphthol-condensed indolylfulgide **15** synthesized by Yokoyama et al., attaching neither antenna nor fluorescent dye, showed the complete on/off switching of the fluorescent ability, because only the C-form emitted fluorescent light.[31] The second on/off switching of fluorescence with fulgide was reported by Rentzepis et al.[32] for a unique indolylfulgide **26** and some other derivatives. The indolyl group of **26** was connected to the alkylidenesuccinic anhydride at the 2-position of indole. It was also reported that the absorption maximum wavelength of the C-form of 2-connected indolylfulgide exhibited solvent effects: in more polar solvents, the absorption maximum was observed at longer wavelength.[33]

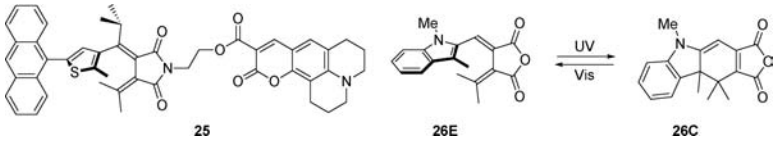

86.5 Supramolecular Properties Controlled by Fulgides

Crowned Fulgides

A fulgide **27** with the benzo-15-crown-5 as the aromatic ring was prepared by Guo et al.[34] Incorporation of alkaline-earth metal cations in the crown-ether moiety resulted in a shift of the absorption of the C-form by more than 40 nm toward shorter wavelengths.

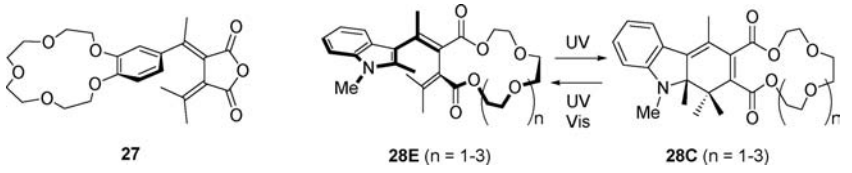

Crowned Fulgenates

Three fulgenates having the crown-ether-like cyclic diester moiety **28** (n = 1, 2, 3) were synthesized by Yokoyama et al.[35] The size-selective incorporation of alkali metal cations, the smaller complexation ability of the C-forms compared to the corresponding *E*-forms, and the on/off of photocyclization of the *E*-form in the absence/presence of the specific alkali metal cation were observed.

Fulgimide with Triplex Hydrogen Bonds

Yokoyama et al.[36] reported that fulgimide **29** changed its ability to form triplex hydrogen bonds with the 2,6-diacylaminopyridine **30** upon photocyclization due to the structural change. While **29E** has enough flexibility around the bismethylenesuccinimide structure to adjust the conformation to permit the triplex hydrogen bonds with **30**, **29C** has little flexibility because it has a maleimide structure. Consequently, the association constant of **29E** with **30** was 855 mol^{-1} dm^3, whereas that of **29C** with **30** was 156 mol^{-1} dm^3 at 21°C in toluene.

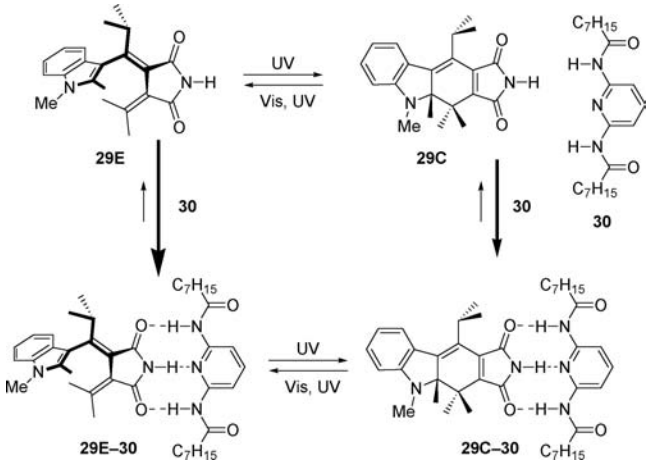

Fulgimides Attached to Peptides

Willner et al.[37] attached a thienylfulgimide to concanavalin A, a protein that forms complexes with pyranoses such as α-D-mannopyranoside, to form **31**. UV irradiation increased the association constant. Also, a thienylfulgide-modified α-chimotrypsin **32** was synthesized by Willner et al.[38] The esterification rate was controllable by photoirradiation.

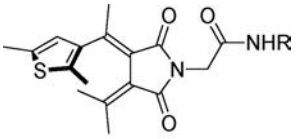

31E: R = Concanavalin A
32E: R = α–Chymotrypsin

86.6 Fulgides for Optical Devices

Nondestructive Readout of Memories

A number of requirements, such as durability, diode laser sensitivity, efficient photoreactivity, etc., are necessary to make use of the thermally irreversible photochromic compounds as photon-mode rewritable optical recording media. Among these requirements, the challenging problem is to make the recording system have a nondestructive readout method. Several methods using fulgides have been proposed to date.

Acid-Base Equilibrium

Although the colored form of dimethylamino-substituted indolylfulgide **33C** in toluene did not revert to **33E** on visible light irradiation,[39] the protonated **33CH**, generated by adding CCl_3CO_2H, restored the photochromic reactivity.[40] In addition, the absorption maximum of **33CH** became shorter than that of **33C** because of the loss of the electron-donating ability of the dimethylamino group. If the amount of acid was small, both **33C** and **33CH**, together with **33E** and **33EH**, should exist with the equilibrated amount at the pss in the system. Therefore, the writing was carried out by UV-light irradiation on **33E** and **33EH** while the readout was achieved by visible light of longer wavelength where only **33C** absorbed light but no photoreaction occurred. The erasing was effected by shorter wavelength visible light absorbed by **33CH** because of the equilibrium maintained between **33C** and **33CH**.

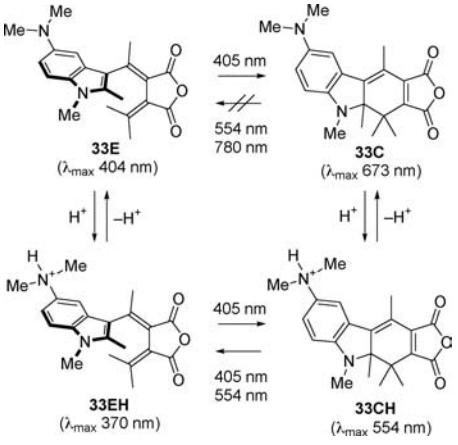

Wavelength Dependency of Discoloration Quantum Yield

Some of the fulgides described have been shown to exhibit quantum yields for decoloration using visible-light irradiation that are wavelength dependent.[41] Yokoyama et al. reported that dimethylaminoindolylfulgide **33C** returned, although very slowly, to **33E** in a PMMA film using visible-light irradiation. The quantum yield for this process was found to decrease when the irradiation was brought about by light of longer wavelength. Surprisingly, the quantum yield was zero although there was still observable absorption. Thus, irradiation at relatively short wavelengths in the absorption of visible region was used to erase the record, whereas irradiation at the far end of the absorption was used to read the record. After 10^5 times of reading the record on the disk with a 784-nm laser, the absorption was still more than 80% of the initial.[42]

Readout with Optical Rotation

Non-racemic mixtures of the chiral compound have the optical rotation values (rotation angles of the linearly polarized light after passing through the material) at wavelengths outside the absorption band. This means that detection of optical rotation can be carried out independently from the photochromic reactions: that is, the record can be read nondestructively. To examine the validity of this idea, Yokoyama et al. measured the change in optical rotation between **15E** and the pss of 366-nm light irradiation. In toluene, the specific rotation of **15E** at 589 nm (sodium D-line) was −572°, while it was −186° at the pss. When **15** is doped in a PMMA film, the net change of optical rotation by repeated alternative UV-VIS photoirradiation was about 0.01° on average.[21]

Readout with Change in IR Absorbance

The reversible change of the structures of the photochromic fulgides by iterative photoirradiation not only changes the absorption spectra of electronic transition but also the IR spectra. Port et al. found that while the fulgide **34E** has a small absorption at 1523 cm,$^{-1}$ **34C** has a medium absorption at that wavenumber. The transmittance of an IR laser of 1534 cm^{-1} was decreased when a dichloromethane solution of **34E** was irradiated with 366-nm light. The reverse process could be brought about by irradiation at 546 nm.[43]

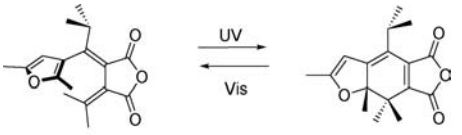

34E **34C**

Fatigue Resistivity

Resistance to fatigue toward the iterative photoirradiation is one of the most important features for a photochromic compound that might be used for optical memory media or switching devices. Diarylethenes are known to be more resistant to fatigue than fulgides. Efforts to improve the durability of fulgides have continued and some important results have recently been obtained.

Elimination of Oxygen from the Photochromic System

The photochromic layer containing a fulgide or a fulgimide can be isolated from air. Matsushima et al. demonstrated that this could be achieved by sticking two glass plates, carrying the photochromic layer on one side, together in the face-to-face manner, and the peripheral sides of the glass plates were sealed with an epoxy resin. The photochromic layer consisted of either (1) a spin-coated polymer containing a fulgide, or (2) an organic glass gel containing a fulgimide. Although the fatigue resistivity of thienylfulgide **23** in polystyrene was not greatly improved, that of furylfulgide **2**, oxazolylfulgide **35** in polystyrene, and furylfulgimide **36** in a gel were enhanced.[44]

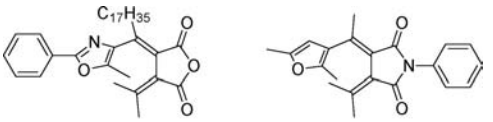

35E **36E**

Trifluoromethyl-Substituted Indolylfulgide

Yokoyama et al. synthesized a trifluoromethyl-substituted indolylfulgide **37**, which was shown to be highly durable toward photoirradiation.[45] Unfortunately, the colorless **37E**[46] was found to undergo undesired thermal rearrangement reactions, although its colored form was thermally stable.[47] Later, Lees et al.[48] clarified the structures of products of the thermal reaction and also the mechanism of their formation. They also synthesized some related fluorinated fulgides[49] as well as introduced the improved synthetic pathway of several indolylfulgides, including **37**.[50]

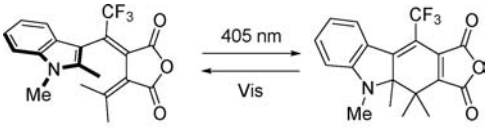

37E[46] **37C**

86.7 Tribochromic Fulgides

Heller et al.[51] reported a unique one-way color change within fulgide derivatives. When the dicyanomethylene-condensed fulgide **38** was recrystallized at the final stage of the synthesis, the first crop of crystals was bright yellow and the second crop was deep red. The structure of the yellow crystals (**38Y**) was determined by x-ray crystallographic analysis. Because both phenyl groups are located on the same side of the molecular plane, the authors called it "folded." When the crystalline compound was ground mechanically or when it was dissolved in solvent, the color changed to dark red (λ_{max} = 503 nm in toluene). The structure of the red crop of crystals, obtained by several methods as the most stable species, was also determined by an x-ray crystallographic analysis (**38R**), and the phenyl groups were found to lie on the opposite side of the molecular plane ("twisted"). As the color change from red to yellow was never achieved, the yellow **38Y** form was described as metastable. The authors termed this as "tribochromism." This effect is different from piezochromism, which involves the stable isomer converting to a metastable species that goes back thermally or by dissolution into the solvent. The tribochromic compounds do never revert to the metastable species; they can only be obtained by synthesis.

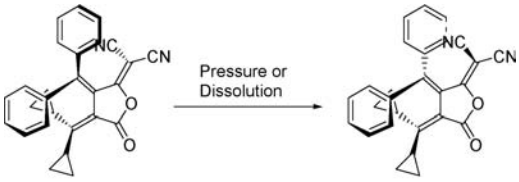

38Y (folded)
metastable form

38R (twisted)
stable form

Although a number of the related compounds have been synthesized, some gave only yellow crystals and others only red crystals. Only **38** gave both the yellow and red crystals, as reported above.

References

1. Stobbe, H., Die fulgide, *Annalen*, 380, 1, 1911.
2. Heller, H.G. and Szewczyk, M., Overcrowded molecules. X. Photoreactions of photochromic (α-phenylethylidene) (substituted methylene) succinic anhydrides, *J. Chem. Soc., Perkin Trans. 1*, 1487, 1974.
3. Darcy, P.J., Heller, H.G., Strydom, P.J., and Whittall, J., Photochromic heterocyclic fulgides. 2. Electrocyclic reactions of (*E*)-α-2,5-dimethyl-3-furylethylidene (alkyl-substituted methylene)-succinic anhydrides, *J. Chem. Soc., Perkin Trans. 1,* 202, 1981.
4. Heller, H.G. and Langan, J.R., Photochromic heterocyclic fulgides. 3. The use of (*E*)-α-(2,5-dimethyl-3-furylethylidene) (isopropylidene)succinic anhydride as a simple convenient chemical actinometer, *J. Chem. Soc., Perkin Trans. 2,* 341, 1981.
5. Yokoyama, Y., Fulgides for memories and switches, *Chem. Rev*, 100, 1717, 2000.
6. Yokoyama, Y., Molecular switches with photochromic fulgides, in *Molecular Switches*, Feringa, B.L., Ed., Wiley-VCH, Weinheim, 2001, chap. 4.
7. (a) Heller, H.G., New fatigue-resistant organic photochromic materials, *Spec. Publ., R. Soc. Chem., Fine Chem. Electron. Ind.*, 60, 120, 1986. (b) Heller, H.G., Fulgides and related systems, in *CRC Handbook of Organic Photochemistry and Photobiology*, Horspool, W.M. and Song, P.-S., Eds., CRC Press, Boca Raton, FL, 1994, chap. 13.
8. Whittall, J., 4+2 Systems: Fulgides, in *Photochromism: Molecules and Systems*, Dürr, H. and Bouas-Laurent, H., Eds., Elsevier, Amsterdam, 1990, chap. 9.
9. Whittall, J., Fulgides and Fulgimides — A promising class of photochrome for application, in *Applied Photochromic Polymer Systems*, McArdle, C.B., Ed., Blackie, Glasgow, 1992, chap. 3.
10. Fan, M., Yu, L., and Zhao, W., Fulgide family compounds: synthesis, photochromism, and applications, in *Organic Photochromic and Thermochromic Compounds, Vol. 1, Main Photochromic Families*, Crano, J.C. and Guglielmetti, R., Eds., Plenum Publishers, New York, 1999, chap. 4.
11. Kaneko, A., Tomoda, A., Ishizuka, M., Suzuki, H., and Matsushima, R., Photochemical fatigue resistances and thermal stabilities of heterocyclic fulgides in PMMA film, *Bull. Chem. Soc. Jpn.*, 61, 3569, 1988.
12. Cabrera, I., Dittrich, A., and Ringsdorf, H., Thermally irreversible photochromic liquid crystal polymers, *Angew. Chem. Int. Ed. Engl.,* 30, 76, 1991.
13. Heller, H.G., Hughes, D.S., Hursthouse, M.B., and Rowles, N.G., Thermally stable fatigue resistant near infrared active photochromic compounds, exemplified by 6-amino-7-cyano-3-(dicyclopropylmethylene) -4-(2,5-dimethyl -3-furyl)-benzofuran-2(3*H*)-one, *J. Chem. Soc., Chem. Commun.*,1397, 2000.
14. Heller, H.G., Koh, K.S. V., Köse, M., and Rowles, N.G., Photochromics by design — The art of molecular tailoring., *Advances in Color Science and Technology,* 4, 6, 2001.
15. Yu, L., Zhu, D., and Fan, M., Synthesis and photochromism of 5-dicyanomethylene-4-isopropylidene-3-[1-(1-*P*-methozy-phenyl-2-methyl-5-phenyl-3-pyrryl)-ethylidene- tetrahyrofuran-2-one, *Mol. Cryst. Liq. Cryst*., 297, 107, 1997.
16. Sun, Z., Hosmane, R.S., and Tadros, M., Fulgides and photochromism. Synthesis of (*E*)- and (Z)-5-dicyanomethylene-4-dicyclopropylmethylene-3- [1-(2,5-dimethyl-3-furyl)ethylidene]tetrahydrofuran-2-one, *Tetrahedron Lett.,* 36, 3453, 1995.
17. Sun, Z. and Hosmane, R.S., Photochromism of fulgides and stereoelectronic factors: Synthesis of (*E*)-4-(3)-adamantylidene-5-dicyanomethylene-3 -(4)-[1-(2,5-dimethylfuryl)ethylidene]tetrahdrofuran-2-one 4 and 4a and (*E*)-4-adamantylidene-3-[2,6-dimethyl-3,5-bis(*p*-diethylaminostyryl)benzylidene]tetrahydrofuran-2,5-dione 10, *J. Heterocyclic Chem.*, 32, 1819, 1995.
18. Yokoyama, Y., Sugiyama, K., Yamada, S., Takimoto, H., and Kurita, Y., Fulgenates. A new class of fulgide-related thermally irreversible photochromic system, *Chem. Lett.*, 749, 1994.

19. Yokoyama, Y., Miyasaka, M., Uchida, S., and Yokoyama, Y., Cyclic fulgenates. Enlargement of quantum yields of coloring reaction of photochromic fulgenates, *Chem. Lett.*, 479, 1995.
20. Yokoyama, Y., Serizawa, T., Suzuki, S., Yokoyama, Y., and Kurita, Y., Fulgenolides. Thermally irreversible photochromic lactones with large quantum yields of photoreactions, *Chem. Lett.*, 17, 1995.
21. Yokoyama, Y., Uchida, S., Yokoyama, Y., Sugawara, Y., and Kurita, Y., Diastereoselective photochromism of an (*R*)-binaphthol-condensed indolylfulgide, *J. Am. Chem. Soc.*, 118, 3100, 1996.
22. Yokoyama, Y., Kurosaki, Y., Sagisaka, T., and Azami, H., Photochromism of (*R*)-binaphthol-condensed benzofurylfulgide and control of properties, *Mol. Cryst. Liq. Cryst. Sect. A*, 344, 223, 2000.
23. Yokoyama, Y., Okuyama, T., Yokoyama, Y., and Asami, M., Highly diastereoselective photochromic cyclization of an indolylfulgide derivative possessing C_2-symmetric chiral diol as an auxiliary, *Chem. Lett.*, 1112, 2001.
24. Badland, M., Cleeves, A., Heller, H.G., Hughes, D.S., and Hursthouse, M.B., Photochromic heteroaromatic thiofulgides and dimethybutanoic acid lactones, *J. Chem. Soc., Chem. Commun.*, 1567, 2000.
25. Cabrera, I., Dittrich, A., and Ringsdorf, H., Thermally irreversible photochromic liquid crystal polymers, *Angew. Chem. Int. Ed. Engl.*, 30, 76, 1991.
26. Allinson, H. and Gleeson, H.F., Physical properties of mixtures of low molar mass nematic liquid crystals with photochromic fulgide guest dyes, *Liq. Crystals,* 14, 1469, 1993.
27. Janicki, S.Z. and Schuster, G.B., A liquid crystal opto-optical switch: nondestructive information retrieval based on a photochromic fulgide as trigger, *J. Am. Chem. Soc.*, 117, 8524, 1995.
28. Yokoyama, Y. and Sagisaka, T., Reversible control of pitch of induced cholesteric liquid crystal by optically active photochromic fulgide derivatives, *Chem. Lett.*, 687, 1997.
29. Sagisaka, T. and Yokoyama, Y., Reversible control of the pitch of cholesteric liquid crystals by photochromism of chiral fulgide derivatives, *Bull. Chem. Soc. Jpn.*, 73, 191, 2000.
30. Walz, J., Ulrich, K., Port, H., Wolf, H.C., Wonner, J., and Effenberger, F., Fulgides as switches for intramolecular energy transfer, *Chem. Phys. Lett.*, 213, 321, 1993.
31. Inada, T., Uchida, S., and Yokoyama, Y., Perfect on/off switching of emission of fluorescence by photochromic reaction of a binaphthol-condensed fulgide derivative, *Chem. Lett.*, 321, 1997.; *Chem. Lett.*, 961, 1997.
32. Liang, Y.C., Dvornikov, A.S., and Rentzepis, P.M., Fluorescent photochromic fulgides, *Res. Chem. Intermed.*, 24, 905, 1998.
33. Liang, Y.C., Dvornikov, A.S., and Rentzepis, P.M., Photochemistry of photochromic 2-indolylfulgides with substituents at the 1'-position of the indolylmethylene moiety, *J. Photochem. Photobiol. A: Chem.,* 146, 83, 2001.
34. Guo, Z., Wang, G., Tang, Y., and Song, X., A crown ether bearing fulgide: the regulation of photochromism by supramolecular effects, *Liebigs Ann.*, 941, 1997.
35. Yokoyama, Y., Ohmori, T., Okuyama, T., Yokoyama, Y., and Uchida, S., Photochromism of fulgenates possessing crown-ether moiety, *Mol. Cryst. Liq. Cryst. Sect. A*, 344, 265, 2000.
36. Okuyama, T., Yokoyama, Y., and Yokoyama, Y., Control of the association of indolylfulgimide with bis(acylamino)pyridine by photochromism, *Bull. Chem. Soc. Jpn.*, 74, 2181, 2001.
37. Willner, I., Rubin, S., Wonner, J., Effenberger, F., and Bäuerle, P., Photoswitchable binding of substrates to proteins: photoregulated binding of α-D-mannopyranose to concanavalin A modified by a thiophenefulgide dye, *J. Am. Chem. Soc.*, 114, 3150, 1992.
38. Willner, I., Lion-Digan, M., Rubin, S., Wonner, J., Effenberger, F., and Bäuerle, P., Photoregulation of α-chymotrypsin activity in organic media: effects of bioimprinting, *Photochem. Photobiol.,* 59, 491, 1994.
39. Yokoyama, Y., Tanaka, T., Yamane, T., and Kurita, Y., Synthesis and photochromic behavior of 5-substituted indolylfulgides, *Chem. Lett.,* 1125, 1991.

40. Yokoyama, Y., Yamane, T., and Kurita, Y., Photochromism of a protonated 5-dimethylaminoindolylfulgide: a model of a non-destructive readout for a photon mode optical memory, *J. Chem. Soc., Chem. Commun.*, 1722, 1991.
41. Yokoyama, Y. and Kurita, Y., Photochromic fulgides applicable to optical information storage — Discovery of new nondestructive readout method, *Nippon Kagaku Kaishi.*, 998, 1992.
42. Matsui, F., Taniguchi, H., Yokoyama, Y., Sugiyama, K., and Kurita, Y., Application of photochromic 5-dimethylaminoindolylfulgide to photon-mode erasable optical memory media with non-destructive readout ability based on wavelength dependence of bleaching quantum yield, *Chem. Lett.*, 1869, 1994.
43. (a) Seibold, M. and Port, H., Mid-infrared recognition of the reversible photoswitching of fulgides, *Chem. Phys. Lett.*, 252, 135, 1996. (b) Seibold, M., Port, H., and Gustav, K., Determination of reaction quantum yields of photochromic fulgides using mid IR spectroscopy: quantitative evaluation and normal mode analysis, *Chem. Phys. Lett.*, 314, 65, 1999. (c) Seibold, M., Handschuh, M., Port, H., and Wolf, H.C., Photochromic fulgides: towards their application in molecular electronics, *J. Lumin.*, 72–74, 454, 1997.
44. Matsushima, R., Nishiyama, M., and Doi, M., Improvements in the fatigue resistances of photochromic compounds, *J. Photochem. Photobiol. A: Chem.,* 139, 63, 2001.
45. Yokoyama, Y. and Takahashi, K., Trifluoromethyl-substituted photochromic indolylfulgide. A remarkable durable fulgides towards photochemical and thermal treatments, *Chem. Lett.*, 1037, 1996.
46. According to the IUPAC nomenclature, the double bond concerning CF_3 group of photocyclizable **37** is *Z*. However, for the easy comparison with other fulgides, it is called **37E** here.
47. Yokoyama, Y. and Takahashi, K., unpublished data, 1996.
48. Wolak, M.A., Sullivan, J.M., Thomas, C.J., Finn, R.C., Birge, R.R., and Lees, W.J., Thermolysis of a fluorinated indolylfulgide features a novel 1,5-indolyl shift, *J. Org. Chem.*, 66, 4739, 2001.
49. Wolak, M.A., Gillespie, N.B., Thomas, C.J., Birge, R.R., and Lees, W.J., Optical and thermal properties of photochromic fluorinated adamantylidene indolylfulgides, *J. Photochem. Photobiol. A: Chem.,* 147, 39, 2002.
50. Thomas, C.J., Wolak, M.A., Birge, R.R., and Lees, W.J., Improved synthesis of indolyl fulgides, *J. Org. Chem.*, 66, 1914, 2001.
51. Asiri, A.M. A., Heller, H.G., Hursthouse, M.B., and Karalulov, A., Tribochromic compounds, exemplified by 3-dicyclopropylmethylene-5-dicyanomethylene-4-diphenylmethylenetetrahydrofuran-2-one, *J. Chem. Soc., Chem. Commun.*, 799, 2000.

87

1,4-Quinone Cycloaddition Reactions with Alkenes, Alkynes, and Related Compounds

Andrew Gilbert
The University of Reading

87.1 Introduction

The photochemistry of quinones has a long history and the earlier literature on the cycloaddition processes was well-referenced in the previous edition of this Handbook.[1] It is, however, felt that it will be useful, particularly for readers new to the subject, to present here a brief general outline of the established mechanistic features of these processes before the more recent activities in this area are considered.

Intersystem crossing between the S_1 and T_1 states of 1,4-quinones is highly efficient and essentially all their photochemistry arises from the lowest excited triplet state. There is the general trend, illustrated in Figure 87.1, that in the cycloaddition reactions of 1,4-quinones, the $^3n,\pi^*$ state yields products from the carbonyl group while reaction at the ethene moiety arises from the $^3\pi,\pi^*$ state. Thus, with ethenes, discrimination between the formation of spiro-oxetanes **1** and cyclobutanes **2** can depend on the nature of the lowest excited triplet state. For example, 1,4-benzoquinone ($^3n,\pi^*$ state 76 kJ mol^{-1} below $^3\pi,\pi^*$ state) yields spiro-oxetanes almost exclusively, whereas 1,4-naphthoquinone, in which the energies of the $^3n,\pi^*$ and $^3\pi,\pi^*$ states are similar, affords both spiro-oxetanes and cyclobutanes. It is to be noted, however, that in general, spiro-oxetane formation is favored by an increase in the electron-donor characteristics of the ethene and that the introduction of electron-donor substituents on the quinone destabilizes the $^3n,\pi^*$ state and can increase its energy above that of the $^3\pi,\pi^*$, resulting in preferred addition at the ethene moiety.

It is widely accepted that the addition reactions of T_1 quinones to S_0 ethenes or ethynes occur either by a pathway involving a triplet exciplex, which collapses to a triplet biradical, or by radical ion formation

0-8493-1348-1/04/$0.00+$1.50

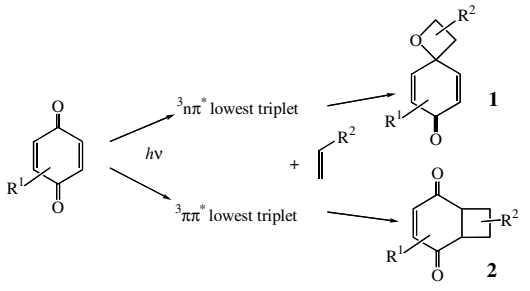

FIGURE 87.1 1,4-Quinone–ethene photocycloadditions.

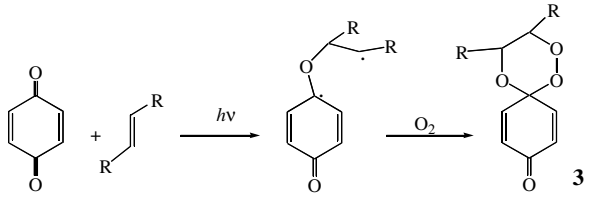

FIGURE 87.2 Trapping of the 1,4-biradical intermediate with oxygen.

and coupling processes. Evidence for the former route in 1,4-benzoquinone /alkene systems has been provided by laser flash photolysis (transients with nanosecond lifetimes assigned to exciplexes)[2] and the determination of isomer ratios of the spiro-oxetanes from *Z*- and *E*-but-2-ene[3] as well as by the trapping of the biradical intermediate with oxygen to give a 1,2,4-trioxane **3** in competition with spiro-oxetane formation (Figure 87.2).[4] The radical ion route is favored in polar solvents, and transients with microsecond lifetimes assigned to contact radical ion pairs have been observed in acetonitrile solution from chloro-1,4-naphthoquinones in the presence of electron-rich ethenes.[5]

It is not the intention in the current account to present a comprehensive review of the literature since the early 1990s, but rather by citing selected publications, to illustrate the breadth of interests in this area of quinone photochemistry and to provide further insight into the detailed mechanisms of these cycloaddition processes.

87.2 Cycloadditions of 1,4-Quinones to Ethene Derivatives

1,4-Benzoquinones and 1,4-Naphthoquinones

Styrene derivatives are commonly used addends in the photocycloaddition studies of 1,4-quinones. With *Z*- and *E*-anethole, 1,4-benzoquinone (BQ), 1,4-naphthoquinone (NQ), and 9,10-anthraquinone in acetonitrile solvent yield spiro-oxetanes in which the *trans*-isomer (e.g., **4** from naphthoquinone) predominates.[6] The process has been studied in detail by CIDNP techniques from which it is deduced that product formation proceeds from triplet radical ion pairs to the triplet biradical, and that there is no significant contribution from direct conversion of exciplex intermediates into the biradicals. Spiro-oxetane formation between simple alkenes and BQ generally has low regioselectivity but this is markedly improved with alkylidene cyclohexanes (Figure 87.3) such that the major isomer can be used as a new access to useful synthetic building blocks.[7] For the BQ/homobenzvalene **5** system, however, where the difference in stability between the intermediate biradicals can be expected to be considerably less, the selectivity ratio for the spiro-oxetanes **6** and **7** is reduced to 3:1, respectively, and the addition to NQ yields only the cyclobutane derivative **8**.[8] Quadricyclane and norbornadiene undergo the same photocycloaddition reaction to BQ, affording the oxolane **9** and the spiro-oxetane **10**.[9] Evidence from CIDNP

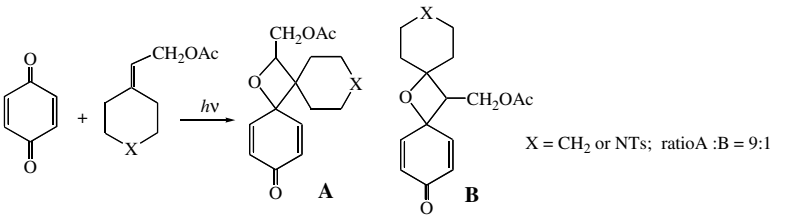

FIGURE 87.3 Photocycloaddition of BQ to alkylidene cyclohexanes.

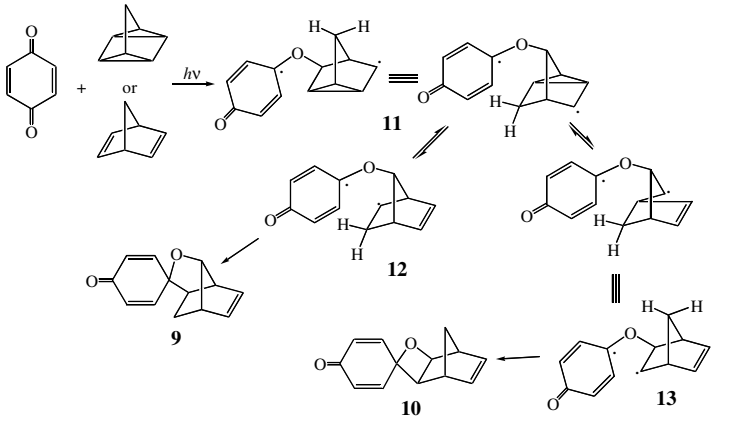

FIGURE 87.4 Photoaddition of BQ to norbornadiene and quadricyclane.

studies leads to the conclusion that the two adducts are formed by geminate processes, as outlined in Figure 87.4, in which the radical ion pair of the quinone and quadricyclane/norbornadiene collapses to the biradical **11**, which undergoes cleavage of the three-membered ring to give the 1,5- and 1,4-biradicals **12** and **13**, which are the respective precursors of the oxolane and the spiro-oxetane.

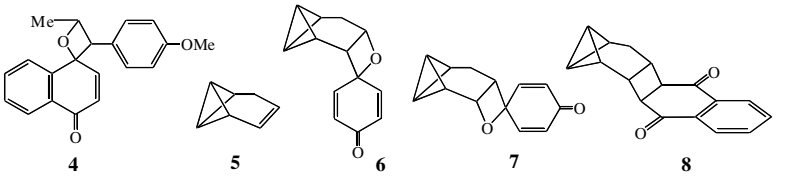

Dibenzoylmethane undergoes a de Mayo-type photoaddition reaction at the carbonyl group of BQ, NQ, and 9,10-anthraquinone to give hydroxyoxetanes that, on further irradiation, afford 1,5-diketones in reasonable yield by a retro-Aldol process.[10] The reaction is outlined in Figure 87.5 for NQ and the addition is reported to be reversed by 254-nm radiation, as is the conversion of the hydroxyoxetane to the 1,5-diketone with 300-nm radiation.

As expected, both duroquinone[11] and 2-acetoxy-1,4-naphthoquinone[12,13] undergo [2π+2π]-photocycloaddition with ethenes to give cyclobutane derivatives. In the former system, the primary adduct **14** from stilbene is reported to be unstable and undergoes oxidation and ring opening to give the cyclooctatriene **15**, while the addition of styrene to the NQ is both regio- and stereo-specific, giving **16**[13] and occurs in high yield in sunlight.[14] Interestingly, ethenes do not undergo [2π+2π]-photocycloaddition to NQs that are 2-substituted with hydroxy, amino, or mercapto groups. Instead, the reaction of these quinones involves [3+2]-addition and gives high yields of 2,3-dihydronapho[2,3-*b*]furan-4,9-diones **17**,[15]

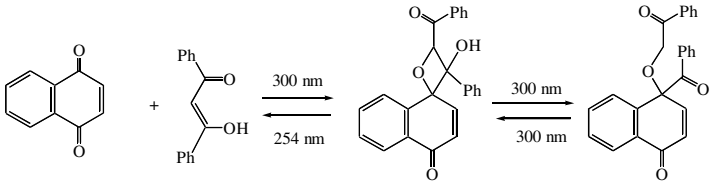

FIGURE 87.5 Photoaddition of BQ to dibenzoylmethane.

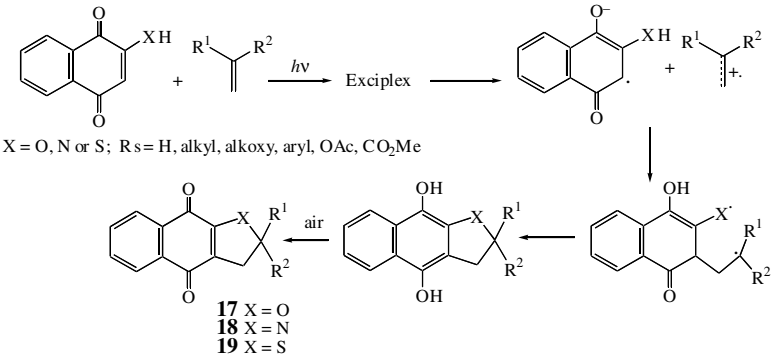

FIGURE 87.6 2-Hydroxy-, amino-, and mercapto-NQ photocycloadditions.

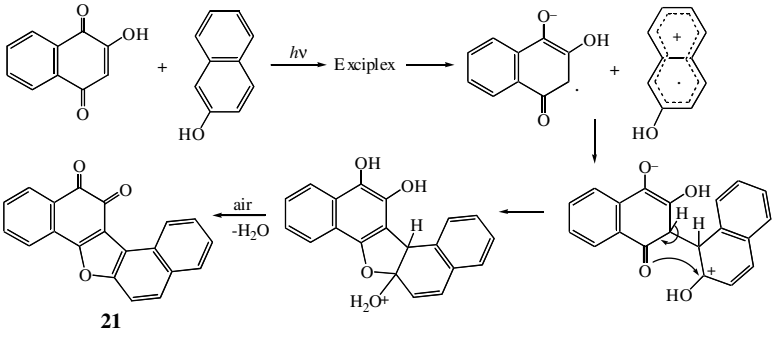

FIGURE 87.7 Photoaddition of 2-hydroxy-NQ to 2-hydroxynaphthalene.

2,3-dihydro-1*H*-benz[*f*]indole-4,9-diones **18**[16] and 2,3-dihydronapho[2,3-*b*]thiophene-4,9-diones 19,[17] respectively. The proposed mechanism of these general processes is summarized in Figure 87.6, and it should be noted that the mercapto-quinone has to be generated *in situ* photochemically from 5-hydroxy-naphth[2,1-*d*]-1,3-oxathiol-2-one **20**. It is relevant to note here that [3+2]-cycloaddition has also been reported for 2-hydroxynaphthalene as the addend with 2-hydroxy-NQ but in this case, the product has the *ortho*-quinone structure **21** and is considered to arise by the mechanism in Figure 87.7.[18] In contrast, 2-methoxy- and 2-acetoxy-naphthalenes yield the [2+2]-adducts **22** with 2-hydroxy-NQ, whereas 1-methoxy-naphthalene behaves like an ethene, giving **23**, presumably by a route similar to that outlined in Figure 87.6.

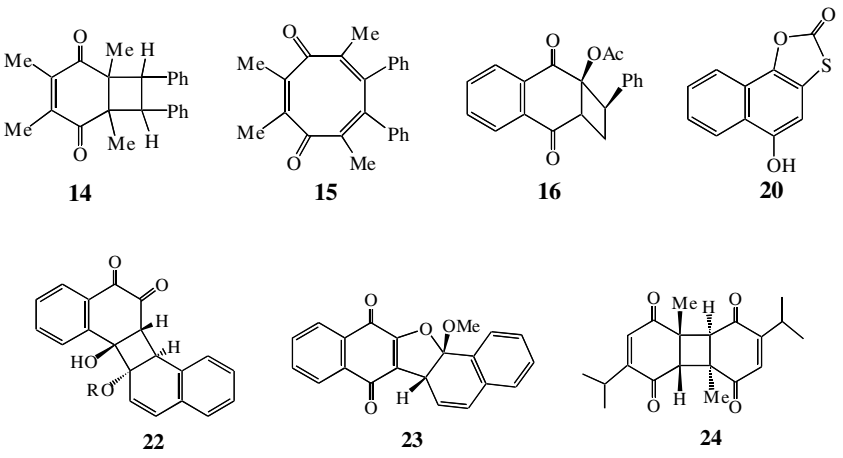

1,4-Quinones also photodimerize by [2π+2π]-cycloaddition and, after some 130 years since the first report of the solid-state photoreaction of thymoquinone, the product has been unambiguously assigned as arising from a regio- and stereo-specific process to give the head-to-tail structure **24**.[19] Intramolecular photodimerization of the di-quinone moiety in **25** occurs to give the tube-like structure **26,** which on exposure to sunlight undergoes a second [2π+2π]- cycloaddition to yield **27**.[20]

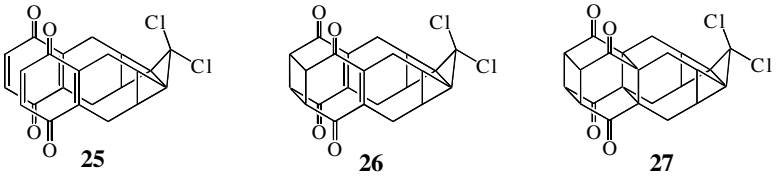

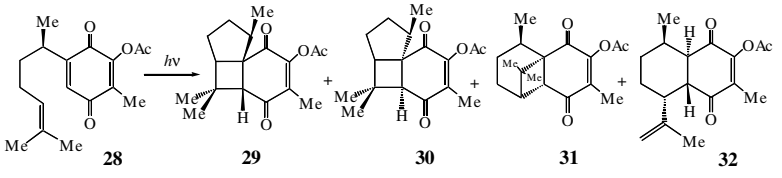

FIGURE 87.8 Intramolecular photocycloaddition of isoperezone.

The intramolecular photoaddition of 1,4-quinone/ethene systems has not attracted much interest in recent years and yet its potential for accessing complex molecular skeletal is appreciable. The reaction with isoperezone acetate **28** is, however, not selective and yields the [2π+2π]-cycloadducts **29**, **30,** and **31,** as well as the ene product **32** in respective ratios of 1.5: 1.0:1.2:4.0 (Figure 87.8).[21] Both allyl and vinyl BQs have interesting photochemistries. In the former series, the biradical **33** produced on irradiation can be readily trapped by a variety of ethenes to give tricyclic adducts **34** in yields dependent on the nature of the R groups on the addend (Figure 87.9).[22] The type of photoreaction that the vinyl BQs undergo is dependent on the position of the aryl group on the ethene substituent.[23] For example, while the 1-phenyl derivative **35** yields the benzofuran **36** in quantitative yield, the styryl compound **37** undergoes [4π+2π]-cyclodimerization, giving **38**, again in quantitative yield, and the 2,2-diphenylvinyl BQ **39** affords 30 to 40% yields of the phenanthrene-1,4-quinones **40** by 6π-photoelectrocyclization.

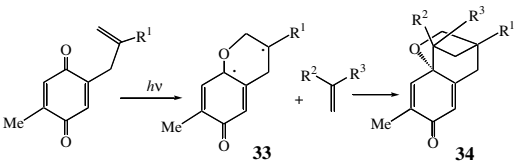

FIGURE 87.9 Trapping of the 1,4-biradical from 2-allyl-BQs with ethenes.

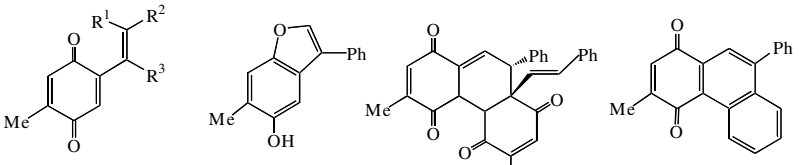

Few studies have been carried out into the photochemistry of 1,4-quinone/1,3-diene systems. It is therefore noteworthy and of appreciable synthetic interest that the [4π+2π]-photoaddition of BQ and NQ to cyclopentadiene and cyclohexa-1,3-diene in dry ethanol in the presence of triethylamine occurs with the opposite stereochemistry to that produced from the thermal reaction and the *exo*-isomers (e.g., **41** from cyclopentadiene and NQ) are obtained in 26 to 81% yields.[24]

Halogenated 1,4-Quinones

In recent years, the photoprocesses of halogenated quinones with ethenes, particularly the additions to chloranil (CA), have attracted appreciable attention. The electron-donor/acceptor characteristics of the ethenes can markedly influence both the site of attack on this quinone and the reaction efficiency; this latter feature can also be significantly dependent on the solvent polarity. These aspects of CA addition photochemistry are illustrated by the examples outlined below.

In benzene solution, the *Z*- and *E*-stilbenes **42** form approximately equal amounts of the two regioisomers of the *trans*-substituted spiro-oxetanes (e.g., **43** from 4-Me-**42**) with CA in yields of 80 to 88%.[25] These addition reactions do not occur in acetonitrile solution and *Z*- and *E*-4-methoxystilbenes do not photoreact with CA in either solvent. However, high yields of the *trans*-spiro-oxetanes **44** are formed from CA with *Z*- or *E*-ethyl cinnamate, ethyl 3-nitrocinnamate, benzalacetone, or chalcone in both benzene and acetonitrile. In contrast, allyl ethyl ether, methyl methacrylate, vinyl acetate, styrene, and α-chlorostyrene all yield cyclobutanes **45** with CA in benzene solution; but under the same conditions, indene and *E*-β-bromostyrene afford spiro-oxetanes.[26] Such variation in reaction site continues to be discussed in terms of the electron-donor/acceptor characteristics of the addends and the role of single electron transfer in the reaction pathway.

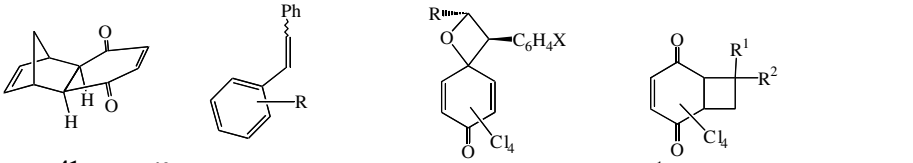

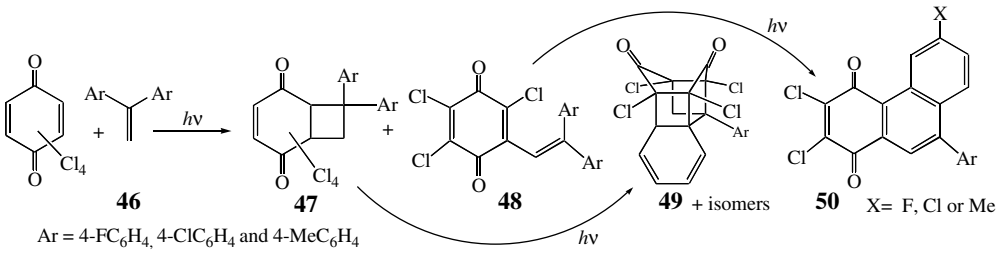

FIGURE 87.10 Photocycloaddition of CA to 1,1-diarylethenes.

It has been shown from a detailed investigation into the formation of spiro-oxetanes from the addition of CA to stilbene and some chloro derivatives in dioxane solution, that specific activation of either the precursor donor/acceptor stilbene/CA complex at 546 nm or the CA carbonyl at 436 nm gives rise to a common electron-transfer mechanism and produces the same regioisomers in identical ratios but with quantum yields of 0.005 and 0.35, respectively.[27] It is concluded from time-resolved (fs/ps) spectroscopy of the former activation that the primary intermediate is the singlet radical ion pair and this unambiguously establishes, for the first time, the electron-transfer mechanism in the Paterno-Büchi process. Direct excitation of the quinone affords the triplet radical ion pair, and this is observed on the nanosecond/microsecond (ns/μs) time scale. The spin multiplicities of the radical ion pairs determine the reaction sequence time scales and thus the efficiencies of their collapse to give the 1,4-biradicals, which are the immediate precursors of the oxetanes. Kinetic studies of these systems have established that the coupling of the triplet radical ions to give the biradical is the crucial step in product formation and must compete with ionic separation, ion exchange, and back electron transfer.[28] Experimental evidence for these conclusions is provided by the marked influence of solvent polarity and donacity, as well as added salt, on the quantum yield of oxetane formation. For example, in dioxane, tetrahydrofuran, and dichloromethane solutions, the quantum yields are 0.34, 0.05, and 0.01, respectively, and with the addition of 0.1*M* tetra-*n*-butylammonium hexafluorophosphate to the tetrahydofuran solution, the value is reduced to 0.01.

The irradiation of benzene solutions of CA in the presence of the 1,1-diarylethenes **46** yields the [2π+2π]-cyclobutane adducts **47** and the substituted quinones **48**, both of which undergo further photochemistry to give the products **49** and **50** of intramolecular arene-ethene cycloaddition and 6π-electrocyclization, respectively (Figure 87.10).[29] It is proposed that products **48** arise from a single electron-transfer process from the donor ethene to the T_1 chloranil, and that the formation of the cyclobutane adducts are formed from the 1,4-biradicals without the involvement of an electron-transfer process. This conclusion is supported by the observation that the ratio of **47**:**48** increases with an increase in both the oxidation potential of the diarylethenes and in the positive ΔG^0 value for electron transfer between the addends; furthermore, the formation of **48** is greatly favored by an increase in solvent polarity.

In contrast to the straightforward photoaddition of homobenzvalene **5** to BQ to give the expected two spiro-oxetanes,[8] the corresponding reaction with CA yields a number of products as outlined in Figure 87.11.[30] The oxolane **51** is photorearranged to **52** by way of a zwitterionic intermediate in a process observed with other cyclohexadienones. The photoaddition of norbornadiene to CA yields the spiro-oxetanes **53** and **54** as well as the tetrahydrofuran derivatives **51** and **55**, but only low yields of the oxetane **53** are formed from CA and quadricyclane (contrast BQ additions). The novel adduct **56** is formed in 67% yield from irradiation of benzene solutions of CA in the presence of norborene.[31] The proposed pathway involves addition of the ethene across the 2,5-positions of the triplet quinone to give the biradical **57** which rearranges to the β-oxoketene **58** and this, in turn, undergoes intramolecular cyclization with concomitant [1,2]-migration of a chlorine atom (Figure 87.12). Similar adducts are formed between CA and cyclopentene and bicyclo[2.1.1]hex-2-ene but in both cases, the major products are the conventional spiro-oxetane and cyclobutane isomers.

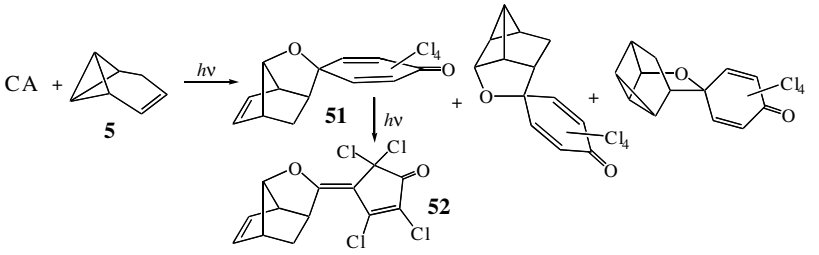

FIGURE 87.11 Photocycloaddition of CA to homobenzvalene.

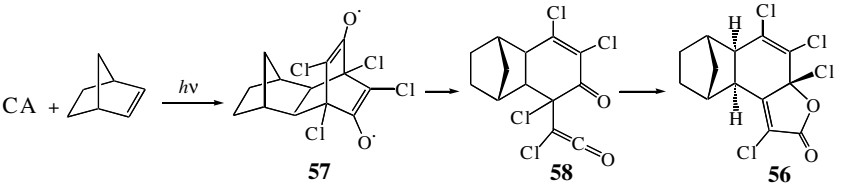

FIGURE 87.12 Photocycloaddition of CA to norbornene.

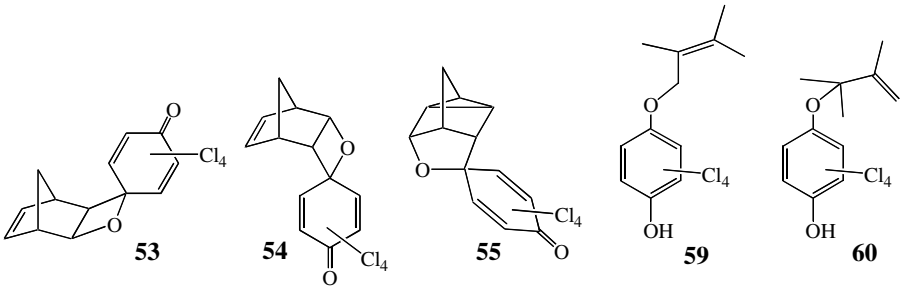

In the presence electron-rich alkenes such as 2,3-dimethylbut-2-ene, irradiation of CA gives the allylethers **59** and **60**, whereas with BQ, a substantial amount of the spiro-oxetane is also formed.[32] The product distribution of the allyl ethers is rationalized by steric effects on the H^+ abstraction and on the recombination of radicals as well as spin densities. The crucial role of solvent polarity in CA photochemistry is well illustrated by the results of a study into the reaction between the quinone and cyclohexanone enol trimethylsilyl ether **61** using time-resolved (ps) spectroscopy.[33] The influence of the solvent occurs following the formation of the radical ion pair ($CA^{-\cdot}$ $\mathbf{61}^{+\cdot}$). The $CA^{-\cdot}$ species is short lived in nonpolar solvents and cyclohex-2-en-1-one and **62** are the reaction products, whereas in acetonitrile, the lifetime is much longer, which allows diffuse separation of the radical ion pair and transference of the TMS to the solvent. The resulting ketyl radical couples to $CA^{-\cdot}$ yielding **63**.

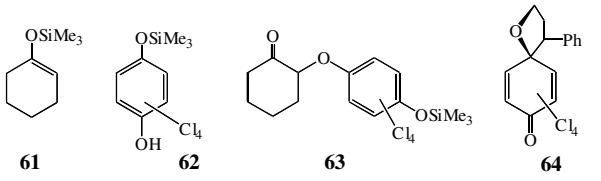

Cyclopropylbenzene is a good electron donor and, not surprisingly, yields triplet radical ion pairs with photoexcited CA.[34] In dichloromethane, these intermediates lead to the spiro-tetrahydrofuran adduct **64** in 68% yield, but in acetonitrile, this drops to 5%. Both NQ and 2,3-dichloro-NQ react similarly with cyclopropylbenzene on irradiation and again the yields of adducts corresponding to **64** are very dependent on solvent polarity.

A wide variety of ethenes undergo photoreaction with 2-mono- and 2,3-dihalogeno-NQs. For example, with arylethenes, [2π+2π]-cyclobutane adduct isomers are formed from styrene, 1,1-diphenylethene undergoes photosubstitution giving products analogous to **48,** and *E*-stilbene yields spiro-oxetanes.[13]

87.3 Cycloadditions of 1,4-Quinones to Ethyne Derivatives

The photocycloadditions of ethynes to 1,4-quinones are directly analogous to those of ethenes and, in general, similar influences affecting the site of reaction and the efficiency of the process operate in both systems. The oxetenes formed by addition of ethynes to the carbonyl group are unstable under ambient conditions and undergo ring opening to yield quinone methides as outlined in Figure 87.13.

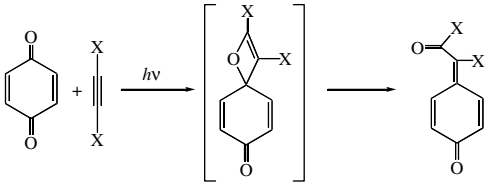

FIGURE 87.13 Photocycloaddition of ethynes to BQ.

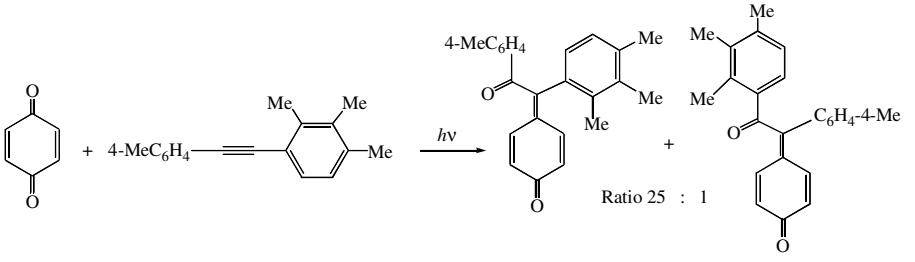

FIGURE 87.14 Photocycloaddition of BQ to diarylethynes.

Arylethynes are commonly used in the studies of these processes and the additions of 2,5-dichloro-BQ to methyl-substituted diphenylacetylenes have been investigated in detail by time-resolved (picosecond/nanosecond) spectroscopy to ascertain the role of radical ion pairs in the formation of the 1,4-biradical precursor of the spiro-oxetene.[35] Irradiation at 532 nm in the charge-transfer absorption band of this system in dichloromethane solution results in spontaneous electron transfer to give the singlet radical ion pair; but from the low quantum yield of adduct formation (*ca.* 1×10^{-3}), it is evident that the rapid decay of this species arises from back electron transfer. Direct excitation of the quinone (at 355 nm) yields the triplet radical ion pair, which may couple to the triplet biradical, dissociate to free ions, or undergo back electron transfer: in this case, the quantum yield of adduct formation is 0.1. However, from unsymmetrical diarylacetylenes, both routes give good yields of the same quinone methides with high regioselectivity (e.g., Figure 87.14); this establishes the same sequence of reactive intermediates. Crystalline 1:2 electron donor/acceptor complexes of these diarylacetylene/quinone systems have been prepared and characterized by x-ray crystallography.[36] Excitation of these crystals at either 355 or 532 nm leads to mixtures of the isomeric quinone methide adducts in ratios very similar to those reported from solution. Time-resolved diffuse reflectance spectroscopy again shows that the radical ion pair is the

reaction intermediate from both wavelengths of activation. It is indeed noteworthy that a pair of dissimilar reactants has the appropriate orientation for [2π+2π]-coupling in the crystals of the complex.

It appears that the addition of ethynes to the carbonyl group in quinones is more efficient than the corresponding ethene process because irradiation of BQ or NQ in the presence of the eneyne **65** preferentially yields quinone methides.[37] The photoaddition of 1,4-bis(phenylethynyl)benzene to BQ in dichloromethane solution gives the quinone methide **66**.[38] However, the expected cyclobutene formation between duroquinone and 1,4-diethynylbenzene is somewhat more complex and affords not only **67**, but also the ring-opened isomer **68** as well as the 2:1 adducts **69** and **70** in yields of 17, 19, 15, and 30%, respectively.[39]

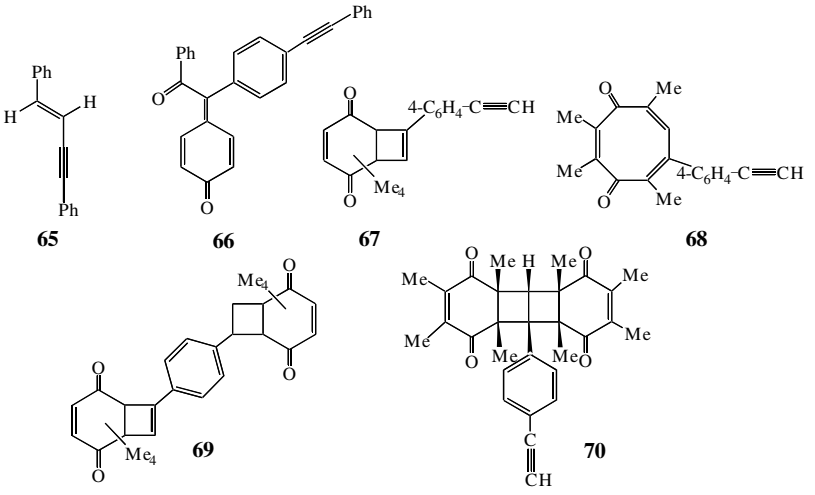

References

1. Creed, D., 1,4-Quinone cycloaddition reactions with alkene, alkynes and related compounds, in *CRC Handbook of Organic Photochemistry and Photobiology*, Horspool, W. M. and Song, P.-S., Eds., CRC Press, Boca Raton, FL, 1995, 280.
2. Schnapp, K.A., Wilson, R.M., Ho, D.M., Caldwell, R.A., and Creed, D., Benzoquinone-olefin exciplexes: the observation and chemistry of the *p*-benzoquinone-tetraphenylallene exciplex, *J. Am. Chem. Soc.*, 112, 3700, 1990.
3. Bunce, N.J. and Hadley, M., On the mechanism of oxetane formation in the photocycloaddition of *p*-benzoquinone to alkenes, *Can. J. Chem.*, 53, 3240, 1975.
4. Wilson, R.M., Wunderly, S.W., Walsh, T.F., Musser, A.K., Outcault, R., Geiser, F., Gee, S. K., Brabender, W., Yerino, D., Conrad, T.T., and Tharp, G.A., Laser photochemistry: trapping of the olefin-quinone preoxetane intermediates with molecular oxygen and chemistry of the resulting 1,2,4-trioxanes, *J. Am. Chem. Soc.*, **1**04, 4429, 1982.
5. Maruyama, K. and Imahori, H., Photoreactions of halogeno-1,4-naphthoquinones with electron-rich alkenes, *J. Chem. Soc., Perkin Trans. 2*, 257, 1990.
6. Eckert, G. and Goez, M., Photoinduced electron-transfer reactions of aryl olefins. 1. Investigation of the Paterno-Buchi reaction between quinones and anetholes in polar-solvents, *J. Am. Chem. Soc.*, 116, 11999, 1994.
7. Ciufolini, M.A., Riverafortin, M.A., and Byrne, N.E., Regioselective photocycloadditions of benzoquinones to alkylidenecyclohexanes — a new synthetic resource, *Tetrahedron Lett.*, 34, 3505, 1993.
8. Christl, M. and Braun, M., [2+2] Photocycloadditions of homobenzvalene, *Liebigs Ann.-Recl.*, 1135, 1997.

9. Goez, M. and Frisch, I., Photocycloadditions of quinones with quadricyclane and norbornadiene — a mechanistic study, *J. Am. Chem. Soc.*, 117, 10486, 1995.
10. Kim, A.R., Kim, K.J., Shim, S.C., and Kim, S. S., Formation of 1,5-diketones from the photoaddition of 1,3-diphenyl-1,3-propanedione to *p*-benzoquinones, *Bull. Korean Chem. Soc.*, 18, 1125, 1997; Kim, S.S., Lim, S.J., Lee, J.M., and Shim, S.C., Photochemical formation of 1,5-diketones from dibenzoylmethane and some quinones, *Bull. Korean, Chem. Soc.*, 20, 531, 1999.
11. Kim, A.R., Kim, S.S., Yoo, D.J., and Shim, S.C., Photoaddition reactions of duroquinone to phenyl substituted ethylenes, *Bull. Korean. Chem. Soc.*, 18, 665, 1997.
12. Senboku, H., Kajizuka, Y., Kobayashi, K., Tokuda, M., and Suginome, H., Photoinduced molecular transformations. 160. Furan annelation of 2-hydroxynaphthoquinone involving photochemical addition and radical fragmentation: xeclusion of the intermediacy of [2+2] cycloadduct in a one-pot formation of furanoquinones by the regioselective 3+2 photoaddition of hydroxyquinones with alkenes, *Heterocycles*, 44, 341, 1997.
13. Cleridou, S., Covell, C., Gadhia, A., Gilbert, A., and Kamonnawin P., Photocycloaddition of arylethenes to 2-substituted-1,4-naphthoquinones and reactions of the cyclobutane adduct isomers, *J. Chem. Soc., Perkin Trans. 1*, 1149, 2000.
14. Covell, C., Gilbert, A., and Richter, C., Sunlight-induced regio- and stereo-specific ($2\pi + 2\pi$) cycloaddition of arylethenes to 2-substituted-1,4-naphthoquinones, *J. Chem. Res.*, 316, 1998.
15. Kobayashi, K., Kanno, Y., and Suginome, H., Photoinduced molecular-transformations. 141. New one-step general-synthesis of benzofuran-4,7-diones by the regioselective (3+2) photoaddition of 2-hydroxy-1,4-benzoquinones with various alkenes, *J. Chem. Soc., Perkin Trans. 1*, 1449, 1993; Kobayashi, K., Shimizu, H., Sasaki, A., and Suginome, H., Photoinduced molecular-transformations. 140. New one-step general-synthesis of naphtho[2,3-b]furan-4,9-diones and their 2,3-dihydro derivatives by the regioselective [3+2] photoaddition of 2-hydroxy-1,4-naphthoquinones with various alkynes and alkenes — application of the photoaddition to a 2-step synthesis of maturinone, *J. Org. Chem.*, 58, 4614, 1993; Suginome, H., Kamekawa, H., Sakurai, H., Konishi, A., Senboku, H., and Kobayashi, K., Photoinduced molecular-transformations. 145. Regioselective [3+2]-photoadditions of 2-hydroxyphenanthrene-1,4-dione with electron-rich alkenes and phenylacetylene — new one-step synthesis of 9,10-dihydrophenanthro-[2,3-b]furan-7,11-diones and 2-phenylphenanthro[2,3-b]furan-7,11-dione, *J. Chem. Soc., Perkin Trans. 1*, 471, 1994.
16. Kobayashi, K., Takeuchi, H., Seko, S., Kanno, Y., Kujime, H., and Suginome, H., Photoinduced molecular transformations. 142. One-step synthesis of 1*H*-benz[f]indole-4,9-diones and 1*H*-indole-4,7-diones by a regioselective photoaddition of 2-amino-1,4-naphthoquinones and 2-amino-1,4-benzoquinones with alkenes, *Helv. Chim. Acta,* 76, 2942, 1993.
17. Suginome, H., Kobayashi, K., Konishi, A., Minakawa, H., and Sakurai, H., One-step synthesis of 2,3-dihydronaphtho[2,3-b]thiophene-4,9-diones by a new regioselective [3+2] photoaddition of photogenerated 2-mercapto-1,4-naphthoquinone with alkenes, *J. Chem. Soc., Chem. Commun.*, 807, 1993.
18. Suginome, H., Konishi, A., Sakurai, H., Minakawa, H., Takeda, T., Senboku, H., Tokuda, M., and Kobayashi, K., Photoinduced molecular-transformations. 156. New photoadditions of 2-hydroxy-1,4-naphthoquinones with naphthols and their derivatives, *Tetrahedron*, 51, 1377, 1995.
19. Robbins, R.J. and Falvey, D.E., Stereochemistry of the solid-state photodimerization of thymoquinone, *Tetrahedron Lett.*, 34, 3509, 1993.
20. Banwell, M.G., Hockless, D.C.R. and Walter, J.M., Construction of a tube-like molecule via sequential cyclopropylidene dimerisation and intramolecular [π2s+π2s] cycloaddition reactions, *J. Chem. Soc., Chem. Commun.*, 1469, 1996.
21. Yuste, F., Barrios, H., Diaz, E., Enriquez, R.G., Gonzalez-Gutierrez, L., Ortiz, B., Sanchez-Obregon, R., and Walls, F., The ultraviolet irradiation of isoperezone acetate. 2D NMR structure elucidation, *Nat. Prod. Lett.*, 8, 181, 1996.
22. Iwamoto, H. and Takuwa, A., Photochemical-reaction of allyl-1,4-benzoquinones — trapping of biradical intermediates with olefins, *Chem. Lett.*, 5, 1993.

23. Iwamoto, H., Takuwa, A., Hamada, K., and Fujiwara, R., Intra- and intermolecular photocyclization of vinylbenzo-1,4-quinones, *J. Chem. Soc., Perkin Trans. 1*, 575, 1999.
24. Pandey, B. and Dalvi, P.V., Photoinduced *exo*-selective Diels-Alder reactions, *Angew. Chem. Int. Ed. Engl.*, 32, 1612, 1993.
25. Xu, J.H., Wang, L.C., Xu, J.W., Yan, B.Z., and Yuan, H.C., Photoinduced reactions of chloranil with stilbene derivatives and α,β–unsaturated carbonyl-compounds, *J. Chem. Soc., Perkin Trans. 1*, 571, 1994.
26. Xu, J.H., Song, Y.L., Zhang, Z.G., Wang, L.C., and Xu, J.W., Photoinduced addition reactions of chloranil with alkenes — factors influencing the reaction site, *Tetrahedron*, 50, 1199, 1994.
27. Sun, D.L.L, Hubig, S.M., and Kochi, J.K., Oxetanes from [2+2] cycloaddition of stilbenes to quinone via photoinduced electron transfer, *J. Org. Chem.*, 64, 2250, 1999.
28. Hubig, S.M., Sun, D.L., and Kochi, J.K., Photodynamics of the Paterno-Büchi cycloaddition of stilbene to quinone. Unusual modulation of electron-transfer kinetics by solvent and added salt, *J.Chem. Soc., Perkin Trans. 2*, 781, 1999.
29. Xue, J., Xu, J.W., Yang, L., and Xu, J.H., Photoinduced reactions of chloranil with 1,1-diarylethenes and product photochemistry-intramolecular [2+2] (*ortho*-)cycloadditions of excited enedione's C=C double bond with substituted benzene ring, *J. Org Chem.*, 65, 30, 2000.
30. Braun, M., Christl, M., Deeg, O., Rudolph, M., Peters, E.M., and Peters, K., Photocycloadditions of chloranil to homobenzvalene, norbornadiene and quadricyclane, *Eur. J. Org. Chem.*, 2093, 1999.
31. Braun, M., Christl, M., Peters, E.M., and Peters, K., Photochemical reactions of chloranil with norbornene, bicyclo[2.1.1]hex-2-ene and cyclopentene. A novel intermolecular photocycloaddition, *J. Chem. Soc., Perkin Trans. 1*, 2813, 1999.
32. Kokubo, K., Masaki, T., and Oshima, T., Steric effects in photoinduced electron transfer reaction of halogenated 1,4-benzoquinones with donor olefins, *Org. Lett.*, 2, 1979, 2000.
33. Bockman, T.M., Perrier, S., and Kochi, J.K., Dehydrosilylation versus α-coupling in the electron-transfer of enol silyl ethers to quinones — strong solvent effect on photogenerated ion-pairs, *J. Chem. Soc., Perkin Trans. 2*, 595, 1993.
34. Takahashi, Y., Endoh, F., Ohaku, H., Wakamatsu, K., and Miyashi, T., Triplet-state electron-transfer reactions of phenylcyclopropane with quinones, *J. Chem. Soc., Chem. Commun.*, 1127, 1994.
35. Bosch, E., Hubig, S.M. and Kochi, J.K., Paterno-Büchi coupling of (diaryl)acetylenes and quinone via photoinduced electron transfer, *J. Am. Chem. Soc.*, 120, 386, 1998.
36. Bosch, E., Hubig, S.M., Lindeman, S.V., and Kochi, J.K., Photoinduced coupling of acetylenes and quinone in the solid state as preorganized donor-acceptor pairs, *J. Org. Chem.*, 63, 592, 1998.
37. Kim, S.S., So, M.H., and Park, S.K., Photoaddition reactions of 1,4-diphenylbut-1-en-3-yne to *p*-quinones, *J. Photosci.*, 3, 61, 1996.
38. Kim, S.S., O, K. J., and Shim, S.C., Photoaddition of p-quinones to 1,4-diethynylbenzenes, *Bull. Korean Chem. Soc.*, 15, 270, 1994.
39. Kim, S.S., Kim, A.R., Joong, K., Yoo, D.J., and Shim, S,C., Photoaddition reaction of 1,4-diethynylbenzene to tetramethyl-1,4-benzoquinone and photochemical transformation of the photoadducts, *Chem. Lett.*, 787, 1995; Kim, S.S., Kim, A.R., Yoo, D.J., and Shim, S.C., Photoaddition reactions of some alkynes to duroquinone and photochemical transformation of the photoadducts, *Bull. Korean Chem. Soc.*, 16, 797, 1995.

88

The "Photochemical Friedel-Crafts Acylation" of Quinones: From the Beginnings of Organic Photochemistry to Modern Solar Chemical Applications

Michael Oelgemöller
Bayer CropScience K.K.

Jochen Mattay
Universität Bielefeld

88.1 Introduction

Due to their diverse biological activity and importance as natural products,[1] quinones and their derivatives have attracted constant interest in terms of synthetic organic photochemistry, as can be seen by a number of summarizing reviews.[2] Among the broad variety of applications, the photochemical reaction between a quinone and an aldehyde has been intensively studied over the past 100 years. This review provides an

0-8493-1348-1/04/$0.00+$1.50

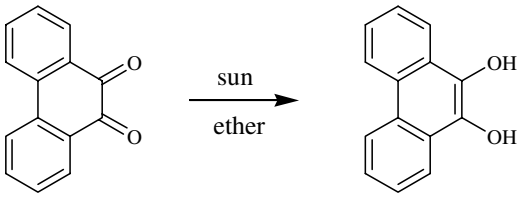

1 **2**

SCHEME 1

overview of the photoacylation of quinones from the discovery by Heinrich Klinger in 1888 to modern solar chemical applications by Mattay and co-workers. To account for the historical development of the photochemical techniques and consequently this application, selected synthetic key-features (e.g., radiation source, solvents applied) are summarized in tables for many of the reported examples.

88.2 Discovery and Early Solar Chemical Studies: 1886–1934

The discovery of the photochemical acylation of quinones with aldehydes dates back to the beginnings of modern organic photochemistry in the late 19th century.[3] During that time, organic photochemistry was closely linked to the use of natural sunlight as the only source of available radiation and thus took place mainly on the rooftops of the chemical institutes and/or in southern countries (as, for example, at Giacomo Ciamician's roof laboratory in Bologna, Italy[3a]).

Discovery and First Reports by Heinrich Klinger: 1886–1911

In 1886, Heinrich Klinger (Bonn, Germany) observed the photoreduction of 9,10-phenanthrenquinone (**1**) in ether to its corresponding dihydroquinone (**2**) and acetaldehyde (Scheme 1).[4]

His interest in photochemistry was thereby stimulated by the accidental discovery of the photochemical reduction of the diketone benzil to hydrobenzoin.[4] In an attempt to obtain the assumed isomer "isobenzil" from a solution of benzil in wet ether, he observed the not-always reproducible precipitation of a crystalline material, which he later correctly assigned to a 2:1 complex of hydrobenzoin and benzil. In his publication, he described in detail the frustrating and time-consuming search for the missing factor that caused the reduction, until he finally noticed that those reaction tubes, in which the reduction took place, were exposed to direct sunlight in the early morning hours.* Klinger also mentioned the experimental difficulties an early photochemist had to deal with and, for instance, reported heavy destructions of some of his flasks (filled with volatile ethereal solutions)[4] or apologized for presenting limited or older data due to bad weather conditions or due to total loss of his reaction flask during a storm.[5]

As an extension of his work, he studied the influence of the solvent on the photoreaction. When he finally replaced the solvent ether with acetaldehyde and later with other aldehydes, he observed — to his own surprise — a different, new kind of photoreaction (Scheme 2), which led him to the following astonishing conclusion: "In this case the effect of light is a strange and synthetic one, best to my knowledge so far only found in a living plant; in so far a balanced one as the two compounds combine to one, in which the quinone appears reduced and the aldehyde oxidized.**" The photoproducts, monoesters of

*Original text:[4a] *"Den wirklichen Grund jener Veränderung des Benzils aufzufinden, gelang mir erst nach längerer Zeit, da zufälliger Weise die Röhren mit Benzillösung in einem fast nach Norden gelegenem Zimmer aufgestellt waren und nur die an den Fenstern stehenden in den Morgenstunden directes Sonnenlicht erhalten konnten, dessen Einfluss desshalb anfangs gar nicht in Betracht gezogen wurde."*

**Original text:[5a] *"Die Wirkung des Lichtes ist in diesem Fall eine ganz eigenartige, synthetische, wie sie meines Wissens bisher nur in der lebenden Pflanze beobachtet wurde; eine insofern ausgleichende, als die beiden Substanzen sich zu einer Verbindung vereinigen, in welcher das Chinon als reducirt, der Aldehyd dagegen als oxydirt erscheint."*

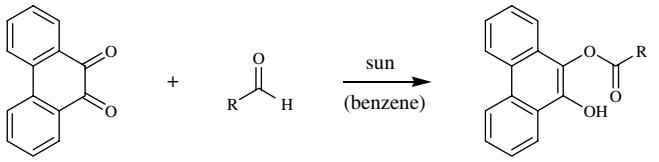

1 **3** (R = Me, *i*-Bu, Ph) **4** (58-96%)

SCHEME 2

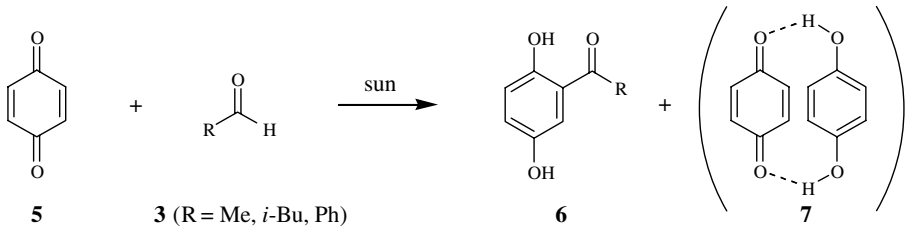

5 **3** (R = Me, *i*-Bu, Ph) **6** **7**

SCHEME 3

TABLE 88.1 Photoreactions of Quinones and Aldehydes as Reported by Klinger[5,6]

Quinone	Aldehyde (R)	Conditions	Ester (**4**) (%)	Acylated Hydroquinone (**6**) (%)	Ref.
1	Me	Sun, several days	58	—	5
1	*i*-Bu	Sun, several days	64–69	—	5
1	Ph	Sun, 3–4 h, benzene	96	—	5
5	Ph	Sun, n.g.[b]	—	n.g.[a,b]	6a
5	*i*-Bu	Sun, n.g.[b]	—	n.g.[a,b]	6a
5	Me	Sun, 3 months	—	Good[a,b]	6b
1	*o*-HOC_6H_4	Sun, *ca.* 5 weeks, benzene	90	—	6c
1	**10**	Sun, 14 days, benzene	n.g.[b]	—	6c
1	*p*-$MeOC_6H_4$	Sun, 2–3 months, benzene	n.g.[b]	—	6c
1	2-Furyl	sun, 53 days, benzene	Low[b]	—	6c

[a] Quinhydrone (**7**) as side-product.
[b] n.g.: illumination period and/or yields not specified or not given.

phenanthrene hydroquinone (**4**), were obtained in moderate to good yields after relatively short illumination times (Table 88.1).[5] In most cases, the aldehyde served as reagent and solvent, but benzene proved to be a suitable dilutant. Klinger also investigated a simple wavelength dependency of the photoacylation using aqueous solutions of inorganic salts as filters (i.e., cuprous ammonium sulfate and potassium dichromate solutions). Based on his observations, he noted that the photoreaction was most pronounced in the blue region, whereas with potassium dichromate the photoreaction proceeded about 30 to 40 times slower.[5]

Klinger also investigated the photoreaction of 1,4-benzoquinone (**5**) for which he expected analogue monoesters.[5] Based on skilled derivatization experiments, the products from this reaction turned out to be acylated hydroquinones **6** accompanied by quinhydrone (**7**) as a major side-product (Scheme 3; Table 88.1).[6] He also studied control reactions in the dark, which yielded only trace amounts of quinhydrone (**7**) after several months, unambiguously proving that light was essential for the activation.[6a]

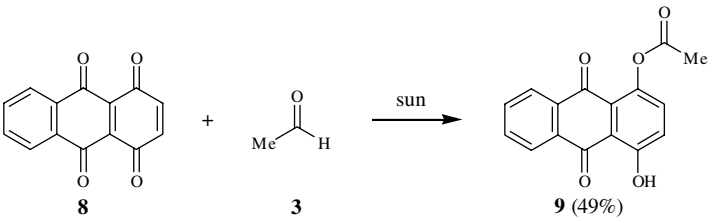

SCHEME 4

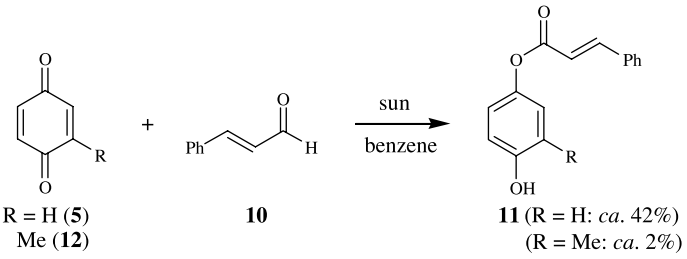

SCHEME 5

Further Early Solar Chemical Experiments: 1920–1934

In 1921, 33 years after Klinger's discovery, Dimroth and Hilcken reported a similar transformation of quinizarinquinone (**8**) with acetaldehyde.[7] Exposure to direct sunlight for 12 days gave the corresponding monoester **9** in 49% yield (Scheme 4). However, when they repeated the experiment during the less light intensive autumn season over an extended period of 1.5 months, they obtained a mixture of quinizarin (the reduction product of **8**) and the monoester **9**.

A few years later in 1930, another example of the photochemical acylation was described by the Italian (photo)chemists Bargellini and Monti in Rome.[8] When a benzene solution of benzoquinone (**5**) and cinnamaldehyde (**10**) was illuminated for 1 month with direct sunlight, the corresponding hydroquinone monoester (**11**) was isolated in about 42% yield (Scheme 5). This observation must have been surprising because it obviously conflicts with earlier findings by Klinger, who had obtained acylated hydroquinones (**6**) instead (*vide supra*).[6] Another example of this reaction came about 5 years later from the University of Torino in Italy. Angeletti and Migliardi exposed a benzene solution of toluquinone (**12**) and cinnamaldehyde (**10**) to sunlight over a period of *ca.* 6 months and obtained the corresponding monoester **11** (*ca.* 2%) along with cinnamic acid (*ca.* 14%) and toluohydroquinone (*ca.* 8%), respectively.[9a] The formation of the latter two compounds was assigned to a dominant photochemical redox reaction, whereas photoacylation was suspected to play only a minor role. Due to steric blocking by the methyl group in **12**, regioselective ester formation was suggested, although analytical proof was missing. Inspired by the original work of Klinger on phenanthrenequinone (**1**), Sircar and Sen examined similar reactions with acenaphthenequinone (**13**) in 1931 in Calcutta, India.[10] They had launched a detailed comparison study on the *thermal* transformations of these two quinones (**1** vs. **13**) and expanded it to the photoacylation of **13** with several aromatic aldehydes. Exposure of mixtures of **13** with salicyl-, cinnam-, benz-, or anisaldehyde in benzene over several weeks yielded the monoesters **14** (Scheme 6; Table 88.2).

Along with all these promising and successful early experiments, a few unsuccessful or rather unusual results were reported as well. In 1930, the American scientists Bogert and Howells (New York) tried to apply the photoacylation protocol to the synthesis of dibenzoylbenzohydroquinone from monobenzoylated **5** and benzaldehyde.[11] However, these authors seemed to be rather skeptical of the young discipline

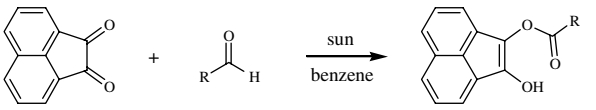

13 **3** **14**

SCHEME 6

TABLE 88.2 Early Photoreactions of Quinones and Aldehydes[7-10]

Quinone	Aldehyde (R)	Conditions	Ester (%)	Ref.
8	Me	Sun, 12 d	49	7
5	**10**	Sun, 1 month, benzene	*ca.* 42	8
12	**10**	Sun, 6 months, benzene	*ca.* 2[a]	9a
13	*o*-HOC_6H_4	Sun, *ca.* 1 month, benzene	n.g.[b]	10
13	10	Sun, 40 d, benzene	n.g.[b]	10
13	Ph	Sun, 15 d, benzene	n.g.[b]	10
13	*p*-$MeOC_6H_4$	Sun, 20 d, benzene	n.g.[b]	10

[a] Several other products (see text). [b] n.g.: yields not given.

of photochemistry because they discontinued their single attempt simply because no crystals were formed during the illumination.*

Later, in 1934, Angeletti and Baldini obtained neither acylated hydroquinones (as **6**) nor hydroquinone monoesters (as **11**) when they exposed a benzene solution of toluquinone (**12**) and benzaldehyde to sunlight over a period of *ca.* 6 months.[9b] In addition to a larger amount of unknown material, they identified benzoic acid (3.3%), toluohydroquinone (*ca.* 16%), and trace amounts of the dibenzoylester of toluohydroquinone as photoproducts, respectively.

88.3 Solar Chemical Studies by Alexander Schönberg: 1939–1957

In 1937, Alexander Schönberg, an emigrant from National Socialistic Germany, was appointed Professor at the University of Cairo in Egypt, where he naturally found extremely suitable conditions for solar chemical reactions. His comprehensive work on light-induced reactions earned him the general recognition as a pioneer in preparative photochemistry.[12]

Only 2 years after his appointment, Schönberg suggested an alternative structure for the photoproducts obtained from phenanthrenequinone (**1**) and aromatic aldehydes (Scheme 7).[13a] In contrast to Klinger's original report,[5] he favored a cyclic acetal structure (**15**). Taking into account the limitations of analytical chemistry of the time, his assignment was reasonably based on further transformations into compounds already reported in the literature. In particular, the suspected photoproduct **15** obtained with *p*-chlorobenzaldehyde gave, after methylation with diazomethane and hydrolysis with sodium hydroxide, and in addition to 9,10-dihydroxyphenanthrene (**2**), a crystalline compound that he assigned to the known methyl *p*-chlorobenzoate.[13a,b] In addition, the photoproduct itself did not show a colored complex with ferric chloride,** at that time a commonly accepted proof for phenols.[14] The assignment to the cyclic acetal structure was adopted and further propagated by his former co-worker Ahmed Mustafa.[15]

*Original text:[11] *"After standing for many days the solution became quite dark, but no crystalline material separated and the experiments were discontinued."*

**This result was, in fact, indirectly reported by Moore and Waters.[16] Schönberg himself did not mention this particular ferric chloride test in his early publications.[13a-c]

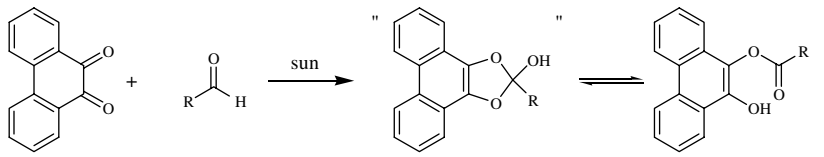

SCHEME 7

Although Schönberg later proposed an existing ring-chain tautomerization between the two structures **15** and **4**,[13d] Moore and Waters reported chemical and IR-spectroscopic evidence (e.g., by *direct* comparison with an authentic sample donated by Schönberg) for the originally assigned monoester (**4**) structure in 1953.[16] These authors also repeated Schönberg's methylation experiment with diazomethane followed by hydrolysis with potassium hydroxide and obtained benzoic acid and 9-hydroxy-10-methoxyphenanthrene, the expected cleavage products of **4** (Scheme 12; *vide infra*). However, Schönberg and Mustafa continued to favor their tautomerization scenario. Another 10 years later, in 1963, Rubin ended this longstanding debate, for example, with the help of modern NMR-spectroscopy, in favor of the monoester structure (**4**).[2e,17]

During more than two decades (1939 to 1960) of their work on the photoacylation reaction, Schönberg and Mustafa studied a variety of different *ortho*-quinone/aldehyde pairs (Chart 1; Table 88.3). Among these numerous examples, three systems deserve further mention.

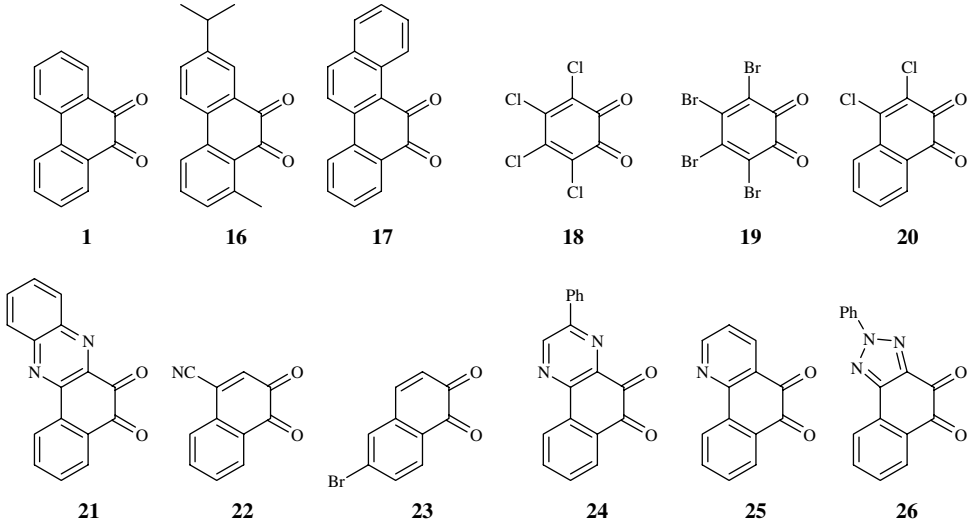

CHART 1

1,2-Benzophenazine-3,4-quinone (**21**) did not yield the expected pale yellow or yellow-colored products, but formed deep purple crystals after photolysis in the presence of anis- or benzaldehyde, respectively.[13e] In ethyl benzoate solutions, the photoproducts showed thermochromism: at 0°C the solutions were purple-brown, whereas upon heating to 170°C, they changed to orange. Because this effect was found to be reversible, Schönberg suggested an existing enol imine–enamine (**27**/**28**) tautomerization (Scheme 8),* which was known for 3,4-dihydroxy-1,2-benzophenazine at that time.[18]

*Schönberg himself used the term lactam-lactim tautomerization.[13e]

TABLE 88.3 Photoacylation Reactions Yielding Esters Studied by Schönberg and Mustafa,[13,15] and Others[16-20a]

Quinone	Aldehyde (R)	Conditions	Ester (%)	Ref.
1	Ph	Sun, 4 d	86	13a
1	*p*-ClC_6H_4	Sun, 2 d, benzene	90	13a
1	2,4-$(MeO)_2C_6H_3$	Sun, 10 d, benzene	n.g.[a]	13b
1	2-MeO-1-naphthyl	Sun, 6 d, benzene	n.g.[a]	13b
1	*p*-(*i*-Pr)C_6H_4	Sun, 10 d, benzene	n.g.[a]	13b
16	*p*-$MeOC_6H_4$	Sun, 13 d, benzene	n.g.[a,b]	15a
17	Ph	Sun, 3 months, benzene	n.g.[a,b]	15a
17	*p*-$MeOC_6H_4$	Sun, 1 month, benzene	n.g.[a,b]	15a
1	9-Anthryl	Sun, 20 d, benzene	*ca.* 100	15c
16	9-Anthryl	Sun, 20 d, benzene	n.g.[a,b]	15c
17	9-Anthryl	Sun, 20 d, benzene	*ca.* 100[b]	15c
1	2-Quinoline	Sun, 3 d, benzene	*ca.* 100	15c
18	Me	Sun, 3 d, benzene	n.g.[a]	13d
18	Ph	Sun, 10 d, benzene	70	13d
18	*p*-MeC_6H_4	Sun, 10 d, benzene	n.g.[a]	13d
18	*p*-$MeOC_6H_4$	Sun, 5 d, benzene	*ca.* 100	13d
18	**10**	Sun, 7 d, benzene	n.g.[a]	13d
19	*p*-MeC_6H_4	Sun, 20 d, benzene	n.g.[a]	13d
19	*p*-$MeOC_6H_4$	Sun, 4 d, benzene	n.g.[a]	13d
20	*p*-$MeOC_6H_4$	Sun, 2 d, benzene	n.g.[a,b]	13d
21	*p*-$MeOC_6H_4$	Sun, 10 d, benzene	*ca.* 70[b,c]	13e
21	Ph	Sun, 10 d, benzene	*ca.* 65[b,c]	13e
22	*p*-$MeOC_6H_4$	Sun, 7 d, benzene	40[b]	13f
22	*p*-$NO_2C_6H_4$	Sun, 7 d, benzene	82[b]	13f
22	**10**	Sun, 7 d, benzene	39[b]	13f
23	Ph	Sun, 1 d, benzene	72[b]	15d
23	*m*-MeC_6H_4	Sun, 1 d, benzene	68[b]	15d
23	*p*-MeC_6H_4	Sun, 1 d, benzene	76[b]	15d
23	*o*-$MeOC_6H_4$	Sun, 7 d, benzene	65[b]	15d
23	*p*-$MeOC_6H_4$	Sun, 7 d, benzene	82[b]	15d
23	*o*-ClC_6H_4	Sun, 7 d, benzene	64[b]	15d
1	*o*-$CHOC_6H_4$	Sun, 6 d, benzene	72	15d
1	*m*-$CHOC_6H_4$	Sun, 4 d, benzene	65	15d
1	*p*-$CHOC_6H_4$	Sun, 4 d, benzene	78	15d
1	3-Pyrenyl[d]	Sun, 8 d, benzene	73	15d
24	Ph	Sun, 7 d, benzene	75[b]	15d
24	*m*-MeC_6H_4	Sun, 10 d, benzene	68[b]	15d
24	*p*-MeC_6H_4	Sun, 5 d, benzene	78[b]	15d
24	*o*-$MeOC_6H_4$	Sun, 5 d, benzene	46[b]	15d
24	*p*-$MeOC_6H_4$	Sun, 10 d, benzene	71[b]	15d
24	*o*-ClC_6H_4	Sun, 10 d, benzene	53[b]	15d
25	Ph	Sun, 10 d, benzene	84[b]	15e
25	*p*-$MeOC_6H_4$	Sun, 8 d, benzene	89[b]	15e
25	*p*-MeC_6H_4	Sun, 15 d, benzene	80[b]	15e
25	*o*-ClC_6H_4	Sun, 12 d, benzene	61[b]	15e
26	*p*-$MeOC_6H_4$	Sun, 7 d, benzene	*ca.* 76[b]	15f
26	3,4-$(EtO)_2C_6H_3$	Sun, 10 d, benzene	*ca.* 80[b]	15f
36	Ph	Sun, 60 d, benzene	44	13g
32	*p*-$NO_2C_6H_4$	Sun, 10 d, benzene	38	19
33	*p*-$MeOC_6H_4$	Sun, 1 d, benzene	56	19
34	Me	Sun, 1 d, benzene	42	19
34	*p*-$MeOC_6H_4$	Sun, 1 d, benzene	51	19
35	Me	sun, 1 d, benzene	82	19
1	Ph	UV-lamp,[e] 75 h, benzene	86	16
1	*p*-$MeOC_6H_4$	UV-lamp,[e] 70 h, benzene	*ca.* 100	16

TABLE 88.3 Photoacylation Reactions Yielding Esters Studied by Schönberg and Mustafa,[13,15] and Others[16-20a] (continued)

Quinone	Aldehyde (R)	Conditions	Ester (%)	Ref.
38	Ph	UV-lamp,[e] 4 d, benzene	35	16
1	Ph	HP Hg-lamp,[f] n.g.[a]	n.g.[a]	17a
38	Ph	HP Hg-lamp,[g] 3 h	35	20a

[a] n.g.: experimental details and/or yields not given.
[b] Regioisomer not assigned (most likely mixtures).
[c] Compounds show enol imine-enamine tautomerization (Scheme 8).
[d] 3-Pyrenealdehyde.
[e] UV lamp (300 W).
[f] High-pressure Hg-lamp (1000 W).
[g] High-pressure Hg-lamp (125 W).

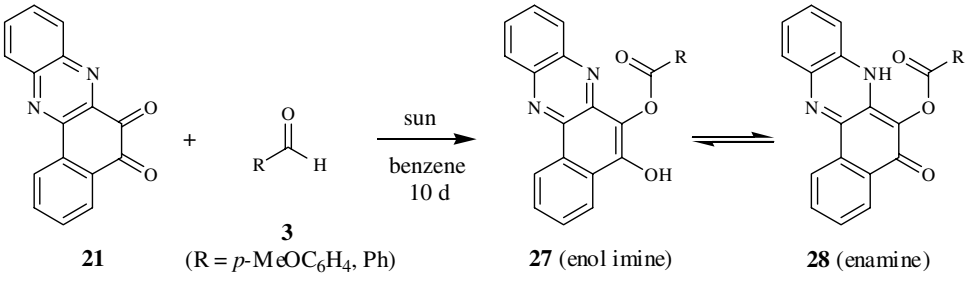

21 **3** (R = *p*-MeOC$_6$H$_4$, Ph) **27** (enol imine) **28** (enamine)

SCHEME 8

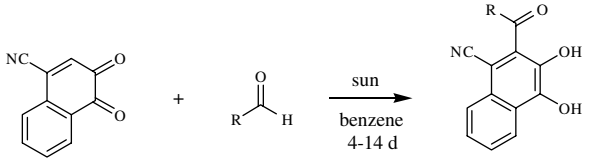

22 **3** (R = Me, Et) **29** (40, 17%)

SCHEME 9

When 4-cyano-1,2-naphthoquinone (**22**) was used as the starting material, the chemoselectivity of the photoacylation depended strongly on the aldehyde used.[13f] Aromatic aldehydes as well as cinnamaldehyde (**10**) gave the expected monoesters (Table 88.3) in moderate to good yields of 39 to 82%. On the other hand, illumination in the presence of aliphatic aldehydes (acetaldehyde or propionaldehyde) led to the isolation of acylated hydroquinones (**29**) as sole products, although the yields were poor at 17 and 40%, respectively (Scheme 9; Table 88.4).[13f] Schönberg did not explain this phenomenon but pointed out similarities to the photoreaction of 1,4-benzoquinone (**5**) with acetaldehyde giving its acylated hydroquinone,[6] and chloranil (**38**) with benzaldehyde giving its corresponding monoester (*vide infra*).[16]

The differing chemoselectivity in the case of 4-cyano-1,2-naphthoquinone (**22**) was striking and, thus, Awad and Hafez later investigated the influence of substituents at the 4-position in more detail (Chart 2).[19]

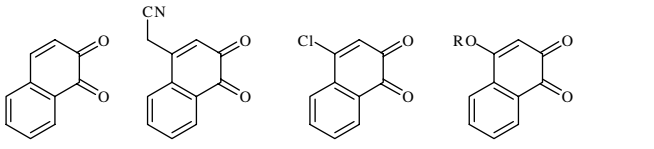

30 **31** **32** **33** (R = 2-Naphthyl)
34 (R = 3,5-$[CH_3]_2C_6H_3$)
35 (R = 2,5-$[CH_3]_2C_6H_3$)

CHART 2

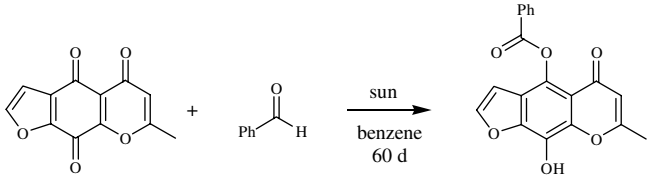

36 **3** **37** (44%)

SCHEME 10

In contrast to Schönberg's original report,[13f] these authors were, however, unable to obtain any photoproducts from the reaction of acetaldehyde with either 1,2-naphthoquinone (**30**), 4-cyanomethyl-1,2-naphthoquinone (**31**), or 4-chloro-1,2-naphthoquinone (**32**), respectively. In all other cases examined (with **33**, **34**, and **35**), isomeric mixtures of the corresponding monoesters were obtained in moderate to good yields of 38 to 82% (Table 88.3). Thus, acylation at the C–C double bond of the quinone was concluded to occur solely with strong electron-withdrawing groups present in the 4-position, whereas other substituents were expected to favor the formation of monoesters. The chemoselectivity of this reaction was later explained in more detail by Bruce[23] and Maruyama and Takuwa.[28,29]

When acylation at the C–C double bond of the 1,4-quinone became impossible, formation of the corresponding monoesters occurred instead. As a further example reported by Schönberg, exposure of a solution of khellinquinone (**36**) and benzaldehyde in benzene to sunlight over 2 months gave the ester **37** in 44% yield (Scheme 10).[13g] The regioselectivity of this photoinduced reaction was confirmed by further derivatization and independent *thermal* synthesis of **37**.

Likewise, chloranil (**38**) gave its corresponding monobenzoate **39** in 35% yield upon irradiation (Scheme 11), as demonstrated by Moore and Waters. Because the formation of a cyclic acetal is impossible in this case, these authors used this transformation as a further proof against Schönberg's postulated cyclic acetal structure (**14**).[16]

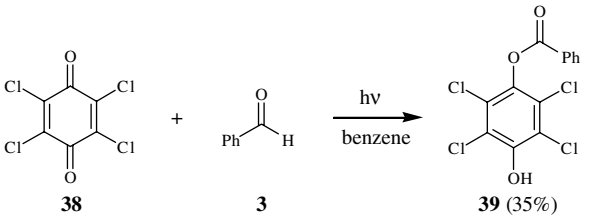

38 **3** **39** (35%)

SCHEME 11

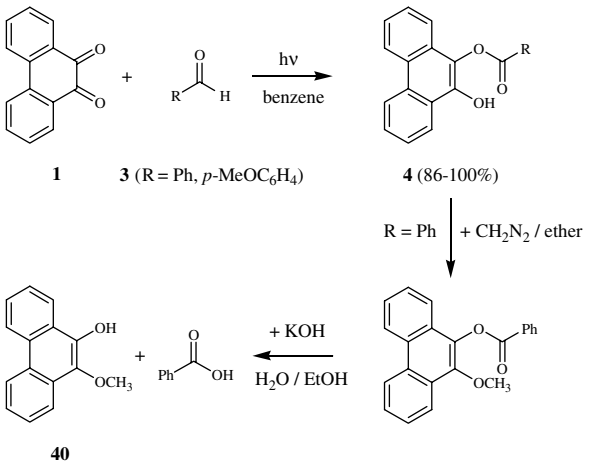

1 **3** (R = Ph, *p*-$MeOC_6H_4$) **4** (86-100%) **40**

SCHEME 12

88.4 Laboratory Studies Using Artificial Light Sources

With the development of suitable artificial light sources[12,21] photochemistry finally moved into laboratories and became independent of varying weather and radiation conditions. Additionally, separation techniques and analytical tools improved, which allowed the isolation and assignment of secondary photoproducts.

Early Mechanistic Proposals: 1953–1965

Accounting for the high yields of the photoacylation of **1** with aromatic aldehydes (Scheme 12), Moore and Waters suggested "a photochemical chain reaction of very long chain-length", initiated via hydrogen abstraction from the aldehyde by the excited quinone (see Scheme 14: *out-of-cage scenario*).[16] However, quantum yield data and effects of inhibitors did not support this proposal as, for example, a quantum yield for the disappearance of the quinone (Φ_d) of $\Phi_d = 1$ has been reported for irradiation of **1** in benzaldehyde at 436 nm.[2e,17]

In contrast, however, Rubin independently demonstrated for a model ester (**4**, R = Ph) that the photoreaction was reversible and phenanthrenequinone (**1**) was obtained in 34% yield with a conversion of 70%.[17b]

Already one year after Moore and Water's mechanistic proposal, Schenck and co-workers favored an alternative *in-cage scenario* (see Scheme 14).[20] They had studied the photochemical acylation of chloranil (**38**)[20a] with benzaldehyde and of 1,4-naphthoquinones[20b] with acetaldehyde (Scheme 13; Table 88.4), respectively. In all cases, quantum yields (Φ) were found to be low, with $\Phi < 0.2$ (for **38**) and $\Phi < 1$ (for

TABLE 88.4 Photoacylation Reactions Yielding Acylated Hydroquinones (Acyl. HQ) Studied by Schönberg[13] and Schenck[20]

Quinone	Aldehyde (R)	Conditions	Acyl. HQ (%)	Ref.
22	Me	Sun, 4 d, benzene	40	13f
22	Et	Sun, 14 d, benzene	17	13f
41	Me	UV lamp,[a] n.g.[b]	50	20b
42	Me	UV lamp,[a] n.g.[b]	n.g.[b]	20b

[a] UV lamp (not specified).
[b] n.g.: experimental details and/or yields not given.

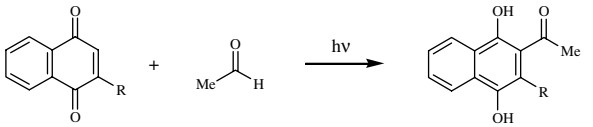

SCHEME 13

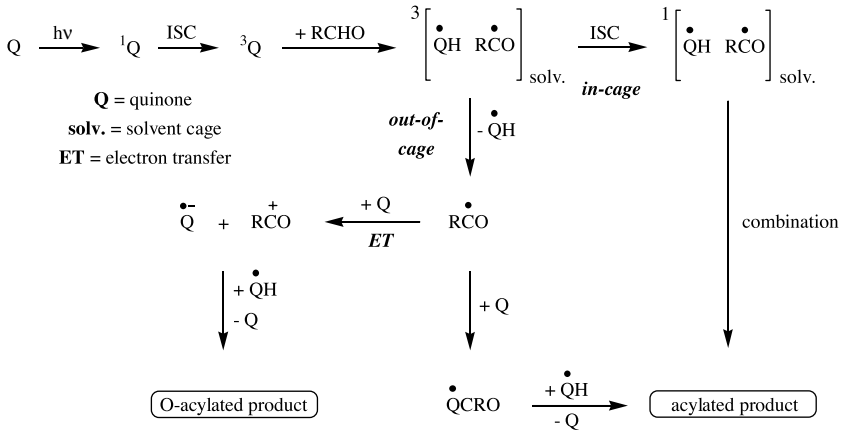

SCHEME 14

41) disfavoring a radical chain mechanism. For the naphthoquinone/acetaldehyde pair, these authors also excluded an initial Photo-Fries rearrangement of a monoester intermediate,[22] although experimental details were not given.

A *thermal* acylation via a radical chain sequence was achieved for chloranil (**38**) and benzaldehyde (similar to Scheme 11) at elevated temperatures using benzoyl peroxide as a radical initiator. As an example, the monoester **39** was readily obtained in yields of 75 to 80% at 120°C. Thus, Schenck concluded that a free radical chain mechanism during photolysis should occur solely at higher temperatures.[20a]

Mechanistic and Synthetic Studies by J. Malcolm Bruce: 1965–1974

In 1965, Bruce and co-workers launched a detailed mechanistic study on the photoinduced acylation of para-benzoquinone (**5**).[23] Careful analysis of the reaction products revealed that in addition to the acylated hydroquinone (**6**), a larger amount of the corresponding unsubstituted hydroquinone (**44**) was formed. As a minor by-product, the monoester **45** was additionally obtained in 0.6% yield (Scheme 15). In a number of experiments under various conditions, Bruce furthermore demonstrated that the acylated hydroquinone **6** was unambiguously not formed from the monoester **45** via an initial Photo-Fries rearrangement.[22]

Upon irradiation at *ca.* −70°C, **6** was isolated in 72% yield, almost identical with the 76% yield obtained in a parallel run at 15°C. Hence, Bruce concluded that an *in-cage-controlled* radical combination might play only a minor role in the mechanistic scenario (see Scheme 14). To further verify this assumption, Bruce irradiated a solution of benzoquinone and acetaldehyde in the presence of several scavengers, of which 1,1-diphenylethylene (**46**) proved to be the most suitable one. Along with a small amount of compound **6**, an isomeric mixture of the *thermally* unstable trapping product **47** was isolated in 39% yield (Scheme 15).[23b] That free radical intermediates were involved was further indicated by the *thermal*

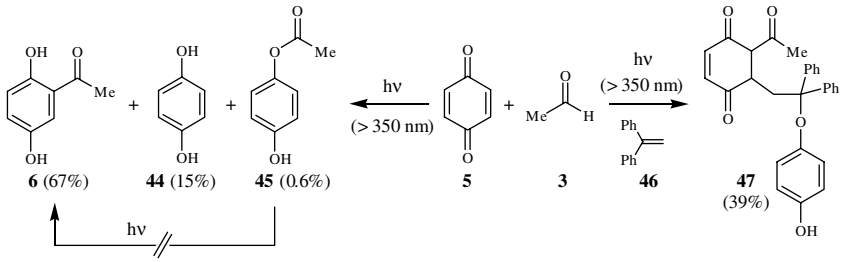

SCHEME 15

generation of acyl radicals initiated by di-*t*-butyl diperoxalate. With benzoquinone (**5**) and this perester in the molar ratio of 2:1 in acetaldehyde, acetylquinol (**6**) was isolated in 37% yield. In the presence of added quinol **44** and a sufficient excess of perester to oxidize it completely to quinone, the yield increased to 69%, thus supporting sequences involving disproportionation of radical intermediates. With only $^1/_{10}$ molar equivalent of the perester, the yield of **6** dropped to 6%, indicating that the initial aldehyde is most likely not the sole source for hydrogen abstraction.[23a,b] In conclusion, Bruce favored an *out-of-cage scenario* (Scheme 14) for the 1,4-benzoquinone/acetaldehyde pair.

In the following years, Bruce and co-workers expanded their studies to a number of 1,4-quinone/aldehyde couples (Chart 3; Table 88.5).[23c-g] For the quinones **53**, **54**, and **56**, acylation also occurred in the dark but these *thermal* reactions were very significantly slower and gave rather sluggish mixtures when compared to the photoreactions. By consequently varying the substitution pattern of both reaction partners, Bruce concluded that the chemoselectivity for the acylation of *para*-quinones was influenced by three main factors.[2b,c]

1. The nucleophilicity of the acyl radical,[24] because with decreasing nucleophilicity of the derived acyl radical, the formation of monoesters (**45**) became favored. For example, whereas most aliphatic acyl radicals predominantly gave acylated hydroquinones (**6**) with benzoquinone (**5**), the more electrophilic aromatic acyl radical carrying electron-withdrawing substituents in *para*-position all gave the corresponding esters (**45**).
2. The redox properties of the quinone:[25] Quinones with high reduction potentials preferentially gave their esters (**45**). For example, 2,3-dicyano-1,4-benzoquinone (**55**) exclusively yielded its corresponding monoester (**45**) when irradiated in acetaldehyde, thus reflecting its high reduction potential of $E_{1/2}$ = 0.71 V (in MeCN vs. SCE[25a]).
3. The observation that cinnamaldehyde and acrolein exclusively gave the corresponding monoesters (**11**) suggested that the oxidation potential of the acyl radical intermediate was of importance.[24] Thus, if the balance between the redox properties of quinone and acyl radical is appropriate for a *thermal* electron transfer (ET) to occur, the corresponding acyl cation and quinone radical cation are generated, which leads to ester formation (Scheme 14).

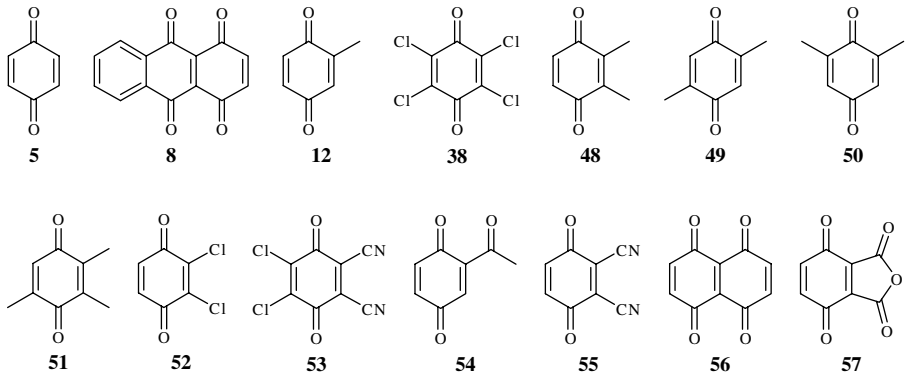

CHART 3

TABLE 88.5 Photoreactions of 1,4-Quinones and Aldehydes as Reported by Bruce.[a,23]

Quinone	Aldehyde (R)	HQ (%)	Acyl. HQ (%)	Ester (%)	Bisacyl. HQ (%)	Ref.
5	Me	15	67	0.6	—	23b
5[b]	Me	n.d.[c]	72	n.d.[c]	—	23b
5	Me	n.d.[c]	76	n.d.[c]	—	23b
5[d]	Me	n.d.[c]	84	n.d.[c]	—	23d
5[e]	Me	24	61	n.d.[c]	—	23d
38	Me	trace	1[f]	80	—	23c
12	Me	25	29 (2,5)[g] 20 (2,6)[g]	—	1 (2,3,5)[g]	23d
48	Me	13	32	—	—	23d
49	Me	26	29	—	16	23d
50	Me	27	39	—	23	23d
51	Me	—	4	—	—	23d
52	Me	4	53	—	—	23d
53[l]	Me	40	—	45	—	23d
54[h,l]	Me	23 (**6**)	8 (2,5)[g] 12 (2,6)[g]	—	—	23d
5	*t*-Bu	25	56	—	4 (2,5)	23d
5[d]	Ph	16	49	15	—	23d
5[d]	*p*-(*t*-BuC_6H_4)	16	70	—	—	23d
5[d]	*p*-MeC_6H_4	7	39	—	—	23d
5[d]	*p*-MeOC_6H_4	—	58	7	—	23d
5[d]	*p*-$NO_2C_6H_4$	—	—	54	—	23d
5[d]	**10**	4	—	69	—	23d
8	Me	17	—	83[i]	—	23d
8[d]	*t*-Bu	32	—	56[i]	—	23d
8	Ph	28	—	52[i]	—	23d
8[d]	*p*-MeOC_6H_4	30	—	37[i]	—	23d
8[d]	*p*-$NO_2C_6H_4$	69	—	6[i]	—	23d
5[d]	*p*-CHOC_6H_4	—	2	40	—	23e
5[d]	*p*-CNC_6H_4	—	10	56	—	23e
5[d]	*p*-$CF_3C_6H_4$	84[j]	—	12	—	23e
55	Me	35	—	64	—	23e
56[l]	Me	16	—	36	—	23e
57	Me	—	—	*ca.* 46	—	23e
61	Me	—	64 (2,5+2,8)[k]	—	—	23e
5[d]	CH_2 = CH	—	—	38	—	23e
5[d]	MeCH = CH	—	28	22	—	23e
5	MeCH = CH	—	50	50	—	23e
70	Me	14	28	7	—	23g
70	Ph	9	21	14	—	23g

[a] Irradiation conditions: tungsten lamp (300 W), Pyrex filter, *ca.* 15°C; HQ = hydroquinone.
[b] At −70°C.
[c] n.d.: not determined.
[d] In benzene.
[e] In water.
[f] See Scheme 18.
[g] Position at C2 occupied by the quinone substituent.
[h] Monoacylated starting material (see Scheme 16).
[i] Similar to Scheme 4.
[j] As quinhydrone (similar to **7**).
[k] As 4:1 mixture, not assigned.
[l] Reaction also occurred in the dark.

In some cases examined, diacylated compounds were isolated in yields up to 23% and a *thermal* oxidation-reduction equilibrium between the monoacylated product and the initial quinone, followed by a rapid, secondary acylation of the intermediary generated acylated quinone was suggested to explain their formation. Secondary acylation was indeed demonstrated with acetyl-1,4-benzoquinone (**54**), and acetaldehyde and the corresponding diacylated products **58** and **59** were isolated in 20% total yield (Scheme 16).[23d]

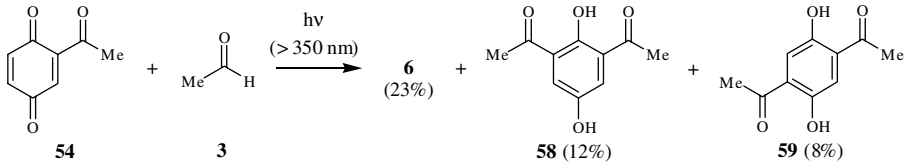

SCHEME 16

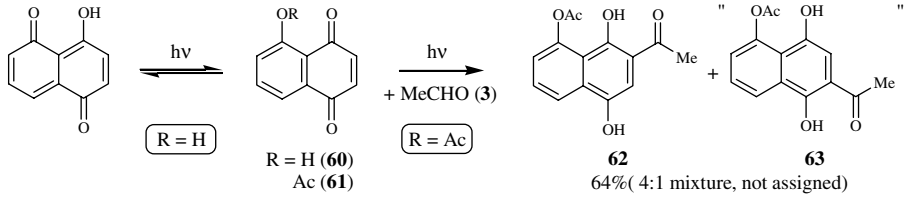

SCHEME 17

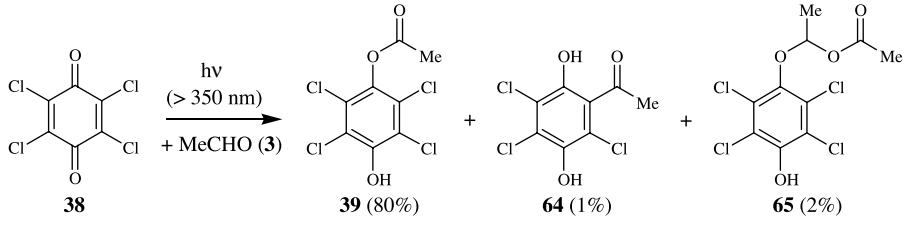

SCHEME 18

Juglone (**60**) did not undergo the photochemical acylation,[23e] indicating a rapid, deactivating *intramolecular* hydrogen-transfer (phototautomerization) process.[26] When the hydrogen bonding site was blocked as for the corresponding acetyl-derivative (**61**), irradiation in acetaldehyde gave a 4:1 mixture (not assigned) of the two regioisomeric hydroquinones **62** and **63** in 64% yield (Scheme 17).[23e] However, recent studies on this transformation indicated that in case of the 2,5-regioisomer **63**, subsequent rearrangement of the acetyl group via a [1,5]-migration occurs (*vide infra*), which remained unrecognized in Bruce's experiments.[33g]

Bruce and Ellis also reinvestigated the photoinduced acylation of chloranil (**38**) to explain the quantitative yield of paraldehyde formed during irradiation.[23c] Careful analysis of the reaction mixture led to the identification of two minor products (Scheme 18): trichloroacetylquinol (**64**) and acetoxyethyl ether (**65**). Whereas the latter was explained via the attack of an acyl radical at the initial aldehyde or alternatively via hydrogen abstraction from paraldehyde, respectively, the formation of **64** was rationalized through expulsion of a chlorine atom from the quinone **38**, followed by rapid reduction of the generated acylated quinone. The released chlorine radical subsequently abstracts a suitable hydrogen to give hydrogen chloride, which is then involved in the generation of paraldehyde.

When *t*-butyl-1,4-benzoquinone (**66**) was used as the starting quinone, reorganization of the *t*-butyl group occurred during photolysis in acetaldehyde (Scheme 19).[23f] The product composition was somewhat sensitive to the amount of water present during the experiment (Table 88.6). In particular, whereas the dihydrobenzodioxepinol **67** was obtained in 80% yield upon irradiation in dry acetaldehyde, a similar run in aqueous aldehyde gave 72% of the alcohol **68** as main product. Because **67** remained photostable

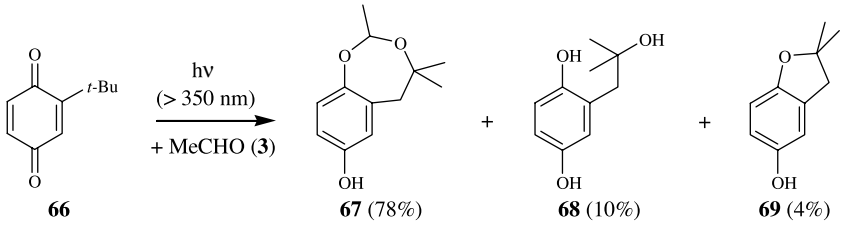

66 **67** (78%) **68** (10%) **69** (4%)

SCHEME 19

TABLE 88.6 Photoreactions Involving the *t*-Butyl-1,4-benzoquinone (**66**)/Acetaldehyde Pair[23f]

Conditions	**67** (%)	**68** (%)	**69** (%)
Aldehyde, 8 d	78	10	4
Aldehyde, $MgSO_4$, 8 d	80	10	—
Aldehyde, 1.6 vol-% H_2O, 4 d	—	72	—

under similar irradiation conditions, an interconversion into **68** was ruled out. 2,5-Di-*t*-butylated quinone similarly gave its corresponding dioxepinol in 38% yield (along with 6% of its hydroquinone **44**), whereas the 2,6-regioisomeric analogue remained almost completely photostable.

In contrast to the light-induced reaction, *thermal* generation of acyl radicals with di-*t*-butyl diperoxalate gave small amounts of the regioisomeric acylated hydroquinones. Thus, *intramolecular* hydrogen abstraction from the *t*-butyl group preceded *intermolecular* hydrogen abstraction from the aldehyde during photolysis. The final photoproducts arise from nucleophilic attack of either aldehyde (to **67**) or water (to **68**), respectively.[23f,27]

Bruce and co-workers further extended their studies on the photoacylation to 4,4′-diphenoquinone derivatives.[23g] Irradiation of the parent diphenoquinone (**70**) in acetaldehyde gave results similar to those found with 1,4-benzoquinone (**5**) and a mixture of hydroquinone (**71**), monoester (**72**), and acylated hydroquinone (**73**) was obtained. The increased amount of monoacetate **72** reflects the higher oxidation potential of the diphenoquinone and thus a greater contribution via the electron-transfer mechanism (*vide supra*). Irradiation of **70** in benzaldehyde gave analogous products (Table 88.5). In contrast, whereas photolysis of 3,3′,5,5′-tetramethyldiphenoquinone in acetaldehyde gave the corresponding hydroquinone in 80% yield, together with some biacetyl, the tetra-*t*-butyl analogue was entirely photostable.[23g]

Mechanistic and Synthetic Studies by Kazuhiro Maruyama and Akio Takuwa: 1972–1990

Between 1972 and 1990, Maruyama and Takuwa reinvestigated the mechanistic scenario of the photoacylation for several quinone/aldehyde pairs.[28,29] For 9,10-phenanthrenequinone (**1**), Maruyama was able to show, via CIDNP investigations and in comparison with other hydrogen donors (e.g., ethers, alkyl benzenes, xanthene), that the photoacylation precedes via the unstable vibrationally excited 1,2-photoadduct **74** (Scheme 21).[28a,f] Subsequent rearrangement through dissociation into singlet radical pairs leads to the stable 1,4-adduct, the monoester **4**. CIDNP effects due to *in-cage* coupling products were generally observed for photoreactions involving **1**. The same mechanism was proposed on the basis of analogue CIDNP examinations for 1,4-benzo- (**5**) and 1,4-naphthoquinone (**41**), which both gave acylated hydroquinones.[28e] Quantum yield determinations for the latter two cases revealed that the acylated hydroquinone **43** of 1,4-naphthoquinone acts as a quencher since the quantum yield significantly drops with increasing conversion. In contrast, quantum yields stayed constant during irradiation involving 1,4-benzoquinone (**5**).[28e]

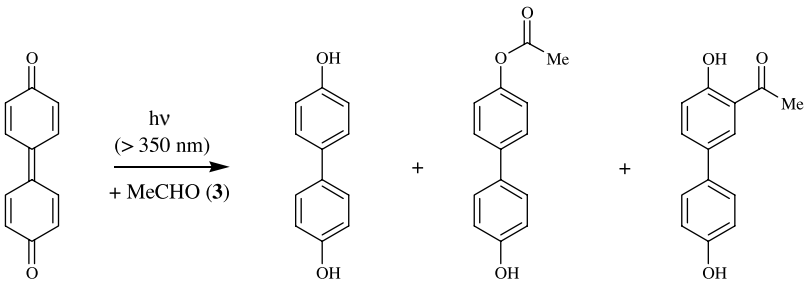

70 **71** (14%) **72** (7%) **73** (28%)

SCHEME 20

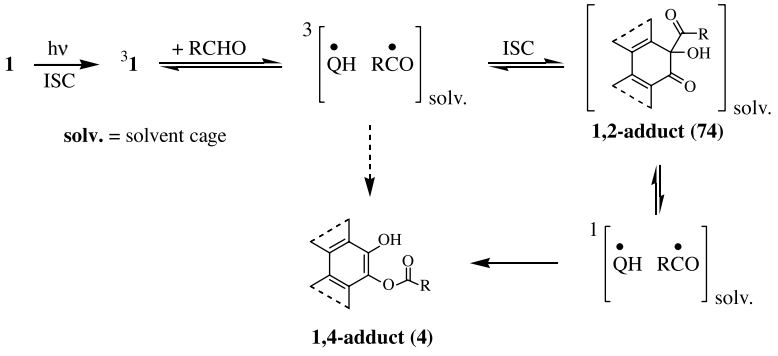

SCHEME 21

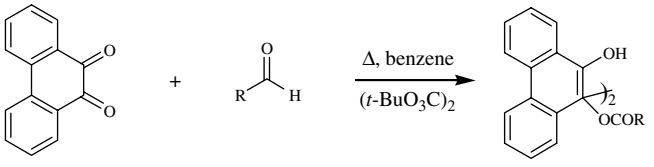

1 **3** **75** (66-90%)

SCHEME 22

Further proof for an *in-cage* process came from the *thermal* generation of acyl radicals and consequent comparison of the product spectrum with that obtained from the photoreaction. In contrast to the photoacylation (and also to Schenck's *thermal* reaction involving chloranil,[20a] *vide supra*), *thermal* reactions of various acyl radicals with ground state 9,10-phenanthrenequinone (**1**) gave *ca.* 1:1 mixtures of the isomeric dimers **75** (Scheme 22), thus disproving a similar *out-of-cage* scenario in the photochemical case.[28h]

In detailed experimental studies on substituted 1,2-naphthoquinones, Maruyama and Takuwa were able to study the role of the aldehyde with respect to the chemoselectivity (Scheme 23; Chart 4; Table 88.7). Irradiation of benzene solutions of various 1,2-naphthoquinones and aliphatic aldehydes gave 3-acyl-1,2-naphthalenediols (**29**) and the 1,2-naphthalenediol monoacyl esters (**76**).[28c,29a] On the contrary, only the latter regioisomeric monoesters were formed in the reaction of 1,2-naphthoquinones with aromatic

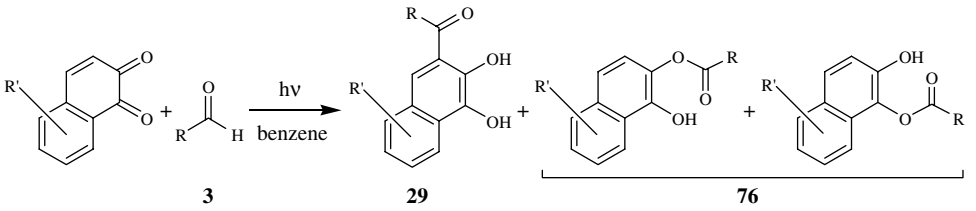

SCHEME 23

aldehydes.[29b] This remarkable regioselectivity difference was ascribed to the decreasing nucleophilic character of the aroyl radical in the order: $CH_3\dot{C}=O > CH_2=CH\dot{C}=O > Ph\dot{C}=O$.[29a,b]

A special case was the irradiation of 3-substituted 1,2-naphthoquinones with aliphatic aldehydes (Scheme 24).[28c,29a,b] Photolysis of the 3-halogenated derivatives afforded the corresponding monoesters (**76**) as the main products. Additionally, large amounts of paraldehyde (*ca.* 90%) were obtained, which accounted for the formation of hydrogen halide during the course of the reaction. In line with this observation, small amounts (1 to 3%) of 3-acyl-1,2-naphthalenediols (**29**) were isolated, unambiguously proving partial replacement of the halogen. Furthermore, 3-halogeno-4-acyl-1,2-naphthoquinones (**79**) were obtained in yields of 2 to 5% and an *in situ* oxidation was suggested to explain their formation. The corresponding 3-methyl-1,2-naphthoquinone (**78**) gave a mixture of its monoesters (**76**) and the 4-acylated quinone (**79**), respectively.

The photochemical reaction of 1,2-naphthoquinone (**30**) with acetaldehyde was reinvestigated to further determine the relative contribution of *in-cage* and *out-of-cage* mechanisms as a function of the temperature.[28j] At 22°C, the *C*-acylated product (**29**) was obtained in 22% along with 34% of the *O*-acylated monoesters (**76**). In addition, the diacylated compound **80** was isolated in 0.9% yield. Its formation was ascribed to an *out-of-cage* process, as proven by CIDNP investigations and by comparison with the results obtained by *thermal* generation of acyl radicals. Thus, the amount of **80** formed during the photoacylation was determined at various temperatures and was used as a measure of the participation of the *out-of-cage* mechanism. Below *ca.* 4°C, **80** could not be detected in the reaction mixture, thus indicating that the photoacylation proceeds exclusively via the *in-cage* pathway. At elevated temperatures, the amount of *out-of-cage* product **80** was estimated as 6.7% (20°C), 7.7% (22°C), 19.4% (50°C), 27.8% (70°C), and 36.6% (90°C), respectively.

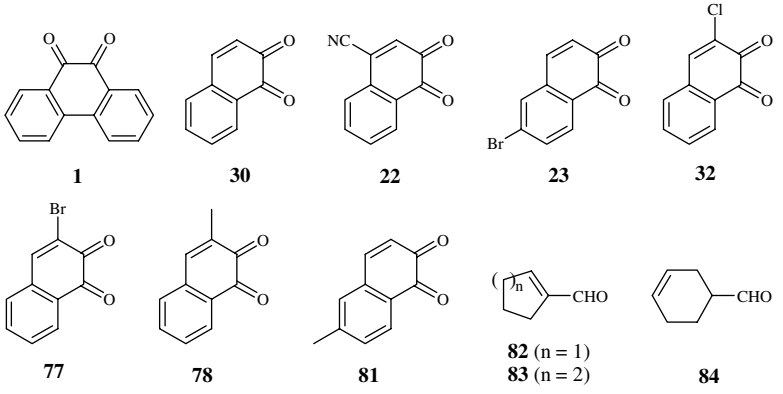

CHART 4

When glyoxals (**85**) were used as starting materials and irradiated in the presence of 9,10-phenanthrenequinone (**1**), the corresponding monoesters were again obtained as sole products in yields of 35 to 50% (Scheme 26). Hence, decarbonylation followed the initial hydrogen abstraction step. Remarkably,

TABLE 88.7 Photoreactions of 1,2-Quinones and Aldehydes as Reported by Maruyama and Takuwa[a,28,29]

Quinone	Aldehyde (R)	Ester (%)	Acyl. HQ (%)	Ref.
1	Me	100	—	28a
1	Et	100	—	28a
1	Pr	100	—	28a
1	*i*-Pr	100	—	28a
1	Bu	100	—	28a
1	*i*-Bu	100	—	28a
1	Ph	100	—	28a
1	*p*-$MeOC_6H_4$	100	—	28a
1	*p*-$NO_2C_6H_4$	*ca.* 100	—	28a
1	*m*-$NO_2C_6H_4$	*ca.* 100	—	28a
1	**10**	*ca.* 100	—	28a
1	3,4-$(CH_2O_2)C_6H_3$	*ca.* 100	—	28a
1	PhCO	85 (**4**)[b]	—	28a,b
30	Me	39[c]	24	28c,29a
30	Et	14[c]	19	28c,29a
30	Pr	7[c]	20	28c,29a
30	*i*-Pr	27.5[c]	5	28c,29a
30	Bu	15.5[c]	8.1	28c,29a
30	*i*-Bu	16[c]	8	28c,29a
30	C_5H_{11}	12.3[c]	12.3	28c,29a
30	C_6H_{13}	19[c]	10.2	28c,29a
30	C_7H_{15}	26.2[c]	14	28c,29a
30	C_8H_{17}	16.4[c]	10	28c,29a
30	C_9H_{19}	15.4[c]	8.6	28c,29a
22	Me	11.6[c]	22.5	28c,29a
22	Et	11[c]	49.5	28c,29a
22	Pr	3[c]	29	28c,29a
22	*i*-Pr	5.4[c]	32	28c,29a
22	Bu	7.4[c]	31	28c,29a
22	C_5H_{11}	5.3[c]	28	28c,29a
22	C_6H_{13}	4.6[c]	28.8	28c,29a
22	C_7H_{15}	6.2[c]	28.7	28c,29a
22	C_8H_{17}	3.1[c]	17.6	28c,29a
22	C_9H_{19}	5.1[c]	22	28c,29a
23	Me	16.9[c]	38	28c,29a
23	Et	24[c]	25.7	28c,29a
23	Pr	28.8[c]	25.8	28c,29a
23	*i*-Pr	40.4[c]	15.4	28c,29a
23	Bu	26.9[c]	18.1	28c,29a
23	*i*-Bu	27.7[c]	16.6	28c,29a
23	C_5H_{11}	33.6[c]	22.4	28c,29a
23	C_6H_{13}	25[c]	20	28c,29a
23	C_7H_{15}	29.7[c]	23.2	28c,29a
23	C_8H_{17}	30.3[c]	20.8	28c,29a
23	C_9H_{19}	36.7[c]	11.5	28c,29a
81	Me	6[c]	10	28c,29a
81	Et	13.9[c]	15.2	28c,29a
81	Pr	11.5[c]	10.4	28c,29a
81	*i*-Pr	31.9[c]	7.8	28c,29a
81	Bu	15.4[c]	13.5	28c,29a
81	*i*-Bu	21[c]	10	28c,29a
81	C_5H_{11}	11[c]	17.4	28c,29a
81	C_6H_{13}	9.2[c]	14	28c,29a
81	C_7H_{15}	4.7[c]	4.4	28c,29a
81	C_8H_{17}	20.2[c]	13.8	28c,29a
81	C_9H_{19}	7.6[c]	9.8	28c,29a

TABLE 88.7 Photoreactions of 1,2-Quinones and Aldehydes as Reported by Maruyama and Takuwa[a,28,29] (continued)

Quinone	Aldehyde (R)	Ester (%)	Acyl. HQ (%)	Ref.
32	Me	38.7[c]	4.9[d] (1[e])	28c,29a
32	Et	28.9[c]	– (3.6[e])	28c,29a
32	Pr	24.4[c]	– (4.6[e])	28c,29a
32	*i*-Pr	33.5[c]	– (5.9[e])	28c,29a
32	Bu	27.7[c]	3.1[d] (5.9[e])	28c,29a
32	*i*-Bu	32.2[c]	4.2[d] (1.5[e])	28c,29a
32	C_5H_{11}	29.3[c]	n.g.[d] (n.g.[e])	28c,29a
32	C_6H_{13}	32.4[c]	3.8[d] (8.2[e])	28c,29a
32	C_7H_{15}	14.1[c]	– (5.1[e])	28c,29a
32	C_8H_{17}	20.7[c]	5.2[d] (9.4[e])	28c,29a
32	C_9H_{19}	21.8[c]	5.3[d] (5.5[e])	28c,29a
77	Me	18.6[c]	trace[d] (2.4[e])	28a,28b
77	Et	8.1[c]	– (8.3[e])	28c,29a
77	Pr	10.8[c]	– (4.2[e])	28c,29a
77	*i*-Pr	14.7[c]	– (5.2[e])	28c,29a
77	Bu	25.5[c]	3[d] (8.8[e])	28c,29a
77	*i*-Bu	21.8[c]	2.2[d] (6.8[e])	28c,29a
77	C_5H_{11}	20.1[c]	2.5[d] (6.9[e])	28c,29a
77	C_6H_{13}	10.2[c]	– (7.5[e])	28c,29a
77	C_7H_{15}	6.5[c]	– (2.1[e])	28c,29a
77	C_8H_{17}	8.5[c]	2.5[d] (3.6[e])	28c,29a
77	C_9H_{19}	8.5[c]	3[d] (3[e])	28c,29a
78	Me	17[c]	6.5[d]	28c,29a
30	Ph	29[c]	—	29b
30	*p*-$NO_2C_6H_4$	39[c]	—	29b
30	*m*-$NO_2C_6H_4$	31[c]	—	29b
30	*p*-MeC_6H_4	23[c]	—	29b
30	*p*-$MeOC_6H_4$	26[c]	—	29b
30	3,4,5-$(MeO)_3C_6H_2$	14[c]	—	29b
23	Ph	47[c]	—	29b
23	*p*-$NO_2C_6H_4$	49[c]	—	29b
23	*m*-$NO_2C_6H_4$	39[c]	—	29b
23	*p*-MeC_6H_4	35[c]	—	29b
23	*p*-$MeOC_6H_4$	54[c]	—	29b
23	2,5-$(MeO)_2C_6H_3$	65[c]	—	29b
23	3,4,5-$(MeO)_3C_6H_2$	15[c]	—	29b
23	2,4,6-$Me_3C_6H_2$	41[c]	—	29b
23	2,4,6-$(i\text{-Pr})_3C_6H_2$	19[c]	—	29b
22	Ph	21[c]	—	29b
22	*p*-$NO_2C_6H_4$	39[c]	—	29b
22	*m*-$NO_2C_6H_4$	35[c]	—	29b
22	*p*-MeC_6H_4	16[c]	—	29b
22	*p*-$MeOC_6H_4$	26[c]	—	29b
22	3,4,5-$(MeO)_3C_6H_2$	27[c]	—	29b
22	2,4,6-$Me_3C_6H_2$	55[c]	—	29b
32	Ph	26[c]	—	29b
32	**10**	25[c]	—	29b
32	*p*-$NO_2C_6H_4$	44[c]	—	29b
32	*m*-$NO_2C_6H_4$	26[c]	—	29b
32	*p*-MeC_6H_4	40[c]	—	29b
32	*p*-$MeOC_6H_4$	26[c]	—	29b
77	Ph	21[c]	—	29b
77	**10**	20[c]	—	29b
77	*p*-$NO_2C_6H_4$	17[c]	—	29b
77	*m*-$NO_2C_6H_4$	15[c]	—	29b
77	*p*-MeC_6H_4	22[c]	—	29b

TABLE 88.7 Photoreactions of 1,2-Quinones and Aldehydes as Reported by Maruyama and Takuwa[a,28,29] (continued)

Quinone	Aldehyde (R)	Ester (%)	Acyl. HQ (%)	Ref.
77	*p*-$MeOC_6H_4$	20[c]	—	29b
81	Ph	38[c]	—	29b
81	**10**	35[c]	—	29b
81	*p*-$NO_2C_6H_4$	23[c]	—	29b
81	*m*-$NO_2C_6H_4$	24[c]	—	29b
81	*p*-MeC_6H_4	41[c]	—	29b
81	*p*-$MeOC_6H_4$	53[c]	—	29b
30	CH_2 = CH	47[c]	—	29b
23	CH_2 = CH	72[c]	—	29b
22	CH_2 = CH	51[c]	—	29b
30	MeCH = CH	42[c]	—	29b
22	MeCH = CH	28[c]	—	29b
30	*trans*-PrCH = CH	16[c]	—	29b
23	*trans*-PrCH = CH	43[c]	—	29b
22	*trans*-PrCH = CH	20[c]	—	29b
30	**82**	37[c]	—	29b
23	**82**	30[c]	—	29b
22	**82**	8[c]	—	29b
30	**83**	28[c]	—	29b
23	**83**	41[c]	—	29b
30	**10**	57[c]	—	29b
23	**10**	39[c]	—	29b
22	**10**	58[c]	—	29b
30	*cyclo*-C_5H_9	25[c]	8	29b
23	*cyclo*-C_5H_9	37[c]	14	29b
22	*cyclo*-C_5H_9	6[c]	21	29b
30	*cyclo*-C_6H_{11}	34[c]	9	29b
23	*cyclo*-C_6H_{11}	36[c]	20	29b
22	*cyclo*-C_6H_{11}	8[c]	17	29b
30	CH_2 = C_9H_{17}	11[c]	8	29b
23	CH_2 = C_9H_{17}	32[c]	12	29b
22	CH_2 = C_9H_{17}	6[c]	25	29b
30	PhC_2H_4	33[c]	5	29b
23	PhC_2H_4	43[c]	18	29b
22	PhC_2H_4	8[c]	32	29b
30	**84**	34[c]	5	29b
23	**84**	42[c]	12	29b
22	**84**	17[c]	10	29b

[a] Irradiation conditions: benzene, high-pressure Hg lamp (300–500 W), with and without filters.
[b] After decarbonylation prior to ester formation, see Ref. 28b.
[c] Regioisomeric mixture, not assigned.
[d] As 4-acylated quinone due to *in situ* oxidation (see Scheme 24).
[e] Yield of dehydrohalogenated acylated hydroquinone.

the hydrogen transfer process was found to be reversible as proven by CIDNP investigations. Owing to the stability of the acyl radical intermediate *t*-butylglyoxal partly underwent secondary decarbonylation yielding the *t*-butylether **86** in 12% yield.[28b]

Decarbonylation was also reported when 1,2-naphthoquinone (**30**) was irradiated in the presence of phenyl- (R = H) or diphenylacetaldehyde (R = Ph).[28i] The initial benzylated or diphenylmethylated product **87** underwent rapid oxidation and isomerization during usual work-up, affording the quinone methides **88** as main products. In the case of diphenylacetaldehyde, acetylation of the reaction mixture with acetic anhydride gave the diacetylated product **89** of the primary addition product (**87**; R = Ph). In addition, when the product mixtures were quickly separated, the corresponding quinone intermediates

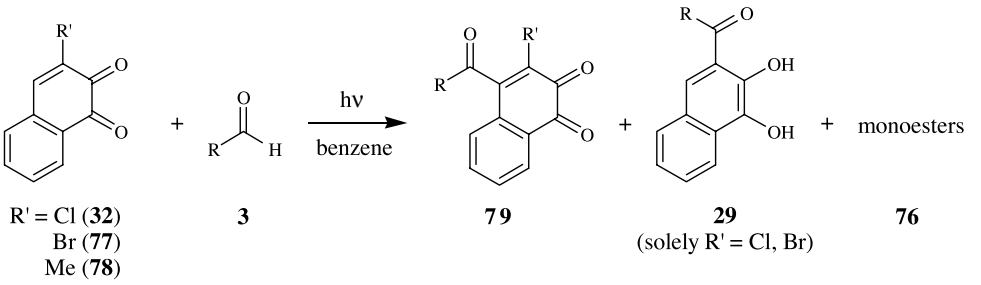

SCHEME 24

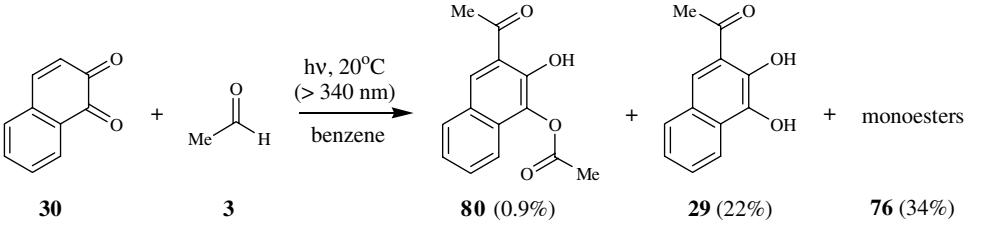

SCHEME 25

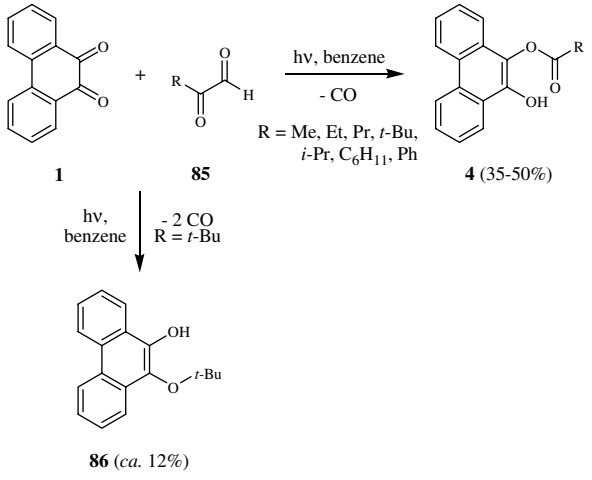

SCHEME 26

90 were isolated and characterized (yields are indicated in *italics* in Scheme 27). Whereas phenylacetaldehyde (R = H) gave a mixture of benzylated and benzoylated products with 1,2-naphthoquinone, diphenylacetaldehyde (R = Ph) exclusively yielded decarbonylation products. This finding correlates convincingly with the stability of the acyl radical intermediate.[24] The different regioselectivity of the addition of acyl vs. benzyl radicals was sufficiently interpreted on the basis of the charge density of the involved radicals.[28l] Maruyama and Takuwa furthermore demonstrated that the isomerization process **90** → **88** on silica gel proceeded much faster for the benzylated adduct (**90**; R = H).[28i]

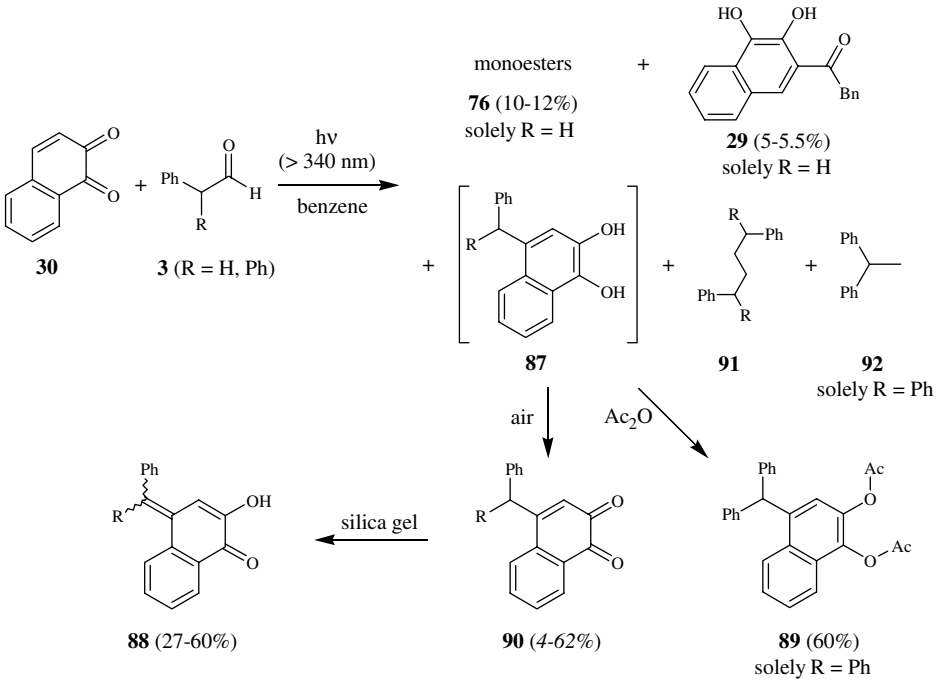

SCHEME 27

A third type of decarbonylation was found during the photolyses of various alkyl-substituted 1,2-benzoquinones (**93**) with acetaldehyde (Scheme 28; Table 88.8).[28k] Although the corresponding acylated hydroquinones (**94**) and monoesters (**95**) were still found as major products, dimers of cyclopentadienone (**96**), generated via photodecarbonylation of the quinones, were obtained for 3,5-di-*t*-butyl- (**93**; $R,^1$ R^3 = *t*-Bu, R^2 = H) and 3-*t*-butyl-5-methyl-1,2-benzoquinone (**93**; R^1 = *t*-Bu, R^2 = H; R^3 = Me) in low yields, respectively. In contrast to other *ortho*-quinones studied (*vide supra*), mechanistic investigations revealed that 1,2-benzoquinones **93** react through the *out-of-cage* pathway because no CIDNP signal was observed. This explanation was further confirmed by experiments involving *thermally* generated acyl radicals. With di-*t*-butyl diperoxyoxalate at 38°C, the acylated hydroquinone (**94**) was found as main product in 26% yield in addition to the monoester-pair (**95**) with 7% and a diacylated compound (similar to **80** in Scheme 25) with 6%. The latter substrate was formed via secondary acylation from the *C*-acylated product (**94**) as shown in an independent experiment.

A novel type of photoproduct was observed for *ortho*-chloranil (**18**).[28d] Whereas various aldehydes studied gave the expected monoesters (**98**) in moderate to good yields, *iso*- and 2-ethylbutyraldehyde afforded the tetrachloro-3,3-dialkyl-2,3-dihydro-benzo[1,4]-dioxin-2-ols **99** (Scheme 29). The formation of these unusual products was explained by initial abstraction of the tertiary methine hydrogen in preference to the formyl hydrogen, followed by rapid transformation into the 1,4-adduct **99**.

In 1990, Takuwa described an interesting modification of the photoacylation protocol.[29c] Upon irradiation of an acetonitrile/benzene solution of 1,2-naphthoquinone (**30**) and acetaldehyde, 3-acetyl-1,2-naphthalenediol (**29**) was isolated in 7% yield. The yield could be significantly increased when irradiations were performed in the presence of a metal perchlorate. Among the various perchlorates used, magnesium perchlorate (1 equivalent) gave the highest yield (30%). Similar yields of 25 to 29% were obtained with

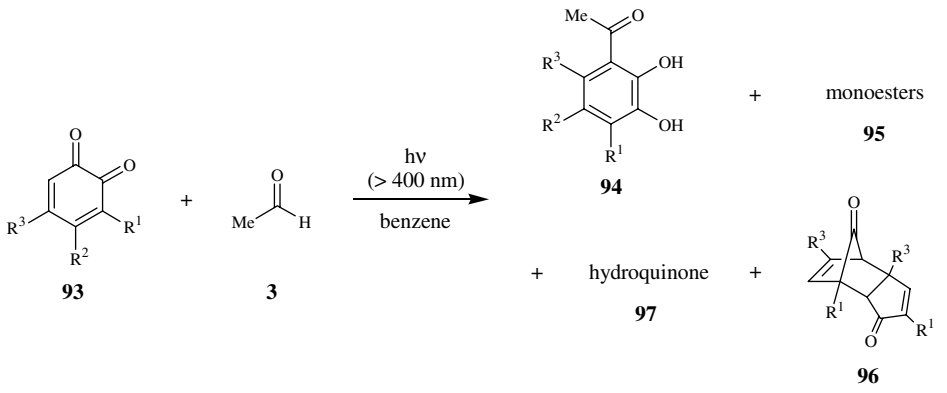

93 **3** **94** **95** **97** **96**

SCHEME 28

TABLE 88.8 Photoreactions Involving 1,2-Benzoquinones (**93**) and Acetaldehyde[a,28k]

R¹	R²	R³	**94** (%)	**95** (%)	**97** (%)	**96** (%)
H	*t*-Bu	H	20	20	—	—
t-Bu	H	*t*-Bu	6	36	22	4.5
t-Bu	H	Me	12	14	—	1

[a] Irradiation conditions: benzene, high-pressure Hg lamp (300 W), filter (>400 nm).

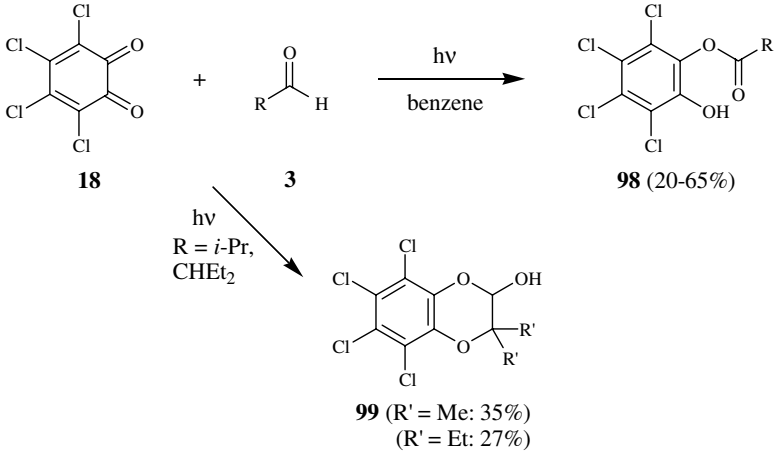

18 **3** **98** (20-65%)

99 (R' = Me: 35%)
(R' = Et: 27%)

SCHEME 29

other aldehydes (Scheme 30; Table 88.9). Because tetrabutylammonium perchlorate gave only 5% yield, the presence of a metal cation was found essential for the activation process.*

As an extension of their studies, Maruyama described the photoacylation of 1,4-naphthoquinone (**41**) with α,β-unsaturated aliphatic aldehydes (Scheme 31; Table 88.10).[28g] In contrast to 1,4-benzoquinone

*However, the same experiments in pure benzene gave mixtures of acylated hydroquinones (**29**) and monoesters (**76**) in yields of 8.1–24% and 7–39% (Table 88.7), respectively.[29a]

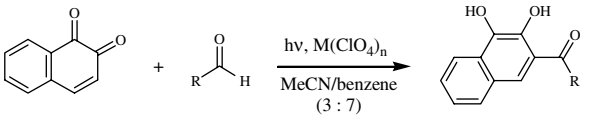

30 **3** **29** (9-30%)

SCHEME 30

TABLE 88.9 Photoreactions of 1,2-Benzoquinone (**30**) in the Presence of Metal Perchlorates[a,29c]

R	$M(ClO_4)_n$	**29** (%)	R	$M(ClO_4)_n$	**29** (%)
Me	none	7	Me	$Ce(ClO_4)_3$[b]	21
Me	$LiClO_4$	9	Me	n-Bu_4NClO_4	5
Me	$Mg(ClO_4)_2$	30	Et	$Mg(ClO_4)_2$	29
Me	$Ca(ClO_4)_2$[b]	16	Pr	$Mg(ClO_4)_2$	27
Me	$Co(ClO_4)_2$[b]	28	Bu	$Mg(ClO_4)_2$	25
Me	$Ni(ClO_4)_2$[b]	18	Me[c]	none	24[d]

[a] Irradiation conditions: MeCN/benzene (3:7), high-pressure Hg-lamp (300 W), Pyrex, 15 h.
[b] As hydrate.
[c] In pure benzene.
[d] Beside 39% of monoesters **76** [29a].

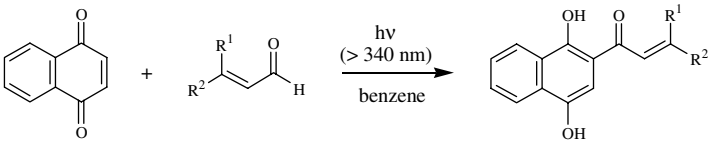

41 **100** **43** (43-53%)

SCHEME 31

TABLE 88.10 Photoreactions of 1,4-Naphthoquinone (**41**) with α,β-Unsaturated Aldehydes[a,29g]

R^1	R^2	**43** (%)
Me	H	53
Me	Me	43
Pr	H	48

[a] Irradiation conditions: high-pressure Hg lamp (300 W), Pyrex, 2,7-dimethyl-3,6-diazacyclohepta-1,6-dieneperchlorate (0.2% solution) filter, 20 to 25 h.

(*vide supra*), irradiations in benzene solutions selectively gave the corresponding acylated hydroquinones (**43**) in yield between 43 and 53%. The photoproducts served as starting materials for the synthesis of α- and β-lapachones (*vide infra*).

Synthetic Studies by George A. Kraus and Others: 1986–2002

From 1992, Kraus and co-workers explored the synthetic value of the photochemical acylation of 1,4-quinones (Scheme 32; Table 88.11),[30] and developed it as a suitable alternative to existing *thermal* Friedel-Crafts acylations.[30c,d] During their studies on the pyranoquinone skeleton, they initially used the classical Friedel-Crafts approach but the poor solubility of some of the starting materials, the drastic reaction

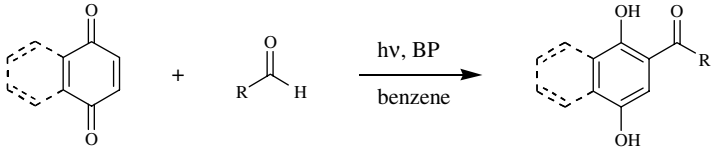

5/41 **3** **6/43** (12-88%)

SCHEME 32

TABLE 88.11 Photoreactions of 1,4-Quinones and Aldehydes as Reported by Kraus[30]

Quinone	Aldehyde (R)	Conditions[a]	Acyl. HQ (%)	Ref.
5	Pr	HP Hg lamp, benzene, 5 d	82	30a
5	Ph	HP Hg lamp, benzene, 5 d	60	30a
5	MeCH=CH	HP Hg lamp, benzene, 5 d	52	30a
5	**10**	HP Hg lamp, benzene, 5 d	65	30a
5	*o*-$MeOC_6H_4$	HP Hg lamp, benzene, 5 d	62	30a
5	2-Furyl-CH=CH	HP Hg lamp, benzene, 5 d	32	30a
41	Pr	HP Hg lamp, benzene, 5 d	77	30a
41	Ph	HP Hg lamp, benzene, 5 d	88	30a
41	MeCH=CH	HP Hg lamp, benzene, 5 d	65	30a
101	Ph	HP Hg lamp, benzene, 5 d	0	30b
101	Ph	HP Hg lamp, BP, benzene, 5 d	61	30b
5	*o*-ClC_6H_4	HP Hg lamp, BP, benzene, 5 d	78	30b
5	*o*-$MeOC_6H_4$	HP Hg lamp, BP, benzene, 5 d	72	30b
5	*o*-MeC_6H_4	HP Hg lamp, BP, benzene, 5 d	65	30b
5	*o*-$MeO_2CC_6H_4$	HP Hg lamp, BP, benzene, 5 d	58	30b
5	*p*-$MeOC_6H_4$	HP Hg lamp, BP, benzene, 5 d	77	30b
5	*p*-ClC_6H_4	HP Hg lamp, BP, benzene, 5 d	73	30b
5	*p*-MeC_6H_4	HP Hg lamp, BP, benzene, 5 d	79	30b
5	*p*-$CHOC_6H_4$	HP Hg lamp, BP, benzene, 5 d	42	30b
5	*p*-FC_6H_4	HP Hg lamp, BP, benzene, 5 d	61	30b
41	*o*-ClC_6H_4	HP Hg lamp, BP, benzene, 5 d	60.4	30b
41	*o*-FC_6H_4	HP Hg lamp, BP, benzene, 5 d	68	30b
41	*o*-MeC_6H_4	HP Hg lamp, BP, benzene, 5 d	57	30b
41	*p*-MeC_6H_4	HP Hg lamp, BP, benzene, 5 d	70	30b
41	*p*-ClC_6H_4	HP Hg lamp, BP, benzene, 5 d	65	30b
5	*p*-$NO_2C_6H_4$	HP Hg lamp, benzene, 5 d	0	30d
5	*o*-$NH_2C_6H_4$	HP Hg lamp, benzene, 5 d	0	30d
5	*o*-ClC_6H_4	HP Hg lamp, benzene, 5 d	61	30d
5	*o*-FC_6H_4	HP Hg lamp, benzene, 5 d	68	30d
5	*p*-MeC_6H_4	HP Hg lamp, benzene, 5 d	70	30d
5	*p*-ClC_6H_4	HP Hg lamp, benzene, 5 d	65	30d
41	CH_2=CH	HP Hg lamp, benzene, 5 d	12	30d
41	**10**	HP Hg lamp, benzene, 5 d	65	30d

[a] HP Hg: benzene, high-pressure Hg lamp (not specified), Pyrex; BP: benzophenone mediated.

TABLE 88.12 Benzophenone-Mediated Photoacylations of 1,4-Benzoquinone (**5**) in SC-CO_2[a,30e]

Aldehyde (R)	Co-solvent	Pressure (psi)	Time (days)	Acyl. HQ (%)
Ph	5% *t*-BuOH	4672	3	49
Ph	5% *t*-BuOH	4548	2	44
Ph	none	6055	2	44
Pr	none	1191	2	53
Pr	none	1492	2	41
Pr	none	1946	2	41
Pr	none	3042	2	50
Pr	none	5860	2	60
Pr	none	8180	2	65
Pr	5% *t*-BuOH	5735	2	81

[a] Conditions: Xenon arc lamp (150 W), Pyrex.

conditions, and the modest yields forced them to examine alternative pathways.* In contrast to the results reported by Klinger or Bruce (*vide supra*), the formation of monoesters was, however, never described by Kraus.

A major improvement in the photochemical approach was achieved by the addition of catalytic amounts of benzophenone (BP). Applying this *mediated* procedure, the yields generally increased and several, so-far unreactive, quinones could be activated for the acylation. As an example, 5,8-dimethoxy-1,4-naphthoquinone (**101**) remained unreactive upon irradiation in benzene and in the presence of benzaldehyde, but when using a catalytic amount of benzophenone, the acylated hydroquinone was readily obtained in 61% yield.[30b]

A major disadvantage of Kraus's procedure in terms of an environmentally benign method involved the use of benzene (or alternatively acetonitrile) as solvent. Supercritical carbon dioxide (SC-CO_2) was recently reported as an alternative solvent and was applied to the benzophenone-mediated photoacylation of 1,4-benzoquinone (**5**) with benzaldehyde or butyraldehyde, respectively.[30e] High yields of up to 81% were achieved at higher CO_2 pressure, or with the addition of 5% *t*-butyl alcohol as co-solvent (Table 88.12); the latter is necessary due to the limited solubility of the quinone in SC-CO_2. Despite these achievements, this technique suffers from technical disadvantages (e.g., high pressure or small reactor volume), especially for a large-scale application.

Another benzophenone-mediated photoacylation was reported by Kobayashi and co-workers for 2-aryl- and 2-alkylamino-1,4-naphthoquinones (**102**).[31a] The photoinduced acylation was achieved in moderate to high yields of 54 to 89% with various aromatic and aliphatic aldehydes solely in the presence of 2 equivalents of benzophenone (Scheme 33; Table 88.13). No acylation occurred in the absence of the mediator, whereas the yields significantly decreased when only 1 equivalent was used. In one exemplary case, benzophenone was re-isolated in 85% yield. Furthermore, careful analysis of the crude product mixture confirmed the absence of any significant degradation products of BP (e.g., benzopinacol, benzhydrol). Based on these findings it was concluded that triplet-excited benzophenone is involved in the hydrogen abstraction step. The primarily formed acylated hydroquinones (**105**) were readily oxidized during work-up to give the corresponding quinones (**103**). Most of these derivatives underwent further quinone–imine tautomerization to **104**.

The initial formation of the hydroquinone was confirmed with the diphenylamino derivative (**106**) as starting material and further transformation into its diester (**107**) with acetic anhydride (Scheme 34).[31a] Additionally, oxidation by air in the presence of $FeCl_3$ gave the corresponding 3-acyl-1,4-naphthoquinone (similar to **103**).

*However, Kraus incorrectly stated about the photoacylation:[30a] *"Isolated examples of this reaction have been reported."*

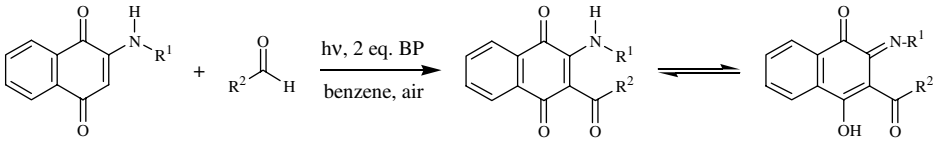

102 **3** **103** (quinone) **104** (imine)

SCHEME 33

TABLE 88.13 Benzophenone-Mediated Photoacylations of 2-Aryl- and 2-Alkylamino-1,4-naphthoquinones[a,31a]

Quinone (R^1)	Aldehyde (R^2)	Time (h)	**103** (quinone) (%)	**104** (imine) (%)
Ph	Et	8	—	89
Ph	Me	8	—	79
Ph	Pr	9	—	82
Ph	Ph	5	68	—
o-$MeOC_6H_4$	Et	15	—	76
$MeOC_2H_4$	Pr	4	—	54

[a] Conditions: benzene, high-pressure Hg lamp (500 W), Pyrex.

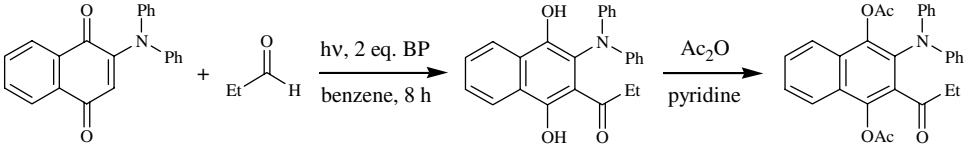

106 **3** **105** (not isolated) **107** (88% overall)

SCHEME 34

TABLE 88.14 Photoreactions of 1,4-Quinones and Aldehydes as Reported by Kobayashi[a,31b,c]

Quinone	Aldehyde (R)	Ref.	Quinone	Aldehyde (R)	Ref.
5	Et	31b	**41**	*o*-HOC_6H_4	31c
5	Ph	31b	**41**	2-HO-5-MeC_6H_3	31c
41	Et	31b	**41**	2-HO-5-ClC_6H_3	31c
41	Pr	31b	**41**	2-HO-5-BrC_6H_3	31c
41	Ph	31b	**41**[b]	2-HO-4-$MeOC_6H_3$	31c

[a] Conditions: benzene, high-pressure Hg lamp (500 W), Pyrex, *ca.* 4 days.
[b] $Mg(ClO_4)_2$ mediated, MeCN/benzene (3:7).[29c]

Kobayashi furthermore adopted the photochemical acylation procedure described by Kraus[30a] as an important key step in the synthesis of several quinone derivatives (details are given in Section 88.7; *vide infra*),[31b,c] and in all of these cases, the acylated hydroquinones were used without any purification. Table 88.14 summarizes the reported details.

To control the site of the acylation step, Tachikawa developed a highly *regioselective* procedure using unsymmetrically substituted 1,4-naphthoquinones (**108**) with bromo or chloro substituents at the C–C double bond (Scheme 35; Table 88.15).[32a] The excellent regioselectivity was achieved through replacement

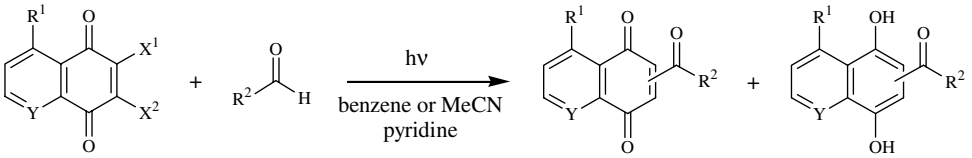

108/111 **3** **109** **110**

SCHEME 35

TABLE 88.15 Regioselective Acylations of Halogen-Substituted 1,4-Naphthoquinones[a,32]

Starting Materials					Conditions		Yields		
R^1	Y	X^1	X^1	**3** (R^2)	Solvent	Time (h)	**109** (%)[b]	**110** (%)[b]	Ref.
MeO	CH	H	H	Pr	Benzene	8	6.5 (2,8)[c]	15.0 (2,8)[c]	32a
							8.7 (2,5)[c]	22.1 (2,5)[c]	
MeO	CH	H	H	Pr	MeCN	8	1.7 (2,8)[c]	10.4 (2,8)[c]	32a
							2.0 (2,5)[c]	13.6 (2,5)[c]	
MeO	CH	Br	H	Pr	Benzene	8	42.2	15.2	32a
MeO	CH	Br	H	Pr	MeCN	8	25.1	15.0	32a
MeO	CH	H	Br	Pr	Benzene	8	46.2	20.3	32a
MeO	CH	H	Br	Pr	MeCN	8	38.3	15.4	32a
H	CH	Cl	H	Pr	Benzene	8	32.9	32.2	32a
H	CH	Cl	H	Pr	MeCN	8	21.1	21.6	32a
MeO	CH	H	H	C_9H_{19}	Benzene	8	7.3 (2,8)[c]	14.6 (2,8)[c]	32a
							5.6 (2,5)[c]	31.5 (2,5)[c]	
MeO	CH	Br	H	C_9H_{19}	Benzene	8	54.9	20.7	32a
MeO	CH	H	Br	C_9H_{19}	Benzene	8	50.0	32.3	32a
H	CH	Cl	H	C_9H_{19}	Benzene	8	29.1	34.5	32a
H	N	H	H	Pr	Benzene	3	6.9 (1,6)[d]	15.0 (1,6)[d]	32b
							4.4 (1,7)[d]	12.0 (1,7)[d]	
H	N	Cl	H	Pr	Benzene	1	15.2	46.6	32b
H	N	H	Cl	Pr	Benzene	1	4.9	40.4	32b
H	N	Br	H	Pr	Benzene	1	23.3	52.2	32b
H	N	H	Br	Pr	Benzene	1	27.1	37.6	32b
H	N	H	H	C_9H_{19}	Benzene	3	4.4 (1,6)[d]	11.6 (1,6)[d]	32b
							5.2 (1,7)[d]	9.0 (1,7)[d]	
H	N	Cl	H	C_9H_{19}	Benzene	1	19.6	28.4	32b
H	N	H	Cl	C_9H_{19}	Benzene	1	9.6	30.4	32b
H	N	Br	H	C_9H_{19}	Benzene	1	12.4	48.8	32b
H	N	H	Br	C_9H_{19}	Benzene	1	10.0	38.9	32b

[a] Conditions: high-pressure Hg lamp (not specified), $CuSO_4 \cdot 5H_2O$ (sat. solution) filter.
[b] Yields of diacetates.
[c] Acyl group at C-2.
[d] Quinolinequinones with N-1.

of the halogen by the acyl group. In most cases, mixtures of the acylated hydroquinones (**109**) and the corresponding acylated quinones (**110**) were obtained in moderate to good total yields. This finding was explained by disproportionation of the acylated radical intermediates. The procedure was further extended to photochemical acylations involving *mono*-halogen substituted quinolinequinones (**111**).[32b] The efficiency of the regiocontrol was demonstrated by comparison with the *non*-halogenated parent compounds ($X^1 = X^2 = H$) and mixtures of both regioisomeric pairs of acylated hydroquinones (**109**) and quinones (**110**) were obtained. However, the 2,5- (from **108**) or 1,6-regiosiomers (from **111**) were always slightly preferred in the *non*-activated cases.

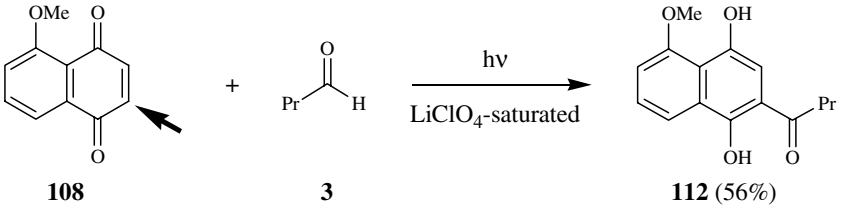

108 **3** **112** (56%)

SCHEME 36

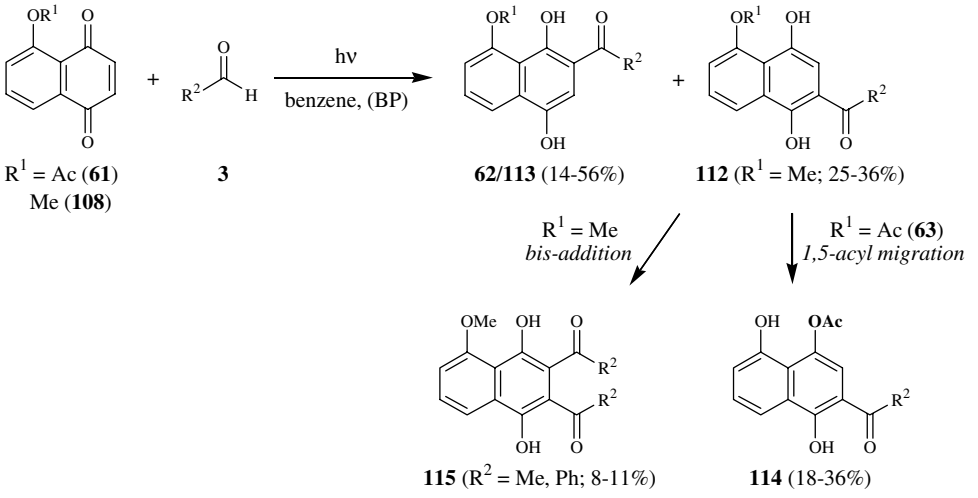

R^1 = Ac (**61**) Me (**108**) **3** **62/113** (14-56%) **112** (R^1 = Me; 25-36%)

115 (R^2 = Me, Ph; 8-11%) **114** (18-36%)

SCHEME 37

A different regioselectivity concept has been achieved by Mattay and co-workers via saturation of the solution with lithium perchlorate prior to photolysis.[33a,b] This was demonstrated for the unsymmetrically substituted 5-methoxy-1,4-naphthoquinone (**108**) by irradiation in $LiClO_4$-saturated butyraldehyde. Only the 2,5-regioisomer (**112**) was obtained in 56% yield, whereas the corresponding 2,8-regioisomer (**113**) could not be detected in the reaction mixture (Scheme 36). The directing effect of the additives was explained by selective complexation of the lithium cation and consequent alteration of the LUMO properties of the quinone. Hence, this phenomenon parallels the results on acceleration of the addition efficiency by metal perchlorates as reported by Takuwa (*vide supra*).[29c]

Mattay and co-workers studied various photoinduced acylations involving the unsymmetrically substituted 1,4-quinones **108** and **61** and, in all cases studied, mixtures of the two regioisomeric hydroquinones were isolated in moderate to good total yields of 59 to 84% (Scheme 37, Table 88.16).[33] In correlation with the nucleophilic character of the corresponding acyl radicals,[29a,b] but in contrast to Tachikawa's results,[32a] aliphatic aldehydes predominantly gave the 2,8-regioisomers (**113**). Only in the presence of benzaldehyde was the 2,5-regioisomer (**112**) formed as the major regioisomer in 36% yield; this differing regioselectivity was explained by the more electrophilic character of the aroyl radical.[29a,b]

With both naphthoquinones, remarkable side reactions have been observed (Scheme 37). Although Bruce had already studied the photoinduced acylation of the acetylated naphthoquinone **61**, for which he assigned the corresponding acylated hydroquinone pair (*vide supra*),[23e] more recent studies revealed that further 1,5-acyl migration of the 2,5-regioisomer (**63** → **114**) occurred.[33g] From the photoacylation of the methoxy derivative **108**, diacylated products (**115**) were obtained with acetaldehyde and benzaldehyde, respectively.

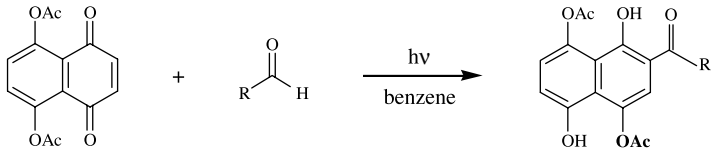

116 **3** **117** (58-60%)

SCHEME 38

TABLE 88.16 Photoacylation of Substituted 1,4-Naphthoquinones **61**, **108**, and **116**[a,33]

Quinone (R^1)	Aldehyde (R^2)	**62/113** (%)	**112** (%)	**114/117** (%)	**115** (%)	Ref.
61 (Ac)	Me	43	—	36[b]	—	33c,
61 (Ac)	Et	41	—	18[b]	—	33c,g
61 (Ac)	Pr	42	—	34[b]	—	33c,g
108 (Me)	Me	34	28	—	8	33f
108 (Me)	Et	56	28	—	—	33f
108 (Me)[c]	Pr	53	25	—	—	33e
108 (Me)	Ph	14	36	—	11	33e
116	Et[d]	—		60	—	33c
116	Pr[d]	—		60	—	33c
116	*i*-Pen[d]	—		58	—	33c

[a] Conditions: benzene, RPR-4190 lamps (419 ± 10 nm) or high-pressure Hg lamp (150 W).
[b] 1,5-Acyl group migration not recognized in Ref. 23e,33c.
[c] Benzophenone mediated.
[d] 15–17% non-rearranged product in the crude reaction mixture.

1,5-Acyl migration was also observed for the diacetylated 5,8-dihydroxy-1,4-naphthoquinone derivative **116**. Upon irradiation in benzene and in the presence of various aliphatic aldehydes, the corresponding acylated products **117** were obtained in yields of 58 to 60% (Scheme 38; Table 88.16). The acetyl group in the 5-position rearranged during the photoacylation; but in all cases, the non-rearranged acylation product was observed in 15 to 17% yield in the crude product mixture. Most reasonably, and supported by the side-selectivity of the rearrangement, the acyl migration follows the monoacylation step (photochemically or thermally).

Following the original protocols described by Kraus,[30] Mattay and co-workers examined numerous photoacylations of 1,4-quinones for which they introduced the term "Photo-Friedel-Crafts acylation".[33] In all cases, the corresponding acylated products were obtained in moderate to good yields (Table 88.17). Because these authors were particularly interested in a large-scale solar chemical outdoor application of the acylation reaction,[33h] they replaced the toxic solvents (benzene or acetonitrile) with nontoxic *t*-butyl alcohol.

A remarkable exception was the irradiation of 1,4-naphthoquinone (**41**) in the presence of benzaldehyde, and the dibenzoylated compound (**118**) was isolated as a side product in yields of 14 to 17% (Scheme 39).[33e] However, in an independent experiment it was shown that secondary addition occurred from the monoacylated product (**43**) itself and not (as originally proposed by Bruce for 1,4-benzoquinone[23d]) from an *in situ*-generated acylated quinone.

In the case of 1,4-benzoquinone (**5**), good evidence for an electron-transfer (ET) key-step from the acyl radical to a ground-state quinone was found when the *t*-butyl ester **119**, a trapping product characteristic for acyl cations,[24] was obtained during photolysis in *t*-butyl alcohol. This ester was not detected when 1,4-naphthoquinone (**41**) was applied, thus supporting the striking difference in the chemoselectivity of the acylation for both 1,4-quinones.

TABLE 88.17 Photoreactions of 1,4-Quinones and Aldehydes as Reported by Mattay[33]

Quinone	Aldehyde (R)	Conditions[a]	Acyl. HQ (%)	Ref.
41	Et	HP Hg lamp, benzene	79	33e
41	Pr	HP Hg lamp, benzene	78	33e
41	Pr	HP Hg lamp, toluene	35	33e
41	Pr	Rayonet (419 nm), *t*-BuOH	84	33c
41	*p*-CNC_6H_4	HP Hg lamp, benzene	63	33e
41	*p*-ClC_6H_4	HP Hg lamp, benzene, BP[b]	58	33e
41	*p*-$CHOC_6H_4$	HP Hg lamp, MeCN, BP[b]	42	33e
5	2,4-$(MeO)_2C_6H_3$	Rayonet (419 nm), *t*-BuOH	66	33c
50	2,4-$(MeO)_2C_6H_3$	Rayonet (419 nm), *t*-BuOH	60	33c

[a] Conditions: high-pressure Hg lamp (150 W) or RPR-4190 lamps (419 ± 10 nm), Pyrex, *ca.* 5 days.
[b] BP: benzophenone mediated.

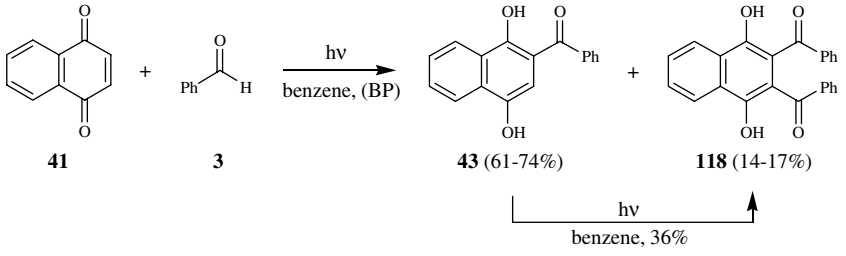

SCHEME 39

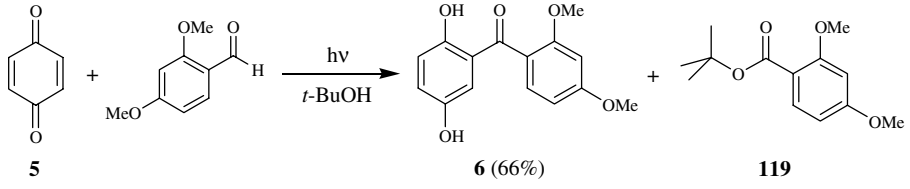

SCHEME 40

To account for the contradictory results on the mechanism of the photoacylation, Mattay and coworkers stated that "Comparing the available data from the literature it can be concluded that both in-cage and out-of-cage mechanisms operate more-or-less simultaneously depending on the specific reaction conditions of each irradiation experiment (i.e., temperature, solvent, quinone/aldehyde applied)."[33f] Hence, in-cage and out-of-cage scenarios can be seen as the extreme mechanistic cases.

88.5 Modern Solar Chemical Applications

Recently, the call for "sustainable developments," reduction of CO_2 emission, and the growing requirement for environmentally friendly technologies has led to increasing interest in (and remembrance of) the sun as an environmentally friendly energy and light source. As shown by the pioneering work of Klinger and Schönberg (*vide supra*), quinones are especially versatile substrates for the use of sunlight, and the photochemical acylation can thus be utilized in the field of *green photochemistry*[34] using modern solar chemical reactors.[35] The principle of a line-focusing parabolic trough collector (PROPHIS) is illustrated as an example in Scheme 41.[33d]

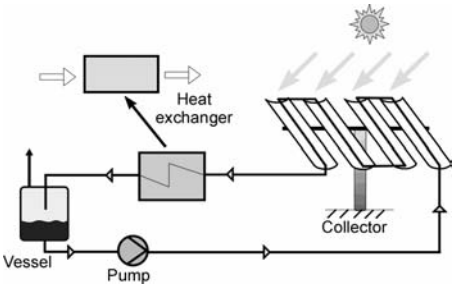

SCHEME 41

TABLE 88.18 Solar Chemical Reactions of 1,4-Quinones and Aldehydes as Reported by Mattay[33d,f]

Quinone	Aldehyde (R)	Reactor	CF (suns)	Radiation Kind	Area (m^2)[a]	Time (h)	Photons (mol)[b]	Conv. (%)
41	Pr	PROPHIS	*ca.* 15	Direct	24	24	298.8	90
5	2,4-$(MeO)_2C_6H_3$	PROPHIS	*ca.* 15	Direct	3	*ca.* 19	20.1	7
5	2,4-$(MeO)_2C_6H_3$	CRC	1–2	Direct, diffuse	3	17	41.6	17
5	2,4-$(MeO)_2C_6H_3$	Flat-bed	1	Direct, diffuse	3	*ca.* 20	n.g.[c]	3.6

[a] Reflecting mirror area (max. for PROPHIS: 32 m^2).
[b] Amount of photons collected within 300–500 nm.
[c] n.g.: not given.

Mattay and co-workers recently realized the first solar chemical large-scale application of the photoacylation reaction.[33] Illumination of a *t*-butanol/acetone solution of 1,4-naphthoquinone (**41**; 500 g) with butyraldehyde (**3**; R = Pr) using a PROPHIS sunlight-concentrating system[35a,b] (MAN-Helioman, concentration factor CF = 15 suns; 24 m^2 mirror area) gave the acylation product **43** within 3 days (Germany, August 1996) and in 90% yield without large amounts of by-products. During the experimental phase, the three concentrating troughs (24-m^2) collected almost 300-mol photons in the important absorption region (within the solar spectrum) of 1,4-quinones between 300 and 500 nm.

Furthermore, the solar chemical reaction of 1,4-benzoquinone (**5**) with 2,4-dimethoxybenzaldehyde (**3**; R = 2,4-$(MeO)_2C_6H_3$) was explored to compare different sunlight-collecting systems (Table 88.18). In parallel runs under standardized conditions, the line-focusing parabolic trough collector (PROPHIS; CF = 15), the compound parabolic collector (CPC; CF = 1–2), and the double sheet flat-bed reactor (CF = 1) gave relatively low conversion rates to **6** of 7%, 17%, and 3.6%, respectively, mainly caused by bad weather conditions.[35b] The CPC and flat-bed systems represent stationary, low concentrating collectors that can also use part of the diffuse solar radiation, which accounts for about 60% of the sunlight in central Europe. Consequently, the influence of the radiation type was reflected in the conversion ratio of 30:70 (PROPHIS vs. CPC), which showed good agreement with the calculated 35:65 ratio of direct (used by PROPHIS) vs. direct+diffuse radiation (used by CPC). This ratio additionally matched with the number of collected photons for each system as the PROPHIS-plant collected 20.1 mol of photons in the 300- to 500-nm range, the CPC reactor 41.6 mol, giving a ratio of 33:67.

88.6 Miscellaneous

A unique example of an *intramolecular* version of the photoinduced acylation has been reported by Thomson and co-workers.[36] These authors examined the extractives of the tree Blue Mahoe (*Hibiscus elatus*, Malvaceae) to explain the intensive color change of its freshly cut wood from blue-gray or pink-gray to light yellow or buff-gray on exposure to light. A number of sesquiterpenoid ketones (hibiscones A–D) and *ortho*-naphthoquinones (hibiscoquinones A–D) have been isolated and identified. Among the

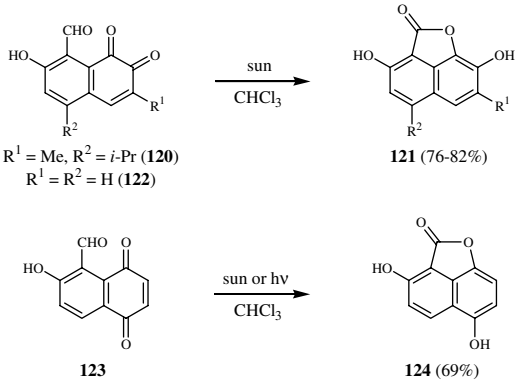

SCHEME 42

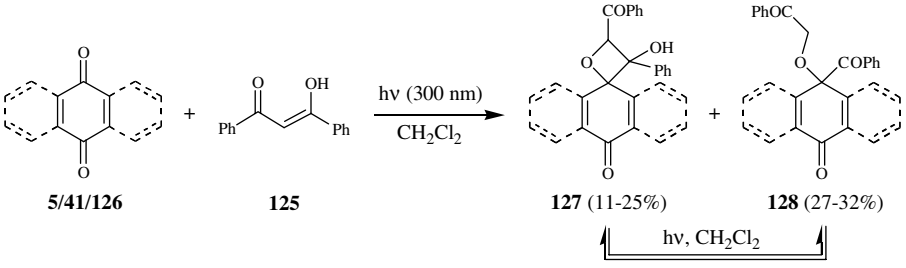

SCHEME 43

ortho-naphthoquinones, especially the pink colored hibiscoquinones A (**120**) was extremely photolabile and reacted quickly in daylight to the corresponding colorless lactone **121** (Scheme 42). This *intramolecular* photoacylation even occurred in the solid state. Thomson and co-workers furthermore compared hibiscoquinones A (**120**) with the related *ortho*- and *para*-quinone aldehydes **122** and **123**. Whereas the *ortho*-quinone **122** readily underwent the photoacylation reaction on exposure to sunlight, the *para*-quinone **123** cyclized slowly to **124** in daylight, but rapidly on irradiation with a medium-pressure mercury lamp. Because the content of hibiscoquinones A (**120**) in the heartwood of *Hibiscus elatus* is usually small, the color change was suggested to originate primarily from photoreduction of the hibiscoquinones in general.

Recently, photochemical [2+2]-additions of dibenzoylmethane (**125**) to quinones have been described by Kim and co-workers,[37] and because acylation-like products were obtained, the reaction will be described here. Although the product composition and spectrum depended on the quinone applied, 1,5-diketones were obtained in all cases examined. Upon irradiation in dichloromethane, the 1,4-quinones **5**, **41**, and anthraquinone (**126**) gave mixtures of the *spiro*-oxetane **127** and the 1,5-diketone **128**, the latter formed via subsequent retro-Aldol cleavage, in yields of 11 to 15% and 27 to 32% (Scheme 43; Table 88.19), respectively.[37a,c] Remarkably, the photoproducts were *inter*-convertible, as demonstrated by independent irradiations under identical conditions.

However, t*etra*-substituted quinones behaved differently, and mixtures of the regioisomeric 1,5-diketones **131** and **132** were isolated in moderate yields (Scheme 44; Table 88.19).[37a,c] The formation of **131** was explained through a competing [2+2]-cycloaddition of **125** to the C–C double bond of the quinone, followed by subsequent ring-opening.

In contrast, when halogenated *ortho*-quinones were used as starting materials, 1,4-dioxenes (**133**) were obtained as major products as well as small amounts of the 1,5-diketones **134** (Scheme 45; Table 88.19).[37b]

TABLE 88.19 Photoreactions of Quinones with Dibenzoylmethane (**125**)[a,37]

Quinone	Time	Main (%)	Minor (%)	Ref.
5	2 days	27 (128)	25 (127)	37a
41	110 h	27 (128)	15 (127)	37c
125	60 h	32 (128)	11 (127)	37c
128	5 days	25 (131)	—	37a
38	120 h	24 (132)	13 (131)	37c
129	120 h	10 (132)	7 (131)	37c
18	7 days	18 (133)	7 (134)	37b
19	7 days	12 (133)	5 (134)	37b
1	3 days	25 (135)	3 (136)	37b
13	4 days	27 (135)	6 (136)	37b

[a] Conditions: CH_2Cl_2, Rayonet (300 ± 10 nm).

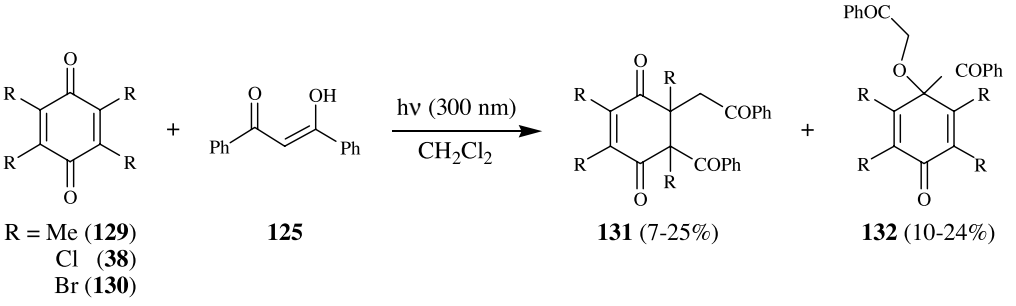

SCHEME 44

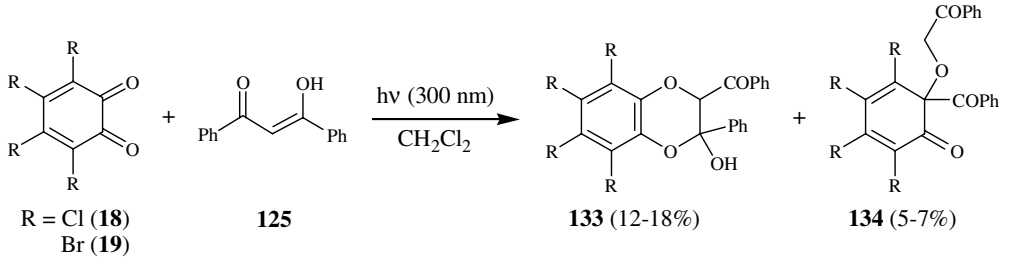

SCHEME 45

9,10-Phenanthenequinone (**1**) and acenaphthenequinone (**13**) behaved differently and photoaddition of **125** gave the 1,5-diketone **135** as major product beside the 1,5-ketoester **136** (Scheme 46; Table 88.19). The preferential formation of **135** was rationalized by comparison of the 1,4-biradical intermediates involved.[37b]

When dibenzoylmethane (**125**) was replaced by 1,3-cyclohexanedione and dichloromethane by methanol, photoaddition to benzoquinone (**5**) to give the *spiro*-oxetane (similar to **127**) fell to 2% and instead methylation to the corresponding methoxycyclohexenone occurred.[37d]

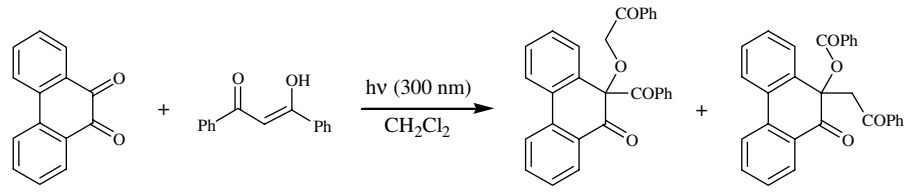

1 (likewise **13**) **125** **135** (25%) **136** (3%)

SCHEME 46

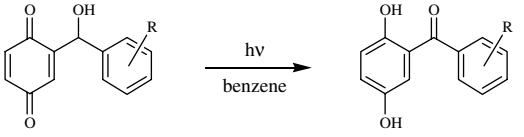

137 (R = 4-Me, 3-Me, 2-Me or 4-F) **6** (35.6-45.4%)

SCHEME 47

Acylated hydroquinones were additionally formed through an *intramolecular* oxidation/reduction reaction of α-hydroxy-benzyl-1,4-benzoquinones (**137**). Irradiation in benzene solution gave the corresponding hydroquinones **6** in moderate yields (Scheme 47).[38] In contrast to **137**, acylated quinones (such as **54**) undergo a multitude of photochemical transformations (e.g., dimerizations).[39]

88.7 Synthetic Applications

Although acylated quinones are known as important natural compounds and useful key intermediates in organic synthesis,[1] only a few examples incorporating photoacylation have been reported up to the present time. Most commonly acylated quinones are prepared via Friedel-Crafts acylation,[40] persulfate oxidation,[41] Fries-[42] or Photo-Fries rearrangement,[43] but many of these *classical* methods suffer from aggressive reaction conditions, the formation of undesired by-products, and certain limitations concerning the starting materials (availability or functionalities). Because some of these disadvantages additionally conflict with the currently increasing interest in environmentally friendly technologies, the photoinduced acylation may serve as a mild and potential future alternative[44] and is therefore often regarded as a "photochemical alternative to certain Friedel-Crafts reactions"(G. A. Kraus)[30c,d] or the "Photo-Friedel-Crafts acylation" (J. Mattay).[33c-f]

Because 1,2-naphthoquinone (**30**) is highly sensitive to acid and heat, Takuwa and Kai applied the $Mg(ClO_4)_2$-mediated acylation to the synthesis of 3-alkylated-1,2-naphthoquinones (**138**).[29c] The photochemically generated acylated hydroquinones **29** were readily transferred into the corresponding alkylquinones in moderate overall yields via a sequence of Clemmensen reduction and oxidation with Fremy's salt (Scheme 48; see Table 88.9 for R).

Maruyama and Naruta completed the syntheses of the naturally occurring α- and β-lapachones and their analogues (**139** and **140**) based on the photoacylation.[28g] Starting from 1,4-naphthoquinone (**41**) and suitable α,β-unsaturated aliphatic aldehydes, theses potent *anti*-microbial and *anti*-tumor agents[1] were conveniently obtained in four to five steps (Scheme 49; see Table 88.10 for R^1, R^2).

As described by Kobayashi and co-workers,[31b] 4,7-dioxo-4,7-dihydrobenzo[*b*]thiophene-2-carboxylates (**143**) are readily available in a one-pot procedure from acylated 1,4-hydroquinones (**54**) and mercaptoacetates (**142**) using 1-trimethylsilylimidazole as a protecting reagent as well as a base (Scheme 50; see Table 88.14 for R^1). Likewise, the corresponding dihydronaphthothiophene carboxylates

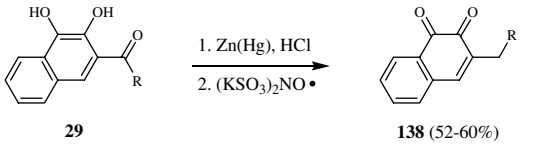

29 **138** (52-60%)

SCHEME 48

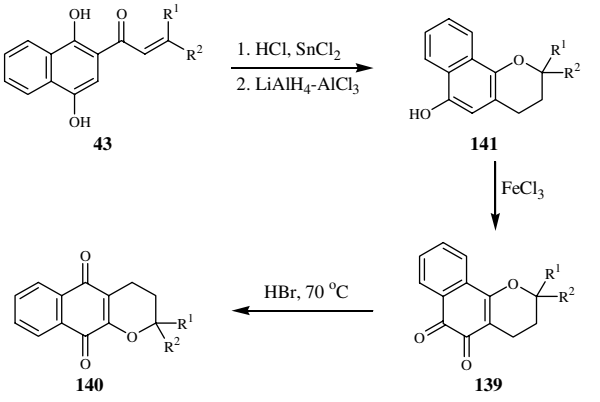

43 **141** **140** **139**

SCHEME 49

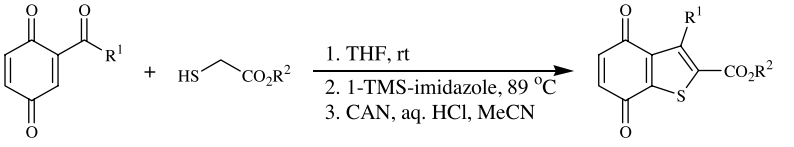

54 **142** **143** (69-90%)

SCHEME 50

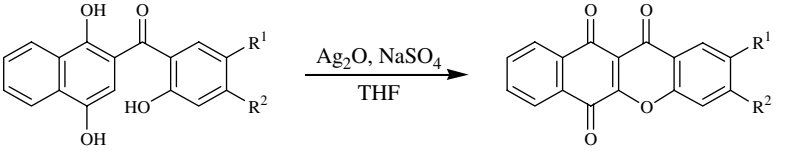

43 **144** (40-50%; including photoacylation step)

SCHEME 51

have been prepared in moderate to good yields of 53 to 84%, but oxidation with CAN was not required in this case.[31b] Recently, Kobayashi reported the synthesis of symmetric benzo [1,2-*b*: 5, 4-*b*′] dithiophene-4,8-diones starting from **143**.[31d]

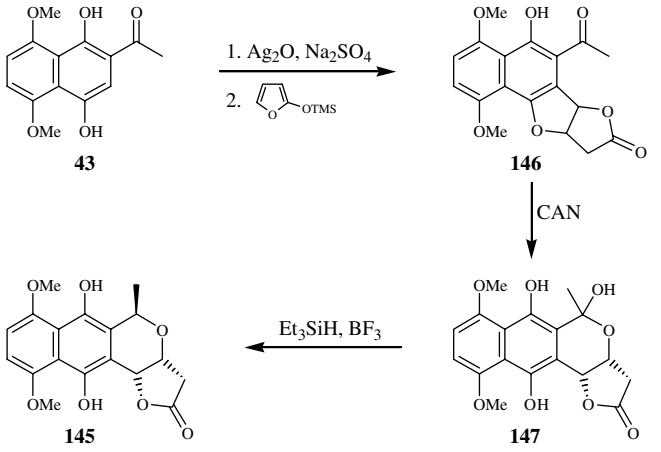

SCHEME 52

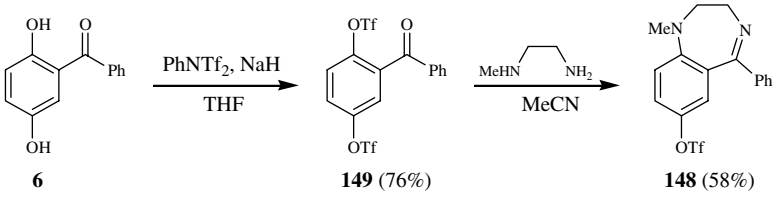

SCHEME 53

Kobayashi and co-workers further developed a simple pathway to benzo[*b*]xanthene-6,11,12-trione derivatives (**144**) involving the photoinduced acylation of naphthoquinone (**41**).[31c] Subsequent oxidative cyclization with an excess amount of Ag_2O gave the xanthenequinone derivatives in moderate overall yields (Scheme 51; see Table 88.14 for R,[1] R[2]).

Due to their strong antibiotic activity, pyranonaphthoquinones (e.g., *frenolicin B* or *kalafungin*) have attracted ongoing attention in synthetic organic chemistry.[45] Kraus and co-workers applied the benzophenone-mediated photoacylation of 5,8-dimethoxy-1,4-naphthoquinone (**101**) to the synthesis of the *kalafungin* analogue **145** (Scheme 52).[30d] Because many pyranonaphthoquinones require regioselective acylation of the unsymmetrically substituted 5-methoxy-1,4-naphthoquinone (**108**) to its 2,8-regioisomer (**113**),[45d] Tachikawa's procedure may represent the method of choice.[32]

Bruce and co-workers furthermore used the photochemical acylation for the synthesis of the benzodiazepine skeleton (Scheme 53).[46] Benzodiazepines (e.g., diazepam [Valium]) are widely used as antianxiety agents, which makes them attractive target molecules.[47] Transformation of **6** (R = Ph) into its bistriflate (**149**) and subsequent reaction with *N*-methylethylenediamine afforded the diazepine **148**. The conversion of the remaining triflate into either nitriles or esters was subsequently accomplished using suitable organopalladium compounds.[46]

Chart 5 shows the structures of various interesting target molecule that have been either synthesized or might be accessible via acylated hydroquinones. Among these examples are the enantiomeric naphthoquinones *alkannin* (**150**) and *shikonin* (**151**),[48] 1-aminoanthraquinones (**152**),[49] the 1,6-dihydroxyantharaquinone *chrysophanol* (**153**) and its isomeric 1,8-dihydroxy analogue *aloesaponarin I* (**154**),[50] 1,3-disubstituted naphthopyrandiones (**155**),[51] isoquinoline-5,8-diones (**156**),[52,53] the related *11-deoxydaunomycinone* (**157**) and (±)-*auramycinone* (**158**),[54,55] 5,8-dihydroxythioflavanone (**159**),[56,57] and benzophenothiazinone derivatives (**160**).[58]

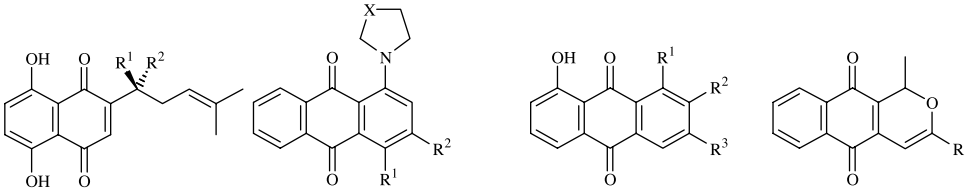

R^1 = H, R^2 = OH (**150**)
R^1 = OH, R^2 = H (**151**)

X = CH_2, CH_2O (**152**)

R^1 = OH, R^2 = H, R^3 = Me (**153**)
R^1 = Me, R^2 = CO_2Me, R^3 = OH (**154**)

(**155**)

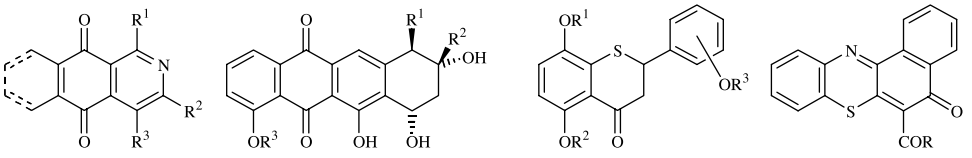

(**156**)

R^1 = H, R^2 = CO_2Me, R^3 = Me (**157**)
R^1 = CO_2Me, R^2 = Me, R^3 = H (**158**)

(**159**)

(**160**)

CHART 5

Acknowledgments

The authors would like to thank Dr. Jürgen Ortner, Dr. Christian Jung, Dr. Christian Sattler, Dipl.-Chem. Jens Otto Bunte, Dr. Christian Schiel, Mrs. Arja Gaestel, and Dr. Maurizio Fagnoni for their help in the preparation of this manuscript.

References

1. (a) Owton, W.M., The synthesis of quinones, *J. Chem. Soc., Perkin Trans. 1*, 2409–2420, 1999; (b) Thomson, R.H., *Naturally Occurring Quinones IV*, Blackie, Glasgow, 1996; (c) Thomson, R.H., The total synthesis of naturally occurring quinones, in *Total Synthesis of Natural Products*, Apsimon, J., Ed., John Wiley & Sons, New York, 1992; (d) Thomson, R.H., *Naturally Occurring Quinones III, Recent Advances*, Chapman & Hall, London, 1987; (e) Bérdy, J., Aszalos, A., Bostian, N., and McNitt, K.L., *CRC Handbook of Antibiotic Compounds. Quinone and Similar Antibiotics*, Vol. 3, CRC Press, Boca Raton, FL, 1980; (f) Patai, S., Ed., *The Chemistry of the Quinonoid Compounds*, John Wiley & Sons, New York, 1974; (g) Thomson, R.H., *Naturally Occurring Quinones*, 2nd ed., Academic Press, New York, 1971; (h) Morton, R.A., Ed., *Biochemistry of Quinones*, Academic Press, New York, 1965.
2. (a) Maruyama, K. and Osuka, A., Recent advances in the photochemistry of quinones, in *The Chemistry of the Quinonoid Compounds*, Patai, S. and Rappoport, Z., Eds., John Wiley & Sons, New York, 1988, Vol. 2, chap. 13, 759–878; (b) Bruce, J.M., Photochemistry of quinones, in *The Chemistry of the Quinonoid Compounds*, Patai, S., Ed., John Wiley & Sons, New York, 1974, Vol. 1, chap. 9, 465–538; (c) Bruce, J.M., Light-induced reactions of quinones, *Quart. Rev.*, 21, 405–428, 1967; (d) Hageman, H.J., Organisch photochemische Reaktionen; an funktionellen Gruppen; an der C=O-Doppelbindung; Chinone, in *Methoden der organischen Chemie (Houben-Weyl)*, Müller, E., Ed., Thieme, Stuttgart, 1975, Vol. IV/5b: Photochemie, Part II, 941–985; (e) Rubin, M.B., Photochemistry of *o*-quinones and α-diketones, *Fortschr. Chem. Forsch.*, 13, 251–306, 1969; (f) Mukherjee, T., Photo and radiation chemistry of quinones, *Proc. Indian Natl. Sci. Acad., Part A*, 66, 239–265, 2000.

3. For a number of excellent historical reviews, see (a) Roth, H.D., Die Anfänge der organischen Photochemie, *Angew. Chem.*, 101, 1220–1234, 1989; The beginnings of organic photochemistry, *Angew. Chem. Int. Ed. Engl.*, 28, 1193–1207, 1989; (b) Roth, H.D., A brief history of photoinduced electron transfer and related reactions, *Topics Curr. Chem.*, 156, 1–19, 1990; (c) Roth, H.D., Twentieth century developments in photochemistry. Brief historical sketches, *Pure Appl. Chem.*, 73, 395–403, 2001; (d) Roth, H.D., Selected developments in the 20th century photochemistry: historical sketches, *EPA Newslett.*, 71, 37–57, 2001.
4. (a) Klinger, H., Ueber das Isobenzil und die Einwirkung des Sonnenlichts auf einige organische Substanzen, *Ber. Dtsch. Chem. Ges.*, 19, 1862–1870, 1886; (b) Klinger, H., in *Sitzungsber. Niederrhein. Ges. Natur Heilkde.*, 225-227, 1885; (c) Klinger, H., in *Sitzungsber. Niederrhein. Ges. Natur Heilkde.*, 224, 1883.
5. (a) Klinger, H., Ueber die Einwirkung des Sonnenlichts auf organische Verbindungen, *Justus Liebigs Ann. Chem.*, 249, 137–146, 1888; (b) Klinger, H., in *Sitzungsber. Niederrhein. Ges. Natur Heilkde.*, 31, 1888.
6. (a) Klinger, H. and Standke, O., Ueber die Einwirkung des Sonnenlichts auf organische Verbindungen, *Ber. Dtsch. Chem. Ges.*, 24, 1340–1346, 1891; (b) Klinger, H. and Kolvenbach, W., Die Bildung von Acetohydrochinon aus Acetaldehyde und Benzochinon im Sonnenlicht, *Ber. Dtsch. Chem. Ges.*, 31, 1214–1216, 1898; (c) Klinger, H., Über Synthesen durch Sonnenlicht, *Justus Liebigs Ann. Chem.*, 382, 211–221, 1911.
7. Dimroth, O. and Hilcken, V., Über Anthradichinone und Anthratrichinone, *Ber. Dtsch. Chem. Ges.*, 54, 3050–3074, 1921.
8. Bargellini, G. and Monti, L., Reazione fra chinone e aldeide cinnamica sotto l'influenza della luce, *Gazz. Chim. Ital.*, 60, 474–478, 1930.
9. (a) Angeletti, A. and Migliardi, C., Reazione fra toluochinone e aldeide cinnamica per l'influenza della luce, *Atti Accad. Sci. Torino*, *Cl. Sci. Fis. Mat. Nat.*, *Series I*, 70, 326–330, 1934/1935; (b) Angeletti, A. and Baldini, V., Reazione fra toluochinone e aldeide benzoica per l'influenza della luce, *Gazz. Chim. Ital.,* 64, 346–350, 1934.
10. (a) Sircar, A.C. and Sen, S.C., Studied in the acenaphthenquinone series, *J. Ind. Chem. Soc.*, 8, 605–612, 1931; (b) Sircar, A.C. and Sen, S.C., Untersuchungen in der Acenaphthenchinonreihe, *Chem. Zentralbl.*, 103, 1528, 1932.
11. Bogert, M.T. and Howells, H.P., The chemistry of the para-quinones. A contribution to the solution of the "Pechmann dyes" problem, *J. Am. Chem. Soc.*, 52, 837–850, 1930.
12. (a) Schönberg, A., in *Präparative organische Photochemie*, Springer, Berlin, 1958; (b) Schönberg, A., Schenck, G.O. and Neumüller, O.A., in *Preparative Organic Photochemistry*, Springer, Berlin, 1968.
13. (a) Schönberg, A. and Moubacher, R., Photo-reactions. Part IV. Photo-reaction between phenanthraquinone and aromatic aldehydes. A new passage from phenanthraquinone to fluorenone, *J. Chem. Soc.*, 1430–1432, 1939; (b) Schönberg, A. and Mustafa, A., Photochemical reactions in sunlight. XII. Reactions with phenanthraquinone, 9-arylxanthens and diphenyl triketone, *J. Chem. Soc.*, 997–1000, 1947; (c) Schönberg, A. and Mustafa, A., Reactions of non-enolizable ketones in sunlight, *Chem. Rev.*, 40, 181–200, 1947; (d) Schönberg, A., Latif, N., Moubasher, R., and Sina, A., Photochemical reactions in sunlight. XVI. (a) Photo-reduction of phenylglyoxylic acid. (b) Photo-reactions between aldehydes and o-quinones. (c) Reactions between o-quinones and ethylenes in the dark and in the light, *J. Chem. Soc.*, 1364–1369, 1951; (e) Schönberg, A., Mustafa, A., and Zayed, S.M. A.D., Experiments with 1,2-benzophenazine-3,4-quinone. Thermochromic effects based on lactam-lactim tautomerism, *J. Am. Chem. Soc.*, 75, 4302–4304, 1953; (f) Schönberg, A., Awad, W.I., and Mousa, G.A., Photochemical reactions in sunlight. XVII. Experiments with 4-cyano-1,2-naphthoquinone, *J. Am. Chem. Soc.*, 77, 3850–3852, 1955; (g) Schönberg, A. and Sidky, M.M., Photochemical reactions in sunlight. XX. Photoreaction between benzaldehyde and khellinquinone, *J Org. Chem.*, 22, 1698–1699, 1957.

14. See, for example, Pawellek, D., Ein- und mehrwertige Phenole; C. Trennung, Analytik und Stabilisierung; II. Analytik; a) Chemische Methoden; 5. Farbreaktionen, in *Methoden der organischen Chemie (Houben-Weyl)*, Müller, E., Ed., Thieme, Stuttgart, 1976, Vol. VI/1c: Phenole, Part II, 1204–1205.
15. (a) Mustafa, A., Reactions in sunlight of (a) phenanthraquinone, retenequinone and chrysenequinone with ethylene; (b) retenequinone and chrysenequinone with aromatic aldehydes; and (c) *o*-formylbenzoic acid with iso-propyl alcohol, *J. Chem. Soc.*, S83–S86, 1949; (b) Mustafa, A., Reactions of 9-anthraldehyde in sunlight, *Nature (London)*, 166, 108–109, 1950; (c) Mustafa, A., Reactions in sunlight of certain diketones with ethylenes and aromatic aldehydes. Photopolymerisation of 9-anthraldehyde, *J. Chem. Soc.*, 1034–1037, 1951; (d) Mustafa, A., Harhash, A.H.E.H., Mansour, A.K.E., and Omran, S.M.A.E., Photochemical addition and photochemical dehydrogenation reactions in sunlight, *J. Am. Chem. Soc.*, 78, 4306–4309, 1956; (e) Mustafa, A., Mansour, A.K., and Shalaby, A.F.A.M., Photochemical reactions in sunlight. Experiments with benzo(h)quinoline-5,6-quinone, monoimine and monoxime derivatives in sunlight and in dark, *J. Am. Chem. Soc.*, 81, 3409–3413, 1959; (f) Mustafa, A., Mansour, A.K., and Zaher, H.A.A., Photochemical reactions in sunlight. Experiments with 2-N-phenyl-α,β-naphtho-1,2,3-triazolequinone and monoxime derivative in sunlight and in dark, *J. Org. Chem.*, 25, 949–950, 1960.
16. Moore, R.F. and Waters, W.A., The photochemical addition of benzaldehyde to quinones, *J. Chem. Soc.*, 238–240, 1953.
17. (a) Rubin, M.B., Photochemical reactions of diketones. The 1,4-addition of ethers to 9,10-phenanthrenequinone, *J. Org. Chem.*, 28, 1949–1952, 1963; (b) Rubin, M.B. and Zwitkowits, P., Photochemical reactions of diketones. II. The 1,2-addition of substituted toluenes to 9,10-phenanthrenequinone, *J. Org. Chem.*, 29, 2362–2368, 1964; (c) Rubin, M.B. and Zwitkowits, P., Polar Effects in free radical reactions. The mechanism of photochemical addition of ethers and substituted toluenes to 9,10-phenanthrenequinone, *Tetrahedron Lett.*, 2453–2457, 1965.
18. (a) Badger, G.M., Pearce, R.S., and Pettit, R., Polynuclear heterocyclic systems. II. Hydroxy-derivatives, *J. Chem. Soc.*, 3204–3207, 1951; (b) for a general review on imine-enamine tautomerizations, see Kurasawa, Y., Takada, A., and Kim, H.S., Tautomerism and isomerism of heterocycles [2], *Heterocycles*, 41, 2057–2093, 1995.
19. Awad, W.I. and Hafez, M.S., Studies on 4-substituted-β-naphthoquinones, *J. Am. Chem. Soc.*, 80, 6057–6060, 1958.
20. (a) Schenck, G.O. and Koltzenburg, G., Zur Photochemie des Chloranils, *Angew. Chem.*, 66, 475, 1954; (b) Schenck, G.O. and Koltzenburg, G., Zur Photochemie der Chinone, *Naturwiss.*, 41, 452, 1954.
21. (a) Scharf, H.-D., Fleischhauer, J., and Aretz, J., Apparative Hilfsmittel; Allgemeines zur Ausführung photochemischer Reaktionen, in *Methoden der organischen Chemie (Houben-Weyl)*, Müller, E., Ed., Thieme, Stuttgart, 1975, Vol. IV/5a: Photochemie, Part I, 41–89; (b) Schenck, G.O., Probleme präparativer Photochemie, *Angew. Chem.*, 64, 12–23, 1952.
22. For some selected reviews on Photo-Fries rearrangements, see (a) Martin, R., Uses of the Fries rearrangement for the preparation of hydroxyarylketones. A review, *Org. Prep. Proc. Int.*, 24, 373–435, 1992; (b) Pfau, M. and Julliard, M., Reactions photochimiques des esters aromatiques, *Bull. Chem. Soc. Fr.*, 785–802, 1977; (c) Bellus, D., Photo-Fries rearrangement and related photochemical [1,j]-shifts (j = 3,5,7) of carbonyl and sulfonyl groups, *Adv. Photochem.*, 8, 109–159, 1971.
23. (a) Bruce, J.M. and Cutts, E., The mechanism of the light-induced reaction between 1,4-benzoquinone and acetaldehyde, *J. Chem. Soc., Chem. Commun.*, 2–3, 1965; (b) Bruce, J.M. and Cutts, E., Light-induced and related reactions of quinones. I. The mechanism of formation of acetylquinol from 1,4-benzoquinone and acetaldehyde, *J. Chem. Soc. (C)*, 449–458, 1966; (c) Bruce, J.M., and Ellis, J.N., Light-induced and related reactions of quinones. II. Reactions involving chloranil and acetaldehyde, *J. Chem. Soc. (C)*, 1624–1627, 1966; (d) Bruce, J.M., Creed, D., and Ellis, J.N., Light-induced and related reactions of quinones. IV. Reactions of some p-quinones with aliphatic and aromatic aldehydes, *J. Chem. Soc. (C)*, 1486–1490, 1967; (e) Bruce, J.M. and Dawes, K., Light-

induced and related reactions of quinones. V. Substituent effects in light-induced reactions between *p*-quinones and aldehydes, *J. Chem. Soc. (C)*, 645–648, 1970; (f) Bruce, J.M. and Chaudhry, A.-U.-H, Light-induced and related reactions of quinones. IX. *t*-Butyl-1,4-benzoquinones, *J. Chem. Soc., Perkin Trans. 1*, 372–379, 1972; (g) Bruce, J.M. and Chaudhry, A.-U.-H., Light-induced and related reactions of quinones. XI. 4,4′-Diphenoquinones, *J. Chem. Soc., Perkin Trans. 1*, 295–297, 1974.

24. (a) Chatgilialoglu, C., Crich, D., Komatsu, M., and Ryu, I., Chemistry of acyl radicals, *Chem. Rev.*, 99, 1991–2069, 1999; (b) Caronna, T. and Minisci, F., The chemistry of acyl radicals, *Rev. React. Species Chem.*, 1, 263–318, 1976.
25. For a number of redox potentials of quinones, see (a) Ulrich, H. and Richter, R., Die para-Chinone der Benzol- und Naphthalin-Reihe; C. Charakterisierung und Bestimmung von p-Chinonen. II. Durch physikalische Methoden; (b) Polarographie (Oxidationspotential), in *Methoden der organischen Chemie (Houben-Weyl)*, Müller, E. and Grundmann C., Eds., Thieme, Stuttgart, 1976, Vol. VII/3a: Chinone, Part I, 730–732; (c) Chambers, J.Q., Electrochemistry of quinones, in *The Chemistry of the Quinonoid Compounds*, Patai, S., Ed., John Wiley & Sons, New York, 1974, Vol. 1, chap. 14, 737–791; (c) Peover, M.E., A polarographic investigation into the redox behaviour of quinones: the roles of electron affinity and solvent, *J. Chem. Soc.*, 4540–4549, 1962.
26. (a) Formosinho, S.J. and Arnaut, L.G., Excited-state proton transfer reactions. II. Intramolecular reactions, *J. Photochem. Photobiol. A: Chem.*, 75, 21–48, 1993; (b) Rommel, E. and Wirz, J., The photoenol tautomer of 5-methyl-1,4-naphthoquinone, *Helv. Chim. Acta*, 60, 38–42, 1977; (c) Chiang, Y., Kresge, A.J., Hellrung, B., Schünemann, P., and Wirz, J., Flash photolysis of 5-methyl-1,4-naphthoquinone in aqueous solution: kinetics and mechanism of photoenolization and of enol trapping, *Helv. Chim. Acta*, 80, 1106–1121, 1997.
27. (a) Orlando Jr., C.M., Mark, H., Bose, A.K. and Manhas, M.S., Photoreactions. IV. Photolysis of t-butyl-substituted p-benzoquinones, *J. Am. Chem. Soc.*, 89, 6527–6532, 1967; (b) Orlando, Jr., C.M., Mark, H., Bose, A.K., and Manhas, M.S., Photoreactions.V. Mechanism of the photorearrangement of alkyl-*p*-benzoquinones, *J. Org. Chem.*, 33, 2512–2516, 1968; (c) Farid, S., Biradical trapping with sulphur dioxide: sulphinic acids from the photoreaction of t-butyl-p-benzoquinone with sulphur dioxide, *J. Chem. Soc., Chem. Commun.*, 73–74, 1971; (d) Farid, S., Photolysis of *t*-butyl-*p*-quinones: competing 1,4- and 1,5-dipolar cycloadditions of the photoproduct to nitriles and ketones, *J. Chem. Soc., Chem. Commun.*, 303–304, 1970.
28. (a) Maruyama, K., Takuwa, A., Otsuki, T., and Kako, S., Syntheses of 9-acyloxy-10-hydroxyphenanthrenes by photochemical reaction, *Bull. Inst. Chem. Res., Kyoto Univ.*, 50, 348–353, 1972; (b) Maruyama, K. and Takahashi, G., Photochemical reaction of 9,10-phenanthrenequinone with glyoxals, *Chem. Lett.*, 295–298, 1973; (c) Maruyama, K. and Takuwa, A., 3-Acyl-1,2-naphthoquinols from the photo-induced reaction of 1,2-naphthoquinone derivatives with aliphatic aldehydes, *Chem. Lett.*, 471–474, 1974; (d) Maruyama, K., Miyazawa, T., and Kishi, Y., A novel type of adducts in the photochemical reactions of *o*-chloranil with aldehydes, *Chem. Lett.*, 721–724, 1974; (e) Maruyama, K. and Miyagi, Y., Photo-induced condensation reaction of *p*-quinones with aldehydes, *Bull. Chem. Soc. Jpn.*, 47, 1303–1304, 1974; (f) Maruyama, K., Otsuki, T., and Naruta, Y., Photochemical reaction of 9,10-phenanthrenequinone with hydrogen donors. Behavior of radicals in solution as studied by CIDNP, *Bull. Chem. Soc. Jpn.*, 49, 791–795, 1976; (g) Maruyama, K. and Naruta, Y., Syntheses of α- and β-lapachones and their homologues by way of photochemical side chain introduction to quinone, *Chem. Lett.*, 847–850, 1977; (h) Maruyama, K., Sakurai, H., and Otsuki, T., The addition reaction of acyl radicals to 9,10-phenanthrenequinone in the presence of the corresponding aldehydes. A support for the in-cage mechanism of the photochemical reaction of 9,10-phenanthrenequinone with aldehydes, *Bull. Chem. Soc. Jpn.*, 50, 2777–2779, 1977; (i) Maruyama, K., Takuwa, A., and Soga, O., Photochemical reaction of 1,2-naphthoquinone with arylacetaldehydes. Products and their intramolecular isomerization, *Chem. Lett.*, 1097–1100, 1979; (j) Maruyama, K., Takuwa, A., Matsukiyo, S., and Soga, O., Mechanism of light-induced reductive acetylation of 1,2-naphthoquinone with acetaldehyde, *J. Chem. Soc., Perkin Trans. 1*, 1414–1419,

1980; (k) Takuwa, A., Iwamoto, H., Soga, O., and Maruyama, K., The formation of acetylcatechol in the photochemical reaction of *o*-benzoquinones with acetaldehyde, *Bull. Chem. Soc. Jpn.*, 55, 3657–3658, 1982; (l) Takuwa, A., Soga, O., and Maruyama, K., The photochemical reaction of 1,2-naphthoquinone with hydrogen donors. An explanation of the coupling sites of alkyl and acyl radicals to 1,2-naphthosemiquinone radical, *J. Chem. Soc.*, *Perkin Trans. 2*, 409–411, 1985.

29. (a) Takuwa, A., The photochemical reaction of 1,2-naphthoquinone with aldehydes. II. The photoaddition reactions of aliphatic aldehydes to 1,2-naphthoquinones, *Bull. Chem. Soc. Jpn.*, 49, 2790–2799, 1976; (b) Takuwa, A., The photochemical reaction of 1,2-naphthoquinone with aldehydes. III. The reactions with aromatic aldehydes and α,β-unsaturated aliphatic aldehydes, *Bull. Chem. Soc. Jpn.*, 50, 2973–2981, 1977; (c) Takuwa, A. and Ryoji, K., Convenient synthesis of 3-acyl and 3-alkyl-1,2-naphthoquinones, *Bull. Chem. Soc. Jpn.*, 63, 623–625, 1990.
30. (a) Kraus, G.A. and Kirihara, M., Quinone photochemistry. A general synthesis of acylhydrochinones, *J. Org. Chem.*, 57, 3256–3257, 1992; (b) Kraus, G.A. and Liu, P., Benzophenone-mediated conjugated additions of aromatic aldehydes to quinones, *Tetrahedron Lett.*, 35, 7723–7726, 1994; (c) Kraus, G.A., Kirihara, M., and Wu, Y., A photochemical alternative to certain Friedel-Crafts reactions, in *Benign by Design. Alternative Synthetic Design for Pollution Prevention*, Anastas, P.T. and Farris, C.A., Eds., ACS Symposium Series 577, American Chemical Society, Washington D.C., 76–83, 1994; (d) Kraus, G.A., Maeda, H., Lui, P., Melekhov, A., and Lu, Y., A photochemical alternative to certain Friedel-Crafts reactions, in *Green Chemistry: Frontiers in Benign Chemical Syntheses and Processes*, Anastas, P.T. and Williamson, T.C., Eds., Oxford University Press, Oxford, 1998, chap. 4, 72–86; (e) Pacut, R., Grimm, M.L., Kraus, G.A., and Tanko, J.M., Photochemistry in supercritical carbon dioxide. The benzophenone-mediated addition of aldehydes to α,β-unsaturated carbonyl compounds, *Tetrahedron Lett.*, 42, 1415–1418, 2001.
31. (a) Kobayashi, K., Suzuki, M., Takeuchi, H., Konishi, A., Sakurai, H., and Suginome, H., Photoinduced molecular transformations. 146. Photoacylation and photoalkylation of 2-arylamino- and 2-alkylamino-1,4-naphthoquinones, *J. Chem. Soc.*, *Perkin Trans. 1*, 1099–1104, 1994; (b) Kobayashi, K., Yoneda, K., Uchida, M., Matsuoka, H., Morikawa, O., and Konishi, H., An improved method for the preparation of 4,7-dioxo-4,7-dihydrobenzo[b]thiophene-2-carboxylates from 2-acyl-1,4-benzoquinones and mercaptoacetates, *Heterocycles*, 55, 2423–2430, 2001; (c) Kobayashi, K., Matsunaga, A., Mano, M., Morikawa, O., and Konishi, H., A new route to benzo[b]xanthene-6,11,12-trione derivatives based on the photoinduced o-hydroxybenzoylation of 1,4-naphthoquinone, *Heterocycles*, 57, 1915–1918, 2002; (d) Kobayashi, K., Ogata, T., Miyamoto, K., Morikawa, O., and Konishi, H., Synthesis of benzo[1,2-*b*: 5,4-*b′*]dithiophene-4,8-dione derivatives, *Heterocycles,* 60, 1689–1695, 2003.
32. (a) Tachikawa, N., Photochemically induced regio-selective acylation of quinones, *Chem. Express*, 1, 587–590, 1986; (b) Tachikawa, N., Photochemically induced regio-selective acylation of quinolinequinones, *Chem. Express*, 3, 33–36, 1988.
33. (a) Mattay, J., Hoffmann, R., Langer, K., Oelgemöller, M., and Schiel C., Untersuchungen zur Nutzung solarer Energien zur Synthese von Wirkstoffen und Zwischenprodukten, in *Solare Chemie und Solare Materialforschung - Ergebnisse der ersten Förderphase des Schwerpunktes 5 in der nordrhein-westfälischen Arbeitsgemeinschaft Solar*, Becker, M. and Funken K.-H., Eds., Verlag C.F. Müller, Heidelberg, 1997, 234–241; (b) Schiel, C., Oelgemöller, M., and Mattay, J., Regioselective photoacylation of substituted naphthoquinones, *J. Inf. Rec.*, 24, 257–260, 1998; (c) Schiel, C., Oelgemöller, M., and Mattay, J., Photoacylation of electron-rich quinones: an application of the photo-Friedel-Crafts reaction, *Synthesis*, 1275–1279, 2001; (d) Schiel, C., Oelgemöller, M., Ortner, J., and Mattay, J., Green photochemistry: the solar-chemical photo-Friedel-Crafts acylation of quinones, *Green Chem.*, 3, 224–228, 2001; (e) Oelgemöller, M., Schiel, C., Mattay, J., and Fröhlich, R., The photo-Friedel-Crafts acylation of 1,4-naphthoquinones, *Eur. J. Org. Chem.*, 2465–2474, 2002; (f) Oelgemöller, M., Schiel, C., Ortner, J., and Mattay, J., The solarchemical "Photo-Friedel-Crafts acylation" of quinones; in *AG Solar Nordrhein-Westfalen —- Solare Chemie und Solare*

Materialforschung — Förderzeitraum 1995-2001, AG Solar NRW, Projektträger ETN, Ed., Forschungszentrum Jülich GmbH, 2002, chap. 2.2, CD-ROM, ISBN 3-89336-306-8; (g) Schiel, C., Photochemische Acylierung von Chinonen und ihre solartechnische Anwendung, Ph.D. thesis, University of Bielefeld, 2002; (h) Mattay, J., Von der Laborsynthese zur Solarchemie, *Chem. unserer Zeit*, 36, 98–106, 2002.

34. For some selected examples of the *green photochemistry* concept, see (a) Griesbeck, A.G. and Bartoschek, A., Sustainable photochemistry: solvent-free singlet oxygen-photooxygenation of organic substrates embedded in porphrin-loaded polystyrene beads, *J. Chem. Soc., Chem. Commun.*, 1594–1595, 2002; (b) Albini, A., Fagnoni, M., and Mella, M., Environment-friendly organic synthesis. The photochemical approach, *Pure Appl. Chem.*, 72, 1321–1326, 2000; (c) Griesbeck, A.G., Kramer, W., and Oelgemöller, M., Photoinduced decarboxylation reactions — radical chemistry in water, *Green Chem.*, 1, 205–207, 1999; (d) Covell, C., Gilbert, A., and Richter, C., Sunlight-induced regio- and stereo-specific ($2\pi+2\pi$) cycloaddition of arylethenes to 2-substituted-1,4-naphthoquinones, *J. Chem. Res. (S)*, 316–317, 1998.
35. (a) Esser, P., Pohlmann, B., and Scharf, H.-D., The photochemical synthesis of fine chemicals with sunlight, *Angew. Chem. Int. Ed. Engl.*, 33, 2009–2023, 1994; (b) Funken, K.-H. and Ortner, J., Technologies for the solar photochemical and photocatalytic manufacture of specialities and commodities: a review, *Z. Phys. Chem.*, 213, 99–105, 1999; (c) Funken, K.-H., Ortner, J., Riffelmann, K.-J., and Sattler, C., New developments in solar photochemistry, *J. Inf. Rec.*, 24, 61–68, 1998; (d) Lede, J., and Pharabod, F., Chimie solaire dans le monde et en france, *Entropie*, 204, 47–55, 1997.
36. (a) Ferreira, M.A., King, T.J., Sadaquat, A., and Thomson, R.H., Naturally occurring quinones. 27. Sesquiterpenoid quinones and related compounds from hibiscus elatus: crystal structure of hibiscone C (gmelofuran), *J. Chem. Soc., Perkin Trans. 1*, 249–256, 1980; for *intramolecular* reactions of 1,4 benzoquinones, see (b) Bruce, J.M. and Creed, D., Light-induced and related reactions of quinones. Part VI. Reactions of some p-quinones carrying formyl groups. *J. Chem. Soc. (c),* 649–653, 1970.
37. (a) Kim, A.R., Kyeong, J.K., Shim, S.C., and Kim, S.S., Formation of 1,5-diketones from the photoaddition of 1,3-diphenyl-1,3-propanedione to p-benzoquinones, *Bull. Korean Chem. Soc.*, 18, 1125–1126, 1998; (b) Chang, J.A., Kim, A.R., and Kim, S.S., Photochemical formation of 1,5-diketones from dibenzoylmethane and *o*-quinones, *Bull. Korean Chem. Soc.*, 19, 917–919, 1998; (c) Kim, S.S., Lim, J.S., Lee, J.M., and Shim, S.C., Photochemical formation of 1,5-diketones from dibenzoylmethane and some quinones, *Bull. Korean Chem. Soc.*, 20, 531–534, 1999; (d) Kim, S.S., Chang, J.A., Kim, A.R., Mah, Y.J., Kim, H.J., and Kang, C., Photochemical formation of 3-methoxycyclohex-2-en-1-ones from 1,3-cyclohexanedione and 2-allyl-3-hydroxycyclohex-2-en-1-one in methanol in the presence of quinones, *J. Photosci.*, 7, 111–114, 2000.
38. (a) Abdulla, K.A., Abdul-Rahman, A.L., Al-Hamdany, R., and Al-Saigh, Z.Y., Preparation and light induced reactions of substituted 1,4-benzoquinone, *J. Prakt. Chem.*, 324, 498–504, 1982; for more detailed studies on this transformation, see (b) Bruce, J.M. and Knowles, P., Light-induced and related reactions of quinones. Part III. Light-induced reactions of some monosubstituted 1,4-benzoquinones, *J. Chem. Soc. (c),* 1627–1634, 1966; (c) Bruce, J.M., Creed, D., and Dawes, K., Light-induced and related reactions of quinones. Part VII. Cleavage and isomerization of some (1-hydroxyalkyl)-1,4-benzoquinones. *J. Chem. Soc. (c),* 2244–2252, 1971; (d) Bruce, J.M., Chaudhry, A.-u.-h., and Dawes, K., Light-induced and related reactions of quinones. Part X. Further studies with hydroxymethyl-, vinyl-, and (2-ethoxycarbonylethyl)-1,4-benzoquinones, *J. Chem. Soc., Perkin Trans. 1,* 288–294, 1974.
39. (a) Maruyama, K., Iwamoto, H., Soga, O., Takuwa, A., and Osuka, A., Photochemical reaction of 2-alkenoyl-3-alkoxy-1,4-benzoquinones. Formation of 5H-pyrano[4,3,2-de][1,3]benzodioxin derivatives, *Chem. Lett.,* 1675–1678, 1985; (b) Maruyama, K., Iwamoto, H., Soga, O., Takuwa, A., and Osuka, A., Photochemical reaction of 2-alkenoyl-1,4-quinones. Formation of chromone derivatives, *Chem. Lett.,* 595–598, 1985; (c) Maruyama, K., Iwamoto, H., Soga, O., and Takuwa, A.,

Photochemical reaction of 2-alkenoyl-3,5-dimethyl-1,5-benzoquinones with alcohol, *Chem. Lett.,* 1343–1346, 1984; (d) Maruyama, K., Muraoka, M., and Naruta, Y., Photo-oxygenation of 2-alkenoyl-1,4-quinones by atmospheric oxygen. Formation of stable cyclic peroxides, *J. Chem. Soc., Chem. Comm.,* 1282–1284, 1980; (e) Miyagi, Y., Maruyama, K., and Yoshimoto, S., The chemical conversion of the photo-dimer of 2-acetyl-5-methyl-1,4-benzoquinone. The determination of the regiochemistry of the dimer, *Bull. Chem. Soc. Jpn.,* 53, 2962–2965, 1980; (f) Maruyama, K. and Narita, N., Photochemical dimerization of 2-acyl-1,4-benzoquinones in the presence of rose bengal, *J. Org. Chem.,* 45, 1421–1424, 1980; (g) Maruyama, K. and Narita, N., Photochemical reaction sensitized by dyes in heterogeneous phase, *Chem. Lett.,* 1211-1212, 1979; (h) Miyagi, Y., Maruyama, K., Ishii, H., Mizuno, S., Kakudo, M., Tanaka, N., Matsuura, Y., and Harada, S., The photochemical dimerization of 2-acyl-1,4-quinones, *Bull. Chem. Soc. Jpn.,* 52, 3019–3026, 1979; (i) Maruyama, K., Narita, N., and Miyagi, Y., Photochemical reaction of 2-acetyl-1,4-benzoquinone in the presence of rose bengal, *Chem. Lett.,* 1033–1034, 1978; (j) Miyagi, Y., Kitamura, K., Maruyama, K., and Chow Y.L., Photochemical dimerization of 2-acyl-1,4-quinones, *Chem. Lett.,* 33–36, 1978.

40. (a) Yonezawa, N., Hino, T., and Ikeda, T., New approaches in Friedel-Crafts type carbon-carbon bond formation using novel types of Friedel-Crafts mediators, in *Recent Research Developments in Organic Chemistry*, Pandalai, S.G., Ed., Transworld Research Network, Trivandrum, 1998, Vol. 1, 213–223; (b) Olah, G.A., Definition and scope: acylation (including halogenation and related reactions), in *Friedel-Crafts and Related Reactions*, Olah, G.A., Ed., Wiley, New York, 1963, Vol. 1, chap. 2, Section IV, 91–169; (c) Gore, P.H., Aromatic ketone synthesis, in *Friedel-Crafts and Related Reactions*, Olah, G.A., Ed., Wiley, New York, 1964, Vol. 3, chap. 31, 1–381; (d) Kurosawa, E., Quinones. I. The syntheses of acetyl-*p*-benzoquinone derivatives and 2-acetylnaphthoquinone, *Bull. Chem. Soc. Jpn.*, 34, 300–304, 1961.
41. Kraus, G.A. and Melekhov, A., A direct route to acylhydroquinones from α-keto acids and α-carboxamido acids, *Tetrahedron Lett.*, 39, 3957–3960, 1998.
42. (a) Boyer, J.L., Krum, J.E., Myers, M.C., Fazal, A.N., and Wigal, C.T., Synthetic utility and mechanistic implications of the Fries rearrangement of hydroquinone diesters in boron trifluoride complexes, *J. Org. Chem.*, 65, 4712–4714, 2000; (b) Amin, G.C. and Shah, N.M., 2,5-Dihydroxyacetophenone, *Org. Synth.*, 42, 42–43, 1948.
43. (a) Sharam, P.K. and Khanna, R.N., Photo-Fries rearrangement: rearrangement of benzoyloxy compounds, *Monatsh. Chem.*, 116, 353–356, 1985; (b) Escobar, C., Fariña, F., Martinez-Utrilla, R., and Paredes, M.C., Polycyclic hydroxyquinones. 1. Photo-Fries rearrangement of polyacetoxynaphthalenes; Application to the synthesis of some acetylnaphthazarin derivatives, *J. Chem. Res. (S)*, 266–267, 1977; *J. Chem. Res. (M)*, 3154–3168, 1977; (c) Park, K.K., Lee, H.J., Kim, E.H., and Kang, S.K., Facile synthesis and photo-Fries rearrangement of 2-benzoyl-4-benzoyloxyphenol leading to dibenzoyldihydroxybenzene derivatives, *J. Photochem. Photobiol A: Chem.,* 159, 17–21, 2003.
44. For an introduction on *green chemistry*, see Tundo, P., Anastas, P., Black, D. StC., Breen, J., Collins, T., Memoli, S., Miyamoto, J., Polyakoff, M., and Tumas, W., Synthetic pathways and processes in green chemistry. Introductory overview, *Pure Appl. Chem.*, 72, 1207–1228, 2000.
45. (a) Brimble, M.A., Synthetic studies towards pyranonaphthoquinone antibiotics, *Pure Appl. Chem.*, 72, 1635–1639, 2000; (b) Brimble, M.A., Nairn, M.R., and Prabaharan, H., Synthetic strategies towards pyranonaphthoquinone antibiotics, *Tetrahedron*, 56, 1937–1992, 2000; (c) Brimble, M.A., Duncalf, L.J., and Nairn, M.R., Pyranonaphthoquinone antibiotics — isolation, structure and biological activity, *Nat. Prod. Rep.*, 16, 267–281, 1999; (d) de Koning, C.B., Giles, R.G.F., and Green, I.R., Naphthopyranquinones. Confirmation of the structures of the ventiloquinones E, G and J by synthesis, *J. Chem. Soc., Perkin Trans. 1*, 2743–2748, 1991; (e) Kraus, G.A. and Shi, J., A versatile intermediate for the synthesis of pyranoquinone antibiotics, *J. Org. Chem.*, 55, 1105–1106, 1990; (f) Uno, H., Allylation of 2-alkanoyl 1,4-quinones with allysilanes and allystannanes. Efficient synthesis of pyranonaphthoquinone antibiotics, *J. Org. Chem.*, 51, 350–358, 1986.
46. Kraus, G.A. and Maeda, H., A direct preparation of 1,4-benzodiazepines. The synthesis of medazepam and related compounds via a common intermediate, *Tetrahedron Lett.*, 35, 9189–9190, 1994.

47. (a) Thurston, D.E. and Bose, D.S., Synthesis of DNA-interactive pyrrolo[2,1-c][1,4]benzodiazepines, *Chem. Rev.*, 94, 433–465, 1994; (b) Schütz, H., *Benzodiazepines II. A Handbook*, Springer-Verlag, Berlin, 1989; (c) Roth, H.J., Kleemann, A., and Beisswenger, T., *Pharmaceutical Chemistry, Drug Synthesis*, Vol. 1, Ellis Horwood, Chichester, 1988; (d) Mohiuddin, G., Reddy, P.S., Ahmed, K., and Ratnam, C.V., Recent advantages in the synthesis of annelated 1,4-benzodiazepines, *Heterocycles*, 24, 3489–3530, 1986.
48. (a) Couladouros, E.A., Strongilos, A.T., Papageorgiou, V.P., and Plyta, Z.F., A new efficient route for multigram asymmetric synthesis of alkannin and shikonin, *Chem.-Eur. J.*, 8, 1795–1803, 2002; (b) Papageorgiou, V.P., Assimopoulou, A.N., Couladouros, E.A., Hepworth, D., and Nicolaou, K.C., The chemistry and biology of alkannin, shikonin and related naphthazarin natural products, *Angew. Chem. Int. Ed. Engl.*, 38, 270–300, 1999; (c) Nicolaou, K.C. and Hepworth, D., Concise and efficient total syntheses of alkannin and shikonin, *Angew. Chem. Int. Ed. Engl.*, 37, 839–841, 1998; (d) Tanoue, Y., Terada, A., and Sugyō, Y., Cycloshikonin and its derivatives. A synthetic route of shikonin, *J. Org. Chem.*, 52, 1437–1439, 1987.
49. Kobayashi, K., Uchida, M., Watanabe, S., Takanohashi, A., Tanmatsu, M., Morikawa, O., and Konishi, H., Synthesis of 1-amino and 1-hydroxy-9,10-anthraquinone derivatives based on reaction sequences between 2-acetyl-1,4-naphthoquinone and enamines, *Tetrahedron Lett.*, 41, 2381–2384, 2000.
50. (a) Uno, H., Masumoto, A., Honda, E., Nagamachi, Y., Yamaoka, Y., and Ono, N., Intramolecular aldol-type condensation between side chains of naphthoquinones: biomimetic synthesis of 1,6- and 1,8-dihydroxyanthraquinones, *J. Chem. Soc., Perkin Trans. 1*, 3189–3189, 2001; (b) Uno, H., Nagamachi, Y., Honda, E., Masumoto, A., and Ono, N., Regioselective preparation of 1,6- and 1,8-dihydroxy-9,10-anthraquinones from the common intermediates: synthesis of aloesaponarin I and K1115A, *Chem. Lett.*, 1014–1015, 2000.
51. Nguyen Van, T., Kesteleyn, B., and De Kimpe, N., Synthesis of 1,3-disubstituted naphtho[2,3-c]pyran-5,10-diones, *Tetrahedron*, 57, 4213–4219, 2001.
52. Kobayashi, K., Takanohashi, A., Watanabe, S., Morikawa, O., and Konishi, H., One-pot synthesis of isoquinoline-5,8-dione derivatives from acylquinones and enamines, *Tetrahedron Lett.*, 41, 7657–7660, 2000.
53. (a) Kubo, A. and Saito, N., Synthesis of isoquinolinequinone antibiotics, in *Studies in Natural Products Chemistry. Vol. 10: Stereoselective Synthesis*, Rahman, A.-U., Ed., Elsevier, Amsterdam, 1992, Part F, 77–145; (b) Ozturk, T., Alkaloids containing an isoquinolinequinone unit, in *Alkaloids: Chemistry and Biology*, Cordell, G.A., Ed., Academic, San Diego, Vol. 53, 119–238, 2000.
54. (a) Naruta, Y., Nishigaichi, Y., and Maruyama, K., Tandem Michael/Diels-Alder addition as a new strategy toward tetracyclic systems: synthesis of 11-deoxyanthracyclinones, *J. Org. Chem.*, 53, 1192–1199, 1988; (b) Uno, H., Naruta, Y., and Maruyama, K., Syntheses of (±)-aklavinones. Application of the stereocontrolled "zipper" bicyclo-cyclization reaction, *Tetrahedron*, 40, 4741–4725, 1984.
55. (a) Arcamone, F., *Doxorubicin*, Academic Press, New York, 1981; (b) El Khadem, H.S., Ed., *Anthracycline Antibiotics*, Academic Press, New York, 1982.
56. Konieczny, M.T., Horowska, B., Kunikowski, A., Konopa, J., Wierzba, K., Yamada, Y., and Asao, T., Synthesis and reactivity of 5,8-dihydroxythioflavone derivatives, *J. Org. Chem.*, 64, 359–364, 1999.
57. Harborne, J.B., Ed., *Flavonoids: Advances in Research*, Chapman & Hall, London, 1993.
58. Ueno, Y., Shiraki, H., Koshitani, J., and Yoshida, T., The photochemical reaction of 5*H*-benzo[a]phenothiazin-5-ones with aldehydes, *Synthesis*, 313–314, 1980.
59. For other "Photo-Friedal-Crafts reactions", see (a) Martens, J., Praefcke, K., and Schulze, U., Intramoleulare Photo-Friedel-Crafts-Reaktionen; ein neues Syntheses-Prinzip für Heterocyclen, *Synthesis,* 532–533, 1976; (b) Bryce-Smith, D., Deshpande, R., Gilbert, A., and Grzonka, J., Acid-catalysis of photochemical reactions, *Chem. Commun.,* 561–562, 1970.

89

Photoisomerism of Azobenzenes

Helmut Knoll
Universität Leipzig

89.1 Introduction

The parent molecule of aromatic azo compounds is azobenzene, whose UV/VIS spectroscopic features and photochemistry are basically determined by the azo group -N = N- in conjugation with two phenyl substituents. The most important applications of azobenzene derivatives (azobenzenes) are their use as dyestuffs. Azo dyes absorb visible light and generally show remarkable light-fastness, which is due to an effective deactivation mechanism of the excited-state molecules that includes photoisomerization. Zollinger[1] has discussed this aspect from the viewpoint of dyestuff chemistry.

The double bond between the two nitrogen atoms gives rise to *E*-or *Z*-configuration of the two substituents. In the following, the more general terms "*E*" and "*Z*" will be used, although the terms "*trans*" and "*cis*" are still in use and unequivocally distinguish the two geometric isomers of azobenzenes. This chapter describes the photochromism of azobenzenes; that is, the interconversion of both isomers by light; see Figure 89.1. The thermal *Z*→*E* isomerization reaction is also included because it is more or less effective in photochemical reaction systems of azobenzenes.

Rau[2,3] reviewed the literature on the photoisomerism of azobenzenes more than a decade ago as did Suginome.[4] This chapter summarizes the essential knowledge up to the present day and describes the latest findings. A historical survey will not be given; instead, recent papers and review articles will be cited as references. The reader is referred to the literature therein. The progress of experimental techniques and of theoretical calculations within the past decade permits a more detailed investigation and description of the dynamics of the processes given in Figure 89.1. By means of new synthetic procedures, many complex molecules with azobenzene as a building block have been prepared, which makes them accessible for manipulation by light and heat on a molecular level.

0-8493-1348-1/04/$0.00+$1.50

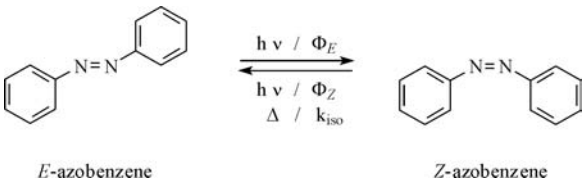

FIGURE 89.1 $E \rightarrow Z$ and $Z \rightarrow E$ isomerization of azobenzene by light (hν) with quantum yields Φ_E and Φ_Z, respectively, and $Z \rightarrow$E isomerization by heat (Δ) with the rate constant k_{iso}.

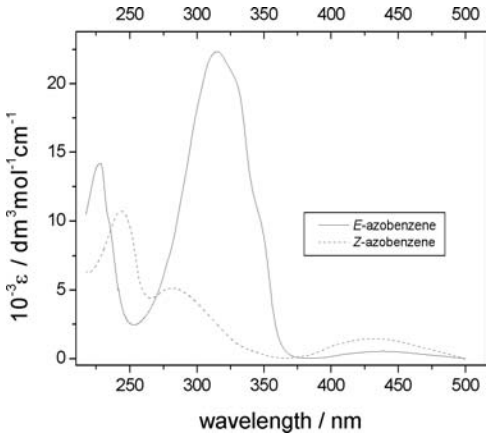

FIGURE 89.2 Absorption spectra of *E*- and *Z*-azobenzene in ethanol. (Adapted from Jaffé, H.H. and Orchin, M., *Theory and Applications of Ultraviolet Spectroscopy*, John Wiley & Sons, New York, 1962.)

In the following section, the UV/VIS spectroscopy of azobenzenes, the knowledge of which is a prerequisite for photochemical isomerization reactions, is described. Conditions and quantum yields of the photoisomerization will be dealt with in Section 89.3 for the azobenzene molecule and some of its derivatives. The mechanism of these simple light-induced unimolecular reactions (i.e., the dynamics of molecular changes) has only recently been studied directly by means of experimental laser spectroscopy methods. The results obtained thus far are summarized and compared with conclusions from quantum chemical calculations in Section 89.4. Thermal $Z \rightarrow E$ isomerization reactions influence the concentration ratio of *E*- and *Z*-isomers in the photostationary state on irradiation of azobenzenes. They are described separately in Section 89.5. Finally, a selection of interesting prospective applications of the photoisomerism of azobenzenes is presented in Section 89.6.

89.2 UV/VIS Spectroscopy of Azobenzenes

Rau classified azobenzenes as azobenzene-type, aminobenzene-type, and pseudostilbene-type molecules according to their UV/VIS spectra, based on different energies for the transitions of n- and π-electrons into the π*-obitals.[2,3]

Azobenzene-Type Molecules

The stable *E*-isomer of the parent molecule azobenzene shows a low-intensity $n \rightarrow \pi^*$ band ($\lambda_{max} = 444$nm/ $\varepsilon \approx 440$ dm^{3}mol^{-1}cm^{-1}) in the visible (VIS) and a high-intensity $\pi \rightarrow \pi^*$ band ($\lambda_{max} = 316$ nm/$\varepsilon \approx 22\,000$) in the UV[5] (see Figure 89.2). The bands are well separated. Changes in the substitution on azobenzene by various groups, except for an amino group, and changing the solvent have only minor effects.

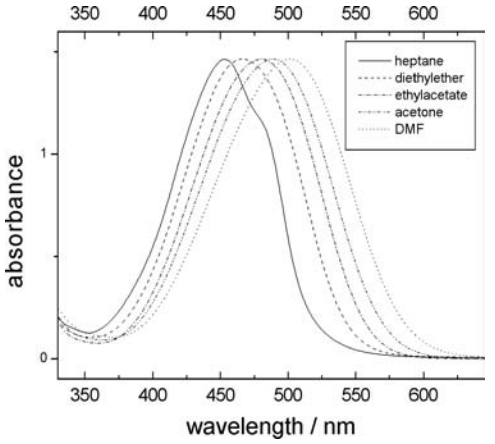

FIGURE 89.3 Absorption spectra of 4-(diethylamino)-4′-nitroazobenzene (about 5×10^{-5} mol dm^{-3} matched to equal absorbance) in solvents of different polarity (DMF = dimethylformamide).

The *Z*-isomer of azobenzene can be isolated by chromatographic separation of the *E*/*Z*-mixture after irradiation of *E*-azobenzene at low temperatures.[5,6] It shows higher intensity of the n→π* band (λ_{max} = 437 nm//ε = 1100) and blue-shifted π→π* bands (λ_{max} = 270 nm//ε = 5000 "sh," λ_{max} = 247nm/ε = 11,500)[5] (see Figure 89.2).

Aminoazobenzene-Type Molecules

The n→π* and π→π* bands of *E*-aminoazobenzene-type molecules are less clearly separated. Moreover, polar solvents lower the transition energy, in particular that of the n→π* band so that π→π* and n→π* bands may overlap and appear as one band.

Pseudostilbene-Type Molecules

Substitution of 4-aminoazobenzene by an electron-withdrawing substituent such as the nitro group in the 4′-position lowers the energy of the $^1(\pi\pi^*)$ state of the *E*-isomers. These donor/acceptor-substituted ("push-pull") azobenzenes find application as dyes with colors shifted toward the red. Here, the sequence of the $^1(n\pi^*)$ and $^1(\pi\pi^*)$ states can be reversed in energy, and the spectrum of the *E*-isomer is dominated by the π→π* band. The charge-transfer character of such low-lying $^1(\pi\pi^*)$ states causes a strong dependence of the band maximum (λ_{max}) on the substituent in the 4-position with another unchanged substituent at the 4′-position. Replacing the simple amino group with the diethylamino group in 4-(amino)-4′-nitroazobenzene brings about an increase in the band maximum of 50 to 60 nm in hexane and acetonitrile, respectively.[8,9] If, accordingly, in 4-phenylaminoazobenzene, the hydrogen atom in the 4′-position is replaced with the nitro group, an increase of λ_{max} of more than 50 nm in acetonitrile and even 70 nm in dimethylsufoxide was observed.[10] For a given azobenzene dye, the absorption maxima are dependent on the solvent polarity. The π→π* band maximum of 4-(diethylamino)-4′-nitroazobenzene changes from 453 nm in heptane to 502 nm in dimethylformamide (see Figure 89.3).

This behavior of λ_{max} or E_{max} (E_{max} = hc/λ_{max} with Planck′s constant h and velocity of light c) and the dependence on varying substituents or different solvents can be correlated with the Hammet σ_P parameter[10] and the Kamlet-Taft π* parameter,[8] respectively. With protic solvents and in aqueous solutions, the dependence of the π→π* band maxima on polarity and water content is less clear. The effect of water on the position of the low-energy band in two 4-(donor)-4′-nitroazobenzenes was studied in polyethyleneglycol/water mixtures. Although the polarity of the mixture obviously increased with increasing water content, the λ_{max} values showed a maximum. This could be due to an increased probability of

hydrogen bonding at the electron lone pairs of nitrogen atoms, in particular reducing the pushing ability of the amino group.[11]

Azobenzenes do not emit noticeably at room temperature, but all three types show fluorescence in strong acids at 77K.[12] Modern experimental techniques, however, allow one to study the very weak fluorescence of azobenzene and azobenzene functionalized molecules even at room temperature.[13–15] Görner et al.[16] observed a transient after laser flash photolysis of donor/acceptor-substituted azobenzenes which they assigned to the lowest energy triplet state of the *E*-isomer. Recent studies were directed at examining the behavior of the transient absorption of the singlet excited states of both geometric isomers with respect to time (see Section 89.4).

In aminoazobenzene and 4,4′-donor/acceptor-substituted azobenzenes, the *Z*- form prepared by photoisomerization is more or less thermally instable. Therefore, and due to the overlapping spectra of the *E*- and the *Z*-isomer, the latter can be prepared in a pure state only in some cases. A photostationary state(PSS) with a mixture of *Z*- and *E*- isomers is established on irradiation with conventional lamps. In particular, in rigid matrices or at low temperatures, the PSS can be maintained for some time in the dark to allow recording of the UV/VIS spectra. Assumptions are necessary, both to derive the UV/VIS spectrum of the *Z*-form and to calculate the quantum yields of isomerization (see Section 89.3). The *Z*-pseudostilbene-type molecules generally exhibit lower absorbance and red-shifted, low-energy absorption bands.[17] In methanol/water mixtures with about molar hydrochloric acid, the aminoazobenzene-type molecules and donor/acceptor-substituted azobenzenes become protonated. In the spectra of 4-(phenylamino)-azobenzenes, the long-wavelength band shifts bathochromically to 530–540 nm.[10]

89.3 Photoisomerization of Azobenzenes: Conditions and Quantum Yields

Quantum yields Φ_E and Φ_Z of the $E \rightarrow Z$ and $Z \rightarrow E$ photoisomerization of azobenzenes, respectively, can be determined by steady irradiation monitoring of the absorbance and its dependence on time during the approach to the PSS, or from the absorbance in the PSS. The *E*/*Z*-isomer concentration ratio in the PSS is determined by the incident light I_0, the extinction coefficients ε_E and ε_Z of both isomers, the quantum yields Φ_E and Φ_Z, and the rate constant k_{iso} of the thermal $Z \rightarrow E$ isomerization (see Equation 89.1).[10,18,19]

Photoisomerization of the parent azobenzene molecule has been fairly well studied.[2,3] It is brought about by UV light in the $E \rightarrow Z$ direction and with visible light ($\lambda > 400$ nm) in the $Z \rightarrow E$ direction. As the *Z*-isomer can be isolated, in this special case, isomerization can be studied starting with either the *E*- or the *Z*-isomer. Average quantum yield data are $\Phi_E = 0.25$ and $\Phi_Z = 0.52$ for excitation at 436 nm, and $\Phi_E = 0.11$ and $\Phi_Z = 0.44$ for excitation at 313 nm in n-hexane, respectively.[20] The sum of Φ_Z and Φ_E is not unity, which is usually taken as an indication that both isomerization reactions do not occur on the same potential energy surface. More interesting is the fact that Φ_E is larger for excitation with lower-energy light ($n \rightarrow \pi^*$) compared to excitation with higher-energy light ($\pi \rightarrow \pi^*$). This behavior is an example of a violation of Kasha's rule, which assumes complete deactivation to the lowest excited state before other deactivation and reaction processes occur (see Section 89.4). However, sterically hindered or cyclic azobenzenes, which cannot rotate, give quantum yields independent of the excitation energy. Quantum yields between 0.2 and 0.3 for the *E*-isomer and between 0.5 and 0.6 for the *Z*-isomer were determined.[2] Moreover, photoisomerisation can be sensitized by aromatic triplet sensitizers. The quantum yield of the triplet *E*-isomer is 0.015 while, starting with the triplet *Z*-isomer, a quantum yield of about unity was measured.[6]

Because thermal $Z \rightarrow E$ isomerization can occur, determining quantum yields of aminoazobenzenes is more difficult. They can be determined if the photostationary state shows a different absorbance compared to the starting pure *E*-isomer and if k_{iso} can be measured. 4-Diethylaminoazobenzene and 4-(diethylamino)-4′-methoxyazobenzene gave $\Phi_E > 0.7$ on excitation at 436 nm but lower values of <0.4 were obtained using 366 nm and shorter wavelengths when these were determined at room temperature.[18]

E→*Z* and *Z*→*E* Photoisomerization of Pseudostilbenes

The sum of the quantum yields $\Phi_Z + \Phi_E \approx 1$ was determined for 4-diethylaminoazobenzenes with different substituents at the 4′-position. The value of Φ_Z increased on increasing the electron-withdrawing power of the 4′-substituents or by increasing the solvent polarity.[18] For a series of 4-phenylaminoazobenzenes with different 4′-electron-withdrawing substituents, Φ_E on the order of 10^{-2} was measured from the absorbance in the PSS by means of the Equation 89.1:

$$I_0\ (1 - 10^{-A})\ \Phi_{E\rightarrow Z} = k_{iso}[Z]_0\ N(V/1000) \qquad (89.1)$$

where I_0 is the incident light (quanta per time), k_{iso} is the thermal isomerization constant, $[Z]_0$ is the concentration of the *Z*-isomer in the PSS, N is Avogadro′s number, and V is the sample volume in milliliters (ml).[10] Equation 89.1 was derived by assuming negligible absorbance of the *Z*-isomer at 400 nm. Equations for the determination of both quantum yields Φ_E and Φ_Z at any irradiation wavelength can be found in the literature and are derived from measurements at the PSS or by measurements on approaching the PSS.[18,19] In studies of polyfunctional molecules, photosensitive metal complexes and azobenzene units were combined. Photoisomerization quantum yields of Ru(II) and Rh(III)complexes with azobenzene-bridged bis(terpyridine) ligands strongly depended on the metal, polarity, viscosity, donor site of the solvents, and size of the counterions.[21,22]

89.4 Mechanism of the Photoisomerization of Azobenzenes

Azobenzene

It was shown by sensitization experiments that *E*→*Z* and *Z*→*E* isomerization can proceed via the triplet state. As the quantum yield for sensitized and direct photoisomerization are different, it was concluded that direct photoisomerization proceeds mainly — if not completely — via singlet excited states.[6] From the observation that $\Phi_Z + \Phi_E < 1$ and from nonlinear Arrhenius plots, it was concluded that more than one excited state is involved. As photoisomerization shows the same quantum yields irrespective of ($n\rightarrow\pi^*$) or ($\pi\rightarrow\pi^*$) excitation in the case of azobenzenes unable to rotate, it was assumed that isomerization occurs from the $^1(n\pi^*)$ state.[2,3]

Since the beginning of the debate on the mechanism of azobenzene photoisomerization, two limiting cases were discussed: rotation around the azo bond with a reduced bond order in analogy to stilbenes, or inversion in the plane due to rehybridization of one azo-nitrogen with small changes of the azo π-bond (Figure 89.4).

This discussion stimulated quantum chemical calculations of potential energy surfaces for both isomerization paths in the ground and excited states. The potential energy diagrams of Monti et al.,[23] calculated by means of an early *ab initio* method with configuration interaction (CI), were the basis of discussion for a long time. Their results were generally interpreted as follows: excitation into the $^1(n\pi^*)$ state of both isomers leads to inversion as this reaction coordinate has a minimum half way between *E* and *Z*, where the slope is steeper on the *Z*-side. Energetically, this minimum is near the maximum of the ground state and near the triplet state, where a fast deactivation to the ground state is possible. This conclusion is in accordance with the lack of vibrational structure of the ($n\rightarrow\pi^*$) absorption bands of both isomers, which means that the Franck-Condon states are apart from a minimum. So far, the potential energy curve of the inversion pathway is qualitatively in accordance with most recent quantum chemical calculations (see Figures 89.5A and 89.5B). Because Monti et al.[23] calculated a significant maximum for the rotation path (in contrast to recent calculations, see Figure 89.5A), rotation was hardly discussed anymore for $n\rightarrow\pi^*$ excitation. They found[23] that after population of the $^1(\pi\pi^*)$ state in both isomers, an energetic downhill molecular change is possible only on the rotation pathway where avoided crossings with the rotational coordinate of the $^1(n\pi^*)$ state on both the *E* and the *Z* sides give two minima. At these minima, bifurcation is postulated, which channels deactivation 1:1 into the $^1(n\pi^*)$ and the ground state. This idea is in accord

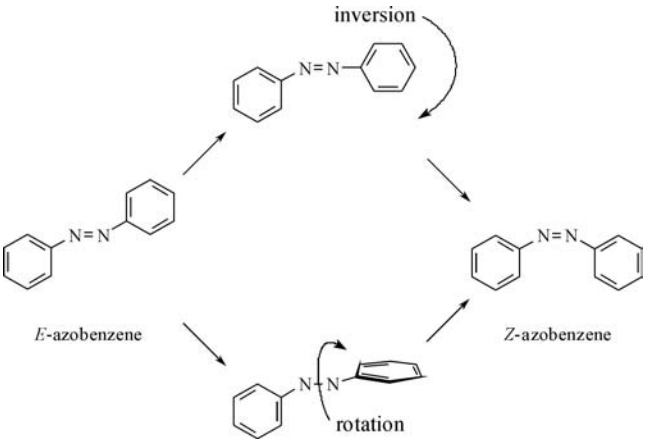

FIGURE 89.4 Rotation and inversion mechanism of azobenzene.

with lower quantum yields Φ_E and Φ_Z after excitation into the $^1(\pi\pi^*)$ state as the $^1(n\pi^*)$ state is bypassed, partly. Therefore, the inversion mechanism should hold irrespective of the excitation path. Rau[19] developed a deviating schematic potential energy diagram. An energetic minimum on the rotation path can be reached that is coupled with the ground state. Accordingly, isomerization on the rotation path after excitation into the $^1(\pi\pi^*)$ state was assumed.

New results of calculations as well as picosecond (ps)- and femtosecond (fs) laser spectroscopy studies have extended the basis for mechanistic discussions. Nägele et al.[24] performed fs transient absorption measurements of the photoisomerization in the $^1(n\pi^*)$ state. They found a very rapid formation of a transient (170 fs after exciting the *Z*-isomer, 320 fs starting from *E*-isomer) and a slower component (2 ps) in both cases. This ultrafast isomerization indicates that the reaction should proceed on a barrierless gradual (inversion) pathway in the direction of a minimum with a steeper slope on the *Z*-side as calculated by Monti et al.[23]

Exciting the $^1(\pi\pi^*)$ state of *E*-azobenzene in n-hexane, Lednev et al.[25] observed transient absorptions at 370 to 450 nm. The decay with a fast (*ca.* 1 ps) and a slower (13 ps) component were assigned to the decay of the $^1(\pi\pi^*)$ state and a bottleneck state of $^1(n\pi^*)$ or $^1(\pi\pi^*)$, respectively. From these bottleneck states, return to the ground state, at least partly on the rotational pathway, and formation of the *Z*-isomer seems possible. Reformation of the ground state occurs with a time constant of 15 ps, similar to the slower decay component of the $^1(\pi\pi^*)$ state. In a second study, Lednev et al.[26] excited both the $^1(n\pi^*)$ state and the $^1(\pi\pi^*)$ state of the *E*-isomer at different energies above the origin. When the $^1(n\pi^*)$ state was excited just above the origin, a transient at 400 nm decayed with a time constant of 2.5 ps, which is attributed to the inversion pathway. An additional fast component with 600 fs when excited >6000cm^{-1} above the origin may arise from motions along other coordinates. After excitation to the $^1(\pi\pi^*)$ state, a transient absorption at 400 nm was observed, which decayed with a major component of 0.9 ps and a weaker component of *ca.* 15 ps. The 400-nm transient rises synchronously with the decay of another band at 475 nm within 200 fs. Again, deactivation of the $^1(\pi\pi^*)$-state via the rotational pathway with the possible formation of the *Z*-isomer is assumed.

In a time-resolved Raman study, Fujino et al.[27] observed an N = N stretch frequency of a 410-nm transient assigned to the vibrationally excited $^1(n\pi^*)$ state. The value of 1427 cm^{-1} is close to that of the ground state. These authors concluded that isomerization occurs by inversion with almost unchanged azo bond and question the theory of a rotational pathway.

Despite the very low fluorescence quantum yields at room temperature, stationary fluorescence spectra and time-resolved fluorescence decay of azobenzene could be studied with high-performance laser and detection equipment. Fujino et al.[15] obtained fluorescence ($n\leftarrow\pi^*$) and ($\pi\leftarrow\pi^*$) bands, which are good mirror images of the corresponding absorption bands, and lifetimes of 110 fs ($^1\pi\pi^*$) and 500 fs($^1n\pi^*$).

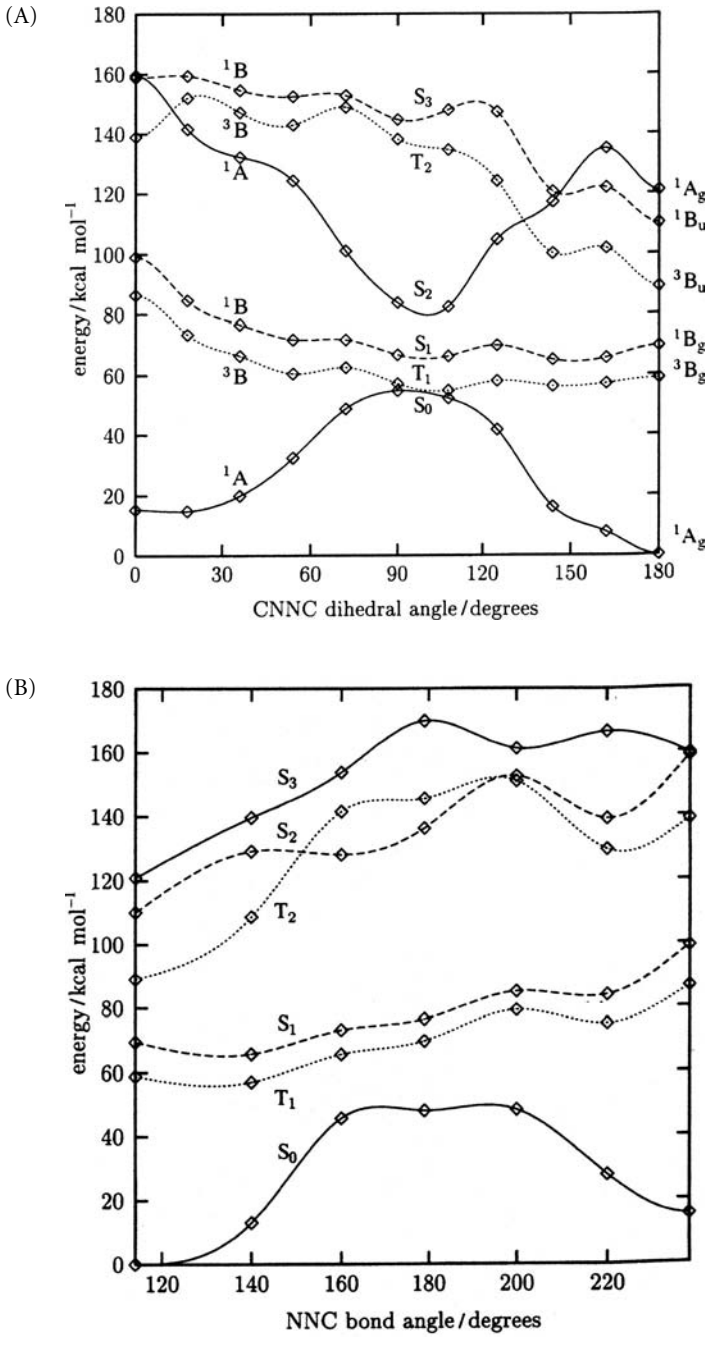

FIGURE 89.5 (A) Potential energy curves for the torsion pathway, CIPSI energies. Left-hand side, *Z*-isomer; right-hand side, *E*-isomer. (B) Potential energy curves for the inversion pathway, CIPSI energies. Left-hand side, *E*-isomer; right-hand side, *Z*-isomer. (From Cattaneo, P. and Persico, M., *Phys. Chem. Chem. Phys.*, 1, 4739, 1999. Reproduced with permission of The Royal Society of Chemistry on behalf of the PCCP Owner Societies.)

Primarily from a comparison of the fluorescence quantum yields, an $^1n\pi^* \leftarrow {}^1\pi\pi^*$ electronic relaxation quantum yield of almost unity was derived. Therefore, these authors concluded that a significant contribution of the rotation pathway starting directly from the $^1(\pi\pi^*)$ state does not exist.

The discussion of all these experimental results refers to and was influenced by the potential energy curves of Monti et al.[23] Now, more recent theoretical studies with more reliable quantum chemical *ab initio* methods are available. By means of CASSCF and multireference perturbation theory, Cattaneo and Persico[28] support the current view that inversion is the preferred pathway for ground-state thermal isomerization and probably also after $n\rightarrow\pi^*$ excitation, although their potential energy curve of the rotation pathway of the $^1(n\pi^*)$ state does not show a significant maximum (see Figure 89.5A).

They find that two states are important in the $\pi\rightarrow\pi^*$ photochemistry of *E*-azobenzene; see Figure 89.5A (2^1A and 2^1B on the rotation path). From the conical intersection at transoid geometry, as well as from the *Z*-isomer, a fast geometrical relaxation into the minimum of $^1(\pi\pi^*)$ should allow isomerization to proceed on the rotational pathway. Ishikawa et al.[29] performed CASSCF–multireference single and double excitation (MRSD) CI calculations and obtained similar results. They found a conical intersection between the $^1(n\pi^*)$ and ground states near the midway of the rotation coordinate. It was concluded that the transition occurs in the vicinity of this conical intersection. Calculated nitrogen–nitrogen bond orders are significantly reduced in the $^1(n\pi^*)$ states of both isomers compared to the ground state. This result is *not* in accord with conclusions from excited-state Raman experiments.[27]

It appears that these recent quantum chemical calculations support the possible contribution of the rotation pathway of the photochemical $E\rightarrow Z$ and $Z\rightarrow E$ isomerizations from the $^1(n\pi^*)$ state. However, these quantum chemical results on potential surfaces of electronically excited states must still be handled with caution. The vertical transition energies, which can be considered a probe for the reliability of the theoretical calculations, do not fully reproduce experimentally determined data and not all geometry parameters could be optimized.[28,29]

89.5 Thermal *Z*→*E* Isomerization

For the parent compound azobenzene and some monosubstituted derivatives, the *Z*-isomers can be isolated at low temperatures. Therefore, rate constants k_{iso} could be determined, starting with the *Z*-isomers in these cases. Arrhenius activation energies between 88 and 100 $kJmol^{-1}$ and A-factors between 10^{12} and $3 \times 10^{13} s^{-1}$ were determined.[30] The *Z*-isomers in particular of donor/acceptor-substituted ("push-pull") azobenzenes are less stable and must be prepared photochemically as short-lived intermediates from the stable *E*-isomers by pulsed or steady irradiation, depending on their lifetime. The formation of *Z*-isomers is indicated by the bleaching of the sample because *Z*-isomers exhibit generally lower absorbance. The return of the original absorbance is followed in the dark. It occurs according to a clean, first-order reaction in homogeneous solution. Whitten and Schanze et al.[8,31] studied thermal $Z\rightarrow E$ isomerization rate constants k_{iso} of "push-pull" azobenzenes. They considered their remarkable solvent dependence as an indication for the rotation mechanism, where a dipolar transition state with a strongly reduced azo bond order would be stabilized in polar solvents. The same effect of an increase of k_{iso} has been found using substituents with increasing +I-effect.[9] Depending on the solvent, lifetimes $\tau_z = 1/k_{iso}$ of microseconds to seconds were determined by means of conventional microsecond flash photolysis. A linear relation between the energy of the absorption maximum of the *E*-isomer E_{max} and $\ln k_{iso}$ was determined in aprotic solvents. It was explained by a similar trend of the charge transfer during electronic excitation of the *E*-isomer and the charge transfer in the transition state of the thermal $Z\rightarrow E$ isomerization.[31] In the case of lifetimes τ_z greater than several seconds, photostationary states with absorbances significantly different from the pure *E*-isomer can be established experimentally and quantum yields can be determined. In this way, Marcandalli et al. determined quantum yields for both $E\rightarrow Z$ and $Z\rightarrow E$ isomerization of 4-diethylaminoazobenzenes with varying 4′-substituent, which add up to unity. These authors could not verify a viscosity effect of the rate and concluded that the inversion mechanism holds.[18]

4-(Phenylamino)-4′-nitroazobenzene with the bulky phenyl group at the amino nitrogen turned out to be a better candidate to detect a rate decreasing viscosity effect as an indication of the rotational pathway. A decrease in k_{iso} with increasing bulk viscosity was determined, comparing simple solvents with highly viscous polyglycols, applying a multilinear regression analysis and taking the polarity of the solvents (E_{max}) into account.[9,11]

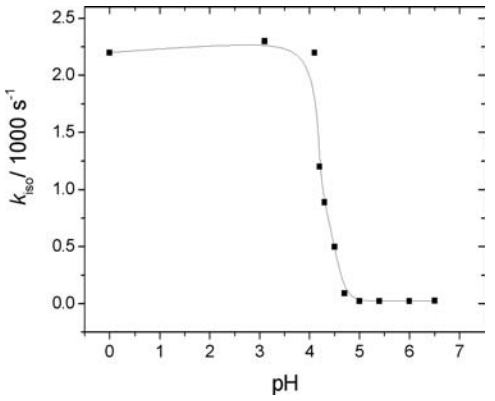

FIGURE 89.6 Plot of the thermal $Z \rightarrow E$ isomerization rate constant k_{iso} of 4-(phenylamino)-4′-nitro-azobenzene in acetone/H_2O (1:1, v:v) vs. pH, established by addition of concentrated HCl (the line is a guide for the eye; $pK_S \approx 4.2$ can be estimated).

In aqueous solutions, protonation of one of the nitrogen atoms — preferably at the N = N double bond — causes a considerable reduction in the activation barrier.[32] Inversely, hydroxide ions decrease the reaction rate.[33] To study thermal $Z \rightarrow E$ isomerization rates of unprotonated azobenzenes in aqueous solutions, the pH of the solution should be clearly above the threshold where protonation influences the rate. The dependence of k_{iso} of 4-(phenylamino)-4′-nitroazobenzene on H_3O^+ concentration in acetone/water (1:1, v/v) mixtures corresponds to a titration curve (see Figure 89.6).[9,34] The flash-photolytic preparation of thermally unstable *Z*-isomers offers the interesting possibility of determining their pK_S-data by means of kinetic experiments.

In aqueous solutions, λ_{max} of the *E*-isomer is strongly influenced by hydrogen bonding. Despite decreasing λ_{max}, indicating apparently lower polarity (see 89-3), the rate constants k_{iso} of the *Z*-isomer continuously increase with increasing water content in poly(ethylene oxide)/water solutions. This is only in part due to the concomitantly decreasing bulk viscosity. By comparing H_2O and D_2O solutions, separating the solvent isotope viscosity effect, there is a significantly higher isomerization rate in H_2O. A dynamic hydrogen-bonding effect was postulated, assuming that the higher frequency in hydrogen-bond making and breaking in H_2O compared to D_2O increases the frequency of electron density fluctuations, which are favorable for approaching the bipolar transition state.[11]

This strong solvent dependence of the absorption maximum λ_{max} and the thermal $Z \rightarrow E$ isomerization rate constants k_{iso} of "push-pull" azobenzenes were used as "spectroscopic" and "kinetic" probes to study aqueous microheterogeneous solutions of surfactants and lipids.[9,11,31,35] The λ_{max} of the stable *E*-isomer indicates that it is solubilized at the head group/water interface, probably more or less aligned with the nitro group to the water side. It was shown that the isomerization rates in solutions of increasing surfactant concentrations decrease with increasing micelle size.[9] The decreasing and vanishing kinetic solvent isotope effect $k_{iso,H_2O}/k_{iso,D_2O}$ (KSIE) indicates decreased accessibility of water to the probe molecules.[9] Interesting non-Arrhenius behavior of k_{iso} of "push-pull" azo dyes was observed in aqueous solutions of triblock copolymers of the poly(ethylene oxide)–poly(propylene oxide)–poly(ethylene oxide) type, which behave as non-ionic surfactants with strong temperature-dominated aggregation behavior. With increasing temperatures, S-shaped Arrhenius plots were obtained, which give decreasing rate constants with increasing temperature due to micelle formation in an intermediate temperature range[11,35] (Figure 89.7).

On structure changes, these "kinetic probes" sensitively reflect the increasing microviscosity and decreasing water content in the microenvironment of the probe molecules, as indicated by decreasing KSIE. In some cases, critical micellization temperatures (cmt) can be derived from these plots. Such systems can be considered as models for the interplay of reaction rates and structure changes in biology.

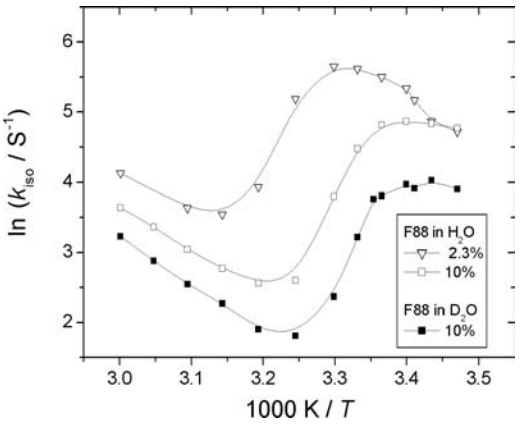

FIGURE 89.7 Arrhenius plots of thermal $Z \rightarrow E$ isomerization rate constants k_{iso} of 4-(phenylamino)-4′-nitroazobenzene in aqueous solutions of the triblock copolymer F88 (poly(ethylene oxide)$_{96}$–poly(propylene oxide)$_{39}$–poly(ethylene oxide)$_{96}$), reflecting micelle formation on increasing temperature. Lines are guides for the eye.

Calculations on transition states of the thermal $Z \rightarrow E$ isomerizations of "push-pull" azobenzenes also became available. *Ab initio* methods, including solvent effects based on continuum models, were applied to 4-(amino)-4′-nitroazobenzene and 4-(dimethylamino)-4′-nitroazobenzene.[36,37] These calculations showed that the transition-state structure of the rotation path was stabilized by the solvent. However, the transition state of the inversion path of the "pull" group is lower in energy than the transition state for the rotation path. Moreover, for 4-(dimethylamino)-4′-nitroazobenzene, the authors concluded that the reaction proceeds by a mechanism of a mixture of the two limiting cases: inversion and rotation.[37] The expected specific solvent interaction with a dipolar transition state, however, cannot be treated with continuum models.

Asano and co-workers studied the effect of pressure on the thermal $Z \rightarrow E$ isomerization of 4-(dimethylamino)-4′-nitroazobenzene in an effort to test the effect of bulk viscosity of the medium on isomerization reactions with respect to reaction rate theories.[38]

Semi-empirical ZINDO calculations showed that the HOMO of 4-phenylaminoazobenzene and 4-(phenylamino)-4′-nitroazobenzene is mainly at the amino nitrogen and the LUMO is localized at the nitrobenzene moiety, confirming the charge-transfer character of the $\pi \rightarrow \pi^*$ absorption band. Protonation at the azo nitrogen leads to a LUMO that is mainly localized at the azo nitrogens. Protonation appears to stabilize the LUMO in accordance with the observed bathochromic shift.[10]

89.6 Applications of the Photoisomerization of Azobenzenes

The change in the absorption spectrum and the molecular structure on photoisomerization of azobenzenes can be used for practical applications. The literature on possible applications in photoresponsive materials was reviewed up to 1988 by Rau.[2] Important contributions by Japanese workers, for example, on light-driven potassium ion transport through membranes by means of crown ethers with a photofunctional azobenzene cap, were recently summarized by Shinkai.[39] Moreover, light-manipulation of other super molecules based on azobenzene photoisomerization is described in the book by Feringa.[40] The $E \rightarrow Z$ *p*hotoisomerization for the preparation of thermally unstable *Z*-isomers for use as "kinetic probes" in microheterogeneous media was described in Section 89.5.

Many studies have been directed toward utilizing azobenzene photochromism in optical data storage devices. However, thermal $Z \rightarrow E$ isomerization limits the stability of the *Z*-isomer and causes information loss. Application of low temperatures is not an alternative for practical reasons. Embedding the photoactive molecules into more rigid matrices improves the stability of such photoswitches. Azobenzene included in microporous zeolites of different structures, such as $AlPO_4$-5 and ZSM-5, shows reversible

photoswitching behavior between the *E* and *Z* states, which is indicated by a remarkable refractive index change for use in all-optical microswitches.[41] Azobenzene-containing melamine resins turned out to be materials with high thermal, optical, and mechanical stability for holographic information storage.[42] First attempts to use thin films of azobenzene-functionalized dendrimers with 32 azobenzene groups in the periphery for holographic materials yielded diffraction efficiencies up to about 20%. The quantum yield of each photoactive unit was not dependent on the total number of azobenzene units present.[43] Other authors studied the light orientation of the azobenzene groups of dendrimers under the action of linearly polarized light.[44,45]

All-optical switching of selectively reflected colors based on isomerization of an azobenzene compound and subsequent change in transmittance were investigated by Ikeda et al.[46] It was found that small amounts of achiral photochromic dopants, as 4,4′-di-n-alkylazobenzenes in cholesteric liquid crystals, accomplished a photo-rewritable, full-color image recording.[47] Molecular switches based on stereoisomers of chiral photoresponsive molecules have the advantage over photochromic systems. The feasibility of nondestructive readout of an optical recording system was demonstrated by monitoring the optical rotation at wavelengths remote from the wavelengths of the actinic light necessary for switching. Azobenzene containing peptide oligomers was used for this purpose.[48]

Liquid crystal forming molecules with donor/acceptor azobenzene units induced and increased the rate of thermal isotropic→nematic phase transition by several orders of magnitude compared to alkoxyl-type azobenzene liquid crystals. These materials suggest their prospective application in real-time holographic materials.[49]

In another field of current activity, the aggregation behavior of amphiphile molecules is modified and controlled by photoswitching of azobenzenes that are covalently linked as a component of some part or all the amphiphilic molecules. Japanese workers collected a large amount of data on photosensitive artificial membranes based on azobenzene derivatives.[50]

Fast osmotic shrinkage of lipid membranes after photoisomerization of azobenzene derivatives and subsequent structure ordering have been demonstrated.[51] Depending on the ratio of azobenzene units containing amphiphiles to other amphiphiles, H-aggregate formation of the azobenzene moieties can occur. The *E*→*Z* isomerization by UV irradiation leads to "catastrophic" destruction of vesicles in the case of azobenzene aggregate or cluster formation.[52] Photochemical switching of vesicle formation in a mixture of an azobenzene-modified cationic surfactant and sodium dodecylbenzenesulfate brought about disruption of the vesicles into larger aggregates on *E*→*Z* isomerization.[53] Wavelength-programmed solute release from photosensitive liposomes based on the photochromism of azobenzene containing lipids was shown by Bisby et al.[54] An azobenzene containing cationic surfactant increased its critical micellization concentration (cmc) from 2.7 m*M* in the *E*-form to 8.2 m*M* in the *Z*-form. In this way, oily substances could be released or up taken by switching between the *E*- and *Z*-forms. The solubilizing capacity could also be varied.[55] Another azobenzene–surfactant also shows the expected increase in the cmc (0.13 m*M* compared to 0.34 m*M*) and of the average area per molecule on the surface (0.60 compared to 0.74 nm^2 per molecule) on switching from pure *E*-isomer to a *Z*-rich mixture on irradiation.[56]

Light control of dynamic surface tension was demonstrated in a mixture of sodium dodecylsulfate and 4,4′-bis(trimethylammonium)hexyloxyazobenzene bromide. A decrease of 25 mN/m was determined on *E*→*Z* isomerization by UV irradiation. Aggregation in the bulk and mass transport of the surfactant to the surface of the solution differ between the isomers. This phenomenon can be used to trigger the release of droplets of aqueous solutions from capillaries.[57] Calix[4]resocinarene derivatives substituted with azobenzenes exhibited reversible precipitation/dissolution in dilute methanol solution upon alternate UV and VIS light irradiation due to the low solubility of the all-*trans* isomer.[58]

The photoisomerism of azobenzenes is one working principle in the regulation of structure and function of biomolecules by light as, for example, the binding of proteins and stimulation of enzyme activity.[59] Photoisomerism of azobenzenes has also been applied to the regulation of bioreactions. By photoregulation of a template-dependent DNA polymerase reaction using photoresponsive oligonucleotides as modulators, DNA of predetermined length is selectively produced from one template DNA.[60]

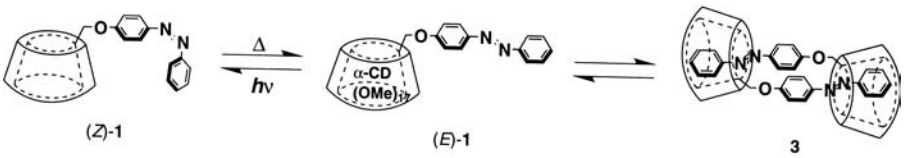

FIGURE 89.8 Monomer(*E*)-1/dimer(3) equilibrium of a permethylated α-cyclodextrin-azobenzene dyad. The equilibrium is disturbed by (*E*)-1→(*Z*)-1 photoisomerization and may be reformed after thermal (*Z*)-1→(*E*)-1 isomerization. (From Fujimoto, T., Nakamura, A. Inoue, Y., Sakata, Y., and Kaneda, T., *Tetrahedron Lett.*, 42(45), 7987, 2001. Reprinted with permission from Elsevier Science. Copyright 2001.)

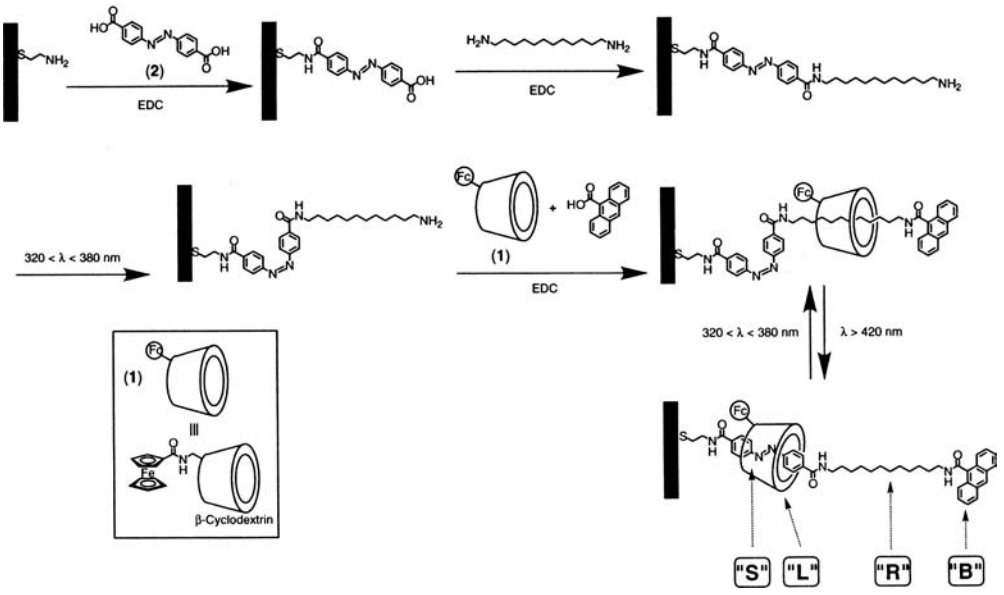

FIGURE 89.9 Organization of the "molecular train" (MT) assembly on a gold electrode and its photoinduced translocation. The MT assembly consists of a station S, a railway R, a locomotive L, and a barrier B (see text). (From Willner, I., Pardo-Yissar, V., Katz, E., and Ranjit, K., *J. Electroanalytical Chemistry,* 497, 172, 2001. Reprinted with permission from Elsevier Science. Copyright 2001.)

The *Z*→*E* isomerization of an azobenzene moiety in the side chain of oligonucleotides reversibly photoregulates the formation and dissociation of the duplex, which is destabilized after switching into the *Z*-form.[61]

Molecular opto-electronic assemblies, which consist of a functionalized gold electrode with a photoisomerizable redox-activated monolayer, enables amperometric transduction of the photonic information recorded by the interface.[62] On-off operation of superstructure formation of hermaphroditic cyclodextrin derivatives is brought about by disturbing the monomer/dimer equilibrium of *E*-azobenzene structures by photoisomerization. When the structures have the *Z*-form, the dimer dissociates. The thermal *Z*→*E* isomerization can be enhanced by heating in favor of the dimer formation (Figure 89.8).[63]

An impressive example of a "molecular machine" was presented by Willner et al.[64] (Figure 89.9). Using the base 1-ethyl-3(3-dimethylaminopropyl)carbodiimide (EDC), a super molecule attached at a gold electrode was synthesized in a stepwise fashion. Here *E*→*Z* photoisomerization of the azobenzene moiety is a necessary step already in the synthetic procedure. By switching photolytic wavelengths between 320–380 and >420 nm, respectively, the movement of the shuttle is activated between the *E*-azobenzene "station" site and an alkyl-chain "railway" component. The distance between the redox active ferrocene label from the electrode is indicated by a chronoamperic response.

All these examples demonstrate the possibility of manipulating self-assembling structures of amphiphiles and artificial supramolecular structures, respectively, by reversible photoswitching between *E*- and *Z*-azobenzene structures. Advancements in the direction of real practical applications will depend on demonstrating the usefulness and stability of such systems.

References

1. Zollinger, H., *Colour Chemistry*, VCH Verlagsgesellschaft mbH, Weinheim, 1987, 253.
2. Rau, H., Photoisomerizations of azobenzenes, in *Photochemistry and Photophysics*, Rabek, J.F., Ed., CRC Press, Boca Raton, FL, 1990.
3. Rau, H., Azo Compounds, in *Photochromism. Molecules and Systems*, Dürr, H. and Bouas-Laurent, H., Eds., Elsevier, Amsterdam, 1990, 165..
4. Suginome, H., *E,Z*-isomerisation of imines, oximes and azo compounds, in *CRC Handbook of Organic Photochemistry and Photobiology*, Horspool, W.M. and Song, P.-S., Eds., CRC Press, Boca Raton, FL, 1995.
5. Forber, C.L., Kelusky, E.C., Bunce, N.J., and Zerner, M.C., *J. Am. Chem. Soc.*, 107, 5884, 1985.
6. Bartolus, P. and Monti, S., *Cis-trans* photoisomerization of azobenzene. solvent and triplet donor effects, *J. Phys. Chem.*, 83, 648, 1979.
7. Jaffé, H.H. and Orchin, M., *Theory and Applications of Ultraviolet Spectroscopy*, John Wiley & Sons, New York, 1962, 430.
8. Schanze, K.S., Mattox, T.F., and Whitten, D.G., Solvent effects upon the thermal *cis-trans* isomerization and charge-transfer absorption of 4-(diethylamino)-4′-nitroazobenzene, *J. Org. Chem.,* 48, 2808, 1983.
9. Gille, K., Knoll, H., and Quitzsch, K., Rate constants of the thermal *cis-trans* isomerization of azobenzene dyes in solvents, acetone/water mixtures and in microheterogeneous surfactant solutions, *Int. J. Chem. Kinetics*, 31, 337, 1999.
10. Makaita, S., Saito, A., Hayashi, M., Yamada, S., Yoda, K., Otsuki, J., and Takido, T., Electronic spectra of push-pull 4-phenylaminobenzene derivatives, *Bull. Chem. Soc. Jpn.,* 73, 1525, 2000.
11. Wang, R. and Knoll, H., Rate constants of the thermal *cis→trans* isomerization of azo dyes as kinetic probes in aqueous solutions of poly(ethylene glycols) and poly(ethylene oxide)-poly(propylene oxide)-poly(ethylene oxide) block copolymer F88, *Langmuir*, 17, 2907, 2001.
12. Bisle, H., Römer, M., and Rau, H., Der Einfluß der Kopplung von $^1(n,\pi^*)$- und (π,π^*)-Zuständen auf die Fluoreszenzfähigkeit von Azobenzolen, *Ber. Bunsenges. Phys. Chem.*, 80, 301, 1976.
13. Tamai, N. and Miyasaka, H., Ultrafast dynamics of photochromic systems, *Chem. Rev.*, 100, 1875, 2000.
14. Tsuda, K., Dol, G.C., Gensch, T., Hofkens, J., Latterini, L., Weener, J.W., Meijer, E.W., and De Schryver, F.C., Fluorescence from azobenzene functionalized poly(propylene imine) dendrimers in self-assembled supramolecular structures, *J. Am. Chem. Soc.*, 122, 3445, 2000.
15. Fujino, T., Arzhantsev, S.Y., and Tahara, T., Femtosecond time-resolved fluorescence study of photoisomerization of *trans*-azobenzene, *J. Phys. Chem. A*, 105, 8123, 2001.
16. Görner, H., Gruen, H., and Schulte-Frohlinde, D., Laser flash photolysis study of substituted azobenzene. Evidence for a triplet state in viscous media, *J. Phys. Chem.,* 84, 3031, 1980.
17. Kobayashi, S., Yokoyama, H., and Kamei, H., Substituent and solvent effects on electronic absorption spectra and thermal isomerization of push-pull-substituted *cis*-azobenzenes, *Chem. Phys. Lett.*, 138, 33, 1987.
18. Marcandalli, B., Seves A., Dubini-Paglia, E., and Beltrame, P.L., Photochemical *trans-cis* isomerization of some 4-diethylaminoazobenzenes, *Dyes and Pigments*, 14, 79, 1990.
19. Rau, H., Further evidence for rotation in the π,π^* and inversion in the $n\pi^*$ photoisomerization of azobenzenes, *J. Photochem.*, 26, 221, 1984.
20. Bortolus, P. and Monti, S., *Cis-trans* photoisomerization of azobenzene-cyclodextrin inclusion complexes, *J. Phys. Chem.,* 91, 5046, 1987.

21. Yukata, T., Kurihara, M., Kubo, K., and Nishihara, H., Novel photoisomerization behavior of Rh binuclear complexes involving an azobenzene-bridged bis(terpyridine) ligand, *Inorg. Chem*. 39, 3438, 2000.
22. Yutaka, T., Mori, I., Kurihara, M., Mizutani, J., Kubo, K., Furusho, S., Matsumura, K., Tamai, N., and Nishihara, H., Synthesis, characterization and photochemical properties of azobenzene-conjugated Ru(II) and Rh(III) bis(terpyridine) complexes, *Inorg. Chem.,* 40, 4986, 2001.
23. Monti, S., Orlandi, G., and Palmieri, P., Features of the photochemically active state surfaces of azobenzene, *Chem. Phys.,* 71, 87, 1982.
24. Nägele, T., Hoche, R., Zinth, W., and Wachtveitl, J., Femtosecond photoisomerization of *cis*-azobenzene, *Chem. Phys. Lett.,* 272, 489, 1997.
25. Lednev, I.K., Ye, T.-Q., Hester, R.E., and Moore, J. N., Femtosecond time-resolved UV-visible absorption spectroscopy of trans-azobenzene in solution, *J. Phys. Chem*., 100, 13338, 1996.
26. Lednev, I.K., Ye, T.-Q., Matousek, P., Towrie, M., Foggi, P., Neuwahl, F.V.R., Umapathy, S., Hester, R.E., and Moore, J. N., Femtosecond time-resolved, UV-visible absorption spectroscopy of *trans* azobenzene: dependence on excitation wavelength, *Chem. Phys. Lett.,* 290, 68, 1998.
27. Fujino, T. and Tahara, T., Picosecond time-resolved Raman study of *trans*-azobenzene, *J. Phys. Chem. A*, 104, 4203, 2000.
28. Cattaneo, P. and Persico, M., An *ab initio* study of the photochemistry of azobenzene, *Phys. Chem. Chem. Phys.*, 1, 4739, 1999.
29. Ishikawa, T., Noro, T., and Shoda T., Theoretical study on the photoisomerization of azobenzene, *J. Chem. Phys.,* 115, 7503, 2001.
30. Talaty, E.R. and Fargo, J.C., Thermal *cis-trans* isomerization of substituted azobenzenes: a correction of the literature, *J. Chem. Soc., Chem. Commun.,* 65, 1967.
31. Shin, D.M., Schanze, K.S. and Whitten, D.G., *J. Am. Chem. Soc.,* 111, 8494, 1989.
32. Sokalski, W.A., Góra, R.W., Bartkowiak, W., Kobulynski, P., Sworakowski, J. and Lesczynski, J., New theoretical insight into the thermal cis-trans isomerization of azo compounds: protonation lowers the activation barrier, *J. Chem. Phys.,* 114, 5504, 2001.
33. Sanchez, A. and de Rossi, R.H., Effect of hydroxide ion in the cis-trans thermal isomerization of azobenzene derivatives, *J. Org. Chem.*, 60, 2974, 1995.
34. Gille, K., Untersuchungen zur thermischen *cis-trans* Isomerisierung von Azofarbstoffen in homogenen und mikrodispersen fluiden Medien, Theses, Universität Leipzig, 1998.
35. Gille, K., Knoll, H., Rittig, F., Fleischer, G., and Kärger, J., Study of structure formation in aqueous solutions of poly(ethylene oxide)-poly(propylene oxide)-poly(ethylene oxide) block copolymers by measuring rate constants of the thermal *cis-trans* isomerization of an azobenzene dye and self-diffusion of copolymer molecules, *Langmuir*, 15, 1059, 1999.
36. Cimiraglia, R., Asano, T., and Hofmann, H.-J., Mechanism of the thermal *Z/E* isomerization of aromatic azo compounds. Relation between rotation and inversion states, *Gazz. Chim. Ital.*, 126, 1996, 679.
37. Kikuchi, O., Azuki, M., Inadomi, Y., and Morihashi, K., *Ab initio* GB study of solvent effect on the *cis-trans* isomerization of 4-dimethylamino-4′-nitroazobenzene, *Theochem*, 468, 95, 1999.
38. Asano, T., Cosstick, K., Furuta, H., Matsuo, K., and Sumi, H., Effects of solvent fluctuations on the rate of thermal *Z/E* isomerizations of azobenzenes and *N*-benzylidenes, *Bull. Chem. Soc. Jpn.*, 69, 551, 1996.
39. Shinkai, S., Switchable molecular receptors and recognition processes: from photoresponsive crown ethers to allosteric sugar sensing systems, in *Molecular Switches*, Feringa, B.L., Ed., Wiley-VCH, 2001, 281.
40. Feringa, B.L., Ed., *Molecular Switches*, Wiley-VCH, 2001.
41. Hoffmann, K., Resch-Genger, U., and Marlow, F., Photoinduced switching of nanocomposites consisting of azobenzene and molecular sieves: investigation of the switching states, *Micropor. Mesopor. Mater.,* 41, 99, 2000.
42. Stracke, A., Wendorff, J.H., Mahler, J., and Rafler, G., *Macromolecules*, 33, 2605, 2000.

43. Archut, A., Vögtle, F., De Cola, L., Azzellini, G.C., Balzani, V., Ramanujam, P.S., and Berg, R.H., Azobenzene-functionalized cascade molecules: photoswitchable supramolecular systems, *Chem.-Eur. J.,* 4, 699, 1998.
44. Patton, D., Park, M., Wang, S., and Advincula, R.C., Evanescent waveguide and photochemical characterization of azobenzene-functionalized dendrimer ultrathin films, *Langmuir*, 18, 1688, 2002.
45. Bobrovsky, A.Y., Pakhomov, A.A., Zhu, X.-M., Boiko, N.I., Shibaev, V.P., and Stumpe, J., Photochemical and photoorientational behaviour of liquid crystalline carbosilane dendrimer with azobenzene terminal groups, *J. Phys. Chem. B*, 106, 540, 2002.
46. Lee, H.-K., Doi, K., Harada, H., Tsutsumi, O., Kanazawa, A., Shiono, T., and Ikeda, T., Photochemical modulation of color and transmittance in chiral nematic liquid crystal containing an azobenzene as a photosensitive chromophore, *J. Phys. Chem. B*, 104, 7023, 2000.
47. Moriyama, M., Song, S., Matsuda, H., and Tamaoki, N., Effects of doped dialkylbenzenes on helical pitch of cholestic liquid crystal with medium molecular weight: utilisation for full-colour image recording, *J. Mater. Chem.*, 11, 1003, 2001.
48. Feringa, B.L., Van Delden, R.A., Koumura, N., and Geertsema, E.M., Chiroptical molecular switches, *Chem. Rev.,* 100, 1789, 2000.
49. Tsutsumi, O., Kanazawa, A., Shiono, T., Ikeda, T., and Park L.-S., Photoinduced phase transition of nematic liquid crystals with donor-acceptor azobenzenes: mechanism of the thermal recovery of the nematic phase, *Phys. Chem. Chem. Phys.,* 1, 1999, 4219.
50. Anzai, J.-I. and Osa, T., Photosensitive artificial membranes based on azobenzene and spirobenzopyran derivatives, *Tetrahedron*, 50, 4039, 1994.
51. Tanaka, M., Jutila, A., and Kinnunen, P.K., Static and kinetic investigations of the structural ordering of phospholipid membranes doped with azobenzene derivative, *J. Phys. Chem. B*, 102, 5358, 1998.
52. Song, X., Perlstein, J.,and Whitten, D.G., Supramolecular aggregates of azobenzene phospholipids and related compounds in bilayer assemblies and other microheterogeneous media: structure, properties and photoreactivity, *J. Am. Chem. Soc.,* 119, 9144, 1997.
53. Sakai, H., Matsumura, A., Yokoyama, S. and Abe, M., Photochemical switching of vesicle formation using an azobenzene-modified surfactant, *J. Phys. Chem. B*, 103, 10737, 1999.
54. Bisby, R.H., Mead, C., and Morgan, C.G., Wavelength-programmed solute release from photosensitive liposomes, *Biochem. Biophys. Res. Commun.,* 276, 169, 2000.
55. Orihara, Y., Matsumura, A., Saito, Y., Ogawa, N., Saji, T., Yamaguchi, A., Sakai, H., and Abe, M., Reversible release control of an oily substance using photoresponsive micelles, *Langmuir*, 17, 6072, 2000.
56. Kang, H.-C., Lee, B.M., Yoon, J., and Yoon, M., Synthesis and surface active properties of new photosensitive surfactants containing the azobenzene group, *J. Colloid Interface Sci.*, 231, 255, 2000.
57. Shin, J.Y. and Abbott, N.L., Using light to control dynamic surface tensions of aqueous solutions of water soluble surfactants, *Langmuir*, 15, 4404, 1999.
58. Ichimura, K., Fukushima, N., Fujimaki, M., Kawahara, S., Matsuzawa, Y., Hayashi, Y., and Kudo, K., Macrocyclic amphiphiles. 1. Properties of calix[4]resorcinarene derivatives substituted with azobenzenes in solutions and monolayers, *Langmuir*, 13, 6780, 1997.
59. Willner, I. and Rubin, S., Steuerung der Struktur und Funktion von Biomakromolekülen durch Licht, *Angew. Chem.,* 108, 419, 1996; *Angew. Chem. Int. Ed. Engl.,* 35, 367, 1996.
60. Yamazawa, A., Liang, X., Asanuma, H., and Komiyama, M., Photoregulation of the polymerase reaction by oligonucleotides bearing an azobenzene, *Angew. Chem.*, 112, 2446, 2000; *Angew. Chem. Int. Ed. Engl.,* 39, 2357, 2000.
61. Asanuma, H., Liang, X., and Komiyama, M., *Meta*-aminoazobenzene as a thermoinsensitive photoregulator of DNA-duplex formation, *Tetrahedron Lett.*, 41, 1055, 2000.
62. Willner, I. and Willner B., Layered molecular optoelectronic assemblies, *J. Mater. Chem.,* 8, 2543, 1998.

63. Fujimoto, T., Nakamura, A., Inoue, Y., Sakata, Y., and Kaneda, T., Photoswitching of the association of a permethylated α-cyclodextrin-azobenzene dyad forming a janus[2]pseudorotaxane, *Tetrahedron Lett.,* 42, 7987, 2000.
64. Willner, I., Pardo-Yissar, V., Katz, E., and Ranjit, K., A photoactivated 'molecular train´ for optoelectronic applications: light stimulated translocation of a ß-cyclodextrin receptor within a stoppered azobenzene-alkyl chain supramolecular monolayer assembly on a Au-electrode, *J. Electroanal. Chem.*, 497, 172, 2001.

90

Photochemical Reactivity of α-Diazocarbonyl Compounds

Tevye C. Celius
Johns Hopkins University

Yuhong Wang
Johns Hopkins University

John P. Toscano
Johns Hopkins University

90.1 Introduction and Applications of α-Diazocarbonyl Compounds

The chemistry of α-diazocarbonyl compounds is closely associated with the Wolff rearrangement[1–5] (see Scheme 1), a versatile reaction that has found wide application in diverse areas of research and technology ranging from long-standing use in organic synthesis[6] to recent examples in surface science.[7] The Arndt-Eistert synthesis utilizes the Wolff rearrangement of α-diazoketones to ketenes in the homologation of carboxylic acids.[6] Wolff rearrangement of cyclic diazoketones leading to ring contraction has been particularly useful in the synthesis of strained small-ring compounds,[8] including four- and six-membered heterocycles.[9] The synthetic applications of ketene nucleophilic[10,11] and electrophilic reactions[12] have also been extensively studied. Ketene radical addition,[5,13–20] bisketene reactions,[5,21] and the chemistry of highly stable silyl-substituted ketenes[22,23] are also active areas of research.

The most extensive application of α-diazocarbonyl compounds is in the lithographic production of integrated circuits used by the computer industry. The majority of photoresist materials involved in this process are α-diazoketone derivatives.[24,25] Upon photolysis, these compounds form ketenes that subsequently react with water to produce carboxylic acids. The difference in carboxylic acid and diazoketone solubility is then utilized to pattern electronic devices.

0-8493-1348-1/04/$0.00+$1.50

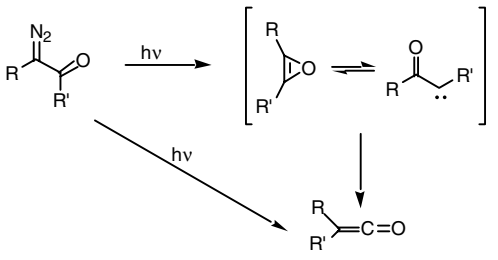

SCHEME 1

Recently, photoinduced Wolff rearrangements have been explored as potential methods of generating DNA cleavage reagents.[26–28] α-Diazoketones absorb UVA (320 to 400 nm) light to produce highly electrophilic ketenes that have intrinsic reaction selectivity toward nucleophilic nucleobases such as guanine and adenine.

As a result of the wide applicability of α-diazoketones, much effort has been applied to understanding the mechanistic pathways available to this class of compounds. Several possible intermediates (e.g., α-carbonylcarbenes, oxirenes, and excited-state species) have played a central role in the proposed mechanisms of the Wolff rearrangement. This chapter examines both experimental and theoretical work that has furthered our understanding of the mechanisms underlying the complex reactivities of these systems.

90.2 Reactive Species Involved in the Wolff Rearrangement

The mechanism of the Wolff rearrangement has been proposed as either the concerted loss of nitrogen and rearrangement to a ketene, or the stepwise loss of nitrogen to give an intermediate carbene (or oxirene) that then rearranges to give ketene (Scheme 1). Carbenes have been detected both directly and indirectly, but the oxirene intermediate has been much more elusive and only indirect evidence is available.

The ketene products of the Wolff rearrangement are by far the most thoroughly characterized and well understood of the reactive species involved.[29] Ketenes are known to undergo both nucleophilic and electrophilic addition reactions, as well as various types of cycloaddition reactions. Of particular interest are the reactions of ketenes with water, alcohols, and amines.

The ketene hydration reaction has been examined recently by time-resolved spectroscopic techniques.[30–34] Intermediate enols have been directly observed in solution,[35–38] although this is not generally the case because ketene hydration is usually slower than enol tautomerization. The hydration rate constants of representative groups of ketenes[30–34,39–41] in aqueous solutions have been obtained and their reactivities rationalized.

The mechanism of the ketene-alcohol addition reaction[30,38,42] depends on the reaction conditions. A time-resolved UV-VIS (TRUV-VIS) study has shown that, under normal photolysis conditions, 2-diazo-1,3-indandione (**1**)[43] in alcohols forms diester **4** via the secondary photolysis of ester **3**. However, under laser drop photolysis conditions,[44] where the laser intensity is very high, the formation of diester **4** occurs via intermediate **5** (Scheme 2).

Spectroscopic methodologies have provided a wealth of information concerning the amination of ketenes.[45,46] Scaiano and co-workers have measured rate constants for ketene reactions with various classes of amines in acetonitrile.[46] The reaction rate is influenced by the basicity of the amine as well as by steric factors in both the ketene and the amine. Ketene amination has also been studied by time-resolved infrared (TRIR) spectroscopy.[47,48] The strong ketene IR band near 2100 cm^{-1} makes it an excellent candidate for study by this spectroscopic technique. Scaiano, Wagner, Lusztyk, and co-workers provided evidence[47] for the first nucleophilic attack being rate determining and that the transition state involves an enol amide. They further found that the asymmetric stretching IR band of substituted ketenes

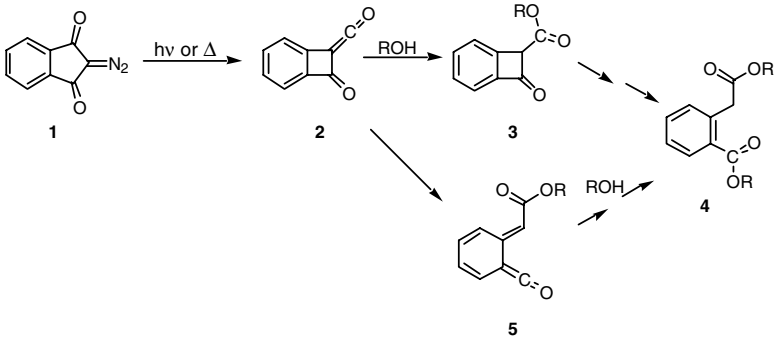

SCHEME 2

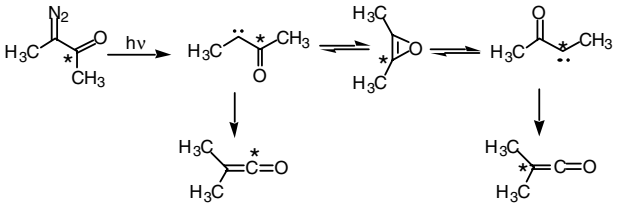

SCHEME 3

correlates with the inductive parameter of the substituent, but not field or resonance effect parameters. For more stable ketenes, such as $PhMe_2SiCH{=}C{=}O$, the rate of amination is found to be second or third order in amine concentration, by both calculation[49,50] and experiment.[51] Cyclic intermediates have therefore been proposed for these cases.

Recently, other photochemical and thermal retro-Wolff rearrangements have been examined by several researchers.[52–55] Under flash vacuum and pulsed pyrolysis conditions, Wentrup and co-workers observed the formation of (cyanovinyl)ketenes from aza fulvenones.[56] Additionally, Moore and co-workers have done extensive work on the gas-phase photochemistry and molecular dynamics on the C_2H_2O surface using state-resolved spectroscopic methods.[57]

A persistent question concerning the Wolff rearrangement is whether or not an alternate intermediate, such as an excited state of the diazo precursor[58–61] or an oxirene,[62,63] is involved. Carbonylcarbenes have been detected in low-temperature matrices by electron spin resonance (ESR)[64–70] and FTIR[71–75] spectroscopies. Evidence for the participation of oxirenes[62,63] comes from experiments[76–79] in which diazoketones labeled at the carbonyl carbon rearrange to form ketenes that possess a label at both carbon atoms (Scheme 3). Similar results were obtained in studies of unsymmetrically substituted diazoketones.[80,81] The direct observation of oxirene intermediates, however, has been more elusive. Initial reports of oxirene detection[82,83] were later called into question.[84,85] Bodot and co-workers have advanced evidence for the existence of dimethyloxirene and its deuterated analogue by low-temperature FTIR methods.[86,87]

90.3 Singlet vs. Triplet Reactivity

Previous classical studies have clearly indicated that the Wolff rearrangement takes place in the singlet rather than triplet manifold.[88,89] For example, Jones and Ando found that the photolysis of diazoacetone **6** in olefin solution leads only to Wolff rearrangement products (Scheme 4). Carbene adducts, however, were isolated upon triplet-sensitized photolysis, demonstrating that the singlet state of either the diazo precursor or the carbene is involved in the Wolff rearrangement.

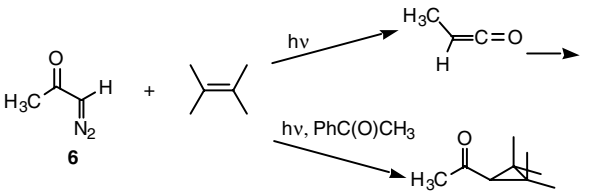

SCHEME 4

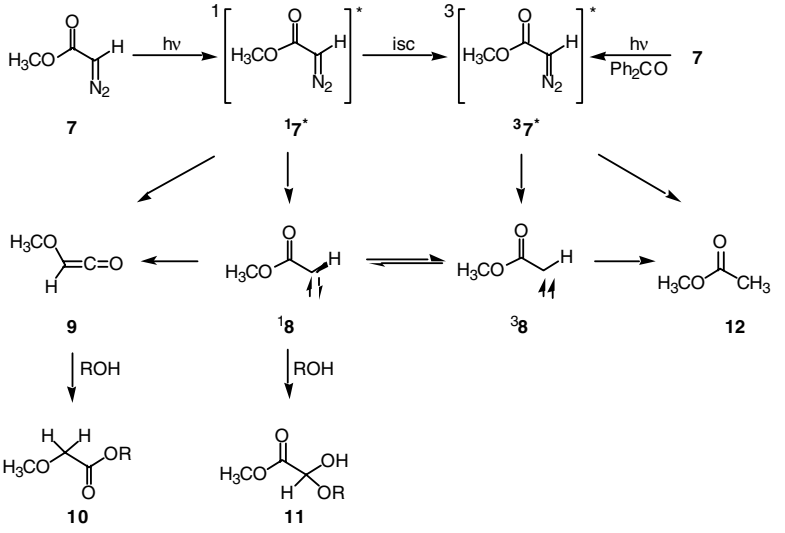

SCHEME 5

Further insight into the multiplicity of the species involved was obtained by Tomioka and co-workers in their thorough study of the photochemistry of methyl diazoacetate **7** (Scheme 5). They demonstrated that direct photolysis of **7** produces an excited singlet state (^{1}**7***) that may suffer Wolff rearrangement concurrent with nitrogen extrusion to yield ketene **9**, lose nitrogen to form the singlet carbene ^{1}**8,** or intersystem cross to give the triplet diazoester ^{3}**7***. The ketene and singlet carbene intermediates are both trapped by alcohol, but give different products, **10** and **11**, respectively. Reduction product **12** is clearly derived from a triplet species, ^{3}**7***, ^{3}**8**, or both, because its yield is enhanced upon triplet-sensitized photolysis but is suppressed by the triplet quencher piperylene, following direct photolysis.

The alcohol insertion product **11** is still formed upon sensitized photolysis of **7**, demonstrating that the triplet carbene ^{3}**8** can interconvert to the singlet carbene ^{1}**8**. Hutton and Roth previously demonstrated, by low-temperature ESR spectroscopy, that ^{3}**8** is the ground state of the carbene.[67] Thus, Tomioka's results show that the more reactive singlet carbene is close in energy to the triplet ground state. In addition, because formation of ketene **9** is suppressed upon triplet sensitization of **7** in neat alcohol, any singlet carbene that is formed must react with neat alcohol faster than it can undergo Wolff rearrangement.

90.4 Role of Conformation

Several studies have indicated that the conformation of the diazo precursor plays a critical role in the pathway of the Wolff rearrangement. Kaplan and co-workers were the first to demonstrate that diazocarbonyl compounds exist as an equilibrium mixture of *syn* and *anti* forms and that concerted rearrangement

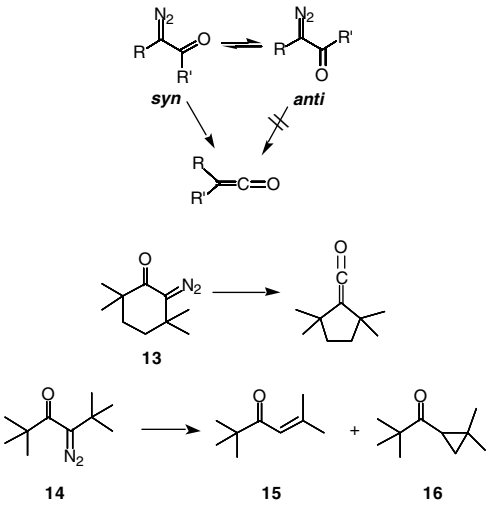

SCHEME 6

is facile from the *syn* conformation, but less likely in the *anti* form (Scheme 6).[90,91] They found that photolysis of 3,3,6,6-tetramethyl-2-diazocyclo-1-hexanone (**13**), which is locked in the *syn* conformation, leads almost exclusively to the Wolff rearrangement product. On the other hand, photolysis of 2,2,5,5-tetramethyl-4-diazo-3-hexanone (**14**), which exists predominantly in the *anti* conformation, produces no ketene.[92] Instead, only carbene derived products, mainly **15** and **16**, are obtained (Scheme 6)

In general, Kaplan and co-workers found that the *syn* form is highly preferred in alkyl diazoketones, but that the *syn* and *anti* forms are present in approximately equal amounts in the case of diazoacetic esters.[90,91] These conformational preferences might be the underlying reason that intermolecular carbene chemistry is much more prevalent in carbene esters than in simple ketocarbenes.[1–5,93]

Tomioka and co-workers expanded on Kaplan's work in their investigation of a series of compounds, including diazoketones **17** and **18**, which exist predominantly in the *syn* conformation.[94] Direct photolysis of these compounds in methanol results almost exclusively in Wolff rearrangement-derived products. However, triplet-sensitized photolysis results in a significant decrease in Wolff rearrangement along with the appearance of carbene-derived products. These results support Kaplan's hypothesis that diazocarbonyl conformation is preserved in the singlet excited state and that rearrangement occurs in concert with nitrogen loss from the *syn* conformer.

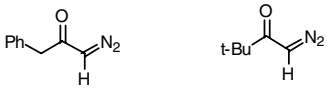

90.5 Spectroscopic Studies of Intermediates Involved in the Wolff Rearrangement

TRUV-VIS spectroscopy is an established method that has been routinely applied to the study of carbene chemistry.[95–100] Obviously, to study an intermediate of interest by absorption spectroscopy, it must possess a useful chromophore in the UV-VIS region. To study spectroscopically "invisible" carbenes, Platz and co-workers introduced the pyridine-ylide probe methodology.[48,101] Here, carbenes without useful absorptions react with probes such as pyridine to form strongly absorbing ylides from which kinetic data can be derived.[48,100,101]

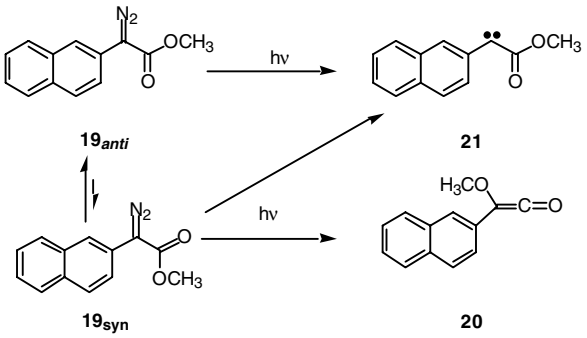

SCHEME 7

Recently, TRUV-VIS studies have made significant contributions to understanding the chemistry of carbonylcarbenes and to clarifying the mechanism of the Wolff rearrangement.[93] Aromatic substituents adjacent to the carbene center significantly prolong the carbene lifetime. For example, phenylcarbomethoxycarbene[102] has a lifetime of 461 ns and 2-naphthyl(carbomethoxy)carbene[103] has a lifetime of 2.2 μs in Freon-113 (1,1,2-tricloroflurоethane). On the other hand, non-aryl carbenes, such as carboethoxycarbene,[104] dicarbomethoxycarbene[105] and its mono- and di-sulfur analogues,[106] and simple ketocarbenes,[107] have lifetimes of only several nanoseconds in the same solvent.

TRUV-VIS studies have also provided evidence to support the role of conformation in the rearrangement reaction.[93] For example, a series of simple diazoketones $RCON_2H$, where R = H, Me, *i*-Pr, and *t*-Bu, has been examined by laser flash photolysis methods[107] and also by picosecond transient grating spectroscopy.[108] Within this series, as the steric bulk of R increases, the extent of the *anti* diazoketone conformer present at equilibrium decreases relative to the *syn* conformer. Consistent with a direct rearrangement pathway leading to ketene via only the *syn* conformer, the amount of trappable carbene intermediate decreases as R becomes more bulky.

The role of diazocarbonyl precursor conformation has also been addressed recently by nanosecond TRIR methods with which the kinetics of the rearrangement process can be monitored directly.[109,110] When excited-state contributions are important, the ketene growth rate will be unresolvable on the nanosecond timescale (assuming a diazocarbonyl excited-state lifetime beyond the time resolution [50 ns] of the TRIR experiments performed). Thus, ketene production from only an excited state is indicated by a fast, unresolvable increase in ketene IR absorbance following laser photolysis. Production only from a relaxed carbene intermediate, on the other hand, would be revealed by a rate of ketene growth equal to that of carbene decay. For diazoester **19**, the observed rate of ketene growth is equal to the rate of carbene decay, clearly demonstrating that ketene **20** arises entirely from carbene **21** (Scheme 7).

This result is in excellent agreement with the alcohol-trapping experiments of Platz and co-workers,[103] who isolated essentially only carbene-derived adducts and with the calculations of Zhu et al.[111] Those calculations indicated that diazoester **19** is planar and exists almost entirely (99%) in conformations in which the diazo and carbonyl groups are *anti*. Thus, the preferred conformation of **19** leads to efficient carbene production upon photolysis with very little, if any, direct rearrangement to ketene **20**.

The lack of excited state involvement for **21** is in contrast to the behavior in systems that have substantial equilibrium concentrations of the *syn* conformer. To examine the effect that conformation has on ketene growth kinetics, 4-diazo-3-isochromanone (**22**),[109] a cyclic analogue (phenyl version) of **21** that is locked in the *syn* conformation, was also recently studied by TRIR spectroscopy. In this case, a carbene IR band is observed at 1686 cm^{-1} that decays with a lifetime of 526 ± 50 ns in Freon-113. The ketene IR band at 2116 $cm,^{-1}$ however, in dramatic contrast to the data observed with acyclic diazocarbonyl **21**, is produced faster than the experimental time resolution. Ketene **24,** therefore, is formed entirely from a non-carbene source, presumably the excited state of **22** (Scheme 8). In agreement with this hypothesis, oxygen and methanol quench carbene **23**, but they leave the initial intensity of the ketene IR band unaffected. These

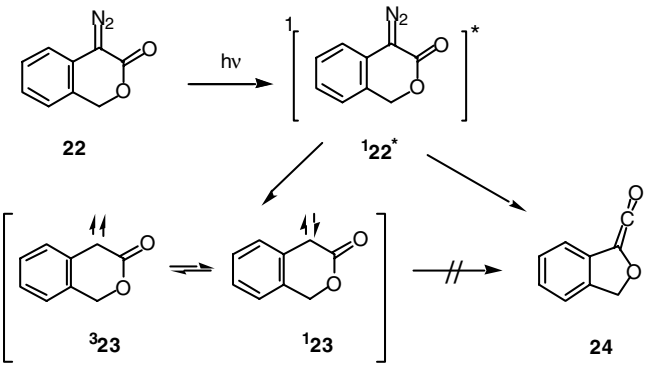

SCHEME 8

results are consistent with other photochemical studies of **19** and the related diazo-naphthoquinones **25**[112,113] and **26.**[114]

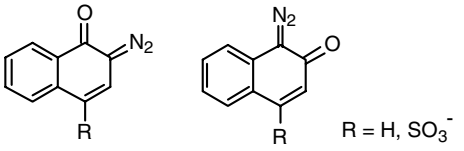

The photoinduced Wolff rearrangement of 5-diazo-1,3-dioxan-4,6-dione has also been examined by TRIR methods.[115] These ultrafast measurements, conducted in a PMMA matrix, revealed that the formation of the ketene rearrangement product was complete within 20 ps; a carbonylcarbene was not detected in this study.

Due to the complication of alternate pathways involved in the photochemistry of diazo compounds or diazirines, new strategies for carbene generation from non-nitrogenous precursors have been studied. Phenyliodonium ylides[116] (**27**) and methyl-8-chloro-3a,7a-methanoindan-8-carboxylates[117] (**28**) are alternative precursors to dicarboethoxycarbene and carbomethoxychlorocarbene, respectively. Photoreactions from these precursors presumably will not be plagued by the excited-state chemistry observed for the diazo compounds and diazirines.

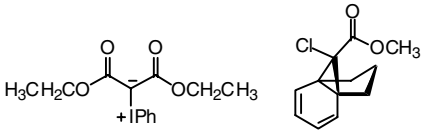

90.6 Computational Studies of the Intermediates Involved in the Wolff Rearrangement

The intermediates involved in the Wolff rearrangement have also been probed computationally. Whether oxirene is a real minimum or a transition state on the potential energy surface is extremely sensitive to the theoretical method used. Schaefer, Radom, and co-workers have calculated the C_2H_2O potential

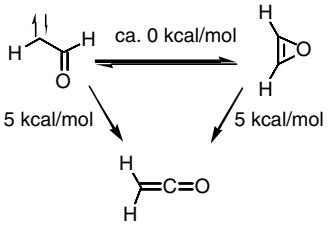

SCHEME 9

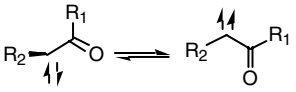

SCHEME 10

energy surface, which includes formylmethylene, oxirene, and ketene, at several levels of *ab initio* theory.[118,119] At their highest level of theory (CCSD(T)/ccpVTZ or CCSD(T)fc/TZ2P(f,d)), they found that there is little or no barrier separating singlet formylmethylene and oxirene, but that both of these intermediates must pass over a 5-kcal mol^{-1} energy barrier to form ketene (Scheme 9). A more recent computational study using density functional theory,[120] on the other hand, predicts oxirene to be a transition state using the B3LYP or the B97-1 hybrid functionals. However, with the B97-2 hybrid functional, oxirene is predicted to be a minimum with formylmethylene 2.1 kcal mol^{-1} lower in energy than oxirene. The Wolff rearrangement barrier is predicted to be 2.9 kcal mol^{-1}.

More recently, Scott, Platz, and Radom have performed *ab initio* calculations on a series of carbonylcarbenes at the G3(MP2)//B3LYP level of theory.[121] In contrast to formylcarbene, carbohydroxycarbene, and carbomethoxycarbene, they predict that chloro- and fluoro-substituted carbonylcarbenes have singlet ground states and that the carbomethoxychlorocarbene will have a singlet-triplet splitting of −3.82 kcal mol^{-1}. (A negative sign indicates that the singlet is of lower energy.) They also predict that the barrier to Wolff rearrangement for the chloro- and fluoro-substituted cases is between 14 and 18 kcal mol^{-1} compared to 2.4 to 7.2 kcal mol^{-1} for the parent carbonylcarbene.

90.7 Solvent and Substituent Effects on the Singlet–Triplet Energy Gap

Calculations[118,119] predict that the triplet states of simple carbonylcarbenes exist in planar conformations while the lowest-lying singlet state is nonplanar with a closed shell configuration (Scheme 10). This orthogonal orientation of the singlet allows donation of the in-plane oxygen lone pair of the carbonyl group to the empty p orbital of the carbene center. In addition, this arrangement also allows the filled σ^2 orbital of the carbene to be in conjugation with the π–system of the carbonyl group. These electron interactions dramatically lower the singlet energy and the singlet–triplet splitting relative to carbenes without adjacent carbonyl groups. Several factors, such as substituent[122–125] and solvent effects,[126] can influence the singlet–triplet splitting and consequently the carbene reactivity.

One complication in the study of carbonylcarbenes is that they generally have a triplet ground state, but the chemistry of the Wolff rearrangement occurs on the singlet surface. As discussed, calculations[121] predict that carbomethoxychlorocarbene possesses a singlet ground state due to the stabilization of the singlet carbene by chlorine subtitution.[127–132] The Wolff rearrangement of this carbene, therefore, is not complicated by the surface crossings required by other triplet ground-state carbonylcarbenes. In agreement with these calculations, carbomethoxychlorocarbene generated in a low-temperature matrix was observed to have a singlet ground state and its rearrangement chemistry has been examined.[117]

Bally, McMahon, and co-workers have recently reported thorough low-temperature spectroscopic and computational studies of the singlet and triplet states of carbene **21**.[111] Very interestingly, they observe reversible interconversion of ^{1}**21** and ^{3}**21** in argon matrices. The barrier between the two spin states is presumably due to the pronounced change in conformation of the carbomethoxy group and may be enhanced in a solid matrix environment.

The solvent dependence of the singlet–triplet energy gap (ΔG_{ST}) for carbene **21** has recently been examined by TRIR spectroscopy and computational methods.[126] The TRIR experiments suggest that ^{3}**21** is favored enthalpically in hexane, but that the singlet is favored in acetonitrile. The preferential stabilization of the singlet carbene is the result of its increased dipole moment in polar solvents and is consistent with the zwitterionic nature of singlet carbenes. The magnitude of the observed solvent effect (approximately 1 kcal mol^{-1}) is comparable to that observed experimentally[133–136] and computationally[137–140] for other carbene systems. Variable-temperature TRIR experiments provide estimates of ΔH_{ST} and ΔS_{ST}, and suggest that solvent and geometrical effects on the entropy of singlet and triplet carbenes can offset the entropic differences arising from spin multiplicity. Density functional calculation using the polarizable continuum solvation model reproduces the general trends in enthalpic differences observed experimentally.[126]

The effects of aromatic substitution on the singlet–triplet gap of substituted phenyl(carbomethoxy)carbene have also been examined by TRIR and computational methods.[123] The *p*-nitro analogue is predicted to have a triplet ground state with a $\Delta G_{ST} = 6.1$ kcal mol^{-1} and the *p*-amino analogue is predicted to have a singlet ground state with $\Delta G_{ST} = -2.8$ kcal mol^{-1}. Predictions of $\Delta G_{ST} = -3.9$ and 1.6 kcal mol^{-1} in the gas phase for the *p*-methoxy and *p*-methyl cases, respectively, have also been made. To model the effects of solvent on the splitting energy, the polarizable continuum model (PCM) was used and predicts ΔG_{ST} of −3.9 and 1.3 kcal mol^{-1}, respectively, in acetonitrile. No solvent perturbations were observed in the TRIR spectra for the parent and *p*-dimethylamino cases, which is consistent with the ground state lying greater than ±2 kcal mol^{-1} from the next electronic state as predicted by the above calculations. Solvent perturbations, however, were observed in the TRIR spectra of the *p*-methoxy and *p*-methyl cases, which is consistent with their ground states lying less than ±1 kcal mol^{-1} away from the next available electronic states. All of these results are consistent with the expected effects of substitution on the benzylic stabilization of carbenes.

90.8 Conclusions

Recent studies of α-diazocarbonyls have helped to clarify their chemistry and have confirmed previous hypotheses concerning the mechanism of the Wolff rearrangement. Clearly, it has been shown that the reaction is mediated in the singlet manifold and that the conformation of the diazocarbonyl precursor has a very significant effect on the resulting photochemistry. It is interesting to note that a reaction discovered at the beginning of the last century is still receiving attention and stimulating new experiments, even at the dawning of a new century.

References

1. Rodina, L.L., and Korobitsyna, I.K., Wolff Rearrangement, *Usp. Khim.*, 36, 611, 1967.
2. Kirmse, W., *Carbene Chemistry 2nd ed.*, Academic Press, New York, 1971.
3. Baron, W.J., DeCamp, M.R., Hendrick, M.E., Jr., M.J., Levin, R.H., and Sohn, M.B., in *Carbenes*, Vol. 1, Jones, M.J. and Moss, R.A., Eds., 1973, 4.
4. Marchand, A.P. and Brockway, N.M., Carbalkoxycarbenes, *Chem. Rev.*, 74, 431, 1974.
5. Meier, H. and Zeller, K.P., Wolff Rearrangement of α-Diazo Carbonyl Compounds, *Angew. Chem. Int. Ed. Engl.*, 14, 32, 1975.
6. March, J., Advanced Organic Chemistry: Reactions, Mechanisms and Structure, 4th ed., Wiley-Interscience, New York, 1992.
7. Pitters, J.L., Griffiths, K., Kovar, M., Norton, P.R., and Workentin, M.S., Reactive Intermediates on Metal Surfaces: A Ketene Monolayer on Single Crystal Platinum Generated by Photolysis of Pyridyl α-Diazo Ketones, *Angew. Chem. Int. Ed. Engl.*, 39, 2144, 2000.

8. Redmore, D. and Gutsche, C.D., Carbocyclic Ring Contraction Reactions, *Adv. Alicyclic Chem.*, 3, 1, 1971.
9. Wentrup, C., Heilmayer, W., and Kollenz, G., α-Oxo Ketenes - Preparation and Chemistry, *Synthesis*, 1219, 1994.
10. Kabir, S.H., Seikaly, H.R. and Tidwell, T.T., Acid-Catalyzed Hydration of Di-*tert*-Butylketene, *J. Am. Chem. Soc.*, 101, 1059, 1979.
11. Tidwell, T.T., Alkylation and Silylation of Directed Enolates from Diethylketene and Organometallic Reagents, *Tetrahedron Lett.*, 4615, 1979.
12. Tidwell, T.T., Ketene Chemistry: The Second Golden Age, *Acc. Chem. Res.*, 23, 273, 1990.
13. Oehlers, C., Temps, F., Wagner, H.G., and Wolf, M., Kinetics of the Reaction of Hydroxyl Radicals with Ketene [CH_2CO], *Ber. Bunsen-Ges. Phys. Chem.*, 96, 171, 1992.
14. Wallington, T.J., Ball, J.C., Straccia, A.M., Hurley, M.D., Kaiser, E.W., Dill, M., Schneider, W.F., and Bilde, M., Kinetics and Mechanism of the Reaction of Cl Atoms with CH_2CO (Ketene), *Int. J. Chem. Kinet.*, 28, 627, 1996.
15. Huang, W.-W., Henry-Riyad, H., and Tidwell, T.T., Reactions of the "Stable" Nitroxyl Radical TEMPO with Ketenes: Formation of a Unique Peroxidic Source of Aminyl Radicals, *J. Am. Chem. Soc.*, 121, 3939, 1999.
16. Carter, J., Fenwick, M.H., Huang, W.-W., Popik, V.V., and Tidwell, T.T., Addition of the Nitroxyl Radical TEMPO to 1-Naphthylketene: Formation of an Unusual Adduct, *Can. J. Chem.*, 77, 806, 1999.
17. Allen, A.D., Cheng, B., Fenwick, M.H., Givehchi, B., Henry-Riyad, H., Nikolaev, V.A., Shikhova, E.A., Tahmassebi, D., Tidwell, T.T., and Wang, S., Ketene Reactions with the Aminoxyl Radical TEMPO: Preparative, Kinetic and Theoretical Studies, *J. Org. Chem.*, 66, 2611, 2001.
18. Woodward, R.B. and Hoffmann, R. *The Conservation of Orbital Symmetry*; Academic Press, New York, 1970.
19. Sung, K. and Tidwell, T.T., Theoretical Study of the Reactivity of Ketene with Free Radicals, *J. Org. Chem.*, 63, 9690, 1998.
20. Allen, A.D., Fenwick, M.F., Henry-Riyad, H., and Tidwell, T.T., Nitroxyl Radical Reactions with 4-Pentenyl- and Cyclopropylketenes: New Routes to 5-Hexenyl- and Cyclopropylmethyl Radicals, *J. Org. Chem.*, 66, 5759, 2001.
21. Allen, A.D., Fenwick, M.H., Jabri, A., Rangwala, H., Saidi, K., and Tidwell, T.T., Generation, Observation and Free Radical Reactivity of Aliphatic Bisketenes: The Solution to a Long-Standing Problem, *Org. Lett.*, 3, 4095, 2001.
22. Leigh, W.J., Kerst, C., Boukherroub, R., Morkin, T.L., Jenkins, S.I., Sung, K., and Tidwell, T.T., Substituent Effects on the Reactivity of the Silicon-Carbon Double Bond. Substituted 1,1-Dimethylsilenes from Far-UV Laser Flash Photolysis of α-Silylketenes and (Trimethylsilyl)Diazomethane, *J. Am. Chem. Soc.*, 121, 4744, 1999.
23. Morkin, T.L., Leigh, W.J., Tidwell, T.T., and Allen, A.D., Direct Detection of Wiberg's Silene (1,1-Dimethyl-2,2-Bis(Trimethylsilyl)Silene) and Absolute Rate Constants for Its Reactions in Solution, *Organometallics*, 20, 5707, 2001.
24. Reiser, A., *Photoreactive Polymers: The Science and Technology of Resists*, Wiley, New York, 1989.
25. Reichmanis, E., Frank, C.W., and O'Donnell, J.H., *Irradiation of Polymeric Materials: Processes, Mechanisms and Applications*, American Chemical Society, Washington, D.C., 1993.
26. Nakatani, K., Isoe, S., Maekawa, S., and Saito, I., Photoinduced DNA Cleavage by Designed Molecules with Conjugated Ene-Yne-Ketene Functionalities, *Tetrahedron Lett.*, 35, 605, 1994.
27. Nakatani, K., Maekawa, S., Tanabe, K., and Saito, I., α-Diazo Ketones as Photochemical DNA Cleavers: A Mimic for the Radical Generating System of Neocarzinostatin Chromophore, *J. Am. Chem. Soc.*, 117, 10635, 1995.
28. Nakatani, K., Shirai, J., Sando, S., and Saito, I., Guanine Specific DNA Cleavage by Photoirradiation of Dibenzoyldiazomethane-Oligonucleotide Conjugates, *J. Am. Chem. Soc.*, 119, 7626, 1997.
29. Tidwell, T.T., *Ketenes*, Wiley, New York, 1995.

30. De Lucas, N.C., Andraos, J., Netto-Ferreira, J.C., and Scaiano, J.C., Laser Flash Photolysis Study of the Reactivity of α-Ketenylbenzocyclobutenone with Water and Alcohols, *Tetrahedron Lett.*, 36, 677, 1995.
31. Andraos, J. and Kresge, A.J., Flash Photolytic Generation and Study of Ketenes: Acid-Catalyzed Hydration in Aqueous Solution, *J. Photochem. Photobiol., A: Chem.*, 57, 165, 1991.
32. Jones, M., Jr. and Kresge, A.J., Flash Photolytic Generation and Reactivity of Phenyl(Methylthio)Ketene in Aqueous Solution, *J. Org. Chem.*, 57, 6467, 1992.
33. Jefferson, E.A., Kresge, A.J., and Paine, S.W., Acid-Catalyzed Hydrolysis of 4-Diazoisothiochroman-3-One. Comparison with the Acyclic Analog and the Corresponding Oxygen System, *Can. J. Chem.*, 75, 56, 1997.
34. Chiang, Y., Jefferson, E.A., Kresge, A.J., and Popik, V.V., Flash Photolytic Investigation of 4-Diazoisothiochroman-3-One in Aqueous Solution: Observation of a Short-Lived Carboxylic Acid Enol, *J. Am. Chem. Soc.*, 121, 11330, 1999.
35. Chiang, Y., Kresge, A.J., Pruszynski, P., Schepp, N.P., and Wirz, J., Mandelic Acid Enols: Determination of the Acidity in Aqueous Solutions and Estimation of Keto-Enol Equilibrium Constants and CH Acidity of Mandelic Acid, *Angew. Chem.*, 102, 810, 1990.
36. Chiang, Y., Kresge, A.J., Popik, V.V., and Schepp, N.P., The Mandelic Acid Keto-Enol System in Aqueous Solution. Generation of the Enol by Hydration of Phenylhydroxyketene and Phenylcarboxycarbene, *J. Am. Chem. Soc.*, 119, 10203, 1997.
37. Andraos, J., Chiang, Y., Kresge, A.J., Pojarlieff, I.G., Schepp, N.P., and Wirz, J., The α-Cyano-α-Phenylacetic Acid Keto-Enol System. Flash Photolytic Generation of the Enol in Aqueous Solution and Determination of the Keto-Enol Equilibrium Constants and Acid Dissociation Constants Interrelating All Keto and Enol Forms in that Medium, *J. Am. Chem. Soc.*, 116, 73, 1994.
38. Chiang, Y., Kresge, A.J., Prusynski, P., Schepp, N.P., and Wirz, J., Mandelic acid enols: Determinations of the acidity in aqueous solutions and estimation of keto enol equilibrium constants and C-H acidity of mandelic acid, *Angew. Chem. Int. Ed. Engl.,* 29, 792, 1990.
39. Allen, A.D. and Tidwell, T.T., Kinetics and Mechanism of Hydration of Alkyl Ketenes, *J. Am. Chem. Soc.*, 109, 2774, 1987.
40. Allen, A.D., Kresge, A.J., Schepp, N.P., and Tidwell, T.T., Hydration Reactivity of Ketenes Generated by Flash Photolysis, *Can. J. Chem.*, 65, 1719, 1987.
41. Allen, A.D., Stevenson, A., and Tidwell, T.T., Hydration Reactivity of Persistent Conjugated Ketenes, *J Org. Chem.*, 54, 2843, 1989.
42. Cava, M.P. and Spangler, R.J., 2-(Carbomethoxy)Benzocyclobutenone. Synthesis of a Photochemically Sensitive Small-Ring System by a Pyrolytic Wolff Rearrangement, *J. Am. Chem. Soc.*, 89, 4550, 1967.
43. Banks, J.T. and Scaiano, J.C., Laser Drop and Low Intensity Photolysis of 2-Diazo-1,3-Indandione: Evidence for a Propadienone Intermediate, *J. Photochem. Photobiol., A: Chem.*, 96, 31, 1996.
44. Banks, J.T. and Scaiano, J.C., The Laser-Drop Method: A New Approach to Induce Multiple Photon Chemistry with Pulsed Lasers. Examples Involving Reactions of Diphenylmethyl and Cumyloxyl Radicals, *J. Am. Chem. Soc.*, 115, 6409, 1993.
45. De Lucas, N.C., Netto-Ferreira, J.C., Lusztyk, A.J., Wagner, B.D., and Scaiano, J.C., Reactivity of Fluorenylideneketene towards Amines. A Laser Photolysis Study with Ultraviolet and Infrared Detection, *Tetrahedron Lett.*, 38, 5147, 1997.
46. De Lucas, N.C., Netto-Ferreira, J. C. Andraos, J., and Scaiano, J.C., Nucleophilicity toward Ketenes: Rate Constants for Addition of Amines to Aryl Ketenes in Acetonitrile Solution, *J. Org. Chem.*, 66, 5016, 2001.
47. Wagner, B.D., Arnold, B.R., Brown, G.S., and Lusztyk, J., Spectroscopy and Absolute Reactivity of Ketenes in Acetonitrile Studied by Laser Flash Photolysis with Time-Resolved Infrared Detection, *J. Am. Chem. Soc.*, 120, 1827, 1998.
48. Platz, M.S., Modarelli, D.A., Morgan, S., White, W.R., Mullins, M., Celebi, S., and Toscano, J.P., Lifetimes of Alkyl- and Dialkylcarbenes in Solution, *Prog. React. Kinet.*, 19, 93, 1994.

49. Allen, A.D. and Tidwell, T.T., Amination of Ketenes: Kinetic and Mechanistic Studies, *J. Org. Chem.*, 64, 266, 1999.
50. Raspoet, G., Nguyen, M.T., Kelly, S., and Hegarty, A.F., Amination of Ketenes: Evidence for a Mechanism Involving Enols of Amides as Intermediates, *J. Org. Chem.*, 63, 9669, 1998.
51. Sung, K. and Tidwell, T.T., Amination of Ketene: A Theoretical Study, *J. Am. Chem. Soc.*, 120, 3043, 1998.
52. Barton, T.J. and Groh, B.L., Thermal Extrusion of Dimethylsilanone from (Hydridosilyl)Ketenes. A Retro-Wolff Rearrangement, *J. Am. Chem. Soc.*, 107, 7221, 1985.
53. Barton, T.J. and Paul, G.C., Silathione (Me_2Si:S) Extrusion in the Thermolysis of Silylthioketenes, *J. Am. Chem. Soc.*, 109, 5292, 1987.
54. Lovejoy, E.R., Kim, S.K., Alvarez, R.A., and Moore, C.B., Kinetics of Intramolecular Carbon Atom Exchange in Ketene, *J. Chem. Phys.*, 95, 4081, 1991.
55. Lovejoy, E.R. and Moore, C.B., Structures in the Energy Dependence of the Rate Constant for Ketene Isomerization, *J. Chem. Phys.*, 98, 7846, 1993.
56. Qiao, G.G., Meutermans, W., Wong, M.W., Traeubel, M., and Wentrup, C., (Cyanovinyl)Ketenes from Azafulvenones. An Apparent Retro-Wolff Rearrangement, *J. Am. Chem. Soc.*, 118, 3852, 1996.
57. Moore, C.B., Spiers Memorial Lecture. State-Resolved Studies of Unimolecular Reactions, *Faraday Disc.*, 102, 1, 1995.
58. Rando, R.R., Conformational and Solvent Effects on Carbene Reactions, *J. Am. Chem. Soc.*, 92, 6706, 1970.
59. Rando, R.R., Conformational and Medium Effects on Intramolecular Carbene Reactions, *J. Am. Chem. Soc.*, 94, 1629, 1972.
60. Wulfman, D.S., Poling, B., and McDaniel, R.S., Jr., Metal Salt Catalyzed Carbenoids. X. Mechanisms of the Photochemical Reaction of Dimethyl Diazomalonate with Cyclohexene and Methylcyclohexene as a Function of Temperature, *Tetrahedron Lett.*, 4519, 1975.
61. Tomioka, H., Kitagawa, H., and Izawa, Y., Photolysis of N,N-Diethyldiazoacetamide. Participation of a Noncarbenic Process in Intramolecular Carbon-Hydrogen Insertion, *J. Org. Chem.*, 44, 3072, 1979.
62. Torres, M., Lown, E.M., Gunning, H.E., and Strausz, O.P., 4n π Electron Antiaromatic Heterocycles, *Pure Appl. Chem.*, 52, 1623, 1980.
63. Lewars, E.G., Oxirenes, *Chem. Rev.*, 83, 519, 1983.
64. Sander, W., Bucher, G., and Wierlacher, S., Carbenes in Matrixes: Spectroscopy, Structure and Reactivity, *Chem. Rev.*, 93, 1583, 1993.
65. Maier, G. and Reisenauer, H.P., Carbenes in Matrices: Spectroscopy, Structure and Photochemical Behavior, *Advances in Carbene Chemistry*, 3, 115, 2001.
66. Trozzolo, A.M., Electronic Spectroscopy of Arylmethylenes, *Acc. Chem. Res.*, 1, 329, 1968.
67. Hutton, R.S. and Roth, H.D., Electron Paramagnetic Resonance Spectra of Carbalkoxycarbenes. Geometric Isomerism in Ground-State Triplets, *J. Am. Chem. Soc.*, 100, 4324, 1978.
68. Murai, H., Torres, M., and Strausz, O.P., A Quintet-State Triplet-Triplet Radical Pair, *J. Am. Chem. Soc.*, 102, 5104, 1980.
69. Murai, H., Ribo, J., Torres, M., and Strausz, O.P., Perfluoroacetylmethylmethylene and Its Quintet Radical Pair: Isolation and ESR Detection, *J. Am. Chem. Soc.*, 103, 6422, 1981.
70. Torres, M., Safarik, I., Murai, H., and Strausz, O.P., Detection of Keto-, Thioxo- and Iminocarbenes and the Quintet State Triplet-Triplet Ketocarbene Radical Pairs, *Rev. Chem. Intermed.*, 7, 243, 1986.
71. Hayes, R.A., Hess, T.C., McMahon, R.J., and Chapman, O.L., Photochemical Wolff Rearrangement of a Triplet Ground State Carbene, *J. Am. Chem. Soc.*, 105, 7786, 1983.
72. McMahon, R.J., Chapman, O.L., Hayes, R.A., Hess, T.C., and Krimmer, H.P., Mechanistic Studies on the Wolff Rearrangement: The Chemistry and Spectroscopy of Some α-Keto Carbenes, *J. Am. Chem. Soc.*, 107, 7597, 1985.
73. Murata, S., Ohtawa, Y., and Tomioka, H., Matrix Studies of the Photolysis of (O-Carbomethoxyphenyl)Diazomethane. Direct Observation of Carbonyl Ylide and Its Photoinduced Valence Tautomerization, *Chem. Lett.*, 853, 1989.

74. Torres, M., Clement, A., and Strausz, O.P., Low-Temperature Photolysis of Diazoketones: The Conformational Isomerism of Benzoylphenylmethylene and the IR Spectrum of Anthronylidene, *Res. Chem. Intermed.*, 13, 1, 1990.
75. Bucher, G. and Sander, W., Direct Observation of the Cyclopropene-Vinylcarbene Rearrangement. Matrix Isolation of Bicyclo[3.1.0]Hexa-3,5-Dien-2-Ones, *J. Org. Chem.*, 57, 1346, 1992.
76. Thornton, D.E., Gosavi, R.K., and Strausz, O.P., Mechanism of the Wolff Rearrangement. II, *J. Am. Chem. Soc.*, 92, 1768, 1970.
77. Csizmadia, I.G., Font, J., and Strausz, O.P., Mechanism of the Wolff Rearrangement, *J. Am. Chem. Soc.*, 90, 7360, 1968.
78. Frater, G. and Strausz, O.P., Mechanism of the Wolff Rearrangement III, *J. Am. Chem. Soc.*, 92, 6654, 1970.
79. Zeller, K.P., Thermal and Photochemical Nitrogen Cycloelimination, *Angew. Chem. Int. Ed. Engl.*, 11, 781, 1977.
80. Matlin, S.A. and Sammes, P.G., Oxocarbene-Oxirene Equilibrium, *J. Chem. Soc., Chem. Commun.*, 11, 1972.
81. Tomioka, H., Okuno, H., Kondo, S., and Izawa, Y., Direct Evidence for Ketocarbene-Ketocarbene Interconversion, *J. Am. Chem. Soc.*, 102, 7123, 1980.
82. Torres, M., Bourdelande, J.L., Clement, A., and Strausz, O.P., Argon-Matrix Isolation of Bis(Trifluoromethyl)Oxirene, Perfluoromethylethyloxirene and Their Isomeric Ketocarbenes, *J. Am. Chem. Soc.*, 105, 1698, 1983.
83. Tanigaki, K. and Ebbesen, T.W., Dynamics of the Wolff Rearrangement of Six-Membered Ring O-Diazoketones by Laser Flash Photolysis, *J. Phys. Chem.*, 93, 4531, 1989.
84. Barra, M., Fisher, T.A., Cernigliaro, G.J., Sinta, R., and Scaiano, J.C., On the Photodecomposition Mechanism of O-Diazonaphthoquinones, *J. Am. Chem. Soc.*, 114, 2630, 1992.
85. Laganis, E.D., Janik, D.S., Curphey, T. J., and Lemal, D.M., Photochemistry of Perfluoro-3diazo-2-butanone, *J. Am. Chem. Soc.*, 105, 7457, 1983.
86. Debu, F., Monnier, M., Verlaque, P., Davidovics, G., Pourcin, J., Bodot, H., and Aycard, J. P., Photolysis of 3Diazo-2-butanone Isolated in Rare Gas Matrices; Evidence and Identification of Dimethyloxirene, *C.R. Acad. Sci., Ser. 2*, 303, 897, 1986.
87. Bachmann, C., N'Guessan, T.Y., Debu, F., Monnier, M., Pourcin, J., Aycard, J.P., and Bodot, H., Oxirenes and Ketocarbenes from α-Diazoketone Photolysis: Experiments in Rare Gas Matrices. Relative Stabilities and Isomerization Barriers from MNDOC-BWEN Calculations, *J. Am. Chem. Soc.*, 112, 7488, 1990.
88. Padwa, A. and Layton, R., Photochemical Decomposition of α-Diazoacetophenone in Hydroxylic Solvents, *Tetrahedron Lett.*, 2167, 1965.
89. Jones, M., Jr. and Ando, W., Formation of Cyclopropanes via the Photosensitized Decomposition of Aliphatic α-Diazo Ketones, *J. Am. Chem. Soc.*, 90, 2200, 1968.
90. Kaplan, F. and Meloy, G.K., Structure of Diazoketones. A Study of Hindered Internal Rotation, *J. Am. Chem. Soc.*, 88, 950, 1966.
91. Kaplan, F. and Mitchell, M.L., Conformational Control of Decomposition Paths of α-Diazoketones, *Tetrahedron Lett.*, 759, 1979.
92. Newman, M.S. and Arkell, A., Decomposition of a Hindered α-Diazo Ketone, *J. Org. Chem.*, 24, 385, 1959.
93. Toscano, J. P., Laser Flash Photolysis Studies of Carbonyl Carbenes, *Advances in Carbene Chemistry*, 2, 215, 1998.
94. Tomioka, H., Okuno, H., and Izawa, Y., Mechanism of the Photochemical Wolff Rearrangement. The Role of Conformation in the Photolysis of α-Diazo Carbonyl Compounds, *J. Org. Chem.*, 45, 5278, 1980.
95. Griller, D., Nazran, A.S., and Scaiano, J. C., Flash Photolysis Studies of Carbenes and Their Impact on the Skell-Woodworth Rules, *Tetrahedron*, 41, 1525, 1985.

96. Schuster, G.B., Structure and Reactivity of Carbenes Having Aryl Substituents, *Adv. Phys. Org. Chem.*, 22, 311, 1986.
97. Moss, R.A. and Turro, N.J., Laser Flash Photolytic Studies of Arylhalocarbenes, *Kinet. Spectrosc. Carbenes Biradicals*, 213, 1990.
98. Platz, M.S. and Maloney, V.M., Laser Flash Photolysis Studies of Triplet Carbenes, *Kinet. Spectrosc. Carbenes Biradicals*, 239, 1990.
99. Moss, R.A., Absolute Kinetics of Intramolecular Alkylcarbene Reactions, *Advances in Carbene Chemistry*, 1, 59, 1994.
100. Jackson, J.E. and Platz, M.S., Laser Flash Photolysis Studies of Ylide-Forming Reactions of Carbenes, *Advances in Carbene Chemistry*, 1, 89, 1994.
101. Jackson, J.E., Soundararajan, N., Platz, M.S., and Liu, M.T.H., Pyridine Ylide Formation by Capture of Phenylchlorocarbene and *tert*-Butylchlorocarbene. Reaction Rates of an Alkylchlorocarbene by Laser Flash Photolysis, *J. Am. Chem. Soc.*, 110, 5595, 1988.
102. Fujiwara, Y., Tanimoto, Y., Itoh, M., Hirai, K., and Tomioka, H., Laser Flash Photolysis Studies of Methoxycarbonyl Phenyl Carbene and Its Derived Carbonyl Oxide at Room Temperature, *J. Am. Chem. Soc.*, 109, 1942, 1987.
103. Wang, J.L., Likhotvorik, I., and Platz, M.S., A Laser Flash Photolysis Study of 2-Naphthyl(Carbomethoxy)Carbene, *J. Am. Chem. Soc.*, 121, 2883, 1999.
104. Toscano, J.P., Platz, M.S., Nikolaev, V., and Popic, V., Carboethoxycarbene. A Laser Flash Photolysis Study, *J. Am. Chem. Soc.*, 116, 8146, 1994.
105. Wang, J.L., Toscano, J.P., Platz, M.S., Nikolaev, V., and Popik, V., Dicarbomethoxycarbene. A Laser Flash Photolysis Study, *J. Am. Chem. Soc.*, 117, 5477, 1995.
106. Snoonian, J.R. and Platz, M.S., The Photochemistry of Sulfur Analogues of Dialkyldiazomalonates, *J. Phys. Chem. A*, 104, 9276, 2000.
107. Toscano, J.P., Platz, M.S., and Nikolaev, V., Lifetimes of Simple Ketocarbenes, *J. Am. Chem. Soc.*, 117, 4712, 1995.
108. Toscano, J.P., Platz, M.S., Nikolaev, V., Cao, Y., and Zimmt, M.B., The Lifetime of Formylcarbene Determined by Transient Absorption and Transient Grating Spectroscopy, *J. Am. Chem. Soc.*, 118, 3527, 1996.
109. Wang, Y. and Toscano, J.P., Time-Resolved IR Studies of 4-Diazo-3-Isochromanone: Direct Kinetic Evidence for a Non-Carbene Route to Ketene, *J. Am. Chem. Soc.*, 122, 4512, 2000.
110. Wang, Y., Yuzawa, T., Hamaguchi, H., and Toscano, J. P., Time-Resolved IR Studies of 2-Naphthyl(Carbomethoxy)Carbene: Reactivity and Direct Experimental Estimate of the Singlet/Triplet Energy Gap, *J. Am. Chem. Soc.*, 121, 2875, 1999.
111. Zhu, Z., Bally, T., Stracener, L.L., and McMahon, R.J., Reversible Interconversion between Singlet and Triplet 2-Naphthyl(Carbomethoxy)Carbene, *J. Am. Chem. Soc.*, 121, 2863, 1999.
112. Andraos, J., Chiang, Y., Huang, C.G., Kresge, A.J., and Scaiano, J.C., Flash Photolytic Generation and Study of Ketene and Carboxylic Acid Enol Intermediates in Aqueous Solution, *J. Am. Chem. Soc.*, 115, 10605, 1993.
113. Oishi, S., Watanabe, Y., and Kuriyama, Y., Photodecomposition Mechanism of O-Diazonaphthoquinones Studied by Laser Flash Photolysis with Infrared Detection, *Chem. Lett.*, 2187, 1994.
114. Vleggaar, J.J.M., Huizer, A.H., Kraakman, P.A., Nijssen, W.P.M., Visser, R.J., and Varma, C.A.G.O., Photoinduced Wolff-Rearrangement of 2-Diazo-1-Naphthoquinones: Evidence for the Participation of a Carbene Intermediate, *J. Am. Chem. Soc.*, 116, 11754, 1994.
115. Lippert, T., Koskelo, A., and Stoutland, P.O., Direct Observation of a Photoinduced Wolff Rearrangement in Pmma Using Ultrafast Infrared Spectroscopy, *J. Am. Chem. Soc.*, 118, 1551, 1996.
116. Camacho, M.B., Clark, A.E., Liebrecht, T.A., and DeLuca, J.P., A Phenyliodonium Ylide as a Precursor for Dicarboethoxycarbene: Demonstration of a Strategy for Carbene Generation, *J. Am. Chem. Soc.*, 122, 5210, 2000.
117. Likhotvorik, I., Zhu, Z., Tae, E.L., Tippmann, E., Hill, B.T., and Platz, M.S., Carbomethoxychlorocarbene: Spectroscopy, Theory, Chemistry and Kinetics, *J. Am. Chem. Soc.*, 123, 6061, 2001.

118. Scott, A.P., Nobes, R.H., Schaefer, H.F., III, and Radom, L., The Wolff Rearrangement: The Relevant Portion of the Oxirene-Ketene Potential Energy Hypersurface, *J. Am. Chem. Soc.*, 116, 10159, 1994.
119. Vacek, G., Galbraith, J.M., Yamaguchi, Y., Schaefer, H.F., III, Nobes, R.H., Scott, A.P., and Radom, L., Oxirene: To Be or Not to Be?, *J. Phys. Chem.*, 98, 8660, 1994.
120. Wilson, P.J., and Tozer, D.J., A Kohn-Sham Study of the Oxirene-Ketene Potential Energy Surface, *Chem. Phys. Lett.*, 352, 540, 2002.
121. Scott, A.P., Platz, M.S., and Radom, L., Singlet-Triplet Splittings and Barriers to Wolff Rearrangement for Carbonyl Carbenes, *J. Am. Chem. Soc.*, 123, 6069, 2001.
122. Geise, C.M. and Hadad, C.M., Computational Study of the Electronic Structure of Substituted Phenylcarbene in the Gas Phase, *J. Org. Chem.*, 65, 8348, 2000.
123. Geise, C.M., Wang, Y., Mykhaylova, O., Frink, B.T., Toscano, J.P., and Hadad, C.M., Computational and Experimental Studies of the Effect of Substituents on the Singlet-Triplet Energy Gap in Phenyl(Carbomethoxy)Carbene, *J. Org. Chem.*, 67, 3079, 2002.
124. Tomioka, H., Okuno, H., and Izawa, Y., Carbenes in a Rigid Matrix. Substituent Effects on the Temperature Dependence of α-Carbonylcarbene Reactions, *J. Chem. Soc., Perkin Trans. 2*, 1636, 1980.
125. Tomioka, H., Hirai, K., Tabayashi, K., Murata, S., Izawa, Y., Inagaki, S., and Okajima, T., Neighboring Group Participation in Carbene Chemistry. Effect of Neighboring Carboxylate Group on Carbene Reactivities, *J. Am. Chem. Soc.*, 112, 7692, 1990.
126. Wang, Y., Hadad, C.M., and Toscano, J.P., Solvent Dependence of the 2-Naphthyl(Carbomethoxy)Carbene Singlet-Triplet Energy Gap, *J. Am. Chem. Soc.*, 124, 1761, 2002.
127. Carter, E.A. and Goddard, W.A., III, Correlation-Consistent Singlet-Triplet Gaps in Substituted Carbenes, *J. Chem. Phys.*, 88, 1752, 1988.
128. Shin, S.K., Goddard, W.A., III, and Beauchamp, J.L., Singlet-Triplet Energy Gaps in Chlorine-Substituted Methylenes and Silylenes, *J. Phys. Chem.*, 94, 6963, 1990.
129. Murray, K.K., Leopold, D.G., Miller, T.M., and Lineberger, W.C., Photoelectron Spectroscopy of the Halocarbene Anions: Fluorocarbene Ion(1-), Chlorocarbene Ion(1-), Bromocarbene Ion(1-), Iodocarbene Ion(1-), Difluorocarbene Ion(1-) and Dichlorocarbene Ion(1-) (HCF-, HCCl-, HCBr-, HCl-, CF_2- and CCl_2-), *J. Chem. Phys.*, 89, 5442, 1988.
130. Bucher, G., Scaiano, J.C., and Platz, M.S., in *Landolt-Bornstein*; Springer, Berlin, 1998; Vol. Group II, Vol.18, Subvolume E2.
131. Ge, C.S., Jang, E.G., Jefferson, E.A., Liu, W., Moss, R.A., Wlostowska, J., and Xue, S., The Kinetic Range of Carbene-Pyridine Ylide Forming Reactions, *J. Chem. Soc., Chem. Commun.*, 1479, 1994.
132. Moss, R.A., Dynamics of Intramolecular Carbenic Rearrangements, *Pure Appl. Chem.*, 67, 741, 1995.
133. Eisenthal, K.B., Turro, N.J., Aikawa, M., Butcher, J.A., Jr., DuPuy, C., Hefferon, G., Hetherington, W., Korenowski, G.M., and McAuliffe, M.J., Dynamics and Energetics of the Singlet-Triplet Interconversion of Diphenylcarbene, *J. Am. Chem. Soc.*, 102, 6563, 1980.
134. Sitzmann, E.V., Langan, J., and Eisenthal, K.B., Intermolecular Effects on Intersystem Crossing Studied on the Picosecond Timescale: The Solvent Polarity Effect on the Rate of Singlet-to-Triplet Intersystem Crossing of Diphenylcarbene, *J. Am. Chem. Soc.*, 106, 1868, 1984.
135. Langan, J.G., Sitzmann, E.V., and Eisenthal, K.B., Picosecond Laser Studies on the Effect of Structure and Environment on Intersystem Crossing in Aromatic Carbenes, *Chem. Phys. Lett.*, 110, 521, 1984.
136. Eisenthal, K.B., Turro, N.J., Sitzmann, E.V., Gould, I.R., Hefferon, G., Langan, J., and Cha, Y., Singlet-Triplet Interconversion of Diphenylmethylene. Energetics, Dynamics and Reactivities of Different Spin States, *Tetrahedron*, 41, 1543, 1985.
137. Khan, M.I. and Goodman, J.L., Picosecond Optical Grating Calorimetry of Singlet Methylene in Benzene, *J. Am. Chem. Soc.*, 117, 6635, 1995.
138. Moss, R.A., Yan, S., and Krogh-Jespersen, K., Modulation of Carbenic Reactivity by π-Complexation to Aromatics, *J. Am. Chem. Soc.*, 120, 1088, 1998.

139. Krogh-Jespersen, K., Yan, S., and Moss, R.A., *Ab Initio* Electronic Structure Calculations on Chlorocarbene-Ethylene and Chlorocarbene-Benzene Complexes, *J. Am. Chem. Soc.*, 121, 6269, 1999.
140. Ruck, R.T. and Jones, M., Jr., Solvent Perturbs the Reactivity of *tert*-Butylcarbene, *Tetrahedron Lett.*, 39, 2277, 1998.

91

Carbene Formation by Extrusion of Nitrogen

Aboel-Magd A. Abdel-Wahab
Assiut University

Saleh A. Ahmed
Assiut University

Heinz Dürr
Universität des Saarlandes

91.1 Introduction

The chemistry of reactive intermediates has always occupied a significant place in all branches of chemistry. Carbenes, as an example of these intermediates, have been the subject of many interesting studies concerning generation, reaction mechanism, selectivity, multiplicity, and even stability studies. It is no exaggeration to claim a major role for these fascinating species in the modern chemist's armory for the synthesis of a large number of interesting compounds.

In the past decade or so,[1,2] our understanding of carbene chemistry has advanced dramatically with the preparation of persistent triplet diarylcarbenes[3] and the isolation of heteroatom-substituted singlet carbenes.[4] From this and other work it is clear that the common statement that carbenes only occur as reactive intermediates is no longer valid. Stable carbenes have attracted little attention until quite recently, when two groups announced the discovery of phosphinocarbenes as a distillable red oil in 1988[5] and imidazo-2-ylidene as high-melting crystals in 1991.[6] However, these carbenes are stabilized by substituents with a heteroatom connected to the carbenic atom and thus have a singlet ground state.

Surprisingly, except for the article by Zimmerman and Paskovich in 1964 dealing with dimesitylcarbene,[7] no serious attempts to generate stable triplet carbenes appeared in the literature until the account in 1990 by Tomioka.[3]

The correct name of carbenes is obtained by attaching either the prefix "carbena" or the suffix "ylidene" to the name of the skeleton from which it is derived. Carbenes are neutral compounds with a divalent carbon atom with only six electrons in the valence shell and in which the two non-bonded electrons may be either paired (singlet) or unpaired (triplet). Considering the simple carbene –C:–, the carbon atom can be either linear or bent; each geometry is describable by a certain degree of hybridization. The linear geometry implies an sp-hybridized carbene center with two non-bonding degenerate orbitals (p_x and p_y). Bending the molecule breaks this degeneracy and the carbon atom adopts sp^2-hybridization. The p_y orbital (p_π) remains almost unchanged while the p_x orbital is stabilized because it acquires some s character.[1] The influence of substituents on the carbene ground-state multiplicity can easily be analyzed in terms of electronic and steric effects.[1] The multiplicity of the ground state of a carbene is related to the energy of the σ and p orbitals. The singlet ground state is favored by a large σ–p separation. Hoffman found that a value of at least 2 eV is necessary to impose a singlet ground state, whereas a value below 1. 5 eV leads to a triplet ground state.[1,8]

0-8493-1348-1/04/$0.00+$1.50

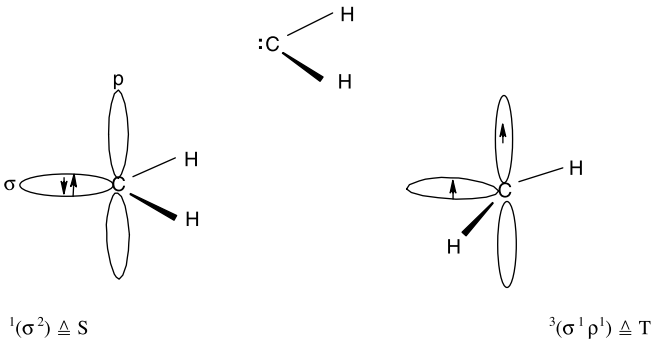

Singlet and triplet carbene

As illustrated above, a carbene can exist, in principle, as a singlet $^1(\sigma^2)$ or as a triplet $^3(\sigma^1 p^1)$ species.[8,9] Higher excited configurations are possible but do not play a major role in preparative experiments. Whereas triplet carbenes exhibit radical-like reactivity, singlet carbenes are expected to show nucleophilic as well as electrophilic behavior because of the lone pair and vacant orbital. Due to their electron deficiency, carbenes, in general, have only fleeting existence and usually behave as transient electrophilic intermediates. However, Wanzlick, after a long debate, was the first one to realize in the early 1960s that electron deficiency of the carbene center can be reduced by electron donation of the appropriate substituent (e.g., amino), resulting in stabilized and less-reactive carbenes with nucleophilic properties.[10] Since the description of stable carbenes by Bertrand and Arduengo, the exploration of their chemical reactivity both experimentally and theoretically has become a major area of current main group chemistry.

In 1991, Arduengo comprehensively characterized a stable, crystalline nucleophilic (singlet) carbene. Since then, numerous derivatives have been reported, including 1. More recently, in 1997, Tomioka isolated the persistent electrophilic triplet carbene 2.[3,11]

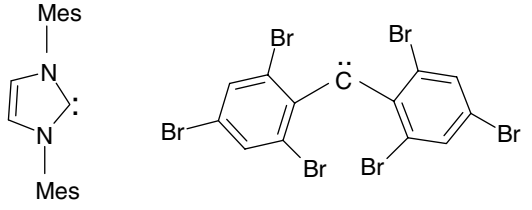

1 **2**

Theoretical approaches have been applied to understand the features that are responsible for the stability of imidazole (in)-2-ylidine. Density Functional theory (DFT) was applied in this respect.[12]

Studies examining the relationship between structure and reactivity have shown that thermodynamic stabilization (electronic conjugation effect) usually plays an important role in stabilizing the singlet state and it can become less reactive to such an extent that it can be isolated under ambient conditions.

On the other hand, kinetic stabilization (steric protection) is more effective in stabilizing the triplet counterpart because the introduction of bulky groups around the carbene center results in an increase in the carbene bond angle and therefore must make ΔG_{ST} larger. In this case, the triplet state is thermodynamically stabilized with respect to the singlet.[3,13]

This chapter focuses on the generation of carbenes by extrusion of nitrogen (Tables 91.1 through 91.8). Several other methods are possible, such as the formation from tosylhydrazone salts, oxiranes, aziridines, dioxolanes, and pyrazolenines from cyclopropanes by photocycloelimination, from transition-metal carbene complexes or by α-elimination, from α,α-dihalogen compounds,[14,15] or from base treatment of *N*-nitrosocarbamate.[16]

TABLE 91.1 UV Absorption and Quantum Yields of Photoinduced N_2 Extrusion from Diazo Compounds

Diazo Compound	λ_{max} (nm)	ε	Quantum Yield φ_{N_2}	Ref.
CH_2N_2	~410	3	4	17b
$H_3C\text{-}CH{=}N_2$	440	3.5	—	17b
	470	3.5		
$H_5C_6\text{-}CH{=}N_2$	491	26		17c
	275	22000		
$(C_5H_6)_2C{=}N_2$	526	101	0.78	17d
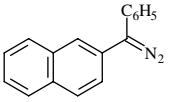	288	21300	0.69	17d
	513	100		
	287	20600		
$H_5C_2OOC\text{-}CH{=}N_2$	360	21	0.66	17d
	269	7110		
	247	7650		
$H_5C_6\text{-}CO\text{-}CH{=}N_2$	294	13500	0.46	17d
	250	12300		
$4\text{-}H_3C\text{-}C_6H_4\text{-}CO\text{-}CH{=}N_2$	297	16800	0.42	17d
	260	13200		
$4\text{-}H_3CO\text{-}C_6H_4\text{-}CO\text{-}CH{=}N_2$	304	24100	0.36	17d
$4\text{-}O_2N\text{-}C_6H_4\text{-}CO\text{-}CH{=}N_2$	307	13300	0.18	17d
	264	15500		
$4\text{-}Cl\text{-}C_6H_4\text{-}CO\text{-}CH{=}N_2$	299	14500	0.41	17d
	257	15200		
$3\text{-}O_2N\text{-}C_6H_4\text{-}CO\text{-}CH{=}N_2$	297	14200	0.22	17d
$2\text{-}H_3CO\text{-}C_6H_4\text{-}CO\text{-}CH{=}N_2$	288	13000	0.49	17d
	252	12300		
$(H_5C_6\text{-}CO)_2C{=}N_2$	275	16600	0.31	17d
	256	22200		
$H_5C_6\text{-}CO\text{-}CN_2\text{-}COOCH_3$	274	10100	0.35	17d
	253	10700		
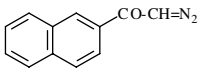	301	11500	0.31	17d
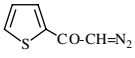	309	19700	0.36	17d
	261			
$ClCH{=}N_2$	458	—		17e
	518	—		
	545	—		
	301	3310	0.24	17d
	318			18
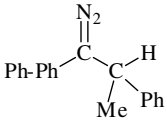	514			
	322			18
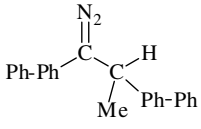	516			

TABLE 91.1 UV Absorption and Quantum Yields of Photoinduced N_2 Extrusion from Diazo Compounds (continued)

Diazo Compound	λ_{max} (nm)	ε	Quantum Yield φ_{N_2}	Ref.
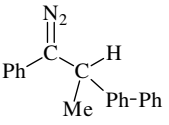	285 513			
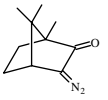	252	12000		17d
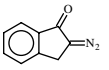	321 256	12150 19000	0.14	17d
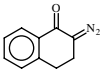	326 260	12000 9780	0.21	17d
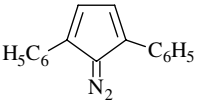	404 468 318 270	2800 4000 5900 10600	—	17f
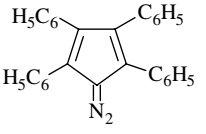	390 335 285 230	2800 13000 17700 26900	—	17f
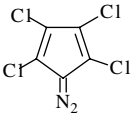	355 310 305	19500 20500 21400	—	17f
N_2=CH-CO-$(CH_2)_4$-CO-CH=N_2	270 248	17300 19000	0.34	17d
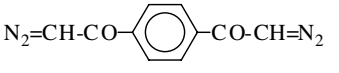	311 264	22500 17500	0.15	17d
N_2=CH-CO-CO-CH=N_2	318 270	11700 15900	0.31	17d
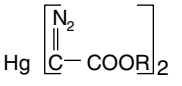	280 264	107 24900	—	17g

Carbenes, as reactive species, are detected by flash spectroscopy. This method is also used to directly measure the rate constant of the addition reactions of free carbenes to olefins. UV absorption spectroscopy of chlorophenylcarbene (Figure 91.1) generated from 3-chloro-3-phenyldiazirine (Scheme 1) and its rate of addition to different olefins have been measured (see Table 91.2), for example, at 77K and 293K in isooctane.[17a]

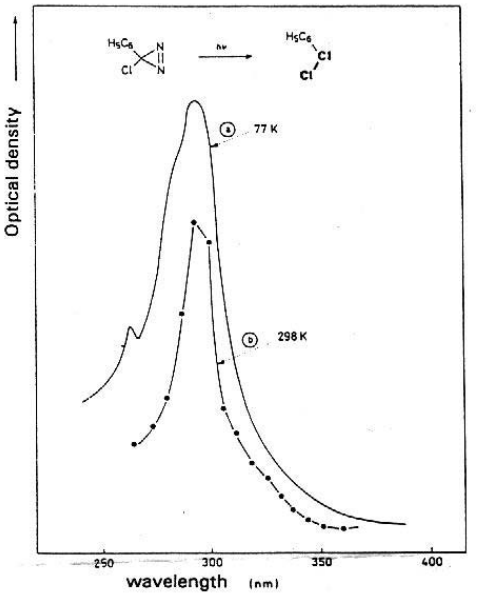

FIGURE 91.1 Ultraviolet absorption spectrum of chlorophenylcarbene in (a) methylpentane at 77K; (b) isooctane at 20°C. (Adapted from Zeller, K.-P. andGuel, H., Houben-Weyl, *Methoden der Org. Chemic*, Band E 19b/1, Regitz, M., Georg Thieme Verlag, Stuttgartt and New York, 1989, chap. 2.)

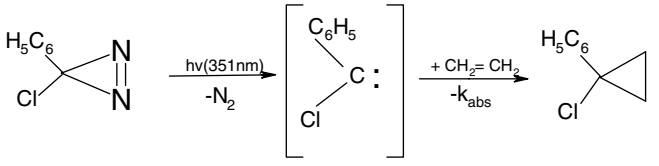

3 **4** **5**

SCHEME 1

TABLE 91.2 Addition Reaction Constants of Chlorophenylcarbene 4 with Olefins

Alkene	K_{abs} (1 mol^{-1} s^{-1})[a]	K_{abs}^{rel} [b]	...-cyclopropane
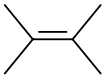	2.8×10^8	1.00	1-Chlor-1-phenyl-tetramethyl-...
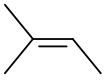	1.3×10^8	0.46	3-Chlor-3-phenyl-1, 1, 2-trimethyl-...
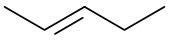	5.5×10^6	0.020*	1-Chlor-3-ethyl-2-methyl-1-phenyl-...
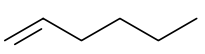	2.2×10^6	0.0079	2-Butyl-1-chlor-1-phenyl-...

[a] Experimental error ± 10%. [b]Relative equlibrium constants/absolute equilibrium constants.

Source: Adapted from Zeller, K.-P. and Guel, H., Methoden der Org. Chemie, Band E 19b/1, Regitz. M., Gerog Thieme Verlag, Stuttard, New York, 1989, chap. 2.

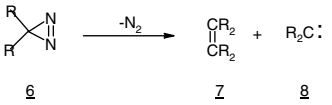

SCHEME 2

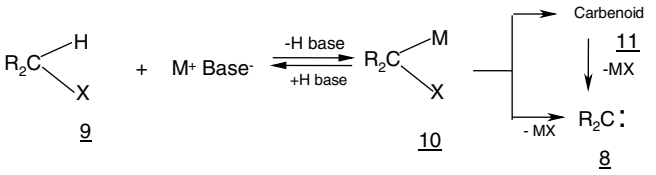

SCHEME 3

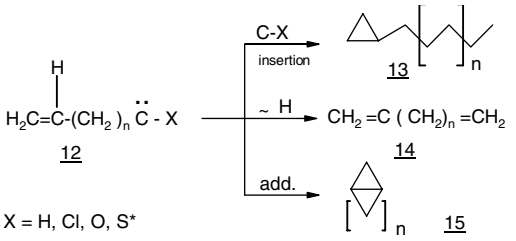

*C-X insertion is not included in this survey, because the emphasis is on the synthetic use of carbene chemistry

SCHEME 4 Intramolecular reactions.

A further method available for the study of triplet carbenes exclusively is ESR spectroscopy. CIDNP experiments are used as well to investigate the spin state of carbenes in solution. Generation of a carbene from 3*H*-diazirine or diazo compounds by thermolysis or photolysis with evolution of nitrogen yields a free carbene (Schemes 1 and 2).

Other methods involving base–-nduced α-elimination from haloalkanes often include the formation of a carbenoid (Scheme 3).

Relative reactivity of olefins with bromophenylcarbene generated either (1) by irradiation of 3-bromo-3-phenyldiazirine or (2) from base-induced α-elimination of α,α-dibromotoluene in the presence and in the absence of 18-crown-6 showed that addition of 18-crown-6 (via the complex of carbene with KCl/KO-*t*-butanolate) as well as photolysis of diazirine afforded the free carbene.[19] α-Elimination normally proceeds via carbenoids (Scheme 3).

The relative reactivities of alkenes with bromophenylcarbene are given in Table 91.3.[19-21]

Carbenes can react either (1) intramolecularly or (2) intermolecularly. The basic reactions are addition and insertion. Triplet carbenes can also react via an abstraction mechanism. As typical examples, the intra- and intermolecular reactions with a double bond are shown in Schemes 4 and 5, respectively.

As a matter of convenience, the generation of each type of carbene will be treated separately.

TABLE 91.3 Relative Reactivities of Alkenes with Bromophenylcarbenes

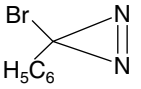

H_5C_6-$CHBr_2$/ $(CH_3)_3C$-OK/ $(CH_3)_3C$-OH, 25°C

Alkene		With 18-Crown-6	Without 18-Crown-6
	4.4	4. 1	1.6
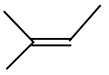	2.5	2.4	1.3
	1.0	1.0	1. 0
	0. 53	0. 50	0. 29
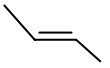	0. 25	0. 24	0. 15

Source: Adapted from Zeller, K.-P. andGuel, H., Houben-Weyl, *Methoden der Org. Chemic*, Band E 19b/1, Regitz, M., Georg Thieme Verlag, Stuttgartt and New York, 1989, chap. 2. See also-Moss, R.A. andPilkiewicz, F.G., *J. Am. Chem. Soc.*, 96, 5632, 1974; Moss, R.A., Joyce, M.A., and Juselton, J.K., *Tetrahedron Lett.*, 4621,1975.

TABLE 91.4 Effect of Substituents on Rate Constant (K_q) for Addition of Haloarylcarbenes to Alkenes

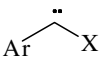

		K_q ($M^{-1}s^{-1}$)	
		$Me_2C{=}CMe_2$	$CH_2{=}CClCN$
Ph	F	$1.6 \times 10^{8,a}$	$1.2 \times 10^{8,b}$
Ph	Cl	$2.8 \times 10^{8,a}$	$2.1 \times 10^{8,b}$
Ph	Br	$3.8 \times 10^{8,a}$	$3.3 \times 10^{8,b}$
p-$MeOC_6H_4$	Cl	$1.4 \times 10^{7,b}$	—
p-MeC_6H_4	Cl	$1.2 \times 10^{8,b}$	—
p-ClC_6H_4	Cl	$3.3 \times 10^{8,b}$	—
p-$CF_3C_6H_4$	Cl	$1.5 \times 10^{9,b}$	—

[a] From Tomioka, H., *Carbene Chemistry,* Vol. 2 Brinker, U.H., Ed., JAI Press, 1998, 175–214; Cox, D.P., Gould, I.R., Hacker, N.P., Moss, R.A., and Turro, N.J., *Tetrahedron Lett.,* 24, 5313, 1983.

[b] Tomioka, H., *Carbene Chemistry,* Vol. 2 Brinker, U.H., Ed., JAI Press, 1998, 175–214; Moss, R.R., Fan, H., Handel, L.M., Shen, S., Wloshtowska, J., Wlostowski, M., and Krogh-Jespersen, K., *Tetrahedron Lett.,* 28, 4779, 1987.

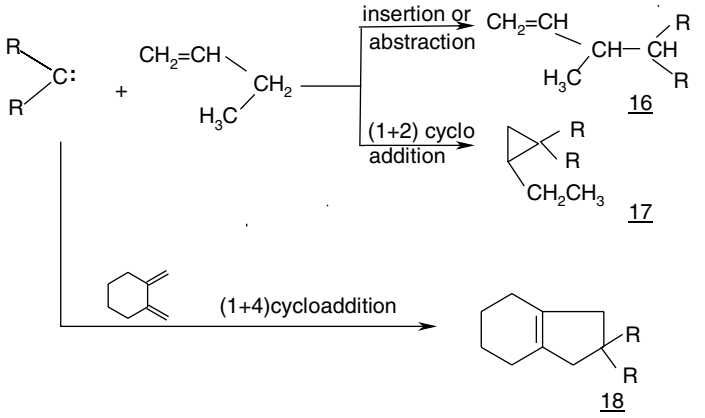

SCHEME 5 Intermolecular reactions. [1+4]-cycloaddition is not dealt with in detail.

91.2 Formation of Carbenes

Carbene of Coordination Number 1

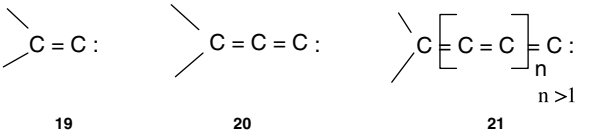

19 **20** **21**

Alkylidene **Alkenylidene** **Alkpolyenylidene**

Type 1 carbenes $R_2C(=C)_n=C:$ ($n = 0 \rightarrow \infty$) are mainly formed by methods that include α-elimination, although thermal extrusion of nitrogen was reported from tetrazolones[23] and 1-aryl-2-diazo-2-oxo-1-silylethane[24] or from 2,3-bis[*N*-nitrosoacyl-amino]-1,1-diphenylcyclopropane[25] (Scheme 6).

Carbenes of Coordination Number 2

Acyclic Homocarbenes (Methylene, Alkyl-, Dialkyl-, Alkenyl-, and Alkynylcarbenes)

3H-Diazirine.

Herzberg and collaborators[26-28] provided the first experimental evidence that a meta-stable, bent singlet was initially produced from diazoalkane and decayed to a ground-state triplet.[29,30] The liquid-phase chemistry of methylene, for example, is simple in comparison with its gas-phase chemistry. However, hot molecules produced by extremely exothermic reactions of methylene play a minor role in the gas phase. Carbenes have been used on countless occasions to make three-membered rings via [1+2]-cycloaddition.

Photolysis and thermolysis of suitably substituted diazirines could be considered an ideal method for the generation of free methylene as well as for alkyl- and dialkylcarbenes. Diazirines are preferred precursors compared to acyclic diazo compounds because of their stability and ease of handling.[31]

The parent 3*H*-diazirine reveals a weak absorption (ε_{max} = 200) in the range of 280 to 350 nm. Photolysis of 3*H*-diazirine in a xenon matrix at 4 K (Scheme 7) gives triplet ground-state methylene; at 77 K, subsequent dimerization and irradiation afford ethenyl radicals.[32-34]

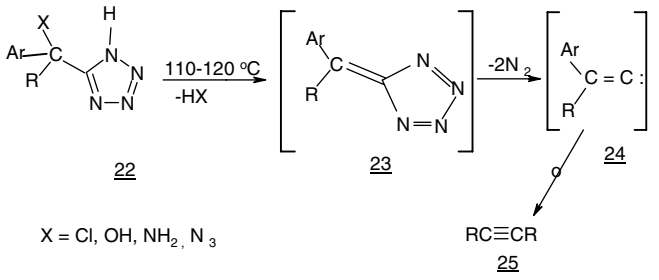

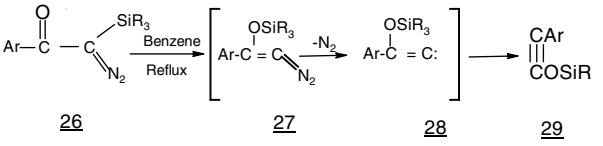

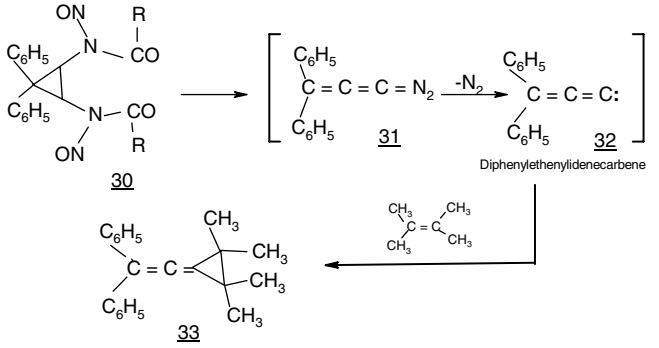

SCHEME 6

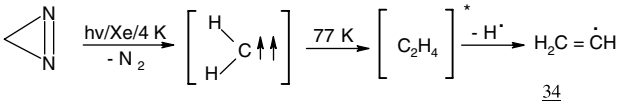

SCHEME 7

The singlet–triplet energy difference of methylene was found to be about 7.5 kcal.mol^{-1}.[35] Direct photolysis of 3*H*-diazirine in chloroform gives 1,1,2-trichloroethane (92% yield) by carbon chlorine insertion, while in the presence of tetradecane, the carbon-hydrogen insertion product 1,1,1,-trichloroethane is formed. These are illustracted in Scheme 8 and identification was carried out using CIDNP NMR measurements to demonstrate the formation of singlet biradicals.[36,37]

In acetonitrile as solvent, irradiation of diazirine gives a nitrile-ylide as a primary product with an absorption at 280 nm (Scheme 9). The ylide was characterized by Turro[38,39] using the pulsed laser technique. It undergoes 1,3-cycloaddition reactions with diethyl acetylenecarboxylate.[40]

An interesting finding was obtained with 3-isopropyl-, 3-*t*-butyl-, and 3- (1-methyl -1-phenylethyl-3*H*-diazirine (Scheme 10). Sensitized photolysis of **40** gives similar results to those obtained by thermolysis either in the gas phase or in decalin (Table 91.6). However, direct photolysis of **40** in benzene

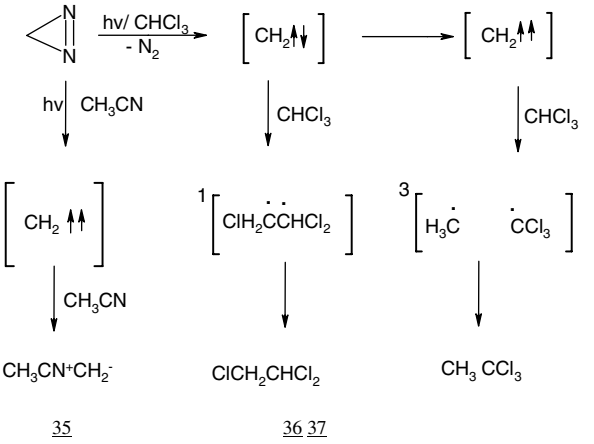

SCHEME 8

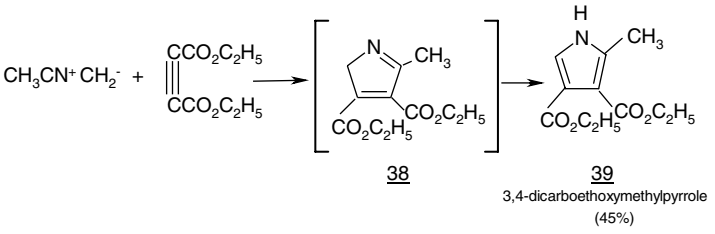

SCHEME 9

leads to similar products but in different ratios. This can be explained by the formation of an electronically excited, less-selective carbene upon direct photolysis, [15,41-44] a result supported by the work of Frey and Stevens.[43]

Diazoalkanes.

As early as 1901, Hantzsch and Lehmann[45] and Staudinger and Kupfer[46] reported on the photochemical and thermal decomposition of diazomethane to afford methylene. Subsequently, Hine[47] and Doering [48] started the **era** of carbene chemistry and excellent reviews were published.[49,50] Compared to other methods, the generation of carbene from diazoalkanes finds wide application despite the toxicity and the tendency of low-molecular-weight diazoalkanes to explode. Diazoalkanes show a weak UV absorption band between 300 and 500 nm, assigned to a forbidden n,π^* transition. Photoexcitation of the long-wavelengh bands of diazo compounds results in an excited singlet state, which may react as shown in Scheme 11.

The rate of disappearance of the diazo compound, that is, the quantum yield of the photolysis, should be independent of the nature and concentration of reactants. This is the criterion for the intermediacy of free radicals. Diazomethane shows a weak UV absorption band between 300 and 500 nm and a sharp band between 200 and 260 nm.[49-52] Photolysis into this band brings about elimination of nitrogen and produces methylene (Scheme 12).

An important new reaction in the chemistry of carbenes is its addition to fullerenes. Addition of CR_2, generated from diazoalkane by the loss of N_2, to pent-hex and hex-hex edges of C_{60}, both with retention and breakage of the carbon-carbon edge bond takes place. The stereochemistries and stabilities of $C_{60}(CR_2)_n$ were investigated.[53]

TABLE 91.5 Thermodynamic Data and Lifetimes of Several Singlet Carbenes.[3]

Carbene	ΔG_{ST} [a] (kcal/mol)	ΔH_f [b] (kcal/mol)	ΔE_{stab} [c] (kcal/mol)	Lifetime [d]	Solvent	Decay Kinetic
$:CCl_2$	–13.5	—	27	10 μs	Cyclohexane	—
$:CF_2$	–56.6	–46	63	~2 ms	Gas	2
PhCOMe	—	—	—	15-30 μs	3-Methyl-pentane	1
ClCOMe	—	–22	60	—	—	—
F COMe	—	–53	74	~1 ms	Pentane	2
$(MeO)_2C:$	–77	–61	80	~2 ms	Pentane	2
$MeCNMe_2$	—	—	93	—	—	—
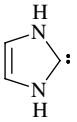 (IM)	–79.4	—	—	•	—	—

[a] Estimated by *ab initio* calculations.
[b] Heat of formation determined either empirically or semiempirically.
[c] Calculated by the isodesmic reaction ($CH_2 + CH_3X + CH_3Y \rightarrow CXY + 2CH_4$) for carbene CXY.
[d] Lifetime in solution at room temperature.

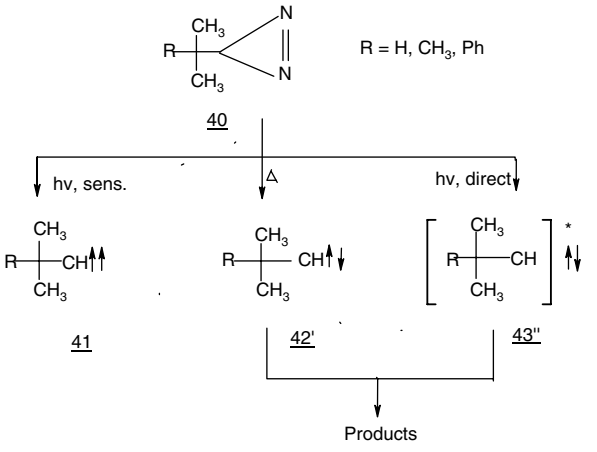

SCHEME 10

Scheme 13 shows the addition of CR_2 to pent-hex and hex-hex edges of C_{60} (46) with retention and breakage of the carbon-carbon edge bond. The movement of the double bond character onto pent-hex edges in the pent-hex bond-intact isomer and the hex-hex bond-broken isomer is indicated.[53]

Evolution of nitrogen from higher diazoalkanes gives the corresponding alkylcarbenes that may undergo (1) intramolecular insertion into β-CH bonds; (2) [1,2]-hydride, alkyl, or aryl shifts; or (3) intramolecular addition in the presence of double bonds as shown in Scheme 14.

By comparison, thermolysis of 1-diazo-2-methylpropane gave only methyl-cyclopropane (33%) and isobutene (67%). Many other carbenes were generated via thermolysis and/or photolysis of the corresponding

TABLE 91.6 Photo- and Thermal Decomposition of 3-*t*-Butyl-3H-diazirine

Condition	1,1-Dimethylcyclopropane	2-Methyl-2-butene
Gas phase, hν	51.0	49.0
Benzene, hν, 25°C	44.7	53.3
Thioxanthone, hν, 25°C	90.8	9.2
Gas phase, 160°C	92.0	8.0
Decalin, 180°C	88.4	11.6

Source: Kirmse, W., *Carbene Chemistry*, Academic Press, New York, 1971; Mansor, A.M. and Stevens, I.D.R., *Tetrahedron Lett.*, 1733, 1966.

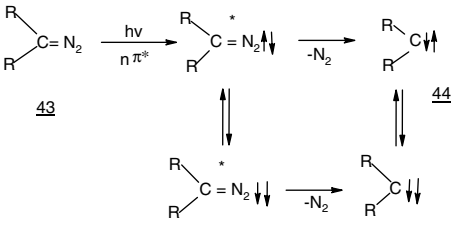

SCHEME 11

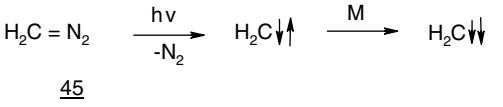

SCHEME 12

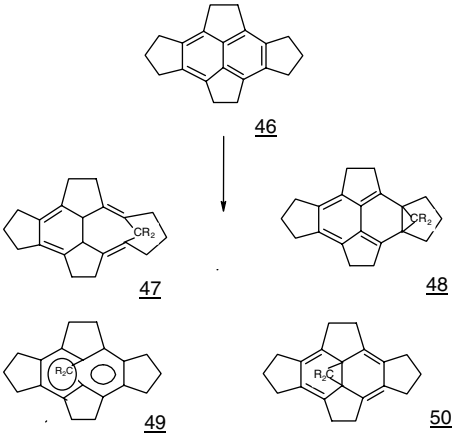

SCHEME 13

diazo precursors (see References 51, 52, 54, and 55). Kirmse and Horn[54] found, in a study of the catalytic, thermal, and photolytic decomposition of diazoalkanes in various solvents, that similar to diazirines, the photodecomposition gave a less-selective intermediate than the thermal reactions. Broadly speaking, it

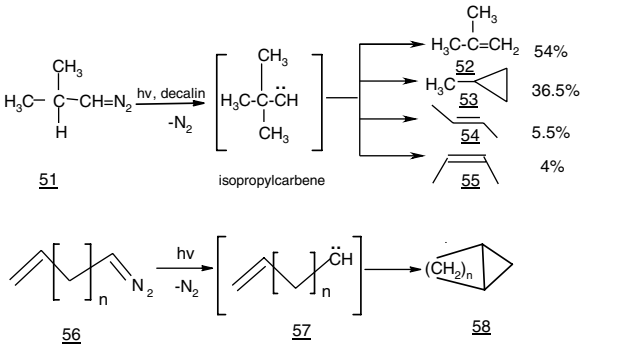

SCHEME 14

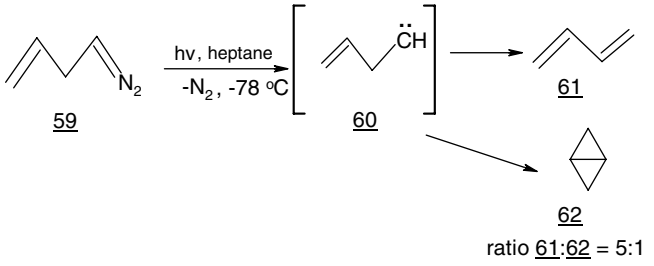

SCHEME 15

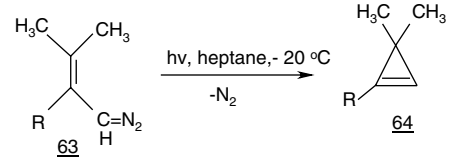

R = CH_3	70 %
C_6H_5	60 -80 %
p-$CH_3OC_6H_4$	90 %

SCHEME 16

can be said that free carbenes are formed from diazo compounds in photochemical and thermal reactions, whereas all other methods yield carbenoids.

Alkenylcarbenes

The situation completely changes when the intramolecular double bond is α,β to the carbene carbon atom or held in close proximity by steric or structural factors. With few exceptions, it can be stated that if a singlet carbene can undergo internal cycloaddition or insertion, it will not be possible to trap it efficiently with an external reagent.[56] In general, the bicyclo[n.1.0] systems are formed. Some other reaction pathways can predominate, as for example, with 3-diazo-1-propene (Scheme 15).[57] In addition, generation of α-alkenyl carbenes in the absence of nucleophilic reagents leads to the formation of cyclopropenes in high yield[58,59] (Scheme 16).

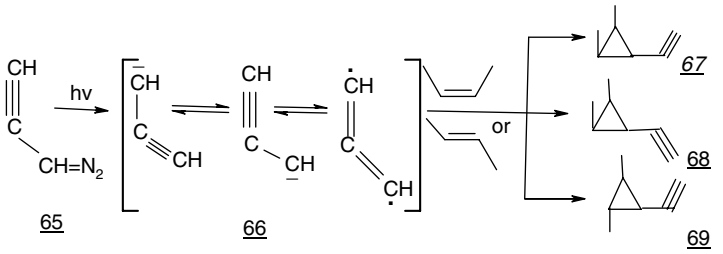

SCHEME 17

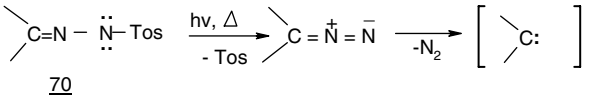

SCHEME 18

Alkynylcarbenes

Skell and Klebe reported in 1960 that photolysis of diazopropyne **65** in *E*- and *Z*-2-butene (Scheme 17) gives a carbene that is slightly nonstereospecific and a mixture of three cyclopropanes (**67**, **68**, and **69**) in the ratios of 4:2.5:1, respectively, with *Z*-2-butene being isolated.[60]

Bamford–Stevens Reaction (Methylene–Alkyl-Dialkylcarbenes).

Thermolysis and/or photolysis of tosylhydrazone salts, accessible by condensation of *p*-toluene-sulfonylhydrazine with aldehydes or ketone, gives rise to elimination of the sulfinate salts and forms the intermediate diazo compound (Scheme 18). Generation of free carbenes by this method is sometimes in doubt and, as a consequence, this method is not included in this chapter except when generation of a carbene from the diazirine or diazo compound is not available.[15,61]

Isocyclic Carbenes

Different cyclopropyl-, cyclobutyl-, cyclopentyl-, cyclohexyl-, cycloheptyl- (or higher) carbenes are known.[56] A survey is provided in the literature.[62] In general, the shift of an alkyl group results in ring expansion (Scheme 19).[56]

Thermolysis or photolysis of cubylphenylcarbene **85** in the presence of ethanol (Scheme 20) affords two isomers of ethoxyhomocubene, **87** and **88**.[65,66] Also, cyclopentyl-,[67] cyclohexyl-.[67] and cycloheptylcarbene[68] are generated, primarily through a Bamford-Stevens reaction to produce a mixture of products (Scheme 21).

Cycloalkenylcarbenes

Cycloalkenylcarbenes are carbenes that contain a cyclic side group. Tolane is the major decomposition product from the decomposition of diphenylcyclopropene diazomethane and a minor product is formed via normal ring expansion[68] (Scheme 22). Cycloheptatrienylcarbene yields only benzene, acetylene, and heptafulvene in addition to cyclooctatetraene[69] (Scheme 23).

Cycloalkylidenecarbene

Optically active cyclopropylidenes afford optically active allenes (Scheme 24).[70,71] Decomposition of diazocyclopentane and diazocyclohexane leads only to cyclopentene and cyclohexene, respectively, but their

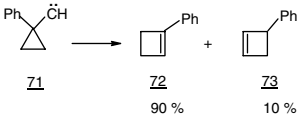

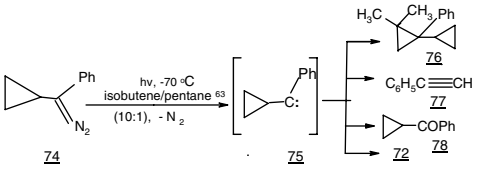

72:76:(77 + 78) = 27 %:34 %:1.9 %

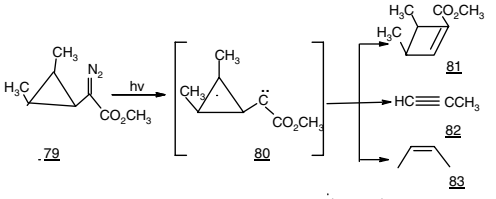

81:(82 + 83) = 57%:3%

SCHEME 19

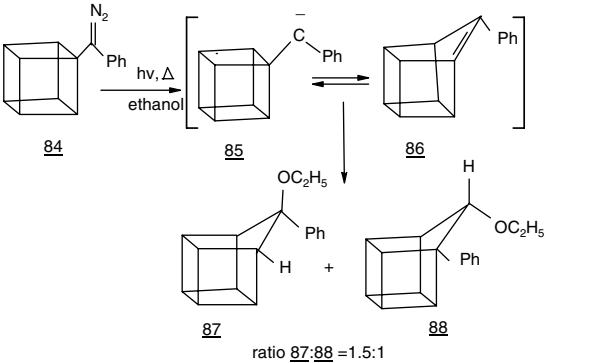

ratio 87:88 =1.5:1

9-ethoxy-9-phenylhomocubane 9-ethoxy-1-phenylhomocubane

SCHEME 20

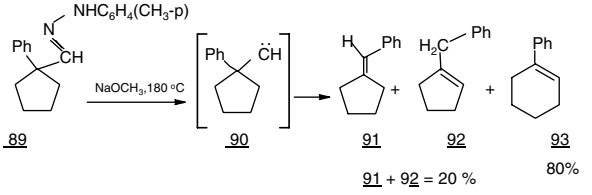

91 + 92 = 20 %

80%

SCHEME 21

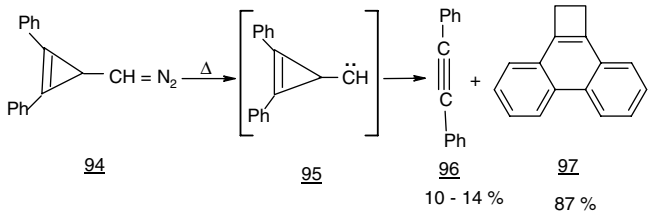

SCHEME 22

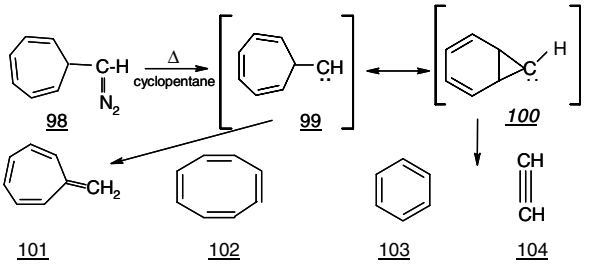

SCHEME 23

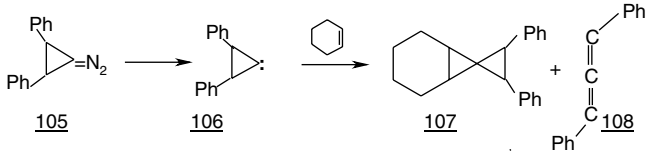

SCHEME 24

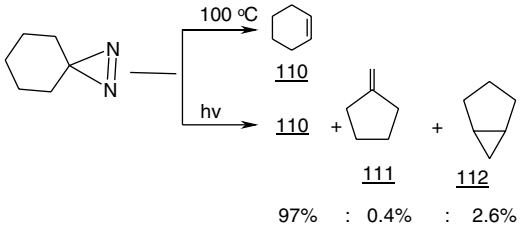

SCHEME 25

isomers, cyclopentyl- and cyclohexyldiazirine, show different behavior, depending on the method of generation (Scheme 25). However, photolysis is less selective than thermal decomposition.[72,73] Higher cycloalkylidenes have been generated through methods that do not involve free carbenes.[73]

Cycloalkenylidenes

This class of carbenes is of special interest because the carbene carbon is attached to a conjugated α,β-unsaturated system. Within this definition, a different series of cycloakenylidenes can be constructed that

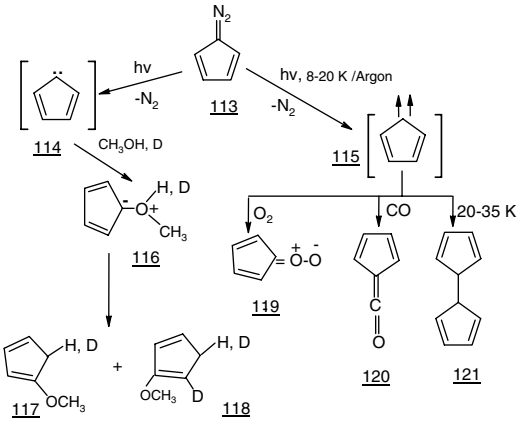

SCHEME 26

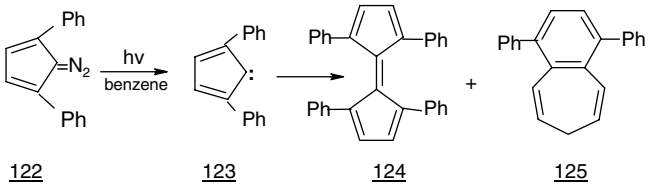

SCHEME 27

contain a total of [4n] or [4n+2] electrons.[74] The resonance structure of these carbenes shows that carbenes A and E have nucleophilic centers and carbenes B, C, and D have electrophilic centers.

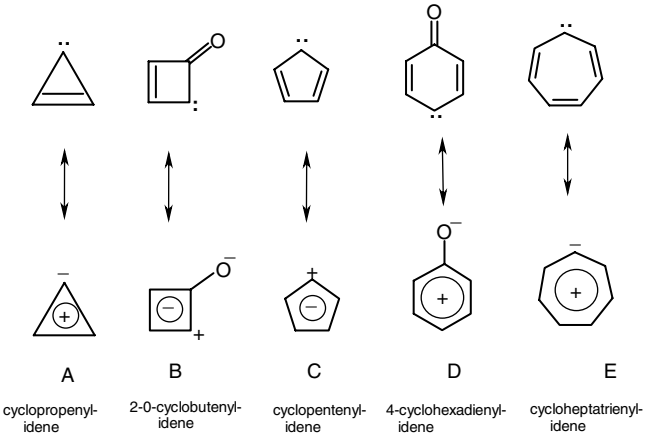

A variety of phenyl-substituted cyclopentadienylidenes have been examined. Irradiation of 5-diazocyclopentadiene at 8 to 20K in argon afforded a triplet carbene,[75,76] while irradiation at 293K in methanol gave a mixture of 1- and 2-methoxy-1,3-cyclopentadiene quantitatively[77] (**117** and **118**, Scheme 26). Irradiation of 5-diazo-1,4-diphenyl-1,3-cyclopentadiene in benzene produced, in addition to the dimer 1,1′-4,4′-tetraphenylfulvene (**124**, 6%); 1,4-diphenyl-7*H* -benzocycloheptatriene (**125,** Scheme 27).[78]

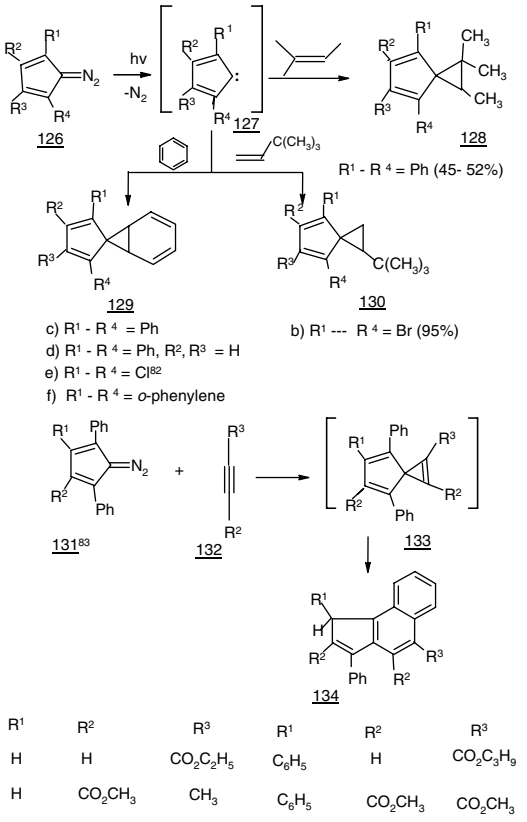

SCHEME 28

Tetrasubstituted 5-diazocyclopentadienes have received attention as a route to spirocyclopropane adducts upon irradiation in alkenes (Scheme 28).[79-81]

Photolysis of 2,5-di-*t*-butyl-3-diazo-6-oxo-1,4-cyclohexadiene at λ = 480 nm (sun lamps) in 2,3-dimethyl-2-butene gave the spiro compound **135** in 80% yield.[84]

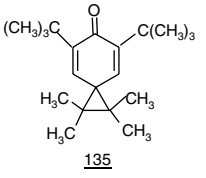

135

Interestingly, the catalytic activity of some platinum complexes toward decomposition of diazo compounds is influenced by the oxidation state of the metal and the type of diazo compound under study. For example, 9-diazofluorene is decomposed either catalytically or stoichiometrically, in the presence of the platinum (0) complex [Pt (C_2H_4) $(PPh_3)_2$], to the corresponding azine while the dicationic complex *cis*-[Pt $(PPh_3)_2(CH_2CN)_2$]•$[BF_4]_2$ catalyzes the formation of the corresponding olefin.[85]

Arylcarbenes

Arylcarbenes are probably the most intensively studied carbenes. Arylcarbenes have a triplet ground state, as shown by ESR and/or CIDNP experiments.[86] Singlet ground-state arylcarbenes are also known.[87,88] Arylcarbenes can be subdivided into (1) monoarylcarbenes, (2) diarylcarbenes, and (3) carbenes in which the carbene carbon is a part of the aromatic system (A, B, and C, respectively).

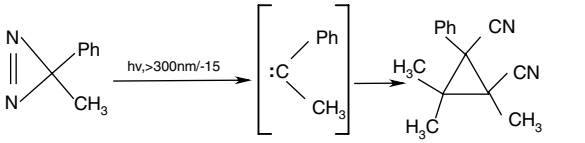

146 147 148 37%[94]

SCHEME 29

TABLE 91.7 Substituent Effects on Properties of Diarylcarbenes[3]

Carbene	K_{eq} [a]	ΔG_{ST} [b] (kcalmol)	Lifetime[c]	Solvent
BA	≥4000	≥5.2	250 μs	PhH
DCFL	1000	4.1	–10 ns	MeCN
DPC	200	3.2	1.5 μs	c-C_6H_{12}
FL	20	1.9	1.7 ns	MeCN
BFL	5	1.0	260 ps	c-C_6H_{12}
DMFL	~0.03	~–2	51 ns	PhH
XA	≤0.0002	≤–5	50 μs	C_5H_{12}

[a] $K_{eq} = K_{ST}/K_{TS}$, where K_{TS} and K_{ST} are the rates of intersystem crossing that could be measured by picosecond time-resolved laser spectroscopic measurements.
[b] Determination by $\Delta G_{ST} = RT \ln K_{eq}$.
[c] Lifetime (τ) or half-life ($t_{1/2}$) in solution at room temperature.

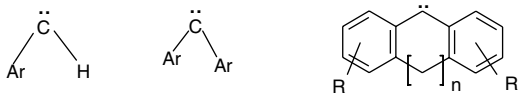

It has been observed that anthryl groups can act as excellent reservoirs for the unpaired electrons as well as relatively effective kinetic protectors for carbene.

Recent growing interest in triplet carbenes as potential organic ferromagnets[89] adds a practical meaning to this project.

Stabilization of triplet carbenes is shown to be better accomplished by steric protection than by electronic effect. However, the latter strategy can be used to stabilize singlet carbenes.[90]

Diazirines.

Diazirines have been used by many authors for the generation of arylcarbenes. Diazirines can directly be decomposed to give carbenes or rearrange to their diazo isomers, which in turn affords the carbene. Several examples are known and are illustrated in Scheme 29.[91,92]

Cyclopropylmethylchlorocarbene **149** and dicyclopropylmethylchlorocarbene **150** give only [1,2]-hydrogen shift products (**151** and **152**) with K_H (absolute rate constant for the [1,2]-H shifts) = 2.0 x 10^7 and 1.3 x10^7, respectively (Scheme 30).[95]

Photolysis of diazirine **157** (X = MeO) gave alkenes **158** and the [1,2]-carbon shift product **159** in the ratio of 1.67, similar to the product ratio obtained by thermolysis (Scheme 31).[96,97]

Sulfur ylides generated by photolysis or thermolysis of diazirines (Scheme 32) can be utilized for synthesis of β-lactams antibiotics and other natural products.[98,99]

Carbenes generated by irradiation of diazirines containing a photoreactive diazirine and mono- and disaccharides such as **167** were used for photoimmobilization of biomolecules on polystyrene.[100]

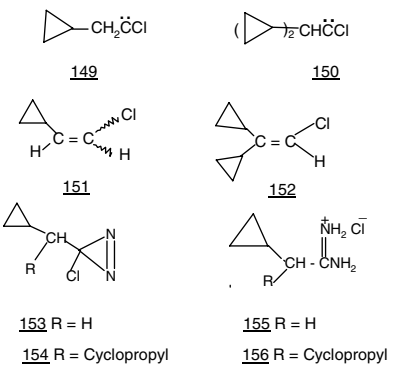

SCHEME 30

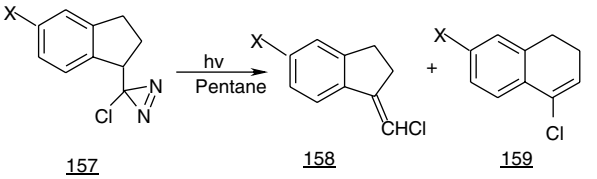

SCHEME 31

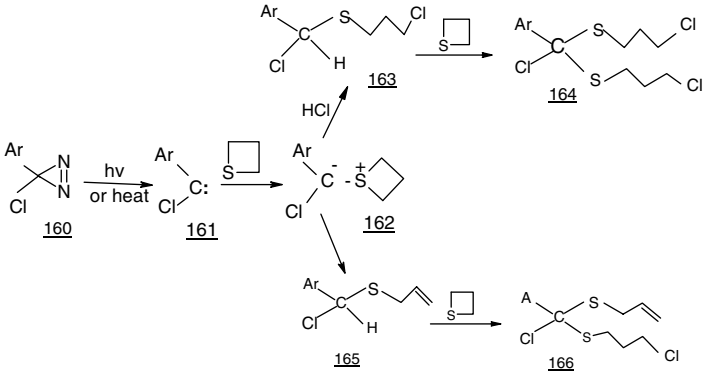

a, Ar = Ph; b, Ar = *p*-MeC$_6$H$_5$; c, Ar = *p*-ClC$_6$H$_5$

SCHEME 32

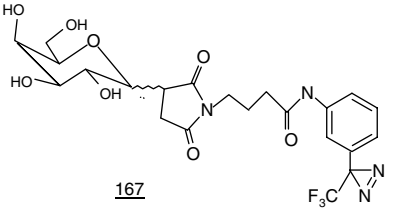

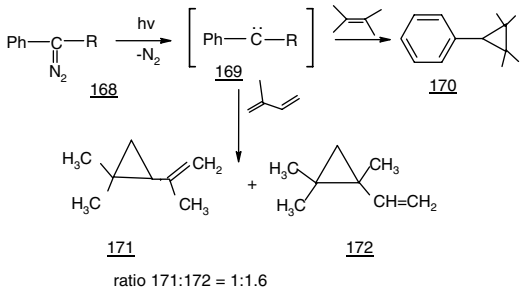

SCHEME 33

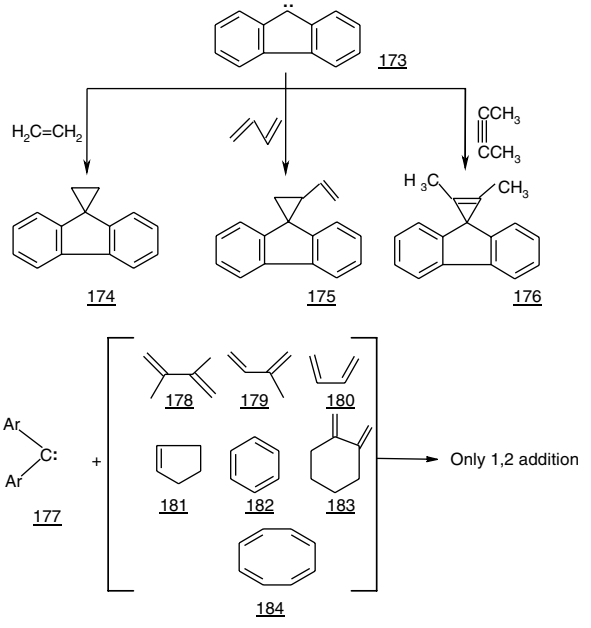

SCHEME 34

Diazo Compounds.

Diazo compounds decompose with extrusion of nitrogen under the effect of light or heat to produce carbenes. Phenylcarbene[101,102] as well as diphenylcarbene[102] possess triplet ground states that are in equilibrium with the singlet configurations.

Decomposition of phenyldiazomethane in olefins (Scheme 33) leads to the formation of cyclopropanes.[28,103] The reaction is largely stereospecific (>96%) and there is only a slight preference for the phenyl group to end up *syn* to the groups attached to the olefins. Fluorenylidenes are of special interest in the field of carbene chemistry. A large number of fluorenylidene derivatives have been prepared and subjected to extensive studies. Diphenylcarbene represents a compound bridged by an infinite chain. Fluorenylidene has two aryl groups connected by a zero bridge. Fluorenylidene seems to be an exceptional carbene (unlike diphenylcarbene) in that it adds easily and without complications to a variety of olefins.[104,105]

Again, an equilibrium state exists between the triplet and singlet states at ambient temperature. Neither fluorenylidene nor diphenylcarbene can be induced to add in a 1,4 fashion to dienes such as **178** to **184**[106] (Scheme 34).

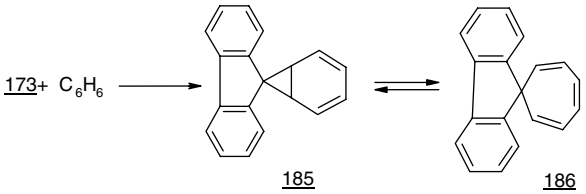

SCHEME 35

Fluorenylidene attacks benzene to give a mixture of the valence isomers norcaradiene **185** and cycloheptatriene **186** (Scheme 35).[107a]

Other aryl or diarylcarbenes are known, such as **187** through **194**. The carbene **187** is similar to diphenylcarbene in its properties.

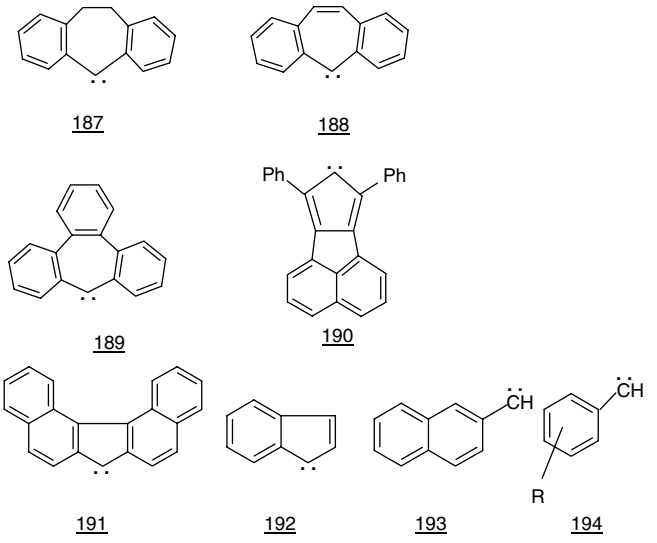

Carbene **190** underwent [1+2]- as well as [1+4]-cycloaddition with 2,3-dimethyl-1,3-butadiene (Scheme 36). It was regarded as a nucleophilic singlet carbene in its addition to styrene.[108]

A few di- and polycarbenes are known, and most were studied by spectroscopic techniques. The dicarbenes 201 and 203 are generated by irradiation of the corresponding bisdiazo precursors. Reaction of 201 in toluene with 1,1-diphenylethene gives 202, while 203 undergoes addition to benzene with ring expansion to yield 204 (Scheme 37).[107b,c]

Oxygen-Containing Carbenes

This section includes carboalkoxy- and ketocarbenes. The Wolff rearrangement[2,15,109] is common to both keto- and carboalkoxycarbenes. This intramolecular reaction is of special significance in the Arndt-Eistert synthesis of homologous acids and esters as well as in the synthesis of strained small rings.

Carboalkoxycarbenes undergo both insertion and cycloaddition. Carbomethoxy-carbene **206** inserts into the α- and β-position of diethyl ether in the ratio of 4:1 to give **207** and **209** in addition to **208**, which may be formed via an ylide[110] (Scheme 38).

Cycloaddition of **206** to olefins has been demonstrated to be stereospecific on addition to cyclic or asymmetric double bonds (Scheme 39) to give mainly the less-hindered *exo*-adduct **210**.[111,112]

Interestingly, sensitized photolysis of dicyanocarbene in cyclooctatetraene leads to the [1,4]- addition product **212** as well as the major [1,2]-adduct **213** (Scheme 40).[113]

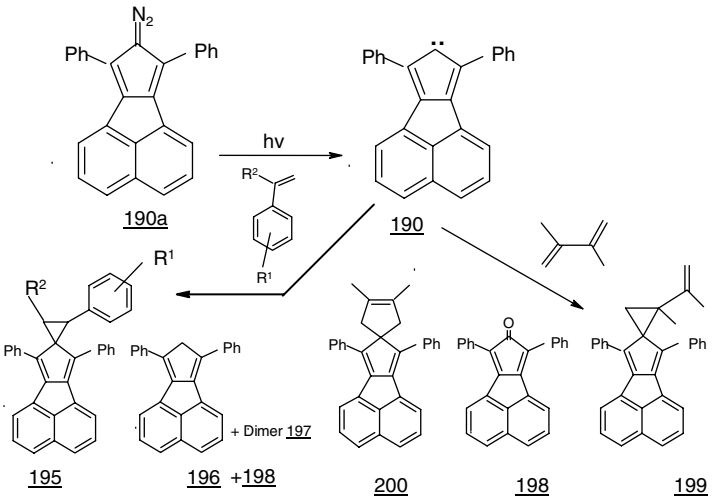

SCHEME 36

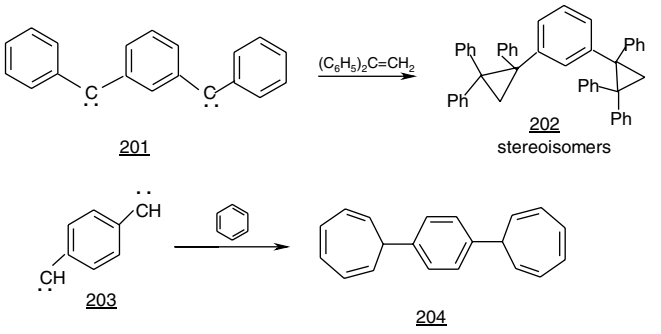

SCHEME 37

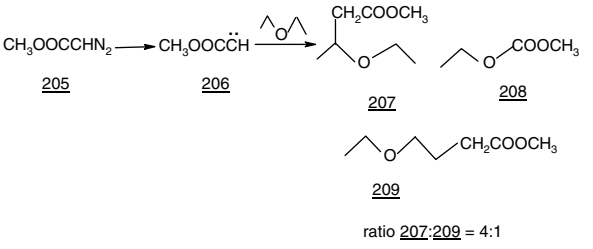

SCHEME 38

Ketocarbenes are most prone to Wolff rearrangement; for example, **217** is formed as a product of the rearrangement of **216** during photolysis of **214**[114,115] (Scheme 41).

However, photolysis of diazoketone **218** in cyclohexene affords adduct **219,** presumably because of the low mobility of an amide in the Wolff rearrangement (Scheme 41).[116]

Several other oxygen-containing carbenes are known, such as carbenes **220** through **225**.[110]

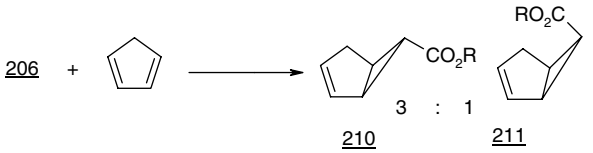

SCHEME 39

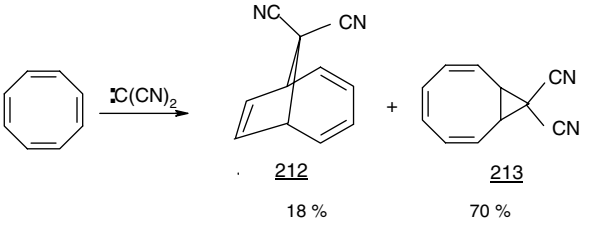

SCHEME 40

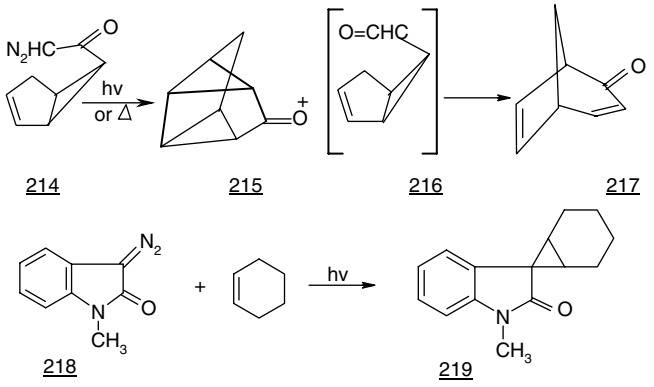

SCHEME 41

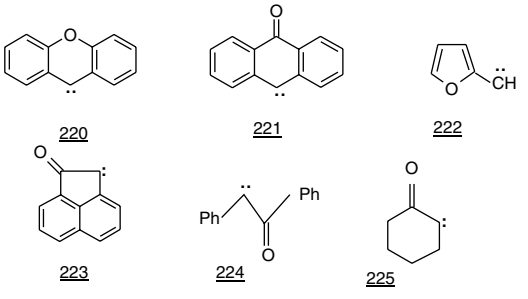

Halogen-Containing Carbenes

Most of the work on halocarbenes is concerned with carbenoids. Pyrolysis of chlorodiazomethane leads to a less-selective intermediate than its carbenoid counterpart.[117] Addition to 2-butene is stereospecific, but the *syn/anti* ratios in various olefins is markedly different.[117]

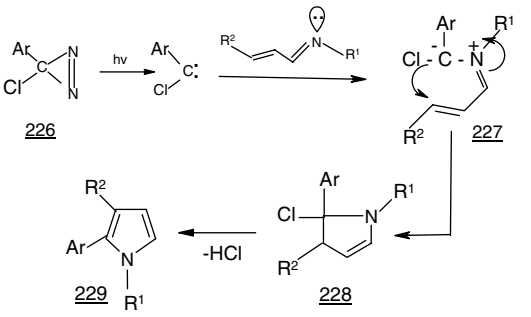

SCHEME 42

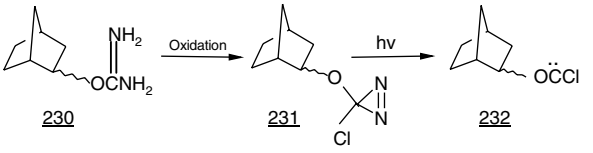

SCHEME 43

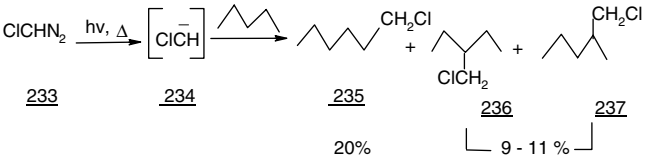

SCHEME 44

The first room-temperature stable triplet carbene 2,2′,4,4′,6,6′-hexabromophenylcarbene was generated from the corresponding diazo derivative, to be a model for chemically stable organic high-spin molecules.[3]

In general, the stable triplet carbene unit is supposed to serve as a useful building block for an extended super-high-spin molecular system and organic super-paramagnets.[118] All arylchlorodiazirines 226 were prepared by oxidation of the corresponding benzamidine hydrochloride with sodium hypochlorite in DMSO. Laser flash photolysis (LFP) of arylchlorodiazirines in the presence of substituted vinylpyridines yield substituted vinylpyridinium ylides (λ = 540 nm), an intermediate 227 of useful synthetic value for a variety of biologically active nitrogen-containing heterocycles (Scheme 42).[119,120]

LFP of arylchlorodiazirine in isooctane in the presence of vinylpyridines yields substituted vinylpyridine ylides that undergo [1,5]-cyclization.

*Ex*o- and *endo*-2-norbornyloxychlorocarbene **232** were generated photochemically from the corresponding diazirine **233** (Scheme 43).[121]

Photochemically or thermally generated carbenes, unlike most carbenoids, undergo the insertion reaction easily. These results are consistent with the involvement of a free halocarbene in its singlet state (Scheme 44).

Difluorocarbene, prepared by thermolysis or photolysis of difluorodiazirine, yields 1,1-difluorocyclopropanes via stereospecific addition to olefins, again consistent with a singlet ground state.[122] The relative reactivities of alkenes with bromophenylcarbene are shown in Table 91.3.

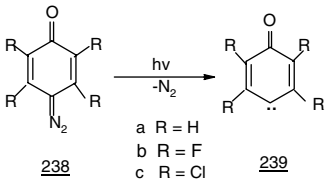

238 239

SCHEME 45

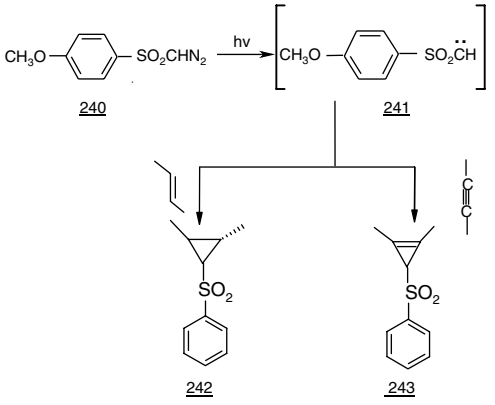

240 241 242 243

SCHEME 46

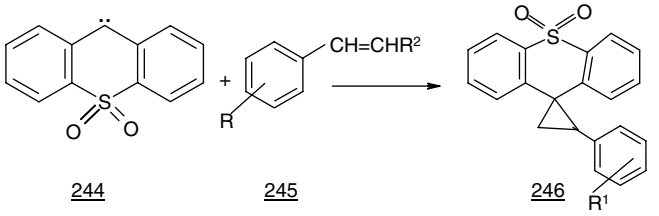

244 245 246

SCHEME 47

The 4-oxo-2,3,5,6-tetrafluoro- and tetrachloro-cyclohexa-2,5-dienylidenes **239** were prepared and investigated as an interesting class of highly electrophilic carbenes (Scheme 45).[123]

Sulfur-Containing Carbenes

Sulfur-containing carbenes are known and review articles have been published.[124,125] The diazo precursors are prepared either by the action of weak bases on the appropriate *N*-nitrosocompound[126] or by the use of diazo transfer reactions.[127,128] The sulfonylcarbene **241** undergoes an addition reaction to olefins and acetylenes (Scheme 46) to give **242** and **243**, respectively.[14,128,129]

The chemistry of the polynuclear-ring, sulfur-containing carbene thioxathen-ylidene-*S*,*S*-dioxide **244** indicates easy cycloaddition to styrenes.[130] It reacts from its singlet state and behaves as an electrophilic carbene (Scheme 47).

The photochemistry of a series of bis(sulfonyl)diazomethanes was investigated in solution and in low-temperature matrices (Scheme 48).[131]

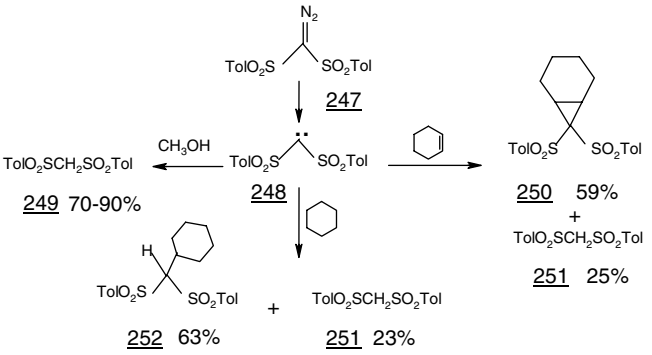

SCHEME 48

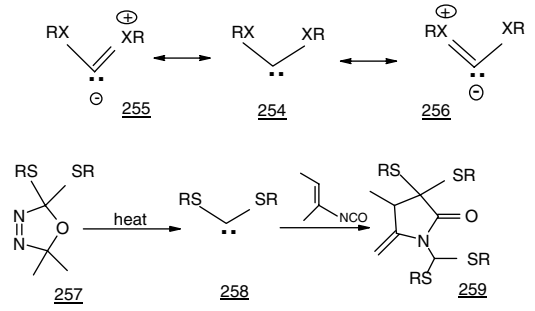

SCHEME 49

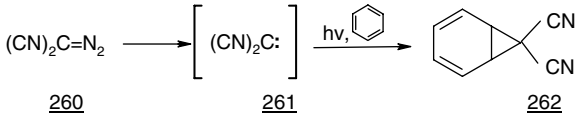

SCHEME 50

Recently, bis(alkylthio)carbenes **258** have been added to the list of nucleophilic carbenes that are useful 1,1-dipole equivalents in reactions with vinyl isocyanates **253**. Substituted hydroindolones, isatins, and hydroquinolines can be prepared by the addition of these carbenes to vinyl isocyanates (Scheme 49).[132,133]

Nitrogen -Containing Carbenes

The unusual stability of imidazolylidene is largely attributed to the accumulated electron density on the nitrogen centers as well as the C4–C5 double bond that surrounds the carbene center, protecting the imidazolylidene from nucleophilic additions and kinetically stabilizing the molecule. Also, imidazolin-2-ylidene (IMH_2) and even bis(diisopropylamino)carbene (IPC) have been isolated as stable crystals. This indicates that unsaturation in the imidazole ring is not required to produce a stable nitrogen-substituted carbene.[3]

Cyanocarbenes, for example, have a triplet ground state, as confirmed by ESR spectroscopy.[134] Their stereospecific[25] addition to olefins gives cyclopropanes. The benzene adduct is norcaradiene (**262**), not cycloheptatriene (Scheme 50).[135]

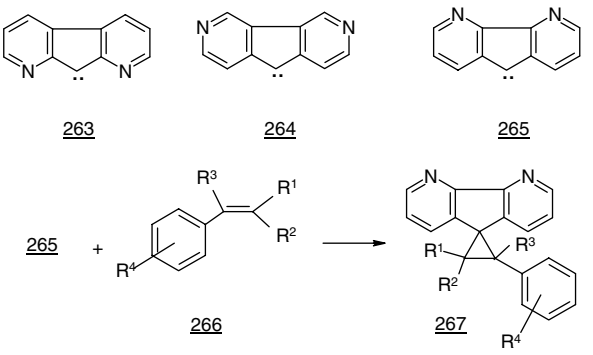

SCHEME 51

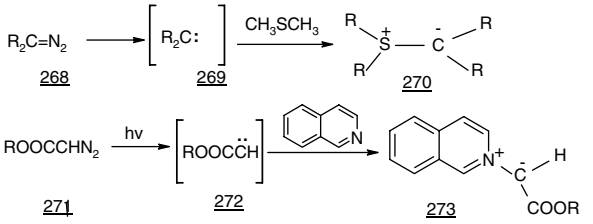

SCHEME 52

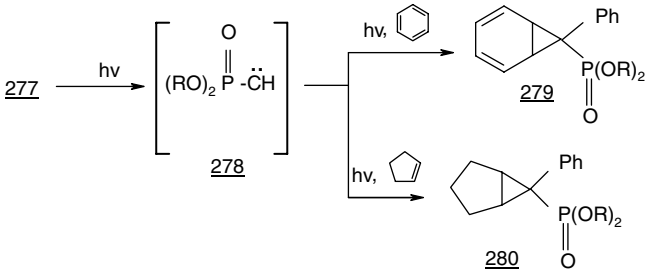

SCHEME 53

Mono- and dinitro-diazomethane are known.[136,137] Diazofluorenylidenes **263** to **265** add to styrenes and other olefins, mainly affording cyclopropanes **267** (Scheme 51).[108,138,139]

Reviews of nitrogen-containing carbenes are available.[1,3,140] Although only a few stable ylides have been made from keto- or carbalkoxycarbenes, **269** and **272** form a stable ylides with alkyl sulfides[141] and isoquinoline,[142] such as **270** and **273**, respectively (Scheme 52).

Phosphorus-Containing Carbenes[143]

Generation of phosphorus-containing carbenes from the corresponding diazo precursors is known. Phosphinocarbene (PC) has been also isolated as distillable oil and shown to react either as a carbene or a phosphaacetylene.[1,3]

Addition to olefins and benzene leads to cyclopropanes **280**, insertion products and norcaradienes **279** (Scheme 53).[144,145]

TABLE 91.8 Stability of Carbenes 283 and 284 and Their Diazo Precursors 281 and 282

	R^1	R^2	R^3	Diazo Stability	Carbene Stability
281, 283a	*i*-Pr_2N	*i*-Pr_2N	$SiMe_3$	bp 85–90°C, 10^{-2} mmHg	bp 75–80°C, 10^{-2} mmHg Several weeks at 25° C
281, 283b	Tmp[a]	*i*-Pr_2N	$SiMe_3$	Few minutes at 25°C	Several weeks at 25°C
281, 283c	Tmp[a]	*i*-Pr_2N	$Si(i\text{-}Pr)_3$	Several days at 25°C	Several weeks at 25°C 1h at 35°C
281, 283d	Tmp[a]	Ph	$SiMe_3$	Few minutes at 25°C	Few hours at 25°C
282, 284a	*i*-Pr_2N	*i*-Pr_2N	PR_2H[+b]	Not observed at 25°C	mp 88°C Indefinitely at 25°C
282, 284b	*i*-Pr_2N	*i*-Pr_2N	PR_2Cl[+b]	Not observed at 25°C	Few days at 25°C in solution

[a] Tmp = 2, 2, 6, 6-tetramethylpiperidino. [b]R = N*i*-Pr_2.

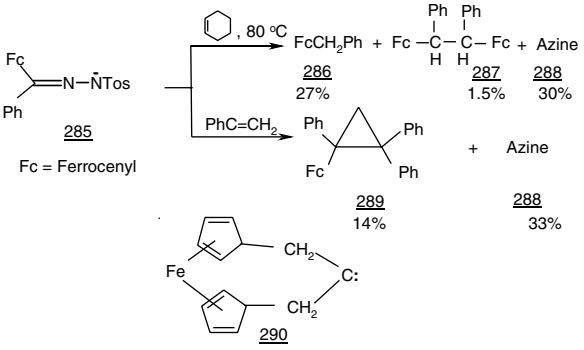

SCHEME 54

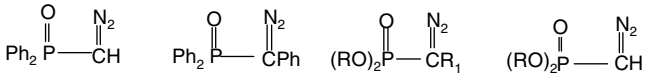

Phosphorus-containing carbenes insert into the OH bond of methanol and undergo a Wolff-type rearrangement. The ease of insertion and addition depends on the group attached to the carbene carbon atom.[144]

Bulky substituents kinetically stabilize phosphinocarbenes, but the stability of carbene is often inversely proportional to that of the diazo precursor.

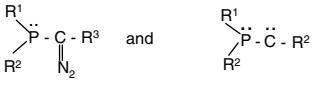

281 and 282 283 and 284

Carbene Containing Other Elements

Several diazo compounds, carbene precursors, containing iron, silicon, cadmium, zinc, germanium, lead, tin, mercury, silver, or lithium are known. Ferrocenylphenylcarbene and ferrocenylmethylcarbene are found to behave similar to diphenylcarbene in their reactions with olefins (Scheme 54).[146-148]

Silicon-containing carbenes, such as trimethylsilydiazomethane (**291**), afforded cyclopropanes **292** and **293** on catalyzed decomposition (Scheme 55).[149]

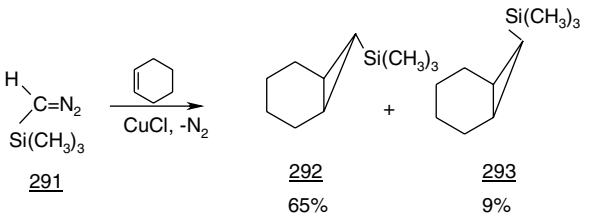

SCHEME 55

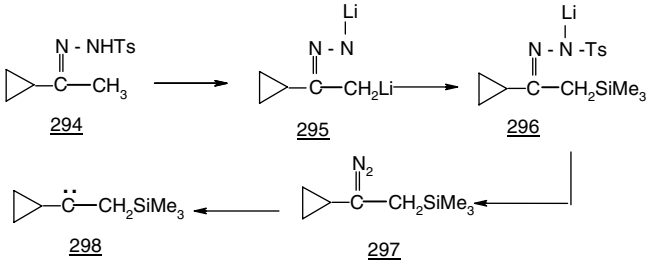

SCHEME 56

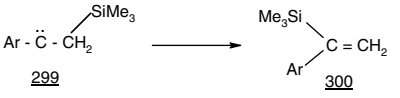

SCHEME 57

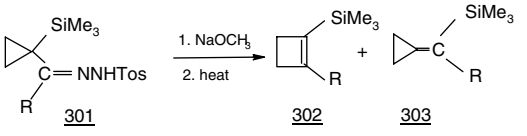

SCHEME 58

The chemistry of carbenes containing trimethylsilyl groups in the vicinity of the carbenic center has great interest.

The tosylhydrazone salt pyrolysis method was used for generation of the diazocompound and carbene (Scheme 56).[150]

Additionally, the trimethyl group is quite prone to migrate to carbon centers or activates hydrogen toward hydride migration to the carbene center (Scheme 57).[151] Computational studies show a substantial interaction of the vaccant carbene orbital with the adjacent C–Si bond (Scheme 58).[151] Concerted loss of molecular nitrogen and rearrangement remains a possibility.[150]

Carbenes containing ferrocenyl substituents $(Fc)_2$ are summarized and the reactivity of these carbenes was explored (Scheme 59).[10]

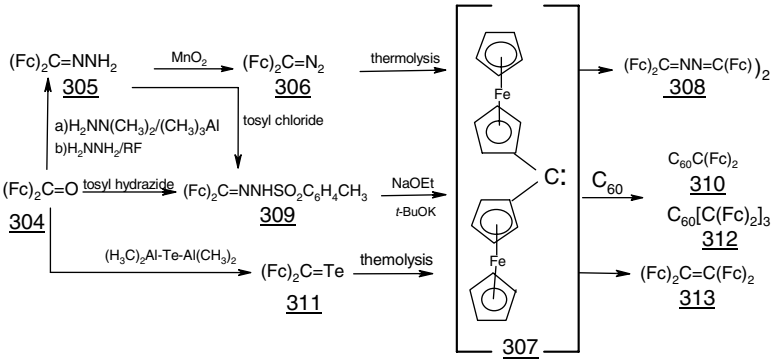

SCHEME 59

References

1. Bourissou, D., Guerret, O., Gabbai, F.P., and Bertrand, G., Stable Carbenes, *Chem. Rev.*, 100, 39, 2000.
2. Regitz, M., Stable carbenes — illusion or reality, *Angew. Chem. Int. Ed. Engl.*, 30, 674, 1991.
3. Tomioka, H., Persistent Triplet Carbenes, in *Advances in Carbene Chemistry*, Vol. 2, Brinker, U.H., JAI Press, Inc, 1998, 175–214.
4. Herman,W. A. and Kocher, C.,N-Heterocyclic carbenes, *Angew. Chem. Int. Ed. Engl.*, 36, 2162, 1997.
5. (a) Dixon, D.A., Dobss, K.D., Arduengo, III, A.J., and Bertrand, G., Electronic structure of λ^5-phosphaacetylene and corresponding triplet methylene, *J. Am. Chem. Soc.*, 113, 8782, 1991; (b) Soleihavoup, M., Baceiredo, A., Treutler, O., Ahlrichs, R., Nieger, M., and Bertrand, G., Synthesis and x-ray crystal structure of $[(\text{iso-Pr}_2\text{N})_2\text{P (H)CP (N-iso-Pr}_2)_2]^+\text{CF}_3\text{SO}_3^-$, a carbene, a cumulene, or a phosphaacetylene, *J. Am. Chem. Soc.*, 114, 10959, 1992.
6. Arduengo, A.J., III, Rasikadias, H.V., Dixon, D.A., Harlow, R.L., Klooster, W.T., and Koetzle, T.F., Electron distribution in stable carbene, *J. Am. Chem. Soc.*, 116, 6812, 1994.
7. (a) Heinemann, C., Müller, T., Apeloig, Y., and Schwarz, H., On the question of stability, conjugation and aromaticity in imidazol-2-ylidenes and their silicon analogs, *J. Am. Chem. Soc.*, 118, 2023, 1996; (b)Boehme, C. and Frenking, G., Electronic structure of stable carbenes, silylenes and germylenes, *J. Am. Chem. Soc.*, 118, 2039, 1996.
8. Hoffman, R., Trimethylene and the addition of methylene to ethylene, *J. Am. Chem. Soc.*, 90, 1475, 1968.
9. (a) Symous, M., *Chemical and Biochemical Aspects of Electron — Spin Resonance Spectroscopy*, Van Nostrand Reinhold, New York, 1978; (b) *Determination of Organic Structures by Physical Methods*, Vol. 3, Nachod, F.C. and Zuckermann, J.J., Eds., Academic Press, New York, 1971.
10. Bildstein, B., Carbenes with ferrocenyl substituents, *J. Organometallic Chemistry*, 618, 28, 2001.
11. Hopkins, J.M., Bowdridge, M., Robertson, K., Cameron, S., Jenkins, H.A., and Clyburne, J.A.C., Generation of azines by the reaction of nucleophilic carbene with diazo-alkanes, *J. Org. Chem.*, 66, 5713, 2001.
12. Cheng, M.J. and Hu, C.-H., Computational study on the stability of imidazol-2-ylidenes and imidazolin-2-ylidenes, *Chem. Phys. Lett.,* 349 (5-6), 477, 2001.
13. Hu, Y., Hiral, K., and Tomioka, H., Effect of para substituents on the molecular and electronic structures of sterically congested triplet diphenylcarbenes*, J. Phys. Chem. A*, 103, 9280, 1999.
14. Moss, R.A. and Jones, I., Jr., *Carbenes I and II*, John Wiley & Sons, NewYork, 1973.
15. Kirmse, W., *Carbene Chemistry*, Academic Press, New York, 1971.

16. (a) Regitz, M. and Maas, G., *Diazo Compounds, Properties and Synthesis*, Academic Press, London, 1986; (b) Zimmerman, H.E. and Paskovich, D.H., A study of hindered divalent carbon species and diazo compounds, *J. Am. Chem. Soc.*, 86, 2149, 1964.
17. (a) Gould, I.R., Turro, N J., Butcher, J., Jr., Doubleday, C., Jr., Hacker, N.P., Lehr, G.F., Moss, R.A., Cox, D.P., Guo, W., Munjal, R.C., Perez, L.A., and Fedorynski, M., Time resolved flash-spectroscopic investigations of the reactions of singlet arylhalocarbenes, *Tetrahedron,* 41, 1787, 1985; (b) Brinton, R.K. and Volman, D.H., The ultraviolet absorption specrta of gaseous diazomethane and diazoethane. Evidence for the existence of ethylidene radicals in diazoethane photolysis, *J. Chem. Phys.*, 19, 1934, 1951; (c) Closs, G.D. and Moss, R.A., Carbenoid formation of acrylcyclopropanes from olefins, benzal bromides and organolithium compounds and from photolysis of aryldiazomethanes, *J. Am. Chem. Soc.*, 86, 4042, 1964; (d) Kirmse, W. and Horner, L., Quantenausbeuten der Photolyse Aliphatischer Diazoverbindungen, *Liebigs Ann. Chem.*, 625, 34, 1959; (e) Closs, G.L. and Coyle, J.J., The halogenation of diazomethane. Study of the reactivities of carbeness derived from halodiazomethanes, *J. Am. Chem. Soc.*, 87, 4270, 1965; (f) Dürr, H., and Scheppers, G., Reaktionen von Carbena-cyclopentadienen mit Cyclohepta-trienen, *Liebigs Ann. Chem.*, 740, 63, 1970; (g) Strausz, O. P., Do Minh, T., and Fout, J.J., The formation and reactions of monovalent carbon intermediates. II. Further studies on the decomposition of diethyl-mercury-bisdiazoacetate, *J. Am. Chem. Soc.*, 90, 1930, 1968.
18. Garcia-Garibay, M.A., Shin, S., and Sanrame, C.N., Engineering reactions in crystalline solids: prediction of molecular carbene rearrangement, *Tetrahedron*, 56, 6729, 2000.
19. Moss, R.A. and Pilkiewicz, F.G., Crown ethers in carbene chemistry. The generation of free phenylhalocarbenes, *J. Am. Chem. Soc.*, 96, 5632, 1974.
20. Moss, R.A., Joyce, M.A., and Huselton, J.K., The olefinic selectivity of dibromocarbene, *Tetrahedron Lett.,* 4621, 1975.
21. Stang, P.I. and Magnum, M.G., Unsaturated carbenes from primary vinyl triflates. The nature of vinylidene carbene intermediates, *J. Am. Chem. Soc.*, 91, 6478, 1975.
22. (a) Cox, D.P., Gould, I.R., Hacker, N.P., Moss, R.A., and Turro, N.J., Absolute rate constant for the addition of halophenylcarbene to alkenes; a reactivity- selectivity relation, *Tetrahedron Lett.*, 24, 5313, 1983. (b) Moss, R.R., Fan, H., Handel, L.M., Shen, S., Wloshtowska, J., Wlostowski, M., and Krogh-Jespersen, K., Chloroacrylonitrile, a detector substrate for carbene nucleophilicity, applications to phenylhalocarbene, *Tetrahedron Lett.*, 28, 4779, 1987.
23. Berhinger, H. and Mainer, M., Ein neuer Abbau des Tetrazol-rings-Acetylen aus substituierten 5-Methyl-1H-tetrazolen, *Tetrahedron Lett.*, 1663, 1966.
24. Mass, G. and Bruckmann, R., Preparation of 1-aryl-2-siloxyalkynes from silylated α-diazocarbonyl compounds, *J. Org. Chem.*, 50, 2801, 1985.
25. Northington, D.J. and Jones, W.M., Diphenyldiazoalkenyll diazotate, *Tetrahedron Lett.*, 317, 1971.
26. Hezberg, G. and Shoosmith, J., Spectrum and structure of the free methylene radical, *Nature,* 183, 1801, 1959.
27. Herzberg, G., The spectra and structure of free methyl and free methylene radical, *Proc. Roy. Soc. London Ser. A,* 262, 291, 1961.
28. Herzberg, G. and John, J.W.C., The spectrum and structure of singlet CH_2, *Proc. Roy. Soc. London Ser. A,* 295, 107, 1966.
29. Braun, W.A., Bass, A.M., and Pelling, M., Flash photolysis of ketene in diazomethane: the production and reaction kinetics of triplet and singlet methylene, *J. Chem. Phys.*, 52, 5931, 1970.
30. Borodko, Y.G., Shilov, A.E., and Shteinmann, A.A., Molecular nitrogen activation, *Dokl. Akad. Nauk. SSSR*, 168, 581, 1966; *Chem. Abstr.,* 65, 8198, 1966.
31. Liu, M.T., The thermolysis and photolysis of diazines, *Chem. Soc. Rev.*, 11, 127, 1981.
32. Bernheim, R.A., Berhard, H.W., Wang, P.S., Wood, K.S., and Skell, P.S., ^{13}C Hyperfine interaction in CD_2, *J. Chem. Phys.*, 54, 4120, 1971.
33. Wasserman, E., Kuck, V.J., Hutton, R.S., Anderson, E.P., and Yager, W.A., ^{13}C Hyperfine interaction and geometry of methylene, *J. Chem. Phys.*, 54, 13309, 1971.

34. Bernheim, R.A. and Chien, S.H., EPR of methylene-temperature dependence in xenon matrix, *J. Chem. Phys.*, 66, 5703, 1977.
35. Shavitt, I., Geometry and singlet-triplet energy gap in methylene: a critical review of experimental and theoretical determinations, *Tetrahedron*, 41, 1533, 1985.
36. Roth, H.D., Reaction of methylene in solutions. Selective abstraction reactions of $^1CH_2$ and $^3CH_2$, *J. Am. Chem. Soc.,* 93, 4935, 1971; Roth, H.D., Chemically induced nuclear spin polarization in the study of carbene reaction mechanisms, *Acc. Chem. Res.,* 10, 85, 1977.
37. Turro, N.J. and Cha, Y., Spectroscopic and chemical evidences for methylene singlet-triplet intersystem crossing in solution, *Tetrahedron Lett.*, 27, 6149, 1986.
38. Turro, N.J., Cha, Y., and Gould, I.R., Reactivity and intersystem crossing of singlet methylene in solution, *J. Am. Chem. Soc.*, 109, 2101, 1987.
39. Turro, N.J., Cha, Y., Gould,, I.R., Padwa, A., Gasdaska, J.R., and Tomos, M., Carbene and silicone routes toward a simple nitrile ylide. Spectroscopic, kinetic and chemical characterization, *J. Org. Chem.*, 50, 4417, 1985.
40. Padwa, A., Gasdaska, I.R., Tomas, M., Turro, N.J., Cha, Y., and Gould, I.R., Carbene and silicone routes as methods for the generation and dipolar cycloaddition reactions of methylnitrilylide, *J. Am. Chem. Soc.*, 108, 6739, 1986.
41. Mansor, A.M. and Stevens, I.D.R., Hot radical effects in reactions, *Tetrahedron Lett.*, 1733, 1966.
42. Shang, K.T. and Shechter, U., Roles of multiplicity and electronic excitation on intermolecular reactions of alkyl-carbenes in condensed phase, *J. Am. Chem. Soc.*, 101, 5082, 1979.
43. Frey, H.M. and Stevens, I.D.R., The photolysis of 3-t-butyl-diazine, *J. Chem. Soc.,* 1301, 1965.
44. Kraska, A.R., Chang, S.T., Mosely, C.C., and Shechterr, H., The effects of multiplicity and excitation on the behavior of 2-methyl-2-phenyl-propylidene. The intermolecular chemistry of 2,2-diphenylpropylidene, *Tetrahedron Lett.*, 23, 1627, 1982.
45. Hantzsch, A. and Lehman, M., Über Derivate des Isodiazomethans, *Ber. Dtsch. Chem. Ges.,* 34, 2506, 1901.
46. Staudinger, H. and Kupfer, O., Über Reaktionen des Methylens. III. Diazomethan, *Ber. Dtsch. Chem. Ges.,* 45, 501, 1912.
47. Hine, J., Carbon dichloride as an intermediate in the basic hydrolysis of chloroform. A mechanism for substitution reactions at a saturated carbon atom., *J. Am. Chem. Soc.*, 72, 2438, 1950.
48. Doering, W.V.E. and Hoffmann, A.K., The addition of dichlorocarbene to olefins, *J. Am. Chem. Soc.*, 67, 6162, 1952.
49. Kirmse, W., Neues über Carbene, *Angew. Chem.*, 73, 161, 1961.
50. Dürr, H., Triplet-intermediates from diazo-compounds — Carbenes, *Topics Curr. Chem.*, 55, 87, 1975.
51. Figurea, J.M., Fernandez, E., and Avila, J., Photolysis of diazo-n-propane. A route for the photochemical activation of propylene, *J. Phys. Chem.*, 78, 1348, 1974.
52. Figurea, J.M., Perez, J.M., and Wolf, A.P., Photolysis of diazo-n-butane, *J. Chem. Soc., Faraday Trans. I*, 1905, 1975.
53. Brian, W., David, L.K., Structure and stabilities of adducts of carbenes and fullerenes, *J. Mol. Struct. (Theochem)*, 548, 61, 2001.
54. Kirmse, W. and Horn, K., Vergleich der katalytischen und photolytischen Zersetzung von Diazoalkanen, *Chem. Ber.*, 100, 2698, 1967.
55. Zeller, K.-P. and Guel, H., Houben-Weyl, *Methoden der Org. Chemie*, Band E 19b/1, Regitz, M., Georg Thieme Verlag, Stuttgart, New York, 1989, chap. 2.
56. Baron, W.J., De Camp, M.R., Hendrick, M.E., Jones, M., Jr., Levin, H., and Sohn, M.B., *Carbenes I*; Jones, M. and Moss, R.A., Eds., John Wiley & Sons, New York, 1973, chap. 1.
57. Lemal, D.M., Menger, F., and Clark, G.W., Bicyclobutane, *J. Am. Chem. Soc.,* 85, 2529, 1963.
58. Closs, G.L., Closs, l.E., and Böll, W.A., The base-induced pyrolysis of tosylhydrazones of α,β-unsaturated aldehydes and ketones. A convenient synthesis of some alkylcyclopropanes, *J. Am. Chem. Soc.*, 85, 3796, 1963.

59. Arnold, D.R., Humphreys, R.W., Leigh, W.J., and Palmer, G.E., Electronic excited state of small ring compounds — cyclopropene, vinylcarbene, *J. Am. Chem. Soc.*, 98, 6225, 1976.
60. Skell, P.S. and Klebe, J., Structure and properties of propargylene C_3H_2, *J. Am. Chem. Soc.*, 82, 241, 1960.
61. Shapiro, R.H., Alkenes from tosylhydrazones, *Org. React.*, 23, 405, 1976.
62. Bockes, F. and Brinker, U.H., *Carbene (oide) Carbine*, Houben Weyl, Vol E 19b/1, Thieme Verlag, Stuttgart, 1989.
63. Moss, R.A. and Wetter, W.P., Cyclopropylphenylcarbene — thermal control of intermolecular addition, *Tetrahedron Lett.*, 22, 997, 1981.
64. Galluci, R. and Jones, M., Jr., The Stereochemistry of intramolecular reactions of cyclopropylcarbenes. *J. Am. Chem. Soc.*, 98, 7704, 1976.
65. Eaton, P.E. and Hoffmann, K.-L., 9-Phenyl- (9)-monocarbene — probably the most twisted olefin yet known and the carbene 1-phenyl-9-homocubylidene, its rearrangement product, *J. Am. Chem. Soc.*, 109, 5285, 1987.
66. Moss, R.A., Fantina, M.E., and Munjal, R.C., Intermolecular addition of cyclobutylchlorocarbene, *Tetrahedron Lett.*, 1277, 1979.
67. Wilt, J.W., Kostruic, J.M., and Orlowski, R.C., Ring-size effects in the neophyl rearrangement. V. The carbenoid decomposition of 1-phenyl-cycloalkane-carboxaldehyde tosylhydrazones, *J. Org. Chem.*, 30, 1052, 1965.
68. White, E.H., Meier, G.E., Graeve, R., Zirngibl, U., and Friend, E.W., The synthesis and properties of diphenyl-cyclopropenyldiazomethane and a structure assignment of the so-called diphenyltetrahedrane, *J. Am. Chem. Soc.*, 88, 611, 1966.
69. Zimmerman, H.E. and Sousa, L.R., Cycloheptatrienyldiazomethane. Its synthesis and behavior; C_3H_8 chemistry, correlation diagrams and nodal properties, *J. Am. Chem. Soc.*, 94, 834, 1972.
70. Jones, W.M. and Walbrick, J.M., Effects of solvent on the cyclopropylidene-alkene conversion, *J. Org. Chem.*, 34, 2217, 1969.
71. Jones, W.M. and Wilson, Jr., J.W., The stereochemistry of the cyclopropane-alkene conversion, *Tetrahedron Lett.*, 1587, 1965.
72. Frey, H.M. and Scaplehorn, A.W., Thermal decomposition of the diazirines. II. 3, 3-Tetramethylenediazirine, 3, 3-pentamethylenediazirine and 3, 3-diethyl-diazirine, *J. Chem. Soc. (A)*, 968, 1966.
73. Friedman, L. and Shechter, H., Transannular and hydrogen rearrangement reactions in carbenoid decomposition of diazocycloalkanes. *J. Am. Chem. Soc.*, 83, 3159, 1961.
74. Dürr, H., Reactivity of cycloalkenecarbenes, *Topics Curr. Chem.*, 40, 103, 1973.
75. Chapman, O.L., Photochemistry of diazocompounds and azides in argon, *Pure Appl. Chem.*, 51, 331, 1979.
76. Baird, M.S., Dunkin, I.R., Hacker, N., Poliakoff, M., and Turner, J.J., Cyclopentadienylidene — a matrix isolation study exploiting photolysis with unpolarized and plane-polarized light, *J. Am. Chem. Soc.*, 103, 5190, 1981.
77. Kirmse, W, Loosen, K., and Sluma, H. D., Carbenes and the O-H bond: cyclopentadienylidene and cycloheptatrienylidene, *J. Am. Chem. Soc.*, 103, 5935, 1981.
78. Dürr, H. and Scheppers, G., Addition von Carbena-cyclopentadienen an Benzol, *Liebigs Ann. Chem.*, 734, 141, 1970.
79. Dürr, H. and Scheppers, G., Reaktion des photochemisch erzeugten Carbens 1,2,3,4-Tetraphenyl-5-carbena-cyclopentadien-(1. 3) mit Olefinen, *Chem. Ber.*, 100, 3236, 1967.
80. Dürr, H. and Bujnoch, W., Gezielte Erzeugung von Triplett-carbena-cyclopenta-dienen durch "Energy Transfer", *Tetrahedron Lett.*, 1433, 1973.
81. Dürr, H. and Scheppers, G., Photochemische Synthese von substituierten 5H- und 7H-Benzocycloheptenen, *Angew. Chem.*, 80, 359, 1968.
82. Mc Bee, E.T. and Sienkowski, K.J., The preparation and photolysis of tetrabromodiazocyclopentadiene, *J. Org. Chem.*, 38, 1340, 1973.

83. Dürr, H. and Schrader, L., Eine neue Benzo-cyclopropen Synthese, *Angew. Chem.*, 81, 426, 1969.
84. Koser, G.F. and Pirkle, H.W., *J. Org. Chem.*, 32, 1992, 1967.
85. Bertani, R., Biasiolo, M., Darini, K., Michelin, R.A., Mozzon, M., Viisentin, F., and Zanotto, L., Catalytic transformation of diazo compounds promoted by, Pt (0) and dicationic Pt (II) complexes, *J. Organomet. Chem.*, 642, 32, 2002.
86. Trozzolo, A.M. and Wasserman, E., *Carbenes II, Moss*, R.A. and Jones, M., Jr., Eds., John Wiley & Sons, New York, 1975, 185.
87. Chuang, C., Lapin, S.C., Schrock, A.K., and Schuster, G.B., Dimethoxy-fluorenylidene — a ground state singlet carbene, *J. Am. Chem. Soc.*, 107, 3238, 1985.
88. Lapin, S.C. and Schuster, G. B., Chemical and physical properties of 9-xanth-ylidene — a ground state singlet aromatic carbene, *J. Am. Chem. Soc.*, 107, 424, 1985.
89. Itakura, H. and Tomioka, H., Generation and characterization of triplet anthryl (aryl)carbenes, *Org. Lett.*, 2, 2995, 2000.
90. Itakura, H., Mizuno, H., Hirai, K., and Tomioka, H., Generation, characterization and kinetics of triplet di[1,2,3,4,5,6,7,8-octahydro-1,4:5,8-di-(ethano)anthryl]carbene, *J. Org. Chem.*, 65, 8797, 2000.
91. Chedekel, M.R., Skoglund, M., Kreeger, R.L., and Shechter, H., Solid state chemistry — discrete trimethylsilylmethylene, *J. Am. Chem. Soc.*, 98, 7864, 1976.
92. Meier, H., *Chemistry of Diazirines II*, Liu, M.T.H., Ed., CRC Press, Boca Raton, FL, 1987, chap. 6.1.
93. Liu, M.T.H. and Ramakrishnan, K., Thermal decomposition of phenylmethyl-diazirine — effect of solvent on product distribution, *J. Org. Chem.,* 42, 3450, 1977.
94. Cox, D.P., Moss, R.A., and Terpenski, J., Exchange reactions of halodiazirines — synthesis of fluorodiazirines, *J. Am. Chem. Soc.*, 105, 6513, 1983.
95. Moss, A.R. and Ma, W., Rearrangements of cyclopropylmethyl-chlorocarbene and dicyclopropyl-chlorocarbene, *Tetrahedron Lett.,* 42, 8923, 2001.
96. Moss, R.A., Ma, W., Zheng, F., and Sauers, R.R., Probing charge alteration in the -mediated rearrangement of 1-indanylchlorocarbene, *Tetrahedron Lett.,* 42, 1419, 2001.
97. (a) Moss, R.A. and Ma, Y., The 1, 2-diphenylethyl cation via carbene fragmentation, *Tetrahedron Lett.*, 42, 6045, 2001; (b) Naito, I., Uryu, T., Sasaki, H., Ishikawa, T., Kobayashi, S., Kamato, I., and Oku, A., *J. Photochem. Photobiol., A: Chem.*, 140, 33, 2001.
98. Romashin, Y.N., Liu, M.T.H., and Bonneau, R., Sulfur ylides generated from the reaction of arylchlorocarbenes with trimethylenesulfide, *Tetrahedron Lett.,* 42, 207, 2001.
99. (a) Trost, B.M. and Melvin, Jr., L.S., *Sulfur Ylides*, Academic Press, New York, 1975; (b) Ando, W, in *The Chemistry of Diazonium and Diazo Groups*, Patai, S., Ed., John Wiley & Sons, New York, 1978.
100. Chevolot, Y., Martins, J., Milosevic, N., Leonard, D., Zeng, S., Malissard, M., Berger, E.G., Maier, P., Mathieu, H.J., Crout, D.H.G., and Sigrist, H., Immobilisation on polystyrene of diazirine derivatives of mono-and disaccharides, *Biorg. Med. Chem.*, 9, 2953, 2001.
101. Kuzai, M., Luerssenn, H., and Wentrup, C., ESR-spectroscopischer Nachweis thermisch erzeugter Triplet — Nitrene und photochemisch erzeugter Triplet- Cycloheptatrienylidene, *Angew. Chem.*, 98, 476, 1986.
102. Wentrup, C., *Arylcarbene* in Houben Weyl B E 19/1, 848, Thieme Verlag, Stuttgart, 1989, 848.
103. Gutsche, C.D., Bacham, G.L., and Coffey, R.S., Chemistry of bivalent carbon intermediates. IV. Comparative intermolecular and intramolecular reactivities of phenylcarbene to various bond types, *Tetrahedron*, 18, 617, 1962.
104. Jones, M., Jr. and Rettig, K.R., Some properties of triplet fluorenylidene — detection of singlet state, *J. Am. Chem. Soc.*, 87, 4015, 1965.
105. D'yakonov, I.A., Dushina, V.P. and Goldonikov, Reaction of 9-diazofluorene with trimethylvinyl-silane, *Zh. Obsch. Khim.*, 39, 923, 1969; *J. Gen. Chem., USSR*, 39, 887, 1969.
106. Jones, M., Jr., Ando, W., Hendrick, M.E., Kukzycki, A., Howey, P.M., Hummel, K.M. and Malamennt, D.S., Irradiation of methyl-diazomalonate in solution — reactions of singlet and triplet carbenes with carbon-carbon double bonds, *J. Am. Chem. Soc.*, 94, 7469, 1972.

107. (a) Dürr, H. and Kober, H., Photochemistry of small ring compounds — new spirocaradienes. Reversible norcaradiene–cycloheptatriene valence isomerization, *Angew. Chem. Int. Ed. Engl.*, 10, 342, 1971; (b) Murray, R.W. and Kaplan, M.L., Sigmatropic reactions in the 1, 4-bis (cycloheptatrienyl)benzene isomers, *J. Am. Chem. Soc.,* 88, 3527, 1966; (c) Muraharashi, S.I., Yoshimura, Y.Y., and Moritani, I., Quintet carbenes: *m*-phenylene-bis(phenylmethlene) and *m*-phenylene-bis(methylene), *Tetrahedron*, 28, 1385, 1972.
108. Dürr, H., Abdel-Wahab, A.A., Ismail, M.T., and Mohamed, O.S., Multiplicity and selectivity of cyclopent[*a*]acenaphthylenylidene, *J. Photochem. Photobiol., A: Chem.,* 132, 167, 2000.
109. Weygand, F. and Bestman, H.J., Neue präparative Methoden der Org. Chemie III. Synthesen unter Verwedung von Diazoketonen, *Angew. Chem*., 72, 535, 1960.
110. Maas G., *Organooxycarbonylcarbene*, in Houben Weyl, B. E. 19b/ Part 2, p. 1134, Thieme Verlag, Stuttgart.
111. Warkentin, J., Singelton, E., and Edger, J.F., Reactions of ethyl diazoacetate with cyclopentadiene; synthesis of the epimeric ethyl bicyclo[3.1.0]hex-2-ene-6-carboxylate, *Can. J. Chem*., 43, 3456, 1965.
112. Skell, P.S. and Etter, R.M., Steric determination in reactions of ethoxy-carbonylcarbene: norcaranecarboxylic acid, *Proc. Chem. Soc*., 433, 1961.
113. Pan, W., Hendrick, M.E., and Jones, M., Jr., Triplet carbenes and cyclooctatetraene, *Tetrahedron Lett.,* 40, 3085, 1999.
114. Freeman, P.K. and Kupar, D.G., Synthesis of bicyclo[3.2.1]-octa-3, 6-dien-2-one. An unusual valence isomerization, *Chem. Ind. (London),* 424, 1965.
115. Meinwald, J. and Wahl, Jr., G.H., Tetracyclo[3.3.0.0^{2,8}0^{4,6}]octan-3-one, *Chem. Ind. (London),* 425, 1965.
116. Moriconi, E.J. and Murray, J.J., Pyrolysis and photoysis of 1-methyl-3-diazooxidole. Base decomposition of isatin-2-tosylhydrazone, *J. Org. Chem*., 29. 3577, 1964.
117. Closs, G.L. and Schwartz, G.M., Carbenes from alkyl halides and organolithium compounds. II. The reactivity of chlorocarbene in its addition to olefins, *J. Am. Chem. Soc*., 82, 5729, 1960.
118. Sato, K., Shiomi, D., Takui, T., Itoh, K., Hattori, M., Hirai, K., and Tomioka, H., Persistent high-spin carbene (S = 3) as studied by 2D-ESTN spectroscopy, *Synth. Met.,* 103, 2269, 1999.
119. Bonneau, R., Romashin, Y.N., and Liu, M.T.H., Laser flash photolysis studies of nitrogen ylides generated by the reaction of arylchlorocarbenes with substituted vinylpyridines and 1-azabuta-1,3-dienes, *J. Photochem. Photobiol., A: Chem.,* 126, 31, 1999.
120. Romashin, Y.N., Liu, M.T.H., Ma, W., and Moss, R.A., New synthesis of
121. 2,2′-heteroarylpyrroles from heteroarylchlorocarbenes, *Tetrahedron Lett.,* 40, 7163, 1999.
122. Moss, R.A., Zheng, F., Sauers, R.R., and Toscano, J.P., The 2-norbornyl cation via fragmentation of exo- and *endo*-2-norbornyloxychlorocarbenes*, J. Am. Chem. Soc.* 123, 8109, 2001.
123. Mitsch, R.A., Difluorodiazirine. III. Synthesis of difluorocyclopropanes, *J. Am. Chem. Soc*., 87, 758, 1965.
124. Sander, W., Hubert, R., Kraka, E., Grafenstein, J., and Cremer, D., 4-Oxo-2,3,5,6-tetrafluorocyclohexa-2,5-dienylidene, *Chem.-Eur. J*., 6, 4567, 2000.
125. Van Leusen, A.M. and Strating, J., Chemistry of sulfonyldiazomethanes, *Quart. Rep. Sulfur. Chem*., 5, 67, 1970.
126. Schank, K., *Organothio-Sulfinyl-and Sulfonyl-carbene*, Houben Weyl, E 19b/Teilband 2, Thiema Verlag, Stuttgart, 1989.
127. Van Leusen, A.M. and Strating, J., Chemistry of α-diazosulfones. V. The synthesis of arylsulfonyldiazomethanes and alkylsulfonyldiazomethanes, *Recl. Trav. Chim. Pays-Bas*, 84, 151, 1965.
128. Regitz, M., *Transfer of Diazo Groups, Newer Methods of Preparative Organic Chemistry*, Vol. VI, Academic Press, New York, 1971.
129. Van Leusen, A.M., Mulder, R.J., and Strating, J., Chemistry of α-diazosulfone. IX. Synthesis of sulfonylcyclopropanes by addition of a sulfonylcarbene to alkenes*, Recl. Trav. Chim. Pays-Bas*, 86, 225, 1967.

130. Abramovitch, R.A. and Roy, J., Reactions of benzenesulfonylcarbene, *J. Chem. Soc., Chem. Commun*., 542, 1965.
131. Abdel-Wahab, A.A., Doss, S.H., Frühauf, E.M., Dürr, H., Gould, I.R., and Turro, N.J., Carbenadibenzocycloheptane —steady-state and time resolved spectroscopic laser studies, *J. Org. Chem*., 52, 434, 1987.
132. Sander, W., Strehl, A., and Winkler, M., Photochemistry of bis(sulfonyl) diazomethanes, *Eur. J. Org. Chem*., 3771, 2000.
133. Rigby, J.H., Laurent, S., Dong, W., and Danca, M.D., Bis(alkylthio)carbenes as novel reagents for organic synthesis, *Tetrahedron*, 56, 10101, 2000.
134. Rigpy, J.H. and Danca, M.D., Rapid construction of isatin derivatives via addition of bis(alkylthio)carbenes to aryl isocyanates, *Tetrahedron Lett.*, 40, 6891, 1999.
135. Ciganek, E., Dicyanocarbene, *J. Am. Chem. Soc*., 88, 1974, 1966.
136. Ciganek, E., 7,7-Dicyanonorcaradienes, *J. Am. Chem. Soc*., 87, 652, 1965.
137. Schöllkopf, U. and Markusch, P., Preparation of dinitrodiazomethane by nitration of nitrodiazomethane, *Angew. Chem. Int. Ed. Engl.*, 8, 612, 1969.
138. Schöllkopf, U., Tonne, P, Schäfer, H., and Markusch, P., Synthesen von Nitro-diazo-essigsäureestern, Nitro-cyan- und Nitro-trifluoromethyl-diazomethan, *Liebigs Ann. Chem.,* 722, 45, 1969.
139. Li, Y.Z. and Schuster, G.B., Photochemistry of 9-diazo-3,6-diazofluorene: through-space or through-bond transmission of electronic effects, *J. Org. Chem*., 52, 3957, 1987.
140. Mohamed, O.S., Dürr, H., Ismail, M.T., and Abdel-Wahab. A.A., A route to 4,5-diazofluorenylidene: preparation, photo- and thermal reactions of 9-diazo-fluorene, *Tetrahedron Lett*., 30, 1935, 1989.
141. Heydt, H. and Regitz, M., *Carbene mit einer N-funktion am Carben C-atom*, Houben Weyl, E 19b/2. Thieme Verlag, Stuttgart, 1989, 1785.
142. Ando, W., Yagihara, T. Tozune, S., and Migita, T., Formation of stable sulfonium ylides via photodecomposition of diazocarbonyl compounds in dimethyl sulfide, *J. Am. Chem. Soc*., 91, 2786, 1964.
143. Zugravesku, I., Rucinschi, E., and Surpateanu, G., The action of carbenes on *N*-heterocycles (1), *Tetrahedron Lett*., 941, 1970.
144. Heydt, H. and Regitz, M., *Phosphocarbene oder Azido-carbene*, Houben Weyl, E 19b/2, Thieme Verlag, Stuttgart, 1989, 1822.
145. Regitz, M., Scherer, H., and W., Anschütz, W., Uber die Reaktivität von Phosphoro-and Phosphinylcarbenen, *Tetrahedron Lett*., 753, 1970.
146. Günther, H., Tunggal, B.D., Regitz, M., Scherer, H., and Keller, T., Application of carbon 13 resonance spectroscopy. 2. Two new norcaradiene–cycloheptatriene equlibria, *Angew. Chem. Int. Ed. Engl.*, 10, 563, 1971.
147. Sonoda, A,. Moritani, I., Saraie, T., and Wada, T., Reactions of ferrocenyl carbenes. 3. Thermal decomposition of acylferrocene tosylhydrazone sodium salt, *Tetrahedron Lett*., 2943, 1969.
148. Sonoda, A. and Moritani, I., Reaction of ferrocenyl-carbene. III. Additions of some α-ferrocenylcarbenes to 1,1-diphenylethylene, *Bull. Chem. Soc. Jpn*., 43, 3522, 1970.
149. Sonoda, A. and Moritani, I. Reaction of Ferrocenyl-carbene. IV. Synthesis of [3]ferrocenophan-2-one tosylhydrazone and thermal decomposition of its sodium salt, *J. Organomet. Chem*., 26, 133, 1971.
150. Seyferth, D., Dow, A.W., Menzel, H., and Flood, T.C., Trimethylsilyldiazo-methane and trimethylsilylcarbene, *J. Am. Chem. Soc*., 90, 1080, 1968.
151. Creary, X. and Butchko, M.A., β-Trimethylsilyl cyclopropylcarbenes, *J. Org. Chem.,* 66, 1115, 2001.
152. Creary, X. and Butchko, M.A., β-Silylcarbenes from isolable diazosilanes, *J. Org. Chem*., 67, 112, 2002.

92

The Photochemistry of Diazirines

Tevye C. Celius
Johns Hopkins University

John P. Toscano
Johns Hopkins University

92.1 Introduction

Paulsen[1] and Schmitz and Ohme[2] synthesized the first alkyl diazirines independently in 1960. The cyclic structure of diazirines was then determined in 1962.[3,4] Almost immediately after their synthesis, diazirines were recognized as potentially useful photochemical and thermal precursors to carbenes. Unlike their valence isomers (diazo compounds), diazirines are relatively stable to most organic reagents and are reasonably stable in dilute solutions. As a result, the photolysis and thermolysis of diazirines has been studied extensively. Several reviews have been written on earlier experimental work.[5–8] This chapter focuses on recent experimental and theoretical progress.

92.2 Spectral Properties of Diazirines

Diazirines contain an N–N double bond constrained in a three-membered ring and have strong absorptions in both the infrared and ultraviolet/visible regions. The N=N stretching vibration of diazirines appears between 1560 and 1630 cm^{-1}.[8] In general, diazirines have an electronic absorption band between 310 and 350 nm ($n\pi^*$), and a second absorption below 200 nm.[8] Associated with the $n\pi^*$ transition is a weak fluorescence.[9,10] The fluorescence lifetime of adamantyldiazirine is on the order of 240 ps with a fluorescence quantum yield of about 0.0012 at ambient temperature.[10] (The lifetime increases with decreasing temperature.)

92.3 General Photoreactions of Diazirines

The most important photoreactions of diazirines are the generation of carbenes and the valence isomerization to linear diazo compounds (Scheme 1). At first glance, these appear to be straightforward processes; but under closer scrutiny, several experimental observations introduce complications.

The first indication that the mechanism is not as simple as the one outlined in Scheme 1 is that the product distributions from thermolysis of alkyl diazirines are markedly different from those of photolysis.

0-8493-1348-1/04/$0.00+$1.50

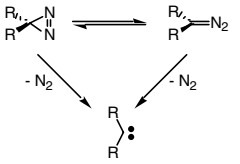

SCHEME 1

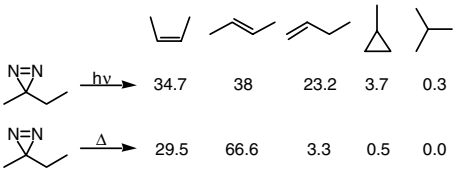

SCHEME 2

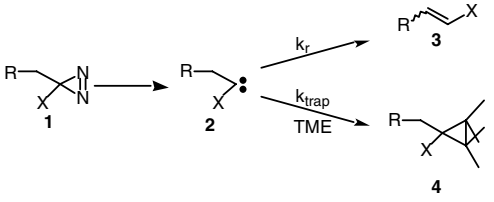

SCHEME 3

An example of such differences is shown in Scheme 2.[6,11–14] The simplest explanation of these results is that different intermediates are involved in the photolysis and thermolysis reactions. Numerous other examples of such systems have been reported in the literature.[6,11,15–21]

Another experimental observation indicative of the involvement of a second intermediate comes from carbene trapping studies. At high concentrations of carbene trap, apparent intramolecular rearrangements are not completely averted. If intramolecular rearrangement products are derived solely from a carbene intermediate, the ratio of trapped products to rearrangement products should increase linearly with increasing concentrations of carbene trap (Scheme 3). However, such trapping experiments have been carried out on a number of diazirines and show curved relationships between the product ratio and trap concentration.[22–29] Additionally, if trapping experiments are performed on non-nitrogenous precursors such as cyclopropylphenanthrenes, linear relationships are now observed.[18,26,30–35]

92.4 Mechanisms for the Photochemical Reactions of Diazirines

In light of the above results, the involvement of another intermediate is required but the question of its identity remains. A number of intermediates have been proposed, including a carbene-olefin complex (COC),[22] an excited carbene,[36] a diazo compound,[37] an excited-state diazirine,[9] and a biradical.[38–41] These proposed intermediates are potentially involved in two types of mechanisms: the COC mechanism and the rearrangement in the excited-state (RIES) mechanism.

The COC mechanism was originally proposed to explain the negative activation energies observed for carbene-olefin addition reactions.[42,43] Later, Liu and Tomioka used this mechanism to explain the curved correlations between the ratio of trapping products to rearrangement product and concentration of carbene trap.[22,23,44] They proposed that the second intermediate was a COC in equilibrium with the initially generated carbene intermediate (Scheme 4).

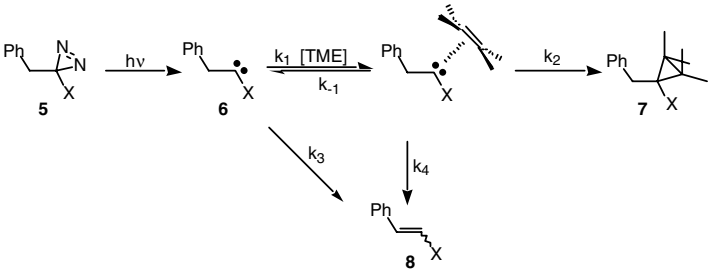

SCHEME 4

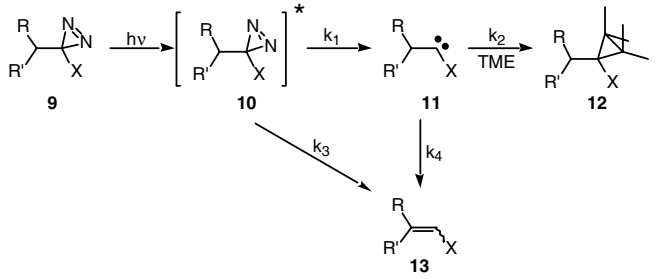

SCHEME 5

Application of the steady-state approximation predicts that the ratio of rearrangement to trapping products (**8**:**7**) will be linearly correlated with the inverse of the olefin concentration (Equation 92.1). This correlation is in excellent agreement with the experimental results.[22,44]

$$\frac{rearrangement}{trapping} = \frac{\mathbf{8}}{\mathbf{7}} = \frac{k_4}{k_2} + \frac{k_3(k_{-1} + k_4 + k_2)}{k_1 k_2 [TME]} \tag{92.1}$$

Although the COC mechanism can explain the experimental observations, there are two problems that have not been resolved. First, a carbene-olefin complex has never been experimentally detected. Second, modern *ab initio* calculations do not predict free energy minima corresponding to COCs in the reaction of chlorocarbenes with olefins.[45–48] They do, however, predict thermally stable π–complexes between benzene and carbenes, indicating that a COC mechanism might be operative if reactions are run in aromatic solvents.[48–51]

The remaining proposed intermediates involve rearrangement from the excited diazirine. This type of explanation was first put forward by Frey[52] and then more recently by Platz and co-workers.[9,10,37,53–55] In this mechanism, an intermediate is formed from the excited diazirine that leads directly to the rearrangement products (Scheme 5). This second intermediate is not defined in the kinetic scheme, but it has been proposed to be an excited carbene,[36] a biradical,[38] a diazo compound,[37] or the excited diazirine itself.[7,27] All of these proposed intermediates are thought to allow for concomitant extrusion of nitrogen and rearrangement.

Again, application of the steady-state approximation predicts that the ratio of rearrangement to trapping products (**13**:**12**) will be linearly correlated with the inverse of the olefin concentration (Equation 92.2).

$$\frac{\mathbf{13}}{\mathbf{12}} = \frac{k_3}{k_1} = \frac{k_4(k_1 + k_3)}{k_1 k_2 [TME]} \tag{92.2}$$

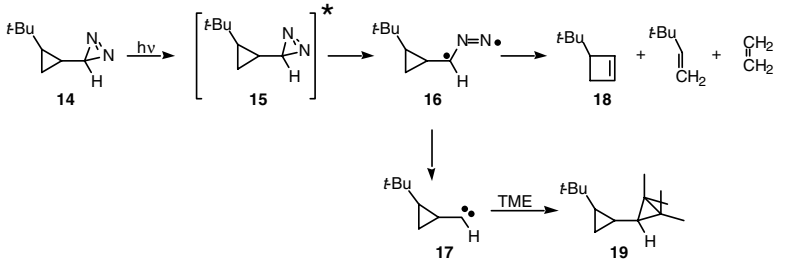

SCHEME 6

Numerous experiments have been performed on different diazirines in search of additional evidence for the RIES mechanism. These have included cyclobutylhalodiazirines,[29] *t*-butylchlorodiazirine,[28] 2,2-dimethylcyclopropylchlorodiazirine,[56] and *trans-t*-butylcyclopropyldiazirnine.[38,57] Of particular interest are the experiments on *t*-butylchlorodiazirine,[28] 2,2-dimethylcyclopropylchlorodiazirine,[56] and *trans-t*-buytlcyclopropyldiazirine.[38,57] When trapping experiments are performed on these systems, it is clearly demonstrated that some of the products are formed exclusively from a second intermediate and therefore lend support to the RIES mechanism.

In the case of *trans-t*-butylcyclopropyldiazirine, Platz and co-workers have proposed an open diazirine biradical (**16**) as the partitioning intermediate (Scheme 6). In the alkene trapping experiments, only a very small change in yield of **18** is observed, indicating that it is derived almost solely from the proposed biradical **16**.[38] Based on theoretical predictions, it is argued that biradical **16** is formed after passage through a conical intersection connecting the first and second singlet excited states. Passage through such an intersection would allow the biradical to be correlated directly with the ground-state products and starting materials.[38]

This scheme is in excellent agreement with the observation that the fluorescence lifetime increases with decreasing temperature,[38] indicative of the fluorescence being in competition with other excited-state processes. This competition in the excited state is further supported by the observation that the fluorescence intensity of diazirines that cannot rearrange, such as adamantyldiazirine and diazirine, fluoresce more strongly than those that can rearrange.[38] Platz and co-workers have performed fluorescence-lifetime measurements on adamantyldiazirine and determined that the barrier to other excited-state processes is between 2.7 and 2.9 kcal mol^{-1}.[10] Additionally, they observed no solvent dependence on the measured fluorescence lifetime, suggesting that the primary nonradiative processes of the first excited singlet state are intramolecular in nature.[10]

92.5 Isomerization of Diazirines to Diazo Compounds

Early experiments on the isomerization of diazirine were controversial. The gas-phase experiments of Amrich and Bell identified diazomethane as a reaction product and concluded that it was formed from isomerization of the starting diazirine.[58] Moore and Pimentel, however, conducted labeling experiments in a solid nitrogen matrix and determined that the diazomethane was formed from recombination of methylene and molecular nitrogen.[59]

Seburg and McMahon have performed matrix isolation experiments on both 3-methyldiazirine and diazoethane in an attempt to observe ethylidene.[60] They were unsuccessful in detecting the desired carbene but did observe isomerization of diazoethylene to 3-methyldiazirine. When matrix-isolated diazoethylene was photolyzed at 8K, ethene and 3-methyldiazirine were observed as the major products in a ratio of 10:1. Additionally, unlike Moore and Pimentel,[59] Seburg and McMahon did not observe isotopic label scrambling when the photolyses were conducted in an $^{15}N_2$ matrix.

Bonneau and Liu performed time-resolved UV-VIS and standard spectroscopic experiments to determine the quantum yield for formation of carbenes and diazo compounds from several diazirines.[61] In

the case of adamantyldiazirine, the quantum yields for formation of the corresponding carbene and diazo compounds were both 50%. The carbenes and diazo compounds, therefore, are formed in a 1-to-1 ratio. The quantum yields for formation of diazo compounds from isopropylchlorodiazirine and *n*-butylchloroaziridine were measured to be 10 to 13% and 10 to 15%, respectively. Bonneau and Liu used these results to argue that, for the isopropyl and *n*-butyl cases, conversion to the diazo compounds is not efficient enough to be the necessary "second" intermediate in the RIES mechanism.

In further agreement with the above results, the photoisomerization of benzylchlorodiazirine to the corresponding diazo compound has been observed using time-resolved infrared spectroscopy.[26] Additionally, the quantum yield of photoisomerization was determined to be 0.075, indicating that such an inefficient process would not likely be the source of the curvature observed in the olefin trapping experiments.

The partitioning of carbene and diazo formation from the photolysis of adamantyldiazirine has been determined by trapping experiments with C_{60}.[62] C_{60} reacts specifically with diazo compounds to yield fulleroids and with carbenes to form methanofullerenes. Photolysis of adamantyldiazirine in the presence of C_{60} gives carbene- and diazo-derived products in a ratio of 49:51, respectively, in excellent agreement with previous results.[37,61]

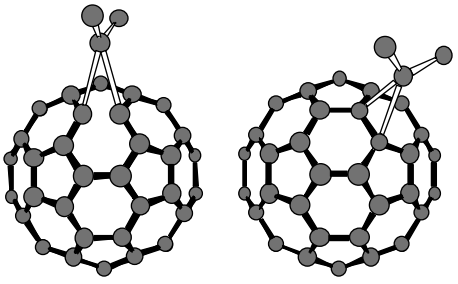

Fulleroid **Methanofullerene**

Most recently, this methodology has been extended to the isopropylchlorodiazirine and chloromethylchlorodiazirine systems.[63] For isopropylchlorodiazirine, the carbene, the diazo compound, and the RIES alkene products were formed in 5, 13, and 82% yields, respectively. These results are in excellent agreement with previous laser flash photolysis experiments[61] and quantum yield determinations.[37] For chloromethylchlorodiazirine, carbene and alkene from RIES are formed in 36 and 64% yields, respectively. Additionally, the *E*/*Z* ratio for the alkene is 28:72. Again, these results are in excellent agreement with earlier experiments.[24]

92.6 Computational Investigations

Surprisingly, there have been relatively few theoretical investigations of the photochemistry of diazirines in comparison to the plethora of experimental studies. In 1978, Devaquet[39] and co-workers performed *ab initio* calculations and in 1985 a semiempirical study was reported by Jug and co-workers.[40] Almost a decade later, Olivucci and Robb performed a multi-configuration, self-consistent-field (MC-SCF) study on the reaction mechanism for photolysis of diazirine using the 6-31G* basis set.[41] Using a six electrons in six orbitals active space, they mapped out the potential energy surfaces corresponding to the ground state, the first and second singlet excited states, and the first triplet state. The key features of their calculations are outlined in Figure 92.1.

Photolysis promotes the ground-state diazirine **DZ**(S_0) to the first excited singlet state **DZ**(S_1). A transition state connects **DZ**(S_1) to conical intersection $\mathbf{CI_1}$, leading to ground-state diazomethane **DM**(S_0). Another conical intersection $\mathbf{CI_2}$ connects the first excited-state diazomethane **DM**(S_1) with ground-state carbene and nitrogen. Finally, a third conical intersection $\mathbf{CI_3}$ connects the second excited-state

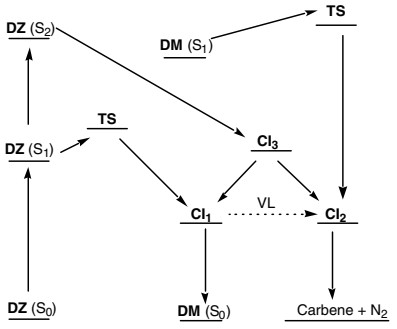

FIGURE 92.1 Schematic of the ground, first excited singlet, and second excited singlet surfaces of diazirine. DZ = diazirine, DM = diazomethane, TS = transition state, CI = conical intersection, and VL = vibrational leakage.

diazirine to the S_1 surface. Diazomethane is proposed to be produced directly from **DZ**(S_1) through $\mathbf{CI_1}$. Formation of methylene and nitrogen comes exclusively from $\mathbf{CI_2}$. Three pathways from **DZ**(S_1) to $\mathbf{CI_2}$ are proposed despite the fact that a transition state connecting them could not be located. The first pathway to $\mathbf{CI_2}$ requires vibrational leakage (VL) from $\mathbf{CI_1}$. The second route requires population of **DZ**(S_2) after promotion to **DZ**(S_1), potentially by passing through $\mathbf{CI_3}$ followed by passage through $\mathbf{CI_2}$. The third route is passage directly from **DZ**(S_1) to $\mathbf{CI_2}$. The barrier separating **DZ**(S_1) and $\mathbf{CI_2}$ is determined to be less than 4 kcal mol^{-1} and might be dynamically preferred over passage through $\mathbf{CI_1}$. Finally, the triplet manifold is concluded not to play a significant role because spin-orbit coupling is very weak.

Hadad, Gustafson, Platz, and co-workers have also performed calculations on the diazirine and adamantyldiazirine systems at the CIS level of theory using a 6-31G* basis set.[10] They arrived at somewhat different conclusions than those described by Olivucci and Robb. First, they were unable to find minima corresponding to diazirine and adamantyldiazirine on the first or second excited singlet surfaces. They also found a point that corresponds to a minimum on both the first and second excited-state surfaces rather than a conical intersection. They suggested that these differences might be the result of the orbitals that were chosen for the active space.

Olivucci and Robb have also performed calculations on the dimethydiazirine system at the CASSCF and CASMP2 levels of theory using the 6-31G* and cc-pVDZ basis sets.[64] They were unable to find any evidence for concerted extrusion of nitrogen and rearrangement on either the ground- or excited-state surfaces. The only reaction path they were able to locate begins on the excited-state surface, passes over a 1.0-kcal mol^{-1} barrier and then through a conical intersection leading to dimethyldiazirine on the ground-state surface. Passage through the conical intersection imparts the molecule with enough energy to pass over the 31.0-kcal mol^{-1} barrier to give ground-state carbene and nitrogen. The carbene can then easily rearrange to propene.

More recently, Arenas and co-workers studied the diazirine system at the complete active space, self-consistent field (CASSCF) level of theory using the cc-pVDZ basis set to map the potential energy surfaces with the critical points recalculated at the CASPT2/cc-pVDZ level.[65] The active space used for these calculations was 12 electrons in 10 orbitals. Additionally, they performed limited direct dynamic trajectory calculations on the S_1 and S_2 surfaces. The key features of the potential energy surfaces are depicted in Figure 92.2.

Two conical intersections $\mathbf{CI}_1$ and $\mathbf{CI}_2$ are located, connecting the three surfaces ($\mathbf{S_0}$, $\mathbf{S_1}$, and $\mathbf{S_2}$). Two transition states are found on the S_0 surface: $\mathbf{TS}_1$ connects the ground-state diazirine **DZ**(S_0) with dissociation products and $\mathbf{TS}_2$ connects **DZ**(S_0) with ground-state diazomethane **DM**(S_0). A transition state connecting **DM**(S_0) with dissociation products is not expected because it requires passage near $\mathbf{CI}_1$, an unfavorable process. Similar to the results obtained by Hadad and co-workers,[10] the stationary points corresponding to diazirine **DZ**(S_1) and diazomethane **DM**(S_1) on the first excited surface are found to be first-order saddle points. Both of these lead directly to $\mathbf{CI}_1$. A molecule that passes through $\mathbf{CI}_1$ would then have enough energy to pass over the barrier to dissociation products. This mechanism is in agreement

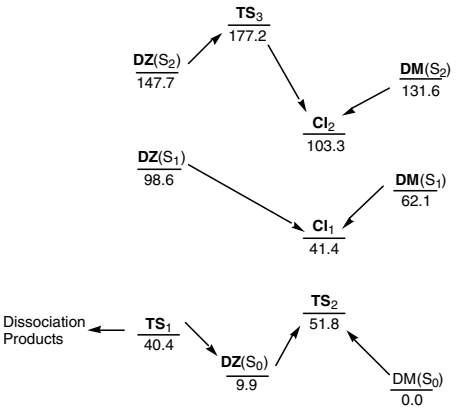

FIGURE 92.2 Schematic of the ground, first excited singlet, and second excited singlet surfaces of diazirine. DZ = diazirine, DM = diazomethane, TS = transition state, and CI = conical intersection. Relative energies are given in kilocalories per mole (kcal mol^{-1}).

with the experimental results of Moore and Pimentel[59] because it requires photochemical generation of diazomethane from diazirine to arise from carbene and molecular nitrogen. Again, on the second excited surface, the stationary points for diazirine **DZ**(S_2) and diazomethane **DM**(S_2) are first-order saddle points. These two saddle points are separated by transition state $\mathbf{TS}_3$ and conical intersection $\mathbf{CI}_2$. Trajectory calculations were performed, starting from various points on the second excited surface. Regardless of the precursor, the observed products were always singlet carbene and molecular nitrogen. The differences in results from earlier work are again suggested to be the result of the orbitals chosen for the active space.

92.7 Conclusion

A great deal of experimental and theoretical effort has gone into understanding the deceptively complicated photochemistry of diazirines. Despite the disagreements between some of the theoretical experimental investigations, most of the evidence points to rearrangement chemistry occurring via the RIES mechanism, with some contribution from carbene complexation possible in aromatic solvents.

References

1. Paulsen, S.R., 3,3-Dialkyldiaza-1-Cyclopropene, *Angew. Chem.*, 72, 781, 1960.
2. Schmitz, E. and Ohme, R., New Diaziridine Synthesis, *Angew. Chem.*, 73, 220, 1961.
3. Schmitz, E., Ohme, R., and Schmidt, R.D., Cyclic Diazo Compounds. IV. Structure Proof of the C-N-N Three-Membered Ring, *Ber.*, 95, 2714, 1962.
4. Pierce, L. and Dobyns, V., Molecular Structure, Dipole Moment and Quadrupole Coupling Constants of Diazirine, *J. Am. Chem. Soc.*, 84, 2651, 1962.
5. Liu, M.T. H. *Chemistry of Diazirines. A 2 Volume Set*; CRC Press, Boca Raton, FL, 1987.
6. Frey, H.M., Photolysis of the Diazirines, *Pure Appl. Chem.*, 9, 527, 1964.
7. Liu, M.T.H., The Thermolysis and Photolysis of Diazirines, *Chem. Soc. Rev.*, 11, 127, 1982.
8. Winnewisser, M., Moller, K., and Gambi, A in *Chemistry of Diazirines*,Vol. 1, Liu, M.T.H., Ed., CRC Press, Boca Raton, FL, 1987, 19.
9. Modarelli, D.A., Morgan, S., and Platz, M.S., Carbene Formation, Hydrogen Migration and Fluorescence in the Excited States of Dialkyldiazirines, *J. Am. Chem. Soc.*, 114, 7034, 1992.
10. Buterbaugh, J.S., Toscano, J.P., Weaver, W.L., Gord, J.R., Hadad, C.M., Gustafson, T.L., and Platz, M.S., Fluorescence Lifetime Measurements and Spectral Analysis of Adamantyldiazirine, *J. Am. Chem. Soc.*, 119, 3580, 1997.

11. Frey, H.M. and Stevens, I.D.R., The Photolysis of 3-*tert*-Butyldiazirine, *J. Chem. Soc.*, 3101, 1965.
12. Frey, H.M. and Stevens, I.D.R., Hot Radical Effects in an Intramolecular Insertion Reaction, *J. Am. Chem. Soc.*, 84, 2647, 1962.
13. 13.Mansoor, A.M. and Stevens, I.D.R., Hot Radical Effects in Carbene Reactions, *Tetrahedron Lett.*, 1733, 1966.
14. Frey, H.M., The Photolysis of the Diazirines, *Adv. Photochem.*, 4, 225, 1966.
15. Kirmse, W. and Wedel, B., Carbenes from Gem-Dihalides, *Annalen der Chemie, Justus Liebigs*, 666, 1, 1963.
16. Chang, K.T. and Shechter, H., Roles of Multiplicity and Electronic Excitation on Intramolecular Reactions of Alkylcarbenes in Condensed Phase, *J. Am. Chem. Soc.*, 101, 5082, 1979.
17. Fukushima, M., Jones, M., Jr., and Brinker, U.H., *tert*-Butylcarbene from 1,1-Diiodoneopentane, *Tetrahedron Lett.*, 23, 3211, 1982.
18. Fox, J.M., Scacheri, J.E.G., Jones, K.G.L., Jones, M., Jr., Shevlin, P.B., Armstrong, B., and Sztyrbicka, R., Phenylcarbene Rearrangement as a Source of Real Carbenes, *Tetrahedron Lett.*, 33, 5021, 1992.
19. Bonneau, R. and Liu, M.T.H., in *Advances in Carbene Chemistry*, Vol. 2, Brinker, U.H., Ed., JAI Press, Stamford, CT, 1998.
20. Platz, M.S., in *Advances in Carbene Chemistry*, Vol. 2, Brinker, U.H., Ed., JAI Press, Stamford, CT, 1998.
21. Merrer, D.C. and Rober, A.M., Kinetics of Intramolecular Carbene Reactions, *Adv. Carbene Chem.*, 3, 53, 2001.
22. Tomioka, H., Hayashi, N., Izawa, Y., and Liu, M.T.H., Photolysis of 3-Chlorodiazirine in the Presence of Alkenes. Kinetic Evidence for Intervention of a Carbene-Alkene Intermediate in Addition of Chlorocarbene to Alkene, *J. Am. Chem. Soc.*, 106, 454, 1984.
23. Liu, M.T. H., Soundararajan, N., Paike, N., and Subramanian, R., Thermolysis and Photolysis of 3-Chloro-3-Benzyldiazirines in Alkenes; Evidence for a Carbene-Alkene Complex, *J. Org. Chem.*, 52, 4223, 1987.
24. Bonneau, R., Liu, M.T. H., Kim, K.C., and Goodman, J.L., Rearrangement of Alkylchlorocarbenes: 1,2-H Shift in Free Carbene, Carbene-Olefin Complex and Excited States of Carbene Precursors, *J. Am. Chem. Soc.*, 118, 3829, 1996.
25. Liu, M.T.H. and Subramanian, R., Addition of an Electrophilic Carbene to an Electron-Deficient Olefin. Kinetics of Benzylchlorocarbene-Diethyl Fumarate Reaction, *Tetrahedron Lett.*, 26, 3071, 1985.
26. Nigam, M., Platz, M.S., Showalter, B.M., Toscano, J. P., Johnson, R., Abbot, S.C., and Kirchoff, M.M., Generation and Study of Benzylchlorocarbene from a Phenanthrene Precursor, *J. Am. Chem. Soc.*, 120, 8055, 1998.
27. LaVilla, J.A. and Goodman, J.L., Photolysis of Alkylhalodiazirines: Two Pathways for Vinyl Halide Formation, *Tetrahedron Lett.*, 31, 5109, 1990.
28. Moss, R.A. and Liu, W., An Unusually Strict Product Partition of an Excited Diazirine-Carbene System, *J. Chem. Soc., Chem. Commun.*, 1597, 1993.
29. Moss, R.A. and Ho, G.J., Carbon and Hydride Migrations of Cyclobutylhalocarbenes, *J. Phys. Org. Chem.*, 6, 126, 1993.
30. Click, H.C., Likhovorik, I.R., and Jones, M., Jr., A Photochemical Source of Real Alkylcarbenes, *Tetrahedron Lett.*, 36, 5715, 1995.
31. Ando, W., Sekiguchi, A., Hagiwara, T., Migita, T., Chowdhry, V., Westheimer, F.H., Kammula, S.L., Green, M., and Jones, M., Jr., Photochemical Decomposition of Trimethylsilyl Diazoacetates in Alcohols, *J. Am. Chem. Soc.*, 101, 6393, 1979.
32. Robert, M., Likhotvorik, I., Platz, M.S., Abbot, S.C., Kirchoff, M.M., and Johnson, R., Laser Flash Photolysis Study of Alkylhalocarbenes Generated from Non-Nitrogenous Precursors, *J. Phys. Chem. A*, 102, 1507, 1998.
33. Pezacki, J.P., Pole, D.L., Warkentin, J., Chen, T., Ford, F., Toscano, J., Fell, J., and Platz, M.S., Laser Flash and Dual Wavelength Photolysis of 3,4-Diaza-2,2-Dimethoxy-1-Oxa[4.5]Spirooct-3-Ene.

Migration of Hydrogen and Carbon in Cyclobutylidene and in the Excited State of Its Precursor, *J. Am. Chem. Soc.*, 119, 3191, 1997.
34. Camacho, M.B., Clark, A.E., Liebrecht, T.A., and DeLuca, J.P., A Phenyliodonium Ylide as a Precursor for Dicarboethoxycarbene: Demonstration of a Strategy for Carbene Generation, *J. Am. Chem. Soc.*, 122, 5210, 2000.
35. Farlow, R.A., Thamattoor, D.M., Sunoj, R.B., and Hadad, C.M., Rearrangement Pathways of 2-Hydroxy-2-Methylpropylidene: An Experimental and Computational Study, *J. Org. Chem.*, 67, 3257, 2002.
36. Warner, P.M., On Carbene Alkene Complexes, *Tetrahedron Lett.*, 25, 4211, 1984.
37. White, W.R., III and Platz, M.S., Concurrent Hydrogen Migration and Nitrogen Extrusion in the Excited States of Alkylchlorodiazirines, *J. Org. Chem.*, *57*, 2841, 1992.
38. Platz, M.S., Huang, H., Ford, F., and Toscano, J., Photochemical Rearrangements of Diazirines and Thermal Rearrangements of Carbenes, *Pure Appl. Chem.*, 69, 803, 1997.
39. Bigot, B., Ponec, R., Sevin, A., and Devaquet, A., Theoretical *Ab Initio* SCF Investigation of the Photochemical Behavior of Three-Membered Rings. 1. Diazirine, *J. Am. Chem. Soc.*, 100, 6575, 1978.
40. Mueller-Remmers, P.L. and Jug, K., SINDO1 Study of Photochemical Reaction Mechanisms of Diazirines, *J. Am. Chem. Soc.*, 107, 7275, 1985.
41. Yamamoto, N., Bernardi, F., Bottoni, A., Olivucci, M., Robb, M.A., and Wilsey, S., Mechanism of Carbene Formation from the Excited States of Diazirine and Diazomethane: An MC-SCF Study, *J. Am. Chem. Soc.*, 116, 2064, 1994.
42. Moss, R.A. and Turro, N.J., in *Kinetics and Spectroscopy of Carbenes and Biradicals*, Platz, M.S., Ed., Plenum Press, New York, 1990, 213.
43. Turro, N.J., Lehr, G.F., Butcher, J.A., Jr., Moss, R.A., and Guo, W., Temperature Dependence of the Cycloaddition of Phenylchlorocarbene to Alkenes. Observation of Negative Activation Energies, *J. Am. Chem. Soc.*, 104, 1754, 1982.
44. Liu, M.T.H., Energy Barrier for 1,2-Hydrogen Migration in Benzylchlorocarbene, *J. Chem. Soc., Chem. Commun.*, 982, 1985.
45. Houk, K.N., Rondan, N.G., and Mareda, J., Are π-Complexes Intermediates in Halocarbene Cycloadditions?, *J. Am. Chem. Soc.*, 106, 4291, 1984.
46. Blake, J.F., Wierschke, S.G., and Jorgensen, W.L., Variational Transition State for the Reaction of Cl_2C: With Ethylene and the Thermodynamics of Carbene Additions, *J. Am. Chem. Soc.*, 111, 1919, 1989.
47. Keating, A.E., Garcia-Garibay, M.A., and Houk, K.N., Origins of Stereoselective Carbene 1,2-Shifts and Cycloadditions of 1,2-Dichloroethylidene: A Theoretical Model Based on CBS-Q and B3LYP Calculations, *J. Am. Chem. Soc.*, 119, 10805, 1997.
48. Krogh-Jespersen, K., Yan, S., and Moss, R.A., *Ab Initio* Electronic Structure Calculations on Chlorocarbene-Ethylene and Chlorocarbene-Benzene Complexes, *J. Am. Chem. Soc.*, 121, 6269, 1999.
49. Moss, R.A., Yan, S., and Krogh-Jespersen, K., Modulation of Carbenic Reactivity by.Pi.-Complexation to Aromatics, *J. Am. Chem. Soc.*, 120, 1088, 1998.
50. Ruck, R.T. and Jones, M., Jr., Solvent Perturbs the Reactivity of *tert*-Butylcarbene, *Tetrahedron Lett.*, 39, 2277, 1998.
51. Khan, M.I. and Goodman, J.L., Picosecond Optical Grating Calorimetry of Singlet Methylene in Benzene, *J. Am. Chem. Soc.*, 117, 6635, 1995.
52. Frey, H.M. and Stevens, I.D.R., The Photolysis of 3-Methyldiazirine (Cyclodiazoethane), *J. Chem. Soc.*, 1700, 1965.
53. Modarelli, D.A. and Platz, M.S., Interception of Dimethylcarbene with Pyridine: A Laser Flash Photolysis Study, *J. Am. Chem. Soc.*, 113, 8985, 1991.
54. Modarelli, D.A. and Platz, M.S., Experimental Evidence for Ethylidene-D4, *J. Am. Chem. Soc.*, 115, 470, 1993.

55. Ford, F., Yuzawa, T., Platz, M.S., Matzinger, S., and Fuelscher, M., Rearrangement of Dimethylcarbene to Propene: Study by Laser Flash Photolysis and *Ab Initio* Molecular Orbital Theory, *J. Am. Chem. Soc.*, 120, 4430, 1998.
56. Moss, R.A., Liu, W., and Krogh-Jespersen, K., Kinetics of the Competitive 1,2-Carbon Migrations of an Unsymmetrically Substituted Cyclopropylchlorocarbene, *J. Phys. Chem.*, 97, 13413, 1993.
57. Huang, H. and Platz, M.S., Intermolecular Chemistry of a Cyclopropylcarbene and Its Mechanistic Implications, *Tetrahedron Lett.*, 37, 8337, 1996.
58. Amrich, M.J. and Bell, J.A., Photoisomerization of Diazirine, *J. Am. Chem. Soc.*, 86, 292, 1964.
59. Moore, C.B. and Pimentel, G.C., Matrix Reaction of Methylene with Nitrogen to Form Diazomethane, *J. Chem. Phys.*, 41, 3504, 1964.
60. Seburg, R.A. and McMahon, R.J., Photochemistry of Matrix-Isolated Diazoethane and Methyldiazirine: Ethylidene Trapping?, *J. Am. Chem. Soc.*, 114, 7183, 1992.
61. Bonneau, R. and Liu, M.T.H., Quantum Yield of Formation of Diazo Compounds from the Photolysis of Diazirines, *J. Am. Chem. Soc.*, 118, 7229, 1996.
62. Akasaka, T., Liu, M.T.H., Niino, Y., Maeda, Y., Wakahara, T., Okamura, M., Kobayashi, K., and Nagase, S., Photolysis of Diazirines in the Presence of C_{60}: A Chemical Probe for Carbene/Diazomethane Partitioning, *J. Am. Chem. Soc.*, 122, 7134, 2000.
63. Wakahara, T., Niino, Y., Kato, T., Maeda, Y., Akasaka, T., Liu, M.T.H., Kobayashi, K., and Nagase, S., A Nonspectroscopic Method to Determine the Photolytic Decomposition Pathways of 3-Chloro-3alkyldiazirine Carbene, Diazo and Rearrangement in the Excited State, *J. Am. Chem. Soc.*, 124, 9465, 2002.
64. Bernardi, F., Olivucci, M., Robb, M.A., Vreven, T., and Soto, J., An *Ab Initio* Study of the Photochemical Decomposition of 3,3-Dimethyldiazirine, *J. Org. Chem.*, 65, 7847, 2000.
65. Arenas, J.F., Lopez-Tocon, I., Otero, J.C., and Soto, J., Carbene Formation in Its Lower Singlet State from Photoexcited 3H-Diazirine or Diazomethane. A Combined CASPT2 and *Ab Initio* Direct Dynamics Trajectory Study, *J. Am. Chem. Soc.*, 124, 1728, 2002.

93

Photomechanistic Aspects of Bicyclic Azoalkanes: Triplet States, Photoreduction, and Double Inversion

Waldemar Adam
University of Würzburg

Alexei V. Trofimov
University of Würzburg
and
Russian Academy of Sciences

93.1 Introduction

This contribution is preceded by an earlier chapter, which covered the main topics of the photochemistry of cyclic azoalkanes for over three decades. Herein, we address the following mechanistic aspects of cyclic azoalkane photochemistry: (1) the generation of azoalkane triplet states on direct irradiation and their photochemical transformations, and (2) the double inversion of the molecular skeleton in the formation of housane during photochemical nitrogen extrusion.

The studies reviewed herein have disclosed that the photochemistry of cyclic azoalkanes depends on spin multiplicity. While the singlet excited states of azoalkanes lead exclusively to the cleavage of the α-C–N bond with subsequent nitrogen extrusion and housane formation, their triplet states undergo β-C–C bond rupture followed by azirane formation. Another prominent feature of the triplet-state photochemistry is the photoreduction of bicyclic azoalkanes by hydrogen donors. For this process, direct hydrogen-atom transfer and charge-transfer mechanisms have been documented.

The double inversion of the molecular skeleton upon thermal and photochemical denitrogenation, first observed for the parent 2,3-diazabicyclo[2.2.1]hept-2-ene, DBH (**1**), constitutes a unique stereoselective process, much under mechanistic dispute for almost four decades. The mechanistic alternatives for the denitrogenation process pertain to whether the diazenyl (^{1}**DZ**) or the nitrogen-free cyclopentane-1,3-diyl (^{1}**DR**) biradical intervenes in the product-branching point to afford the diastereomeric housane

0-8493-1348-1/04/$0.00+$1.50

TABLE 93.1 Photophysical Properties[a] of Bicyclic Azoalkanes

	1 (DBH)	2 (DBO)	3a	4a
$^1\tau$	0.15	682	2.4	2.9
$^3\tau$	<1	≥7	630	580
Φ_{ISC}	~0	~0	~0.5	0.59
Φ_{fl}	<0.001	~0.5	0.02	0.02
Φ_{ph}	0.00	0.00	0.052	0.035
Φ_r	1.0	0.02	0.59	0.75
E_S	84.5	76	78.1	78.8
E_T	62.0	~53	62.4	63.1
ΔE_{ST}	22.5	~23	15.7	15.7
IP	8.83	8.19	8.41	8.35

[a] Lifetimes (in ns) of singlet ($^1\tau$) and triplet ($^3\tau$) excited states, quantum yields of intersystem crossing (Φ_{ISC}), fluorescence (Φ_{fl}), phosphorescence at 77K (Φ_{ph}), and nitrogen-extrusion reaction (Φ_r), energies (in kcal mol^{-1}) of singlet (E_S) and triplet (E_T) excited states, S_1T_1 energy gap (ΔE_{ST}), and lowest vertical ionization potentials (IP in eV). [b] Data taken from Ref. 3b.

products. This long-standing mechanistic query has recently been addressed in terms of medium and substituent effects on the diastereoselectivity in the photochemical denitrogenation. Herein, we consider recent developments, which confirm the intermediacy of the diazenyl biradical ^{1}**DZ** in the photolysis of the DBH-type bicyclic azoalkanes.

93.2 Triplet-State Photochemistry of Bicyclic Azoalkanes

Direct Generation of Triplet-Excited Bicyclic Azoalkanes and Their Photophysical Behavior

The bicyclic derivatives 2,3-diazabicyclo[2.2.1]hept-2-ene, DBH (**1**), and 2,3-diazabicyclo[2.2.2]oct-2-ene, DBO (**2**), serve as instructive probes for the photochemical and photophysical properties of azoalkanes in view of their contrasting behavior. While derivatives of DBH (**1**) readily extrude molecular nitrogen from their excited states with quantum yield close to unity,[a,] DBO (**2**) and most of its derivatives are "photoreluctant," that is, they exhibit very low decomposition yields.[4b,5] With a few exceptions, substituents in the DBH and DBO molecules do not significantly alter the photochemical properties of the parent molecules.[3] Despite the contrasting photochemical reactivity of DBH (**1**) and DBO (**2**), their photophysical characteristics are similar. For both **1** and **2**, the intersystem crossing is inefficient and triplet lifetimes are very short; consequently, these azoalkanes do not phosphoresce, either in solution or even in matrix at 77K.[3b]

DBH (**1**)

DBO (**2**)

The DBH derivative **3a** constitutes the first case for which direct spectroscopic characterization of the *long-lived* (0.63 μs) triplet state was achieved,[3a] in view of the efficient singlet-to-triplet intersystem crossing (Φ_{isc} *ca.* 0.5). This unprecedented finding stimulated further studies on the azoalkanes **3** through **9** in an effort to define the essential structural requirements for the exceptional photophysical features of azoalkane **3a**.[3b] This work[3b] reports, for the first time, the phosphorescence emission spectra of azoalkanes (**3**, **4a**, **6a**, **8**, and *para*-substituted [*p*-F and *p*-Br] derivatives **3c**] at 77K. As representative cases, the photophysical properties of azoalkanes **3a** and **4a** are compared in Table 93.1 with those of

DBH (**1**) and DBO (**2**). It is noteworthy that the lowest triplet states of all azoalkanes **3** through**9** have been found to fall in the narrow range of 62.5 ± 1 kcal mol^{-1}. The n,π* character of the lowest azoalkane triplet state[3b] determines the photochemical reactivity, which is discussed below.

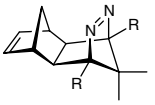

3a (R = H)
3b (R = Me)
3c (R = Ph)

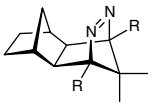

4a (R = H)
4b (R = Me)
4c (R = Ph)

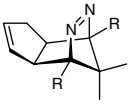

5a (R = H)
5b (R = Me)
5c (R = Ph)

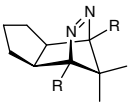

6a (R = H)
6b (R = Me)
6c (R = Ph)

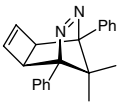

7

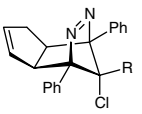

8a (R = Me)
8b (R = Cl)

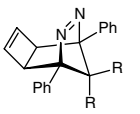

9a (R = H)
9b (R = Me)

The zeolite environment dramatically alters the photophysical properties of azoalkanes. Thus, the intersystem -crossing efficiency of DBH, negligible in liquid solution and glass matrix, may be significantly enhanced in a zeolite interior through the heavy-atom[7a] or orbital-confinement[7b] effects. A large heavy-atom perturbation, imposed by the Tl^+ cation on $S_1 \rightarrow T_1$ intersystem crossing in the parent DBH, has been recently reported. This was manifested by the phosphorescence emission of DBH in TlY zeolite at 77K, observed for the first time. Recently, the first observation of DBH phosphorescence even at room temperature has been reported in the metal-free theta-1 zeolite.[7b] This was attributed to the orbital confinement, imposed by the spatial constraints of the rigid zeolite cavity, which enhances the intersystem crossing efficiency.

Triplet-State Reactions of Bicyclic Azoalkanes

β-C–C Bond Cleavage

The various photoreactions of the bicyclic azoalkanes **3** are summarized in Scheme 1. On direct irradiation, the azoalkanes **3** do not only afford the housanes **10** through the typical singlet-state α-CN-bond cleavage and subsequent denitrogenation, but also yield the aziranes **11** through β-CC-bond breakage and rearrangement.

The increased formation of the aziranes **11** on triplet sensitization with benzophenone and suppression of these rearrangement products by the triplet quenchers *trans*-piperylene and 1,3-cyclohexadiene show that these photoproducts are derived from the triplet-state azoalkanes ^{3}**3*** on β-CC-bond cleavage.[8a] The larger amount of housanes **10** at higher temperatures[8a] suggests that the intersystem-crossing process ^{1}**3*** $\rightarrow$ ^{3}**3*** competes effectively with denitrogenation in the singlet-excited azoalkanes ^{1}**3***. Because intersystem crossing should not be significantly dependent on temperature, the temperature effect has been rationalized in terms of an activation barrier for α-CN-bond cleavage in the singlet-excited azoalkanes ^{1}**3***.

From the temperature dependence of the direct and sensitized photolysis of azoalkanes **3**, the activation energies were estimated to be ≥3.3 kcal mol^{-1} and ≥10.5 kcal mol^{-1} for α-CN-bond breakage in the singlet and triplet states, and ≥7.9 kcal mol^{-1} for the β-CC-bond cleavage in the triplet state.[8a]

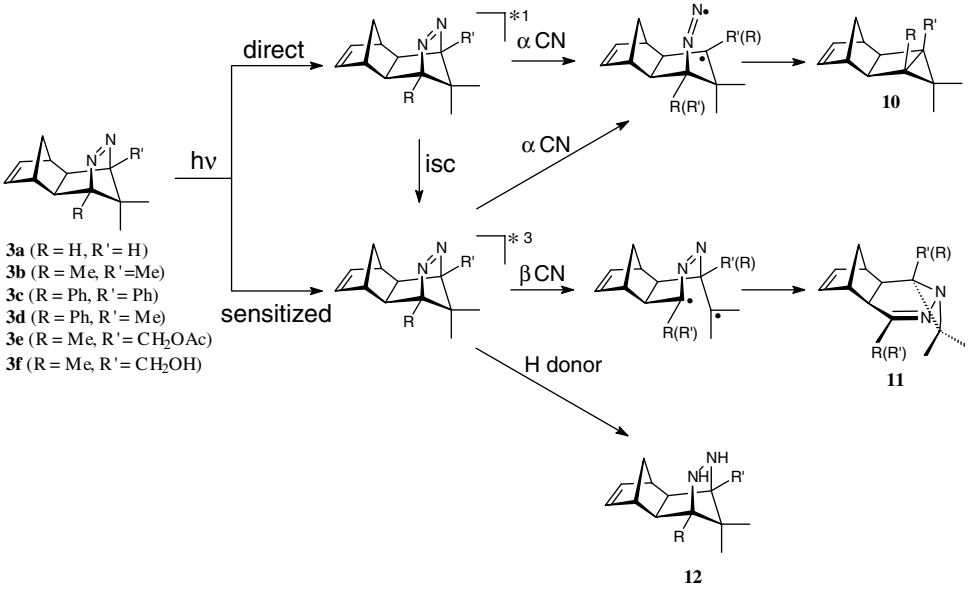

SCHEME 1

Subsequent studies[8b,c] exposed a pronounced medium effect on the product distribution. In the liquid-phase photolysis[8b] of the azoalkanes **3a,b**, for which the triplet channel competes effectively with the singlet-state deazetation, the product distribution depends significantly on the type of solvent. In contrast, the azoalkanes **3c,d**, with efficient denitrogenation in the singlet state, do not display solvent-dependent photobehavior. Thus, the aziranes **11** are produced almost exclusively in polar protic solvents, while housane formation is predominant in nonpolar solvents. It should be noted that the observed solvent dependence derives from bulk medium interactions, as similar product distributions are exhibited by the hydroxy-substituted derivative **3f** and azoalkane **3b** in benzene.[8b] Evidently, the intramolecular hydroxy functionality in the azoalkane **3f** does not influence the photochemistry of the triplet azo chromophore.

Selective formation of the azirane **11** from the triplet-excited azoalkanes **3** in polar media is rationalized in terms of solvent stabilization of the more polar transition state for the β-CC-bond cleavage vs.that for the α-CN-bond scission.[8b] This solvent polarity effect, observed for the liquid-phase photolysis of azoalkanes **3**, is similar to the photochemical behavior of the azoalkane **3a** in the interior of the zeolites.[8c] The polar zeolite environment enhances the formation of azirane **11a** compared to the solution photochemistry in benzene. In contrast to zeolites, the formation of azirane **11a**, a triplet-state product, is completely suppressed in the crystalline state and the housane **10a**, a singlet-state product, is formed selectively.[8c]

Photoreduction

As mentioned, the lowest triplet state of bicyclic azoalkanes is of the n,π* type, similar to that of the carbonyl chromophore. Consequently, the chemical reactivity of the azoalkane triplet state should be characteristic for the n,π* triplets; that is, it should be prone to hydrogen abstraction. Indeed, photoreduction of bicyclic azoalkanes (*cf.* Scheme 1) through intermolecular hydrogen abstraction and charge transfer has been reported.[8b,] As illustrated exemplarily in Table 93.2 for the DBH-type azoalkane 3a,[9] the rate constants for the reaction of the azoalkane ^{3}(n,π*) state with hydrogen donors are rather high. Thus, the formation of azirane **11**, the triplet-state photolysis product, may be almost totally suppressed and hydrazine **12** (*cf.* Scheme 1) is formed in high yields. Noteworthy is the fact that only azoalkanes with high quantum yields of intersystem crossing (Φ_{ISC} *ca.* 0.5) undergo photoreduction,[9c] which implies that the azoalkane triplet states are responsible for this process.

TABLE 93.2 Rate Constants (k_r) and Product Yields for the Reaction of the $^3(n, \pi^*)$-Excited Azoalkane 3a with Hydrogen Donors

Hydrogen Donor	k_q (10^7 $M^{-1}s^{-1}$)	Product yield (%) 10	11	12
None	—	54	46	—
1,4-Cyclohexadiene	2.4	23	3	74
Tributyltin hydride	3.5	<34	—	>66
Benzhydrol	1.9	5	—	95
n-Butylamine	—	20	9	71
Diethylamine	—	20	—	80
Triethylamine	15	40	—	60
Diphenylamine	130	—	—	—
Triphenylamine	66	—	—	—

Note: Data taken from Ref. 9.

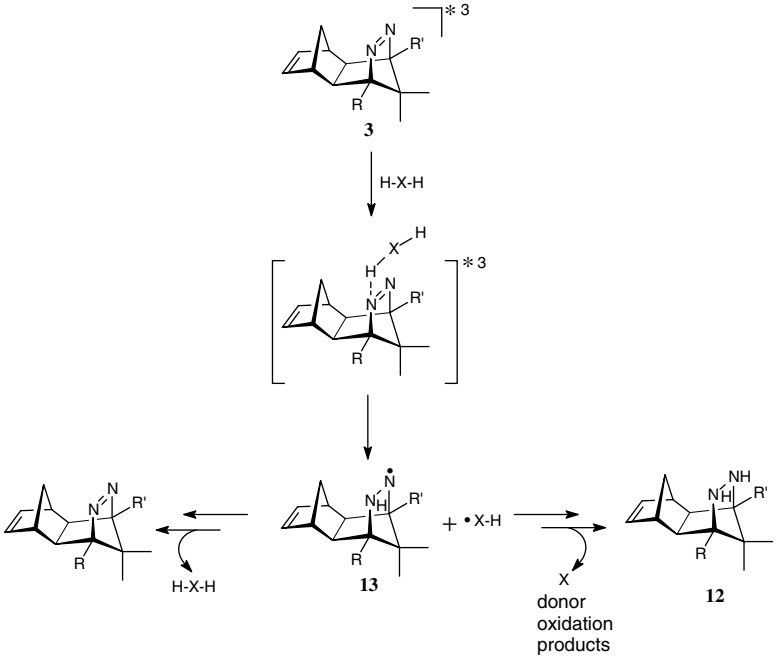

SCHEME 2

Different mechanisms have been proposed for the photoreduction of azoalkanes by a number of hydrogen donors (1,4-cylohexadiene, alcohols, stannanes, and silanes) and amines. While direct hydrogen abstraction operates for the former group of donors,[9b] amines react with the triplet azoalkanes by charge transfer.[9a,c] The mechanistic details of photoreduction by the direct hydrogen donors depend on the donor structure;[9b] however, intervention of the hydrazinyl radical **13** (Scheme 2) is a common feature of these photoreduction processes.

In contrast, photoreduction by amines obeys a general mechanism (Scheme 3) that involves a charge-transfer process.[9c] It should be noted that the azoalkane **3c**, which exhibits a low intersystem crossing (Φ_{ISC} *ca.* 0.1), resists photoreduction.[9c] The efficiencies of photoreduction for the azoalkanes **3** by amines

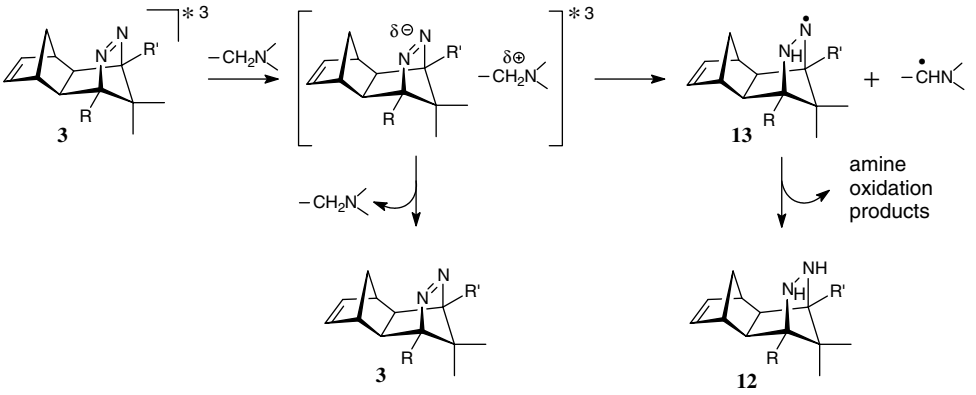

SCHEME 3

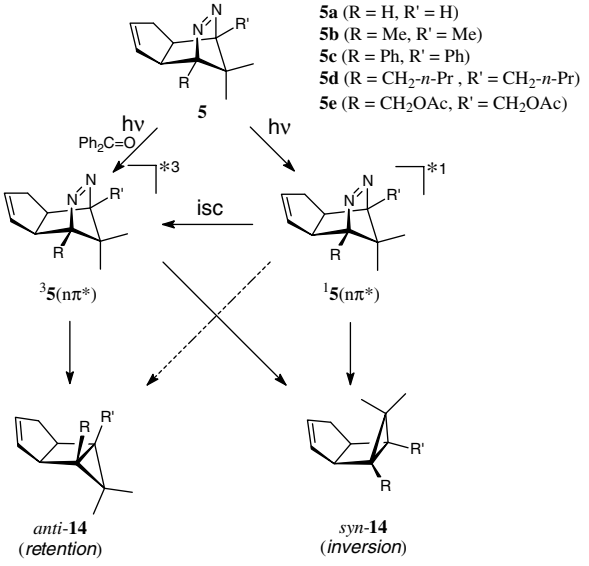

SCHEME 4

follow the same trend (primary ≈ tertiary >> secondary) as observed for benzophenone; the latter also exhibits the lowest photoreduction efficiency with secondary amines. This fact establishes the same general photochemical behavior of the azo and carbonyl n,π* triplet states.

α-CN-Bond Cleavage in Triplet and Singlet States

Definitive for triplet-state photochemistry, the α-CN-bond cleavage has been recently disclosed in the direct irradiation of azoalkanes **5**. A prominent feature of the photolysis of azoalkanes **5** (Scheme 4) is the fact that the *syn*/*anti* product diastereoselectivity depends on temperature and bridgehead substitution. The temperature dependence of the *direct* photolysis of azoalkanes **5** stems from the competition between the singlet and triplet reaction channels (Scheme 4), the latter dominating at low temperature. Mechanistic details of this diastereoselective process is considered below, subsequent to a general discussion on the stereochemical inversion phenomenon in the photochemical nitrogen extrusion.

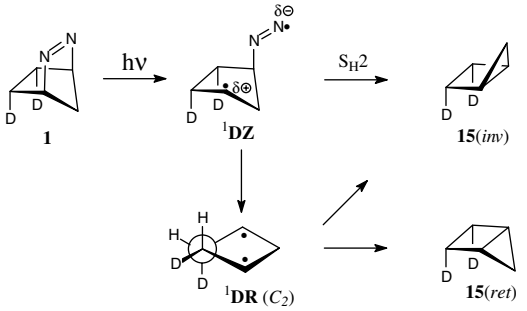

SCHEME 5

93.3 Stereochemical Double Inversion in Photochemical Nitrogen Extrusion

Liquid-Phase Photolysis of DBH-Type Azoalkanes

The inversion of stereochemistry upon nitrogen extrusion from diazabicyclo[2.2.1]heptenes, DBH (**1**), constitutes an intriguing stereoselective process. More than 30 years ago, it was reported that in the gas-phase thermolysis of *exo*-deuterated diazabicyclo[2.2.1]heptene (*exo*-d_2-**1**), the inverted *exo*-deuterated housane bicyclo[2.1.0]pentane [**15**(*inv*)] was formed as the major product.[2a] Subsequently, it was also shown that, in the liquid-phase photolysis, the inversion dominates.[2b]

The persisting mechanistic query on this nitrogen extrusion concerns stepwise versus concerted breakage of the two C–N bonds in DBH (**1**): the stepwise CN-bond rupture necessarily implicates a nitrogen-containing intermediate, namely the diazenyl biradical **DZ**, whereas the concerted process passes through the nitrogen-free **DR** species (Scheme 5).

Nitrogen loss from the singlet ^{1}**DZ** biradical along the S_H2 trajectory leads to the inverted housane **15**(*inv*); the N_2 molecule is displaced homolytically through rearside attack by the radical center. Alternatively, the nitrogen-free singlet ^{1}**DR** biradical affords both the inverted and the retained housanes **15**(*inv*) and **15**(*ret*). To account for the loss of stereoselectivity of the ^{1}**DZ** intermediate, a bifurcation in the product-forming step has been proposed (Scheme 5), in which nitrogen extrusion to the singlet ^{1}**DR** biradical competes with the inversion process (S_H2 mechanism).

A recent computational study on the *thermolysis* of the parent DBH has concluded that the lower-energy pathway of deazetation is the concerted expulsion of N_2 directly to the ^{1}**DR** species.[11] The observed stereoselection, namely more **2**(*inv*) than **2**(*ret*), was interpreted in terms of the dynamic effects of the nonstatistical ^{1}**DR** biradical intermediate.

Computational[12] and experimental[13] evidence exist in favor of the stepwise nitrogen elimination in the photolysis of azoalkanes, which implicate the intervention of a diazenyl radical species. Thus, a recent theoretical study on the parent DBH discloses the singlet diazenyl biradical ^{1}**DZ** as the lowest-energy transient on n,π^* excitation.[12] Similarly, computational results on the photolysis of azomethane suggest a stepwise mechanism for the denitrogenation.[14] Indeed, simple symmetry considerations in terms of the Dauben-Salem-Turro theory on photochemical transformations[15] predict a stepwise process.[13c]

The mechanistic implications of the above computational study[12] on the photodenitrogenation of DBH are shown in Scheme 6. Passage of the n,π^*-excited singlet DBH through the conical intersection generates first the ^{1}**DZ**(*exo-ax*) biradical as *bona fide* intermediate, which relaxes to the ^{1}**DZ**(*exo-eq*) species. The latter leads to the inverted housane by means of rearside attack along the S_H2 coordinate. Alternatively, the ^{1}**DZ**(*exo-ax*) intermediate loses N_2 to afford initially the puckered singlet 1,3-cyclopentanediyl biradical ^{1}**DR**(puckered), which is predestined to cyclize into the retained housane (stereochemical memory effect). In competition, the ^{1}**DR**(puckered) transient relaxes to the C_2-symmetric ^{1}**DR**(C_2) biradical, from which the retained and inverted housanes are produced in equal amounts.

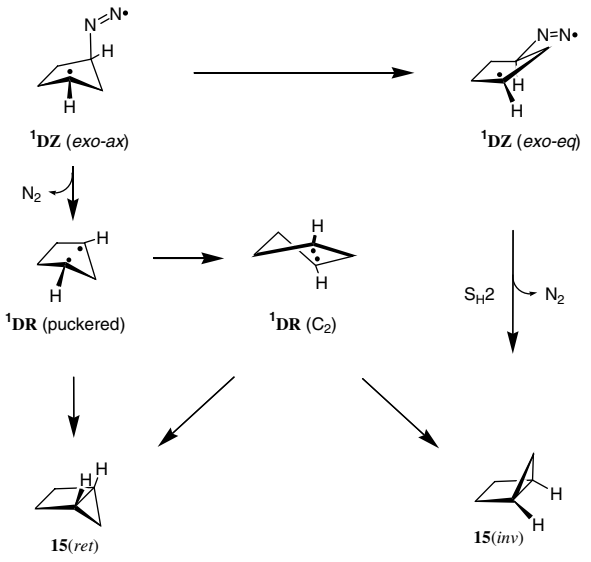

SCHEME 6

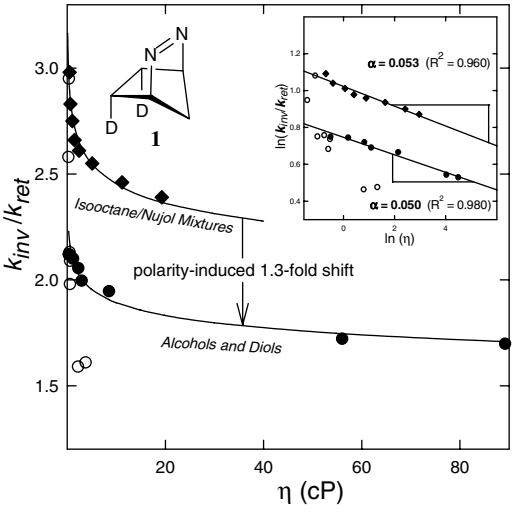

FIGURE 93.1 Viscosity dependence of the k_{inv}/k_{ret} ratio in the DBH (**1**) photolysis (λ = 333 nm) as a function of solvent at 20°C and 1 atm for alcohols and diols {●}, isooctane/nujol mixtures {◆}, and aprotic solvents of different polarity {○} (for details, *cf.* ref 16c); the insert displays the double-logarithmic plots of the viscosity *versus* k_{inv}/k_{ret} data (η expressed in cP).

The stepwise mechanism with the unsymmetrical singlet diazenyl biradical ^{1}**DZ** as pivotal intermediate is corroborated by the viscosity effects observed for the inversion (k_{inv}) and retention (k_{ret}) channels in liquid-phase DBH photolysis. In a more viscous solvent, the inversion process along the S_H2 trajectory is slowed down due to frictional impediment on the inversion motion (flap mode) of the methylene bridge, which is manifested by the decrease of the inversion/retention ratio i.e., k_{inv}/k_{ret} (*cf.* Figure 93.1). Conversely, for the concerted denitrogenation process, no viscosity effect on the k_{inv}/k_{ret} ratio should be expected, because similar motions of the methylene bridge to form the inverted [**15**(*inv*)] and retained

[**15**(*ret*)] housanes from the C_2-symmetric[17] ^{1}**DR** biradical would experience the same frictional impediment in the liquid medium.[16]

As is evident from Figure 93.1, the $\boldsymbol{k}_{inv}/\boldsymbol{k}_{ret}$ ratio exhibits the same viscosity profiles in polar protic (alcohols and diols) and nonpolar aprotic (Nujol/isooctane mixtures) media, but the two curves are shifted relative to one another by a constant factor of *ca.* 1.3. This becomes especially evident from the linear double-logarithmic plots of $\ln(\boldsymbol{k}_{inv}/\boldsymbol{k}_{ret})$ vs. $\ln(\eta)$ [*cf.* insert in Figure 93.1]. In both cases, the $\boldsymbol{k}_{inv}/\boldsymbol{k}_{ret}$ ratio depends on the viscosity to the same fractional power, *i. e.*, $\boldsymbol{k}_{inv}/\boldsymbol{k}_{ret} = const x \eta^{-\alpha}$; α takes the value 0.050 ± 0.002 for both solvent series (*cf.* insert in Figure 93.1).[16c] This viscosity behavior has been rationalized in terms of the free-volume model for the molecular reorganization,[16] in which the α value constitutes a characteristic parameter of the chemical transformation, namely the fraction of molecular volume involved in the rearrangement process.

The similar viscosity profiles of the $\boldsymbol{k}_{inv}/\boldsymbol{k}_{ret}$ ratio in protic and aprotic solvents (Figure 93.1) manifest the same free-volume requirements (the same α) and thereby reflect similar frictional impositions on the stereoselective inversion in the DBH photolysis in these media. The 1.3-fold shift of the $\boldsymbol{k}_{inv}/\boldsymbol{k}_{ret}$ curve for the alcohols and diols relative to that for the isooctane/Nujol mixtures is due to bulk polarity rather than hydrogen-bonding effects.[16c] The decrease in the $\boldsymbol{k}_{inv}/\boldsymbol{k}_{ret}$ ratio in polar media is accounted for by the lower dipole moment of the transition state for denitrogenation compared to that of the diazenyl biradical ^{1}**DZ**.[16c]

Clearly, the α value depends primarily on substituents in the molecule that suffer major displacement during the reaction, while substituents distant from the reaction center should have little effect. Hence, the dependence of the α value on substitution in various parts of the molecule should provide pertinent information on the motion of substituents during the chemical transformation and thereby offer valuable mechanistic details.

Table 93.3 compiles the experimental α data for the photolysis of azoalkanes **1, 16, 5b**, and 17.[16] As expected, the lowest α value (0.050 ± 0.003) is observed for the unsubstituted (parent) DBH **1**. As is evident from Table 93.3, dimethyl substitution in the methylene bridge (azoalkane **16**) increases the α value *ca.* threefold (0.146 ± 0.005) compared to the parent **1**. This is also expected because in a more viscous solvent, the inversion process (k_{inv}) along the S_H2 trajectory should be slowed down mainly due to frictional impediment on the inversion motion (flap mode) of the methylene bridge. Substitution in the methylene bridge should enhance the frictional imposition by the liquid medium on the flap mode of the skeletal inversion.

Furthermore, inspection of Table 93.3 reveals the following mechanistically important fact: bridgehead substitution (azoalkane **17**) leads to an additional increase of α, which takes the value 0.27 ± 0.01, the latter value is *ca.* two times higher than that of the merely methylene-bridge-substituted azoalkane **16** and *ca.* five times higher compared to parent DBH **1**. This observation shows that, in addition to the flap motion of the methylene bridge, the displacements of the bridgehead substituents are also of importance for the skeletal inversion during nitrogen extrusion.

Interesting is the finding that the cyclopentene annelation does not cause a large difference in the α values for azoalkane **5b** compared to **17** (*cf.* Table 93.2). Evidently, the annelated cyclopentene ring in the bicyclic **5d** is sufficiently distant from the reaction site such that it exercises little influence on the skeletal inversion process.

DBH Photolysis in Supercritical Fluids: Pressure Dependence of the Diastereoselectivity

As seen from Figure 93.2, the diastereoselectivity in the DBH photolysis in supercritical fluids (sc-CO_2 and sc-C_2H_6) depends on pressure.[18]The increase of pressure up to 200 bar leads to a *ca.* 2.3-fold decrease of the stereoselectivity (k_{inv}/k_{ret} ratio) in sc-CO_2 and sc-C_2H_6. Analysis of the observed pressure dependence in terms of collisional (self-diffusion coefficient) and frictional (viscosity) effects discloses that frictional impositions by the fluid media account best for the experimental observations. This is consistent with the experimental observations on solvent effects for liquid-phase DBH photolysis.[16]

TABLE 93.3 The α Values for the Photochemical Skeletal Inversion

Reactant	α [a]
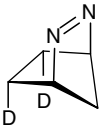 **1**	0.050 ± 0.003 (Refs 16a,c)
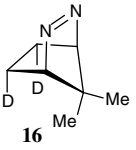 **16**	0.146 ± 0.005 (Ref 16e)
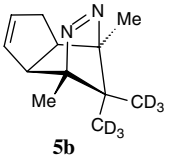 **5b**	0.20 ± 0.01 (Ref 16d)
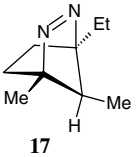 **17**	0.27 ± 0.01 (Ref 16b)

[a] The α value refers to the fraction of molecular volume involved in the rearrangement process (for details, cf. text).

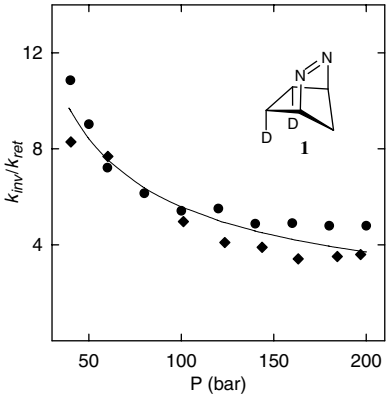

FIGURE 93.2 Pressure dependence of the k_{inv}/k_{ret} ratio (data taken from ref 18) for the photolysis (λ = 333 nm) of DBH (**1**) in supercritical carbon dioxide (◆) and ethane (●) at 50 °C.

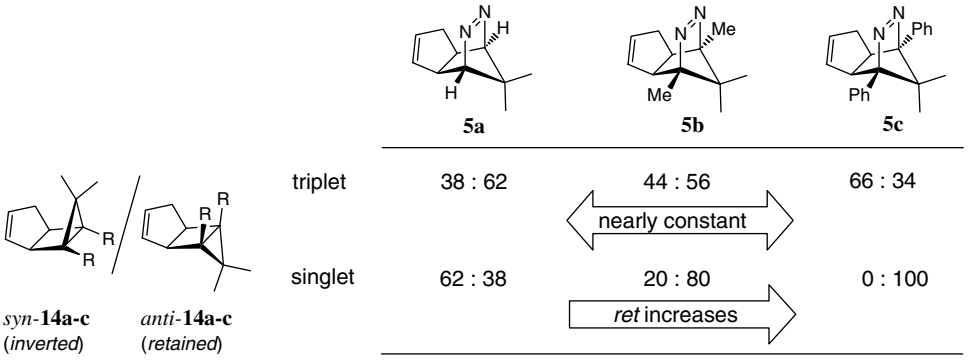

SCHEME 7

Temperature and Substitution Effects

The dependence of the diastereoselectivity on spin multiplicity exhibits different structural effects for the rotationally symmetric (azoalkanes **5a,b,c**) and rotationally unsymmetric (azoalkanes **5d,e**) bridgehead substitutions.[10b,c] The bridgehead substituents in azoalkanes **5a,b,c** are *rotationally symmetric* in the sense that both sides of the 1,3-cyclopentanediyl ring are equally sterically shielded on rotation of the substituents about the bridgehead position; conversely, the *n*-propyl and the acetoxymethyl groups at the bridgehead positions of the azoalkanes **5d** and **5e** are rotationally unsymmetric. Furthermore, the effect of long-range steric interactions between the annellated ring and the *gem*-dimethyl-substituted methylene bridge has been recently exposed.[10c]

Rotationally Symmetric Bridgehead Substitution

As mentioned, the temperature dependence of the diastereoselectivity (*syn*/*anti* ratio) in the photodenitrogenation of azolkanes **5** (*cf.* Scheme 4) manifests a competition between the singlet (high temperature) and triplet (low temperature) reaction channels in the direct photolysis. More explicitly, the observed change-over in the reaction path with temperature stems from the temperature dependence of the α-CN-bond cleavage in the singlet-excited azoalkanes **5**: at high temperatures (20 to 40°C), α scission is efficient, whereas at low temperatures (−20 to −75°C), it no longer competes effectively with the essentially temperature-independent (barrierless) intersystem crossing (Scheme 4).[10] The triplet pathway of the photodenitrogenation at low temperatures is evidenced by the same product distribution for the direct and benzophenone-sensitized photolysis under the same temperature conditions.[10]

Scheme 7 summarizes the results on the product distribution for the triplet and singlet photolysis channels of the azoalkanes **5a,b,c**. For the triplet reaction path, two characteristic features are evident from Scheme 7: the low diastereoselectivity and the small substituent effect on the latter. Thus, for **5a**, merely a small preference for the retained product has been found, whereas for **5c** an inverted housane is slightly favored (Scheme 7). The low stereoselectivity suggests the intervention of a thermally equilibrated *planar* biradical **DR** in the triplet process, which affords similar amounts of the inverted (*syn*) and retained (*anti*) housanes **14** upon ring closure.[10] Expectedly, for the planar **DR** intermediate, the substituent effects on the inversion and retention channels should be similar. In contrast, the singlet reaction channel exhibits a pronounced dependence on bridgehead substitution. In the latter case, the amount of the *anti* diastereomer (retention) follows the order Ph > Me > H (Scheme 7); that is, the larger the substituents, the more retained housane is formed. This stereochemical memory is interpreted in terms of the inertia (mass) effect of the substituents and steric interaction (size) between the substituents at the bridgehead and the methylene bridge during the deazetation step of the *exo-axial* [^{1}**DZ**(*exo-ax*)] and *exo-equatorial* [^{1}**DZ**(*exo-eq*)] conformations of the diazenyl biradical **DZ** (Scheme 8).[10,12b] The larger mass imparts a drag (inertia) on the bridgehead substituent during the inversion, whereas the larger size imposes a higher steric barrier in moving the bridgehead substituents past the *gem*-dimethyl

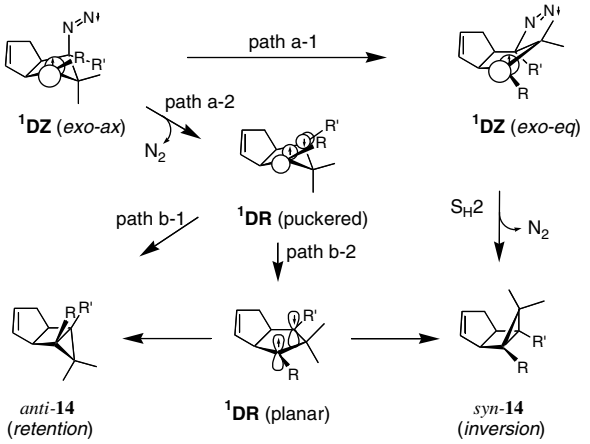

SCHEME 8

bridge; both expectedly slow down the conformational changes and promote nitrogen loss from the original geometry.

To qualitatively rationalize the bridgehead-substituent effect, it suffices to consider the two extreme cases, which are the unsubstituted derivative **5a** and the diphenyl case **5c**. Scheme 8 displays two bifurcation steps, namely, path a-1/a-2 and path b-1/b-2. For **5a**(H/H), both the mass drag and the steric hindrance are minimal on the conformational change along path a-1 and most of the singlet-state denitrogenation proceeds by the S_H2 mechanism to afford mainly inverted housane *syn*-**14a**(*inv*). Because substantial amounts of retained housane *anti*-**14a**(*ret*) are produced, denitrogenation along path a-2 must compete, but beyond this point it is difficult to assess even qualitatively what happens stereochemically because no information is available on the relative importance of the path b-1 vs. path b-2 in the subsequent bifurcation step. If one assumes that all of the ^{1}**DR**(puckered) relaxes to ^{1}**DR**(planar) along path b-2 (no memory effect), on the basis of the observed product ratios,[10b] *ca.* one third of the direct photolysis goes through the S_H2 process and the remaining two thirds through the thermally equilibrated ^{1}**DR**(planar) biradical. In contrast, the stereochemical analysis of the **5c**(Ph/Ph) case is straightforward because only the retained housane *anti*-**14c**(*ret*) is obtained; that is, complete stereochemical memory. In this case, both the mass and steric factors operate so efficiently that only the a-2 and b-1 paths are pursued by the respective biradicals ^{1}**DZ**(*exo-ax*) and ^{1}**DR**(puckered); the conformational changes in the a-1 and b-2 steps are too slow to compete with the a-2 and b-1 paths.

Rotationally Unsymmetric Bridgehead Substitution

Contrary to the rotationally symmetric bridgehead substitution (azoalkanes **5a,b,c**), which leads to the unselective triplet reaction channel and selective formation of *anti*-configured (retained) housanes (Scheme 7), the direct photolysis of the rotationally unsymmetric bridgehead-substituted azoalkanes **5d,e** is moderately diastereoselective for *both* the singlet and triplet modes of photolysis (Scheme 9), as evidenced by the *syn*/*anti* (inversion/retention) ratio. Thus, the photolysis of **5d,e** affords under singlet conditions (high-temperature direct photolysis) predominantly the retained housanes *anti*-**14d,e** (*syn*/*anti* 21:79 for housane **14d** and 33:67 for **14e**); while under triplet conditions (low-temperature direct or benzophenone-sensitized photolysis), the inverted diastereomer *syn*-**14d,e** is favored (*syn*/*anti* 61:39 for **14d** and 70:30 **14e**).

This unprecedented inversion for the triplet pathway is rationalized in terms of the unsymmetric nature of the *n*-propyl and acetoxymethyl substituents in regard to rotation about the bridgehead position of the planar cyclopentane-1,3-diyl triplet biradicals ^{3}**DR**(**d,e**); *cf.* Scheme 9. For the lower-energy conformation of the ^{3}**DR**(**d,e**) biradical, the X fragments of the bridgehead substituents points, for steric reasons, away from the annellated cyclopentene ring and are preferably located on the upper side of the

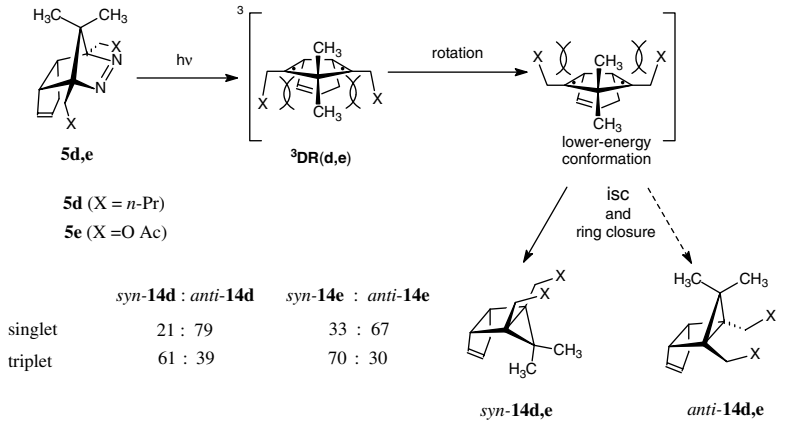

SCHEME 9

diyl ring. After intersystem crossing (ISC) of the triplet biradicals ^{3}**DR**(**d,e**) to the singlet biradicals ^{1}**DR**(**d,e**), the *gem*-dimethyl-substituted methylene bridge may tilt either downward or upward, too close to the respective diastereomeric *syn* and *anti* housanes (Scheme 9). The preference for the *syn* housane comes from the steric interactions of the upper methyl group on the methylene bridge with the two bridgehead substituents in their lower-energy conformation (located above the diyl plane), which directs the tilting motion of the methylene bridge downward in favor of the *syn* housane.

Long-Range Steric Effects

Usually the triplet photolysis mode of azoalkanes **5a,b,c** affords poor product selectivity with a slight preference for the retained housane *anti*-**14a** (H/H in bridgehead), for which the *syn*/*anti* ratio is 38:62. This slight preference for retention has recently[10c] been mechanistically attributed to the steric interactions between the annellated cyclopentene ring and the *gem*-dimethyl-substituted methylene bridge during the ring closure of the planar nitrogen-free triplet biradical ^{3}**DR**. It may be anticipated that an increase in the steric interactions between the remote annellated ring and the *gem*-dimethyl-substituted methylene bridge should raise the energy barrier of the ^{3}**DR** → *syn*-**14a** cyclization and, consequently, the formation of *anti* housane should be enhanced. That this is actually the case has been demonstrated[10c] for the photodenitrogenation of the saturated azoalkane derivative **18** (Scheme 10). Whereas in the direct photolysis (singlet-excited process), the *syn/anti*-**19** housane ratio (*syn/anti* 53:47 for **19** vs. 62:38 for **14**) is nominally affected by this structural change, for the benzophenone-sensitized photolysis (triplet-excited process), essentially exclusively (*syn/anti* 6:94 for **19** vs.38:62 for **14**) the *anti*-**19** housane is observed.

Scheme 10 provides a pictorial rationale for the essentially exclusive *anti* stereoselectivity in the photolysis of azoalkane **18** under triplet conditions. After intersystem crossing (ISC) to the singlet biradical ^{1}**DR**, the direction of the ring closure to the diastereomeric housanes **19** is controlled by steric effects between the *gem*-dimethyl-substituted methylene bridge and the annellated ring. This steric interaction is more effective for the bulkier annellated cyclopentane ring during the puckering motion of the ring closure in the resulting ^{1}**DR**(**18**) biradical, such that the *anti*-**19** (path a) rather than *syn*-**19** (path b) is pursued in high preference (Scheme 10).

Acknowledgments

We express our deep gratitude to all our colleagues and co-authors whose names appear in the references of the original publications. The generous financial support from the *Deutsche Forschungsgemeinschaft*, the *Volkswagen Stiftung,* and the *Fonds der Chemischen Industrie* is gratefully appreciated.

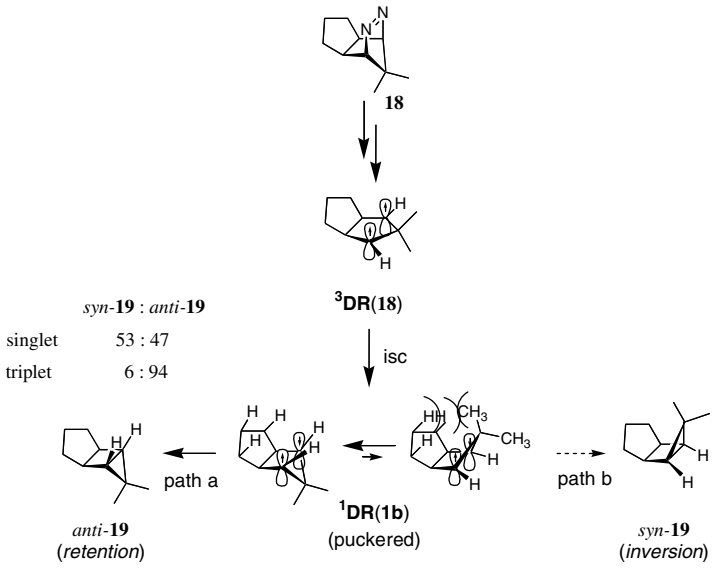

SCHEME 10

References

1. Adam, W. and Sahin, C., Photochemical decomposition of cyclic azoalkanes, in *CRC Handbook of Organic Chemistry and Photobiology*; Horspool, W.M. and Song, P.-S., Eds., CRC Press, Boca Raton, FL, 1995, 937–953.
2. (a) Roth, W.R. and Martin, M., Stereochemistry of the 1,2-cycloaddition to the bicyclo[2.1.0] system, *Tetrahedron Lett*, 47, 4695, 1967; (b) Roth, W.R. and Martin, M., Stereochemistry of the thermal and photochemical decomposition of 2,3-diazabicyclo[2.2.1]hept-2-ene, *Liebigs Ann. Chem.*, 702, 1, 1967.
3. (a) Adam, W., Nau, W.M., Sendelbach, J., and Wirz, J., Identification of a remarkably long-lived azoalkane triplet state, *J. Am. Chem. Soc.*, 115, 12571, 1993; (b) Adam, W., Fragale, G., Klapstein, D., Nau, W., and Wirz, J., Phosphorescence and transient absorption of azoalkane triplet states, *J. Am. Chem. Soc.*, 117, 12578, 1995.
4. (a) Solomon, B.S., Thomas, T.F.,, and Steel, C., Primary processes in the photochemistry of diazabicyclic compounds, *J. Am. Chem. Soc.*, 90, 2249, 1968; (b) Clark, W.D.K. and Steel, C., Photochemistry of 2,3-diazabicyclo[2.2.2]oct-2-ene, *J. Am. Chem. Soc.*, 93, 6347, 1971.
5. (a) Rau, H., Spectroscopic properties of organic azo compounds, *Angew. Chem. Int. Ed. Engl.*, 12, 224, 1973; (b) Bisle, H. and Rau, H., Fluorescence of noncyclic azo compounds with a low-lying $^1(n,\pi^*)$ state, *Chem. Phys. Lett.*, 31, 264, 1975.
6. (a) Engel, P.S., Horsey, D.W., Scholz, J.N., Karatsu, T., and Kitamura, A., Intramolecular triplet energy transfer in ester-linked bichromophoric azoalkanes and naphthalenes, *J. Phys. Chem.*, 96, 7524, 1992; (b) Caldwell, R.A., Helms, A.M., Engel, P.S., and Wu, A., Triplet energy and lifetime of 2,3-diazabicyclo[2.2.2]oct-1-ene, *J. Phys. Chem.*, 100, 17716, 1996.
7. (a) Uppili, S., Marti, V., Nikolaus, A., Jockusch, S., Adam, W., Engel, P.S., Turro, N.J., and Ramamurthy, V., Heavy-cation-induced phosphorescence of alkanones and azoalkanes in zeolites as hosts: induced S_1 (n,π^*) to T_1 (n,π^*) intersystem crossing and S_0 to T_1 (n,π^*) absorption, *J. Am. Chem. Soc.*, 122, 11025, 2000; (b) Márquez, F., Martí, V., Palomares, E., García, H., and Adam, W., Observation of azo chromophore fluorescence and phosphorescence emissions from DBH by applying exclusively the orbital confinement effect in siliceous zeolites devoid of charge-balancing cations, *J. Am. Chem. Soc.*, 124, 7264, 2002.

8. (a) Adam, W., Nau, W.M., and Sendelbach, J., Temperature dependence on the α versus β bond cleavage in the direct and triplet-sensitized photolysis of azoalkanes of the 2,3-diazabicyclo[2.2.1]hept-2-ene type, *J. Am. Chem. Soc.*, 116, 7049, 1994; (b) Adam, W., Moorthy, J.M., Nau, W., and Scaiano, J.C., Solvent effect on the product distribution in the photochemical pathways of a C-N versus b C-C cleavage of n,π* triplet-excited azoalkanes, *J. Am. Chem. Soc.*, 119, 5550, 1997; (c) Adam, W., Garcia, H., Marti, V., Moorthy, J.N., Peters, K., and Peters, E.-M, Photochemical denitrogenation of norbornene-annelated 2,3-diazabicyclo[2.1.1]hept-2-ene-type azoalkanes: crystal-lattice versus zeolite-interior effects, *J. Am. Chem. Soc.*, 122, 3536, 2000.
9. (a) Adam, W., Moorthy, J.N., Nau, W.M., and Scaiano, J.C., Photoreduction of azoalkane triplet states by hydrogen atom and charge transfer, *J. Org. Chem.*, 61, 8722, 1996; (b) Adam, W., Moorthy, J.N., Nau, W.M., and Scaiano, J.C., Photoreduction of azoalkanes by direct hydrogen abstraction from 1,4-cylohexadiene, alcohols, stannanes, and silanes, *J. Org. Chem.*, 62, 8082, 1996; (c) Adam, W., Moorthy, J.N., Nau, W.M., and Scaiano, J.C., Charge-transfer-induced photoreduction of azoalkanes by amines, *J. Am. Chem. Soc.*, 119, 6749, 1997.
10. (a) Adam, W., Garcia, H., Marti, V., and Moorthy, J.N., Homolytic substitution (S_H2) versus triplet biradical (ISC) in the photochemical denitrogenation of a DBH azoalkane: temperature-dependent *syn*/*anti* diastereoselectivity as a mechanistic probe for the doubly-inverted housane, *J. Am. Chem. Soc.*, 121, 9475, 1999; (b) Adam, W., Garcia, H., Diedering, M., Marti, V., Olivucci, M., and Palomares, E., Stereochemical memory in the temperature-dependent photodenitrogenation of bridgehead-substituted DBH-type azoalkanes: inhibition of inverted-housane formation in the diazenyl biradical through the mass effect (inertia) and steric hindrance, *J. Am. Chem. Soc.*, 124, 12192, 2002; (c) Diedering, M., Mechanistische Untersuchungen zum Einfluß der Viskosität und Polarität des Lösungsmittels sowie des Substitutionsmusters auf das Produktverhältnis bei der Photolyse von Azoalkanen vom DBH Typ, prospective Ph.D. thesis, University of Würzburg, Würzburg, 2002.
11. Reyes, M.B. and Carpenter, B.K., Mechanism of thermal deazetization of 2,3-diazabicyclo[2.2.1]hept-2-ene and its reaction dynamics in supercritical fluids, *J. Am. Chem. Soc.*, 122, 10163, 2000.
12. (a) Yamamoto, N., Olivucci, M., Celani, P., Bernardi, P., and Robb, M.A., An MC-SCF/MP2 study of the photochemistry of 2,3-diazabicyclo[2.2.1]hept-2-ene: production and fate of diazenyl and hydrazonyl biradicals, *J. Am. Chem. Soc.*, 120, 2391, 1998; (b) Olivucci, M., unpublished data, 2002.
13. (a) Porter, N.A., Landis, M.E., and Marnett, L.J., Photolysis of unsymmetric azo compounds, *J. Am. Chem. Soc.*, 93, 795, 1971; (b) Green, J.G., Dubay, G.R., and Porter, N.A., A nitrogen-15 CIDNP investigation of dialkyl azo compounds: evidence for *tert*-alkyl diazenyl radicals, *J. Am. Chem. Soc.*, 99, 1264, 1977; (c) Adam, W., Oppenländer, T., and Zang, G., Photochemistry of the azoalkanes 2,3-diazabicyclo[2.2.1]hept-2-ene and spiro[cyclopropane-7,1'-[2,3]-diazabicyclo[2.2.1]hept-2-ene]: on the question of one-bond vs. two-bond cleavage during the denitrogenation, cyclization vs. rearrangement of the 1,3-biradicals and double inversion, *J. Org. Chem.*, 50, 3303 1985; (d) Adam, W., Denninger, U., Finzel, R., Kita, F., Platsch, H., Walter, H., and Zang, G., Comparative study of the pyrolysis, photoinduced electron transfer (PET), and laser-jet and 185-nm photochemistry of alkyl-substituted bicyclic azoalkanes, *J. Am. Chem. Soc.*, 114, 5027, 1992; (e) Diau, E.W.-G., Abou-Zied, O.K., Scala, A.A., and Zewail, A.H., Femtosecond dynamics of transition states and the concept of concertedness: nitrogen extrusion of azomethane reactions, *J. Am. Chem. Soc.*, 120, 3245, 1998.
14. Liu, R., Cui, Q., Dunn, K.M., and Morokuma, K., *Ab initio* molecular orbital study of the mechanism of photodissociation of trans-azomethane, *J Chem. Phys.*, 105, 2333, 1996.
15. Dauben, W.G., Salem, L., and Turro, N.J., Classification of photochemical reactions, *Acc. Chem. Res.*, 8, 41, 1975.
16. (a) Adam, W., Grüne, M., Diedering, M., and Trofimov, A.V., Temperature and viscosity dependence in the stereoselective formation of inverted housane for the photochemical nitrogen loss from the deuterium-stereolabeled parent diazabicyclo[2.2.1]hept-2-ene, *J. Am. Chem. Soc.*, 123,

7109, 2001; (b) Adam, W., Martí, V., Sahin, C., and Trofimov, A.V. Stereoselective formation of inverted housane in the denitrogenation of the diazenyl biradical photolytically derived from a stereolabeled diazabicyclo[2.2.1]hept-2-ene with bridgehead substituents as a function of solvent- and temperature-varied viscosity, *Chem. Phys. Lett.*, 340, 26, 2001; (c) Adam, W., Diedering, M., and Trofimov, A.V., Solvent effects in the photodenitrogenation of the azoalkane diazabicyclo[2.2.1]hept-2-ene: viscosity- and polarity-controlled stereoselectivity in the housane formation from the diazenyl biradical *Phys. Chem. Chem. Phys.*, 4, 1036, 2002; (d) Adam, W., Diedering, M., and Trofimov, A.V., Photochemical versus thermal skeletal inversion: viscosity-controlled photodenitrogenation of a bridgehead-substituted DBH-type azoalkane and thermal *syn*-to-*anti* housane isomerization *J. Am. Chem. Soc.*, 124, 5427, 2002; (e) Adam, W., Diedering, M., Sajimon, M.C., and Trofimov, A.V., unpublished data, 2002.

17. Sherrill, C.D., Seidl, E.T., and Schaefer III, H.F., Closs's biradical: some surprises on the potential energy hypersurface, *J. Phys. Chem.*, 96, 3712, 1992.
18. Adam, W., Diedering, M., and Trofimov, A.V., Pressure dependence of the stereoselectivity in the photodenitrogenation of diazabicyclo[2.2.1]hept-2-ene in supercritical fluids: evidence for the diazenyl biradical, *Chem. Phys. Lett.*, 350, 453, 2001.

94

E,Z-Isomerization and Accompanying Photoreactions of Oximes, Oxime Ethers, Nitrones, Hydrazones, Imines, Azo- and Azoxy Compounds, and Various Applications

Hiroshi Suginome
Hokkaido University

0-8493-1348-1/04/$0.00+$1.50

94.1 Brief Historical Background

Oximes, nitrones, hydrazones, imines, and azo compounds having either a nitrogen–carbon or nitrogen–nitrogen double bond in the *Z* or *E* configuration exhibit a wide variety of photochemical reactions. In particular, the reversible *E,Z*-photoisomerization of azobenzene and its derivatives has recently attracted considerable attention by virtue of their potential for technological applications. This chapter briefly presents an overview of the *E,Z*-photointerconversions that are the primary photoreactions of these groups of compounds. The accompanying diverse photochemical reactions are also described.

The first recorded example of the *E,Z*-isomerization of a CN double bond was that of oximes by Hantzsch in Zürich, who reported in 1890 that *E,Z*-isomerization took place when the tolylphenyl ketone oxime or α-anisylphenyl ketone oxime was irradiated.[1] Subsequent to this study, Ciamician and Silber at Bologna reported that when *E-o-* and *p*-nitrobenzaldehyde oximes, as suspensions in benzene, were exposed to sunlight, they were converted to the corresponding *Z*-nitrobenzaldehyde oximes.[2] This report was confirmed and extended to O-methyloximes by Brady and Dunn in London (Scheme 1).[3] Stoermer also found a similar photochemical *E,Z*-photoisomerization with certain ketoximes.[4]

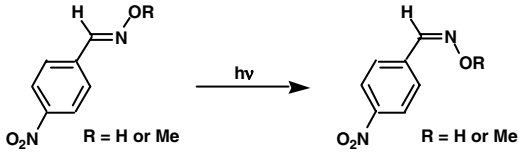

SCHEME 1

Subsequent to Thiele's preparation of azomethane, the first azoalkane, and the observation on its thermal decomposition to give ethane and nitrogen in 1909,[5] Ramsperger first reported in 1928 that azomethane similarly decomposed to ethane and nitrogen upon irradiation with monochromatic light.[6] Studies on the photochemistry of azoalkanes since then, especially those by Ausloos,[7] Bartlett,[8] and Steel[9] and their colleagues between 1950 and the 1960s were primarily concerned with the mechanistic aspects of nitrogen elimination in connection with the behavior of the generated biradicals.

Sophisticated mechanistic details concerning the elimination of the nitrogen from azoalkanes are still being reported to this day.[10]

The first report concerning the photochemical *E,Z*-isomerization of the NN double bond was made by Hartley in 1937.[11] His work dealt with azobenzene and its derivatives because these compounds have greater stability than azoalkanes. The possibility of isomerism in azobenzenes had been discussed for many years prior to this report. He thus succeeded in isolating *Z*-azobenzene, w;hich thermally reverted to *E*-azobenzene. The physical and chemical properties of the *Z*-isomer were measured (Scheme 2). In subsequent years, the photoisomerization was found to be general for azobenzenes and their naphthalene or heterocyclic derivatives. Some 25 years later, Hutton and Steel found that *E,Z*-photoisomerization was a general reaction of even the simple azoalkanes.[12]

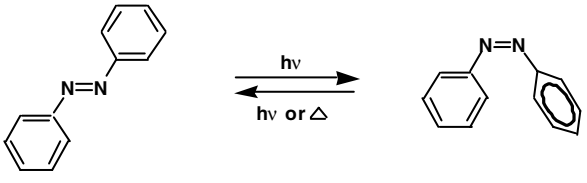

SCHEME 2

The photochemical *E,Z*-isomerization of imines carrying alkyl, aryl, or acyl substituents at the nitrogen of their CN group, on the other hand, was reported much later. This was due to the fact that the energy

barrier to interconversion was normally small for imines and that, at ambient temperatures, a thermal reversion from the *Z*-form to the more stable *E*-form readily takes place. Fischer and Frei thus reported in 1957 that the irradiation of some diarylimines in solution at −100°C induced a change in the UV spectrum and led to photoequilibrium.[13] The spectrum of the starting solution was restored by allowing the solution to warm up to ambient temperature. They correctly interpreted this change in the spectra as being due to *E,Z*-interconversions of the imines (Scheme 3).

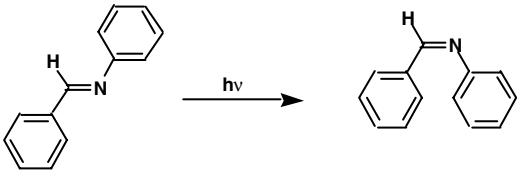

SCHEME 3

Since the 1960s, numerous investigations have been carried out on the nature of the CN and NN double bond photoisomerization and the competitive nature of the *E,Z*-isomerization with other processes, such as photocyclization, photoreduction and photorearrangement. The variety of substrates studied included oxime, oxime ethers, aliphatic and aromatic azo compounds, azoxy compounds, hydrazones, and Schiff bases. The accumulated results were the subjects of several comprehensive and thorough review articles by Wettermark,[14] Padwa,[15] Pratt,[16] Griffiths,[17] Engel,[9] Dürr,[18] and Taylor.[92]

A notable application of *E,Z*-photoisomerization of azobenzene since the late 1960s involves the construction of a great number of photoresponsive molecules, including polymers, peptides, and crown ethers. The most impressive developments in the past 10 years involved the constructions of new photoresponsive molecules containing azobenzene units, including photoresponsive dendrimers and liquid crystals for technological devices such as optical switching as well as new photoreactions of imines and oximes. The irradiation of complex molecules carrying an azobenzene function is accompanied by profound reversible conformational changes; these photoresponsive molecules have great potential for application to a number of technological problems related to photocontrol.

94.2 *E,Z*-Photoisomerization and the Accompanying Reactions of Oximes, Oxime Ethers, Nitrones, and Hydrazones

Oximes and Oxime Ethers

An isolated -C=N-OH group in saturated oximes in a hydrocarbon solvent gives rise to a band at 192–200 nm (ε; 7800–9440),[19] which has been assigned to the $\pi\pi^*$ transition.[19] The corresponding O-methyl oxime also revealed absorption at a similar wavelength and with a similar intensity (cyclohexanone O-methyl oxime; 201 nm; ε; 7000).[20] No distinct low-intensity band or shoulder attributable to a $n\pi^*$ transition has been observed, and any weak $n\pi^*$ band occurring near 190 nm should be submerged in the $\pi\pi^*$ band.

In 1963, de Mayo and colleagues found that arylaldoximes, such as benzaldoxime in protic solvents, undergo a Beckmann-type photorearrangement to give the corresponding amide upon irradiation through quartz.[20] The major reaction for energy dissipation was, however, *E,Z*-photoisomerization. They suggested, based on a variety of experimental evidence, that the amides are produced from an oxaziridine intermediate formed from an excited oxime as outlined in Scheme 4. The intermediacy of the oxaziridine in this rearrangement was subsequently confirmed by de Mayo[20] as well as by Oine and Mukai.[21]

Subsequent to this discovery, the formation of amides and lactams was found to be the major competing photoreaction of oximes; Just and colleagues found that the irradiation of a methanolic solution of cyclohexanone oxime gave caprolactam.[22] We found that the chirality of the migrating carbon center α to the hydroxyimino group in the formation of lactams in the photo-Beckmann rearrangement is

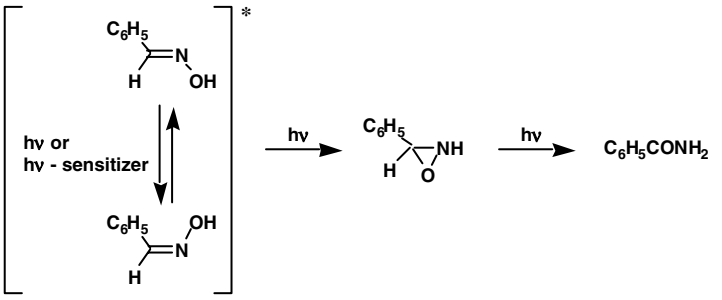

SCHEME 4

retained[23a–j] with one exception;[23k] typically, 5α-cholestan-6-one oxime gives a 1:1 ratio of the two corresponding 5α-lactam isomers, while 5β-cholestan-6-one oxime gives a 1:1 ratio of two 5β-lactam isomers in the photo-Beckmann rearrangement. Based on this and other evidence, we have proposed the path of the photo-Beckmann rearrangement in terms of a simple scheme (Scheme 5) involving photochemical *E,Z*-isomerization, followed by transformations of the excited singlet *E*- and *Z*-oximes into oxaziridine intermediates, and reorganization of the resulting singlet excited oxaziridines to the lactams in a fully concerted manner.[23a–c] A number of five- to eight-membered steroidal lactams were subsequently synthesized by photo-Beckmann rearrangements.[23d–j]

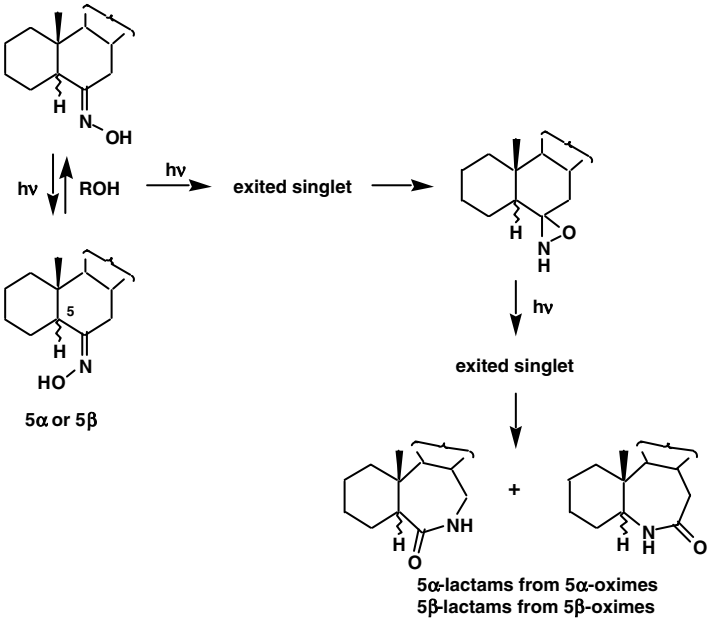

SCHEME 5

The oxime ethers (such as outlined in Scheme 6) are attractive candidates for mechanistic studies concerning the *E,Z*-photoisomerization of imines *(vide infra)* because the presence of the alkoxyl group drastically reduces the rates of thermal interconversion ($K \times 10^{-3}$ at 60°C) and allows mechanistic studies to be carried out at ambient temperatures.[24] Padwa and Albrecht studied photochemical *E,Z*-isomerization regarding the carbon-nitrogen bond of O-methyl oxime ethers in some detail.[24] They found that upon direct irradiation of the O-methyl oximes of acetophenone, a photostationary state *Z*:*E* ratio of

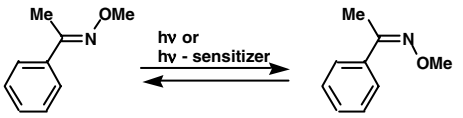

SCHEME 6

2.20 can be achieved. Photoisomerization about the CN double bond of the oxime ethers could also be induced by triplet excitation. A photostationary state vs. the triplet energy of the sensitizer plot indicates: (1) a high-energy region in which the stationary state ratio is *ca*. 1.5; (2) a gradual increase in the *Z:E* ratio from 72 down to 59 kcal of the triplet energy; and (3) a sharp decrease from 59 to 54 kcal. The latter two observations are explained by a non-vertical excitation of the acceptor, as in the case of stilbene photochemistry. Because direct irradiation could not be quenched with a high concentration of piperylene, an electronically excited singlet appears to be the reactive state in direct irradiation. The O-methyl oxime ether of 2-acetophenone has also been reported to undergo facile *Z,E*-photoisomerisation.[24b] The composition of the photostationary state appears to be concentration dependent, with the *Z*-isomer predominating at low concentration. Fluorescence quenching studies and photosensitization experiments gave evidence for the involvement of a singlet state.[24b] The photoisomerization of some α-oxo-oxime ethers was also investigated in some detail.[25]

More recently, Tokumaru and collaborators found that the O-methyl ether of an aromatic ketone oxime, 2-acetylanthracene oxime O-methyl ether, upon irradiation in benzene underwent one-way *Z,E*-isomerization through a quantum chain process in the triplet state[26a] (Scheme 7). The kinetics of the triplet-state isomerization and the potential energy surface of the triplet state were studied by transient spectroscopy. A quantum yield as high as 22 at a concentration of 1.35×10^{-3} *M* was obtained. According to their calculation, the T_1 potential-energy curves of the substrate are in agreement with the rotation mechanism for one-way isomerization.[26b]

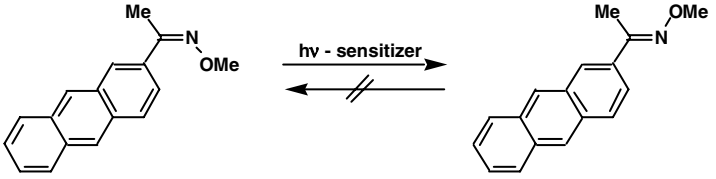

SCHEME 7

The photochemical reactions of some acyclic β,γ-unsaturated oxime O-methyl ethers, such as 2,2,4-trimethyl-1-phenylpent-3-en-1-one oxime O-methyl ether, were found to undergo only *E,Z*-isomerization and no ADPM rearrangement was observed.[27]

Nitrones

Koyano and Tanaka found that *E*-to-*Z*- and *Z*-to-*E*-photoisomerization takes place upon the irradiation of a solution of α-cyano-α,*N*-diphenylnitrone in the presence of a triplet sensitizer, while the irradiation of *E*- or *Z*-forms of the nitrone in the absence of a sensitizer resulted in the formation of the corresponding oxaziridine.[28] These results indicated that photochemical $E \rightarrow Z$ and $Z \rightarrow E$ isomerization take place from the triplet-excited nitrone, while the photochemical formation of the oxaziridine takes place from a singlet-excited nitrone (Scheme 8).

α,β-Unsaturated Oximes

Conjugation of the hydroxyimino group with a CC double bond results in the appearance of a highly intense absorption near 236–260 nm ($\varepsilon = 1.1–2.6 \times 10^4$),[19,29] probably assignable to $\pi\pi^*$ transitions.

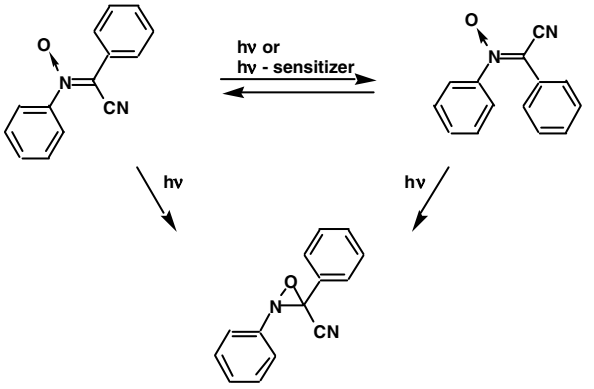

SCHEME 8

Subsequent to some early studies concerning the photoreactions of α,β-unsaturated ketone oximes, Bonet and collaborators reported that the photolysis of 17β-hydroxyandrost-1,5-dien-3-one oxime in methanol gave the corresponding lactam arising from a photo-Beckmann rearrangement as outlined in Scheme 9.[30]

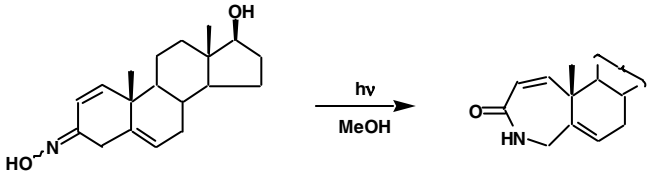

SCHEME 9

A more systematic investigation on the photoreactions of steroidal α,β-unsaturated cyclic ketone oximes as model substrates was carried out by Suginome and collaborators.[31–34] The steroidal substrates studied included the oximes of steroidal 1-en-3-one, 2-en-1-one, 2-en-4-one, 3-en-2-one, 4-en-3-one, 5-en-4-one, and 5-en-6-one. These oximes were found to react in the following ways on irradiation in protic solvents: (1) *E,Z*-isomerization of the hydroxyimino group, (2) a photo-Beckmann rearrangement to give lactams (Scheme 10), (3) an addition to the α, β-double bond, and (4) a new rearrangement to isoxazoline derivatives, although this was restricted to a single example.

Thus, while the excited oximes, such as those of steroidal-4-en-3-one, 4-en-6-one, 5-en-4-one, and 5-en-7-one, having a constrained CC double bond at a ring junction, lead to a photo-Beckmann rearrangement to give either the corresponding enamine-type lactam or enamide (Scheme 10),[31] the excited oximes with more flexible CC double bonds at a non-ring junction (such as the oximes of 5α-cholest-1-en-3-one, 2-en-3-one, and 3-en-2-one) dissipate the excited energy by photoisomerization in preference to the photo-Beckmann rearrangement. This yields transient *trans*-isomers from which stereospecific additions of protons or methanol to the *trans*-CC double bonds take place (Scheme 11).

While the factor that controlled the regioselectivity of the photo-Beckmann rearrangement of steroidal α,β-unsaturated oximes remains obscure, the different regioselectivity in the lactam formation may originate from a stereoelectronic effect — the relative geometry between a lone pair on the nitrogen and the migrating CC bond in the oxaziridine intermediate.

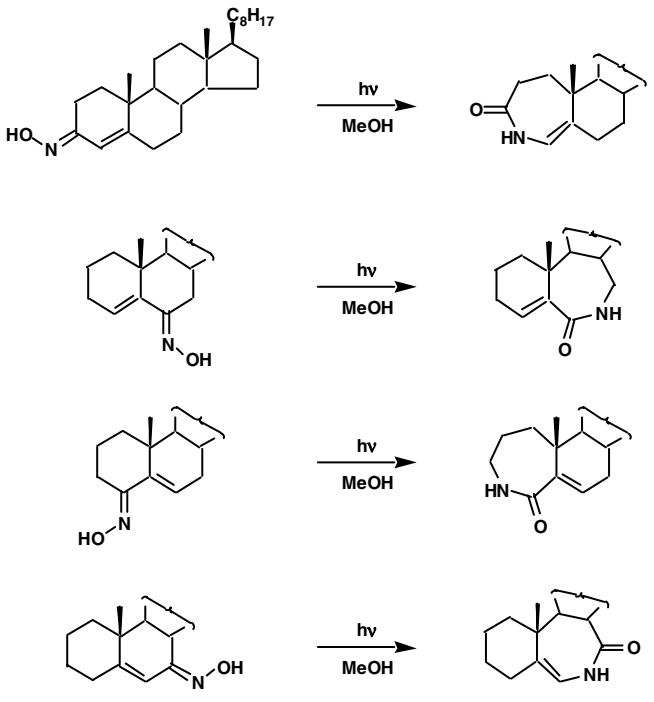

SCHEME 10

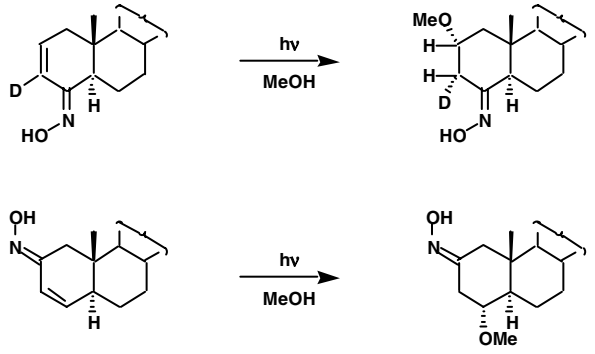

SCHEME 11

5α-Cholest-1-en-3-one oxime and its 4,4-dimethyl derivative behaved differently upon irradiation.[32] Thus, the irradiation of 5α-cholest-1-en-3-one oxime or its 4,4-dimethyl derivative in a protic or an aprotic solvent gave isoxazole derivatives (determined by x-ray), arising from an unprecedented rearrangement. These products were accompanied by 1β-methoxy-oximes arising from stereospecific addition of methanol (Scheme 12).

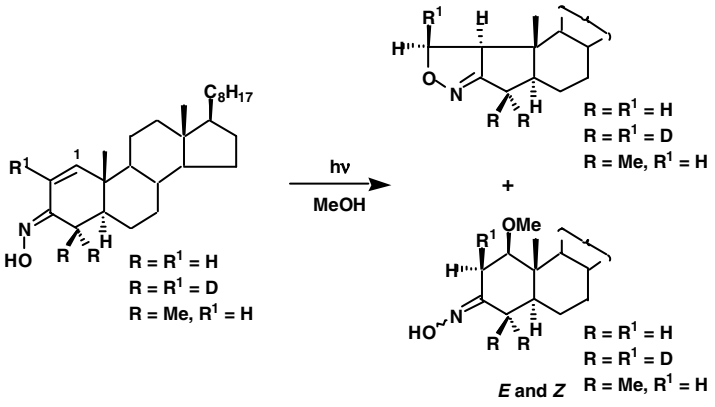

SCHEME 12

The pathway leading to the isoxazoles from the excited enone oximes, based on the results of deuterium labeling, is outlined in Scheme 13;[32] excited oximes generate a twisted ground-state intermediate in which the CC bond is twisted by more than 90°. Stereospecific protonation by either the hydroxyimino proton or by a protic solvent then takes place at C2 of the reactive twisted intermediate from the rear side to give carbocation, since the front side is blocked by the ring. A significant portion of the proton bonded to C2 would be the hydroxyimino proton because the isoxazoline is formed even in dry hexadeuteriobenzene. A carbocation in which the nitrogen lone pair on the C2–C3 bond is oriented in an appropriate geometry for fragmentation may immediately give a nitrile oxide by cleavage of the C2–C3 bond. An intramolecular stereospecific 1,3-dipolar addition of nitrile oxide may give the isoxazoline.

The stereochemistry of the photoaddition of methanol to the cycloalkenone oximes, as disclosed by deuterium labeling, indicates that the adducts are formed by a *syn*-addition to the twisted double bond of the ground-state intermediate from the rear side, as outlined in Scheme 13. The carbocation D fragments to give nitrile oxide E before it is trapped by methanol to give the adduct. The effect of the alkyl group attached to C1 is profound. The irradiation of the 1-methyl derivative of 5α-cholest-1-en-3-one oxime in either a protic or aprotic solvent gave 1-methylene-5α-cholestan-3-one oxime arising from an unprecedented photodeconjugation of α,β–enone oximes into the β,γ -isomers, as outlined in Scheme 14.[33] Neither the expected isoxazole derivative (Scheme 13) nor the unsaturated lactam that arises

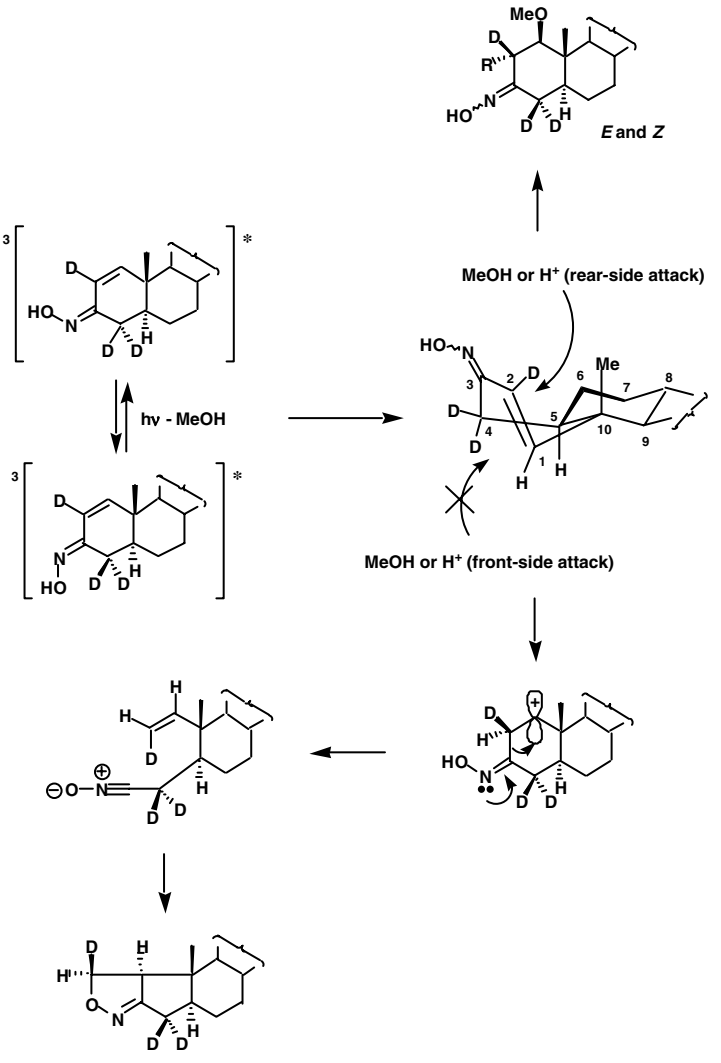
MeO
D
R
HO
N
D D H
E and Z
MeOH or H+ (rear-side attack)
3
*
hν - MeOH
Me
MeOH or H+ (front-side attack)

SCHEME 13

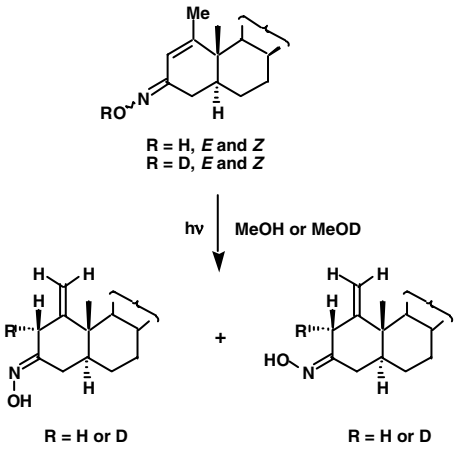

SCHEME 14

from a photo-Beckmann rearrangement was formed. Deuterium labeling studies on the photoreactions of 1-methyl-5α-cholest-1-en-3-one oxime established that either a proton or a deuteron is stereospecifically introduced at the 2α-position of the steroidal oxime in this photodeconjugation. A pathway to the 1-methylene derivative that involves the stereospecific addition of either a proton or deuteron to the photogenerated, twisted double bond of the oximes from the rear side of the steroidal framework, followed by the loss of a proton or deuteron from the 1-methyl group of the resulting carbocation intermediate, is outlined in Scheme 15.

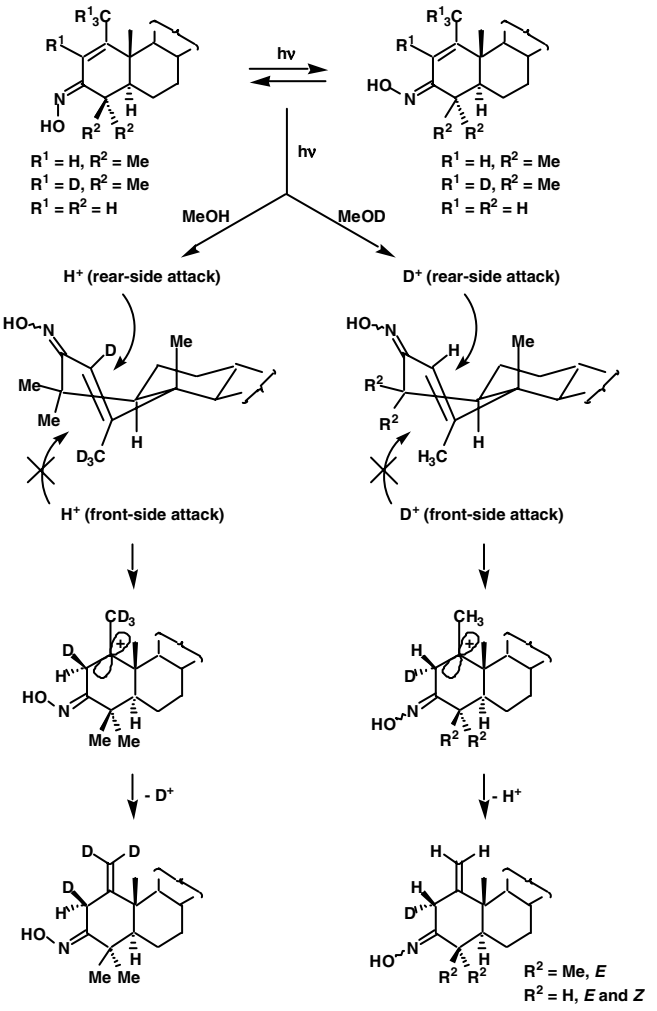

SCHEME 15

The irradiation of 5β-cholest-1-en-3-one in methanol gave 1α-methoxy-5β-cholestan-3-one arising from the photoaddition of methanol, accompanied by the corresponding ketone and a product derived from a skeletal rearrangement of the ketone.[34] Deuterium labeling studies confirmed that the formation of the methanol adduct again involves a stereospecific *syn*-addition of methanol to the photogenerated, twisted, ground-state double bond of the oxime from the rear side of the steroid framework, as indicated by the formation of the 1α-methoxy-steroid (Scheme 16).

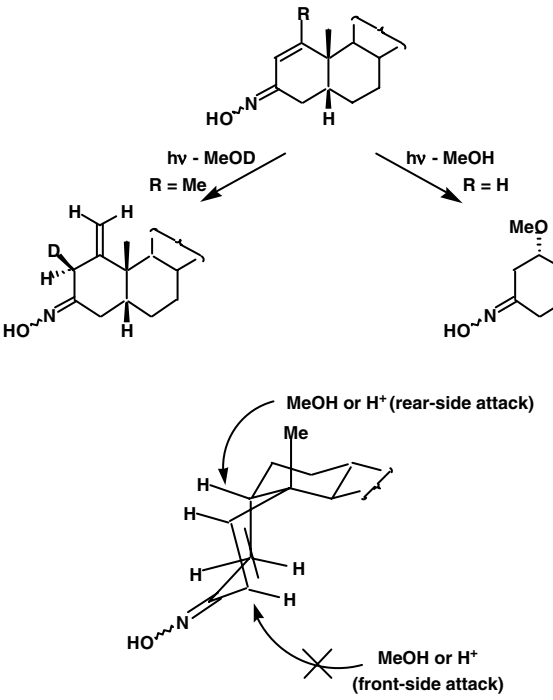

SCHEME 16

The irradiation of 1-methyl-5β-cholest-1-en-3-one oxime in methanol gave almost exclusively 1-methylene-5β-cholestan-3-one oxime, arising from photodeconjugation.[34] A deuterium labeling study established that deuterium is stereospecifically introduced at the 2β-position of the oxime in the photodeconjugation in deuteriomethanol, while deuterium is stereospecifically introduced at the 2α-position in the photodeconjugation of its 5α-isomer, as mentioned above (Scheme 16). The results are fully parallel with the pathway concerning the above-mentioned photodeconjugation of the 5α-isomer. Neither the isoxazole derivative nor the unsaturated lactam is formed in these photoreactions.

β,γ-Unsaturated Oximes

The photoreaction of β,γ-unsaturated oximes was first reported in 1977 by Nitta and collaborators.[35] They found that a highly constrained cyclic β,γ–unsaturated ketone oximes, such as substituted tricyclo[3.2,1.$0^{2,7}$]oct-3-en-8-one oxime in acetonitrile upon irradiation with 254-nm light, resulted in an aza-di-π-methane (ADPM) rearrangement involving the hydroxyimino group to give tetracyclo[3.3.0.$0^{2,8}$ $0^{4,6}$]octane-3-one skeleton, as outlined in Scheme 17.[35a] They also reported that a less-constrained substituted tricyclo[3.3.1.$0^{2,8}$]nona-3-en-6-one oxime with a hydroxyimino group in a larger ring failed to give any product arising from an ADPM rearrangement, but gave the corresponding lactam arising from a photo-Beckmann rearrangement, as outlined in Scheme 18.[35b] Steroidal β,γ-unsaturated ketone oximes, such as 4,4-dimethylcholest-5-en-3-one oxime, behave like saturated cyclic ketone oximes, as expected by the photoreaction of the parent ketone (Scheme 19).[36] Apart from the photoreaction of the constrained oximes, the only photoreaction of acyclic β,γ-unsaturated systems found until the middle of the 1990s

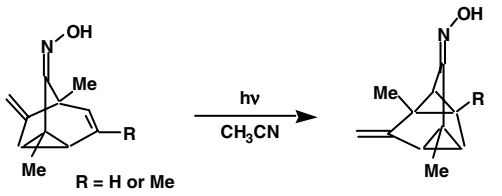

SCHEME 17

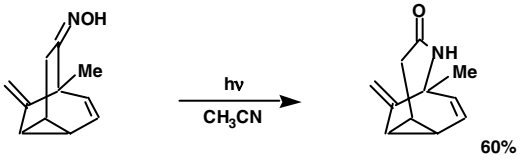

SCHEME 18

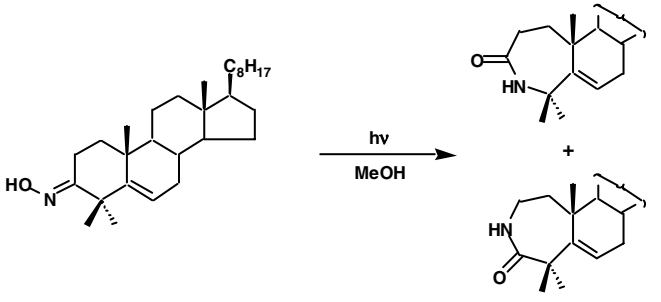

SCHEME 19

was *E,Z*-isomerization;[27] the oximes usually showed no ADPM reactivity. However, in 1994, Armesto, Horspool, and collaborators found that while direct or sensitized irradiation of acyclic oximes, such as the 2,2-dimethyl-4,4-diphenyl-but-3-enal oxime and its methyl ether (Scheme 20, **1** and **2**), showed no ADPM reactivity, the acetate of the oxime **2** and oximes, such as 2-methyl-4,4-diphenyl-2-vinylbut-3-enal oximes and its methyl ether (Scheme 20, **3** and **4**), underwent the ADPM rearrangement to give the corresponding cyclopropyl derivatives upon direct or sensitized irradiation.[37]

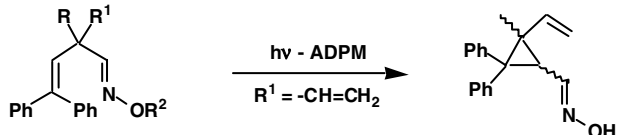

1; R = R^1 = Me, R^2 = H
2; R = R^1 = R^2 = Me
3; R = Me, R^1 = -CH=CH_2; R^2 = H
4; R = R^2 = Me, R^1 = -CH=CH_2
5; R = R^1 = Ph, R^2 = H

SCHEME 20

In contrast to the acyclic DPM process, which occurs from the singlet state in most cases, these ADPM rearrangements of the oximes take place from their excited triplet state.

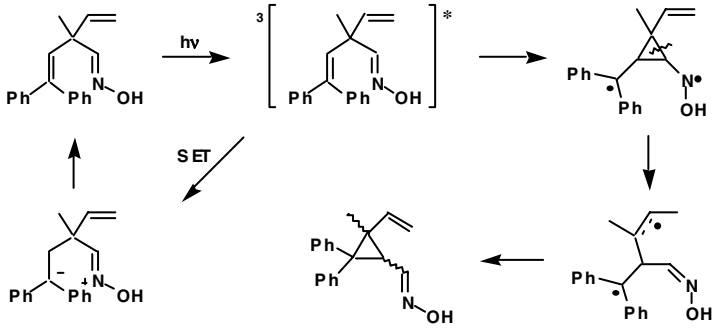

SCHEME 21

The mechanism for the ADPM rearrangement of the oximes proposed by the authors is outlined in Scheme 21. Thus, the ADPM rearrangement from an excited triplet of the oxime to the cyclopropyl derivative via a 1,3-biradical competes with the SET process, leading back to the starting material. If the energy barrier for the conversion of the excited state to the 1,3-biradical is lower than that for the SET process by virtue of its sufficient stabilization, the ADPM process dominates to give cyclopropyl products. The stability of the intermediate 1,3-biradical is crucial to allow the ADPM rearrangement to compete with the SET process that reverts to the starting material. The replacement of the methyl group attached to the central carbon of the oximes by substituents, such as a vinyl or a phenyl group (Scheme 20, **5**), provides stability for the 1,3-biradical.

Armesto and collaborators also reported that the irradiation of ketoximes, such as (*E*)-2,2-dimethyl-1,4,4-triphenylbut-3-en-1-one oxime, resulted in the formation of the new dihydroisoxazoles.[38,39] According to the authors, this cyclization is controlled by a SET process from the alkene moiety to the hydroxyimino group, as outlined in Scheme 22. Cyclization within the zwitterionic biradical, followed by back electron transfer and hydrogen migration affords the final product.

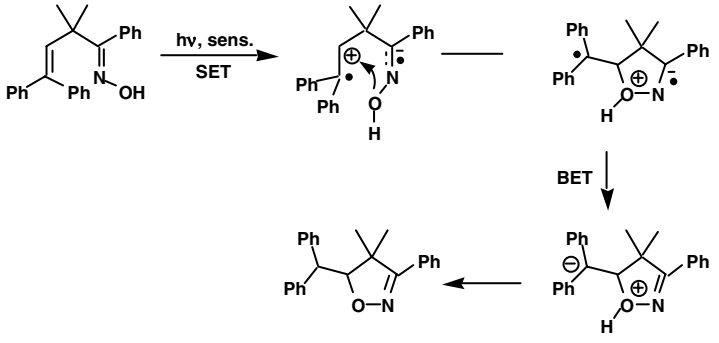

SCHEME 22

Armesto, Horspool, and co-workers also found a new photochemical 1,3-migration of the hydroxyimino groups in β,γ-unsaturated oximes, although it is restricted to a very limited number of the oximes with all of the correct parameters;[40] acetophenone-sensitized irradiation of the oxime acetate of 2,2-dimethyl-3-phenylbut-3-enal brought about an efficient conversion (81%) to 4-methyl-3-phenylpent-3-enal oxime acetate, as outlined in Scheme 23. This rearrangement is the first example of a 1,3-migration of a C=N group in a 1-aza-diene system. In this rearrangement, one of the radical centers in the intermediate 1,4-biradical is stabilized by conjugation with a phenyl ring.

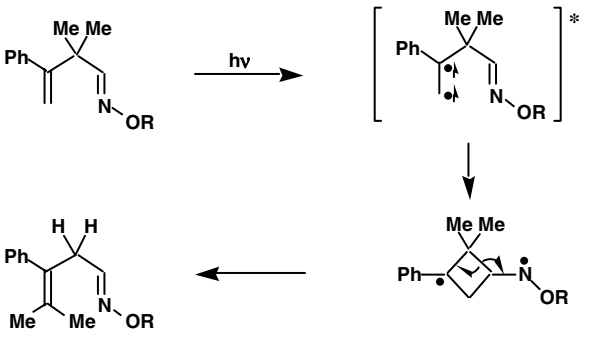

SCHEME 23

γ,δ-Unsaturated Oximes

Armesto, Horspool, and collaborators reported in 1996 that the 9,10-dicyanoanthracene (DCA)-sensitized irradiation of acyclic γ,δ-unsaturated oxime, such as 6,6-diphenylhex-5-en-2-one oxime, underwent a novel photochemical cyclization, yielding the corresponding 5,6-dihydro-4*H*-2,2-oxazine, as outlined in Scheme 24.[41] The mechanism proposed to account for this cyclization by the authors is outlined in Scheme 25. The excitation of DCA, followed by SET from the hydroxyimino group to the sensitizer, generates the radical cation intermediate. The cyclization affords a new radical cation. Proton transfer from the cation to the DCA radical anion, followed by hydrogen abstraction, forms the observed product.

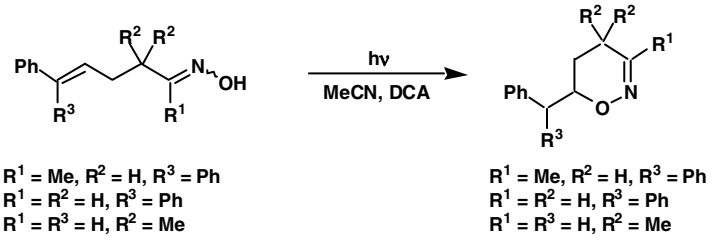

SCHEME 24

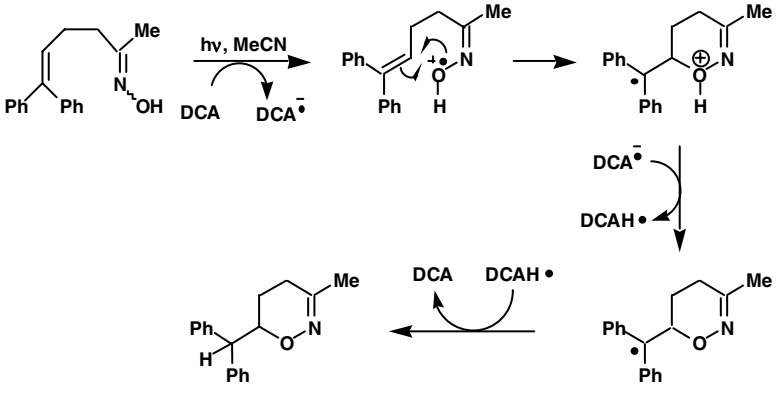

SCHEME 25

The photocyclization of γ,δ-unsaturated oximes enlarges the synthetic utility of the photochemical reaction of oximes.

Hydrazones

The photochemical *E,Z*-isomerization of phenylhydrazones has also been investigated.[42–46] The introduction of a nitro group to the *N*-aryl group of pyridine-2-aldehyde phenylhydrazone[44] enhances the quantum yield of the photoisomerization of the *E*-isomer to the *Z*-isomer in benzene, but decreases the quantum yield to zero for the reverse process.[44,45] Thus, a direct irradiation of the *E*-isomer of pyridine-2-aldehyde 4-nitrophenylhydrazone in benzene resulted in a complete one-way isomerization to the *Z*-form, the stability of which apparently arises from an intramolecular hydrogen bond between the nitrogen of the pyridine ring and NH (Scheme 26).[44,45]

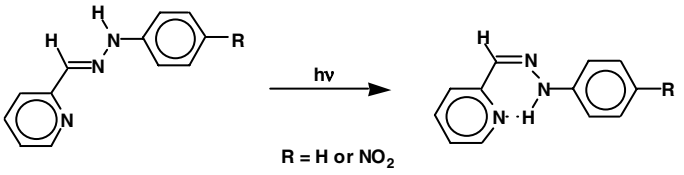

SCHEME 26

Meanwhile, the photoreactions of some alicyclic and aromatic hydrazones and their acetyl derivatives were investigated by Suginome and Uchida, disclosing photochemical reactions other than the *E,Z*-isomerization.[47–49]

An isolated –C=N-NH_2 group of hydrazones in the UV spectrum gives rise to a band at 198 nm (ε = 3900) in methanol, assignable to the $\pi\pi^*$ transition.[47] The photolysis of an alicyclic ketone, 3β-acetoxy-5α-androstan-17-one hydrazine, was found to lead to NN-bond homolysis to give rise to the corresponding azines in the presence or absence of oxygen (Scheme 27).[47] Thus, *E,Z*-isomerization and NN-bond homolysis are the major photoreactions of excited alicyclic ketone hydrazones.

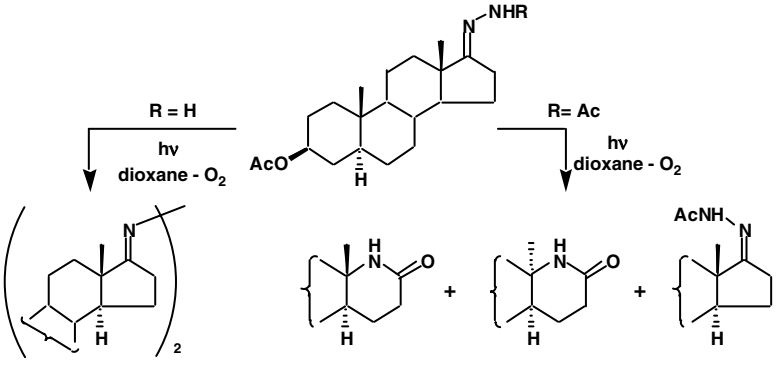

SCHEME 27

Steroidal cyclic ketone acetyl hydrazones, on the other hand, behaved differently upon photolysis; an unprecedented formation of lactams was found in the photolysis of some steroidal acetylhydrazones in the presence of oxygen.[47,48] The irradiation of 3β-acetoxy-5α-androstan-17-one acetyl hydrazone in dioxan in the presence of oxygen afforded 17-oxo-17α-aza-D-homosteroid and its 13α-isomer in low yields, while if oxygen was excluded, none of these lactams were formed (Scheme 27).[47] A pair of γ-lactams is also formed from its D-nor homologue.[48] Although the details of the multistep process for the lactam

formation were not defined, the path most probably involves the formation of an oxaziridine intermediate, followed by rearrangement to the lactams, as outlined in Scheme 28,[47] since the corresponding oxime yields the same lactam pair arising from the photo-Beckmann rearrangement.[23k]

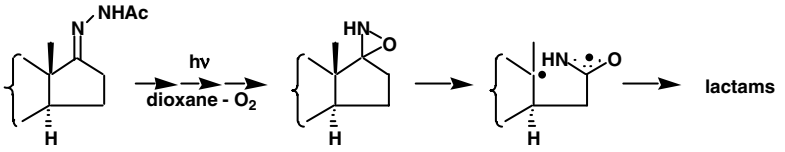

SCHEME 28

Monochromatic light-induced reactions of aromatic ketone hydrazones and acetyl derivatives were also investigated in an effort to compare with those of the alicyclic ketone hydrazones.[49] Benzophenone hydrazone and its 4-substituted derivatives exhibit two strong absorption maxima due to $\pi\pi^*$ transitions in dioxan, one at 277 nm and the other at 223–234 nm. The acetyl derivative also exhibited two absorption maxima due to $\pi\pi^*$ transitions, which are stronger than the hydrazones.

The irradiation of the hydrazone of benzophenone in carbon tetrachloride in the presence of oxygen with 273-nm monochromatic light generated from a grating spectro-irradiator gave rise to the corresponding azine arising from NN-bond homolysis. On the other hand, the irradiation of the acetylhydrazone of benzophenone in the presence of oxygen gave rise to the corresponding hydroperoxide, which was transformed spontaneously into benzophenone upon isolation (Scheme 29). 4-Substituted derivatives of benzophenone hydrazone and the acetyl derivatives behaved similarly.[49]

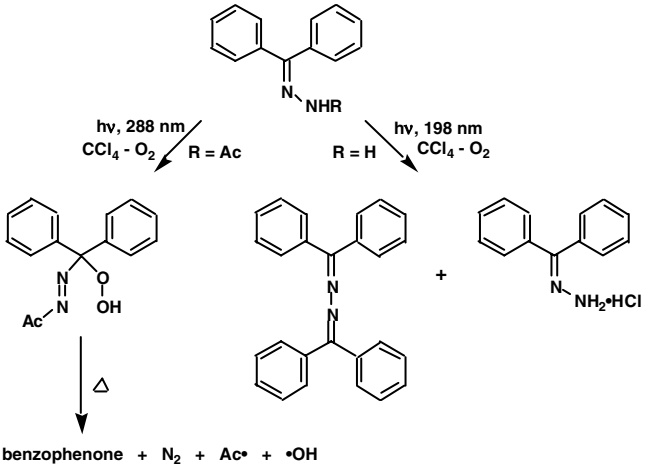

SCHEME 29

Recently, Armesto, Horspool, and collaborators reported a novel photochemical cyclization of acyclic β,γ-unsaturated tosylhydrazone leading to dihydropyrazoles.[39] The acetophenone-sensitized irradiation of the 3,3-dimethyl-5.5-diphenylpent-4-en-2-one tosylhydrazone yielded the dihydropyrazole in 75% yield. The reaction path, analogous to the oxime cyclization mentioned above, involves SET from the alkene moiety to the substituent on the terminal nitrogen as outlined in Scheme 30.[39]

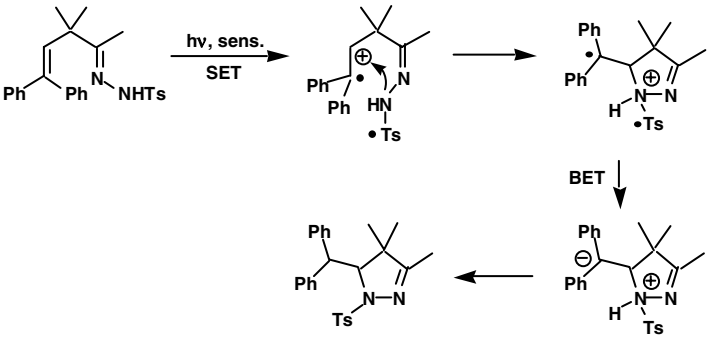

SCHEME 30

94.3 *E,Z*-Photoisomerization and the Accompanying Reactions of Imines

An isolated azomethine chromophore in alkylimines gives rise to two absorption bands in the UV region of the spectrum at about 230–260 nm ($\varepsilon \approx ca.\ 2 \times 10^2$) and at 170–180 nm ($\varepsilon \approx 10^4$). The former was assigned to the $n\pi^*$ transition band and the latter to the $\pi\pi^*$ transition.[14] Aryl substituted imines absorb at longer wavelength.[50] They exhibit a number of bands; band positions depend on the substituents on the aromatic ring. These bands have been interpreted as being of $\pi\pi^*$ and charge-transfer type;[50] benzylideneaniline exhibits an intense absorption maximum at 252 nm and a shoulder at 315 nm. The absorption attributable to the $n\pi^*$ transition has not been unambiguously assigned and may be submerged in the $\pi\pi^*$ band. It was shown that the absorption spectrum of benzylideneaniline is distinctly different from that of stilbene and azobenzene. It was proved that *E*-benzylideneaniline exists in a conformation in which the PhC=N moiety is planar, but the plane of the *N*-phenyl ring makes an angle with the rest of the molecule. This allows conjugation with the lone-pair electron on the nitrogen atom, but reduces the conjugation between the phenyl rings through the CN double bond. The angle of rotation in the *E*-isomer in the gas, solution, and solid phases was estimated by various techniques to be in the 30 to 55°.[51] It seems to be generally agreed that the aniline ring of the *Z*-form is also rotated.

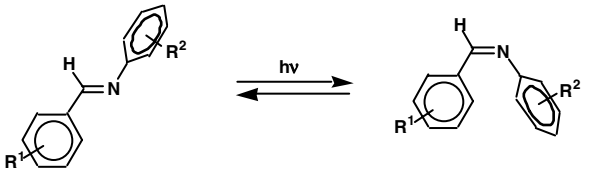

SCHEME 31

In 1957, Fischer and Frei found that the irradiation of some diarylamines in solution at −100°C induced distinct changes in the UV spectra of the solutions, with the changes leading to an equilibrium.[13] Allowing the solutions to warm up to room temperature restored the spectrum of the original isomer. This report was the first spectroscopic observation of the *E,Z*-photoisomerization of imines. They estimated the thermal relaxation to have an activation energy of 16 to 17 kcal mol^{-1}, which was appreciably lower than those of azobenzene and stilbene (23 and 42 kcal mol^{-1}, respectively). Later, Wettermark and co-workers demonstrated that *E,Z*-isomerism of *N*-benzylideneaniline and related compounds can take place even at room temperature (Scheme 31).[52] At this temperature, thermal relaxation proceeds with a half-life of about one second. They obtained the range of activation energies of $Z \rightarrow E$ thermal relaxation for a number of derivatives of *p*-substituted *N*-benzylideneaniline.

The formation of the *Z*-forms of benzylideneaniline and its derivatives was also observed in matrices at 77K by ^{1}H-NMR,[53a] ^{13}C-NMR,[53b] UV spectroscopy, and IR spectroscopy in Nujol at 77K[53c] and in solution at room temperature by flash photolysis.[53d]

The photochemistry of salicylideneanilines suffers from competing reversible photoreactions involving transfer of the phenolic proton to the imino nitrogen, along with the formation of the corresponding *o*-quinoid forms (photochromism)[52a,54a–d] or a zwitterion.[54e]

Many simple imines are susceptible to facile hydrolysis to give their parent ketones in the presence of even a trace of moisture. The small amount of ketones generated affects the results of the photoreaction of imines. Thus, a major activity in investigating the photochemical behavior of imines has been on imine derivatives, such as O-alkyl oximes and hydrazones, which are less susceptible to hydrolysis. Extensive studies were thus carried out on the *E,Z*-photoisomerization of the configurationally stable oxime ethers, which have already been described (*vide supra)*.[24–27]

A 2-anthryl substituent attached to an imine double bond, as in the case of the corresponding oxime O-methyl ether, was found to affect the photostationary *E*:*Z*-ratio upon low-temperature, triplet-sensitized irradiation. Thus, while *Z*-2-anthrylmethylidene aniline undergoes one-way $Z \rightarrow E$ isomerization upon triplet-sensitized irradiation, the triplet-sensitized irradiation of benzylidene-2-aminoanthracene in an EPA matrix affords a photostationary *E,Z*-mixture rich in the *E* isomer under the same reaction conditions (Scheme 32).[26,55]

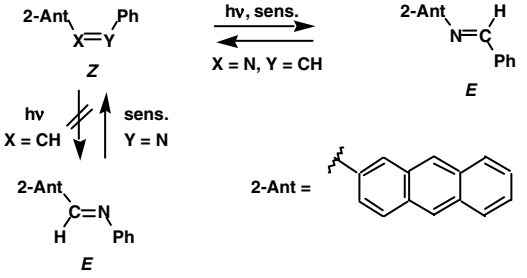

SCHEME 32

Comprehensive reviews concerning the photochemistry of the carbon–nitrogen double bond were published in the mid 1970s.[15,16]

Two decades ago, Armesto, Horspool, and collaborators demonstrated that acyclic 1-aza-1,4-dienes undergo an acetophenone-sensitized aza-di-π-methane (ADPM) rearrangement analogous to the di-π-methane (Zimmerman) rearrangement;[56] the direct irradiation in *t*-butanol or acetophenone-sensitized irradiation in benzene of moisture-sensitive imines of 2,2-dimethyl-4,4-diphenylbut-3-enal with UV light resulted in the formation of a cyclopropyl imine as a single product arising from an ADPM rearrangement, as outlined in Scheme 33. In contrast to the DPM rearrangement, which takes place from the excited singlet in most cases, the ADPM reaction takes place from the excited triplet state with a quantum yield of 2.6×10^{-3} in a typical example.

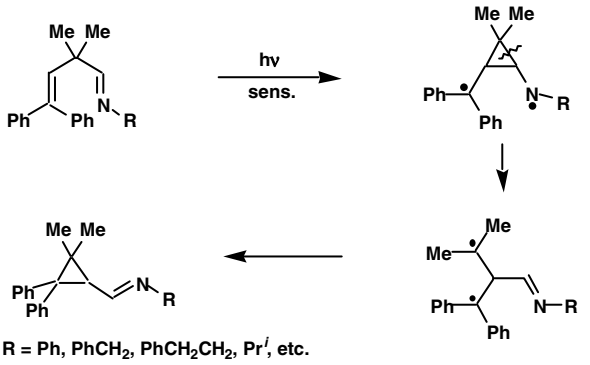

R = Ph, PhCH$_2$, PhCH$_2$CH$_2$, Pr^i, etc.

SCHEME 33

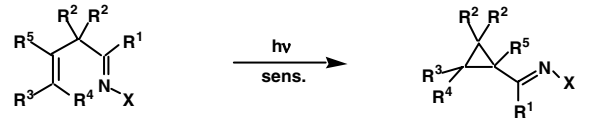

X = R, OCOR or NHCOR
R^1 = H or Me
R^2 = Me or Ph
R^3 = Ph, Me, CH=CH$_2$ or CN
R^4 = Ph, Me or H
R^3 = R^5 = -(CH$_2$)$_3$-, -(CH$_2$)$_4$-, -(CHPh)$_2$-,

SCHEME 34

Since the discovery of the reaction, extensive investigations have disclosed that the photorearrangement is very general in acyclic 1-aza-1,4-dienes (Scheme 34).[57] The reaction was recently extended to β,γ-oximes.[37]

Thus, the scope of this reaction for the synthetic utility has been considerably expanded.

94.4 *E-Z* Isomerization of Azo Compounds

Azoalkanes

Azoalkanes exhibit absorption bands in two regions: one in the 320–380 nm (ε = 10–150) region and other in the 200-nm region (ε = 1000).[9a,58] The weak, longer wavelength band has been assigned to the nπ* transition and the stronger, shorter wavelength band to the nσ* transition. Bathochromic and hypsochromic effects of the nπ* band are observed in going from *E*-azoalkanes to the *Z*-isomer; *E*-azoisopropane exhibits the nπ* band at 360 nm with ε = 14.5, while the *Z*-isomer exhibits the corresponding absorption at 380 nm with ε = 140 in nonpolar solvents.[9a,59]

The principal reactions of azo compounds upon irradiation with UV light are either the elimination of nitrogen to give alkyl radicals or *E,Z*-isomerization. Until the 1950s, studies on the photoreaction of aliphatic azo compounds largely focused on the elimination of nitrogen in the gas phase.[17,60] For example, the photolysis of azoisopropane in the gas phase generates isopropyl radicals and nitrogen with unit quantum efficiency (Scheme 35).[61] Many aliphatic azo compounds, such as 2,2′-azoisobutyronitrile,[62] that readily generate alkyl radicals upon irradiation or pyrolysis have been used as initiators of such radical reactions as polymerization and radical cyclization in organic syntheses.

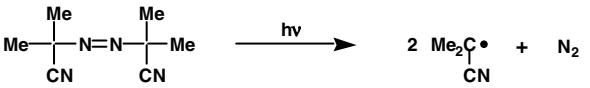

SCHEME 35

However, in 1964, Hutton and Steel found that irradiation into the nπ* band of *E*-azomethane in solution at room temperature caused a decrease in the quantum yield of nitrogen formation to 0.17 and led to *E,Z*-photoisomerization, as detected by UV and ^{1}H-NMR spectroscopy (Scheme 36).[12] More energetic irradiation into the nπ* band of aliphatic *E*-azoalkanes, such as azoisopropane, using UV light in the 200-nm region led to the elimination of nitrogen along with the formation of vibrationally excited alkyl radicals.[63]

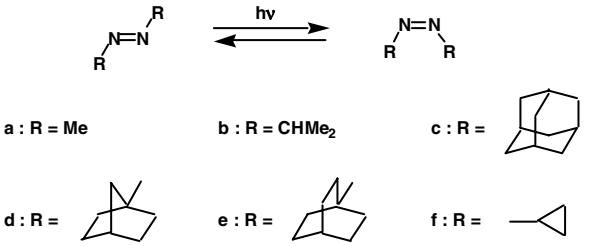

SCHEME 36

Subsequently, Arin and Steel as well as Mill and Stringham found that *E,Z*-isomerization is an important general process competing with dissociation and that many of the photogenerated *Z*-isomers undergo remarkably facile thermal decomposition to give nitrogen and alkyl radicals.[63,64] The irradiation of *E*-azomethane at 25°C in benzene gives the *Z*-isomer with a quantum yield $\Phi_{E\rightarrow Z}$ of 0.42.; the quantum yield $\Phi_{Z\rightarrow E}$ of the reverse reaction was found to be 0.45.[65] The steric effect and the nature of the incipient radical largely govern the stability of *Z*-azoalkenes. *Z*-Azo-2-methyl-2-propane decomposes with an activation energy of 23 kcal mol^{-1}, some 20 kcal mol^{-1} less than that of the *E*-isomers.[64a] The activation energy of the thermal decomposition of *Z*-azoisopropane[64b] is 41 kcal mol^{-1}, which is only about 8 kcal mol^{-1} less than that of the *E*-isomer, while the *Z*-isomer of azobis(1,1-dimethyl-2-propene) decomposes at −120°C.[9a,64c] This mechanism, *E,Z*-isomerization followed by thermal decomposition of the unstable *Z*-isomer to give alkyl radicals, was found to be general for symmetric[66] and unsymmetric azo compounds.[67]

The *Z*-isomer, having considerable steric bulk and a high energy of decomposition due to the generation of high-energy radicals, is expected to be stable and can be thermally isomerized to the *E*-form without the loss of nitrogen. Thus, Engel and colleagues synthesized *Z*-di-1-adamantyldiazene and *Z*-di-1-norbornyldiazene by UV irradiation of the corresponding *E*-isomers in toluene at 0°C (Scheme 36).[68] The quantum yields of nitrogen eliminationin these *E,Z*-isomerizations were extremely low. Engel and Gerth also synthesized *Z*-azacyclopropane via irradiation of the corresponding *E*-isomer with 313-nm light (Scheme 36). It exhibited extraordinary thermal stability toward elimination of nitrogen.[69] Similarly, an eight-membered cyclic *E*-azoalkane was synthesized by Overberger and colleagues, as outlined in Scheme 37.[70] The formation of a seven-membered cyclic *E*-azoalkane has been reported;[71] the direct irradiation (403 nm, nπ* band) or the triplet-sensitized irradiation of 1,4-dihydronaphtho [1,8-de][1,2]-diazepine resulted in a smooth isomerization to the *E*-isomer, while irradiation of either the *E*- or *Z*-isomer with 313-nm light (ππ* band) induced a clear removal of nitrogen to give acenaphthene via a biradical, as outlined in Scheme 38.

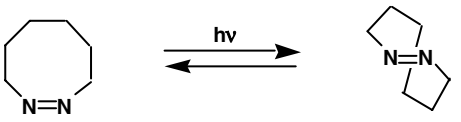

SCHEME 37

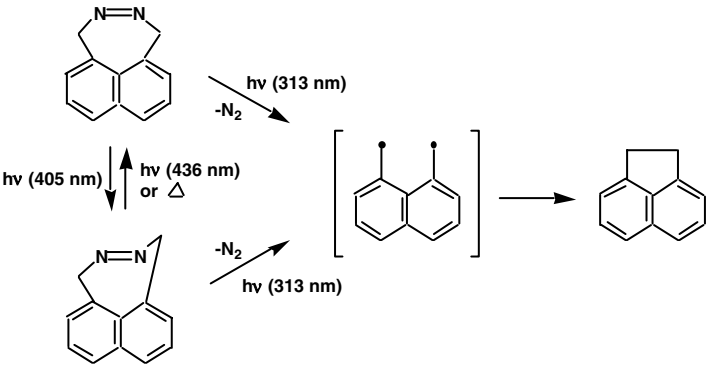

SCHEME 38

The mechanism by which *E*- and *Z*-azo compounds are interconverted remains unclarified. $\Phi_{E,Z}$ for *E*-azopropane and *E*-azocumene over the +20 to −190°C temperature range indicated no significant barriers to isomerization.[9] Theoretical studies indicated that the mechanism involving rotation about the NN double bond is the preferred pathway for the $n\pi^*$ state, whereas that involving in-plane motion of the substituent group is the preferred one for the $^3\pi\pi^*$ state.[72]

The investigation of *E,Z*-isomerization of azo compounds by triplet sensitization up to the 1980s has been summarized by Engel.[9b]

Azoarenes

E- and *Z*-azobenzenes exhibit three absorptions at longer wavelength.[17,58,73] The lowest-energy bands assignable to their $n\pi^*$ transitions occur at approximately 440 nm ($\varepsilon = 500$) in the *E*-isomer and at 430 nm ($\varepsilon = 1500$) in the *Z*-isomer, respectively. Their second absorption bands occur at 314 nm ($\varepsilon = 17000$) in the *E*-isomer and at 280 nm ($\varepsilon = 5100$) in the *Z*-form. The highest-energy absorption band occurs in the 230–240-nm region for both isomers. The marked hypsochromic shift of the absorption band in the *Z*-isomer is due to the nonplanar conformation of the *Z*-isomer in solution.[17,58] The introduction of an electron-donating substituent to the azobenzene system results in the appearance of the absorption bands in the visible region (azo dyes).

The direct irradiation of aromatic azo compounds in solution brings about *E,Z*-isomerization; but, in contrast to azoalkanes, the elimination of nitrogen to give aryl radicals is negligible (see Scheme 2). This is due to the stronger CN-bond and lower excited-state energy. A full understanding of the nature of the excited state associated with the photoisomerization of azobenzene is more difficult than hydrocarbon analogues, such as stilbene, because of the involvement of an additional $n\pi^*$ state. (Readers should refer to a review article with regard to this aspect.[17])

Subsequent to the discovery and identification of the thermally unstable *Z*-isomer of azobenzene by Hartley (see Scheme 2),[11] the crystal structures of the *E*- and *Z*-isomers were determined by Robertson.[74] The benzene ring of the *Z*-isomer of azobenzene is rotated by 56° from the planar position and the distance between the 4 and 4′-carbons is shortened from 9.0 Å in the *E*-isomer to 5.5 Å in the *Z*-isomer. Since then, the generality of the photoisomerization reaction has been demonstrated with a variety of

azobenzene derivatives.[75] A convenient isolation procedure of *Z*-azobenzene, *Z*-2,2′-azopyridine and azonaphthalenes using column chromatography has been described.[76]

The proportion of the *Z*-isomer at the photostationary state is increased if the wavelength of light applied is not absorbed by the *Z*-isomer. Fischer and colleagues showed that the proportion of *Z*-azobenzene at the photostationary state increased to 91% with 365-nm light, while it was only 37% with unfiltered UV light, because the *E*-isomer has a much higher extinction coefficient than the *Z*-isomer.[77]

The quantum efficiency of *E,Z*-isomerization was studied by several investigators.[77,78] Among them, the quantum yields determined by Zimmerman are: for the ultraviolet band, $\Phi_{Z,E} = 0.42$, $\Phi_{E,Z} = 0.11$; for the visible band, $\Phi_{Z,E} = 0.4.8$; $\Phi_{E,Z} = 0.24$.[78]

Although the mechanism of the photoisomerization of azobenzene may involve either twisting around the central NN double bond in the excited state (rotation mechanism) or inversion at one of the nitrogen atoms (inversion mechanism), this has been a subject of debate.[79] Evidence has recently been reported for the involvement of an inversion mechanism for $n\pi^*$ excitations.[80] An *E,Z*-photoisomerization took place when *E*-2,19-dithia[3,3](4,4′)-*trans*-diphenyldiazeno(4)phane 1 in benzene was irradiated. This

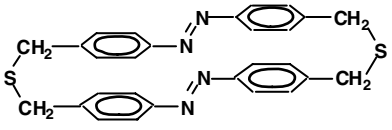

1

was taken as unequivocal proof for an inversion mechanism of azobenzene because a planar inversion in this molecule is possible while rotation should be severely hindered. The quantum yields were found to be wavelength independent, in contrast to those of the parent azobenzene. Further evidence was reported[80b] that normal azobenzenes isomerize via an inversion from the $n\pi^*$ state, but that upon $\pi\pi^*$ excitation a rotational feature becomes important. Evidence for the involvement of an inversion mechanism has also been obtained from a study of a substituted azobenzene.[80c]

The activation energy of the thermal reversion of *Z*-azobenzenes to their *E*-forms has been shown to be *ca*. 24 kcal mol^{-1} for a wide range of derivatives. This value is some 13 kcal mol^{-1} lower than that observed for the isomerization of stilbene, thus suggesting an inversion mechanism.[81]

More recently, it was shown that the thermal $Z \rightarrow E$ isomerization of a *Z*-isomer of azobenzene-bridged azacrown ether (**5** *Z*, Scheme 53) took place via an inversion mechanism[82] because the isomerization via rotation was severely hindered in this molecule.

A fundamental study of the sensitized photochemical *E,Z*-isomerization of azobenzene in solution was again carried out.[83]

The photochemistry of 4-diethylamino- and 4-diethylamino-4′-methoxyazobenzene was studied as reasonable models for commercially useful mono-azo dyes.[84] It was concluded that the lowest singlet and triplet states of these azobenzene derivatives are only capable of geometrical isomerization, whereas hydrogen abstraction takes place from the high-lying triplet state of both the *E*- and *Z*-forms of these dyes.[84]

Karatsu and co-workers recently reported that, like the corresponding oxime O-methyl ether and imine,[26] a 2-anthryl group attached to an azo group appreciably influenced the *Z*:*E* ratio, rich in the *E*-isomer, at the photostationary state; 2-phenylazoanthracene in an EPA matrix in the presence of eosin as a triplet sensitizer upon irradiation at 273K with 520-nm light resulted in a 9:1 *E*:*Z*-mixture of the isomers.[55]

94.5 *E,Z*-Isomerization of Azoxy Compounds and Nitrosoalkane Dimers

Like azo compounds, aromatic aliphatic or mixed azoxy compounds, represented by the general formula $R\text{-}N^+(\text{-}O^-)\text{=}N\text{-}R'$ (R, R′ = alkyl or aryl), exist in *E*- and *Z*-forms. Nitrosoalkane dimers, represented by

the general formula R-$N^+(-O^-)$=$N^+(-O^-)$-R (R = alkyl) are also able to exist in two interconvertible *E*- and *Z*-geometrical forms.

Although studies of the action of light on azoxy compounds were initiated at the turn of the last century, little attention was paid to the photochemical *E,Z* isomerization for the initial 60 years.

Azoxyarenes

Since the discovery of azoxybenzene by Zinin,[85] which dates back to as early as 1841, *E*-azoxybenzene was prepared either by the reduction of nitrobenzene[86] or by the oxidation of *E*-azobenzene[87] with peracetic acid.

Wacker was the first to report that paper impregnated with 1,1′-azoxynaphthalene turned red upon exposure to sunlight and to propose the formation of an "oxy-azo" compound.[88] Subsequently, Knipscheer reported that azoxybenzene, impregnated in sheets of filter paper, rearranged to 2-hydroxyazobenzene upon exposure to sunlight (Scheme 39; X = H).[89] Cumming and co-workers subsequently found that this rearrangement also took place when azoxybenzenes in various solvents were irradiated with ultraviolet light.[90] Bigelow[91] has reviewed the early development of the chemistry of azoxybenzene, including the action of light. The development of the photochemical reactions including *E,Z*-isomerizations until the late 1960s has been summarized by Spence, Taylor, and Buchardt.[92]

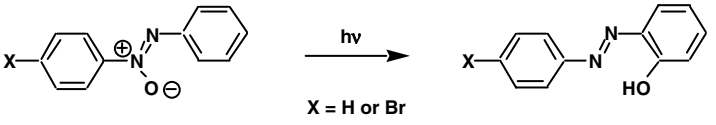

SCHEME 39

Badger and Buttery then demonstrated that unsymmetrical azoxybenzene and azoxynaphthalene derivatives rearranged (5 to 15% yields) to the corresponding *o*-hydroxyazo compounds, the oxygen atom migrating from nitrogen to the remote aromatic nucleus, upon exposure to sunlight for 1 month; α-4-bromoazoxybenzene rearranged to give 4-bromo-2-hydroxyazobenzene (Scheme 39; X = Br).[93] This result suggested the process outlined in Scheme 40 involving an intramolecular transfer of oxygen. The intramolecularity was further proved by ^{15}N or ^{18}O labeling studies (Scheme 41 and Scheme 42)[94,95] and by a study using azoxybenzene substituted with alkyl groups (Scheme 43).[96]

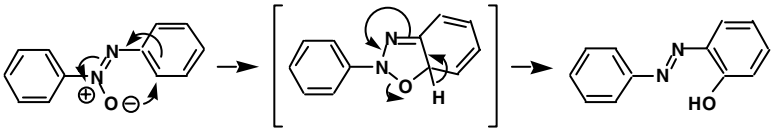

SCHEME 40

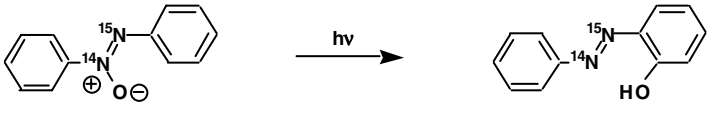

SCHEME 41

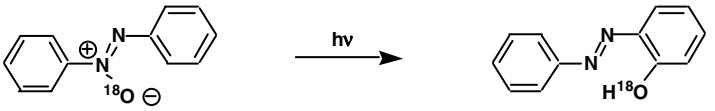

SCHEME 42

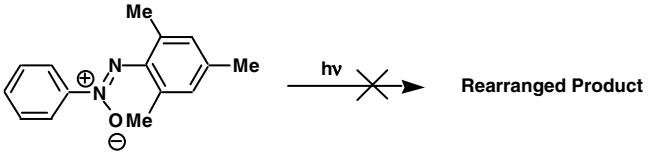

SCHEME 43

Like azo compounds, *E,Z*-isomerization should have taken place in the photoirradiation of the azoxy compounds. However, the reported formation of 2-hydroxyazobenzene mentioned above required either prolonged sunlight irradiation or UV light irradiation at a temperature of 150 to 200°C, although the inefficiency of the rearrangement suggested some other competitive energy dissipation process. In fact, a paper published by Müller in 1932 reported that isoazoxybenzene in alcohol was transformed into normal azoxybenzene upon UV irradiation at 0°C.[97]

An excited state leading to oxygen transfer and *E,Z*-isomerization of azoxybenzene was first reported by Tanikaga.[98] The UV spectrum of azoxybenzene in ethanol shows an absorption maximum at 323 nm ($\varepsilon = 14700$) assignable to the $\pi\pi^*$ band, but the $n\pi^*$ band is submerged under the $\pi\pi^*$ band. The direct irradiation of *E*-azoxybenzene with light longer than 300 nm resulted in the formation of 2-hydroxyazobenzene, together with *E*- and *Z*-azoxybenzenes, while the irradiation in ethanol in the presence of benzophenone as a triplet sensitizer resulted in the formation of azobenzene. Based on these results, Tanikaga concluded that the formation of 2-hydroxyazobenzene and *E*- and *Z*-azoxybenzene takes place from the excited $\pi\pi^*$ singlet state of azoxybenzene.

The mechanism of the photoreduction of azoxybenzene to azobenzene in the presence of benzophenone was rationalized by Monroe and Wamser to involve the transfer of a proton from the ketyl radical, generated from excited benzophenone via hydrogen abstraction from the solvent to azoxybenzene, followed by dehydration (chemical sensitization).[99]

Mauser and collaborators then proved spectrophotometrically that *E*- azoxybenzene in methanol isomerises to *Z*-azoxybenzene upon irradiation with 313 nm light and the *Z*-form is converted back to the *E*-form under the action of light or in the dark. The *E*-isomer rearranged to 2-hydroxyazobenzene in a parallel reaction.[100]

In 1964, Webb and Jaffe found that the irradiation of a substituted *E*-azoxybenzene at low temperature resulted in an *E,Z*-equilibrium mixture from which the corresponding *Z*-isomer was isolated by adsorption chromatography for the first time.[101] Thermal *Z,E*-isomerization seems to be suppressed at this low temperature. Rhee and Jaffe then made a photo- and thermochemical study of the *E,Z*-isomerization of azoxybenzene. They reported that the activation energy of the *E,Z*-isomerization of azoxybenzene was 25 kcal mol^{-1} in 95% ethanol and 19 kcal mol^{-1} in heptane (Scheme 44). The quantum yields for the photoisomerization in heptane or ethanol were 0.11 for $E \rightarrow Z$ and 0.60 for $Z \rightarrow E$ and were independent of the wavelength of irradiation in the 330- to 370-nm range.[102]

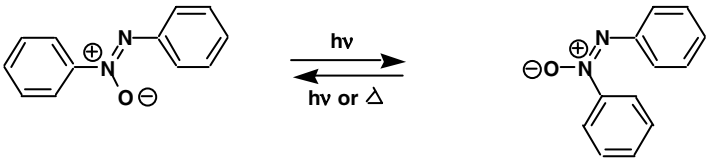

SCHEME 44

Among several studies made from the 1970s to the 1980s on the mechanistic details of the photorearrangement,[103–108] Bunce and collaborators[106] concluded that the rearrangement involves an intermediate formed by an intramolecular electrophilic substitution by the azoxy oxygen, originally proposed by Badger and Buttery.[93] They also argued,[101,106] based on their quenching experiment and INDO calculations, that the excited state responsible for the azoxybenzene rearrangement is the $n\pi^*$ singlet and not the $\pi\pi^*$ singlet assumed by Tanikaga.

More recently, Albini and collaborators took up the problem.[108] They investigated the photoreactions in alcohol and in benzene of six azobenzenes bearing methoxy or dimethylamino group(s) at the *para*- and/or *para′*- positions. They found significant solvent and wavelength effects for the rearrangement, which occurred for all except the disubstituted derivatives (Scheme 45). The process involves a Badger intermediate, which either reverts to the starting material or is transformed into the final *o*-hydroxyazobenzene via a diazonium ion that can be trapped with 2-naphthol (Scheme 46). The effect of wavelength of irradiation also seems to be significant in those azoxybenzenes having electron-donating group(s); 1,2-oxygen shift from (4-methoxyphenyl)phenyldiazene-2-oxide to the isomeric 1-oxide in ethanol upon Pyrex-filtered light irradiation is general for the azoxybenzenes bearing an electron-donating group (Scheme 45). The oxygen transfer, which probably involves an oxadiazirine intermediate 2, is a one-way

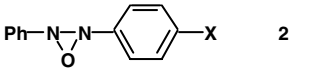

2

X = NMe_2, OMe

process in every case, transferring the oxygen atom distant from the ring bearing the electron-donating group. On the other hand, the photorearrangement to 2-hydroxyazobenzene in ethanol takes place upon irradiation with quartz-filtered light (Scheme 45).

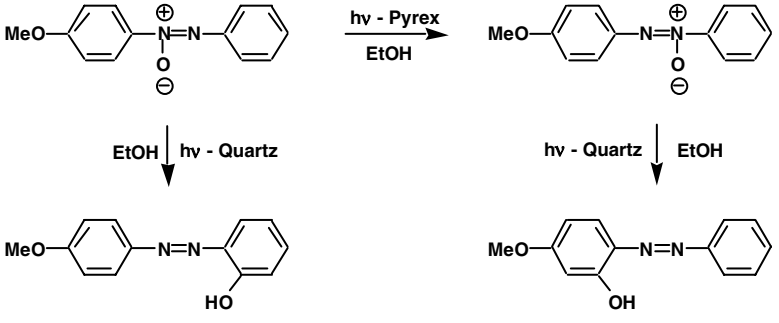

SCHEME 45

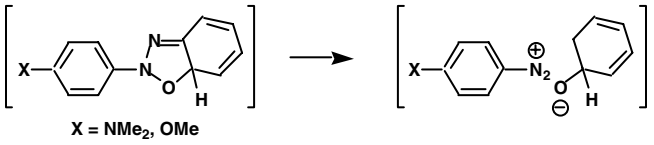

SCHEME 46

Based on the solvent and substituent effects on the electronic spectra, the quantum yields, and the product distribution, it was concluded that the azoxy rearrangement takes place from a $\pi\pi^*$ CT (charge-transfer) state rather than the $n\pi^*$ state as suggested by Bunce.

Azoxyalkanes

Lythgoe and co-workers synthesized azoxymethane and other azoxyalkanes.[109] The photolysis of azoxymethane led to a decomposition to give nitrogen, nitrous oxide, methane, and ethane (Scheme 47).[110] Azoxy-*t*-butane stabilized by *t*-butyl groups, however, resulted in the formation of 1,3-di-*t*-butyloxadiaziridine upon UV irradiation at 10°C (Scheme 48).[111]

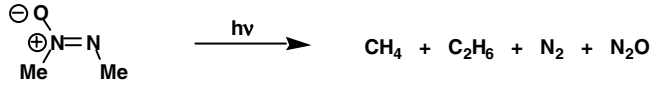

SCHEME 47

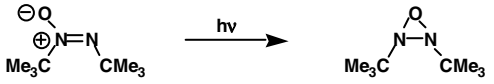

SCHEME 48

Nitrosoalkane Dimers

Many nitrosoalkanes and nitrosoarenes exist as dimers at room temperature. In 1976, Gowenlock and Trotman carried out a unique investigation on the isolation of *E*- and *Z*-isomers of the nitrosoalkane dimer.[112] They prepared two isomers, A and B, of dimeric nitrosomethane generated by the photolysis and pyrolysis of *t*-butyl nitrite vapor by trapping them on the surface of the apparatus. The less-stable isomer A was transformed into isomer B upon heating or by dissolving it in a solvent. They formulated the A and B forms as *Z*- and *E*-isomers of diazine dioxides **3**. The diazine dioxide structure for the nitroso dimers was later confirmed by NMR spectroscopy by Freeman.[113]

3*E* **3*Z***

Many nitrosoalkane dimers in solution are in equilibrium with nitrosoalkane monomers at room temperature. De Boer and collaborators demonstrated that the photolysis of nitrosoalkane dimers in solution results in the formation of the corresponding nitroxides, as proved by ESR spectroscopy (Scheme 49).[114] The formation involves a combination of alkyl radicals generated from excited nitrosoalkanes with ground-state nitrosoalkanes.

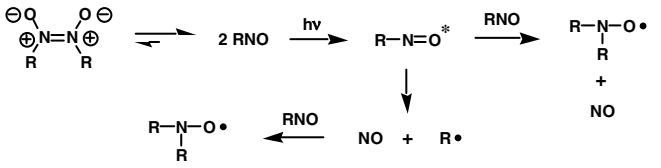

SCHEME 49

94.6 Applications

Synthesis

The ground-state synthesis of imines, oximes, and azo compounds invariably produces the more stable *E*-isomers and photochemical isomerization is practically the only means for preparing their less-stable *Z*-isomers,[76] as in the case of olefins such as stilbene. For example, the pharmacologically active *Z*-isomer of isonicotinaldehyde was prepared by photoisomerization (Scheme 50).[115] A less stable *E*-isomer of methyl *p*-nitrophenylhydroximate O-methyl ether can be isolated in 38% yield by UV irradiation of the *Z*-isomer in benzene, followed by preparative TLC (Scheme 51).[116]

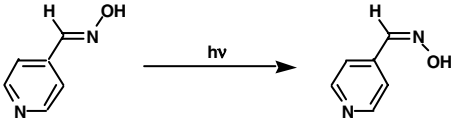

SCHEME 50

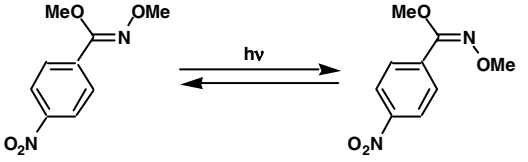

SCHEME 51

The *E,Z*-photostationary ratio is largely governed by the relative extinction coefficient of the absorptions of the two isomxxsers at the wavelength used for direct irradiation.[24,77] Isomerization can also be achieved by triplet sensitization, in which the relative values of the triplet energies are important in governing the ratio of the isomers.[24]

Photoreactions of Azobenzenes Adsorbed on Polymer or Silica Film

The photochemical and photophysical behavior of azobenzene adsorbed on polymer or silica films has been reported recently;[117] azobenzene adsorbed in water-swollen Nafion-H^+ (Nafion is a polymer consisting of a perfluorinated backbone and short pendant chains terminated by sulfonic acid groups) exhibited strong fluorescence. The irradiation resulted in the formation of benzo[*c*]cinnoline and benzidine in quantitative yield, while azobenzene incorporated into a methanol-swollen Nafion-H^+ membrane did not emit fluorescence but merely underwent *E,Z*-isomerization. Thus, solvent–swollen Nafion is useful in the selective phototransformation of azobenzene. According to the authors, protonated azobenzene molecules are located at the fluorocarbon/water interface in water-swollen Nafion-H^+ *Z*-Azobenzene formed on these membranes resulted in cyclization to give the observed products (Scheme 52).

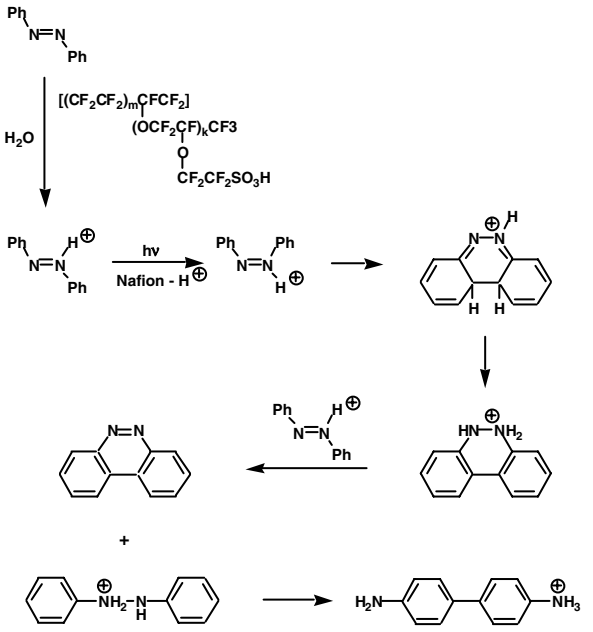

SCHEME 52

On the other hand, an azobenzene derivative was recently used as a photoresponsive probe to examine photoreactions in constrained media.[118] *E,Z*-photoisomerization was observed over the temperature range of 80 to 300K when a cationic azobenzene derivative, *p*-(ω-dimethylhydroxyethylammonioethoxy)-azobenzene, adsorbed on an aluminum-containing mesoporous silica film as a nano-reactor for photoreactions, was irradiated with 350-nm light. The results indicated that mesoporous silica films can be exploited as a nano-reaction vessel over a wide temperature range for photochemical reactions.

Photoresponsive Molecules Containing an Azobenzene Unit

The photoinduced *E,Z*-isomerization of azobenzene, which is a typical photochromic molecule,[119] has attracted considerable attention of chemists since the 1970s when several research groups recognized the usefulness of photoinduced *E,Z*-isomerization of azobenzene as a new tool to enforce reversible changes in the conformation of a lamellar multibilayer,[120] a synthetic bilayer membrane,[121] cyclodextrins,[123] crown ethers,[124–129] gelators,[135,136] enzyme regulators,[139,151] dendrimers,[141–145] polypeptides,[122,146–153] and polymers[154–157] with a variety of intentions. The applications have recently expanded from the field of molecular recognition to that of bio- and material sciences and technology such as liquid crystal displays and devices, reversible optical data storage systems, holographic gratings, etc. Thus, considerable efforts have been devoted to investigations concerning the constructions and properties of photoresponsive molecular systems having azobenzene units, especially in the past two decades.

Photoresponsive Crown Ethers

Shinkai and colleagues have synthesized a number of photoresponsive azobenzene-bridged crown ethers and studied their functions. In general, 70 to 80% of the photoresponsive molecules containing the *E*-azobenzene unit can be converted to the *Z*-isomer upon irradiation with UV light ($330 < \lambda < 380$ nm). The *E*-isomer is quantitatively regenerated, either thermally or upon irradiation with visible light ($\lambda >$ 420 nm). Because of space limitations, only a few of the results in this area are highlighted in this review.

Thus, in their first study, Shinkai and colleagues prepared the azobenzene-bridged azacrown ether **4** and found that the binding efficiency of **4** for alkali-metal ions can be modified by *E,Z*-photoisomerization (Scheme 53). The result was rationalized in terms of a photoinduced expansion of the azacrown ether

size.[124a] Similarly, they prepared the *E*-isomer of a new photoresponsive cryptand **5** containing a 2,2′-azopyridine bridge that can bind heavy-metal ions such as Cu^{2+}, Ni^{2+}, Co^{2+}, and Hg^{2+} from aqueous solution into the organic phase, whereas the photo-generated *Z*-isomer is unable to bind such ions (Scheme 53).[125]

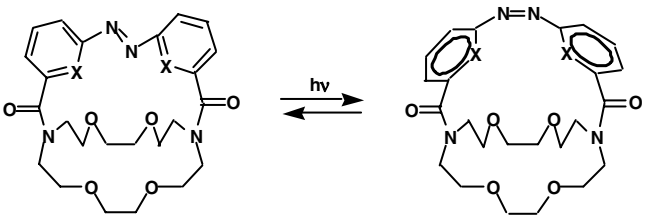

SCHEME 53

In contrast, the *E*-isomer of azobenzenophane crown ether **6** totally lacks the ability to extract metal ions, whereas the *Z*-isomer is able to bind alkali-metal cations (Scheme 54).[126]

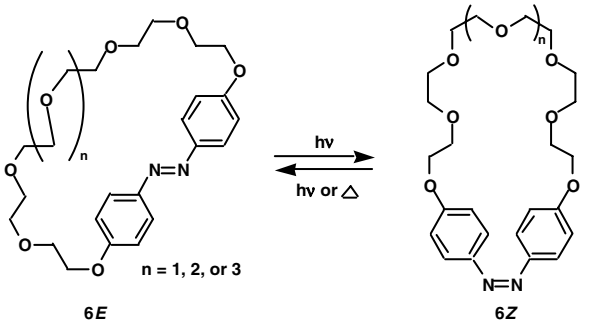

SCHEME 54

The *Z*-form of the photoresponsive crown ether **7**, prepared by Shiga and colleagues, lacks affinity for alkali-metal ions, whereas the *E*-form is reactive in this process.[124b] The *E*-isomer of a bis-crown ether **8** and the photoisomerized *Z*-isomer (Scheme 55) exhibit a contrasting ion-extraction ability;[127] the ratio (*E*:*Z*) of extractability for Na^+ against that for K^+ is 238-fold. Rb^+ and Cs^+ are also extracted by **8*Z*** more efficiently that by **8*E***.

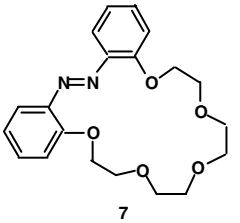

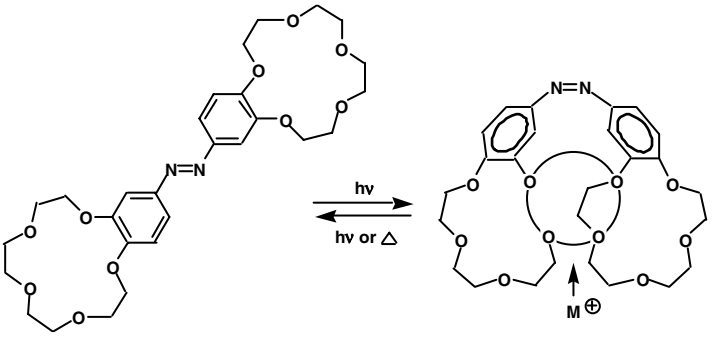

SCHEME 55

Moreover, the rate of the K^+ transport across a liquid (*o*-dichlorobenzene) membrane was found to be suppressed by light when a hydrophobic counterion was used, whereas it was accelerated by light when a relatively hydrophilic counterion was used. The ion-binding ability of the *E*-form of the photoresponsive crown ether **9** changes upon irradiation as a consequence of an intramolecular interaction between the ammonium group and the crown ether in the *Z*-isomer, as outlined in Scheme 56.[128]

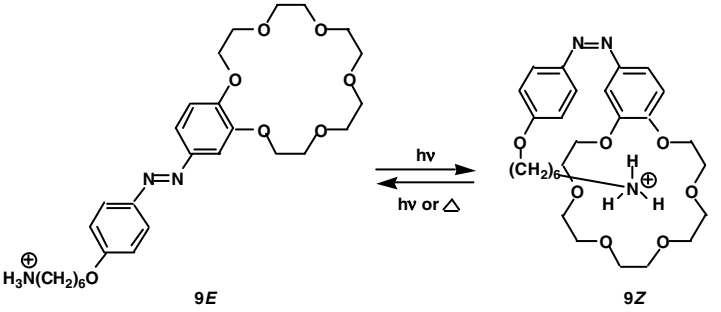

SCHEME 56

Similarly, the ion-binding properties of the crown ether **10** are appreciably altered upon *E,Z*-photoisomerization.[129]

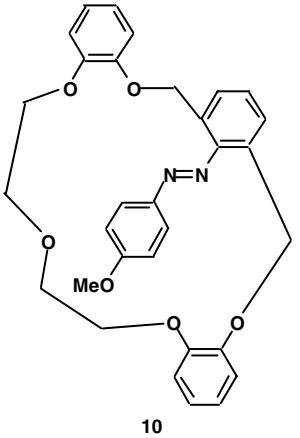

In another attempt, azobenzene-appended γ-cyclodextrin **11** was prepared. Upon the irradiation with 320- to 390-nm light, 70% of the *E*-isomer in water isomerized to the *Z*-isomer, which exhibited an enhanced binding ability for (−)-borneol and (+)-fenchone.[130] Benzo-18-crown-6 **12** linked to a phenol was synthesized. Upon irradiation by UV light, the azo linkage isomerized to the *Z*-isomer. It slowly reverted to the *E*-form in the dark and rapidly upon irradiation with visible light. An enhanced extraction of Ca^{2+} by the *Z*-isomer has been observed. The *Z* structure constitutes a "photoresponsive anion cap."[131]

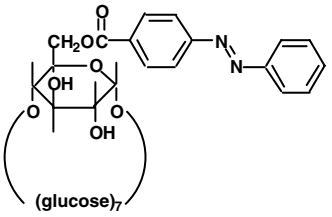

11

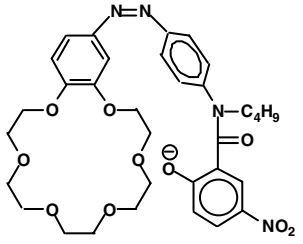

12

A polymer-bearing pendant photoresponsive crown ether **13** was prepared and the effects of photoirradiation on metal ion extraction was examined. There was little effect on the extractability for Na^+ and K^+ but a significant decrease for Rb^+ and Cd^+.[132]

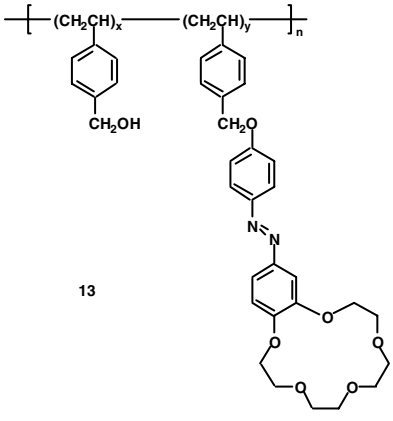

13

Readers interested in this application of the photoisomerization of azo compounds should refer to the review articles[133] and the original papers.[134]

Photoresponsive Gelators

Photoresponsive steroids containing an azobenzene moiety were synthesized and their functions as a gelator[135] were studied by Shinkai and collaborators.[136a] The sol–gel transition of the steroidal gelator– butanol system could be controlled by UV and visible light irradiation, which induced the reversible *E,Z*-isomerization of

the azo unit (Scheme 57). Shinkai and collaborators then prepared more than 19 cholesterol derivatives containing a variety of azobenzene moieties coupled to a steroidal structure through an ester linkage.[136b] Among them, cholesterol derivatives bearing a *p*-alkoxyazobenzene group acted as gelators of various organic fluids. The gel formed from the *E*-isomer was found to be converted to the sol when *E,Z*-isomerization was brought about on irradiation. This process could be repeated reversibly.

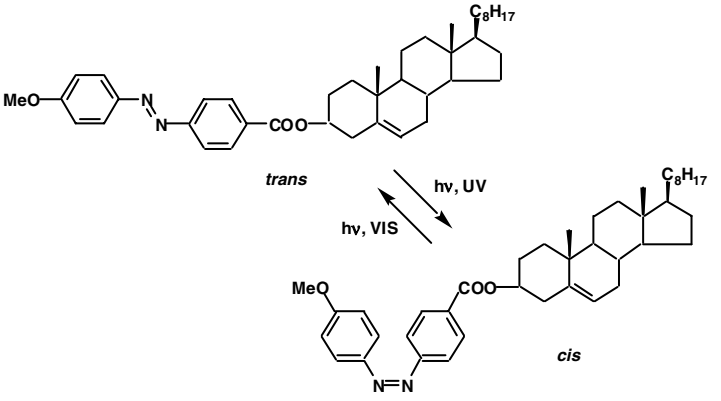

SCHEME 57

Photoresponsive Cyclophane

The synthesis of a photoresponsive, water-soluble azobenzenophane and the photoresponsive association properties for mono- and dicarboxylate guest molecules were studied by Shinkai and collaborators.[137] It was found that the guest recognition ability of the cyclophane was affected by photo-irradiation, which induced a change in its cavity shape generated by *E,Z*-isomerism of the azobenzene moieties (Scheme 58).

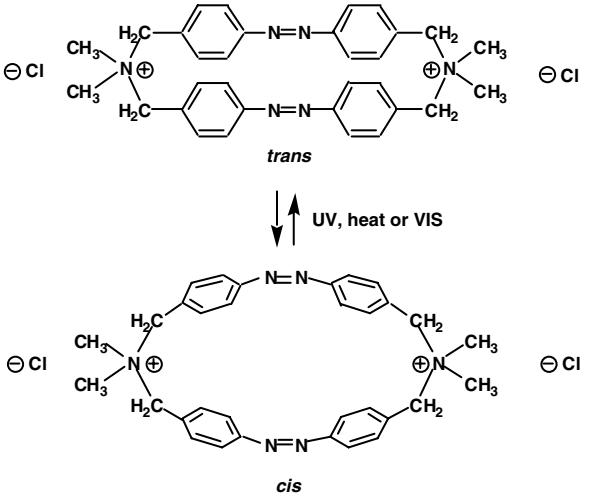

SCHEME 58

Tamaoki and co-workers have reported the synthesis of several azobenzenophanes, and their most recent work includes the synthesis of [1,1]-(3,3′)–azobenzenophane, in which two azobenzene units are connected by $-CH_2-$ chains at the *meta* positions.[138] They isolated the three isomers, *EE*, *EZ*, and *ZZ*, (Scheme 59) and determined the crystal structures. The x-ray crystal structures disclosed slightly and

highly distorted conformations for the *EE* and *EZ* isomers, respectively. The *ZZ* isomer, however, is not strained and this is in agreement with the thermal stability of the isomers in solution.

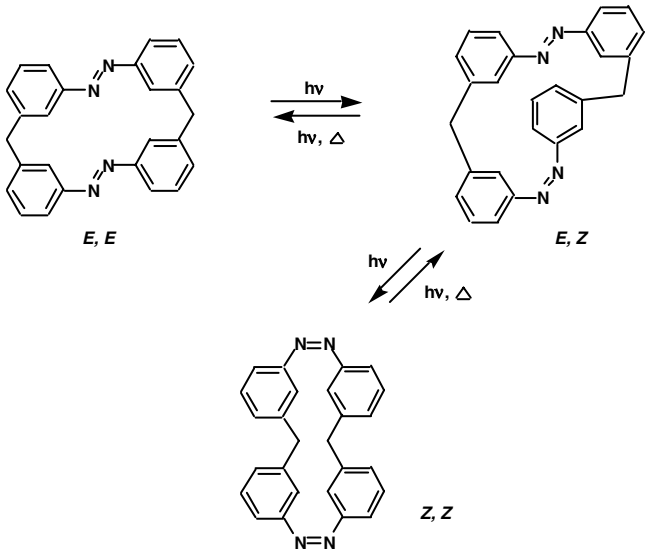

SCHEME 59

Photochromic Enzyme Inhibitors

Photocontrol of enzyme functions is an important area of current research. The aldehyde **14** and the boronic acid **15,** both bearing an azobenzene group, were designed.[139] In these molecules, the head consists of a primary recognition moiety for reversible binding in the enzyme active site. The tail is a photochromic moiety for controlling enzyme functions in a photoswitchable manner. These photochromic molecules were shown to be reversible, photoregulatable inhibitors of several enzymes such as cysteine and serine proteases; the irradiation of a solution containing papain and *trans*-**15** with $300 > \lambda > 370$-nm light resulted in a photostationary state of 83% of *cis*-**15** and a 5 times increase in the enzyme activity. The original activity level was subsequently restored by irradiation with visible light that converted the *cis*-isomer back to its *trans*-configuration.

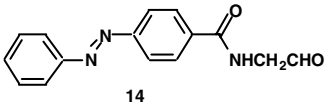

14

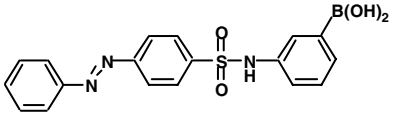

15

Light-Gated Receptor

A bis(boronic acid)-based receptor bearing an azobenzene moiety has been synthesized. The photocontrol of the saccharide-binding properties by the change of distance between two boronic acid groups was found to be possible by *E,Z*-photoisomerization of the azobenzene unit[140] (Scheme 60).

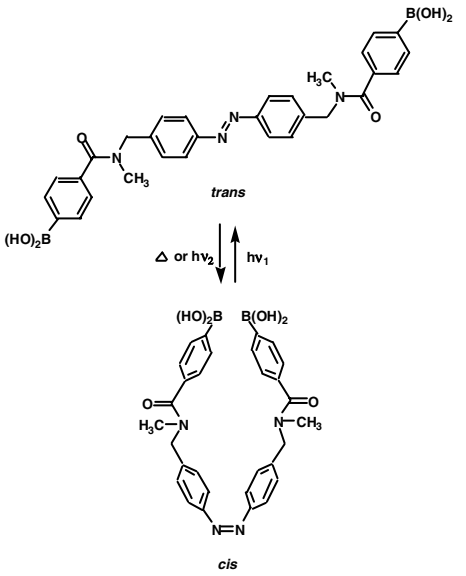

SCHEME 60

Photoresponsive Dendrimers

Dendrimers belong to a new class of multi-branched macromolecules[141] and have attracted much attention in recent years as photoresponsive molecules. This interest stems from the fact that the precise placement of a photoactive group in a well-defined macromolecule is possible, and predictable control of the reversible photoinduced molecular change for altering their function can be expected for these molecules.

Thus, a number of photoresponsive dendrimers with photochromic azobenzene units in the exterior,[142] interior,[143] periphery,[144] or whole[145] of the structure have been designed and prepared with different intentions.

Junge and MacGrath synthesized benzyl aryl ether dendrimers with azobenzene central linkers.[143a] The irradiation of the *E*-dendrimers in dichloromethane with 350-nm light resulted in clean isomerization to *Z*-isomers, which reverted to *E*-isomers upon exposure to bright sunlight for a period of only several seconds (Scheme 61).

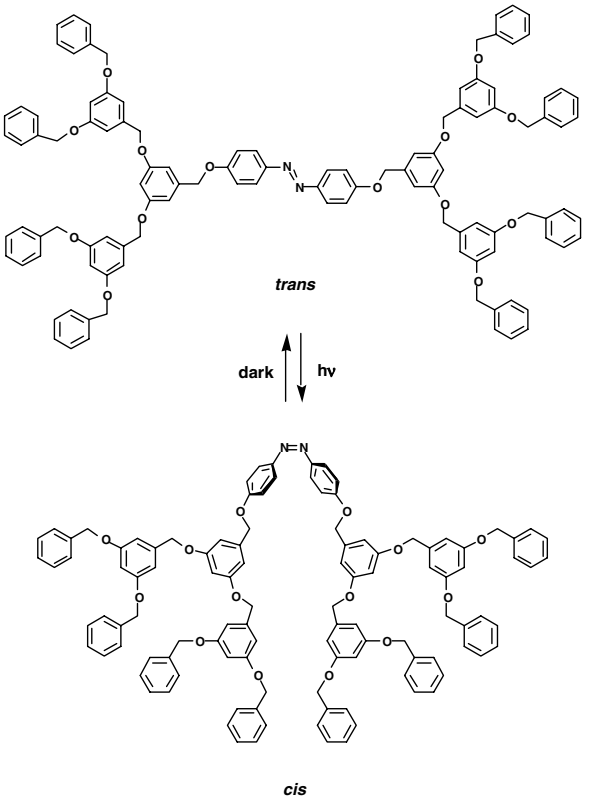

Scheme 61

SCHEME 61

Jiang and Aida reported on the synthesis of even more highly branched aryl ether dendrimers (*trans*-LnAZO, where n denotes the number of aromatic layers, 1, 3–5) with azobenzene in the center of the molecules.[143b] Upon UV irradiation at 21°C, these *E*-dendrimers isomerized to *Z*-isomers, which slowly reverted to the *E*-form in the dark. Remarkably, IR irradiation appreciably accelerated reversion to the *E*-form, and this reversion depended on the size of the dendrimers; the rate of the isomerization of *Z*-L5AZO to the *E*-form **16** was 260 times faster than that of thermal isomerization at 21°C in the dark, while, in sharp contrast, no effects were observed upon IR irradiation for the isomerization of smaller homologues, such as *Z*-L1AZO,**17** and *Z*-L3AZO.

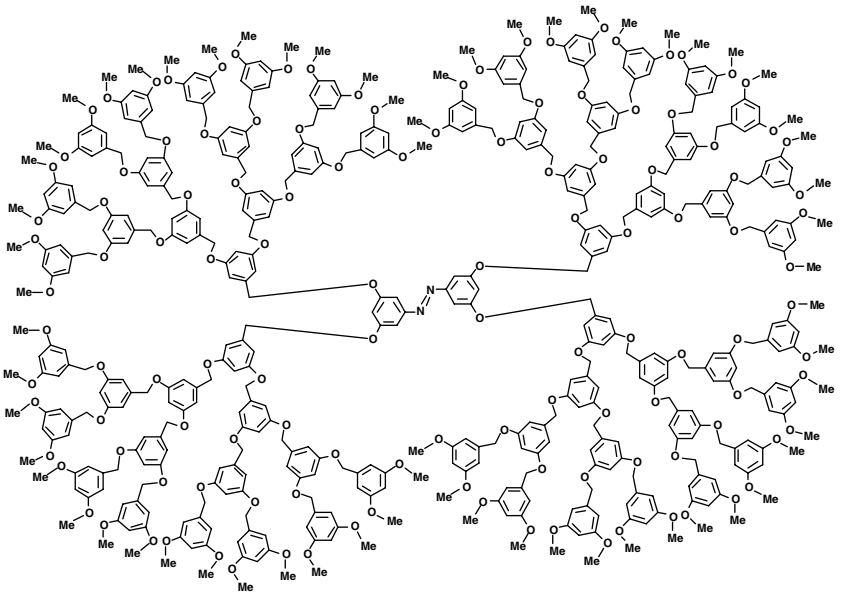

16

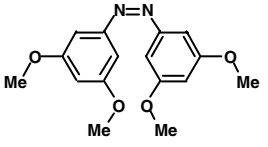

***cis*-L*1*AZO**

17

According to the authors, intramolecular energy transfer from the aromatic rings of the dendrimer matrix, which absorbed the infrared energy, excites the central azobenzene chromophore and accelerates the *Z,E*-isomerization. Thus, low-energy photons may serve for the chemical transformation of molecules such as dendrimers with the azobenzene unit in the center.

More recently, the preparation of dendrimer **18**, which contains three interior azobenzene units radially configured about the core unit, was reported.[143c] All four possible states (*EEE, EEZ, EZZ*, and *ZZZ)* with regard to the azobenzene chromophore were detected in solution and exhibited different physical properties. Thus, the dendrimer undergoes multiple discrete property changes upon an external stimulus of the interior groups.[143c]

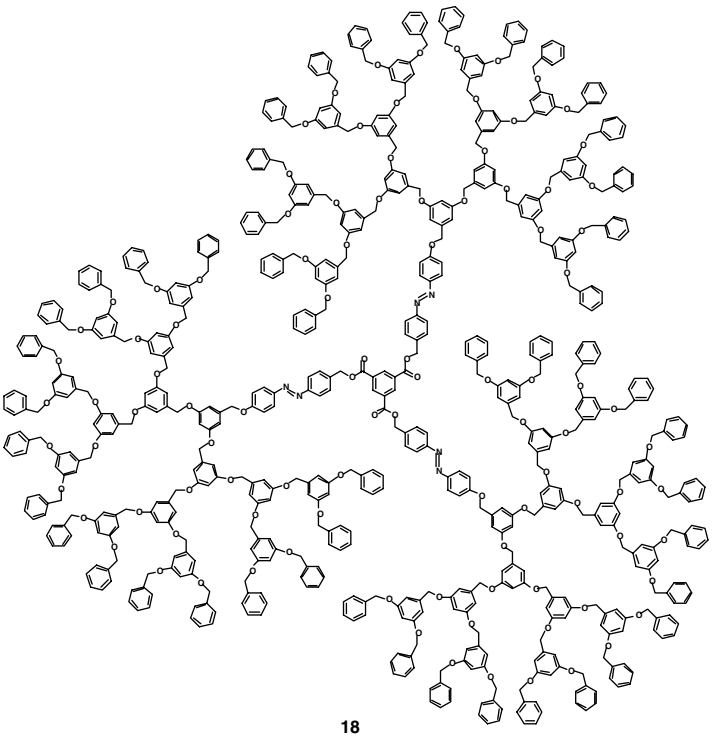

18

Photoresponsive Polypeptides

Polypeptides can exist in disordered or regularly folded structures, such as α-helix and β-structures. Among photoresponsive polymers, chiral polypeptides bearing photochromic units, such as an azobenzene or spiropyran group in their side chain, occupy a special position, because the change of the chiroptical properties in their photoisomerisation upon irradiation can be correlated with their conformational changes involving their backbone secondary structure and their conformation of the side chain bearing the photochromic groups. Any study on the behavior of these photoresponsive polypeptides should be of considerable value for a deeper understanding of some important biological processes and for the development of devices, such as chiroptical switches and sensors.

The exploitation of the *E,Z*-isomerization of the azoaromatic group for conformational problems was first studied in the 1960s. Goodman and Falxa synthesized copolypeptides of L-*p*-(phenylazo)phenylalanine with γ-benzyl-*L*-glutamate. They found that photoisomerization of the azobenzene group in synthetic polypeptides resulted in changes in the ORD spectra due to changes in the conformation.[-146]

A decade later, Ueno and collaborators synthesized a number of copolymers, such as those of *p*-phenylazobenzyl-*L*-aspartate and β-benzyl-*L*-aspartate and studied their conformational change by means of CD spectrometry.[147]

Ciardelli and co-workers, on the other hand, synthesized polymers of *L*-glutamic acid containing azobenzene or stilbene groups in the side chain (Scheme 62) and studied the relationship between their secondary structure and the photochromic behavior.[148,149]

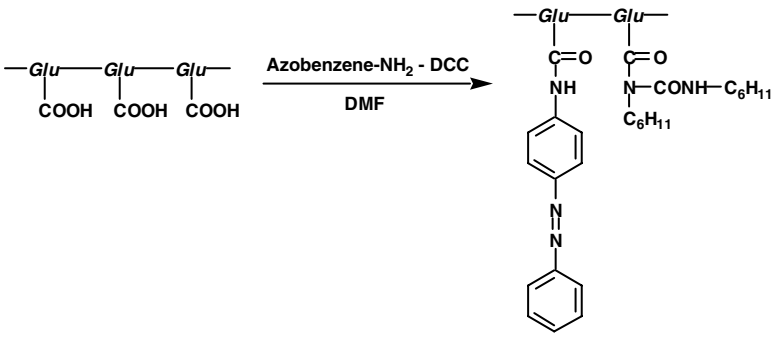

SCHEME 62

Subsequent to these investigations, many investigations on the synthesis of polypeptides bearing azobenzene groups in their side chain and correlations between their photoisomerization and the change of the chiroptical properties associated with their conformation were carried out by several groups of investigators. Italian investigators reviewed these investigations, carried out until the 1980s,; any readers interested in this subject are advised to refer to the available review articles.[150,153] A few recent examples are mentioned below.

Photoregulation of the hydrolysis activity of a modified enzyme-containing azobenzene group was recently reported. Thus, Imanishi and collaborators prepared a semi synthetic mutant, phospholipase A_2, which replaced Trip[3] with nonnatural aromatic amino acids, such as *p*-phenylazo-*L*-phenylalanine, by a semi synthetic method.[151] While a modified AzoF-AMPA having an *E*-configuration of the azophenylalanine unit lost hydrolysis activity for phospholipid membranes, AzoF-AMPA with a *Z*-configuration generated by UV light irradiation recovered hydrolytic activity. The change in the enzyme activity is ascribed to a conformational change of the mutant proteins.[151]

Fissi and colleagues recently reported the preparation of a new azo-modified poly(*L*-lysine) **19,** in which the azobenzene units are linked to the Lys side chains by means of a sulfonamide function.[152] In contrast to azo-modified poly(*L*-lysine) containing azobenzene units linked to the Lys side chains by means of an amide function, **20**, the new polypeptide, in hexafluoro-2-propanol, adopted a random-coil conformation, irrelevant of the configuration of the azobenzene units. However, the addition of co-solvents, such as methanol, to the solution resulted in the system being able to respond to light, giving rise to reversible photoinduced random coil/α-helix conformational transitions. Thus, poly{N^{ε}–[(phenylazophenyl)sulfonyl]-*L*-lysine} may have potential as a material for designing sensors, optical and chiroptical switches and devices that can be photomodulated.

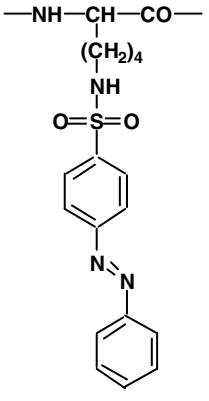

19

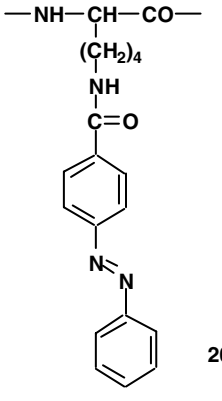

20

Readers interested in more detailed aspects of work in this area are referred to a recent comprehensive review article.[153]

Photoresponsive Polymers

In 1966, Lovrien was the first to propose photoresponsive polymers in which photochromic units, such as azobenzene chromophores, are parts of the polymers.[154] He envisioned that isomerization of the photoresponsive units in the polymer by light energy may influence the conformation of the polymers, thereby resulting in a reversible change of the polymers in solution. He found that the viscosity of an aqueous solution of copolymers of methacrylic acid and *N*-(2,2′-dimethoxyazobenzene)acrylamide increased upon UV light irradiation. The photoisomerization of the azobenzene units to the *Z*-configuration led the polymer coil to expand due to a decrease in the hydrophobic interaction between the azobenzene chromophores.

Since the 1970s a great number of photoresponsive polymers have been designed and prepared. The physical and chemical properties of these polymers in conjunction with their reversible conformational change upon photoirradiation have been examined. This work was aimed at the reversible control of their properties.

Among various photoisomeric units, azobenzene has been most widely used to construct photoresponsive polymers, as is apparent in applications to the field of polypeptides, already separately discussed in the previous section.

Concerning the polymers, Irie and collaborators prepared a number of polyamides with azobenzene groups in the backbone (e.g., **21**).[155] The viscosity of the polyamides in a polar solvent decreased upon irradiation and returned to the initial value in the dark.

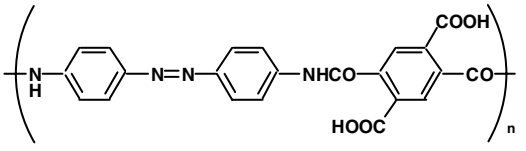

21

The development of some fundamental and practical aspects of the area until the 1990s has been summarized in several comprehensive review articles.[156,157]

Some examples of the recent progress in this area are discussed below.

Müller and Zentel prepared several copolymers by copolymerization of hexylisocyanate with seven new chiral azo chromophores with an isocyano functionality (e.g., **22**). The co-polyisocyanates with the azo side chains possess a helical conformation. The interplay of the chiral side chains and the helical main chains in the polymers were studied by chiroptical methods.[158]

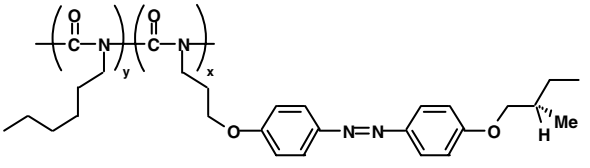

22

Yamamoto and co-workers recently prepared a polyrotaxane **23** composed of an azobenzene-containing polyester and γ-cyclodextrin. While a DMSO solution of the polymer underwent *E,Z*-photoisomerization upon UV irradiation, the reverse *Z,E*-photoisomerization did not take place upon irradiation with visible light under ordinary conditions. In contrast, cyclodextrin-free polyester **24** having azobenzene groups, prepared in a similar manner, underwent *E,Z*-photoisomerization with UV light and reverse

Z,E-photoisomerization with visible light.[159] According to the authors, intramolecular N····H-O- hydrogen bonds between a *Z*-azo group and a hydroxyl group of the isomerized polyrotaxane molecules retarded the photoinduced *Z,E*-photoisomerization.

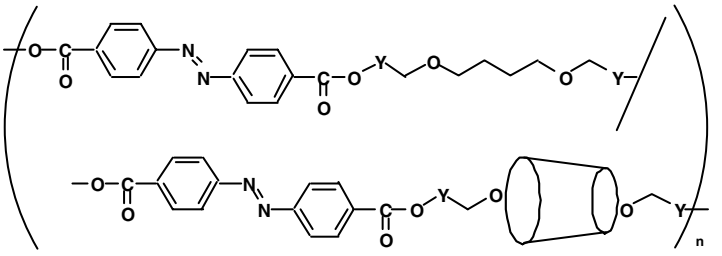

Y = $-CH(CH_2OH)-$ (0.79 : $-CH_2-CH(OH)-$ 0.21)

23

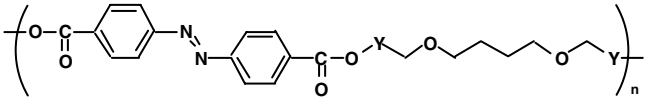

Y = $-CH(CH_2OH)-$ (0.62 : $-CH_2-CH(OH)-$ 0.38)

24

Preparation of hydrogen-bonded complexes, composed of poly(4-vinylpyridine-co-styrene and 4-[(4-octylphenylazo)phenoxy]butanoic or hexanoic acid, has been reported by Kato and colleagues.[160] The polymeric complexes behave like side-chain liquid-crystalline polymers and caused reversible photoinduced phase transitions due to *E,Z*-isomerization of an azobenzene moiety in the guest molecules.

Materials for Optical Devices and SAM-Modified Electrodes, etc.

A potential technological exploitation of the reversible *E,Z*-isomerization of materials containing azo units has attracted growing attention over the past decade and the subject was reviewed in 1993.[163] A variety of the attempts include liquid-crystal displays and devices,[161] nonlinear optics,[162] optical switching and data storage,[163–168] holographic grating, etc.

Tachibana designed a molecule **25** that functions as an organic switching device by a photoinduced change in the conductivity of a Langmuir-Blodgett (LB) film composed of a charge-transfer complex between TCNQ and the pyridinium cation bearing an azobenzene unit.[164] About 25% of the *E*-isomer isomerized to the *Z*-form upon 356-nm light irradiation, and the *E*-isomer reverted to the *Z*-isomer upon 436-nm light irradiation. The measured conductivity of the LB film increased by aproximately 30% for a 25:75 *Z/E* mixture, compared to the pure *E*-isomer.

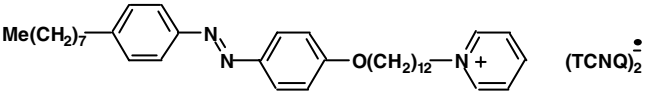

25

Ikeda and Tsutsumi synthesized three azobenzene derivatives **26**. Liquid-crystal films formed from these azobenzenes exhibited a nematic phase in the *E*-isomer and no LC (liquid crystal) phase in the *Z*-isomers. *E,Z*-photoisomerization of these azobenzenes with a laser pulse resulted in a nematic-to-isotropic phase transition with a rapid optical response of 200 microseconds.[165]

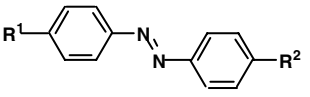

$R^1 = n\text{-}C_4H_9$; R^2 = MeO-
$R^1 = R^2 = n\text{-}C_8H_{17}O$-
$R^1 = -(CH_2\text{-}CH)_n-$; $R^2 = C_2H_5O$-
C=O
$O(CH_2)_6O$-

26

Öge and Zentel designed a ferroelectric LC side-chain copolymer containing both azo and mesogenic units. A change in the ferroelectricity in the LC polymer was observed upon UV irradiation.[166]

Fujishima and collaborators have devised an information storage system using Langmuir-Blodgett films containing an azobenzene unit.[167a] The LB film was prepared by depositing 4-octyl-4′(5-carboxy-pentamethyleneoxy)azobenzene **27** onto SiO_2 glass. Scheme 63 outlines the data-storage system based on

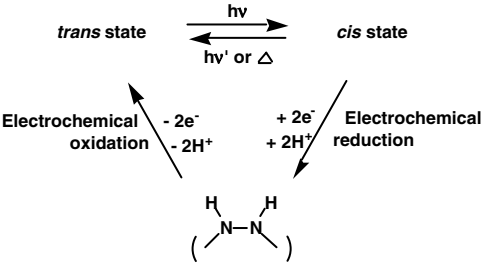

SCHEME 63

the combination of photochemical isomerization and electrochemical reduction — oxidation processes. Irradiation of *trans*-state LB films in aqueous solution by a He-Cd laser (325 nm) induced *E,Z*-isomerization. The potential of the film was then switched to a voltage where only the *cis*-azobenzene unit was reduced to the hydrazobenzene derivative. This was converted electrochemically back to the original *trans*-state. The stored data could be detected by the difference in the UV absorption. The advantage of this system is to remove the possibility of any undesirable thermal re-isomerization of the *Z*-isomer in the photoprocess. The authors also investigated the structures and properties of several related SAM and LB films.[167b–d]

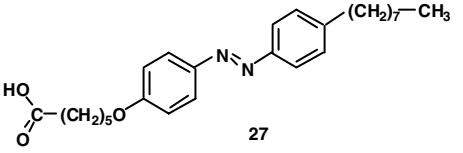

27

The design of a system for photoswitching 'on' and 'off' coordination sites in a self-assembled monolayer (SAM) containing an azopyridine unit has recently been reported by Cook and co-workers.[168] The required SAM was prepared by depositing an unsymmetrical disulfide **28** having 4-(arylazo)pyridine and phenoxy moieties onto an 8-nm-thick film of gold supported on a quartz glass slide. Scheme 64 outlines the system for the evanescent field-driven SAM photoswitch. Zinc tetraphenylporphyrin (ZnTPP) was

then coordinated to the pyridine nitrogen atom in the *trans*-form film. Direct or 365-nm waveguided-light illumination of the coordinated SAM films resulted in photoisomerization to the *cis*-form film, releasing the coordinated ZnTPP. Further irradiation with 439-nm light effected the *Z,E*-isomerization. Thus, a three-step cycle involving the waveguided, light-induced release of metallomacrocycles within a SAM was achieved.

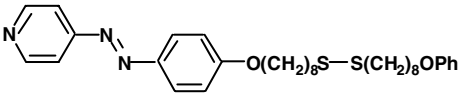

28

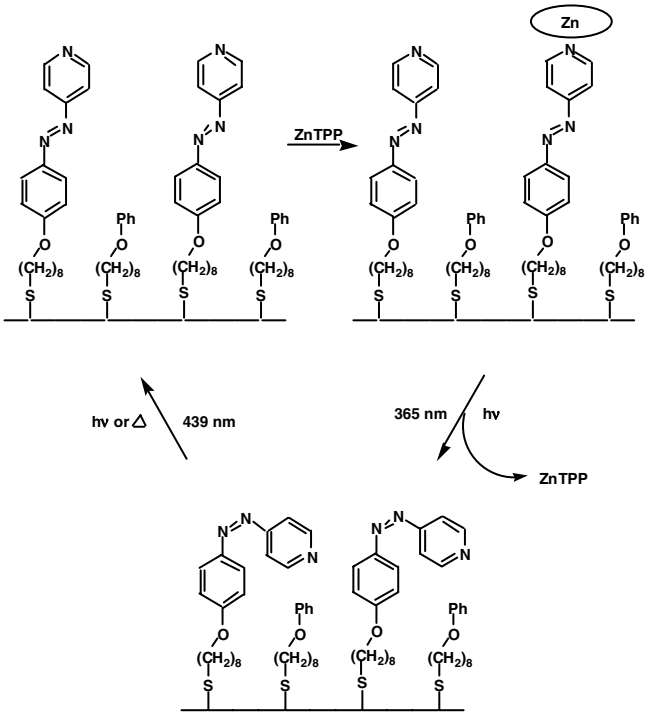

SCHEME 64

SAMs containing an azobenzene moiety have also been used to modify the electrochemical properties of electrodes by several investigators.[169] Thus, Uosaki and collaborators constructed a SAM by depositing an alkyl thiol molecule containing ferrocene and azobenzene moieties on gold electrode surface (Scheme 65).[169] They found that the charge-transfer rate of the ferrocene group in the SAM could be reversibly controlled by electro- and photochemical isomerization between *E,Z*-forms of the azobenzene moiety in the SAM.

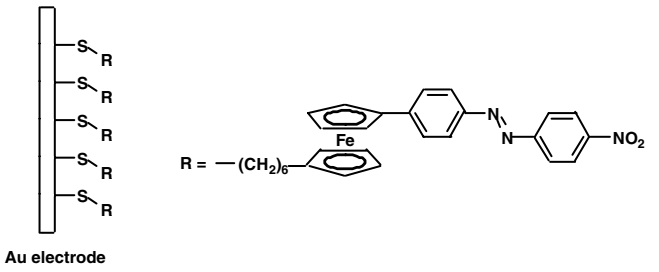

SCHEME 65

Various LB and SAM films and vesicles containing an azobenzene unit have been prepared, and their structures and functions have been investigated to seek new functional materials.[170]

Meanwhile, a self-assembled alternating multilayer film, composed of a bipolar amphiphile, 4,4′-bis[(12-(trimethylammonio)dodecyl)oxy]azobenzene dibromide **29** and an anionic polyelectrolyte poly(vinyl sulfate, potassium salt) on a pre-coated fused silica substrate, was prepared. The effects of added salt on the photochemical isomerization of the azobenzene unit in the self-assembled multilayer films were investigated.[171]

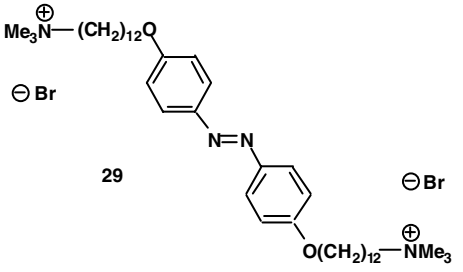

Acknowledgments

The author wishes to thank Dr. Hisanori Senboku for his kind assistance in preparing the diagrams.

References

1. Hantzsch, A., Die stereochemisch-isomerin Oximes des *p*-Tolyl-Phenylketones. *Ber.*, 23, 2325, 1890; *idem*, Üeber stereoisomere Ketoxime, 24, 51, 1891.
2. Ciamician, G. and Silber, P., Chemische Lichtwirkungen, *Ber.*, 36, 4266, 1903.
3. Brady, O.L. and Dunn, F.P., The isomerism of the oximes. II. The nitrobenzaldoximes, *J. Chem. Soc.*, 103, 1619, 1913; Brady, O.L. and McHugh, G.P., The isomerism of the oximes. Part XVI. The action of ultraviolet light on aldoximes and their derivatives, *J. Chem. Soc.*, 125, 547, 1924.
4. Stoermer, R., Über die Umlagerung der stabilen Stereoisomeren in labile durch ultraviolettes Light (II)., *Ber.*, 44, 637, 1911.
5. Thiele, J., Über Hydrazo- und Azomethan, *Ber.*, 42, 2575, 1909.
6. Ramsperger, H., The photochemical decomposition of azomethane, *J. Am. Chem. Soc.*, 50, 123, 1928.
7. For example, see (a) Steacie, E.W.R., *Atomic and Free Radical Reactions*, Reinhold, New York, 1954, 376; (b) Rebbert, R.W. and Ausloos, P., The photolysis and radiolysis of $CH_3N_2CH_3$ and $CH_3N_2CH_3$-$CD_3N_2CD_3$ mixtures, *J. Phys, Chem.*, 66, 2253, 1962.

8. For example, see Nelson, S.F. and Bartlett, P.D., Azocumene. I. Preparation and decomposition of azocumene. Unsymmetrical coupling products of the cumyl radical, *J. Am. Chem. Soc.*, 88, 137, 1966; Bartlett, P.D. and McBride, J.M., Configuration, conformation and spin in radical pairs, *Pure Appl. Chem.*, 15, 89, 1967.
9. (a) Engel, P.S. and Steel, C., Photochemistry of aliphatic azo compounds in Solution, *Acc. Chem. Res.*, 5, 242, 1972; (b) Engel, P.S., Mechanism of the thermal and photochemical decomposition of azoalkanes, *Chem. Rev.*, 80, 99, 1980.
10. (a) Adam, W., Garcia, H., Marti, V., and Moorthy, J.N., Homolytic substitution (S_H2) versus triplet diradical (ISC) in the photochemical denitrogenation of a DBH azoalkane: temperature-dependent *syn/anti* diastereoselectivity as a mechanistic probe for the doubly inverted housane, *J. Am. Chem. Soc.*,121, 9475, 1999 and papers cited therein; (b) Adam, W., Marti, V., Sahin, C., and Trofimov, A.V., Viscosity-controlled stereoselective inversion in the photochemical denitrogenation of a stereolabeled diazabicyclo[2.2.1]heptane (DBH)-type azoalkane, *J. Am. Chem. Soc.,* 122, 5002, 2000.
11. Hartley, G.S., The *cis*-form of azobenzene, *Nature*, 140, 281, 1937.
12. Hutton, R.F. and Steel, C., Photoisomerization of azomethane, *J. Am. Chem. Soc.*, 86, 745, 1964.
13. Fischer, E. and Frei, Y., Photoisomerization equilibria involving the C=N double bond, *J. Chem. Phys.*, 27, 808, 1957.
14. Wettermark, G., Photochemistry of the carbon-nitrogen double bond, in *The Chemistry of the Carbon-Nitrogen Double Bond,* Patai, S., Ed., Interscience, New York, 1969, 565.
15. Padwa, A., Photochemistry of the carbon-nitrogen double bond, *Chem. Rev.*, 77, 37, 1977.
16. Pratt, A.C., The chemistry of imines, *Chem. Soc. Rev.*, 6, 63, 1977.
17. Griffiths, J., Photochemistry of azobenzene and its derivatives, *Chem. Soc. Rev.*, 1, 481, 1972.
18. Dürr, H. and Ruge, B., Triplet states from azo compounds, *Top. Curr. Chem.*, 66, 55, 1976.
19. (a) Orenski, P.J. and Clossan, W.D., The ultraviolet absorption spectra of oximes, *Tetrahedron Lett.*, 3629, 1967; (b) Suginome, H., Takahashi, H., and Masamune, T., The photo-Beckmann rearrangement of 3a,5-cyclo-5α-cholestan-6-one oxime, *Bull. Chem. Soc. Jpn.*, 45, 1836, 1972.
20. (a) Amin, J.H. and de Mayo, P., The irradiation of aryl aldoximes, *Tetrahedron Lett.*, 1585, 1963; (b) Izawa, H., de Mayo, P., and Tabata, T., The Photochemical Beckmann rearrangement, *Can.J. Chem.*, 47, 51, 1969.
21. Oine, T. and Mukai, T., Evidence for the formation of oxaziridines during the irradiation of oximes, *Tetrahedron Lett.*, 157, 1969.
22. (a) Taylor, R.T., Douek, M., and Just, G., Photolysis of oximes, *Tetrahedron Lett.*, 4143, 1966; (b) Cunningham, M., Ng Lim, L.S., and Just, G., Photochemistry of oximes. III. Photochemical Beckmann rearrangement, *Can.J. Chem.*, 49, 2891, 1971.
23. (a) Suginome, H. and Takahashi, H., Stereochemical aspects of the photo-Beckmann rearrangement. Stereochemical integrity of the terminus of the migrating carbon in the photo-Beckmann rearrangements of 5α- and 5β-cholestan-6-one oximes, *Bull. Chem. Soc. Jpn.*, 48, 576, 1975; (b) Suginome, H. and Yagihashi, F., Photoinduced transformations. 36. Stereochemical integrity of the terminus of the migrating carbon in the photo-Beckmann rearrangements of some cholestanone oximes, *J. Chem. Soc., Perkin Trans. 1*, 2488, 1977; (c) Suginome, H., Takahashi, H., and Masamune, T., The photo-Beckmann rearrangement of 3α,5-cyclo-5α-cholestane-6-one oxime, *Bull. Chem. Soc. Jpn.*, 45, 1836, 1972; (d) Suginome, H. and Takahashi, Y., Photoinduced transformations. 41. Photo-Beckmann rearrangement of some cholestane-3-one oximes with methyl groups attached to the α-carbon, *J. Chem. Soc., Perkin Trans. 1,* 2921, 1979; (e) Suginome, H., Takeda, H., and Masamune, T., The photo-Beckmann rearrangement of A-nor-5α-cholestan-3-one oxime, *Bull. Chem. Soc. Jpn.,* 52, 269, 1979; (f) Suginome, H. and Shea, C.-M., Synthesis of α-hydroxy lactams by photorearrangement of cyclic α-hydroxy ketone oximes, *Synthesis*, 229, 1980; (g) Suginome, H. and Uchida, T., Photoreaction of D-nor-5α-androstan-16-one oxime, a steroidal cyclobutanone oxime, *Bull. Chem. Soc. Jpn.*, 53, 2292,1980; (h) Suginome, H. and Shea, C.-M., Photoinduced transformations. 50. The photo-Beckmann rearrangement of 3a,5-cyclo-5a-cholestan 7-one oxime,

a β,γ-cyclopropyl ketone oxime, *J. Chem. Soc., Perkin Trans. 1,* 2268, 1980; (i) Suginome, H., Yabe, T., and Osawa, E., Photoinduced transformations. LXI. Syntheses of some six-membered and eight-membered lactams of the β-homo- and α-nor-β,β-dihomocholestane series by the photo-Beckmann rearrangement, *J. Chem. Soc., Perkin Trans. 1,* 931, 1982; (j) Suginome, H., Furukawa, K., and Orito, K., Photoinduced molecular transformations. 119. Photochemical nitrogen insertion into bicyclo[2.2.1]heptanones; the photochemistry of oximes of (+)-fenchone and (+)-camphor, *J. Chem. Soc., Perkin Trans. 1,* 917, 1991; (k) Suginome, H. and Uchida, T., Photo-Beckmann rearrangements of oximes of androsterone and 13α-androsterone, *Bull. Chem. Soc. Jpn.*, 47, 687, 1974.

24. (a) Padwa, A. and Albrecht, F., Photochemical *syn-anti* isomerization about the carbon-nitrogen double bond, *J. Am. Chem. Soc.*, 96, 4849, 1974; (b) Padwa, A. and Albrecht, F., *J. Org. Chem.*, 39, 2361, 1974.
25. Baas, P. and Cerfontain, H., Photochemistry of α-oxo-oximes. 3. Photoisomerization of some α-oxo-oxime ethyl ethers, *J. Chem. Soc., Perkin Trans. II*, 151, 1979.
26. (a) Arai, T., Furuya, Y., Furuuchi, H., and Tokumaru, K., One-way *Z*→*E* isomerization around the double bond of N-methoxy-1-(2-anthryl)ethanimine in the excited triplet state. Direct observation of one-way isomerization from *Z* triplet to *E* triplet of the C=N bond, *Chem. Phys. Lett.*, 21, 597, 1993; (b) Segawa, K., Kikuchi, O., Arai, T., and Tokumaru, K., Photochemical *E,Z*-isomerization of aryl-substituted methanimines. AM1-CI potential energy curves along the CN double bond twisting and the N atom in plane inversion, *J. Mol. Struct. (Theochem)*, 343, 133, 1995.
27. Pratt, A.C. and Abdul-Majid, O., Photochemistry of the carbon-nitrogen double bond. 2. An investigation of the 3-methylenepropan-1-imine and 3-oxopropan-1-imine chromophores, *J. Chem. Soc., Perkin Trans. 1,* 359, 1987.
28. Koyano, K. and Tanaka, I, The photochemical and thermal isomerization of *trans*- and *cis*-α-cyano-α-phenyl-N-phenylnitrones, *J. Phys. Chem.*, 69, 2545, 1965.
29. Suginome, H., Kaji, M., Ohtsuka, T., Yamada, S., Ohki, T., Senboku, H., and Furusaki, A., Photo-induced molecular transformations. 130. Novel stereospecific photorearrangement and stereospecific addition of methanol in steroidal α,β-unsaturated cyclic ketone oximes, *J. Chem. Soc., Perkin Trans. 1*, 427, 1992.
30. Repolles, J., Servera, F. and Bonet, J.-J., Photochemische umwandlung des oxims von 3-oxo-17β-acetoxy-$\Delta^{1,5}$-androstadien, *Helv. Chim. Acta,* 57, 2454, 1974.
31. Suginome, H., Kaji, M., and Yamada, S., Photo-induced molecular transformations. 87. Regiospecific photo-Beckmann rearrangement of steroidal α, β-unsaturated ketone oximes: synthesis of some steroidal enamino lactams, *J. Chem. Soc., Perkin Trans. 1,* 321, 1988.
32. Suginome, H., Ohshima, K., Ohue, Y., Ohki, T., and Senboku, H., Photoinduced molecular transformations. 149. Stereospecific photoaddition and photorearrangements of oximes of some steroidal α, β-unsaturated cyclic ketones and their deuterio derivatives, *J. Chem. Soc., Perkin Trans. 1,* 3229, 1994.
33. Suginome, H., Ohki, T., Nagaoka, A., and Senboku, H., Photoinduced molecular transformations. 133. New photoinduced deconjugation of steroidal α,β-unsaturated cyclic ketone oxime into the β,γ-isomer involving stereospecific proton transfer, *J. Chem. Soc., Perkin Trans. 1,* 1849, 1992.
34. Suginome, H., Nagaoka, A., and Senboku, H., Photoinduced molecular transformations. P134. Photoinduced stereospecific addition of methanol to 5β–cholest-1-en-3-one oxime and photoinduced deconjugation of its 1-methyl derivative involving stereospecific proton transfer, *J. Chem. Soc., Perkin Trans. 1*, 3103, 1992.
35. (a) Nitta, M., Inoue, O., and Tada, M., A photorearrangement of 6-methylenetricyclo[3.2.1.$0^{2,7}$]oct-3-en-8-one oxime derivatives: di-π-methane type rearrangement involving an oxime moiety, *Chem. Lett.,* 1065, 1977; (b) Nitta, M., Kasahara, I., and Kobayashi, T., Aza-di-π-methane rearrangement involving an oxime group, *Bull. Chem. Soc. Jpn.,* 54, 1275, 1981.
36. Suginome, H., Maeda, N., Takahashi, Y., and Miyata, N., The photo-Beckmann rearrangement of steroidal β, γ-unsaturated ketone oximes, *Bull. Chem. Soc. Jpn.,* 54, 846,1981.

37. (a) Armesto, D., Ramos, A., and Mayoral, E.P., The aza-di-π-methane rearrangement of β,γ-unsaturated oximes, *Tetrahedron Lett.*, 35, 3785, 1994; (b) Armesto, D., Ortiz, M.J., Ramos, A., Horspool, W.M., and Mayoral, E.P., A study of the competition between the di-π-methane and the aza-di-π-methane processes in 2-vinyl-β,γ-unsaturated oxime derivatives. The novel aza-di-π-methane reactivity of β,γ-unsaturated oximes, *J. Org. Chem.*, 59, 8115,1994; (c) Armesto, D. and Ramos, A., Photochemical synthesis of oxime acetates derivatives of 1-carbaldehydobicyclo[n,1.0] alkanes by the aza-di-π-methane rearrangement, *Tetrahedron,* 49, 7159, 1993.
38. Armesto, D., Ramos, A., Ortiz, M.J., Mancheno, M.J., and Mayoral, E.P., Novel photocyclization of β,γ-unsaturated oximes, *Recl. Trav. Chim. Pays-Bas*, 114, 514, 1995.
39. Armesto, D., Ramos, A., Ortiz, M.J., Horspool, W.M., Mancheno, M.J., Caballero, O., and Mayoral, E.P., Novel photochemical behaviour of the oximes and hydrazones of β,γ-unsaturated carbonyl compounds*, J. Chem. Soc., Perkin Trans. 1,* 1535, 1997.
40. Armesto, D., Gallego, M., Horspool, W.M., and Ramos, A., A study on the scope of the photochemical 1,3-migration of oximino groups in β,γ–unsaturated oximes and oxime derivatives, *J. Chem. Soc., Perkin Trans. 1*, 107, 1996.
41. Armesto, D., Austin, M.A., Griffiths, O.J., Horspool, W.M., and Carpintero, M., A novel photochemical synthesis of 5,6-dihydro-4*H*-1,2-oxazines by DCA-sensitized irradiation of γ,δ-unsaturated oximes, *J. Chem. Soc., Chem. Commun.,* 2715, 1996.
42. Schulte-Frohlinde, D., Quantenausbeuten bei der Photochemischen *syn* → *anti*-Umlagerung der Pyridin-Aldehyd-(2)-phenylhydrazone, *Liebigs Ann. Chem.*, 615, 114, 1958.
43. Condorelli, G., Costanzo, L.L., Pistara, S., and Giuffrida, S., The photochemical isomerization of 2-naphthaldehydephenylhydrazone, *Zeitsch. Phys. Chem. Neue Folge*, 90, 58, 1974.
44. Condorelli, G., Constanzo, L.L., Alicata, L., and Giuffrida, A., The photochemical isomerization of the pyridine-2-aldehyde 4-nitrophenylhydrazone, *Chem. Lett.*, 227, 1975.
45. Condorelli.G., Costanzo, L.L., Giuffrida, A., and Pistara, S., On the mechanism of the photoisomerization of the benzaldehyde and its derivative 4-nitrophenylhydrazones, *Zeitsch. Phys. Chem. Neue Folge*, 96, 97, 1975.
46. Courtot, P., Pichon, R., and Le Saint, J., Photochromise par isomerization syn-anti de phenylhydrazone-2 de tricetones-1,2,3 et de dicetones-1,2 substituees, *Tetrahedron Lett.*, 1181, 1976.
47. (a) Suginome, H. and Uchida, T., Photochemical rearrangement of steroidal hydrazone and acylhydrazone, *Tetrahedron Lett.*, 73, 2289, 1973; (b) Suginome, H. and Uchida, T., Photo-induced transformations. 44. Formation of lactams in the photolysis of some steroidal acetylhydrazones in the presence of oxygen, *J. Chem. Soc., Perkin Trans. 1,* 1356, 1980.
48. Suginome, H., Uchida, T., Kizuka, K., and Masamune, T., Synthesis and photoreaction of *D*-nor 5α-androstan-16-one acetylhydrazone in the presence of oxygen, *Bull. Chem. Soc. Jpn.*, 53, 2285, 1980.
49. Suginome, H. and Uchida, T., Monochromatic light-induced reactions of benzophenone hydrazones and the *N*-acetyl derivatives in carbon tetrachloride in the presence of oxygen, *Bull. Chem. Soc. Jpn.*, 53, 3225, 1980.
50. (a) El-Bayoumi, M.A., El-Aasser, M., and Abdel-Halim, F., Electronic spectra and structures of Schiff's bases. I. Benzanils, *J. Am. Chem. Soc.,* 93, 586, 1971; (b) El-Aasser, M., Abdel-Halim, F., and El-Bayoumi, M.A., *J. Am. Chem. Soc.*, 93, 590, 1971.
51. (a) Bürgi, H.B. and Dunitz, J.D., Crystal and molecular structures of benzylideneaniline, benzylideneaniline-*p*-carboxylic acid and *p*-methoxybenzilidene-*p*-nitroaniline, *Helv. Chim. Acta,* 53, 1747, 1970; (b) Bally, T., Haselbach, E., Lanyiova, J., Marschner, E., and Rossi, M., Concerning the conformation of isolated benzilideneaniline, *Helv. Chim. Acta,* 59, 486, 1976; (c) Traetteberg, M., Hilmo, I., Abraham, R.J. and Ljunggren, S., The molecular structure of N-benzylideneaniline, *J. Mol Struct.,* 48, 395, 1978; (d) Akaba, R., Tokumaru, K., and Kobayashi, T., Electronic structures and conformations of *N*-benzylideneanilines. I. Electronic absorption spectral study combined with CNDO/S CI calculations, *Bull, Chem. Soc. Jpn.*, 53, 1993, 1980; (e) Akaba, R., Tokumaru, K.,

Kobayashi, T., and Utsunomiya, C., Electronic structures and conformations of *N*-benzylideneamilines. II. Photoelectron spectral study, *Bull Chem. Soc. Jpn*., 53, 2002, 1980.

52. (a) Anderson, D.G. and Wettermark, G, Photoinduced isomerization of anils, *J. Am. Chem. Soc*., 87, 1433, 1965; (b) Wettermark, G., Weinstein, J., Sousa, J.,and Doglioti, L., Kinetics of *cis-trans* isomerization of *para*-substituted N-benzylidene anilines, *J. Phys. Chem*., 69, 1584, 1965.
53. (a) Kobayashi, M., Yoshida, M., and Minato, H., Configuration of the photoisomers of benzylideneanilines, *J. Org. Chem*., 41, 3322, 1976; (b) Yoshida, M. and Kobayashi, M., Configuration and conformation of the photoisomers of *N*-[*p*-(dimethylamino)benzylidene]anilines, *Bull. Chem. Soc. Jpn*., 54, 2395, 1981; (c) Lewis, J.W., and Sandorfy, C., An infrared study of the photoisomerization of N-benzilideneaniline, *Can. J. Chem*., 60, 1720, 1982; (d) Kanamaru, N. and Kimura, K., Photoinduced isomerization of benzalaniline, *Mol. Photochem*., 5, 427, 1973.
54. (a) Cohen, M.D. and Schmidt, G.M.T., *J. Phys. Chem*., 66, 2442, 1962; (b) Wettermark, G. and Dogliotti, L., Transient species in the photolysis ofanils, *J. Chem. Phys.*, 40, 1486, 1964; (c) Potashnik, R. and Ottolenghi, M, Photoisomerization of photochromic anils, *J. Chem. Phys.*, 51, 3671, 1969; (d) Rossenfeld, T., Ottolenghi, M., and Meyer, A.Y., Photochromic anils. Structure of photoisomers and thermal relaxation processes, *Mol. Photochem*., 5, 39, 1973; (e) Lewis, J.W. and Sandorfy, C., A spectroscopic study of proton transfer and photochromism in *N*-(2-hydroxybenzylidine)aniline, *Can. J. Chem*., 60, 1738, 1982. and papers cited therein.
55. Karatsu, T., Shiga, T., Kitamura, A., Arai, T., Sakuragi, H., and Tokumaru, K., Effect of substitution of a 2-anthryl group at the N=N and N=C unsaturated bonds on their photoisomerization in the triplet state, *Chem. Lett*., 825, 1994.
56. (a) Armesto, D., Martin, J. A.F., Perez-Ossorio, R., and Horspool, W.M., A novel aza-di-π-methane rearrangement. The photoreaction of 4,4-dimethyl-1.6.6-triphenyl-2-aza-hexa-2.5-diene, *Tetrahedron Lett.,* 23, 2149, 1982; (b) Armesto, D., Horspool, W.M., Martin, J.-A.F., and Perez-Ossorio, R., The synthesis and photochemical reactivity of β,γ–unsaturated imines. An aza-di-π-methane rearrangement of 1-azapenta-1,5-dienes, *J. Chem. Res. (S)*, 46, 1986.
57. (a) Armesto, D., Langa, F., Martin, J.-A.F., Perez-Ossorio, R., and Horspool, W.M., Studies on the scope of the aza-di-π-methane rearrangement of β,γ-unsaturated imines, *J Chem. Soc., Perkin Trans. 1,* 743, 1987; (b) Armesto, D., Horspool.W. M., Langa, F., and Perez-Ossorio, R., Substitution effects on the aza-di-π-methane rearrangement of imines, *J. Chem. Soc., Perkin Trans. 2,* 1039, 1987; (c) Armesto, D., Horspool, W.M., and Langa, F., The aza-di-π-methane rearrangement of 1-aryl-4,4-dimethyl-6,6-diphenyl-2-azahexa-2,5-dienes. The influence of substituents on the *N*-benzyl group, *J. Chem. Soc., Perkin Trans. 2*, 903, 1989; (d) Armesto, D., Horspool, W.M., Mancheno, M.J., and Ortiz, M.J., Chemically efficient aza-di-π-methane photoreactivity with novel stable derivatives of β,γ–unsaturated compounds, *J. Chem. Soc., Perkin Trans. 1,* 2325, 1992, and papers cited in Reference 37.
58. (a) Rubin, M.B., Hart, R.R., and Keubler, N.A., Electronic states of the azoalkanes, *J. Am. Chem. Soc*., 89, 1564, 1967; (b) Rau, H., Spectroskopische Eigenshaften Organischer Azoverbindungen, *Angew. Chem*., 85, 248, 1973.
59. Calvert, J.G., Pitts, Jr., J.N., *Photochemistry*, Wiley, New York, 1967, 450.
60. For a review see Ref. 59, p.462.
61. Abram, I.I., Milne, G.S., Solomon, B.S., and Steel, C., The photochemistry of aliphatic azo compounds. The role of triplets and singlets in their photochemistry, *J. Am. Chem. Soc*., 91, 1220,1969.
62. For example, see (a) Back, R. and Sivertz, C., The photolysis of 2,2′-azo-bis-isobutyronitrile, *Can. J. Chem*., 32, 1061, 1954; (b) Roy, J.-C., Nash, J.R., Williams, Jr., R.R., and Hamill, W.H., Diffusion kinetics; The photolysis of azo-bis-isobutyronitrile, *J. Am Chem. Soc.*, 78, 519, 1956; (c) Smith, P. and Rosenberg, A.M., The kinetics of the photolysis of 2,2′-azo-bis-isobutyronitrile, *J. Am. Chem. Soc.*, *81*, 2037, 1957.
63. Arin, M.L. and Steel, C., Photochemistry of azoisopropane in the 2000-Å region, *J. Phys. Chem*., 76, 1685, 1972

64. (a) Mill, T. and Stringham, R.S., Photoisomerization of azoalkanes, *Tetrahedron, Lett*., 1853, 1969; (b) Fogel, L.D., Rennert, A.M., and Steel, C., Thermal decomposition and isomerization of *cis*-azoisopropane, *J. Chem. Soc., Chem. Commun*., 536, 1975; (c) Engel, P.S. and Bishop, D.J., Thermolysis of *cis* and *trans* azoalkanes, *J. Am. Chem. Soc*., 97, 6754, 1975.
65. For example, see Baird, N C. and Swenson, J.R., Quantum organic photochemistry. IV. The photoisomerization of diimide and azoalkanes, *Can. J. Chem.*, 51, 3097, 1973.
66. Engel, P.S. and Bartlett, P.D., The sensitized photolysis of acyclic azo compounds. Singlet energy transfer, *J. Am. Chem. Soc*., 92. 5883, 1970.
67. Porter, N.A., Marnett, L.J., Lochmüller, C.H., Closs, G.L., and Shobataki, M., Application of chemically induced dynamic nuclear polarization to a study of the decomposition of unsymmetric azo compounds, *J. Am. Chem. Soc*., 94, 3664, 1972.
68. (a) Engel, P.S., Melaugh, R.A., Page, M.A., Szilagyi, S., and Timberlake, J.W., Stable *cis* dialkyldiazenes (azoalkanes): *cis*-di-1-adamantyldiazene and *cis*-di-1-norbornyldiazene, *J. Am. Chem. Soc*., 98, 1976; (b) Chae, W.K., Baughman, S.A., Engel, P.S., Bruch, M., Özmeral, C., Szilagyi, S., and Timberlake, J.W., Decomposition and isomerization of bridgehead *cis* 1,2-diazenes (azoalkanes), *J. Am. Chem. Soc*., 103, 4824, 1981.
69. Engel, P.S. and Gerth, D.B., Azocyclopropane, *J. Am. Chem. Soc*., 103, 7689, 1981.
70. Overberger, C.G., Chi, M.-S., Pucci, D.G., and Barry, J.A., *trans*-Azo linkages in eight-, nine- and ten-membered cyclic azo compounds, *Tetrahedron Lett*., 4565, 1972; Overberger, C.G. and Chi, M.-S., Photochemical isomerization of eight-membered azo compounds, *J. Org. Chem*., 46, 303, 1981.
71. (a) Gisin, M. and Wirz, J., Photolysis of the azo-precursors of 2,3- and 1,8-naphthoquinodimethane, *Helv. Chim. Acta,* 59, 2273, 1976; (b) Pagin, R.M., Burnett, M.N. and Dodd, J.R., Photochemistry of 1,4-dihydronaphtho[1,8-de][1,2]diazepine. Preparation and electron spin resonance observation of the unsubstituted 1,8 naphthoquinodimethane, *J. Am. Chem. Soc*., 99, 1972, 1977.
72. Thompson, A.M., Goswami, P.C., and Zimmerman, G.L., Kinetic analysis of the photochemistry of alkyldiazenes in hydrocarbon solution. The quasi-steady state, *J. Phys. Chem*., 83, 314, 1979.
73. Beveridge, D.L. and Jaffe, H.H., The electronic structure and spectra of *cis*- and *trans*-azobenzene, *J. Am. Chem. Soc*., 88, 1948, 1966.
74. (a) Robertson, J.M., Crystal structure and configuration of the isomeric azobenzene, *J. Chem. Soc.,* 232, 1939; (b) Hampton, G.C. and Robertson, J.M., Bond lengths and resonance in the *cis*-azobenzene molecule, *J. Chem. Soc.,* 409, 1941.
75. For example, see Brod, W.R., Gould, J.H., and Wyman, G.M., The relation between the absorption spectra and the chemical constitution of dyes. XXV. Phototropism and *cis-trans* isomerism in aromatic azo compounds, *J. Am. Chem. Soc*., 74, 4641, 1952.
76. (a) Cook, A.H., The preparation of some *cis*-azo-compounds, *J. Chem. Soc*., 876, 1938; (b) Campbell, N., Henderson, A.W., and Taylor, D., Geometrical isomerism of azo-compounds, *J. Chem. Soc*., 1281, 1953; (c) Frankel, M., Wolovsky, R., and Fisher, E., Geometrical isomerism of the azonaphthalenes, *J. Chem. Soc*., 3441, 1955.
77. Fischer, E., Frankel, M., and Wolovsky, R., Wavelength dependence of photoisomerization equilibria in azo compounds, *J. Chem. Phys*., 23, 1367, 1955.
78. Zimmerman, G., Chow, L.-Y., and Paik, U.-J., The photochemical isomerization of azobenzene, *J. Am. Chem. Soc.*, 80, 3528, 1958.
79. For example, see Gegiou, D., Muszkat, K.A., and Fischer, E., Temperature dependence of photoisomerization. V. The effect of substituents on the photoisomerization of stilbenes and azobenzenes, *J. Am. Chem. Soc*., 90, 3907, 1968.
80. (a) Rau, H. and Lüddecke, E., On the rotation-inversion controversy on photoisomerization of azobenzenes. Experimental proof of inversion, *J. Am. Chem. Soc*., 104, 1616, 1982; (b) Rau, H., Further evidence for rotation in the π,π^* and inversion in the n,π^* photoisomerization of azoben-

zenes, *J. Photochem*., 26, 221, 1984; (c) Tanaka, T., Sueishi, Y., Yamamoto, S., and Nishimura, N, Pressure dependence of the photostationary *trans/cis* concentration ratio of 4-dimethylamino-4′-niroazobenzene. A new method of evaluating the reaction volume, *Chem. Lett*., 1203, 1985.

81. Talaty, E.R. and Fargo, J.C., Thermal *cis-trans*-isomerization of substituted azobenzenes : a correction of the literature, *J. Chem. Soc., Chem. Commun., 65*, 1967.
82. (a) Shinkai, S., Kusano, Y., Shigematsu, K., and Manabe, O., On the rotation versus the inversion mechanism in the thermal isomerization of *cis*-azobenzenes, *Chem. Lett.,* 1303, 1980; (b) Asano, T., Okada, T., Shinkai, S., Shigematsu, K., Kusano, Y., and Manabe, O., Temperature and pressure dependences of thermal *cis*-to-*trans* isomerization of azobenzenes which evidence an inversion mechanism., *J. Am. Chem. Soc.,* 103, 5161, 1981.
83. Ronayette, J., Arnaud, R., Lebourgeois, P., and Lemaire, J., Isomérisation photochimique de lázobenzene en solution. I. *Can.J Chem.*, 52, 1848, 1974; Ronayette, J., Arnaud, R., and Lemaire, J., Isomérisation photosensibilisée par des colorants et photoréduction de l´azobenzene en solution. II. *Can. J. Chem*., 52, 1858, 1974.
84. Albini, A., Fasani, E., and Pietra, S., The photochemistry of azo dyes. Photoisomerization versus photoreduction from 4-diethylaminoazobenzene and 4-diethylamino-4′-methoxyazobenzene, *J. Chem. Soc., Perkin Trans. II*, 1021, 1983.
85. Zinin, N., Uber das azobenzid und die nitrobenzinsäure, *J. Prakt. Chem.*, 36, 93, 1841.
86. (a) Busch, M. and Schulz, K., Zur katalytischen reduktion von nitroverbindungen, *Ber.*, 62,1458,1929; (b) Bigelow, H.E. and Palmer, A., Azoxybenzene, *Org. Syn.,* Coll. Vol. II, 57, 1943.
87. For example, see (a) D'Ans, J. and Kneip, A., Über organische persäuren, *Ber*., 48, 1136, 1915; (b) Badger, G.M., Buttery, R.G., and Lewis, G.E., Aromatic azo-compounds. I. Oxidation of *cis*- and *trans*-azobenzene, *J Chem. Soc.,* 2143, 1953 and the subsequent papers.
88. Wacker, L., Über das α-azoxynaphtalin, *Ann. Chem*., 317, 375, 1901.
89. Knipscheer, M.H.M., Transpositions intramoleculaires des azoxybenzenes, *Recl. Trav. Chim. Pays-Bas*, 22, 1,1903.
90. Cumming, W.M. and Ferrier, G.S., The reaction of azoxy-compounds. I. The action of light., *J. Chem. Soc*., 2374, 1925.and the subsequent papers.
91. Bigelow, H.E., Azoxy compounds, *Chem. Rev*., 9, 117,1931.
92. Spence, G.G., Taylor, E.C., and Buchardt, O., The photochemical reactions of azoxy compounds, nitrones and aromatic amine N-oxides, *Chem. Rev*., 70, 231,1970.
93. Badger, G.M. and Buttery, R.G., Aromatic azo-compounds. VI. The action of light on azoxy compounds., *J. Chem. Soc.,* 2243, 1954.
94. Shemyakin, M.M., Maimind, V.J., and Vaichunite, B.K., A study of the Wallach rearrangement and related reaction, *Chem. Ind., (London).,* 755, 1958.
95. (a) Oae, S., Fukumoto, T., and Yamaguchi, T., *Bull. Chem. Soc. Jpn*., 34, 1873, 1961; (b) Oae, S., Fukumoto, T., and Yamagami, M., Mechanism of Wallach rearrangement, *Bull. Chem. Soc. Jpn.,* 36, 601, 1963.
96. Lewis, G.E. and Reiss, J.A., Photochemical reactions of azo compounds. VIII. Photochemical rearrangement of 2,2′-dimethylazoxybenzene, *Aust. J. Chem.,* 19, 1887, 1966.
97. Müller, E., Hory, E., Krüger, W., and Kreutzmann, E., Stereomerie von azoxybenzolen, *Ann. Chem.,* 493, 166, 1932.
98. (a) Tanikaga, R., Photoreduction of azoxybenzene to azobenzene, *Bull. Chem. Soc. Jpn.,* 41, 1664, 1968; (b) Tanikaga, R., Photochemical rearrangement of azoxybenzene to 2-hydroxyazobenzene and *cis-trans* isomerization, *Bull. Chem. Soc. Jpn.,* 41, 2151, 1968.
99. Monroe, B.M. and Wamser, C.C., Photoreduction of azoxybenzene by chemical sensitization, *Mol. Photochem*., 2, 213, 1970.
100. Mauser, H., Gauglitz, G., and Stier F., Zur Photochemie des azoxybenzols, *Liebigs Ann. Chem* 739, 84, 1970.
101. Webb.D.L. and Jaffe, H.H., *cis*-Azoxybenzenes. II. Photoequilibrium studies of azoxybenzenes, *Tetrahedron Lett.,* 1875,1964.

102. Rhee, S.-B. and Jaffe, H.H., Photochemical and thermal *cis-trans* isomerization of azoxybenzene, *J. Am. Chem. Soc.*, 95, 5518, 1973.
103. Neiman, L.A., Smolyakov, V.S., and Saluvere, T., Mechanism of the photoisomerization of aromatic azoxy compounds, *Zh. Org. Khim.,* 9,. 2382, 1973 (Russian).
104. Goon, D.J.W., Murray, N.G., Schoch, J.P., and Bunce, N.J., Evidence against a hydrogen abstraction mechanism in the photorearrangement of azoxybenzene to 2-hydroxyazobenzene, *Can. J. Chem.* 51, 3827, 1973.
105. Squire, R.H. and Jaffe, H.H., Photochemical reaction with a preequilibrium step. Acid-catalyzed photochemical Wallach rearrangement, *J. Am. Chem. Soc.*, 95, 8188, 1973.
106. Bunce N.J., Schoch, J.P., and Zerner, M.C., Photorearrangement of azoxybenzene to 2-hydroxyazobenzene. Evidence for electrophilic substitution by oxygen, *J. Am. Chem. Soc.*, 99, 7986, 1977.
107. Gegiou, D., Tsoka, A., and Hadjoudis, E., Photorearrangement of azoxybenzene to 2-hydroxyazobenzene. A flash photolysis study, *J. Photochem.,* 9, 216, 1978.
108. Albini, A., Fasani, E., Moroni, M., and Pietra, S., The photochemistry of some methoxy and dimethylamino derivatives of azoxybenzene, *J. Org. Chem.,* 51, 88, 1986.
109. Langley, B.W., Lythgoe, B., and Rayner, L.S., Macrozamin. III. Azoxymethane and some simple analogues, *J. Chem. Soc.,* 4191, 1952.
110. Gowenlock, B.G., Azoxycompounds. 1. The photolysis of azoxymethane, *Can. J. Chem.,* 42, 1936, 1964.
111. Hecht, S.S. and Greene, F.D., Di-*t*-butyloxadiaziridine, the cyclic form of an azoxy group. Ring-chain isomerism in three-membered ring, *J. Am. Chem. Soc.*, 89, 6761, 1967.
112. Gowenlock, B.G. and Trotman, J., Geometrical isomerism of dimeric nitrosomethane, *J. Chem. Soc.*, 4190, 1955.
113. Freeman, J.P., The nuclear magnetic resonance spectra and structure of aliphatic azoxy compounds, *J. Org. Chem.,* 28, 2508, 1963.
114. Mackor, A., Wajer, T.A. J.W., de Boer, T.J., and van Voorst, J.D.W., C-nitroso compounds. I. The formation of nitroxides by photolysis of nitroso compounds as studied by electron spin resonance, *Tetrahedron Lett.,* 2115, 1966.
115. Posiomek, E.J., Photochemical isomerization. Synthesis of *anti*-isonicotinaldehyde oxime derivatives, *J. Pharm. Sci.*, 54, 333, 1965.
116. Ogino, K., Matsumoto, T., and Kozuka, S., Photoisomerization of substituted O-methyl-*p*-nitrobenzohydroxymates, *Me. Fac. Eng., Osaka Univ.*, 16, 1545, 1979. (*Chem. Abstr.*, 92, 58910, 1980)
117. Tung, C.-H. and Guan, J.-Q., Modification of photochemical reactivity by Nafion. Photocyclization and photochemical *cis-trans* isomerization of azobenzene, *J. Org. Chem*. 61, 9417, 1996.
118. Ogawa, M., Kuroda, K. and Mori, J., Aluminium-containing mesoporous silica films as nano-vessels for organic photochemical reactions*, J. Chem. Soc., Chem. Commun.,* 2441, 2000.
119. Concerning a general introduction and the definition of the term, see Bouas-Laurent, H. and Dürr, H., Organic photochromism, (IUPAC Technical report), *Pure Appl. Chem.*, 73, 639, 2001.
120. Balasubramanian, D., Subramani, S., and Kumar, C., Modification of a model membrane structure by embedded photochrome, *Nature (London),* 254, 252, 1975.
121. (a) Kano, K., Tanaka, Y., Ogawa, T., Shimomura, M., Okahata, Y., and Kunitake, T., Photoresponsive membranes. Regulation of membrane properties by photoreversible *cis-trans* isomerization of azobenzenes, *Chem. Lett.*, 421, 1980; (b) Kunitake, T., Nakashima, N., Shimomura, M., Okahata, Y., Kano, Y., and Ogawa, T., Unique properties of chromophore-containing bilayer aggregates: enhanced chirality and photochemically induced morphological change, *J. Am. Chem. Soc.*, 102, 6642, 1980.
122. (a) Pieroni, O., Houben, J.L., Fissi, A., Costantino, P., and Ciardelli, F., Reversible conformational changes induced by light in poly (L-glutamic acid) with photochromic side chains, *J. Am. Chem. Soc.*, 102, 5913, 1980; (b) Ueno, A., Takahashi, K., Anzai, J., and Osa, T., Photocontrol of polypeptide helix sense by *cis-trans* isomerism of side-chain azobenzene moieties, *J. Am. Chem. Soc.*, 103, 6410, 1981.

123. Ueno, A., Tomita, Y., and Osa, T., Photoresponsive binding ability of azobenzene-appended γ-cyclodextrin, *Tetrahedron Lett.*, 24, 5245, 1983, and references cited therein.
124. (a) Shinkai, S., Nakaji, T., Nishida, Y., Ogawa, T., and Manabe, O., Photoresponsive crown ethers. 1. *Cis-trans* isomerism of azobenzene as a tool to enforce conformational changes of crown ethers and polymers, *J. Am. Chem. Soc.,* 102, 5860, 1980; (b) Shiga, M., Takagi, M., and Ueno, K., Azo-crown ethers. The dyes with azo group directly involved in the crown ether skeleton, *Chem. Lett.*, 1021, 1980.
125. Shinkai, S., Kouno, T., Kusano, Y., and Manabe, O., Photoresponsive crown ethers. 7. Proton and metal ion catalyses in the *cis-trans* isomerization of azopyridines and an azopyridine-bridged cryptand.*J. Chem. Soc., Perkin Trans. I*, 2741, 1982.
126. Shinkai, S., Minami, T., Kusano, Y., and Manabe, O., Photoresponsive crown ethers. 8. Azobenzenophane-type "switched-on" crown ethers which exhibit an all-or-nothing change in ion-binding ability, *J. Am. Chem. Soc.*, 105, 1851, 1983.
127. Shinkai, S., Nakaji, T., Ogawa, T., Shigematsu, K., and Manabe, O., Photoresponsive crown ethers. 2. Photocontrol of ion extraction and ion transport by a bis (crown ether) with a butterfly-like motion, *J. Am. Chem. Soc.*, 103, 111, 1981.
128. Shinkai, S., Ishihara, M., Ueda, K., and Manabe, O., On-off-switched crown ether-metal ion complexation by photoinduced intramolecular ammonium group 'tail-biting', *J. Chem. Soc., Chem. Commun.*, 727, 1984.
129. Shinkai, S., Miyazaki, K., and Manabe, O., A photochemically "switched-on" crown ether containing an intramolecular 4-methoxyphenylazo substituent, *Angew. Chem. Int. Ed. Engl.*, 24, 866, 1985.
130. Ueno, A., Tomita, Y., and Osa, T., Photoresponsive binding ability of azobenzene-appended γ-cyclodextrin, *Tetrahedron Lett.*, 24, 5245, 1983.
131. Shinkai, S., Minami, T., Kusano, Y., and Manabe, O., Photoresponsive crown ethers. 5. Light-driven ion transport by crown ethers with a photoresponsive anion cap, *J. Am. Chem. Soc.*, 104, 1967, 1982.
132. Shinkai, S., Ishihara, M., and Manabe, O., Photoresponsive crown ethers. XVII. Metal extraction with a polymer bearing pendent photoresponsive crown ethers., *Polym.J. (Tokyo).*, 17, 1141, 1985.
133. (a) Shinkai, S. and Manabe, O., Photoresponsive crown ethers, *Yukigoseikagaku* (in Japanese), 40, 92, 1982; (b) Shinkai, S. and Manabe, O., Host guest complex chem. 3. Photocontrol of ion extraction and ion transport by photofunctional crown ethers, *Top. Curr. Chem.*, 121, 67, 1984; (c) Ueno, A. and Osa, T., Photocontrol of molecular functions, *Yukigoseikagaku* (in Japanese), 38, 207, 1980.
134. Shinkai, S., Yoshida, T., Manabe, O., and Fuchita, Y., Photoresponsive crown ethers. 20. Reversible photocontrol of association-dissociation equilibria between azobis (benzo-18-crown-6) and diammonium cation, *J. Chem. Soc., Perkin Trans. 1*, 1431, 1988, their earlier papers and the references cited therein.
135. For recent reviews, see (a) Terech, P. and Weiss, R.G., Low molecular mass gelators of organic liquids and the properties of their gels, *Chem. Rev.*, 97, 3133, 1997; (b) van Esch, J.H. and Feringa, B.L., New functional materials based on self-assembling organogels: from serendipity towards design, *Angew. Chem. Int. Ed. Engl.,* 39, 2263, 2000.
136. (a) Murata, M., Aoki, M., Nishi, T., Ikeda, A., and Shinkai, S., New cholesterol-based gelators with light- and metal-responsive functions, *J. Chem. Soc., Chem. Commun.,* 1715, 1991; (b) Murata, K., Aoki, M., Suzuki, T., Harada, T., Kawabata, H., Komori, T., Ohseketo, F., Ueda, K., and Shinkai, S., Thermal and light control of the sol-gel phase transition in cholesterol-based organic gels. Novel herical aggregation modes as detected by circular dichroism and electron microscopic observation, *J. Am. Chem. Soc.,* 116, 6664, 1994.
137. (a) Shinkai, S., Yoshioka, A., Nakayama, H., and Manabe, A., Photochemically activated cyclophane, *J. Chem. Soc., Perkin Trans. 2,* 1905, 1990.
138. Norikane, Y., Kitamoto, K., and Tamaoki, N., [1,1](3,3′)-Azobenzenophane: novel crystal structure and *cis-trans* isomerization of distorted azobenzene, *Org. Lett.*, 4. 3907, 2002, and theearly papers cited therein.

139. Westmark, P.R., Kelly, J. P., and Smith, B.D., Photoregulation of enzyme activity. Photochromic, transition-state-analogue inhibitors of cysteine and serine proteases, *J. Am. Chem. Soc.*,115, 3416, 1993.
140. Shinmori, H., Takeuchi, M., and Shinkai, S., A novel light-gated sugar receptor, which shows high glucose selectivity, *J. Chem. Soc., Perkin Trans. 2,* 847, 1998.
141. Zeng, F. and Zimmerman, S.C., Dendrimers in supramolecular chemistry: from molecular recognition to self-assembly, *Chem. Rev.*, 97, 1681, 1997; (b) Archut, A. and Vögtle, F., Functional cascade molecules, *Chem. Soc. Rev.*, 27, 233, 1998.
142. (a) Mekelburger, H.-B., Rissanen, K., and Vögtle, F., Repetitive synthesis of bulky dendrimers — A reversibly photoactive dendrimer with six azobenzene side chains, *Chem. Ber.*,126, 1161, 1993, and papers cited therein; (b) Nagasaki, T., Tamagaki, S., and Ogino, K., Syntheses and characterization of photochromic dendrimers including a 1,3-alternate carix[4]arene as a core and azobenzene moieties as branches, *Chem. Lett.*, 717, 1997.
143. (a) Junge, D.M. and McGrath, D.V., Photoresponsive dendrimers, *J. Chem. Soc., Chem. Commun.*, 857, 1997; (b) Jiang, D.-L. and Aida, T., Photoisomerization in dendrimers by harvesting of low-energy photons, *Nature*, 388,454, 1997; (c) Junge, D.M. and McGrath, D.V., Photoresponsive azobenzene-containing dendrimers with multiple discrete state, *J. Am. Chem. Soc.*, 121, 4912, 1999.
144. Archut, A., Azzellini, G.C., Balzani, V., Cola.L. D., and Vögtle, F., Toward photoswitchable dendritic hosts. Interaction between azobenzene-functionalized dendrimers and eosin, *J. Am. Chem. Soc.*, 120, 12187, 1998.
145. Yokoyama, S., Nakahama, T., Otomo, A., and Mashiko, S., Preparation and assembled structure of dipolar dendrons based electron donor/acceptor azobenzene branching, *Chem. Lett.*, 1137, 1997.
146. Goodman, M. and Falxa, M.L., Conformational aspects of polypeptide structure. XXIII. Photoisomerization of azoaromatic polypeptides, *J. Am. Chem. Soc.,* 89, 3863, 1967.
147. For example, see Ueno, A., Anzai, J., Osa, T., and Kodama, Y., Light-induced conformational changes of polypeptides. Photoisomerization of azoaromatic polypeptides, *Bull. Chem. Soc. Jpn.*, 52, 549, 1979, and the subsequent papers.
148. Ciardelli, F., Carlini, C., Sorano, R., Altomare, A., Pieroni, O., Houben, J.L., and Fissi, A., Light-induced conformational changes in chiral polymers with photochromic side chains, *Pure Appl. Chem.*, 56, 329, 1984.
149. Pieroni, O., Fissi.A., Houben, J.L., and Ciardelli, F., Photoinduced aggregation changes in photochromic polypeptides, *J. Am. Chem. Soc.*, 107, 2990, 1985.
150. Ciardelli, F., Pieroni.O., Fissi.A., Carlini, C., and Altomare, A., Photoresponsive optically active polymers — A review, *Br. Polymer J.*, 21, 97, 1989.
151. Ueda, T., Murayama, K., Yamamoto, T., Kimura, S., and Imanishi, Y., Photo-regulation of hydrolysis activity of semisynthetic mutant phospholipases A_2 replaced by non-natural aromatic amino acids, *J. Chem. Soc., Perkin Trans. 1,* 225, 1994.
152. Fissi, A., Pieroni, O., Balestreri, E., and Amato, C., Photoresponsive polypeptides. Photomodulation of the macromolecular structure in poly(N^{ε} ((phenylazophenyl)sulfonyl)-L-lysine)., *Macromolecules*, 29, 4680, 1996.
153. (a) Pieroni, O., Fissi, A., and Popova, G., Photochromic polypeptides, *Prog. Polym. Sci.,* 23, 81, 1998; (b) Pieroni, O., Fissi, A., Angelini, N., and Lenci, F., Photoresponsive polypeptides, *Acc. Chem. Res.,* 34, 9, 2001.
154. Lovrien, R., The photoviscosity effect, *Proc. Nat. Acad. Sci.*, 57, 236, 1967.
155. For example, see Irie, M., Hirano, K., Hashimoto, S., and Hayashi, K., Photoresponsive polymers. 2. Reversible solution viscosity change of polyamides having azobenzene residues in the main chain, *Macromolecules,* 14, 262, 1981, and the subsequent papers.
156. (a) Irie, M., Photoresponsive polymers, *Adv. Polym Sci.*, Fujita, H., Ed., Springer Verlag, Berlin, 1990, 27–67; (b) Irie, M., Properties and applications of photoresponsive polymers, *Pure Appl. Chem.*, 62, 1495, 1990.
157. Kumar, G.S. and Neckers, D.C., Photochemistry of azobenzene-containing polymers, *Chem. Rev.*, 89, 1915, 1989.

158. Müller, M. and Zentel, R., Interplay of chiral side chains and herical main chains in polyisocyanates, *Macromolecules*, 29, 1609, 1996.
159. Yamaguchi, I., Osakada, K., and Yamamoto, T., Pseudopolyrotaxane composed of an azobenzene polymer and γ-cyclodextrin. Reversible and irreversible photoisomerization of the azobenzene groups in the polymer chain, *J. Chem. Soc., Chem. Commun.,* 1335, 2000.
160. Kato, T., Hirota, N., Fujishima, A., and Frecht, J.M.J., Supramolecular hydrogen-bonded liquid-crystalline polymer complexes. Design of side-chain polymers and a host-guest system by noncovalent interaction, *J. Polymer Sci.: Part A: Polymer Chem.,* 34, 57, 1996.
161. (a) Seki, T., Tamaki, T., Suzuki, Y., Kawanishi, Y., and Ichimura, K., Photochemical alignment regulation of nematic liquid crystal by Langmuir-Blodgett layers of azobenzene polymers as "command surfaces," *Macromolecules*, 22, 3505, 1989; (b) Ichimura, K. Photoalignment of liquid-crystal systems, *Chem. Rev.,* 100, 1847, 2000; (c) Tamaoki, N., Cholesteric liquid crystals for color information technology, *Adv. Mater.*, 13, 1135, 2001.
162. (a) Lin, W., Lin, W., Wong, G.K., and Marks, T.J., Supramolecular approaches to second-order nonlinear optical materials. Self-assembly and microstructural characterization of intrinsically acentric [(aminophenyl) azo] pyridinium superlattices, *J. Am. Chem. Soc.,* 118, 8034, 1996; (b) Delaire, J. A., and Nakatani, K., Linear and nonlinear optical properties of photochromic molecules and materials, *Chem. Rev.*, 100, 1817, 2000.
163. Feringa, B.L., Jager, W.F., and de Lange, B., Organic materials for reversible optical data storage, *Tetrahedron,* 49, 8267, 1993.
164. (a) Tachibana, H., Nakamura, T., Matsumoto, M., Komizu, H., Manda, E., Niino, H., and Yabe, A. Kawabata, Y., Photochemical switching in conductive Langmuir-Blodgett films, *J. Am. Chem. Soc.,* 111, 3080, 1989; (b) Tachibana, H., Azumi, R., Nakamura, T., Matsumoto, M., and Kawabata, Y., New types of photochemical switching phenomena in Langmuir-Blodgett films, *Chem. Lett.,* 173, 1992.
165. Ikeda, T. and Tsutsumi, O., Optical switching and image storage by means of azobenzene liquid-crystal films, *Science*, 268, 1873, 1995.
166. Öge, T. and Zentel, R., Manipulation of the ferroelectricity in LC polymers via photomechanical isomerization of azobenzene moieties, *Macromol. Chem. Phys.,* 197, 1805, 1996.
167. (a) Liu, Z.F., Hashimoto, K., and Fujishima, A., Photoelectrochemical information storage using an azobenzene derivative, *Nature*, 347, 658, 1990; (b) Wang, R., Iyoda, T., Jiang, L., Hashimoto, K., and Fujishima, A., Molecular arrangement in an azobenzene-terminated self-assembled monolayer film, *Chem. Lett.,* 1005,1996; (c) Wang, R., Jiang, L., Iyoda, T., Tryk, D.A., Hashimoto, K., and Fujishima, A., Investigation of the surface morphology and photoisomerization of an azobenzene-containing ultrathin film, *Langmuir*, 12, 2052, 1996; (d) Enomoto, T., Hagiwara, H., Tryk, D.A., Liu, Z.-F., Hashimoto, K., and Fujishima, A., Electrostatically induced isomerization of azobenzene derivatives in Langmuir-Blodgett films, *J. Phys. Chem.B.*,101, 7422, 1997; (e) Wang, R., Iyoda, T., Tryk, D.A., Hashimoto, K., and Fujishima, A., Electrochemical modulation of molecular conversion in an azobenzene-terminated self-assembled monolayer film: an *in situ* UV-visible and infrared study, *Langmuir*, 13, 4644, 1997.
168. Cook, M.J., Nygard, A.-M., Wang, Z., and Russell, D.A., An evanescent field driven monomolecular layer photoswitch: coordination and release of metallated macrocycles, *J. Chem. Soc., Chem. Commun.*,1056, 2002, and papers cited therein.
169. Kondo, T., Kanai, T., and Uosaki, K., Control of the charge-transfer rate at a gold electrode modified with a self-assembled monolayer containing ferrocene and azobenzene by electro- and photochemical structural conversion of *cis* and *trans* forms of the azobenzene moiety, *Langmuir,* 17, 6317, 2001, and papers cited therein.
170. (a) Wang, R., Iyoda, T., Jiang, L., Tryk, D.A., Hashimoto, K., and Fujishima, A., Structural investigation of azobenzene-containing self-assembled monolayer films, *J. Electroanal. Chem.*, 438, 213, 1997; (b) Einaga, Y., Sato, O., Iyoda, T., Fujishima, A., and Hashimoto, K., Photofunctional vesicles containing Prussian Blue and azobenzene, *J. Am. Chem. Soc.,* 121, 3745, 1999; (c) Einaga, Y., Gu,

Z.-Z., Hayami, S., Fujishima, A., and Sato, O., Reversible photoinduced switching of magnetic properties at room temperature of iron oxide particles in self-assembled films containing azobenzene, *Thin Solid Films*, 374, 109, 2000.

171. Hong, J.–D, Park, E.-S., and Park, A.-L., Effects of added salt on photochemical isomerization of azobenzene in alternate multilayer assemblies: bipolar amphiphile-polyelectrolyte, *Langmuir*, 15, 6515, 1999, and papers cited therein.

95

Novel Di-π-methane Rearrangements Promoted by Photoelectron Transfer and Triplet Sensitization

Diego Armesto
Universidad Complutense of Madrid

Maria J. Ortiz
Universidad Complutense of Madrid

Antonia R. Agarrabeitia
Universidad Complutense of Madrid

95.1 Introduction

The di-π-methane (DPM) reaction of 1,4-alkenes and its counterpart (the oxa-di-π-methane [ODPM] rearrangement of β,γ-unsaturated ketones) have been known for more than 30 years.[1a–i,1l] The large number of studies devoted to these two reactions by different research groups during three decades show that these reactions are very general and usually take place with high chemical and quantum yields, affording cyclopropane derivatives that, in many instances, are difficult to obtain, or not available, by alternative routes. Both reactions show a high degree of diastereoselectivity, or even enantioselectivity in some instances. Therefore, it is not surprising that these rearrangements have been applied in the synthesis of complicated molecules that are difficult to prepare by alternative reaction paths. In particular, the ODPM reaction has been applied as the key step in the synthesis of some natural products by routes that compete with conventional alternatives.[1g,1i,1l,2] Some comprehensive reviews of this subject have been published in the past 25 years or so, summarizing the mechanistic aspects, scope, and synthetic applications of these rearrangements.[1a–i,1l]

Despite the large number of studies carried out on the DPM and ODPM rearrangements since the discovery of the DPM reaction in 1967 by Zimmerman et al.,[5] it was necessary to wait 10 years before the reaction was extended to other 1,4-unsaturated systems, particularly to CN double bond derivatives. The first example of a 1-aza-di-π-methane rearrangement (1-ADPM) was reported by Nitta et al.[6] in a study of the photoreactivity of highly constrained tricyclic oximes. However, the reaction was limited to

0-8493-1348-1/04/$0.00+$1.50

a few compounds, and attempts to extend the rearrangement to other related systems were unsuccessful. The first examples of 1-ADPM reactions in acyclic CN double bond derivatives were reported by Armesto et al.[7] in 1982 in the triplet-sensitized irradiation of a series of β,γ-unsaturated imines that yielded the corresponding cyclopropyl imines regioselectively. The studies in this area have demonstrated that the 1-ADPM rearrangement is as general as the DPM and ODPM counterparts.[1j-n] The reaction has been extended to different CN double bond derivatives, such as oxime esters, semicarbazones, and hydrazones.[1j-m]

As a result of the studies carried out by different research groups worldwide on these three types of di-π-methane reactions, the majority of organic photochemists considered that the photoreactivity of 1,4-unsaturated systems was well established and totally predictable in most cases and, therefore, there was very little to uncover in this area of research.

However, studies recently carried out in our laboratory have demonstrated that some of the ideas firmly established about the photoreactivity of these compounds are incorrect. Thus, the normal photochemical reactivity of β,γ-unsaturated aldehydes reported in books and monographs is decarbonylation.[1c,1i,8] However, our results demonstrate that many β,γ-unsaturated aldehydes undergo the oxa-di-π-methane rearrangement even more efficiently than the corresponding methyl ketones, which is contrary to popular belief.[9] Alternative reaction modes, such as 1,3-formyl migration and decarbonylation, that take place via the T_1 excited state and, therefore, are not Norrish Type I processes, have also been uncovered.[9c] These novel photoreactions of aldehydes are discussed in a separate chapter.

On the other hand, di-π-methane rearrangements have been considered the paradigm of reactions that take place exclusively in the excited state.[1a-l] Concerted or biradical mechanisms were postulated to justify these rearrangements in all the cases studied.[1a-l] There were no data that suggested the involvement of other intermediates in these processes. However, our results on the photoreactivity of 1-aza- and 2-aza-1,4-dienes, using electron-acceptor sensitizers, demonstrate that the 1-ADPM and 2-aza-di-π-methane (2-ADPM) rearrangements can occur via radical-cation intermediates in the ground state. Under these conditions, 2-aza-1,4-dienes rearrange to *N*-vinylaziridines in the first example of a reaction of the di-π-methane type that yields heterocyclic products. Finally, recent studies demonstrate that DPM and 1-ADPM rearrangements also occur in the ground state of radical-anion intermediates.

In our opinion, these results have modified some of the ideas firmly established for many years on the photoreactivity of β,γ-unsaturated systems and demonstrate that a considerable research effort remains necessary in order to rationalize the photo-behavior of these compounds. The following sections summarize our findings in the area of SET-sensitized di-π-methane reactions.

95.2 The 2-Aza-di-π-methane Rearrangement

As mentioned, the large number of studies on the photochemical reactivity of β,γ-unsaturated compounds, carried out by many different research groups worldwide, demonstrated that DPM rearrangements are very general for a variety of 1,4-unsaturated systems, such as, 1,4-dienes, β,γ-unsaturated aldehydes and ketones, and different 1-aza-1,4-diene derivatives.[1] However, up to 1997, the literature was devoid of studies describing the photoreactivity of the closely related 2-aza-1,4-diene derivatives. This was somewhat surprising considering that Mariano and co-workers had previously documented the interesting SET-promoted photocyclization reactions of iminium salts derived from 2-aza-1,4-dienes.[10] The interesting results obtained in our studies on the 1-ADPM rearrangement and also Mariano's precedents prompted us to explore the photoreactivity of 2-aza-1,4-dienes.

The first compound selected for this study was the azadiene **1**. Previous studies demonstrated that tetraphenyl-substitution in positions 3 and 5 of the β,γ-unsaturated system promotes efficient DPM, ODPM, and 1-ADPM reactions in acyclic 1,4-dienes,[11] β,γ-unsaturated aldehydes,[9b] and 1-aza-1,4-dienes,[12] respectively. Based on these precedents, the 2-azadiene **1** was considered to be a suitable candidate to undergo rearrangement of the di-π-methane type. Triplet-sensitized irradiation of azadiene **1**, using acetophenone, for 25 min, afforded two new products that were identified as the cyclopropyl imine **2** (11%) and the vinylaziridine **3** (3%) (Scheme 1). Compound **2** hydrolyzes to the corresponding cyclopropyl amine during isolation.[13]

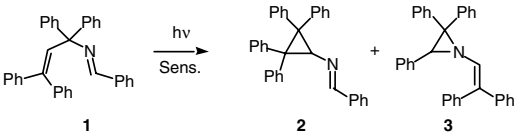

SCHEME 1

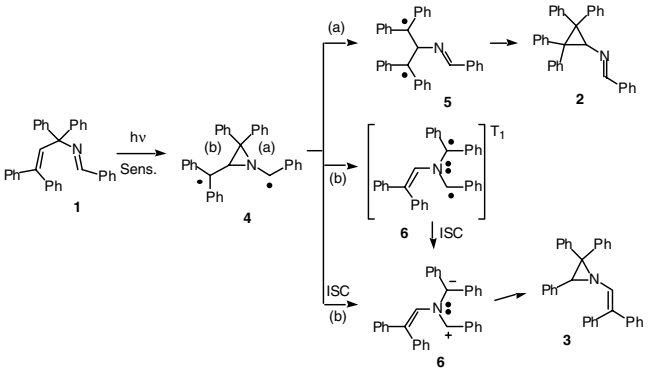

SCHEME 2

Direct irradiation of **1**, for 10 h, also afforded the cyclopropyl imine **2** (4%). Qualitatively, the direct irradiation reaction is less efficient than the triplet-sensitized process. In addition, the direct irradiation photoreaction of **1** is quenched by 1,3-cyclooctadiene, suggesting that the rearrangement occurs via the triplet excited state.

The formation of **2** and **3** can be justified by a conventional biradical mechanism similar to those normally used to rationalize the previously reported di-π-methane processes, as shown in Scheme 2. This involves generation of the aziridinyl-dicarbinyl biradical **4**. Cleavage of the CN bond labeled (a) in **4** affords the highly stabilized 1,3-biradical **5**, which yields the major product **2** (path a). The alternative fragmentation of the C–C bond in **4** generates the intermediate **6**, the precursor of the *N*-vinylaziridine **3** (path b). It is interesting to note at this point that intermediate **6** could be either a triplet 1,3-biradical or a singlet azomethine ylide, depending on whether or not ISC (intersytem crossing) occurs prior to bond cleavage in **4**. Only the singlet azomethine ylide is capable of undergoing cyclization to form **3**. As far as we are aware, this is the case in a di-π-methane reaction where a zwitterion can be postulated as a possible intermediate.[13b-c] The photoreaction of **1** represents the first example of a 2-aza-di-π-methane rearrangement (2-ADPM) that takes place via a three-membered ring heterocyclic biradical and brings about the formation of a heterocyclic product. This result is of importance because previous attempts to observe the formation of oxiranes by the ODPM rearrangement were unsuccessful.[14]

The study was extended to azadienes **7a,7b**, **8**, **9**, and **10a,10b**. Triplet-sensitized irradiation of compounds **7a**, **7b**, and **8** afforded the corresponding cyclopropyl imines **11a**, **11b**, and **12**, respectively, in low yield. In these instances, the corresponding *N*-vinylaziridines were not formed.[13b]

The results obtained in the triplet-sensitized irradiation of compounds **1**, **7a**, **7b**, and **8** indicate that the 2-ADPM rearrangement takes place in 2-aza-1,4-dienes with different substitution patterns, affording cyclopropyl imines in low isolated yields. Attempts to increase product yields resulted in destruction of the starting material. In one case only (compound **1**), the corresponding regioisomer, the *N*-vinylaziridine **3**, has been obtained. The reasons for this regioselectivity remain unclear but it is obvious that methyl substitution at the methane carbon in the 2-aza-1,4-diene system suppresses the formation of the corresponding *N*-vinylaziridines.

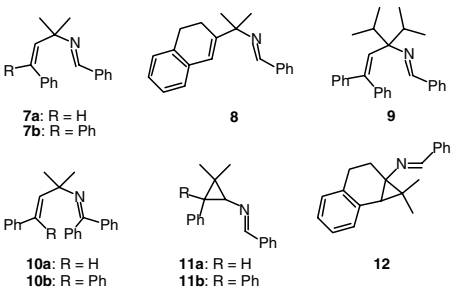

The absence of the heterocyclic regioisomer in these reactions is particularly surprising in the case of azadiene **7a**. According to the mechanism postulated for the 2-ADPM rearrangement (Scheme 2), the ring opening of the aziridinyl-dicarbinyl biradical intermediate **13** should afford the 1,3-biradicals **14** and **15** of comparable stability, the precursors of **11a** and the aziridine **16**, respectively (Scheme 3).[13b]

A possible explanation for the absence of **16** could be found by considering that intermediates **14** and **15** should be triplet biradicals. Intersystem crossing in **14** would afford a singlet biradical that cyclizes to the cyclopropyl imine **11a**. However, intersystem crossing within biradical **15** would yield the zwitterionic intermediate **17**, which is not stabilized by phenyl substitution, as in the case of **6** (Scheme 2). Literature precedents[15] show that nonstabilized 1,3-dipolar intermediates similar to **17** do not cyclize to three-membered heterocycles but undergo different reactions yielding a complex mixture of products. This interpretation is speculative at this point and it will be necessary to carry out additional studies to establish the accuracy of this proposal.

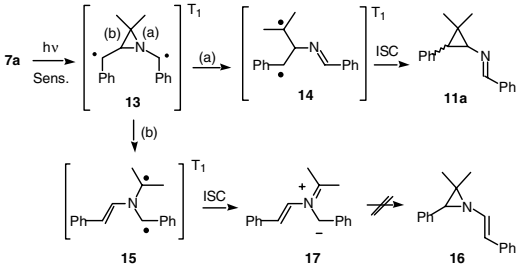

SCHEME 3

Azadienes **9**, **10a**, and **10b** have substitution patterns that promote DPM rearrangements efficiently.[11] However, triplet-sensitized irradiation of these compounds afforded recovered starting material and a complex mixture of products in which the corresponding cyclopropyl imines or *N*-vinylaziridines were not present. These results demonstrate that the 2-ADPM reaction has features that make it different from other versions of the rearrangement studied previously. In particular, the lack of reactivity of ketoimines **10** is surprising because the stability of biradical intermediates **18** should be comparable to, or even greater than, the corresponding intermediates derived from aldimines **7**. The absence of 2-ADPM products in the irradiation of azadienes **10** could be due to the presence of two phenyl rings at C1 of the azadiene system that would favor the preferential ring opening of the aziridinyl intermediates **18** by breaking bond (b) to afford the 1,3-biradicals **19** (Scheme 4). Intersystem crossing in **19** would give the zwitterionic intermediates **20**, which could decompose to a mixture of products instead of undergoing cyclization to the corresponding vinylaziridines (Scheme 4).

In summary, our results on the triplet-sensitized photochemistry of a series of 2-aza-1,4-dienes have uncovered the first examples of 2-ADPM rearrangements yielding cyclopropyl imines. In the case of azadiene **1**, the *N*-vinylaziridine **3** was also obtained in the first example of a di-π-methane rearrangement

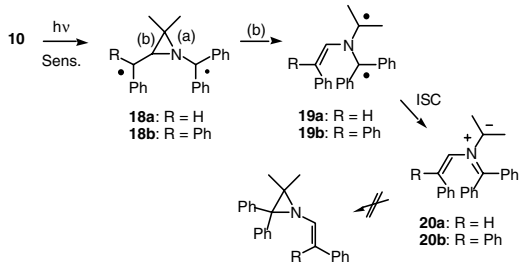

SCHEME 4

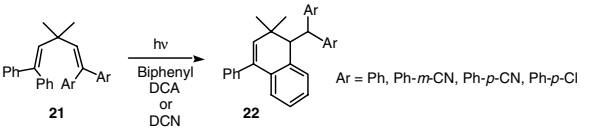

SCHEME 5

that yields a heterocyclic product. However, the 2-ADPM reaction presents special features that make it different from other versions of the rearrangement previously described. Further studies will be necessary to understand the mechanistic aspects of the 2-ADPM rearrangement and the factors that control the influence of substitution on the outcome of the reaction.

95.3 Di-π-methane Rearrangements *via* Radical-cation Intermediates

The studies carried out on di-π-methane for many years involved the direct or triplet-sensitized irradiation of 1,4-unsaturated systems. The results obtained show that, in general terms, acyclic 1,4-dienes undergo the DPM reaction in the singlet excited state while cyclic and polycyclic dienes are reactive as triplets.[1a,1d,1f,1h,1l] The ODPM, 1-ADPM, and 2-ADPM counterparts only occur in the triplet excited state of β,γ-unsaturated carbonyl compounds,[1a-c,1e,1g,1i,1l] 1-aza-1,4-dienes,[1j-n] and 2-aza-1,4-dienes,[1m,1n,13] respectively. An attempt to observe di-π-methane reactions promoted by SET sensitization was unsuccessful. Thus, Zimmerman and Hoffacker[16] carried out a study on the photoreactivity of 1,4-dienes **21** using 9,10-dicyanoanthrathene (DCA) or 1,4-dicyanonaphthalene (DCN) as electron-acceptor sensitizers. The results obtained show that these compounds undergo intramolecular cyclization to yield dihydronaphthalenes **22** (Scheme 5). The corresponding DPM products are not produced in these photoreactions.

2-ADPM Rearrangements via Radical-cation Intermediates

Based on the above precedent, we were interested in carrying out a study on the DCA-sensitized reactivity of 2-aza-1,4-dienes **1**, **7a,7b**, **8**, **9**, and **10a,10b** to determine whether these compounds would behave similarly to the 1,4-dienes reported by Zimmerman or undergo alternative reactions. The results obtained were unexpected and have opened novel and very interesting lines of research.

DCA-sensitized irradiation of **1**, in acetonitrile for 25 min, using biphenyl as co-sensitizer, afforded the *N*-vinylaziridine **3** (11%) and the cyclopropyl imine **23** (19%), as shown in Scheme 6.[13] This result was very surprising because it represents the first examples of SET-promoted di-π-methane reactions (a 2-ADPM rearrangement generating **3** and an aryl-di-π-methane reaction affording **23**) that take place

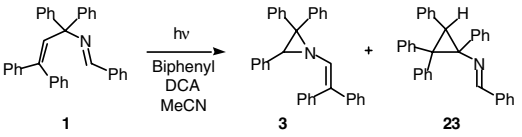

SCHEME 6

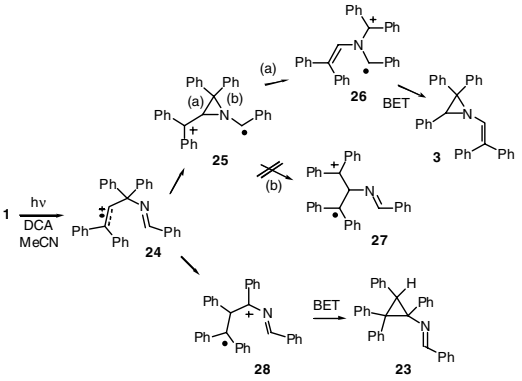

SCHEME 7

via radical-cation intermediates in the ground state. As mentioned previously, di-π-methane reactions were considered the paradigm of processes that took place in the excited state only.[1] In addition, it is also worth noting that the vinylaziridine **3** is formed in both the triplet- and DCA-sensitized irradiations of **1**.

The mechanism shown in Scheme 7 was proposed to account for the formation of these two products. This involves the generation of an olefin-localized cation-radical intermediate **24** that bridges by CN bond formation to give the aziridinyl cation-radical **25**. Ring opening in **25** by path (a) generates **26**, which by back electron transfer and biradical cyclization yields **3**. The alternative ring opening of **25** by path (b), which would have produced the corresponding cyclopropyl imine, does not occur probably because the intermediate radical-cation **27** is less stable than **26**. A competitive route, involving phenyl migration in **24**, generates the cation-radical **28**, the precursor of **23** (Scheme 7).

The study was extended to azadienes **7a,7b**, **8**, **9**, and **10a,10b**.[13b] DCA-sensitized irradiation of **7a** yielded the corresponding vinylaziridine **16**, exclusively, in low yield. However, azadiene **7b** gave a complex mixture of products in which the corresponding aziridine was not present. The lack of 2-ADPM reactivity of **7b** is difficult to explain at this point.

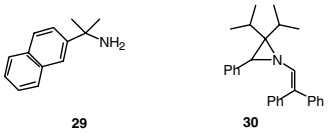

Compound **8** is also unreactive in the 2-ADPM mode. DCA-sensitized irradiation of **8** afforded the naphthalene derivative **29**, resulting from aromatization of the dihydronaphthalene unit and hydrolysis of the CN double bond. This result shows, under these conditions, that oxidation of the cyclohexene moiety takes preference over the 2-ADPM rearrangement. Despite these negative results, compound **9** yielded the aziridine **30** in 14% yield after only 15 min of irradiation.

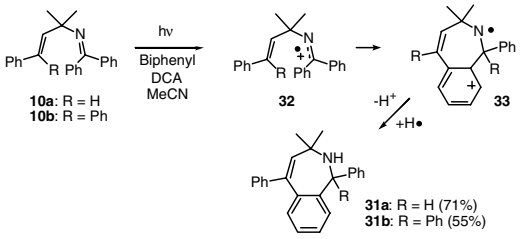

SCHEME 8

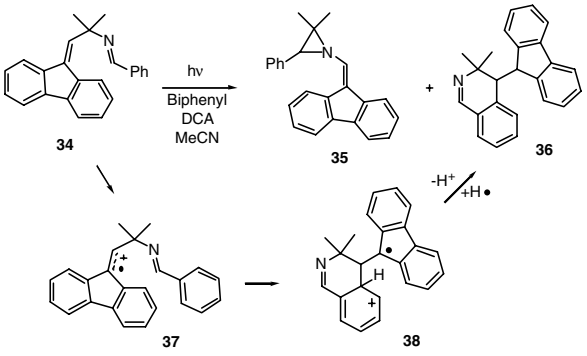

SCHEME 9

DCA-sensitized irradiation of compounds **10a** and **10b** for short periods of time afforded the corresponding dihydrobenzoazepines **31a** and **31b**, respectively, in high isolated yields (Scheme 8). The corresponding *N*-vinylaziridines are not generated in these processes, showing that diphenyl substitution at C1 in ketoimines **10** allows an alternative cyclization route to form dihydrobenzoazepines to take place in preference to 2-ADPM rearrangement. The formation of **31** is consistent with a mechanism involving the generation of an imine-localized radical-cation **32** that, by electrophilic attack on the phenyl ring at C5, yields intermediate **33**, the precursor of **31** (Scheme 8). The high yields of products obtained in the DCA-sensitized irradiation of **10** suggest that this methodology might be applicable to the synthesis of dihydrobenzoazepines from β,γ-unsaturated ketoimines.

Finally, the study was extended to azadiene **34**.[13] Irradiation of **34** under the above conditions, for 1 h, yielded the vinylaziridine **35** (24%) and the dihydroisoquinoline **36** (16%), as shown in Scheme 9. The formation of **36** can be explained by a pathway in which a cation-radical **37**, centered on the olefin unit, undergoes electrophilic attack on the phenyl ring at C1, affording intermediate **38**, the precursor of **36** (Scheme 9).

The results summarized above demonstrate that the novel 2-ADPM rearrangement of 2-aza-1,4-dienes to form *N*-vinylaziridines via radical-cation intermediates is not restricted to compound **1** but can be extended to azadienes **7a**, **9**, and **34**. The SET-sensitized irradiation of azadienes **10a,10b** and **34** afford dihydrobenzoazepines **31a,31b** and dihydroisoquinoline **36**, respectively, showing that alternative cyclization paths are open to the radical-cation intermediates, in addition to the 2-ADPM reaction. Something worth noting regarding the formation of compounds **23**, **31a,31b**, and **36** is that, while compounds **31a,31b** result from radical-cations centered in the imine moiety, the aryl-di-π-methane product **23** and the dihydroisoquinoline **36** are formed from radical-cations centered in the alkene unit. This is somewhat surprising and demonstrates that two different radical-cation intermediates can be generated from the alkene and imine functional groups, which have different ionization potentials.

The comparison between the results obtained in the triplet-sensitized and the SET-sensitized irradiation of 2-aza-1,4-dienes shows that there are clear differences between these two reactions. Probably the most significant of these is the observed regiochemistry. Thus, while the triplet reaction yields cyclopropyl imines, SET-promoted rearrangement affords the corresponding *N*-vinylaziridines. Although the reasons for the triplet regioselectivity are still unclear, formation of the vinylaziridines can be easily explained based on the differences in stability between the two possible radical-cation intermediates resulting from ring opening of the intermediate aziridinyl radical-cation (Scheme 7). Another important difference has been observed in the reactions of **7b** and **9**. Thus, while **7b** undergoes the triplet 2-ADPM rearrangement in low yield, the corresponding aziridine is not formed via radical-cation intermediates. On the other hand, azadiene **9** yields the aziridine **30** in the SET-sensitized reaction but does not rearrange under triplet sensitization. These results are difficult to interpret at this point, but they clearly show that the structural factors that control these two reactions are very different.

In summary, our studies of the triplet-sensitized photoreactions of 2-aza-1,4-dienes have allowed us to uncover the first examples of 2-ADPM rearrangements that yield cyclopropyl imines. In the case of azadiene **1**, the reaction also affords the *N*-vinylaziridine **3**. This is the first example of a di-π-methane rearrangement that yields a three-membered ring heterocyclic photoproduct. However, azadienes with substitution patterns that promote efficient DPM, ODPM, and 1-ADPM reactions do not undergo the 2-ADPM rearrangement. A possible reason for this difference might be due to the unique involvement of azomethine ylides in the 2-ADPM rearrangement.

A more significant conclusion of this study is that 2-ADPM rearrangements can also take place under SET-sensitized irradiation conditions to generate *N*-vinylaziridines regioselectively. In the case of azadiene **1**, cyclopropyl imine **23**, resulting from an aryl-di-π-methane reaction via a radical-cation intermediate, is observed. This result demonstrates that DPM processes can also occur by way of radical-cation intermediates. Alternative cyclization modes have been detected, in some instances yielding dihydrobenzoazepines and dihydroisoquinolines. It is our belief that the results coming from these studies have led to new views of an old but still important photochemical rearrangement process.

1-ADPM Rearrangements via Radical-cation Intermediates

The results obtained in the SET-sensitized irradiation of 2-aza-1,4-dienes using DCA as an electron-acceptor sensitizer suggested that other β,γ-unsaturated compounds could also participate in di-π-methane type rearrangements via radical-cation intermediates. To test this proposal, we have carried out a study on a series of 1-substituted-1-aza-1,4-dienes. The compounds selected for this study were the β,γ-unsaturated imines **39a**, **39b**, and **40a**. DCA-sensitized irradiation of these imines in acetonitrile, using biphenyl as co-sensitizer, yielded the corresponding cyclopropyl imines **41a**, **41b**, and **42a**, which hydrolyze to the corresponding cyclopropane carbaldehydes during isolation.[17]

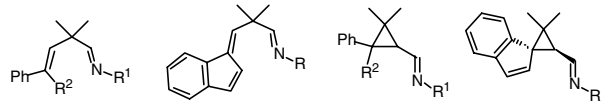

39a: R^1 = Ph, R^2 = H
39b: $R^1 = R^2$ = Ph
39c: R^1 = OAc, R^2 = H
39d: R^1 = OAc, R^2 = Ph
39e: R^1 = OMe, R^2 = H
39f: R^1 = OMe, R^2 = Ph

40a: R = Ph
40b: R = OAc
40c: R = OMe

41a: R^1 = Ph, R^2 = H
41b: $R^1 = R^2$ = Ph
41c: R^1 = OAc, R^2 = H
41d: R^1 = OAc, R^2 = Ph
41e: R^1 = OMe, R^2 = H

42a: R = Ph
42b: R = OAc
42c: R = OMe

These results clearly demonstrate that di-π-methane rearrangements via radical-cation intermediates are not restricted to 2-aza-1,4-dienes but can be extended to 1-aza-1,4-dienes. The mechanism shown in Scheme 10 is proposed to account for the formation of **41b**. This involves the generation of radical-cation **43**, which bridges to afford the cyclopropyl cation-radical **44**. Ring opening by bond (a) cleavage generates **45**. Back electron transfer in **45**, followed by biradical cyclization, yields **41b**. The alternative

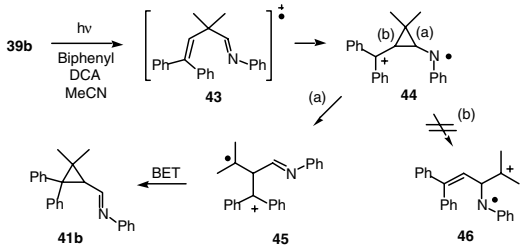

SCHEME 10

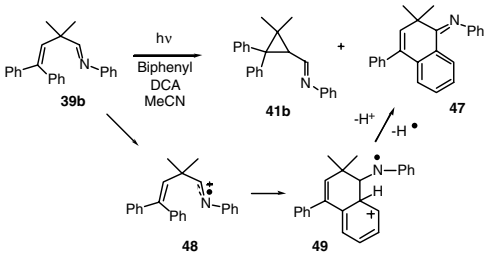

SCHEME 11

cleavage of bond (b), which would have yielded the corresponding aziridine, is not observed, probably due to the fact that the resulting radical-cation **46** is less stable than **45**.

Irradiation of imine **39b** afforded, in addition to the cyclopropyl imine **41b**, the dihydronaphthalene derivative **47** (Scheme 11). This result shows that two different reaction paths are open to the radical-cation intermediate derived from **39b**. The first involves 1-ADPM rearrangement leading to **41b** and the other is the intramolecular cyclization affording **47**. A possible mechanism to justify the formation of **47** involves electrophilic attack of a radical-cation centered in the CN double bond **48** to one of the phenyl ring at C5, affording the intermediate **49**, which loses a proton and a hydrogen radical to yield **47** (Scheme 11). The formation of **47** is similar to the reaction described in the study of the electron-acceptor sensitized photoreactions of 1,4-dienes **21**, which yield dihydronaphthalenes **22**.[16] However, dienes **21** do not undergo radical-cation rearrangements of the di-π-methane type.

An alternative cyclization of the radical-cation intermediate has been observed in the irradiation of **40a** that affords, in addition to the cyclopropane **42a**, the dihydroquinoline **50**.[17b] The formation of **50** is in agreement with a mechanism involving the generation of the radical-cation centered in the CC double bond **51**. Intramolecular cyclization in **51**, by electrophilic attack on the phenyl ring attached to the nitrogen atom, generates the intermediate **52**, which by aromatization and hydrogen abstraction yields **50** (Scheme 12).

The study was extended to β,γ-unsaturated oxime acetates and oxime ethers that do not hydrolyze to the corresponding aldehydes during isolation. Previous studies on the triplet photoreactivity of 1-substituted 1-aza-1,4-diene derivatives have demonstrated that oxime acetates undergo the 1-ADPM rearrangement more efficiently than the corresponding imines.[12] However, oxime ethers do not rearrange on triplet-sensitized irradiation.[18] Therefore, it was considered of interest to explore the photoreactivity of these compounds under DCA-sensitized conditions to determine possible analogies or differences between the triplet- and DCA-sensitized reactivity of these substrates. The compounds selected for this study were the oxime acetates **39c**, **39d**, **40b**, and the oxime ethers 3**9e**, **39f**, **40c**, structurally related to the imines **39a,39b** and **40a**. DCA-sensitized irradiation of oxime acetates **39c**, **39d**, and **40b** for variable times afforded the corresponding cyclopropanes **41c**, **41d**, and **42b**, respectively, resulting from 1-ADPM

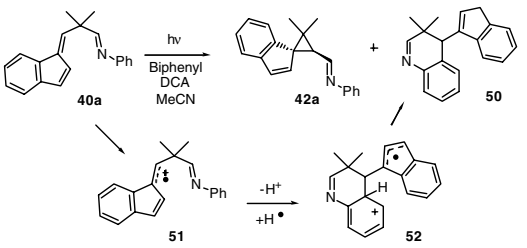

SCHEME 12

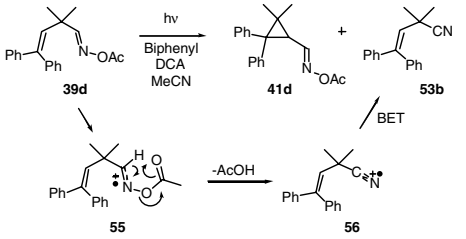

SCHEME 13

rearrangements.[17] The qualitative efficiencies of the reactions of oxime acetates and the yields of products are clearly higher than those for the corresponding imines.

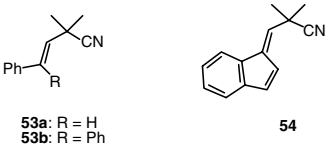

SET-sensitized irradiations of **39c, 39d**, and **40b** also afforded, in addition to the corresponding cyclopropanes, the nitriles **53a**, **53b**, and **54**, respectively, resulting from elimination of acetic acid.[17b]

This elimination reaction cannot be considered a thermal process because it does not occur in the triplet-sensitized irradiation of oxime acetates. The mechanism shown in Scheme 13 for compound **39d** is proposed to account for the formation of these nitriles. It involves the generation of a radical-cation centered on the CN double bond **55**, followed by elimination of acetic acid to afford the radical-cation **56**, which yields the nitrile **53b** by back electron transfer (Scheme 13).

In the case of oxime acetate **40b**, the dihydroisoxazole **57** was obtained in addition to the cyclopropane **42b** and the nitrile **54**. A possible mechanism to justify the formation of **57** is shown in Scheme 14. This involves the generation of the radical-cation **58** that by intramolecular cyclization affords the radical-cation **59**. Elimination of acetic acid in **59** yields **57**.

DCA-sensitized irradiation of oxime ethers **39e** and **40c** afforded the corresponding cyclopropanes **41e** and **42c** in low yield.[17] However, for unknown reasons, irradiation of compound **39f** under these conditions gave a complex mixture of products in which the corresponding 1-ADPM product was not present. Irradiation of oxime ether **40c** also afforded the [4+4]-cycloadduct **60**.[17b] The mechanism shown in Scheme 15 could justify the formation of **60**. This involves the generation of a radical-cation/radical-anion pair **61**. Intramolecular cyclization of the radical-cation within the solvent cage generates the intermediate **62**, which undergoes intermolecular cyclization, to yield the observed product (Scheme 15).

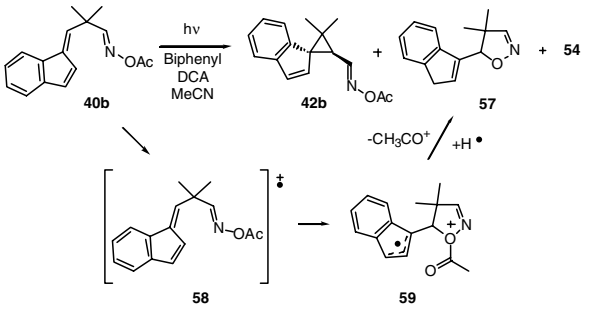

SCHEME 14

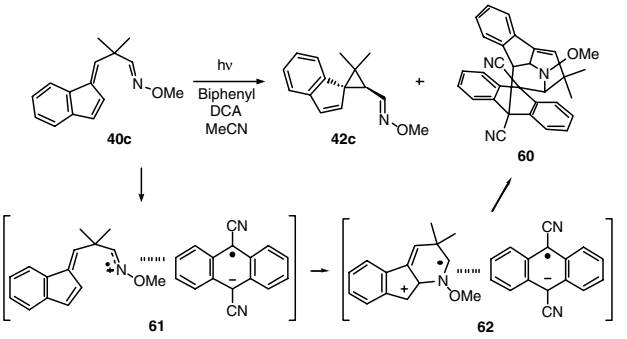

SCHEME 15

The results obtained in the DCA-sensitized irradiation of β,γ-unsaturated oxime acetates and oxime ethers show that the 1-ADPM rearrangement via radical-cation intermediates is not limited to β,γ-unsaturated imines but can be extended to hydrolytically stable CN double bond derivatives. Something worth mentioning in this study is that a previous report showed that β,γ-unsaturated oxime ethers do not undergo the 1-ADPM rearrangement on direct or triplet-sensitized irradiations,[18] but compounds **39e** and **40c** rearrange via radical-cation intermediates, although in low yields. Finally, alternative reactions of the radical-cation intermediates, affording nitriles, dihydroquinolines, dihydronaphthalenes, dihydroisoxazoles, and [4+4]-cycloadducts, have been observed in some instances.

Another interesting observation in this study is that, while the dihydronaphthalene derivative **47** and the nitriles **53a**, **53b**, and **54** are formed from radical-cations centered in the CN double bond, the dihydroquinoline **50** results from a radical-cation centered in the alkene unit. These observations are in agreement with similar results obtained in the study of the photochemical reactivity of 2-aza-1,4-dienes under SET-sensitized conditions and suggest that two different radical-cations intermediates can be generated from functional groups with different ionization potentials.

The 1-ADPM rearrangement and the alternative reaction modes of 1-substituted-1,4-dienes via radical-cation intermediates described above have an obvious mechanistic interest. However, the yield of products in these reactions is considerably lower than in the triplet-sensitized photoreactions of these compounds, with the exception of oxime ethers **39e** and 4**0c**; therefore, the synthetic utility of these reactions is limited. However, this inconvenience can be overcome using alternative electron-acceptor sensitizers. Recent results show that replacing DCA by dicyanodurene (DCD) as an electron-acceptor sensitizer and biphenyl as a co-sensitizer, results in a considerable increase in the yields of 1-ADPM photoproducts.[17b] Thus, for example, DCA-sensitized irradiation of **39c**, for 2.5 h, affords cyclopropane **41c** in 15% yield, whereas using DCD as the sensitizer, this compound is obtained in 60% yield after

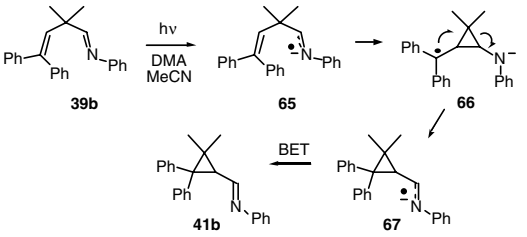

SCHEME 16

only 1 h of irradiation. Similar enhancements in the yield of 1-ADPM photoproducts have been observed in most of the cases studied.[17b] Furthermore, the nitriles **53a**, **53b**, and **54**, obtained in the DCA-sensitized irradiation of oxime acetates **39c**, **39d**, and **40b**, are not obtained under DCD-sensitization conditions.

In summary, our investigations on the photochemical reactivity of β,γ-unsaturated imines, oxime acetates, and oxime ethers using electron-acceptor sensitizers have allowed us to describe the second example of di-π-methane rearrangements that take place via radical-cation intermediates in the ground state. In some instances, alternative reactions of these intermediates have been observed, yielding nitriles, dihydroquinolines, dihydronaphthalenes, dihydroisoxazoles, and cycloaddition products. Some of the products obtained in these SET-promoted reactions arise from radical-cations centered in the alkene unit while others are formed from radical-cations centered in the CN double bond. The yield of 1-ADPM photoproducts increases considerable when DCD is used as electron-acceptor sensitizer instead of DCA. Finally, the reactions of the di-π-methane type observed in the SET-sensitized irradiations of 1-aza- and 2-aza-1,4-dienes are important because these rearrangements have been considered for many years as the paradigm of processes that took place in the excited state only. Our results show that these rearrangements can also occur in the ground state of radical-cation intermediates. In our opinion, the studies summarized above have opened new lines of research in the area of di-π-methane reactions.

95.4 Di-π-methane Rearrangements *via* Radical-Anion Intermediates

The aryl-di-π-methane, 1-ADPM, and 2-ADPM rearrangements via radical-cation intermediates observed in the DCA-sensitized irradiations of 1-aza- and 2-aza-1,4-dienes suggested the possibility that these reactions could also occur via radical-anion intermediates. To test this proposal we have carried out a study on the photoreactivity of 1-aza-1,4-dienes **39a**, **39b**, **40a**, and **63** using *N*,*N*-dimethylaniline (DMA) as electron-donor sensitizer. Irradiation of **39a**, **39b**, **40a**, and **63**, in acetonitrile, under these conditions, afforded the corresponding cyclopropyl imines **41a** (21%), **41b** (15%), **42a** (11%), and **64** (15%), respectively, that hydrolyzed to the corresponding aldehydes during isolation.[19] These results demonstrate that the 1-ADPM rearrangement of azadienes **39a**, **39b**, **40a**, and **63** can be promoted by DMA, a well-known electron-donor sensitizer.[20] A possible mechanism to account for the formation of the cyclopropyl imines is shown in Scheme 16 for compound **39b**. It involves generation of the radical-anion **65** that bridges to form the cyclopropyl radical-anion **66**. The rearrangement in **66** generates **67**, which, by back electron transfer, yields **41b** (Scheme 16).

However, previous studies show that compound **39b** undergoes 1-ADPM rearrangement very efficiently in the triplet excited state.[7b] Because DMA has a triplet energy of 68.4 kcal mol^{-1},[20] efficient triplet energy transfer to the alkene unit is a possibility to take into account in these reactions. Therefore, the question that arises is whether the 1-ADPM rearrangements of compounds **39a**, **39b**, **40a**, and **63** occur by triplet energy transfer or by SET via radical-anions. To answer this question, the DCA-sensitized irradiation of compounds **39a**, **39b**, and **40a** was carried out in hexane, a nonpolar solvent that should not favor the generation of radical-anions. Under these conditions, the corresponding cyclopropanes **41a** (2%), **41b** (2%), and **42a** (4%) were also obtained but the yields of products were considerably lower

than in the runs carried out in acetonitrile.[19] This result support the involvement of radical-anions in these rearrangements when the reaction is carried out in acetonitrile. However, in the case of compound **63**, the yield of cyclopropane **64** in hexane and acetonitrile were comparable, thus casting doubt on whether or not these reactions are taking place via triplet sensitization or SET.

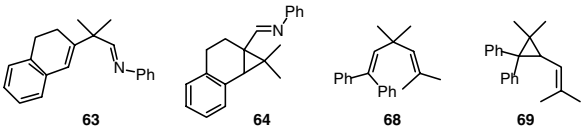

Trying to arrive at a definitive answer to this question, the study was extended to the 1,4-diene **68**. In a previous study, Zimmerman and Pratt[21] reported the efficient DPM rearrangement of **68** on direct irradiation to give cyclopropane **69** in good yield. However, the rearrangement was very inefficient when the irradiation was carried out using benzophenone as triplet sensitizer. Therefore, compound **68** was considered to be a perfect candidate to determine whether DMA was acting as a triplet energy donor or as an electron donor. DMA-sensitized irradiation of **68**, in acetonitrile, afforded **69** in 34% yield. When the reaction was carried out in hexane, **69** was obtained in 22% yield. However, benzophenone-sensitized irradiation of **68**, in hexane, for the same period of time gave **69** in 5% yield only, in agreement with the earlier results. The drastic decrease in the yield of product in the reactions run in hexane caused by changing the sensitizer from DMA to benzophenone cannot by explained by less efficient triplet energy transfer from the benzophenone to the diene **68** because the triplet energy of benzophenone (69.2 kcal mol^{-1})[20] is comparable to the value reported for the DMA (68.4 kcal mol^{-1}).[20] Therefore, the results obtained in the study of the photoreactivity of diene **68** clearly support the involvement of radical-anions in the DMA-sensitized irradiation. Considering that the CN double bond in compounds **39a**, **39b**, **40a**, and **63** should be a better electron acceptor than the diphenylvinyl unit in **68**, it is logical to assume that the rearrangement of **39a**, **39b**, **40a**, and **63** also occurs via similar radical-anion intermediates. However, the absence of a solvent polarity effect on the efficiency of photoreactions of **63** and **68** is surprising. A possible explanation for the strong influence of the solvent polarity in the case of compounds **39a**, **39b**, and **40a** and the small influence of this effect for compounds **63** and **68** is shown in Scheme 17 for compound **39b**.

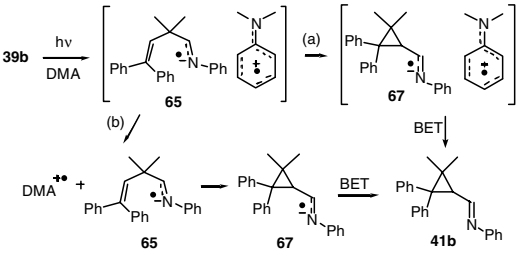

SCHEME 17

Thus, the very fast rearrangement of the radical-anion **65** within solvent cages (Scheme 17, path a) could justify the absence of solvent polarity effect. In cases in which this intermediate escapes from the cage before rearrangement occurs (Scheme 17, path b), a significant influence of the polarity of the solvent would have been observed. This is the situation in DMA-sensitized reactions of **39a**, **39b**, and **40a**.[19]

The results summarized above demonstrate that 1-ADPM, 2ADPM, and DPM reactions can take place via radical-cation and radical-anion intermediates. These observations have modified some of the ideas firmly established for many years on the photoreactivity of β,γ-unsaturated systems, opening new lines of research in an area in which, due to the large number of studies carried out for more than 30 years,

apparently there were very few things to uncover. Further studies are underway to determine the scope and possible synthetic applications of these novel reactions and to rationalize the photo-behavior of these compounds.

References

1. For reviews see (a) Hixson, S.S., Mariano, P.S., and Zimmerman, H.E., The di-π-methane and oxa-di-π-methane rearrangements, *Chem. Rev.*, 73, 531–551, 1973; (b) Dauben, G.W., Lodder, G., and Ipaktschi, J., Photochemistry of β,γ-unsaturated ketones, *Top. Curr. Chem.,* 54, 73–114, 1975; (c) Houk, K.N., The photochemistry and spectroscopy of β,γ-unsaturated carbonyl compounds, *Chem. Rev.*, 76, 1–74, 1976; (d) Zimmerman, H.E., The di-π-methane (Zimmerman) rearrangement, in *Rearrangements in Ground and Excited States*, Vol. 3, de Mayo P., Ed., Academic Press, New York, 1980, 131–166; (e) Schuster, D.I., Photochemical rearrangements of β,γ-enones, in *Rearrangements in Ground and Excited States*, Vol. 3, de Mayo, P., Ed., Academic Press, New York, 1980, 167–279; (f) De Lucchi, O. and Adam, W., Di-π-methane photoisomerizations, in *Comprehensive Organic Synthesis*, Vol. 5, Trost, B.M., Fleming, I., and Paquette, L.A., Eds., Pergamon Press, Oxford, 1991, 193–214; (g) Demuth, M., Oxa-di-π-methane photoisomerizations, in *Comprehensive Organic Synthesis*, Vol. 5, Trost, B.M., Fleming, I., and Paquette, L.A., Eds., Pergamon Press, Oxford, 1991, 215–237; (h) Zimmerman, H.E., The di-π-methane rearrangement, in *Organic Photochemistry,* Vol. 11, Padwa, A., Ed., Marcel Dekker, New York, 1991, 1–36; (i) Demuth, M., The Oxa-di-π-methane rearrangement, in *Organic Photochemistry*, Vol. 11, Padwa, A., Ed., Marcel Dekker, New York, 1991, 37–109; (j) Armesto, D., The aza-di-π-methane rearrangement, in *CRC Handbook of Organic Photochemistry and Photobiology*, Horspool, W.M. and Song, P.-S., Eds., CRC Press, Boca Raton, FL, 1995, 915–930; (k) Armesto, D., Influence of nitrogen incorporation on the photoreactivity of some unsaturated systems, *EPA Newsletter*, 53, 6–21, 1995; (l) Zimmerman, H.E. and Armesto, D., Synthetic aspects of the di-π-methane rearrangement, *Chem. Rev.*, 96, 3065–3112, 1996; (m) Armesto, D., Ortiz, M.J., and Agarrabeitia, A.R., Novel photoreactions of azadienes and related compounds. Synthetic applications and mechanistic studies, in *Advanced Functional Molecules and Polymers*, Vol. 1, Nalwa H.S., Ed., Gordon and Breach, Amsterdam, 2001, 351–379; (n) Armesto, D., Ortiz, M.J., and Agarrabeitia, A.R., Recent advances in di-π-methane photochemistry. A new look at a classical reaction, in *Photochemistry of Organic Molecules in Isotropic and Anisotropic Media*, Ramamurthy, V. and Schanze, K.S., Eds., Marcel Dekker, New York, 2003, 1–41.
2. Ciganek, E., The photoisomerization of dibenzobicyclo[2.2.2]octatrienes, *J. Am. Chem. Soc.*, 88, 2882–2883, 1966.
3. (a) Demuth, M. and Hinsken, W., Extensions of the tricyclooctanone concept. A general principle for the synthesis of linearly and angularly annelated triquinanes, *Angew. Chem. Int. Ed. Engl.*, 24, 973–975, 1985; (b) Demuth, M. and Hinsken, W., The first total synthesis of enantiomerically pure (−)-silphiperfol-6-en-5-on, *Helv. Chim. Acta*, 71, 569–576, 1988.
4. Paquette, L.A., Kang H.-J., and Ra, C.S., Stereocontrolled access to the most highly condensed pentalenolactone antibiotic. From cycloheptatriene to pentalenolactone P methyl ester, *J. Am. Chem. Soc.*, 114, 7387–7395, 1992.
5. Zimmerman, H.E., Binkley, R.W., Givens, R.S., and Sherwin, M.A., Mechanistic organic photochemistry. XXIV. The mechanism of the conversion of barrelene to semibullvalene. A general photochemical process, *J. Am. Chem. Soc.*, 89, 3932–3933, 1967.
6. Nitta, M., Kasahara, I., and Kobayashi T., Aza-di-π-methane rearrangement involving an oxime group, *Bull. Chem. Soc. Jpn.,* 54, 1275–1276, 1981.
7. (a) Armesto, D., Martin, J.F., Perez-Ossorio R., and Horspool, W.M., A novel aza-di-π-methane rearrangement. The photoreaction of 4,4-dimethyl-1,6,6-triphenyl-2-azahexa-2,5-diene, *Tetrahedron Lett.,* 23, 2149–2152, 1982; (b) Armesto, D., Horspool, W.M., Martín J.F., and Perez-Ossorio, R., The synthesis and photochemical reactivity of β,γ-unsaturated imines. An aza-di-π-methane rearrangement of 1-azapenta-1,4-dienes, *J. Chem. Res. (S)*, 46–47, 1986; *(M)*, 0631–0648, 1986.

8. Tsuji, T. and Nishida, S., Preparation of cyclopropyl derivatives, in *The Chemistry of Functional Groups, The Chemistry of the Cyclopropyl Group, Part 1*, Patai, S. and Rappoport, Z., Eds., John Wiley & Sons, New York, 1987, chap. 7, 347.
9. (a) Armesto, D., Ortiz, M.J., and Romano, S., The oxa-di-π-methane rearrangement of β,γ-unsaturated aldehydes, *Tetrahedron Lett.*, 36, 965–968, 1995; (b) Armesto, D., Ortiz, M.J., Romano, S., Agarrabeitia, A.R., Gallego, M.G., and Ramos, A., Unexpected oxa-di-π-methane rearrangement of β,γ-unsaturated aldehydes, *J. Org. Chem.*, 61, 1459–1466, 1996; (c) Armesto, D., Ortiz, M.J., Agarrabeitia A.R., and Aparicio-Lara S., Diastereoselective synthesis of cyclopropanecarbaldehydes, *Synthesis*, 1149–1158, 2001.
10. Mariano, P.S., SET-induced inter- and intramolecular additions to iminium cations, in *CRC Handbook of Organic Photochemistry and Photobiology*, Horspool, W.M. and Song, P.-S., Eds., CRC Press, Boca Raton, FL, 1995, 867–878.
11. Zimmerman, H.E., Boetcher, R.J., and Braig, W., Accentuation of di-π-methane reactivity by central carbon substitution. Mechanistic and exploratory organic photochemistry. LXXV., *J. Am. Chem. Soc.*, 95, 2155–2163, 1973.
12. Armesto, D., Horspool, W.M., Langa, F., and Ramos, A., Extension of the aza-di-π-methane reaction to stable derivatives. Photochemical cyclization of β,γ-unsaturated oxime acetates, *J. Chem. Soc., Perkin Trans. 1*, 223–228, 1991.
13. (a) Armesto, D., Caballero, O., and Amador, U., Novel photorearrangements of 2-aza-1,4-dienes to produce vinylaziridines and cyclopropylimines, *J. Am. Chem. Soc.* 119, 12659–12660, 1997; (b) Caballero, O., Sintesis y reactividad fotoquimica de 2-aza-1,4-dienos, Ph.D. thesis, Universidad Complutense de Madrid, Madrid (Spain), 2001; (c) Armesto, D., Caballero, O., Ortiz, M.J., Agarrabeitia, A.R., Martin-Fontecha, M., and Torres, R., Novel photoreactions of 2-aza-1, 4-dienes in the triplet excited state and via radical-cation intermediates. 2-Aza-di-π-methane rearrangements yielding cyclopropylimines and *N*-vinylaziridines, *J. Org. Chem.,* 68, 2003, in press.
14. (a) Adam, W., Berkessel, A., Hildenbrand, K., Peters, E.-M., Peters, K., and von Schnering, H.G., The photochemistry of bis(2,2-diphenylvinyl) ether: a search for the 3-oxa-di-π-methane rearrangement, *J. Org. Chem.*, 50, 4899–4909, 1985; (b) Adam, W., Berkessel, A., and Krimm, S., Photochemical decarbonylation of 2,2,4,4-tetramethyl-6-oxabicyclo[3.1.0]hexan-3-one: an entry into the diradical manifold of the novel 3-oxa-di-π-methane rearrangement, *J. Am. Chem. Soc.,* 108, 4556–4561, 1986.
15. (a) Grigg, R., Thornton-Pett, M., and Yoganathan, G., Cycloaddition reactions of aldimines of 1,5-ketoaldehydes. Applications in the synthesis of polycyclic nitrogen heterocycles, *Tetrahedron*, 55, 1763–1780, 1999; (b) Pearson, W.H. and Clark, R.B., Formation and cycloaddition of nonstabilized *N*-unsubstituted azomethine ylides from (2-azaallyl)stannanes and (2-azaallyl)silanes, *Tetrahedron Lett.*, 40, 4467–4471, 1999.
16. Zimmerman, H.E. and Hoffacker, K.D. Novel radical cation reactions of bichromophoric systems. Transannular aryl migrations; mechanistic and exploratory organic photochemistry, *J. Org. Chem.*, 61, 6526–6534, 1996.
17. (a) Ortiz, M.J., Agarrabeitia, A.R., Aparicio-Lara, S., and Armesto, D., The novel 1-aza-di-π-methane rearrangement of 1-substituted-1-aza-1,4-dienes promoted by DCA-sensitization, *Tetrahedron Lett.*, 40, 1759–1762, 1999; (b) Armesto, D., Ortiz, M.J., Agarrabeitia, A.R., Aparicio-Lara, S., Martin-Fontecha, M., Liras, M., and Martinez-Alcazar, M.P., Photochemical reactivity of 1-substituted-1-aza-1,4-dienes promoted by electron-acceptor sensitizers. Di-π-methane rearrangements and alternative reactions via radical-cation intermediates, *J. Org. Chem.*, 67, 9397–9405, 2002.
18. Pratt, A.C. and Abdul-Majid, Q., Photochemistry of the carbon-nitrogen double bond. 2. An investigation of the 3-methylenepropan-1-imine and 3-oxopropan-1-imine chromophores, *J. Chem. Soc., Perkin Trans. 1*, 359–364, 1987.
19. Armesto, D., Ortiz, M.J., Agarrabeitia, A.R., and Martin-Fontecha, M., Di-π-methane reactions promoted by SET from electron-donor sensitizers, *J. Am. Chem. Soc.*, 123, 9920–9921, 2001.

20. Kavarnos, G.J. and Turro N.J., Photosensitization by reversible electron transfer: theories, experimental evidence and examples, *Chem. Rev.*, 86, 401–449, 1986.
21. Pratt, A.C. and Zimmerman H.E., Unsymmetrical substitution and the direction of the di-π-methane rearrangement. Mechanistic and exploratory organic photochemistry. LVI., *J. Am. Chem. Soc.*, 92, 6259–6267, 1970.

96

Photochromic Nitrogen-Containing Compounds

Saleh A. Ahmed
Assiut University

Aboel-Magd A. Abdel-Wahab
Assiut University

Heinz Dürr
University of Saarland

96.1 Introduction and Definition

Photochromism is an exemplary field of photochemistry that deals with photochemical reactions that are reversibly thermally or photoinduced. This term is made up of two parts — photo (light) and chroma (color) — and the suffix "ism" indicates the phenomenon. Photochromism literally means coloration by light. It has received considerable attention ever since its discovery toward the end of the 19th century, both for organic or inorganic substances, and is still an active field of research, primarily because of its actual and potential applications and for its paramount importance in biological phenomena.[1–6]

Photochromism[7–11] is a reversible transformation of a single chemical species between two states, whose absorption spectra are recognizably different, brought about, in at least one direction, by electromagnetic radiation (Equation 96.1).

$$A\,(\lambda_1) \underset{\Delta \text{ or } h\nu_2}{\overset{h\nu_1}{\rightleftharpoons}} B(\lambda_2) \quad \text{(unimolecular process)} \tag{96.1}$$

Species A is transformed into the higher-energy form B as a result of irradiation with light. The reverse reaction to reform A usually occurs as a spontaneous thermal process, but may also be light induced. Equation 96.1 holds only for unimolecular reactions. More recently, bimolecular photochromic systems, based on a cycloaddition or cycloreversion,[12–14] have also been discovered.

$$A\,(\lambda_1) + B(\lambda_2) \underset{\Delta \text{ or } h\nu_2}{\overset{h\nu_1}{\rightleftharpoons}} C(\lambda_3) \quad \text{(bimolecular process)} \tag{96.2}$$

0-8493-1348-1/04/$0.00+$1.50

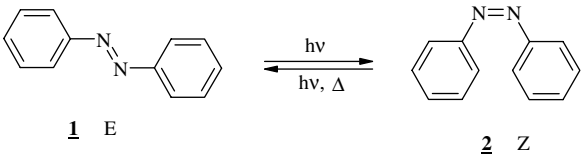

1 E **2** Z

SCHEME 1

The photochromic[1–7,15] systems illustrated in Equation 96.1 can be classified into several groups on the basis of a photochemically induced primary step:

1. *Z,E*-(*cis,trans*)-isomerization
2. Tautomerism
3. Pericyclic reactions
4. Homolytic bond cleavage
5. Electron transfer reactions

This chapter discusses only *N*-containing photochromic molecules. However, it covers many classes of photochromic systems. Therefore, photochromism based on triplet-triplet absorption of stilbenes, thioindigo, bianthrylidenes, fulgides, and salicylates (only briefly) is not discussed. Nitrogen-containing photochromic systems are dealt with if the reacting fragment of the molecule contains nitrogen. One exception is made for the very important spiropyrans (*vide infra*).

96.2 *Z,E*-(*cis-trans*)-Isomerization

Azobenzenes

When the double bond of azo compounds is excited either directly or via sensitizers, a reversible *Z,E*-isomerization is observed.[16–18]

Azobenzene isomerization normally is a very clean reaction (Scheme 1). In the presence of oxygen, slow photooxidation to azobenzene occurs.[16]

E,Z-isomerization can be induced by a direct (singlet) or sensitized (triplet) route from the n,π^* or π,π^* state. The thermal back-reaction from the *Z*-isomer is slow in azobenzene and fast in amino- or aminonitro-substituted azobenzenes (pseudo-stilbenes). The color change is more in intensity than in wavelength.[16–18] In geometrically locked azobenzene (i.e., in **3**, **4**, and **5**), the *Z*-form might be stable and cannot isomerize (Scheme 2).[18]

Compounds of type 4 show identical quantum yields $\phi_{E,Z}$ when excited either in the n,π^* or π,π^* state.

More recently, so-called photoresponsive crown ethers have also been prepared and, in these too, the light-sensitive behavior is based on *Z,E*-isomerization.[17,18] The study of azo-groups in polymers[18b-d] has been undertaken recently. Switching processes have been an intensively studied domain in recent years as show in some recent papers.[18e,18f] *Z,E*-isomerization also plays an important role in simpler compounds such as benzylidene anilines[17b] and azomethines. The latter are of importance in biological systems such as rhodopsin in the human eye.[1–5]

96.3 Pericyclic Reactions

Pericyclic reactions are among the most important processes that allow for the design and construction of photochromic systems, and a large number of photochromic organic molecules utilize pericyclic reactions as the bases for photochromic materials.

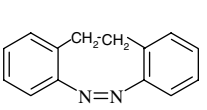

3

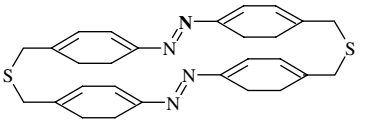

4

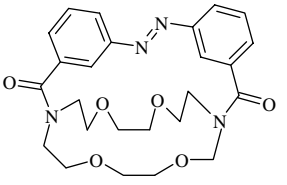

5

SCHEME 2

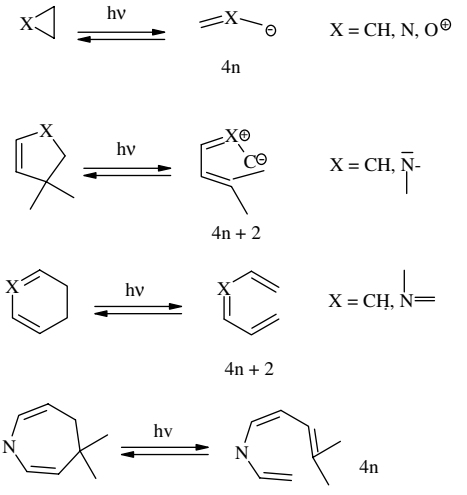

SCHEME 3

Electrocyclization

Electrocyclic reactions have proved especially suitable as a structural unit for photochromic systems. Scheme 3 shows four different types of ring-opening reactions. However, only a few of the many possible electrocyclizations are important with regard to application.

4n-System

Here, the three-membered heterocycles have an outstanding role. Griffin and co-workers prepared a new class of stable carbonyl ylides from epoxydiphenylsuccinimde **6** and diphenylepoxymaleic anhydride **7**.[19] Colors are generated when the bicyclic oxides **6** and **7** are irradiated at 77K. In rigid matrices (2-methyltetrahydrofuran), ring opening affords the ylides **8** and **9.** The colors of **8** and **9** persist after the matrix is warmed, softens, and appears to become fluid (130 to 140K).

10 **11**

SCHEME 4

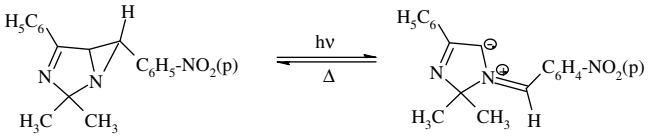

12 **13**

SCHEME 5

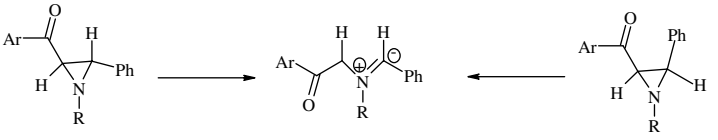

14 **15** **16**

SCHEME 6

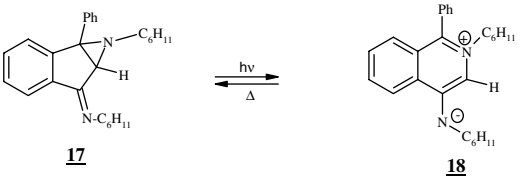

17 **18**

SCHEME 7

8 **9**

Color is not visible at ambient temperature in fluid 2-methyltetrahydrofuran; however, **8** and **9** are stable in the solid state even at room temperature.

In the analogous way, the nitrones **10** can be converted by irradiation into the oxaziridines **11** (Scheme 4). The latter are powerful oxidizing agents, highly reactive, and in most cases they cannot be isolated. The reverse reaction takes place upon heating. Here, the open form **10** is more stable. Interesting photochromic molecules of the aziridine type have been found by Cromwell[20] and Tap Do Minh and Trozzolo et al.[21–23] Aziridines show photochromic behavior in the crystalline state although some systems

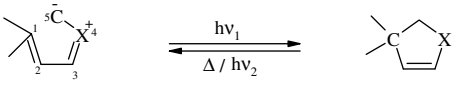

19 **20**

SCHEME 8

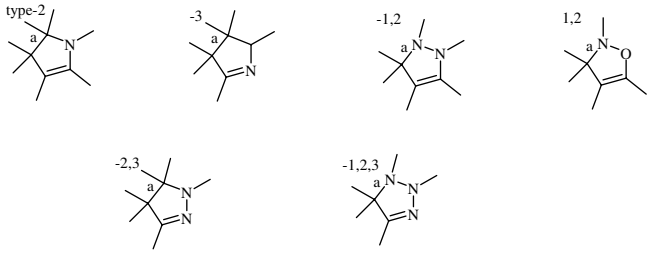

SCHEME 9 The numbers show the positions of the heteroatoms in aza-pentadiene, thus classifying the molecule as type 2-system etc.

are also photochromic in solution. An especially efficient photochromic system is found in the bicyclic aziridine **12**, which undergoes a light-induced reaction according to Scheme 5 to give monocyclic **13.**[21–23]

Cromwell and co-workers[20] discovered the photochromism of arylaziridines some time ago. Padwa and Hamilton[24] investigated the photochromism of glasses at 77K in the arylaziridine system **14**, **16**. On warming slowly, the colors fade and the aziridine is regenerated.

All attempts to obtain colored species by carrying out the irradiation in solution failed. Lown and Matsumoto[25] as well as Padwa and Vega[26] investigated another class of photochromic aziridines based on 1,3-electrocyclization.

4n+2 Systems (5 Atoms, 6 Electrons n = 1)

A very efficient photochromic system was discovered in 1979 by Dürr and Hauck.[27,28] It is based on the electrocyclic ring closure of azapentadienes to azacyclopentenes.

Nitrogen or oxygen can be in different positions (1 to 5) of the azapentadiene system. Thus, a great versatility is available as far as different classes of five-membered heterocycles are concerned. The different photochromic compounds based on this intercoversion are given in Scheme 9.

This scheme shows the classification (types) and characteristic structural features of the new photochromic system (a: σ-bond formed upon 1,5-electrocyclization). According to the position of the heteroatom in the aza-pentadiene, fragments are classified as type 2, etc.[7,27,28]

Type 2 System

Systems of type 2 can be regarded as "1,3-dipoles of an allylic type."[28] The organic chemist's entire armory has been brought to bear on the study of 1,3-dipolar cycloadditions[29] but despite this, it is only quite recently that the reaction has been successfully used in an effective photochromic system.

A new photochromic system whose structural basis are the spiro-dihydroindolizines[27] was found and studied intensively.[27,28,30–33] It can be prepared easily by different routes[30–33] and a typical path is shown in Scheme 10. When spirocyclopropenes with the general structure **21**[30] are allowed to react with pyridine or pyridazine derivatives, photochromic [1,8-a]dihydroindolizines **25** (Y = CH or Y = N, respectively) are formed.[34–36]

Compounds with a very wide range of absorption wavelength can be synthesized using this "cyclopropene route." The photochromic properties are not linked, however, to spiro-dihydroindolizines; simpler systems (diphenyl derivatives) can also be prepared easily. Thus, by introducing a variety of

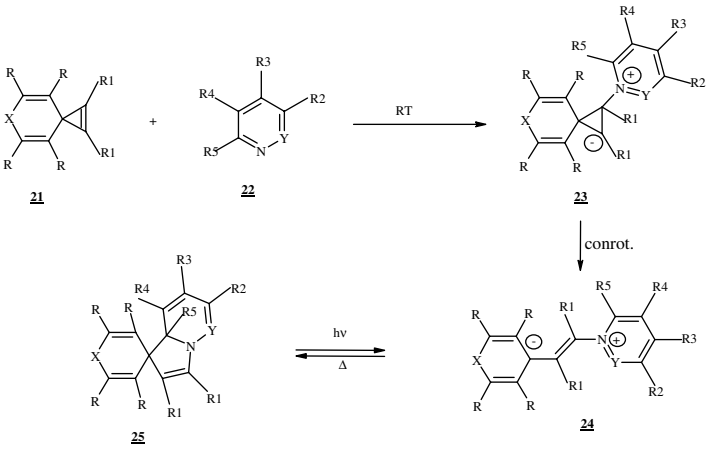

21 + **22** → **23** (RT); **23** → **24** (conrot.); **24** ⇌ **25** (hν / Δ)

SCHEME 10 Cyclopropene route to **24** and **25**. Solvent: CH_2Cl_2/ether; temperature: 25°C; yield: 12 to 89%.

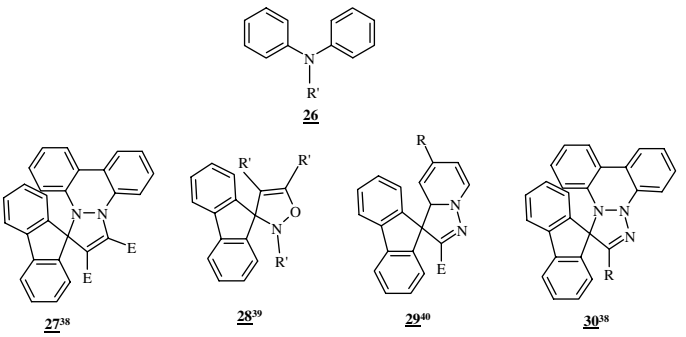

26

27[38] **28**[39] **29**[40] **30**[38]

SCHEME 11

different substituents in all positions of **25**, molecules with tailor-made properties are accessible. Crown ether-linked dihydroindolizines can be made that allow special effects due to host, guest, or supramolecular assemblies.[34]

Type 3 System

On irradiation, systems of the type such as **20** in the presence of oxygen give indoles. However, owing to subsequent thermal reactions, such as sigmatropic H-shifts (and possibly oxidation) at moderate or high temperature, irreversible secondary reactions occur to yield di-and tetrahydroindolizines and the system therefore cannot be regarded as being reversibly photochromic.[37]

Mixed systems (1,2; 2,3-; 1,2,3.)

Mixed photochromic systems such as **27** through **30** can be synthesized as well. A survey of typical examples is given below.

Biphotochromic systems containing (1) two DHI-molecules,[41] (2) a DHI- and a salicylideneanil,[42] and (3) DHI-spirooxazine have also been prepared.

Applying one of the above four synthetic routes in combination with the same or a second approach can lead to biphotochromic systems.[41,42] In principle, these are symmetrical systems such as DHI-DHI **31** and unsymmetrical systems such as DHI_a-DHI_b, photochromic systems(**32** or **33**) are possible (see Scheme 12).

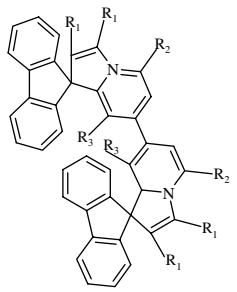

31

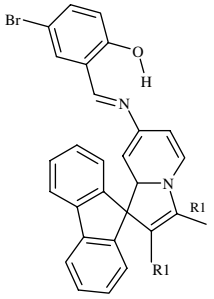

32

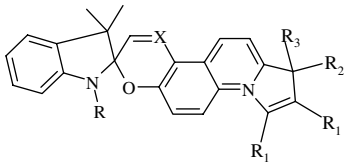

33

SCHEME 12

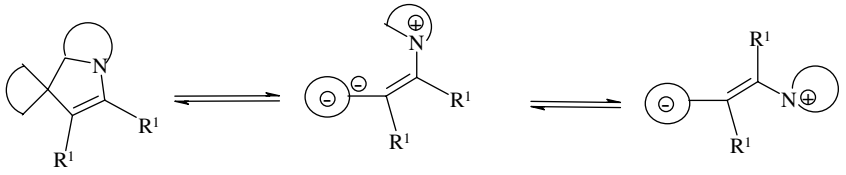

25 *E*-**24** *Z*-**24**

SCHEME 13

A typical system for an unsymmetrical photochromic compound is molecule **32**. It is prepared by reaction of **21** with pyridosalicylidenanil.[42] Recently, unsymmetrical biphotochromic molecules combining spiroxazine-and spirodihydroindolizine structures have been prepared.[43]

1,5-Electrocyclization

The UV spectra of the dihydroindolizines **25**, X = CH, and dihydropyrrolo[1,2-b]pyridazine **25**, X = N, usually have absorption maxima in the near-UV between 360 and 410 nm. The betaines **35** produced by photochemical ring opening absorb at about 505 to 726 nm.

The σ-bonds in the various azoheterocycles that undergo photochemical cleavage are marked in Scheme 9. These cases differ significantly from the ring opening of the cyclopentenyl anion because, in previous molecules, no anion is formed. The photoproduced compounds from these electroneutral, five-membered heterocycles are zwitterions or betaines in all cases.

The ring opening of **25** occurs easily in solution, in polymers, and in rigid matrices at room temperature. In some cases, ring opening was also observed in the crystalline state.

Dürr and co-workers[35b] recently discovered the first intramolecular trapping of the key intermediate in the formation of indolizine photochromic compounds. Therefore, the reaction of substituted spirocyclopropenes with 1-(3,5-dinitrophenyl)-3,4-dihydroisoquinolines afforded not only the expected tetrahydroindolizines (THI) **26** but also novel fluorenespiroazanorcaradiene dyes **27,** which were proved to be formed via 1,6-electrocyclization as shown in Scheme 14.

Multiplicity of the Photochemical Reaction 25 → 24

The photochemical reaction for the ring opening of **25** to **24** was demonstrated to proceed via an excited singlet or a fast-reacting triplet state that does not undergo bimolecular quenching (for details, see Ref. 36 and 44a). The determination of the quantum yield for ring opening **25** → **24** was carried out using nonlinear optimization methods (details in Reference 45). The values for ϕ_R are on the order of 0.4 to

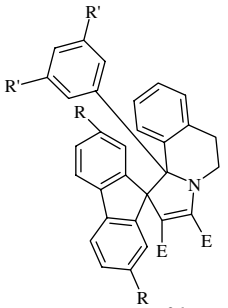

26

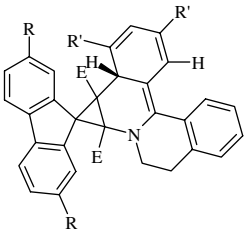

27

SCHEME 14

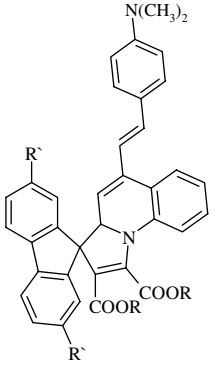

25A

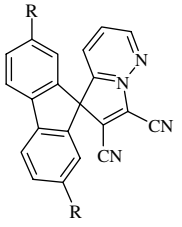

25B

SCHEME 15 Structure of the P_r chromophore of phytochrome.

0.8 for the forward reaction and 0.1 for the back reaction. The quantum yields are also wavelength dependent.

We have also shown that the amino-styryl –DHI **25A** undergoes ring opening to a blue betaine **25A′** showing for the first time fluorescence from the colored form. This has been used to develop *destruction*-free, dual-mode storage systems or switches.[44] Using films of **25A** in PMMA, a single molecule fluorescence was detected.[44] The use of the long-lived colored form, produced by irradiation of **25B** allowed the development of a holographic data storage system.[44] The photochemical switch based on the DHIs **25** is now well established.

An important system belonging to the class of five-membered heterocyclic interconversions are the phytochromes (P_R), which have been studied by Schaffner and Braslavsky et al.[46] These systems play an important biochemical role in regulating plant growth.[46]

4n + 2 System: (6 Atoms, 6 Electrons)

An electrocyclic (4n + 2)-reaction (n = 1) is also found in the spiropyrans **29**[47–50] as shown in Scheme 15. UV irradiation of the colorless or slightly yellow spiro compounds **29** leads to cleavage of the CO bond to give the open-chain molecule **30** that absorbs strongly in the visible region. These highly interesting photochromic spiropyrans have been studied very intensively.[1,50] This system has also led to a number of practical applications. Braeuchle et al., among others, have shown that an unstable intermediate with an orthogonally bridged structure is formed during ring opening of nitrobenzo-spiran at 4.2K.[51]

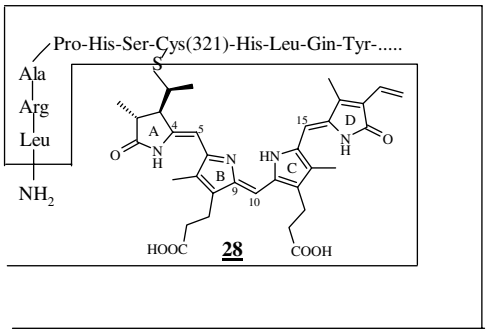

28

SCHEME 16

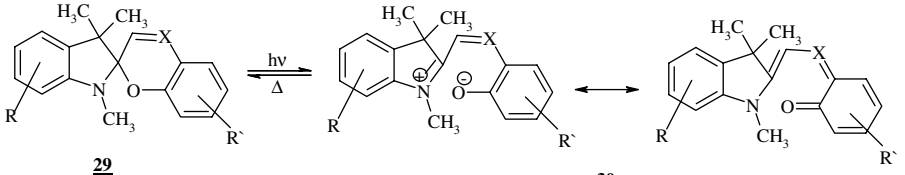

29 **30**

SCHEME 17 R and R′ can be a large number of organic groups; each ring can also contain several substituents.

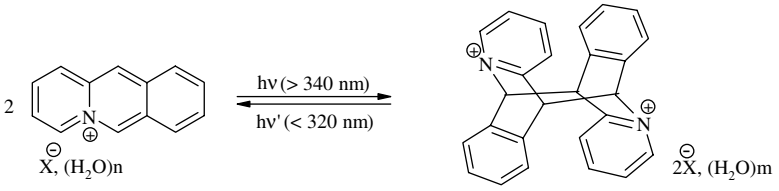

37 **38**

SCHEME 18

If in Scheme 17 X is N, the molecules **29** belong to the class of spirooxazines.[52–58] This photochromic system undergoes very fast ring opening to the colored form **30** with good quantum yield ($\phi_{R=}$ 0.2 to 0.8) in solution and in films. The color rapidly fades thermally. No photochromism is observed in the crystalline state. The spiroxazines have recently been studied with regard to solvatochromism,[58d] sol-gel inclusion,[58c] and semiempirical caclulations.[58a] In connection with good, long-term photostability, spirooxazines are of great commercial value. They belong to the best N-containing photochromic systems used today.[57] Recently, a series of spirooxazines has been investigated and their photochemical[58] properties have been discussed in detail. Related electrocyclizations were also studied with 1-nitro-2-aryl-alkenes.[59]

1,7-Electrocyclization

Recently, Dürr and co-workers[36,60] reported a new photochromic 8π-process based on an azaheptatriene 1,7-electrocyclization **31, 32**. This type of photochromic systems is formed by a pericyclic process. Other

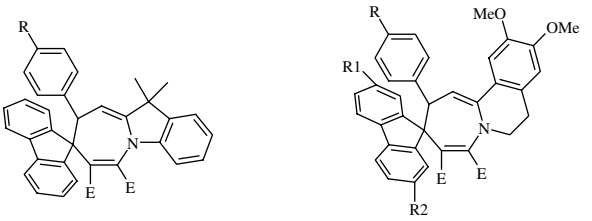

31 **32**

SCHEME 19

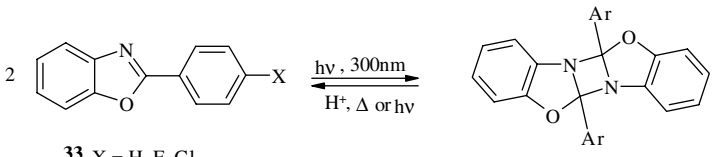

33 X = H, F, Cl **34** "ht"

SCHEME 20

reports on 8π-seven-atom photochromic systems (4n) are rare.[60] Only a very few molecules have been described and the reversibility of the processes involved has been established.[2]

Cycloadditions

[2 + 2]-Cycloadditions

The photodimerization of 2-phenylbenzooxazole **33** produces a head-tail photodimer **34** involving two carbon-nitrogen double bonds.[61]

The photodimer **34** is labile in fluid solution but thermally stable in the solid state at room temperature. This system has been proposed as a system for light-energy conversion, because the thermal reversion of the photodimer to the starting material **33** releases 116 kJ mol.$^{-1}$ A similar reversible [2+2]-cycloaddition has been reported for 1,1′-polymethylene-bisthymines (n = 2 to 6). The dimerization (λ = 300 nm) can be reversed by irradiation with 254-nm light.[62]

[4 + 4]-Cycloaddition

2-Aminopyridine as the HCl-salt can undergo a [4+4]-photodimerization.[63] The diphosphate or dimethanesulfate of the dimer **36** can be cleaved by short wavelength irradiation. Chandross has used this reversible photoreaction, employing crystals of the dimer, to write holographic gratings.[64] In a [4+4]-cycloaddition, acridinium bromide **37** gave **38**.[65] Related studies were carried out with polymethylene-linked acrizidinium salts.[66]

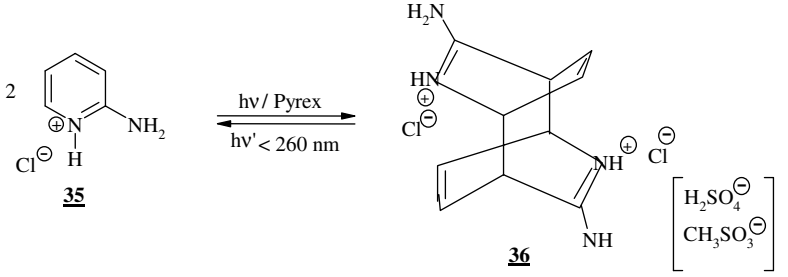

35 **36**

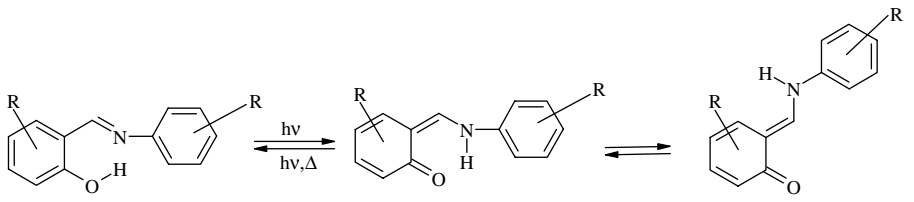

39
enol form

40
Keto form

SCHEME 21

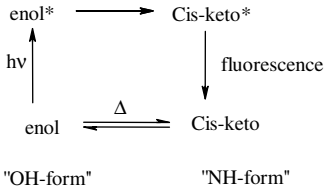

SCHEME 22

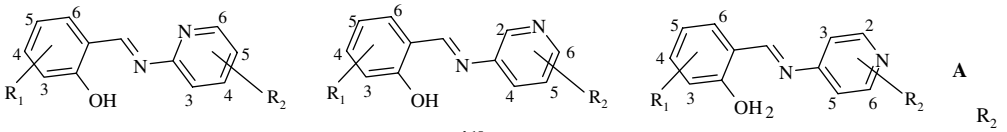

41a
salicylidene-2-aminopyridines

41b
salicylidene-3-aminopyridines

41c
salicylidene-4-aminopyridines

SCHEME 23

96.4 Tautomerism

Light-induced tautomerism can occur within the salicylidene-anilines in the form of prototropic rearrangements such as **39** → **40.**[67–72]

These molecules are photochromic in the crystalline state (α and β modification) and in rigid glasses. The large Stokes shift (F-spectrum) is explained by proton transfer in the excited state. The mechanism has been studied in great detail.[73]

Similar behavior is found in 2-, 3-, or 4-(salicylideneamino) pyridines.[73,74] However, compounds **41a,b,c** show only thermochromism in the crystalline state. In rigid glasses at low temperature, salicylideneanilines **41** are also photochromic.

Some theoretical studies,[74e] photochromism in sol-gel systems, and photochromic switching of salicylideneanils were reported recently.[67–74]

A related tautomerization occurs in aromatic nitro compounds **42.** It is designated as an acid/nitro phototautomerization (Scheme 24).[73]

An interesting tautomerism occurs in benzotriazoles (TINUVIN)* that are used as light filters in dye protection.[75] The tautomerism processes in porphyrins are the basis of a photochromic reaction used in hole burning.[76a] This process has been used for making a molecular computer. Dithizonates were used as photochromic materials in ophthalmic lenses.[76b]

*TINUVIN is the commercial name for benzotriazoles, which are used as light stabilizers in polymers and dyes.

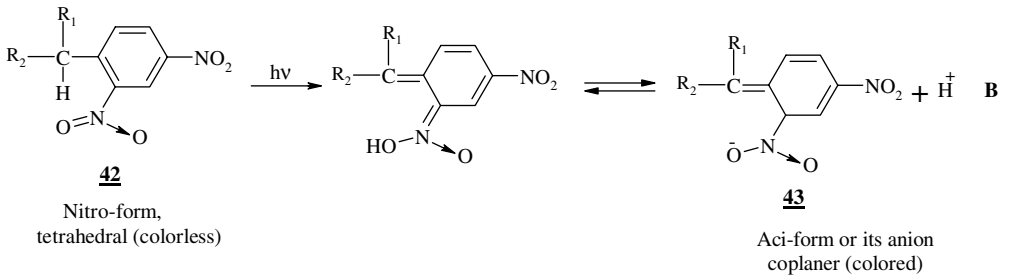

42

Nitro-form,
tetrahedral (colorless)

43

Aci-form or its anion
coplaner (colored)

SCHEME 24

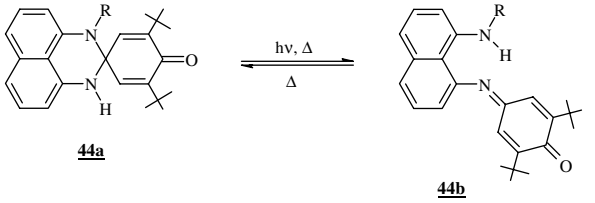

44a **44b**

SCHEME 25

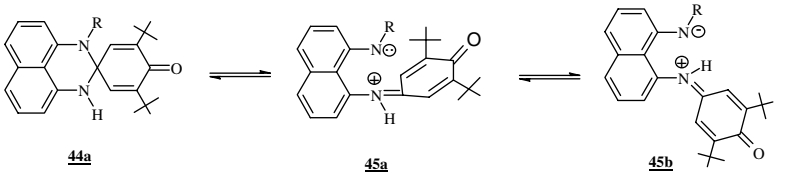

44a **45a** **45b**

SCHEME 26

Valence and prototropic tautomeric reactions are among the most important mechanisms that govern transformations of a broad variety of photochromic organic systems.[3,4] Until recently, no examples of photochromic compounds have been reported whose photochromic behavior was due to a combination of these two tautomeric reactions. Such a combination, which is characteristic of ring-chain/tautomerism,[77] a sigmatropic reaction, has been implemented in the photochromic and thermochromic rearrangements of a novel type of heterocyclic photochromes, derivatives of 2,3-dihydro-2-spiro-4′-(di-*tert*-butylcyclohexadien-one)perimidine **44a** and its analogues.[78] The occurrence of a proton transfer step is in accord with the fact that the *N,N′*-dimethyl derivative of **44a** exhibits no photochromic properties.

UV irradiation of an octane solution of **44a** (R = H or alkyl) changes its color from yellowish to deep blue. The initial spectrum is slowly restored at room temperature (the effective lifetime of the colored form at room temperature is about 10^4 s). The mechanism of the photochromic reaction involves cleavage of a C-N bond in the first singlet excited state of **45a**, followed by the conformational rearrangement of the resultant zwitterionic (biradical) intermediate **45b** that precedes the final step of the intramolecular proton transfer (Scheme 26).

It has, therefore, been concluded that any further modification of the photochromic compound **44a** should be associated with structural variations in its 2,3-dihydroperimidine moiety. In the course of subsequent studies, the spirocyclohexadienones **44a** have been found to display photo-and thermochromic properties.[77]

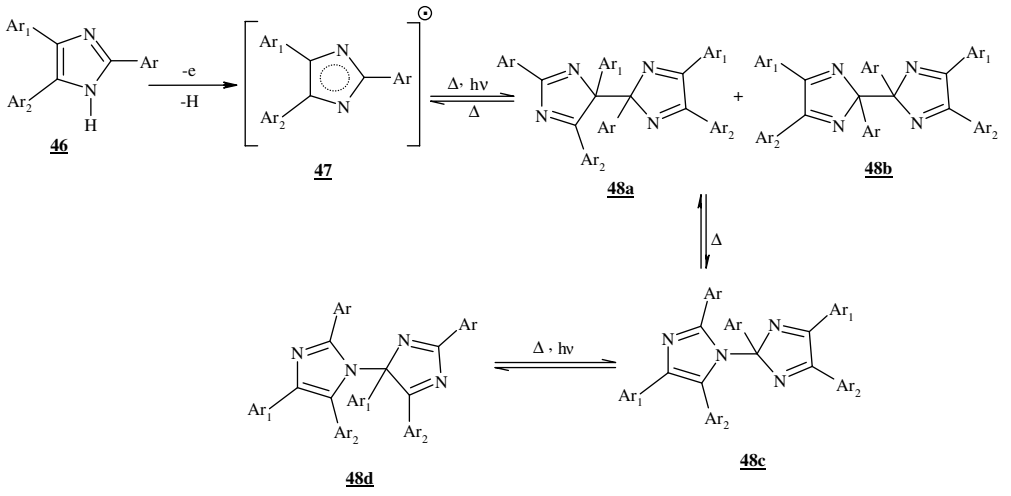

SCHEME 27

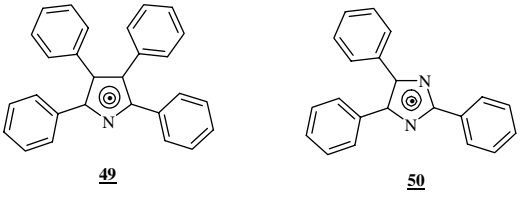

SCHEME 28

96.5 Dissociation/Homolytic Cleavage of Bonds

Homolytic and heterolytic dissociation processes play a role in the field of reactions responsible for the photochromic properties of various chemical compounds.[79]

Imidazoles **46** under oxidative condition form dimers **48** that are photochromic both in the crystalline state and in solution.[80] A long-lived intermediate **47** was assumed to be responsible for the observed purple color and the radical nature was proved by ESR methods.[80]

Typical examples of this type include the cleavage reactions of octaphenyl-1,1′-bipyrrolyl and of hexaphenyl-1,1′-biimidazolyl, which on exposure to light yield the colored free radicals **49** and **50**, respectively. These reactions form the basis of a photochromic system.[81] Photochromism is observed both in the crystalline state and in solution.

96.6 Electron Transfer/Redox Photochromism

The best photochromic system based on an electron transfer reaction is undoubtedly that of AgCl, which is decomposed by light according to Equation 963.[82]

$$\mathrm{AgCl} \xrightarrow{h\nu} \mathrm{Ag} + \dot{\mathrm{Cl}} \qquad (96.3)$$

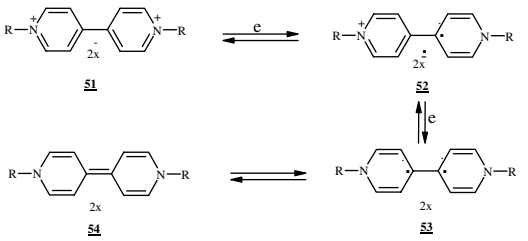

SCHEME 29

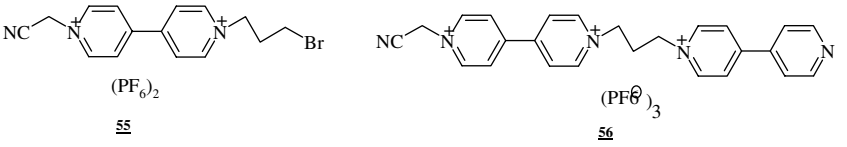

SCHEME 30

The photochromic mechanisms of redox-photochromic compounds are usually difficult to determine because they are often multicomponent systems. However, the methylene blue/iron sulfate system [83] is relatively well understood.

Nanasawa[84] has reported studies on new photochromic viologens such as 4,4′-bipyridine **51**, 2,2′-bipyridine, and 1,10-phenanthroline based on electron transfer. The colorless viologens composed of diquaternary salts turn into a violet-blue radical-anion **52** by one-electron reduction[81–86] and are further reduced to the yellowish quinonoid **54** via the biradical **53**. New results in crown ether containing viologenes,[84e] in the crystalline state[84c] as well as in polymer[84a,b,d,] were reported recently.

We have demonstrtaed that viologen dications **55** and bisviologen trications **56** (X = PF_6^-) in polyvinylpyrrolidone films give blue radical-cations on irradiation being thermally reversible, thus showing clear photochromism of this system.[87]

96.7 Application of Photochromic Materials

The inherent properties of photochromic systems make them suitable for use in many different areas. Thus, applications are directly dependent upon the color change caused by the molecular and electronic structures of the two species (A, B) and their corresponding absorption or emission spectra.

Typical applications include:

- Variable-transmission optical materials such as the photochromic ophthalmic lenses
- Camera filters
- Fluid flow visualization
- Optical information storage
- Novelty items (toys, T-shirts, etc.)
- Authentication systems (security printing inks)
- Cosmetics

Properties such as conductivity, refractive index, electrical moment, dielectric constant, chelate formation, ion dissociation, phase transitions, solubility, and viscosity can be changed as well. Certain physical changes that occur when the photochromic entity is chemically attached to the macromolecular backbone of polymers are of special interest. Some examples of possible applications utilizing these physical or chemical changes that accompany the observed shift in the absorption maxima are given below:

TABLE 96.1 Applications of Photochromic Materials

Control and Measurements of Radiation Intensities	Contrast Effects	Recording and Storage of Information
Optical filters	Masks for contrast equalization in photography	Imaging
Lenses	Film material	Instantaneous imaging material
Glasses		Office copying materials
Cuvettes	Amplifying contrast in projected images	Microfilm
	Projection screens	
Radiation protection equipment	Projection walls	Microfilm copying materials
Glasses		Sprays
Spectacles	Production of printing plates and circuit boards	Digital information
Films	Photoresists	Slow storage
Containers	Photopolymers	Bulk data storage (archives, etc.)
Protection from sun	Solar energy conversion	Holography
Protection from flash exposure, lasers, etc.	Energy storage	Storage disks
		Storage films
Document preservation		Crystals
Temperature indicators		Data display system
		Display screens (image screens)
Actinometry, dosimetry		Molecular computers
Actinometer		Q-switches (for lasers)
Dosimeter		Molecular electronics

Adapted from Reference 31a.

TABLE 96.2 Spectral Parameters of the Colored Forms of NOSI Compounds in Toluene at 294K

Compound		λ_{max}/nm	$\varepsilon_{max}/10^{-3}$dm^{-3} mol^{-1} cm^{-1} Fischer's Method	Intensity Variation
NOSI1	R=H	592 ± 1	NA[a]	31 ± 3
NOSI2		560 ± 1	32 ± 2	32 ± 3
NOSI3	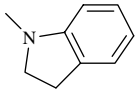	583 ± 1	48 ± 3	45 ± 4
NOSI4	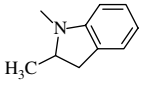	588 ± 1	43 ± 2	43 ± 4

[a] NA: not applicable.

- Optoelectronic systems (semi-conductor modulated by photochromic pigments).
- Reversible holographic systems.
- Photochemically switchable enzymatic systems.
- Nonlinear optical devices

The use of photochromic molecules such as spirooxazines in combination with chromenes in ophthalmic plastic lenses has been a major commercial breakthrough for photochromic molecules. Thus, these molecules are manufactured worldwide; leading firms include Ttransitions, Rodenstock, and Essilor (see Tables 96.1, 96.2, and 96.3). Practical use in dental materials has been reported as well.

Some commercial applications as well as potential applications of simple and very sophisticated applications are collected in Table 96.1 while some selected properties of commercially interesting molecules are given in Tables 96.2 and 96.3.

TABLE 96.3 Kinetic and Photochemical Parameters of NOSI Compounds at 352 nm in Toluene at 294K

Compound	ϕ_B/ϕ_A	$\phi_A + \phi_B = \phi_A$	$k(s^{-1})$
NOSI1	NA	0.23 ± 0.10	0.270 ± 0.010
NOSI2	0.03 ± 0.01	0.42 ± 0.20	0.044 ± 0.002
NOSI3	<0.04[a]	0.20 ± 0.10	0.077 ± 0.004
NOSI4	0.07 ± 0.05	0.85 ± 0.20	0.099 ± 0.004

[a] Measured in polyurethane matrix.
Adapted from Reference 58.

The application of photochromics in data storage, information recording, and holographic data storage is very promising and commercial applications in this field are anticipated in the near future.

Optical computers using photochromes are under active study. So, the field is moving forward and promises a series of applications to be marketed in the near future.

References

1. Brown, G.H., *Photochromism*, Wiley Interscience, New York, 1971.
2. Dürr, H. and Bouas-Laurent, H., Eds., *Photochromism — Molecules and Systems,* Elsevier, Amsterdam,1990.
3. El'tsov, A.V., *Organic Photochromes*, Plenum, New York, 1990.
4. McArdle, C.B., Ed., *Applied Photochromic Polymer Systems*, Blackie, New York, 1992.
5. Crano, J.C. and Guglielmetti, R.J.,Eds., *Photochromic and Thermochromic Compounds,* Vols. I and II., Plenum Press, New York, 1999.
6. Fritsche, M., *Compt. Rend. Acad. Sci.*, 69, 1035, 1868.
7. Dürr, H., Perspektiven auf dem Gebiet der Photochromie: 1,5-Elektrocyclisierung von heteroanalogen Pentadienyl-anionen als Basis eines neuartigen Systems, *Angew. Chem.*, 101, 427, 1989, *Angew. Chem. Int. Ed. Engl.*, 28, 413, 1989; Dürr, H., A new photochromic system: potential limitations and perspectives, *Pure Appl. Chem.*, 62, 1477, 1990.
8. Osuka, A., Fujikane, D., Shinmori, H., Kobatake, S., and Irie, M., Synthesis and photoisomerization of dithienylethene-bridged diporphyrins, *J. Org. Chem.*, 66, 3913, 2001.
9. Irie, M., Diarylethenes for memories and switches, *Chem. Rev.*, 100, 1685, 2000, and the references therein.
10. Horii, T., Abe, Y., and Nakao, R., Theoretical quantum chemical study of spironaphthoxazines and their merocyanines; thermal ring-opening reaction and geometric isomerization, *J. Photochem. Photobiol., A: Chem.*, 144, 119, 2001.
11. Ortica, F., Levi, P., Gugielmetti, R.J., Mazzucato, U., and Favaro, G., Photokinetic behaviour of biphotochromic supramolecular systems. 2. A bis-benzo-[2*H*]-chromene and a spirooxazine-chromene with a (*Z*-)ethenic bridge between each moiety, *J. Photochem. Photobiol., A: Chem.*, 139, 133, 2001, and the references therein.
12. Dürr, H. and Ma, Y., *Deutsche Offenlegungsschrift,* 4444 244.09, 1994; Ma, Y., Cortellaro, G., and Dürr, H., Preparation of photochromic molecules with polymerizable organic functionalities, *Synthesis*, 294, 1995; Dürr, H., Nitrogen-containing photochromic systems, *Handbook of Organic Photochemistry and Photobiology,* Horspool, W.M., Song, P.-S., Eds., CRC Press, Boca Raton, FL, 1995, 1121; Irie, M., *ibid*,, 1995; Bleisinger, H., Scheidhauer, P., Dürr, H., Wintgens, V., Valat, P., and Kossanyi, J., Photophysical properties of biphotochromic dihydroindolizines. Ring opening into extended betaines, *J. Org. Chem.*, 63, 990, 1998; Fromm, R., Born, R., Dürr, H, Kannengießer, J., Breuer, H-D, Valat, P., and Kossanyi, J., Spirodihydroazafluorenes-a new type of *cis*-fixed photochromic molecule with rigid region B showing extremely fast back reaction, *J. Photochem. Photobiol., A: Chem.*, 135, 85, 2000; Ahmed, S.A., Hartmann, Th., Huch, V., Dürr.H., and Abdel-Wahab, A.A., Synthesis of IR-sensitive photoswitchable molecules: photochromic 9′-styrylquinolinedihydroindolizines, *J. Phys. Org. Chem.*, 13, 539, 2000;

Ahmed, S.A., Photochromism of dihydroindolizines. II. Synthesis and photophysical properties of new photochromic IR-sensitive photoswitchable substituted fluorene-9′-styrylquinoline- dihydroindolizines, *ibid.*, 15, 392, 2002; Ahmed, S.A., Abdel-Wahab, A.A., and Dürr, H., Steric substituent effects of new photochromic tetrahydroindolizines leading to tunable photophysical behavior of the colored betaines, *J. Photochem. Photobiol., A: Chem.*, 154, 131, 2003.

13. Heller, H.G. and Jottaway, M., Intramolecular (4+4) photocycloaddition reactions of the photochromic compounds, 3,4-bis(9-anthrylmethylene)tetrahydrofuran-2,5-dione and its 5-dicyanomethylene derivative, *J. Chem. Soc., Chem. Commun.*, 479, 1995; Stauffer, M.T., Grosko, J.A.K., Ismail, Z., and Weber, S.G., Optical switching of the redox activity of a hydroxychromene, *ibid,,* 1695, 1995; Van Gemert, B. and Knowles, D.B., U.S. Patent, 5 395 567, 1995; Malatesta, V., Renzi, F., Wis, M.L., Montanari, L., Milosa, M., and Scotti, D., Reductive degradation of photochromic spirooxazines. Reaction of the merocyanine forms with free radicals, *J. Org. Chem.*, 60, 5446, 1995; Wilkinson, F., Worrall, D.R., Hobley, J., Janzen, L., Williams, S.L., Langley, A.J., and Matousek, P., Picosecond time-resolved spectroscopy of the photocolouration reaction of photochromic naphthoxazine-spiro-indolines, *J. Chem. Soc., Faraday Trans.,* 92, 1331, 1996.
14. Luchina, V.G., Sychev, I. Yu., Shienok, A.I., Zaichenko, N.L., and Marevtsev, V.S., Photochromism of spironaphthooxazines having electron-donor substituents, *J. Photochem. Photobiol., A: Chem.*, 93, 173, 1996; Chamontin, K., Lokshin, V., Samat, A., Guglielmetti, R.J., Dubest, R., and Aubard, J., Synthesis and photochromic properties of new spiro[azahomoadamantane-naphthoxazines], *Dyes Pigm.*, 43, 119,1999; Nakao, R., Horii, T., Kushino, Y., Shimaoka, K., and Abe, Y., Synthesis and photochromic properties of spironaphth[1,2-b]oxazine containing a reactive substituent, *ibid.*, 52, 95, 2002.
15. Articles: Murray, R.D., *Silverless Imaging Systems, Neblette's Handbook Photogr. Reprogr.,* 7th ed., 1977, 397; Barachevskii, A.S., Lashkov, G.I., and Tsekhomskii, V.A., Photochromism and Its use, *Izd. Khimiya, Moscow*, 1977; Heller, H.G., The development of photochromic compounds for use in optical in formation stores, *Chem. Ind.* (London), 193, 1978; *Chem. Abstr.,* 89, 1978; Workshop in Photochromism, ISOP I, Les Embiez, France, 1993; ISOP II, Clearwater Beach, FL, 1996 and ISOP III, Fukuoka, Japan, 1999; Workshop on Photochromics, Xth IUPAC Symposium on Photochemistry, Interlaken, 1984; Marcus, L.H., Photochromic materials. June 1976-May 1980 (citations from the NTIS data base), Gov. Rep. Announce. Index (U.S.) 80, 5760, 1980; Photochromic materials June 1970–June 1980 (citations from the Engineering Index data base), *Chem. Abstr.*; 94, 130192r, Photochromic materials June 1976-May 1980 (citations from the NTIS database), *Chem. Abstr.*, 94, 130193s, Photochromic materials. June 1974-May 1980 (citations from the International Aerospace Abstracts data base), *Chem. Abstr.,* 94, 130196v (1981); Kholmanskii, A.V. and Dyumaev, K.M., The nature of the primary photochemical step in spiropyranes, *Russ. Chem. Rev*; 50, 305, 1981; El'tsov, A.V., Bren, V.A., and Gerasimenko, Y.E., *Organic Photochromic Substances,* P.P. Khimiya, Leningradskoe, Otdelenie, Leningrad, 1982, 285; *Chem. Abstr.,* 99, 1983, B: 4775y; Smets, G., Photochromic phenomena in the solid phase, *Adv. Polym. Sci.,* 50, 17, 1983; Fischer, E., Photochromism and other reversible photoreactions in the dianthrylidenes and implications regarding environmental control of photoreactions, color-structure correlations and other points, *Rev. Chem. Intermed.,* 5, 393, 1984; Ayyangar, N.R., Srinivasan, K.V. C., *Chem. Rev.*, 36, 39, 1989; Hu, A.T. and Lee, H-J., *Phys. Sci. Eng.,* 21, 185, 1997; Maeda, S., Spirooxazines, *Organic Photochromic and Thermochromic Compounds*, Crano, J.C. and Guglielmetti, R.J, Eds., Plenum Publishing; New York, 85, 1999; Kawata, S. and Kawata, Y., Three-dimensional optical data storage using photochromic materials, *Chem. Rev.,* 100, 1777, 2000; Ichimura, K., Photoalignment of liquid-crystal systems, *Chem. Rev.,* 100, 1847, 2000; Tamai, N., Miyasaka, H., Ultrafast dynamics of photochromic systems, *Chem. Rev.*, 100, 1875, 2000; Berkovic, G., Krongauz, V., and Weiss, V., Spiropyrans and spirooxazines for memories and switches, *Chem. Rev.,* 100, 1741, 2000; Delaire, J.A. and Nakatani, K., Linear and nonlinear optical properties of photochromic molecules and materials, *Chem. Rev.*, 100, 1817, 2000; Malatesta, V., Hobley, J., and Salemi-Devaux, C., The chemistry of photomerocyanines, *Mol. Cryst. Liq. Cryst. Sci.,* 344, 69, 2000; Yi, Yu-R. and Lee,

In-Ja., Photoreactions of spirophenanthrooxazine dispersed in polystyrene film at room temperature, *J. Photochem. Photobiol., A: Chem.*, 151, 89, 2002.

16. Rau, H., Azo compounds, in *Photochromism-Molecules and Systems*, Dürr, H. and Bouas-Laurent, H., Eds., Elsevier, Amsterdam, 1990, chap.4.
17. Shinkai, S., Okawa, T., Kusano, Y., Manabe, O., Kikuwa, K., Goto, T., and Matsudo, T., Photoresponsive crown ethers.5. Light-driven ion transport by crown ethers with a photoresponsive anionic cap, *J. Am. Chem. Soc.,* 104, 1960, 1982;(b) Ball, P. and Nicholls, C.H., Photochromism of the azo tautomer of 4-phenylazo-1-naphthol and its *o*-methyl ether in solvents and polymer substrates, *Dyes Pigm.*, 6, 13, 1985; (c) Amato, C., Fissi, A., Vaccari, L., Balestrei, E., Pieroni, O., and Felicioli, R., Modulation of a proteolytic enzyme activity by means of a photochromic inhibitor, *J. Photochem. Photobiol., A: Chem.*, 28, 71, 1995; (d) Wang, Y., Q, Yu.H. Z., Mu, T., Zhao, C.X., and Liu, Z.E.F., Photochromic and electrochemical behavior of a crown-ether-derived azobenzene monolayer assembly, *J. Electroanal. Chem.,* 438, 127, 1997; (e) Tanaka, M. and Yonezawa, M., Photochemical regulation of ion transport through "quasi-channels" embedded in black lipid membrane, *Mater. Sci. Eng.,* C4, 297, 1997; (f) Kinoshita, T., Photoresponsive membrane systems, *J. Photochem. Photobiol., A: Chem.*, 42, 12, 1998; (g) Aoshima, Y., Egami, C., Kawata, Y., Sugihara, O., Tsuchimori, M., Watanabe, O., Fujimura, H., and Okamoto, N., Two-way optical memory for azobenzene-containing urethane-urea copolymer films, *Optics Comm*., 165, 177, 1999; (h) Angiolini, L., Caretti, D., Giorgini, L., Salatelli, E., Altomare, A., Carlini, C., and Solaro, R., Optically active polymethacrylates with side-chain-lactic acid residues connected to push-pull azobenzene chromophores, *Polymer*, 41, 4767, 2000; (i) Tomov, A.V. and Voitenkov, A.I., All-optical modulation in azo-dye-doped polymer waveguides, *Optics Comm.,* 174, 133, 2000; (j) Buruiana, T., Buruiana, E.C., Arinei, A., and Grecu, I., Synthesis and characterization of some polyurethane cationomers with photochromic azoaromatic groups, *ibid.*, 37, 343, 2001; (k) Yuxia, Z., Zhao, L., Ling, Q., Jianfen, Z., and Jiayun, Z., Synthesis and characterization of a novel nonlinear optical polyurethane polymer, *Eur. Polym.J.*, 37, 455, 2001; (l) Xie, H., Liu, Z., Huang, X., and Guo, J., Synthesis and non-linear optical properties of four polyurethanes containing different chromophore groups*., ibid*, 37, 497, 2001; (m) Matusi, T., Nagata, T., Ozaki, M., Fujii, A., Onada, M., Teraguchi, M., Masuda, T., and Yoshino, K., Novel properties of conducting polymers containing azobenzene moieties in side chain, *Synth. Metals*, 119, 299, 2001
18. Labasky, J., Mikes, F., and Kalal, J., The photochromism of spiropyrans bound on side chains of soluble polymers, *Polym. Bull.,* 4, 711, 1981; (b) Henry D. and Lecrivain, C., (Corning S.A., Fr.) WO 2001092372; (c) Pieroni, O., Fissi, A., and Ciardelli, F., Photochromic poly(-amino acid)s: photomodulation of molecular and supramolecular structure, *React. Funct. Polym.*, 26, 185, 1995; (d) Shinkai, E. and Manabe, O., *Top. Curr. Chem.,* 121, 67, 1984; (e) Altomare, A., Solaro, R., Angiolini, L., Caretti, D., and Carlini, C., Photoresponsive properties of optically active (meth)acrylic homopolymers with pendent-lactic acid or alanine residues connected to 4-aminoazobenzene, *Polymer*, 36, 3819, 1995; (f) Usui, M., Shindo, Y., Suzuki, Y., and Yamagishi, T., Syntheses and reactions of diazaanthracenophanes. 8. Syntheses and photochromism of diazaanthracenoparacyclophanes having a substituent on a phenyl ring, *Dyes Pigm.*, 30, 55, 1996; (g) Röttger, D. and Rau, H., Photochemistry of azobenzenophanes with three-membered bridges *J. Photochem. Photobiol., A: Chem.*, 101, 205, 1996; (h) Kurihara, S., Nomiyama, S., and Nonaka, T., *Proc. SPIE-Int. Soc. Opt. Eng.,* 4107, 69, 2000; (i) Nagata, T., Matsui, T., Ozaki, M., Yoshino, K., and Kajzar, F.; (j) Novel optical properties of conducting polymer-photochromic polymer systems, *Synth. Metals*, 119, 607, 2001; (k) Bobrovsky, A. Yu., Boiko, N.I., and Shibaev, V.P., Dual photochromism of copolymers containing two different types of photoisomerizable side groups, *J. Photochem. Photobiol., A: Chem.*, 138, 261, 2001; (l) Kim, S.-H., Suh, H.-J., Cui, J.-Z., Gal, Y.-S., Jin, S.-H., and Koh, K., Crystalline-state photochromism and thermochromism of new spiroxazine, *Dyes Pigm.*, 53, 251, 2002.
19. Griffin, G.W., Nishiyama, K., and Ishikawa, K., A potential precursor for 2,3-diphenyloxirene, *J. Org. Chem*., 71, 180, 1977.

20. Cromwell, N.H. and Cauglhilan, J.A., Ethylene imine ketones, *J. Am. Chem. Soc.*, 67, 2225, 1945; Cromwell, N. H. and Hocksma, H., Ethylene imime ketones. IV. Isomerism and absorption spectra, *J. Am. Chem. Soc.,* 71, 708, 1949.
21. Trozzolo, A.M., Yager, W., Griffin, G., Kristinsson, H., and Sarkar, I., Direct evidence for the formation of diphenylmethylene in the photolysis of triphenyl- and teraphenyloxirane, *J. Am. Chem. Soc.,* 89, 3357, 1967; Do Minh, T. and Trozzolo, A.M., Photochromic aziridines. I. Mechanism of photochromism in 1,3-diazabicyclo[3.1.0]hex-3-enes and related aziridines, *J. Am. Chem. Soc.,* 94, 4046, 1972.
22. Trozzolo, A.M., Leslie, T.M., Sarpotdar, A.S., Small, A.D., Ferraudi, G.J., Do Minh, T., and Hartless, R.L., Photochemistry of some three membered ring heterocyles, *Pure Appl. Chem.,* 51, 261, 1979.
23. Trozzolo, A.M., Sarpotar, A.S., Leslie, T.M., Hartless, R.L., and Do Minh, T., The photochemistry of aryl substituted three-membered hetrocycles, *Mol. Cryst. Liq. Cryst.,* 50, 201, 1979.
24. Padwa, A. and Hamilton, L., *J. Heterocyclic Chem.,* 4, 118, 1967.
25. Lown, J. W. and Matsumoto, K., Thermally disallowed valence tautomerization of an indano[1,2-b]aziridine to an isoquinolinium imine, *J. Org. Chem.,* 36, 1405, 1971.
26. Padwa, A. and Vega, E., Photochromic aziridines. The photochemical valence tautomerization and cycloaddition reactions of a substituted indano[1,2-b]aziridine, *J. Org. Chem.,* 40, 175, 1975.
27. Hauck, G. and Dürr, H., *Angew. Chem.,* 91, 1010, 1979; *Angew. Chem. Int. Ed. Engl.,* 18, 945, 1979; Dürr, H. and Hauck, G., *Deutsche Offenlegungs Schrift,* 29 06 193, 1979; Dürr, H., 4n + 2 Systems based on 1,5-electrocyclization, in *Photochromism — Molecules and Systems,* Dürr, H. and Bouas-Laurent, H., Eds., Elsevier, Amsterdam, 1990, 210.
28. Dürr, H., *Wiss. Zeitschr. TH Leuna- Merseburg.,* 26, 664, 1984; Dürr, H., *Praxis d. Naturwiss.*, 40, 22, 1991; Dürr, H., Kranz, C., and Kilburg, H., Supramolecular aggregates and ion binding in photochromic molecules, *Mol. Cryst. Liq. Cryst.*, 298, 89, 1997; Deniel, M.H., Tixier, J., Lavabre, D., Micheau, J.C., and Dürr, H., Kinetic modelling of the photochromism of dihydroindolizines, *Mol. Cryst. Liq. Cryst.,* 298, 129; 1997; Rustemeyer, F. and Dürr, H., A simple qualitative nicotine-test for demonstration in lectures, *EPA Newsletter*, 66, 37,1999; Gogritchiani, E., Samsoniya, Sh., and Dürr, H., Preparation of bis-[spirofluorene-9,4-(1-aza-cyclopentene[1,5a]indoline-8′-yl] sulfone, *Org. Prep.*, 32, 29, 2000; Samsoniya, Sh.A., Gogritchiani, E.O., and Katsadze, E.G., New indole derivates synthesis of photochromic 2-arylindole systems, *Chem. Heterocyclic Compounds,* 1562, 2000; Fedorova, O.A., Fedorov, Y.V., Andrenjktima, E.N., Bobrovsky, M.B., Gromov, S., Alfimov, M.V., Born, R., and H. Dürr., Novel 2-styryl thiazoles and dihydroindolizines in cooperating 15-crown-5-ethers, private communication, 2002.
29. For a review, see Taylor, E.C. and Turchi, I.J., 1,5-Dipolar cyclizations, *Chem. Rev.,* 79, 181, 1979; Huisgen, R., 1,5-Electrozyklisierungen — ein wichtiges Prinzip der Heterozyklenchemie, *Angew. Chem.,* 92, 979, 1980.
30. Dürr, H., Gombler, W., and Sergio, R., *Angew. Chem.,* 84, 215, 1972; Dürr, H. and Gleiter, R., *Angew. Chem.*, 94, 591, 1978; *Angew. Chem. Int. Ed. Engl.,* 17, 1978; Gross, H. and Dürr, H., Neue Synthese von Spiro(1,8a)dihydroindolizinen; ein neues, photochemisch schaltbares System, *Angew. Chem.*, 94, 204, 1982; *Angew. Chem. Int. Ed. Engl.,* 21, 216, 1982; Dürr, H., Gross, H., and Hauck, G., New heterocyclic systems from electrophilic cyclopropenes and N-nucleophiles, *Chem. Ber.,* 116, 856, 1983; Dürr, H., Gross, H., and Zils, K.D., *Deutsche Offenlegungs Schrift Pat.* 32 20 275 A 1 1983; Pozzo, J.L., Bouas-Laurent, H., Deffieux, A., Seidler.D., and Dürr, H., Living free-radical polymerization process. A new approach towards well-defined photochromic (co)polymers, *Mol. Cryst. Liq. Cryst.*, 298, 161,1997; Gogritchiani, E., Hartmann, Th., Palm, B., Samsoniya, Sh., and Dürr, H., Photochromic nucleic base units for nucleic acid labelling, *J. Photochem. Photobiol., B: Biol.,* 67, 18, 2002.
31. (a) Dürr, H., Gross, H., Zils, K.D., Hauck, G., and Hermann, H., Novel photochromic systems: tetra-, hexa- and octahydroindolizines, *Chem. Ber.,* 116, 3915, 1983; (b) Dürr, H., Jönsson, H.P., Scheidhauer, P., Münzmay; T., and Spang, P., *Deutsche Offenlegungs Schrift Pat.* 3521432 5, 1985; (c) Dürr, H., Janzen, K.P., Thome, A., and Braun, B., *Deutsche Offenlegungs Schrift Pat.* 3521432

5, 1988; (d) Dürr, H., Perspectives in photochromism: a novel system based on the 1,5-electrocyclization of heteteroanalogous pentadienyl, *Angew. Chem*., 101, 427, 1989*; Angew. Chem. Int. Ed. Engl.*, 28, 413, 1989; (e) Dürr, H. and Abdel-Wahab, A.A., Photochemical key steps, *Org. Synthesis,* 151, 1994.

32. Spang, P. and Dürr, H., Photochrome Systeme nach Mass: Erste bichromophore Spiro-1,8a-dihydroindolizine, *Angew. Chem.,* 96, 227, 1984; Dürr, H. and Spang, P., *Deutsche Offenlegungs Schrift Pat.* 32 20 2571, 1984; Münzmay, T., Spang, P., Holderbaum, M., Dürr, H., Raabe, E., and Krüger, C., Photochchromie einfacher 1,8a-dihydroindolizine bzw. 1,8a-dihydro-azaindolizine, *Chem. Ber.,* 121, 843, 1988.
33. Dürr, H., Schommer, C., and Münzmay, T., Dihydropyrazolopyridine und bis(dihydroindolizine) — neuartige mono- und difunktionelle photochrome Systeme, *Angew. Chem.*, 98, 565, 1986; *Angew. Chem. Int. Ed. Engl.,* 25, 572, 1986.
34. Dürr, H., Thome, A., Kilburg, H., Bossmann, S., Blasius, E., Janzen, K., and Kranz, C., Supramolecular effects in photochromism: properties of crownether modified dihydroindiolizines, *J. Phys. Org. Chem.,* 5, 689, 1992; Dürr, H., Photochromism — from the molecular to the supramolecular system, *Chimia*, 48, 514, 1994; Dürr, H., Amlung, M., Rustemeyer, F., and Tan, Y; Photochrome Verbindungen in Polymermatrices, *Deutsche Offenlegun-gsschrift*, 198 349 408, 1998.
35. (a) Burtscher, P., Dürr, H., Rheinberger, V., and Salz, U., Photochrome Dentalmaterialien (Fa. IVOCLAR) *German Patent* 195200160, 1995; (b) Bouas-Laurent, H. and Dürr, H., Organic photochromism, *Pure Appl. Chem.,* 73, 639, 2001; (c) Fromm, R., Ahmed, S.A., Hartmann, Th., Huch, V., Abdel-Wahab, A.A., and Dürr, H., A new photochromic system based on a pyridazinopyrrolo[1,2-b]pyridazine with ultrafast thermal decoloration, *Eur. J. Org. Chem.,* 4077, 2001; (d) Tan, Y., Ahmed, S.A., Dürr, H., Huch, V., and Abdel-Wahab, A.A., First intramolecular trapping and structural proof of the key intermediate in the formation of indolizine photochromics, *J. Chem. Soc., Chem. Commun.,* 1246, 2001.
36. Andreis, C., Dürr, H., Wintgens, V., Valat, P., and Kossanyi, J., New aspects of the photophysical properties of 1′H-2′,3′-dimethoxycarbonyl-spiro[fluorene-9,1′-pyrrolo[2,1-a]quinoline, *Chem. Eur. J.*, 3, 509, 1997; Weber, C., Rustemeyer, F., and Dürr, H., A light driven switch based on photochromic dihydroindolizines, *Adv. Mater.*, 10, 1348, 1998; Ma, Y., Weber, C., Hartmann, Th., Dürr, H., Krüger, C., and Kossanyi, J., Access to indoline-azepines — a new halochromic system for information recording, *Synthesis*, 1812, 2001.
37. Grellmann, K. H., Kühnle, W., Weller, H., and Wolf, T., Photochemical formation of dihydrocarbazoles from diphenylamines and their thermal rearrangement and disproportionation reactions, *J. Am. Chem. Soc.*, 103, 6889, 1981; Grellmann, K. H., Schmitt, M., and Weller, H., The photoinduced stereospecific formation of 9-ethyl-1,4a-dimethyl-4,4a-dihydrocarbazole from N-ethyl-2,6-dimethyldiphenylamine and its photoreactions, *J. Chem. Soc., Chem. Commun.,* 591, 1982; Schultz, A.G., Photochemical six-electron heterocyclization reactions, *Acc. Chem. Res.,* 16, 210, 1983; Minkin, V, I. and Komissarov, V. N., Perimidinespirocyclohexadienones a novel photo- and thermochromic system, *Mol. Cryst. Liq. Cryst.,* 297, 205, 1997; Sworakowski, J., Nespurek, S., Lipinski, J., and Lewanowicz, A., On the mechanism of bleaching reactions in a photochromic dihydropyridine derivative, *J. Photochem Photobiol., A: Chem.*, 129, 81, 1999; Ziane, O., Casalegno, R., and Corval, A., Multistep photoinduced proton transfer in crystalline 2-(2′,4′-dinitrobenzyl)pyridine, *Chem. Phys.,* 250, 199, 1999; Zhao, J., Zhao, B., Liu, J., Xu, W., and Wang, Z., Spectroscopy study on the photochromism of Schiff bases N,N′-bis(salicylidene)-1,2-diaminoethane and N,N′-bis(salicylidene)-1,6-hexanediamine, *Spectrochim. Acta*, 57, 149, 2001.
38. Dürr, H., Thome, A., Steiner, U., Ulrich, T., Krueger, C., and Raabe, E., 1H-Benzo(c)pyrazolo(1,2-a)cinnolines: A novel photochromic system, *J. Chem. Soc., Chem. Commun.,* 338, 1988; Ahmed, S.A, Preparation, characterization and photophysical studies of new photochromic di and tetrahydroindolizines, Ph.D thesis, Assiut University, Egypt, 2000.
39. Gilchrist, T.L. and Rees, C.W., Thermolysis of salts of 2-substituted acrylic acids. Novel reductions of a vinyl bromide, *J. Chem. Soc.,* C, 779, 1968; Bach, V., Dipolma thesis, University of Saarbücken, 1984.

40. Dürr, H., Schommer, C., and Münzmay, T., Dihydropyrazolopyridine und bis(dihydroindolizine) — neuartige mono- und difunktionelle photochrome systeme, *Angew. Chem.,* 98, 565, 1986 and *Angew. Chem. Int. Ed. Engl.,* 25, 572, 1986; Schommer, C., *Ph.D thesis,* University of Saarbrücken, 1987.
41. Dürr, H. and Spang, P., Photochrome Systeme nach Mass: erste bichromophore Spiro-1,8a-dihydroindolizine, *Angew. Chem.,* 96, 277, 1984; *Angew. Chem. Int. Ed. Engl.,* 23, 142, 1984; Weber, C., Dürr, H., and Bonneau, R., Calixochromes: synthesis, structure, supramolecular effects of biphotochromic Calix[4]arenes, *Synthesis*, 1005, 1999.
42. Holderbaum, M., Dürr, H., and Hadjoudis, E., Novel bi-photochromic systems: dihydroindolizines with a Schiff base moiety, *J. Photochem. Photobiol., A: Chem.,* 58, 37, 1991.
43. Dürr, H., Ma, Y., and Cortellaro, G., Preparation of photochromic molecules with polymerizable organic functionalities, *Synthesis*, 294, 1995.
44. Gross, H., Dürr, H., and Rettig, W., Photochromic systems. 8. Emission spectra of photochromic spiro[1,8a]dihydroindolizines and mechanism of the electrocyclic ring opening reaction, *J. Photochem.,* 26, 165, 1984; Hartmann, Th., Vom 5-Ring zum 7-Ring, Synthese, Photophysikalische Eignschaften Photochromer Dihydropyrrolizidine, -Dihydroindolizine und Tetrahydroazepinisochinotine. Ph.D thesis, University of Saarland, 2001.
45. Bär, R., Gauglitz, G., Benz, R., Polster, J., Spang, P., and Dürr, H., Photokineticsche Untersuchungen an photochromen Systemen der Dihydroindolizine, *Z. Naturforsch.,* A39, 662, 1984.
46. Braslavsky, S., Holzwarth, A.R., and Schaffner, K., Konformationsanalyse, Photophysik und photochemie der gallenpigmente; Bilirubin- und biliverdindimethylester und verwandte lineare tetrapyrrole, *Angew. Chem.,* 95, 670, 1984; *Angew. Chem., Int. Ed. Engl.,* 22, 656, 1983.
47. Bergmann, E.D., Weizmann, A., and Fischer, E., Structure and polarity of some polycyclic spirans, *J. Am. Chem. Soc.*, 72, 5009, 1950; Salemi, C., Giusti, G., and Guglielmetti, R.J., DABCO effect on the photodegradation of photochromic compounds in spiro[indoline-pyran] and spiro[indoline-oxazine] series, *J. Photochem. Photobiol., A: Chem.,* 86, 247, 1995; Zhou, J., Zhao, F., Li, Y., Zhang, F., and Song, X., Novel chelation of photochromic spironaphthoxazines to divalent metal ions, *J. Photochem. Photobiol., A: Chem.*, 91, 193, 1995; Srinivasan, M.P. and Lau, K.K. S., Molecular orientation in mixed LB films containing photochromic molecules, *Thin Solid Films*, 307, 266, 1997.
48. Fischer, E. and Hershberg, Y., Formation of colored forms of spirans by low-temperature irradiation, *J. Chem. Soc.,* 3129, 1954; Chamontin, K., Lokshin, V., Samat, A., Guglielmetti, R.J., Dubset, R., and Aubard, J., Synthesis and photochromic properties of new spiro[azahomoadamantane-naphthoxazines], *Dyes Pigm.*, 43, 119, 1999.
49. Bercovici, T., Heiligman-Rim, R., and Fischer, E., Photochromism in spiropyrans. VIII. Photochromism in acidified solutions, *Mol. Photochem.*, 23, 189, 1969; Minkovska, St., Kolev, K., Jeliazkova, B., and Deligeorgiev, T., Photochemical properties of a photochromic naphthoxazine upon UV irradiation in the presence of transition metal ions, *Dyes Pigm.*, 39, 25, 1998; Hattori, H. and Uryu, T., Synthesis and properties of photochromic liquid-crystalline polyacrylates containing a spirooxazine group, *J. Polym. Sci.,* 37, 3513, 1999; Gabbutt, C.D., Hepworth, J.D., Heron, B.M., Partington, S.M., and Thomas, D.A., Synthesis and spectroscopic properties of some merocyanine dyes, *Dyes Pigm.*, 49, 65, 2001.
50. Guglielmetti, R., in *Photochromism — Molecules and Systems,* Dürr, H. and Bouas-Laurent, H., Eds., Elsevier, Amsterdam, 1991, chap. 8.; Zhou, J., Sui, Q., and Huang, B; Photoinduced self-assembly of the supramolecular photochromic systems _ photoinduced dimer formation of the inclusion complexes of an indolinospiropyran with CDs, *J. Photochem. Photobiol., A: Chem.*, 117, 129, 1998; Tanaka, M., Kamada, K., Ando, H., Kitagaki, T., Shibutani, Y., and Kimura, K., Synthesis and photochromism of crowned spirobenzothiapyran: facilitated photoisomerization by cooperative complexation of crown ether and thiophenolate moieties with metal ions, *J. Org. Chem.*, 65, 4342, 2000; Nakatsuji, S., Ogawa, Y., Takeuchi, S., Akutsu, H., Yamada, J., Naito, A., Sudo, K., and Yasuoka, N., Novel photo-responsive organic spin systems: preparation and properties of norbornadienes and spiropyrans with TEMPO radical substituents, *J. Chem. Soc., Perkin Trans. 2*, 1969, 2000; Nespurek, S. and Sworakowski, J., Molecular current modulator consisting of conjugated

polymer chain with chemically attached photoactive side groups, *Thin Solid Films,* 393, 168, 2001; Ock, K., Jo, N., Kim, J., Kim, S., and Koh, K., Thin film optical waveguide type UV sensor using a photochromic molecular device, spirooxazine, *Synth. Metals*, 117, 131, 2001.

51. (a) Gehrtz, M., Bräuchle, C., and Volitländer, J., Photochromic forms of 6-nitrobenzospiropyran. Emission spectroscopic and ODMR investigations, *J. Am. Chem. Soc.,* 104, 2094, 1982; (b) Lenoble, C. and Becker, R.S., Photophysics, photochemistry, kinetics and mechanism of the photochromism of 6′-nitroindolinospiropyran, *J. Phys. Chem.,* 90, 62, 1986; (c) Häupl, T., Zimmermann, T., Hermann, R., and Brede, O., The photoisomerization of spiro[cyclohexadiene-indoline] via an intramolecular charge transfer state, *Chem. Phys. Lett*., 291, 215, 1998; (d) Tagaya, H., Nagaoka, T., Kuwahara, T., Karasu, M., Kadokawa, J., and Chiba, K., Preparation and photochromism of sulfonated spiropyran-silica nanocomposites, *Microporous Mesoporous. Mater.,* 21, 395, 1998; (e) Casades, I., Constantine, S., Cardin, D., Garcia, H., Gilbert, A., and Marquez, F., "Ship-in-a-Bottle." Synthesis and photochromism of Spiropyrans encapsulated within zeolite Y supercages, *Tetrahedron,* 56, 6951, 2000; (f) Tanaka, M., Nakamura, M., Salhin, A.M.A., Ikeda, T., Kamada, K., Ando, H., Shibutani, Y., and Kimura, K., Synthesis and photochromism of spirobenzopyran derivatives bearing an oxymethyl crown ether moiety: metal ion-induced switching between positive and negative photochromisms, *J. Org. Chem.,* 66, 1533, 2001; (g) Osnishi, Y., Yoshimoto, S., and Kimura, K., Novel compounds producing a photochromic spiropyran on heating, *J. Photochem. Photobiol., A: Chem.*, 141, 57, 2001.
52. Chu, N.Y., Photochromism of spiroindolinonaphthoxazine. I. Photophysical properties, *Can. J. Chem.,* 62, 300, 1983; Fox, R.E., Res. Rep. and Test., Final Report Contr. AF 41, 657, 1962, AD 444226; Antipin, S.A., Petrukhin, A.N., Gostev, F.E., Marevtsev, V.S., Titov, A.A., Barachevsky, V.A., Strokach, Yu, P., and Sarkisov, O.M., Femtosecond transient absorption spectroscopy of non-substituted photochromic spirocompounds, *Chem. Phys. Lett*., 331, 378, 2000.
53. Ono, H. and Osada, T., Photochromic Compound and Compounds, U.S. Patent 3562 172, 1971; Luchina, V.G., Sychev, I. Yu., Shienok, A.I., Zaichenko, N.L., and Marevtsev, V.S., Photochromism of spironaphthooxazines having electron-donor substituents, *J. Photochem. Photobiol., A: Chem.*, 93, 173, 1996.
54. Pottier, E., Du Best, R., Guglielmetti, R.J., Taridieu, P., Kellmann, A., Tfibel, F., Lenoir, P., and Aubard, J., Substituent, heteroatom and solvent effects on the thermal-bleaching kinetics and absorption spectra of photomerocyanines issued from spiro(indoline-oxazines), *Helv. Chim. Acta*, 73, 303, 1990; Hori, T., Tagaya, H., Nagaoka, T., Kadokawa, J., and Chia, K., Photochromism of sulfonated spiropyran in a silica matrix, *Appl. Surf. Sci.,* 121/122, 530, 1997.
55. Hovery, R.J., Chu, N.Y., Piusz, P.G., and Fudsmann, C.H., Photochromic Compounds, U. S. Patent 4342, 668, 1982; Kawanishi, Y., Seki, K., Tamaki, T., Sakuragi, M., and Suzuki, Y., Tuning reverse ring closure in the photochromic and thermochromic transformation of 1′,3′,3′-trimethyl-6-nitrospiro[2*H*-1-benzopyran-2,2′-indoline] analogues by ionic moieties, *J. Photochem. Photobiol., A: Chem.,* 109, 237, 1997.
56. Melzig, M. and Martinuzzi, G., Photochromic subst., *PCT Int. Appl*. WO 85 02 619, 1985.
57. Chu, N.Y., 4n + 2 systems: spiroxazines, in *Photochromism — Molecules and Systems*, Dürr, H. and Boaus-Laurent, H., Eds., Elsevier, Amsterdam, 1990,. chap. 10.
58. (a) Wilkinson, F., Hobely, J., and Naftaly, M., Photochromism of spiro-naphthoxazines: molar absorption coefficients and quantum efficiencies, *J. Chem. Soc., Faraday Trans.,* 88, 1511, 1992; (b) Goto, K., Kega, H., and Ichmura, K., Alignment photocontrol of a liquid crystal by spirooxazines monolayer, *Mol. Cryst. Liq. Cryst. Sci*., 345, 293, 2000; (c) Favaro, Ortica, F., and Favaro, G., Effect of gel-trapping on spectral properties and relaxation dynamics of some spiro-oxazines, *J. Phys. Chem.,* 104, 12179, 2000; (d) Metelotsa, A.V., Micheau, J.C., Voloshin, N.A., Voloshina, E.N., and Minkin, V.I., Kinetic and thermodynamic investigations of the photochromism and solvatochromism of semipermanent merocyanines, *J. Phys. Chem. A*, 105, 8417, 2001; (e) G., Levi, D., Ortica, F., Samat, A., Guglielmetti, R., and Mazzucato, U., Photokinetic behaviour of bi-photochromic supramolecular systems; 3. Compounds with chromene and spirooxazine units linked through ethane, ester and acetylene bridges, *J. Photochem. Photobiol., A: Chem.*, 149, 91, 2002.

59. Sousa, J., Weinstein, A., and Bluhm, A.L., The photochromism of 1-aryl-2-nitroalkenes, *J. Org. Chem.*, 34, 3320, 1969; Humphry-Baker, R.A., Salisbury, K., and Wood, G.P., Photochemical reactions of an α,β-unsaturated nitro compound, *J. Chem. Soc., Perkin Trans. 2*, 659, 1978; Zhou, J., Ting, Yi,. and Song, X., Investigation of the chelation of a photochromic spiropyran with Cu(II), *J. Photochem. Photobiol., A: Chem.,* 87, 37, 1995; Marevtsev, V.S. and Zaichenko, N.L., Peculiarities of photochromic behaviour of spiropyrans and spirooxazines, *J. Photochem. Photobiol., A: Chem.*, 104, 197, 1997; Tanaka, M., Kamada, K., Ando, H., Kitagaki, T., Shibutani, Y., Yajima, S., Sakamoto, H., and Kimura, K., Metal-ion stabilization of photoinduced open colored isomer in crowned spirobenzothiapyran, *J. Chem. Soc., Chem. Commun.,* 1453, 1999; Lee, J., Park, E., and Yoon, C., Suzuki coupling reaction of 6-iodo- or 6,8-diiodospiropyran: synthesis of spiropyran analogs, *Tetrahedron. Lett.*, 42, 8311, 2001.
60. Dürr, H., Photochromism of dihydroindolizines and related systems, in *Organic Photochromic and Thermochromic Compounds,* Vol. I, Crano, J.C., Guglielmetti, R.J., Eds., Plenum Press, New York, 1999, 223; Tan, Y., Hartmann, Th., Huch, V., Dürr, H., and Kossanyi, J., A new photochromic 8π-system based on an azaheptatriene – tetrahydroazepinoisoquinoline electrocyclization, *J. Org. Chem.,* 66, 1130, 2001.
61. Yano, E., Tatsura, K., and Ikegami, K., *Proc. of the XXth IUPAC Symp. on Photochem.,* Abstracts, Bologna, 1988, 232.
62. Beukers, R. and Berends, W., Effects of ultraviolet irradiation on nucleic acid and their components, *Biochem. Biophys. Acta*, 41, 550, 1960; 49, 181, 1961; Leonard, N.J., Mc Credie, R.S., Logne, M.W., and Cundall, R., Synthetic spectroscopic models related to coenzymes and base pairs. XI. Solid state ultraviolet irradiation of 1,1′-trimethylenebisthymine and photosensitized irradiation of 1,1′-polymethylenebisthymines, *J. Am. Chem. Soc.,* 95, 2320, 1973.
63. Ayer, W.A., Hayatsu, R., De Mayo, P., Peid, S.T., and Stothers, J.B., The photodimers of α-pyridones, *Tetrahedron Lett.,* 648, 1961; Taylor, E. and Kan, R.O., Photochemical dimerization of 2-amino-pyridines and 2-pyridines, *J. Am. Chem. Soc.,* 85, 776, 1963.
64. Tomlinson, W.J., Chandross, E.A., Frok, R.L., Pryde, C.A., and Lamola, A.A., *Appl. Optics*, 11, 543, 1972.
65. Bradscher, C.R., Beavers, L.E., and Jones, J.H., Acridinum salts, *J. Org. Chem.,* 22, 1740, 1957; Chandross, E.A., Frok, R.L., Lamola, A.A., and Tomlinson, N.J., Optical Storage Devices, U.S. Patent 3668 663, 1972.
66. Wagner, J., Bending, J., and Kreysig, D., Mechansimus der reversiblen intramolekularen [π4s + π4s] — Photocycloaddition von α,ω- Bis-(acridiziniumyl)-alkanen, *J. Prakt. Chem.,* 326, 747 and 757, 1984; Lahlou, S., Bitit, N., and Desvergne, J.-P., Syntheses and photoreactivity of new bisanthracenes incorporating one or two nitrogen atoms in the linkage, *J. Chem. Res.,* 302, 1998.
67. (a) Senier, A. and Shepheard, F.G., Studies in phototropy and thermotropy. I. Arylidene- and naphthylidene-amines, *J. Am. Chem. Soc.*, 95, 1943, 1909; 101, 1950, 1912; (b) Hadjoudis, E., Dziembowska, T., and Rozwadowski, Z., Photoactivation of the thermochromic solid di-anil of 2-hydroxy-5-methyl-isophthalaldehyde in cyclodextrin, *J. Photochem. Photobiol., A: Chem.*, 128, 97, 1999; (c) Hirai, M., Yuzawa, T., Haramoto, Y., and Nanasawa, M., Synthesis and photochromic behavior of methylmethacrylate copolymers having anils as pendant, *React. Funct. Polym.*, 45, 175, 2000; (d) Pang, S. and Liang, Y., Photochromic behavior of 2,4-dihydroxy-*N*-octadecylbenzylideneamine in Langmuir-Blodgett film, *Mat. Chem. Phys.*, 71, 103, 2001.
68. De Gaouck, V. and Le Fevre, R.J.W., The phototropy of anils and a note on the phototropy of solutions of the leuco-cyanides of malachite- and brilliant-greens, *J. Chem. Soc.*, 1457, 1939; Elmali, A. and Elerman, Y., Structure and conformation of N-(2-methyl-5-chlorophenyl)salicylaldimine, *J. Mol. Struct.*, 442, 31, 1998; Shen, M.Y., Zhao, L.Z., Goto, T., and Mordzinski, A., Photochromism in salicylideneaniline (SA) single crystals, *J. Luminescence*, 87–89, 667, 200; Elmali, A., Elerman, Y., and Teyrek, C.T., Conformational study and structure of *N*-(2,5-methylphenyl)salicylaldimine, *J. Mol. Struct.,* 443, 123, 1998; Kabak, M., Elmali, A., Elerman, Y., and Durlu, T.N., Conformational study and structure of bis-*N,N′-p*-bromo-salicylideneamine-1,2-diaminobenzene, *J. Mol. Struct.,* 553, 187, 2000.

69. Hadjoudis, E. and Hayon, E., Flash photolysis of some photochromic *N*-benzylideneanilines, *J. Phys. Chem.*, 74, 3184, 1970; Grabowska, A., Kownacki, K., Karpiuk, J., Dobrin, S., and Kaczmarek, L., Photochromism and proton transfer reaction cycle of new internally H-bonded Schiff bases, *Chem. Phys. Lett.*, 267, 132, 1997; Kabak, M., Elmali, A., and Elerman, Y., Tautomeric properties, conformations and structure of *N*-(2-hydroxyphenyl)-4-amino-3-penten-2-one, *J. Mol. Struct.*, 470, 295, 1998.
70. Rosenfeld, T., Ottolenghi, M., and Meyer, A.Y., Photochromic anils. Structure of photoisomers and thermal relaxation process, *Mol. Photochem.,* 5, 39, 1973; Lambi, E., Gegiou, D., and Hadjoudis, E., Thermochromism and photochromism of N-salicylidenebenzylamines and N-salicylidene-2-aminomethylpyridine, *J. Photochem. Photobiol., A: Chem.*, 86, 241, 1995; Goto, T. and Tashiro, Y., Photochromism of *N*-salicylideneaniline single crystal, *J. Luminescence.,* 72–74, 921, 1997.
71. Miller, L.J. and Margerum, D.J., *Tech. Chem.* (New York), 3, 557, 1971; Jaques, P., Biava, J.P., Goursot, A., and Faure, J., Investigation of tautomersim and photochromism exhibited by series of hydroxyazodyes. 1. Spectroscopic study and conformational analysis of fundamental states, *Chim. Phys. Phys. Chim. Biol.,* 76, 56, 1979; Jaques, P., Investigations of tautomersim and photochromism exhibited by a series of hydroxyazoic cationic dyes. II. Kinetic behavior, *Chim. Phys. Phys. Chim.*, 79, 352, 1982; Jaques, P., Substituent effects on the tautomersim and photochromism exhibited by a series of hydroxyazo cationic dyes for polyester fibers, *Dyes Pigm.*, 5, 351, 1984.
72. Lewis, J.W. and Sandorfy, J.W., A spectroscopic study of proton transfer and photochromism in *N*-(2-hydroxybenzylidene)aniline, *Can. J. Chem.*, 60, 1738, 1982; Becker, R.S., Lenoble, C., and Zein, A., A comprehensive investigation of the photophysics and photochemistry of salicylideneaniline and derivatives of phenylbenzothiazole including solvent effects, *J. Phys. Chem.*, 91, 3509, 1987; Pistolis, G., Gegiou, D., and Hadjoudis, E., Effect of cyclodextrin complexation on thermochromic Schiff bases, *J. Photochem. Photobiol., A: Chem.,* 93, 179, 1996.
73. Hadjoudis, E., Toutomerism by hydrogen transfer in anils, aci-nitro and related compounds, in *Photochromism-Molecules and Systems*, Dürr, H. and Bouas-Laurent, H., Eds., Elsevier, Amsterdam, 1990, chap. 17.
74. (a) Hadjoudis, E., Moustakali-Mavridis, I., and Xexakis, J., Effect of crystal and molecular structure on the thermochromism and photochromism of some salicylidene-2-aminopyridine, *Isr. J. Chem.,* 18, 202, 1979; (b) Moustakali-Mavridis, I., Hadjoudis, E., and Mavridis, A., Structure of thermochromic Schiff bases. II. Structures of N-salicylidine-3-aminopyridine and *N*-(5-methoxysalicylidene)-3-aminopyridine, *Acta Crystallogr.*, B36, 1126, 1980; (c) Hadjoudis, E., Photochromism and thermochromsim of *N*-salicylideneanilines and *N*-salicylideneaminopyridine, *J. Photochem.*, 17, 355, 1981; (d) Knyazhansky, M.I., Melelitsa, A.V., Lketskii, M.E., Millov, A.A., and Besugliy, S.O., The structural transformations and photo-induced processes in salicylidene alkylimines, *J. Mol. Struct.,* 526, 65, 2000; (e) Zgierski, M.Z. and Grabowska, A., Theoretical approach to photochromism of aromatic Schiff bases: A minimal chromophore salicylidene methylamine, *J. Chem. Phys.,* 113, 7845, 2000; (f) Hadjoudis, E., Verganelakis, V., Trapalis, C., and Kordas, G., *Mol. Eng.,* 8, 459, 2000; g) Poineau, F., Nakatani, K., Delaire, J.A., *Mol. Cryst. Liq. Cryst.*, 344, 89, 2002.
75. Kramer, H.E.A., Tautomerism by hydrogen transfer in salicylate, triazoles and oxazoles, in *Photochromism — Molecules and Systems*, Dürr, H. and Bouas-Laurent, H., Eds., Elsevier, Amsterdam, 1990.
76. (a) Wild, U., Spectral hole-burning, in *Photochromism — Molecules and Systems*, Dürr, H. and Bouas-Laurent, H., Eds., Elsevier, Amsterdam, 1990, chap. 28; (b) Meriwether, L.S. and Breitner, E.C., The photochromism of metal dithizonates, *J. Am. Chem. Soc.,* 87, 4448, 1965.
77. Volter, R.E. and Flitsch, W., R*ing-Chain Tautomerism*, Plenum Press, New York, 1985.
78. Minkin, V.I. and Komissarov, N., *Mol. Cryst. Liq. Cryst.,* 297, 205, 1979; Komissarov, V.N., Kharlanov, V.A., Ukhin, L.Yu., and Minkin, V.I., Detection of a ring-chain rearrangement of spiroperimidines in their ground and excited states, *Dokl. Akad. Nauk SSSR*, 301, 902, 1988; Salbeck, J., Komissarov, V.I., Minkin, V.I., and Daub, J., Molecular switching by eIectron transfer — the spiroperimidine/quinoneimine system, *Angew Chem. Int. Ed. Engl.,* 31, 1498, 1992; Komissarov, V.N., Gruzdeva, E.N., Kharlanov, V.A., Kogan, V.A., and Minkin, V.I., Synthesis, photo and thermochromic properties of derivatives of cyclohexa-2,5-dienoquinazolines, *Zh. Org. Khim.,* 29, 2030,

1993; Minkin, V. and Komissarov, V.N., Perimidinespirocyclohexadienones — a novel photo- and thermchromic system, *Mol. Cryst. Liq. Cryst.,* 297, 205, 1997; Metelitsa, A.V., Komissarov, V.N., Knyazhansky, M.I., and Minkin, V.I., New photochromic bisspirocyclic systems, *Mol. Cryst. Liq. Cryst.,* 297, 205, 1997; Kharlanov, V.A., Effect of molecular oxygen on the kinetics of dark transformation of quinonimine structure and spiran structure for photochromic spirans of perimidine series, *Zh. Org. Khim*., 35, 631, 1999.

79. Eigenmann, G., in *Photochromism*, Brown, G.H., Ed., New York, 1971, 433; Bertelson, R.C., *ibid*, 1971, 49; Aldag, R., in *Photochromism — Molecules and Systems*, Dürr, H. and Bouas-Laurent, H., Eds., Elsevier, Amsterdam, 1990, 713,.
80. Dreyer, J.F. and Baltzer, D.H., U.S Patent 3,436, 353, 1969; Maeda, K., Chinone, A., and Hayashi, T., The photochromism, thermochromism and piezochromism of dimers of tetraphenylpyrryl, *Bull. Chem. Soc. Jpn.,* 43, 429, 1970.
81. Blinder, S.M. and Lord, N.W., Electron spin resonance of tetraphenylpyrryl radical, *J. Chem. Phys*., 36, 540, 1961.
82. Gliemeroth, G. and Mader, K.H., Phototropes glass, *Angew. Chem.,* 82, 421, 1970; *Angew. Chem., Int. Ed. Engl.*, 9, 434, 1970.
83. Parker, C.A., Photoreduction of methyleneblue. Some preliminary experiments by flash photolysis, *J. Chem. Phys.*, 63, 26, 1959.
84. (a) Nanasawa, M., Kaneko, M., and Kamogawa, H., Effect of temperature on the color developed by near ultraviolet light for 4,4′-bipyridinium salts (viologens) embedded in poly(1-vinyl-2-pyrrolidone) matrix, *Bull. Chem. Soc. Jpn.,* 66, 2443, 1993; (b) Bhowmik, P.K., Molla, A.H., Han, H., Gangoda, M.E., and Bose, R.N., Lyotropic liquid crystalline main-chain viologen polymers: homopolymer of 4,4′-bipyridyl with the ditosylate of *trans*-1,4-cyclohexanedimethanol and its copolymers with the ditosylate of 1,8-octanediol, *Macromolecules*, 31, 621,1998; (c) Polishchuk, I.Yu., Grineva, L.G., Polishchuk, A.P., and Chernega, A.N., Products of quaternization of 4,4′-bipyridine with halogenated carboxylic acids. Synthesis, structure and photoreduction in the crystalline state, *Russ. J. Gen. Chem*., 68, 609, 1998; (d) Suzuki, M., Kimura, M., Hanabusa, K., and Shirai, H., Reversible color changes induced by photosensitized charge separation in partially quaternized poly(1-vinylimidazole)-bound ruthenium(II) complex and viologen films, *Eur. Polym. J*., 35, 977, 1999; (e) Kuwabara, T., Sugiyama, M., and Nanasawa, M., Photochromism of viologens included in crown ether cavity, *J. Photochem. Photobiol.*, 73, 469, 2001; (f) Nanasawa, M., in *Organic Photochromic and Thermochromic Compounds*, Vol. 1, Kluwer Academic, New York, 1999, 341.
85. Bockman, T.M. and Kochi, J.K., Isolation and oxidation-reduction of methylviologen cation radicals. Novel disproportionation in charge-transfer salts by x-ray crystallography, *J. Org. Chem.,* 55, 4127, 1990; Isoda, Y., Kawai, H., Muta, S., and Nagamura, T., Time-resolved ion-pair charge transfer fluorescence of bipyridinium salts in various microenvironments, *J. Photochem. Photobiol., A: Chem.*, 97, 113, 1997; Jin, J-J, Uchida, T., Kuwabara, T., Hirai, M., and Nanasawa, M., Synthesis of covalently linked ferric tris(bipyridyl)-viologen molecule and photo coloration in poly(vinylalcohol), *J. Am. Chem. Soc.,* 123, 87, 1999; Nanasawa, M., Miwa, M., Hirai, M., and Kuwabara, T., Synthesis of viologens with extended π-conjugation and their photochromic behavior on near-IR absorption, *J. Org. Chem.*, 65, 593, 2000; Kuwabara, T., Sugiyama, M., and Nanasawa, M., Photochromism of viologens included in crown ether cavity, *J. Photochem. Photobiol., A: Chem.*, 73, 469, 2001; Liddell, P.A., Kodis, G., Moore, A.L., Moore, T.A., and Gust, D., Photonic switching of photoinduced electron transfer in a dithienylethene-porphyrin-fullerene triad molecule, *J. Am. Chem. Soc.*, 124, 7668, 2002.
86. Nagamura, T. and Isoda, Y., Novel photochromic polymer films containing ion-pair charge-transfer complexes of 4,4′-bipyridinium ions for optical recording, *J. Chem. Soc., Chem. Commun.,* 72, 1991.
87. Schild, V., Synsitizer und Akzeptor Diaden und Triaden, Ph.D. Thesis, University of Saarland, 2001.

97

Photoisomerization of Some Nitrogen-Containing Hetero-Aromatic Compounds

James W. Pavlik
Worcester Polytechnic Institute

This chapter deals with the photoisomerization reactions of pyrazoles, 1,2,4-oxadiazoles, pyridine, and its simple derivatives and pyridinium cations. The photochemistry of nitrogen-containing heteroaromatic compounds that also contain sulfur are considered in another chapter.

97.1 Pyrazole Photochemistry

The photochemistry of 1-methylpyrazoles has been of considerable interest since it was reported that 1-methylpyrazole **1** undergoes photoconversion to 1-methylimidazole **3**. This transposition was rationalized in terms of a ring contraction ring-expansion mechanism shown in Scheme 1 involving the intermediacy of 2-(*N*-methylimino)-2*H*-azirine **2** formed by cyclization of a photochemically generated biradical species. This mechanism would result in a transposition pathway involving interchange of only the N2 and C3 atoms of the pyrazole ring as shown in Scheme 2. The ring-scrambling pattern resulting from the N2–C3 interchange shown in Scheme 2 has been referred to as the P_4 pattern.[2]

Although the intermediacy of acylazirines has been demonstrated in the analogous isoxazole-oxazole phototransposition,[3] iminoazirines such as **2** have not been detected in a pyrazole→imidazole reaction and thus this mechanistic suggestion has never been confirmed.

The existence of an additional reaction pathway was confirmed by Beak and co-workers, who reported (see Scheme 3) that 1,3,5-trimethylpyrazole **5** phototransposes to 1,2,5-trimethylimidazole **6**, a product that can result from the 2,3-interchange pathway and 1,2,4-trimethylimidazole **7**, a product which cannot be formed by this pathway.[4,5] The formation of the latter product was suggested to occur (Scheme 4) by a pathway involving initial electrocyclic ring closure, heteroatom migration via [1,3]-sigmatropic shift of nitrogen, and rearomatization of the resulting 2,5-diazabicyclo[2.10]pentene to provide **7**.

Barltrop and colleagues[6] also observed that 3-cyano-1,5-dimethylpyrazole **8** undergoes photoisomerization to yield **9** and **10** (Scheme 5), which can be formed by the 2,3-interchange pathway and the one-step nitrogen

0-8493-1348-1/04/$0.00+$1.50

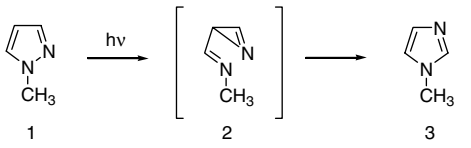

SCHEME 1

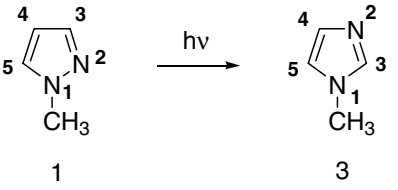

SCHEME 2

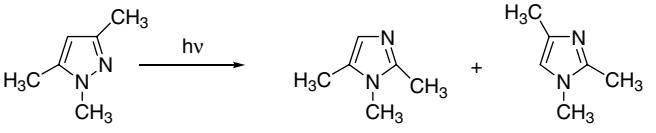

SCHEME 3

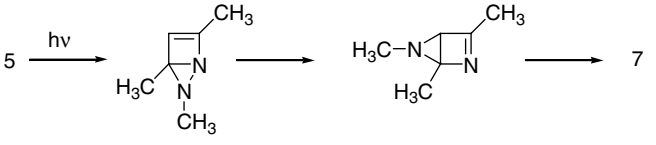

SCHEME 4

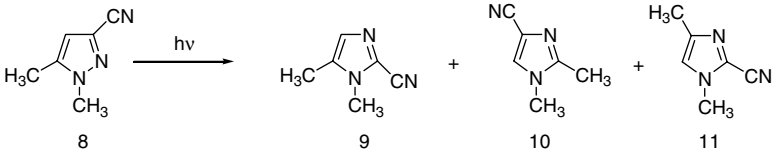

SCHEME 5

walk mechanism, respectively, and **11,** which cannot be formed by either of these pathways but was suggested to arise by the double nitrogen walk mechanism shown in Scheme 6. Such a double walk process has also been observed in the photochemistry of cyanothiophenes[7] and cyanopyrroles.[2b,8]

The mechanistic pathways implicated by these reactions are shown in Scheme 7, which shows how the ring atoms transpose by each pathway.

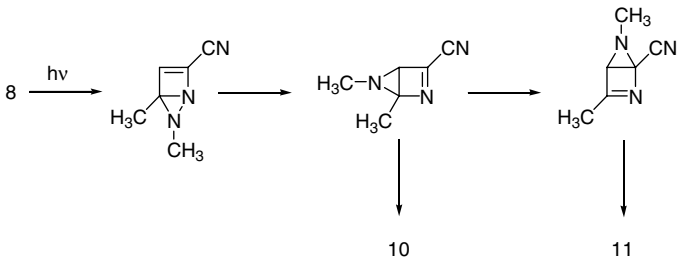

SCHEME 6

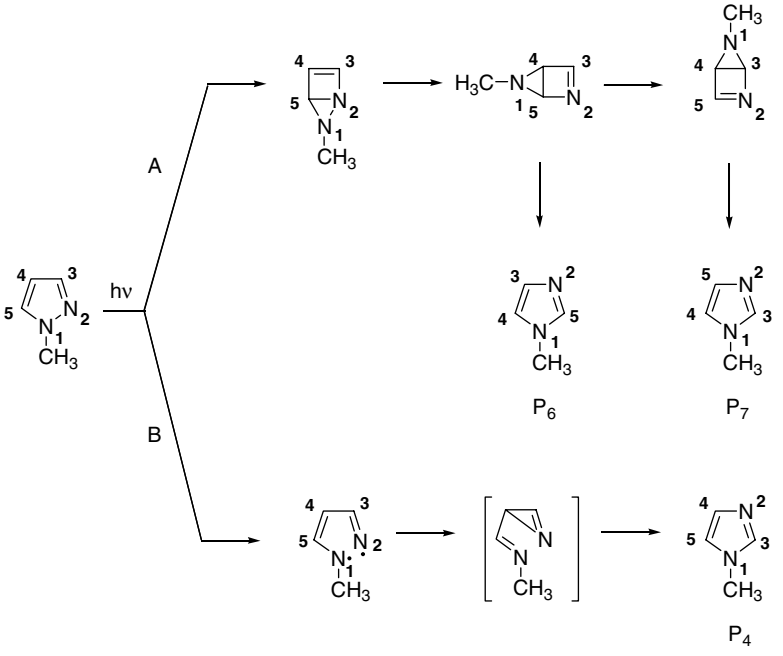

SCHEME 7

According to this interpretation, the photochemistry of 1-methylpyrazoles involves competition between electrocyclic ring closure (path A, Scheme 7) and cleavage of the N1–N2 bond (path B, Scheme 7). Path A results in the formation of a 1,5-diazabicyclo[2.1.0]pentene intermediate that undergoes one or two sigmatropic shifts of nitrogen, followed by rearomatization of the two isomeric 2,5-diazabicyclo[2.1.0]pentene species to yield 1-methylimidazoles with two different ring scrambling patterns referred to as P_6 and P_7.[2] It is interesting to note that because only pyrazole-to-imidazole transpositions have been observed, the [1,3] sigmatropic shift of nitrogen must take place away from the azetine nitrogen to form a 2,5-diazabicyclo species but not in the opposite direction toward the azetine nitrogen to yield an isomeric 1,5-diazabicyclic species and eventually a pyrazole-to-pyrazole transformation. Alternatively, path B leads to a species that can be viewed as a biradical that is the precursor of the 1-methylimidazole in which the P_4 scrambling pattern involves only interchange of the N2 and C3 atoms.

The photochemistry of 1-methylpyrazoles **12** through **14**, in which the various ring carbons are systematically labeled with a second methyl group, has also been studied.[9] The primary products shown in Scheme 8, and the results of deuterium labeling studies shown in Scheme 9 confirm that these dimethylpyrazoles undergo only pyrazole-to-imidazole phototransposition by as many as three distinct pathways.

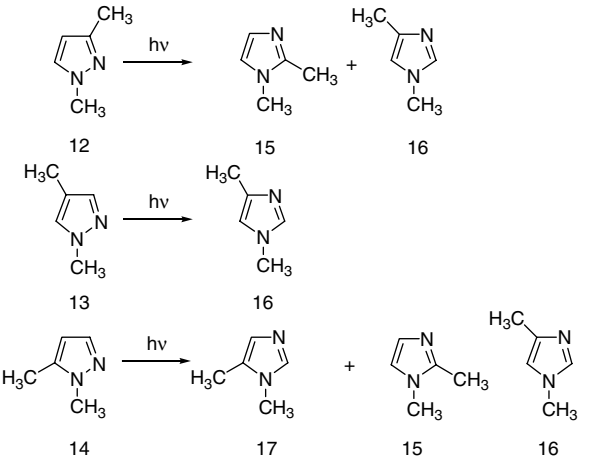

SCHEME 8

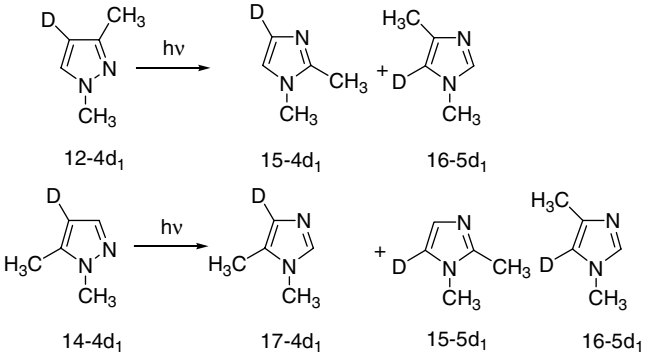

SCHEME 9

Thus, whereas 1,5-dimethylpyrazole **14** transposes by the P_4, P_6, and P_7 pathways to yield 1,5-, 1,2-, and 1,4-dimethylimidazoles **17**, **15**, and **16**, respectively, 1,3-dimethylpyrazole **12** transposes only via the P_4 and P_6 pathways to form 1,2- and 1,4-dimethylimidazoles **15** and **16**, respectively. Finally, 1,4-dimethylpyrazole **13** transposes to a single product, 1,4-dimethylimidazole **16**, presumably via the P_4 N2–C3 interchange pathway.

To study the phototransposition with minimum substituent perturbation, the phototransposition chemistry of 3,4-dideuterio-1-methylpyrazole **1-3,4d$_2$** was also studied.[9] This labeling pattern allows distinction between the three pathways because Scheme 7 shows that conversion of **1**→**2** via the P_4, P_6, or P_7 pathways is accompanied by transposition of C5 of the reactant to ring position 5, 2, or 4 in the product.

After less than 10% photoconversion of **1-3,4d$_2$**, ^{1}H NMR analysis revealed that the product consisted of a mixture of **2-2,4d$_2$**, **2-4,5d$_2$,** and **2-2,5d$_2$,** confirming that **1-3,4d$_2$** undergoes phototransposition via the P_4, P_6, and P_7 pathways in a ratio of 4.8:6.5:1.0. Thus, the phototransposition of 1-methylpyrazole **1** to 1-methylimidazole **2** is considerably more complicated than originally suggested.

A key mechanistic step in the formation of the P_6 and P_7 imidazoles is electrocyclic ring closure leading to a transient 1,5-diazabicyclo[2.1.0]pentene. Convincing evidence for the existence of this species is available. Thus, whereas irradiation of 1-methyl-5-phenylpyrazole **18** in methanol results in the formation

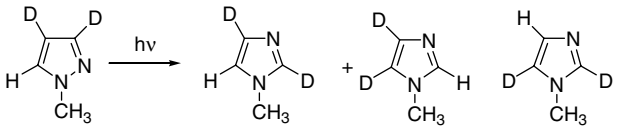

SCHEME 10

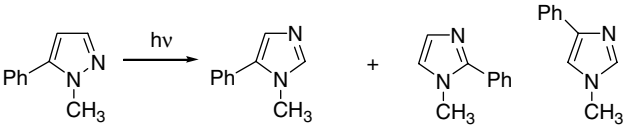

SCHEME 11

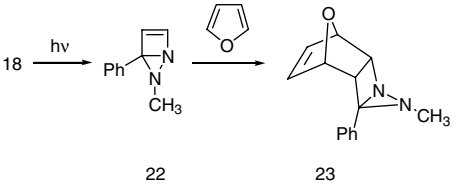

SCHEME 12

of the anticipated P_4, P_6 and P_7 imidazoles **19** through **21** in the chemical and quantum yields shown in Scheme 11, irradiation of **18** in neat furan led only to the pyrazole-furan [4+2] adduct **23**.[10] The formation of this product is consistent with furan trapping of a photochemically generated 1,5-diazabicyclopentene species **22** as shown in Scheme 12.

In addition to phototransposition, *N*-substituted pyrazoles have also been observed to undergo two photocleavage reactions to yield enaminonitrile and enaminoisocyanide photoproducts. Thus, 1-methyl-4-phenylpyrazole **24** phototransposes regiospecifically to the P_4 product 1-methyl-4-phenylimidazole **25** and to the two photocleavage products (*E,Z*)-3-(*N*-methylamino)-2-phenylpropenenitrile **26** and (*E,Z*)-2-(*N*-methylamino)-1-phenylethenylisocyanide **27** in the chemical and quantum yields shown in Scheme 13.[10,11] Furthermore, these photocleavage pathways are not limited to the reactions of **24**, they are involved in all other pyrazole to imidazole photoreactions investigated.

Direct irradiation of *Z*-enaminonitrile **26** and *Z*-enaminoisocyanide **27** shows (Scheme 14) that both undergo *Z*→*E* isomerization and photocyclization to 1-methyl-4-phenylimidazole **25**, the P_4 transposition product. In addition, cyclization of **27** to **25** was observed when the former was heated to 80°C. Although the quantum yields shown in Scheme 14 reveal that the photocyclization of enaminonitrile **26** to imidazole **25** is a very inefficient reaction, chemical and quantum yields show that the photocleavage-photocyclization pathway via an isocyanide intermediate is a major route for the P_4 phototransposition reaction.[10] Furthermore, it has been shown that this pathway is general for a variety of other pyrazoles that bear hydrogen at the C3 ring position.

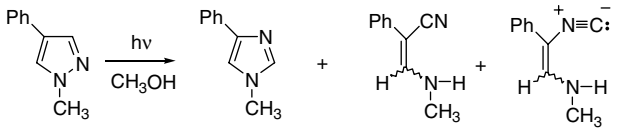

	24	25	26	27
%	- 20.5	17.2	12.0	68.1
Φ	0.200+/-0.003	0.037+/-0.002	0.008+/-0.001	0.114+/-0.001

SCHEME 13

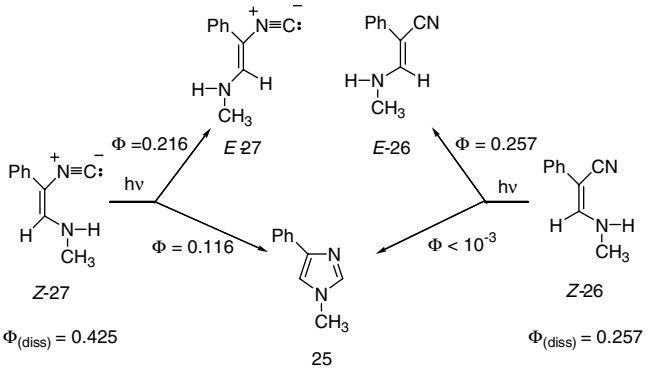

SCHEME 14

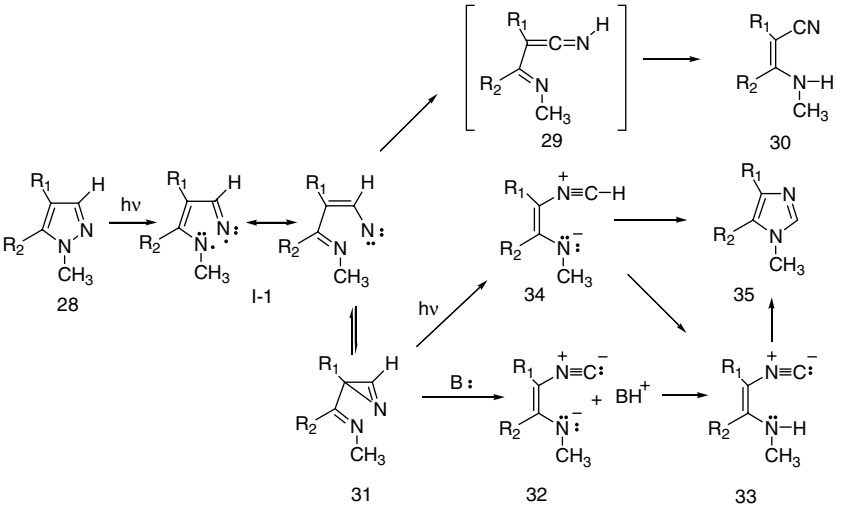

SCHEME 15

From these studies, a general mechanistic scheme for the P_4 N2–C3 interchange pathway is emerging. As shown in Scheme 15, photocleavage of the N1–N2 bond in **28** is suggested to result in the formation of a species I-1 that was described as either a biradical or as a β-iminovinyl nitrene. The isomerization of terminal vinyl nitrenes to nitriles is a well-documented reaction.[12] Accordingly, nitrene I-1 would be

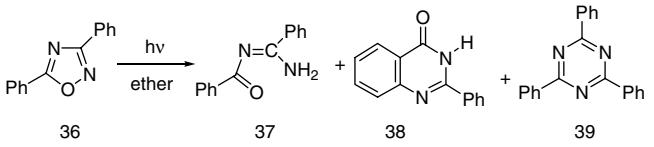

36 37 38 39

SCHEME 16

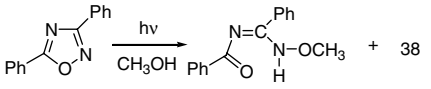

36 40

SCHEME 17

expected to rearrange as shown in Scheme 15 to the enaminonitrile photocleavage product **30**, plausibly by way of iminoketeneimine **29**. In addition, vinyl nitrene I-1 would also be expected to be in equilibrium with the isomeric iminoazirine **31**,[13] which could isomerize to the enaminoisocyanide **33**, a known precursor of imidazole **35**, the P_4 phototransposition product. This reaction requires proton transfer from carbon in **31** to nitrogen in **33**. Although in the case of acylazirines[14] and thioformylazirines[15] this proton transfer requires an added base, pyrazoles and certainly imidazoles are sufficiently basic to act in this capacity. Alternatively, electrocyclic ring opening of azirine **31** would be expected to yield nitrile ylide **34**,[16] which could undergo direct cyclization to the P_4 imidazole **35** or proton transfer resulting in the formation of the isocyanide **33**. If azirine **31** is formed in the ground state, calculations suggest that in the absence of deprotonation by a base, the most likely reaction pathway is back to the pyrazole. Calculations also reveal that excitation to the S_1 surface is accompanied by an increase in the carbon-carbon bond length from 1.49 to 1.74Å. Accordingly, if an azirine-like structure is reached on the reaction coordinate before crossing to the S_0 surface, the excited species would be expected to undergo facile conversion to the nitrile ylide rather than resulting in an isolable product.

97.2 1,2,4-Oxadiazole Photochemistry

Irradiation of an ethereal solution of diphenyl-1,2,4-oxadiazole **36** with quartz-filtered light from a medium-pressure Hg lamp was reported to result (Scheme 16) in the formation of a photoreduced product **37** in 31% yield, a photoisomerization product **38** in 5% yield, and an interesting ring-expansion product **39** in 0.5% yield.[17] When the irradiation was carried out in methanol solvent, the major product (Scheme 17) was identified as the 1:1 methanol adduct **40** (or its tautomer) in 40% yield and **38** in 7.5% yield.[18] Thus, irradiation of **36** results in homolysis or heterolysis of the O–N bond in the oxadiazole.

Cleavage of the O–N bond also dominates the photochemistry of isoxazoles.[3] In this case (Scheme 18), cleavage of isoxazole **41** is followed by ring contraction to the acylazirine **42** and subsequent ring expansion to the oxazole **43** in which the N2 and C3 atoms of the isoxazole ring have been interchanged.

By analogy with isoxazole chemistry, 1,2,4-oxadiazoles **44** might also be expected to undergo phototransposition by the ring contraction–ring expansion pathway shown in Scheme 19 leading to the formation of 1,3,4-oxadiazole **46** via diazirine **45**. This reaction has been studied in detail by Vivona[19] and colleagues and found to occur in greater than trace quantities only when a tautomerizable group (NH_2, $NHCH_3$, NHPh, or OH) is present at the C3 position of the 1,2,4-oxadiazole ring, as shown in Scheme 20.[20–22] Thus, direct excitation of 1,2,4-oxadiazoles **47** through **55** at 254 nm in methanol solution led to the formation of 1,3,4-oxadiazoles **56** through **64** in yields of approximately 10%. The phototransposition of **47** through **56** could not be quenched with added penta-1,3-diene (E_T = 62.5 kcal mol^{-1}) or

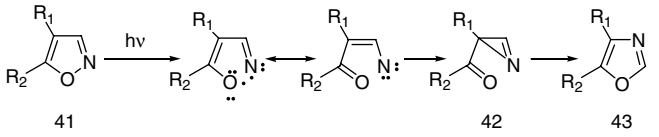

41 42 43

SCHEME 18

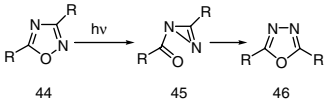

44 45 46

SCHEME 19

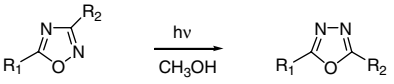

	R1	R2	
47	Ph	NH_2	56
48	$pCH_3C_6H_4$	NH_2	57
49	$pCH_3OC_6H_4$	NH_2	58
50	$pClC_6H_4$	NH_2	59
51	$PhCH_2$	NH_2	60
52	Ph	$NHCH_3$	61
53	n-C_8H_{17}	NH_2	62
54	n-$C_{11}H_{23}$	NH_2	63
55	Ph	OH	64

SCHEME 20

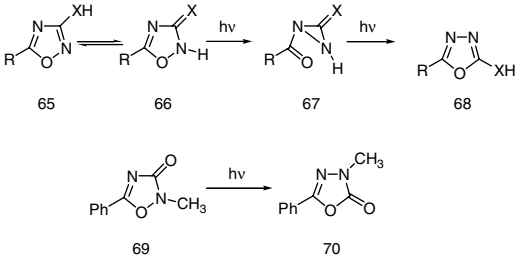

65 66 67 68 69 70

SCHEME 21

sensitized by diphenylacetylene (E_T = 62.5 kcal mol^{-1}) and thus presumably does not involve the triplet state of the reactant.

Because of the necessity of the tautomerizable group at C3 of the reactant, it was suggested that a tautomeric form **66** of the oxadiazole **65** or intermediate **67** (Scheme 21) might be involved in this phototransposition.[21] The photoconversion of 2-methyl-5-phenyl-f^4-1,2,4-oxadiazolin-3-one **69** to 3-methyl-5-phenyl-f^4-1,3,4-oxadiazolin-2-one **70** is consistent with this suggestion.

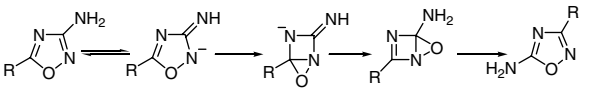

SCHEME 22

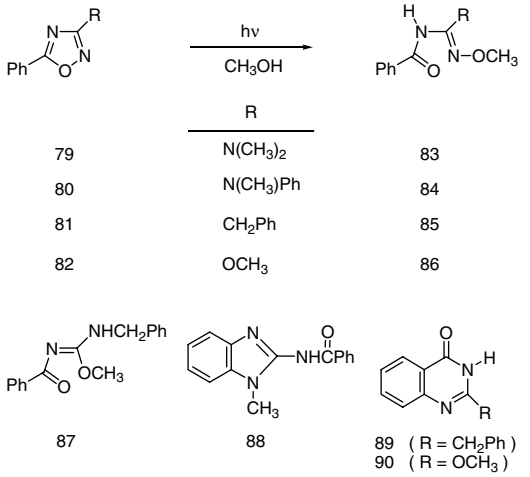

SCHEME 23

Interestingly, irradiation of 3-amino-5-alkyl-1,2,4-oxadiazoles **53** or **54** at 254 nm in methanol containing a small quantity of base such as triethylamine (TEA) or aqueous sodium bicarbonate leads to the formation of 1,3,4-oxadiazoles **62** or **63** and also to 5-amino-3-alkyl-1,2,4-oxadiazoles **77** and **78**, respectively, as shown in Scheme 22.[22]

It has been suggested that photochemically excited **53** or **54** is deprotonated by the base, resulting in the formation of the anionic species **71** or **72**, respectively, which undergo electrocyclic ring closure between N2 and C5 to give the stabilized anions **73** and **74**, respectively. Oxygen migration and reprotonation then provides **75** and **76**, from which the observed phototransposition products **77** or **78** arise by rearomatization.

In contrast, when the C3 substituent is not tautomerizable, as in the case of **79** through **82** in Scheme 23, irradiation at 254 nm in methanol solvent led to the solvent adducts **83** through **86**, respectively; and in the case of **81**, to a second adduct **87**. In addition, irradiation of **80–82** also resulted in the formation of the cyclized products **88–90**, respectively.[20]

The products shown in Scheme 23 can be rationalized in terms of photocleavage of the O–N bond in **79** through **82**, resulting in a species that can be viewed as a zwitterion **Ia** or as a β-acyliminonitrene **Ib** (Scheme 9). The observed products then result from reactions typical of an electrophilic nitrogen.[20] Thus, reaction with the nucleophilic solvent (Scheme 24) leads to **83** through **86**; a 1,2-shift of the benzyl group from carbon to nitrogen in the nitrene formed from **81** would provide the carbodiimide **91**, which would react with methanol to form **87**; electrophilic attack on the phenyl ring in the C3 substituent of **80** results in the benzimidazole **88**; or electrophilic attack on the C5 phenyl group in **81** or **82** would provide quinazolines **89** or **90**.

When the substituent at C3 of the 1,2,4-oxadiazole ring is a participating three-atom side chain, new reaction pathways become available.[23–27] Thus, irradiation of 1,2,4-oxadiazoles **92a,b,-c** at 254 nm in methanol solvent also resulted in the formation of benzimidazoles **94a,b** or benzoxazole **94c** (Scheme 25).

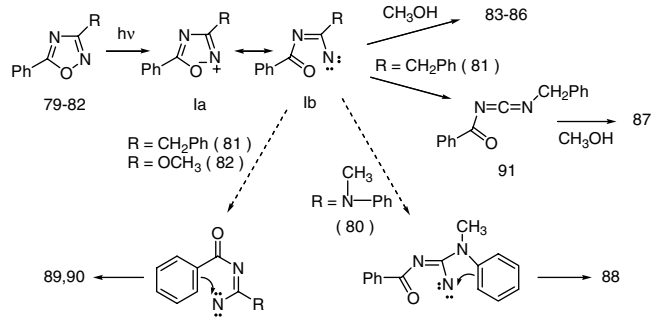

SCHEME 24

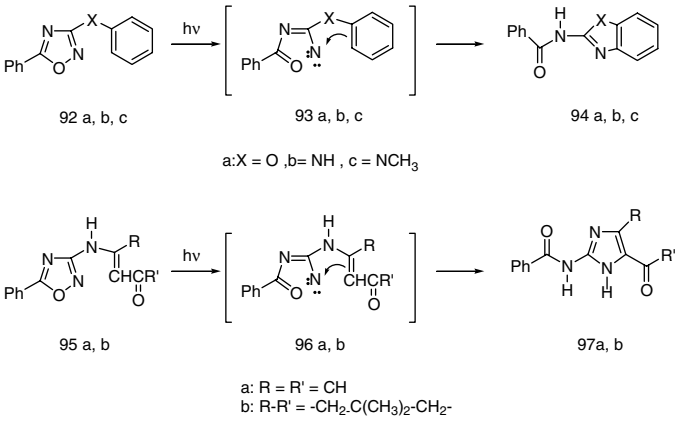

SCHEME 25

Similarly, enanimoketones **95a,b** photoisomerize to imidazoles **97a,b**.[23] These reactions can also be rationalized by photocleavage of the O–N bond of the oxadiazole ring and electrophilic attack by the electron deficient nitrogen in **93a,b,c** or **96a,b**.

The photochemistry of 3-benzoylamino-5-methyl-1,2,4-oxadizole **98** and 3-acetylamino-5-phenyl-1,2,4-oxadiazole **99** has also been investigated (Scheme 26).[24–27]

Upon direct excitation at 254 nm, **98** gave quinazolinone derivative **101**, which was suggested to result from initial hetero-electrocyclic ring closure to yield **100** followed by ring opening. This reaction can be quenched by added penta-1,3-diene and was suggested to involve the triplet state of the aroylamino group. Direct irradiation of 3-acetylamino **99** at 254 nm gave the 3-benzoylamino isomer **98**, which was converted to **101** under the conditions of the irradiation. The photoconversion of **99** could not be quenched by added penta-1,3-diene, and its conversion to **98** was assumed to involve the intermediacy of singlet nitrene **102**. Interestingly, triplet-sensitized excitation of **99** using phenylacetylene or diphenylacetylene led to the direct formation of quinazolinone **101** without the intermediacy of **98**. This conversion was suggested to involve the intermediacy of the triplet nitrene **102**. The triplet-sensitized irradiation of 5-phenyl-1,2,4-oxadiazoles can be used as a synthetic route to various 2-substituted quinazolin-2-ones.[27]

The conversion of oxadiazoles to quinazolin-4-ones can also be achieved by electron-transfer sensitization.[28] For example, 9,10-diphenylanthracene (DAN)-sensitized irradiation at 313 nm of 5-aroyl-3-methoxy-1,2,4-oxadiazoles **103ab,c,d** and 5-aroyl-3-phenyl-1,2,4-oxadiazoles **106a,b,c,d** resulted in the formation of quinazolin-4-ones **104a,b,c,d** and **107a,b,c,d**, respectively, and photoreduced products **105a,b,c,d** and **108a,b,c,d**, respectively. In these reactions, neither singlet nor triplet sensitization is

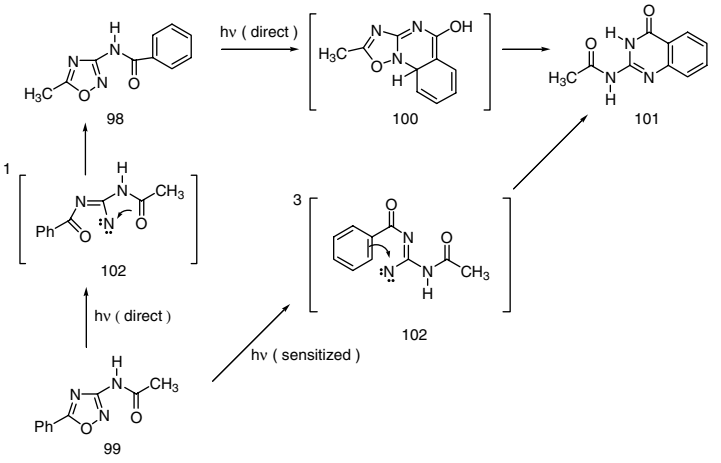

SCHEME 26

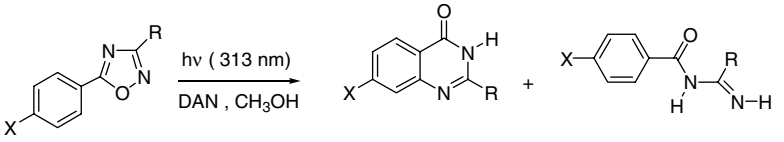

103 a-d (R = OCH_3)
106 a-d (R = Ph)

104 a-d (R = OCH_3)
107 a-d (R = Ph)

105 a-d (R = OCH_3)
108 a-d (R = Ph)

a: X = H; b: x = CH_3; c: x = CN; d: x = Cl

SCHEME 27

feasible. These reactions can also be achieved by direct excitation of **103a,b,c** at 313 nm in methanol solvent containing an excess of triethylamine (TEA).[28] Under these conditions, **103a,b,c** gave **104a,b,c** in yields of 50 to 60% and photoreduced products **105a,b,c** in approximately 30% yield. Similarly, **106a** provided quinazolin-4-one **107a** in 36% yield, along with a trace quantity of the photoreduced product **108a**. These reactions are envisioned to occur by cleavage of the N–O bond in the 1,2,4-oxadiazole radical anion formed either by electron transfer from the excited sensitized (DAN) to the ground state of the 1,2,4-oxadiazole or from TEA to the excited singlet state of the 1,2,4-oxadiazole.

97.3 Pyridine Photochemistry

Introduction and Background

The photochemistry of six-membered aromatic compounds has been of considerable interest since it was shown that benzene and its simple derivatives undergo photo-valence isomerization and phototransposition.[29–32] The photochemistry of the important heteroaromatic compound pyridine **109** is of interest because it has an $S_2(\pi, \pi^*)$ state similar to benzene and a lower-lying $S_1(n, \pi^*)$ state not available to benzene. Accordingly, pulsed excitation of pyridine in neutral solution led to the observation of two transients with decay components of 2.2 ps, assigned to motion along the π,π^* reaction pathway, and 23 ps that represents the nonradiative, nonreactive decay pathway of S_1 leading to intersystem crossing to the $T(\pi,\pi^*)$ state or to chemical reaction.[33]

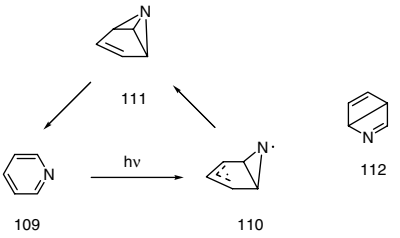

SCHEME 28

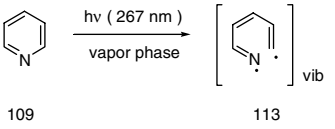

SCHEME 29

Excitation of aromatic molecules such as benzene or pyridine with excess energy results in a dramatic decrease in their fluorescence yields due to the availability of an extremely rapid nonradiative deactivation pathway.[34] This phenomenon has been termed the "channel three" process. For pyridine **109**, the onset of channel three deactivation occurs at ~1600 cm^{-1} above the S_1 origin.[35] This deactivation was originally thought to involve a concerted pathway, originating from a vibrationally excited S_1 aromatic molecule, leading to the ground state of a bicyclic prefulvene biradical. In the case of pyridine **109** (Scheme 28), this species would be azaprefulvene **110,** which could rearomatize to pyridine **109,** either directly or via azabenzvalene **111** in an energy wasting process. More recently, it has been proposed that channel three deactivation might involve direct S_1–S_0 internal conversion resulting in a vibrationally excited ground-state species geometrically disposed to undergo isomerization to the prefulvene isomer.

Time-Resolved Studies

The nonradiative transitions in pyridine vapor have been studied using femtosecond, time-resolved mass spectroscopy.[36] In these experiments, pyridine vapor was excited with a femtosecond light pulse of 277 nm, which is below (~300 cm^{-1}) the channel three threshold. Time-resolved mass spectroscopy revealed a fast decay component of 400 fs, which describes the initial motion on the pyridine potential surface and shows components of 3.5 and 15 ps, which were assigned to the formation of Dewar-pyridine **112** and azabenzvalene **111**, respectively (Scheme 28).[36]

These processes have also been studied using ultra-fast electron diffraction.[37] In this case, a femtosecond light pulse of 267 nm was used to excite pyridine **109** vapor into the S_1 (n, π^*) state with an excess energy of ~2700 cm^{-1}, well above the ~1600 cm^{-1} threshold for channel three behavior. Sequentially delayed ultra-short electron pulses were then used to probe the ensuing structural dynamics.

Interestingly, the results were not consistent with either direct $S_1 \rightarrow S_0$ internal conversion to a vibrationally excited ground-state molecule or with valence isomerization-mediated internal conversion. Instead, surprisingly, the results indicate that the primary product is a hot ring-opened biradical **113** (Scheme 29) formed via cleavage of a CN bond.

The deactivation pathway for excited pyridine **109** in solution phase has been studied using femtosecond transient absorption spectroscopy.[33] According to these studies, excitation of pyridine **109** in acetonitrile with a femtosecond pulse of 266 nm results in the population of vibrationally excited $S_1(n,\pi^*)$ and $S_2(\pi,\pi^*)$ molecules. The S_2 $(\pi,\pi^*)_{vib}$ relaxes to its equilibrium geometry in less than 100 fs. This vibrationally relaxed $S_2(\pi,\pi^*)$ molecule can either undergo internal conversion to the S_1 (n,π^*) state in

109
S_2 (π,π*)

110

SCHEME 30

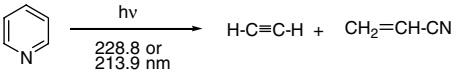

109 114 115

SCHEME 31

greater than 10ps or, more rapidly (~2.2 ps), can isomerize to the azaprefulvene **110** (Scheme 30) by passing over the barrier in the S_2 state and crossing the conical intersection. Previous calculations on pyridine also suggest the existence of an azaprefulvene structure formed from the $S_2(\pi,\pi^*)$ excited state.[38] This prefulvene species **110** can revert to the ground state of pyridine **109** in greater than 2 ns by passing over the barrier and crossing over to the ground state of pyridine **109**. These studies also conclude that $S_1(n,\pi^*)$ pyridine can decay via intersystem crossing to the $T_1(\pi,\pi^*)$ triplet state and by interconversion to other isomers. Although earlier theoretical studies indicated that the potential energy surfaces of both $S_1(n,\pi^*)$ and $S_2(\pi,\pi^*)$ have a crossing point along the isomerization coordinate to the azaprefulvene, these studies show that the barrier from the $S_1(n,\pi^*)$ surface is too high for this isomerization to occur. It was concluded, however, that $S_1(n,\pi^*)$ pyridine can interconvert to other isomers.

Continuous Excitation Studies

The vapor-phase photochemistry of pyridine **109** under conditions of continuous irradiation has been studied at various wavelengths. Little or no decomposition of pyridine was observed upon irradiation at 254 nm and no gaseous products were detected after irradiation at 265 or 248 nm.[39] Upon irradiation at 228.8 or 213.9 nm, however, pyridine **109** was converted to acetylene **114** and acrylonitrile **115** (Scheme 31).

Irradiation of pyridine **109** in butane solution at −15°C with light of 254 nm has been shown to result in the formation of Dewar-pyridine **112,** which was characterized and observed to have a half-life of 36 minutes at 0°C and 2 minutes at ambient temperatures.[41] Alternatively, if pyridine is irradiated in water[42,43] or in aqueous sodium borohydride, the initially formed **112** undergoes hydration to **116** and ring opening to form 5-amino-2,4-pentadienal **117** or reduction to provide 2-azabicyclo[2.2.0]hex-5-ene **118**, respectively (Scheme 32).

Irradiation of pyridine **109** matrix isolated in argon at 8K gave rise to hydrogen cyanide and cyclobutadiene **119** as secondary photoproducts.[44] It was assumed that these products arise from photofragmentation of the initially formed Dewar-pyridine **112** (Scheme 33).

Irradiation of 2-methylpyridine **120** vapor (10 to 15 Torr) led to the formation (Scheme 34) of both 3-methylpyridine **121** and 4-methylpyridine **122** in a ratio of 10:1.[45]

Within the $\pi\rightarrow\pi^*$ transition absorption band, the quantum yields for the formation of **121** and **122** increased by a factor of 6 when the excitation wavelength is decreased from 266 nm (0–0) to 238 nm.[45] These results are typical for channel three behavior. No conversion of 2-methylpyridine **120** was observed upon irradiation in the $n\rightarrow\pi^*$ transition at either 280 or 290 nm. It was suggested that the conversion of **120** to **121** and **122** proceeds via an azaprismane intermediate.[45]

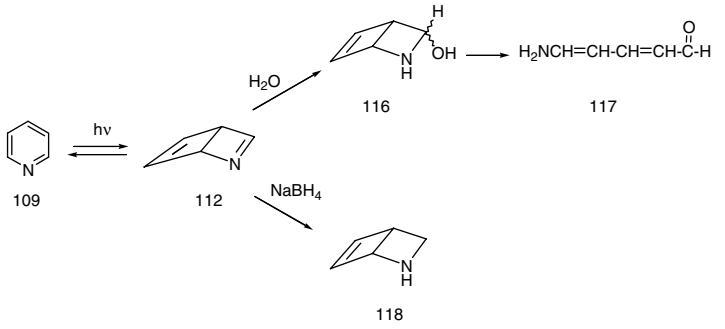

SCHEME 32

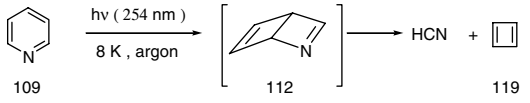

SCHEME 33

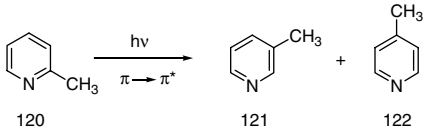

SCHEME 34

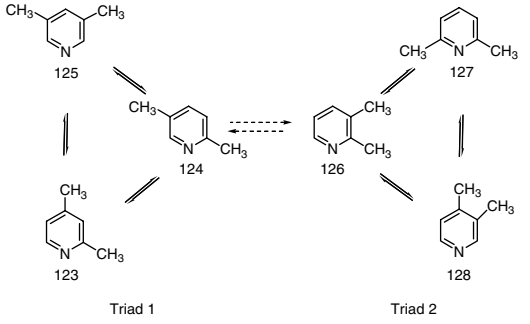

SCHEME 35

Dimethylpyridines were also reported to undergo phototransposition in the gas phase. These reactions were also suggested to occur by way of azaprismane intermediates.[46]

The photochemistry of dimethylpyridines in the vapor phase has been reinvestigated with substantially different results and conclusions.[47] According to these studies, irradiation of the six dimethylpyridines **123** through **128** at 254 nm in the vapor phase results in phototransposition and photodemethylation or, in one case, photomethylation of a dimethylpyridine to a trimethylpyridine.

Based on the major transposition products observed, the six isomers can be divided into the two triads shown in Scheme 35. The first triad consists of 2,4-dimethyl-**123**, 2,5-dimethyl-**124**, and 3,5-dimethyl-**125**,

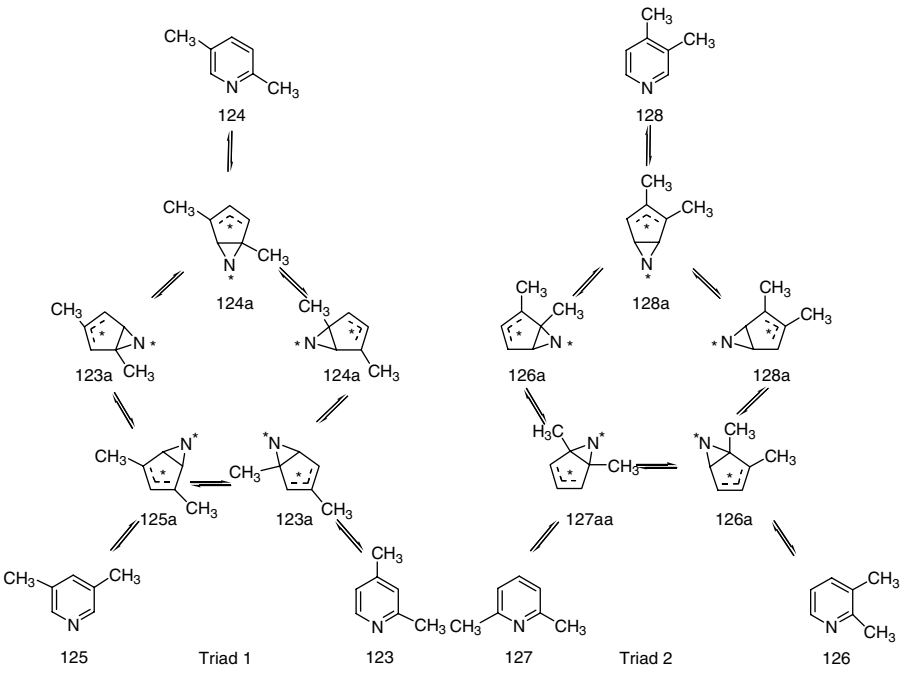

SCHEME 36

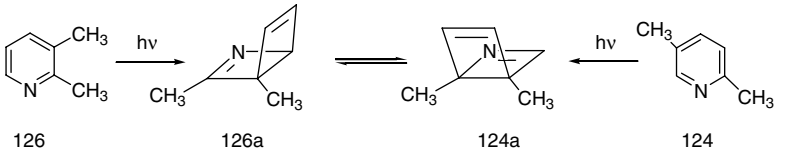

SCHEME 37

while the second triad includes 2,3-dimethyl-**126**, 2,6-dimethyl-**127**, and 3,4-dimethylpyridine **128**. These intra-triad interconversions were suggested to occur (Scheme 36) via 2,6-bonding, originating from a vibrationally excited $S_2(\pi,\pi^*)$ state of the dimethylpyridine, resulting in the formation of the dimethyl-azafulvene intermediates shown in Scheme 36. Subsequent nitrogen migration and rearomatization then allows interconversion of the three members of each triad. The unsubstituted azaprefulvene **110** was also suggested to result from the $S_2(\pi,\pi^*)$ state of pyridine generated by pulsed excitation.[33] In that case, sigmatropic nitrogen migration would not lead to a distinguishable product after rearomatization.

In addition to these intra-triad reactions, 2,5-dimethylpyridine **124**, a member of triad 1, was observed to interconvert with 2,3-dmethylpyridine **126**, a member of triad 2 (Scheme 35). As illustrated in Scheme 37, these inter-triad interconversions were shown to occur via interconverting Dewar-pyridine intermediates **124a** and **126a**, which were detected by ^{1}H-NMR spectroscopy after irradiation of the dimethylpyridines in CD_3CN at −30°C. These inter-triad reactions involving Dewar-pyridine intermediates were enhanced by dilution of the dimethylpyridine vapor with nitrogen, by irradiation with light of wavelength >290 nm, and took place in the condensed phase at low temperature. These facts indicate that Dewar-pyridine formation occurs from an excited state of lower energy than the first excited singlet (π,π^*) state. These observations do not seem to be consistent with the suggestion based on calculations that isomerization to the Dewar-pyridine can involve a Möbius-pyridine on the higher-energy π,π^* potential energy surface.[48]

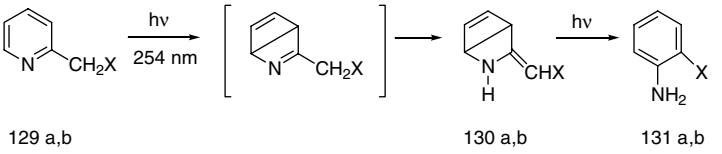

SCHEME 38

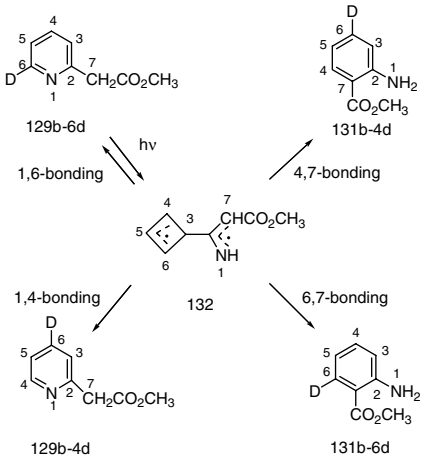

SCHEME 39

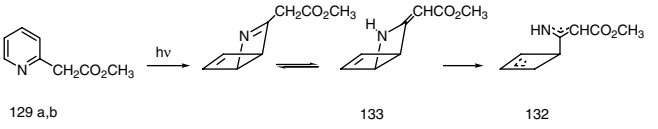

SCHEME 40

Dewar-pyridine derivatives have been implicated as intermediates or isolated as products in other photoreactions of pyridine derivatives in solution phase. Irradiation of pyridine derivatives **129a,b** (Scheme 38) at 254 nm in ether/*t*-butyl alcohol solvent led to the formation of aniline derivatives **131a,b** via Dewar-pyridine tautomers **130a,b**.[49] The tautomer **130b** was isolated when **129b** was irradiated in aqueous sodium hydroxide and was shown to be photochemically converted to **131b** upon irradiation in diethyl ether solution.[50]

The photochemistry of **129b-6d** was also studied.[51] After 80% conversion of the reactant (Scheme 39), the rearranged product was shown to consist of equal amounts of **131b-4d** and **131b-6d** (Scheme 39) while the unconverted reactant consists of the original **129b-6d** and 10% of the rearranged reactant **129b-4d**. The mechanism suggested to account for the conversion of the 2-substituted pyridine **129b** to the methylanthranilate product **131b** and to explain the observed deuterium scrambling (Scheme 39) involves formation and cyclization of intermediate **132**. Presumably, **132** is not formed directly from the pyridine reactant **129b** but from the Dewar-pyridine tautomer **133** as shown in Scheme 40.

Polyperfluoroalkyl substitution greatly stabilizes both Dewar-pyridine and azaprismane valence isomers. Irradiation of pentakis(pentafluoroethyl)pyridine **134** in perfluoro-n-pentane with light of $\lambda >$

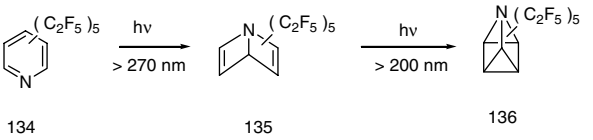

SCHEME 41

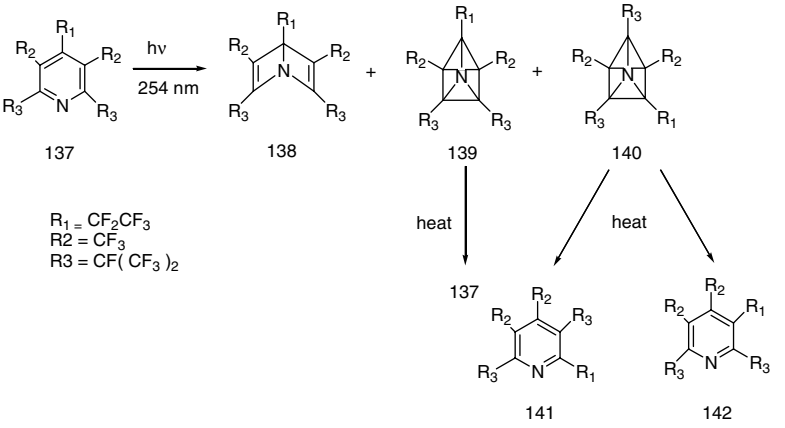

SCHEME 42

270 nm (Scheme 41) gave the 1,4-bonded Dewar isomer **135** in 95% yield. Irradiation with light of $\lambda >$ 220 nm led to the formation of the azaprismane **136**, pentakis(pentafluoroethyl)-1-azatetracyclo[2,2,0,0,$^{2}0^{3,5}$]hexane in 91% yield, apparently by way of the Dewar-isomer **135**. Both isomers are thermally quite stable with boiling points of 176°C and 184°C, respectively. Indeed, **135** was reported to have a half-life, $t_{1/2}$ = 104 h at 170°C.[52,53]

The perfluoroalkyl-substituted pyridine **137** (Scheme 42) contains four different ring labels, provided nitrogen is included. Irradiation of this compound at 254 nm resulted in the formation of a small yield of the 1,4-bonded Dewar-pyridine **138** and larger yields of the azaprismane derivatives **139** and **140**, which were thermally converted back to **137** or to pyridines **141** and **142**, respectively. The conversion of **137** $\rightarrow$ **138** $\rightarrow$ **139** is straightforward; the formation of **140** from **137** requires rearrangement. The pathway suggested, as shown in Scheme 43, involves initial formation of the 2,5-bonded Dewar-pyridine **143**, which isomerizes to the 1,4-bonded isomer **144** via a 1,3-shift. Ring closure then leads to the observed azaprismane **140**.[54,55]

It is interesting to note that these conversions indicate a strong preference for formation of the 1,4-bonded Dewar-pyridine isomer despite the prediction that the 2,5-isomer is the more stable isomer. The conversion of pyridine **145** (Scheme 44) to the 1,4-bonded Dewar-pyridine **146** is another example of this preference.[56]

When pyridine derivatives **147**, **148**, and **149** (Scheme 45) were irradiated at 254 nm using a slow transference technique, however, the 2,5-bonded Dewar-pyridines were the major or only valence isomers formed.[57] All of these Dewar-pyridine isomers rearrange at 160°C to the corresponding pyridine. Preference for 2,5-bonding was also observed in the photoisomerizations of tri-*t*-butylpyridines **155**, **156**, and **157** to the Dewar-pyridine **158**, **159**, and **160** shown in Scheme 46. As expected, preference is for the 2,5-bonded Dewar isomers, in which steric interference of the three adjacent t-butyl groups is minimized.

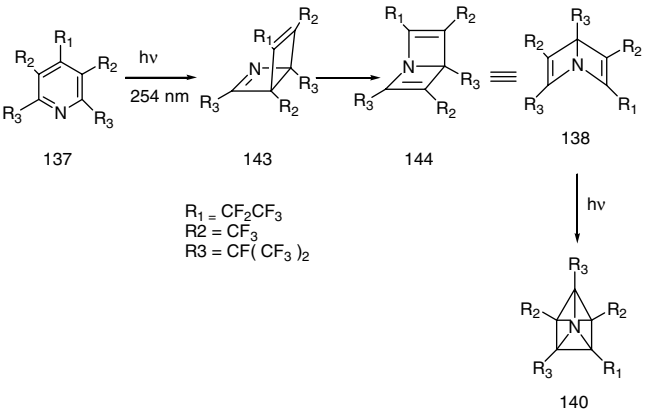

SCHEME 43

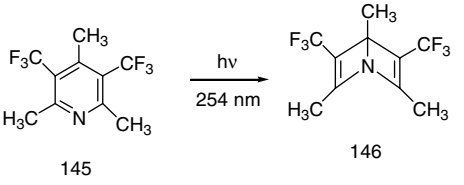

SCHEME 44

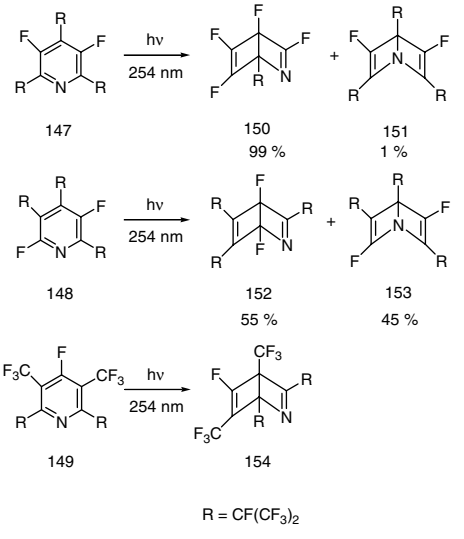

SCHEME 45

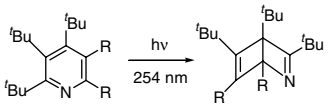

155 R = CO_2CH_3 158
156 R = CF_3 159
157 R = CN 160

SCHEME 46

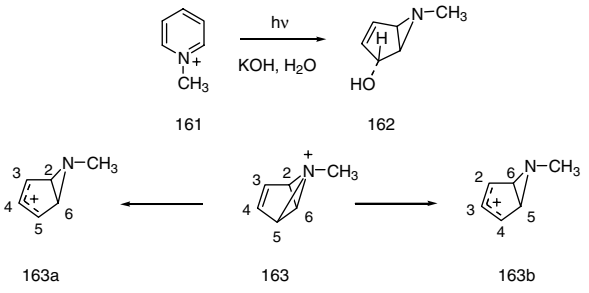

161 162

163a 163 163b

SCHEME 47

97.4 Pyridinium Cation Photochemistry

Some years ago it was shown that *N*-methlypyridinium chloride **161** undergoes photohydration to yield 6-methylazabicyclo[3.1.0]hex-3-en-2-0l **162** (Scheme 47). This product appeared to result from formation and hydration of an azabicyclohexenyl cation.

Labeling experiments, however, revealed that, in some cases, 1,2-shifts of nitrogen precede nucleophilic capture of the bicyclic cation. These shifts are consistent with formation and statistical opening of a 1-methylazoniabenzvalene **163**, resulting in the formation of unrearranged and rearranged azabicyclohexenyl cations **163a** and **163b**, respectively, which are both captured by water.[58]

Recent experimental and theoretical studies indicate that 2,6-bridging is the primary photochemical event and that azabicyclohexenyl cation **163b** can be captured by solvent or be converted to the azoniabenzvalene cation **163**. In addition to opening to **163b** as previously suggested, it also appears that **163** can be intercepted directly by nucleophilic attack at its allylic bridgehead positions.[59]

2,6-Bridging, which must arise via the π,π^* state of the pyridinium ring, is quite different from Dewar-pyridine formation observed upon irradiation of neutral pyridine, in which the lower-energy n,π^* state is also accessible. Indeed, transient absorption spectroscopy following pulsed excitation of the pyridinium cation in acetonitrile revealed that the slower decay component, associated with decay of the n,π^* state is totally missing while the first component due to motion along the π,π^* reaction pathway remains practically unchanged.[33] Taken together, these results suggest that the $S_2(\pi,\pi^*)$ state of pyridine leads to the 2,6-bridged isomer while the $S_1(n,\pi^*)$ state or some state derived from it, gives rise to the Dewar-valence isomer. It is interesting to note that in the case of benzene, Dewar-benzene formation requires excitation to a state of higher energy (i.e., $S_2(\pi,\pi^*)$,[60] while in the case of pyridine and its dimethyl derivatives, Dewar formation is enhanced by population of an excited state that is of lower energy than the first (π,π^*) state.[47]

In addition to the mechanistic interest of the photoreactions of pyridinium cations, the bicyclic products have several interesting features. Both the *N*-alkyl group and OH group adopt the *exo* orientation with respect to the bicyclic skeleton. Furthermore, the photochemical step fixes the relative configuration of the three new stereogenic carbon atoms. It is now recognized that photohydration of *N*-substituted pyridinium cations provides a powerful approach to a variety of synthetically useful materials.[61–65]

References

1. Tiefenthaler, H., Dorschelen, W., Goth, H., and Schmid, H., Photoisomerisierung von pyrazolen und indazolen zu imidazolen-bzw, benzimadazolen und 2-aminobenzonitrilen, *Helv. Chim. Acta*, **50**, 2244, 1967.
2. For a discussion of permutation pattern analysis in aromatic phototransposition chemistry and its application to the analysis of the phototransposition reactions of five-membered heteroaromatics, see (a) Barltrop, J.A. and Day, A.C., Ring permutations: a novel approach to aromatic phototransposition reactions, *J. Chem. Soc., Chem. Commun.*, 177, 1975; and (b) Barltrop, J., Day, A.C., Moxon, P.D, and Ward, R.R., Permutation patterns and the phototranspositions of 2-cyanopyrroles, *J. Chem. Soc., Chem. Commun.*, 786, 1975.
3. Padwa, A., Photochemical rearrangements of five membered ring heterocycles, in *Rearrangements in Ground and Excited States*, Vol. 3, de Mayo, P., Ed., Academic Press, New York, 1980, 501.
4. Beak, P., Miesel, J.L., and Messer, W.R., The photoisomerization of 1,4,5-trimethylimidazole and 1,3,5-trimethylpyrazole, *Tetrahedron Lett.*, 5315, 1967.
5. Beak, P. and Messer, W.R., Photorearrangements of some *N*-methyldiazoles, *Tetrahedron*, 25, 3287, 1969.
6. Barltrop, J.A., Day, A.C., Mac, A.G., Shahrisa, A., and Wakamatsu, S., Competing pathways in the phototransposition of pyrazoles, *J. Chem. Soc.*, *Chem. Commun.*, 604, 1981.
7. (a) Barltrop, J.A., Day, A.C., and Irving, E., Phototransposition of cyanothiophenes: permutation pattern analysis and the chemical trapping of an intermediate 5-thiabicyclo[2.10]pent-2-ene, *J. Chem. Soc., Chem. Commun.,* 881, 1979; (b) Barltrop, J.A., Day, A.C., and Irving, E., Cyano-substituted thiabicyclo[2.1.0]-pent-2-enes: reactions and relevance to cyanothiophene phototransposition, *J. Chem. Soc.*, *Chem. Commun.*, 966, 1979.Barltrop, J.A., Day, A.C., and Ward, R.W., Phototransposition of 2-cyanopyrroles: evidence for the intermediacy of 5-azabicyclo[2.1.0]pent-2-enes, *J. Chem. Soc., Chem. Commun.*, 131, 1978.
8. Pavlik, J. W. and Kurzweil, E.M., Phototransposition chemistry of 1-methylpyrazole. Deuterium, methyl and fluorine substitution, *J. Org. Chem.,* 56, 6313, 1991.
9. Pavlik, J.W. and Kebede, N., Photochemistry of phenyl-substituted 1-methylpyrazoles, *J. Org. Chem.*, 62, 8325, 1997.
10. Pavlik, J.W., Kebede, N., Bird, N.P., Day, A.C., and Barltrop, J.A., Phototransposition chemistry of 1-methyl-4-phenylpyrazole. A new intermediate on the p_4 pathway, *J. Org. Chem.*, 60, 8138, 1995.
11. Hassner, A., Vinyl azides and nitrenes, in *Azides and Nitrenes. Reactivity and Utility*, Scriven, E.F.V., Ed., Academic Press, Orlando, FL, 1984, 35.
12. Hassner, A. Wiegand, N.H., and Gottlieb, H.E., Kinetics of thermolysis of vinyl azides. Empirical rules for formation of azirine and rearranged nitriles, *J. Org. Chem.,* 51, 3176, 1986.
13. Isomura, K., Hirose, Y., Shuyama, H., Abe, S., Ayabe, G.-i., and Taniguichi, H., Unusual formation of oxazoles by base or acid-catalyzed ring opening of 2-acyl-2H-azirines, *Heterocycles*, 9, 1207, 1978.
14. Pavlik, J.W., Tongcharoensirikul, P., and French, K.M., Phototransposition chemistry of 4-substituted isothiazoles. The P_4 permutation pathway, *J. Org. Chem.*, 63, 5592, 1998.
15. Padwa, A., Azirine photochemistry, *Acc. Chem. Res.*, 9, 371, 1976.
16. Newman, H., Photochemistry of 3,5-diphenyl-1,2,4-oxadiazole, I. Photolysis in aprotic media, *Tetrahedron Lett.*, 2417, 1968.
17. Newman, H., Photochemistry of 3,5-diphenyl-1,2,4-oxadiazoles. II. Photolysis in protic media, *Tetrahedron Lett.*, 2421, 1968.
18. For a review, see Vivona, N. and Buscemi, S., Photoinduced molecular rearrangements of O-N bond containing five-membered heterocycles. An assay for 1,2,4- and 1,2,5-oxadiazoles, *Heterocycles*, 41, 2095, 1995.
19. Buscemi, S., Cicero, M., Vivona, N., and Caronna, T., Photochemical behavior of some 1,2,4-oxadiazole derivatives, *J. Chem. Soc., Perkin Trans. 1*, 1313, 1988.

20. Buscemi, S., Cicero, M. Vivona, N., and Caronna, T., Heterocyclic photorearrangements. Photochemical behavior of some 3,5-disubstituted 1,2,4-oxadiazoles in methanol at 254 nm, *J. Heterocyclic Chem.*, 25, 931, 1988.
21. Buscemi, S., Pace, A., Pibiria, I., and Vivona, N., Competing ring-photoisomerization pathways in the 1,2,4-oxadiazole series. An unprecedented ring-degenerate photoisomerization, *J Org. Chem.,* 67, 6253, 2002.
22. Buscemi, S. and Vivona, N., Heterocyclic photorearrangements. Photoinduced rearrangements of 1,2,4-oxadiazoles substituted by an XYZ side chain sequence, *J. Heterocyclic Chem.*, 25, 1551, 1988.
23. Buscemi, S. and Vivona, N., Heterocyclic photorearrangements — photoinduced rearrangements of some 3-aroylamino-5-methyl-1,2,4-oxadiazoles, *Heterocycles*, 29, 737, 1989.
24. Buscemi, S., Macaluso, G., and Vivona, N., Heterocyclic photorearrangements — photochemical behavior of some 3-acetylamino-5-aryl-1,2,4-oxadiazoles. A photoinduced *iso*-heterocyclic rearrangement, *Heterocycles*, 29, 1301, 1989.
25. Buscemi, S., Cusmano, G., and Gruttadauria, M., Heterocyclic photorearrangements. Photoinduced rearrangement of 3-styryl-1–2,4-oxadiazoles, *J. Heterocyclic Chem.*, 27, 861, 1990.
26. Buscemi, S. and Vivona, N., Heterocyclic photorearrangements. Some investigations of the photochemical behavior of 3-acylamino-1,2,4-oxadiazoles. Synthesis of the quinazolin-4-one system, *J. Chem. Soc., Perkin Trans. 2*, 187, 1991.
27. Buscemi, S., Pace, A., Vivona, N., Caronna, T., and Galia, A., Photoinduced single electron transfer on 5-aryl-1,2,4-oxadiazoles: some mechanistic investigations in the synthesis of quanazolin-4-ones, *J. Org. Chem.*, 64, 7028, 1999.
28. van Tamelen, E.E. and Papas, S.P., Chemistry of Dewar benzene. 1,2,5-Tri-*t*-butylbicyclo[2.2.0]hexa-2,5-diene, *J. Am. Chem. Soc.*, 84, 3789, 1962.
29. Wilzbach, K.E. and Kaplan, L., Photoisomerization of tri-*t*-butylbenzenes. Prismane and benzvalene isomers, *J. Am. Chem. Soc.*, 87 4004, 1965.
30. Kaplan, L. and Wilzbach, K.E., Benzvalene, the tricyclic valence isomer of benzene, *J. Am. Chem. Soc.*, 89, 1031, 1967.
31. Wilzbach, K.E. and Kaplan, L., Photoisomerization of dialkylbenzenes, *J. Am. Chem. Soc.,* 86, 2307, 1964.
32. Chachisvilis, M. and Zewail, A.H., Femtosecond dynamics of pyridine in the condensed phase: valence isomerization by conical intersections, *J. Phys. Chem.A.*, 103, 7408, 1999.
33. Kaplan, L. and Wilzbach, K.E., Photolysis of benzene vapor. Benzvalene formation at wavelengths 2537–2370, *J. Am. Chem. Soc.,* 90, 3291, 1968.
34. Villa, E., Amirav, A., and Lim, E.C., Single-vibronic-level and excitation-energy dependence of radiative and nonradiative transitions in jet-cooled S_1 pyridine, *J. Phys. Chem.* 92, 5393, 1988.
35. Dongping, Z., Diau, E.W.-G., Bernhardt, T.M., DeFeyler, S., Roberts, J.D., and Zewail, A.H., Femtosecond dynamics of valence-bond isomers of azenes: transition states and conical intersections, *Chem. Phys. Lett.*, 298, 129, 1998.
36. Lobastov, V.A., Srinivasan, R., Goodson, B.M., Ruan, C.-Y., Feenstra, J.S., and Zewail, A.H., Ultrafast diffraction of transient molecular structures in radiationless transitions, *J. Phys. Chem. A.,* 50,11159, 2001.
37. Sobolewski, A.L. and Domcke, W., Photophysically relevant potential energy functions of low-lying singlet states of benzene, pyridine and pyrazine: an *ab initio* study, *Chem. Phys. Lett.,* 180, 381, 1991.
38. Linnell, R.J. and Noyes, W.A., Photochemical studies. XLIV. Pyridine and mixtures of acetone and pyridine, *J. Am. Chem. Soc.*, 73, 3986, 1951.
39. Mathias, E. and Heicklen, J., The gas phase photolysis of pyridine, *Mol. Photochem.*, 4, 483, 1972.
40. Wilzbach, K.E. and Rausch, D.J., Photochemistry of nitrogen heterocycles. Dewar pyridine and its intermediacy in photoreduction and photohydration of pyridine, *J. Am. Chem. Soc.*, 92, 2178, 1970.
41. Joussot-Dubien, J. and Houdard, J., Reversible photolysis of pyridine in aqueous solution, *Tetrahedron Lett.*, 4389, 1967.

42. Joussot-Dubien, J. and Houdard-Peyrere, J., Photolyse de la pyridine en solution aqueous, *Bull Soc. Chim. Fr.*, 2619, 1969.
43. Chapman, O.L., MacIntosh, C.L., and Pacansky, J., Cyclobutadiene, *J. Am. Chem. Soc.*, 95, 614, 1973.
44. Roebke, W., Gas phase photolysis of 2-picoline, *J. Phys. Chem.,* 74, 4198, 1970.
45. Caplain, S. and Lablache-Combier, A., Gas phase photochemistry of picolines and lutidines, *J. Chem. Soc., Chem. Commun.,* 1018, 1969.
46. Pavlik, J.W., Kebede, N., Thompson, M., Day, A.C., and Barltrop, J.A., Vapor-phase photochemistry of dimethylpyridines, *J. Am. Chem. Soc.*, 121, 5666, 1999.
47. Cao, Z., Zhang, Q., and Peyerimhoff, S.D., Theoretical characterization of photoisomerization channels of dimethylpyridines on the singlet and triplet potential energy surfaces, *Chem.-Eur. J.,* 7, 1927, 2001.
48. Ogata, Y. and Takagi, K., Photoisomerization of 2-pyridylacetonitrile to anthranilonitrile, *J. Am. Chem. Soc.*, 96, 5933, 1974.
49. Ogata, Y. and Takagi, K., Photochemistry of 2-picolines in alkaline media. Intermediacy of Dewar-pyridines and their methides, *J. Org. Chem.,* 43, 944, 1978.
50. Takagi, K. and Ogata, Y., Photoisomerization of substituted 2-methylpyridines to *ortho*-substituted anilines, *J. Chem. Soc., Perkin Trans. 2*, 1148, 1977.
51. Barlow, M.G., Dingwall, J.G., and Haszeldine, R.N., Valence-bond isomers of heterocyclic compounds: isomers of pentakis-(pentafluoroethyl)pyridine, *J. Chem. Soc., Chem. Commun.*, 1580, 1970.
52. Barlow, M.G., Haszeldine, R.N., and Dingwall, J.G. Valence-bond isomer chemistry. IV. The valence-bond isomers of pentakis-(pentafluoroethyl)pyridine, *J. Chem. Soc., Perkin Trans. 1*, 1542, 1973.
53. Chambers, R.D., Middleton, R., and (in part) Corbally, R.P., Transposition in aromatic rings, *J. Chem. Soc., Chem. Commun.*, 731, 1975.
54. Chambers, R.D. and Middleton, R., Photochemistry of halogenocarbon compounds. 3. Rearrangements involving azaprismanes, *J. Chem. Soc., Perkin Trans. 1*, 1500, 1977.
55. Kobayashi, Y., Ohsawa, A., Baba, M., Sato, T., and Kumadaki, I., Studies on organic fluorine compounds. XX. Synthesis and reactions of a substituted Dewar pyridine, *Chem. Pharm. Bull.*, 24, 2219, 1976.
56. Chambers, R.D. and Middleton, R., Stable 2-azabicyclo[2.2.0]hexa-2,5-diene derivatives, *J. Chem. Soc., Chem. Commun.,* 154, 1977.
57. Kaplan, L., Pavlik, J.W., and Wilzbach, K.E., Photohydration of pyridinium ions, *J. Am. Chem. Soc.*, 94, 3283, 1972.
58. King, R.A., Lüthi, H.P., Schaefer, III, H.F., Glarner, F., and Burger, U., The photohydration of *N*-alkylpyridinium salts: theory and experiment, *Chem.-Eur. J.,* 7, 1734, 2001.
59. Bryce-Smith, D. Gilbert, A., and Robinson, D.A., Direct transformation of the second excited singlet state of benzene into Dewar benzene, *Angew. Chem. Int. Ed. Engl.*, 10, 745, 1971.
60. See, for example, (a) Glarner, F., Acar, B., Etter, I., Damiano, T., Acar, E.A., Bernardinelli, G., and Burger, U., The photo-hydration of *N*-glycosyl pyridinium salts and of related pyridinium N,O-acetate, *Tetrahedron*, 56, 4311, 2000; (b) Acar.E. A., Glarner, F., and Burger, U., Aminocyclopentitols from *N*-alkylpyridinium salts. A photochemical approach, *Helv. Chim. Acta*, 81 1095, 1998; (c) Glarner, F., Thornton, S.R., Schaerer, D., Bernardinelli, G., and Burger, U., 6-Azabicyclo[3.1.0]-hex-3-en-2-ol derivatives, photochemically generated building blocks for bicyclic β-lactams, *Helv. Chim. Acta*, 80, 121, 1997; (d) Cho, S.J., Ling, R., Kim, A., and Mariano, P.S., A versatile approach to the synthesis of (+)-mannostatin A analogues, *J. Org. Chem.*, 65, 1575, 2000; (e) Ling, R. and Mariano, P.S., A demonstration of the synthetic potential of pyridinium salt photochemistry by its application to a stereocontrolled synthesis of (+)-mannostatin A, *J. Org. Chem.*, 63, 6072, 1998; (f) Ling, R., Yoshida, M., and Mariano, P.S., Exploratory investigations probing a preparatively versatile, pyridinium salt photoelectrocyclization-solvolytic aziridine ring opening sequence, *J. Org. Chem.,* 61, 4439, 1996.

98

Photochemistry of Thiazoles, Isothiazoles, and 1,2,4-Thiadiazoles

James W. Pavlik
Worcester Polytechnic Institute

98.1 Introduction and Historical Review

The photochemistry of five-membered heteroaromatic compounds containing two heteroatoms has been of interest[1] since the first report that *N*-methylpyrazole **1** (Scheme 1) undergoes photoconversion to *N*-methylimidazole **2**.[2] Subsequent mechanistic studies revealed that this formally simple isomerization is mechanistically quite complex,[3–8] involving competition between the two pathways shown in Scheme 2. These include the electrocyclic ring closure–heteroatom migration pathway (A) that leads to imidazole **2a**, with interchange of the N2 and C4 ring atoms, and **2b**, with interchange of both N2–C3 and C4–C5. Alternatively, photocleavage of the N1–N2 bond initiates a second primary pathway (B) that leads to imidazole **2c** with interchange of the N2 and C3 atoms of the pyrazole ring. This pathway, which is enhanced by substitution at C4 of the pyrazole ring, is known to involve enaminonitrile **3** and enaminoisonitrile **4** intermediates.

The photoisomerization of isothiazole **5** to thiazole **6** (Scheme 3) was the first reported phototransposition in the isothiazole-thiazole heterocyclic system.[9] Later work published during the period 1971 to 1978 by Lablache-Combier and co-workers,[10] by Vernin and colleagues,[11–17] and by Maeda and Kojima[18–21] also showed that methylisothiazoles phototranspose to methylthiazoles and that phenyl-substituted isothiazoles and thiazoles also undergo phototransposition reactions. A surprising finding, however, was that phenylisothiazoles were not observed to react via the N2–C3 interchange pathway, an important pathway in pyrazole photochemistry. Furthermore, a common conclusion of these studies was that these photoisomerizations proceed by way of tricyclic zwitterionic intermediates, which had no counterparts in pyrazole photochemistry.

98.2 Mechanistic Studies

Methylisothiazoles and Methylthiazoles

Reinvestigation showed that methylisothiazoles **7**, **8**, and **9** (Table 98.1) undergo phototransposition in ethanol solvent to yield methylthiazoles **10, 11,** and **12** in the yields shown in Scheme 4.[22] Thus, although 5-methylisothiazole had been previously reported to transpose to 5-methylthiazole **12**, 3-methylisothiazole

0-8493-1348-1/04/$0.00+$1.50

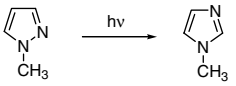

SCHEME 1

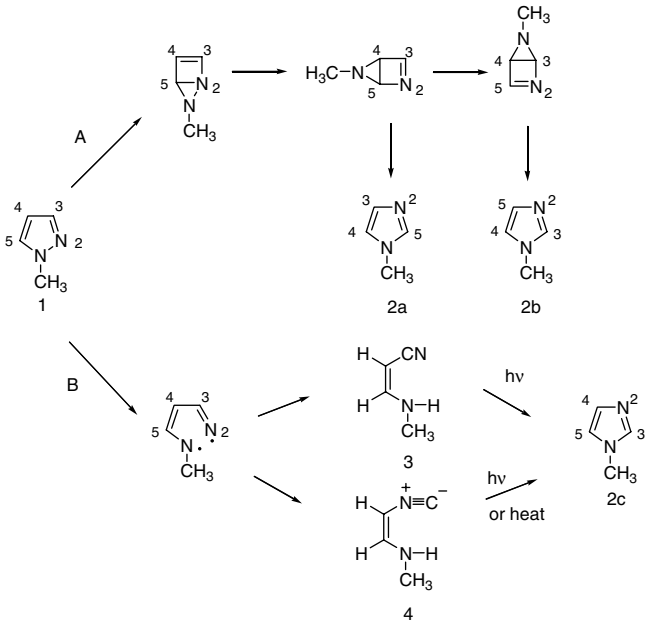

SCHEME 2

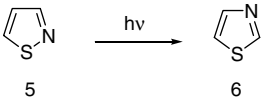

SCHEME 3

7, and 4-methylthiazole **2**,[10] the latter two products could not be detected in the reaction mixture. All of the products formed (Scheme 4) can be viewed as the result of N2–C3 interchange reactions. This indicates that the methylisothiazole-to-methylthiazole transposition is mechanistically analogous to the N2–C3 interchange reaction observed for pyrazole-to-imidazole photoisomerization. Accordingly, it is not necessary to invoke the intermediacy of tricyclic zwitterions as intermediates in these reactions.[22]

Although methylthiazoles do not undergo phototransposition in a variety of neutral solvents, methylthiazolium cations **10H**$^+$ through **12H**$^+$, formed by dissolving methyl-thiazoles **10** through **12** in trifluoroacetic acid (TFA), do undergo phototransposition (Scheme 5) to methylisothiazolium ions **9H**$^+$, **7H**$^+$, and **8H**$^+$, respectively. These N2–C4 interchange reactions are consistent with the electrocyclic ring closure–heteroatom migration mechanism (Scheme 6) in which the heteroatom migrates regiospecifically toward the positively charged azetine nitrogen. This regiospecificity is in contrast to that observed in the neutral 1-methylimidazoles, in which the heteroatom only migrates away from the azetine ring nitrogen to give only imidazole-to-imidazole transpositions.

TABLE 98.1 UV Absorption Maxima for Methylisothiazoles and Methylthiazoles in Hexane Solution

Compound	λ max (nm)	ε(at 254 nm)
 7	260	6000
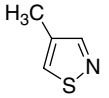 8	261	6000
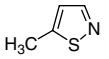 9	260	5000
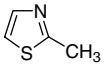 10	259	4500
 11	258	5500
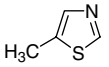 12	258	4500

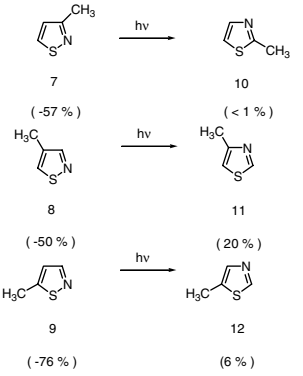

SCHEME 4

Phenylisothiazoles and Phenylthiazoles

Interconversions in Benzene Solution

Vernin and colleagues conducted extensive studies of the phototransposition chemistry of phenylisothiazoles **13**, **14**, and **15** and phenylthiazoles **16**, **17**, and **18** in benzene solution (see also Table 98.2).[12–17]

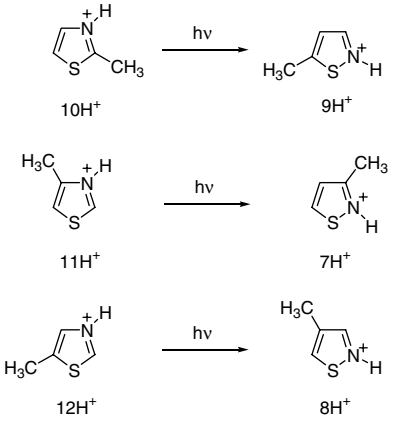

SCHEME 5

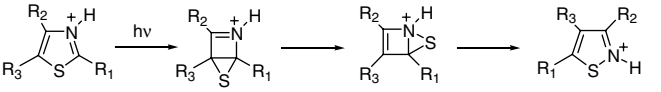

SCHEME 6

From these studies, they concluded that although most of the products observed could be explained by the electrocyclic ring closure–heteroatom migration mechanism, the apparent conversion of 5-phenylthiazole **18** to 5-phenylisothiazole **15** and 3-phenylisothiazole **13** could not occur by this mechanistic pathway. Accordingly, Vernin et al. concluded that one mechanistic pathway could not account for the formation of all products and suggested that phenylisothiazoles **13**, **14**, and **15** and phenylthiazoles **16**, **17**, and **18** react by the electrocyclic ring closure–heteroatom migration mechanism and by the mechanism postulated by Kellog[23] to account for the interchange of any two ring atoms in the 5-membered ring.

Later work, however, showed that 5-phenylthiazole **18** transposes to 4-phenylisothiazole **14** but that 5-phenylisothiazole **15** and 3-phenylisothiazole **13** are not formed in this reaction. As a consequence, it is not necessary to invoke the Kellogg mechanism to explain the formation of any products in the photoreactions of phenylthiazoles or phenylisothiazoles.[24]

According to the observed photochemical products and the results of deuterium labeling studies, the six isomeric phenylisothiazoles **13**, **14**, and **15** and phenylthiazoles **16**, **17**, and **18** can be organized into a tetrad of four photochemically interconverting isomers and a dyad in which 5-phenylthiazole **18** phototransposes to 4-phenylisothiazole **14** (Scheme 7), the only isomer that did not yield a transposition product upon irradiation in benzene solution. In addition to transposing to members of the tetrad, the transposition of 5-phenylisothiazole **15** to 5-phenylthiazole **18**, the first member of the dyad, in less than 1% yield, was the only observed conversion between the tetrad and dyad. This conversion was assumed to occur via the N2–C3 interchange reaction pathway.[24]

The photoisomerizations within the tetrad are consistent with the electrocyclic ring closure–heteroatom migration mechanistic pathway shown in Scheme 8. According to this mechanism, photochemical excitation of any member of the tetrad is predicted to result in electrocyclic ring closure, leading to the formation of azathiabicyclo[2.1.0] pentene intermediates. The four bicyclic intermediates, and hence the four members of the tetrad, are interconvertible via 1,3-sigmatropic shifts of sulfur around the four sides of the azetine ring. Thus, sulfur migration followed by rearomatization allows sulfur insertion into the four different sites in the carbon–nitrogen sequence.

TABLE 98.2 UV Absorption Maxima for Phenylisothiazoles and Phenylthiazoles

Compound	λ max (nm)	ε max	Solvent
 13	271	17,370	cyclohexane
 14	268 240	9,985 8,810	methylcyclohexane methanol
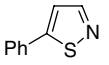 15	265	15,090	methylcyclohexane
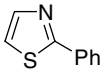 16	285	14,290	cyclohexane
 17	254 252	14,600 13,370	methylcyclohexane methanol
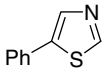 18	274	13,309	cyclohexane

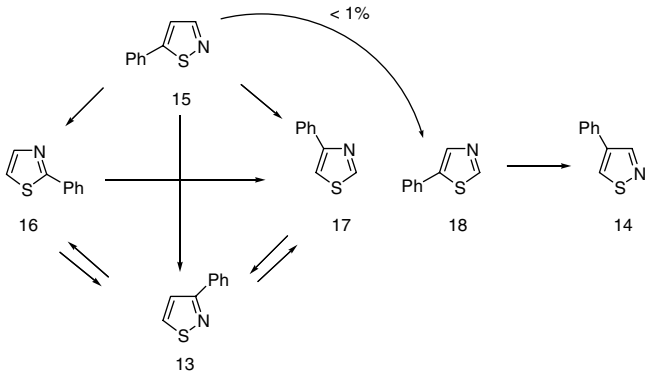

SCHEME 7

Insertion of sulfur between ring positions C1 and C4, or betweem C1 and C2 of the 3-phenylazetine ring leads to the same compound, 5-phenylthiazole **18**. Similarly, insertion of a sulfur atom between N3 and C4, or between N3 and C2, leads to 4-phenylisothiazole **14**. Accordingly, because of the symmetry of the 3-phenylazetine ring, only a dyad results. This symmetry is removed, however, in the case of

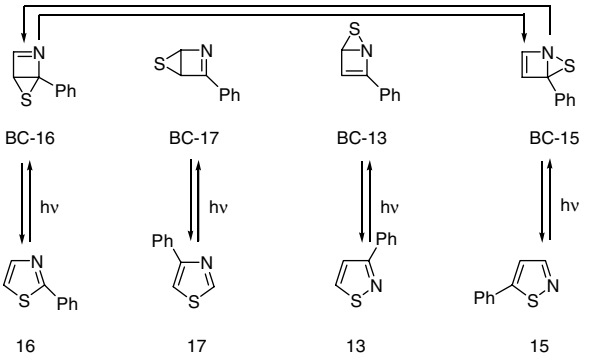

SCHEME 8

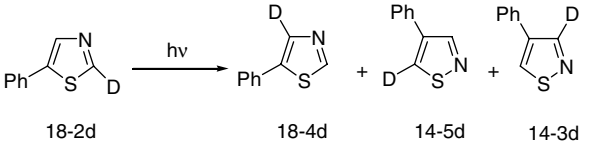

SCHEME 9

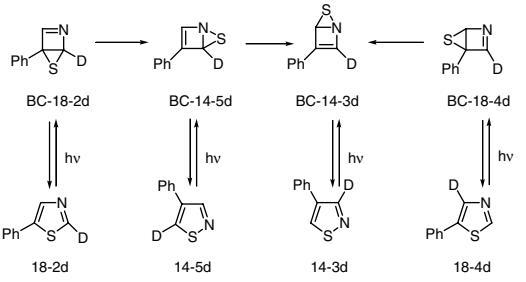

SCHEME 10

2-deuterio-5-phenylthiazole **18-2d**. Hence, deuterium labeling expands the dyad into a tetrad. As expected, irradiation of 2-deuterio-5-phenylthiazole **18-2d** resulted in the formation of three isomeric products (i.e., 4-deuterio-5-phenylthiazole **18-4d**, 5-deuterio-4-phenylisothiazole **14-5d,** and 3-deuterio-4-phenylisothiazole **14-3d** (Scheme 9). These deuterium-labeling results are entirely consistent with the electrocyclic ring closure-heteroatom migration mechanism shown in Scheme 10.

Photodeuteration Studies

Maeda and Kojima studied the photochemistry of phenylisothiazoles **13**, **14**, and **15** and phenylthiazoles **16**, **17**, and **18** in benzene or ether saturated with D_2O.[18–21] They reported that 2-phenylthiazole **16**, 4-phenylthiazole **17**, and 5-phenylisothiazole **15** each phototranspose under these conditions to 3-phenylisothiazole **13** with deuterium incorporation at ring position 4. Irradiation of 2-phenylthiazole **16** also led to the formation of 4-phenylthiazole **17** but without deuterium incorporation. Finally, they reported that none of the reactants undergo photodeuteration prior to transposition.

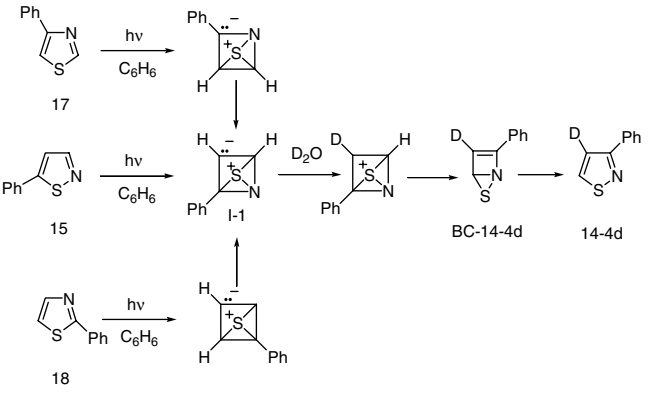

SCHEME 11

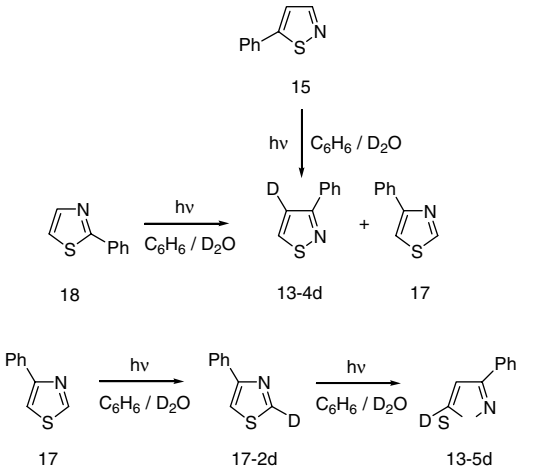

SCHEME 12

Maeda and Kojima argued that deuterium incorporation demands a carbanion intermediate. They, therefore, rejected the electrocyclic ring closure–heteroatom migration mechanism and concluded that all three reactants isomerize to 3-phenylisothiazole **13** via a common tricyclic zwitterionic intermediate I-1 (Scheme 11) that reacts with D_2O with deuterium incorporation. Thus, according to these workers, the carbanion intermediate responsible for deuterium incorporation is on the reaction pathway leading from 4-phenylthiazole **17**, 5-phenylisothiazole **15**, and 2-phenylthiazole **18** to 3-phenylisothiazole **14**.

Later work,[24] shown in Scheme 12, confirmed that 3-phenylisothiazole **13** is formed with deuterium incorporation at C4 upon irradiation of either 2-phenylthiazole **18** or 5-phenylisothiazole **15** in benzene/D_2O but revealed that **13** is formed with approximately twice the extent of deuterium incorporation from the latter reactant. Furthermore, it was also shown that 4-phenylthiazole **17** undergoes photodeuteration at C_2 when irradiated in benzene/D_2O more rapidly than it transposes to 3-phenylisothiazole **13**. Upon further irradiation, the initially formed 2-deuterio-4-phenylthiazole **17-2** transposes to 5-deuterio-3-phenyl-isothiazole **13-5d** without additional incorporation of deuterium.

These results show that, within the tetrad (Scheme 8), the intermediate that incorporates deuterium is on the reaction pathway leading from 2-phenylthiazole **16** and 5-phenylthiazole **15** to 3-phenylisothiazole **13** but is not on the pathway leading from 4-phenylthiazole **17** to 3-phenylisothiazole **13.** Accordingly,

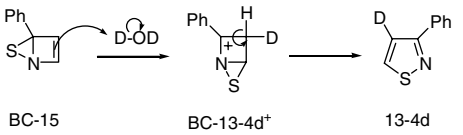

SCHEME 13

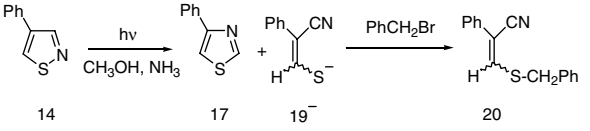

SCHEME 14

although Maeda and Kojima concluded that the photodeuteration reactions demanded the intermediacy of tricyclic zwitterionic intermediates, these results actually preclude their involvement in the phototransposition pathway.

These results can be rationalized by the electrocyclic ring closure–heteroatom migration mechanism (Scheme 8) by assuming that **BC-15** (Scheme 13), formed by electrocyclic ring closure of 5-phenylisothiazole **15,** undergoes deuteration with simultaneous sulfur migration to yield **BC-13–4d**$^+$. This accounts for the greater deuterium incorporation when 3-phenylisothiazole **13** is formed from 5-phenylisothiazole **15** than from 2-phenylthiazole **16**. From 5-phenylisothiazole **15**, all molecules of 3-phenylisothiazole **13** must arise via **BC-15**; (i.e., **15** + hν → **BC-15** → **BC-13** → **13** with deuterium incorporation. From 2-phenylthiazole **16**, however, 3-phenylisothiazole **13** may be formed by the pathway **16** + hυ → **BC-16** → **BC-15** → **BC-13** → **13** with deuterium incorporation or by the pathway **16** + hυ → **BC-16** → **BC-17** → **BC-13** → **13** without passing through **BC-15** and, hence, without deuterium incorporation.

These results reveal that both isothiazoles and pyrazoles phototranspose by the electrocyclic ring closure–heteroatom migration mechanism and that tricyclic zwitterionic intermediates, once thought to be important in thiazole and isothiazole photochemistry, need not be invoked.

The N2-C3 Interchange Pathway: The Effect of Added Base

A significant difference between the photochemistry of pyrazoles and the photoreactions of phenylisothiazoles in benzene solutions is the almost complete absence of transposition of the latter via the N2-C3 interchange reaction pathway. Indeed, although 4-phenylisothiazole **14** is expected to be the most reactive isomer by this pathway, it is the only isomer that was not observed to yield a phototransposition product upon irradiation in benzene solution. This is not due to the low reactivity of the isomer because the quantum yield for disappearance of this compound ($\Phi = 0.41$) indicates that it is the most reactive of the phenylisothiazole isomers.

In contrast to the reactivity in benzene solution, when 4-phenylisothiazole **14** was irradiated in methanol containing a small quantity of base such as aqueous NH_3 or triethylamine (TEA),[24] the N2-C3 interchange product, 4-phenylthiazole **17**, was obtained in 90% yield (Scheme 14), with a small amount of the deprotonated photocleavage product **19**$^-$ that was trapped by reaction with benzylbromide to yield the (*E/Z*)-benzylthioether **20**. Conversion of **14-5d** to **17-5d** under these conditions confirmed that the transposition occurs via the N2-C3 interchange pathway. Although phototransposition is enhanced by the addition of base to the reaction medium, if the reaction is carried out in methanol containing HCl, phototransposition is completely quenched, and the only product observed is a large yield of the photocleavage product **19H** (Scheme 15).

Convincing evidence for the intermediacy of an isocyanide cleavage product in the N2-C3 interchange transposition was obtained by studying the photochemistry of 4-benzylisothiazole **21**

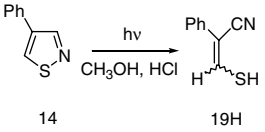

SCHEME 15

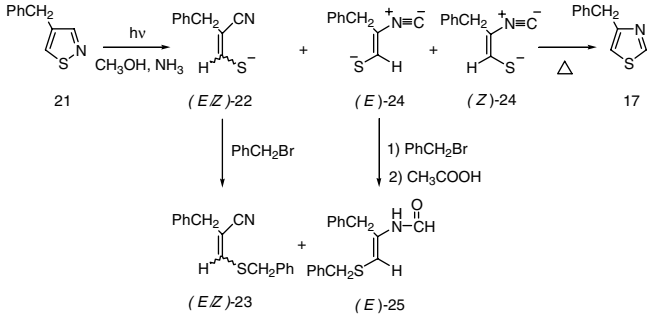

SCHEME 16

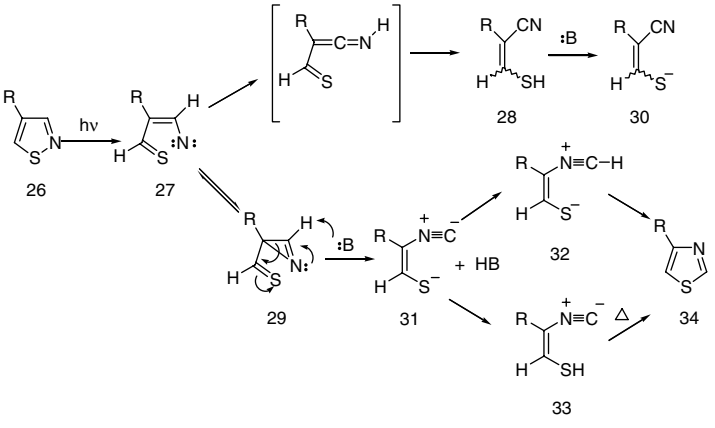

SCHEME 17

(Scheme 16). Irradiation in methanol-NH_3 led to the formation of 4-benzylthiazole **17**, the N2-C3 interchange product, and to the nitrile photocleavage product **22**, which was trapped as the benzylthioether **23**, and to the formation of the (*E*) isocyanide photocleavage product (*E*)-**24**, which was trapped by reaction with benzylbromide followed by hydrolysis to yield (*E*)-formamide (*E*)-**25** and the (*Z*)-isocyanide photocleavage product (*Z*)-**24**, which was thermally converted to the observed phototransposition product **17**.

Mechanistically, it was suggested that the N2-C3 interchange reaction was initiated by photocleavage of the S–N bond in **26,** resulting (Scheme 17) in the formation of β-thioformylvinyl nitrene **27** that is expected to rearrange to the cyanothiol photocleavage product **28** and also to be in equilibrium with an undetected thioformylazirine **29**. In the absence of an external base, β-thioformylvinyl nitrene **27** is thus converted totally to cyanothiol **28**. As a result, upon irradiation in benzene or methanol containing HCl, 4-substituted isothiazoles only undergo photocleavage to cyanothiols. In the presence of NH_3 or TEA,

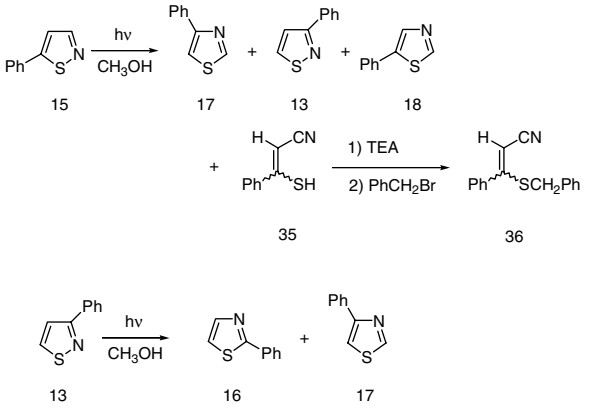

SCHEME 18

the base converts cyanothiol **28** to cyanosulfide **30** and, more importantly, the base can also deprotonate azirine **29**, resulting in its conversion to isocyanide **31**.

The fate of the isocyanide was suggested to depend on the nature of the substituent originally at C4 of the isothiazole ring. If the substituent is aromatic, the isocyanide is reprotonated at the isocyanide carbon to yield **32**, which spontaneously cyclizes to the 4-subsituted thiazole **34**, the observed N2-C3 interchange transposition product. If the substituent is not aromatic, **31** is reprotonated at sulfur to provide **33**, which has a higher energy barrier to cyclization. In these cases, the isocyanosulfides can be observed spectroscopically and can be trapped as their *N*-formylaminobenzyl thioether derivatives.

Although the photochemistry of 4-substituted isothiazoles is dominated by reactions initiated by cleavage of the S–N bond, as shown in Scheme 17, 5-phenyl- and 3-phenylisothiazoles **15** and **13**, react by competing photochemical pathways.[26] As shown in Scheme 18, 5-phenylisothiazole **15** undergoes phototransposition in methanol by the electrocyclic ring closure–heteroatom migration pathway to yield 4-phenylthiazole **17** in 6% yield and 3-phenylisothiazole **13** in 2% yield, and by the N2-C3 interchange pathway to yield 5-phenylthiazole **18** in 23%. The yield of **18**, the N2-C3 interchange product, was increased to 34% upon addition of TEA to the reaction medium, and to 42% when the irradiation of **15** was carried out in the more polar solvent, 2,2,2,-trifluoroethanol containing TEA. In addition to phototransposition, 5-phenylisothiazole **15** was also reported to undergo photocleavage to cyanothiol **35** that was trapped as its benzylthioether **36**. 3-Phenylisothiazole **13** also phototransposes by both reaction pathways; but without hydrogen at C3, the N2-C3 interchange pathway is not enhanced by the addition of a base.

These results indicate that the photochemistry of pyrazoles and isothiazoles can be understood in terms of one general mechanistic scheme involving competition between the electrocyclic ring closure–heteroatom migration and the N2-C3 interchange pathways. Although in the case of isothiazoles the addition of a base substantially alters the competition between these pathways, similar effects are not observed in pyrazole photochemistry. Presumably this is because pyrazoles and imidazoles are already sufficiently basic to deprotonate the azirine as shown in Scheme 17.

Phenyl-1,2,4-Thiadiazoles

Phenyl-substituted 1,2,4-thiadiazoles (see Table 98.3) undergo a variety of photoreactions, including photofragmentation, phototransposition, and a unique photo-ring expansion reaction.[26] As shown in Scheme 19, irradiation of 5-phenyl-1,2,4-thiadiazole **35** in acetonitrile solvent with light of Î > 290 nm results in the formation of benzonitrile **39**, the photofragmentation product, 3-phenyl-1,2,4-thiadiazole **36**, the phototransposition product, and phenyl-1,3,5-triazine **41** and diphenyl-1,3,5-triazine **42**, the two photo-ring expansion products. 3-Methyl-5-phenyl-1,2,4-thiadiazole **37** reacted similarly to yield

TABLE 98.3 UV Absorption Maxima for Phenyl Substituted 1,2,4-Thiadiazoles

Compound	λ max (nm)	ε max	Solvent
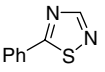 35	273 273	13,880 13,870	cyclohexane acetonitrile
 36	264	10,200	cyclohexane
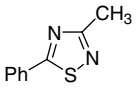 37	278	14,100	acetonitrile
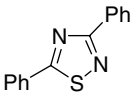 38	255	6190	cyclohexane

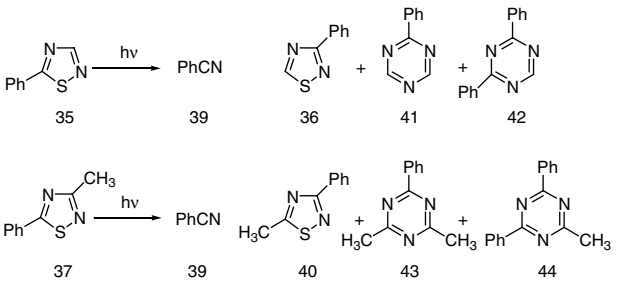

SCHEME 19

benzonitrile **39**, 5-methyl-3-phenyl-1,2,4-thiadiazole **40**, dimethylphenyl-1,3,5-triazine **43**, and methyldiphenyl-1,3,5-triazine **44**.

The phototransposition of **35** to **36** (and of **37** to **40**) can be explained by the electrocyclic ring closure-heteroatom migration mechanism shown in Scheme 20. Thus, photoexcitation of **35** is predicted to result in electrocyclic ring closure resulting in the formation of bicyclic species **BC-35**. 3-Phenyl-1,2,4-thiadiazole **36** can be formed by one or two sigmatropic shifts of sulfur, followed by aromatization. Reaction in the opposite direction would lead back to **35** via the intermediacy of **BC-35′**. Experiments using ^{15}N-labeling confirmed that sulfur can undergo sigmatropic shifts around all four sides of the diazetine ring in this bicyclic species. Thus (Scheme 21), irradiation of 5-phenyl-1,2,4-thiadiazole-4-^{15}N (**35-4-^{15}N**) led to the formation of 5-phenyl-1,2,4-thiadiazole-2-^{15}N (**35-2-^{15}N**), 3-phenyl-1,2,4-thiadiazole-4-^{15}N (**36-4-^{15}N**), and 3-phenyl-1,2,4-thiadiazole-2-^{15}N (**36-2-^{15}N**).

Bicyclic species **BC-35** was also suggested to undergo sulfur elimination. As shown in Scheme 22, sulfur elimination from ^{15}N-labeled **BC-35** would provide an equilibrium mixture of **45a** and **45b,** which could undergo complete fragmentation to a 1:1 mixture of benzonitrile-^{14}N (**39-^{14}N**) and benzonitrile-^{15}N (**39-^{15}N**). Alternatively, it was also suggested that **45a** and **45b** could undergo [4 + 2]-cycloaddition

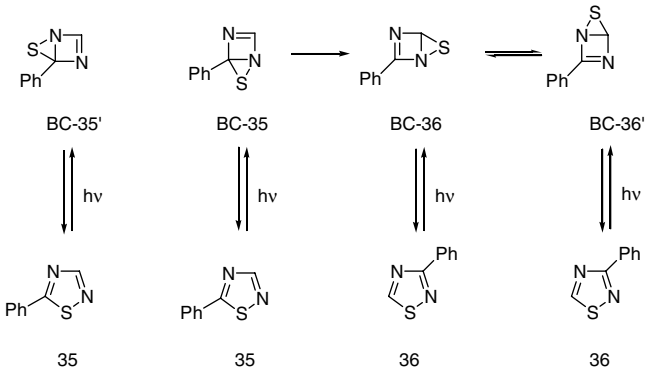

SCHEME 20

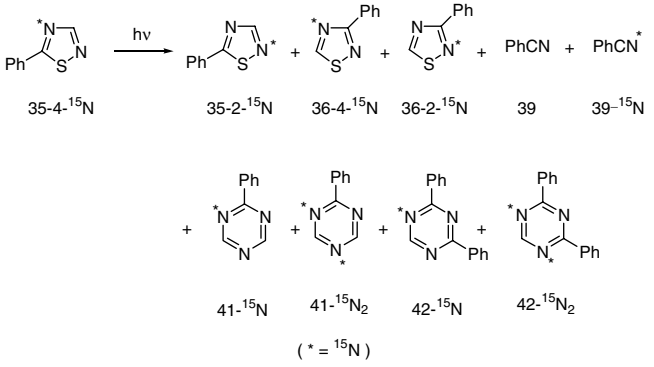

SCHEME 21

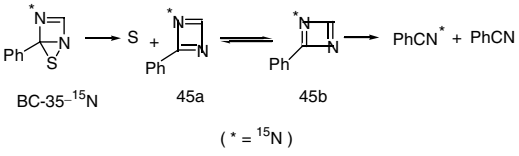

SCHEME 22

(Scheme 23), leading to unstable tricyclic adducts **46** and **47**, the suggested precursors of the 1,3,5-triazine ring expansion products. The tricyclic adducts **46** and **47** can eliminate benzonitrile-^{15}N (**39-^{14}N**), leading to a 1:1 mixture of mono- and di-^{15}N-labeled phenyl-1,3,5-triazine **41-^{15}N** and **42-^{15}N$_2$**. These predicted 1:1 ratios are very close to the experimentally determined ratios.[26]

3-Phenyl-1,2,4-thiadiazole **37** was found to react exclusively by the photofragmentation pathway, leading to benzonitrile. Experiments using ^{15}N-labeling showed that irradiation of 3-phenyl-1,2,4-thiadiazole-2-^{15}N (**37-2-^{15}N**) results in the formation of only benzonitrile-^{15}N **39-^{15}N** without transposition to 3-phenyl-1,2,4-thiadiazole-4-^{15}N (**37-4-^{15}N**). This led to the conclusion that photochemically excited 3-phenyl-1,2,4-thiadiazole **39** does not undergo electrocyclic ring closure but reacts only by the more efficient photofragmentation pathway.

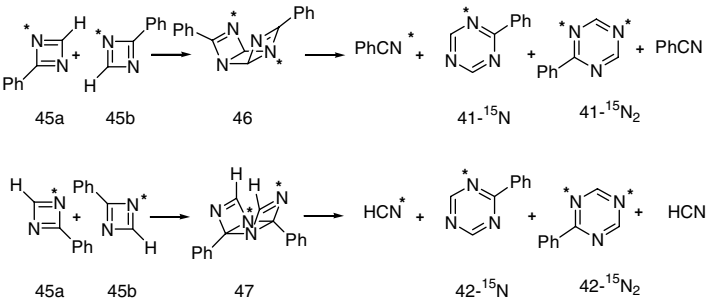

SCHEME 23

References

1. Lablache-Combier, A., Photoisomerization of five membered heterocyclic compounds, in *Photochemistry of Heterocyclic Compounds*, Buchardt, O., Ed., Wiley, New York, 1976, 123; Padwa, A., Photochemical rearrangements of five membered ring heterocycles, in *Rearrangements in Ground and Excited States*, Vol. 3, de Mayo, P., Ed., Academic Press, New York, 1980, 501; Lablache-Combier, A., Photorearrangement of nitrogen-containing arenes, in *CRC Handbook of Photochemistry and Photobiology*, Horspool, W.M. and Song, P.-S., Eds., CRC Press, Boca Raton, FL, ,1994, 1063; Pavlik, J.W., The photochemistry of pyrazoles and isothiazoles, in *Organic Photochemistry*, Ramamurthy, V. and Schanze, K., Eds., Marcel Dekker, New York, 1997; 57.
2. Tiefenthaler, H., Dorschelen, W., Goth, H., and Schmid, H., Photoisomerisierung von pyrazolen und indazolen zu imidazolen-bzw. benzimidazolen und 2-aminobenzonitrilen, *Helv. Chim. Acta*, 50, 2244, 1967.
3. Pavlik, J.W. and Kurzweil, E.M., Phototransposition chemistry of 1-methylpyrazole. Deuterium, methyl and fluorine substitution, *J. Org. Chem*., 56, 6313, 1991.
4. Connors, R.E., Pavlik, J.W., Burns, D.S., and Kurzweil E.M., A theoretical investigation of the pyrazole phototransposition, *J. Org. Chem*., 56, 6321, 1991.
5. Connors, R.E., Burns, D.S., Kurzweil, E.M., and Pavlik, J.W., The temperature dependent phototransposition chemistry of 1,5-dimethylpyrazole and 1,2-dimethylimidazole, *J. Org. Chem*., 57, 1937, 1992.
6. Pavlik, J.W., Connors, R.E., Burns, D.S., and Kurzweil, E.M., Phototransposition chemistry of 1-phenylpyrazole. Experimental and computation studies, *J. Am. Chem*. Soc., 115**,** 7654, 1993.
7. Pavlik, J.W., Kebede, N., Bird, N.P., Day, A.C., and Barltrop, J.A., Phototransposition chemistry of 1-methyl-4-phenylpyrazole. A new intermediate on the P_4 pathway, *J. Org. Chem*., 60, 8138, 1995.
8. Pavlik, J.W. and Kebede, N., Photochemistry of phenyl substituted 1-methyl-pyrazoles, *J. Org. Chem*., 62, 8325, 1997.
9. Catteau, J.P., Lablache-Combier, A., and Pollet, A., Isothiazole photoisomerization, *J. Chem. Soc., Chem. Commun*., 1018, 1969.
10. Lablache-Combier, A. and Pollet, A., Photoreactions of methylisothiazoles, *Tetrahedron*, 28, 3141, 1972.
11. Vernin, G., Dou, H.J.M., and Metzger, J., Photoisomérisation des aryl-2-thiazoles, *Compt. Rend. Acad. Sci. Paris*, 271, 1616, 1970.
12. Vernin, G., Poile, J.C., Metzger, J., Aune, J.P., and Dou, H.J.M., Isomérisation photochimique des phénylthiazoles et phénylisothiazoles, *Bull. Soc. Chim. Fr.*, 1101, 1971.
13. Vernin, G., Riou, C., Dou, H.J.M., Bouscasse, L., Metzger, J., and Loridan, G., Transposition photochemique en série héterocyclique. Arylthiazoles et isothiazoles isomèrs, *Bull. Soc. Chim. Fr.*, 1743, 1973.

14. Riou, C. Vernin, G., Dou, H.J.M., and Metzger, J., Les réactions de transposition photochemique en séne hétérocyclique. II. Photoisomérisation du phenyl-2-deutéro-5-thiazole et du phényl-2-methyl-4-thiazole. Influence des solvants et d'additifs divers sur la photoisoérisation du phenyl-2-thiazole. Résultats experimentaux, *Bull. Soc. Chim. Fr.*, 2673, 1972.
15. Vernin, G., Jauffred, R., Richard, C., Dou, H.J.M., and Metzger, J., Reaction of thiazoyl-2-yl and benzothiazol-2-yl radicals with aromatic compounds, *J. Chem. Soc., Perkin Trans. 2*, 1145, 1972.
16. Riou, C., Poile, J. C., Vernin, G., and Metzger, J., Les réactions de transposition photochimique en série hétérocyclique. IV. Photoisomérization des phényl-méthylthiazole et isothiazoles isomers, *Tetrahedron*, 30, 879, 1974.
17. Vernin, G., Poite, J.C., Dou, H.J.M., Metzger, J., and Vernin, G., Etude des radicaux methyl-3-isothiazolyl-5-en série aromatique, *Bull. Soc. Chim. Fr.*, 3157, 1972.
18. Kojima, M. and Maeda, M., Photorearrangements of 2,5- and 2,4-diphenylthiazole, *J. Chem. Soc., Chem. Commun.*, 386, 1970.
19. Maeda, M. and Kojima, M., Mechanism of the photorearrangements of phenylthiazoles, *Tetrahedron Lett.*, 3523, 1973.
20. Maeda, M., Kawahara, A., Kai, M., and Kojima, M. Reaction pathway in the photorearrangements of phenylisothiazoles, *Heterocycles*, 3, 389, 1975.
21. Maeda, M. and Kojima, M., Mechanism of the photorearrangements of phenylisothiazoles, *J. Chem. Soc., Perkin Trans. 1*, 685, 1978.
22. Pavlik, J.W., Pandit, C.R., Samuel, C.J., and Day, A.C., Phototransposition chemistry of methylisothiazoles and methylthiazoles, *J. Org. Chem*, 58, 3407, 1993.
23. Kellogg, R.M., Photochemistry of thiophenes. X. Model for the photochemically induced valence bond isomerizations of thiophenes, *Tetrahedron Lett.*, 1429, 1972.
24. Pavlik, J.W., Tongcharoensirikul, P., Bird, N.P., Day, A.C., and Barltrop, J.A., Phototransposition chemistry of phenylisothiazoles and phenylthiazoles I. Interconversions in benzene solution, *J. Am. Chem. Soc.*, 116, 2292, 1994.
25. Pavlik, J.W., Tongcharoensirikul, P., and French, K.M., Phototransposition chemistry of 4-substituted isothiazoles. The P_4 permutation pathway, *J. Org. Chem.*, 63, 5592, 1998.
26. Pavlik, J.W. and Tongcharoensirikul, P., Photochemistry of 3- and 5-phenylisothiazoles. Competing phototransposition pathways, *J. Org. Chem.*, 65, 3626, 2000.
27. Pavlik, J.W., Changtong, C., and Tsefrikas, V.M., Photochemistry of phenyl substituted 1,2,4-thiadiazoles. Phototransposition, photofragmentation and photo-ring expansion. ^{15}N-labeling studies, *J. Org. Chem.,* 68, 4855, 2003.

99

Photochemistry of *N*-Oxides

Angelo Albini
University of Pavia

Maurizio Fagnoni
University of Pavia

99.1 Introduction

The large class of *N*-oxides includes the nitrogen-containing compounds formally obtained by adding an oxygen atom forming a covalent bond with the nitrogen lone pair. Since the electron pair is donated by the nitrogen atom, charges are indicated in the *N*-oxide functionality, N^+ -O^- (or, in the older literature, the donative bond is indicated by an arrow directed toward the electron-receiving oxygen, N→O), although this does not necessarily means that *N*-oxides have a zwitterionic character.[1]

Indeed, (formal) *N*-oxidation does not affect different classes of nitrogen-containing compounds in the same way, and it is important to distinguish different classes of such compounds. This can be conveniently done by making reference to the hybridization of the nitrogen atom before oxidation, although some confusion in the nomenclature can be found in the literature and leads to the following classification. Amines (nitrogen sp^3-hybridized) form amine *N*-oxides (only in the case of the trialkyl derivatives, see formula **1** in Equation 99.1).

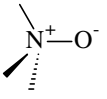

1 (99.1)

Imines, azo derivatives, and heteroaromatic compounds (nitrogen sp^2–hybridized) form nitrones (**2**), azoxy derivatives (**3**), and heteroaromatic *N*-oxides (**4**), respectively. Nitriles (nitrogen *sp*-hybridized) form nitrile *N*-oxides (**5**, Equation 99.2).

0-8493-1348-1/04/$0.00+$1.50

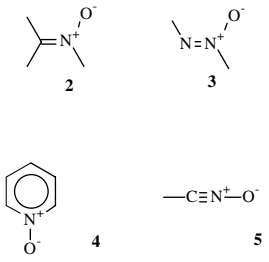

2 **3** **4** **5** (99.2)

These compounds differ greatly in their chemical and physical properties, including, as discussed below, the structure of their electronic excited states, but interestingly share the characteristic of exhibiting a photochemistry different from that of the corresponding non-oxidized derivatives. Such photochemistry is often, although by no means necessarily, more efficient than that of the non-oxidized compounds and usually consists of the cleavage or some transformation of the *N*-oxide function itself, involving either the N^+-O^- bond or a C–N bond α to the *N*-oxide group or both of them. Indeed, the *N*-oxide function is one of the few to which monomolecular photochemistry is quite generally associated, making this class of compounds one of those for which photoreactivity was noticed early (more than a century ago)[2] and to which a large and continuing interest has been devoted.[1,3-6]

All of the compounds considered above are obviously closed-shell species, as is every organic molecule. It is important to distinguish such compounds, to which the name of *N*-oxide applies, from *N*-oxyl radicals (or "nitroxides", **6**, see Equation 99.3), that is, the products formally resulting from the homolysis of the OH bond in dialkylhydroxylamines.

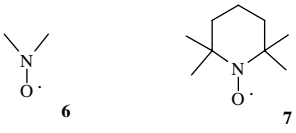

6 **7** (99.3)

Although there is some confusion in the literature about the nomenclature, these are odd-electron species unrelated to the above *N*-oxides. Some of these radicals are endowed with an uncommon persistence, such as shown in the indefinite stability of many 2,2,6,6-tetramethylpiperidine *N*-oxyl (TEMPO, **7**) derivatives.[7,8] This has led to their widespread use as radical traps, particularly for carbon-centered radicals generated in thermal and photochemical reactions.[9,10] *N*-oxyl radicals and their photochemical reactions are not discussed in this chapter.

Likewise, photochemical reactions of *N*-oxides are considered in the following, not the use of *N*-oxides in photochemistry. Therefore, the use of nitrones, in particular of cyclic polysubstituted cyclic nitrones such as 5,5-dimethylpyrroline *N*-oxide (DMPO, **8**, see Equation 99.4), as radical traps for oxygen-centered radicals, in particular the hydroxyl radical or the superoxide anion,[11-13] is not discussed here. In fact, these nitrones are used for determining the mechanism of photoinduced oxidation reactions, for example, in lipid photooxidation[14] or in oxidative DNA damage[15,16] but are not undergoing a photochemical reaction under such circumstances.

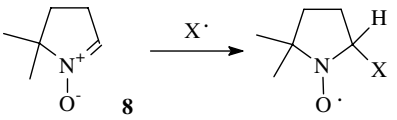

8 (99.4)

99.2 Tertiary Amine *N*-Oxides

Aliphatic tertiary amines easily give the corresponding *N*-oxides. These derivatives, just like aliphatic amines, do not absorb above 200 nm and their photochemical properties have not been investigated, at least in solution. When a different light-absorbing moiety is present in the molecule, a reaction can take place at the *N*-oxide function, even if this is not directly involved in light absorption. A typical case is that of benzyldimethylamine *N*-oxide (**9**, Equation 99.5), which has been found to undergo the Meisenheimer rearrangement to the corresponding *O*-benzylhydroxylamine, not only thermally but also photochemically, a result that has been taken as support of the radical mechanism of the rearrangement.[17]

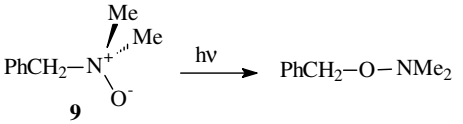

9 (99.5)

Some alkaloid *N*-oxides have been found to react photochemically, either with rearrangement to hydroxylamines, as with protopine (**10**) and allocryptopine *N*-oxides,[18] or with conversion to amides, as with canadine (**11**) and xylopine *N*-oxides (see Equation 99.6).[19]

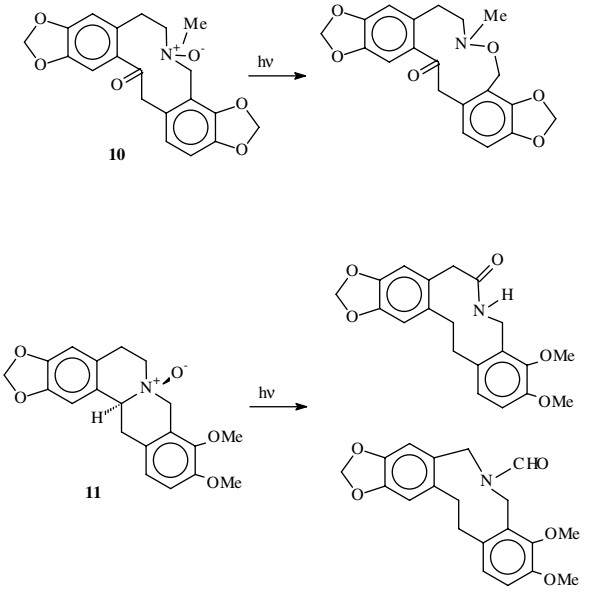

(99.6)

N-Oxidation has an important effect on the absorption spectrum of *N,N*-dialkylanilines (e.g., **12**, see Equation 99.7). The substituent is no longer an electron-donating group and both a hypso- and a hypochromic shift take place.[20] In this case, irradiation causes hydrogen transfer to the solvent, as well as attack on the side chain leading to amides and dealkylated anilines.[21]

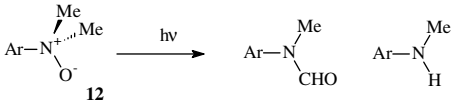

12 (99.7)

This has been observed with dialkylaminoazobenzenes *N*-oxides, that, when irradiated in 11*M* sulfuric acid, cyclize to the corresponding benzo[*c*]cinnoline, the *N*-oxide group in this case serving as an oxidant of the dihydrobenzophenanthrene intermediate.[22]

99.3 Nitrones and Azoxy Compounds

Different from the case of tetrahedral amine *N*-oxides, linking an oxygen atom to the sp^2-hybridized nitrogen, pertaining to the planar moiety of imines, azo compounds, and heterocycles completely changes the electronic structure with the introduction of a further conjugated *p* electron pair. In these compounds, the lowest-energy absorption band is thus a $\pi\pi^*$ transition with strong internal charge-transfer character. In general, this band is red shifted with respect to the corresponding imine, although it is not always distinguishable, particularly in compounds containing further conjugation. Due to the charge-transfer nature, the band is blue-shifted in polar and protic solvents.[23,24]

Two main classes of photoreactions have been observed with such compounds, *E,Z*-isomerization, ubiquitous with open-chain derivatives, rearrangement (typically cyclization) (see Equation 99.8); photocycloaddition occurs rarely. It has been demonstrated in some cases and is probably generally valid that *E,Z*-isomerization occurs via the triplet, cyclization via the singlet excited state.[25]

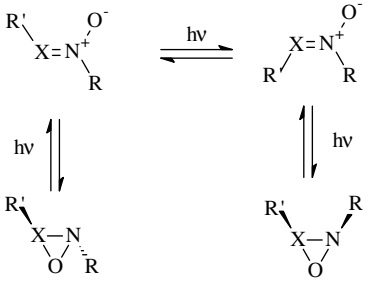

X = CR", N (99.8)

[π^4]-Electrocyclic ring closure would be the expected reaction for such derivatives. Indeed, both aliphatic[26] and aromatic nitrones[27-29] undergo cyclization to oxaziridines. The quantum yield is approximately 0.5.[30] This is, in fact, a useful entry for such three-membered heterocycles, provided that the short-wavelength component is removed from the irradiation source by filters, as the oxazirine is itself photolabile (see, for example, the aliphatic nitrone **13**, Equation 99.9).

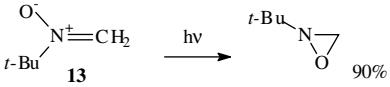

(99.9)

Starting from cyclic nitrones, bicyclic oxaziridines,[31,32] as well as spiro-oxaziridines[33,34] have been obtained. Some examples of stereospecific rearrangement have been reported,[31,35] although this is not always the case. The result may be altered both by photoisomerization of the nitrone (for open-chain derivatives)[27] and by isomerization of the oxaziridine,[26] the latter process occurring also via reversible photoisomerization to the nitrone.[36] Furthermore, an enantiomeric excess has been obtained upon photocyclization of some nitrones in chiral solvents at −78°C.[37] Likewise, irradiation of some azine *N*-oxides has been studied. As an example, cyclic azine *N*-oxide **14** undergoes firstly π^4 electrocyclic ring closure and the resulting diazetine *N*-oxide fragments, possibly via rearrangement to the oxaziaziridine and cleavage to a diazoketone (see Equation 99.10).[38]

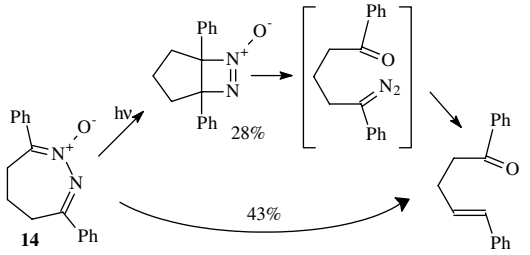

(99.10)

As mentioned, the oxaziridines are, in turn, photolabile and when products such as amides are obtained, these are often rationalized as being formed via such three-membered heterocycles, even if these are not directly observed. Such reactions may involve cleavage of the NO bond to give a biradical and in this connection it should be mentioned that addition of 2-methyl-2-butene to a diphenylcyanonitrone (**15**) has been found to occur through such a mechanism (see Equation 99.11).[39]

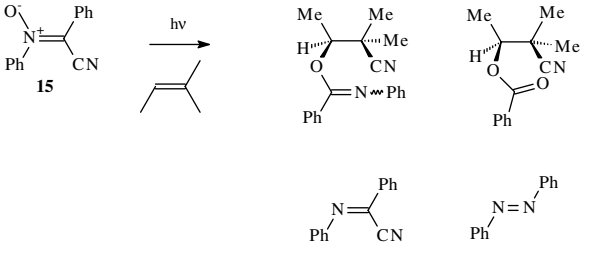

(99.11)

In a similar way, azoxy derivatives cyclize to oxadiaziridines (see Equation 99. 8, X = N). Here, however, the reaction is limited to aliphatic derivatives, both open chain[40,41] and cyclic,[42-44] even if the resulting fused oxadiaziridines may have limited stability. At any rate, cyclization is usually thermally and/or photochemically reversible and the transient formation of oxadiaziridines may be also involved when either *E,Z*- or positional isomerizations of the azoxy derivatives are the observed final result. Likewise, products from further photochemical rearrangement or fragmentation of oxadiaziridines may be obtained.

Diarylazoxy[45-49] as well as arylalkylazoxy[50] derivatives, on the other hand, undergo a different photorearrangement. In this case, 2-hydroxyazobenzenes are formed, a reaction that bears a loose likeness to the (thermal) Wallach rearrangement to 4-hydroxyazobenzenes (see Equation 99.12). The photorearrangement involves exclusively attack of the oxygen atom to the *ortho* position in the aromatic ring far from the *N*-oxide function (when such positions bear a substituent, the reaction fails) and occurs via an intermediate, apparently a dihydrobenzooxadiazole. This either reverts back to the azoxy compound, or gives the final hydroxyazobenzene, either via a hydrogen shift, subject to both acid and basic catalysis, or via a fragmentation-recombination mechanism where an aryldiazonium cation (which can be trapped) is formed.

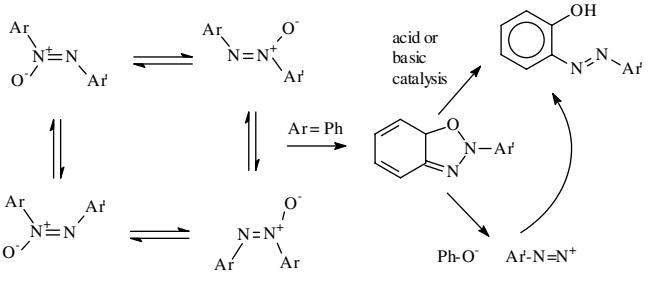

(99.12)

Due to the reversibility of the first step of the rearrangement, the overall yield of the hydroxyazo compound undergoes a marked solvent effect and, likewise, the proportion of the paths followed in the second part of rearrangement depend on solvent polarity. This rearrangement has also been observed upon irradiation in the solid state of a tetra-(*t*-butyl)-substituted azoxybenzene and apparently then mainly proceeds via a diazonium cation.[51] Substituents with a strong electron-withdrawing or electron-donating effect (e.g., 4-dimethylamino) slow the above reaction and a different process, positional isomerization reasonably via an oxadiaziridine, becomes more important. The latter process shows little solvent dependence.

1,3-Diaryltriazene 1-oxides (**16**, Equation 99.13; tautomeric with 3-hydroxytriazenes **17**) are photochemically cleaved, giving finally the products from fragment recombination, *viz.* biphenyls and azoxybenzenes, as well as the products from the secondary photolysis of the latter derivatives.[52]

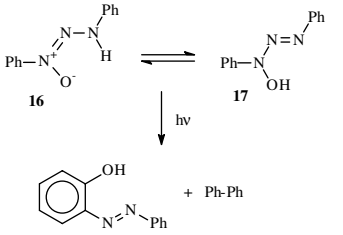

(99.13)

$[\pi^2+\pi^2]$-Cycloaddition would appear a further possibility for nitrones or azoxy derivatives, at least in suitable intramolecular models. However, methathesis and no cycloaddition was observed with proximate, *syn*-periplanar bis-diazene *N,N*-dioxides (in the mono *N*-oxides elimination predominates).[53-55] Interestingly, cyclization to an oxadiazirine occurred in preference to cycloaddition in other rigid systems possessing a geometry seemingly favorable to addition, such as azoxy **18** (see Equation 99.14).[56] Finally, nitrones can be prepared photochemically. Arylbenzyl nitrones have been prepared through the photosensitized (with cyanoanthracene or 10-methylacridinium perchlorate) oxidation of dibenzylhydroxylamines, the active species being the superoxide anion.[57,58] as well as by the photoreaction of nitro(hetero)aromatics with styrene.[59]

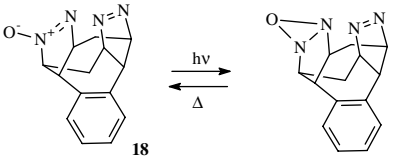

(99.14)

99.4 Five- and Seven-Membered Heterocyclic *N*-Oxides

The photochemistry of five- and seven-membered heterocyclic *N*-oxides is most often related to that observed with nitrones. Thus, rearrangement to bicyclic oxaziridines has been documented in a number of cases. Both with 2*H*- and with 4*H*-imidazole *N*-oxides, rearrangement to the corresponding oxaziridines has been reported.[60,61] The *N,N*-dioxide of the latter heterocycle (**19**, n = 1, see Equation 99.15) undergoes two consecutive photorearrangements to give the *cis*- and *trans*-isomers of the tricyclic derivative.

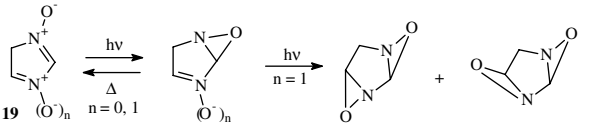

(99.15)

More often, products that can be envisioned as resulting from further reaction of oxaziridines are isolated. As an example, lactams are obtained from 1-alkyl-1,2,4-triazole 4-oxides,[62] 1-alkylbenzimidazole 3-oxides (in protic medium)[63] or 3*H*-indole 1-oxides.[64] Alternatively, ring-cleaved lactams are obtained from 1-alkylbenzimidazole 3-oxides in aprotic solvents,[63] and from 1*H*-tetraarylimidazole 3-oxides.[65]

With polyaza heterocycles, positional isomerism of the *N*-oxide function is often observed, as is the case with (benzo)thiadiazoles,[66,67] benzofuroxans,[68] and benzotriazoles.[69] There are indications that such reactions involve a ring-opening/ring-closure mechanism. In particular, with benzofuroxan (**20**, Equation

99.16), 1,2-dinitrosobenzene has been directly observed by irradiation in Ar or Xe matrices.[70,71] Noteworthy, photolysis of benzofuroxan in wet acetonitrile gives 1*H*-azepine-2,7-dione (**21**), a reaction that has been rationalized as involving cleavage to a bis-nitrile oxide.[72]

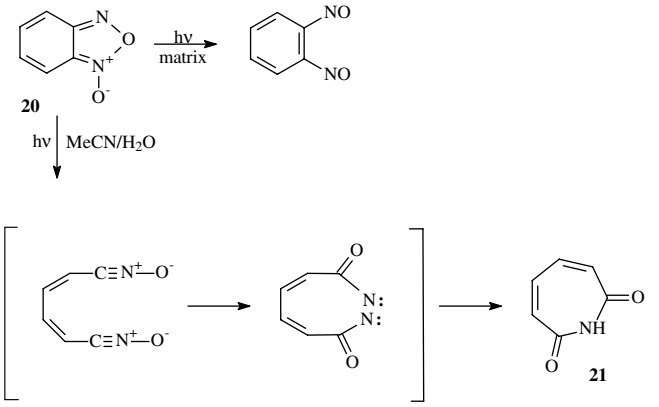

(99.16)

3,5-Diaryl-1,2,4-oxadiazole 4-oxides undergo photochemical cleavage to give, in addition to an arylnitrile, a nitrosocarbonyl intermediate that can be trapped by dienes[73] and 2,2-dimethyl-2*H*-benzimidazole 1,3-dioxide cleaves to *O*-(2-nitrosophenyl)acetone oxime.[74]

An example of the complex chemistry occurring upon irradiation of a seven-membered heterocycle is shown below for the case of the sedative chlordiazepoxide **22** (see Equation 99.17), where both ring contraction and expansion occur.[75]

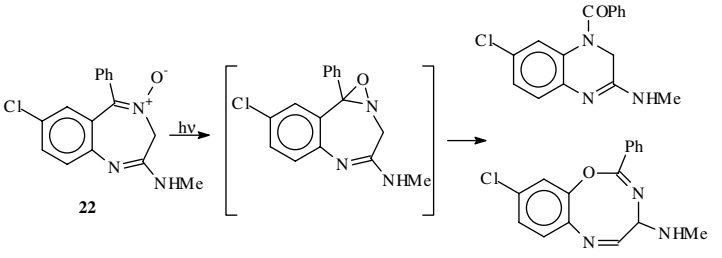

(99.17)

On the other hand, some photochemical syntheses of heterocyclic *N*-oxides exists, typical being the cyclization of *o*-nitrophenylazo dyes to give 2-aryl-2*H*-benzotriazoles under basic conditions.[76]

99.5 Photorearrangement of Six-Membered Heterocyclic *N*-Oxides

Six-membered heterocyclic *N*-oxides depart more strongly in their photochemical behavior from that observed with nitrones. Also in this case, the lowest excited singlet state is a $\pi\pi^*$ state with internal charge-transfer character from an essentially oxygen-centered *p* orbital to the ring.[77,78] With pyridine 1-oxide and other monocyclic *N*-oxides, the transition is clearly discernible as a weak band that shows a marked blue shift in polar and protic solvents. With azanaphthalene and azaanthracene *N*-oxide, the transition is strong, tends to become blurred with the following bands, and shows decreased solvatochromism. Azaanthracene *N*-oxides and derivatives containing further fused rings fluoresce and in general show photophysical properties increasingly similar to that of carbocyclic aromatics, while maintaining a photochemical reactivity centered on the *N*-oxide group. The quantum yield of reaction is largely dependent on structure and conditions, typically ranging between 0.05 and 0.5.[3] Two kinds of photoprocesses occur,

rearrangement (proceeding only from the singlet) and deoxygenation, which proceeds at least in some cases via the triplet. The latter reaction will be discussed in a following section in connection with the use of *N*-oxides as oxidizing species. The observed reactions are, in part, related to those occurring with nitrones, in the sense that most of the processes occurring can be envisaged as arising from further evolution of a primarily formed oxaziridine. However, the situation is profoundly different. With nitrones, oxaziridines have been actually isolated in a large number of cases and their further thermal or photochemical transformation has been demonstrated. With heterocyclic *N*-oxides, on the contrary, oxaziridines have never been isolated. The reactions are surely monophotonic and in most cases no intermediate is detected. Thus, although a high-quality computational study on the subject is still lacking, it appears that the oxaziridine structure (**23″** in Equation 99.18) corresponds to no minimum of the potential energy surface connecting the excited state to the final products, in all of which, however, the oxygen atom becomes bonded to the carbon atom in α (or to carbon atoms further away). Therefore, the rearrangement is expected to proceed over some biradical (**23**) or zwitterionic (**23′**) structure, which however represents no minimum. The main paths identified in simple *N*-oxides is indicated in Equation 99.18.

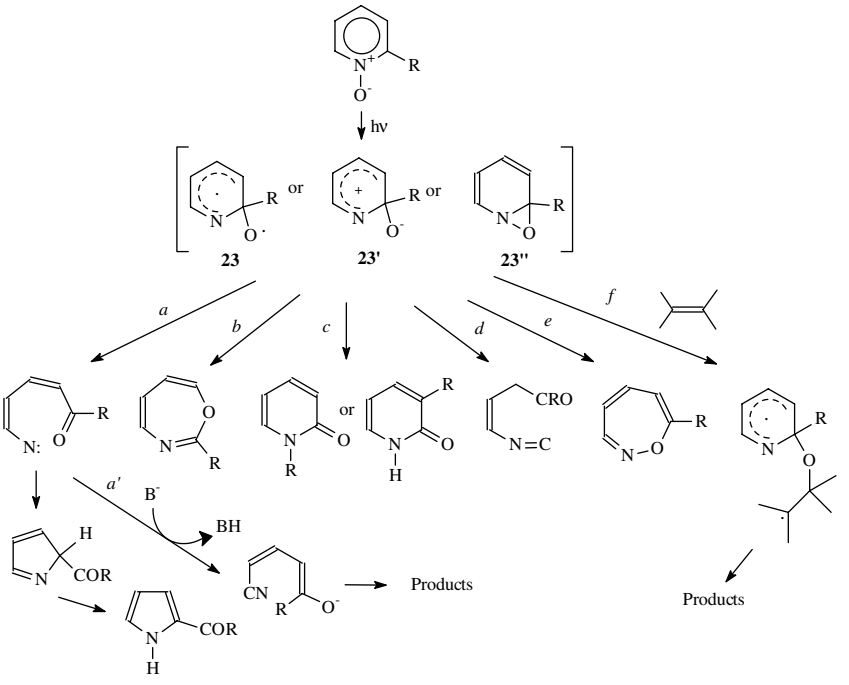

(99.18)

This includes cleavage of the CN bond (path *a*), insertion of the oxygen atom between C_α and C_β with expansion to an oxazepine ring (*b*), formation of a lactam (*c*), cleavage of the CC bond (path *d*), and insertion of the oxygen atom between the nitrogen atom and the vicinal carbon (path *e*, not observed with monocyclic *N*-oxides). Trapping reactions with evidence of the biradical or zwitterionic nature of the intermediate have been also obtained in some cases (see path *f*).

Irradiation of the parent of the series, pyridine 1-oxide (**24**, see Equation 99.19), gives only a tiny amount of an isolable product, 2-formylpyrrole, while intractable tars account for the major part of the converted reagent. Similar results are obtained with alkyl-substituted derivatives.[79,80] This has been attributed to the formation of nitrene **25** (compare path *a* in Equation 99.18), which readily polymerizes. In accord with this hypothesis, carrying out the irradiation in basic aqueous solution, the nitrene is deprotonated to give a conjugate anion (**26**), which can be detected by flash photolysis or trapped by amines to give an unsaturated aminonitrile (path *a′*).[81,82]

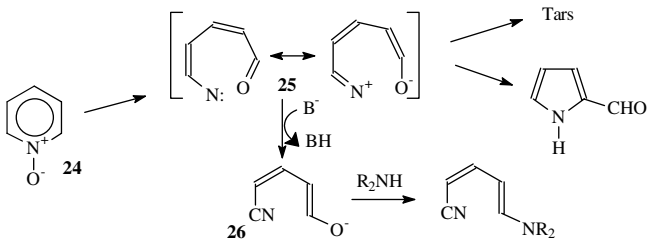

(99.19)

A different ring cleavage occurs with pentachloropyridine 1-oxides, which give pentachlorobutadienylisocyanate.[83] Rearranged heterocycles are obtained in medium to high yield from pyridine 1-oxide bearing conjugating substituents, such as cyano or phenyl. The main processes are ring contraction to 2-acylpyrroles and ring expansion to 1,3-oxazepines.[84,85] The latter products (≥80% with tetra- and pentaphenylpyridine 1-oxides) undergo thermal or acid-catalyzed rearrangement to 1-acylpyrroles and 3-hydroxypyridines, which are in some cases the products obtained from the work-up of the raw photolysate.

As for diazine *N*-oxides, pyridazine 1-oxides cleave in a way formally analogous to that of pyridine 1-oxide, to yield 4-diazobut-2-en-1-ones identified by flash photolysis and from these intermediates both nitrogen-conserving products (5-acylpyrazoles) and products resulting from the corresponding carbene (cyclopentylketones and furans).[86,87] On the other hand, pyridazine 1,2-dioxide undergoes cleavage of the NN bond and rearrangement to finally give 3,4-dihydroisoxazolo[4,5-*d*]isoxazole and isoxazole.[88] With pyrimidine 1-oxides, both ring contraction to 4-acylimidazoles[89] and ring cleavage to acylaminoacrylonitriles[90] have been observed. 1,2,4-Triazine 4-oxide follows the first path, giving 1,2,4-triazoles.[91] 4-Acylimidazoles are often formed form pyrazine-1-oxides,[92] while 1,4-pyrazine 1,4-dioxide (in aqueous solution) gives 2,5-dihydroxypyrazine.[93]

With azanaphthalene *N*-oxides, the photochemistry becomes simpler and is dominated by two processes, *viz.* ring enlargement to benzoxazepines in aprotic solvents (compare path *b* in Eq. 99.18) and rearrangement to lactams (path *c*) in protic solvents. Thus, the parent quinoline 1-oxide and many derivatives give 3,1-benzoxazepines (Equation 99.20),[94-98] and, likewise, isoquinoline 2-oxides give 1,3-benzoxazepines (too sensitive to be isolated from the parent system).[94,98-100]

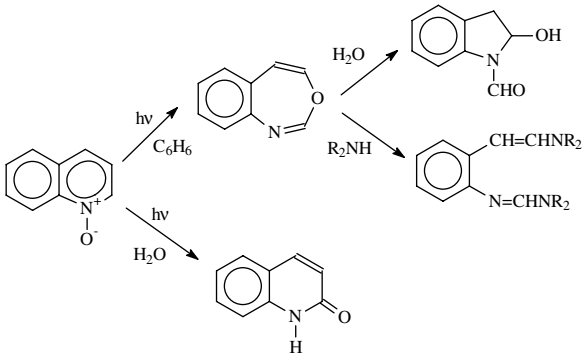

(99.20)

Several substituted quinoxaline 1-oxides give 3,5,1-benzoxadiazepine[101,102] and 4-phenylquinazoline 3-oxide gives the corresponding 1,3,5-benzoxadiazepine in aprotic media.[103] The photoproducts are moisture sensitive and easily add nucleophiles, and their isolation requires careful work-up. As an example,

parent 3,1-benzoxadiazepine can be obtained by bulb-to-bulb distillation of the photolysate from quinoline 1-oxide in benzene and easily adds water and amines,[94] (and ring-contracted derivatives are often directly obtained)[104] while isomeric 1,3-benzoxapine has not been obtained in the pure state, but only as the adduct with amines.[94] The presence of some substituents such as phenyl, cyano, methoxy, and trifluoromethyl at the iminoether moiety makes the benzoxapines much more stable and allows easier isolation. Ring fragmentation is less often observed than with azabenzene *N*-oxides. However, examples of this are the formation of an open-chain isocyanide from parent quinoxaline 1-oxide (**27**, X = H, Equation 99.21) as well as its 3-methoxy derivative (**27**, X = OMe) [101] and the 3-carbamate,[105,106] and likewise from 3-methoxyquinoline 1-oxide (compare path *d* in Eq. 99.18).[97]

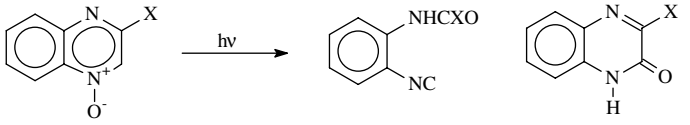

27

in C_6H_{12}	X = H	65%	27%
	X = OMe	80%	
in H_2O	X = H		90%
	X = OMe		95%

(99.21)

Another fragmentation reaction leads to the formation of diazoketones from 1,4-diphenylphthalazine 2-oxide.[86] Benzo-1,2,3-triazine 3-oxide[107] and cinnoline 2-oxide[108] also undergo ring fragmentation.

On the other hand, rearrangement to lactams is generally observed in a good yield in protic solvents, for example, carbostyril from quinoline[3] and isocarbostyril from isoquinoline[109] *N*-oxides. Exceptions are the above-mentioned *N*-oxides containing a conjugating substituent in the α position; in that case, ring enlargement remains the main process and the final products result from solvent addition to such derivatives. When the substituent in the α position is an alkyl group, however, the rearrangement to lactams occurs and the alkyl group migrates either to the nitrogen atom or to the β position (as does a deuterium atom in α).[110] An application of such a rearrangement is the preparation of the alkaloid ravenine (**28**, see Equation 99.22), a *N*-methyl-4-alkoxycarbostyril from the corresponding 2-methylquinoline 1-oxide.[111]

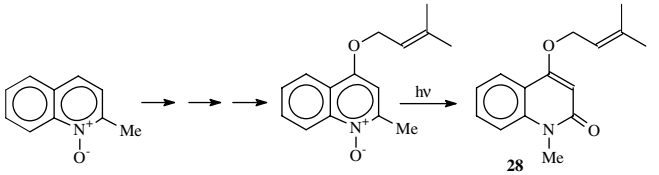

28

(99.22)

The solvent dependent photochemistry extends also to the phenanthrene and anthracene series, with some interesting variations. In apolar solvents, both 1- and 4-azaphenanthrene *N*-oxides rearrange to the corresponding naphthoxazepines, while phenanthridine gives only phenanthridone.[112] However, 6-aryl- and 6-cyanophenanthridine 5-oxides do undergo ring enlargement to dibenzoxazepines (see Equation 99.23).[113-115] In polar solvents, all of these *N*-oxides rearrange to lactams. Noteworthy is that with 6-alkylphenanthridine 5-oxides, 5-alkylphenanthridones are formed, except when a strongly stabilized group such as a benzyl is the substituent; in that case, the group is eliminated in the rearrangement.[113,116] This is an indication of the development of biradical/zwitterionic character during the rearrangement (compare formulae **23**, **23′** in Equation 99.18), which has been also evidenced through various reactions of 6-cyanophenanthridine 5-oxide. This adds ethanol when this is the solvent and alkenes when these are present (see Equation 99.23, compare path *t* in Equation 99.18).[114,117]

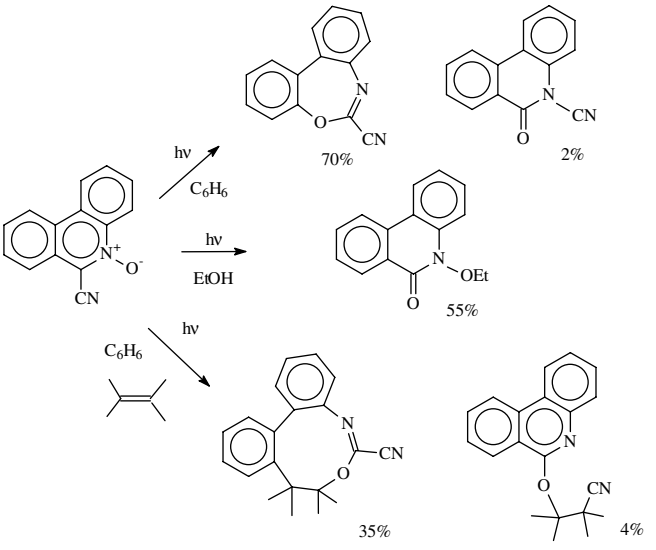

(99.23)

Among azaanthracene *N*-oxides, acridine and phenazine derivatives have been extensively investigated. Some acridine 10-oxides, such as the 9-chloro- and 9-cyano-substituted derivatives, give the corresponding dibenzo-1,2-oxazepines and it may be that products of similar structure are formed and then further converted with other derivatives.[118] Parent acridine 10-oxide gives a mixture of cycloheptatrienoindoles in apolar solvents and 11-methoxy-5,11-dihydrodibenzo[*b,e*]-1,4-oxazepine, which could arise by addition of the alcohol to a primarily formed dibenzo-1,2-oxazepine, in methanol (compare path *e* in Equation 99.18). Furthermore, oxepinoquinoline, with migration of the oxygen atom to the neighboring ring, are found in acetonitrile-water.[119] Phenazine 5-oxides tend to give azepinonbenzimidazoles and minor amounts of 5-(2-benzoxazolyl)pentadienenitrile in aprotic media, with a larger proportion of oxepinoquinoxalines in protic solvents (Equation 99.24).[120]

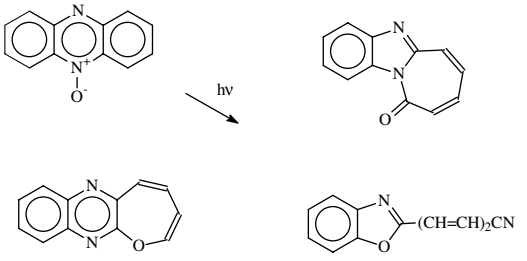

(99.24)

The study of several substituted derivatives has shown that the rearrangement to acylbenzimidazoles involves rotation of the carbocyclic ring, as if the intermediate were a *spiro*-oxocyclohexadienylbenzimidazole; whereas in the rearrangement to the oxepine, no rotation occurs and the oxygen atom inserts between the close-lying atoms.[121,122]

With both benzo[*a*]acridine[123] and benzo[*a*]phenazine 7-oxides,[124] a photorearrangement occurs and the oxygen atom migrates toward the naphthalene ring, forming annulenes with two fused seven-membered rings. Benzo[*a*]phenazine 12-oxide in part gives the same product as the 7-oxide, along with a larger amount of naphthoimidazoloazepinones where the oxygen atom has migrated toward the 7-oxide

ring. Some *N*-oxides of important polyazaheteroaromatics, such as purine and pteridine, have also been studied photochemically, usually in water, where tautomerism with the *N*-hydroxy form is important. Deoxygenation tends to predominate under such conditions (see below), but some of the rearrangements discussed above have also been observed, such as positional isomerism of the *N*-oxide function (with purines),[125] rearrangement to lactams (with purines[126,127] and pteridines),[128] and cleavage of the pyrimidine ring (with some purines[129] and a pyrazolopyrimidine).[130]

A photochemical synthesis of *N*-oxides, that of phenazine *N*-oxides from acylated *o*-nitrodiphenylamines, has also been reported.[131]

99.6 Photoinduced Deoxygenation of Heterocyclic *N*-Oxides

As mentioned, reduction to the corresponding heterocycle occurs along with the various rearrangements upon irradiation of *N*-oxides. The role of this reaction changes greatly, from practically negligible to quantitative, depending on both structure and conditions. As one might expect, the fraction of the deoxygenation process with respect to the overall photoreaction increases in more easily reduced substrates, *viz.* in polycyclic vs. monocyclic *N*-oxides, in polyaza *N*-(poly)oxides, and in electron-withdrawing substituted *N*-oxides.[3] Thus, deoxygenation is, as a rule, more important (20 to 50%) with pyridazine and pyrazine than with pyridine (≤5%) *N*-oxides and tends to become the only photoreaction with *N*-oxides such as those of benzoylpyridine,[132] benzo[*c*]cinnoline,[133] and nitrophenazine.[134] Likewise, using a good hydrogen donor as the solvent favors deoxygenation: phenazine *N*-oxide rearranges in most solvents but is mainly reduced in methanol.[120] Tautomerism to the *N*-hydroxy form, as observed in 2-pyridone[135,136] and 2-thiopyridone 1-oxide[137,138] or in purine and alloxazine *N*-oxides,[139] also favors deoxygenation. The photodeoxygenation of 1-deazapurine 3-oxide has been proposed as an actinometer in view of the expeditious fluorimetric determination of the heterocyclic compound in the presence of the *N*-oxide.[140] There has been some discussion about the mechanism involved in deoxygenation or oxygen transfer to an acceptor, be it the medium or a specifically added reagent. Probably, there is no uniform answer and different mechanisms operate. A rationalization that has been considered is that rearrangement occurs from the singlet and deoxygenation occurs from the triplet. A triplet reaction involving hydrogen abstraction from the solvent appears to operate in the photodeoxygenation of benzoylpyridine 1-oxides[132] as well as of some diazine *N,N′*-dioxides (see below)[3] and triplet-sensitized *N*-deoxygenations have been documented.[141] A second mechanism involves electron transfer to the excited *N*-oxide, followed by proton transfer; this appears to operate in the photoreduction of 2-nitrophenazine 10-oxide by amine (in this case via the singlet).[134] A third possibility envisages oxygen transfer as occurring on the same path as rearrangement, *viz.* as involving a rearranged intermediate such as an oxaziridine; this route has been followed particularly in the case of 6-cyanophenanthridine 5-oxide.[115]

Obtaining a selective and effective *N*-deoxygenation is susceptible to two kinds of applications. The first is the use of photochemistry for deoxygenating *N*-oxides, a process that is efficient in the presence of suitable oxygen acceptors such as boron trifluoride,[142] triphenylphosphine,[143] triphenylphosphite,[144] or amines,[134] and is synthetically useful when occurring selectively, leaving unaffected other potentially reducible moieties such as a nitro group (as is well known, nitration of the *N*-oxides is usually much more expeditious than that of the corresponding heterocycles).

Second, heterocyclic *N*-oxides (typically benzodiazine of polycyclic polyazine *N*-oxides) can be used as mild photochemical oxidants. Under these conditions, reactions such as the hydroxylation of aromatics[145-147] but also of alkanes,[148] the epoxidation of alkenes,[146] the oxidation of epoxides to ketones,[149] of phosphine sulfides to phosphine oxides,[150] as well as the oxidative dealkylation of amines[151] can be carried out. Intramolecular variations have been found in the photochemistry of papaverine *N*-oxide (**29**, see Equation 99.25), which gives the typical medium-dependent rearrangements in neat organic solvents but intramolecular hydroxylation of the benzyl group in the presence of trifluoroacetic acid,[152,153] and in the case of some nucleoside derivatives, which upon irradiation in the presence of a *N*-oxide gives the radical cation, in turn attacked by the hydroxyl group of the sugar moiety to form a cyclonucleoside.[154,155]

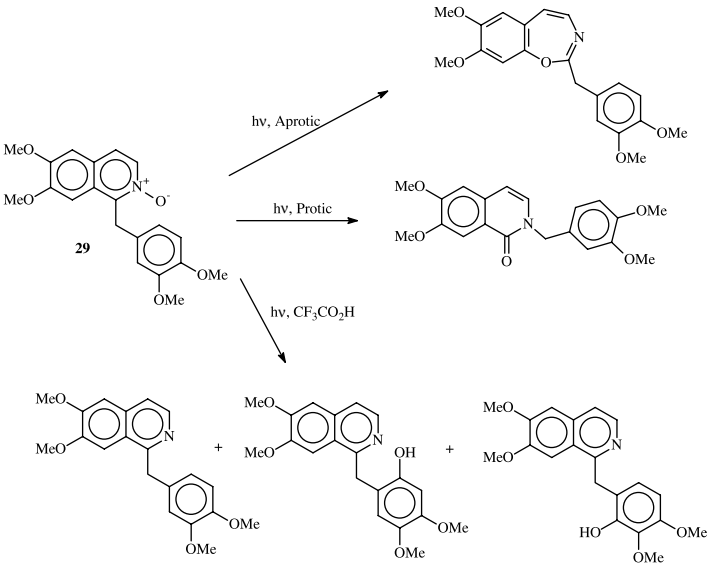

(99.25)

The use of the *N*-oxides as oxidizing agents obviously reiterates the question of the mechanism. Apart from the electron-transfer path that is operative when using *N*-oxides that are very good acceptors, such as pyrimido[5,4-*g*]pteridinetetraone *N*-oxides (**30**, see Equation 99.26)[154] or tirazapamine (**31**),[156] with good donors such as amines and nucleosides, the oxidation is probably the result of the generation of some "activated" oxygen species.

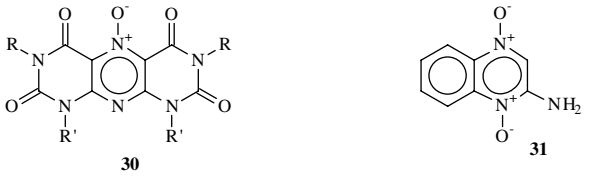

(99.26)

The fact that alkanes are oxidized suggested that atomic oxygen is liberated[157] and also the attack on aromatic hydrocarbons[158-160] seems to differ from reaction via hydroxyl radicals. Actually, the hydroxylation of aromatics by this path has been considered as a model for biochemical oxidation.

Recently, however, there has been increased interest in *N*-oxides for the generation of hydroxyl radicals in aqueous solution. This process has been reported for some nitrated *N*-oxides[161] but is most often observed for tautomeric *N*-oxides, where the *N*-hydroxy form is significant.[135-140] The main application is in photobiology, as specific sources of hydroxyl radicals for DNA damage, both strand break and base modifications. *N*-Hydroxy-2-pyridone and 2-pyridinethione,[162] *N*-hydroxy-4-(4-chlorophenyl)thiazole-2(3*H*)-thione,[163] and pyrimido[5,4-*g*]pteridinetetraone *N*-oxide (for which the path followed depends on conditions)[164] and related *N*-oxides[165] have been used for this purpose.

An oxygen transfer reaction is presumably the origin of the successful photo-cross-linking of several polymers containing heterocyclic *N*-oxide moieties in the backbone or with *N*-oxides as additives[166-168] as well as for photolithography.[169]

99.7 Nitrile *N*-Oxides

Nitrile *N*-oxides are reactive intermediates that are usually generated *in situ* through an elimination reaction. These are rarely stable enough to allow the study of their photochemical behavior. When this

is possible, as with sterically hindered arylnitriloxides, irradiation has been found to cause rearrangement to either acylnitrenes or isocyanates, both of which can be characterized via adducts to suitable traps.[170] Acetonitrile oxide has been generated by means of photolysis of an aziridine, addition of oxygen, and fragmentation of the resulting 5*H*-dioxazole.[171]

References

1. Albini, A. and Pietra, S., *Heterocyclic N-Oxides*, CRC Press, Boca Raton, FL, 1992.
2. Wacker, L., On α-azoxynaphthalene, *Liebigs Ann. Chem.*, 317, 375, 1901.
3. Albini, A. and Alpegiani, M., Photochemistry of the *N*-oxide function, *Chem. Rev.*, 84, 43, 1984.
4. Spence, A.G., Taylor, E.C., and Buchardt, O., The photochemical reactions of azoxy compounds, nitrones and aromatic amine *N*-oxides, *Chem. Rev.*, 70, 231, 1970.
5. Buchardt, O., Amine and imine *N*-oxides, in *Houben Weil Handb. Org. Chem.: Photochemistry*, G. Thieme Verlag, Stuttgart, Vol. 4/5b, 1975, 1282.
6. Bellamy, F. and Streith, J., The photochemistry of aromatic *N*-oxides: a critical review, *Heterocycles*, 4, 1931, 1976.
7. Keane, J.F.N., Newer aspects of the synthesis and chemistry of nitroxide spin traps, *Chem. Rev.*, 78, 37, 1978.
8. Marque, S., Fischer, H., Baier, E., and Studer, A., Factors influencing the C-O bond homolysis of alkoxyamines: effect of H-bonds and polar substituents, *J. Org. Chem.*, 66, 1146, 2001.
9. Root, K.S., Hill, C.L., Lawrence, L.M., and Whitesides, G.M., The mechanism of formation of Grignard reagents. Trapping of free alkyl radicals intermediates by reaction with tetramethylpiperidine *N*-oxyl, *J. Am. Chem. Soc.*, 111, 5405, 1989.
10. Keana, J.F.W., Dinenstein, R.J., and Beitis, F., Photolytic studies on 4-hydroxy-2,2,6,6-tetramethylpiperidine-1-oxyl, a stable nitroxide free radical, *J. Org. Chem.*, 36, 209, 1971.
11. Buettner, G.R., Spin trapping: ESR parameters of spin adducts, *Free Rad. Biol. Med.*, 3, 259, 1987.
12. Finkelstein, E., Rosen, G.M., and Rauchman, E.J., Spin trapping of superoxide and hydroxyl radical: practical aspects, *Acta Biochem. Biophys.*, 200, 1, 1980.
13. Li, A.S.W. and Chignell, C.F., STDBII a database for storing, retrieving and analysing spin trapping data on an IBM or Macintosh personal computer, *Res. Chem. Intermed.*, 14, 235, 1990.
14. Albro, P.W., Bilski, P., Corbett, J.T., Schroeder, J.L., and Chignell, C.F., *Photochem. Photobiol.*, 66, 316, 1997.
15. Adam, W., Arnold, M.A., Grimm, G.N., Saha-Moeller, C.R., Dall'Acqua, F., Miolo, G., and Vedaldi, D., 4-*tert*-Butylperoxylmethyl-9-methoxypsoralen as intercalating photochemical alkoxyl-radical source for oxidative DNA cleavage, *Photochem. Photobiol.*, 68, 511, 1998.
16. Adam, W., Groer, P., Mielke, K., Sha-Moeller, C.R., Hutterer, R., Kiefer, W., Nagel, V., Schneider, F.W., Ballmaier, D., Schleger, Y., and Epe, B., Photochemical and photobiological studies with acridine and phenanthridine hydroperoxides in cell-free DNA, *Photochem. Photobiol.* 66, 26, 1997.
17. Schheollkopf, U., Patsch, M., and Schafer, M., Indication of the radicalic course of the Meisenheimer rearrangement, *Tetrahedron Lett.*, 2515, 1964.
18. Iwasa, K. and Takao, N., The pyrolysis and photolysis of the protopine type alkaloids, *Heterocycles*, 20, 1535, 1983.
19. Chinnasamy, P., Minard, R.D., and Schamma, M., The photolysis of berbine *N*-oxides, *Tetrahedron*, 36, 1515, 1980.
20. Colonna, M. and Risaliti, A., UV spectra and character of the *N*-O bond in 2- and 4-phenylpyridine *N*-oxide, *Ann. Chim. (Rome)*, 48, 1395, 1958.
21. Albini, A., Fasani, E., Moroni, M., and Pietra, S., Photochemical decomposition of 4-arylazo- and 4-arylazoxy-*N,N*-dialkylaniline *N*-oxides, *J. Chem. Soc., Perkin Trans. 2*, 1439, 1986.
22. Lewis, G.E. and Reiss, G.A., Formation and characterization of 2-dimethylaminobenzo[*c*]cinnoline, *Aust. J. Chem.*, 19, 1887, 1966.

23. Ghersetti, L., Maccagnani, G., Mangini, A., and Montanari, F., Infrared and ultraviolet absorption spectra of pyridine *N*-oxides, *J Heterocyclic Chem.*, 6, 859, 1969.
24. Kubota, T., Electronic spectra and electronic structure of some basic heterocyclic *N*-oxides, *Bull. Chem. Soc. Jpn.*, 35, 946, 1962.
25. Koyano, K. and Tanaka, I., Photochemical and thermal isomerization of *trans* and *cis* α-cyano-α-phenyl-*N*-phenylnitrones, *J. Phys. Chem.*, 69, 2545, 1965.
26. Druelinger, M.L., Shelton, R.W., and Lammert, S.R., Photochemistry of methylenenitrones and related compounds, *J. Heterocyclic Chem.* 13, 1001, 1976.
27. Splitter, J.S., Su, T.M., Ono, H., and Calvin, M. Orbital symmetry control in the nitrone-oxaziridine system, *J. Am. Chem. Soc.*, 93, 4075, 1971.
28. Ning, R.Y., Field, G.F., and Sternbach, L.H., Quinoxaline and 1,4-benzodiazepines. XLVI. Photochemistry of nitrones and oxaziridines, *J. Heterocyclic Chem.,* 7, 745, 1970.
29. Ono, H., Splitter, J.S., and Calvin, M., The effect of phenyl substituent in the nitrogen inversion barrier in a 2-phenyloxaziridine, *Tetrahedron Lett.*, 4107, 1973.
30. Koyano, K., Suzuki, H., Mori, Y., and Tanaka, I., Quantum yield of photorearrangement of nitrones, *Bull. Chem. Soc. Jpn.*, 43, 3582, 1970.
31. Black, D.S.C. and Watson, K.G., Photorearrangement of some bicyclic oxaziridines, *Aust. J. Chem.*, 26, 2502, 1973.
32. Suginome, H., Mizuguchi, T., and Masamune, T., Formation of an oxazirine by the irradiation and benzoylation of (22S, 25S)-*N*-acetyl-11a-aza-C-homo-5α-veratra-11a, 13(17)diene-3β, 11β, 23 β-triol-11a-oxide, *Bull. Chem. Soc. Jpn.*, 50, 987, 1977.
33. Aurich, H.G. and Grigo, U., Photochemistry of oxindolinilydeneamine *N*-oxides, *Chem. Ber.*, 109, 3849, 1976.
34. Oliveros, E., Antoun, H., Rivière, N., and Lattes, A., Comparison between the thermal and photochemical rearrangement of spirooxaziridines, *J. Heterocyclic Chem.*, 13, 623, 1976.
35. Bapat, J.B., Black, D.S. C., Stereoselective photorearrangement of a pyrroline *N*-oxide, *J. Chem. Soc., Chem. Commun.*, 73, 1967.
36. Bjørgo, N.J., Boyd, R.D., Campbell, R.M., and Neill, D.C., Photoracemization at a chiral pyramidal nitrogen centre, *J. Chem. Soc., Chem. Commun.*, 162, 1976.
37. Boyd, D.R. and Neill, D.C., Asymmetric synthesis of a pyramidal nitrogen centre in a chiral medium, *J. Chem. Soc., Chem. Commun.* 51, 1977.
38. Williams, W.M. and Dolbier, W.R., Photochemical reaction of cyclic azine monoxides, *J. Am. Chem. Soc.*, 94, 3955, 1972.
39. Sehgal, R.K. and Griffin, G.W., Novel photocycloaddition of electron deficient nitrones to 2-methyl-2-butene, *Liebigs Ann. Chem*., 513, 1997.
40. Greene, F.D. and Hecht, S.S., Oxadiaziridines. Synthesis, valence isomerization and reactivity, *J. Org. Chem.*, 35, 2842, 1970.
41. Taylor, K.G., Isaac, S.R., and Swigert, J.L., Photolytic isomerization of azoxyalkanes, *J. Org. Chem.*, 41, 1146, 1976.
42. Squillacote, M.E., Bergman, A., De Felippis, J., and West, E.M., Thermal stability of *cis*-oxadiaziridines, *Tetrahedron Lett.*, 28, 275, 2987.
43. Olsen, H. and Pedersen, C.L., Photochemical isomerisation of bicyclo *cis*-1,2-diazene *N*-oxides to oxadiaziridines, *Acta Chem. Scand.*, B36, 701, 1977.
44. Dolbier, W.R., Matsui, K., Michl, J., and Horak, D.V., 2, 2-dimethylisoindene and 5, 5-dimethylbenzobicyclo[2.1.0]pent-2-ene, *J. Am. Chem. Soc.*, 99, 3876, 1977.
45. Albini, A., Fasani, E., Moroni, M., and Pietra, S., Photochemistry of some methoxy and dimethylamino derivatives of azoxybenzene, *J. Org. Chem.*, 51, 88 1986.
46. Bunce, N.J., Schoch, J.P., and Zerner, M.C., Photorearrangement of azoxybenzene to 2-hydroxyazobenzene. Evidence for electrophilic substitution by oxygen, *J. Am. Chem. Soc.*, 99, 7986, 1977.
47. Bunce, N.J., A new mode of photoreaction in the azoxybenzene series, *Can. J. Chem.*, 53, 3477, 1977.

48. Goon, D.J.W., Murray, N.G., Schoch, J.P., and Bunce, N.J., Evidence against a hydrogen abstraction mechanism in the photorearrangement of azoxybenzene to 2-hydroxyazobenzene, *Can. J. Chem.*, 51, 3827, 1973.
49. Bunce, N.J., Goon, D.J.W., and Schoch, J.P., Synthesis and photolysis of some naphthylazoxy compounds, *J. Chem. Soc., Perkin Trans. 1*, 688, 1976.
50. Taylor, K.G. and Riehl, T., Synthesis of new azoxy compounds by photolytic isomerization, *J. Am. Chem. Soc.*, 94, 250, 1972.
51. Döpp, D. and Muller, D., Solid state photolysis. Photocleavage of a sterically hindered azoxybenzene into aryldiazonium phenoxide, *Tetrahedron Lett.*, 3863, 1978.
52. Nour-El-Din, A.M., Mohamed, S., K., and Döpp, D., Photochemical behavior of 1,3-diaryltriazene 1-oxides, *Bull. Chem. Soc. Jpn.*, 69, 131, 1996.
53. Exner, K., Hochstrate, D., Keller, M., Klärner, F.G., and Prinzbach, H., Proximate, *syn*-periplanar diazene/diazene substrates: N=N and ON=N/N=NO photomethathesis reactions, *Angew. Chem., Int. Ed. Engl.*, 35, 2256, 1996.
54. Exner, K., Fischer, G., Lugan, M., Fritz, H., Hunkler, D., Keller, M., Knothe, L., and Prinzbach, H., Proximate, *syn*-periplanar diazene/diazene(di)oxy, diazeneoxy/diazene(di)oxy and diazenedioxy/diazenedioxy skeletons: syntheses, [2+2] photocycloadditions, metathesis, *Eur. J. Org. Chem.*, 787, 2001.
55. Fischer, G., Fritz, H., Rihs, G., Hunkler, D., Exner, K., Knothe, L., and Prinzbach, H., Proximate, *syn*-periplanar, rigid imine (nitrone)/ene- and diazene (diazeneoxy)/ene systems: synthesis, homoconjugate reactivity and photochemistry, *Eur. J. Org. Chem.*, 743, 2000.
56. Cullman, O., Vögtle, M., Stelzer, F., and Prinzbach, H., Proximate, *syn*-periplanar bisdiazenes/bisdiazeneoxides — synthesis, photochemistry, *Tetrahedron Lett.*, 39, 2303, 1998.
57. Ohba, Y., Kubo, K., Igarashi, T., and Sakurai, T., Mechanism of the 10-methylacridinium ion-sensitized photooxidation of *N,N*-dibenzylhydroxylamine and its derivatives in acetonitrile, *J. Chem. Soc., Perkin Trans. 2*, 491, 2001.
58. Sakurai, T., Yokono, M., Komiya, K., Masuda, Y., and Inoue, H., Cyanoanthracenes sensitizes photooxidation of *N, N*-dibenzylhydroxylamine and its derivatives: free-energy dependence of back-electron transfer rates in geminate pairs, *J. Chem. Soc., Perkin Trans. 2*, 2515, 1994.
59. D'Auria, M., Photochemical reaction of nitroarenes with styrene, *J. Photochem. Photobiol., A: Chem.*, 79, 67, 1994.
60. Gainsford, G.J. and Woolhouse, A.D., Facile photoisomerization of 2*H*-imidazole *N*-oxides to 1,3-diaza-6-oxabicyclo[3.1.0]hex-3-enes and synthesis of a 1,3-diaza-4,7dioxatricyclo[4-1-0.0]heptane, *J. Heterocyclic Chem.*, 29, 803, 1992.
61. Nechepurenko, I.V., Petrenko, O.P., Grigor'ev, I.A., and Volodarskii, L.B., Photochemical isomerisation of 4*H*-imidazole *N*-oxides and *N,N*-dioxides, *Russ. J Org. Chem.*, 33, 705, 1997.
62. Timpe, H.J. and Becher, H.G.O., The photochemistry of isoelectronic 1,2,4-triazole 4-*N*-oxide and 4-imino-1,2,4-triazolium ylide, *J. Prakt. Chem.*, 314, 324, 1972.
63. Ogata, M., Matsumoto, H., Takahashi, S., and Kano, H., Photolysis of 1-benzyl-2-ethylbenzimidazole 3-oxides, *Chem. Pharm. Bull.*, 18, 964, 1970.
64. Döpp, D., Photoisomerization and acidolysis of 3,3-dimethyl-3*H*-indole 1-oxides, *Chem. Ber.*, 109, 3849, 1976.
65. Woolhouse, A.D., Photoisomerization of tetraaryl-1*H*-imidazole 3-oxides, *Aust. J. Chem.*, 32, 2059, 1979.
66. Pedersen, C.L., Lohse, C., and Poliakoff, M., Photolysis of benzo[*c*]-1,2,5-thiadiazole 2-oxide. Spectroscopic evidence for the reversible formation of 2-thionitrosonitrobenzene, *Acta Chem. Scand.*, B32, 625, 1978.
67. Braun, H.P., Zeller, K.P., and Meier, H., Photolysis of 1, 2,3-thiadiazole 2-oxide, *Liebigs Ann. Chem.*, 1257, 1975.
68. Calzaferri, G., Gleiter, R., Knauer, K.H., Martin, H.D., and Schmidt, E., Photochromism of 4-substituted benzofuroxans, *Angew. Chem. Int. Ed. Engl.*, 13, 86, 1974.

69. Serve, M.P., Feld, W.N., Seybold, P.C., and Steppel, R.N., Synthesis of 1-methyl-1,2,3-benzotriazole 2-oxide, *J. Heterocyclic Chem.*, 12, 811, 1975.
70. Dunkin, I.R., Lynch, M.A., Boulton, A.J., and Henderson, N., 1,2-Dinitrosobenzene in argon matrices at 14K, *J. Chem. Soc., Chem. Commun*., 1178, 1991.
71. Hacker, N.P., Benzofuran photochemistry: direct observation of 1,2-dinitrosobenzene by steady-state spectroscopy. A new photochromic reaction, *J. Org. Chem.*, 56, 5216, 1991.
72. Hasegawa, M. and Takabatake, T., Photoreactions of benzofuroxan, *J. Heterocyclic Chem.*, 28, 1079, 1991.
73. Quadrelli, P., Mella, M., and Caramella, P., A photochemical generation of nitrosocarbonyl intermediates, *Tetrahedron Lett.*, 40, 797, 1999.
74. Latham, D.W. S., Meth-Cohn, O., Suschitzky, H., and Herbert, J.A.L., Conversion of benzofurazan *N*-oxide into 2*H*-benzimidazoles and some unusual reactions of 2*H*-benzimidazoles, *J. Chem. Soc., Perkin Trans. 1*, 470, 1977.
75. Cornelissen, P.J.G., Beijersbergen van Henegouwen, G.M. J., and Gerritsma, K.W., Photochemistry of 1,4-benzodiazepines. Chlordiazepoxide, *Int. J. Pharm.*, 3, 205, 1985.
76. Baik, W., Yoo, C.H., Koo, S., Kim, H., Hwang, Y.K., Kim, B.H., and Lee, S.W., Photostimulated reductive cyclization of *o*-nitrophenylazo dyes using sodium hydroxide in isopropyl alcohol. A new synthesis of 2-aryl-2*H*-benzotriazoles, *Heterocycles*, 51, 1779, 1999.
77. Scholz, M., Electronic structure of pyridine *N*-oxide, *J. Prakt. Chem.*, 323, 571, 1981.
78. Scholz, M., MO calculations of electronic spectra of pyridine *N*-oxide. A critical review, *J. Prakt. Chem.*, 324, 85, 1982.
79. Bellamy, F., Streith, J., and Fritz, H., Photochemical behavior of monosubstituted pyridine *N*-oxide in water, *Nouv. J. Chem.*, 3, 115, 1979.
80. Bellamy, F. and Streith, J., Effect of copper salts on the photochemistry of monosubstituted pyridine *N*-oxides, *J. Chem. Res. (S)*, 18, 1979.
81. Lohse, C., Hagedorn, L., Albini, A., and Fasani, E., Photochemistry of pyridine *N*-oxide, *Tetrahedron*, 44, 2591, 1988.
82. Buchardt, O., Christensen, J.J., Nielsen, P.E., Koganty, R.R., Finsen, L., Lohse, C., and Becher, J., Photochemical ring-opening of pyridine *N*-oxide to 5-oxo-2-pentenenitrile and/or 5-oxo-3-pentenenitrile, *Acta Chem. Scand.,* B34, 31, 1980.
83. Ager, E., Chivers, G.E., and Suschitzky, H., Photochemistry of pentachloropyridine *N*-oxide and some of its derivatives, *J. Chem. Soc., Perkin Trans. 1*, 1125, 1973.
84. Ischikawa, M., Kaneko, C., Yokoe, L., and Yamada, S., Photolysis of 2, 6-dicyanopyridine 1-oxide, *Tetrahedron,* 25, 295, 1969.
85. Buchardt, O., Pedersen, C.L., and Harrit, N., Light-induced ring expansion of pyridine *N*-oxides, *J. Org. Chem.*, 37, 3592, 1972.
86. Tomer, K.B., Harrit, N., Rosenthal, I., Buchardt, O., Kumler, P.L., and Creed, D., Photochemical behaviour of aromatic 1,2-diazine *N*-oxides, *J Am. Chem. Soc.*, 95, 7402, 1973.
87. Tsuchiya, T., Arai, H., and Igeta, H., Formation of cyclopropenylketones and furans from pyridazine *N*-oxide by irradiation, *Tetrahedron*, 29, 2747, 1973.
88. Ohsawa, A., Arai, H., Igeta, H., Akimoto, T., and Tsuji, A., The photoisomerization of pyridazine 1,2-dioxide; formation of 3a,6a-dihydroisoxazolo[1,2*d*]isoxazole, *Tetrahedron*, 35, 1267, 1979.
89. Roeterdink, F., van der Plas, H.C., and Kandijs, A., Photochemistry of pyrimidine *N*-oxides, *Recl. Trav. Chim. Pays-Bas*, 94, 16, 1975.
90. Streith, J., Leibovici, C., and Martz, P., Photochemistry of pyrimidine *N*-oxides, *Bull. Soc. Chim. Fr.*, 4152, 1971.
91. Neunhöffer and Böhnisch, V., Reactions of 1,2,4-triazine 4-oxides, *Liebigs Ann. Chem.*, 153, 1976.
92. Ikekawa, N., Honma, Y., and Kenkyusho, R., Photochemical reactions of pyrazine *N*-oxides, *Tetrahedron Lett.*, 1197, 1967.
93. Kawata, H., Niizuma, S., and Kokubun, H., Photochemistry of pyrazine *N*-dioxide in aqueous solution, *J. Photochem.*, 13, 261, 1980.

94. Albini, A., Bettinetti, G., and Minoli, G., On 1,3-benzoxazepine and 3,1-benzoxazepine, *Tetrahedron Lett.*, 3761, 1979.
95. Buchardt, O., Kumler, P.L., and Lohse, C., Photolysis of phenylquinoline *N*-oxides in solution. Solvent influence on the product distribution, *Acta Chem. Scand.*, 21, 1841, 1967.
96. Kaneko, C., Yamada, S., and Ishikawa, M., Irradiation of *N*-oxides of α-cyanoazanaphthalenes in aprotic solvents, *Tetrahedron Lett.*, 2145, 1966.
97. Albini, A., Fasani, E., and Maggi Dacrema, L., Photochemistry of methoxy substituted quinoline and isoquinoline *N*-oxides, *J. Chem. Soc., Perkin Trans. 1*, 2738, 1980.
98. Kaneko, C., Hayashi, S., and Kobayashi, Y., Photolysis of 2-(trifluoromethyl)quinoline 1-oxides and isoquinoline 2-oxides, *Chem. Pharm. Bull.*, 22, 2147, 1974.
99. Simonsen, O., Lohse, C., and Buchardt, O, The photolysis of 1-phenyl- and 1-cyano-substituted isoquinoline *N*-oxides to benz[*f*][1, 3]oxazepines, *Acta Chem. Scand.*, 24, 268, 1970.
100. Bremmer, J.B. and Wiryachitra, P., The photochemistry of papaverine *N*-oxide, *Aust. J. Chem.*, 26, 437, 1973.
101. Albini, A., Colombi, R., and Minoli, G., Photochemistry of quinoxaline 1-oxide and some of its derivatives, *J. Chem. Soc., Perkin Trans. 1*, 974, 1978.
102. Kaneko, C., Yamada, S., Yokoe, I., and Ishikawa, M., Study of the stable photoproducts derived from quinoline 1-oxide and quinoxaline 1-oxide, *Tetrahedron Lett.*, 1873, 1967.
103. Field, G.F. and Sternbach, L.H., Quinazoline and 1,4-benzodiazepines. XLII. Photochemistry of some *N*-oxides, *J. Org. Chem.*, 33, 4438, 1968.
104. Kaneko, C., Yamamoto, A., and Hashiba, M., Ring contraction reactions of methylquinoline 1-oxide 5-carboxylates via the corresponding benz[*a*]-1,3-oxazepines. A facile synthesis of methyl indole-4-carboxylate and its derivatives, *Chem. Pharm. Bull.*, 27, 946, 1979.
105. Kurasawa, Y. and Takada, A., Progress in the chemistry of quinoxaline *N*-oxides and *N,N′*-dioxides, *J. Heterocyclic Chem.*, 32, 1085, 1995.
106. Burrel, A., Cox, J.M., and Savins, e.g., Quinoxaline precursors of fungitoxic benzimidazolylcarbamates: syntheses and photochemical induced transformations, *J. Chem. Soc., Perkin Trans. 1*, 2707, 1973.
107. Horspool, W.M., Kershaw, J.R., Murray, A.W., and Stevenson, G.M., Photolysis of 4-substituted 1,2,3-benzotriazine 3-oxides, *J. Am. Chem. Soc.,* 85, 2390, 1973.
108. Horspool, W.M., Kershaw, J.R., and Murray, A.W., Photolysis of 4-methylcinnoline 1- and 2-oxides, *J. Chem. Soc., Chem. Commun.*, 345, 1973.
109. Lohse, C., Primary photoprocesses in isoquinoline 2-oxide, *J. Chem. Soc., Perkin Trans. 2*, 229, 1972.
110. Buchardt, O., Tomer, K.B., and Madsen, V., A photochemical 1,2-deuterium shift. Irradiation of quinoline *N*-oxide-2d_1, *Tetrahedron Lett.*, 1311, 1971.
111. Kaneko, C., Naito, T., Hashiba, M., Fujii, H., and Somei, M., A new synthesis of ravenine and related alkaloids by means of a photo-rearrangement reaction of 4-alkoxy-2-methylquinoline 1-oxides, *Chem. Pharm. Bull.*, 27, 1813, 1979.
112. Albini, A., Bettinetti, G., and Minoli, G., Photochemistry of some azaphenanthrene *N*-oxides, *J. Chem. Soc., Perkin Trans. 1*, 1159, 1980.
113. Albini, A., Fasani, E., and Frattini, V., Medium and substituent effect on the photochemistry of phenanthridine *N*-oxides. Is an intermediate of biradical character involved in the photorearrangement of heterocyclic *N*-oxides?, *J. Chem. Soc., Perkin Trans. 2*, 235, 1988.
114. Kaneko, C., Hayashi, R., Yamamori, M., Tokumura, K., and Itoh, M., Photochemical reactions of 6-cyanophenanthridine 5-oxide, *Chem. Pharm. Bull.*, 26, 2508, 1978.
115. Tokumura, K., Goto, H., Kashibara, H., Kaneko, C., and Itoh, M., Formation and reaction of an oxaziridine intermediate in the photochemical reaction of 6-cyanophenanthridine 5-oxide at low temperature, *J. Am. Chem. Soc.*, 102, 5643, 1980.
116. Taylor, E.C. and Spence, G.G., Group migration in the photolysis of 6-substituted phenanthridine *N*-oxides, *J. Chem. Soc., Chem. Commun.*, 767, 1966.
117. Albini, A., Fasani, E., and Buchardt, O., Radicaloid intermediates in the photochemistry of 6-cyanophenanthridine 5-oxide, *Tetrahedron Lett.*, 23, 4849, 1982.

118. Yamada, S. and Kaneko, C., Photochemistry of acridine 10-oxide: synthesis and reaction of dibenz[*c, f*]oxazepines, *Tetrahedron*, 33, 1273, 1979.
119. Yamada, S., Ishikawa, M., and Kaneko, C., Photochemistry of acridine *N*-oxides, *Chem. Pharm. Bull.*, 23, 2818, 1973.
120. Albini, A., Bettinetti, G., and Pietra, S., Photoreaction of phenazine 5-oxide, *Tetrahedron Lett.*, 3657, 1972.
121. Albini, A., Bettinetti, G., and Pietra, S., Photoisomerization of substituted phenazine *N*-oxides, *Gazz. Chim. Ital.*, 105, 15, 1975.
122. Albini, A., Barinotti, G., Bettinetti, G., and Pietra, S., The effect of substituents on the photoisomerization of phenazine *N*-oxide, *J. Chem. Soc., Perkin Trans. 2*, 238, 1977.
123. Kaneko, C., Yamada, S., and Ishikawa, M., Synthesis of dibenzo[*c, g*]-2,5diaza-1,6-oxido[10]annulene and 12-methyldibenz[*c, g*]-2-aza-1,6-oxido[10]annulene, *Tetrahedron Lett.*, 2539, 1970.
124. Albini, A., Barinotti, A., Bettinetti, G., and Pietra, S, The photoisomerization of benzo[*a*]phenazine *N*-oxides, *Gazz. Chim. Ital.*, 106, 871, 1976.
125. Lam, F.L., Brown, G.B., and Parham, J.C., Photoisomerization of 1-hydroxy to 3-hydroxyxanthine. Photochemistry of related 1-hydroxypurines, *J. Org. Chem.*, 39, 1391, 1974.
126. Lam, F.L. and Parham, J.C., Photochemistry of purine 3-oxides in hydroxylic solvents, *Tetrahedron*, 38, 2371, 1982.
127. Lam, F.L. and Parham, J.C., Photochemistry of 1-hydroxy- and 1-methoxyhypoxanthines, *J. Org. Chem.*, 38, 2397, 1973.
128. Lam, F.L. and Lee, T.C., Photochemistry of some pteridine *N*-oxides, *J. Org. Chem.*, 43, 167, 1978.
129. Lam, F.L. and Parham, J. C., The photoreaction of 6-methyl and 6,9-dimethylpurine 1-oxides, *J. Am. Chem. Soc.*, 97, 2839, 1975.
130. Bose, S.N., Kumar, S., Davies, J.M., Sethi, S.M., and McCloskey, J.A., Conversion of formycin into the fluorescent isoguanosine analogue 7-amino-3-(β–D-ribofuranosyl)-1*H*-pyrazolo[4,3*d*]pyrimidin-5(4*H*)-one, *J. Chem. Soc., Perkin Trans. 1*, 2421, 1984.
131. Fasani, E., Pietra, S., and Albini, A., The photocyclization of *N*-acyl-2-nitrodiphenylamines to phenazine *N*-oxides, *Heterocycles,* 33, 573,1992.
132. Albini, A., Fasani, E., and Frattini, V., Photochemistry of 2- and 4-benzoylpyridine *N*-oxides, *J. Photochem.*, 37, 355, 1975.
133. Tanigaka, R., Photoreduction of azoxybenzene to azobenzene, *Bull. Chem. Soc. Jpn.*, 41, 1664, 1968.
134. Pietra, S., Bettinetti, G., Albini, A., Fasani, E., and Oberti, R., Photochemical reactions of 2-nitrophenazine 10-oxide with amines, *J. Chem. Soc., Perkin Trans. 2*, 185, 1978.
135. Aveline, B.M. and Redmond, R.W., Selective photoexcitation of the thione and thiol forms in *N*-hydroxypyridine-4(1*H*)thione. A tautomeric heteroaromatic system, *J. Am. Chem. Soc.*, 121, 9977, 1999.
136. Aveline, B.M., Kochevar, I.E., and Redmond, R.W., Photochemistry of *N*-hydroxy-2(1*H*)-pyridone, a more selective source of hydroxyl radicals than *N*-hydroxypyridine-2(1*H*)-thione, *J. Am. Chem. Soc.*, 118, 10124, 1996.
137. Adam, W., Ballmaier, D., Epe, B., Grimm, G.N., and Saha-Möller, C.R., *N*-hydroxypyridinethiones as photochemical hydroxy radical sources for oxidative DNA damage, *Angew. Chem. Int. Ed. Engl.*, 34, 2156, 1995.
138. Reszka, K.J. and Chignell, C.F., EPR study of photoproduction of hydroxyl radicals by *N*-hydroxypyridine-2-thione using 5,5-dimethyl-1-pyrroline *N*-oxide in aqueous solution, *Photochem. Photobiol.*, 61, 269, 1995.
139. Gladys, M. and Knappe, W.R., Stepwise photoreduction of (iso)alloxazine *N*-oxides, *Z. Naturforsch.*, 29b, 549, 1974.
140. Blaney, R., Al-Nakib, T., Davies, R., and Jeremy, H., A fluorogenic actinometer for nucleic acid photochemistry utilizing 1-deazapurine 3-oxide, *Photochem. Photobiol.*, 57, 380, 1993.
141. Tokumura, K. and Matsuhita, Y., Triplet-sensitized deoxygenation reaction of 6-cyanophenanthridine 5-oxide in ethanol, *J. Photochem. Photobiol., A: Chem.*, 140, 27, 2001.

142. Hata, N. Ono, Y., and Kawaki, M., Photoinduced deoxygenation reaction of heterocyclic *N*-oxides, *Chem. Lett.*, 25, 1975.
143. Kaneko, C., Yamamori, M., Yamamoto, A., and Hayashi, R., Irradiation of aromatic amine oxides in dichloromethane in the presence of triphenylphosphine. A facile deoxygenation procedure of aromatic amine *N*-oxides, *Tetrahedron Lett.*, 2799, 1978.
144. Kaneko, C., Yamamoto, A., and Gomi, M., A facile method for the preparation of 4-nitropridine and -quinoline derivatives. Reduction of aromatic amine *N*-oxides with triphenylphosphite under irradiation, *Heterocycles*, 12, 227, 1979.
145. Igeta, H., Tsuchiya, T., Yamada, M., and Arai, H., Photoinduced oxygenation of aromatics by pyridazine *N*-oxides, *Chem. Pharm. Bull.*, 16, 767, 1968.
146. Tsuchiya, T., Arai, H., and Igeta, H., Photoinduced oxygenation by pyridazine *N*-oxides. II. Formation of epoxides from ethylenic compounds, *Tetrahedron Lett.,* 2213, 1970.
147. Sako, M., Shimada, K., Hirata, K., and Makai, Y., Photochemical hydroxylation of benzene derivatives by pyrimido[5,4-*g*]pteridine *N*-oxide, *Tetrahedron Lett.*, 26, 6493, 1985.
148. Schneider, H.J. and Sanerbrey, R., Photo-oxidation of alkanes with *N*-oxides, *J. Chem. Res. (S)*, 14, 1987.
149. Ito, Y. and Matsuura, T., The reaction of epoxides with oxygen-transfer reagents, *J. Chem. Soc., Perkin Trans. 1*, 1871, 1981.
150. Bharaway, R.K. and Davidson, R.S., The use of *N*-oxides to photoinduce the oxidative desulfurization and deselenation of pentacovalent phosphorous, *J. Chem. Res. (S)*, 406, 1987.
151. Sako, S., Shimada, K., Hirota, K., and Maki, Y., Photochemical oxygen atom transfer reaction by heterocyclic *N*-oxides involving a single electron transfer process. Oxidative demethylation of *N,N*-dimethylaniline, *J. Am. Chem. Soc.*, 108, 6039, 1986.
152. Suau, R., Rico-Gomez, R., Souto-Bachiller, F.A., Rodriguez-Rodriguez, L.A., and Ruiz, M.L., Efficient photoinduced electron transfer in papaverine *N*-oxide: regioselective intramolecular hydroxylation of papaverine as an alternative disconnection for the synthesis of cularine alkaloids, *Tetrahedron Lett.*, 36, 2653, 1995.
153. Souto-Bachiller, F.A., Perez-Inestrosa, E., Suau, R., Rico-Gomez, R., Rodriguez-Rodriguez, L.A., and Coronado-Perez, M.E., Photochemistry and photophysics of papaverine *N*-oxide, *Photochem. Photobiol.*, 70, 875, 1999.
154. Sako, M., Makino, T., Kitade, Y., Hirota, K., and Maki, Y., *N*6-substituent effect on the photooxidation of 2',3'-*O*-isopropylideneadenosines with a pyrimido[5,4-*g*]pteridinetetraone *N*-oxide, *J. Chem. Soc., Chem. Commun.*, 1704, 1986.
155. Sako, C., Shimada, K., Hirota, K., and Maki, Y., Photochemical intramolecular cyclization of purine and pyrimidine nucleosides induced by an electron acceptor. Chemical evidence for the generation and reactivity of adenosyl cation radicals, *J. Chem. Soc., Perkin Trans. 1*, 1801, 1992.
156. Poole, J.S., Hadad, C.S., Platz, M.S., Fredin, Z.P., Pickard, L., Guerrero, E.L., Kessler, M., Chowdhury, G., Kotandeniya, D., and Gates, K.S., Photochemical electron transfer reactions of tirazapamine, *Photochem. Photobiol.*, 75, 339, 2002.
157. Strub, H., Strehler, C., and Streith, J., Photoinduced nitrene, carbene and atomic oxygen transfer reaction starting from the corresponding pyridinium *N*-, *C*- and *O*-ylides, *Chem. Ber.*, 120, 355, 1987.
158. Akhatar, N.M., Boyd, D.R., Neill, J.D., and Jerina, D.M., Stereochemical and mechanistic aspects of sulfoxides, epoxides, arene oxides and phenol formation by photochemical oxygen atom transfer from aza-aromatic *N*-oxides, *J. Chem. Soc., Perkin Trans. 1*, 1693, 1980.
159. Lucien, E. and Greer, A, Electrophilic oxidant produced in the photodeoxygenation of 1,2-benzodiphenylene sulfoxide, *J. Org. Chem.*, 66, 4576, 2001.
160. Ogawa, Y., Iwasaki, S., and Okuda, S., Photochemical aromatic hydroxylation by aromatic amine *N*-oxides, remarkable solvent effect on the NIH-shift, *Tetrahedron Lett.*, 22, 3637, 1981.
161. Botchaway, S.W., Chakrabarti, S., and Makrigiorgios, G.M., Novel visible and ultraviolet light photogeneration of hydroxyl radicals by 2-methyl-4-nitroquinoline *N*-oxide (MNO) and 4,4′-dinitro-(2,2′)bipyridyl *N,N′*-dioxide (DBD), *Photochem. Photobiol.*, 67, 635, 1998.

162. Adam, W., Marquardt, S., and Saha-Möller, C.R., Oxidative DNA damage in the photolysis of *N*-hydroxy-2-pyridone, a specific hydroxyl-radical source, *Photochem. Photobiol.,* 70, 287, 1999.
163. Adam, W., Hartung, J., Okamoto, H., Saha-Möller, C.R., and Spehar, K., *N*-Hydroxy-4-(4-chlorophenyl)thiazole-2(3*H*)thione as a photochemical hydroxyl radical source. Photochemistry and oxidative damage of DNA (strand breaks) and 2′-deoxyguanosine (8-oxodG formation), *Photochem. Photobiol.*, 72, 619, 2000.
164. Maki, Y., Makino, T., Hirota, K., and Sako, M., Distinct solvent-dependence in the photoreactions of purine nucleosides with pyrimido[5,4-*g*]pteridinetetraone *N*-oxide. Possible generation of hydroxyl radical from the excited *N*-oxide in alcohols, *Heterocycles*, 35, 325, 1993.
165. Sako, M., Takeda, Y., Hirota, K., and Maki, Y., Synthesis and DNA photo-cleaving activity of novel heterocyclic *N*-oxide — acridine hybrid molecular, *Heterocycles*, 42, 31, 1996.
166. Decout, J.L., Lablache-Combier, A., and Loucheux, C., Photocrosslinking in polymers and copolymers containing pyridine *N*-oxide groups, *J. Polym. Sc., Polym. Chem. Ed.,* 18, 2371, 1980.
167. Decout, J.L., Lablache-Combier, A. and Loucheux, C., Photocrosslinking in polymers and copolymers containing various amine *N*-oxide groups, *J. Polym. Sc., Polym. Chem. Ed.*, 18, 2391, 1980.
168. Booker, R.A., *In situ* hardening with pyridine *N*-oxide and aldehyde precursors, *U.S. Patent* 4504578 A, 1985; *Chem. Abstr.*, 102, 157941e, 1985.
169. Hiraoka, H. and Welsch, L.W., Deep UV photolithography with composite photoresists containing poly(olefin)sulfones, *Org. Coat. Appl. Polym. Sci. Proc.*, 48, 48, 1983.
170. Just, G. and Zehetner, W., Photolysis of podocarponitrile oxide and mesitonitrile oxide, *Tetrahedron Lett.*, 3389, 1967.
171. Inui, H. and Murata, S. Photochemical generation of acetonitrile oxide via C-N bond cleavage of 3-methyl-2-(4-nitrophenyl)-2*H*-azirine, *J. Chem. Soc., Chem. Commun.*, 1036, 2001.

100

A New Look at Pyridinium Salt Photochemistry

Patrick S. Mariano
University of New Mexico

100.1 Overview

Interest in the area of pyridinium salt photochemistry dates back to the 1960s, a time when intense efforts were underway to probe the mechanistic details of photoinduced, benzene valence bond isomerization reactions. Amid this flurry of activity is found a single report in 1972 by Kaplan, Pavlik, and Wilzbach[4], describing the novel, bicyclic aziridine forming, photohydration reaction of N-methylpyridinium chloride. Many years passed before another study, in 1983 and focused on pyridinium salt single electron transfer photochemistry, led to the tangential observation that the bicyclic aziridines, arising by excited-state cyclizations of pyridinium salts, participate in acid catalyzed ring opening reactions to produce functionalized aminocyclopentenes. This area again remained uncultivated for many years until the pyridinium salt photocyclization and bicyclic aziridine ring-opening processes were finally investigated in a more thorough manner. The more recent efforts, starting in the mid-1990s, have finally uncovered the unique synthetic value of this chemistry.

In this review, the results of early studies in this area will be presented first in order to establish the background and context of the recent studies of pyridinium salt photocyclization and bicyclic aziridine ring-opening reactions. The overall aim of the presentation is to show how these processes can be used as key steps in synthetic routes to simple, yet interesting natural and non-natural products.

100.2 Early Studies of Pyridinium and Pyrylium Salt Photochemistry

An intense series of highly competitive investigations in the 1960s led to a comprehensive picture of excited state valence bond isomerization reactions of benzene and its substituted derivatives.[1] The principal products of the generally inefficient benzene photoreactions are benzvalene, Dewar-benzene and

0-8493-1348-1/04/$0.00+$1.50

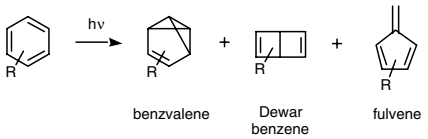

SCHEME 1

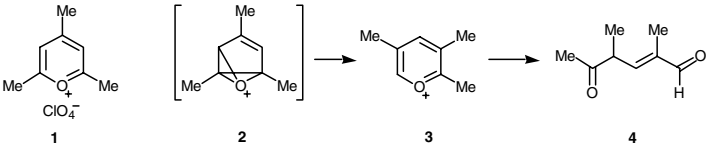

SCHEME 2

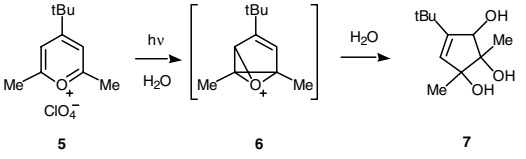

SCHEME 3

fulvene (Scheme 1). Stimulated by these observations, studies were initiated in the early 1970s to probe the photochemical properties of heteroatom analogs of benzene. Early independent investigations by Baltrop[2] and Pavlik[3] and their co-workers demonstrated that pyrylium salts undergo photoinduced ring isomerization and ring-opening reactions. For example, irradiation of 2,4,6-trimethylpyrylium perchlorate (**1**) was found to result in the formation of its 2,3,5-trimethyl isomer **3** along with the unsaturated keto-aldehyde **4** when water is present in the reaction mixtures (Scheme 2). In a similar vein, the cyclopentenetriol **7** was observed as the major primary product formed upon irradiation of an aqueous solution of the *t*-butyl-pyrylium salt **5** (Scheme 3). Both of these processes were proposed to involve the intermediary of oxabenzvalene cations **2** and **6**. Ring opening of these intermediates would form isomerized pyrylium salts while their hydrolytic cleavage would lead to the triol. 4-Hydroxypyrylium salts, formed by *in situ* protonation of 4-pyranones, have similar excited-state reactivity profiles. This is exemplified by the photochemical conversion of the 2,3,6-trimethyl-4-hydroxypyrylium salt **8** to the cyclopentenediol **9** by irradiation at 0°C in 50% aq. H_2SO_4 (Scheme 4). At elevated temperature, **9** undergoes a dark, acid-catalyzed reaction to produce the furfuryl ketone **10**.

Of comparable interest, yet receiving much less attention, was the early report by Kaplan, Pavlik and Wilzbach[4] that N-methylpyridinium chloride undergoes photoinduced cyclization to produce the bicyclic aziridine **14** upon irradiation in aqueous base solution (Scheme 5). The structure and stereochemistry of the product of this reaction, along with those generated by irradiation of ring-deuteriated and methyl-substituted analogs, led these workers to propose that the process is initiated by excited-state electrocyclization. The bicyclic-aziridine cation **11** formed in this manner undergoes least-hindered addition of hydroxide (Scheme 5). To account for partial scrambling of the carbon skeleton in these photoreactions, Kaplan and co-workers suggested that the initially formed cation **11** undergoes competitive isomerization (**11** → **13**) via the azabenzvalene cation **12**. As a consequence, it was proposed that product distributions from photoreactions of ring-deuteriated and methylated pyridinium salts are governed by the relative rates of hydroxide capture and 1,5-migrations of the key cation intermediates (e.g., **11** and **13**).

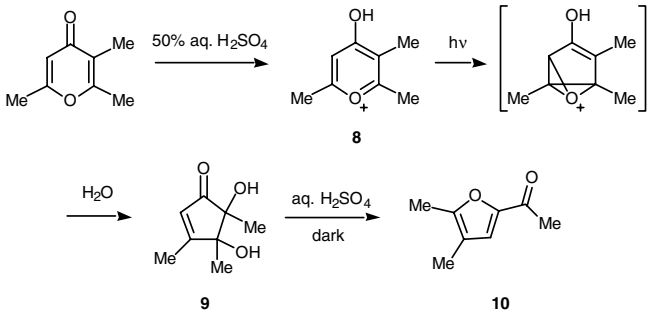

SCHEME 4

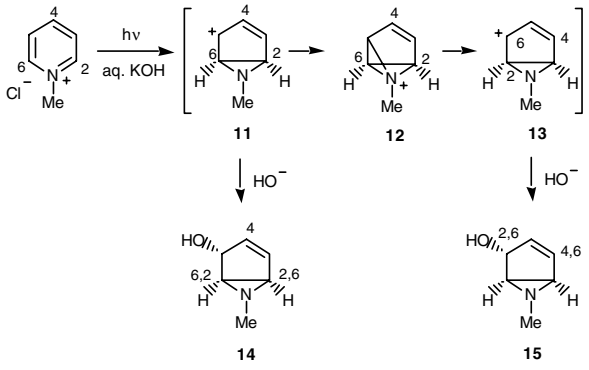

SCHEME 5

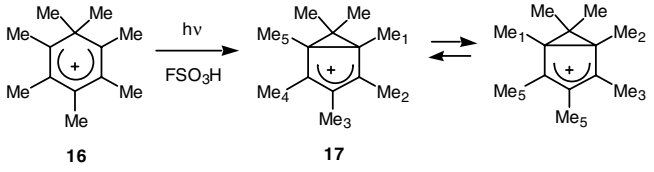

SCHEME 6

The photocyclization reactions of pyridinium and pyrylium salts are initiated by excited-state 2,6-bonding. These processes are analogous to 1,3-diradical forming photocyclization reactions of benzenes.[1] Also, these pyridinium and pyrylium excited-state processes can be visualized as photo-Nazarov cyclizations of cyclohexadienyl cations, which result in the formation of heteroatom substituted bicyclo[3.1.0]hexenyl cations.[5]

In the early investigations summarized above, benzvalene oxonium and ammonium ion intermediates were invoked to explain how ring carbon scrambling occurs in the initially formed bicyclic allyl cation intermediates. Although reasonable, rationalizations for these skeletal rearrangements do not necessarily require the intermediacy of benzvalene-like onium ions. Winstein,[6] in his early studies of carbocation photochemistry, showed that the heptamethyl bicyclo[3.1.0]hexenyl cation **17** (Scheme 6), generated by photocyclization of the corresponding cyclohexadienyl cation **16**, undergoes exceptionally rapid ($\Delta G^{\pm}$ = 9 kcal mol^{-1}) ring isomerization. The NMR-detected, fivefold degenerate rearrangement of this cation, occurring even at low temperatures, suggests that the suprafacial 1,5-migration with inversions at the

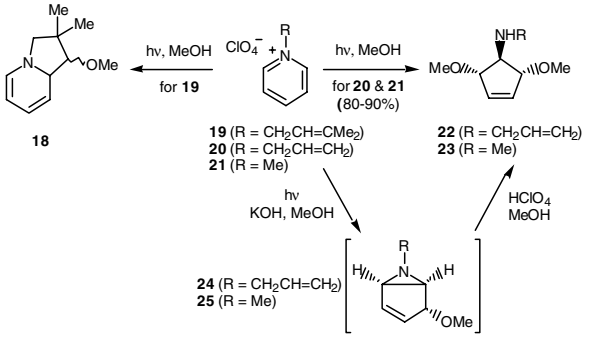

SCHEME 7

migrating carbon is an exceedingly facile process. Thus, similar pathways not involving the intermediacy of benzvalene onium ions might be responsible for isomerization reactions of the initially formed bicyclic allyl cations in the photochemistry of pyrylium and pyridinium salts.

A number of years passed, following the first report describing the photocyclization reaction of N-methylpyridinium chloride, before this process was again investigated. In the interim, interest in the general field of photochemistry shifted away from benzene valence bond isomerizations to other synthetically relevant processes. During this time, numerous efforts focused on photochemical reactions that are driven by excited-state singlet electron transfer (SET). Owing to the large excited-state reduction potentials of pyridinium and related N-heteroaromatic salts, these substances readily participate in SET-photochemical reactions with suitable electron donors.[7] Another perspective of pyridinium salt photocyclization processes was opened by observations made in a 1983 study by Mariano and co-workers[8] of SET-promoted photoreactions of N-heteroaromatic salts. An example of this is found in the photochemistry of N-prenylpyridinium perchlorate **19**, which undergoes smooth SET-promoted cyclization to form indolizidine **18**. In contrast, the N-allyl derivative **20** is efficiently transformed to the aminocyclopentene **22** upon irradiation in MeOH (Scheme 7). In a similar fashion, the aminocyclopentene **23** is produced by irradiation of N-methylpyridinium perchlorate **21** in MeOH.

The aminocyclopentene products of these pyridinium salt photoreactions were shown to arise by acid-catalyzed methanolytic aziridine ring opening of bicyclic aziridine intermediates. Accordingly, treatment of the bicyclic aziridines **24** and **25**, produced by irradiation of basic MeOH solutions of the salts **20** and **21**, with catalytic quantities of $HClO_4$ in MeOH led to smooth formation of the respective aminocyclopentenes **22** and **23**. Thus, when base is not included in pyridinium salt photoreaction mixtures, the initially formed photocyclization products are N-protonated bicyclic aziridines, which are subject to nucleophile-induced cleavage at their allylic aziridine centers.

100.3 Recent Studies of Pyridinium Salt Photocyclization: Bicyclic Aziridine Ring-Opening Processes

As has become the pattern in this area, it took a decade before the synthetic significance of the pyridinium salt photocyclization–aziridine ring opening sequence was finally recognized. As pointed out in the 1996 publication by Mariano and co-workers,[9] a two-step methodology (Scheme 8) can be employed in the stereocontrolled preparation of a variety of symmetric and differentially functionalized aminocyclopentenes. For example, these workers found that irradiation of the N-substituted pyridinium perchlorates **26** in aqueous or methanolic base solutions leads to efficient formation of the bicyclic-aziridinyl alcohols or ethers **27** (Scheme 9). Acid-catalyzed ring opening of the photoproducts, using a number of different nucleophiles, results in production of the *trans,trans*-aminocyclopentenes **28**.

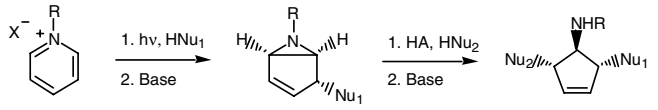

SCHEME 8

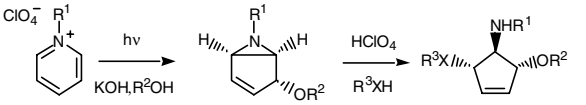

26 $\left\{\begin{array}{l} R^1 = nC_3H_5, \\ CH_2CONH_2, \\ \text{or } CH_2CH_2OH \end{array}\right\}$ **27** $\{R^2 = H, Me\}$ **28** $\left\{\begin{array}{l} R^3X = OMe, OH, \\ OAc, \text{ or } SAc \end{array}\right\}$

SCHEME 9

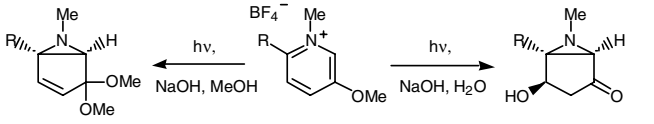

29 R = H, 6%
R = Me, 41%
R = Et, 77%

30

31 R = H, < 5%
R = Me, 38%
R = Et, 40%

SCHEME 10

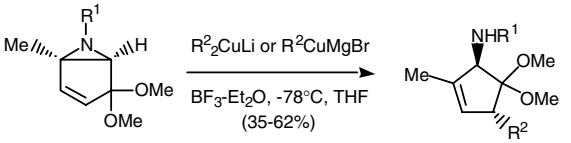

(R^1 = Et or $CH_2CH{=}CH_2$) (R^2 = Me, nBu, $CH{=}CH_2$)

SCHEME 11

Very similar (in some cases, identical) observations were reported in a 1998 publication by Burger and co-workers.[10] More novel are the recent findings by Penkett and Simpson[11] that irradiation of 3-alkoxypyridinium salts in aqueous alcohol solutions gives rise to bicyclic ketals. As depicted in Scheme 10, irradiation of the 3-methoxy salts **30** gives use to ketals **29** in yields that are highly dependent on the nature of the C6 substituent. In addition, β-hydroxyketones **31** are produced when the corresponding methoxy-substituted pyridinium salts are irradiated in aqueous base solutions (Scheme 10). Penkett and Simpson have also demonstrated the bicyclic ketal photoproducts participate in anti-S_N2' reactions with organocopper reagents to afford novel aminocyclopentene adducts (Scheme 11).[12]

Another interesting feature of the pyridinium salt photocyclization reactions is pointed out by the observation made by Mariano and his co-workers[9] that products resulting from intramolecular nucleophilic

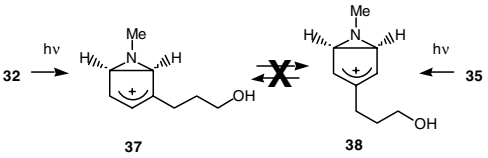

SCHEME 13

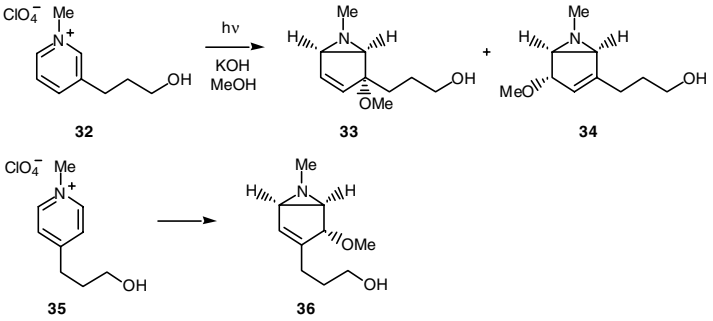

SCHEME 12

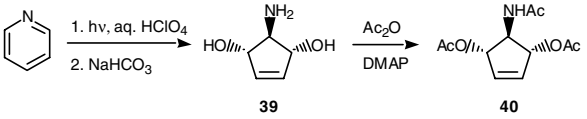

SCHEME 14

capture of intermediate azabicyclic allyl cations, are not formed in these processes. This feature is exemplified by photoreactions of N-tethered alcohol and amide substrates **26** (Scheme 9) which only yield products arising by addition of the external nucleophiles (MeOH and H_2O) to the cation intermediates formed by excited state 2,4-bonding. This trend extends to substrates that possess hydroxyalkyl side chains appended to C3 or C4 of the N-heteroaromatic nucleus. For example, the bicyclic alcohols **33** and **34** are the sole products formed when a basic MeOH solution of 1-methyl-3-hydroxypropylpyridinium perchlorate (**33**) is irradiated (Scheme 12). Similarly, the 4-hydroxypropyl analog **35** is transformed to the solvent incorporation adduct **36** exclusively under these photoreaction conditions.

It is interesting to note as an aside that the above photocyclization reactions are not attended by ring reorganization (i.e., no crossover formation of **36** from **32** or **33** + **34** from **35**). This result contrasts with the early observations of Kaplan and co-workers[4] and suggests that the initially formed bicyclic allyl cation intermediates **37** and **38** (Scheme 13) do not interconvert by 1,5-nitrogen migration on the intermolecular methanol addition time scale.

Another significant and synthetically relevant observation was made in studies probing the photochemical reactivity of N-protonated pyridines. Mariano and co-workers[9] have demonstrated that irradiation of a solution of pyridine in aqueous perchloric acid at 45 to 70°C results in clean generation of the cyclopentene aminodiol **39**, isolated as its triacetyl derivative **40** (Scheme 14). Despite the fact that the quantum efficiency of this reaction is low, the process can be used to prepare 1–2 g quantities of 40 following 1–2 day irradiation periods.

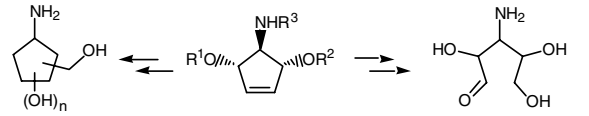

SCHEME 15

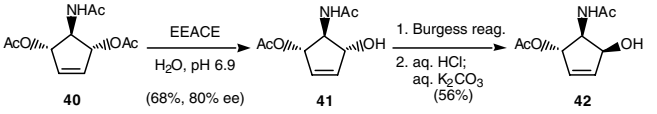

SCHEME 16

100.4 Applications of Pyridinium Salt Photochemistry to the Synthesis of Biomedically Relevant Targets

The pyridinium salt photocyclization–aziridine ring opening reactions described above introduce remarkably high levels of molecular, functional, and stereochemical complexity into the reacting substances. As a consequence of this characteristic, a number of synthetic applications of this chemistry can be envisaged. For example, the aminocyclopentene formed by these sequences contain functionality at each of the five contiguous ring carbons. Consequently, these substances are ideal intermediates in synthetic routes targeted at the biomedically interesting aminocyclopentitol class of natural and non-natural products (Scheme 15). In addition, the $\Delta^{1,2}$-alkene moiety and differentiable C3 and C5 substituents make the aminocyclopentenes suitably disposed for ring-opening reactions, which can be used to elaborate stereochemically defined, terminally differentiated five-carbon acyclic arrays. In this way, pyridinium salt photochemistry can be employed as key steps in concise sequences for the preparation of aminoaldopentoses and higher amino-sugar analogs (Scheme 15).

Studies conducted thus far to develop synthetic applications of this chemistry have relied heavily on the earlier finding that the *trans,trans*-amidocyclopentenyl acetate **40** can be prepared readily by irradiation of pyridine in aqueous acid solution (Scheme 14).[9] This substance is functionally similar to compounds that have been converted to non-racemic mono-alcohols by enzymatic desymmetrization processes. Thus, treatment of diacetate **40** with the electric eel acetylcholinesterase (EEACE) was found to generate the mono-ester **41** in a 68% yield and 80% ee (Scheme 16).[13] In addition, Mariano and co-workers have demonstrated that stereochemical diversity can be introduced into the aminocyclopentene ring system using hydroxyl inversion procedures.[9,13] An example of this is found in the conversion of **41** to its *cis-trans*-diastereomer **42**[13] by employment of the amide directed inversion method developed by Wipf and co-workers[14] (Scheme 16). These observations have established the foundation for applications of pyridinium salt photochemistry to the synthesis of the biomedically important aminocyclopentitols and aminoaldopentoses shown in Schemes 17, 18 and 19.[13,15–17]

100.5 Summary

Without doubt, it is possible to characterize the developments made in the area of pyridinium salt photochemistry as slow and "far between." More recent investigations of this chemistry have begun to uncover its synthetic significance. However, a number of questions pertaining to the mechanism of the photocyclization process, the factors governing the rates of ring isomerization, and the regiocontrol of nucleophilic addition to the unsymmetrically substituted cation intermediates still need to be answered before the full potential of this unique excited-state process can be elaborated.

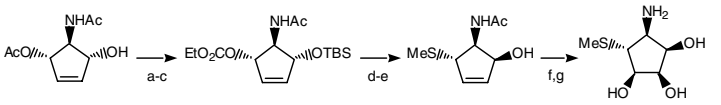

(a) TBSCl, imidaz; (b) NaOMe, MeOH; (c) EtO_2COCl;
(d) TMSSMe, Pd(0); (e) TBAF; (f) OsO_4, TMEDA; (g) 4 N HCl

SCHEME 17

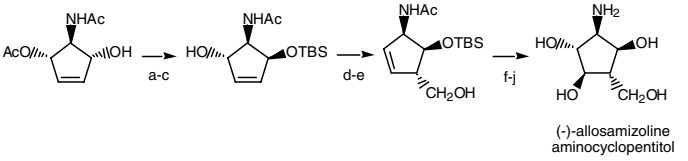

(a) Burgess reag.; aq HCl; aq K_2CO_3; (b) TBSCl, imidaz; (c) NaOMe, MeOH; (d) KH; Bu_3SnCH_2I
(e) BuLi; (f) TBAF; ,(g) $Me_3C(OMe)_2$, PTSA,; (h) MCPBA; (i) 0.5 N NaOH; (j) 4 N HCl

SCHEME 18

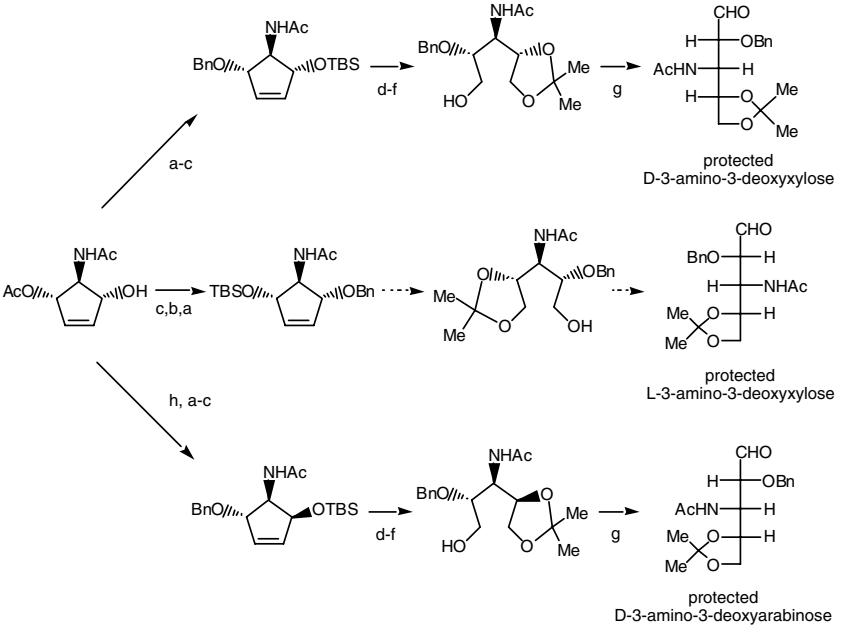

(a) TBSCl, imidaz; (b) NaOMe, MeOH; (c) BnBr; (d) O_3; $NaBH_4$; (e) TBAF;
(f) $Me_2C(OMe)_2$, PTSA; (g) Swern Oxid; (h) Burgess reag; aq HCl; aq K_2CO_3

SCHEME 19

Acknowledgments

The author expresses deep appreciation to his enthusiastic, hard-working, and productive co-workers Haiyan Lu, Rong Ling, Zhuoyi Su, and Mutsuo Yoshida, and Ling Song whose studies in the area of pyridinium salt photochemistry established the basis for the results presented in this review. Also, the generous financial support given to the author's research program in this area by the Petroleum Research Fund of the American Chemical Society and the National Institutes of Health is acknowledged.

References

1. Bryce-Smith, D. and Gilbert, A., The organic photochemistry of benzene, *Tetrahedron*, **32**, 1309, 1976.
2. Baltrop, J.A., Dawes, K., Day, A.C., and Summers, A.J.H., Photohydrolysis of 2,4,6-trimethylpyrylium perchlorate. Evidence for isomerization to an oxoniabenzvalene intermediate, *J. Chem. Soc., Chem. Commun.*, 1240, !972; Baltrop, J.A., Dawes, K., Day, A.C., Nutall, S.J., and Summers, A.J.H., Light induced 1,2-transposition and 2,6-bonding in 4-ethyl-2,6-dimethylpyrylium perchlorate, *J. Chem. Soc., Chem. Commun.*, 410, 1973; Baltrop, J.A., Dawes, K., Day, A.C., and Summers, A.J.H., Photochemistry of 4-*tert*-butyl-2,6-dimethylpyrylium perchlorate. Evidence for an oxoniabenzvalene intermediate, *J. Am. Chem. Soc.,* 95, 2406, 1973.
3. Pavlik, J.W. and Clennan, E.L., Photochemical rearrangements of pyrylium cations, *J. Am. Chem. Soc.,* 95, 1697, 1973; Pavlik, J.W. and Kwong, J., Photochemical rearrangements of neutral and protonated 2-pyrones, *J. Am. Chem. Soc.,* 95, 7914, 1973; Pavlik, J.W., Bolin, D.R., Bradford, K.C., and Anderson, W.G., Photoisomerization of 4-hydroxypyrylium cations. Furyl cation formation, *J. Am. Chem. Soc.,* 99, 2816, 1977; Pavlik, J.W. and Spada, A.P., Photo-ring contraction of 4-hydroxypyrylium cations, *Tetrahedron Lett.*, 4441, 1979.
4. Kaplan, L., Pavlik, J.W., and Wilzbach, K.E., Photohydration of pyridinium ions, *J. Am. Chem. Soc.*, 94, 3283, 1972.
5. Childs, R.F., Sakai, M., and Winstein, S., The observation and behavior of the pentamethylcyclopentadienylmethyl cation, *J. Am. Chem. Soc.*, 90, 7144, 1968.
6. Childs, R.F. and Winstein, S., Ring opening and fivefold degenerate scrambling in hexa- and heptamethylbicyclo[3.1.0]hexenyl cations, *J. Am. Chem. Soc.,* 90, 7146, 1968.
7. Mariano, P.S. and Stavinoha, J.L., Synthetic aspects of photochemical electron transfer reactions, *Synthetic Organic Photochemistry,* Horspool, W.M, Ed.,Plenum, New York, 1984.
8. Yoon, U.C., Quillen, S.L., Mariano, P.S., Swanson, R., Stavinoha, J.L., and Bay, E., Exploratory and mechanistic aspects of the electron transfer photochemistry of olefin-*N*-heteroaromatic cation systems, *J. Am. Chem. Soc.,* 105, 1204, 1983.
9. Ling, R., Yoshida, M., and Mariano, P.S., Exploratory investigations probing a preparatively versatile, pyridinium salt photoelectrocyclization-solvolytic aziridine ring opening sequence, *J. Org. Chem.*, 61, 4439, 1996.
10. Acar, E.A., Glarner, F., and Burger, U., Aminocyclopentitols from N-alkylpyridinium salts. A photochemical approach, *Helv. Chim. Acta.*, 81, 1095, 1998.
11. Penkett, C.S. and Simpson, I.D., New methods of preparing cyclopentenone ketals. The photosolvolysis of 3-alkoxypyridinium tetrafluoroborates, *Synlett.*, 93, 1999; Penkett, C.S., and Simpson, I.D., Photosolvolysis reactions of 3-alkoxypyridinium tetrafluoroborate salts, *Tetrahedron*, 55, 6183, 1999.
12. Clive, S., Penkett, C.S., and Simpson, I.D., The stereoselective addition of organocuprates to cyclopentenyl aziridine derivatives, *Tetrahedron Lett.*, 42, 1179, 2001.
13. Ling, R. and Mariano, P.S., A demonstration of the synthetic potential of pyridium salt photochemistry by its application to a stereocontrolled synthesis of (+)-mannostatin A, *J. Org. Chem.*, 63, 6072, 1998.

14. Cho, J.C., Ling, R., Kim, A., and Mariano, P.S., A versatile approach to the synthesis of (+)-mannostatin A analogs, *J. Org. Chem.*, 65, 1574, 2000.
15. Wipf, P. and Miller, C.P., Stereospecific synthesis of peptide analogs with allo-threonine and D-allo-threonine residues, *J. Org. Chem.* 58, 1575, 1993.
16. Lu, H., Mariano, P.S., and Lam, Y.-F., A concise synthesis of the (−)-allosamizoline aminocyclopentitol based on pyridinium salt photochemistry, *Tetrahedron Lett.*, 42, 4755, 2001.
17. Lu, H., Su, Z., Song, L., and Mariano, P.S., A novel approach to the synthesis of amino-sugars. Routes to selectively protected 3-amino-3-deoxy-aldopentoses based on pyridinium salt photochemistry, *J. Org. Chem.*, 67, 2002.

101

The Dynamics and Photochemical Consequences of Aminium Radical Reactions

Ung Chan Yoon
Pusan National University

Zhuoyi Su
University of New Mexico

Patrick S. Mariano
University of New Mexico

101.1 Overview

Single electron transfer (SET) is now recognized as a key mechanistic event in a wide variety of ground- and excited-state chemical and biochemical processes.[1–5] Organic photochemistry is one discipline where this recognition has profoundly impacted the understanding of mechanistic pathways and the development of new reactions.[6] Owing to the large driving force for SET in the electronic excited states vs. ground states, radical ion formation is often one of the most efficient pathways for excited-state deactivation.

0-8493-1348-1/04/$0.00+$1.50

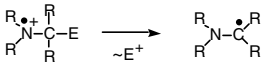

SCHEME 1

TABLE 101.1 Estimated Oxidation Potentials, $E^o(+)$ of Selected Amines, Amides, and Carbamates

Amine	$E^o(+)$ (V)	Amine	$E^o(+)$ (V)
Me_2NPh	+0.45	$PhCH_2CH_2N(Me)CO_2Me$	+1.61
Me_3N	+0.82	$PhCH_2CH_2N(CH_2SiMe_3)CO_2Me$	+1.45
Et_3N	+0.79	MeNHPh	+0.25
n-Bu_3N	+0.62	Me_3SiCH_2NHPh	+0.10
Me_2NCOMe	+1.82	$Me_3SiCH_2CH_2NPh_2$	+0.30
n-Bu_2NCO_2Me	+1.52	$Me_3SiCH_2NPh_2$	+0.07

From Miller, L.L., Nordblum, G.D., and Mayeda, E.A., *J.-Org. Chem.*, **37**, 916, 1972; Mann, C.K., and Barnes, K.K., *Electrochemical Reactions in Non-Aqueous Systems.*, Marcel Dekker, New York, 1970.

Consequently, in contrast to classical photochemical reactions, SET-promoted excited-state processes are controlled by the nature and rates of secondary reactions of charged radical intermediates.

α-Heterolytic fragmentation reactions are the most common types of decay pathways open to ion radicals. These fragmentation reactions play a pivotal role in SET photochemistry. Departure of an electrofugal or nucleofugal group from a respective cation or anion radical often competes with back electron transfer or alternative reaction modes to generate a carbon-centered radical intermediate in routes for product formation. Therefore, knowledge about the dynamics of ion radical fragmentation reactions and their dependence on structure, substituents, and the reaction medium is crucial for the design of new and efficient SET photochemical processes.

This review[7–9] focuses on α-heterolytic fragmentation reactions of aminium radicals (Scheme 1), which are derived by one-electron oxidation of amines. In these fragmentation processes, electrofugal groups are transferred to either Lowry-Brønsted or Lewis bases to produce α-amino radicals. The review concentrates on the results of investigations that have provided information about the dynamics of important aminium radical fragmentation reactions, including deprotonation, demetallation, retro-Aldol fragmentation and decarboxylation. Included in the discussion are examples that show how the rates of aminium radical cleavage influence the nature and efficiencies of photochemical reactions involving amine substrates.

101.2 Redox Properties of Amines

Amines are among the most easily oxidized classes of neutral organic substances. This is reflected by their low oxidation potentials (Table 101.1). As expected, oxidation potentials of amines are significantly altered by N-substituents. Accordingly, amines bearing N-substituents that are capable of stabilizing the formed aminium radicals have lower oxidation potentials as compared to those with N-electron-withdrawing substituents. Resonance stabilization caused by N-aryl substituents lowers the oxidation potential of amines by nearly 0.4 V while alkoxycarbonyl or acyl substitution raises the oxidation potential by *ca.* 0.9 to 1 V. A less dramatic effect is seen for substituents that inductively stabilize the aminium radical. This is exemplified by the only slight decrease in the oxidation potential of tertiary amines caused by α-alkyl substitution (e.g., Me_3N, +0.82 V; Et_3N, +0.79 V; nBu_3N, +0.62 V).

In contrast, other types of α–substituents can lead to large stabilization of amine cation radicals. For example, Yoshida[10] and Cooper[11] have demonstrated that α–trialkylsilylamines and α–trialkylsilylcarbamates have significantly lower oxidation potentials than their non-silicon substituted counterparts.

This phenomenon, observed also for allyl- and benzylsilanes,[12,13] is attributed to hyperconjugative stabilization of the aminium radicals by interaction of the half-vacant nitrogen nonbonding *p*-orbital with the carbon-silicon σ–orbital.[14] α–Silyl substitution also causes a significant decrease in the oxidation potentials of ethers by as much as 0.9 eV.[15,16] This effect is strongly dependent on molecular geometry, being larger in cases where the C–Si bond is oriented to overlap well with the half-vacant oxygen orbital.

101.3 Photochemical Generation of Aminium Radicals

Owing to their low oxidation potentials, amines serve as potent electron donors in photoinduced SET processes. SET occurs at near diffusion controlled rates from amines to acceptors, which have excited-state reduction potentials that are higher than the oxidation potential of the amines. Three common methods have been used to promote excited state SET oxidation of amines. These include (1) SET to the excited state of acceptors, which participate as substrates in photochemical reactions with the amine (e.g., α,β-unsaturated ketones); (2) SET to the excited-state acceptors, which serve as sensitizers (e.g., cyanoarenes) for photochemical reactions occurring between amines and other substrates; and (3) SET to preformed radical cations. The third method, in which amines are converted to aminium radicals without simultaneous in-cage generation of substrate or sensitizer anion radicals, is known as redox photosensitization.[19] In contrast, the former two methods lead to direct formation of contact ion radical pairs (CIRP) or solvent-separated ion radical pairs (SSIRP), whose lifetimes and behavior depend on the polarity of the medium. Polar solvents facilitate cage escape of the ion radicals, leading to generation of fully solvated free ion radical intermediates.

101.4 Chemical Reactions of Aminium Radicals

Aminium radicals have a rich history as reactive intermediates in organic chemistry. The nature and rates of aminium radical reactions play a major role in governing the chemoselectivities, regioselectivities, and efficiencies of a wide variety of amine oxidation processes. Perhaps the most common reaction mode open to tertiary aminium radicals is α-CH deprotonation, which results in the production of neutral α-amino radicals (Scheme 2). Closely related to α-CH deprotonation are other α-heterolytic fragmentation reactions in which electrofugal groups are lost to Lowry-Brønsted or Lewis bases. One example of this reaction type is base-induced retro-Aldol cleavage of cation radicals derived from tertiary β-aminoalcohols. Decarboxylation, with or without simultaneous deprotonation, is another common reaction of aminium radicals derived from SET oxidation of α-amino acids or their carboxylates. Finally, silophile-promoted α-desilylation of α-trialkylsilylaminium radicals is the last type of reaction pathway commonly

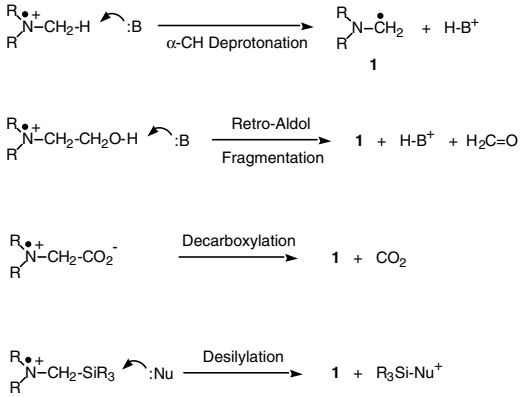

SCHEME 2

observed for these reactive intermediates. In all cases, the driving force for fragmentation of the aminium radical is provided by a combination of factors, including (1) delocalization of the N-centered positive charge density into the α-C-H, α-C-C, or α-C-SiR_3 σ-bonds, and (2) the thermodynamics associated with formation of carbonyl π-bonds or silicon-silophile σ-bonds.

101.5 α-CH Deprotonation of Aminium Radicals

Direct Measurement of Deprotonation Rates

Studies probing the structural, spectroscopic, and chemical characteristics of aminium radicals have been discussed in a thorough earlier review by Nelsen and co-workers.[20] The cationic and radical nature of these intermediates combine to define their chemical properties. The N-H protons of primary and secondary aminium radicals generally are more acidic (pKa *ca.* 7) than their neutral amine (pK_a *ca.* 35) or charged ammonium ion (pKa *ca.* 11) counterparts.[21] Consequently, cation radicals derived from SET oxidations of primary and secondary amines typically undergo rapid N-H-deprotonation to generate neutral aminyl radicals. By employing kinetic ESR techniques, Ingold[22] has determined that the rate constants for N-H proton transfer from the Me_2NH cation radical to solvents varies from 10^5 to 10^6 M^{-1} s^{-1}.

Tertiary aminium radicals also are acidic, owing to the presence of α-CH protons. As a result, the most common reaction mode open to these charged radicals is α-CH deprotonation, leading to generation of α-amino radicals (Scheme 2). The importance of this process in electrochemical and SET photoinduced oxidation reactions of amines has stimulated a number of detailed studies aimed at elucidating the kinetics of base-promoted α-CH deprotonation of tertiary aminium radicals. In an early investigation, Das and Von Sonntag[23] used pulse radiolysis methods to determine that the pKa of the N-centered radical cation derived from trimethylamine is *ca.* 8 in H_2O (Scheme 3). In addition, this effort established that the bimolecular rate constant for proton transfer from this aminium radical to Me_3N is 7×10^8 M^{-1} s^{-1}. Equally informative results have come from another early kinetic investigation of ferricyanide oxidation reactions of 1,4-dihydropyridines and N-methylacridanes by Bruice and co-workers.[24,25] Kinetic analysis of these reactions demonstrated that rate-limiting deprotonation of the aminium radical intermediates **2,** with imidazole and acetate as bases, occurs with rate constants in the 1×10^7 M^{-1} s^{-1} range (Scheme 4). The primary kinetic isotope effect of 4.4 and Brønsted β-value of 0.2 measured for this process suggest that the transition states for proton transfer in these processes lie close to the aminium radical reactants rather than the α-amino radical products.

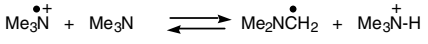

SCHEME 3

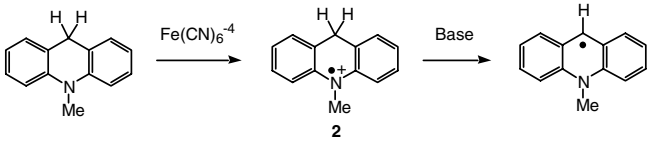

SCHEME 4

A more thorough evaluation of the dynamics of tertiary aminium radical α-CH deprotonation reactions has come from relatively recent studies employing stopped-flow, time-resolved laser flash photolysis, and electrochemical techniques. In one effort, Dinnocenzo and Banach[26] examined acid-base reactions of the stable aminium radical **3**, prepared by SET oxidation of N,N-dianisyl-N-methylamine (Scheme 5). Using stopped-flow kinetic methods, these workers showed that the bimolecular rate constants for α-deprotonation of **3** by four quinuclidine bases **4** in MeCN are (1) in the range of 1×10^2 to 6×10^4 M^{-1}

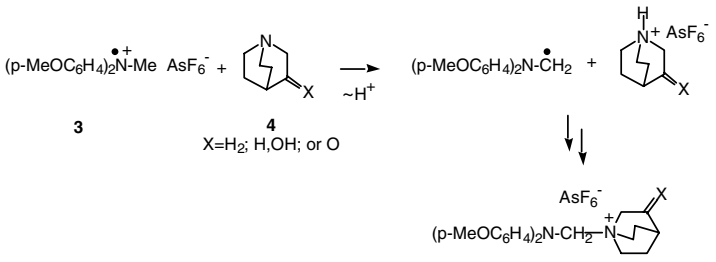

SCHEME 5

s^{-1} and (2) associated with a primary deuterium isotope effect (NCH_3 vs. NCD_3) of 6 to 7.8. Also, the rate constants were found to be linearly dependent on the pKa values of the quinuclidines, providing a Brønsted β-value of 0.63. Thus, the rates of α-CH deprotonation of **3** parallel the thermodynamic driving force associated with base strength.

More typically, aminium radicals are unstable species that can be detected and studied only by using ultra-fast kinetic methods. An example of this is found in the time-resolved laser spectroscopic investigation of anilinium radicals conducted by Mariano, Falvey, and co-workers.[27] Laser flash photolysis (LFP) of a solution of N,N-dimethylaniline (DMA) and 1,4-dicyanobenzene (DCB) leads to generation of the respective free ion radical intermediates **5** and **6** (X = H). In the absence of added bases, these free ion radical transients undergo diffusion-controlled, second-order decay by back electron transfer (Scheme 6). α-CH deprotonation of anilinium radical **6** (R = H) by the weak bases n-Bu_4NOAc and n-$Bu_4NO_2CCF_3$ occurs with respective second-order rate constants of 3.1×10^5 and 8×10^4 M^{-1} s^{-1} and a deuterium isotope effect (NCH_3 vs. NCD_3) of 3.6 (for n Bu_4NOAc). To probe the driving force dependence of the rates of this process, *p*-OMe, *p*-Me, *p*-CF_3-substituted dimethylanilines were subjected to LFP studies. The substituents were found to have a pronounced effect on the rates of n-Bu_4NOAc-induced deprotonation (k(*p*-OMe) = 2.0×10^4 M^{-1} s^{-1}, k(*p*-Me) = 1.1×10^5 M^{-1} s^{-1}, k(*p*-CF_3) = 2.5×10^6 M^{-1} s^{-1}). These effects are well correlated with the control of the oxidation potentials of the aniline derivatives by groups at the *para*-position. A cyclic voltammetry study of *p*-substituted N,N-dimethylanilines by Parker and Tilset[28] led to the same general conclusions about the substituent dependence of α-CH deprotonation rates.

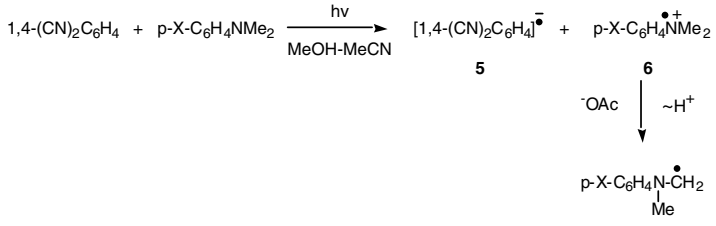

SCHEME 6

Substituents located on the α-carbon center can also influence the rates of aminium radical α-CH deprotonation through a combination of steric and electronic effects. This issue was probed by Mariano, Falvey, and co-workers[27] in studies with N-substituted-N,N-diphenylamines **7** (Scheme 7, Table 101.2). Aminium radicals **8**, produced by photoinduced SET from the amines **7** to DCB, undergo deprotonation by n-Bu_4NOAc with rate constants in the region of *ca.* 1×10^6 M^{-1} s^{-1}. Interestingly, alkyl substitution at the α-carbon retards deprotonation while conjugating substituents at this position bring about an acceleration in the rate of deprotonation.

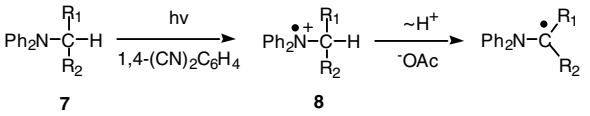

7 **8**

SCHEME 7

TABLE 101.2 Rate Constants for α-CH Deprotonation of Diphenylaminium Radicals **8** by n-Bu_4NOAc

R_1, R_2 in **8**	K ($M^{-1}s,^{-1}$ 25°C)
H, H	9.5×10^5
H, CH_3	2.3×10^5
CH_3, CH_3	1.7×10^5
Ph, H	3.2×10^6
$CH{=}CH_2$, H	2.6×10^6
C≡CH, H	7.0×10^7

Studies by Saveant and co-workers[29] provide a more comprehensive picture of how steric and electronic effects govern the rates of aminium radical α-CH deprotonation. In this account, a combination of double potential step chronoamperometry, cyclic voltammetry, and laser flash photolysis methods were used to measure the rates of 9-CH deprotonation of aminium radicals **9**, produced by SET oxidation of 9-substituted-N-methylacridanes (Scheme 8). Amines with differing base strength and steric constraints were employed as bases. The data (Table 101.3) clearly show that the deprotonation rate constants are significantly reduced when sterically encumbering substituents are present at C-9 of the acridanium

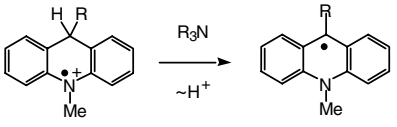

9

SCHEME 8

TABLE 101.3 Rate Constants for 9-CH Deprotonation of Acridanium Radicals **9** by Amine Bases

R in Acridanium Radical **9** (pKa)	Amine Bases (pKa)	Log Deprotonation Rate Constant (M^{-1} s^{-1})
H (0.8)	2-Chloropyridine (6.3)	4.1
CH_3 (1.5)	2-Chloropyridine	3.3
Ph (1.2)	2-Chloropyridine	3.5
H	Pyridine (12.3)	6.5
H	Piperidine (18.9)	9.4
CH_2Ph (1.7)	3,5-Dimethylpyridine (14.7)	4.8
CH_2Ph	2,6-Dimethylpyridine (15.4)	3.4

From Anne, A., Hapiot, P., Moiroux, J., Neta, P., and Saveant, J.-M., *J. Am. Chem. Soc.*, **114**, 4694, 1992.

radical or on the base. In addition, the rates correlate closely with the pKa values of both the bases and amine cation radicals.

The results emanating from the studies described above have demonstrated that nitrogen and α-carbon substituents control the kinetic α-CH acidities of aminium radicals. It is clear that the kinetic acidities of these reactive intermediates, like those of other CH-proton donors, parallel thermodynamic acidities as reflected by their pKa values. As the empirical relationship developed by Nicholas and Arnold[30] shows, the pKa of an aminium radical is determined by both the oxidation potentials (E^o) of the parent amine (a measure of the aminium radical stability) and the bond dissociation energy (BDE) of the cleaved α-CH bond in the amine (a measure of the stability of the α-amino radical formed by deprotonation). In line with this formulation, electron-donating groups on nitrogen lower acidity by decreasing the energy of the aminium radical. The electronic effects of α-substituents on acidity operate through their control of α-amino radical stability.

Another important feature of aminium radical deprotonation reactions is revealed by comparing the results from independent investigations by Saveant[31] and Peters[32–35] of N-methylacridane cation radical deprotonation reactions. Under the conditions used in the electrochemical and laser flash photolysis experiments carried out by Saveant, the free N-methylacridanium radical is observed. This species undergoes deprotonation by base in a diffusion-governed encounter process. Using d-isotope effects, Saveant showed that deprotonation of this free aminium radical occurs preferentially at C9 of the acridane ring. Earlier picosecond LFP studies by Peters revealed that proton transfer between the SET-photogenerated N-methylacridanium radical and arylketone anion radicals can also occur in contact ion radical pairs (CIRP). Interestingly, Peters found that in the CIRP generated by photoinduced SET between benzophenone and N-methylacridane, proton transfer occurs selectively from the N-methyl position of the acridanium radical. These contrasting observations suggest that the site of deprotonation in aminium radicals can be strongly influenced by the environment in which the deprotonation process occurs, that is, whether it takes place in a diffusion encounter manner or within a highly organized ion radical pair. In the latter case, the lowest energy orientation of the charged radical partners can influence deprotonation regioselectivities.

Relative Rates of Aminium Radical α-CH Deprotonation Based on Photoproduct Distributions

Information about the relative kinetic acidities of aminium radicals has also come from a number of studies probing product distributions of SET-promoted photochemical reactions. One of the earliest investigation in this area was conducted by Cohen and co-workers,[36] in which product distributions of SET-induced photoreactions of unsymmetrically substituted tertiary amines were used to gain information about how alkyl substituents affect the rates of aminium radical α-CH deprotonation. Irradiation of solutions of 4-benzoylbenzoic acid containing a variety of tertiary amines leads to formation of dealkylation products (Scheme 9). In these processes, the initially formed aminium radical **10** transfer a proton to the 4-benzoylbenzoic acid anion radical to generate an α-amino radical, which then donates an electron to another 4-benzoylbenzoic acid molecule. Hydrolysis of iminium ions **11**, formed in this manner, then gives carbonyl and secondary amine products. The results of these studies qualitatively indicate that dealkylation occurs preferentially at the less alkyl-substituted α-carbon.

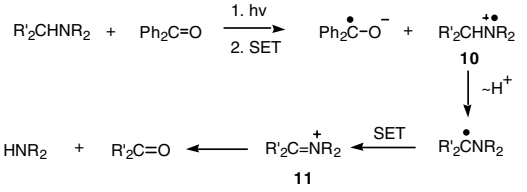

SCHEME 9

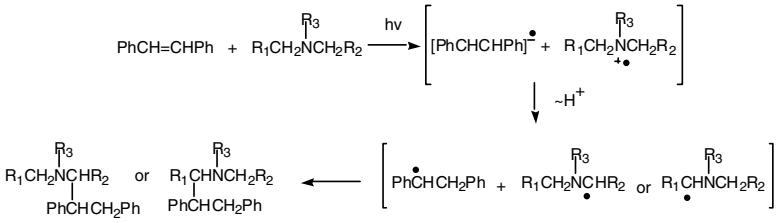

SCHEME 10

TABLE 101.4 Relative α-CH Kinetic Acidities of Tertiary Aminium Radicals Derived from SET-Induced Stilbene Photoadditions of R_2NCH_2R'

R′ in R_2NCH_2R'	Relative Deprotonation Rates
H	1.1
CH_3	0.5
$CH_2CH_2CH_3$	0.5
CO_2Me	2.3
Ph	1.0
$CH{=}CH_2$	0.5
C≡CH	>110

From Lewis, F.D. and Ho, T.L., *J. Am. Chem. Soc.,* **102**, 1751, 1980; Lewis, F.D., Ho, T.L., and Simpson, J.T., *J. Org. Chem.,* **46**, 1077, 1981; Lewis, F.D., Ho, T.I., and Simpson, J.T., *J. Am. Chem. Soc.*, **104**, 1924, 1982.

Detailed investigations of the SET photochemistry of tertiary amine–stilbene systems by Lewis and co-workers[37–39] have elucidated a number of factors that govern the relative rates of α–deprotonation reactions of aminium radicals. As shown in Scheme 10, photoreactions of stilbene with unsymmetrically substituted tertiary amines in acetonitrile proceed via pathways in which contact ion radical pairs (CIRP), generated by excited-state SET, undergo proton transfer to yield radical pair precursors of stilbene–amine photoadducts. By careful analysis of the product distributions, Lewis has determined the relative kinetic α-CH acidities of the intermediate aminium radicals (Table 101.4).

These data show that both steric and electronic factors contribute in determining the kinetic acidities of tertiary aminium radicals. Proton transfer in the stilbene-amine CIRP requires that the α-CH bond be aligned parallel to the half-vacant *p*-orbital on nitrogen in the aminium radical. Lewis has proposed that the energy of the transition state for proton transfer in the CIRP is influenced by steric strain associated with internal interactions between alkyl groups in the amine cation radical component.[37–38] In addition, the energies of transition states for proton transfer in these CIRPs should be governed by steric interactions between the tightly aligned ion radical partners. As a result, transition state energies should vary with the nature of the α–carbon in the following manner: methyl < primary < secondary. Importantly, steric effects of alkyl substituents appear to be more important than electronic effects in controlling the rates of proton transfer from aminium radicals in contact ion radical pairs.

The influence of electronic effects on aminium radical α-CH kinetic acidities has been observed in product distribution studies of Mariano and co-workers.[40–41] These workers found that irradiation of β-aminoethyl-substituted cyclohexenones **12** leads to formation of mixtures of regioisomeric products **14**. The SET promoted photocyclization reactions proceed via the intermediacy of zwitterionic biradicals **13.** Intramolecular proton transfer between the aminium and enone anion radical moieties in **13** is followed by radical coupling to give spirocyclic aminoketones **14** (Scheme 11). The relative rates of aminium radical

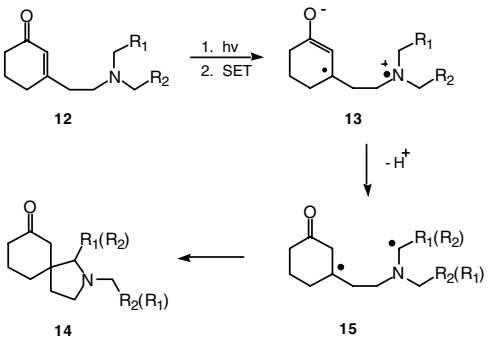

SCHEME 11

TABLE 101.5 Relative α-CH Kinetic Acidities of Tertiary Aminium Radicals Derived from SET-Induced Photocyclizations of the R_2NCH_2R' Amine Moiety in Amino-Enones **12**

R′ in R_2NCH_2R'	Relative Deprotonation Rates
H	0.01
CH_3	0.02
$CH_2CH_2CH_3$	0.1
CO_2Me	0.5
Ph	1.0
$CH = CH_2$	1.9
C≡CH	3.9

From Xu, W., Zhang, X.M., and Mariano, P.S., *J. Am. Chem. Soc.*, **113**, 8863, 1991; Xu, W. and Mariano, P.S., *J. Am. Chem. Soc.*, **113**, 1431, 1991.

α-deprotonation (Table 101.5), obtained from analysis of the product ratios, indicate that the radical stabilizing ability of α–substituents (C≡CH > CH = CH_2 > Ph > CO_2Me > TMS > Me > H) plays a key role in determining the aminium radical kinetic acidities in these cases.

A comparison of the product distribution results obtained from studies of the stilbene–amine and aminoethylcyclohexenone photoreactions shows that steric and electronic effects contribute differently in determining aminium radical kinetic acidities. Product distribution analysis of SET-induced stilbene–tertiary amine photoadditions suggests that alkyl substitution leads to decreased rates of α-CH proton transfer from the tertiary aminium radicals to the stilbene anion radical within contact ion radical pairs. As mentioned, this effect is likely due to steric hindrance that raises the energy of early transition states for proton transfer when the stilbene anion radical is tightly associated with the aminium radical. In this pair, the aminium radical exists in a stereoelectronically preferred conformation **16** (Figure 101.1), having good overlap between the half-vacant nitrogen *p*-orbital and filled α-CH σ–orbital. The fact that proton transfer in the stilbene–amine photoreaction occurs in a contact ion radical pair, whose rigid structure (i.e., relative orientation of negative and positive radical partners) is governed by the need for maximum charge neutralization,[42,43] could cause kinetic acidities to be more sensitive to steric factors.

In contrast, α-CH proton transfer in SET-promoted photoreactions of tethered amino-enones occurs in an intramolecular fashion. The proton transfer transition states **17** (Figure 101.1) are significantly different from those involved in the stilbene–amine CIRP. The intramolecular nature of proton transfer in the enone–amine zwitterionic biradicals disfavors coplanar alignment of the aminium radical α–CH σ–orbital and nitrogen *p*-orbital. This conformational requirement could very well lead to a minimization

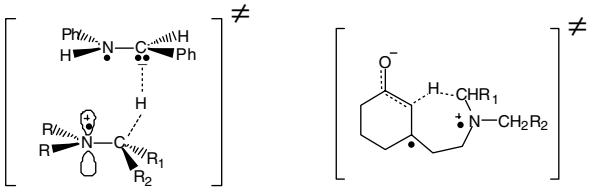

16 **17**

FIGURE 101.1 Proton transfer transition states involved in stilbene–amine and tethered amino–enone photoreaction pathways.

of steric effects on the proton transfer process. Also, proton transfer in this case occurs to a less basic anion radical than in the stilbene–amine system and this may translate into a later, more α–amino-radical-like transition state for proton transfer. As a result, electronic (radical stabilizing) properties of substituents may be more dominant in governing the relatives rates of proton transfer in amino–enone zwitterionic biradicals. Consistent with this proposal is the observation that kinetic acidities observed for intramolecular proton transfer in the amine–enone derived zwitterionic biradicals closely parallel thermodynamic acidities as judged by estimated relative pKa values.[30]

101.6 Desilylation Reactions of α-Trialkylsilylaminium Radicals

Laser Flash Photolysis Measurements of Desilylation Rates

α-Silylamines are more easily oxidized than their non-silicon-containing counterparts (Table 101.1). This is attributable to an aminium radical stabilizing interaction between a high-energy α-CSi orbital and the half filled *p*-orbital on nitrogen. This effect also results in kinetic instabilty because the α-CSi bond is weakened and the silicon is made more electropositive by the orbital interaction. As a consequence, silophiles promote C–Si bond cleavage in α-silylaminum radicals, resulting in the formation of carbon centered α-amino radicals.

Mariano, Falvey, Yoon, and Su[27,44] probed the dynamics of aminium radical desilylation using time-resolved laser flash photolysis studies of SET photoreactions of 1,4-dicyanobenzene (DCB) and N-silylmethylanilines **18** (Scheme 12). Interestingly, the rate of desilylation of the anilinium radical **19** (R = Me), formed by SET from the corresponding aniline to DCB, is slow and not competitive with back-SET (BSET) when weak silophiles such as MeCN are present. However, in the presence of good silophiles, such as MeOH or water, desilylation of **19** (R = Me) occurs more rapidly than either BSET or α-deprotonation. Second-order rate constants for the desilylation processes are found to parallel the silophilicity of the silophile (e.g., 8.9×10^5 M^{-1} s^{-1} for MeOH and 1.3×10^6 M^{-1} s^{-1} for H_2O, and 3.1×10^9 M^{-1} s^{-1} for fluoride ion in MeCN).

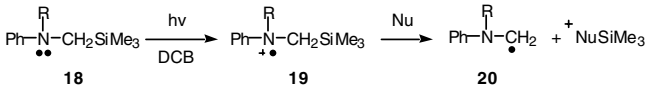

18 **19** **20**

SCHEME 12

In a fashion similar to amine cation radical α-CH-deprotonation reactions, the presence of electron-withdrawing substituents on nitrogen results in a significant enhancement of the rates of desilylation of α-silylaminium radicals. This is seen in comparisons of the second-order rate constants for methanol-promoted desilylation of anilinium radicals **19** having N-methyl (R = Me, 9×10^5 M^{-1} s^{-1}), N-ethoxycarbonyl

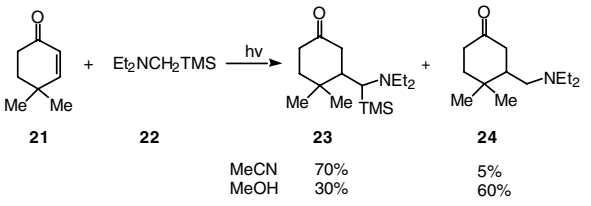

SCHEME 13

(R = CO_2Et, 2×10^7 M^{-1} s^{-1}), and N-acetyl (R = COMe, 6×10^7 M^{-1} s^{-1}) substituents. Because an N-electron-withdrawing group pronouncedly increases the oxidation potential of the silylaniline **19** while having little effect on the stability of the resulting α-amino radical **20**, the rate acceleration is attributable to destabilization of the amine cation radical.

The Influence of Desilylation Rates on SET Photoreactions of α–Silylamines

The results of early studies by Mariano, Yoon, and co-workers[45,46] demonstrated that SET-promoted photoreactions of α-silylamines are governed in unique ways by the relative rates of aminium radical desilylation and deprotonation. An example is found in the photoaddition reactions of silylamine **22** and cyclohexenone **21** (Scheme 13). The polarity and protic nature of solvents used for this process govern the relative efficiencies for formation of the TMS and non-TMS photoadducts **23** and **24**. Production of the TMS-adduct **23** is favored when the photoreaction is conducted in low-polarity aprotic solvents (e.g., MeCN) while the non-TMS-adduct **24** predominates in processes occurring in high-polarity protic media (e.g., MeOH). A more detailed study of this phenomenon demonstrates that the non-TMS to TMS adduct ratio (**24**:**23**) increases as the polarity of the solvent increases. This trend is even more pronounced when the solvents are comprised of a series of alcohols of varying nucleophilicity (MeOH > EtOH > n-PrOH > *t*-BuOH). Finally, this effort shows that salts also exhibit a similar effect on the non-TMS to TMS adduct ratio. For example, the **24**:**23** ratio from photoreactions of enone **21** with silylamine **22** in MeCN increases significantly as the concentration of $LiClO_4$ is increased. On the other hand, increasing the concentration of amine **22** results in decrease of the adduct ratio (**24**:**23**).

These observations suggest that the nature of photoreactions of cyclohexenone-silylamine systems is controlled by factors that govern the chemical reactivity of the intermediate aminium radicals. A reaction sequence involving the intermediacy of different types of enone anion and amine cation radical pairs is proposed to account for these results (Scheme 14). The reaction is initiated by SET from the silylamine **22** to triplet excited state of **21**, generating a solvent-separated ion radical pair (SSIRP) **25**. Proton transfer in one route to the TMS–adduct **23** requires that a contact ion radical pair (CIRP) **26** form first. In aprotic solvents of low polarity, formation of the CIRP would be favored, owing to the fact that stabilization between the oppositely charged radicals is more effective than with the solvent. α-Proton transfer from the most kinetically acidic site (see above) in the aminium radical to the enone anion radical occurs in the CIRP to generate the caged radical pair **29,** which undergoes radical coupling to give the TMS–adduct **23**. In polar protic solvents (MeOH), transformation of SSIRP to free radical ions (**27** and **28**) would be more facile due to strong solvation of the radical ions by H-bonding and dipole interactions. Salts, especially those that contain an oxophilic metal cation (Li^+), have a similar effect on enhancing free radical ion formation. Two possible reaction pathways are available to the solvated free α–silylaminium radical **28**. When the concentration of amine **22** (a base) is low and the solvent is highly silophilic, desilylation of **28** is expected to predominate over deprotonation. This yields the α-amino radical **30**. On the other hand, when the amine concentration is high, deprotonation of **28** becomes competitive with desilylation and a mixture of **30** and the TMS-containing radical **31** is produced**.** Conjugated addition of **30** or **31** to the ground state of enone **21** then gives rise to the respective non-TMS or TMS–adduct **24** or **23**.

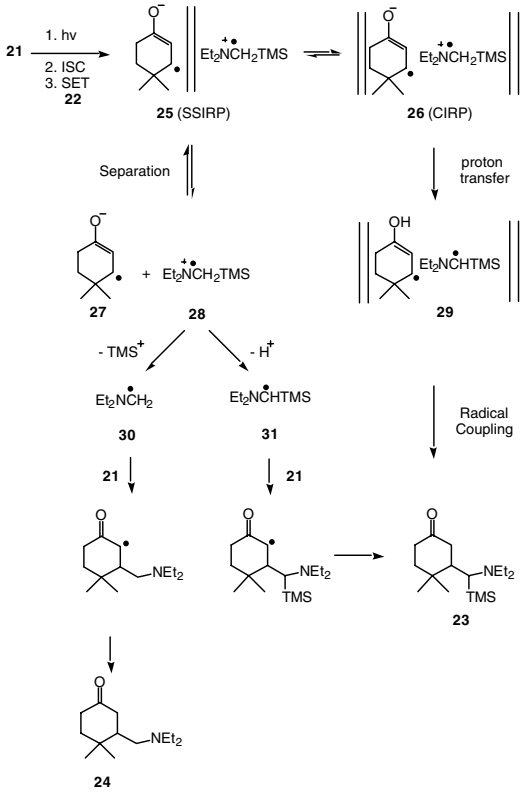

SCHEME 14

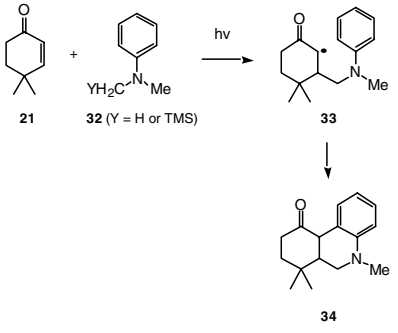

SCHEME 15

To further investigate the modes of C–C bond formation (specifically the competition between radical coupling and radical conjugate addition routes) in the SET-promoted photoaddition of amines to conjugated enones, Mariano and co-workers[47] designed a system in which intramolecular trapping of the putative α-ketoradical would reveal the operation of the radical conjugate addition mechanism (Scheme 15). For this purpose, photoaddition reactions of N,N-dimethylaniline and its silyl analog **32** (Y = H or TMS) were investigated. The observed formation of the tricyclic adduct **34** in photoreactions of the silyl-aniline in polar silophilic solvents indicates that the keto-radical **33** is an intermediate in this

process. Also, it shows that the radical conjugate addition pathway is a competitive, if not exclusive, pathway followed in photoreactions proceeding through the intermediacy of free ion radical intermediates.

That base strength of the enone anion radical **27** is an important factor governing the relative rates of deprotonation, and desilylation of the silylaminium radical **28** is further evidenced by additional observations made in related photochemical studies. For example, 9,10-dicyanoanthracene (DCA) SET-sensitized photoaddition reaction of silylaniline **32** (R = TMS) and cyclohexenone **21** in MeCN leads to near-exclusive production of the non-TMS-containing tricyclic ketone **34**. In this case, desilylation of the intermediate anilinium radical predominates over deprotonation even when the solvent is not highly silophilic because the DCA anion radical is a very weak base. In addition, non-TMS-containing adducts are generated exclusively in direct SET-promoted photoaddition reactions of silylamine **22** in the weakly silophilic solvent MeCN with a variety of acceptors, including DCA,[48] acenaphthenoquinone,[49] and N-methylphthalimide.[50] Thus, unlike the anion radicals of conjugated enones, which have a pKa value of *ca.* 10 (H_2O),[51,52] those of DCA (pKa < 0),[53,54] α-diketones (pKa *ca.* 5),[51] and phthalimides (pKa < 7)[52] are much less basic.

The ability to control the nature and regiochemistry of fragmentation reactions of silylamine cation radicals by the choice of solvent has served as a key component in the design of new and highly efficient SET-promoted photocyclization reactions. This is demonstrated by observations made in studies of photochemical transformations of the silylaminoethyl-cyclohexenones **35** and **36** (Scheme 16), where cyclizations occur to give non-TMS products cleanly on direct irradiation in MeOH or DCA-sensitized irradiation in MeCN. In contrast, TMS-containing spirocyclic products are formed exclusively when MeCN is used as solvent for the direct irradiation reactions.[40,55] The much higher degrees of chemoselectivity in these processes as compared to their intermolecular counterparts are presumably due to the fact that low amino–enone concentrations of *ca.* 1×10^{-3} *M* are used in the intramolecular systems. Consequently, amine induced deprotonation of the intermediate amine cation radical is less favorable.

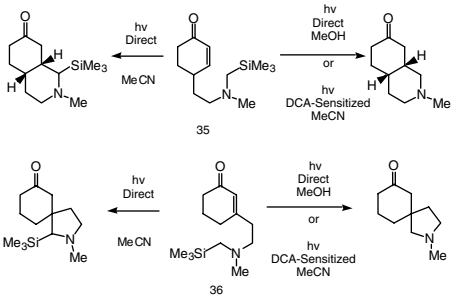

SCHEME 16

101.7 Heterolytic Cleavage of Aminium Radicals Derived from β-Aminoalcohols

Davidson and co-workers[56] were the first to observe that aminium radicals, derived by SET oxidation of β-aminoalcohols, undergo C–C bond-cleaving fragmentation by a pathway that is analogous to a retro-Aldol process (Scheme 17). Both the mechanistic features and chemical and biochemical applications of this process have received much attention. An analysis[57–61] of the thermochemical and electrochemical properties of β-aminoalcohols indicates that the bond dissociation energy of the cleaving C–C bond in the aminium radical **38** is much lower than that in the parent neutral molecule **37**. Thus, retro-Aldol-like fragmentations have high thermodynamic driving forces. In a related manner, thermochemical calculations suggest that the corresponding C–C bond in the 1,2-diamine radical cation is slightly weaker than that in amino alcohol derived aminium radicals.[62,63]

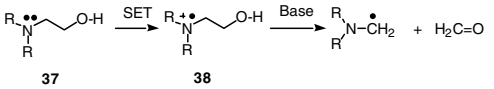

SCHEME 17

Base-Induced Retro-Aldol Cleavage of β-Aminoalcohol Derived Aminium Radicals

Investigations by Schanze[64,65] have demonstrated that retro-Aldol fragmentation of β-aminoalcohol-derived aminium radicals takes place relatively slowly in the absence of base and that this process is accelerated by the addition of bases. Schanze and co-workers observed that the rate constants for deprotonation of aminium radicals, derived from the β-hydroxyanilines $ArNHCH_2CH(Ph)OH$, by pyridine fall in the range of 10^5 to 10^7 M^{-1} s.$^{-1}$ When the hydroxyl hydrogen in these cation radicals is replaced by deuterium, kinetic isotope effects in the range of 1.3 to 4 are observed, and the magnitude of these effects is inversely related to the basicity of the proton acceptor. Furthermore, rate data for deprotonation reactions of these aminium radicals with substituted pyridines can be fitted to the Brønsted relationship. Thus, the mechanism for retro-Aldol fragmentation of β-aminoalcohol cation radicals most likely involves base-induced deprotonation in concert with C–C bond cleavage.

Similar results have come from laser flash photolysis studies by Su and co-workers.[44] This effort probed the kinetics of acetate-induced fragmentation reactions of cation radicals derived by photoinduced SET from a variety of β-anilinoethanols **39** (Scheme 18) to 1,4-dicyanobenzene. The data demonstrate that, like in related α-CH deprotonation and desilylation reactions, substituents that destabilize the β-hydroxyanilinium radical enhance the rates of retro-Aldol cleavage. (e.g., **39** ($R_1 = R_2 = H$) (X = OMe), k = 2.8×10^4 $M^{-1}s^{-1}$; (X = H), k = 4.1×10^4 $M^{-1}s^{-1}$; (X = CF_3), k = 3.1×10^5 $M^{-1}s^{-1}$). In addition, alkyl substitution at the R_1 position slows fragmentation (e.g., **39** (R_1 = Me, R_2 = H, X = H), k = 3.3×10^4 $M^{-1}s^{-1}$) and phenyl substitution at the R_2 position accelerates the process (e.g., **39** (R_1 = H, R_2 = Ph, X = H), k = 3.1×10^5 $M^{-1}s^{-1}$).

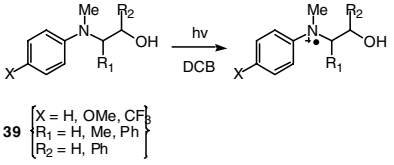

SCHEME 18

A comparison of the rate constants for acetate-induced α-CH deprotonation of anilinium radicals (**6**, Scheme 6) with those for retro-Aldol fragmentation of related β-hydroxyanilinium radicals promoted by the same base gives rise to a perplexing conclusion. Specifically, the α-CH deprotonation rates are larger than those for retro-Aldol cleavage in comparably substituted anilinium radicals. Yet, retro-Aldol fragmentation is the predominant pathway followed. This finding suggests that β-hydroxyanilinium radicals are inherently less reactive than related anilinium radicals, which do not have β-hydroxy substitution. A possible source for this effect might be a through-space interaction of the filled oxygen sp^3-orbital and half filled nitrogen *p*-orbital, which would stabilize the hydroxyl-substituted charged radical intermediates.

101.8 Decarboxylation Reactions of Aminium Radicals Derived from α-Amino Carboxylates

SET Pathways in the Photoinduced Decarboxylation of α-Heteroatom Substituted Carboxylates

Early investigations of the photochemistry of α-heteroatom substituted carboxylates **40** (Scheme 19) concentrated on the operation of SET processes. These substances possess two potential electron donor sites. SET from the carboxylate moiety leads to formation of an acyloxy radical **41** while SET from the heteroatom center gives rise to a zwitterionic radical **42**. Subsequent loss of carbon dioxide from either of these intermediates yields the same carbon-centered, heteroatom-stabilized radical **43**. The critical factors determining which of these pathways is responsible for the SET-promoted decarboxylation reactions of substrates in this family is (1) the relative oxidation potentials of the two potential donor moieties and (2) the relative rates of decarboxylation of intermediates **41** and **42**. Redox potential data indicate that electron transfer from sulfur (E(+) = *ca.* 0.4 V) and nitrogen (E(+) = ca. 0.7 V) centers to acceptors should be thermodynamically more favorable than from carboxylate groups (E(+) = *ca.* 1.4 V).

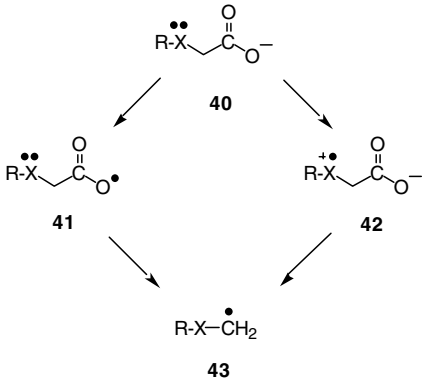

SCHEME 19

Ohga and co-workers[66,67] carried out an interesting study that provides important information about the nature of decarboxylation reactions of α-heteroatom-substituted carboxylates. It is known that the singlet excited state of N-methyl-2-phenyl-1-pyrrolinium perchlorate (**44**) (Scheme 20) participates as an acceptor in SET-promoted photochemical reactions.[67–69] As expected, irradiation of this salt in the presence of a variety of α-heteroatom substituted carboxylates leads to efficient formation of substituted pyrrolidines **45**. The adducts are generated by sequential SET, decarboxylation, radical coupling pathways. Moreover, Stern-Volmer analysis of data obtained from fluorescence quenching of **44** by reversible SET from α-heteroatom-substituted and simple carboxylates clearly shows that SET is more favorable from nitrogen and sulfur centers than from the carboxylate grouping. For example, near-diffusion-limited fluorescence quenching is observed for $HSCHMeCO_2$ and $H_2NCH_2CO_2$, whereas quenching by acetate occurs an order of magnitude more slowly.

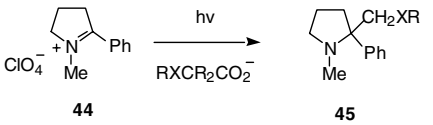

SCHEME 20

Stern-Volmer analysis of excited-state emission quenching data has also been used by Davidson and co-workers[70,71] to probe SET pathways involved in photoinduced decarboxylation reactions of α-thio- and α-amino-substituted carboxylic acids. In this study, Davidson compared k_q values for benzophenone triplet excited state quenching by the substituted carboxylic acids with those for quenching by related heteroatom electron donors not containing the carboxylic acid function. The data obtained reveal a striking similarity between these rate constants, strongly suggesting that SET from the heteroatom is the predominant mode of triplet benzophenone quenching by the α-thio- and α-amino-substituted carboxylic acids.

Laser flash photolysis techniques have been employed to evaluate the dynamics of decarboxylation reactions of cation radicals derived from α–aminocarboxylates.[44,72] In one report,[44] variously substituted aminium radicals **47** were generated by laser flash excitation of anilinocarboxylates **46** (Scheme 21) in MeCN solutions containing the acceptor, 1,4-dicyanobenzene. These transients undergo fast, first-order decay by a pathway involving loss of carbon dioxide. The rate constants for decarboxylation were found to be in the range of 8×10^5 to 4×10^6 s^{-1}. In addition, the rates show the same dependence on nitrogen, α-alkyl and α-phenyl substituents, as do the related α-CH deprotonation, α-desilylation, and retro-Aldol cleavage reactions.

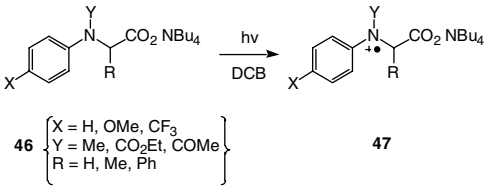

SCHEME 21

The nature and concentration of added metal cations play a major role in governing the rates of decarboxylation of anilinocarboxylate-derived aminium radicals. For example, the rate of decarboxylation of the tetrabutylammonium derivative of **47** (X = R = H, Y = Me) decreases from 4.1×10^6 s^{-1} to 3×10^5 s^{-1} when the concentration of added $CsClO_4$ is increased from 1 to 100 m*M*. Also, $LiClO_4$ has a greater effect on lowering the decarboxylation rate than does $CsClO_4$ (1.1×10^6 s^{-1} vs. 2.9×10^6 s^{-1} at 10 m*M*, respectively) and $Ca(ClO_4)_2$ greatly retards this process (8×10^4 s^{-1}at 10 m*M*). These observations suggest that the aminium carboxylate decarboxylation reaction is dependent in a predictable manner on the oxophilic nature of metal cations and that free carboxylates lose carbon dioxide faster than do their metal cation-ligated analogs.

The Influence of Decarboxylation Rates on SET-Photoreactions of α–Amino Carboxylates

The data presented above demonstrate that the rates of α-heterolytic fragmentation reactions of aminium radicals are principally governed by the nature of the leaving electrofugal group. In addition, nitrogen and side-chain substituents in these reactive intermediates also contribute in governing the rates of these processes. The speed with which aminium radical α-heterolytic cleavage occurs plays a significant role in determining the chemical yields (see above) and quantum efficiencies of SET-promoted photoaddition and photocyclization reactions of amine substrates. In these excited-state reactions, fragmentation in the direction of product formation competes with photon wasting, back electron transfer to generate ground states of the amine reactants. As a consequence of this competition, the quantum efficiencies of reactions of structurally related amines should correlate with the rates of α-heterolytic cleavage. A demonstrative example of this relationship is found in the photochemistry of the N-(aminoethyl)phthalimides **48** (Scheme 22).[44] Irradiation of these substrates in MeOH solutions containing either 0.3 *M* n-Bu_4NOAc or n-Bu_4NClO_4 results in production of the corresponding tricyclic-amidols **49**. These products arise by pathways involving initial intramolecular SET from the amine to the excited phthalimide. This is followed

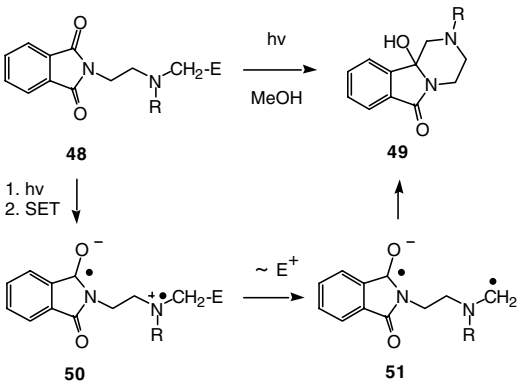

SCHEME 22

by fragmentation of aminium radical **50** and C–C bond formation in the resulting biradical **51**. The quantum yields of these cyclization reactions display a dramatic dependence on the nature of the electrofugal group in a manner that parallels aminium radical fragmentation rates (e.g., for **48** (R = Me, E = H, with 0.3 *M* n-Bu_4NOAc) $\phi = 0.003$, for **48** (R = Me, E = TMS, 0.3 *M* n-Bu_4NClO_4) $\phi = 0.039$, and for **48** (R = Me, E = CO_2NBu_4, 0.3 *M* n-Bu_4NClO_4) $\phi = 0.32$).

Acknowledgments

The authors express their deep appreciation to their enthusiastic, hard-working, and productive coworkers whose studies in the area of amine electron transfer photochemistry established the basis for the results presented in this review. Also, the generous financial support given to the PSM research group by the National Institutes of Health and the National Science Foundation and to the UCY research group by the Korea Science and Engineering Foundation (Basic Research Program 2001-1-12300-006-3, International Cooperative Research Program, and CBM of POSTECH) is acknowledged.

References

1. Eberson, L., *Electron Transfer Reactions in Organic Chemistry*, Springer-Verlag, New York, 1987.
2. Mayo, S.L., Ellis, W.R., Crutchley, R.J., and Gray, H.B., Long-range electron-transfer in heme-proteins, *Science*, 233, 948, 1986.
3. McLendon, G., Long-distance electron-transfer in proteins and model systems, *Acc. Chem. Res.*, 21, 160, 1988.
4. Poulos, T. and Finsel, B., Heme enzyme structure and function, *Peptide Protein Revs.*, 4, 115, 1984.
5. Hollen, D., Hoganson, C., Windsor, M.W., Schenck, C.C., Parsons, W.W., Migus, A., Fork, R.L., and Shank, C.V., Subsecond and picosecond studies of electron transfer intermediates in Rhodopseudomonas sphaeroides reaction center, *Biochim. Biophys. Acta*, 592, 461, 1980.
6. Mariano, P.S. and Stavinoha, J.L., Synthetic aspects of photochemical electron transfer reactions, in *Synthetic Organic Photochemistry*, Horspool, W.M., Ed. Plenum Press, London, 1984, chap. 3, 145.
7. Pienta, N.J., Amines, thiols and thioethers. heteroatomic electron donors, in *Photoinduced Electron Transfer*, Fox, M.A. and Chanon, M., Eds., Part C, Elsevier, New York, 1988.
8. Lewis, F.D., Proton transfer reactions of photogenerated radical ion pairs, *Acc. Chem. Res.*, 19, 401, 1986.
9. Yoon, U.C., Mariano, P.S., Givens, R.S., and Atwater, B.W., Photoinduced electron transfer chemistry of amines and related electron donors, *Advances in Electron Transfer Chemistry, Vol. 4,* Mariano, P.S., Ed. JAI Press, Greenwich, CT, 1994, 117.

10. Yoshida, J., Maekawa, T., Murata, T., and Matsunaga, S., Electrochemical oxidation of organosilicon compopunds. The origin of the β-silicon effect in electron transfer reactions of silicon substituted heteroatom compounds. electrochemical and theoretical studies, *J. Am. Chem. Soc.*, 112, 1962, 1990.
11. Cooper, B.E. and Owen, W.J., Silicon carbon bond hyperconjugation in cation radicals. Lower oxidation potentials of N-(trimethylsilylmethyl)-aromatic amines, *Organametal. Chem.*, 29, 33, 1971.
12. Yoshida, J., Murata, T., and Isoe, S., Electrochemical oxidation of organosilicon compounds. Oxidative cleavage of carbon-silicon bond in allylsilanes and benzylsilanes, *Tetrahedron Lett.*, 27, 3373, 1986.
13. Koizumi, T., Fuchigami, T., and Nonaka, T., Anodic oxidation of (trimethylsilyl)methanes with π-electron donor substituents in the presence of nucleophiles, *Bull. Chem. Soc. Jpn.,* 62, 219, 1989.
14. Yoshida, J. and Isoe, S., Electrochemical oxidation of organo-silicon compounds. electrochemical oxidation of α-silylcarbamates, *Tetrahedron Lett.,* 28, 6621, 1987.
15. Yoshida, J., Murata, T., and Isoe, S., Electrochemical oxidation of organosilicon compounds. Electrochemical oxidation of alpha-silylethers. remarkable effect of silicon on oxidation potentials and reaction pathways, *J. Organometal. Chem.,* 345, C23, 1988.
16. Yoshida, J., Murata, T., and Isoe, S., Electrochemical oxidation of organosilicon compounds. Electrochemical oxidation of 1-phenylthio-1-trimethylsilyl alkanes, *Chem. Lett.,* 631, 1987.
17. Miller, L.L., Nordblum, G.D., and Mayeda, E.A., A simple comprehensive correlation of organic oxidation and ionization potentials, *J. Org. Chem.*, 37, 916, 1972.
18. Mann, C.K. and Barnes, K.K. *Electrochemical Reactions in Non-Aqueous Systems.,* Marcel Dekker, New York, 1970.
19. Majima, T., Pac, C., Nakasone, A., and Sakurai, H., Redox-phtosensitized reactions. aromatic hydrocarbon-photosensitized electron transfer reactions of furan, methylated furans and indene with *p*-dicyanobenzene, *J. Am. Chem. Soc.*, 103, 499, 1981.
20. Chow, Y.L., Danen, W.C., Nelsen, S.F., and Rosenblatt, D., Non-aromatic aminium radicals, *Chem. Rev.*, 78, 243, 1978.
21. Fessenden, R.W., and Neta, P., Electron spin resonance spectra of di- and trimethylaminium radicals, *J. Phys. Chem.*, 76, 2857, 1972.
22. Malatesta, V. and Ingold, K.U., Kinetic applications of electron spin resonance spectroscopy. aminium radicals, *J. Am. Chem. Soc.,* 95, 6400, 1973.
23. Das, S. and Von Sonntag, C.Z., The oxidation of trimethylamine by OH radicals in aqueous solution as studied by pulse radiolysis, electron spin resonance and product analysis, *Naturforsch.*, 416, 505, 1986.
24. Powell, M.F., Wu, J.C., and Bruice, T.C., Ferricyanide oxidation of dihydropyridines and analogs, *J. Am. Chem. Soc.*, 106, 3850, 1984.
25. Sinha, A. and Bruice, T.C., Rate determining general base catalysis in an obligate Le oxidation of a dihydropyridine, *J. Am. Chem. Soc.*, 106, 7291, 1984.
26. Dinnocenzo, J.P. and Banach, T.E., Deprotonation of amine cation radicals. A direct experimental approach, *J. Am. Chem. Soc.*, 111, 8646, 1989.
27. Zhang, X., Yeh, S.-R., Hong, S., Freccero, M., Albini, A., Falvey, D.E., and Mariano, P.S., Dynamics of α-CH deprotonation and α-desilylation reactions of tertiary amine cation radicals, *J. Am. Chem. Soc.*, 116, 4211, 1994.
28. Parker, V.D. and Tilset, M., Facile proton transfer reactions of N,N-dimethylaniline cation radicals, *J. Am. Chem. Soc.,* 113, 8778, 1991.
29. Anne, A., Hapiot, P., Moiroux, J., Neta, P., and Saveant, J.-M., Dynamics of proton transfer from cation radicals. Kinetic and thermodynamic acidities of cation radicals of NADH analogs, *J. Am. Chem. Soc.*, 114, 4694, 1992.
30. Nicholas, A.M. D. and Arnold, D.R., Thermochemical parameters for organic radicals and radical ions. Protonation of hydrocarbon radicals in the gas phase, *Can. J.Chem.,* 60, 2165. 1982.

31. Anne, A., Fraoua, S., Hapiot, P., Moiroux, J., and Saveant, J.-M., Steric and kinetic isotope effects in the deprotonation of cation radicals of NADH synthetic analogs, *J. Am. Chem. Soc.*, 117, 7412, 1995.
32. Simon, J.D. and Peters, K.S., Solvent effects on the picosecond dynamics of the photoreduction of benzophenone by aromatic amines, *J. Am. Chem. Soc.*, 103, 6403, 1981.
33. Manring, L.E. and Peters, K.S., Picosecond dynamics of proton transfer, *J. Am. Chem. Soc.*, 107, 6452, 1985.
34. Simon, J. D. and Peters, K.S., Picosecond dynamics of ion-pairs. The effect of hydrogen bonding on ion pair intermediates, *J. Am. Chem. Soc.*, 104, 6542, 1982.
35. Simon, J. D. and Peters, K.S., Na^+ and Li^+ effects on the photoreduction of benzophenone. A picosecond absorption study, *J. Am. Chem. Soc.*, 105, 4875, 1983.
36. Cohen, S.G. and Stein, N.M., Kinetics of photoreduction of bezophenones by amines. Deamination and dealkylation of amines, *J. Am. Chem. Soc.,* 93, 6542, 1971.
37. Lewis, F.D. and Ho, T.L., Selectivity of tertiary amine oxidations, *J. Am. Chem. Soc.,* 102, 1751, 1980.
38. Lewis, F.D., Ho, T.L., and Simpson, J.T., Photochemical addition of tertiary amines to stilbene. Stereoelectronic control of tertiary amine oxidation, *J. Org. Chem.,* 46, 1077, 1981.
39. Lewis, F.D., Ho, T.I., and Simpson, J. T., Photochemical addition of tertiary amines to stilbene. Free radical and electron transfer mechanisms for amine oxidation, *J. Am. Chem. Soc.*, 104, 1924, 1984.
40. Xu, W., Zhang, X.M., and Mariano, P.S., Single electron transfer promoted photocyclization reactions of aminoalkyl cyclohexenones. Mechanistic and synthetic features of the process involving the generation and reactions of amine cation and alpha-amino radicals, *J. Am. Chem. Soc.*, 113, 8863, 1991.
41. Xu, W. and Mariano, P.S., Substituent effects on amine cation radical acidity. Regiocontrol of β-(aminoethyl)cyclohexenone photocyclizations, *J. Am. Chem. Soc.*, 113, 1431, 1991.
42. Wagner, P.J., Kemppainen, A.E., and Jellinek, T., Type II photoreactions of phenyl ketones. Competitive charge transfer in dialkylamino ketones, *J. Am. Chem. Soc.,* 94, 7512, 1972.
43. Wagner, P.J and Ersfeld, D.A., Solvent specific photochemistry involving intramolecular amino ketone triplet exciplexes, *J. Am. Chem. Soc.,* 98, 4516, 1976.
44. Su, Z., Mariano, P.S., Falvey, D.E., Yoon, U.C,. and Oh, S.W., Dynamics of anilinium radical α-heterolytic fragmentation processes. Electrofugal group, substituent and medium effects on desilylation, decarboxylation and retro-Aldol cleavage pathways, *J. Am. Chem. Soc.*, 120, 10676, 1998.
45. Hasegawa, E., Xu, W., Mariano, P.S., Yoon, U.C., and Kim, J.U., Electron transfer induced photoadditions of the silylamine Et_2NCH_2TMS to α,β-unsaturated cyclohexenones. Dual reaction pathways based on ion pair selective cation radical chemistry, *J. Am. Chem. Soc.*, 110, 8099, 1988.
46. Yoon, U.C., Kim, J.U., Hasegawa, E., and Mariano, P.S., Electron transfer photochemistry of α-silylamine cyclohexenone systems. Medium effects on reaction pathways followed, *J. Am. Chem. Soc.*, 109, 4421, 1987.
47. Zhang, X.M. and Mariano, P.S., Mechanistic details for SET promoted photoadditions of amines to conjugated enones arising from studies of aniline-cyclohexenone photoreactions, *J. Org. Chem.*, 56, 1655, 1991.
48. Hasegawa, E., Brumfield, M.A., Mariano, P.S., and Yoon, U.C., Photoadditions of ethers, thioethers and amines to 9,10-dicyanoanthracene by electron transfer pathways, *J. Org. Chem.*, 53, 5435, 1988.
49. Yoon, U.C., Kim, Y.C., Choi, J.J., Kim, D.U., Mariano, P.S., Cho, I.S., and Jeon, Y.T., Photoaddition reactions of acenaphthylenedione with α-silyl n-electron donors via triplet single electron transfer desilylation and triplet hydrogen atom abstraction pathways, *J. Org. Chem.,* 57, 1422, 1992.
50. Yoon, U.C., Kim, H.J., and Mariano, P.S., Electron transfer induced photochemical reactions in imide $RXCH_2TMS$ systems. Photoadditions of α-trimethylsilyl substituted heteroatom containing compounds to phthalimides, *Heterocycles*, 29, 1041, 1989.
51. Hayon, E., Ibata, J., Lichtin, N.N., and Simic, M., Electron and hydrogen atom attachment to aromatic carbonyl compounds in aqueous solution. Absorption spectra and dissociation constants of ketyl radicals, *J. Phys. Chem.*, 76, 2072, 1972.

52. Lilie, J. and Henglein, A., Pulsradiolytische Messung und LCAO-Berechnung der Absorptionspektren und pK-Werte Frein Radikale mit Konjugierten Doppelbindungen, *Ber. Bunsenyes. Phys. Chem.*, 73, 170, 1969.
53. Kellet, M.A., Whitten, D.G., Gould, I.R., and Bergmark, W.R., Surprising differences in the reactivity of cyanoaromatic radical anions generated by photoinduced electron transfer, *J. Am. Chem. Soc.*, 113, 358, 1991.
54. Lewis, F.D. and Petisce, J. R., Proton transfer reactions of photogenerated cyanoaromatic methylaromatic radical ion pairs, *Tetrahedron,* 42, 6207, 1986.
55. Xu, W., Jeon, Y.T., Hasegawa, E., Yoon, U.C., and Mariano, P.S., Novel electron transfer photocyclization reactions of alpha-silylamine alpha,beta-unsaturated ketone and ester systems, *J. Am. Chem. Soc.*, 111, 406, 1989.
56. Davidson, R.S. and Orton, S.P., Photoinduced electron transfer reactions. fragmentation of 2-aminoethanols, *J. Chem. Soc., Chem. Commun.*, 209, 1974.
57. Okamoto, A., Snow, M.S., and Arnold, D.R., Radical ions in photochemistry. Photosensitized (electron transfer) carbon-carbon bond cleavage of radical cations. The diphenylmethyl system, *Tetrahedron,* 42, 6175, 1986.
58. Popierlarz R. and Arnold, D.R., Radical ions in photochemistry. Carbon-carbon bond cleavage of radical cations in solution. Theory and application, *J. Am. Chem. Soc.,* 112, 3068, 1990.
59. Wayner, D.D. M., McPhee, D.J., and Griller, D., Oxidation and reduction potentials of transient free radicals, *J. Am. Chem. Soc.,* 110, 132, 1988.
60. Griller, D., Martinho Sinoes, J.A., Mulder, P., and Wayner, D.D.M., Unifying the solution thermochemistry of molecules, radicals and ions, *J. Am. Chem. Soc.,* 111, 7872, 1989.
61. Brady, W. and Gu, Y.Q., Cycloadditions of (Arylalkylamino)ketenes with cycloalkenes, *J. Org. Chem.,* 54, 2834, 1989.
62. Gaillard, E.R. and Whitten, D.G., Photoinduced electron transfer bond fragmentations, *Acc. Chem. Res.*, 29, 292, 1996.
63. Gan, H., Kellett, M.A., and Whitten, D.G., Novel intermolecular and intramolecular photochemical reactions initiated by excited state electron transfer processes, *J. Photochem. Photobiol., A: Chem.,* 82, 211, 1994.
64. Wang, Y., Hauser, B.T., Rooney, M.M., Burton, R.D., and Schanze, K.S., Ligand to ligand charge transfer photochemistry, *J. Am. Chem. Soc.,* 115, 5675, 1993.
65. Burton, R.D., Bartberger, M.D., Zhang, Y., Eyler, J.R., and Schanze, K.S., Carbon-carbon bond fragmentation in aminoalcohol radical cations. Kinetics, Thermodynamic correlations and mechanism, *J. Am. Chem. Soc.,* 118, 5655, 1996.
66. Kurauchi, T. and Ohga, K., Electron transfer initiated photoreactions of 1-methyl-2-phenyl-1-pyrrolinium perchlorate with α-heteroatom substituted alkanoate anions, K, *Bull. Chem. Soc. Jpn.,* 59, 897, 1986.
67. Kurauchi, T. and Ohga, K., Decarboxylative photoaddition of 3-butenoate anion to 1-methyl-2-phenyl-1-pyrrolinium perchlorate via an electron transfer reaction, *Bull. Chem. Soc. Jpn.,* 58, 2711, 1985.
68. Mariano, P.S., Stavinoha, J., and Bay, E., Photochemistry of iminium salts. Electron transfer mechanisms for singlet quenching and photoaddition of n-electron donating alcohols and ethers, *Tetrahedron,* 37, 3385, 1981.
69. Stavinoha, J., Bay, E., Leone, A. and Mariano, P.S., Photochemistry of iminium salts in the presence of n-electron donating alcohols and ethers, *Tetrahedron Lett.,* 3455, 1980.
70. Brimage, D.R.G. and Davidson, R.S., Photoreactions of polycyclic aromatic hydrocarbons with N-aryglycines, *J. Chem. Soc., Perkins Trans. 1,* 496, 1973.
71. Davidson, R.S. and Steiner, P.R., Mechanism of the photoinduced decarboxylation of carboxylic acids sensitized by aromatic ketones and quinones, *J. Chem. Soc., Perkin Trans. 2,* 1357, 1972.
72. Hug, G., Bonifacic, M., Asmus, K., and Armstrong, D., Fast decarboxylation of aliphatic amino acids induced by 4-carboxybenzophenone triplets in aqueous solutions. A nanosecond laser flash photolysis study, *J. Phys. Chem.,* 104, 6674, 2000.

102

Remote Functionalization by Alkoxyl Radicals Generated by the Photolysis of Nitrite Esters: The Barton Reaction and Related Reactions of Nitrite Esters

Hiroshi Suginome
Hokkaido University

102.1 Definition of the Reaction and a Short Historical Background

The photolysis of organic nitrites of appropriate constitution and conformation in solvents such as benzene, toluene, or acetonitrile transforms them into δ-nitroso alcohols via a homolytic fission of the O–N bond of their nitrosoxy group, followed by an intramolecular δ-hydrogen abstraction of the resulting alkoxyl radicals to generate a δ-carbon radical that combines with the generated nitric oxide. The nitroso alcohols are isolated as δ-hydroxyimino alcohols via a spontaneous thermal isomerization or the nitroso-dimers[1] (Scheme 1). This transformation has been named the "Barton reaction."[2]

Thompson and colleagues initiated spectroscopic as well as photochemical investigations of organic nitrites in the vapor phase during the 1930s at Oxford.[3] The interpretation of the primary mode of the photochemical decomposition of nitrite esters by Thompson, however, differed from what has now become established as the primary process for nitrite photolysis. Subsequent to Thompson's study, Coe

0-8493-1348-1/04/$0.00+$1.50

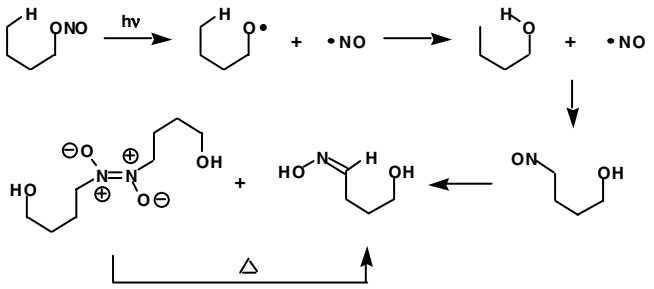

SCHEME 1

and Doumani reinvestigated the vapor-phase photolysis of *t*-butyl nitrite, confirming that the products of photolysis were acetone and nitrosomethane[4] (Scheme 2). They interpreted the results in terms of a concerted photochemical molecular rearrangement of *t*-butyl nitrite because no ethane was detected in this photolysis.

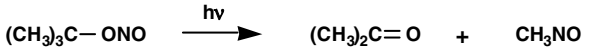

SCHEME 2

Gray and Style proposed, for the first time, that the primary step of nitrite photolysis is the homolysis of the ONO bond, based on their study on the photolysis of methyl nitrite.[5] The process was entirely analogous to a mechanism that had already been proposed for the gas-phase pyrolysis of organic nitrites by Steacie.[6] Tarte then undertook an extensive investigation of the photolysis of primary, secondary, and tertiary alkyl nitrites, believing that his results could be accommodated by either of the two possible mechanisms,[7] depending on the wavelength of the incident light and the structure of the alkyl nitrite.

Since these early studies on nitrite photolysis, a number of extensive synthetic and physicochemical studies on the photodissociation of steroidal alcohol nitrite esters and simple alkyl nitrites, such as *t*-butyl nitrite (as summarized by Calvert and Pitts, Jr.[8]), established that the primary reaction of the photolysis of nitrite esters in solution is the homolysis of the ONO bond of their nitrosoxy groups to give alkoxyl radicals and nitric oxide (Scheme 3).

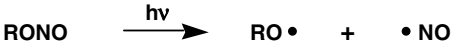

SCHEME 3

The sophistication of the physicochemical details of the photodissociation process of the ONO bond of prototype alkyl nitrites, such as methyl, ethyl, and *t*-butyl nitrites,[9a] (and the SNO bond of thionitrites[10]) in the gas phase,[9b] in matrix isolated states,[11] in adsorbed states[9a] and at a shorter wavelength band (S_2 state),[12] etc. is continuing today through newer techniques. These aspects are beyond the present discussion.

The photochemistry of nitrite esters, however, became the subject of considerable attention by organic chemists when Barton ingeniously showed its usefulness for organic synthesis in the beginning of the 1960s.[1] He and his colleagues showed that the photolysis of suitably constituted steroidal alcohol nitrites provoked an intramolecular exchange of the NO of the nitrite group with a hydrogen atom attached to a carbon atom in the δ-position, as mentioned above. This reaction has been shown not only to be one of the most useful photochemical processes for the selective functionalization of an unactivated carbon atom in organic synthesis, but has also led to a renaissance of the concept of remote functionalization

by an intramolecular reaction, such as the Hofmann-Löffler-Freytag reaction.[13] This led to the general recognition of the utility of photochemical and radical reactions in organic synthesis.

The historical and mechanistic aspects and the synthetic applications of the reaction have been the subject of a number of comprehensive review articles by Barton[14] himself, as well as his pupils.[2,15]

102.2 Mechanism of the Barton Reaction

Alkyl nitrites, which can readily be prepared either by reactions of the corresponding alcohols with nitrosyl chloride in pyridine[1] or by an exchange reaction between the alcohols and *t*-butyl nitrite,[16] exhibits UV absorptions in two regions: a broad, unstructured band centered at ca. 210 nm (ε = 1000 to 1700) and a structured band at ca. 360 to 380 nm (ε = ca. 80).[8,17] The absorption at the longer wavelength band (S_1) is assigned to the ($n\pi^*$) transition; that at the shorter wavelength band (S_2) is assigned as being due to a $\pi\pi^*$ transition and possibly higher excited states.[8,9b,18] The irradiation of the weak $n\pi^*$ band causes a homolysis of the ONO bond to give the corresponding alkoxyl radicals and nitric oxide with a quantum yield of 0.7, as proved by the photolysis of steroidal nitrite esters in methanol with 365-nm monochromatic light.[17] A quantum yield of 0.76 was also reported for the photolysis of octyl nitrite in heptane.[19] A quantum yield less than unity in the solution photolysis of the nitrites may indicate the reversibility of the primary process of the dissociation. The photodissociation of *t*-butyl nitrite at 193 nm using a newer technique has recently been reported.[12]

The thermolysis of nitrite esters in solution, on the other hand, resulted in the decomposition of nitrite esters and did not lead to any homolysis of the ONO bond. This was attributed to ionic decomposition due to protonation of the ONO group with adventitious protons as an impurity in the solution.[20]

Alkoxyl radicals thus generated intramolecularly abstract a hydrogen that is appropriately located. A number of experiments with a variety of cyclic and acyclic systems[2,15,21,22] have established that hydrogen abstraction involving a six-membered cyclic transition state is preferred over that involving five- or seven-(and more) membered cyclic transition states; the alkoxyl radical generated by the photolysis of the nitrite of 5-phenylpentanol abstracts a hydrogen attached to the δ-carbon, but not a hydrogen attached to the ε-carbon, to generate stabilized benzyl radicals[21] (Scheme 4). On the basis of a number of results in the steroid field, together with an inspection of Dreiding models, the most appropriate distances between an alkoxy radical and a carbon bearing a hydrogen atom to be abstracted have been estimated to be in the 2.5 to 2.7 Å range.[23]

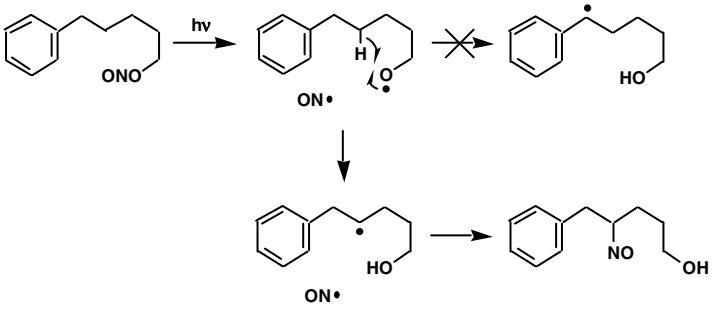

SCHEME 4

Carbon-centered radicals thus generated then combine with nitric oxide to form nitroso compounds, which readily isomerize to afford the corresponding oximes (or nitrosodimers[24]). Quantum-yield studies of the overall process cited above[8,17] indicated that this free radical reaction is not a chain process. The behaviors of the nitric oxide generated in the solution was studied by using labeled nitrites;[25,26] the photolysis of an equimolecular mixture of ^{15}N nitrite A and ^{14}N nitrite B gave a mixture of two products (arising from intramolecular hydrogen abstraction) in which ^{15}N and ^{14}N were completely scrambled

in the two products[25,26] (Scheme 5). It was thus concluded that a cage structure in which NO is kept in the solvent cage during the entire process does not exist. A similar mass spectrometric determination on the nitrite recovered after partial completion of the photolysis showed that no scrambling took place at this stage. These experiments indicated that non-cage combinations take place after hydrogen abstraction, although the primary homolysis step is a cage process, as outlined in Scheme 6.[25]

In agreement with this mechanism, 18-iodopredonisolone 21-acetate, but not the 18-oxime, is obtained when predonisolone 11β-nitrite 21-acetate in benzene is photolyzed in the presence of iodine (Scheme 7).[27]

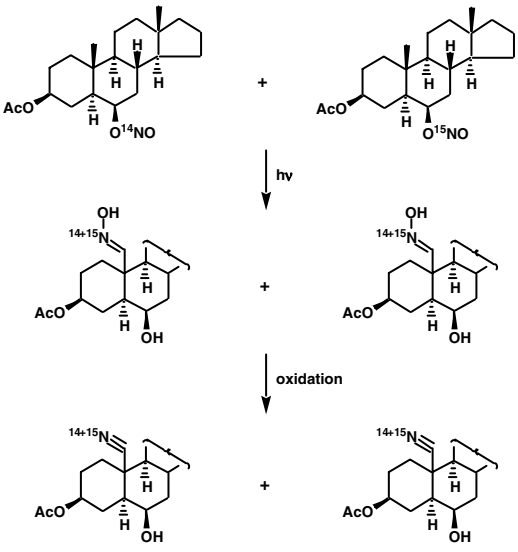

SCHEME 5

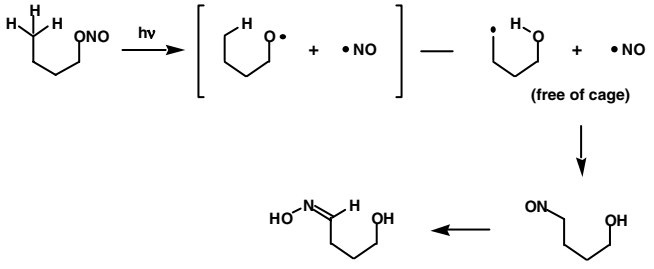

SCHEME 6

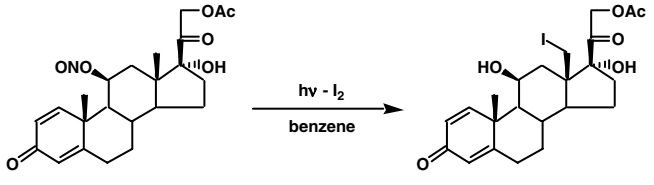

SCHEME 7

102.3 Synthetic Applications

Because angular methyl groups and alkoxyl radicals with a 1,3-diaxial relationship in a rigid steroid and some terpenoid molecules ideally satisfy hydrogen abstraction through a 6-membered cyclic transition state, the Barton reaction has most successfully been applied to the field of steroids and some di- and triterpenoids. By this reaction, functional groups can, in principle, be introduced into the unactivated angular 10β- or 13β-methyl groups of steroids. As shown in Scheme 8, a hydrogen attached to the 13β-carbon can be abstracted by an alkoxyl radical at C11, C15, or C20 and a hydrogen attached to the 10β-carbon from an alkoxyl radical at C2, C4, C6, or C11. Thus, a one-step introduction of functionality into an unactivated position can be achieved.

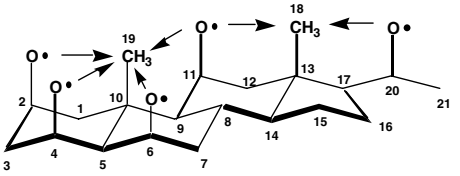

SCHEME 8

Potier, Motherwell, and their colleagues[28] recently devised a new version of the Barton reaction in which the functionalisation of the10b-methyl of steroids can be achieved by irradiating a solution with visible light instead of ultraviolet light. The method employs O-alkylthiohydroxamates,[29] which have also been proved to be efficient precursors for the generation of alkoxyl radicals. Thus, the irradiation of 6-O-acylthiohydroxamate in benzene containing an equimolecular amount of thionitrite as a donor of NO with a 250-W tungsten lamp gave the nitroso dimer corresponding to the product obtainable by the photolysis of 6β-ol nitrite, in 41% yield (Scheme 9).

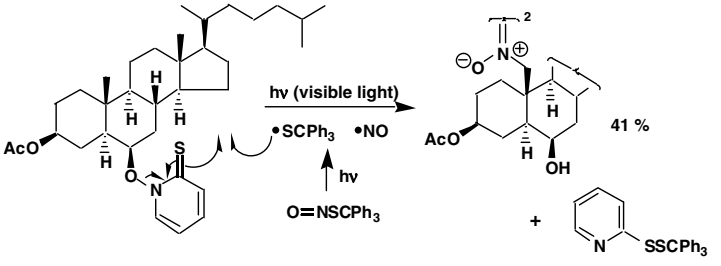

SCHEME 9

Suginome and collaborators have discovered a tandem Barton-remote-functionalization through the photochemical nitro-nitrosoxy rearrangement.[30] Thus, photolysis of 6β-nitrocholest-4-ene in methanol with 254-nm light gave 19-hydroxyiminocholest-4-en-6β-ol and its 5-ene-4β-ol isomer, along with accompanying formations of cholest-4-en-6-one and cholest-4-en-6β-ol. The isomeric 4β-nitrocholest-5-ene reacted in an entirely analogous manner, as outlined in Scheme 10. The products are formed via successive reactions; homolysis of CN, recombination of generated NO_2 to give nitrites, and the Barton reaction.

In the following, some representative examples among the numerous applications of this reaction found over four decades are presented. For more details of each example of functionalization, readers should consult the review articles and original papers cited:[2,15]

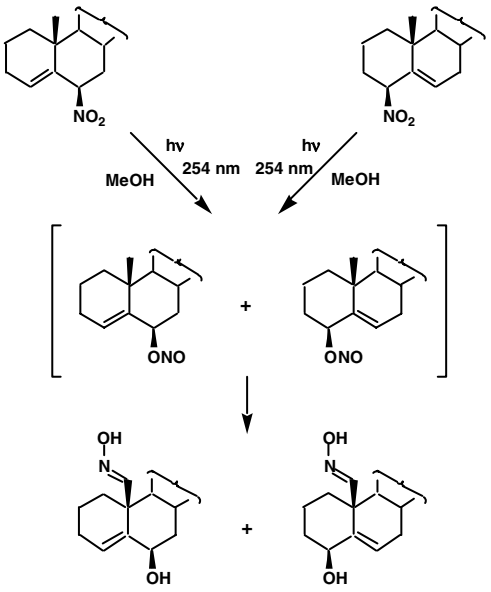

SCHEME 10

1. Functionalization of 10β-Me of a steroid from the 2β-ol nitrite[31] (Scheme 11)

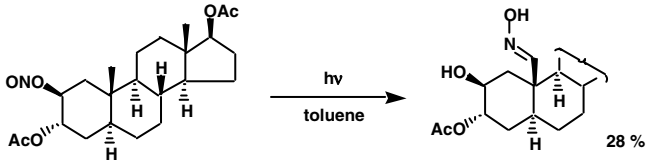

SCHEME 11

2. Functionalization of 10β-Me of a steroid from the 6β-ol nitrite[1,28] (Schemes 9 and 12)

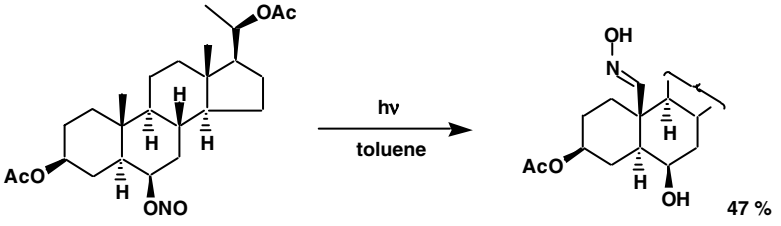

SCHEME 12

3. Functionalization of 10β- and 13β-Me of steroids from the 10β-ol nitrite: synthesis of aldosterone acetate[32,33] (Schemes 13 and 14)

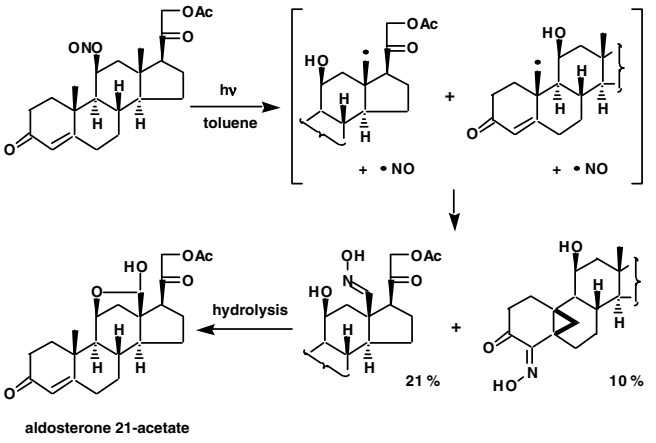

SCHEME 13

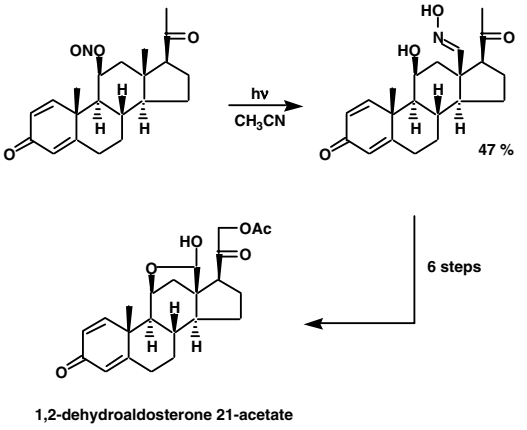

SCHEME 14

These examples are the most well-known applications of the reaction found by Barton as well as by his colleagues. The irradiation of corticosterone acetate nitrite affords aldosterone acetate oxime, which with nitrous acid gives aldosterone 12-acetate (Scheme 13). The overall yield, however, is rather low (15%) because an attack by the 11β-alkoxyl radical on C19 competes with the desired attack on C18. The incorporation of the 1,2-double bond into the nitrite could avoid an undesired C19 attack by the radical; a far better yield (47%) of 19-oxime was achieved, as shown in Scheme 14. These examples of the functionalization may indicate that the Barton reaction is sensitive to structural changes and that the distance and conformation requirements between the alkoxyl radical and the methyl group, which are in a 1,3-diaxial relationship, is rather strict (Scheme 14).

4. Functionalisation of 14α-Me of a steroid from steroidal 7α-ol nitrite[34] (Scheme 15)

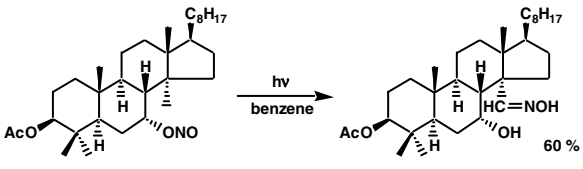

SCHEME 15

5. Functionalization of 13α-Me from steroidal 20α-ol nitrite: synthesis of deoxofukujusonorone[35] (Scheme 16)

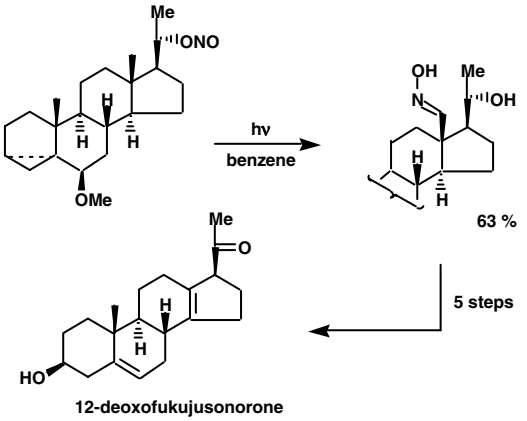

SCHEME 16

6. Functionalization of an angular methyl of terpenoid[36] (Scheme 17)

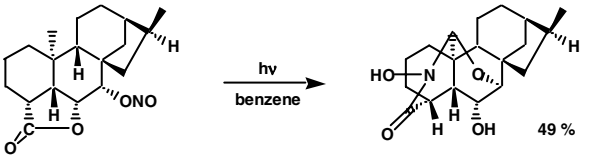

SCHEME 17

102.4 Accompanying Reactions to the Barton Reaction in the Photolysis of Nitrite Esters

The reactions described here compete with the Barton reaction in the photolysis of nitrites when the alkoxyl radical and the hydrogen to be abstracted are not ideally disposed for the Barton reaction. Representative examples, including the formation paths in each competing reaction, are shown in the schemes below. The fundamental nature of these competitive reactions of alkoxyl radicals generated from simple alcohols has been extensively investigated.[37] The competing reactions occasionally predominate over the Barton reaction (Scheme 24) or comprise an exclusive reaction (Schemes 18 through 23 and 26), which can be used for synthetic purposes. Among these reactions, the β-cleavage is frequently the predominant reaction. Since the 1970s, we have found a variety of new processes in which the β-cleavage of alkoxyl radicals takes place in a highly selective manner. We obtained the first concrete evidence for the reversibility of β-fragmentation.[38] Although little attention was drawn to its potential in synthesis until the 1970s, we recognized that the β-cleavage of alkoxyl radicals is as useful as intramolecular hydrogen abstraction in organic synthesis and have shown the usefulness by synthesizing a variety of natural products using β-cleavage of alkoxyl radicals (generated from alkyl hypoiodites) as the key step. This topic is dealt with in a separate chapter.[39]

β-Fragmentation and Epimerization of Alkoxyl Radicals

β-Cleavage takes place especially readily when the cleavage relieves some strain, such as cyclopropanoxyl and cyclobutanoxyl radicals, or provides stabilized carbon-centered radicals, such as those conjugated with a heteroatom or tertiary and allyl radicals, as outlined in the following examples.

1. β-Fragmentation of cyclopropanol nitrites[40,41] (Scheme 18)

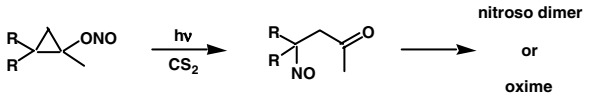

SCHEME 18

2. β-Fragmentation of cyclobutanol nitrite[42] (Scheme 19)

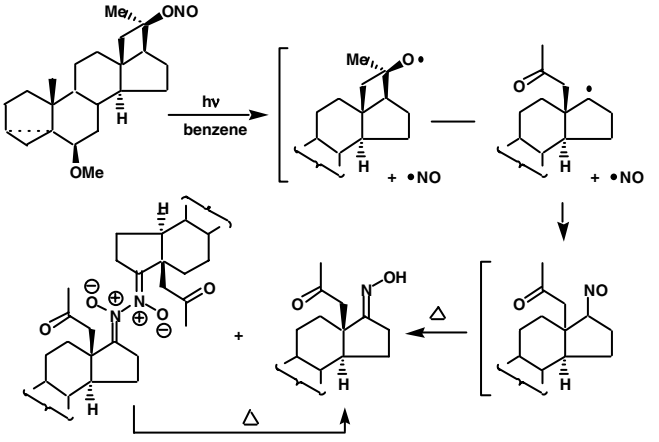

SCHEME 19

3. β-Fragmentation of N-acyl-3-nitrosoxypiperidine ring[43] (Scheme 20)

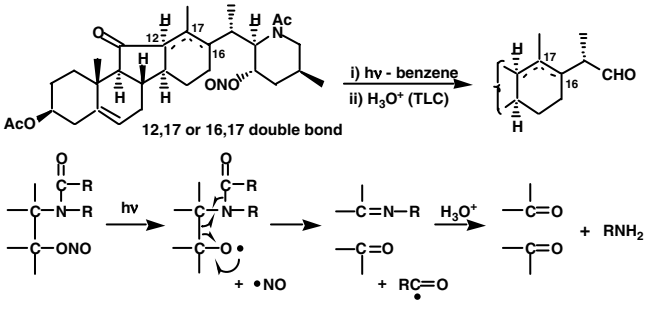

SCHEME 20

4. Formation of cyclic hydroxamic acids[42b,44] (Scheme 21)

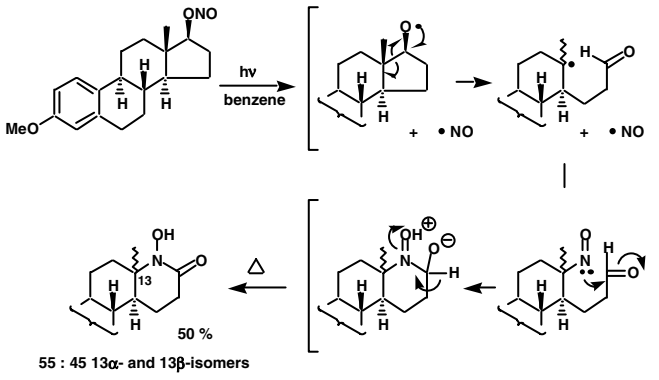

SCHEME 21

5. Formation of cyclic nitrone[17,45] (Scheme 22)

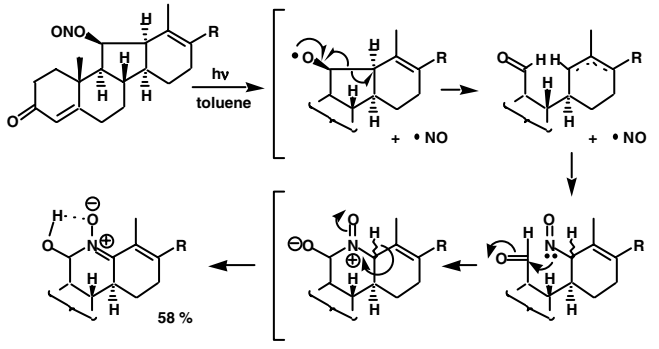

SCHEME 22

6. Formation of spiroisoxazolines[46] (Scheme 23)

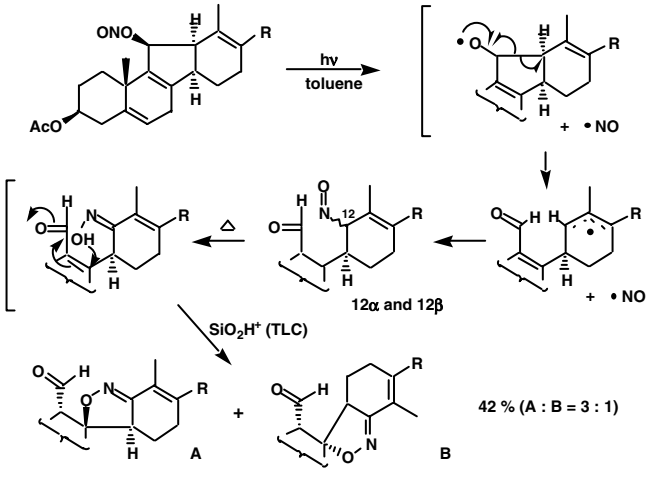

SCHEME 23

7. Epimerization of alkoxyl radicals[38,47] (Schemes 24 and 25)

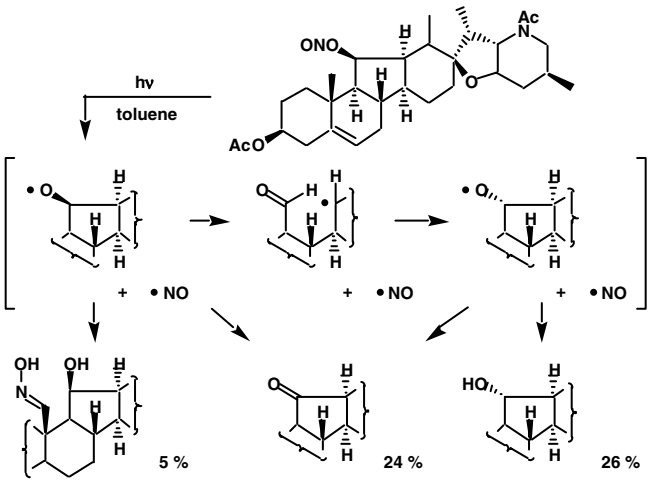

SCHEME 24

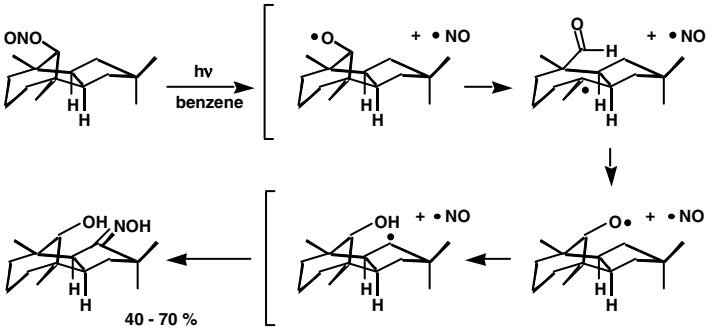

SCHEME 25

8. β-Fragmentation of β-silyl alkoxyl radicals[48] (Scheme 26)

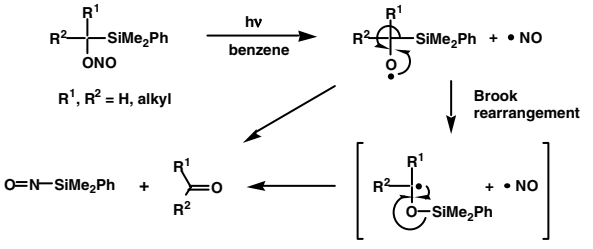

SCHEME 26

Intramolecular Addition of the Alkoxyl Radicals to the CC Double Bond[49]

1. The formation of oxirane[50,51] (Schemes 27 and 28)

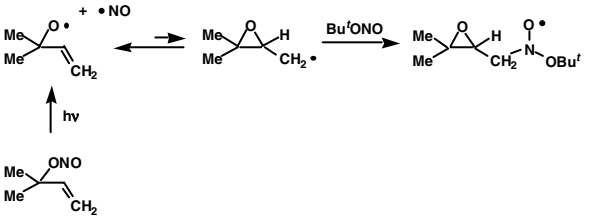

SCHEME 27

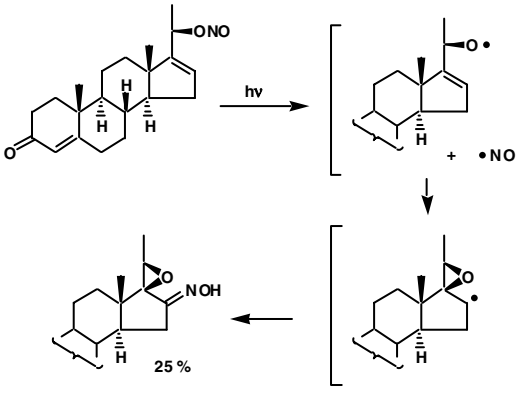

SCHEME 28

2. The formation of a tetrahydrofuran ring[51,52] (Scheme 29).

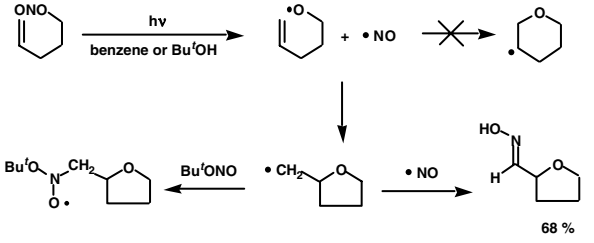

SCHEME 29

Disproportionation or α-Hydrogen Fission

The photolysis of cyclic secondary alcohol nitrites is sometimes accompanied by the formation of the corresponding cyclic ketones via loss of the α-hydrogen of the alkoxyl radicals arising from either disproportionation or, less likely, α-hydrogen fission.

Intermolecular Hydrogen Abstraction

The parent alcohols are formed as a by-product via hydrogen abstraction from another molecule when the above-mentioned reactions are inefficient.

The untimely death in 1998 of Derek Barton, the inventor of the reaction, is a great loss to organic photochemistry and radical chemistry.

The Barton reaction is considered to be one of the classics of the photo- and radical reactions in organic chemistry. Although its application to synthesis is rather limited today, the reaction has had a great impact on organic chemists in general and has aroused the interest and imagination of synthetic organic chemists for photo- and radical reactions, in particular. It has contributed to the considerable development of these research fields, as we see today.

Acknowledgments

The author thanks Dr. H. Senboku for his assistance in preparing the diagrams.

References

1. Barton, D.H.R., Beaton, J.M., Geller, L.E., and Pechet, M.M., A new photochemical reaction, *J. Am. Chem. Soc.,* 82, 2640, 1960; *ibid.,* A new photochemical reaction, 83, 4076, 1961.
2. Nussbaum, A.L. and Robinson, C.H., Some recent developments in the preparative photolysis of organic nitrites, *Tetrahedron,* 17, 35, 1962.
3. Purkis, C.H. and Thompson, H.W., The photochemistry of nitrates, nitrites and nitro-compounds. II, *Trans. Faraday Soc.,* 32. 1466, 1936; Thompson, H.W. and Dainton, F.S., The photochemistry of alkyl nitrites. III, *Trans. Faraday Soc.,* 33, 1546, 1937.
4. Coe, C.S. and Doumani, T.F., Photochemical decomposition of *t*-butyl nitrite, *J. Am. Chem. Soc.,* 70, 1516, 1948.
5. Gray, J.A. and Style, D.W.G., Photolysis of methyl nitrite, *Trans. Faraday Soc.,* 48, 1137, 1952.
6. Steacie, E.W.R. and Show, G.T., The homogeneous unimolecular decomposition of gaseous alkyl nitrites. II. The decomposition of ethyl nitrite, *J. Chem. Phys.,* 2, 345, 1934.
7. Tarte, P., Recherches experimentales sur la decomposition photochimique des nitrites d'alkyles, *Bull. Soc. Roy Sci. Liege,* 22, 226, 1953.
8. Calvert, J.G. and Pitts, J.N., Photochemistry, Wiley, New York, 1966, p.480.
9. See, For example, (a) Jenniskens, H.G., Phillippe, L., Essenberg, W., van Kadodwala, M., and Kleyn, A.W., *t*-Butyl nitrite surface photochemistry: the transition submonolayer to multilayer behavior, *J. Chem. Phys.,* 108, 1688, 1998 and references cited therein; Fieberg, J.E., Szulczewski, G.J., and White, J.M., Trimodal velocity distributions of nitric oxide for ultraviolet photodissociation of CH_3ONO adsorbed on Ag(III), *Chem. Phys. Lett.,* 290, 268, 1998; Jenniskens, H.G., Phillippe, L., Kadodwala, M., and Kleyn, A.W., The wavelength dependence of *t*-butyl nitrite surface photochemistry, *J. Phys. Chem., B,* 102, 8736, 1998; (b) Keller, B.A., Felder, P., and Huber, J.R., Molecular beam photodissociation study of methyl nitrite in the near-ultraviolet region, *J. Phys. Chem.,* 91, 1114, 1987, and papers cited therein; Mestdagh, J.M., Berdah, M., Dimicoli, I., Mons, M., Meynadier, P., D'Oliveira, P., Piuzzi, F., Visticot, J.P., Jouvet, C., Lardeuxdedonder, C., Martrenchard-barra, S., Soep, B., and Solgadi, D., Observation of an indirect pathway in the femtosecond study of alkyl nitrite photodissociation in the S1 state, *J. Chem. Phys.,* 103, 1013, 1995, and papers cited therein.
10. Kennedy, G.R, Ning, C.-L., and Pfab, J., The 355 nm photodissociation of jet-cooled CH_3SNO: Alignment of the NO photofragment, *Chem. Phys. Lett.,* 292, 161, 1998.
11. See, for example, Jacox, M.E. and Rook, F.L., Photodecomposition of methyl nitrite trapped in solid state, *J. Phys. Chem.,* 86, 2899, 1982
12. Finke, H., Spieker, H., and Andresen, P., The photodissociation of *t*-butyl nitrite at 193 nm, *J. Chem. Phys.,* 110, 4777, 1999.
13. (a) Hofmann, A.W., Ueber die einwirkung des broms in alkalisher lösung auf die amine, *Ber,* 16, 558,1883; *ibid.,* Zur kenntniss der coniin-gruppe, 18, 5 and 109, 1985; (b) Löffler, K. and Freytag,

C., Über eine neue bildungsweise von N-alkylierten Pyrrolidin, *Ber.,* 42, 3427, 1909; (c) Corey, E.J. and Hertler, W.R., A study of the formation of haloamine and cyclic amines by the free radical chain decomposition of *N*-haloammonium ions (Hofmann-Löffler reaction), *J. Am. Chem. Soc.,* 82, 1657, 1960.; (d) Wolff, M.E., Cyclization of N-halogenated amines (The Hofmann-Löffler reaction), *Chem. Rev.,* 63, 55, 1963.

14. Barton, D.H.R., The use of photochemical reactions in organic synthesis, in *Organic Photochemistry,* Vol. 2. Butterworths, London, 1968, chap. 1.
15. (a) Akhtar, M., Some recent developments in the photochemistry of organic nitrites and hypohalites, in *Advances in Photochemistry,* Vol. 2. Noyes, W.A., Hammond, G.S., and Pitts, Jr., J.N., Eds., Interscience, New York, 1964, 263; (b) Hesse, R.H., Barton reaction, in *Advances in Free Radical Chemistry,* 13, 83, 1969; (c) Chow, Y.L., Photochemistry of nitro and nitroso compounds, in *The Chemistry of Amino, Nitroso, Nitro Compounds and Their Derivatives,* Patai, S., Ed., Wiley, New York, 1982, 241.
16. Doyle, M.P., Terpstra, J.W., Pickering, D.M., and LePoire, R.A., Hydrolysis, nitrosyl exchange and synthesis of alkyl nitrites, *J. Org. Chem.,* 48, 3379, 1983.
17. Suginome, H., Mizuguchi, T., Honda, S., and Masamune, T., Photoinduced transformations. 33. Mechanism of photoinduced rearrangement of a (22S, 25S)-N-acetylveratr-13(17)-enin-11-yl nitrite, a fused cyclopentyl nitrite, to a nitrone, *J. Chem. Soc., Perkin Trans. 1,* 927, 1977.
18. For an early study, see Tanaka, M., Tanaka J., and Nagakura, S., The electronic structures and electronic spectra of some aliphatic nitroso compounds, *Bull. Chem. Soc. Jpn.,* 39, 766, 1966.
19. Kabasakalian, P. and Townley, E.R., Photolysis of nitrite esters in solution. I. Photochemistry of n-octyl nitrite, *J. Am. Chem. Soc.,* 84, 2711, 1962.
20. Barton, D.H.R., Ramsay, G.C., and Wege, D., Photochemical transformations. XXI. A comparison of the photolysis and pyrolysis of organic nitrites, *J. Chem. Soc. C,* 1915, 1967.
21. Kabasakalian, P., Townley, E.R., and Yudis, M.D., Photolysis of nitrite esters in solution. II. Photochemistry of aromatic alkyl nitrites, *J. Am. Chem. Soc.,* 84, 2716, 1962.
22. Breslow, R., Biomimetic chemistry, *Chem. Soc. Rev.,* 1, 553, 1972.
23. Heusler, K. and Kalvoda, J., Intramolecular free-radical reactions, *Angew, Chem. Int. Ed. Engl.,* 3, 525, 1964.
24. See Suginome, H., Chapter 109 in this Handbook
25. Akhtar, M. and Pechet, M.M., The mechanism of the Barton reaction, *J. Am. Chem. Soc.,* 86, 265, 1964.
26. Suginome, H., Mizuguchi, T., and Masamune, T., Photoinduced transformations. 32. Scrambling of unlabelled and [^{15}N] nitrogen monoxide in the photo-induced rearrangement of (22S, 25S)-5-veratr-13(17)-enin-11-yl nitrites to nitrones, *J. Chem. Soc., Perkin Trans. 1,* 2365, 1976.
27. Akhtar, M., Barton, D.H.R., and Sammes, P.G., Some radical exchange reactions during nitrite ester photolysis, *J. Am. Chem. Soc.,* 87, 4601, 1965.
28. Girard, P., Guillot, N., Motherwell, W.B., and Potier, P., Observations on the reaction of O-acylthiohydroxamates with thionitrite esters: a novel free radical chain reaction for decarboxylative amination, *J. Chem. Soc., Chem. Commun.,* 2385,1995.
29. Beckwith, A.L.J. and Hay, B.P., Generation of alkoxyl radicals from N-alkoxypyridinethiones, *J. Am. Chem. Soc.,* 110,4415, 1988; 111, 230, 1989; Barton, D.H.R. and Ramesh, M., Generation and fate of nondecarboxylating acyloxy radicals derived from the photolysis of acyl derivatives of N-hydroxy-2-thiopyridine, *Tetrahedron Lett.,* 31, 949, 1990.
30. Suginome, H., Takakuwa, K., and Orito, K., Functionalisation of unactivated carbon involving photochemical intramolecular rearrangement of nitro group attached to tetrahedral carbon to nitrosooxy group, *Chem. Lett.,* 1357, 1982.
31. Wolff, M.E. and Morioka, T., C-19 Functional steroids. III. 2,19-disubstituted androstane and cholestane derivatives, *J. Org. Chem.,* 30, 423, 1963.
32. Barton, D.H.R. and Beaton, J.M., A synthesis of aldosterone acetate, *J. Am. Chem. Soc.,* 82, 2641, 1960; ibid., 83, 4083, 1961.

33. Barton, D.H.R., Basu, N.K.J., Day, M., Hesse, R.H., Pechet, M.P., Starratt, A.N., Improved synthesis of aldosterone, *J. Chem. Soc., Perkin Trans. 1,* 2243, 1975.
34. Bentley, T.J., McGhie, J.F. and Barton, D.H.R., The synthesis of 32-oxygenated lanostane derivatives, *Tetrahedron Lett.,* 2497, 1965.
35. Suginome, H., Nakayama, Y., and Senboku, H., Photoinduced molecular transformations. 131. Synthesis of 18-norsteroids, deoxofukujusonorone and the related steroids based on a selective b-scission of alkoxyl radicals as the key step, *J. Chem. Soc.,* 1837, 1992.
36. Hanson, J.R., The chemistry of the tetracyclic diterpenoids. II. The shape of ring B of the kaurenolides, *Tetrahedron,* 22, 1701, 1966.
37. Gray, P. and Williams, A., The thermochemistry and reactivity of alkoxyl radicals, *Chem. Rev.,* 59, 239. 1959; Bacha, J.D. and Kochi, J.K., Polar and solvent effects in the cleavage of *t*-alkoxyl radicals, *J. Org. Chem.,* 30, 3272, 1965; Walling, C. and Padwa, A., Positive halogen compounds. VI. Effects of structure and medium on the β-scission of alkoxyl radicals, *J. Am. Chem. Soc.,* 85,1593, 1963, and the references cited in these papers.
38. Suginome, H., Sato, N., and Masamune, T., Photolysis of nitrites of 3-*O, N*-diacetyl-22,27-imino-17,23-oxidojervan-5-ene-3-11- and 3,11-diols, *Tetrahedron Lett.,* 1557, 1967; Suginome, H., Sato, N., and Masamune, T., Some observation on photolysis of fused cyclopentyl nitrites, *Bull. Chem. Soc. Jpn.,* 42, 215, 1969.
39. See Suginome, H., Chapter 109 in this book.
40. Depuy, C.H., Jones, H.L., and Gibson, D.H., Cyclopropanols. VIII. Low-temperature thermolysis of cyclopropyl nitrites, *J. Am. Chem. Soc.,* 90, 5306, 1968.
41. Depuy, C.H., The chemistry of cyclopropanols, *Acc. Chem. Res.,* 1, 41, 1968.
42. (a) Suginome, H. and Nakayama, Y., Photoinduced molecular transformations. 132. A two-step intramolecular transposition of the 17β-acetyl group of pregnan-20-one to C-18 through the formation of cyclobutanols by the reaction of the excited carbonyl, followed by a selective β-scission of alkoxyl radicals generated from them, *J. Chem. Soc., Perkin Trans. 1,* 1843, 1992; (b) Suginome, H. and Uchida, T., Photoinduced rearrangement of a steroidal cyclobutyl nitrite; anomalous β-scission of a cyclobutanoxyl radical, *J. Chem. Soc., Chem. Commun.,* 701,1979.
43. Suginome, H., Murakami, M., and Masamune, T., A new photochemical fragmentation of nitrogen heterocycles, *J. Chem. Soc., Chem. Commun.,* 343,1966.
44. (a) Robinson, C.H., Gnoj, O., Mitchell, A., Wayne, R., Townley, E., Kabasakalian, P., Oliveto, E.P., and Barton, D.H.R., The photolysis of organic nitrites. II. Synthesis of steroidal hydroxamic acids, *J. Am. Chem. Soc.,* 83, 1771, 1961; (b) Robinson, C.H., Gnoj, O., Mitchell, A., Oliveto, E.P., and Barton, D.H.R., The photochemical rearrangement of steroidal 17-nitrites, *Tetrahedron,* 21, 743, 1965; (c) Suginome, H., Yonekura, N., Mizuguchi, T., and Masamune, T., On the mechanism of the formation of steroidal cyclic hydroxamic acid in the photolysis of steroidal 17-ol nitrite, *Bull. Chem. Soc. Jpn.,* 50, 3010, 1977; (d) Suginome, H., Maeda, N., and Kaji, M., Photoinduced transformations. 60. Photoinduced rearrangements of cholesteryl nitrites with monochromatic light, *J. Chem. Soc., Perkin Trans. 1,* 111, 1982.
45. Suginome, H., Sato, N., and Masamune, T., Photochemical formation of cyclic nitrone from nitrite of a fused 5-membered ring alcohol, *Tetrahedron,* 27, 4863, 1971.
46. Suginome, H., Thuneno, T., Sato, N., Maeda, N., Masamune, T., Shimanouchi, H., Tsuchida, Y., and Sasada, Y., Photoinduced transformations. XXX. Photorearrangement of (22S,25S)-N-acetylveratra-5,8,13(17)-trienine-3β,11β,23β-triol 3,23-diacetate 11-nitrite, a fused cyclopentenyl nitrite, to two spiroisooxazolines, *J. Chem. Soc., Perkin Trans. 1*, 1297,1976.; Suginome, H., Maeda, N., and Masamune, T., Photoinduced transformations. XXXI. Photoinduced rearrangement of (22S,25S)-N-acetyl-5a-veratra-8,13(17)-dienine-3b,11b,23b-triol 3,23-diacetate 11-nitrite to two spiro-isoxazolines, *J. Chem. Soc., Perkin Trans. 1,* 1312, 1976.
47. Nickon, A., Iwadare, T., McGuire, F.J., Mahajan, J.R., Narang, S.A., and Umezawa, B., The structure, stereochemistry and genesis of α-caryophyllene alcohol (apollan-11-ol), *J. Am. Chem. Soc.,* 92, 1688, 1970.

48. Paredes, M.D. and Alonso, R., On the radical Brook rearrangement. Reactivity of α-silyl alcohols, α-silyl alcohol nitrite esters and β-haloacylsilanes under radical-forming conditions, *J. Org. Chem.,* 65, 2292, 2000.
49. For a review, see Surzur, J.M., Radical cyclizations by intramolecular additions, in *Reactive Intermediates,* Vol. 2. Abramovitch, R.A., Ed., Plenum Press, New York, 1982, chap. 3.
50. Nussbaum, A.L., Wayne, R., Yuan, E., Sarre, O.Z., and Oliveto, E.P., Photolysis of organic nitrites. VIII. Intramolecular addition to a double bond, *J. Am. Chem. Soc.,* 87, 2451, 1965.
51. Grossi, L. and Strazzari, S., Oxaranylmethyl radicals: EPR detection by spin trapping, *J. Chem. Soc., Chem. Commun.,* 917, 1997.
52. Rieke, R.D. and Moore, N.A., The cyclic addition of hetero radicals. II. Cyclic additions of alkoxyl radicals in alkenes, *J. Org. Chem.,* 37, 413, 1972.

103

Photochemical Reactivity of Pyridones

Scott McN. Sieburth
Temple University

103.1 Introduction

Pyridone photochemistry has been extensively studied because of the important and interesting β-lactam and cyclooctadiene products (see Scheme 2), the dominance of a short-lived singlet excited state in most of the photochemistry, interesting substituent effects, and an absence of solvent effects. A number of reviews have included aspects of pyridone photochemistry[1–6] but no comprehensive discussion has been published. The breadth of 2-pyridone photoreactivity stands in contrast to its thermal stability, reluctant partners in Diels-Alder reactions, for example.[3,7] The 4-pyridones have provided less useful photochemical reactivity and, consequently, have been the subject of fewer studies.

Pyridones take two constitutional forms: 2-pyridones and 4-pyridones, **2** and **3** (Scheme 1). These two parent structures have tautomers, the corresponding hydroxypyridines **1** and **4**. These solvent-sensitive equilibria strongly favor the pyridone form.[8–10] Photochemically induced tautomerism has also been extensively studied.[11,12]

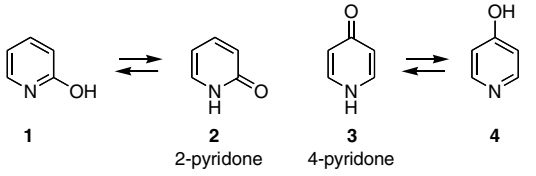

SCHEME 1 The two pyridone structures and their tautomers

103.2 2-Pyridone Photochemistry

Overview

First described in 1960,[13] the most accessible photoproduct of 1-methyl-2-pyridone **5** is a dimer, with a *trans*-head-to-tail structure **6** (Scheme 2). Photoisomerization of 2-pyridone to give the 2-aza-bicyclo[2.2.0]hex-5-en-3-one **7** competes with dimerization. Both of these products are derived from a short-lived (ca. 0.2 ns) singlet excited state[14] generated by irradiation above 300 nm, typically using a Pyrex

0-8493-1348-1/04/$0.00+$1.50

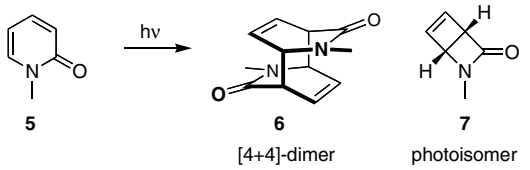

SCHEME 2 Irradiation of 1-methyl-2-pyridone yields both dimer and isomerization products

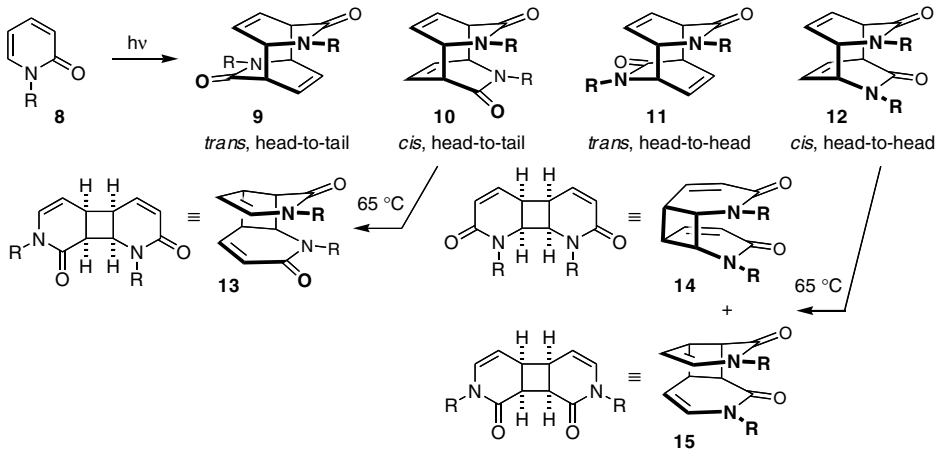

SCHEME 3 Photodimerization can lead to four [4+4]-dimers but the head-to-head products are rare. *Cis*-isomers undergo a facile Cope rearrangement.[16]

filter. High-, medium-, and low-pressure mercury lamps have been employed, as well as a 300-nm fluorescent lamp setups such as the Rayonet photoreactor.[15] In general, triplet sensitization leads to other photoproducts (Schemes 8, 11, and 13). The competition between isomerization to give **7** and dimerization to give **6**, from the same transient intermediate, results in a concentration-dependent reaction. Studies in several laboratories have found that the dimerization dominates at concentrations above 0.1 *M* and isomerization is the major product at or below 0.01 *M*.[16] The quantum yield for the formation of **7** has been determined to be 0.6%.[14,17,18] It has been noted that [2+2]- and [4+2]-products are not formed during 2-pyridone photodimerizations.[16] Nevertheless, [2+2]-products can be produced with excellent regioselectivity by the proper choice of co-reactant and reaction conditions (Schemes 11, 12, and 13).

Both dimerization and isomerization reactions are essentially solvent insensitive, proceeding at similar rates and giving similar product ratios when run in water,[16] alcohols,[16] acetonitrile,[18] ethers,[18] or benzene[16] (see Figure 103.3). Moreover, a marked insensitivity of the photoreaction to oxygen has been noted.[17,19]

Photodimerization

Regio- and Stereochemistry

While the major reaction product is generally the *trans* head-to-tail dimer **6** (**9**, Scheme 3) and this can often be purified directly by crystallization, it was noted by several authors that additional dimeric structures were also formed.[14,19] Careful analysis of the mixture by Nakamura and co-workers led to the identification of all three of the other *cis/trans* and head-to-head [4+4]-isomers (**10**, **11**, and **12**).[16]

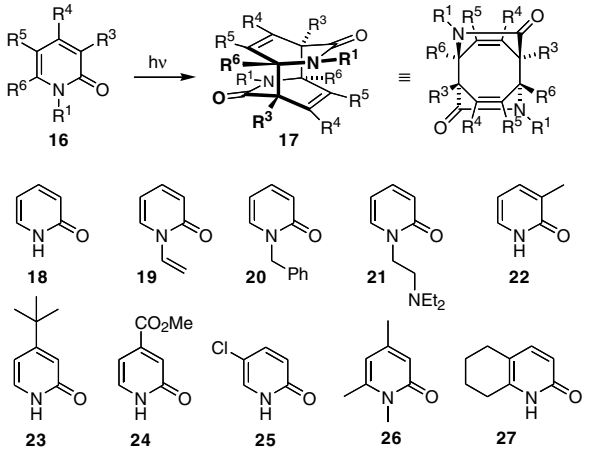

FIGURE 103.1 Examples of 2-pyridones that undergo [4+4]-photodimerization.

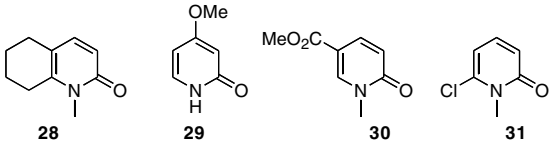

FIGURE 103.2 Examples of 2-pyridones that do not undergo [4+4]-photodimerization.

Nakamura also demonstrated a very simple method for differentiating the *cis*-isomers **10** and **12** from the *trans*-isomers **9** and **11**. Heating the dimers to 65°C results in a very facile [3,3]-rearrangement of the *cis*-1,5-cyclooctadienes to cyclobutanes. The C_2 symmetric **10** can form only one product **13**, whereas the *meso*-**12** leads to nearly equal quantities of two different Cope products **14** and **15**. *trans*-Isomers **9** and **11** are stable under these conditions.

Substituent Effects

The photodimerization reaction is highly tolerant of substitution (Figure 103.1). The dimer of the parent 2-pyridone **18** has been reported several times,[19–21] in isolated yields of up to 54%.[19] This *trans*-head-to-tail dimer is highly crystalline, precipitating during the photoreaction. An alkyl group on nitrogen, R^1 removes intermolecular hydrogen bonding and greatly enhances the solubility of the photodimer. Methyl substitution is tolerated at every ring position (e.g., **22** and **26**),[20,21] and even a 4-*t*-butyl group (**23**) does not prevent [4+4]-dimerization (35%[17]). Chlorine substitutions at R,[3] R^4, and R^5 (**25**) are individually compatible with [4+4]-photodimerization.[19] Photodimers from 2-pyridones with alkene substitution on nitrogen (**19**) have been reported,[18] and the presence of a proximal amino group (**21**) does not hinder dimer formation.[20] Multiple substitution is possible but steric limitations undoubtedly exist. Tetrahydroquinolone **27** readily yields a highly insoluble photodimer,[22,23] but the corresponding *N*-methyl congener **28** (Figure 103.2) does not photodimerize.[23,24]

Other notable incompatibilities with the [4+4]-dimerization reaction are 2-pyridones with 4-alkoxy (**29**),[25] 5-carboalkoxy (**30**),[26] and 6-chloro groups (**31**).[27] These incompatibilities are caused by alternative photochemical reaction paths (see Figure 103.6 and Scheme 14), although 4-alkoxy-2-pyridone **29** will undergo [4+4]-photocycloadditions with other pyridones (Scheme 4).[28,29]

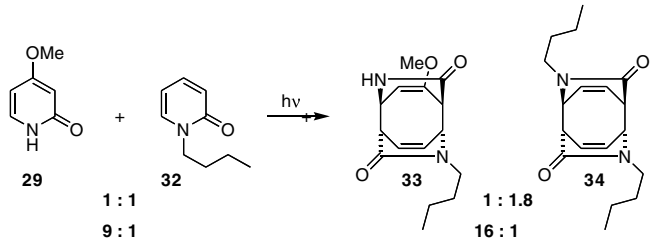

SCHEME 4 Cross-[4+4]-cycloaddition of 4-methoxy-2-pyridone **29**[28,29]

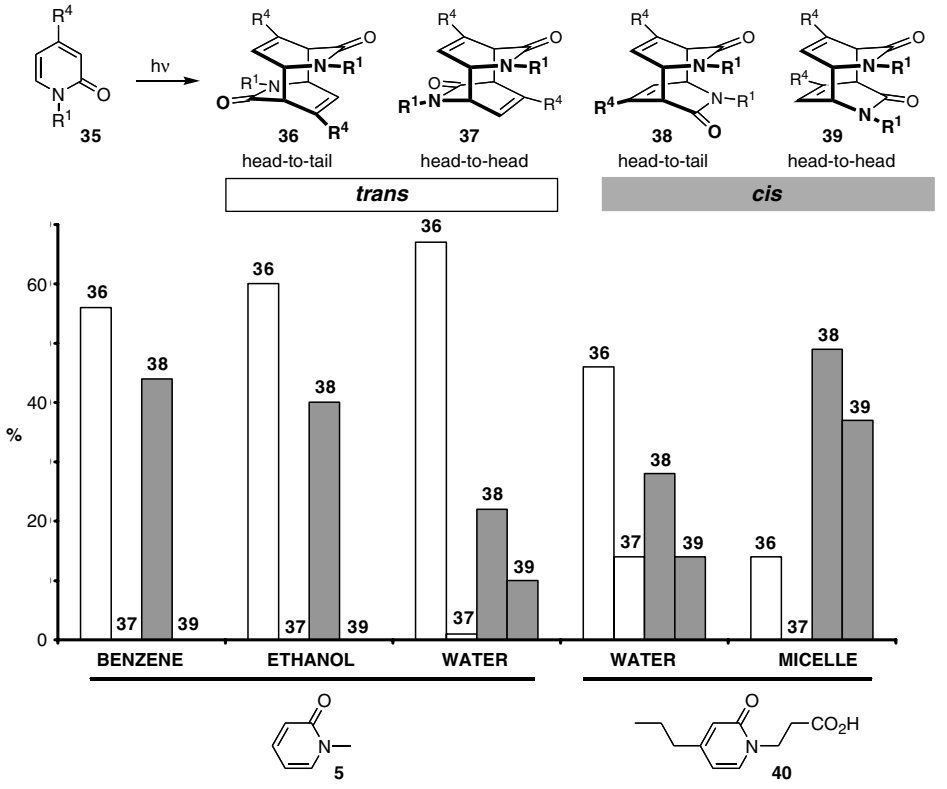

FIGURE 103.3 Solvent effects on the ratio of dimerization products **36**, **37**, **38**, and **39.**[30–32]

Alkoxy substitution at C4 leads to photoisomerization by eliminating the dimerization reaction (see Figure 103.6). It does not, however, prevent cross-[4+4]-cycloaddition with other pyridones (Scheme 4).[28,29] An equimolar mixture of **29** with 1-butyl-2-pyridone **32** led to a mixture of the cross product **33** and the known dimer **34**. Dimerization of **32** dominates, possibly because the UV light is largely absorbed by **32**. Systematic increases in the relative amount of **29** led to an increase in the amount of the cross product **33**. The excess **29** is recovered unchanged.

Solvent and Medium Effects

Solvent has little effect on pyridone dimerization, Figure 103.3. For 1-methyl-2-pyridone **5**, benzene and ethanol as solvent yield a nearly identical mixture of *trans*- and *cis*-head-to-tail isomers **36** and **38**, favoring the former. Only in water are head-to-head isomers **37** and **39** formed, favoring the *cis*-**39**. A similar result in water (and in alcohol) is observed for the 4-propyl-2-(2-pyridonyl) propionic acid **40**. Alignment of pyridone **40** in micelles can be used to give a high proportion of the *cis*-isomers **38** and **39**.[30–32]

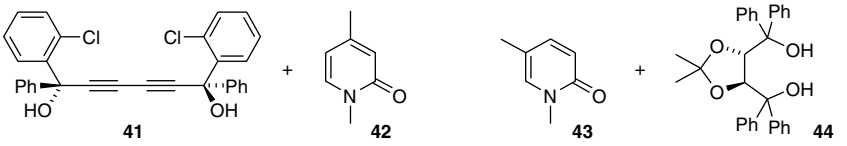

FIGURE 103.4 Pyridones crystallized with hosts **41** and **44** undergo *trans* head-to-tail photodimerization.[33]

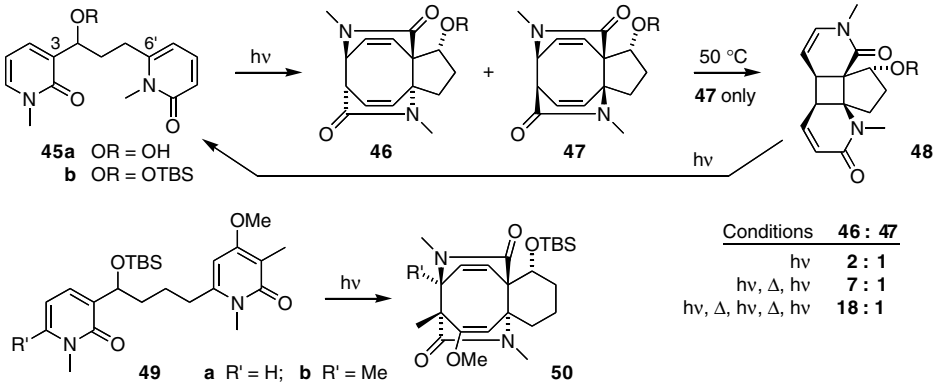

SCHEME 5 Intramolecular 2-pyridone cycloadditions.[35–37]

Photodimerization of 2-pyridones in the solid state has only been reported for pyridones co-crystallized with a chiral host, the 1:2 mixture of **41**/**42** and the 1:1 mixture of **43**/**44** (Figure 103.4). The resulting *trans*-head-to-tail dimers are formed in high yield but are centrosymmetric and achiral.[33]

Intramolecular [4+4]-Cycloaddition

Intramolecular [4+4]-photocycloaddition of 2-pyridones is accommodated with appropriate tether length and points of attachment (Scheme 5). When the tether is linked at the 3- and 6′- positions (**45** and **49**), it reinforces the preferred head-to-tail cycloaddition. With a three-atom chain, the cycloaddition of **45** yields a 2:1 mixture of *trans*- and *cis*-isomers, similar to the intermolecular reaction.[34] A tether alcohol **45a** has little effect on the formation of stereogenic centers during the cycloaddition and yields two diastereomers for both **46** and **47**, epimeric at the alcohol carbon. Protection of the alcohol as the sterically demanding *t*-butyldimethylsilyl (TBS) ether (**45b**) leads to only **46** and **47**.

A highly *trans*-selective cycloaddition of **45** can be achieved utilizing the thermal instability of the *cis*-isomer (see Scheme 3). Heating the 2:1 mixture of **46** and **47** to 50°C results in Cope rearrangement of *cis*-**47** but does not alter **46**. This rearrangement of **47** generates an α,β-unsaturated carbonyl moiety. Irradiation of the resulting mixture cleaves **48**, regenerating **45,** and leads to a **46**:**47** mixture of 7:1. Another cycle of heat and light converts this mixture to an 18:1 ratio while maintaining a good isolated yield.[35]

A four-carbon tether (**49a**) yields only the *trans*-isomer. This is likely due to a high level of strain in the polycyclic product **50a**. The crystal structure of a dihydro derivative of **50a** found the tether-derived cyclohexane to be in a boat conformation, a substantial contribution to the strain of this adduct.[36] An analog carrying an additional methyl group at a carbon involved in bond formation, **49b**, does not undergo cycloaddition.[37]

Highly selective formation of *cis*-cycloadduct **53** from three-carbon tethered pyridones can be achieved through intermolecular hydrogen bonding. Compound **51a**, lacking nitrogen substitution, yields exclusively the *cis*-**53a** when the photochemistry is conducted in benzene or toluene, but only the *trans*-isomer **52a** when the reaction is run in DMSO or methanol.[38] Solvent and concentration studies were consistent

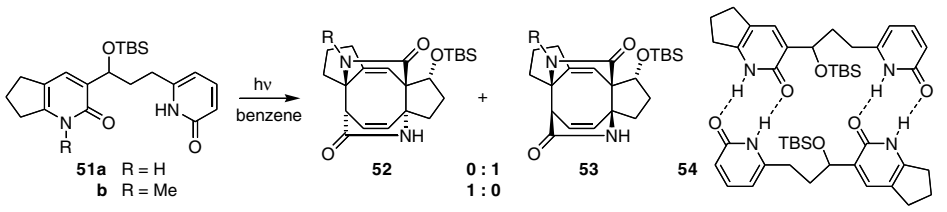

SCHEME 6 *cis*-Selective cycloaddition with hydrogen-bonded pyridones.[38–40]

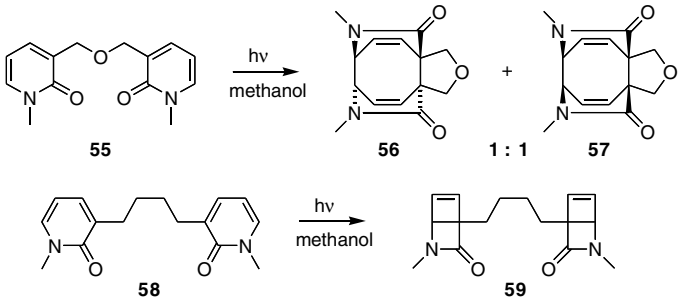

SCHEME 7 Tether-directed head-to-head photocycloaddition.[41–43]

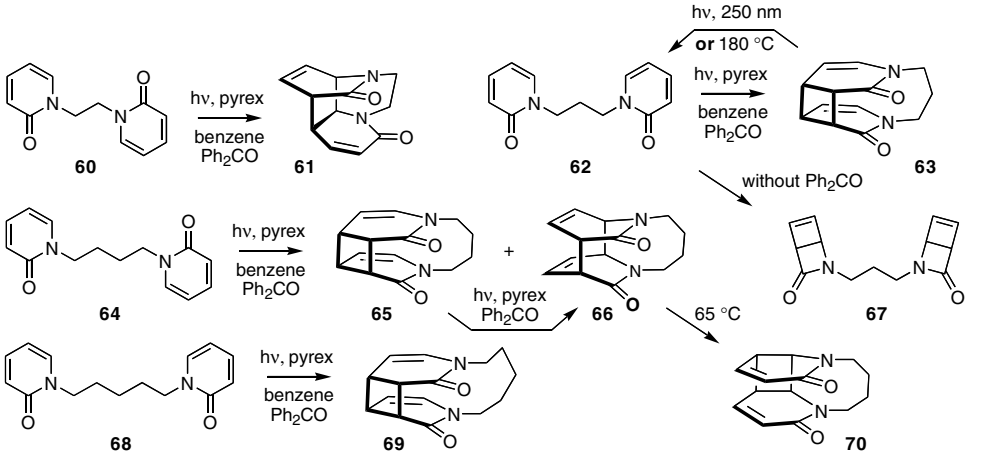

SCHEME 8 *N,N*-Tethered pyridones and triplet sensitized cycloadditions.[44]

with involvement of a hydrogen bonded dimer **54**, aligning both molecules for *cis*-cycloaddition.[38,39] In keeping with this analysis, a single methyl substitution **51b** provides only the *trans*-isomer **52b**, regardless of the reaction solvent.[38,40]

Tethering of 2-pyridones can enforce the non-preferred head-to-head regiochemistry. For a three-atom tether, this cycloaddition is highly efficient but without stereoselectivity, for both the head-to-head tethered **55**[41] (Scheme 7) and the tail-to-tail tethered isomer.[42] The four-carbon tethered **58**, however, only undergoes isomerization.[43]

Tethering the pyridones at nitrogen has been explored with tether lengths of two through five carbons (Scheme 8).[44] Only the longest lengths are compatible with the [4+4]-cycloadduct and other products dominate. Benzophenone sensitization is utilized for most of these reactions. The two-carbon tethered

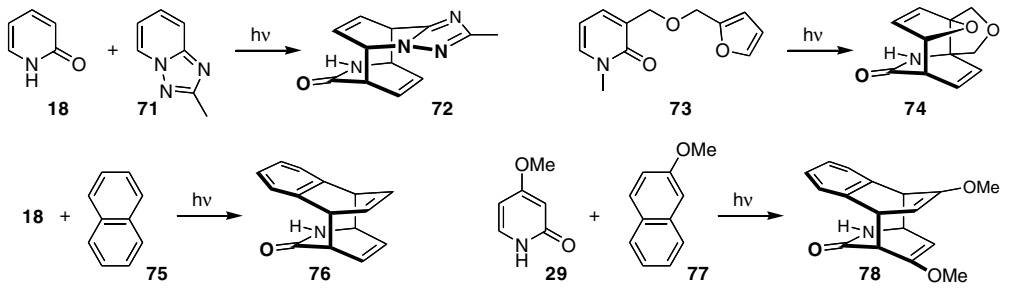

SCHEME 9 Photocycloadditions of 2-pyridones with other aromatics.[45–47]

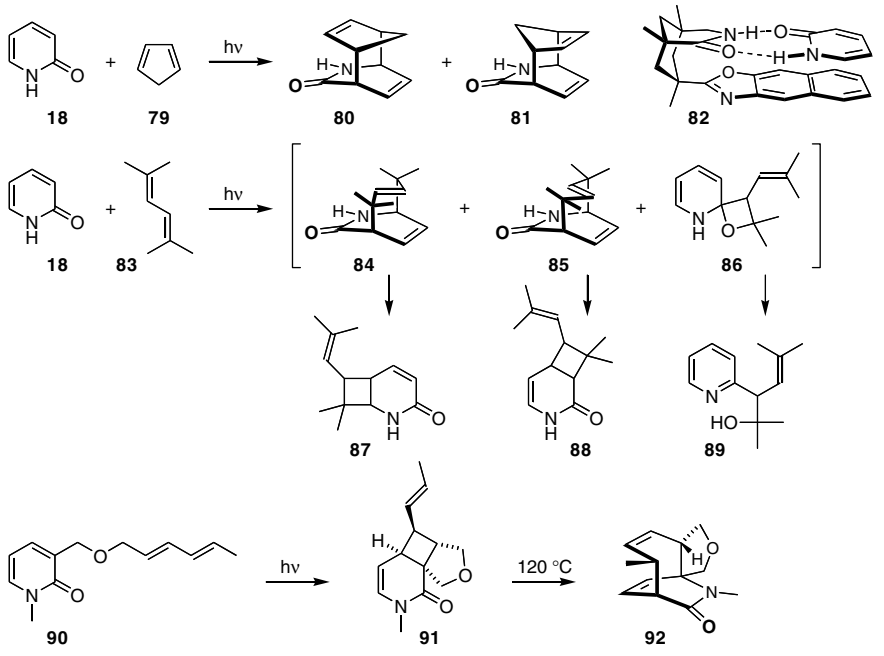

SCHEME 10 Cycloaddition of 2-pyridones with *s-cis* and *s-trans* 1,3-dienes.[48–52]

structure **60** leads to the [4+2]-adduct **61**. Three carbons (**62**) give the [2+2]-adduct **63** involving only the C3,C4 alkenes. Without triplet sensitization, the Dewar pyridones **67** are formed from **62**. Adduct **63** reverts to starting pyridones **62** at 180°C or when irradiated with 250-nm light. The same type of [2+2]-adduct (**65**) is also formed from the four-carbon tethered pyridones **64**, accompanied by the *cis* head-to-head [4+4]-adduct **66**. Irradiation of the [2+2]-adduct **65** converts it to **66**. Heating the [4+4]-adduct **66** to 65°C leads to a Cope rearrangement and the new cyclobutane **70**. The [2+2]-adduct **69** is formed when the tether length is five atoms.

Other [4+4]-Cycloadditions

Pyridones and Other Aromatics

In addition to dimerizations, 2-pyridones undergo [4+4]-photocycloadditions with other aromatics and with 1,3-dienes (Schemes 9 and 10). Triazolopyridine **71** will photodimerize,[45] but when mixed with pyridone **18** yields significant amounts of cross product **72**.[46] Intermolecular reactions of pyridones with

furans has not been reported but intramolecular cycloaddition of **73** yields the *trans* [4+4]-cycloadduct **74** as well as the *cis*-isomer (10:3).[47] Naphthalene **75** and pyridone **18** yield the *cis*-adduct **76**, whereas the three-atom tethered intramolecular reaction gives a mixture of *cis*- and *trans*-isomers.[47] A mixture of 4-methoxy-2-pyridone **29** and 2-methoxynaphthalene **77** gives a single product **78**.[47]

Pyridones and 1,3-Dienes

2-Pyridones and 1,3-dienes also undergo [4+4]-cycloadditions. For *s-cis*-1,3-dienes like cyclopentadiene **79**, *trans*- and *cis*-adducts **80** and **81** are formed in good yield.[48,49] The hydrogen bonded complex of the pyridone to the enantiomerically pure scaffold **82** leads to enantiomerically enriched [4+4]-adducts with cyclopentadiene, in up to 87% *ee*.[50]

When the 1,3-dienes are largely or exclusively in the *s-trans*-conformation, such as with diene **83**, pyridone **18** leads to three products, **87**, **88**, and **89**.[48,49] The two cyclobutane products **87** and **88** derive from Cope rearrangement of the highly strained [4+4]-photocycloaddition adducts **84** and **85**, a mechanism precedented by photocycloadditions of 1,3-dienes with other aromatic species.[51] Pyridine **89** may be formed from oxetane **86**. When the 1,3-diene is delivered intramolecularly (**90**), the only photoproduct is **91**, presumably via an intermediate relating to **85**. In contrast with the chemistry of the *cis*-pyridone dimers (Scheme 3), cyclobutane **91** thermally rearranges to the cyclooctadiene **92**.[52]

Isomerization

Substituent Effects

When 2-pyridones are irradiated in dilute solution, generally below 0.01 *M*, they isomerize to 2-azabicyclo[2.2.0]hex-5-en-3-ones **93** in high chemical yields but low quantum yields.[14] A wide variety of substituents are compatible with this isomerization. The unsubstituted **18** and 1-alkenyl **94** have been isomerized (46%[25,53] and 60%[18] yields, respectively). Isomerization is reasonably efficient with pentamethyl **95** (45%) and tetrachloro **96** (70%). Electron-donating groups at C3 do not inhibit isomerization (**97**, 36%[25]; **98**, 62%[54]). For pyridones with chiral C3 and C5 substituents, isomerization yields diastereomeric mixtures from **99** (100%, 2:1[55]), **100** (59%[56]), and **101** (93%, 2.5:1[56]).

Two substitutions of 2-pyridones have been identified as preventing [4+4]-dimerization but compatible with isomerization, the 5-carboalkoxy group (**30**[26]) and the 4-alkoxy group (**102** and **103**) (Figure 103.6). The effect of the 4-alkoxy group was first observed with ricinine **102**, a naturally occurring toxin.[25] A broad set of 4-oxygen substitutions have been utilized, **103**.[53,55,57–60]

Enantioselective Isomerizations

The enantioselective preparation of pyridone photoisomers has been described by several laboratories, motivated in part by the importance of β-lactams as antibiotics. Lipase hydrolysis of racemic **104** and similar Dewar pyridones has led to resolutions with high enantiomeric purities.[53,60] Isomerization of pyridones when complexed to the chiral scaffold **106** gave the isomerized product with good to excellent levels of enantioselectivity.[50]

Two different approaches to control of the photoisomerization in the solid state have also been very successful. Complexes of 2-pyridones with a chiral host, such as the 1:1 complex of **41** and **107**, gave high *ee* levels even at significant conversion.[33] Pyridones with a 4-benzyloxy group, **108**, were found to crystallize in a chiral space group. Irradiation of these crystals gave excellent levels of asymmetric induction, but only at rather low levels of conversion.[61] This solid-state reaction has been analyzed computationally[62] (see Figure 103.7).

[2+2]-Cycloadditions

Intermolecular [2+2]-Cycloadditions

Irradiation of 2-pyridone in the presence of electron-poor alkenes leads to products of [2+2]-cycloaddition, both from direct and triplet-sensitized conditions (Scheme 11). Unsensitized irradiation of acrylonitrile

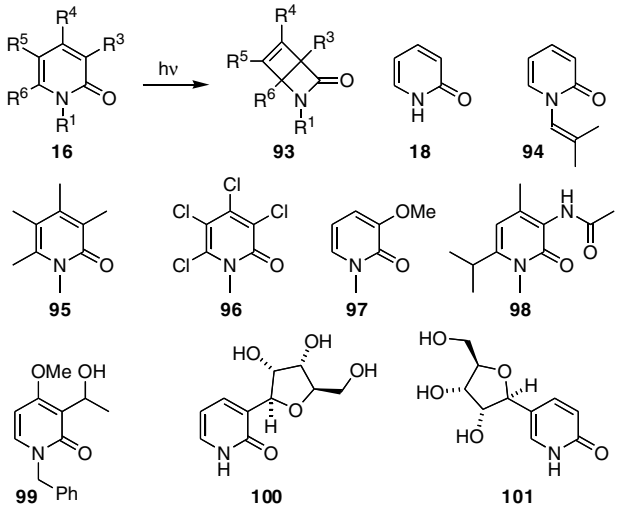

FIGURE 103.5 Examples of 2-pyridones that undergo photoisomerization to 2-aza-bicyclo[2.2.0]hex-5-en-3-ones **93**.

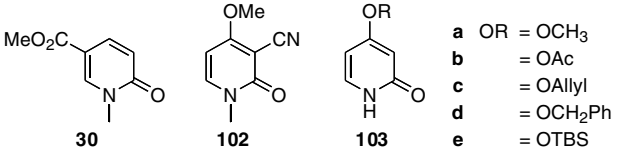

FIGURE 103.6 Pyridones that yield Dewar pyridones but do not dimerize.

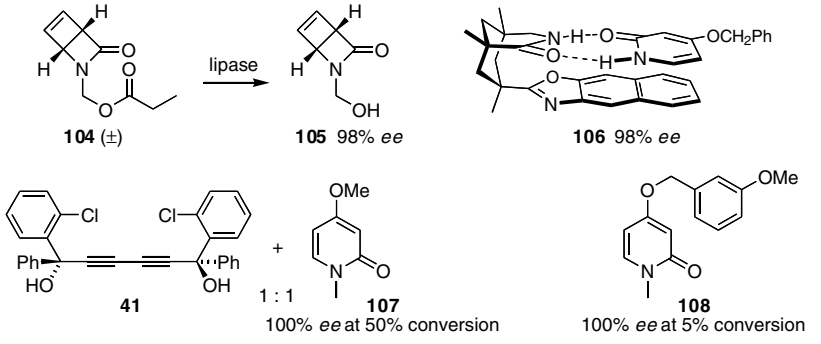

FIGURE 103.7 Preparation of enantiomerically pure Dewar pyridones has been accomplished by resolution (**105**),[53,60] use of a chiral host (**106**),[50] in the solid state by co-crystallization (**41** + **107**)[33] and with asymmetric crystals (**108**).[61]

109 with 2-pyridone **18** leads to two products, cyclobutane **110** (41%) and the eight-membered lactam **111** (4%).[63] Substituting pentadienyl ester **112** yields a mixture of products **113**, **114**, and **115** with good regioselectivity, but derived from reaction at both alkenes of the ester and both alkenes of the pyridone.[64] Yields of up to 54% for isomers **113** have been realized. Di-, tri-, and tetrachloroethene **114** undergo [2+2]-cycloaddition with pyridone when the reactions are sensitized with benzophenone or xanthone,

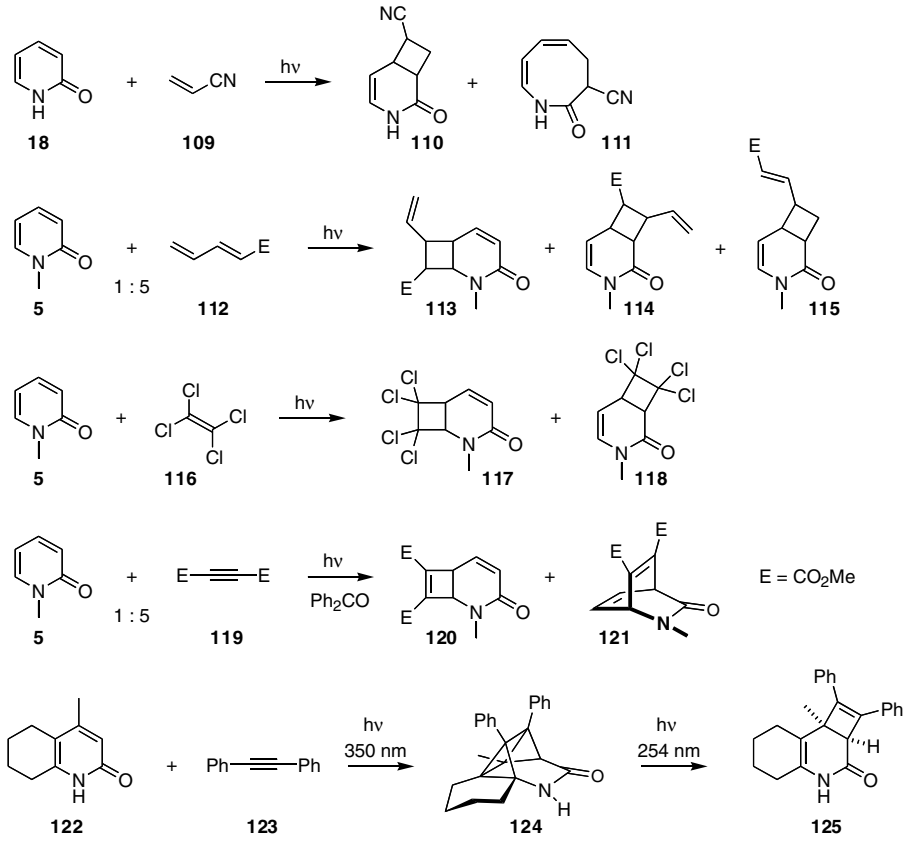

SCHEME 11 Cycloaddition reactions of 2-pyridone with alkenes and alkynes.[63–67]

giving product mixtures derived from reaction at both alkenes of the pyridone. Tetrachloroethene **116** and 1,1-dichloroethene both undergo cycloaddition without sensitization, but trichloroethene does not.[65] Intermolecular addition of dimethyl acetylenedicarboxylate **119** occurs with a triplet sensitizer, yielding a cyclobutene adjacent to the nitrogen, **120** and the [4+2]-adduct **121**, both in modest yield.[66] Combination of tetrahydroquinolones such as **122** with diphenylacetylene **123**, without triplet sensitization, yields the pentacyclic **124**.[23,24,67] Irradiation of **124** at shorter wavelengths leads to the cyclobutene adduct **125**.

Pyridones with 4-alkoxy substitution do not dimerize, but they do photoisomerise (Figure 103.6) and they will undergo [2+2]-cycloaddition with a variety of alkenes, (Scheme 12).[68–72] Most alkenes react at the C3–C4 double bond of the pyridone, with the more substituted end of the alkene attached to C4 of the pyridone, **127** and **130**. Many of these products have been shown to eliminate methanol on treatment with base, regenerating the pyridone ring unsaturation (e.g., **128**). When the alkene has an electron-withdrawing group such as ester **131**, the major (but not exclusive) site of reaction is the C5–C6 bond, to give **132**. Allene **134** reacts in the standard way to give **135**,[71] but a more efficient route to **135** using diketene **137** has been reported.[72]

Intramolecular [2+2]-Cycloadditions

Alkenes have been tethered to pyridones at nitrogen (Scheme 13),[73] and at C3[74] and C4.[75] Triplet-sensitized reaction of unsaturated esters **138** leads to [2+2]-cycloaddition at the nearby pyridone double bond, for tether lengths of two to five carbons. When the ester attachment is reversed, **140**, no cycloaddition is observed. Alkoxy-substituted pyridones react with simple alkenes (compare with Scheme 12) tethered at

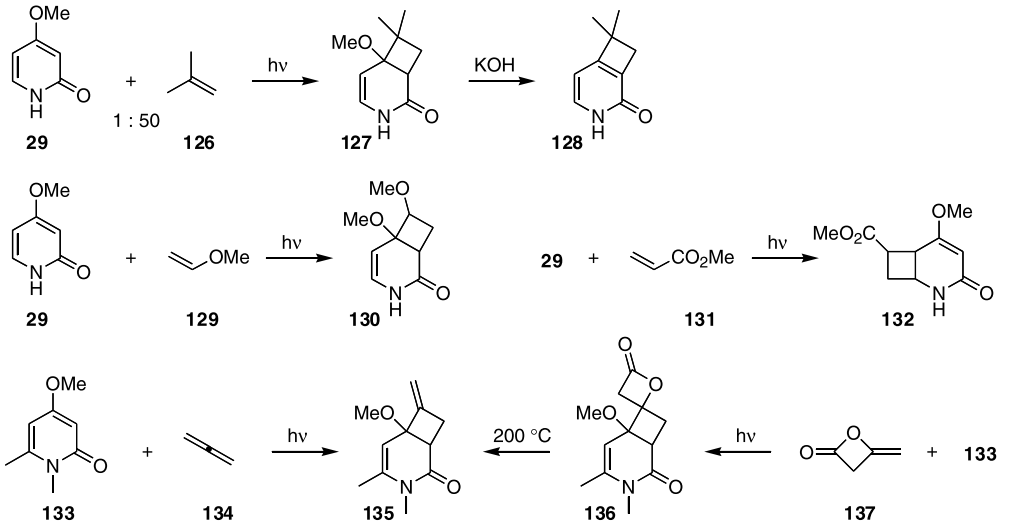

SCHEME 12 Cycloaddition of 4-alkoxy-2-pyridones with alkenes.[68–72]

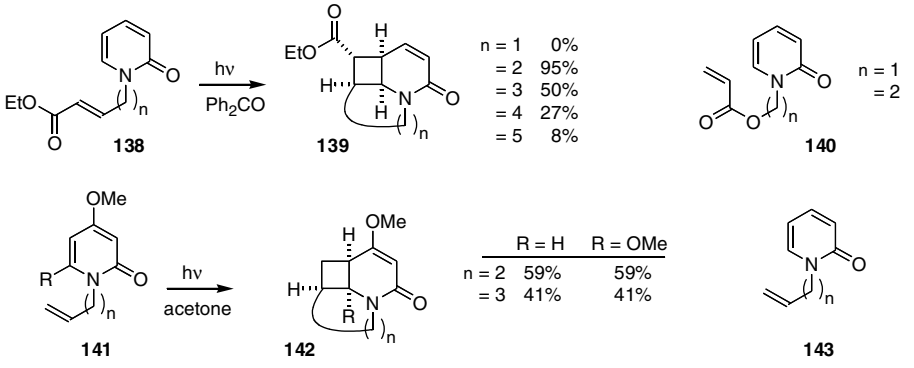

SCHEME 13 Intramolecular [2+2]-cycloadditions of 2-pyridones.[73–75]

nitrogen, **141**.[73] Both 4-methoxy and 4,6-dimethoxy substitution are acceptable. Similar pyridones **143** lacking the alkoxy groups do not undergo cycloaddition.[73]

Other Reactions

Substituent Effects

When 2-pyridone carries a chlorine or a bromine at C6 (**31**), irradiation leads to electrocyclic ring opening to give **144** (Scheme 14). The observed products are consistent with elimination of HCl and addition of methanol to a ketene. Both (*E*)-and (*Z*)-**146** as well as (*E*)-**147** are isolated.[27]

Pyridones carrying an *N*-alkenyl substituent such as **94** photodimerize (Figure 103.1) and photoisomerize (Figure 103.5),[18] but in water the alkene undergoes hydration to give **149**.[18,76] Performance of this reaction in the presence of perchloric acid leads to an isolable intermediate **148**. When the alkene is a styrene, (*E*),(*Z*)-isomerization and stilbene-like cyclization reactions are also observed.[77,78]

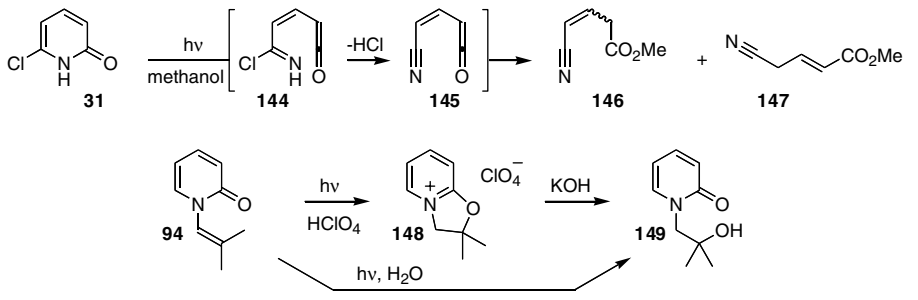

SCHEME 14 Photoisomerization of 6-chloro-2-pyridone[27] and photohydration of *N*-alkenyl pyridones.[18,76]

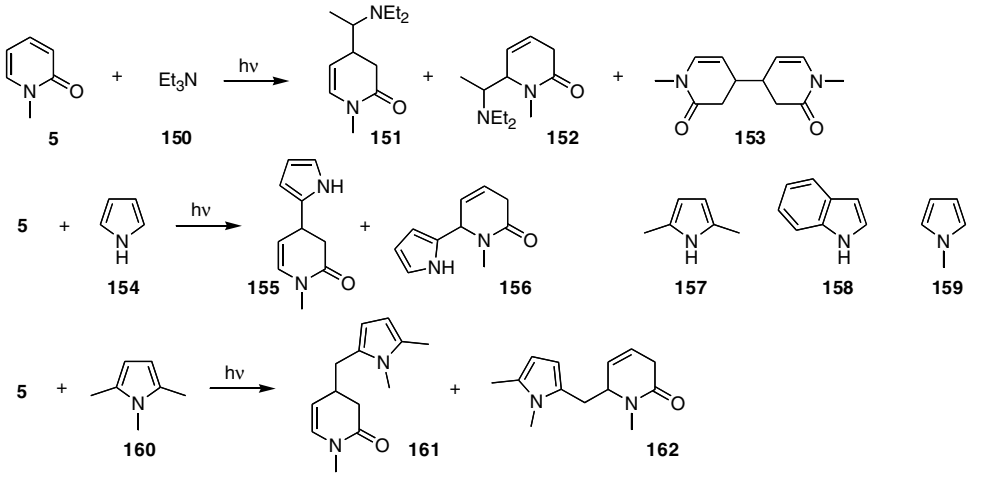

SCHEME 15 Photoreaction of 2-pyridone with aliphatic and heterocyclic amines.[79–81]

Pyridones with Aliphatic and Aromatic Amines

Photoreaction of 2-pyridone with aliphatic and aromatic amines leads to addition of the amines at C4 and C6 to give mixtures of dihydropyridone products (Scheme 15). All of these reactions appear to derive from a single electron transfer process. Tertiary aliphatic amines such as triethylamine **150** yield pyridones **151** and **152** (2:1) plus the reductively coupled pyridone dimer **153**.[79] Pyrrole **154** leads to a similar mixture of 4- and 6-substituted dihydropyridones **155** and **156** (1:1).[80] Dimethylpyrrole **157** and indole **158** lead to analogous products of 4- and 6-substition of the pyridone (at C3 of the pyrrole **157**). *N*-Methyl pyrrole **159**, however, does not yield photoproducts. When the *N*-methyl pyrrole is alkyl substituted at C2 (**160**), addition to the pyridone yields **161** and **162** (1:1).[81]

Pyridones with Singlet Oxygen

The addition of singlet oxygen to 2-pyridones leads to oxygenated products derived from intermediates **163** (Scheme 16). All reported examples carry alkyl substitution of the pyridone at C3 (**164**) or C6 (**26**). Acidic hydrolysis (methanolysis) of these intermediates yield dicarbonyl products **165** and **166**.[82]

N-Heteroatom Pyridones

When the pyridone carries an *N*-heteroatom group, homolytic cleavage occurs.[83,84] Irradiation of benzyloxy pyridone **167** leads to quantitative formation of **168** and benzaldehyde. The *N*-piperidinyl **170**

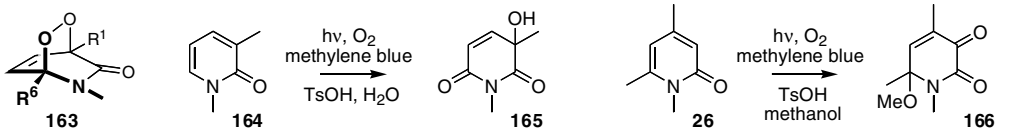

SCHEME 16 Singlet oxygen addition to 2-pyridones.[82]

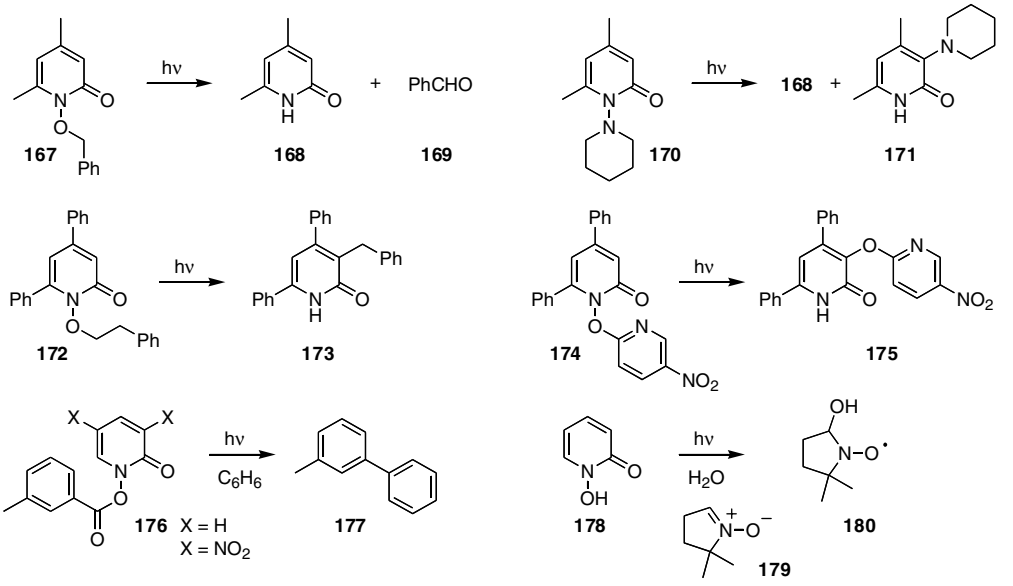

SCHEME 17 Homolytic photocleavage of *n*-alkoxy-2-pyridones.[83–91]

also yields **168**, plus 3-piperidiyl pyridone **171**.[83] A broad survey of this reaction, employing 4,6-diphenylpyridones such as **172** and **174** found similar products.[85,86] A singlet excited state is the source of the N–O bond cleavage.[87] With benzene as solvent, the cleavage can be used to generate and trap aryl radicals, leading to biphenyl synthesis from **176** in good to moderate yields. The dinitropyridone gave somewhat higher yields.[88] Irradiation of *N*-hydroxy pyridone **178** generates hydroxyl radical cleanly and with solvent dependent quantum yields of 0.25 to 0.6.[89] The hydroxyl radical can be trapped with the spin trap **179** and has been shown to damage DNA.[90,91]

103.3 4-Pyridone Photochemistry

In contrast to 2-pyridones, 4-pyridones have little productive chemistry. Both **181a** and **181b** are reported to be unreactive.[92] Nicotinamide metabolite **182** has been found to interact photochemically with cellulose to yield a fluorescent product and in alcohol solution to give an aldehyde.[93,94] When two 4-pyridones are held in close proximity, **183**, a [2+2]-photocycloaddition occurs.[95] Product **184** is not photostable, with ambient light promoting photocleavage to return **183**.

The 4-pyridones can also isomerize to 2-pyridones. For the 1,2,6-trimethyl-3,5-diaryl-4-pyridones such as **185**, the isomerization to **186** and **187** occurs from the singlet excited state[96–98] (Scheme 18).

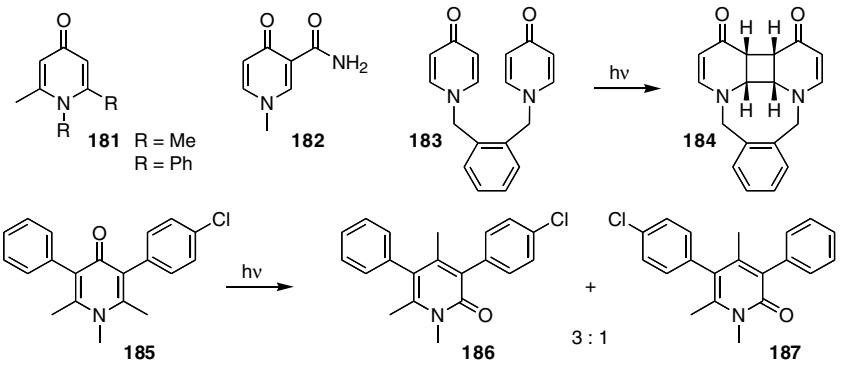

SCHEME 18 Photochemistry of 4-pyridones.[92–98]

References

1. Schönberg, A., Photodimerizations involving formation of eight-membered rings, in *Preparative Organic Photochemistry,* Springer-Verlag, New York, 1968, 97–104.
2. Trecker, D.J., Photodimerizations, *Org. Photochem.,* 2, 63–116, 1969.
3. Tieckelmann, H., Pyridinols and pyridones, in *Heterocyclic Compounds*, Abramovitch, R.A., Ed., John Wiley & Sons, New York, 1974, 597–1180.
4. McCullough, J.J., Photoadditions of aromatic compounds, *Chem. Rev.,* 87, 811–860, 1987.
5. Bouas-Laurent, H. and Desvergne, J.-P., Cycloaddition reactions involving 4n electrons: (4+4) cycloaddition reactions between unsaturated conjugated systems, in *Photochromism: Molecules and Systems*, Dürr, H. and Bouas-Laurent, H., Eds., Elsevier, New York, 1990, 561–630.
6. Sieburth, S. McN., The Inter- and intramolecular [4 + 4]-photocycloaddition of 2-pyridones and its application to natural product synthesis, in *Advances in Cycloaddition*, Harmata, M., Ed., JAI, Greenwich, CT, 1999, 85–118.
7. Afarinkia, K., Vinader, V., Nelson, T.D., and Posner, G.H., Diels-Alder cycloadditions of 2-pyrones and 2-pyridones, *Tetrahedron,* 48, 9111–9171, 1992.
8. Beak, P., Energies and alkylations of tautomeric heterocyclic compounds: old problems — new answers, *Acc. Chem. Res.,* 10, 186–192, 1977.
9. Wong, M.W., Wiberg, K.B., and Frisch, M.J., Solvent effects. 3. Tautomeric equilibria of formamide and 2-pyridone in the gas phase and solution: an *ab initio* SCRF study, *J. Am. Chem. Soc.,* 114, 1645–1652, 1992.
10. Johnson, C.D., Pyridines and their benzo derivatives: structure, in *Comprehensive Heterocyclic Chemistry II*, Katritzky, A.R., Rees, C.W., and Scriven, E.F.V., Eds., Pergamon, New York, 1996, 1–36.
11. Sobolewski, A.L. and Adamowicz, L., Photophysics of 2-hydroxypyridine: an *ab initio* study, *J. Phys. Chem.,* 100, 3933–3941, 1996.
12. Lapinski, L., Nowak, M.J., Fulara, J., Les, A., and Adamowicz, L., Relation between structure and tautomerism in diazinones and diazinethiones: an experimental matrix isolation and theoretical *ab initio* study, *J. Phys. Chem.,* 96, 6250–6254, 1992.
13. Taylor, E.C. and Paudler, W.W., Photodimerization of some α,β-unsaturated lactams, *Tetrahedron Lett.,* No. 25, 1–3, 1960.
14. Sharp, L.J., IV and Hammond, G.S., Photoreactions of N-methyl-2-pyridone, *Mol. Photochem.,* 2, 225–250, 1970.
15. Southern New England Ultraviolet, 550 E Main St # 29, Branford, CT 06405.
16. Nakamura, Y., Kato, T., and Morita, Y., Structures of the four possible [4+4]-cycloaddition products formed on photodimerization of *N*-alkyl-2-pyridones, *J. Chem. Soc., Perkin Trans. 1*, 1187–1191, 1982.

17. Matsushima, R. and Terada, K., Photoreactions of alkylated 2-pyridones, *J. Chem. Soc., Perkin Trans. 2*, 1445–1448, 1985.
18. Mariano, P.S. and Leone, A.A., Excited-state chemistry of 1-alkenyl-2-pyridones. exploratory and mechanistic investigations and kinetic analysis of photocyclization reactions involving conversion of the *N*-vinylamide to oxazolium ylide function, *J. Am. Chem. Soc.,* 101, 3607–3617, 1979.
19. Dilling, W.L., Tefertiller, N.B., and Mitchell, A.B., Organic photochemistry. xii. the photodimerization and photoisomerization of 2-pyridone and its monochloro derivatives, *Mol. Photochem.,* 5, 371–409, 1973.
20. Paquette, L.A. and Slomp, G., Derivatives of *trans*-3,7-diazatricyclo[4.2.2.$2^{2,5}$]dodecane, *J. Am. Chem. Soc.,* 85, 765–769, 1963.
21. Taylor, E.C. and Kan, R.O., Photochemical dimerization of 2-aminopyridines and 2-pyridones, *J. Am. Chem. Soc.,* 85, 776–784, 1963.
22. Brown, J.N., Towns, R.L.R., and Trefonas, L.M., Crystal and molecular structure of the photodimer of 5,6,7,8-tetrahydro-2-quinolone, *J. Am. Chem. Soc.,* 93, 7012–7015, 1971.
23. Meyers, A.I. and Singh, P., Photoaddition of diphenylacetylene to tetrahydro-2-quinolones, *J. Org. Chem.,* 35, 3022–3030, 1970.
24. Meyers, A.I. and Singh, P., Photocycloaddition of diphenylacetylene to a 2-pyridone, *J. Chem. Soc., Chem. Commun.*, 576–577, 1968.
25. De Selms, R.C. and Schleigh, W.R., Heterocyclodieneone photochemistry I. Photo-2-pyridone (2-Aza-3-oxobicyclo[2.2.0]hex-5-ene), *Tetrahedron Lett.,* 3563–3566, 1972.
26. Nakano, H. and Hongo, H., Synthesis and high-pressure Diels-Alder cycloadditions of 6-methoxycarbonyl-3-oxo-2-azabicyclo[2.2.0]hex-5-ene, *Chem. Pharm. Bull.,* 41, 1885–1887, 1993.
27. Kaneko, C., Fujii, H., and Kato, K., Photochemistry of 6-chloro-2-pyridones: the first example for electrocyclic ring opening of the pyridone ring system, *Heterocycles,* 17, 395–400, 1982.
28. Sieburth, S. McN. and Lin, C.-H., Intermolecularly selective [4+4]-photocycloaddition of 2-pyridone mixtures, *Tetrahedron Lett.,* 37, 1141–1144, 1996.
29. Sieburth, S. McN., Lin, C.-H., and Rucando, D., Selective intermolecular photo-[4 + 4]-cycloaddition with 2-pyridone mixtures. 2. Preparation of (1α,2β,5β,6α)-3-butyl-9-methoxy-3,7-diazatricyclo[4.2.2.$2^{2,5}$]dodeca-9,11-diene-4,8-dione, *J. Org. Chem.,* 64, 950–953, 1999.
30. Kato, T. and Nakamura, Y., Micellar alignment effect on the photodimerization of 2-pyridones, *Heterocycles,* 16, 135, 1981.
31. Nakamura, Y., Kato, T., and Morita, Y., A micellar alignment effect in the photodimerizations of *N*-ω-carboxyalkyl-2-pyridones and their 4-alkyl derivatives in micelle or reversed micelle, *Tetrahedron Lett.,* 22, 1025–1028, 1981.
32. Kato, T., Nakamura, Y., and Morita, Y., Reactions using micellar systems. IV. Regioselectivity in the photodimerizations of 2-pyridones in micelles and reversed micelles, *Chem. Pharm. Bull.,* 31, 2552–2563, 1983.
33. Toda, F. and Tanaka, K., Enantioselective photoconversion of pyridones into β-lactam derivatives in inclusion complexes with optically active host compounds, *Tetrahedron Lett.,* 29, 4299–4302, 1988.
34. Sieburth, S. McN., Hiel, G., Lin, C.-H., and Kuan, D.P., Intramolecular [4+4]-photocycloaddition of 2-pyridones tethered by a three-carbon chain: studies on the formation of cycloadducts and control of stereogenesis 3, *J. Org. Chem.,* 59, 80–87, 1994.
35. Sieburth, S. McN. and Lin, C.-H., Stereocontrol of 2-pyridone [4+4]-photocycloaddition: a thermal-photochemical cycle to produce exclusively trans cycloadducts, *J. Org. Chem.,* 59, 3597–3599, 1994.
36. Sieburth, S. McN., Boat *versus* half-chair cyclohexyl rings: determinants of conformational preference, *J. Chem. Soc., Chem. Commun.*, 1663–1664, 1994.
37. Sieburth, S. McN., Chen, J., Ravindran, K., and Chen, J.-l., A 2-pyridone photo-[4 + 4]-approach to the taxanes, *J. Am. Chem. Soc.,* 118, 10803–10810, 1996.

38. Sieburth, S. McN., McGee Jr., K.F., and Al-Tel, T.H., Fusicoccin ring system by [4 + 4]-cycloaddition. control of diastereoselectivity through hydrogen bonding, *J. Am. Chem. Soc.,* 120, 587–588, 1998.
39. Sieburth, S. McN. and McGee, K.F., Jr., Solvent-dependent stereoselectivity of bis-2-pyridone [4 + 4]-photocycloaddition is due to H-bonded dimers, *Org. Lett.,* 1, 1775–1777, 1999.
40. McGee, K.F., Jr., Al-Tel, T.H., and Sieburth, S. McN., Fusicoccin synthesis by intramolecular [4+4]-photocycloaddition of 2-pyridones: stereocontrol of the cycloaddition and elaboration of the pentacyclic product, *Synthesis*, 1185–1196, 2001.
41. Sieburth, S. McN. and Siegel, B., Tether-enforced reversal of regioselectivity: head-to-head [4 + 4]-photocycloaddition of 2-pyridones, *J. Chem. Soc., Chem. Commun.*, 2249–2250, 1996.
42. Li, T., Yin, T., and. Sieburth, S. McN., SUNY Stony Brook, unpublished results.
43. Al-Tel, T.H., Qiu, Z., and Sieburth, S. McN., SUNY Stony Brook, unpublished results.
44. Nakamura, Y., Zsindely, J., and Schmid, H., Photocyclisierungen von 1,1′-Polymethylen-di-2-pyridonen, *Helv. Chim. Acta,* 59, 2841–2854, 1976.
45. Nagano, T., Hirobe, M., Itoh, M., and Okamoto, T., Reversible photodimerization of 2-methyl-s-triazolo[1,5-a]pyridines, *Tetrahedron Lett.*, 3815–3818, 1975.
46. Nagano, T., Hirobe, M., and Okamoto, T., [4πs + 4πs]-Photocycloadditions of 2-methyl-s-triazolo[1,5-a]pyridines to pyridones, *Tetrahedron Lett.,* 3891–3894, 1977.
47. Sieburth, S. McN., McGee, K.F., Jr., Zhang, F., and Chen, Y., Photoreactivity of 2-pyridones with furan, benzene and naphthalene. Inter- and intramolecular photocycloadditions, *J. Org. Chem.,* 65, 1972–1977, 2000.
48. Sato, E., Ikeda, Y., and Kanaoka, Y., Photoaddition of 2-pyridones to conjugated dienes, *Heterocycles,* 28, 117–120, 1989.
49. Sato, E., Ikeda, Y., and Kanaoka, Y., Photoaddition of 2-pyridones and 2-quinolones to conjugated dienes, *Liebigs Ann. Chem.*, 781–788, 1989.
50. Bach, T., Bergmann, H., and Harms, K., Enantioselective photochemical reactions of 2-pyridones in solution, *Org. Lett.,* 3, 601–603, 2001.
51. Sieburth, S. McN. and Cunard, N.T., The [4+4]-cycloaddition and its strategic application in natural product synthesis, *Tetrahedron,* 52, 6251–6282, 1996.
52. Sieburth, S. McN. and Zhang, F., Intramolecular photocycloaddition of 1,3-dienes with 2-pyridones, *Tetrahedron Lett.,* 40, 3527–3530, 1999.
53. Hongo, H., Iwasa, K., Kabuto, C., Matsuzaki, H., and Nakano, H., Preparation of optically active photopyridone by lipase-catalyzed asymmetric resolution, *J. Chem. Soc., Perkin Trans. 1*, 1747–1754, 1997.
54. Furrer, H., Preparation and reactions of 3-oxo-2-azabicyclo[2.2.0]hex-5-enes and of 3-oxo-1,2,4,6-tetramethyl-2,5-diazabicyclo[2.2.0]hexane, *Chem. Ber.,* 105, 2780–2790, 1972.
55. Katagiri, N., Sato, M., Yoneda, N., Saikawa, S., Sakamoto, T., Muto, M., and Kaneko, C., Cycloadditions in syntheses. 28. 2-Azabicyclo[2.2.0]hexan-3,5-dione and its derivatives: synthesis and transformation to azetidin-2-ones., *J. Chem. Soc., Perkin Trans. 1*, 1289–1296, 1986.
56. Wenska, G., Skalski, B., Gdaniec, Z., Adamiak, R.W., Matulic-Adamic, J., and Beigelman, L., Photophysical and photochemical properties of C-linked ribosides of pyridin-2-one, *J. Photochem. Photobiol. A: Chem.,* 133, 169–176, 2000.
57. Kaneko, C., Shiba, K., Fujii, H., and Momose, Y., Syntheses and ring-opening reactions of 5-alkoxy- and 5-acetoxy-3-oxo-2-azabicyclo[2.2.0]hex-5-enes, *J. Chem. Soc., Chem. Commun.*, 1177–1178, 1980.
58. Katagiri, N., Sato, M., Saikawa, S., Sakamoto, T., Muto, M., and Kaneko, C., 2-Azabicyclo[2.2.0]hexane-3,5-dione, a new building block for carbapenem nuclei, *J. Chem. Soc., Chem. Commun.*, 189–190, 1985.
59. Kaneko, C., Katagiri, N., Sato, M., Muto, M., Sakamoto, T., Saikawa, S., Naito, T., and Saito, A., Cycloadditions in syntheses. 27. *rel*-(1*R*,4*R*,5*S*)-5-hydroxy-2-azabicyclo[2.2.0]hexan-3-one and its

derivatives: synthesis and transformation to azetidin-2-ones., *J. Chem. Soc., Perkin Trans. 1*, 1283–1288, 1986.
60. Nakano, H., Iwasa, K., Kabuto, C., Matsuzaki, H., and Hongo, H., Lipase catalyzed resolution and absolute configuration of photopyridones, *Chem. Pharm. Bull.,* 43, 1254–1256, 1995.
61. Wu, L.-C., Cheer, C.J., Olovsson, G., Scheffer, J.R., Trotter, J., Wang, S.-L., and Liao, F.-L., Crystal engineering for absolute asymmetric synthesis through the use os *meta*-substituted aryl groups, *Tetrahedron Lett.,* 38, 3135–3138, 1997.
62. Garcia-Garibay, M.A., Houk, K.N., Keating, A.E., Cheer, C.J., Leibovitch, M., Scheffer, J.R., and Wu, L.-C., Computational prediction of the enantioselectivity of a solid-state photoreaction, *Org. Lett.,* 1, 1279–1281, 1999.
63. Somekawa, K., Shimou, T., Tanaka, K., and Kumamoto, S., A novel type of adducts in the photochemical reactions of 2-pyridones with cyanoethylenes, *Chem. Lett.*, 45–46, 1975.
64. Suishu, T., Tsuru, S., Shimo, T., and Somekawa, K., Singlet and triplet photocycloaddition reactions of 2-pyridones with propenoate and 2,4-pentadienoates and the frontier molecular orbital analysis, *J. Heterocycl. Chem.,* 34, 1005–1011, 1997.
65. Somekawa, K., Imai, R., Furukido, R., and Kumamoto, S., Photoadducts of 2-pyridones with chloroethylenes and their derivatives, *Bull. Chem. Soc. Jpn.,* 54, 1112–1116, 1981.
66. Somekawa, K., Okumura, Y., Uchida, K., and Shimo, T., Preparation of 2-azabicyclo[2.2.2]octa-5,7-dien-3-ones and 7-azabicyclo[4.2.0]octa-2,4-dien-8-ones *via* addition reactions of 2-pyridones, *J. Heterocycl. Chem.,* 25, 731–734, 1988.
67. Meyers, A.I. and Singh, P., Photocycloaddition to 2-pyridones. II. Photoisomerization of an azahomoquadricyclane to a cyclobutenopyridone, *Tetrahedron Lett.*, 4073–4076, 1968.
68. Fujii, H., Shiba, K., and Kaneko, C., Photocycloadditions of 4-methoxy-2-pyridone to olefins and synthesis of 1,2-dihydrocyclobuta[c]pyridin-3(4*H*)-ones, *J. Chem. Soc., Chem. Commun.*, 537–538, 1980.
69. Kaneko, C., Momose, Y., Maeda, T., Naito, T., and Somei, M., Reactions of 6-methoxy-3-azabicyclo[4.2.0]octan-2-one and its 7-substituted derivatives, *Heterocycles,* 20, 2169–2172, 1983.
70. Kaneko, C., Naito, T., Momose, Y., Shimomura, N., Ohashi, T., and Somei, M., A novel three-carbon annelation method for pyridine derivatives, *Chem. Pharm. Bull.,* 31, 2168–2171, 1983.
71. Kaneko, C., Shimomura, N., Momose, Y., and Naito, T., Photocycloaddition of 4-methoxyquinolin-2(1H)-one and related compounds to allene: synthesis of 1-methylene-1,2-dihydrocyclobuta[c]quinolin-3(4*H*)-one and related compounds, *Chem. Lett.*, 1239–1242, 1983.
72. Chiba, T., Kato, T., Yoshida, A., Moroi, R., Shimomura, N., Momose, Y., Naito, T., and Kaneko, C., Photoaddition of 2-quinolone and 2-pyridone derivatives to diketene: on the regioselectivity of the photoaddition, *Chem. Pharm. Bull.,* 32, 4707–4720, 1984.
73. Kaneko, C., Uchiyama, K., Sato, M., and Katagiri, N., Novel annelation method to pyridine and isoquinoline by photochemical means, *Chem. Pharm. Bull.,* 34, 3658–3671, 1986.
74. Somekawa, K., Okuhira, H., Sendayama, M., Suishu, T., and Shimo, T., Intramolecular [2 + 2] photocycloadditions of 1-(ω-alkenyl)-2-pyridones possessing an ester group on the olefinic carbon chain, *J. Org. Chem.,* 57, 5708–5712, 1992.
75. Kaneko, C., Suzuki, T., Sato, M., and Naito, T., Cycloadditions in syntheses. XXXII. Intramolecular photocycloaddition of 4-(ω-alkenyloxy)quinolin-2-(1*H*)-one: Synthesis of 2-substituted cyclobuta[*c*]quinolin-3(4*H*)-ones, *Chem. Pharm. Bull.,* 35, 112–123, 1987.
76. Mariano, P.S. and Leone, A., Kinetic analysis and solvent polarity effects on the ylide-forming photocyclization reaction of 1-vinyl-2-pyridones, *J. Am. Chem. Soc.,* 100, 3947–3949, 1978.
77. Mariano, P.S., Leone, A.A., and Krochmal, E., Jr., Novel Photocyclization Reactions of 1-vinyl-2-pyridones leading to oxazolo[3,2-a]pyridinium salts, *Tetrahedron Lett.,* 2227–2230, 1977.
78. Mariano, P.S., Krochmal, E., Jr., and Leone, A., Stilbene like photocyclizations of 1-phenylvinyl-2-pyridinones. Preparation of 4H-benzo[a]quinolizin-4-ones, *J. Org. Chem.,* 42, 1122–1125, 1977.

79. Ohmiya, S., Noguchi, M., Chen, C.Y., Murakoshi, I., and Otomasu, H., Intermolecular photoaddition reaction of aliphatic *tert*-amines to *N*-alkyl-2-pyridones, *Chem. Pharm. Bull.,* 37, 2516–2518, 1989.
80. Ohmiya, S., Noguchi, M., Ina, S., Kubo, H., and Otomasu, H., Photoaddition reaction of pyrroles and indoles to *N*-methyl-2-pyridone, *Chem. Pharm. Bull.,* 40, 854–857, 1992.
81. Sakurai, N. and Ohmiya, S., Photoaddition reaction of 1,2-dialkylindoles and -pyrroles to 1-methyl-2-pyridone *via* proton transfer from the 2-methylene group of the indole or pyrrole, *J. Chem. Soc., Chem. Commun.*, 297–298, 1993.
82. Sato, E., Ikeda, Y., and Kanaoka, Y., Photosensitized oxygenation of 2-pyridones, *Heterocycles,* 25, 65–68, 1987.
83. Furrer, H., Photochemistry of 1-alkoxy- and 1-dialkylamino-2-pyridones, *Tetrahedron Lett.*, 2953–2956, 1974.
84. Yoshioka, N. Andoh, C., Kubo, K., Igarashi, T., and Sakurai, T., Competitive occurrence of homolytic N-O and-heterolytic C-O bond cleavage in excited-state 1-(arylmethyloxy)-2-pyridones, *J. Chem. Soc., Perkin Trans. 2*, 1927–1932, 2001.
85. Katritzky, A.R., Chapman, A.V., Cook, M.J., and Millet, G.H., Novel thermal and photochemical rearrangements of *N*-substituted 2-pyridones, *J. Chem. Soc., Chem. Commun.*, 395–396, 1979.
86. Katritzky, A.R., Chapman, A.V., Cook, M.J., and Millet, G.H., *N*-Oxides and related compounds. 60. Novel thermal and photochemical rearrangements of *N*-substituted 2-pyridones, *J. Chem. Soc., Perkin Trans. 1*, 2743–2754, 1980.
87. Sakurai, T., Obana, T., Inagaki, T., and Inoue, H., Internal and external heavy-atom effects on the photolysis of 1-benzyloxy-2-pyridone, *J. Chem. Soc., Perkin Trans. 2*, 535–538, 1989.
88. Taylor, E.C., Altland, H.W., Kienzle, F., and McKillop, A., Thallium in organic synthesis. XLI. Synthesis of 1-substituted 2(1*H*)-pyridones. New synthesis of unsymmetrical biphenyls *via* photochemical nitrogen-oxygen bond cleavage of 1-aroyloxy-2(1*H*)-pyridones, *J. Org. Chem.,* 41, 24–27, 1976.
89. Aveline, B.M., Kochevar, I.E., and Redmond, R.W., Photochemistry of N-hydroxy-2(1*H*)-pyridone, a more selective source of hydroxyl radicals than *N*-hydroxypyridine-2(1*H*)-thione, *J. Am. Chem. Soc.,* 118, 10124–10133, 1996.
90. Adam, W., Marquardt, S., and Saha-Moller, C.R., Oxidative DNA damage in the photolysis of *N*-hydroxy-2-pyridone, a specific hydroxyl-radical source, *Photochem. Photobiol.,* 70, 287–291, 1999.
91. Adam, W., Hartung, J., Okamoto, H., Marquardt, S., Nau, W.M., Pischel, U., Saha-Möller, C.R., and Spehar, K., Photochemistry of N-isopropoxy-substituted 2(1*H*)-pyridone and 4-*p*-tolylthiazole-2(3*H*)-thione: alkoxyl-radical release (spin-trapping, EPR and transient spectroscopy) and its significance in the photooxidative induction of DNA strand breaks, *J. Org. Chem.,* 67, 6041–6049, 2002.
92. Sugiyama, N., Sato, Y., and Kashima, C., Photoreaction of 2,6-diphenyl-4*H*-thiopyran-4-one and its related compounds, *Bull. Chem. Soc. Jpn.,* 43, 3205–3209, 1970.
93. Abelson, D. and Boyle, A., Photochemistry of a nicotinamide metabolite, N'-methyl-4-pyridone-3-carboxamide, *Nature (London),* 197, 460–462, 1963.
94. Abelson, D., Parthe, E., Lee, K.W., and Boyle, A., Spectral and biological changes induced in nicotinic acid and related compounds by ultraviolet light, *Biochem. J.,* 96, 840–852, 1965.
95. Johnson, B.L., Kitahara, Y., Weakley, T.J.R., and Keana, J.F.W., Intramolecular [2+2]-photocycloaddition of juxtaposed 4-pyridone moieties, *Tetrahedron Lett.,* 34, 5555–5558, 1993.
96. Ishibe, N. and Masui, J., Photoisomerization of 4-pyridones to 2-pyridones, *J. Am. Chem. Soc.,* 96, 1152–1158, 1974.
97. Ishibe, N. and Yutaka, S., Heavy-atom effect in photoisomerization of 4-pyrones and 4-pyridones, *J. Org. Chem.,* 43, 2138–2143, 1978.
98. Ishibe, N., Yutaka, S., Masui, J., and Ihda, N., Substituent effect on selectivity in photoisomerization of 4-pyrones and 4-pyridones, *J. Org. Chem.,* 43, 2144–2148, 1978.

104

Reversible Photodimerization of Pyrimidine Bases

Yoshiaki Inaki
Osaka University

104.1 Photochemistry of DNA

UV irradiation of DNA is known to cause damage to the genetic information. DNA contains four nucleic acid bases where purine bases such as adenine and guanine are stable to UV light, but pyrimidine bases of thymine (uracil in RNA) and cytosine are unstable to UV light. Thymine bases in DNA undergo photodimerization via UVirradiation at 270 nm to form the photodimer. The photodimerization occurs at a thymidine sequence where the thymine bases stack with each other (Figure 104.1).[1–3] However, the photodimers in DNA are cleaved and regenerated by the action of an enzyme *in vivo*. There are four stereoisomeric dimers possible by linkage of two thymines to form a cyclobutane ring across the C5–C6 double bonds: *cis-syn*, *cis-anti*, *trans-syn*, and *trans-anti* (Figure 104.2).[4–7] The photodimerization in solution gives four kinds of isomers, but the photodimer from DNA is only the *cis-syn* isomer (Figure 104.1).

The reversible photoreaction was found to be controlled by the regulation of the UV wavelength. The thymine compound has a UV absorption with a high extinction coefficient at 270 nm. The absorbance

0-8493-1348-1/04/$0.00+$1.50

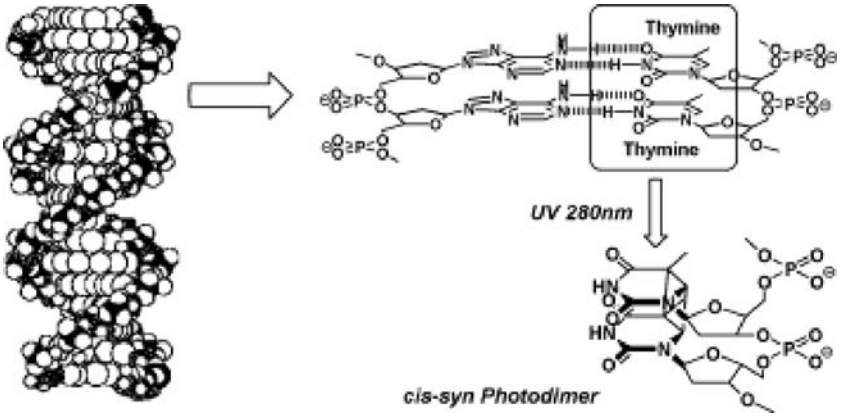

FIGURE 104.1 Photodimerization of thymine in DNA.

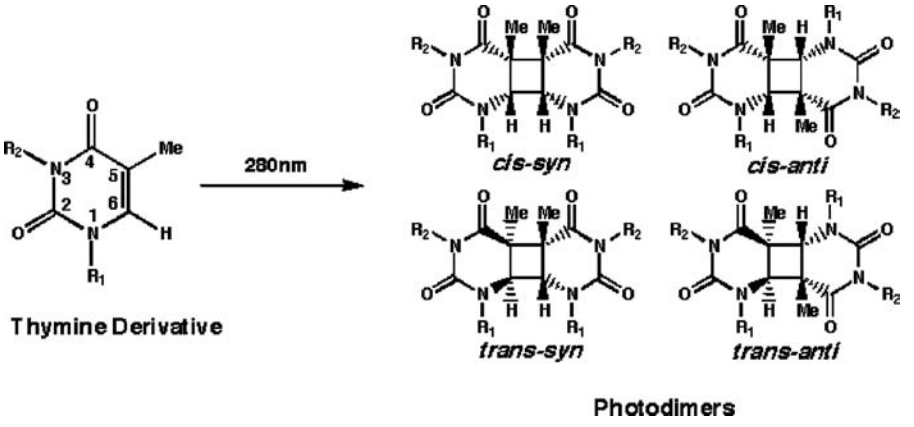

FIGURE 104.2 Isomers of thymine photodimers formed in solution.

of the thymine bases at 270 nm decreases on photodimerization, but increases again by the photosplitting of the photodimer on irradiation at short wavelength around 240 nm (Figure 104.3). Using white light, the photoreaction will be saturated below 100% conversion because the photodimerization is an equilibrium reaction and a photostationary state is achieved. If monochromatic UV light of 270 nm or UV light with wavelengths above 270 nm, using a cut-off filter, the photodimerization gives one photodimer. The driving force for the photosplitting reaction of the thymine photodimer is the steric repulsions of the methyl groups at C5 of the thymine. However, photosplitting is not observed for the photodimer of uracil, which has no methyl group at C5. The wavelength of 240 nm is the isosbestic point of the thymine and the thymine photodimer, and the quantum yield of the photosplitting reaction is very high (*ca.* 1). Therefore, UV irradiation at 240 nm of the photodimer causes complete photosplitting.

Thymine derivatives[8–11] are very resistant to UV irradiation in dilute solution because the triplet state is the precursor of the photodimer and intersystem crossing of thymine is very low.[12–18] The yield of the photodimer in solution is low, but a high yield of photodimer can be obtained with acetone as the sensitizer. In DNA polymers and solid state, however, the photodimerization reaction is fast and proceeds through the singlet state. The photodimerizations of thymine oligomers and polymers were studied in the presence of isoprene as a triplet quencher. The photodimerization of the thymine, monomeric and dimeric model, were quenched by isoprene, but the photodimerization of a polymer with thymine units was not quenched. This result appears to indicate that the photodimerization of aggregated thymine compounds occurs almost completely from the singlet state.[19–29]

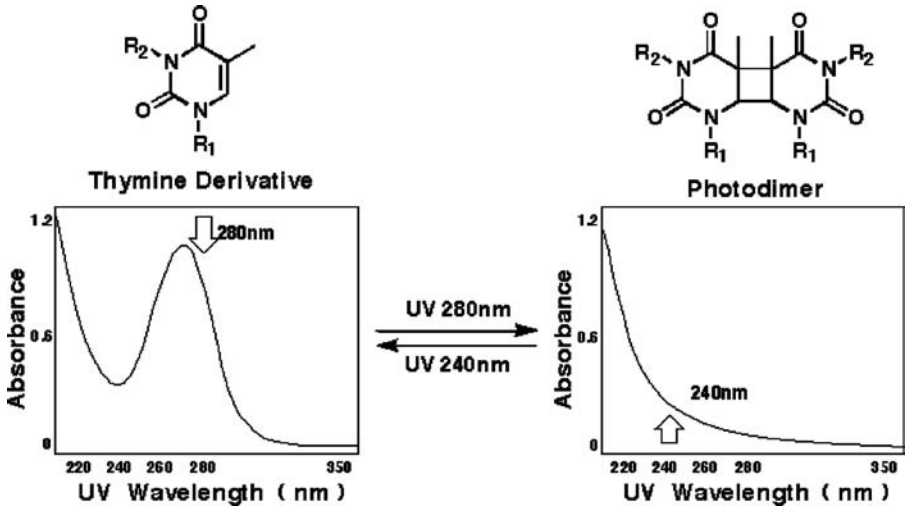

FIGURE 104.3 Reversible photodimerization and UV absorption of thymine derivatives.

The solubility of the thymine derivatives in alkaline solution or organic solvents can be changed by photodimerization or photodissociation. In addition, both the conversions of thymine units to the photodimer and the reverse photoreaction can be followed by monitoring the decrease and increase in absorbance at 270 nm, respectively. The reversible photodimerization of thymine derivatives therefore can be applied to negative or positive type photo-resist materials[30–47] and a photo-recording system by controlling the wavelength of UV light.[48–61] This system may satisfy the requirements for a high-resolution resist or for a high-density photorecording system due to the reversible photoreaction and monitoring in the far-UV. For applications of the thymine system, it is necessary to investigate the reactivity of thymine derivatives in thin solid films.

This chapter deals with the crystal structure and photodimerization reaction of thymine derivatives and the reversible photodimerization reactions in crystals and films.[48–61]

104.2 Photodimerization of 1-Alkylthymine in a Solid Film

Reversible Photodimerization

The photodimerization of thymine is reversible, depending on the wavelength of irradiating UV light. Polymer and monomer derivatives of thymine therefore can be used as reversible photosensitive materials such as reversible photo-resists and reversible photo-recording systems. For high sensitivity and completely reversible photoreactive materials, it is necessary to study the reversible photodimerizations and the conformation of the thymine derivatives in the solid film. There are troublesome problems for these studies. For the investigation of the photodimerization, the thymine compounds need to form a transparent film in an amorphous state. On the other hand, single crystals are necessary for the studies of conformation by x-ray structural analysis. For 1-*n*-alkylthymines and ester derivatives of thymine with long alkyl chains, transparent films and single crystals were obtained as discussed below.

Thymine compounds with long alkyl chains (Figure 104.4) gave the photodimer efficiently in a spin-coat film by irradiation at 280 nm. Figure 104.5 shows a typical repeatable reversible photodimerization of 1-*n*-hexadecylthymine (**C16**) in a solid film. The thin film was obtained by spin coating onto a quartz plate from chloroform solution, followed by drying overnight under reduced pressure. Irradiation with UV light was carried out by a spectro-irradiator (CRM-FA) at 280 nm for dimerization and 240 nm for splitting reactions. The energy irradiated was 8.0 (mJ/count) at 280 nm and 2.0 (mJ/count) at 240 nm. The photodimerization was followed by measuring the UV spectra at 270 nm. Photodimerization of

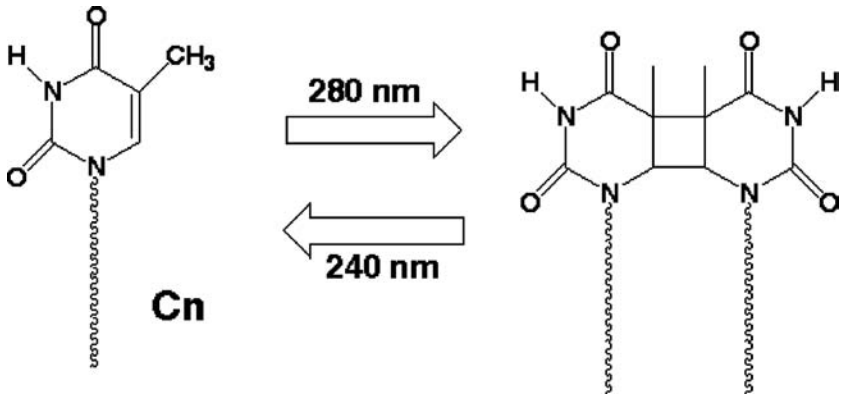

FIGURE 104.4 Reversible photodimerization of the 1-*n*-alkylthymine.

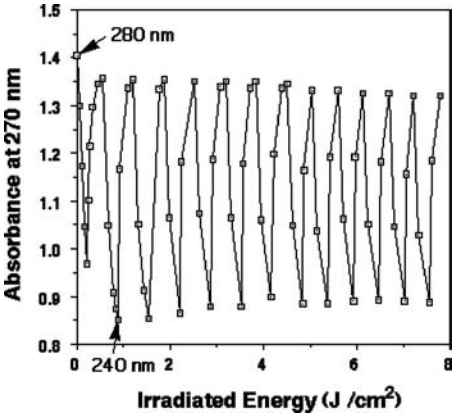

FIGURE 104.5 Typical repeated reversible photodimerization (1-*n*-hexadecylthymine in spin-coated film).

1-*n*-alkylthymine depends on the length of the alkyl chain. The results of the photodimerization are plotted in Figure 104.6. The reaction was fast at the beginning of the reaction but slowed in the later stages. In this case, the decyl (**C10**) compound had the fastest photodimerization reaction rate.

Annealing of the Thin Film

Annealing of the spin-coat film was found to affect the photodimerization of the 1-*n*-alkylthymine. Figure 104.7 is the result of photodimerisation of 1-*n*-tetradecylthymine (**C14**) in a thin film. Annealing for 1 min at 100°C below the melting temperature (123°C) caused an acceleration of the fast photodimerization reaction in the initial reaction stage, but the overall conversion decreased (Figure 104.7b). The photodimerization did not occur in the film after annealing for 4 min (Figure 104.7e). This finding suggests that annealing for 1 min enhanced the reactive site for the fast reaction in the film. However, annealing for 4 min changed the system to an inactive site.

Powder X-ray Diffraction

The powder x-ray diffraction (XRD) was measured for the spin-coat film of 1-*n*-tetradecylthymine (**C14**) and the annealed films (Figure 104.8). The spin-coat film had only a broad peak (a), suggesting an amorphous state. New peaks appeared on annealing the film for 1 min (b) the large peak at $2\theta = 4.360°$

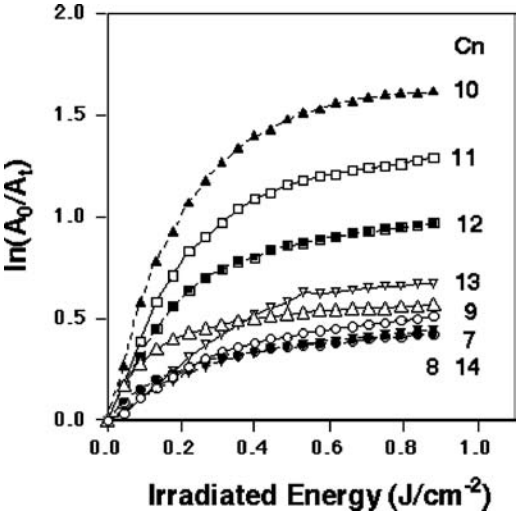

FIGURE 104.6 First rates of photodimerization for heptyl (**C7**) to tetradecyl (**C14**) derivatives of thymine.

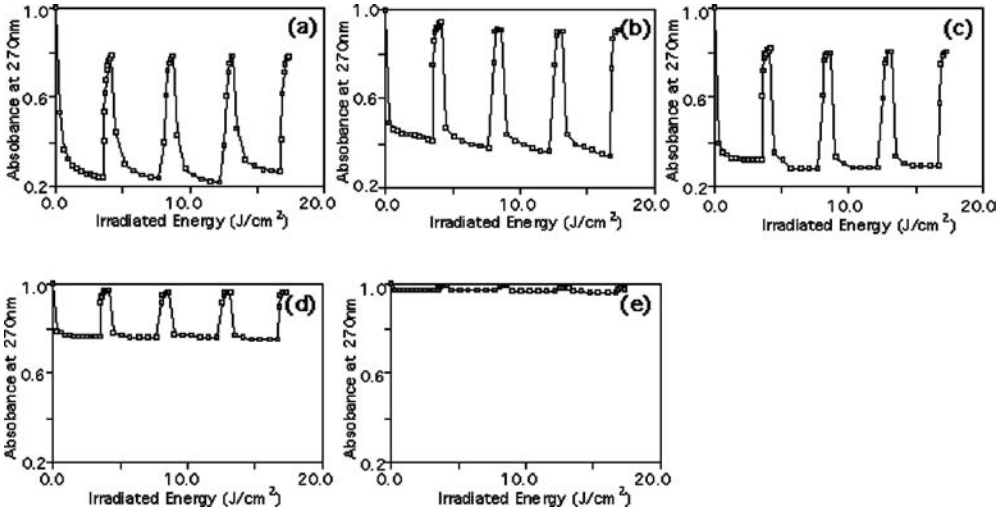

FIGURE 104.7 Reversible photodimerization on thin films in several annealing times for 1-*n*-tetradecylthymine. Annealing time (min): a: 0, b: 1, c: 2, d: 3, and e: 4.

on low angle and small peaks at 8.660°, 17.320°, 21.680°, and 26.080°. By additional annealing for 1 min, all peaks grew larger and the crystalline parts increased (c). Moreover, new peaks at $2\theta = 4.800$Åã and 9.620° appeared. These new peaks indicated that the thin film already had begun to shift to the next structure. After annealing for 3 min, the first five peaks derived from the first structure became smaller and the two new peaks grew bigger (d). For the 4-min annealed thin film, the peak at $2\theta = 4.360°$ was quite small and other four peaks on a higher angle disappeared gradually (e). Finally the first five peaks vanished completely and only the two peaks at $2\theta = 4.800°$ and 9.620° remained (f, annealing for 5 min). Annealing of the amorphous state of the spin-coat film caused crystallization of the thymine compound to give **Structure I**, which is very active toward photodimerization. Prolonged annealing, however, causes deformation of **Structure I** to **Structure II**, which is inactive for the photodimerization.

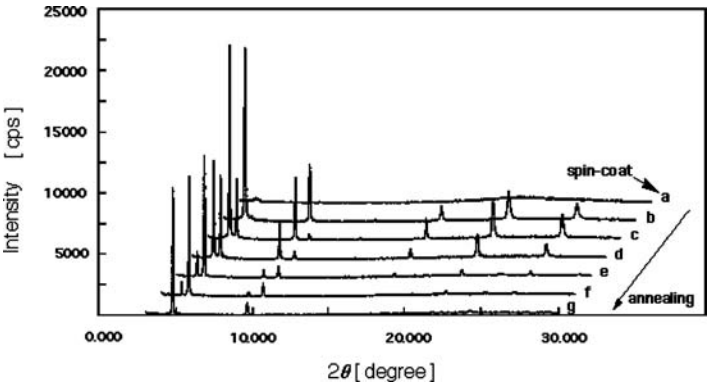

FIGURE 104.8 X-ray powder diffraction on thin films in several annealing times for 1-*n*-tetradecylthymine. Annealing time (min): a: 0, b: 1, c: 2, d: 3, e: 4, f: 5, and g: 10.

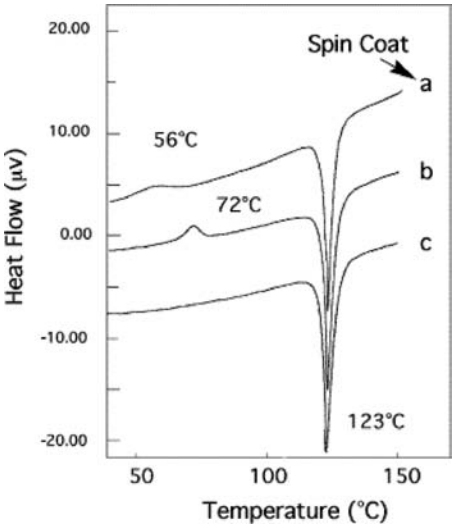

FIGURE 104.9 Differential thermal analysis of thin film for 1-*n*-tetradecylthymine in several annealing times. a: 0 min (spin-coated), b: 2 min, and c: 10 min's annealing.

Thermal Analysis of the Thin Films

Each transition point of the amorphous state to **Structure I** and **Structure I** to **Structure II** was obtained by a differential thermal analysis (DTA) study (Figure 104.9). Samples were prepared by removal from the quartz plate. The trace (a), without annealing, shows a broad exothermic peak at around 56°C and a large endothermic peak at 123°C (the melting point). The peak at 56°C should be the crystallization point of **Structure I**. The thin film, after annealing for 1 min (b), shows an exothermic peak at 72°C and the same endothermic peak at 123 °C as the spin-coat film (a). The exothermic peak at 72°C for (b) should be the deformation point from **Structure I** to **Structure II**. Only the endothermic peak at 123°C was observed for the thin film after annealing for 10 min (c). This indicates that **Structure II** is formed and this is confirmed from the powder x-ray analysis in Figure 104.8.

TABLE 104.1 Isomer Ratio of Photodimers for 1-*n*-Tetradecylthymine in Several States

	cis-syn	*cis-anti*	*trans-syn*	*trans-anti*
Solution	0.85	0.76	1.00	0.95
Spin-coated	0.14	0.32	0.98	1.00
2min annealed	0.06	0.16	0.23	1.00

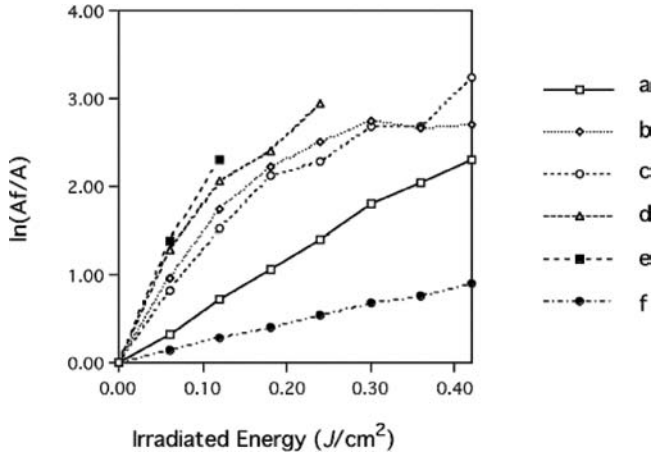

FIGURE 104.10 Splitting rate of photodimer on thin film in several annealing times. Annealing time (min): a: 0, b: 1, c: 2, d: 3, e: 4, and f: spin-coated thin film for *trans-anti* dimer

Isomers of the Photodimers

The photodimerization of thymine in solution gives four isomeric photodimers (Figure 104.2), but the spin-coat film of 1-*n*-alkylthymine from chloroform solution gave the *trans-syn* and *trans-anti* photodimers as the main products (Table 104.1, 1-*n*-tetradecylthymine). On the other hand, the photodimerization of the 2 min annealed film gave only the *trans-anti* photodimer. As mentioned below, the *trans-syn* and *trans-anti* photodimers were obtained by the photodimerization of needles obtained by crystallization from acetonitrile solution. Therefore, the spin-coated film may contain crystals that are the same as the needles from acetonitrile solution. The structure of the thymine in the annealed film may be the same as the plates obtained by crystallization from ethyl acetate solution because the crystals from ethyl acetate gave only the *trans-anti* photodimer.

Reverse Reaction in Spin-Coated Film

Splitting of the photodimer by irradiation at 240 nm also depends on the state of the films. Annealing of the spin-coat film (a to e) caused an acceleration of the reverse reaction as shown in Figure 104.10 for 1-*n*-octylthymine. In the same figure, the results of the reverse reaction for the film prepared from the solution of photodimer (f) obtained by photodimerization of crystal from ethyl acetate are also plotted. This film gave a slower reaction compared to the annealed film. As mentioned below, rotation of the thymines in the crystal during photodimerization may cause strain within the crystal. The strain in the crystal may be the driving force for the reverse reaction. However, the strain in the crystal disappears on dissolution and, therefore, the splitting reaction in solution is slow.

TABLE 104.2 Polymorphism and Properties of 1-*n*-Octylthymine

Crystal Structure	Solvent	Shape	Photo-reaction	Isomers	DSC
Form I	ethyl acetate	plate	Yes	*trans-anti*	108.0, 119.9
Form II	ethanol	plate	No	—	120.1
Form III	acetonitrile	needle	Yes	*trans-anti*, *trans-syn*	59.3, 120.1
Form IV	DMF	plate	No	—	122.6

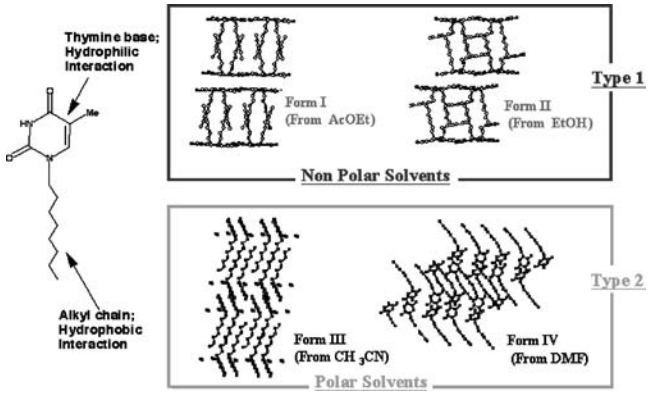

FIGURE 104.11 Formation of crystals in various solvents.

104.3 Crystal Structure and Photodimerisation of 1-Alkylthymine

Solvent Effect on Crystal Structure of 1-*n*-Octylthymine

The polymorphism found in crystals of 1-alkylthymines is related to the length of the alkyl chains and to the solvent used for crystallization. Alkylthymines have two sites for interaction: the thymine base for hydrogen bonding and stacking interactions and the alkyl group for hydrophobic interaction. The polarity of the solvents used for crystallization affects the structure of crystals. Four kinds of crystal structures were found for 1-*n*-octylthymine from x-ray crystal analysis as tabulated in Table 104.2. In less polar solvents (ethyl acetate and ethanol) compared with acetonitrile and DMF, 1-*n*-octylthymine forms **Type 1** crystals (**Form I** and **Form II**) (Figure 104.11).) In the **Type 1** crystals, hydrogen-bonded thymine bases form a plane and the alkyl chains form aggregates to give a bilayer. The bilayers form crystals by the stacking interaction of thymine bases. In the more polar solvents (acetonitrile and DMF), however, 1-*n*-octylthymine forms **Type 2** (**Form III** and **Form IV**) crystals (Figure 104.11). In the **Type 2** crystals, plates of thymine bases are not formed but alkyl chains aggregate regularly. Plates from an ethyl acetate solution (**Form I**) and needles from an acetonitrile solution (**Form III**) gave photodimers. The other crystals (**Forms II** and **IV**) did not give photodimers.

Crystal Obtained from Ethyl Acetate[54]

Photodimerization of 1-*n*-octylthymine in a single crystal obtained from ethyl acetate was very fast and gave only one photodimer. The crystal structure determined by the results of x-ray analysis suggested this to be the *trans-syn* photodimer. However, the photodimer was identified as the *trans-anti* isomer from the NMR spectrum.

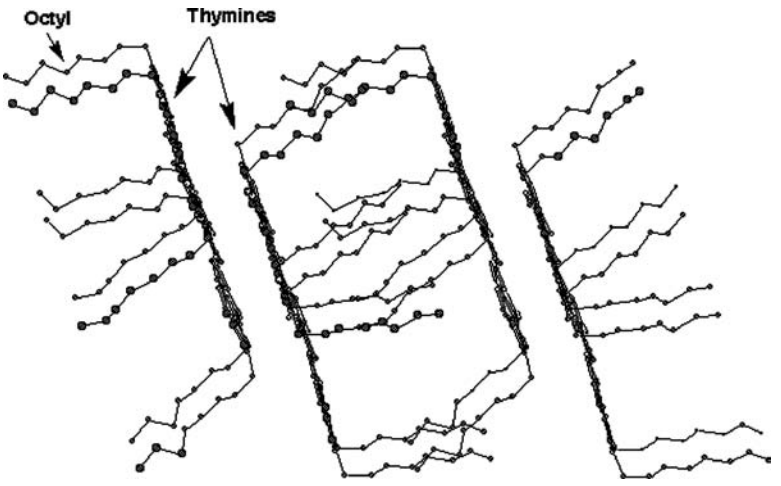

FIGURE 104.12 Lamella structure of 1-*n*-octylthymine (**Form I**).

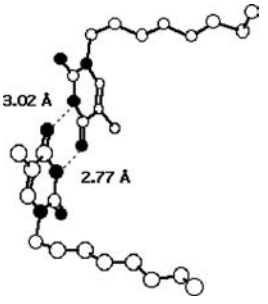

FIGURE 104.13 Two thymine derivatives associated with hydrogen bonding.

The crystal is a layer structure consisting of a hydrophilic layer of thymine bases and a hydrophobic layer of long alkyl groups (Figure 104.12, **Form I**). The distance between the two planes formed by the thymine bases was almost 3.3 Å. Moreover, the long alkyl chain groups aggregate and form a hydrophobic layer. The thymine bases are in the same plane and associated by hydrogen bonding in the plane (Figure 104.13). The thymine molecule faces another thymine in an opposite plane in a head-to-head arrangement (Figure 104.14). As shown in the Figure 104.14, two thymine bases on opposite planes are in the position of *trans-syn*. Therefore, the distance and the orientation of the two thymine bases in this crystal suggest that the *trans-syn* photodimer should be the dominant photodimer.

The plate crystals, obtained by recrystallization from ethyl acetate, were irradiated with UV light. The process of the photoreaction was confirmed from UV, IR, and NMR spectra. The conversion was calculated from the NMR spectra in $CDCl_3$ from the peaks of the 6-H of the photodimer and the original thymine. After UV irradiation of the plate crystal for 3 hours, a 98.3% yield of a single photodimer was obtained. The dimerization was rapid because the reaction proceeded through the singlet state. The isomer was identified as *trans-anti* from chemical shifts of the 5-CH and 6-H in the NMR spectra. This isomer is different from the *trans-syn* isomer predicted from the crystal structure.

If the photodimerization occurs face-to-face between the stacked thymines, the photodimer should be the *trans-syn* isomer. However, the photodimer obtained was the *trans-anti* isomer, suggesting another mechanism of photodimerization. The photocyclization of a diene compound is known to occur by disrotatory motion, although the thermal cyclization occurs by a conrotatory motion.[62] If the photodimerization of thymine bases in the crystal occurred by disrotatory motion, the product should be the

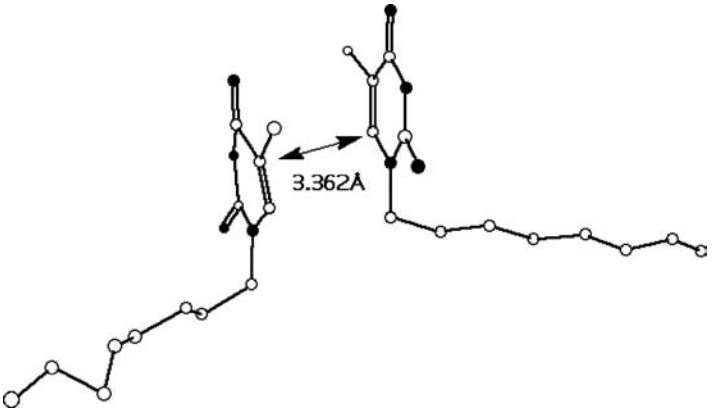

FIGURE 104.14 Two opposite thymine derivatives in the position of *trans-syn.*

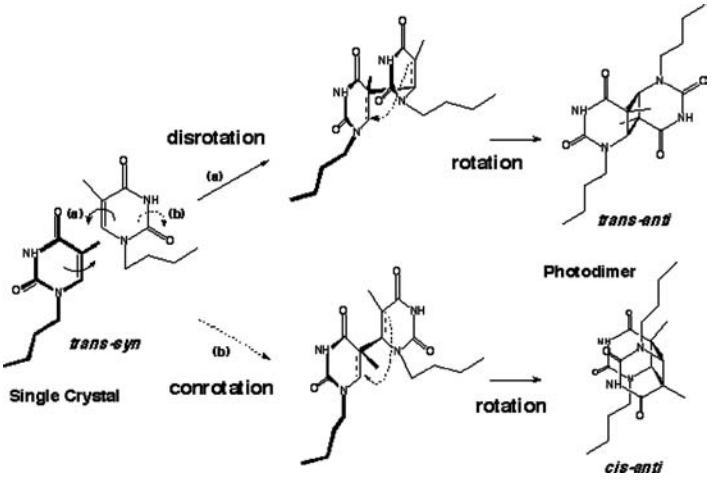

FIGURE 104.15 Probable mechanism of photodimerization of 1-*n*-octylthymine in crystal state from two opposite thymine derivatives in the position of *trans-syn.*

trans-anti isomer. This mechanism of disrotation may be possible because the motion of the molecule is fixed in the crystal by the interaction of the long alkyl chains.

The probable mechanism of the photodimerization is illustrated in Figure 104.15. When the thymine bases in the crystal rotate in the disrotatory manner (path a), the first bond is formed between C5 and C6′ in a *cis*-conformation. After rotation of the thymine in the plane, the second bond is formed between C6 and C5′, giving the *trans-anti* photodimer. By the conrotatory motion of thymine bases (path b), however, the *cis-anti* photodimer should be formed through the *trans*-type intermediate.

Crystal Obtained from Ethanol[55]

Figure 104.16 shows a molecular packing structure of 1-*n*-octylthymine crystallized from ethanol (**Form II**). The crystal is a double-layer structure consisting of a hydrophilic layer of thymine bases and a hydrophobic layer of long alkyl groups. The distance between the two planes formed by the thymine bases was about 3.3 Å. The long alkyl chain groups aggregate weakly and form a hydrophobic layer. Therefore, hydrogen bonding and van der Waals forces of the thymine bases are the main driving forces to form the crystal.

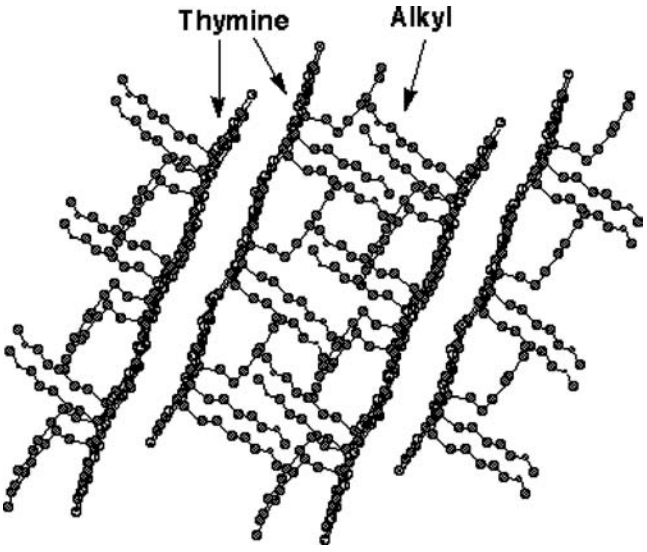

FIGURE 104.16 Lamella structure of 1-*n*-octylthymine crystallized from ethanol (**Form II**).

Irradiation with UV light (280 nm) of the crystal from ethyl acetate gave the photodimer with 98.7% conversion.[54] On the other hand, crystals from ethanol gave no photodimers under the same reaction conditions. These results of photodimerization in single crystals correspond with the results from the photoreaction in thin films. **Structure I** of the spin-coated film gave the photodimer, but the **Structure II** formed by annealing gave no photodimer. The differences between these photoreactivities will be clarified by the molecule orientation in the crystal structure obtained from x-ray structure analysis studies.

The transition points of the **Form I** to **Form II** were obtained by a differential thermal analysis (DTA) study. On the trace from **Form I** (ethyl acetate), a small endothermic peak was found at 106°C and an exothermic peak was found at 111°C. A large endothermic peak at 122°C should be the melting point. On the trace from **Form II** (ethanol), a broad endothermic peak is shown at 100°C and a large endothermic peak at 122°C. The small endothermic peaks at around 100°C can be assigned to the melting of the *n*-octyl chain. The differences of temperature between the two crystals forms may be caused by the difference of assembly for each long alkyl chain (Figure 104.17). Long alkyl chains cross each other in **Form II** but the chains are parallel in **Form I**. To make sure that the peaks at 106° and 111°C for **Form I** are the transition point, DTA was measured for the annealed crystal. **Form I** was heated to 110°C and cooled to 50°C. The DTA trace for the annealed crystal showed a similar DTA trace to **Form II**. This result indicated that **Form I** (ethyl acetate) transformed to **Form II** (ethanol).

Crystal Obtained from Acetonitrile[56]

Crystallization of 1-*n*-octylthymine from acetonitrile solution gave needles and plates. The plates of 1-*n*-octylthymine obtained by slow evaporation of acetonitrile were the same form as the plates from ethanol solution (**Form II**). Needles of 1-*n*-octylthymine were obtained by crystallization from acetonitrile solution. The form of the needles (**Form III**) was greatly different from those crystals obtained from ethyl acetate (**Form I**) and ethanol solutions (**Form II**). The needles contained acetonitrile in the cavity in a molar ratio of 1:1 (thymine: acetonitrile). As the *z* value was 2, one unit cell includes two thymine molecules and two acetonitrile molecules. Figure 104.18 shows the arrangement of the *ab* and *cb* planes. The thymine bases stacked on the *c* axis but did not completely overlap. The lamella structure consists of the hydrophilic and hydrophobic layers. The hydrophilic layer was composed of thymine bases and acetonitrile, and the hydrophobic layer of the long alkyl chains. The two layers were conjugated by hydrogen bonding and they contributed to the stability of the hydrophilic layer.

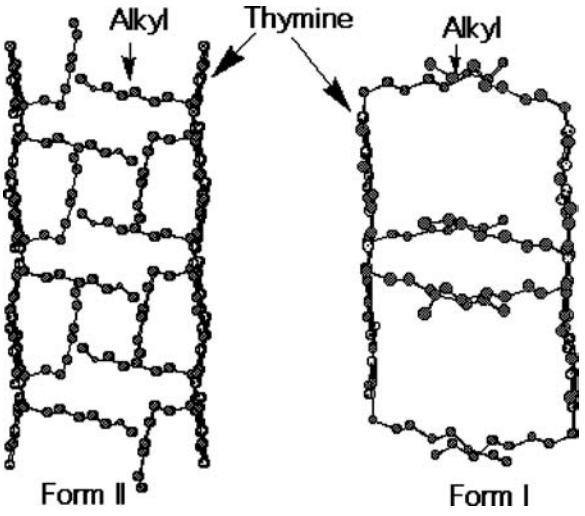

FIGURE 104.17 Packing of long alkyl chains in crystals: [a]; **Form II** (ethanol); and [b] **Form I** (ethyl acetate).

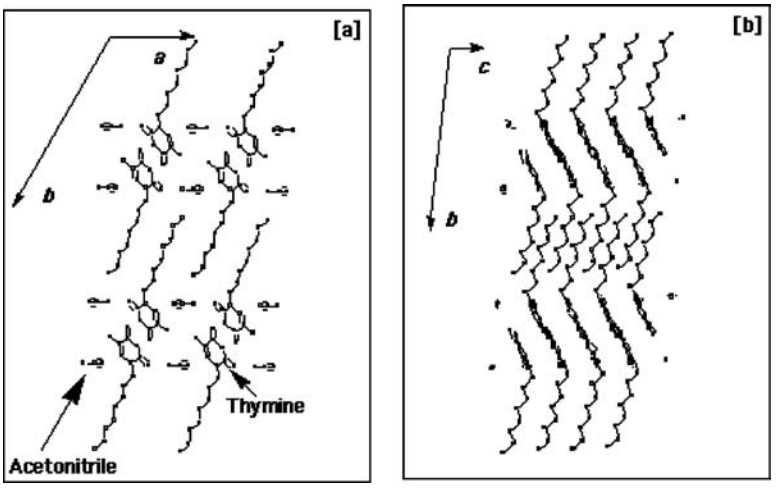

FIGURE 104.18 Molecular arrangement of 1-*n*-octylthymine in needles (**Form III**): [a] *ab* Plane and [b] *bc* Plane.

Irradiation with UV light around 280 nm of the needles obtained from the acetonitrile solution gave the photodimer. The NMR spectrum suggests the formation of two kinds of photodimers. The two isomers were identified as the *trans-anti* and *trans-syn* isomeric dimers by comparison of the NMR spectra of the isolated photodimers.[54]

The mechanism for the formation of the two photodimers was postulated from the form of the needles. There are two orientations of the thymine pairs that form photodimers in the needles from acetonitrile solution. One is in the *trans-anti* orientation. As shown in Figure 104.19, thymines in a *trans-anti* orientation (**a** in Figure 104.19) rotate for the reaction between C5 and C5′ and rotate again for the formation of the photodimer, giving the *trans-syn* isomer. The other orientation is *cis-syn* (**b** in Figure 104.19) and gives the *trans-anti* photodimer by rotation of thymines during the photodimerization reaction. As illustrated in Figure 104.20, the thymines rotate outside to give the *cis-syn* orientation of the intermediate that gives the *trans-anti* photodimer by reaction between C6 and C5′ with internal rotation. If the thymines rotate inside, the photodimer should be *cis-anti*. The rotation inside, however, may be inhibited by steric hindrance of the methyl groups of thymine. Therefore, only small amounts of the *cis-anti*

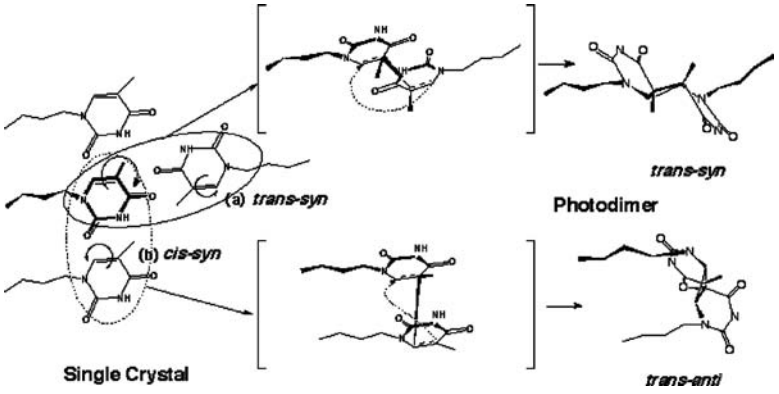

FIGURE 104.19 Mechanisms of photodimerization for 1-*n*-octylthymine in needles: [a] Orientation of *trans-anti* giving *trans-syn* photodimer; [b] orientation of *cis-syn* giving *trans-anti* photodimer.

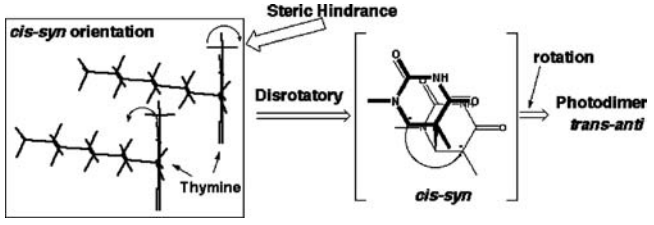

FIGURE 104.20 Illustration of disrotatory motion from *cis-syn* orientation to *cis-syn* intermediate.

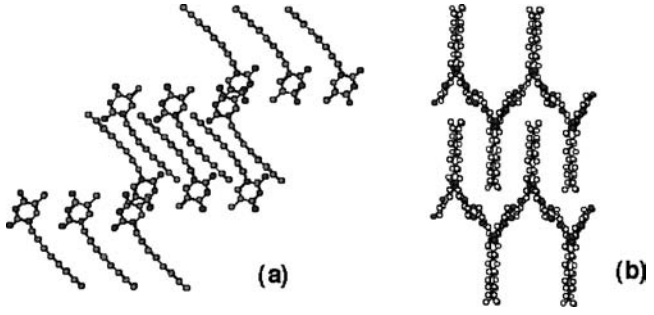

FIGURE 104.21 Molecular packing of 1-*n*-octylthymine (**Form IV** from DMF) along b axis (a) and a axis (b).

photodimer were obtained. In both pairs, the thymines gave the photodimers by disrotatory motion in the crystals during the photodimerization reaction. If conrotatory motion occurred during the photodimerization, another isomers would have been obtained.

Crystals Obtained from DMF[58]

Single-crystal of 1-*n*-octylthymine was obtained from DMF (*N*,*N*-dimethylformamide) solution. Figure 104.21 shows molecular packing of 1-*n*-octylthymine (**Form IV**) along *b* axis (a) and *a* axis (b). The thymine rings in crystal are not stacked but crossed at about 60° as shown in Figure 104.22. Moreover, the terminal methyl group of the molecule is closely located to the double bond of the thymine base in the molecule with the distance of 3.62 Å, and the terminal methyl group of the molecule is closely located to the thymine base of the molecule. Then two molecules in the crystal of 1-*n*-octylthymine form a pair instead of a helix.

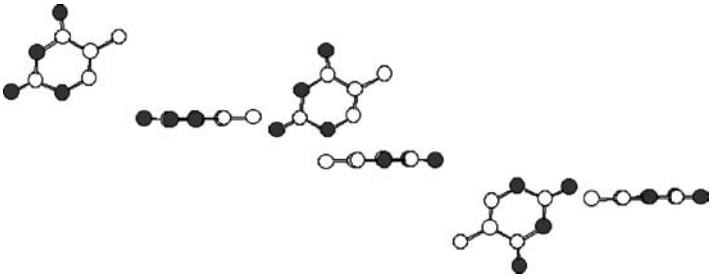

FIGURE 104.22 Thymine bases in **Form IV** crystal.

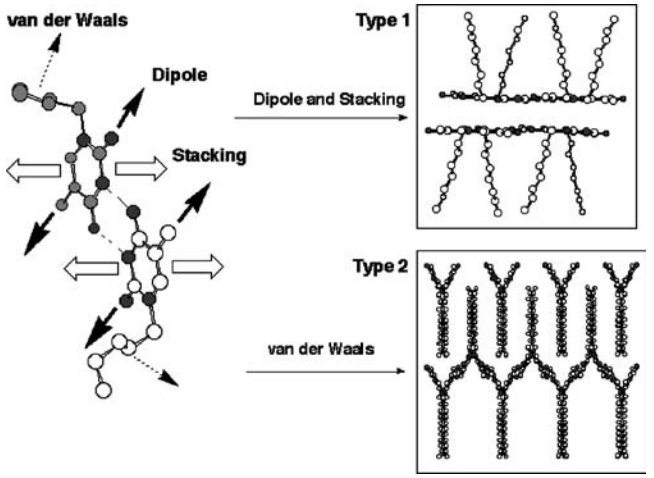

FIGURE 104.23 Interactions and crystallizations of 1-*n*-alkylthymine.

UV light was irradiated on the single crystal obtained from DMF for 1-*n*-octylthymine using an optical fiber with a cutoff filter (above 280 nm). The photodimerization of the thymine bases was followed by UV spectra at 270 nm in chloroform solution. A decrease in UV absorption at 270 nm, however, was not detected after irradiation for 2 days.

Crystal Structure and Photodimerization of 1-*n*-Octylthymine: Summary

Crystal Structure

Polymorphism of 1-*n*-octylthymine is related to polarity of solvent used for crystallization. Two types of crystals (**Type 1** and **Type 2**) are obtained, depending on solvent used. In both types, a hydrogen bonded-pair of thymine may be formed at first during crystallization from solution. For the formation of **Type 1** crystals, the hydrogen-bonded pairs associate to form stacked plates by dipole and stacking interaction, followed by association of the alkyl chains between two plates by van der Waals interaction to give **Type 1** crystals (Figure 104.23). In the case of **Type 2** crystals, alkyl chains of the hydrogen-bonded pairs crystallized by van der Waals interaction without stacking of thymine bases or formation of plates.

In **Form I** (**Type 1**), any interaction was found between the hydrogen-bonded pairs in the same plane (Figure 104.24). However, stacking interactions of thymine bases were found between the hydrogen-bonded base pairs on the opposite planes as shown in Figure 104.25.

Ethyl acetate (dielectric constant = 6.02 at 20°C, Dipole Moment = 1.88 D) and ethanol (dielectric constant = 23.8 at 20°C, Dipole Moment = 1.68 D) are aprotic and nonpolar solvents. The 1-*n*-octylthymine in these solvents forms hydrogen-bonded pairs, and then form double layers by the stacking interaction of thymine bases. Finally, the double layers aggregate by van der Waals interaction to form

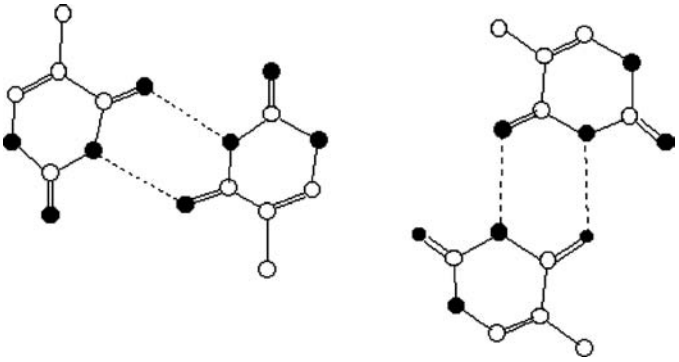

FIGURE 104.24 Hydrogen bonding of 1-*n*-octylthymine in a plane of **Form I**.

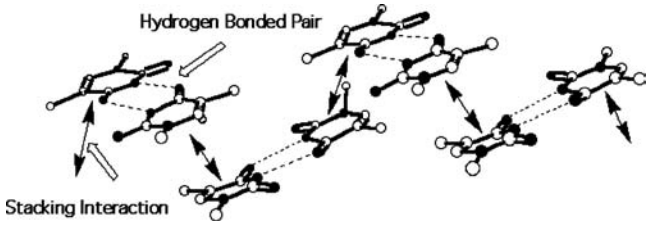

FIGURE 104.25 Stacking interaction between hydrogen-bonded pairs of thymine (**Form I**).

crystals. In these solvents, the stacking interaction of thymine bases take priority over the van der Waals interactions of the alkyl chain. In **Form I** from ethyl acetate, the interaction of the long alkyl chain is weak and rotation of the thymine base in crystal is possible; that is important for photodimerization. The structure of crystal obtained from ethanol (**Form II**) is similar to the crystal from ethyl acetate (**Form I**), but the interaction of the long alkyl chain is stronger than the crystal from ethyl acetate because the polarity of ethanol is higher than that of ethyl acetate. Therefore, the strong interaction of the long alkyl chain in **Form II** inhibits the rotation of the thymine base during photodimerization reaction.

In **Form III** from acetonitrile (**Type 2**), both stacking of the thymine bases and crystallization of the alkyl chains are found. Acetonitrile (dielectric constant = 37.5 at 20°C, Dipole Moment = 3.44 D) is an aprotic and polar solvent. Also, in acetonitrile, thymines form hydrogen-bonded pairs at first. For the association of the hydrogen-bonded pairs, the stacking interaction of thymine bases and the van der Waals interaction of the long alkyl chains occur at the same time. In this crystal, acetonitrile interacts with C2-O of thymine to give an inclusion crystal. Rotation of the thymine bases in crystal is possible because included acetonitrile is mobile. The formation of the inclusion crystal may be kinetic control, but slow evaporation of acetonitrile gives thermodynamically stable plates.

In the **Form IV** (**Type 2**) crystal, the hydrogen-bonded pairs are not parallel to each other (Figure 104.22). Therefore, the formation of the plane structure by stacking interaction of thymine bases is impossible. DMF (dielectric constant = 36.71 at 25°ãC, Dipole Moment = 3.86 D) is an aprotic and polar solvent as well as a good solvent for nucleic acid bases as DMSO. Therefore, the stacking interaction of the hydrogen-bonded pairs is weak because the thymine bases form the complex with DMF. Then, the long alkyl chains of the 1-*n*-octylthymine crystallize by van der Waals interaction. In DMF, the van der Waals interaction of the alkyl chain takes priority over the stacking interaction of thymine bases. In the crystal from DMF, inclusion of DMF molecules dose not occur because the DMF molecule is larger than acetonitrile. Rotation of the thymine bases in the crystal is impossible because molecules are packed closely by strong interaction of the long alkyl chains in the crystal.

TABLE 104.3 Factors Determining the Activity of 1-*n*-Octylthymine for the Photodimerization

	Form I	Form II	Form III	Form IV	Ref.
Thymine - Thymine (Å)	3.40	4.34	4.47, 4.71	4.36, 4.56	Fig. 27
Thymine – Methyl (Å)					Fig. 28
[Thymine] 5C	4.26	3.86	7.34	3.64	
6C	4.55	3.86	6.90	3.60	
5Me	5.14	3.86	7.80	3.86	
DSC(°C)	108.9, 119.9	120.1	59.3, 120.1	122.6	

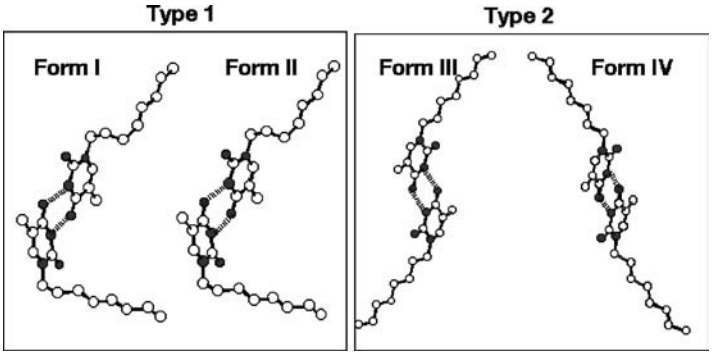

FIGURE 104.26 Hydrogen bonded pairs of 1-*n*-octylthymine for **Form I**, **Form II**, **Form III,** and **Form IV.**

Photodimerization

Intensive studies concerning topochemical reactions have been reported on the photodimerization of cinnamic acid and its derivatives. Schmidt and co-workers proposed a geometrical criterion for the photodimerization in the crystalline state: that the reacting double bonds should be situated within about 4.2 Å of each other and aligned parallel.[63] In the case of the photoactive single crystal of 1-*n*-octylthymine obtained from acetonitrile solution (**Form III**), however, the distance between the reacting double bonds of the thymine bases was 4.47 Å.[56] It is difficult to apply Schmidt's rule to the photodimerization of the 1-*n*-octylthymine crystals. Therefore, it is necessary to determine the feature within the crystal of 1-*n*-octylthymine for the photodimerization reaction in the crystalline state.

From the crystal structure of 1-*n*-octylthymine, we will study the factors determining the activity of the crystals for the photodimerization. The possible factors for the crystal structure are summarized in Table 104.3. An important feature of the thymine compounds is the hydrogen bonding between the thymine bases. The hydrogen bonding of the thymine bases does not directly influence the photoactivity, but is important for the stability of the crystal structure. The crystallization of 1-*n*-octylthymine from nonpolar solvents may begin from the hydrogen bonding of the thymine bases, followed by stacking of the thymine bases and aggregation of the long alkyl chains. Figure 104.26 shows the hydrogen-bonded pairs for four crystal forms of 1-*n*-octylthymine. In **Type 1** (**Form II** and **I**), the long alkyl chains extend in the same direction from the plane of the hydrogen-bonded thymine bases. On the other hand, in the case of **Type 2** (**Form III** and **Form IV**), the long alkyl chains extend in the opposite direction from the plane of the hydrogen-bonded thymine bases. The direction of the long alkyl chain may determine the aggregation of the long alkyl chains and, therefore, the crystal structure. The interaction of the solvent with the molecules may cause a change in the direction of the long alkyl chain during crystallization in solution.

The most important factor of the crystal structure for the photoactivity should be the distance between the C5–C6 double bonds of the thymine bases, as proposed by Schmidt and co-workers.[63] Two facing thymine bases in the crystals are shown in Figure 104.27 for four crystal forms of 1-*n*-octylthymine, and

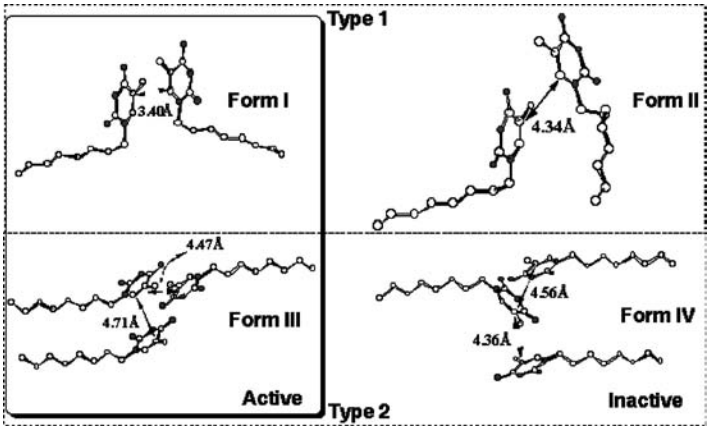

FIGURE 104.27 Facing thymine bases in **Form I**, **Form II**, **Form III**, and **Form IV**.

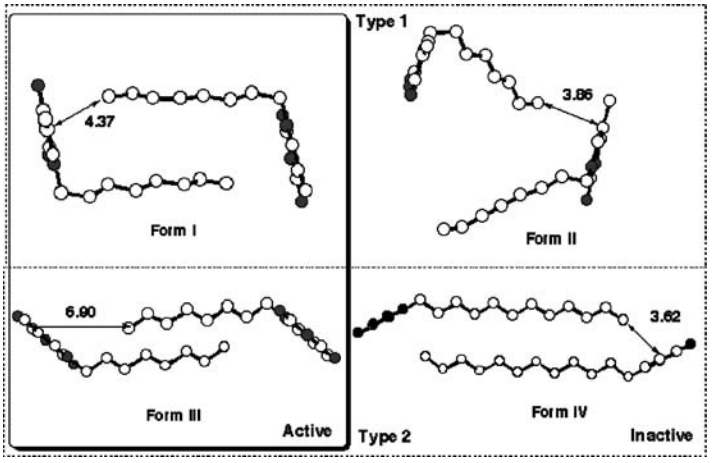

FIGURE 104.28 The nearest neighboring molecules of 1-*n*-octylthymine for **Form I**, **Form II**, **Form III**, and **Form IV**.

the distances between the adjacent double bonds of thymine bases are tabulated in Table 104.3. The distances between the thymine bases in **Form IV** are 4.36 Å and 4.56 Å, which are longer than the distance of the photoactive **Form I** (3.40 Å) but shorter than the distance of the photoactive **Form III** (4.47 and 4.71 Å). Therefore, the distance between the double bonds of the thymine bases is not the main factor for the photodimerization of thymine bases in crystal.

As mentioned, the characteristic of the crystal structure for **Form IV** is the presence of the terminal methyl group in the vicinity of the double bond in the thymine base. The nearest neighboring terminal methyl group and thymine bases are picked out from the crystal structure of 1-*n*-octylthymine for **Forms I**, **II**, **III**, and **IV** in Figure 104.28 and the distances are tabulated in Table 104.3. The distances between the methyl group and the thymine base (C5) are long for the photoactive **Form I** (4.26 Å) and **Form III** (7.34 Å), but are short for the inactive **Form II** (3.86 Å) and **Form IV** (3.64 Å). The terminal methyl group of the alkyl chain should be important for the photodimerization of the thymine bases, although the methyl group did not participate directly in the photodimerization.

The DSC curves of 1-*n*-octylthymine indicate the stability of the crystals (Figure 104.29). The inactive crystals of **Form II** and **Form IV** gave only one peak at high temperature (around 120°C). The photoactive crystals of **Form I** and **Form III**, however, had one more peak in the DSC. **Form III**, including acetonitrile molecules, released the acetonitrile at 59.3°C. This was followed by melting at 120.1°C. **Form III** underwent

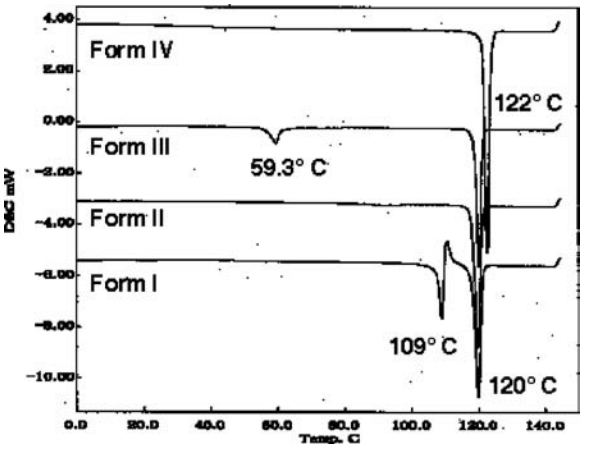

FIGURE 104.29 DSC of 1-*n*-octylthymine for **Form I**, **Form II**, **Form III,** and **Form IV**.

photodimerization but became inactive after annealing at 100°C. **Form I** was also active for the photodimerization but became inactive after annealing at 100°C. Then, the unstable crystals suggested by the DSC curves were active for the photodimerization.

Photodimerizations and crystal structures of 1-*n*-octylthymine are summarized as follows. In photoactive **Form I**, the distance between the double bonds of the thymine bases is short (3.40 Å) and the terminal methyl group of the alkyl chain is not near the thymine base (4.26 Å). The DSC data of **Form I** indicates that the crystals are unstable and change to the stable **Form II**. Consequently, the thymine bases in **Form I** can rotate in the crystal to give the photodimer. In photoactive **Form III** from acetonitrile, the distance between the photoactive double bonds of the thymine base was 4.36 Å, which was longer than the 4.2 Å of Schmidt's rule. However, the distance between the methyl group and the thymine base (C5) is long enough (7.34 Å) to permit the disrotatory motion of the thymine bases in the crystal. The DSC data also supports the instability of the crystal in **Form III**. Therefore, the crystal of **Form III** is active for photodimerization to give the photodimer.

When the terminal methyl group of the long alkyl chain is close to the double bond of the thymine bases, the terminal methyl group of the alkyl chain could block the rotation of the thymine bases during photodimerization. The DSC data indicated that the crystals of **Forms II** and **IV** were stable and could not transform to another crystal form. Therefore, the blocking of the disrotatory motion of the thymine base by the terminal methyl group of the alkyl chain was concluded to be the reason of the inactivity for the photodimerization of **Form II** and **Form IV**. The distance between the terminal methyl group and the C5–C6 double bond of the thymine bases is a measure of the blocking effect of the methyl group on the disrotatory motion of the thymine base.

Effects of Chain Length on Crystal Structure and Isomer Ratio of Photodimer[60]

Crystal Structure

The polarity of solvents determines the type of crystal for 1-alkylthymine: **Type 1** or **Type 2**. The chain length of the alkyl group is also an important factor for the determination of the crystal type (Figure 104.30). **Type 1** crystals were obtained for 1-alkylthymines with short alkyl chains such as **C5**. With the increase of chain length, both **Type 1** and **Type 2** crystals were obtained from **C8** to **C10**. For **C9** and **C10**, **Type 2** crystals were too unstable to isolate, but the DSC data indicated the presence of two crystal forms. For 1-alkylthymine with long alkyl chains above **C11**, only **Type 2** crystals were obtained. Crystallization of 1-alkylthymine is competitive crystallization of thymine bases with alkyl chains (Figure 104.23). For compounds with short alkyl chains, thymine bases crystallized in preference to alkyl chains to form **Type 1** crystals. For compounds with long alkyl chains, the alkyl chains crystallized in preference to thymine bases to form **Type 2** crystals.

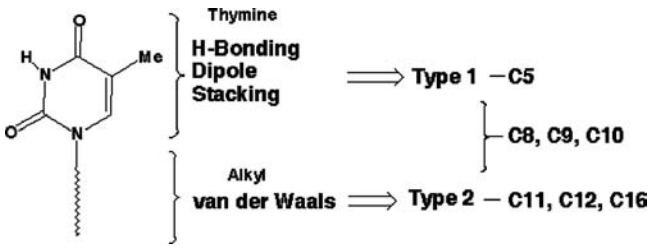

FIGURE 104.30 Interactions and crystallization of 1-*n*-alkylthymine.

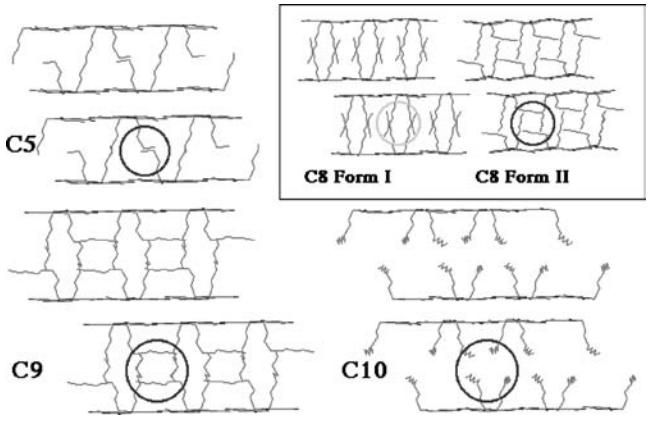

FIGURE 104.31 Molecular packing of **Type 1** crystals for **C5**, **C8**, **C9,** and **C10**.

Crystal structures of **Type 1** for **C5**, **C9**, and **C10** are shown in Figure104.31 along with the data for **C8**. In **Type 1** crystals, the hydrogen-bonded thymines form a parallel plane by stacking interactions and form sheets by van der Waals interactions of the alkyl chains. The style of aggregation of alkyl chains depends on the length of the alkyl chains (circles in Figure 104.31). This figure suggests that there is no significant interaction of the alkyl chains for **C10** between the bilayers of the thymine bases. This fact indicates that hydrogen-bonded pairs of thymines are first formed during crystallization from solution, followed by formation of two plates by dipole and stacking interactions (**Type 1** in Figure 104.31). Finally, the crystal was formed by van der Waals interaction of the alkyl chains between two plates. When the alkyl chains are long, the van der Waals interaction of the alkyl chains is strong enough to form a regular arrangement of the alkyl chain to give **Type 2** crystals.

Isomer Ratio of Photodimers

Photodimerization of 1-*n*-alkylthymine in solution gave four isomeric photodimers (Figure 104.2 and Table 104.1). **Type 1** crystals of 1-*n*-octylthymine (**C8**) (**Form I**), obtained from ethyl acetate, gave only the *trans-anti* isomer and **Form III** crystals, obtained from acetonitrile, gave two photodimers. In **Type 1** crystals, the length of the alkyl chain was found to affect the isomer ratio of photodimers (Table 104.4). In the case of 1-*n*-pentylthymine (**C5**) and 1-*n*-nonylthymine (**C9**), irradiation gave the *trans-syn* photodimer. **Type 1** crystals of 1-*n*-undecylthymine (**C10**) gave a mixture of photodimers, *trans-anti* and *trans-syn*. The photodimerization for **C8** was efficient (98%) but conversions of **C5**, **C9,** and **C10** were low, around 30%. The length of the alkyl chain should relate to aggregation of the alkyl chains in the **Type 1** crystals. Thus, types of aggregation may affect the isomer ratio of the photodimers formed. The conformation of facing thymines for photodimerization is *trans-syn.* This is the same for **C5**, **C8**, **C9**, and **C10**. The conformation of the thymines, therefore, cannot explain the differences of type and ratio of the photodimers obtained. The key factor must be the length of the alkyl chains.

TABLE 104.4 Conversion and Isomer Ratios of Photodimerization in Single Crystals

Compound	Solution	Penthyl(C5)	Octyl(C8)	Nonyl(C9)	Decyl(C10)
Conversion(%)	—	30	98	30	40
cis-syn	0.85	—	—	—	—
cis-anti	0.76	—	—	—	—
trans-syn	1.00	1.0	—	1.0	0.7
trans-anti	0.95	—	1.0	—	0.3

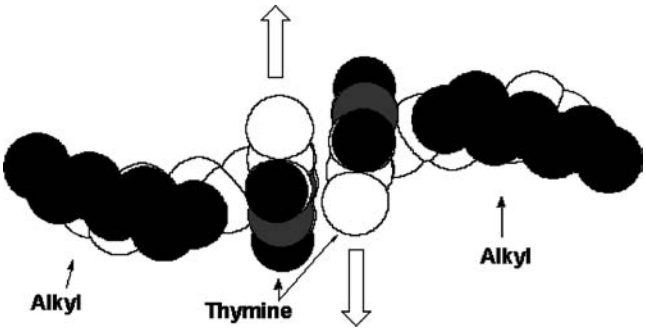

FIGURE 104.32 Restriction of rotation by terminal methyl groups for 1-*n*-octylthymine (**C8**).

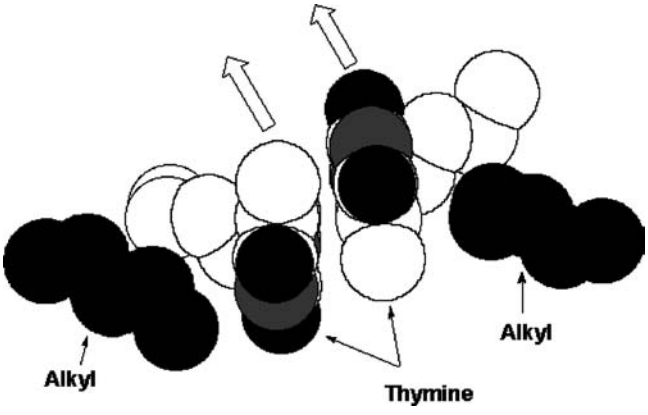

FIGURE 104.33 Restriction of rotation by terminal methyl groups for 1-*n*-pentylthymine (**C5**).

Figure 104.32 shows active thymine bases and surrounding alkyl groups in a space-filling model for **C8**. In this model, the terminal methyl group of the alkyl chain is closely located to the thymine base. The distance of the methyl group to N3 of the thymine was 3.6 Å and to C5 was 4.3 Å. The methyl groups inhibit rotation of the thymine bases and permit only one direction of rotation for two thymine bases, as in Figure 104.32. Permitted rotations of thymine bases during photodimerization may give the *trans-anti* photodimer.

In the case of **C5** (Figure 104.33), the blocking effect of the terminal methyl group permits rotation of the thymine bases in the same direction. The permitted directions of rotation for **C5** must be in a parallel sense, as shown in Figure 104.33. This is, however, opposite to the direction for **C8**. Different isomers of the photodimer (*trans-syn*) were obtained for **C5** than from **C8** as a result of the difference in rotation. The allowed direction of rotation for **C9** was the same as for **C5**.

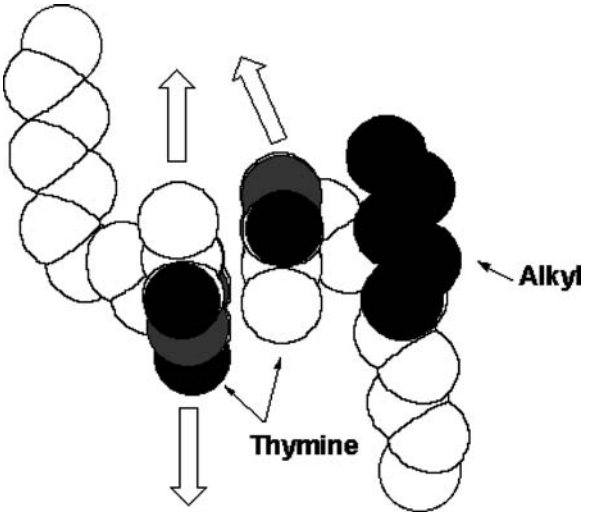

FIGURE 104.34 Restriction of rotation by terminal methyl groups for 1-*n*-pentylthymine (**C10**).

In the case of **C10**, there are no alkyl chains near the thymine base on the left and rotation of the thymine base can take place (Figure 104.34). However, rotation of the thymine base on the right is inhibited by the terminal methyl group of the alkyl chain that is in the same plane. The allowed rotation of the thymine on the right can only be in an upward direction. Then, two isomers of the photodimers, *trans-syn* and *trans-anti*, can be obtained for **C10** (Table 104.4).

Crystal structures of **Type 1** are similar for **C5**, **C8**, **C9**, and **C10**, except for the interactions of the alkyl chains. Alkyl chains play an important role in forming different isomers of the photodimers. Terminal methyl groups of the alkyl chains are close to the thymine bases and inhibit rotation of the bases during photodimerization within the crystals.

104.4 Ester Derivatives of Thymines Having Long Alkyl Chains

Photodimerization in Thin Solid Films[59]

The reversible photodimerizations of the ester derivatives of thymines (Figure 104.35) were studied in thin solid films that were prepared by spin coating from chloroform solution. Figure 104.36 shows typical repeated photodimerizations of tridecyl (**ES13**) ester derivatives of thymine in thin solid films. The absorbance of the UV spectra at 270 nm decreased on irradiation at 280 nm, indicating the formation of the photodimer and increased again by irradiation at 240 nm, suggesting the photosplitting of the photodimer (a in Figure 104.36). After annealing of the thin solid film at 100°C, the photodimerization was negligible, suggesting a structural change within the thin solid films (b in Figure 104.36).

Figure 104.37 shows the first and the second photodimerizations of the decyl ester (**ES10**) in the thin solid film (a, b, c) with the data in solution (e) and in polymer film (d). The rate of the photodimerization in chloroform solution was slow but proceeded completely (e). The photodimerization of thymine derivatives in solution is known to proceed by way of the triplet excited state. The short lifetime of the singlet state and the inefficient intersystem crossing are the reasons for the slow reaction rate for photodimerization of thymine in solution. The photodimerization was studied in the polymer film using poly(vinyl acetate) (PVAc) (d). The polymer film was obtained from a chloroform solution of the ester derivatives of thymine and poly(vinyl acetate) by spin coating on a quartz plate. The rate of photodimerization in poly(vinyl acetate) was faster than the rate in chloroform solution. In the polymer matrix, photodimerization occurs from associated thymine bases via the singlet state with a higher quantum yield than that from the triplet-state reaction.

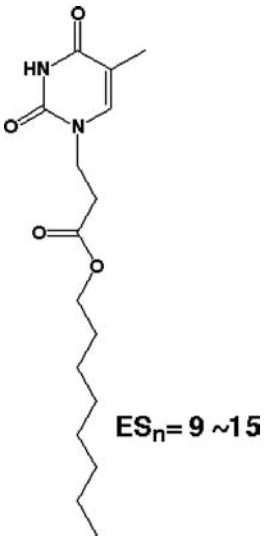

FIGURE 104.35 Ester derivatives of thymine.

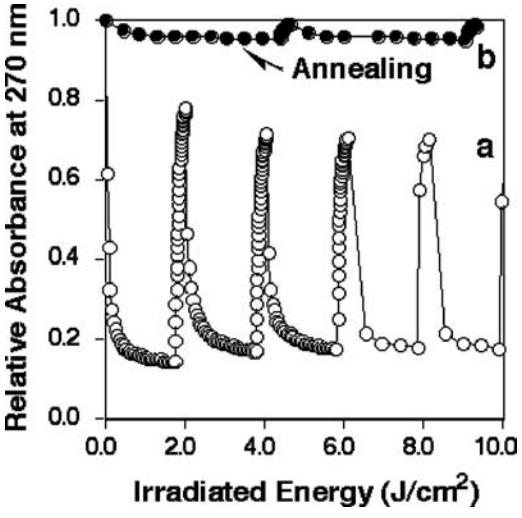

FIGURE 104.36 Typical repeated photodimerizations of tridecyl 2-(thymin-1-yl)-propionate (**ES13**) in thin solid film: (a) spin-coat film and (b) after annealing at 100°C

Repeated reversible photodimerizations in the spin-coated film were studied for nonyl (**ES9**), decyl (**ES10**), undecyl (**ES11**), dodecyl (**ES12**), tridecyl (**ES13**), tetradecyl (**ES14**), and pentadecyl (**ES15**) 2-(thymin-1-yl)-propionates. Decay of the photodimerization was observed for all except **ES12** and **ES13**. The conversions of the first photodimerization from **ES9** to **ES15** are plotted in Figure 104.38. Initially, the photodimerization was fast, up to about 0.5 J/cm^2 of irradiation energy; then the rate slows. The initial fast reactions of [**ES10**, **ES11**] were similar to the rate of [**ES9**]. Interestingly, the slower reactions above 0.5 J/cm^2 of [**ES10**, **ES11**] were faster than slower process for [**ES9**]. The initial rates of the first photodimerization of [**ES12**, **ES13**] were very fast and the conversion for **ES13** reached 90% within 0.5 J/cm^2. For [**ES14**, **ES15**], the initial rates were faster than the rates of [**ES10**, **ES11**], but the final conversions were lower than those of [**ES10**, **ES11**]. From these results, the rates of the first photodimerization in Figure 104.38 can be divided into four classes — [**ES9**], [**ES10**, **ES11**], [**ES12**, **ES13**], and [**ES14**, **ES15**] — according to the slopes of the curves shown in Figure 103.38.

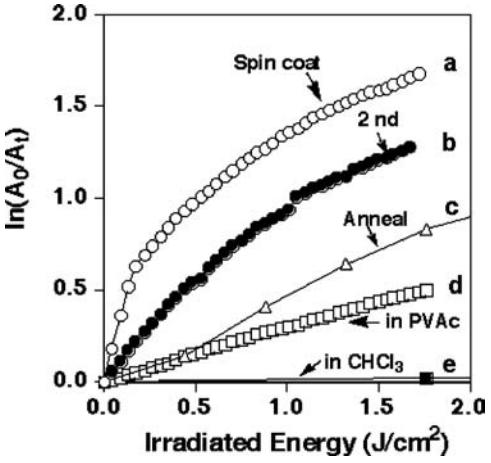

FIGURE 104.37 Conversions of the photodimerizations for decyl 2-(thymin-1-yl)-propionate (**ES10**) in various states under UV irradiation at 280 nm: (a) spin-coat film, (b) after photo splitting, (c) after annealing at 100°C, (d) in poly(vinyl acetate) film, and (e) in chloroform solution.

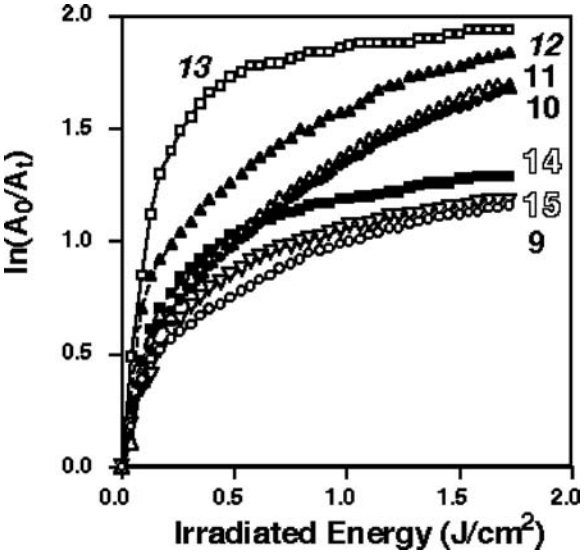

FIGURE 104.38 Conversions of the first photodimerization in the spin-coat film from **ES9** to **ES15**. UV irradiation: 280 nm. The numbers are the carbon number of the alkyl chain.

Photodimerization in Annealed Solid Films

Annealing is carried out at 100°C above the melting point for the spin-coated thin films. The first photodimerizations after annealing are shown in Figure 104.39. The reactivities of **ES10** and **ES11** were decreased by the annealing and become the same as shown by **ES9**. The curves in this figure can be classified into three groups; [**ES9**, **ES10**, **ES11**], [**ES12**, **ES13**], and [**ES14**, **ES15**]. The remarkable change observed for **ES12** and **ES13** after annealing was the absence of photodimerization. This result suggests that the structure of the thin film changes on annealing.

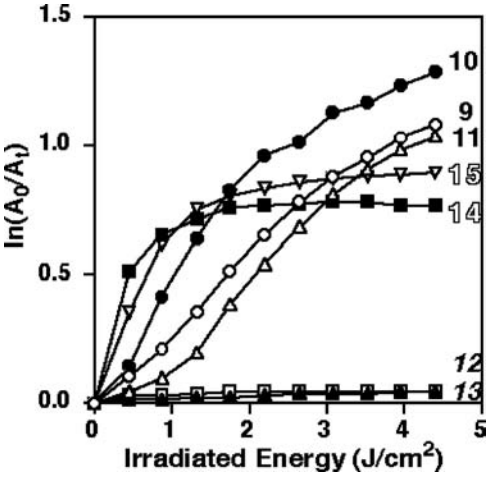

FIGURE 104.39 The first photodimerizations after annealing at 100°C. UV irradiation: 280 nm. The numbers are the carbon number of the alkyl chain.

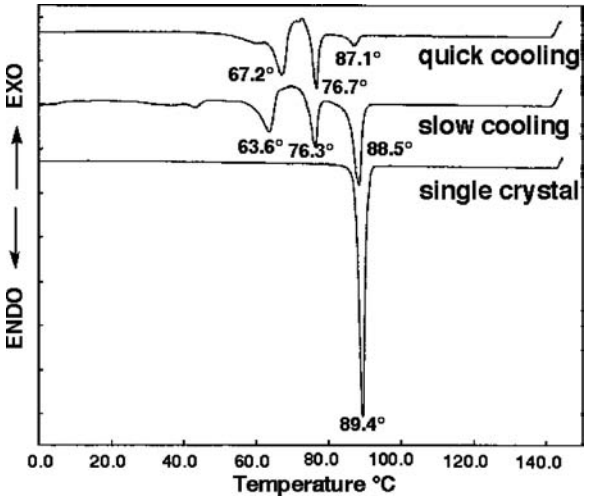

FIGURE 104.40 DSC curves for **ES10**. Heating: 5°/min. (a) Single crystal, (b) after slow cooling (3°/min) of the melt, and (c) after quick cooling (100°/min) of the melt.

DSC of the Ester Derivatives of Thymine

The results of the photodimerization for the ester derivatives of thymine in thin solid films suggested the presence of several crystal structures. Differential scanning calorimetry (DSC) measurements were carried out for the crystals obtained from benzene solution. The measurements were carried out for single crystals, for solids obtained after slow cooling (3°/min) of the melt and for the solid after rapid cooling (100°/min) of the melt.

The patterns of DSC curves for **ES10** and **ES11** were similar to that shown in Figure 104.40 for **ES10**. The peak at 89.4°C of the single crystal (a) was split into three peaks at 63.6°, 76.3°, and 88.5°C by slow cooling of the melt (b). Quick cooling of the sample (c) gave also three peaks (67.2°, 76.7°, and 87.1°C), but the ratios of these peaks were different from that of slow cooling. The results suggested that the single crystal became a mixture of crystals by melting. In the x-ray powder diffraction patterns of **ES10** (Figure 104.41), the cast film from chloroform solution (a) showed small peaks of crystal and strong

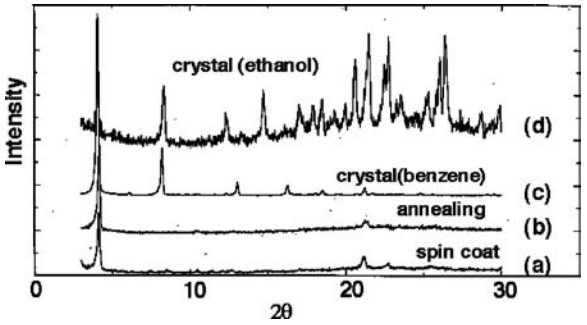

FIGURE 104.41 X-ray powder diffraction patterns for **ES10**. (a) The thin film cast from chloroform solution, (b) after annealing at 100°C (melting), (c) the single crystal from benzene, and (d) the single crystal from ethanol.

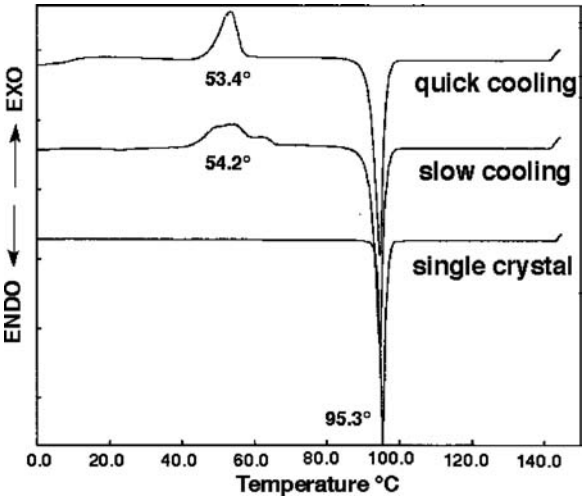

FIGURE 104.42 DSC curves for **ES12**. Heating: 5°/min. (a) The single crystal, (b) the solid after slow cooling (3°/min) of the melt, and (c) the solid after quick cooling (100°/min) of the melt.

peaks of interplanar spacing at 21.3 Å and 4.18 Å. However, the small peaks of crystal were different from the peaks of single crystals (c from benzene and d from ethanol). Melting of the single crystal gave no peaks of crystals but strong peaks of the interplanar spacing at 21.3 Å and 4.18 Å, suggesting the formation of a layered structure.

The DSC curves of the group [**ES12**, **ES13**] show similar curves as that shown in Figure 104.42 for **ES12.** A broad exothermic peak at 54.2°C in addition to a sharp endothermic peak at 94.7°C for the slow cooling sample of **ES12** (b) was observed. However, an additional endothermic peak was not shown for the peak of the single crystal (a). The exothermic peak around 54°C should be the melting of amorphous parts to form the crystal. The result indicated that the slow and the quick cooling gave the same hydrogen-bonded structure of thymines but also gave an amorphous part by aggregation of the alkyl chains. The melting point of the single crystals for **ES13** was 95.8°C. The compounds in this group gave similar patterns of x-ray powder diffraction. In the x-ray powder diffraction patterns, small peaks of the cast film from chloroform solution are the same as the peaks of single crystal from benzene. Melting of the film gave no peaks showing of crystals but gave strong peaks of interplanar spacing at 22.6 Å and 24.8 Å suggesting the formation of the bilayer structure. The DSC and the x-ray powder diffraction for the group [**ES14**, **ES15**] gave similar results as the data of the group [**ES12**, **ES13**]. The melting points of the single crystals for **ES14** and **ES15** were 97.2°C and 99.0°C, respectively.

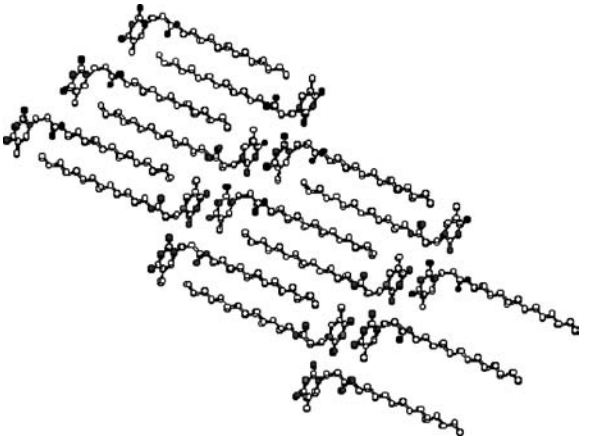

FIGURE 104.43 Crystal structures of decyl 2-(thymin-1-yl)-propionate (**ES10**) viewed along *a* axis.

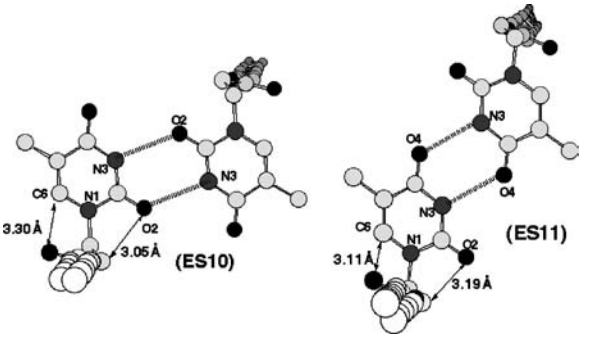

FIGURE 104.44 Racemic pairs connected by hydrogen bonds for (a) ES10 and (b) ES11.

Crystal Structure of the Ester Derivatives

Plates of decyl (**ES10**) and dodecyl (**ES12**) 2-(thymin-1-yl)-propionates and needles of nonyl (**ES9**), undecyl (**ES11**) and tridecyl (**ES13**) 2-(thymin-1-yl)-propionates were obtained from benzene solutions. Figure 104.43 shows the molecular packing of **ES10**. The crystal structure of **ES10** was the same as the structure of other ester derivatives with alkyl chains (**ES12**) containing even numbers of carbons. The only difference was the length of the *b* axis. The molecular packing of **ES11** was the same as the structures of the compounds having odd-numbered alkyl chains (**ES9**, **ES11**, and **ES13**) again apart from the length of the *b* axis. These structures show bilayer structures of the polar thymine bases and the nonpolar alkyl chains. For both structures, the thymine bases were hydrogen bonded.

The style of hydrogen bonding between thymines for the ester derivatives of the even-numbered alkyl chains (**ES10** and **ES12**) was different from the style for the compound with the odd-numbered alkyl chains (**ES9**, **ES11** and **ES13**). Figure 104.44 shows the hydrogen bonding pairs of the ester derivatives of thymine for **ES10** and **ES11**. In the crystals of **ES11** and of the odd-numbered alkyl chain derivatives, the hydrogen bonding formed between N3-H and O4 (Figure 104.44b), which was the usual hydrogen bonding observed in DNA (Watson-Crick type[64]). On the contrary, the hydrogen bonding for **ES10** and **ES12** was formed between N3-H and O2 (Figure 104.44a), which is the reversed Watson-Crick type.[65] The lengths of the hydrogen bonds, however, were 2.8 Å for both crystals. Watson-Crick type hydrogen bonding of thymine bases is more stable than the reversed Watson-Crick type because the basicity of O4 is higher than the basicity of O2[66] and the first protonation occurs at O4 of uracil.[67] The hydrogen bonding

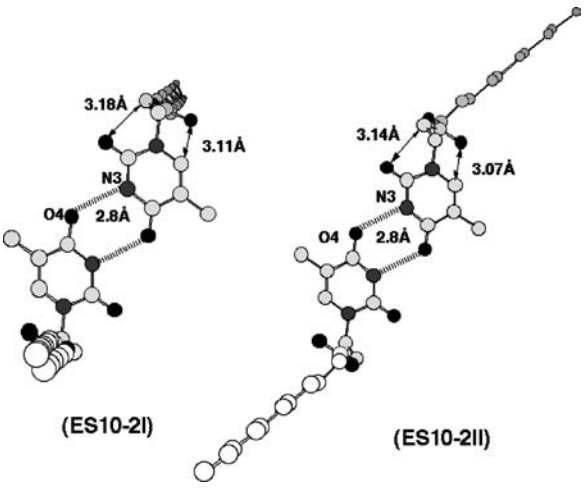

FIGURE 104.45 Two racemic pairs connected by hydrogen bonds for ES10–2. (a) ES10-2I and (b) ES10-2II.

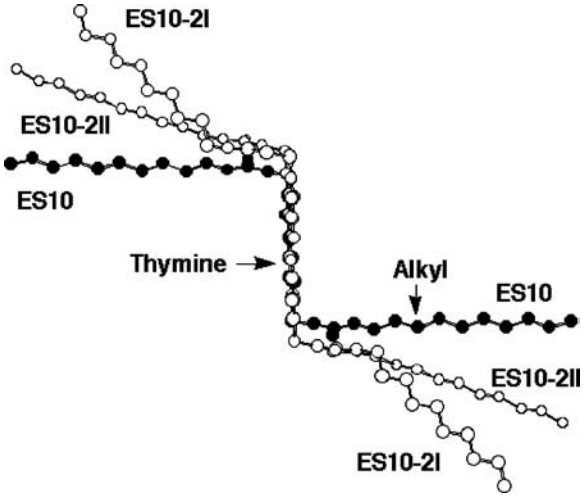

FIGURE 104.46 Three kinds of base pairs for **ES10**, **ES10-2I** and **ES10-2II.**

at O4, in preference to O2, was also shown for thymine monohydrate crystals[68] and 1-(2-hydroxyethyl)uracil[69] where water or the hydroxyl group formed the hydrogen bonds with O4 instead of O2. The unstable hydrogen bonds in **ES10** may be formed by blocking of O4 because of the absence of a hydroxyl group in **ES10**.

From ethanol solution, needles of decyl 2-(thymin-1-yl)propionate (**ES10–2**) were obtained. The crystal structure of **ES10–2** consists of two independent molecules forming a racemic pair. Figure 104.45 shows two kinds of conformations (**I** and **II**) in the crystal. The hydrogen bonds of the thymine bases in this crystal were formed between O4 and N3-H (Watson-Crick type) that is the same seen with derivatives with odd-numbered alkyl chain (Figure 104.44b). One base pair **I** (Figure 104.45a) shows a similar conformation to **ES11** where the alkyl chain is perpendicular to the thymine ring. The alkyl chains of the other base pair **II** (Figure 104.45b), however, were in an extended conformation.

In Figure 104.46, the angles of the alkyl chains from the thymine ring for three base pairs (**ES10**, **ES10-2I,** and **ES 10-2II**) were compared. The highest angle was **ES10-2I** (138°) and the lowest was **ES10** (93°).

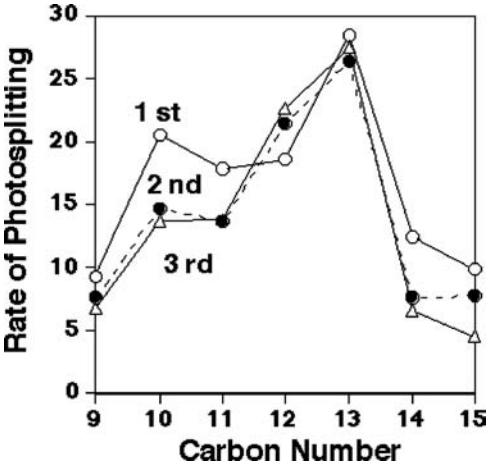

FIGURE 104.47 The initial rate of the photosplitting against the carbon number of the alkyl chains: (°) the first, (l) the second, and (Í) the third photosplitting. UV irradiation: 240 nm.

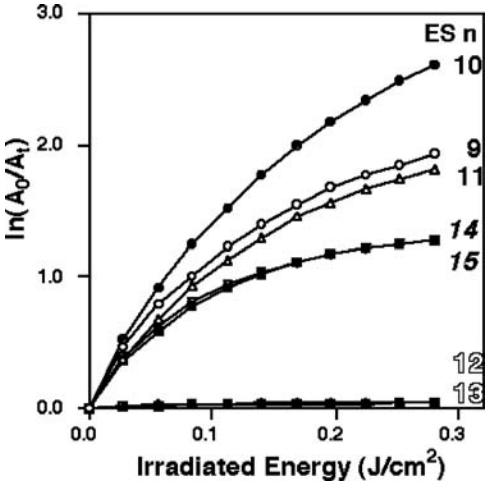

FIGURE 104.48 The conversions of the photosplitting of the photodimer in the annealed film from **ES9** to **ES15**. UV irradiation: 240 nm. The numbers are the carbon number of the alkyl chain.

However, the angles of the carboxyethyl group from the thymine were similar for the three pairs because of the interactions between the carbonyl group of the ester and C6 of the thymine base and between the carbonyl group at C2 of the thymine base and the α-methylene of the ester group (Figure 104.44). A higher dihedral angle of the alkyl chains from the thymine ring for **ES10-2** should result in a loose interaction of the molecules to form stable hydrogen bonds.

Photosplitting of the Photodimer

The thymine photodimers formed by UV irradiation at 280 nm in thin solid films were monomerised by UV irradiation at 240 nm. Figure 104.47 shows the results of photosplitting of **ES9** to **ES15**. The fastest reaction of photosplitting was observed for **ES13**. The dependence of the first photosplitting on the carbon number in Figure 104.47 was similar to that of the photodimerization in Figure 104.38, but the rates for **ES10** and **ES11** were fast compared with the case of the photodimerization. The photosplitting of the photodimer formed in the annealed film gave also irregularity for **ES12** and **ES13** (Figure 104.48).

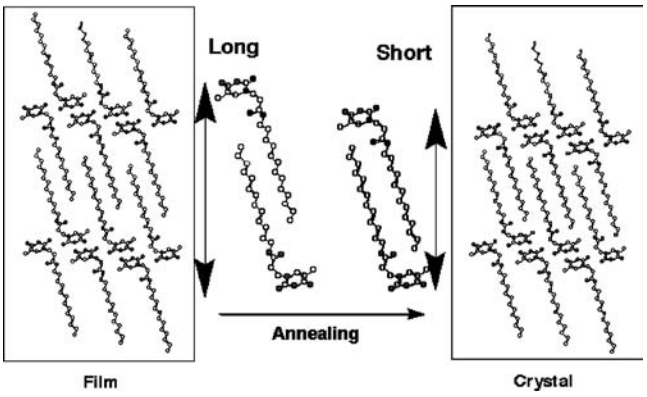

FIGURE 104.49 Illustration of the layered structure in the thin solid film and the crystal structure of **ES13**.

Summary of Photodimerization and Photosplitting of Ester Derivatives of Thymine

The results of the photodimerization and photosplitting reactions in thin solid films raises three questions: (1) classification of the first photodimerization reactions to four groups, (2) the fastest reaction for **ES13** and (3) absence of photodimerization by annealing of **ES12** and **ES13**. These questions will be made clear by crystal structure, DSC, and x-ray powder diffraction for the thin solid film as follows.

Photodimerization in Solid Film

For the photodimerization of the thymine derivatives in thin solid films, the essential factor is the rotation of the thymine bases during photodimerization. The data of the powder x-ray diffraction of the thin film indicated that the film has a layered structure. The layered structure should be formed by loose interaction of the alkyl chain of the hydrogen-bonded thymine pairs. The layered structure of the film is illustrated and compared with the crystal structure for **ES13** (Figure 104.49), where the distance between the layers in the thin solid film is longer than that of the crystals as supported by the powder x-ray diffraction. In the layered structure of the thin film, the rotation of the thymine bases should be possible, because the distance between the thymine and the terminal methyl group of alkyl chain is sufficiently long. With this arrangement the thymine compounds in the layered structure of the thin solid films are able to undergo photodimerization. The alkyl chain length may influence the arrangement of the layered structure and the photodimerizations are affected by the length of the alkyl chain (Figure 104.38). The thin solid films of the third group [**ES12**, **ES13**] had high activity for the first photodimerization. The photodimerization of the thymine bases should be fast in the layered structure of this group, where the thymine bases are arranged suitably for photodimerization and the rotation of the thymines is possible.

Annealing of the Film

The DSC data indicated that the thin solid films of **ES9** contain mixtures of two crystals, even if the crystals are formed after annealing. In the case of the second group [**ES10**, **ES11**], the thin solid films of this group contain three crystals when crystallization occurred in the film. Therefore, the photodimerization of these groups occurred after annealing of the film.

The third and fourth groups [**ES12**, **ES13**] and [**ES14**, **ES15**] are different from the former two groups. The single crystals melt at around 100°C and reform the same crystalline state on cooling. Recrystallization is accompanied by the formation of an amorphous part. The crystals formed by cooling should be inactive for photodimerization, although the amorphous part is active. The amorphous part of [**ES12**, **ES13**] may be small while that of [**ES14**, **ES15**] may be large.

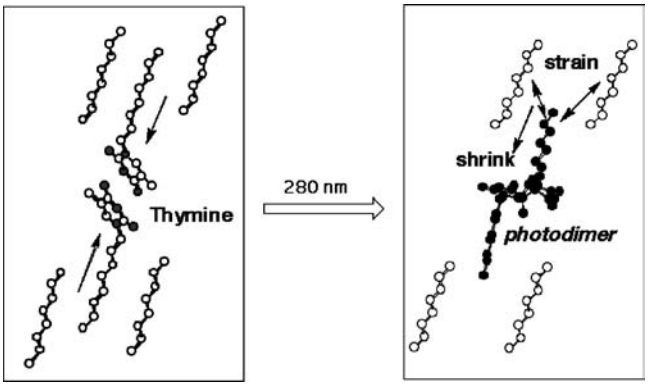

FIGURE 104.50 The induced strain during the photodimerization of thymine bases in the crystal (illustration).

Photosplitting

As shown in Figure 104.47, the rates of the first photosplitting increase with an increase in the length of the alkyl chains and decreases after **ES13**. Photosplitting of the thymine photodimer in solution is caused by steric repulsion of the C5-methyl groups of the thymine base. On the other hand, the photosplitting in the solid state is caused by the strain within the crystal lattice in addition to the strain of the C5-methyl groups. The reason is that the photodimerization of thymine bases with long alkyl chains in crystals induces the rotation of the thymine bases, thus involving strain in the crystal as illustrated in Figure 104.50. When the alkyl chains are long, the strain within the crystal lattice becomes strong because the interaction of the alkyl chains increases with the increase in the length of the chain. The rate of the photosplitting reaction should increase with lengthening alkyl chain. The reason for the slow reaction of [**ES 9**] and [**ES14**, **ES15**] is not clear, but low yields of photodimers may not cause high strain in the thin solid films.

104.5 Conclusion

Reversible photodimerizations of 1-*n*-alkylthymine in single crystals depend on the crystal structures. However, the orientation of the thymine bases in the single crystal does not correspond to the isomer of the photodimer formed because thymines undergo disrotatory motion during the photodimerization process in the single crystals. The most important factor of the crystal structure for the photodimerization is the distance between the thymine base and the terminal methyl group of alkyl chain because this can influence the rotation of the thymine bases.

The rate of photodimerization of thymine bases in thin solid films is fast in the amorphous areas. Annealing of the film cause crystallization to give inactive crystals. Alkylthymines with chains around C_{10} show polymorphism and the thin solid films contain many crystalline forms. Therefore, the films of thymine compound with C_{10} chains are very active for photodimerization.

Acknowledgments

The author would like to express his grateful acknowledgment to Dr. Norimitu Thonai and Dr. Eiko Mochizuk who obtained the results in this chapter. The author gratefully acknowledges the invaluable discussions with Prof. Mikiji Miyata and Prof. Yasusi Kai.

References

1. Wang, S.Y., Reversible behavior of the ultra-violet irradiated deoxyribonucleic acid and its apurinic acid, *Nature*, 188, 844,1960.
2. Setlow, R.B. and Carrier, W.L., The identification of UV-induced thymine dimers in DNA by absorbency measurements, *J. Photochem. Photobiol.*, 2, 49, 1963.
3. Patrick, M.H. and Rahn, R.O., Photochemistry of DNA and polynucleotides: Photoproducts, *Photochemistry and Photobiology of Nucleic Acids, Vol. II*, Wang, S.Y., Ed., Academic Press, New York, 1976, 35.
4. Fisher, G.J. and Johns, H.E., Pydimidine photodimers, *Photochemistry and Photobiology of Nucleic Acids, Vol. I,* Wang, S.Y., Ed., Academic Press, New York, 1976, 225.
5. Wagner, P.J. and Bucheck, D.J., Photodimerization of thymine and uracil in acetonitrile, *J. Am. Chem. Soc.*, 92, 181, 1970.
6. Weinblum, D., Determination of the quantum yield of reversal in crystalline dimethyl thymine dimer, syn head to head, *Photochem. Photobiol.*, 12, 509, 1970.
7. Otten, J.G., Yeh, C.S., Byrn, S., and Morrison, H., Solution phase photodimerization of tetramethyluracil. Further studies on the photochemistry of ground-state aggregates, *J. Am. Chem. Soc.*, 99, 6353, 1977.
8. Takemoto, K. and Inaki, Y., Synthetic nucleic acid analogs: Preparation and their interaction, *Advances in Polymer Science, Vol. 41*, Springer-Verlag, Berlin, Heidelberg, 1981, 1.
9. Takemoto, K. and Inaki, Y., The preparation of nucleic acid analogs, *Functional Monomers and Polymers*, Takemoto, K., Inaki, Y., and Ottenbrite, R.M., Eds., Marcel Dekker, New York, 1987, 149.
10. Inaki, Y. and Takemoto, K., Functionality and applicability of synthetic nucleic acid analogs, *Current Topics in Polymer Science, Vol. I*, Ottenbrite, R.M., Utracki, L.A., and Inoue, S., Eds., Hanser Pub., New York, 1987, 79.
11. Inaki, Y., Synthetic Nucleic Acid Analogs, *Progress Polymer Science, Vol 17*, Vogl, O., Ed., Pergamon Press, New York, 1992, 515.
12. Elad, D,. Rosenthal, I., and Sasson, S., Solution photodimerization of 1,3-dimethyluracil, *J. Chem. Soc.*, 1971, 2053.
13. Lamola, A.A., Gueron, M., Yamane, T., Eisinger, J., and Shulman, R.G., *J. Chem. Phys.,* 47, 2210, 1967.
14. Wienblum, D., Radiolysys of the dimer of dimethylthymine in the crystalline state, *Rad. Res.*, 39, 731, 1969.
15. Kleopfer, R. and Morrison, H., Organic photochemistry. XVII. The solution-phase photodimerization of dimethylthymine, *J. Am. Chem. Soc.*, 94, 255, 1972.
16. Wang, S.Y., Humidity and photochemistry, *Nature*, 200, 879, 1960.
17. Weinblum, D. and Johns, H.E., Isolation and properties of isomeric thymine dimer, *Biochim. Biophys. Acta*, 114, 450, 1966.
18. Lisewski, R. and Wierzchowski, K.L., Solid state photochemistry of thymine, its N-methylated derivatives and orotic acids in KBr matrices, *Photochem. Photobiol.*, 11, 327, 1970.
19. Kita, Y., Inaki, Y., and Takemoto, K., Photochemical reactions on the synthetic polymers containing thymine bases, *J. Polymer Sci., Polymer Chem. Ed.*, 18, 427, 1980.
20. Kita, Y., Uno, T., Inaki, Y., and Takemoto, K., Photochemical reactions on synthetic polymers with pendant thymine bases: Effect of solvents, *J. Polymer Sci., Polymer Chem. Ed.*, 19, 477, 1981.
21. Kita, Y., Uno, T., Inaki, Y., and Takemoto, K., Photochemical reactions on the acrylic and methacrylic copolymers containing thymine bases, *J. Polymer Sci., Polymer Chem. Ed.*, 19, 1733, 1981.
22. Kita, Y., Uno, T., Inaki, Y., and Takemoto, K., Photochemical reactions on synthetic polymers having pendant thymine bases in polymethacrylate film, *J. Polymer Sci., Polymer Chem. Ed.*, 19, 2347, 1981.
23. Inaki, Y., Suda, Y., Kita, Y., and Takemoto, K., Photochemical reactions on oligo- and polyethyleneimines which contain pendant thymine bases, *J. Polymer Sci., Polymer Chem. Ed.*, 19, 2519, 1981.

24. Kita, Y., Uno, T., Inaki, Y., and Takemoto, K., Photochemical reactions on the synthetic polymers containing thymine bases in the presence of adenine derivatives, *J. Polymer Sci., Polymer Chem. Ed.*, 19, 3315, 1981.
25. Suda, Y., Inaki, Y., and Takemoto, K., Photoreaction of poly(amino acid)s containing thymine moieties as side groups, *Nucleic Acids Res., Sym. Ser.*, 12, 169, 1983.
26. Suda, Y., Inaki, Y., and Takemoto, K., Photodimerization of pendant thymine bases in thymine containing poly-L-lysine derivatives, *J. Polymer Sci., Polymer Chem. Ed.*, 21, 2813, 1983.
27. Suda, Y., Inaki, Y., and Takemoto, K., Photoinduced conformational change of thymine containing poly-lysine derivatives, *J. Polymer Sci., Polymer Chem. Ed.*, 22, 623, 1984.
28. Suda, Y., Kono, M., Inaki, Y., and Takemoto, K., Photochemical reactions on oligo- and polyethyleneimine containing pendant thymine bases: Effects of spacer, *J. Polymer Sci., Polymer Chem. Ed.*, 22, 2427,1984.
29. Suda, Y., Inaki, Y., and Takemoto, K., Photodimerization of pendant thymine bases in thymine containing isopoly-L-lysine derivatives, *Polymer J.*, 16, 303, 1984.
30. Inaki, Y., Fukunaga, S., Suda, Y., and Takemoto, K., Synthesis and photochemical reaction of polymethacrylate derivatives containing 6-cyanouracil, *J. Polymer Sci., Polymer Chem. Ed.*, 24, 119, 1986.
31. Takemoto, K. and Inaki, Y., Photodimerization of thymine-containing polymers: applicability to reversible photoresists, *J. Macromol. Sci. Chem., A25*, 757, 1988.
32. Inaki, Y., Moghaddam, M.J., Kanbara, K., and Takemoto, K., Pyrimidine polymers as high resolution, high sensitivity deep-UV photoresists, *J. Photopoly. Sci. Technol.*, 1, 28, 1988.
33. Moghaddam, M.J., Hozumi, S., Inaki, Y., and Takemoto, K., Synthesis and photochemical reactions of polymers containing thymine photodimer units in the main chain, *J. Polym. Sci. Part A, Polymer Chem.*, 26, 3297, 1988.
34. Inaki, Y., Photochemistry of pyrimidine derivatives as lithographic materials, *Polym. Mater. Sci. Eng.*, 60, 165, 1989.
35. Inaki, Y., Aoki, N., Honda, K., Minami, T., and Takemoto, K., Photo-imaging systems containing leuco dyes and haloganated polymers, *J. Photopolym. Sci. Technol.*, 2, 153, 1989.
36. Moghaddam, M.J., Hozumi, S., Inaki, Y., and Takemoto, K., Syntheses and photoreactions of poly(methacrylate)s containing thymine bases, *Polymer J.*, 21, 203, 1989.
37. Moghaddam, M.J., Kanbara, K., Hozumi, S., Inaki, Y., and Takemoto, K., Syntheses and photochemical reactions of bis-thymine derivatives, *Polymer J.*, 22, 369, 1990.
38. Moghaddam, M.J., Inaki, Y., and Takemoto, K., Photolysis of polyamides containing thymine photodimer units in the main chain and application to deep-UV positive type photoresists, *Polymer J.*, 22, 468, 1990.
39. Inaki, Y., Horito, H., Matsumura, N., and Takemoto, K., Acid sensitive polymers of pyrimidine derivatives for chemical amplification resists, *J. Photopolym. Sci. Technol.*, 3, 417, 1990.
40. Horito, H., Inaki, Y., and Takemoto, K., Photochemistry and acid sensitivity of pyrimidine polymers, *J. Photopolym. Sci. Technol.*, 4, 33, 1991.
41. Inaki, Y., Acid sensitive pyrimidine polymers for chemical amplification resist, *Polym. Mater. Sci. Eng.*, 66, 109, 1992.
42. Mochizuki, E., Masuda, K., Wada, T., and Inaki, Y., Photodimerization of thymine derivatives in ionomer matrix, *J. Photopolym. Sci. Technol.*, 6, 131, 1993.
43. Sugiki, T., Wada, T., and Inaki, Y., Synthesis of polymers containing pyrimidine base as chemically amplified resist, *J. Photopolym. Sci. Technol.*, 8, 9, 1995.
44. Inaki, Y., Moghaddam, M.J., and Takemoto, K., Pyrimidine derivatives as lithographic materials, *Polymers in Microlithography Materials and Process*, Reichmanis, E., MacDonald, S.A., and Iwayanagi, T., Eds, ACS Symp. Ser., 412, 303, 1989.
45. Inaki, Y., Matsumura, N., Kanbara, K., and Takemoto, K., UV and x-ray sensitive polyurethanes containing pyrimidine photodimers, *Polymers for Microelectronics*, Tabata, Y., Mita, I., Nonogaki, S., Horie, K., and Tagawa, S., Eds., Kodansha-VCH, Tokyo, 1990, 91.

46. Inaki, Y., Matsumura, N., and Takemoto, K., Acid sensitive pyrimidine polymers for chemical amplification resists, *Polymers for Microelectronics*, Thompson, L.F., Willson, G., and Tagawa, S., Eds, ACS Symp. Ser., 537, 142, 1994.
47. Inaki, Y., Thymine polymers as high resolution photoresists and reversible photo-recording materials, *Polymer News*, 17, 367, 1992.
48. Inaki, Y., Wang, Y., Kubo, M., and Takemoto, K., Reversible photorecording system: ordered thymine derivatives having long alkyl chain, *J. Photopolym. Sci. Technol.*, 4, 259, 1991.
49. Inaki, Y., Wang, Y., Saito, T., and Takemoto, K., Reversible photochemical reactions of thymines having long alkyl chain, *J. Photopolym. Sci. Technol.*, 5, 567, 1992.
50. Inaki, Y., Wang, Y., Kubo, M., and Takemoto, K., Reversible photochemical reactions of thymines having long alkyl chain, *Chemistry of Functional Dyes*, Yoshida, Z. and Shirota, Y., Eds., Mita, Osaka, 1993, 365.
51. Tohnai, N., Sugiki, T., Mochizuki, E., Wada, T., and Inaki, Y., Photodimerization and crystal structure of long alkyl thymine derivatives, *J. Photopolym. Sci. Technol.*, 7, 91, 1994.
52. Tohnai, N., Miyata, M., and Inaki, Y., Solid state photodimerization of thymine derivatives: xylene derivatives, *J. Photopolym. Sci. Technol.*, 9, 63, 1996.
53. Sugiki, T., Thonai, N., Wang, Y., Wada, T., and Inaki, Y., Photodimerizations and crystal structures of thymine derivatives having a long alkyl chain connected with a carbamate bond, *Bull. Chem. Soc. Jpn.*, 69, 1777, 1996.
54. Tohnai, N., Inaki, Y., Miyata, M., Yasui, N., Mochizuki, E., and Kai, Y., Photodimerization of thymine derivatives in single crystal, *J. Photopolym. Sci. Technol.*, 11, 59, 1998.
55. Tohnai, N., Inaki, Y., Miyata, M., Yasui, N., Mochizuki, E., and Kai, Photoreactive and inactive crystals of 1-alkylthymine derivatives, *Bull. Chem. Soc. Jpn.*, 72, 851, 1999.
56. Tohnai, N., Inaki, Y., Miyata, M., Yasui, N., Mochizuki, E., and Kai, Y., Photodimerization of 1-alkylthymines crystallized from acetonitrile solution, *Bull. Chem. Soc. Jpn.*, 72, 1143, 1999.
57. Inaki, Y., Mochizuki, E., Donoue, H., Miyata, M., Yasui, N., and Kai, Y. Intramolecular photodimerization of bisthymine compounds *J. Photopolym. Sci. Technol.*, 12, 725, 1999.
58. Mochizuki, E., Yasui, N., Kai, Y., Inaki, Y., Tohnai, N., and Miyata, M., Structures and photodimerizations of 1-alkylthymine crystals obtained from *N, N*-dimethylformamide, *Bull. Chem. Soc. Jpn.*, 73, 1035, 2000.
59. Mochizuki, E., Yasui, N., Kai, Y., Inaki, Y., Wang, Y., Saito, T., Tohnai, N., and Miyata, M., Reversible photodimerization of ester derivatives of thymine having long alkyl chain in solid film, *Polymer J.*, 32, 492, 2000.
60. Inaki, Y., Mochizuki, E., Yasui, N., Miyata, M., and Kai, Y., Crystal structure and photodimerization of 1-alkylthymine: effect of long alkyl chain on isomer ratio of photodimer, *J. Photopolym. Sci. Technol.*, 13, 177, 2000.
61. Mochizuki, E., Yasui, N., Kai, Y., Inaki, Y., Wang, Y., Saito, T., Tohnai, N., and Miyata, M., Crystal structure of long alkyl 2-(thymin-1-yl)propionates: style of hydrogen bonding and dependence on the alkyl chain length, *Bull. Chem. Soc. Jpn.*, 74, 193, 2001.
62. Woodward, R.B. and Hoffmann, R., Stereochemistry of electrocyclic reactions, *J. Am. Chem. Soc.*, 87, 395, 1965.
63. Cohen, M.D. and Schmidt, G.M. J.,Topochemistry. 1. A survey, *J. Chem. Soc.*, 1996, 1964
64. Watson, J.D. and Crick, F.H.C., Molecular structure of nucleic acid, *Nature*, 171, 737, 1953
65. Hoogsteen, K., *Acta Cryst.*, The structure of crystals containing a hydrogen-bonded complex of 1-methylthymine and 9-methyladenine, 12, 822, 1959.
66. Haschemeyer, A.E.V. and Sobell, H.M.,The crystal structure of a hydrogen bonded complex of adenosine and 5-bromouridine, *Acta Cryst.*, 18, 525, 1965.
67. Katz, L., Tomita, K., and Rich, A., The crystal structure of the intermolecular complex 9-ethyladenine: 1-methyl-5-bromouracil, *Acta Cryst.*, 21, 754, 1966.

68. Voet, D. and Rich, A., The crystal structures of purines, pyrimidines and their intermolecular complexes, *Progress in Nucleic Acid Research and Molecular Biology*, Vol. 10, Davidson, J.N. and Cohn, W.E., Eds., Academic Press, New York, 1970, 183.
69. Green, D.W., Mathews, F.S., and Rich, A., The crystal and molecular structure of N-methyluracil, *J. Biol. Chem.*, 237, 3573, 1962.

105

Photocycloaddition of Halogenated Pyrimidines to Benzene and its Related Compounds: Cycloaddition and the Electrocyclic Rearrangement of the Adducts

Koh-ichi Seki
Health Sciences University of Hokkaid

Kazue Ohkura
Health Sciences University of Hokkaid

0-8493-1348-1/04/$0.00+$1.50

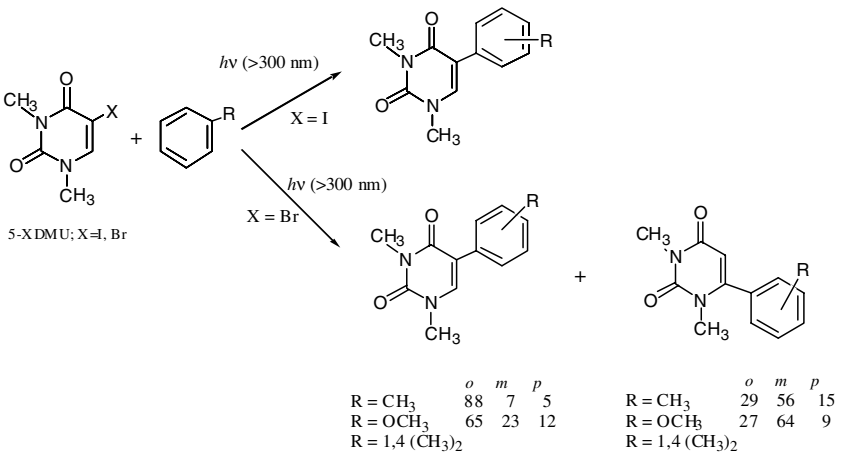

SCHEME 1

105.1 Introduction

The chemical modification of nucleic bases is recognized as one of the most promising approaches for developing bioactive substances such as anticancer and antiviral agents.[1]

The photochemistry of 5-bromouracil and its derivatives has been studied extensively in relation to radiation chemistry, radio-sensitization, and photobiology,[2] but little attention has been paid from a synthetic point of view.

This chapter deals with the photoaddition reactions of halogenated pyrimidines with benzene derivatives.

105.2 Acid-Catalyzed Electrophilic Aromatic Photosubstitution Reactions with 5-Halo-1,3-dimethyluracils

UV irradiation of 5-bromo-1,3-dimethyluracil (5-BrDMU) in benzene (**1a**) afforded 5-pheny-1,3-dimethyluracil (5-PhDMU), while prolonged irradiation of the solution afforded not only the corresponding 5-phenyl-1,3-dimethyluracils (5-PhDMU) but also the unexpected 6-phenyl isomer (6-PhDMU).[3] Similar results were obtained from the reaction of the uracil with substituted benzenes (Scheme 1). Detailed studies revealed that formation of the 6-aryl isomers (6-ArDMU) was effected by hydrogen bromide generated during the photoreaction.[4,5] It was suggested that the 5-isomers (5-ArDMU) are the products obtained through the excited singlet states, while 6-ArDMUs are produced via the excited triplet states. The anomalous 6-arylation was also effected by the addition of TFA. Noteworthy is the fact that 5-substitution occurred mainly at the *ortho*-position of the substituted benzenes while 6-arylation took place most favorably at the *meta*-position.

The isomer distribution for 5-ArDMU's was analogous to those typically observed in aromatic photosubstitution reactions.[6] On the other hand, few reports have appeared on the *meta*-oriented aromatic photosubstitution reaction, the primary example being the photoinduced proton exchange in benzenes[7] that proceeds via an electrophilic aromatic photosubstitution reaction.[8] In the case of either the 5-chloro- or 5-fluoro-1,3-dimethyluracil (5-ClDMU, 5-FDMU),[9,10] addition of TFA simply promoted 5-arylation (photo-Friedel-Crafts reaction), while the addition of a bromide (*p*-dibromobenzene, 1,2-dibromoethane, benzyl bromide, HBr) to the solution induced the *meta*-oriented 6-arylation (Scheme 2).[11]

It is proposed that 5-substitution is explicable by a mechanism involving an electron transfer from a benzene ring (**1x**) to **5-XDMU**-H$^+$ (X = Br, Cl, F), while 6-ArDMUs are derived from the direct coupling

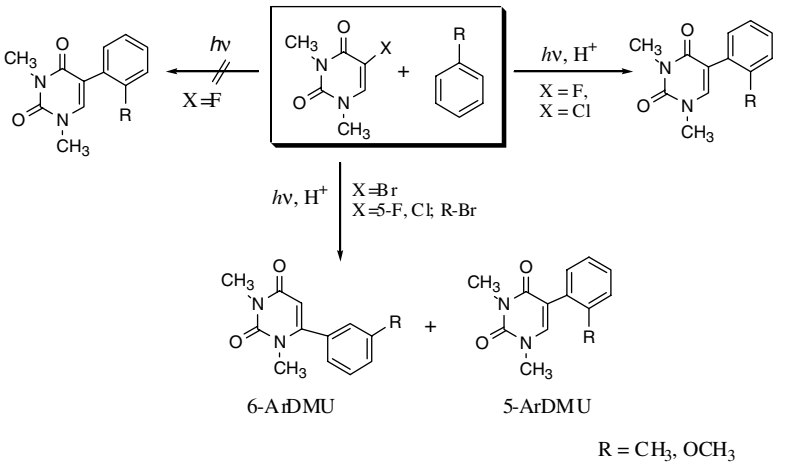

SCHEME 2

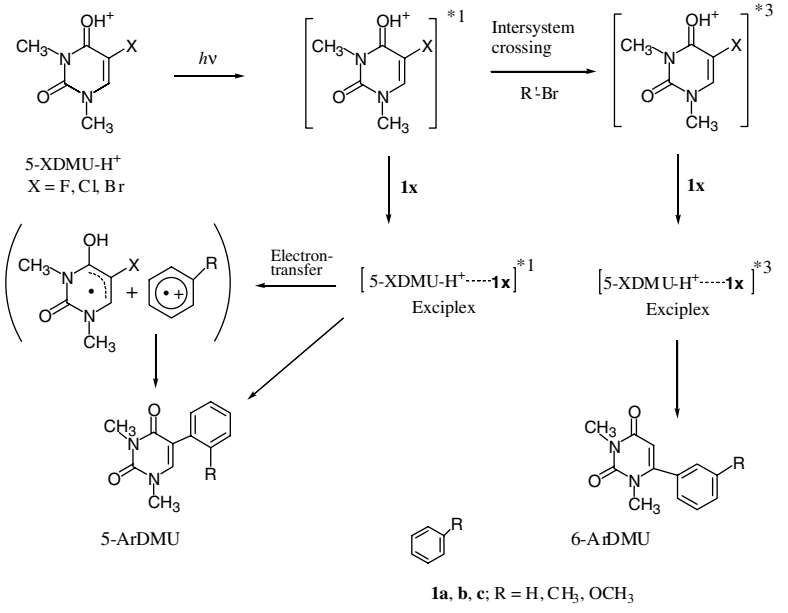

SCHEME 3

between the excited **5-XDMU**-H^+ in the triplet state and **1x** in the ground state or through the triplet exciplex (Scheme 3).

105.3 Acid-Catalyzed Photoreaction of 6-ClDMU with Benzene and Its Derivatives: Synthesis of Cyclooctapyrimidine-2,4-diones

This acid-catalyzed photoreaction has successfully been applied to 6-chloro-1,3-dimethyluracil (6-ClDMU).

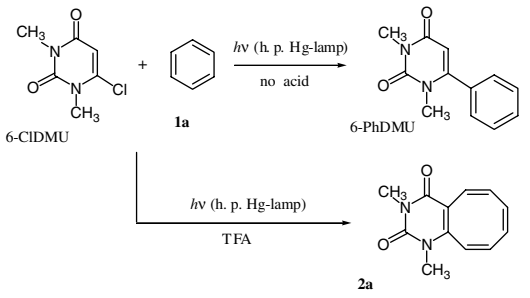

SCHEME 4

TABLE 105.1 Photolysis of 6-Chloro-1,3-dimethyluracil in Benzene in the Presence of Various Acids

Hg Lamp	Acid (equiv. mol)	Yields[a] (%) 6-PhDMU	Yields[a] (%) 2a	6-ClDMU(%) consumed
h-p	none	33	—	11
h-p	TFA (2)	3.8	62	41
h-p	TFA (48)	3.3	32	69
l-p	none	25	17	15
l-p	TFA (2)	25	17	32
l-p	TFA (48)	9	38	24
h-p	H_2SO_4 (48)	61	—	28
h-p	AcOH (2)	16	6	21
h-p	AcOH (48)	14	10	28
h-p	$ZnCl_2$ (2)	18	39	71
h-p	H_2SO_4 (0.05)	24	24	79
h-p	H_2SO_4 (1.25)	61	—	28

[a] Yields are reported on the basis of 6-ClDMU consumed.

UV irradiation of 6-ClDMU in a solution of benzene (**1a**) afforded 6-PhDMU through a substitution reaction. In sharp contrast, addition of TFA (2 molar equiv) to the reaction mixture induced [1,2]-photocycloaddition to give cyclooctapyrimidine (**2a**) in high yield (Scheme 4).[12] Among the various acids examined, trifluoroacetic acid (TFA) gave the best result for the formation of **2a** (Table 105.1).[13]

The photoreaction with monosubstituted benzenes (toluene **1b**, anisole **1c,** and fluorobenzene **1d**) in the presence of TFA at room temperature afforded the corresponding cyclooctapyrimidines (**2xn**: **x** = **b**, **c**, **d**; **n** = **i**, **ii**, **iii**, **iv**, **v**, and **vi** for substitution at 5, 6, 7, 8, 9, and 10) (Scheme 5, Table 105.2).

The photoreaction with *p*-xylene (**1e**) furnished predominantly the 5,8-dimethyl derivative (**2ei**) at low temperature (−58°C), while **2ei** and the 7,10-dimethyl derivative (**2eii**) were produced in the ratio of 1:3 at −25°C (Scheme 6).[14]

Similarly, UV irradiation of 6-ClDMU in mesitylene (**1f**) in the presence of TFA at −25°C for 5 h gave 5,7,9-trimethyl derivative (**2fi**) (20%) and 6,8,10-methyl isomer (**2fii**) (34%) in appreciable yields (Scheme 7).[15]

The UV spectrum of 6-ClDMU (λ_{max} 264 nm; 0.08 m*M*) shifted ca. 6 nm to the red in cyclohexane on the addition of TFA (9 molar equiv.) to the solution. This new spectrum was insensitive to added **1a**, whereas the fluorescence of this solution (emission λ_{max} at 330 nm with excitation at 285 nm) was quenched with **1a** (1.7 m*M*). Furthermore, addition of the triplet quencher piperylene to the reaction mixture of **1a** was ineffective in initiating the formation of **2a**, suggesting that the present cycloaddition may precede via the singlet excited state of protonated 6-ClDMU. This presumably occurs at either O-4 or the charge-transfer complex of 6-ClDMU and TFA.[13]

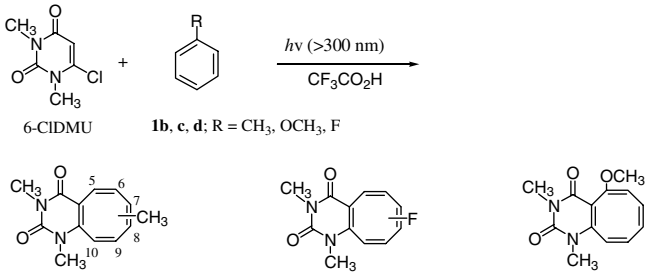

SCHEME 5

TABLE 105.2 Photoreaction of 6-ClDMU in Monosubstituted Benzenes (1x) in the Presence of TFA

1x/x	Reaction Time (h)/lamp	TFA (mmol)	Yields[a] (%) of 6-ArDMU [Isomer ratio (%); [*o*, *m*, *p*]]	Yields[a] (%) of $2x_n$ [Isomer ratio (%); n = i, ii, iii, iv, v, vi]	Consumed 1 (%)
a	10/h-p	50	10	49	42
b	5/h-p	2	6	73	15
			[100, —, —]	[—, 21.5, 23, 37, —— 18.5]	
c	10/l-p	2	34.5 [66, 14, 20]	8 [100, —, —, —, —, —]	50
d	5/l-p	2	19 [58, 26, 16]	42 [13, 34, 16, 19.5, 17.5, —]	29

[a] Yields are reported on the basis of **1** consumed.

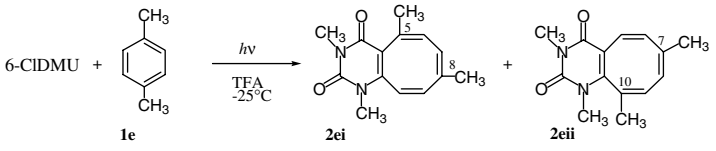

SCHEME 6

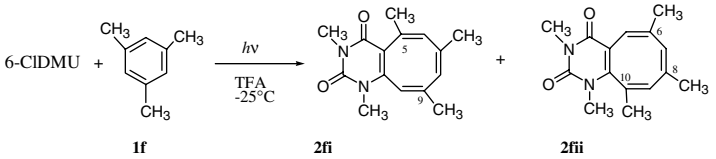

SCHEME 7

105.4 Acid-Catalyzed Photorearrangement of Cyclooctapyrimidines: Synthesis of (6a,1-d)Pentalenopyrimidine

Cyclooctatetraenes are one of the most interesting and well studied non-benzenoid $(CH)_n$ families that provide a considerable variety of isomeric strained compounds.[16,17] This section deals with the photochemical modification of cyclooctapyrimidines.

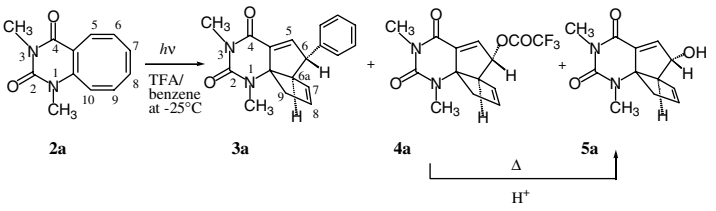

SCHEME 8

UV irradiation of a solution of cyclooctapyrimidine-2,4-dione (**2a**) in benzene with a 500 W high-pressure mercury lamp either at room temperature or at low temperature (−25°C) in the absence of TFA did not induce any reaction. Similarly, irradiation in the presence of 2 molar equivalents of TFA also gave no photoproduct.

However, it was found that at low temperature (−25°C) a photorearrangement product began to appear as the amount of TFA was increased. When a large excess of TFA (10 molar equiv) was used, tricyclic compounds 9*H*-6,6a-dihydro-1,3-dimethyl- 6-phenylpentaleno[6a,1-d]pyrimidine-2,4-dione (**3a**), 10,12-diaza-10,12-dimethyl-9,11- dioxotricyclo[6.4.0.0^{1,5}]dodeca-3,7-dien-6-yl 2,2,2-trifluoroacetate (**4a**), and 6-hydroxypentaleno[6a,1-d]pyrimidine (**5a**) were obtained in 55%, 5%, and 23% yields, respectively (Scheme 8).[18] When the reaction was performed in cyclohexane, the formation of **3a** could not be detected and the predominant product was trifluoroacetate (**4a**). Similarly, UV irradiation of the C-methyl derivatives (**2bii**, **iv**, **v**) in frozen benzene containing TFA gave varying yields of trifluoroacetoxypentaleno[6a,1-d]pyrimidines (**4b**) and/or phenyl derivative (**3b**) (Scheme 9).

The tri-C-methyl derivative (**2fii**) under similar conditions, furnished 7-methylene-1,3,6,9-tetramethylpentaleno[6a,1-*d*]pyrimidine-2,4-dione (**6fii**) in appreciable yield. Each of these structures contains a methyl group attached to the same carbon as the parent compound.

The participation of a di-π-methane process[19,20] through the benzocyclobutapyrimidine intermediate (**8bii**, **9bii**; R = CH_3) was ruled out (Scheme 10) by the fact that reaction with the 6-isomer (**2bii**) gave neither **3bii** nor **4bii**, but produced **3biii** and **4biii**.

The formation of these tricyclic compounds (**3**, **4**, and **5**) was explained in terms of a [π4s + π2a] type rearrangement[21] of the cyclooctatetraene moiety into the semibullvalene intermediate (**8**) or (**9**), followed by subsequent ring opening of the cyclopropane moiety through protonation. The MO of **2a,** on which the effect of TFA was neglected, showed that the LUMO (Figure 105.1A) has a large extension over C4a and C10a, and the next LUMO (NLUMO) (Figure 105.1B) extends largely over C7, C8, C9, and C10, supporting the [π4s + π2a] process.[22]

The role of acid in the photoreaction was studied using UV-spectroscopy. Sequential addition of TFA (0 to 10 molar equiv.) to a solution of **2a** in cyclohexane decreased the UV absorbance at λ_{max} 249 nm (ε = 10400) to ε = 9960 and increased the λ_{max} 307 nm (ε = 1640) to ε = 1820 with isosbestic points at 242 and 248 nm. Addition of aqueous potassium carbonate (2 molar equiv. to TFA added) returned the spectrum to its original form, suggesting that **2a** forms a charge-transfer complex with TFA. The other C-methylcyclooctapyrimidines (**2b**, **e**, **f**) that underwent the rearrangement showed similar spectroscopic behavior.

The effect of TFA on **2a** was investigated further using NMR spectroscopy. The signals due to C10a, C6, C9, and C4a were shifted downfield upon the addition of TFA, while the signals due to C5 and C10 were shifted upfield. The chemical shifts change drastically in the region of the plot where the amounts of TFA are increased from 0 to 3 molar equiv.. The changes, however, in the region where TFA is increased above 5 molar equiv. are minimal (Figure 105.2).

These results demonstrate that the presence of excess amounts of TFA is required for formation of the charge-transfer complex that is responsible for the photorearrangement into the semibullvalene intermediate (**8b** or **9b**). When **2a** was irradiated in the presence of TFA-*d*, significant amounts of deuterium

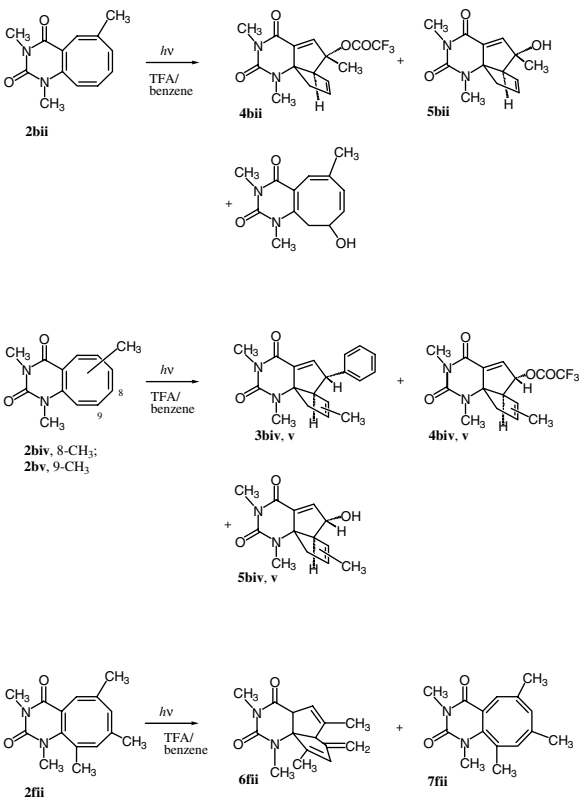

SCHEME 9

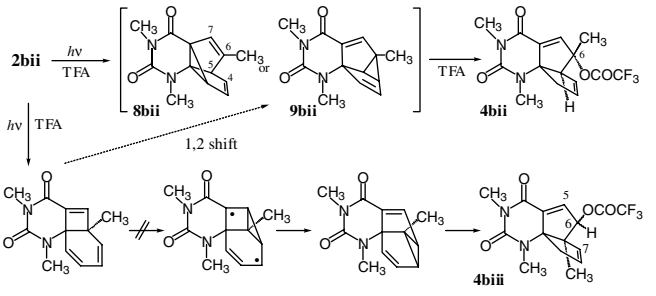

SCHEME 10

were incorporated into **3a**, and **4a** at C9 (50% for **3a**, and 94% for **4a**), suggesting that the resulting intermediate undergoes either a Friedel-Craft reaction or the addition of TFA to give the phenypentaleno[6a,1-*d*]pyrimidine (**3a**) or trifluoroacetoxy pentaleno[6a,1-*d*]pyrimidine (**4a**). Protonation of **8b** (or **9b**) would generate the carbocation center at C6 with the cleavage of the cyclopropane ring, which couples with benzene to form the ultimate product (**3a**), while the addition of TFA would lead to the formation of **4a**.

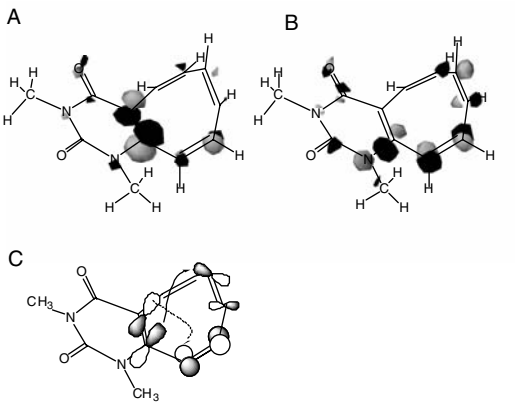

FIGURE 105.1 The molecular orbitals of **1a**: The LUMO(A) , THE NLUMO (B), and the possible MO interaction (C).

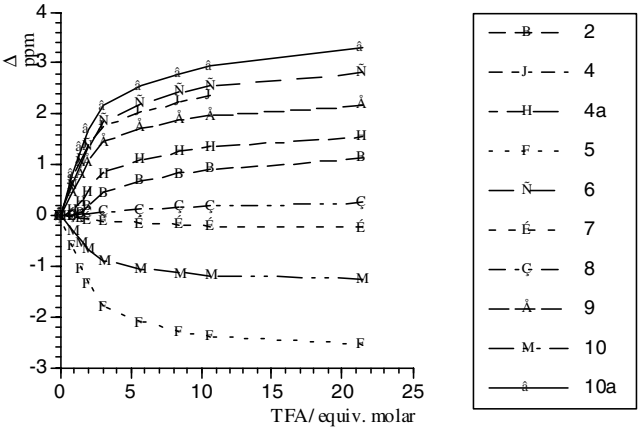

FIGURE 105.2 Changes in the ^{13}C-NMR chemical shifts of **2a** by the addition of TFA.

105.5 Synthesis of the Tautomeric Isomers of Cyclooctapyrimidines and their Photorearrangement

Photorearrangement of Cyclooctapyrimidine in the Absence of Acid: Synthesis of the Tautomer (*p*-Xylene)

UV irradiation of a solution of 1,3,5,8-tetramethylcyclooctapyrimidine (**2ei**) in benzene in the absence of an acid at room temperature for 1 h effected bond-switching to produce the tautomer (**7ei**)[23] as an equilibrium mixture with the starting material (1:10) (isolated by column chromatography on silica gel) (Scheme 11). Prolonged irradiation (4 h) of the solution was ineffective in altering the product ratio. No formation of other valence isomers was detected under the reaction conditions (Scheme 2).[16] Upon heating in the dark, transformation into cyclobutaquinazoline (**10ei**) occurred through an intramolecular Diels-Alder reaction.

Similar irradiation of 1,3,5,7,9- and 1,3,6,8,10-pentamethylcyclooctapyrimidine-2,4-diones (**2fi**, **2fii**) gave the corresponding tautomeric isomers (**7fi**, **7fii**).[24] Upon being kept in the dark at room temperature, the former (**7fi**) (half life, 30 min) was transformed into cyclobutaquinazoline (**11fi**) with competitive reversion into **7fi**, while the latter (**7fii**) reverted to **2fii** with half-life of 8 h.

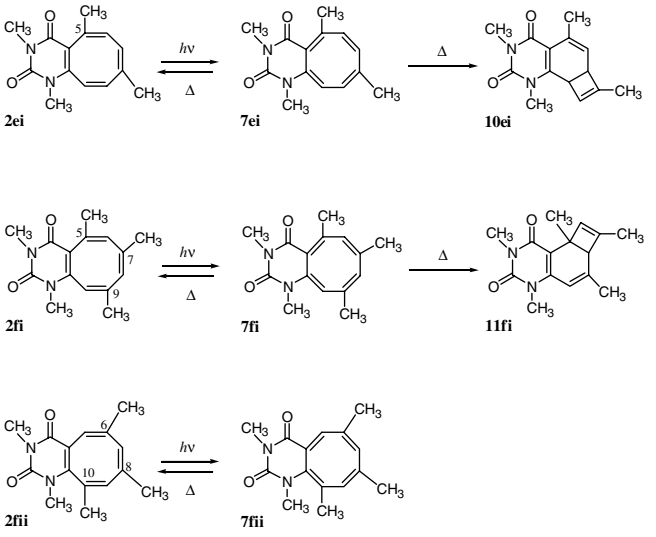

SCHEME 11

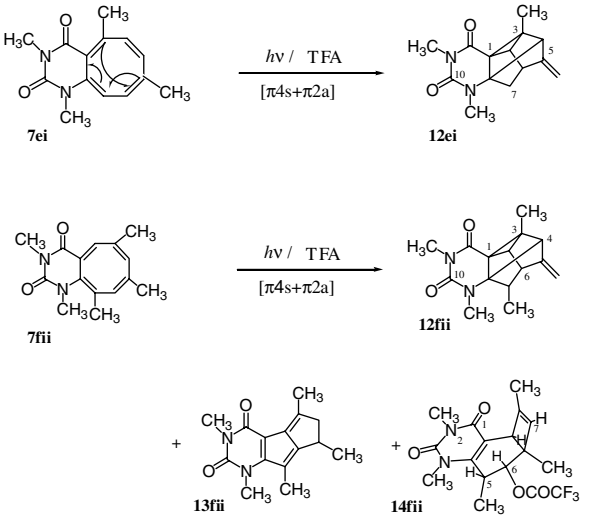

SCHEME 12

Acid-Catalyzed Photorearrangement of Tautomer (7) in the Presence of TFA ([π4s + π2a] Reaction)

UV irradiation of **7ei** (6,8,10-methyl) in the presence of TFA gave rise to the formation of 9,11-diazapentacyclo[6.4.0.0.^{1,3}0.^{2,5}0^{4,8}]dodecane (**12ei**) as the major product.

Similar photolysis of **7fii** (6,8,10-trimethyl) in benzene in the presence of TFA for 18 h furnished 9,11-diazapentacyclo[6.4.0.0.^{1,3}0.^{2,5}0^{4,8}]dodecane (**12fii**) as the major product, together with pentaleno[2,1-*d*]pyrimidine (**13fii**) and a cyclobutaquinazoline derivative (**14fii**).[25,26]

The formation of these pentacyclic compounds (**12**) was explained by the analogous mechanism employed for the photorearrangement of cyclooctapyrimidines (**2**) involving a [π4s + π2a] process (Figure 105.3).[22] Through this process, **7** would be transformed into the semibullvalene intermediate

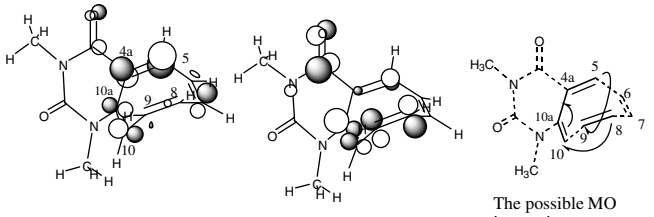

FIGURE 105.3 The molecular orbitals of **7a**.

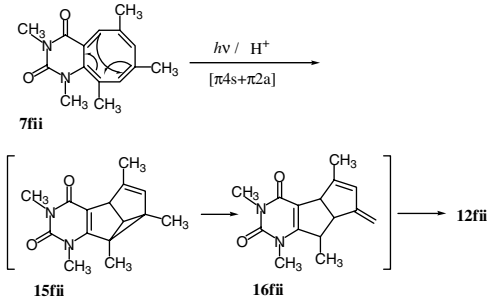

SCHEME 13

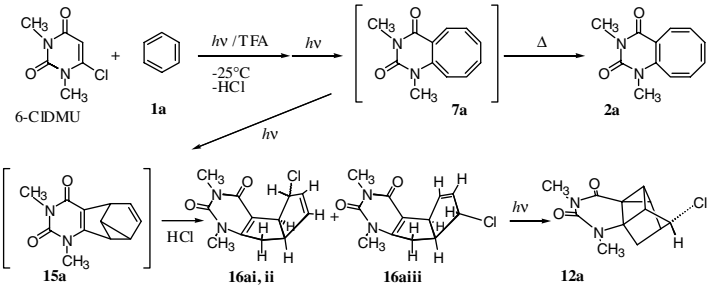

SCHEME 14

(**15fii**), followed by subsequent ring opening of the resulting cyclopropane moiety through protonation.[27] Subsequent intramolecular [2+2]-coupling of the resulting pentalenopyrimidine (**16fii**) would ultimately lead to its transformation into **12fii** (Scheme 13).

Although the synthesis or the detection of the tautomer of the simple cyclooctapyrimidine (**2a**) derived from **1a** was unsuccessful, photolysis of 6-ClDMU in frozen benzene (−25°C) in the presence of TFA resulted in the formation of pentalenopyrimidine derivatives (**16ai**, **ii, iii**) and a diazapentacyclo[6.4.0.0^{1,3}.0^{2,6}.0^{4,8}]dodecane derivative (**12a**) in moderate yields (Scheme 14).[28] These results indicate that the tautomer (**7a**) may be involved in the present reaction as the key intermediate.

UV irradiation of the pentalenopyrimidine (**16aiii**) gave **12a**.[29]

These results substantiate the mechanism that pentacyclic compounds (**12x**) are derived from the tautomeric isomer (**7x**) by way of the semibullvalene intermediate (**15x**) followed by rearrangement to pentalenopyrimidine (**16x**). Thus, the present work demonstrates that pentacyclo[6.4.0.0.^{1,3}0.^{2,6}0^{4,8}]dodecanes (**3x**)

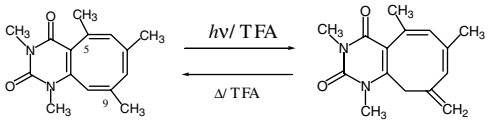

2fi **17fi**

SCHEME 15

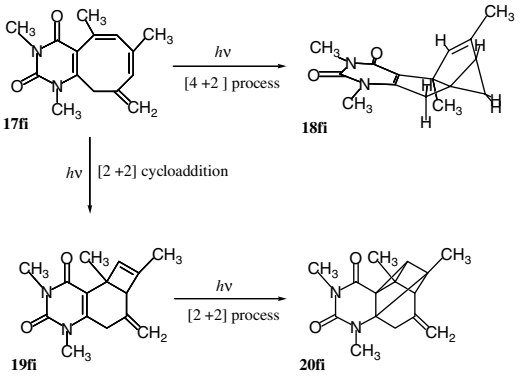

17fi **18fi** **19fi** **20fi**

SCHEME 16

are products from the initial *ortho*-cycloaddition, but not from the *meta*-cycloaddition between 6-ClDMU and a benzene.[30]

105.6 Acid-Catalyzed Sigmatropic Rearrangements

Synthesis of 9-Methylenecyclooctapyrimidine

As described above, UV irradiation of cyclooctapyrimidines (**2x**) in the absence of an acid undergoes bond-switching to form the corresponding tautomers. In contrast, in the presence of TFA, photoisomerization of **2x** bearing a methyl group at C9 or C10 proceeds in a different manner.

Upon irradiation in the presence of TFA at room temperature for 1 h, **2fi** was quantitatiely transformed into the *exo*-methylene derivative (**17fi**) (Scheme 15).[15,26]

No deuterium uptake into **17fi** was observed when **2fi** was irradiated in the presence of TFA-*d*, suggesting that the present process can be regarded as an acid-catalyzed sigmatropic reaction.

In the presence of TFA, **17fi** was exclusively converted back to **2fi** in the dark.

Photorearrangement of *exo*-Methylenecyclooctapyrimidine

Irradiation of **17fi** at room temperature for 30 min effected the competitive synthesis of **18fi** (25%) through a [4+2]-process and cyclobutaquinazoline **19fi** (75%) via a [2+2]-process (at the stage when 35% of **2fi** had been consumed). Cyclobuta[*f*]quinazoline (**19fi**) was further converted to **20fi** *via t*he secondary [2+2]-process (Scheme 16).[15,26]

It is suggested that the NLUMO of **17fi** consists of 6π electrons developing over the carbon atoms C5–C9 and the *exo*-methylene carbon, which is responsible for the formation of **18fi** through the [π4s + π2a] orbital interaction (Figure 105.4). This process is regarded as analogous to that reported for the photo-transformation of vitamin D_3 into suprasterol I and II.[31,32]

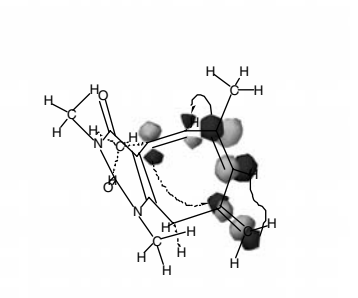

FIGURE 105.4

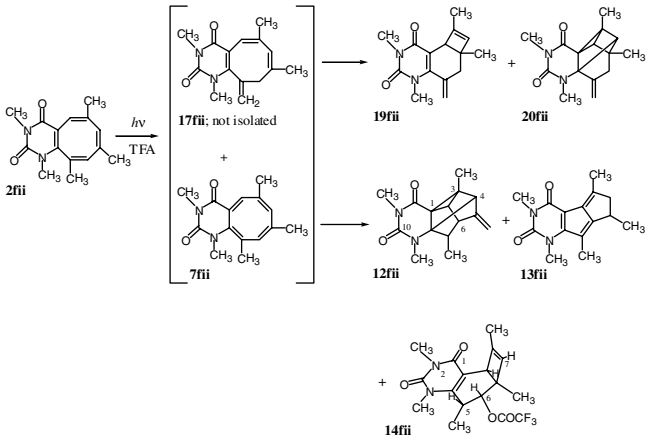

SCHEME 17

The 6,8,10-methylyclooctapyrimidine (**2fii**) is much less sensitive to UV irradiation than the 5,7,9-methyl isomer (**2fi**). Nonetheless, prolonged irradiation of **2fii** resulted in the competitive formation of its valence isomers (**19fii**, **20fii**), apparently through the *exo*-methylene intermediate (**17fii**) by way of a sigmatropic rearrangement, though not isolated, with pentalenopyrimidines (**12fii**, **13fii**) through the tautomer (**7fii**) (Scheme 17).[26]

Photoreaction of 6-ClDMU with *p*-xylene (**1e**) and *m*-xylene (**1g**) in the presence of TFA furnished the 6-methylenediazapentacyclo[6.4.0.0^{1,3}.0^{2,5}.0^{4,8}]dodecanes (**20eiii**, **20giii**)[33] together with 5-methylenediazapentacyclo[6.4.0.0^{1,3}.0^{2,6}.0^{4,8}]dodecane derivatives (**12ei**, **12fi**) (Scheme 18).[34] Due to the presence of the *exo*-methylene group at C6, these compounds (**20eiii**, **20giii**) can be regarded as originating from the 9-*exo*-methylene derivatives (**17eiii, 17giii**), although their isolation or detection has not yet been achieved (see Scheme 19).

Photorearrangement of Cyclobutapyrimidines

As described above, each pentacyclo[6.4.0.0^{1,3}.0^{2,5}.0^{4,8}]dodecane (**2a**-**d**) includes a methylene group at C6 or C7 as a component, suggesting that the presence of a methylene group at C6 or C7 in the precursory cyclobutaquinazoline may be important for the construction of the ring system (Scheme 19).[35]

Recently, it was shown that the hydrochlorinated cyclobutaquinazolines (**19fii-cCl**,[35] **19fii-tCl**,[36] **19a-Cl**[30]), which have no *exo*-methylene group, underwent cycloaddition to give the corresponding pentacyclododecane derivatives (**20fii-cCl**, **20fii-tCl**, **20a-Cl**).

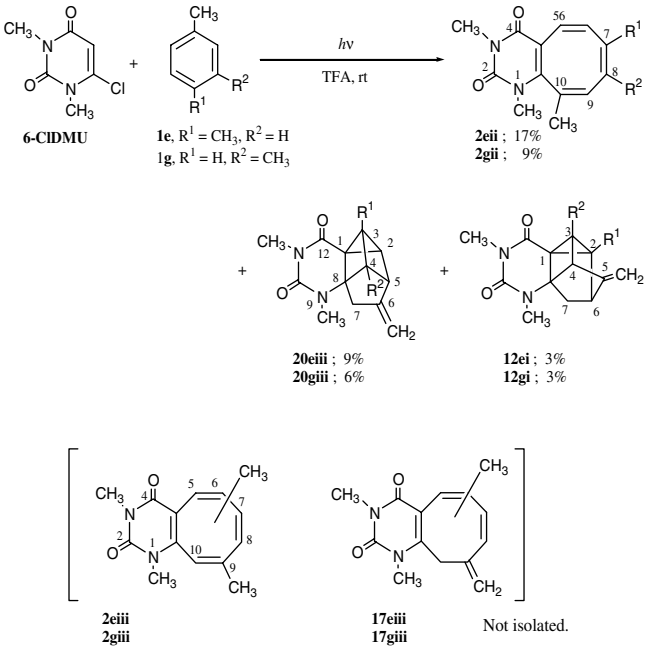

SCHEME 18

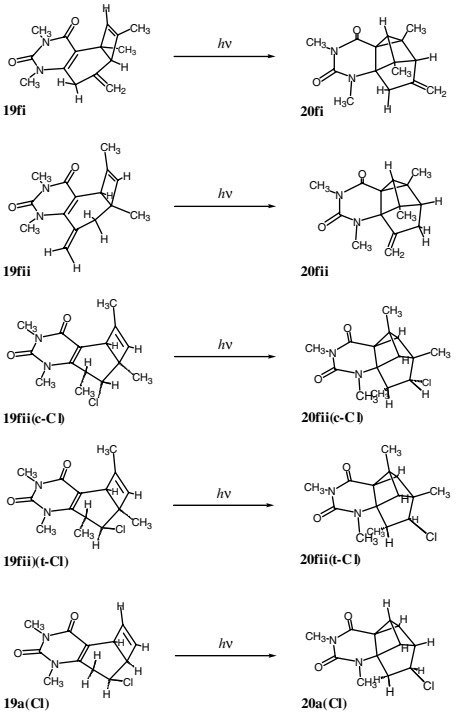

SCHEME 19

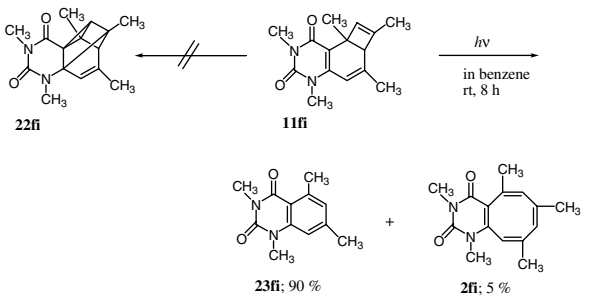

SCHEME 20

In contrast, UV irradiation of **11fi**, which retains the double bond between C5 and C6, resulted in the cleavage of the cyclobutene ring to produce propyne and quinazoline (**23fi**) in place of the anticipated pentacyclododecane (**22fi**) (Scheme 20). These findings indicate that the removal of the C5–C6 double bond may be essential for the formation of pentacyclo[6.4.0.0^{1,3}.0^{2,5}.0^{4,8}]dodecanes.

105.7 Summary

The present chapter describes various aspects of photoreaction with halouracils and benzenes, as listed below.

1. Aromatic photosubstitution, including acid-catalyzed photosubstitution reaction (photo-Friedel-Crafts reaction)
2. Anomalous aromatic photosubstitution regarded as related to an electrophilic aromatic photosubstitution reaction
3. Photocycloaddition of 6ClDMU to benzenes
4. Valence isomerization of the cycloadduct that could be explained in terms of (a) acid-catalyzed sigmatropic rearrangement, (b) [2 + 2] cycloaddition, (c) [π4s + π2a]-type cycloaddition, (d) [π4s + π2a] type electrocyclic reaction
5. Synthesis of various novel cycloadducts, including highly strained polycyclic compounds, through these various photochemical processes

Noteworthy is that a majority of these photoreactions take place only in the presence of acids (TFA). Thus, the present studies provide not only useful methods for modifying the pyrimidine ring, but also incorporate a novel photoreaction wherein the presence of acid can be employed to switch the photochemical behavior via a novel acid-catalyzed photoreaction.[37]

References

1. Périgaud, C., Gosselin, G., and Imbach, J.–L., Nucleoside analogues as chemotherapeutic agents: a review, *Nucleosides Nucleotides*, 11, 903, 1992.
2. Hutchinson, F., The lesions produced by ultraviolet light in DNA containing 5-bromouracil, *Quart. Rev. Biophys.*, 6, 201, 1973; Wang, S.Y., *Photochemistry and Photobiology of Nucleic Acids*, Vol. 1, Wang, S.Y., Ed., Academic Press, New York, 1976, chap. 6; Matsuura, T., Saito, I., Sugiyama, H., and Shinmura., Organic chemical approach to photo-cross-links of nucleic acids to proteins, *Pure Appl. Chem.*, 52, 2705, 1980; Shetlar, M.D., Cross-linking of proteins to nucleic acid by ultraviolet light, *Photochem. Photobiol. Rev.*, 5, 105, 1980; Celewicz, L., Photochemical coupling of 5-bromo-1,3-dimethyluracil and its 6-alkyl derivatives to 3-methylindole and N$^{\alpha}$-acetyl-L-tryptophan methyl ester, *J. Photochem. Photobiol., B: Biol.*, 3, 565, 1989.
3. Seki, K., Bando, Y., and Ohkura, K., Photolysis of 5-bromo-1,3-dimethyluracil in substituted benzenes, *Chem. Lett.*, 195, 1986.

4. Seki, K., Matsuda, K., and Ohkura, K., Photoreaction of 5-bromo-1,3-dimethyluracil with 1,4-xylene. The effect of acid, *Chem. Lett*., 175, 1987.
5. Seki, K., Matsuda, K., Bando, Y., and Ohkura, K., Photolysis of 5-bromo-1,3-dimethyluracil in substituted benzenes, *Chem. Pharm. Bull*., 36, 4737, 1988.
6. Ohkura, K., Terashima, M., Kanaoka, Y., and Seki, K., New aspects of the aromatic photosubstitution with iodopyridines, *Chem. Pharm. Bull*., 41, 1920, 1993.
7. Havinga, E. and Cornelisse, J., Aromatic photosubstitution reactions, *Pure Appl. Chem.,* 47, 1, 1976; Pàrkànyi, C., Aromatic photosubstitutions, *Pure Appl. Chem.,* 55, 331, 1983.
8. Fleming, I., *Frontier Orbitals and Organic Chemical Reactions*, John Wiley & Sons, New York, 1976, 225–227.
9. Ohkura, K., Matsuda, K., and Seki, K., Acid-catalyzed photoreaction of 5-chloro-1,3-dimethyluracil with substituted benzenes, *Heterocycles*, 32, 1371, 1991.
10. Seki, K. and Ohkura, K., Acid-catalyzed photosubstitution of 5-fluoro-1,3-dimethyluracil with substituted benzenes, *Nucleosides Nucleotides*, 11, 521, 1992.
11. Seki, K., Ohkura, K., Fukai, Y., and Terashima, M., Effect of bromides on the anomalous photoarylation of 5-halo-1,3-dimethyluracils, *Heterocycles*, 42, 341, 1996.
12. Seki, K., Kanazashi, N., and Ohkura, K., Acid-catalyzed photoreaction of 6-chloro-1,3-dimethyluracil in benzene; synthesis of cyclooctapyrimidine-2,4-dione, *Heterocycles*, 32, 229, 1991.
13. Ohkura, K., Kanazashi, N., and Seki, K., Synthesis of cyclooctapyrimidine-2,4-diones by photocycloaddition of 6-chloro-1,3-dimethyluracil to benzenes in the presence of trifluoroacetic acid, *Chem. Pharm. Bull*., 41, 239, 1993.
14. Ohkura, K. and Seki, K., unpublished data.
15. Ohkura, K., Nishijima, K., Sakushima, A., and Seki, K., Photochemistry of 9,10-dihydro-1,3,5,7-tetramethyl-9-methylenecyclooctapyrimidine-2,4-dione; synthesis of novel ring systems through electrocyclic reaction, *Heterocycles*, 53, 1247, 2000.
16. Scott, L.T. and M. Jones, J.R., Rearrangements and interconversions of compounds of the formula $(CH)_n$, *Chem. Rev*., 72, 181,1972.
17. Hassenrück, K., Martin H., and Walsh R., Consequences of strain in $(CH)_8$ hydrocarbons, *Chem. Rev*., 89, 1125, 1989.
18. Ohkura, K., Noguchi, Y., and Seki, K., Acid-catalyzed photorearrangement of 1,3-dimethylcyclooctapyrimidine-2,4-dione into 10,12-diazatricyclo-[6.4.0.0^{1,5}]dodeca-3,7-diene-9,11-diones, *Heterocycles*, 49, 59, 1998.
19. Zimmerman, H.E., The di-π-methane rearrangement, in *Organic Photochemistry*, Vol. 11, Padwa A., Ed., Marcel Dekker, New York, 1991, 1–36.
20. Bender, C.O., Dolman, D., and Murphy G.K., The photochemistry of 8-cyano-2,3-benzobicyclo[4.2.0]octa-2,4,7-triene, *Can. J. Chem*., 66, 1656, 1988.
21. Woodward, R.B. and Hoffmann, R., The conservation of orbital symmetry, Verlag Chemie GmbH, Weinheim/Bergstr, 1970.
22. Ohkura, K. and Seki, K., Photoinduced transannular reaction of 1,3-dimethylcyclo-octapyrimidine-2,4-diones, *Photochem. Photobiol*., 75, 579, 2002.
23. Photo-induced bond switching in substituted cyclooctatetraenes has been reported; Anet, F.A.L. and Bock, L.A., Photochemical interconversion of cyclooctatetraene bond shift isomers, *J. Am. Chem. Soc*., 90, 7130, 1968.
24. Ohkura, K., Nishijima, K., Uchiyama, S., Sakushima, A., and Seki, K., Photochemical synthesis and characterization of the tautomers of 1,3,5,7,9- and 1,3,6,8,10-pentamethylcyclooctapyrimidine-2,4-diones, *Heterocycles*, 54, 65, 2001.
25. Ohkura, K., Nishijima, K., Uchiyama, S., Sakushima A., and Seki K., Acid-catalyzed photorearrangement of the bond-switching isomer of a pentamethylcyclooctapyrimidine-2,4-dione, *Heterocycles*, 55, 1015, 2001.
26. Ohkura K., Nishijima K., and Seki, K., Electrocyclic rearrangement of pentamethyl-cyclooctapyrimidine-2,4-diones: reaction pathway into a 9,11-diazapenta-cyclo[6.4.0.0.^{1,3}0.^{2,5}0^{4,8}]dodecane sys-

tem and a 9,11-diazapentacyclo-[6.4.0.0.^{1,3}0.^{2,6}0^{4,8}]dodecane system, *Photochem. Photobiol.*, 74, 385, 2001.

27. Bender, C.O., Bengston, D.L., Dolman, D., Herle, C.E., and O'Shea, S.F., Substituent effects in arosemibullvalene photochemistry: the methylcyclopropane rearrangement of 1,8-dimethylbenzosemibullvalene, *Can. J. Chem.* 60, 1942, 1982.
28. Ohkura, K., Noguchi, Y., and Seki, K., Acid-catalyzed photoreaction of 6-chloro-1,3-dimethyluracil in frozen benzene: formation of novel cycloadducts, tetrahydropentaleno[1,2-*e*]pyrimidine-2,4-dione derivatives, *Chem. Lett.*, 99, 1997.
29. Ohkura, K., Noguchi, Y., and Seki, K., Photorearrangement of the *ortho*-cycloadduct of 6-chloro-1,3-dimethyluracil to benzene through [π4s+π2a] photocycloaddition, *Heterocycles*, 46, 141, 1997.
30. Ohkura, K., Noguchi, Y., and Seki, K., Acid-catalyzed photoreaction of 6-chloro-1,3-dimethyluracil in frozen benzene: formation of photocycloadducts and their isomerization through photo-Diels-Alder reaction, *Heterocycles*, 47, 429, 1998.
31. Dauben, W.G., Bell, I., Hutton, T.W., Law, G.F., Rheiner Jr., A., and Urscheler, H., Structure of suprasterol II, *J. Am. Chem. Soc.*, 80, 4116, 1958.
32. Dauben, W.G. and Baumann, P., Photochemical transformations. IX. Total structure of suprasterol II, *Tetrahedron Lett.*, 565, 1961.
33. Ohkura, K., Kanazashi, N., Okamura, K., Date, T., and Seki, K., A new ring system from photocycloaddition of 6-chloro-1,3-dimethyluracil to *p*- and *m*-xylene. Formation of 6-methylene-9,11,x-trimethyl-9,11-diazapentacyclo-[6.4.0.0^{1,3}.0^{2,5}.0^{4,8}]dodecane-10,12-diones, *Chem. Lett.*, 667, 1993.
34. Seki, K., Ohkura, K., Hiramatsu, H., Aoe, K., and Terashima, M., Acid-catalyzed photoreaction of 6-chloro-1,3-dimethyluracil to *p*- and *m*-xylene: Formation of novel photo-cycloadducts, 6-methylene-9,11,x-trimethyl-9,11-diaza-pentacyclo-[6.4.0.0^{1,3}.0^{2,5}.0^{4,8}]dodecane-10,12-diones and 5-methylene-9, 11, x-trimethyl-9,11-diazapentacyclo [6.4.0.0^{1,3}.0^{2,6}.0^{4,8}]dodecane-10,12-diones, *Heterocycles*, 44, 467, 1997.
35. Ohkura, K., Nishijima, K., Kuge, Y., and Seki, K., Synthesis of 9,11-diazapentacyclo-[6.4.0.0.^{1,3}0.^{2,5}0^{4,8}]dodecane-2,4-diones, *Heterocycles*, 56, 235, 2002.
36. Ohkura, K., Nishijima, K., and Seki, K., Acid-catalyzed photoreaction of 6-chloro-1,3-dimethyluracil and mesitylene: formation of photocycloadducts and their characterization, *Chem. Pharm. Bull.,* 49, 384, 2001.
37. Bryce-Smith, D. and Gilbert, A., The organic photochemistry of benzene. II, *Tetrahedron*, 40, 2459,1976; Ohashi, M., Yoshino, A., Yamazaki, K., and Yonezawa, T., Use of the zinc chloride in the 1,2-photoaddition of acrylonitrile to benzene, *Tetrahedron Lett.*, 3395, 1973; Tada, M., Saiki, H., Miura, K., and Shinozaki, H., The photoreaction of benzyl 1-cycloalkenyl ketone in acidic or protic media, *Bull. Chem. Soc. Jpn.*, 49, 1666, 1976; Mori, T., Wada, T., and Inoue, Y., Perfect switching photoreactivity by acid: photochemical decarboxylation versus transesterification of methyl cyclohexanecarboxylate, *Org. Lett.*, 2, 3401, 2000.

106

The Photochemistry of Thioamides and Thioimides

Masami Sakamoto
Chiba University

Takehiko Nishio
University of Tsukuba

106.1 Introduction

The photochemistry of thiocarbonyl compounds has been extensively studied over the past three decades and many new photochemical reactions have been developed.[1–7] Thiocarbonyl compounds, such as thioketones and thioesters, show considerably high photochemical reactivity toward (2+2)-cycloaddition and hydrogen abstraction by thiocarbonyl sulfur. Simple thioamides are generally inert toward photolysis; however, in contrast, cyclic thioamides and arylthioamides show considerable reactivity in a variety of photochemical reactions such as photochemical (2+2)-cycloaddition with various alkenes, and which provides a method for the synthesis of a new C–C bond. The thioimides are more reactive than thioamides toward the photochemical cycloaddition to multiple bonds and hydrogen abstraction by thiocarbonyl sulfur atom. Most thioamides are conveniently prepared by sulfurization of the corresponding amides with thionation reagents such as Lawesson's reagent or phosphorous pentasulfide. Monothioimides or dithioimides are usually provided by thionation of the corresponding imides with the same thionation reagents or acylation of the corresponding thioamides. The photochemical reaction of thioamides and thioimides provides not only a new photochemical aspect in the area of organic photochemistry but also a useful synthesis of nitrogen-containing heterocycles. Some reviews for thione photochemistry, including thioamides and thioimides, have been reported; therefore, the photochemical reactions in this chapter are limited to those developed in the past ten years.[8–11]

106.2 Photochemical (2+2)-Cycloaddition Reaction of Thioamides and Thioimides

Photochemical (2+2)-photocycloaddition of thiocarbonyl compounds with multiple bonds is a well-studied reaction. Thioamides undergo both inter- and intramolecular photocycloaddition reactions with alkenes to afford a variety of adducts (Scheme 1). The aminothietanes (II), formed as the primary

0-8493-1348-1/04/$0.00+$1.50

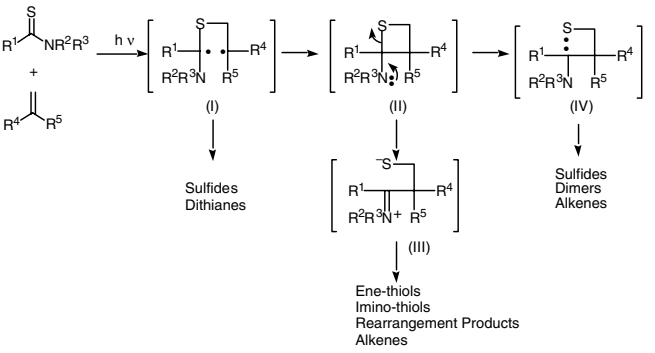

SCHEME 1

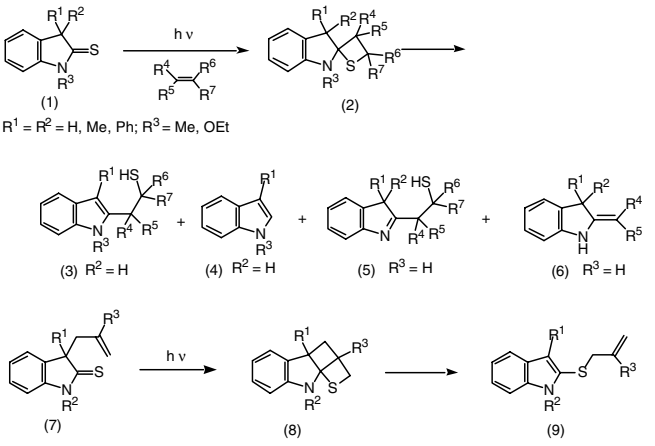

SCHEME 2

products via biradical (I), are generally unstable and undergo C–S bond cleavage of the thietane ring, leading to zwitterions (III) or diradicals (IV), followed by subsequent reactions. The instability of aminothietanes (II) may be due to the participation of lone-pair electrons on the nitrogen atom. Therefore, suppressing the participation will stabilize the aminothietanes. In fact, thietanes derived from thioimides (R^2 or R^3 = acyl group), in which the nitrogen atoms are cross-conjugated with a carbonyl or thiocarbonyl group, show considerable stability and many thietane derivatives are isolated. The photochemical cycloaddition of thioamides and thioimides with multiple bonds provides a facile route for the formation of new C–C bonds of nitrogen-containing heterocycles.

Irradiation of indoline-2-thiones (1) in the presence of alkenes gives 2-alkyl-3*H*-indoles and 2-alkylindoles (3–6) through the ring cleavage of the intermediates, spirocyclic aminothietanes (2), initially derived by (2+2)-cycloaddition of the C=S bond and alkenes (Scheme 2).[12] Intramolecular photoaddition has been also reported in the photoreaction of (7), in which allyl indole sulfide (9) is obtained.[13] The highly strained aminothietane intermediate (8) is proposed as the key intermediate in the reaction.

Photolysis of isoindoline-1-thiones (10), which are the structural isomer of indoline-2-thiones, brings about cycloaddition with various electron-rich and electron-deficient alkenes, yielding tricyclic isoindoline derivatives (12).[14] The plausible mechanism for this transformation is explained (Scheme 3) and involves amino-thietane intermediate (11), which undergoes ring opening to form zwitterions followed by further reaction. In contrast to the photoreaction of (10), stable thietanes (14, 16) are formed by the

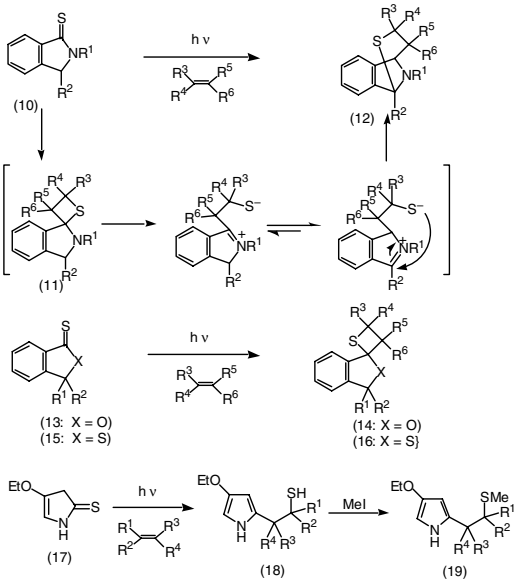

SCHEME 3

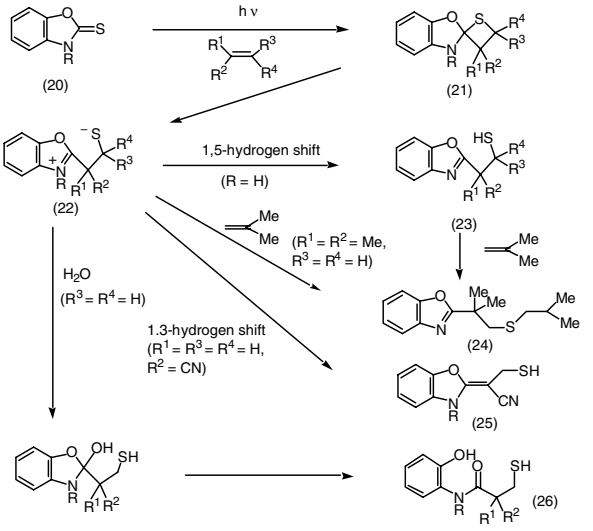

SCHEME 4

photoreaction of isobenzofuran-1-thione (13, X = O) and isobenzothiophene-1-thione (15, X = S) in the presence of alkenes.[15]

Irradiation of a benzene solution of 4-ethoxy-2,5-dihydro-1*H*-pyrrole-2-thione (17) and electron-rich alkenes gives 2-(mercaptoalkyl)pyrroles (18), which are alkylated with methyl iodide to give (19).[16]

Photochemical addition of benzoxazoline-2-thiones (20) to alkenes affords the 2-substituted benzooxazolines (23–25) or ring-opened products (26), depending on the substituent R and the alkenes used. The formation of these products may be rationalized in terms of zwitterionic intermediate (22), from ring-opening of an aminothietane (21), formed by regioselective (2+2)- photoaddition of the C=S bond of (20) to the C = C bond of the alkene (Scheme 4).[17,18]

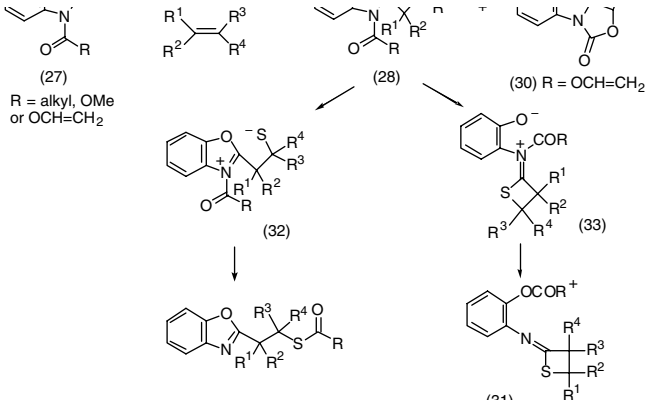

SCHEME 5

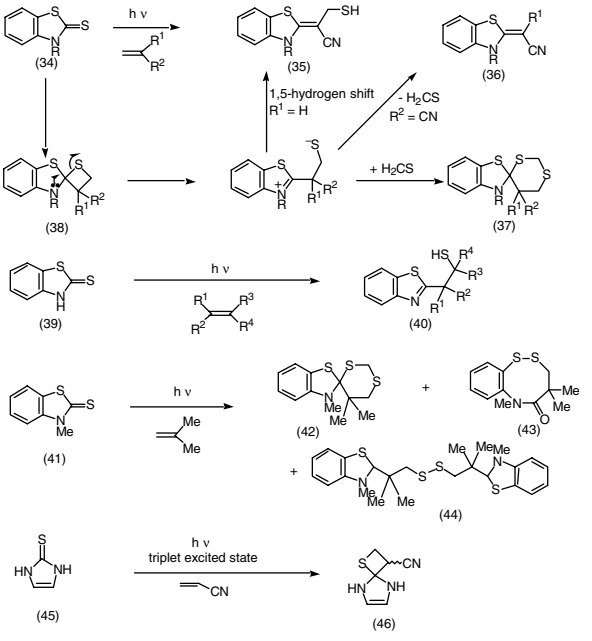

SCHEME 6

On the other hand, *N*-acylbenzoxazoles-2-thiones (27, R = alkyl) also photocycloadd to alkenes regioselectively to give the 2-substituted benzoxazoles (29) and/or the iminothietanes (30) by intramolecular trapping of zwitterionic intermediate (32) and (33), respectively (Scheme 5).[18,19] Stable aminothietanes (28) have been isolated and characterized from the photoaddition of *N*-methoxycarbonylbenzoxazole-2-thiones (27, R = OMe) to alkenes. Furthermore, the *N*-vinyloxycarbonyl derivatives (27, R=O-CH=CH_2) undergoes intramolecular (2+2)-cycloaddition to give the analogous multi-fused aminothietane (31).[20]

Irradiation of benzothiazoline-2-thiones (34) and acrylonitrile affords 2-alkylidenethiazoles (35) (Scheme 6). On the other hand, two products (36, 37) are formed by the photoaddition of (34) with 1,1-disubstituted alkenes such as methacrylonitrile and methyl methacrylate.[21] Aminothietanes (38) is proposed as intermediates in these photoreactions. Thioformaldehyde formed by the decomposition of the intermediate has been detected by its trapping by a diene. Photocycloaddition reaction of *N*-unsubstituted

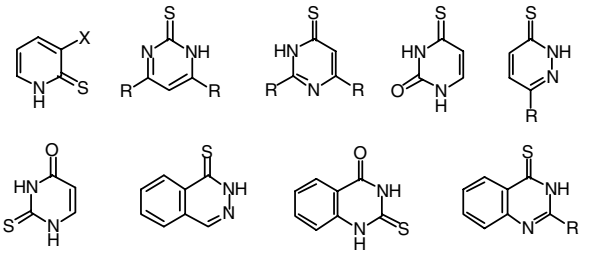

FIGURE 106.1

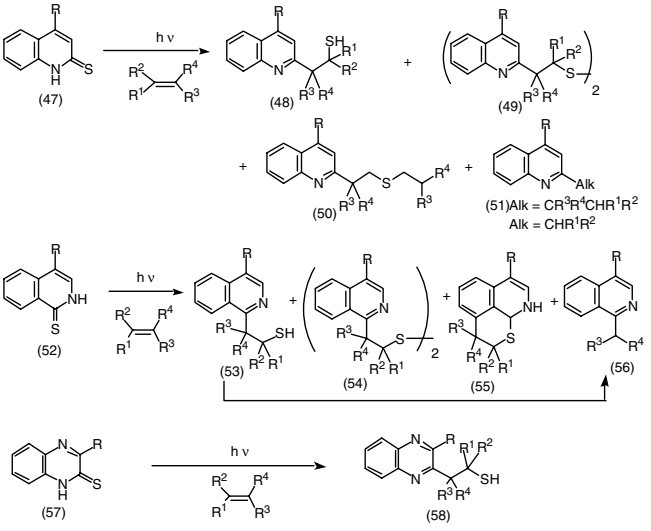

SCHEME 7

benzothioazole-2-thione (39) and electron-rich alkenes gives 2-substituted benzothiazole (40), whereas that of *N*-methyl derivatives (41) to isobutene gives three types of products (42–44) via aminothietanes.[22] Laser flash photolysis has been used to show that the triplet excited state of (45) is involved in the addition reaction which occurs to electron-deficient alkenes such as acrylonitrile, giving thietane (46).[23]

Photoreaction of six-membered thioamides, such as pyridinethiones, pyrimidinethiones, pyridazinethiones, thiouracils, thiouridines and their benzo-analogs (Figure 106.1), gives a variety of types of adducts in the presence of alkenes where thietanes are believed to be intermediates. Most of the reactions are already documented in previous reviews.[8–11]

Photochemical reaction of benzo-analogs, quinoline-2-thiones (47), in the presence of a variety of alkenes gives 1:1 photoadducts via a thietane intermediate (Scheme 7). Irradiation of (47) in the presence of electron-deficient alkenes gives thiols (48) and affords 1:2 adducts (50) with alkyl vinyl ether. On the other hand, irradiation with other electron-rich alkenes, such as isobutene or tetramethylethylene, gives various products (48–51). The transpositional isomer, isoquinoline-2-thiones (52), also give many types of adducts (53–56) upon irradiation in the presence of electron-rich alkenes.[24–27]

Thietanes are also intermediates in the photoreaction of quinoxaline-2-thiones (57) with alkenes, leading to 2-substituted quinoxalines (58).[28] This behavior is strikingly different from the photoreaction of the oxo-analogs, quinoxalin-2-ones, which undergo photoaddition to carbon-nitrogen double bonds.

Thiobarbiturates (59) undergo (2+2)-cycloaddition with alkenes to give the thietanes (60) and the methylene derivatives (61) by secondary photolysis involving elimination of either thioacetone or thioformaldehyde (Scheme 8).[29,30] Dithiobarbiturate and trithiobarbiturate undergo analogous reactions.

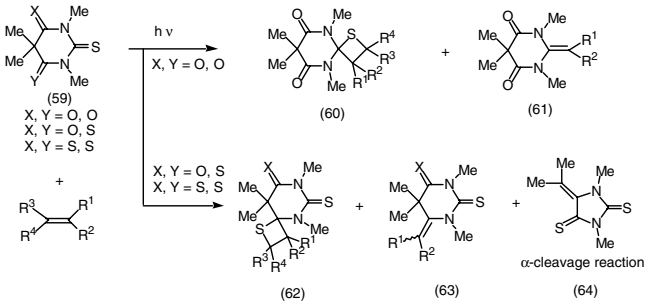

SCHEME 8

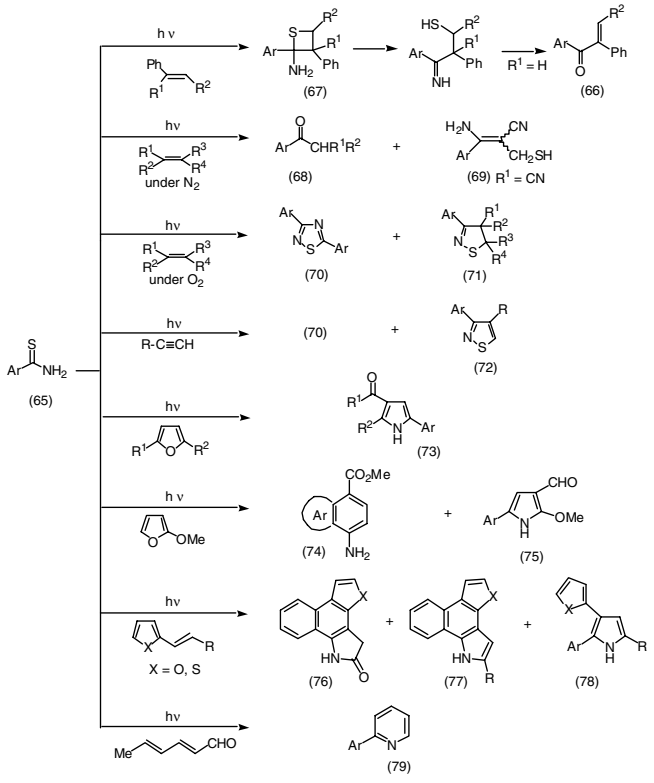

SCHEME 9

For trithiobarbiturate, a competing conversion to dithiohydantoin (64) occurs in all cases, accompanied by the formation of (62) and (63), possibly involving a α-cleavage reaction adjacent to the gem-dimethyl group, reclosure to form a sulfur heterocycle and subsequent carbon-carbon bond formation with exclusion of sulfur.

The formation of enones (66) by irradiation of the arylcarbothioamides (65) in the presence of styrene derivatives proceeds by initial formation of the thietane (67): this conversion provides a potentially valuable route for the arylation of simple alkenes as shown in (Scheme 9).[31] Several types of photoproducts are obtained by the irradiation of (65) in the presence of alkenes. The type of product obtained depends on the alkenes used and the reaction conditions.

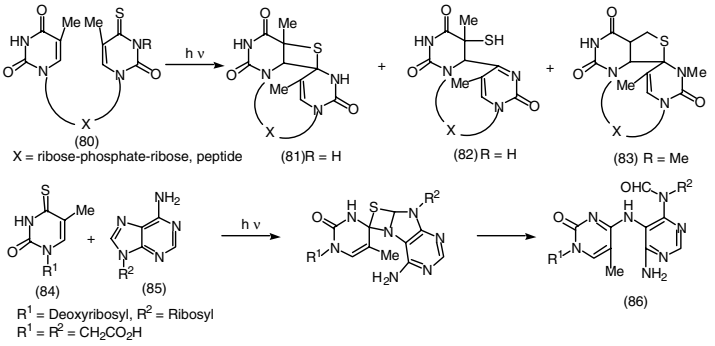

SCHEME 10

Irradiation of (65) with tetramethylethylene under nitrogen atmosphere gives arylketone (68) and thiol (69).[32] The reaction takes a different course in the presence of oxygen and yields 1,2,4-thiadiazoles (70) and isothiazolines (71, 72); a pathway via a nitrile sulfide has been proposed. Irradiation of (65) in the presence of five-membered heteroaromatics such as furan, thiophene, and pyrrole in benzene regioselectively gives the corresponding 3-aroyl derivatives (73). For the formation of aroylfurans, cycloaddition of the C–N bond with furan was proposed.[33–36] Photolysis with 2-methoxyfuran yields unstable thietanes, which rearrange to give moderate yields of benzo-fused arene derivatives (74) and pyrrole derivatives (75).[31,37,38] The intermediacy of the thietane is suggested from the formation of the fused furan derivatives (76–78) that are produced from irradiation of thiobenzamide with 2-vinylfurans or thiophenes.[39,40] Irradiation of (65) in the presence of aldehyde gives tetracyclic imidazole,[41] and pyridine derivatives (79) are obtained by the photolysis in the presence of a dienal (Scheme 9).[42]

Intramolecular photocycloaddition is also reported to occur in the thiothymidine thymidinyl phosphates (80, R = H) and this gives the thietane (81) and the ring-opened thiol (82) (Scheme 10).[43,44] The importance of this process is related to lesion in DNA. Irradiation of (80, R = Me) gives a new type of photoproduct (83) in the nucleic acid series that involves attack of the thiocarbonyl across the propene moiety of the thymidine ring.[45] Irradiation at 366 nm in aqueous solution of the thiothymine (84) in the presence of adenine derivative (85) results in the formation of the adduct (86); this is formed presumably by way of the (2+2)-cycloaddition reaction between the C=S and the C=N bonds.[46] Intermolecular (2+2)-cycloaddition is also reported in the photoreaction of (84) with pyrimidinone derivative.[47] Intramolecular photocycloaddition also occurs between thymine and 6-thioinosine derivatives tethered with ribose-phosphate-ribose and thietanes are obtained.[48–50]

Many mono- and dithioimides show high reactivity toward intra- and intermolecular (2+2)-cycloaddition with alkenes. Introduction of an acyl group to the amide function shares the lone-pair electrons of the nitrogen atoms with carbonyl and thiocarbonyl groups; also, the acyl group of aminothietane decreases the activity for the ring-opening reaction. Therefore, stable thietanes are isolated in many cases. This reaction provides a powerful method to synthesize nitrogen-containing heterocycles by efficient modeling of the starting materials.

Irradiation of the acyclic imides (87) proceeds by (2+2)-cycloaddition to yield thietane-fused β-lactams (88) (Scheme 11).[51] Because the mechanism involves the 1,4-diradical intermediate, a more efficient reaction occurs when R^2 is not hydrogen. Furthermore, when the achiral imide (87, R^1 = H, R^2 = Me, and R^3 = Ph) crystallizes in a chiral fashion and the solid-state photoreaction gives an optically active product.[52] Irradiation of a benzene solution of *N*-[(*R*)-phenyl]-*N*-tigloylthiobenzamide, possessing an intramolecular chiral handle, does not show diastereoselectivity and gives four stereoisomeric β-lactams. On the contrary, high diastereoselectivity has been observed in the corresponding solid-state photoreaction.[53] The intramolecular (2+2)-cycloaddition is observed in β,γ-unsaturated thioimides (89) which have been converted photochemically into the 2-thiabicyclo[2.1.0]pentanes (90) in high yield.[54]

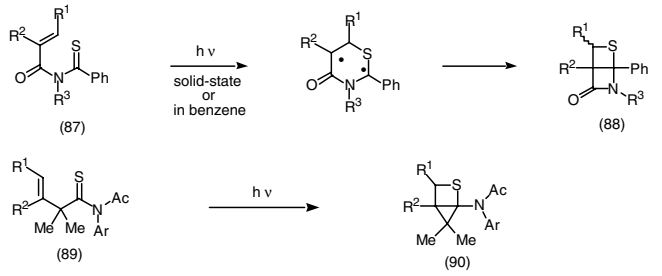

SCHEME 11

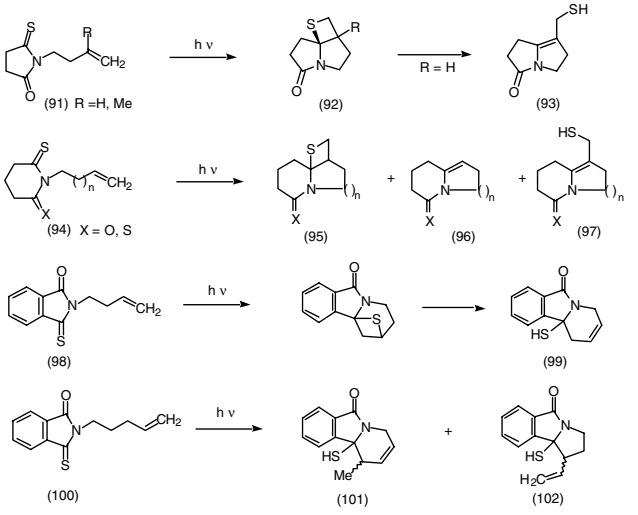

SCHEME 12

Cyclic thioimides (91) undergo intramolecular photocycloaddition in a regiospecific manner to afford spirocyclic amidothietanes (92) (Scheme 12).[55,56] These highly strained multicycles undergo a subsequent ring-opening reaction to furnish fused pyrrolidinones (93). Intramolecular photoreaction of *N*-(4-alkenyl)- or *N*-(4-alkenyl)-glutarimides (94) gives thietanes (95) and their fission products (96, 97).[57] Similarly, intramolecular thietane formation is observed in the photolysis of cyclic monothioimides (98) and the isoindole derivatives (99) were isolated through the photolabile thietanes. On the other hand, photolysis of (100) gives (101) and (102) via hydrogen abstraction by thiocarbonyl sulfur atom.[58]

Photoreaction of monocyclic monothioimides (103) gives lactams (104) and thioester (105), in which the products are dependent on the substituents on the alkenes and the ring size of thiolactam chromophore (Scheme 13).[59] Photoproducts (104) and (105) are formed via 7-membered biradical intermediate and another type of (2+2)-cycloaddition leads to bicyclic lactam (106).

Acyclic thiocarbamates (107) also give thietane formation on irradiation. This reaction is followed by ring opening, leading to oxylanes (108) (Scheme 14).[60] Irradiation of monocyclic thiocarbamates or dithiocarbamates (109) gives tricyclic β-lactams (110) and β-thiolactones (112).[61] The formation of (112) is reasonably explained via a zwitterionic intermediate (111). Irradiation of *N*-(β,γ-unsaturated carbonyl)-thiocarbamates and -dithiocarbamates (113) also promotes (2+2)-thietane formation and subsequently yields bicyclic lactams (114) and γ-thiolactone derivatives (115).[62] Similar reactivity is also shown in the solid state and absolute asymmetric synthesis is performed by the photoreaction of acyclic *N*-(β,γ-unsaturated carbonyl)thionocarbamate (116), leading to optically active thiolactones (117).[63]

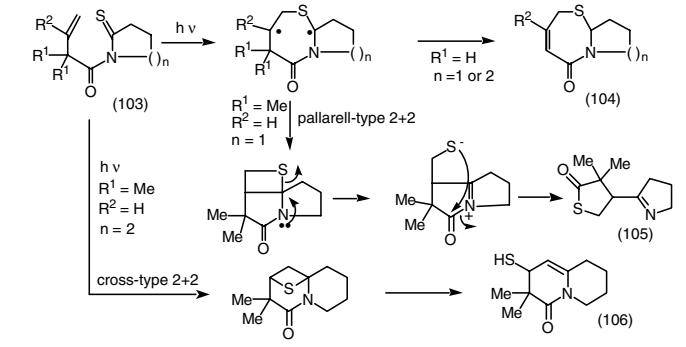

SCHEME 13

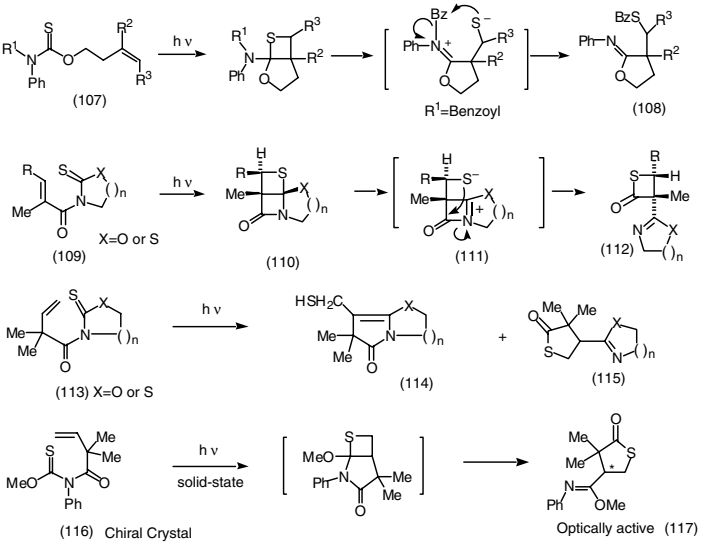

SCHEME 14

Irradiation of many other cyclic, semi-cyclic, and acyclic thioimides in the presence of variety alkenes, alkynes, allenes, or ketenes gives the corresponding thietanes by intermolecular reaction.[8–11]

106.3 Photochemical Hydrogen Abstraction of Thioamides and Thioimides

Photochemical hydrogen abstraction of a thiocarbonyl function is a common reaction. While thioamides generally do not show this photochemical reactivity, thioimides do undergo hydrogen abstraction by the thiocarbonyl sulfur of (C=S)-N chromophore from the β-, γ-, and δ-positions to yield various heterocycles.

A rare example has been reported for the hydrogen abstraction reaction of thioamides. Irradiation of amide (118) proceeds by β-hydrogen abstraction to generate a 1,3-diradical intermediate by a 1,3-hydrogen shift. Two reaction pathways are observed. One is the formation of thioenamides (119); the other is cyclization of a 1,5-diradical intermediate to yield pyrrole derivatives (120) (Scheme 15).[64]

In another case, β-hydrogen abstraction of acyclic monothioimides followed by cyclization leads to aziridine derivatives. When acyclic monothioimides (121) are irradiated at room temperature, thioketones

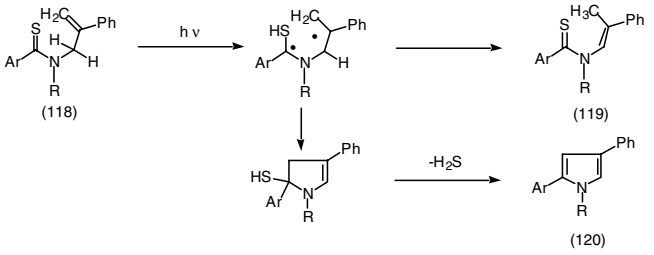

SCHEME 15

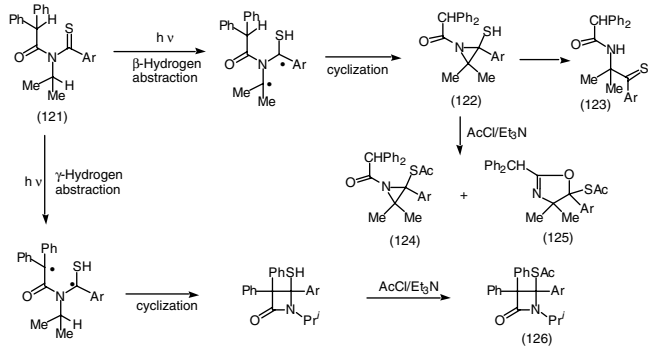

SCHEME 16

(123) are formed via ring-opening reaction of unstable mercaptoaziridines (122) (Scheme 16). Irradiation of (121) at low temperature, followed by acetylation, gives the stable aziridine (124) and rearranged oxazolidines (125). The β-lactams (126) are also obtained via γ-hydrogen abstraction, followed by cyclization.[65]

Furthermore, three achiral monothioimides (121) (Ar = Ph, 4-ClPh, and 4-MeOPh derivatives) crystallize in a chiral fashion and the solid-state photolysis followed by acylation gives optically active aziridines (124), oxazolidines (125), and β-lactams (126).

Hydrogen abstraction has been reported in *N*-acylthionocarbamates and dithiocarbamates (127) leading to cyclization products (128) and (129).[66] The formation of (129) is reasonably explained in terms of ring-opening reaction followed by an α-cleavage reaction of the C=S group. The resulting carbene is trapped intramolecularly to yield (129) (Scheme 17 and see also Scheme 21). Irradiation of 1-acylindoline-2-thiones (130) gives the deacylation products (131) via a γ-hydrogen abstraction. The ketene formed by this fission process is trapped by ethanol to yield the corresponding esters (132).[12] Similar deacylation involving a γ-hydrogen abstraction has been observed in the photolysis of *N*-acyl-2-thionothiazolidines.[67]

Photolysis of the monothioimides (133) gives γ-lactams (134) and disproportionation products (135, 136) via a 1,5-diradical intermediate generated by δ-hydrogen abstraction. Thioamides (137) are obtained via γ-H abstraction (Scheme 18).[68] Irradiation of *N*-(3-phenylpropionyl)-2-pyrrolidinethione, in which R^3 and R^4 substituents are tethered, gives isomers of pyrrolopyrrolidone.

Photolysis of 1-(ω-arylalkyl)cyclic thioimides (138) (X = O, S; m = 1, 2; Ar = Ph, 2-furyl) gives a pair of stereoisomers of 1-azabicycloalkanes (139, 140) in moderate yields (Scheme 19).[69] Similarly, phenylalkylcyclic dithioimides (141) (m = 1, 2; n = 2–4) give 2-azabicycloalkanes (142) and disproportionation products (143) on irradiation.

Irradiation of thiouracil tethered by peptide or ribose-phosphate (144) at 366 nm in water results in the formation of the products (145, 146) (Scheme 20).[45,49,70]

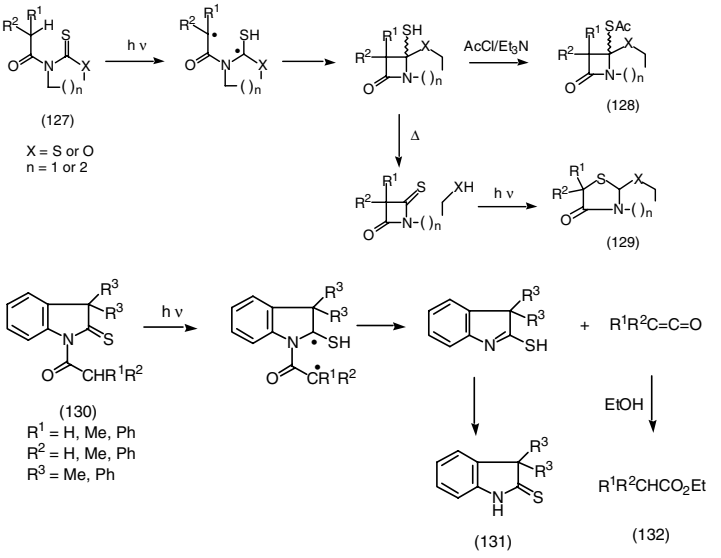

SCHEME 17

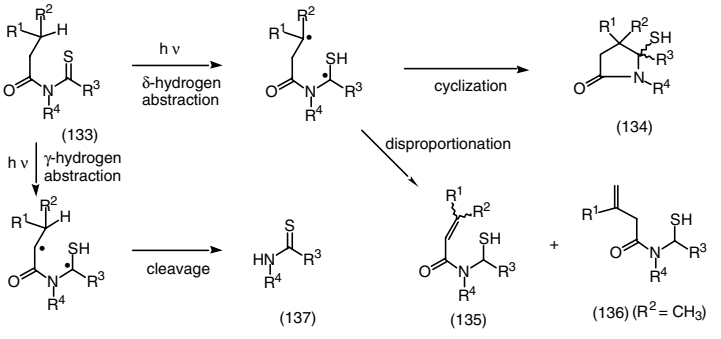

SCHEME 18

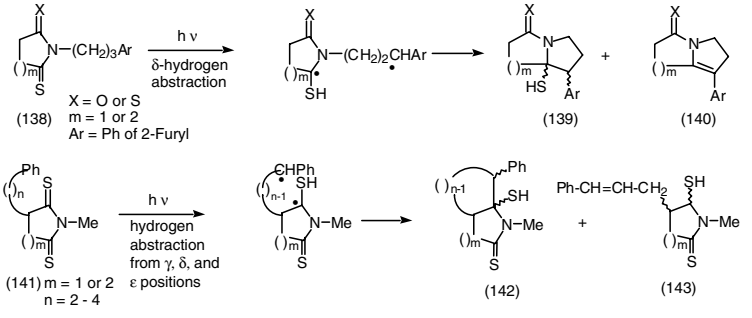

SCHEME 19

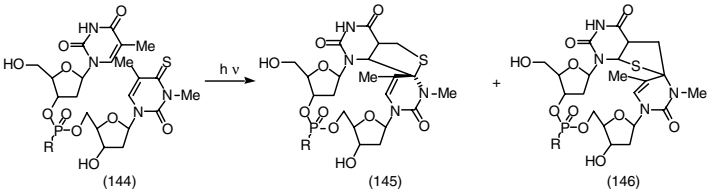

(144) (145) (146)

SCHEME 20

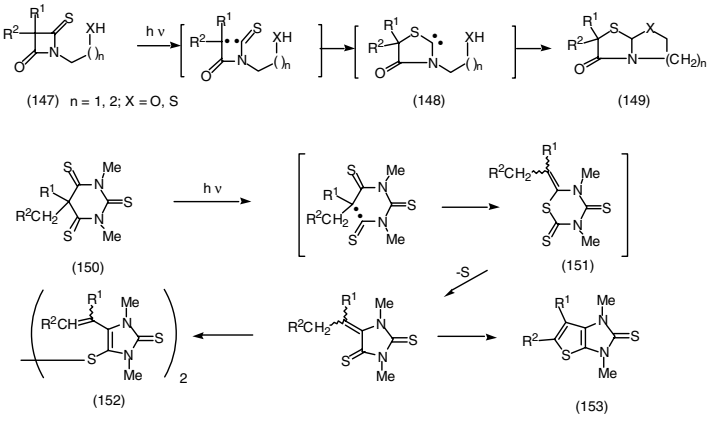

(147) n = 1, 2; X = O, S (148) (149)

(150) (151)

(152) (153)

SCHEME 21

106.4 Miscellaneous Photoreactions of Thioamides and Thioimides

The Norrish Type I reaction (α-cleavage reaction) is a common process in carbonyl photochemistry. It is quite rare, however, in thiocarbonyl photochemistry. One of the reasons for this difference is that the C=S system has a lower triplet energy than that of the C=O analogs. Some strained thiocarbonyl compounds are known to undergo C-(C=S) bond cleavage in four-membered thioketone and thioesters.[7–9] Photolysis of four-membered thioimides (147) also promotes an α-cleavage reaction leading to thiacarbene (148) and this is trapped intramolecularly by thiol or alcohol to give bicyclic lactams (149) (Scheme 21).[66] Another example is reported for the six-membered trithiobarbiturate (150) leading to thiohydantoin (152) and a small amount of the imidazolinothiophene derivative (153). The reaction mechanism is explained in terms of initial formation of a 1,6-biradical intermediate, α-cleavage of the thiocarbonyl group, and this is followed by recyclization to (151). Ring contraction by loss of a sulfur atom leads to (152) and (153).[25]

Irradiation of indoline-2-thiones (154) in the presence of Et_3N yields the desulfurization products, indolines (155), along with Et_2NCSMe (Scheme 22). The photodesulfurization reactions can be explained by a sequential electron/proton-transfer mechanism from amine to the excited indoline-2-thione (154).[71]

Primary thioamides (156) are photolyzed by UV light in nitrogen to the corresponding nitriles with evolution of H_2S (Scheme 23). Irradiation in the presence of oxygen gives nitriles, amides, carboxylic acids, and 3,5-disubstituted 1,2,4-thiadiazoles (157), together with S, SO_2 and SO_4^{2-} but no H_2S. Secondary thioamides (158) and tertiary thioamides (159) are stable under both conditions. Singlet oxygen reacts with secondary and tertiary thioamides to form the corresponding amides with expulsion of S.[72]

Examples of photocyclization involving the thiocarbonyl group have been reported. The 2-substituted benzothiazoles (161) are prepared in this way from *o*-halogenothiobenzanilides (160) via a

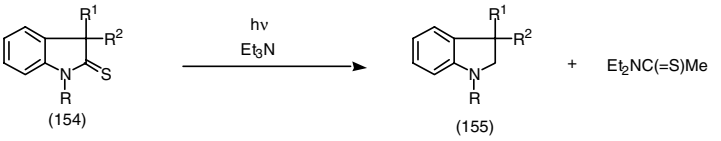

SCHEME 22

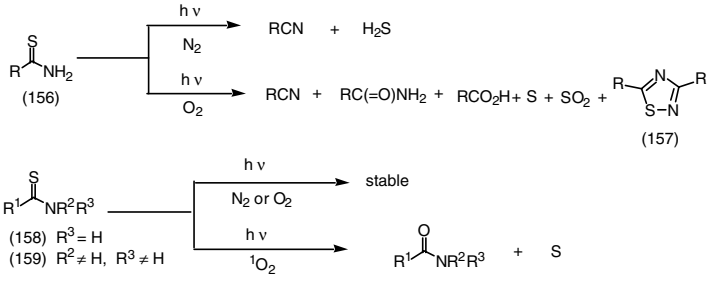

SCHEME 23

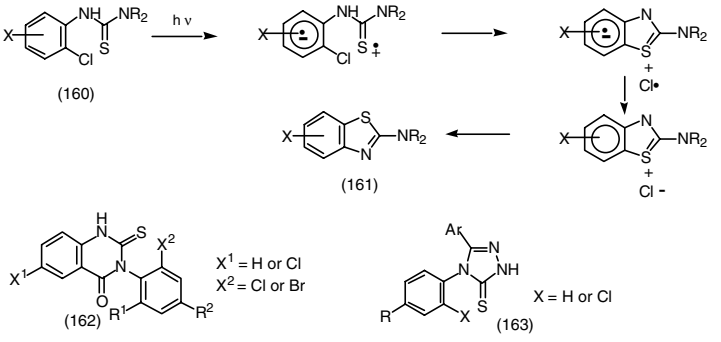

SCHEME 24

dehydrohalogenation initiated by electron transfer (Scheme 24).[73] Similarly, cyclization is observed in the photoreaction of 2-thiaquinazolinediones (162) and 4-(2-haloaryl)-5-aryl-1,2,4-triazol-3-thiones (163).[74,75]

Irradiation of 2,5-dihydro-1*H*-pyrrole-2-thiones (164) in the presence of triethylamine gives desulfurization products, pyrroles (165), or reduction products, pyrrolidine-2-thiones (166), depending on the substituent on the nitrogen atom. This reaction can be explained by a sequential electron/proton-transfer mechanism from the amine to the excited pyrrole thione (Scheme 25).[16]

Photolysis of a benzene solution of acyclic monothioimides (167) proceeds via δ-hydrogen abstraction, leading to δ-lactams (Scheme 18).[68] However, irradiation of (167) in the solid state affords only thioamides (169) and the corresponding acid (170), where the mechanism via the 1,3-oxazetidinium ion (168) is proposed (Scheme 26).[76,77]

Irradiation of 2-methyl-4-phenyl-substituted benzaldehyde thiosemicarbazones (171) leads to the corresponding Δ^2-1,2,4-triazoline-5-thione derivatives (173) through the formation of stable 1,2,4-triazolidine-5-thione derivatives (172) (Scheme 27).[78] Irradiation of *N*-acylthiourea (174) in the presence of triethylamine gives thiourea (175) and benzothiazoles (176) via an electron-transfer mechanism.[79] A photochemically induced Dimroth rearrangement has been reported in the 1,2-thiazolino[5.4-*d*]-1,2-thiazoline-3,6-dithione (177) and yields the 3*H*,6*H*-1,2-dithiolo[4.3-*c*]-1,2-dithiole (178).[80]

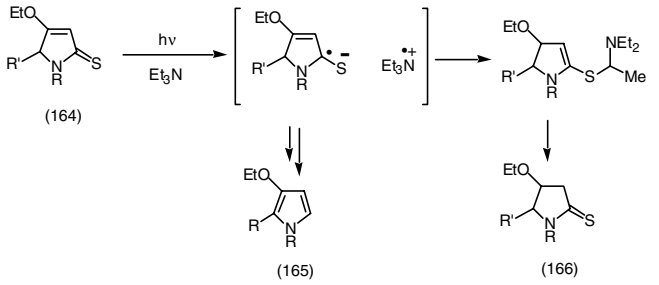

SCHEME 25

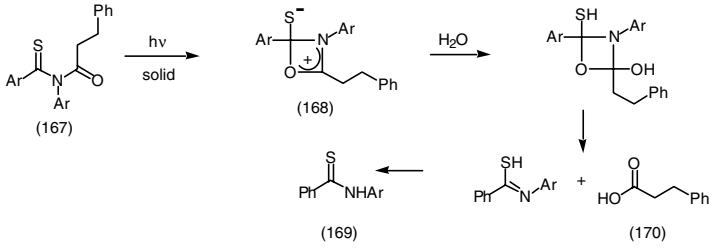

SCHEME 26

106.5 Photoreactions of Conjugated Thioamides

The singlet $\pi\pi^*$ excited state of the *N,N*-disubstituted thioamides (179) is responsible for conversion to the thioazetidinones (180) accompanied by the fragmentation product (181) (Scheme 28). This product is presumed to be formed by a hydrogen abstraction path to afford the zwitterionic intermediate.[81] Furthermore, *N,N*-dibenzyl-1-cyclohexenecarbothioamide (179, R^1-R^2 = -$(CH_2)_4$-) crystallizes in a chiral fashion and the photolysis in the solid state leads to exclusive production of optically active thioazetidinone (180) in 94% enantiomeric yield.[82–84]

Unsymmetrically substituted *N*-benzyl-*N*-isopropyl-α,β-unsaturated thioamides (182) exist in an equilibrium between two rotamers owing to the rotation of the C(=S)–N bond. The free energy of activation lies in the range 18.4 to19.5 kcal mol^{-1}. Irradiation in benzene solution induces hydrogen abstraction by the alkenyl carbon from both the benzyl and isopropyl groups to give a β-thiolactam (183) and 1,3,5-dithiazinane products (185) as products, respectively. In the solid state, however, photolysis causes hydrogen abstraction from only the isopropyl group to give isomeric β-thiolactam (184).[85]

Photochemical isomerization of monosubstituted α,β-unsaturated thioamides (186) gives iminothietanes, *N*-(2-thietanylidene)amines (187), in good yields. The iminothietanes revert quantitatively to the starting materials on heating (Scheme 29).[86]

Photochemical (*E,Z*)-isomerization of *N,N*-disubstituted tigloylthioamide (179) occurs in solution and in the solid state.[81,82] Furthermore, photochemical (*E,Z*)-isomerizability of cinnamothioamide derivatives (188) in the solid state has been reported. Crystallographic analysis reveals that the isomerizability in the solid state partially depends on their molecular conformation in the crystal.[87] In addition, it is found that the packing coefficient has correlation with the isomerizability; a smaller value of the packing coefficient causes an increased formation of (*Z*)-isomers.

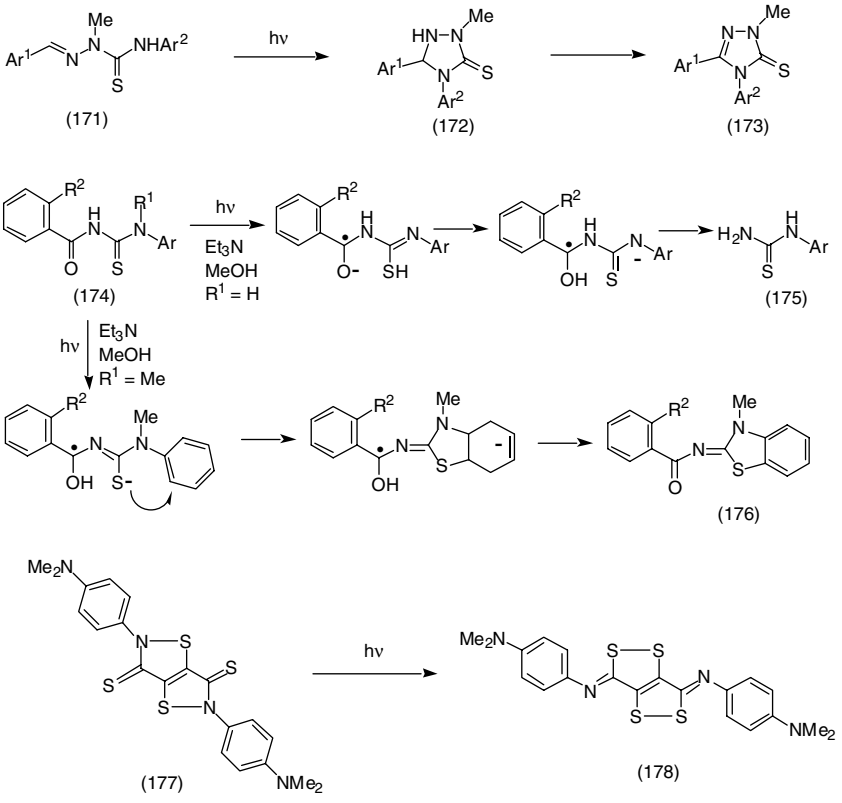

SCHEME 27

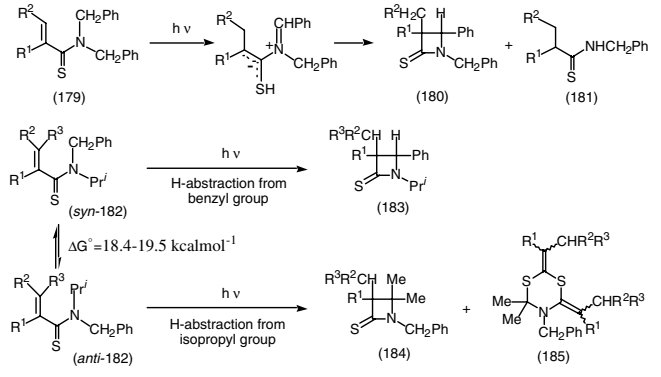

SCHEME 28

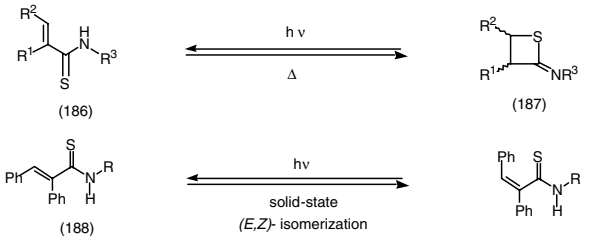

SCHEME 29

References

1. Ohno, A., Photocycloaddition of thiocarbonyl compounds to olefins and related reactions, *Int. J Sulfur Chem.,* Part B, 6, 183, 1971.
2. Ohno, A., Thiones in *Organic Chemistry of Sulfur*, Oae S., Ed., Plenum, New York, 189, 1977.
3. Coyle, J.D., Photochemistry of organic sulphur compounds, *Chem. Soc. Rev.*, 4, 523, 1975.
4. Coyle, J.D., The photochemistry of thiocarbonyl compounds, *Tetrahedron*, 41, 5393, 1985.
5. de Mayo, P., Thione photochemistry and the chemistry of the S_2 state, *Acc. Chem. Res.*, 9, 52, 1976.
6. Turro, N.J., Ramamurthy R., Cherry W., and Farneth W., The effect of wavelength on organic photoreactions in solution. Reactions from upper excited states, *Chem. Rev.,* 78, 125, 1978.
7. Ramamurthy, V., Thiocarbonyl photochemistry, in *Organic Photochemistry*, Padwa A., Ed., Marcel Dekker, New York, Vol. 7, 231–329, 1985.
8. Machida, M., Oda, K., Sato, E., and Kanaoka, Y., Photoreaction of nitrogen-thiocarbonyl systems, *J. Synth. Org. Chem. Jpn. (Yuki Gosei Kagaku Kyokai-shi),* 44, 1071, 1986.
9. Sakamoto, M., Fujita, T., Watanabe, S., and Nishio, T., Photochemical reaction of thioamides and thioimides, *J. Synth. Org. Chem. Jpn. (Yuki Gosei Kagaku Kyokai-shi),* 52, 685, 1994.
10. Nishio, T. and Sakamoto, M., Photochemistry of thioamides, *Rev. Heteroatom Chem.*, 12, 23, 1995.
11. Sakamoto, M. and Nishio, T., Photochemistry of thioimides, *Rev. Heteroatom Chem*, 12, 53, 1995.
12. Nishio, T. and Oka, M., Synthesis of indole derivatives by [2+2] photocycloaddition of indoline-2-thiones with alkenes and photodesulfurization of indoline-2-thiones, *Helv. Chim. Acta*, 80, 388, 1997.
13. Nishio, T., Photochemical rearrangement of 3-allylindoline-2-thiones to 2-allylthioindoles, *J. Chem. Res. (S)*, 204, 1989.
14. Nishio, T. and Okuda, N., Photoreactions of isoindoline-1-thiones with alkenes: unusual formation of tricyclic isoindolines, *J. Org. Chem.,* 57, 4000, 1992.
15. Nishio, T., Photoreactions of 1,3-dihydroisobenzofuran-1-thiones and 1,3-dihydro-2-benzothiophene-1-thiones with alkenes, *J. Chem. Soc., Perkin Trans. 1*, 561, 1995.
16. Nishio, T., Photochemical synthesis of pyrrole derivatives by desulfurization of 2,5-dihydro-1*H*-pyrrole-2-thiones and [2+2] cycloaddition of 2,5-dihydro-1*H*-pyrrole-2-thiones with alkenes, *J. Chem. Soc., Perkin Trans. 1*, 885, 1997.
17. Nishio, T., Mori Y., Iida I., and Hosomi A., Photoaddition of benzoxazole-2-thiones with alkenes, *J. Chem. Soc., Perkin Trans. 1*, 921, 1996.
18. Nishio, T., Photoaddition of *N*-acylbenzoxazole-2-thiones to alkenes, *J. Chem. Soc., Perkin Trans. 1*, 1007, 1998.
19. Nishio, T., Photochemical reactions of *N*-acylbenzoxazole-2-thiones, *J. Chem. Soc., Perkin Trans. 1*, 3039, 2000.
20. Nishio, T., Photocycloaddition of *N*-alkoxycarbonylbenzoxazole-2-thiones to alkenes: isolation of stable aminothietanes, *J. Chem. Soc., Perkin Trans. 1*, 1151, 1999.

21. Nishio, T., Mori, Y., and Hosomi, A., Photochemical reactions of benzothiazole-2-thiones, *J. Chem. Soc., Perkin Trans. 1,* 2197, 1993.
22. Nishio, T., Mori Y., Iida, I,. and Hosomi, A., Photocycloaddition of benzothiazole-2-thiones to alkenes, *Helv. Chim. Acta*, 77, 981, 1994.
23. Alam, M.M. and Ito, O., Energy transfer, electron transfer, and addition reactions of triplet state of 1,3-dihydroimidazole-2-thiones investigated by laser flash photolysis, *Bull. Chem. Soc. Jpn.,* 72, 339, 1999.
24. Nishio, T. and Omote, Y., Photo-induced carbon-carbon bond formation: reactions of 2-thiopyridones and 2-quinolinethiones with alkenes, *Synthesis,* 54, 1986.
25. Sato, E., Ikeda, Y., and Kanaoka, Y., Photo-induced reactions. Photochemistry of conjugated nitrogen-thiocarbonyl systems. Photoaddition of quinoline-, isoquinoline- and phthalazinethione systems to olefins, *Chem. Pharm. Bull.*, 38, 1205, 1990.
26. Sato, E., Ikeda, Y., and Kanaoka, Y., Photoinduced reactions. Photochemistry of conjugated nitrogen-thiocarbonyl systems. Two-fold photoaddition of vinyl ethers to aza-aromatic thiones, *Chem. Pharm. Bull.*, 35, 3641, 1987.
27. Sato, E., Ikeda, Y., and Kanaoka, Y., Photochemistry of conjugated nitrogen-thiocarbonyl systems. Photoaddition of olefins to quinoline-, isoquinoline-, and phthalazinethione systems, *Chem. Lett.*, 237, 1987.
28. Nishio, T., Photocycloaddition of quinoxaline-2(1*H*)-thiones to alkenes, *Helv. Chim. Acta,* 75, 487, 1992.
29. Takechi, H. and Machida, M., Photoreactions of thiobarbiturates. Intermolecular cycloaddition with alkenes and ring contraction reaction of trithiobarbiturate, *Chem. Pharm. Bull.*, 45, 1, 1997.
30. Oda, K., Takahashi, H., and Machida, M., Photochemical transformation of trithiobarbiturate into thiohydantoin and imidazolinothiophene derivatives, *Heterocycles*, 50, 159, 1999.
31. Oda, K., Machida, M., and Kanaoka, Y., Photochemistry of the nitrogen-thiocarbonyl systems. 18. Photoreaction of arenecarbothioamides with styrenes: the regioselective photoinduced acylation at the α-position of styrenes, *Synlett,* 603, 1992.
32. Oda, K., Machida, M., and Kanaoka, Y., Photoreaction of benzenecarbothioamide with olefins. Synthesis of isothiazole derivatives and phenones, *Heterocycles,* 30, 983, 1990.
33. Oda, K., Sakai, M., Ohno, K., and Machida, M., Photochemistry of nitrogen-thiocarbonyl systems. 33. Photoreaction of arenecarbothioamides with furan. Facile synthesis of pentagonal di- and triheterocyclic compounds, *Heterocycles*, 50, 277, 1999.
34. Oda, K. and Machida, M., Photochemistry of the nitrogen-thiocarbonyl systems. Photoreaction of arenecarbothioamides with 5-membered heteroaromatics. The regioselective photoinduced aroylation at the 3-position of 5-membered heteroaromatics, *Chem. Pharm. Bull.,* 41, 1299, 1993.
35. Oda, K., Tsujita, H., Ohno, K., and Machida, M., Photochemistry of the nitrogen-thiocarbonyl systems. 24. Photoreactions of thiobenzamide with various substituted furans: regioselective β-benzoylation and transformation of furans to other aromatic compounds, *J. Chem. Soc., Perkin Trans. 1*, 2931, 1995.
36. Oda, K. and Machida, M., Photochemistry of the nitrogen-thiocarbonyl systems. 20. Photoreaction of thiobenzamide with furans in methanol. Facile construction of the arylpyrrole ring system, *J. Chem. Soc., Chem. Commun.,* 437, 1993.
37. Oda, K. and Machida, M., Benzannulation of heteroaromatics by photoreaction of arenecarbothioamides with 2-methoxyfuran, *J. Chem. Soc., Chem. Commun.,* 1477, 1994.
38. Oda, K., Sakai, M., and Machida, M., Photochemistry of the nitrogen-thiocarbonyl systems. 30. Intermolecular photoaddition reaction of arenecarbothioamides to 2-methoxy- and 2-(trimethylsiloxy)furans. Facile synthesis of arene-fused aminobenzoates by novel photoinduced benzannulation, *Chem. Pharm. Bull.*, 45, 584, 1997.
39. Oda, K., Tsujita, H., Sakai, M., and Machida, M., Photochemistry of the nitrogen-thiocarbonyl systems. Photoreaction of thiobenzamide with 2-vinylfuran analogs. Facile synthesis of tetracyclic indole system, *Heterocycles,* 42, 121, 1996.

40. Oda, K., Tsujita, H., Sakai, M., and Machida, M., Photochemistry of the nitrogen-thiocarbonyl systems. Photoreaction of arenecarbothioamides with 2-vinylfuran analogs. The formation of tetracyclic indoles and 2,3-diaryl-2-pyrrolin-5-ones, *Chem. Pharm. Bull.,* 46, 1522, 1998.
41. Oda, K., Saka,i M., Tsujita, H., and Machida, M., Photochemistry of the nitrogen-thiocarbonyl system. 29. Photoreaction of benzenecarbothioamide with aldehydes. Facile synthesis of tetracyclic imidazoles, *Synth. Commun.,* 27, 1183, 1997.
42. Oda, K., Nakagami, R., Nishizono, N., and Machida, M., Pyridine ring formation through the photoreaction of arenecarbothioamides with diene-conjugated carbonyl compounds, *J. Chem. Soc., Chem. Commun.,* 2371, 1999.
43. Clivio, P., Fourrey, J.L., and Gasche, J., DNA photodamage mechanistic studies: characterization of a thietane intermediate in a model reaction relevant to "6–4 lesions," *J. Am. Chem. Soc.,* 113, 5481, 1991.
44. Clivio, P., Fourrey, J.-L., and Gasche, J., Novel insight into the stereochemical pathway leading to (6–4) pyrimidine-pyrimidone photoproducts in DNA, *Tetrahedron Lett.,* 33, 1615, 1992.
45. Clivio, P., Fourrey, J.-L., Szabo, T., and Stawinski, J., Photochemistry of di(deoxyribonucleoside) methylphosphonates containing N^3-methyl-4-thiothymine, *J. Org. Chem.,* 59, 7273, 1994.
46. Saintome, C., Clivio P., Favre, A., and Fourrey J.-L., Photochemistry of 4-thiothymine derivatives in the presence of *N*-9-substituted-adenine derivatives: formation of *N*-6-formamidopyrimidines, *J. Org. Chem.,* 62, 8125, 1997.
47. Clivio, P. and Fourrey, J.-L., Photochemistry of the thio analog of the DNA (6–4) photoproduct Dewar valence isomer: structure of a new photoproduct, *Tetrahedron Lett.,* 39, 275, 1998.
48. Woisard A. and Favre, A., Hammerhead ribozyme tertiary folding: intrinsic photolabeling studies, *J. Am. Chem. Soc.,* 114, 10072, 1992.
49. Clivio, P., Guillaume, D., Adeline, M.-T., and Fourrey, J.-L., A photochemical approach to highlight backbone effects in PNA, *J. Am. Chem. Soc.,* 119, 5255, 1997.
50. Saintome, C., Clivio, P., Favre, A., Fourrey, J.-L., and Riche, C., RNA photolabeling mechanistic studies: x-ray crystal structure of the photoproduct formed between 4-thiothymidine and adenosine upon near UV irradiation, *J. Am. Chem. Soc.,* 118, 8142, 1996.
51. Sakamoto, M., Yanase, T., Fujita, T., Watanabe, S., Aoyama, H., and Omote, Y., Thietane-fused β-lactams via photochemical cycloaddition reaction of *N*-(α,β-unsaturated carbonyl)thioamides, *J. Chem Soc., Perkin Trans. 1.,* 403, 1991.
52. Sakamoto, M., Hokari, N., Takahashi, M., Fujita, T., Watanabe, S., Iida, I., and Nishio, T., Chiral thietane-fused β-lactam from an achiral monothioimide using the chiral crystal environment, *J. Am. Chem. Soc.,* 115, 818, 1993.
53. Sakamoto, M., Takahashi, M., Hokari, N., Fujita, T., and Watanabe, S., Solid-state photochemistry: diastereoselective synthesis of thietane-fused β-lactams from an acyclic monothioimide with a chiral group, *J. Org. Chem.,* 59, 3131, 1994.
54. Sakamoto, M., Shigematsu, R., Fujita, T., and Watanabe, S., Photochemical isomerization of β,γ–unsaturated thioimides to 2-thiabicyclo[2.1.0]pentanes, *J. Chem. Soc., Chem. Commun.,* 91, 1992.
55. Machid,a M., Oda, K., and Kanaoka Y., Intramolecular photocycloaddition of thiosuccinimides with alkenyl *N*-side chains: synthesis of strained multicyclic spiro-thietanes, *Chem. Pharm. Bull.,* 33, 3552, 1985.
56. Padwa, A., Jacque, M.N., and Schmidt, A., Intramolecular photocycloaddition of cyclic thioimides as a method for heterocyclic synthesis, *Org. Lett.,* 3, 1781, 2001.
57. Oda, K., Ishioka, T., Fukuzawa, Y., Nishizono, N., and Machida, M., Photochemistry of *N*-3-butenyl- and *N*-4-pentenylglutarimides: intramolecular thietane formation and the fission of thietane ring, *Heterocycles,* 53, 2781, 2000.
58. Oda, K., Machida, M., and Kanaoka, Y., Photochemistry of the nitrogen-thiocarbonyl systems. Photochemistry of *N*-but-3-enyl thiophthalimides. Intramolecular thietane formation, *Chem. Pharm. Bull.,* 40, 585, 1992.

59. Sakamoto, M., Watanabe, S., Fujita, T., and Yanase, T., Photochemical reactions of semicyclic monothioimides. A novel photocyclization of *N*-(β,γ–unsaturated carbonyl)thioamides, *J. Org. Chem.,* 55, 2986, 1990.
60. Sakamoto, M., Yoshiaki, M., Takahashi, M., Fujita, T., and Watanabe, S., Photochemical isomerization of *O*-allyl and *O*-3-bet-3-enyl thiocarbamates, *J. Chem. Soc., Perkin Trans. 1,* 373, 1995.
61. Sakamoto, M., Yoshiaki, M., Takahashi, M., Fujita, T., and Watanabe, S., Photochemical synthesis of tricyclic β-lactams and their isomerization to β-thiolactones, *J. Chem. Soc., Perkin Trans. 1,* 2938, 1994.
62. Sakamoto, M., Obara, K., Fujita, T., and Watanabe, S., A novel photochemical isomerization of *N*-(2′,2′-dimethyl-3′-butenoyl) cyclic dithiocarbamates, cyclic thionocarbamates, and thiolactams to thiolactones, *J. Org. Chem.,* 57, 3735, 1992.
63. Sakamoto, M., Takahashi, M., Arai, T., Shimizu, M., Yamaguchi, K., Mino, T., Watanabe, S., and Fujita, T., Solid-state photochemical reaction of achiral *N*-(β, γ-unsaturated carbonyl)thionocarbamate to optically active thiolactone in the chiral crystalline environment, *J. Chem. Soc., Chem. Commun.,* 2315, 1998.
64. Aoyama, H., Photochemical reaction of thiobenzamides bearing an allylic substituent on the nitrogen atom: double-bond migration via tandem 1,4- and 1,6-hydrogen shift, *J. Chem. Soc., Perkin Trans. 1*, 1851, 1997.
65. Sakamoto, M., Takahashi, M., Shimizu, M., Fujita, T., Nishio, T., Iida, I., Yamaguchi, K., and Watanabe, S., "Absolute" asymmetric synthesis using the chiral crystal environment: photochemical hydrogen abstraction from achiral acyclic monothioimides in the solid state, *J. Org. Chem.,* 60, 7088, 1995.
66. Sakamoto, M., Watanabe, S., Fujita, T., Aoyama, H., and Omote, Y., Photochemical reactions of *N*-acyldithiocarbamates and *N*-acylthiocarbamates, *J. Chem. Soc., Perkin Trans. 1,* 2541, 1991.
67. Burton, L.P.T. and White, J.D., Photochemical activation of the carboxyl group via *N*-acyl-2-thionothiazolidines, *Tetrahedron Lett.,* 21, 3147, 1980.
68. Sakamoto, M., Tohnishi, M., Fujita, T., and Watanab,e S., Photochemical reactions of *N*-acyldithiocarbamates and *N*-acylthiocarbamates, *J. Chem. Soc., Perkin Trans. 1*, 347, 1991.
69. Oda, K., Fukuzawa, Y., Ohno, K., Machida, M., and Kanaoka, Y., Photochemistry of the nitrogen-thiocarbonyl systems. 21. Photoreaction of 1- and 3-aralkylalicyclic thioimides: facile syntheses of various azabicycloalkanes via Norrish type II process, *Heterocycles*, 36, 71, 1993.
70. Clivio, P., Guillaume, D., Adeline, M.-T., Hamon, J., Riche, C., and Fourrey, J.-L., Synthesis and photochemical behavior of peptide nucleic acid dimers and analogues containing 4-thiothymine: unprecedented (5–4) photoadduct reversion, *J. Am. Chem. Soc.,* 120, 1157, 1998.
71. Nishio, T., Okuda, N., and Kashima, C., Photochemical desulfurization of indoline-2-thiones, *J. Chem. Soc., Perkin Trans. 1,* 141, 1991.
72. Crank, G. and Mursyidi, A., Photochemical reactions of thioamides, *J. Photochem. Photobiol., A: Chem.*, 53, 301, 1990.
73. Muthusamy, S., Paramasivam, R., and Ramakrishnan, V.T., Photochemical synthesis of 2-substituted benzothiazoles, *J. Heterocyclic Chem.,* 28, 759, 1991.
74. Muthusamy, S. and Ramakrishnan, V.T., A facile photochemical synthesis of 12*H*-benzothiazolo[2,3-*b*]quinazolin-12-ones, *Synth. Commun.,* 22,519, 1992.
75. Jayanthi, G., Muthusamy, S., Paramasivam, R., Ramakrishnan, V.T., Ramasamy, N.K., and Ramamurthy, P., Photochemical synthesis of s-triazolo[3,4-b]benzothiazole and mechanistic studies on benzothiazole formation, *J. Org. Chem.,* 62, 5766, 1997.
76. Fu, T.Y., Scheffer, J.R., and Trotter, J., A new mechanism for the photocleavage of monothioimides, *Tetrahedron Lett.,* 35, 3235, 1994.
77. Fu, T.Y., Scheffer, J.R., and Trotter, J., Photocleavage reaction of monothioimides, *Acta Cryst.,* C54, 103, 1998.
78. Buscemi, S. and Gruttadauria, M., Photocyclization reaction of some 2-methyl-4-phenyl-substituted aldehyde thiosemicarbazones. Mechanistic aspects, *Tetrahedron*, 56, 999, 2000.

79. Muthusamy, S. and Ramakrishnan, V.T., Photoreaction of *N*-arylcarbonyl-*N′*-arylthiourea derivatives, *J. Photochem. Photobiol., A: Chem.*, 116, 103, 1998.
80. Fanghaenel, E., Kordts, B., Richter, A.M., and Dutschmann, K., Lewis-acid and photochemically induced Dimroth rearrangement of 3*H*,6*H*-2,5-bis(p-*N*,*N*-dimethylaminophenyl)1,2-thiazolino[5,4-d] 1,2-thiazoline-3,6-dithione, *J. Prakt. Chem.,* 332, 387, 1990.
81. Sakamoto, M., Kimura, M., Shimoto, T., Fujita, T., and Watanabe, S., Photochemical reaction of *N*,*N*-dialkyl-α,β-unsaturated thioamides, *J. Chem. Soc., Chem. Commun.,* 1214, 1990.
82. Sakamoto, M., Takahashi, M., Arai, W., Mino, T., Yamaguchi, K., Fujita, T., and Watanabe, S., Solid-state photochemistry: absolute asymmetric β-thiolactam synthesis from achiral *N*,*N*-dibenzyl-α,β-unsaturated thioamides, *Tetrahedron,* 56, 6795, 2000.
83. Sakamoto, M., Takahashi, M., Kamiya, K., Yamaguchi, K., Fujita, T., and Watanabe, S., Crystal-to-crystal solid-state photochemistry: absolute asymmetric β-thiolactam synthesis from an achiral α,β-unsaturated thioamide, *J. Am. Chem. Soc.,* 118, 10664, 1996.
84. Sakamoto, M., Takahashi, M., Kamiya, K., Arai, W., Yamaguchi, K., Fujita, T., and Watanabe, S., X-ray crystallographic analysis and photochemical reaction of asymmetrically substituted α,β–unsaturated thioamides, *J. Chem. Soc., Perkin Trans. 1*, 3731, 1998.
85. Sakamoto, M., Takahashi, M., Arai, W., Kamiya, K., Yamaguchi, K., Fujita, T., and Watanabe, S., X-ray crystallographic analysis and the photochemical reaction of *N*-benzyl-*N*-methylmethacrylthioamide in solution and the solid state, *J. Chem. Soc., Perkin Trans. 1,* 3633, 1999.
86. Sakamoto, M., Ishida, T., Fujita, T., and Watanabe, S., Photochemical isomerization of *N*-monosubstituted α,β-unsaturated thioamides to iminothietanes, *J. Org. Chem.*, 57, 2419, 1992.
87. Kinbara, K. and Saigo, K., Photochemical *EZ*-isomerization of α,β-unsaturated amides and thioamides in the solid state, *Bull. Chem. Soc. Jpn.,* 69, 779, 1996.

107

Manipulating Photochemical Reactions

Arunkumar Natarajan
Tulane University

Lakshmi S. Kaanumalle
Tulane University

V. Ramamurthy
Tulane University

107.1 Introduction

Over a period of time we have learned to control thermal reactions. This control is often achieved by variation of temperature, pressure, and solvent and with the help of catalysts. Because the activation barrier for photochemical reactions is small, temperature is expected to have only a minor influence. Yet it can be a valuable tool. Solvents, by influencing the stability of products and/intermediates, play an important role in thermal reactions. In addition to such effects, solvents, by influencing the closeness and ordering of excited states, would have a profound effect on photochemical reactions. Solvents with special properties (e.g., with a heavy atom) may also control the spin configuration of the reactive state, a feature we rarely consider in ground-state reactions. Wavelength and the mode of excitation have a significant influence on photoreactions. They help to place molecules in various excited states of different energy and spin. Further, photoreactions are susceptible to control by addends such as cations and Lewis acids that would control the ordering of excited states by interacting with lone pairs present in a carbonyl chromophore. Because most photochemical reactions occur at room temperature, one could preorganize reacting molecules prior to excitation. Such a templating influence is much more difficult to achieve in thermal reactions because temperature has a significant negative effect on the pre-association of molecules. This chapter discusses how one can exploit these features to manipulate the known photochemical behavior of various chromophores. One or two examples are provided for each category to illustrate the concept.

0-8493-1348-1/04/$0.00+$1.50

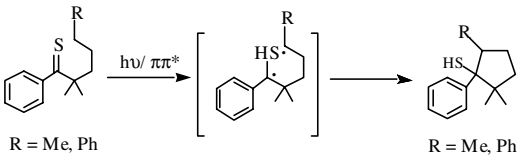

SCHEME 1

107.2 Wavelength Effect

Wavelength effects in solution might arise due to two factors: (1) reactions from upper excited states (singlet and triplet) and (2) ground-state structural features.[1] The tri*vial* wavelength effect would be absorption by products, which is not considered here. One could visualize wavelength as a tool to expand the number and types of reactions a given molecule might undergo. Generally, most reactions occur from the lowest excited singlet and triplet states. Only if a molecule fulfills certain conditions will reaction from upper excited singlet and triplet states take place; however, this happens only with a few molecules. There are several methods that are adopted to acquire sufficient concentrations of molecules in the upper excited state.

Reactions from Upper Excited Singlet States

Thiocarbonyl compounds have a large energy gap between S_1 and S_2 (> 30 kcal mol^{-1}) and have lower and upper excited states with different electronic configuration ($n\pi^*$ and $\pi\pi^*$).[2] Because of these, the S_2 state of thiones has a long lifetime (10^{-11} sec in hydrocarbon solvents and 10^{-10} sec in perfluoro hydrocarbon solvents), allowing them to react from the upper singlet states. They undergo both intra- and intermolecular reactions from S_2.

Thiocarbonyls, their structure permitting, undergo distinct wavelength-dependent intramolecular hydrogen abstraction reactions. The course of hydrogen abstraction and subsequent product formation are related to the substituents on the thiocarbonyl function and the wavelength of excitation.[2,3] While in carbonyls γ-hydrogen is the most common one, in thiocarbonyls abstraction occurs from the β, γ, δ, and ε positions. Aryl alkyl thiones containing saturated hydrocarbon alkyl chains, upon excitation to the $S_2(\pi\pi^*)$ state, yield cyclopentane thiols via a δ-hydrogen abstraction from the alkyl chain (Scheme 1). This reaction does not occur upon irradiation into the $S_1(n\pi^*)$ band. Successful quenching of the reaction by singlet quenchers and unsuccessful triplet sensitization are taken to support $S_2(\pi\pi^*)$ as the reactive state. Aryl alkyl thiones lacking δ-hydrogens do not undergo any photoreaction. However, when an ethereal oxygen atom replaces the δ-carbon, photochemical hydrogen abstraction occurs from carbons adjacent (ε and/or γ) to the oxygen atom (Scheme 2) as a result of activation of the neighboring hydrogens by the heteroatom. ε-Hydrogen abstraction leads to six-membered ring thiols, while γ-hydrogen abstraction leads to cyclization (cyclobutanethiols) and cleavage (olefin) products. Whereas the γ-hydrogen abstraction can be initiated by light of short and long wavelength, ε-hydrogen abstraction is wavelength specific and occurs only upon excitation to the S_2 state.

Adamantanethione adds to both electron-rich and -poor olefins upon excitation to the S_1 level.[2,3] The addition is nonstereospecific and regioselective (Scheme 3). Based on sensitization and quenching studies, the above addition has been established to occur via the triplet state (T_1). The quantum yield of the isolated adduct is low (10^{-4}). Upon excitation to S_2, adamantanethione adds to both electron-rich and -poor olefins to yield thietanes. These additions are stereospecific and regioselective (Scheme 4). Note that the characteristics of additions are different from the one occurring from the $n\pi^*$ triplet state. Based on sensitization and quenching studies and the nature of products formed, the reactive state has been identified to be the S_2 state.

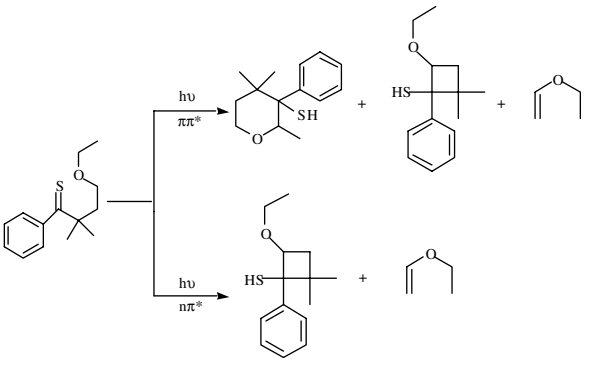

SCHEME 2

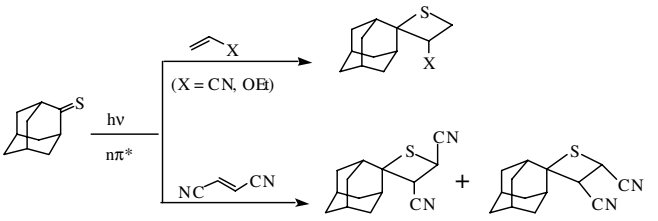

SCHEME 3

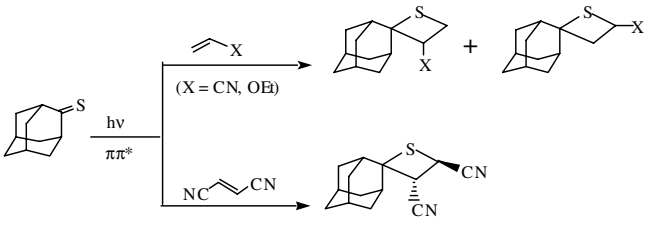

SCHEME 4

Reactions from Upper Excited Triplet States

An approach to produce upper triplets is via direct excitation into S_n followed by intersystem crossing. Except in cases where T_2 is below S_1, this approach is not successful. An alternative method for producing these higher triplet states involves direct excitation via $T_1 \rightarrow T_n$ absorption. In this method, a population of the lowest triplet state produced initially is converted to the higher triplet state using a second light source. Sufficient concentrations of molecules in the T_1 state are accumulated using either low-temperature matrices or high-intensity light sources.

An elegant illustration of the low-temperature matrix technique is provided by the photochemistry of pleiadene precursor **1** (Scheme 5).[4] Compound **1** rearranges to pleiadene (**2**) only after population of an upper triplet state by biphotonic excitation in rigid glasses at 77K. It is important to note that solution irradiation both at room and low temperatures leads to no reaction, and that triplet sensitization in solution is similarly ineffective. The reaction was achieved only in matrices at 77K using both UV and visible radiation sources simultaneously in a biphotonic process, or with a single UV source in a monophotonic

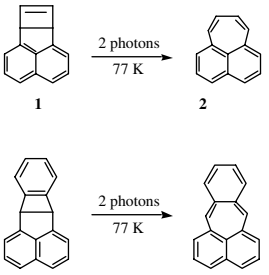

SCHEME 5

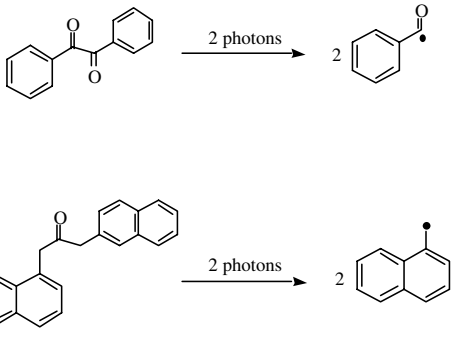

SCHEME 6

process, at wavelengths much shorter than that required to populate S_1. In the two-photon excitation experiments, the product yield has been maximized by tuning the visible source to wavelengths appropriate for known naphthalene $T_1 \rightarrow T_n$ absorption maxima (~400–415 nm). The proposed mechanism for the above two light source experiments involves UV absorption followed by relaxation to a long-lived T_1 state (3.3 sec for 1 at 77K), triplet-triplet absorption of the visible photon to populate a higher triplet state T_n, from which steps leading to the chemical reaction occur.

While matrix isolation spectroscopy is experimentally simple, it only allows unimolecular processes. Because diffusion is severely restricted, no bimolecular process can occur at low temperatures in a matrix. To allow such reactions, the upper excited-state chemistry needs to be conducted at room temperature in isotropic solution media. The high-intensity light sources required to produce high concentrations of excited states are achieved through the use of lasers.

In the two-laser (two-color) technique, two lasers of different wavelengths, firing sequentially, are employed to produce the upper states of molecules.[5] The first laser produces the lowest excited state of the molecule and the second laser selectively excites these molecules into an upper level. By this approach a variable delay can be introduced between the two photons to allow the lower excited state concentration to build up. Using a tunable laser, the wavelength of the second photon can be adjusted to correspond to the absorption maximum of the lower excited state. Because excited singlets (S_1) are too short-lived in comparison with the laser pulse duration to allow for efficient upper singlet production, the two-laser setup is better suited for populating upper triplets than upper singlets.

An illustration of the above technique is found in the cleavage reactions of several carbonyl and aromatic systems that do not cleave in solution when irradiated with conventional light sources (Scheme 6).[6] For example, benzil does not cleave when populated to the T_1 ($\pi\pi^*$) state by either direct excitation or triplet sensitization. However, generation of a higher triplet through excitation of T_1 results in α-cleavage.

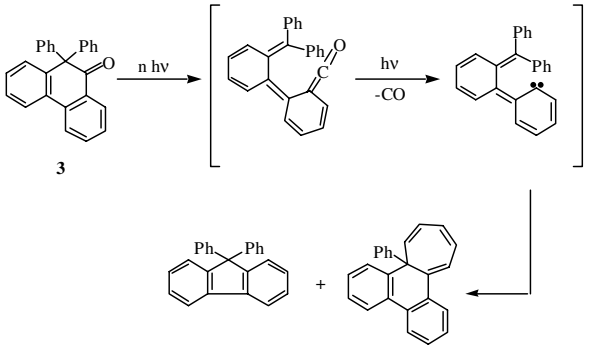

SCHEME 7

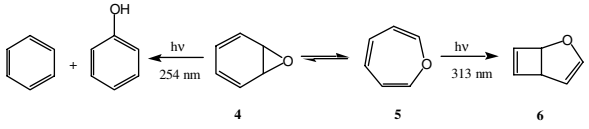

SCHEME 8

The two-laser (two-color) technique described above provides excellent spectroscopic information on the transients produced during the formation of products from upper excited states. However, isolation of the products of a photoreaction by this approach could be tedious. For product isolation, a "laser jet" apparatus is often used.[7] In this laser jet technique, a high-velocity microjet of a solution of material to be irradiated is injected into the focal region of an argon ion laser beam. The typical microjet flow rates can be controlled and the sample recycled as many times as necessary to bring the reaction to completion. Consequently, isolation of significant quantities of products is possible. Usually, a high-intensity CW argon ion laser is used to excite molecules. In this method, sufficient concentrations of molecules in their S_1 or T_1 states are trapped within a "microbubble" so that they can absorb a second photon. Reactions generally occur from the upper excited states. The ketone **3** shown in Scheme 7 is stable to low-intensity light (Rayonet reactor). However, when irradiated with an argon ion laser under laser jet conditions, it yields the product shown in Scheme 7, believed to be derived via T_n.[8]

Wavelength Effects due to Ground-State Structural Features

When there is more than one type of molecule in the medium with different absorption characteristics and photobehaviors, there is likely to be a wavelength effect. The two types of molecules need not be distinctly different molecules; they could be geometric isomers or conformational isomers in thermal equilibrium.

Irradiation of benzene oxide in ether solution with light of wavelength above 310 nm gave **6** as the only product (Scheme 8).[9] On the other hand, irradiation at 254 nm at −80°C gave benzene and phenol. This wavelength dependence has its origin in the equilibrium that exists between the open and closed forms of benzene oxide. The cyclic triene **5** absorbs at longer wavelength and results in product **6** when irradiated at >313 nm. At lower temperature, the benzene oxide exists in the closed form, which absorbs at shorter wavelength. Hence, 254-nm excitation gives a different set of products characteristic of the closed form.

The interconverting structures need not be structural isomers as in the above example, but could in fact be conformational isomers. As shown in Scheme 9, *cis*-1,3,5-hexatriene can exist in three conformations. In the ground state, equilibrium between the three conformers occurs. Upon excitation, equilibration is prevented in the excited state and each one gives its own product (Scheme 9).[10]

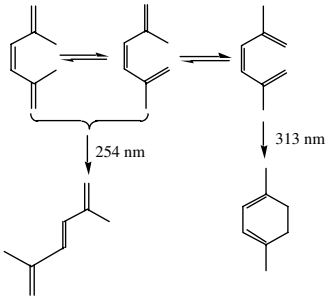

SCHEME 9

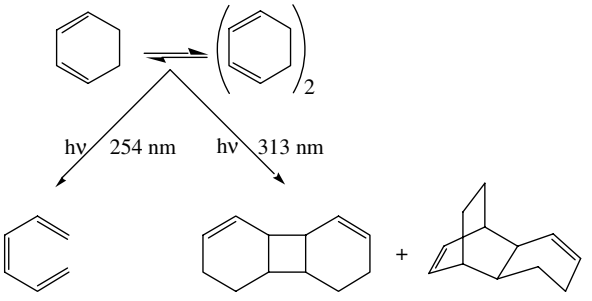

SCHEME 10

Equilibrium between monomer and aggregates with different absorption characteristics is likely to result in wavelength-dependent chemistry. For example, 1,3-cyclohexadiene upon irradiation with 254-nm light gives 1,3,5-hexatriene as the only product; but irradiation at 313 nm produces dimers (Scheme 10).[11] Upon irradiation at 254 nm, mainly the monomer is expected, while at 313 nm the dimer is excited with the two yielding different products.

Yet another possibility is the presence of a charge-transfer (CT) complex in equilibrium with the reactant. If the CT complex and the uncomplexed reactant have different absorption characteristics as well as different photochemistries, wavelength-dependent chemistry is likely to result. The chemistry of styrenes aptly illustrates this point.[12] Styrenes form ground-state complexes with oxygen molecules, with the CT complex having a weak absorption shifted to the red of the absorption due to the olefin $\pi\pi^*$ transition. When an oxygen-saturated acetonitrile solution of the styrene derivative is irradiated with light of wavelength 254 nm (into the olefin absorption band), two dimers (via photocycloaddition) are obtained. However, when the excitation wavelength is shifted to 366 nm, the benzaldehyde is obtained as one of the major products (Scheme 11). The latter is believed to result from the excitation of the styrene–oxygen complex.

107.3 Mode of Excitation (Direct vs. Triplet Sensitization)

When a reactant is excited to the S_1 state, depending on the rate of intersystem crossing and reactivity of S_1 and T_1, products from both S_1 and T_1 or S_1 alone or T_1 alone may result. One could resort to triplet sensitization to obtain products only from T_1. If the intersystem crossing quantum yield from S_1 to T_1 is negligible one could obtain different products upon direct excitation and triplet sensitization (Scheme 12).[13]

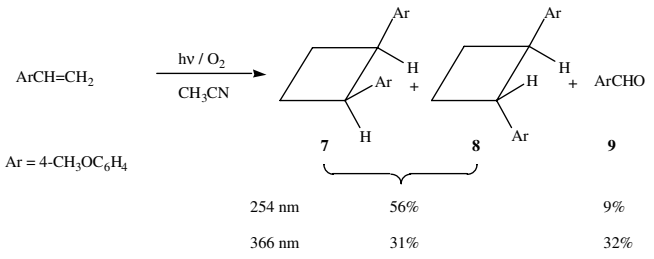

SCHEME 11

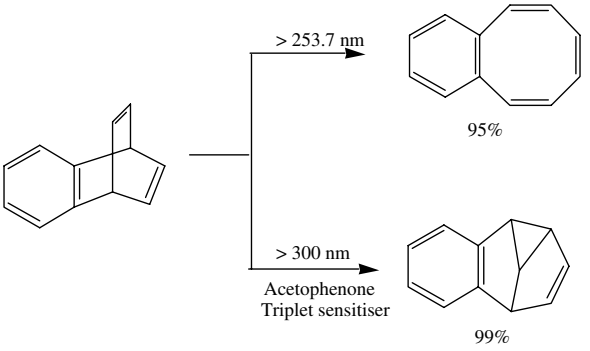

SCHEME 12

107.4 Solvent Effects

Heavy-Atom Solvents

Solvents containing heavy atoms such as bromine and iodine can be used to promote singlet–triplet crossings in the excited state of the reactants. Most common solvents used in this context are alkyl halides such as propyl bromide and propyl iodide.

Heavy-atom solvents are often used to influence the product distributions when different products are obtained from S_1 and T_1. For example, acenaphthylene gives different dimers from S_1 and T_1 (Scheme 13).[14] The *trans*-isomer, the one arising from T_1, is formed in excess in solvents with the heavier atom. For example, the ratios of *cis*/*trans* in cyclohexane containing 10% n-butyl chloride, 10% n-butyl bromide, and 10% *n*-butyl iodide are 2.37, 0.73, and 0.25, respectively. Because the spin-orbit coupling parameter increases in the same order as the percentage of the *trans*-isomer (chloride < bromide < iodide), the heavy-atom solvent is believed to favor intersystem crossing from S_1 to T_1 of the reactant acenaphthylene.

Polar Solvents

Carbonyl compounds have close-lying $n\pi^*$ and $\pi\pi^*$ states with different photochemical properties. If the ordering of the two states can be controlled externally, then one could obtain, at will, products from the two states. One approach is to make use of a polar medium. If the ordering of the two states is different in polar and nonpolar solvents, different products would be obtained in these solvents. Even olefins have two states ($\pi\pi^*$ and doubly excited $\pi^*\pi^*$) of different polarizability. When these two states are nearby, the photochemistry could be solvent dependent.

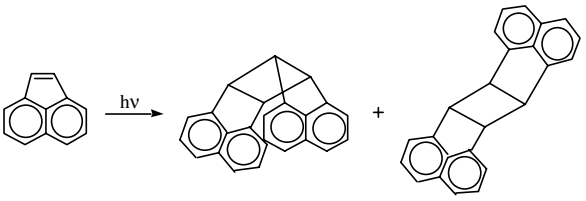

S_1 : 100 : 0

T_1 : 1 : 9

Solvent	Cis/trans dimer
Cyclohexane	4.97
n-Butyl chloride	2.37
n-Propyl bromide	0.41
Ethyl iodide (10% mole %)	0.25

SCHEME 13

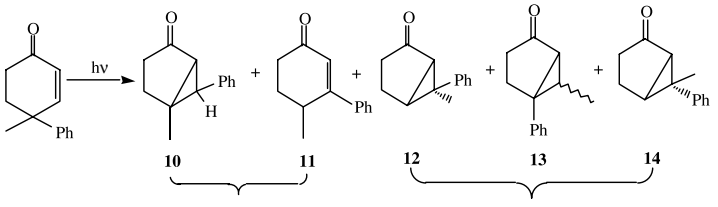

Benzene	100	0
Acetonitrile	58	42
Formamide	38	62

SCHEME 14

For example, 4-methyl-4-phenyl-2-cyclohexenone upon irradiation yields several products (Scheme 14).[15] Two of these products derive from a triplet of $n\pi^*$ character and three of them from a triplet of $\pi\pi^*$ character. As indicated in the scheme, in the nonpolar solvent benzene, only $n\pi^*$-derived products are formed; whereas in more polar acetonitrile and formamide, $\pi\pi^*$-derived products are also obtained.

Solvents not only have an influence on the ordering of excited states but may also alter the reaction pathway taken by intermediates. For example, while the quantum yield of addition of diphenylvinylene carbonate to 2,5-dimethyl-2,4-hexadiene in hexane is 0.5, that in acetonitrile is <0.001 (Scheme 15); that is, adduct is formed in hexane but not in acetonitrile.[16] The reaction in both solvents proceeds via an exciplex. In nonpolar solvents, the exciplex yields the adduct while in polar solvents, electron transfer occurs, which leads to energy wastage.

Protic Solvents

The quantum yield of the Norrish-Yang reaction product from valerophenone (Scheme 16) is significantly enhanced in *t*-butanol (1.00) with respect to benzene (0.42).[17] In addition to the rate increase, the

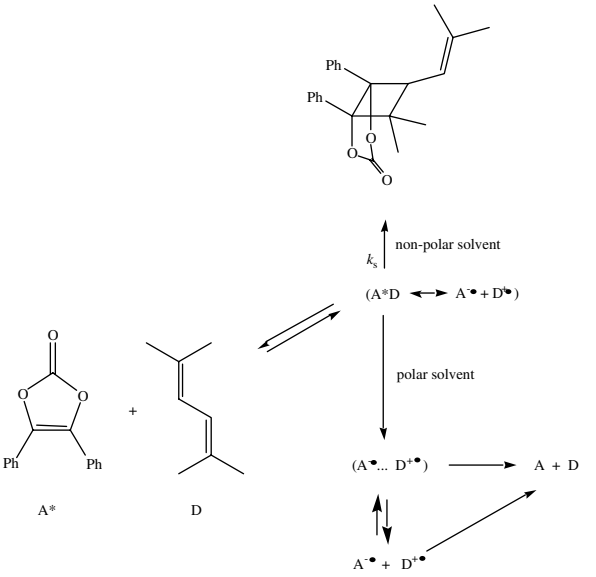

SCHEME 15

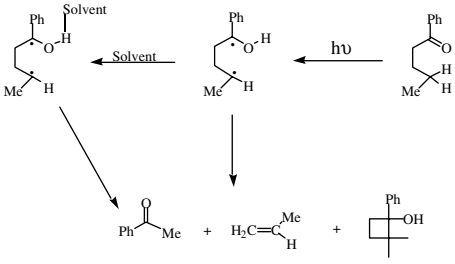

SCHEME 16

elimination (E) to cyclization (C) products ratio changed between the two solvents (C/E+C in benzene = 4 and *t*-butanol = 2; Scheme 16). These changes are consistent with hydrogen bonding between the solvent *t*-butanol and the intermediate in the 1,4-biradical. Hydrogen bonding shuts down the reverse hydrogen transfer and favors the elimination over cyclization.

Strong hydrogen bonding to the reactive carbonyl chromophore often alters the ordering of the $n\pi^*$ and $\pi\pi^*$ states. Similar to polar solvents, in a protic hydrogen-bonding medium, the $\pi\pi^*$ state becomes the reactive state. The hydrogen bonding could be even more powerful than a polar solvent in lowering the $\pi\pi^*$ state below the $n\pi^*$ state, which is illustrated by the photobehavior of the dienone **15** (Scheme 17).[18] While in ethanol α-cleavage characteristic of $n\pi^*$ state occurs (ketene product), in trifluoroethanol a product characteristic of the $\pi\pi^*$ state is obtained (bicyclic product). Apparently, polarity alone is not enough to bring out the $\pi\pi^*$ reactivity of the dienone; a strong hydrogen bonding or a proton donating solvent is needed.

Consider the intramolecular cycloaddition of an enone to an alkene illustrated in Scheme 18.[19] The two adducts that are formed derive via the conformers A and B shown in Scheme 19. Of the two conformers, A is of lower energy in systems that do not form intramolecular hydrogen bonding. A single diastereomeric adduct is obtained when the proximal substituent is $OSiEt_3$. However, when the proximal substituent is OH, the selectivity is reversed, suggesting that intramolecular hydrogen bonding, favoring the conformer B controls the photoaddition. The extent of selectivity depends on the solvent. While in

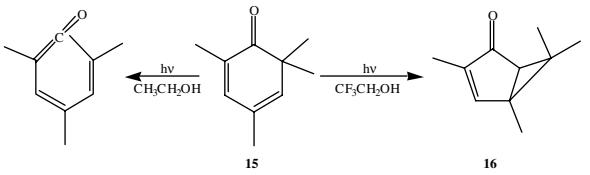

SCHEME 17

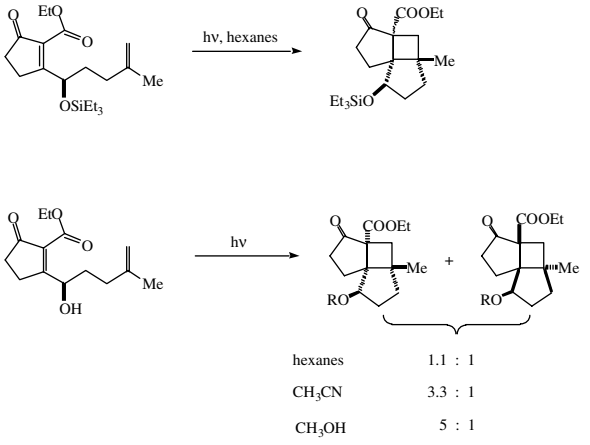

SCHEME 18

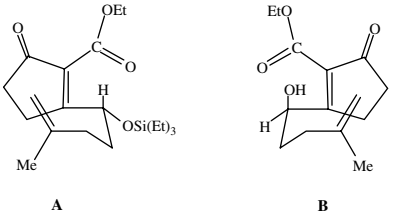

SCHEME 19

non-hydrogen-bonding solvents (hexane and methylene chloride) the adduct formed from conformer B is favored, in the hydrogen-bonding solvent methanol, the selectivity is slightly favored toward the adduct from conformer A.

Fluorinated Solvents

Owing to the fact that the C–F compared to a C–H bond is stronger (the dissociation energy of a C–F bond is 129 kcal mol^{-1} while that for a C–H bond is 100 kcal mol^{-1}), perfluorinated solvents are generally inert. Fluorinated solvents are therefore the best medium when one wishes to avoid hydrogen abstraction reactions, which occur to some degree in almost any solvent. A remarkable influence of perfluoro solvents on the S_2 lifetime of thiones and on the T_1 lifetime of benzophenone at room temperature have been noted. Xanthione in hexane has an S_2 lifetime of 25 picoseconds while in perfluorohexane, the lifetime is 162 picosecond.[20] The triplet lifetime of benzophenone in cyclohexane is 5 microseconds while in perfluoromethylcyclohexane it is 0.7 milliseconds.[21] An increase of three orders is observed. The quantum

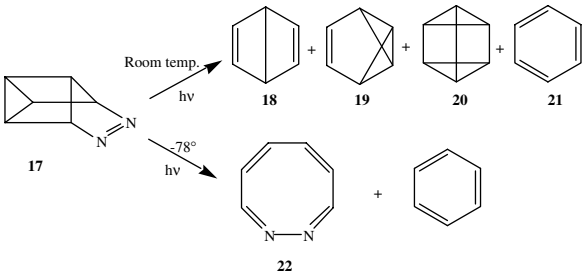

Temperature (°C)	21	18	19	20	22
22	30	45	6	11	8
0	30	34	3	5	31
- 35	20	5	-	-	75
- 78	10	-	-	-	90

SCHEME 20

yield of phosphorescence of benzophenone in perfluoromethylcyclohexane at room temperature reaches as high as 0.1.

Singlet oxygen also has a significantly long lifetime in perfluorinated solvents, although the origin of this effect is different from the one observed in the case of thiones and carbonyls. While in benzene, singlet oxygen $^1\Delta_g$ has a lifetime of 32 microseconds, in perfluorobenzene the lifetime is 3900 microseconds!.[22] In hydrocarbon solvents, the singlet oxygen relaxes nonradiatively by a specific interaction with a C–H bond, which does not occur (or only very weakly) with the C–F bond.

107.5 Temperature Effects

Even excited-state reactions can have small activation energies. If this is the case, the photoreaction could be sensitive to the temperature at which the photolysis is conducted. The azoalkane **17**, when photolyzed at −78°C, yields a single product, diazacyclooctatetraene (Scheme 22).[23] On the other hand, when photolyzed at room temperature, benzene isomers are obtained. Diazacyclooctatetraene **22** is derived from the triplet state of azoalkane **17**. At low temperature (−78°C), when the cleavage from S_1 state is slow the intersystem crossing to T_1 occurs readily to yield the triplet product diazacyclooctatetraene. At room temperature, the S_1 gains enough activation energy to extrude nitrogen, resulting in highly strained benzene isomers. The energy of activation for nitrogen extrusion from S_1 is determined to be ~6 kcal mol^{-1}.

107.6 Use of Lewis Acids and Metal Ions

The $\pi\pi^*$ reactivity of a carbonyl chromophore could be induced and the $n\pi^*$ reactivity could be prevented provided the $n\pi^*$ state is pushed well above the energy of the $\pi\pi^*$ state. An approach to achieve this goal has been to protonate the carbonyl chromophore.[24] In an acidic medium, the $n\pi^*$ band of a neutral carbonyl is substantially blue-shifted as a result of one of the two pairs of n-electrons being bonded to the proton. On the other hand, the $\pi\pi^*$ band is red-shifted. As a result, the lowest excited energy state is $\pi\pi^*$ in character. The probability of intersystem crossing from the singlet to the triplet manifold is reduced in protonated carbonyl compounds owing to the energy of the $n\pi^*$ triplet being above that of the $\pi\pi^*$ singlet. Thus, the chemistry occurs essentially from an S_1 of $\pi\pi^*$ character. While acids are quite useful to effect protonation of a carbonyl compound and the photochemistry from the $\pi\pi^*$ state of the protonated carbonyl is clean, the isolation of primary products is troublesome. Due to this complication, instead of using strong Brønsted acids, most often Lewis acids are used to achieve the same goal.

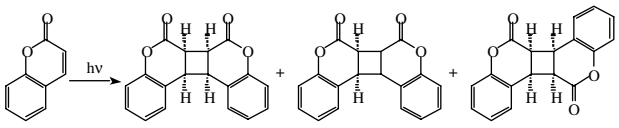

	23	**24**	**25**
None	20	71	10
In presence of BF_3	0	10	90

SCHEME 21

Coumarins, upon direct excitation, yield a mixture of the syn-head-head (**23**), *anti*-head-head (**24**) and *syn*-head-tail (**25**) dimers (Scheme 21).[25] At moderate coumarin concentration (0.2 *M*) when the reaction occurs mainly from the triplet state, the major product (75%) in methylene chloride is *anti*-head-head dimer. This dimer is believed to arise from the $n\pi^*$ triplet of coumarin. Irradiation of coumarin–BF_3 complexes under similar concentration conditions gave the *syn*-head-tail dimer (**25**) as the major product (90%). There is a reversal in the geometry of the dimer formed in the absence and presence of the Lewis acid BF_3. This change is attributed to the lowering of the energy of the $\pi\pi^*$ state of coumarin by BF_3 complexation.

2-Naphthaldehyde has a non-fluorescent lowest $n\pi^*$ excited singlet.[26] However, in presence of Mg^{2+}, this becomes fluorescent. This change in the photophysics is attributed to the switching of the order of the $n\pi^*$ and $\pi\pi^*$ states. In acetonitrile, in the absence of $Mg(ClO_4)_2$, the S_1 is $n\pi^*$ in nature, which has a high rate of intersystem crossing to the triplet manifold. On the other hand, in the presence of $Mg(ClO_4)_2$, the S_1 state is $\pi\pi^*$ in character.

Intramolecular photocycloadditions of 1,n-dienes can be achieved by the use of Cu^+ ions. Cu^+ serves as a removable tether to preorganize the ene chromophores. Cu^+ triflate-catalyzed photoreactions of alkenes involve light absorption by preformed alkene–Cu^+ complexes. The Cu^+–alkene triflate complex generally shows two strong absorption bands (230–240 nm and 260–290 nm) while the uncomplexed alkenes are nearly transparent in this region. Because of this effect even if only a small percentage of alkene exists in the complexed state, only the complex will react. This cycloaddition reaction is run most often under catalytic conditions.

Irradiation of the diene in Scheme 22 as a Cu^+ triflate complex yields the intramolecular adducts. In the absence of the Cu^+ ,the intramolecular [2+2]-addition is very inefficient. The addition reaction in the presence of Cu^+ triflate is often *endo-exo* selective. One such example is also shown in Scheme 22.

107.7 Use of Chiral Sensitizers and Chiral Auxiliaries

Induction of chirality to obtain enantiomerically or diastereomerically enriched materials is achieved by several approaches:[27] (1) absorption of circularly polarized light by a racemate, causing different reaction rates for the enantiomers; (2) reactions in chiral medium such as chiral solvent; (3) the use of an enantiomerically pure sensitizer; and (4) the use of enantiomerically pure materials, that is, photochemically reactive components attached to an enantiomerically pure auxiliary. The first two methods have not yielded product with more than a few percent enantiomeric excess (*ee* < 5%). Chiral sensitization has yielded, in a few select examples, moderate *ee* (~15–65%), while the chiral auxiliary approach has yielded high diastereomeric excess (*de*). In this approach, because there is a chiral center in the reactant, the products are formed as diastereomers. Removal of the chiral auxiliary results in an enantiomerically enriched product.

cis-Diphenylcyclopropane is achiral while the *trans*-isomer is chiral. Energy- or electron-transfer sensitized irradiation of *cis*-diphenylcyclopropane in isotropic solvents provides the *trans*-isomer as a

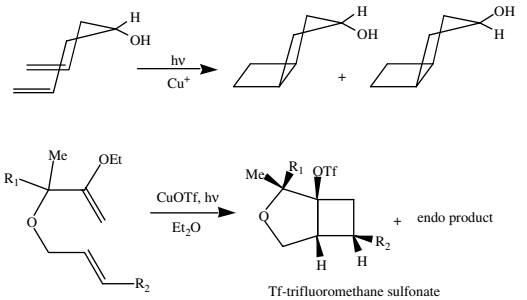

R_1	R_2	exo : endo
Me	Me	2.5 : 1
Me	Ph	100 : 0
Me	$CH{=}CHCH_3$	2.2 : 1
Bn	$CH{=}CHCH_3$	100 : 0

SCHEME 22

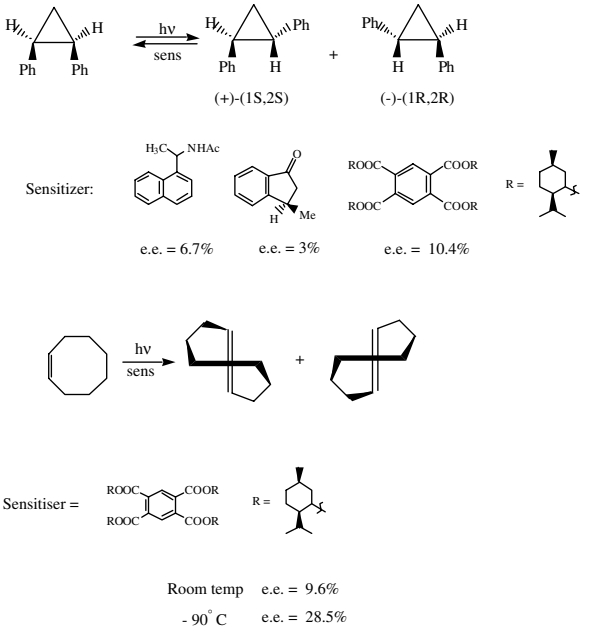

SCHEME 23

racemic mixture. However, the photoisomerization upon sensitization with a chiral sensitizer results in the *trans*-isomer with an *ee* of ~5 to 10% (Scheme 23).[29]

Achiral *cis*-cyclooctene upon singlet sensitization yields chiral *trans*-cyclooctene. While achiral sensitizers yield a racemic *trans*-cyclooctene, chiral sensitizers yield enantiomerically enriched *trans*-cyclooctene (Scheme 23).[30] The highest *ee* reported (73%) thus far is with optically active (−) tetramenthyl-1,2,4,5-benezene tetracarboxylate at −110°C in diethyl ether. The extent of *ee* depends on temperature, pressure, and solvent.

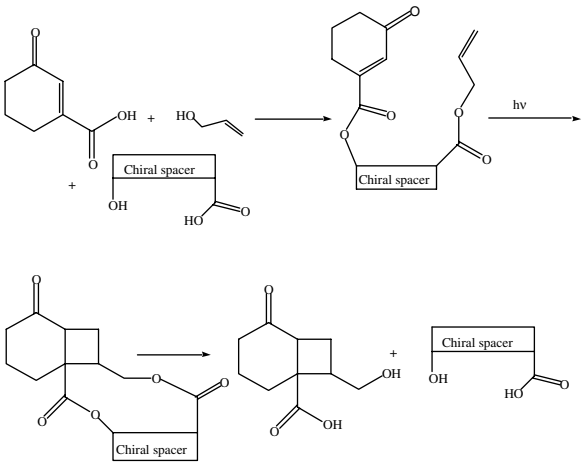

SCHEME 24

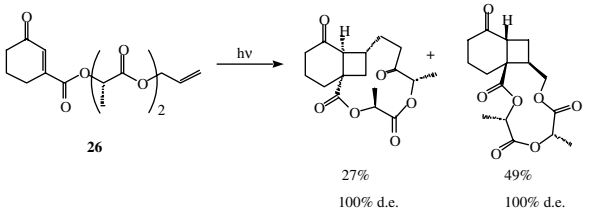

SCHEME 25

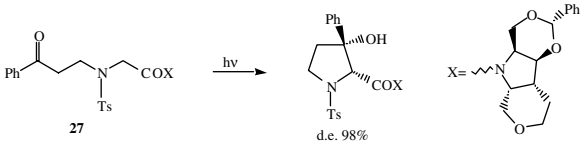

SCHEME 26

An alternate approach to chiral sensitization is to tie the chiral component and the reactant through a covalent bond.[31] This traditionally popular synthetic strategy is known as the chiral auxiliary approach. The best examples of this strategy are found in bimolecular photoaddition reactions. The chiral auxiliary could be either on the reactant to be excited or on the ground state molecule reacting with the excited-state species.

For this method to be a success, the chiral auxiliary should be an easily attachable and removable group (Scheme 24).[32] The dimalic ester substrate **26** gave head-head and head-tail adducts. What is remarkable is that both adducts are formed as single diastereomer (Scheme 25). Removal of the chiral auxiliary gave a single enantiomer in each case. This route is useful because the inexpensive chiral auxiliary is used as a temporary linker and can easily be removed after photocycloaddition.

The chiral auxiliary method yields exceptionally high *de* values even during intramolecular hydrogen abstraction reactions of carbonyl systems. A single isomer of highly substituted cyclopentanols was obtained when the chirally modified aryl alkyl ketones **27** shown in Scheme 26 were irradiated.[33]

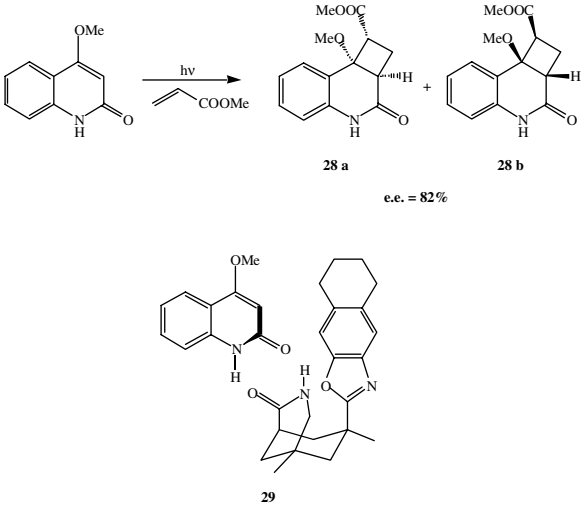

SCHEME 27

107.8 Templating Effect

By a templating effect we mean that the reactants are prearranged for the reaction and the photoreaction becomes more selective or a reaction that would not occur otherwise takes place in the presence of the template. Best templating effects are achieved in organized/confined media, which is discussed in the next section. In this section we provide examples that illustrate a strategy that can be adopted to achieve selective chemistry.

Consider the addition of vinyl acetate to the quinolone shown in Scheme 27.[34] Addition to excited quinolone could take place from either prochiral face resulting in a diastereomeric mixture of **28**. Chiral amide **29** is able to hold the quinolone in a good orientation so that the addition occurs only to one of the two prochiral faces (Scheme 27). Hydrogen bonding between the amide and quinolone plays an important role in this operation. The *ee* obtained is fairly high with several olefins (>80%). The fact that the binding constants between the chiral amide and quinolone are high and the chiral amide is recoverable makes this a novel approach.

A modification of the above approach is one where one of the reactants is covalently linked to the chiral amide. Paterno-Buchi reaction of benzaldehyde under normal conditions would proceed equally from the two prochiral faces of the carbonyl chromophore.[35] If one wishes to control the addition, "somehow" one needs to distinguish between the two faces. This is done by the templating effect — that is, the olefin is steered to approach the carbonyl preferentially from one face by the use of external forces. The example shown in Scheme 28 illustrates this concept. The olefin dihydropyridone, when pre-associated to the carbonyl with the help of hydrogen bonding to the chiral amide, undergoes addition selectively from one face. A diastereomeric ratio of 95:5 is achieved in toluene while that in acetonitrile is 50:50. The importance of pre-organizing the dihydropyridone prior to exciting the carbonyl is evident from the fact that when the chiral amide is modified so that it cannot selectively form hydrogen bonds with the dihydropyridone, the diastereomeric ratio is 50:50.

Cinnamate esters in solution undergo geometric isomerization much more efficiently than dimerization. Consistent with this, the diaminotriazine-substituted cinnamate ester **30**, upon irradiation in solution, undergoes mainly geometric isomerization, with minor amounts of several dimers being formed upon prolonged irradiation. When the irradiation is conducted in the presence of the template, substituted barbituric acid **31**, three dimers were formed with much higher quantum yield (Scheme 29).[36] The hydrogen bonding complementary nature of the diaminotriazine unit and barbituric acid unit is exploited

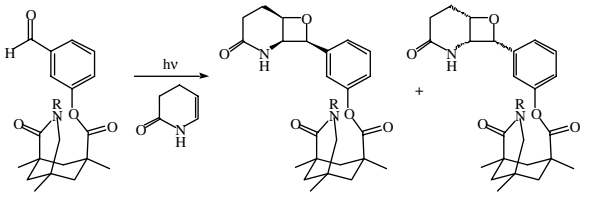

Acetonitrile 0% d.e.

Toluene 90% d.e.

SCHEME 28

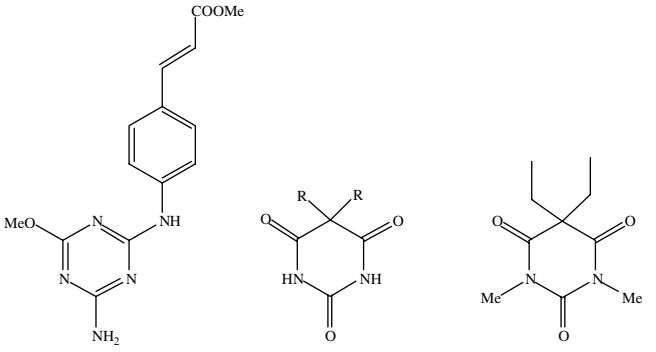

30 **31** (R = hexyl) **32**

Quantum yields of photodimers (x 0.001)

dimers*	**30**	0.5 equiv of **31**	0.5 equiv of **32**
33	0.7	2.3	0.7
34	0.1	0.6	0.1
35	<0.1	0.8	<0.1

*for structure of dimers see scheme 30

SCHEME 29

in this templating operation (Scheme 30). When the hydrogen-bonding ability of the barbituric acid unit was eliminated by alkylation of the amino groups (**32**), no enhancement in the dimerization occurred.

107.9 Influence of Organized Media

Chemists have long recognized the important role that the reaction medium plays in controlling the rates, product distributions, and stereochemistry of organic reactions. Recently, much effort has been directed toward the use of organized media to modify the photochemical reactivities achieved with isotropic liquids.[37] A principal goal of such studies is to utilize the order of the medium to increase the rate and selectivity of a chemical process in much the same way that enzymes modify the reactivity of the substrates to which they are bound. Notable among the many ordered or constrained systems are micelles, microemulsions, liquid crystals, inclusion complexes, monolayers, and solid phases such as porous solids (silica, alumina, clay, and zeolites) and crystals. The differences in chemical reactivities observed in ordered media, compared to isotropic solvent phases, are largely due to the physical restraints

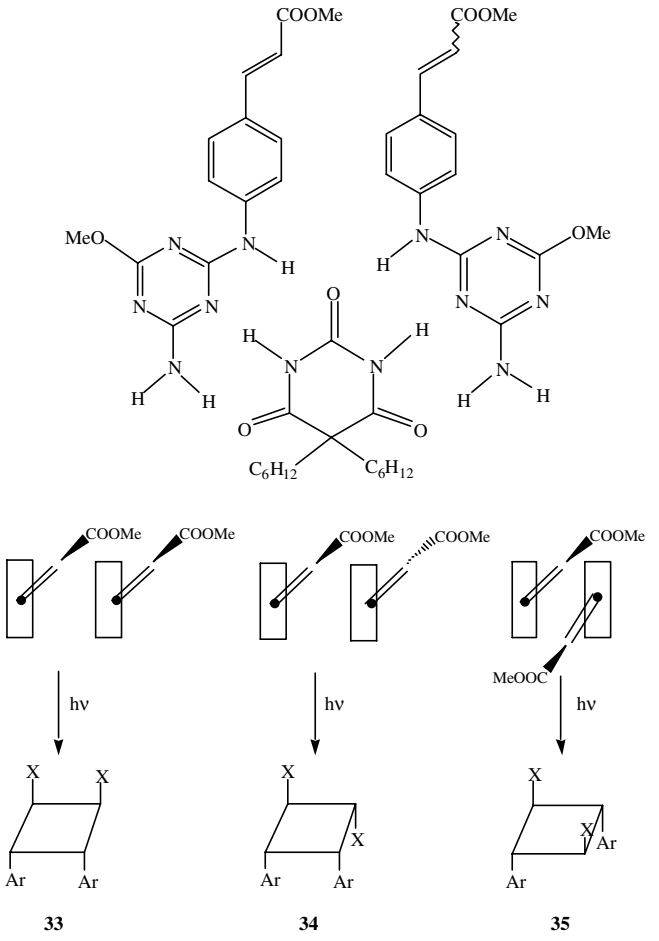

SCHEME 30

imposed by the environment. These include preventing large-amplitude conformational, configurational, and translational changes along the reaction coordinate, modifying diffusional characteristics of reactants, and facilitating alternate reaction pathways. The intrinsic reactivity of a molecule in an ordered medium is frequently of secondary importance in comparison to features such as site symmetry, nearest neighbor separation, and other geometric considerations. In organized media, the very familiar electronic and dipolar effects and hydrogen bonding of solution chemistry are replaced by structural and topological factors that frequently result in degrees of selectivity or stereospecificity of product formation that are not observed in solution. A few examples employing micelles, cyclodextrins, silica, and zeolite surfaces and liquid crystals as media are presented in this section.

Photochemistry of dibenzyl ketones has been examined in a number of organized media. Photolysis of 3-(4-methylphenyl)-1-phenylacetone (MeDBK) results in a 1:2:1 mixture of three products shown in Scheme 31.[38] Photolysis of the same molecule solubilized in a micelle (hexadecyltrimethylammonium chloride) gives a single product (AB). This remarkable change in product distribution is due to the cage effect brought forth by the micellar structure. The change in product distribution occurs at or above the critical micelle concentration.

Photocycloaddition of 3-*n*-butylcyclopentanone in the presence of 1-hexene in organic solvents gives two adducts **36** and **37** in a 1:1 ratio (Scheme 32).[39] However, irradiation in a potassium dodecanoate micelle yields the isomer **37** as the major product, consistent with the notion that a micellar interface

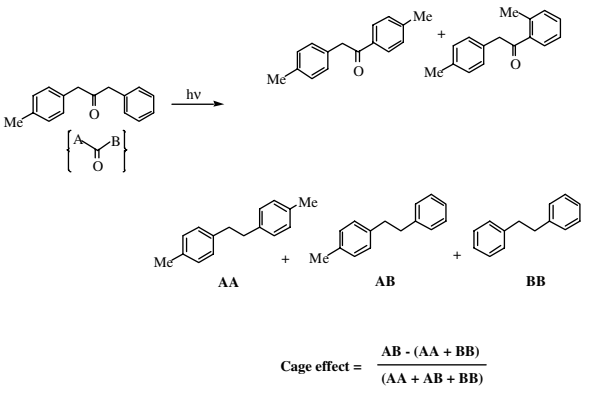

SCHEME 31

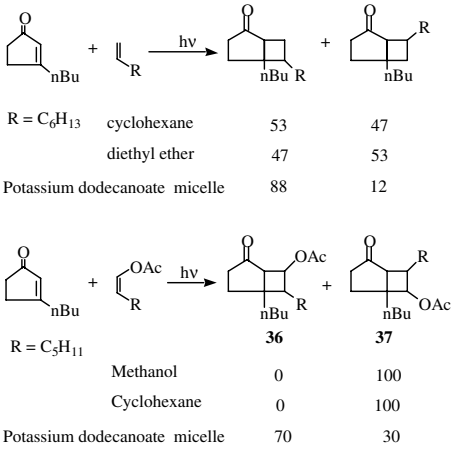

SCHEME 32

helps orient the reactant molecules. When the orientation of the reactive olefin is further fixed with a hydrophilic group, as when the olefin is heptenyl acetate instead of 1-heptene, a dramatic switch in the regiochemistry of the product is observed.

Upon irradiation, in acetonitrile/aqueous solution, of 1-cyanonapthalene in the presence of *all trans*-farnesyl acetate, the latter undergoes only *cis,trans*-isomerization via an electron-transfer process.[40] No products from any other reactions were isolated. However, when the same combination of molecules was irradiated in sodium dodecyl acetate micellar solution, the main product was the result of intramolecular cyclization (Scheme 33). The cyclization is stereo- and regioselective to yield a *trans*-fused product in which the water molecule has added stereoselectively. Such an amazing selective cyclization occurs only in a micellar medium.

Irradiation of the (S)-tropolone 2-methyl butyl ether shown in Scheme 34 in solution yields a 1:1 diastereomeric mixture.[41] Clearly, in solution the presence of a chiral auxiliary in proximity to a reactive center has no influence on the product stereochemistry. When irradiated within NaY zeolite, the same molecule gave the cyclized product in ~53% diastereomeric excess. The smaller and controlled space of the zeolite supercage apparently has forced the establishment of communication between the chiral center and the reaction site.

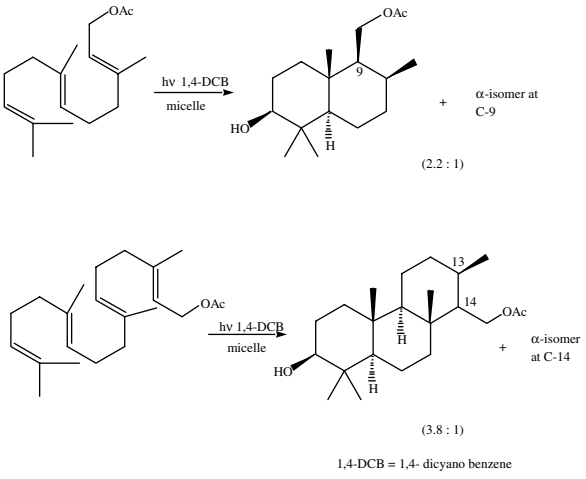

SCHEME 33

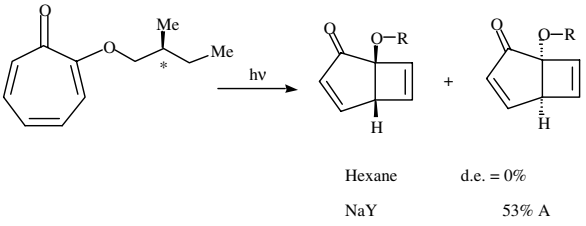

SCHEME 34

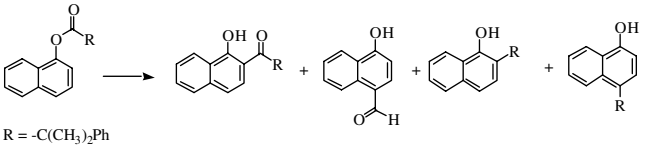

Hexane	28	15	9	14
NaY	99%	--	--	--

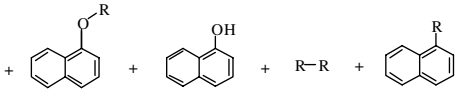

Hexane	0	13	15	6
NaY	99%	--	--	--

SCHEME 35

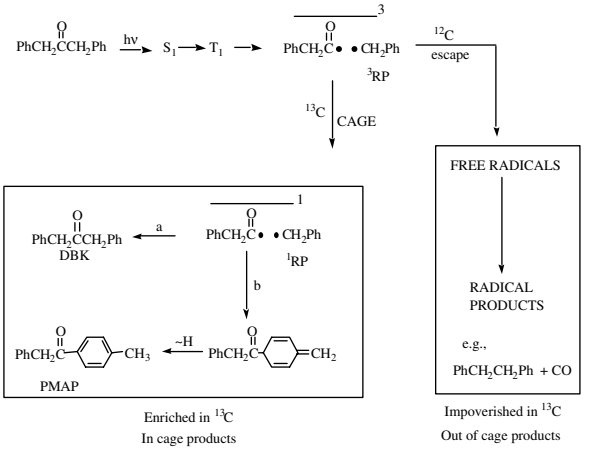

SCHEME 36

An impressive illustration of the influence of the medium on the photo-Fries reaction product distribution can be found in Scheme 35.[42] Remarkably, whereas in solution eight products are formed, within NaY zeolite a single product dominates the product mixture. Cations present within zeolites help to anchor the reactants, intermediates, and products to the surfaces of the zeolite and control the reactivity of the intermediates. In this case, the cation binding not only forced the phenyl acyl radical to react at the *ortho*-position preferentially but also prevented it from decarbonylation.

The difference in the nature of the reaction cavity provided by an isotropic solvent and a micelle is nicely demonstrated by the isotope enrichment observed during the photolysis of DBK. This process can be understood using the detailed mechanism for cleavage process presented in Scheme 36.[43] α-Cleavage of the triplet excited DBK results in a triplet geminate primary radical pair ($C_6H_5CH_2^{\bullet}$ and $C_6H_5CH_2CO^{\bullet}$, PRP^3). This initial radical pair loses CO to generate the secondary radical pair ($2C_6H_5CH_2^{\bullet}$, SRP). The two benzylic SRP combine to yield the final product, 1,2-diphenylethane. An option, unavailable in isotropic solution to the PRP^3, becomes available within a micellar reaction cavity. If the PRP^3 is constrained long enough to allow intersystem crossing to the singlet state PRP^1, it can recombine with rearrangement to yield 1-phenyl-4-methylacetophenone (PMAP) or without rearrangement to afford the parent DBK. In a micelle, the triplet-to-singlet intersystem crossing of PRP^3 competes with the decarbonylation process and the cage escape. The rate of decarbonylation of the phenylacetyl radical has been established to be 6.4×10^6 s^{-1} at room temperature and the rate of cage escape from the micelle has been estimated to be around 10^6 s^{-1}. Intersystem crossing facilitated by the hyperfine interaction between ^{13}C nuclei at the carbonyl carbon (or the benzylic position) and the unpaired electron spin could occur on the microsecond timescale. Because ^{12}C nuclei do not enhance intersystem crossing, the competition between decarbonylation and intersystem crossing of PRP^3 to PRP^1 can only occur in molecules containing ^{13}C nuclei. Based on the established mechanism for the nuclear hyperfine-induced intersystem crossing, one would expect a higher yield of PRP^1 from molecules containing ^{13}C nuclei and decarbonylation from those with ^{12}C nuclei. This selective process would be expected to yield ^{13}C-enriched DBK and PMAP. This has been demonstrated by photolysis of DBK that is 48% enriched in ^{13}C at the carbonyl carbon. After 90% photolysis, the CO carbon of the remaining DBK has 62% ^{13}C as compared to 48% at the start. Similar enrichment in PMAP was also noted. The absence of such effects in homogeneous solutions is due to the short lifetime of the solvent cage, which is much shorter ($<10^{-10}$ s) than that of a micelle ($\sim 10^{-6}$ s). Within the short time of the solvent cage, nuclear hyperfine coupling will not be able to induce intersystem crossing of PRP^3 to form PRP.[1]

107.10 Summary

This chapter provides examples where the established excited-state behavior of organic molecules has been altered by various techniques. Singlet–triplet control via sensitization and the heavy-atom effect are well-established, common methods used routinely by photochemists. Wavelength effects, although specific to chromophores, can be useful. Reactions from upper excited states continue to be unique and novel. Among the various solvents used, perfluorinated ones have unusual properties and should be used as reaction media especially when the chromophore reacts with hydrogenated solvents. Control via the templating effect is truly novel and imaginative. This approach will gain strength in the coming years when better understanding is reached about "weak interactions." Controlling reactions via cation–organic interactions in organic solvents, unfortunately, is a technically difficult one. Given the potential of this method, more attention needs to be paid to this system. Of the various approaches, the ones employing organized media have received considerable attention. Even in these, organic crystals, micelles, and zeolites show more promise than others in terms of product selectivity.

References

1. Turro, N.J., Ramamurthy, V., Cherry, W., and Farneth, W., The Effect of Wavelength on Organic Photoreactions in Solution. Reactions from Upper Excited States, *Chem. Rev.*, 78, 125–145, 1977.
2. (a) de Mayo, P., Thione Photochemistry and the Chemistry of the S_2 State, *Acc. Chem. Res.*, 9, 52–59, 1976; (b) Ramamurthy, V., Thiocarbonyl Photochemistry, in *Organic Photochemistry*, A. Padwa, Ed., Marcel Dekker: New York, 1985, Vol. 7, 231–338; (c) Ramamurthy, V., Rao, N.B., and Rao, P.V., Solution Photochemistry of Thioketones, in *CRC Handbook of Organic Photochemistry and Photobiology*, W.M. Horspool and P.-S. Song, Eds., CRC Press, Boca Raton, FL, 1995, 775–792; (d) Rao, P.V., Rao, N.B., and Ramamurthy, V., Thiocarbonyls: Photochemical Hydrogen Abstraction Reactions, in *CRC Handbook of Organic Photochemistry and Photobiology*, W.M. Horspool and P.-S. Song, Eds., CRC Press, Boca Raton, FL, 1995, 793–802; (e) Maciejewski, A. and Steer, R.P., The Photophysics, Physical Photochemistry and Related Spectroscopy of Thiocarbonyls, *Chem. Rev.*, 93, 67–98, 1993.
3. (a) Couture, A., Ho, K., Hoshino, M., de Mayo, P., Suau, R., and Ware, W.R., Thione Photochemistry: Intramolecular Cyclization of Aralkyl Thiones from S_2, *J. Am. Chem. Soc.*, 98, 6218–6225, 1976; (b) Lawrence, A.H., Liao, C.C., de Mayo, P., and Ramamurthy, V., Thione Photochemistry: Mechanism of the Short Wavelength Cycloaddition of Adamamtanethione: Evidence for an Excimer Derived from S_2, *J. Am. Chem. Soc.,* 98, 3572–3579, 1976; (c) Lawrence, A.H., Liao, C.C., de Mayo, P., and Ramamurthy, V., Thione Photochemistry: Cycloaddition in a Saturated Alicyclic System, *J. Am. Chem. Soc.*, 98, 2219–2226, 1976.
4. (a) Michl, J. and Kolc, J., A Photochemical Electrocyclic Reaction Requiring an Upper Triplet State, *J. Am. Chem. Soc.*, 92, 4148–4150, 1970; (b) Meinwald, J., Samuelson, G.E., and Ikeda, M., Naphtho[1,8]bicyclo[3.2.0]hepta-2,6-diene. Synthesis and Rearrangement to Pleiadiene, *J. Am. Chem. Soc.*, 92, 7604–7606, 1970; (c) Kolc, J. and Michl, J., Photochemical Synthesis of Matrix-Isolated Pleiadene, *J. Am. Chem. Soc.*, 92, 4147–4148, 1970.
5. (a) McGimpsey, W.G., Chemical and Photophysical Processes of Transients Derived from Multiphoton Excitation: Upper Excited States and Excited Radicals, in *Molecular and Supramolecular Photochemistry*, V. Ramamurthy and K. Schanze, Eds., Marcel Dekker, New York, 1998, Vol. 2, 249–306; (b) Scaiano, J.C., Johnston, L.J., McGimpsey, W.G., and Weir, D., Photochemistry of Organic Reaction Intermediates: Novel Reaction Paths Induced by Two-Photon Laser Excitation, *Acc. Chem. Res.*, 21, 22–29, 1988.
6. (a) Guerin, B., Johnston, L.J., and Quach, T., Photochemistry of Singlet and Upper Triplet States of Dibenzocycloheptadienone, *J. Org. Chem.*, 53, 2826–2829, 1988; (b) Johnston, L.J. and Scaiano, J. C., One- and Two-Photon Processes in the Photochemistry of 1,3-Bis(1-napthyl)-2-propanone:

An Example of a "Reluctant" Norrish Type I Reaction, *J. Am. Chem. Soc.*, 109, 5487–5491, 1987; (c) McGimpsey, W.G. and Scaiano, J.C., A Two-Photon Study of the "Reluctant" Norrish Type I Reaction of Benzil, *J. Am. Chem. Soc.*, 109, 2179–2181, 1987.

7. Wilson, R.M. and Schnapp, K.A., High-Intensity Laser Photochemistry of Organic Molecules in Solution, *Chem. Rev.*, 93, 223–249, 1993.
8. Wilson, R.M., Romanova, T.N., Azadnia, A., Krause Bauer, J.A., and Johnson, R.P., The Argon Laser-Jet Initiated, Multiple-Photon (Reluctant), Electrocyclic Ring Opening of 10,10-Diphenyl-9-(10*H*)-phenanthrenone: A Carbene and Biradical Modeling Study, *Tetrahedron Lett.*, 35, 5401–5404, 1994.
9. Holovka, J.M. and Gardner, P.D., Photolysis and Photoisomerization of the Benzene Oxide-Oxepin System, *J. Am. Chem. Soc.*, 89, 6390–6391, 1967.
10. Courtot, P. and Rumin, R., Processus Concurrents de Photoisomerisation D'Hexatrienes Polymethyles : Effet de Longueur D'Onde, *Tetrahedron*, 32, 441–446, 1976.
11. Bahurel, Y.L., MacGregor, D.J., Penner, T.L., and Hammond, G.S., Mechanisms of Photochemical Reactions in Solution. LXXI. Photochemistry of 1,3-Cyclohexadiene at Long Wavelength, *J. Am. Chem. Soc.*, 94, 637–638, 1972.
12. (a) Kojima, M., Sakuragi, H., and Tokumaru, K., Electron Transfer Resulting from Excitation of Contact Charge Transfer Complexes of Some Styrene Derivatives and Oxygen. The Role of Oxygen as an Electron Acceptor, *Bull. Chem. Soc. Jpn.*, 62, 3863–3868, 1989; (b) Onodera, K., Furusawa, G.-I., Kojima, M., Tsuchiya, M., Aihara, S., Akaba, R., Sakuragi, H., and Tokumaru, K., Mechanistic Considerations on Photoreaction of Organic Compounds via Excitation of Contact Charge Transfer Complexes with Oxygen, *Tetrahedron*, 41, 2215–2220, 1985.
13. Rabideau, P.W., Hamilton, J.B., and Friedman, L., Photoisomerization of Mono- and Dibenzobarrelenes, *J. Am. Chem. Soc.*, 90, 4465–4466, 1968.
14. (a) Cowan, D.O. and Drisko, R.L. E., The Photodimerization of Acenaphthylene. Heavy-Atom Solvent Effects, *J. Am. Chem. Soc.*, 92, 6281–6285, 1970; (b) Cowan, D.O. and Drisko, R.L.E., The Photodimerization of Acenaphthylene. Mechanistic Studies, *J. Am. Chem. Soc.*, 92, 6286–6291, 1970.
15. Dauben, W.G., Spitzer, W.A., and Kellogg, M.S., The Photochemistry of 4-Methyl-4-phenyl-2-cyclohexenone. The Effect of Solvent on the Excited State, *J. Am. Chem. Soc.*, 93, 3674–3677, 1971.
16. Lewis, F.D. and Hoyle, C.E., 1,2-Diarylethylene-Diene Exciplexes. Solvent-Induced Changes in Chemical and Physical Processes, *J. Am. Chem. Soc.*, 99, 3779–3786, 1977.
17. a) Wagner, P.J., Polar Solvent Enhancement of the Quantum Efficiency of Type II Photoelimination, *Tetrahedron Lett.*, 18, 1753–1756, 1967; (b) Wagner, P.J., Kelso, P.A., Kemppainen, A.E., McGrath, J.M., Schott, H.N., and Zepp, R.G., Type II Photoprocesses of Phenyl Ketones. A Glimpse at the Behavior of 1,4 Biradicals, *J. Am. Chem. Soc.*, 94, 7506–7512, 1972.
18. (a) Griffiths, J. and Hart, H., A New General Photochemical Reaction of 2,4-Cyclohexadienones, *J. Am. Chem. Soc.*, 90, 5296–5298, 1968; (b) Hart, H. and Takino, T., Irradiation of Eucarvone in Polar Media, *J. Am. Chem. Soc.*, 93, 720–725, 1971.
19. Crimmins, M.T. and Choy, A.L., Solvent effects on diastereoselective intramolecular [2+2] photocycloadditions : Reversal of selectivity through intramolecular hydrogen bonding, *J. Am. Chem. Soc.*, 119, 10237–10238, 1997.
20. (a) Maciejewski, A., The Application of Perfluoroalkanes as Solvents in Spectral, Photophysical and Photochemical Studies, *J. Photochem. Photobiol. A: Chem.*, 51, 87–131, 1990; (b) Ho, C.-J., Motyka, A.L., and Topp, M.R., Picosecond Time-Resolved S_2 to S_o Fluorescence of Xanthione in Different Fluid Solvents, *Chem. Phys. Lett.*, 158, 51–59, 1989.
21. Parker, C.A., Triplet State Processes in Fluid Solution, *Berichte der bunsengesellschaft*, 764–772, 1970.
22. (a) Hurst, J.R. and Schuster, G.B., Nonradiative Relaxation of Singlet Oxygen in Solution, *J. Am. Chem. Soc.*, 105, 5756–5760, 1983; (b) Ogilby, P.R. and Foote, C.S., Chemistry of Singlet Oxygen. 42. Effect of Solvent, Solvent Isotopic Substitution and Temperature on the Lifetime of Singlet

Molecular Oxygen ($^1\Delta_g$), *J. Am. Chem. Soc.*, 105, 3423–3430, 1983; (c) Rodgers, M.A.J., Solvent-Induced Deactivation of Singlet Oxygen: Additivity Relationships in Nonaromatic Solvents, *J. Am. Chem. Soc.*, 105, 6201–6205, 1983; (d) Schmidt, R. and Brauer, H.-D., Radiationless Deactivation of Singlet Oxygen ($^1\Delta_g$) by Solvent Molecules, *J. Am. Chem. Soc.*, 109, 6976–6981, 1987.

23. (a) Turro, N.J. and Ramamurthy, V., Photochemistry and Photophysics of a Polycyclic Azoalkane. Solvent and Temperature Effects, *Recl. J. Roy. Neth. Chem. Soc.*, 98, 173–176, 1979; (b) Katz, T.J. and Acton, N., Synthesis of Prismane, *J. Am. Chem. Soc.*, 95, 2738–2739, 1973.
24. Childs, R.F. and Shaw, G.B., The photochemistry of carbenium ions and related species, In *Org. Photochem.*, 11, 111–225, 1991.
25. Lewis, F.D. and Barancyk, S.V., Lewis Acid Catalysis of Photochemical Reactions. 8. Photodimerization and Cross-Cycloaddition of Coumarin, *J. Am. Chem. Soc.*, 111, 8653–8661, 1989.
26. Fukuzumi, S., Satoh, N., Okamoto, T., Yasui, K., Suenobu, T., Seko, Y., Fujitsuka, M., and Ito, O., Change in Spin State and Enhancement of Redox Reactivity of Photoexcited States of Aromatic Carbonyl Compounds by Complexation with Metal Ion Salts Acting as Lewis Acids. Lewis Acid-Catalyzed Photoaddition of Benzyltrimethylsilane and Tetramethyltin via Photoinduced Electron Transfer, *J. Am. Chem. Soc.*, 123, 7756–7766, 2001.
27. (a) Salomon, R.G., Homogeneous Metal-Catalysis in Organic Photochemistry, *Tetrahedron*, 39, 485–575, 1983; (b) Moggi, L., Juris, A., Sandrini, D., and Manfrin, M.F., Photocatalysis by Transition-Metal Coordination Compounds in Homogeneous Phase. II. Photochemical Steps Involving the Organic Substrate, *Rev. Chem. Int.*, 5, 107–155, 1984.
28. (a) Rau, H., Asymmetric Photochemistry is Solution, *Chem. Rev.*, 83, 535–547, 1983; (b) Inoue, Y., Asymmetric Photochemical Reactions in Solution, *Chem. Rev.*, 92, 741–770, 1992; (c) Everitt, S.R. L. and Inoue, Y., Asymmetric Photochemical Reactions in Solution, in *Molecular and Supramolecular Photochemistry*, Ramamurthy, V. and Schanze, K., Eds., Marcel Dekker: New York, 1999, Vol. 3, 71–130.
29. (a) Hammond, G.S. and Cole, R.S., Asymmetric Induction during Energy Transfer, *J. Am. Chem. Soc.*, 87, 3256–3257, 1965; (b) Ouannes, C., Beugelmans, R., and Roussi, G., Asymmetric Induction during Transfer of Triplet Energy, *J. Am. Chem. Soc.*, 95, 8472–8474, 1973; (c) Inoue, Y., Yamasaki, N., Shimoyama, H., and Tai, A., Enantiodifferentiating *Cis-Trans* Photoisomerizations of 1,2-Diarylcyclopropanes and 2,3-Diphenyloxirane Sensitized by Chiral Aromatic Esters, *J. Org. Chem.*, 58, 1785–1793, 1993.
30. (a) Inoue, Y., Yamasaki, N., Yokoyama, T., and Tai, A., Enantiodifferentiating Z-E Photoisomerization of Cyclooctene Sensitized by Chiral Polyalkyl Benzenepolycarboxylates, *J. Org. Chem.*, 57, 1332–1345, 1992; (b) Inoue, Y., Matsushima, E., and Wada, T., Pressure and Temperature Control of Product Chirality in Asymmetric Photochemistry. Enantiodifferentiating Photoisomerization of Cyclooctene Sensitized by Chiral Benzenepolycarboxylates, *J. Am. Chem. Soc.*, 120, 10687–10696, 1998.
31. (a) Buschman, H., Scharf, H.-D., Hoffmann, N., and Esser, P., The Isoinversion Principle — A General Model of Chemical Selectivity, *Angew. Chem. Int. Ed. Engl.*, 30, 477–515, 1991; (b) Pete, J.-P., Asymmetric Photoreactions of Conjugated Enones and Esters, in *Adv. Photochem.*, D.C. Neckers, D.H. Volman, and G. Von Bunan, Eds., John Wiley & Sons, New York, Vol. 21, 135–216, 1996.
32. (a) Faure, S., Blanc, S.P.-L., Piva, O., and Pete, J.-P., Hydroxyacids as Efficient Chiral Spacers for Asymmetric Intramolecular [2+2] Photocycloadditions, *Tetrahedron Lett.*, 38, 1045–1048, 1997; (b) Faure, S., Piva-Le-Banc, S., Bertrand, C., Pete, J.P., Faure, R., and Piva, O. Asymmetric Intramolecular [2 + 2] Photocycloadditions: α-and β-Hydroxy Acids as Chiral Tether Groups, *J. Org. Chem.*, 67, 1061–1070, 2002.
33. (a) Steiner, A., Wessig, P., and Polborn, K., Asymmetric Synthesis of 3-Hydroxyprolines by Photocyclization of C(1')-Substituted N-(2-Benzoylethyl)glycine Esters, *Helv. Chim. Acta*, 79, 1843–1862, 1996; (b) Wessig, P., Asymmetric Synthesis of 3-Hydroxyprolines by Photocyclization of N-(2-Benzoylethyl)glycinamides, *Helv. Chim. Acta*, 77, 829–837, 1994.

34. (a) Bach, T. and Bergmann, H., Enantioselective Intermolecular [2+2]-Photocycloaddition Reactions of Alkenes and a 2-Quinolone in Solution, *J. Am. Chem. Soc.*, 122, 11525–11526, 2000.
35. Bach, T., Bergmann, H., and Harms, K., High Facial Diastereoselectivity in the Photocycloaddition of a Chiral Aromatic Aldehyde and an Enamide Induced by Intermolecular Hydrogen Bonding, *J. Am. Chem. Soc.*, 121, 10650–10651, 1999.
36. Bassani, D.M., Darcos, V., Mahony, S., and Desvergne, J.-P., Supramolecular Catalysis of Olefin [2+2] Photodimerization, *J. Am. Chem. Soc.*, 122, 8795–8796, 2000.
37. *Photochemistry in Organized and Constrained Media*, Ramamurthy, V., Ed., VCH, New York, 1991.
38. (a) Turro, N.J.and Cherry, W.R., Photoreactions in Detergent Solutions. Enhancement of Regioselectivity Resulting from the Reduced Dimensionality of Substrates Sequestered in a Micelle, *J. Am. Chem. Soc.*, 100, 7431–32., 1978; (b) Turro, N.J. and Weed, G.C., Micellar Systems as "Supercages" for Reactions of Geminate Radical Pairs. Magnetic Effects, *J. Am. Chem. Soc.*, 105, 1861–1868, 1983.
39. (a) Berenjian, N., de Mayo, P., Sturgeon, M., Sydnes, L.K., and Weedon, A.C., Biphasic Photochemistry: Micelle Solutions as Media for Photochemical Cycloadditions of Enones, *Can. J. Chem.*, 60, 425–436, 1982; (b) Mayo, P.D. and Sydnes, L.K., Biphasic Photochemistry: Micellar Control of Regioselectivity in Enone Photoannelations, *J. Chem. Soc., Chem. Commun.*, 994–995, 1980; (c) Lee, K. and Mayo, P.D., Biphasic Photochemistry: Micellar Regioselectivity in Enone Dimerisation, *J. Chem. Soc., Chem. Commun..*, 493–495, 1979.
40. Hoffmann, U., Gao, Y., Pandey, B., Klinge, S., Warzecha, K.-D., Kruger, C., Roth, H.D., and Demuth, M., Light-Induced Polyene Cyclizations via Radical Cations in Micellar Medium, *J. Am. Chem. Soc.*, 115, 10358–10359, 1993.
41. Joy, A., Uppili, S., Netherton, M.R., Scheffer, J.R., and Ramamurthy, V., Photochemistry of a Tropolone Ether and 2,2-Dimethyl-1-(2*H*)-Naphthalenones within a Zeolite: Enhanced Diastereoselectivity via Confinement., *J. Am. Chem. Soc.,* 122, 728–729, 2000.
42. Gu, W., Warrier, M., Ramamurthy, V., and Weiss, R.G., Photo-Fries Reactions of 1-Naphthyl Esters in Cation Exchanged Zeolite Y and Polyethylene Media., *J. Am. Chem. Soc.*, 121, 9467–68, 1999.
43. (a) Turro, N.J., Influence of Nuclear Spin on Chemical Reactions: Magnetic Isotope and Magnetic Field Effects, *Proc. Natl. Acad. Sci.*, 80, 609–621, 1983; (b) Turro, N.J. and Kraeutler, B., Magnetic Field and Magnetic Isotope Effects in Organic Photochemical Reactions. A Novel Probe of Reaction Mechanisms and a Method for Enrichment of Magnetic Isotopes, *Acc. Chem. Res.*, 13, 369–77, 1980; (c) Gould, I.R., Turro, N.J., and Zimmt, M.B., Magnetic Field and Magnetic Isotope Effects on the Product of Organic Reactions, in *Adv. Phys. Org. Chem.*, V. Gold and D. Bethell, Eds., Academic Press, London, Vol. 20, 1–53, 1984.

108

Endoperoxides: Thermal and Photochemical Reactions and Spectroscopy

Axel G. Griesbeck
University of Cologne

Murthy S. Gudipati
University of Maryland

108.1 Introduction

Cyclic saturated or unsaturated dialkylperoxides are termed endoperoxides with 1,2-dioxetanes as exceptions that are normally not grouped in the endoperoxide family.[1] The prefix *endo* has only historical reasons[2] and by no means indicates stereochemical properties, thus the term "*exo*peroxides" should be avoided. Common useage also comprises monocyclic dialkylperoxides and bi- and polycyclic compounds. The central structural feature determining the thermal, the photochemical, and also the redox behavior of endoperoxides is the oxygen–oxygen single bond. In most thermal or photochemical processes, homolytic OO bond cleavage follows activation; redox processes are mostly initiated by one-electron reduction followed by mesolytic cleavage or a subsequent secondary electron transfer.[3] The bond dissociation energy of the OO bond in unstrained or moderately strained endoperoxides is approx. 37 kcal mol^{-1} and, thus, these compounds are prone to thermal decomposition.[4] It is commonly accepted that the peroxide chromophore is characterized by a broad $\pi^*\sigma_{oo}^*$ transition with a low extinction coefficient.[5] An increase in ring strain induces a blue shift of this absorption (1,2-dioxetanes — not counted as endoperoxides — are yellow compounds with λ_{max} around 450 nm). Unstrained endoperoxides exhibit absorption in the region of λ_{max} = 300–350 nm, higher strained or unsaturated endoperoxides absorb from 350 up to 400 nm with extinction coefficients of 10–15 M^{-1} cm^{-1}. From the reactivity point of view, it is appropriate to arrange endoperoxides into unsaturated and saturated compounds, that is, endoperoxides with the peroxy linkage in allylic position and saturated analogs. The additional double bond in unsaturated endoperoxides gives rise to secondary reactions preceding the primary cleavage of the oxygen–oxygen single bond. The thermal and photochemical behavior of different types of endoperoxides

0-8493-1348-1/04/$0.00+$1.50

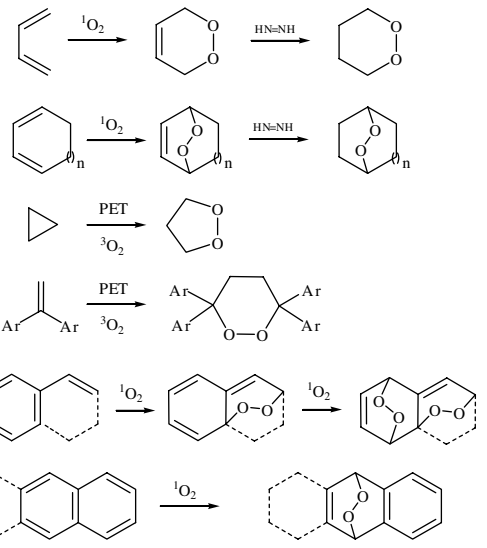

SCHEME 1

are outlined herein. Theoretical interpretation of the photochemistry of aromatic endoperoxides has been the subject of some controversy in the past few years few years and this is presented in detail in the last part of this review.

108.2 Synthesis

There are several synthetic approaches to endoperoxide structures. One of the most important routes is the singlet oxygen [4+2]-cycloaddition to acyclic or cyclic 1,3-dienes and hetero-analogs.[6] In some cases, also autoxidation ("type I process") can lead to endoperoxides but these processes often lack selectivity and have poor product stability.[7] For several applications, Lewis-acid-catalyzed peroxidations of 1,3-dienes results in high product yields.[8] Saturated endoperoxides are easily available from their unsaturated precursors by double-bond reduction with diimide.[9] 1,2-Dioxolanes (five-membered endoperoxides) are accessible by photoinduced electron-transfer reaction with cyclopropanes and trapping of the trimethylene radical cations by triplet oxygen.[10] A similar approach to saturated six-membered ring peroxides involves the photochemically induced one-electron oxidation of arylated alkenes and subsequent dimerization/triplet oxygen addition.[11] This reaction is superior for electron-donor substituted 1,1-diarylethylenes resulting in 3,3,6,6-tetraaryl-1,2-dioxanes.[12] The singlet oxygen route to monocyclic unsaturated endoperoxides (1,2-dioxenes) is possible from a large variety of substituted 1,3-butadienes.[13]

The solvent dependence of these [4+2]-cycloadditions has been intensively studied.[14] Cyclic 1,3-dienes and heteroanalogs are obviously more reactive and a multitude of endoperoxides have been generated by singlet oxygen addition to these substrates. Even vinylarenes (styrene, stilbene, vinylnaphthalene, vinylheteroarenes) can react with singlet oxygen to give monoadducts, which rapidly add another equivalent of singlet oxygen to give *bis*-endoperoxides.[15] Alkylated benzene or naphthalene derivatives are converted into doubly unsaturated endoperoxides by singlet oxygenation.[16] Naphthalene and higher arenes give monoadducts with singlet oxygen that can be applied in retro [4+2]-cycloadditions and thus store electronically excited oxygen.[17] In addition to photochemical reactions thermal pathways to endoperoxides also exist: hydrogen peroxide can be used as a *bis*-nucleophile and substitute two appropriate leaving groups (halogen, hydroxy, and activated hydroxy groups, respectively).[1]

By reaction with silver acetate, 1,n-bromohydroperoxides are converted into endoperoxides with (n+2) ring atoms.[18] Similar to the classical oxymercuration, intramolecular peroxymercuration of unsaturated (homoallylic or higher homologs) hydroperoxides can also serve as an efficient path to endoperoxides.[19]

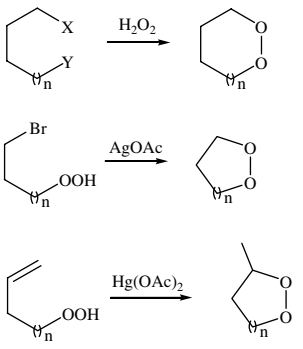

SCHEME 2

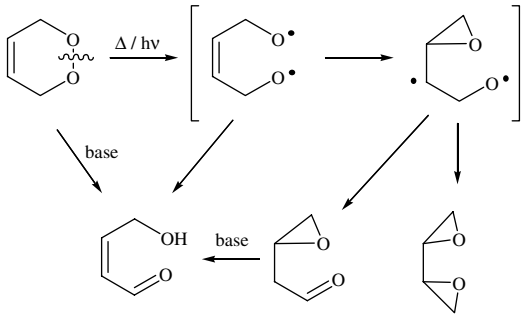

SCHEME 3

108.3 Thermal and Photochemical Reactions

Aliphatic Unsaturated Endoperoxides

Due to the presence of an additional double bond in the starting material, alkoxy radicals generated by thermal or photochemical reactions can react in an intramolecular fashion to give *bis*-epoxides.[20] This symmetric path can be accompanied by a hydrogen transfer process, which leads to hydroxyenones, equivalent to the base-catalyzed Kornblum-DeLaMare process.[21] Alternatively, initiated by cleavage of two CO single bonds (either stepwise via a peroxy radical or concertedly) singlet oxygen is produced in a cycloreversion process and the diene substrate is regenerated.[22] A third (dissymmetric) path leads to the formation of epoxycarbonyl compounds involving the formation of the OO-biradical and subsequent ring formation and 1,2-hydrogen transfer reaction (see Scheme 3).[23]

A series of experimental and theoretical studies indicate that the two symmetric pathways, *bis*-epoxide and singlet oxygen formation, respectively, are initiated by two different excited states.[24,25,]

The OO cleavage path seems to originate from the dissociative $\pi^*\sigma_{oo}^*$ transition at relatively long wavelength, whereas the retrocleavage path results from a $\pi\pi^*$ transition of the unsaturated part of the molecule in a shorter wavelength region. In the absence of an additional CC double bond, no cycloreversion can be observed, whereas photoinduced isomerization processes were observed from saturated as well as from saturated endoperoxides. Dufraisse and co-workers published the first report on the photoisomerization of an unsaturated endoperoxide.[26] They investigated the endoperoxide from 2,3,4,5-tetraphenylfulvene and a series of substituted 2,3,4,5tetraphenyl-cyclopenta-2,4-dienes **1**. From these substrates the syn *bis*-epoxides **2** were formed efficiently and with high chemoselectivity (Scheme 4).

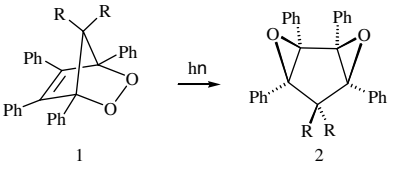

1 2

SCHEME 4

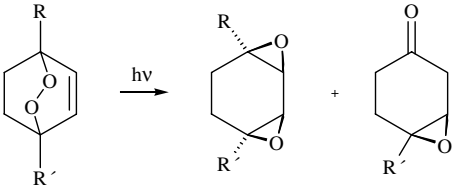

3 (a: R = Me, R = *i*Pr) 4 5

SCHEME 5

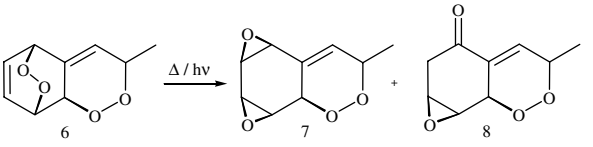

6 7 8

SCHEME 6

In contrast to the commonly observed, highly selective photochemical reactions, thermal rearrangements of endoperoxides often lead to more complex mixturex of products.[27] A naturally occurring compound, the terpene endoperoxide ascaridole (**3a**) rearranges into isoascaridole (**4a**) upon irradiation (long-wavelength excitation at 366 nm) while similar cyclohexadiene endoperoxides **3** result in mixtures of bis-epoxides **4** and epoxyketones **5** upon thermolysis (Scheme 5).[28]

A systematic study was performed by Carless and co-workers on the photochemical behavior of endoperoxides derived from cyclohexadiene, cycloheptadiene, and cyclooctadiene.[29] They found that epoxyketones are preferentially formed over *bis*-epoxides and that this trend is more pronounced in the photolysis than in the thermal isomerization of these compounds. The mechanism of these reactions is state dependent. After direct excitation as well as thermal activation, a singlet excited state is generated that can proceed by a concerted $[\sigma^2+\pi^2]$-cycloaddition to give the *bis*-epoxide.[30] Alternatively, a dioxyl biradical can be formed as a short-lived singlet intermediate. The latter species is a more likely intermediate for the corresponding triplet process, which has been also described in several examples.[28] Actually, triplet-triplet energy transfer can increase the efficiency of the photoisomerization in comparison with direct excitation. In the triplet path, an intermediate triplet dioxyl radical might constitute a longer-lived intermediate enabling a stronger competition of hydrogen migration (leading to epoxyketones) with the formation of the *bis*-epoxides. An increase in the endoperoxide ring strain often facilitates the ring opening, as seen in the *bis*-endoperoxide **6** where the more strained peroxy bridge opens more efficiently upon photolysis and results in a 1:2 mixture of *bis*-epoxide **7** and epoxyketone **8** (Scheme 6).[31]

Various applications of the endoperoxide-epoxide rearrangements in the multistep total synthesis of natural products are reported in the literature,[32] for example, the synthesis of stemolide, a natural *syn*-diepoxide with antileukemic activity.[33] A photochemical route from arenes to inositol intermediates was

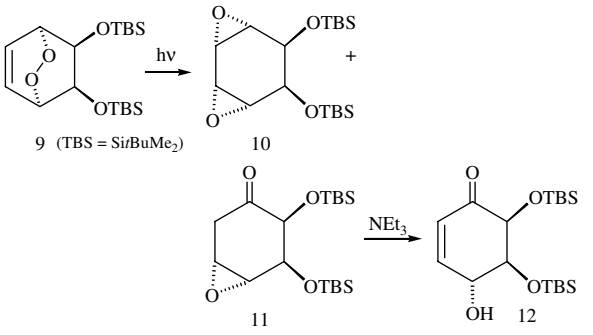

SCHEME 7

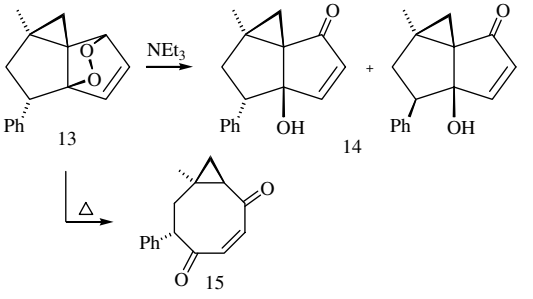

SCHEME 8

described using the photooxidation of substituted *cis*-cyclohexa-3,5-diene-1,2-diols and subsequent photolytic isomerization of the endoperoxide **9** to the *bis*-epoxide **10** and two diastereoisomeric β,γ-epoxyketones **11** (only one shown). The latter compounds can rearrange by base catalysis to give γ-hydroxyenones **12** (Scheme 7).[34]

In addition to photolytic or thermolytic conditions, the endoperoxide rearrangement to *bis*-epoxides can also be conducted in a catalytic version in the presence of metaloporphyrins (e.g., cobalt(II) tetraphenylporphyrin).[35] An illustrative difference between base-catalyzed (Kornblum-DeLaMare reaction)[21] and thermal rearrangement of a cyclopentadiene-derived endoperoxide **13** was described recently.[36] When **13** was treated with a base at low temperature, two diastereoisomeric hydroxyenones **14** resulted, whereas the eight-membered (ring-enlarged) enedione **15** was formed as the major rearrangement product from **13** when kept at room temperature for a longer time (Scheme 8).

The synthesis and chemistry of endoperoxides **17** derived from 3,4-dihydroazulene-1-one **16** was studied by Balci and co-workers.[37] Three regioisomeric products **17a**,**b**,**c** derived from the singlet oxygen photoooxygenation of **16**, which were subjected to solution thermolysis as well as to CoTPP-catalyzed ring opening. All endoperoxides resulted in the same *bis*-epoxide **18a** as the major product, indicating a thermal endoperoxide–endoperoxide isomerization. This isomerization was not detected for the corresponding 1-methoxy-1,2,3,4-tetrahydroazulene, indicating the special role of the carbonyl group in **17** for isomerization processes (Scheme 9).[38]

Aliphatic Saturated Endoperoxides

The thermolysis of the 3,3,6,6-tetramethyl-1,2-dioxane **19** results in the formation of ethylene and acetone.[39] Studies on the stereoselectivity of the alkene formation using deuterium labels at C4 and C5

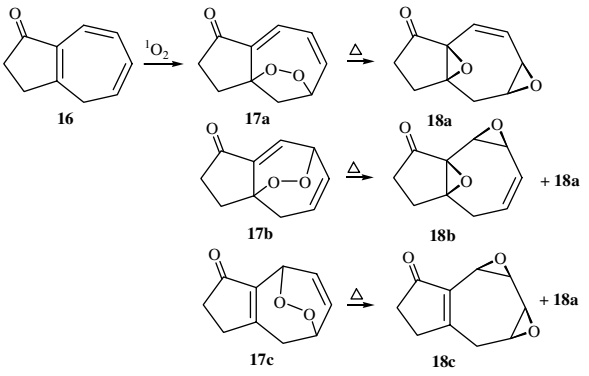

SCHEME 9

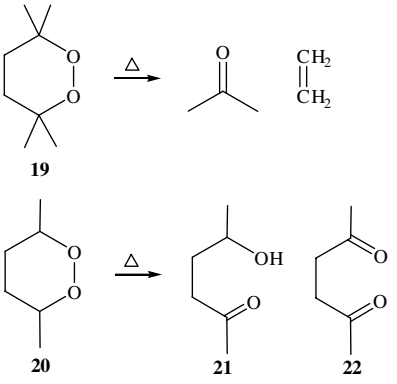

SCHEME 10

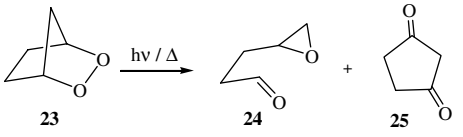

SCHEME 11

revealed that the β-scission occurs from two different conformers, leading to *cis*- and *trans*-alkenes. Permethylation of the C_α-positions is crucial for this process; for example, 3,6-dimethyl-1,2-dioxane **20** results in a hydrogen shift and a dehydrogenation product **21** and **22**, respectively, upon thermolysis (Scheme 10).[40]

The bicyclic endoperoxide **23** (from cyclopentadiene and subsequent diimide reduction)[9] thermally rearranged to two products (**24**, **25**) by hydrogen migration or dehydrogenation without β-scission.[41] The major photoproduct from 2,3-dioxa[2.2.1]heptane **23** is the 4,5-epoxypentanal **24** as also observed from gas- or solution-phase thermolysis (Scheme 11). An extended study on homologous bicyclic endoperoxides revealed comparable behavior under gas-phase thermolysis conditions.[42] Studies on the photolysis of saturated bicyclic endoperoxides showed similarities to the thermolytic behavior, which are interpreted via intermediate dioxyl radicals resulting from the homolysis of the OO bond. Saturated

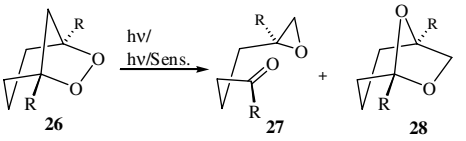

SCHEME 12

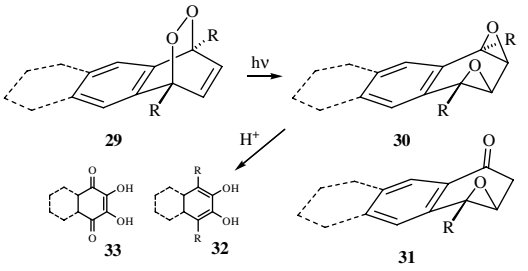

SCHEME 13

bicyclic peroxides have been investigated by Bloodworth and Eggelte.[43] Thermal and photochemical activation in several cases results in divergent processes due to different thermal or electronic states (singlet/triplet) of the initial generated dioxyl biradicals.

Under identical photochemical conditions, [n.2.1]peroxides (n = 3, 4, 5) afforded mainly the corresponding epoxyaldehydes, whereas gas-phase thermolysis resulted in ketoaldehydes in high yields. Concerning the multiplicity of the intermediary generated dioxyl biradical, the photolysis of the 6,7-dioxa[3.2.1]heptane **26** (R = H) is most illustrative. Upon triplet-sensitized photolysis in the presence of benzophenone, a rearranged product 6,8-dioxabicyclo[3.2.1]octane **28** is formed as the major product. Due to the spin multiplicity of the initially formed triplet 1,5-O,O-biradical, the formation of the carbonyl group with concerted CO bond cleavage generates a triplet 1,3-C,O-biradical that cannot directly form a new single bond and alternatively reacts with the carbonyl group in a [2+2]-cycloaddition. In contrast, the direct photolysis at lower wavelengths gives preferentially the epoxyaldehyde **27**. In this case, the singlet 1,3-C,O-biradical can directly combine without spin-barrier. An analogous effect was reported for the dimethyl analog, 1,5-dimethyl-6,7-dioxabicyclo[3.2.1]octane **26b** (R = Me), whose benzophenone-sensitized irradiation provided an elegant photochemical synthesis of the pheromone frontalin (Scheme 12).[44]

Aromatic Endoperoxides

The benzoannulated endoperoxides **29** derived from naphthalene and anthracene derivatives (endoperoxides of the 1,4-type termed *benzo*-endoperoxides) exclusively give *syn-bis*-epoxides **30** when irradiated at long wavelength ($\lambda > 366$ nm) (see Scheme 13).[45,46,] Formation of the corresponding epoxyketone **31** was solely observed from the tetramethyl-substituted **29** when the reaction was triplet sensitized.[47] The acid-catalyzed isomerization of *bis*-epoxides to give phenol derivatives **32**[45b,46b] and 2,3-dihydroxynaphtho- and anthraquinones **33** via the bridgehead methoxy-substituted endoperoxides **29**, respectively, is synthetically useful.[45a,46a]

Reactive *syn-bis*-epoxides available from the anthracene-endoperoxides by low-temperature irradiation at long wavelength could be thermally isomerized to benzocyclobutenic diethers and other products.[48] A new kind of isomerization of aromatic endoperoxides, which is initiated by a Grob-fragmentation step, was described recently for anthracene and naphthalene *bis*-epoxides.[49] The photochemistry of aromatic

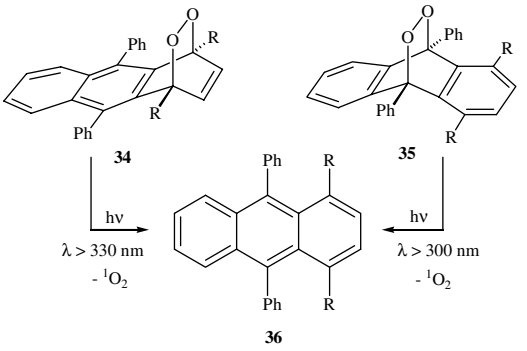

SCHEME 14

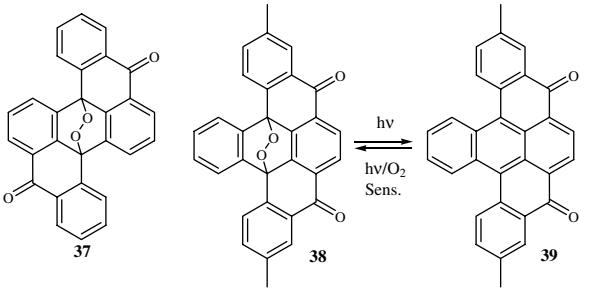

SCHEME 15

endoperoxides (or, more pre*cis*ely, endoperoxides with annulated aromatic rings) is striking because not only do several reaction modes compete but also higher excited singlet states seem to be involved. The photoinduced cleavage of endoperoxides into singlet oxygen and the deoxygenated arene occurs upon irradiation at short wavelength. Thus, the high-energy excitation of the endoperoxide of 9,10-diphenylanthracene ($\lambda < 300$ nm) leads to photodissociation, whereas low-energy excitation ($\lambda > 300$ nm) leads to photoisomerization. Similar effects were observed with endoperoxides from anthracene and 9,10-dimethylanthracene.[50] For another substrate, the *benzo*-endoperoxide **34** (R = Me), cycloreversion from even higher excited singlet states S_3 and S_4 was postulated (Scheme 14).[51]

With the endoperoxide of heterocoerdianthrone **37**, the quantum yield of the (irreversible) photolytic decomposition becomes extremely small and the (reversible) photoinitiated cleavage to singlet oxygen and the arene establishes an efficient photochromic system.[52] A further improvement of this concept was achieved with the blue dimethylhomeocoerdianthrone **38**. This compound gave the colorless endoperoxide **39** by sensitized photooxygenation that reverts back quantitatively to the starting material **38** on irradiation at 313 nm (Scheme 15).[53]

The mechanism of the photochemical cycloreversion of endoperoxides has been a matter of debate. It was originally proposed that the CO bonds break simultaneously in a concerted fashion after electronic excitation of the endoperoxide.[54] From the relatively "slow" evolution of hydrocarbon ($\tau_2 = 1.6$ to 95 ps) compared to the very short lifetime of excited states ($\tau_1 \sim 3$ ps), it was concluded later that the photocycloreversion occurs in two steps (for a detailed discussion of the state-selectivity question, see Section 108.4). The first step is thus an ultrafast CO bond cleavage followed by the slow decay of the resulting 1,6-OC-singlet biradical to the ground state of the arene and singlet oxygen.[55] Laser-induced fluorescence[56] and transient absorption studies[57] have been used to measure the lifetimes of the intermediates; the shortest ones were detected for **39** ($\tau_1 < 0.35$ ps; $\tau_2 = 1.6 \pm 0.5$ ps). Photolysis at 275 nm of the anthracene endoperoxide in argon matrices at 15K resulted in cycloreversion exclusively.[58]

108.4 Spectroscopic and Theoretical Studies

Historical Perspective

Kearns and Khan predicted in 1969, using state and orbital correlation diagrams, that excitation of 1,3-cyclopentadiene endoperoxide (CPO) into S_1 or T_1 states leads to a barrierless rearrangement through OO homolytic bond cleavage and that the cycloreversion from these states has to circumvent a barrier.[54,59] However, a barrierless cycloreversion to generate cyclopentadiene and singlet molecular oxygen (O_2, $a^1\Delta_g$) was predicted by Kearns and Khan when CPO is excited into the higher singlet. These authors also generalized their predictions to aromatic endoperoxides and forecast that the family of endoperoxides should undergo wavelength-dependent dual photochemistry. Ironically, to date, dual photochemistry of CPO has not been experimentally proven. Nine years later, Rigaudy et al. reported wavelength-dependent photochemistry of 9,10-diphenylanthracene-9,10-endoperoxide (DPAPO).[60] They found that irradiation at 253.7 nm results in cycloreversion as the major channel and irradiation at longer wavelengths ($\lambda >$ 280 nm) leads to OO homolysis and rearrangement products. Around the same time, Brauer and co-workers had shown that photocycloreversion of dibenzo[*aj*]perylene-8,16-dione endoperoxide (HCDPO) occurs from the S_2 state and not from the S_1 or T_1 states.[61] Thus, three publications on three different molecules, consistent with each other on the dual photochemistry, lead to the general belief and acceptance that aromatic or aliphatic endoperoxides undergo photochemistry from higher excited electronic states,[62] consequently not in line with the photochemical interpretation of Kasha's rule: "the emitting electronic level of a given multiplicity is the lowest excited level of that multiplicity, (regardless of which state of a given multiplicity is excited)".[63]

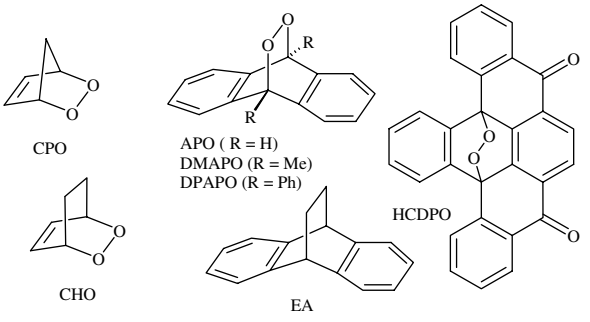

Later on, more insight into the mechanistic aspects of endoperoxides photochemistry was obtained from time-resolved picosecond and femtosecond studies.[64] Unusually long risetimes of 40 to 95 ps, unexpected for a concerted and barrierless S_n ($n \geq 2$) photocycloreversion (should have been <3 ps), have been interpreted in terms of a biradical intermediate through a non-concerted cleavage of one of the CO bonds and due to a barrier which slows down the cycloreversion during the second CO bond cleavage. Thus, until recently, all the experimental findings sought their interpretation based on cycloreversion from higher excited states and OO homolytic rearrangement from the first excited singlet state of aliphatic and aromatic endoperoxides. If, on the other hand, the photocycloreversion occurs from the S_1 state, then the risetime of 40 to 95 ps is not very surprising. Two important underlying assumptions for the unusual photochemistry of endoperoxides were: the S_1 state has $\pi^*_{OO} \rightarrow \sigma^*_{OO}$ character and the S_2 state has $\pi^*_{OO} \rightarrow \sigma^*_{CO}$ character.

Recent Developments

Recent spectroscopic and theoretical studies[58,65] on anthracene-9,10-endoperoxide (APO) and 9,10-dimethylanthracene-9,10-endoperoxides (DMAPO) have shown that the well-accepted assignment of the electronic states based on the one and only empirical theoretical work carried out by Kearns and Khan[59,54]

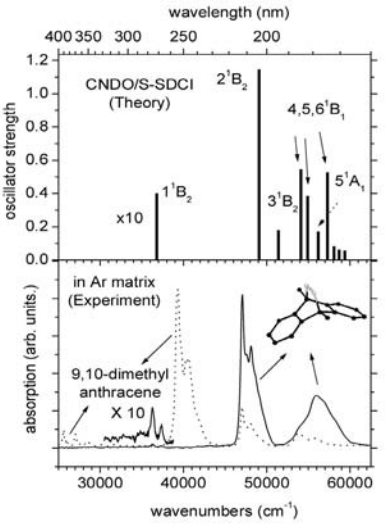

FIGURE 108.1 Bottom: Absorption spectra of DMAPO (solid line) and the cycloreversion product DMA obtained after photolysis at 275 nm, measured from the same sample using VUV synchrotron radiation. Top: Semiempirical predictions using CNDO/S (singly and doubly excited configurations included — SDCI) method.[58]

in 1969 and experimental observations of Brauer et al.[61] are not consistent with the spectroscopic data and semiempirical predictions.[64] Although it is convenient to think that the OO homolysis occurs through the $\pi^*_{OO} \rightarrow \sigma^*_{OO}$ character of the lowest excited singlet state (S_1), as accepted and believed earlier, this has been shown to be wrong in the case of the aromatic anthracene-endoperoxides APO and DMAPO.[58] Their assignment that the S_1 of APO and DMAPO should be the 1^1B_2 state with $\pi\pi^*$ (aromatic) character located around 275 nm in DMAPO is based on the semiempirical predictions that are in excellent agreement with the experimental data (Figure 108.1). Several consistency checks were carried out: (1) the nearly one-to-one correspondence between the predicted and observed energies of the singlet states of APO and DMAPO (Figure 108.1), (2) excellent agreement between the predicted and experimentally derived oscillator strength of the band at 210 nm due to the 2^1B_2 state of APO, (3) experimental observation of the theoretically predicted triplet states around 450 nm, (4) excellent agreement between the electronic states of APO and its isoelectronic molecule 9,10-dihydro-9,10-ethanoanthracene, and (5) successful application of exciton model to interpret the electronic states (singlet and triplet) of APO and EA.

Thus, the absorption due to triplet states detected at ~450 nm was attributed to the OO bond homolysis and subsequent rearrangement for the long-wavelength photochemistry and the normal $\pi\pi^*$ excitation into the first singlet (S_1) state for the cycloreversion reaction. These results lead to some controversy.[65,66] As discussed in these articles, it was proposed that to understand the photochemistry of endoperoxides, correlating the electronic states of the reactants and products alone (adiabatic approximation) may not be sufficient; rather, a non-adiabatic curve crossing needs to be considered seriously. That is, instead of a static picture of excited stationary states and their energies, a dynamic treatment including the evolution of the electronic excited states needs to be taken into account.

The spectroscopy and photochemistry of aliphatic endoperoxides should be clearly differentiated from the aromatic endoperoxides. The MOs containing significant coefficients on the non-dioxygen bridge and the dioxygen chromophore lie energetically very close to each other in aliphatic endoperoxides as, for example, in the case of CPO. They can even mix strongly. In such a case, the electronic states with MOs localized on the dioxygen bridge can become the lowest excited singlet states in accordance with the predictions of Kearns and Khan. However, for aromatic endoperoxides like APO, the MOs localized on the OO moiety are much further separated in energy compared to the MOs localized on the aromatic

units. Further, due to exciton-like interactions, the electronic states resulting from MOs localized on the aromatic units will be further stabilized to lower energies.[67] Due to the fact that the σ^* and π^* orbitals of the dioxygen bridge have very small overlap with the rest of the molecule, the OO bridge behaves like a sub-chromophore. This fact further supports the above-mentioned analysis.

Recently, Sevin and McKee carried out an extensive reaction pathway study using *ab initio* and DFT methods on reactions of 1,3-cyclohexadiene with singlet oxygen.[68] They located several transition states for the reaction pathways and computed the electronically excited states of 1,3-cyclopentadiene endoperoxides (CPO) and 1,3-cyclohexadiene endoperoxides (CHO), respectively. Their results for CPO disagree with the results of Klein and Gudipati, obtained using semiempirical (CNDO/S) methods.[58] On the other hand, the analysis of the electronic states of CPO by Sevin and McKee does not agree with the empirical predictions of Kearns and Khan either. Sevin and McKee conclude that their TD-DFT results for CPO and CHO indicate that photorearrangement should take place from $S_0 \rightarrow S_1$ excitation and photocycloreversion should take place from $S_0 \rightarrow S_2$ excitation, in accordance with earlier results.[54,59] In their analysis of the electronically excited states using the TD-B3LYP/6-31+G(d) method, they show that for CPO the $S_0 \rightarrow S_1$ transition at 290 nm has predominantly $\pi^*_{OO} \rightarrow \pi^*_{CC}$ character; hence, the OO bond would not be weakened and consequently may lead to cycloreversion. In Kearns and Khan's work, cycloreversion of CPO is predicted to occur from S_2. Further, Sevin and McKee analyze that the $S_0 \rightarrow S_2$ transition in CPO at 248 nm leads to a much weaker OO bond, which would favor rearrangement,[68] Kearns and Khan predicted rearrangement from S_1.[54,59]

Aromatic endoperoxides, on the other hand, are expected to show less discrepancy between semiempirical and *ab initio* theoretical predictions. The main reason is the grouping of the MOs that are localized primarily on the aromatic rings near the Fermi level, resulting in the MOs containing contributions from the dioxygen bridge to lie far above the unoccupied MOs and far below in the occupied MOs. Further, semiempirical methods have been tested on innumerable aromatic molecules and found to be very reliable.[69] Due to the importance of the theoretical work to interpret the mechanism of endoperoxide photochemistry, high-level *ab initio* quantum chemical treatment of the aliphatic and aromatic endoperoxides, including the evolution of the excited states, is needed. Ideally, thorough CASSCF-level computations on CPO and anthracene-9,10-endoperoxide (APO), the smallest aliphatic and aromatic endoperoxides, respectively, would end the present controversy.

References

1. Kropf, H., Organische Peroxo-Verbindungen, *Houben-Weyl* (Methoden der Organischen Chemie), E13/ part 1 and 2, Thieme, Stuttgart, New York, 1988.
2. Hock, H., Lang, S., and Knauel, G., Autoxydation von Kohlenwasserstoffen, X. Über Peroxyde von Benzolderivaten, *Chem. Ber.*, 83, 227, 1950.
3. (a) Clennan, E.L. and Foote, C.S., in *Organic Peroxides,* Ando, W., Ed., Wiley, New York, 1992, 255; (b) Balci, M., Bicyclic endoperoxides and synthetic applications, *Chem. Rev.,* 81, 91, 1981.
4. Baldwin, A.C., in *The Chemistry of Peroxides,* Patai, S., Ed., Wiley, New York, 1983, 97.
5. Silbert, L.S., in *Organic Peroxides*, Swern, D., Ed., Vol. II, Wiley, New York, 1971.
6. (a) Adam, W., Bosio, S., Bartoschek, A., and Griesbeck, A.G., Photooxygenation of 1,3-dienes, *CRC Handbook of Photochemistry,* Horspool, W.M. and Song, P.-S., Eds., CRC Press, Boca Raton, FL,; (b) Saito, I. and Matsuura, T., in *Singlet Oxygen,* Wasserman, H.H. and Murray, R.W., Eds., Academic Press, New York, 1979, chap. 10.
7. (a) Hock, H. and Depke, F., Autoxidation of hydrocarbons. XVI. Peroxides from cyclopentadiene and cyclohexadiene, *Chem. Ber.*, 84, 349, 1951; (b) Hock, H., Lang, S., and Knauel, G., Autoxidation of hydrocarbons. X. Peroxides of benzene derivatives, *Chem. Ber.*, 83, 227, 1950; (c) Yin H., Havrilla C.M., Morrow J.D., and Porter, N.A., Formation of isoprostane bicyclic endo*peroxides* from the autoxidation of cholesteryl arachidonate, *J. Am. Chem. Soc.*, 124, 7745, 2002; (d) Pryor, W.A. and Stanley, J.P., A suggested mechanism for the production of malonaldehyde during the autoxidation of polyunsaturated fatty acids. Nonenzymatic production of prostaglandin endo*peroxides* during autoxidation, *J. Org. Chem.*, 40, 3615, 1975.

8. (a) Barton, D.H.R., Haynes, R.K., Leclerc, G., Magnus, P.D., and Menzies, I.D., New reactions of triplet oxygen which avoid the spin barrier, *J. Chem. Soc., Perkin Trans. 1*, 2055, 1975; (b) Haynes, R.K. and Hilliker, A.E., Photoinduced reactions of 3β-acetoxycholesta-5,7-diene, 3β-acetoxycholest-5-ene, tetraphenylcyclopentadiene and 1,1-diphenylethylene with oxygen in the presence of phenylselenenyl bromide, *Tetrahedron Lett.*, 509, 1986.
9. Adam, W. and Eggelte, H.J., Cyclic peroxides. 58. 2,3-Dioxabicyclo[2.2.2]octane by selective reduction of double bonds with azodicarboxylate, *Angew. Chem.*, 89, 762, 1977.
10. (a) Mizuno, K., Kamiyama, N., and Otsuji, Y., Photooxygenation of 1,2-diarylcyclopropanes: formation of 3,5-diaryl-1,2-dioxolanes via photoinduced electron transfer, *Chem. Lett.*, 477, 1983; (b) Mizuno, K., Kamiyama, N., Ichinose, N., and Otsuji, Y., Photooxygenation of 1,2-diarylcyclopropanes via electron transfer, *Tetrahedron*, 41, 2207, 1985.
11. Gollnick, K. and Schnatterer, A., Formation of 1,2-dioxanes by electron-transfer photooxygenation of 1,1-disubstituted ethylenes, *Tetrahedron Lett.*, 2735, 1984.
12. Mattes, S. and Farid, S.L., Photochemical electron-transfer reactions of olefins and related compounds, *Org. Photochem.*, 6, 233, 1983.
13. (a) Kondo, T., Matsumoto, M., and Tanimoto, M., Microwave and NMR studies of the structure and the conformational isomerization of 3,6-dihydro-1,2-dioxin, *Tetrahedron Lett.,* 3819, 1978; (b) Gollnick, K. and Griesbeck, A., Interactions of singlet oxygen with 2,5-dimethyl-2,4-hexadiene in polar and non-polar solvents. Evidence for a vinylog ene-reaction, *Tetrahedron*, 40, 3235, 1984.
14. (a) Aubry, J.-M., Mandard-Cazin, B., Rougee, M., and Benasson, R.V., Kinetic studies of singlet oxygen [4+2]-cycloadditions with cyclic 1,3-dienes in 28 solvents, *J. Am. Chem. Soc.*, 117, 9159, 1995; (b) Gollnick, K. and Griesbeck, A., Interactions of singlet oxygen with 2,5-dimethyl-2,4-hexadiene in polar and non-polar solvents. Evidence for a vinylog ene-reaction, *Tetrahedron*, 40, 3235, 1984; (c) Griesbeck, A.G., Fiege, M., Gudipati, M.S., and Wagner, R., Photooxygenation of 2,4-dimethyl-1,3-pentadiene: solvent dependence of the chemical (ene reaction and [4+2]-cycloaddition) and physical quenching of singlet oxygen, *Eur. J. Org. Chem.*, 2833, 1998.
15. (a) Matsumoto, M. and Kuroda, K., Solvent effect in reaction of singlet oxygen with conjugated dienes, *Synth. Commun.*, 987, 11, 1981; (b) Yancheng, Z. and Foote, C.S., Photooxidation of substituted indenes at low temperature, *Tetrahedron Lett.*, 6153, 1986; (c) Burns, P.A. and Foote, C.S., Chemistry of singlet oxygen. XXIV. Low temperature photooxygenation of 1,2-dihydronaphthalenes, *J. Org. Chem.*, 41, 908, 1976.
16. van den Heuvel, C.J.M., Steinberg, H., and de Boer, T.J., The photooxidation of mono- and dimethylnaphthalenes by singlet oxygen, *Recl. Trav. Chim. Pays-Bas*, 99, 109, 1980.
17. Rigaudy, J., Photooxidation of aromatic derivatives, *Pure Appl. Chem.*, 16, 169, 1968.
18. Bloodworth, A.J. and Eggelte, H.J., Prostaglandin endoperoxide model compounds. 1. Synthesis of (n + 5)-bromodioxabicyclo[n.2.1]alkanes, *J. Chem. Soc., Perkin Trans. 1*, 1375, 1981.
19. Nixon, J.R., Cudd, M.A., and Porter, N.A., Cyclic peroxides by intramolecular peroxymercuration of unsaturated hydroperoxides, *J. Org. Chem.*, 43, 4048, 1978.
20. See, for example, Sengul, M.E. and Balci, M., Thermolysis and CoII-tetraphenylporphyrin-catalyzed decomposition of substituted cycloheptatriene endoperoxides: a new synthetic approach to substituted dihydrooxepines, *J. Chem. Soc., Perkin Trans. 1*, 2071, 1997.
21. Kornblum, N. and DeLaMare, H.E., The base catalyzed decomposition of a dialkyl peroxide, *J. Am. Chem. Soc.*, 73, 880, 1951.
22. See, for example, Schaffner, K., Schmidt, R., and Brauer, H.D., Photochromism based on the reversible reaction of singlet oxygen with aromatic compounds, *Mol. Cryst. Liq. Cryst. Sci. Technol.*, 246, 119, 1994.
23. See, for example, de Meijere, A., Kaufmann, D., and Erden, I., Photooxidation of dispiro[2.0.2.4]deca-7,9-diene and its analogs: synthesis and properties of new nonenolizable cyclohex-2-ene-1,4-diones, *Tetrahedron*, 42, 6487, 1986.
24. Srinivasan, R., Brown, K.H., Ors, J.A., White, L.S., and Adam, W., Organic photochemistry with 6-7 eV photons: Ascaridole, *J. Am. Chem. Soc.,* 101, 7424, 1979.

25. Drews, W., Schmidt, R., and Brauer, H.-D., The photolysis of the endoperoxide of 9,10-diphenylanthracene, *Chem. Phys. Lett.,* 70, 84, 1980.
26. Dufraisse, C., Rio, G., and Basselier, J.-J., Isophotooxydes cyclopentadieniques, *Compt. Rend. Acad. Sci. Paris,* 246, 1640, 1958.
27. Basselier, J.-J. and Leroux, J.P., Rearrangements thermiques et photochimiques des photooxydes de tetraphenyl-2,3,4,5-cyclopentadienes-2,4. Influence des substituants metheniques, *Bull. Soc. Chim. Fr.,* 4448, 1971.
28. Maheshwari, K.K., de Mayo, P., and Wiegand, D., Photochemical rearrangement of diene endoperoxides, *Can. J. Chem.,* 48, 3265, 1970.
29. Carless, H.A.J., Atkins, R., and Fekarurhobo, G.K., Thermal and photochemical reactions of unsaturated bicyclic endoperoxides, *Tetrahedron Lett.,* 26, 803, 1985.
30. Basselier, J.-J. and Leroux, J.P., Rearrangements thermiques et photochimiques des photooxydes de tetraphenyl-2,3,4,5-cyclopentadienes-2,4. Influence des substituants metheniques, *Bull. Soc. Chim. Fr.,* 4448, 1971.
31. Carless, H.A.J., Atkins, R., and Fekarurhobo, G.K., Polyoxygenated cyclohexenes from aromatic compounds: selective reactions of bis(endoperoxides), *J. Chem. Soc., Chem. Commun.,* 139, 1985.
32. Adam, W. and Balci, M., Cyclic polyepoxides. Synthetic, structural and biological aspects, *Tetrahedron,* 36, 833, 1980.
33. van Tamelen, E.E. and Taylor, E.G., Total synthesis of stemolide, *J. Am. Chem. Soc.,* 102, 1202, 1980.
34. Carless, H.A.J., Billinge, J.R., and Oak, O.Z., Photochemical routes from arenes to inositol intermediates: the photooxidation of substituted cis-cyclohexa-3,5-diene-1,2-diols, *Tetrahedron Lett.,* 30, 3113, 1989.
35. (a) Boyd. J.D., Foote, C.S., and Imagawa, D.K., Synthesis of 1,2;3,4-diepoxides by catalyzed rearrangement of 1,4-endoperoxides, *J. Am. Chem. Soc.,* 102, 3641, 1980; (b) Balci, M. and Sutbeyaz, Y., CoTPP catalysed rearrangement of 1,4-endoperoxides, *Tetrahedron Lett.,* 24, 311, 1983.
36. Griesbeck, A.G., Deufel, T., Peters, K., Peters, E.-M., and von Schnering, H.G., Singlet oxygen photooxygenation of tricyclo[4.3.0.$0^{1,3}$]nona-6,8-dienes and bicyclo[4.3.0]nona-1(6),7-dienes: characterization of the primary reaction products and subsequent transformations, *J. Org. Chem.*, 60, 1952, 1995.
37. Akbulut, N., Menzek, A., and Balci, M., Thermolysis and CoTPP-catalyzed rearrangement of endoperoxides derived from 2.3-dihydro-1(2H)azulenone. A new endoperoxide-endoperoxide rearrangement, *Tetrahedron. Lett.,* 28, 1689, 1987.
38. Celik, M., Akbulut, N., and Balci, M., Synthesis and chemistry of endoperoxides derived from 3,4-dihydroazulene-1(*2H*)-one: an entry to cyclopentane-annellated tropone derivatives, *Helv. Chim. Acta,* 83, 3131, 2000.
39. Adam, W. and Sanabia, J., Prostanoid endoperoxide model compounds: 1,6-diradicals in the thermolysis and photolysis of 1,2-dioxanes and cyclic peroxides, *J. Am. Chem. Soc.*, 99, 2735, 1977.
40. Bloodworth, A.J. and Baker, D.S., Dehydrogenation of cyclic and bicyclic secondary alkyl peroxides during flash vacuum pyrolysis, *J. Chem. Soc., Chem. Commun.,* 547, 1981.
41. Salomon, R.G., Salomon, M.F., and Coughlin, D.J., Prostaglandin endoperoxides. 6. A polar transition state in the thermal rearrangement of 2,3-dioxabicyclo[2.2.1]heptane, *J. Am. Chem. Soc.*, 100, 660, 1978.
42. Bloodworth, A.J., Baker, D.S., and Eggelte, H.J., Formation of dicarbonyl compounds in the flash vacuum pyrolysis of saturated bicyclic peroxides, *J. Chem. Soc., Chem. Commun.,* 1034, 1982.
43. Bloodworth, A.J. and Eggelte, H.J., Photolysis of saturated bicyclic peroxides, *Tetrahedron Lett.,* 25, 1525, 1984.
44. Wilson, R.M. and Rekers, J.W., Decomposition of bicyclic endoperoxides: an isomorphous synthesis of frontalin via 1,5-dimethyl-6,7-dioxabicyclo[3.2.1]octane, *J. Am. Chem. Soc.,* 103, 206, 1981.
45. (a) Rigaudy, J., Deletang, C., and Basselier, J.-J., Autoxydation photosensibilisee du dimethoxy-1,4 naphtalene: le photooxyde et ses produits de transformation, *Compt. Rend. Acad. Sci. Paris,* 268, Serie C, 344, 1969; (b) Rigaudy, J., Maurette, D., and Nguyen Kim Cuong, Autoxydation photo-

sensibilisee du dimethyl-1,4 naphtalene: le photooxyde et sa photo-isomerisation, *Compt. Rend. Acad. Sci. Paris,* 273, Serie C, 1553, 1971.

46. (a) Rigaudy, J., Cohen, N.C., and Nguyen Kim Cuong, Photooxydes "benzo" des anthracenes dialcoxyles en 1-4. Leur photo-isomerisation en *bis-epoxydes, Compt. Rend. Acad. Sci. Paris,* 264, Serie C, 1851, 1967; (b) Rigaudy, J., Caspar, A., Lachgar, M., Maurette, D., and Chassagnard, C., Photoisomerisations d' 1,4-endoperoxydes et de 1,2;3,4-diepoxydes derives de 1,4-dimethylanthracenes, *Bull. Soc. Chim. Fr.,* 129, 16, 1992.
47. Rigaudy, J., Lachgar, M., and Saad, M.M.A., Photoisomerization of 1,4-endoperoxides derived from 1,2,3,4-tetramethylanthracenes and 1,2,3,4-tetramethylnaphthalene, *Bull. Soc. Chim. Fr.,* 131, 177, 1994.
48. Defoin, A., Baranne-Lafont, J., and Rigaudy, J., Transformations photochimiques d'endoperoxydes derives d'hydrocarbures aromatiques polycycliques. II. Cas de l'endoperoxyde d'anthracene: Di- et tetraepoxydes derives, *Bull. Soc. Chim. Fr.,* 145, 1984.
49. Rigaudy, J. and Lachgar, M., Anthracenic and naphthalenic vic-diepoxides. A new kind of isomerization going through fragmentation, *Tetrahedron Lett.*, 38, 2267, 1997.
50. Schmidt, R., Schaffner, K., Trost, W., and Brauer, H.-D., Wavelength-dependent and dual photochemistry of the endoperoxides of anthracene and 9,10-dimethylanthracene, *J. Phys. Chem.,* 88, 956, 1984.
51. Schmidt, R., Brauer, H.-D., and Rigaudy, J., Reactions originating from different upper excited singlet states: the photocycloreversion of the endoperoxides of 1,4-dimethyl-9,10-diphenylanthracene, *J. Photochem.,* 34, 197, 1986.
52. Brauer, H.-D., Drews, W., and Schmidt, R., A new photochromic system of unusual high thermal stability, *J. Photochem.,* 12, 293, 1980.
53. Schmidt, R., Drews, W., and Brauer, H.-D., Wavelength-dependent photostable or photoreversible photochromic system, *J. Phys. Chem.,* 86, 4909, 1982.
54. Kearns, D.R. and Khan, A.U., Sensitized photooxygenation reactions and role of singlet oxygen, *Photochem. Photobiol.*, 10, 193, 1969.
55. Jesse, K., Markert, R., Comes, F.J., Schmidt, R., and Brauer, H.-D., Picosecond photochemistry: the mechanism of photocycloreversion of aromatic endoperoxides, *Chem. Phys. Lett.,* 166, 95, 1990.
56. Jesse, K. and Comes, F.J., Rate parameters for the two-step photofragmentation of aromatic endoperoxides in solution, *J. Phys. Chem.,* 95, 1311, 1991.
57. Ernsting, N.P., Schmidt, R., and Brauer, H.-D., Subpicosecond transient absorption studies of the photocycloreversion of an aromatic endoperoxide, *J. Phys. Chem.,* 94, 5252, 1990.
58. Klein, A., Kalb, M., and Gudipati, M.S., New assignment of the electronically excited states of anthracene-9,10-endoperoxide and its derivatives: A critical experimental and theoretical study, *J. Phys. Chem. A*, 103, 3843, 1999.
59. Kearns, D.R., Selection rules for singlet-oxygen reactions. Concerted addition reactions, *J. Am. Chem. Soc.*, 91, 6554, 1969.
60. Rigaudy, J., Breliere, C., and Scribe, P., Photochemistry of 9,10-diphenylanthracene endoperoxide, *Tetrahedron Lett.*, 687, 1978.
61. Schmidt, R., Drews, W., and Brauer, H.-D., Photolysis of the endoperoxide of heterocoerdianthrone — A concerted, adiabatic cycloreversion originating from an upper excited singlet-state, *J. Am. Chem. Soc.*, 102, 2791, 1980.
62. Freyer, W. and Leupold, D., A multichromophoric tetraanthraporphyrazine based on involvement of molecular singlet oxygen, *J. Photochem. Photobiol., A: Chem.*, 105, 153, 1997.
63. Kasha, M., Characterization of electronic transitions in complex molecules, *Discuss. Faraday Soc.*, 14, 1950.
64. Jesse, K.J., Structural impacts on the photodissociation dynamics of aromatic endoperoxides in solution, *Chem. Phys. Lett.*, 264, 193, 1997.

65. Gudipati, M.S. and Klein, A., Reply to the comment on "New assignment of the electronically excited states of anthracene-9,10-endoperoxide and its derivatives: A critical experimental and theoretical study," *J. Phys. Chem. A*, 104, 166, 2000.
66. Brauer, H.-D. and Schmidt, R., Comment on "New assignment of the electronically excited states of anthracene-9,10-endoperoxide and its derivatives: A critical experimental and theoretical study," *J. Phys. Chem. A*, 104, 164, 2000
67. Gudipati, M.S., Exciton, exchange and through-bond interactions in multichromophoric molecules: an analysis of the electronic excited states, *J. Phys. Chem.*, 98, 9750, 1994.
68. Sevin, F. and McKee, M.L., Reactions of 1,3-cyclohexadiene with singlet oxygen. A theoretical study, *J. Am. Chem. Soc.*, 123, 4591, 2001.
69. Fabian, J., Diaz, L.A., Seifert, G and Niehaus, T., Calculation of excitation energies of organic chromophores: a critical evaluation, *J. Mol. Struct. (THEOCHEM)*, 594, 41, 2002.

109

Reaction and Synthetic Application of Oxygen-Centered Radicals Photochemically Generated from Alkyl Hypohalites

Hiroshi Suginome
Hokkaido University

109.1 Brief Historical Background

Alkyl hypohalites (ROX; X = Cl, Br, I), a class of molecules that can be prepared from the corresponding alcohols by a variety of methods,[1] dissociate to alkoxyl and halogen radicals with high efficiency upon irradiation with light of wavelength longer than 300 nm (Scheme 1).

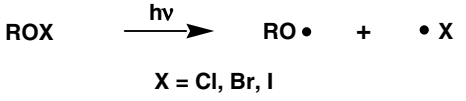

SCHEME 1

Methyl and ethyl hypochlorites, the first alkyl hypohalites known, were prepared by Sandmeyer in 1885.[2] Chattaway and Backeberg of Oxford subsequently reported the preparation of alkyl hypochlorites such as propyl, isopropyl, and *t*-butyl hypochlorites in 1923[3] and observed that although the primary and secondary hypochlorites are very unstable and decompose rapidly at room temperature, the tertiary hypochlorites, such as *t*-butyl hypochlorite, prepared by the reaction of chlorine, sodium hydroxide, and

0-8493-1348-1/04/$0.00+$1.50

t-butyl alcohol, are moderately stable pale-yellow liquids that can be distilled without decomposition.[3] Moreover, they found that *t*-butyl hypochlorite decomposed upon exposure to bright sunlight to give methyl chloride and acetone (Scheme 2). During the following years, simple alkyl hypochlorites received attention, principally as free-radical chlorinating reagents and oxidants (as summarized in review articles by Anbar and Ginsburg[1a] and by Walling[4]). *t*-Butyl hypochlorite converts toluene into benzyl chloride and the allylic position of olefins is chlorinated.[5]

SCHEME 2

Since this early work, studies from the late 1950s until the 1960s by Walling,[6–8] Green,[9] Kochi[10] and their collaborators using *t*-alkyl hypohalites disclosed some fundamental characteristics of the principal radical chain reactions, such as intermolecular hydrogen abstraction and β-scission of intermediate alkoxyl radicals in hypohalite photolysis. This work was summarized in a review article by Kochi.[11]

The photochemistry of alkyl hypohalites, however, has attracted considerable attention from organic chemists since the 1960s when Barton and colleagues,[12] a group of Swiss chemists,[13,14] as well as Mills and Petrow[15] demonstrated that alkyl hypochlorites and hypoiodites can be utilized in a manner parallel to the organic nitrites for the functionalization of an unactivated carbon atom based on a concept delineated by Barton.[16,17] The photolysis of steroidal hypohalites with appropriate constitution provoked an intramolecular exchange of the halogen of the ROX group with a hydrogen atom attached to a carbon atom in the δ-position (Scheme 3). An analogous intramolecular δ-hydrogen abstraction of long-chain hypochlorites (Walling and Padwa,[18] Green,[9] and Jenner[19]) and hypobromites (Mihailovic[20]) were also reported. Both the mechanistic and synthetic aspects of remote functionalization via the photolysis of hypohalites have been the subjects of comprehensive review articles by Akhtar[21] as well as by Heusler and Kalvoda.[1b,14]

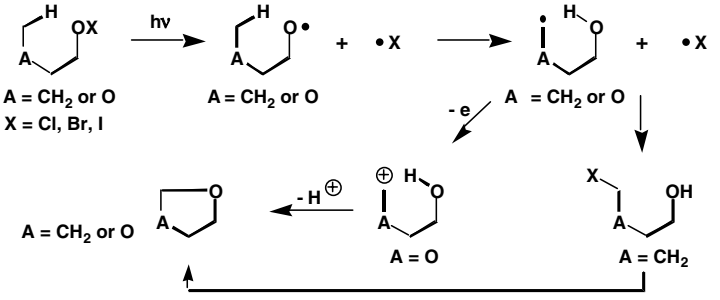

SCHEME 3

A more recent investigation by Suginome and collaborators has demonstrated that the selective fragmentation of alkoxyl radicals, one of the principal reactions of these species, can be utilized as the key step in the synthesis of a variety of molecules, including several natural products.[22] Subsequently, Suarez and colleagues have also demonstrated the utility of the (diacetoxyiodo)benzene/iodine procedure[23] in the hypoiodite photolysis in a series of articles.

109.2 Photochemistry of *t*-Alkyl Hypohalites

Alkyl hypochlorites, as prototype alkyl hypohalites, in carbon tetrachloride exhibit two absorption peaks in the ultraviolet region: one at about 260 nm and the other at about 310–320 nm.[12,24] Specifically, 3β-acetoxy-20-methylallopregnan-20-ol hypochlorite in carbon tetrachloride exhibits two absorption maxima

at 258 nm (ε = 107) and 318 nm (ε = 9.5). Although the corresponding hypobromites reveal similar absorptions, the peaks are displaced to longer wavelengths; *t*-butyl hypobromite exhibits an absorption maximum at 280 nm (ε = 120) and a long-tail absorption extending into the visible region.[7c] The UV spectra of alkyl hypoiodites, which are non-isolated species, have not been reported. Their absorption maxima, however, should appear at even longer wavelengths. Homolysis of the RO–X bond takes place when alkyl hypohalites in an inert solvent are irradiated with light of wavelength >300 nm.[25]

Homolysis is also initiated by azoisobutyronitrile or by thermolysis.[4,6] This characteristic of alkyl hypohalites differs from those of the corresponding nitrites in solution;[17] homolysis of the ON bond in solution can only be achieved by photolysis.

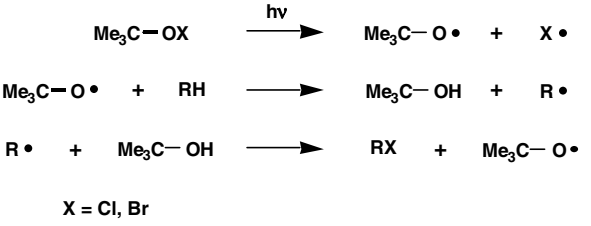

SCHEME 4

The competitive nature of the principal reactions of the alkyl hypohalites was investigated using *t*-butyl hypochlorite[26] and hypobromite as the prototypes.[7c] Walling and collaborators found that *t*-butyl hypochlorite and hypobromite are efficient free-radical chlorinating agents for saturated aliphatic hydrocarbons (Scheme 4).[6,7] They also investigated the photoinduced allylic chlorination of olefins with *t*-butyl hypochlorite, for which there have been sporadic reports from the 1940s until the 1950s, in great detail.[7] They found that a variety of olefins react with *t*-butyl hypochlorite via a photoinduced radical chain process to give a good yield of allylic chlorides in preference to an addition to give β-chloroalkyl *t*-butyl ethers.

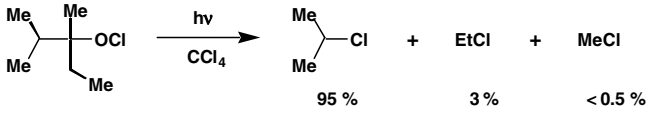

SCHEME 5

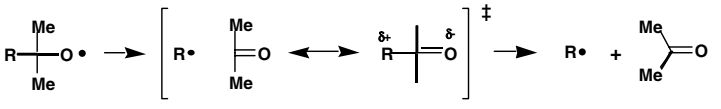

SCHEME 6

Another principal competing reaction of *t*-alkyl hypohalites in a photoinduced reaction is a β-fragmentation of the alkoxyl radicals to give alkyl halides and ketones. The factors that affect the relative rates of ejection of the alkyl radical in the β-fragmentation of alkoxyl radicals has been extensively investigated by Walling, Green, Kochi, and their collaborators[8–10] by carrying out the photodecomposition of a variety of *t*-alkyl hypochlorites. The results indicated increasing β-fragmentation in the order methyl < ethy l< isopropyl < benzyl < *t*-butyl (Scheme 5). The high degree of selectivity found in the β-fragmentation of alkoxyl radicals can be attributed to polar effects in the transition state[10,11] (Scheme 6). Studies with some aliphatic alcohol hypochlorites by Green and collaborators[9] indicated that intermolecular hydrogen abstraction from cyclohexene as the solvent competes poorly with β-fragmentation

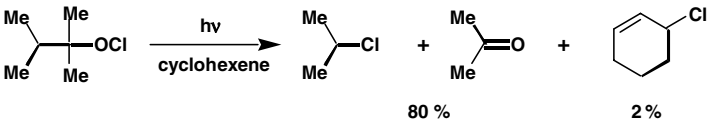

SCHEME 7

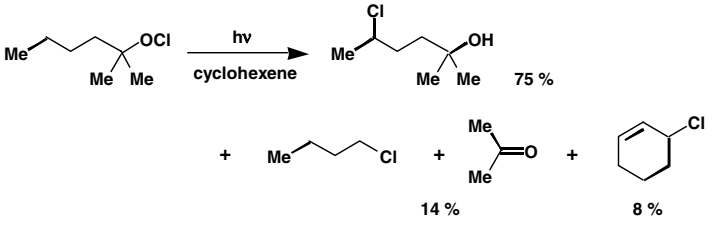

SCHEME 8

(Scheme 7). The results outlined in Scheme 8 also clearly indicate that intramolecular hydrogen abstraction by the alkoxyl radical via a six-membered transition state predominates over fragmentation and intermolecular allylic hydrogen abstraction. For more details concerning this subject, readers should refer to the original literature and also to a review article.[11]

109.3 Synthetic Applications of Oxygen-Centered Radicals Photochemically Generated from Hypohalites

Among the competing principal reactions of alkoxyl radicals, intramolecular hydrogen abstraction and β-fragmentation have been extensively and successfully used in organic synthesis. This situation is in contrast to the case of carbon-centered radicals in which intramolecular radical addition has been most successfully exploited in synthesis.[27] Some representative examples of the synthetic application are described below. The literature covers up to the beginning of 2002.

Preparation of Alkyl Hypobromites

Alkyl hypobromites can be prepared by the reaction of alcohols with either aqueous hypobromous acid[7c] or silver oxide-bromine or mercuric oxide-bromine[28] in an appropriate solvent. The proposed reaction sequence for hypobromite formation is shown in Scheme 9. Bromine oxide as the intermediate has been isolated and characterized.[29,30]

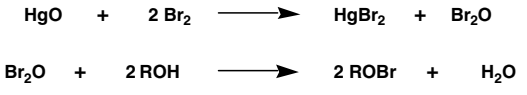

SCHEME 9

In situ Preparation of Alkyl Hypoiodites

Although alkyl hypochlorites and hypobromites are isolable species, alkyl hypoiodites are not isolable. They can only be prepared *in situ,* either by the reaction of alcohols with metal acetates or oxide and iodine in solution, or by the reaction of alcohols with a hypervalent iodine compound and iodine in

solution. Irradiation of the solution generates oxygen-centered radicals at room temperature. Active species in the formation of hypoiodites from metal acetate–iodine and hypervalent iodine-iodine reagents are considered to be acetyl hypoiodite, CH_3COOI, while active species in hypoiodite generation from mercuric oxide–iodine reagent should be iodine oxide, I_2O. The method for generating hypoiodites is thus occasionally reflected in the reaction products.

Metal Acetate–Iodine Reagents

The hypoiodites can be generated from alcohols with iodine and metal acetates, such as silver, mercuric,[31] or lead acetate.[13] Among them, an iodine and lead tetraacetate combination, proposed by Meystre and collaborators in 1961,[13] was most extensively used to generate the hypoiodites *in situ* in the 1960s and 1970s.[14] The combination of mercuric or lead acetate and iodine initially generates acetyl hypoiodite,[31] analogous to the formation of acetyl hypochlorite,[32,33] which reacts with steroidal alcohols to give hypoiodites,[13] as outlined in Scheme 10.

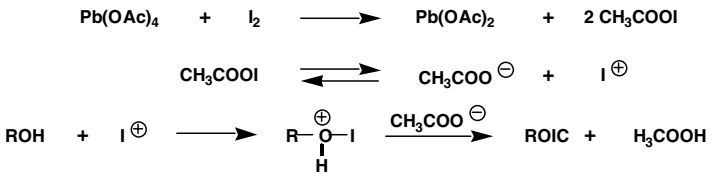

SCHEME 10

Mercury (II) Oxide–Iodine Reagent

The reaction of alcohols with this reagent in solvents, such as carbon tetrachloride or benzene, generates alkyl hypoiodites at room temperature. The reactive species, which reacts with alcohol, should be non-isolable I_2O, since isolable Br_2O is formed by an analogous reaction of HgO and Br_2 (Scheme 11).[29,30] The products that arose from a dark reaction of alkenes with this reagent, reported by Goosen[31] and our numerous results concerning β-fragmentation reactions described in this chapter are indeed best rationalized in terms of the intermediacy of iodine oxide. An excess of iodine oxide occasionally gives products from reactions with carbon-centered radical intermediates. This powerful reagent was initially used by Barton and collaborators[12] in the 1960s and then extensively by us from the 1970s.

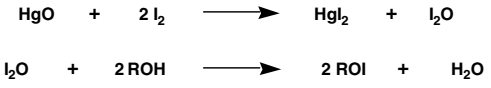

SCHEME 11

Hypervalent Iodine–Iodine Reagents

The combination of organic hypervalent iodine compounds, such as (diacetoxyiodo)benzene (DIB) or iodosylbenzene, PhI = O, with iodine, proposed by Suarez in the mid 1980s, was extensively used by his group for the hypoiodite reaction.[23] As in the case of lead tetraacetate–iodine, the alkyl hypoiodites were assumed to be formed by the reaction of alcohols with acetyl hypoiodite produced *in situ* by the reaction of DIB with iodine at room temperature. The reaction of the alcohols with acetyl hypoiodite generates the alkyl hypoiodite (Scheme 12). The acetoxy ion is occasionally incorporated into the reaction products.

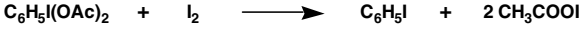

SCHEME 12

Diphenylselenium Hydroxyacetate–Iodine Reagent

This selenium reagent, $Ph_2Se(OH)OAc$, was also proposed by Suarez in 1988.[34] The reaction is carried out in cyclohexane at the reflux temperature (80°C). The active species in the formation of alkyl hypoiodites could again be acetyl hypoiodite.

Other Reagents

The hypoiodites can also be prepared *in situ* from alcohols with *t*-butyl hypochlorite and iodine, with *t*-butyl hypoiodite, with N-bromosuccinimide and iodine, and with N-iodosuccinimide, etc.

Remote Functionalization by Hypohalites

Remote Functionalization by Hypochlorites and Hypobromites

Akhtar and Barton[12] demonstrated a successful remote functionalization in the photolysis of a steroidal hypochlorite in 1960 (outlined in Scheme 13). The photolysis with Pyrex-filtered light of 3β-acetoxy-6α-methylcholestan-6β-ol hypochlorite, prepared from the parent 6β-ol and chlorine monoxide in dry benzene, gave a chlorohydrin, which was treated with a base to give the 6,19-oxide in 50% yield,[12] through a radical chain process.[6] Thus, functional groups can be introduced into the unactivated angular 10β- or 13β-methyl groups of steroids by the photolysis of hypohalites, as in the photolysis of nitrites.[16,17] An analogous photoinduced reaction of hypobromites of cedrol and the related bicyclo[3.2.1]octanes generated with mercury(II) oxide and bromine was reported.[35]

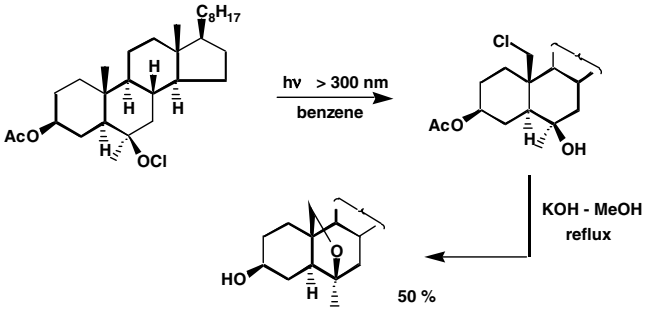

SCHEME 13

Remote Functionalization by Hypoiodites

Although alkyl hypoiodites cannot be isolated, they are even more convenient and powerful for generating alkoxyl radicals for remote functionalisation.[12,14,16] They are prepared *in situ* from alcohols and lactols. The stability for the base-catalyzed heterolytic decomposition of secondary hypohalites is in the order hypoiodites > hypobromites > hypochlorites. Moreover, the reactivity of hypoiodites (and iodine) with ketones or carbon-carbon double bonds under neutral conditions decreases in comparison with that of hypochlorites or hypobromites.[14] Remote functionalization can be achieved by irradiating a solution of a hypoiodite prepared *in situ* by one of the methods mentioned above. Remote functionalization via photolysis of an alkyl hypoiodite was designated a "hypoiodite reaction" by Heusler and Kalvada.[14] It is not clear whether the hypoiodite reaction involved a chain process similar to the one postulated for hypochlorite photolysis. Scheme 14 illustrates the positions of the alkoxyl radicals by which the hydrogen in 10β- and 13β-methyl groups can be abstracted to give the carbon radical. The most favorable O–C separation for the intramolecular abstraction of hydrogen was estimated to be 2.5 to 2.7 Å by a Swiss group on the basis of the results concerning the remote functionalization of a number of hypoiodites of rigid systems, such as steroids (*vide infra*) and an inspection of Dreiding models.[14] In the following, some representative examples among the numerous applications of the hypoiodite reaction to remote functionalization are outlined.

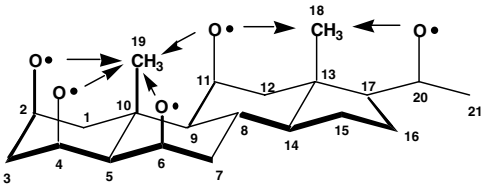

SCHEME 14

Functionalization of 10β-Me of a Steroid from the 6β-ol Hypoiodite Generated with Mercury(II) Oxide and Iodine[12] (Scheme 15)

A light-induced reaction of steroidal hypoiodites prepared by the reaction of a steroidal alcohol with iodine oxide generated from mercury(II) oxide–iodine generally gives a five-membered oxide, which should be formed by an intramolecular S_N2 or S_H2 reaction of intermediate 19-iodide, as outlined in Scheme 15.

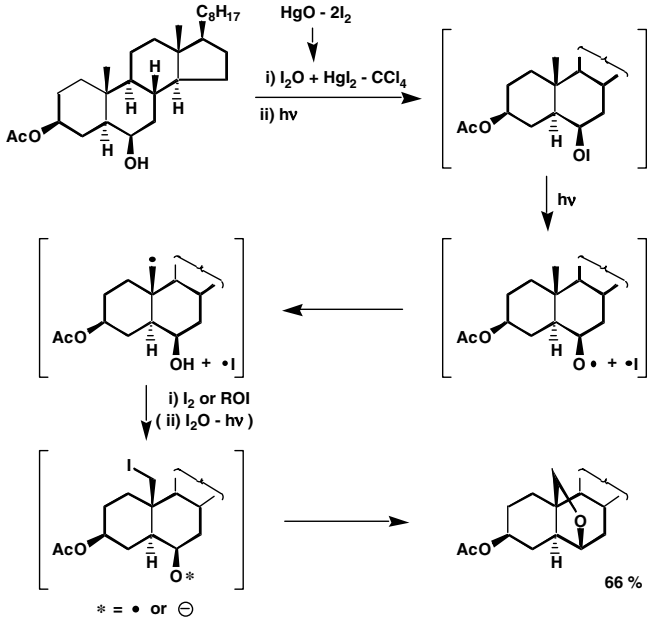

SCHEME 15

Functionalization of 10β-Me of a Steroid from the 6β-ol Hypoiodite Generated by Lead Tetraacetate and Iodine (Schemes 16 and 17)

Among the numerous results reported by the Swiss group, two typical examples of remote functionalization with this reagent are outlined in Schemes 16 and 17. The products of the remote functionalization of steroids by the hypoiodite reaction are either the five-membered oxide (Scheme 16) or the α-lactol acetate (Scheme 17), depending on the relative disposition between the relevant alkoxyl radical and the iodine attached to C18 or C19 of a conformer of the first-formed intermediate monoiodide. Thus, the five-membered oxide is an exclusive product[14] in the example outlined in Scheme 16, because the iodomethyl group can adopt an orientation that is appropriate for an S_H2 or S_N2 displacement of the iodine by the 6β-alkoxyl radical or ion, to give the observed oxide, as shown in Scheme 18. On the other hand, the α-lactol acetate is an exclusive product in the example[36] outlined in Scheme 17, because the preferred orientation of the iodomethyl group with respect to the 4β-hydroxyl in the first-formed intermediate

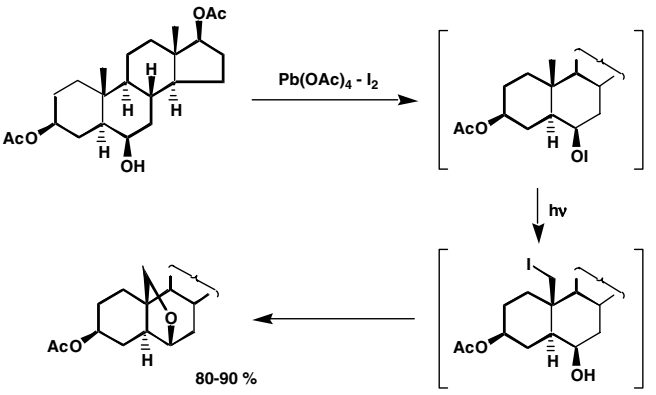

SCHEME 16

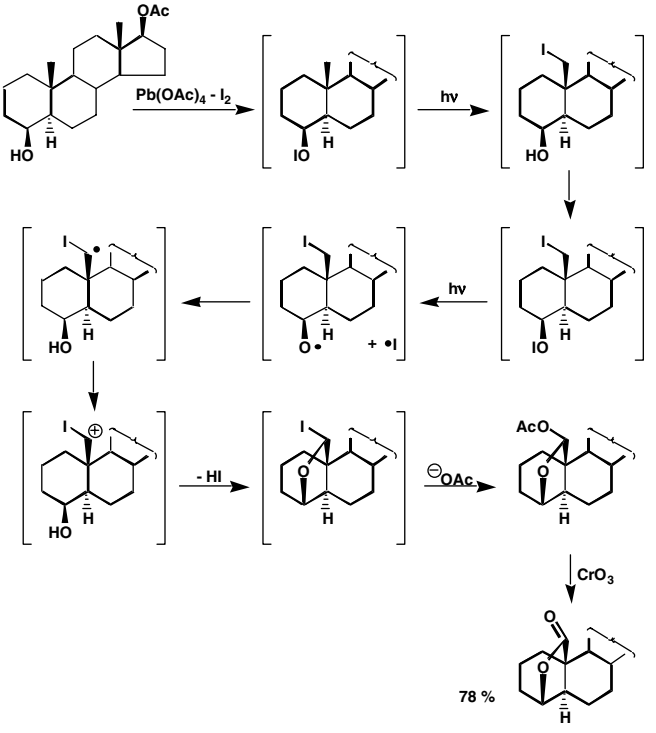

SCHEME 17

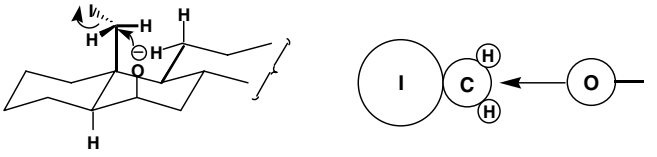

SCHEME 18

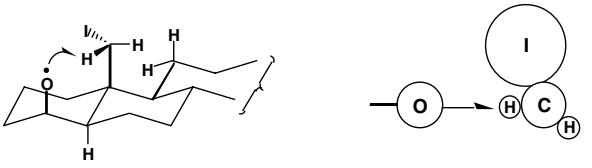

SCHEME 19

monoiodide does not allow any displacement of the iodine by the 4β-hydroxyl; however, it is appropriate for the second intramolecular hydrogen abstraction by the 4β-alkoxyl radical to give the iodo-oxide (Scheme 19), the iodine on which is displaced by an acetoxy ion to give a lactol acetate. Its oxidation with chromium trioxide then readily results in a transformation into the corresponding lactone. Analogously, the product of the hypoiodite reaction of the 20β-hydroxysteroid was the corresponding 18,20β-α-lactol acetate, which was isolated as the corresponding lactone by oxidation with chromium trioxide in 72% yield.[37]

For a thorough discussion concerning this subject, including more examples and accompanying reactions, the readers should consult the comprehensive review articles.[1b,14,21]

Functionalization of 18β-Me of* D-*homo*-C-*norsteroids from the 20β-ol Hypoiodite Generated with Mercury(II) Oxide and Iodine[38]

The photolysis of *D*-homo-*C*-norsteroid 20β-ol hypoiodites gives the corresponding cyclic ethers, which are formed via an intramolecular hydrogen abstraction from their 18β-methyl group by the 20β-alkoxyl radical, as outlined in Scheme 20.

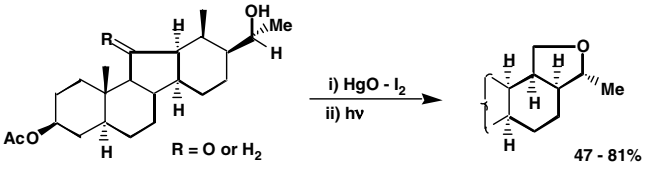

SCHEME 20

"Billiard Reaction" in the Hypoiodite Photolysis[39]

The "billiard reaction," a second intramolecular hydrogen abstraction from a 1,3-diaxially located methyl group by a carbon-centered radical, initially generated by an alkoxyl radical was observed in the remote functionalization of certain triterpenoids and diterpenoids by a thermal hypoiodite reaction with lead tetraacetate–iodine by Wenkert and Milari in 1967.[39a,b] Recent work by Suarez indicates that similar results can be achieved by the photolysis of hypoiodites in the presence of (diacetoxyiodo)benzene–iodine[39c] (Scheme 21). Scheme 22 outlines the reaction path.

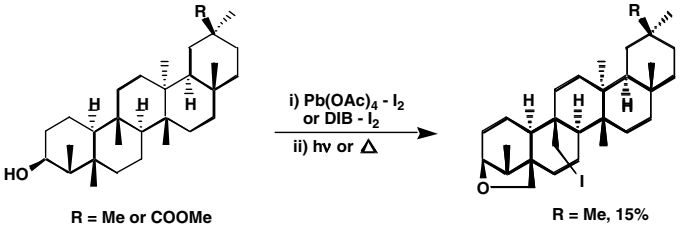

SCHEME 21

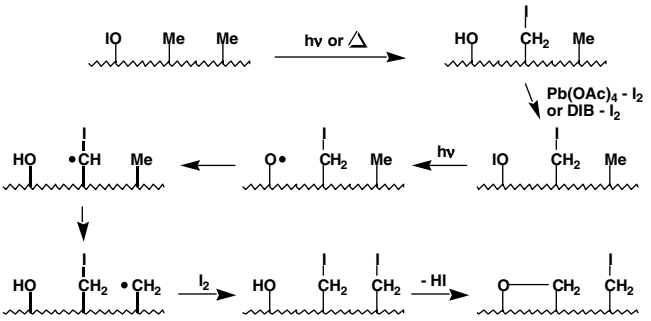

SCHEME 22

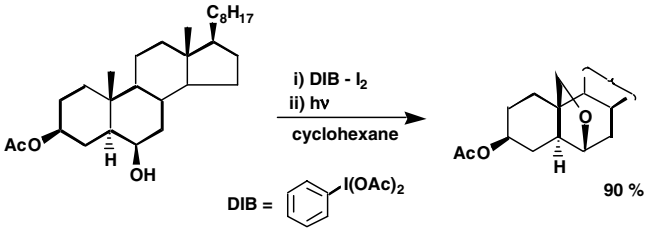

SCHEME 23

Functionalization of 10β-Me of Steroids by (Diacetoxyiodo)benzene (DIB) and Iodine[23]

Suarez and colleagues[23] have shown that each one equivalent of DIB and iodine in cyclohexane reacts with steroidal alcohols to produce the corresponding hypoiodites, and that irradiation of the solution with visible light gives cyclic ethers and monoiodo-alcohol derivatives as the major products arising from intramolecular hydrogen abstraction. Two examples[23] concerning the functionalization of the 10β-methyl group of a steroid from the 6β-ol and 4β-ol hypoiodites and an example[39c] of the remote functionalization of (−)-*cis*–nopiol reported by Suarez are outlined in Schemes 23, 24, and 25. These results should be compared with the products from the lead tetraacetate–iodine procedure outlined in Schemes 16 and 17. The products are more complicated as a result of the double intramolecular hydrogen abstraction processes.

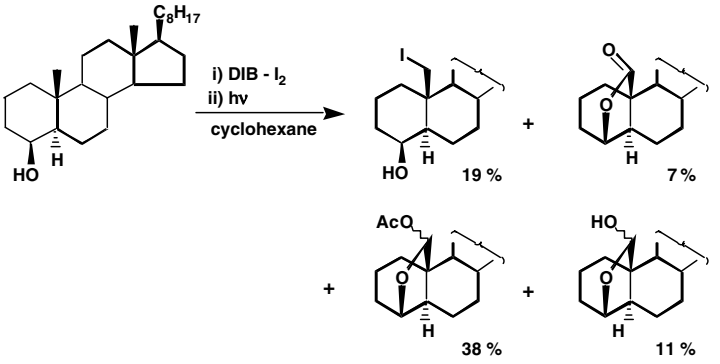

SCHEME 24

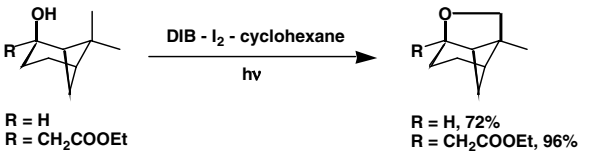

SCHEME 25

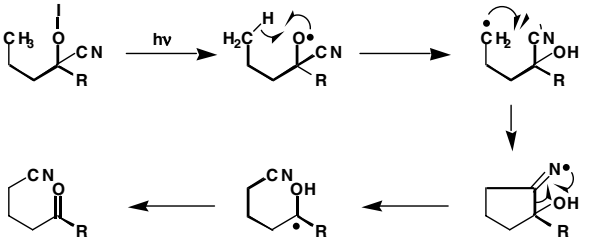

SCHEME 26

The Oxidative Cyanohydrin–Cyanoketone Rearrangement

An especially interesting example of the hypoiodite reaction is the oxidative cyanohydrin–cyanoketone rearrangement,[14,40] which is represented by the general pathway outlined in Scheme 26. The hypoiodite reaction of 20-hydroxy-20-cyanosteroids gives the 18-cyanoketones arising from a 1,4 shift of the cyano group accompanied by the loss of two atoms of hydrogen[14] (Scheme 27).

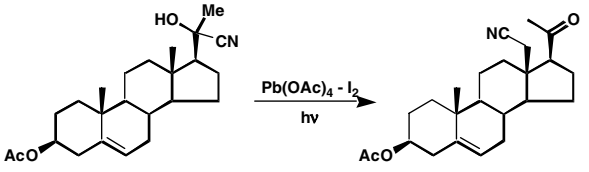

SCHEME 27

Intramolecular Functionalization via a Many-Membered Cyclic Transition State

Successful intramolecular hydrogen abstraction via a many-membered cyclic transition state by alkoxyl radicals generated by the photolysis of hypohalites has recently been reported; alkoxyl radicals generated by the irradiation of hypoiodites of 5α-cholestan-7α-yl-(hydroxymethyl)-phenyl acetates and propionates, respectively, abstracted a hydrogen from the remote C25 of the cholestane side chain to give novel macrocyclic ether lactones, which gave 5α-cholestane-7α,25-diol by reduction with Na and liquid ammonia (as outlined in Scheme 28[41]). A similar one-step introduction of a carbonyl group to C15 of the 5α-androstane skeleton, based on a long-range intramolecular hydrogen abstraction by alkoxyl radicals, generated by the irradiation of 5α-androstane esters carrying a benzhydryl group in carbon tetrachloride containing mercury(II) oxide and iodine, is outlined in Scheme 29. The proposed reaction path is also illustrated here.[42] Suginome and collaborators also reported a one-step double introduction of a carbon-carbon double bond and oxygen functions to ring C of 5α-steroid skeletons, based on a long-range intramolecular hydrogen abstraction by alkoxyl radicals generated from the esters of 5α-cholestan-3α-ol carrying a benzhydryl group.[42]

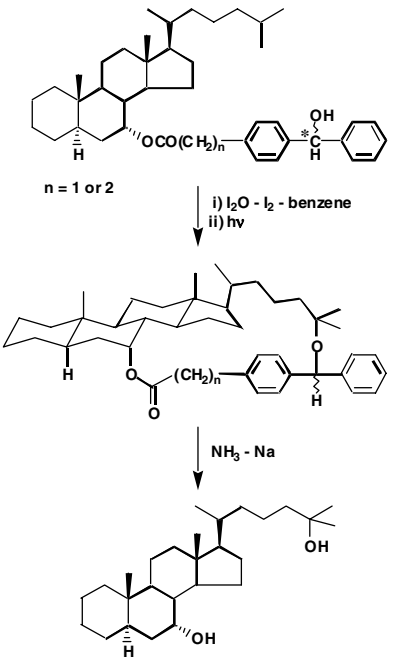

SCHEME 28

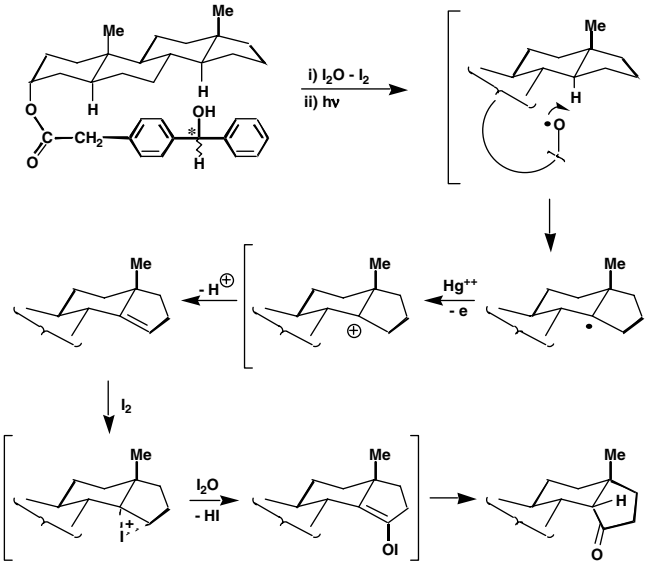

SCHEME 29

These results indicate that hypoiodite photolysis with mercury (II) oxide and iodine reagent is a powerful method that is applicable to even remote functionalization involving a many-membered transition state, because alkoxyl radicals are considered to be repeatedly generated from the regenerated hypoiodites in a solution containing an excess of the reagent.

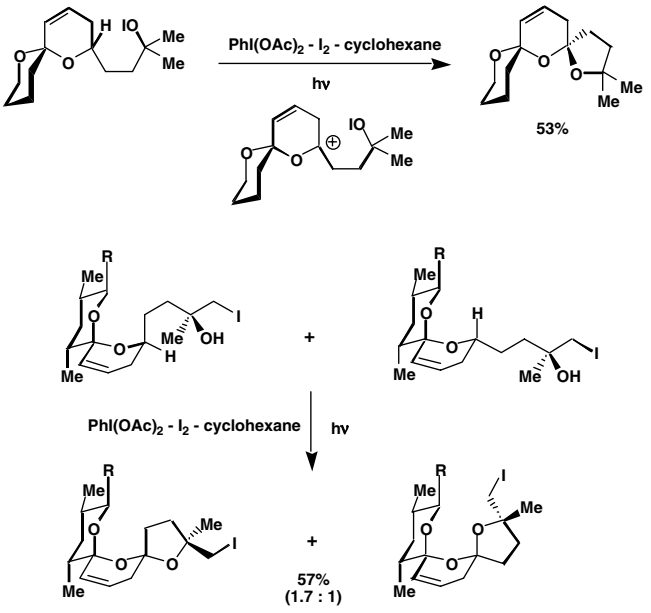

SCHEME 30

Formations of Cyclic and Spiro Acetals by a Tandem Intramolecular Hydrogen Abstraction-Cyclization Process (Schemes 30 through 36)

The application of hypoiodite photolysis for remote functionalization has been mostly in the steroid field. There has been, however, a resurgence of applications in the field of spiroacetal-type compounds. The reaction was originally found in 1966 by Mihailovic and collaborators, who described remote functionalization by a thermal reaction of alcohols with lead tetraacetate.[43]

Thus, two groups of investigators reported that the irradiation of certain oxygen heterocycles having a hydroxyalkyl side chain in cyclohexane in the presence of (diacetoxyiodo)benzene and iodine at room temperature gave bis-spiroacetals in good yields[23b,44] (Scheme 30). Subsequent work showed that similar reaction conditions could be applied to the synthesis of a number of five- and six-membered cyclic acetals from γ- and ε-hydroxyethers[45] (Scheme 31). The formation of a cyclic acetal was also found in the hypoiodite reaction of hydroxysteroid with mercury(II) oxide and iodine[46] (Scheme 32).

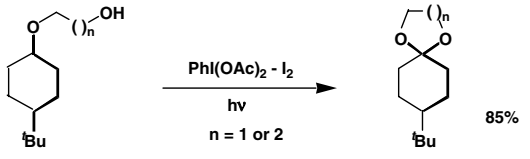

SCHEME 31

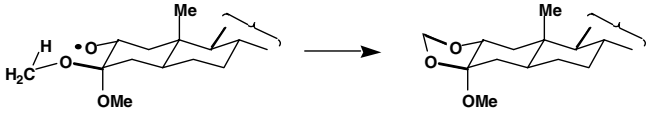

SCHEME 32

More recently, spiroacetal formation has been successfully exploited by Suarez and collaborators in the synthesis of a number of chiral spiroacetals and dispiroacetals from carbohydrates[47] (Schemes 33, 34, and 35). The approach was also used to synthesize anomeric spironucleosides[48] (Scheme 36). The best yields were achieved with the DIB-iodine reagent. Some typical examples are shown in Schemes 30 through 36.

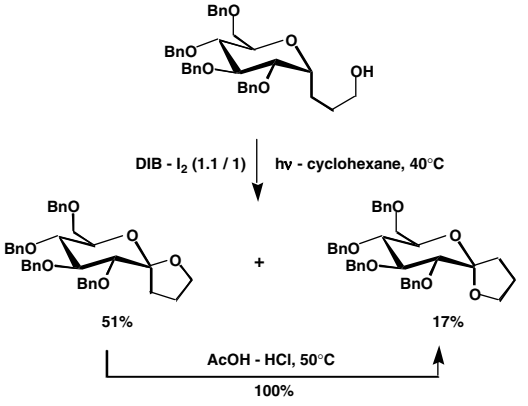

SCHEME 33

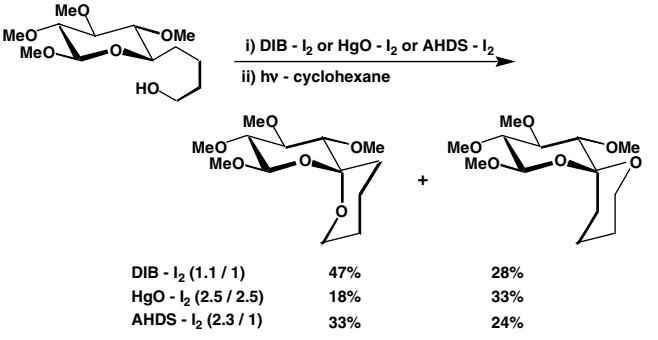

SCHEME 34

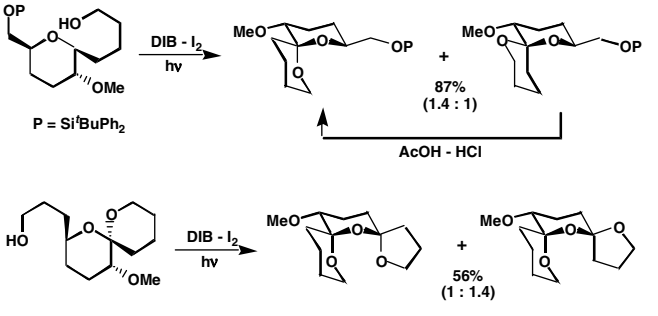

SCHEME 35

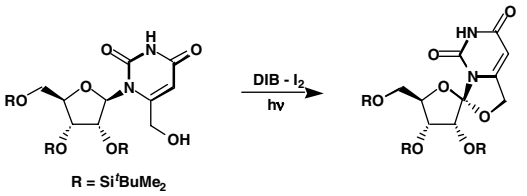

SCHEME 36

A notable feature of the remote functionalization of γ-hydroxyethers is that six-membered rings can be formed by intramolecular hydrogen abstractions through a seven-membered cyclic transition state. This exceptional regioselectivity in intramolecular hydrogen abstraction by oxygen-centered radicals can be attributed to the effect of the ethereal oxygen; one-electron oxidation of carbon radicals, generated by intramolecular hydrogen abstraction involving seven-membered cyclic transition state, to the corresponding carbocation is influenced by the ethereal oxygen atom, as suggested by Mihailovic.[43]

The acceleration of carbocation formation implies that spiroacetal formation may take place by the cyclization of a carbocation intermediate, but not by cyclization through an iodohydrin intermediate.

β-Fragmentation and Its Synthetic Application

In contrast to the intramolecular hydrogen abstraction mentioned above, fragmentation, another principal reaction of alkoxyl radicals, was seldom used in organic synthesis until the 1970s. An analysis of the numerous examples reported in the past and our own results concerning the photochemistry of alkyl nitrites[17] and hypohalites indicated that the direction of β-fragmentation in unsymmetrical substrates is the outcome of an interplay of multiple factors, such as the relative thermodynamic stability of the resultant radicals, ring strain, and stereoelectronic factors.

This situation is in contrast to the heterocyclic cleavage of bonds, such as the ring-fusion bond in bicyclic compounds, in which the cleavage requires a bifunctional substrate with strict stereoelectronic constraints.[49] Nevertheless, β-scission is frequently not only the predominant reaction, but also takes place in a highly selective manner and comprises an exclusive reaction when the alkoxyl radical and the hydrogen to be abstracted are not ideally disposed for intramolecular hydrogen abstraction. The β-scission is especially enhanced in the hypoiodite reaction when alkoxyl radicals appear to be repeatedly generated from the regenerated parent alcohol by excess reagent. Since the 1980s, Suginome and colleagues have shown that a variety of molecules, including natural products, can be synthesized using the β-scission of alkoxyl radicals generated by the photolysis of hypoiodites as the key step.

In the following, the type of the reaction and the formation paths, together with some representative examples of the synthesis, when they are necessary, are outlined. These selected examples may indicate that the β-scission of alkoxyl radicals takes place in a very selective manner and has become an integral part of synthetic strategies. For more details, readers should consult the original papers.

Cascade Radical Rearrangement Triggered by a Selective β-Fragmentation of Alkoxyl Radicals Generated by the Photolysis of Cyclic Alcohol Hypoiodites

The irradiation of hypoiodites generated *in situ* from cyclic alcohols with an excess of mercury(II) oxide and iodine with Pyrex-filtered light results in the formation of novel iodo-esters, arising from cascade radical rearrangements triggered by a selective β-fragmentation of the corresponding alkoxyl radicals, as shown by two examples outlined in Schemes 37 and 38.[51] The photolysis of cyclopentanol as a prototype cyclic alcohol under similar conditions gave rise to 5-iodopentyl formate corresponding to the steroidal formates.[51,52b]

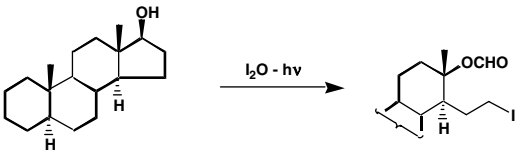

SCHEME 37

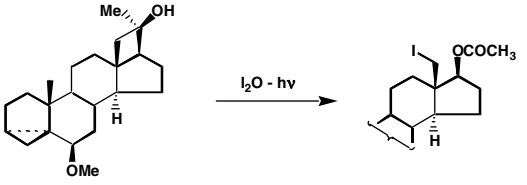

SCHEME 38

Mechanism of the Formation of the Iodo-Formates

Labeling studies using ^{18}O applied to the hypoiodites derived from androstan-17β-ol[51a] and cyclopentanol[51b] (Schemes 39 and 40) in which ^{18}O-labeled mercury (II) oxide as the source of $I_2{}^{18}O$ was used, proved that the ^{18}O was specifically incorporated in the formyl group of the formates, and that no ^{18}O was incorporated in the oxasteroid derived from it.

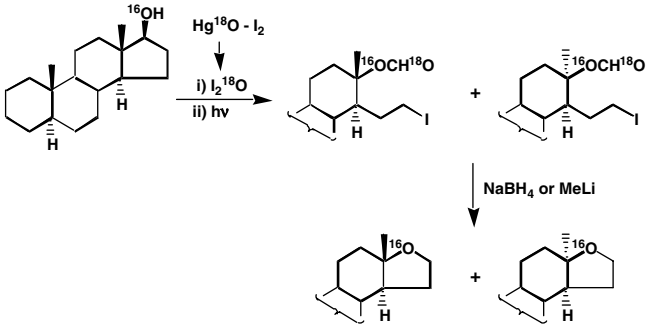

SCHEME 39

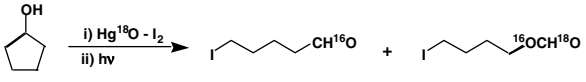

SCHEME 40

The pathway of the formation of the iodo-formates based on the ^{18}O labeling results thus involves the following sequence: (a) a selective β-fragmentation of the alkoxyl radical (A) to give a carbon-centred radical (B) bearing a carbonyl; (b) its cyclization to give a tetrahydropyranyl radical (c) followed by the one-electron oxidation to a tetrahydropyranyl cation (E) or one-electron oxidation of (B) to a tertiary carbocation (D), followed by the cyclization to (E); (c) its reaction with iodine oxide to form the second hypoiodite (F) and (d) a regioselective β-fragmentation of the secondary alkoxyl radical (G) generated from (F) to give the formate through (H), as outlined in Scheme 41.

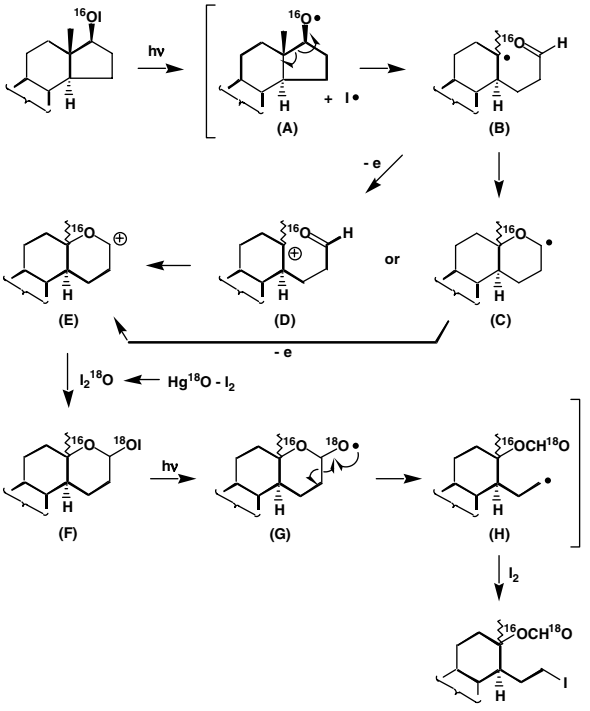

SCHEME 41

A Two-Step Transformation of Hydroxysteroids into Oxasteroids

This cascade radical rearrangement to the esters, followed by cyclization to cyclic ethers, comprises a new method of transforming hydroxy steroids into oxasteroids under essentially neutral conditions. A number of hydroxysteroids have been converted into oxasteroids. Another example is outlined in Scheme 42.[50a,52]

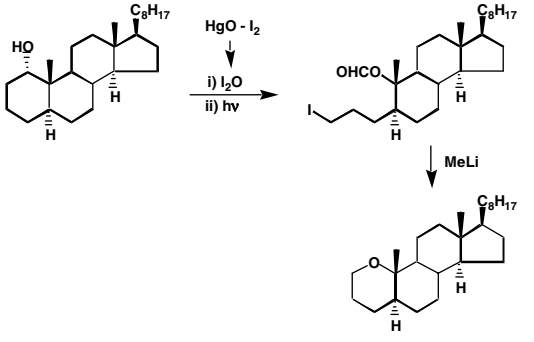

SCHEME 42

The Selective β-Fragmentation of Alkoxyl Radicals Generated by the Photolysis of Lactol Hypoiodites

The above-mentioned pathway for the formation of formates involves β-fragmentation of the second alkoxyl radicals generated from the hypoiodites cyclic alcohols. In fact, the irradiation of hypoiodites generated *in situ* from lactols prepared from appropriate ketones by the standard method in the presence of an excess amount of mercury(II) oxide-iodine and pyridine in benzene resulted in selective β-fragmentation to yield iodo-formates.[53] This fragmentation, which was found to be general in the alkoxyl radicals generated from the lactols, is of considerable value for organic synthesis, as shown below.

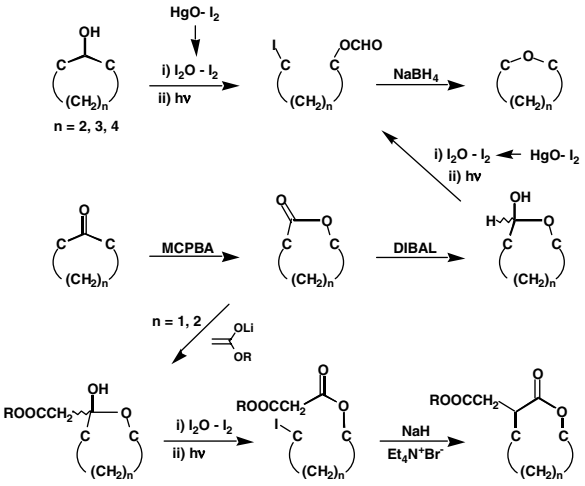

SCHEME 43

A New Four-Step Transformation of Cyclic Ketones into Cyclic Ethers[53]

Scheme 43 outlines a versatile method for transforming cyclic ketones as starting materials into cyclic ethers with the same ring size via four steps. The method is applicable not only to synthesize oxasteroids, but also to synthesize cyclic ethers in general. Among examples of the transformation of a number of cyclic ketones, such as steroidal ketones, adamantanone,[54] and camphor,[55] etc. into the corresponding cyclic ethers. Three are outlined in Schemes 44, 45, and 46.

An interesting application of the method, in which 5α,6β-dihydroxypregnane was transformed into 6-oxa-5β–pregnane-3,20-dione, has recently been reported.[56]

1. The transformation of a steroidal ketone into an oxasteroid and the ring contraction[52] (Scheme 44)

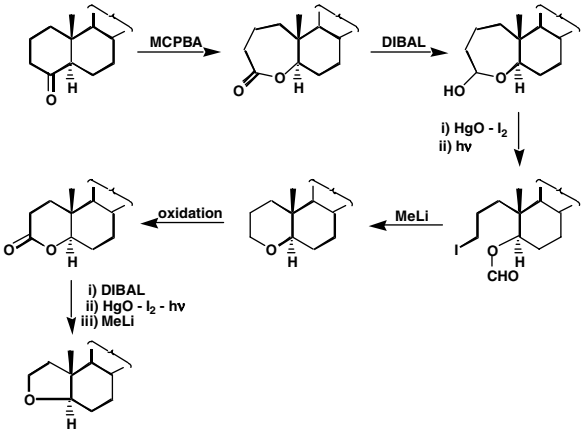

SCHEME 44

2. New stereo- and regioselective synthesis of (±) sesamin[57] (Scheme 45)

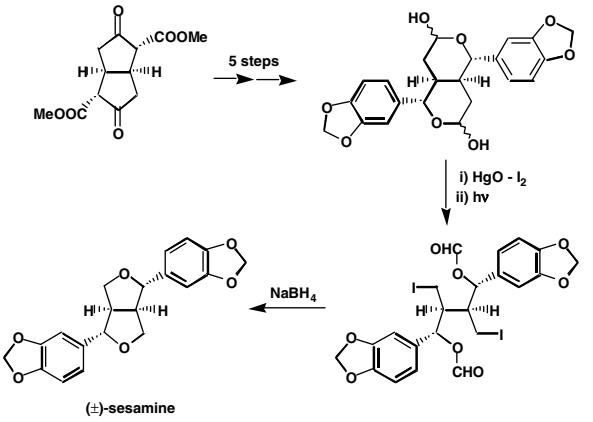

SCHEME 45

3. The transformation of steroids into 18- and 19-norsteroids[58] (Scheme 46)

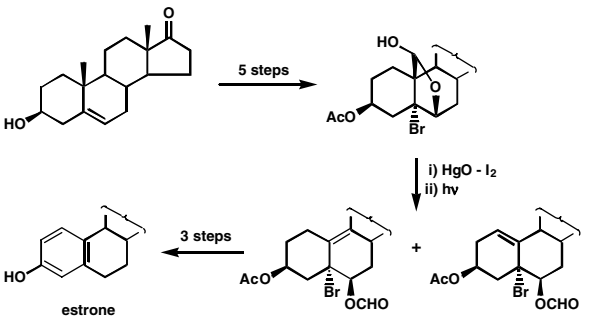

SCHEME 46

One-Carbon Intercalation of γ- and δ-Lactones

The reaction of γ- and δ-lactones with lithioalkyl acetate gave alkyl-(2-hydroxytetrahydrofuran-2-yl) acetates or their pyranyl homologs. The photolysis of the hypoiodites results in a selective endocyclic β-fragmentation of the corresponding alkyl radicals to give alkyl iodoalkylpropanedioates. Treatment of the iodo esters with tetraethyl ammonium bromide and sodium hydride gives the corresponding δ- or γ-lactones (Scheme 43).[59]

Transformation of Cyclic Ethers into ω-Iodoalkyl Formates and of Aldehyde Cyclic Acetals into α,ω-Alkanediol Esters by Hypothetical Iodoxyl Radical[60]

The photolysis of cyclic ethers with an excess of $HgO\text{-}I_2$ reagent in benzene gives the corresponding iodoalkyl formates in one step; tetrahydrofuran can be transformed into ω-iodoalkyl formate in 31% yield (Scheme 47). Aldehyde cyclic acetals lead to monoesters of α,ω-alkanediols in one step (Scheme 48). The formation of the products can be rationalized by postulating iodoxyl radical participation, as outlined in the schemes.

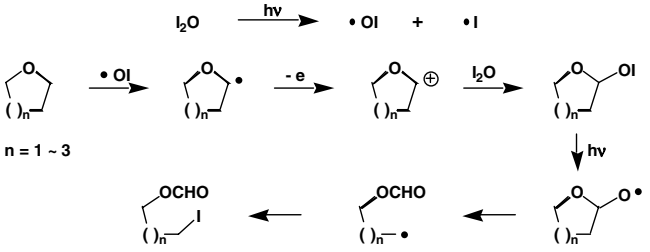

SCHEME 47

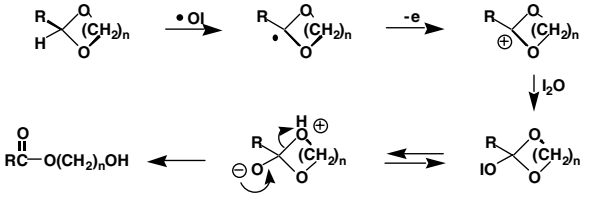

SCHEME 48

Substitution of a Carbonyl Group of Cyclic Ketones by a Heteroatom; Synthesis of Aza-, Oxa, Thia-, Selena-, and Tellurasteroids[53,61]

The iodo-formates obtained as described above are useful intermediates, which can be further transformed into cyclic amines, cyclic sulfides, cyclic tellurides, and cyclic selenides by the sequences outlined in Scheme 49.[61] A variety of heterosteroids have been synthesized from the corresponding steroidal ketones by these methods.[61]

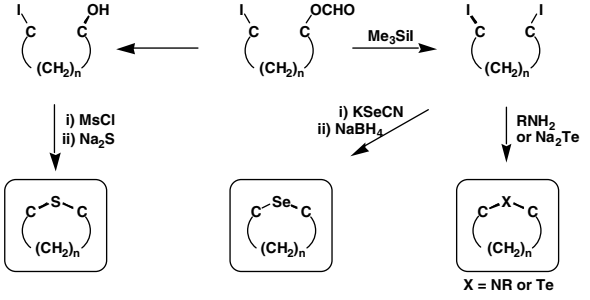

SCHEME 49

The Transformations of Carbohydrates by Selective β-Fragmentation

During the past decade, Suarez and collaborators have made use of the above-mentioned selective fragmentation of alkoxyl radicals generated from lactols. They reported on the preparation of four-carbon chiral building blocks of the D- and L-erythrose types by β-fragmentation of the anomeric alkoxyl radicals generated from the protected D- and L-arabinose, D-ribose and 2-deoxy-D-ribose in the presence of DIB-iodine or iodosylbenzene-iodine reagent, as outlined in Scheme 50.[62] When the starting carbohydrates bear an alkoxyl group, the fragmentation reaction in the presence of DIB-iodine terminates at the acetate stage, because the oxidation of the generated carbon radical to the carbocation, which traps acetoxy group, is facilitated.

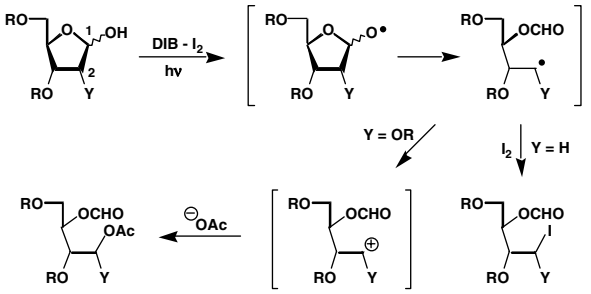

SCHEME 50

Schemes 51, 52, and 53 outline an extension of the method by the tandem β–fragmentation-cyclization sequence to modify the carbohydrates by the iodosylbenzene-iodine reagent instead of DIB-iodine. Thus, the transformations of D-ribofuranose to 3-O-formyl-α-D-erythrofuranose (Scheme 51),[63,64] furanose to cyclic ketoses, such as alduronic acid lactones (Scheme 52),[65] and carbohydrates to five- and-six-membered azasugars (Scheme 53) can be achieved.[66] β-Fragmentation of carbohydrate suitably substituted by azide group resulted in the formation of chiral nitriles (Scheme 54).[67]

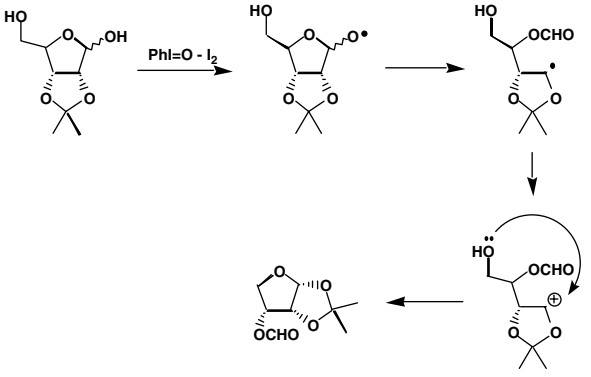

SCHEME 51

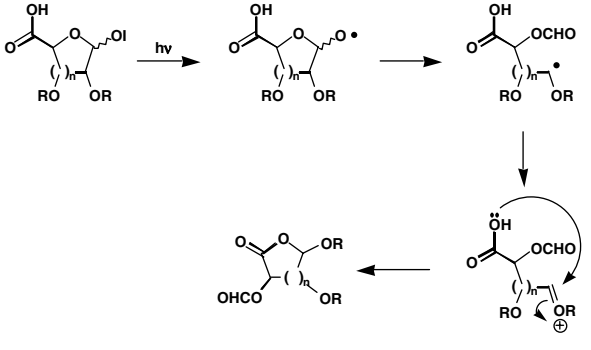

SCHEME 52

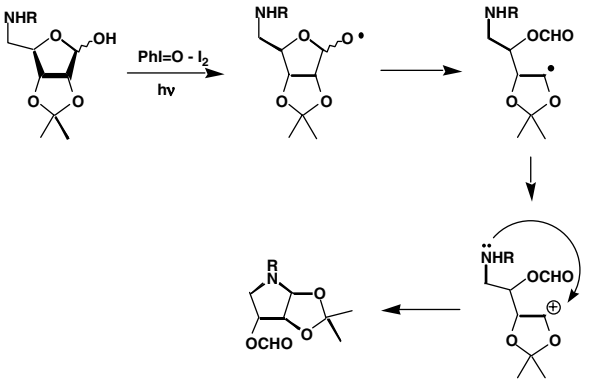

SCHEME 53

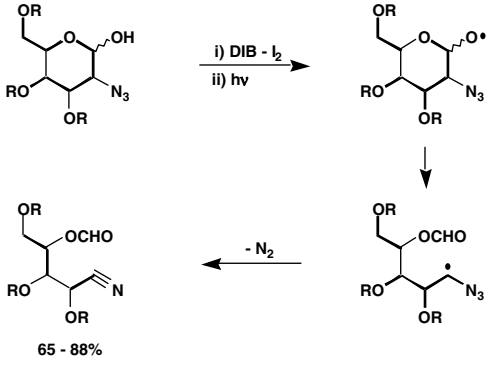

SCHEME 54

The Synthesis of 3-Substituted γ-Lactones

3-Substituted γ-lactones including some pheromones can be synthesized in three steps from cyclic 1,4-diketones. The key step is a selective β-fragmentation of lactols, as outlined in Scheme 55.[68]

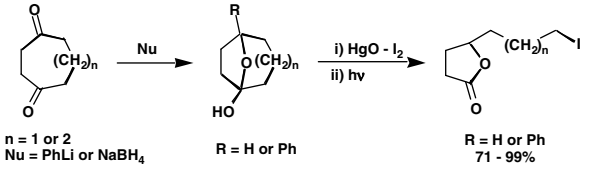

SCHEME 55

New General Synthesis of medium-ring lactones via a Regioselective β-Fragmentation of Alkoxyl Radicals Generated from Catacondensed Lactols

Suginome and collaborators further extended the above-mentioned regioselective β-fragmentation to the synthesis of medium-ring lactones in 1985. The irradiation of the hypoiodites of catacondensed lactols gives lactones arising from a regioselective cleavage of the inner bond of the systems.[69] The reduction of iodo-lactones with tributyltin hydride gives medium-ring lactones in high yields, as outlined in Scheme 56. A number of nine- to eleven-membered lactones were synthesized from 6/5, 6/6, 7/5, 7/6, and 8/5 fused lactols by this method. Scheme 57 outlines a ring expansion of steroidal substrate and Scheme 58

outlines a new four-step synthesis of a racemic phoracantholide from cyclohexanone trimethylsilyl enol ether by this method.

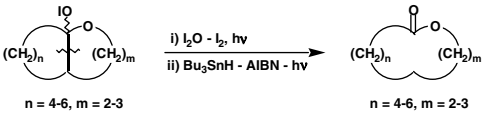

SCHEME 56

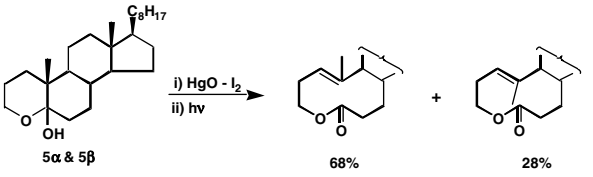

SCHEME 57

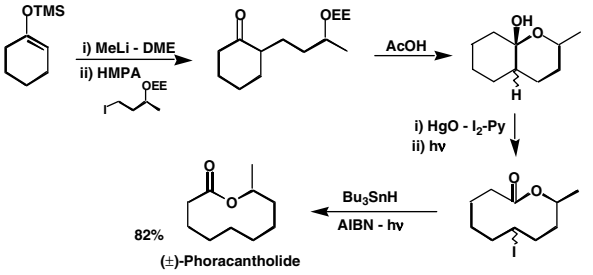

SCHEME 58

Subsequently, a similar ring expansion of steroidal substrates with (diacetoxyiodo)benzene-iodine reagent was reported by Suarez and collaborators,[70] and the method was applied to natural product synthesis.[70] Meanwhile, Suarez has studied products formed in a ring-expansion reaction in the presence of oxygen. Thus, while the photolysis of lactol in the presence of DIB-iodine gave a mixture of lactones in 85% yield, molecular oxygen scavenged the intermediary carbon-centered radical to give an epoxy product in 35% yield, together with the ring-expansion products in 14% yield, as outlined in Scheme 59.[70]

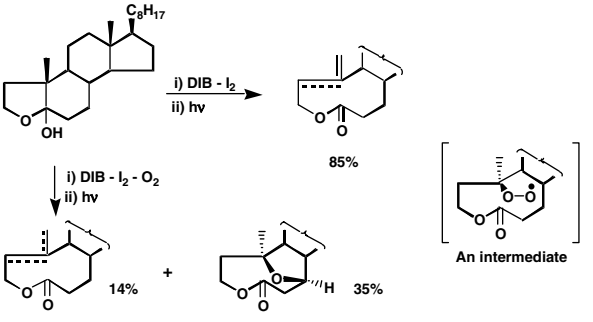

SCHEME 59

Similarly, the photolysis of a lactol in the presence of molecular oxygen afforded a lactone incorporated by oxygen, as outlined in Scheme 60.[71]

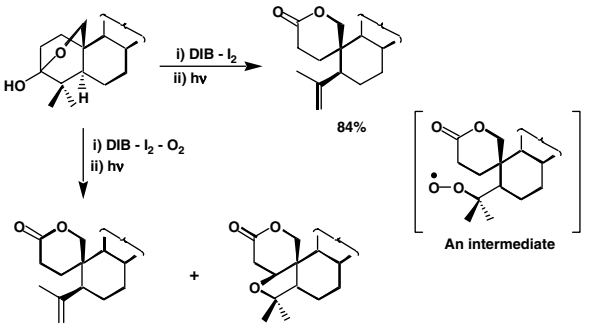

SCHEME 60

It has been reported that the treatment of a hydroxytricycloundecenone derivative, which exists largely in the form of a hydroxyketone in solution (90%), with DIB-iodine in cyclohexane, followed by the photolysis resulted in the formation of a iodolactone arising from a β-fragmentation in 76 to 82% yield[72] (Scheme 61).

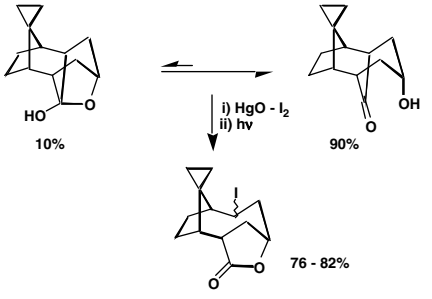

SCHEME 61

New General Synthesis of Macrolides via β-Fragmentation of Alkoxyl Radicals Generated from Lactol–Hydroxyketone Equilibrium

11- to 17-Membered macrolides can analogously be synthesized by photolysis of the hypoiodites of open-hydroxy ketones, as outlined in Scheme 62.[73] The iodo-lactones mentioned here are believed to be formed either via a regioselective β-fragmentation of alkoxyl radicals generated from the lactol, which is in equilibrium with the hydroxy ketone form or, although less likely, via a consecutive homolytic process — an intramolecular homolytic addition of the alkoxyl radicals to the carbonyl carbon followed by a fragmentation of the bridged bond of the generated alkoxyl radicals. It then traps an iodine atom to give iodo-macrolides.

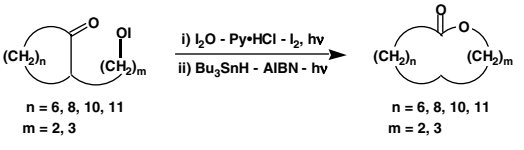

SCHEME 62

(±)-Recifeiolide, a natural 12-membered macrolide, was synthesized from cyclooctanone based on this process, as outlined in Scheme 63.[74]

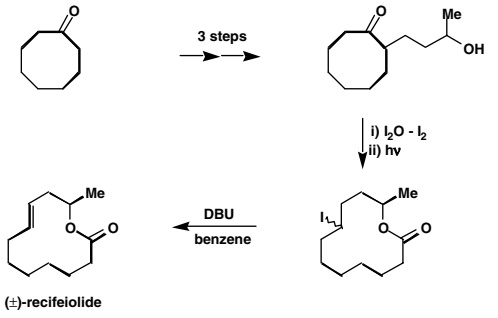

SCHEME 63

The Formation of Cyclic Imides by β-Fragmentation of Bicyclic Carbinolamides

According to Suarez and collaborators, the photolysis of the hypoiodites of certain bicyclic carbinolamids in the presence of DIB-iodine leads to fragmentation to give cyclic imides, as outlined in Scheme 64.[34b,75] The cleavage, however, appears not to be as selective as the cleavage of lactols.

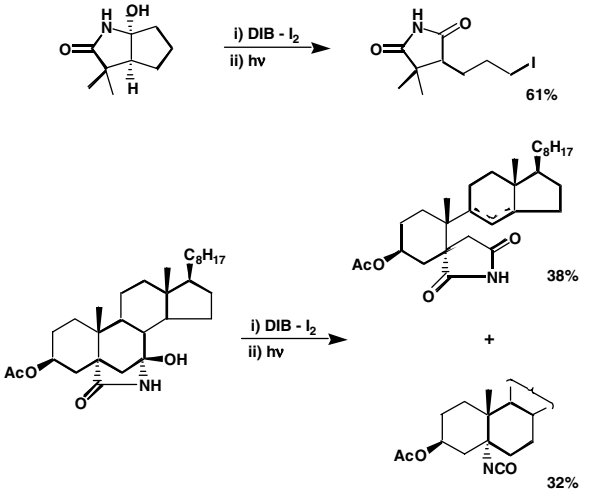

SCHEME 64

The General Synthesis of Medium and Macrocyclic Ketones Based on Ring Expansion by the Photolysis of the Hypoiodites of Bicyclic Alcohols

A medium or macrocyclic ketone can generally be synthesized by selective β-fragmentation of alkoxyl radicals generated from the hypoiodites prepared from catacondensed bicyclic alcohols, analogous to the synthesis of the macrolides mentioned above. The products of the ring expansion are either iodo ketone and/or olefinic ketones (as outlined in general Scheme 65).[76] In contrast to the established ring expansion involving an ionic cleavage, such as retro-Aldolization, the synthesis can be carried out under virtually neutral conditions, and no extra functional group is necessary for the cleavage. Schemes 66 and 67 outline the new synthesis of (±)-muscone[76] and (±)-caryophyllene[77] based on this method as the key step.

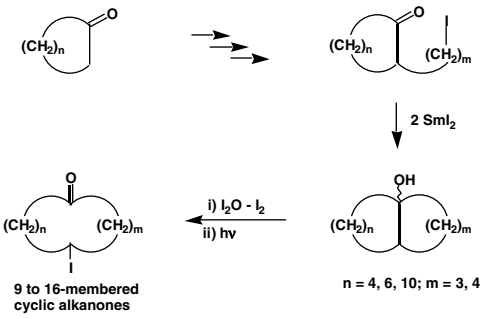

SCHEME 65

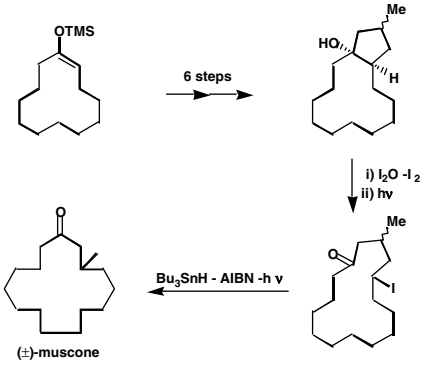

SCHEME 66

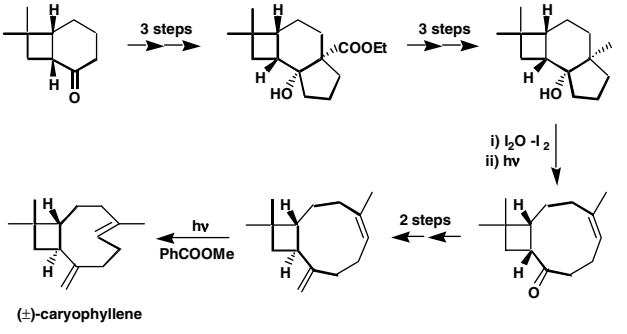

SCHEME 67

An interaction of the intermediate carbon-centered radical (A) with a neighboring carbon-carbon bond in this ring expansion leads to a transannular radical cyclization; the treatment of the unsaturated decanols with (diacetoxyiodo) benzene-iodine followed by irradiation underwent fragmentation of intermediate allyloxy radicals (A) to give the bicyclo[5.3.0]decanones (40–78%) and to give the 7,5,5-tricyclic compound (81%) by way of a "Billiard reaction," as outlined in Scheme 68.[78]

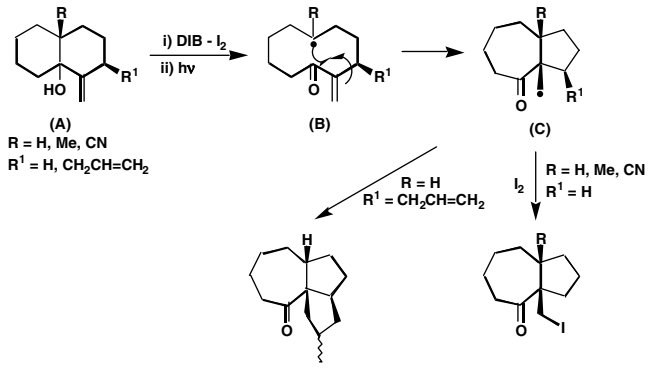

SCHEME 68

It has been reported that, while ring expansion by ionic fragmentation of a bicyclo[3.3.0]octanol could not be achieved, an alkoxyl radical generated from the octanol resulted in a selective β-cleavage of the fused bond to give a functionalized bridged cyclooctane derivative[79] (Scheme 69).

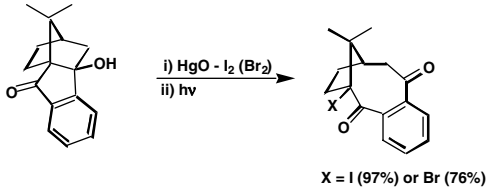

SCHEME 69

The Construction of 5/7, 5/8, 6/7, and 6/8 Bicyclic Systems Based on [2+2]-Photoaddition of Cyclic Enones with Enol Ethers of Cyclic Ketones Followed by a β-Fragmentation of Alkoxyl Radicals Generated from the Resulting Cyclobutanols

Functionalized bicyclo [x.y.0]alkanes (x = 5 or 6; y = 7 or 8) can be synthesized by the irradiation of hypoiodites prepared by [2+2]-photoaddition of cyclic enones with the trimethylsilyl enol ethers of cyclic ketones (as outlined in general in Scheme 70).[80] Scheme 71 outlines the new total synthesis of (±)-α-himachalene based on this method as the key step.[81]

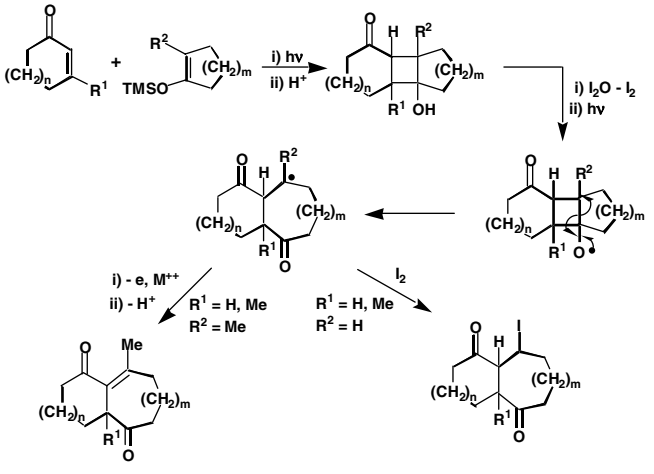

SCHEME 70

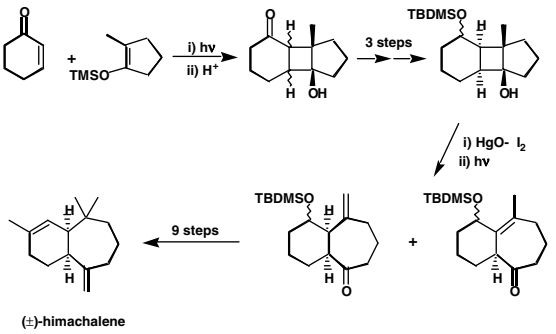

SCHEME 71

Two-Carbon Ring Expansion of Cyclic Ketones through [2+2]-Photoaddition-β-Fragmentation Sequence[82]

Two-carbon ring expansions of the five-, six,- and seven-membered rings of β-indanone, β-tetralone, and β-suberone can be achieved via a sensitized [2+2]-photoaddition of the trimethylsilyl enol ethers of the cyclic ketones with acrylonitrile or methyl acrylate followed by β-fragmentation of the alkoxyl radicals generated from the hypoiodites of the resulting cyclobutanols and mercury(II) oxide-iodine, as outlined in Scheme 72. The ring expansion of the cyclobutanol derived from β-indanone enol ether and acrylonitrile gave an α,β-unsaturated nitrile.

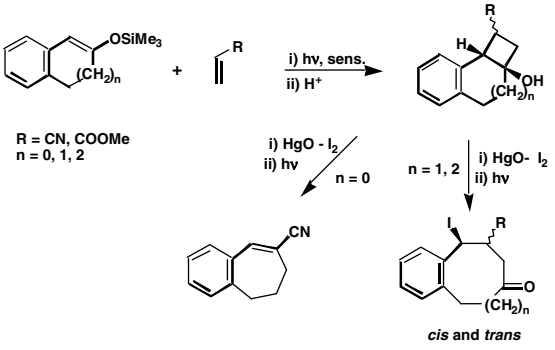

SCHEME 72

Analogous ring expansion via β-fragmentation of cyclobutanoxyl radicals derived from the photoadducts between α- or β-naphthyl trimethylsilyl ether and acrylonitrile or methyl acrylate resulted in the formation of a benzohomotropone after treatment with a base.

Thus, these ring-expansion experiments have confirmed that the β-fragmentation of the cyclobutanoxyl radicals generated from the [2+2]-photoadducts takes place selectively at their ring-fused bonds.

Insertion of Oxygen Atom of Alkoxyl Radical Generated from Fused Cyclic Alcohols by Tandem β-Fragmentation-Cyclization

Suginome and collaborators have found that heterocyclic compounds can be formed by insertion of the oxygen atom of alkoxyl radicals into alicyclic compounds; the insertion takes place through a tandem β-fragmentation-cyclization sequence.

The Formation of Fused Furan Rings via Tandem β-Fragmentation-Cyclization of Cyclobutanoxyl Radicals Generated from [2+2]-Photoadducts Derived from 4-Hydroxycoumarin, 3-(or 4-)-Hydroxyquinolinone or 2-Hydroxynaphthoquinone withA alkenes

The [2+2]-photoaddition of aromatic lactones and lactams with an enolized 1,3-dicarbonyl group with alkenes, followed by photolysis of the hypoiodites generated from the resulting cyclobutanols, induced regioselective β-fragmentation of the corresponding cyclobutanoxyl radicals. This results in a transformation of the cyclobutane rings into furan rings via the incorporation of the alkoxyl oxygen. For example, photolysis of the hypoiodites derived from the [2+2]-photoadducts of 4-hydroxycoumarin (R = H; X = O)[83] or 4-hyroxyquinolin-2(2*H*)-one (R = H; X = NMe)[84a] with alkenes underwent a regioselective β-fragmentation of their non ring-fusion bond to give furocoumarins (X = O), furochromones (X = O), furo[3,2-*e*]quinolin-4-(5H)-ones (X = NMe), and furo [2,3-*b*]quinolin-4(9*H*)-ones (X = NMe), as outlined in Scheme 73.[83,84a] The analogous furanoheterocycles were formed from the [2+2]-photoadduct of 4-hydroxy-1-phenyl- [1,8]-naphthyridin-2(1*H*)-one with alkenes.[84b] The intermediate carbon-centered radical arising from the fragmentation may well be in equilibrium with a resonance-stabilized heteroaromatic radical A. This explains why the observed fragmentation is preferred over ring expansion.

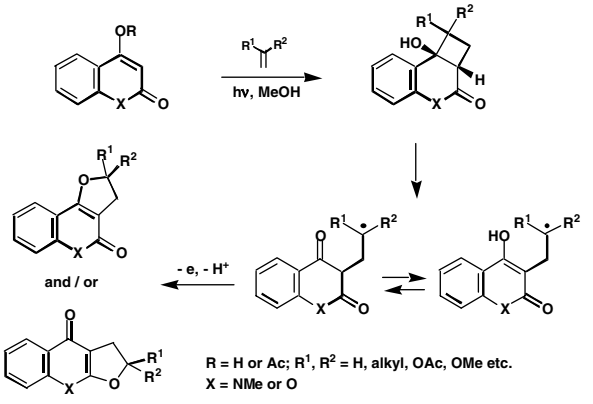

SCHEME 73

The photolysis of the hypoiodites of cyclobutanols derived from the [2+2]-photoadducts of 3-hydroxyquinolin-2(1*H*)-one with alkenes induced β-fragmentation at the outer bonds of the corresponding cyclobutanoxyl radicals to give furo[2,3-*c*]quinolin-4(5*H*)-ones in 5 to 50% yields with an accompanying formation of products arising from a ring expansion, as outlined in Scheme 74.[85]

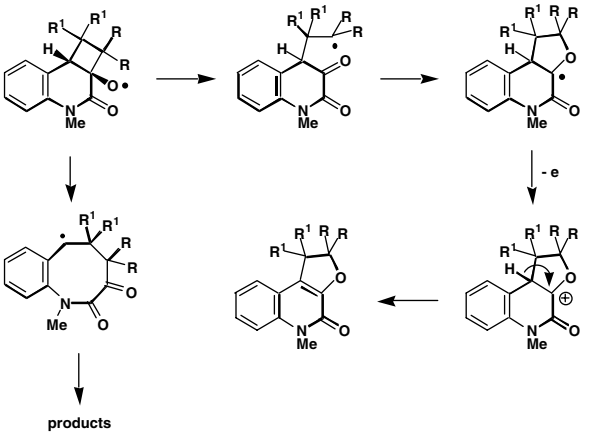

SCHEME 74

The photolysis of the hypoiodite generated from a cyclobutanol derived from the [2+2]-photoaddition of 4-hydroxy-1(2*H*)-isoquinolinone with an electron-deficient alkene in the presence of mercury(II) oxide and iodine resulted in a β-scission at the ring-fusion bond of the cyclobutanoxyl radical to give a 3,6-epoxybenzazocinone derivative in 76% yield (Scheme 75).[86] A weaker aromatic stabilization and destabilization by the cyano substituent in the carbon-centered radical arising from a fragmentation at the non-fusion bond led to ring expansion.

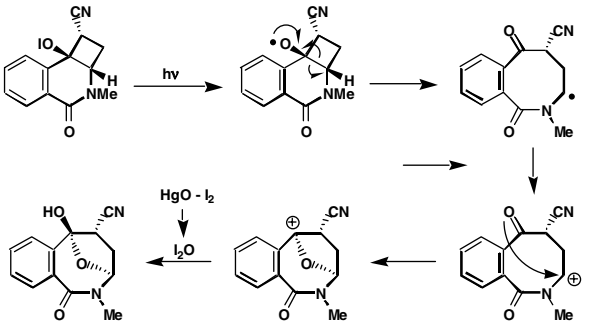

SCHEME 75

The photolysis of the hypoiodites generated from the cyclobutanols, derived from the [2+2]-photoaddition of 2-hydroxynaphthoquinone with alkenes (A) and of 2-aminonaphthoquinone with vinyl arenes (B) in the presence of mercury(II) oxide and iodine induced regioselective β-fragmentations of the cyclobutanoxyl radicals to give a 2,3-dihydronaphtho[2,3-*b*]furan-4,9-dione and its [1,2-*b*]furan-4,5-dione isomer[87](Scheme 76).

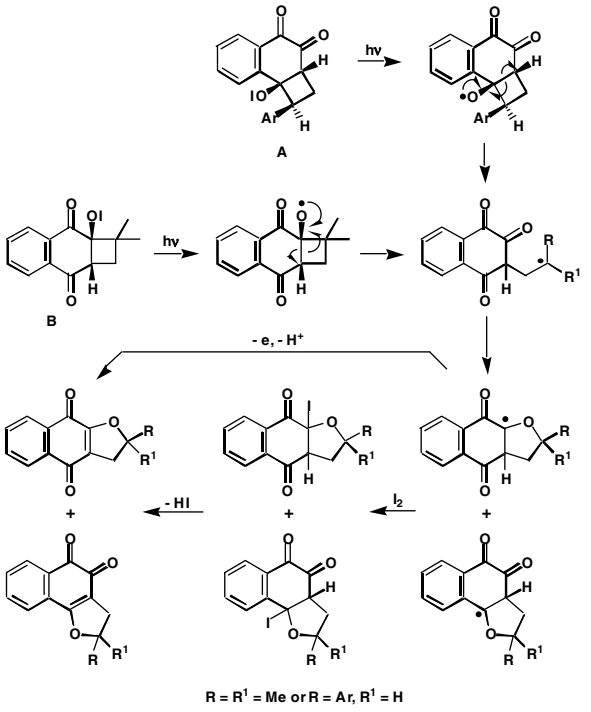

SCHEME 76

The Formation of Cyclic Anhydrides via β-Fragmenation of Steroidal α-Axoalkoxyl Radicals

Irradiation of the hypoiodites of five- or six-membered cyclic α-ketols in the presence of mercury(II) oxide and iodine resulted in the formation of the corresponding cyclic anhydrides or α-hydroxy ε–lactones arising from regioselective β-fragmentation of the bond between the carbonyl and the carbon carrying an alkoxyl radical[88] (Schemes 77 and 78). An ^{18}O labeling study indicated that an oxygen atom in mercury(II) oxide is incorporated in the hydroxy group and the ring oxygen of the hydroxy ε-lactones. A rationalization for the observed incorporation of ^{18}O to the ring in all of the products is outlined in Scheme 79.

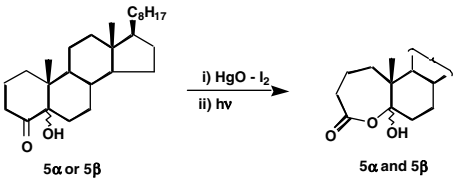

SCHEME 77

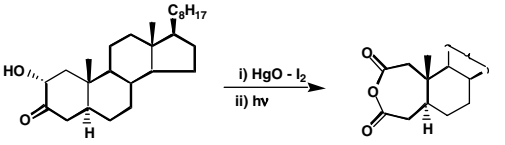

SCHEME 78

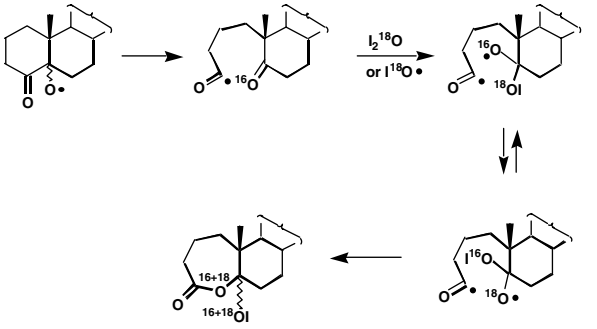

SCHEME 79

New Synthesis of Isobenzofuran-1(3H)-ones (Phthalides) via a Cascade Radical Process Involving Double β-Fragmentation of Alkoxyl Radicals[89]

The photolysis of the hypoiodites of 1-ethylbenzocyclobuten-1-ols, prepared by a treatment of the 1-ols with mercury(II) oxide and iodine gives the corresponding phthalides in good yields (Scheme 80). The pathway is outlined in Scheme 81.[89a] The principal feature of this process is an intramolecular combination of a carbocation or, less likely, a carbon-centered radical with a carbonyl oxygen generated by a regioselective β-fragmentation of the alkoxyl radicals. The photolysis of the hypoiodite of benzocyclobuten-1-ol gives simply a cleaved product; the alkyl group attached to C1 of cyclobutenol is necessary in order to keep the conformation appropriate for cyclization to give the furan ring. The reaction can also be achieved by lead tetraacetate oxidation.[89b] This lactone formation by an expulsion of the alkyl radical was applied to a two-step general synthesis of 3-substituted dihydroisocoumarins from the lactols.[89c]

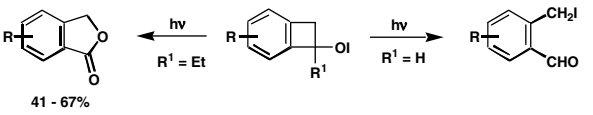

SCHEME 80

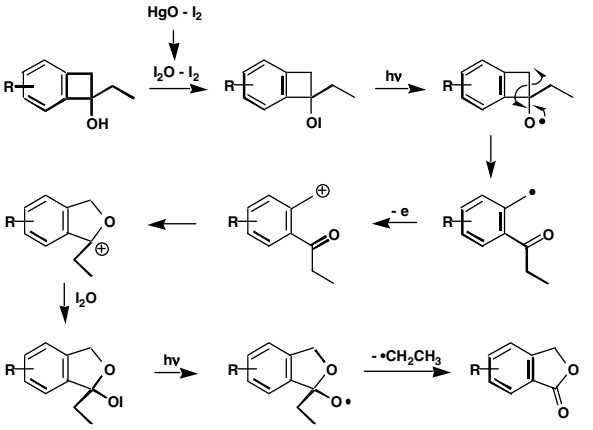

SCHEME 81

1. Synthesis of 3-(ω-iodoalkyl)phthalides.[89a,89b] Scheme 82 outlines the synthesis of phthalides bearing a four- or five-carbon chain at C3 from catacondensed 1,2-dihydrocyclobuten-1-ol hypoiodites.

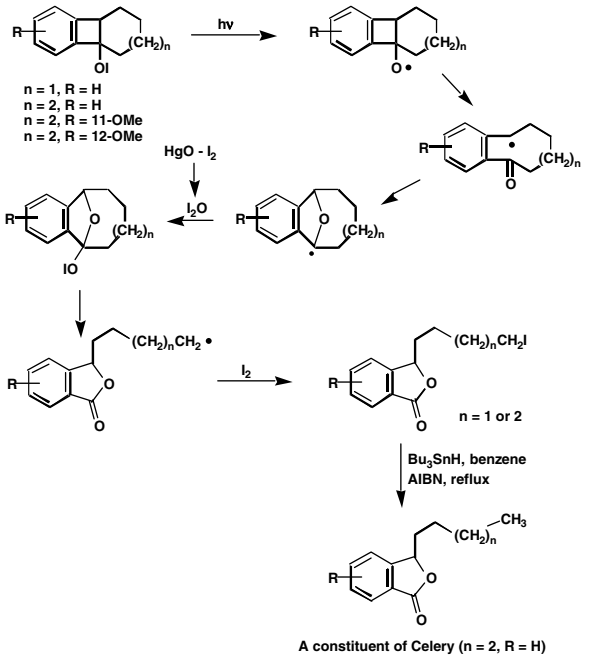

SCHEME 82

2. New synthesis of naphthalide lignans, taiwanin C and justicidin E.[90] Scheme 83 outlines a new synthesis of taiwanin C and justicidin E based on the cascade β-fragmentation strategy.

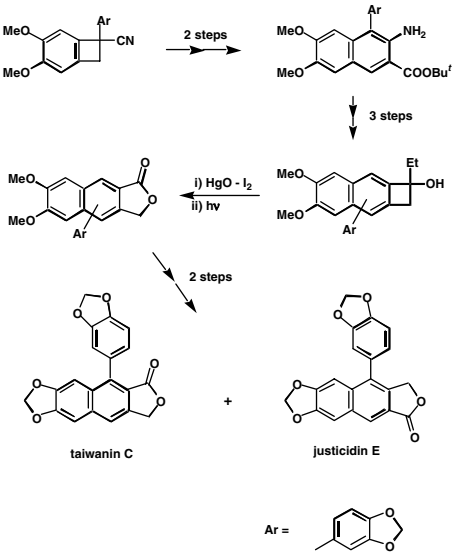

SCHEME 83

Oxygen Insertion by Tandem β-Fragmentation-Cyclization of Alkoxyl Radicals

Oxasteroids arising from tandem β-fragmentation and cyclization are products in the photolysis of the hypoiodites generated from 3-hydroxy-Δ^5-steroids and lead tetraacetate-iodine, as outlined in Scheme 84. The path of the formation of the oxasteroids is outlined in Scheme 85; one-electron oxidation of the intermediate radicals arising from the cyclization of allylic radicals generates the oxonium ions, which trap acetic acid to give the products.[91]

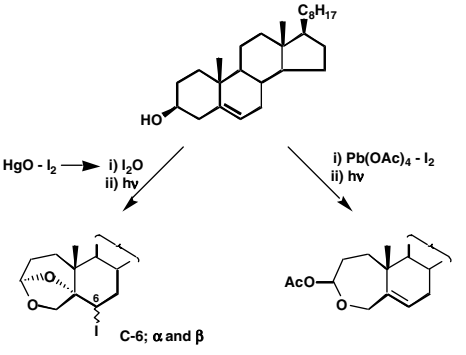

SCHEME 84

On the other hand, when mercury (II) oxide instead of lead tetraacetate is used to generate the hypoiodites, 3a,5-epoxy-4-oxa-A-homo-5a-steroids are the products, as outlined in Scheme 84. An ^{18}O labeling study using $Hg^{18}O$ and iodine and an analysis of the extent of ^{18}O incorporation by mass spectrometry showed that the oxygen of mercury (II) oxide is incorporated into the epoxy oxygen of the products (31–61%).[92] Based on these labeling results, the pathway of the formation is rationalized as outlined in Scheme 85.

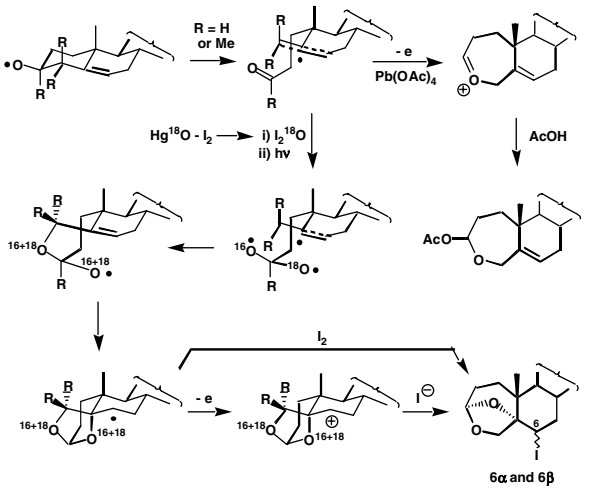

SCHEME 85

Intramolecular Additions of Alkoxyl Radicals to Carbon–Carbon Double Bonds

The intramolecular additions of alkoxyl groups to carbon–carbon double bonds to give β-iodo-alkyl ethers from alkyl hypoiodites under photolytic conditions have been reported. Suginome and collaborators found that the formation of α-iodoepoxides arising from an intramolecular α, β-addition of an allylic alkoxyl radical is a major general process in the photolysis of tertiary and some secondary allylic alcohol hypoiodites in the presence of mercury (II) oxide and iodine in benzene.[93] Thus, 5-hydroxy-5β-cholest-3-ene gave epimeric α-iodoepoxides in a ratio of 10:1 in 86% yield as outlined in Scheme 86. Similar reaction of 1-alkylcyclohex-2-en-1-ols gave a mixture of *cis*- and *trans*-α-iodoepoxides (Scheme 87). The addition of pyridine dramatically enhanced the yield of the addition product. The yields of the α-iodoepoxides obtained from the photolysis of 1-alkylcyclohex-2-en-1-ols and the ratios of *cis*- to *trans*-isomers are summarized in Table 109.1.

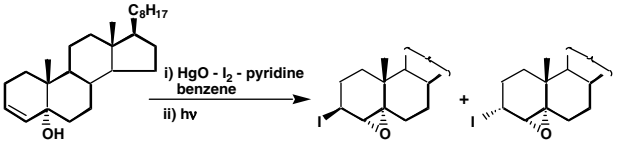

SCHEME 86

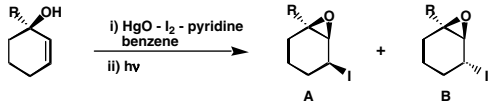

SCHEME 87

It has been reported that epoxides arising from an intramolecular γ,δ–*trans*-additions of homoallylic alkoxyl group are the major products in the photolysis of the hypoiodites of several seven-membered cyclic steroidal homoallylic alcohols, such as *A*-homocholest-4a-ene-3-ols,[94] *A*-homo-5α–cholest-1-en-4-ols,[95] and *B*-homocholest-5-en-7a-ols[93] in the presence of mercury (II) oxide and iodine in benzene;

TABLE 109.1 Ratio of A:B Combined Yield(%)

Me	1:0	61
Bu	5:1	99
Bu^t	7:1	46
Ph	4:1	84

the irradiation of the hypoiodites of 3α- and 3β-methyl-*A*-homo-4a-cholesten-3-ols in the presence of mercury(II) oxide-iodine gave 3α,5-epoxy-3β-methyl-4aβ-iodo-*A*-homo-5β-cholestane and its 3β,5-epoxy isomer in high yields, as outlined in Scheme 88.[96]

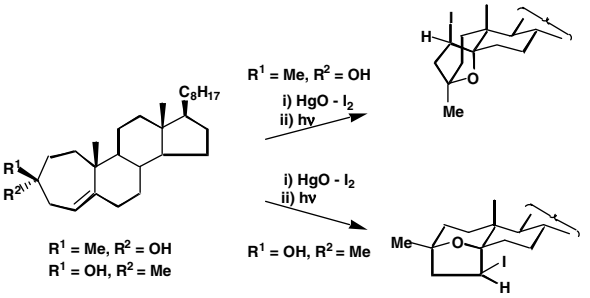

SCHEME 88

The steric effects for the addition *vs* the β-fragmentation pathway seems to be of importance. Thus, irradiation of the hypoiodites of a sesqiterpene, widdrol, which has a structural unit corresponding to the A- and B-rings of 3 methyl-*A*-homo-4a-cholesten-3β-ol, except that it has *gem*-dimethyl groups on the carbon corresponding to C6 of the steroids, resulted in exclusive β-fragmentation of the corresponding 3β-alkoxyl radical and gave a cyclic ether having iodine, but no products from intramolecular addition were formed[97] (Scheme 89). The sharp contrast in the results obtained for the steroids can be rationalized in terms of steric effects. Thus, a transition state leading to the rigid intermediate radical involves a 1,3-diaxial interaction between the angular methyl and one of the *gem*-dimethyl groups; therefore, the addition would be slower and result in the observed β-fragmentation.

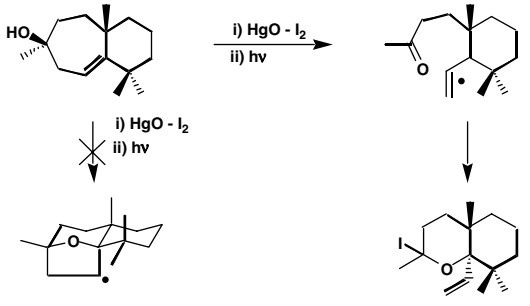

SCHEME 89

It has been reported that *t*-butyl hypoiodite adds to alkenes via a bridged iodonium ion intermediate in a *trans* manner in benzene to give β-iodo-ethers in the dark.[98] Unlike the addition in nitrite photolysis,[17] thermal ionic additions may take place in hypoiodite photolysis. The additions in the steroids, even under photolytic conditions, can be rationalized in terms of an ionic *trans*-addition of alkyl hypoiodites via bridged iodonium ions, although a homolytic mechanism cannot be excluded.

Intramolecular heterolytic additions of the hypoiodites of bishomoallyl alcohols *under photolytic conditions* have been proved:[99] while alkoxyl radicals generated from the photolysis of steroidal bishomoallyl alcohol nitrite resulted in products arising from a β-fragmentation, the corresponding hypoiodite in the presence of mercury (II) oxide and iodine in benzene at room temperature in the dark and in the photolysis gave a spirotetrahydrofuran derivative that arose from addition via bridged iodonium ions in high yield, as outlined in Scheme 90. Thus, if the double bonds are appropriately located, the ionic intramolecular addition is preferred to the β-fragmentation, even in the photolysis of hypoiodites of alcohols, such as steroidal 17β-ols,[50] which form alkoxyl radicals very susceptible to β–fragmentation.

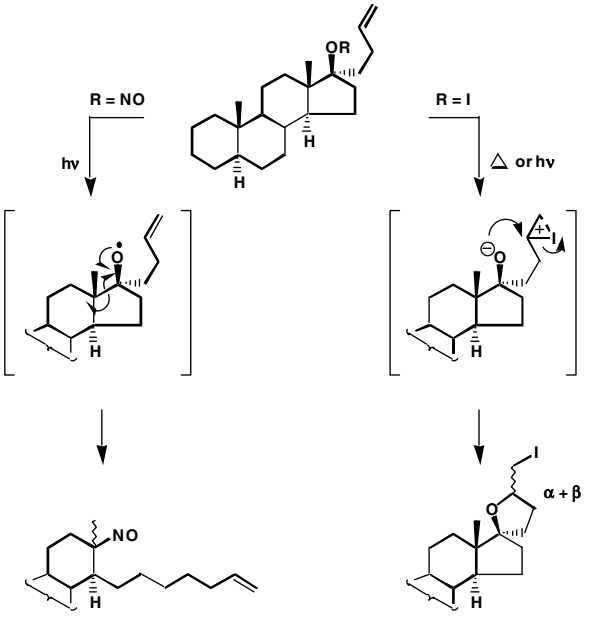

SCHEME 90

Reaction of Iminoxyl Radicals

Horspool and collaborators recently found that the irradiation of β, γ–unsaturated oximes in benzene in the presence of either HgO-I_2 or DIB-I_2 resulted in the formation of a *peri*-naphthisoxazoles in 55 to 77% yields, as outlined in Scheme 91.[100] The path of the formation involves the generation of an iminoxyl radical formed from a homolytic fission of the OI bond of the oxime hypoiodites, followed by its intramolecular cycloaddition to the aryl group to afford the product.[100]

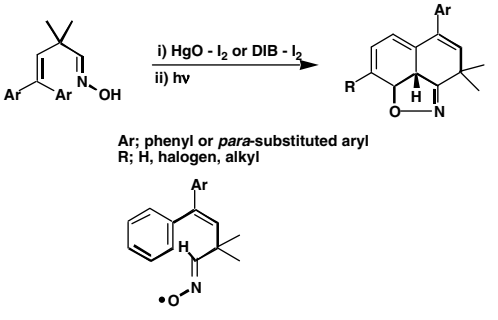

SCHEME 91

109.4 Conclusions

The past half a century has witnessed that alkoxyl radicals are highly reactive, unique chemical species and are as important and useful as carbon-centered radicals in organic synthesis. The usefulness of intramolecular hydrogen abstraction and β-fragmentation of alkoxyl radicals in synthesis is believed to be comparable to the intramolecular addition of carbon-centered radicals. This chapter is an attempt to bring together the diverse photochemical reactions of hypohalites, which are the most powerful and convenient precursors of alkoxyl radicals.

Acknowledgment

The author wishes to thank Dr. H. Senboku for his kind assistance in preparing diagrams.

References

1. For reviews, see (a) Anbar, M. and Ginsburg, D., Organic hypohalites, *Chem. Rev.,* 54, 925, 1954; (b) Heusler, K., and Kalvoda, J., Selective functionalisation of the angular methyl group and further transformation to 19-norsteroids, in *Organic Reactions in Steroid Chemistry*, Fried, J. and Edwards, J.A., Eds., van Nostrand Reinhold, New York, 1972, chap. 12.
2. Sandmeyer, T., Üeber den Aethylester der Unterchlorigen Säure, *Ber.*, 18, 1767, 1885; Üeber Aethyl- und Methylhypochlorit, *Ber.,* 19, 857, 1886.
3. Chattaway, F.D. and Backeberg, O.G., Alkyl hypochlorites, *J. Chem., Soc.*, 2999, 1923.
4. For a review, see Walling, C., *Free Radicals in Solution*, Wiley, New York, 1957, 388.
5. Kenner, J., Oxidation and reduction in chemistry, *Nature*, 156, 370, 1945; Teeter, H.M., Bachman, R.C., Bell.E.W., and Cowan, J.C., Reactions of *t*-butyl hypochlorite with vegetable oils and derivatives, *Ind. Eng. Chem.*, 41, 849, 1949.
6. (a) Walling, C. and Jacknow, R.B., Positive halogen compounds. I. The radical chain halogenation of hydrocarbons by *t*-butyl hypochlorite, *J. Am. Chem. Soc.*, 82, 6108; (b) Walling, C. and Jacknow, R.B., Positive halogen compounds. II. Radical chlorination of substituted hydrocarbons with *t*-butyl hypochlorite, *J. Am. Chem. Soc.,* 82, 6113, 1960.
7. (a) Walling, C. and Thaler, W., Positive halogen compounds. III. Allylic chlorination with *t*-butyl hypochlorite. The stereochemistry of allylic radicals, *J. Am. Chem. Soc.*, 83, 3877, 1961; (b) Walling, C. and Fredricks, P.S., Positive halogen compounds. IV. Radical reactions of chlorine and *t*-butyl hypochlorite with some small ring compounds, *J. Am. Chem. Soc.*, 84, 3326, 1962; (c) Walling, C. and Padwa, A., Positive halogen compounds. V. *t*-Butyl hypobromite and two new techniques for hydrocarbon bromination, *J. Org. Chem.*, 27, 2976, 1962.
8. Walling, C. and Padwa, A., Positive halogen compounds. VI. Effects of structure and medium on the β-scission of alkoxyl radicals, *J. Am. Chem. Soc.*, 85, 1593, 1963 and subsequent papers.
9. Greene, F.D., Savitz, M.L., Osterholtz, F.D., Lau, H.H., Smith, W.N., and Zanet, P.M., Decomposition of tertiary alkyl hypochlorites, *J. Org. Chem.*, 28, 55, 1963.
10. (a) Kochi, J.K., Chemistry of alkoxyl radicals: cleavage reactions, *J. Am. Chem. Soc.*, 84, 1193, 1962; (b) Bacha, J.D. and Kochi, J.K., Polar and solvent effects in the cleavage of *t*-alkoxyl radicals, *J. Org. Chem.*, 30, 3272, 1965.
11. Kochi, J.K., Oxygen radicals, in *Free Radicals*, Vol II, Kochi, J.K., Ed., Wiley, New York, 1973, chap. 23.
12. Akhtar, M. and Barton, D.H.R., Reactions at position 19 in the steroid nucleus. A convenient synthesis of 19-norsteroids, *J. Am. Chem. Soc.*, 86, 1528, 1964.
13. Meystre, Ch., Heusler, K., Kalvoda, J., Wieland, P., Anner, G., and Wettstein, A., Neue Substitutionsreactionen bei Steroiden, *Experientia*, 17, 475, 1961.
14. For reviews, see (a) Heusler, K. and Kalvoda, J., Intramolecular free-radical reactions, *Angew. Chem. Int. Ed. Engl.,* 3, 525, 1964; (b) Kalvoda, J. and Heusler, K., Die Hypoiodit-Reaction, *Synthesis*, 549, 1971.

15. Mills, J.S. and Petrow, V., The rearrangement of steroid hypochlorites: Preparation of 6-methylandrost-5-ene-3β,17β,19-triol, *Chem. Ind. (London)*, 946, 1961.
16. Barton, D.H. R., Geller, J.M., and Pechet, M.M., A new photochemical reaction, *J. Am. Chem. Soc.,* 83, 4076, 1961.
17. See Chapter 102 in this book.
18. Walling, C. and Padwa, A., Intramolecular chlorination with long chain hypochlorites, *J. Am. Chem. Soc.*, 83, 2207, 1961.
19. Jenner, E.L., Intramolecular hydrogen abstraction in primary alkoxyl radical, *J. Org. Chem.*, 27, 1031, 1962.
20. Mihailovic, M.L., Cekovic, Z., and Stankovic, J., Oxidation with metal oxide-halogen reagents. Cyclization of primary and secondary aliphatic alcohols to tetrahydrofurans, *J. Chem. Soc., Chem. Commun.,* 981,1969.
21. Akhtar, M., Organic nitrites and hypohalites, in *Advances in Photochemistry*, Vol. 2, Noyes, W.A. Hammond, G.S., and Pitts, Jr., J.N., Eds., Interscience, New York, 1964.
22. Suginome H., New developments in photoinduced radical reactions in organic synthesis, in *Modern Methodology in Organic Synthesis*, Shono, T. Ed., Kodansha, Tokyo, 1992, 245.
23. (a) Concepcion, J.I., Francisco, C.G., Hernandez, R., Salazar, J.A., and Suarez, E., Intramolecular hydrogen abstraction. Iodosobenzene diacetate, an efficient and convenient reagent for alkoxy radical generation, *Tetrahedron Lett.*, 25, 1953, 1984; (b) de Armas, P., Concepcion.J.I., Francisco, C.G., Hernandez, R., Salazar, J.A., and Suarez, E., Intramolecular hydrogen abstraction. Hypervalent organoiodine compounds, convenient reagents for alkoxyl radical generation, *J. Chem. Soc., Perkin Trans. 1*, 405, 1989. and their subsequent papers.
24. Anbar, M. and Dostrovsky, *I.,* Ultraviolet absorption spectra of some organic hypohalites, *J. Chem. Soc.*, 1105, 1954.
25. Gray, P. and Williams, A., The thermochemistry and reactivity of alkoxyl radicals, *Chem. Rev.*, 59, 539, 1959.
26. Teeter, H.M. and Bell, E.W., *t*-Butyl hypochlorite, *Organic Synthesis*, 32, 20, 1952.
27. c.f. Remaiah, M., Radical reactions in organic synthesis, *Tetrahedron*, 43, 3541, 1987.
28. Brun, P. and Waegell, B., Heterocyclization intramoleculaire d'alcools possedant un squelette cedranique. Oxydation par l'oxide de mercure et le brome, *Tetrahedron,* 32, 1137, 1976.
29. (a) Brenschende, W. and Schumaker, H., Über das bromoxyd Br_2O, *Z. Physikal. Chem.*, 29B, 356, 1935; (b) Brenschede, W. and Schumaker, H.J., Über die Darstellung und einige Eigenshaften eines bromoxyds von der formel Br_2O, *Z. Anorg. Chem.,* 226, 370, 1936; (c) Jennings, P.W. and Ziebarth, T.O., On the mechanism of the modified Hunsdieker, *J. Org. Chem.*, 34, 3216, 1969.
30. Suginome, H., Mercury(II) oxide/bromine, in *Encyclopedia of Reagents for Organic Synthesis*, Paquette, L.A., Ed., Wiley, Chichester,1995, 3260.
31. Forbes, C.P., Goosen, A., and Laue, H.A.H., Hypoiodite reaction: the reaction of mercuric oxide-iodine reagent with olefins, *J. S. African Chem. Inst.*, 25, 144, 1972; Forbes, C.P., Goosen, A., and Laue, H.A.H, Hypoiodite reaction: mechanism of the reaction of mercury(II) oxide-iodine with olefins, *J. Chem. Soc., Perkin Trans. 1,* 2346, 1974.
32. Chen, E.M., Keefer, R.M., and Andrews, L.J., *J. Am. Chem. Soc.*, 89, 428, 1967.
33. Anbar, M. and Dostrovsky, I., A kinetic study of the formation and hydrolysis of *t*-butyl hypochlorite, *J. Chem. Soc.*, 1094, 1954.
34. (a) Dorta, R.L., Francisco, C.G., Freire, R., and Suarez, E., Intramolecular hydrogen abstraction. The use of organoselenium reagents for the generation of alkoxyl radicals, *Tetrahedron Lett.,,* 29, 5429, 1988; (b) Dorta, L., Francisco, C.G., and Suarez.E., A selenurane derivative promotes β-fragmentation of carbinolamides leading to cyclic imides, *Tetrahedron Lett.,* 35, 1083, 1994.
35. Bensadoun, N., Brun, P., Casanova, J., and Waegell, B., Stereoelectronic control in the β-fragmentation reaction of alkoxyl radicals. An empirical predictable rule, *J. Chem. Res. (S)*, 236, 1981 and *(M)*, 2601, 1981.

36. Heusler, K., Kalvoda, J., Wieland, P., Anner, G., and Wettstein, A., Reactionen von Steroid-Hypoioditen. IV. Über den Verlauf intramolecularer Substitutions Reactionen, insbezondere bei 2β- and 4β-Hydroxysteroiden, *Helv. Chim. Acta,* 45, 2575, 1962.
37. Meystre, Ch., Heusler, K., Kalvoda, J., Wieland, P., Anner, G., and Wettstein, A., Reactionen von Steroid-Hypoioditen. II. Über die Herstellung 18-oxygenierter Pregnenverbindungen, *Helv. Chim. Acta,* 45, 1317, 1962.
38. (a) Suginome, H., Yonekura, N., and Masamune, T., The transformation of jervine into 18-functional C-nor-D-homosteroids, *Bull. Chem. Soc. Jpn.,* 53, 210, 1980; (b) Suginome, H., Ono, H., and Masamune, T., The transformation of jervine into 18-functional *D*-homo-*C*-norsteroids. IV. The transformation of jervine into (20 *R*)-18, 20β-epoxy-3β-hydroxy-17β-ethyletiojervan-18-one 3-acetate via (20 *R*)-18, 20β-epoxy-3β-hydroxy-12α, 17β ethyletiojervan-11-one 3-acetate, *Bull. Chem. Soc. Jpn.,* 54, 852, 1981.
39. (a) Wenkert, E. and Mylari, B.L., Intramolecular, long-range oxidation at saturated carbon centers, *J. Am. Chem. Soc.*, 89, 174, 1967; (b) Ceccherelli, P., Curini, M., Marcotullio, M.C., Mylari, B.L., and Wenkert, E., Iodohydrins and tetrahydrofurans from lead tetraacetate-iodine oxidation of terpenic alcohols, *J. Org. Chem.*, 51, 1505, 1986; (c) Dorta, R.L., Francisco, C.G., Hernandez, R., Salazar, J., and Suarez, E., Intramolecular hydrogen abstraction,(Diacetoxyiodo)benzene, a useful reagent for the remote functionalization of non-activated carbon atoms, *J. Chem. Res.(S)*, 240, 1990; (*M*), 1836, 1990.
40. (a) Kalvoda, J., Meystre, Ch., and Anner, G., Reactionen von Steroid-Hypoioditen. VIII. 1,4-Verschiebung der Nitrilgruppe (18-Cyano-pregnane), *Helv. Chim. Acta,* 49, 424, 1966; (b) Kalvoda, J., Reaction von Steroid-Hypoioditen. IX. Beitrag zum Mechanisms der oxydativen Cyanhydrin-Cyanketon-Umlagerung, *Helv. Chim. Acta,* 51, 267, 1968; (c) Kalvoda, J., A new type of intramolecular group-transfer in steroid photochemistry. A contribution to the mechanism of the oxidative cyanohydrin–cyano-ketone rearrangement, *J. Chem. Soc., Chem. Commun.*, 1003, 1970.
41. Orito, K., Satoh, S., and Suginome, H., Photoinduced transformations. 153. Long-range intramolecular hydroxylation of C(25) of the cholestane side chain, *J. Chem. Soc., Perkin Trans. 1*, 63, 1995.
42. (a) Orito, K., Ohto, M., and Suginome, H., A long-range intramolecular functionalization by alkoxyl radicals; a long-range intramolecular oxygenation of C(15) of the androstane skeleton, *J. Chem. Soc., Chem. Commun.*, 1074, 1990; (b) A Wagner-Meerwein rearrangement of the cholestane skeleton induced by a long-range intramolecular hydrogen abstraction by alkoxyl radicals; the first example of long-range intramolecular addition of an alkoxyl radical to a carbon-carbon double bond, *J. Chem. Soc., Chem. Commun.*, 1076, 1990; (c) Orito, K., Ohto, M., Sugawara, N., and Suginome, H., Long-range intramolecular functionalization by alkoxyl radicals; long-range intramolecular double functionalization of ring C of cholestane and androstane skeletons, *Tetrahedron Lett.*, 31, 5921, 1990.
43. Mihailovic, M.L. and Miloradovic, M., The reaction of lead tetraacetate with some acyclic hydroxyethers, *Tetrahedron*, 22, 723, 1966.
44. (a) Baker, R. and Brimble, M.A., Chemistry of bis-spiroacetals. Synthesis of the 1,6,8-trioxadispiro [4.1.5.3] pentadecane ring system, *J. Chem. Soc., Perkin Trans. 1*, 125, 1988; (b) Baker, R., Brimble, M.A., and Robinson, J.A., Determination of the stereochemistry of 2,2,-dimethyl-1,6,8-trioxadispiro(4.1.5.3)pentadec-13-ene formed by two sequential cyclization reactions using high field ^{1}H NMR. spectroscopy, *Tetrahedron Lett.*, 26, 2115, 1985; (c) Brimble, M.A., Williams, G.M., and Baker, R., Chemistry of bis-spiroacetals: Synthesis of *cis*- and *trans*-1-(2-methyl-1,6,8-trioxadispiro[4.1.5.3]pentadec-13-en-2-yl) methanol, *J. Chem. Soc., Perkin Trans. 1*, 2221, 1991. (d) Brimble, M.A. and Williams, G.M., Synthesis of the bis-spiroacetal moiety of 17-epi-20-deoxysalinomycin, *J. Org. Chem.*, 57, 5818, 1992.
45. Furuta, K., Nagata, T., and Yamamoto, H., A direct synthesis of cyclic acetals from β– or γ-hydroxyethers by means of C-H activation, *Tetrahedron Lett.,* 29, 2215, 1998.

46. Suginome, H., Satoh, G., Wang, J.B., Yamada, S., and Kobayashi, K., Photoinduced molecular transformations. 106. The formation of cyclic anhydrides via regioselective β-scission of alkoxy radicals generated from 5- and 6-membered α-hydroxy cyclic ketones, *J. Chem. Soc., Perkin Trans. 1*, 1239,1990.
47. (a) Martin, A., Salazar, J.A., and Suarez, E., Synthesis of chiral spiroacetals from carbohydrates, *J. Org. Chem*., 61, 3999, 1996; (b) Dorta, R.L., Martin, A., Salazar, J.A., Suarez, E., and Prange, T., Synthesis of chiral dispiroacetals from carbohydrates, *J. Org. Chem*., 63, 2251, 1998.
48. Gimisis, T., Castellari, C., and Chatgilialoglu, C., A new class of anomeric spironucleosides, *J. Chem. Soc., Chem. Commun.,* 2089, 1997.
49. Shibuyama, M., Jaishi, F., and Eschenmoser, A., A fragmentation approach to macrolides: (5-*E*, 9-*E*)-6-methyl-5,9-undecadien-11-olide, *Angew. Chem. Int. Ed. Engl.,* 18, 635, 1979.
50. (a) Suginome, H. and Yamada, S., Photoinduced transformations. 73. Transformations of five-(and six-) membered cyclic alcohols into five-(and six-) membered cyclic ethers — A new method of a two-step transformation of hydroxysteroid into oxasteroid, *J. Org. Chem*., 49, 3753, 1984; (b) Suginome, H. and Nakayama, Y., Photoinduced molecular transformations. 132. A two-step intramolecular transposition of the 17β-acetyl group of pregnan-20-one to C-18 through the formation of cyclobutanols by the reaction of the excited carbonyl, followed by a selective β-scission of alkoxyl radicals generated from them, *J. Chem. Soc., Perkin Trans. 1,* 1843, 1992.
51. (a) Suginome, H., Yamada, S., and Miyaura, N., Mechanism of the photoinduced rearrangement of 5α-androstan-17β-ol hypoiodite to 13α- and 13β- formyloxy-16-iodo-13,16-seco-*D*-nor-5α-androstane in the presence of HgO and I_2. An ^{18}O labeling study, *Chem. Lett.,* 55, 1983; (b) Suginome, H. and Senboku, H., Photoinduced molecular transformations. 154. On the mechanism of the formation of the 5-iodopentyl formate in the photolysis of cyclopentanol hypoiodite in solution in the presence of mercury(II) oxide-iodine, *Tetrahedron*, 50, 13101,1994.
52. (a) Suginome, H. and Kondoh, T., Photoinduced molecular transformations. 136. Reactions of alkoxyl radicals generated from hypoiodites of 3β-hydroxy-7-oxo-Δ^5-steroids. Synthesis of some functionalized oxasteroids, *J. Chem. Soc., Perkin Trans. 1*, 3119, 1992; (b) Suginome, H. and Yamada, S., Synthesis of some five- and six-membered oxasteroids of cholestane series by ring contraction and the mass spectrometric fragmentation of oxasteroids, *Bull. Chem. Soc. Jpn.,* 60, 3453, 1987.
53. Suginome, H. and Yamada, S., Photoinduced transformations. 77. A four-step substitution of a carbonyl group of steroidal ketones by an oxygen atom. A new method for the synthesis of cyclic ethers, *J. Org. Chem*., 50, 2489, 1985.
54. Suginome, H. and Yamada, S., The replacement of the carbonyl group of adamantanone by an oxygen or sulfur atom and the one-step transformation of 2-methyladamantan-2-ol into 2-oxaadamantane; An efficient new synthesis of 2-oxa- and 2-thiaadamantane, *Synthesis,* 741, 1996.
55. Suginome, H. and Yamada, S., Replacement of a carbonyl group of camphor by an oxygen atom. Synthesis of 1,7,7,-trimethyl-2-oxabicyclo [2,2,1] heptane, *Bull. Chem. Soc. Jpn.,* 58, 3055, 1985.
56. Nicoletti, D., Ghini, A.A., Brachet-Cota, A.L., and Burton, G., Simple synthetic approach to 6-oxasteroids. Synthesis of 6-oxa-5β-pregnane-3,20-dione, *J. Chem. Soc., Perkin Trans. 1,* 1089, 1995.
57. (a) Suginome, H., Orito, K., Yorita, K., Ishikawa, M., Shimoyama, N., and Sasaki, T., Photoinduced molecular transformations.157. A new stereo and regioselective synthesis of 2,6-diaryl-3,7-dioxabicyclo-[3.3.0] octane lignans involving a β-scission of alkoxyl radicals as the key step. New total synthesis of (±)-sesamin,(±)-eudesmin, and (±)-yangambin, *J. Org. Chem*, 60, 3052, 1995; (b) Orito, K., Sasaki, T., and Suginome, H, Photoinduced molecular transformations. 158. A total synthesis of (±)-methyl piperitol: an unsymmetrically substituted 2,6-diaryl-3,7-dioxabicyclo [3.3.0] octane lignan, *J. Org. Chem*., 60. 6208, 1995.
58. (a) Suginome, H., Senboku, H., and Yamada, S., Photoinduced molecular transformations. 112. Transformation of steroids into ring-A-aromatized steroids and 19-norsteroids involving a regioselective β-scission of alkoxyl radicals : synthesis of two marine natural products, 19-nor-5α-cholestan-3β–ol and 19-norcholest-4-en-3-one, and new synthesis of estrone and 19-nortestosterone, *J. Chem. Soc., Perkin Trans. 1*, 2199, 1990; (b) Suginome, H., Nakayama, Y., and Senboku, H.,

Photoinduced molecular transformations. 131. Synthesis of 18-norsteroids. deoxofukujusonorone and the related steroids, based on a selective β-scission of alkoxyl radicals as the key step, *J. Chem. Soc., Perkin Trans. 1*, 1837, 1992.

59. Kobayashi, K., Minakawa, H., Sakurai, H., Kujime, S., and Suginome, H., Photoinduced molecular transformations. 144. One-carbon intercalation of γ- and δ-lactones involving the β-scission of alkoxy radicals as the key step: synthesis of δ- and ε-lactones with α-substituents, *J. Chem. Soc., Perkin Trans. 1,* 3007, 1993.
60. Suginome, H. and Wang, J.B., Photoinduced molecular transformations. 113. One-step transformations of cyclic ethers into ω-iodoalkyl formates and of aldehyde cyclic acetals into monoesters of α,ω-alkanediols by iodoxyl radical*, J. Chem. Soc., Perkin Trans. 1*, 2825, 1990.
61. (a) Suginome, H. and Wang, J.B., Replacement of an 11-carbonyl group of 11-oxo steroide by an oxygen atom. A new partial synthesis of 11-oxaprogesterone, *Bull. Chem. Soc. Jpn.*, 62, 193, 1989; (b) Suginome, H., Yamada, S., and Wang, J.B., Photoinduced molecular transformations. 107. A versatile substitution of a carbonyl group of steroidal ketones by a heteroatom. The synthesis of aza, oxa-, thia-, selena- and tellurasteroids, *J. Org. Chem.,* 55, 2170, 1990; (c) Suginome, H. and Wang, J.B., Transformation of epiandrosterone into 3-oxa-,3-thia-, 3-selena-,and 3-aza-17-oxaandrostanes of the 5α-series based on β-scission of alkoxyl radicals, *Steroids*, 55, 353, 1990.
62. Armas, d.P., Francisco, C.G., and Suarez, E, Reagents with hypervalent iodine: formation of convenient chiral synthetic intermediates by fragmentation of carbohydrate anomeric alkoxy radicals, *Angew. Chem. Int. Ed. Engl.*, 31, 772, 1992.
63. Armas, D.P., Francisco, C.G., and Suarez, E., Fragmentation of carbohydrate anomeric alkoxyl radicals. Tandem β-fragmentation-cyclization of alcohols, *J. Am. Chem. Soc.*, 115, 8865, 1993.
64. Dorta, R.L., Francisco, C.G., and Suarez, E, Organoselenium reagents in the tandem β-fragmentation-cyclization of carbohydrate anomeric alkoxyl radicals, *Tetrahedron Lett.,* 35, 2049, 1994.
65. Francisco, C.G., Martin C.G., and Suarez, E., Fragmentation of carbohydrate anomeric alkoxyl radicals. A new general method for the synthesis of alduronic lactones, *J. Org. Chem.*, 63, 2099, 1998.
66. Francisco, C.G., Freire, R., Gonzalez, C.C., and Suarez, E., Fragmentation of carbohydrate anomeric alkoxy radicals. Synthesis of azasugars, *Tetrahedron Asymm.*, 8, 1971, 1997.
67. Hernandez, R., Leon, E.I., Moreno, P., and Suarez, E, Radical fragmentation of β-hydroxy azides. Synthesis of chiral nitriles, *J. Org. Chem.*, 62, 8974, 1997.
68. Kobayashi, K., Sasaki, A., Kanno, Y., and Suginome, H., A new route to γ-substituted γ-lactones and δ-lactones based on the regioselective β-scission of alkoxyl radicals generated from transannular hemiacetals, *Tetrahedron*, 47, 7245, 1991.
69. Suginome, H. and Yamada, S., New general synthesis of medium ring-lactones via a regioselective β-scission of alkoxyl radicals generated from catacondensed lactols, *Tetrahedron*, 43, 3371, 1987.
70. (a) Arencibia, M.T., Freire, R., Perales, A., Rodriguez, M.S., and Suarez, E., Hypervalent organoiodine compounds: radical fragmentation of oxabicyclic hemiacetals. Convenient synthesis of medium-sized and spiro 1H lactones, *J. Chem. Soc., Perkin Trans. 1*, 3349, 1991; (b) Kaino, M., Naruse, Y., Ishihara, K., and Yamamoto, H., Stereospecific cyclization of vinyl ether alcohols. Facile synthesis of (−)-lardolure, *J. Org. Chem.*, 55, 5814, 1990.
71. Boto, A., Freire, R., Hernandez, R., Suarez, E., and Rodriguez, M.S., Tandem β–fragmentation–hydrogen abstraction reaction of alkoxy radicals in steroidal systems, *J. Org. Chem.,* 62, 2975, 1997 and their early papers cited therein.
72. Lee, J., Oh, J., Jin, S., Choi, J., Atwood, J.L., and Cha, J. K., Fragmentation of alkoxy radicals and oxidative elimination of alicyclic iodides, *J. Org. Chem.*, 59, 6955,1994.
73. Suginome, H. and Yamada, S., Simple new synthesis of macrolides by a four atom ring expansion of cyclic ketones through a consecutive intramolecular homolytic addition-β-scission of alkoxyl radicals. A new entry to the synthesis of 15-pentadecanolides, *Chem. Lett.*, 245, 1988.
74. Suginome, H. and Ihizawa, A., A new synthesis of (±)-recifeiolide based on a consecutive intramolecular homolytic addition and β-scission of alkoxyl radicals, Thesis, Hokkaido University, 1991.

75. Hernandez, R., Marrero, J.J., Melian, D., and Suarez, E., Hypervalent organoiodine reagents in the β-fragmentation of bicyclic carbinolamides leading to imides, *Tetrahedron Lett.,* 29, 6661,1988.
76. (a) Akhtar, M. and Marsh, S., Synthesis of a medium-size ring via alkoxy radical decomposition, *J. Chem. Soc*., 937, 1966; (b) Suginome, H. and Yamada, S., A simple new synthesis of macrocyclic ketones: a new entry to the synthesis of exaltone and (±)-muscone, *Tetrahedron Lett*., 28, 3963, 1987.
77. Suginome, H., Kondoh, T., Gogonea, C., Singh, V., Goto, H., and Õsawa, E, Photoinduced molecular transformations. 155. General synthesis of macrocyclic ketones based on a ring expansion involving a selective β-scission of alkoxyl radicals, its application to a new synthesis of (±)-isocaryophyllene and (±)-caryophyllene, and a conformational analysis of the two sesquiterpenes and the radical intermediate in the synthesis by MM3 calculations, *J. Chem. Soc., Perkin Trans. 1*, 69, 1995.
78. (a) Ellwood, C.W. and Pattenden, G., Sequential alkoxy radical fragmentation-transannular radical cyclisation-radical ring expansion reactions. A new approach to bicyclo [6.3.0] undecanones, *Tetrahedron Lett.,* 32, 1591, 1991; (b) Mowbray, C.E. and Pattenden, G., Polycyclic construction via cascade radical fragmentation-transannulation-cyclisation processes, *Tetrahedron Lett*., 34, 127, 1993.
79. Saicic, R.N., Synthesis of bridged cyclooctane derivatives via alkoxy radical fragmentation. *Tetrahedron Lett.,* 38, 295, 1997.
80. Suginome, H., Nakayama, Y., Harada, H., Hachiro, H., and Orito, K., A new synthesis of a functionalized bicyclo[5.4.0] undecane skeleton based on a sequence involving [2+2] photoaddition and regioselective β-scission of alkoxyl radicals from the resulting cyclobutanols, *J. Chem. Soc., Chem. Commun*., 451, 1994;
81. Suginome, H. and Nakayama, Y., Photoinduced molecular transformations.150. A new total synthesis of (±)-α-himachalene based on a sequence involving [2+2] photoaddition and regioselective β-scission of alkoxyl radicals generated from the resulting cyclobutanols, *Tetrahedron,* 26, 7771, 1994;
82. (a) Suginome, H., Liu, C.F., Tokuda, M., and Furusaki, A., Photoinduced transformations. 76.Ring expansion through a [2+2] photoaddition–β-scission sequence; the photorearrangement of *endo*-4-cyanotricyclo[6.4.0.02,5]dodeca-1(12),6,8,10-tetraen-5-yl hypoiodite to 4-cyanotricyclo[6.4.0.02,4]dodeca-1(12),6,8,10-tetraen-5-one, *J. Chem. Soc., Perkin Trans. 1*, 327, 1985; (b) Suginome, H., Itoh, M., and Kobayashi, K., Photoinduced molecular transformations.Part 87.Ring expansion through [2+2] photocycloaddition-β-scission sequence; synthesis of benzohomotropones from 1- and 2-naphthols and methyl acrylate, *J. Chem. Soc., Perkin Trans. 1*, 491, 1988; (c) Suginome, H., Takeda, T., Itoh, M., Nakayama, Y., and Kobayashi, K., Photoinduced molecular transformations. 152. Ring expansion based on a sensitized [2+2] photoaddition of enol ethers of cyclic ketones with olefins, followed by a β-scission of alkoxyl radicals generated from the resulting cyclobutanols. Two-carbon ring expansion of β-indanone, β-tetralone and β-suberone, *J. Chem. Soc., Perkin Trans. 1*, 49, 1995.
83. Suginome, H., Liu, C.F., Seko, S., Kobayashi, K., and Furusaki, A., Photoinduced molecular transformations. 100. Formation of furocoumarins and furochromones via a β-scission of cyclobutanoxyl radicals generated from [2+2] photoadducts from 4-hydroxycoumarin and acyclic and cyclic alkenes. X-ray crystal structures of penta [3.4] cyclobuta [1,2-*d*] pyran-6(6a*H*)-one, *cis*-(±)-6b,8,9,9a-tetrahydro-6*H*,7*H*-cyclopenta[4,5]furo[3,2-*c*] [1]benzopyran-6-one, and *cis*-1,2,2a,8b-tetrahydro-8b-hydroxy-1,1,2,2-tetramethyl-3*H*-benzo [*b*] cyclobuta [*d*] pyran-3-one, *J. Org. Chem*., 53, 5952, 1988.
84. (a) Suginome, H., Kobayashi, K., Itoh, M., Seko, S., and Furusaki A., Photoinduced molecular transformations. 110. Formation of furoquinolinones via β-scission of cyclobutanoxyl radicals generated from [2+2] photoadducts of 4-hydroxy-2-quinolone and acyclic and cyclic alkenes. X-ray crystal structure of (6aα, 6bβ, 10aβ, 10bα)-(±)-10b-acetoxy-6a,6b,7,8,9,10,10a,10b-octahydro-5-methylbenzo [3,4] cyclobuta [1,2-*c*] quinolin-6(5*H*)-one, *J. Org. Chem*., 55, 4933, 1990; (b) Senboku, H., Takashima, M., Suzuki, M., Kobayashi, K., and Suginome, H., Photoinduced molecular

transformations. 159. Formation of some furonaphthyridinones by selective β-scission of cyclobutanoxyl radicals generated from [2+2] photoadducts of 4-hydroxy-1-phenyl [1,8] naphthyridin-2(1*H*)-one with alkenes, *Tetrahedron,* 52, 6125, 1996.

85. Kobayashi, K., Suzuki, M., and Suginome, H., Photoinduced molecular transformations. 128. Regioselective [2+2] photocycloaddition of 3-acetoxyquinolin-2(1*H*)-one with alkenes and formation of furo [2,3-*c*] quinolin-4(5*H*)-ones, 1-benzazocine-2,3-diones, and cyclopropa [*d*] benz [1] azepine-2,3-diones via a β-scission of cyclobutanoxyl radicals generated from the resulting [2+2] photoadducts, *J. Org. Chem*., 57, 599, 1992.
86. Suginome, H., Kajizuka, Y., Suzuki, M., Senboku., H., and Kobayashi, K., Photoinduced molecular transformations. 147. [2 + 2] Photoaddition of protected 4-hydroxy-1(2*H*)-isoquinolinone with an electron-deficient alkene and the formation of a 3,6-epoxy-3,4,5,6-tetrahydro-2-benzazocin-1(2*H*)-one via a β-scission of cyclobutanoxyl radicals generated from the resulting photoadduct, *Heterocycles,* 37, 283, 1994.
87. (a) Senboku, H., Kajizuka, Y., Kobayashi, K., Tokuda, M., and Suginome, H., Photoinduced molecular transformations. 160. Furan annelation of 2-hydroxynaphthoquinone involving photochemical addition and radical fragmentation; exclusion of the intermediacy of [2+2] cycloadduct in a one-pot formation of furanoquinones by the regioselective 3+2 photoaddition of hydroxyquinones with alkenes, *Heterocycles*, 44, 341, 1997; (b) Kabayahsi, K., Sasaki, A., Takeuchi, H., and Suginome, H., Photoinduced transformations. Part 127. A new [2+2] photoaddition of 2-amino-1,4-naphthoquinone with vinylarenes and the synthesis of 2,3-dihydronaphtho 2,3-dihydronaphtho [1,2-*b*] furan-4,5-diones and 2,3-dihydronaphtho [2,3-*b*] furan-4,9-diones by β-scission of alkoxyl radicals generated from the resulting photoadducts, *J. Chem. Soc., Perkin Trans. 1*, 115,1992.
88. (a) Suginome, H., Wang, J.B., and Satoh, G., Regioselective β-scission of α-oxoalkoxyl radicals: a novel formation of α-hydroxy-ε-lactone by photolysis of steroidal α-oxoalcohol hypoiodites in the presence of mercury (II) oxide and iodine, *J. Chem. Soc., Perkin Trans. 1*, 1553, 1989; (b) Suginome, H., Satoh, G., Wang, J.B., Yamada, S., and Kobayashi, K, Photoinduced molecular transformations. 106. The formation of cyclic anhydrides via regioselective β-scission of alkoxyl radicals generated from 5- and 6- membered α-hydroxy cyclic ketones, *J. Chem. Soc., Perkin Trans. 1*, 1239, 1990.
89. (a) Kobayashi, K., Itoh, M., Sasaki, A., and Suginome, H., New short step general synthesis of isobenzofuran-1(3*H*)-ones (phthalides) based on a single or double β-scission of alkoxyl radicals generated from 1-ethylbenzocyclobuten-1-ols: synthesis of some natural phthalides, *Tetrahedron*, 47, 5437, 1991; (b) Kobayashi, K., Shimizu, H., Itoh, M.M., and Suginome, H., An efficient synthesis of 5,7-dihydroxy-4-methylisobenzofuran-1(3*H*)-one, a metabolite of *aspergillus flavus* and a key intermediate in the synthesis of mycophenolic acid, *Bull. Chem. Soc. Jpn.*, 63, 2435,1990; (c) Kobayashi, K., Konishi, A., Kanno, Y., and Suginome, H., Photoinduced molecular transformations. 137. A new general synthesis of 3-substituted (1*H*)-3,4-dihydrobenzo [2] pyran-1-ones (3,4-dihydroisocoumarins) via radical and photochemical fragmentations as the key step.*J. Chem. Soc., Perkin Trans. 1*, 111,1993
90. Kobayashi, K., Kanno, Y., Seko, S., and Suginome, H., Photoinduced molecular transformations. 135. New synthesis of taiwanin C and justicidin E based on a radical cascade process involving β-scission of alkoxyl radicals generated from 3-aryl-1-ethyl-1,2-dihydrocyclobuta [*b*] naphthalen-1-ols prepared by thermolysis of (Z)-*t*-butyl 3-3-(bicyclo [4.2.0] octa-1,3,5-trien-7-yl) propenoates, *J Chem. Soc., Perkin Trans. 1*, 3119, 1992.
91. Suginome, H., Washiyama, H., and Yamada, S., The transformation of cyclic alcohols into cyclic acetals through a new oxygen atom insertion by photolysis in the presence of lead tetraacetate and iodine, *Bull. Chem. Soc. Jpn*., 60, 1071, 1987.
92. Suginome, H., Seki, Y., Yamada, S., Orito, K., and Miyaura, N., Photo-induced transformations. 79. On the mechanism of the formation of oxasteroids via photo- and thermally-induced rearrangement of 3-hydroxy-Δ^5-steroid hypoiodites in the presence of mercury(II) oxide and iodine. An oxygen-18 labeling study. *J. Chem. Soc., Perkin Trans. 1*, 1431, 1985.

93. Suginome, H. and Wang, J.B., Intramolecular β,γ-addition of allylic alkoxyl radicals. A new general synthesis of α-iodoepoxides by photolysis of allylic alcohol hypoiodites in the presence of mercury(II) oxide, iodine and pyridine in benzene, *J. Chem. Soc., Chem. Commun.,* 1629, 1990.
94. Suginome, H., Isayama, S., Maeda, N., Furusaki, A., and Katayama, C., Photo-induced transformations. 57. The formation of bridged oxabicyclic compounds by intramolecular radical addition of oxyl radicals generated from some *A*-homo-4a-cholesten-3-ol hypoiodites, *J. Chem. Soc., Perkin Trans. 1*, 2963, 1981.
95. Suginome, H., Yamamoto, Y., and Orito, K., Photoinduced molecular transformations. 106. Intramolecular addition vs β-scission of oxyl radicals generated from *A*-homo-5a-cholest-1-en-4α- and 4β-ol hypoiodites and 4-methyl-*A*-homo-5a-cholest-1-en-4α-and 4β-ol hypoiodites, *J. Chem. Soc., Perkin Trans. 1*, 1033, 1990.
96. Suginome, H., Ohtsuka, T., Orito, K., Jaime, C., and Osawa, E., Photoinduced transformations. 69. The formation of bridged oxabicyclic compounds by intramolecular radical addition of oxyl radicals generated from *B*-homocholest-5-en-7α-ol hypoiodites, *J. Chem. Soc., Perkin Trans. 1*, 575, 1984.
97. Takahashi, H., Ito, M., Suginome, H., and Masamune, T., Photoinduced rearrangement of widdrol hypoiodite, *Chem. Lett*., 901, 1979.
98. Glover, S.A. and Goosen, A., Synthesis of β-iodo-*t*-butyl and methyl ethers from the reaction of alkenes with *t*-butyl and methyl hypoiodites, *Tetrahedron Lett*., 21, 2005, 1980.
99. (a) Suginome, H., Senboku, H., and Tsunetoshi, A., Efficient formation of a spirotetrahydrofuran ring by the ionic cyclization of bishomoallyl tertiary alcohols via their hypoiodites, *J. Chem. Soc., Perkin Trans. 1,* 2917, 1992; (b) Kraus, G.A. and Thurston, J., Alkoxyl radicals in organic synthesis. A novel approach to spiroketals, *Tetrahedron Lett*., 28, 4011, 1987.
100. Barnes, J.C., Horspool, W.M., and Hynd, G., A new synthetic path to *peri*-naphthisoxazoles by oxidative intramolecular cyclization of some β,γ-unsaturated oximes, *J. Chem. Soc., Chem. Commun.,* 425, 1999.

110

Photochemistry of Hypervalent Iodine Compounds

Tsugio Kitamura
Saga University

110.1 Introduction

This chapter deals with the photochemical reactions of hypervalent iodine compounds, especially organoiodine(III) species. Although there has been an increasing interest in the synthetic use of hypervalent iodine compounds,[1–12] the photochemical study is very limited. Recently, remarkable progress has been made in the use of diaryliodonium salts as photoinitiators for cationic polymerization and as photoacid generators for imaging systems. On the other hand, the photochemical applications of hypervalent iodine compounds to organic synthesis have been found in the reactions accompanying generation of alkyl and alkoxy radicals, carbene formation, halogenation, and arylation.

110.2 Photochemistry of Diaryliodonium Salts and Related Iodonium Salts

The photochemistry of diaryliodonium salts has been investigated extensively for use in cationic polymerization and microlithographic applications (chemical amplification).[13–20] In principle, these applications are based on the generation of a strong acid by the photolysis as shown in Scheme 1.

Typically, diaryliodonium salts exhibit an intense absorption band in the 230- to 260-nm region ($\varepsilon \sim 17{,}000\ M^{-1}\cdot cm^{-1}$) as shown in Table 110.1.[21] Electron-donating substituents on the aromatic rings induce a bathochromic shift while electron-withdrawing substituents shift the UV absorption to shorter wavelengths.

Direct photolysis of diphenyliodonium triflate in acetonitrile, as shown in Equation 110.1, gives iodobenzene, 2-, 3-, and 4-iodobiphenyls, benzene, acetanilide, and biphenyl. In addition to these products, triflic acid is also formed.

0-8493-1348-1/04/$0.00+$1.50

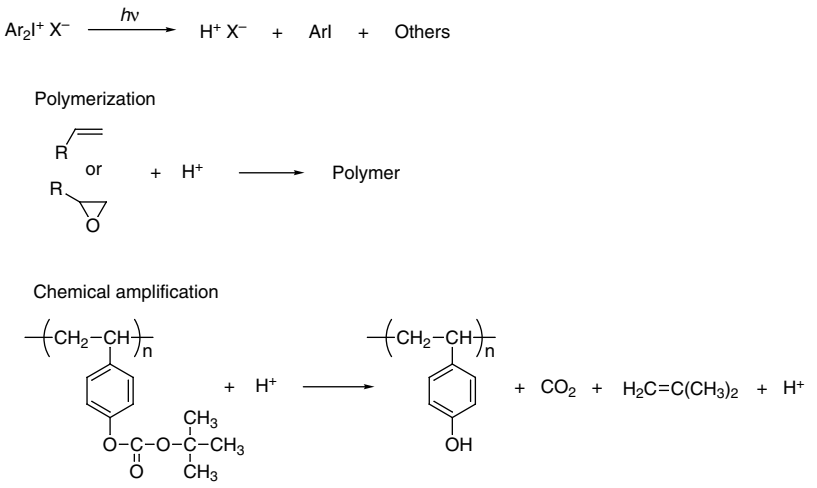

SCHEME 1 Application of diaryliodonium salts photochemistry.

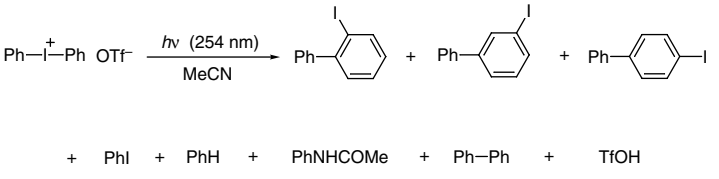

(110.1)

The mechanistic studies have been demonstrated by product analysis, analysis of the polymer formed, and by the detection of the intermediates.[22–47]

The photolysis of diphenyliodonium salts has been proposed to occur by both heterolytic and a homolytic cleavage of the carbon–iodine bonds (Scheme 2). Excitation by irradiation produces the excited singlet diphenyliodonium salt. This species can undergo a heterolytic cleavage, leading to a caged pair of phenyl cation and iodobenzene. Intersystem crossing from the excited singlet state leads to the excited triplet state, which can undergo homolysis to a caged pair of iodobenzene radical cation and phenyl radical. Each of the corresponding caged pairs of reactive intermediates undergoes further reactions leading to products. Detection of the reactive intermediates was made using flash photolysis.

When diphenyliodonium salts are photolyzed, acids species are generated by several reaction paths as shown in Scheme 3. These acids are the predominant species responsible for cationic polymerization and photodepolymerization.

Photosensitized decomposition of diphenyliodonium salts occurs mostly through electron transfer, as shown in Scheme 4. Another mechanism via triplet energy transfer is possible for specific photosensitizers

The photochemistry of alkenyl(phenyl)iodonium tetrafluoroborates in methanol as well as 2,2,2-trifluoroethanol, dichloromethane, and toluene has been investigated (Equation 110.2).[48–50] Homolysis as well as heterolysis of both bonds, the vinylic C–I bond and the aromatic C–I bond, occur. The predominant formation of styryl cation accounts for the product derived from nucleophilic substitution, elimination, and rearrangement, as shown in Scheme 5.

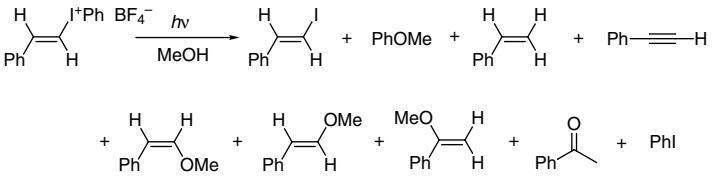

(110.2)

TABLE 110.1 UV Spectra of Diaryliodonium Salts

Structure	Anion	λ_{max}, nm (ε_{max})[a]
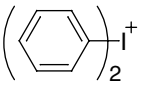	BF_4^-	227 (17,800)
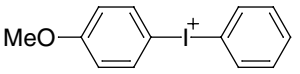	BF_4^-	246 (15,400
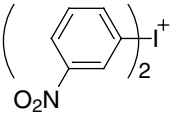	AsF_6^-	215 (35,000) 245 (17,000)
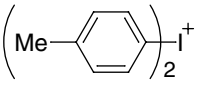	BF_4^-	236 (18,000)
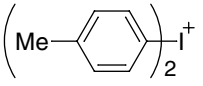	PF_6^-	237 (18,200)
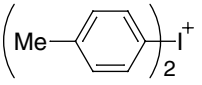	AsF_6^-	237 (17,500)
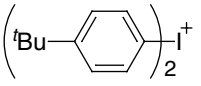	BF_4^-	238 (20,800)
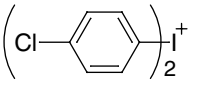	AsF_6^-	240 (23,000)
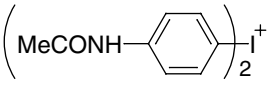	AsF_6^-	275 (30,000)
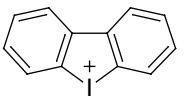	AsF_6^-	264 (17,300)

[a] In MeOH.

Photolysis of alkynyl(phenyl)iodonium salts results in the major formation of products derived from homolysis of the carbon–iodine bonds, such as iodoalkynes, iodobenzene, and phenylalkynes as the major reaction paths (Equation 110.3).[51]

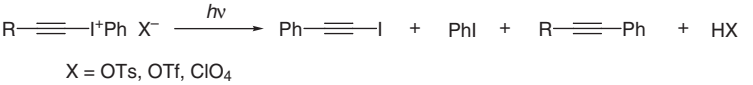

(110.3)

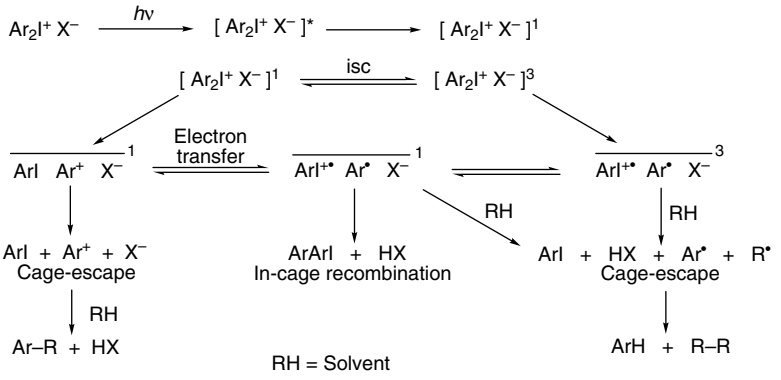

SCHEME 2 Mechanism for product formation from direct photolysis of diaryliodonium salts.

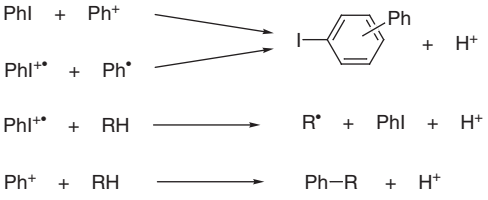

SCHEME 3 Acid generation.

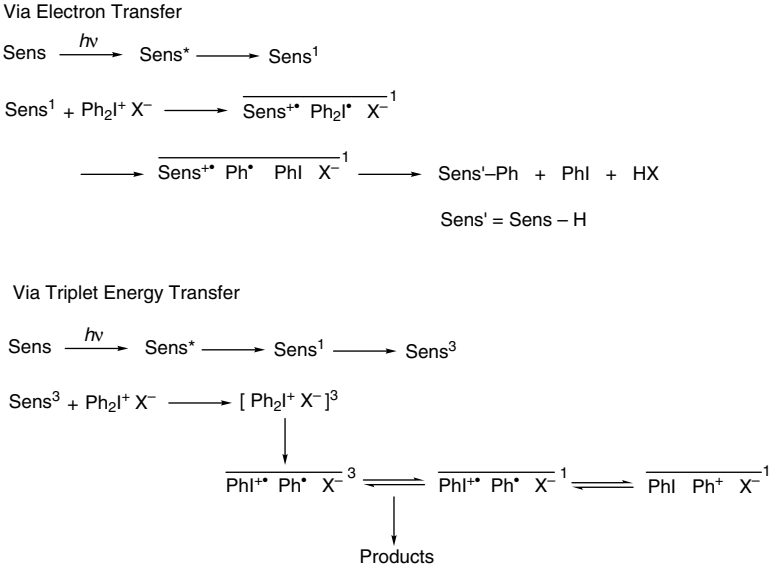

SCHEME 4 Photosensitized decomposition of diphenyliodonium salts.

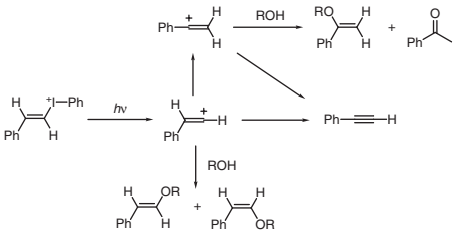

SCHEME 5

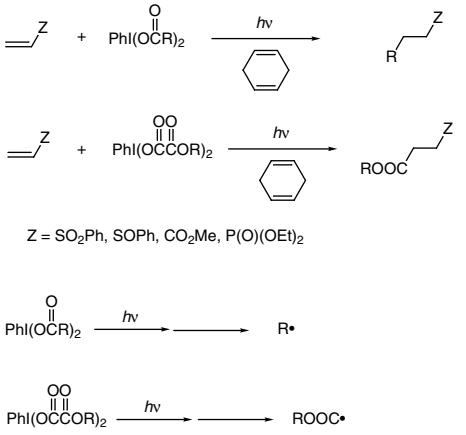

SCHEME 6

110.3 Application to Organic Synthesis

Generation of Alkyl Radicals[52–63]

(Diacetoxyiodo)benzene and [bis(trifluoroacetoxy)iodo]benzene generate radicals under photochemical conditions. These [bis(acyloxy)iodo]benzenes are efficient radical initiators for the polymerization of 2-[2-((dimethylamino)ethyl)methacrylate, methyl methacrylate, and styrene. Under photochemical conditions, [bis(acyloxy)iodo]benzenes readily produce free radicals that, in the presence of a hydrogen donor such as 1,4-cyclohexadiene, react with electron-deficient alkenes to give reductive addition products, as shown in Scheme 6.

Further applications of this procedure are found in the radical alkylation of nitrogen heterocycles, *C*-nucleosides, and disulfides, and in the cyclization of the radicals to yield heterocycles.

Generation of Alkoxy Radicals[64–73]

Photolysis of (diacetoxyiodo)benzene with alcohols in the presence of iodine leads to the generation of alkoxy radicals that can undergo fragmentation, rearrangement, or cyclization. The generation of an alkoxy radical is accomplished in the following way (Scheme 7). The acetyl hypoiodite initially forms and converts alcohols to alkyl hypoiodites. Under photochemical conditions with visible light, the alkyl hypoiodites generate the alkoxy radicals by I–O bond homolysis.

For example, photolysis of steroidal hemiacetals with (diacetoxyiodo)benzene and iodine in the absence of oxygen affords medium-sized lactones as a result of alkoxy radical fragmentation (Equation 110.4).[65]

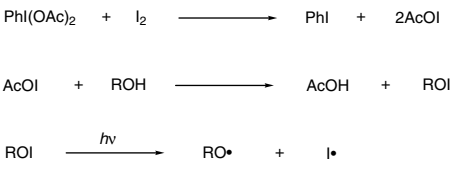

SCHEME 7

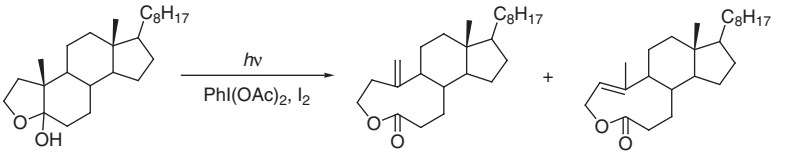

(110.4)

Halogenation[74–80]

Dichloroiodobenzene and 1-chlorobenziodoxoles were used as reagents for chlorination under photochemical conditions. The chlorination of alkanes or alkenes using this method proceeds via a radical mechanism (Equations 110.5 through 110.7). Special interest is given to the selective chlorination of a steroid derivative bearing dichloroiodo group at an appropriate position (Equation 110.8).[75]

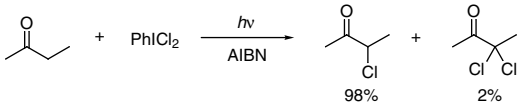

(110.5)

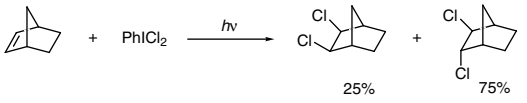

(110.6)

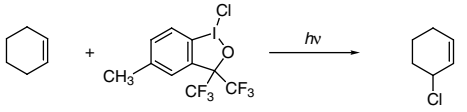

(110.7)

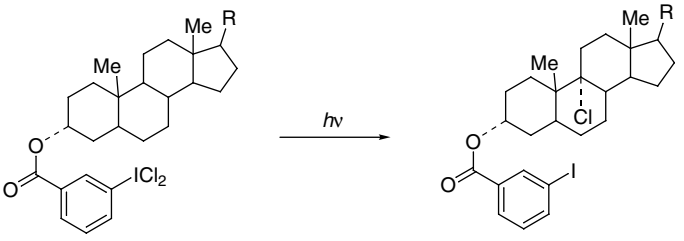

(110.8)

Carbene Precursors[81–84]

Iodonium ylides can serve as precursors of carbenes under photochemical, thermal, or catalytic conditions. For example, phenyliodonium bis(trifluoromethylsulfonyl)methide under photochemical conditions affords the cycloaddition product with cyclohexene, the CH insertion products with aromatic substrates, and the ylide transfer product from pyridine, as shown in Scheme 8.[82–84]

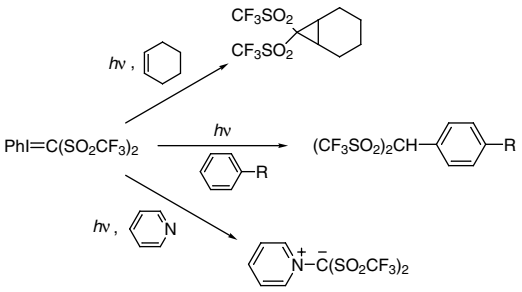

SCHEME 8

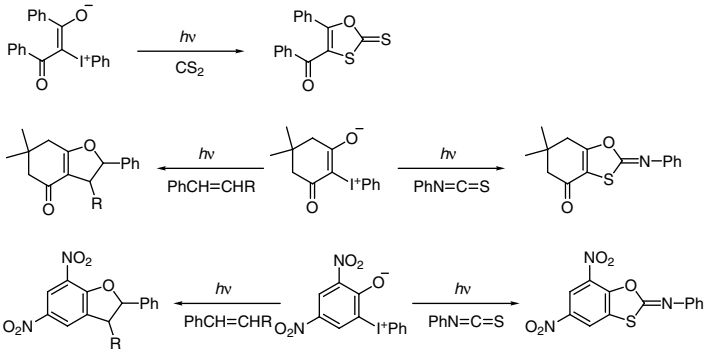

SCHEME 9

Synthesis of Heterocyclic Compounds[81,85,86]

Another use of iodonium ylides is as a synthetic route to heterocyclic compounds (Scheme 9). Iod**o**nium ylides can be photochemically converted to oxathiole-2-thiones in the presence of CS_2. In the presence of phenyl isothiocyanate or styrenes, the iodonium ylides undergo photochemical conversion to 2-phenyliminooxathioles, dihydrofurans, and dihydrobenzofurans, respectively. Many other interesting reactions of iodonium ylides based on the photochemical approach are also reported in the literature.

Phenylation[87]

Diphenyliodonium chloride and tetrafluoroborate undergo light-catalyzed reaction with triphenylphosphine to give tetraphenylphosphonium salts (Equation 110.9).

$$Ph_2I^+X^- \quad + \quad Ph_3P \xrightarrow{h\nu} Ph_4P^+X^- \quad + \quad PhI \tag{110.9}$$

References

1. Banks, D.F., Organic polyvalent iodine compounds, *Chem. Rev.*, 66, 243, 1966.
2. Koser, G.F., Hypervalent halogen compounds, in *The Chemistry of Functional Groups, Supplement D*, Patai, S. and Rappoport, Z., Eds., John Wiley & Sons, New York, 1983, part 1, chap. 18.
3. Koser, G.F., Halonium ions, in *The Chemistry of Functional Groups, Supplement D*, Patai, S. and Rappoport, Z., Eds., John Wiley & Sons, New York, 1983, part 2, chap. 25.
4. Varvoglis, A., Polyvalent iodine compounds in organic synthesis, *Synthesis*, 709, 1984.

5. Moriarty, R.M. and Vaid, R.K., Carbon–carbon bond formation via hypervalent iodine oxidations, *Synthesis*, 431, 1990.
6. Varvoglis, A., *The Organic Chemistry of Polycoordinated Iodine*, VCH Publishers, New York, 1992.
7. Prakash, O. and Singh, S.P., Iodobenzene diacetate and related hypervalent iodine reagents in the synthesis of heterocyclic compounds, *Aldrichimica Acta*, 27, 15, 1994.
8. Stang, P.J. and Zhdankin, V.V., Organic polyvalent iodine compounds, *Chem. Rev.*, 96, 1123, 1996.
9. Varvoglis, A., Chemical transformations induced by hypervalent iodine reagents, *Tetrahedron*, 53, 1179, 1997.
10. Varvoglis, A., *Hypervalent Iodine in Organic Synthesis*, Academic Press, London, 1997.
11. Kitamura, T. and Fujiwara, Y., Recent progress in the use of hypervalent iodine reagents in organic synthesis. A review, *Org. Prep. Proc. Int.*, 29, 409, 1997.
12. Moriarty, R.M. and Prakash, O., Synthesis of heterocyclic compounds using organohypervalent iodine reagents, *Adv. Heterocyclic Chem.*, 69, 1, 1998.
13. Crivello, J.V., Photoinitiated cationic polymerization, in *UV Curing: Science and Technology*, Pappas, S.P., Ed., Technology Marketing Corporation, Stamford, CT, 1978, 23.
14. Crivello, J.V., Cationic polymerization — Iodonium and sulfonium salt photoinitiators, *Adv. Polym. Sci.*, 62, 3, 1984.
15. Ito, H. and Willson, C.G., Applications of photoinitiators to the design of resists for semiconductor manufacturing, in *Polymers in Electronics*, Davidson, T., Ed., American Chemical Society, Washington, D.C., 1984, 11.
16. Pappas, S.P., *UV Curing: Science and Technology*, Vol. 2, Technology Marketing Corp., Norwalk, CT, 1985.
17. Pappas, S.P., Photoinitiation of cationic and concurrent radical-cationic polymerization. V, *Progr. Org. Coat.*, 13, 35, 1985.
18. Yagci, Y. and Schnabel, W.R., Light-induced cationic polymerization, *Makromol. Chem., Macromol. Symp.*, 13/14, 161, 1988.
19. Willson, C.G. and Bowden, M.J., Recent advances in organic resist materials. 2, *CHEMTECH*, 19, 182, 1989.
20. Ito, H. and Ueda, M., Recent advances in the design of chemical amplification resists, *J. Photopolym. Sci. Technol.*, 2, 1, 1989.
21. Crivello, J.V. and Lam, J.H.W., Diaryliodonium salts. A new class of photoinitiators for cationic polymerization, *Macromolecules*, 10, 1307, 1977.
22. Knapczyk, J.W., Lubinkowski, J.J., and McEwen, W.E., Photolysis of diphenyliodonium salts in alcohol solutions, *Tetrahedron Lett.*, 35, 3739, 1972.
23. Foster, D.L.D., Hobbs, P.D., and Magnus, P.D., Photolysis of diaryliodonium salts in aqueous alkaline solution, *Tetrahedron Lett.*, 4793, 1972.
24. Pappas, S.P., Pappas, B.C., Gatechair, L.R., and Jilek, J.H., Photoinitiation of cationic polymerization. IV. Direct and sensitized photolysis of aryl iodonium and sulfonium salts, *Polym. Photochem.*, 5, 1, 1984.
25. Pappas, S.P., Pappas, B.C., Gatechair, L.R., and Schnabel, W., Photoinitiation of cationic polymerization. II. Laser flash photolysis of diphenyliodonium salts, *J. Polym. Sci., Polym. Chem. Ed.*, 22, 69, 1984.
26. DeVoe, R.J., Sahyun, M.R. V., Serpone, N and Sharma, D.K., Transient intermediates in the photolysis of iodonium cations, *Can. J. Chem.*, 65, 2342, 1987.
27. DeVoe, R.J., Sahyun, M.R.V., Schmidt, E., Serpone, N., and Sharma, D.K., Electron transfer sensitized photolysis of onium salts, *Can. J. Chem.*, 66, 319, 1988.
28. Fouassier, J. P., Burr, D., and Crivello, J.V., Time-resolved laser spectroscopy of the sensitized photolysis of iodonium salts, *J. Photochem. Photobiol., A: Chem.*, 49, 317, 1989.
29. Tilley, M., Pappas, B., Pappas, S.P., Yagci, Y., Schnabel, W., and Thomas, J.K., Laser flash photolysis studies on iodonium and sulfonium salts, *J. Imaging Sci.*, 33, 62, 1989.
30. Dektar, J.L. and Hacker, N.P., Photochemistry of diaryliodonium salts, *J. Org. Chem.*, 55, 639, 1990.

31. Devoe, R.J., Sahyun, M.R.V., Schmidt, E., and Sharma, D.K., Photooxidation of 9,10-diethoxyanthracene: mechanistic dichotomies between homogeneous solution and reverse-micelle photoprocesses, *Can. J. Chem.*, 68, 612, 1990.
32. Dektar, J.L. and Hacker, N.P., Comparison of the photochemistry of diarylchloronium, diarylbromonium, and diaryliodonium salts, *J. Org. Chem.*, 56, 1838, 1991.
33. Hacker, N.P., Leff, D.V., and Dektar, J.L., The photochemistry of diphenyliodonium halides: evidence for reactions from solvent-separated and tight ion pairs, *J. Org. Chem.*, 56, 2280, 1991.
34. Grushin, V.V., Demkina, I.I., and Tolstaya, T.P., Unified mechanistic analysis of polar reactions of diaryliodonium salts, *J. Chem. Soc., Perkin Trans. 2*, 505, 1992.
35. Bi, Y. and Neckers, D.C., Photochemical reaction of halogenated xanthene dye with diaryliodonium salts, *J. Photochem. Photobiol., A: Chem.*, 74, 221, 1993.
36. Timpe, H.-J., Ulrich, S., and Fouassier, J.-P., Photochemistry and use of decahydroacridine-1,8-diones as photosensitizers for onium salt decomposition, *J. Photochem. Photobiol., A: Chem.*, 73, 139, 1993.
37. Kampmeier, J.A. and Nalli, T.W., Initiation of cationic polymerization of cyclic ethers by redox radical-chain reactions of onium salts, *J. Org. Chem.*, 59, 1381, 1994.
38. Bi, Y. and Neckers, D.C., A visible light initiating system for free radical promoted cation polymerization, *Macromolecules*, 27, 3683, 1994.
39. Kunze, A., Muller, U., Tittes, K., Fouasier, J.P., and Morlet-Savary, F., Triplet quenching by onium salts in polar and nonpolar solvents, *J. Photochem. Photobiol. A: Chem.*, 110, 115, 1997.
40. Muneer, R. and Nalli, T.W., Use of diaryliodonium/phosphine radical-chain chemistry for visible photoinitiation of cationic polymerizations. trimethyl phosphite as a co-initiator of the ring-opening polymerization of cyclohexene oxide, *Macromolecules*, 31, 7976, 1998.
41. Eckert, G. and Goez, M., CIDNP investigation of radical decay pathways in the sensitized photolysis of triphenylsulfonium salts, *J. Am. Chem. Soc.,* 121, 2274, 1999.
42. Goez, M., Eckert, G., and Mueller, U., Sensitized photolysis of iodonium salts studied by CIDNP-solvent dependence and influence of lipophilic substituents, *J. Phys. Chem. A*, 103, 5714, 1999.
43. Muller, U. and Zucker, I., Sensitized proton formation using lipophilic substituted iodonium salts, *J. Photochem. Photobiol., A: Chem.*, 120, 93, 1999.
44. Gu, H., Zhang, W., Feng, K., and Neckers, D.C., Photolysis of ((3-(trimethylsilyl)propoxy)phenyl)phenyliodonium salts in the presence of 1-naphthol and 1-methoxynaphthalene, *J. Org. Chem.*, 65, 3484, 2000.
45. Hartwig, A., Harder, A., Luhring, A., and Schroder, H., (9-Oxo-9H-fluoren-2-yl)iodonium hexafluoroantimonate(V) — a photoinitiator for the cationic polymerization of epoxides, *Eur. Polym. J.*, 37, 1449, 2001.
46. Selvaraju, C., Sivakumar, A., and Ramamurthy, P., Excited state reactions of acridinedione dynes with onium salts: mechanistic details, *J. Photochem. Photobiol., A: Chem.*, 138, 213, 2001.
47. Gu, H., Ren, K., Grinevich, O., Malpert, J.H., and Neckers, D.C., Characterization of iodonium salts differing in the anion, *J. Org. Chem.*, 66, 4161, 2001.
48. Gronheid, R., Lodder, G., Ochiai, M., Sueda, T., and Okuyama, T., Thermal and photochemical solvolysis of (*E*)- and (*Z*)-2-phenyl-1-propenyl(phenyl)iodonium tetrafluoroborate: benzenium and primary vinylic cation intermediates, *J. Am. Chem. Soc.*, 123, 8760, 2001.
49. Gronheid, R., Lodder, G., Ochiai, M., Sueda, T., and Okuyama, T., Thermal and photochemical solvolysis of (*E*)- and (*Z*)-2-phenyl-1-propenyl(phenyl)iodonium tetrafluoroborate: Benzenium and primary vinylic cation intermediates, *J. Am. Chem. Soc.*, 123, 8760, 2001.
50. Gronheid, R., Lodder, G., and Okuyama, T., Photosolvolysis of (*E*)-styryl(phenyl)iodonium tetrafluoroborate. Generation and reactivity of a primary vinyl cation, *J. Org. Chem.*, 67, 693, 2002.
51. Kitamura, T., Tanaka, T., and Taniguchi, H., Photolysis of alkynyl(phenyl)iodonium salts. Remarkable solvent effect and generation of acids, *Chem. Lett.*, 2245, 1992.
52. Georgiev, G., Kamenska, E., Christov, L., Sideridou-Karayannidou, I., Karayannidis, G., and Varvoglis, A., (Diacetoxyiodo)benzene and [bis(trifluoroacetoxy)iodo]benzene as photoinitiators for radical and cationic polymerization, *Eur. Polym. J.*, 28, 207, 1992.

53. Togo, H., Aoki, M., and Yokoyama, M., Facile radical decarboxylative alkylation of heteroaromatic bases using carboxylic acids and trivalent iodine compounds, *Tetrahedron Lett.*, 32, 6559, 1991.
54. Togo, H., Aoki, M., and Yokoyama, M., Alkylation of aromatic heterocycles with oxalic acid monoalkyl esters in the presence of trivalent iodine compounds, *Chem. Lett.*, 1691, 1991.
55. Vismara, E., Torri, G., Pastori, N., and Marchiandi, M., A new approach to the stereoselective synthesis of C-nucleosides via homolytic heteroaromatic substitution, *Tetrahedron Lett.*, 33, 7575, 1992.
56. Togo, H., Aoki, M., and Yokoyama, M., Reductive addition of alkyl radical to phenyl vinyl sulfone, *Chem. Lett*., 2169, 1992.
57. Togo, H., Aoki, M., Kuramochi, T., and Yokoyama, M., Radical decarboxylative alkylation onto heteroaromatic bases with trivalent iodine compounds, *J. Chem. Soc., Perkin Trans. 1*, 2417, 1993.
58. Togo, H., Aoki, M., and Yokoyama, M., Reductive addition to electron-deficient olefins with trivalent iodine compounds, *Tetrahedron*, 36, 8241, 1993.
59. Togo, H., Muraki, T., and Yokoyama, M., Preparation of adamantyl sulfides with [bis(1-adamantanecarboxy)iodo]arenes and disulfides, *Synthesis*, 115, 1995.
60. Togo, H., Hoshina, Y., Nogami, G., and Yokoyama, M., Radical reactions with trivalent iodine compounds, *Yuki Gosei Kagaku Kyokaishi*, 55, 90, 1997.
61. Togo, H., Hoshina, Y., Muraki, T., Nakayama, H., and Yokoyama, M., Study on radical amidation onto aromatic rings with (diacyloxyiodo)arenes, *J. Org. Chem.*, 63, 5193, 1998.
62. Togo, H., Harada, Y., and Yokoyama, M., Preparation of 3,4-dihydro-2,1-benzothiazine 2,2-dioxide skeleton from N-methyl 2-(aryl)ethanesulfonamides with (diacetoxyiodo)arenes, *J. Org. Chem.*, 65, 926, 2000.
63. Togo, H. and Katohgi, M., Synthetic uses of organohypervalent iodine compounds through radical pathways, *Synlett*, 565, 2001.
64. De Armas, P., Concepcion, J.I., Francisco, C.G., Hernadez, R., Salazar, J.A., and Suarez, E., Intramolecular hydrogen abstraction. Hypervalent organoiodine compounds, convenient reagents for alkoxy radical generation, *J. Chem. Soc., Perkin Trans. 1*, 405, 1989.
65. Arencibia, M.T., Freire, R., Perales, A., Rodriguez, M.S., and Suarez, E., Hypervalent organoiodine compounds: radical fragmentation of oxabicyclic hemiacetals. Convenient synthesis of medium-sized and spiro lactones, *J. Chem. Soc., Perkin Trans. 1*, 3349, 1991.
66. Galatsis, P. and Millan, S.D., Use of iodobenzene diacetate for the synthesis of α-iodoepoxides, *Tetrahedron Lett.*, 32, 7493, 1991.
67. Boto, A., Betancor, C., Prange, T., and Suarez, E., Fragmentation of alkoxy radicals: tandem β-fragmentation-cycloperoxyiodination reaction, *Tetrahedron Lett.*, 33, 6687, 1992.
68. Boto, A., Betancor, C., Hernandez, R., Rodriguez, M.S., and Suarez, E., Sequential alkoxy radical fragmentation. A one-step method for breaking two 1,3-positioned carbon-carbon bonds, *Tetrahedron Lett*., 34, 4865, 1993.
69. Mowbray, C.E. and Pattenden, G., Polycycle construction via cascade radical fragmentation-transannulation-cyclization processes, *Tetrahedron Lett*., 34, 127, 1993.
70. Courtneidge, J.L., Lusztyk, J., and Page, D., Alkoxy radicals from alcohols. Spectroscopic detection of intermediate alkyl and acyl hypoiodites in the Suarez and Beebe reactions, *Tetrahedron Lett.*, 35, 1003, 1994.
71. Boto, A., Betancor, C., Prange, T., and Suarez, E., Fragmentation of alkoxy radicals: tandem β-fragmentation-cycloperoxyiodination reaction, *J. Org. Chem.*, 59, 4393, 1994.
72. Boto, A., Betancor, C. ,and Suarez, E., Sequential alkoxy radical fragmentation-cyclopropylcarbinyl rearrangement. Synthesis of highly functionalized eleven-membered rings, *Tetrahedron Lett*., 35, 5509, 1994.
73. Boto, A., Betancor, C., and Suarez, E., Hypervalent iodine reagents: synthesis of a steroidal orthoacetate by a radical reaction, *Tetrahedron Lett*., 35, 6933, 1994.
74. Tanner, D.D. and Van Bostelen, P.B., Free-radical chlorination reactions of iodobenzene dichloride, *J. Org. Chem*., 32, 1517, 1967.

75. Breslow, R., Corcoran, R.J., Snider, B.B., Doll, R.J., Khanna, P.L., and Kaleya, R., Selective halogenation of steroids using attached aryliodide templates, *J. Am. Chem. Soc.*, 99, 905, 1977.
76. Dneprovskii, A.S., Krainyuchenko, I.V., and Temnikova, T.I., Reaction of carbonyl compounds with phenylchloroiodonium chloride, *Zh. Org. Khim.*, 14, 1514, 1978.
77. Amey, R.L. and Martin, J.C., Synthesis and reaction of substituted arylalkoxyiodinanes: formation of stable bromoarylalkoxy and aryldialkoxy heterocyclic derivatives of tricoordinate organoiodine(III), *J. Org. Chem.*, 44, 1779, 1979.
78. Amey, R.L. and Martin, J.C., Identity of the chain-carrying species in halogenations with bromo- and chloroarylalkoxyiodinanes: selectivities of iodinanyl radicals, *J. Am. Chem. Soc.*, 101, 3060, 1979.
79. Moskovkina, T.V. and Vysotskii, V.I., Reaction of aryl aliphatic 1,5-diketones with (dichloroiodo)benzene, *Zh. Org. Khim.*, 27, 833, 1991.
80. Andreev, V.A., Anfilogova, S.N., Pekkh, T.I., and Belikova, N.A., Acylation and chlorination of *cis*-3,4-dimethylbicyclo[4.3.0]nona-3,7-diene, *Zh. Org. Khim.*, 29, 142, 1993.
81. Hadjiarapoglou, L.P., The chemistry of photolytically and thermally generated α-ketocarbenes from iodonium ylides of β-diketones, *Tetrahedron Lett.*, 28, 4449, 1987.
82. Zhu, S. and Chen, Q., Phenyliodonium bis(perfluoroalkanesulfonyl)methide: synthesis and reactions as a precursor of bis(perfluoroalkanesulfonyl)carbene, *J. Chem. Soc., Chem. Commun.*, 1459, 1990.
83. Zhu, S. Chen, Q., and Kuang, W., Phenyl iodonium bis(perfluoroalkanesulfonyl)methide-dimethyl sulfoxide adduct. Its formation and x-ray structural analysis, *J. Fluorine Chem.*, 60, 39, 1993.
84. Zhu, S., Synthesis and reactions of phenyliodonium bis(perfluoroalkanesulfonyl)methides, *Heteroatom Chem.*, 5, 9, 1994.
85. Papadopoulou, M., Spyroudis, S., and Varvoglis, A., 1,3-Oxathiole-2-thiones from the reaction of carbon disulfide with zwitterionic iodonium compounds, *J. Org. Chem.*, 50, 1509, 1985.
86. Spyroudis, S.P., Photochemical reactions of 2,4-dinitro-6-phenyliodonium phenolate with alkenes, alkynes and aromatic compounds, *J. Org. Chem.*, 51, 3453, 1986.
87. Ptitsyna, O.A., Pudeeva, M.E., Belkevich, N.A., and Reutov, O.A., Photochemical reaction of arylation of triphenylphosphine by diaryliodonium fluoroborates, *Dokl. Akad. Nauk SSSR*, 143, 383, 1965.

111

Photolysis of Short-Lived Transient Species in Solutions: Product Analysis Studies

Akihiko Ouchi
Research Institute for Green Technology
National Institute of Advanced Industrial Science and Technology

111.1 Introduction

Lasers are ideal light sources for studying organic photochemical reactions, so much so that they are widely used in spectroscopic studies. However, product analysis studies of organic laser-induced reactions have not been carried out as much as spectroscopic studies. For product analysis studies, it is necessary to conduct reactions with high efficiency, compared with spectroscopic studies, in order to determine the yields of photochemical products by GC and/or HPLC analyses. This can be accomplished by applying precise control of the irradiation of light using four major characteristics of lasers that differ from conventional light sources; that is, light intensity, monochromaticity, coherency, and intermittence (for pulse lasers).

Using these characteristics of lasers, photochemical reactions that cannot be conducted with conventional light sources can be brought about,[1,2] and a multiphoton reaction is one of these processes. Multiphoton reactions can be classified in two categories: (1) stepwise reactions through short-lived transient species (Path 1 in Scheme 1) and (2) reactions by concerted multiphoton absorptions (Path 2 in Scheme 1). In many cases, Path 1 predominates when the substrates are complex organic compounds. The transient species can be either long-lived excited states, such as triplet states, or chemical species, such as radicals, carbenes, nitrenes, and thermally unstable molecules.

0-8493-1348-1/04/$0.00+$1.50

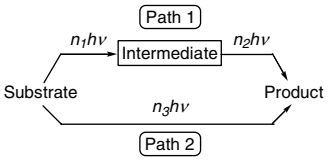

SCHEME 1

Product analysis studies of the photochemical reactions of such transient species have been conducted using various lasers and techniques. Such studies not only complement spectroscopic studies to give a better understanding of multiphoton reactions, but also give new methods for the study of short-lived transient species.

111.2 Photolysis Techniques

Laser Photolysis

This method comprises simple irradiations of substrate solutions in reaction vessels by continuous or pulsed lasers. For the continuous irradiation of high-intensity pulse lasers, the laser-drop photolysis technique[3] and a flow system with a short optical path length have been used.

In general, the high-intensity character of lasers is considered the most important factor for efficient multiphoton reactions. However, matching the wavelength of the lasers to both starting materials and intermediate species is also necessary to obtain high efficiency in the reactions. When pulse lasers are used, laser pulse width and the timing of the generation of the intermediates must be considered, in addition to wavelength matching; the intermediates must be generated within the same laser pulse for successive photon absorptions.

Laser-Jet Photolysis

This method was developed to conduct high-intensity, continuous laser photolysis.[4] However, this technique can be used also for the optimization of laser wavelength to both starting materials and intermediates and for the matching of the timing of the intermediate generation and laser irradiation. Figure 111.1 shows an experimental setup of a laser-jet apparatus. The solution of sample is pumped through a glass capillary with an internal diameter of 50 to 100 μm and the focus of a focused continuous laser is set on the liquid stream just below the outlet of the capillary. In general, 333-, 351-, and 364-nm emissions of argon ion lasers are used at the same time. However, when only one wavelength of the laser is needed, a prism can easily separate the three distinct emissions. The matching of the laser wavelength to both starting materials and intermediates can be often accomplished by using all the three laser emissions. By changing the internal diameter of the capillary and the flow rate, irradiation times can be varied between 10 and 100 μs. Multiple irradiations of the solution is also possible by recycling of the solution. However, the laser intensity of this method is much less than that of pulse lasers.

Time-Delayed, Two-Color Pulse Laser Photolysis

This technique has been used often in flash photolysis experiments but has not been used much in product analysis studies. Figure 111.2 shows a diagrammatic experimental setup of the method. The concept of this method is to generate intermediates with the first laser pulse and photolyze the intermediates with the second laser pulse. The wavelength of the first laser pulse can be adjusted to the absorption of starting materials and that of the second laser pulse to the absorption of the intermediates. The maximum yield of the photochemical products of the intermediates should be obtained if the second laser pulse irradiates when the concentration of the intermediate becomes maximum.

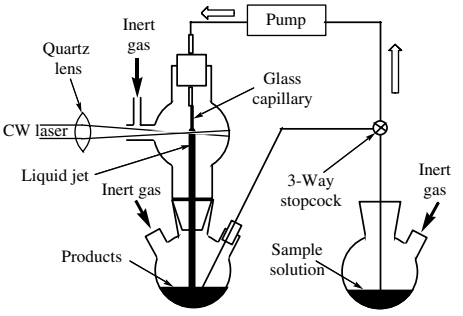

FIGURE 111.1

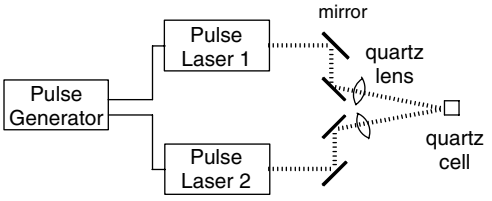

FIGURE 111.2

111.3 Selected Examples

Photolysis of Triplet Species

Scheme 2 shows an example of the photolysis of a triplet state.[5] The reaction was conducted under high-intensity, laser-jet conditions. The triplet state of **1** is further excited to a higher state, which gave products **3** and **4** via biradical **2**. Compound **3** is formed by the reaction of **2** with solvent benzene and **4** is formed by a decarboxylation followed by a series of reactions shown in the scheme.

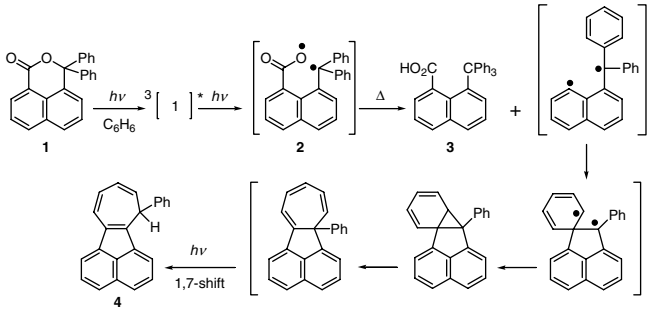

SCHEME 2

When cyclobutene **5** is irradiated with an XeCl excimer laser (308 nm), compounds **6** and **7** are formed (Scheme 3).[6] It was revealed that **6** is formed by the excitation of the triplet state of **5** whereas **7** was formed from higher singlet states. The transient spectrum of **5** shows a triplet absorption maximum at 440 nm with its maximum intensity appearing 3.9 μs after the laser pulse. The time-delayed, two-color pulse laser photolysis technique using an XeCl and 440-nm laser pulses showed the increase in the ratio of the yields **6**:**7**.

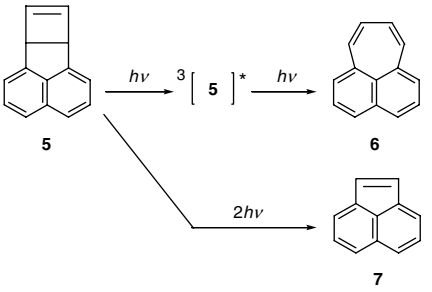

SCHEME 3

Scheme 4 shows the cleavage of the P–OAr bond in **8** from higher excited states, in contrast to the PO–Ar bond cleavage that occurs by a one-photon process.[7] The excited state that is populated by the second photon absorption is still not clear at the moment. However, participation of a triplet state is most likely because the heavy-atom effect of phosphorus is expected and the photolysis in alkane solution reduces the possibility of charge-transfer processes.

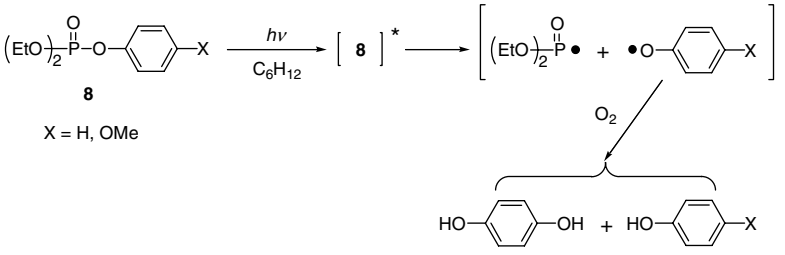

SCHEME 4

Further examples of the reactions from higher triplet states are shown in a review.[8]

Photolysis of Radicals

Radicals are also further photolyzed to give products. Scheme 5 shows the photolysis of benzil **9** that is conducted by the laser-jet technique in CCl_4, giving **12**, **13**, and **14** as photoproducts.[9] Compound **14** is a photochemical product of the benzyl radical **10**, which is generated by a two-photon process from **9**. The laser-jet reactions of diphenylmethyl radicals in CCl_4 and alcoholic solvents are also reported.[10]

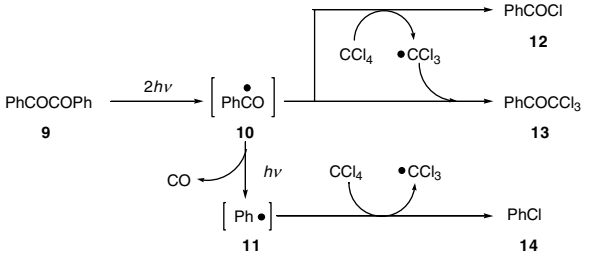

SCHEME 5

Scheme 6 is an interesting example of radical photolysis conducted by the laser-jet technique.[11] Radical **16** is generated by a two-photon reaction of **15**. When radical **16** absorbs another photon in CH_2Cl_2, it gives **18**, similar to the reaction shown in Scheme 5. However, when **16** is photolyzed in MeOH, the excited radical **16b** ionizes to cation **17**, which reacts with MeOH to give **19**. Similar reactions are also observed with 1-naphthyl[12] and 4-biphenylmethyl radicals.[13]

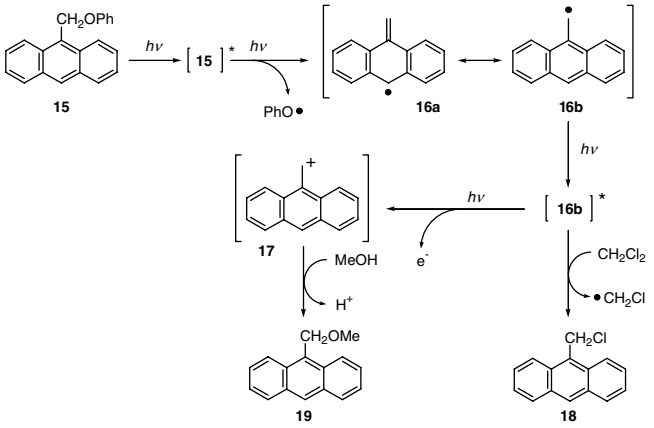

SCHEME 6

Scheme 7 shows another example of radical photolysis, in which radical **21** is the intermediate that undergoes the second photolysis.[14] Laser-drop photolysis of **20** shows the formation of **22**, which is confirmed by GC-MS analysis. The presence of radical **21** is observed by flash photolysis experiments using a 266-nm pulse laser. Similar reactions of 1,*n*-dihaloalkanes have been the subject of a review.[15]

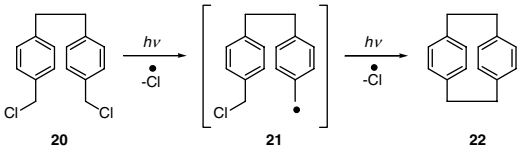

SCHEME 7

Further examples of such reactions brought about on the photolysis of radicals have also been reviewed.[8]

Photolysis of Carbenes and Nitrenes

Scheme 8 shows a two-photon reaction of bis(diazo) compound **23** conducted with a 248-nm pulse laser. Monocarbene **24** is generated as an intermediate and further photolyzed to biscarbene **25** within the same laser pulse, which undergoes intramolecular coupling to **26** and **27**.[16] Compounds **26** and **27** are not observed in conventional light photolysis.

Scheme 9 is the result of an experiment using a KrF excimer laser (248 nm) to bring about photolysis of diazide **28**. Diazide **28** is photolyzed to the mononitrene **29** and then to dinitrene **30a**, which tautomerizes into biradical **30b**. Intermediates **30a** and **30b** undergo polymerization and form a violet solid **31**.[17]

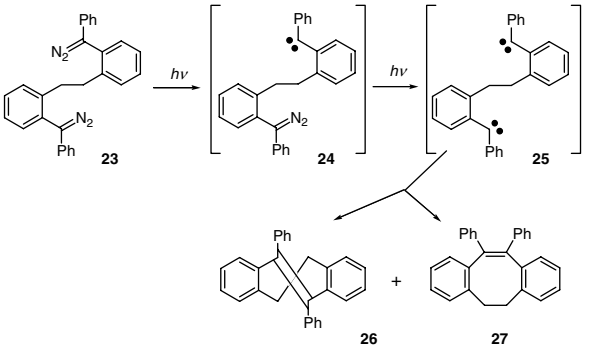

SCHEME 8

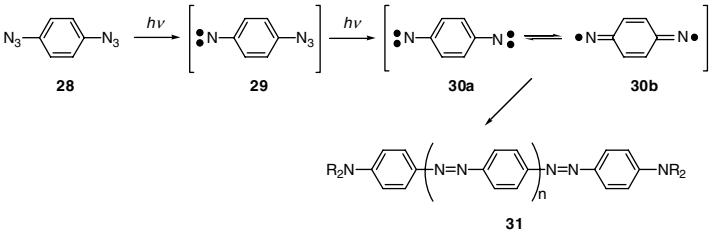

SCHEME 9

Photolysis of Unstable Molecules

Most of the photolyses of unstable compounds is directed toward the behavior of ketenes. Scheme 10 shows a laser-drop photolysis of diazo compound **32**. Ketene **33** is formed and further photolyzed to **34**, to which two alcohol molecules add to give the stable diester **35**.[18]

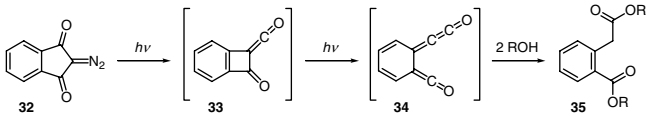

SCHEME 10

Scheme 11 is a laser-jet photolysis of the intermediate ketene **37** generated from **36** by a multiphoton process.[19] In addition to the formation of **39**, photochemical decarbonylation of **37** also occurs under photolysis conditions to give carbene **38**, which forms **40**. Similar examples on the photolysis[20] and photochemical decarbonylation[21] of ketenes have been reported.

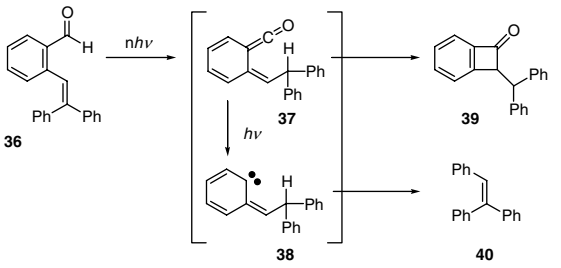

SCHEME 11

The reaction shown in Scheme 12 was studied using the time-delayed, two-color pulse laser photolysis technique.[22] An unstable *o*-quinodimethane derivative **42** is photochemically generated from substituted indanone **41**. The *o*-quinodimethane derivative **42** is further photolyzed to **43** and **44**. In the case of simple 308-nm laser photolysis, the ratio of the yields **44**:**43** is 2.54, whereas the ratio changes to 3.93 when the time-delayed, two-color photolysis technique is used. In the two-color photolysis, the first laser used is a 308-nm laser pulse and the second is a 480-nm laser pulse that is irradiated 2 μs after the first laser pulse. The wavelength of the second laser is adjusted to the absorption maximum of **42**.

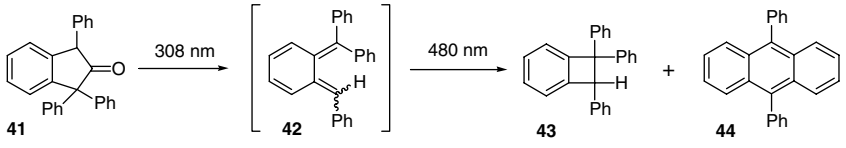

SCHEME 12

Scheme 13 is another example of a time-delayed, two-color pulse laser photolysis.[23] The unstable ketene **46** was generated by the first KrF laser pulse irradiation, which gave **47** by the addition of H_2O. However, with successive 337-nm laser pulse irradiations, **50**, **51**, **53**, and **54** are formed through the sequence of reactions shown in the scheme. The yields of **47**, **50**, **51**, **53**, and **54** were very dependent on the delay time of the two laser pulses.

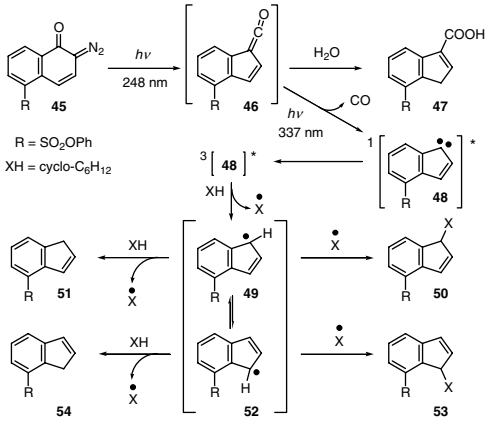

SCHEME 13

111.4 Improving the Efficiency of the Photochemical Reactions of Short-Lived Transient Species

A systematic study of the increase of the efficiency in the photochemical reactions of transient species has been reported using 1,8-bis(substituted-methyl)naphthalenes **55** (Scheme 14).

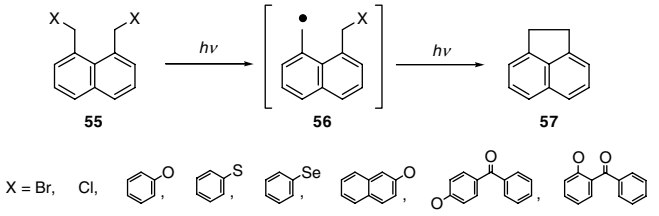

SCHEME 14

A simple laser photolysis of **55** (X = Br, Cl) using XeCl (308 nm), KrF (248 nm), and ArF (193 nm) excimer lasers shows that the yield of the two-photon product acenaphthene **57** decreases in the order KrF > XeCl > ArF.[24,25] By analogy with the photolysis of 1-halomethylnaphthalenes,[26] **55** is excited to its S_1, S_2, and S_3 states by the irradiation of XeCl, KrF, and ArF excimer lasers, respectively, and the energy dissipation from each excited state is shown in Scheme 15.[25] The presence of the intermediate monoradical **56** is confirmed by nanosecond flash photolysis experiments.[27]

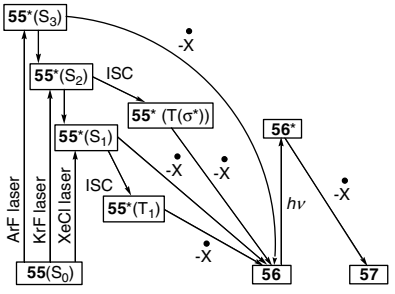

SCHEME 15

When **55** is excited to the S_1 state by the XeCl laser pulse, it undergoes intersystem crossing (ISC) to the T_1 state. The lifetime of the T_1 state is expected to be 0.5 to 0.7 μs, so that the monoradical **56** is generated at least 0.5 to 0.7 μs after the irradiation by the first laser pulse. However, this time range is larger than the pulse width of the XeCl laser (17 ns); thus, **56** has a very small chance of absorbing the second photon. This explains the low yield of the two-photon product **57** by the XeCl laser photolysis (*cf.* Scheme 15: **55***(S_1) → **55***(T_1) → 56).

KrF laser photolysis of **55** gives a very fast generation of **56** through its S_2 state and successive ISC to the T(σ*) state. The high yield of **57** by the excitation of **55** to its S_2 state is explained by the efficient generation and succeeding second photon absorption of **56** within the same laser pulse (30 ns) (*cf.* Scheme 15: **55***(S_2)→**55***(T(σ*))→**56**).

The use of halogen atoms for leaving groups X decreases the yield of **57** due to the high reactivity of the eliminated halogen atoms.[24a,25]

The above results indicate several problems in the photolysis of short-lived intermediates, including:

1. Wavelength matching. Starting materials and intermediates have different absorptions so that when the wavelength of lasers is optimized for the photolysis of the starting compounds, it is not the ideal wavelength for the intermediates and vice versa.

2. Photolysis timing. When pulse lasers are used, the generation of intermediates and successive photolyses have to be conducted within the same laser pulse.
3. Energy transfer. In the case of **55**, photons are absorbed by the naphthalene moiety and the energy is transferred to the cleaving C-X bond that is not directly connected to the naphthalene ring. For efficient energy transfer, cleaving bonds should be directly connected to the chromophores.
4. Secondary reactions. Suppression of the reactivity of the cleaved leaving groups is necessary to minimize secondary reactions.

These problems can be improved by two means: (1) improving the photolysis technique and (2) by chemical modification of the substrates.

Increasing the Photochemical Efficiency by Improvement of Photolysis Technique

Laser-jet and time-delayed, two-color pulse laser photolysis techniques can be used to overcome problems 1 and 2 above. In the case of the laser-jet technique, the three emissions (333, 351, and 364 nm) of an argon ion laser can be used at the same time for the wavelength matching of the starting materials and the intermediates; in general, the shorter wavelength is suitable for the photolysis of starting materials and the longer wavelength for the intermediates. The irradiation time is generally 10 to 100 μs, which is sufficient for the generation of intermediates and for conducting successive photolysis. In the case of the time-delayed, two-color pulse laser photolysis technique, the wavelength of the first and the second laser pulses can be matched with the starting material and the intermediate, respectively, and the second laser pulse can be fired at the time when the concentration of the intermediate is at its maximum.

Laser-Jet Photolysis

In the reaction shown in Scheme 14, the low yield of **57** by the excitation to the S_1 state is explained by the difference of the timing between the laser pulse irradiation (17 ns) and the generation of **56** (> 0.5–0.7 μs). By the laser-jet photolysis technique using an argon ion laser (using all 333-, 351-, and 364-nm emissions), the irradiation time of the laser to **55** can be prolonged to *ca.* 100 μs so that the timing problem can be solved. Furthermore, the 333-nm emission is suitable for the photolysis of **55,** and the 351- and 364-nm lines are good for the photolysis of **56**.

There are no standards for the comparison of the efficiency between pulse laser photolysis and laser-jet photolysis. However, when the efficiency is compared with parameters — yield of **57**/photon and yield of **57**/fluence (photons·m^{-2}·s^{-1}) — the laser-jet photolysis technique showed an increase of both parameters by three orders of magnitude compared with that in the simple XeCl laser photolysis.[25,28] A similar trend was also observed when the leaving group X is changed to OPh, SPh, and SePh.[29]

Time-Delayed, Two-Color Pulse Laser Photolysis

Time-delayed, two-color pulse laser photolysis is applied to the reaction of **55** (Scheme 14). An XeCl (308 nm) (first laser pulse) and an XeF (351 nm) (second laser pulse) excimer laser pulse are irradiated successively to **55** (X = Cl) with varying delay times.[25,30] The result is shown in Figure 111.3. The horizontal

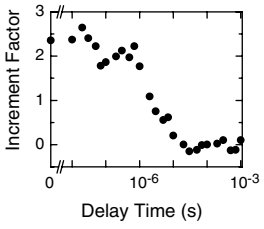

FIGURE 111.3 Increment factor of **57** as a function of the delay time of the two laser pulses.

axis of the figure shows the delay time of the two lasers and the vertical axis shows the Increment Factor (IF), which is defined as (A − B)/B, where A is the yield of **57** obtained by the time-delayed, two-color pulse laser photolysis and B is the yield of **57** obtained by the simple XeCl laser photolysis. An interesting feature in Figure 111.3 is that the IF, which reflects the concentration of **56**, shows two maxima: at 0 to 30 ns and and at 0.2 to 0.5 μs. The maximum at 0.2 to 0.5 μs is explained by the formation of **56** via the T_1 state and that at 0 to 30 ns is rationalized in terms of direct formation of **56** from the S_1 state (*cf.* Scheme 15: **55***(S_1) → **56**). A similar trend is also observed when the leaving group X is OPh, SPh, and SePh.[31] In the case of SPh, the IF increases to 8.

Improving the Photochemical Efficiency by Chemical Modification of Substrates

By using OPh, SPh, and SePh groups as the leaving group X in the reaction of **55**, the two leaving groups can be directly excited by the same wavelength because they have identical absorptions. This solves problems 1 and 2. Problem 3 is also solved because the chromophore of these leaving groups is directly connected to the cleaving bonds. The stability of the OPh, SPh, and SePh radicals is expected to be greater, especially for SPh and SePh, so that problem 4 can be also overcome. The photolysis of **55** (X = OPh, SPh, SePh) shows considerable improvement in the yield of **57**, which shows the maximum yield of 72% by simple KrF excimer laser photolysis using PhS leaving groups.[32] The presence of intermediate **56** was confirmed by nanosecond flash photolysis experiments.[33] However, when X is Se, the monoradical **56** prefers to exist as the bridged structure **58**, which is supported by semi-empirical MO calculations.[29] The photolysis can be conducted at longer wavelengths using an XeF (351 nm) excimer laser when 4-benzoyloxyphenoxy and 2-benzoyloxyphenoxy groups are used for the leaving groups.[32]

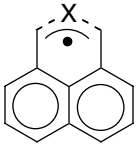

58

111.5 Applications

Synthetic Applications

o-Quinodimethane **62** can be generated from 1,2-bis(substituted-methyl)benzenes **59** (X = O, S, Se) via monoradical **60** by a two-photon process using excimer laser photolysis (Scheme 16). The conventional precursors of **62** often used in organic synthesis generally need several steps for preparation, whereas **59** can be synthesized in one step in good yield from commercially available 1,2-bis(bromomethyl)benzene.

The effects of laser fluence, substrate concentration, and optical path were investigated by simple laser photolysis of KrF, XeCl, and XeF excimer lasers.[34] The yield of **64** increased with the decrease of the concentration of **59**, with the decrease of the length of the optical path, and with the increase of the fluence of the laser. The maximum yield of **64** obtained by irradiation of the KrF excimer laser was 48% at room temperature and 60% at 60°C. The decrease in length of the optical path for increasing product yields has considerable synthetic importance because the increase in laser intensity often results in the destruction of the reaction vessel.

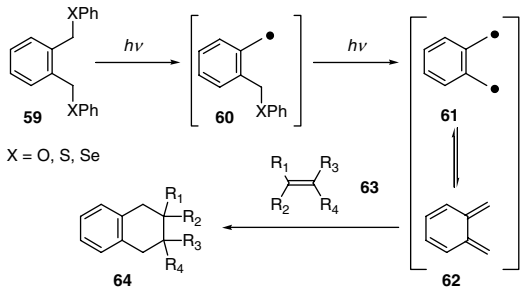

SCHEME 16

Mechanistic Studies

Photochemical Efficiency of the Photolysis of *o*-Quinodimethane in Solution at Room Temperature

As shown in Scheme 17, the KrF laser photolysis of **59-Se** in the absence of olefins yielded benzocyclobutene **65** and *o*-quinodimethane spiro dimer **66**. The formation of **65** is explained by the initial generation of **62** from **59-Se** via a two-photon process and the successive one-photon reaction of **62**, within the same pulse of the KrF laser.[35] The thermal dimerization of **62** to **66** is known to occur even at −150°C in an organic solid matrix.[36a,b] This photochemical reaction of **62** was never conducted in solution at room temperature; thus, its photochemical efficiency remains unknown.

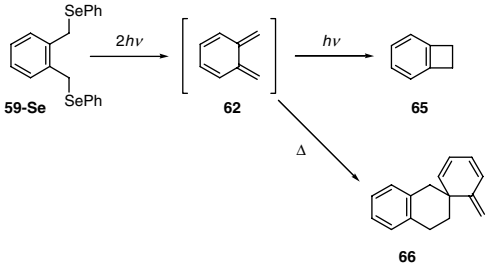

SCHEME 17

A time-delayed, two-color pulse laser photolysis of **59-Se** was conducted using KrF and XeCl (or XeF) excimer lasers. The result of this is shown in Figure111.4.[35,37] This figure shows that the yield of **65** is maximum at *ca.* 20 ms, whereas that of **66** achieves its minimum at the same delay time. The yield of **65** at each delay time reflects the concentration of **62** so that the result indicates that the concentration of **62** becomes a maximum at 20 ms. Figure 111.4c shows that **62** decreases with second-order kinetics, which is consistent with the flash photolysis experiment of which **62** is generated from different precursors.[38]

The photochemical efficiency of the formation of **65** from **62** is obtained by analysis of the delay-time dependence of the yield of **65**. An interesting result in this experiment is that a wavelength effect on the formation of **65** was observed when XeCl (308 nm) (Figure 111.4a) and XeF (351 nm) (Figure 111.4b) excimer lasers were used as the second laser. Although the molar absorption coefficient of **62** at 351 nm is threefold larger than that at 308 nm,[36b,c] the yield of **65** was 2.5-fold higher when the 308-nm laser was used instead of the 351-nm laser. Participation of the higher excited state S_2 [36a,b,d] for the photochemical conversion of **62** to **65** is postulated but the $S_0 \rightarrow S_2$ transition is still not explicitly observed by spectroscopic means. It is probably buried under the more intense $S_0 \rightarrow S_1$ band. The wavelength effect of the second laser in the time-delayed, two-color pulse laser photolysis supports this theoretical prediction.

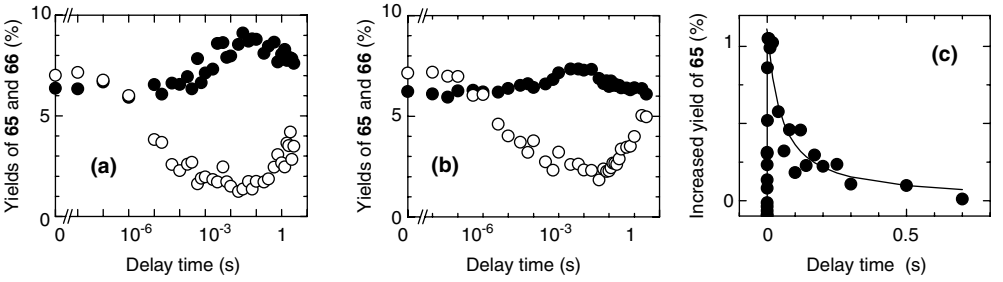

FIGURE 111.4 Yields of **65** and **66** (a,b) and increased yield of **65** (c) as a function of the delay time of the two laser pulses. Combination of the two lasers: KrF – XeCl (a), KrF – XeF (b). **65**: closed circle; **66**: open circle.

Determination of Kinetic Constants of Fast Reactions

Although the cycloaddition of **62** with alkenes (**63**) and alkynes is one of the well-investigated reactions, the rate constant for cycloaddition in solution at room temperature has not been reported thus far. This may be due to the difficulty in conducting the experiments spectroscopically. The rate constant for the cycloaddition of **62** and maleic anhydride **67** in solution at room temperature is determined by product analyses using the time-delayed, two-color pulse laser photolysis technique (Scheme 18).[39] Compound **62** is generated via irradiation of a KrF laser pulse to **59-Se** in the presence of **67**. The cycloaddition of **62** to **67** yields the adduct **68** (Path 1), together with the thermal products of **62**[38c] (Path 2). The cycloaddition is quenched by the decomposition of the remaining **62** by the second XeCl laser pulse, which is irradiated after varied delay times between 0 and 0.1 s. The rate constant for the cycloaddition of **62** and **67** is obtained by analyzing the delay-time dependence of the yield of **68**, which is found to be $2.1 \times 10^5\ M^{-1}\cdot s^{-1}$.

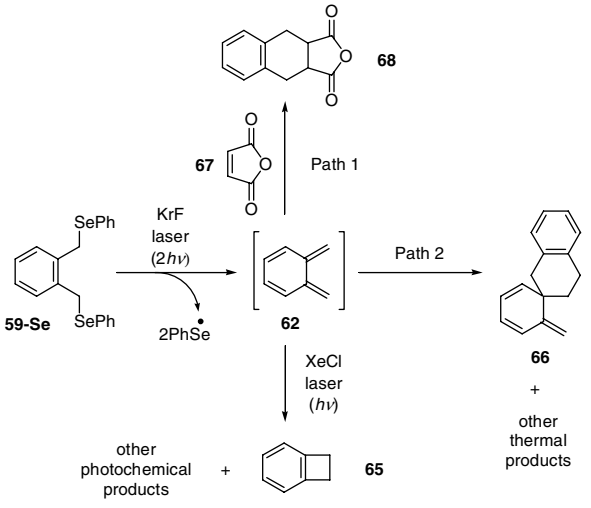

SCHEME 18

References

1. Wilson, R.M. and Schnapp, K.A., High-intensity Laser photochemistry of organic molecules in solution, *Chem. Rev.*, 93, 223–249, 1993.
2. Johnston, L.J., Photochemistry of radicals and biradicals, *Chem. Rev.*, 93, 251–266, 1993.
3. Banks, J.T. and Scaiano, J.C., The laser-drop method: a new approach to induce multiple photon chemistry with pulsed lasers. Examples involving reactions of diphenylmethyl and cumyloxy radicals, *J. Am. Chem. Soc.*, 115, 6409–6413, 1996.
4. Wilson, R.M., Schnapp, K.A., Hannemann, K., Ho, D.M., Memarian, H.R., Azadnia, A., Pinhas, A.R., and Figley, T.M., High intensity, argon ion laser-jet photochemistry, *Spectrochim. Acta*, 46A, 551–558, 1990.
5. Wilson, R.M., Schnapp, K.A., Glos, M., Bohne, C., and Dixon, A.C., High-intensity, laser-jet photochemistry: photodecarboxylation of 3,3-diphenyl-1*H*,3*H*-naphtho[*cd*][2]pyran-1-one, *J. Chem. Soc., Chem. Commun.*, 149–150, 1997.
6. Plaas, D. and Schäfer, F.P., Laser photochemistry of aromatic substituted cyclobutanes and cyclobutenes, *Chem. Phys. Lett.*, 131, 528–533, 1986.
7. Nakamura, M., Ouchi, A., Miki, M., and Majima, T., Photochemical P-O bond fission of aryl diethyl phosphates by a resonant two-photon reaction, *Tetrahedron Lett.*, 42, 7447–7449, 2001.
8. McGimpsey, W.G., Chemical and photophysical processes of transients derived from multiphoton excitation: upper excited states and excited radicals, *Mol. Supramol. Photochem.*, 2, 249–306, 1998.
9. Adam, W. and Schulte Oestrich, R., Two-photon cleavage of benzil in the laser-jet: intermolecular reaction of transient benzoyl and *tert*-butoxy radicals in the photolysis of *tert*-butyl peroxide mixtures, *J. Am. Chem. Soc.*, 115, 3455–3457, 1993.
10. (a) Adam, W. and Kita, F., Photochemistry of the 9-hydroxyxanthenyl radical in the laser-jet: evidence for photochemically induced, regioselective radical coupling, *J. Am. Chem. Soc.*, 116, 3680–3683, 1994; (b) Adam, W., Kita, F., and Schulte Oestrich, R., Two-photon chemistry in the laser jet: generation of radical intermediates and their photochemical transformations, *J. Photochem. Photobiol., A: Chem.*, 80, 187–197, 1994; (c) Adam, W. and Walther, B., Multiple-photon chemistry in the benzophenone photoreduction during laser-jet photolysis: effect of alcohol solvent on cross-coupling *versus* hydrogen abstraction of the electronically excited hydroxydiphenylmethyl radical, *Tetrahedron*, 52, 10399–10404, 1996.
11. Adam, W., Schneider, K., Stapper, M., and Steenken, S., Multiple-photon chemistry of 9-(phenoxymethyl)- and 9, 10-bis(phenoxymethyl)anthracenes in the laser-jet: generation, photochemistry and time-resolved laser-flash spectroscopy of anthracenyl radicals and pulse radiolysis of 9-(bromomethyl)anthracene, *J. Am. Chem. Soc.*, 119, 3280–3287, 1997.
12. Adam, W., Schneider, K., and Steenken, S., Multiple-photon chemistry in the laser-jet: photochemistry and time-resolved laser-flash spectroscopy of the 1-naphthylmethyl radical, *J. Org. Chem.*, 62, 3727–3733, 1997.
13. Adam, W. and Schneider, K., Multiple-photon chemistry in the laser-jet: photochemistry of the 4-biphenylmethyl radical, *J. Chem. Soc., Perkin Trans. 2*, 441–444, 1997.
14. Miranda, M.A., Font-Sanchis, E., Pérez-Prieto, J., and Scaiano, J.C., The 4, 4′-(1, 2-ethanediyl)bis-benzyl biradical: its generation, detection and (photo)chemical behavior in solution, *J. Org. Chem.*, 66, 2717–2721, 2001.
15. Miranda, M.A., Pérez-Prieto, J., Font-Sanchis, E., and Scaiano, J.C., One- vs two-photon processes in the photochemistry of 1,*n*-dihaloalkanes, *Acc. Chem. Res.*, 34, 717–726, 2001.
16. (a) Hannemann, K. and Wirz, J., Preparative UV-laser photochemistry: a biscarbene intermediate in the synthesis of a 5,6-dihydrodibenzo[*a, e*]cyclooctene containing a *trans*-double bond, *Angew. Chem. Int. Ed. Engl.*, 27, 853–855, 1988; (b) Hannemann, K., Wirz, J., and Riesen, A., Conventional and laser photolysis of a bisdiazo compound, *Helv. Chim. Acta*, 71, 1841–1857, 1988.

17. Ohana, T., Ouchi, A., Moriyama, H., and Yabe, A., Preparation of polykis azobenzene by photolysis of 1,4-diazidobenzene with excimer laser radiation, *J. Photochem. Photobiol., A: Chem.*, 72, 83–86, 1993.
18. Banks, J.T. and Scaiano, J.C., Laser drop and low intensity photolysis of 2-diazo-1,3-indanone: evidence for a propadienone intermediate, *J. Photochem. Photobiol., A: Chem.*, 96, 31–33, 1996.
19. Wilson, R.M., Patterson, W.S., Austen, S.C., Ho, D.M., and Bauer, J. A.K., Orbital symmetry governed reactions under high-intensity argon laser-jet conditions: the involvement of a [1, 5_s] sigmatropic shift in the photocyclization of an *o*-alkenylbenzaldehyde to a benzocyclobutenone, *J. Am. Chem. Soc.*, 117, 7820–7821, 1995.
20. Adam, W. and Patterson, W.S., High-intensity laser-jet photochemistry: formation of benzocyclobutenedione from 1, 2, 3-indantrione *via* transient targeting, *J. Org. Chem.*, 60, 7769–7773, 1995.
21. Wilson, R.M., Romanova, T.N., Azadnia, A., Bauer, J.A.K., and Johnson, R.P., The argon laser-jet initiated, multiple-photon (reluctant), electrocyclic ring opening of 10, 10-diphenyl-9-(10*H*)-phenanthrenone: a carbene and biradical modeling study, *Tetrahedron Lett.*, 35, 5401–5404, 1994.
22. Netto-Ferreira, J.C., Wintgens, V., and Scaiano, J.C., Photochemistry of 1,1,3-triphenyl-2-indanone. Spontaneous and photochemical decay of *ortho*-xylylenes, *Tetrahedron Lett.*, 30, 6851–6854, 1989.
23. Bendig, J. and Mitzner, R., Laser photolysis of naphthoquinone diazide in cyclohexane — Two-laser chemistry, *Ber. Bunsenges. Phys. Chem.*, 98, 1004–1008, 1994.
24. (a) Ouchi, A. and Yabe, A., A laser-specific C-C bond formation of bichromophoric compounds, *Tetrahedron Lett.*, 31, 1727–1730, 1990; (b) Ouchi, A. and Yabe, A., A remarkable wavelength dependence on the laser-induced two-photon C-C bond formation, *Tetrahedron Lett.*, 33, 5359–5362, 1992.
25. Ouchi, A., Koga, Y., and Adam, W., Two-photon laser-induced reaction of 1,8-bis(halomethyl)naphthalenes from different excited states and transient targeting of its intermediate by time-delayed, two-color photolysis and argon ion laser-jet photolysis techniques, *J. Am. Chem. Soc.*, 119, 592–599, 1997.
26. (a) Johnston, L.J. and Scaiano, J.C., Generation, spectroscopy and reactivity of excited 1-naphthylmethyl radicals, *J. Am. Chem. Soc.*, 107, 6368–6372, 1985; (b) Tokumura, K., Udagawa, M., and Itoh, M., Two-step laser excitation fluorescence study of the reactions of the 1-naphthylmethyl radical produced in the 248-nm KrF laser photolysis of 1-(chloromethyl)naphthalene in hexane at room temperature, *J. Phys. Chem.*, 89, 5147–5149, 1985; (c) Kelley, D.F., Milton, S.V., Huppert, D., and Rentzepis, P.M., Formation kinetics and spectra of aromatic radicals in solution, *J. Phys. Chem.*, 87, 1842–1843, 1983; (d) Hilinski, E.F., Huppert, D., Kelley, D.F., Milton, S.V., and Rentzepis, P.M., Photodissociation of haloaromatics: detection, kinetics and mechanism of arylmethyl radical formation, *J. Am. Chem. Soc.*, 106, 1951–1957, 1984.
27. Ito, O., Alam, M.M., Ouchi, A., and Koga, Y., Laser flash photolysis of 1,8-bis(halomethyl)naphthalenes, *J. Photochem. Photobiol., A: Chem.*, 97, 19–23, 1996.
28. Adam, W. and Ouchi, A., Two-photon chemistry of 1,8-bis(bromomethyl)naphthalene in the laser-jet: generation of acenaphthene by intramolecular C-C bond formation, *Tetrahedron Lett.*, 33, 1875–1878, 1992.
29. Ouchi, A. and Adam, W., Laser-jet photolysis of 1,8-bis(substituted-methyl)naphthalenes: the effect of heteroatom leaving groups on the two-photon C-C bond formation, *J. Chem. Soc., Chem. Commun.*, 628–629, 1993.
30. Ouchi, A. and Yabe, A., Time-delayed, two-color excimer laser photolysis of 1,8-bis(halomethyl)naphthalenes, *Chem. Lett.*, 945–946, 1995.
31. Ouchi, A. and Koga, Y., Time-delayed, two-color excimer laser photolysis of 1,8-bis(substituted-methyl)naphthalenes with Group 16 atom leaving groups, *Tetrahedron Lett.*, 36, 8999–9002, 1995.
32. Ouchi, A. Yabe, A., and Adam, W., Highly efficient C-C bond formation in the two-photon chemistry of 1,8-bis(substituted-methyl)naphthalenes by direct excitation of photoactive leaving groups, *Tetrahedron Lett.*, 35, 6309–6312, 1994.

33. Ouchi, A., Koga, Y., Alam, M.M., and Ito, O., Laser flash photolysis of 1,8-bis(substituted-methyl)naphthalenes, *J. Chem. Soc., Perkin Trans. 2*, 1705–1709, 1996.
34. (a) Ouchi, A. and Koga, Y., KrF excimer laser photolysis of 1,2-bis(substituted-methyl)benzenes in the presence of alkenes and acetylene; two-photon formation of *o*-quinodimethane and its cycloaddition with dienophiles, *J. Chem. Soc., Chem. Commun.*, 2075–2076, 1996; (b) Ouchi, A. and Koga, Y., A facile synthesis of tetra- and dihydronaphthalene derivatives by excimer laser photolysis of 1,2-bis(substituted-methyl)benzenes in the presence of olefins and acetylene, *J. Org. Chem.*, 62, 7376–7383, 1997.
35. Ouchi, A. and Koga, Y., Effect of irradiation timing and wavelength in the time-delayed, two-color photolysis of 1,2-bis[(phenylseleno)methyl]benzene: transient targeting of *o*-quinodimethane in room-temperature solutions, *J. Org. Chem.*, 63, 6780–6781, 1998.
36. (a) Flynn, C.R. and Michl, J., Photochemical preparation of *o*-xylylene from 1,4-dihydrophthalazine in rigid glass, *J. Am. Chem. Soc.*, 95, 5802–5803, 1973; (b) Flynn, C.R. and Michl, J., π,π-Biradicaloid hydrocarbons: *o*-xylylene. Photochemical preparation from 1,4-dihydrophthalazine in rigid glass, electronic spectroscopy and calculations, *J. Am. Chem. Soc.*, 96, 3280–3288, 1973; (c) Fujiwara, M., Mishima, K., Tamai, K., Tanimoto, Y., Mizuno, K., and Ishii, Y., Spectroscopic studies on photochemical formation of *o*-xylylene in solution, *J. Phys. Chem. A*, 101, 4912–4915, 1997; (d) Tseng, K.L. and Michl, J., An approach to biradical-like species: spectroscopy of *o*-xylylene in argon matrix, *J. Am. Chem. Soc.*, 99, 4840–4842, 1977.
37. Ouchi, A., Sakuragi, M., Kitahara, H., and Zandomeneghi, M., Determination of the photochemical efficiency of *o*-quinodimethane ring closure in room temperature solutions by using time-delayed, two-color photolysis technique, *J. Org. Chem.*, 65, 2350–2357, 2000.
38. (a) Scaiano, J.C., Wintgens, V., and Netto-Ferreira, J.C., Mechanistic studies of the photogeneration and photochemistry of *ortho*-xylylenes, *Pure Appl. Chem.*, 62, 1557–1564, 1990; (b) Roth, W.R., Biermann, M., Dekker, H., Jochems, R., Mosselman, C., and Hermann, H., Das Energieprofil des *o*-Chinodimethan-Benzocyclobuten-Gleichgewichtes, *Chem. Ber.*, 111, 3892–3903, 1978; (c) Trahanovsky, W.S. and Macias, J.R., Direct observation of *o*-xylylene (*o*-quinodimethane) in solution. Dimerization kinetics of some *o*-quinodimethanes, *J. Am. Chem. Soc.*, 108, 6820–6821, 1986.
39. Ouchi, A., Li, Z., Sakuragi, M., and Majima, T., A two-color laser photolysis method for determining reaction rates of short-lived intermediates by product analysis: application to the *o*-quinodimethane problem, *J. Am. Chem. Soc.,* 125, 1104–1108, 2003.

112

Action Spectroscopy: General Problems

Edward D. Lipson
Syracuse University

112.1 Introduction

Action spectroscopy is a general approach toward identifying the receptor pigment for a particular photobiological response or effect. The early identification of major chromophores, such as rhodopsin and chlorophyll, depended on comparison of the action spectra for vision and photosynthesis, respectively, with the absorption spectra of candidate pigments.

It is remarkable how few chromophore types with intrinsic photochemistry are employed in photobiological systems.[1,2] A basic list consists of the following:

1. Retinal pigments (in rhodopsins)
2. Tetrapyrroles (including chlorophylls, and phycobiliproteins including phytochromes)
3. Flavin and pterin accessory chromophores (in cryptochrome and phototropin pigments; these are blue-light receptors in plants and microorganisms and, in the case of cryptochromes, in animals too)
4. Hypericin pigments[2]
5. The *p*-coumaric acid chromophore of the photoactive yellow protein (PYP) of *Ectothiorhodospira halophila*[3,4] (now reclassified *Holorhodospira halophila,* see Chapter 123)

This focus in this chapter is on analytical methods for measuring action spectra, with emphasis on those derived from fluence-response data. For a set of examples, the reader can consult studies of *Phycomyces,* not only studies of its phototropism[5–7] but also of the light–growth response,[8,9] carotene synthesis,[10] and differentiation,[11] as well as studies of other blue-light systems.[12–16] The later studies on *Phycomyces* employed formal data analysis methods — including error analysis (and error propagation[17])

0-8493-1348-1/04/$0.00+$1.50

in the curve fitting and parameter estimation — as summarized elsewhere,[18] so that error bars could be assigned to the points in the action spectra derived from the fluence-response raw data points and their error bars.

For other representative action spectra, the reader is referred to the following chapters in this volume and to the major photobiology journals: *Photochemistry and Photobiology, Journal of Photochemistry and Photobiology, B: Biology,* and *Photochemical and Photobiological Sciences*. There are also a number of review articles that give various perspectives on action spectroscopy.[18–27] For practical advice on light sources and radiometry, the reader should consult standard photobiology texts.[28–30]

112.2 Alternative Types of Action Spectra

The most elementary type of action spectrum consists of a graph of some response or effect as a function of wavelength, under conditions where the photon fluence is maintained constant at all wavelengths. This convenient approach, however, can be confounded by the frequent circumstance that the response may depend nonlinearly on the fluence (or fluence rate). For example, if at some wavelengths the response is in a saturation region, then the action spectrum will be "clipped" (*viz.* peaks flattened) at those wavelengths; similarly, other types of nonlinearities will produce other distortions. Accordingly, a preferred way of obtaining an action spectrum — provided that the experimenter is willing and able to apply the additional effort needed — is to derive it from fluence-response curves (sometimes called dose-response curves, by analogy with pharmacology). In this way, one essentially obtains a graph of sensitivity, rather than response, as a function of wavelength. Operationally, for each wavelength, the photon fluence required to achieve a standard response level is determined and then the reciprocal of that photon fluence is plotted as a measure of sensitivity. The graph so obtained is sometimes called an "equal-response action spectrum," which is not subject to the nonlinear distortions above and is, therefore, more likely to represent the absorption spectrum of the responsible chromophore (subject to various considerations specified below).

112.3 Photophysics

After a chromophore absorbs a photon, a number of alternative photophysical events may ensue. These can be represented graphically by a "Jablonski diagram" depicting transitions among the electronic, vibrational, and rotational states of the pigment molecule.[31] Upon absorption of a photon, the molecule is promoted from the ground state (usually of singlet character, and designated, therefore, as S_0) to an excited electronic state (also singlet, and designated S_1, S_2, etc.); the molecule generally becomes excited with respect to vibrational and rotational motions, as well (the corresponding energy spacings among these states are progressively lower than those between electronic states). The molecule then de-excites rapidly by internal conversion and vibrational relaxation to the lowest excited singlet level S_1, before there is time for photochemistry to take place. Consequently, regardless of the wavelength of the incident photon that excited the molecule, the molecular excitation relaxes rapidly to the bottom vibrational levels based on S_1. Then, the relevant photochemistry proceeds directly from S_1 or — following intersystem crossing from the singlet to the triplet manifold — from the lowest triplet state T_1, provided that the excitation energy has not been dissipated in the meantime by internal conversion or fluorescence.

112.4 Illumination Units

Fluence-response curves are sometimes measured using broadband rather than monochromatic light, because higher fluence rates are achievable with broadband filters, and unless one is trying to study the wavelength dependence of a particular response or effect, it may be more representative of natural illumination conditions to use broadband light covering the range of sensitivity. For example, in studies of photogravitropism "threshold curves" of *Phycomyces* wild-type and mutant strains,[6,32] it is customary

to employ broadband blue illumination at fluence rates extending over a 10-decade range. With broadband illumination, the units pertain to energy fluence rather than photon fluence. The energy units are J m^{-2} for fluence and J m^{-2} s^{-1} (or, equivalently, W m^{-2}) for fluence rate. In action spectroscopy, however, one must use monochromatic light (occasionally in combination with polychromatic background light; see Chapter 113). It is then preferable to use photon units: photons m^{-2} for fluence, and photons m^{-2} s^{-1} for fluence rate.

112.5 Conditions for Measurement and Interpretation of Action Spectra

The shape of an action spectrum may be distorted significantly from the absorption spectrum of the responsible pigment. To obviate such distortions, the experimenter should strive to satisfy the following conditions insofar as possible:[24,27]

1. The quantum efficiency (or quantum yield) — defined as the probability that a particular type of event of photobiological or photochemical interest occurs as the result of absorption of a photon — should be independent of wavelength.
2. The absorption spectrum of the receptor pigment should be the same whether measured *in vivo* or *in vitro*.
3. Screening or shading pigments, as well as scattering effects, should not cause significant wavelength-dependent distortion. Scattering is generally stronger at shorter wavelengths, but the trend is a gradual one and normally would not obscure the key features of an action spectrum; instead, scattering tends to superpose a sloping baseline, which can be largely eliminated, if desired, by using a suitable scattering reference.
4. When an action spectrum is derived from fluence-response curves, the condition of reciprocity should be valid over the range of fluence rates and exposure times used. In other words, the response should depend on the product of fluence rate and exposure time but should not otherwise depend on either factor.
5. Light should not be totally absorbed by the sample for any wavelength under study. More specifically, an ample fraction of the incident light (a practical guideline is 50%) should reach the receptor pigment region under all conditions.

112.6 Reciprocity

For measurements employing continuous illumination, the stimulus strength is given by the fluence rate. With pulse illumination, however, the fluence can be adjusted by varying the exposure time (pulse width) and the fluence rate. Considering the kinetics of photochemical and subsequent dark reactions, it is preferable in most circumstances to maintain the exposure time constant and vary the fluence rate. In general, though, one should establish the range of validity of reciprocity between exposure time and fluence rate (see above).

112.7 Fundamental Derivations

For action spectroscopy with pulse illumination, assume that the response R can be expressed as a function of the product of four variables:

$$R = R\left(\phi \sigma_1 I_1 \Delta t\right) \tag{1}$$

where ϕ is the quantum efficiency (or quantum yield), σ_1 is the cross section (see below) at wavelength λ_1, I_1 is the fluence rate (note that the traditional symbol I stands for "intensity," which is sometimes used

informally in place of fluence rate; however, according to strict radiometric terminology, intensity is defined as the power per unit solid angle), and Δt is the exposure time (pulse duration). The fluence is given by $F_l = I_l \Delta t$.

To derive an equal-response action spectrum from fluence-response curves, the first step is to specify a "criterion" response level. Then, for each wavelength, the fluence (or fluence rate) needed to produce that standard response should be determined. Choices for the criterion response include the following:

1. Some fixed absolute level
2. A percentage (typically 50%) of the maximum response level, which may depend on wavelength
3. The maximum response (peak) level, for those instances where the response descends at high fluence after reaching a peak
4. The absolute threshold fluence rate (often extrapolated downward to the baseline from the linearly rising part of the fluence-response curve; note that an alternative approach that should be avoided would be to try to find the limiting fluence at which there just begins to be a perceptible response; the difficulty is that this measure is highly susceptible to experimental noise and subjective judgment; see below for a further discussion of threshold measurements)

If fluences $F_{\lambda 1}$ and $F_{\lambda 2}$ elicit the same response level — the criterion response — and if one assumes that Δt is the same in both experiments (or, if reciprocity applies, one can correct for the different values of Δt), then the argument of the function in Equation 1 is the same for both experiments at these two wavelengths, λ_1 and λ_2. If the quantum efficiency ϕ is assumed to be the same at both wavelengths, then

$$\frac{\sigma_{\lambda_1}}{\sigma_{\lambda_2}} = \frac{F_{\lambda_2}}{F_{\lambda_1}} \tag{2}$$

It is assumed implicitly that the fluence response curves are monotonic, or at least that the corresponding criterion response points on the curves are chosen (otherwise, if the fluence-response curve were, for example, bell-shaped, there would be two values of fluence with the same response value, and one could conceivably err by choosing noncorresponding points on curves for different wavelengths). From Equation 2, it is evident that the cross section at any wavelength λ is inversely proportional to the applied fluence that produces the criterion response at that wavelength, or $\sigma_\lambda \propto F_\lambda^{-1}$.

If, instead, the response is measured as a function of fluence rate rather than fluence, then a derivation similar to that above, starting from the equation

$$R = R\left(\phi \sigma_1 I_1\right) \tag{3}$$

leads to the relation

$$\frac{\sigma_{\lambda_1}}{\sigma_{\lambda_2}} = \frac{I_{\lambda_2}}{I_{\lambda_1}} \tag{4}$$

or

$$\sigma_\lambda \propto I_\lambda^{-1}$$

112.8 Relationship between Extinction Coefficient and Cross Section

The extinction coefficient ε is used in conventional spectrophotometry and measured in the traditional units of L mol^{-1}cm^{-1}. It can be related by a conversion factor to a quantity from physics, the absorption

cross section (introduced in the previous section), in traditional units of cm^2. The ratio between the fluence rate I transmitted through a spectrophotometric sample and the incident intensity I_0 can be derived from the following relations:

$$\frac{I}{I_0} = 10^{-\varepsilon c \ell} = e^{-\sigma n \ell} \tag{5}$$

where c is the molar concentration of the pigment, ℓ is the internal path length through the cuvette (usually 1 cm), σ is the absorption cross section, and n is the pigment concentration in units of molecules per cm^3. The expression in the first exponent, $\varepsilon c \ell$, represents the absorbance, A.

The extinction coefficient and the cross section are, therefore, interrelated by the following conversion formula:

$$\varepsilon = 2.62 \times 10^{20}\ \sigma \tag{6}$$

where ε is in units of L mol^{-1} cm^{-1}, and σ is in cm^2. As an example of applying this conversion formula, consider riboflavin (or other flavin), which has an extinction coefficient of 1.25×10^4 L mol^{-1} cm^{-1} (at ~450 nm); then $\sigma = 4.8 \times 10^{-17}$ cm^2. This represents the effective target area the chromophore presents for absorption of light. As another example, rhodopsin, with an extinction of 4×10^4 L mol^{-1} cm^{-1} (at ~500 nm) has $\sigma = 1.5 \times 10^{-16}$ cm^2.

112.9 Derivation of Action Spectrum from Fluence-Response Curves

Shown in Figure 112.1 is a set of five idealized fluence-response curves. In the following discussion, it will be demonstrated how action spectra can be derived from such curves. The hypothetical response is presumed to be measured as a function of the photon fluence; alternatively, fluence rate could have been chosen as the independent variable. The fitting function of the form $ax/(x+b)$, where x stands for the fluence (or fluence rate), is plotted for the five wavelengths on both logarithmic (a) and linear (b) scales for x. In this example, wavelength λ_3 is the most effective, because the least amount of light is required to achieve the criterion response level, chosen here to be half of the maximum response. Conversely, λ_5 is the least effective. So, when this set of "data" is converted into an action spectrum, the ordinate representing the sensitivity, or effectiveness, will be high for λ_3 and low for λ_5.

In the semilogarithmic plot (Figure 112.1a), the curves have the same sigmoidal shape and differ only by lateral displacement. The symmetrical sigmoidal shape is a property of the hyperbolic saturation function, which is frequently used to fit fluence-response curves and other types of stimulus-response relationships in sensory physiology,[33,34] in photochemical kinetics,[35] and in other areas of biophysics and biology, including the well-known Michaelis–Menten enzyme kinetics (see below).

The procedure for deriving the action spectrum (Figure 112.2) from these curves is straightforward. The action spectrum ordinate, often labeled as "relative quantum effectiveness," or just "effectiveness," is simply the reciprocal of the fluence required to produce a criterion response (see Equation 2 and Equation 4) as a function of wavelength. Some authors choose instead to label the ordinate in "relative units," for example, by normalizing several action spectra to the wavelength of maximal effectiveness of one of them. However, it is preferable to retain the proper physical units of m^2 mol^{-1}. If fluence rate-response curves are used instead as the basis for the action spectra, then the corresponding reciprocal units for the "effectiveness" are m^2 s mol^{-1}. In the former case — based on fluence rather than fluence rate — the units of the action spectrum ordinate are reciprocal to the fluence units, which are essentially m^{-2} (apart from dimensionless entities such as photons or moles of photons). Consequently, the action spectrum physical units are m^2, indicating that some kind of area quantity is involved. This dimensionality corresponds specifically to that of a cross section (see relationship, above, between extinction coefficient and cross section).

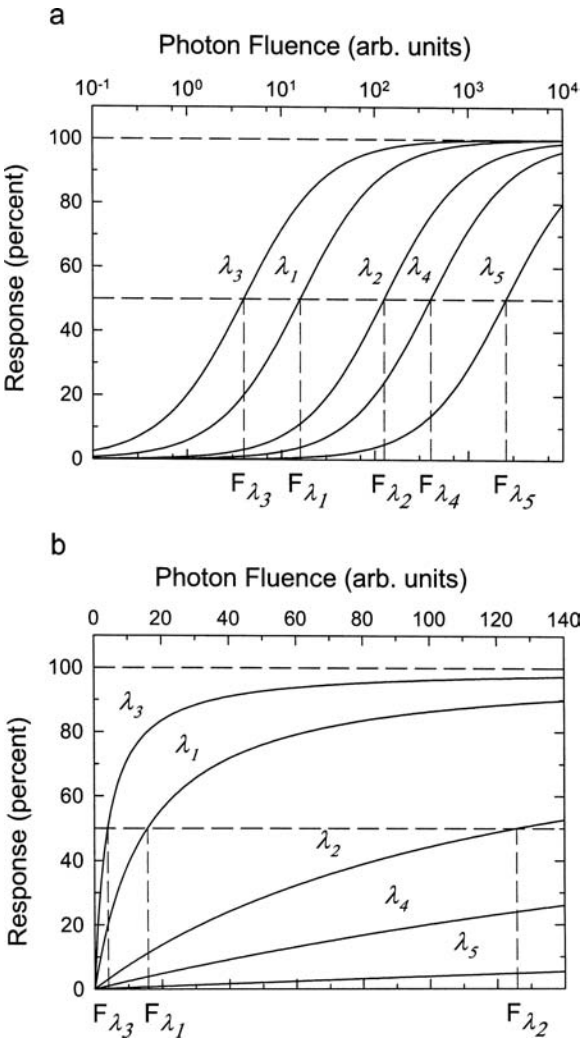

FIGURE 112.1 Generic fluence-response curves for five wavelengths (λ_1 through λ_5) shown on logarithmic (a) and linear (b) scales for photon fluence. The curves represent the hyperbolic saturation function of the form $ax/(x+b)$, where x is the fluence (also denoted in this chapter by the symbol F) (see top row of Table 1). On a semilogarithmic scale (a), the curves have the same sigmoidal shape (see functions in Rows 4 and 5 of Table 112.1). The fluence F needed to produce the standard criterion response (here chosen to be 50%) at each wavelength is shown by the vertical dashed lines. The designation of "arbitrary units" on the abscissa scales above each graph means that no importance should be given to the absolute numbers used in this example, and, implicitly, that fluence rate could be used instead of fluence if continuous rather than pulse illumination were employed; the actual units of photon fluence would be mol m^{-2}. If photon fluence rate were used instead, the units would be mol m^{-2} s^{-1}.

For a given application, one has to decide between plotting the action spectrum on a logarithmic or linear ordinate. In *Phycomyces*, with a sensitivity range exceeding 10 decades, it is particularly appropriate to plot such action spectra on a logarithmic ordinate.[6,32] This choice is advantageous for comparing action spectra to one another or to absorption spectra of putative receptor pigments. Spectra that differ only by a scale factor will have identical shapes on a logarithmic scale (and will be displaced by the logarithm of the scale factor). Now, if such spectra were identical, apart from a scale factor, they could be forced to have the same shape on a linear scale too, simply by normalizing them at any wavelength of choice (thereby, superposing the spectra completely). The practical problem, however, is that in the usual case,

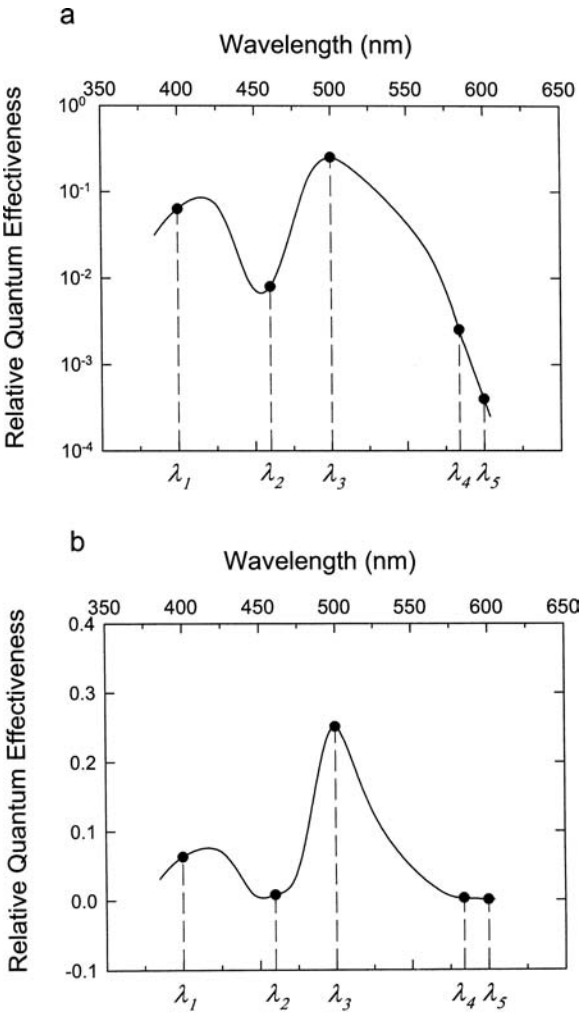

FIGURE 112.2 Five-point action spectrum derived from the fictitious fluence-response curves shown in Figure 112.1. The relative quantum effectiveness, shown on logarithmic (a) and linear (b) scales, is simply the reciprocal of the photon fluence F required at each wavelength to achieve the criterion response, as indicated in Figure 112.1.

when spectra are similar but not identical, choosing one wavelength or another for normalization will lead to different relative shapes. Such ambiguity and subjectivity are avoided by doing the comparison on a logarithmic scale. On the other hand, using a linear ordinate scale has the advantage that it is the more familiar way of viewing absorption spectra, for example, the chart records from commercial spectrophotometers.

The abscissa of an action spectrum is usually presented as a wavelength scale. On the basis of quantum mechanical principles, it would be preferable to use an energy rather than a wavelength scale; the two are related reciprocally according to the relation $E = hc/\lambda$, where E is the energy of a photon of wavelength λ, h is Planck's constant, and c is the speed of light. When an action or absorption spectrum is plotted as a function of energy, the positions of peaks are linearly related to transitions between the energy levels corresponding to molecular states (as on a Jablonski diagram; see above)). This is particularly worthwhile in the case of rhodopsin-type pigments in animals — as well as in halophilic bacteria and algae — because such pigments have spectra of standard shape, except for lateral shifts in the energy of maximum

TABLE 112.1 Representative Functions for Fluence-Response Curve Fits

Description	Function	References
Hyperbola	$\frac{ax}{x+b}$	11
Two hyperbolas plus a constant[a]	$\frac{ax}{x+b}+\frac{cx}{x+d}+h$	11, 36
Hill function	$\frac{ax^n}{x^n+b^n}$	7
Sigmoid[b]	$\frac{a}{1+\exp\left[n(k-u)\ln 10\right]}$	7
Sigmoid[b]	$\frac{a}{2}\left[1+\tanh\left\{n(u-k)\frac{\ln 10}{2}\right\}\right]$	7
Hill plus hyperbola[c]	$\frac{ax^n}{x^n+b^n}+c\log\left(\frac{x}{d}\right)+\sqrt{c^2\log^2\left(\frac{x}{d}\right)+k^2}$	10, 37

[a] This function consists of a sum of two hyperbolas plus an optional constant, h. The coefficients *a* and *c* may be positive or negative for saturation components that rise or fall, respectively.

[b] These two equivalent functions are derivable from the Hill function (familiar in the context of ligand binding for hemoglobin, for example) in the third row, with the substitutions $u = \log x$ and $k = \log b$. They represent the sigmoidal shape taken on by the Hill function when plotted on a semilogarithmic scale, i.e., plotted against log *x* instead of *x*. In the special case with $n = 1$, these sigmoidal functions are equivalent to the hyperbola function in the top row (see Figure 112.1). In general, the Hill exponent does not need to be an integer.

[c] The last two terms together comprise a hyperbola when plotted on a *logarithmic* scale for x. Note that this usage of hyperbola is different from that in the top row function. The hyperbola here has a horizontal asymptote for small *x* and a slant asymptote with slope 2*c* for large *x*.

Source: After Lipson, E.D., in *Biophysics of Photoreceptors and Photomovements in Microorganisms*, Plenum, New York; London, 1991, 293. With permission.

absorption and vertical shifts in the absolute extinction or effectiveness. Nevertheless, most action and absorption spectra are plotted customarily on a wavelength scale for the abscissa, in keeping with the usual display from spectrophotometers.

112.10 Additional Fitting Functions

The hyperbolic saturation function of the form $ax/(x+b)$ often arises in biophysical and biochemical applications. It is more obvious that this represents a hyperbola, if it is written in a double-reciprocal form, as in a Lineweaver–Burk transformation of the Michaelis–Menten enzyme kinetics that employs this type of function. Other contexts where this function appears are monomolecular photochemical kinetics[35] and visual physiology.[33,34] In the present context of action spectroscopy, *x* would stand for the fluence or, in some cases, the fluence rate. When $x = b$, the function is at the half-maximum level that is often chosen to be the criterion response. So, when one performs least-squares fits using such a function, the parameter *b* is the estimate of the fluence needed for the criterion response, and the effectiveness (action spectrum ordinate) is just b^{-1}.

Given in Table 112.1 are several functional forms that are useful for fitting fluence-response curves. These are all based on the hyperbolic saturation function given above and shown in the top row of the

table. In certain cases, fluence-response curves have a two-component (biphasic) structure. The first component reaches a plateau, as shown in Figure 112.1, and then, at high fluence, a second component appears that may or may not approach saturation at the maximum available fluence. For such a two-component curve, if saturation is reached for the second component, then the function in the second row of Table 112.1 may apply, perhaps with the addition of exponents n (often attributable to cooperativity) for each component, as in the Hill function in the third row. Otherwise, if saturation is not reached at some or all wavelengths, then the function in the last row of Table 112.1 may be useful. The second and third terms of that function together have the shape of a hyperbola when plotted on a semilogarithmic scale (i.e., with abscissa log x). Note that this hyperbola, with a (rising) slant asymptote at high fluence, is unrelated to the hyperbola functions (for linear axes) in the first and second rows.

The functions in Table 112.2 depend nonlinearly upon their parameters (unlike the case of a polynomial, for example, where the coefficients are linear parameters). Therefore, it is appropriate to use nonlinear least-squares data-analysis methods. These are widely available and are specifically incorporated in graphical packages such as SigmaPlot® (SPSS Science) and Origin® (OriginLab Corporation). For applications, like the present one of deriving action spectrum values from fluence-response curves, that require error propagation methods, it is important to have the *variance-covariance matrix* of the parameter estimates obtained by least-squares methods. This matrix is made available in Origin® but not yet in SigmaPlot® (Version 8). For those preferring to develop their own data analysis programs, a valuable resource is the *Numerical Recipes* series of books and software (http://www.nr.com), which includes source code in Fortran, Pascal, C, and C++ programming languages for various numerical analysis problems including nonlinear regression (nonlinear least squares), applicable here.

112.11 Null and Threshold Action Spectra

Another way to measure action spectra is to employ a balance or null method, in which the criterion response is zero, but there is no need to work at absolute threshold levels. For example, two lights, one a fixed "reference" light and the other a variable "test" light, could be applied, as appropriate, from opposite directions or in temporal alternation, in such a way that no net response occurs. Examples for action spectroscopy on *Phycomyces* are balance experiments on phototropism[6] and null experiments on the light–growth response.[8,9]

In general, when sigmoidal and other functions are fit to fluence-response curves for the purpose of action spectroscopy, there is another clear choice for criterion response besides the half-maximum (50%) level, namely, a "threshold" response level. However, as mentioned above, thresholds (defined as the highest fluence at which there is no apparent response) per se are difficult to measure because of signal-to-noise considerations at low response levels. A more practical measure of the threshold can be defined operationally as the fluence at which the tangent line at the inflection point (or midpoint) intersects the baseline. This level is generally somewhat higher than the actual threshold, but it has the advantages of being much better defined and easier to measure. For a fluence-response curve, or component thereof, described by the Hill function (third row of Table 112.1), the operational threshold fluence is smaller than the midpoint fluence by a factor of $e^{-2/n}$. In the special case when $n = 1$ (top two rows of Table 112.1), the factor is just e^{-2}. On a $\log_{10}$ scale, this threshold fluence is displaced to the left of the midpoint fluence by 0.869/n "log units".

112.12 Conclusions

This brief chapter on action spectroscopy has given some practical methodology for obtaining action spectra from fluence-response data. Special mention was made of applications in the field of blue-light effects, in which action spectroscopy remains particularly active, mainly because, in most organisms with blue-light response, the responsible pigments remain to be isolated and identified.

In this chapter, we did not delve into action spectroscopy for photochromic receptors, such as phytochrome, a complex topic dealt with in many of the references on action spectroscopy cited in the introduction. Photochromic systems, and others with significant kinetic complexity, call for a mathematical approach termed "analytical action spectroscopy" by Hartmann.[23]

Beyond the key recommendation of basing action spectra on fluence-response curves, readers are encouraged to apply formal data analysis techniques, including error analysis, for analyzing experimental results in action spectroscopy research. Details on such methods are available elsewhere.[18]

References

1. Delbrück, M., Light and life III, *Carlsberg Res. Commun.*, 41, 299, 1976.
2. Lipson, E.D. and Horwitz, B.A., Photosensory reception and transduction, in *Sensory Receptors and Signal Transduction*, Spudich, J. and Satir, B., Academic Press, New York, 1991, p. 1.
3. Meyer, T.E. et al., Properties of a water-soluble, yellow protein isolated from a halophilic phototrophic bacterium that has photochemical activity analogous to sensory rhodopsin, *Biochem.*, 26, 418, 1987.
4. Schlichting, I. and Berendzen, J., Out of the blue: the photocycle of the photoactive yellow protein, *Struct.*, 5, 735, 1997.
5. Galland, P. and Lipson, E.D., Action spectra for phototropic balance in *Phycomyces blakesleeanus*: dependence on reference wavelength and intensity range, *Photochem. Photobiol.*, 41, 3, 323, 1985.
6. Galland, P. and Lipson, E.D., Modified action spectra of photogeotropic equilibrium in *Phycomyces blakesleeanus* mutants with defects in genes *madA*, *madB*, *madC*, and *madH*, *Photochem. Photobiol.*, 41, 3, 331, 1985.
7. Ensminger, P.A., Chen, X., and Lipson, E.D., Action spectra for photogravitropism of *Phycomyces* wild type and three behavioral mutants (L150, L152, and L154), *Photochem. Photobiol.*, 51, 6, 681, 1990.
8. Ensminger, P.A. and Lipson, E.D., Action spectra of the light-growth response in three behavioral mutants of *Phycomyces*, *Planta*, 184, 4, 506, 1991.
9. Ensminger, P.A., Schaefer, H.R., and Lipson, E.D., Action spectra of the light-growth response of *Phycomyces*, *Planta*, 184, 498, 1991.
10. Bejarano, E.R. et al., Photoinduced accumulation of carotene in *Phycomyces*, *Planta*, 183, 1, 1990.
11. Corrochano, L.M. et al., Photomorphogenesis in *Phycomyces*: fluence-response curves and action spectra, *Planta*, 174, 315, 1988.
12. Baskin, T.I. and Iino, M., An action spectrum in the blue and ultraviolet for phototropism in alfalfa, *Photochem. Photobiol.*, 46, 127, 1987.
13. Presti, D.E. and Galland, P., Photoreceptor biology of *Phycomyces*, in *Phycomyces*, Cerdá-Olmedo, E. and Lipson, E.D., Cold Spring Harbor Laboratory, Cold Spring Harbor, New York, 1987, p. 93.
14. Galland, P. and Senger, H., The role of flavins as photoreceptors, *J. Photochem. Photobiol. B:Biol.*, 1, 277, 1988.
15. Schmid, R., Idziak, E.-M., and Tuennermann, M., Action spectrum for the blue-light-dependent morphogenesis of hair whorls in *Acetabularia mediterrania*, *Planta*, 171, 96, 1987.
16. De Fabo, E.C., Harding, R.W., and Shropshire, W., Action spectrum between 260 and 800 nanometers for the photoinduction of carotenoid biosynthesis in *Neurospora crassa*, *Plant Physiol.*, 57, 440, 1976.
17. Baird, D.C., *Experimentation: An Introduction to Measurement Theory and Experiment Design*, 3rd ed., Prentice Hall, Upper Saddle River, NJ, 1994.
18. Lipson, E.D., Action spectroscopy, in *Biophysics of Photoreceptors and Photomovements in Microorganisms*, Lenci, F., Ghetti, F., Colombetti, G., Häder, D.-P., and Song, P.-S., Plenum, New York; London, 1991, p. 293.
19. Coohill, T.P., Action spectra revisited, *J. Photochem. Photobiol. B:Biol.*, 13, 1, 95, 1992.

20. Foster, K.W., Action spectroscopy of photomovement, in *Photomovement*, Häder, D.-P. and Lebert, M., Elsevier, Amsterdam, 2001, p. 51.
21. Coohill, T.P., Action spectra again, *Photochem. and Photobiol.*, 54, 5, 859, 1991.
22. Galland, P., Action spectroscopy, in *Blue Light Responses: Phenomena and Occurrence in Plants and Microorganisms*, Senger, H., CRC Press, Boca Raton, FL, 1987, p. 37.
23. Hartmann, K.M., Action spectroscopy, in *Biophysics*, 2nd ed., Hoppe, W., Lohmann, W., Markl, H., and Ziegler, H., Springer-Verlag, Heidelberg, 1983, p. 115.
24. Jagger, J., *Introduction to Research in Ultraviolet Photobiology*, Prentice-Hall, Englewood Cliffs, NJ, 1967.
25. Schäfer, E. and Fukshansky, L., Action spectroscopy, in *Techniques in Photomorphogenesis*, Smith, H. and Holmes, M.G., Academic Press, New York, 1984, p. 109.
26. Schäfer, E., Fukshansky, L., and Shropshire, W., Jr., Action spectroscopy of photoreversible pigment systems, in *Photomorphogenesis*, Shropshire, W., Jr., Mohr, H., and Zimmermann, M.H., Springer-Verlag, Heidelberg, 1983, p. 39.
27. Shropshire, W., Jr., Action spectroscopy, in *Phytochrome*, Mitrakos, K. and Shropshire, W., Jr., Academic Press, New York, 1972, p. 162.
28. Häder, D.-P. and Tevini, M., *General Photobiology*, Pergamon Press, Oxford, 1987.
29. Björn, L.O., *Photobiology: The Science of Light and Life*, Kluwer Academic Publishers, Dordrecht, 2002.
30. Smith, K.C., *The Science of Photobiology*, 2nd ed., Plenum Press, New York, 1989.
31. Grossweiner, L.I., Photophysics, in *The Science of Photobiology*, 2nd ed., Smith, K.C., Plenum Press, New York, 1989, p. 1.
32. Galland, P. and Lipson, E.D., Light physiology of *Phycomyces* sporangiophores, in *Phycomyces*, Cerdá-Olmedo, E. and Lipson, E.D., Cold Spring Harbor Laboratory, Cold Spring Harbor, NY, 1987, p. 49.
33. Naka, K.I. and Rushton, W.A.H., S-potentials from colour units in the retina of fish (Cyprinidae), *J. Physiol.*, 185, 536, 1966.
34. Williams, T.P. and Gale, J.G., "Compression" of retinal responsivity: V-log I functions and increment thresholds, in *Visual Psychophysics and Physiology*, Armington, J.C., Academic Press, New York, 1978, p. 129.
35. Lipson, E.D. and Presti, D., Graphical estimation of cross sections from fluence-response data, *Photochem. Photobiol.*, 32, 383, 1980.
36. Galland, P., Orejas, M., and Lipson, E.D., Light-controlled adaptation kinetics in *Phycomyces*: evidence for a novel yellow-light absorbing pigment, *Photochem. Photobiol.*, 49, 493, 1989.
37. Trad, C.H. and Lipson, E.D., Biphasic fluence-response curves and derived action spectra for light-induced absorbance changes in *Phycomyces* mycelium, *J. Photochem. Photobiol. B:Biol.*, 1, 169, 1987.

113

Action Spectroscopy: Ultraviolet Radiation

Thomas P. Coohill
Siena College

113.1 Introduction to Ultraviolet Radiation

Ultraviolet (UV) radiation is that portion of the electromagnetic spectrum that extends from the lower wavelength limit of human vision (usually defined as 380 to 400 nm) to wavelengths as short as about 10 nm, where it overlaps the x-ray region. In the natural environment, the shortest wavelength of sunlight that can be routinely measured at the earth's surface is about 290 nm, largely due to the absorption properties of ozone and other atmospheric gases. So, the only environmentally relevant UV region is from 290 to 380 nm. However, artificial UV sources, such as certain fluorescent lamps, mercury and xenon arcs, and lasers, are readily available and extend the possibility of exposure of biological specimens to UV down to wavelengths of about 190 nm. Below 190 nm, air (oxygen) and water begin to absorb UV heavily, making it difficult to expose biological samples except under extreme conditions (e.g., in a vacuum). Hence, the focus of UV photobiology is mainly on the effects on biological processes due to exposure to photons in the wavelength range of 190 to 380 nm.[1]

113.2 Division of the Ultraviolet Region for Photobiological Studies

Vacuum UV (10 to 190 nm)

Photons in the "vacuum" UV (VUV) are heavily absorbed by water and oxygen (in air), both of which become essentially transparent (more than 50% transmission, for a 1 cm path length) to UV at wavelengths above 190 nm. Because of this limited penetration, VUV damage to cells is usually confined to

0-8493-1348-1/04/$0.00+$1.50

a narrow region (a few micrometers) near the cell surface. The energies of single photons in this region are above 6.5 eV, sufficient to ionize many biomolecules. Because the biological effects due to ionizing photons are different from those due to nonionizing photons, the VUV often causes different types of cellular and molecular damage. Thus, VUV effects can be qualitatively different from those of other UV regions.

UV-C (190 to 290 nm)

The shorter-wavelength end of the UV-C (190 nm) is the wavelength region where air and water become transparent. The longer-wavelength limit (290 nm) is the shortest solar UV wavelength easily measured at the earth's surface. Thus, all of the UV-C is environmentally irrelevant. However, research in the UV-C range was central in elucidating many important features of cell functioning. DNA, the genetic material, has peak absorption near 260 nm that falls by a factor of six by 290 nm. This fact, combined with the readily available 254 nm "germicidal" UV fluorescent source, allowed for simple experimental molecular manipulation of DNA, and UV-C photobiology was central in establishing the then-new field of molecular biology.

UV-B (290 to 320 nm)

The shorter-wavelength limit (290 nm) of the UV-B region can be defined as the shortest UV wavelength routinely measurable at the earth's surface, where it is about 1 million-fold less prevalent than 320 nm radiation. The longer-wavelength limit (320 nm) is where ozone and other atmospheric components begin to (more than 50%) attenuate sunlight appreciably. This absorption prevents much of the significant DNA damage that would result if no ozone layer existed. DNA absorption rapidly decreases by more than four orders of magnitude from 290 nm to 320 nm.[2] Nevertheless, absorption of UV-B photons by DNA contributes to a wide variety of bioeffects. The UV-B, which constitutes less than 0.3% of the total sunlight spectrum, is responsible for most of the damage inflicted on organisms by sunlight.

UV-A (320 to 380 nm)

The shorter-wavelength limit of the UV-A (320 nm) can be defined as that wavelength at which ozone becomes transparent. The longer-wavelength limit (380 nm) is where human vision begins, and the UV ends. The UV-A region is also biologically effective and causes cellular death, mutation, and DNA damage, although the primary chromophores for these effects may be non-DNA sensitizers that are chemically matched to the photon energy and act as intermediates in relaying the absorbed energy to DNA.[3] UV-A exposures from sunlight are considerable, constituting about 8% of the total sunlight spectrum.

Terrestrial Solar UV (290 to 380 nm)

This region is easily defined as the wavelength bracket that is the limit of human vision (380 nm) at the long-wavelength end and the effective limit of the solar UV reaching the earth's surface at the short-wavelength (290 nm) end. This is the environmentally relevant UV region and is, of course, the UV-B plus the UV-A regions.

113.3 Absorption of UV by Cells

The responses of biological samples to UV can be greatly affected by their absorption properties. Beginning at the cellular level, it can be seen in Table 113.1 that 200 nm UV-C, for example, is absorbed only slightly by viruses (about 30%), more so by bacterial cells (about 70%), and entirely by mammalian cells (more than 90%). This absorption is due mainly to the presence of endogenous molecules that absorb heavily in the UV-C. At longer wavelengths, cell absorption decreases. The absorption of two important biomolecules, the genetic material DNA and protein, are compared in Figure 113.1. Both molecules begin

TABLE 113.1 Percent Transmission to the Center of Selected Cells and Viruses in the Ultraviolet

Biological sample	Diameter (μm)	Wavelength (nm) 200	250	300	350
Bacteriophage (T_2)	0.1	74	86	100	100
Herpes simplex virus	0.15	66	80	100	100
Bacterial cell	1	33	78	98	100
Yeast cell	5	1.6	69	97	100
Mammalian cell (spherical)	20	10[a]	20	91	96
Mammalian tissue (100 μm thick)	—	—	10[b]	39	66

[a] See also Coohill, T.P., in *Topics in Photomedicine*, Plenum, New York, 1984, p. 1.
[b] See also Coohill, T.P., *Photochem. Photobiol.,* 54, 859, 1990.

Note: All values are approximate. Values at λ above 300 nm can vary widely due to the presence of endogenous chromphores (see also Coohill, T.P., in *Topics in Photomedicine*, Plenum, New York, 1984, p. 1).

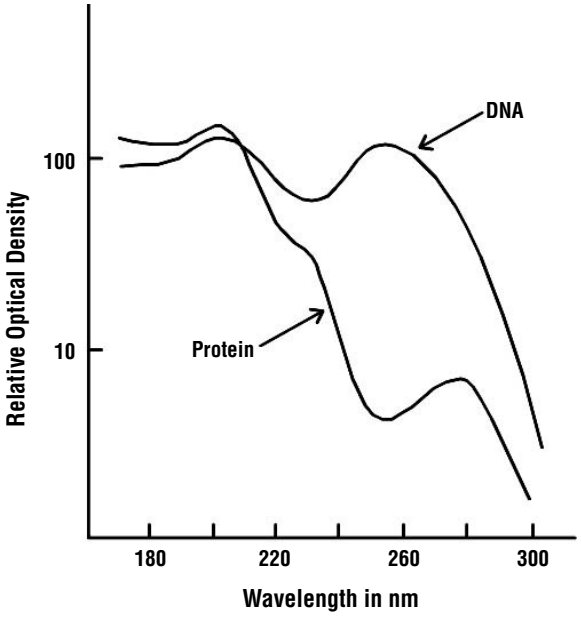

FIGURE 113.1 The absorption spectra of DNA and protein (bovine serum albumin). Both curves are for a 1% solution and 1 cm pathlength.

to absorb appreciably in the UV-B region and substantially in the UV-C region. In a weight-by-weight comparison, DNA absorbs about 20-fold as much 260 nm radiation as does protein. Therefore, the absorption of even homogenates of mammalian cells is similar in the wavelength range 220 to 290 nm to that of DNA. The absorbance (a logarithmic function) of such homogenates is seven times higher at 240 nm compared to 300 nm. As the UV wavelength decreases below 220 nm, proteins and nucleic acids contribute greatly to the total cellular absorption. At wavelengths below 190 nm, water and oxygen absorption prevails. In addition to these macromolecules, some cells contain certain pigments that can alter cellular absorption significantly, even at the longest UV wavelengths. Also, cellular particles and organelles can absorb and scatter UV radiation and, at some wavelengths, shield the center of the cell from a significant portion of the incident beam. Such cytoplasmic screening can alter measured bioeffects to a large degree, especially in the UV-C region, and must be considered when cellular exposure is

attempted.[4] Such concerns are important, because biological cells and tissues will absorb radiation in a wavelength-dependent manner and alter the exposure of the target accordingly. Therefore, the absorption properties of cells are not merely a summation of the individual absorptions of their component molecules.

113.4 Absorption by Tissue

Much of the direct absorption of UV by tissues such as the human skin can be accounted for by the presence of endogenous pigments, especially melanin, hemoglobin, carotenes, and keratin, and exogenous pigments and drugs. Because skin is such a heterogeneous material, UV can be reflected, absorbed, scattered, and rescattered. This means that the direct component of the UV beam is augmented by additions from photons scattered and reflected back into the beam pathway. Hence, at any tissue depth, the sum of the total UV exposure is the direct plus the diffuse. At wavelengths below 300 nm, absorption by tissue rapidly increases, making all but the first few cell layers of the skin essentially opaque to radiation below about 290 nm.

113.5 Action Spectroscopy

Differences in Effects with Wavelength

An action spectrum (AS) is simply defined as the measurement of a biological effect as a function of wavelength. Crude AS was first used in the 19th century to help identify chlorophyll as the chromophore most responsible for the growth of plants. In this century, more sophisticated methods refined the analysis of AS so that it is now possible, in some instances, to make a reasonable determination of the molecule that is likely to contain the chromophore responsible for the response being studied (see Chapter 112). It is this latter usage that was among the first methods that pointed to DNA as the genetic material. This was possible, because small unicellular organisms, such as bacteria, had relatively high transmission rates for UV and, thus, met the rather stringent criteria[5] for a reliable analysis called an analytical action spectrum (AAS). An AAS can only be claimed if the AS corresponds closely to the absorption spectrum of the suspected molecule.

UV-C (190 to 290 nm) Action Spectra

Because some molecules absorb heavily in the UV, certain bioresponses are highly dependent on the wavelengths to which the cell is exposed. In 1930, Gates (Figure 113.2) reported[6] that the AS for bacterial cell death closely followed the absorption of nucleic acid, not protein, which was then widely believed to be the genetic material. In retrospect, this was the first clear evidence that DNA was the genetic material. It should be remembered that an AS could not distinguish between DNA and RNA as the target molecules, because both have similar absorption spectra. However, an AS for a photoproduct exclusive to DNA, such as the thymine dimer, can. Although conducting AS analysis utilizing small cells is somewhat simple, it is difficult to extend these studies to larger (e.g., mammalian) cells because of the substantial absorption of UV by large cells and tissues (Table 113.1). Two other AS in the UV-C region for cell death, one for mammalian tissue and one for individual mammalian cells, are shown in Figure 113.2.[5] Experiments utilizing hanging-drop mammalian tissue samples failed to produce an AS with the fine structure of those studies that utilized bacteria, because the tissue was essentially opaque to radiation near the peak of DNA absorption (260 nm). Thus, the target molecule (DNA) was shielded to an extent such that the shape of the AS did not parallel the absorption spectrum of the target. The advent of single-cell mammalian culture techniques and the unique flattened geometry that mammalian cells assume when in monolayer culture allowed for these studies to begin. Thus, AS for killing of cultured mammalian cells reported data similar to those with bacteria, but the peak was shifted to about 270 nm. This discrepancy can be accounted for by looking at the absorption properties of single mammalian cells and considering, as is the case in bacteria, that the likely target molecule for cell killing is also DNA that resides in the

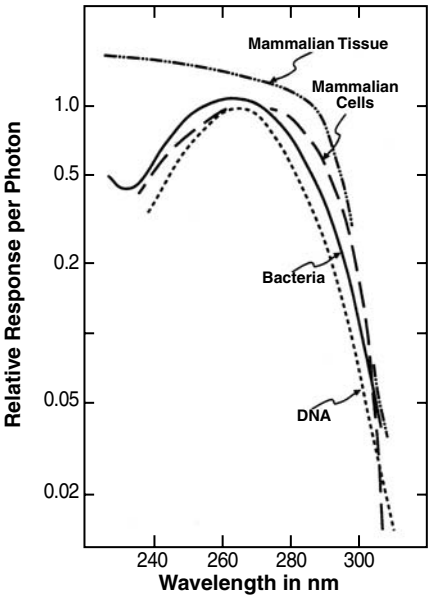

FIGURE 113.2 UV action spectra for the killing of bacteria, mammalian cells, and mammalian tissue. Also represented is the absorption spectrum for DNA. Note that the fine structure inherent in the analytical action spectra for bacteria and mammalian cells is absent in the case of the essentially opaque mammalian cell.

nucleus. This means that the UV beam had to traverse half of the cell, on average, to strike its target. In bacteria, this distance is small enough to allow one to neglect absorption effects; in mammalian cells, the absorption is substantial. An AS for the production of pyrimidine dimers caused by UV exposure to the DNA in mammalian cells matched the action spectrum for cell death. Therefore, DNA was considered responsible for mammalian cell lethality in the 220 to 290 nm region.[7] However, if detailed knowledge of scattering and absorption events before the beam reaches the target is not known, or if the identification of the target is unsure, then any attempt to "correct" or interpret the data generated is suspect. In some cases, it may be useful to modify the incident beam such that the center of the cell, rather than the cell surface, always receives the same exposure.

Not all UV-C AS follow DNA absorption. For example, the loss of saxitoxin binding to sodium channels in rodent cells, or sodium conduction loss in frog cells or lobster axons, or the UV-induced termination of beating by embryonic chick heart aggregates, all follow an AS similar to the absorption spectra of protein moieties.[7] In addition, UV-C AS for highly pigmented tissue (such as plants) shows little correspondence to the absorption of any chromophore. The latter is due to the high degree of absorption of UV-C, which essentially rules out useful AAS in this region for cells and tissues that absorb most of the incident radiation before it can reach the target molecule. Thus, UV-C AS is useful for small or relatively transparent cell studies, but is of limited use for multicellular or highly pigmented samples. Even if a chromophore cannot be identified, an AS still shows the effect of separate wavelengths on a biological response and, as such, is of some use in predicting results due to exposure. Studies of human skin exposure to UV-C (e.g., skin cancer or erythema) show, on average, an essentially flat response in the UV-C region, or in some cases a lessening of effect at shorter wavelengths, that is probably due to limited penetration of the UV beam.

UV-B and UV-A (290 to 380 nm) Action Spectra

It was widely thought that experimental work in the UV-C and UV-B (wavelength range 190 to 320 nm) could be extrapolated to predict photobiological responses in the UV-A (320 to 380 nm). This is not the

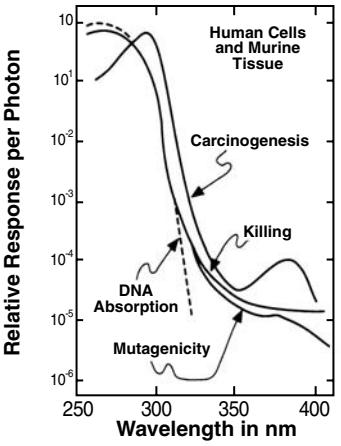

FIGURE 113.3 UV action spectra for human cell killing and mutagenesis and carcinogenic AS for mouse skin.

case, and UV-A AS are more complex than predicted.[3] Here, even events such as cell mutation, which surely involve the genetic material, can be affected at fluences that appear to be below those necessary to affect DNA in these wavelength regions. Details of the divergence of several AS for human cell photoresponses from the DNA absorption spectrum as the curves shift to longer wavelengths in the UV-A are given in Figure 113.3. In the UV-C, cell killing and mutagenesis follow the absorption spectrum of DNA, and carcinogenesis shows a decrease in effect at shorter wavelengths. The UV-B is a transition region from the highly damaging UV-C to the less damaging UV-A region. In the UV-A region, all of the biological parameters are affected at levels that are not fully explainable by the absorption properties of DNA. The absolute absorption of moieties in the DNA molecule is difficult to measure at wavelengths above 320 nm because of scattering and contamination by extraneous chromophores.[2] It is thought that if the absorption is not intrinsic to DNA, then an intermediate molecule may be involved that absorbs the incident UV-A photon and transfers the effect to DNA.

The motivation for focusing on studies of the effects of UV-A and UV-B, the solar UV wavelength region, is provided by three observations. First, many cells and tissues are more transparent to terrestrial solar UV than to UV-C, especially in the UV-A region; thus, this region should be more amenable to AS analysis. Second, research suggested that the nature of the primary and secondary chromophore, photoproducts, and mechanisms for cellular response to solar UV appears, in some cases, to be different from those elucidated for wavelengths shorter than about 300 nm. For example, in contrast to their marked sensitivity to UV-C, certain photosensitive human cell lines, such as xeroderma pigmentosum cells (XP), exhibit the same sensitivity to UV-A as normal cells.[8] Third, solar UV impacts a large number of important bioresponses, such as skin cancer, plant growth, cellular survival and mutagenesis, etc. Research in this area should ultimately reveal the nature of biological responses to a portion of the radiation present in a normal environmental setting.[9,10]

113.6 Carcinogenesis

The role of solar UV in human skin cancer has long been established. Squamous and basal cell carcinomas are believed to be the result of chronic UV exposure. The expression of these cancers is highly dependent on skin type and individual predisposition. The carcinogenic data in Figure 113.3 is mainly a composite drawn from the analysis of De Gruijl and van der Leun[11] and incorporates 12 separate studies utilizing mice. This AS shows major effects in the UV-C and UV-B regions, and falls off rapidly in the UV-A compared to the UV-B in solar radiation (about a factor of 35) — the contribution of UV-A to carcinogenesis is significant. As shown, however, the major cause of UV-induced cancer is the UV-B component of sunlight.

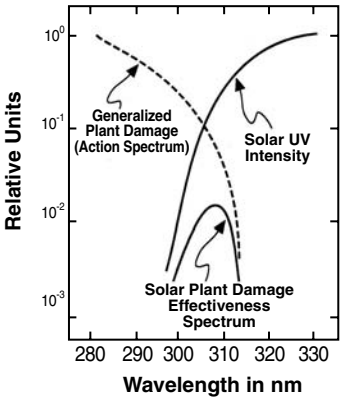

FIGURE 113.4 An AS for generalized plant damage, the terrestrial solar UV intensity spectrum, and a solar plant damage effectiveness spectrum obtained by combining the previous two spectra.

113.7 Polychromatic Action Spectra (PAS)

Some scientists, perhaps realizing the futility of attempting to construct monochromatic AAS using multicellular organisms, reported AS that employs polychromatic sources.[12] These studies vary from irradiating the affected system with additional single wavelengths added to an ambient background, to generating a set of data using polychromatic sources that employ cut-off filters at successively shorter wavelengths. The polychromatic system is complex and tends to obscure individual chromophores, but it is the experimental setup closest to natural field conditions. A major advantage of using polychromatic radiation in the development of PAS is that interactions of biological responses to different wavelengths (usually unknown) are empirically incorporated into the composite spectrum. In addition, highly pigmented tissues, such as plants, have a large variety of chromophores that interacts to give a total effect. Here, PAS can give a composite view of the organism's response, even for such complex parameters as "generalized plant response,"[12] and many other field measurements.

In a recent paper, Sutherland[13] described mathematical procedures for calculating the biological effects from exposing samples to polychromatic (especially ultraviolet) radiation. His analysis included a variety of fluence-response functions and presented an approach for predicting total effect and analyzing subtle differences between classical action spectrum analysis and biological weighting functions.

113.8 Effectiveness Spectra (ES)

It is also possible to estimate the damage to a biological system by exposure to UV by combining AS for a given effect with a known ambient exposure.[14] These are called effectiveness spectra (ES), and they give at least a first approximation to the effects of UV on the studied system. One such ES spectrum is shown in Figure 113.4, which charts the AS for generalized plant damage[12] and the ambient solar UV. The product of these two curves is the solar plant damage ES. From this chart, one can see that the UV-B region is the most damaging, with a peak at about 308 nm. Although solar intensity increases by a factor of 10 from 310 to 330 nm, the biological response decreases more rapidly over the same wavelength range so that the overall effect is less.

Cullen[15] and his coworkers, using spectrally resolved model calculations of water-column photosynthesis (and its inhibition by UV), were able to generate simple mathematical functions that allowed researchers to add environmentally relevant variables and generate results that predict total yield that matches field measurements.

113.9 Constraints

Finally, it should be pointed out that even if all of the constraints necessary to produce a detailed AS are adhered to, experimental variables usually limit the reliability of any AS. These variables include but are not limited to the following:

1. Spectral purity of the radiation source (including the bandwidth of any "monochromate radiation")
2. Accuracy of the dosimetry measurements
3. Presence of endogenous or exogenous "nonparticipating" chromophores
4. Presence of ambient (even microenvironmental) condition
5. Time in the life cycle (cellular) or growth cycle (developmental) of the exposed organism
6. Geometry of the cell or tissue when irradiated
7. Availability of proper nutrients
8. Presence of water stress in plant studies
9. Occurrence of numerous extraneous conditions

References

1. Jagger, J., *Introduction to Research in Ultraviolet Photobiology*, Prentice-Hall, Englewood Cliffs, NJ, 1967.
2. Sutherland, J.C. and Griffin, K.P., Absorption spectrum of DNA for wavelengths greater than 300 nm, *Radiat. Res.,* 41, 399, 1981.
3. Coohill, T.P., Peak, M.J., and Peak, J.G., The effects of the ultraviolet wavelengths present in sunlight on human cells *in vitro, Photochem. Photobiol.,* 46, 1043, 1987.
4. Coohill, T.P., Knauer, D.J., and Fry, D.G., The wavelength dependence of changes in cell geometry on the sensitivity to ultraviolet radiation of mammalian cellular capacity, *Photochem. Photobiol.,* 30, 565, 1979.
5. Coohill, T.P., Action spectra again?, *Photochem. Photobiol.,* 54, 859, 1990.
6. Gates, F.L., A study of the bactericidal action of ultraviolet light. III. The absorption of ultraviolet light by bacteria, *J. Gen. Physiol.*, 14, 31, 1930.
7. Coohill, T.P., Action spectra for mammalian cells *in vitro*, in *Topics in Photomedicine*, Smith, K.C., Ed., Plenum, New York, 1984, p. 1.
8. Keyse, S.M., Moss, S.H., and Davies, K.J.G., Action spectra for inactivation of normal and Xeroderma pigmentosum human skin fibroblasts by ultraviolet radiations, *Photochem. Photobiol.*, 37, 307, 1983.
9. Jagger, J., *Solar-UV Actions on Living Cells*, Praeger, New York, 1985.
10. Peak, M.J. and Peak, J.G., Use of action spectra for identifying molecular targets and mechanisms of action of solar ultraviolet light, *Physiol. Plan.*, 58, 367, 1983.
11. de Gruijl, F.R. and van der Leun, J., Action spectra for photocarcinogenesis, in *Biological Responses to UV-A Radiation*, Urbach, F., Ed., Valdenmar, Overland Park, KS 1992.
12. Flint, S.D. and Caldwell, M.M., A biological weighting function for ozone depletion research with higher plants, *Physiol. Plan.*, 117, 137, 2003.
13. Sutherland, J.C., Biological effects of polychromatic light, *Photochem. Photobiol.*, 76, 164, 2002.
14. Coohill, T.P., Ultraviolet action spectra (280 to 380 nm) and solar effectiveness spectra for higher plants, *Photochem. Photobiol.,* 50, 451, 1989.
15. Cullen, J.J, Davis, R.F., Huot, Y., and Lehmann, M.K., Simple functions describing the effects of UV on daily water column photosynthesis, presented at the 30th annual meeting of the American Society for Photobiology (Abstr. 205, p. 71), Quebec City, Canada, July, 2002.

114

Environmental UV Action Spectroscopy

Francesco Ghetti
Istituto di Biofisica CNR

Costanza Bagnoli
Istituto di Biofisica CNR

114.1 Introduction

In the last two decades of the past century, the presence in the atmosphere of ozone-depleting substances (CFCs, HCFCs, halons, carbon tetrachloride, etc.) has been reducing the ozone concentration in the stratosphere over high and mid-latitudes of both hemispheres. Ozone concentration in the atmosphere is very low (about 3 parts in 10 millions), and that of the total ozone column is equivalent to that of 3 mm at standard temperature and pressure. Nevertheless, its optical density is about 45 at the absorption maximum around 255 nm, about 13 at 280 nm, and goes to 0 at 320 nm. Therefore, the stratospheric layer, which contains approximately 90% of the total ozone, has the function of a protective filter for the Earth's surface, fully cutting off solar radiation under 280 nm and greatly reducing UV-B radiation (280 to 315 nm).

The reduction of stratospheric ozone was recognized as the main cause of the increase in UV-B irradiance at the Earth's surface. From meteorological measurements at several sites distributed over mid- and high latitudes of both hemispheres, this increase was estimated to be in the range of 6 to 14% in the last 20 years. Also, spectral measurements performed at various sites in Europe, North and South America, Antarctica, and New Zealand correlated an UV-B radiation increase with ozone decline.[1]

UV-B has various direct adverse effects on human health (skin cancer, immunosuppression, eye disorders), terrestrial plants and aquatic organisms [DNA alterations, photosynthesis inhibition, reduced growth, photoresponsiveness suppression (see Chapter 116)]. Moreover, due to the differences in UV-B sensitivity and adaptation among the various species, shifts in species composition may occur as a consequence of increased UV-B radiation, thus leading indirectly to alterations in ecosystems.[2–4]

Being clear that the above-mentioned ozone-depleting compounds are almost exclusively of industrial source, nations have agreed (Montreal Protocol, 1987) on the gradual elimination of these substances. Since the first half of the 1990s, their abundance in the atmosphere is slowly declining. However, even models based on the most optimistic scenarios predict that the return to normal ozone levels will take several decades.[5] Moreover, the observation that other atmospheric gases, with an abundance that depends on anthropic activities, may affect stratospheric ozone concentration, and the uncertainties due to the ongoing climate change make it difficult to reliably predict future UV trends.[1] The reader is also referred

0-8493-1348-1/04/$0.00+$1.50

to Kondratyev and Varotsos[6] for a complete discussion of the basic aspects of ozone variability in the atmosphere.

114.2 Radiation Amplification Factors

As the enhancement of solar UV-B is highly wavelength specific and increases when the wavelength decreases, action spectroscopy plays a central role in assessing the effects of ozone depletion on the biosphere. The effectiveness spectrum (ES) obtained by determining the convolution product of an action spectrum for a biological effect with a given solar irradiance spectrum, originated by a particular ozone-depletion scenario, indicates the biological significance of the change in solar UV-B (see Chapter 113). A useful measure of the overall effect of a particular irradiation condition (E) is the biologically active irradiance (E_{BA}) defined as the area under the ES curve:

$$E_{BA} = \int AS(\lambda)E(\lambda)d\lambda$$

The radiation amplification factor (RAF) is a convenient indicator for correlating the sensitivity of a biological effect to different UV exposures caused by various levels of ozone depletion.[5,6] For small variations (about 1 to 10%) of ozone concentration (OC), the RAF can be defined as follows:

$$RAF = - (\Delta E/E)/(\Delta OC/OC)$$

i.e., the ratio between the relative increase in active irradiance and the corresponding relative decrease in ozone concentration. For larger ozone changes, a more accurate relation is as follows:

$$RAF = - \ln(E_2/E_1)/\ln(OC_2/OC_1)$$

where the index denotes a particular situation of ozone concentration and the corresponding biologically active irradiance. As a decrease in ozone is accompanied by an increase in E, in both formulas, the minus sign is used to give positive values of the RAF. RAFs are useful for comparing, at a glance, the UV sensitivity of various biological processes, but they must be used with some caution, because they constitute an oversimplified representation both of the complex radiative transfer in the atmosphere and the biological action of UV radiation.[5]

114.3 Polychromatic Exposures

Ecologically relevant studies aimed to determine action spectra require the careful consideration of various experimental features, such as treatment duration (short exposures may not allow for the observance of overall response of the organism), use of suitable samples (*in vitro* studies can have limitations for extrapolation to the performance of the whole organism), presence of reciprocity effects, and irradiation patterns. For a comprehensive discussion on the correct methodology with which to determine ecologically significant action spectra, the reader is referred to Holmes.[7]

We only want to focus here on the importance of using irradiation conditions not too far from the present levels of natural radiation or those under predictable ozone depletion scenarios. Using extraterrestrial or such high irradiances that the organisms are irreversibly damaged certainly produces a clear effect, but this is not meaningful for a realistic assessment of ozone depletion consequences. Not only radiation intensity but also spectral composition are crucial. Monochromatic action spectra can provide indications on the effects of UV-B without interference due to processes induced by other radiation bands. And, they are useful in demonstrating a direct photochemical effect on a specific target. For example, the action spectrum for DNA cyclobutyl pyrimidine dimer formation in alfalfa seedlings shows that the damage extends well into UV-A up to about 370 nm.[8] However, studies conducted using

monochromatic irradiation do not allow for photoregulated compensatory mechanisms that occur in nature, such as photorepair[9] and the induction of protective UV-absorbing compounds.[10,11] A complementary approach, which takes into account information from monochromatic and polychromatic irradiation conditions, seems to be more appropriate to describe the complex biological responses to UV of whole, intact organisms.

Sun simulators (also known as phytotron), which allow irradiation conditions and climatic factors to be reproduced at any time and disturbing agents to be excluded, are promising tools for overcoming the difficulties of outdoor studies.[12–14] The employment of a wide range of modern lamp types and different filter combinations allow for the spectral quality and the intensity of natural global radiation to be obtained and for the appropriate shaping of the short-wave cutoff.[15,16]

Notwithstanding the complexity of experiments under natural radiation, various spectral studies have been performed by removing increasingly larger portions of the solar UV spectrum by means of different combinations of long-pass filters,[17–19] or by supplementing UV radiation by means of appropriate fluorescent lamps.[20,21] Recently, a sophisticated irradiation system was described, which uses filters and supplementary UV lamps and can provide computer-controlled modulated changes in any radiation band between about 250 and 730 nm.[22–24]

114.4 Determination of Action Spectra from Polychromatic Exposures

Two different approaches were proposed for extracting an action spectrum from experimental data obtained with polychromatic exposures in which UV irradiance is varied by means of filter combinations with progressively decreasing cutoff wavelength. Differential action spectroscopy (DAS) takes into account the spectral bands given by the difference in irradiance of two filter combinations with successive cutoff wavelength. Assuming that different spectral bands supplement one another in producing the observed effect, it is possible to estimate the weighted contribution of each band by dividing the differences in response to the treatment by the corresponding differential irradiances. Finally, the action spectrum is derived by plotting the weighted effects as a function of the average wavelength of the corresponding band. As UV action spectra tend to exponentially increase with decreasing wavelength, the main limit of this method is given by the potentially large variability of the response in the range of each differential band, which could significantly alter the shape of the resulting action spectrum.[25] This limit, however, is also present for monochromatic action spectroscopy, when using currently available interference filters. The differential method can be improved by using several irradiance levels for each differential band, thus reducing statistical errors and allowing correct shaping of the action spectrum.[7]

If DAS reduces the problem to the monochromatic situation, the other approach proposed by Rundel[25] is a deconvolution technique in which it is assumed that the action spectrum [which, in this case, can be defined as the "biological weighting function" (BWF)[26]] is an analytical continuous function $\varepsilon(\lambda)$, and the predicted system response R_i to the ith irradiation regime $E_i(\lambda, t)$ can be expressed as a function, F, of the biologically active irradiance integrated over the irradiation time:

$$R_i = F\left[\iint_{t,\lambda} \varepsilon(\lambda) E_i(\lambda, t)\, d\lambda\, dt\right]$$

Once a functional form for $\varepsilon(\lambda)$ has been chosen depending on a given number of parameters, the latter can be determined by means of iterative calculations to minimize the differences between each R_i and the corresponding measured response. The limit of this method is that the *a priori* choice of the form of $\varepsilon(\lambda)$ and the functional relationship F between response and exposure is critical for the correct determination of the action spectrum. However, the use of multivariate statistical analysis (such as, for example, principal component analysis) allows more detailed BWFs to be obtained.[26,27]

References

1. United Nations Environment Program (UNEP), World Meteorological Organization (WMO), Scientific assessment of ozone depletion: 2002 — Executive summary (Final), http://www.unep.org/ozone/pdf/execsumm-sap2002.pdf.
2. Longstreth, J., de Gruijl, F.R., Kripke, M.L., Abseck, S., Arnold, F., Slaper, H.I., Velders, G., Takizawa, Y., and van der Leun, J.C., Health risks, *J. Photochem. Photobiol. B: Biol.*, 46, 20, 1998.
3. Caldwell, M.M., Björn, L.O., Bornmann J., Flint S.D., Kulandaivelu, G., Teramura A.H., and Tevini, M., Effects of increased solar ultraviolet radiation on terrestrial ecosystems, *J. Photochem. Photobiol. B: Biol.*, 46, 40, 1998.
4. Häder, D.-P., Kumar, H.D., Smith, R.C., and Worrest, R.C., Effects on aquatic ecosystems, *J. Photochem. Photobiol. B: Biol.*, 46, 53, 1998.
5. Madronich, S., McKenzie, R.L., Björn, L.O., and Caldwell, M.M., Changes in biologically active UV radiation reaching the Earth's surface, *J. Photochem. Photobiol. B: Biol.*, 46, 5, 1998.
6. Kondratyev, K.Ya. and Varostos, C., *Atmospheric ozone variability,* Springer Praxis, Mason, J., Chichester, 2000.
7. Holmes, M.G., Action spectra for UV-B effects on plants: monochromatic and polychromatic approaches for analysing plant responses, in *Plant and UV-B: responses to environmental change*, Lumsden, P.J. (Ed.), Cambridge University Press, Cambridge, 1997, p. 31.
8. Quaite, F.E., Sutherland, B.M. and Sutherland, J.C., Action spectrum for DNA damage in alfalfa lowers predicted impact of ozone depletion, *Nature*, 358, 576, 1992.
9. Sinha, R.P. and Häder, D.-P., UV-induced DNA damage and repair: a review, *Photochem. Photobiol. Sci.*, 1, 225, 2002.
10. Rozema, J. and Björn, L.-O. (Eds.), Evolution of UVB absorbing compounds in aquatic and terrestrial plants, *J. Photochem. Photobiol. B: Biol.*, Special Issue, 66, 2002.
11. Häder, D.-P., Lebert, M., Sinha, R.P., Barbieri, E. and Helbling, E.W., Role of protective repair mechanisms in the inhibition of photosynthesis in marine microalgae, *Photochem. Photobiol. Sci.*, 1, 809, 2002.
12. Ghetti, F., Hermann, H., Häder, D.-P., and Seidlitz, H.K., Spectral dependence of the inhibition of photosynthesis under simulated global radiation in the unicellular green alga *Dunaliella salina*, *J. Photochem. Photobiol. B:Biol.,* 48, 166, 1999.
13. Ries, G., Heller, W., Puchta, H., Sandermann Jr., H., Seidlitz, H.K. and Hohn, B., Elevated UV-B radiation reduces genome stability in plants, *Nature*, 406, 98, 2000.
14. Ibdah, M., Krins, A., Seidlitz, H.K., Heller, W., Strack, D., and Vogt, T., Spectral dependence of flavonol and betacyanin accumulation in *Mesembryanthemum crystallinum* under enhanced UV radiation, *Plant, Cell and Environment*, 25, 1145, 2002.
15. Thiel, S., Döhring, T., Köfferlein, M., Kosak, A., Martin, P., and Seidlitz, H.K., A phytotron for plant stress research: how far can artificial lighting compare to natural sunlight?, *J. Plant Physiol.*, 148, 456, 1996.
16. Döhring, T., Köfferlein, M., Thiel, S., and Seidlitz, H.K., Spectral shaping of artificial UV-B irradiation for vegetation stress research, *J. Plant Physiol.* 148, 115, 1996.
17. Searles, P.S., Caldwell, M.M., and Winter, K., The response of five tropical dicoltyledon species to solar ultraviolet-B radiation, *Am.J. Bot.*, 82, 445, 1995.
18. Boucher, N.P. and Prézelin, B.B., Spectral modeling of UV inhibition of *in situ* Antarctic primary production using a field-derived biological weighting function, *Photochem. Photobiol.*, 64, 407, 1996.
19. Hermann, H., Häder, D.-P., and Ghetti, F., Inhibition of photosynthesis by solar radiation in *Dunaliella salina*: relative efficiencies of UV-B, UV-A and PAR, *Plant, Cell and Environment*, 20, 359, 1997.
20. Caldwell, M.M., Gold, W.G., Harris, G., and Ashurst, C.W., A modulated lamp system for solar UV-B (280–320 nm) supplementation studies in the field, *Photochem. Photobiol.,* 37, 479, 1983.

21. McLeod, A.R., Outdoor supplementation systems for studies of the effects of increased UV-B radiation, *Plant. Ecol.*, 128, 1, 1997.
22. Holmes, M.G., An outdoor multiple wavelength system for the irradiation of biological samples: analysis of the long-term performance of various lamps and filter combinations, *Photochem. Photobiol.*, 76, 158, 2002.
23. Cooley, N.M., Truscott, H.M.F., Holmes, M.G., and Attrige, T.H., Outdoor ultraviolet polychromatic action spectra for growth responses of *Bellis perennis* and *Cynosurus cristatus*, *J. Photochem. Photobiol. B: Biol.*, 59, 64, 2000.
24. Holmes, M.G. and Keiler, D.R., A novel phototropic response to supplementary ultraviolet (UV-B and UV-A) radiation in the siliquas of oilseed rape (*Brassica napus* L.) grown under natural conditions, *Photochem. Photobiol. Sci.*, 1, 890, 2002.
25. Rundel, R.D., Action spectra and estimation of biologically effective UV radiation, *Physiol. Plant.*, 58, 380, 1983.
26. Cullen, J.J. and Neale, P.J., Biological weighting functions for the effects of ultraviolet radiation on aquatic systems, in *The Effects of Ozone Depletion on Aquatic Ecosystems*, Häder, D.-P., Ed., Academic Press, San Diego, CA, and R.G. Landes Company, Austin, TX, 1997, chap.6.
27. Cullen, J.J., Neale, P.J., and Lesser, M.P., Biological weighting function for the inhibition of phytoplankton photosynthesis by ultraviolet radiation, *Science*, 258, 646, 1992.

115

Action Spectroscopy for Photosensory Processes

Masakatsu Watanabe
National Institute for Basic Biology

115.1 Introduction

Action spectroscopy (Chapter 112) is primarily a crucial methodology for experimentally estimating the absorption spectra and, thus, the chemical nature, of the (sometimes unidentified) photoreceptor molecules[1] involved in various light-dependent chemical and biological reactions. Technically, the development and extensive collaborative use (Table 115.1) of the Okazaki Large Spectrograph (OLS),[2] at the National Institute for Basic Biology (NIBB), Okazaki, Japan, and of computerized video image analysis methods[3,4] are especially noteworthy.

For a definition of and comprehensive information about the major categories of plant and microbial photosensory processes, i.e., photomovement and photomorphogenesis, the reader is referred to the chapters in this volume (e.g., Chapters 120 to 124) and also to other textbooks.[5,6]

The aim in this chapter is to provide the reader with a selected set of representative action spectral documentation in a way that enables the reader to easily grasp the overview of the present status of our knowledge. For this aim, after showing some typical action spectra, most of the materials are presented in tabular form, closely coupled with a figure that shows the distribution of spectral sensitivities with respect to phylogenetically arranged taxonomic groups.

115.2 Action Spectra for Photosensory Processes

Major Types of Photosensory Action Spectra

Five major types of photosensory action spectra and examples of them are shown in Figure 115.1:

1. *UV-B~C type*,[1] for which the putative UV-B receptor is not yet chemically identified
2. (*UV-B~C), UV-A, blue type*,[7] for which several flavoprotein photoreceptors (cryptochromes, phototropins, photoactivated adenyl cyclase, AppA, and WC-1)[8–13] were successfully identified and characterized in the last decade

0-8493-1348-1/04/$0.00+$1.50

TABLE 115.1 List of Action Spectral Data for Photosensory Processes

Entry Number	Organism	Response Type	Sign[a]	Wavelength Range[b]	Peaks and Shoulders (nm)	Ref.
		Photomovement				
	Eubacteria					
1	*Beggiatoa*	Phobic	-	B	430	16
	Archaebacteria					
2	*Halobacterium*	Phobic	-	UV-A, B	380, 480	17
3	*Halobacterium*	Phobic	+	G	592	18
	Cyanobacteria					
4	*Anabaena*	Taxis	+	B, O, R	440, 600, 620–650, 670	19
5	*Phormidium*	Taxis	+	Y, R	560, 670	20
6	*Phormidium*	Phobic	+	UV-A, B, G, R	390, 490, 560, 610	20
7	*Synechococcus*	Taxis	+	G, Y, R, FR	530, 570, 640, 680, 720, 740	126[f]
8	*Synechocystis*	Taxis	+	Y, R, FR	560, 660, 730	123[f]
	Red Algae					
9	*Porphyridium*	Taxis		V, B	416, 443, 467–477	21
	Slime Molds					
10	*Dictyostelium*	Taxis in amoebae	+	V, B, G, Y, R	405, 450, 520, 580, 640	22
11	*Physarum*	Taxis; O_2- generation	-; +	UV-B~C, UV-A, B	260, 370, 460	23[f]
12	*Physarum*	Taxis	-	UV-B~C, UV-A, B, FR	270, 350, 460, 750	116[f]
	Zygomycetes					
13	*Phycomyces*	Tropic balance with reference (450; 507 nm)	+	UV-A, B	383, 394, 455, 477; 383, 455	24
14	*Phycomyces*	Tropism in sporangiophores	+	UV-A, B	370, 445, 470	25
	Diatoms					
15	*Pleurosira*	Chloroplast migration	-; +	G; B	540; 450	121[f]

	Xanthophyceae					
16	*Vaucheria*	Tropism	+	V, B	415, 430, 450, 480	26
17	*Vaucheria*	Chloroplast accumulation	+	B	470	27
	Brown Algae					
18	*Ectocarpus*	Taxis in gametes	+	UV-A, B	380, 430, 450, 460	28
19	*Pseudochorda*	Taxis in zoospores		B	420, 460	29[f]
	Cryptomonads					
20	*Cryptomonas*	Taxis	+	B, Y	490, 560	30
21	*Cryptomonas*	Taxis	+	UV-B~C, B, Y	280, 430, 480, 560	113[f]
	Protozoa					
22	*Blepharisma*	Phobic	-	B, G, Y	473, 491, 538, 580	31
23	*Blepharisma*	Phobic	-	B, G, Y	493, 538, 580	32
24	*Ophryoglena*	Taxis	+	B, G, O	420, 540, 590	129
25	*Paramecium*	Accumulation; membrane depolarization	+; +	B, G	420, 560	33
26	*Stentor*	Phobic; membrane depolarization	-; +	G, R	560, 610	34
27	*Stentor*	Taxis	-	R	610–620	35
	Dinoflagellates					
28	*Alexandrium*	Taxis	+	UV-B~C, B, G	260, 420, 460, 500	122[f]
29	*Gymnodinium*	Phobic; taxis	-; +	UV-B~C, B	280, 450	36
30	*Peridinium*	Taxis	+	R	640	37
	Euglenoids					
31	*Euglena*	Phobic	+	UV-A, B	370, 440, 470	38
32	*Euglena*	Phobic	-	UV-B~C, UV-A, B	280, 370, 440, 480	120[f]
	Prasinophyceae					
33	*Platymonas*	Taxis	+; -	UV-B~C, UV-A, V, B	275, 333, 405, 450, 495	39
	Green Algae					
34	*Boergesenia*	Tropism	-	UV-A, B	380, 430, 443, 470	40
35	*Bryopsis*	Tropism	-	UV-B~C, UV-A	260, 310	112[f]
36	*Chlamydomonas*	Taxis	+	B, G	443, 503	41

TABLE 115.1 List of Action Spectral Data for Photosensory Processes (continued)

Entry Number	Organism	Response Type	Sign[a]	Wavelength Range[b]	Peaks and Shoulders (nm)	Ref.
37	*Chlamydomonas*	Photoreceptor current	+	B, G	475, 510; (470, 500)	131
38	*Cosmarium, Micrasterias*	Phobic; taxis		B, R	440, 670	42
39	*Dunaliella*	Phobic; taxis	+, -; +	B, G	510; 450–460	43[f]
40	*Mesotaenium*	Chloroplast rotation		UV-A, B, R(/FR)	366, 450, 650	44
41	*Mougeotia*	Chloroplast rotation	+/-	R/FR	679, 717	45
	Ferns					
42	*Adiantum*	Chloroplast redistribution	+	B, R(/FR)	420, 450, 480, 680	46[f]
43	*Adiantum*	Tropism; polarotropism	+	R(/FR)	662; 680	47[f]
	Angiospermeae					
44	*Arabidopsis*	Enhancement of phototropism	+	UV-A, R	378, 669	48
45	*Avena*	Tropism; growth	+; -	UV-A, B	360, 440, 470	49
46	*Hordeum*	Streaming in root hair	+	UV-A, B, G	366, 433–465; 540	50
47	*Medicago*	Tropism	+	UV-B, UV-A, B	280, 380, 450	51[f]
48	*Phaseolus*	Membrane depolarization	+	UV-A, B	380, 420, 460	118[f]
49	*Zea*	Induction of geotropism	+	R	640	52
		Photomorphogenesis				
	Photosynthetic Bacteria					
50	*Rhodobacter, Erythrobacter*	Bchl and carotenoid synthesis	-	B	470	53
51	*Roseobacter*	Bchl and carotenoid synthesis	-	V, Y, FR	400, 575, 770	54
	Cyanobacteria					
52	*Anabaena*	Germination	+	R	620–630	55
53	*Anabaena*	Intracellular cAMP	+; -	FR; R, B, UV-A	720; 660	128[f]
54	*Chlorogloeopsis*	MAA synthesis	+	UV-B	310	131
55	*Tolypothrix*	Phycoerythrin synthesis	+	B, G	480, 540	56[f]
	Red Algae					
56	*Chondrus*	MAA (shinorine) synthesis	+	UV-A	345	132

	Ascomycetes					
57	*Gelasinospora*	Sexual induction	+	UV-B~C, B	280, 350, 370, 420, 440, 460, 480	57[f]
58	*Leptosphaerulina*	Sexual induction	+	UV-B~C, UV-A	265, 287, 300	58
59	*Neurospora*	Conidiation rhythm	-	UV-A, V, B	375, 415, 465, 485	59
60	*Rhodotorula*	Carotenoid synthesis	+	UV-B~C, UV-A, V	280, 340, 370, 400	60[f]
	Bacidiomycetes					
61	*Coprinus*	Sexual induction	+	UV-B~C, UV-A, B	260, 280, 370, 440	61[f]
62	*Polyporus*	Styrylpyrone synthesis	+	UV-A, B	380, 440	62
	Fungi imperfectiae					
63	*Alternaria*	Conidiation	+; -	UV-B; UV-A, B	300, 320; 385, 420, 447, 478	63
64	*Fusarium*	Catotenoid synthesis	+	UV-A, B	380, 430, 455, 475	64
65	*Mycobacterium*	Carotenoid synthesis	+	UV-B~C, UV-A,B	280, 370, 410, 445, 470	65
66	*Verticillium*	Absorbance change and carotenoid synthesis	+	UV-A, B	384	66
	Slime Molds					
67	*Physarum*	Acid from glucose	-	UV-A, B	390, 465, 485	67
68	*Physarum*	Sporulation	+	UV-B~C, UV-A, B, FR	(270, 350, 460), 750	116[f]
69	*Physarum*	Fragmentation	+	UV-A, B, FR(/R)	350, 450, 750	127[f]
	Zygomycetes					
70	*Phycomyces*	Macrophore formation	+	UV-A, B, G	383, 431, 477, 514	68
71	*Phycomyces*	Beta-carotene synthesis	+	UV-A, V, B, G	394, 416, 450, 491, 530	69
72	*Phycomyces*	Sexual fusion	-	UV-A, V	370, 410	114[f]
	Diatoms					
73	*Thalassioiosira*	Gene expression of FCP	+	UV-A, B, G, Y, R, FR	380, 430, 520, 560, 660, 760	124[f]
	Dinoflagellates					
74	*Gyrodinium*	MAA synthesis	+	UV-B	310	133
	Brown Algae					
75	*Laminaria*	Egg production		UV-A, V, B	380, 412, 435, 480	70
76	*Scytosiphon*	Night break of erect thallus formation	-	V, B	414, 442, 480	71
77	*Dictyota*	Egg release	+	UV-A, B	366, 464, 491	72

TABLE 115.1 List of Action Spectral Data for Photosensory Processes (continued)

Entry Number	Organism	Response Type	Sign[a]	Wavelength Range[b]	Peaks and Shoulders (nm)	Ref.
	Euglenoids					
78	*Euglena*	Synthesis of Chl; alkaline DNase, etc.	+	B, R	433, 631	73
	Green Algae					
79	*Acetabularia*	Hair whorl formation	+	UV-A, B	370, 425, 470	74
80	*Chlamydomonas*	Gametogenesis	+	UV-A, B	370, 450	75
81	*Chlamydomonas*	Division	-	V, G	400, 500	76
82	*Chlamydomonas*	Carbonic anhydrase synthesis	+	B	460	77[f]
83	*Chlamydomonas*	Rhodopsin synthesis	+	G	500	78
84	*Chlamydomonas*	Resetting clock in illuminated cells		B, R	450–480, 650–670	79[f]
85	*Chlamydomonas*	Resetting clock in cells in darkness		G, R	520, 660	80[f]
86	*Chlamydomonas*	Flagellation in a mutant	-	V, R	400, 660	81[f]
87	*Chlorella*	Chl and ALA synthesis in glucose bleached	+	UV-A, B	370, 440, 480	82
88	*Scenedesmus*	Chl a,b synthesis in autotrophic cells		B, G	450, 500	83
89	*Scenedesmus*	Chl synthesis (LIR[c]) in heterotrophic cells	+	B	450–480	84
90	*Scenedesmus*	Chl synthesis; cell growth (VLIR[d])	-; +	V, R	408, 645	84
	Charophyceae					
91	*Nitella*	Germination (VLIR[d])	+	R	669	85
	Mosses					
92	*Marchantia*	Rhizoid formation	+(/-)	R(/FR)	650	86
	Ferns					
93	*Adiantum*	Division	+	UV-A, B	370, 460	87
94	*Adiantum*	Germination	-	UV-B, UV-A, B	275, 390, 440	88[f]
95	*Adiantum*	Apical growth	-	UV-A, B	370, 450, 470–480	89
96	*Onoclea*	Germination	+/-	R/FR	660/730	90
97	*Dryopteris*	Germination	+/-	R/FR	660/730	91
	Angiospermeae					
98	*Arabidopsis*	Hypocotyl growth (HIR[e]) in WT; *hy-2*	-	UV-A, B, R, FR; UV-A, B	375, 450, 625, 725; 375, 450	92[f]

99	*Arabidopsis*	Germination	+/-	R/FR	660/720–740	93
100	*Arabidopsis*	Hypocotyl growth (HIR[e]) in *phyB*; *phyAphyB*	-	B, FR; B	400, 460,750; 400, 460	125[f]
101	*Arabidopsis*	Germination in *phyB*; *phyA*	+/-	V, B, R; R/FR	400, 460, 660/730	115[f]
102	*Arabidopsis*	Hypocotyls grow CRY-1 overexpressor	-	B	440, 450, 470, 485	134
103	*Armoracia*	Adventitious shoots from hairy roots	+	UV-A, B, R	380, 460, 680	94[f]
104	*Cuscuta*	Haustoria formation	+	FR (/R)	740 (/660)	117[f]
105	*Daucus*	Anthocyanin synthesis in cultured cells	+	UV-B~C	280	95[f]
106	*Daucus*	Expression of PAL; CHS	+	UV-B~C; UV-B~C, UV-A	280; 280, 330	111[f]
107	*Daucus*	Promoter activity of PAL gene	+	UV-B~C	280	119[f]
108	*Egeria*	Membrane hyperpolarization	+	B, R	400, 450, 650, 700	96[f]
109	*Haplopappus*	Anthocyanin synthesis in cultured tissue	+	UV-A, B	372, 438	97
110	*Lactuca*	Germination	+/-	R/FR	660/730	98
111	*Lactuca*	Germination (HIR[e])	-	B, FR	470, 720	99
112	*Lactuca*	Hypocotyl growth (HIR[e])	-	UV-A, B, FR	363, 441, 716	100
113	*Lemna*	Flowering	-	R, FR	640, 730	101[f]
114	*Pharbitis*	Flowering in etiolated seedlings	-	R	660	102[f]
115	*Phaseolus*	Gene expression (Cab, etc.)	+	V, G, R	400, 510, 660	103[f]
116	*Raphanus*	Hypocotyl growth	-	B, R, FR	455, 515, 630–660, 705–735	104
117	*Sinapis*	Hypocotyl growth (HIR[e])	-	B, R, FR	448, 655, 716	105
118	*Sorghum*	Anthocyanin synthesis	+	UV-B, UV-A, B, R	290, 385, 480, 650	106
119	*Triticum*	Flowering in light-grown plants	+	R, FR	660, 716	107
120	*Triticum*	Chl a,b synthesis	+	R	650	108

[a] + = positive (phototaxis), step-down or photoattractant (photophobic reaction), induction or stimulation (of photomophogenetic reactions); - = negative (phototaxis), step-up or photorepellent (photophobic reaction), suppression or inhibition (of photomorphogenetic reactions).

[b] B = blue; G = green; R = red; FR = far-red.

[c] LIR = low irradiance reaction.

[d] VLIR = very low irradiance reaction.

[e] HIR = high irradiance reaction.

[f] Work done at the Okazaki Large Spectrograph (OLS), National Institute for Basic Biology (NIBB), Okazaki, Japan; these and other works done there are listed at http://www.nibb.ac.jp/%7Elspectro/papers.htm and http://www.nibb.ac.jp/%7Elspectro/reviews.htm.

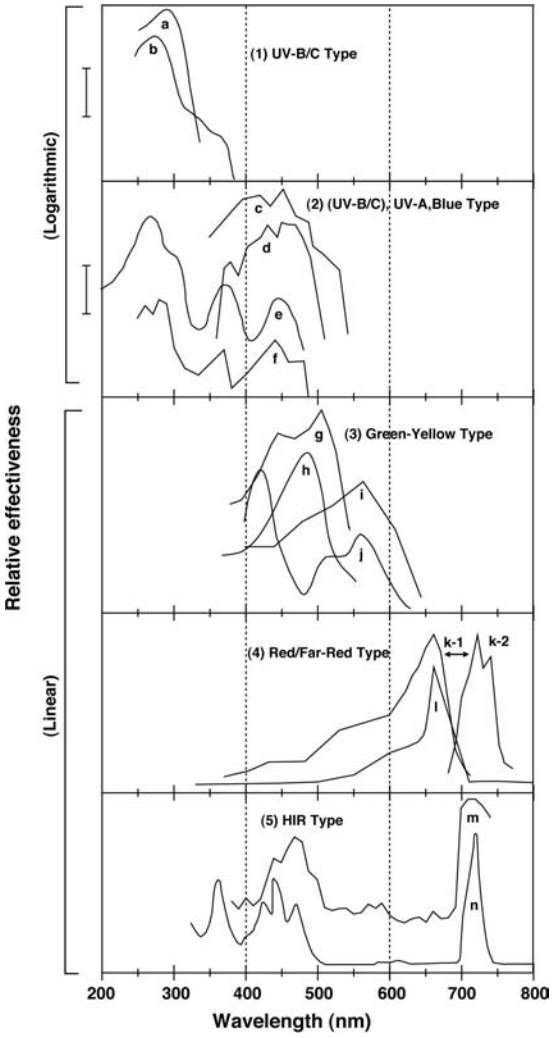

FIGURE 115.1 Major types of photosensory action spectra and examples. (1) *UV-B C type*: (a) induction of anthocyanin synthesis in *Sorghum* (Angiospermae) [entry number (EN), 118 in Table 115.1] (Curve was replotted after Yatsuhashi, H. and Hashimoto, T., *Photochem. Photobiol.*, 41, 673, 1985); (b) induction of carotenoid synthesis in *Rhodotorula* (Ascomycetes) (EN 60) (Curve was replotted after Tada, M., Watanabe, M., and Tada, Y., *Plant Cell. Physiol.*, 31, 241, 1990.). (2) *(UV-B C), UV-A, blue type:* (c) phototaxis in *Ectocarpus* gametes (brown alga) (EN 18) (Curve was replotted after Kawai, H., Mueller, D.G., Foelster, E., and Haeder, D.-P., *Planta*, 182, 292, 1990.); (d) induction of carotenoid synthesis in *Phycomyces* (Zygomycetes) (EN 71) (Curve was replotted after Bejarano, E.R., Avalos, J., Lipson, E.D., and Cerda-Olmedo, E., *Planta*, 183, 1, 1991.); (e) photoavoidance in *Physarum* (slime mold) (EN 11) (Curve was replotted after Ueda, T., Mori, Y., Nakagaki, T., and Kobatake, Y., *Photochem. Photobiol.*, 48, 705, 1988.); (f) sexual induction in *Coprinus* (Basidiomycetes) (EN 61) (Curve was replotted after Durand, R. and Furuya, M., *Plant Cell. Physiol.*, 26, 1175, 1985.). (3) *Green yellow type*: (g) phototaxis in *Chlamydomonas* (green alga) (EN 36) (Curve was replotted after Nultsch, W., Throm, G., and Rimscha, I.V., *Arch. Mikrobiol.*, 80, 315, 1971.); (h) photoavoidance in *Halobacterium* (archaebacterium) (EN 2) (Curve was replotted after Takahashi, T. and Tsuda, M., *Protein Nucl. Acid Enz.*, 34, 452, 1989.); (i) phototaxis in *Cryptomonas* (cryptomonad) (EN 20) (Curve was replotted after Watanabe, M. and Furuya, M., *Plant Cell. Physiol.*, 15, 413, 1974.); (j) induction of membrane depolarization in *Paramecium* (protozoa) (EN 25) (Curve was replotted after Matsuoka, K. and Nakaoka, Y., *J. Exp. Biol.*, 137, 477, 1988.). (4) *Red/far-red type*: (k-1) induction and (k-2) its cancellation of germination in *Arabidopsis* (Angiospermae) (EN 99) (Curve was replotted after Shropshire, W., Klein, W.H., and Elstad, V.B., *Plant Cell. Physiol.*, 2, 63, 1961.); (l) suppresion of flowering in *Pharbitis* (Angiospermae) (EN 114) (Curve was replotted after Saji, H., Vince-Prue, D., and Furuya, M., *Plant Cell. Physiol.*, 24, 1183, 1983.). (5) *HIR type*: (m) suppression of germination in *Lactuca* (Angiospermae) (EN 111) (Curve was replotted after Gwynn, D. and Scheibe, J., *Planta*, 106, 247, 1972.); (n) suppression of hypocotyl growth in *Lactuca* (Angiospermae) (EN 112) (Curve was replotted after Hartmann, K.M., *Z. Naturforsch.*, 22b, 1172, 1967.). Vertical bars beside the ordinates of (1) and (2) indicate one $\log_{10}$ unit.

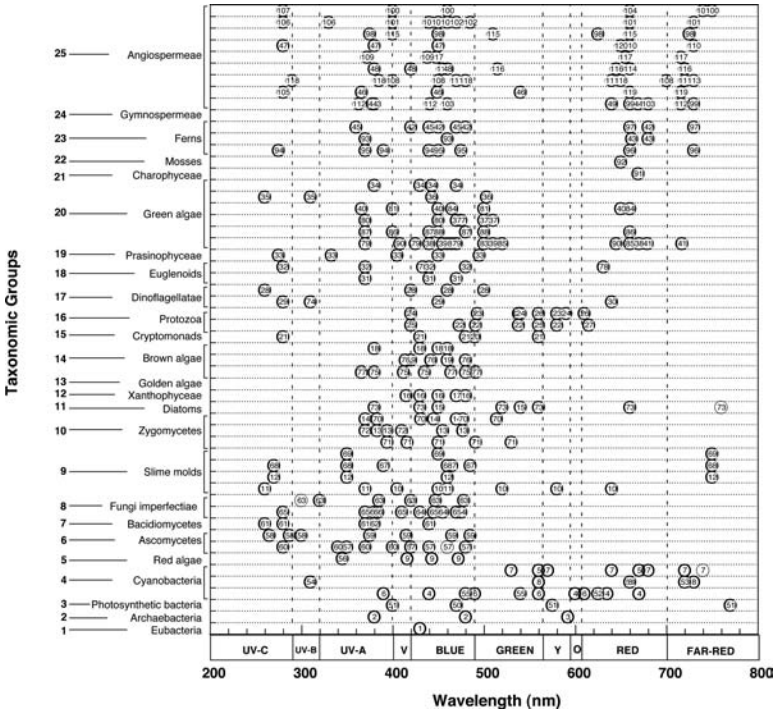

FIGURE 115.2 Distribution of action spectral peak wavelengths with respect to phylogenetically arranged taxonomic groups. The number in each datum point corresponds to the entry number in Table 115.1.

3. *Green yellow type*, for some cases (e.g., g and h in Figure 115.1), of which rhodopsins[14] are established as the photoreceptors
4. *Red/far-red type*,[1,15] in which "/" means a reversible mutually canceling effect between Red and Far-Red lights, and for which phytochrome, a photoisomerizable chromoprotein, is the established and well-characterized photoreceptor (Chapters 129 and 130)
5. *HIR type*,[1,15,92,100,125] often observed in the case of long-term irradiations of plant materials; HIR standing for "High Irradiance Reaction," because a strong dependency of the light effect on fluence rate ("irradiance") is generally observed

Distribution of Action Spectral Peak Wavelengths with Respect to Phylogenetically Arranged Taxonomic Groups

The distribution of action spectral peak wavelengths with respect to phylogenetically arranged taxonomic groups is shown in Figure 115.2.

Recent demonstrations of red/far-red-type responses in microorganisms such as cyanobacteria, slime mold, and diatom are especially clear. Hopefully, together with Table 115.1 below, the information presented in Figure 115.2 can help the reader to think about trends of evolution of photoreceptors, find out new problems to solve, and find suitable experimental materials for his or her own research.

List of Action Spectral Data for Photosensory Processes

A list of 120 selected sets of action spectral data for photosensory processes (photomovement and photomorphogenesis) in the same phylogenetical order of taxonomic groups as shown in Figure 115.2 is presented in Table 115.1.

115.3 Prospects

Future evolution of action spectroscopy research would include the following:

1. Extensive use of photosensitivity mutants, including gene-manipulated organisms,[92,109,110,115,125,130,134] as well as chemical manipulation of contents and characteristics of (sometimes putative) photoreceptors by means of inhibitors and analogs
2. Development and extensive collaborative use of even more efficient, innovative irradiation and observation systems than the ones now available[2]
3. Rapid exchange, retrieval, and analysis of action spectral data on the combined bases of a well-organized action spectral database to be constructed and the worldwide digital communication networks which are already available

Acknowledgments

The author cordially thanks M. Kubota for assistance in preparing Table 115.1; M. Iseki and S. Matsunaga for assistance in preparing Figure 115.1 and Figure 115.2; and H. Kawai for phylogenetical arrangement of the taxonomic groups in Figure 115.2 and Table 115.1.

A substantial part of the works cited here was supported by the National Institute for Basic Biology (NIBB) Cooperative Research Program for the Use of the Okazaki Large Spectrograph (OLS) (Table 115.1).

References

1. Mohr, H., Criteria for photoreceptor involvement, in *Techniques in Photomorphogenesis.* Smith, H. and Holmes, M.G., Eds., Academic Press, London, 1984, p. 13.
2. Watanabe, M., Furuya, M., Miyoshi, Y., Inoue, Y., Iwahashi, I., and Matsumoto, K., Design and performance of the Okazaki Large Spectrograph for photobiological research, *Photochem. Photobiol.*, 36, 491, 1982.
3. Takahashi, T. and Kobatake, Y., Computer-linked automated method for measurement of the reversal frequency in phototaxis of *Halobacterium halobium*, *Cell. Struct. Function*, 7, 183, 1982.
4. Haeder, D.-P. and Lebert, N., Real time computer-controlled tracking of motile microorganisms, *Photochem. Photobiol.*, 42, 509, 1985.
5. Haeder, D.-P. and M. Lebert, Eds., *Photomovement,* Elsevier, Amsterdam, 2001.
6. Kendrick, R.E. and Kronenberg, G.H.M., Eds., *Photomorphogenesis in Plants*, 2nd ed., Kluwer Academic Publishers, Dordrecht, 1994.
7. Senger, H., Ed., *Blue Light Responses: Phenomena and Occurrence in Plants and Microorganisms*, Vols. I and II, CRC Press, Boca Raton, FL, 1987.
8. Cashmore, A.R., Jarillo, J.A., Wu, Y.-J., and Liu, D., Cryptochromes: blue light receptors for plants and animals, *Science*, 284, 760–765, 1999.
9. Briggs, W.R. et al., The phototropin family of photoreceptors, *Plant Cell.*, 13, 993–997, 2001.
10. Iseki, M., Matsunaga, S., Murakami, A., Ohno, K., Shiga, K., Yoshida, K., Sugai, M., Takahashi, T., Hori, T., and Watanabe, M., A blue-light-activated adenylyl cyclase mediates photoavoidance in *Euglena gracilis*, *Nature*, 415, 1047–1051, 2002.
11. Masuda S. and Bauer C.E., AppA is a blue light photoreceptor that antirepresses photosynthesis gene expression in *Rhodobacter sphaeroides*, *Cell.*, 110, 613–623, 2002.
12. Froelich, A.C., Liu, Y., Loros, J.J., Dunlap, J.C., White Collar-1, a circadian blue light photorecptor, binding to the *frequency* promoter, *Science,* 297, 815–819, 2002.
13. He, Q., Cheng, P., Yang, Y., Wang, L., Gardner, K., and Liu, Y., White Collar-1, a DNA binding transcription factor and a light sensor, *Science*, 297, 840–843, 2002.

14. Spudich, J.L., Color-sensitive vision by haloarchaea, in *Photomovement*, Haeder, D.-P. and Lebert, M., Eds., Elsevier, Amsterdam, 2001, pp. 151–178.
15. Sage, L.C., *Pigment of the Imagination*, Academic Press, San Diego, 1992.
16. Nelson, D.C. and Castenholz, R.W., Light responses of *Beggiatoa, Arch. Microbiol.*, 131, 146, 1982.
17. Takahashi, T. and Tsuda, M., Photoreceptors of phototaxis of *Halobacteria*; sensoryrhodopsins and phoborhodopsin, *Protein Nucl. Acid Enz.*, 34, 452, 1989.
18. Tomioka, H., Takahashi, T., Kamo, N., and Kobatake, Y., Action spectrum of the photoattractant response of *Halobacterium halobium* in early logarithmic growth phase and the role of sensory rhodopsin, *Biochim. Biophys. Acta*, 884, 578, 1986.
19. Nultsch, W., Schuchart, H., and Hoehl, M., Investigations on the photo tactic orientation of *Anabaena variabilis*, *Arch. Microbiol.*, 122, 85, 1979.
20. Nultsch, W., Photosensing in cyanobacteria, in *Sensory Perception and Transduction in Aneural Organisms*, Colombetti, G., Lenci, F., and Song, P.-S., Eds., Plenum Press, New York, 1985, p. 147.
21. Nultsch, W. and Schuchart, H., Photo movement of the red alga *Porphyridium cruentum* 2. photo taxis, *Arch. Microbiol.*, 125, 181, 1980.
22. Hong, C.B., Haeder, M.A., Haeder, D.-P., and Poff, K.L., Phototaxis in *Dictyostelium discoideum* amoebae, *Photochem. Photobiol.*, 33, 373, 1981.
23. Ueda, T., Mori, Y., Nakagaki, T., and Kobatake, Y., Action spectra for superoxide generation and UV and visible light photoavoidance in plasmodia of *Physarum polycephalum*, *Photochem. Photobiol.*, 48, 705, 1988.
24. Galland, P. and Lipson, E.D., Action spectra for phototropic balance in *Phycomyces blakesleeanus* dependence on reference wavelength and intensity range, *Photochem. Photobiol.*, 41, 323, 1985.
25. Curry, G.M. and Gruen, H.E., Action spectra for the positive and negative phototropism of phycomyces sporangiophores, *Proc. Natl. Acad. Sci. USA*, 45, 797, 1959.
26. Kataoka, H., Phototropism in *Vaucheria geminata* I. The action spectrum, *Plant Cell. Physiol.*, 16, 427, 1975.
27. Blatt, M.R., The action spectrum for chloroplast movements and evidence for blue light photo receptor cycling in the alga *Vaucheria*, *Planta*, 159, 267, 1983.
28. Kawai, H., Mueller, D.G., Foelster, E., and Haeder, D.-P., Phototactic responses in the gametes of the brown alga *Ectocarpus siliculosus*, *Planta*, 182, 292, 1990.
29. Kawai, H., Kubota, M., Kondo, T., and Watanabe, M., Action spectra for phototaxis in zoospores of the brown alga *Pseudochorda gracilis*, *Protoplasma*, 161, 17, 1991.
30. Watanabe, M. and Furuya, M., Action spectrum of phototaxis in a cryptomonad alga *Cryptomonas* sp., *Plant Cell. Physiol.*, 15, 413, 1974.
31. Scevoli, P., Bisi, F., Colombetti, G., Ghetti, F., Lenci, F., and Passarelli, V., Photomotile responses of *Blepharisma Japonicum* I: action spectra determination and time-resolved fluorescence of photoreceptor pigments, *J. Photochem. Photobiol. B: Biol.*, 1, 75, 1987.
32. Matsuoka, T., Matsuoka, S., Yamaoka, Y., Kuriu, T., Watanabe, Y., Takayanagi, M., Kato, Y., and Taneda, K., Action spectra for step-up photophobic response in *Blepharisma, J. Protozool.*, 39, 498, 1992.
33. Matsuoka, K. and Nakaoka, Y., Photoreceptor potential causing phototaxis of *Paramecium bursaria*, *J. Exp. Biol.*, 137, 477, 1988.
34. Fabczak, S., Fabczak, H., Tao, N., and Song, P-S., Photosensory transduction in ciliates I. An analysis of light-induced electrical and motile responses in *Stentor coeruleus*, *Photochem. Photobiol.*, 57, 696, 1993.
35. Song, P.-S., Haeder, D.-P., and Poff, K.L., Photo tactic orientation by the ciliate *Stentor coeruleus*, *Photochem. Photobiol.*, 32, 781, 1980.
36. Forward, R.B., Jr., Phototaxis by the dinoflagellate *Gymnodinium splendens* Lebour, *J. Protozool.*, 21, 312, 1974.
37. Liu, S.-M., Haeder, D.-P., and Ullrich, W., Photoorientation in the freshwater dinoflagellate *Peridinium gatunense* nygaard, *FEMS Microbiol. Ecol.*, 73, 91, 1990.

38. Barghigiani, C., Colombetti, G., Franchini, B., and Lenci, F., Photobehavior of *Euglena gracilis*; Action spectrum for the step-down photophobic response of individual cell, *Photochem. Photobiol.*, 29, 1015, 1979.
39. Halldal, P., Ultraviolet action spectra of positive and negative phototaxis in *Platymonas subcordiformis, Physiol. Plant*, 14, 133, 1961.
40. Ishizawa, K. and Wada, S., Action spectrum of negative phototropism in *Boergesenia forbesii*, *Plant Cell. Physiol.*, 20, 983, 1979.
41. Nultsch, W., Throm, G., and Rimscha, I.V., Phototaktische Untersuchungen an *Chlamydomonas reinhardii* Dangeard in homokontinuierlicher Kultur, *Arch. Mikrobiol.*, 80, 315, 1971.
42. Wenderoth, K. and Haeder, D.-P., Wavelength dependence of photo movement in desmids, *Planta*, 145, 1, 1979.
43. Wayne, R., Kadota, A., Watanabe, M., and Furuya, M., Photomovement in *Dunaliella salina* fluence rate-response curves and action spectra, *Planta*, 184, 515, 1991.
44. Gaertner, R., Die Bewegung des *Mesotaenium*-Chloroplasten im Starklichtbereich II. Aktionsdichroismus und Wechselwirkungen des Photoreceptors mit Phytochrom, *Z. Pflanzenphysiol.*, 63, 428, 1970.
45. Haupt, W., Die Chloroplastendrehung bei *Mougeotia* I. Ueber den quantitativen und qualitativen Lichtbedarf der Schwachlichtbewegung, *Planta*, 53, 484, 1959.
46. Yatsuhashi, H., Kadota, A., and Wada, M., Blue-and red-light action in photoorientation of chloroplasts in *Adiantum* protonemata, *Planta*, 165, 43, 1985.
47. Kadota, A., Koyama, M., Wada, M., and Furuya, M., Action spectra for polaro tropism and photo tropism in protonemata of the fern *Adiantum capillus-veneris*, *Physiol. Plant*, 61, 327, 1984.
48. Janoudi, A.-K. and Poff, K.L., Action spectrum for enhancement of phototropism by *Arabidopsis thaliana* seedlings, *Photochem. Photobiol.*, 56, 655, 1992.
49. Elliott, W.M. and Shen-Miller, J., Similarity in dose responses action spectra and red light responses between phototropism and photo-inhibition of growth, *Photochem. Photobiol.*, 23, 195, 1976.
50. Keul, M., Action spectrum of photodinesis within barley root hairs *Hordeum vulgare*, *Z. Pflanzenphysiol.*, 79, 40, 1976.
51. Baskin, T.I. and Iino, M., An action spectrum in the blue and UV for phototropism in alfalfa, *Photochem. Photobiol.*, 46, 127, 1987.
52. Suzuki, T. and Fujii, T., Spectral dependence of the light-induced geotropic response in *Zea* roots, *Planta*, 142, 275, 1978.
53. Takamiya, K.-I., Shioi, Y., Shimada, H., and Arata, H., Inhibition of accumulation of bacteriochlorophyll and carotenoids by blue light in an aerobic photosynthetic bacterium *Roseobacter denitrificans* during anaerobic respiration, *Plant Cell. Physiol.*, 33, 1171, 1992.
54. Iba, K. and Takamiya, K.-I., Action spectra for inhibition of light of accumulation of bacteriochlorophyll and carotenoid during aerobic growth of photosynthetic bacteria, *Plant Cell. Physiol.*, 30, 471, 1989.
55. Braune, W., C phyco cyanin the main photo receptor in the light dependent germination process of *Anabaena* akinetes, *Arch. Microbiol.*, 122, 289, 1979.
56. Ohki, K., Watanabe, M., and Fujita, Y., Action of near UV and blue light on the photocontrol of phycobiliprotein formation; a complementary chromatic adaptation, *Plant Cell. Physiol.*, 23, 651, 1982.
57. Inoue, Y. and Watanabe, M., Perithecial formation in *Gelasinospora reticulispora* 7. action spectra in UV region for the photo induction and the photo inhibition of photo inductive effect brought by blue light, *Plant Cell. Physiol.*, 25, 107, 1984.
58. Leach, C.M., An action spectrum for light induced sexual reproduction in the ascomycete fungus *Leptosphaerulina trifolii*, *Mycologia*, 64, 475, 1972.
59. Sargent, M.L. and Briggs, W.R., The effect of light on a circadian rhythm of conidiation in *Neurospora*, *Plant Physiol.*, 42, 1504, 1967.

60. Tada, M., Watanabe, M., and Tada, Y., Mechanism of photoregulated carotenogenesis in *Rhodotorula minuta* VII. Action spectrum for photoinduced carotenogenesis, *Plant Cell. Physiol.*, 31, 241, 1990.
61. Durand, R. and Furuya, M., Action spectra for stimulatory and inhibitory effects of UV and blue light on fruit-body formation in *Coprinus congregatus*, *Plant Cell. Physiol.*, 26, 1175, 1985.
62. Vance, C.P., Tregunna, E.B., Nambudiri, A.M.D., and Towers, G.H.N., Styryl pyrone biosynthesis in *Polyporus hispidus*, Part 1, Action spectrum and photo regulation of pigment and enzyme formation, *Biochim. Biophys. Acta*, 343, 138, 1974.
63. Kumagai, T., Action spectra for the blue and near ultraviolet reversible photoaction in the induction of fungal conidiation, *Physiol. Plant*, 57, 468, 1983.
64. Rau, W., Untersuchungen uber die lichtabhangige Carotinoidsynthese.I. Das Wirkungsspektrum von *Fusarium aquaeductum., Planta*, 72, 14, 1967.
65. Howes, C.D. and Batra, P.P., Mechanism of photo induced carotenoid synthesis further studies on the action spectrum and other aspects of carotenogenesis, *Arch. Biochem. Biophys.*, 137, 175, 1970.
66. Hsiao, K.C. and Bjorn, L.O., Light induced absorbance changes in the fungus *Verticillium agaricinum*, *Physiol. Plant*, 55, 73, 1982.
67. Schreckenbach, T., Walckhoff, B., and Verfuerth, C., Blue light receptor in a white mutant of *Physarum polycephalum* mediates inhibition of spherulation and regulation of glucose metabolism, *Proc. Natl. Acad. Sci. USA*, 78, 1009, 1981.
68. Corrochano, L.M., Galland, P., Lipson, E.D., and Cerda-Olmedo, E., Photomorphogenesis in phycomyces fluence-response curves and action spectra, *Planta*, 174, 315, 1988.
69. Bejarano, E.R., Avalos, J., Lipson, E.D., and Cerda-Olmedo, E., Photoinduced accumulation of carotene in phycomyces, *Planta*, 183, 1, 1991.
70. Luening, K. and Dring, M.J., Reproduction growth and photosynthesis of gametophytes of *Laminaria saccharina* grown in blue and red light, *Mar. Biol.*, 29, 195, 1975.
71. Dring, M.J. and Luening, K., A photoperiodic response mediated by blue light in the brown alga *Scytosiphon lomentaria, Planta*, 125, 25, 1975.
72. Kumke, J., Beitraege zur Periodizitaet der Oogon-Entleerung bei *Dictyota dichotoma* (Phaeophyta), *Z. Pflanzenphysiol.*, 70, 191, 1973.
73. Egan, J.M., Jr., Dorsky, D., and Schiff, J.A., Events surrounding the early development of *Euglena gracilis* var *bacillaris* chloroplasts, Part 6, Action spectra for the formation of chlorophyll lag elimination in chlorophyll synthesis and appearance of TPN dependent triose phosphate dehydrogenase and alkaline DNase activities, *Plant Physiol.*, 56, 318, 1975.
74. Schmid, R., Idziak, E.-M., and Tunnermann, M., Action spectrum for the blue-light-dependent morphogenesis of hair whorls in *Acotabularia medeterranea*, *Planta*, 171, 96, 1987.
75. Weissig, H. and Beck, C.F., Action spectrum for the light-dependent step in gametic differentiation of *Chlamydomonas reinhardtii*, *Plant Physiol.*, 97, 118, 1991.
76. Muenzner, P. and Voigt, J., Blue light regulation of cell division in *Chlamydomonas reinhardtii*, *Plant Physiol.*, 99, 1370, 1992.
77. Dionisio, M.L., Tsuzuki, M., and Miyachi, S., Blue light induction of carbonic anhydrase activity in *Chlamydomonas reinhardtii*, *Plant Cell. Physiol.*, 30, 215, 1989.
78. Foster, K.W., Saranak, J., and Zarrilli, G., Autoregulation of rhodopsin synthesis in *Chlamydomonas reinhardtii*, *Proc. Natl. Acad. Sci. USA*, 85, 6379, 1988.
79. Johnson, C.H., Kondo, T., and Hastings, J. W., Action spectrum for resetting the circadian phototaxis rhythm in the CW 15 strain of *Chlamydomonas*. II. Illuminated cells, *Plant Physiol.*, 97, 1122, 1991.
80. Kondo, T., Johnson, C.H., and Hastings, J.W., Action spectrum for resetting the circadian phototaxis rhythm in the CW15 strain of *Chlamydomonas*, *Plant Physiol.*, 95, 197, 1991.
81. Nakamura, S., Watanabe, M., Hatase, K., and Kojima, M.K., Light inhibits flagellation in a *Chlamydomonas* mutant, *Plant Cell. Physiol.*, 31, 399–401, 1990.

82. Oh-hama, T. and Senger, H., Spectral effectiveness in chlorophyll and 5 amino levulinic-acid formation during regreening of glucose bleached cells of *Chlorella protothecoides*, *Plant Cell. Physiol.*, 19, 1295, 1978.
83. Thielmann, J., Galland, P., and Senger, H., Action spectra for photosynthetic adaptation in *Scenedesmus obliquus* I. Chlorophyll biosynthesis under autotrophic conditions, *Planta*, 183, 334, 1991.
84. Thielmann, J. and Galland, P., Action spectra for photosynthetic adaptation in *Scenedesmus obliquus* II. Chlorophyll biosynthesis and cell growth under heterotrophic conditions, *Planta*, 183, 340, 1991.
85. Sokol, R.C. and Stross, R.G., Phytochrome-mediated germination of very sensitive oospores, *Plant Physiol.*, 100, 1132, 1992.
86. Otto, K.-R. and Halbsguth, W., Stimulation of primary rhizoid formation on gemmae of *Marchantia polymorpha* as caused by light and IAA, *Z. Pflanzenphysiol.*, 80, 197, 1976.
87. Wada, M. and Furuya, M., Action spectrum for the timing of photo induced cell division in *Adiantum capillus-veneris* gametophytes, *Physiol. Plant*, 32, 377, 1974.
88. Sugai, M. and Furuya, M., Action spectrum in UV and blue light region for the inhibition of red-light-induced spore germination in *Adiantum capillus-veneris*, *Plant Cell. Physiol.*, 26, 953, 1985.
89. Kadota, A., Wada, M., and Furuya, M., Apical growth of protonemata in *Adiantum capillus-veneris* 3. Action spectra for the light effect on dark cessation of apical growth and the intracellular photoreceptive site, *Plant Sci. Lett.*, 15, 193, 1979.
90. Towill, L.R. and Ikuma, H., Photo control of the germination of *Onoclea* spores, Part 1. Action spectrum, *Plant Physiol.*, 51, 973, 1973.
91. Mohr, H., Die Beeinflussung der Keimung von Farnsporen durch Licht und andere Faktoren, *Planta*, 46, 534, 1956.
92. Goto, N., Yamamoto, K.T., and Watanabe, M., Action spectra for inhibition of hypocotyl growth of wild-type plants and of the hy2 long-hypocotyl mutant of *Arabidopsis thaliana* l, *Photochem. Photobiol.*, 57, 867, 1993.
93. Shropshire, W., Klein, W.H., and Elstad, V.B., Action spectra of photomorphogenic induction and photoinactivation of germination in *Arabidopsis thaliana*, *Plant Cell. Physiol.*, 2, 63, 1961.
94. Saitou, T., Tachikawa, Y., Kamada, H., Watamabe, M., and Harada, H., Action spectrum for light-induced formation of adventitious shoots in hairy roots of horseradish, *Planta*, 189, 590, 1993.
95. Takeda, J. and Abe, S., Light-induced synthesis of anthocyanin in carrot cells in suspension IV. The action spectrum, *Photochem. Photobiol.*, 56, 69, 1992.
96. Tazawa, M., Shimmen, T., and Mimura, T., Action spectrum of light-induced membrane hyperpolarization in *Egeria densa*, *Plant Cell. Physiol.*, 27, 163, 1986.
97. Lackmann, I., Action spectra of anthocyanin synthesis in tissue cultures and seedlings of *Haplopappus gracilis* D., *Planta*, 98, 258, 1971.
98. Borthwick, H.A., Hendreicks, S.B., Toole E.H., and Toole, V.K., Action of light on lettuce-seed germination, *Bot. Gaz*, 115, 205, 1954.
99. Gwynn, D. and Scheibe, J., An action spectrum in the blue for inhibition of germination of lettuce seed, *Planta*, 106, 247, 1972.
100. Hartmann, K.M., Ein Wirkungsspektrum der Photomorphogenese unter Hochenergiebedingungen und seiner Interpretation auf der Basis des Phytochroms (Hypokotylwachstumshemmung bei *Lactuca sativa* L.), *Z. Naturforsch.*, 22b, 1172, 1967.
101. Lumsden, P.J., Saji, H., and Furuya, M., Action spectra confirm two separate actions of phytochrome in the induction of flowering in *Lemna paucicostata* 441, *Plant Cell. Physiol.*, 28, 1237, 1987.
102. Saji, H., Vince-Prue, D., and Furuya, M., Studies on the photoreceptors for the promotion and inhibition of flowering in dark-grown seedlings of *Pharbitis nil* choisy, *Plant Cell. Physiol.*, 24, 1183, 1983.
103. Sasaki, Y., Yoshida, K., and Takimoto, A., Action spectra for photogene expression in etiolated pea seedlings, *FEBS Lett.*, 239, 199, 1988.

104. Jose, A.M. and Vince-Prue, D., Action spectra for the inhibition of growth in radish hypocotyls, *Planta*, 136, 131, 1977.
105. Beggs, C.J., Holmes, M.G., Jabben, M., and Schaefer, E., Action spectra for the inhibition of hypocotyl growth by continuous irradiation in light and dark grown *Sinapis alba* seedlings, *Plant Physiol.*, 66, 615, 1980.
106. Yatsuhashi, H. and Hashimoto, T., Multiplicative action of a UV-B photoreceptor and phytochrome in anthocyanin synthesis, *Photochem. Photobiol.*, 41, 673, 1985.
107. Carr-Smith, H.D., Johnson, C.B., and Thomas, B., Action spectrum for the effect of day-extensions on flowering and apex elongation in green light-grown wheat *Triticum aestivum* L., *Planta*, 179, 428, 1989.
108. Virgin, H.I., Action spectra for chlorophyll formation during greening of wheat *Triticum aestivum* leaves in continuous light, *Physiol. Plant*, 66, 277, 1986.
109. Deng, X.-W., Matsui, M., Wei, N., Wagner, D., Chu, A.M., Feldmann, K., and Quail, P.H., *COP1*, an *Arabidopsis* regulatory gene, encodes a protein with both a zinc-binding motif and a G_{beta} homologous domain, *Cell*, 71, 791, 1992.
110. Chory, J., Out of darkness: mutants reveal pathways controlling light-regulated development in plants, *Trends Genet.*, 9, 167–172, 1993.
111. Takeda, J., Obi, I., and Yoshida, K., Action spectra of phenylalanine ammonia-lyase and chalcone synthase expression in carrot cells in suspension, *Physiol. Plant*, 91, 517–521, 1994.
112. Iseki, M. and Wada, S., Action spectrum in the ultraviolet region for phototropism of *Bryopsis* rhizoids, *Plant Cell. Physiol.*, 36, 1033–1040, 1995.
113. Erata, M., Kubota, M., Takahashi, T., Inoue, I., and Watanabe, M., Ultrastructure and phototactic action spectra of two genera of cryptophyte flagellate algae, *Cryptomonas* and *Chroomonas*, *Protoplasma*, 188, 258–266, 1995.
114. Yamazaki, Y., Kataoka, H., Miyazaki, A., Watanabe, M., and Ootaki, T., Action spectra for photoinhibition of sexual development in *Phycomyces blakesleeanus*, *Photochem. Photobiol.*, 64, 387–392, 1996.
115. Shinomura, T., Nagatani, A., Hanzawa, H., Kubota, M., Watanabe, M., and Furuya, M., Action spectra for phytochrome A- and B-specific photoinduction of seed germination in *Arabidopsis thaliana*, *Proc. Natl. Acad. Sci. USA*, 93, 8129–8133, 1996.
116. Nakagaki, T., Umemura, S., Kakiuchi, Y., and Ueda, T., Action spectrum for sporulation and photoavoidance in the plasmodium of *Physarum polycephalum*, as modified differentially by temperature and starvation, *Photochem. Photobiol.*, 64, 859–862, 1996.
117. Furuhashi, K., Tada, Y., Okamoto, K., Sugai, M., Kubota, M., and Watanabe, M., Phytochrome participation in induction of haustoria in *Cuscuta japonica*, a holoparasitic flowering plant, *Plant Cell. Physiol.*, 38, 935–940, 1997.
118. Nishizaki, Y., Kubota, M., Yamamiya, K., and Watanabe, M., Action spectrum of light pluse-induced membrane depolarization in pulvinar motor cells of *Phaseolus*, *Plant Cell. Physiol.*, 38, 526–529, 1997.
119. Takeda, J., Ozeki, Y., and Yoshida, K., Action spectrum for induction of promoter activity of phenylalanine ammonia-lyase gene by UV in carrot suspension cells, *Photochem. Photobiol.*, 66, 464–470, 1999.
120. Matsunaga, S., Hori, T., Takahashi, T., Kubota, M., Watanabe, M., Okamoto, K., Masuda, K., and Sugai, M., Discovery of signaling effect of UV-B/C light in the extended UV-A/blue-type action spectra for step-down and step-up photophobic responses in the unicellular flagellate alga *Euglena gracilis*, *Protoplasma*, 201, 45–52, 1998.
121. Furukawa, T., Watanabe, M., and Shihira-Ishikawa, I., Green- and blue-light-mediated chloroplast migration in the centric diatom, *Pleurosira laevis*, *Protoplasma*, 203, 214–220, 1998.
122. Horiguchi, T., Kawai, H., Kubota, M., TakahashiI, T., and Watanabe, M., Phototactic responses of four marine dinoflagellates with different types of eyespot and chloroplast, *Phycol. Res.*, 47, 101–107, 1999.

123. Choi, J.-S., Chung, Y.-H., Moon, Y.-J, Kim, C., Watanabe, M., Song, P.-S., Joe, C.-O, Bogorad, L., and Park, Y.M., Photomovement of the gliding cyanobacterium *Synechocystis* sp. PCC 6803, *Photochem. Photobiol.*, 70, 95–102, 1999.
124. Leblanc, C., Falciatore, A., Watanabe, M., and Bowler, C., Semi-quantitative RT-PCR analysis of photoregulated gene expression in marine diatoms, *Plant Mol. Biol.*, 40, 1031–1044, 1999.
125. Shinomura, T., Uchida, K., and Furuya, M., Elementary processes of photoperception by phytochrome A for high-irradiance response of hypocotyl elongation in *Arabidopsis*, *Plant Physiol.*, 122, 147–156, 2000.
126. Kondou, Y., Nakazawa, M., Higashi, S-I., Watanabe, M., and Manabe, K., Equal-quantum action spectra indicate fluence-rate-selective action of multiple photoreceptors for photomovement of the thermophilic cyanobacterium *Synechococcus elongatus*, *Photochem. Photobiol.*, 73, 90–95, 2001.
127. Kakiuchi, Y., Takahashi, T., Murakami, A., and Ueda, T., Light irradiation induces fragmentation of the plasmodium, a novel photomorphogenesis in the true slime mold *Physarum polycephalum*: action spectra and evidence for involvement of the phytochrome, *Photochem. Photobiol.*, 73, 324–329, 2001.
128. Ohmori, M., Terauchi, K., Okamoto, S., and Watanabe, M., Regulation of cAMP-mediated photosignaling by a phytochrome in the cyanobacterium *Anabaena cylindrica*, *Photochem. Photobiol.*, 75, 675–679, 2002.
129. Cadetti, L., Marroni, F., Marangoni, R., Kuhlmann, H.-W., Gioffre, D., and Colombetti, G., Phototaxis in the ciliated protozoan *Ophryoglena flava*: dose effect curves and action spectrum determination, *J. Photochem. Photobiol. B: Biol.*, 57, 41–50, 2000.
130. Sineshchekov, O.A., Jung, K.-H., and Spudich, J.L., Two rhodopsins mediate phototaxis to low- and high-intensity light in *Chlamydomonas reinhardtii*, *Proc. Natl. Acad. Sci. USA*, 99, 8689–8694, 2002.
131. Portwich, A. and Garcia-Pichel, F., A novel prokaryotic UVB photoreceptor in the cyanobacterium *Chlorogloepsisi* PCC6912, *Photochem. Photobiol.*, 71, 493–498, 2000.
132. Kraebs, G., Bischof, K., Hanelt, D., Karsten, U., and Wiencke, C., Wavelength-dependent induction of UV-absorbing mycosporine-like amino acids in the red alga *Chondrus crisps* under natural solar radiation, *J. Exp. Mar. Biol. Ecol.*, 268, 69–82, 2002.
133. Klisch, M. and Haeder D.-P. Wavelength dependence of mycosporine-like amino acid synthesis in *Gyrodinium dorsum*, *J. Photochem. Photobiol. B. Biol.*, 66, 60–66, 2002.
134. Ahmad, M., Grancher, N., Heil, M., Black, R.C., Giovani, B., Galland, P., and Lardemer, D., Action spectrum for cryptochrome-dependent hypocotyl growth inhibition in *Arabidopsis*, *Plant Physiol.*, 129, 774–785, 2002.

116

Photoecology and Environmental Photobiology

Donat-P. Häder
Friedrich-Alexander-Universität Erlangen-Nürnberg

116.1 Introduction

Light is used by photosynthetic organisms as an energy source to produce organic substances in the process of photosynthesis. Solar radiation is harvested by the photosynthetic pigments chlorophyll *a* and the accessory pigments, including phycobilins, carotenoids, and other chlorophylls (*b, c, d*). Completely independent from this process, plants and other photosynthetic (and also nonphotosynthetic) organisms utilize light as an environmental information source with which they select and optimize their positions in their habitats. This selection is governed by two aims. On the one hand, the organisms try to obtain sufficient solar energy for efficient photosynthesis that can be brought about by aquatic motile microorganisms, e.g., by moving toward the water surface.[1] On the other hand, unfiltered solar radiation at the surface may be detrimental for many photosynthetic organisms, and their delicate photosynthetic apparatuses may be damaged by excessive solar energy, particularly in the UV range.[2] Many photosynthetic organisms try to solve this dilemma by using antagonistic responses to light and other environmental clues to optimize their positions dynamically over time.

116.2 Orientation Mechanisms in Plants and Microorganisms

Motile microorganisms use active propulsion or passive movement mechanisms based on buoyancy[3] to select suitable habitats. But, sessile higher plants are also capable of adjusting their organs (roots, stems, leaves, flowers) with respect to light.[4]

Orientation Mechanisms in Higher Plants

The classical orientation mechanisms in higher plants with respect to light are photonasty and phototropism.[5] Plant shoots show positive phototropism (bending toward the light source) at low fluence rates,

0-8493-1348-1/04/$0.00+$1.50

and they show negative phototropism (bending away from the light source) at higher fluence rates. Roots perform negative or no phototropism, and leaves orient themselves perpendicular or at other angles to the impinging light beam (plagio- or diaphototropism) (see Chapter 133). In some higher plants, the leaves track the sun during its daily cycle so that the leaf area is mostly perpendicular to the impinging light rays.[6]

Photonastic movements are independent of the light direction and follow a built-in direction, e.g., flower opening or stomata movements follow predefined patterns and are elicited by changes in the light quality or quantity. The photoreceptor pigments involved in these responses are independent from the photosynthetic pigments and include phytochrome and flavoproteins (see Chapters 130, 132, and 133).

Photoorientation in Microorganisms

Motile microorganisms rely on external factors and endogenous rhythms[7,8] to control the movements in their habitats. Major sources of information are gravity,[9,10] chemical gradients (such as oxygen or carbon dioxide),[11,12] temperature (gradients),[13] magnetic field lines,[14–16] and electric currents.[17,18] Light is one of the major clues for microorganisms. Photophobic responses, phototaxis, and photokinesis are three responses of microorganisms with respect to steady state light quality, quantity, direction, or changes in these parameters[19] (for details, see Chapters 120, 121, and 122).

Photomorphogenetic Reactions

Microorganisms and higher plants show morphological changes in dependence of the impinging light quality and quantity,[20] e.g., germinating seedlings elongate in darkness or shaded conditions to reach a niche with sufficient irradiation for optimal growth conditions.[21] Likewise, leaf form, thickness, and area, as well as stomata and chloroplast density and position, can be controlled by ambient light.[22,23] The pigment concentration as well as the quantitative ratio between various light harvesting pigments employed in photosynthesis can be governed by the irradiance or wavelength distribution of solar radiation. In cyanobacteria, the ratio between the green-light-absorbing phycoerythrin and the red-light-absorbing phycocyanin is rapidly altered when the organisms are grown in red or green light (chromatic adaptation).[24,25]

116.3 Ecological Consequences of Photomovement

The movement responses of individual organisms may result in a mass movement of populations and accumulation of organisms in favorable light environments. Positive phototaxis guides a population toward the light source (water surface), and negative phototaxis guides away from detrimental excessive surface irradiation. Often, upward movement is supported by negative gravitaxis.[9] This response has the advantage in that it works in darkness or in murky waters so that the photosynthetic organisms get to the surface even without seeing the light. Often, several responses operate antagonistically, e.g., in the green flagellate *Euglena*, negative gravitaxis is countered by negative phototaxis. The result is an accumulation of the cells at a certain depth. In the case of this flagellate, the optimal depth is at a fluence rate of 30 W m^{-2}, which also corresponds with its requirements for optimal photosynthesis.[26]

Photophobic responses result in accumulations of organisms in light fields or in dark areas, depending on whether the response is elicited when the organisms experience a step-up or a step-down in irradiance. At low irradiances, filamentous gliding cyanobacteria cross dark–light boundaries without a response. In contrast, leaving a light field will result in a reversal of movement. This behavior causes the organisms to accumulate in light fields (light trap).[27] The same organism shows the opposite response at high irradiances, causing the filaments to leave the irradiated areas and accumulate in the shade. These fine-tuned antagonistic reactions allow the organisms to precisely select optimal light conditions. The ciliate *Stentor* is easily killed within minutes by exposure to unfiltered solar radiation.[28] The cells protect themselves by step-up photophobic responses.[29] Consequently, in nature, the organisms are found in the shade of leaves or other objects.

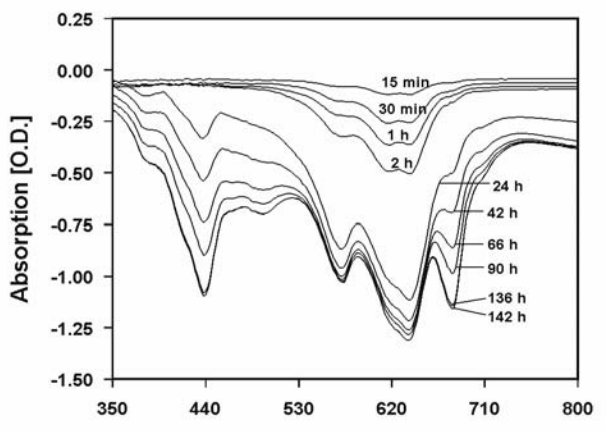

FIGURE 116.1 Absorption difference spectra of *Oscillatoria tenuis* after increasing times of exposure to UV radiation. Spectra are obtained by subtracting the initial absorption spectrum of the unirradiated sample from each spectrum of the irradiated samples. (From Donkor, V.A. and Häder, D.-P., *Aquatic Microbiol. Ecol.*, 11, 143, 1996. With permission.)

In photokinesis, the actinic steady state light intensity modulates the velocity of movement[30–32] and, thus, governs the time spent in dark or lit areas in the environment.[33] A higher swimming speed in light compared to in darkness causes the organisms to spend less time in irradiated areas and more time in darkness. This can be taken to its extreme: cells moving in light and stopping in darkness will result in the population eventually accumulating in dark areas of their habitats. The opposite behavior results in leaving dark areas and accumulating in bright areas. Some organisms settle on and stick to surfaces when irradiated and start moving again when in darkness. There are many deviations in the light-dependent movement patterns of microorganisms, and some do not even fit the definitions described above.

116.4 Excessive Light Stress

Obviously, photosynthetic biomass production is suboptimal under low light conditions. The break-even point between photosynthetic oxygen production and respiratory oxygen uptake (light compensation point) is different for different organisms: shade-adapted organisms need less light for a positive net production than do high-light-adapted ones.[34]

By several molecular mechanisms, excessive light exposure causes stress in many photosynthetic organisms. Excitation energy, which cannot be used by chlorophyll *a* in the photosynthetic reaction center, can be passed to oxygen that normally occurs in its triplet state. Upon uptake of the excitation energy from the excited chlorophyll, oxygen reaches its singlet state, which is fairly short-lived but aggressive, and can destroy proteins, lipids, and other biomolecules in its vicinity.

Solar energy can be absorbed by a number of cellular pigments and can then be used to form reactive oxygen species, including superoxide radicals ($O_2^{\bullet -}$), hydroxyl radicals ($OH^{\bullet}$), hydrogen peroxide (H_2O_2), and singlet oxygen ($^1O_2$) and other radicals, all of which can be destructive for cellular organelles and biomolecules.

Solar energy can also directly bleach cellular chromoproteins, such as the photosynthetic accessory pigments, including chlorophylls, carotenoids, and the algal phycobilins (Figure 116.1). The highly energetic, short-wavelength UV radiation (UV-A 315 to 400 nm and UV-B 280 to 315 nm) is effective in causing damage to cellular targets. Solar UV-B also breaks down proteins, especially those with high concentrations of aromatic amino acids, which strongly absorb around 280 nm. The even more detrimental UV-C does not play an ecological role because it is almost quantitatively absorbed in the atmosphere.

Another target of solar UV radiation is the nuclear and plastidic DNA. Mainly, UV-B causes the formation of cyclobutane dimers, such as thymine-thymine dimers. Shorter-wavelength UV-C mainly causes the formation of 6–4 photoproducts, pyrimidine hydrates, and DNA-protein cross-links.

116.5 Defense Systems against Excessive Solar Radiation

Higher plants and photosynthetic microorganisms developed a number of effective defense mechanisms to limit damage caused by excessive solar radiation. One strategy relies on habitat selection. Low-light-adapted plants select niches in their habitats in the shade. The distribution of macroalgae in the tidal zone is governed by the availability of solar radiation.[35] Many of the delicate and shade-adapted Rhodophytes are found in the understory of kelps in the subtidal zone, where they are never reached by unfiltered solar radiation. Vertical migration of motile phytoplankton organisms and protection in the shade of floating objects were mentioned above. The earliest organisms with oxygenic photosynthesis were the cyanobacteria, which are believed to have developed before a protective oxygen layer was present in the troposphere.[36] Also, the stratospheric ozone layer, which absorbs most of the detrimental solar UV-B radiation, was built up only later. These organisms are believed to have developed deep down in the water column or in endolithic habitats.

Most photosynthetic organisms developed protective pigments to absorb solar UV radiation before it can hit sensitive cellular targets. Scytonemins are yellow-brown lipid-soluble dimeric pigments located in the extracellular sheath of certain cyanobacteria growing in extreme habitats mostly exposed to high light intensities; these substances have been proposed to serve as UV-B sunscreens.[37,38] Other cyanobacteria and many eukaryotic phytoplankton organisms produce mycosporine-like amino acids (MAAs), which are water-soluble substances characterized by a cyclohexenone or cyclohexenimine chromophore conjugated with the nitrogen substituent of an amino acid or its imino alcohol, having absorption maxima ranging from 310 to 360 nm and an average molecular weight of around 300.[39]

Reactive oxygen species (ROS) and other radicals are effectively quenched by carotenoids, tocopherols, ascorbate, and reduced glutathione, supported by antioxidant enzymes, including superoxide dismutase (SOD), catalase, glutathione peroxidase (GSH-Px), and the enzymes involved in the ascorbate–glutathione cycle to detoxify ROS, such as ascorbate peroxidase (APX), monodehydroascorbate reductase (MDHAR), dehydroascorbate reductase (DHAR), and glutathione reductase (GR).[40]

The photosynthetic apparatus is protected by several mechanisms. Carotenoids absorb access excitation energy and dissipate it thermally (see above). Some photosynthetic organisms developed the xanthophyll cycle to improve this protective mechanism.[41] The photosynthetic electron transport is downregulated at the site of the D1 protein in Photosystem II. This mechanism, called photoinhibition, is found in algae and higher plants.[42,43] Many photosynthetic organisms show a typical midday decrease in the photosynthetic yield around noon. This pattern is believed to be mainly due to dynamic photoinhibition. In marine algae, this pattern is complicated by the tidal rhythm, so that the highest irradiance stress occurs when low tide coincides with high solar angles.[44,45] When exposed to excessive solar radiation, the quantum yield of PS II decreases. Upon short-term exposure, this process may be reversible within minutes or hours, while long-term exposure may cause irreversible damage. Regeneration is brought about by resynthesis of the damaged and cleaved D1 protein. Using pulse amplitude modulated (PAM) fluorescence, a number of fluorescence parameters can be determined, from which the photosynthetic quantum yield can be calculated (Figure 116.2).

If not repaired, UV-induced damage of the DNA can potentially result in mutations and death of the cells affected. Several mechanisms were developed to detect and repair damaged regions. In excision repair, the damaged site is cleaved, e.g., by an endonuclease, and excised by an exonuclease.[46] The gap is closed by a polymerase and a ligase. Photoreactivation is based on the photolyase enzyme, which utilizes the energy of UV-A/blue photons to split pyrimidine dimers.[47] If these systems fail to repair the damage, postreplication repair is another chance to regenerate the original state of the DNA.[48]

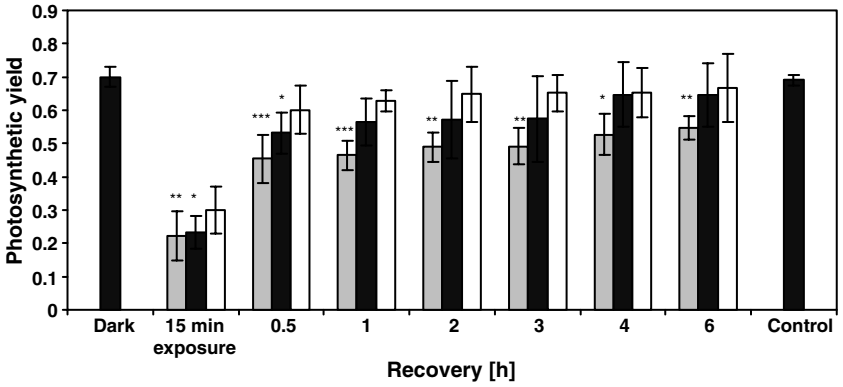

FIGURE 116.2 Effective photosynthetic quantum yield of *Enteromorpha linza* measured after 30 min dark adaptation, 15 min exposure, and after increasing recovery times in the shade, calculated as (*Fm*' - *Ft*)/*Fm*'. Gray bars denote the specimens exposed to unfiltered solar radiation. Black bars denote the specimens exposed to UV-A and PAR. White bars represent the specimens exposed to PAR only. The data are mean values of eight measurements and SE. The values for unfiltered solar radiation and under the 320 nm cutoff filter treatments are statistically significantly different from the PAR-only values (395 nm cutoff) in each set with $^{***}P < 0.001$, $^{**}P < 0.01$, or $^{*}P < 0.1$, respectively, as indicated by the student's *t*-test. Irradiances for the experiment were as follows: PAR 349 W m^{-2}, UV-A 44.15 W m^{-2}, and UV-B 1.34 W m^{-2}. (From Häder, D.-P., Lebert, M., and Helbling, E.W., *J. Photochem. Photobiol. B: Biol.* 62, 43, 2001. With permission.)

References

1. Carlile, M.J., Positioning mechanisms — the role of motility, taxis and tropism in the life of microorganisms, in *Contempory Microbiological Ecology*, Ellwood, C.D.C., Lathan, M., Hedger, J.N., Lynch, J.M., and Slater, J.H., Eds., Academic Press, London, 1980, p. 55.
2. Zonneveld, C., Photoinhibition as affected by photoacclimation in phytoplankton: a model approach, *J. Theor. Biol.*, 193, 115, 1998.
3. Walsby, A.E., Mechanisms of buoyancy regulation by planktonic cyanobacteria with gas vesicles, in *The Cyanobacteria*, Fay, P. and Van Baalen, C., Eds., Elsevier, Amsterdam; New York, 1987, p. 385.
4. Iino, M., Phototropism in higher plants, in *Photomovement. Comprehensive Series in Photosciences*, Häder, D.-P. and Lebert, M., Eds., Elsevier, Amsterdam, New York, 2001, p. 659.
5. Wagner, G., The physiology of tropisms, in *Progress in Botany: Genetics, Cell Biology and Physiology, Ecology and Vegetation Science*, Behnke, H.-D., Esser, K., Kadereit, J.W., Lüttge, U., and Runge, M., Eds., Springer-Verlag, Heidelberg, 1998, p. 396.
6. Koller, D., Solar navigation by plants, in *Photomovement. Comprehensive Series in Photosciences*, Häder, D.-P. and Lebert, M., Eds., Elsevier, Amsterdam; New York, 2001, p. 833.
7. Lebert, M., Porst, M., and Häder, D.-P., Circadian rhythm of gravitaxis in *Euglena gracilis*, *J. Plant Physiol.*, 155, 344, 1999.
8. Hasegawa, K., Tsukahara, Y., Ishizaki, S., Shimamoto, M., Nakamura, T., Sohma, M., and Sato, T., Contribution of the cAMP-dependent signal pathway to circadian synchrony of motility and resting membrane potential in *Paramecium*, *Photochem. Photobiol.*, 67, 256, 1998.
9. Häder, D.-P. and Lebert, M., Graviperception and gravitaxis in algae, *Adv. Space Res.*, 27, 861, 2001.
10. Richter, P.R., Schuster, M., Wagner, H., Lebert, M., and Häder, D.-P., Physiological parameters of gravitaxis in the flagellate *Euglena gracilis* obtained during a parabolic flight campaign, *J. Plant Physiol.*, 159, 181, 2002.
11. Porterfield, D.M., Orientation of motile unicellular algae to oxygen: oxytaxis in *Euglena*, *Biol. Bull.*, 193, 229, 1997.

12. van Houten, J., Signal transduction in chemoreception, in *Sensory Receptors and Signal Transduction*, Spudich, J.L. and Satir, B.H., Eds., John Wiley & Sons, New York, 1991, p. 65.
13. Wolf, R., Niemuth, J., and Sauer, H., Thermotaxis and protoplasmic oscillations in *Physarum plasmodia* analysed in a novel device generating stable linear temperature gradients, *Protoplasma*, 197, 121, 1997.
14. Emura, R., Ashida, N., Higashi, T., and Takeuchi, T., Orientation of bull sperms in static magnetic fields, *Bioelectromag.*, 22, 60, 2001.
15. Keim, C.N., Lins, U., and Farina, M., Elemental analysis of uncultured magnetotactic bacteria exposed to heavy metals, *Can. J. Microbiol.*, 47, 1132, 2001.
16. Davies, E., Olliff, C., Wright, I., Woodward, A., and Kell, D., A weak pulsed magnetic field affects adenine nucleotide oscillations, and related parameters in aggregating *Dictyostelium discoideum* amoebae, *Bioelectrochem. Bioenerg.*, 48, 149, 1999.
17. Clarkson, N., Davies, M.S., and Dixey, R., Diatom motility: the search for independent replication of biological effects of extremly low-frequency electromagnetic fields, *Int. J. Radiat. Biol.*, 75, 387, 1999.
18. Machemer-Röhnisch, S., Machemer, H., and Bräucker, R., Electric-field effects on gravikinesis in *Paramecium*, *J. Comp. Physiol.* A, 179, 213, 1996.
19. Häder, D.-P., Photomovement, in *Encyclopedia of Plant*, Haupt, W. and Feinleib, M.E., Eds., Springer-Verlag, Heidelberg, 1979, p. 268.
20. Chory, J., Light modulation of vegetative development, *Plant Cell*, 9, 1225, 1997.
21. von Arnim, A. and Deng, X.-W., Light control of seedling development, *Ann. Rev. Plant Physiol.*, 47, 215, 1996.
22. Weller, J.L., Beauchamp, N., Huub, L., Kerckhoffs, L.H.J., Platten, J.D., and Reid, J.B., Interaction of phytochromes A and B in the control of de-etiolation and flowering in pea, *Plant J.*, 26, 283, 2001.
23. Mazzella, M.A. and Casal, J.J., Interactive signalling by phytochromes and cryptochromes generates de-etiolation homeostasis in *Arabidopsis thaliana*, *Plant, Cell and Environ.*, 24, 155, 2001.
24. Murakami, A., Fujita, Y., Nemson, J.A., and Melis, A., Chromatic regulation in *Chlamydomonas reinhardtii*: time course of photosystem stoichiometry adjustment following a shift in growth light quality, *Plant Cell Physiol.*, 38, 188, 1997.
25. Palenik, B., Chromatic adaptation in marine *Synechococcus* strains, *Appl. Environ. Microbiol.*, 67, 991, 2001.
26. Häder, D.-P., Polarotaxis, gravitaxis and vertical phototaxis in the green flagellate, *Euglena gracilis*, *Arch. Microbiol.*, 147, 179, 1987.
27. Häder, D.-P., Photomovement, in *The Cyanobacteria*, Fay, P. and van Baalen, C., Eds., Elsevier, Amsterdam; New York, 1987, p. 325.
28. Häder, D.-P. and Häder, M.A., Effects of solar radiation on motility in *Stentor coeruleus*, *Photochem. Photobiol.*, 54, 423, 1991.
29. Song, P.-S., Häder, D.-P., and Poff, K.L., Step-up photophobic response in the ciliate, *Stentor coeruleus*, *Arch. Microbiol.*, 126, 181, 1980.
30. Iwatsuki, K., *Stentor coeruleus* shows positive photokinesis, *Photochem. Photobiol.*, 55, 469, 1992.
31. Cohn, S.A., Light dependent effects on diatom motility, *Mol. Biol. Cell*, 4, 168a, 1993.
32. Song, P.-S. and Poff, K.L., Photomovement, in *The Science of Photobiology*, Smith, K.C., Ed., 1989, p. 305.
33. Häder, D.-P., Ecological consequences of photomovement in microorganisms, *J. Photochem. Photobiol.*, 1, 385, 1988.
34. Boardman, N.K., Comparative photosynthesis of sun and shade plants, *Ann. Rev. Plant Physiol.*, 28, 355, 1977.
35. Lüning, K., Ed., *Seaweeds. Their environment, biogeography and ecophysiology*, John Wiley & Sons, New York, 1990.
36. Garcia-Pichel, F., Solar ultraviolet and the evolutionary history of cyanobacteria, *Origins Life Evol. Biosphere*, 28, 321, 1998.

37. Garcia-Pichel, F. and Castenholz, R.W., Characterization and biological implications of scytonemin, a cyanobacterial sheath pigment, *J. Phycol.*, 27, 395, 1991.
38. Sinha, R.P., Klisch, M., Gröniger, A., and Häder, D.-P., Ultraviolet-absorbing/screening substances in cyanobacteria, phytoplankton and macroalgae, *J. Photochem. Photobiol. B: Biol.*, 47, 83, 1998.
39. Gröniger, A., Sinha, R.P., Klisch, M., and Häder, D.-P., Photoprotective compounds in cyanobacteria, phytoplankton and macroalgae — a database, *J. Photochem. Photobiol. B: Biol.*, 58, 115, 2000.
40. Foyer, C.H., Descourvieres, P., and Kunert, K.J., Protection against oxygen radicals: an important defence mechanism studied in transgenic plants, *Plant Cell Environ.*, 17, 507, 1994.
41. Niyogi, K.K., Grossman, A.R., and Björkman, O., *Arabidopsis* mutants define a central role for the xanthophyll cycle in the regulation of photosynthetic energy conversion, *Plant Cell*, 10, 1121, 1998.
42. Krause, G.H. and Weis, E., Chlorophyll fluorescence and photosynthesis: the basics, *Ann. Rev. Plant Physiol.*, 42, 313, 1991.
43. Häder, D.-P., Kumar, H.D., Smith, R.C., and Worrest, R.C., Effects on aquatic ecosystems, UNEP Environmental Effects Panel Report, 1998, p. 86.
44. Hanelt, D., Li, J., and Nultsch, W., Tidal dependence of photoinhibition of photosynthesis in marine macrophytes of the South China Sea, *Bot. Acta*, 107, 66, 1994.
45. Häder, D.-P., Lebert, M., and Helbling, F.W., Effects of solar radiation on the Patagonian macroalga *Enteromorpha linza* (L.) J. Agardh — Chlorophyceae, *J. Photochem. Photobiol. B: Biol.*, 62, 43, 2001.
46. Blakefield, M.K. and Harris, D.O., Delay of cell differentiation in *Anabaena aequalis* caused by UV-B radiation and the role of photoreactivation and excision repair, *Photochem. Photobiol.*, 59, 204, 1994.
47. Dany, A.-L., Douki, T., Triantaphylides, C., and Cadet, J., Repair of the main UV-induced thymine dimeric lesions within *Arabidopsis thaliana* DNA: evidence for the major involvement of photoreactivation pathways, *J. Photochem. Photobiol. B: Biol.*, 65, 127, 2001.
48. Moreau, P.L., Role of *Escherichia coli* RecA protein in SOS induction and post-replication repair, *Biochimie*, 67, 353, 1985.

117

Chemistry and Spectroscopy of Chlorophylls

Hugo Scheer
Universität München

117.1 Introduction

The chlorophylls (Chl) and bacteriochlorophylls (BChl) comprise a group of more than 50 tetrapyrrolic pigments with common structural elements and functions.[1,2] Chemically, they are defined as Mg-complexes of cyclic tetrapyrroles of the porphyrin (Figure 117.1b), chlorin (Figure 117.1a), or bacteriochlorin (Figure 117.1b) oxidation state, all bearing a fifth, isocyclic ring, and most of them esterified at C-17[3] by the diterpenoid alcohol, phytol (Phy) (Figure 117.1a). However, an increasing number of structural variations have become obvious that do not strictly follow this definition (Section 117.2).

In a more biological definition, those of the above pigments and their derivatives are chlorophylls, which function in photosynthetic light harvesting or energy transfer. This excludes precursors or degradation products that conform to the chemical definition, and *vice versa*, it includes several pigments that deviate from the chemical definition but are functional in photosynthesis. Among them are the pheophytins (Phe) and bacteriopheophytins (BPhe) lacking the central Mg, a [Zn]-BChl *a* in which it is replaced by zinc, and the *c*-type chlorophylls [or more strictly speaking, chlorophyllides (Chlid), because they are generally are not esterified at C-17[3]]. There also exists a relatively small number of hydroporphyrins that are structurally related but functionally unrelated to chlorophylls, *viz*. the sex determinant(?) bonellin in *Bonellia* viridis,[3] a structurally yet uncertain component of the visual system of deep-sea fish,[4] and antioxidants(!) from several clams and diatoms.[5] Heavy-metal derivatives of chlorophylls were isolated from plants growing on media enriched in the respective metals.[6] Open-chain tetrapyrroles derived of chlorophylls were identified as breakdown products of chlorophylls[7] but also as bioluminescent pigments in krill.[8]

0-8493-1348-1/04/$0.00+$1.50

Chlorin Esterifying alcohols (R_{17}3)

Pigment	Abbreviation	R_3	R_7	R_8	R_{12}	$R_{13^2\alpha}$	R_{13^2b}	R_{17^3}	R_{20}	M	Funct..	Occurence
Chlorophyll a	Chl a	C_2H_3	CH_3	C_2H_5	CH_3	$COOCH_3$	H	Phy^1	H	Mg	RC, LHC	C CA G R P
Chlorophyll a'	Chl a'	C_2H_3	CH_3	C_2H_5	CH_3	H	$COOCH_3$	Phy	H	Mg	RC type I	C CA G R P
[8-Vinyl]-chlorophyll a	[8-Vinyl]-Chl a	C_2H_3	CH_3	C_2H_3	CH_3	$COOCH_3$	H	Phy	H	Mg	RC, LHC	CB(II)
[8-Hydroxyethyl]-chlorophyll a_F	[8^1-OH]-Chl a_F	C_2H_3	CH_3	C_2H_4OH	CH_3	$COOCH_3$	H	Far	H	Mg	RC type I	GS
Chlorophyll b	Chl b	C_2H_3	CHO	C_2H_5	CH_3	$COOCH_3$	H	Phy	H	Mg	LHC	CB(II) GA P
[8-Vinyl]-chlorophyll b	[8-Vinyl]-Chl b	C_2H_3	CHO	C_2H_3	CH_3	$COOCH_3$	H	Phy	H	Mg	LHC	CB(II)
Chlorophyll d	Chl d	CHO	CH_3	C_2H_5	CH_3	$COOCH_3$	H	Phy	H	Mg	RC, LHC	$CB(II)^2$
Chlorophyll d'	Chl d'	CHO	CH_3	C_2H_5	CH_3	H	$COOCH_3$	Phy	H	Mg	RC type I	$CB(II)^2$
Pheophytin a	Phe a	C_2H_3	CH_3	C_2H_5	CH_3	$COOCH_3$	H	Phy	H	H_2	RC typeII	C CA G R P
Bacteriochlorophyll c	BChl c	CHOH-CH_3	CH_3	$CH_2CH_n(CH_3)_{3-n}$	CH_3/C_2H_5	H	H	Far/others	CH_3	Mg	LHC	GN,GS
Bacteriochlorophyll d	BChl d	CHOH-CH_3	CH_3	$CH_2CH_n(CH_3)_{3-n}$	CH_3/C_2H_5	H	H	Far/others	H	Mg	LHC	GN,GS
Bacteriochlorophyll e	BChl e	CHOH-CH_3	CHO	$CH_2CH_n(CH_3)_{3-n}$	CH_3/C_2H_5	H	H	Far/others	CH_3	Mg	LHC	GS

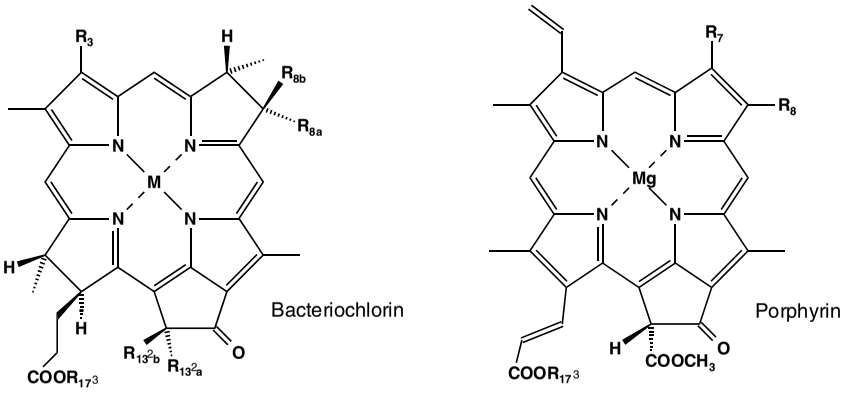

Pigment	Abbreviation	R_3	R_7	R_{8a}/R_{3b}	R_{13^2a}	R_{13^2b}	R_{17^3}	M	Function	Occurence
Bacteriochlorophyll a	BChl a	$COCH_3$		C_2H_5/H	$COOCH_3$	H	Phy (sometimes others)	Mg	RC, LHC	PB GN GS
Bacteriochlorophyll a'	BChl a'	$COCH_3$		C_2H_5/H	H	$COOCH_3$	Phy	Mg	RC type I	PB
[Zn]-Bacteriochlorophyll a	Zn-BChl a	$COCH_3$		C_2H_5/H	$COOCH_3$	H	Phy	Zn	RC, LHC	PB[3]
Bacteriochlorophyll b	BChl b	$COCH_3$		= CH-CH_3	$COOCH_3$	H	Phy (sometimes others)	Mg	RC, LHC	PB
Bacteriochlorophyll g	BChl g	C_2H_3		= CH-CH_3	$COOCH_3$	H	Far	Mg	RC, LHC	HB
Bacteriochlorophyll g'	BChl g'	C_2H_3		= CH-CH_3	H	$COOCH_3$	Far	Mg	RC type I	HB
Bacteriopheophytin a	BPhe a	$COCH_3$		C_2H_5/H	$COOCH_3$	H	Phy	H_2	RC type II	PB GN
Bacteriopheophytin b	BPhe b	$COCH_3$		= CH-CH_3	$COOCH_3$	H	Phy	H_2	RC type II	PB
Chlorophyll(ide) c_1	Chl(ide) c_1		CH_3	C_2H_5			H	Mg	LHC	CB(II) CA
Chlorophyll(ide) c_2	Chl(ide) c_2		CH_3	C_2H_3			H	Mg	LHC	CB(II) CA
Chlorophyll(ide) c_3	Chl(ide) c_3		$COOCH_3$	C_2H_5			H	Mg	LHC	CB(II) CA
[8-Vinyl]-protochlorophyllide a[4]	[8-Vinyl]-PChlid a[4]		CH_3	C_2H_3			H	Mg	LHC	CB(II) CA

FIGURE 117.1 Structures of chlorophylls and their functions in photosynthesis. a) Chlorin-type chlorophylls derived of the *trans-17,18-dihydroporphyrin* macrocyle (left) and a selection of esterifying alcohols at C-17[3]; b) bacteriochlorin-type chlorophylls (left) and porphyrin-type chlorophylls (right) derived of the *trans-7,8,17,18-tetrahydroporphyrin* and the fully unsaturated porphyrin macrocyle, respectively. The [8-vinyl] pigments are often also termed "divinyl" chlorophylls. The bacteriochlorophylls c, d, and e, which are chlorins, comprise a complex mixture of pigments with varying R_8, R_{12}, and R_{17^3}, and of epimers at C-3[1]. *The* stereochemistry at C-13[2] of most c-type chlorophylls is uncertain. Chl c_3 is probably a mixture with $R_8 = C_2H_3$ and C_2H_5.

Footnotes: 1) 2,6-Phytadienol in RC of green sulfur bacteria; 2) *Acaryochloris marina* and possibly some other species; 3) *Acidiphilium rubrum* and related species; 4) No 17[1],17[2] double bond, this pigment is also termed [Mg-3,8-divinyl]-pheoporphyrin a_5-13[3]-monomethylester; 5) abbreviations used: C = cyanobacteria including cyanelles (Glaucophyta), C(II) = nonclassical (Type II) cyanobacteria, CA = chromophyte algae, G = green algae, GN = green nonsulfur bacteria (*Chloroflexus*), GS = green sulfur bacteria, P = plants, PB = purple bacteria, R = red and cryptophyte algae.

117.2 Chlorophyll Structures and Functions

Chlorophylls function in photosynthetic organisms as light-harvesting pigments in antenna complexes (LHC)[9] and as electron carriers in reaction centers (RC) that carry out the light-driven electron transfer across the photosynthetic membrane.[10] A Chl *a* molecule of unknown function is also present in the electrogenic cytochrome b_6/f complex located between the two photosystems, PSII and PSI, of oxygenic organisms.[11,12]

A wide variety of chlorophylls (Figure 117.1) were identified in the various types of LHC, which are probably polyphyletic.[13] This number is increasing with advances in microbiology and improved analytical techniques, and some of the more recently discovered pigments are, by no means, "exotic." The most striking examples are [8-vinyl]-Chl *a* and *b*, often referred to as "divinyl" Chl *a* and *b*, respectively. In marine prochlorophytes, they are responsible for a sizeable amount of the earth's photosynthetic CO_2 fixation.[14] BChl with Zn as central metal has recently been found in several acidophilic purple bacteria as the main LHC pigment.[15] While most of the recently identified heavy-metal chlorophylls (e.g., Cu, Ag) are deleterious to photosynthesis,[6] [La]-Chl *a* has been suggested to be beneficial.[16] In LHC of anoxygenic bacteria, alcohols other than phytol were frequently found at C-17[3] (Figure 117.1). A number of C-20 terpenoid alcohols other than phytol were identified in purple bacteria, C-15 terpenoid alcohols in heliobacteria, and these and other alcohols, including unbranched ones, in green bacteria. The *c*-type Chls generally do not carry a long-chain esterifying alcohol at C-17[3]. However, some do, and among them, an unusual lipid ester was recently identified[17] (Figure 117.1).

By contrast, there are only two types of RC, which are probably monophyletic.[10] In all RC, chlorophylls act as primary electron donors (generally designated Pxxx, with xxx giving the wavelength of the red-most absorption maximum) and also as primary electron acceptors. In the Type I RC, into which the core antenna is integrated, the secondary acceptors are chlorophylls as well, while in Type II RC, the secondary acceptors are pheophytins lacking the central Mg. One of the four BChl in purple bacterial RC (which are of Type II), is also implicated in triplet energy transfer to carotenoids, e.g., in the light protection.[18] Chl *a* is found in the RC of nearly all organisms capable of oxygenic photosynthesis, together with Phe *a* in PS II RC. They are replaced by [8-vinyl]-Chl *a* (and possibly [8-vinyl]-Phe *a*) in the oxygenic marine *Prochlorococcus* species, and by BChl *a*, *b*, or *g* in most anoxygenic bacteria. BPhe *a* and BPhe *b* replace Phe *a* in the Type II RC of purple bacteria containing BChl *a* and BChl *b*, respectively, as major pigments. Additional, more specialized chlorophylls were identified in RC.[19] Chl *a*′, *viz.* the 13[2]-epimer of Chl *a*, has long been known as a component of PSI RC and was recently identified as one pigment of the dimeric primary donor of PSI, P700.[20] BChl *g*′ was found in the RC of heliobacteria. Because they are of Type I, too, a BChl *g*/BChl *g*′ heterodimer was suggested, in analogy, as primary donor in these phototrophic prokaryotes. A Chl *a*-type pigment, [8[1]-OH]-Chl *a*, is discussed as the first electron acceptor (A_0) in PSI. In the oxygenic prokaryote, *Acaryochloris marina*, Chl *d* replaces at least part of the Chl *a*, and Chl *d*′ replaces Chl *a*′. Recently, an autotrophic mutant of a cyanobacterium was described, in which 50% of the Chl *a*/Phe *a* content of PSII RC was replaced by Chl *b*/Phe *b*.[21] In the RC and the LHC of several *Acidiphilium* species, [Zn]-BChl *a* replaces BChl *a*.[15] The BChl of the purple bacterium, *Rhodospirillum rubrum*, contains geranylgeraniol as the esterifying alcohol, while the BPhe *a* of RC is esterified with phytol.[22]

Exchange experiments showed that a surprising variety of modified chlorophylls can be incorporated into the various pigment-protein complexes, often with distinct specificities of the individual binding sites.[23–27] It remains a challenge to understand these binding specificities, as well as the functional significance of the various aforementioned "specialized" chlorophylls on a molecular level.

117.3 Spectroscopy

The absorption spectra of cyclic tetrapyrroles are generally described by the four-orbital model first proposed by Gouterman for cyclic tetrapyrroles, resulting in four possible electronic transitions[28,29] that are generally each split into two vibrational bands. In the fully unsaturated porphyrin-type pigments like

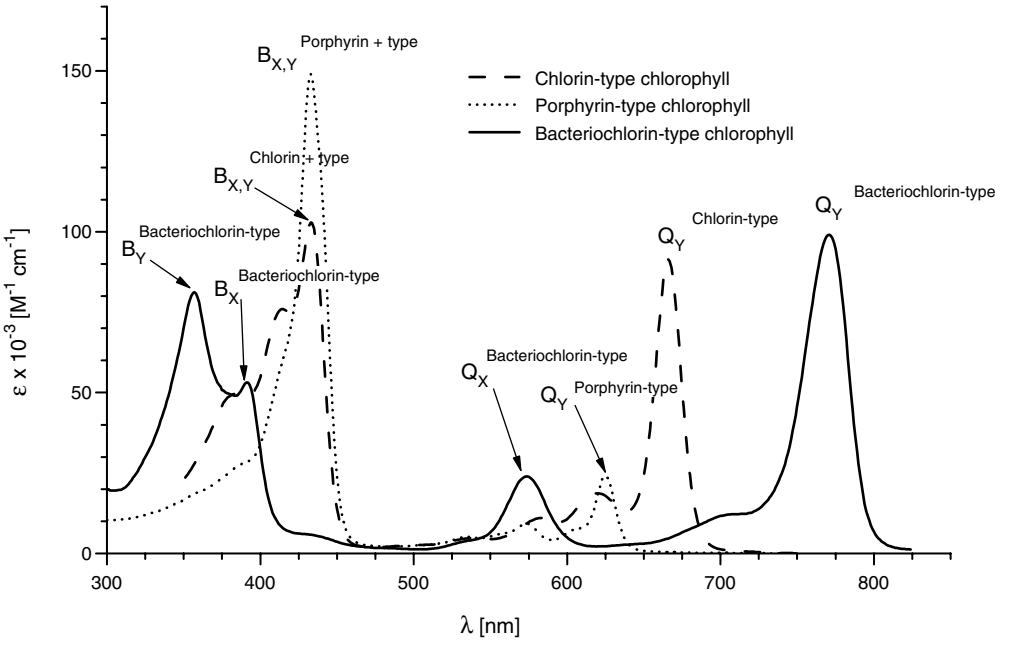

FIGURE 117.2 Type-spectra of chlorophylls.

Chl *c*, the two transitions in the visible (Q_y, Q_x) are only weakly allowed, while two in the blue or near-UV spectral region (B_y, B_x) are intense ($\varepsilon_{max} \approx 3 \times 10^5$). The Q_y-band is less forbidden ($\varepsilon_{max} \approx 10^5$) and progressively red-shifted in chlorin- and bacteriochlorin-type chlorophylls (Figure 117.2). These pigments have, therefore, two regions of intense absorptions in the red to near-IR (Q_y) and in the blue to near-UV spectral ranges (Soret or *B*-bands). The Q_x-band remains weak in the chlorins but is moderately intense in the bacteriochlorins. Because in the latter, the B_x- and B_y-bands are also well separated, all four canonical transitions are clearly discernible in the bacteriochlorophylls. The significance of this fact was first realized by Scherz et al., who used it, subsequently, as a sensitive environmental probe.[30,31]

Absorption spectroscopy after extraction is the most common method for (B)Chl quantitation.[32–34] The solution spectra of the more common chlorophylls are summarized in Table 117.1. Monomeric (B)Chls are highly fluorescent, and phosphorescence was observed for many pigments. Both are quenched *in situ*, and the degree and dynamics of fluorescence quenching are valuable indicators for photosynthetic processes.[35,36]

In (B)Chl proteins, the *Q*-bands are generally red-shifted and hyperchromic. Aggregation was recognized as a major factor of these changes, based on x-ray structures[20,37,38] and a large number of aggregation studies in various environments (see Section 117.4). It is generally accompanied by an induction of strong optical activity, with conservative as well as nonconservative excitonic bands.[39–41] While point charges (which are important in linear polyenes) seem to play only a minor role as "spectral modifiers," conformational changes can induce considerable red shifts[42,43] and optical activity.[44] Interactions with nearby aromatic amino acids were recognized as another important factor.[45]

The intense absorptions in the visible and NIR spectral regions are an important factor in photosynthetic light harvesting. However, the bands are narrow, and there is only moderate absorptivity in the green spectral region, where the light flux is often highest. In antennas, (B)Chls are, therefore, almost always supplemented by additional light-harvesting pigments, in particular, in microorganisms.[9] The lowest excited electronic state, ^{1}S, of (B)Chls absorbs in the red region close to the ground-state absorption.[46] Excited state dynamics were studied, in solution and in pigment-protein complexes, by high-resolution spectroscopy, in the time[47–48] and frequency domains,[49,50] by nonlinear absorption techniques[51] and, more recently, by single molecule spectroscopy.[52] The absorption spectra of triplets and anion and

TABLE 117.1 Absorption Maxima of Main Chlorophylls

		of Chlorophyll [λ_{max} (nm) ($\varepsilon/10^{-3}$)]				of Pheophytin [λ_{max} (nm)]			
Parent Pigment	Type Spectrum	Q_Y	Q_X	B_Y	B_X	Q_Y	Q_X	B_X	B_Y
Chlorophyll *a*[a]	Chlorin	662 (100.9) (DE)		434		667	535, 505	408	
Chlorophyll *b*[a]	Chlorin	644 (62) (DE)		454		655	525	412	
Chlorophyll *c*[b]	Porphyrin	626	576	444		650	592, 579	532	433
Chlorophyll *d*[c]	Chlorin	687 (98.3) (DE)		446 (87.4)		638	586, 564	525	417
Bacteriochlorophyll *a*[d]	Bacteriochlorin	770 (96) (DE)	577 (20.9)	358 (73.4)	391 (48.1)	749	525	385	357
Bacteriochlorophyll *b*[e]	Bacteriochlorin	794 (106) (DE)	578 (25)	368 (81)	408 (78)	776	528	398	368
Bacteriochlorophyll *c*[f]	Chlorin	660 (91) (DE)	622 (15.9)	432 (142)	412 (72.6)	664	547, 515	408	
Bacteriochlorophyll *d*[f]	Chlorin	650 (89.9) (DE)	612 (12.5)	425 (116)	406 (69)	658	548, 505	406	
Bacteriochlorophyll *e*[g]	Chlorin	649 (48.9) (A)		462 (185)		654	534	439	
Bacteriochlorophyll *g*[h]	Bacteriochlorin	762 (76) (A)	567	405	365	753	518	396	388

cation radicals feature generally broader and less-structured absorptions.[53,54] The cation radical of the primary donor of purple bacterial RC has an intense and narrow near-infrared band characteristic of mixed-valence complexes, and a less-intense feature is also seen in Chl *a* containing oxygenic reaction centers.[55] There is, furthermore, an electronic absorption band at much longer wavelengths, assigned to charge-transfer absorptions in the cation radical.[56] Radical ions and triplets were studied widely in reaction centers by optical, magnetic resonance, and vibrational spectroscopy, in order to obtain selective information on the pigments involved in electron transfer (see Ref. 10 for a list of the leading references).

Many types of chlorophyll show, in solution, a fairly efficient intersystem crossing from the ^{1}S to the lowest triplet (^{1}T) state. Accordingly, they are good sensitizers for singlet oxygen. This potentially damaging effect is neutralized in photosynthetic organisms by an efficient triplet and $^1O_2$-quenching by carotenoids. Carotenoid-less mutants are, therefore, prone to photodynamic killing at high light intensities in the presence of oxygen. On the other hand, triplet formation and their intense red and NIR absorptions in the therapeutic window, render chlorophylls and, in particular, bacteriochlorophylls, good candidates for photodynamic therapy (and photodiagnosis) of certain types of cancer.[57,58]

117.4 Aggregates

Several modes of aggregation are known in chlorophylls. Because the process was implicated as an important factor in the stability, structure formation, and spectral properties of (B)Chls in their functional native environments, it was studied widely (for leading references, see Refs. 41, 59, 60). One type of aggregation can be induced by interactions of the central Mg of one pigment with a peripheral donor group of another. This mechanism is of particular importance in hydrophobic environments. It is also a factor in BChl *c*, *d*, and *e* aggregation in the chlorosome, the major antenna of green and brown bacteria, which contains only very little protein.[61] Dispersive and π,π interactions are probably more important in other aggregation types of (B)Chl, because aggregation here occurs equally well with the metal-free (bacterio)pheophytins. This process was studied, in particular, in aqueous-organic solvent mixtures,[41] in micelles, and in vesicles.[60] Large micellar aggregates are formed in aqueous systems, and aggregation is important on surfaces.

117.5 Reactivity

Chlorophyll chemistry before 1991 was treated in a comprehensive review article[62] (the recent advances were covered in a review of Senge[63]). Some of the early and more recent works are summarized in Figure 117.3. Only few details are given here, and the reader is referred to the cited references. While most of the early work was focused on the chemistry of chlorophylls as photosynthetic pigments, it has become of interest lately, with regard to their potentials in photodynamic therapy.[57,58]

Dark Reactions of the Aromatic Macrocyclic System

A large variety of redox reactions is known for the (B)Chls and related (hydro)porphyrins.[62,64] The reductions generally involve methine bridges but are often followed by rearrangements of the system. Reductions at the pyrrolenine-peripheral double-bonds are important in the dark biosynthesis of (B)Chls, which for the dark reaction, is carried out by enzymes related to nitrogenase.[65] Chemical equivalents of such reductions are only known for simple porphyrins, and the more gentle diimide reaction yields the *cis*-isomer. Alternatively, oxidation to *vic*-diols followed by pinacol rearrangement to ketones leads formally to hydroporphyrins.[66,67] Isomerization of endo- into exocyclic double-bonds would yield similar results but only the inverse process is experimentally known in the conversion of BChls *b* and *g* to the respective chlorins, [3-acetyl]-Chl *a* and Chl *a*.[68,69] The electrochemistry of (B)Chls shows several one-electron redox reactions of the macrocyclic π system. Pigments containing other central metals show redox reactivities of the metal, the macrocycle, or both.[70,71]

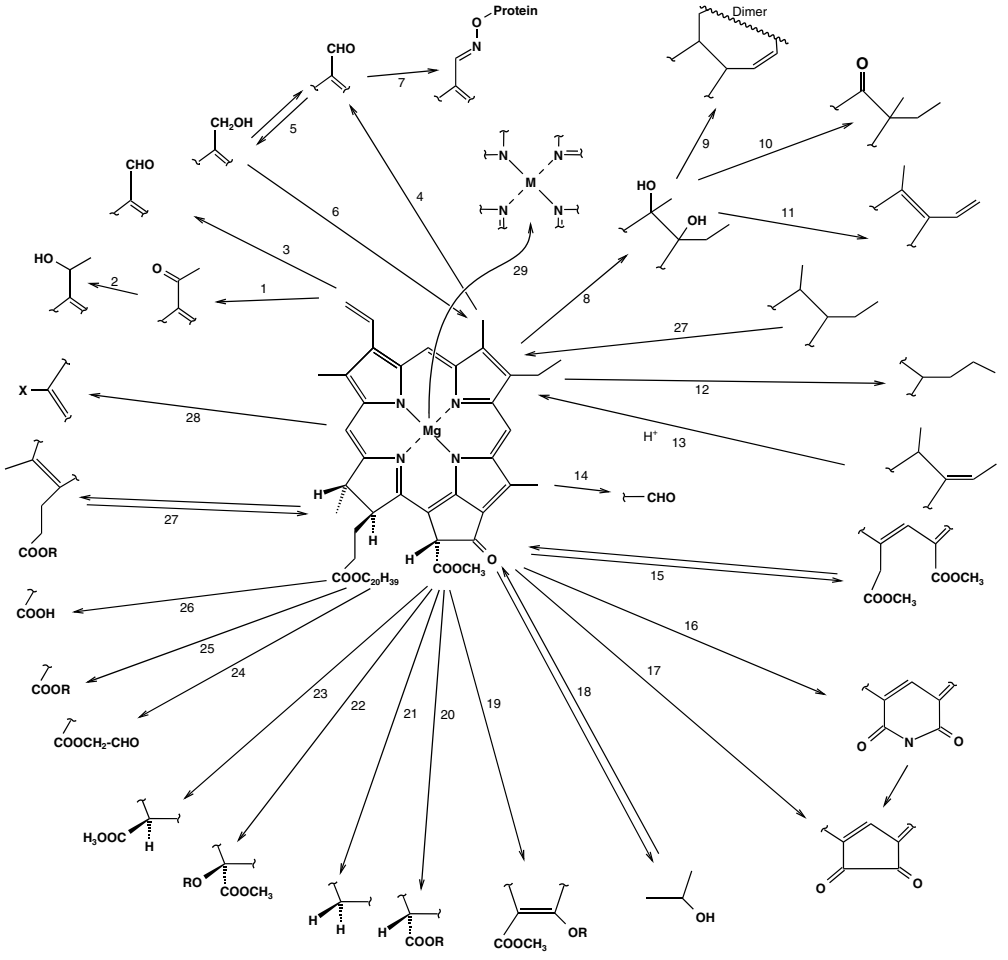

FIGURE 117.3 Schematic overview of chemical modifactions of the chlorophyll side chains and the central metal. For natural variations, see Figure 117.1. References: 1,2) Ref. 91; 3) Ref. 92; 4) Ref. 91; 5,6) Refs. 93–95; 7) Ref. 96; 8) Refs. 66, 97; 9) Ref. 98; 10) Refs. 66, 97; 11) Refs. 99–100; 12) Refs. 101, 102; 13) Refs. 68, 69; 14) Ref. 103; 15) Refs. 99, 100; 16) Ref. 104; 17) Ref. 103; 18) Ref 105; 19) Refs. 103, 106–108; 20) Refs. 109, 110; 21) Ref. 111; 22) Ref. 112; 23) Ref. 113; 24) Snigula and Scheer, unpublished (O_3); 25) Refs. 110, 114–116; 26) Ref. 117; 27) Refs. 118–120; (all reductions proceed with wrong stereochemistry); 28) Refs. 72, 122, 123; 29) Refs. 31, 73.

Substitution reactions are dependent on the relative electron densities, like in other aromatic systems. Electrophilic substitutions at methine bridges next to reduced rings are studied well.[72] The central Mg is easily lost in the presence of acid. Mg and a variety of other metals were (re)introduced into Phes of the chlorin and porphyrin type[73] and into BPhe.[74]

Ring opening to bile pigments, in particular at the C-5 position, was recognized as a critical step in chlorophyll degradative metabolism, because the linear tetrapyrroles are much less phototoxic than the cyclic ones. In contrast to the ring opening of the Fe porphyrins, the hemes, the bridging methine is retained in this process.[7,75] In green plants, Chl *b* is converted first to Chl *a*, while degradation products of both were identified in green algae. Another ring opening at C-20 gives rise to linear tetrapyrroles involved in the bioluminescence of *Euphausid* shrimps.[8]

Reactions of Peripheral Substituents

The peripheral groups of (B)Chls react as they would in similarly substituted simpler aromatic systems. There is a considerable long-range influence of other substituents that have an origin that is not fully understood. A variety of reactions are known at the isocyclic ring, and many are related to the presence of an enolizable β-ketoester system and to "peripheral crowding." The β-ketoester system can compete with the central N_4-cavity for chelation of metals. Conjugation reactions with amino acids, sugars, or other biological materials are of considerable interest for affinity labeling and the design of photo drugs. Useful handles are the 17^3-propionic acid groups *via* esterification or amide formation, C-13^2 via hydroxylation, C-3^1 and, in particular, C-7^1 (in Chl *b*), and C-8^1 (in BChl *b* and *g*) (see Figure 117.3).

Photochemistry

Light-induced redox reactions are important for the biological function of chlorophylls in RC and for the biosynthesis of Chl *a*; a photochemical ring opening may be involved in the breakdown of (B)Chls. Metalloporphyrins and chlorins are photoreduced in a two-electron reaction, e.g., by amines or thiols, at the methine bridges,[76] the former products rearrange to *cis*-chlorins.[64] The light-dependent protochlorophyllide reductase performs a *trans*-reduction at Ring *D* of the porphyrin precursor, protochlorophyllide, which structurally resembles the *c* chlorophylls. In spite of a large body of work, the structures of the intermediates are still unknown. With the recent development of reconstitution methods,[77] the photoreduction of chlide was characterized. A photoreaction of unknown mechanism has been reported for a rare water-soluble Chl protein from *Chenopodium*.[78]

One-electron redox reactions are most important in photosynthetic RC. BChls *a*, *b*, and *g*, and Chl *a*, and in certain bacteria, also [Zn]-BChl *a* or Chl *d*, act as electron donors. The same or similar (B)Chls act as primary and secondary acceptors in Type I RC, while in Type II RC, the secondary acceptors are the respective metal-free (B)Phe.[10] (B)Chl-sensitized reductions of redox partners, in particular, across membranes are of considerable interest as model reactions for photosynthesis. These reactions were also studied in solution in covalently linked systems like caroteno-chlorophyllo-quinones and more elaborate systems.[79]

Most photooxidative ring-opening reactions of Chls of the chlorin-type cleave the macrocycle at the C-20 methine bridge. But, cleavage at the C-5 bridge was reported for a Cd-pheophytin.[80] There is currently no evidence that the biodegradation involves light (see Section 117.6). The photosensitized oxidations of (B)Chl are of growing interest in photodynamic applications, e.g., in tumor therapy. However, little is known on the fate of the sensitizer, which in many cases, is irreversibly bleached.[81] Yet another type of photoreaction is demetalation ("photopheophytinization"), on what little is known.[82]

117.6 Metabolism

The starting point for the biosynthesis of chlorophylls is 5-amino-levuIinate (ALA), which in most photosynthetic organisms is formed from glutamate and in animals and purple bacteria from glycine and succinyl CoA. Dimerization leads to the monopyrrole, porphobilinogen, which then tetramerizes to protoporphyrin in a step involving the rotation of one of the pyrrole rings (for leading references, see Ref. 83). The specific part of Chl biosynthesis (Figure 117.4) starts with the insertion of Mg, followed by the formation of the isocyclic ring, reduction of the macrocycle (except for Chl *c*), and esterification. In angiosperms, the reduction *via* the so-called light protochlorophyllide reductase, is a photoreaction (see above). Several modified cyclic tetrapyrroles were identified during the biodegradation of chlorophylls. The subsequent crucial step in removing these phototoxic compounds is the ring opening to bile pigments, which in the currently studied cases in plants and green alga, is an enzymatic reaction that does not require light. These and the following reactions on the resulting open-chain tetrapyrroles were recently studied in some detail.[7,75]

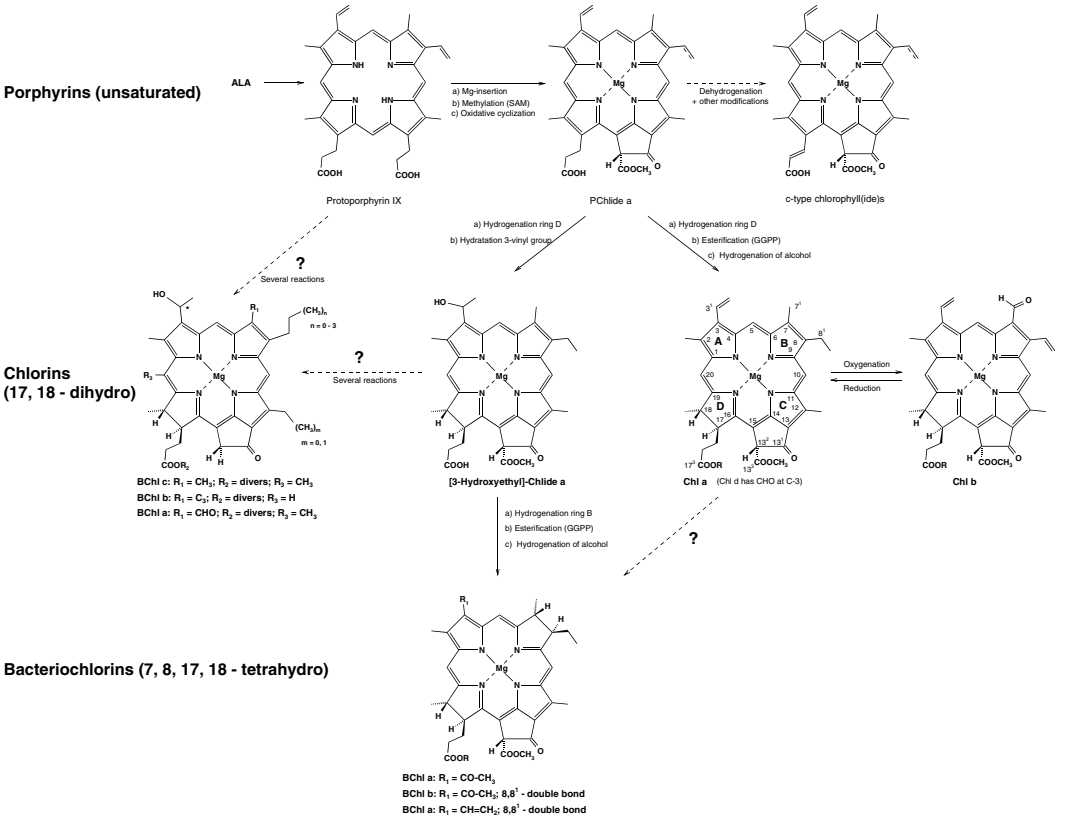

FIGURE 117.4 The biosynthesis of various chlorophylls from the common precursor, protoporphyrin IX**.**

117.7 Abbreviations

BChl	bacteriochlorophyll
BPhe	bacteriopheophytin
B_x, B_y	higher-energy absorption bands of tetrapyrroles in the Vis/UV spectral range
Chl	chlorophyll
ε	molar extinction coefficient [M^{-1} cm^{-1}]
Far	farnesol
GGPP	geranyl-geranyl pyrophosphate
IC	internal conversion
ISC	intersystem crossing
λ	wavelength (nm)
NIR	near-infrared spectral range (700 to 1200 nm)
nmr	nuclear magnetic resonance
Phe	pheophytin
Phy	phytol
Q_x, Q_y	low-energy absorption bands of tetrapyrroles in the Vis/NIR spectral region
RC	reaction center (Type I and Type II relate to the homologies with PSI and PSII, respectively)
UV	ultraviolet spectral range (200 to 400 nm)
Vis	visible spectral range (400 to 700 nm)

117.8 Nomenclature

IUPAC numbering is used throughout (see Figure 117.1a).

Acknowledgments

The work of the author was supported by the Deutsche Forschungsgemeinschaft, Bonn; the Hans-Fischer Gesellschaft, München; the German–Israel Foundation, Jerusalem; and the VW foundation, Hannover.

References

1. Scheer, H., Chlorophylls, Boca Raton, FL, CRC Press LLC, 1991.
2. Grimm, B., Porra, R., Rüdiger, W., and Scheer, H., *Biochemistry, Biophysics, and Biological Functions of Chlorophylls,* Kluwer, Dordrecht, In press.
3. Ballantine, J.A., Psaila, A.F., Pelter, A., Murray-Rust, P., Ferrito, V., and Jaccarini, V. The structure of bonellin and its derivatives, Unique Physiologically active chlorins from the marine *Bonellia viridis*., *J. Chem. Soc. Perkin I*, 1080, 1980.
4. Douglas, R.H., Partridge, J.C., Dulai, K., Hunt, D., Mullineaux, C.W., Tauber, A.Y., and Hynninen, P.H., Dragon fish see using chlorophyll, *Nature*, 393, 423, 1998.
5. Watanabe, N., Yamamoto, K., Ihshikawa, H., Yagi, A., Sakata, K., Brinen, L.S., and Clardy, J., New chlorophyll-A-related compounds isolated as antioxidants from marine bivalves, *J. Nat. Prod.*, 56, 305, 1993.
6. Küpper, H., Setlik, I., Spiller, M., Küpper, F.C., and Prasil, O., Heavy metal-induced inhibition of photosynthesis: targets of *in vivo* heavy metal chlorophyll formation, *J. Phycol.*, 38, 1, 2001.
7. Kräutler, B. and Matile, P., Solving the riddle of chlorophyll breakdown, *Acc. Chem. Res.*, 32, 35, 1999.
8. Shimomura, O., Structure of the light emitter in krill (*Euphaisia pacifica*) bioluminescence, *J. Amer. Chem. Soc.*, 110, 2683, 1988.
9. Green, B. and Parson, W., *Light-harvesting antennas in photosynthesis,* Kluwer, Dordrecht, In press.
10. Deisenhofer, J. and Norris, J.R., *The Photosynthetic Reaction Center,* Academic Press, New York, 1993.
11. Pierre, Y., Breyton, C., Lemoine, Y., Robert, B., Vernotte, C., and Popot, J.-L. On the presence and role of a molecule of chlorophyll *a* in the cytochrome b_6f complex, *J. Biol. Chem.*, 272, 21,901, 1997.
12. Peterman, E.J., Wenk, S.O., Pullerits, T., Palsson, L.O., van Grondelle, R., Dekker, J.P., Rogner, M., and van Amerongen, H., Fluorescence and absorption spectroscopy of the weakly fluorescent chlorophyll *a* in cytochrome b_6f of *Synechocystis* PCC6803, *Biophys. J.*, 75, 389, 1998.
13. Scheer, H., The pigments, in *Light-Harvesting Antennas in Photosynthesis*, Green, B. and Parson, W., Eds., Kluwer, Dordrecht, the Netherlands, in press, 2003.
14. Goericke, R. and Repeta, D., The pigments of *Prochlorococcus marinus*: the presence of divinyl-chlorophyll a and b in a marine procaryote., *Limnol. Oceanogr.*, 37, 425, 1992.
15. Kobayashi, M., Akiyama, M., Yamamura, M., Kise, H., Takaichi, S., Watanabe, T., Shimada, K., Iwaki, M., Itoh, S., Ishida, N., Koizumi, M., Kano, H., Wakao, N., and Hiraishi, A., Structural determination of the novel Zn-containing bacteriochlorophyll in *Acidiphilium rubrum*, *Photomed. Photobiol.*, 20, 80, 1998.
16. Wang, Q., Huang, B., Guan, Z., Yang, L., and Li, B., Speciation of rare earth elements in soil by sequential extraction than HPLC coupled with visible and ICP-MS detection, *Fresenius' J. Anal. Chem.*, 370, 1041, 2001.
17. Garrido, J.L., Otero, J., Maestro, M.A., and Zapata, M., The main nonpolar chlorophyll c from *Emiliana huxleyi* (Prymnesiophyceae) is a chlorophyll c_2-monogalactosyldiacylglyceride ester: a mass spectrometry study, *J. Phycol.*, 36, 497, 2000.
18. Angerhofer, A., Bornhäuser, F., Aust, V., Hartwich, G., and Scheer, H., Triplet energy transfer in bacterial photosynthetic reaction centres, *Biochim. Biophys. Acta*, 1365, 404, 1998.

19. Kobayashi, M., Akiyama, M., Watanabe, T., and Kano, H., Exotic chlorophylls as key components of photosynthesis, *Curr. Topics Plant Biol.*, 1, 17, 1999.
20. Jordan, P., Fromme, P., Witt, H.T., Klukas, O., Seanger, W., and Krauss, N., Three-dimensional structure of cyanobacterial photosystem I at 2.5 ANG resolution, *Nature,* 411, 909, 2001.
21. Xu, H., Vavilin, D., and Vermaas, W., Chlorophyll b can serve as the major pigment in functional photosystem II complexes of cyanobacteria, *Proc. Natl. Acad. Sci. USA*, 98, 14,168, 2001.
22. Walter, E., Schreiber, J., Zass, E., and Eschenmoser, A., Bakteriochlorophyll a_{GG} und Bakteriophäophytin a_P in den photosynthetischen Reaktionszentren von *Rhodospirillum rubrum G9.*, *Helv. Chim. Acta*, 62, 899, 1979.
23. Scheer, H. and Hartwich, G., Bacterial reaction centers with modified tetrapyrrole chromophores, in *Anoxygenic Photosynthetic Bacteria*, Blankenship, R., Madigan, M.T., and Bauer, C.E., Eds., Kluwer, Dordrecht, 1995, p. 649.
24. Herek, J.L., Fraser, N.J., Pullerits, T., Martinsson, P., Polvika, T., Scheer, H., Cogdell, R.J., and Sundström, V., Mechanism of B800->B850 energy transfer mechanism in bacterial LH2 complexes investigated by B800 pigment exchange, *Biophys. J.*, 78, 2590, 2000.
25. Davis, C.M., Parkes-Loach, P.S., Cook, C.K., Meadows, K.A., Bandilla, M., Scher, H., and Loach, P.A., Comparison of the structural requirements for Bacteriochlorophyll binding in the core light-harvesting complexes of *Rhodospirillum rubrum* and Rhodobacter sphaeroides using reconstitution methodology with Bacteriochlorophyll analogs, *Biochemistry*, 35, 3072, 1996.
26. Paulsen, H., Chlorophyll a/b-binding proteins, *Photochem. Photobiol.*, 62, 367, 1995.
27. Bassi, R., Croce, R., Cugini, D., and Sandona, D., Mutational analysis of a higher plant antenna protein provides identification of chromophores bound into multiple sites, *Proc. Natl. Acad. Sci. USA*, 96, 10056, 1999.
28. Weiss, C., *Optical Spectra of Chlorophylls*, Vol. 3, Dolphin, D., Ed., Academic Press, New York, 1978, chap. 3.
29. Noy, D., Fiedor, L., Hartwich, G., Scheer, H., and Scherz, A., Metal-substituted bacteriochlorophylls. 2. Changes in redox potentials and electronic transition energies are dominated by intramolecular electrostatic interactions, *J. Am. Chem. Soc.*, 120, 3684, 1998.
30. Noy, D., Yerushalmi, R., Brumfeld, V., Ashur, I., Scheer, H., Baldridge, K.K., and Scherz, A., Optical absorption and computational studies of [Ni]-Bacteriochlorophyll *a*. New insight into charge distribution between metal and ligands, *J. Am. Chem. Soc.*, 122, 3937, 2000.
31. Hartwich, G., Fiedor, L., Simonin, I., Cmiel, E., Schaefer, W., Noy, D., Scherz, A., and Scheer, H., Metal-Substituted Bacteriochlorophylls.1. Preparation and influence of metal and coordination on spectra, *J. Am. Chem. Soc.*, 120, 3675, 1998.
32. Porra, R.J., Recent advances and re-assessments in chlorophyll extraction and assay procedures for terrestrial, aquatic, and marine organisms, including recalcitrant algae, in *Chlorophylls*, Scheer, H., Ed., CRC Press LLC, Boca Raton, FL, 1991, p. 31.
33. Oelze, J. Analysis in bacteriochlorophylls, *Meth. Microbiol.*, 18, 257, 1985.
34. Porra, R.J., The chequered history of the development and use of simultaneous equations for the accurate determination of chlorophylls a and b**,** *Photosynth. Res.*, 73, 149, 2002.
35. Krause, G.H. and Jahns, P., Pulse amplitude modulated chlorophyll fluorometry and its application in plant science, in *Light-Harvesting Antennas in Photosynthesis,* Green, B. and Parson, W., Eds., Kluwer, Dordrecht, in press.
36. Nedbal, L., Chlorophyll fluorescence as a reporter, in *Biochemistry and Biophysics of Chlorophylls,* Grimm, B., Porra, R., Rüdiger, W., and Scheer, H., Eds., Kluwer, Dordrecht, in press,
37. McDermott, G., Prince, S.M., Freer, A.A., Hawthornthwaite-Lawless, A.M., Papiz, M.Z., Cogdell, R.J., and Isaacs, N.W., Crystal structure of an integral membrane light-harvesting complex from photosynthetic bacteria, *Nature*, 374, 517, 1995.
38. Parson, W.W. and Warshel, A., Simulations of electron transfer in bacterial reaction centers, in *The Photosynthetic Reaction Center*, Vol. II, Deisenhofer, J. and Norris, J.R., Eds., Academic Press, 1993, p. 23.

39. Sauer, K., Primary events and the trapping of energy, in *Bioenergetics of Photosynthesis*, Govindje, Academic Press, New York, 1975, chaps. 3, 115.
40. Cogdell, R.J. and Scheer, H., Circular dichroism of light-harvesting complexes from purple photosynthetic bacteria, *Photochem. Photobiol.*, 42, 669, 1985.
41. Scherz, A., Rosenbach-Belkin V., Michalski T.J., and Worcester D.L., Chlorophyll aggregates in aqueous solutions, in *Chlorophylls*, Scheer, H., Ed., CRC Press LLC, Boca Raton, FL, 1991, p. 237.
42. Barkigia, K.M. and Fajer, J., Models of photosynthetic chromophores: molecular structures of Chlorins and Bacteriochlorins in *The Photosynthetic Reaction Center*, Vol. II, Deisenhofer, J. and Norris, J.R., Eds., Academic Press, New York, 1993, p. 513.
43. Kalisch, W.W. and Senge, M.O., Synthesis and structural characterization of nonplanar Tetraphenylporphyrins with graded degree of β-ethyl substitution, *Tetrahedron Lett.*, 32, 1183, 1996.
44. Wolf, H. and Scheer, H., Stereochemistry and chiroptic properties of pheophorbides and related compounds, *Ann. NY Acad. Sci.*, 206, 549, 1973.
45. Olsen, J. D., Sockalingum, G.D., Robert, B., and Hunter, C.N., Modification of a hydrogen bond to a bacteriochlorophyll a molecule in the light-harvesting I antenna of *Rhodobacter sphaeroides*, *Proc. Natl. Acad. Sci. USA*, 91, 7124, 1994.
46. Teuchner, K., Stiel, H., Leupold, D., Scherz, A., Noy, D., Simonin, I., Hartwich, G., and Scheer, H., Fluorescence and excited state absorption in modified pigments of bacterial photosynthesis: a comparative study of metal-substituted bacteriochlorophylls a, *J. Luminesc.*, 72–74, 612, 1997.
47. Fleming, G.R. and van Grondelle, R., Femtosecond spectroscopy of photosynthetic light-harvesting systems, *Curr. Opinion in Struct. Biol.*, 7, 738, 1997.
48. Sundström, V. and Grondelle van, R., Kinetics of excitation transfer and trapping in purple bacteria, in *Anoxygenic Photosynthetic Bacteria*, Blankenship, R., Madigan, M.T., and Bauer, C.E., Eds., Kluwer, Dordrecht, 1995, p. 349.
49. Jankowiak, R. and Small, G.J., Spectral hole burning: a window on excited state electronic structure, heterogeneity, electron-photon coupling, and transport dynamics of photosynthetic units, in *The Photosynthetic Reaction Center*, Vol. II, Deisenhofer, J. and Norris, J.R.., Eds., Academic Press, New York, 1993, p. 133.
50. Reinot, T., Hayes, J.M., and Small, G.J., Fundamentals on non-photochemical hole burning spectroscopy and its applications to complex systems, *Photon. Sci. News*, 6, 83, 2000.
51. Leupold, D., Lokstein, H., and Hoffmann, P., Structure–function relationships in the higher plant photosynthetic antenna complex LHC as revealed by non-linear laser spectroscopy — the problem of "chlorophyll forms," *Trends Photochem. Photobiol.*, 6, 43, 1999.
52. Ketelaars, M., van Oijen, A.M., Matsushita, M., Kohler, J., Schmidt, J., and Aartsma, T.J., Spectroscopy on the B850 band of individual light-harvesting 2 complexes of *Rhodopseudomonas acidophila*.I. Experiments and Monte Carlo simulations, *Biophys. J.*, 80, 1591, 2001.
53. Davis, M.S., Forman, A., Hanson, L.K., Thornber, J.P., and Fajer, J., Anion and cation radicals of Bacteriochlorophyll and Bacteriopheophytin b. Their role in the primary charge separation of *Rhodopseudomonas viridis*, *J. Phys. Chem.*, 83, 3325, 1979.
54. Clarke, R.H., The Chlorophyll Triplet State and the Structure of Chlorophyll Aggregates, in *Light Reaction Path of Photosynthesis,* Fong, F.K., Ed., Springer-Verlag, Heidelberg, 196, 1982.
55. Parson, W.W., *Electron transfer in reaction centers*, in *Chlorophylls,* Scheer, H., Ed., CRC Press, Boca Raton, FL, 1991, p. 1153.
56. Parson, W.W., Nabedryk, E., and Breton, J., Mid- and near IR electronic transitions of P+: new probes of resonance interactions and structural asymmetry in reaction centers, in *The Photosynthetic Bacterial Reaction Center II. Structure, Spectroscopy, and Dynamics*, Breton, J. and Verméglio, A., Eds., Plenum Press, NATO ASI Series. Ser. A.: Life Sciences, New York, 1992, p. 67.
57. Spikes, J.D. and Bommer, J.C., Chlorophyll and related pigments as photosensitizers in biology and medicine, in *Chlorophylls,* Scheer, H., Ed., CRC Press, Boca Raton, FL, 1991, p. 1181.
58. Moser, J.G., Photodynamic Tumor Therapy: 2nd and 3rd Generation Photosensitizers, American Chemical Society, 1998.

59. Katz, J.J., Oettmeier, W., and Norris, J.R., Organization of antenna and photo-reaction centre Chlorophylls on the molecular level, *Phil. Trans. Royal Soc.*, 273, 227, 1976.
60. Agostiano, A., Catucci, L., Colafemmina, G., della Monica, M., and Scheer, H., Relevance of the phytyl chain of the chlorophylls on the lamellar phase formation and organization, *Biophys.J.*, 84, 189, 2000.
61. Van Rossum, B.-J., Steensgaard, D.B., Mulder, F.M., Boender, G.J., Schaffner, K., Holzwarth, A.R., and de Groot, H.J.M., A refined model of the chlorosomal antennae of the green bacterium *Chlorobium tepidum* from proton chemical shift constraints obtained with high-field two-dimensional and three-dimensional MAS NMR dipolar correlation, *Biochemistry*, 40, 1587, 2001.
62. Hynninen, P.H., Chemistry of chlorophylls: modifications, in *Chlorophylls*, Scheer, H., Ed., CRC Press LLC, Boca Raton, FL, 1991, p. 145.
63. Senge, M.O., Wiehe, A., and Ryppa, C., Synthesis, reactivity and structure of chlorophylls, in *Biochemistry and Biophysics of Chlorophylls,* Grimm, B., Porra, R., Rüdiger, W., and Scheer, H., Eds., Kluwer, Dordrecht, in press.
64. Scheer, H., Synthesis and stereochemistry of hydroporphyrins, in *The Porphyrins*, Vol., II, Dolphin, D., Ed., Academic Press, New York, 1978, Part B, p. 1.
65. Fujita, Y. and Bauer, C.E., Reconstitution of light-independent protochlorophyllide reductase from purified BchL and BchN-BchB subunits, *J. Biol. Chem.*, 275, 23,583, 2000.
66. Pandey, R.K., Shiau, F.Y., Isaac, M., Ramaprasad, S., Dougherty, T.J., and Smith, K.M., Substituent effects in tetrapyrrole subunit reactivity and pinacol-pinacolone rearrangements: *vic*-dihydroxychlorins and *vic*-dihydroxybacteriochlorins, *Tetrahedron Lett.*, 33, 7815, 1992.
67. Scheer, H. and Inhoffen, H.H., Hydroporphyrins: reactivity, spectroscopy and hydroporphyrin analogues, in *The Porphyrins*, Vol. II, Dolphin, D., Ed., Academic Press, New York, 1978, p. 45.
68. Steiner, R., Cmiel, E., and Scheer, H., Chemistry of bacteriochlorophyll b — Identification of some (photo)oxidation products, *Z. Naturforsch. C*, 38, 748, 1983.
69. Kobayashi, M., Hamano, T., Akiyama, M., Watanabe, T., Inoue, K., Oh-oka, H., Amesz, J., Yamamura, M., and Kise, H., Light-independent isomerization of bacteriochlorophyll g to chlorophyll a catalyzed by weak acid *in vitro*, *Anal. Chim. Acta*, 365, 199, 1998.
70. Watanabe, T. and Kobayashi, M., Electrochemistry of chlorophylls, in Chlorophylls, Scheer, H., Ed., CRC Press LLC, Boca Raton, FL, 1991, p. 287.
71. Geskes, C., Hartwich, G., Scheer, H., Maentele, W., and Heinze, J., Electrochemical and spectroelectrochemical investigation of metal-substituted bacteriochlorophyll a, *J. Am. Chem. Soc.*, 117, 7776, 1995.
72. Kureishi, Y. and Tamiaki, H., Synthesis and self-aggregation of zinc 20-halochlorins as a model for bacteriochlorophylls c/d, *J. Porph. Phthalocyan.*, 2, 159, 1998.
73. Urumov, T., *Metallkomplexe von Chlorophyllderivaten.,* Dissertation, TU München, 1975.
74. Hartwich, G., Fiedor, L., Simonin, I., Cmiel, E., Schäfer, W., Noy, D., Scherz, A., and Scheer, H., Metal-substituted bacteriochlorophylls: I. Preparation and influence of metal and coordination on spectra, *J. Amer. Chem. Soc.*, 120, 3675, 1998.
75. Gossauer, A. and Engel, N., Chlorophyll catabolism — structures, mechanisms, conversions., *J. Photochem. Photobiol.B.*, 32, 141, 1996.
76. Scheer, H. and Katz, J.J., Structure of the Krasnovskii photoreduction product of chlorophyll *a*, *Proc. Natl. Acad. Sci. USA*, 71, 1626, 1974.
77. Klement, H., Helfrich, M., Schoch, S., and Rüdiger, W., Pigment-free NADPH:protochlorophyllide oxidoreductase from *Avena sativa* L: purification and substrate specificity, *Eur.J. Biochem.*, 265, 862, 1999.
78. Oku, T. and Tomita, G., The photoconversion of *Chenopodium* chlorophyll protein, *Photochem. Photobiol.*, 25, 199, 1977.
79. Steinberg-Yfrach, G., Rigaud, J.L., Durantini, E.N., Moore, A.L., Gust, D., and Moore, T.A., Light-driven production of ATP catalysed by F_0F_1-ATP synthase in an artificial photosynthetic membrane, *Nature*, 392, 479, 1998.

80. Curty, C., Engel, N., Iturraspe, J., and Gossauer, A., Mechanism of photooxygenation of the Cd (II) complex of pyropheophorbide a methyl ester, *Photochem. Photobiol.*, 61, 552, 1995.
81. Fiedor, J., Fiedor, L., Kammhuber, N., Scherz, A., and Scheer, H., Photodynamics of the bacteriochlorophyll-carotenoid system.2. Influence of central metal, solvent and ,-carotene on photobleaching of bacteriochlorophyll derivatives, *Photochem. Photobiol.*, 76, 145, 2002.
82. Seely, G.R., Photochemistry of chlorophylls *in vitro*, in *The Chlorophylls*, Vernon, L.P. and Seely, G.R., Eds., Academic Press, New York, 1966, p. 523.
83. Beale, S. Enzymes of chlorophyll biosynthesis., *Photosynth. Res.*, 60, 43, 1999.
84. Smith, J.H.C. and Benitez, A., Chlorophylls: analysis in plant material, in *Moderne Methoden der Pflanzenanalyse*, Paech, K. and Tracey, M.V., Eds., Springer-Verlag, Heidelberg, 1955, Part 4, p. 142.
85. Jeffrey, S.W., Mantoura, R.F.C., and Wright, S.W.E., Phytoplankton pigments in oceanography, UNESCO Publications, Paris, 1997.
86. Miyashita, H., Adachi, K., Kurano, N., Ikemoto, H., Chihara, M., and Miyachi, S., Pigment composition of a novel oxygenic photosynthetic prokaryote containing chlorophylli d as the major chlorophyll, *Plant Cell Physiol.*, 38, 274, 1997.
87. Sauer, K., Smith, J.R.L., and Schultz, A.J., The dimerization of chlorophyll a, chlorophyll b, and bacteriochlorophyll in solution, *J. Am. Chem. Soc.*, 88, 2681, 1966.
88. Stanier, R.Y. and Smith, J.H.C. The chlorophylls of green bacteria, *Biochim. Biophys. Acta*, 41, 478, 1960.
89. Borrego, C.M., Arellano, J.B., Abella, C.A., Gillbro, T., and Garcia-Gil, J., The molar extinction coefficient of bacteriochlorophyll *e* and the pigment stoichiometry in *Chlorobium phaeobacteroides*, *Photosynth. Res.*, 60, 257, 1999.
90. Van de Meent, E.J., Kobayashi, M., Erkelens, C., van Veelen, P.A., Amesz, J., and Watanabe, T., Identification of 8^1-hydroxychlorophyll *a* as a functional reaction center pigment in heliobacteria, *Biochim. Biophys. Acta*, 1058, 356, 1991.
91. Tamiaki, H., Omoda, M., and Kubo, M., A novel approach toward bacteriochlorophylls-e and f, *Bioorg. Med. Chem. Lett.*, 9, 1631, 1999.
92. Fischer, R., Engel, N., Henseler, A., and Gossauer, A., Synthesis of Chlorophyll a labeled at C(3^2) from Pheophorbide a methyl Ester, *Helv. Chim. Acta*, 77, 1046, 1994.
93. Scheumann, V., Helfrich, M., Schoch, S., and Rüdiger, W., Reduction of the formyl group of zinc pheophorbide b *in vitro* and *in vivo*: a model for the chlorophyll b to a transformation, *Z. Naturforsch.,* 51c, 185, 1996.
94. Scheumann, V., Reduction von Chlorophyll b zu Chlorophyll a *in vitro* and *in vivo.* München, Ludwig-Maximilians-Universität, 1999.
95. Oba, T., Masada, Y., and Tamiaki, H., Convenient preparation of pheophytin from plant extract through the C7-reduced intermediate, *Bull. Chem. Soc. Jpn*, 70, 1905., 1997.
96. Rau, H.K., Snigula, H., Struck, A., Scheer, H., and Haehnel, W., Design, synthesis and properties of synthetic chlorophyll proteins, *Eur. J. Biochem.*, 268, 3284, 2001.
97. Pandey, R.K., Recent advances in photodynamic therapy, *J. Porph. Phthalocyan.*, 4, 368, 2000.
98. Kozyrev, A.N., Zheng, G., Shibata, M., Alderfer, J.L., Dougherty, T.J., and Pandey, R.K., Thermolysis of vic-dihydroxybacteriochlorins: a new approach for the synthesis of chlorin-chlorin and chlorin-porphyrin dimers, *Org. Lett.*, 1, 1193, 1999.
99. Gerlach, B., Brantley, S.E., and Smith, K.M., Novel synthetic routes to 8-vinyl chlorophyll derivatives, *J. Org. Chem.*, 63, 2314, 1998.
100. Zheng, G., Dougherty, T.J., and Pandey, R.K. A simple and short synthesis of divinyl chlorophyll derivatives, *J. Org. Chem.*, 64, 3751, 1999.
101. Tamiaki, H., Tomida, T., and Miyatake, T., Synthesis of methyl bacteriopheophorbide-d with 8-propyl group, *Bioorg. Med. Chem. Lett.*, 7, 1415, 1997.
102. Oba, T. and Tamiaki, H., Molecular requirement of chlorosomal chlorophylls. Self-organization of a chlorophyll derivative possessing a hydroxyl group at Ring II, *Photochem. Photobiol*, 67, 295, 1998.

103. Kozyrev, A.N., Dougherty, T.J., and Pandey, R.K., LiOH promoted allomerization of pyropheophorbide a. A convenient synthesis of 13^2-oxopyropheophorbide a and its unusual enolization, *Chem. Comm.*, 481, 1998.
104. Zheng, G., Graham, A., Shibata, M., Missert, J.R., Oseroff, A.R., Dougherty, T.J., and Pandey, R.K., Synthesis of beta-galactose-conjugated chlorins derived by enyme metathesis as galactin-specific photosensitizers for photodynamic therapy, *J. Org. Chem.*, 66, 8709, 2001.
105. Holt, A.S., Reduction of chlorophyllides, chlorophylls and chlorophyll derivatives by sodium borohydride, *Plant Physiol.*, 34, 310, 1959.
106. Falk, H., Hoornaert, G., Isenring, H.P., and Eschenmoser, A., Über Enolderivate der Chlorophyllreihe: Darstellung von 13,^{2}17^3-cyclophäophorbid enolen, *Helv. Chim. Acta*, 58, 2347, 1975.
107. Scheer, H. and Katz, J.J., Peripheral metal complexes: chlorophyll isomers with magnesium bound to the ring -ketoester system, *J. Amer. Chem. Soc.*, 100, 561, 1978.
108. Wasielewski, M.R., Norris, J.R., Shipman, L.L., Lin, C.P., and Svec, W.A., Monomeric chlorophyll a enol — evidence for its possible role as the primary electron donor in photosystem I of plant photosynthesis, *Proc. Natl. Acad. Sci. USA*, 78, 2957, 1981.
109. Shinoda, S. and Osuka, A., Transesterification of the.alpha.-keto ester in methyl pheophorbide-a, *Tetrahedron Lett.*, 37, 4945, 1996.
110. Fischer, M.J., Darstellung fluorierter Bakteriochlorophyll- und Bakteriopheophytin-Derivate und ihr Einbau in das photosynthetische Reaktionszentrum von *Rhodobacter sphaeroides* R26 als Spinsonden. München, Ludwig-Maximilians-Universität, 1997.
111. Pennington, F.C., Strain, H.H., Svec, W.A., and Katz, J.J., Preparation and properties of pyrochlorophyll a, methyl-pyrochlorophyllide a, pyropheophytin a and methyl-pyropheophorbide a derived from dhlorophyll by decarbomethoxylation, *J. Amer. Chem. Soc.*, 86, 1418, 1964.
112. Woolley, P.S., Moir, A.J., Hester, R.E., and Keely, B.J., A comparative study of the allomerization reaction of chlorophyll a and bacteriochlorophyll a, *J. Chem. Soc. Perkin 2*, 1998, 1833, 1998.
113. Mazaki, H., Watanabe, T., Takahashi, T., Struck, A., and Scheer, H., Epimerization of chlorophyll derivatives. V. Effects of the central magnesium and ring substituents on the epimerization of chlorophyll derivatives, *Bull. Chem. Soc., Jpn.*, 65, 3080, 1992.
114. Borovkov, V.V., Gribkov, A.A., Kozyrev, A.N., Brandis, A.S., Ishida, A., and Sakata, Y., Synthesis and properties of pheophorbide-quinone compounds, *Bull. Chem. Soc. Jpn.*, 65, 1533, 1992.
115. Fiedor, L., Rosenbach-Belkin, V., Sai, M., and Scherz, A., Preparation of tetrapyrrole-amino acid covalent complexes, *Plant Physiol. Biochem.*, 34, 393, 1996.
116. Kammhuber, N., Bakteriochlorophyll-derivate als neuartige Sensibilisatoren für die photodynamische therapie von Tumoren: Darstellung und screening, München, Ludwig-Maximilians-Universität, 1999.
117. Rosenbach-Belkin, V., *The Primary Reactants in Bacterial Photosynthesis Modeling by in vitro Preparation*, Rehovot, Weizmann Institute of Science, dissertation, 1988.
118. Whitlock, H.W., Hanauer, R., Oester, M.Y., and Bower, B.K., *J. Amer. Chem. Soc.*, 91, 7485, 1969.
119. Senge, M.O., Kalisch, W.W., and Runge, S. Conformationally distorted chlorins via diimide reduction of nonplanar porphyrins, *Tetrahedron*, 54, 3781, 1998.
120. Wolf, H. and Scheer, H., Photochemische Hydrierung von Phäoporphyrinen: 7,8-*cis* Phäophorbide, *Liebig's Ann. Chem.*, 1973, 1710, 1973.
121. Smith, J.R.L. and Calvin, M., Studies on the chemical and photochemical oxidation of Bacteriochlorophyll, *J. Amer. Chem. Soc.*, 88, 4500, 1966.
122. Woodward, R.B. and Skaric, V., A new aspect of the chemistry of Chlorins, *J. Amer. Chem. Soc.*, 83, 4676, 1961.
123. Senge, M. and Senger, H. Enzymatic chlorination of chlorophylls using chloroperoxidase, *Biochim. Biophys. Acta,* 977, 177, 1989.

118

Photosynthetic Reaction Centers

Paul Mathis
CEA-Saclay

118.1 Presentation of Reaction Centers

General Properties, Composition, and Isolation

In plants, algae, and photosynthetic bacteria, the photosynthetic apparatus converts light energy into chemical energy. This machinery is an assembly of membrane proteins, in which the action of light starts in an "antenna," an ensemble of pigments (chlorines such as chlorophylls, polyenes such as carotenoids, and phycobilins) embedded in proteins. The antenna absorbs light and funnels excitation energy toward large specific proteins named reaction centers, where photoinduced charge separation takes place. Reaction centers (RC) can thus be considered as microscopic photocells that realize the first steps of energy conversion. In this system, all elementary processes take place rapidly (in less than 1 ps for pigment-to-pigment energy transfer, in less than 3 ps for primary electron transfer), so that the overall quantum yield is higher than 90%, with only a small fraction of excitation being lost by internal conversion, by fluorescence (less than 2%), or by conversion to the triplet state (less than 4%). For many years, RCs were simply hypothesized as specific sites in the photosynthetic membrane, but progress in membrane biochemistry has led to their effective isolation as large proteins made of several polypeptides (from two in the simplest case of nonsulfur green bacteria to at least 12 in Photosystem I and Photosystem II of oxygenic organisms) and of several pigment molecules (all RCs contain at least six chlorin-type molecules and one or more carotenoids). They contain several chemical groups implicated in electron transfer (these groups are called "redox centers": quinones, hemes, iron-sulfur centers, Mn atoms, amino acid residues of polypeptides, etc.).

Several classes of reaction centers (Table 118.1) are found among the various photosynthetic biological organisms.[1] Their basic mode of functioning is always the same: excitation energy arriving from the antenna is trapped by the primary electron donor P [which is most often, and perhaps always, a well-defined aggregate of two molecules of (bacterio)chlorophyll, often named "special pair"]; excitation of P is followed by several steps of electron transfer on the acceptor side, and P^+ is then re-reduced by an electron donor. Several classes of RCs will be briefly presented, starting with the best-known RC, that of purple bacteria.

0-8493-1348-1/04/$0.00+$1.50

TABLE 118.1 Sequences of Electron Carriers in Various Classes of Photosynthetic Reaction Centers, Ranging from Most Terminal Donors (Top) to Most Terminal Acceptors (Bottom)

Purple Bacteria		Photosystem II		Photosystem I		Green Sulfur Bacteria, Heliobacteria	
		H_2O	+810				
		$(Mn)_4$	+1000				
Cyt *c*	+350	Tyr Z	+1100	Pc or Cyt *c*	+360	Cyt *c*	+360
P $(BChl)_2$	+490	P-680	+1200	P-700	+490	P-840	+420
I (Bpheo)	-600	*I* (Pheo)	-600	A_0 (Chl *a*)	-1000	A_0 (BChl)	-1100
				A_1 (vit K_1)	-850	A_1 quinone)(?)	?
Q_A (MQ)	-300	Q_A (PQ)	–100	(FeS)X	-700	(FeS)"X"	-800
Q_A (UQ)	–100						
Q_B (UQ)	+50	Q_B (PQ)	+50	(FeS)A,B	-550	(FeS)"A,B"	-600
				Ferredoxin	-420	Ferredoxin	?

Note: MQ, UQ, PQ: menaquinone, ubiquinone, plastoquinone, respectively; Pc: plastocyanin; (FeS): iron–sulfur center; I: intermediate electron acceptor; Other symbols: see text. The numbers are redox midpoint potentials Em (versus the normal hydrogen electrode), in mV.

Purple Bacteria

The reaction center of purple bacteria serves as a general model for all classes of RCs, because it was isolated as a pure protein a long time ago. Its structural and functional properties were studied in detail by biochemical and spectroscopic methods, and its structure was determined at atomic resolution by x-ray crystallography, providing a firm basis for site-specific mutations, for theoretical calculations of spectroscopic properties and of electron transfer kinetics, etc.[2–4]

The RC is made of three polypeptides: L, M, H (MW: 32, 34, and 28 kDa, respectively). L and M make up the core of the reaction center. They carry the cofactors: four bacteriochlorophylls, two bacteriopheophytins, two quinones of species-dependent chemical nature, and one nonheme Fe^{2+} atom. In many species of bacteria, the RC also includes a bound tetraheme *c*-type cytochrome of about 12 kDa MW (when it is absent, its function of electron donation to P^+ is fulfilled by a soluble *c*-type cytochrome). Proteins and cofactors are organized, as sketched in Figure 118.1. The RC is endowed with an approximate C_2 symmetry in structure that is not found in the function. The primary donor *P* is a dimer of bacteriochlorophylls, a so-called "special pair," in that the two molecules are held in close proximity by the *L* and *M* subunits; they are in electronic interaction without establishing any chemical link. Recent developments in the structural analysis of RCs dealt with refinements of the structure and with possible structural changes coupled to electron transfer.[5,6]

Excitation by energy transfer from the antenna brings *P* to its lowest excited state P^*, permitting the fast ($t_{1/2} = 2$ ps) transfer of an electron to the bacteriopheophytin located on the L branch (the involvement of bacteriochlorophyll B_L is still a matter of debate). The electron is then transferred to the quinone Q_A with $t_{1/2} \approx 200$ ps, and from there to the quinone Q_B ($t_{1/2}$ in the microsecond time domain). The quinone Q_A functions as a one-electron carrier, but Q_B functions as a two-electron, two-proton carrier. After its full reduction by two electrons and two protons, Q_B (in the form of an hydroquinone) leaves the reaction center and diffuses in the membrane to reduce another redox protein, the cytochrome *b/c* complex, while another oxidized quinone from the membrane binds at the Q_B site. P^+ is re-reduced by a *c*-type cytochrome. The *c*-type cytochrome is reduced by the *b/c* complex in a complicated mechanism involving transmembrane proton movement. Altogether, the RC functions as a proton pump, transferring protons against their concentration gradient across the membrane, while the electron flow is mainly cyclic.

Photosystem II

In oxygen-evolving organisms, such as plants, algae, and cyanobacteria, the photosynthetic membranes contain two types of RCs, called Photosystem I and Photosystem II. The latter presents strong analogies

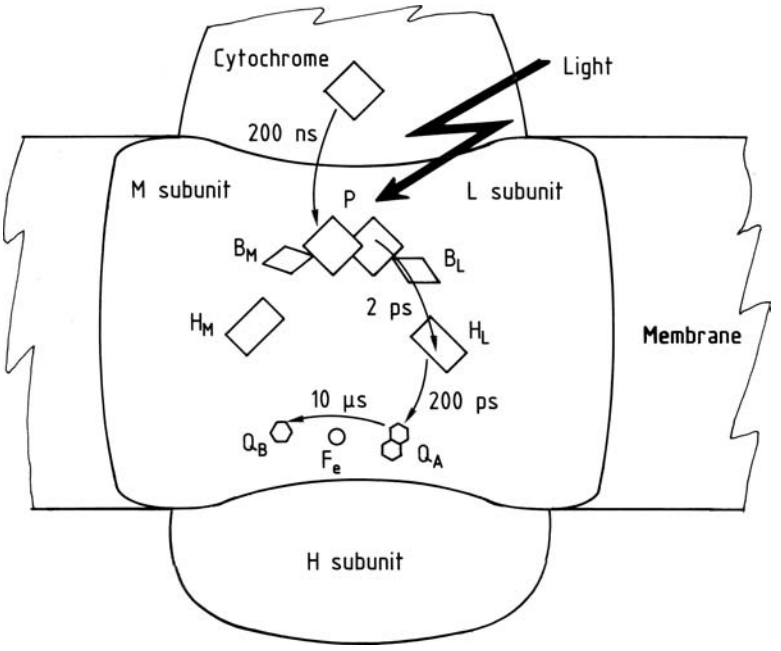

FIGURE 118.1 The *Rhodopseudomonas viridis* reaction center, with approximate half-times of the three major steps of electron transfer on the active acceptor branch, and of one step from the cytochrome moiety (only partly drawn). Membrane thickness: about 35 Å. (Inspired from Deisenhofer, J. and Michel, H., *EMBO J.*, 8, 2149, 1989.)

with the RC of purple bacteria.[1,7,8] The inner part of the reaction center is built from two polypeptides (named D1 and D2) of about 32 kDa, which are homologous to L and M. The sequence of electron acceptors is similar: pheophytin → quinone Q_A → quinone Q_B. Both quinones are plastoquinone A, and their functional properties are like their bacterial counterparts. Specific inhibitors block electron transfer by binding specifically at the Q_B site in competition with plastoquinone. Several of them are used as herbicides: dichlorophenyl-dimethylurea and other urea derivatives, triazines, etc. Many of them also bind at the Q_B site in purple bacteria.

The Photosystem II reaction center,[9] however, differs from the RC of purple bacteria in at least three important respects:

1. It performs water oxidation, resulting in O_2 evolution and in proton release. The redox equilibrium $2H_2O \rightarrow 4H^+ + 4e^- + O_2$ has an Em of +0.82 V at pH 7. The reaction is pulled by the oxidized primary donor P^+ (named P-680$^+$ in Photosystem II). P-680 is a "special pair" of chlorophyll *a* molecules, but these molecules are not as close as in purple bacteria, and they are surrounded by two other chlorophyll *a*, so that P-680 can also be described as a "special tetramer." The P-680/P-680$^+$ redox couple must have an Em (perhaps around +1.2 V) much more positive than +0.82 V, in order to oxidize water irreversibly. P-680$^+$ is directly reduced by a tyrosine residue named TyrZ; it is Tyr 161 of the polypeptide D1. Oxidized TyrZ then oxidizes a cluster of four manganese atoms, which is the catalytic site for water oxidation. A histidine residue is probably involved in the process, which also requires Ca^{2+} and Cl^- ions. The details of the structure and mechanism of this ensemble are still under intense investigation.[10,11]
2. The Photosystem II reaction center is highly complex because it contains at least 10 polypeptides. In addition to D1 and D2, there are the two subunits of cytochrome b_{559}, two chlorophyll-proteins named CP47 and CP43, several hydrophobic polypeptides of unknown function, and three peripheral proteins located at the water oxidizing site (MW: 33, 24, and 16 kDa).

3. The Photosystem II RC is susceptible to degradation by an excess of light in a process called photoinhibition. In the dark, the process is followed *in vivo* by a recovery that requires specific protein synthesis. Photoinhibition is usually thought to be an adaptive protective mechanism avoiding permanent photodamages.

For a long time, the Photosystem II RC could not be crystallized, perhaps because of its complexity or because of its inherent instability. Hypothetical structural models were proposed, based on its partial similarity with the RC of purple bacteria. Two-dimensional crystals were studied by electron crystallography, leading to a reasonable structure.[12] It is only recently that the Photosystem II RC from thermophilic cyanobacteria was crystallized in a three-dimensional manner. A structure was published at the resolution of 3.8 Å,[13] and data acquired at high resolution by the same laboratory are being analyzed.

Photosystem I

The other reaction center from oxygenic organisms, Photosystem I,[7,14–16] is organized according to the same basic principles as other RCs (see Figure 118.1) but with important differences. It was crystallized from the thermophilic bacterium *Synechococcus elongatus* (like Photosystem II), and its structure was determined at a resolution of 2.5 Å.[17,18] It includes 12 protein subunits and 123 cofactors: 96 molecules of chlorophyll *a*, two phylloquinones (also named vitamin K_1), 22 carotenoids, and three 4Fe-4S clusters. The core of the RC is made of two large polypeptides (PSI-A and PSI-B, of about 83 kDa each) that carry the pigment molecules which serve as undissociable antenna, and they carry most of the redox-active cofactors: the primary donor P-700 (a special pair of chlorophyll *a*), the primary acceptor A_0 (a specialized chlorophyll *a*), the secondary acceptor A_1 (phylloquinone), and a low-potential 4Fe-4S iron-sulfur center named F_X, which is held at the interface between the two large polypeptides. After absorption of a photon and subsequent steps of energy transfer, P-700 becomes excited; an electron then goes from P-700* to A_0, and then to A_1, and then to F_X, and from there to a small polypeptide (PSI-C) holding two 4Fe-4S centers (F_A and F_B), which serve as a relay toward the physiological electron acceptor, a soluble 2Fe-2S ferredoxin (replaced by flavodoxin in some cases). All the electron acceptors have a low Em (see Table 118.1). To complete the electron path, P-700$^+$ is re-reduced by a soluble acceptor (plastocyanin or cytochrome *c*-553) on the membrane side opposite that of ferredoxin action. The successive steps of electron transfer are rapid and difficult to analyze in detail. A cycle is completed in a few microseconds.

The structure of the Photosystem I RC is nearly symmetrical, with an approximate symmetry axis running from the center of P-700 to the center of F_X. The electron acceptors A_0 and A_1 have symmetrically located counterparts, also chlorophyll *a* and phylloquinone, which were first postulated to be inactive but might well play a role in electron transfer.[19] Two additional chlorophyll *a* molecules are located between P-700 and A_0 (and its symmetric counterpart). These molecules have not been identified as discrete intermediates in electron transfer, but they might be involved in facilitating electron transfer from P-700* to A_0. It should also be mentioned that the roles of most of the protein subunits are still not understood; several serve for the docking of ferredoxin or of plastocyanin, but many small hydrophobic polypeptides have no obvious functions.

Green Sulfur Bacteria and Heliobacteria

Like the purple bacteria, these classes of bacteria have only one type of reaction center, but it greatly resembles the Photosystem I RC of oxygenic organisms.[20] Their RCs are still poorly known, because their study is extremely difficult, but their sequence of electron carriers, as far as it is known, is similar to that of Photosystem I,[21,22] with small chemical differences in the structure of the chlorin pigments and a tendency to have lower redox potentials (see Table 118.1). They contain quinones of the menaquinone family, but all functional tests failed in showing a function for them; it is thus hypothesized that electron transfer goes directly from A_0 to F_X.[23] Like in Photosystem I, the RC core is made of two large polypeptides that carry about 30 molecules of antenna pigments, in addition to the redox centers involved in primary photochemistry. These polypeptides, however, have an identical sequence of amino acids,[24] and it is

usually assumed that the RC has a symmetrical structure, whereas other RCs have a pseudo-symmetry axis. It is also supposed, but not demonstrated, that the electron leaving P-840 has an equal probability of using two equivalent paths to reach the FeS center F_X. Although they are not well known, these classes of RCs play a key role in the speculations concerning the evolution of photosynthesis.

Altogether, it is possible to classify all of the types of photosynthetic RCs according to the structure of their protein matrix, to the nature and corresponding redox properties of their redox centers, to the size and chemistry of their antenna pigments.[1,8,20,25] Purple bacteria and Photosystem II RCs are named Type II or pheophytin-quinone-type RCs. Their RC core is made of small polypeptides holding a small antenna; they have two quinones (Q_A and Q_B) functioning in series, and they operate at a rather high redox potential (not mentioned yet, the RC of green nonsulfur bacteria has similar properties). Green sulfur bacteria, heliobacteria, and Photosystem I of oxygenic organisms are Type I or FeS-type RCs, characterized by a large protein core holding a large number of antenna pigments; they operate at a low redox potential, and their most characteristic electron acceptors are iron–sulfur clusters.

118.2 Methods for Studying Structural and Functional Properties

Biochemical Methods: Proteins

Reaction centers are complex membrane proteins, and their study requires appropriate biochemical methods that are only briefly mentioned here:

- The isolation of reaction centers requires treatment of the membranes by detergents, followed by classical purification methods such as centrifugation, chromatography, etc. (see, e.g., Reference 26). Their polypeptidic composition is determined by dissociation of pure RCs with sodium dodecyl sulfate, followed by gel electrophoresis under denaturing conditions.
- The sequencing of polypeptides is done directly for rather small polypeptides or, more generally, by sequencing the corresponding genes. Eventual processing of the preprotein can be checked by comparison with N- or C-terminal partial sequences of the polypeptide.
- The crystallization of RCs in view of structure determination by x-ray crystallography requires special methods that have worked successfully for two kinds of purple bacteria (*Rhodopseudomonas viridis* and *Rhodobacter sphaeroides*) and for Photosystems I and II of thermophilic cyanobacteria.

Successful methods for the biochemical manipulation of RCs have been developed progressively during the last 20 years: site-directed mutagenesis [for four purple bacteria (*R. capsulatus*, *R. sphaeroides*, *Rps. viridis* and *Rvx. gelatinosus*), for several species of cyanobacteria, and for the green alga (*Chlamydomonas reinhardtii* [27])], protein extraction (or denaturation) followed by reconstitution (this was especially successful for the iron–sulfur centers of Photosystem I and for the peripheral polypeptides of Photosystem II), etc. Selective pigment extraction, modification and reconstitution are also in progress.

Optical Spectroscopy

Methods of optical spectroscopy are especially important, because they provide plentiful information on RCs, in which pigments are involved directly in energy or electron transfer, and in which redox centers also have characteristic optical properties.[28]

Absorption Spectroscopy

All photosynthetic pigments have intense and distinctive absorption spectra, in relation to the ability of each of them to capture specific parts of the solar light spectrum.[29] The pigments chlorophylls and bacteriochlorophylls belong to the chemical group of chlorins. Their reduced symmetry compared to porphyrins results in a strong Q_Y band absorbing well into the red or IR, the position of which is highly sensitive to the local environment of the molecule.[30,31] From a single chemical molecular species, such as chlorophyll *a* (Figure 118.2) or bacteriochlorophyll *b* (Figure 118.3), complex spectra are thus obtained

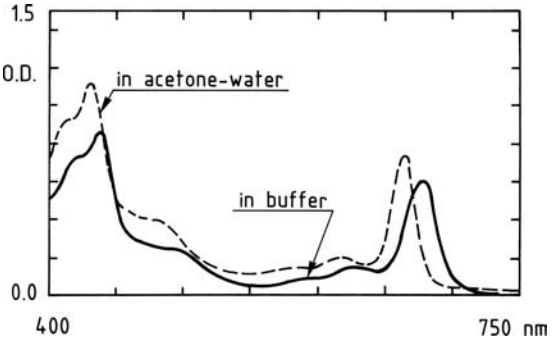

FIGURE 118.2 Absorption spectra of (a): Photosystem I reaction centers from the cyanobacterium *Synechocystis 6803*, isolated with the detergent dodecylmaltoside (kindly provided by Dr. H. Bottin); (b): the same material (same pigment concentration) extracted with an acetone–water (80:20) mixture.

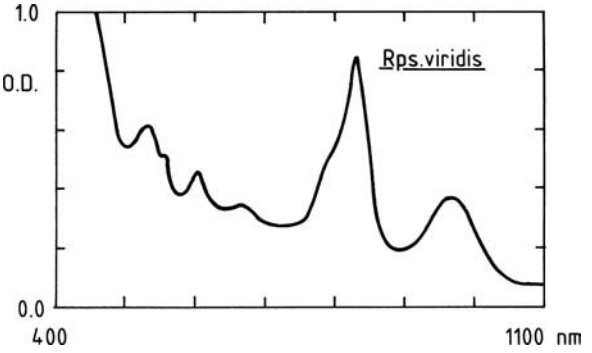

FIGURE 118.3 Absorption spectrum of a suspension of *Rhodopseudomonas viridis* reaction centers (plus 100 μM Na ascorbate) dispersed by a detergent (LDAO). The absorption band at 970 nm is due to the primary donor *P*, and the large massif around 820 nm is mainly due to the two bacteriochlorophylls other than *P*, and to the two bacteriopheophytins. (Reaction centers kindly provided by Dr. J. Breton.)

as a result of pigment–pigment or pigment–protein interactions. This effect is especially clear for the primary donor *P* in purple bacteria (Figure 118.3). Absorption spectroscopy thus remains a basic technique in separation procedures, to check for the good state and the purity of samples.

Difference Spectra and Kinetic Properties

Absorption of light results in the formation, in RCs, of excited states and, after charge separation, of reduced and oxidized species. The molecules involved experience a change in their absorption spectrum that can be detected with a high sensitivity by differential absorption spectroscopy.[28] This technique is often coupled to flash excitation and to time-resolved detection (as shown in Figure 118.4), permitting the identification of successive partners in energy or electron transfer (from the difference spectra), kinetics of the successive steps, and the factors that control the reactions. This methodology is in constant development, especially in terms of time resolution, because the pump–probe methods provide a resolution well below 1 ps.[32–34]

Fluorescence

Fluorescence spectroscopy has been used for a long time to investigate energy transfer in photosynthetic membranes.[35] Spectral and time-resolved properties can be studied. Fluorescence is still of interest in many cases (e.g., for the screening of photosynthetic mutants), but its impact is especially important in the study of Photosystem II, because the fluorescence yield of chlorophyll *a* in photosynthetic membranes

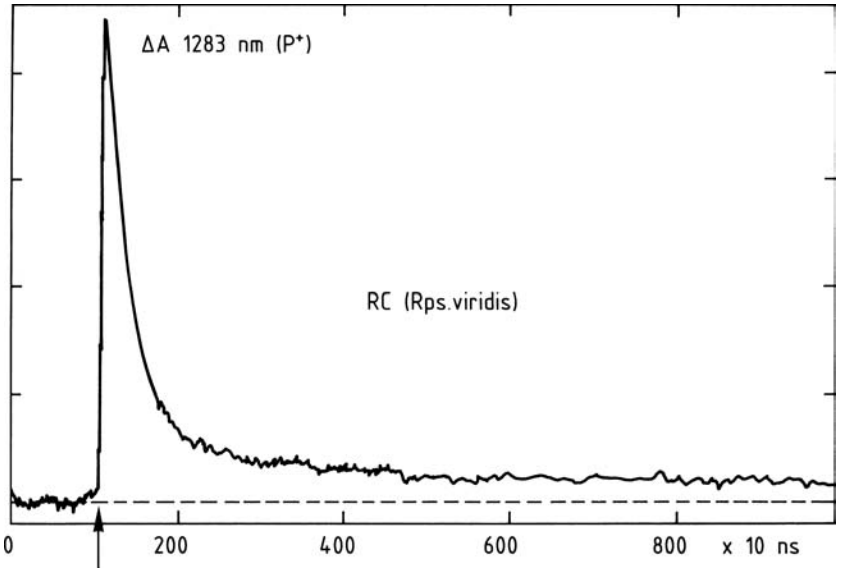

FIGURE 118.4 Absorption change at 1283 nm due to the oxidation of *P* by a flash, followed by its re-reduction by an electron coming from the high-potential heme of the tetraheme cytochrome in *Rhodopseudomonas viridis* reaction centers, at 287 K, at an ambient redox potential of about +200 mV (see Reference 48).

is dependent on several properties of the Photosystem II reaction center: (1) the redox state of Q_A and, by way of consequence, properties related to electron transfer from Q_A to Q_B (herbicide binding and resistance, photoinhibition, etc.); and (2) properties more related to the water-oxidizing enzyme and to the *in vivo* functioning of photosynthesis, such as the pH inside thylakoids or defects in the manganese cluster.[36,37] Also informative on the state of Photosystem II, thermoluminescence is a technique in development, because it can be used *in vivo* with cells or leaves, without isolating reaction centers or membranes.

Vibrational Spectroscopy

Molecular vibrations can be studied by infrared absorption or by Raman scattering spectroscopy. Both methods are fairly classical for the study of small molecules, but their utilization for the complex molecules involved in reaction centers was made possible only by recent developments in lasers and in detectors technology. Resonance Raman spectroscopy is mostly informative on the mode of binding of cofactors (pigments, redox centers) to polypeptides.[38] Fourier transform infrared (FTIR) spectroscopy is used mainly in a differential mode to investigate the structural changes that are coupled to electron transfer, involving polypeptides, cofactors, water molecules, etc. Most studies were conducted on RCs of purple bacteria, in which differential FTIR spectra were recorded for the oxidation of *P*, reduction of bacteriopheophytin, reduction of Q_A or Q_B, oxidation of cytochrome, etc. (see e.g., References 39, 40). These difference spectra have a rich content of information (as exemplified in Figure 118.5) that starts to be unraveled, often by comparisons with model molecules *in vitro* or by selective labeling with stable isotopes (^{13}C, ^{15}N, ^{18}O).

Other Optical Methods

The large number of questions raised by the structure–function relations in RCs, and the wealth of their optical properties, led to intensive use of many methods that cannot be examined here (see Reference 28). Let us briefly mention a few of them. Linear dichroism with oriented samples or coupled to photoselection gives access to the relative and absolute orientations of practically all the cofactors in RCs.[41] Circular dichroism allows for the probing of the interactions between pigments or between pigments and proteins. Several methods give access to properties of excited states: phosphorescence (for triplet states), hole burning (for singlet excited states), the Stark effect (in absorption or fluorescence)

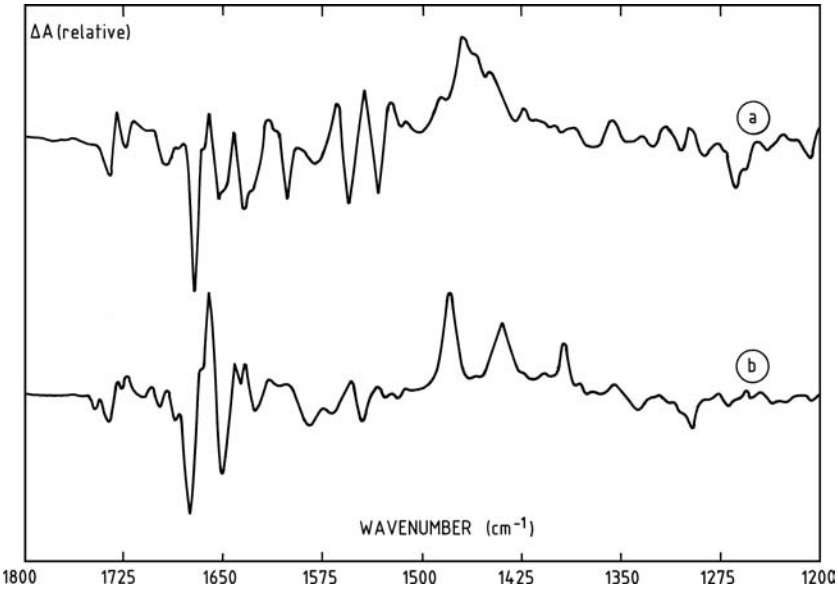

FIGURE 118.5 FTIR difference spectra ("light" minus "dark") of reaction centers of *Rhodobacter sphaeroides* (a) and *Rhodopseudomonas viridis* (b), at 10°C. The spectra are due to the reduction of Q_A (Q_A^- minus Q_A). Q_A is ubiquinone-10 in (a) and menaquinone in (b). The features between 1380 and 1500 cm^{-1} are attributable to the quinone anion, while the features around 1530 to 1570 cm^{-1} are due to an indirect effect of Q_A reduction on the protein. (Spectra kindly provided by Dr. E. Nabedryk.)

for evaluation of the charge–transfer character of singlet excited states, etc. Most of these methods are useful complements to x-ray crystallography, by the kind of information they provide, and by the fact that they can be used more simply on mutants, on intact membranes, or on noncrystallized RCs.

Electron Paramagnetic Resonance

Electron paramagnetic resonance (EPR) is a method that is extremely important for structural and functional studies of RCs. Detailed, authoritative presentations were published for the method and for its applications to RCs (see, e.g., References 42, 43). Briefly, it can be said that EPR detects three types of molecular states, all of which have a nonzero spin: triplet states, radical ions (cations or anions), and centers possessing transition metals. These states are relevant to the functioning of reaction centers.

The triplet state of *P*, designated ^3P, is populated as a result of charge recombination in the primary radical pair P^+I^-. Under conditions of normal functioning, this radical pair is extremely short-lived (under 1 ns) because of a rapid electron transfer from the primary acceptor to the secondary acceptor. When that transfer is made impossible, usually because the secondary acceptor is prereduced or absent, the radical pair may live between 10 and 100 ns, and decay primarily by charge recombination with high probability (10 to 100%) of populating the state ^3P. This artifactual reaction is extremely informative with regard to interactions between *P* and the primary electron acceptors and to the structural properties of *P*: orientation, degree of symmetry of the pair, etc. It is, thus, frequently studied, mainly by EPR spectroscopy.[44]

Radicals are formed in electron transfer reactions involving organic molecules such as chlorins [*P*, (bacterio)chlorophylls, (bacterio)pheophytins], quinones (Q_A, Q_B, A_1 of Type I RCs), tyrosine (TyrZ and TyrD in Photosystem II), carotenoids, etc. Classical EPR spectroscopy, now complemented by more elaborate techniques such as pulse EPR, ENDOR, or high-field EPR, is the most efficient way to study them (see examples of applications in References 3, 4, 14, 42–45).

EPR is the major tool for determining the redox state of metal centers and of some of their structural properties. Many of them participate in secondary steps of electron transfer in RCs: iron–sulfur-centers

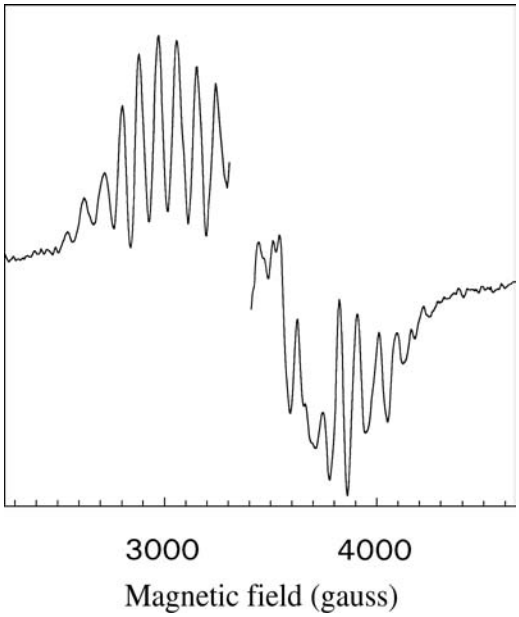

FIGURE 118.6 EPR spectrum measured in Photosystem II membranes at 10 K (X-band at 9.45 GHz; modulation amplitude: 25 G): difference between a sample illuminated at 200 K and a sample kept in darkness, before freezing to 10 K. The spectrum is attributed essentially to the S_2 state of the $(Mn)_4$ water-oxidizing enzyme. (Data kindly provided by Dr. A. Boussac.)

(in low-potential Type I RCs), cytochromes (in purple bacteria and in Photosystem II), Mn cluster in the water-oxidizing enzyme of Photosystem II, etc. Each is EPR-detectable at low temperature in one or several of its redox states: the reduced state for iron–sulfur centers, the oxidized state for cytochromes. The situation is more complex for the Mn cluster, which includes four Mn ions[10,11,46] (see Figure 118.6). X-ray absorption (near-edge structure and extended fine structure) is used in conjunction with EPR to derive a hypothetical structure in each of the redox states of the cluster.[10]

Electrochemical Properties

Midpoint redox potentials of the redox centers bound to the RCs polypeptides are essential properties that determine their functional behavior. They naturally define the possible directions of electron flow, but they are also implicated in controlling the rates of electron transfer steps and the energetic yield of photoconversion. Redox midpoint potentials are measured by classical methods, where a potential is imposed electrically or chemically, and the redox state of the studied couple is measured, usually by a spectroscopic technique such as EPR or UV-visible absorption spectroscopy. The approximate redox potentials of redox centers are given in Table 118.1, in a manner that emphasizes similarities between classes of reaction centers. Several values are not known precisely, mainly because they are too positive (donor side of Photosystem II) or too negative (first acceptors of Photosystem I and of other Type I RCs). Midpoint potentials depending on pH are given for pH = 7.0. The table clearly shows that electron-accepting and electron-donating sides can be classified into two separate classes that share common features. This has been recognized for a long time, and the more recent findings on green sulfur and on heliobacteria lead to valuable hypotheses on the phylogeny of photosynthetic organisms.[8,20,25]

Facts and Questions

The availability of detailed crystallographic three-dimensional structures for several classes of RCs makes these proteins interesting objects. They already served as models for membrane proteins, since they were

the first of them to provide a three-dimensional structure at nearly atomic level. They are also important for the study of electron transferring proteins in general because of the possibility to trigger charge separation precisely with a short pulse of light and for the study of electron transfer reactions with many spectroscopic methods.

It should be kept in mind, however, that the relationships between the structure and the function of RCs include a large number of unresolved basic problems that are the motivations of a strong research effort.

In the best-known purple bacteria, understanding of the primary electron transfer events is still rudimentary: why is a dimer needed as primary electron donor, what is the function of the monomeric bacteriochlorophyll located on the active branch, what makes possible a high yield of charge separation even at low temperature, why are there two branches in the RC structure and why is only one of them active?

How can a better knowledge of plant reaction center be arrived at? To what extent can the knowledge acquired on purple bacteria be used to better understand Photosystems I and II? What is the mechanism of water oxidation, a key biological process that proves difficult to unravel?

Electron transfer from Q_A to Q_B in purple bacteria and in Photosystem II is sensitive to many parameters, including the presence of a metal center (most often Fe^{2+}). How does this step work? How is it coupled to H^+ movements? Are there privileged paths for H^+ around Q_B? Are there well-defined structural changes of the protein during the process, as indicated in a seminal paper?[47]

Generally, the description of function in RCs is limited to the cofactors (pigments and redox centers). Apart from scaffolding, what are the roles of the protein? How are its structural changes coupled to electron transfer? In order to receive satisfying answers, all of these basic questions will require concerted multidisciplinary approaches in the future.

References

1. Nitschke, W. and Rutherford, A.W., Photosynthetic reaction centers: variations on a common structural theme?, *Trends Biochem. Sci.*, 16, 241, 1991.
2. Deisenhofer, J. and Michel, H., The photosynthetic reaction center from the purple bacterium *Rhodopseudomonas viridis*, *EMBO J.*, 8, 2149, 1989.
3. Feher, G., Allen, J.P., Okamura, M.Y., and Rees, D.C., Structure and function of bacterial photosynthetic reaction centers, *Nature*, 339, 111, 1989.
4. Hoff, A.J. and Deisenhofer, J., Photophysics of photosynthesis, *Physics Rep.*, 287, 1, 1997.
5. Stowell, M.H.B., McPhillips, T.M., Rees, D.C., Soltis, S.M., Abresch, E., and Feher, G., Light-induced structural changes in photosynthetic reaction center: implications for mechanism of electron transfer, *Science*, 276, 812, 1997.
6. Lancaster, C.R.D. and Michel, H., Refined structural structures of reaction centers from *Rhodopseudomonas viridis* in complexes with the herbicide atrazine and two chiral atrazine derivatives also lead to a new model of the bound carotenoids, *J. Mol. Biol.*, 286, 883, 1999.
7. Mathis, P. and Rutherford, A.W., The primary reactions of photosystems I and II of algae and higher plants, in *Photosynthesis*, Amesz, J., Ed., Elsevier, Amsterdam; New York, 1987, chap.4.
8. Rutherford, A.W. and Nitschke, W., Photosystem II and the quinone-iron-containing reaction centers: comparisons and evolutionary perspectives, in *Evolution of Biological Energy Conservation*, Baltscheffsky, H., Ed., VCH Publishers, Weinheim, Germany, 1994, chap. 6, p. 143.
9. Diner, B.A. and Babcock, G.T., Structure, dynamics, and energy conversion efficiency in Photosystem II, in *Oxygenic Photosynthesis: The Light Reactions*, Ort, D.R. and Yocum, C.F., Eds., Kluwer, Dordrecht, 1966, chap. 12.
10. Yachandra, V.K., Sauer, K., and Klein, M.P., Manganese cluster in photosynthesis: where plants oxidize water to dioxygen, *Chem. Rev.*, 96, 2927, 1996.
11. Tommos, C. and Babcock, G.T., Oxygen production in Nature: a light-driven metalloradical enzyme process, *Acc. Chem. Res.*, 31, 18, 1998.

12. Rhee, K.-H., Morris, E.P., Barber, J., and Kühlbrandt, W., Three-dimensional structure of the plant photosystem II reaction center at 8 Å resolution, *Nature*, 396, 283, 1998.
13. Zouni, A., Witt, H.T., Kern, J., Fromme, P., Krauß, N., Saenger, W., and Orth, P., Crystal structure of photosystem II from *Synechococcus elongatus* at 3.8 Å resolution, *Nature*, 409, 739, 2001.
14. Golbeck, J.H., Structure, function and organization of the Photosystem I reaction center complex, *Biochim. Biophys. Acta*, 895, 167, 1987.
15. Sétif, P., Energy transfer and trapping in Photosystem I, in *The Photosystems: Structure, Function and Molecular Biology,* Barber, J., Ed., Elsevier, Amsterdam; New York, 1992, chap. 12.
16. Brettel, K., Electron transfer and arrangement of the redox cofactors in photosystem I, *Biochim. Biophys. Acta*, 1318, 322, 1997.
17. Krauss, N., Hinrichs, W., Witt, I., Fromme, P., Pritzkow, W., Dauter, Z., Betzel, C., Wilson, K.S., Witt, H.T., and Saenger, W., Three-dimensional structure of system 1 of photosynthesis at 6 Å resolution, *Nature*, 361, 326, 1993.
18. Jordan, P., Fromme, P., Witt, H.T., Klukas, O., Saenger, W., and Krauss, N., Three-dimensional structure of cyanobacterial photosystem I at 2.5 Å resolution, *Nature*, 411, 909, 2001.
19. Guergova-Kuras, M., Boudreaux, B., Joliot, A., Joliot, P., and Redding, K., Evidence for two active branches for electron transfer in photosystem I, *Proc. Natl. Acad. Sci. U.S.A.*, 98, 4437, 2001.
20. Nitschke, W., Mattioli, T., and Rutherford, A.W., The FeS-type photosystems and the evolution of photosynthetic reaction centers, in *Origin and Evolution of Biological Energy Conversion*, Baltscheffsky, H., Ed., VCH Publishers, Weinheim, Germany, 1994, chap. 7.
21. Hauska, G., Schoedl, T., Remigny, H., and Tsiotis, G., The reaction center of green sulfur bacteria, *Biochim. Biophys. Acta,* 1507, 260, 2001.
22. Neerken, S. and Amesz, J., The antenna reaction center complex of heliobacteria: composition, energy conversion and electron transfer, *Biochim. Biophys. Acta,* 1507, 278, 2001.
23. Brettel, K., Leibl, W., and Liebl, U., Electron transfer in the heliobacterial reaction center: evidence against a quinone-type electron acceptor functioning analogous to A_1 in photosystem I, *Biochim. Biophys. Acta*, 1363, 175, 1998.
24. (a) Büttner, M., Xie, D.L., Nelson, H., Pinther, W., Hauska, G., and Nelson, N., Photosynthetic reaction center genes in green sulfur bacteria and in Photosystem I are related, *Proc. Natl. Acad. Sci. U.S.A.*, 89, 8135, 1992; (b) Liebl, U., Mockensturm-Wilson, M., Trost, J.T., Brune, D.C., Blankenship, R.E., and Vermaas, W., Single core polypeptide in the reaction center of the photosynthetic bacterium *Heliobacillus mobilis*: structural implications and relations to other photosystems, *Proc. Natl. Acad. Sci. U.S.A.*, 90, 7124, 1993.
25. Blankenship, R.E., Origin and early evolution of photosynthesis, *Photosynthesis Res.*, 33, 91, 1992.
26. Gingras, G., A comparative review of photochemical reaction center preparations from photosynthetic bacteria, in *The Photosynthetic Bacteria*, Clayton, R.K. and Sistrom, W.R., Eds., Plenum Press, New York, 1978, chap. 6.
27. Hippler, M., Redding, K., and Rochaix, J.-D., *Chlamydomonas* genetics, a tool for the study of bioenergetic pathways, *Biochim. Biophys. Acta*, 1367, 1, 1998.
28. Mathis, P., Optical techniques in the study of photosynthesis, in *Methods in Plant Biochemistry*, Vol. 4, Bowyer, J., Ed., Academic Press, New York, 1990, chap. 8.
29. Lichtenthaler, H.K., Chlorophylls and carotenoids: pigments of photosynthetic membranes, in *Methods in Enzymology*, 148, 351, 1987.
30. Scheer, H., *Chlorophylls*, CRC Press, Boca Raton, FL, 1991.
31. Hoff, A.J. and Amesz, J., Visible absorption spectroscopy of chlorophylls, in *Chlorophylls*, Scheer, H., Ed., CRC Press, Boca Raton, FL, 1991, pp. 723–738.
32. Vos, M.H. and Martin, J.-L., Femtosecond processes in proteins, *Biochim. Biophys. Acta*, 1411, 1, 1999.
33. van Brederode, M. and van Grondelle, R., New and unexpected routes for ultrafast electron transfer in photosynthetic reaction centers, *FEBS Lett.*, 455, 1, 1999.

34. Arnett, D.C., Moser, C.C., Dutton, P.L., and Scherer, N.F., The first events in photosynthesis: electronic coupling and energy transfer dynamics in the photosynthetic reaction center from *Rhodobacter sphaeroides*, *J. Phys. Chem.*, 103, 2014, 1999.
35. Govindjee, J. and Fork, D.C., *Light Emission in Plants and Bacteria*, Academic Press, New York, 1985.
36. Horton, P., and Bowyer, J.R., Chlorophyll fluorescence transients, in *Methods in Plant Biochemistry*, Vol. 4, Bowyer, J.R., Ed., Academic Press, New York, 1990, chap. 9.
37. Krause, G.H. and Weis, E., Chlorophyll fluorescence and photosynthesis: the basics, *Annu. Rev. Plant Physiol. Plant Mol. Biol.*, 42, 313, 1991.
38. Lutz, M. and Mäntele, W., Vibrational spectroscopy of chlorophylls, in *Chlorophylls*, Scheer, H., Ed., CRC Press, Boca Raton, FL, 1991, pp. 855–902.
39. Breton, J. and Nabedryk, E., Protein-quinone interactions in the bacterial photosynthetic reaction center: light-induced FTIR difference spectroscopy of the quinone vibrations, *Biochim. Biophys. Acta*, 1275, 84, 1996.
40. Nabedryk, E., Light-induced Fourier transform infrared difference spectroscopy of the primary electron donor in photosynthetic reaction centers, in *Infrared Spectroscopy of Biomolecules*, Mantsch, H.H. and Chapman, D., Eds., Wiley, New York, 1996, chap. 3.
41. Breton, J. and Verméglio, A., Orientation of photosynthetic pigments *in vivo*, in *Photosynthesis: Energy Conversion by Plants and Bacteria*, Govindjee, J., Ed., Academic Press, New York, 1982, chap. 4.
42. Hoff, A.J., Applications of ESR in photosynthesis, *Phys. Rep.*, 54, 75, 1979.
43. Hoff, A.J., Advanced EPR: applications in biology and biochemistry, Elsevier, Amsterdam; New York, 1989.
44. Budil, D.E. and Thurnauer, M.C., The chlorophyll triplet state as a probe of structure and function in photosynthesis, *Biochim. Biophys. Acta*, 1057, 1, 1991.
45. Ivancich, A., Mattioli, T.A., and Un, S., Effect of protein microenvironment on tyrosyl radicals. A high-field (285 GHz) EPR, resonance Raman, and hybrid density functional study, *J. Am. Chem. Soc.*, 121, 5743, 1999.
46. Carrell, T.G., Tyryshkin, A.M., and Dismukes, G.C., An evaluation of structural models for the photosynthetic water oxidizing complex derived from spectroscopic and x-ray diffraction signatures, *J. Biol. Inorg. Chem.*, 7, 2, 2002.
47. Stowell, M.H.B., McPhillips, T.M., Rees, D.C., Soltis, S.M., Abresch, E., and Feher, G., Light-induced structural changes in photosynthetic reaction center: implications for mechanism of electron–proton transfer, *Science*, 276, 812, 1997.
48. Ortega, J.M. and Mathis, P., Electron transfer from the tetraheme cytochrome to the special pair in isolated reaction centers of *Rhodopseudomonas viridis*, *Biochemistry*, 32, 1141, 1993.

119

Biological Incorporation of Alternative Quinones into Photosystem I

T. Wade Johnson*
The Pennsylvania State University

John H. Golbeck
The Pennsylvania State University

119.1 Introduction

All well-characterized photosynthetic reaction centers contain quinone molecules. Type II reaction centers, such as Photosystem II (PS II), contain two quinones, one that functions as a bound one-electron acceptor, and the other that functions as a mobile two-electron (and two-proton) accumulator. In PS II, plastoquinone-9 (PQ-9) serves the role of the mobile quinone, which shuttles electrons to Photosystem I (PS I) via the cytochrome $b_6 f$ complex. Type I reaction centers, such as PS I of cyanobacteria and green plants, contain two bound phylloquinones (PhQ — vitamin K_1, 2-methyl-3-phytyl-1,4-naphthoquinone).[1–4] One or both PhQ molecules function as one-electron acceptor, shuttling electrons from the primary acceptor A_0 (a chlorophyll *a* monomer), to F_X (a [4Fe-4S] cluster).[5] PhQ neither becomes protonated as part of the electron transfer process nor diffuses from the PS I complex as part of its normal function. The drop in Gibbs free energy from A_0 to F_X is estimated to be ca. 250 mV[6] to 320 mV.[7,8] Thus, PhQ plays an important role as an intermediate in the early stages of electron transfer in PS I.[8]

Phylloquinone has become a focus of a variety of structure function relationships due to its central role in electron transfer. The PhQ molecules can be extracted from PS I using dry or water-saturated diethyl ether[9,10] or using hexane containing 0.3% methanol.[11,12] Water-saturated ether extraction also removes a significant number of antenna chlorophylls, and all of the carotenoids (and probably lipids), while leaving the iron–sulfur clusters unaffected. As might be expected, both extraction procedures block room-temperature electron transfer from A_0 to the iron–sulfur clusters.[4,9] Reconstitution of one PhQ fully restores electron transfer from A_0 to the iron–sulfur clusters.[13] Iwaki and coworkers reported that PhQ could be replaced by a variety of quinones with appropriate redox potentials.[14] Moreover, an assortment of non-native quinones can be inserted into the PhQ binding site *in vitro*.[15,16] In particular,

* Currently at Susquehanna University.

0-8493-1348-1/04/$0.00+$1.50

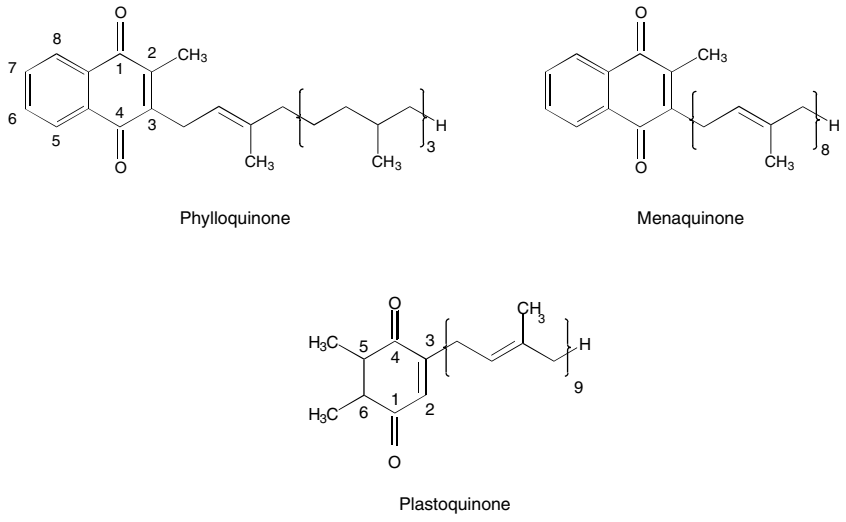

FIGURE 119.1 Structure of phylloquinone, menaquinone-8, and plastoquinone-9.

artificial quinones (benzo- naphtho-, anthraquinones) and quinoid compounds added *in vitro* to chemically extracted PS I bind to the PhQ site and are capable of forward electron transfer.[13,17,18] Biggins suggested that in addition to energetic considerations, a necessary structural constraint was the presence of an alkyl tail.[19] However, a recent review supported the assessment that a quinone head group of appropriate redox potential is alone capable of restoring electron transfer from A_0 to the iron–sulfur clusters.[16]

In this chapter, we focus on protocols that were developed for modifying or replacing PhQ *in vivo*. This method utilizes the biosynthetic machinery of the cell to replace PhQ with PQ-9, a molecule otherwise associated with PS II, and with a variety of naphthoquinone derivatives. We will first identify candidates for genes responsible for the biosynthetic pathway of PhQ. It will be shown that inactivation of these genes disallows PhQ production. We will then describe the physiological and bioenergetic changes that result from the insertion of PQ-9 and naphthoquinone derivatives into the PhQ binding site. These derivatives will be shown to result from a specific gene inactivation or from *in vivo* feeding of (naphtho- and anthra-) quinones to living cells.

119.2 Phylloquinone Biosynthetic Pathway

The only known function of PhQ in cyanobacteria and plants is to function as an electron transfer cofactor in PS I. In spite of its importance in cyanobacteria, the biosynthetic route of PhQ was not previously elucidated. Many prokaryotes contain the metabolic pathway for the biosynthesis of menaquinone (MQ), a PhQ-like molecule (Figure 119.1). In certain bacteria, MQ is used during fumarate reduction in anaerobic respiration.[20,21] In green sulfur bacteria and in heliobacteria, MQ may function as a loosely bound secondary electron acceptor in the photosynthetic reaction center.[22] The genes encoding enzymes involved in the conversion of chorismate to MQ were cloned in a variety of organisms. MQ differs from PhQ only in the tail portion of the molecule: an unsaturated C-40 side chain is present, rather than a mostly saturated C-20 phytyl side chain. Therefore, the synthesis of the naphthalene rings in PhQ and MQ involves similar steps in both pathways.

Given that PhQ biosynthesis is comparable to MQ biosynthesis, the starting molecule for the naphthoquinone nucleus is isochorismate (Figure 119.2), which is ultimately derived from shikimic acid. The first committed step involves the loss of pyruvate and carbon dioxide with the attachment of 2-oxoglutarate to the benzene ring.[23] The next two steps involve stripping the aromatic ring of the hydroxyl group and subsequently attaching a CoA to the aromatic carboxylate group. A succinyl moiety provides the C-2 through C-4 carbons in the formation of the second aromatic ring, which is catalyzed by DHNA

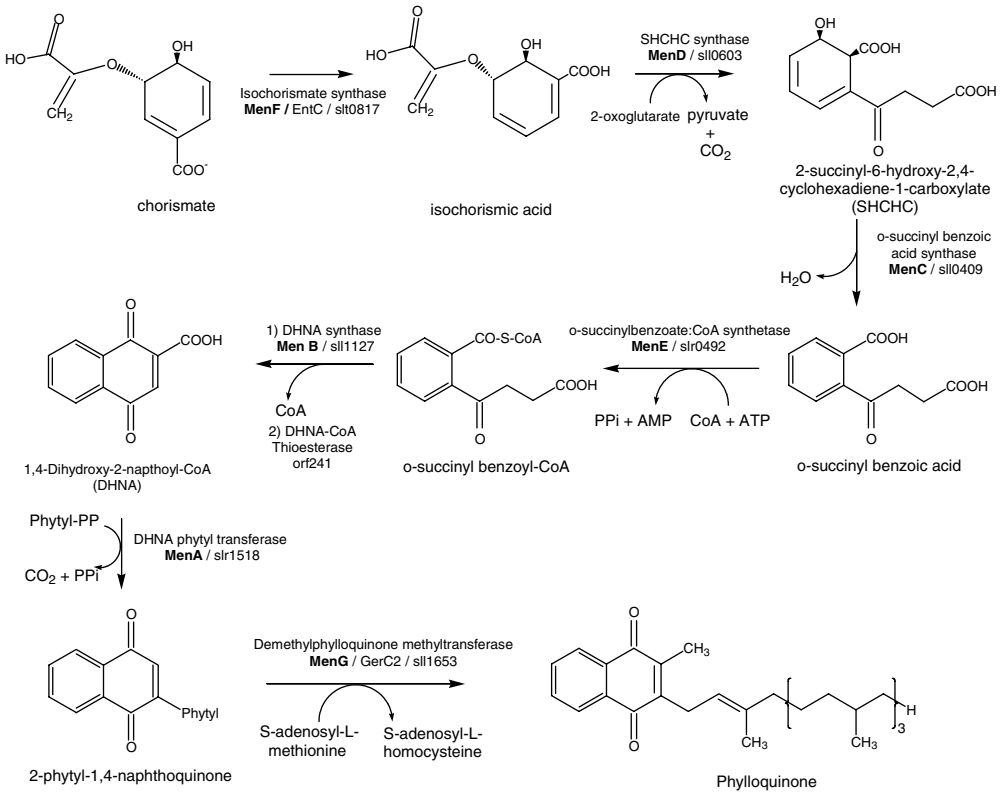

FIGURE 119.2 Proposed biosynthetic pathway of phylloquinone in *Synechocystis* sp. PCC 6803. The genes responsible for the biosynthesis of menaquinone were initially described in *E. coli*. The homologs of these genes were identified in the genome sequence of *Synechocystis* sp. PCC 6803, and *menA*, *menB*, *menD*, *menE*, and *menG* were confirmed by experiment.

synthase with subsequent removal of the CoA by a thioesterase. Both quinone oxygens are derived from water, not from molecular oxygen.[24] At this point, the naphthoquinone head group of PhQ is essentially formed. The biosynthesis of the phytyl tail is thought to be generated from acetyl-CoA through the mevalonate pathway to form geranylgeranyl pyrophosphate.[25] This molecule is then hydrogenated to phytyl pyrophosphate using NADPH as the contributing electron donor.[26] The synthesis of the PhQ phytyl tail and the MQ isoprenoid tail is treated in greater detail in the literature.[27] The remaining steps involve attaching a phytyl group in the C-3 position, with loss of pyrophosphate and carbon dioxide from the pyrophosphate-phytyl group and carboxylate, respectively. Finally, the demethyl-PhQ is methylated, with the methyl group derived from L-methionine, at the C-2 position.

The search for the proteins involved in the PhQ biosynthetic pathway in *Synechocystis* sp. PCC 6803 begins with a search for the genes involved in MQ biosynthesis in other organisms. The genes encoding enzymes involved in the conversion of chorismate to MQ were cloned in *Escherichia coli*[28–34] and *Bacillus subtilis*.[35–38] Specific genes involved in the pathway were identified in spinach[39] and *Bacillus stearothermophilus*.[40] MQ biosynthetic genes were also identified by homology in a variety of other genomes (Table 119.1), including *Haemophilus influenzae* and *Arabidopsis thaliana*.[41] The genome database for *Synechocystis* sp. PCC 6803[42] contains homologs for several genes that encode enzymes for MQ biosynthesis: *menF* (isochorismate synthase), *menD* (2-succinyl-6-hydroxy-2,4-cyclohexadiene-1-carboxylate synthase), *menE* (*O*-succinylbenzoic acid-CoA ligase), *menB* (DHNA synthase), and *menA* (identified as a MQ biosynthesis protein). Possible homologs of *menC* and ORF241 (the DHNA thioesterase) were also identified in database searches. The proposed pathway is illustrated in Figure 119.2. We will focus here

TABLE 119.1 Percent Identity and Percent Homology of Enzymes of Proposed Homologous Genes in the PhQ Biosynthetic Pathway of *Synechocystis* sp. PCC 6803 to Menaquinone Genes in Four other Organisms: *Escherichia coli*, *Bacillus subtilis*, *Haemophilus influenza*, and *Arabidopsis thaliana*

	Percentage Identity and Homology Compared to *Synechocystis* sp. PCC 6803 (%H/%I)			
Gene	*Escherichia coli*	*Bacillus subtilis*	*Haemophilus influenza*	*Arabidopsis thaliana*
menD	49/32	52/33	42/29	42/28
menC	37/22	40/23	42/25	46/26
menE	42/25	42/24	40/27	46/29
menB	78/64	79/67	82/70	67/54
orf241	42/28	45/25	[a]	43/25
menA	44/26	42/20	41/24	46/30
menG	50/30	51/33	[a]	44/32

[a] No homologous proteins were identified.

on the dedicated steps to PhQ synthesis from isochorismate, involving products of the *menD*, *menC*, *menE*, *menB*, ORF241, *menA*, and *menG* genes. The product of the *menF* gene is involved as a dedicated step, even considering that isochorismate also participates in the synthesis of serine and enterochelin.[60] Each protein in the PhQ biosynthetic pathway was examined individually for domain/active site homologies between *Synechocystis* sp. PCC 6803 and organisms ranging from bacteria to higher plants. The phylogenetic tree was determined for each gene product, suggesting overall evolutionary ties among organisms.

In general, the phylogenetic tree comparisons for *menD*, *menC*, *menE*, *menB*, and *menA* indicate that *Synechocystis* sp. PCC 6803 (*Syn*) and *B. subtilis* (*BSU*) tend to be paired first. *E. coli* (*Eco*) and *H. influenza* (*HIN*) also tend to form an initial pair throughout the biosynthetic pathway. Those two first pairs (*Syn*/*BSU* and *Eco*/*HIN*) are usually joined before *A. thaliana* (*Art*) intersects. The *Syn* enzymes tend to be more closely conserved with other bacteria, with *Art* showing the greatest discrepancy in protein alignment.

The *menD* (SHCHC synthase) and *menC* (o-succinyl benzoic acid synthase) genes are the first two genes coding for enzymes that are likely to be involved exclusively in PhQ biosynthesis. Starting with isochorismic acid, SHCHC synthase produces 2-succinyl-6-hydroxy-2,4-cyclohexadiene-1-carboxylate (SHCHC), with the subsequent enzyme o-succinyl benzoic acid synthase producing o-succinyl benzoic acid. Both *menD* genes from *E. coli*[28] and *B. subtilis*[37] were cloned. The *menC* gene was also cloned in *E. coli*[30] and *B. subtilis*.[36,43] The protein alignment of SHCHC synthase from both organisms shows a 42 to 52% similarity. The similarity is 37 to 46% for o-succinyl benzoic acid synthase (Table 119.1). Protein alignments for SHCHC synthase show a highly conserved *N*-terminal domain. This domain may be part of the active site or a possible substrate-binding site for 2-oxoglutarate, which is consumed in the reaction with pyruvate and carbon dioxide released as side products. O-succinyl benzoic acid synthase (*menC*) has no well-defined domains that can be identified as active sites. However, there are several sets of residues that have complete identity in the direction of the *C*-terminal end. The reaction involves loss of an hydroxyl from the substrate without cofactor involvement, and this may suggest that a smaller less-conserved active site may be present.

The largest enzyme in the pathway is o-succinyl benzoate:CoA synthetase, which has ca. 450 residues and is encoded by the *menE* gene The homology comparison of the sequence of this protein in *Synechocystis* sp. PCC 6803 to other organisms is lower compared to the other protein similarities probed in this pathway. There is a *C*-terminal region of identity that could represent the active site domain. This generally basic domain has conserved hydrophobic, basic, and hydroxyl amino acids from residues 350 to 400 and also contains two conserved proline residues. The enzyme attaches a CoA while utilizing the energy of hydrolysis of ATP (to AMP). This suggests that there may be several domains that perform different aspects of the enzyme function.

The *menB* gene product (DHNA synthase) is the most conserved protein within the PhQ biosynthetic pathway among different organisms (Table 119.1). The *menB* gene in *A. thalina* has the lowest identity

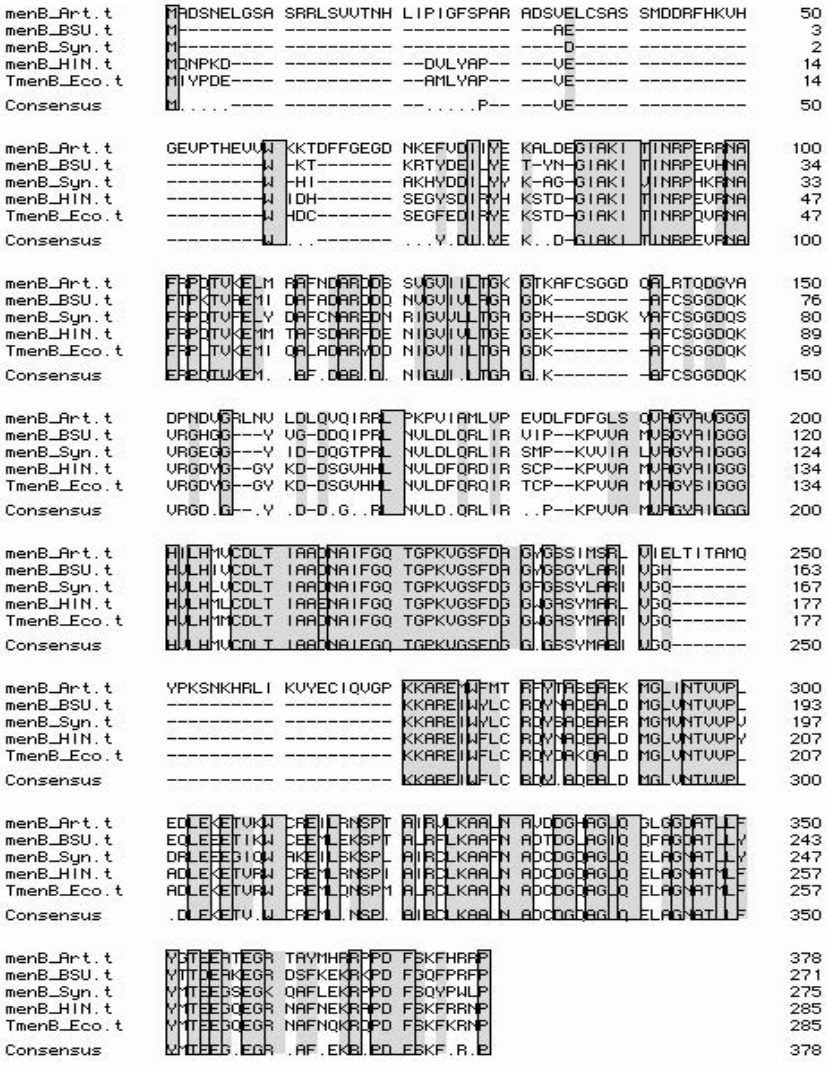

FIGURE 119.3 Homology comparison of the *menB* gene. Abbreviations for each organism: Art is *Arabidopsis thaliana*, BSU is *Bacillus subtilis*, Eco is *E. coli*, HIN is *Haemophilus influenza*, and Syn is *Synechocystis* sp. PCC 6803.

at 54%, which may be due to the presence of an intron in the *N*-terminal region (Figure 119.3). The overall homology of the bacterial proteins is about 80%. The *C*-terminal half is highly conserved. Given the high degree of similarity, the second ring closure can be considered a critical step, converting a substituted benzene ring into naphthoquinone. DHNA synthase is the only step that does not produce by-products or consume high-energy cofactors. This suggests that the enzyme mechanism is refined, hence imparting a high degree of functional and structural similarity between species.

Given the small amount of information on *orf241*, we will only acknowledge that it is a likely component of the MQ/PhQ biosynthetic pathway. The homology is relatively low among the organisms compared (Table 119.1). It is thought to be a thioesterase that releases CoA from DHNA-CoA.

The DHNA phytyl transferase encoded in the *menA* gene is clearly an important step, and it differentiates the production of PhQ from MQ in *Synechocystis* sp. PCC 6803. The homology comparisons among organisms are surprisingly similar, given that DHNA phytyl transferase in *Synechocystis* sp. PCC 6803 transfers to the naphthoquinone a C-20 mostly saturated phytyl tail, whereas in other bacterial organisms, it transfers an unsaturated C-40 group.

The *menG* gene codes for a demethyl-PhQ methyl transferase. The gene involved in the PhQ biosynthetic pathway has proven difficult to identify because methylation is a common cellular reaction and is performed by many enzymes on a variety of substrates.[44] Although the homology comparison among organisms is comparable to other enzymes in this pathway, the protein alignment fails to yield a consistent domain for the active site.

Genes involved in PhQ biosynthesis of *Synechocystis* sp. PCC 6803 were thus identified. The percent homology and identity among organisms vary significantly, leading to tentative identification. To prove that these proposed genes code for enzymes involved in the biosynthetic pathway of PhQ, several were selected for gene disruption studies.

119.3 Phylloquinone Biosynthetic Pathway Gene Disruption

Five of the seven identified genes (*menA, menB, menD, menE*, and *menG*) in the PhQ biosynthetic pathway were disrupted. With the pathway interrupted at specific points, our goals were to characterize the physiology of the mutant cells and to study the effect on PS I electron transfer.

The *menB* and *menA* genes were chosen for the first set of inactivation studies. The *menB* gene encodes DHNA synthetase, which is responsible for the biosynthesis of the naphthoquinone head group. By disrupting the *menB* gene, we hoped to prevent the synthesis of a molecule that would be capable of binding in the PhQ site. We expected that *menB* gene inactivation would lead to an empty PhQ binding site. The *menA* gene was chosen for disruption as a complement to the *menB* gene. The *menA* gene encodes phytyl transferase, which is responsible for displacing the carboxy group with a phytyl group. According to Itoh and coworkers, tail-less naphthoquinones are capable of binding to the PhQ site.[16] By disrupting the *menA* gene, synthesis halts at the production of DHNA, which we thought might be incorporated into the PhQ binding site. This could allow us to determine if phytylation is a necessary precondition for binding, and whether the naphthoquinone head group, with an appropriate redox potential, is the only requirement for function. The results of these mutations are discussed in the next section.

The *menD* and *menE* genes were chosen for the next set of inactivation studies. The *menD* gene was chosen because its product was thought to be the first dedicated step in the pathway. The *menE* gene was chosen to confirm the gene's assignment, given the relatively low sequence homology. Isochrosmate, the product from the previous step (coded by *menF*), is an intermediate found in many other pathways and yet has been recently determined necessary for PhQ biosynthesis.[60]

The identification of the *menG* gene was difficult, and after careful consideration of several potential methylases in a variety of genomes, disruption as the open reading frame *sll1653* in *Synechocystis* sp. PCC 6803 confirmed its involvement in the PhQ biosynthetic pathway.[45,55] This disruption is important, not only in identifying the proper methylase, but also for generating demethyl-PhQ, a potentially interesting substitute for PhQ in PS I.

119.4 Results of Phylloquinone Pathway Gene Disruption

The *menA* and *menB* genes were inactivated by disrupting and partially removing the targeted gene with an antibiotic resistance cassette, thereby preventing a fully functional enzyme from being translated.[46] High-performance liquid chromatography coupled with detection by UV-Vis (HPLC/UV-Vis) and mass spectroscopy (LC-MS) showed that pigments extracted from membranes and PS I trimers of the *menA* and *menB* deletion mutant strains lacked detectable levels of PhQ. Therefore, one immediate conclusion was that the *menA* and *menB* genes in the *Synechocystis* sp. PCC 6803 genome code for phytyl transferase and DHNA synthase, respectively, in the PhQ biosynthetic pathway. However, interesting observations were made regarding function. The *menA* and *menB* deletion mutant strains continued to grow photoautotrophically, albeit with increased doubling times, indicating that photosynthesis was still functional. Plastoquinone-9 (PQ-9) was found by HPLC/UV-Vis and LC-MS analysis in extracted pigments of PS I

trimers from the *menA* and *menB* deletion mutant strains but not from the wild type. Using low-temperature electron paramagnetic resonance (EPR) spectroscopy, it could be shown that an electron derived from P700 reduced the terminal iron–sulfur clusters, F_A/F_B. Additionally, steady state electron transfer rates of cytochrome c_6 to flavodoxin in PS I complexes from the *menA* and *menB* deletion mutant strains were about 80% that of the wild type. This led us to two possible conclusions: (1) that the PhQ-binding site is bypassed as the electron is transferred from A_0 to the iron–sulfur clusters or (2) that a foreign molecule is recruited into the PhQ binding site, and that it participates as a cofactor in forwarding the electron transfer.

A series of careful magnetic resonance experiments identified a foreign quinone as this intermediate cofactor in PS I.[47] Initially, a semiquinone anion radical (Q^-) was observed transiently by EPR spectroscopy at X-band (9 GHz) when living whole cells of the *menA* and *menB* deletion mutant strains were illuminated with white light. The molecule responsible for this radical was not only capable of accepting an electron from P700, but also, it was able to discharge electrons forward to the iron–sulfur clusters. When the radical was photoaccumulated at low temperatures and studied at higher microwave frequencies (34 GHz), the larger *g*-anisotropy hinted that the quinone contained a single benzoquinone ring rather than a naphthoquinone ring. Also, the prominent hyperfine splittings due to the 2-methyl group of PhQ[48] were missing. ENDOR spectroscopy showed that Q^- remained the same in the *menA* and *menB* deletion mutant strains, and there were two asymmetric methyl groups on the molecule. These structural features are consistent with the identity of the intermediate cofactor as PQ-9. Spin-polarized transient EPR at three microwave frequencies (X, Q, and W-bands) indicated that the vector connecting the quinone carbonyls is pointed toward P700, which is the same orientation as in native PhQ.[49] Pulsed EPR techniques indicated that the distance from P700 and Q^- is 25.3 Å, which is close to the $P700^+$ and A_1^- distance.[50,51] Hence, Q^- is the same orientation and distance from P700 as PhQ. The accumulated magnetic resonance data, therefore, prove that Q^- is PQ-9, and that it is likely bound to the same site as PhQ.

We next focused on the kinetics of electron transfer in PS I complexes from the *menA* and *menB* deletion mutant strains. Electron transfer rates are sensitive to distance, Gibbs free energy, and reorganization energies among donor and acceptor pairs. The replacement of PhQ with PQ-9 translated into changes in forward and backward electron transfer rates through the quinone. In particular, the forward electron donation from the PhQ^- to F_X slowed by about a factor of 10 relative to the wild type. In wild-type PS I, the charge recombination between $P700^+$ and $[F_A/F_B]^-$ is multiphasic after a saturating flash.[6] When measured in the absence of an external electron acceptor, the reduction of $P700^+$ is biphasic, with typical lifetimes of 10 to 30 ms and 80 to 100 ms. The reduction of $P700^+$ in *menA* and *menB* deletion mutant strains reduction are also biphasic, with lifetimes of ca. 3 and ca. 10 ms. The 30-fold increase in the $P700^+$ reduction kinetics in the *menA* and *menB* deletion mutant strains was confirmed using CW EPR spectroscopy. The 3 ms phase has proven to be a highly useful characteristic that allows one to determine whether PQ-9 or PhQ is in the binding site. The changes in the electron transfer kinetics are explained by a change in the redox potential of PQ-9. It is estimated to be ca. +95 mV more oxidizing than PhQ, resulting in a thermodynamically "uphill" electron transfer step from Q^- to F_X.[6]

The *menD* and *menE* genes code for enzymes that function and reside earlier in the PhQ biosynthetic pathway. These genes were targeted for gene inactivation due to the possibility that there may be an alternative pathway that circumvents the *menD* and *menE* gene inactivations. The *menD* and *menE* deletion mutant strains were similarly engineered by inserting an antibiotic-resistant cassette into the gene.[52] The physiological characteristics of the *menD* and *menE* deletion mutant strains were found to be similar to the *menA* and *menB* deletion mutant strains. The cells grew at a fraction of the wild-type rate, and all showed high light sensitivity, a lower chlorophyll content *a* per cell, and a lower ratio of PS I:PS II. All of the mutant strains had comparable rates of whole-chain and PS II oxygen evolution. Using LC-MS and HPLC-UV/Vis detection of extracted pigments we showed that the mutant strains did not contain PhQ in the thylakoid membrane or the purified PS I complexes. As with the *menB* deletion mutant strain, PQ-9 was identified in PS I complexes by Q-band EPR spectroscopy. A 3 ms lifetime was also observed for the kinetic back-reaction. Therefore, similar to the *menA* and *menB* deletion mutant strains, PQ-9 is recruited into the PhQ binding site of PS I in the *menD* and *menE* deletion mutant

strains. We therefore find the same general physiological and phenotypic responses when PQ-9 is in the PhQ binding site of PS I, regardless of which gene in the PhQ biosynthetic pathway is inactivated. A corollary of this conclusion is that no alternative pathways exist for the biosynthesis of PhQ in *Synechocystis* sp. PCC 6803.

119.5 High-Light-Tolerant Strains of *menB* and *menD* Mutant Strains

All of the original PhQ biosynthetic pathway mutant strains (including *menA*, *menB*, *menD* and *menE*) have a low content of PS I and a low chlorophyll content per cell, and they are sensitive to high-light intensities.[46, 52–54] Previously known as the *menB* mutant strain, the original *menB*18 deletion mutant strain is high-light sensitive and was used for the experiments described here. Two high-light-tolerant strains were isolated from the *menD* and *menB* deletion mutant strains. Colonies of the mutant strains were streaked onto BG11 agar plates containing antibiotics and were placed under high-light intensities (160 μM m^{-2} s^{-2}). The *menD*-R1 and *menB*26 mutant strains were two of several isolates that could grow under high-light intensities. The latter mutation also occurred spontaneously in liquid cultures grown under normal-light intensities (40 to 60 μM m^{-2} s^{-2}), in which the cells were recultured continually for many generations. Presumably, these high-light-tolerant, suppressor mutations can be generated in any of the PhQ biosynthetic pathway gene disruption mutations. To prevent the development of high-light tolerance, liquid cultures should only be grown for two to five generations under low-light intensities (5 μM m^{-2} s^{-2}). Cells stored on BG11 plates in low light have not been found to become high-light tolerant.

Approximately 20 *menB* deletion mutant strains were characterized for growth rate, PS I to PS II ratio, PhQ/PQ-9 content, and oxygen evolution.[54] Of the 20, 10 were high-light tolerant. The other strain, *menB*26, was selected for robustness, the ability to tolerate high-light intensities, and the ability to grow in the presence of supplemented (benzo-, naphtho-, and anthra-) quinones. This trait was necessary for the naphthoquinone feeding experiments described later. The other strains did not have the ability to thrive in liquid cultures containing low levels (10 μM) of supplemented quinone.

The doubling time of the *menD*-R1 mutant strain (30 h) was comparable to the wild type (26 h), which grows nearly three times faster than the *menD* mutant strain (80 h).[52,54] Both the *menB*18 and *menB*26 mutant strains had comparable doubling times (over 70 h). Additionally, *menB*26, unlike *menB*18, was more tolerant of quinones added to the liquid growth media. The *menB*18 strain tended to die or enter an early stationary phase upon addition of quinones.

The high-light tolerant *menD*-R1 and *menB*26 strains are otherwise similar to the original high-light sensitive *menD* and *menB*18 strains.[54] All mutant strains contain active PQ-9 in the PhQ binding site, and the chlorophyll content per cell is reduced to 67 to 85% that of the wild type. To determine if the quinone-binding pocket contained a secondary site mutation, the appropriate regions of the *psaA* and *psaB* genes were sequenced and found to be identical to the wild type, *menD*, and *menB*18 strains. The quinone-to-chlorophyll ratio for all mutant strains is similar to that of the wild type, 1:50.

The differences that arise between the original mutant strains (*menD* and *menB*18) and the high-light-tolerant strains (*menD*-R1 and *menB*26) relate to the PS I to PS II ratio.[54] Phenotypic differences are noted in several ways. Shown in Figure 119.4 is the 77 K fluorescence emission of whole cells on a equal cell number basis; the 720 nm emission is characteristic of PS I, while the 685/695 nm emission is characteristic of PS II. When compared to the wild type, the original *menD* strain and the original *menB*18 strains reduced ratios of PS I:PS II. This is also true of the *menA* and *menE* mutant strains (not shown). The high-light-tolerant *menD*-R1 and *menB*26 strains have PS I:PS II ratios comparable or greater than those of the wild type. Oxygen evolution rates provide a striking example in the differences in the high-light-tolerant strains relative to the wild-type strains and the *menD* and *menB*18 mutant strains. Under the growth conditions of these experiments, the wild type, and the *menD*, *menB*18, and *menE* mutant strains have approximately a 1:3 ratio of water-to-bicarbonate whole-chain oxygen evolution versus PS II oxygen evolution alone. In the high-light-tolerant strains, this ratio drops to ca. 1:1. Whole-chain

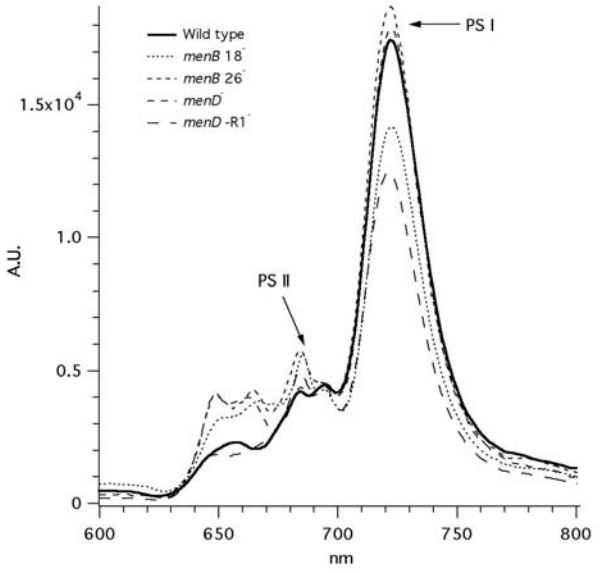

FIGURE 119.4 Fluorescence emission spectra at 77 K of whole cells from *Synechocystis* sp. PCC 6803 wild type, *menB* mutant strains, and *menD* mutant strains. Spectra were recorded at the same cell density and normalized relative to PS II. Each spectrum was the average of the four measurements performed in duplicate. The excitation wavelength was 435 nm, which excites mostly chlorophyll. PS II and its accessory pigments exhibit emission maxima at 685 and 695 nm; PS I has a maximum emission at 721 nm.

electron transfer rates decrease 86% and 58% in the *menD*-R1 and *menB*26 strains, compared to the original strains (*menD* and *menB*18), respectively. The PS II oxygen evolution levels of *menD*-R1 and *menB*26 decreased to 30% and 49% of the levels in the original *menD* and *menB*18 mutant strains, respectively. The change in oxygen evolution for *menD*-R1 and *menB*26, coupled with the 77 K fluorescent measurements, indicate that the cell has downregulated the amount of PS II. The lower level of PS II per cell generates less reductant under high-light conditions, an amount that can be adequately processed by the lower amount of PS I. This leads to a lower level of stress on the cells under high-light conditions, which, in turn, allows the cells to grow.

119.6 Modification of Phylloquinone through Gene Inactivation

A novel PhQ derivative was introduced biologically into the PhQ binding site by inactivating a specific methyltransferase coded by the *menG* gene, one that methylates the naphthoquinone ring ortho to the phytyl tail.[55] Mass spectrometric measurements show that pigments extracted from PS I complexes of the *menG* mutant strain lack the $m/z = 450$ peak characteristic of PhQ and instead reveal an $m/z = 436$ peak characteristic of 2-phytyl-1,4-naphthoquione. EPR spectroscopy of the photoaccumulated semiquinone Q^- signal in PS I complexes showed the presence of a hyperfine doublet that indicated the presence of an H in place of the CH_3 group ortho to the phytyl tail.

Unlike PQ-9 containing mutant strains, the phenotype of the demethyl-PhQ mutant strain is similar to the wild type.[55] The doubling times of the *menG* deletion mutant strain under photoautotrophic and mixotrophic conditions are the same as those of the wild type. The chlorophyll content is also comparable. The steady state rates of electron transport for PS I complexes of the *menG* deletion mutant strain were virtually identical to those of the wild type. Transient EPR shows that the lifetime for the forward electron transfer from Q^- to the iron–sulfur clusters slowed from a lifetime of 290 ns in the wild type to 600 ns

in the *menG* deletion strain. This would be expected if the redox potential of 2-phytyl-1,4-naphthoquinone were +50 to +60 mV more oxidizing than PhQ. The lifetime of the $P700^+[F_A/F_B]^-$ backreaction also decreased from 80 ms in the wild type to 20 ms in the *menG* deletion mutant strain.

119.7 *In Vivo* Recruitment of Media-Supplemented Naphthoquinones

Success at genetically disrupting the PhQ biosynthesis pathway allowed us to embark on a project aimed at the biological replacement of the native PhQ with alternative quinones. The initial gene disruptions resulted in a PQ-9 molecule occupying the PhQ site of PS I. These mutant strains allowed us to introduce a variety of phytylated benzyl- and naphthoquinone in order to probe the structural requirements for quinones to function in PS I. This method has proven to be a useful adjunct to PhQ removal by organic solvents[16,19,56,57] and has additional advantages because it allows physiological observations of living cells. We found that it is possible to introduce phytylated quinones into the PhQ site *in vivo* by utilizing the phytyltransferase in the *menB* mutant strain and the methyltransferase in the *menA* mutant strain and by selecting tolerant strains (Figure 119.2).[53] For example, the *menB*26 mutant strain prevents the naphthoquinone head group from forming, yet it allows phytylation of a quinone supplemented in the growth medium. Because the *menA* mutant strain is incapable of phytylation, it serves as a control to determine if the supplemented quinone head group alone is capable of displacing PQ-9 and functioning in forward electron transfer.[53]

To assess the stability of PhQ over time and to gauge the relative binding of PQ-9, an *in vivo* PhQ pulse experiment was conducted on the living *menB*26 cells. Within 15 min of the addition of PhQ to the growth media, PQ-9 was completely displaced by PhQ in PS I. Hence, PhQ must enter the PhQ binding site by diffusion, and it must displace the resident PQ-9. This rapid incorporation of PhQ suggests a significant difference in the affinity of the binding site for PhQ and PQ-9. This displacement of the loosely bound PQ-9 is the key for incorporating alternative phytylated quinones.

Reincorporation of PhQ was also achieved by supplementing the *menB*26 growth media with the enzymatic product of DHNA synthetase, 2-CO_2-1,4-naphthoquinone, which resulted in a 94% replacement of PQ-9 with PhQ.[53] The Chl:Q_{total} in the supplemented *menB*26 deletion mutant strain is comparable to that of the wild type. This proves that phytyltransferase (the *menA* gene product) and methylase (*menG* gene product) remain functional in the mutant strains. Furthermore, PQ-9 is retained when the *menA* deletion mutant strain is supplemented with 2-CO_2-1,4-naphthoquinone. Because the *menA* gene codes for phytyltransferase, we concluded that the phytyl group is important for binding the quinone into the site.

Reincorporation of PhQ also occurs with compounds such as 2-CH_3-1,4-naphthoquinone.[53] Supplementation with the deuterated derivative of 2-CD_3-1,4-naphthoquinone yields a d-PhQ product that still contains the CD_3 moiety. This shows that the deuterated methyl group is unaffected by the phytyl- and methyltransferase enzymes. The addition of 1,4-napthoquinone led to the detection by LC-MS of a mixture of phytylated and phytylated/methylated molecules.[53] However, there was clear EPR evidence for *in vivo* incorporation of 1,4-naphthoquinone into the PhQ site with an orientation similar to that of PhQ in the wild type. This was an unexpected result, considering that previous *in vitro* incorporation of 1,4-naphthoquinone in solvent-extracted PS I complexes led to the incorporation of 1,4-naphthoquinone with an altered orientation.[49,58]

It may even be possible to incorporate 1,2-naphthoquinone into the PhQ site.[54] Growth media supplementation with unsubstituted 1,2-naphthoquinone led to an admixture of phytylated and methylated/phytylated naphthoquinone molecules as well as to the retention of significant amounts of PQ-9 when assayed by LC-MS. The replacement of PQ-9 with phytylated 1,2-naphthoquinone was therefore low (<50%) in the *menB*26 mutant strain. The chlorophyll-to-quinone ratio was 63, which is higher than that for the wild-type Chl:Q_T of 42.[59] This suggests, although it does not prove, the presence of a subpopulation of PS I that lacks a bound quinone molecule. The contribution of the 3 ms $P700^+$

backreaction drops to <10% in the 1,2-naphthoquinone supplemented cells. Two new phases were observed, with lifetimes of 10 ms and 34 ms in a 1:1 ratio, totaling 50% of the total decay. Photoaccumulation of Q^- at 200 K revealed a complex EPR spectrum, suggesting that PQ-9 and a 1,2-naphthoquinone derivative are reduced. More work is obviously required, but this experiment hints at the promise of biological incorporation of novel quinones into the PhQ binding site of PS I.

Finally, a double gene knockout of the *menB* and *menG* genes has been generated (*menBG*). This mutant strain has the potential to phytylate naphthoquinones without additional methylation. The *menBG* mutant strain should allow for comparisons of novel, phytylated quinones in the PhQ binding site, with or without an accompanying methyl group. The *menBG* mutant strain, therefore, adds an additional option for probing the structure and function of molecules in the PhQ binding site of PS I.

Acknowledgments

T.W.J. gratefully acknowledges support from Professor Parag Chitnis. This work was supported by grants from the National Science Foundation (MCB-0117079) and the United States Department of Energy (DE-FG-02-98-ER20314).

References

1. Malkin, R., On the function of two vitamin K molecules in the PSI electron acceptor complex, *FEBS Lett.*, 208, 343, 1986.
2. Schoeder, H.U. and Lockau, W., Phylloquinone copurifies with the large subunit of photosystem I, *FEBS Lett.*, 199, 23, 1986.
3. Takahashi, Y., Hirota, K., and Katoh, S., Multiple forms of P_{700}-chlorophyll *a*-protein complexes from *Synechococcus* sp. PCC 6803: The iron, quinone, and carotenoid contents, *Photosynth. Res.*, 6, 183, 1985.
4. Biggins, J. and Mathis, P., Functional role of vitamin K in photosystem I of the cyanobacterium *Synechocystis* 6803, *Biochemistry*, 27, 1494, 1988.
5. Brettel, K., Electron transfer from A_1^- to an iron-sulfur center with $t_{1/2}$ = 200 ns at room temperature in photosystem I. Characterization by flash absorption spectroscopy, *FEBS Lett.*, 239, 93, 1988.
6. Semenov, A.Y., Vassiliev, I.R., van der Est, A., Mamedov, M.D., Zybailov, B., Shen, G., Stehlik, D., Diner, B.A., Chitnis, P.R., and Golbeck, J.H., Recruitment of a foreign quinone into the A_1 site of Photosystem I. Altered kinetics of electron transfer in phylloquinone biosynthetic pathway mutants studied by time-resolved optical, EPR and electrometric techniques, *J. Biol. Chem.*, 275, 23,429, 2000.
7. Brettel, K., Electron transfer and arrangement of the redox cofactors in photosystem I, *Biochim. Biophys. Acta*, 1318, 322, 1997.
8. Brettel, K. and Leibl, W., Electron transfer in photosystem I, *Biochim. Biophys. Acta*, 1507, 100, 2001.
9. Itoh, S., Iwaki, M., and Ikegami, I., Extraction of vitamin K_1 from photosystem I particles by treatment with diethyl ether and its effect on the A_1^- EPR signal and system I photochemistry, *Biochim. Biophys. Acta*, 893, 508, 1987.
10. Itoh, S. and Iwaki, M., Vitamin K_1 restores the turnover of FeS centers in the ether-extracted spinach PS I particles, *FEBS Lett.*, 243, 47, 1989.
11. Rustandi, R.R., Snyder, S.W., Feezel, L.L., Michalski, T.J., Norris, J.R., Thurnauer, M.C., and Biggins, J., Contribution of vitamin K_1 to the electron spin polarization in spinach photosystem I, *Biochemistry*, 29, 8030, 1990.
12. Sétif, P., Ikegami, I., and Biggins, J., Light-induced charge separation in Photosystem I at low temperature is not influenced by vitamin K_1, *Biochim. Biophys. Acta*, 894, 146, 1987.
13. Iwaki, M. and Itoh, S., Electron transfer in spinach photosystem I reaction center containing benzo-, naphtho- and anthraquinones in place of phylloquinone, *FEBS Lett.*, 256, 11, 1989.

14. Iwaki, M. and Itoh, S., Reaction of reconstituted acceptor quinone and dynamic equilibration of electron transfer in the photosystem I reaction center, *Plant Cell Physiol.*, 35, 983, 1994.
15. Kumazaki, S., Iwaki, M., Ikegami, I., Kandori, H., Yoshihara, K., and Itoh, S., Rates of primary electron transfer reactions in the photosystem I reaction center reconstituted with different quinones as the secondary acceptor, *J. Phys. Chem.*, 98, 11,220, 1994.
16. Itoh, S., Iwaki, M., and Ikegami, I., Modification of photosystem I reaction center by the extraction and exchange of chlorophylls and quinones, *Biochim. Biophys. Acta*, 1507, 115, 2001.
17. Iwaki, M. and Itoh, S., Function of quinones and quinonoids in green-plant photosystem I reaction center, *Adv. Chem. Ser.*, 228, 163, 1991.
18. Iwaki, M. and Itoh, S., Structure of the phylloquinone-binding (Q_ϕ) site in green plant photosystem I reaction centers: the affinity of quinones and quinonoid compounds for the Q_ϕ site, *Biochemistry*, 30, 5347, 1991.
19. Biggins, J., Evaluation of selected benzoquinones, naphthoquinones, and anthraquinones as replacements for phylloquinone in the A_1 acceptor site of the photosystem I reaction center, *Biochemistry*, 29, 7259, 1990.
20. Iverson, T.M., Luna-Chavez, C., Cecchini, G., and Rees, D.C., Structure of the *Escherichia coli* fumarate reductase respiratory complex, *Science*, 284, 1961, 1999.
21. Luna-Chavez, C., Iverson, T.M., Rees, D.C., and Cecchini, G., Overexpression, purification, and crystallization of the membrane-bound fumarate reductase from *Escherichia coli*, *Protein Exp. Purif.*, 19, 188, 2000.
22. Hauska, G., Schoedl, T., Remigy, H., and Tsiotis, G., The reaction center of green sulfur bacteria, *Biochim. Biophys. Acta*, 1507, 260, 2001.
23. Campbell, I.M., Robins, D.J., Kelsey, M., and Bentley, R., Biosynthesis of bacterial menaquinones (vitamins K_2), *Biochemistry*, 10, 3069, 1971.
24. Snyder, C.D. and Rapoport, H., Biosynthesis of bacterial menaquinones. Origin of quinone oxygens, *Biochemistry*, 9, 2033, 1970.
25. Rohmer, M., Knani, M., Simonin, P., Sutter, B., and Sahm, H., Isoprenoid biosynthesis in bacteria: a novel pathway for the early steps leading to isopentenyl diphosphate, *Biochem. J.*, 295, 517, 1993.
26. Schultz, G., Soll, J., Fiedler, E., and Schultz-Siebert, D., Synthesis of prenylquinones in chloroplasts, *Physiol. Plant*, 64, 123, 1985.
27. Reategui, R.F., Phylloquinone in the photosynthetic activity of *Synechocystis* sp. PCC 6803, Master's thesis, Iowa State University, 1998.
28. Palaniappan, C., Sharma, V., Hudspeth, M.E., and Meganathan, R., Menaquinone (vitamin K_2) biosynthesis: evidence that the *Escherichia coli menD* gene encodes both 2-succinyl-6-hydroxy-2,4-cyclohexadiene-1-carboxylic acid synthase and alpha-ketoglutarate decarboxylase activities, *J. Bacteriol.*, 174, 8111, 1992.
29. Sharma, V., Suvarna, K., Meganathan, R., and Hudspeth, M.E., Menaquinone (vitamin K_2) biosynthesis: nucleotide sequence and expression of the *menB* gene from *Escherichia coli*, *J. Bacteriol.*, 174, 5057, 1992.
30. Sharma, V., Meganathan, R., and Hudspeth, M.E., Menaquinone (vitamin K_2) biosynthesis: cloning, nucleotide sequence, and expression of the *menC* gene from *Escherichia coli*, *J. Bacteriol.*, 175, 4917, 1993.
31. Daruwala, R., Kwon, O., Meganathan, R., and Hudspeth, M.E., A new isochorismate synthase specifically involved in menaquinone (vitamin K_2) biosynthesis encoded by the *menF* gene, *FEMS Microbiol. Lett.*, 140, 159, 1996.
32. Sharma, V., Hudspeth, M.E., and Meganathan, R., Menaquinone (vitamin K_2) biosynthesis: localization and characterization of the *menE* gene from *Escherichia coli*, *Gene*, 168, 43, 1996.
33. Suvarna, K., Stevenson, D., Meganathan, R., and Hudspeth, M.E., Menaquinone (vitamin K_2) biosynthesis: localization and characterization of the *menA* gene from *Escherichia coli*, *J. Bacteriol.*, 180, 2782, 1998.

34. Wu, G., Williams, H.D., Zamanian, M., Gibson, F., and Poole, R.K., Isolation and characterization of *Escherichia coli* mutants affected in aerobic respiration: the cloning and nucleotide sequence of *ubiG*. Identification of an S-adenosylmethionine-binding motif in protein, RNA, and small-molecule methyltransferases, *J. Gen. Microbiol.*, 138, 2101, 1992.
35. Driscoll, J.R. and Taber, H.W., Sequence organization and regulation of the *Bacillus subtilis menBE* operon, *J. Bacteriol.*, 174, 5063, 1992.
36. Hill, K.F., Mueller, J.P., and Taber, H.W., The *Bacillus subtilis menCD* promoter is responsive to extracellular pH, *Arch. Microbiol.*, 153, 355, 1990.
37. Palaniappan, C., Taber, H., and Meganathan, R., Biosynthesis of o-succinylbenzoic acid in *Bacillus subtilis*: identification of *menD* mutants and evidence against the involvement of the alpha-ketoglutarate dehydrogenase complex, *J. Bacteriol.*, 176, 2648, 1994.
38. Taber, H.W., Dellers, E.A., and Lombardo, L.R., Menaquinone biosynthesis in *Bacillus subtilis*: isolation of *men* mutants and evidence for clustering of *men* genes, *J. Bacteriol.*, 145, 321, 1981.
39. Kaipling, S., Soll, J., and Schultz, G., Site of methylation of 2-phytyl-1,4-naphthoquinol in phylloquinone (vitamin K_1) synthesis in spinach chloroplasts, *Phytochemistry*, 23, 89, 1984.
40. Koike-Takeshita, A., Koyama, T., and Ogura, K., Identification of a novel gene cluster participating in menaquinone (vitamin K_2) biosynthesis. Cloning and sequence determination of the 2-heptaprenyl-1,4-naphthoquinone methyltransferase gene of *Bacillus stearothermophilus*, *J. Biol. Chem.*, 272, 12,380, 1997.
41. www.genome.ad.jp, http://www.genome.ad.jp/dbget-bin/www_bget?path:syn00130.
42. Kaneko, T., Sato, S., Kotani, H., Tanaka, A., Asamizu, E., Nakamura, Y., Miyajima, N., Hirosawa, M., Sugiura, M., Sasamoto, S., Kimura, T., Hosouchi, T., Matsuno, A., Muraki, A., Nakazaki, N., Naruo, K., Okumura, S., Shimpo, S., Takeuchi, C., Wada, T., Watanabe, A., Yamada, M., Yasuda, M., and Tabata, S., Sequence analysis of the genome of the unicellular cyanobacterium *Synechocystis* sp. strain PCC 6803. II. Sequence determination of the entire genome and assignment of potential protein-coding regions, *DNA Res.*, 3, 109, 1996.
43. Guest, J.R., Menaquinone biosynthesis: mutants of *Escherichia coli* vitamin K_2 requiring 2-succinylbenzoate, *J. Bacteriol.*, 130, 1038, 1977.
44. Voet, D. and Voet, J.G., *Biochemistry*, 2nd ed., John Wiley & Sons, New York, 1995.
45. Shen, G. and Bryant, D.A., personal communication.
46. Johnson, T.W., Shen, G., Zybailov, B., Kolling, D., Reategui, R., Beauparlant, S., Vassiliev, I.R., Bryant, D.A., Jones, A.D., Golbeck, J.H., and Chitnis, P.R., Recruitment of a foreign quinone into the A_1 site of photosystem I. I. Genetic and physiological characterization of phylloquinone biosynthetic pathway mutants in *Synechocystis* sp. PCC 6803, *J. Biol. Chem.*, 275, 8523, 2000.
47. Zybailov, B., van der Est, A., Zech, S.G., Teutloff, C., Johnson, T.W., Shen, G., Bittl, R., Stehlik, D., Chitnis, P.R., and Golbeck, J.H., Recruitment of a foreign quinone into the A_1 site of photosystem I. II. Structural and functional characterization of phylloquinone biosynthetic pathway mutants by electron paramagnetic resonance and electron-nuclear double resonance spectroscopy, *J. Biol. Chem.*, 275, 8531, 2000.
48. Klughammer, C., Klughammer, B., and Pace, R., Deuteration effects on the *in vivo* EPR spectrum of the reduced secondary photosystem I electron acceptor A_1 in cyanobacteria, *Biochemistry*, 38, 3726, 1999.
49. Van der Est, A., Prisner, T., Bittl, R., Fromme, P., Lubitz, W., Möbius, K., and Stehlik, D., Time-resolved X-, K-, and W-band EPR of the radical pair state $P_{700}^{\bullet+}A_1^{\bullet-}$ of photosystem I in comparison with $P_{865}^{\bullet+}Q_A^{\bullet-}$ in bacterial reaction centers, *J. Phys. Chem. B*, 101, 1437, 1997.
50. Bittl, R., Zech, S.G., Fromme, P., Witt, H.T., and Lubitz, W., Pulsed EPR structure analysis of photosystem I single crystals: localization of the phylloquinone acceptor, *Biochemistry*, 36, 9774, 1997.
51. Zech, S.G., van der Est, A.J., and Bittl, R., Measurement of cofactor distances between $P_{700}^{\bullet+}$ and $A_1^{\bullet-}$ in native and quinone-substituted photosystem I using pulsed electron paramagnetic resonance spectroscopy, *Biochemistry*, 36, 9774, 1997.

52. Johnson, T.W., Naithani, S., Zybailov, B., Jones, A.D., Golbeck, J.H., and Chitnis, P.R., The *menD* and *menE* homologues code for 2-succinyl-6-hydroxyl-2,4-cyclohexadiene-1-carboxylate synthase and O-succinylbenzoic acid-CoA ligase in the phylloquinone biosynthetic pathway of *Synechocystis* sp. PCC 6803, *Biochim. Biophys. Acta,* 1557, 67, 2003.
53. Johnson, T.W., Zybailov, B., Jones, A.D., Bittl, R., Zech, S., Stehlik, D., Golbeck, J.H., and Chitnis, P.R., Recruitment of a foreign quinone into the A_1 site of Photosystem I. *In vivo* replacement of plastoquinone-9 by media-supplemented naphthoquinones in phylloquinone biosynthetic pathway mutants of *Synechocystis* sp. PCC 6803, *J. Biol. Chem.*, 276, 39,512, 2001.
54. Johnson, T.W., Phylloquinone Biosynthetic Pathway, Ph.D. dissertation, Iowa State University, 2000.
55. Sakuragi, Y., Zybailov, B., Shen, G., Jones, A.D., Chitnis, P.R., van der Est, A., Bittl, R., Zech, S., Stehlik, D., Golbeck, J.H., and Bryant, D.A., Insertional inactivation of the *menG* gene, encoding 2-phytyl-1,4-naphthoquinone methyltransferase of *Synechocystis* sp. PCC 6803, results in the incorporation of 2-phytyl-1,4-naphthoquinone into the A_1 site and alteration of the equilibrium constant between A_1 and F_X in Photosystem I, *Biochemistry*, 41, 394, 2002.
56. Rustandi, R.R., Snyder, S.W., Biggins, J., Norris, J.R., and Thurnauer, M.C., Reconstitution and exchange of quinones in the A_1 site of photosystem I. An electron spin polarization electron paramagnetic resonance study, in *Biochim. Biophys. Acta,* 1101, 311, 1992.
57. Ikegami, I., Itoh, S., Warren, P.G., and Golbeck, J.H., Reconstitution of the photosystem I secondary quinone acceptor (A_1) in the P_{700}-F_X core isolated from *Synechococcus* PCC 6301, *Plant Cell Physiol.*, 34, 849, 1993.
58. Sieckman, I., Van der Est, A., Bottin, H., Sétif, P., and Stehlik, D., Nanosecond electron transfer kinetics in photosystem I following substitution of quinones for vitamin K_1 as studied by time resolved EPR, *FEBS Lett.*, 284, 98, 1991.
59. Fromme, P., Jordan, P., and Krauß, N., Structure of photosystem I, *Biochim. Biophys. Acta*, 1507, 5, 2001.
60. Sakuragi, Y. and Bryant, D.A., personal communication.

120

Photomovements of Microorganisms: An Introduction

Giovanni Checcucci
Istituto di Biofisica CNR

Antonella Sgarbossa
Istituto di Biofisica CNR

Francesco Lenci
Istituto di Biofisica CNR

120.1 Introduction

There is no need to emphasize that without light, life on our planet as we know it would not exist. Solar radiation, in fact, is a fundamental source of energy for all photosynthetic organisms and microorganisms, and photosynthesis is one of the most important biological processes on earth, which, by consuming carbon dioxide and liberating oxygen, has made the world into the livable place we know today. Light is also a sensory stimulus that provides vital information on the environment to all living beings, terrestrial and aquatic, diurnal and nocturnal, prey and predators, to creatures provided with "eyes" and nervous systems, as well as to aneural life forms like plants, fungi, and unicellular microorganisms, such as bacteria, algae, and protozoa.

Many freely motile microorganisms are provided with a photoreceptor apparatus able to perceive the quantity and the quality of light (propagation direction, fluence rate, spectral composition, polarization) in the environment and to transform the absorption of a photon into a biophysical/biochemical signal that can be recognized, elaborated, and transduced to the motor apparatus. Light constitutes, therefore, an information signal that controls their movement and eventually brings the cells to accumulate into settings in which the illumination conditions are best for their growth, survival, and development.[1]

In this chapter, we will focus our attention on the general features of photomovements of freely motile microorganisms, referring to the chapters of other authors for deeper insight into some of the most important case studies (see Chapters 116 and 121–124).

120.2 Photobehavioral Responses of Microorganisms

The main photobehavioral responses are, according to the terminology of Diehn et al.,[2] photophobic reactions, phototaxis, and photokinesis.

In photophobic responses, the sensory stimulus consists of a sudden change in light intensity, which elicits a transient variation in the motor activity of the microorganisms. Step-up and step-down photophobic responses are caused by a step-wise increase or, respectively, decrease in photon flux. Usually,

0-8493-1348-1/04/$0.00+$1.50

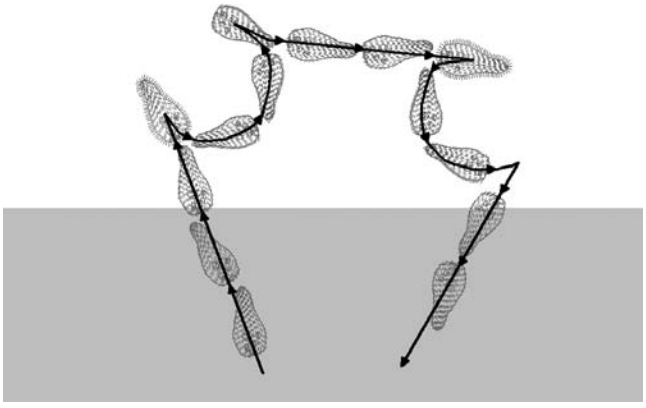

FIGURE 120.1 The step-up photophobic response exhibited by a cell (namely, in this case, the ciliate *Blepharisma japonicum*) upon crossing a dark(gray)-light(white) border.

both photophobic responses consist of a brief cessation of forward movement (stop response) followed by a random change of the direction of movement or, mainly in bacteria, by a variation of the frequency of tumbling/movement inversion. The response pattern depends on the morphology of the microorganism and is independent of light direction. A photophobic response can typically last for several seconds or even a few minutes, after which the microorganism can become adapted to the new illumination conditions. When a swimming cell crosses a dark-light (light-dark) border, it can experience a sudden change in light intensity that triggers a step-up (step-down) photophobic response. The final outcome of these sensory reactions is an avoidance of the lighted (shady) region and accumulation in shaded (lightened) areas (photodispersal or, respectively, photoaccumulation). Usually step-up photophobic reactions occur with a time lag with respect to the stimulus application. This delay decreases with increasing photon flux density and depends on the stimulating wavelength. Similarly, in the case of a step-down photophobic response, the stimulus, now an abrupt decrease in light intensity, finally brings the cells to escape from shadowed areas and to accumulate in lighted regions (photoaccumulation). In Figure 120.1, a schematic reconstruction of a step-up photophobic response is presented.

Phototaxis results from the detection of the direction of light propagation and is a directional response. It is defined as positive or negative according to whether the oriented movement is toward or away from the source. Such a response implies the existence of a sophisticated photoreceptor apparatus. To perceive the position of the light source, in fact, an asymmetry in the photoreceptor apparatus, which allows the cell to sense the vectorial characteristics of the light signal, is required. This can be accomplished, for instance, by means of a single photosensing unit coupled to a screening device that periodically shades the photoreceptor proper.

In photokinesis, light intensity affects the absolute value of the microorganism velocity. If the velocity increases (decreases) when the organism is exposed to light, photokinesis is positive (negative) and causes photodispersal (photoaccumulation).

It is worth noting that the same organism may be able to exhibit more than one photoresponse, which, in some cases, causes the same result (e.g., photodispersal induced by negative phototaxis and step-up photophobic responses) and, in other cases, depends on the environmental illumination condition (e.g., positive or negative phototaxis elicited by low- or high-light intensities).

Consequently, photoaccumulation and photodispersal of cell populations can be the result of phobic, kinetic, and tactic responses, and drawing conclusions on behavioral strategies can be difficult.

Reported in Figure 120.2 is a schematic block diagram of a typical experimental apparatus for measuring photomotile responses in microorganisms. Monitoring IR radiation, which is not perceived by the microorganisms, allows the operator to observe the cells without "disturbing" them. To quantitatively measure photoresponses, population methods and single-cell track (usually computer-assisted[3]) analyses

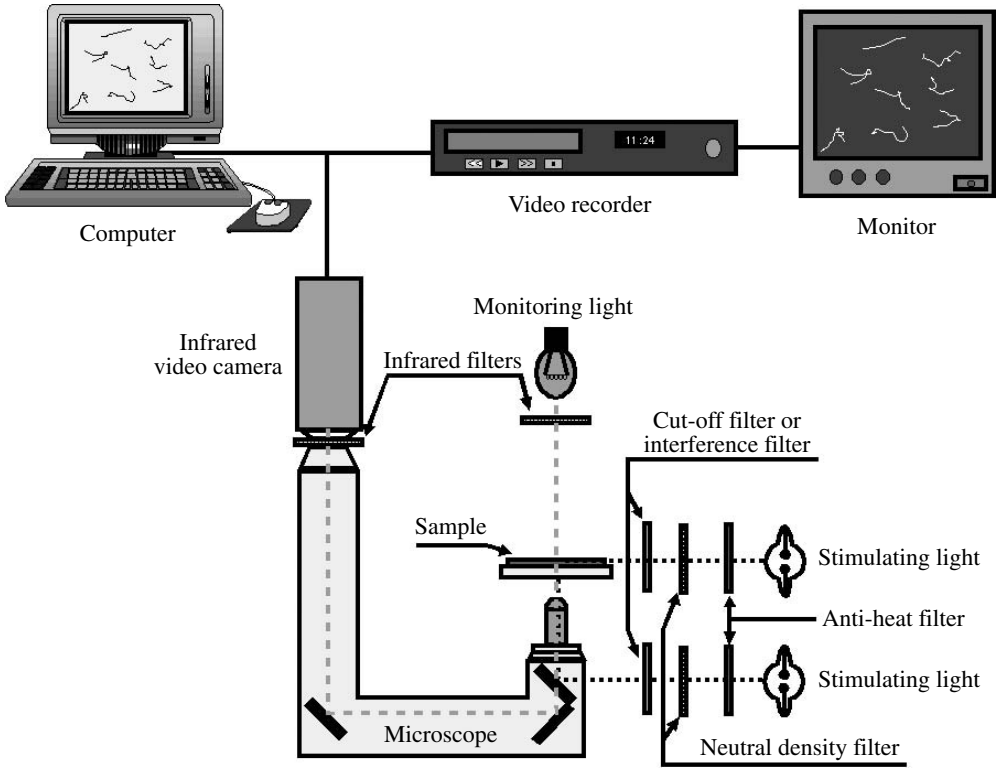

FIGURE 120.2 A typical experimental apparatus for studying photobehavioral responses in microorganisms.

are currently used. Both have advantages and drawbacks, and here, we only want to point out that these measurements deserve an accurate choice of meaningful parameters with which to reliably discriminate among different reactions. As explained above, photodispersal (photoaccumulation) may result not only from true negative (positive) phototaxis but also from a series of step-up (step-down) photophobic reactions, as well as from positive (negative) photokinesis. A still useful, even if "old-fashioned," experimental setup to discriminate between, for example, step-up photophobic responses and negative phototaxis, was used in the case of ciliate *Stentor coeruleus*[4,5] and is reported in Figure 120.3.

Photomotile responses allow photosynthetic bacteria and microalgae to gather in environments in which light is bright enough to efficiently drive the photosynthetic process but, at the same time, not too intense to lead to photoinhibition or photobleaching. However, even for microorganisms that do not harvest and convert light energy directly for their metabolism, like ciliates, for example, light can be an environmental cue to accumulate into habitats that can be favorable for reproduction or propitious for their prey and, in general, for food.[6] In microorganisms containing endogenous photosensitizers, used as defensive pigments against predators (e.g., *Blepharisma japonicum* and *Stentor coeruleus*, see Chapter 122), even relatively dim light can cause severe damage. Their ability to escape lighted spots is directly linked to their survival.[7]

Some microorganisms, finally, have been shown to be able to perceive and transduce short-wavelength ultraviolet radiation (UV-B = 280 – 315 nm). As in aquatic ecosystems and, in particular, in microorganisms, UV-B has been shown to impair photosynthetic activity, curb growth and metabolic rates, damage DNA, spoil photo- and gravi-orientation in the water column, and hurt cell viability and motility (see Chapter 116). This ability of cells to elaborate UV-B photons as environmental sensory stimuli can directly lead the cells into sheltered areas, thus avoiding harmful UV irradiation.[8,9]

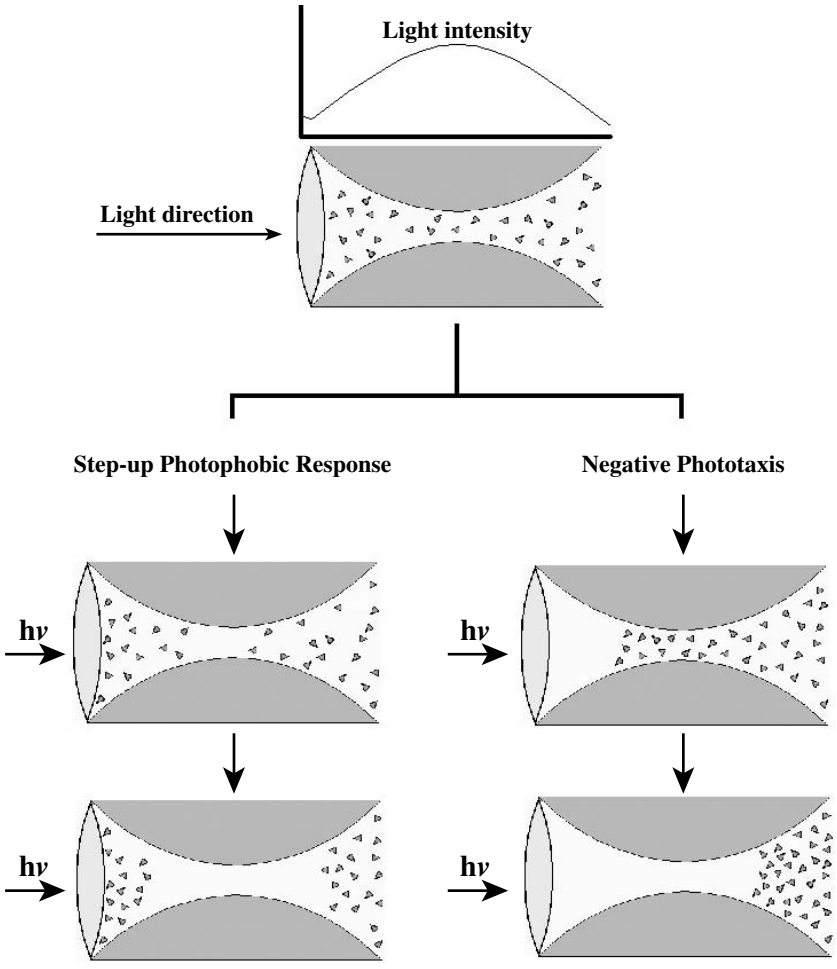

FIGURE 120.3 Cell distribution in the light field produced by a convex lens in the case of negative phototaxis and step-up photophobic responses.

120.3 Photosensory Transduction Chains

In Figure 120.4, the block diagram of the photosensory transduction chain is reported: following absorption of a photon, the photosensing chromophore undergoes molecular modifications leading to the formation of the signaling state that triggers the transduction chain, eventually acting on the motor apparatus.

In what follows, we will go through the different blocks, trying to highlight the main and most promising experimental approaches to the different problems. It is worth noting that because of their intrinsic multidisciplinary character, most key problems encountered in these kinds of studies can best be faced using different experimental techniques and methodologies.

To identify the chromophore responsible for the absorption of the photon triggering the whole photosensory process, action spectroscopy[10] is an unmatched, effective nondestructive technique (see Chapter 115). If not affected by artifacts (screening and reflecting organelles, energy transfer processes, multiple sensing chromophores, etc.) and not made unreliable by wrongly choosing the behavioral parameters describing photoresponsiveness, the structure of an action spectrum is proportional to that

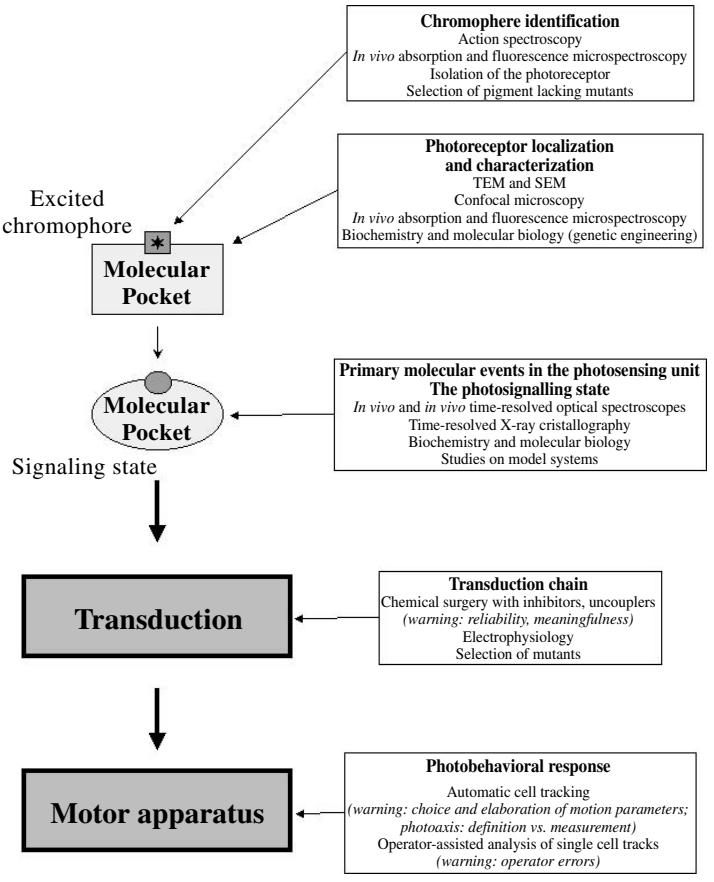

FIGURE 120.4 The photosensory transduction chain in photomotile microorganisms.

of the chromophore absorption spectrum. Action spectra, moreover, relate photoresponsiveness to the wavelength of the stimulating light, thus directly linking the functional absorption of photons by the presumed photoreceptor pigment to the observed physiological reaction. Even if it has some limitations and can be painstakingly time-consuming, nonetheless, action spectroscopy provides direct information about the photoreceptor pigment, is noninvasive, usually requires simple and nonexpensive instrumentation, and is one of the most, and once the only one, used techniques for studying photoresponses in microorganisms.

Whenever it is possible to extract the chromophore, or better, to isolate the integral photoreceptor unit, all chemical, biochemical, and physicochemical assays can be used to carefully characterize the structural and functional properties of the chromophore. The chromophore, for instance, can be purified by HPLC, and its molecular weight and structure can be determined by mass, IR, and NMR spectroscopy.[11,12] Information on the apoprotein–chromophore complex, as another example, can be obtained by means of column chromatographies, mono- and bidimensional gel electrophoresis, and enzymatic assays. When reliable hypotheses are available on the chemical nature of the sensing chromophore, specific inhibitors of its biosynthesis can advantageously be employed.[13]

Mutants lacking one or more photopigments can allow discrimination, which is responsible for the photobehavioral reaction. In mutants with a photosensing unit deprived of the light-detecting chromophore (blind mutants), exogenous addition of chromophores restoring the photoresponse can bring identification of the nature of the molecule with the role of perception and transduction of light stimuli.[14]

Electron microscopy and *in vivo* absorption and emission microspectroscopy and confocal microscopy allow detailed morphological information on the photoreceptor unit to be obtained and the spectroscopic characteristics of the candidate sensing chromophores in their physiological molecular environment to be determined. *In vivo* absorption and emission microspectroscopy and confocal microscopy also permit the photosensing units to be localized within the cell and, in some cases, the maps of their spatial and spectral distributions to be determined.

Time-resolved optical spectroscopies *in vitro*, x-ray crystallography, and microspectroscopies *in vivo* can provide thorough information on the kind and the time-scale of primary molecular reactions occurring in the photoreceptor unit, up to some tiny detail of molecular rearrangements following the absorption of the photon.[15]

These studies on biological structures and substructures can profitably be complemented with studies on model systems. Artificial models of natural photoreceptors have, in fact, been widely utilized, with the aims of elucidating the molecular mechanisms of light-driven biological processes[16] and of devising synthetic tools able to mimic the performance of biological light detectors and transducers and suitable for technological applications.[17] The study of model photosensing and phototransducing systems not only helps clarify the relationships between light-induced modifications in the photopigment and subsequent biophysical/biochemical signal transduction steps but can also yield impressive advancements in natural pigments-based photonic devices for applications in holography, neural network optical computing, and optical memories[18,19] (see Chapters 134, 135, and 139).

Mutants deficient in one or more biochemical pathways, or engineered organisms, can supply data for understanding the molecular machinery operating in the transduction process. Similar figures can be achieved by means of chemical surgery with metabolic drugs, such as, for example, inhibitors and uncouplers. Of course, any drug can severely affect not only the specific pathway presumed to be involved in the sensory process but also many others, and cell viability in general, so that extreme care has to be taken to avoid unreliable results and misleading conclusions.

Electrophysiological techniques, in particular, patch-clamp, may be difficult to use with microorganisms, the dimensions of which vary from a few hundreds to a few μm. They are the only techniques (with the exception of some special fluorescent probes, like ion-specific fluorescent indicators), however, that allow photoelectric effects, like light-induced membrane depolarizations, action potentials, and photic receptor potentials, to be measured. Then, these data can be related to light-induced modification of the motor (flagella and cilia) activity.[20]

Electrophysiological studies are also possible on intact cells, by performing photoelectric measurements in cell suspensions.[21]

Chromophores

As photomotile microorganisms belong to almost every phyletic group that includes unicellular organisms, it is not unexpected that a multiplicity of chromophores with completely different molecular structures and spectroscopic features can act as the prosthetic group of the photoreceptor. To whatever class the organisms belong, in order to be able to detect light over a large range of the solar spectrum, their chromophores usually have broad absorption bands with high molecular extinction coefficients. In some cases, the spectral sensitivity can be widened, if different chromophores, absorbing in contiguous spectral ranges, are spatially assembled in molecular frameworks to maximize the collective interaction among them.

The presently known chromophores are 4-hydroxy-cinnamic acid (e.g., in *Ectothiorhodospira halophila*, now reclassified as *Halorhodospira halophila* see Chapter 123), carotenoids (e.g., retinal in *Halobacterium salinarum*, see Chapter 124), pterins and flavins (e.g., in *Euglena gracilis*, see Chapter 115), and dianthronic molecules (e.g., stentorin in *S. coeruleus* and blepharismins in *B. japonicum*, see Chapter 122).

These chemically different chromophores undergo different, early, light-induced molecular transformations: photoinduced charge transfer (flavins, stentorin, and blepharismins), *cis-trans* photoisomerization (retinals, 4-hydroxy-cinnamic acid), and energy transfer (pterins–flavins).

Primary Reactions and Signaling States

A chromophore acts as a photosensing-phototransducing biological device, because it is not isolated but rather embedded in and interacting with a molecular framework (an apoprotein, in most cases) that "senses" the molecular modifications induced by light in the chromophore and, in its turn, gives rise to the signaling state.[22] The intermolecular interactions between the chromophore and its surrounding microenvironment (its "molecular pocket") can severely affect its photophysical and photochemical properties, the probability of radiationless and radiative transitions from the first excited singlet and triplet states, and the yields of energy and charge transfer processes from excited and metastable states. Study of them can, therefore, lead to the formulation of hypotheses on the primary mechanisms operating in the photosensing-phototransducing process.

Photoreceptor Organelles

A chromophore coupled to a transducing protein without any further "superstructure" is a simple photosensory system seldom found in microorganisms. Instead, to efficiently harvest and transduce the information carried by light, in most microorganisms, the photosensors are organized in ordered structures, with complexity that amazingly varies between prokaryotes and eukaryotes and within eukaryotes. This wide variety of ordered structures is due not only to their different origins, generally regarded as polyphyletic even within the same class, but also to their functional requirements. The photoreceptor organelles must usually operate over a wide range of light incidence angles and intensities and discriminate between different wavelengths to reduce the environmental noise. Above all, it must match the cell morphology and locomotion pattern, especially if detection of the direction of light is required. In phototactic (able to perceive the direction of light) flagellated microalgae, the essential components of a photoreceptor apparatus are the stigma (or eyespot) and the photoreceptor proper. The main role of the stigma is, thanks to the helical movement of the cell, to periodically shade the photosensing structure, so that the stigma–photosensor system constitutes a highly directional apparatus. The modulation of the photic stimulus on the photosensor allows the cell to track the light source and correct its trajectory, finally pointing toward (positive phototaxis) or away from (negative phototaxis) the light source.[23]

In ciliates, the capability of responding to directional light stimuli depends on the structural properties of the photoreceptor (see Chapter 122), and different subcellular organelles have been suggested to be decisive factors in photomovements of the cells: from pigment granules to stigmas, from watchglass (Lieberkuehn) to composed crystalline organelles.[24]

In bacteria, finally, the photoreceptor molecules can be embedded into the cell membrane (as is the case of sensory rhodopsins in *H. salinarum,* see Chapter 124) or can simply be located in the cytoplasm (as is the case of PYP in *H. halophila*, see Chapter 123).

Dark Steps

As shown in the block diagram of Figure 120.4, the light stimulus is converted by the photoreceptor, through its primary molecular reactions, into an intracellular signal that must travel up to the motor apparatus in order to alter the motile behavior of the cell. The intracellular events of the signal transduction chain triggered but not directly driven by the photic stimulus are called "dark steps." In general, they encompass processes for signal amplification without adding noise and feedback mechanisms, in order to extend dynamic ranges, improve accuracy, prevent overloads, and prevent signal reduction and uncontrolled fluctuations.[25]

The large variety of photoreceptor systems of unicellular microorganisms entails a wide diversity of possible mechanisms of signal transduction. Moreover, notwithstanding their apparent "simplicity," microorganisms show a significant richness and complexity of sensory pathways originated by the need to balance multiple environmental signals (oxygen, carbon and nitrogen sources, pH, light, etc.), to move toward or maintain themselves in the optimum environment for growth.

Among bacteria, the halophilic archaebacterium *H. salinarum* has been thoroughly studied, and many of the molecular processes at the basis of its phototransducing mechanisms were clarified (see Chapter 124). In this cell, the light stimulus is transduced through mechanisms similar to those discovered in bacterial chemotaxis. The sensory rhodopsins I and II play their roles of photosensors, thanks to their complexation with the corresponding transducer proteins, HtrI and HtrII, respectively, all of them inserted into the membrane. The transducer proteins modulate the kinase activity that, in turn, controls, through a cytoplasmic phosphoregulator, probably a fumarate molecule, the flagellar motor switching which is placed in the membrane.[26]

In the case of the purple-sulfur bacterium *H. halophila*, the molecular mechanisms responsible for signal generation were comprehensively studied and clarified (see Chapter 123), but the signal transduction pathway from PYP to the flagella still needs to be identified.

As far as microalgae are concerned, the structural components and the signaling cascade initiated by the photoreceptor excitation have not yet been definitely ascertained (see Chapter 121). Electrophysiology measurements can provide crucial complementary information on the light-initiated and light-dependent processes in green flagellated algae. Unfortunately, algal cells do not usually exceed 10 to 20 μm in diameter, which makes microelectrode recording problematic. In several cases, however, thanks to the asymmetric localization of the signal sources within the cell, the photoinduced electrical signals involved in phototaxis and photophobic response in green flagellates could be measured extracellularly from individual cells and from cell suspensions.[21]

In *C. reinhardtii*, different lines of evidence point to the presence of heterotrimeric G-proteins for coupling between the rhodopsin and the ion channels. In analogy to the invertebrate visual system, IP_3 may be a good candidate for a messenger, mediating activation of the ion channels in the plasma membrane.[27]

Recently, in the photoreceptor organelle of *Euglena gracilis*, a new type of blue-light receptor flavoprotein, photoactivated adenylyl cyclase (PAC) (see Chapters 115 and 121), was discovered and biochemically characterized, indicating cAMP as the second messenger for step-up photophobic response of this green alga. It constitutes a unique case of a protein performing two different functions simultaneously: photoreception and transduction (cAMP synthesis catalysis).[28]

Among ciliates, particularly interesting are the cases of *B. japonicum* and *S. coeruleus*, for the richness of the data available and because of the difficulty in depicting a unitary framework. In fact, two main hypotheses are, at present, available. The first hypothesis was that, following light stimulation, an intracellular increase of proton concentration could lead to the opening of calcium channels, indirectly by depolarizing the membrane or directly by altering the conductance of specific calcium channels.[29] More recent results cast doubt on this simple model, suggesting the involvement of amplification and transduction steps similar to those operating in the visual process of metazoans. The fact that in *B. japonicum* and *S. coeruleus* the light-induced ciliary beating stop occurs with a delay up to 1 sec (significantly long in comparison with the millisecond lag-time of mechanoresponses in the same organisms) has been considered indicative of specific time-limiting biochemical processes involving G-proteins and second messengers as cGMP or IP_3.[30–32] Among the most important questions to clarify in this framework is the mechanism of G-protein activation in *B. japonicum* and *S. coeruleus*. The presently available experimental results bring us to hypothesize that the G-protein could be activated by the intracellular pH variation following the release of protons from the photoreceptor, but a direct interaction between the excited photoreceptor and the G-protein cannot be discarded, even though its nature is currently unknown (see Chapter 122). It is, finally, worth noting that a substantial number of data allow us to set up a satisfactory picture of the electrophysiological basis of photosensory transduction in *B. japonicum* and *S. coeruleus*.[20]

120.4 Concluding Remarks

This introductory chapter should provide basic knowledge for better understanding and enjoying the following chapters devoted to the photobehaviors of some characteristic unicells. In those chapters,

further details about the richness of the chromophore molecular structures and pockets and of the "dark steps" involved in microorganism photosensory perception and transduction will be presented.

In nature, of course, light is not the only environmental signal affecting the behavior of microorganisms, and their motile responses result from the integration of "internal needs" (such as, for instance, metabolism and cell cycle) with a diversity of external stimuli (chemical, mechanical, gravitational, photic, etc.). Integrated investigations of their motile responses to different environmental signals (chemical and photic, for example) might, therefore, offer clues for a deeper understanding of sensory processes in microorganisms.

Finally, we would like to retake a general consideration on the lack of an unitary description of the mechanisms at the basis of photomovements of microorganisms.[33] At present, it looks like (as it does for almost every single unicell) an *ad hoc* model holds: specific photosensing chromophores embedded in and interacting with particular molecular pockets, distinctive signaling states triggering unique and different molecular cascades. The question then becomes, is the cause of such a multiplicity of interpretations a consequence of our low level of knowledge and understanding or is it an intrinsic feature of these natural phenomena?

References

1. Häder, D.-P. and Lebert, M., *Photomovements*, Comprehensive Series in Photosciences, Vol. 1, Häder, D.-P. and Jori, G., Eds., Elsevier, Amsterdam; New York, 2001.
2. Diehn, B., Feinleib, M.E., Haupt, W., Hildebrand, E., Lenci, F., and Nultsch, W., Terminology of behavioral responses of motile microorganisms, *Photochem. Photobiol.*, 26, 559, 1977.
3. Takahashi, T., Computer-aided analysis of movement responses of microorganisms, in *Image Analysis: Methods and Applications*, Häder, D.-P., Ed., CRC Press LLC, Boca Raton, FL, 2001, p. 423.
4. Song, P.-S., Häder, D.-P., and Poff, K.L., Phototactic orientation by the ciliate, *Stentor coeruleus*, *Photochem. Photobiol.*, 32, 781, 1980.
5. Song, P.-S., Häder, D.-P., and Poff, K.L., Step-up photophobic response in the ciliate, *Stentor coeruleus*, *Arch. Microbiol.*, 126, 181, 1980.
6. Ricci, N., The behavior of ciliated protozoa, *Anim. Behav.*, 40, 1048, 1990.
7. Giese, A.C., *Blepharisma:The Biology of a Light-Sensitive Protozoan*, Stanford University Press, Stanford, CA, 1973.
8. Lenci, F., Checcucci, G., Ghetti, F., Gioffré, D., and Sgarbossa, A., Sensory perception and transduction of UV-B radiation by the ciliate *Blepharisma japonicum*, *Biochim. Biophys. Acta*, 1336, 23, 1997.
9. Matsunaga, S., Hori, T., Takahashi, T., Kubota, M., Watanabe, M., Okamoto, K., Masuda, K., and Sugai, M., Discovery of signalling effect of UV-B/C for step-down and step-up photophobic responses in the unicellular flagellate alga *Euglena gracilis*, *Protoplasma*, 201, 45, 1998.
10. Ghetti, F. and Checcucci, G., Action spectroscopy, in *Light as Energy Source and Information Carrier in Plant Physiology*, Jennings, R. et al., Eds., Plenum Press, New York, 1996, p. 275.
11. Hoff, W.D., Düx, P., Hård, K., Devreese, B., Nugteren-Roodzant, I.M., Crielaard, W., Boelens, R., Kaptein, R., Van Beeumen, J., and Hellingwerf, K.J., Thiol ester-linked p-coumaric acid as a new photoactive prosthetic group in a protein with rhodopsin-like photochemistry, *Biochemistry*, 33, 13,959, 1994.
12. Checcucci, G., Shoemaker, R.K., Bini, E., Cerny, R., Tao, N., Hyon, J.-S., Gioffré, D., Ghetti, F., Lenci, F., and Song, P.-S., Chemical structure of blepharismin, the photosensor pigment for *Blepharisma japonicum*, *J. Am. Chem. Soc.*, 119, 5762, 1997.
13. Barsanti, L., Passarelli, V., Lenzi, P., and Gualtieri, P., Elimination of photoreceptor (paraflagellar swelling) and the photoreception in *Euglena gracilis* by means of the carotenoid biosynthesis inhibitor nicotine, *J. Photochem. Photobiol.*, 135, 1992.
14. Yan, B., Takahashi, T., Johnson, R., Derguini, F., Nakanishi, K., and Spudich, J.L., All-*trans*/13-*cis* isomerization of retinal is required for phototaxis signaling by sensory rhodopsins in *Halobacterium halobium*, *Biophys..J.*, 57, 807, 1990.

15. Genick, U.K., Borgstahl, G.E.O., Ng, K., Ren, Z., Pradervand, C., Burke, P.M., Srajer, V., Teng, T.-Y., Schildkamp, W., McRee, D.E., Moffat, K., and Getzoff, E.D., Structure of a protein photocycle intermediate by millisecond time-resolved crystallography. *Science*, 275, 1471, 1997.
16. Lenci, F., Angelini, N., Ghetti, F., Sgarbossa, A., Losi, A., Vecli, A., Viappiani, C., Taroni, P., Pifferi, A., and Cubeddu, R., Spectroscopic and photoacoustic studies of hypericin embedded in liposomes as a photoreceptor model, *Photochem. Photobiol.*, 62, 199, 1995.
17. Pieroni, O., Fissi, A., Angelini, N., and Lenci, F., Photoresponsive polypeptides, *Acc. Chem. Res.*, 34, 9, 2001.
18. Birge, R.R., Chen, Z., Govender, D., Gross, R.B., Hom, S.B., Izgi, K.C., Stuart, J.A., Stuart, J.R., and Vought, B.W., Biomolecular photonics based on bacteriorhodopsin, in *CRC Handbook of Organic Photochemistry and Photobiology*, Horspool, W.A. and Song, P.-S., Eds., CRC Press LLC, Boca Raton, FL, 1568, 1995.
19. Willner, I., Photoswitchable biomaterials: en route to optobioelectronic systems, *Acc. Chem. Res.*, 30, 347, 1997.
20. Wood, D.C., Electrophysiology and light responses in *Stentor* and *Blepharisma*, in *Photomovements*, Vol. 1, Häder, D.-P. and Lebert, M., Eds., Comprehensive Series in Photosciences, Häder, D.-P. and Jori, G., Eds., , Elsevier, Amsterdam; New York, 2001, p. 505.
21. Sineshchekov, O.A., Govorunova, E.G., Der, A., Keszthely, L., and Nultsch, W., Photoelectric responses in phototactic flagellated algae measured in cell suspension, *J. Photochem. Photobiol. B: Biol.*, 13, 119, 1992.
22. Hellingwerf, K.J., Key issue in the photochemistry and signalling-state formation of photosensor proteins, *J. Photochem. Photobiol. B: Biol.*, 54, 94, 2000.
23. Kreimer, G., Light perception and signal modulation during photoorientation of flagellated green algae, in *Photomovements*, Vol. 1, Häder, D.-P. and Lebert, M., Eds., Comprehensive Series in Photosciences, Häder, D.-P. and Jori, G., Eds., Elsevier, Amsterdam; New York, 2001, p. 193.
24. Kuhlmann, H.-W., Do phototactic ciliates make use of directional antennas to track the direction of light?, *Eur. J. Protistol.*, 34, 244, 1998.
25. Block, S.M., Biophysical principles of sensory transduction, in *Sensory Transduction*, The Rockfeller University Press, New York, 1992, p. 1.
26. Barak, R., Giebel, I., and Eisenbach, M., The specificity of fumarate as a switch factor of the bacterial flagellar motor, *Mol. Microbiol.*, 19, 139, 1995.
27. Suzuki, T., Narita, K., Yoshihara, K., Nagai, K., and Kito, Y., Phosphatidyl inositol-phospholipase C in squid photoreceptor membrane is activated by stable metarhodopsin via GTP-binding protein Gq, *Vision Res.*, 35, 1995, p. 1011.
28. Iseki, M., Matsunaga, S., Murakami, A., Ohno, K., Shiga, K., Yoshida, K., Sugai, M., Takahashi, T., Hori, T., and Watanabe, M., A blue-light-activated adenylyl cyclase mediates photoavoidance in *Euglena gracilis*, *Nature*, 415, 1047, 2002.
29. Lenci, F., Ghetti, F., and Song, P.-S., Photomovements of ciliates, in *Photomovements*, Vol. 1, Häder, D.-P. and Lebert, M., Eds., Comprehensive Series in Photosciences, Häder, D.-P. and Jori, G., Eds., Elsevier, Amsterdam; New York, 2001.
30. Fabczak, H., Walerczyk, M., Groszynskaand, B., and Fabczak, S., Light induces inositol trisphosphate elevation in *Blepharisma japonicum*, *Photochem. Photobiol.*, 69, 254, 1999.
31. Matsuoka, T., Moriyama, N., Kida, A., Okuda, K., Suzuki, T., and Kotsuki, H., Immunochemical analysis of a photoreceptor protein using anti-IP3 receptor antibody in the unicellular organism, *Blepharisma*, *J. Photochem. Photobiol., B: Biol.*, 54, 131, 2000.
32. Walerczyk, M. and Fabczak, S., Additional evidence for the cyclic GMP signalling pathway resulting in the photophobic behavior of *Stentor coeruleus*, *Photochem. Photobiol.*, 74, 829, 2001.
33. Sgarbossa, A., Checcucci, G., and Lenci, F., Photoreception and photomovements of microorganisms, *Photochem. Photobiol. Sci.*, 1, 459, 2002.

121

Photoreception in Microalgae

Laura Barsanti
Istituto di Biofisica CNR

Valtere Evangelista
Istituto di Biofisica CNR

Paolo Gualtieri
Istituto di Biofisica CNR

Vincenzo Passarelli
Istituto di Biofisica CNR

121.1 Introduction

Information is essential for all forms of life — so it is important to understand how information is perceived, how it is stored, how it is passed on, and how it is used by organisms as they live and reproduce. In the world of photosynthetic microorganisms, where virtually all life depends on solar energy, light becomes a source of information, used to orient microorganisms spatially and to guide their movements or growth. The full exploitation of this information necessitates proper perceiving devices, able to change the small signal represented by the light falling upon them into a larger signal and response of an entirely different physical nature, i.e., these devices must perform perception, transduction, and amplification.

The most primitive photoreceptors are represented by extensive two-dimensional patches of photopigment, which probably exist in the Chlorophyta; whereas more complex photoreceptors, such as three-dimensional crystals of proteins, are present in the Euglenophyta and Chrysophyta. The photosensory proteins in these algal structures occur only in small amounts because they are used to detect light not to collect it. They are concentrated in photoreceptive structures and do not contribute to the color of the organism. This is an important consideration because a primary, historical criterion for algal taxonomy and phylogeny has been bulk pigment composition. Yet, sensory pigments played no role in these determinations, because it is generally believed that different algal groups have different photosensory pigments; furthermore, the association of particular sensory pigments with particular algal groups was based largely upon the examination of only one or a few species.

For a long time, the behavior of microalgae in response to light stimuli attracted the attention of scientists, who hoped that the simplicity of the material would make this phenomenon easy to investigate. On the contrary, the undertaking turned out to be more difficult than expected, and to date, a clear

0-8493-1348-1/04/$0.00+$1.50

understanding of the phenomenon has still to be attained, while the comprehension of the visual process in humans is extensive. Initial ideas on the chemical nature of receptors for photobehavioral responses were gained by measurements of their spectral sensitivity. Action spectroscopy results were then screened and supported by other methods, such as biochemistry, absorption spectroscopy, and molecular biology, that integrated different investigative approaches and shed more light on photoreceptive pigments.

In this chapter, we present a classification of algae and photosensitive apparatus, explain the theoretical basis of their functioning, introduce the methods used to study visual pigments and to compare their different performances, and conclude with a survey of the visual pigments thus far characterized in algae, emphasizing gaps and discrepancies in current knowledge. Our approach will be focused only on the "vision" phenomenon in motile microalgae, i.e., the processing (transduction) of a photic stimulus into an oriented movement; for an overall survey of other phenomena still controlled by photoreceptors, e.g., phototropism, photomorphogenesis, and circadian clock setting, the reader is referred to Chapters 132 and 133 of this book. For more detailed insight into the different photoreceptors evolved in algae, which regulate their growth and development, the reader is referred to the review by Hegemann.[1]

121.2 Phylogenesis and Classification of Algae

The algae are a polyphyletic, noncohesive, and artificial assemblage of O_2-evolving, photosynthetic organisms that includes macroalgae and other highly diverse groups of microorganisms known as microalgae. Most algae are aquatic in fresh or marine waters, but some species may be found growing in such diverse habitats as tree trunks, snowbanks, hot springs, and even within desert rocks. They can be motile and unicellular or pluricellular and nonmotile at some stage of their life cycle. The number of algal species was estimated at between one to 10 million, and most are microalgae. This assemblage of organisms includes prokaryotic blue-green algae (cyanobacteria), prochlorophytes, and eukaryotic algae. Eukaryotic algae represent a minimum of five phyletic assemblages: green algae, red algae, euglenoids, chromophyte algae, and dinoflagellates (Figure 121.1). In eukaryotic algae, which represent at least five distinct evolutionary lineages, there are also protists, traditionally recognized as fungi and protozoa.[2]

All biologists agree that unicellular eukaryotes have prokaryotic ancestors. Among the algae, fossil records show the blue-green algae lineage arising early in the Precambrian period. Euglenoids, red and green lineages, date from the middle to late Precambrian period. Chromophyte algae are first seen in the Paleozoic period. While, dinoflagellates date from early to late Mesozoic period.[3–5]

Historically, the major groups of algae are classified into divisions (equivalent to the zoological phylum) on the basis of pigmentation, chemical nature of photosynthetic storage product, photosynthetic membranes (thylakoid) organization and other features of the chloroplasts, chemistry and structure of cell wall, number, arrangement and ultrastructure of flagella (if any), and the occurrence of any other special features.[6] The information in Figure 121.2 can help us summarize the phylogenetic relationship of microalgae. The starting point of this scheme is an ancestral prokaryote that gave rise to at least two types of organisms: a blue-green alga[7] and an ancestral heterotrophic flagellate.[8] The derivative of the ancestral prokaryote captured a coccoid blue-green alga cell and retained it as a symbiont. As result, the blue-green alga became a system of thylakoids. This association eventually gave rise to red algae. Thereafter, a single-cell red alga was taken up by an ancestral flagellate, so generating chromophytes. Another symbiotic affair between a blue-green alga and an ancestral flagellate gave origin to green algae, and successively to Land Plants. Euglenoids are considered a direct derivative of the ancestral flagellate, with successive symbiotic events for taking up chloroplasts. Finally, the ancestral flagellates, with a relatively recent acquisition of a plastid, generated dinoflagellates.[9,10] Among the approximately 2500 described species of blue-green algae, there are unicellular coccoid, colonial, and filamentous forms, with or without branching or differentiation of specialized cells, such as akinetes (spores) and heterocysts (anaerobic N_2-fixing cells). Eukaryotic microalgae, basically flagellate, also contain some members that are nonmotile (e.g., coccoid) or filamentous, although flagellate stages may be involved in reproduction. Most are unicellular, although a range of colonial types that can be found in the Chlorophyceae and palmmelloid phases are present in the Cryptophyceae.[11]

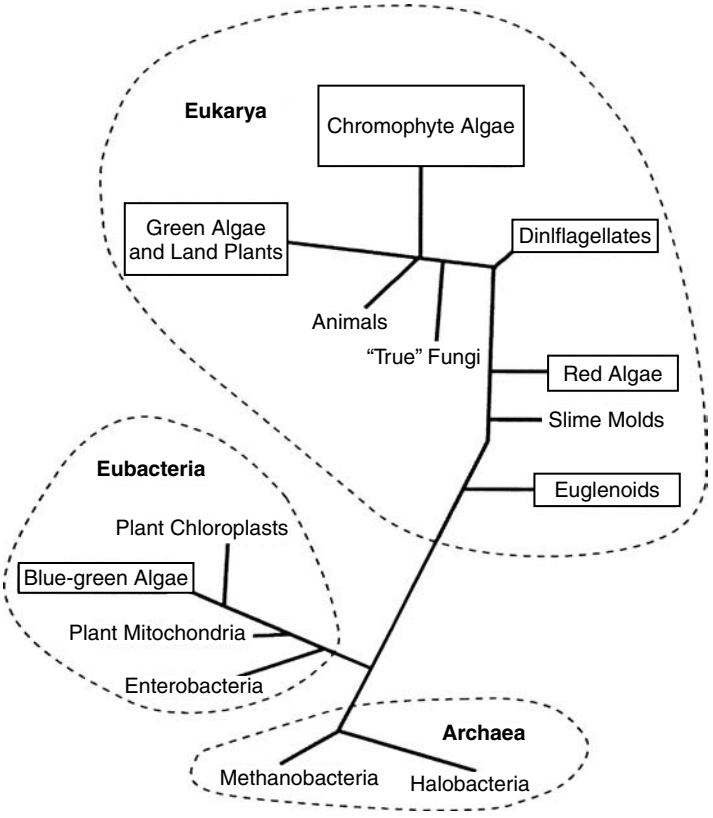

FIGURE 121.1 Phylogenetic relatedness of some group of algae. Lengths of segments are proportional to evolutionary distance based on analysis of ribosomal RNA gene sequences (modified from Gualtieri, 2001).

Eukaryotic cells are usually provided with at least one flagellum, and there may be as many as six.[12] The basic number is two, but in some species, only one emerges from the cell. There is normally one nucleus, although two are found in some dinoflagellates. The cell is covered by a basic plasma membrane; in addition to it, there may be scales or spines, a cell wall, a complex pellicle, or a theca.[13]

121.3 Classification of Photosensitive Apparatus

True vision involves production of a focused image of the external world, and the optical requirements for an eye probably cannot be satisfied by microorganisms, requiring true multicellularity with cell specialization and division of labor. Still, microalgae "eyes" have many similarities with the complex vision systems of higher organisms, because they possess optics, photoreceptors, and signal transduction chain components. The essential elements of these "eyes" are the screening devices, for example, the eyespot, and the detector, i.e., the photoreceptors. Often, the photoreceptor cannot be identified by optical microscopy, while the eyespot can be seen easily because of its size and color, usually orange-red. Sometimes the eyespot function is performed by the whole cell body, and the photosensitive function is demanded by the whole cell membrane.

The eyespot is a roundish shield, inwardly or outwardly concave, and made up of one or more layers of lipidic globules closely packed. The individual globules are not membrane bound, and the eyespot as a whole is not bound to any membrane. These globules principally contain carotenoids that can play the shading role thanks to their strong absorbance.[14] Although the pigments of the eyespot are always

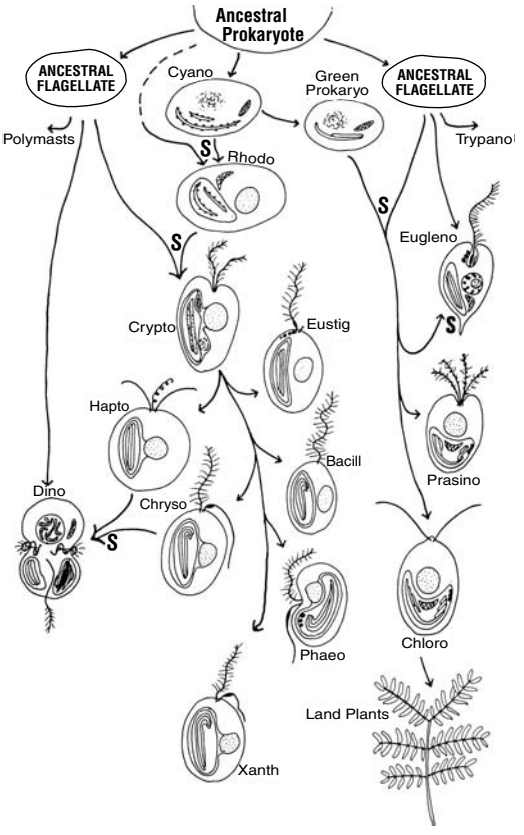

FIGURE 121.2 Phylogenetic relationships of algal groups. S indicates that a symbiotic event occurred (modified from Gualtieri, 2001).

synthesized inside a chloroplast, the globules can be located near its surface or be completely separated from the chloroplast. The photoreceptor, when visible, appears as a swelling of the basal portion of one flagellum or as a separate organelle (the ocellus).

Dodge[15] grouped the different kinds of eyespots into four categories. Keeping in mind this classification, the structure of the photoreceptive systems, and the optical design and molecular organization of photoreceptive proteins, we can divide the photosensitive apparatus of algae into three types[16]:

- Type I, single layer: A single layer of photoreceptor molecules is present inside the whole cell membrane or is located in just the patch of membrane that covers the eyespot. The eyespot, if present, is independent of the flagella and generally multilayered and inwardly concave. If the eyespot is absent, the whole cell body performs the shading function. This means that algae perceive light, even though their photoreceptive systems are not visible.
- Type II, multiple layers: Photoreceptor molecules form a multilayered membrane structure or a three-dimensional membrane protein crystal. The eyespot is outwardly concave and is located close to this structure.
- Type III, multiple layers plus lens: The photoreceptor is more specialized and can be considered an ocelloid. It consists of a lens of complex design and a retinoid. Between the lens and the retinoid, a chamber lined by the plasma membrane is interposed. The eyespot is a pigmented cup wrapping the retinoid.

121.4 Theoretical Considerations

No physical quantity regulates and stimulates the developments of microalgae as strongly as light. Light is electromagnetic radiation characterized by its quality (different wavelengths) and intensity. To measure both parameters and react to them, the microalgae photoreceptor system has to satisfy three main requirements: it should be a photon counter, it should detect either spatial or temporal patterns of light, and it should transmit the detected signal in order to modify the cell behavior. The interpretation of these photoreactions rests upon two postulates:

1. Only the light actually absorbed is effective.
2. Only one quantum is involved in a primary reaction.

Keeping these two postulates in mind, in the following, we discuss a few general principles concerning the functional properties of photoreceptors.

Sensitivity

The ability to perceive and adapt to changing light conditions is critical to the life and growth of photosynthetic microorganisms. Light quality and quantity vary on any given day because of changes in the cloud cover and pollution. Competition for light in an aquatic environment may be particularly fierce because of shading among the different organisms and rapid absorption of light in the water column. Hence, detecting light as low as possible (i.e., a single photon) becomes an adaptive advantage, because a photosynthetic organism in dim light can obtain more metabolic energy if it is able to move to more lighted and suitable areas.

For detecting the direction of light of a specific spectral range, a photoreceptor demands a high density of chromophore molecules (with a high absorption cross section and low thermal noise) organized in a lattice structure. For detecting patterns of light, the number and location of photoreceptors having fixed size and exposure time must be viewed according to the pattern of motion of microalgae. For transmitting the detected signal, a photoreceptor must generate a potential difference, or a current.[17]

All known photoreception systems (those identified with no doubts) are based on rhodopsin-like protein molecules embedded in a membrane (i.e., packed chromophores showing the same parallel orientation relative to the plane of the membrane surface). They can generate a proton motive force or current, thus controlling ion fluxes. The simplest photoreception system consists of a patch of these molecules in the plasma membrane (Type I). In the cases examined,[18] the density of packing of these molecules appears to be about 20,000 to 30,000 molecules/μm^2 of membrane, with a molar absorption coefficient ε of 40,000 to 60,000 M^{-1} cm^{-1} and a dark noise (see after) approximately equal to zero. The number of embedded molecules per μm^2 of membrane, the absorption cross section, and the dark noise are at the best of theoretical limits. Nevertheless, the fraction of photon absorbed from a single layer of these molecules is less than 0.05% (each layer contributes approximately 0.005 OD).

Let us calculate how many photons this simple but real photoreception system can absorb (Type I). On a sunny day, 10^{18} photons per square meter per second per nanometer are emitted by the sun; on a cloudy day, the number of photons lowers to 10^{17}.[19] This means that a photoreceptor of 1 μm^2 can catch at most 10^8 photons per second in its 100 nm absorbance window on the sunniest day. Considering absorption and reflection effects of water, we can correct this figure to 10^7 photons per second striking the photoreceptor surface.[19] Because only 0.05% of the incident radiation will be effectively absorbed by a single-layer photoreceptor, the amount of photons lowers to about 10^3 photons per second. In the case of microalgae, which often use "sequential sampling" (see after), the true signal consists of the number of photons absorbed by the photoreceptor when it is illuminated (for about 400 ms) minus the number of photons absorbed by the photoreceptor when it is shaded by a 50% screen (for about 600 ms). In the case of the sunniest day, the highest signal is about 100 photons per second, which lowers to about 10 photons per second on a cloudy day. Even on the sunniest day, the number of photons absorbed for detecting light direction is very low. Because this photoreceptor does not form any image but detects

only light intensity, this amount of photons is enough; however, this photoreceptor must possess a very low threshold and a very low or negligible dark noise. As a matter of fact, Schaller and coworkers[20] demonstrated that single photons induce transient direction changes and that fluence rates as low as 1 photon $cell^{-1}$ sec^{-1} can actually lead to a persistent orientation in *Chlamydomonas* (Chlorophyceae).

Strategies evolved to increase the sensitivity of a photoreceptor, such as stacking many pigment-containing membranes in the direction of the light path (*Euglena gracilis* is a wonderful example of such a solution) or exploiting the reflecting properties of the eyespot, as in *Chlamydomonas*[21,22] and in different species of dinoflagellates.[23] The effectiveness of the multilayer strategy was experimentally tested by researchers of the W.M. Keck Center of the Syracuse University (R.R. Birge, personal communication). The absorption value recorded on a preparation of precisely ordered bacteriorhodopsin multilayers was close to that recorded on the photoreceptor crystal of Euglena,[24] which consists of more than 100 layers of proteins.[25]

Noise

The ability to detect light is limited by noise.[26,27] Organisms must deal with noise of various kinds:

- Dark noise is the noise inherent in a receptor, constant and independent of light level. It arises from thermal and molecular noises.
- Photon noise (also known as shot noise) is due to the quantum nature of the light stimulus and to the resulting statistical fluctuation in the capture of a photon. This noise can be accurately estimated as the square root of the number of photons captured.
- Response noise leads to random variations in the locomotory response of the microorganism. Response noise can be further divided into motor noise, in which variations occur in locomotion from one time to another in an individual; and developmental noise, in which variations occur between individuals, as a bias to turn toward one side.
- Environmental noise consists of extraneous signals arising from sources other than those of the true signal.

In general, photoreceptors have a noise signal even in absence of a true signal. The problem is to decide whether or not a signal is present, when a given intensity is observed. In the simplest case, the problem becomes that of determining the threshold intensity upon which to make the decision. Usually, a situation is not so well defined that an optimal threshold intensity can be chosen, because the signal and noise distributions overlap. The degree of overlapping is measured by the signal-to-noise (S/N) ratio. Another complication is that the cost of missing a signal may be different from the cost of falsely concluding that a signal is present. For example, the cost of missing an alarm call may be death, whereas the cost of falsely sensing light is only a waste of time and energy. Because in the case of microalgae the cost of missing an alarm is negligible, the evolutive pressure lowered the probability of sensing a false signal.

Let us calculate the number of distinguishable intensities, **I**, in an algal photoreceptor in such a way as to relate intensity and noise.[28] The light stimulus that maximizes information transmission is intrinsically random and has a standard deviation of $\mathbf{S}_{sd}$. Then, if a photoreceptor has a noise level of $\mathbf{N}_{sd}$, the number of distinguishable intensity levels can be estimated. We assume that two intensity levels must differ by $2N_{sd}$ to be distinguishable, and this corresponds to approximately 95% reliability. Therefore, the number of distinguishable intensity levels is closely related to the ratio of the variances of the signal and noise, as in the following:

$$I \cong (1 + S_{sd}^2/N_{sd}^2)^{1/2}$$

In microalgae, the number of intensity levels is reduced to two (dark and light), so we can write:

$$S_{sd}/N_{sd} \cong 2$$

On the basis of this equation and, once calculated, the number of photons on the sunniest and cloudiest days, we can state that the simplest photoreceptor system of most microalgae could recognize light from

dark even on a cloudy day, but this is possible only if the dark noise is close to zero. In the case of higher levels of dark noise, such recognition is impossible, even on the sunniest days.

Direction

To determine the direction of a light source, a microalga must possess a light detector and a light screen to provide directional selectivity. Such a screen can be an absorbing element that prevents light coming from a certain direction from reaching the detector or a refractive element that focuses light onto the detector only from specific directions.[19]

Most bacteria (prokaryotes) are too small compared to the wavelength of light to create differential light intensity; hence, they cannot determine the direction of a light source. Still, these microorganisms can use light but can only measure its intensity and move in a light-intensity gradient. Gliding filamentous prokaryotes that move slowly can compare light intensity at different positions and make directed turns. In contrast, microalgae are large enough to determine light direction and move along a beam of light by scanning the environment with their directionally sensitive receptor as they rotate while swimming.

Guiding

To determine the orientation of a stimulus field, an organism has to measure the stimulus intensity at different positions. The two fundamental alternative strategies for obtaining information are as follows[19]:

1. Stimulus sampling by multiple separated receptors positioned on different parts of the organism surface — In this case, the organism directly measures the spatial gradient by comparing the intensities at different positions.
2. Sequential sampling by a single receptor that moves from one place to another — In this situation, the organism directly measures a temporal gradient, then infers the spatial gradient from the information on the movements of the receptor.

The simultaneous comparison of signals requires widely spaced receptors to detect intensity gradients, which makes large body size advantageous. On the other hand, sequential sampling requires a coherent pattern of movement, such as locomotion in a helical path. Sequential sampling also requires some form of memory to allow for comparison with previously recorded intensities.

Another fundamental distinction is based on whether an organism is able to make turns in its motion path, which will direct it toward its destination. Depending on the characteristics of the stimulus and the abilities of the microorganism, guiding may be direct, in the sense of taking a straight-line path to the destination, or indirect, as in the case of a biased random walk, to reach the vicinity of the destination.

Phototaxis is the behavior that involves orientation in response to light stimuli that carry the information. This behavior consists of a migration oriented with respect to the stimulus direction, which is established and maintained by direct turns. (Phototaxis is different from phototropism. Phototropism is frequently used for the behavior in which the organisms respond to the light with an oriented growth.) Photokinesis is the behavior that comprises undirected responses dependent on the intensity or temporal changes in intensity of the stimulus.

Trajectory Control

Control characteristics, and thus behavioral peculiarities, are connected with the functioning of the propelling structure of the cell.[14] If the cell is asymmetric, it advances spinning along its axis; it can correct its trajectory only by sudden steering obtained by changing the insertion angle of flagella. This behavior can be attributed to all heterokont (e.g., *Euglena*) or monocont microalgae. In the case of a symmetric cell, it can accomplish a gradual smooth correction of its trajectory going forward without spinning (or rotating for a long period), and displacing the baricenter of the motor couple. This behavior can be attributed to all isokont cells (e.g., *Chlamydomonas*).

121.5 Photoreceptive Proteins

Nature evolved a limited number of photoreceptive molecules in the different evolutionary branches of the tree of life because of the closely similar needs of organisms to detect the external world. Two photoreceptor molecules are considered as underlying "vision" in microalgae: rhodopsins and flavins.

Rhodopsins

These retinal-based proteins seem to be used by motile algae (in their vegetative and reproductive stages) as well as in the motile stages of sessile macroalgae, because they must respond rapidly on a time scale of milliseconds to seconds as environmental conditions change or as the organism changes position relative to its static surroundings. The photoreception systems based on rhodopsins are fast, hence, the intracellular response is immediately reset so that the system is prepared for a new light signal. Evidence for a retinal-based photoreceptor was reported in one lineage of prokaryotes (*Leptolyngbya* sp.,[29] *Anabaena* sp.,[30]) and in at least three lineages of eukaryotic algae (*Chlamydomonas* sp.,[31] *Dunaliella* sp.,[32] *Spermatozopsis* sp.,[33] *Volvox* sp.,[34] *Euglena* sp.,[35] *Ochromonas* sp.,[36] and *Silvetia* sp.[37]).

We will present, in detail, the case of *Euglena*. The investigations so far performed on this microalga led to conflicting results on the nature of its photoreceptor, leaving open the debate of flavin versus rhodopsin. The flagellate *Euglena gracilis* dwells in natural shallow ponds and uses sunlight as a source of energy and information. Its chloroplasts are the energy-supplying devices, whereas a simple but sophisticated system is used as a light detector. This system consists of a locomotory flagellum, a stigma, and a photoreceptor.[38–40] In general, as the cell rotates while swimming, the stigma comes between the light source and the photoreceptor, thus modulating the light that reaches it and regulating the steering of the locomotory flagellum. This configuration of stigma, photoreceptor, and flagellum can be considered a simple but complete visual system.

The photoreceptor, a three-dimensional proteic crystal, is composed of a stack of more than 100 crystalline sheets with a regular organization of component proteins. Fourier analysis suggests that the unit cells of proteic subunits within these sheets have a parallelogram shape. The dimensions of the monoclinic unit cell (or distorted hexagon, because , = 107°) of the sheet are about 50 Å × 40 Å. The layer seems to be constituted of the same protein, and the height of this integral membrane protein is about 70 Å. No other proteic structures or peripheral proteins could be seen between the layers.[25]

In 1989, Gualtieri and coworkers,[24] and subsequently in 1992, Crescitelli and coworkers,[41] measured the absorption spectrum of a single *Euglena* paraflagellar swelling. Due to the great similarity between these spectra and the absorption curve of rhodopsin ·-band centered around 510 nm, both research groups suggested a pigment based on a rhodopsin-like protein. Successive experiments on inhibition of the formation of the swelling and cellular photo-orientation by means of hydroxylamine and nicotine showed that retinal is the chromophore present in the photoreceptor.[42,43] The extraction of retinal from intact cells and from photoreceptors isolated from demembranated cells further strengthened the hypothesis of a rhodopsin-like protein.[35] The estimated number of proteins, on the basis of the number of retinal molecules and of photoreceptor integrated optical density, is about 10^7 molecules. In 1997, Barsanti and coworkers reported the presence of a photochromic pigment in the paraflagellar swelling of *Euglena gracilis*, which undergoes repeated and reversible fluorescence changes with a determinate kinetics.[44] According to these authors, the paraflagellar swelling possesses optical bistability, i.e., the nonfluorescent parent form (first conformer) of its molecules upon photoexcitation generates a fluorescent stable intermediate (second conformer) that can be photochemically driven back to the parent form. The quantum yields of the forward and reverse reactions are almost the same and close to unit.[44] In 2000, Barsanti et al.[45] isolated the photoreceptors of Euglena in very high yield (see Figure 1 in Barsanti et al.[45]) and performed the purification of the photoactive protein from this sample. Spectroscopically, the 27 kDa protein they obtained showed a well-defined absorption band centered around 510 nm. This spectrum can be superimposed on the *in vivo* absorption spectrum recorded on the photoreceptor by Gualtieri et al.[24] and by James et al.[41] and on the absorption spectrum of sensory rhodopsin II from *Natronobacterium pharaonis*.[46]

To confirm the hypothesis that the extracted protein was a rhodopsin-like protein, it was treated with hydroxylamine and sodium borohydride. The former is known to combine with retinal molecules released in the bleaching of rhodopsin or to displace the retinal from opsin to form oximes; the latter reacts rapidly with bleached rhodopsin in solution by reducing the retinylidene linkage. The effect of both compounds on the protein was comparable: both produced a dramatic fading of the absorption band centered around 510 nm. This clearly indicated that the chromophore is an aldehyde, possibly the extracted retinal. Moreover, the emission features of the native protein reproduced exactly the *in vivo* photoreceptor photocycle, with a nonfluorescent parent form and a green-fluorescent stable intermediate. All of these experimental data allowed Gualtieri's group to identify the crystalline paraflagellar swelling as the true rhodopsin-based photoreceptor of *Euglena gracilis*.

Flavoproteins

The proposition that these proteins could function as a near-UV-visible-light detector dates back more than 40 years. Despite the ubiquity and ancient origins of flavins, their role in acquiring information from the radiation environment still remains a complex area of study. Apart from difficulties in their identification, much of the reason for the lack of understanding lies in their diversity of function.

Most of the investigations to verify the presence of flavoproteins in microalgae were performed on the genus *Euglena*. The literature contains an extensive choice of papers on this argument, but we will limit our references to the most recent works. Häder and Lebert[47] reported a case of phototaxis reconstruction in *E. gracilis* strains with low flavin content by adding riboflavin and roseoflavin, the latter shifting the action spectrum to longer wavelength. Recently, Iseki et al.[48] biochemically characterized a new type of blue-light receptor flavoprotein, a photoactivated adenyl cyclase, in the photoreceptor organelle of *Euglena*. They concluded that this protein, with a molecular mass of 400,000 and FAD as prosthetic group, is the major constituent of the *Euglena* photoreceptor. It acts as photoreceptor for the step-up photophobic response (transition from dark to light), but it is not involved in the step-down photophobic response (transition from light to dark).

Even though the isolation procedure of Iseki and colleagues had a poor yield of paraflagellar bodies (see Figure 1 in Iseki et al.[48]), the authors were able to isolate and purify a 400K flavoprotein with a $(105K)_2(90K)_2$ heterotetrameric structure. By immunostaining *Euglena* cells with a polyclonal antibody against oligopeptides synthesized in accordance with the carboxyterminal sequence of the protein polypeptides, they localized the 105K subunit in the paraflagellar body. The purified flavoprotein was identified as a photoactivated adenylyl cyclase; this protein has no apparent transmembrane helices, does not possess a photocycle, and is not fluorescent under native conditions, because the fluorescence of the protein-bound flavin was quenched by the surrounding protein matrix. In our opinion, the protein isolated by Iseki et al. is not consistent with the ultrastructure characteristics[25] and the fluorescence behavior of *Euglena* photoreceptor,[44] which possesses a clearly detectable emission and undergoes an unquestionable photocycle.[44] Another fluorescent protein might therefore be present in this organelle to justify its fluorescence. The disappearance of the phobic response[48] may not necessarily mean that this protein is the light-detecting protein, because it could act as an amplification factor, as one of the segments of the phototactic response chain. This means that the photodetecting role could be assigned to another protein, and nothing prevents us from saying that this role may be played by the protein isolated by Barsanti et al.[45]

121.6 Methods for Studying Photoreceptor Proteins

Here, we briefly describe and compare spectroscopic and biochemical techniques that were used to define the light-absorbing properties of visual pigments, either *in vivo* (single cell or cell population) or *in vitro* (extracted material). To provide a clear perspective on the efficacy of different techniques as tools for the study of photoreceptive structures, a discussion of the pros and cons, the advantages and limitations, of each technique is included (see also Chapter 9).

Action Spectroscopy

Action spectroscopy represents the classic way to investigate photopigments. By means of action spectroscopy, the photosensitivity of a cell at different wavelengths can be measured, thus providing information on the nature of the pigments involved in photoreception[49] (see Chapters 1 and 4). It is still a common belief that this approach represents the only feasible way to study the photosensory pigments of a large number of species. However, direct measure of an action spectrum is much more difficult than that of an absorption spectrum. Moreover, action spectra may not be directly correlated with the absorption peaks of the pigments involved in photoreception, because light scattering can cause several errors.[50] When many pigments with similar absorption characteristics in the same visible range are present, action spectroscopy often fails to discriminate between them. Even when there is only one predominant pigment, it is not always possible to identify it. To obtain more reliable results, threshold action spectra should be preferred. They eliminate adaptation phenomena and screening modulation, limiting the utilization of action spectroscopy, which is limited to the study of changes or increases in the photosensitivity of a mutant cell, after the exogenous addition of a presumptive photoreceptor pigment the cell lacks.[51] It may be hasty to indicate the nature of a photoreceptor only on the basis of data obtained from action spectroscopy. This is especially true in the case of photoreceptors, such as rhodopsins, which have retinal as the chromophoric group. Retinal absorption can be fine-tuned by amino acid charges of the retinal pocket, which allows the entire spectrum between 360 and 635 nm to be covered.[52,53] Moreover, the presence or formation of photointermediates may shift the absorption maxima and make the interpretation of the action spectrum difficult.

Absorption and Fluorescence Microspectroscopy

These techniques do not disturb the integrity of the organism or subcellular components, and allow the examination of an uninjured system with its physiological functions intact [41,54]. The spectroscopic overshadowing of one pigment by another cannot occur since each pigment is packed in a different structure. Thus, cellular structures can be easily correlated with pigment type by direct observation. It is possible to make exact quantitative determinations of a) various reactions at the time of their occurrence in the sample, b) the progressive changes in these reactions, and c) their relationships to different conditions in the external medium [55]. Because of the fundamental connection between optical parameters and properties of molecular structures, microspectroscopy allows assessments of minute changes in the state of the molecules of various substances in the organism, the degree of their aggregation, and the interconversions of various forms of pigments and other important biochemical compounds with characteristic spectra. In many cases the lability and reversibility of such changes make microspectroscopy the only possible method of investigation. There is virtually no light scattering problem associated with microspectroscopic measurements, even if the analyzed structure has a dimension of one μm. Obviously, the absorption spectrum cannot provide adequate information about the photochemical action of photons as a function of their fundamental energy; however, the identification of the chromophores in the photoreceptive structures does provide information about possible mechanisms of energy transfer. The measurements are very difficult when small changes in absorption have to be measured in the presence of a strong total signal (luminous background), since photon noise is proportional to the square root of the intensity of the incident light. Then, fluorescence spectroscopy is recommended: it can achieve more reliable results compared to absorption spectroscopy, since the background emission is much reduced. In this case the sensitivity of detection is not limited by the signal-to-noise ratio, but rather by the presence, virtually unavoidable, of fluorescent contaminants [55,56].

Biochemical and Spectroscopic Study of Extracted Visual Pigments

Extraction of visual pigments (chromophore and/or protein), either by means of detergents such as digitonin and Triton [57], or by organic solvents, could be the best method for providing large quantities of photoreceptive pigments in an accessible "*in vitro*" form for subsequent detailed biochemical analysis.

Such samples allow a very accurate determination of spectroscopic parameters. Spectroscopy of solubilized pigment may be complicated, however, by the simultaneous extraction of several other pigments in the cell, which cause distortion of absolute spectra and necessitate special procedures of purification. These problems can be solved by separating the different pigments after extraction, e.g., by High Performance Liquid Chromatography (HPLC) and final identification with Gas Chromatograpy - Mass Spectrography (GC-MS) for chromophores [58], or affinity chromatography for proteins [59]. Since the pigment extraction permanently removes the identifying link to a particular cell structure and may change the spectroscopic properties of a receptor because native interactions are disrupted, these detrimental factors mandate a careful evaluation of the results obtained by this method.

Molecular Biology Investigations

DNA hybridization is useful in attempting to determine phylogenetic interrelationship between species. The rationale is that similarities between DNA structure correlate to interrelatedness. It is used to detect and isolate specific sequences and to measure the extent of homology between nucleic acids [60]. It represents an alternative to the study of visual pigments at the protein level, since the genes encoding these proteins can be identified, their sequences determined, and the comparative genetic information assessed. Genomic Southern blot hybridization is used to probe the genomes of a variety of species in a manner analogous to that reported for other protein families. The potential for using bovine rhodopsin opsin complementary DNA (cDNA) probe to identify homologous genes in other species was demonstrated by Martin et al. [61]. These authors identified coding regions of bovine opsin that are homologous with visual pigment genes of vertebrate, invertebrate, and phototactic unicellular species. Successful application of this method requires closely homologous genes, and in general additional criteria, such as protein sequence information, is desirable for eliminating false positives on Southern blots. A molecular biology approach has been used also by Sineshchekov et al. [62] in *Chlamydomonas*. These authors identified gene fragments with homology to the archaeal rhodopsin apoprotein genes in the expressed sequence-tag data bank of *C. reinhardtii*. Two quite similar genes were identified having almost all the residues in the retinal-binding site of bacteriorhodopsin. The authors suspected that these genes were related to the putative retinal-based pigments already suggested for *Chlamydomonas* [63].

However, to show that the pigments are a part of the genuine signaling system, ideally one would like to delete each gene by using homologous recombination, but it is not easy to do such gene knockouts in any algal species. The problem can be overcome partially by using RNA interference (RNAi) technology to preferentially suppress the synthesis of the pigments to convincingly show that the pigment is a genuine segment of the algal phototactic response.

121.7 Concluding Remark

Understanding the molecular mechanism used by algal cells to "see the light," as we have tried to explain, is a very difficult task. At least a century has been wasted without any success. It is discouraging to think that even if the algae are not as intelligent as men are, they have "understood" very well how to orientate themselves in their light environment, and do it very efficiently. Maybe the compass mechanism they use is too simple for our complex brain…

References

1. Hegemann, P., Algal sensory photoreceptors, J. Phycol., 37, 668, 2001.
2. Norton T.A., Andersen R.A. and Melkonian, M., Algal Biodiversity, *Phycologia* 35, 308, 1996.
3. Andersen, R.A., Algae, in Maintaining Cultures for Biotechnology and Industry, Hunter-Cevera, J.C. and Belt, A., Eds., Academic Press, San Diego, 1996, 29.
4. Doolittle R.F., Molecular evolution: computer analysis of protein and nucleid acid sequences, *Methods in Enzymology, vol.* 183, Academic Press, Inc., San Diego, California, 1990.

5. Woese, C.R., Kandler, O., and Wheelis, M.L., Towards a natural system of organisms: proposal for the domains Archaea, Bacteria, and Eucarya, *Proc. Natl. Acad. Sci. USA*, 87, 4576, 1990.
6. Van de Hoeck, C., Mann, D., Jahns, H.M., *An Introduction to Phycology.* Cambridge University Press, Cambridge, 1994.
7. Cavalier-Smith, T., The origin of eukaryotes and archaebacterial cells, *Ann. New York Acad. Sci.,* 503, 17, 1987.
8. Margulis, L., *Origin of eukaryotic cell,* Yale University Press, New Haven, 1970.
9. Dodge, J., The phytoflagellates: Fine structure and phylogeny, in *Biochemistry and Physiology of protozoa,* Levandosky, M. and Hutner, S.H., Eds., Academic Press, New York, 1979, chap.2.
10. Gunderson, J. H., Elwood, H., Ingold, A., Kindle, K., and Sogin, M.L., Phylogenetic relationship between chlorophytes, chrysophytes, and oomycetes, *Proc. Natl. Acad. Sci.* USA, 84, 5823, 1987.
11. Metting, F.B., Biodiversity and application of microalgae, *J. Ind. Microbiol.*, 17, 477, 1996.
12. Moenstrup, O., Flagellar structure in algae: a review, with new observation particularly on the Chrisophyceace, Phaeophyceae, Euglenophyceae, and Reckertia, Phycologia, 21, 427, 1982.
13. Bold, H.C., and Wynne, M.J., *Introduction to the algae*, 2th ed., Prentice-Hall Inc., Englewood Cliffs, New Jersey, 1985.
14. Omodeo, P., The photoreceptive apparatus of flagellated algal cells, in *Photoreceptor and Sensory Transduction in Aneural Organisms,* Lenci F., and Colombetti, G., Eds., Plenum Press, New York, 1980, 127.
15. Dodge, J., Photosensory systems in eukaryotic algae, in *Evolution of the Eye and Visual System,* Cronly-Dillon, J.R., and Gregory, R.L., Eds., Macmillan Press, London, 1991, chap. 15.
16. Gualtieri, P., Morphology of photoreceptor systems in microalgae, *Micron*, 32, 411, 2001.
17. Walne, P.L., and Gualtieri, P., Algal Visual Proteins: An Evolutionary Point of View, *Crit. Rev. Plant Sci.,* 13, 185, 1994.
18. Krebs, W., and Kuhn, H., Structure of isolated bovine rod outer segment membrane, *Exp. Cell. Res.*, 25, 511, 1977.
19. Dusenbery, D.B., *Sensory Ecology.* Freeman, New York, 1992.
20. Schaller, K. David, R., and Uhl, R., How *Chlamydomonas* keeps track of the light once it has reached the right phototactic orientation, *Biophys.J.,*73, 1562, 1997.
21. Kreimer, G., and Melkonian, M., Reflection confocal laser scanning microscope of eyespot in flagellated green algae, *Eur.J. Cell Biol.,* 53, 101, 1990.
22. Schaller, K., and Uhl, R., A Microspectrophotometric study of the shielding proprieties of eyspot and cell body in *Chlamydomonas, Biophys.J.*,73, 1573, 1997.
23. Kreimer, G., Reflective proprierties of different eyespot types in dinoflagellates, *Protist,* 150, 311, 1999.
24. Gualtieri, P., Barsanti, L., and Passarelli, V., Absorption spectrum of a single isolated paraflagellar swelling of *Euglena gracilis*, *Biochim. Biophys. Acta*, 993, 293, 1989.
25. Walne, P.L., Passarelli, V., Barsanti, L., and Gualtieri, P., Rhodopsin: a photopigment for phototaxis in Euglena gracilis, *Crit. Rev. Plant Sci.,* 17, 559, 1998.
26. Barlow, H.B., The physical limits of visual discrimination, in *Photophysiology*, Giese A., Ed., Academic Press, 1964, 84.
27. Aho, A.C., Donner, K., Hyden, C., Larsen, L.O., and Reuter, T., Low retinal noise in animals with low body temperature allows high visual sensitivity, *Nature*, 334, 348, 1988.
28. Snyder, A.W. Laughlin, S.B. and Stavenga, D.G., Information capacity of eyes, *Vision Res.,* 17, 1163, 1977.
29. Albertano, P., Barsanti, L., Passarelli, V., and Gualtieri, P., A complex photoreceptive structure in the cyanobacterium *Leptolyngbya* sp., *Micron*, 31, 27, 2000.
30. Jung, K.-H., and Spudich, J., Microbial rhodopsins: transport and sensory proteins throughout the three domains of life, in *CRC Handbook of Organic Photochemistry and Photobiology*, Horspool, W.M., and Lenci, F., Eds., CRC Press, Inc., Boca Raton, 2002, chap. 13.

31. Deininger, W., Kroger, P., Hegemann, U., Lottspeich, F., and Hegemann, P., Chlamyrhodopsin represents a new type of sensory photoreceptor, *The EMBO Journal*, 14, 5849, 1995.
32. Wayne, R., Kadota, A., Watanabe, M., and Furuya, M., Photomovement in *Dunaliella salina*: fluence rate-response curves and action spectra, *Planta*, 184, 515, 1991.
33. Kreimer, G., Marner, F.J., Brohsonn, U., Melkonian M., Identification of 11-cis and all-trans-retinal in the photoreceptive organelle of a flagellate green alga, *FEBS Letters*, 293, 49, 1991.
34. Ebnet, E., Fischer, M., Deininger, W., and Hegemann, P., Volvoxrhodopsin, a light-regulated sensory photoreceptor of the spheroidal green alga *Volvox carteri*, *The Plant Cell*, 11, 1473, 1999.
35. Gualtieri, P., Pelosi, P., Passarelli, V., and Barsanti, L., Identification of a rhodopsin photoreceptor in *Euglena gracilis*, *Biochim. Biophys. Acta,* 1117, 55, 1992.
36. Walne, P.L., Passarelli, V., Lenzi, P., Barsanti, L., and Gualtieri, P., Isolation of the flagellar swelling and identification of retinal in the phototactic flagellate *Ochromonas danica* (Chrysophyceae), *J. Euk. Microbiol.*, 42, 7, 1995.
37. Gualtieri, P., and Robinson, K.R., A rhodopsin-like protein in the plasma membrane of *Silvetia compressa* eggs, *Photochem. Photobiol.*, 75, 76, 2002.
38. Gualtieri, P., Barsanti, L., Passarelli, V., Verni, F., and Rosati, G., A look into the reservoir of *Euglena*: SEM investigation of the flagellar apparatus, *Micron Microscop. Acta*, 21, 131, 1990.
39. Rosati, G., Verni, F., Barsanti, L., Passarelli, V., and Gualtieri, P., Ultrastructure of the apical zone of *Euglena gracilis*: photoreceptors and motor apparatus, *Electron Microsc. Rev.*, 4, 319, 1991.
40. Verni, F., Rosati, G., Lenzi, P., Barsanti, L., Passarelli, V., and Gualtieri, P., Morphological relationship between paraflagellar swelling and paraxial rod in *Euglena gracilis*, *Micron Microscop. Acta, 23, 37, 1992.*
41. James, T.W., Crescitelli, F., Loew, E.R., and McFarland, W.N., The eyespot of *Euglena gracilis*: a microspectrophotometric study, *Vision Res.,* 32, 1583, 1992.
42. Barsanti, L., Passarelli, V., Lenzi, P., and Gualtieri, P., Elimination of photoreceptor (paraflagellar swelling) and the photoreception in *Euglena gracilis* by means of the carotenoid biosynthesis inhibitor nicotine, *J. Photochem. Photobiol.*, 13, 135, 1992.
43. Barsanti, L., Passarelli, V., Lenzi, P., Walne, P.L., Dunlap, J. R., and Gualtieri, P., Effects of hydroxylamine, digitonin and Triton X-100 on photoreceptor (paraflagellar swelling) and photoreception of *Euglena gracilis*, *Vision Res.*, 33, 2043, 1993.
44. Barsanti, V., Passarelli, V., Walne, P.L., and Gualtieri, P., In vivo photocycle of the *Euglena gracilis* photoreceptor, *Biophys.J.*, 72, 545, 1997.
45. Barsanti, L., Passarelli, V., Walne, P.L., and Gualtieri, P., The photoreceptor protein of *Euglena gracilis*, *FEBS Letters*, 482, 247, 2000.
46. Scharf, B., Pevec, B., Hess, B., and Engelhard, M., Blue halorhodospin from *Natronobacterium pharaonis*: wavelength regulation by anions, Eur.J. Biochem., 206, 359, 1992.
47. Häder, D.-P., and Lebert, M., The photoreceptor of phototaxis in the photosynthetic falgellate *Euglena gracilis*, *Photochem. Photobiol.*, 68, 260, 1998.
48. Iseki, M., Matsunaga, S., Murakami, A., Ohno, K., Shiga, K., Yoshida, K., Sugai, M., Takahashi, T., Hori, T., and Watanabe, M., A blue-light-activated adenylyl cyclase mediates photoavoidance in *Euglena gracilis*, *Nature*, 415, 1047, 2002.
49. Lipson, E., Action spectroscopy, in *Biophysics of Photoreceptors and Photomovements in Microorganisms*, Lenci, F., Ghetti, F., Colombetti, G., Häder, D.-P., and Song, P.-S., Eds., Plenum Press, New Colombetti, G., Häder, D.-P., and Song, P.-S., Eds., Plenum Press, New York, 1991, 293.
50. Latimer, P., Apparent shifts of absorption bands of cell suspension and selective light scattering, *Science*, 127, 29, 1957.
51. Hegemann.P., Hegemann, U., and Foster, K.W., Reversible bleaching of *Chlamydomonas reinhardtii* rhodopsin in vivo, *Photochem. Photobiol.*, 48, 123, 1988.
52. Nathans, J. Determinants of visual pigment absorbance: role of charged amino acids in the putative transmembrane segment. *Biochem.* 29, 937–942, 1990.

53. Kochendoerfer, G., Lin, S.W., Sakmar, T.P., and Mathies, R.A., How color vision proteins are tuned, *TIBS*, 24, 300, 1999.
54. Strother, G.K. and Wolken, J.J. In vivo absorption spectra of *Euglena*: chloroplast and eyespot.*J. Protozool.*, 8, 261, 1961.
55. Gualtieri, P. Microspectroscopy of photoreceptor pigments in flagellated algae. *Critical Rev. Plant Sci.*, 9, 6, 474–495, 1991.
56. Gualtieri, P. Molecular biology by means of digital microscopy. *Micron and Microsc. Acta*, 23, 239–257, 1992.
57. Fong, S.L., Tsin, A.T. C., Bridges, C.D. B., and Liou, G.I. Detergents for extraction of visual pigments: types, solubilization and stability, in *Methods in Enzymology*, 81, Biomembranes, part H, Packer, L., Ed., Academic Press, 1982, 133–140.
58. Foster, R.G., Garcia-Fernandez, G.M. Provencio, I., and DeGrip, W.J. Opsin localization and chromophore retinoids identified within the basal brain of the lizard *Anolis carolinensis.J. Comp. Physiol.* A, 33–45, 1993.
59. Litman, B.L. Purification of Rhodopsin by concanavalin A affinity chromatography, in *Methods in Enzymology*, 81, Biomembranes, part H, Packer, L., Ed., Academic Press, 1982, 150–153.
60. Krebs, M.P., Spudich.E. N., Khorana., H.G., and Spudich.J.L. Synthesis of a gene for sensory rhodopsin I and its functional expression in *Halobacterium halobium*. *Proc. Natl. Acad. Sci.* USA, 90, 3486–3490, 1993.
61. Martin, R.L, Wood, C., Baehr, W., and Applebury, M. Visual pigment homologies revealed by DNA hybridization. *Science* 232, 1266–1269, 1986.
62. Sineshchekov, O.A., Jung, K.-H., and Spudich, J.L., Two rhodopsins mediate phototaxis to low- and high-intensity light in Chalmydomonas reinhardtii, PNAS, 99, 8689, 2002.
63. Sineshchekov, O.A., and Govorunova, e.g., Rhodopsin-mediated photosensing in green flagellated algae, *Trends Plant Sci.*, 4, 58, 1999.

122

Photomovements in Ciliates

Roberto Marangoni
Istituto di BioFisica CNR

Sabina Lucia
Istituto di BioFisica CNR

Giuliano Colombetti
Istituto di BioFisica CNR

122.1 Introduction

Ciliates are one of the most important components of the food chain on our planet: they constitute, in fact, a relevant fraction of the total microzooplankton and represent the main food of zooplankton and higher aquatic organisms.[1] Along evolution, ciliates (and protozoa in general) discovered and occupied new ecological niches (acting as primary and secondary consumers) and became the link between the *microbial loop* (the food chain in the microscopic world) and the *macrobial loop* (the chain involving higher organisms), because they are the preferred food of the larval stages of fishes, crustaceans. This was exploited in water culture systems for fishes and other organisms. Ciliates (and protozoa in general) represent the connecting ring through which energy and organic matter produced by the primary producers are transferred to secondary consumers.[3]

Ciliates are diffused everywhere in the world and have colonized almost all aquatic environments: from freshwaters to salt marshes, from the sea to lagoons and other hypersaline or saltish ponds. They can even be found in soil. Their contribution to the ecology of the planet is fundamental; for instance, being natural predators of flagellated algae and bacteria, they are often able to stop the exponential growth of these organisms.

The evolutionary success of ciliates is a direct consequence of their high plasticity and adaptation capability. In fact, ciliates are often much more complex than cells of pluricellular organisms, which are, on the other hand, more specialized.

The integration of these organisms in their environment is remarkable, as shown by their enhanced capability to perceive and react to external physical (light, temperature, pressure, etc.) and chemical (such as food attractants) stimuli. This allows them to explore the environment searching for the best conditions for survival, be it looking for food or avoiding potentially harmful situations.

Ciliates integrated in the same cell many different functions that in higher organisms are carried out by different cells; they can, in fact, perceive simultaneously different stimuli, elaborate them, and respond

0-8493-1348-1/04/$0.00+$1.50

with a suitable motile reaction. This integration capability has prompted some to call ciliates "walking neurons."

Among the environmental stimuli, light certainly is one of the most important. After all, almost all living species evolved in a world dominated by light. It is somehow intriguing, however, to understand why ciliates evolved the capability of altering their motion in response to luminous stimuli. In fact, different from some bacterial species or from green algae, they cannot use light as a source of energy. They can, however, use light as a source of information; in some cases, this is used to avoid harmful light levels; in other cases, this can tell them where a photosynthetic prey is more likely to be found. The study of photomotile reactions of ciliates is, therefore, quite useful for obtaining clues on the functioning of ecological systems.

The investigation of the photomotile responses in these organisms requires careful attention; many stimuli, in fact, are often present at the same time, so that it is necessary to be able to isolate the response relative to only one stimulus, and rule out the contribution of others. In the study of photomotile reactions, this is usually done by trying to keep under control, as much as possible, all the environmental conditions (temperature, pH, chemicals) and by varying the characteristics of light (fluence rate, spectral composition, polarization) at will.

In the present section, we will start by describing the different types of photomotile responses in ciliates, then we will move on to a short description of the photoreceptor organelles and will consider in some detail phototaxis and possible light-tracking mechanisms. We will then briefly consider the main experimental techniques used in this field of research and will discuss some aspects of the photosensory transduction chain (for a general introduction, see Chapter 9). At the end of this chapter, we will give a somewhat more detailed description of the state of the art of our knowledge on two case studies, that were investigated by our research group in the last years.

122.2 Photomotile Responses

There is general consensus that photomotile responses can be divided into three main types[4,5]:

- *Photokinesis*, where the average speed of microorganisms is affected by light exposure
- *Photophobic reactions*, where the microorganisms perform an avoiding reaction when the ambient light intensity suddenly increases (*step-up photophobic response*) or decreases (*step-down photophobic response*)
- *Phototaxis*, where a microorganism exposed to unidirectional light orients its motion toward (positive phototaxis) or away from (negative phototaxis) the light source

Some further classifications can be used, for example, *diaphototaxis* (i.e., the orientation orthogonal to light direction) shown by *Urotricha* sp.,[6] but we will not consider them further in what follows.

As we have seen above, photomotile responses in ciliates are not easily understood from an evolutionary and adaptive point of view, they are complex and often vary with the stage of the life cycle or with the degree of starvation. Among photomotile responses, the most interesting, for its implication from an evolutionary and adaptative point of view, is surely phototaxis, because it controls the movement of cell populations in the water column and across large areas of the oceans. Photomovements can contribute to cell survival, because, even if ciliates are not photosynthetic, their preferred food is often constituted by algae or other photosynthetic organisms that move to illuminated regions; therefore, the capability of tracking light for a ciliate can be useful to track food.

The sensitivity to light varies considerably among ciliates: some ciliates do not respond to light or perform only photophobic reactions but not phototaxis; some others are phototactically responsive only during a particular phase of their life cycle, or they are responsive only when starved but not after food uptake. An interesting correlation exists between phylogenetic relationships, photomotile behavior, and the ultrastructural photoreceptive elements: phylogenetical clusters of ciliates often show similar photobehavior.[7]

Many ciliates have life cycles formed by several different stages, in which they can change cell shape and functions. Some of these stages, such as cysts, are defensive and are entered only when the surrounding environment changes toward unfavorable conditions. In these stages, ciliates transform into much simpler cells, in which subcellular organelles or ultrastructural elements seems to be "packed" or, sometimes, disappear: cilia are suppressed, and the cell shows, of course, no motile responses in this stage.

Besides defensive stages, there are other stages in which the ciliate can be photoresponsive or not. For example, the ciliate *O. flava*, which we will discuss in detail later, shows a strong positive phototactic response during the stage of *theront*, when the cell is starved; while in the stage of *trophont* (immediately after food uptake), it shows no photoresponsiveness.

It is apparent, therefore, that the investigation of the photomotile reactions in ciliates is often strictly related to their stage in the life cycle, besides being strongly affected by the environmental conditions; the results obtained in a system can, thus, hardly be generalized.

Photoreceptor Organelles

Photoresponsive ciliates have a large variety of photoreceptor structures. In some cases, there is no apparent organelle dedicated to light detection. In other cases, stigma-like structures may be present, and in a few cases, more complex structures are found, as in *Porpostoma notatum*, which bears a composed crystalline organelle,[8] or in all species of the genus *Ophryoglena*, which possess a watchglass organelle, called Lieberkühn organelle.[7]

Among the photoresponsive ciliates that do not seem to have specialized photoreceptor organelles, there is *Paramecium bursaria* that is transparent, and when *Chlorella* deprived, it shows "*in vivo*" no detectable candidate pigment, as determined by microspectrophotometry or microfluorometry. Even if there is strong evidence in favor of the presence of a rhodopsin-like photoreceptor pigment,[9,10] no strong indication has been found on a possible spatial arrangement of it that could justify the existence of a directional antenna. Rhodopsin-like pigment is, in fact, localized on the cell cilia and on the ventral part of the cell body.[10] In the marine heterotrich ciliate *Fabrea salina*, there are two candidate photopigments, a rhodopsin-like molecule localized on the cell membrane, and a hypericin-like molecule localized in pigment granules that are just below the cell membrane and in certain cases in conjunction with it. Both molecules can be responsible for the photoresponses of this ciliate (positive phototaxis and photophobic step-down reaction), but both are uniformly diffused, and no proper photoreceptor organelle can be detected. Shown in Figure 122.1 is the structure of such pigment granules, with detail that shows the intimate junction between the granule and the cell membrane, which can suggest a functional meaning. Similar structures can also be found in *Blepharisma japonicum* and *Stentor coeruleus.*[11,12]

Other ciliates, like *Chlamydodon mnemosyne* and *Nassula citrea,* show the presence of a stigma-like organelle, made by a cluster of colored vesicles.[13] Its function as photoreceptive organelle is, however, dubious, because cells that possess a low amount of these vesicles are still capable, in certain cases, of performing phototaxis.[7] Probably, similar to what happens in flagellated algae, the stigma-like structure is not the photoreceptor proper, but acts, more likely, as a screening device that may help orient cells toward light.

A typical representative of ciliates possessing watchglass organelles is *Ophryoglena flava* (Figure 122.2), which will be treated in detail in the last section of this chapter. Behavioral experiments showed that the Lieberkühn organelle is involved in tracking light direction,[13] but its role and the orientation mechanism are still debated. The removal of this organelle from the cells, in fact, causes a significant, but not total, reduction of the phototactic responsiveness of the cells that recover their phototactic activity within 24 h, a time period that is long enough for a new Lieberkühn organelle to form.

The ciliate *Porpostoma notatum* belongs to the group of ciliates bearing complex photoreceptive organelle composed by alternate layers of cytoplasm and flattened crystals. This kind of receptor reminds the structure of a quarter-wave optical reflector, described in the stigma of some flagellated algae, such as *Chlamydomonas reinhardtii.*[14,15] In this alga, it was suggested that the stigma may be involved in the

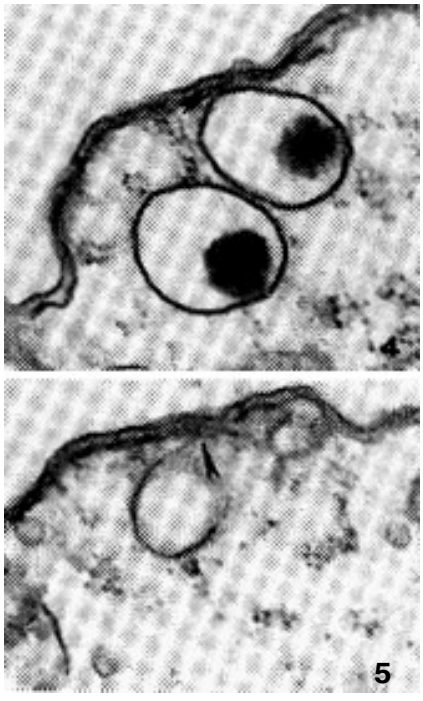

FIGURE 122.1 Pigment granules in *Fabrea salina*, and, below, a detail of the intimate association of them with the cell membrane.

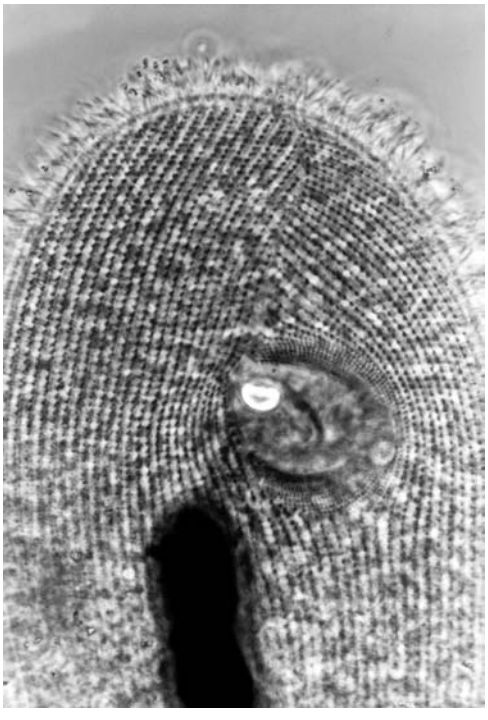

FIGURE 122.2 Detail of the Lieberkün organelle in *Ophryoglena flava*.

orientation of cells toward light. This is based upon calculations of the amount of light reflected by the quarter-wave structure on the photoreceptor that depends on the orientation of the cell body with respect to unilateral light; this, together with the helical swimming of the cells, gives rise to a directional detector.

Light-Tracking Strategies

The word "phototaxis" usually indicates the following:

- From a "sensorial" point of view, the perception of the light propagation vector
- From a "motile" point of view, the capability to actively orient cell swimming with respect to light direction

These two definitions are apparently equivalent, but this requires a more thorough consideration. There are orientation strategies in which the cells use the light propagation vector as input but do not actively control the swimming direction. A possible approach to this problem is to model the swimming behavior of microorganisms as a random walk. In such a model, the trajectories described by the cells can often be simply approximated by using straight-line segments connected together. Three independent variables can completely describe the motile behavior of such models: cell speed, frequency of directional changes, and distribution of the angles of directional changes (i.e., the probability to choose a defined angle at each directional change). By setting the parameters in a suitable way, a simple computer program can easily generate tracks that are similar to the real ones. In these conditions, the simulated cells move randomly and uniformly along all possible directions. Phototaxis can be simply simulated by introducing a directional anisotropy in one of these parameters:

- If the bias is set on speed, the cells will move *rapidly* only when they are swimming along certain defined directions.
- If the bias is set on frequency of directional changes, the cells will *hold* a defined direction once they have found it by chance.
- If the bias is set on the distribution of the angles of directional changes, the cells will *choose*, at each step, angles that reduce the angular distance between the swimming direction and the light direction; this can be considered as the true, active, orientation mechanism.

These three mechanisms lead to an orientation of the trajectories of the cells with respect to light direction and, in all cases, light direction represents the input signal. With respect to the definitions given in the literature, only the last mechanism should be called phototaxis, while the others are usually known as photokinesis and klinokinesis, respectively. In practice, it is difficult to distinguish experimentally the parameter primarily involved in the orientation mechanism. There are, in fact, some experimental problems and sources of noise that can make it difficult to decide if one is dealing with a "true" phototaxis or not:

- The finite dimensions of the experimental chamber that can greatly influence the swimming of the cells
- The finite (and often low) number of cells present in the experimental sample
- The limited possibility of exactly reconstructing single cell trajectories for a sufficient time — this is essentially due to technical problems: the experimental techniques currently used to track cells do it for a time too short to have statistical significance; sometimes, they are unable to always follow the same cell, so that what appears to be a single trajectory is actually the summation of the trajectories described by different cells
- The image digitalization, which transforms continuous trajectories into discrete ones; the choice of the frequency of spatial sampling is of fundamental importance for the measurement of the random walk parameters that strongly depend on it

Because of these difficulties, the problem of the orientation mechanism has been studied only in a theoretical way, but with few practical applications. In a work of Marangoni et al.,[16] the problem of

orientation strategy was discussed in terms of biased random walk, with a practical application to the phototaxis of the marine ciliate *Fabrea salina*. In this work, the authors, starting from the experimental result that this ciliate did not show photokinesis, studied two possible orientation models: in one (M1), the cells are able to correct their swimming direction; in the second model (M2), the cells can only vary the frequency of directional changes, locking their swimming to light direction, once it has been found by chance. By means of computer simulations, the authors generated virtual populations of cells that used the M1 or M2 orientation models: the response of these simulated populations to unidirectional light was determined, in order to detect possible different macroscopic behaviors. The authors proved that, depending on the orientation parameter chosen, these two models have different macroscopic behaviors, even though they produce similar simulated single cell trajectories. Comparison with the experiments suggested that *F. salina* performs phototaxis using an M2 mechanism. This conclusion was confirmed by other studies, where real single cell trajectories were analyzed (Marangoni et al., in preparation). It is not easy to conclude if the phototactic response of *F. salina* is a "true" phototaxis or a klinokinesis: polarograms (i.e., the distribution of the cells' fraction moving along a direction) measured during a phototaxis experiment are significant, but this protozoa seems to be unable to actively modify the swimming direction; on the contrary, it is more reasonable that it decreases the frequency of directional changes once it is already swimming in a direction close to that of light. Preliminary measurements on the freshwater ciliate *O. flava* seem to show, on the contrary, that this ciliate is capable of actively orienting toward the light source.

These different behaviors might result from the different ultrastructural organizations of the photoperceptive organelle. The existence in *O. flava* of a specific watchglass organelle, which can act as directional antenna, may confer to this organism a direction control system. On the contrary, *F. salina* does not have any oriented structure (see above), and it is, therefore, unable to actively change its swimming direction. In this case, we can hypothesize that the cell body shape, which is not symmetric, could be responsible for the motion directionality under unilateral illumination.

Further studies are being carried on to clarify this point and to better understand the phototactic orientation mechanisms in ciliates.

122.3 Experimental Techniques

Action spectra determination has certainly been one of the most used approaches to gain hints as to the nature of the photoreceptor pigments involved in the photomotile response (see Chapters 112 and 115). To put it schematically, an action spectrum is a measure of the relative effectiveness of the different wavelengths in inducing the desired photoresponse. A thorough discussion of the theory underlying action spectra determination[17–20] goes beyond the purpose of this chapter, and therefore, we will limit ourselves to a short discussion of the meaningfulness of the results that this methodology can give.

Let us assume that after absorption of a photon of light the photoreceptor pigment P undergoes a series of dark reactions, say,

$$P \xrightarrow{h\nu} P^* \xrightarrow{k_1} P_1 \xrightarrow{k_2} \ldots\ldots \xrightarrow{k_i} P_i \xrightarrow{k_j} P_j \longrightarrow \ldots$$

if P_j is the signaling state for the photoresponse, its concentration will be directly related to the intensity of the response. In its turn, P_j depends on the number of P molecules that underwent the expected photoreactions (say, a photoisomerization) and from the constants of the various dark reactions. For a mole of pigment, the rate constant k_1 of the primary photoreaction, $P^* \rightarrow P_1$, depends on the light fluence rate, on the molar extinction coefficient of P, ε, and on the quantum efficiency ϕ of the phototransformation, so that $k_{1\lambda} = I \cdot \varepsilon_\lambda \cdot \phi_\lambda$, where ε and ϕ depend on the energy of the impinging photon. If the ks are the same at two different wavelengths λ, then the amounts of the signaling state P_j will also be equal, and consequently, the same will hold for the measured photoresponses. If the quantum efficiencies do not strongly depend on λ, we have that $k_{\lambda a} = k_{\lambda b}$ or $R_{\lambda a} = R_{\lambda b} \Rightarrow \varepsilon_{\lambda a}:\varepsilon_{\lambda b} = 1/F_{\lambda a}:1/F_{\lambda b}$, where R represents

the measured photoresponse. To say it in different words, if a certain wavelength λ_a is more effective than another λ_b, a lower number of photons at λ_a than at λ_b will be needed to elicit the same response *R*. This is the main conclusion of a simplified theory of action spectra, which only holds if certain requirements are fulfilled. The first requirement is that the signaling state be formed from *P* according to the scheme given above. If, on the contrary, P_j is formed, as shown in the scheme,

$$P \xrightarrow{h\nu} P^* \xrightarrow{k_1} P_1 \xrightarrow{k_2} \ldots\ldots \xrightarrow{k_i} P_i \xrightarrow{h\nu} P_i^* \xrightarrow{k_j} P_j \longrightarrow \ldots.$$

by light absorption of one of the intermediates, say P_i, then its amount will not only depend on k_1 but also on k_j, and subsequently, the action spectrum will reflect the absorption properties of both forms and will be limited to the spectral region where both species absorb.

Further requirements are that λ-dependent light scattering must be small, and that shading effects between the photoreceptor pigments be negligible.

When all these conditions are verified, an action spectrum gives useful information on the *in vivo* absorption spectrum of the photoreceptor pigment. This spectrum is then compared to known absorption spectra of photoreceptor pigments in a database, and conclusions can then be drawn on the nature of the molecules involved. An unambiguous identification of a photoreceptor pigment, however, cannot normally be obtained by relying only on action spectra determination, and other experimental evidence is required, such as pigment isolation and characterization, possibly accompanied by gene isolation and cloning.

If the photoreceptor pigment is localized, as is the case in Euglena, microspectrophotometry can give reliable information on its nature.[21] If the pigment is fluorescent, steady state and time-resolved spectrofluorometry and microspectrofluorometry can help in getting hints on its chemical structure and on possible de-excitation pathways.[22,23] Microfluorescence and confocal microscopy can be used to reveal the pigment location in the cell, even if the pigment is not fluorescent, by linking it to fluorescent antibodies, as done, for instance, in *Paramecium bursaria*[11] and in *Fabrea salina*.[22] Fluorescent antibodies can also be used for immunoblotting or immunocytochemistry to identify the photoreceptor molecules or other components of the sensory transduction chain.[11,24] The high spatial resolution of electron microscopy allowed detailed investigation of the structure of the pigment granules in *Stentor*,[11] Blepharisma,[12] and *Fabrea*,[25] while the chemical structure of blepharismin, the chromophore of *B. japonicum*, was determined by NMR.[26]

Molecular biology has been hardly utilized in this field of study in ciliates, but the genome sequences of some ciliates should soon be available. This could make it possible to search them for the presence of putative photoreceptor genes and, as already done for some flagellates, to try to express these genes in bacteria and to study the spectroscopic and biochemical properties of the proteins for which they code. Another, more interesting, possibility might be to block the synthesis of this pigment *in vivo* (for instance, by means of the RNAi technique[27]) and to study the light response in cells thus modified.

122.4 Photosensory Transduction Chain

Photoreceptor Pigments

The identification and isolation of the photoreceptor pigments in ciliates is still an open problem; in a few cases, in particular in some heterotrichs such as *Stentor coeruleus* and *Blepharisma japonicum*, a good amount of information is available, also thanks to the fact that in these cells, the presumed photoreceptor pigments, which belong to the family of hypericin-like molecules, are present in large quantities. Just to give an idea, while in cells like *Euglena gracilis* or *Chlamydomonas reinhardtii* the amount of photoreceptor molecules per cell is estimated to be of the order of 10^6–10^7, in these ciliates, that are deeply colored, a reasonable estimate may be as high as 10^9–10^{10} (Lenci, private communication). This makes it, of course, relatively easier to isolate and purify the photoreceptor molecules, even if, as we are going to see in the

following, not all the questions have been satisfactorily answered. It may be interesting to note that the large amount of pigments present poses a problem: why is it necessary to have such a large amount of pigments for a photosensory system? The metabolic cost for the synthesis of these molecules is probably high, and one could think that this may be evolutionarily justified only if it gives the cells a higher chance of survival in their environment. Both *Stentor* and *Blepharisma* may be killed by an exposure to prolonged illumination just because of the presence of these pigments, though blue *Blepharisma* require much higher doses than red *Blepharisma*. It is also true that blepharismin, the chromophore found in *Blepharisma*, can act as a defensive substance against predators.[28] This does not seem to be true of stentorin (which is the chromophore of *Stentor*), but the defensive role of stentorin is less investigated. It was also suggested that only a small subset of the pigment present could play the role of light sensing, but this answer, in fact, leaves open all the problems indicated before. For a more detailed discussion on this point, see Wood.[29]

Both stentorin and blepharismin chromophores have chemical proprieties and structures similar to those of hypericin and are substituted forms of phenanthroperylene quinones.[30] In *B. japonicum*, five homologs of the chromophore blepharismin were isolated.[31,32] Under the action of light, this chromophore changes its chemical structure *in vitro*[26] and *in vivo*,[33,34] becoming oxidized, and it also changes its absorption spectrum; in fact, living cells change their red color to a bluish one, similar to that of *Stentor*. In this oxidized form, it is called oxyblepharismin, and its chemical structure is more similar to that of stentorin and hypericin than to that of the dark form, blepharismin. Strangely enough, both forms of pigments seem to be able to activate the photosensory transduction in *Blepharisma*, at least according to the action spectra determined. In fact, the action spectra for the step-up photophobic response of red and blue cells overlap well the absorption spectra of blepharismin and oxyblepharismin, respectively.[33,34]

Though the chemical, physical, and photophysical properties of the chromophore in *Blepharisma* were widely investigated, there is not yet a consensus on the structure of the protein moiety of the photoreceptor. Two photoreceptor proteins, one with a molecular weight of about 30 KDa[35] and another with a molecular weight of about 200 KDa[36] were isolated in this ciliate. According to the Japanese authors, the protein they isolated is a monomer, as shown by denaturation experiments.[31] The situation seems to be better known in *Stentor*, where two chromoproteins, called stentorin-1 and stentorin-2, respectively, were isolated. Stentorin-1 can be easily extracted with ethanol from cell suspensions, is strongly fluorescent, and has a peak in absorption at 608 nm. It is a small complex composed of at least two heterologous subunits corresponding to apparent molecular weights of 46 kDa and 52 kDa.[37] Stentorin-2, which is more difficult to isolate, is also composed of two subunits; it is thought to be the functional receptor. In particular, the subunit called stentorin-2B, covalently bound to the chromophore, has a molecular weight of 50 kDa.[38]

In other ciliates, which show photomotile responses, the picture is even less clear. In some cases, the formation of pigmented structures seems to depend on the nutritional state of the cells. This is true, for example, in *Chlamydodon mnemosyne*, where phototaxis and pigment granules appear at the same time when the cells are starved for 24 to 48 h.[39] In this ciliate, the action spectrum for negative phototaxis[40] resembles the absorption spectrum of flavins. Furthermore, the wavelengths efficiently exciting the fluorescence of a region of the plasma membrane adjacent to the stigma of the cell[39] coincide reasonably well with the peaks in the action spectrum for negative phototaxis.[40] However, it should be noted that the fluorescence faded so rapidly that it was not possible to measure a fluorescence excitation spectrum. Also in *Loxodes*,[41] the action spectrum of photomotile reactions, determined using the rate of escape from oxic water to quantify photoresponsiveness, suggests a flavin as the photoreceptor. This is further supported by the fact that when *Loxodes* pigment is illuminated in the presence of O_2, the superoxide ion O_2^- is photodynamically produced, as is reasonably expected by a flavin, which is an efficient photosensitizer of a wide range of substrates. In other ciliate, it is not clear where the receptor pigments might be localized, as is the case for *Fabrea salina* or *Ophryoglena flava*. Until now, no attempt to isolate and characterize these photoreceptor proteins was described.

The hypothesis that rhodopsin-like molecules could be involved in photoreception in ciliates was put forward in the early 1990s by Japanese researchers[42,10] who suggested the presence of this pigment in the colorless ciliate *Paramecium bursaria*, based on the results of biochemical and immunocytochemical experiments. The authors were able to extract retinal by using HPLC[42] and to isolate a rhodopsin-like protein from *P. bursaria*.[10] The HPLC elution profile of the extract showed four peaks. Three of these were comparable to the peaks derived from the elution of standard all-*trans*, 9-*cis*, 11-*cis*, and 13-*cis*-retinal. The presence of 9-*cis*-retinal was ascribed by the authors to a thermal isomerization taking place during the separation process. The copresence of other isomers in light-adapted and in dark-adapted cell extracts does not allow for any conclusion to be drawn as to the process of retinal isomerization in *P. bursaria*; in other words, it is not possible to establish whether the isomerization process is similar to that of higher organisms or to that of *Halobacterium salinarum*. The rhodopsin hypothesis is further supported by other experiments with hydroxylamine, where the phototactic response decreased to about 30% of untreated samples. Furthermore, a polyclonal antibody raised in rabbit against frog rhodopsin was found by immunoelectrophoresis to cross-react with a 63 kDa protein of *P. bursaria,* and when the cells were treated with an anti-frog-rhodopsin antibody obtained from rabbit, the measurements of immunofluorescence microscopy, made using FITC-conjugated goat anti-rabbit IgG (FITC = fluorescein isothiocyanate), showed intense cell fluorescence, especially in the cilia. Similar results were obtained by immuno-electron microscopy. These results and those obtained by electrophysiological recordings in ciliated and deciliated cells give further evidence that the pigment is a rhodopsin, and that a great part of this pigment is localized into the cilia in the antero-ventral region of *P. bursaria*.[10]

There is also some evidence that a rhodopsin-like molecule could be the photoreceptor pigment for phototaxis in *Fabrea salina*, as will be discussed below.

Dark Reactions Steps in the Sensory Transduction Chain

Not much is known of the primary photophysical events taking place after photon absorption. If the pigment belongs to the rhodopsin family, the primary event is most likely a photoisomerization. In the case of hypericin-like pigments, as in *Stentor* and *Blepharisma* (and possibly *Fabrea salina*), some primary photophysical events of the photosensory transduction chain were possibly identified, the main hypothesis being that of an electron transfer from the pigment singlet excited state.[43,44]

The knowledge of the molecular steps of the sensory transduction chain in ciliates is limited to some indirect proofs obtained in *B. japonicum*, in *S. coeruleus*,[45] and in *P. bursaria*.[46] The main idea behind this approach is to test the effects of some metabolic drugs known to inhibit more or less specifically some steps of the sensory transduction chain of vertebrates and invertebrates. In some experiments, cells were treated with 8-Br-cGMP or *N*-2-*o*-dibutyryl-cGMP, which are membrane-penetrating, slowly hydrolyzable analogs of cGMP, with the final effect of an increase of cGMP intracellular levels. When exposed to light, the cells showed a decreased responsiveness to light stimulation and an increased latency time, T_L, defined as the time between light stimulation and the stop reaction.[47,48] This latency time seems to be characteristic of the photophobic responses and resembles the latency time occurring in intracellular recordings of action potentials. Furthermore, chemicals known to lower the activity of PDE (phosphodiesterase) brought about an effect similar to that caused by cGMP analogs. In fact, in *B. japonicum* and in *S. coeruleus*, the incubation with IBMX (isobutylmethylxanthine), a specific inhibitor of PDE, decreased the percentage of cells that react to light stimuli and increased the latency T_L. In *B. japonicum*, a similar effect was induced by the treatment with CTX (cholera toxin) or with PTX (pertussis toxin). Treatments of cells of *S. coeruleus* with theophylline (1,3-dimethylxanthine) and with zaprinast (1,4-dihydro-5-[2-propoxyphenyl]-7H-1,2,3-triazolo[4,5-*d*]pyrimidine-7-one), a highly specific cGMP-PDE inhibitor, have the same effect as IBMX. Zaprinast seems to be the most effective drug in affecting the photophobic response. In *B. japonicum* and in *S. coeruleus*, LY 83583, an inhibitor of guanylate cyclase, which should lower the cytoplasmatic level of cGMP, caused a marked increase in responsiveness to light stimulation and a reduction of the latency time T_L.

In *P. Bursaria*, the injection of GDP-beta-S abolished the light-induced inward current,[46] and a GTP-binding protein (57 kDa) was detected by immunostaining.

To summarize, these results could suggest that the photosensory transduction chain in these ciliates is similar to that of vertebrates.

However, results of other experiments on *B. japonicum* seem to complicate this picture. In fact, the photobehavior of this ciliate is also affected by treatment with chemicals, such as neomycin, heparin, and Li^+ ions, that bind phosphoinositides interfering with the phospholipase (PLC) activity and, thus, reducing the inositol and diacylglycerol intracellular levels. The parameters measured in this set of experiments are the latency time T_L, and the inverse of the light-stimulus intensity eliciting photophobic responses in 50% of the cell population.[49] Neomycin, heparin, and Li^+ have similar effects, causing an increase of T_L and of the light intensity eliciting the required (50%) response with respect to the controls. The effect depends on the concentration of the drug and incubation time. Mastoparan, which activates small G-proteins and increases inositol triphosphate levels ($InsP_3$), mimics the effect of light in *B. japonicum* cells. For instance, the administration of 0.5 μM mastoparan in the close vicinity of a dark-adapted cell in control medium elicited a ciliary reversal with a latency time similar to that of the photophobic response. The effect of mastoparan, together with the results obtained by immunoblotting on extracts of the cortex fraction of the cells,[49] demonstrates that *B. japonicum* possesses a G-protein.

These results could suggest that in *B. japonicum* the transduction chain resembles the invertebrate visual transduction chain, where the activated G-protein activates PLC that in turn produces $InsP_3$.

In summary, the photobehavior of *B. japonicum* seems to depend on two different mechanisms. One is linked to cGMP intracellular level and PDE activity, as is the case in vertebrates, and the other is linked to the activation of a G-protein and $InsP_3$ concentration, as in invertebrates.

It may be interesting to recall that in ventral photoreceptor cells of *Limulus*, the photoreceptor current has three different components that are controlled by three different enzymatic pathways, using three different terminal transmitters (cGMP, cAMP, and $InsP_3$). Until now, the details of these enzymatic pathways were not clarified, and it is not known whether there is a unique photoreceptor or distinct photoreceptors for each different pathway.[50] It is thus possible that phototransduction in ciliates follows the same mechanisms as in *Limulus*.

We think it may be appropriate at this point to make some general comments on the use of drugs and the interpretation of their effects in ciliates and, more in general, on microorganisms. Ciliates are unicellular microorganisms, meaning that, unlike photoreceptor cells of higher organisms, phototransduction is not the main or only function of the cell. Furthermore, many different physiological pathways probably have the same final output, a voltage-dependent inward Ca^{2+} current, and some intermediates could be common between different pathways, be they sensorial or not. Chemicals act by modifying the intracellular level of these intermediates and their effects on ciliates could not be as specific as in other organisms. This problem is, e.g., less important in rod cells, because almost all enzymatic pathways are involved in photosensory transduction. Even if the measure of the latency time of the photophobic response, T_L, should give reasonably unambiguous information on the effect of drugs in these ciliates, intracellular recordings of currents or voltage changes and molecular biological experiments could help in confirming this interpretation.

122.5 Two Case Studies

In the following, we will summarize the results obtained by our research group on two ciliates, *F. salina* and *O. flava*.

Fabrea Salina

Fabrea salina is a heterotrich marine ciliate found only in concentrated saltwater that actively swims along a left-handed helix. It belongs to the same order as the photomotile ciliates *Stentor coeruleus* and *Blepharisma japonicum*, but it is different from them in that it is not apparently pigmented. The cells

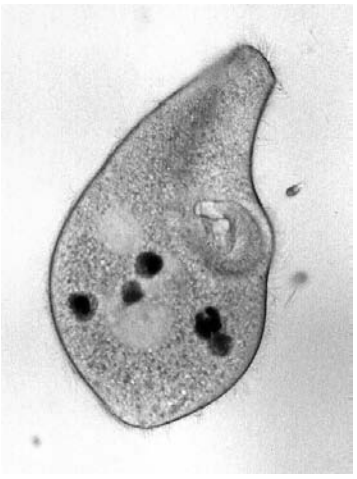

FIGURE 122.3 A view of *Fabrea salina* taken under optic microscope (original magnification × 200): the adoral zone of membranelles and the digestive vacuoles are clearly visible.

have a typical pear-shaped body, the surface of which is densely covered with cilia; the adoral zone is characterized by a deep spiral-shaped invagination, on the edge of which adoral membranelles can easily be seen (Figure 122.3). The cell cytoplasm of the cells grown in our laboratory is apparently colorless; sometimes green food vacuoles, containing the rests of ingested *D. salina* cells, are visible (Figure 122.3). The motion of *F. salina* in the dark can be simply described as a random walk: the cells move along straight lines interrupted by sudden directional changes. *F. salina* reacts to light stimuli by showing step-down photophobic reactions and positive phototaxis but apparently no photokinesis. Phototaxis depends only on light direction and cannot be induced by spatial gradients of light. A discussion of the possible mechanisms by which the cells can track light direction was given in Section 122.2.2. Because the cells respond to light stimuli, they must possess one or more photoreceptor pigments. The phototactic sensitivity curve of *F. salina* given in W/m^2 units as a function of the fluence rate at 600 nm can be fitted by a hyperbolic function of the form $R = (R_m \cdot I)/(I + I_{R/2})$, where R is the phototactic response, I is the light fluence rate, R_m is the level of saturation of the response; $I_{R/2}$, the light fluence rate corresponding to half maximum response, is of the order of 1.0 W/m^2.

As we already mentioned, one of the main techniques used to try and have some hints as to the possible nature of the photoreceptor pigment is action spectrum determination. The equal-response action spectrum calculated on the basis of the dose–response curves is shown in Figure 122.4.[51] This action spectrum is similar to that of photoaccumulation and membrane depolarization of the colorless ciliate *P. bursaria*.[9] As we have seen, in this system, there are indications of the presence of a rhodopsin-like pigment. The similarity between the action spectra of *F. salina* and *P. bursaria* might suggest that the photoreceptor pigment of *F. salina* is a rhodopsin-like molecule. It is, however, difficult to understand why there are two peaks in the action spectrum, if the pigment is a rhodopsin. It could be that two different photoreceptors are present in *F. salina*. If so, they must drive the same sensory transduction chain, as we were unable to find any experimental condition in which the responses at 420 and 580 nm could be affected to a different extent. Foster[20] recalculated the action spectrum of *F. salina* and concluded that it is compatible with the sum of two rhodopsins. However, it should be noted that the authors of the paper cited by Foster decided not to use his method to determine the action spectrum because of the high level of errors involved.

The saturation level of the dose response curves at 420 is higher than that at 580 nm, indicating that blue light is more efficient than green-orange light in inducing cell orientation toward light. At the same fluence rate, white light is as efficient as colored light in inducing phototaxis; this indicates that if there are two different pigments, they do not interfere with each other, and it is likely that *F. salina* cannot discriminate the colors of light.

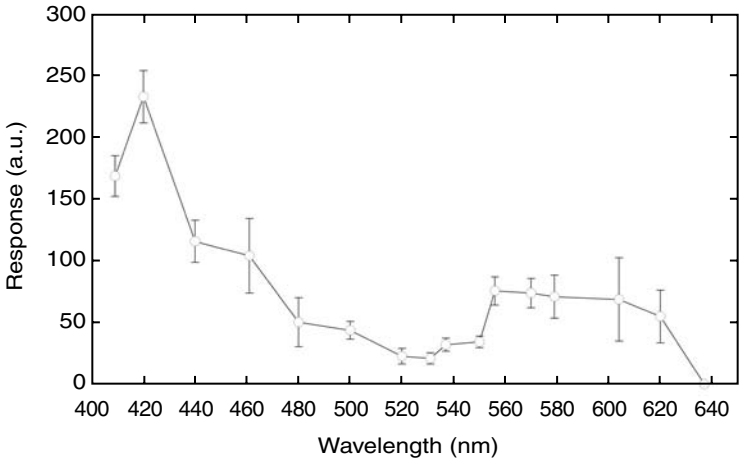

FIGURE 122.4 Action spectrum for the positive phototaxis in *Fabrea salina*.

The possibility that a rhodopsin might be the pigment for phototaxis in *F. salina* prompted us to use immunofluorescence to reveal the presence of a rhodopsin-like molecule on its plasma membrane.

Our study shows that there is immunostaining of *F. salina* cells with a polyclonal antiserum raised in sheep against bovine rhodopsin. The role of specific antibodies in cell staining is demonstrated by the evidence that incubation with FITC-labeled nonimmune sheep serum does not alter the endogenous cell-fluorescence. This implies that none of the serum components, other than the antibodies, is able to nonspecifically bind the cell membrane and that the cell fixation procedure does not alter the membrane permeability in such a way as to allow free access of the fluoresceinated serum molecules to the cytosol.[52] In addition, the binding of the antiserum to the cell membrane was established by confocal microscopy.[22] The theoretical possibility that antibodies other than the anti-opsin are present in the sheep antiserum and able to bind unknown antigens at the cell surface is negligible. Although these findings are consistent with the presence of a rhodopsin antigen activity on the plasma membrane of *F. salina*, they do not unequivocally prove the identity of the protozoan surface antigen to a rhodopsin molecule.

We then ran preliminary experiments looking for the possible presence of a rhodopsin-like gene in *F. salina* by means of the PCR (polymerase chain reaction), performed using two different pairs of primers, based, respectively, on the rhodopsin sequence of the halophilic archæobacterium *H. salinarum* and on the more conserved regions of known rhodopsin sequences of higher organisms. The latter pair of primers allowed the amplification of a sequence in *F. salina* corresponding to a fragment of a rhodopsin-like gene, more similar to the genes of higher organisms and of some flagellated algae than to those of *Halobacteria*.[53]

F. salina possesses, however, another type of pigment. In fact, fluorescence microscopy and imaging of living cells reveal a hardly detectable emission, but dead cells (either treated with various chemicals or dried) are characterized by a strong red fluorescence indicating the presence of an endogenous fluorescent pigment.[22] Single-cell microspectrofluorometry, fluorescence imaging, and laser confocal microscopy studies, together with time-gated fluorescence spectroscopy of cell suspensions, were performed in order to investigate the nature of this pigment and its topological localization. The fluorescence emission spectrum at different excitation wavelengths (from 337 to 425 nm) exhibits two peaks: the main one in the range 590 to about 615 nm, depending on the cell treatment, and the other one at about 655 nm. The time decay of fluorescence shows three distinct components, with lifetimes ranging from a few hundred picoseconds to some nanoseconds, and relative contributions varying with the chemical treatment. Time-gated spectroscopy also allows us to observe differences in the spectral features of the distinct emitting species. Laser confocal microscopy reveals that the pigment is localized just below the cell membrane. The spectral and temporal fluorescence features of the endogenous pigment present in *F.*

salina are similar to the ones of blepharismin, the pigment of *Blepharisma japonicum,*[54] thus suggesting that the *F. salina* pigment might be a hypericin-like pigment, too. The fact that the red fluorescence becomes detectable after cell death suggests a possible photoreceptor role of the pigment in living cells, where most of the energy absorbed by the pigment could be funneled into physiologically active processes, such as a light-induced motile response, and not be available for fluorescence. After death, damage to the cell structures could favor energy dissipation mainly via fluorescence. A similar situation was described in the case of *Blepharisma*, in which damage and rupture of the cell membrane cause a strong increase in emission intensity.[54] For the pigment present in *Fabrea*, as already for blepharismin, the change from nonradiative to radiative deactivation mechanisms can probably be related to differences in the environment of the pigment, which in living cells is embedded in granules, and after cell death could be, at least in part, released.

To summarize, *F. salina* contains two different types of pigments, one probably a rhodopsin and the other a hypericin-like pigment. Though the phototaxis action spectrum is similar to that of *Paramecium bursaria* and, therefore, by analogy, suggestive of a rhodopsin, its shape is not fully incompatible with a hypericin pigment, even though the structure of the spectrum, especially at the red wavelengths, is much less resolved.

There are, however, other pieces of evidence that may indirectly suggest a role for a rhodopsin photoreceptor in *Fabrea salina*. In fact, preliminary experiments have shown that phototaxis is drastically reduced in the presence of hydroxylamine, which is known to interfere with the retinal-lysine binding in rhodopsins, and is strongly affected in the presence of zaprinast, a specific inhibitor of the phosphodiesterase known to be an essential component of the sensory transduction in vertebrate vision. In both cases, cell motility is not affected by the presence of the drugs.

Moreover, we also have indirect evidence that phototaxis is strongly dependent on the conductance state of the membrane.[55] Cells were exposed to potassium concentrations higher than those of the growth medium (from 20 to 60 mM); for about 5 h their swimming changed, going to a tumbly behavior; after this time, the cells, on the average, resumed normal swimming. This is considered typical of cells with the membrane potential of which transiently depolarizes and then goes back to normal, thanks to a change of potassium (and possibly other ions) channel conductance. This has been shown to be true in *Paramecium caudatum* cells.[56] In this condition, the phototactic response of *F. salina* increases at least by a factor of two, while the step-down photophobic reaction disappears. In *P. bursaria*, intracellular recording of photoreceptor potential showed that light stimulation affects membrane conductance.[57] It is thus reasonable to infer that phototaxis is controlled by membrane channel conductance changes. This might, in turn, be related to the action of a rhodopsin-like pigment that could trigger upon illumination a chain of events ultimately leading to opening or closing of ion channels, as happens with rhodopsin in vertebrates and in invertebrates.

In summary, the body of evidence currently available for *F. salina* indicates that these cells possess two different types of putative photoreceptors, a rhodopsin-like and a hypericin-like pigment. The hypothesis that a rhodopsin pigment is responsible for phototaxis is supported by several pieces of evidence based on the similarity of its action spectrum to that of *P. bursaria*, by the effect of metabolic inhibitors such as hydroxylamine and zaprinast, by gene analysis, and by the suggested effect of light on membrane conductance.

Ophryoglena Flava

As we have seen, several histophagous ciliates, belonging to the order Hymenostomatida, among which *Ophryoglena flava* (Figure 122.5), contain a watchglass organelle, the so-called Lieberkühn's organelle, and show a clear phototactic response to light, the sign of which depends on the state of cell starvation.[8] Cells are negatively phototactic in the well-fed state, and positively phototactic during mild starvation. In order to get information on the dependence of phototaxis on light fluence rate, with attention to the possible emergence of negative phototaxis at high fluence rates, and on possible chromatic effects of the photoreceptor pigment, we determined the fluence-rate response curves in mildly starved, positively

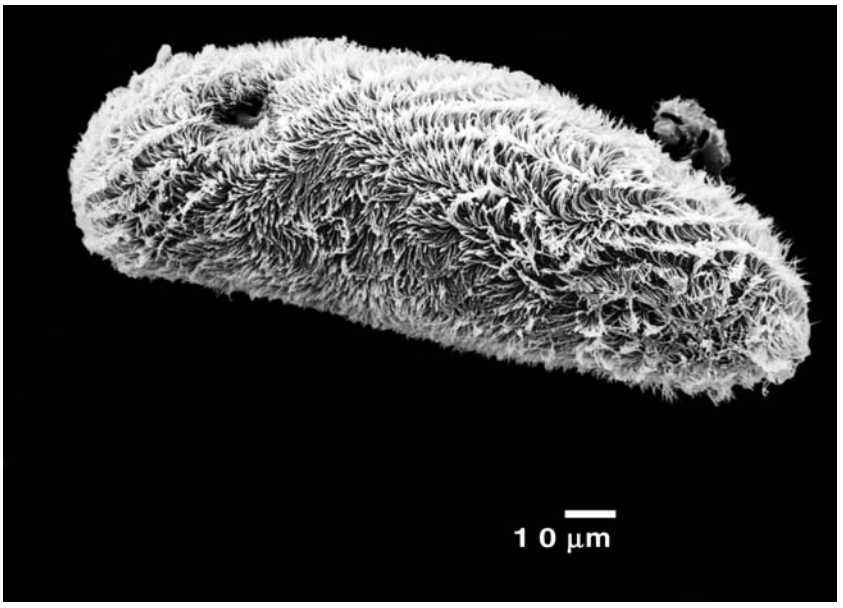

FIGURE 122.5 SEM of the freshwater ciliate *Ophryoglena flava*. The adoral zone is clearly visible.

phototactic, cells of *Ophryoglena flava* in white light and in broadband blue and red light. We then measured fluence-rate response under narrow-band quasi-monochromatic light in the wavelength range 400 to 650 nm. On the basis of these curves, we determined the action spectrum for positive phototaxis (Figure 122.6).[58]

The general trend of the fluence rate-response curve shows that, within the irradiance range investigated, there is no decline of positive phototaxis with light fluence rate. The curve can be fitted by a simple hyperbolic saturation function, and the saturation value is comparable to those obtained under broadband and narrow-band excitation light.[58] This indicates that in our experimental conditions, there is no negative phototaxis, no receptor pigment bleaching, and no saturation of the light tracking system. The first two conclusions are straightforward: if negative phototaxis was elicited at high-light irradiances, we should expect a bell-shaped fluence rate-response, which is not our case; the same holds true in the case of bleaching of the photoreceptor pigment. The third point needs some more discussion. There is general consensus that phototaxis requires some mechanism of light tracking from the cells; the simplest one is that brought about by a periodical shading of the photoreceptor pigment by some screening device. In the case of colorless ciliates, such as *O. flava*, the shading structure is probably the cell body. At high-light irradiances, the cell body could be unable to provide the modulation required to detect light direction (cfr. the argument as discussed by Selbach et al.[40]) because of a sort of overloading of the photoreceptor. In the case of *C. mnemosyne*, which is also a colorless ciliate, the authors report a white light irradiance of 10 Klux as the turning point of the fluence rate-response curve.[40] Even if it is difficult to compare Klux and W/m,^{2} we can use a rough conversion factor given by Lenci and Colombetti,[4] according to whom a white light of 10^2 Klux from a tungsten lamp with a color temperature of about 3000 K corresponds to approximately 60 W/m.^{2} By applying this conversion factor to the present case, the inversion irradiance found by Selbach et al.[40] is of the order of 6 W/m,^{2} whereas *O. flava* shows no decline in positive phototaxis up to 25 W/m.^{2} This could indicate that the light-tracking mechanism of *O. flava* is more robust than that of *C. mnemosyne*, due, for example, to a higher screening capability of its cell body, or that in the case of *C. mnemosyne*, there is some bleaching of the photoreceptor pigments. Moreover, the saturation behavior of the fluence rate-response curve together with the observation that cells continue to show phototaxis even when kept under unilateral illumination for long times is a strong indication that cells do not adapt to this kind of stimulus.

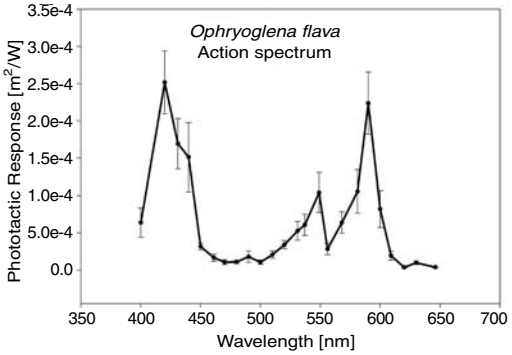

FIGURE 122.6 Action spectrum for the positive phototaxis in *O. flava*.

The fluence rate-response curves in broadband blue and red light are characterized by the same hyperbolic shape as in *F. salina*; they have the same saturation level within the experimental error ($R_{m_{blue}}$ = 0.14, $R_{m_{red}}$ = 0.18); the $I_{R/2}$ parameter in blue light is significantly smaller than that in red light ($I_{R/2blue}$ = 0.03 W/m^2, $I_{R/2red}$ = 0.18 W/m^2), indicating that the cells are more sensitive to blue than to red light. The fact that fluence rate-response curves in white light and broadband blue and red light follow the same trend, that they can be fitted by the same hyperbolic saturation function. and that at the same fluence rate white light is as efficient as colored light in inducing cell orientation toward light indicates that there is no chromaticity effect (in other words, *O. flava* cannot discriminate the colors of light) and that the pigments act independently of each other.

Also, the fluence rate-response curves in narrow-band monochromatic light follow the same hyperbolic saturation behavior, while the saturation level is the same for all wavelengths, within experimental errors. This indicates that if there is more than one type of photoreceptor pigment, they are functionally equivalent (same fluence rate-response curve, same saturation level). A simpler, and perhaps simplistic, solution is that we are dealing with only one type of pigment.

It may be interesting to compare the value of $I_{R/2}$ calculated for *Ophryoglena* in red light, which is of the order of 0.2 W/m^2 with that measured in *Fabrea* (see above), which is of about 1.0 W/m^2.

The action spectrum shown in Figure 122.6 clearly has two major peaks, one at 420 nm and one at 590 nm; a third, minor peak, is possibly present at about 560 nm. This action spectrum resembles, in its two major peaks, the ones measured for photoaccumulation and membrane depolarization in *P. bursaria*, and also that for phototaxis in *F. salina*, though in the latter case there is no well-defined peak in the green-orange region of the spectrum but rather a broad, unresolved band. In the cases of *P. bursaria* and of *F. salina*, a rhodopsin-like receptor pigment was proposed, as discussed above. One could thus tentatively conclude that the pigment responsible for phototaxis in *O. flava* might be a rhodopsin-like molecule, as well. This tentative conclusion faces, however, the same problem as in *F. salina*; no rhodopsin-like molecule can give rise to two peaks in the action spectrum, and the only alternative explanation is that *O. flava* possesses two spectroscopically different, but functionally equivalent, rhodopsins. It should also be noted that there is a similarity between the action spectrum of *O. flava* and that of the *B. japonicum* or *S. coeruleus*. There is, however, no indication that *O. flava* might contain hypericin-like pigments, and preliminary measurements carried out with microspectrofluorometry show no detectable presence of such pigments. Moreover, electron microscopy did not reveal any structure comparable to the pigment granules containing hypericin-like pigments, commonly found in heterotrich ciliates.

122.6 Conclusions

To summarize what is known of the nature of the photoreceptor pigments involved in photomotile responses in ciliates, the results reported in the literature seem to roughly indicate three main types of photoreceptor pigments.[58]

In *Loxodes striatus* and *C. mnemosyne*, it was suggested that the pigment involved might be a flavin. For *S. coeruleus* and *B. japonicum* (probably the best-known and most thoroughly investigated ciliates), from the point of view of photoreception, there is consensus that the pigment responsible for photomotile responses in the former and photophobic step-up response in the latter is due to hypericin-like molecules, stentorin and blepharismin, respectively. In the case of *P. bursaria*, there is some convincing evidence that a rhodopsin-like molecule is present in the cells. It should be noted, as briefly discussed above, that the presence of such a molecule is not *per se* a proof that it also plays the role of photoreceptor pigment, and that if a single rhodopsin is present, it should give rise to only one peak in the action spectrum. In *P. bursaria*, however, there are two peaks that might point to two different rhodopsins, a blue one and a red one, essentially equivalent. Now, the idea that in such a unicellular organism there may be more than one rhodopsin is not surprising; after all, a much smaller cell, such as *Halobacterium salinarum* contains four different rhodopsins,[59] two of which play different receptor roles. The same arguments also hold true for the case of *F. salina*, where there is some evidence in favor of the presence of a rhodopsin molecule, and where a hypericin-like pigment is present. In the case of *O. flava*, the action spectrum resembles those of *F. salina* and *P. bursaria* except for the presence of the smaller peak at about 540 nm. In this ciliate, no hypericin-like molecule was detected, for which we can tentatively say that the action spectrum might give some indication that a rhodopsin is present, but further work is necessary to substantiate this hypothesis.

The results reported and discussed above allow us to conclude that ciliates probably evolved more than one type of photoreceptor pigment and that the most common photoreceptors likely belong to the families of flavins, rhodopsins, and hypericins.

The way in which these photoreceptor molecules seem to be organized in photoreceptor structures and how these structures control the motile apparatus to generate motile responses to light, is apparently linked with the phylogenetic group, reflecting similar adaptation necessities of the organisms. Probably, the light perception strategies properly belong to the evolutionary necessities of survival and best fitness with the surrounding environment.

References

1. Repak, A.J., Suitability of selected bacteria and yeasts in growing the estuarian heterotrich ciliate *Fabrea salina* (Henneguy), *J. Protozool.*, 23, 219, 1986.
2. Ricci, N., Microhabitats of ciliates specific adaptation to different substrates, *Limnol. Oceanogr.*, 34, 1089, 1989.
3. Finlay, B.J. and Fenchel, T., Ecology: role of ciliates in natural environment, in *Ciliates: Cells as Organisms*, Hausmann, K., Ed., G.F. Verlag, Stuttgart, 1996, p. 417.
4. Lenci, F. and Colombetti, G., Photobehaviour of microorganisms: a biophysical approach, *Annu. Rev. Bioeng.*, 7, 341, 1978.
5. Colombetti, G. and Marangoni, R., Mechanisms and strategies of photomovements in flagellates, in *Biophysics of Photoreceptors and Photomovements in Microorganisms,* Lenci, F., Ghetti, F., Colombetti, G., Haeder, D.P., and Song, P.S., Eds., Plenum Press, New York, 1991, p. 53.
6. Kuhlmann, H.W., Phototaxis in ciliates, in *Progress in Protozoology*, Hausmann, K. and Hulsmann, N., Eds., Fischer, Stuttgart, 1994, p. 134.
7. Kuhlmann, H.W., Photomovements in ciliated protozoa, *Naturwissenschaften*, 85, 143, 1998.
8. Kuhlmann, H.W., Braucker, R. and Schepers, A.G., Phototaxis in *Porpostoma notatum*, a marine scuticociliate with a composed crystalline organelle, *Europ.J. Protistol.* 33, 295, 1997.
9. Matsuoka, K. and Nakaoka, Y., Photoreceptor potential causing phototaxis of *Paramecium bursaria*, *J. Exp. Biol.*, 137, 477, 1988.
10. Nakaoka, Y., Tokioka, R., Shinozawa, T., and Fujita, J., Photoreception of Paramecium cilia: localization of photosensitivity and binding with anti-frog IgG, *J. Cells Science*, 99, 67, 1991.
11. Matsuoka, T., Tokumori, D., Kotsuki, H., Ishida, M., Matsushita, M., Kimura, S., Itoh, T., and Checcucci, G., Analyses of structure of photoreceptor organelle and blepharismin-associated protein in unicellular eukaryote *Blepharisma*, *Photochem. Photobiol.*, 72, 709, 2000.

12. Tao, N.B., Deforce, L., Romanowski, M., Mezakeuthen, S., Song, P.S., and Furuya, M., *Stentor* and *Blepharisma* photoreceptors: structure and function, *Acta Protozool.*, 33, 199, 1994.
13. Kuhlmann, H.W., Do phototactic ciliates make use of directional antennas to track the direction of light? *Eur. J. Protistol.,* 34, 244, 1998.
14. Foster, K.W. and Smyth, R., Light antenna in phototactic algae, *Microbiol. Rev.*, 44, 572, 1980.
15. Kreimer, G., Cell biology in phototaxis in flagellate algae, *Int. Rev. Cytology*, 148, 229, 1994.
16. Marangoni, R., Preosti, G., and Colombetti, G., Phototactic orientation mechanism in the ciliate *Fabrea salina*, as inferred from numerical simulations, *J. Photochem. Photobiol.: B*, 54, 185, 2000.
17. Hartmann, K.M., Action spectroscopy, in *Biophysics*, Hoppe, W., Lohomann, W., Markl, H., and Ziegler, H., Eds., Springer-Verlag, Berlin, 1983, p. 115.
18. Lipson, E., Action spectroscopy, in *Biophysics of Photoreceptors and Photomovements in Microorganisms*, Lenci, F., Ghetti, F., Colombetti, G., Häder, D.P., and Song, P.S., NATO-ASI Series, Eds., Plenum Press, New York, 1991, p. 293.
19. Ghetti, F. and Checcucci G., Action spectroscopy in microorganism photomovements, in *Biophysics of Photoreception*, Taddei-Ferretti, C., Ed., World Scientific, Singapore, 1997, p. 38.
20. Foster, K.W., Action spectroscopy of photomovement, in *Photomovement*, Haeder, D.P. and Jori, G., Eds., Elsevier, Amsterdam; New York, 2001, p. 51.
21. Barsanti, L., Passarelli, V., Walne, P.L., and Gualtieri, P., *In vivo* photocycle of the *Euglena gracilis* photoreceptor, *Biophys. J.*, 72, 545, 1997.
22. Marangoni, R., Cubeddu, R., Taroni, P., Valentini, G., Sorbi, R., Lorenzini, E., and Colombetti, G., Microspectrofluorometry, fluorescence imaging and confocal microscopy of an endogenous pigment of the marine ciliate *Fabrea salina*, *J. Photochem. Photobiol.: B*, 34, 183, 1996.
23. Angelini, N., Cubeddu, R., Ghetti, F., Lenci, F., Taroni, P., and Valentini, G., In vivo spectroscopic study of photoreceptor pigments of *Blepharisma japonicum* red and blue cells, *Biochim. Biophys. Acta*, 1231, 247, 1995.
24. Fabczak, H., Groszynska, B., and Fabczak S., Light regulation of protein phosphorylation in *Blepharisma japonicum*, *Acta Protozool.*, 40, 311, 2001.
25. Marangoni, R., Gobbi, L., Verni, F., Albertini, G., and Colombetti, G., Pigment granules and hyperycin-like fluorescence in the marine ciliate *Fabrea salina*, *Acta Protozool.*, 35, 177, 1996.
26. Checcucci, G., Shoemaker, R.K., Bini, E., Cerny, R., Tao, N.B., Hyon, J.S., Gioffré, D., Ghetti, F., Lenci, F., and Song, P.S., Chemical structure of blepharismin, the photosensor pigment for *Blepharisma japonicum*, *J. Am. Chem. Soc.*, 119, 5762, 1997.
27. Montgomery, M.K., Xu, S., and Fire, A., RNA as a target of double-stranded RNA-mediated genetic interference in *Caenorhabditis elegans, Proc. Natl. Acad. Sci. USA*, 95, 15502, 1998.
28. Harumoto, T., Miyake, A., Ishikawa, N., Sugibayashi, R., Zenfuku, K., and Iio, H., Chemical defense by means of pigmented extrusomes in ciliate *Blepharisma japonicum*, *Eur. J. Protistol.*, 34, 458, 1998.
29. Wood, D.C., Electrophysiology and light responses in Stentor and Blepharisma, in *Photomovement*, Haeder, D.P. and Jori.G., Eds., Elsevier, Amsterdam; New York, 2001, p. 51.
30. Falk, H., From the photosensitizer hypericin to the photoreceptor stentorin. The chemistry of phenanthroperylene quinones, *Angew. Chem. Int. Ed.*, 38, 3116, 1999.
31. Maeda, M., Naoki, H., Matsuoka, T., Kato, Y., Kotsuki, H., Utsumi, K., and Tanaka, T., Blepharismin 1–5, novel photoreceptor from the unicellular organism *Blepharisma japonicum*, *Tetrahedron Lett.*, 38, 7411, 1997.
32. Spitzner, D., Hofle, G., Klein, I., Pohlan, S., Ammermann, D., and Jaenicke, L., On the structure of oxyblepharismin and its formation from blepharismin, *Tetrahedron Lett.*, 39, 4003, 1998.
33. Checcucci, G., Damato, G., Ghetti, F., Lenci, F., Action spectra of the photophobic response of the blue and red forms of *Blepharisma japonicum*, *Photochem. Photobiol.*, 57, 686, 1993.
34. Matsuoka, T., Matsuoka, S., Yamaoka, Y., Kuriu, T., Watanabe, Y., Takayanagi, M., Kato, Y., and Taneda, K., Action spectra for step-up photophobic response in *Blepharisma*, *J. Protozool.*, 39, 498, 1992.
35. Gioffrè, D., Ghetti, F., Paradiso, C., Dai, R., and Song, P.S., Isolation and characterization of the presumed photoreceptor protein of *Blepharisma japonicum*, *Photochem. Photobiol.*, 58, 275, 1993.

36. Matsuoka, T., Muratami, Y., and Kato, Y., Isolation of blepharismin-binding 200 kDa protein responsible for behavior in *Blepharisma*, *Photochem. Photobiol.*, 57, 1042, 1993.
37. Kim, I.H., Rhee, J.S., Huh, J.W., Florell, S., Faure, B., Lee, K.W., Kahsai, T., Song, P.S., Tamai, N., Yamazaki, T., and Yamakazi, I., Structure and function of the photoreceptor stentorins in *Stentor coeruleus*. I. Partial characterization of the photoreceptor organelle and stentorins, *Biochim. Biophys. Acta*, 1040, 43, 1990.
38. Dai, R.K., Yamazaki, T., Yamazaki, I., and Song, P.S., Initial spectroscopic characterization of the ciliate photoreceptor stentorin, *Biochim. Biophys. Acta*, 1231, 58, 1995.
39. Selbach, M. and Kuhlmann, H.W., Structure, fluorescent properties and proposed function in phototaxis of the stigma apparatus in the ciliate *Chlamydodon mnemosine*, *J. Exp. Biol.*, 202, 919, 1999.
40. Selbach, M., Häder, D.-P., and Kuhlmann, H.W., Phototaxis in *Chlamydodon mnemosyne*: determination of the illuminance-response curve and the action spectrum, *J. Photochem. Photobiol: B*, 49, 35, 1999.
41. Finlay, B.J. and Fenchel, T., Photosensitivity in the ciliated protozoon *Loxodes*: pigment granules, absorption and action spectra, blue light perception, and ecological significance, *J. Protozool.*, 33, 534, 1986.
42. Tokioka, R., Matsouka, K., Nakaoka, Y., and Kito, Y., Extraction of retinal from *Paramecium bursaria*, *Photochem. Photobiol.*, 53, 149, 1991.
43. Lenci, F., Ghetti, F., and Song, P.S., Photomovement in ciliates, in *Photomovement*, Haeder D.-P. and Jori, G., Eds., Elsevier, Amsterdam; New York, 2001, p. 51.
44. Sgarbossa, A., Checcucci, G., and Lenci F., Photoreception and photomovements of microorganisms, *Photochem. Photobiol. Sci.*, 1, 459, 2002.
45. Fabczak, H., Protozoa as model system for studies of sensory light transduction: photophobic response in the ciliate *Stentor* and *Blepharisma*, *Acta Protozool.*, 39, 171, 2000.
46. Shinozawa, T., Hashimoto, H., Fujita, J., and Nakaoka, Y., Participation of GTP-binding protein in the photo-transduction of *Paramecium bursaria*, *Cell Struct. Funct.*, 21, 469, 1996.
47. Fabczak, H., Tao, N.B., Fabczak, S., and Song, P.S., Photosensory transduction in ciliates. IV. Modulation of the photomovement response of *Blepharisma japonicum* by cGMP, *Photochem. Photobiol.*, 57, 889, 1993.
48. Walerczyk, M. and Fabczak, S., Additional evidence for the cyclic GMP signaling pathway resulting in the photophobic behavior of *Stentor coeruleus*, *Photochem. Photobiol.*, 74, 829, 2001.
49. Fabczak, H., Contribution of phosphoinositide-dependent signalling to photomotility of *Blepharisma* ciliate, *J. Photochem. Photobiol. B: Biol.,* 55, 120, 2000.
50. Dorlochter, M. and Stieve, H., The Limulus ventral photoreceptor: light response and the role of calcium in a classic preparation, *Prog. Neurobiol.*, 53, 451, 1997.
51. Marangoni, R., Puntoni, S., Favati, L., and Colombetti, G., Phototaxis in *Fabrea salina*. 1. Action spectrum determination, *J. Photochem. Photobiol. B*, 23, 149, 1994.
52. Podestà, A., Marangoni, R., Villani, C., and Colombetti, G., A rhodopsin-like molecule on the plasma-membrane of *Fabrea salina*, *J. Eukaryot. Microbiol.*, 41, 565, 1994.
53. Boscarelli, C., Bettini, P., Marangoni, R., Colombetti, G., and Buiatti, M., Identification of a rhodopsin-like gene sequence in the ciliate *Fabrea salina*, in *From Structure to Information in Sensory System*, Taddei-Ferretti, C. and Musio, C., Eds., World Scientific, Singapore, 1998.
54. Cubeddu, R., Taroni, P., Valentini, G., Ghetti, F., and Lenci, F., Time-gated fluorescence imaging of *Blepharisma* red and blue cells, *Biochim. Biophys. Acta*, 1143, 327, 1993.
55. Puntoni, S., Marangoni, R., Gioffre, D., and Colombetti, G., Effects of Ca^{2+} and K^{+} on motility and photomotility of the marine ciliate *Fabrea salina*, *J. Photochem. Photobiol. B*, 43, 204, 1998.
56. Machemer, H., Cellular behaviour modulated by ions: electrophysiological implications, *J. Protozool.*, 36, 463, 1989.
57. Nakaoka, Y., Kinugawa, K., and Kurotani, T., Ca^{2+}-dependent photoreceptor potential in *Paramecium bursaria*, *J. Exp. Biol.*, 131, 107, 1987.

58. Cadetti, L., Marroni, F., Marangoni, R., Kuhlmann, H.W., Gioffre, D., and Colombetti, G., Phototaxis in the ciliated protozoan *Ophryoglena flava*: dose-effect curves and action spectrum determination, *J. Photochem. Photobiol. B*, 57, 41, 2000.
59. Hoff, W.D., Jung, K.H., and Spudich, J.L., Molecular mechanism of photosignaling by archaeal sensory rhodopsins, *Annu. Rev. Biophys. Biomed.*, 26, 223, 1997.

123

Photoactive Yellow Protein, the Prototype Xanthopsin

Johnny Hendriks
University of Amsterdam

Klaas J. Hellingwerf
University of Amsterdam

123.1 Introduction

Discovery and Biological Context of the Photoactive Yellow Protein

In 1985 several ferredoxins and other chromophoric proteins from the halophilic phototrophic bacterium *Ectothiorhodospira halophila* were isolated.[1] One of the "other chromophoric proteins" was yellow and was named "photoactive yellow protein" in a subsequent study.[2] *E. halophila* was reclassified in 1996 to its current name *Halorhodospira halophila*.[3] *H. halophila* is a unicellular prokaryote, or more specifically, a phototrophic purple sulfur spirillum that deposits sulfur extracellularly. It was first isolated and classified from salt-encrusted mud taken from the shores of Summer Lake, Lake County, Oregon.[4,5] Later, it was also isolated from the extremely saline lakes of the Wadi el Natrun in Egypt.[6] Both locations are salt lakes, and *H. halophila* only thrives in extremely salty environments.

0-8493-1348-1/04/$0.00+$1.50

As a phototrophic organism, *H. halophila* exploits the free energy available from light to survive. However, like most organisms, *H. halophila* is not immune to the effects of UV radiation. It is, therefore, essential for *H. halophila* to find a place to live where there is enough light to grow but where the amount of UV radiation is at a minimum. Like most phototrophic organisms, *H. halophila* has mechanisms to perceive the available light climate. It is not only attracted by (infra)red (i.e., photosynthetic) light, but it also has a blue-light response that steers it away from potentially harmful places, rich in blue light. This blue-light repellent response has a wavelength dependence that fits the absorption spectrum of the photoactive yellow protein (PYP).[7] This is the first evidence that PYP is the sensor in the blue-light response of *H. halophila*. Further evidence for the function of PYP in *H. halophila* can be provided via genetic techniques. However, their application in extremophilic prokaryotes like *H. halophila* is not well developed, which is why genetic proof for the function of PYP is not yet available.

Interestingly, the function of PYP is similar to that of the sensory rhodopsins, and in particular, to sensory rhodopsin II, which is also a sensor for a negative tactile response to blue light (in *Halobacterium salinarum*, an archaebacterium that can also be found in salt lakes). The family of the rhodopsins is a large family. Its members are found in all kingdoms of life, from unicellular organisms to complex ones such as *Homo sapiens sapiens*. It is the most extensively studied family of photoactive proteins available. Its best-known members are the visual rhodopsins, which allow us to see, and bacteriorhodopsin, which is a light-activated proton pump found in *H. salinarum*. Sensory rhodopsins are close relatives to bacteriorhodopsin and can be found in the same organism. In fact, the most notable difference between bacteriorhodopsin and the sensory rhodopsins is their function. Bacteriorhodopsin provides the cell with means of harvesting light energy, whereas the sensory rhodopsins are light detectors that make sure the organisms can find a location where bacteriorhodopsin can do its work safely. The possible similarity between PYP and the sensory rhodopsins was already noted after the first characterization of PYP.[2] There is, however, one major difference with sensory rhodopsins that boosted the study of PYP— it is highly water soluble, whereas the rhodopsins, being membrane proteins, are not. As we shall see later, PYP and the sensory rhodopsins belong to structurally completely different families of proteins, which are only similar in function. For more information on the rhodopsins, the reader is referred to several excellent reviews on this topic.[8–10]

Xanthopsins: The Family of Photoactive Yellow Proteins

Halorhodospira halophila is not the only organism in which a photoactive yellow protein has been discovered. There are five other organisms — all purple bacteria — that also contain a protein similar to PYP from *H. halophila*. This family of photoactive yellow proteins was named the Xanthopsin family.[11] Presently, the six known Xanthopsins can be divided into three subgroups, according to their mutual similarity in primary structure. The first group is formed by proteins found in *Halorhodospira halophila* (synonymous to *Ectothiorhodospira halophila*),[1] *Rhodothalassium salexigens* (synonymous to *Rhodospirillum salexigens*),[12] and *Halochromatium salexigens* (synonymous to *Chromatium salexigens*).[13] The second group is formed by proteins found in *Rhodobacter sphaeroides*,[11] and *Rhodobacter capsulatus*.[14] The third group consists of a single protein found in *Rhodospirillum centenum*.[15] In the latter, the Xanthopsin is the amino-terminal domain of a larger phytochrome-like protein.

Though all these Xanthopsins can absorb blue light, their roles in various organisms differ. In *H. halophila*, PYP induces a photophobic tactile response.[7] For *Rb. sphaeroides*, genetic evidence is available that indicates that the blue-light-induced photophobic tactile response in that organism is not mediated by the Xanthopsin present in that organism, provided no genetic redundancy exists.[16] The Xanthopsin found in *Rs. centenum* regulates chalcone synthase gene expression.[15] These different functions of the Xanthopsin members coincide with the subgroup assignments. Though the function of all the known Xanthopsins has not yet been elucidated, it is likely that the members within the different subgroups of Xanthopsins, distinguished based on sequence similarity, have a similar function, while these functions differ between the subgroups.

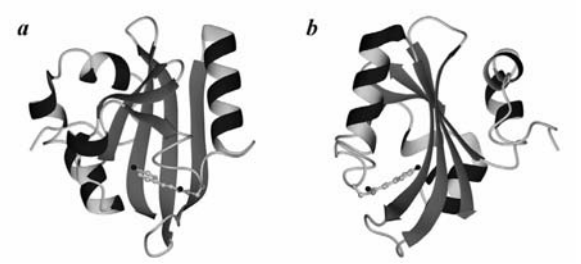

FIGURE 123.1 *Tertiary structure of the Photoactive Yellow Protein*. Two orientations of a ribbon representation of the Photoactive Yellow Protein from *Halorhodospira halophila* are presented. Panel *a* clearly shows the β-sheet with the chromophore in front of it. Shown in Panel *b* is a side view of the orientation in Panel *a*, visualizing both sides of the β-sheet. The figure was prepared using the program MOLMOL[82] using the structure coordinate file deposited at the Protein Data Bank[50] (http://www.rcsb.org/pdb) with PDB ID: 2PHY.[20] The program POV-Ray™ (http://www.povray.org) was used to render the images.

Photoactive Yellow Protein: The Prototypical PAS Domain

As described above, PYP is part of a family of proteins named Xanthopsins, which thus far have only been identified in proteobacteria. Nevertheless, PYP also shows striking similarities to the much larger family of PAS domains. These PAS domains were identified in proteins from all three kingdoms of life, i.e., in the *Bacteria*, the *Archaea*, and the *Eucarya*. PAS is an acronym formed from the names of the proteins in which the PAS motive was first recognized:[17] the *Drosophila* period clock protein (PER), the vertebrate aryl hydrocarbon receptor nuclear translocator (ARNT), and the *Drosophila* single-minded protein (SIM).

Proteins containing PAS domains are predominantly involved in signal transduction. Over 200 proteins have been identified that contain a PAS domain.[18] Most of these are receptors, signal transducers, or transcriptional regulators. Strikingly, at present, PAS domains have only been identified in the cytoplasmic compartment. PAS domains are usually present in proteins with a multidomain architecture. Furthermore, a single protein can have more than one PAS domain. In fact, proteins were identified containing up to six. In contrast, the entire photoactive yellow protein from *H. halophila* can be considered a single PAS domain. As it is the first protein from the PAS domain family for which the three-dimensional structure was elucidated, it was proposed that PYP is the structural prototype of the PAS domain fold.[19]

123.2 Structure

The backbone of photoactive yellow protein contains an α/β-fold with a six-stranded antiparallel β-sheet as a scaffold, which is flanked by several helices.[20] The loop containing helices α3 and α4, and the loop containing helix α5, fold on top of the central β-sheet to form the major hydrophobic core and a pocket in which the chromophore resides. The *N*-terminal segment, containing helices α1 and α2, folds behind the central β-sheet to form a smaller hydrophobic core. The tertiary structure is shown more clearly in Figure 123.1, where in Panel *a,* the structure is oriented such that the β-sheet is oriented similar to the schematic drawing shown in Figure 123.2. The view in Panel *b* of Figure 123.1 shows how the different α-helix-containing loops fold around the central β-sheet.

In photoactive proteins, the chromophore is at the heart of its functional characteristics. The type of chromophore in a photoactive protein typically corresponds with the wavelength range in which the holoprotein needs to be active.[21] In agreement with this, the Xanthopsins were shown to use an aromatic chromophore. This chromophore was identified in *Halorhodospira halophila* in 1994 as 4-hydroxycinnamic acid, covalently bound to the apoprotein via a thiol ester linkage with Cys69.[22,23]

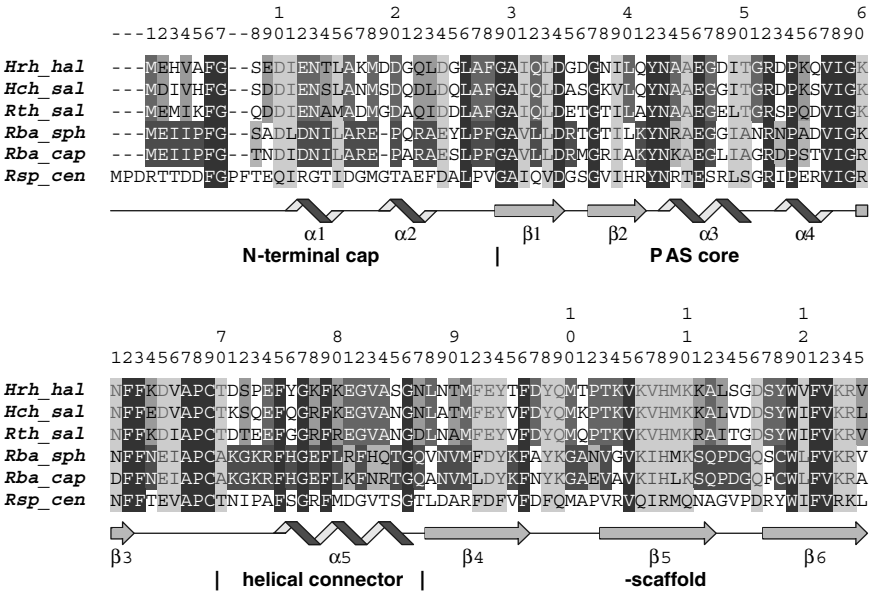

FIGURE 123.2 *Sequence alignment of the Xanthopsins.* An alignment of all currently known Xanthopsins is presented, where the following abbreviations stand for the organism in which the Xanthopsin was found, with the accession number for the primary sequence in parentheses: `Hrh_hal`, *Halorhodospira halophila* (X98887); `Hch_sal`, *Halochromatium salexigens* (P81046); `Rth_sal`, *Rhodothalassium salexigens* (X98888); `Rba_sph`, *Rhodobacter sphaeroides* (AJ002398); `Rba_cap`, *Rhodobacter capsulatus* (AF064095); and `Rsp_cen`, *Rhodospirillum centenum* (AF064527). Only the residues from `Hrh_hal`, `Hch_sal`, and `Rth_sal` are correctly numbered, for the correct numbering of the other sequences, you need to correct for deletions (Residue 19 in `Rba_sph` and `Rba_cap`) and insertions (up to Residue 8 in `Rsp_cen`) in the sequence. The location of the α-helices and β-strands for the `Hrh_hal` sequence are shown via cartoons below the sequence alignment, together with the names of the PAS-domain, subdomains.

The color code for the alignment is as follows. The base color is a white highlight with black letter; any other color has a special meaning for the alignment. Residues that are conserved throughout the currently known Xanthopsins have a black highlight and white letter. Residues that have conserved substitutions are shown with a light gray highlight. Residues that are conserved for the Xanthopsin subgroup containing `Hrh_hal`, `Hch_sal`, and `Rth_sal`, but are not conserved in all currently known Xanthopsins, have a medium dark gray highlight with white letter. If they are part of conserved substitutions for all Xanthopsins, they have a light gray highlight with medium dark gray letter. Conserved substitutions in this subgroup are given a medium gray highlight. Residues that are conserved for the Xanthopsin subgroup containing `Rba_sph` and `Rba_cap`, but are not conserved in all currently known Xanthopsins, have a dark gray highlight with white letter. If they are part of conserved substitutions for all Xanthopsins, they have a light gray highlight with dark gray letter. Conserved substitutions in this subgroup are given a medium light gray highlight.

This figure was prepared using information obtained from several alignments performed with ClustalW[83] (http://www.ebi.ac.uk/clustalw/).

Primary, Secondary, and Tertiary Structure

The chromophore plays a crucial role in the activity of PYP. The amino acids containing atoms that line the chromophore pocket are (in the order in which they appear in the sequence): Val120, Val122, Ile31, Tyr42, Glu46, Thr50, Arg52, Phe62, Val66, Ala67, Cys69, Thr70, Phe96, Asp97, Tyr98, and Met100. This pocket is completely buried in the major hydrophobic core of the protein and has no direct contact with solvent.

In the ground state of PYP, the phenolic oxygen of the chromophore is deprotonated.[23,24] The resulting negative charge of the phenolate is completely buried in the hydrophobic core of the protein and is

stabilized via a hydrogen-bonding network and by the positive charge of the nearby Arg52.[20,25,26] The negative charge of the phenolate is delocalized over the chromophore via an extensive π-orbital system. The hydrogen-bonding network is made up of the residues Tyr42, Glu46, and Thr50, where O_{η} from Tyr42 and $O_{\varepsilon,2}$ from Glu46 form a direct hydrogen bond with the chromophore. $O_{\gamma,1}$ from Thr50 hydrogen bonds with O_{η} from Tyr42 but does not line the chromophore pocket.

Solution Structure vs. Crystal Structure

Until now, we only looked at the structure of PYP in the confines of a crystal lattice. *In vivo*, the protein is located in the cytoplasm, where it may have more freedom for dynamical alterations in its structure, and where it may be more like the conditions used for most *in vitro* experiments. It is, therefore, relevant to know whether there are differences between its structure in a crystal and in aqueous solution. It is important, however, to keep in mind that in the intact cell, the protein may also be confined or partly constrained in its movements by, e.g., a transducer protein. The *in vivo* situation may, therefore, be a situation that is in between the situation in the crystal lattice and the situation in solution.

The solution structure of PYP was determined via multidimensional NMR spectroscopy.[27] This structure is similar to the structure determined with x-ray crystallography. When one compares the elements of secondary structure in the two structures, it turns out that most are present in both, though they may start and end one to two residues earlier or later. Different are helix α2 and the π-helix, which are not defined in the solution structure. There are three poorly defined regions in the solution structure comprising residues 1–5, 17–23, and 113–117. This is caused by lack of structural constraints in the NMR dataset, which might be caused by fast internal motions in those regions, or in other words, by high side-chain or backbone mobility.[27] In the crystal structure, the same regions also have higher values for the B-factor, which expresses the mean-square fluctuations of atoms from their average positions.

From an ensemble of structures, such as those obtained with NMR or via molecular dynamics, it is possible to determine eigenvectors that describe the path along which the different protein elements may move.[28,29] Using these eigenvectors, or modes of flexibility, it is possible to transform the solution structure into the crystal structure, indicating that the observed differences are within the confines of the intrinsic flexibility of the protein. This is further corroborated by the fact that when PYP is crystallized in the $P6_5$ space group,[29] instead of the $P6_3$ space group,[20] these structures are different but are within the confines of the intrinsic modes of flexibility of the protein.

The structure determined with NMR confirms the presence of the hydrogen-bonding network in the chromophore-binding pocket. However, there is one striking difference with the crystal structure. Residue Arg52 is present in two conformations: One in which Arg52 is clustered about 4 Å above the aromatic ring of the chromophore; and the other in which the guanidinium group of Arg52 positioned about 4 Å above the aromatic ring of Tyr98.[27] This latter position is in line with the observation that positively charged amino groups like to pack within 3.4 to 6 Å of the centroids of aromatic rings (the so-called -stacking[30]). The conformation for Arg52 and Tyr98 found in the crystal is different from the two conformations for Arg52 and the conformation of Tyr98 found in solution.

The Xanthopsins Compared

The Xanthopsins can be divided into three subgroups based on their primary structure. Subgroup I contains Xanthopsins found in *Halorhodospira halophila*, *Rhodothalassium salexigens*, and *Halochromatium salexigens*. Subgroup II contains Xanthopsins found in *Rhodobacter sphaeroides* and *Rhodobacter capsulatus*. Subgroup III contains the Xanthopsin found in *Rhodospirillum centenum*. The primary structures within the subgroups are similar, with identities around 75% (87% similarity, i.e., including conserved substitutions) in pair-wise alignments. In a comparison of Xanthopsins from Subgroup I with Xanthopsins from other groups, the alignments become worse with identities around 45% (67% similarity). Comparison of Xanthopsins from Subgroup II with those from Subgroup III provides even poorer results, with identities around 33% (57% similarity). When all currently known Xanthopsins are aligned, an identity of 23% (46% similarity) is obtained.

Because the Xanthopsin subgroups were defined based on sequence similarity, these results should not be surprising. However, by looking at subdomains of the sequence alignments, better insight is obtained on which domains make up a Xanthopsin and which domains are important for the function the Xanthopsin has in the organism it resides in. Above, PYP was proposed to be a prototype for the PAS domain. The family of PAS domains is large and spans all three kingdoms of life. A PAS domain is not so much defined by its primary structure but more by its secondary and tertiary structural elements. The PAS domain can be divided into four subdomains: the *N*-terminal cap, the PAS core, the helical connector, and the β-scaffold. In PYP from *Halorhodospira halophila*, these subdomains comprise residues 1–28, 29–69, 70–87, and 88–125, respectively.[19] Thus, the *N*-terminal cap contains helices α1 and α2; the PAS core contains the β-strands, β1, β2, and β3, and the helices α3 and α4; the helical connector contains helix α5; and the β-scaffold contains the β-strands, β4, β5, and β6. The residues that form the chromophore pocket are all contained within the PAS core and β-scaffold, which are sandwiched together.

Within the Xanthopsin subgroups, no distinction can be made between the degrees of homology between the different PAS subgroups, indicating that the mutations are spread evenly over the entire protein. However, in a comparison of all Xanthopsins, a clear distinction can be made between the PAS subgroups when looking at the percentage of similarity. The PAS-core and β-scaffold have similarities of 66 and 50%, respectively, whereas the *N*-terminal cap and helical connector have similarities of 25 and 34%, respectively. This suggests that the PAS-core and β-scaffold are what makes a Xanthopsin, and that the *N*-terminal cap and the helical connector determine the specific function of a particular Xanthopsin. When the same analysis is done with only the Xanthopsin Subgroups I and II, the picture becomes slightly different. The PAS-core is best conserved with a similarity of 71%, the *N*-terminal cap and β-scaffold have similarities of 50 and 53%, respectively, and the helical connector has a similarity of 33%. The most remarkable difference here is that the *N*-terminal cap has a considerably increased percentage of similarity that has become close to the one of the β-scaffold. This difference can be explained by the fact that Xanthopsins from Subgroups I and II are complete proteins, whereas the Xanthopsin from Subgroup III is a subdomain of a larger protein. This could indicate that the *N*-terminal cap may play an important part in signal transduction, because this is probably one of the biggest differences between Xanthopsins from Subgroups I plus II, as compared with Subgroup III.

123.3 Photoactivity of the Xanthopsins

Photoactivity of the Xanthopsins expresses itself in the form of a photocycle. When a Xanthopsin in the ground state absorbs a photon of the proper wavelength, structural changes occur in the protein that lead to a signaling state that can be "read" by the organism in which it resides. Within a second, the Xanthopsin spontaneously returns to its stable ground state. This self-regenerative cycle requires only that the holoprotein be in hydrated form, and it does not require the presence of a membrane, additional proteins, or cofactors, etc. Most Xanthopsin research is focused on this photocycle or a part of it. The best-studied Xanthopsin by far is PYP from *Halorhodospira halophila*. Therefore, the photocycle of this protein will be discussed in detail.

The Basic Photocycle

Models of the photocycle of PYP have become more complex over the years (see Figure 123.3). Nonetheless, the key states involved are as follows:

1. The ground- or dark-adapted state, pG, in which the chromophore is deprotonated and the isomerization state of the chromophore is *trans*
2. A spectrally red-shifted state, pR, that is formed on a nanosecond timescale (In this state, the chromophore is still deprotonated, but its configuration changed to *cis*.)
3. A spectrally blue-shifted state, pB, with respect to the ground state, which is formed on a microsecond timescale (This species is presumed to be the signaling state of the photoreceptor. It is

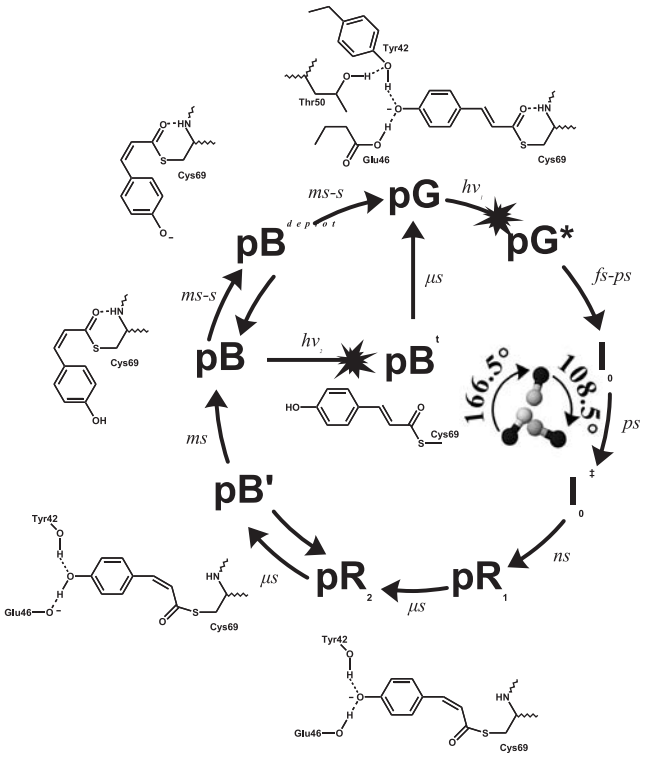

FIGURE 123.3 *Up-to-date description of the photocycle of PYP.* An up-to-date complete description of the photocycle events at room temperature is shown. In addition, the chromophore and its interactions with the protein were added. The drawings represent the situation in the intermediate it is placed next to. For the primary events, the rotation of the carbonyl group is illustrated instead. This inset was prepared using the program MOLMOL[82] using the structure coordinate file deposited at the Protein Data Bank[50] (http://www.rcsb.org/pdb) with PDB ID: 2PHY,[20] 3PYP,[44] 2PYR.[49] The program POV-Ray™ (http://www.povray.org) was used to render the image.

stable enough to allow for a signal to be processed by the organism. In pB, the chromophore has become protonated, while it retains the *cis* configuration. The holoprotein subsequently recovers to its ground state on the millisecond timescale.)

These three major steps — isomerization, protonation change, and recovery — are also observed in the sensory rhodopsins, which have a similar cellular function as PYP but are structurally different. It is interesting to note that although the Xanthopsins and sensory rhodopsins evolved separately, the photochemical mechanism they use to generate a signal from an absorbed photon is essentially the same.

Photocycle Nomenclature

Over the years, several nomenclatures for the photocycle intermediates were introduced. As the photocycle models become more complex, so does the nomenclature. Unfortunately, there is not a single nomenclature that is able to handle all the new intermediates being discovered. Also, not all intermediates are related to color changes of the chromophore. All the different nomenclatures contain the above-mentioned three basic photocycle species and can, therefore, be compared using these three species as a reference. Initially, the ground, red-shifted, and blue-shifted states were called *P*, I_1, and I_2.[31] In 1995, the names pG, pR, and pB were introduced by Hoff et al.[32] Yet another nomenclature[33] was introduced in 1996, in which these species were called PYP, PYP_L, and PYP_M, based upon the photocycle nomenclature of bacteriorhodopsin. The nomenclatures are made even more complicated by the use of additional subscripts that state a specific property of the species (e.g., the absorption maximum). Such a property

can be dependent on the measurement conditions used. As a consequence, different subscripts are used for the same species. Furthermore, an increasing number of different techniques are used to analyze the photocycle. As a result, more photocycle species are discovered that were previously undetectable. To provide these new intermediates a new name that fits logically within one of the existing nomenclatures is close to impossible.

Experimental Context

It is of crucial importance to take the experimental context of an experiment into consideration when comparing different experiments. Four different experimental parameters are of basic importance: temperature, nature of the solvent, mesoscopic context (or phase), and illumination conditions. The first, temperature, is obviously important when comparing kinetic experiments. But, temperature may also allow one to trap certain photocycle species[33,34] and prevent others from being formed. The second, the nature of the solvent, is also very important and is usually different between different experiments. Though pH is probably the most important solvent feature that has an effect on, e.g., the kinetics of the photocycle,[35,36] other solvent features, such as hydrophobicity of the solvent,[31] type and concentration of solutes present,[31,37] and the nature of the solvent (e.g., water versus deuterium oxide[35]) also can have their effects on the data. The third experimental parameter is the mesoscopic context or phase. In the crystalline phase (or lattice), no large structural change is observed in the protein upon formation of the signaling state, whereas when the protein is in solution, such a significant overall structural change is observed.[38] Furthermore, illumination conditions can have pronounced effects on the data, particularly, its color and intensity are important. The choice of wavelength can have an effect on which photocycle species are formed.[33,34] Also, the duration of the excitation pulse can have an effect. Longer illumination allows the possibility of photoactivation of photocycle species other than the ground state[39] and may lead to hysteresis effects in the recovery (Gensch et al., unpublished). The probe beam can also influence the data.

Mutants and Hybrids

PYP can be engineered genetically, via site-directed mutagenesis, and chemically, e.g., through the use of chromophore derivatives. The types of proteins obtained in these two approaches are referred to as mutant and hybrid, respectively. Many of the residues that interact with the chromophore (e.g., Tyr 42, Glu46, and Thr50) have already been mutated, and various chromophore analogs, particularly with ring substituents, have been used for holoprotein reconstitution.

123.4 The Photocycle of Photoactive Yellow Protein

Initial Events

In the first basic step of the photocycle of PYP, the chromophore isomerizes. The description of this process is still a puzzle. Though several models were suggested, it is not clear which, if any, of these models is correct. Nevertheless, several features are known. At least two different fluorescent states are formed after photoexcitation of PYP. One of these fluorescent states has a chromophore configuration that is different from the ground state configuration, which presents as an anisotropy difference with respect to the ground state.[40] It is unclear if both fluorescent states are actual photocycle intermediates that lead to progression of the photocycle, are photocycle dead ends, or are both (i.e., upon formation they can return to the ground state directly or indirectly via the photocycle).

The first step in the photocycle is completed upon formation of pR. At least one photocycle intermediate is formed between the excited (fluorescent) state and pR at room temperature. This intermediate, called I_0, is formed on a picosecond timescale and decays to pR on a nanosecond timescale. An additional intermediate with similar absorption characteristics as those of I_0, called $I_0^{\ddagger}$, exists between I_0 and pR.[40,41] At cryogenic temperatures, more intermediates can be distinguished. Here a branched pathway exists,

with each branch containing two intermediates, one of which can be assigned to the room temperature intermediate I_0. The two branches join upon formation of pR. Because the absorption characteristics of the intermediates of one of the branches are similar to those of the ground state, it is difficult to confirm their existence at room temperature. Nevertheless, this has been suggested for one of them.[42]

A bias for one of the branches in the low-temperature photocycle can be obtained via adjustment of the excitation wavelength. The branch with the I_0-like intermediate is preferred when shorter wavelengths are used for excitation.[34,43] It is, however, unclear if this is caused by the characteristics of PYP or by the fact that the I_0 intermediate can be photoconverted back to pG, which occurs at longer wavelengths. Similarly, the PYP_H intermediate can be photoconverted back to pG, which occurs at shorter wavelengths.[33] Here, we are confronted with one of the pitfalls of cryotrapping photocycle intermediates. The photoactivity of the protein is not limited to its ground state. Photocycle intermediates are photoactive as well. To accumulate a cryotrapped intermediate, the sample is usually illuminated for an extended period of time. As a result, the intermediate being cryotrapped is also illuminated and can thus be photoactively converted as well. The intermediate may return to the ground state. However, it is also possible that other intermediates, not normally part of the photocycle, are formed. Such an intermediate may be the fluorescent species F_{430}, which is possibly formed from the PYP_H intermediate.[34] It is, therefore, vital to take into account the illumination conditions when interpreting and comparing results obtained with cryotrapping.

Though the correct spectroscopic identification of the different intermediates is important, it is more interesting to understand their structural bases. From what is known, it is clear that the protein part shows little structural change during the first step of the photocycle. Also, the aromatic ring of the chromophore stays more or less at the same position.[44–46] The only way to facilitate isomerization of the chromophore under these conditions is by rotating the thiol-ester carbonyl. This carbonyl flip can be interpreted as a double isomerization around the $C_7 = C_8$ double bond and the C_9–S_γ single bond, i.e., the chromophore configuration changes from $C_7 = C_8$-*trans* C_9–S_γ-*cis* to $C_7 = C_8$-*cis* C_9–S_γ-*trans*. This model was first introduced on the basis of low-temperature FTIR spectroscopy,[47] and later confirmed.[38,45,48]

PYP is the first protein for which the structure of photocycle intermediates has been determined with x-ray crystallography. The structure of two intermediates from the first step in the photocycle was determined, i.e., PYP_{BL} and pR. For both intermediates, the structural changes are limited to the immediate surroundings of the chromophore. The structure of the PYP_{BL} intermediate was obtained via cryotrapping and resolved with a resolution of 0.85 Å. Based on the temperature and illumination conditions used, together with measurement of the absorption spectrum of the sample, it was concluded that PYP_{BL} was the cryotrapped intermediate.[44] However, it cannot be excluded that PYP_{HL} was also formed and, thus, that a mixture of intermediates was present. From the resolved structure, it is evident that the chromophore is in a *cis* configuration, be it a distorted one that has barely crossed the *trans* to *cis* transition point. The most important conclusion from this structure is that the chromophore is isomerized in such a way as to cause as little as possible movement of the chromophore within the chromophore pocket. Isomerization is achieved by rotating the carbonyl function 166.5° (see inset Figure 123.3), with respect to the aromatic ring, breaking the hydrogen bond between the carbonyl function and the backbone amide group of Cys69.

The structure of the pR intermediate was obtained via time-resolved x-ray crystallography at near room temperature, with 1.9 Å resolution.[49] The structure was determined from the 1 ns time-slice of a dataset encompassing time-slices up to 1 ms. Though initially the obtained structure was assigned to pR, this was revised in a subsequent paper describing the complete dataset of the time-resolved x-ray diffraction experiment.[46] The recorded 1 ns time-slice overlapped with the excitation laser pulse, which could result in the presence of multiple intermediates that are in photoequilibrium. Besides pG and pR, intermediates that occur between these two in the photocycle could also be present. The structure deposited at the Protein Data Bank[50] (http://www.rcsb.org/pdb) with PDB ID: 2PYR[49] has been refined, but was not updated or replaced. Where in the deposited structure the hydrogen-bonding network is

disrupted, in the refined structure, the hydrogen-bonding network stays intact, as is also suggested by experiments with other techniques, e.g., 47, 48. However, the position of the chromophore carbonyl function remains similar. The deposited pR structure has a completely *cis* isomerized chromophore for the $C_7 = C_8$ double bond. In this structure, the carbonyl function rotated an additional 108.5° with respect to the cryotrapped intermediate PYP_{BL} (see inset Figure 123.3). This may allow the formation of a hydrogen bond between the carbonyl and the backbone amide of Tyr98.

Recently, an extensive study on the photoexcitation and isomerization of PYP was published.[26] In this study, a combination of molecular dynamics simulation techniques and time-dependent density functional theory calculations were used. Several interesting results were obtained. Out of five separate simulations that were performed of the excited state, two showed a twisted configuration of the chromophore, and in three, the chromophore retained its *trans* configuration. This could explain the two different excited states observed in the ultrafast absorption measurement (see above).

The (free) energy content of PYP increased 120 to 160 $kJ \cdot mol^{-1}$ upon formation of pR.[51,52] This means that about half the energy of an absorbed photon is stored in the holoprotein at this point (a photon with a wavelength of 446 nm has an energy content of 268 $kJ \cdot mol^{-1}$). This amount of energy should then be enough to drive the remainder of the photocycle. This also implies that half the energy of the absorbed photon is lost in, e.g., thermal relaxations. FTIR analysis of the cryotrapped intermediates in the first step of the photocycle, suggests that there is little structural difference between these intermediates.[45] Thus, small movements induced by thermal relaxations may dictate the exact isomerization route of the chromophore.

Signaling State Formation and Ground State Recovery

In the signaling state, PYP interacts with a putative transducer protein to signal the cell that a blue photon was absorbed. Therefore, this state needs to have a relatively long lifetime to allow for this communication. Because the interacting transducer protein was not yet identified, all experiments have so far been performed on the purified PYP. It is possible that certain characteristics of the signaling state will change when transducer protein is added. An example of the effect that a transducer protein can have on a photosensor can be observed in sensory rhodopsin I. Here, in the absence of the transducer protein, the sensor protein acts as a proton pump, while in the presence of the transducer protein, the proton pump activity is lost.[53] Also, the pH dependence of the photocycle kinetics changes upon removal of the transducer protein.[53] This does not imply that measurements on just the isolated photosensor are obsolete. On the contrary, any differences between the characteristics in the absence and presence of the accompanying transducer may lead to a better understanding of how a signal might be transmitted.

In the formation of the signaling state of PYP, two key events were identified. One is protonation of the chromophore, neutralizing its negative charge, and the other is structural change of the protein. In the last basic step of the photocycle, the ground state is recovered, i.e., the chromophore has to be deprotonated and re-isomerized, and the protein part has to return to its ground state structure. Though knowledge about the formation of the signaling state increased significantly over the past few years, little is known about the specifics of the recovery of the ground state.

The Photocycle Model

Recently, photocycle models changed significantly with respect to events that occur after the formation of the pR intermediate (pre-pR events are discussed in detail in Section 123.4.1). Much of the early work assumed a simple three-state photocycle model, i.e., with the pG, pR, and pB states only. In these models, formation of the signaling state, pB (from pR), was described as a kinetically biexponential and as a monoexponential event. Actually, the first detailed analysis of the photocycle of PYP[37] postulated a photocycle containing an additional intermediate with similar spectral properties as pB, because of the observed biexponential kinetic character of pB formation. However, this model was abandoned in a

subsequent paper.[31] Recently, the intermediate pB′ was introduced as an intermediate in the pR to pB photocycle step based on results obtained with FTIR spectroscopy.[38] A subsequent detailed laser-induced transient UV/Vis spectroscopic kinetic analysis of the photocycle confirmed the existence of this intermediate and showed it has spectroscopic properties similar to those of pB.[35] Here, it was also revealed that the pB′ intermediate is in equilibrium with pR, which explains the previously observed biexponential character of the pR to pB photocycle step.[37,54]

Recovery of the ground state can be achieved spontaneously in the dark or light-induced via an accelerated path. In the latter, a photon absorbed by pB′ and pB, photoisomerizes the chromophore, thereby allowing a thousand-fold increase in the rate of recovery, with respect to the rate of recovery in the dark.[55] It may be useful to note that the measuring light can also induce this branching reaction, and hence, influence data.Though for the dark recovery, it has been suggested that before isomerization can take place, the chromophore must first be deprotonated and, thus, an intermediate must exist between pB and pG,[56] This was not experimentally demonstrated until recently, in an extensive series of measurements of the kinetic deuterium isotope effect of photocycle transitions in PYP.[35]

Structural Relaxation of pR

Recently, it was found that additional relaxation events in the protein occur after pR formed.[57,58] Through the use of the transient grating and pulsed-laser photoacoustic methods, it was shown that a μs dynamic component exists during the lifetime of pR. This indicates that after the structural changes in and immediately around the chromophore are completed, additional structural changes occur in the protein away from the chromophore. Thus, pR can be split into the two intermediates pR_1 and pR_2. Though the transition from pR_1 to pR_2 is claimed to be spectrally silent, a similar transition was observed earlier in UV/Vis data.[54] However, as this transition only contributed a small amount to the total signal, no confident assignment could be made, and the feature was not further discussed. In a recent analysis of UV/Vis data,[35] reaction kinetics were obtained that fit the pR_1 to pR_2 transition observed via transient grating. Though the obtained spectra for both pR intermediates are similar, pR_1 seems to have a slightly higher extinction coefficient than pR_2, whereas the λ_{max} values are indistinguishable.

Protonation Change upon pB′ Formation

The first event that takes place after the formation of the pR intermediate is protonation of the chromophore, which results in the formation of pB′. Because the UV/Vis spectroscopic properties of pB′ are similar to those of pB, the first experimental evidence for the existence of this intermediate was obtained in FTIR measurements.[38] It was shown that deprotonation of Glu46 and protonation of the chromophore are simultaneous events, which are followed by a structural change of the protein. Because the absorption changes monitored with UV/Vis spectroscopy mainly represent changes of the chromophore and its immediate surroundings and far less of the structure of the surrounding protein, it is difficult to distinguish between pB′ and pB on the basis of UV/Vis spectroscopy. With proof for the existence of a pB′ intermediate available, it was incorporated in a photocycle model, which was used to analyze UV/Vis data in a study on the kinetic deuterium isotope effect in the photocycle of PYP.[35] From these analyses, it was evident that pR and pB′ exist in an equilibrium that shifts toward pB′ upon going to the extremes of pH (both low and high). The observed kinetic Deuterium Isotope Effect is in line with a proton transfer from Glu46 to the chromophore for the whole pH range that was investigated (pH 5 to 11). However, for the return reaction, the situation is more complex. Here, formation of pR from pB′ can occur via different routes, dependent on pH.

With the reversible character of the pR to pB′ transition, a plausible explanation for the biexponential behavior of pB formation, previously observed with UV/Vis spectroscopy,[37,54] is now available. The shift of this equilibrium toward pB′, when going to the pH extremes, also explains the shift toward monoexponential behavior for the formation of pB at these latter pH values.

Structural Change upon pB Formation

From the strongly nonlinear Arrhenius kinetics of the recovery reaction of pG,[59] it was concluded that the signaling state of PYP is at least partly unfolded. In a mutant with the first 25 *N*-terminal amino acids removed,[60] the deviation from normal Arrhenius behavior was largely gone. Therefore, it seems that the *N*-terminal region of PYP is largely responsible for the large structural change upon formation of the signaling state. Several other methods, like, e.g., CD, NMR, fluorescence, and FTIR spectroscopy, confirmed this partial unfolding.

Hydrogen–deuterium (H/D) exchange measurements, in particular, contributed to the insight into the structural change that is at the basis of signaling state formation in PYP. Whereas a buried hydrogen atom may take days to exchange, an exposed hydrogen atom may be exchanged within seconds. PYP contains 235 potentially exchangeable hydrogen atoms, 42 of which are from (de)protonatable groups. In a study with electrospray ionization mass spectrometry,[61] it was shown that in the dark, less hydrogen atoms were exchanged for deuterium atoms compared to an experiment performed in the presence of light. Also, in apoPYP, 29 potential exchange sites resist exchange, which can be interpreted as that 29 or less of the 42 (de)protonatable groups are deprotonated. Additionally, it may mean that apoPYP has a certain degree of structure, depending on the actual number of deprotonated groups. The light-induced H/D exchange was independently confirmed using FTIR difference spectroscopy.[61] Though these experiments show that there is a difference between the ground and signaling state of PYP with respect to H/D exchange protection, they do not pinpoint the areas of the protein responsible for the observed differences. However, it is possible to obtain more specific information with NMR spectroscopy.[62] Even though it was only possible to obtain specific information for the backbone amide exchangeable hydrogen of 51 residues, 14 of these showed a significant change in protection (i.e., resistance against exchange) upon formation of the signaling state pB, i.e., only two less than the number predicted by mass spectrometry, which was not limited to the backbone amide hydrogen atoms. The residues with the most significant loss in protection are Phe28, Glu46, and Thr70. The latter two are close to the chromophore, whereas Phe28 is close to Glu46.

In an NMR study of the pB intermediate in solution, it was shown that pB exhibits structural and dynamic disorder with respect to the ground state.[63] Interestingly, a subsequent NMR study of pB_{dark} formation[62] showed that pB_{dark} and the photocycle intermediate pB are similar. It was also made clear that upon formation of pB_{dark}, the protein can be divided into three parts: a relatively stable core (residues 32–41, 80–94, and 113–122) and two areas that display large structural perturbation; the *N*-terminus (residues 6–18, and 26–29); and the area around the chromophore binding site (residues 42–58, 69–78, and 95–100). As discussed above, the structural perturbations of the *N*-terminus are largely responsible for the observed non-Arrhenius behavior of the photocycle kinetics. Furthermore, the NMR data suggest that the pB intermediate is a mixture of structurally perturbed forms and a form structurally similar to the ground state, or more specifically, similar to the pB crystal structure.[64]

The trigger for the major structural change upon formation of pB is the formation of a buried negative charge on Glu46 when it donates its proton to the chromophore.[38] After formation of pB′, the buried negative charge, initially located on the chromophore, is centered on Glu46. Whereas on the chromophore, the negative charge can be effectively neutralized by delocalization of the charge, the hydrogen-bonding network, and possibly the positive charge on Arg52. On Glu46, the buried negative charge cannot be effectively neutralized. This leads to a stress situation within the protein, which can be relieved via several routes. One is return to the pR state, reflecting the reversible nature of pB′ formation (see above). Other routes lead to the formation of pB. The extent of the structural change upon formation of the pB intermediate depends on the route taken. One route to take to relieve the buried negative charge is to expose it to solvent, which requires structural change of the protein. Another route is to protonate the Glu46, but not via the chromophore, because that would lead to the reformation of pR. Once Glu46 is protonated, the stress situation is relieved, and a large structural change is no longer necessary. Because protonation changes play a key role, it is to be expected that these events are pH dependent. Thus, depending on the pH, one route may dominate over the other. In fact, a pH dependence of the extent

of structural change was observed to coincide with protonation of Glu46 (J. Hendriks and A. Xie et al., unpublished results). Of course, both routes to pB mentioned here assume that pB′ is formed as an intermediate. It is also possible that a direct, or alternative, route from pR to pB exists. In such a route, Glu46 may stay protonated, i.e., it does not donate a proton to the chromophore. The chromophore then becomes protonated only after exposure to the solvent, or via another residue (e.g., Tyr42). Such a route would require little structural change of the protein and might be preferred in the crystal environment. All mentioned routes are possibilities, and depending on the conditions, one particular route may dominate. The key factor in all these routes is what happens to the protonation state of Glu46 and the chromophore. In fact, it was shown that for the Glu46Gln mutant in solution, the structural change upon formation of pB is significantly less compared to the wild-type situation.[38] In this mutant, Residue 46 can no longer donate a proton to the chromophore, and thus, no buried negative charge is formed on Residue 46, and hence, less driving force for structural change is generated. Though Residue 46 plays an essential role in the amount of structural change that takes place, other residues may also have influence, e.g., His108 also has influence on the extent of structural change, as it was shown that the mutant His108Phe exhibits less structural change compared to the wild-type protein.[65]

The pH dependence of structural change was also shown to exist via transient probe binding,[66] showing less structural change at low pH. Together with experiments monitoring the pH-dependent net proton uptake and release of PYP during pB formation,[67] and pH-dependent FTIR results (J. Hendriks and A. Xie et al., unpublished results), it is likely the pK_a of Glu46 in pB is 5.5, where above pH 5.5 more structural change occurs than below pH 5.5.

In a recent molecular dynamics study, the effect of protonation of the chromophore by Glu46 on the stability of the protein was simulated.[68] Though the simulation was run for only 4 ns after the proton transfer, it is clear that this event induces structural changes in the protein. For one, the proton transfer causes the hydrogen-bonding network with the chromophore to collapse, which results in a shift of the negative charge, which becomes localized on Glu46, an energetically unfavorable situation. Furthermore, the *N*-terminal domain is affected in the simulation as well as α-helix 3. These domains were also shown to be involved in structural change based on NMR measurements (see above and Craven et al.[62]).

Recovery of the Ground State

During the recovery of the ground state of PYP, several events have to take place. The chromophore has to re-isomerize to the *trans* form, the protonation states of several residues and the chromophore have to be changed, and the protein needs to return to its original fold. Though these are seemingly distinct steps, until recently, they appeared to occur simultaneously. On the basis of measurements of the kinetic deuterium isotope effect,[35] it was shown that deprotonation of the chromophore occurs before its isomerization. Hence, an intermediate named pB^{deprot} is formed "en route" from pB to pG. Though deprotonation of the chromophore aids the re-isomerization of the chromophore tremendously,[69] this re-isomerization is still a rate-controlling step, in which the protein fold likely plays a crucial part. The pB^{deprot} intermediate is, therefore, characterized by a deprotonated chromophore and a folding state that allows re-isomerization of the chromophore. This latter characteristic is important, as this intermediate possibly has an absorption spectrum similar to that of the ground state of PYP and not one that is similar to the pB intermediate at high pH, which also has a deprotonated chromophore but has its absorption maximum around 430 nm.[35,67] An absorption spectrum similar to the ground state for the pB^{deprot} intermediate also explains why it was not observed before.

When re-isomerization of the chromophore is accelerated with a short flash of 350 nm light, the rate of recovery of the ground state is increased a thousand-fold.[55] In this branching reaction, an intermediate pB^t is formed instantaneously on the nanosecond timescale. A slight blue shift of pB^t, with respect to pB, can be explained by the difference in isomerization state of the chromophore, i.e., *cis* (pB) versus *trans* (pB^t). No other intermediates are observed with UV/Vis spectroscopy in going from pB^t to pG, indicating that change of the protein fold and the protonation state of several residues can be achieved quickly once the chromophore is isomerized. The existence of this branching reaction can influence data

because of the presence of light that can be absorbed by any of the pB intermediates. This may allow recovery kinetics to appear faster than they really are in the absence of this probe light.[70] This light accelerated recovery can be exploited in the study of the very-slow recovery variants, like M100A.

Several studies were done to study refolding of PYP. Mostly, these studies employ a denaturant to aid the initial unfolding of the protein. The exception is an NMR study,[63] where recovery of the ground state was measured solely on the basis of light-induced unfolding of the protein. For the recovery, a differential refolding was observed where the central β-sheet and parts of the α-helical structure refold slightly faster, after which the region around the chromophore returns to the ground state fold. The differences between the rates are small, and it is unclear if the accompanying error allows one to differentiate between the rates. But, the observed trend is in line with the idea that in order to facilitate re-isomerization of the chromophore, the chromophore not only needs to be deprotonated, but also the protein needs to be in a relatively folded state.

In a study utilizing the denaturants urea and guanidinium·HCl, refolding was studied in unfolded ground state protein and in the unfolded signaling state.[71] The major difference between these two denatured forms of the protein is the isomerization state of the chromophore. Where refolding from the denatured ground state is a monoexponential event, refolding from the denatured signaling state is a biexponential event. Here, the fast component is identical to refolding from the denatured ground state, and the slow exponent has a rate similar to the photocycle ground-state recovery rate under similar conditions. This indicates that after the signaling state renatures, it recovers to the ground state through normal photocyclic events. Interestingly, extrapolation of the obtained refolding kinetics to the absence of denaturant shows close to a thousand-fold faster rate for refolding for protein with the chromophore in the *trans* state compared to protein with the chromophore in the *cis* state. This is similar to the rate difference observed between the ground state recovery in the dark and photoactivated ground state recovery via the branching reaction.[55]

Similar experiments with the acid denatured state of PYP were also performed.[72] Similar results as with the denaturants as described above were obtained, where refolding from the acid denatured state with the chromophore in the *trans* state, i.e., pB_{dark}, is three to five orders of magnitude faster compared to the acid denatured state with the chromophore in the *cis* state. Interestingly, it was shown with temperature denaturation that, when in the acid denatured state, the chromophore is in the *cis* state, and the protein is more stable than when the chromophore is in the *trans* state. Furthermore, it was shown that the acid denatured state with the chromophore in the *cis* state is similar to the photocycle intermediate pB.

For a few mutants of PYP, a dramatic decrease in recovery rate was observed, i.e., Glu46Asp,[73] Met100Ala,[74] and Met100Leu.[75] This indicates that Glu46 and Met100 are important for recovery. Met100 is important for the re-isomerization of the chromophore, as indicated by the dramatic increase in rate of recovery when the chromophore is photochemically re-isomerized in the Met100Ala mutant.[74] In a recent study, it was argued that the electron-donating character of the residue at position 100 influences the rate of recovery through interaction with another residue, most likely Arg52.[76] With the Glu46Asp mutant, such a dramatic increase in recovery rate was not observed upon photochemical re-isomerization of the chromophore.[73] As such, it is likely that Glu46 is important for refolding of the protein, though it may still be involved in dark re-isomerization of the chromophore.

123.5 Spectral Tuning of Photoactive Yellow Protein

Tuning of the UV/Vis absorption band of PYP, away from the values of neutral or anionic coumaric acid, is of interest for several reasons. First, there is the tuning of the absorption band of the ground state structure. Here, the contribution of specific structural characteristics must be analyzed. However, during the photocycle of PYP, the absorption spectrum changes as well. These changes, therefore, contain valuable information regarding the chromophore and its surroundings in the respective photocycle states. A proper understanding of the tuning of PYP will, therefore, aid in understanding events that occur during the photocycle.

Ground State Tuning

The interaction of the chromophore and protein part of PYP produces an absorption band with 446 nm as its maximum. As the free chromophore, *trans*-4-hydroxycinnamic acid, has an absorption maximum at 284 nm (in aqueous solvent around neutral pH),[77] this interaction of the chromophore with the protein induces a large red shift. Several specific interactions can be distinguished. For one, the thiol ester link of the chromophore with Cys69 causes a red shift of ~5713 cm^{-1} (from 284 to 339 nm). This follows from a comparison of the absorption maximum of 4-hydroxycinnamic acid and the denatured form of PYP in aqueous solution at pH 7.[78] An additional red shift of 4310 cm^{-1} (from 339 to 397 nm) occurs when the chromophore becomes deprotonated, which follows from a comparison of the absorption maximum of the denatured form of PYP in aqueous solution at pH 7 and 11.[78] This leaves a red shift of ~2767 cm^{-1} (from 397 to 446 nm) that is due to interactions with the protein. Though this description is illustrative, it does not provide specific insight regarding the nature of the interactions between the chromophore and the protein.

In a recent study, a closer look was taken at the mechanisms that lead to the spectroscopic tuning of PYP in its ground state.[25] Two model compounds were used for comparison, i.e., a propyl ester and a propyl-thiol ester of 4-hydroxycinnamic acid. The thiol ester model compound was consistently red-shifted by ~1000 cm,$^{-1}$ with respect to the ester model compound, irrespective of the protonation state of the chromophore. With regard to tuning in PYP, three tuning contributions were considered, i.e., a medium effect of the protein matrix (700 cm^{-1}), a counterion effect (5300 cm^{-1}), and a hydrogen-bonding effect (~1600 cm^{-1}). The medium effect of the protein matrix takes into account nonspecific solvent effects. For the model compounds, the absorption maximum shifted with the solvent that was used, e.g., for the thiol ester model compound, the absorption maximum ranged from 34,800 cm^{-1} (287 nm) in pentane to 31,500 cm^{-1} (317 nm) in pyridine. This difference is mainly caused by differences in the dielectric constant and refractive index between the solvents. To determine the medium effect in PYP, these values were estimated for the protein. Absorption maxima of the thiol ester model compound in hexane and protein were calculated. Note that only the solvent properties of the protein are considered here (the counterion and hydrogen-bonding effects are not). This leads to a contribution of ~700 cm^{-1} to the tuning of the chromophore in the protein. The counterion effect considers the difference in position of the counterion of the thiol ester model compound in solution (sodium ion at 2.5 Å in a straight line from the phenolate oxygen bond) and in the protein (position of Arg52 in the crystal structure PDB ID: 2PHY[20]). Here, protein solvent conditions were used in the calculation of the absorption maxima. This leads to a contribution of ~5300 cm^{-1} to the tuning of the chromophore. The hydrogen-bonding effect was determined by placing methanol at the positions of the hydroxy groups of residues Tyr42, Glu46, and Thr50, which are involved in the hydrogen-bonding network with the chromophore, in the calculations. By comparing the situation incorporating the medium effect of the protein matrix and the counterion effect, with the situation that also takes into account the hydrogen-bonding effect, the contribution of the latter was calculated as a blue shift of ~1600 cm^{-1}. Furthermore, with regard to the counterion effect, an interesting observation was made. The position of the Arg52 is such that it appears that the counterion is infinitely far apart from the chromophore, i.e., it does not contribute to the tuning. Movement of the counterion toward the thiol ester linkage would result in a red shift, whereas movement toward the phenolate oxygen would result in a blue shift. From NMR measurements[27] and molecular dynamics studies,[26] it is evident that Arg52 may have two distinct positions in the ground state. Here, the two distinct positions obtained with the molecular dynamics studies result in a difference of 20 nm between the absorption maxima of the two conformers.[26]

When the hydrogen-bonding network in PYP is weakened (by replacing the bridging hydrogen atoms with deuterium atoms), a small red shift is observed, which would be expected when the hydrogen-bonding effect contributes a smaller blue shift to the total tuning. Furthermore, the residues involved in the hydrogen-bonding network (Tyr42, Glu46, and Thr50) were altered through mutagenesis. Mutants in Tyr42, Glu46, and Thr50 result in red shifts (e.g., Tyr42Ala, Tyr42Phe, Glu46Gln, Glu46Ala, Thr50Val, and Thr50Ala[36,73,79–81]) reflecting the weaker hydrogen-bonding effect in these mutants. In some mutants

though, protein stability was severely affected, as indicated by a major, additional, blue-shifted absorption band (Tyr42Phe, Tyr42Ala, and Glu46Ala).

Several mutants of residue Arg52 were also prepared. The Arg52Ala mutant is slightly red shifted,[36] while the Arg52Gln mutant shows no shift of the absorption maximum.[79] As described above, removal of the counterion would not lead to a change in absorption maximum, which is what is observed in the Arg52Gln mutant. A small red shift that is observed in the Arg52Ala mutant may be explained by a more open structure of the chromophore-binding pocket, possibly allowing a solvent cation to act as a counterion.

Spectral Tuning in Photocycle Intermediates

The negative charge on the chromophore is most effectively delocalized if the chromophore is planar. During isomerization, planarity is lost, and the negative charge is not as efficiently delocalized, which results in a red shift of the absorption spectrum. This would explain why the intermediates I_0 and $I_0^{\ddagger}$ are more red shifted than pR, as in those intermediates, isomerization was not yet completed, and the chromophore may be in a twisted form. In pR, the chromophore is still not quite planar due to steric hindrance between the carboxylic oxygen and atoms of the phenolate ring,[68] explaining the red shift. Additionally, in pR, the chromophore contracted ~0.5 Å,[68] while the structure of the protein is similar to that of the ground state. Such a contraction could lead the counterion Arg52 to become located closer to the phenolate oxygen of the chromophore, which would also lead to a red shift.

Protonation of the chromophore leads to a large blue shift, which is what is observed. In pB′, the structure of the protein is still similar to that of pR, and thus to the ground state. Therefore, interactions with the protein are likely. When pB is formed, the structure of the protein has dramatically changed (in solution), where the interaction of the protein with the chromophore has likely diminished, which is also illustrated by the slight additional blue shift of the pB intermediate with respect to pB′. However, even though the chromophore has become more exposed in pB, its absorption maximum is still slightly red shifted compared to the situation in denatured protein.[71] The chromophore is, therefore, still tuned in pB, through interactions with the protein. The presence of these interactions is further demonstrated by the pK_a of the chromophore in pB, which is ~10 and not 8.7 as is the case in fully denatured protein.[35]

Before re-isomerization can take place, the chromophore needs to be deprotonated first. This leads to a large red shift, with respect to pB, as is demonstrated by the pB spectrum at high pH, where its absorption maximum shifts to ~430 nm.[35,67] However, for isomerization to take place, the folding state of the protein also needs to be correct. When that condition is also met, we refer to the intermediate pB^{deprot}. As an intermediate with an absorption maximum of 430 nm has not been observed during the recovery of PYP, it is unlikely that the absorption spectrum of pB^{deprot} is similar to that of pB at high pH. More likely is that, due to interaction with the protein, the absorption band of pB^{deprot} is even more similar to that of the ground state.[35]

123.6 Summary and Future Perspective

After excitation of the ground state of PYP, a twisted, excited state configuration will be formed that results in formation of the I_0 photocycle intermediate. In this latter intermediate, the chromophore has already achieved the *cis* configuration, though it is still twisted. Further relaxation in the protein leads to formation of $I_0^{\ddagger}$ and, subsequently, pR. Isomerization is achieved with a minimal amount of movement of the chromophore, i.e., through a concerted rotation around several bonds that can be described as a $C_7 = C_8$-*trans* C_9-S_γ-*cis* to $C_7 = C_8$-*cis* C_9-S_γ-*trans* multiple-bond isomerization, or "a rotation" of the chromophore carbonyl oxygen. Isomerization of the chromophore increases the probability of a proton transfer from Glu46 to the chromophore. When this occurs, the intermediate pB′ is formed. As a result, the negative charge — which was stabilized when it resided on the chromophore via delocalization, a hydrogen-bonding network, and a counterion — now resides on Glu46, where it is localized. This is an energetically unfavorable situation resolved by formation of pB, in which structural changes took place

in the *N*-terminal domain and around the chromophore. Particularly, the involvement of the more or less independently folded *N*-terminus in the partial unfolding is remarkable. Together with the sequence comparisons within the PAS domains, this may suggest that the *N*-terminus is important for signaling. The extent of these structural changes depends on sample conditions and can range from very little structural change in crystals, at low temperature, and in insufficiently hydrated films, to large structural changes in solution and sufficiently hydrated films.

After formation of the signaling state, the photocycle enters the recovery phase. For recovery to take place, the chromophore has to be re-isomerized, and the protein needs to return to its ground state fold. Before re-isomerization can take place, the chromophore needs to be deprotonated, and the protein needs to adopt a specific fold that allows for the re-isomerization to take place. This situation is represented by the pB^{deprot} intermediate, which is in equilibrium with pB. In addition to this recovery in the dark, it is also possible to re-isomerize the chromophore photochemically, which results in a rate of recovery that is three orders of magnitude faster than dark recovery.

Through the years, PYP has become popular as a model system. This is easily demonstrated by a literature search with the key words "Photoactive Yellow Protein." Where only a few years ago, the search result would contain mostly papers on PYP itself, nowadays, studies on many other proteins are included, for which PYP is seen as a model or reference system. Three areas of research in particular are relevant for this role-model function:

1. The study of signaling state formation in PAS-domains
2. The study of functional protein unfolding
3. The study of the primary photochemistry of photoreceptors

This popularity is based on the favorable handling characteristics, the availability of high-resolution structures, and the relatively simple structure of the chromophore of PYP.

Nevertheless, several additional fields may benefit from efforts made to understand the details of signaling in PYP. The first is molecular dynamics modeling, because this approach may benefit from the availability of transient reference structures from time-resolved x-ray diffraction. Furthermore, recently a number of biophysical approaches were used to estimate the rate of translational diffusion of PYP in its ground and signaling states. As the values obtained varied among the techniques used (e.g., K.J. Hellingwerf, J. Hendriks, and T. Gensch[84]), further detail about the assumptions and approximations used in these techniques may be revealed.

Beyond all this, of course, the field of signal transduction in photobiology could benefit enormously from the detailed insight into the mechanism that leads to signal generation within PYP. However, that aspect will blossom only when additional signal transduction components that link PYP to the flagellar apparatus are identified.

References

1. Meyer, T.E., Isolation and characterization of soluble cytochromes, ferredoxins and other chromophoric proteins from the halophilic phototrophic bacterium *Ectothiorhodospira halophila*, *Biochim. Biophys. Acta*, 806, 1, 175–183, 1985.
2. McRee, D.E., Meyer, T.E., Cusanovich, M.A., Parge, H.E., and Getzoff, E.D., Crystallographic characterization of a photoactive yellow protein with photochemistry similar to sensory rhodopsin, *J. Biol. Chem*., 261, 29, 13,850–13,851, 1986.
3. Imhoff, J.F. and Suling, J., The phylogenetic relationship among *Ectothiorhodospiraceae*: a reevaluation of their taxonomy on the basis of 16S rDNA analyses, *Arch. Microbiol*., 165, 2, 106–113, 1996.
4. Raymond, J.C. and Sistrom, W.R., The isolation and preliminary characterization of a halophilic photosynthetic bacterium, *Arch. Mikrobiol.*, 59, 1, 255–268, 1967.
5. Raymond, J.C. and Sistrom, W.R., *Ectothiorhodospira halophila*: a new species of the genus *Ectothiorhodospira*, *Arch. Mikrobiol.*, 69, 2, 121–126, 1969.

6. Imhoff, J.F., Hashwa, F., and Trüper, H.G., Isolation of extremely halophilic bacteria from the alkaline Wadi Natrun, Egypt, *Arch. Hydrobiol.*, 84, 381–388, 1978.
7. Sprenger, W.W., Hoff, W.D., Armitage, J.P., and Hellingwerf, K.J., The eubacterium *Ectothiorhodospira halophila* is negatively phototactic, with a wavelength dependence that fits the absorption spectrum of the photoactive yellow protein, *J. Bacteriol.*, 175, 10, 3096–3104, 1993.
8. Spudich, J.L., Yang, C.S., Jung, K.H., and Spudich, E.N., Retinylidene proteins: structures and functions from archaea to humans, *Annu. Rev. Cell Dev. Biol.*, 16, 365–392, 2000.
9. Hoff, W.D., Jung, K.H., and Spudich, J.L., Molecular mechanism of photosignaling by archaeal sensory rhodopsins, *Annu. Rev. Biophys. Biomol. Struct.*, 26, 223–258, 1997.
10. Balashov, S.P., Photoreactions of the photointermediates of bacteriorhodopsin, *Israel J. Chem.*, 35, 3–4, 415–428, 1995.
11. Kort, R., Hoff, W.D., Van West, M., Kroon, A.R., Hoffer, S.M., Vlieg, K.H., Crielaand, W., Van Beeumen, J.J., and Hellingwerf, K.J., The xanthopsins: a new family of eubacterial blue-light photoreceptors, *EMBO J.*, 15, 13, 3209–3218, 1996.
12. Meyer, T.E., Fitch, J.C., Bartsch, R.G., Tollin, G., and Cusanovich, M.A., Soluble cytochromes and a photoactive yellow protein isolated from the moderately halophilic purple phototrophic bacterium, *Rhodospirillum salexigens*, *Biochim. Biophys. Acta*, 1016, 3, 364–370, 1990.
13. Koh, M., Van Driessche, G., Samyn, B., Hoff, W.D., Meyer, T.E., Cusanovich, M.A., and Van Beeumen, J.J., Sequence evidence for strong conservation of the photoactive yellow proteins from the halophilic phototrophic bacteria *Chromatium salexigens* and *Rhodospirillum salexigens*, *Biochemistry*, 35, 8, 2526–2534, 1996.
14. Jiang, Z. and Bauer, E.C., Genetic characterization of photoactive yellow protein from *Rhodobacter capsulatus*, unpublished, 1998.
15. Jiang, Z., Swem, L.R., Rushing, B.G., Devanathan, S., Tollin, G., and Bauer, C.E., Bacterial photoreceptor with similarity to photoactive yellow protein and plant phytochromes, *Science*, 285, 5426, 406–409, 1999.
16. Kort, R., Crielaard, W., Spudich, J.L., and Hellingwerf, K.J., Color-sensitive motility and methanol release responses in *Rhodobacter sphaeroides*, *J. Bacteriol.*, 182, 11, 3017–3021, 2000.
17. Nambu, J.R., Lewis, J.O., Wharton, K.A., Jr., and Crews, S.T., The Drosophila single-minded gene encodes a helix-loop-helix protein that acts as a master regulator of CNS midline development, *Cell*, 67, 6, 1157–1167, 1991.
18. Taylor, B.L. and Zhulin, I.B., PAS domains: internal sensors of oxygen, redox potential, and light, *Microbiol. Mol. Biol. Rev.*, 63, 2, 479–506, 1999.
19. Pellequer, J.L., Wager-Smith, K.A., Kay, S.A., and Getzoff, E.D., Photoactive yellow protein: a structural prototype for the three-dimensional fold of the PAS domain superfamily, *Proc. Natl. Acad. Sci. USA*, 95, 11, 5884–5890, 1998.
20. Borgstahl, G.E., Williams, D.R., and Getzoff, E.D., 1.4 Å structure of photoactive yellow protein, a cytosolic photoreceptor: unusual fold, active site, and chromophore, *Biochemistry*, 34, 19, 6278–6287, 1995.
21. Hellingwerf, K.J., Hoff, W.D., and Crielaard, W., Photobiology of microorganisms: how photosensors catch a photon to initialize signalling, *Mol. Microbiol.*, 21, 4, 683–693, 1996.
22. Hoff, W.D., Dux, P., Hard, K., Devreese, B., Nugteren-Roodzant, I.M., Crielaard, W., Boelens, R., Kaptein, R., van Beeumen, J., and Hellingwerf, K.J., Thiol ester-linked p-coumaric acid as a new photoactive prosthetic group in a protein with rhodopsin-like photochemistry, *Biochemistry*, 33, 47, 13,959–13,962, 1994.
23. Baca, M., Borgstahl, G.E., Boissinot, M., Burke, P.M., Williams, D.R., Slater, K.A., and Getzoff, E.D., Complete chemical structure of photoactive yellow protein: novel thioester-linked 4-hydroxycinnamyl chromophore and photocycle chemistry, *Biochemistry*, 33, 48, 14,369–14,377, 1994.
24. Kim, M., Mathies, R.A., Hoff, W.D., and Hellingwerf, K.J., Resonance Raman evidence that the thioester-linked 4-hydroxycinnamyl chromophore of photoactive yellow protein is deprotonated, *Biochemistry*, 34, 39, 12,669–12,672, 1995.

25. Yoda, M., Houjou, H., Inoue, Y., and Sakurai, M., Spectral tuning of photoactive yellow protein. Theoretical and experimental analysis of medium effects on the absorption spectrum of the chromophore, *J. Phys. Chem. B*, 105, 40, 9887–9895, 2001.
26. Groenhof, G., Lensink, M.F., Berendsen, H.J., Snijders, J.G., and Mark, A.E., Signal transduction in the photoactive yellow protein. I. Photon absorption and the isomerization of the chromophore, *Proteins: Struct., Function, Gen.*, 48, 2, 202–211, 2002.
27. Dux, P., Rubinstenn, G., Vuister, G.W., Boelens, R., Mulder, F.A., Hard, K., Hoff, W.D., Kroon, A.R., Crielaard, W., Hellingwerf, K.J., and Kaptein, R., Solution structure and backbone dynamics of the photoactive yellow protein, *Biochemistry*, 37, 37, 12,689–12,699, 1998.
28. van Aalten, D.M., Hoff, W.D., Findlay, J.B., Crielaard, W., and Hellingwerf, K.J., Concerted motions in the photoactive yellow protein, *Protein Eng.*, 11, 10, 873–879, 1998.
29. van Aalten, D.M.F., Crielaard, W., Hellingwerf, K.J., and Joshua-Tor, L., Conformational substates in different crystal forms of the photoactive yellow protein — Correlation with theoretical and experimental flexibility, *Protein Sci.*, 9, 1, 64–72, 2000.
30. Scrutton, N.S. and Raine, A.R., Cation-pi bonding and amino-aromatic interactions in the biomolecular recognition of substituted ammonium ligands, *Biochem. J.*, 319, Pt. 1, 1–8, 1996.
31. Meyer, T.E., Tollin, G., Hazzard, J.H., and Cusanovich, M.A., Photoactive yellow protein from the purple phototrophic bacterium, *Ectothiorhodospira halophila*. Quantum yield of photobleaching and effects of temperature, alcohols, glycerol, and sucrose on kinetics of photobleaching and recovery, *Biophys. J.*, 56, 3, 559–564, 1989.
32. Hoff, W.D., Matthijs, H.C.P., Schubert, H., Crielaard, W., and Hellingwerf, K.J., Rhodopsin(s) in eubacteria, *Biophy. Chem.*, 56, 1–2, 193–199, 1995.
33. Imamoto, Y., Kataoka, M., and Tokunaga, F., Photoreaction cycle of photoactive yellow protein from *Ectothiorhodospira halophila* studied by low-temperature spectroscopy, *Biochemistry*, 35, 45, 14,047–14,053, 1996.
34. Hoff, W.D., Kwa, S.L.S., van Grondelle, R., and Hellingwerf, K.J., Low temperature absorbance and fluorescence spectroscopy of the photoactive yellow protein from *Ectothiorhodospira halophila*, *Photochem. Photobiol.*, 56, 529–539, 1992.
35. Hendriks, J., van Stokkum, I.H.M., and Hellingwerf, K.J., Deuterium isotope effects in the photocycle transitions of the Photoactive Yellow Protein, *Biophys. J.*, 84, 1180–1191, 2003.
36. Genick, U.K., Devanathan, S., Meyer, T.E., Canestrelli, I.L., Williams, E., Cusanovich, M.A., Tollin, G., and Getzoff, E.D., Active site mutants implicate key residues for control of color and light cycle kinetics of photoactive yellow protein, *Biochemistry*, 36, 1, 8–14, 1997.
37. Meyer, T.E., Yakali, E., Cusanovich, M.A., and Tollin, G., Properties of a water-soluble, yellow protein isolated from a halophilic phototrophic bacterium that has photochemical activity analogous to sensory rhodopsin, *Biochemistry*, 26, 2, 418–423, 1987.
38. Xie, A., Kelemen, L., Hendriks, J., White, B.J., Hellingwerf, K.J., and Hoff, W.D., Formation of a new buried charge drives a large-amplitude protein quake in photoreceptor activation, *Biochemistry*, 40, 6, 1510–1517, 2001.
39. Gensch, T., Hellingwerf, K.J., Braslavsky, S.E., and Schaffner, K., Photoequilibrium in the primary steps of the photoreceptors phytochrome A and photoactive yellow protein, *J. Phys. Chem. A*, 102, 28, 5398–5405, 1998.
40. Gensch, T., Gradinaru, C.C., van Stokkum, I.H.M., Hendriks, J., Hellingwerf, K.J., and van Grondelle, R., The primary photoreaction of photoactive yellow protein (PYP): anisotropy changes and excitation wavelength dependence, *Chem. Phys. Lett.*, 356, 3–4, 347–354, 2002.
41. Ujj, L., Devanathan, S., Meyer, T.E., Cusanovich, M.A., Tollin, G., and Atkinson, G.H., New photocycle intermediates in the photoactive yellow protein from *Ectothiorhodospira halophila*: picosecond transient absorption spectroscopy, *Biophys. J.*, 75, 1, 406–412, 1998.
42. Imamoto, Y., Kataoka, M., Tokunaga, F., Asahi, T., and Masuhara, H., Primary photoreaction of photoactive yellow protein studied by subpicosecond-nanosecond spectroscopy, *Biochemistry*, 40, 20, 6047–6052, 2001.

43. Masciangioli, T., Devanathan, S., Cusanovich, M.A., Tollin, G., and el-Sayed, M.A., Probing the primary event in the photocycle of photoactive yellow protein using photochemical hole-burning technique, *Photochem. Photobiol.*, 72, 5, 639–644, 2000.
44. Genick, U.K., Soltis, S.M., Kuhn, P., Canestrelli, I.L., and Getzoff, E.D., Structure at 0.85 Å resolution of an early protein photocycle intermediate, *Nature*, 392, 6672, 206–209, 1998.
45. Imamoto, Y., Shirahige, Y., Tokunaga, F., Kinoshita, T., Yoshihara, K., and Kataoka, M., Low-temperature Fourier transform infrared spectroscopy of photoactive yellow protein, *Biochemistry*, 40, 30, 8997–9004, 2001.
46. Ren, Z., Perman, B., Srajer, V., Teng, T.Y., Pradervand, C., Bourgeois, D., Schotte, F., Ursby, T., Kort, R., Wulff, M., and Moffat, K., A molecular movie at 1.8 Å resolution displays the photocycle of photoactive yellow protein, a eubacterial blue-light receptor, from nanoseconds to seconds, *Biochemistry*, 40, 46, 13,788–13,801, 2001.
47. Xie, A., Hoff, W.D., Kroon, A.R., and Hellingwerf, K.J., Glu46 donates a proton to the 4-hydroxycinnamate anion chromophore during the photocycle of photoactive yellow protein, *Biochemistry*, 35, 47, 14,671–14,678, 1996.
48. Brudler, R., Rammelsberg, R., Woo, T.T., Getzoff, E.D., and Gerwert, K., Structure of the II early intermediate of photoactive yellow protein by FTIR spectroscopy, *Nat. Struct. Biol.*, 8, 3, 265–270, 2001.
49. Perman, B., Srajer, V., Ren, Z., Teng, T., Pradervand, C., Ursby, T., Bourgeois, D., Schotte, F., Wulff, M., Kort, R., Hellingwerf, K., and Moffat, K., Energy transduction on the nanosecond time scale: early structural events in a xanthopsin photocycle, *Science*, 279, 5358, 1946–1950, 1998.
50. Berman, H.M., Westbrook, J., Feng, Z., Gilliland, G., Bhat, T.N., Weissig, H., Shindyalov, I.N., and Bourne, P.E., The Protein Data Bank, *Nucl. Acids Res.*, 28, 1, 235–242, 2000.
51. van Brederode, M.E., Gensch, T., Hoff, W.D., Hellingwerf, K.J., and Braslavsky, S.E., Photoinduced volume change and energy storage associated with the early transformations of the photoactive yellow protein from *Ectothiorhodospira halophila*, *Biophys. J.*, 68, 3, 1101–1109, 1995.
52. Takeshita, K., Hirota, N., Imamoto, Y., Kataoka, M., Tokunaga, F., and Terazima, M., Temperature-dependent volume change of the initial step of the photoreaction of photoactive yellow protein (PYP) studied by transient grating, *Journal of the Am. Chem. Soc.*, 122, 35, 8524–8528, 2000.
53. Spudich, E.N. and Spudich, J.L., The photochemical reactions of sensory rhodopsin I are altered by its transducer, *J. Biol. Chem.*, 268, 22, 16,095–16,097, 1993.
54. Hoff, W.D., van Stokkum, I.H., van Ramesdonk, H.J., van Brederode, M.E., Brouwer, A.M., Fitch, J.C., Meyer, T.E., van Grondelle, R., and Hellingwerf, K.J., Measurement and global analysis of the absorbance changes in the photocycle of the photoactive yellow protein from *Ectothiorhodospira halophila*, *Biophys. J.*, 67, 4, 1691–1705, 1994.
55. Hendriks, J., van Stokkum, I.H., Crielaard, W., and Hellingwerf, K.J., Kinetics of and intermediates in a photocycle branching reaction of the photoactive yellow protein from *Ectothiorhodospira halophila*, *FEBS Lett.*, 458, 2, 252–256, 1999.
56. Demchuk, E., Genick, U.K., Woo, T.T., Getzoff, E.D., and Bashford, D., Protonation states and pH titration in the photocycle of photoactive yellow protein, *Biochemistry*, 39, 5, 1100–1113, 2000.
57. Takeshita, K., Imamoto, Y., Kataoka, M., Mihara, K., Tokunaga, F., and Terazima, M., Structural change of site-directed mutants of PYP: new dynamics during pR state, *Biophys. J.*, 83, 3, 1567–1577, 2002.
58. Takeshita, K., Imamoto, Y., Kataoka, M., Tokunaga, F., and Terazima, M., Themodynamic and transport properties of intermediate states of the photocyclic reaction of photoactive yellow protein, *Biochemistry*, 41, 9, 3037–3048, 2002.
59. van Brederode, M.E., Hoff, W.D., Van Stokkum, I.H., Groot, M.L., and Hellingwerf, K.J., Protein folding thermodynamics applied to the photocycle of the photoactive yellow protein, *Biophys. J.*, 71, 1, 365–380, 1996.
60. van der Horst, M.A., van Stokkum, I.H., Crielaard, W., and Hellingwerf, K.J., The role of the *N*-terminal domain of photoactive yellow protein in the transient partial unfolding during signalling state formation, *FEBS Lett.*, 497, 1, 26–30, 2001.

61. Hoff, W.D., Xie, A., Van Stokkum, I.H., Tang, X.J., Gural, J., Kroon, A.R., and Hellingwerf, K.J., Global conformational changes upon receptor stimulation in photoactive yellow protein, *Biochemistry*, 38, 3, 1009–1017, 1999.
62. Craven, C.J., Derix, N.M., Hendriks, J., Boelens, R., Hellingwerf, K.J., and Kaptein, R., Probing the nature of the blue-shifted intermediate of photoactive yellow protein in solation by NMR: Hydrogen–deuterium exchange data and pH studies, *Biochemistry*, 39, 47, 14392–14399, 2000.
63. Rubinstenn, G., Vuister, G.W., Mulder, F.A., Dux, P.E., Boelens, R., Hellingwerf, K.J., and Kaptein, R., Structural and dynamic changes of photoactive yellow protein during its photocycle in solution, *Nat. Struct. Biol.*, 5, 7, 568–570, 1998.
64. Genick, U.K., Borgstahl, G.E., Ng, K., Ren, Z., Pradervand, C., Burke, P.M., Srajer, V., Teng, T.Y., Schildkamp, W., McRee, D.E., Moffat, K., and Getzoff, E.D., Structure of a protein photocycle intermediate by millisecond time-resolved crystallography, *Science*, 275, 5305, 1471–1475, 1997.
65. Kandori, H., Iwata, T., Hendriks, J., Maeda, A., and Hellingwerf, K.J., Water structural changes involved in the activation process of photoactive yellow protein, *Biochemistry*, 39, 27, 7902–7909, 2000.
66. Hendriks, J., Gensch, T., Hviid, L., van Der Horst, M.A., Hellingwerf, K.J., and van Thor, J.J., Transient exposure of hydrophobic surface in the photoactive yellow protein monitored with nile red, *Biophy. J.*, 82, 3, 1632–1643, 2002.
67. Hendriks, J., Hoff, W.D., Crielaard, W., and Hellingwerf, K.J., Protonation/deprotonation reactions triggered by photoactivation of photoactive yellow protein from *Ectothiorhodospira halophila*, *J. Biol. Chem.*, 274, 25, 17,655–17,660, 1999.
68. Groenhof, G., Lensink, M.F., Berendsen, H.J., and Mark, A.E., Signal transduction in the photoactive yellow protein. II. Proton transfer initiates conformational changes, *Proteins: Struct., Function, and Genet.*, 48, 2, 212–219, 2002.
69. Sergi, A., Gruning, M., Ferrario, M., and Buda, F., Density functional study of the photoactive yellow protein's chromophore, *J. Phys. Chem. B*, 105, 19, 4386–4391, 2001.
70. Miller, A., Leigeber, H., Hoff, W.D., and Hellingwerf, K.J., A light-dependent branching-reaction in the photocycle of the yellow protein from *Ectothiorhodospira-Halophila*, *Biochim. Biophys. Acta*, 1141, 2–3, 190–196, 1993.
71. Lee, B.C., Pandit, A., Croonquist, P.A., and Hoff, W.D., Folding and signaling share the same pathway in a photoreceptor, *Proc. Natl. Acad. Sci.U.S.A.* 98, 16, 9062–9067, 2001.
72. Lee, B.C., Croonquist, P.A., and Hoff, W.D., Mimic of photocycle by a protein folding reaction in photoactive yellow protein, *J. Biol. Chem.*, 276, 48, 44,481–44,487, 2001.
73. Devanathan, S., Brudler, R., Hessling, B., Woo, T.T., Gerwert, K., Getzoff, E.D., Cusanovich, M.A., and Tollin, G., Dual photoactive species in Glu46Asp and Glu46Ala mutants of photoactive yellow protein: a pH-driven color transition, *Biochemistry*, 38, 41, 13,766–13,772, 1999.
74. Devanathan, S., Genick, U.K., Canestrelli, I.L., Meyer, T.E., Cusanovich, M.A., Getzoff, E.D., and Tollin, G., New insights into the photocycle of *Ectothiorhodospira halophila* photoactive yellow protein: photorecovery of the long-lived photobleached intermediate in the Met100Ala mutant, *Biochemistry*, 37, 33, 11,563–11,568, 1998.
75. Sasaki, J., Kumauchi, M., Hamada, N., Oka, T., and Tokunaga, F., Light-induced unfolding of photoactive yellow protein mutant M100L, *Biochemistry*, 41, 6, 1915–1922, 2002.
76. Kumauchi, M., Hamada, N., Sasaki, J., and Tokunaga, F., A role of methionine100 in facilitating PYP(M)-decay process in the photocycle of photoactive yellow protein, *J. Biochem.*, 132, 2, 205–210, 2002.
77. Aulin-Erdtman, G. and Sandén, R., Spectrographic contributions to Lignin chemistry, *Acta Chem. Scand.*, 22, 1187–1209, 1968.
78. Kroon, A.R., Hoff, W.D., Fennema, H.P., Gijzen, J., Koomen, G.J., Verhoeven, J.W., Crielaard, W., and Hellingwerf, K.J., Spectral tuning, fluorescence, and photoactivity in hybrids of photoactive yellow protein, reconstituted with native or modified chromophores, *J. Biol. Chem.*, 271, 50, 31,949–31,956, 1996.

79. Mihara, K., Hisatomi, O., Imamoto, Y., Kataoka, M., and Tokunaga, F., Functional expression and site-directed mutagenesis of photoactive yellow protein, *J. Biochem.*, 121, 5, 876–880, 1997.
80. Brudler, R., Meyer, T.E., Genick, U.K., Devanathan, S., Woo, T.T., Millar, D.P., Gerwert, K., Cusanovich, M.A., Tollin, G., and Getzoff, E.D., Coupling of hydrogen bonding to chromophore conformation and function in photoactive yellow protein, *Biochemistry*, 39, 44, 13,478–13,486, 2000.
81. Imamoto, Y., Koshimizu, H., Mihara, K., Hisatomi, O., Mizukami, T., Tsujimoto, K., Kataoka, M., and Tokunaga, F., Roles of amino acid residues near the chromophore of photoactive yellow protein, *Biochemistry*, 40, 15, 4679–4685, 2001.
82. Koradi, R., Billeter, M., and Wuthrich, K., MOLMOL: a program for display and analysis of macromolecular structures, *J. Mol. Graphics*, 14, 1, 51–55, 1996.
83. Thompson, J.D., Higgins, D.G., and Gibson, T.J., CLUSTAL W: improving the sensitivity of progressive multiple sequence alignment through sequence weighting, position-specific gap penalties and weight matrix choice, *Nucl. Acids Res.*, 22, 22, 4673–4680, 1994.
84. Hellingwerf, K.J., Hendriks, J., and Gensch, T., Photoactive Yellow Protein, a new type of photoreceptor protein: Will this "Yellow Lab" bring us where we want to go?, *J. Phys. Chem.*, 107, 1082–1094, 2003.

124

Microbial Rhodopsins: Transport and Sensory Proteins throughout the Three Domains of Life

Kwang-Hwan Jung
University of Texas

John L. Spudich
University of Texas

124.1 Summary

Archaeal rhodopsins, photoactive seven transmembrane helix proteins that use all-*trans* retinal as their chromophore, have been known for three decades and extensively studied in extreme halophiles. In the past 3 years, microbial genome sequencing and environmental genomics revealed archaeal rhodopsin homologs in the other two domains of life as well, namely, Bacteria and Eucarya. Microorganisms containing these genes inhabit diverse environments, including salt flats, soil, freshwater, and the world's oceans. They comprise a broad phylogenetic range of microbial life, including haloarchaea, proteobacteria, cyanobacteria, fungi, and algae. Analyses of the new microbial rhodopsins by genetic, biochemical, and structural techniques are beginning to reveal a variety of photosensory signaling and light-driven transport mechanisms in diverse life forms.

124.2 Introduction

In the 1970s and early 1980s, four rhodopsins were discovered in the cytoplasmic membrane of the archaeon *Halobacterium salinarum*: the light-driven ion pumps bacteriorhodopsin (BR[1]) and halorhodopsin (HR[2,3]), and the phototaxis receptors sensory rhodopsin I (SRI[4]), and sensory rhodopsin II (SRII[5]). Many laboratories extensively characterized this family of proteins with a battery of diverse techniques, because they provide excellent model systems for the two fundamental functions of membranes: active transport and sensory signaling. Twenty-nine variants of BR, HR, SRI, and SRII were documented in related extremely halophilic archaea, such as *Natronomonas pharaonis* and *Haloarcula vallismortis*. Members of the "archaeal rhodopsin family" were generally assumed to be only in the haloarchaea and appeared to be restricted to the extreme halophilic environments of solar evaporation ponds and other regions of near-saturated salt concentration.

0-8493-1348-1/04/$0.00+$1.50

Our understanding of the abundance and diversity of this family was radically transformed by findings over the past 3 years. Genome projects on a number of microbes revealed archaeal rhodopsin homologs in the other two domains of life as well, namely, bacteria and eukaryotes. Organisms containing these homologs live in such diverse environments as soil, freshwater, and ocean waters, and they include a broad range of microbial life, including proteobacteria, cyanobacteria, fungi, and algae (Table 124.1). Analysis of the sequences of the new microbial rhodopsins, their heterologous expression and study, and spectroscopic analysis of environmental samples showed that they fulfill ion transport and sensory functions in these organisms. The purpose of this review is to summarize what we learned regarding the rapidly expanding group of retinylidene pigments we now call the "microbial rhodopsin family."

124.3 Microbial Rhodopsins

Archaeal Rhodopsins

As evidenced by the many incisive articles in this issue, the archaeal rhodopsins rank among the best-understood membrane proteins in terms of structure and function. Atomic resolution structures, which exist for only a handful of membrane proteins, were obtained from electron and x-ray crystallography of three of the archaeal rhodopsins: bacteriorhodopsin,[6–8] halorhodopsin,[9] and recently, sensory rhodopsin II (NpSRII from *N. pharaonis*[10,11b,11c]). The transport and sensory rhodopsins share a common design of seven transmembrane helices forming an interior pocket for the chromophore all-*trans* retinal. The retinal binding pocket is comprised of residues from each of the seven helices, and it is the conservation of these residues that provides the most definitive identification of archaeal rhodopsin homologs in other organisms. Conservation outside of the pocket is sparse but recognizable (Figure 124.1). Even between members of the archaeal branch, conservation outside the pocket is limited. For example, the *N. pharaonis* phototaxis receptor NpSRII is 27% identical to BR in amino acid sequence and exhibits typically ~40% identity with other sensory rhodopsins; all four archaeal rhodopsins exhibit ~80% identity in the 22 residues that form the retinal binding pockets in BR, HR, and NpSRII. In the new rhodopsins, 55 to 75% identity is found in retinal binding pocket residues (Figure 124.1).

The functions of the four archaeal rhodopsins were well characterized. BR (λ_{max} 568 nm) and HR (λ_{max} 576 nm) are light-driven ion pumps for protons and chloride, respectively, absorbing maximally in the green-orange region of the spectrum.[12,13] Their electrogenic transport cycles provide energy to the cell under conditions in which respiratory electron transport activity is low. Accordingly, their production in the cells is induced when oxygen is depleted in late exponential/early stationary phase cultures. BR and HR hyperpolarize the membrane to generate a positive outside membrane potential, thereby creating inwardly directed proton motive force. HR further contributes to pH homeostasis by hyperpolarizing the membrane by electrogenic chloride uptake rather than proton ejection, thereby providing an electrical potential for net proton uptake, which is especially important in alkaline conditions.

SRI and SRII are phototaxis receptors controlling the cell's swimming behavior in response to changes in light intensity and color.[14] SRI (λ_{max} 587 nm) is also induced in cells in late exponential/early stationary phase and attracts the cells to orange light, which is useful to the transport rhodopsins. To avoid guiding the cells into light containing harmful near-UV radiation, SRI has a color-discriminating mechanism that ensures that the cells will be attracted to orange light only if that light is not accompanied by near-UV wavelengths.[15] The mechanism is based on photochromic reactions. If SRI absorbs a single photon (maximal absorption in the orange), it produces a photointermediate species called SRI-M or S_{373} (λ_{max} 373 nm) that is interpreted by the cell's signal transduction machinery as an attractant signal. However, if S_{373} is photoexcited, it generates a repellent signaling photointermediate. Therefore, single-photon excitation of SRI, such as occurs in orange light, attracts the cells, whereas two-photon excitation, as occurs in white light, repels the cells. SRII absorbs in the mid-visible range (λ_{max} 487 nm) and appears to serve only a repellent function.[16] It is the only rhodopsin in *H. salinarum* produced in cells during vigorous aerobic grow when light is not being used for energy and is best avoided.

TABLE 124.1 List of microbial rhodopsins with database accession numbers. (BR: bacteriorhodopsin, HR: halorhodopsin, SRI & II: sensory rhodopsin I & II, NR: *Neurospora* rhodopsin, CSRA & B: *Chlamydomonas* sensory rhodopsin A & B)

Species and Name	Accession#	Comments
Archaea		
Haloarcula argentinensis BR	D31880	H^+ pump
Haloarcula japonica BR	AB029320	H^+ pump
Haloarcula sp. (Andes) BR	S76743	H^+ pump
Haloarcula vallismortis BR	D31882	H^+ pump
Haloarcula vallismortis HR	D31881	Cl^- pump
Haloarcula vallismortis SRI	D83748	Phototaxis
Haloarcula vallismortis SRII	Z35308	Phototaxis
Halobacterium salinarum BR	V00474	λ_{max} 568 nm, H^+ pump
Halobacterium salinarum HR	D43765	λ_{max} 576 nm, Cl^- pump
Halobacterium salinarum SRI	L05603	λ_{max} 587 nm, phototaxis (attractant/repellent)
Halobacterium salinarum SRII	U62676	λ_{max} 487 nm, phototaxis (repellent)
Halobacterium mex BR	D11056	H^+ pump
Halobacterium port BR	D11057	H^+ pump
Halobacterium port HR	D43766	Cl^- pump
Halobacterium shark BR	D11058	H^+ pump
Halobacterium shark HR	D43765	Cl^- pump
Halobacterium sp. AUS-1 BR	J05165	H^+ pump
Halobacterium sp. AUS-1 SRII	AB059748	Phototaxis
Halobacterium sp. AUS-2 BR	S56354	H^+ pump
Halobacterium sp. SG1 BR	X70291	H^+ pump
Halobacterium sp. SG1 HR	X70292	Cl^- pump
Halobacterium sp. SG1 SRI	X70290	Phototaxis
Halorubrum sodomense BR	D50848	H^+ pump
Halorubrum sodomense HR	AB009622	Cl^- pump
Halorubrum sodomense SRI	AB009623	Phototaxis
Haloterrigena sp. Arg-4 BR	AB009620	H^+ pump
Haloterrigena sp. Arg-4 HR	AB009621	Cl^- pump
Natronomonas pharaonis HR	J05199	Cl^- pump
Natronomonas pharaonis SRII	Z35086	λ_{max} 497 nm, phototaxis (repellent)
Eubacteria		
Anabaena sp. PCC7120	AP003592	Also known as *Nostoc*, λ_{max} 543 nm, photosensory
Magnetospirillum magnetotacticum	—	genome.ornl.gov/microbial/mmag
γ-proteobacterium (BAC31A8)	AF279106	λ_{max} 527 nm, H^+ pump
γ-proteobacterium (HOT75m4)	AF349981	λ_{max} = 490 nm, H^+ pump
Fungi		
Botrytis cinerea	AL115930	
Botryotinia fuckeliana	—	cogeme.ex.ac.uk
Cryptococcus neoformans	—	www.genome.ou.edu/cneo.html
Fusarium sporotrichioides	BI187800	
Gibberella zeae	—	cogeme.ex.ac.uk
Leptosphaeria maculans	AF290180	
Mycosphaerella graminicola	AW180117	Two homologs are present
Neurospora crassa NR	AF135863	λ_{max} = 534 nm
Algae		
Chlamydomonas reinhardtii CSRA	AF508965	Photomotility for high-light intensity
Chlamydomonas reinhardtii CSRB	AF508966	Photomotility for low-light intensity
Pyrocystis lunula	AF508258	Dinoflagellate
Guillardia theta	AW342219	Cryptomonad

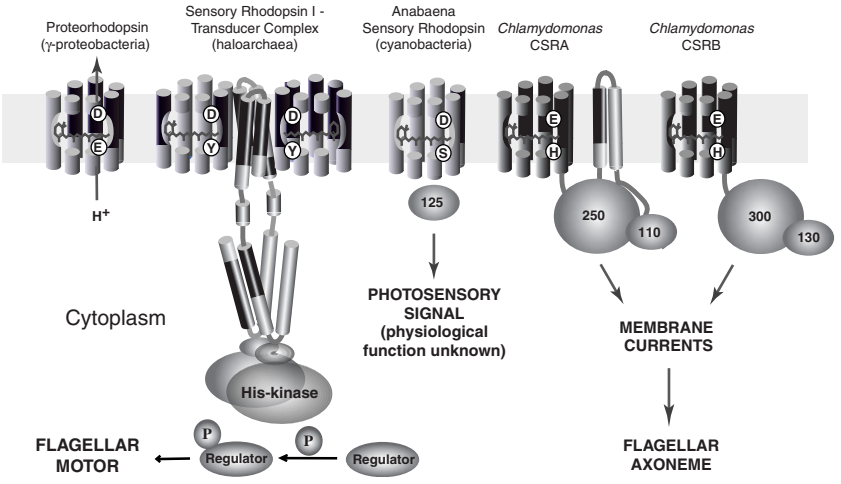

FIGURE 124.1 Diversity among the archaeal-type rhodopsins. Domains of the two sensory rhodopsins from *Chlamydomonas reinhardtii,* CSRA and CSRB, compared with those for proteorhodopsin and sensory rhodopsin I (in a dimeric complex with its cognate dimeric transducer) from haloarchaea, and a cyanobacterial sensory rhodopsin from *Anabaena*. The domains for CSRA, CSRB, and *Anabaena* sensory rhodopsin are based on known crystal structures of microbial rhodopsins and secondary structure predictions. The drawing for the sensory rhodopsin I transducer, HtrI, is based on biochemical data and secondary structure predictions. All of the rhodopsins shown were demonstrated to contain an all-*trans* retinal chromophore covalently linked to a conserved lysine residue in the seventh transmembrane helix. Amino acid variations within or near the retinal-binding pocket contribute to differences in the absorption spectrum of each pigment or specialized function. Residues in the third transmembrane helix of bacteriorhodopsin that are important for proton translocation (Asp85 and Asp96), and the amino acid differences at their corresponding positions in the other rhodopsins, are highlighted. For CSRA and CSRB, the numbers correspond to the number of amino acid residues in each domain. The cyanobacterial sensory rhodopsin and its cognate 125-residue putative transducer protein are based on Reference 34.

Comparison of the primary sequence (Figure 124.1) gives hints to distinguishing properties of different microbial rhodopsins, but most properties cannot be deduced from primary structure alone. An exemplary case is that of NpSRII, which is unusual in that its maximal absorption is shifted 70 to 90 nm to the blue of the other archaeal pigments.[17] Mutagenic substitution of 10 residues, in or near the retinal-binding pocket with their corresponding BR residues, produced only a 28 nm red shift of the NpSRII absorption maximum.[18,19] Structural differences responsible for the shift are evident in the 2.4 Å resolution structure.[11] One notable change is a displacement of the guanidinium group of Arg72 by 1.1 Å coupled with a rotation away from the Schiff base in NpSRII. This increase in distance reduces the influence of Arg72 on the counterion, thus strengthening the Schiff base–counterion interaction, shifting the absorption to shorter wavelengths. In addition, the position of the positive charge destabilizes the excited state, contributing further blue shift.[20] Arg72 is repositioned as a consequence of several factors, including movement of its helix backbone by 0.9 Å and the cavity created by changes from BR: Phe208 → Ile197, Glu194 → Pro183, and Glu204 → Asp192. Hence, the spectral tuning results from precise positioning of retinal-binding pocket residues and the guanidinium of Arg72, which could not be deduced from primary structure but required atomic-resolution tertiary structure information.

Differences between Sensory and Transport Rhodopsins

A fundamental question is how the common design of microbial rhodopsin proteins adapted to carry out their two distinct functions (Figure 124.2). Transport rhodopsins function independently of interaction with other proteins and translocate ions through an intramolecular channel. The archaeal sensory rhodopsins, on the other hand, transmit signals by protein–protein interaction with transducer proteins that control cytoplasmic enzymatic activity.[21–23] In HsSRI and HsSRII, the receptors form a molecular

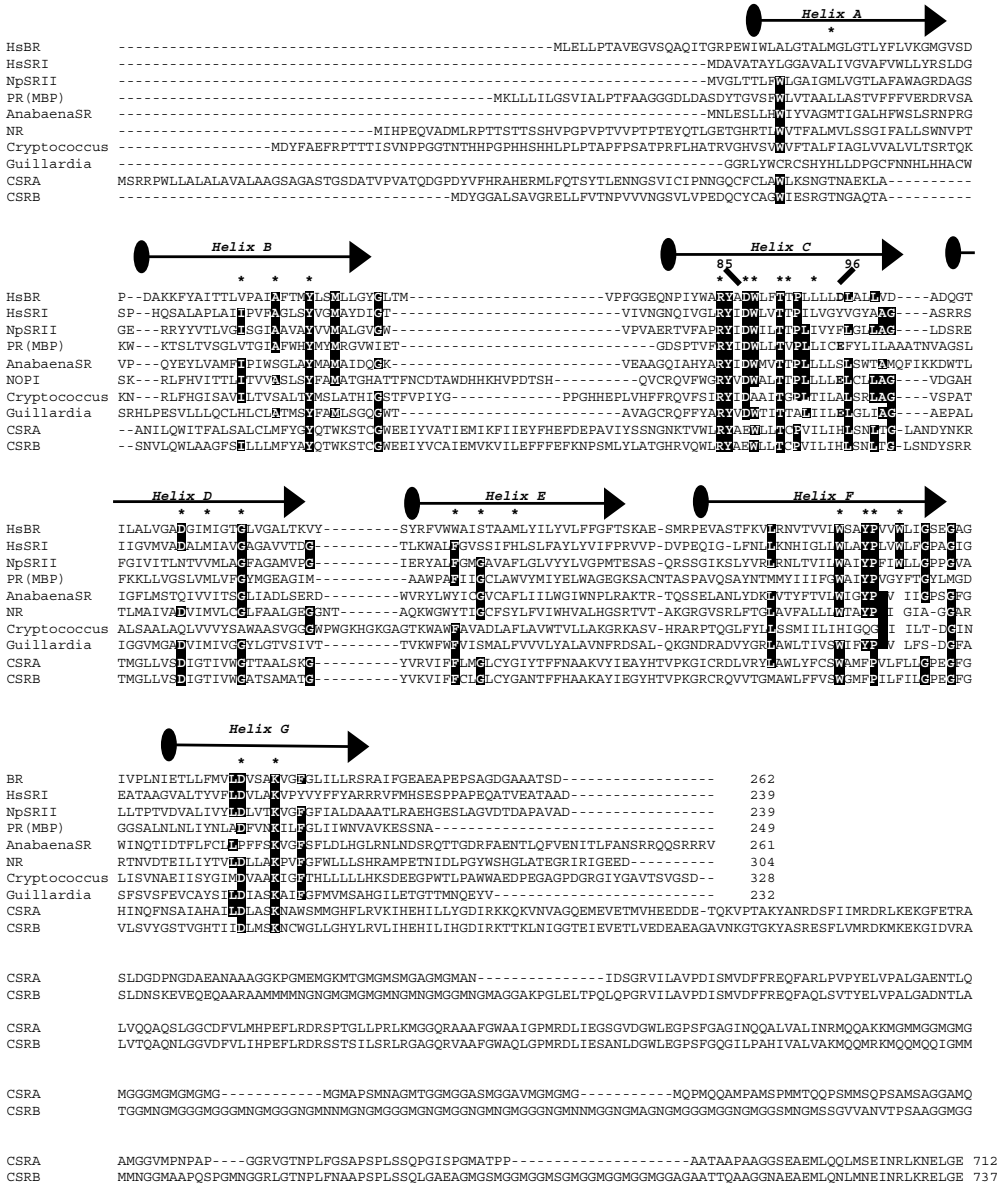

FIGURE 124.2 Primary sequence comparison of the microbial rhodopsins. (Hs: *Halobacterium salinarum*, Np: *Natronomonas pharaonis,* BR: bacteriorhodopsin, SR: sensory rhodopsin, PR: proteorhodopsin, NR: *Neurospora* rhodopsin, CSRA and CSRB: *Chlamydomonas* sensory rhodopsins A and B) Conserved residues are marked with black boxes, and residues in the retinal-binding pocket are marked with an asterisk.

complex with their cognate integral membrane transducer proteins, HtrI and HtrII, respectively, which, in turn, modulate a cytoplasmic phosphorylation[24] pathway that controls the cell's motility apparatus. Deletion and chimera experiments with the *H. salinarum* transducers showed that the interaction specificities of SRI with HtrI and SRII with HtrII are determined by the transmembrane helices of the Htr subunits,[25,26] indicating that interaction occurs within or near the membrane. A fragment of NpHtrII lacking most of the cytoplasmic domain interacts with NpSRII *in vitro*,[27,28] and functionally *in vivo*,[29] supporting that transmembrane helix–helix interactions occur also in the *N. pharaonis* pair and is seen in NpSRII/NpHtrII cocrystals (IIc).

Important to the analysis of the new rhodopsins is whether clues can be found in their primary sequences and spectroscopic properties as to whether they carry out transport or sensory functions. One difference in the primary sequence between BR, HR, and the SRs stands out. Asp96 in BR functions as a proton donor, returning a proton to the Schiff base from the cytoplasmic side of the protein during the pumping cycle. This proton transfer improves the pumping efficiency of BR by accelerating the decay of its unprotonated Schiff base photocycle intermediate, M, and is present in all BR homologs in the haloarchaea. In the sensory rhodopsins, the corresponding M intermediates are signaling states of the receptor proteins (demonstrated unequivocally only for HsSRI), and longer M lifetimes increase the signaling efficiencies of the receptors. Accordingly, each of the five known sensory rhodopsin sequences lacks a carboxylate residue at the position corresponding to Asp96 and contains Tyr or Phe instead. The residue corresponding to Asp85, which is the proton acceptor from the Schiff base, is a carboxylate residue in BR, SRI, and SRII, and in each of the newly identified rhodopsins (Figure 124.1). HR, not shown in the figure, does not produced an unprotonated Schiff base intermediate in its photocycle and, therefore, does not contain a carboxylic acid residue in the positions corresponding to Asp96 and Asp85. It is likely that the presence of a carboxylate at the position corresponding to Asp96 in BR is necessary, but not sufficient, for identification of a new rhodopsin as a proton pump.

More than order-of-magnitude faster photocycling rates distinguish the transport from the sensory pigments; the latter, in fact, were initially called "slow-cycling rhodopsins" for this reason.[4,30] The transport rhodopsins are characterized by photocycles typically <30 ms, whereas sensory rhodopsins are slow-cycling pigments with photocycle halftimes typically >300 ms.[31] This large kinetic difference is functionally important, because a rapid photocycling rate is advantageous for efficient ion pumping, whereas a slower cycle provides more efficient light detection, because signaling states persist for longer times.

Bacterial Rhodopsins

Proteorhodopsins

A gene encoding a bacterial homolog of the archaeal rhodopsins was revealed by genomic analysis of environmental samples of marine picoplankton from Monterey Bay, California.[32] The gene was functionally expressed in *Escherichia coli* and bound retinal to form an active, light-driven proton pump. The rRNA sequence on the same DNA fragment identified the organism as an uncultivated γ-proteobacterium (the SAR86 group), and the expressed protein was named proteorhodopsin. A phylogenetic comparison with archaeal rhodopsins placed proteorhodopsin on an independent long branch. The new rhodopsin (λ_{max} 527 nm) exhibited a photochemical reaction cycle with intermediates and kinetics characteristic of archaeal proton-pumping rhodopsins. The efficient proton pumping and rapid photocycle (15 ms halftime) of the new pigment strongly suggests that proteorhodopsin functions as a proton pump in its natural environment.

Retinylidene pigmentation with photocycle characteristics identical to that of the *E. coli*-expressed proteorhodopsin gene was subsequently demonstrated by flash spectroscopy in membranes prepared from Monterey Bay picoplankton.[33] Estimated from flash-induced absorbance changes, a high density of proteorhodopsin in the SAR86 membrane is indicated by the data, arguing for a significant role of the protein in the physiology of these bacteria. The flash photolysis data provided direct physical evidence for the existence of proteorhodopsin-like pigments and endogenous retinal molecules in the prokaryotic fraction of the Monterey Bay coastal surface waters. Furthermore, genomic analysis of bacterioplankton of Antarctica and the central North Pacific Ocean near Hawaii (both surface and 75 m deep waters) revealed proteorhodopsin variants in these different ocean environments. The Hawaiian deep proteorhodopsin variant exhibits a blue-shifted absorption (λ_{max} 490 nm) matching the blue-shifted incident light at that depth. Therefore, the protein pigments comprising this family are spectrally tuned to different habitats, absorbing light at different wavelengths in accordance with light available in the environment. The abundance and widespread presence of proteorhodopsin variants throughout the world's oceans indicate proteorhodopsin light-driven proton pumping is a globally significant oceanic microbial process (33b).

Anabaena Sensory Rhodopsin

A rhodopsin pigment in a cyanobacterium establishes that sensory rhodopsins also exist in eubacteria. A gene encoding a homolog of the archaeal rhodopsins was found via a genome sequencing project of *Anabaena (Nostoc)* sp. PCC7120 at Kazusa Institute, Japan (http://www.kazusa.or.jp/). The opsin gene was expressed in *E. coli* and bound all-*trans* retinal to form a pink pigment (λ_{max} 543 nm). The *Anabaena* rhodopsin in *E. coli* membranes exhibited a photochemical reaction cycle with an M-like photointermediate and 110 ms half-life at pH 6.8.[34]

The opsin gene and another open reading frame separated by 16 base pairs under the same promoter were found in the genome. This operon is predicted to encode a 261-residue (opsin) and a 125-residue (14 kDa) protein. The rate of the photocycle is increased ~20% when the *Anabaena* rhodopsin and the soluble protein are coexpressed in *E. coli*,[34] indicating physical interaction between the two proteins. We also confirmed binding of 14 kDa protein to *Anabaena* rhodopsin by affinity enrichment measurements and Biacore interaction analysis. The pigment did not exhibit detectable proton transport activity when expressed in *E. coli*, and Asp96, the proton donor of BR, is replaced with Ser86 in *Anabaena* rhodopsin. These observations are compelling in that *Anabaena* opsin functions as a photosensory receptor in its natural environment, and that the 125-residue cytoplasmic soluble protein transduces a signal from the receptor, unlike the archaeal sensory rhodopsins that transmit signals by transmembrane helix–helix interactions with integral membrane transducers.

Magnetospirillum Rhodopsin

Genome sequencing of the α-proteobacterium *Magnetospirillum magnetotacticum* revealed a microbial opsin gene (Table 124.1), preceded by a homolog of *brp*, which encodes an enzyme for synthesis of retinal from β-carotenene in *H. salinarum*.[35] The two-gene operon contains a single promoter.

Eukaryotic Rhodopsins

Fungal Rhodopsins

A sequencing project on the genome of the filamentous fungus *Neurospora crassa* revealed the first of the eukaryotic homologs designated NOP-1.[36] A search of genome databases currently in progress indicates the presence of archaeal rhodopsin homologs in various fungi, including plant and human pathogens — Ascomycetes: *Botrytis cinerea, Botryotinia fuckeliana* (anamorph *Botrytis cinerea*), *Fusarium sporotrichioides, Gibberella zeae* (anamorph *Fusarium graminearum*), *Leptosphaeria maculans*, *Mycosphaerella graminicola* (two opsin homologs); and Basidiomycetes: *Cryptococcus neoformans*. Each of these organisms contains genes predicted to encode proteins with the retinal-binding lysine in the seventh helix and high identity in the retinal-binding pocket. The Asp Schiff base counterion and proton acceptor (Asp85 in BR) are conserved among all fungal opsin homologs, and the carboxylate proton donor specific to proton pumps (Asp96 in BR) is also either Asp or Glu, except in *Cryptococcus*, which contains an Ala residue.

The *nop-1* gene was heterologously expressed in the yeast *Pichia pastoris*, and it encodes a membrane protein that forms with all-*trans* retinal a green light-absorbing pigment (λ_{max} 534 nm) with a spectral shape and bandwidth typical of rhodopsins.[37] Laser flash kinetic spectroscopy of the retinal-reconstituted NOP-1 pigment (i.e., *Neurospora* rhodopsin) in *Pichia* membranes revealed that it undergoes a seconds-long photocycle with M and O intermediates spectrally similar to intermediates detected in BR and SRII.

The physiological function of *Neurospora* rhodopsin has not yet been identified. Based on the long lifetime of the intermediates in its photocycle and its apparent lack of ion transport activities (at least when heterologously expressed[38]), it seems likely to serve as a sensory receptor for one or more of the several different light responses exhibited by the organism, such as photocarotenogenesis or light-enhanced conidiation. *Neurospora* is nonmotile, but phototaxis by zoospores of the motile fungus *Allomyces reticulatus* was shown to be retinal dependent,[39] and therefore, photomotility modulation is a likely photosensory function of rhodopsins in this particular fungal species.

Algal Rhodopsins

Recently, we identified short cDNA sequences in an EST database at Kazusa Institute (http://www.kazusa.or.jp/) and, based on this information, cloned two archaeal-type opsin genes from a cDNA library (provided from the *Chlamydomonas* Genetics Center). A microbial rhodopsin homolog gene is also present in *Guillardia theta,* which is a small biflagellate organism considered a protozoan and an alga (Figure 124.1) and is also found in the dinoflagellate *Pyrocystis lunula*. The *csoA* and *csoB* (*Chlamydomonas* sensory opsin A and B) genes encode 712 and 737 amino acid proteins (Figure 124.1). The *N*-terminal 300 residues have a significant homology to archaeal rhodopsins with seven transmembrane helices and the conserved retinal binding pocket (Figure 124.1). The *Chlamydomonas* rhodopsins provide the first examples of evolution fusing the microbial rhodopsin motif with other domains.

Early work established that the green alga *Chlamydomonas* uses retinylidene receptors for photomotility responses. Restoration of photomotility responses by retinal addition to a pigment-deficient mutant of *Chlamydomonas reinhardtii* first indicated a retinal-containing photoreceptor.[40] Subsequent *in vivo* reconstitution studies with retinal analogs prevented from isomerizing around specific bonds ("isomer-locked retinals") in several laboratories further established that the *Chlamydomonas* rhodopsins governing phototaxis and the photophobic response have the same isomeric configuration (all-*trans*), photoisomerization across the C13–C14 double bond (all-*trans* to *13-cis*), and 6-*s*-*trans* ring-chain conformation (coplanar) as the archaeal rhodopsins.[41–45]

The proteins encoded by *csoA* and *csoB* complexed with retinal (called CSRA and CSRB) are the first of the eukaryotic archaeal-type rhodopsins for which we can assign physiological roles.[46] We found by RNA*i* suppression of gene expression that the *Chlamydomonas* rhodopsins CSRA and CSRB mediate photomotility responses (phototaxis and photophobic reactions) to high- and low-intensity light, respectively. The functions of the two rhodopsins were demonstrated by analysis of electrical currents and motility responses in transformants with RNA*i* directed against each of rhodopsin genes. CSRA has an absorption maximum near 510 nm and mediates a fast photoreceptor current that saturates at high-light intensity. In contrast, CSRB absorbs maximally at 470 nm and generates a slow current saturating at low-light intensity.[46] The saturation at different light fluence levels extends the range of light intensity to which the organism can respond.

A protein that binds radiolabeled retinal was isolated from *Chlamydomonas* eyespot preparations.[47] For several years, this abundant protein in the eyespot membranes was considered the photoreceptor for photomotile responses.[48] However, its gene-predicted primary sequence, as well as that of a similar *Volvox* protein,[49] suggest two to four transmembrane helices and no homology to archaeal opsins. Moreover, recently, the so-called "chlamyrhodopsin" was ruled out as a photoreceptor pigment for phototaxis or photophobic responses in *Chlamydomonas*.[50]

Opsin-Related Proteins

Several other genes in the fungi *N. crassa* (YRO2), *Aspergillus nidulans*, *Saccharomyces cerevisiae*, *Schizosaccharomyces pombe*, *Coccidioides immitis*, *Coriolus versicolor*, and in the plant *Sorghum bicolor* (Corn) encode proteins that exhibit significant homology to microbial rhodopsins, but they are missing the critical lysine residue in the seventh helix that forms the covalent linkage with retinal. The microbial-opsin-related proteins are, therefore, not likely to form photoactive pigments with retinal. The most conserved region in these proteins is along Helix C, E, and the middle of Helix F. It is intriguing that one of the yeast opsin-related proteins, HSP30 (heat shock protein 30), is implicated as interacting with a proton transport protein, the H^+ATPase. HSP30 downregulates stress stimulation of H^+ATPase activity under heat shock conditions.[51,52] Probably, the conformational switching properties of the archaeal rhodopsins were preserved in these opsin-related proteins, while the photoactive site was lost and replaced presumably by another input module, such as a protein–protein interaction domain.

124.4 Future Directions

Because microbial rhodopsins are present in all three domains of life, progenitors of these proteins may have existed in the early phases of evolution, before the divergence of archaea, eubacteria, and eukaryotes.

Is so, light-driven ion transport as a means of obtaining cellular energy may well have predated the development of photosynthesis and represents one of the earliest means by which organisms tapped solar radiation as an energy source. As more rhodopsins are identified, their evolution and dissemination into such a wide variety of organisms, whether by divergence from a common progenitor or horizontal gene transfer, should become clearer.

There is much work to be done to understand the physiological roles and molecular mechanisms of the rhodopsins so far identified in the various microbial species. It seems likely that we will see even more members of this family, as genomic sequencing becomes ever more rapid. The vast majority of microbial species have never been cultivated in a laboratory. Therefore, the use of microbial rhodopsin probes in environmental genomics, which expands the search for orthologous genes in uncultivated organisms, is likely to be especially fruitful.

References

1. Oesterhelt, D. and Stoeckenius, W., Functions of a new photoreceptor membrane, *Proc. Natl. Acad. Sci. USA*, 70, 10, 2853, 1973.
2. Schobert, B. and Lanyi, J.K., Halorhodopsin is a light-driven chloride pump, *J. Biol. Chem.*, 257, 17, 10,306, 1982.
3. Matsuno-Yagi, A. and Mukohata, Y., Two possible roles of bacteriorhodopsin; a comparative study of strains of *Halobacterium halobium* differing in pigmentation, *Biochem. Biophys. Res. Commun.*, 78, 1, 237, 1977.
4. Bogomolni, R.A. and Spudich, J.L., Identification of a third rhodopsin-like pigment in phototactic *Halobacterium halobium*, *Proc. Natl. Acad. Sci. USA*, 79, 20, 6250, 1982.
5. Takahashi, T., Tomioka, H., Kamo, N., and Kobatake, Y., A photosystem other than PS370 also mediates the negative phototaxis of *Halobacterium halobium*, *FEMS Microbiol. Lett.*, 28, 161, 1985.
6. Grigorieff, N., Ceska, T.A., Downing, K.H., Baldwin, J.M., and Henderson, R., Electron-crystallographic refinement of the structure of bacteriorhodopsin, *J. Mol. Biol.*, 259, 3, 393, 1996.
7. Luecke, H., Schobert, B., Richter, H.T., Cartailler, J.P., and Lanyi, J.K., Structure of bacteriorhodopsin at 1.55 Å resolution, *J. Mol. Biol.*, 291, 4, 899, 1999.
8. Essen, L., Siegert, R., Lehmann, W.D., and Oesterhelt, D., Lipid patches in membrane protein oligomers: crystal structure of the bacteriorhodopsin-lipid complex, *Proc. Natl. Acad. Sci. USA*, 95, 20, 11,673, 1998.
9. Kolbe, M., Besir, H., Essen, L.O., and Oesterhelt, D., Structure of the light-driven chloride pump halorhodopsin at 1.8 Å resolution, *Science*, 288, 5470, 1390, 2000.
10. Kunji, E.R., Spudich, E.N., Grisshammer, R., Henderson, R., and Spudich, J.L., Electron crystallographic analysis of two-dimensional crystals of sensory rhodopsin II: a 6.9 Å projection structure, *J. Mol. Biol.*, 308, 2, 279, 2001.
11. (a) Luecke, H., Schobert, B., Lanyi, J.K., Spudich, E.N., and Spudich, J.L., Crystal structure of sensory rhodopsin II at 2.4 angstroms: insights into color tuning and transducer interaction, *Science*, 293, 5534, 1499, 2001. (b) Royant, A., Nollert, P., Edman, K., Neutze, R., Landau, E.M., Pebay-Peyroula, E., and Navarro, J., X-ray structure of sensory rhodopsin II at 2.1-Å resolution, *Proc. Natl. Acad. Sci. USA*, 98, 10131, 2001. (c) Gordeliy, V.I., Labahn, J., Moukhametzianov, R., Efremov, R., Granzin, J., Schlesinger, R., Buldt, G., Savopol, T., Scheidig, A.J., Klare, J.P., Engelhard, M., Molecular basis of transmembrane signalling by sensory rhodopsin II-transducer complex, *Nature,* 419, 6906, 484, 2002.
12. Varo, G., Analogies between halorhodopsin and bacteriorhodopsin, *Biochim. Biophys. Acta*, 1460, 1, 220, 2000.
13. Oesterhelt, D., The structure and mechanism of the family of retinal proteins from halophilic archaea, *Curr. Opinion Struct. Biol.*, 8, 4, 489, 1998.
14. Hoff, W.D., Jung, K.H., and Spudich, J.L., Molecular mechanism of photosignaling by archaeal sensory rhodopsins, *Annu. Rev. Biophys. Biomol. Struct.*, 26, 223, 1997.

15. Spudich, J.L. and Bogomolni, R.A., Mechanism of colour discrimination by a bacterial sensory rhodopsin, *Nature*, 312, 5994, 509, 1984.
16. Takahashi, T., Yan, B., Mazur, P., Derguini, F., Nakanishi, K., and Spudich, J.L., Color regulation in the archaebacterial phototaxis receptor phoborhodopsin (sensory rhodopsin II), *Biochemistry*, 29, 36, 8467, 1990.
17. Tomioka, H. and Sasabe, H., Isolation of photochemically active archaebacterial photoreceptor, pharaonis phoborhodopsin from *Natronobacterium pharaonis*, *Biochim. Biophys. Acta*, 1234, 2, 261, 1995.
18. Kamo, N., Shimono, K., Iwamoto, M., and Sudo, Y., Photochemistry and photoinduced proton-transfer by pharaonis phoborhodopsin, *Biochemistry (Moscow)*, 66, 11, 1277, 2001.
19. Shimono, K., Iwamoto, M., Sumi, M., and Kamo, N., Effects of three characteristic amino acid residues of pharaonis phoborhodopsin on the absorption maximum, *Photochem. Photobiol.*, 72, 1, 141, 2000.
20. Ren, L., Martin, C.H., Wise, K.J., Gillespie, N.B., Luecke, H., Lanyi, J.K., Spudich, J.L., and Birge, R.R., Molecular mechanism of spectral tuning in sensory rhodopsin II, *Biochemistry*, 40, 46, 13,906, 2001.
21. Seidel, R., Scharf, B., Gautel, M., Kleine, K., Oesterhelt, D., and Engelhard, M., The primary structure of sensory rhodopsin II: a member of an additional retinal protein subgroup is coexpressed with its transducer, the halobacterial transducer of rhodopsin II, *Proc. Natl. Acad. Sci. USA*, 92, 7, 3036, 1995.
22. Yao, V.J. and Spudich, J.L., Primary structure of an archaebacterial transducer, a methyl-accepting protein associated with sensory rhodopsin I, *Proc. Natl. Acad. Sci. USA*, 89, 24, 11,915, 1992.
23. Zhang, W., Brooun, A., Mueller, M.M., and Alam, M., The primary structures of the Archaeon *Halobacterium salinarium* blue light receptor sensory rhodopsin II and its transducer, a methyl-accepting protein, *Proc. Natl. Acad. Sci. USA*, 93, 16, 8230, 1996.
24. Rudolph, J., Tolliday, N., Schmitt, C., Schuster, S.C., and Oesterhelt, D., Phosphorylation in halobacterial signal transduction, *EMBO J.*, 14, 17, 4249, 1995.
25. Perazzona, B., Spudich, E.N., and Spudich, J.L., Deletion mapping of the sites on the HtrI transducer for sensory rhodopsin I interaction, *J. Bacteriol.*, 178, 22, 6475, 1996.
26. Zhang, X.N., Zhu, J., and Spudich, J.L., The specificity of interaction of archaeal transducers with their cognate sensory rhodopsins is determined by their transmembrane helices, *Proc. Natl. Acad. Sci. USA*, 96, 3, 857, 1999.
27. Sudo, Y., Iwamoto, M., Shimono, K., and Kamo, N., Pharaonis phoborhodopsin binds to its cognate truncated transducer even in the presence of a detergent with a 1:1 stoichiometry, *Photochem. Photobiol.*, 74, 3, 489, 2001.
28. Schmies, G., Engelhard, M., Wood, P.G., Nagel, G., and Bamberg, E., Electrophysiological characterization of specific interactions between bacterial sensory rhodopsins and their transducers, *Proc. Natl. Acad. Sci. USA*, 98, 4, 1555, 2001.
29. Jung, K.H., Spudich, E.N., Trivedi, V.D., and Spudich, J.L., An archaeal photosignal-transducing module mediates phototaxis in *Escherichia coli*, *J. Bacteriol.*, 183, 21, 6365, 2001.
30. Spudich, J.L., Zacks, D.N., and Bogomolni, R.A., Microbial sensory rhodopsins: photochemistry and function, *Isr. J. Photochem.*, 35, 495, 1995.
31. Spudich, J.L., Yang, C.S., Jung, K.H., and Spudich, E.N., Retinylidene proteins: structures and functions from archaea to humans, *Annu. Rev. Cell Dev. Biol.*, 16, 365, 2000.
32. Beja, O., Aravind, L., Koonin, E.V., Suzuki, M.T., Hadd, A., Nguyen, L.P., Jovanovich, S.B., Gates, C.M., Feldman, R.A., Spudich, J.L., Spudich, E.N., and DeLong, E.F., Bacterial rhodopsin: evidence for a new type of phototrophy in the sea, *Science*, 289, 5486, 1902, 2000.
33. (a) Beja, O., Spudich, E.N., Spudich, J.L., Leclerc, M., and DeLong, E.F., Proteorhodopsin phototrophy in the ocean, *Nature*, 411, 6839, 786, 2001. (b) Wang, W.W., Sineshchekov, O.A., Spudich, E.N., and Spudich, J.L., Spectroscopic and photochemical characterization of deep ocean proteorhodopsin, *J. Biol. Chem.*, in press, 2003.

34. Jung, K.H., Trivedi, V.D., and Spudich, J.L., Demonstration of a sensory rhodopsin in eubacteria, *Mol. Microbiol.*, 47, 6, 1513, 2002.
35. Peck, R.F., Echavarri-Erasun, C., Johnson, E.A., Ng, W.V., Kennedy, S.P., Hood, L., DasSarma, S., and Krebs, M.P., brp and blh are required for synthesis of the retinal cofactor of bacteriorhodopsin in *Halobacterium salinarum*, *J. Biol. Chem.*, 276, 8, 5739, 2001.
36. Bieszke, J.A., Braun, E.L., Bean, L.E., Kang, S., Natvig, D.O., and Borkovich, K.A., The nop-1 gene of Neurospora crassa encodes a seven transmembrane helix retinal-binding protein homologous to archaeal rhodopsins, *Proc. Natl. Acad. Sci. USA*, 96, 14, 8034, 1999.
37. Bieszke, J.A., Spudich, E.N., Scott, K.L., Borkovich, K.A., and Spudich, J.L., A eukaryotic protein, NOP-1, binds retinal to form an archaeal rhodopsin-like photochemically reactive pigment, *Biochemistry*, 38, 43, 14,138, 1999.
38. Brown, L.S., Dioumaev, A.K., Lanyi, J.K., Spudich, E.N., and Spudich, J.L., Photochemical reaction cycle and proton transfers in *Neurospora* rhodopsin, *J. Biol. Chem.*, 276, 35, 32,495, 2001.
39. Saranak, J. and Foster, K.W., Rhodopsin guides fungal phototaxis, *Nature*, 387, 6632, 465, 1997.
40. Foster, K.W., Saranak, J., Patel, N., Zarilli, G., Okabe, M., Kline, T., and Nakanishi, K., A rhodopsin is the functional photoreceptor for phototaxis in the unicellular eukaryote *Chlamydomonas*, *Nature*, 311, 5988, 756, 1984.
41. Sineshchekov, O.A., Govorunova, E.G., Der, A., Keszthelyi, L., and Nultsch, W., Photoinduced electric currents in carotenoid-deficient *Chlamydomonas* mutants reconstituted with retinal and its analogs, *Biophys. J.*, 66, 6, 2073, 1994.
42. Takahashi, T., Yoshihara, K., Watanabe, M., Kubota, M., Johnson, R., Derguini, F., and Nakanishi, K., Photoisomerization of retinal at 13-ene is important for phototaxis of *Chlamydomonas reinhardtii*: simultaneous measurements of phototactic and photophobic responses, *Biochem. Biophys. Res. Commun.*, 178, 3, 1273, 1991.
43. Sakamoto, M., Wada, A., Akai, A., Ito, M., Goshima, T., and Takahashi, T., Evidence for the archaebacterial-type conformation about the bond between the beta-ionone ring and the polyene chain of the chromophore retinal in chlamyrhodopsin, *FEBS Lett.*, 434, 3, 335, 1998.
44. Lawson, M.A., Zacks, D.N., Derguini, F., Nakanishi, K., and Spudich, J.L., Retinal analog restoration of photophobic responses in a blind *Chlamydomonas reinhardtii* mutant. Evidence for an archaebacterial like chromophore in a eukaryotic rhodopsin, *Biophys. J.*, 60, 6, 1490, 1991.
45. Hegemann, P., Gartner, W., and Uhl, R., All-*trans* retinal constitutes the functional chromophore in *Chlamydomonas* rhodopsin, *Biophys. J.*, 60, 1477, 1991.
46. Sineshchekov, O.A., Jung, K.H., and Spudich, J.L., Two rhodopsins mediate phototaxis to low- and high-intensity light in *Chlamydomonas reinhardtii*, *Proc. Natl. Acad. Sci. USA*, 99, 13, 8689, 2002.
47. Deininger, W., Kroger, P., Hegemann, U., Lottspeich, F., and Hegemann, P., *Chlamyrhodopsin* represents a new type of sensory photoreceptor, *EMBO J.*, 14, 23, 5849, 1995.
48. Hegemann, P., Vision in microalgae, *Planta*, 203, 3, 265, 1997.
49. Ebnet, E., Fischer, M., Deininger, W., and Hegemann, P., Volvoxrhodopsin, a light-regulated sensory photoreceptor of the spheroidal green alga *Volvox carteri*, *Plant Cell*, 11, 8, 1473, 1999.
50. Fuhrmann, M., Stahlberg, A., Govorunova, E., Rank, S., and Hegemann, P., The abundant retinal protein of the *Chlamydomonas* eye is not the photoreceptor for phototaxis and photophobic responses, *J. Cell Sci.*, 114, Pt 21, 3857, 2001.
51. Zhai, Y., Heijne, W.H., Smith, D.W., and Saier, M.H., Jr., Homologues of archaeal rhodopsins in plants, animals and fungi: structural and functional predications for a putative fungal chaperone protein, *Biochim. Biophys. Acta*, 1511, 2, 206, 2001.
52. Piper, P.W., Ortiz-Calderon, C., Holyoak, C., Coote, P., and Cole, M., Hsp30, the integral plasma membrane heat shock protein of *Saccharomyces cerevisiae*, is a stress-inducible regulator of plasma membrane H(+)- ATPase, *Cell Stress Chaperones*, 2, 1, 12, 1997.

125

Photochemical Aspect of Rhodopsin

Yoshinori Shichida
Kyoto University

Toru Yoshizawa
Kyoto University

125.1 Introduction

The visual transduction process in rod photoreceptor cells for scotopic vision begins with absorption of a photon by a rhodopsin molecule, which is a seven-transmembrane α-helical protein having 11-*cis*-retinal as a chromophore. Light isomerizes the 11-*cis*-retinal into all-*trans* form,[1] resulting in conformational changes of the protein moiety to form an enzymatically active intermediate, metarhodopsin II (meta II).[2–4] The meta II then activates retinal G protein, transducin,[3,4] which in turn, activates the signal transduction cascade that eventually generates an electrical response of the rod photoreceptor cells.[5]

Rhodopsin is one of the members of G protein-coupled receptors (GPCRs) in the sense that it can activate retinal G protein, transducin. However, it is unique in the sense that it can be activated not by chemical stimulus but by light, a physical stimulus. Several lines of evidence indicated that rhodopsin exhibits an extremely high photosensitivity, an effective activation of G protein, and an inert character in the dark.[6] These properties are the parts of the molecular mechanisms in which a rod photoreceptor cell works as a single photon counter with an extremely low level of noise in the dark. Because the functional expression of the photoreceptor cell is totally different from those of the cells that are activated by hormones, neurotransmitters, and so on, the molecular mechanism of G protein activation by rhodopsin was thought to be somewhat different from those by other ligand-binding GPCRs.[7] However, accumulated evidence reveals that the chromophore of rhodopsin acts as an inverse agonist,[8,9] and light fulfils a role in converting the inverse agonist into the agonist, all-*trans*-retinal, within the protein moiety, suggesting that the G protein activation mechanism is similar between rhodopsin and other GPCRs. Therefore, elucidation of the activation mechanism of the G protein by rhodopsin would give insight into the common mechanism of G protein activation by GPCRs. In this chapter, we summarize the structural and spectroscopic studies of rhodopsin, focusing on the role of the chromophore in the mechanisms of photon absorption and G protein activation by rhodopsin.

0-8493-1348-1/04/$0.00+$1.50

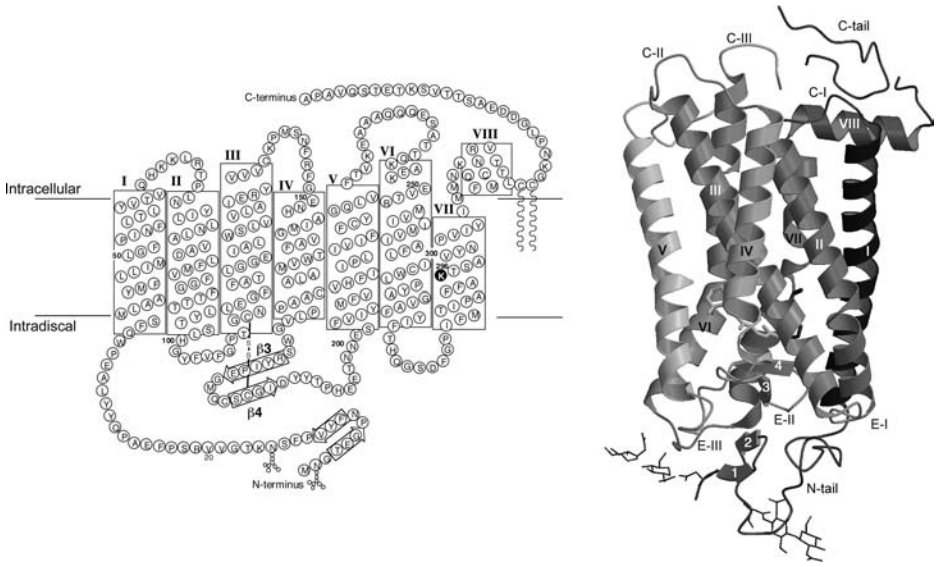

FIGURE 125.1 Structure of bovine rhodopsin. Secondary structure of rhodopsin is shown in (a). The three-dimensional structure of rhodopsin is shown in (b).[17] The coordinate (IF88) was retrieved from the Protein Data Bank.

125.2 Structures of Retinal Chromophore and its Binding Site in Rhodopsin

As already described, rhodopsin is a ~40 kDa membrane protein that consists of a single polypeptide opsin and a chromophore, 11-*cis*-retinal.[1] Opsin contains seven transmembrane α-helices, the structural motif typical of the GPCRs.[10] The primary structure (amino acid sequence) of bovine rhodopsin was first determined in 1983 by three groups, based on sequencing the peptide fragments[11,12] and complementary DNA (cDNA) cloning.[13] Then the helical alignment of bovine rhodopsin was determined by means of electron cryomicroscopy using a two-dimensional rhodopsin crystal.[14,15] Recently, a three-dimensional crystal of bovine rhodopsin was successfully developed,[16] and its atomic structure was analyzed by x-ray crystallography (Figure 125.1).[17] This provides a comprehensive structural basis for giving insight into the functional roles of rhodopsin.

Because it is an essential function for rhodopsin to receive a visible light, elucidation of the mechanism regulating the absorption maximum of rhodopsin (spectral tuning mechanism of rhodopsin) is important. Opsin and 11-*cis*-retinal show no absorbance at the visible region, but binding of 11-*cis*-retinal to the opsin causes generation of rhodopsin having absorption maximum at about 500 nm.

Earlier studies indicated that 11-*cis*-retinal forms a protonated Schiff base with Lys296 of opsin,[11,12,18] and the proton on the Schiff base is stabilized by a negatively charged glutamate at position 113 (Glu113).[19–21] Crystal structure of rhodopsin confirmed that the retinal is really bound to Lys296, and Glu113 is located at 3.2 Å from the Schiff base nitrogen.[17]

The structural information on such a short distance between the Schiff base and the counterion has led to confusion among researchers. This is because many researchers believed that a water molecule should be present between the Schiff base and the counterion, as in the case of bacteriorhodopsin.[22] In general, pKa of a Schiff base is higher than that of a glutamate, so that a proton on the Schiff base should be transferred to the glutamate if these two molecules interact directly with each other. Moreover, there is ample evidence that a water molecule is present and forms a hydrogen-bonding network near the Schiff base and the counterion.[23–25] Therefore, a water molecule was speculated to be located between the Schiff

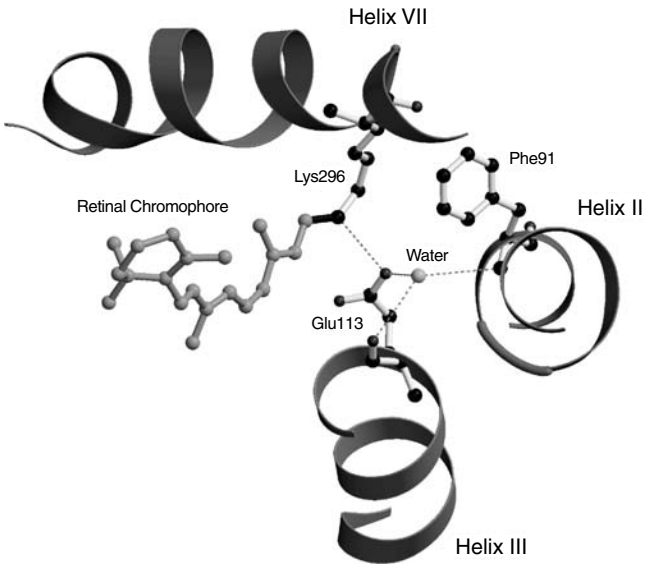

FIGURE 125.2 Water molecule in chromophore binding site.[27] The water molecule is located not between the Schiff base and the counterion, but on the carboxyl and peptide carbonyl groups of Glu113. The coordinate (IL9H) was retrieved from the Protein Data Bank.

base and the counterion, even in the theoretical model of the rhodopsin[26] constructed on the basis of the three-dimensional Cα-structure model of the transmembrane helices of opsin.[10]

Recently, the spatial resolution of the diffraction of the rhodopsin crystal was improved to visualize water molecules in the rhodopsin molecule.[27] The results showed that a water molecule is located not in between the Schiff base and the counterion, but on the carboxyl and peptide carbonyl groups of the glutamate at position 113 (Figure 125.2). These results suggest that the water molecule would have a role of stabilizing the proton on the Schiff base by reducing the negative charge of the carboxylate of the glutamate.

The crystal structure of rhodopsin also shows that the second extracellular loop forms an antiparallel β-sheet, and that one of the strands (β4) is in the proximity of the chromophore (Figure 125.1).[17] This indicates that a part of the second extracellular loop forms a chromophore binding site. Furthermore, one of the oxygen atoms of Glu181 is located close (about 4.5 Å) to the C12 position of retinal, which could affect the absorption characteristics of the chromophore. Our recent study clearly showed the existence of a water molecule between the side chains of Glu181 and Ser186.[27] The location of the water molecule is significant in terms of the mechanism of color regulation in retinal proteins, including cone visual pigments. In the long-wavelength cone visual pigments (human green and red), a histidine residue at the position of the Glu181 in bovine rhodopsin was demonstrated to bind a chloride ion,[28] shifting the absorption maximum to the red.[29–31] The presence of the water molecule in these chloride-binding pigments was suggested by our FTIR study on the chicken red pigment (iodopsin).[32] Moreover, our recent study of squid retinal photoisomerase retinochrome showed that Glu181 can directly act as a counterion of the protonated Schiff base.[33] In bovine rhodopsin, Glu181 is located in the middle of a cluster of three polar residues, Tyr191, Tyr192, and Tyr268, with hydroxyl groups that cover a part of the retinal binding pocket near C9. Thus, we found a continuous hydrogen-bonding network that lies in the extracellular side of the chromophore-binding site, covering a distance of >17 Å from the hydroxyl group of Tyr192 to the peptide amide of Phe91.[27] This observation of the network implies that replacement of a single amino acid at a given position in this region would induce long-range effects on the spectral properties of visual pigments.

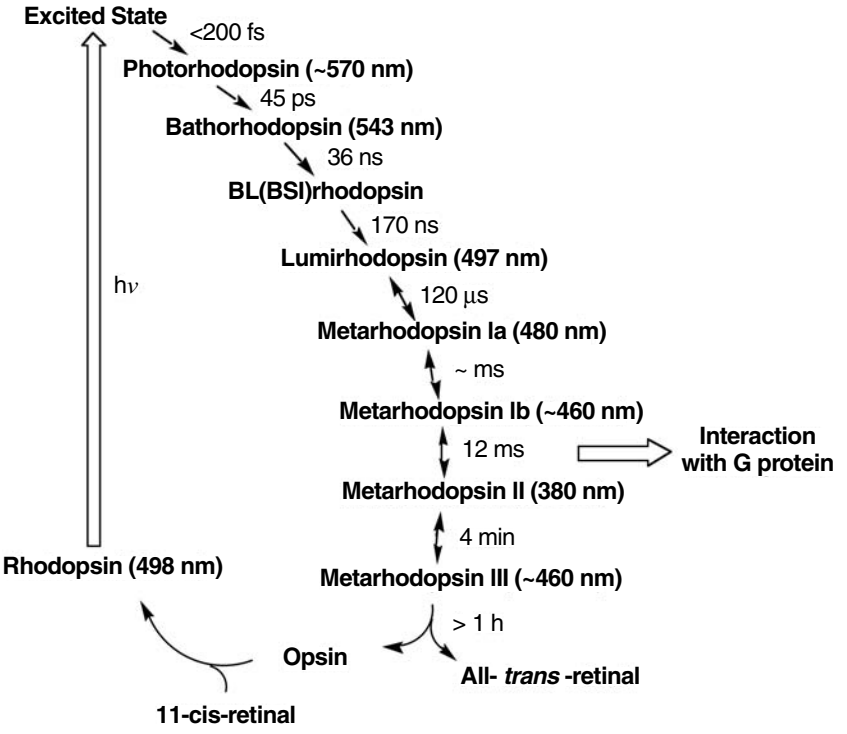

FIGURE 125.3 Photobleaching process of bovine rhodopsin. The times denoted at the right-hand side of the arrows are decay time constants of the intermediates. The absorption maxima of rhodopsin and its intermediates are shown in parentheses.

125.3 *Cis-Trans* Isomerization Mechanism of Chromophore in Rhodopsin

On absorption of light, rhodopsin changes its absorption maximum from 500 to 380 nm, fading in color from red to pale yellow. This photobleaching process of rhodopsin is composed of photoreaction (photochemical reaction) and subsequent thermal reactions. How efficiently the photoreaction occurs is closely connected with a trapping yield of light signal, that is, the absolute photosensitivity of rhodopsin, while subsequent thermal reactions are important for generating an active state that transduces a light signal to a retinal G protein. Because the chromophore acts as an intrinsic probe to monitor conformational changes of the protein during the thermal reactions of rhodopsin, each step of the change was confirmed by detection of an intermediate state having specific absorption spectrum. Historically, low-temperature spectroscopy was applied to detect the distinctive intermediate states, such as bathorhodopsin, lumirhodopsin, metarhodopsin I to III.[1,34] Subsequently, kinetic experiments using an ultrashort laser pulse identified photorhodopsin as the primary intermediate[35] and then observed the excited state of rhodopsin.[36] Recent kinetic experiments using laser photolysis at room temperature and time-resolved low-temperature spectroscopy showed that other intermediates exist between the originally identified intermediates.[37,38] Thus, the bleaching process of rhodopsin could be summarized in Figure 125.3.

The initial event of rhodopsin after absorption of a photon is now confirmed to be a *cis-trans* isomerization of the retinal chromophore. Originally, the *cis-trans* isomerization hypothesis was based on the experimental facts that irradiation of rhodopsin at liquid nitrogen temperature yields a photo-steady-state mixture containing rhodopsin, bathorhodopsin, and isorhodopsin (Figure 125.4).[34] Because rhodopsin and isorhodopsin contain 11-*cis*- and 9-*cis*-retinals, respectively, as their chromophores, bathorhodopsin should have an intermediate configuration, that is, a twisted all-*trans*-retinal,

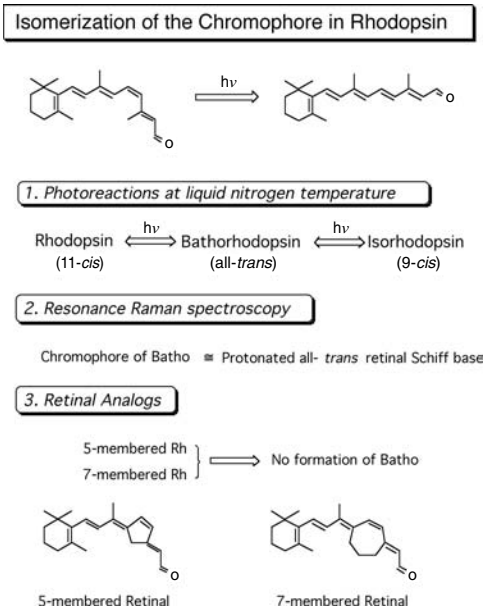

FIGURE 125.4 Experimental evidence that supports the *cis-trans* isomerization of the retinal chromophore of rhodopsin as an initial event after absorption of a photon.

as its chromophore. Later experiments using resonance Raman spectroscopy indicated that the chromophore of bathorhodopsin is similar to the protonated all-*trans*-retinal Schiff base in solution.[39] The more sophisticated evidence that the *cis-trans* isomerization is essential for the formation of bathorhodopsin was obtained from the experiments using retinal analogs with 11–12 double bonds fixed by ring structures. That is, no formation of bathorhodopsin is observed when 11–12 double bonds are fixed.[40,41]

Several lines of evidence indicated that photoreceptor cells are able to respond to a single photon stimulus. The pioneering studies by Dartnall[42] showed that the quantum yields of isomerization of rhodopsins are extraordinarily high (0.67) compared with those of the protonated retinylidene Schiff base in organic solution (~0.2).[43] Therefore, it is of interest to investigate how efficiently the isomerization occurs.

Because the high quantum yield originates from the high-rate isomerization, which competes with other relaxation processes in the excited state of rhodopsin, ultrafast laser spectroscopies were applied to investigate the isomerization process of the retinal chromophore. Picosecond time-resolved spectroscopy was applied to the photochemistry of rhodopsin, and the formation of the primary intermediates was reported, such as photorhodopsin and bathorhodopsin at room temperature.[35,44,45] However, the time resolution needed to be improved in order to detect the *cis-trans* isomerization process in the excited state of rhodopsin. The direct observation of the rhodopsin excited state was reported in 1991, in which the primary intermediate photorhodopsin formed from the excited state of rhodopsin within 200 fs.[36] Later, the effects of oscillatory features with a period of 550 fs (60 cm^{-1}) on the formation kinetics of photorhodopsin,[46] were observed, suggesting that the primary step in vision is a vibrationally coherent process.

The femtosecond spectroscopies described above are so-called transient absorption (pump probe) spectroscopy. To probe the excited-state dynamics of rhodopsin, however, the absorption spectroscopy may not be advantageous, because other spectral features, such as ground-state depletion and product absorption, are possibly superimposed on the excited-state spectral features in the data obtained. In order to monitor the excited-state dynamics of rhodopsin more directly, we attempted to apply femtoseconds up-conversion spectroscopy to detect it in real time.[47,48]

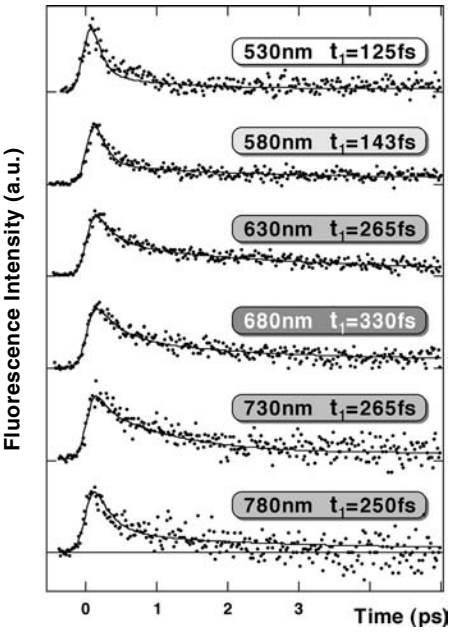

FIGURE 125.5 Fluorescence dynamics of bovine rhodopsin excited at 430 nm and monitored at 530, 580, 630, 680, 730, and 780 nm. The photon counts at maximum position for each monitoring wavelength are 133, 145, 204, 169, 106 and 60, respectively. Smooth curves are the best fits obtained by deconvolution procedure with the instrumental response function (full width of half maximum: 210 fs). Three kinetic components are used in the fitting: fs (125 to 330 fs), early ps (1.0 to 2.4 ps) and >50 ps components, among which the fs component is major (58 to 87%). The fs components are shown in the figure. (Modified from Kandori, H., Furutani, Y., Nishimura, S., Shichida, Y., Chosrowjan, H., Shibata, Y., and Mataga, N., *Chem. Phys. Lett.*, 334, 271, 2001.)

Shown in Figure 125.5 are the fluorescence dynamics of rhodopsin excited at 430 nm and observed at various wavelengths.[48] In addition to the observed decay curves, smooth curves simulated by superposing exponential decay function, taking into consideration the instrumental response, are indicated. The decay kinetics clearly showed nonexponential nature, where components of femtoseconds (125 to 330 fs) and early picoseconds (1.0 to 2.3 ps) were predominantly obtained as the best fit. The rises of fluorescence were rapid, and the fs components of the fluorescence at blue (530 and 580 nm) and red (780 nm) sides of the spectrum decayed faster than those at the center. These results suggest that the conversion from the Frank–Condon state to the fluorescence state occurs within the time resolution of the apparatus (<100 fs), owing to coupling with intrachromophore high-frequency modes; and faster initial decay is due to the sharpening of the band shape caused by a decrease of amplitudes of high-frequency modes along the reaction coordinate of twisting.[48] It should be noted that the average amplitude of the fs components among six wavelengths was about 70%, being close to the quantum yield of photoisomerization of rhodopsin (0.67). Thus, the components in the 100 fs regime are probably correlated with the ultrafast coherent isomerization process, which leads to formation of photorhodopsin within 200 fs. On the other hand, the slow components (~30%) in the ps regime would originate from the nonreactive excited state of rhodopsin.

In order to get more insight into the excited state dynamics of rhodopsin, we analyzed the excited-state dynamics of rhodopsin by means of FTOA (Fourier transform optical absorption) method.[49,50] In this method, the time-correlation function between the wavepacket of the Franck–Condon state and that at a certain time after propagation from the Franck–Condon state, was calculated by Fourier transform of absorption spectrum of rhodopsin that was measured by conventional spectrophotometer. It was then used for estimating the propagation of wavepacket in the excited state.

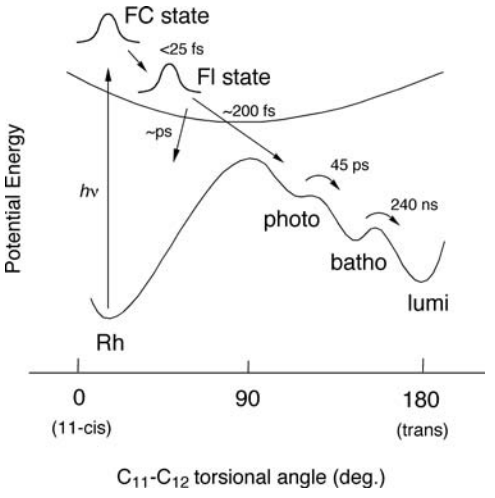

FIGURE 125.6 The primary process of rhodopsin.

The results showed that the wavepacket rapidly moves from the Franck–Condon state within about 25 fs, and it goes to the ground state at about 170 fs. The lifetime of the excited state of rhodopsin estimated by this calculation is in agreement with that directly observed by means of fs spectroscopy.[48]

We then investigated the excited-state dynamics by analyzing deuterium substitution effects for hydrogen atoms bonded to C11 and C12 of the retinal chromophore.[51] The substitution effects do not appear significantly in the excited-state dynamics until about 60 fs, but they appear after 60 fs. The mode of isomerization at C11–C12 double bond would couple with the mode of hydrogen-out-of-plane and, therefore, isomerization would start at about 60 fs after photon absorption of rhodopsin.

The primary process of rhodopsin is summarized in Figure 125.6. Rhodopsin goes to the Franck–Condon state (FC state) by photon absorption. Then, the Franck–Condon state moves rapidly to a fluorescent state (Fl state) within 25 fs. The fluorescent state then goes to the ground state intermediate photorhodopsin, within about 200 fs.

125.4 Protein-Directed Isomerization Mechanism of Rhodopsin

After the *cis-trans* photoisomerization of the retinal chromophore, rhodopsin changes its protein conformation to a G-protein-activating state. Because the conformational change of the protein needs chemical-free energy, light energy absorbed by the chromophore should be converted to chemical energy.

Because formations of photorhodopsin and bathorhodopsin after photon absorption of rhodopsin are extremely rapid (200 and 45 ps, respectively), it is easily believed that only minor rearrangements of amino acid residues constituting the chromophore-binding site would occur. The isomerization causes an extension of the longitudinal length of the chromophore, resulting in a highly twisted conformation of the chromophore in the restricted chromophore binding pocket. This may cause an elevation of the potential energy.[34] In fact, calorimetric study showed that about 60% of photon energy (~30 kcal) is stored as an increase in enthalpy.[52]

In order to get insight into chromophore conformation of the primary intermediates as well as the energy storage mechanism, we conducted the picosecond laser photolysis experiments using rhodopsin analogs having retinal analogs, as shown in Figure 125.7.[41,53] All the analogs have a locked structure of the C11–C12 double bond but differ from each other in the manner of prohibition of the isomerization around the C11–C12 double bond.

The five-membered ring is a completely planar and rigid ring, so that C11–C12 double bond cannot be distorted any more. The picosecond experiments of the five-membered rhodopsin (Rh5) showed that

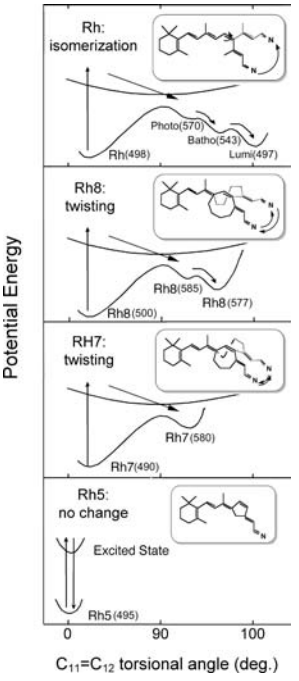

FIGURE 125.7 Ground- and excited-state potential surfaces along the 11-ene torsional coordinate of the chromophore of rhodopsin (Rh), eight-membered rhodopsin (Rh8), seven-membered rhodopsin (Rh7), and five-membered rhodopsin (Rh5).[53] Values in parentheses denote difference absorption maxima between original pigments and the respective intermediates. Dotted structures for Rh8 and Rh7 simply denote the formation of transoid double bonds in the ring. (Modified from Mizukami, T., Kandori, H., Shichida, Y., Chen, A.H., Derguini, F., Caldwell, C.G., Biffe, C.F., Nakanishi, K., and Yoshizawa, T., *Proc. Natl. Acad. Sci. USA*, 90, 4072, 1993.)

only the excited state was produced and went back to the original state. On the other hand, a seven-membered ring is a relatively flexible ring, and the 11–12 double bond or the nearby single bonds can be distorted to some extent. The experimental results of the seven-membered rhodopsin (Rh7) showed formation of a photorhodopsin-like intermediate from the excited state, and the intermediate went back to the original state directly. The eight-membered rhodopsin that has more flexible conformation in eight-membered ring went to an excited state and converted to photorhodopsin-like and then to bathorhodopsin-like intermediates. These results clearly show that the formation of the primary intermediates depends on the flexibility of the 11–12 double bond. From these results, we have two important conclusions: One is that the primary intermediates have a highly twisted all-*trans* chromophore in the restricted chromophore binding pocket. This means that the light energy is converted to a potential energy, owing to the distortion of the retinal chromophore. The other is that the appearance of the early intermediate is dependent on the flexibility of the moiety comprising the C11–C12 double bond and the photoisomerization proceeds by sequential interaction between the chromophore and the protein, resulting in stepwise relaxation of the highly strained all-*trans* retinal chromophore. That is, the isomerization of the chromophore is protein directed.

125.5 Changes in Chromophore–Opsin Interaction in Bleaching Process of Rhodopsin

The state that activates retinal G protein was thought to be Meta II,[2–4] the conformation of the protein that was investigated by various techniques with great enthusiasm. The most prominent difference

between Meta II and the other intermediates is their protonation states of the Schiff base chromophore, that is, Meta II is the only intermediate with a retinylidene Schiff base that is deprotonated.[54] As already described, the proton on the Schiff base in rhodopsin mediates the interaction between the chromophore and the counterion E113. Thus, the transfer of the proton to the counterion results in the loss of interaction, inducing a flexible conformation near the Schiff base.[8] Recently, important experimental evidence was reported from site-directed spin-labeling studies, where a separation in cytoplasmic ends between Helices III and VI, as rigid bodies, occurs upon formation of Meta II.[55] The separation between the helices then unmasks the G protein-binding sites located in the third cytoplasmic loop (C-III in Figure Chapter 125.1).[56] Thus, the next investigation was how the energy stored in the chromophore can transfer the protein moiety for inducing the helical movements of the protein.

Recently, an important finding about the energy transfer from the chromophore to the protein was obtained by cross-linking studies using a retinal analog having a diazo-keto residue as a photoaffinity substituent in its β-ionone ring.[57] The reconstituted rhodopsin with the retinal analog as its chromophore was irradiated with a ultraviolet light, resulting in cross-link of the β-ionone ring and we can crosslink the β-ionone ring with nearby amino acid residue. Before the cross-link, we prepared several intermediates of the reconstituted rhodopsin by irradiation at various temperatures, and then, these intermediates were irradiated with ultraviolet light to cross-link the β-ionone ring with nearby amino acid residue. Then, the protein moiety was cleaved by CNBr, followed by separation of the peptides to be analyzed.

In the rhodopsin state, the β-ionone ring was cross-linked with the tryptophan at position 265 of the Helix VI. This result is consistent with that previously reported using different retinal analog.[58] Then, we performed the cross-linking experiments in the intermediate states. In bathorhodopsin state, the same tryptophan residue was cross-linked, suggesting that the β-ionone ring does not move during the *cis-trans* photoisomerization of the chromophore. We previously reported on the basis of an experiment using the fluorinated retinal analogs, that the isomerization of the chromophore would proceed by movement of the half of the polyene chain containing the Schiff base.[59] Thus, it is reasonable to speculate that the first rearrangement of the amino acid residues would occur near the protonated Schiff base in the chromophore. Then, we applied the cross-linking experiments to the lumirhodopsin state and found that the alanine residue at position 169 of Helix 4 was newly cross-linked.[57] From these results, the β-ionone ring changes its cross-linked position from Helix VI to Helix IV during the batho-to-lumi transition. Although the previous studies using the ring-truncated retinal analogs already suggested the change of the protein conformation near the β-ionone ring region of the chromophore,[60] the present results demonstrate that the more dramatic changes in chromophore–opsin interaction occurs in the lumirhodopsin state. The cross-linked residue did not change during the lumi-to-Meta I and Meta I-to-Meta II transitions.[57] These results indicate that the relative position between the β-ionone ring of the chromophore and the Ala169 did not change. However, analog studies suggested the occurrence of the protein conformational changes near the 9-methyl group of the chromophore during the lumi-to-Meta I transition[61] and that of the deprotonation of the Schiff base chromophore during the meta I-to-meta II transitions, respectively.

Figure 125.8 shows a schematic drawing of the structures of rhodopsin, bathorhodopsin, lumirhodopsin and metarhodopsin II, the active state of rhodopsin.[57] Rhodopsin has an 11-*cis*-retinal as its chromophore. It forms a protonated Schiff base with Lys296 of the helix VII and the β-ionone ring of the chromophore interacts with Trp265 of the helix VI. The β-ionone ring becomes cross-linked to Ala169 in helix IV when bathorhodopsin converts to lumirhodopsin. Our experiments suggest that flip-over of the β-ionone ring of the chromophore causes loss of interaction between β-ionone ring and the tryptophan residue and pushes the helix III to the outside. This would be the reason why helices III and VI change their positions. In other words, the large movements of the chromophore trigger conformational changes of the helices to interact with G protein.

To further understand the molecular mechanism of light absorption and G protein activation by rhodopsin, it is important to determine structural changes in the bleaching process of rhodopsin at atomic resolution. Recent success of the preparation of the rhodopsin crystal enables us to determine the crystal structure of the intermediates upon irradiation of the crystal at adequate temperature.[27]

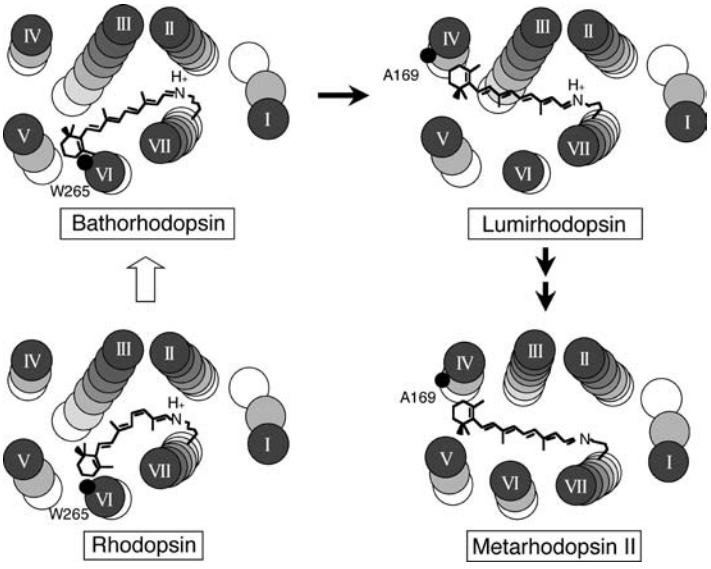

FIGURE 125.8 Opsin conformational movements triggered by 11-*cis* to all-*trans* photoisomerization of the chromophore.[57] In rhodopsin and bathorhodopsin, the β-ionone ring is close to Trp265 in Helix VI, but in lumirhodopsin and metarhodopsin II, it becomes cross-linked to Ala169. Thus, during the batho-to-lumi transition, the β-ionone ring of the chromophore flips over in the helical bundle using the energy stored as a highly strained chromophore structure in bathorhodopsin.

Therefore, we will be in a stage that mechanisms of photon absorption and G protein activation by rhodopsin will be elucidated at atomic resolution.

Acknowledgments

The authors thank Dr. Tetsuji Okada for help preparing Figure 125.1 and Figure 125.2. The authors also thank Drs., T. Okada, H. Kandori, A. Terakita, and H. Imai for their valuable discussions during the preparation of the manuscript. This work is supported in part by Grants-in-Aid for Scientific Research from the Japanese Ministry of Education, Culture, Sports, Science, and Technology.

References

1. Wald, G., Molecular basis of visual excitation, *Science*, 162, 230, 1968.
2. Fukada, Y. and Yoshizawa, T., Activation of phosphodiesterase in frog rod outer segment by an intermediate of rhodopsin photolysis. II, *Biochim. Biophys. Acta,* 675, 195, 1981.
3. Emeis, D., Kuhn, H., Reichert, J., and Hofmann, K.P., Complex formation between metarhodopsin II and GTP-binding protein in bovine photoreceptor membranes leads to a shift of the photoproduct equilibrium, *FEBS Lett*,, 143, 29, 1982.
4. Bennett, N., Michel-Villaz, M., and Kuhn, H., Light-induced interaction between rhodopsin and the GTP-binding protein. Metarhodopsin 2 is major photoproduct involved, *Eur. J. Biochem.,* 127, 97, 1982.
5. Yau, K.W., Phototransduction mechanism in retinal rods and cones. The Friedenwald Lecture, *Invest. Ophthalmol. Vis. Sci.*, 35, 9, 1994.
6. Baylor, D., How photons start vision; *Proc. Natl. Acad. Sci. USA* 93, 560, 1996.
7. Gether, U. and Kobilka, B.K., G protein-coupled receptors. II. Mechanism of agonist activation, *J. Biol. Chem.* 273, 17, 979, 1998.

8. Robinson, P.R., Cohen, G.B., Zhukovsky, E.A., and Oprian, D.D., Constitutively active mutants of rhodopsin, *Neuron*, 9, 719, 1992.
9. Han, M., Lou, J., Nakanishi, K., Sakmar, T.P., and Smith, S.O., Partial agonist activity of 11-*cis*-retinal in rhodopsin mutants, *J. Biol. Chem.*, 272, 23,081, 1997.
10. Baldwin, J.M., Schertler, G.F., and Unger, V.M., An alpha-carbon template for the transmembrane helices in the rhodopsin family of G-protein-coupled receptors, *J. Mol. Biol.*, 272, 144, 1997.
11. Hargrave, P.A., McDowell, J.H., Curtis, D.R., Wang, J.K., Juszczak, E., Fong, S.L., Rao, J.K., and Argos, P. The structure of bovine rhodopsin, *Bioph. ys. Struct. Mech.*, 9, 235, 1983.
12. Ovchinnikov Iu, A., Abdulaev, N.G., Feigina, M., Artamonov, I.D., and Bogachuk, A.S., [Visual rhodopsin. III. Complete amino acid sequence and topography in a membrane], *Bioorg. Khim.* 9, 1331, 1983.
13. Nathans, J. and Hogness, D.S., Isolation, sequence analysis, and intron-exon arrangement of the gene encoding bovine rhodopsin, *Cell*, 34, 807, 1983.
14. Schertler, G.F., Villa, C., and Henderson, R., Projection structure of rhodopsin, *Nature,* 362, 770, 1993.
15. Unger, V.M., Hargrave, P.A., Baldwin, J.M., and Schertler, G.F., Arrangement of rhodopsin transmembrane alpha-helices, *Nature* 389, 203, 1997.
16. Okada, T., Le Trong, I., Fox, B.A., Behnke, C.A., Stenkamp, R.E., and Palczewski, K., X-ray diffraction analysis of three-dimensional crystals of bovine rhodopsin obtained from mixed micelles, *J Struct Biol* 130, 73, 2000.
17. Palczewski, K., Kumasaka, T., Hori, T., Behnke, C.A., Motoshima, H., Fox, B.A., Le Trong, I., Teller, D.C., Okada, T., Stenkamp, R.E., Yamamoto, M., and Miyano, M., Crystal structure of rhodopsin: A G protein-coupled receptor, *Science*, 289, 739, 2000.
18. Bownds, D., Site of attachment of retinal in rhodopsin, *Nature*, 216, 1178, 1967.
19. Zhukovsky, E.A. and Oprian, D.D., Effect of carboxylic acid side chains on the absorption maximum of visual pigments, *Science* 246, 928, 1989.
20. Sakmar, T.P., Franke, R.R., and Khorana, H.G., Glutamic acid-113 serves as the retinylidene Schiff base counterion in bovine rhodopsin, *Proc. Natl. Acad. Sci. USA*, 86, 8309, 1989.
21. Nathans, J., Determinants of visual pigment absorbance: identification of the retinylidene Schiff's base counterion in bovine rhodopsin, *Biochemistry*, 29, 9746, 1990.
22. Luecke, H., Richter, H.T., and Lanyi, J.K., Proton transfer pathways in bacteriorhodopsin at 2.3 angstrom resolution, *Science,* 280, 1934, 1998.
23. Rafferty, C.N. and Shichi, H., The involvement of water at the retinal binding site in rhodopsin and early light-induced intramolecular proton transfer, *Photochem. Photobiol.*, 33, 229, 1981.
24. Nagata, T., Terakita, A., Kandori, H., Kojima, D., Shichida, Y., and Maeda, A., Water and peptide backbone structure in the active center of bovine rhodopsin, *Biochemistry,* 36, 6164, 1997.
25. Deng, H., Huang, L., Callender, R., and Ebrey, T., Evidence for a bound water molecule next to the retinal Schiff base in bacteriorhodopsin and rhodopsin: a resonance Raman study of the Schiff base hydrogen/deuterium exchange, *Biophys. J.*, 66, 1129, 1994.
26. Pogozheva, I.D., Lomize, A.L., and Mosberg, H.I., The transmembrane 7-alpha-bundle of rhodopsin: distance geometry calculations with hydrogen bonding constraints, *Biophys. J.*, 72, 1963, 1997.
27. Okada, T., Fujiyoshi, Y., Silow, M., Navarro, J., Landau, E.M., and Shichida, Y., Functional role of internal water molecules in rhodopsin revealed by x-ray crystallography, *Proc. Natl. Acad. Sci. USA*, 99, 5982, 2002.
28. Wang, Z., Asenjo, A.B., and Oprian, D.D., Identification of the Cl(-)-binding site in the human red and green color vision pigments, *Biochemistry*, 32, 2125, 1993.
29. Knowles, A., The effects of chloride ion upon chicken visual pigments, *Biochem. Biophys. Res. Commun.*, 73, 56, 1976.
30. Fager, L.Y. and Fager, R.S., Halide control of color of the chicken cone pigment iodopsin, *Exp. Eye Res.*, 29, 401, 1979.

31. Shichida, Y., Kato, T., Sasayama, S., Fukada, Y., and Yoshizawa, T., Effects of chloride on chicken iodopsin and the chromophore transfer reactions from iodopsin to scotopsin and B-photopsin, *Biochemistry*, 29, 5843, 1990.
32. Hirano, T., Imai, H., Kandori, H., and Shichida, Y., Chloride effect on iodopsin studied by low-temperature visible and infrared spectroscopies, *Biochemistry*, 40, 1385, 2001.
33. Terakita, A., Yamashita, T., and Shichida, Y., Highly conserved glutamic acid in the extracellular IV–V loop in rhodopsins acts as the counterion in retinochrome, a member of the rhodopsin family, *Proc. Natl. Acad. Sci. USA*, 97, 14,263, 2000.
34. Yoshizawa, T. and Wald, G., Prelumirhodopsin and the bleaching of visual pigment, *Nature*, 197, 1279, 1963.
35. Shichida, Y., Matuoka, S., and Yoshizawa, T., Formation of photorhodopsin, a precursor of bathrhodopsin, detected by a picosecond laser photolysis at room temperature, *Photochem. Photobiol.*, 7, 221, 1984.
36. Schoenlein, R.W., Peteanu, L.A., Mathies, R.A., and Shank, C.V., The first step in vision: femtosecond isomerization of rhodopsin, *Science*, 254, 412, 1991.
37. Hug, S.J., Lewis, J.W., Einterz, C.M., Thorgeirsson, T.E., and Kliger, D.S., Nanosecond photolysis of rhodopsin: evidence for a new, blue-shifted intermediate, *Biochemistry*, 29, 1475, 1990.
38. Tachibanaki, S., Imai, H., Mizukami, T., Okada, T., Imamoto, Y., Matsuda, T., Fukada, Y., Terakita, A., and Shichida, Y., Presence of two rhodopsin intermediates responsible for transducin activation, *Biochemistry*, 36, 14, 173, 1997.
39. Oseroff, A.R. and Callender, R.H., Resonance Raman spectroscopy of rhodopsin in retinal disk membranes, *Biochemistry*, 13, 4243, 1974.
40. Mao, B., Tsuda, M., Ebrey, T.G., Akita, H., Balogh-Nair, V., and Nakanishi, K., Flash photolysis and low temperature photochemistry of bovine rhodopsin with a fixed 11-ene, *Biophys. J.*, 35, 543, 1981.
41. Kandori, H., Matuoka, S., Shichida, Y., Yoshizawa, T., Ito, M., Tsukida, K., Balogh-Nair, V., and Nakanishi, K., Mechanism of isomerization of rhodopsin studied by use of 11-*cis*-locked rhodopsin analogues excited with a picosecond laser pulse, *Biochemistry*, 28, 6460, 1989.
42. Dartnall, H.J., The photosensitives for visual pigments in the presence of hydroxylamine, *Vision Res.*, 8, 339, 1967.
43. Becker, R.S., A comprehensive investigation of the mechanism and photophysics of isomerization of a protonated and unprotonated Schiff base of 11-*cis*-retinal, *J. Am. Chem. Soc.*, 107, 1477, 1985.
44. Busch, G.E., Applebury, M.L., Lamola, A.A., and Rentzepis, P.M., Formation and decay of prelumirhodopsin at room temperatures, *Proc. Natl. Acad. Sci. USA*, 69, 2802, 1972.
45. Green, B.H., Monger, T.G., Alfano, R.R., Aton, B., and Callender, R.H., *Cis-trans* isomerisation in rhodopsin occurs in picoseconds, *Nature*, 269, 179, 1977.
46. Wang, Q., Schoenlein, R.W., Peteanu, L.A., Mathies, R.A., and Shank, C.V., Vibrationally coherent photochemistry in the femtosecond primary event of vision, *Science*, 266, 422, 1994.
47. Chosrowjan, H., Mataga, N., Shibata, Y., Tachibanaki, S., Kandori, H., Shichida, Y., Okada, T., and Kouyama, T., Rhodopsin emission in real time: a new aspect of the primary event in vision, *J. Am. Chem. Soc.*, 120, 9706, 1998.
48. Kandori, H., Furutani, Y., Nishimura, S., Shichida, Y., Chosrowjan, H., Shibata, Y., and Mataga, N., Excited-state dynamics of rhodopsin probed by femtosecond fluorescence spectroscopy, *Chem. Phys. Lett.*, 334, 271, 2001.
49. Kakitani, T., Hatano, Y., Shichida, Y., Imamoto, Y., Tokunaga, F., and Kakitani, H., Excited state dynamics of retinal proteins as studied by Fourier transform of optical absorption spectrum-I. Development of analytical method, *Photochem. Photobiol.*, 56, 977, 1992.
50. Kakitani, T., Matsuda, N., Hatano, Y., Shichida, Y., and Kakitani, H., Excited state dynamics of retinal proteins as studied by Fourier transform of optical absorption spectrum-II. Theoretical analysis of wavepacket propagation of rhodopsin, *Photochem. Photobiol.* 56, 989, 1992.

51. Kakitani, T., Akiyama, R., Hatano, Y., Imamoto, Y., Shichida, Y., Verdegem, P., and Lugtenburg, J., Deuterium substitution effect on the excited-state dynamics of rhodopsin, *J. Phys. Chem.*, 102, 1334, 1998.
52. Cooper, A., Energy uptake in the first step of visual excitation, *Nature*, 282, 5313, 1979.
53. Mizukami, T., Kandori, H., Shichida, Y., Chen, A.H., Derguini, F., Caldwell, C.G., Biffe, C.F., Nakanishi, K., and Yoshizawa, T., Photoisomerization mechanism of the rhodopsin chromophore: picosecond photolysis of pigment containing 11-*cis*-locked eight-membered ring retinal, *Proc. Natl. Acad. Sci. USA*, 90, 4072, 1993.
54. Matthews, R.G., Hubbard, R., Brown, P.K., and Wald, G., Tautomeric forms of metarhodopsin, *J. Gen. Physiol.*, 47, 215, 1963.
55. Farrens, D.L., Altenbach, C., Yang, K., Hubbell, W.L., and Khorana, H.G., Requirement of rigid-body motion of transmembrane helices for light activation of rhodopsin, *Science*, 274, 768, 1996.
56. Yamashita, T., Terakita, A., and Shichida, Y., Distinct roles of the second and third cytoplasmic loops of bovine rhodopsin in G protein activation, *J. Biol. Chem.*, 275, 34,272, 2000.
57. Borhan, B., Souto, M.L., Imai, H., Shichida, Y., and Nakanishi, K., Movement of retinal along the visual transduction path, *Science*, 288, 2209, 2000.
58. Zhang, H., Lerro, K., Yamamoto, T., Lien, T., Sastry, L., Gawinowicz, M., and Nakanishi, K., The location of the chromophore in rhodopsin: a photoaffinity study, *J. Am. Chem. Soc.,* 116, 10,165, 1994.
59. Shichida, Y., Ono, T., Yoshizawa, T., Matsumoto, H., Asato, A.E., Zingoni, J.P., and Liu, R.S., Electrostatic interaction between retinylidene chromophore and opsin in rhodopsin studied by fluorinated rhodopsin analogues, *Biochemistry*, 26, 4422, 1987.
60. Okada, T., Kandori, H., Shichida, Y., Yoshizawa, T., Denny, M., Zhang, B.W., Asato, A.E., and Liu, R.S., Spectroscopic study of the batho-to-lumi transition during the photobleaching of rhodopsin using ring-modified retinal analogues, *Biochemistry*, 30, 4796, 1991.
61. Shichida, Y., Kandori, H., Okada, T., Yoshizawa, T., Nakashima, N., and Yoshihara, K., Differences in the photobleaching process between 7-*cis*- and 11-*cis*-rhodopsins: a unique interaction change between the chromophore and the protein during the lumi-meta I transition, *Biochemistry*, 30, 5918, 1991.

126

The Bleaching of Visual Pigments

Thomas Ebrey
University of Washington

126.1 Introduction

The focus of this chapter is on the series of photochemical transformations of vertebrate visual pigments, after the initial photoproduct has been formed, that lead to the pigment losing its color as the chromophore, retinal, is hydrolyzed from its Schiff base linkage. This sequence of events is often called the bleaching of the visual pigment, and the members of the sequence are called the bleaching intermediates or the photoproducts. The intermediates are usually defined by their absorption maxima, but are also characterized by their vibrational spectra, either the vibrations of the chromophore, the apoprotein, or even of the bound water molecules in the pigment.

There are five families of vertebrate visual pigments, some found mostly in rods, others mostly in cones, but there seem to be exceptions for every family.[1] So, while one cannot accurately talk about "rod" or "cone" pigments, it is convenient to talk about members of the RH1 (rhodopsin) family as "rod" pigments, the Short-Wavelength Sensitive 1 (SWS1) and Mid- and Long-Wavelength Sensitive (M/LWS) as UV/blue cone and green/red cone pigments. The RH2 (rhodopsin-like) and SWS2 (Short Wavelength Sensitive 2) families are not found in mammals and have no tradition of being called rod or cone pigments; like the others, they were found in rods and cones and in the salamander retina in both rods and cones at the same time.[2] It is believed that the bleaching process is similar for all the families, but there are some interesting differences that will be discussed after a more general review.

126.2 Outlines of the Bleaching Process

The literature on the bleaching of the visual pigments has been the topic of several recent reviews.[3–8] In addition, Szundi et al.[9] presented a global analysis of the light-induced kinetics of bleaching; the approach promises to help sort some of the complexities noted below. The following is a rough summary of what characterizes each intermediate. The primary photoproduct, bathorhodopsin, starts to decay within a nanosecond or so after it is formed by the isomerization of the 11-*cis*-retinal chromophore of the pigment to the all-*trans*-conformation. In most pigments, batho rapidly equilibrates with a blue-shifted intermediate (BSI) that decays to lumirhodopsin. Lumi decays to Meta I, which decays to Meta II, which decays

0-8493-1348-1/04/$0.00+$1.50

to Meta III, which then decays finally to all-*trans*-retinal plus opsin. Alternative decay pathways, backreactions, and the effects of various photointermediates interacting with other proteins all change this simple picture. The most important tentative revision is a branching after lumi that decays to Meta I but also can decay directly to a UV-absorbing intermediate, but one distinct from Meta II. This UV species was called Meta I(380) and it decays to the more conventional Meta II.

The primary photoproduct, bathorhodopsin, absorbs at longer wavelengths than rhodopsin, and its vibrational spectrum is unique.[10] The bathochromic shift for the primary photoproduct was seen for every visual pigment investigated and, except for the now considered unlikely model of charge separation for the primary photoreaction,[11] there is no explanation for this universal shift. For bovine rhodopsin, the default visual pigment system, batho decays to and equilibrates with the BSI in about 70 ns in the physiological temperature range.[13] BSI has its absorption maxima at ca. 475 nm.[12] The lifetimes from batho to BSI to lumi are all roughly the same at room temperature.[13,14] While batho is stable at temperatures lower than 130 K, BSI cannot be trapped at low temperatures due to its thermodynamic properties.[14,15] Bovine lumirhodopsin has its absorption maximum at ca. 495 nm.[16,17]

There is some uncertainty as to the rate at which lumi decays to Meta I. This may be because these transitions have not been well characterized spectrally, due to the differences in lifetimes for pigments measured in membranes versus in detergent and, to a lesser extent, the way the data are analyzed. The lifetimes reported for this transition are in the range of 50 to 300 μs at temperatures in the 20 to 27°C range in rods.[17] Meta I absorbs at slightly shorter wavelengths than lumi and has a lower extinction coefficient.[16,18,19] The resonance Raman spectra of lumi, Meta I, and Meta II are distinctive and show that the former is a protonated Schiff base and the latter is deprotonated.[20] If the sample is desiccated sufficiently, then its bleaching is stopped at the Meta I stage.[21]

126.3 Formation and Equilibration of Meta II

The Meta I-to-Meta II transition was perhaps the best studied of the latter portion of the bleaching process. This transition involves the deprotonation of the Schiff base of the chromophore shifting the absorption spectrum from the visible (478 nm for Meta I) to that of Meta II, 380 nm. For most species, Meta II is formed in ca. 1 to 2 ms at room temperature and probably about 70 μs at 37°C[22,23]; it is this time constant that could contribute to the shaping of the kinetics of the receptor potential of rods.[24] The transition from Meta I (and lumi) to Meta II represents a change from a form of rhodopsin that probably has no special affinity to transducin and cannot activate transducin to a form that binds transducin and can catalyze the exchange of GDP for GTP, activating transducin. This binding greatly alters the equilibrium concentration of the two intermediates, shifting it toward Meta II.[25]

There have to be several changes that take place in rhodopsin before it can activate transducin, and these all have to take place by the time of the formation of Meta II. The first change is the photoisomerization of the chromophore from the 11-*cis* to the all-*trans* configuration (see Chapter 125 and Mathies and Lugtenburg[10]). The second required change seems to be the neutralization of the counterion to the protonated Schiff base of the chromophore.[26,27] In vertebrates, this is Glu113 in the bovine rhodopsin residue numbering system. In invertebrates, this residue is a tyrosine or a phenylalanine and is thought to already be neutral in the unphotolyzed pigment.[28] Finally, there is gathering evidence that a substantial conformational change involving at least two of the transmembrane helices of rhodopsin moving apart must occur, at the Meta II stage, for the photolyzed pigment to be able to activate transducin.[29]

Meta II seems to have multiple pathways of decay, either going on to a longer-wavelength intermediate Meta III or decaying directly to the free all-*trans*-retinal plus opsin.[30] The decay of Meta II *in situ* appears to be slow[22,31] and may be the rate-limiting step in the normal regeneration of the visual pigment.

Meta I is in pH- and temperature-dependent equilibrium with Meta II.[18] The observed pH dependence was at first surprising in that one might expect that the equilibrium between a protonated and unprotonated Schiff base would favor the protonated Schiff base with increasing proton concentration. Instead, the equilibrium is shifted toward Meta II with increasing proton concentration. This suggests that the protonation state of one or more groups, other than the Schiff base, can shift the equilibrium from Meta

I to Meta II. It was shown that when light initiates events that lead to Schiff base deprotonation, the proton is transferred to its counterion, Glu113.[32] The Meta I–Meta II transition is identified with this proton transfer. More recently, the x-ray structure of bovine rhodopsin[33] has shown that another carboxylic acid, Glu181, is also close to the Schiff base. Studies on an invertebrate pigment, retinochrome, suggest it can be in its anionic form so that it can, in some circumstances, act as a counterion.[34]

In early reports, the formation of Meta II, monitored spectroscopically at 380 nm, was fitted as a single exponential. Others found the process to be multiexponential, even in ROS (summarized in Abrahamson[35]). More recent reports share the finding that there are two or three components of Meta II formation for rhodopsin in ROS or digitonin at 15 to 25°C (see, e.g., Jäger et al.[36,37]). An explanation for the complexity may lie in the observation, as noted above, that there is a Meta-II-like species formed directly from lumi.[38] In addition, Hofmann and coworkers[39,40] provided convincing evidence for two Meta IIs in series, with the transition to the second involving the picking up of a proton.

126.4 The Role of Protons in Forming Meta II

As noted above, the equilibrium between Meta I and Meta II is pH dependent, with the higher concentration of protons favoring the deprotonated form of the Schiff base (Meta II). Because the formation of Meta II reflects the intraprotein proton transfer between the Schiff base and Glu113,[32] the origin of the pH dependence of this equilibrium is not obvious; it must reflect the role of another protonatable groups. The Meta I/Meta II equilibrium was studied in detail by Liebman and coworkers,[41,42] who made careful measurements of the thermodynamics and kinetics of the Meta I to Meta II transition between pH 5.9 and 8.1. Their results suggested that a single proton is taken up during the formation of Meta II. Note that with this technique, only protons taken up or released that control the Meta I/Meta II equilibrium are measured. Liebman and coworkers called these "essential protons." Arnis and Hofmann[39] examined the kinetics of Meta II formation at different pHs and formulated a model in which Meta II formation is divided into two steps: Schiff base deprotonation/Glu113 protonation and then proton uptake (see below). They proposed that there are two Meta IIs in series, Meta I $\leftrightarrow$ Meta II_a $\leftrightarrow$ Meta II_b, with the proton being taken up in the second step. Thus, of the three exponential phases reported in the 1 μs to 500 ms time range, the fastest can be assigned to the lumi-to-Meta-I transition, while the other two are assigned to the Meta I $\leftrightarrow$ Meta II_a $\leftrightarrow$ Meta II_b. However, an examination of the pH dependence of the Meta I $\leftrightarrow$ Meta II_a $\leftrightarrow$ Meta II_b sequence finds that both components of the Meta I decay are pH dependent,[31] so that an even more complex model than that proposed by Hofmann and co-workers must obtain. A similar need for complexity was found in the careful study of Szundi et al.[44]

Meta II takes minutes to decay. The lifetime of the active form of rhodopsin is not set by the lifetime of Meta II, for soon after it is formed, Meta II is inactivated by being phosphorylated and binding arrestin. Therefore, a discussion of the role of the lifetime of Meta II in controlling physiological processes in rods and cones is misleading, because the "spectroscopic" species is not the active species *in vivo*. *In vivo*, soon after it is formed, most Meta II is inactivated without its absorption spectrum changing.

Stoichiometry of the Protonation Changes Associated with Meta II Formation

The pH dependence of the Meta I/Meta II equilibrium provides evidence of transient protonation changes upon light activation of rhodopsin. Accurate determination of the stoichiometry and the kinetics of proton binding and release from light-activated rhodopsin are complicated by many seemingly contradictory results that may depend on the experimental preparation used. Below, I summarize these results; a more detailed discussion can be found in Kuwata et al.[43] Matthews et al.[19] found that the pK_a of the group that controlled the equilibrium between Meta I and Meta II is ca. 6.4. Several paths of research were then pursued. One line of investigation was to measure, near room temperature, the number of protons taken up or released from light-activated rhodopsin. Emrich[46] was the first to report results with pH-sensitive dyes and found a light-initiated proton uptake for ROS membranes using bromocresol purple as an indicator. Similarly, Wong and Ostroy[47] used a pH indicator dye, bromocresol green, to

measure light-induced changes for rhodopsin in digitonin at low temperatures, e.g., -10°C and found that one proton was taken up during Meta II formation and released later, in times of the order of minutes at 25°C. Bennett[48] reported that over the pH range 6 to 8, two protons are taken up per Meta II formed in ROS membranes at 3°C. At warmer temperatures, the Meta II decays but also loses protons, so that now an "unprotonated" Meta II is formed. The pH changes were measured with a pH electrode. Using the pH-sensitive dye bromocresol purple, washed ROS membranes, and reasonable time resolution (ms at 20°C), Bennett[49] reported that two protons were taken up as Meta II was formed, but that at pHs greater than 5, one of the protons was released before Meta II decayed, so that the H+/Meta II stoichiometry = 2 only at low pHs. Later, Arnis and Hofmann[39,40] found that two protons are taken up per Meta II at pH 6, none for pH 7.5, and a net release at higher pHs.

Another method used to determine the number of protons taken up and released upon Meta II formation is photocalorimetry. Cooper and Converse[50] measured the amount of heat released from a solution of ROS membranes after photolysis in several different buffers with differing heats of proton ionization. They found that there were no protonation changes during Meta II formation at pH = 8.0, and only one proton was taken up during Meta II formation at pH = 5.4.

To summarize, several experiments following light-induced protonation changes with pH-sensitive dyes or pH electrodes,[45,46,51] pH effects on the Meta I/Meta II equilibrium,[42] and photocalorimetric experiments,[50] find that just one proton is taken up in forming Meta II at lower pHs. In contrast, Bennett[52] and Arnis and Hofmann[39] found that up to two protons are taken up per Meta II at lower pHs. While some experiments would only measure the protons that must be taken up to allow Meta II formation (the "essential" protons[42]), others measure all the protons taken up, essential and nonessential. This could explain part of the discrepancy. We tentatively assume that the simpler, more comprehensive set of data is accurate, and that only one proton is taken up in going from Meta I to Meta II in ROS membranes.

Kinetics of the Protonation Changes in Photolyzed Rhodopsin

Several of the techniques used to measure the stoichiometry of the protonation changes were also used to measure the time course with which the proton is taken up during the photolysis of rhodopsin. With measurements taken in ROS membranes or rhodopsin in digitonin,[47,48,53] it was found that proton uptake fairly well matched the Meta-I-to-Meta-II transition rate, although resolution and precision were limited. Bennett[52] reported good time resolution data for proton uptake (bromocresol purple) and Meta II formation (absorbance at 365 nm), and found that they matched. Kaupp et al.[54] used the pH indicator bromocresol purple to show that in sonicated ROS membranes, proton uptake and Meta II formation times were identical at 20°C.

In 1993, Arnis and Hofmann[39] solubilized bovine rhodopsin in two different detergents, octyl glucoside or dodecyl maltoside (in these detergents, Meta II formation is greatly accelerated compared to ROS or digitonin solutions), and showed that at some temperatures, the light-induced proton uptake signal from bromocresol purple lagged significantly behind Meta II formation. Their experiments were performed at such a low temperature (3°C) that their time base was fast enough to detect any possible deprotonation associated with Meta II on the 1 to 10 s time scale. Thus, their plausible explanation is that they are looking at two consecutive Meta IIs, with the uptake of a proton only associated with the formation of the second Meta II. More complex kinetics of proton release and uptake are reported by Szundi et al.[44]

There is another way to potentially follow proton kinetics in intact ROS and that is to use the early receptor potential (ERP) or the early receptor current (ERC). The ERP is a very fast potential/current evoked from oriented photoreceptors with bright flashes (reviewed in Cone and Pak[55] and Sullivan and Shukla[56]). At room temperature, two phases can be easily observed for the ERP, a somewhat faster (sub msec) corneal negative R1 and a bit slower (1 to 10 msec) potential of opposite sign, R2. For rhodopsin, Cone[57,58] showed that the kinetics of appearance of R2 and Meta II were identical within experimental error (this correlation was also reported by Spalink and Stieve[59] for bovine retinas at 37°C). This finding, along with R2's temperature dependence, led Cone[57,58] to propose that R2 was due to charge movements associated with the Meta-I-to-Meta-II transition. (R1 was similarly linked to the RH to Meta I transitions.)

Cone[57,58] argued that because R2 is caused by charge movement associated with Meta II formation, and because it is known that at least one proton is taken up when Meta II is formed, that such a proton uptake could contribute to the charge movement associated with Meta II formation. (Movement of charged groups or dipoles within the pigment could also contribute to the observed electrical signal and must be the source of R1.) Two recent studies seemed to demonstrate this assignment. Dickopf et al.[37] studied oriented ROS membrane fragments incorporated into lipid vesicles. They found that the rise of the light-evoked electrical current could be resolved into two components with similar time constants, 1.1 and 3.0 ms at 22°C, pH = 7.8. Together, these probably correspond to R2; R1 was not observed, perhaps because the recording method used makes very fast events difficult to detect. The photocurrent's amplitude and time course were pH dependent, with the amplitude falling with increasing pH. These changes seemed to track the pH dependence of the amplitude Meta II produced, although both determinations did not quite match what was reported in other studies. However, this may be because of the unusual environment of the rhodopsin, in sonicated membrane fragments attached to a lipid support membrane. Sullivan[60] titrated the R2 component for rhodopsin expressed and then incorporated into HEK293S cells. He found that ¾ of the R2 amplitude disappeared upon raising the pH with a pK_a of 6.3, again suggesting that a large part of R2 is due to proton uptake by the photolyzed rhodopsin in forming Meta II.

In summary, using three kinds of techniques for measuring proton kinetics — pH electrode, pH sensitive dyes, and the shape of the R2 component of the ERP — it was found that the formation of Meta II is intimately and kinetically associated with the uptake of a proton. Arnis and Hofmann[39] showed that in some unusual circumstances, proton uptake can lag behind Meta II formation. Moreover, titration data for the equilibrium between Meta I and Meta II, along with the titration of the fast photocurrent due to proton uptake associated with Meta II formation, proved that the pK_a of the group binding the proton is approximately 6.4 in 150 mM salt.

Site of Proton Uptake

Arnis and coworkers[40] showed that the light-induced proton uptake by rhodopsin was completely abolished in a mutant in which Glu134 was changed to a neutral residue. The authors reasonably enough argued that this shows that Glu134 is the site of proton uptake. The uptake of a proton by Glu134, located on the cytoplasmic surface of the pigment,[33] would be of the right sign to contribute to the R2 photovoltage from rods. In addition, using FTIR spectroscopy, Fahmy et al.[61] recently showed that Glu134 is likely deprotonated in the dark but is protonated in Meta II in the presence of transducin. Can we identify Glu134 as the site that, when it takes up a proton, shifts the equilibrium between Meta I and Meta II toward Meta II? This seems plausible. Because Arnis et al. worked in the context that there were two protons taken up in Meta II formation, they had to posit that the alteration of one locus for proton uptake, Glu134, affected the second locus. If we assume that there is only one proton taken up, then this awkward problem disappears. Although it appears the proton uptake site is Glu134, other residues may be involved, and so to avoid making premature conclusions, we will call the proton uptake group, Z.

126.5 The Bleaching Intermediates of the "Cone" Pigments

The photochemical transformations of pigments other than rhodopsins are not as well studied, but an increasing number of contributions to this area of inquiry has been made. The best-studied M/LWS pigments are chicken P571 (iodopsin) and gecko P521. Low-temperature experiments showed that chicken iodopsin (562 nm) forms bathoiodopsin (640 nm) upon light absorption (see Shichida and Yoshizawa, Chapter 125, Reference 10). When the temperature is raised to -180°C, bathoiodopsin reverts to iodopsin instead of going on to lumi as rhodopsin does.[52] At warmer temperatures, a lumiiodopsin is formed.[63] An unusual feature of the M/LWS family is that almost all members use the binding of chloride to shift the spectrum to longer wavelengths and to raise the pK of the pigment's Schiff base. Many other properties are also affected by the chloride, such as the reversion mentioned just above.[64] Another example

is that the equilibrium between the batho product and the BSI product of gecko P521 is chloride dependent.[65] It was proposed that the bleaching of iodopsin is accompanied by the release of Cl^-,[64] but so far, there is no direct evidence for this. Analogues of most of the other bleaching intermediates were seen for iodopsin[63,66] and gecko P521.[73]

There are several recent papers on the very short wavelength SWS1 pigment family. The UV-absorbing members of this family seem to have an unprotonated Schiff base linkage, while the longer wavelength ("blue," Abs. Ma. 400 to 440 nm) probably all have protonated Schiff bases.[67,68] Birge and coworkers studied the bleaching sequence of both types of pigments[68,69] and developed a fascinating story that indicates that both types of pigments have bathochromically shifted primary photoproducts (i.e., we can still call them bathorhodopsins). And for the UV pigment with its initially unprotonated Schiff base, by at least the lumi stage, the Schiff base becomes protonated.

With respect to members of the other pigment families, the Kyoto group[63] purified and studied chicken[70] and gecko[71] RH2 pigments and the chicken SWS2 pigment.[72] All seem to have the same set of bleaching intermediates as the rhodopsin-type (RH1) pigments.

Acknowledgment

This work was supported in part by NIH grant EYO1323.

References

1. Ebrey, T.G. and Koutalos, Y., Vertebrate photoreceptors, *Prog. Retin. Eye Res.*, 20, 49, 2001.
2. Ma, J., Znoiko, S., Othersen, K.L., Ryan, J.C., Das, J., Isayama, T., Kono, M., Oprian, D.D., Corson, D.W., Cornwall, M.C., Cameron, D.A., Harosi, F.I., Makino, C.L., and Crouch, R.K., A visual pigment expressed in both rod and cone photoreceptors, *Neuron*, 32, 451, 2001.
3. Kliger, D.S. and Lewis, J.W., Spectral and kinetic characterization of visual pigment photointermediates, *Isr. J. Chem.*, 35, 289, 1995.
4. Shichida, Y., Visual pigment: photochemistry and molecular evolution, in *The Retinal Basis of Vision*, Toyoda, J., Ed., Elsevier, Amsterdam; New York, 1999, p. 23.
5. Shichida, Y. and Imai, H., Amino acid residues controlling the properties and functions of rod and cone visual pigments, in *Rhodopsins and Phototransduction*, Vol. 224, Novartis Foundation Symposium, 1999, p. 142.
6. Hofmann, K.P., Signaling states of photoactivated rhodopsin, in *Rhodopsins and Phototransduction*, Vol. 224, Novartis Foundation Symposium, 1999, p. 158.
7. Lewis, J.W. and Kliger, D.S., Absorption spectroscopy in studies of visual pigments: spectral and kinetic characterization of intermediates, *Methods Enzymol.*, 316, 164, 2000.
8. Hofmann, K.P., Late photoproducts and signaling states of bovine rhodopsin, in *Handbook of Biological Physics*, Vol. 3, Stavenga, D.G., DeGrip, W.J., and Pugh, E.N., Jr., Ed., Elsevier, Amsterdam: New York, 2000, p. 91.
9. Szundi, I., Lewis, J.W., and Kliger, D.S., Deriving reaction mechanisms from kinetic spectroscopy. Application to late rhodopsin intermediates, *Biophys. J.*, 73, 688, 1997.
10. Mathies, R.A. and Lugtenburg, J., The primary photoreaction of rhodopsin, in *Handbook of Biological Physics 3*, Stavenga, D.G., DeGrip, W.J., and Pugh, E.N., Jr., Ed., Elsevier, Amsterdam; New York, 2000, p. 55.
11. Honig, B., Ebrey, T., Callender, R.H., Dinur, U., and Ottolenghi, M., Photoisomerization, energy storage, and charge separation: a model for light energy transduction in visual pigments and bacteriorhodopsin, *Proc. Natl. Acad. Sci. USA*, 76, 2503, 1979.
12. Ganter, U.M., Kashima, T., Sheves, M., and Siebert, F., FTIR evidence of an altered chromophore-protein interaction in the artificial visual pigment *cis*-5,6-dihydroisorhodopsin and its photoproducts BSI, lumirhodopsin, and metarhodopsin-I, *J. Am. Chem. Soc.*, 113, 4087, 1991.

13. Lewis, J.W., van Kuijk, F.J., Thorgeirsson, T.E., and Kliger, D.S., Photolysis intermediates of human rhodopsin, *Biochemistry*, 30, 11372, 1991.
14. Lewis, J.W. and Kliger, D.S., Photointermediates of visual pigments, *J. Bioeng. Biomembr.*, 24, 201, 1992.
15. Randall, C.E., Lewis, J.W., Hug, S.J., Bjorling, S.C., Eisner-Shanas, I., Ottolenghi, M., Sheves, M., Friedman, M., and Kliger, D.S., A new photolysis intermediate in artificial and native visual pigments, *J. Am. Chem. Soc.*, 113, 3473, 1991.
16. Hubbard, R., Brown, P.K., and Kropf, A., Action of light on visual pigments, *Nature*, 183, 442, 1959.
17. Applebury, M.L., Dynamic processes of visual transduction, *Vision Res.*, 24, 1445, 1984.
18. Lewis, J.W., Winterle, J.S., Powers, M.A., Kliger, D.S., and Dratz, E.A., Kinetics of rhodopsin photolysis intermediates in retinal rod disk membranes. I. Temperature dependence of lumirhodopsin and metarhodopsin I kinetics, *Photochem. Photobiol.*, 34, 375, 1981.
19. Matthews, R.G., Hubbard, R., Brown, P.K., and Wald, G., Tautomeric forms of metarhodopsin, *J. Gen. Physiol.*, 47, 215, 1963.
20. Doukas, A., Aton, B., Callender, R., and Ebrey, T., Resonance Raman studies of bovine metarhodopsin I and metarhodopsin II, *Biochemistry*, 17, 2430, 1978.
21. Nishimura, S., Sasaki, J., Kandori, H., Lugtenburg, J., and Maeda, A., Structural changes in the lumirhodopsin-to-metarhodopsin I conversion of air-dried bovine rhodopsin, *Biochemistry*, 34, 16758, 1995.
22. Ebrey, T.G., The thermal decay of the intermediates of rhodopsin *in situ*, *Vision Res.*, 8, 965, 1968.
23. Baumann, C., The equilibrium between metarhodopsin I and metarhodopsin II in the isolated frog retina, *J. Physiol.*, 279, 71, 1978.
24. Lamb, T.D. and Pugh, E.N., Jr., A quantitative account of the activation steps involved in phototransduction in amphibian photoreceptors, *J. Physiol.*, 449, 719, 1992.
25. Hofmann, K.P., Photoproducts of rhodopsin in the disc membrane, *Photobiochem. Photobiophys.*, 13, 309, 1986.
26. Robinson, P.R., Cohen, G.B., Zhukovsky, E.A., and Oprian, D.D., Constitutively active mutants of rhodopsin, *Neuron*, 9, 719, 1992.
27. Rao, V.K. and Oprian, D.D., Activating mutations of rhodopsin and other G protein-coupled receptors, *Annu. Rev. Biophys. Biomol. Struct.*, 25, 287, 1996.
28. Nakagawa, M., Iwasa, T., Kikkawa, S., Tsuda, M., and Ebrey, T.G., How vertebrate and invertebrate visual pigments differ in their mechanism of photoactivation, *Proc. Natl. Acad. Sci. USA*, 96, 6189, 1999.
29. Farrens, D.L., Altenbach, C., Yang, K., Hubbell, W.L., and Khorana, H.G., Requirement of rigid-body motion of transmembrane helices for light activation of rhodopsin, *Science*, 274, 768, 1996.
30. Blazynski, C. and Ostroy, S.E., Pathways in the hydrolysis of vertebrate rhodopsin, *Vision Res.*, 24, 459, 1984.
31. Ostroy, S.E., Rhodopsin and the visual process, *Biochim. Biophys. Acta*, 463, 91, 1977.
32. Jäger, F., Fahmy, K., Sakmar, T.P., and Siebert, F., Identification of glutamic acid 113 as the Schiff base proton acceptor in the metarhodopsin II photointermediate of rhodopsin, *Biochemistry*, 33, 10878, 1994.
33. Palczewski, K., Kumasaka, T., Hori, T., Behnke, C.A., Motoshima, H., Fox, B.A., Le Trong, I., Teller, D.C., Okada, T., Stenkamp, R.E., Yamamoto, M., and Miyano, M., Crystal structure of rhodopsin: a G protein-coupled receptor, *Science*, 289, 739, 2000.
34. Terakita, A., Yamashita, T., and Shichida, Y., Highly conserved glutamic acid in the extracellular IV-V loop in rhodopsins acts as the counterion in retinochrome, a member of the rhodopsin family, *Proc. Natl. Acad. Sci. USA*, 97, 14263, 2000.
35. Abrahamson, E.W., in *Biochemistry: Physiology of Visual Pigments*, Langer, H., Ed., Springer-Verlag, Heidelberg, 1973, p. 47.
36. Jäger, S., Szundi, I., Lewis, J.W., Mah, T.L., and Kliger, D.S., Effect of pH on rhodopsin photointermediates from lumirhodopsin to metarhodopsin II, *Biochemistry*, 37, 6998, 1998.

37. Dickopf, S., Mielke, T., and Heyn, M.P., Kinetics of the light-induced proton translocation associated with the pH-dependent formation of the metarhodopsin I/II equilibrium of bovine rhodopsin, *Biochemistry*, 37, 16888, 1998.
38. Thorgeirsson, T.E., Lewis, J.W., Wallace-Williams, S.E., and Kliger, D.S., Photolysis of rhodopsin results in deprotonation of its retinal Schiff's base prior to formation of metarhodopsin II, *Photochem. Photobiol.*, 56, 1135, 1992.
39. Arnis, S. and Hofmann, K.P., Two different forms of metarhodopsin II: Schiff base deprotonation precedes proton uptake and signaling state, *Proc. Natl. Acad. Sci. USA*, 90, 7849, 1993.
40. Arnis, S., Fahmy, K., Hofmann, K.P., and Sakmar, T.P., A conserved carboxylic acid group mediates light-dependent proton uptake and signaling by rhodopsin, *J. Biol. Chem.*, 269, 23879, 1994.
41. Parkes, J.H. and Liebman, P.A., Temperature and pH dependence of the metarhodopsin I-metarhodopsin II kinetics and equilibria in bovine rod disk membrane suspensions, *Biochemistry*, 23, 5054, 1984.
42. Gibson, S.K., Parkes, J.H., and Liebman, P.A., Phosphorylation alters the pH-dependent active state equilibrium of rhodopsin by modulating the membrane surface potential, *Biochemistry*, 38, 11103, 1999.
43. Kuwata, O., Yuan, C., Misra, S., Govindjee, R., and Ebrey, T.G., Kinetics and pH dependence of light-induced deprotonation of the Schiff base of rhodopsin: possible coupling to proton uptake and formation of the active form of Meta II, *Biochemistry (Moscow)*, 66, 1283, 2001.
44. Szundi, I., Mah, T.L., Lewis, J.W., Jäger, S., Ernst, O.P., Hofmann, K.P., and Kliger, D.S., Proton transfer reactions linked to rhodopsin activation, *Biochemistry*, 37, 14237, 1998.
45. Hurley, J.B., Spencer, M., and Niemi, G.A., Rhodopsin phosphorylation and its role in photoreceptor function, *Vision Res.*, 38, 1341, 1998.
46. Emrich, H.M., Optical measurements of the rapid pH-change in the visual process during the metarhodopsin I-II reaction, *Z. Naturforsch.*, 26b, 352, 1971.
47. Wong, J.K. and Ostroy, S.E., Hydrogen ion changes of rhodopsin I. Proton uptake during the metarhodopsin I 478 metarhodopsin II 308 reaction, *Archives Biochem. Biophys.*, 154, 1, 1973.
48. Bennett, N., Evidence for differently protonated forms of metarhodopsin II as intermediates in the decay of membrane-bound cattle rhodopsin, *Biochem. Biophys. Res. Commun.*, 83, 457, 1978.
49. Bennett, N., The decay of metarhodopsin II in cattle rod outer segment membranes: protonation and spectral changes, *Biochem. Biophys. Res. Commun.*, 96, 1695, 1980.
50. Cooper, A. and Converse, C.A., Energetics of primary processes in visual exitation: photochemistry of rhodopsin in rod outer segment membranes, *Biochemistry*, 15, 2970, 1976.
51. Schleicher, A. and Hofmann, K.P., Proton uptake by light induced interaction between rhodopsin and G-protein, *Z. Naturforsch.*, 40c, 400, 1985.
52. Bennett, N., Michel-Villaz, M., and Dupont, Y., Cyanine dye measurement of a light-induced transient membrane potential associated with the metarhodopsin II intermediate in rod-outer-segment membranes, *Eur. J. Biochem.*, 111, 105, 1980.
53. Emrich, H.M. and Reich, R., Primary reactions in the visual process. Thermodynamic and kinetic influence of pH on the metarhodopsin I-II transition. Proton consumption as an effect of a conformation change, *Z. Naturforsch.*, 29, 577, 1974.
54. Kaupp, U.B., Schnetkamp, P.P.M., and Junge, W., Rapid calcium release and proton uptake at the disk membrane of isolated cattle rod outer segments. 1. Stoichiometry of light-stimulated calcium release and proton uptake, *Biochemistry*, 20, 5500, 1981.
55. Cone, R.A. and Pak, W.L., The early receptor potential, in *Handbook of Sensory Physiology: Principles of Receptor Physiology*, Vol. 1, Lowenstein, W.R., Ed., Springer-Verlag, Heidelberg, 1971, p. 345.
56. Sullivan, J.M. and Shukla, P., Time-resolved rhodopsin activation currents in a unicellular expression system, *Biophys. J.*, 77, 1333, 1999.
57. Cone, R.A., Early receptor potential: photoreversible charge displacement in rhodopsin, *Science*, 155, 1128, 1967.

58. Cone, R.A., The early receptor potential, in *Proceedings of the International School of Physics "Enrico Fermi"*, Reichardt, W., Ed., Academic Press, New York, 1969, p. 187.
59. Spalink, J.D. and Stieve, H., Direct correlation between the R2 component of the early receptor potential and the formation of metarhodopsin II in the excised bovine retina, *Biophys. Struct. Mech.*, 6, 171, 1980.
60. Sullivan, J.M., Brueggemann, L., and Anumonwo, J.M., Voltage and proton sensitivity of rhodopsin activation, *Biophys. J.*, 80, 19a, 2001.
61. Fahmy, K., Sakmar, T.P., and Siebert, F., Transducin-dependent protonation of glutamic acid 134 in rhodopsin, *Biochemistry*, 39, 10607, 2000.
62. Hubbard, R., Bownds, D., and Yoshizawa, T., The chemistry of visual photoreception, *Cold Spring Harbor Symp. Quantitat. Biol.*, 30, 301, 1965.
63. Shichida, Y. and Imai, H., Amino acid residues controlling the properties and functions of rod and cone visual pigments, in *Rhodopsins and Phototransduction*, Vol. 224, Novartis Foundation Symposium, 1999, p. 142.
64. Imamoto, Y., Kandori, H., Okano, T., Fukada, Y., Shichida, Y., and Yoshizawa, T., Effect of chloride ion on the thermal decay process of the batho intermediate of iodopsin at low temperature, *Biochemistry*, 28, 9412, 1989.
65. Lewis, J.W., Liang, J., Ebrey, T.G., Sheves, M., and Kliger, D.S., Chloride effect on the early photolysis intermediates of a gecko cone-type visual pigment, *Biochemistry*, 34, 5817, 1995.
66. Imai, H., Mizukami, T., Imamoto, Y., and Shichida, Y., Direct observation of the thermal equilibria among lumirhodopsin, metarhodopsin I, and metarhodopsin II in chicken rhodopsin, *Biochemistry*, 33, 14351, 1994.
67. Fasick, J.I., Applebury, M.L., and Oprian, D.D., Spectral tuning in the mammalian short-wavelength sensitive cone pigments, *Biochemistry*, 41, 6860, 2002.
68. Kusnetzow, A., Dukkipati, A., Babu, K.R., Singh, D., Vought, B.W., Knox, B.E., and Birge, R.R., The photobleaching sequence of a short-wavelength visual pigment, *Biochemistry*, 40, 7832, 2001.
69. Dukkipati, A., Kusnetzow, A., Babu, K.R., Ramos, L., Singh, D., Knox, B.E., and Birge, R.R., Phototransduction by vertebrate ultraviolet visual pigments: protonation of the retinylidene Schiff base following photobleaching, *Biochemistry*, 41, 9842, 2002.
70. Imai, H., Imamoto, Y., Yoshizawa, T., and Shichida, Y., Difference in molecular properties between chicken green and rhodopsin as related to the functional difference between cone and rod photoreceptor cells, *Biochemistry*, 34, 10525, 1995.
71. Kojima, D., Imai, H., Okano, T., Fukada, Y., Crescitelli, F., Yoshizawa, T., and Shichida, Y., Purification and low temperature spectroscopy of gecko visual pigments green and blue, *Biochemistry*, 34, 1096, 1995.
72. Imai, H., Terakita, A., Tachibanaki, S., Imamoto, Y., Yoshizawa, T., and Shichida, Y., Photochemical and biochemical properties of chicken blue-sensitive cone visual pigment, *Biochemistry*, 36, 12773, 1997.
73. Liang, J., Govindjee, R., and Ebrey, T., Metarhodopsin intermediates of the Gecko cone pigment P521, *Biochemistry,* 32, 14187, 1993.

127

Studies of the Phosphorylation of Visual Pigments

Zsolt Ablonczy
Medical University of South Carolina

Daniel Knapp
Medical University of South Carolina

Rosalie K. Crouch
Medical University of South Carolina

127.1 Introduction

A key question in the biology of vision is that of the role of phosphorylation in the regulation of the activity of the photosensitive visual pigments.[1–3] There are two types of light-sensitive cells in the retina: rods that are sensitive to dim light and cones that are responsible for color vision. Rhodopsin, the protein that absorbs light in the rod, is the most thoroughly studied of the visual pigments due to its abundance, and it has proven to be a valuable model for the whole G-protein coupled receptor superfamily.[4–7] Two main factors control the activity of rhodopsin: the ligand (or chromophore), which is 11-*cis* retinal,[8,9] and phosphorylation.[10–14] Although rhodopsin phosphorylation was characterized using numerous different methods, currently mass spectrometry is probably the most sensitive analytical tool for its quantitation. We describe here our results from recent studies on the determination of phosphorylation of rhodopsin.

127.2 Visual Pigments and the Visual Cycle

The ligand of visual pigments, 11-*cis* retinal or 3,4-dehydroretinal, is covalently bonded to the rod and cone apoprotein, opsin, and has two roles. First, this molecule acts as a chromophore, positioning the rod or cone opsin to be activated by light of specific wavelengths. Second, this ligand controls the activity of these G-protein coupled receptors by changing the conformation of the protein.[15] In the dark-adapted photoreceptor, the ligand 11-*cis* retinal is covalently bound to the apoprotein opsin, acting as a reverse agonist and locking rhodopsin in its inactive form. Upon excitation with light, the chromophore (11-*cis* retinal) isomerizes to all-*trans* conformation, which now acts as an agonist and initiates structural changes in the protein that lead to activation followed by deactivation by subsequent phosphorylation, dissociation of all-*trans* retinal, dephosphorylation, and regeneration with 11-*cis* retinal (Figure 127.1).

As a first step toward its deactivation, the *C*-terminal end of activated pigment is phosphorylated by the respective kinase. For rhodopsin, that enzyme is rhodopsin kinase (G-protein-coupled receptor kinase 1, GRK1).[16] The phosphorylation sites are the numerous hydroxyl amino acids, serine (S) and threonine

0-8493-1348-1/04/$0.00+$1.50

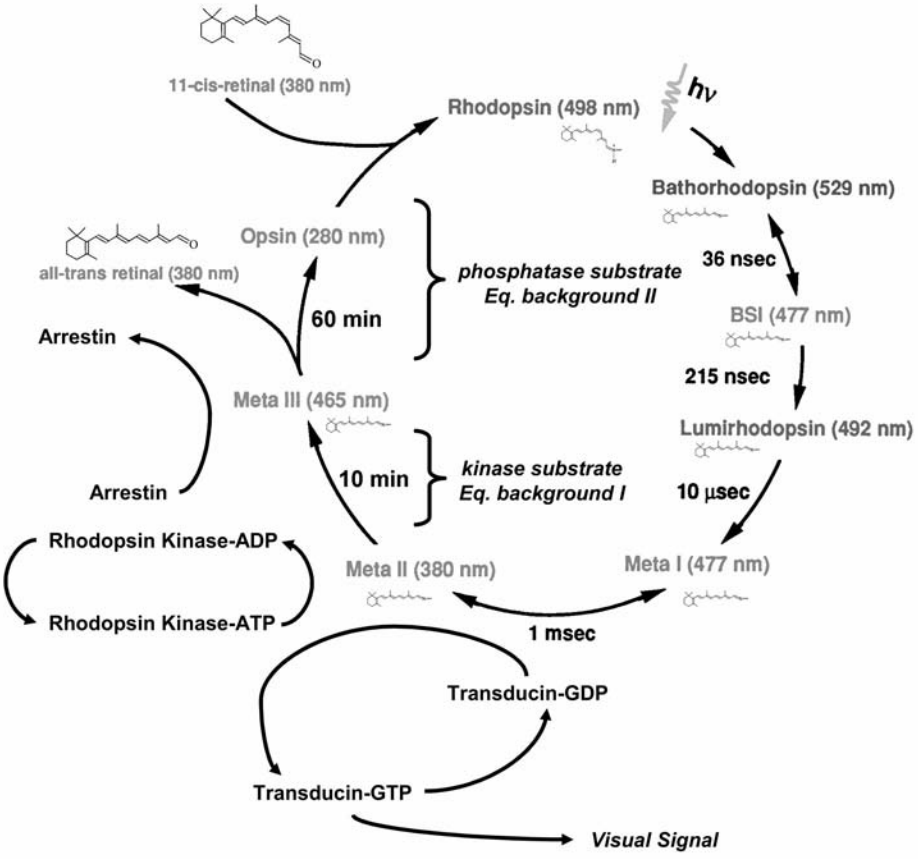

FIGURE 127.1 The photocycle of rhodopsin.

(T), that lie in this region of the protein.[10,17,18] *In vitro*, it was demonstrated that bleached rhodopsin can incorporate up to nine moles of phosphate per mole of bovine rhodopsin.[19] However, the first *in vitro* mass spectrometric experiments identified only single sites of rhodopsin phosphorylation.[10,11] Recently, it was shown by mass spectrometric experiments that *in vivo* phosphorylation involves multiple sites.[14,20,21] Multiple phosphorylation is necessary for a rapid deactivation of rhodopsin and return of visual sensitivity.[13] The key factor in the deactivation process is that the increasing multiplicity of phosphorylation simultaneously decreases the binding strength of transducin[22,23] and increases the binding strength of arrestin.[22,24] Therefore, by multiple phosphorylation, the activity of signal transduction (which requires the binding of transducin) is completely suppressed.[25,26]

After the dissociation of arrestin (initiated by the removal of all-*trans* retinal from the pigment-binding pocket) transducin can again (although to a lesser extent) bind to opsin, as long as it is not regenerated with 11-*cis* retinal.[27–29] This results in the activity generally assigned to bleached opsin.[30,31] In moderate light levels, dephosphorylation and regeneration occur simultaneously,[14] leaving no free bleached opsin (the protein part of rhodopsin) that could potentially activate the signal transduction cascade. Although it is clear that phosphorylation regulates the activity of rhodopsin, the interpretation of the measured levels and multiplicity of phosphorylation, and how it correlates with physiological visual activity measurements, is still an open question. In a recent study, it was shown that the phosphorylation of activated rhodopsin could be correlated to an early phase of a decreasing equivalent background light in the reduction of photoreceptor sensitivity, while the dephosphorylation of opsin correlates to a late phase, diminishing parallel to the regeneration of opsin to rhodopsin and the restoration of visual sensitivity.[14] On the other hand, it has to be noted that phosphorylation does not promote but quenches activity in activated rhodopsin and bleached opsin.[26,32]

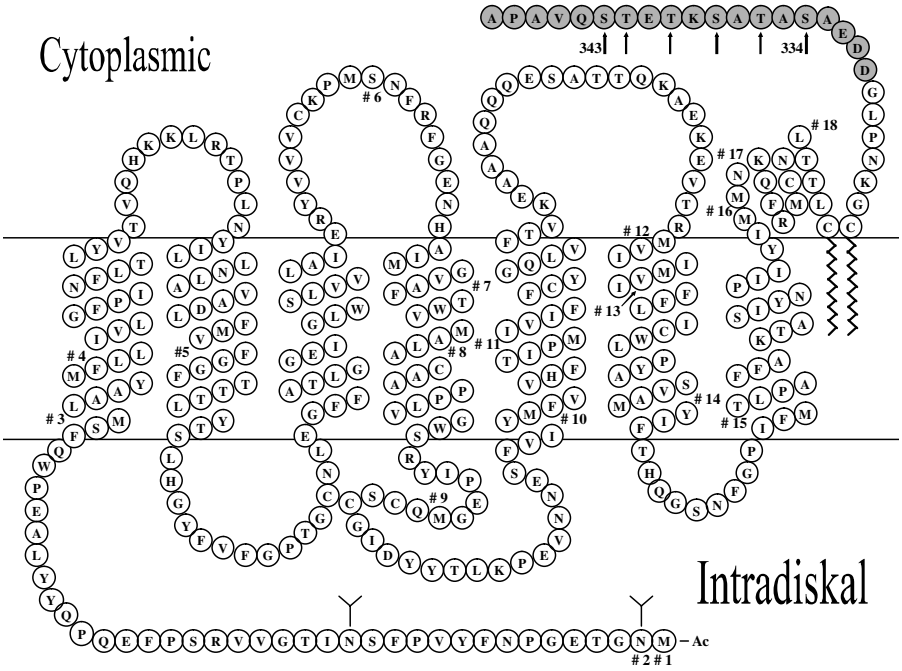

FIGURE 127.2 Two-dimensional model and amino sequence of rat rhodopsin. The sites of CNBr cleavage are marked. The *C*-terminus that can be cleaved with ASPN is shaded. Arrows indicate the possible sites of phosphorylation.

127.3 Mass Spectrometric Studies

We applied a series of mass spectrometric (MS) methods to the analysis of the phosphorylation of rhodopsin.[10,33,34] Our most recent methods employ HPLC-electrospray ionization (ESI) tandem mass spectrometry (MS-MS) using ion-trap mass spectrometers. Our studies were all performed on the rod pigment, rhodopsin. MS is a powerful technique for analyzing the primary structures of proteins. The analytical approach combines enzymatic or chemical fragmentation of the intact proteins and HPLC separation of the digest mixture prior to online MS-MS. Although MS analysis was used for soluble proteins for some years, special methodology had to be developed for the mapping of integral membrane proteins. We employed reduction and alkylation of cysteines prior to the removal of the protein from the membrane, ethanol delipidation, and CNBr digestion as a means to prepare soluble fragments of these hydrophobic materials. By applying these fragment peptide mixtures to a reversed-phase HPLC column in a large volume of a low% organic mobile phase (2.5%), we were able to achieve complete sequence and posttranslational modification mapping with rhodopsin from a single swine eye (~50 μg) (Figure 127.2). We have now used this methodology for mapping rhodopsin from several species.[20,21,33,35,36]

127.4 Rhodopsin Phosphorylation

Phosphorylation is identified by a mass shift of +80 Da for HPO_3 (or its appropriate multiple for multiple phosphorylation) on the rhodopsin *C*-terminal 19-mer fragment that was cleaved by the Asp-N enzyme. In order to identify the sites of phosphorylation, tandem mass spectral data were also collected. Examples of the data obtained are shown in Figure 127.3.

When the animals (rats or mice) were dark-adapted before sacrifice, a 1 to 3% background phosphorylation was observed, similar to the analysis of other laboratories.[21,37] If the animals were in dim light before sacrifice,

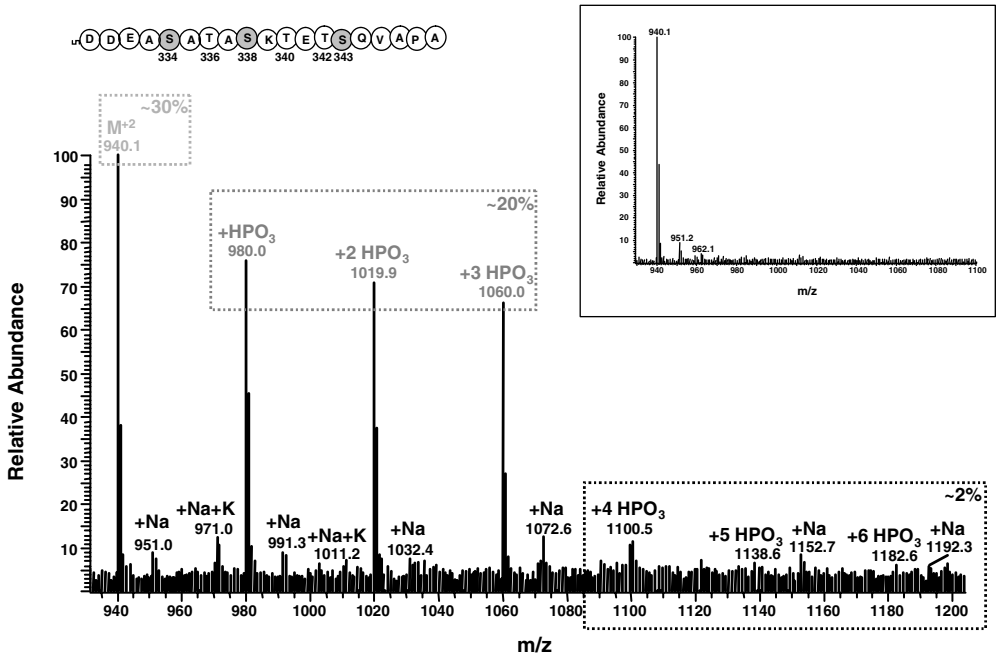

FIGURE 127.3 Phosphorylation pattern of rhodopsin. A mass spectrum of the rat rhodopsin AspN cleavage peptide ion. The ions are doubly charged in samples exposed to 30 min intense visible light (1500 lux) starting at 5 p.m. The sequence indicates the phosphorylation sites, with shading on the most prominent ones. All possible sites were phosphorylated, but up to triple phosphorylation, the levels were elevated. As shown in the insert, dark adaptation completely removes phosphorylation.

the detected phosphorylation levels did not exceed the background.[34] However, if the animals were exposed to moderate or bright light, multiple *in vivo* (mono-hexa) phosphorylation was detected.[20,21] The multiplicity and levels of phosphorylation depended on the light intensity and the available number of sites.

Three main sites of phosphorylation were identified in light-damaged rats: T336, S334, and S338. These animals were kept in light-saturated chambers for extended periods of time. The phosphorylation of the di- and triphosphorylated states was found at various combinations of these sites. Tetraphosphorylation was also present.[21]

Interestingly, porcine retina, dissected in a brightly lit operation room, also showed mono- to triphosphorylation at levels only slightly below those found in light-damaged rats.[20] However, in contrast to rat rhodopsin, which contains six sites, porcine rhodopsin contains eight potential phosphorylation sites. Because all the possible sites may be phosphorylated in a sequential manner, there may be more phosphorylation with the additional potential sites by similar intensities of light. This may be a potential reason for the high level of phosphorylation observed with less-intense light exposure in the porcine model.

127.5 Opsin Phosphorylation

Opsin is the apoprotein of rhodopsin that can result from exposure of the protein to light (termed bleached opsin) or from lack of the availability of the 11-*cis* retinal (termed virgin opsin) (Figure 127.4). There is, however, a physiological difference at these two forms of opsin. Bleached opsin is induced by light exposure of rhodopsin and is phosphorylated by rhodopsin kinase. Bleached opsin was shown to have residual activity that reduces visual sensitivity.[27–30] On the other hand, the characteristics of opsin that has not previously bound 11-*cis* retinal, because it was not available due to a disruption in the retinoid metabolism[38,39] and prior to its developmental occurrence,[40] or because it was unable to bind the ligand and form rhodopsin,[32] are different from those of the opsin resulting from the photoactivation

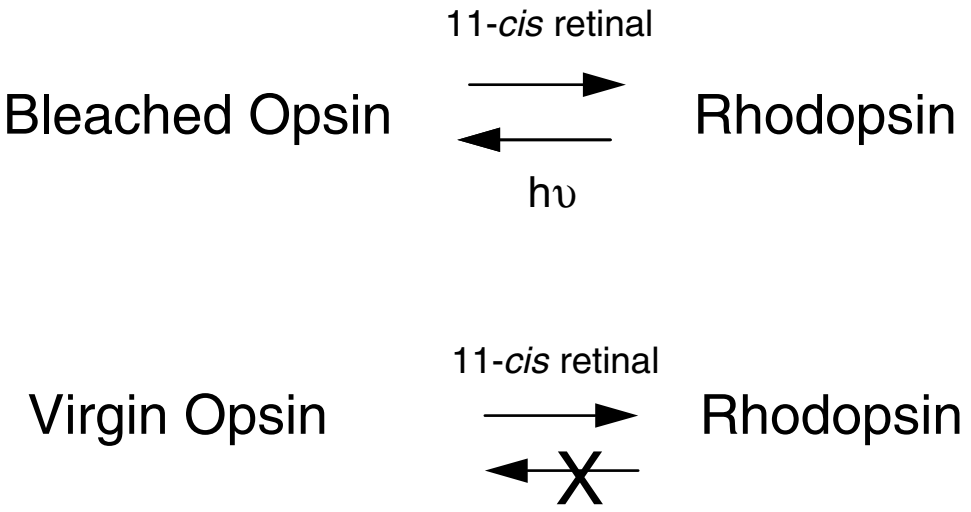

FIGURE 127.4 Bleached versus virgin opsin.

of rhodopsin. This "virgin opsin" is constitutively phosphorylated by an unidentified kinase, and the phosphorylation is only removed if a ligand (e.g., 9- or 11-*cis* retinal) is made available. RPE65 is a major protein of the retinal pigment epithelium (RPE),[41] also identified in cone photoreceptors.[42,43] The photoreceptors of *Rpe65*$^{-/-}$ mice are almost completely depleted of 11-*cis* retinal, resulting in minimal levels of rhodopsin and the deterioration of photosensitivity.[38] This is a useful animal model for the study of "virgin opsin," because almost the full opsin content of the animal has never been exposed to its ligand. The opsin is otherwise structurally intact, and photoreceptor function can be partially restored by supplying exogenous ligand.[36,39,44] The kinetics of the *Rpe65*$^{-/-}$ rods do not resemble those expected of bleached rods,[27,45] but rather those of a dark-adapted rod, showing that, in contrast to bleached opsin, virgin opsin is inactive. In other words, opsin that has never been exposed to its native ligand has the kinetics of a receptor containing its inverse agonist, probably due to its constitutive phosphorylation. Therefore, the constitutive phosphorylation of opsin could possibly be a protective mechanism, shutting off the transduction cascade normally activated by bleached opsin.

Our MS measurements (Figure 127.5) show that the *C*-terminal opsin phosphorylation in dark-adapted *Rpe65*$^{-/-}$ mice was approximately eight-fold higher than in opsin from WT mice (24 versus 3%).[36] This monophosphorylation was independent of light exposure and age (1 month to 18 months) with the most prominent sites of phosphorylation being S334 and S343. However, this constitutive phosphorylation was dose-dependently affected by the administration of 11-*cis* retinal. At 24 h after intraperitoneal 11-*cis* retinal injections, the opsin phosphorylation was significantly reduced in light-exposed and dark-adapted retinas without changing the sites of phosphorylation (to 13 ± 3%). The *in vivo* observations were confirmed under *in vitro* conditions. *In vitro* addition of excess 11-*cis* retinal also resulted in dephosphorylation (10 ± 1%). Similar agonist-independent phosphorylation was reported in other G-protein coupled receptors (bradykinin B_2 receptor,[46] α_2 adrenegeric receptor[47]). The mechanism of the phosphorylation of "virgin opsin" remains to be elucidated. If there is a parallel with agonist-independent desensitization suggested for other G-protein coupled receptors, then protein kinase C may be a candidate, as it is known to phosphorylate rhodopsin,[48] but its role in the visual process *in vivo* is yet unclear.

127.6 Summary

The MS analysis of the *C*-terminus of rhodopsin and opsin uncovered unexpected differences between their phosphorylation patterns. These new results may increase our knowledge of how phosphorylation

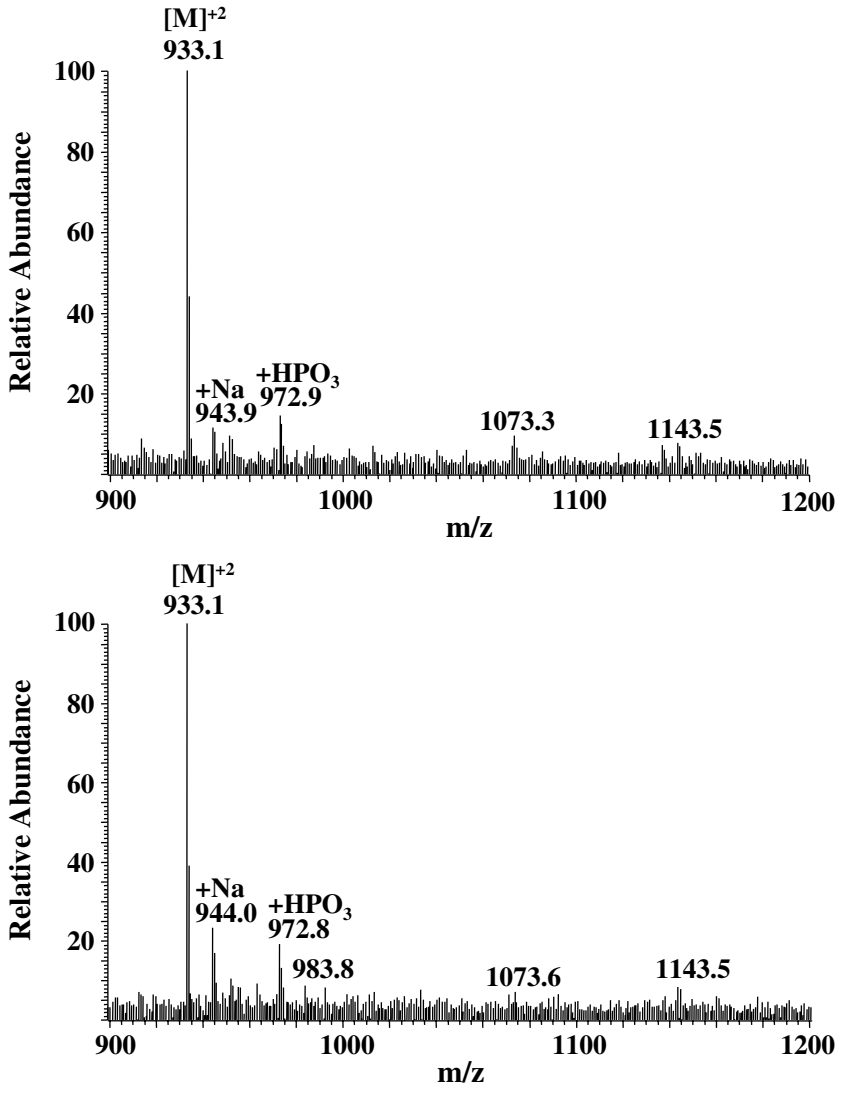

FIGURE 127.5 Phosphorylation pattern of opsin. Mass spectra of the rhodopsin AspN cleavage peptide ion from RPE65-deficient mice. Light exposure (A), 24 h dark-adaptation (B), and age do not influence the level or pattern of opsin phosphorylation.

and the availability of the chromophore mutually regulate the activity of rhodopsin and thereby the physiological responses of the visual signal transduction cascade.

Acknowledgments

Funding was provided by grants from NIH EY-04939 and EY-08239, Office of Naval Research, Foundation Fighting Blindness, and an unrestricted grant to MUSC from Research to Prevent Blindness, Inc., New York, NY. The mass spectrometry was performed in the MUSC Mass Spectrometry Institutional Research Resource Facility.

References

1. Arshavsky, V.Y., Rhodopsin phosphorylation: from terminating single photon responses to photoreceptor dark adaptation, *Trends Neurosci.*, 25, 124, 2002.
2. Baylor, D.A. and Burns, M.E., Control of rhodopsin activity in vision, *Eye*, 12, 521, 1998.
3. Surya, A. and Knox, B.E., Modulation of opsin apoprotein activity by retinal. Dark activity of rhodopsin formed at low temperature, *J. Biol. Chem.*, 272, 21745, 1997.
4. Ballesteros, J.A., Shi, L., and Javitch, J.A., Structural mimicry in G protein-coupled receptors: Implications of the high-resolution structure of rhodopsin for structure-function analysis of rhodopsin-like receptors, *Mol. Pharmacol.*, 60, 1, 2001.
5. Sakmar, T.P., Rhodopsin: a prototypical G protein-coupled receptor, *Prog. Nucleic Acid Res. Mol. Biol.*, 59, 1, 1998.
6. Okada, T. and Palczewski, K., Crystal structure of rhodopsin: implications for vision and beyond, *Curr. Opin. Struct. Biol.*, 11, 420, 2001.
7. Meng, E.C. and Bourne, H.R., Receptor activation: what does the rhodopsin structure tell us?, *Trends Pharmacol. Sci.*, 22, 587, 2001.
8. Crouch, R.K. and Ma, J.-X., The role of vitamin A in visual transduction, in *Vitamin A and Retinoids: An Update of Biological Aspects and Clinical Applications,* Livrea, M.A., Birkhauser, Basel; Boston, 2000, p. 59.
9. McBee, J.K., Palczewski, K., Baehr, W., and Pepperberg, D.R., Confronting complexity: The interlink of phototransduction and retinoid metabolism in the vertebrate retina, *Prog. Retin. Eye Res.*, 20, 469, 2001.
10. Papac, D.I., Oatis, J.E., Crouch, R.K., and Knapp, D.R., Mass spectrometric identification of phosphorylation sites in bleached bovine rhodopsin, *Biochemistry*, 32, 5930, 1993.
11. Ohguro, S., Himi, T., Harabuchi, Y., Suzuki, T., Asakura, K., and Kataura, A., Adult T-cell leukaemia-lymphoma in Waldeyer's ring: a report of three cases, *J. Laryngol. Otol.*, 107, 960, 1993.
12. Ohguro, H., Van Hooser, J.P., Milam, A.H., and Palczewski, K., Rhodopsin phosphorylation and dephosphorylation in vivo, *J. Biol. Chem.*, 270, 14259, 1995.
13. Mendez, A., Burns, M.E., Roca, A., Lem, J., Wu, L.W., Simon, M.I., Baylor, D.A., and Chen, J., Rapid and reproducible deactivation of rhodopsin requires multiple phosphorylation sites, *Neuron*, 28, 153, 2000.
14. Kennedy, M.J., Lee, K.A., Niemi, G.A., Craven, K.B., Garwin, G.G., Saari, J.C., and Hurley, J.B., Multiple phosphorylation of rhodopsin and the in vivo chemistry underlying rod photoreceptor dark adaptation, *Neuron*, 31, 87, 2001.
15. Crouch, R.K., Kefalov, V., Gartner, W., and Cornwall, M.C., Use of retinal analogues for the study of visual pigment function, *Methods in Enzymology*, 343, 29, 2002.
16. Kuhn, H. and Wilden, U., Deactivation of photoactivated rhodopsin by rhodopsin-kinase and arrestin, *J. Recept. Res.*, 7, 283, 1987.
17. Thompson, P. and Findlay, J.B., Phosphorylation of ovine rhodopsin. Identification of the phosphorylated sites, *Biochem. J.*, 220, 773, 1984.
18. Palczewski, K. and Benovic, J.L., G-protein-coupled receptor kinases, *Trends Biochem. Sci.*, 16, 387, 1991.
19. Wilden, U. and Kuhn, H., Light-dependent phosphorylation of rhodopsin: number of phosphorylation sites, *Biochemistry*, 21, 3014, 1982.
20. Ablonczy, Z., Goletz, P., Knapp, D.R., and Crouch, R.K., Mass spectrometric analysis of porcine rhodopsin, *Photochem. Photobiol.*, 75, 316–321, 2002.
21. Ablonczy, Z., Knapp, D.R., Darrow, R., Organisciak, D.T., and Crouch, R.K., Mass spectrometric analysis of rhodopsin from light damaged rats, *Mol. Vis.*, 6, 109, 2000.
22. Gibson, S.K., Parkes, J.H., and Liebman, P.A., Phosphorylation modulates the affinity of light-activated rhodopsin for G protein and arrestin, *Biochemistry*, 39, 5738, 2000.

23. Gibson, S.K., Parkes, J.H., and Liebman, P.A., Phosphorylation alters the pH-dependent active state equilibrium of rhodopsin by modulating the membrane surface potential, *Biochemistry*, 38, 11103, 1999.
24. McDowell, J.H., Robinson, P.R., Miller, R.L., Brannock, M.T., Arendt, A., Smith, W.C., and Hargrave, P.A., Activation of arrestin: requirement of phosphorylation as the negative charge on residues in synthetic peptides from the carboxyl-terminal region of rhodopsin, *Invest. Ophthalmol. Vis. Sci.*, 42, 1439, 2001.
25. Wilden, U., Hall, S.W., and Kuhn, H., Phosphodiesterase activation by photoexcited rhodopsin is quenched when rhodopsin is phosphorylated and binds the intrinsic 48-kda protein of rod outer segments, *Proc. Natl. Acad. Sci. USA*, 83, 1174, 1986.
26. Rim, J. and Oprian, D.D., Constitutive activation of opsin: interaction of mutants with rhodopsin kinase and arrestin, *Biochemistry*, 34, 11938, 1995.
27. Buczylko, J., Saari, J.C., Crouch, R.K., and Palczewski, K., Mechanisms of opsin activation, *J. Biol. Chem.*, 271, 20621, 1996.
28. Surya, A., Foster, K.W., and Knox, B.E., Transducin activation by the bovine opsin apoprotein, *J. Biol. Chem.*, 270, 5024, 1995.
29. Melia, T.J., Cowan, C.W., Angleson, J.K., and Wensel, T.G., A comparison of the efficiency of G protein activation by ligand-free and light-activated forms of rhodopsin, *Biophys. J.*, 73, 3182, 1997.
30. Cornwall, M.C. and Fain, G.L., Bleached pigment activates transduction in isolated rods of the salamander retina, *J. Physiol.*, 480, 261, 1994.
31. Cornwall, M.C., Matthews, H.R., Crouch, R.K., and Fain, G.L., Bleached pigment activates transduction in salamander cones, *J. Gen. Physiol.*, 106, 543, 1995.
32. Li, T., Franson, W.K., Gordon, J.W., Berson, E.L., and Dryja, T.P., Constitutive activation of phototransduction by k296e opsin is not a cause of photoreceptor degeneration, *Proc. Natl. Acad. Sci. USA*, 92, 3551, 1995.
33. Ball, L.E., Oatis, J.E., Jr., Dharmasiri, K., Busman, M., Wang, J., Cowden, L.B., Galijatovic, A., Chen, N., Crouch, R.K., and Knapp, D.R., Mass spectrometric analysis of integral membrane proteins: application to complete mapping of bacteriorhodopsins and rhodopsin, *Protein Sci.*, 7, 758, 1998.
34. Ablonczy, Z., Kono, M., Crouch, R.K., and Knapp, D.R., Mass spectrometric analysis of integral membrane proteins at the subnanomolar level: application to recombinant photopigments, *Anal. Chem.*, 73, 4774, 2001.
35. Knapp, D.R., Crouch, R.K., Ball, L.E., Gelasco, A.K., and Ablonczy, Z., Mass spectrometric analysis of G protein-coupled receptors, *Methods in Enzymol.*, 343, 157, 2002.
36. Ablonczy, Z., Crouch, R.K., Goletz, P., Redmond, T.M., Knapp, D.R., Ma, J.-X., and Rohrer, B., 11-cis Retinal reduces constitutive opsin phosphorylation and improves quantum catch in retinoid deficient mouse rod photoreceptors, *J. Biol. Chem.*, 277, 40491, 2002.
37. Hurley, J.B., Spencer, M., and Niemi, G.A., Rhodopsin phosphorylation and its role in photoreceptor function, *Vision Res.*, 38, 1341, 1998.
38. Redmond, T.M., Yu, S., Lee, E., Bok, D., Hamasaki, D., Chen, N., Goletz, N., Ma, J.-X., Crouch, R.K., and Pfeifer, K., Rpe65 is necessary for production of 11-*cis*-vitamin A in the retinal visual cycle, *Nat. Genet.*, 20, 344, 1998.
39. Van Hooser, J.P., Liang, Y., Maeda, T., Kuksa, V., Jang, G.-F., He, Y.-G., Rieke, F., Fong, H.K.W., Detwiler, P.B., and Palczewski, K., Recovery of visual functions in a mouse model of Leber congenital amaurosis, *J. Biol. Chem.*, 277, 19173, 2002.
40. Ratto, G.M., Robinson, D.W., Yan, B., and McNaughton, P.A., Development of the light response in neonatal mammalian rods, *Nature*, 351, 654, 1991.
41. Hamel, C.P., Tsilou, E., Harris, E., Pfeffer, B.A., Hooks, J.J., Detrick, B., and Redmond, T.M., A developmentally regulated microsomal protein specific for the pigment epithelium of the vertebrate retina, *J. Neurosci. Res.*, 34, 414, 1993.
42. Znoiko, S.L., Crouch, R.K., Moiseyev, G., and Ma, J.-X., Identification of the rpe65 protein in mammalian cone photoreceptors, *Invest. Ophthalmol. Vis. Sci.*, 43, 1604, 2002.

43. Ma, J.-x., Xu, L., Othersen, D.K., Redmond, T.M., and Crouch, R.K., Cloning and localization of rpe65 mRNA in salamander cone photoreceptor cells, *Biochim. Biophys. Acta*, 1443, 255, 1998.
44. Van Hooser, J.P., Aleman, T.S., He, Y.G., Cideciyan, A.V., Kuksa, V., Pittler, S.J., Stone, E.M., Jacobson, S.G., and Palczewski, K., Rapid restoration of visual pigment and function with oral retinoid in a mouse model of childhood blindness, *Proc. Natl. Acad. Sci. USA*, 97, 8623, 2000.
45. Li, Z., Zhuang, J., and Corson, D.W., Delivery of 9-*cis* retinal to photoreceptors from bovine serum albumin, *Photochem. Photobiol.*, 69, 500, 1999.
46. Blaukat, A., Aleman, T.S., He, Y.G., Cideciyan, A.V., Kuksa, V., Pittler, S.J., Stone, E.M., Jacobson, S.G., and Palczewski, K., G protein-coupled receptor-mediated mitogen-activated protein kinase activation through cooperation of Gα(q) and G α (i) signals, *Mol. Cell Biol.*, 20, 6837, 2000.
47. Jewell-Motz, E.A. and Liggett, S.B., G protein-coupled receptor kinase specificity for phosphorylation and desensitization of alpha2-adrenergic receptor subtypes, *J. Biol. Chem.*, 271, 18082, 1996.
48. Greene, N.M., Williams, D.S., and Newton, A.C., Identification of protein kinase c phosphorylation sites on bovine rhodopsin, *J. Biol. Chem.*, 272, 10341, 1997.

128

The Early Receptor Potential and its Analog in Bacteriorhodopsin Membranes

Felix T. Hong
Wayne State University School of Medicine

128.1 Introduction

Almost four decades ago, Brown and Murakami[1,2] discovered a tiny electrical signal in the retina of Cymolgus monkey, when they stimulated the retina with an intense millisecond flash light. The photosignal appeared almost instantaneously upon light stimulation; the latency was undetectable and was estimated to be less than 1 μs (Figure 128.1). This signal was thought to be a new type of bioelectric phenomenon (for earlier reviews, see the literature[3–9]). It was named the early receptor potential (ERP) so as to distinguish it from the then-known receptor potential in the retina — the *a*-wave of the electroretinogram (ERG).[10] The latter has a latency of about 1.7 ms, and was then renamed the late receptor potential (LRP). Unlike LRP, ERP is small in amplitude and requires a significantly more intense flash light to elicit. While LRP can be abolished by anoxia or by other treatments that disrupt the supply of metabolic energy, ERP persists under these rough treatments.

ERP consists of two separate signal components: R1 and R2. The fast component, R1, has a cornea-positive polarity, whereas the slow component, R2, has the opposite polarity. R2 can be reversibly inhibited by low temperature, but R1 persists even at -35°C [Figure 128.1(C) through Figure 128.1(E)].[11,12] ERP from cone photoreceptors is similar: it consists of a brief depolarizing phase (R1) followed by a hyperpolarizing R2 phase.[13–15] ERP-like signals were also found in plant leaves and other pigmented animal tissues.[16] ERP and ERP-like photosignals were generically referred to as fast photovoltages or displacement photocurrents.

Before the discovery of ERP, all known bioelectric signals were generated by ionic diffusion. For example, LRP is associated with the light-induced Na^+ influx at the outer segment of the retinal photoreceptor.[17] The latency of ERP is too short to be accounted for by ionic diffusion. Investigators concluded

0-8493-1348-1/04/$0.00+$1.50

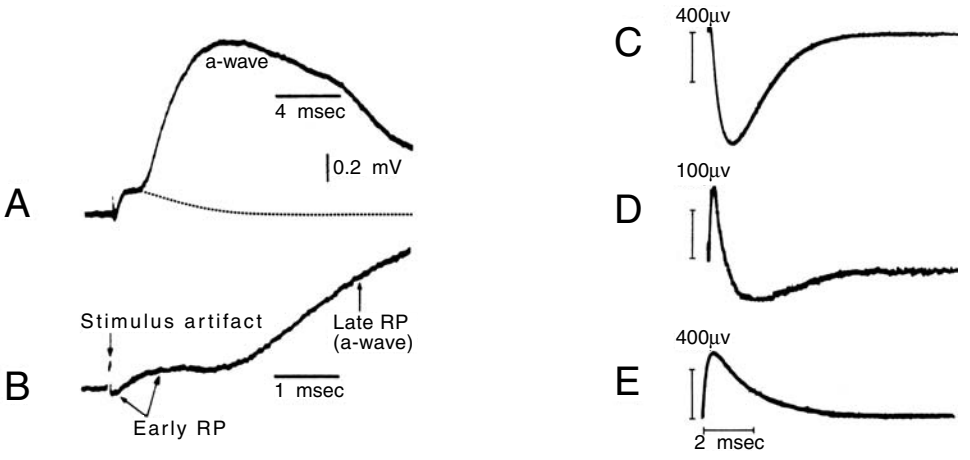

FIGURE 128.1 The early receptor potential from the retina of a Cynmolgus monkey (A and B) and from an albino rat (C, D, and E). In Records A and B, the stimulus was a 20-μs flash, and the ERP appears without an appreciable delay after the light stimulus and merges into the ERG *a*-wave (also known as the late receptor potential). The late receptor potential can be abolished by anoxia, leaving the ERP intact, as shown by the dotted line in Record A. Records C, D, and E show the ERP at 35, 25, and 0°C, respectively. [From Brown, K.T., Watanabe, K., and Murakami, M., *Cold Spring Harbor Symp. Quant. Biol.*, 30, 457, 1965 (A and B); Pak, W.L. and Cone, R.A., *Nature*, 204, 836, 1964 (C,D,E). With permission.]

that ERP is generated by charge displacements caused by a light-induced conformational change of rhodopsin.[18–20] After more than a decade of intense research, investigators were unable to associate ERP with any known physiological function of the retina. ERP was thus regarded as an epiphenomenon — a by-product of photochemical reaction of visual pigment and an evolutionary vestige with no important physiological function. Interests in ERP eventually subsided. However, Pak[6] did not completely rule out the possibility of still unidentified and silent processes intervening between the generation of ERP and the excitation of the rods.

The interest in investigating ERP was revived by the discovery of fabricating artificial black lipid membranes (BLM), by Rudin and his coworkers in 1962.[21] Shortly after, Tien[22] demonstrated a transient photosignal in an artificial BLM reconstituted from a chloroplast extract. Subsequently, similar photosignals appeared in BLM reconstituted with various kinds of organic dyes or pigments, including the chromophore of visual pigments, retinal, and a related compound, retinoic acid[23] (for a recent review, see Tien and Ottova-Leitmannova,[24] Chapter 9). Most of these reconstitution studies involved small organic molecules. The first successful incorporation of a protein molecule into BLM was reported by Takagi and coworkers.[25] The original method of fabricating BLM is not suitable for incorporation of proteins into a BLM because of the use of organic solvents in the process of forming a BLM. Takagi and coworkers used an ingenious technique to incorporate rhodopsin into a BLM. What they did was first incorporate rhodopsin into a monolayer on a specially designed Langmuir trough. A BLM was then formed by fusing two solvent-free monolayers into a bilayer. This method was subsequently improved by Montal and Mueller.[26] A direct observation of ERP-like signal in a reconstituted BLM that contains rhodopsin was reported by Montal and Korenbrot.[27] However, the detected signal was too small to be accurately analyzed. The small amplitude was thought to be the consequence of current shunting caused by a leaky BLM. Enhanced signals were subsequently obtained by Trissl et al.[28] by depositing an oriented layer of visual membrane fragments on a thin (6 μm) Teflon film. The placement of a Teflon film prevents shunting but also precludes the recording of any DC electric signal. They called the ERP-like signal in a reconstituted rhodopsin membrane early receptor current (ERC), because the photosignal was measured as a current instead of a voltage. The ability to detect an electric signal under this condition supported the interpretation that ERP is a manifestation of light-induced charge displacements. In other words,

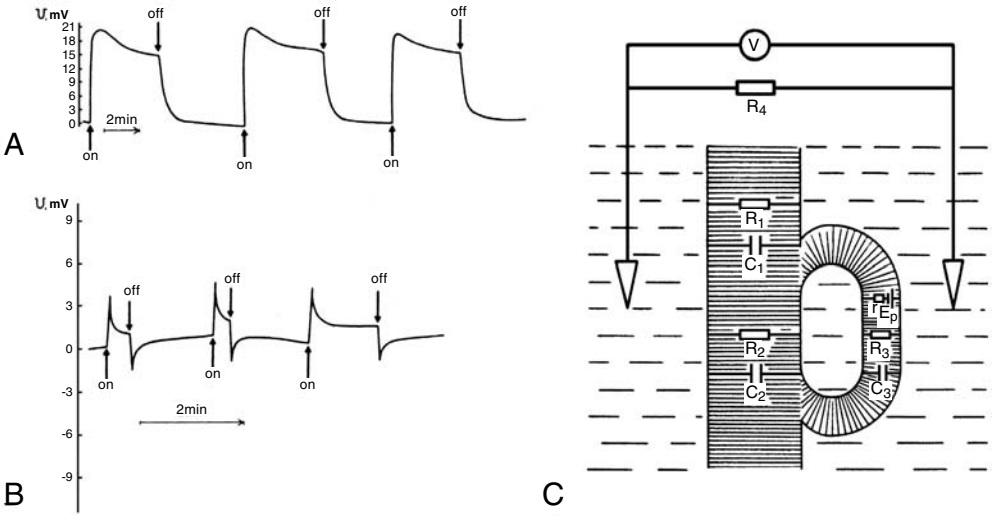

FIGURE 128.2 Differential responsivity. (A) Open-circuit photovoltages of a reconstituted bacteriorhodopsin membrane to a long square-wave light pulse, measured before (Record A) and after (Record B) addition of 0.2 μ*M* of CCCP, are shown. Shunting with an external resistor has a similar effect. The spikes appearing upon the onset and cessation of illumination are known as differential responsivity. (B) An explanation of differential responsivity proposed by Drachev et al. Fusion of bacteriorhodopsin-containing vesicles with the planar BLM is incomplete, thus forming a button-like structure. Capacitors for three regions — regular planar BLM, contact region, and vesicle — are represented by C_1, C_2, and C_3, respectively. Here, C_3 is series capacitor which, together with resistor *r* in the vesicle region, forms a linear high-pass RC filter. [From Drachev, L.A., Kaulen, A.D., Ostroumov, S.A., and Skulachev, V.P., *FEBS Lett.*, 39, 43, 1974 (A, B); Drachev, L.A., Frolov, V.N., Kaulen, A.D., Liberman, E.A., Ostroumov, S.A., Plakunova, V.G., Semenov, A.Yu., and Skulachev, V.P., *J. Biol. Chem.*, 251, 7059, 1976 (C). With permission.]

ERP is a capacitative signal — an AC-coupled electric signal. In contrast, most diffusion-generated bioelectric signals are DC-coupled electric signals. (However, the well-known gating current detected in a squid axon is a voltage-induced displacement current.)

At about the same time, Oesterhelt and Stoeckenius[29] discovered a retinal-containing protein in a halophilic bacterium *Halobacterium salinarum* (formerly *Halobacterium halobium*). This molecule, known as bacteriorhodopsin, resembles rhodopsin in its chemical structure but is actually a photosynthetic pigment — a light-driven proton pump (for recent reviews, see the literature[30–33]). The first report of the photoelectric effect in a reconstituted bacteriorhodopsin membrane was published by Skulachev and coworkers in 1974.[34,35] These investigators first loaded spherical liposomes with bacteriorhodopsin, and then allowed these vesicles to fuse with a planar BLM that did not contain any pigment initially. They then delivered a long square-wave light pulse to illuminate the membrane, and they observed a sustained photovoltage during illumination [Figure 128.2(A)]. This sustained photovoltage reflected mainly the DC-coupled signal caused by a net transport of protons. In addition, they reported a peculiar finding: upon the addition of a proton ionophore CCCP (carbonyl cyanide-*m*-chlorophenylhydrazone), the monotonic waveform was transformed into a signal with a spike at the onset of illumination and an inverted spike at the cessation of stimulation [Figure 128.2(B)]. They interpreted the waveform as being indicative of a peculiar membrane structure that resulted from incomplete fusion of vesicles with a planar BLM [Figure 128.2(C)].[36] Alternatively, Hong[37] interpreted the CCCP-induced waveform change as an indication of the concurrent presence of a light-induced capacitative current, an ERP-like signal, so to speak. Subsequently, by depositing an oriented layer of bacteriorhodopsin membrane fragments on a Teflon film (as in the aforementioned Teflon-supported reconstituted system), Trissl and Montal[38] found a fast electric signal upon illuminating the preparation with a millisecond flash light. What they observed was a signal analogous to R2. Using a microsecond laser light pulse, Hong and Montal[39] reported an even faster signal with a submicrosecond rise time in addition to the R2-like signal. (The rise time was

subsequently determined by Simmeth and Rayfield[40] and by Groma and coworkers[41] to be in the picosecond range.) The slower R2-like component could be reversibly inhibited by low temperature, whereas the faster component persisted at 5°C. They referred to the fast and the slow components as the B1 and the B2 components, respectively, because their temperature sensitivities are similar to that of the R1 and the R2 components, respectively. A sizable literature accumulated during the past quarter century and continues to expand. The literature provides a wealth of information for elucidating ERP, if bacteriorhodopsin can be regarded as a surrogate molecule for rhodopsin. Data from a reconstituted bacteriorhodopsin membrane were easier and faster to collect because of bacteriorhodopsin's legendary stability and cyclicity. Unlike rhodopsin that is bleached by illumination, bacteriorhodopsin is regenerated after illumination via a photocycle. The cyclicity allows a virtually unlimited number of measurements to be made on the same preparation and allows signal averaging to be performed on the measured data. Bacteriorhodopsin can withstand high temperature and extreme acidity and allows experiments to be performed under extreme conditions. The difficulty in collecting quality data of ERP from a unicellular system was recently alleviated by cloning rhodopsin in an expression system using recombinant DNA technology.[42,43]

In this chapter, the focus is on the electrophysiological analysis of ERP based on data of rhodopsin and bacteriorhodopsin, and the mechanistic interpretation. The elucidation of the above-mentioned problems requires a combined electrochemical and electrophysiological approach. The results of our analysis suggest that ERP might function as a molecular switch for visual transduction. A mechanistic explanation will be integrated with the contemporary understanding of the biochemical mechanism of visual transduction. The subject of molecular switches has important technological implications and is discussed in Chapter 134. The lesson so learned also includes how risky it could be if an established electrophysiological technique and an established method of analysis in solution-phase photochemistry were indiscriminately transplanted to heterogeneous photochemistry — a system that involves a membrane phase and two solution phases.

128.2 Mechanistic Models of ERP Generation

Light-induced ion diffusion across the membrane is not sufficiently fast to account for the short latency of ERP. The obvious alternative possibility is light-induced charge displacements. This conclusion is further supported by two experimental observations. Hagins and McGaughy[18] found that the electric current associated with ERP satisfies the following condition:

$$\int_0^\infty I(t)\,dt = 0 \tag{128.1}$$

where $I(t)$ is the time course of the photocurrent. This condition, which suggests that ERP reflects reversible charge displacements in rhodopsin, will be referred to as the zero time-integral condition. Currents generated by diffusion through ion channels do not satisfy this condition, but reversible charge displacements that result in an AC-coupled signal do. The idea of reversible charge displacements was also supported by Cone's finding of the *photoreversal potential* [Figure 128.3(A)]:[20] the visual membrane, which was first enriched with predominantly the metarhodopsin photointermediate from prior illumination, responds to a second light flash with a signal that resembles ERP in waveform but has a reversed polarity. Light stimulation that drives an intermediate back to the ground state may reverse the time-sequence of charge movements.

A commonly envisioned picture of these charge displacements is the movement of charged groups in the amino acid side chains of rhodopsin as a result of a sequence of light-induced conformational changes (photobleaching sequence).[44] Because rhodopsin maintains a fixed orientation with respect to the membrane, such charge movements naturally lead to the formation of an array of transient electric dipoles. The appearance and disappearance of such electric dipoles thus gives rise to a photocurrent that satisfies the

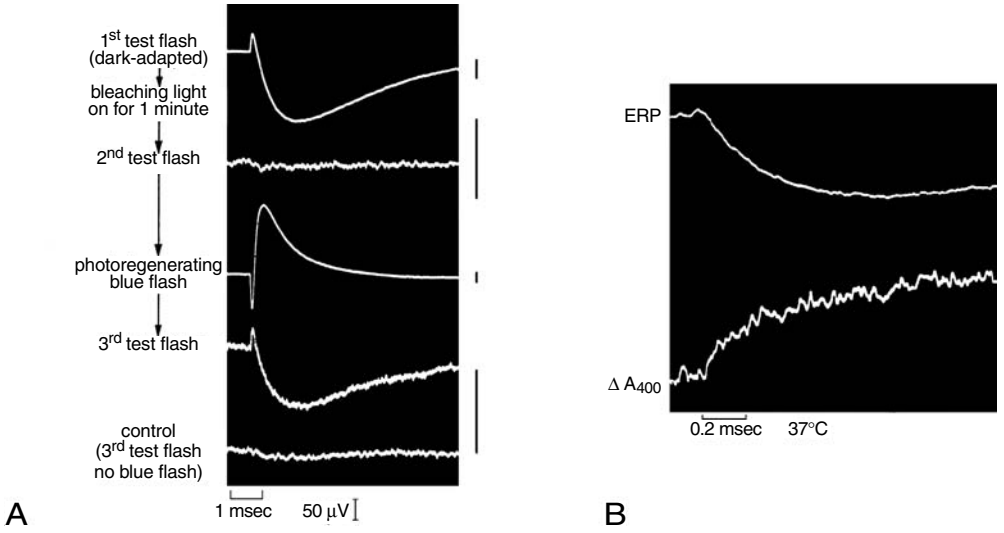

FIGURE 128.3 Salient features of ERP. (A) Photoreversal potential can be elicited by illuminating photointermediates with a blue light flash. Photosignals were measured from excised eye of albino rat at 27°C. Three test flashes contained long wavelengths primarily absorbed by rhodopsin. Blue photoregenerating flash contained wavelengths absorbed by longer-lived intermediates. Control trace was obtained from a second eye, subjected to the same bleaching exposure and test flashes but without the blue flash. (B) The appearance of the R2 component of ERP and the formation of metarhodopsin II are time-correlated. The latter was monitored by absorbance change at 400 nm. The flash duration was 0.1 ms. [From Cone, R.A., *Science*, 155, 1128, 1967 (A); Cone, R.A., in Reichardt, W., Ed., *Proceedings of International School of Physics "Enrico Fermi," Course XLIII*, Academic Press, New York, 1969 (B). With permission.]

zero time-integral condition, Equation 128.1. Illuminating photointermediates with blue light causes a conformational change of rhodopsin in the reversed time-sequence, thus generating the photoreversal potential. This widely accepted mechanistic explanation is known in the ERP literature as the dipole mechanism or, more precisely, the *oriented dipole* (OD) mechanism (Figure 128.4). Thus, in its original form, the dipole mechanism tacitly acknowledged the capacitative nature of ERP; the notion of charge displacements implies charge separation and subsequent recombination. However, this important idea was subsequently forgotten when investigators investigated ERP-like signals in bacteriorhodopsin (see later).

The oriented dipole mechanism is, however, not the only possible mechanism with which to generate charge displacements. In a model membrane system with a membrane-bound magnesium porphyrin (magnesium octaethylporphyrin or amyl ester of magnesium mesoporphyrin IX) and a redox gradient of water-soluble electron acceptor, ferricyanide, and electron donor, ferrocyanide, Hong and Mauzerall[45,46] demonstrated a capacitative photoelectric signal that reflects light-induced electron transfer from magnesium porphyrin to ferricyanide: an heterogeneous electron transfer reaction across a single-membrane–water interface. In this reaction, the separated charges are essentially magnesium porphyrin monocation, in the membrane phase, and ferrocyanide, in the adjacent aqueous phase. While magnesium porphyrin monocation remains essentially fixed in location during the time course of the measured fast photosignal, ferrocyanide ions are free to diffuse. Strictly speaking, the pair does not form an electric dipole in the usual sense. One is a fixed positive charge in the membrane near its surface, whereas the other joins a layer of diffuse negative charges distributed in the double-layer region. Yet, the fast photoelectric signal so generated exhibits all major characteristics of the ERP.[47] Indeed, an interfacial electron transfer (or, more generally, interfacial charge transfer) constitutes another kind of charge separation. When the absorbed photon ejects an electron from the membrane-bound magnesium porphyrin to the aqueous-borne acceptor ferricyanide ion, the oxidized pigment molecule remains in the membrane phase

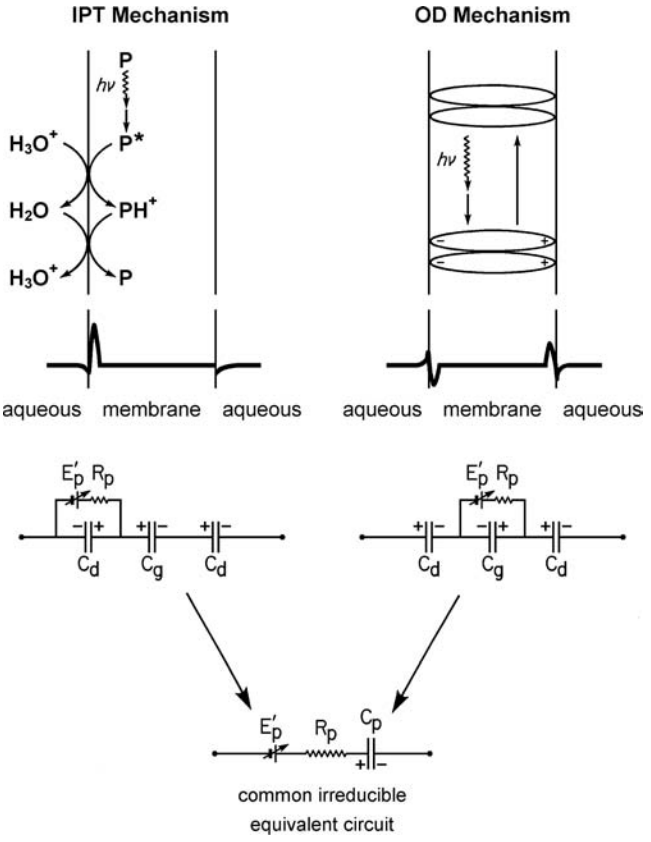

FIGURE 128.4 Interfacial proton transfer (IPT) mechanism and oriented dipole (OD) mechanism. IPT mechanism describes transfer of proton from the adjacent aqueous phase to the membrane phase, while leaving counterion behind in the aqueous phase. Ground-state pigment is designated as *P*. Excited pigment that binds proton from the aqueous phase is designated as *P**. The charge-density profile is also shown, along with two slightly different equivalent circuits. OD mechanism describes light-induced generation of a transient array of oriented electric dipoles, inside the membrane. The diagram is self-explanatory. These two circuits can be further reduced to a common irreducible one (bottom of diagram). (From Hong, F.T., *Bioelectrochem. Bioenerg.*, 5, 425, 1978. With permission.)

and, together with other such molecules, forms a layer of fixed positive surface charges, while electron jumps to ferricyanide to form a mobile counterion. Similarly, when a proton is taken up by photostimulated membrane-bound pigment, the mobile counterion is left behind in the adjacent aqueous phase, and, again, charge separation takes place at the interface. There is no evidence of interfacial electron transfer in visual membranes, but an interfacial proton transfer takes place at the membrane–water surface.

It has long been known that the metarhodopsin-I-to-metarhodopsin-II transition in the photobleaching sequence of rhodopsin involves a net uptake of a single proton from the aqueous phase.[48] Furthermore, Cone[5,49] demonstrated that the R2 component appears at the same time when the photointermediate metarhodopsin I is converted to metarhodopsin II [Figure 128.3(B)]. Ostroy and co-workers[50] further demonstrated that the amplitude of the R2 component varies linearly with the amount of metarhodopsin II produced. Thus, in principle, the R2 component can be generated by interfacial proton transfer. This mechanism will be referred to as the *interfacial proton transfer* (IPT) mechanism (Figure 128.4). At least two components of ERP-like signals could be generated by such a mechanism in bacteriorhodopsin membranes. Being a light-driven proton pump, bacteriorhodopsin is obligated to bind protons from the cytoplasmic side and release them to the extracellular side, thus generating two signal components that reflect charge separation at the two respective membrane–water interfaces. For some time, it was not

clear at which side of the two aqueous phases proton uptake takes place in rhodopsin. Using phospholipid vesicles reconstituted from rhodopsin, Ostrovsky and coworkers[51,52] found that illumination caused a transient pH increase of the bathing solution in a sample of normally oriented vesicles (with the *C*-terminus of rhodopsin facing the bathing solution) but no corresponding pH decrease in a sample of inverted vesicles (with the *N*-terminus of rhodopsin facing the bathing solution). They concluded that the proton uptake takes place at the cytoplasmic side, but no proton uptake or release takes place at the opposite (intradiscal) side. They further concluded that there is no net light-induced proton transport across the membrane. Their observations and conclusions are consistent with the role of rhodopsin being a photon energy sensor rather than a photon energy converter — there is no need to move protons all the way across the membrane. Although this latter reasoning sounds suspiciously teleological, it makes evolutionary sense.

Thus, in principle, ERP can be generated by the OD or the IPT mechanism. In addition, there is no compelling reason that R1 and R2 must be generated by the same mechanism. The question is: which one is for which? Answering this question requires some understanding of the relationship between the macroscopically measured photosignal and the underlying microscopic mechanistic event. A natural linkage between the two events can be established by equivalent circuit analysis. The two simple models shown in Figure 128.4 offer a starting point. The process of charge separation and recombination in the direction perpendicular to the membrane surface is tantamount to charging and discharging a capacitance. However, the capacitance being charged and discharged is not the ordinary membrane capacitance that is commonly encountered in classical electrophysiology. This can be made clear by analyzing the two models in terms of Guoy–Chapman's theory of diffuse double layers.[47,53] The two models give rise to two slightly different equivalent circuits (Figure 128.4). Notably, the charge distribution patterns on the three elementary capacitances — one geometric capacitance of the inert bilayer and two diffuse double-layer capacitances — are different. These patterns are also different from those of an ordinary membrane capacitance. That the three distinct patterns cannot be converted into one another was established by a simple geometric argument published elsewhere.[54,55] However, on a macroscopic level, these two equivalent circuits are equivalent to the same common irreducible equivalent circuit shown at the bottom of Figure 128.4. The most salient feature of this circuit is the inclusion of a capacitance C_p that is connected in series to the photogenerator, E_p. In contrast, the ordinary membrane capacitance, C_m is connected in parallel to E_p. Thus, C_p is fundamentally different from C_m (not shown in Figure 128.4). C_p was named *chemical capacitance*, because charging or discharging of this capacitance is accomplished by photochemical reactions instead of physical flows of ions. Here, we shall not pursue the theoretical implications of the subtle difference between C_p and C_m, as detailed analysis can be found in the literature.[54,55]

128.3 An Apparent Paradox

The above analysis suggests that the OD and the IPT mechanisms are electrically indistinguishable. However, the differentiation can be made by chemical means. In the formation of a transient oriented electric dipole, the separated pair of charges remains on the same molecule, and their locations remain correlated. The charge recombination, therefore, follows a first-order kinetics of chemical reaction. But when the charge separation takes place across the membrane–water interface, one of the separated charges quickly gets lost in the adjacent aqueous phase because of rapid ionic cloud relaxation in water, while the other remains fixed in the membrane phase at the surface. The locations of the pair of separated charges become quickly decorrelated, and the recombination thus follows a second-order or a pseudo first-order kinetics (the two charges that recombine need not be the two from the same pair that was previously separated). For the interfacial proton transfer during the metarhodopsin I to Metarhodopsin II transition, proton is one of the two reactants. By virtue of the law of mass action, the reaction is expected be strongly pH-dependent. Thus, the recombination — a proton rerelease back to the aqueous phase on the same surface — is expected to be a second-order process in an unbuffered aqueous solution. But, it will be a pseudo-first-order process if the aqueous phase is buffered; the pseudo-first-order rate

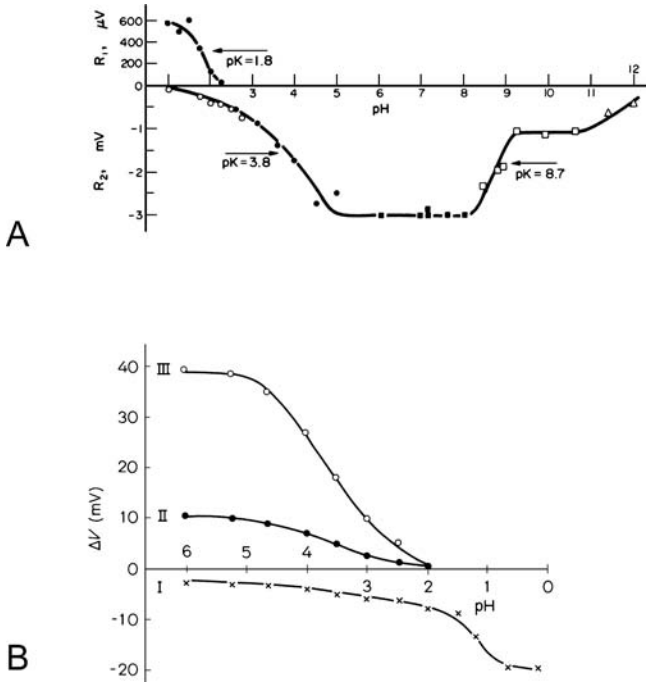

FIGURE 128.5 pH dependence of amplitudes of fast photovoltages from rhodopsin (A) and bacteriorhodopsin (B), measured under open-circuit conditions. ERP was decomposed into R_+ (i.e., R1) and R2. Analogous signal from bacteriorhodopsin was decomposed into Components I, II, and III. [From Trissl, H.-W., *Photochem. Photobiol.*, 29, 579, 1979 (A); Drachev, L.A., Kaulen, A.D., Khitrina, L.V., and Skulachev, V.P., *Eur. J. Biochem.*, 117,461, 1981 (B). With permission.]

constant is expected to be pH-dependent, possibly linearly. Actually, Cone[20] and Ostroy[9] once considered proton uptake as a possible mechanism, but the idea was eventually abandoned presumably because R2 had not exhibited the expected pH dependence (summarized in Reference 6).

The availability of reconstitution techniques for incorporating rhodopsin into a BLM made it possible to reexamine this problem under rigorously controlled conditions in a reduced system — the major advantage of the reductionist approach. Figure 128.5(A) shows the amplitude of R1 and R2 components as a function of the aqueous pH, measured in a reconstituted rhodopsin membrane.[44] However, no striking pH dependence was evident. A similar result was found in a reconstituted bacteriorhodopsin membrane [Figure 128.5(B)].[38,56] In both cases, the amplitudes are largely pH insensitive, except at pH below 2 (and above 8). When pH approaches 2 and below, R2 declines in amplitude, while R1 rises reciprocally. Similarly, as Components II and III of a bacteriorhodopsin membrane decline, the amplitude of Component I increases. If we identify Component I as the R1 analog, whereas Component II or III is identified as the R2 analog, the similarity becomes apparent. This lack of pH sensitivity runs against our intuitive expectation. The reciprocal relationship between R1 and R2 amplitudes also looks suspiciously correlated. The apparent paradox thus demands an explanation.

The investigation of reconstituted model systems greatly facilitated detailed kinetic analysis of fast photovoltages, but the initial results did not clear the apparent paradox, instead, they compounded the puzzle. It was found that the observed relaxation time constants differ drastically from laboratory to laboratory. The discrepancies between laboratories amount to a factor as much as 1000 and could hardly be explained by variations of common experimental conditions such as temperature, pH, etc. (see Table 1 in Okajima and Hong[57]). Apparently, the variation of a hidden parameter is the culprit. Using the same type of reconstitution method previously used by Trissl and Montal,[38] Hong and Montal[39] found that the measured time course of the ERP-like signal of a bacteriorhodopsin membrane under an open-circuit

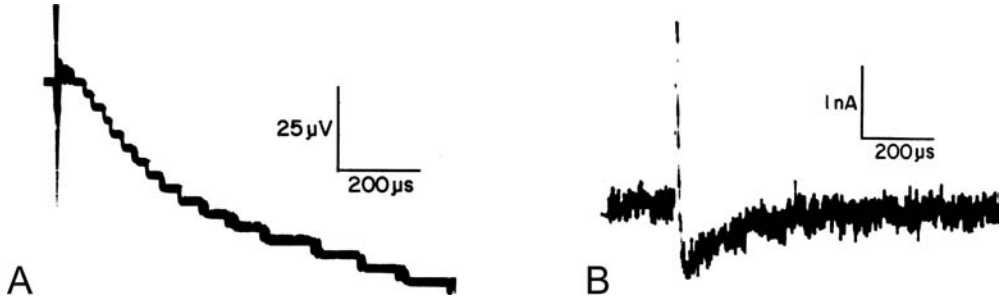

FIGURE 128.6 ERP-like photosignals measured from a reconstituted bacteriorhodopsin membrane under open-circuit conditions (A) and under near-short-circuit conditions (B). The access impedance was 1 kΩ. The light source is a microsecond dye laser pulse. The negative spike in Record A is a stimulus artifact. (From Hong, F.T. and Montal, M., *Biophys. J.*, 25, 465, 1979. With permission.)

condition differs drastically from that measured under a near-short-circuit condition. Specifically, the B1 component is smaller than the B2 component under the open-circuit condition, but the reverse is true under the near-short-circuit condition (Figure 128.6). Furthermore, the apparent relaxation time is considerably faster under the near-short-circuit condition than under the open-circuit condition. Similar observations pertaining to a reconstituted rhodopsin membrane were reported by Ostrovsky's group, when the membrane was short-circuited by shunting (Figure 128.7).[58] The latter observation suggests that changes of measurement conditions — shunting alters the measurement condition — affect the photoelectric kinetics similarly in reconstituted bacteriorhodopsin and rhodopsin membranes.[52] Conventional approaches could offer no satisfactory explanation for the observed kinetic variations. The two questions of how the measurement device interacts with the signal generating system in general and how short-circuiting of the membrane affects the waveform of fast photoelectric signals are readily understood by means of equivalent circuit analysis.

128.4 Equivalent Circuit Analysis

The key to resolving the above-mentioned apparent paradox is to recognize the heterogeneous nature of photochemical reactions in biomembranes. Intuitively, the electric currents generated by photoreactions must interact with the inert supporting structure — the lipid bilayer — as well as the measuring device. Equivalent circuit analysis thus provides a shortcut to a better understanding.

Let us start with the irreducible equivalent circuit, shown in Figure 128.4, that provides a description of the electrical event stemming from heterogeneous photochemical reactions. Additional features representing the inert supporting structure of the lipid bilayer must be added to this circuit [Figure 128.8(A)]. In a reconstituted model membrane, the lipid bilayer portion provides ion channels or leakage pathways for currents to go through the membrane, and the pathways are collectively represented by the membrane resistance, R_m (or its reciprocal, the membrane conductance, $G_m = 1/R_m$). When an ionophore is added to the membrane, R_m decreases. The membrane capacitance, C_m, holds transported charges; the potential across C_m represents the transmembrane voltage (open-circuit voltage). Thus, there are two parallel pathways for electric currents to go through the membrane: the photochemical pathway comprised of the irreducible circuit, as shown in Figure 128.4, and the inert RC circuit (R_mC_m) formed by the bilayer's conductance and capacitance. An additional element, R_s, is added to the photochemical pathway in order to account for the passage of the DC photocurrent. The value of R_s can be set to infinity in the case of visual membranes, because a transmembrane photoconduction pathway does not exist. The parameter R_e is usually referred to as the access impedance. It represents the combined impedance of the input impedance of the measuring device, the impedance of electrodes, and the impedance of the intervening solution between the membrane surfaces and the electrodes. The latter, though small in most electrophysiological measures, can at times become significant, and must be included in the equivalent circuit

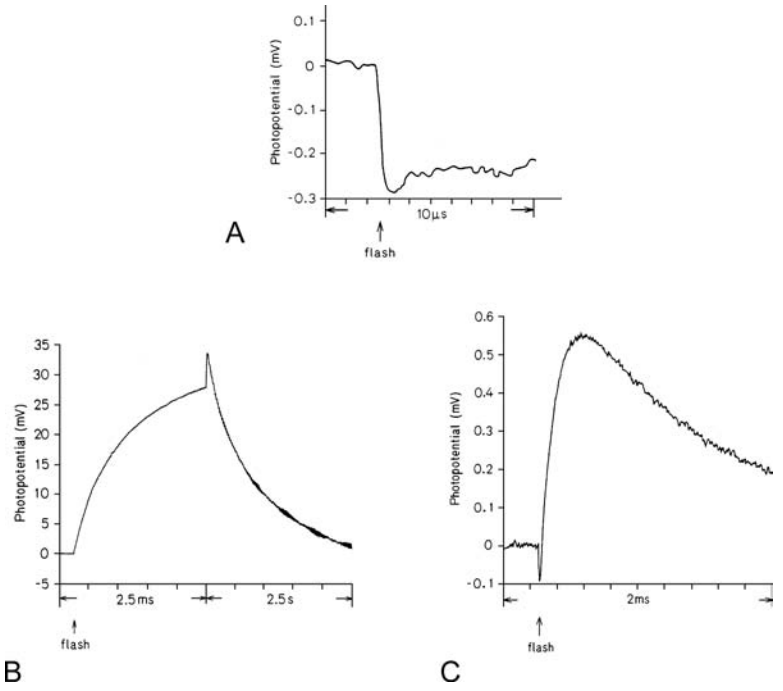

FIGURE 128.7 Effect of shunting on ERP. Rhodopsin was reconstituted into a Collodion membrane. Photosignals were elicited with 15 ns laser pulse at 530 nm (A and B), or at 500 nm (C). Records A and B show ERP at three different time scales. Fast negative Phase I (seen in Record A) corresponds to R1. Slow positive Phases II and III (seen in Record B) correspond to R2. Resistance of Collodion membrane was 50 MΩ-cm^2 in Records A and B but was shunted with external resistance of 2 kΩ-cm^2 in Record C. Experimental conditions in Record C were otherwise identical to those in Records A and B. Amplitude ratio R1/R2 of two components was 0.014 before shunting but became 0.16 after shunting. (From Drachev, L.A., Kalamkarov, G.R., Kaulen, A.D., Ostrovsky, M.A., and Skulachev, V.P., *Eur. J. Biochem.*, 117, 471, 1981. With permission.)

analysis. As far as photocurrent generation is concerned, R_e and R_m are placed in parallel and compete for the passage of photocurrents. It is the neglect of this access impedance that caused almost all of the confusion in the literature of photoelectric effects.

In standard electrophysiological measurements, two conditions are usually considered: voltage-clamp (short-circuit) or current-clamp (open-circuit) conditions. In the case of short-circuit measurements, R_e is much smaller than the combined impedance of R_m and C_m, the photogenerated electric current preferentially goes through R_e, and the R_mC_m circuit drops out of the picture and can be ignored. As expected, the photovoltage is zero or is held at a fixed (clamped) value (dictated by the voltage-clamping amplifier), and what is being measured is the photocurrent. If a brief light pulse is so short as to be effectively a mathematical delta function, an initial surge of photocurrent appears [left panel of Figure 128.8(B)]. The initial spike is then followed by an almost immediate reversal of polarity; the reversed photocurrent then relaxes with a characteristic exponential time constant, τ_p:

$$\frac{1}{\tau_p} = \frac{1}{R_pC_p} + \frac{1}{R_sC_p} \tag{128.2}$$

Because R_s is infinite for a visual membrane, and R_s is much larger than R_p for a bacteriorhodopsin membrane, the value of τ_p becomes approximately $1/R_pC_p$: the intrinsic photoelectric relaxation time constant.

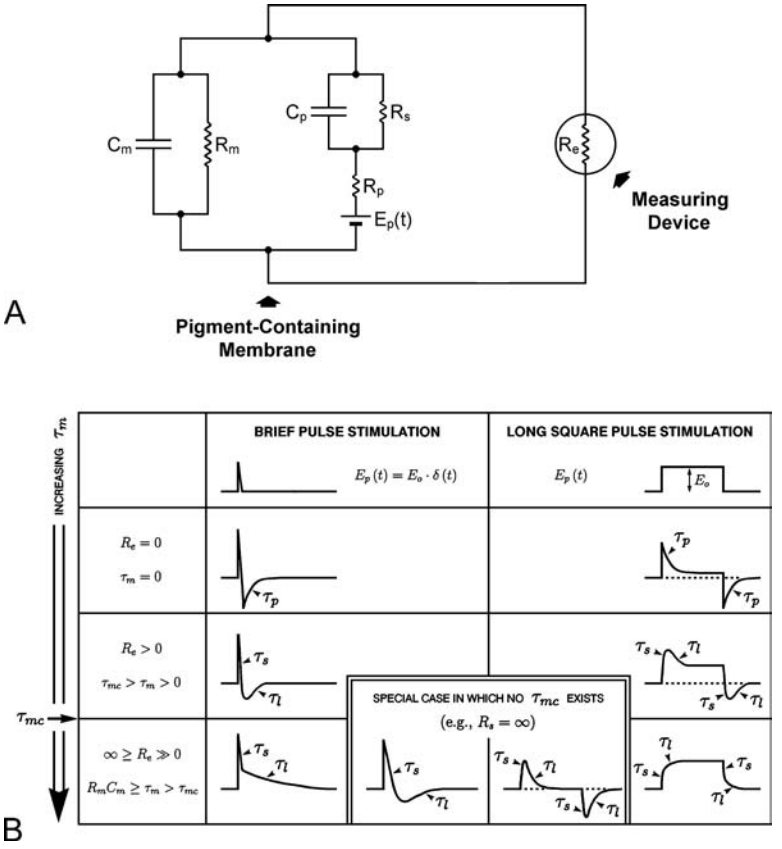

FIGURE 128.8 Universal equivalent circuit for the photoelectric effect, and its predicted responses to two different regimes of illumination. (A) In the equivalent circuit, a photochemical event is represented by an RC network including photoemf $E_p(t)$, internal resistance R_p of $E_p(t)$, chemical capacitance C_p, and transmembrane resistance R_s. With the exception of strictly short-circuit measurements, the time course of the photoelectric signal is further shaped via interaction with another RC network, formed by membrane resistance R_m, membrane capacitance C_m, and access resistance R_e. See text for further explanation. (B) Photosignal relaxation time courses are calculated in accordance with equivalent circuit. Two different regimes of illumination are considered: a brief δ-function-like light pulse and a long square-wave light pulse. Note that the relaxation time course varies with a change of the discharging time constant, τ_m, as defined by Equation 128.4. Under open-circuit conditions (i.e., $R_e = \infty$), the photosignal relaxes with two exponential time constants, τ_s and τ_l, of which the longer one, τ_l, approaches the membrane RC relaxation time constant, R_mC_m. Under short-circuit or near-short-circuit conditions, a photosignal in response to a long square-wave light pulse exhibits "on" spike and "off" spike, as expected in a linear high-pass RC filter. This characteristic waveform may disappear, if τ_m exceeds a critical value, τ_{mc}. (From Hong, F.T., in *Bioelectrochemistry: Ions, Surfaces, Membranes*, Blank, M., Ed., American Chemical Society, Washington, DC, 1980. With permission.)

In the case of open-circuit measurements, R_e is much larger than the combined impedance of R_m and C_m. Therefore, the photocurrent goes almost exclusively to R_mC_m to charge the membrane voltage; only a minute current goes through R_e, just enough to make the photovoltage measurable. The measured photovoltage thus rises abruptly but decays with two time constants: τ_s and τ_l (see References 47 and 55 for a detailed analysis). The longer time constant, τ_l, is nothing but the RC relaxation time constant of the inert structure: $1/R_mC_m$. In a record that captures the long time constant τ_l, the shorter time constant, τ_s, is usually too fast to be detected.

A third condition of measurements can be found when the source impedance of the membrane matches the value of R_e so that neither an open-circuit nor a short-circuit condition is met. The photocurrent thus splits into two branches: one goes to charge the membrane RC network, and the other goes to the

measuring device R_e. The measured quantity could be either the photocurrent or the photovoltage, depending on the configuration of the measuring equipment (the photovoltage is the product of the photocurrent and the access impedance, in accordance with Ohm's law). Again, the photocurrent, $I(t)$, rises abruptly but usually relaxes in two exponential terms:

$$I(t) = \frac{\frac{1}{\tau_s} - \frac{1}{R_s C_p}}{R_e C_m \left(\frac{1}{\tau_s} - \frac{1}{\tau_l}\right)} \int_0^t \frac{E_p(u)}{R_p} \exp\left(\frac{u-t}{\tau_s}\right) du \quad - \quad \frac{\frac{1}{\tau_l} - \frac{1}{R_s C_p}}{R_e C_m \left(\frac{1}{\tau_s} - \frac{1}{\tau_l}\right)} \int_0^t \frac{E_p(u)}{R_p} \exp\left(\frac{u-t}{\tau_l}\right) du \quad (128.3)$$

where $E_p(t)$ is the photo emf representing the photocurrent generator, and τ_m, τ_s, and τ_l are defined by the following equations:

$$\frac{1}{\tau_m} = \frac{1}{R_e C_m} + \frac{1}{R_m C_m} \quad (128.4)$$

$$\frac{1}{\tau_s} = \frac{1}{2}\left[\left(\frac{1}{R_p C_m} + \frac{1}{\tau_p} + \frac{1}{\tau_m}\right) + \sqrt{\left(\frac{1}{R_p C_m} + \frac{1}{\tau_p} + \frac{1}{\tau_m}\right)^2 - 4\left(\frac{1}{R_p C_m R_s C_p} + \frac{1}{\tau_p \tau_m}\right)}\right] \quad (128.5)$$

$$\frac{1}{\tau_l} = \frac{1}{2}\left[\left(\frac{1}{R_p C_m} + \frac{1}{\tau_p} + \frac{1}{\tau_m}\right) - \sqrt{\left(\frac{1}{R_p C_m} + \frac{1}{\tau_p} + \frac{1}{\tau_m}\right)^2 - 4\left(\frac{1}{R_p C_m R_s C_p} + \frac{1}{\tau_p \tau_m}\right)}\right] \quad (128.6)$$

The relaxation time constants, τ_s and τ_l, are neither τ_p nor τ_m but are a mixture of various RC constants. This third condition of measurement — collectively, it covers all measurement conditions that are neither strictly short-circuit nor open-circuit — is by no means fictitious. It could arise unwittingly in many photoelectric measurements. The awareness of its existence usually came as hindsight. Some earlier photocurrent measurements were performed with a picoammeter with an input impedance of about 100 kΩ, which is adequate to measure DC currents or low-frequency AC currents.[44] But, it becomes problematic in high-frequency measurements. The presence of a novel capacitance C_p that is connected in series with the photovoltage source E_p diminishes the source impedance of the membrane to about 20 kΩ. Thus, a current amplifier designed for low-frequency or DC measurements could not meet the condition of low-input impedance (as compared to the source impedance). Under this circumstance, although the measured signal was expressed in the unit of electric current, the measurement condition was actually closer to open circuit than short circuit. Thus, the variations of relaxation kinetics and the discrepancies between different laboratories can be accounted for by the variation of this hidden parameter — the access impedance. However, despite the variation of apparent relaxation time courses, the fundamental parameter τ_p can be recovered by deconvolution and remains unchanged: measurements made at two different access impedances gave rise to essentially the same value of τ_p, although two significantly different time courses of B1 were recorded.[57]

So far, we considered only the time course of photoresponses to a brief delta-function-like light pulse. The equivalent circuit also predicts the time course of photoresponses when the membrane is illuminated with a long square-wave light pulse, such as that shown in Figure 128.2(A) and Figure 128.2(B). In fact, it explains why a monotonic waveform of Figure 128.2(A) can be converted to a waveform with sharp spikes at the onset and the cessation of illumination, when shunting reduces the relaxation time constant τ_m to below a critical value τ_{mc} [right panel of Figure 128.8(B)]. The equivalent circuit predicts a pair of symmetric spikes. Upon closer examination of Figure 128.2(B), a slight asymmetric pattern of the two spikes is revealed. An explanation of this asymmetry is deferred to Chapter 134.

Now, we will explain why R2 exhibits no apparent pH dependence. Because the relaxation of an open-circuit photovoltage reflects mainly the membrane RC relaxation as explained above, it is, therefore, a poor indicator of the intrinsic photokinetic relaxation. Because most previous measurements of fast photoelectric signals were carried out under open-circuit conditions, the apparent lack of pH dependence is thus more expected than surprising.[59] Photoelectric measurements under open-circuit conditions pick up two relaxation time constants: τ_s reflects a distorted intrinsic relaxation, whereas τ_l reflects mainly the RC relaxation of the inert supporting lipid bilayer. Because τ_s and τ_l often differ by as many as six orders of magnitude (cf. Table 1 of Okajima and Hong[57]), they usually do not show up concurrently in the same (single) measurement record. Liu and Ebrey[60] indicated that photovoltages are good for the study of very fast kinetics, because photovoltage measurements are less sensitive to ionic strength and amplifier impedance. Ironically, the perceived merit is actually weakness of the method. The insensitivity to ionic strength is a consequence of the relaxation's tracking of the irrelevant RC relaxation of the supporting bilayer instead of the relevant photochemical relaxation. In fact, while open-circuit measurements failed to detect any ionic strength effect,[38] a near-short-circuit measurement showed demonstrable ionic strength effect.[57] Regarding the sensitivity to amplifier impedance that makes up a major contribution to the access impedance, it is easier to achieve rigorous open-circuit conditions than short-circuit conditions. For example, Hong and Mauzerall measured the fast photosignal of a magnesium-porphyrin BLM at an access impedance of 380 Ω, but the short-circuit condition is still not met rigorously (see Figure 3 of Hong and Mauzerall[61]). That the latter measurement condition was not exactly short-circuit can be seen from the apparent relaxation time course: the photocurrent did not reverse its polarity upon the cessation of the laser pulse, as dictated by the analysis shown in Figure 128.8(B) (the laser pulse ended at around 0.7 μs, but the photocurrent had not reversed its polarity 3 μs after the onset of the laser pulse or 2.3 μs after the cessation of light stimulation.) The sensitivity of short-circuit measurements to the access impedance (which includes the amplifier impedance) is an asset rather than a nuisance, because the access impedance can be tuned to match the source impedance so that the relaxation time course can be deconvoluted more reliably to yield intrinsic kinetics, as we routinely did. Therefore, we called this approach tunable voltage clamp method.[61] It is very difficult, if not impossible, to recover intrinsic kinetic information by deconvoluting an open-circuit photovoltage, mainly because of the low information content regarding intrinsic photochemical processes.

The reciprocal change of amplitude of the B1 and B2 components, as the aqueous pH approaches 2 and below, as shown in Figure 128.5(B), is no coincident but is actually an illusion. This point can be made clear by examining a schematic diagram shown in Figure 128.9. Because of the partial overlap of the decay of B1 and the rise of B2, and because they have opposite polarities, the coexistence of B2 partially cancels the amplitude of B1. Thus, inhibition of B2 leads to an apparent increase of the B1 amplitude. That this is not merely a speculation can be seen in the pH dependence of isolated B1, as compared to that of a composite signal (B1 + B2). Figure 128.10(A) shows reciprocal changes of peak amplitudes of a composite signal when the aqueous pH was varied. Unlike Figure 128.5(B), the composite signal exhibits significant pH sensitivity over a wide pH range, where bacteriorhodopsin remains stable. In contrast, an isolated B1 record shows no trace of pH dependence over the same range [Figure 128.10(B)]. I suspected that the reciprocal changes of the amplitude of the two ERP components could be similarly explained [Figure 128.5(A)]. Actually, a similar reciprocal change of R1 and R2 peaks, as temperature is lowered, was observed by Pak and Cone[12] [Figure 128.1(C) through Figure 128.1(E)]. They correctly attributed the temperature effect to R2 alone. Again, a similar reciprocal change of amplitudes appears in the ERP-like signals from bacteriorhodopsin, as temperature is lowered[62] [Figure 128.10(C)]. However, as shown in Figure 128.10(D), an isolated B1 exhibits almost no temperature dependence. A closer examination reveals that there is a small temperature effect on B1. The small changes shown in Figure 128.10(D) between 5 to 45°C are real and reproducible. The temperature dependence of $1/\tau_p$ on $1/T$ (where T is the absolute temperature) obeys the Arrhenius relationship.[57] Whether similar temperature dependence exists in R1 or not remains a speculation. It is important to realize that such a small temperature dependence could not have been detected at the time when ERP was being actively investigated because of technical difficulties encountered in an *in vivo* measurement

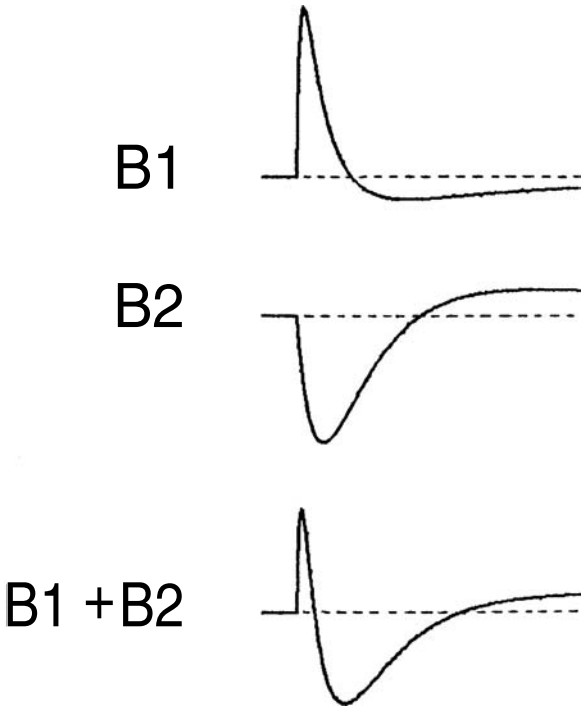

FIGURE 128.9 The decomposition of an ERP-like signal in a reconstituted bacteriorhodopsin membrane, according to equivalent circuit analysis. Each component decays with two exponential time constants, and each satisfies zero time-integral condition Equation 128.1. Note the partial overlapping of the decay of B1 and the rise of B2. (From Okajima, T. and Hong, F.T., *Biophys. J.*, 50, 901, 1986. With permission.)

and because of insufficient signal-to-noise ratio. The recent development of an expression system by Sullivan and Shukla[42,43] offered a hope of seeing such a subtle change. Of course, a prerequisite is the development of a technique to isolate the pure R1 component.

In isolating B1, we used a drastic procedure: multiple oriented bacteriorhodopsin layers were first deposited on a Teflon film, and the preparation was allowed to dry for four days.[63] Such a drastic procedure is almost certainly going to denature rhodopsin. Alternatively, we used chemical modification to suppress B2, but the suppression was not complete because of the limitation of our choice of chemical reagent fluorescamine, which hydrolyzes rapidly.[64] We were able to suppress the B2 component completely within the pH range from 6 to 9 by means of site-directed mutagenesis.[65] Thus, the rhodopsin expression system used by Sullivan and Shukla remains the most promising approach. Still, I must caution here that the conventional approach of curve-fitting the measured signal with multiple exponential relaxation terms almost certainly will not work. The reason will be presented in the next section.

128.5 A Critique on the Multiexponential Analysis

In the literature of photoelectric effects, investigators often used computer-assisted curve-fitting procedure to decompose a transient photoelectric signal into multiple components of exponential decays.[66–68] Each component is then associated with a known spectral transition in the photocycle. Mainstream investigators gradually realized the distortion effect of the membrane RC relaxation process and have begun to acknowledge the presence of the pure membrane RC time constant among the time constants determined by exponential analysis.[60,69–71] But the extent of distortion has not been fully appreciated — just about every time constant is affected.

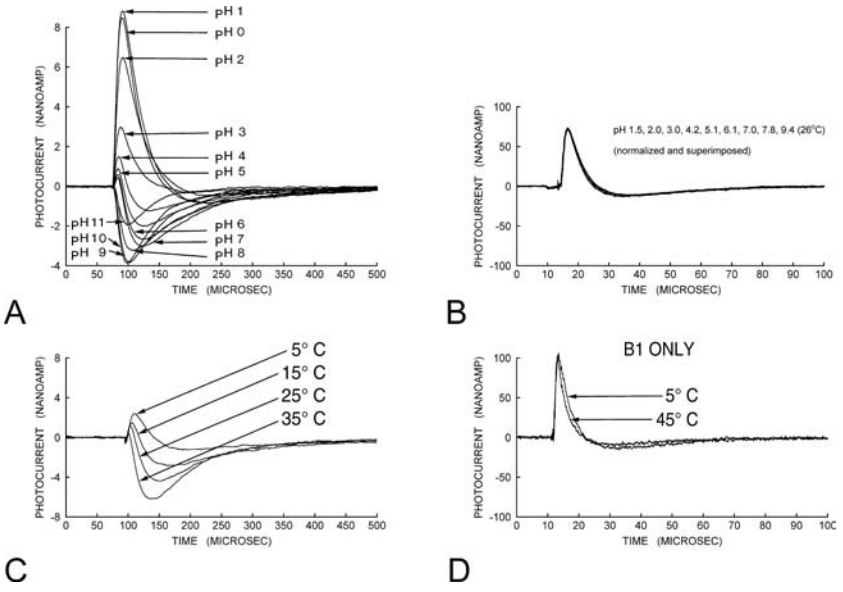

FIGURE 128.10 Effect of pH and temperature on B1 and B2. (A) The data illustrate effects of varying pH on a composite signal consisting of B1 and B2, at 25°C. (B) The data illustrate the total lack of pH dependence of an isolated B1 signal. (C) The data show the temperature dependence of the composite signal (B1 and B2) at neutral pH. (D) The data show a small temperature dependence of an isolated B1 signal. The temperature effect is reversible. For detailed experimental conditions, consult the cited sources. [From Okajima, T. and Hong, F.T., *Biophys. J.*, 50, 901, 1986 (A); Michaile, S. and Hong, F.T., *Bioelectrochem. Bioenerg.*, 33, 135, 1994 (B); Hong, F.T. and Okajima, T.L., in *Biophysical Studies of Retinal Proteins*, Ebrey, T.G., Frauenfelder, H., Honig, B., and Nakanishi, K., Eds., University of Illinois Press, Urbana-Champaign, IL, 1987 (C,D). With permission.]

Although associating each exponential term with a photochemical relaxation process appears to be an innocuous and acceptable practice in solution-phase photochemistry, it is fundamentally flawed to apply the same approach to heterogeneous reactions involving a membrane phase and two aqueous phases for the following reason. A signal component in the form of a single exponential decay obviously cannot possibly satisfy the zero-time integral condition. This can be made clear by examining Figure 128.11, which was constructed to illustrate the generation of a capacitative signal by a single step of charge shift inside the membrane.[72] The charge shift during the transition from state E_i to state E_{i+1} is shown to be represented by an impulsive rise of the photocurrent that decays with a characteristic time constant τ_i. Time integration of the photocurrent thus yields the amount of charges that shifts in the direction perpendicular to the membrane surface as a function of time. It is apparent that the result shows that the charges separated during this transition never recombine [Figure 128.11(C)]. The latter conclusion directly contradicts the notion of capacitative current, because integration of the area under the curve gives rise to a nonzero value, thus violating Equation 128.1. In other words, a capacitative current cannot possibly be represented by a single exponential term without leading to a self-contradiction. In contrast, the waveforms as described in Figure 128.8(B) satisfy the zero time-integral condition.

Common sense in electronics engineering leads to a second objection. The membrane that is capable of generating an ERP-like capacitative current resembles an electronic device in which the current (or voltage) generator is embedded in a thin-film matrix. It is, therefore, inconceivable that the photosignal relaxation can be analyzed and interpreted without, at the same time, considering the interaction between the active current generator and the passive RC network. Here, the RC network is formed by the inert supporting substrate — the phospholipid bilayer membrane. Hagins and Rüppel[8] and Govardovskii[73] once proposed equivalent circuit models (cable models with RC networks) for an intact rod cell and attempted to account for the waveform of ERP. Hochstrate et al.[74] recognized the shaping effect of the

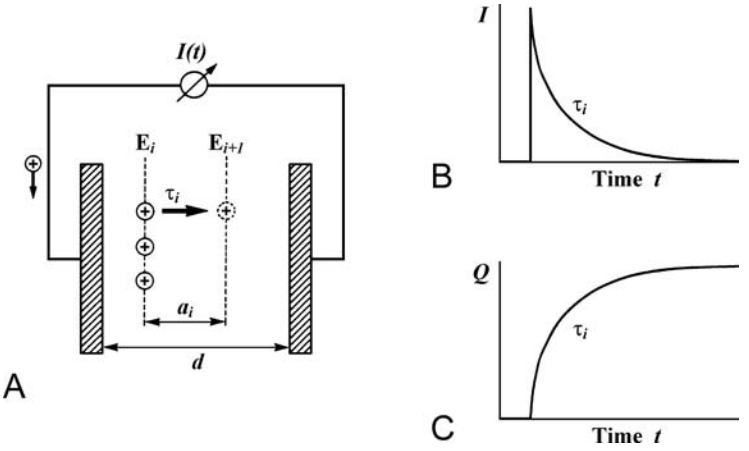

FIGURE 128.11 Principle of capacitative coupling, according to the mainstream approach. (A) Membrane is represented by dielectric layer, which is interposed between two plates of parallel-plate capacitor. Under short-circuit conditions, flash excitation creates an initial unstable state E_i, which relaxes to a stable product state E_{i+1} with the time constant τ_i. (B) The process leads to measurable transient photocurrent I, which decays to zero with same time constant as that of transition $E_i \rightarrow E_{i+1}$. C. Time-integration of the photocurrent generates a curve that represents accumulation of separated charges Q as a function of time. According to this interpretation, capacitance is charged with a rising exponential time course to steady level but is never discharged. Thus, charges are separated but never recombined — a description contradicting the notion of capacitative coupling. (From Läuger, P., *Electrogenic Ion Pumps*, Sinauer Associates, Inc., Sunderland, MA, 1991. With permission.)

RC property of the photoreceptor membrane and proposed a two-capacitor model to account for the ERP waveform. However, they associated the second (series) capacitor with the capacitor of the nonpigmented portion of plasma membrane. As we shall see, this second capacitor exists. It even persists in reconstituted systems, where the distorting effect of nonpigmented plasma membrane is absent, and it can be identified as the chemical capacitance in Figure 128.8(A). The effect of the RC network formed by the photoreceptor membrane (essentially a linear RC filter) on the time course of the observed ERP was also recognized by Brindley and Gardner-Medwin,[75] but was apparently ignored or neglected by most investigators working on the ERP-like signal elicited in reconstituted bacteriorhodopsin membranes.

It is of interest to note that Hodgkin and O'Bryan[13] proposed the following equation to describe the waveform of R1 and R2, measured intracellularly in a turtle cone receptor:

$$j(t) = -NK\delta_o(t) + BNKa_3 \exp(-a_3 t) \tag{128.7}$$

where $\delta_o(t)$ is the unit impulse (δ-function at $t = 0$), B, K, and a_3 are constants, N is the number of excited molecules, and $j(t)$ is the outward current representing the ERP (called early receptor current). Had the parameter B been set to unity, the waveform defined by Equation 128.7 would have satisfied the zero time-integral condition (Equation 128.1).

A lingering question is if multiexponential analysis cannot guarantee a meaningful model, why did most of these models fit the data reasonably well? The answer lies in what it takes to accomplish curve fitting. It is a well-known mathematical fact that any curve can be fit, to any degree of accuracy, with a polynomial function, as long as there is no limit as to how many terms can be used (Weirstrass' theorem). Of course, polynomials are not the only class of function serving this purpose. In effect, just like any three-dimensional vector can be expressed in terms of a linear combination of three orthogonal basis vectors (coordinates), any curve can be expressed with a linear combination of infinitely many orthogonal functions, of which the orthogonal set of polynomials is but one. Deconvolution of a curve in terms of an infinite series of polynomials, of course, makes little physical sense in chemical relaxation; deconvolution in exponential terms makes more sense. The process is tantamount to a Laplace transform, which

converts a function in the time domain into another function in the frequency domain. A peak in the latter curve in the frequency domain represents a discrete exponential decay. As long as there is no noise, the process appears to be innocuous. In the presence of noise, spurious peaks are not uncommon. This is the reason why detailed curve fitting often yields conformational substates,[66] which may or may not be physically meaningful depending on independent corroboration from data obtained by means of a drastically different way — independent corroboration from different laboratories using the same approach is often insufficient. Previously, Gauch[76] presented an illuminating analysis concerning fitting experimental data to a mathematical model. He pointed out that there is a balance between the accuracy and the parsimony of mathematical models. Over-fitting data to a model with an ever-increasing number of parameters can result in fitting the model more to noise than to real data — a well-known fact in systems analysis theory. Therefore, data imposes no constraint on multiexponential analysis. The agreement with data is no proof of the validity of a particular model under consideration. If associating each exponential decay with a chemical relaxation process seems the only possibility, multiexponential analysis will be admissible. This is the reason why applying multiexponential analysis to solution-phase photochemical relaxation never led to any difficulty in interpretation. In the case of heterogeneous photochemical relaxation in a three-phase system, alternative interpretations must be sought for and eliminated before one jumps to the conclusion of proving the model. A detailed discussion of the validity of curve-fitting or model-fitting was published elsewhere.[55,77]

In contrast, in the above-described equivalent circuit analysis, we first separated the individual components by physical means, using various reconstitution methods. Contrary to common impressions, our data of isolated components was subjected to multiexponential analysis to obtain the time constants, such as τ_s and τ_l. These deconvoluted data are then tested with the equivalent circuit. The equivalent circuit imposes a constraint that the investigator cannot manipulate or overcome by "massaging" the data. Equation 128.3 can be simplified by using a brief light pulse so that $E_p(t) = E_0 \cdot \delta(t)$, where $\delta(t)$ is the mathematical delta function:

$$I(t) = A_s \cdot \exp\left(-\frac{t}{\tau_s}\right) - A_l \cdot \exp\left(-\frac{t}{\tau_l}\right) \tag{128.8}$$

where the preexponential factors (amplitudes) satisfy the following relation:

$$\frac{A_s}{A_l} = \frac{\tau_l}{\tau_s} \tag{128.9}$$

For a pure, isolated photoelectric current component, Equation 128.9 must be satisfied. Taken together, Equation 128.8 and Equation 128.9 satisfy the zero time-integral condition (Equation 128.1). It is, therefore, not surprising that the definition of capacitative current provides the crucial constraint. It is also not surprising that the conventional multiexponential analysis is so misleading in membrane-phase photochemistry; capacitative events are a major feature of interfacial photochemistry.

128.6 Molecular Interpretation of Fast Photoelectric Signals

There is little doubt that fast photoelectric signals are electrical manifestation of light-induced charge separation and recombination. For a macromolecule with a multistep reaction sequence as complex as rhodopsin or bacteriorhodopsin, there are many candidates for generating a fast photoelectric signal component. In principle, each step of reversible reaction can contribute a component. Fast photokinetic measurements have a tendency to pick up faster processes. We identified three fast components in reconstituted bacteriorhodopsin membranes: B1, B2, and a B2-like signal, which we called B2′ component. Like B2, the B2′ component is generated by interfacial proton transfer — the proton release and reuptake at the extracellular surface.[62] This does not mean that slower components do not exist. In fact,

other investigators identified many slower components. The problem is that all of these data were subjected to multiexponential analysis alone. It is difficult to make sensible comments other than point out the inadequacy of multiexponential analysis.

The fast rise time of the R1 component of ERP and the corresponding B1 component of its bacteriorhodopsin analog suggest that they are associated with early events in the photobleaching sequence of rhodopsin and the photocycle of bacteriorhodopsin, respectively. Trissl[78] measured the rise time of the R1 component to be about 0.8 μs at 0°C and 1.6 μs at 37°C in an intact cat photoreceptor. The corresponding value of isolated outer segments attached to Millipore filters was 90 ns. Trissl concluded that the R1 component might be associated with an early charge separation as fast as the *cis-trans* isomerization of the retinal chromophore. Using an ultrafast measurement method, Groma and coworkers[41] found the rise time of ERP-like signals from bacteriorhodopsin membranes to be between 2.5 to 5 ps for the forward charge separation (ground-state bacteriorhodopsin to K transition) and 3.5 ps for the charge separation driven by reverse phototransition (K to bacteriorhodopsin). Liu et al.[79] showed that bacteriorhodopsin reconstituted with a modified all-*trans* retinal that cannot isomerize to 13-*cis* retinal does not have this component. Therefore, B1, and perhaps also R1, are mostly likely to be associated with the earliest photolytic event of photoisomerization of the chromophore. By analyzing the temperature dependence of the first-order relaxation time constant of τ_p of the B1 component, Okajima and Hong[57] determined the value of τ_p to be 12.3 ± 0.7 μs and the activation energy to be 2.54 ± 0.24 kcal/mol. These values are not affected by overnight exchange of H_2O/D_2O, a change of ionic strength by replacing 0.1 M of KCl with 3 M of KCl. Note that the latter was not a measurement of rise time but rather the time constant of charge recombination following the initial rise. However, there is no known activation energy among the photocycle intermediates that matches the value of activation energy. Therefore, its molecular interpretation remains unclear.

In our equivalent circuit analysis, the B2 component was found to have the following properties. It is sensitive to pH[57] and to ionic strength[62] of the bathing solutions. Its relaxation kinetics are reversibly slowed by overnight exchange of H_2O/D_2O.[57] It is almost abolished by a water-soluble chemical label, fluorescamine, which specifically attacks primary amine of exposed amino acid residues.[64] This latter finding supports the interpretation that B2 reflects light-induced interfacial proton uptake because fluorescamine quickly hydrolyzes in water and is, therefore, incapable of attacking amino acids buried inside the membrane. It was further found that the B2 component changes polarity at pH 2.7.[80] Below pH 2.7, B2 was found to be sensitive to Cl^- concentration, whereas it was found to be sensitive to Ca^{2+} and Mg^{2+} concentrations above pH 2.7.[81] The R2 component is most likely associated with the light-induced proton uptake of the metarhodopsin-I-to-metarhodopsin-II transition of the photobleaching sequence. No further detailed interpretation could be made on the basis of the existing ERP literature.

More recently, Kaulen[82] attempted to integrate photoelectric data with newly obtained structural information of bacteriorhodopsin. He noted that discrepancies of reported photoelectric measurements exist not only between model membranes constructed by drastically different methods but also in membranes constructed with "analogous" methods. Attempts to seek explanations in terms of different reconstitution methods seem misdirected. The true culprit is probably the exact condition of measurements. However, by continuing to ignore the presence of chemical capacitance, one tends to overlook the resulting reduction of the source impedance at microsecond and submicrosecond time ranges, and the most crucial parameter — access impedance — remains missing in data reporting. Differentiating valid conclusions from dubious ones, based on correlation of photoelectric data with structural data, remains a daunting task for readers.

128.7 Discussion and Conclusions

Most vision researchers treat ERP as an epiphenomenon. Two reasons have often been singled out to discredit the possible physiological importance of ERP: the amplitude of ERP is too small, and the ERP-like signals are ubiquitous. Shortly after the discovery of ERP, similar fast photoelectric signals were found in many different pigment-containing tissues, such as pigmented epithelia of the eyes and chloroplasts.

ERP-like signals were also found in BLM reconstituted with various kinds of pigments or organic dyes, provided that some inherent asymmetry (i.e., a membrane containing a pigment with a fixed orientation or facing two asymmetric aqueous solutions) exists. The ubiquity suggests that ERP is nothing unique for vision and perhaps serves no physiological function. But the reasoning was flawed. In hindsight, the ubiquity is understandable. Most dyes or pigments respond to light stimulation by ejecting electrons, and reverse reactions are common in chemical reactions. Thus, dye or pigment membranes that have some inherent asymmetry always respond to light with a fast photoelectric signal. In hindsight, the fast photoelectric effect is biologically relevant, because the primary event in vision and in photosynthesis is light-induced charge separation. However, these signals cannot be expected to always be functionally significant. Just because stick-like structures are ubiquitous does not mean some cannot be used to write, to point, or to be used as a weapon. Likewise, the ubiquity of ERP-like signals alone does not rule out a possible physiological function. A dismissal of ERP as an epiphenomenon may be premature. In fact, it may remain forever premature until proved otherwise, because absence of evidence is not evidence of absence.

Next, a dismissal of ERP's possible physiological role based on its small amplitude may be misleading. This is because ERP may not be small at the vicinity of the (cytoplasmic) membrane surface, where action is. Physiologists often discussed bioelectric phenomena in terms of transmembrane potentials, but what really matters at the molecular level is the local electric field. In other words, what really matters is the potential gradient across the membrane rather than the transmembrane potential and, in the case of interfacial phenomena, the potential gradient in the diffuse double-layer region: $E = -dV(x)/dx$, where x is the coordinate in the direction perpendicular to the membrane, and $V(x)$ is the electric potential profile. Surface potentials are rather short-ranged in action. Because of charge screening, the potential profile at the vicinity of the membrane surface is steep. This is because the fixed charges on the membrane surface are completed neutralized by the net counterions in the double-layer regions (strictly speaking, it takes counterions of both double layers on opposite sides of the membrane to neutralize the fixed charges on a single surface).[83] As a result, the local electric field fades exponentially, as the distance from the membrane increases, instead of the more gradual fashion prescribed by the inverse-square law. A surface potential is small if viewed from outside of the double-layer regions, but it is locally intense, because the surface potential must drop to zero over a distance that is of the same order as the Debye length. Therefore, the slope of the potential profile must be steep, and the force must be locally intense. Years ago, Hong speculated about the possible appearance and disappearance of a large surface potential accompanying the appearance and disappearance of R2.[53] Hong cited an actual example of a reconstituted membrane that exhibited an open-circuit photovoltage of 1.4 mV, but the calculated surface potential amounted to 50 mV. If a surface potential of this modest amplitude presides over a double layer of a Debye length of the order of 5 Å (a deliberate underestimate), it would give rise to a local electric field comparable to that generated by a transmembrane potential of 600 mV inside the membrane. This speculated surface potential and the associated intense electric field were subsequently observed by Cafiso and Hubbell,[84,85] using a spin-label to probe the local electric field. Thus, the intensity of the local electric field near the membrane surface cannot be judged by the size of the corresponding potential measured externally. The highly localized nature of electric field generated by ERP may just be what is needed for an effective trigger.

Just imagine the requirement of a mechanistic trigger of visual phototransduction. Because a trigger is an event prior to the biochemical amplification process, it must be linear and localized near the site of illuminated rhodopsin. The R2 component fulfills this requirement. It is linear in view of the equivalent circuit presented in this article. Its local nature was demonstrated by Hagins and McGaughy.[19] As mentioned earlier, Ostrovsky and coworkers demonstrated that the proton uptake takes place at the cytoplasmic surface. Furthermore, the polarity of the R2 signal is consistent with a proton binding at the cytoplasmic side.[86] Thus, the surface potential associated with R2 appears at the right place at the right time to trigger binding of transducin to metarhodopsin II. Based on these considerations, Hong[87] proposed a surface potential-based mechanism for triggering the cyclic GMP cascade. The plausibility of a mechanistic switch based on light-induced surface potential was demonstrated by Drain et al.[88] (cited

TABLE 128.1 A Hypothetical ERP-Based Electrostatic Trigger Mechanism

1. The cyclic GMP cascade takes place at the cytoplasmic surface.
2. Binding of transducin to metarhodopsin II leads to its activation.
3. The formation of metarhodopsin II involves the net uptake of a proton at the cytoplasmic side.
4. The rise phase of the ERP R2 component is time-correlated with the formation of metarhodopsin II.
5. The polarity of the R2 component is consistent with the proton uptake at the cytoplasmic surface.
6. The photophosphorylation of rhodopsin at its cytoplasmic surface occurs during the deactivation of visual transduction.
7. The above events are associated with a surface-potential change at the cytoplasmic surface.

Source: From Hong, F.T., *J. Mol. Electron.*, 5, 163, 1989. With permission.

in Figure 32.4 of Hong[89]). Their experimental model membrane shows that a light-induced surface potential can operate like a phototransistor (or light-activated field effect transistor). Thus, the positive surface potential associated with R2 may be the mechanistic "on" trigger of visual phototransduction. By the same line of reasoning, the mechanistic "off" trigger for the termination of the cyclic GMP cascade may be provided by the negative surface potential generated by subsequent photophosphorylation of up to nine amino acid residues at rhodopsin's cytoplasmic domain.[90] The lines of circumstantial evidence suggesting a surface potential-based trigger for the initiation and termination of visual transduction is listed in Table 128.1.

Here, we restrict our consideration to electrostatic interactions. As we shall see in Chapter 134, the real-life situation is, of course, more complex. In addition to electrostatic interactions, other noncovalent bond interactions must be taken into account. But the possible role of ERP should not been overlooked. Investigators familiar with the biochemistry of visual transduction and electrophysiology may argue that ERP plays no such role, because most, if not all, of the biochemical experiments regarding the cyclic GMP cascade were performed in the solution phase, where no membrane potential can be sustained. However, one should not overlook an important difference between ERP and other well-known bioelectric phenomena. While diffusion potentials vanish instantly upon the rupture of a membrane, surface potentials, being localized, persist even in a broken membrane. In fact, the equivalent circuit shown in Figure 128.4 was derived mathematically under a short-circuit condition, which is fulfilled by a broken membrane (see Appendix of Hong[53] or Section 8 of Hong[55] for a rigorous derivation). Cafiso and Hubbell[84,85] once used spin-label to monitor interfacial potentials of vesicles made of rod disk membranes. The same methodology can be used for broken membranes. Therefore, the case remains open until more convincing evidence appears, one way or the other. It is, therefore, of interest to see how a possible role of ERP measures up in light of the current understanding of the biochemical mechanism of visual phototransduction. This topic will be treated in Chapter 134.

As for the role of ERP-like photosignals in bacteriorhodopsin membranes, we can only speculate here. From a bioenergetic point of view, signals such as B2 and B2′ represent processes that are counterproductive; charge recombination has the same effect as internal short-circuiting of a battery. In view of the universal presence of reverse reactions, ERP-like signals cannot be eliminated. However, their presence does not prevent a net light-induced transfer of proton across the bacteriorhodpsin membrane. Although the presence of a reverse reaction implies that the reaction stops upon reaching chemical equilibrium, a light-pumped system, such as the purple membrane, never reaches equilibrium but reaches a steady state; the continuing input of photon energy ensures that the net proton pumping goes forward in spite of reverse reactions. Still, nature strove to minimize the reverse reaction, and nature's strategy is a sophisticated scheme of optimization. We shall also consider how nature enhances solar energy conversion by means of noncovalent bond interactions of photosynthetic components.

Finally, a comment regarding photoelectric effects is in order. The study of ERP and ERP-like photosignals offers a proving ground with which to try various approaches of interpreting the measured photosignals. In this chapter, the peril of extrapolating and transplanting methodology established in the solution phase to a heterogeneous three-phase system as well as the peril of applying methodology established in classical electrophysiology to systems in which light plays a crucial role were pointed out. For over a quarter century, investigators could not reach a consensus regarding the interpretation of

measured photosignals. The dispute eventually subsided, and some investigators viewed both approaches — the multiexponential analysis and the analysis based on the concept of chemical capacitance — as complementary to each other. But a detailed comparison reveals that the two approaches are fundamentally incompatible. Although the present approach requires a more complicated equivalent circuit model than the conventional multiexponential approach, it is more general than the latter. Here, only a single equivalent circuit model is used to explain virtually all electric phenomena arising from light-induced charge separation in membranes. In contrast, an ad hoc model must be concocted for each experimental system in the alternative approach. The latter approach also lacks a predictive power and often leads to conflicting interpretations from different laboratories. In the light of increasing interest in possible technological applications of the photoelectric effect of bacteriorhodopsin and other biopigments, the present approach seems to offer a distinct advantage as a design tool of molecular devices because of its predictive power.

Acknowledgments

The author acknowledges the contribution of the following individuals, whose experimental work on bacteriorhodopsin was cited: Man Chang, Albert Duschl, Brian Fuller, Filbert Hong, Sherie Michaile, Baofu Ni, Ting Okajima, Michelle Petrak, and Wita Wojtkowski. The author is also indebted to his collaborators: Janos Lanyi, Lowell McCoy, Mauricio Montal, and Richard Needleman.

References

1. Brown, K.T. and Murakami, M., A new receptor potential of the monkey retina with no detectable latency, *Nature*, 201, 626, 1964.
2. Brown, K.T., Watanabe, K., and Murakami, M., The early receptor potentials of monkey cones and rods, *Cold Spring Harbor Symp. Quant. Biol.*, 30, 457, 1965.
3. Cone, R.A., The early receptor potential of the vertebrate eye, *Cold Spring Harbor Symp. Quant. Biol.*, 30, 483, 1965.
4. Pak, W.L., Some properties of the early electrical response in the vertebrate retina, *Cold Spring Harbor Symp. Quant. Biol.*, 30, 493, 1965.
5. Cone, R.A. and Pak, W.L., The early receptor potential, in *Handbook of Sensory Physiology, Volume I: Principles of Receptor Physiology*, Loewenstein, W.R., Ed., Springer-Verlag, Heidelberg, 1971, p. 345.
6. Pak, W.L., Rapid photoresponses in the retina and their relevance to vision research, *Photochem. Photobiol.*, 8, 495, 1968.
7. Arden, G.B., Bridges, C.D.B., Ikeda, H., and Siegel, I.M., Mode of generation of the early receptor potential, *Vison Res.*, 8, 3, 1988.
8. Hagins, W.A. and Rüppel, H., Fast photoelectric effects and the properties of vertebrate photoreceptors as electric cables, *Fed. Proc.*, 30, 64, 1971.
9. Ostroy, S.E., Rhodopsin and the visual process, *Biochim. Biophys. Acta*, 463, 91, 1977.
10. Brown, K.T., The electroretinogram: its components and their origins, *Vision Res.*, 8, 633, 1968.
11. Pak, W.L. and Ebrey, T.G., Visual receptor potential observed at sub-zero temperatures, *Nature*, 205, 484, 1965.
12. Pak, W.L. and Cone, R.A., Isolation and identification of the initial peak of the early receptor potential, *Nature*, 204, 836, 1964.
13. Hodgkin, A.L. and O'Bryan, P.M., Internal recordings of the early receptor potential in turtle cones, *J. Physiol.*, 267, 737, 1977.
14. Hestrin, S. and Korenbrot, J.I., Activation kinetics of retinal cones and rods: response to intense flashes of light, *J. Neurosci.*, 10, 1967, 1990.
15. Makino, C.L., Taylor, W.R., and Baylor, D.A., Rapid charge movements and photosensitivity of visual pigments in salamander rods and cones, *J. Physiol.*, 442, 761, 1991.

16. Arden, G.B., Bridges, C.D.B., Ikeda, H., and Siegel, I.M., Rapid light-induced potentials common to plant and animal tissues, *Nature*, 212, 1235, 1966.
17. Penn, R.D. and Hagins, W.A., Signal transmission along retinal rods and the origin of the electroretinographic *a*-wave, *Nature*, 223, 201, 1969.
18. Hagins, W.A. and McGaughy, R.E., Molecular and thermal origins of fast photoelectric effects in the squid retina, *Science*, 157, 813, 1967.
19. Hagins, W.A. and McGaughy, R.E., Membrane origin of the fast photovoltage of squid retina, *Nature*, 159, 213, 1968.
20. Cone, R.A., Early receptor potential: photoreversible charge displacement in rhodopsin, *Science*, 155, 1128, 1967.
21. Mueller, P., Rudin, D.O., Tien, H.T., and Wescott, W.C., Reconstitution of cell membrane structure *in vitro* and its transformation into an excitable system, *Nature*, 194, 979, 1962.
22. Tien, H.T., Light-induced phenomena in black lipid membranes constituted from photosynthetic pigments, *Nature*, 219, 272, 1968.
23. Schadt, M., Photoresponse of bimolecular lipid membranes pigmented with retinal and vitamin A acid, *Biochim. Biophys. Acta*, 323, 351, 1973.
24. Tien, H.T. and Ottova-Leitmannova, A., *Membrane Biophysics: As Viewed from Experimental Bilayer Lipid Membranes (Planar Lipid Bilayers and Spherical Liposomes)*, Elsevier, Amsterdam; New York, 2000.
25. Takagi, M., Azuma, K., and Kishimoto, U., A new method for the formulation of bilayer membranes in aqueous solution, *Annu. Report Biol. Works Faculty of Sci. Osaka Univ.*, 13, 107, 1965.
26. Montal, M. and Mueller, P., Formation of bimolecular membranes from lipid monolayers and a study of their electrical properties, *Proc. Natl. Acad. Sci. USA*, 69, 3561, 1972.
27. Montal, M. and Korenbrot, J.I., Incorporation of rhodopsin proteolipid into bilayer membranes, *Nature*, 246, 219, 1973.
28. Trissl, H.-W., Darszon, A., and Montal, M., Rhodopsin in model membranes: charge displacements in interfacial layers, *Proc. Natl. Acad. Sci. USA*, 74, 207, 1977.
29. Oesterhelt, D. and Stoeckenius, W., Rhodopsin-like protein from the purple membrane of *Halobacterium halobium*, *Nature New Biol.*, 233, 149, 1971.
30. Lanyi, J.K., Progress toward an explicit mechanistic model for the light-driven pump, bacteriorhodopsin, *FEBS Lett.*, 464, 103, 1999.
31. Lanyi, J.K., Bacteriorhodopsin, *Biochim. Biophys. Acta*, 1460, 1, 2000.
32. Lanyi, J.K. and Pohorille, A., Proton pumps: mechanism of action and applications, *Trends Biotechnol.*, 19, 140, 2001.
33. Lanyi, J.K. and Luecke, H., Bacteriorhodopsin, *Curr. Opinion Struct. Biol.*, 11, 415, 2001.
34. Drachev, L.A., Jasaitis, A.A., Kaulen, A.D., Kondrashin, A.A., Liberman, E.A., Nemecek, I.B., Ostroumov, S.A., Semenov, A.Yu., and Skulachev, V.P., Direct measurement of electric current generation by cytochrome oxidase, H-ATPase and bacteriorhodopsin, *Nature*, 249, 321, 1974.
35. Drachev, L.A., Kaulen, A.D., Ostroumov, S.A., and Skulachev, V.P., Electrogenesis by bacteriorhodopsin incorporated in a planar phospholipid membrane, *FEBS Lett.*, 39, 43, 1974.
36. Drachev, L.A., Frolov, V.N., Kaulen, A.D., Liberman, E.A., Ostroumov, S.A., Plakunova, V.G., Semenov, A.Yu., and Skulachev, V.P., Reconstitution of biological molecular generators of electric current, *J. Biol. Chem.*, 251, 7059, 1976.
37. Hong, F.T., Photoelectric and magneto-orientation effects in pigmented biological membranes, *J. Colloid Interface Sci.*, 58, 471, 1977.
38. Trissl H.-W. and Montal M., Electrical demonstration of rapid light-induced conformational changes in bacteriorhodopsin, *Nature*, 266, 655, 1977.
39. Hong, F.T. and Montal, M., Bacteriorhodopsin in model membranes: a new component of the displacement photocurrent in the microsecond time scale, *Biophys. J.*, 25, 465, 1979.
40. Simmeth, R. and Rayfield, G.W., Evidence that the photoelectric response of bacteriorhodopsin occurs in less than 5 picoseconds, *Biophys. J.*, 57, 1099, 1990.

41. Groma, G.I., Hebling, J., Ludwig, C., and Kuhl, J., Charge displacement in bacteriorhodopsin during the forward and reverse bR–K phototransition, *Biophys. J.*, 69, 2060, 1995.
42. Sullivan, J.M. and Shukla, P., Time-resolved rhodopsin activation currents in a unicellular expression system, *Biophys. J.*, 77, 1333, 1999.
43. Shukla, P. and Sullivan, J.M., Normal and mutant rhodopsin activation measured with the early receptor current in a unicellular expression system, *J. Gen. Physiol.*, 114, 609, 1999.
44. Trissl H.-W., Light-induced conformational changes in cattle rhodopsin as probed by measurements of the interface potential, *Photochem. Photobiol.*, 29, 579, 1979.
45. Hong, F.T. and Mauzerall, D., Photoemf at a single membrane-solution interface specific to lipid bilayers containing magnesium porphyrins, *Nature*, 240, 154, 1972.
46. Hong, F.T. and Mauzerall, D., Interfacial photoreactions and chemical capacitance in lipid bilayers, *Proc. Natl. Acad. Sci. USA*, 71, 1564, 1974.
47. Hong, F.T., Charge transfer across pigmented bilayer lipid membrane and its interfaces, *Photochem. Photobiol.*, 24, 155, 1976.
48. Matthews, R.G., Hubbard, R., Brown, P.K., and Wald, G., Tautomeric forms of metarhodopsin, *J. Gen. Physiol.*, 47, 215, 1963.
49. Cone, R.A., The early receptor potential, in *Proceedings of the International School of Physics "Enrico Fermi": Course XLIII*, Reichardt, W., Ed., Academic Press, New York, 1969, p. 187.
50. Gedney, C., Ward, J., and Ostroy, S.E., Isolation and study of rhodopsin and cone responses in the frog retina, *Am. J. Physiol.*, 221, 1754, 1971.
51. Shevchenko, T.F., Kalamkarov, G.R., and Ostrovsky, M.A., The lack of H^+ transfer across the photoreceptor membrane during rhodopsin photolysis, *Sensory Systems (USSR Acad. Sci.)*, 1, 117, 1987 (in Russian).
52. Ostrovsky, M.A., Animal rhodopsin as a photoelectric generator, in *Molecular Electronics: Biosensors and Biocomputers*, Hong, F.T., Ed., Plenum Press, New York, 1989, p. 187.
53. Hong, F.T., Mechanisms of generation of the early receptor potential revisited, *Bioelectrochem. Bioenerg.*, 5, 425, 1978.
54. Hong, F.T. and Okajima, T.L., Electrical double layers in pigment-containing biomembranes, in *Electrical Double Layers in Biology*, Blank, M., Ed., Plenum Press, New York, 1986, p. 129.
55. Hong, F.T., Interfacial photochemistry of retinal proteins, *Prog. Surface Sci.*, 62, 1, 1999.
56. Drachev, L.A., Kaulen, A.D., Khitrina, L.V., and Skulachev V.P., Fast stages of photoelectric processes in biological membranes: I. Bacteriorhodopsin, *Eur. J. Biochem.*, 117, 461, 1981.
57. Okajima, T.L. and Hong, F.T., Kinetic analysis of displacement photocurrents elicited in two types of bacteriorhodopsin model membranes, *Biophys. J.*, 50, 901, 1986.
58. Drachev, L.A., Kalamkarov, G.R., Kaulen, A.D., Ostrovsky, M.A., and Skulachev, V.P., Fast stages of photoelectric processes in biological membranes: II. Visual rhodopsin, *Eur. J. Biochem.*, 117, 471, 1981.
59. Hong, F.T., Displacement photocurrents in pigment-containing biomembranes: artificial and natural systems, in *Bioelectrochemistry: Ions, Surfaces, Membranes*, ACS Advances in Chemistry Series 188, Blank, M, Ed., American Chemical Society, Washington, DC, 1980, p. 211.
60. Liu, S.Y. and Ebrey, T.G., Photocurrent measurements of the purple membrane oriented in a polyacrylamide gel, *Biophys. J.*, 54, 321, 1988.
61. Hong, F.T. and Mauzerall, D., Tunable voltage clamp method: application to photoelectric effects in pigmented bilayer lipid membranes, *J. Electrochem. Soc.*, 123, 1317, 1976.
62. Hong, F.T. and Okajima, T.L., Rapid light-induced charge displacements in bacteriorhodopsin membranes: an electrochemical and electrophysiological study, in *Biophysical Studies of Retinal Proteins*, Ebrey, T.G., Frauenfelder, H., Honig, B., and Nakanishi, K., Eds., University of Illinois Press, Urbana-Champaign, IL, 1987, p. 188.
63. Michaile, S. and Hong, F.T., Component analysis of the fast photoelectric signal from model bacteriorhodopsin membranes. Part I. Effect of multilayer stacking and prolonged drying, *Bioelectrochem. Bioenerg.*, 33, 135, 1994.

64. Okajima, T.L., Michaile, S., and Hong, F.T., Component analysis of the fast photoelectric signal from model bacteriorhodopsin membranes: Part II. Effect of fluorescamine treatment, *Bioelectrochem. Bioenerg.*, 33, 143, 1994.
65. Hong, F H., Chang, M., Ni, B., Needleman, R.B., and Hong, F.T., Component analysis of the fast photoelectric signal from model bacteriorhodopsin membranes: Part III. Effect of the point mutation aspartate 212 → asparagine 212, *Bioelectrochem. Bioenerg.*, 33, 151, 1994.
66. Holz, M., Lindau, M., and Heyn, M.P., Distributed kinetics of the charge movements in bacteriorhodopsin: evidence for conformational substrates, *Biophys. J.*, 53, 623, 1988.
67. Trissl, H.-W., Photoelectric measurements of purple membranes, *Photochem. Photobiol.*, 51, 793, 1990.
68. Yao, B., Xu, D., and Hou, X., Analyses and proofs of multiexponential process of bacteriorhodopsin photoelectric response, *J. Applied Phys.*, 89, 1, 2001.
69. Trissl, H.-W., Dér, A., Ormos, P., and Keszthelyi, L., Influence of stray capacitance and sample resistance on the kinetics of fast photovoltages from oriented purple membranes, *Biochim. Biophys. Acta*, 765, 288, 1984.
70. Wulf, K. and Trissl, H.-W., Fast photovoltage measurements in photosynthesis. I. Theory and data evaluation, *Biospectroscopy*, 1, 55, 1995.
71. Trissl, H.-W. and Wulf, K., Fast photovoltage measurements in photosynthesis. II. Experimental methods, *Biospectroscopy*, 1, 71, 1995.
72. Läuger, P., *Electrogenic Ion Pumps* (Distinguished Lecture Series of the Society of General Physiologists, Volume 5), Sinauer Associates, Sunderland, MA, 1991.
73. Govardovskii, V.I., Mechanism of the generation of the early receptor potential and an electrical model of the rod of the rat retina, *Biophysics (Moscow)*, 23, 520, 1979 (*Biofizika*, 23, 514, 1978).
74. Hochstrate, P., Lindau, M., and Rüppel, H., On the origin and the signal-shaping mechanism of the fast photosignal in the vertebrate retina, *Biophys. J.*, 38, 53, 1982.
75. Brindley, G.S. and Gardner-Medwin, A.R., The origin of the early receptor potential of the retina, *J. Physiol.*, 182, 185, 1966.
76. Gauch, H.G., Jr., Prediction, parsimony and noise, *Am. Sci.*, 81, 468, 1993.
77. Hong, F.T., Molecular sensors based on the photovoltaic effect of bacteriorhodopsin: origin of differential responsivity, *Mater. Sci. Eng. C,* 4, 267, 1997. Reprinted with corrections, *Mater. Sci. Eng. C,* 5, 61, 1997.
78. Trissl, H.-W., On the rise time of the R1-component of the early receptor potential, *Biophys. Struct. Mech.*, 8, 213, 1982.
79. Liu, S.Y., Ebrey, T., Zingoni, J., and Crouch, Fang, J.-M., and Nakanishi, K., Fast photoelectric response from artificial pigments of bacteriorhodopsin, *Biophys. J.*, 51, 134a, 1987 (Abstr.).
80. Hong, F.H. and Hong, F.T., Component analysis of the fast photoelectric signal from model bacteriorhodopsin membranes: Part 4. A method for isolating the B2 component and the evidence for its polarity reversal at low pH, *Bioelectrochem. Bioenerg.*, 37, 91, 1995.
81. Petrak, M. and Hong, F.T., Component analysis of the fast photoelectric signal from model bacteriorhodopsin membranes: Part 5. Effect of chloride ion transport blocker and cation chelators, *Bioelectrochem. Bioenerg.*, 45, 193, 201, 1998.
82. Kaulen, A.D., Electrogenic processes and protein conformational changes accompanying the bacteriorhodopsin photocycle, *Biochim. Biophys. Acta*, 1460, 204, 2000.
83. Hong, F.T., Internal electric fields generated by surface charges and induced by visible light in bacteriorhodopsin membranes, in *Mechanistic Approaches to Interaction of Electric and Electromagnetic Fields with Living Systems*, Blank, M. and Findl, E., Eds., Plenum Press, New York, 1987, p. 161.
84. Cafiso, D.S. and Hubbell, W.L., Interfacial charge separation in photoreceptor membranes, *Photochem. Photobiol.*, 32, 461, 1980.
85. Cafiso, D.S. and Hubbell, W.L., Light-induced interfacial potentials in photoreceptor membranes, *Biophys. J.*, 30, 243, 1980.

86. Bolshakov, V.I., Kalamkarov, G.R., and Ostrovsky, M.A., Photoinduced generation of potential on disc membrane of photoreceptor cell, *Dokl. Akad. Nauk USSR*, 240(5), 1231, 1978 (in Russian).
87. Hong, F.T., Relevance of light-induced charge displacements in molecular electronics: design principles at the supramolecular level, *J. Mol. Electron.*, 5, 163, 1989.
88. Drain, C.M., Christensen, B., and Mauzerall, D., Photogating of ionic currents across a lipid bilayer, *Proc. Natl. Acad. Sci. USA*, 86, 6959, 1989.
89. Hong, F.T., Molecular electronic switches in photobiology, in *Handbook of Organic Photochemistry and Photobiology*, 1st ed., Horspool,W. and Song, P.-S., Eds., CRC Press, Boca Raton, FL, 1995, p. 1557.
90. Wilden, U. and Kühn, H., Light-dependent phosphorylation of rhodopsin: number of phosphorylation sites, *Biochemistry*, 21, 3104, 1982.

129

Phytochrome: Molecular Properties

Seong Hee Bhoo
Kyung Hee University

Pill-Soon Song
Kumho Life & Environmental Science Laboratory

129.1 Introduction

Light is energy and is an information source for plant growth and development. The absolute requirement of light is the key feature that distinguishes the plants from the animals. Phytochromes are the well-characterized plant proteins that perceive the light as an environmental signal to control growth and development. The phytochromes belonging to the principal family of red/far-red light signal-transducing photoreceptors undergo photochromic transformation between the inactive (Pr) and the active (Pfr) forms to mediate the growth and development of plants.[1,2] The red light-absorbing Pr form (λ_{max} 666 nm) and the far-red light-absorbing Pfr form (λ_{max} 730 nm) are manifested by the photoreversible isomerization of the linear tetrapyrrole 3E-phytochromobilin covalently attached to the cystein residue of polypeptides.[3–5] Light signals perceived by phytochromes are transmitted to the downstream, and they trigger gene expression and cellular modification for growth and developmental changes, such as germination, seedling establishment, development of photosynthetic machinery, suppression of shade avoidance, setting of flowering time, and development of reproductive structures.[6,7]

Phytochromes exist as dimers and are known to have two structural subdomains: a globular amino terminal chromophore binding domain (~65 kDa) and a structurally extended carboxy terminal domain (~60 kDa), which are connected by a flexible and protease-sensitive hinge region.[8–10] Each domain has unique functions. The *N*-terminal domain perceives light signals of red/far-red wavelength quality, intensity, duration, and direction. The *N*-terminal domain of phytochromes carries the light sensory motifs required for light signal transduction.[9] The *C*-terminal domain contains the dimerization and regulatory sites.[1] Although the molecular mechanism and biological function of dimerization are not well known, studies indicate that dimerization is crucial for phytochrome action in plants.[11,12] The regulatory sites in the *C*-terminal domain interact with the signal transducer proteins, such as the recently identified Phytochrome Interacting Factor 3 (PIF3),[13,14] Nucleoside Diphosphate Kinase 2 (NDPK2),[15] and Phytochrome Kinase Substrate 1 (PKS1).[16] Some other phytochrome-interacting proteins are being characterized by several laboratories. Several conserved motifs for regulatory roles were identified in the *C*-terminal domain, such as Ser/Thr kinase in the *C*-terminal end and Per-Arnt-Sim (PAS) motifs around

0-8493-1348-1/04/$0.00+$1.50

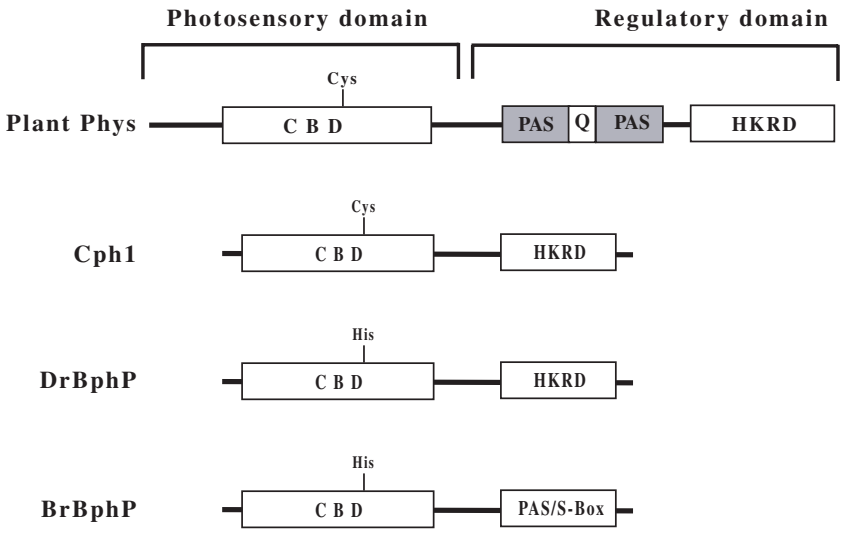

FIGURE 129.1 *Structural and functional motifs of the phytochromes*. Phytochromes have a two-domain structure: the photosensory *N*-terminal domain and the regulatory *C*-terminal domain. Structural and functional motifs of the plant phytochromes, the *Synechocystis* Cph1, and bacteriophytochromes from eubacterial DrBphP and photosynthetic bacterial BrBphP are compared, including the *N*-terminal chromophore-binding domain (CBD) and the *C*-terminal regulatory domain that are connected via the hinge region. The *C*-terminal regulatory domain includes the regulatory core region and the histidine-kinase-related domain (HKRD). The regulatory core region contains Quail box (Q) and two PAS repeat. The DrBphP and BrBphP phytochromes do not have the conserved cysteine residue in the chromophore-binding domain. The His-260, rather than the Cys residue, is the chromophore-binding site in the DrBphP.[19] BrBphP has a Per-Arnt-Sim (PAS) motif in the *C*-terminal domain. The regulatory core region of plant phytochromes, including two PAS motifs, undergoes detectable conformational changes in the phototransformation.

the regulatory core region. Recently identified prokaryotic phytochromes, the cyanobacterial Cph1,[17,18] eubacterial DrBphP,[19,20] and symbiotic bacterial BrBphP,[21] also share similar structural and functional organizations (Figure 129.1).

129.2 Conformational Changes and Surface Topography

The Pr to Pfr phototransformation induces specific changes in the secondary and tertiary structures of phytochromes, and its chromophore topography induces through photoisomerization and interdomain interactions.[22–27] The chromophore appears to move out of its hydrophobic pocket upon Pr to Pfr phototransformation. This chromophore movement is modulated by the helix-forming 6 kDa *N*-terminal peptide and triggers the conformational changes during phototransformation.[28,29] The helix-forming peptide causes a series of conformational changes by interacting directly with the chromophore and possibly with other structural motifs, especially the *C*-terminal motifs. The *N*-terminal domain is known to be more exposed in the Pr form than the Pfr form, and the connecting hinge region is preferentially exposed in the Pfr form.[10] Prokaryotic phytochromes such as Cph1 and DrBphP do not have these structural differences between the Pr and the Pfr forms, primarily because of sequence truncations.[30]

The surface topographies of Pr- and Pfr-phytochromes also exhibit differential exposures and microenvironments around the tryptophan residues. During the phototransformation, subtle conformational changes are detected in the region around Trp-569 and Trp-572.[31] These two tryptophans are located close to the Ser-598 that is preferentially phosphorylated in the Pfr form *in vivo*.[16] Two more tryptophans, Trp-773 and Trp-777, are also modified by HNB-Br preferentially in the Pfr form, indicating that the surroundings of these two Trp residues undergo significant changes and rearrangements of surface

topography during the phototransformation.[24,32] These observations suggest that the light-induced conformational changes and their resultant changes in surface topography are important for interdomain cross-talk in light signal transduction mediated by phytochrome activation.

129.3 Structural Motifs and Interdomain Interactions

Eukaryotic and prokaryotic phytochromes are similar in their structural and functional molecular architectures. Although some structural motifs are missing or are substituted in prokaryotic phytochromes, the chromophore-binding *N*-terminal domains carry determinants for phytochrome individuality followed by functionally interchangeable regulatory *C*-terminal domains (Figure 129.1).[9,18,19,21,33] PAS and kinase motifs in the *C*-terminal domain of plant phytochromes are also identified in prokaryotic phytochromes with similar regulatory functions.[16,21,34] These observations suggest that regulatory motifs in the *C*-terminal domain share common molecular mechanisms for interactions with downstream signaling components.

Recently identified phytochrome-interacting proteins interact with different structural motifs in the *C*-terminal domain. PKS1 interacts with the Ser/Thr kinase motif.[16] PIF3 and NDPK2 interact with the regulatory "Quail box" containing PAS motifs.[13,15] The NDPK2-phytochrome interaction seems to be different from the PIF3-phytochrome interaction. The latter occurs through the interaction between the PAS motifs.[13,15] Both NDPK2 and PIF3 bind to the phytochrome *C*-terminal domains preferentially in the Pfr form.[13,15] Their interactions confirm the preferential exposure of *C*-terminal domain around Trp-773 and Trp-777 in the Pfr form.[32] However, PIF3 and NDPK2 seem to interact differently, in that the NDPK2 interaction requires the *N*-terminal and the *C*-terminal domains for full binding activity.[13,14] PIF3, isolated in yeast using two hybrid screening with the phytochrome *C*-terminal domain as bait, also binds the *N*-terminal domain. It binds more strongly to the full-size phytochrome, indicating that direct interdomain interactions are required for the phytochrome–PIF3 association.[13,14] PKS1 binds to the *C*-terminal Ser/Thr kinase motif independent of the Pr/Pfr phototransformation, suggesting that this motif is not changed during phototransformation.[16] However, PKS1 phosphorylation and phytochrome autophosphorylation are increased 2 to 2.5 times in the Pfr form, indicating that the phosphorylation is an important factor for phytochrome signal transduction through phytochrome-PKS1 interaction. Therefore, phytochrome interacting proteins seem to be recognized by specific *C*-terminal regulatory motifs activated by differential interdomain interactions (Figure 129.2).

The Pfr form of phytochromes is considered to be a biologically active form, in most cases, in higher plants. Recent studies, however, show the possibility that the Pr form of phytochrome could be the active form in some cases. The Pr form of Cph1 exhibits autophosphorylation activity.[18] Also, the Pr form of BrBphP accelerates the synthesis of complete photosynthetic apparatus.[21] The Pr form of Phytochrome B was also suggested to be the regulatory active form in seed germination.[35,36] PIF3 and NDPK2, however, bind preferentially to the Pfr form to regulate phytochrome signaling.[13–15] The Pfr form of DrBphP also exhibited increased autophosphorylation and phosphate transfer activity.[34] This active Pr/active Pfr signaling could be explained by the intermolecular or by the intramolecular pathway in which the photoactivated Pfr signals induce the release of a Pr-specific factor from regulatory motifs.[37] The released Pr-specific factor then transfers "Pr signal" to the downstream signaling components, whereas the phytochrome interacts with a Pfr-specific factor to transfer "Pfr signal" to the downstream of the signal transduction pathway (Figure 129.3).

129.4 Phytochrome Phosphorylation and Signal Transduction

Until recently, the hypothesis that the phytochrome is a kinase has been controversial.[38–40] The finding that the Cph1 has histidine kinase activity triggered the reexamination of plant phytochrome kinase activity and confirmed that plant phytochromes are Ser/Thr kinases.[16,18,41–44] The Ser-7 of Phytochrome A is phosphorylated *in vivo* in Pr and Pfr forms, but the Ser-17 is phosphorylated *in vitro* in the Pr

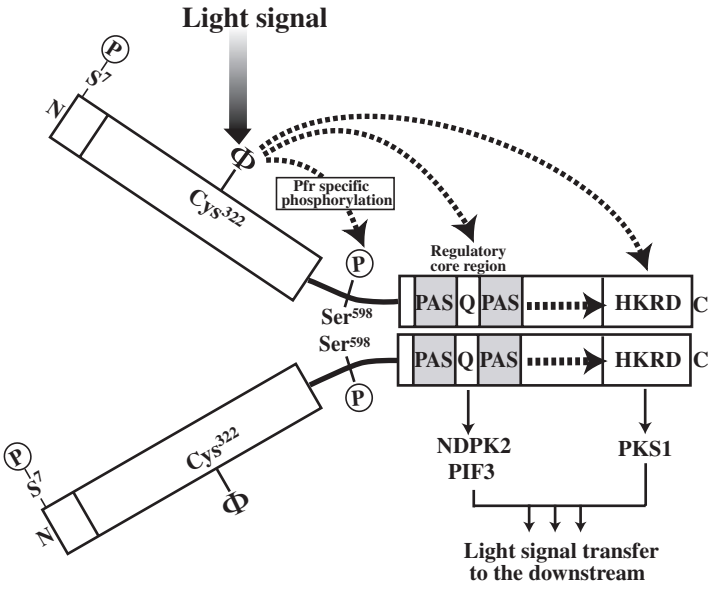

FIGURE 129.2 *Interdomain signal transmission in a dimeric oat phytochrome A*. The Ser-7 is phosphorylated *in vivo*. The Ser-598 is located in the hinge region and phosphorylated preferentially in the Pfr form. The Pfr-dependent conformational changes are generated through the chromophore photoisomerization by absorbing red light (R) in the *N*-terminal domain, and they trigger subtle conformational changes through the whole phytochrome molecule. The conformational signals are subsequently transmitted through the regulatory domain (Q) and HKRD either directly or indirectly to the downstream signal-transducing molecules. The photoactivated or uncovered Quail box (see Figure 129.3) interacts directly with the NDPK2 and the PIF3. The PKS1 seems to associate with the HKRD motif.

form.[45–47] Also, the protein kinase activity of Phytochrome A autophosphorylates Ser-17 (unpublished data). The Ser-598 is light-dependently phosphorylated, mainly in the Pfr form, *in vivo* and transfers the phosphate to the substrate.[47] Mutation of this serine abolishes the light dependency of phosphorylation and phosphate transfer, indicating that the phosphorylation of Ser-598 could be a molecular switch in the interdomain interactions (Figure 129.2).[16]

Phytochrome phosphorylation appears to regulate conformational changes and modulates the cross-talks between the *N*-terminal and *C*-terminal domains as well. Phytochrome interacting proteins might be activated through phosphorylation by phytochrome kinase, regulation of subcellular location, or regulation of interaction with other components. The light-dependent phosphate transfers between Cph1 and Rcp1 in *Synechocystis*,[43] and between DrBphP and DrBphR in *Deinococcus radiodurans*,[34] are well characterized *in vitro*. The phytochrome-mediated photoreversible phosphorylation of PKS1 is similar to the Cph1-Rcp1 phospho-relay system.[16] The PKS1 is phosphorylated about twofold higher on a serine or threonine residue by the Pfr form of phytochrome. The kinase activity of NDPK2 is also increased twofold by the Pfr form of phytochrome.[15] Taken together, light-induced conformational changes accompany the interdomain cross-talks by protein phosphorylation and modulate the signaling through interactions with downstream signaling components (Figure 129.3).

129.5 Evolution of Structural Motifs and Functions of Phytochrome

Until recently, phytochromes were thought to be restricted to photosynthetic organisms.[20,48] However, recent studies based on DNA sequencing databases uncovered many phytochrome-like genes in prokaryotic organisms, such as *Synechocystis*,[17,41] *Bradyrhizobium*,[21] and *Deinicoccus*.[19] Protein sequence comparison shows that the chromophore bearing *N*-terminal domains are conserved in all known phytochromes,

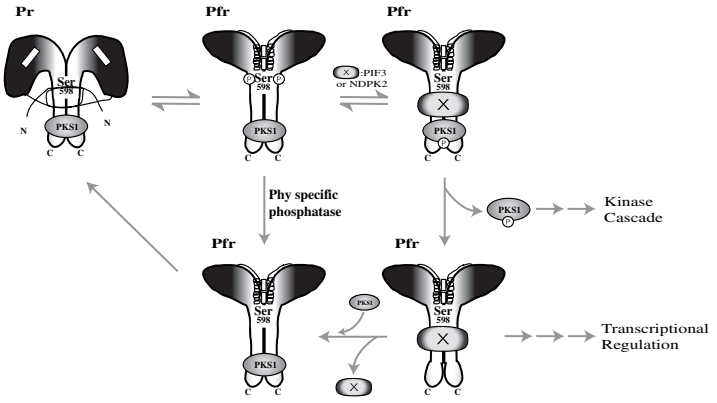

FIGURE 129.3 Conformational changes and interdomain interactions in the phytochrome photoactivation. The photoactivation of the phytochrome includes changes in the domain conformation and in the surface topography triggered by apoprotein–chromophore interactions. The *N*-terminal 6 kDa-peptide region forms an α-helix conformation in the Pfr but a random coil conformation in the Pr. The proximity between the *N*- and the *C*-termini in the Pr form is to depict the covered Quail box and to shield the hinge region. Upon photoactivation, the hinge region is exposed, and the Ser-598 may be phosphorylated. The Pfr phytochrome phosphorylated at Ser-598 is not an active form, but it accelerates the association of the PIF3 or NDPK2 and phosphorylation of the PKS1. The phospho-PKS1 is subsequently released from the photoactivated phytochrome to give light signals to the downstream, presumably through the kinase cascade. The factor X also transmits the signal directly or indirectly to the downstream. The Ser-598 phosphorylation is proposed as a mechanism to desensitize the Pfr activity in combination with an unidentified phytochrome specific protein phosphatase.

but *C*-terminal domains of prokaryotic phytochromes are shorter and missing regulatory motifs of plant phytochromes. The *C*-terminal domains of prokaryotic phytochromes have either a kinase motif or a PAS motif (Figure 129.1). Even though all phytochromes bind bilin-type chromophores covalently to the *N*-terminal domains, bacteriophytochromes, designated as BphPs, seem to bind biliverdin through different binding modes.[19,34] All known eukaryotic phytochromes including Cph1 have the conserved chromophore-binding cystein followed by the conserved histidine that is essential residue for chromophore-binding activity.[49] However, BphPs have no aligned chromophore-binding cystein substituted by hydrophobic residues but have absolutely conserved adjacent histidine (Figure 129.1).[19,34] Biochemical and molecular biological studies suggested that the chromophore attachments of BphPs are through a Schiff's-base-type linkage to a histidine rather than a thio-ether linkage to the cystein, the chromophore attachment site in plant phytochrome and Cph1.[19]

Whereas the phytochromobilin and phycocyanobilin are the chromophores of plant phytochrome and Cph1, BphPs prefer to bind biliverdin as a chromophore with perfect spectral properties except substantial red shift; the absorbance maxima for the Pr and Pfr forms of biliverdin-bound BphPs are at 698 and 750 nm, respectively.[34] This shift can be easily explained by the increased double-bond conjugation in biliverdin as compared to phytochromobilin and phycocyanobilin. A recent report further supports that biliverdin is the chromophore of BphPs. The bacteriophytochrome of *Bradyrhizobium* (BrBphP) binds biliverdin. The BrBphP controls the synthesis of photosynthetic apparatus using 750 nm of light, instead of 730 nm for plant phytochrome and 712 nm for Cph1, for photoconversion.[21] Unlike the case in other BphPs, the *C*-terminal domain of BrBphP has no conserved histidine kinase motif but has an S-box motif that corresponds to a strongly conserved region in PAS motif.[21] This BrBphP seems to transfer the light signals through biliverdin-bound BphP to its downstream component PpsR, the transcription factor that represses the expression of bacteriochlorophyll and light-harvesting II complex structural genes in anaerobic purple bacteria to regulate the photosystem synthesis.[21,50] BphP and PpsR interact using PAS motif present in both proteins, and they transfer light signals directly to the target genes.[21,51] This scheme is conserved during the evolution of phytochromes, in that light signals are transferred directly through a

phytochrome to PIF3, for example, bound to the target genes.[52] The kinase activity of DrBphP for its substrate BphR resembles the kinase activity of plant phytochrome for PKS1.[16,34] Thus, structural motifs as well as functional mechanisms of plant phytochromes evolved from the primitive bacteriophytochromes, suggesting that the bacteriophytochromes are the progenitors of plant phytochromes.

129.6 Conclusions

Although the biochemical and molecular biological properties of phytochromes have been well studied, the three-dimensional structure and light signal transduction pathways are not well understood. The questions as to how phytochromes perceive light signals and how light signals are transmitted to downstream molecules are now beginning to be recognized. One of the proposed models depicts that the phototransformation of the chromophore triggered by light signals modulates the interactions between the chromophore and apoprotein. This is followed by conformational changes throughout the whole phytochrome molecule via interdomain cross-talks or communications within the phytochrome molecules, in analogy to the well-understood rhodopsin visual receptor system in animals.[8,53,54]

Acknowledgments

This work was partly supported by the Plant Metabolism Research Center through Kyung Hee University (to Seong Hee Bhoo), KISTEP, and BioGreen 21 (to Pill-Soon Song).

References

1. Quail, P.H., Boylan, M.T., Park, B.M., Short, T.W., Xu, Y., and Wagner, D., Phytochromes: photosensory perception and signal transduction, *Science*, 268, 675, 1995.
2. Smith, H., Physiological and ecological function within the phytochrome family, *Annu. Rev. Plant Physiol. Plant Mol. Biol.*, 46, 289, 1995.
3. Rudiger, W., Thuemmler, F., Cmiel, S., and Schneider, S., Chromophore structure of the physiologically active form (Pfr) of phytochrome, *Proc. Natl. Acad. Sci. USA,* 80, 6244, 1983.
4. Farrens, D.L., Holt, R.E., Rospendowski, B.N., Song, P.-S., and Cotton, T.M., Surface-enhanced resonance Raman scattering spectroscopy applied to phytochrome and its model compounds, *J. Am. Chem. Soc.*, 111, 9162, 1989.
5. Fodor, S.P.A., Lagarias, J.C., and Mathies, R.A., Resonance Raman analysis of the Pr and Pfr forms of phytochrome, *Biochemistry*, 29, 11141, 1990.
6. Chory, J., Chatterjee, M., Cook, R.K., Elich, T., Fankhauser, C., Li, J., Nagpal, P., Neff, M., Pepper, A., Poole, D., Reed, J., and Vitart, V., From seed germination to flowering, light controls plant development via the pigment phytochrome, *Proc. Natl. Acad. Sci. USA*, 93, 12066, 1996.
7. Smith, H., Phytochromes and light signal perception by plants — an emerging synthesis, *Nature*, 407, 585, 2000.
8. Quail, P.H., An emerging map of the phytochromes, *Plant Cell Environ.*, 20, 657, 1997.
9. Wagner, D., Fairchild, C.D., Kuhn, R.M., and Quail, P.H., Chromophore-bearing N-terminal domains of phytochromes A and B determine their photosensory specificity and differential light lability, *Proc. Natl. Acad. Sci. USA*, 93, 4011, 1996.
10. Lapko, V.M., Jiang, X.-Y., Smith, D.L., and Song, P.-S., Surface topography of phytochrome A deduced from specific chemical modification with iodoacetamide, *Biochemistry*, 37, 12526, 1998.
11. Cherry, J.R., Hondred, D., Walker, J.M., Keller, J.M., Hershey, H.P., and Vierstra, R.D., Carboxy-terminal deletion analysis of oat phytochrome A reveals the presence of separate domains required for structure and biological activity, *Plant Cell*, 5, 565, 1993.
12. Boylan, M., Douglas, N., and Quail, P.H., Dominant negative suppression of Arabidopsis photoresponses by mutant phytochrome A sequences identifies spatially discrete regulatory domains in the photoreceptor, *Plant Cell*, 6, 449, 1994.

13. Ni, M., Tepperman, J.M., and Quail, P.H., PIF3, a phytochrome-interacting factor necessary for normal photoinduced signal transduction, is a novel basic helix-loop-helix protein, *Cell*, 95, 657, 1998.
14. Ni, M., Tepperman, J.M., and Quail, P.H., Binding of phytochrome B to its nuclear signalling partner PIF3 is reversibly induced by light, *Nature*, 400, 781, 1999.
15. Choi, G., Yi, H., Lee, J., Kwon, Y.K., Soh, M.S., Shin, B., Luka, Z., Hahn, T.R., and Song, P.-S., Phytochrome signalling is mediated through nucleoside diphosphate kinase 2, *Nature*, 401, 610, 1999.
16. Fankhauser, C., Yeh, K.-C., Lagarias, J.C., Zhang, H., and Chory, J., PKS1, a substrate phosphorylated by phytochrome that modulates light signaling in Arabidopsis, *Science*, 284, 1539, 1999.
17. Hughes, J., Lamparter, T., Mittmann, F., Hartmann, E., Gartner, W., Wilde, A., and Borner, T., A prokaryotic phytochrome, *Nature*, 386, 663, 1997.
18. Lamparter, T., Mittmann, F., Gartner, W., Borner, T., Hartmann, T., and Hughes, J., Characterization of recombinant phytochrome from the cyanobacterium Synechocystis, *Proc. Natl. Acad. Sci. USA*, 94, 11792, 1997.
19. Davis, S.J., Vener, A.V., and Vierstra, R.D., Bacteriophytochromes: phytochrome-like photoreceptors from nonphotosynthetic eubacteria, *Science*, 286, 2517, 1999.
20. Vierstra, R.D. and Davis, S.J., Bacteriophytochromes: new tools for understanding phytochrome signal transduction, *Semin. Cell Dev. Biol.*, 11, 511, 2000.
21. Giraud, E., Fardoux, J., Fourrier, N., Hannibal, L., Genty, B., Bouyer, P., Dreyfus, B., and Vermeglio, A., Bacteriophytochrome controls photosystem synthesis in anoxygenic bacteria, *Nature*, 417, 202, 2002.
22. Parker, W., Partis, M., and Song, P.-S., N-terminal domain of Avena phytochrome: interactions with sodium dodecyl sulfate micelles and N-terminal chain truncated phytochrome, *Biochemistry*, 31, 9413, 1992.
23. Farrens, D.L., Cordonnier, M.M., Pratt, L.H., and Song, P.-S., The distance between the phytochrome chromophore and the N-terminal chain decreases during phototransformation. A novel fluorescence energy transfer method using labeled antibody fragments, *Photochem. Photobiol.*, 56, 725, 1992.
24. Wells, T.A., Nakazawa, M., Manabe, K., and Song, P.-S., A conformational change associated with the phototransformation of Pisum phytochrome A as probed by fluorescence quenching, *Biochemistry*, 33, 708, 1994.
25. Deforce, L., Tokutomi, S., and Song, P.-S., Phototransformation of pea phytochrome A induces an increase in alpha-helical folding of the apoprotein: comparison with a monocot phytochrome A and CD analysis by different methods, *Biochemistry*, 33, 4918, 1994.
26. Lagarias, J.C. and Mercurio, F.M., Structure function studies on phytochrome. Identification of light-induced conformational changes in 124-kDa Avena phytochrome *in vitro*, *J. Biol. Chem.*, 260, 2415, 1985.
27. Kneip, C., Hildebrandt, P., Schlamann, W., Braslavsky, S.E., Mark, F., and Schaffner, K., Protonation state and structural changes of the tetrapyrrole chromophore during the Pr → Pfr phototransformation of phytochrome: a resonance Raman spectroscopic study, *Biochemistry*, 38, 15185, 1999.
28. Song, P.-S., The molecular topography of phytochrome: chromophore and apoprotein, *J. Photochem. Photobiol.*, 2, 43, 1989.
29. Vierstra, R.D., Quail, P.H., Hahn, T.R., and Song, P.-S., Comparison of the protein conformations between different forms (Pr and Pfr) of native (124 kDa) and degraded (118/114 kDa) phytochromes from *Avena sativa*, *Photochem. Photobiol.*, 45, 429, 1987.
30. Park, C.M., Shim, J.Y., Yang, S.S., Kang, J.G., Kim, J.I., Luka, Z., and Song, P.-S., Chromophore-apoprotein interactions in *Synechocystis* sp. PCC6803 phytochrome Cph1, *Biochemistry*, 39, 6349, 2000.
31. Singh, B.R. and Song, P.-S., A differential molecular topography of the Pr and Pfr forms of native oat phytochrome as probed by fluorescence quenching, *Planta*, 181, 263, 1990.

32. Nakazawa, M., Hayashi, H., Yoshida, Y., and Manabe, K., Identification of surface-exposed parts of red-light- and far-red-light-absorbing forms of native pea phytochrome by limited proteolysis, *Plant Cell Physiol.*, 34, 83, 1993.
33. Quail, P.H., The phytochromes: a biochemical mechanism of signaling in sight, *Bioassays*, 19, 571, 1997.
34. Bhoo, S.H., Davis, S.J., Walker, J., Karniol, B., and Vierstra, R.D., Bacteriophytochromes are photochromic histidine kinases using a biliverdin chromophore, *Nature*, 414, 776, 2001.
35. Reed, J.W., Nagatani, A., Elich, T.D., Fagan, M., and Chory, J., Phytochrome A and phytochrome B have overlapping but distinct functions in Arabidopsis development, *Plant Physiol.*, 104, 1139, 1994.
36. Shinomura, T., Nagatani, A., Chory, J., and Furuya, M., The induction of seed germination in *Arabidopsis thaliana* is regulated principally by phytochrome B and secondarily by phytochrome A, *Plant Physiol.*, 104, 363, 1994.
37. Smith, H., Phytochromes. Tripping the light fantastic, *Nature*, 400, 710, 1999.
38. Kim, I.S., Bai, U., and Song, P.-S., A purified 124-kDa oat phytochrome does not possess a protein kinase activity, *Photochem. Photobiol.*, 49, 319, 1989.
39. Wong, Y.S., McMichael, R.W.J., and Lagarias, J.C., Properties of a polycation-stimulated protein kinase associated with purified Avena phytochrome, *Plant Physiol.*, 91, 709, 1989.
40. Cashmore, A.R., Higher-plant phytochrome: "I used to date histidine, but now I prefer serine," *Proc. Natl. Acad. Sci. USA*, 95, 13358, 1998.
41. Yeh, K.C., Wu, S.H., Murphy, J.T., and Lagarias, J.C., A cyanobacterial phytochrome two-component light sensory system, *Science*, 277, 1505, 1997.
42. Elich, T.D. and Chory, J., Phytochrome: if it looks and smells like a histidine kinase, is it a histidine kinase?, *Cell*, 91, 713, 1997.
43. Yeh, K.C. and Lagarias, J.C., Eukaryotic phytochromes: light-regulated serine/threonine protein kinases with histidine kinase ancestry, *Proc. Natl. Acad. Sci. USA*, 95, 13976, 1998.
44. Reed, J.W., Phytochromes are Pr-specific kinases, *Curr. Opin. Plant Biol.*, 2, 393, 1999.
45. McMichael, R.W.J. and Lagarias, J.C., Phosphopeptide mapping of Avena phytochrome phosphorylated by protein kinases *in vitro*, *Biochemistry*, 29, 3872, 1990.
46. Lapko, V.M., Jiang, X.-Y., Smith, D.L., and Song, P.-S., Posttranslational modification of oat phytochrome A: phosphorylation of a specific serine in a multiple serine cluster, *Biochemistry*, 36, 10595, 1997.
47. Lapko, V.M., Jiang, X.-Y., Smith, D.L., and Song, P.-S., Mass spectrometric characterization of oat phytochrome A: isoforms and posttranslational modifications, *Protein Sci*., 8, 1032, 1999.
48. Hughes, J. and Lamparter, T., Prokaryotes and phytochrome. The connection to chromophores and signaling, *Plant Physiol.*, 121, 1059, 1999.
49. Bhoo, S.H., Hirano, T., Jeong, H.-Y., Lee, J.-G., Furuya, M., and Song, P.-S., Phytochrome photochromism probed by site-directed mutations and chromophore esterification, *J. Am. Chem. Soc.*, 119, 11717, 1997.
50. Gomelsky, M. and Kaplan, S., Genetic evidence that PpsR from Rhodobacter sphaeroides 2.4.1 functions as a repressor of puc and bchF expression, *J. Bacteriol.*, 177, 1634, 1995.
51. Gomelsky, M., Horne, I.M., Lee, H.J., Pemberton, J.M., McEwan, A.G., and Kaplan, S., Domain structure, oligomeric state, and mutational analysis of PpsR, the *Rhodobacter sphaeroides* repressor of photosystem gene expression, *J. Bacteriol.*, 182, 2253, 2000.
52. Martinez-Garcia, J.F., Huq, E., and Quail, P.H., Direct targeting of light signals to a promoter element-bound transcription factor, *Science*, 288, 821, 2000.
53. Song, P.-S., Sommer, D., Wells, T.A., Hahn, T.R., Park, T.-R., and Bhoo, S.H., Light signal transduction mediated by phytochromes: preliminary studies and possible approaches, *Ind.J. Biochem. Biophys.*, 33, 1, 1996.
54. Abdulaev, N.G. and Ridge, K.D., Light-induced exposure of the cytoplasmic end of transmembrane helix seven in rhodopsin, *Proc. Natl. Acad. Sci. USA*, 95, 12854, 1998.

130

Phytochrome Genealogy

Masaki Furuya
University of Tokyo

Norihito Kuno
Hitachi Ltd.

130.1 Introduction

It was very difficult to characterize the molecular structure of large, labile proteins like spectrally photoreversible phytochromes (phy) by the methods of conventional protein chemistry. Our knowledge of the primary structure and biogenesis of phy apoproteins (PHY), however, progressed greatly after the PHY genes (*PHY*) were isolated and sequenced (for reviews, see the literature[1,2]). The first cloning of phy cDNA was the essential step in the molecular approach and was followed by differential screening of *Avena* cDNA clones, using either enriched or depleted probes for *PHY*.[3] Once the sequence of *PHY* genes was known, it became significantly easier to clone *PHY* from other plants. To date, *PHY* genes were isolated not only from various species of seed plants[4] but also ferns,[5] mosses,[6] and algae.[7] Furthermore, recent development of the genome sequencing projects resulted in the discovery of prokaryotic phytochromes in cyanobacteria,[8,9] purple bacteria, nonphotosynthetic eubacteria, and fungi, so that we can discuss the origin and molecular evolution of *PHY*.[10] We are also able to apply various gene technologies to analyze the structure/function *in vitro*[11] and *in vivo*[12] of these tetrapyrrole-sensing photoreceptor proteins.

130.2 Structure and Evolution of Phytochrome Genes

Since the discovery of phy,[13] this red/far-red photoreversible pigment has been spectrophotometrically detected in a wide range of eukaryotic green plants.[14] The universal distribution of phytochromes was further confirmed by the cloning and sequencing of full- or partial-length cDNAs and genomic DNAs of *PHY* genes with seed plants[15] and were extended to various species of lower plants and prokaryotes.[10] The sequence analyses indicate that the *PHY* gene in seed plants contains six exons and five introns, including one intron in each of the two untranslated regions at the 5′ and 3′ ends of the sequence.[15] It also provided evidence for the presence of multiple *PHY* gene families (Figure 130.1). Five *PHY* genes, named *PHYA, PHYB, PHYC, PHYD*, and *PHYE*, were first identified in the Arabidopsis genome,[16,17] and then *PHYA*,[18] *PHYB*,[19] and *PHYC*[20] in rice. Recently published genome sequences of Arabidopsis and rice clearly confirmed the above five *PHY* genes in Arabidopsis genome (The Kazusa *Arabidopsis* data site home page: http://www.kazusa.or.jp/kaos/), and the three in *Oryza sativa* L. ssp. *japonica*.[21] The Arabidopsis *PHY* genes are located on the different chromosomes (Chr.); namely *PHYA* on Chr. 1, *PHYB* on Chr. 2, *PHYC* on Chr. 5, and *PHYD* and *PHYE* on Chr. 4. On the other hand, all three rice *PHY* genes

0-8493-1348-1/04/$0.00+$1.50

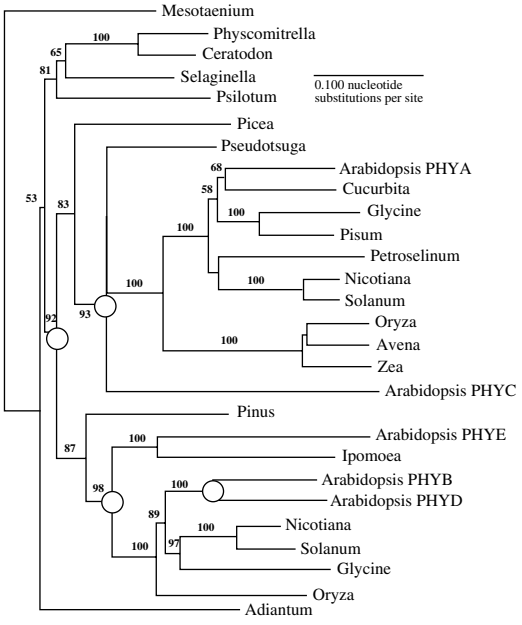

FIGURE 130.1 Phylogenic tree with phytochrome amino acid sequences constructed by the neighbor-joining methods. Branch length shows the genetic distances. Open circles represent gene duplication. Values from 100 bootstrap replicates are given above branches. (From Mathews, S. and Sharrock, R.A., Phytochrome gene diversity, *Plant Cell Env.*, 20, 666, 1997. With permission.)

are located on Chr. 3.[22] Estimated amino acid sequences show only 50% identity each with *PHYA*, *PHYB*, and *PHYC* in Arabidopsis,[16] but the identity with *PHY* from other plants is diverse.[4] In Gymnosperms, two different types of *PHY* genes were identified in *Picea abies* and *Pinus sylvestris*, and they appeared to diverge from the two main lineages of angiosperm phytochromes[23] (Figure 130.1).

The discovery of genes that code for PHY-homologous proteins in prokaryotes gave us great insight into the phy evolution. This example was first identified in the cyanobacteria *Fremyella*.[24] Until now, few mutual domains of phy-related proteins were found in not only cyanobacteria but also in purple bacteria *Rhodospirillum*,[25] nonphotosynthetic bacteria *Deinococcus*,[26] and soil bacterium *Agrobacterium*.[27] These prokaryotic photoreceptors possess the conserved chromophore-bearing domain (CBD) to which the bilin chromophore is covalently attached (Figure 130.2), though there is the exception of a purple bacteria *R. centenum* that possesses the photoactive yellow protein (PYP) domain.[25]

The histidine kinase-related domain (HKRD) is present in the *C*-terminal regulatory region of the plant phy (Figure 130.2). Most bacteriophytochromes also contain histidine kinase domain (HKD) of bacterial two-component system at the *C*-terminal region. Moreover, light-regulated histidine kinase activity was clearly demonstrated in cyanobacterial phy.[8] These results strongly support the concept that phy is a light-modulated kinase.[10]

130.3 Expression of Phytochrome Genes

Since cloned *PHY* genes became available as specific tools, spatial and temporal analyses of gene expression of individual members of the phy family were carried out at various stages of plant development.[15] The mRNA abundance of *PHY* genes was not uniform, depending upon plant species, types of tissues and organs, or environmental conditions where plants grew. For example, in rice seedlings, *PHYA*-mRNA was twofold higher in leaves than in roots when grown in the dark, whereas roots contained higher levels of the mRNA than leaves in fully green plants.[28] In etiolated pea seedlings, the abundance of the *PHYA*-mRNA was significantly higher in the shoot apex and the cotyledons than in the other parts.[29] In transgenic

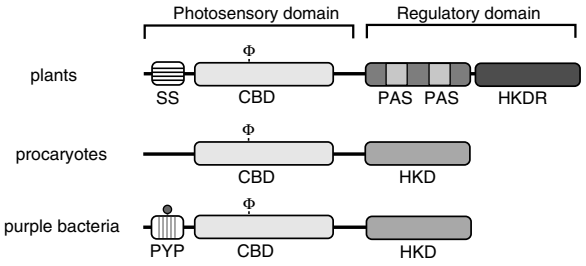

FIGURE 130.2 Domain structures of prokaryotic and plant phytochromes. Phytochromes have two functional domains, the *N*-terminal photosensory domain and the *C*-terminal regulatory domain. CBD, chromophore-bearing domain; HKRD, histidine kinase-related domain; HKD, histidine kinase domain; PAS, Pas (Per/Arndt/Sim) domain; SS, serine-rich domain; PYP, photoactive yellow protein domain similar to PAS domain; **Φ**, bilin-chromophore. (Modified from Frankhauser, C., Phytochromes as light-modulated protein kinases, Figure 1, *Seminars in Cell and Developmental Biology,* 11, 468, 2000. With permission from Elsevier Science.)

Petunia seedlings that have the pea *PHYA*-GUS fusion reporter gene, the expression level of this reporter gene was highest in the apical region, lower in a declining gradient down the hypocotyl, and barely detectable in the root when grown in the dark.[30] This level was red/far-red photoreversibly regulated.[30]

In the early 1980s, workers became aware of the fact[31] that the contents of translatable *PHY*-mRNA measured using an *in vitro* translation system were lowered by exposure of oat to white or red light. This phenomenon was confirmed by quantitative hybridization of *PHY*-mRNA using *PHY*-cDNA as a probe in oat[32] and rice.[33] The photoinduced downregulation of *PHYA* expression was more complex in dicots than in monocots. The single-copy gene coding for pea *PHYA* produces three distinct transcripts differing in the length of the 5′-noncoding sequence, when detected by S1 nuclease protection assay.[34] With respect to the abundance of these three *PHYA*-mRNAs, the shortest and the second shortest transcripts decreased rapidly after brief irradiation with red light, and the red-light-induced effect was reversed by subsequent irradiation with far-red light, indicating a Type II phy regulation.[35] Later, this was confirmed in etiolated Arabidopsis seedlings.[36] Further, when the seedlings of *phya*-deficient Arabidopsis mutant were exposed to far-red light, the far-red-light-induced downregulation of *PHYA* expression was not observed. In the *phyb*-deficient mutant, the red-light-induced downregulation also failed. These results clearly indicated that *phya* and *phyb* mediate the downregulation of *PHYA* expression in Arabidopsis seedlings.[36]

In contrast, *PHYB* and *PHYC* are constitutively expressed, regardless of the environmental light condition, as shown by Northern blot analysis using transcript-specific probes with Arabidopsis[16] and rice.[19] Densitometric analysis shows that *PHYA*-mRNA is fivefold more abundant than *PHYB*-mRNA in etiolated rice seedlings, whereas these two mRNAs are equally abundant in green tissues because of light-induced decline of *PHYA* transcript.[19] In tobacco, expression of *PHYB* gene is regulated mainly, while that of *PHYA* genes is regulated partially at the level of transcription.[37]

Recently, the circadian clock-regulated expression of *PHY* genes in Arabidopsis was clearly demonstrated through the studies of transgenic Arabidopsis plants carrying *PHY* promoter fused to the luciferase (LUC) reporter.[38,39] The transgenic seedlings carrying each *PHY*promoter::LUC showed diurnal rhythmic expression under 12-h-light/12-h-dark photoperiods and, except for *PHYC*::LUC, these oscillations persisted under constant conditions. Moreover, detailed studies of each PHY expression confirmed that expression of all *PHY*s is under the control of the circadian clock. Interestingly, each *PHY* showed the maximum level of mRNA expression at different timings.[39] These results indicated that the plant circadian clock controls the mRNA expression of PHY.

130.4 Application of Phytochrome Genes

Techniques of gene engineering were applied for studies on *in vitro* assembly of variously mutated PHY to a bilin chromophore,[40] overexpression of recombinant *PHY*s in transgenic plants,[41,42] and structure/function analysis of PHY[43] and the linear tetrapyrrole (bilin) chromophore.[11]

The preparation of PHY apoproteins has been most difficult since the discovery of phy, because the chromophore is attached covalently to a cysteinyl residue of photobiologically active holophytochromes.[44] However, the recent success of expressing recombinant *PHYA*-cDNA in bacteria[45] and yeast,[46,47] and *PHYB*-cDNA in yeast[47] made it possible to provide sufficient amounts of each PHY apoprotein with or without the chromophore. Using such PHYs, red/far-red photoreversible adducts of full-length PHYA in pea,[49] oat,[46] and tobacco[48] were synthesized *in vitro*. Furthermore, truncation of the *N*-terminal tail to residue 70 amino acid residues does not appear to be crucial for the assembly,[50] but the deletion of *N*-terminal 80 amino acids or more shows no assembly *in vivo* or *in vitro*.[51] A mutant *phyA* comprised of a deletion of the *C*-terminus to residue 548 showed bilin incorporation and red/far-red photoreversible spectral changes, indicating that the *C*-terminal half domain of PHYA is not required for chromophore assembly *in vitro*[40] and in transgenic plants.[51] The kinetic analysis of the *in vitro* assembly with PHYA[52] and PHYB[48] revealed a similar pseudo-first-order rate constant.

To analyze the structural requirements of bilin chromophore for the photoreversible spectral properties of PhyB, chemically synthesized 20 bilin analogs were reconstituted *in vitro* with PHYB.[11] Each ring of tetrapyrrole has different roles for the assembly; namely, the A-ring of bilin acts mainly as the anchor for ligation to PHYB, whereas the side-chains of the B- and C-rings are crucial to position the bilins properly in the chromophore pocket of PHYB. The side-chain of the D-ring is required for the photoreversible spectral change of the adducts.

Structure and biological function analysis of phy was made extensively using transgenic techniques by expressing a cloned *PHY* gene. Earlier, biological activity of the transgenes was demonstrated only when full-length *PHY* was overexpressed in transgenic plants, while any modification of *PHY* structure fails to induce any biological functions.[41,42] The biological activity of rice phyA in transgenic tobacco seedlings demonstrated clearly that rice PHYA assembles with tobacco phytochromobilin *in vivo* and forms spectrophotometrically active phy,[42] which regulates hypocotyl elongation in transgenic tobacco seedlings.[53] Because the *N*-terminus of PHYA in several plant species is always rich in serine residue, the first 10 serine codons of rice *PHYA* were changed to alanine codons. This mutant *phyA* gene as well as the WT *PHYA* was transferred into the tobacco genome, finding that the serine/alanine mutant responded to dim light with more sensitivity than the wild type (WT).[51]

Phy molecules have two functional domains: the chromophore-bearing photosensory *N*-terminal domain and the signaling *C*-terminal domain. To probe the intramolecular determinants for photosensory specificity of phyA and phyB, the physiological results of reciprocal *PHYA/PHYB* generic chimeras were examined under continuous red and far-red light conditions. The results[43] evidently suggested that *N*-terminal domain determined the photosensory specificity of phyA or phyB for growth responses to far-red or red light, respectively, in Arabidopsis. The far-red light sensitivity of phyA depends on the structure of not only apoproteins but also bilin chromophore. By reconstitution of holophytochrome *in vivo* through feeding various synthetic bilins to chromophore-deficient mutants of Arabidopsis, the requirement for a double bond on the bilin D-ring for rescuing PhyA function was established.[12]

130.5 Conclusions

It is evident that molecular biological approaches using *PHY* genes have opened a promising new way to apply both basic photobiology and applied photosciences. First of all, if the full-length *PHY* genes have not been cloned, it would be impossible to estimate the amino acid sequences of full-length PHY and then, subsequently, the *PHY* gene family. Second, if the different phy subfamilies were not known, the inconsistency between spectrophotometrically measured amounts and states of phy *in vivo* and the physiologically determined responses of phy[2,54] would never be solved. Third, the amounts of phyB, phyC, and others, if any, in plant tissues are so low[55] that the study of their molecular properties by conventional techniques is not possible. The expression of recombinant *PHY* in bacteria and yeasts and the *in vitro* assembly techniques with *PHY*s to the bilin chromophore, however, now provided us with measurable amounts of spectrally active phytochromes for studying their physical and chemical properties. A number of photomorphogenetic mutants were isolated and characterized in terms of relevant genes, finding

chromophore-deficient mutants,[56] apophytochrome-related mutants,[57] and downstream signaling mutants.[58] The application of gene engineering to phytochrome studies has been very fruitful, but new techniques will initiate further development in this field.

References

1. Quail, P.H., Phytochrome: a light-activated molecular switch that regulates plant gene expression, *Annu. Rev. Genet.*, 25, 389, 1991.
2. Furuya, M., Phytochromes: their molecular species, gene families, and functions, *Annu. Rev. Plant Physiol. Plant Mol. Biol.*, 44, 617, 1993.
3. Hershey, H.P., Colbert, J.T., Lissemore, J.L., Barker, R.F., and Quail, P.H., Molecular cloning of cDNA for *Avena* phytochrome, *Proc. Natl. Acad. Sci. USA*, 81, 2332, 1984.
4. Mathews, S. and Sharrock, R.A., Phytochrome gene diversity, *Plant Cell Env.*, 20, 666, 1997.
5. Wada, M., Kanegae, T., Nozoe, K., and Fukuda, S., Cryptogam phytochromes, *Plant Cell Env.*, 20, 685, 1997.
6. Thümmler, F., Beetz, A., and Rüdiger, W., Phytochrome in lower plants. Detection and partial sequence of a phytochrome gene in the moss *Ceratodon purpureus* using the polymerase chain reaction, *FEBS Lett.*, 275, 125, 1990.
7. Lagarias, D.M., Wu, S.-H., and Lagarias, J.C., Atypical phytochrome gene structure in the green algae *Mesotaenium caldariorum*, *Plant Mol. Biol.,* 29, 1127, 1995.
8. Yeh, K.-C., Wu, S.-H., Murphy, J.T., and Lagarias, J.C., A cyanobacterial phytochrome two-component light sensory system, *Science*, 277, 1505, 1997.
9. Hughes, J., Lamparter, T., Mittmann, F., Hartmann, E., Gärtner, W., Wilde, A., and Börner, T., A prokaryotic phytochrome, *Nature*, 386, 663, 1997.
10. Montgomery, B.L. and Lagarias, J.C., Phytochrome ancestry: sensors of bilins and light, *Trends in Plant Sci.*, 8, 357, 2002.
11. Hanzawa, H., Inomata, K., Kinoshita, H., Kakiuchi, T., Jayasundera, K.P., Sawamoto, D., Ohta, A., Uchida, K., Wada, K., and Furuya, M., *In vitro* assembly of phytochrome B apoprotein with synthetic analogs of the phytochrome chromophore, *Proc. Natl. Acad. Sci. USA*, 98, 3612, 2001.
12. Hanzawa, H., Shinomura, T., Inomata, K., Kakiuchi, T., Kinoshita, H., Wada, K., and Furuya, M., Structural requirement of bilin chromophore for the photosensory specificity of phytochromes A and B, *Proc. Nat. Acad. Sci. USA*, 99, 4725, 2002.
13. Butler, W.L. Norris, K.H., Siegelman, H.W., and Hendricks S.B., Detection, assay, and preliminary purification of the pigment controlling photoresponsive development of plants, *Proc. Natl. Acad. Sci. USA*, 45, 1703, 1959.
14. Furuya, M., Biochemistry and physiology of phytochrome, in *Progress in Photochemistry*, Vol. 1, Reinhold, L. and Liweschitz, Y., Eds., John Wiley & Sons, New York, 1968, p. 347.
15. Quail, P.H., Phytochrome genes and their expression, in *Photomorphogenesis in Plants*, 2nd ed., Kendrick, R.E. and Kronenberg, G.H.M., Eds., Kluwer, Dordrecht, 71, 1994.
16. Sharrock, R.A. and Quail, P.H., Novel phytochrome sequences in *Arabidopsis thaliana*: structure, evolution, and differential expression of a plant regulatory photoreceptor family, *Genes Dev.*, 3, 1745, 1989.
17. Clack, T., Mathews, S., and Sharrock, R.A., The phytochrome apoprotein family in Arabidopsis is encoded by five genes: the sequences and expression of *PHYD* and *PHYE*, *Plant Mol. Biol.,* 25, 413, 1994.
18. Kay, S.A., Keith, B., Shinozaki, K., and Chua, N.-H., The sequence of the rice phytochrome gene, *Nucleic Acids Res.*, 17, 2865, 1989.
19. Dehesh, K., Tepperman, J., Christensen, A.H., and Quail, P.H., *phyB* is evolutionarily conserved and constitutively expressed in rice seedling shoots, *Mol. Gen. Genet.*, 225, 305, 1991.
20. Tahir, M., Kanegae, H., and Takano, M., *PHYC* (phytochrome C) gene in rice: isolation and characterization of a complete coding sequence (Accession No. AB018442), *Plant Physiol.*, 118, 1555, 1998.

21. Goff, S.A. et al., A draft sequence of the rice genome (*Oryza sativa* L. ssp. *japonica*), *Science*, 296, 92, 2002.
22. Basu, D., Dehesh, K., Schneider-Poetsch, H.J., Harrington, S.E., McCouch, S.R., and Quail, P.H., Rice PHYC gene: structure, expression, map position and evolution, *Plant Mol. Biol.*, 44, 27, 2000.
23. Clapham, D.H., Kolukisaoglu, H.Ü., Larsson, C.-T., Qamaruddin, M., Ekberg, I., Wiegmann-Eirund, C., Schneider-Poetsh, H.A.W., and von Arnold, S., Phytochrome types in *Picea* and *Pinus*. Expression patterns of PHYA-related types, *Plant Mol. Biol.*, 40, 669, 1999.
24. Kehoe, D.M. and Grossman, A.R., Similarity of a chromatic adaptation sensor to phytochrome and ethylene receptors, *Science*, 273, 1409, 1996.
25. Jiang, Z., Swem, L.R., Rushing, B.G., Devanathan, S., Tollin, G., and Bauer, C.E., Bacterial photoreceptor with similarity to photoactive yellow protein and plant phytochromes, *Science*, 285, 406, 1999.
26. Davis, S.J., Vener, A.V., and Vierstra, R.D., Bacteriophytochromes: phytochrome-like photoreceptors from nonphotosynthetic eubacteria, *Science*, 286, 2517, 1999.
27. Lamparter, T., Michael, N., Mittmann, F., and Esteban, B., Phytochrome from *Agrobacterium tumefaciens* has unusual spectral properties and reveals an N-terminal chromophore attachment site, *Proc. Nat. Acad. Sci. USA,* 99, 11628–11633, 2002.
28. Quail, P.H., Hershey, H.P., Idler, K.B., Sharrock, R.A., Christensen, A.H., Park, B.M., Somers, D., Tepperman, J., Bruce, W.B., and Dehesh, K., Phy-gene structure, evolution, and expression, in *Phytochrome Properties and Biological Action*, Thomas, B. and Johnson, C.B., Eds., NATO ASI Series, Vol. H50, Springer-Verlag, Heidelberg, 1991, p. 13.
29. Tomizawa, K., Masatsuji, E., Ishii, K., Furuya, M., Distribution of type I phytochrome (*phyA*) RNA1 and RNA2 in etiolated pea seedlings, *J. Photochem. Photobiol.*, *B: Biol.*, 11, 163, 1991.
30. Komeda, Y., Yamashita, H., Sato, N., Tsukaya, H., and Naito, S., Regulated expression of a gene-fusion product derived from the gene for phytochrome I from *Pisum sativum* and the *uidA* gene from *E. coli* in transgenic *Petunia bybrida*, *Plant Cell Physiol.*, 32, 737, 1991.
31. Quail, P.H., Phytochrome: a regulatory photoreceptor that controls the expression of its own gene, *Trends Biochem. Sci.*, 9, 450, 1984.
32. Colbert, J.T., Hershey, H.P., and Quail, P.H., Autoregulatory control of translatable phytochrome mRNA levels, *Proc. Natl. Acad. Sci. USA*, 80, 2248, 1983.
33. Kay, S.A., Keith, B., Shinozaki, K., Chye, M.L., and Chua, N.-H., The rice phytochrome gene: structure, autoregulated expression, and binding of GT-1 to a conserved site in the 5′ upstream region, *Plant Cell*, 1, 351, 1989.
34. Sato, N., Nucleotide sequence and expression of the phytochrome gene in *Pisum sativum*: differential regulation by light of multiple transcripts, *Plant Mol. Biol.*, 11, 697, 1988.
35. Tomizawa, K., Nagatani, A., and Furuya, M., Phytochrome genes: studies using the tools of molecular biology and photomorphogenetic mutants: yearly review, *Photochem. Photobiol.*, 52, 265, 1990.
36. Canton, F.R. and Quail, P.H., Both phyA and phyB mediate light-imposed repression of *PHYA* gene expression in Arabidopsis, *Plant Physiol.*, 121, 1207, 1999.
37. Adam, E., Deak, M., Kay, S., Chua, N.-H., and Nagy, F., Sequence of a tobacco (*Nicotiana tabacum*) gene coding for type A phytochrome, *Plant Physiol.*, 101, 1407, 1993.
38. Hall, A., Kozma-Bognár, L., Tóth, R., Nagy, F., and Millar, A.J., Conditional circadian regulation of *PHYTOCHROME A* gene expression, *Plant Physiol.*, 127, 1808, 2001.
39. Tóth, R., Kevei, E., Hall, A., Millar, A.J., Nagy.F., and Kozma-Bognár, L., Circadian clock-regulated expression of phytochrome and cryptochrome genes in Arabidopsis, *Plant Physiol.*, 127, 1607, 2001.
40. Furuya, M., Tomizawa, K., Ito, N., Sommer, D., Deforce, L., Konomi, K., Farrens, D., and Song, P.-S., Biogenesis of phytochrome apoprotein in transgenic organisms and its assembly to the chromophore, in *Phytochrome Properties and Biological Action*, Thomas, B. and Johnson, C.B., Eds., NATO ASI Series, Vol. H50, Springer-Verlag, Heidelberg, 1991, p. 71.
41. Boylan, M.T. and Quail, P.H., Oat phytochrome is biologically active in transgenic tomatoes, *Plant Cell*, 1, 765, 1989.

42. Kay, S.A., Nagatani, A., Keith, B., Deak, M., Furuya, N., and Chua, N.-H., Rice phytochrome is biologically active in transgenic tobacco, *Plant Cell*, 1, 775, 1989.
43. Wagner, D., Fairchild, C.D., Kuhn, R.M., and Quail, P.H., Chromophore-bearing NH_2-terminal domains of phytochromes A and B determine their photosensory specificity and differential light lability, *Proc. Natl. Acad. Sci. USA,* 93, 4011, 1996.
44. Lagarias, J.C. and Rapoport, H., Chromopeptides from phytochrome. The structure and linkage of the Pr form of the phytochrome chromophore, *J. Am. Chem. Soc.*, 102, 4821, 1980.
45. Tomizawa, K., Ito, N., Komeda, Y., Uyeda, T.Q.P., Takio, K., and Furuya, M., Characterization and intracellular distribution of pea phytochrome I polypeptides expressed in *E. coli*, *Plant Cell Physiol.*, 32, 95, 1991.
46. Wahleithner, J.A., Li, L.M., and Lagarias, J.C., Expression and assembly of spectrally active recombinant holophytochrome, *Proc. Natl. Acad. Sci. USA*, 88, 10387, 1991.
47. Ito, N., Tomizawa, K., and Furuya, M., Production of full-length pea phytochrome A (type I) apoprotein by yeast expression system, *Plant Cell Physiol.*, 32, 891, 1991.
48. Kunkel, T., Tomizawa, K., Kern, R., Furuya, M., Chua, N.-H., and Schäfer, E., *In vitro* formation of a photoreversible adduct of phycocyanobilin and tobacco apophytochrome B, *Eur. J. Biochem.*, 215, 587, 1993.
49. Deforce, L., Tomizawa, K., Ito, N., Farrens, D., and Song, P.-S., *In vitro* assembly of apophytochrome and apophytochrome deletion mutants expressed in yeast with phycocyanobilin, *Proc. Natl. Acad. Sci. USA*, 88, 10392, 1991.
50. Cherry, J.R., Hondred, D., Walker, J.M., and Vierstra, R.D., Phytochrome requires the 6-kDa N-terminal domain for full biological activity, *Proc. Natl. Acad. Sci. USA*, 89, 5039, 1992.
51. Stockhaus, J., Nagatani, A., Halfter, U., Kay, S., Furuya, M., and Chua, N.-H., Serine-to-alanine substitutions at the amino-terminal region of phytochrome A result in an increase in biological activity, *Genes Devel.*, 6, 2364, 1992.
52. Li, L. and Lagarias, J.C., Phytochrome assembly: defining chromophore structural requirements for covalent attachment and photoreversibility, *J. Biol. Chem.*, 267, 19204, 1992.
53. Nagatani, A., Kay, S.A., Deak, M., Chua, N.-H., and Furuya, M., Rice type I phytochrome regulates hypocotyl elongation in transgenic tobacco seedlings, *Proc. Natl. Acad. Sci. USA*, 88, 5207, 1991.
54. Furuya, M., Molecular properties and biogenesis of phytochrome I and II, *Adv. Biophys.*, 25, 133, 1989.
55. Sharrock, R.A. and Clack, T., Patterns of expression and normalized levels of the five Arabidopsis phytochromes, *Plant Physiol.*, 129, 1674, 2002.
56. Kohchi, T., Mukougawa, K., Frankenberg, N., Masuda, M., Yokota, A., and Lagarias, J.C., The Arabidopsis hy2 gene encodes phytochromobilin synthase, a ferredoxin-dependent biliverdin reductase, *Plant Cell*, 13, 425, 2001.
57. Reed, J.W., Nagpal. P, Poole, D.S., Furuya, M., and Chory, J., Mutations in the gene for the red/far-red light receptor phytochrome B alter cell elongation and physiological responses throughout Arabidopsis development, *Plant Cell*, 5, 147, 1993.
58. Hudson, M.E., The genetics of phytochrome signalling in Arabidopsis. *Sem. Cell Devel. Biol.*, 11, 475, 2000.

131

Photomorphogenic Mutants of Tomato

Bartolomeo Lercari
Università di Pisa

Lise Bertram
Università di Pisa

131.1 Introduction

Already in the early 20th century, it was shown that light controls growth and development of plants through the action of a signaling photoreceptor separate from the photosynthetic activity.[1,2] These studies provided the starting point of an exciting field of research that was subsequently designated photomorphogenesis. In the natural environment, plants are subjected to an array of external signals, such as temperature, gravity, wind, light, and water conditions. Because plants are anchored by their roots to one place for their entire lives, they have to adapt to various changing environmental conditions where they are located.[3,4] Thus, postembryonic growth and development of plants are characterized by remarkable plasticity that requires plants to have abilities that allow them to integrate and respond to metabolic, developmental, and environmental signals. The plants, to grow and develop optimally, evolved sophisticated systems of receptors and signaling networks that provides them with an enormous ability to perceive and process information from their biotic and abiotic environments. Light is the only source of energy; therefore, it is not surprising that light plays a major signaling role in plant development.

The diverse light-induced responses of plants require precise sensing of quantity, quality, direction, and duration of light.[4] Thus, plants evolved arrays of light-sensing molecules that, according to their action spectra, can be assigned to at least three different photoreceptor classes: red/far-red photoreceptors (phytochromes); blue/UVA photoreceptors (cryptochromes, phototropin, zeaxantin, and rhodopsin?),

0-8493-1348-1/04/$0.00+$1.50

and UVB photoreceptors.[5] The combined actions of several photoreceptors allow a plant to utilize a broad spectrum of solar radiation, from ultraviolet to far-red light, to control different aspects of growth and development from seed germination to flowering. In spite of the diffuse, initial skepticism (for instance, phytochrome was defined as a pigment of imagination), photomorphogenesis developed as a relevant sector of plant physiology. The attribution of a variety of light-regulated responses to a single photoreceptor was and still is one of the problems with photomorphogenic research. Furthermore, genetic analysis has shown that there is a complex web of interactions, not only between the phytochromes but also between phytochromes, UVB, and the UVA-blue-light-absorbing photoreceptors, including redundancy, antagonism, and effector/modulator relationships.[6]

In the present review, we discuss studies in which photomorphogenic tomato mutants implicated specific photoreceptors, and the interaction of signaling pathways was activated by different photoreceptors in various light-dependent responses.

131.2 Functional Photoreceptors of Photomorphogenesis in Higher Plants

Phytochromes

Phytochromes are the best-characterized plant photosensors. Individual plants contain multiple functional phytochromes. Five phytochrome genes were characterized in Arabidopsis *(PHYA, PHYB, PHYC, PHYD, and PHYE)*[7,8] and in tomato (*PHYA, PHYB1, PHYB2, PHYE*, and *PHYF*).[9] Arabidopsis *PHYA, PHYB, PHYC*, and *PHYE* encode proteins that share 46 to 53% amino acid sequence identity, while *PHYD* encoded apoprotein (phyD) shares 80% amino acid sequence identity with phyB, and therefore, it is a member of the same subfamily.[9]

Thus, these five *PHY* genes were assigned to four subfamilies: *A*, *B* (which includes *PHYD*), *C*, and *E*. Phytochromes are dimers composed of two ~125 kDa polypeptides, with each monomer carrying a single chromophore (a linear tetrapyrrole) in its amino terminal domain. The photosensory function of a phytochrome molecule is due to its ability to photointerconvert between two stable isomers, a red-light-absorbing form, Pr (λ_{max} = 660 nm) and a far-red-light-absorbing form, Pfr (λ_{max} = 730 nm). Upon exposure to red light, Pr is converted to Pfr; upon exposure to far-red light, Pfr is converted back to Pr. Under any light conditions, phytochromes are always present in an equilibrium of the two forms that is λ dependent (photoequilibrium) and is established in a few seconds in the presence of enough radiant energy.

The classical phytochrome-mediated responses are induced by a pulse of red light interrupting darkness and reversed by a subsequent immediate pulse of far-red light. These responses include photoregulation of seed germination, inhibition of stem elongation, promotion of cotyledon expansion, flowering, gene expression, etc. Therefore, phytochrome acts as a light-regulated molecular switch, and Pfr, which is formed after a pulse of red light, is generally thought of as being the active form.

Soon after the discovery of phytochrome, the Beltsville group (H. Borthwick, S.B. Hendricks, and M.W. Parker) proposed that phytochrome might be an enzyme, however, determining the identity of this enzymatic activity has proven difficult.[5] Finally, it was demonstrated that phytochrome acts as a serine kinase and can autophosphorylate itself or transphosphorylate its partner proteins.[10] Even the subcellular localization of phytochrome appears to be affected by light.

Recently, it was shown that there is distinct light-dependent nuclear transport of phyA and phyB.[11] In dark-grown seedlings or dark-adapted light-grown plants, phyA and phyB are localized in the cytosol. Nuclear translocation of phyB is inducible by red light and shows the classical red/far-red reversibility characteristic of phytochrome-mediated responses, whereas, import of phyA in the nucleus was induced by far-red light with light pulses or with prolonged irradiation. That de-etiolation requires light-regulated gene expression is in agreement with the light-dependent nuclear translocation of phytochromes, where two phytochrome-signaling proteins, SPA1 and PIF3, were identified. It is worth noting that light

perception by phytochromes in the cytosol activates phototransduction pathways involving Ca^{2+} and cGmp.[12] Thus, it appears that phytochromes activate two distinct but coordinated circuits: cytosolic and nuclear.

Based on biochemical and physiological properties, phytochromes were grouped into two classes, Type I and Type II.[13] Type I phytochrome is light labile, indeed, its Pfr form is unstable, and following red irradiation Pfr is rapidly degraded. It is generally believed that phyA is the only Type I (labile) phytochrome, whereas the remaining phytochrome species constitute Type II (light-stable) phytochrome. The dramatic >100-fold drop in phyA levels in light-grown tissues is furthered by light-induced inhibition of transcription and degradation of mRNA. The phyA protein level is, therefore, regulated by light with coordinated transcriptional and posttranscriptional regulation. As a result of this, phyA accumulates prevalently in etiolated seedlings, whereas the other more stable phytochrome species are predominantly present in light-grown mature plants.

There are at least three distinct modes of phytochrome action that can be distinguished according to their light fluence requirement: the very low fluence responses (VLFR, requiring <0.1 nmol/m^2 light); the low fluence responses (LFRs, requiring 1 mmol/m^2 light); and responses to prolonged red and far-red light known as high irradiance responses (HIR, requiring >10 mmol/m^2).[14] VLFR and HIR to continuous far-red light were attributed to labile phyA, while LFR and HIR to continuous red light were attributed mainly to stable phytochromes.[15] Thus, different phytochrome species have distinct photosensory and physiological roles in controlling plant growth and development. It is worth noting that the above-mentioned conclusions were obtained almost completely from studies with the model plant Arabidopsis and that individual tomato phytochromes may not be hortologous to the Arabidopsis counterpart and have functions similar but not identical to their Arabidopsis homologs.[16,17,18] Furthermore, evidence was provided that angiosperm phytochrome gene subfamilies and different regions of the phytochrome protein are evolving differentially.[19] The fast rate of evolution of the signal transduction/dimerization domain of phytochrome apoprotein is presumably related to acquisition of new molecular functions.[20] Taking into account the fact that *PHY* gene family and size differ significantly among flowering plants, it appears that the extrapolation of the information obtained with Arabidopsis to other species could be misleading.

Blue-UVA Photoreceptors

For more than one century, it has been known that blue light induces phototropic responses in plants. Nowadays, it is well known that blue and UVA regions of the solar spectrum control a large number of responses in plants: inhibition of stem elongation, leaf expansion, stomatal opening, phototropism, and gene expression. But, it was only in the last decade that four blue-light photoreceptors were characterized in plants, cryptochrome 1, cryptochrome 2, phototropin, and zeaxanthin.[21] It is widely believed that the current list of photoreceptors perceiving blue-UVA regions of the spectrum is not complete.[21] On the other hand, all-*trans*-retinal was identified in tomato plants at physiological levels.[22] Because retinal is the ligand of a G-protein-linked receptor, it appears worthwhile to verify whether or not a rhodopsin-like protein can be one of the blue-light photoreceptors in higher plants.

Cryptochromes

Cryptochromes are blue-light photoreceptors found in plants and animals. Already in the year 1950, Galston[23] proposed flavins as the blue-light-absorbing chromophores. But it was only the isolation of an Arabidopsis mutant, *hy4* (now named *CRY1*), that has an elongated hypocotyl in blue light, that allowed for the isolation of the first flavin-type blue-light photoreceptor.[24] The *CRY1*-encoded protein shows substantial homology to prokaryotic DNA photolyases that catalyze blue/UVA-dependent DNA repairing. *CRY1* encodes a 75 kD protein that binds a flavin (FAD) and a pterin chromophore, as do Class I photolyases, but does not have photorepair activity. The results of overexpression studies, in Arabidopsis and tobacco, showed that plants containing elevated levels of cry1 have short hypocotyl in UVA and blue light, further supporting the conclusion that cry1 is a blue receptor mediating blue-light inhibition of

hypocotyl elongation.[25] Mutants at the *CRY1* locus also showed reduced blue-light induction of the expression of several genes. Besides *CRY1,* a second cryptochrome gene, *CRY2,* was isolated in plants and animals. These genes show sequence similarity, mainly in the *N*-terminal photolyase-like domains, but little similarity in their *C*-terminal domains. In plants, the physiological functions of cry1 and cry2 appear to partly overlap — mediated inhibition of hypocotyl elongation, induction of anthocyanin synthesis, and entrainment of the circadian clock[26,27] — whereas only cry2 is involved in the control of cotyledon expansion and flowering timing.[28] In *Adianthum capillus-veneris*, at least two cryptochromes are localized in the nucleus.[29]

Phototropins

It was only in 1995 that a genetic locus, named *NPH1* (Nonphototropic Hypocotyl 1), encoding a plasma membrane protein essential for most phototropic responses to blue light was isolated in Arabidopsis.[30] Since then, a number of phototropin homologs were identified in several species. All the putative phototropin proteins contain in the *N*-terminal two LOV domains (they are activated by light, oxygen, or voltage) that bind FMN as a chromophore and a serine/threonine kinase in the *C*-terminal; they show light-activated autophosporylation.[5] It appears that different phototropins can mediate photropism in response to different fluence rates of light. It was agreed to designate the phototropic photoreceptors as phot1, phot2, and so on.

131.3 Tomato as Model Plant for Photomorphogenesis Studies

Tomato, *Solanum lycopersicum* L., is considered a model plant system alternative to Arabidopsis for the study of photomorphogenesis.[17] Tomato has a growth habit that is different from Arabidopsis, it produces large seeds, seedlings, and fruits that make it easier to use in the laboratory. The phytochrome family of tomato was characterized, and, in particular, the temporal and photoregulated expression of all known tomato phytochrome genes was shown.[31,32,33] The two cryptochrome genes of tomato were cloned and sequenced,[34] and several photomorphogenic mutants are available. Therefore, tomato is now a comparative experimental system to Arabidopsis for studying the functions of phytochromes and cryptochromes throughout the whole plant life cycle — from seed germination to fruit ripening.[35,36]

The Phytochrome Gene Family in Tomato

The genome of the tomato contains five phytochrome genes, each encoding a different apoprotein.[9,20] In tomato, the five cloned phytochrome genes are distributed over different chromosomes of the genome.[37] *PHYA, PHYB1, PHYB2, PHYE*, and *PHYF* are located on Chromosomes 10, 1, 5, 2, and 7, respectively. *PHYA*, *PHYB1*, and *PHYB2* genes are organized into four exons interrupted by three introns.[38,39,40] The five identified tomato phytochrome (*PHY*) genes were designated *PHYA*, *PHYB1*, *PHYB2*, *PHYE*, and *PHYF*, as a function of their amino acid similarity to the five Arabidopsis phytochromes. Tomato *PHYA* fragments and the polypeptides it encodes share 82% nucleotide and 98% amino acid identity with Arabidopsis *PHYA*; tomato *PHYB1* shares 80% nucleotide and 96% amino acid identity with Arabidopsis *PHYB*; tomato *PHYB2* shares 79% nucleotide and 91% amino acid identity with Arabidopsis *PHYB*; tomato *PHYE* shares 79% nucleotide and 88% amino acid identity with Arabidopsis *PHYE*; and tomato *PHYF* shares only 61 to 73% nucleotide and 65 to 72% amino acid with Arabidopsis phytochromes. Tomato *PHYB1* and *PHYB2* share 85% nucleotide and 90% amino acid identity.

Hauser et al.[31] determined the abundance of *PHY* mRNAs for dry seeds and for different organs of seedlings and mature tomato plants. In dry tomato seeds, each of the five *PHY* mRNAs was detectable, *PHYB1* mRNA being predominant. It is worth noting that the amount of *PHY* mRNA in dry tomato seeds is very low (about 1 to 5 μmol/mol mRNA). In greenhouse-grown tomato seedlings, the expression patterns of *PHYB1* and *PHYE* are almost indistinguishable, whereas each of the other *PHY* transcripts differed from one another. Except for *PHYA* mRNA, which shows the highest level in the root, the abundance of all the other *PHY* transcripts is maximal in the hypocotyl. In seedlings the abundance of

each *PHY* mRNA changes two- to threefold among organs. The order of decreasing abundance of the five transcripts in young seedlings is *PHYA* > *PHYB1* = *PHYE* > *PHYB2* > *PHYF*. Mature plants show a different picture. Whereas *PHYA, PHYB1*, and *PHYE* mRNAs display similar patterns of expression in different organs, the levels of *PHYB2* and *PHYF* mRNA show a larger variability, up to 15-fold. In particular, *PHYB2* and *PHYF* are expressed maximally in ripening fruits. The fact that the abundance of each of the five tomato *PHY* shows a significant variability among organs, suggests an organ-dependent biological activity of each phytochrome species.[31]

The same authors[33] subsequently followed the changes of the absolute transcript amount of the five *PHY* throughout the tomato plant life cycle, during a normal day cycle, and in response to light conditions. Their measurements were on whole plant basis; therefore, these data do not provide any further information about the above-mentioned variability of the abundance of each of the five *PHY* mRNAs among organs. Dry seeds contain the lowest amount of mRNAs transcribed from each of the five phytochrome genes. All five transcripts increase by 10- to 1000-fold during the first 24 h after imbibition, irrespective of light conditions. The early and dramatic increase of all five transcripts indicates that, although in dry tomato seeds there are physiological levels of Pfr sufficient to promote dark seed germination,[41] the *PHY* mRNAs occurring in dry tomato seeds are probably not sufficient to provide seedlings growing underground with an amount of photosensors adequate to perceive the small number of photons transmitted through the soil.[33] In darkness, after the peak at 24 h, *PHYA, PHYB1*, and *PHYB2* continue to increase to Day 5, while the abundance of *PHYE* and *PHYF* changes relatively little. After 5 days in darkness, *PHYA* abundance reaches approximately 2500 a mol μg^{-1} poly(A)$^+$-enriched RNA, whereas the abundance of the transcripts of the other *PHY* was more than one order of magnitude lower.

By contrast, when tomato seedlings are grown in greenhouse under natural photoperiod, there is, even though at lower rates, a constant increase in all but *PHYF* mRNAs throughout Day 6. In light-grown seedlings, *PHYA* transcripts are still the most abundant, even with a 10-fold decrease in comparison to etiolated seedlings. The analysis of transcript levels from sowing time to 56-day-old tomato plants shows a similar pattern for the levels of *PHYA, PHYB1, PHYB2*, and *PHYF* transcripts, characterized by a maximum peak at Day 6 followed by a decreasing phase until Day 14 and relatively constant levels thereafter. The data from Hauser et al.[35] suggest that besides the well-established roles of phyA and phyB1, even phyB2 and phyF could have roles in young tomato seedlings. The different pattern of *PHYE* mRNA that increases continuously for 3 weeks after sowing until a maximum plateau is reached that is maintained constant in mature plants suggests a main role of phyE in mature plants. The similarity of *PHYA* and *PHYB2* patterns of expression represented the most unexpected result. Both *PHYA* and *PHYB2* showed largest enhancements in expression after a light-to-dark transfer, the greatest decline following a dark-to-light transfer, and a similar variation during the daily natural light–dark cycle.[33] *PHYA* and *PHYB2* exhibit maximum values around midnight and minimal values around noon. Thus, a gene encoding for the labile phyA shows the same pattern of expression of a gene encoding for the stable phyB2. Characteristically, *PHYB1* transcripts attain maximum level in the afternoon and minimal levels just before dawn. On the other hand, the levels of *PHYE* and *PHYF* transcripts are almost constant during the 24 h. The fact that *PHYA*, *PHYB1*, and *PHYB2* present diurnal-dependent levels of expression, could suggest that these phytochromes are involved in rhythmic responses linked to various environmental parameters.[33]

Cryptochromes Family of Tomato

In tomato, two *CRY* genes — *CRY1* and *CRY2* — were characterized.[34] They map to Chromosomes 4 and 9, respectively, and encode proteins of 679 and 635 amino acids. Tomato cry1 and cry2 apoproteins display higher similarity to Arabidopsis crys than to each other.

Photomorphogenic Mutants of Tomato

Whereas only 10 years ago (in 1992), no mutations were isolated in phytochrome genes, in any plant, nowadays a number of phytochrome and photomorphogenic mutants are available. The availability of

mutations in genes involved in sensing and transducing light signal has contributed much to the fast-paced progress of our understanding of phytochrome functions that occurred in the last few years. Clearly, the fastest and easiest way to isolate photomorphogenic mutant is to screen under different light conditions the phenotype of mutagenized seeds at the seedling stage. Seedling development of higher plants follows two contrasting patterns: photomorphogenesis, which is exhibited in the light, and skotomorphogenesis (dark development or etiolation), which is the pathway followed upon germination in darkness. A seedling growing in darkness is characterized by long hypocotyl, unexpanded, closed, and pale cotyledons on an apical hook, absence of chlorophyll and anthocyanin biosynthesis, and true leaf development. When exposed to light, the seedling switches from skotomorphogenesis to photomorphogenesis, the elongation rate of the hypocotyl decreases, cotyledons green and enlarge, the shoot apical meristem is activated, anthocyanin biosynthesis starts, and the first true leaves emerge. The light-mediated transition from skotomorphogenesis to photomorphogenesis requires photoreceptor-mediated gene expression. Hypocotyl elongation, anthocyanin accumulation, and cotyledon expansion are the light-dependent responses most extensively used for the isolation of photomorphogenic mutants.

In Arabidopsis, there are two general classes of photomorphogenic mutants: light-insensitive mutants and mutants that undergo photomorphogenesis in the dark.[11] Tomato mutants differ substantially from Arabidopsis mutants in many aspects; in particular, no tomato mutants were isolated that exhibited visible photomorphogenic phenotype when the plants are grown in the dark.[17] Therefore, tomato mutants affected in-light regulated physiological responses fall in two different classes in comparison to Arabidopsis. One class includes mutants with impaired photomorphogenesis with a morphology, in the light, that shows aspects of dark-grown plants, while the mutants belonging to the other class show enhanced photomorphogenic responses in the light and etiolated phenotype in the dark. Mutants with a morphology that resembles that of dark-grown plants, although grown in the light, identify positive regulatory components of photomorphogenesis. This class of mutants shows lesions in genes that control chromophore biosynthesis or encode the photoreceptor's apoproteins. Mutants that exhibit enhanced light-dependent responses identify negative regulators of light signal transduction. In tomato, a large number of mutants are available, covering all stages of plant life from seed to fruit ripening and senescence, therefore, a more complete picture about the role of photomorphogenic photoreceptors during entire plant cycle can be depicted.[17]

Tomato Mutants Affected in Light Perception

Several photomorphogenic mutants of tomato were isolated by screening performed under low fluence rate of white, blue, red, or far-red light. In this section, we will describe briefly the molecular nature of the mutations in specific genes encoding photoreceptor apoproteins of mutants that have impaired light perception. Their effects in different phases and photomorphogenic responses of plants during their life cycle will be discussed separately.

Far-red-light insensitive (*fri*^{1} *and fri*^{2}, now named *phyA*), phytochrome-A-deficient mutants of tomato were obtained by treating seeds with ethyl methane sulfonate (EMS).[37] *Fri* mutations and *PHYA* were mapped at the same location on Chromosome 10.[37] Both *fri*^{1} and *fri*^{2} mutants have an identical point mutation in *PHYA*, A_{2327}-to-T.[38] The two *PHYA* mutants produce less than 1% of phyA apoprotein.

With the same mutagenetic approach, three mutant alleles in tomato (*tri*^{1,2,4}) were isolated with slightly longer hypocotyl under white light in comparison to wild type.[37,43] A fourth mutant was isolated as a somaclonal variant of the cv. Money Maker. The *TRI* locus and the *PHYB1* gene locus were located to Chromosome 1, and it was concluded that the *TRI* locus is the gene encoding the apoprotein of phytochrome B1. Each mutation appears to be the result of a different, single-base substitution in *PHYB1* that affects transcript and protein size and abundance.[39] *Tri*^{1} is considered a null mutant, and in the next pages, we will consider only the *tri*^{1} mutant as the *phyB1* mutant. In particular, it was shown that this mutant has a nucleotide substitution that results in a stop signal at codon 92.[39,43]

Subsequently, double mutants *phyA/phyB1* were obtained from segregating populations derived from crosses of the monogenic mutants.[40] The double mutant does not contain immunochemically detectable phyA and phyB1 polypeptides, its phenotype in white light is similar to that of *phyB1* mutant. From M_2

populations, obtained from γ-mutagenized *phyA/phyB1* double mutants, two new mutants were isolated with elongated hypocotyls and reduced anthocyanin content. Both mutants were found to have molecular lesions in *PHYB2* that produced apoproteins lacking a significant part of the *C*-terminal region.[40] The mature plants of the triple mutant *phyA/phyB1/phyB2* were characterized by dramatically elongated stem internodes, fruit trusses, pedicels and peduncles, and by pale stem and leaves.[35,36]

By a combination of phenotypic and PCR-based screening of the back-cross of the triple mutant (*phyA/phyB1/phyB2*) lines to the wild-type, monogenic *phyB2* mutants and double *phyA/phyB2* and *phyB1/phyB2* mutants were isolated. The phenotype of *phyB2* mutant is almost indistinguishable from that of wild-type tomato, as seedlings under red light or as mature plants grown in greenhouse. Furthermore, the effect of *phyB2* mutation on a *phyA* background, i.e., in the case of *phyA/phyB2* double mutation, is limited, almost null. By contrast, the phenotype of double mutant *phyB1/phyB2* showed, in comparison to wild-type or either single mutant, enhanced stem elongation and lower chlorophyll content. At seedling stage, under continuous red light, loss of phyB2 dramatically affected tomato phenotype only in a *phyB1* background.

The progeny from transgenic plants with lowered tomato CRY1 mRNA and protein levels, obtained by using an antisense mRNA approach, show elongated hypocotyl and decreased anthocyanins accumulation under blue light, providing the first direct evidence of a cryptochrome role in tomato photomorphogenesis.[44]

With further studies on M_2 populations, obtained from γ-mutagenized *phyA/phyB1* double mutants, recessive mutants with increased hypocotyl length, reduced chlorophyll content, and retarded hook opening were isolated.[36] These mutants showed reduced responsiveness to blue light in comparison to their *phyA/phyB1* progenitor as a result of lesions in the gene encoding the blue-light receptor Cryptochrome 1. The cross of the triple mutant *phyA/phyB1/cry1* to wild-type allowed the isolation of new photoreceptor mutant combinations: monogenic *cry1* and the double mutants *cry1/phyA* and *cry1/phyB1*.[36] Quadruple mutants were subsequently isolated in F_2 progenies of a cross between *phya/phyB1/phyB2* and *phyA/phyB1/cry1* mutants.[36] The quadruple mutants were characterized by an extreme phenotype: dramatically elongated and severely chlorophyll- and anthocyanin-deficient hypocotyl, and small cotyledons in comparison to all the other genotypes. The quadruple mutant did not survive until seed production. From the comparison of all these genotypes, it appears that cry1, phyA, phyB1, and phyB2 contribute to blue-light-mediated responses.[36]

Important clues concerning photoreceptor function may be uncovered by overexpressing single photoreceptors. Boylan and Quail[45] showed that ectopic expression of oat phyA in tomato induced dramatic phenotypic effects in seedlings (short hypocotyls and elevated anthocyanin contents) and in mature plants (dwarf, with dark green foliage and fruits).

A subclass of photoreceptor mutants includes the phytochrome chromophore-deficient mutants that are impaired in their ability to synthesize the linear tetrapyrrole chromophore of phytochrome.[46] Because all the phytochromes utilize the same chromophore, the chromophore mutants like *aurea* (*au*) and *yellow green-2* (*yg-2*) are affected in several phytochrome species. For instance, in etiolated *au* seedlings, three holophytochrome species are lost.[47] Thus, in etiolated seedlings, there is no spectrophotometrically detectable phytochrome, while mature plants of the *au* mutant contain about 60% of WT phytochrome level.[48] An antibody raised to pea phyB detected the same amount of photoactive phyB in green leaves in both *au* and WT plants.[49] The phenotype of these mutants is characterized by elongated and pale hypocotyl in white light, and even adult plants show more or less dramatic yellow gold color and elongated phenotype, depending on the genetic background.[50,51] In contrast, *au* fruits are normally pigmented. The pale phenotype is due to feedback inhibition of chlorophyll synthesis. The *au* mutant was used extensively for phytochrome signaling studies, because it was thought to be specifically deficient in phyA.[12,52]

Tomato Mutants Affected In Light Signaling

Several light-oversensitive mutants were isolated in tomato: high pigment (*hp-1* and *hp-2*), atroviolacea (*atv*), and intense pigmentation (*Ip*).[17] The *hp-1* locus was mapped to tomato Chromosome 2,[53] whereas the *hp-2* locus was mapped to Chromosome 1.[37] The two mutants did not display light phenotypes in

TABLE 131.1 Percentage of Seed Germination Recorded 5 and 10 Days after Sowing, at 25°C, in Darkness or under Continuous Red, Far-Red or Blue Light (Fluence Rate 5 $\mu molm^{-2}s^{-1}$)

	Dark		Red		Far-Red		Blue	
	5 Days	10 Days	5 Days	10 Days	5 Days	10 Days	5 Days	10 Days
MM	96	97	52	100	0	0	11	81
PhyA	95	96	93	100	1	5	83	89
$phyB_1$	23	31	11	35	0	0	0	3
$phyB_2$	9	11	12	95	0	0	0	0
phyA $phyB_1$	67	83	85	96	12	20	71	87
phyA $phyB_2$	13	16	97	99	1	1	7	11
$phyB_1$ $phyB_2$	4	7	12	85	0	0	0	0
phyA $phyB_1$ $phyB_2$	0	0	16	24	0	0	0	0

darkness, whereas, when grown in the presence of light, they showed shorter hypocotyls, higher anthocyanin accumulation, and more pigmented fruit in comparison to their wild-type; i.e., exaggerated light responsiveness. The analysis of double mutants *phyA hp-1* and *phyB1 hp-1* provided evidence that *hp-1* mutation enhances the effectiveness of both phytochromes.[54,55] On the other hand, it was shown that the *hp-1* phenotype was repressed in the double mutant *au hp-1*, confirming that *hp-1* phenotype requires an active phytochrome. The *hp-1* mutant presents a similar phytochrome content as that of the wild-type tomato. The *HP-2* gene was cloned and found to encode the tomato homolog of DET1 from Arabidopsis.[56] Even in the case of *hp-2* mutant, the mutation is expressed only in the presence of activated functional photoreceptors.

131.4 Photomorphogenic Responses in Different Phases of Tomato Life Cycle

The growth habits and the sizes of tomato plants make it easy to follow the photomorphogenic effects of light and the relative roles of different photoreceptors and of components of the light transduction chains at different stages of plant growth and development. In this review, we will cover seed germination, hypocotyl growth and differentiation, stem growth, and fruit ripening.

Photoregulation of Tomato Seed Germination

Although tomato seed germination in the dark is fairly good, phytochrome involvement was established. Different tomato cultivars show different sensitivities to light.[41,57] For instance, continuous red light promotes the germination of the line UC-105,[58] but the same light significantly decreases the rate of the germination process in the cv Money Maker (Table 131.1). Therefore, we will discuss separately the photoregulation of seed germination of distinct tomato lines.

Seed germination of line UC-105 is promoted, in comparison to the dark, by continuous and cyclic red light, whereas it is inhibited by continuous and cyclic far-red light and by continuous long-wavelength far-red light, 758 nm.[58] In cyclic irradiation, far-red pulses reverse almost completely the promoting effect of the preceding red light pulses. By contrast, seed germination of the *au* mutant, obtained from UC-105 genetic background, is promoted by continuous irradiation with red, far-red, and long-wavelength far-red (758 nm) as well as by cyclic irradiations with red and far-red lights. The promoting effect (in the *au* mutant), and the inhibitory effect (in wild-type) of continuous far-red light does not show photon fluence rate dependence in the range of 0.02 nmol $m^{-2}s^{-1}$ to 20 $\mu mol\ m^{-2}\ s^{-1}$. Consequently, the HIR of phytochrome is not involved.[58] The fluence-rate-independent inhibitory effect of continuous far-red and continuous 758 nm in UC-105 line can be attributed to the removal of almost all the Pfrs from seed cells, and consequently, to the fact that the LFR, requiring high phytochrome photoequilibrium, cannot take place. On the other hand, seed germination in *au* mutant is promoted by irradiation with 758 nm that establishes low phytochrome photoequilibria, <0.001, falling in a range compatible with VLFR of

phytochrome. Thus, it is possible to conclude that seed germination in UC-105 genetic background can be controlled by LFR and VLFR of phytochrome. The fact that the VLFR is manifested only in the *au* mutant that lacks at least three phytochromes, indicates that in WT tomato, some likely act antagonistically to those involved in VLFR. The involvement of LFR in the photocontrol of seed germination of wild-type tomato was confirmed by osmotic presowing treatments given under different light conditions. Unfortunately, seeds of the *au* mutant do not germinate after osmoconditioning.[59] Osmotic presowing treatment (osmoconditioning) is a method widely used to improve germination behavior in many species that we use to study the role of the phytochrome system in the photoregulation of tomato seed germination in UC-105 genetic background. During osmoconditioning of tomato seed, the limited water content of cells allows for phytochrome synthesis and phytochrome photoconversion but does not allow seed germination. Thus, it has been possible to separate the light effects on the phytochrome system from the Pfrs effect on the final physiological response, i.e., seed germination. The osmoconditioning in the dark or under continuous red light induces the capability for seed germination, even under the usually inhibitory far-red light. These results indicate that osmoconditioning in dark and in red light enables the transformation of phytochrome intermediates to Pfr (in the dark) and of old and new Pr to Pfr (in red light), which can exert its action during the osmotic inhibition of seed germination. In other words, the initial action of phytochrome, as far as germination is concerned, occurs during the osmotic treatment and, therefore, cannot be reversed by subsequent continuous far-red light. The same argument explains the inhibition of seed germination induced by far-red light, following osmoconditioning under far-red light. Continuous far-red light during seed osmoconditioning removes almost all the Pfr from the cells, and obviously, the initial action of Pfr, in the LFR mode, cannot occur. Thus, seed germination after osmoconditioning in far-red light is still under the control of the LFR (far-red light reversible) of phytochrome. The involvement of a high irradiance response in the control of seed germination in UC-105 genetic background is therefore excluded.

The analysis of the photoregulation of seed germination in Money Maker (MM) genetic background, i.e., in a genotype in which red light inhibits seed germination, produces a different picture (Table 131.1). Seeds of WT, i.e., MM, show the highest velocity of germination in darkness. Furthermore, only with a delay of several days is a high germination percentage of germinated seeds reached by red- and blue-germinated seeds. In the dark, *phyA* mutant shows a pattern of seed germination similar to wild-type, whereas seed germination of the other phytochrome mutants (*phyB1, phyB2, phyA/phyB1, phyA/phyB2, phyB1/phyB2, phyA/phyB1/phyB2*) is impaired (Table 131.1). Under continuous red light, seed germination velocity of p*hyA, phyA/phyB1,* and *phyA/phyB2* mutants was greater than in wild-type; whereas, those of *phyB2, phyB1, phyB1/phyB2,* and *phyA/phyB1/phyB2* mutants were lower. The fact that only the mutants lacking phyA or phyA in addition to phyB1 or phyB2 show red-light-promoted seed germination in comparison to wild-type, clearly indicates that phyA exerts an antagonistic action toward phyB1 and phyB2, and that phyB2 and phyB1 play major roles in the regulation of tomato seed germination by red light. Under continuous blue light, seed germination of MM is dramatically inhibited in comparison to the dark, by contrast it is promoted in *phyA* and *phyA/phyB1* mutants. These results indicate again an antagonistic action of phyA toward phyB2, the late one appears to have a major role in blue-light-regulated germination of tomato seeds. The fact that continuous far-red light inhibits seed germination in absence of phyA, phyB1, and phyB2 in MM genetic background, clearly indicates that in this cv, the inhibitory effect of continuous far-red does not involve the phyA-mediated HIR but is merely the result of the low photoequilibrium established by this waveband that is below the threshold required for seed germination. Conversely, the fairly good germination in the dark can be ascribed to the substantial levels of dry Pfrs present in dry tomato seeds.

The inhibition of tomato seed germination by far-red light was further studied in *hp-1*, *hp-1/phyA*, and *hp-1/phyB1* mutants.[60] Unfortunately, the genetic backgrounds of these mutants were not reported, making a comparison with the results previously described impossible. Anyway, the analysis of time-dependent effectiveness of far-red light pulse or of continuous far-red light provides the first evidence that an HIR response of phytochrome can be involved in the photoregulation of tomato seed germination. It appears that inhibition of seed germination in *hp-1* mutant of tomato is the result of LFR at an early

stage and of an HIR at a later stage, this one being mediated by phyA. In conclusion, it appears that the phytochrome family of photoreceptors, acting through VLFR, LFR, and HIR, controls tomato seed germination by means of at least four phys (phyA, phyB1, phyB2, and another one phyE or phyF?). PhyA appears to inhibit seed germination by acting antagonistically to phyB1 and phyB2 (Table 131.1), as well by an HIR at a later stage of the germination process. Both phyB1 and phyB2 play crucial roles in sensing red light, and phyB2 has a crucial role in sensing blue light.

Photocontrol of Hypocotyl Elongation Growth

The availability of several photomorphogenic mutants and the use of hypocotyl extension as a model system allowed for a genetic dissection of light sensing in young seedlings of tomato that uncovered many facets of physiological interactions among photoreceptors.[35,36,61–66] For sake of brevity and clarity, we will refer only to selected light conditions.

Continuous Red Light

Inhibition of hypocotyl elongation by low fluence rates of continuous red light is slightly, albeit significantly, reduced in *phyA* mutant, while the loss of phyB1 causes a large and substantial decrease of hypocotyl growth inhibition.[35] No detectable effect of phyB2 is displayed on MM or on a *phyA* background. On the other hand, under red light, a remarkable effect of phyB2 is shown in the absence of phyB1, indicating the presence of partial redundancy between the two phytochromes.[36] When three phytochromes, phyA, phyB1, and phyB2 are absent, the hypocotyl length after several days under different fluence rates of red light is similar to that of WT in the dark.

At first glance, these results could suggest that only the three above-mentioned phytochromes are involved in red-induced inhibition of growth in tomato hypocotyl.[36] A different picture emerges with a different experimental approach that takes into account the fact that in tomato seedlings, blue light is the region of visible light with the strongest effect on hypocotyl elongation; and that activation of blue-light photoreceptors enhances responsiveness to phytochrome.[65] Thus, in an experiment comparing the effects of red and dichromatic red plus blue light in *phyA/phyB1/phyB2* and *phyA/phyB1/phyB2/hp-1* mutants, the data revealed residual phytochrome responses in the *phyA/phyB1/phyB2* triple mutant, suggesting that at least one of the two remaining phytochromes (phyE or phyF) has a role in red-light sensing.[35] In conclusion, as long as red-light-induced inhibition of hypocotyl elongation is concerned, available data indicate that phyB1 and phyB2 mediate the HIR to red light, whereas the small effect of phyA appears to be a multiple LFR independent of the presence of phyB1 and phyB2.

The four mutants in the light signal transduction chains, *hp-1*, *hp-2*, *atv*, and *Ip* showed enhanced inhibition of hypocotyl growth in comparison to WT when grown under continuous red light.[17]

Continuous Far-Red Light

The inhibitory effect of continuous far-red light on hypocotyl elongation was studied in a number of tomato mutants. Under continuous far-red light, the kinetic of hypocotyl growth of *phyB1* mutant is indistinguishable from that of the wild-type, whereas *phyA* and *au* mutants appear to be blind to far-red light (there is no difference in hypocotyl length between *phyA* and *au* seedlings grown in darkness and those grown under continuous far-red light). The obvious conclusion is that phyA is the only phytochrome responsible of the HIR to continuous far-red light. *hp-1, hp-2, atv*, and *Ip* mutants showed enhanced inhibition of hypocotyl growth in comparison to WT when grown under continuous far-red light.[17]

Continuous Blue Light

The effect of continuous blue light on hypocotyl elongation was genetically dissected in tomato by using mutants deficient in phyA, phyB1, and phyB2 and cry 1.[36] From this genetic approach, it appears that it is not possible to obtain reliable evaluation of the contributions of each photoreceptor when single mutants are used. For instance, in previous papers, the kinetics of hypocotyl elongation under blue light showed substantial inhibition of hypocotyl growth in *phyA* and *au* mutants, even though reduced in

comparison to wild-type tomato, whereas the kinetic of hypocotyl growth of *phyB1* mutant was indistinguishable from that of the wild type.[47] These results were only partially confirmed by Weller et al.[36] by using an isogenic series of all mutant combinations among *phyA*, *phyB1*, *phyB2*, and *cry1*. In particular, it was shown that only *phyA* and *cry1* display significant roles in blue-induced inhibition of hypocotyl growth in a WT background. The role of *phyB1* emerges only in the absence of *phyA* and *phyB2*, and furthermore, the effect of *phyB2* is detectable only in the absence of *phyB1*. Phytochrome A and *cry1* act additively to control hypocotyl elongation, and together they are responsible for about 35% of the WT response. Instead, the triple mutant *cry1*/*phyA*/*phyB1* shows a 72% reduction of responsiveness to blue light in comparison to WT. While the quadruple mutant (*cry1*/*phyA*/*phyB1*/*phyB2)* loses totally the responsiveness to monochromatic blue light. Furthermore, the quadruple mutant does not survive long enough to reproduce.

Continuous UV Radiation

The effect of UV radiation on the elongation growth of tomato hypocotyl was characterized by comparing the responses of wild-type and *au* mutant tomato seedlings.[61–63] The experimental evidence provided in several reports suggests different relative roles of phytochrome and of a specific UVB photoreceptor in the UV-induced inhibition of hypocotyl elongation. Both WT and *au* mutant of tomato show similar patterns of the time courses of growth inhibition in response to UV radiation in etiolated as well as in de-etiolated seedlings. UV radiation that includes the UVB part (<320 nm) is the most effective, partial (305 nm cutoff filter) or almost total removal of the UVB band (320 nm filter) produces an intermediate and slower inhibitory effect in the case of a 305 nm filter, while in the presence of a 320 nm filter, a small inhibition of growth was found only in dark-grown hypocotyls. It is worth noting that de-etiolation increases the growth inhibition caused by short UVB radiation, but it decreases inhibition by long (>305 and >320 nm) radiation (by 40 and 90%, respectively). Therefore, it appears that irradiation from sowing time, with yellow light, that establishes a high phytochrome photoequilibrium and does not activate blue-UVA photoreceptors, enhances the UV-dependent inhibition of hypocotyl elongation, probably through a phytochrome-mediated enhancement of responsiveness to signals from UVB photoreceptor. The *au* mutant displays an UVB-mediated inhibition of hypocotyl growth that is usually hidden by the overriding action of phytochrome.[61,62] Therefore, it could be suggested that each of the photoreceptive systems capable of interacting with UVB radiation can acquire a pivotal role in the absence of one another. The presence of one or more photosensors that can substitute for one another is an obvious advantage for the adaptive ability of higher plants.

Photocontrol of Anthocyanins and Flavonoids Accumulation in Tomato Seedlings

Light-dependent anthocyanin synthesis is one of the photomorphogenic responses of tomato seedling that involves action and interaction of several photoreceptors and several modes of action of phytochromes.[63–65] Anthocyanins are absent in dark-grown hypocotyls of tomato, in contrast, significant levels of UV-absorbing compound are present in dark-grown hypocotyls.[65] The involvement of the phytochrome system in light-dependent anthocyanins accumulation was demonstrated by pulse experiments, showing red/far-red reversible and nonreversible responses, involving phyA and phyB1, respectively. The preactivation of blue-light photoreceptors induces a large responsiveness amplification to Pfr,[64] while the preactivation of phytochrome enhances the UVB-induced accumulation of flavonoids.[63] For sake of brevity and clarity, in the next paragraphs, we will refer only to selected light conditions.

Continuous Red Light

In etiolated WT tomato seedlings, the fluence-rate response curve for anthocyanin accumulation with 24 h monochromatic red light shows that is possible to isolate two components: a low fluence rate response (multiple LFR) and a fluence rate-dependent high irradiance response (HIR).[35,36] *Phy A* mutant shows only the R-HIR component and lacks the LFR response to red light. On the contrary, *phyB1* mutant lacks the R-HIR component. Etiolated *phyA phyB1* mutant lacks any detectable response. The absence

of phyB2 does not significantly affect the accumulation of anthocyanins.[36] Obviously, from these results, it is concluded that phyA mediates the LFR to red light, whereas phyB1 mediates the R-HIR. These conclusions were further supported by results obtained with a transgenic tomato line overexpressing the oat *PHYA3* gene.[55]

On the other hand, the results and the consequent attribution of distinct roles to specific phytochromes is completely different, if the seedlings are germinated and grown for several days under continuous red light.[36] The anthocyanin content of 12-day-old tomato hypocotyl is maximal in *phyA* mutant and low when phyB1 is absent alone or in combination with the absence of phyA and phyB2. Even in the absence of phyA and phyB2, the accumulation of anthocyanin is increased in comparison to WT. These results imply an antagonistic action of phyA toward phyB1 and a crucial promoting role of phyB1 on anthocyanin accumulation. The results obtained when phyB2 is absent, alone, or in combination with phyA or phyB1, confirm the negligible contribution of phyB2 under red light.

Continuous Far-Red Light

The dose response curves for anthocyanin accumulation under 24 h monochromatic far-red light, 708 and 728 nm, are similar in WT and *phyB1/phyB2* double mutant. Etiolated hypocotyls of *phyA* and *phyA/phyB1* mutants do not accumulate anthocyanins under a wide range of far-red light irradiance, confirming the need for phyA in FR-HIR mediated responses.[36]

Continuous Blue Light

The synthesis of anthocyanins in etiolated hypocotyl of tomato in response to 24 h irradiation with 10 μmol m^{-2} s^{-1} blue appears to be under the almost total control of phyA and cry1. In the double mutant *phyA/cry1*, there is a reduction of about 95% in anthocyanin accumulation in comparison to WT.[36] The two photoreceptors act additively but at different irradiance ranges: between 0.001 and 3 μmol m^{-2} s^{-1} phyA is the functional photoreceptor, whereas *cry1* is active at irradiances above 3 μmol m^{-2} s^{-1}, thus, providing tomato plants with a wide range of sensitivity to blue light. The effect of *phyB1* is small, and it is manifested only at high irradiances. The effect of *phyB2* is negligible on WT background, but it becomes substantial at high irradiance, when *phyA/phyB1* and *phyA/phyB1/phyB2* mutants are compared. In the quadruple mutant *phyA/phyB1/phyB2/cry1*, there is no measurable synthesis of anthocyanin in response to blue light.[36]

Continuous UV Radiation

The effect of UV radiation on the production of anthocyanins and UV-absorbing compounds was characterized in etiolated hypocotyls of wild-type and *au* mutant tomato seedlings.[65] Only prolonged exposures to UV radiation induce low but detectable levels of anthocyanins in the *au* mutant and large accumulation of the pigments in WT. Further to this, the differences in the time courses of UV-induced accumulation of anthocyanins and UV-absorbing compounds (putatively flavonoids and phenolic acids) indicate that different photoregulatory mechanisms are involved for each of these two groups of pigments.

The dramatic difference found between the wild-type and the *au* mutant strongly indicates the involvement of phytochromes as functional photoreceptors for the photoinduction of anthocyanin accumulation in tomato hypocotyls. The UVB photoreceptor could only marginally replace the action of phytochrome (as far as anthocyanin accumulation is concerned) when the functional phytochrome pool is missing, as in the *au* mutant. The general picture of UV-mediated induction of UV-absorbing compounds shows only one macroscopic difference between wild-type and the *au* mutant of tomato: the higher initial level (in darkness) of these compounds in the wild-type in comparison to the *au* mutant. There is substantial UV-induced accumulation of UV-absorbing compounds in both genotypes, and the largest increment is displayed by *au* mutant, even though the levels in the *au* mutant never reach those of the WT under the same UV exposure. Therefore, the fact that an UVB-absorbing photoreceptor is able to establish high responsiveness for the UV-induced flavonoid accumulation, even in the absence of three phytochromes, i.e., in the *au* mutant, strongly indicate that a UVB photoreceptor plays a crucial role in the photoregulation of UV-absorbing compound accumulation. It appears that in WT hypocotyls,

several photosensors could be involved, while in the *au* mutant, the massive accumulation of UV-absorbing compounds is mediated mainly by a UVB photoreceptor, and the absence of functional phytochromes determines an increase of the effectiveness of UVB photoreceptor.

Tomato seedlings de-etiolated under monochromatic yellow light showed a significant enhancement of shorter UVB wavelength efficiency in production of UV-absorbing compounds in *au* mutant and WT.[63] Irradiation from sowing time, with yellow light, which establishes a high phytochrome photoequilibrium, shortens the apparent lag phase and increases the rate of pigment accumulation, probably through a phytochrome-mediated increase of responsiveness to UVB radiation. The fact that de-etiolated seedlings show faster and enhanced responses, mainly to the shorter wavelengths and, therefore, to the potentially most damaging UV radiation, indicates that the interaction between phytochrome and UVB photoreceptor may have crucial adaptive functions.

Photocontrol of Nuclear Structure of Tomato Hypocotyl

Etiolated hypocotyl of 4-day-old tomato seedlings of WT and *au* mutant of tomato, show different frequencies of chromosome endoreduplication.[66] The cultivar UC-105 (WT) presents a mean cell ploidy level lower than *au*. This could be due to the phytochrome content in the seed, which is very low in the *au* mutant compared to WT, cv. UC-105. It was shown that dry tomato seeds contain physiological levels of phytochrome, and seeds germinating in the dark show 40% of phytochrome in the active Pfr form.[41] Thus, active Pfr in the seed might prevent chromosome endoreduplication during the first phases of germination.

Exposures of 4-day-old tomato seedlings, WT and *au* mutant, to UV or white light influence chromosome endoreduplication and chromatin conformation differently in the two genotypes.[66] A 3 h white light treatment has no effect on the mean ploidy level in the WT, but it increased the ploidy level in the *au* mutant. Therefore, it may be concluded that in the WT, fluorescent white light (mainly blue + red wavebands) has no effect on ploidy levels because of antagonistic effects of different photoreceptors (phytochromes and blue photoreceptors). In fact, in the *au* mutant (which at seedling stage has undetectable phytochrome levels), white light induces higher ploidy levels than darkness, probably because of the action of blue-light photoreceptors, which in this mutant are not opposed by phytochrome. Only in the WT, compared to darkness or white light, are higher ploidy levels induced after exposure to UV for 3 h. The fact that in the *au* mutant UV radiation induces the same chromosome endoreduplication as white light, indicates that the UV effect may be due again to the action of cryptochromes, which are activated by the blue-UVA energy emitted by the UV source or by the action of a specific UVB photoreceptor. White light and UV transiently increased heterochromatin amounts only in the diploid nuclei of WT. It is, therefore, suggested that this response is mediated by phytochrome, because it is lacking in the *au* mutant.

Photocontrol of Regenerative Capability from Tomato Hypocotyl

In tomato hypocotyl, the transition from a genetically totipotent vascular parenchyma cell to different stages of a committed cell, and the subsequent ontogeny of an adventitious shoot, involves developmental events with a molecular nature that is still mostly unknown.[67] Formation of adventitious buds from hypocotyl segments occurs in hormone-free medium, and light is essential during the *in vitro* culture. Hormones added to the growing medium cannot overcome the need for light of hypocotyl explants.[67–70] In tomato hypocotyl, the frequency of shoot formation depends also on light conditions during seedling growth preceding the *in vitro* culture and on the cell's position along the hypocotyl.[70] Light-dependent acquisition of competence is acquired before the transfer of explants *in vitro*. The comparison of the photoregulation of *in vitro* shoot formation from excised hypocotyl of *phyA* and *phyB1* mutants of tomato and their wild-type indicates that the light-dependent acquisition of competence for shoot regeneration in tomato hypocotyl is controlled only by the phytochrome system, and it is mediated at least by two distinct phytochrome species: phyB1 and phyA.[70] The action of phyB1 during seedling growth appears

to be essential, and the lower regenerative capability of middle and basal explants of tomato hypocotyl appears to correlate with phyB1 levels. Furthermore, it appears that phyA and phyB1 are not necessary for LFR- and VLFR-induced acquisition of competence in apical segments of hypocotyl, whereas they are essential for the VLFR of middle and basal segments.[18] The blue-light induction of competence for shoot regeneration does not appear to involve the cryptochrome family, rather it appears to be mediated by the phytochrome system as well. A network of photoreceptor interactions coupled to the effects of the wounds, made to separate the hypocotyl segment hypocotyl, plays a pivotal role in the acquisition of competence for shoot formation and, subsequently, on the expression of this developmental potential.

Photocontrol of Stem Elongation of Green Mature Tomato Plants

The kinetics of stem elongation of 3- to 4-week-old tomato plants were studied by using linear voltage transducers connected to personal computers.[71–73] Thanks to the high sensitivity of the transducers, it was possible to characterize accurately and for several days the time courses of light-induced changes of stem growth in the same tomato plant by measuring: very fast growth responses (in the order of a few minutes); very slow responses (in the order of hours and days); short- and long-lasting responses; and the specific light effects on the different growth phases occurring in the presence of light and in darkness during the daily cycle.

Kinetics of Stem Elongation under 12 h White Light/12 h Dark Cycles

The analysis of short- and long-term stem elongation responses of WT and *au* mutant tomato plants to different photosynthetically active radiation (PAR) provided novel information about stem elongation, even in light conditions similar to those found in the greenhouse by tomato crops.[71] WT plants display PAR-dependent (in the range of 100 to 800 μmol $m^{-2}s^{-1}$) inhibition of growth during the day and during the night. In contrast, the *au* mutant shows a fluence-rate-dependent promotion of growth during the dark periods, in the range of 10 to 400 μmol $m^{-2}s^{-1}$. Large, fast, and opposite changes in stem elongation rate at the light–dark and dark–light transitions are present in both genotypes. The internode elongation rate in the first half of the night is always modest in WT tomato, whereas it increases rapidly in the *au* mutant. Stem elongation rate of WT starts to increase after about 6 h in darkness, showing the typical time course of escape from Pfr-mediated inhibition of elongation by an end-of-day response. Measurements of leaf gas exchange parameters showed no significant differences in all the photosynthetic quantities between WT and *au* mutant, in the range between 100 and 800 μmol $m^{-2}s^{-1}$ PAR. However, PAR levels influence the stem elongation of the two genotypes differently. Even though an adequate photosynthetic level plays a central role in stem growth, the similar photosynthetic behavior of the WT and *au* mutant suggests that photomorphogenic responses are responsible for the differences between the two genotypes. The fluence-rate-dependent inhibition of stem growth is absent in *au* mutant plants also at fluence rates of white light as high as 800 μmol $m^{-2}s^{-1}$. The absence or reduction of fluence-rate-dependent inhibition of stem growth in light-grown and etiolated *au* mutants strongly suggests that phytochrome is one of the functional photoreceptors sensing light quantity in etiolated and in green plants.[71] The PAR-dependent reduction of internode growth displayed during the dark periods by WT tomato is totally absent in the *au* mutant and is, therefore, likely regulated by some of the lacking phytochromes. It appears, therefore, that the fluence-rate-dependent inhibition of stem elongation found in WT plants during the dark period could be the result of an HIR-induced increase in effectiveness of end-of-day response of phytochrome. The fluence-rate-dependent inhibition of elongation in the WT during the light periods might be due to an HIR response that is overriding the promotion of growth induced by the large pool of photosynthates available for stem growth. No PAR-dependent inhibition of elongation was found in the mutant, even at a fluence rate as high as 800 μmol $m^{-2}s^{-1}$. If we take into account that the light-grown *au* mutant contains 60% of the phytochrome found in the WT,[48] and if a direct relationships exists between concentration of phytochrome and extent of the response, the effect of irradiations with 800 μmol $m^{-2}s^{-1}$ on *au* mutant should be similar to that of 480 μmol $m^{-2}s^{-1}$ on WT.

The results presented by Bertram and Lercari[71] show that dose-response curves differ significantly from that expected from these calculations. Therefore, the difference between the two genotypes cannot be explained only on the basis of phytochrome content. Rather, they suggest that the *au* mutant is lacking the fluence-rate-dependent response not because it has a lower concentration of phytochrome, but because it is missing the phytochrome type involved in sensing light quantity. On the other hand, if all functional photoreceptors for the regulation of stem growth were missing in the *au* mutant, one should expect larger growth with higher PAR also during the light period, but this is not the case. Therefore, besides phytochrome, even the blue-light-absorbing photoreceptor is involved in the fluence-rate-dependent photoregulation of stem growth of tomato during the light period.

Kinetics of Stem Elongation following Transfer in Continuous Darkness

Substantial differences in stem growth of green tomato plants transferred to continuous darkness were displayed by different genotypes, showing the decreasing order: *phyB1* > WT = *phyA* > *au* > *hp1*.[73] The differences of stem growth in darkness are due to two factors: the different stem elongation rate and the different duration of the growing phase among the genotypes. In darkness, the stem growth of *au* and *hp1* mutants lasted for about 18 h, whereas it continued for the whole experimental period (36 h) in the other genotypes.

Kinetics of Stem Elongation under Continuous UV Radiation

The UVB irradiation drastically reduced stem growth of 21-day-old tomato plants (4.5 μmol $m^{-2}s^{-1}$ being more effective than 0.1 μmol $m^{-2}s^{-1}$).[73] Both irradiances of UVB induced a detectable reduction of SER after 15 min of irradiation. *PhyA*, *phyB1*, and WT tomato showed similar UVB-induced inhibition of growth, confirming the previous conclusion that UVB-induced inhibition of stem growth in tomato is not mediated by phytochrome.[61,62] Consistent with the above-mentioned results, the *hp1* mutant showed responsiveness to UVB similar to that shown by WT, *phyA*, and *phyB1* mutants.[73] The *au* mutant showed the highest UVB-induced growth inhibition during the 12 h of irradiation with both fluence rates, further confirming that UVB-induced inhibition of stem growth in tomato does not involve phytochrome. The results of dichromatic irradiations UVB + red or UVB + far-red indicate the presence of an addictive effect of UVB photoreceptor and the phytochrome system.

Phytochrome and Tomato Fruit Ripening

Already in 1954, Piringer and Heinze[74] showed that harvested mature-green tomato fruits accumulate a yellow pigment (putatively flavonoids) following a daily exposure of a few minutes to red light. The promoting effect of red-light pulse was almost completely reversed by a following irradiation with far-red light, which is classical evidence for a LFR of phytochrome. The promoting role of the phytochrome system was further supported by a genetic dissection. The *hp1* mutant showed a 13-fold increase in quercetin accumulation in comparison to WT.[53] A comparison of flavonoids content in WT (Money Maker), phyA, phyB1, and *au* mutants grown in a glasshouse, showed the following decreasing order: MM > phyA > phyB1 > *au* (Lercari unpublished data). These different amounts of total flavonoids are resultant of the differences in the patterns of accumulation of distinct molecular species: rutin is the main flavonoid found in MM and phyA, whereas naringenin is the one most present in phyB1 and *au*. The concentration of rutin and quercetin followed the same order: MM > phyA > phyB1 > *au*, whereas narigenin showed the opposite order: *au* > phyB1 > phyA > MM (Lercari, unpublished results). It appears, therefore, that distinct phytochromes can control the accumulation of different flavonoids in tomato fruits.

The fruit of the mutant *hp1* contains enhanced levels of carotenoids and sucrose in comparison to wild-type. Alba et al.[75] demonstrated that fruit-localized phytochromes control lycopene accumulation in tomato pericarp during fruit ripening but do not regulate ethylene biosynthesis and many other aspects of fruit ripening in tomato. Their obvious conclusion was that fruit-localized phytochromes are not global regulators of tomato fruit ripening.

131.5 Conclusions

From the few examples presented in this review and from many other data present in the pertinent literature, it appears that different phytochromes can have distinct functions, and that they act additively or antagonistically toward each other according to their localization in the cell, to cell position in the plant, to the moment of the day, to previous plant history, and to present environmental conditions. Furthermore, it is well established that in tomato, blue light substantially influences the effectiveness of phytochrome-dependent responses. On the other hand, light, acting through phytochrome, enhances the responsiveness of tomato cells to UVB photoreceptor signals. Therefore, by using mutants, which are supposed to provide a simplified experimental system, because they lack one or more component of light signaling, a complex web of signaling networks, which provide tomato plants and likely all the other green plants with an enormous flux of information about the surrounding environment, was unraveled. The continuous input of information-producing signals moving in the signaling web allows for continuous and fine-tuning of plant growth and development. The interacting genes and gene products, creating a complex but flexible, unstable network interposed between the unitary genetic element and the phenotype (epistasis, polygenic, and pleiotropic effects) are integrated with networks that transduce a plethora of internal and external signals.[76] The identification and characterization of "check points" of signal fluxes will probably provide new insight on the mechanisms controlling plant growth and development.

Acknowledgments

We are most grateful to R.E. Kendrick for providing most of the seeds of mutants discussed in this chapter. We appreciate the copyright permission granted from the American Society for Photobiology for the paper.[71]

References

1. Garner, W.W. and Allard, H.A., Effect of the relative length of day and night and other factors of the environment on growth and reproduction in plants, *J. Agr. Res.*,18, 553, 1920.
2. Flint, L.H. and McAlister, E.D., Wavelength of radiation in the visible spectrum inhibiting the germination of light-sensitive lettuce seed, *Smithsonian Inst. Publ. Misc. Coll.*, 94, 1, 1935.
3. Neff, M.N., Frankhauser, C., and Chory, J., Light: an indicator of time and place, *Genes & Develop.*, 14, 257, 2000.
4. McNellis, T. and Deng, X.W., Light control of seedling morphogenetic pattern, *The Plant Cell.*, 7, 1749, 1995.
5. Briggs, W.R. and Olney, M.A., Photoreceptors in plant photomorphogenesis to date. Five phytochromes, two Cryptochromes, one phototropin, and one superchrome, *Plant Physiol.*, 125, 85, 2001.
6. Chory, J. and Wu, D., Weaving the complex web of signal transduction, *Plant Physiol.*, 125, 77, 2001.
7. Sharrock, R.A. and Quail, P.H., Novel phytochrome sequences in *Arabidopsis thaliana*: structure, evolution and differential expression of a plant regulatory photoreceptor family, *Genes Dev.*, 3, 1745, 1989.
8. Clack, T., Mathews, S., and Sharrock, R.A., The phytochrome apoprotein family in *Arabidopsis* is encoded by five genes: the sequences and expression of PHYD and PHYE, *Plant Mol. Biol.*, 25, 413, 1994.
9. Hauser, B.A., Cordonnier-Pratt, M.-M., Daniel-Vedele, F., and Pratt, L.H., The phytochrome gene family in tomato includes a novel subfamily, *Plant Mol. Biol.*, 29, 1143, 1995.
10. Frankhauser, C. et al., PKS1, a substrate posphorylated by phytochrome that modulates light signaling in *Arabidopsis, Science*, 284, 1539, 1999.

11. Nagy, F. and Schäfer, E., Nuclear and cytosolic events of light-induced phytochrome-regulated signaling in higher plants, *EMBO J.*, 19, 157, 2000.
12. Bowler, C., Neuhaus, G., Yamagata, H., and Chua, N.-H., Cyclic GMP and calcium mediate phytochrome phototransduction, *Cell*, 77, 73, 1994.
13. Furuya, M., Phytochromes: their molecular species, gene family and functions, *Annu. Rev. Plant Physiol. Plant Mol. Biol.*, 44, 617, 1993.
14. Mancinelli, A.L., The physiology of phytochrome action, in *Photomorphogenesis in Plants*, 2nd ed., Kendrick, R.E. and Kronenberg, G.H.M., Eds., Kluwer, Dordrecht, 1994, p. 211.
15. Quail, P.H. et al., Phytochromes: photosensory perception and signal transduction, *Science*, 268, 675, 1995.
16. Pratt, L.H., Cordonnier-Pratt, M.-M., Hauser, B., and Caboche, M., Tomato contains two differentially expressed genes encoding B-type phytochromes, neither of which can be considered an ortholog of *Arabidopsis* phytochrome B. *Planta*, 197, 203, 1995.
17. Kendrick, R.E., Kerckhoffs, L.H.J., Van Tuinen, A., and Koornneef, M., Photomorphogenetic mutants of tomato, *Plant Cell Environ.*, 20, 746, 1997.
18. Lercari, B., Manetti., A., and Bertram, L., Temporal and spatial pattern of light-dependent acquisition of competence for shoot formation in tomato hypocotyl. I. Light pulse conditions, *Adv. Hort. Sci.*, 16, 17, 2002.
19. Mathews, S. and Sharrock, R.A., Phytochrome gene diversity, *Plant Cell Environ.*, 20, 666, 1997.
20. Alba, R., Kelmenson, P.M., Cordonnier-Pratt, M.-M., and Pratt, L.H., The phytochrome family in tomato and the rapid differential evolution of this family in angiosperms, *Mol. Biol. Evol.*, 17, 362, 2000.
21. Briggs. W.R. and Huala, E., Blue-light photoreceptors in higher plants, *Annu. Rev. Cell. Dev. Biol.*, 15, 33, 1999.
22. Lorenzi, R., Ceccarelli, N., Lercari, B., and Gualtieri, P., Identification of retinal in higher plants: is a rhodopsin-like protein the blue light receptor? *Phytochemistry*, 36, 599, 1994.
23. Galston, A.W., Riboflavin, light, and the growth of plants, *Science*, 111, 619, 1950.
24. Cashmore, A.R. et al., Chryptochromes: blue light receptors for plants and animals, *Science*, 284, 760, 1999.
25. Lin, C. et al., Expression of an *Arabidopsis* cryptochrome gene in transgenic tobacco results in hypersensitivity to blue, UV-A, and green light, *Proc. Natl. Acad. Sci. USA*, 92, 8423, 1995.
26. Lin, C., Enhancement of blue-light sensitivity of *Arabidopsis* seedlings by a blue-light receptor Chryptochrome 2, *Proc. Natl. Acad. Sci. USA*, 95, 2686, 1998.
27. Somers, D.E., Devlin, P.F., and Kay, S.A., Phytochromes and chryptochromes in the entrainment of the *Arabidopsis* circadian clock, *Science*, 282, 1488, 1998.
28. Guo, H. et al., Regulation of flowering time by *Arabidopsis* photoreceptors, *Science*, 279, 1360, 1998.
29. Imaizumi, T., Kanegae, T., and Wada, M., Cryptochrome nucleocytoplasmatic distribution and gene expression are regulated by light quality in the fern *Adiantum capillus-veneris*, *Plant Cell*, 12, 81, 2000.
30. Liscum, E. and Briggs, W.R., Mutations in the NPH1 locus of Arabidopsis disrupt the perception of phototropic stimuli, *Plant Cell*, 7, 473, 1995.
31. Hauser, B.A., Pratt, L.H., and Cordonnier-Pratt, M.M., Absolute quantification of five phytochrome transcripts in seedlings and mature plants of tomato (*Solanum lycopersicum* L.), *Planta*, 201, 379, 1997.
32. Pratt, L.H. et al., The phytochrome gene family in tomato (*Solanum lycopersicum* L.), *Plant, Cell Environ.*, 20, 672, 1997.
33. Hauser, B., Cordonnier-Pratt, M.-M., and Pratt, L.H., Temporal and photoregulated expression of five tomato phytochrome genes, *Plant J.*, 14, 431, 1998.
34. Perrotta, G. et al., Tomato contains homologues of *Arabidopsis* cryptochromes 1 and 2. *Plant Mol. Biol.*, 42, 765, 2000.

35. Weller, J.L. et al., Physiological interactions of phytochrome A, B1 and B2 in the control of development in tomato, *Plant J.*, 24, 245, 2000.
36. Weller, J.L. et al., Genetic dissection of blue-light sensing in tomato using mutants deficient in cryptochrome 1 and phytochromes A, B1 and B2, *Plant J.*, 25, 427, 2001.
37. van Tuinen, A. et al., The mapping of phytochrome genes and photomorphogenic mutants of tomato, *Theor. Appl. Genet.*, 94, 115, 1997.
38. Lazarova, G.I. et al., Molecular analysis of PHYA in wild-type and phytochrome A-deficient mutant of tomato, *Plant J.*, 14, 653, 1998.
39. Lazarova, G.I. et al., Characterization of tomato PHYB1 and identification of molecular defects in four mutant alleles, *Plant Mol. Biol.*, 38, 1137, 1998.
40. Kerckhoffs, L.H.J. et al., Characterization of the gene encoding the apoprotein of phytochrome B2 in tomato, and identification of molecular lesions in two mutant alleles, *Mol. Gen. Genet.*, 261, 901, 1999.
41. Mancinelli, A.L., Yaniv, Z., and Smith, P., Phytochrome and seed germination. I. Temperature dependence and relative P_{fr} levels in the germination of dark-germinating tomato seeds, *Plant Physiol.*, 42, 333, 1967.
42. van Tuinen, A. et al., Far-red light-insensitive, phytochrome A-deficient mutants of tomato, *Mol. Gen. Genet.*, 246, 133, 1995.
43. Kerckhoffs, L.H.J. et al., Molecular analysis of *tri*-mutant alleles in tomato indicates the *TRI* locus is the gene encoding the apoprotein of phytochrome B1, *Planta*, 199, 152, 1996.
44. Ninu, L. et al., Cryptochrome 1 controls tomato development in response to blue light, *Plant J.*,18, 551, 1999.
45. Boylan, M.T. and Quail, P.H., Oat phytochrome is biologically active in transgenic tomatoes, *Plant Cell*, 1, 765, 1989.
46. Terry, M.J., Phytochrome chromophore-deficient mutants, *Plant, Cell Environ.*, 20, 740, 1997.
47. Kerckhoffs, L.H.J., Physiological functions of phytochromes in tomato: a study using photomorphogenic mutants, Ph.D. thesis. Wageningen Agricultural University, The Netherlands.
48. López-Juez, E. et al., Response of light-grown wild-type and *aurea*-mutant tomato plants to end-of-day far-red light, *J. Photochem. Photobiol. B*, 4, 391, 1990.
49. Sharma, R. et al., Identification of photo-inactive phytochrome A in etiolated seedlings and photoactive phytochrome B in green leaves of the *aurea* mutant of tomato, *Plant J.*, 4, 1035, 1993.
50. Adamse, P. et al., Photophysiology of a tomato mutant deficient in labile phytochrome, *J. Plant Physiol.*, 133, 436, 1988.
51. Lipucci di Paola, M. et al., A phytochrome mutant from tissue culture of tomato, *Adv. in Hort. Sci.* 2, 30, 1988.
52. Neuhaus, G., Bowler, C., Kern, R., and Chua, N.-H., Calsium/Calmodulin-dependent and -independent phytochrome signal transduction pathways, *Cell*, 73, 937, 1993.
53. Yen, H.C. et al., The tomato *high-pigment* (*hp*) locus maps to chromosome 2 and influences plastome copy number and fruit quality, *Theor. Appl. Genet.*, 95, 1069, 1997.
54. Peters, J.L. et al., High-pigment mutants of tomato exhibit high sensitivity for phytochrome action, *J. Plant Physiol.*, 134, 661, 1989.
55. Kerckhoffs, L.H.J. et al., Phytochrome control of anthocyanin biosynthesis in tomato seedlings: analysis using photomorphogenic mutants, *Photochem. Photobiol.*, 65, 374, 1997.
56. Mustilli, A.C. et al., Phenotype of the tomato *high pigment-2* mutant is caused by mutation in the tomato homolog of *Deetiolated* 1, *Plant Cell*, 11, 145, 1999.
57. Mancinelli, A.L., Borthwick, A.H., and Hendricks, S.B., Phytochrome action in tomato-seed germination, *Bot. Gaz.*, 127, 1, 1966.
58. Lercari, B. and Lipucci di Paula, M., Photoregulation of seed germination of wild-type and of an *aurea*-mutant of tomato, *Physiologia Plantarum*, 83, 265, 1991.
59. Lercari, B., Photoregulation of germination in osmoconditioned tomato seed, *Adv. Hort. Sci.*, 5, 112, 1991.

60. Shichijo, C., Katada, K., Tanaka, O., and Hashimoto, T., Phytochrome A-mediated inhibition of seed germination in tomato, *Planta*, 213, 764, 2001.
61. Lercari, B., Sodi, F., and Lipucci di Paola, M.L., Photomorphogenic responses to UV radiation: involvement of phytochrome and UV photoreceptors in the control of hypocotyl elongation in *Lycopersicon esculentum*, *Physiol. Plant*, 79, 668, 1990.
62. Lercari, B. and Sodi, F., Photomorphogenic responses to UV radiation. II: A comparative study of UV effects on hypocotyl elongation in a wild-type and an aurea mutant of tomato (*Lycopersicon esculentum* Mill.), *Photochem. Photobiol.*, 56, 651, 1992.
63. Lercari, B. and Bertram, L., Photomorphogenic responses to UV radiation IV: A comparative study of UVB effects on growth and pigment accumulation in etiolated and de-etiolated hypocotyls of wild-type and *aurea* mutant of tomato (*Lycopersicon esculentum* Mill.), *Plant Biosyst.*, 13, 83, 1997.
64. Drumm-Herrel, H. and Mohr, H., Effect of blue/UV light on anthocyanin synthesis in tomato seedlings in the absence of bulk carotenoids, *Photochem. Photobiol.*, 36, 229, 1982.
65. Brandt, K., Giannini, A., and Lercari, B., Photomorphogenetic responses to UV radiation III: A comparative study of UVB effects on anthocyanin and flavonoid accumulation in wild-type and *aurea* mutant of tomato (*Lycopersicon esculentum* Mill.), *Photochem. Photobiol.*, 62, 1081, 1995.
66. Cavallini, A. et al., White and UV light effects on cell nuclei in the aurea genotype of *Lycopersicon esculentum* M., *Cytobios*, 104, 83, 2001.
67. Pugliesi, C. et al., A histological study of light-dependent shoot regeneration in hypocotyl explants of tomato cultured *in vitro*, *Adv. Hort. Sci.*, 13, 168, 1999.
68. Lercari, B. et al., Photomorphogenic control of shoot regeneration from etiolated and light-grown hypocotyls of tomato, *Plant Sci.*, 140, 53, 1999.
69. Lercari, B. et al., Photocontrol of shoot regeneration from hypocotyls of tomato, in *Plant Biotechnology and In Vitro Biology in the 21st Century*, Altman, A. et al., Eds., Kluwer, Dordrecht, 1999, pp. 69.
70. Bertram, L. and Lercari, B., Phytochrome A and phytochrome B1 control the acquisition of compentence for shoot regeneration in tomato hypocotyl, *Plant Cell Reports*, 19, 604, 2000.
71. Bertram, L. and Lercari, B., Kinetics of stem elongation in light grown tomato plants. Responses to different photosynthetically active radiation levels by wild type and *aurea* mutant tomato, *Photochem. Photobiol.*, 66, 396, 1997.
72. Kerckhoffs, L.H.J., Sengers, M.M.T., and Kendrick, R.E., Growth analysis of wild-type and photomorphogenetic-mutant tomato plants, *Physiologia Plantarum*, 99, 309, 1997.
73. Bertram, L. and Lercari, B., Evidence against the involvement of phytochrome in UVB-induced inhibition of stem growth in green tomato plants, *Photos. Res.*, 64, 107, 2000.
74. Piringer, A.A. and Heinze, P.H., Effect of light on the formation of a pigment in the tomato fruit cuticle, *Plant Physiol.*, 29, 467, 1954.
75. Alba, R., Cordonnier-Pratt, M.-M., and Pratt, L.H., Fruit-localized phytochromes regulates lycopene accumulation independently of ethylene production in tomato, *Plant Physiol.*, 123, 363, 2000.
76. Trewavas, A.J. and Malhò, R., Signal perception and transduction: the origin of the phenotype, *Plant Cell*, 9, 1181, 1997.

132

Phototropism

Paul Galland
Philipps Universität

0-8493-1348-1/04/$0.00+$1.50

132.1 Introduction

Plants and fungi are capable of directing their growth toward or away from light. The phenomenon of oriented plant growth, including phototropism, has been known for centuries, if not millennia. Common people as well as great luminaries from the sciences and arts commented about it or made it the subject of elaborate investigations. Theophrastos (372 to 287 BC), a pupil of Aristotle and acknowledged founder of botany, reported on this and related phenomena, such as leave movements in his volumes, *Inquiry into Plants* and *Growth of Plants*. One may safely conclude that astute observers as the Arabian scientist Hanifa Ad-Dinawari (d. 895 AD) and Albertus Magnus (1200 to 1280), both of whom described the nyktinastic movements of leaves and petals,[1] were also aware of phototropism without explicitly describing it. The well-known sun tracking of sunflowers was mentioned by the French playwright, Jean-Baptiste Molière (1622 to 1673), in his play "Le malade imaginaire."[2]

Altar paintings of the 15th and 16th century are a rich source of plant pictures. While most of these paintings are sufficiently precise to allow their identification, very few, alas, depict the physiological properties of plants. The cathedral of Ghent houses the painting "The adoration of the lamb" (about 1430) by the brothers Hubert and Jan Eyck, in which several inflorescences of the Salomon's seal (*Polygonatum odoratum*) show clear phototropic orientation. The most impressive display of phototropisms of various flowers and shrubs can be found in the painting "Madonna in the grotto" (Louvre, Paris) by Leonardo da Vinci (1452 to 1519). The depicted setting, which is rich in shaded and bright areas including sunflecks, clearly provides the asymmetric illumination required for phototropic bending. That the depicted growth pattern is not accidental is further proven by the fact that Leonardo comments in one of his scientific diaries on the light-seeking and directed growth of tree branches.

Systematic studies of phototropism appear with the beginning of the 19th century. As early as 1817, the Italian Poggioli succeeded in showing that seedlings of *Brassica* and *Raphanus* bend more effectively to blue than to red light.[2] His study represents the first attempt to generate a crude action spectrum. Early investigators were greatly influenced by the developments in physics and photochemistry. Wiesner, who was among the first to use a clinostat and who wrote probably the first long treatise on phototropism,[3] emphasized that the photochemical processes in the plant should obey, in principle, the same physicochemical laws that were described by Bunsen and Roscoe for photochemical reactions of the gases Cl_2 and H_2.[3] Particularly the Bunsen–Roscoe law of reciprocity, which was originally described for the photochemical reactions occurring upon exposure of camera films, had a great impact on the early and later physiologists and is one major reason why investigations of dose-response relationships are usually performed with pulse stimuli rather than with long-term irradiations. In 1878, Vines published the first study on the phototropism of a single-celled organism, the zygomycete *Phycomyces*,[3] after Wilhelm Hoffmeister mentioned in 1867 the phenomenon in his textbook *Die Pflanzenzelle*. The most famous and still quoted work of this period is, however, the book by Charles and Francis Darwin from 1880, *The Power of Movement in Plants*, which includes numerous classic observations including the tip light sensitivity of grass coleoptiles and the distinction between signal perception and signal transduction.

With the discovery of auxins in the 1920s, the field was largely dominated by biochemical and physiological analyses of this growth regulator. The systematic application of action spectroscopy during the second half of the 20th century led to the recognition that phototropisms as well as numerous reactions of photomorphogenesis are controlled by one or more ubiquitous blue-light photoreceptors, since 1980 often called cryptochromes. For several of these investigators, phototropism has been mainly a tool rather than the prime motivation for hunting the then-elusive blue-light receptors. With the isolation of Cryptochrome 1 in 1993 by Ahmad and Cashmore[4] and of phototropin in 1998 by Briggs and associates,[5] rapid advances were made in the blue-light field, which has become amenable to detailed photophysical analysis at the molecular and atomic levels.

Major treatises on phototropism are available for every decade of the past 100 years, so that interested readers can easily get access to historical aspects.[2,6,7] The reviews by du Buy and Nuernbergk[3] cover *in extenso* the literature of the 20th, 19th, and even earlier centuries. The most recent and detailed treatise on phototropism is that by Iino.[8]

132.2 Relation between Phototropism and Growth

Phototropism of Bowing Organisms Requires the Differential Modulation of Growth Rates

Phototropism, the directed growth toward or away from the light source, can be caused by bulging or by bowing (bending). Bulging is typical for moss and fern protonemata, which reorient the apical growth point in response to unilateral light in such a way that the axis of the cells is aligned to the light beam. No differential growth rates of the cell walls are required in this case. Bowing or bending is typical for multicellular organs, such as seedlings, grass coleoptiles, roots, and macromycete fungi, as well as single-celled sporangiophores of the zygomycete fungi, *Phycomyces* and *Pilobolus*. In these organisms, phototropism is caused by differential growth rates of the organ sides proximal and distal to the light source. During bending, the growth rate of the proximal side can be retarded, while the distal side is accelerated relative to the time prior to unilateral irradiation. Such a symmetric redistribution of growth rates was observed for *Zea* coleoptiles, *Pisum* epicotyls, and for sporangiophores of *Phycomyces.*[6,7,9,10] For phototropism to occur, however, it is sufficient if the growth rate of only one side is modulated. For example, when *Avena* coleoptiles are irradiated continuously from one side, then the growth of the proximal side can be arrested completely, while the distal side continues to elongate with the same growth rate.[6,7]

Light-Growth and Dark-Growth Responses: The Phototropism Paradox

Phototropism is related to the so-called light-growth and dark-growth responses that represent transient modulations of the growth rates in response to symmetric or even asymmetric changes of irradiance. In *Avena* coleoptiles, a step up of the fluence rate causes a transient diminution of the growth rate that lasts about 40 min.[10] In *Phycomyces*, a step up of the irradiance elicits a transient increase of the growth rate that subsides after some 40 min.[9,10] A step down of the fluence rate causes in grass coleoptiles a transient increase and in *Phycomyces* a transient decrease of the growth rate.[9,10] The described transient growth responses are not related to the well-known light-induced growth inhibition of hypocotyl growth, which is a nonadaptive response and is not related to phototropism. One can, for example, kinetically separate the phototropism of *Cumumis* seedlings from the blue-light-induced inhibition of stem elongation.[10]

Mutants that affect the phototropism of *Phycomyces* affect, at the same time, the light- and dark-growth responses.[9] The growth responses are thus mechanistically related to phototropism. A fundamental difference between the two responses is that the growth responses are adaptive, while the phototropism is not. With special mechanical devices such as a tropostat,[9] the phototropism can be maintained almost indefinitely, showing that the redistribution of growth rates is nonadaptive. The phototropism paradox appears to hold for all phototropic organisms. The solution of the paradox requires the postulate of "cross-talk" between the proximal and distal sides of the bending organ. Localized autonomous growth reactions cannot possibly explain phototropism, because bending would subside due to the adaptive properties of the growth reactions.

132.3 Perception of Light Direction

Phototropism Requires Spatial Irradiance Differences

A prerequisite for the establishment of differential growth rates is an internal asymmetry of irradiance inside the bending organ. For opaque plant organs like hypocotyls or grass coleoptiles, the proximal side receives a higher irradiance than the distal one. The opaqueness of the material generates a light gradient that translates into differential growth rates. Carotenoids, which contribute to the opaqueness of *Zea* coleoptiles, cause a steeper light gradient and increase, at the same time, the phototropic responsiveness but not, however, the absolute sensitivity.[7,10] It is immaterial how the irradiance difference is generated. One can, for example, irradiate *Avena* coleoptiles with light guides from inside or irradiate only one half

of the organ from above.[2,6–8] Split-field irradiation with filaments of *Vaucheria geminata* yielded similar results, because the filaments always bend to the side of the irradiated area.[2] These experiments demonstrate that the bending organs sense the irradiance difference between the irradiated and the shaded side rather than sense the direction of the light source.

In the transparent sporangiophore of *Phycomyces*, the irradiance difference is caused by its lens property that leads to focusing of unilateral light in a bright band on the distal side. The elevated irradiance in the focal band is responsible for the elevated growth rate at the distal side, causing positive phototropism.[9] Lens effects that are relevant for phototropism also occur in other hyaline cells, such as in chloronemata of ferns and mosses.

The minimal difference of two opposed light sources that can induce bending is called the discrimination threshold. For *Phycomyces*, it is near 8%, while *Avena* coleoptiles can resolve a fluence difference of some 3 to 4%.[10]

Resultant Law

When a phototropic organism is irradiated asymmetrically with two light sources of equal intensity, it bends in a plane bisecting the angle that is formed by the organism and the light sources (Resultantengesetz, resultant law).[3] The zygomycete fungus, *Pilobolus*, is violating this law in that it bends to either one or the other light source, if they form an angle with the sporangiophore that is steeper than 7°.[3]

Polarotropism

Chloronemata of some algae, mosses, and ferns are able to react to plane polarized light. The organisms, which are typically cultured on an agar plate, are irradiated with polarized light from "above," i.e., in a plane perpendicular to the plane of growth. The chloronemata grow perpendicular to the plane of the electric vector of the incident polarized light. Rhizoids of *Dryopteris* grow, however, parallel to it.[2,6] The behavior is explained by the assumption that the photoreceptor is dichroic and localized in the plasmalemma. Depending on the orientation of the electrical vector, an asymmetric distribution of excited photoreceptors (phytochrome) is generated, which in turn, causes a reorientation of the growing tip. The polarotropism of chloronemata represents a special case in that an internal irradiance difference is absent. There is evidence that the photoreceptors of *Phycomyces* are also dichroically oriented.[2,10] In this organism, an internal irradiance asymmetry is, however, prerequisite for phototropic bending.

132.4 Perception of Temporal Irradiance Changes

Visual Range and Temporal Irradiance Changes

In nature, plants and fungi bend in an environment that is continuously changing with respect to irradiance. The internal spatial irradiance differences have, therefore, to be perceived on a fluctuating background. The organism must thus possess a mechanism that adjusts the prevailing sensitivity to the changing background irradiances (range adjustment). The visual range of phototropic organisms is enormous and can cover, as in the case of *Phycomyces*, more than 10 orders of magnitude (see below and Figure 132.2). The capacity for range adjustment is ascribed to sensory adaptation.[11,12] The status of the sensory adaptation (level of adaptation; can be inferred from the prevailing sensitivity that is defined as the reciprocal of the prevailing threshold, or from the phototropic latency, which is discussed below). The molecular mechanisms of sensory adaptation in plants and fungi are practically unknown. Mutant analysis in *Phycomyces* indicates that at least part of the sensory adaptation is processed at the level of the photoreceptor.[11,12]

Phototropic Latency

For dark-adapted organisms, the phototropic latency, i.e., the time that elapses between the onset of the unilateral light pulse and the first observable bending, depends over a wide range on the logarithm of

the fluence. This relationship was investigated for *Phycomyces* and *Avena* coleoptiles.[10] When the pre-adapting light and the unilateral stimulus light are of equal fluence rate, then the lag time is about 4 to 6 min for *Phycomyces*, the exact value depending also on the intensity range and wavelength.[9,11] For *Vaucheria*, the latency is about 1 to 2 min.[2]

Phototropic Dark and Light Adaptation

Beside the fluence of the actinic light, the phototropic latency largely depends on the light pretreatment prior to light stimulus. The light pretreatment determines the status of sensory adaptation, and the phototropic latency can be used to determine the level of adaptation. Protocols for the measurement of the so-called dark-adaptation kinetics employ basically the following treatment: the organisms are irradiated for a "long" time omnilaterally with blue light and are then exposed to unilateral light of variable irradiances of lower fluence rate than the adapting light (step down). The phototropic latency increases with the logarithm of the magnitude of the step down. When the fluence rate of the unilateral light that elicits phototropism is plotted versus the duration of the phototropic latency, one can reconstruct the kinetics of dark adaptation. *Phycomyces*, *Avena*, and *Zea* display for this type of protocol biexponential decay kinetics.[9,11,12]

Protocols for the measurement of light-adaptation kinetics that are based on the measurement of phototropic latencies are elaborate. These kinetics are much faster than the corresponding dark-adaptation kinetics. A characteristic feature of the kinetics for large steps up of the fluence rate is the fact that the level of adaptation appears to overshoot the actual fluence rate, a property that holds true for *Phycomyces* as well as for *Avena* coleoptiles.[10,11] For oat seedlings, there is evidence that the processes that entail sensory adaptation are related to the phosphorylation of the putative photoreceptor.[13]

132.5 Dependence on Irradiance

The irradiance dependence for phototropism can be tested with light pulses or with continuous irradiation. Phototropism was investigated mostly by employing pulses of unilateral light. Only few data exist for phototropism elicited by continuous irradiation. Long-term irradiation is more relevant to the irradiance conditions and responses prevailing in nature. On the other side, irradiation with light pulses has certain analytic advantages and is thus prevalent in the requisite literature.

Pulse-Induced Phototropism: Fluence-Response Curves

Fluence-response curves for the phototropism of grass coleoptiles are complex [Figure 132.1(A)]. For *Avena* coleoptiles, one can distinguish three distinct response types (nomenclature of Iino[7,8]): the first pulse-induced positive phototropism (fPIPP) (called first positive phototropism in the older literature), a pulse-induced negative phototropism (PINP), and the second pulse-induced positive phototropism (sPIPP) (second positive phototropism in the older literature). Provided the fluences are delivered in pulses of short duration (1 to 30 s), then reciprocity holds for the entire range, i.e., 10^{-3} to 10^{4} μmol m^{-2}, including thus fPIPP, sPIPP, and PINP.[7,8] Reciprocity holds for the fPIPP, i.e., the response depends on the product of fluence rate times pulse duration [Figure 132.1(B)].[7,8,14] In contrast, PINP and sPIPP are greatly dependent on the duration of the irradiation. Reciprocity breaks down when the duration of the pulses exceeds a critical duration (above 30 s). In this case, the response becomes greatly time dependent, i.e., long irradiations of low fluences elicit greater bending angles than short irradiations of elevated fluences [Figure 132.1(B)]. This behavior is called time-dependent phototropism (TDP),[7,8] and it corresponds to the "second positive curvature," a term used by earlier authors.[14]

A time-limiting step is responsible for the optimum curve of the fPIPP. When the fluence eliciting the fPIPP of *Arabidopsis* or of *Avena* coleoptiles is delivered by a sequence of small individual pulses instead of a large single one, the response can be substantially increased.[6–8] The response thus depends not only on the number of absorbed quanta but also on the time interval between the individual pulses. The PINP

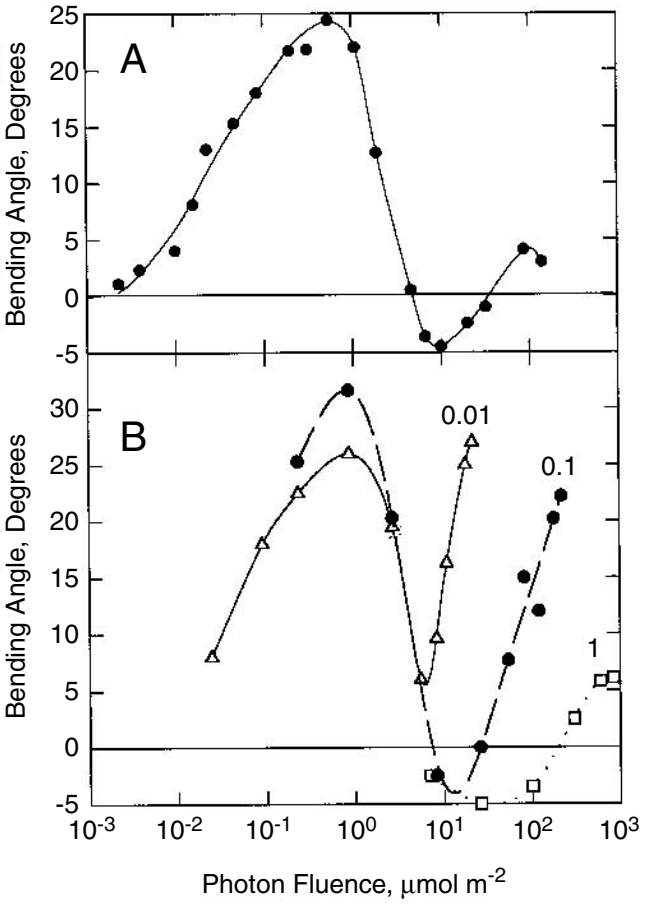

FIGURE 132.1 Photon fluence-response curves for phototropic bending of *Avena* coleoptiles. (A) Coleoptiles were irradiated unilaterally with a blue-light pulse (458 nm) of constant duration (30 s) and variable photon-fluence rates.[14] (B) Irradiation with constant photon-fluence rates (0.01, 0.1, and 1 μmol m^{-2} s^{-1}) and variable pulse duration.[8] Bending angles were measured 2 h after the unilateral light pulse.

is characteristic for *Avena* and is absent for *Zea* coleoptiles. It was, however, observed even in *Phycomyces*[10] and *Vaucheria*.[2,7,8]

Numerous phototropic organisms display fluence-response relationships that are similar to those of grass coleoptiles. These include various monocots and dicots, *Phycomyces*, *Pilobolus*, *Arabidopsis*, *Vaucheria*, and chloronemata of the fern Dryopteris.[2,6–8,10] The fluence-response curves for the phototropism of *Raphanus* seedlings appear less typical in that a classical bell-shaped curve for the first positive phototropism is absent. Kinetic models for the complex dose-response relationships were proposed by several authors.[7,8]

Pulse-Induced Phototropism: Dependence on Adaptation

A preirradiation with a strong pulse of blue light desensitizes transiently *Avena* coleoptiles and causes a shift of the entire bell-shaped fluence-response curve for fPIPP.[7,8] In *Zea* coleoptiles, preirradiation reduces mainly the phototropic responsivity, not however, the absolute threshold. After about 120 min in darkness, the responsivity recovers, and the original bell-shaped curve for the fPIPP is reestablished, indicating that the full sensitivity has recovered.[7,8,11,12] Earlier authors who worked with a sequence of strong conditioning pulses and subsequent unilateral pulses of lesser irradiance similarly found evidence for

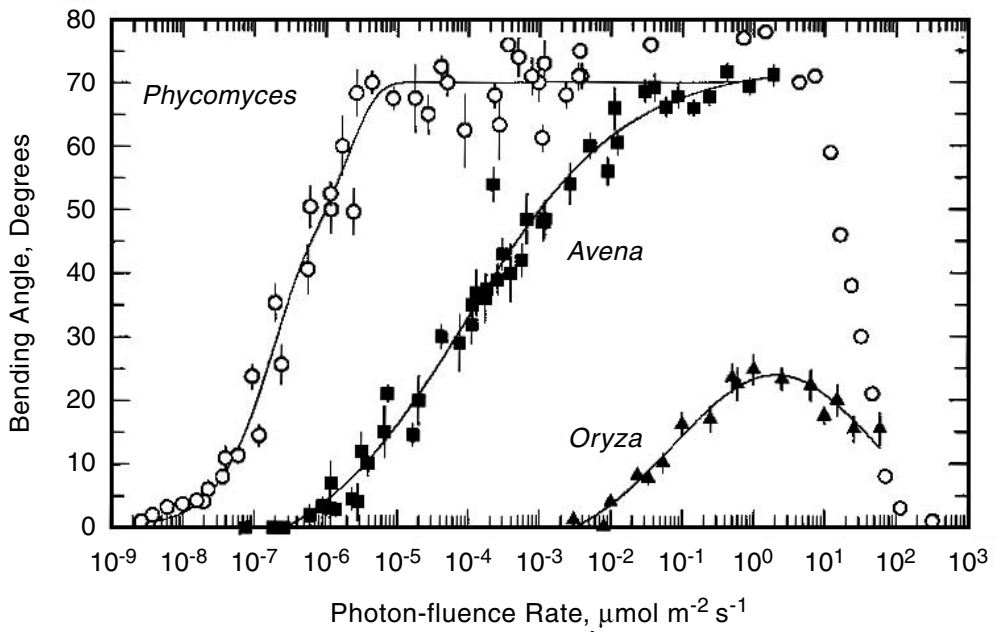

FIGURE 132.2 Photon-fluence rate-response curves for photogravitropic equilibrium. Sporangiophores of *Phycomyces*: unilateral irradiation for 8 h (465 nm)[21]; above 10^{-2} µmol m^{-2} s^{-1}: irradiation for 6 h with broad-band blue light.[22] Coleoptiles of *Avena*: unilateral irradiation for 8 h (465 nm).[20] Coleoptiles of *Oryza*: unilateral irradiation for 5 h with broad-band blue light.[17]

sensitivity recovery in darkness. Such results were obtained with *Avena* and *Zea* coleoptiles, hypocotyls of *Arabidopsis*, and sporangiophores of *Pilobolus.*[7,8,11,12] The desensitizations caused by blue and red light (132.5.3) are mediated by different photoreceptor systems and are distinguished kinetically.

Pulse-Induced Phototropism: Effect of Red Light, Phytochrome

A pretreatment of dark-grown *Avena* or *Zea* coleoptiles with red light exerts a dual effect on fPIPP: it raises the threshold of fluence-response curves; in fact, the entire curve with the ascending and descending arms of the fPIPP is shifted to elevated fluences, and it slightly increases the maximal bending angle[2,6–8].

Red light is thus desensitizing the coleoptiles to subsequent irradiation (rise of threshold) while it enhances the responsiveness (rise of bending angle). The effect requires low fluences and is probably mediated by phytochrome and represent a "very low-fluence response" that can be elicited also with far-red light. An action spectrum for the enhancement of responsiveness made with *Arabidopsis* indicates phytochrome as photoreceptor.[7,8] The effect is mediated mainly by the Pr-form of PhyA. However, PhyB also plays a role when PhyA is absent.[15]

Continuous Irradiation: Fluence-Rate-Response Curves

Continuous unilateral irradiation establishes a photogravitropic equilibrium, in which the two stimuli, light and gravity, balance each other (132.6.2). *Avena* coleoptiles[16] and sporangiophores of *Phycomyces*[9,10] that were irradiated unilaterally for 7 to 8 h show fluence-rate-response curves that can be fitted to raising exponential or hyperbolic functions. For blue light, the threshold values for *Avena* is near 3×10^{-7} and that of *Phycomyces* near 3×10^{-9} µmol m^{-2} s^{-1} (Figure 132.2). For both organisms, maximal bending angles of 70 to 75° are reached. Coleoptiles of *Oryza* possess a threshold near 5×10^{-3} µmol m^{-2} s^{-1} and moderate bending angles of some 25°[17] (Figure 132.2). Fluence-rate-response curves such as those shown in Figure 132.2 are characterized by a low-irradiance threshold and a high-irradiance threshold. At low

fluence rates, the number of hit photoreceptors is limiting; at very high fluence rates, the photoreceptors at the proximal and distal sides are hit at the same rate, and differential growth, i.e., bending, is thus rendered impossible.

Continuous Irradiation: Dependence on Adaptation

Dark adaptation greatly affects the shape of fluence-rate-response curves of phototropism of light-grown *Avena* coleoptiles that are exposed for 2 h to unilateral blue light. With extending periods of darkness prior to unilateral irradiation, the threshold drops exponentially, and the maximal bending angle increases concomitantly. Darkness thus sensitizes (drop of threshold) and enhances the responsiveness (increase of bending angle).[16] The same behaviors are also found for *Phycomyces* (Galland, unpublished).

132.6 Interaction between Gravitropism and Phototropism

In nature and under almost all experimental conditions, phototropism always occurs together with gravitropism. This is unavoidable, because as soon as phototropic bending occurs, a gravitropic stimulus is concomitantly established. Phototropism unaffected by gravitropism can be measured only under weightlessness or on a clinostat, which neutralizes the gravitropic bending, even though it does not eliminate (omnilateral) gravitropic stimulation.

The Effect of Gravity on Pulse-Induced Phototropism

When *Avena* coleoptiles are clinostatted horizontally after phototropic stimulation with pulse stimuli (fPIPP or sPIPP), then phototropic bending occurs faster and greater curvature is observed, showing that gravitropism interferes with the phototropic bending.[6–8] Similar results were also obtained with coleoptiles of *Triticum* and seedlings of *Helianthus*.[6,8] After unilateral light pulses, maximal curvature is normally reached after about 2 h. When *Zea* coleoptiles were kept on a clinostat after the pulse stimulus, the bending could be maintained for over 20 h.[6] The use of clinostatting has to be evaluated with care, because clinostatting before the application of the phototropic stimulus may also affect the phototropic bending.

Photogravitropic Equilibrium

During continuous unilateral irradiation, plants and fungi reach a so-called photogravitropic equilibrium angle. This angle represents an equilibrium of two antagonistic stimuli, i.e., light eliciting positive bending and gravity eliciting negative gravitropism. Time-dependent phototropism (TDP) is, therefore, always the result of two responses. The photogravitropic equilibrium angle of *Phycomyces* could be substantially enhanced by clinostatting the sporangiophores "head-over," i.e., in a plane, where the tip of the sporangiophore is positioned in the center of rotation and the base of the sporangiophore at the circumference. The absolute threshold is, however, not affected by clinostatting,[18] a result that was also obtained with coleoptiles of *Avena*.[16]

Quantitative Relationship between Gravitropism and Phototropism

The threshold value for photogravitropic equilibrium (Figure 132.2) depends on the strength of gravitropic stimulus generated by the earth gravitational field ($1 \times g$). When the earth gravitational field is substituted by centrifugal accelerations that exceed the value of $1 \times$ g, one finds that the threshold raises exponentially with the gravitational stimulus, g. The following empirical relationship was observed for sporangiophores of *Phycomyces*:

$$I = I_0\, a \exp\,(b\, g) \qquad (1)$$

where I is the threshold fluence rate at elevated g, I_0 is the threshold fluence rate at $1 \times g$, g is the centrifugal acceleration (expressed as multiples of the earth's gravitational acceleration), and a and b are adjustable parameters. A linear increase of g results in an exponential increase of the threshold fluence rate ("exponential law").[18]

The exponential relationship is also valid under natural conditions, i.e., for unilateral irradiation of vertical or inclined organisms. The gravitropic stimulus, S, and the elicited response depend (in darkness) on the sine of the initial inclination angle (sine law of Julius Sachs[6]):

$$S = g \sin \gamma \tag{2}$$

where S is the gravitropic stimulus, g is the earth gravitational acceleration, and γ the initial inclination angle. The sine law holds reasonably well for coleoptiles of *Zea* and *Oryza*[19] and *Avena*,[20] and also for the sporangiophores of *Phycomyces*.[21]

To counterbalance the negative gravitropism of an inclined organ with unilateral light, one can choose an experimental setup, in which the unilateral light is always impinging at a right angle. One can then determine the fluence rate that can compensate the negative gravitropism and thus keep the inclined organ permanently in the same straight position. For this setup, one finds that the inclination angle and the compensating fluence rate are also obeying a simple "exponential law," which is described by the following equation:

$$I = I_0 \, a \exp \, (b \times g \sin \gamma) \tag{3}$$

where I is the compensating fluence rate that counterbalances an inclined organ, I_0 is the absolute threshold as determined with fluence-rate-response curves of photogravitropic equilibrium under standard conditions (Figure 132.2), a and b are adjustable parameters, g is the earth gravitational acceleration, and γ is the inclination angle at the beginning and the end of the experiment. The validity of this relation was shown for *Phycomyces*[21] as well as for *Avena* coleoptiles.[20]

In contrast to the experimental setup described above (Equation 132.3), photogravitropic equilibrium is normally established in a dynamic situation, in which the incidence angle of the unilateral light decreases from 90° to values of some 20° (*Phycomyces* and *Avena* in Figure 132.2). The amount of absorbed light depends on the cosine square of the incidence angle (cosine square law). The final photogravitropic equilibrium angle is thus determined by three empirical laws: the sine law, the exponential law, and the cosine square law.[20,21]

132.7 Action Spectra

The spectral sensitivities of various phototropic plants and fungi are listed in Table 132.1. Higher plants and fungi are generally sensitive only to near-UV and blue, not however, to red light. An exception is the phytochrome-mediated phototropism of the mesocotyl of Zea.[6–8] Action spectra for the phototropism of most organisms indicate a ubiquitous flavin-like blue-light receptor with absorption in the UVB, UVA, and blue spectral regions. To date, the only isolated and well-characterized phototropism receptor is phototropin from *Arabidopsis*, a flavin-photoreceptor with kinase activity (see below).

The phototropism and polarotropism of mosses and ferns can be elicited by blue and red light, the latter being mediated by phytochrome. Filaments of the algae *Mougeotia* and *Vaucheria* are bending toward or away from blue light; apical cells of *Mougeotia* can bend toward red light (Table 132.1).

Action Spectra for Pulse-Induced Phototropism

Action spectra for the fPIPP of *Medicago* hypocotyls[32] display a major peak near 450 and smaller peaks near 280 and 370 nm (Figure 132.3). Action spectra for *Avena* coleoptiles display similar peak positions in the near-UV and blue spectral regions.[2,7,8]

TABLE 132.1 Spectral Sensitivities for Phototropism and Polarotropism of Various Organisms

Organism	Organ	Type of Phototropism	Spectral Sensitivity	Ref.
Mougeotia	Filaments	Negative	Blue	2
Mougeotia	Apical cell	Positive	Red	2
Vaucheria	Filaments	Positive	Blue	2
Vaucheria	Filaments	Negative	Blue above 60 Wm^{-2}	23
Boergesinia	Rhizoid	Positive	Blue	2,6
Ceratodon	Chloronema	Polarotropism	Red	24
Funaria	Chloronema	Polarotropism	Red	2,6
Physcomitrium	Chloronema	Positive	Red	2
Physcomitrella	Chloronema	Positive	Blue, red	25
Physcomitrella	Chloronema	Polarotropism	Blue, red	25
Sphaerocarpus	Chloronema	Polarotropism	UVA, blue	2
Sphaerocarpus	Seta	Positive	Blue	2
Adiantum	Chloronema	Positive	Blue, red	26,27
Adiantum	Chloronema	Polarotropism	Blue, red	26,27
Pteridium	Chloronema	Positive	Red	2
Pteris	Chloronema	Polarotropism	Blue	28
Dryopteris	Rhizoids	Negative	Red	2
Dryopteris	Rhizoids	Polarotropism	Red	2
Dryopteris	Chloronema	Positive	Blue, red	2
Dryopteris	Chloronema	Polarotropism	UVA, blue, red	2
Arabidopsis	Hypocotyl	Positive	UVA, blue	29
Avena	Coleoptile	Positive	UVA, blue	2,7
Avena	Coleoptile	Positive	UVB	2,8
Celosia	Hypocotyl	Positive	UVA, blue, green	2
Helianthus	Hypocotyl	Positive	UVA, blue	2
Lepidium	Hypocotyl	Positive	UVA, blue	2
Medicago	Hypocotyl	Positive	UVB, UVA, blue	2
Zea	Mesocotyl	Positive	Red	6–8
Conidiobolus	Conidiophore	Positive	Blue, red	2
Coprinus	Fruiting body	Positive	Blue	30
Entomophthora	Conidiophore	Positive	Blue, red	2
Neurospora	Perithecial beak	Positive	Blue	31
Phycomyces	Sporangiophore	Positive	UVA, blue	9,10
Phycomyces	Sporangiophore	Negative	UVB	9,10
Pilobolus	Sporangiophore	Positive	UVA, blue	2
Pilobolus	Sporangiophore	Negative	UVB	2

Action Spectra for Photogravitropic Equilibrium

Action spectra that were generated on the basis of fluence-rate-response curves (continuous irradiation for several hours) exist mostly for *Phycomyces*.[9] The fine structures of these action spectra differ from those of the balance action spectra in that the UVA peak is much higher. Everett and Thiman[8] analyzed the so-called second positive phototropic response that is time dependent. All of these action spectra have in common a steep drop of the effectiveness above 500 nm.

Mutants of *Phycomyces* with defects in the genes *madB* and *madC* have an about 100-fold greater effect on the near-UV than on the blue-light sensitivity, indicating that more than the photoreceptor may be involved in near-UV and blue-light perception.[9] Similar conclusions can be drawn from the observation that the *nph-2* mutant of *Arabidopsis* affects the blue-light sensitivity more profoundly than the one for near-UV.[29]

The sensitivity to UVB was analyzed in only a few cases. *Phycomyces* shows negative phototropism to wavelengths below 300 nm (Figure 132.3).[33] The UVB sensitivity appears to be mediated by a photoreceptor other than the one mediating near-UV and blue-light phototropism, because mutants with defects in the genes *madD, E, F, G* affect the UVB sensitivity only little, while they almost completely eliminate the near-UV and blue-light sensitivity.[9] Also, the fact that UVB and red light strongly interact

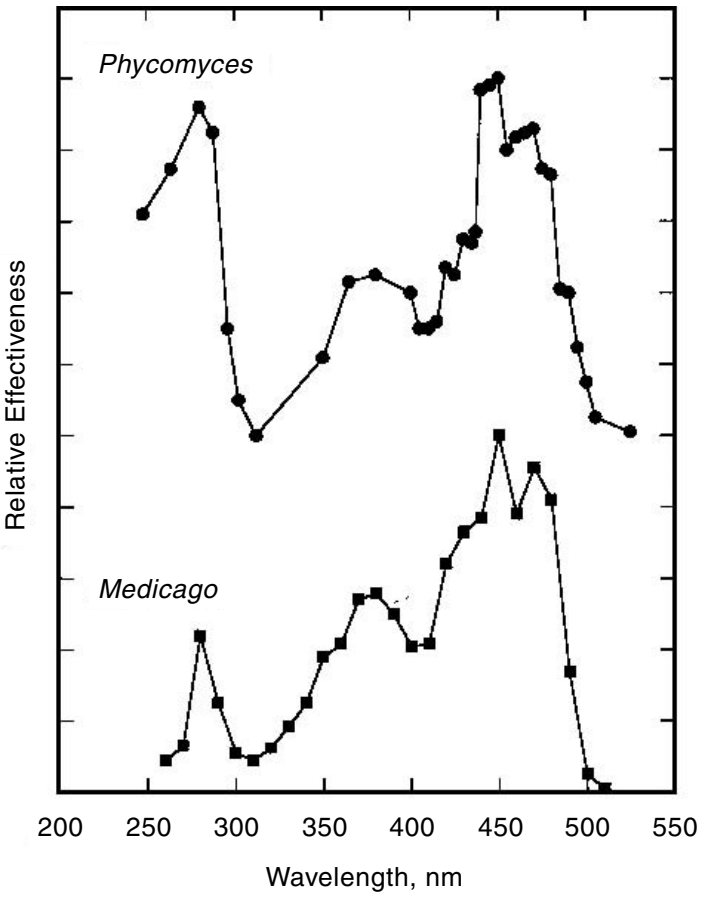

FIGURE 132.3 Action spectra of phototropism. *Phycomyces* sporangiophores: phototropic balance action spectrum. The relative effectiveness was determined by achieving phototropic balance with two opposing light sources consisting of a test light of variable wavelength and a broad-band blue reference light (460 nm). Below 300 nm, the sporangiophores bend away from the UV light.[33] *Medicago* hypocotyls: phototropic action spectrum determined on the basis of first pulse-induced phototropism.[32]

antagonistically in bichromatic irradiation, while red and blue light do not argue for two separate photoreceptor systems.[9]

Action spectra for the phototropism of *Phycomyces* and its related light-growth response display a very small peak near 600 to 610 nm that may indicate the lowest triplet state of a flavin-like blue-light receptor.[2,9] These older observations are pertinent in view of the recent finding that phototropin of *Arabidopsis* probably acts from the lowest excited triplet state.[34]

Action Spectra for Phototropic Balance

When plants or fungi are irradiated bilaterally with two light sources facing each other, they bend toward the light source that they recognize as the subjectively more effective one. Action spectra that were generated with the phototropic balance method display major peaks near 280, 370, and 450, thus indicating the presence of a flavin-like photoreceptor (Figure 132.3). Such action spectra exist for *Avena* coleoptiles,[2,7,16] *Lepidium*, *Helianthus*, and *Celosia*,[2] and *Phycomyces*.[9,10] A puzzling property of the balance action spectra of *Phycomyces* is that the height of near-UV and blue-light maxima depends on the intensity range that is chosen for balance. Near threshold (about 10^{-8} W m^{-2}, 450 nm), the near-UV peak disappears,

while it dominates the blue peak at elevated fluence rates.[9,10] A photoreceptor model implying only a single photoprimary response cannot possibly explain this observation.

132.8 Blue-Light Photoreceptors Controlling Phototropism and Growth

Two types of blue-light receptors were identified that control phototropism and growth of higher plants. These are phototropins (Phot)[5] and cryptochromes (Cry),[4] respectively. Besides phototropin, there must exist another phototropism photoreceptor of *Arabidopsis*, because the *nph1* mutant lacking Phot1 is not completely deficient but is still sensing unilateral light of high irradiance.[5,29] These results indicate that probably two light-signaling pathways are involved in the phototropism of *Arabidopsis*. There are conflicting reports as to whether or not cryptochromes play a role in phototropism. Roles for Cry1 and Cry2 in phototropism, which were inferred for first positive, not however, for second positive phototropism, are presently discussed controversially.[5,29,35]

Phototropins

The *Arabidopsis* phototropins, Phot1 and Phot2 (previously called *nph1* and *npl1*), contain 996 and 915 amino acids, respectively, and possess a *C*-terminal serine/threonine domain and, in addition, two *N*-terminal LOV (light-, oxygen-, voltage-sensitive) domains, each of which noncovalently binds an oxidized flavin mononucleotide (FMN).[5,36] Phot2 (*npl1*) is a paralogue of Phot1 (*nph1*), with about 60% sequence identity and with highly conserved LOV domains.[5,36] The crystal structure of the LOV2 domain of the *Adiantum* phytochrome/phototropin chimeric photoreceptor Phy3 was determined at a resolution of 2.73 Å.[5,36]

Upon irradiation, the FMN undergoes a self-contained photocycle, which entails the generation of a semistable intermediate, a flavin-C(4a)-cysteinyl adduct, that returns in darkness to the ground state. The covalent adduct is formed between the FMN and the cysteine residue, Cys39. In the adduct, which is generated *via* a S1-T1 intersystem crossing, the FMN is reduced, while the cysteine is oxidized.[5,34–37] The photocycle was characterized spectroscopically for the LOV2 domain of Phot1 of *Avena sativa*,[5,36] the LOV1 and LOV2 domains of Phot1 and Phot2 from *Chlamydomonas*,[34,37] *Arabidopsis*, and *Oryza*.[37] Phototropin-related flavoproteins are also present in prokaryotes. The protein YtvA from *Bacillus subtilis* contains a LOV domain with high homology to LOV domains of plant phototropins and similar spectroscopic features.[38]

Phot1 is a membrane-associated 120 kD serine/threonine kinase that undergoes autophosphorylation upon absorption of near-UV and blue light.[5,35,36] Both phototropins thus represent light-activated serine-threonine protein kinases. The formation of the flavin-C(4a)-cysteinyl adduct upon light absorption causes a conformational change of the apoprotein that is believed to activate the kinase activity.[5]

Functions of Phototropins

The phototropins Phot1 and Phot2 mediate phototropism of leaves, flowers, and seedlings,[5] chloroplast movement,[36] and opening of stomata.[39] Phot1 and Phot2 differ with respect to their light sensitivity: while Phot1 mediates phototropism and chloroplast relocation both to low- and high-fluence rates, Phot2 does so only in response to high-fluence rates.[36] The opening of guard cells is also under the redundant control of Phot1 and Phot2, because only double mutants, not single mutants, show the absence of blue-light-induced opening of stomata.[39] In *Arabidopsis*, Phot1 mediates blue-light-induced Ca^{2+}-influx by regulating Ca^{2+} uptake from the apoplast into the cytoplasm.[40] The hypocotyl growth of etiolated seedlings is unaffected by mutations in either of the *nph1* (Phot1) or *nph3* genes (see below).

Photoreceptor-Interacting Proteins and Elements Essential for Phototropism

In *Arabidopsis*, several mutations interrupt the phototropism transduction chain: *nph2* (nonphototropic hypocotyl), *rpt2* (root phototropism), and *nph3* (nonphototropic hypocotyl). *Nph3* codes for a

membrane-associated protein that interacts *via* at least two protein–protein interaction domains with Phot1, likely with its chromophore-binding domain. RPT2 is a signal transducer of the phototropic response in *Arabidopsis*.[5,35] The protein contains putative phosphorylation sites; it belongs to a large gene family that also includes the above-mentioned *nph3* gene.[5,35]

Cryptochromes

Cryptochromes regulate the growth of plant hypocotyls. Cry1 was first isolated from *Arabidopsis*.[4] Beside growth regulation, cryptochromes are also involved in the regulation of circadian rhythm of plants, animals, and cyanobacteria.[5,29] In *Arabidopsis*, cryptochromes are involved in the blue-light-induced inhibition of hypocotyl elongation, the accumulation of anthocyanin,[4] internode and petiole elongation, seed germination, and initiation of flowering time.[4]

Cryptochromes belong to the family of photolyases/cryptochromes. They share with the DNA photolyases (DNA repair enzymes) the chromophore-binding domains without possessing, however, the capacity of photolyases to monomerize pyrimidine dimers upon irradiation.[4,35] Cryptochromes contain as chromophores FAD and methenyltetrahydrofolate, both of which are noncovalently bound.[4,35] *Arabidopsis* possesses two cryptochromes, Cry1 and Cry2, which possess great sequence homology apart from a small *C*-terminal domain. The two cryptochromes differ in their stability: while Cry1 is stable, Cry2 is degraded upon irradiation.[2,29,35] Interestingly, Cry2 is more stable under monochromatic blue than under broad-band blue light.[41]

Because of the phylogenetic relation between cryptochromes and photolyases, it appears likely that cryptochromes also possess an electron transfer as primary photoresponse.[4,35] *In situ* and after isolation cryptochromes exist in a reduced form, because their absorption spectra are semiquinone-like. The action spectrum for hypocotyl inhibition, a Cry1-mediated response, resembles, however, the absorption spectrum of the oxidized form.[41] This observation could indicate that the active form of Cry1 exists *in situ* in the oxidized state, while the inactive form remains reduced.

132.9 Role of Hormones

Auxin, Indole-3-Acetic Acid

Unilateral irradiation of shoots and coleoptiles induces a lateral auxin transport away from the irradiated side and a concomitant asymmetry of auxin, which is a prerequisite for redistribution of growth and, thus, phototropic bending. This so-called Cholodny–Went theory of phototropism[2,6–8] survived several ups and downs and still provides an excellent basis for providing a molecular model for phototropism and also gravitropism of various plant materials.[42]

Red-light-grown *Zea* coleoptiles that are stimulated unilaterally with pulses of blue light display a slower growth rate at the irradiated half and a faster one at the shaded half.[6–8] This asymmetry of growth pattern correlates with an elevated auxin concentration in the shaded half and a reduced content in the irradiated half.[7,8,42] The phototropic growth responses of *Zea* travel basipetally at a speed that is comparable to the velocity of basipetal auxin transport.[43] In accordance with the Cholodny–Went theory, it was found that the establishment of an auxin asymmetry upon irradiation precedes the actual bending.[8,43] Also in accordance with the theory is the observation that saturating doses of exogenous auxin inhibit phototropism.[43] Finally, the *nph4* mutation of *Arabidopsis*, which confers reduced photo- and gravitropism, causes at the same time a reduced sensitivity to exogenously applied auxin.[29]

The lateral translocation can be explained by a light-induced inhibition of basipetal transport.[2,6–8,43] In accordance with this explanation are the observations that the action spectra for phototropism, light-growth response, and light-induced basipetal auxin transport resemble each other.[8,43]

In tobacco, unilateral irradiation caused an about twofold activation of auxin-responsive promoters in the shaded half of the stem relative to the irradiated side,[44] a result that was explained by the redistribution of auxin.[45]

Lateral translocation of exogenous auxin in response to unilateral irradiation was demonstrated early on with hypocotyls of radish and, subsequently, with *Zea* coleoptiles,[2] epicotyls of *Pisum*.[7,8,46] The apical part of coleoptiles (1 mm below the tip) represents the most light-sensitive zone, and at the same time, the zone that is most effective with respect to lateral auxin translocation.[2,6]

Participation of Growth Inhibitors

Tropic bending can, in principle, be generated by translocation of growth inhibitors or growth promoters. The existence of growth inhibitors appears well established for *Raphanus* hypocotyls, in which *cis*- and *trans*-raphanusanins inhibit growth when applied exogenously.[7,8,47] The inhibitor asymmetry is detectable after pulse-induced phototropism.[7,8] Two distinct inhibitors, Raphanusol A and B, are translocated laterally during pulse-induced phototropism.[7,8] The results indicate that in some organisms, phototropism may be exclusively explained by the action of growth inhibitors and their redistribution rather than by the action of growth promoters such as auxin. In seedlings of *Helianthus*, auxin remains evenly distributed after unilateral irradiation. The growth inhibitor, xanthoxin, accumulates, however, on the irradiated side.[7,8]

132.10 Role of Cytoskeleton

In chloronemata of *Ceratodon*, an irradiation with unilateral red light induces a reorientation of actin strands in the apical dome toward the point of the prospective outgrowth.[48] Cell-wall-associated microtubules and their orientations play an important role for growth. The reorientation of microtubules in the outer epidermal wall of *Zea* can be controlled by blue and red light as well as auxine.[49] During phototropism of *Zea*, coleoptiles and *Helianthus* hypocotyls cortical microtubules undergo reorientation.[49] On the irradiated side, the tubules reorient from the transverse to the longitudinal orientation. It is tempting to explain bending in terms of fibril reorientation: the light-induced longitudinal orientation would be less amenable to stretch and could thus explain the reduced growth rate at the irradiated side. A more detailed analysis has, however, shown that such a direct role of fibrils does not hold. While it is true that microtubules respond to phototropic stimulation, they do not control tropic curvature, because the two events can be experimentally separated.[49]

132.11 Transduction Chain: Phosphorylation, Proton Pumps, Calcium Ions

Blue-light irradiation of plant seedlings induces the phosphorylation of a 120 kD plasma membrane associated protein.[50] There is a strong correlation between the phosphorylation of this protein and phototropism.[50] The fluence requirement for the phosphorylation, its asymmetric distribution in the coleoptile after unilateral irradiation,[29] and its correlation with sensitivity changes[13] show that it is related to an early step of the phototropic transduction chain. The phosphorylated protein is the blue-light receptor proper, phototropin, because the photoreceptor mutant, *nph1* of *Arabidopsis* is lacking the phosphorylation, and the mutant is devoid of phototropism.[4,5] Blue light induces in *Neurospora crassa* bending of the protoperithecial beak and the dephosphorylation of a 33 kDa protein. Two mutants, *wc-1* and *wc-2* (white collar), that are defective in all blue-light responses, including phototropism, possess an abnormal dephosphorylation pattern.[51] The white-collar proteins are transcription regulators with PAS and LOV domains[52] that are also involved in the light control and maintenance of the circadian clock.[53]

Cell-wall loosening and a concomitant increase of growth rate can be elicited by acidification. It is assumed that auxin stimulates a plasma membrane H^+-ATPase that causes the acidification. A lateral translocation of auxin during unilateral irradiation would thus lead to differential acidification and thus differential growth. In *Zea* coleoptiles, auxin enhances the exocytosis and the synthesis of H^+-ATPase of the plasma membrane, and also the activation of existing H^+-ATPase was demonstrated.[54,55] The strong and critical points of this so-called acid-growth theory were discussed.[56]

In the epidermis of *Zea* coleoptiles, exogenous auxins elicits a rapid increase of cytosolic free Ca^{2+}, suggesting a role for this ion as second messenger.[57] In *Zea* coleoptiles, Ca^{2+} is translocated during phototropic bending from the convex to the concave side, the major part of the ions probably being located in the apoplast. Auxin transport inhibitors prevent the translocation, indicating that Ca^{2+} and auxin act in the same transduction chain.[58] In *Arabidopsis* and *Nicotiana*, the cytosolic free Ca^{2+} changes transiently about 30 sec after a short pulse of blue light. In the phototropism mutant *nph1*, which lacks the photoreceptor phototropin, this response was greatly affected.[59]

References

1.. Nabielek, R., Biologische Kenntnisse und Überlieferungen im Mittelalter (4. – 15. Jh.), in *Geschichte der Biologie*, Jahn, I., Ed., Gustav Fischer, Jena, 1998, chap. 3.
2.. Pohl, U. and Russo, V.E.A., Phototropism, in *Membranes and Sensory Transduction*, Colombetti, G. and Lenci, F., Eds., Plenum Press, 1984, chap. 7.
3.. du Buy, H.G. and Nuernbergk, E., 1935. Phototropismus und Wachstum der Pflanzen, *Ergebn.d. Biol.*, 12, 325, 1935.
4.. Ahmad, M. and Cashmore, A.R., Seeing blue: the discovery of cryptochrome, *Plant Mol. Biol.*, 30, 851, 1996.
5.. Christie, J.M. and Briggs, W.R., Blue light sensing in higher plants, *J. Biol. Chem.*, 276, 11457, 2001.
6.. Hart, J.W., *Plant Tropisms and Other Growth Movements*, Unwin Hyman, London, 1990.
7.. Iino, M., Phototropism: mechanisms and ecological implications, *Plant Cell Environ.*, 13, 633, 1990.
8.. Iino, M., Phototropism in higher plants, in *Photomovement, ESP Review Series on Photobiology*, Häder, D.-P. and Lebert, M., Eds., Elsevier, Amsterdam; New York, 2001, chap. 23.
9.. Galland, P., Phototropism in *Phycomyces*, in *Photomovement, ESP Review Series on Photobiology*, Häder, D.-P. and Lebert, M., Eds., Elsevier, Amsterdam; New York, 2001, chap. 22.
10. Galland, P., Phototropism of the *Phycomyces* sporangiophore: a comparison with higher plants, *Photochem. Photobiol.*, 52, 233, 1990.
11. Galland, P., Photosensory adaptation in plants, *Bot. Acta,* 102, 11, 1989.
12. Galland, P., Photosensory adaptation in aneural organisms, *Photochem. Photobiol.*, 54, 1119, 1991.
13. Salomon, M., Zacherl, M., Luff, L., and Rüdiger, W., Exposure of oat seedlings to blue light results in amplified phosphorylation of the putative photoreceptor for phototropism and in high sensitivity of the plants to phototropic stimulation, *Plant Physiol.*, 115, 493, 1997.
14. Blaauw, O.H. and Blaauw-Jansen, G., The phototropic responses of *Avena* coleoptiles, *Acta Bot. Neerl.,* 19, 755, 1970.
15. Janoudi, A.K., Konjevic, R., Whitelam, G., Gordon, W., and Poff, K.L., Both phytochrome A and phytochrome B are required for the normal expression of phototropism in *Arabidopsis thaliana* seedlings, *Plant Physiol.*, 101, 278, 1997.
16. Galland, P., Photogravitropic equilibrium in *Avena* coleoptiles: fluence rate-response relationships and dependence on dark adaptation and clinostating, *J. Plant Res.*, 115, 131, 2002.
17. Neumann, R. and Iino, M., Phototropism of rice (*Oryza sativa* L.) coleoptiles: fluence-response relationships, kinetics and photogravitropic equilibrium, *Planta*, 201, 288, 1997.
18. Grolig, F., Eibel, P., Schimek, C., Schapat, T., Dennison, D.S., and Galland, P., Interaction between gravitropism and phototropism in sporangiophores of *Phycomyces*, *Plant Physiol.*, 123, 765, 2000.
19. Iino, M., Tarui, Y., and Uematsu, C., Gravitropism of maize and rice coleoptiles: dependence on the stimulation angle, *Plant Cell Environ.*, 19, 1160, 1996.
20. Galland, P., Tropisms in *Avena* coleoptiles: sine law for gravitropism, exponential law for photogravitropic equilibrium, *Planta*, 215, 779–784, 2002.
21. Galland, P., Wallacher, Y., Finger, H., Hannappel, M., Tröster, S., Bold, E., and Grolig, F., Tropisms in *Phycomyces*: sine law for gravitropism, exponential law for photogravitropic equilibrium, *Planta*, 214, 931, 2002.
22. Lipson, E.D., López-Díaz, I., and Pollock, J.A., Mutants of *Phycomyces* with enhanced tropisms, *Exp. Mycol.*, 7, 241, 1983.

23. Kataoka, H. and Watanabe, M., Negative phototropism in *Vaucheria terrestris* regulated by calcium. III. The role of calcium characterized by use of a high-power argon-ion laser as the source of unilateral blue light, *Plant Cell Physiol.*, 34, 737, 1993.
24. Hartmann, E., Klingenberg, B., and Bauer, L., Phytochrome-mediated phototropism in protonemata of the moss *Ceratodon purpureus* BRID, *Photochem. Photobiol.*, 38, 599, 1983.
25. Jenkins, G.I. and Cove, D., Phototropism and polarotropism of primary chloronemata of the moss *Physcomitrella patens*: response of the wild-type, *Planta*, 158, 357, 1983.
26. Kadota, A., Koyama, M., Wada, M., and Furuya, M., Action spectra for polarotropism and phototropism in protonemata of the fern *Adiantum capillus-veneris*, *Physiol. Plant*, 61, 327, 1984.
27. Kadota, A., Wada, M., and Furuya, M., Phytochrome-mediated polarotropism of *Adiantum capillus-veneris* L. protonema as analyzed by microbeam irradiation with polarized light, *Planta*, 165, 30, 1985.
28. Kadota, A., Kohyama, I., and Wada, M., Polarotropism and photomovement of chloroplasts in the protonema of the ferns *Pteris* and *Adiantum*: evidence for the possible lack of dichroic phytochrome in *Pteris*, *Plant Cell Physiol.*, 30, 523, 1989.
29. Briggs, W.R. and Huala, E., Blue light photoreceptors in higher plants, *Annu. Rev. Cell. Dev. Biol.*, 15, 33, 1999.
30. Borris, H., Beiträge zur Wachstums- und Entwicklungsphysiologie der Fruchtkörper von *Coprinus lagopus*, *Planta*, 22, 28, 1934.
31. Harding, R.W. and Melles, S., Genetic analysis of phototropism of *Neurospora crassa* perithecial beaks using white collar and albino mutants, *Plant Physiol.*, 72, 996, 1983.
32. Baskin, T.I. and Iino, M., An action spectrum in the blue and ultraviolet for phototropism in alfalfa, *Photochem. Photobiol.*, 46, 127, 1987.
33. Curry, G.M. and Gruen, H.E., Action spectra for the positive and negative phototropism of *Phycomyces* sporangiophores, *Proc. Natl. Acad. Sci. USA*, 45, 797, 1959.
34. Holzer, W., Penzkofer, A., Fuhrmann, M., and Hegemann, P., Spectroscopic characterization of flavin mononucleotide bound to the LOV1 domain of phot1 from *Chlamydomonas reinhardtii*, *Photochem. Photobiol.*, 75, 479, 2002.
35. Lin, C., Plant blue-light receptors, *Trends Plant Sci.*, 5, 337, 2000.
36. Briggs, W.R., Beck, C.F., Cashmore, A.R., Christie, J.M., Hughes, J., Jarillo, J.A., Kagawa, T., Kanegae, H., Liscum, E., Nagatanni, A., Okada, K., Salomon, M., Rüdiger, R., Sakai, T., Zakano, M., Wada, M., and Watson, J.C., The phototropin family of photoreceptors, *Plant Cell*, 13, 993, 2001.
37. Kasahara, M., Swartz, T.E., Olney, M.A., Onodera.A., Mochizuki, N., Fukuzawa, H., Asamizu, E., Tabata, S., Kanegae, H., Takano, M., Christie, J.M., Nagatani, A., and Briggs, W.R., Photochemical properties of the flavin mononucleotide-binding domain of the phototropins from *Arabidopsis*, rice, and *Chlamydomonas reinhardtii*, *Plant Physiol.*, 129, 762, 2002.
38. Losi, A., Polverini, E., Quest, B., and Gärtner, W., First evidence for phototropin-related blue-light receptors in prokaryotes, *Biophys.J.*, 82, 2627, 2002.
39. Kinoshita, T., Doi, M., Suetsugu, N., Kagawa, T., Wada, M., and Shimazaki, K., Phot1 and phot2 mediate blue light regulation of stomatal opening, *Nature*, 414, 656, 2001.
40. Babourina, O., Newman, I., and Shabala, S., Blue light-induced kinetics of H^+ and Ca^{2+} fluxes in etiolated wild-type and phototropin-mutant *Arabidopsis* seedlings, *Proc. Natl. Acad. Sci. USA*, 99, 2433, 2002.
41. Ahmad, M., Grancher, N., Heil, M., Black, R.C., Giovani, B., Galland, P., and Lardemer, D., Action spectrum for cryptochrome-dependent hypocotyl growth inhibition in *Arabidopsis*, *Plant Physiol.* 129, 774, 2002.
42. Trewavas, A., Briggs, W.R., Bruinsma, J., Evans, M.L., Firn, R., Hertel, R., Iino, M., Jones, A.M., Leopold, A.C., Pilet, P.E., Poff, K.L., Roux, S.J., Salisbury, F.B., Scott, T.K., Sievers, A., Zieschang, H.E., and Wayne, R., What remains of the Cholodny–Went theory?, *Plant Cell Environ.*, 15, 761, 1992.

43. Iino, M., Auxin and phototropism in maize coleoptiles, in *Plant Cell Walls as Biopolymers with Physiological Functions*, Masuda, Y., Ed., Yamada Science Foundation, Osaka, 1992, p. 211.
44. Li, Y., Hagen, G., and Guilfoyie, T.J., An auxin-responsive promoter is differentially induced by auxin gradients during tropisms, *Plant Cell*, 3, 1167, 1991.
45. Li, Y., Wu, Y.H., Hagen, G., and Guilfoyie, T., Expression of the auxin-inducible GH3 promoter/GUS fusion gene is a useful molecular marker for auxin physiology, *Plant Cell Physiol.*, 40, 675, 1999.
46. Kühn, H. and Galston, A.W., Physiological asymmetry in etiolated pea epicotyls: relation to patterns of auxin distribution and phototropic behavior, *Photochem. Photobiol.*, 55, 313, 1992.
47. Hasegawa, K., Noguchi, H., Iwagawa, T., and Hase, T., Phototropism in hypocotyls of radish. I. Isolation and identification of growth inhibitors, *cis*- and *trans*-raphanusanins and raphanusamide, involved in phototropism of radish hypocotyls, *Plant Physiol.*, 81, 976, 1986.
48. Meske, V. and Hartmann, E., Reorganization of microfilaments in protonemal tip cells of the moss *Ceratodon purpureus* during the phototropic response, *Protoplasma*, 188, 59, 1995.
49. Nick, P., Role of microtubular cytoskeleton, in *Photomovement, ESP Review Series on Photobiology*, Häder, D.-P. and Lebert, M., Eds., Elsevier, Amsterdam; New York, 2001, chap. 24.
50. Short, T.W. and Briggs, W.R., The transduction of blue light signals in higher plants, *Annu. Rev. Plant Physiol. Plant Mol. Biol.*, 45, 143, 1994.
51. Lauter, F.-R. and Russo, V.E.A., Light-induced dephosphorylation of a 33 kDa protein in the wild-type strain of *Neurospora crassa*: the regulatory mutants *wc-1* and *wc-2* are abnormal, *J. Photochem. Photobiol., B: Biol.*, 5, 95, 1990.
52. Ballario, P., Talora, C., Galli, D., Linden, H., and Macino, G., Roles in dimerization and blue light photoresponse of the PAS and LOV domains of *Neurospora crassa* white collar proteins, *Mol. Microbiol.*, 29, 719, 1998.
53. Crosthwaite, S.K., Dunlap, J.C., and Loros, J.J., *Neurospora wc-1* and *wc-2*: transcription, photoresponses, and the origins of circadian rhythmicity, *Science*, 276, 763, 1997.
54. Hager, A., Debus, G., Edel, H.-G., Stransky, H., and Serrano, R., Auxin induces exocytosis and the rapid synthesis of a high-tumover pool of plasma-membrane H^+-ATPase, *Planta,* 185, 527, 1991.
55. Frias, I., Caldeira, M.T., Perex-Castifieira, J.R., Navarro-Avin, J.P., Culianez-Maci, F.A., Kuppinger, O., Stransky, H., Pages, M., Hager, A., and Serrano, R., A major isoform of the maize plasma membrane H^+-ATPase: characterization and induction by auxin in coleoptiles, *Plant Cell,* 8, 1533, 1996.
56. Rayle, D.L. and Cleland, R.E., The acid growth theory of auxin-induced cell elongation is alive and well, *Plant Physiol.*, 99, 1271, 1992.
57. Felle, H., Auxin causes oscillations of cytosolic free calcium and pH in *Zea mays* coleoptiles, *Planta*, 174, 495, 1988.
58. Goswami, K.K.A. and Audus, L.J., Distribution of calcium, potassium and phosphorus in *Helianthus annuus* hypocotyls and *Zea mays* coleoptiles in relation to tropic stimuli and curvatures, *Am. J. Bot.,* 40, 49, 1976.
59. Baum, G., Long, J.C., Jenkins, G.I., and Trewawas, A.J., Stimulation of the blue light phototro-pic receptor NPH1 causes a transient increase in cytosolic Ca^{2+}, *Proc. Natl. Acad. Sci. USA*, 96, 13554, 1999.

133

Building Photonic Proteins

Kenneth J. Rothschild
Boston University and AmberGen, Inc.

Sadanand Gite
AmberGen, Inc.

Sergey Mamaev
AmberGen, Inc.

Jerzy Olejnik
AmberGen, Inc.

133.1 Introduction

Photonic proteins are ubiquitous in the biological world.[1] These include proteins involved in the transduction of light energy into chemical energy, the detection of light for sensing purposes, and the emission of light such as bioluminescence. For example, the major energy input into the biosphere is solar, with the exception of organisms that rely on geothermal energy, such as lithotrophic bacteria living near hydrothermal deep sea vents.[2,3] Many proteins evolved with the function of efficiently capturing the roughly 10^5 Terawatts of solar power that impinges on the earth's surface. This includes the well-known photosynthetic reaction center and light-harvesting proteins found in photosynthetic bacteria, algae, and plants,[4-6] as well as the light-driven bacteriorhodopsin (BR) proton pumps found in archaebacteria such as *Halobacteria salinarum*.[7] Recently, BR-like proton pumps were also discovered in marine bacteria,[8,9] indicating a much wider distribution of this family of light-energy-converting proteins.

Other proteins evolved as light receptors that play a critical role in bacterial phototaxis, plant phototropism, and visual sensing. Examples include the retinylidene-containing visual pigment rhodopsin, a family of G-coupled protein light receptors[10–12] involved in invertebrate and vertebrate vision. In the archaebacterial world, the rhodopsin counterpart, sensory rhodopsin, is also based on isomerization of the retinylidene chromophore, and it mediates phototaxis.[13] Additional examples are the red and far-red light sensing phytochromes receptors of plants[14,15] and the newly discovered phototropins, a family of proteins that mediates blue-light responses in plants.[16,17]

A third class of photonic proteins is made up of those that evolved a light-emitting role, such as the green fluorescent protein (GFP) found in Aequorea (jellyfish) and Renilla (sea pansy).[18] In nature, GFP is excited through radiationless energy transfer by the well-known chemiluminescent protein aequorin, also found in Aequorea. Currently, little is known about the function of GFP as compared to the light signaling function of the extensively studied chemiluminescent firefly luciferase.[19]

In this chapter, we review the new and emerging field of engineering artificial photonic proteins, which complements the classic study of natural photoproteins discussed above. The term artificial photonic

0-8493-1348-1/04/$0.00+$1.50

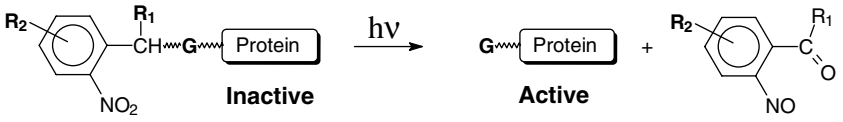

FIGURE 133.1 2-nitrobenzyl mediated photoactivation of proteins. Protein is initially inactivated by attaching 2-nitrobenzyl moiety to group G, involved in protein activity, rendering protein inactive. After illumination, the nitrobenzyl group is removed, the G group is regenerated, and protein becomes active.

proteins as used in this review is meant to represent examples of nonphotonic proteins that were engineered to have photonic functions and also photonic proteins completely designed de novo. Examples include proteins that were engineered to contain reporter groups at specific positions to detect conformational changes or to sense interaction with other biomolecules; proteins with functions that can be activated by light; and proteins that have similar functions to those in nature, including energy conversion, light sensing, and light signaling.

The engineering of artificial photonic proteins is becoming feasible in part because of the emergence of a number of powerful methods aimed at the incorporation of light absorbing, fluorescent, and photocleavable moieties into proteins. In addition to the well-established field of chemical labeling, methods based on genetic engineering, including tRNA-mediated protein engineering (TRAMPE) and protein ligation, have emerged. These techniques offer increasing ability to incorporate nonnative chemical moieties, including unnatural amino acids, into proteins at specific positions. As described in this review, this opened the door to many novel applications of photonic proteins in the fields of molecular biophysics, cell biology, diagnostics, drug discovery, and proteomics.

133.2 Chemical Engineering of Photonic Proteins

By far the simplest method with which to impart photonic properties to any given protein is via chemical labeling. For example, a photonic label can be covalently linked to an exposed lysine or cysteine residues on a target protein using amine-reactive reagents (NHS esters or isothiocyanates) or thiol-reactive reagents (iodoacetamides or maleimides). However, this approach leads to a heterogeneous nonuniform label distribution,[20] and in extreme cases, in complete loss of protein activity. In order to attach a photonic tag to a specific site on the protein, cysteine mutagenesis can be utilized, whereby a single reactive cysteine is incorporated into the protein.[21,22] A label is then attached using SH reactive groups, such as maleimides or iodoacetamides. However, this sometimes requires that native cysteines present in the protein be removed by site-directed mutagenesis, thereby altering its structure and function. Despite these limitations, there are many examples of applications of chemical labeling that led to the production of photonic proteins that fall into a variety of categories as described below.

Photoswitches

Chemical labeling was used extensively to create "photoswitchable" protein conjugates. Such proteins have the property that upon illumination, the photonic labels render the protein active/inactive or change its physicochemical properties. These photonic switches can be further subdivided into two categories: irreversible and reversible photoswitches.

Irreversible Photoactivation

Irreversible photoswitches consist mainly of "caged" proteins that upon illumination undergo a transition from an inactive (resting) to an active state. Normally, caging is accomplished by blocking reactive groups on the protein side chains (labeled G in Figure 133.1) with a photoremovable protective group, such as 2-nitrobenzyl or its derivatives. Upon illumination, the caging group is removed, and the protein activity is restored.

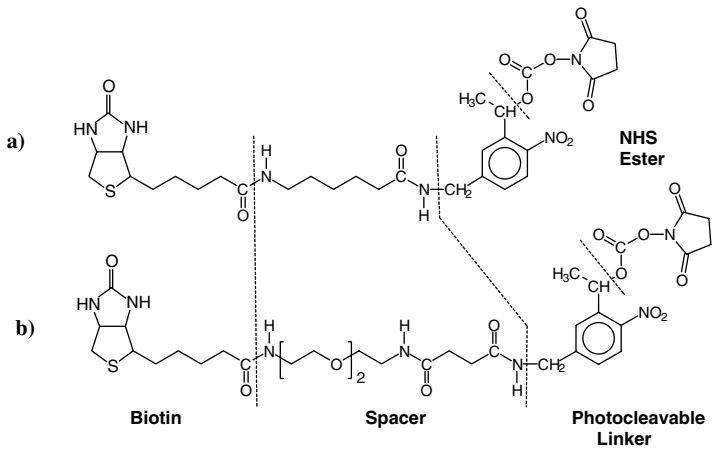

FIGURE 133.2 Design of photocleavable biotin (PC-Biotin) NHS reagents: (a) water insoluble PC-Biotin-NHS, (b) water soluble PC-Biotin NHS. After modification of biomolecule with PC-Biotin and binding of the conjugate to streptavidin, light can be used to release the target biomolecule or reactivate it.

The caging process was successfully employed for a number of proteins as well as for complex biological systems. For example, Thompson et al.[23] showed that up to 15 2-nitrobenzyl residues can be incorporated into bovine serum albumin and ~95% of them can be removed by exposure to near-UV light. Marriott[24,25] used 6-nitroveratryloxy-chloride (NVOC-Cl) to prepare caged G-actin in high yield. The conjugate was characterized by biochemical and absorption spectroscopic methods, in particular, the ability to polymerize into F-actin. Approximately 90% of activity was restored upon illumination with near-UV light. Caged G-actin labeled with tetramethylrhodamine or fluorescein at Cys374 was also prepared and characterized. These caged fluorescent G-actin conjugates can be used to generate fluorescent, polymerization-competent G-actin following light activation. Caged antibodies were first described by Self et al.[26] These conjugates were obtained by performing coupling of 1-(2-nitrophenyl)ethanol (Npe) to proteins using diphosgene. In addition to caging antibodies, the authors also performed caging of antigens and showed that light can be used to modulate the level of antibody-binding sites for antigen, antigen-binding sites for antibody, and antibody-Fc-binding sites for Protein A.

Kossel et al.[27] used 6-nitroveratryloxy-chloride (NVOC-Cl) to inactivate function-blocking monoclonal antibody against brain-derived neurotrophic factor (BDNF). This antibody was then used to study synaptic potentiation in brain slices under controlled concentration of BDNF. This is an example of caged antibody used as a precise spatiotemporal control of endogenous protein levels. The same compound (NVOC-Cl) was used by Minden et al.[28] to cage GAL4VP16, a potent transcriptional activator. The caged protein was then injected into drosophila embryos and used to locally activate the expression of a wide variety of GAL4 UAS transgenes with a brief exposure to near-UV light.

Macromolecular Complexes

Photoactive moieties can also be used to produce light-activated macromolecular complexes such as light-activated ionic pores in membranes. A photocleavable-biotin reagent, PC-biotin-NHS (see Figure 133.2), was synthesized[29] and used to reversibly modify lysine residues of α-hemolysin (α-HL), an exotoxin of *Staphylococcus aureus*, which forms pores in lipid bilayer membranes.[30] When α-hemolysin was incubated with 5- to 20-fold molar excess of PC-biotin-NHS at 0°C and pH 10.5 for 10 min, it exhibited a concentration-dependent loss of hemolytic activity. At 20-fold molar excess of PC-biotin-NHS, the activity was negligible. When the modified α-hemolysin was exposed to long-wavelength UV light (>300 nm) for 10 min, over 80% of its activity was regenerated. This "caging" effect is most likely due to the prevention of proper assembly of the individual α-hemolysin monomers into a heptameric ion channel that spans the lipid bilayer.

Moritz et al.[31] used PC-biotin-labeled antibodies to selectively isolate the γ-tubulin ring complex of *Drosophila*. After capture using streptavidin media, the structure of the complex was studied using electron microscopic tomography and metal shadowing.

As an example of using chemical engineering to produce a much larger light-activatable biomolecular assembly, Pandori et al.[32] used water-soluble photocleavable biotin (see Figure 133.2) to control the infectivity of adenoviral vectors. Upon treatment with PC-biotin, the infectivity of these vectors is almost completely eliminated and can be restored by short exposures to near-UV light (365 nm). This method was used to locally induce the expression of transgenes in the target cells *in vitro* and *in vivo*. This demonstration offers advantages in the field of gene therapy by providing a novel method to control viral infectivity.

Selective Chemical Labeling

In addition to random caging reactions, it is desirable to be able to specifically cage the particular amino acid residue involved in activity. This approach was demonstrated, again with α-HL, by using scanning cysteine mutagenesis and the cysteine specific caging reagent, 2-bromo-2-(2-nitrophenyl)acetic acid (BNPA).[33] Similar methodology was also used to generate caged, unprotected, cysteine-containing or thiophosphorylated peptides in aqueous solution with 2-nitrobenzyl bromides.[34,35] A similar highly directed reaction between a single thiophosphorylated threonine residue in the catalytic subunit of protein kinase A and 4-hydroxyphenacyl bromide was used to generate caged protein kinase A. This caged protein exhibited significantly reduced activity[36] that was restored up to 90% upon near-UV illumination.

Unlike most proteins, where precise control of the caging reaction is difficult to achieve, chemically synthesized peptides can be caged relatively easily at specific amino acids.[37–39] In one case, this approach was used to generate photoactivatable ribonuclease S.[40] This enzyme is composed of two units: S-peptide (Residues 1 to 20) and S-protein (Residues 21 to 124). A series of S-peptides carrying a 2-nitrobenzyl caging group on either Asp, Glu, Gln, or Lys side chains was prepared by chemical synthesis and chimeric RNAse S variants composed of these caged peptides assembled. In one case, a complete inactivation of RNAse S was achieved with 37% activity recovered upon illumination.

Photoactivatable fluorochromes or "caged" fluorescent moieties are useful for visualizing and tracking the movement of macromolecules inside living cells.[41,42] Caged fluorescent tubulin was extensively used to study microtubule formation, dynamics, and movement.[43–45]

Reversible Protein Photoactivation

In contrast to the previous discussion, some photonic protein switches are reversible. Reminiscent of several retinylidene-based rhodopsins, such as Sensory Rhodopsin I,[46,47] most of these systems are based on reversible photoisomerization. In this case, however, the chromophore is based on the azobenzene, cinnamate, or spiropyrane-merocyanine system. The photochemical reactions for these three classes of photonic switches are illustrated in Figure 133.3.

Both azobenzene and cinnamate derivatives were used as early as the 1960s and 1970s to photoregulate enzyme activity. This was accomplished by covalently modifying an enzyme's active site or by tethering these labels to specific enzyme inhibitors.[48] A recent interesting example includes caged thrombin,[49] which was photoactivated intravenously to produce localized thrombosis. Novel peptide-based photoswitchable inhibitors of α-chymotrypsin based on α-ketoester were also recently described.[50] In this case, the utilization of a peptide recognition sequence as well as an azobenzene moiety resulted in tighter binding and better photomodulation properties as opposed to nonpeptide inhibitors conjugated to azobenzene.

Ribonuclease S peptide containing an azobenzene switch at various positions was also recently synthesized and evaluated[51] but did not exhibit efficient photomodulation of activity. In contrast, site-specific incorporation of azobenzene switch into horseradish peroxidase using TRAMPE (for details see Section 133.3) allowed for efficient control of enzymatic activity.[52] Similarly, 90% photomodulation of horseradish peroxidase activity was achieved by covalent conjugation of the enzyme to carboxylated spiropyran dye.[53]

It is well known that the conjugation of proteins to chemical polymers can be used to improve protein stability or change its solubility. Ito et al.[54] conjugated subtilisin to spiropyran carrying polymethacrylate

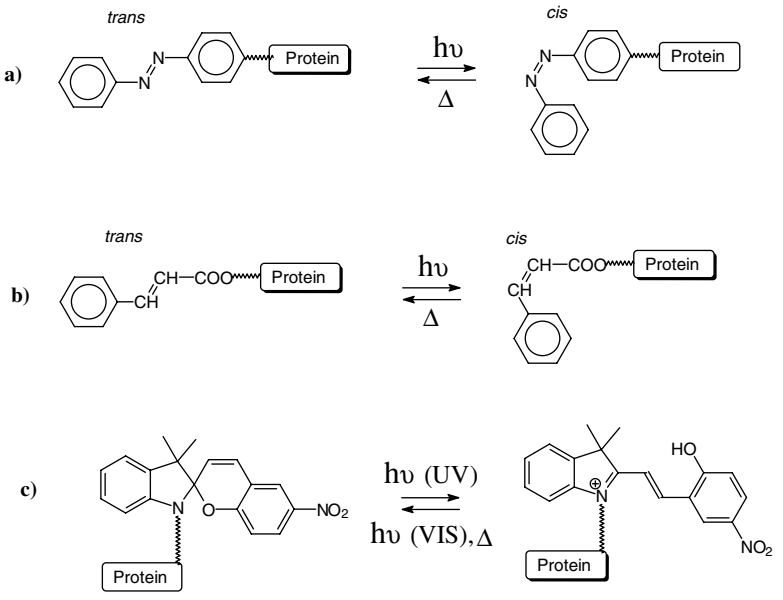

FIGURE 133.3 Reversible protein photoactivation. The attachment of azobenzene (a), cinnamate (b), or spiropyrane-merocyanine (c) to active sites in proteins enables reversible photomodulation of activity. These photoswitches involve reversible *cis-trans* isomerization (a–c) and cyclization (c) reactions.

that rendered the conjugate soluble in toluene while retaining 100% activity. The conjugate was precipitated upon exposure to UV light and could be resolubilized upon exposure to visible light.

In a similar approach, a single cysteine mutant N55C of endoglucanase 12A, was conjugated to the end of linear polymethacrylate grafted with azobenzene.[55] Two different means of azobenzene grafting onto the polymer (amide or ester) resulted in two different enzyme conjugates, which could be activated or deactivated using UV or visible light. Importantly, these conjugated enzymes exhibit ~50% of the activity of the native enzyme in the "on" state, while only 1 to 3% activity is observed in the "off" state.

In addition to photomodulation of enzymatic activity, an azobenzene moiety was incorporated into a model peptide antigen Glu-azoAla-Gly-Gly that allows for photoregulation of the antigen–antibody interaction.[56] More recently, incorporation of an azobenzene moiety was used to photomodulate peptide conformation.[57–62] The reader is referred to a recent review[63] for more examples of photoresponsive peptides produced using azobenzene or spiropyran moieties.

Photonics Probes

In addition to photonic switches, photonic proteins were engineered to contain fluorescent moieties that react to changes in a protein's local environment and to conformational changes. In this section, we review several examples of designing photonic probes that goes beyond simple chemical labeling and cysteine mutagenesis.

Protein Modifications

One novel approach involves incorporation of an epitope tag that assumes a α-helical motif. Furthermore, this tag contains a tetracysteine (CCXXCC) sequence that reacts with a specific fluorophore carrying a biarsenical moiety leading to a fluorescent conjugate.[64] In addition to the originally described reagent that produces a fluoroscein-like fluorescence (FlAsH, fluorescence emitting at 528 nm), two additional biarsenical analogues were developed with emission in the blue (CHoXAsH, 430 nm) and red (ReAsH, 608 nm).[65] A dual color-labeling approach utilizing FlAsH and ReAsH was also recently used for intracellular sequential labeling of connexin-43 and for monitoring its trafficking in and out of gap junctions.[66]

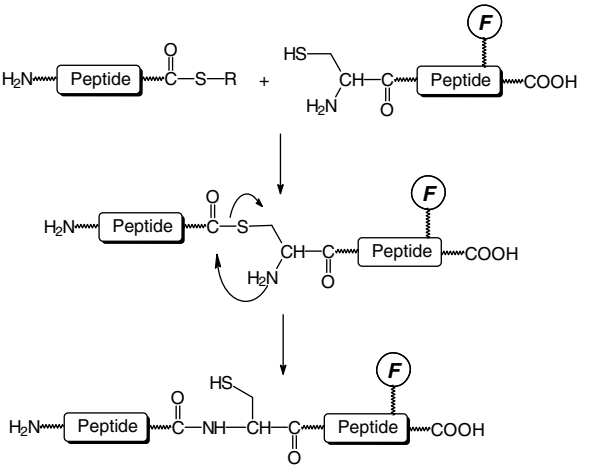

FIGURE 133.4 Incorporation of photonic probes into proteins *via e*xpressed protein ligation (F = fluorescent probe). This approach involves a very specific chemical reaction between thioester on one polypeptide fragment and the N-terminal cysteine moiety on the other. Initial intermediate cysteine thioester is converted into native peptide bond by intramolecular reaction. The original free SH group of the cysteine is also regenerated.

This approach allows for a determination of protein "age" within living cells as well as for a determination of expression level. A similar, environment-sensitive dye was used to monitor intracellular calmodulin conformational changes in response to Ca^{2+} concentration.[67]

An alternative approach to site-specific introduction of photonic probes relies on the selective oxidation of *N*-terminal serine or threonine to an aldehyde followed by specific reaction with aromatic amines or hydrazine derivatives (hydrazides, thiosemicarbazide).[68] Ketone moieties can also be generated by metal-catalyzed transamination reaction.[69]

As discussed previously, chemical synthesis allows a more general method of introducing site-specific photonic probes into polypeptides that is normally not possible using recombinant-DNA-based methods. However, chemical peptide synthesis is limited to peptides of 50 to 100 amino acid residues. In order to circumvent this limitation, an approach termed native chemical ligation[70] was developed, which is based on the chemoselective reaction of unprotected peptide segments in water at pH 7 to form amide-linked polypeptide products.

This approach requires, as illustrated in Figure 133.4, two peptide fragments, one with thioester at the *C*-terminus and the other with the *N*-terminal cysteine. The availability of the thioester peptide segments is facilitated by the discovery of the "defective intein" splicing system.[71,72] This approach was used, for example, to generate a fluorescent biosensor for Abl kinase activity.[73] In this work, the truncated version of the c-Crk-II protein was synthesized bearing rhodamine and fluorescein at two different sites. Upon phosphorylation, a conformational change induced alterations in the FRET signal observed between the two labels. In another example, two fluorescent amino acids with structures based on the nitrobenz-2-oxa-1,3-diazole (NBD) and coumarin fluorophores were incorporated into the Ras binding domain (RBD) of c-Raf1.[74,75] The binding of activated Ras protein could be detected by monitored fluorescence.

Using Native Fluorescent Proteins

Proteins that exhibit fluorescence in their native form were extensively studied and utilized in a variety of applications. One important example is green fluorescent protein[18] (GFP) of *Aequorea victoria* and its mutants (BFP, CFP, YFP), which exhibit blue, cyan, and yellow emissions, respectively.[76] In addition, a novel fluorescent protein, termed DsRed, was recently cloned and characterized.[77] These proteins are unique in having fluorophores formed from the natural amino acid side chains via cyclization. A major application for them is the creation and expression of fluorescent fusion proteins. Such fusion constructs were used in a variety of applications involving *in vitro* and *in vivo* spatial and temporal fluorescence

monitoring, especially involving use of fluorescence resonance energy transfer (FRET). For example, Chan et al.[78] demonstrated that the interactions between individual receptor chains of the tumor necrosis factor receptor (TNFR) family members in a cellular system can be detected using FRET. By fusing CFP and YFP to caspase substrates, apoptotic caspase activity can be monitored within single cells.[79–81] Protein–protein interactions, transport phenomena,[82] and conformational changes[83] in living cells can also be monitored using coexpression of GFP fusions and its variants. A protease assay utilizing two-photon cross-correlation and FRET between GFP and DsRed was described.[84] Unlike FRET, the method of dual-color cross-correlation is not limited to a specific range of distances between the fluorophores. By fusing CFP and YFP to kinase substrate, specific kinase activity inside living cells can be monitored.[85–87] A calmodulin-GFP fusion molecule was used as an *in vivo* real-time FRET-based sensor for monitoring Ca^{2+} concentration.[88]

Besides the GFP family, phycobiliproteins were used in a FRET-mediated FACS assay[89] and to construct a FRET-based glucose sensor.[90] However, a major difficulty with the use of phycobiliproteins is related to their oligomeric structure and the requirement for cofactors.[76]

133.3 tRNA-Mediated Engineering of Photonic Proteins

In addition to chemical engineering and site-directed mutagenesis described in the previous section, an approach based on tRNA-mediated protein engineering (TRAMPE) presents new opportunities for engineering photonic proteins. TRAMPE relies on the following:

1. Development of novel tRNAs and their misaminoacylation with custom-designed amino acids
2. Recognition of special codons by the tRNAs
3. Efficient expression of these modified proteins

Recent progress was made in all these areas (see Rothschild and Gite[91] for a detailed review), and a few representative examples that resulted in the production of photonic proteins are described below.

The Basics of TRAMPE

The pioneering studies of Khorana and Nirenberg in the early 1960s[92,93] provided scientists with the genetic code, the critical information necessary to engineer proteins at the genetic level. In addition, the ability of the translation machinery to accommodate amino acids outside the canonical 20 has been long known.[94] TRAMPE, by exploiting this fact, allows expansion of the genetic code so that custom-designed nonnative amino acids can be selectively introduced into proteins.

Misaminoacylated tRNAs

Early studies using TRAMPE were based on the chemical modification of aminoacyl-tRNAs prepared enzymatically with one of the 20 native amino acids. This approach, referred to here as nonnative amino acid replacement (NAAR), allows specific amino acids in the protein to be replaced by their derivatized analogs. For example, it was demonstrated by Johnson and coworkers that a $tRNA^{Lys}$ enzymatically aminoacylated with lysine could be derivatized with a light-activated cross-linking reagent to form N-ε-(5-azido-2-nitrobenzoyl)-Lys-$tRNA^{Lys}$.[95–97] Using these misacylated tRNAs in a cell-free protein synthesis system enabled investigation of secretory protein translocation across the ER membrane by photo-cross-linking techniques. More recently, effective methods were developed to incorporate nonnative amino acids at a specific point in a protein. This approach, called site-directed nonnative amino acid replacement (SNAAR), is based on the use of stop codons incorporated at specific positions in the DNA coding for proteins and complementary suppressor tRNAs, which cause the stop codon to be read-through.[98,99]

Illustrated in Figure 133.5 is the basic approach for the incorporation of nonnative amino acids at specific locations in a protein. The aminoacylation of a suppressor tRNA (Figure 133.5, top) is accomplished by using methods for chemical aminoacylation of tRNAs or by modifying an aminoacyl-tRNA aminoacylated enzymatically. In the chemical aminoacylation method, the nonnative amino acid of

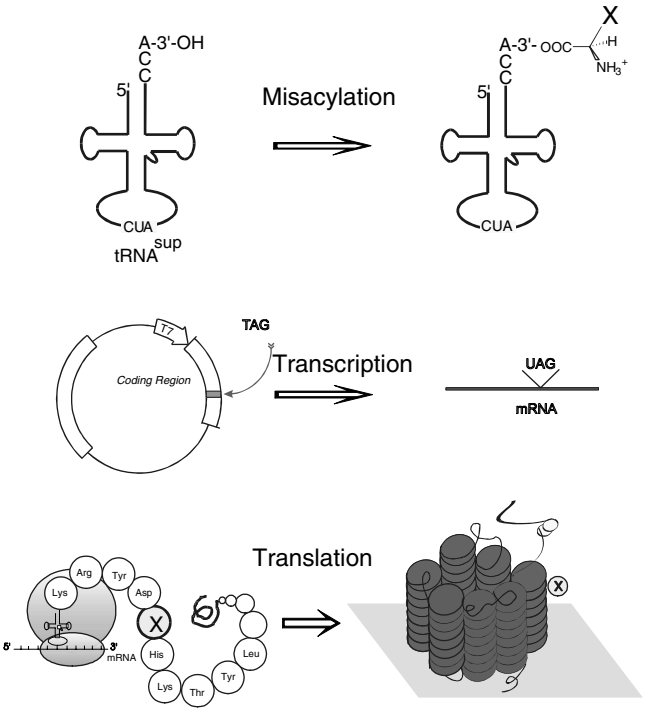

FIGURE 133.5 Steps for the incorporation of a non-native amino acid (X) into a protein by using SNAAR. Top: A suppressor tRNA with an anticodon corresponding to the amber codon UAG is misacylated with a non-native amino acid (X). Middle: The TAG stop codon is transcribed into an mRNA containing the UAG stop signal at a defined position. Bottom: Cell-free translation of the above mRNA results in incorporation of non-native amino acid, X, into the nascent protein at a specific position.

interest is used to acylate the dinucleotide pdCpA and then is ligated to a truncated tRNA.[98,100] In contrast to enzymatic aminoacylation of tRNAs, which is generally limited to only natural amino acids or, in special cases, their analogs, it is possible to aminoacylate tRNAs with any nonnative amino acid by chemical aminoacylation. A third method is to misaminoacylate a tRNA using a native aminoacyl synthetase. However, this latter approach is restricted to a relatively small set of amino acid analogs, such as fluoro-phenylalanine[101] or the proline analog thiaproline.[102] The nonnative amino acid is then targeted to the proper position in the nascent protein by choosing a specific codon (out of the possible 64) that corresponds to the anticodon of the misaminoacylated tRNA. For example, for the purpose of SNAAR, a suppressor tRNA, which acts to suppress a stop codon (i.e., UAG, amber; UAA, ochre; or UGA, opal), can be placed at a specific position in the gene (Figure 133.5, middle). Finally, the protein is synthesized in a cell-free or cellular translation system to which the misaminoacylated tRNA is introduced (Figure 133.5, bottom).

In addition to the aforementioned methods, it is possible to use *in vitro* evolved ribozyme for tRNA aminoacylation.[103] The evolved ribozyme can be programmed for selectivity toward specific tRNAs. This method, therefore, has potential as a means of generating aminoacyl-tRNAs that are charged with nonnatural amino acids.

Frameshift Suppression

To avoid competition between endogenous release factor and suppressor tRNA, a new strategy based on frameshift suppression mutations was developed.[104–106] This strategy, based on the ability of tRNAs with extended anti-codons to suppress frameshift mutations, has two advantages over conventional suppression using the three-base amber, opal, and ochre stop codons: competition between tRNA and release factors (RF) is avoided, and this approach allows more than one unnatural amino acid to be incorporated

into a single protein by using two or more frameshift suppressor tRNAs. In fact, it was shown that not only four-base but even five-base anti-codon tRNAs are able to incorporate unnatural amino acids with efficiency up to 86%.[107–110]

Incorporating Photonic Reporter Groups

One attractive use of TRAMPE is the incorporation of reporter groups into molecules that can provide information about protein structure and conformational changes, especially in membrane proteins not easily analyzed by x-ray crystallography. One of the earliest demonstrations of this capability was the work of Johnson and coworkers, in which they were able to label proteins with fluorescent amino acid derivatives.[111] Cornish et al.[112] reported site-specific incorporation of spin-labeled, fluorescent, and photoactivatable amino acids into T4 lysozyme. More recently, Chamberlin and coworkers incorporated three different fluorescent analogs, 5-hydroxyltryptophan, 7-azatryptophan, and ε-dansyllysine into β-galactosidase.[113] One novel aspect of this work was the use of an *E. coli* S30 extract derived from a mutant strain producing a faulty release factor (RF1). The highest expression yield obtained was for 5'-OH Trp (7.6 μg/ml) using the suppressor $tRNA^{Gly}_{CUA}$, whereas much lower yields were observed for 7-azatryptophan and ε-dansyllysine.

As an example of a similar approach using *in vivo* SNAAR, Turcatti et al.[114,115] incorporated a fluorescent amino acid, 3-*N*-(7-nitrobenz-2-oxa-1,3-diazol-4-yl)-2,3-diaminopropionic acid (NBD-Dpr), at specific sites in the tachykinin neurokinin-2 receptor, a member of the large family of seven α-helix G-protein coupled receptors (GPCRs). The expression system, *Xenopus* oocytes, allowed for functional assays of the receptor. Structural information was obtained by measuring the intermolecular distance between the fluorescent amino acids placed at different sites and a fluorescently labeled heptapeptide antagonist using fluorescence resonance energy transfer (FRET).

Photonic Probes of Electrostatic Environment

The site-specific incorporation of a fluorescent amino acid, Aladan (Alanyl-6-dimethylamino-2-acyl-naphthalene), into soluble and membrane proteins was recently reported using TRAMPE.[116] **Aladan** was shown to be exceptionally sensitive to the polarity of its surroundings and could be incorporated site-selectively at buried and exposed sites, in soluble and membrane proteins. In one example of this capability, Aladan was incorporated at various sites into the Kir2.1 and Shaker potassium channels. These proteins showed normal activity, indicating that the incorporation of Aladan did not interfere with proper folding. In addition, Aladan was incorporated by solid-phase synthesis at four different sites in GB1, a highly thermostable IgG-binding domain that has been extensively characterized. In all cases, the fluorescence emission wavelength was dependent on the site of incorporation and local microenvironment.

N-Terminal Labeling of Nascent Proteins with Fluorescent Groups

A sensitive, nonisotopic, fluorescence-based method for the detection of nascent proteins directly in polyacrylamide gels was reported.[117] A fluorescent reporter group was incorporated at the *N*-terminus of nascent proteins using an *E. coli* initiator $tRNA^{fmet}$ misaminoacylated with methionine modified at the α-amino group. In addition to the normal formyl group, the protein translational machinery accepts BODIPY-FL, a relatively small fluorophore with a high fluorescent quantum yield, as an *N*-terminal modification. A direct visualization of a nascent protein bands with good sensitivity was achieved by using a fluorescence scanner or a conventional UV-transilluminator. This approach eliminates the need for radioactivity and provides rapid detection of the protein bands immediately after electrophoresis without any downstream processing.

C-Terminal Labeling of Nascent Proteins with Fluorescent Groups

Nemoto et al. developed a method for the fluorescence labeling of the *C*-terminal of nascent proteins using fluorescein-puromycin conjugates.[118] The fluorescent analog of puromycin (an antibiotic that inhibits protein synthesis by binding to the A site on the ribosome) forms a bond with the *C*-terminal amino acid residue of the protein but only when the coding sequence does not contain a termination

codon. This method was used to monitor protein–protein interactions by fluorescence polarization.[118] More recently, Doi et al.[119] used this method along with microarrays and fluorescence cross-correlation spectroscopy (FCCS) to monitor protein–protein interactions.

Detecting Ligand Binding, Protein Conformational Changes and Proteolysis

A four-base codon/anticodon (CGGG/CCCG) pair was recently used to incorporate fluorescent amino acid analogues at specific positions in streptavidin.[120] Streptavidin mutants with nonnatural amino acid were found to bind biotin, indicating that they retained their native conformation. When an anthryl group was incorporated at Residue 120, its fluorescence was markedly decreased upon biotin binding due to suppression of energy transfer from excited tryptophan. In addition, when the modified amino acid 7-methoxycoumaryl-alanine was incorporated at this position, the fluorescence intensity was modulated by biotin binding. More recently, this approach was used to incorporate a position-specific fluorophore-quencher pair (β-anthraniloyl-L-α,β-diaminopropionic acid [atnDap] as a fluorophore and *p*-nitrophenylalanine [ntrPhe] as a quencher) into streptavidin.[121] Such an approach holds great promise for designing photonic proteins that can "sense" binding of native and nonnative ligands present at very low concentrations.[122,123]

Another example of the incorporation of two unnatural photonic groups into a single protein was shown by Hecht and coworkers.[124] Dihydrofolate reductase (DHFR) was engineered with a fusion peptide at its *N*-terminus that contains the quencher (*N*β-dabcyl-1,2-diaminopropionic acid) and fluorophore (7-azatryptophan) flanking an HIV-1 protease cleavage site. *In vitro* expression involved use of an amber suppressor tRNA and a four-base anticodon tRNA. The resulting DHFR fusion complex exhibited an increase in fluorescence intensity upon treatment with HIV-protease.

Incorporating Light-Activated Residues

Photonic Switching of Protein Activity

In contrast to chemical labeling (Section 133.2), TRAMPE provides a method for engineering proteins with light-activated residues. For example, in early work, Schultz's group succeeded in engineering a photoactivatable T4 lysozyme by substituting nitrobenzyl caged Asp (NB-Asp) for Asp-20, a residue that is essential for catalytic activity.[125] While the modified protein was completely inactive, photolysis by 350 nm light rapidly restored the activity of lysozyme. More recently, a method for site-specific, nitrobenzyl-induced photochemical proteolysis of proteins expressed in living cells was reported by England et al.[126] This method is based on the chemistry of an unnatural amino acid (2-nitrophenyl)glycine (Npg), and its incorporation into nascent proteins in *Xenopus* oocytes using the *in vivo* nonsense codon suppression approach. This nonnative amino acid has the property that irradiation leads to site-specific, nitrobenzyl-induced photochemical proteolysis (SNIPP) along the polypeptide chain. Rapid inactivation of the voltage-activated Shaker B K^+ channel with incorporated Npg residues was achieved by light-induced cleavage of the structural domain responsible for inactivation. SNIPP was also used to cleave the Cys128-Cys142 disulfide loop of the nicotinic acetylcholine receptor, thereby demonstrating that the integrity of this loop is crucial for function.

An additional example of production using TRAMPE of a reversible photoactivatable enzyme was recently reported by Muranaka et al.[52] Horseradish peroxidase mutants containing L-*p*-phenylazophenylalanine (azoAla) at various positions were synthesized by using an *E. coli* cell-free translation system. Among the several mutants studied, four mutants containing a single azoAla residue at positions 6, 68, 142, and 179 retained peroxidase activity. Interestingly, the activity of the Phe68azoAla mutant was higher when the azobenzene group was in the *cis* form than when in the *trans* form. In contrast, the activity of the Phe179azoAla mutant disappeared when the azobenzene group was photoisomerized to the *cis* form but recovered in the *trans* form.

Light-Activated Channels

Caged proteins are useful in a wide variety of applications, including signal transduction.[24,25,36,37] Although most of the work in this area is based thus far on chemical modification of proteins, as discussed in

Section 133.2, TRAMPE can also be used for incorporation of caged amino acids residues. For example, Philipsson et al.[127] reported incorporation of a caged Cys or Tyr into the transmembrane segment of a membrane protein. The authors used suppressor tRNA to incorporate *o*-nitrobenzyl cysteine or *o*-nitrobenzyl tyrosine (caged Cys or Tyr) into Position 9 of the M2 transmembrane segment of the γ-subunit of the muscle nicotinic ACh receptor expressed in *Xenopus* oocytes. The caged amino acids replaced an endogenous Leu residue that was implicated previously in channel gating. Removal of the caging group from modified protein by UV-irradiation resulted in a substantial increase in the ACh-induced current. In addition, it was found that the incorporation of a bulky nitrobenzyl group does not prevent the assembly or trafficking of the ACh receptor. Similarly, Tong et al.[128] used a similar procedure to incorporate a caged tyrosine residue in place of the natural tyrosine at Position 242 of the inward rectifier channel Kir2.1 expressed in *Xenopus* oocytes. In this case, the tyrosine residue was chosen, because its side chain is known to participate in several distinct signaling pathways, including phosphorylation and membrane trafficking. The protein containing caged tyrosine was activated by exposure to near-UV light.

Monitoring Protein Expression

In addition to custom design of photonic proteins, which normally requires site-specific modifications at particular internal residues, TRAMPE can be used to incorporate photonic moieties at nonspecific positions, such as at random lysine residues or only at the *N*-terminal position of a protein. This approach can be useful in the fields of gene expression, proteomics, and even medical molecular diagnostics. For example, fluorescent labels can be used to monitor *in vitro* or even *in vivo* expression of proteins, to build arrays of proteins with which to detect specific protein–protein or drug–protein interactions, and even to detect genetic defects, which are expressed on the protein level.

Efficient *N*-Terminal Labeling with Photonic Groups

As described in Section 133.3, it is possible to label the *N*-terminus of proteins expressed in a cell-free translation system with a fluorescent tag using *E. coli* initiator $tRNA^{fmet}$.[117] Under optimal conditions, the incorporation of BODIPY-FL was found to be low (1 to 2%), even though it was sufficient to detect nascent proteins with good sensitivity using SDS-PAGE. For this reason, a more efficient method was developed[129] that utilizes an amber initiator suppressor tRNA chemically aminoacylated with a nonnative amino acid conjugate, which is introduced into an *E. coli* S30 cell-free translation system. The normal initiator codon (ATG) of the gene was replaced by an amber codon (TAG) in the DNA template. Using this approach, several fluorophores and affinity tags were incorporated at the *N*-terminus of various proteins, such as α-hemolysin, dihydrofolate reductase, and firefly luciferase. Typically, in this system, the specific labeling achieved was 25 to 50%, while protein yield was around 20% compared to the yield of wild-type protein translation. For the proteins studied, the presence of modifying groups at the *N*-terminus did not affect enzymatic activity. Protein translation was initiated with different labeled amino acids. In one case, lysine carrying two different labels on both amino groups was successfully incorporated at the *N*-terminus. The resulting protein had a fluorophore BODIPY-FL group on the ε-amino group and a biotin or PC-biotin on α-amino group of the *N*-terminal lysine.

Labeling at Specific Amino Acids with TRAMPE

A general method of incorporating fluorophores into nascent proteins can be based on the use of elongator tRNAs (e.g., lysyl-tRNA) misaminoacylated with fluorophores. For example, AmberGen, Inc. developed an approach based on the fluorescent reporter group BODIPY-FL,[130] which is randomly incorporated at lysine positions in the protein chain using an *E. coli* $tRNA^{lys}$ aminoacylated with lysine and modified at the ε-amino group.[131] This particular tRNA is available under the trade name Fluoro-Tect™-$Green_{Lys}$ from Promega Corp (Madison, WI). Similar to BODIPY-FL-Met-$tRNA^{fmet}$, BODIPY-FL-Lys-$trna^{lys}$ enables sensitive detection of cell-free synthesized proteins in a prokaryotic translation system (*E. coli* S30 extract) as well as eukaryotic translation systems (wheat germ and rabbit reticulocyte cell-

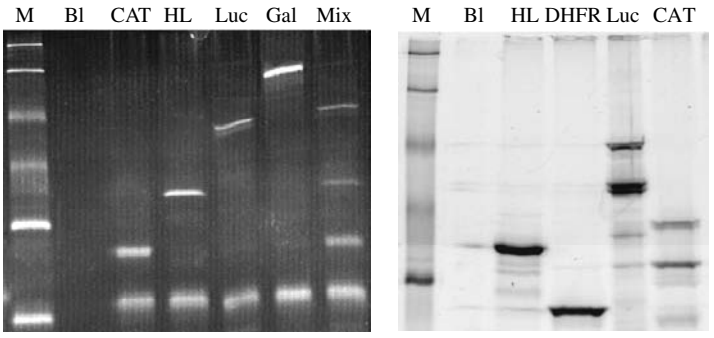

FIGURE 133.6 Fluorescent detection of *in vitro* expressed proteins. (A) Test proteins were labeled with BODIPY-FL-Lys-tRNA^{lys} in TNT wheat germ cell-free expression system and visualized using UV-transilluminator/CCD camera. (B) Test proteins were labeled using BODIPY-FL-Lys-tRNA^{lys} in *E. coli* S30 cell-free expression system and visualized using laser scanner (FluorImager). Lane M - fluorescent molecular weight markers, Bl - negative control-no DNA added; CAT - chloramphenicol acetyltransferase; HL - α-hemolysin; Luc - luciferase; Gal - β-galactosidase; DHFR - dihydrofolate reductase and Mix - a mixture of CAT, HL and Luc DNA.

free translation extracts).[132] Recently, this tRNA was used for high-throughput expression screening of various cDNA constructs.[133]

As an example of its application to monitor cell-free protein expression, shown in Figure 133.6 is the visualization of fluorescent bands from several proteins expressed in wheat germ and *E. coli* translation systems in the presence of BODIPY-FL-lysyl-tRNA^{lys}. In contrast to conventional radioactive detection, these proteins were detected on the gel immediately after SDS-PAGE. In particular, the gels did not require fixing, which normally is at least a 30 min procedure. The detection time using a conventional UV-transilluminator/CCD camera or a laser scanner (FluorImager, Molecular Dynamics) was less than 5 min, compared to several hours for autoradiography.

This tRNA (BODIPY-lysyl-tRNA^{lys}) was recently used to demonstrate the presence of coupled transcription and translation within the nuclei of mammalian cells.[134] This was achieved by incubating permeabilized mammalian cells with lysyl-transfer RNA tagged with BODIPY (BODIPY-lysyl-tRNA^{lys}). Although most nascent polypeptides were found in the cytoplasm, some were found in discrete nuclear sites known as transcription "factories." This coupling is simply explained, if nuclear ribosomes translate nascent transcripts as those transcripts emerge from still-engaged RNA polymerases, much as they do in bacteria.

In addition to nonspecific lysine labeling, Lien et al.[135] reported site-specific incorporation of a fluorescent tag into nascent proteins using a Cys-tRNA^{cys}. After aminoacylation of *E. coli* Cys-tRNA^{cys}, it was modified with a SH-reactive fluorophore (BODIPY-FL). This method may prove valuable when used in conjunction with site-directed mutagenesis to create protein containing single-cysteine residues by which one can prepare the nascent protein containing single fluorophore at a defined position.

Applications of TRAMPE to Molecular Diagnostics

Truncations in a protein can occur due to frameshift and point mutations that result in creating a prematured stop codon in the reading frame of a gene. Such truncated polypeptides can be detected by translating a specific region of the DNA (mRNA) corresponding to the target gene in a cell-free translation system in the presence of radioactive labels (e.g., ^{35}S-methionine or ^{14}C-leucine) and then by analyzing SDS-PAGE and autoradiography. Such an approach, known as the protein truncation test (PTT), was successfully used for the analysis of truncating mutations in a variety of cancer-linked genes, including BRCA1/BRCA2, ATM, MHS2, MLH1, and APC.[136–138] However, in conventional PTT, the use of radioactive isotopes presents several problems, including detection time (>8 h), which is critical for high-throughput analysis. For this reason, it would be highly advantageous to replace radioactivity with a

more rapid means of detection. In order to overcome this, a nonisotopic, high-throughput PTT method was developed using cell-free protein synthesis and incorporating biotin and BODIPY-FL.[131] The incorporation of fluorescent moieties into nascent proteins or protein fragments using TRAMPE allowed for the detection of premature chain-truncating mutations that occur in a variety of tumor suppressor proteins.

133.4 Future Perspectives

In this review, we described many of the emerging tools that can be used to build artificial photonic proteins. They include a repertoire of increasingly versatile and selective molecular engineering techniques for incorporating photonic molecules into nonphotonic proteins, including TRAMPE, chromophore-binding motifs, and selective chemical reactions. The creation of new and useful photonic molecules that can serve as chromophores for photonic proteins, such as isomerizable chromophore and photocleavable caging agents, is also contributing to this goal.

A second convergent path toward building functional photonic proteins not covered in this chapter is the progress occurring in the field of "designer proteins," e.g., de novo design of proteins.[139] The goal of researchers in this area is to develop the ability to build new proteins from the ground up, with specific functional properties, such as receptor, enzymatic, and ion transport. Progress includes the discovery of increasingly shorter amino acid sequences (~20) that fold into well-defined stable structure domains.[140] In addition, progress is also occurring in the understanding of the principles that govern protein folding, cooperativity, and conformational changes.[141] Such structures can serve as scaffolds on which to incorporate photonic moieties that serve as light sensors and light triggers, as discussed in this chapter.

A third factor contributing to the development of artificial photonic proteins is the increasing detail for which the mechanism of natural photonic proteins is understood. For example, in the case of bacteriorhodopsin, one of the most extensively studied photonic proteins, high-resolution three-dimensional structures along with spectroscopic probes of BR and its photocycle intermediates are providing an unprecedented look at hydrogen-bonded proton chains, helix movements, and chromophore isomerization, which underlie the light-driven proton transport function of this protein.[7,142,143] Similar progress is also occurring in the study of the related Sensory Rhodopsin II signal transduction protein and its associated transducer HtRII[144–147] (see Chapter 124) as well as many other light-activated proteins in nature. This knowledge, along with increased understanding of how such proteins fold stably in the membrane[148,149] and possess, in many cases, structural integrity at high temperatures,[150] will provide an increasingly firm basis for constructing biomimetic photonic proteins.

While many of the examples described in this review are already useful for basic research, it is expected that as the ability to build artificial photonic proteins continues to improve, they will find their way into many areas of biotechnology and medicine. One example described in the *Scientific American* article, "Building Doors into Cells," by H. Bayley,[151] is the use of engineered photonic proteins for targeted drug delivery. Using light-activated pores of α-hemolysin as an example , it is proposed that such photonic proteins could be incorporated into liposomes, which would serve as drug delivery vehicles. Once the liposome is distributed throughout the body, the drug can be delivered locally via photoinduced release of the drug from the liposome. A similar strategy applies to light-activated gene therapy, the basis of which was described by Pandori et al.[32]

Photonic proteins are also likely to become critical components of a new generation of biosensors. The ability to design proteins that contain fluorescent molecules at specific positions, such as within a binding pocket or inside a channel, facilitates the detection of specific molecular interactions, as discussed previously. One example where such an approach might be especially attractive and have a major impact is the detection of single nucleotides as an oligonucleotide as it transits through a nanopore. Dramatic progress was recently achieved in this direction by monitoring conductivity changes of oligonucleotides inside such a pore,[152,153] including the engineering of α-hemolysin for this purpose.[154] It is possible to envision a photonic version of a nanopore that could be used for rapid DNA sequencing and mutation detection. In such a system, fluorescence rather than electrical current would be monitored as individual

bases transiting past a molecularly engineered photonic read probe. In such a system, single molecule fluorescence detection could be utilized.[155] An array of such nanopores, each engineered to recognize different small sequences, could also be envisioned.

In the continuing endeavor to build photonic proteins evolve, cutting-edge progress in molecular biology, photochemistry, and photobiology will continue to be relied upon.

Acknowledgments

The authors wish to acknowledge the contributions from the Boston University Molecular Biophysics Laboratory and AmberGen, Inc., whose members contributed to the research described in this chapter, along with many of our collaborators, including H. Bayley, C. Cantor, W. DeGrip, H.G. Khorana, U.L. RajBhandary, J.L. Spudich, and T. Sano, who inspired our interest at an early stage in many of the concepts described here. This work was supported by grants from the NIH (EY05499) to KJR and SBIR awards to AmberGen, Inc., from the Army Research Office and the NIH (GM64912, CA83396, and GM63369). We also wish to thank the Photonics Center at Boston University and its Director, Don Fraser, for encouragement and infrastructure support.

References

1. Le Grand, Y., *An Introduction to Photobiology*, Elsevier, Amsterdam; New York, 1970.
2. Teske, A., Hinrichs, K.U., Edgcomb, V., de Vera Gomez, A., Kysela, D., Sylva, S.P., Sogin, M.L., and Jannasch, H.W., Microbial diversity of hydrothermal sediments in the Guaymas Basin: evidence for anaerobic methanotrophic communities, *Appl. Environ. Microbiol.*, 68, 4, 1994–2007, 2002.
3. Madigan, M.T. and Marrs, B.L., Extremophiles, *Sci. Am.*, 276, 4, 82, 1997.
4. Deisenhofer, J. and Michel, H., Nobel lecture. The photosynthetic reaction centre from the purple bacterium *Rhodopseudomonas viridis*, *EMBO J.*, 8, 8, 2149, 1989.
5. Allen, J.P. and Williams, J.C., Photosynthetic reaction centers, *FEBS Lett.*, 438, 1–2, 5, 1998.
6. Breton, J. and Vermeglio, A., *The Photosynthetic Bacterial Reaction Center II*, Plenum Press, New York, 1992.
7. Rothschild, K.J. and Sonar, S., Bacteriorhodopsin: new biophysical perspectives, in *CRC Handbook of Organic Photochemistry and Photobiology*, Horspool, W.M. and Song, P.-S., Eds., CRC Press LLC, Boca Raton, FL, 1995, pp. 1521–1544.
8. Beja, O., Aravind, L., Koonin, E.V., Suzuki, M.T., Hadd, A., Nguyen, L.P., Jovanovich, S.B., Gates, C.M., Feldman, R.A., Spudich, J.L., Spudich, E.N., and DeLong, E.F., Bacterial rhodopsin: evidence for a new type of phototrophy in the sea, *Science*, 289, 5486, 1902, 2000.
9. Dioumaev, A.K., Brown, L.S., Shih, J., Spudich, E.N., Spudich, J.L., and Lanyi, J.K., Proton transfers in the photochemical reaction cycle of proteorhodopsin, *Biochemistry*, 41, 17, 5348, 2002.
10. Wald, G., Molecular basis of visual excitation, *Science*, 162, 230, 1968.
11. Khorana, H.G., Rhodopsin, photoreceptor of the rod cell. An emerging pattern for structure and function, *J. Biol. Chem.*, 267, 1, 1, 1992.
12. DeGrip, W.J. and Rothschild, K.J., Structure and mechanism of vertebrate visual pigments, in *Molecular Mechanisms in Visual Transduction*, Stravenga, D.G., de Grip, W.J., and Pugh, E.N., Elsevier, Amsterdam; New York, 2000, pp. 1–54.
13. Spudich, J.L., Variations on a molecular switch: transport and sensory signalling by archaeal rhodopsins, *Mol. Microbiol.*, 28, 6, 1051, 1998.
14. Choi, G., Yi, H., Lee, J., Kwon, Y.K., Soh, M.S., Shin, B., Luka, Z., Hahn, T.R., and Song, P.S., Phytochrome signalling is mediated through nucleoside diphosphate kinase 2, *Nature*, 401, 6753, 610, 1999.
15. Smith, H., Phytochromes and light signal perception by plants — an emerging synthesis, *Nature*, 407, 6804, 585, 2000.

16. Briggs, W.R. and Christie, J.M., Phototropins 1 and 2: versatile plant blue-light receptors, *Trends Plant Sci.*, 7, 5, 204, 2002.
17. Swartz, T.E., Wenzel, P.J., Corchnoy, S.B., Briggs, W.R., and Bogomolni, R.A., Vibration spectroscopy reveals light-induced chromophore and protein structural changes in the LOV2 domain of the plant blue-light receptor phototropin 1, *Biochemistry*, 41, 23, 7183, 2002.
18. Tsien, R.Y., The green fluorescent protein, *Annu. Rev. Biochem.*, 67, 509, 1998.
19. Baldwin, T.O., Firefly luciferase: the structure is known, but the mystery remains, *Structure*, 4, 3, 223, 1996.
20. Craig, D.B., Dovichi, N.J., Multiple labeling of proteins, *Anal. Chem.*, 70, 13, 2493, 1998.
21. Hafner, F.T., Kautz, R.A., Iverson, B.L., Tim, R.C., and Karger, B.L., Noncompetitive immunoassay of small analytes at the femtomolar level by affinity probe capillary electrophoresis: direct analysis of digoxin using a uniform-labeled scFv immunoreagent, *Anal. Chem.*, 72, 23, 5779, 2000.
22. Tim, R.C., Kautz, R.A., and Karger, B.L., Ultratrace analysis of drugs in biological fluids using affinity probe capillary electrophoresis: analysis of dorzolamide with fluorescently labeled carbonic anhydrase, *Electrophoresis*, 21, 1, 220, 2000.
23. Thompson, S., Spoors, J.A., Fawcett, M.-C., and Self, C.H., Photocleavable nitrobenzyl-protein conjugates, *Biochem. Biophys. Res. Commun.*, 201, 1213, 1994.
24. Marriott, G., Caged protein conjugates and light-directed generation of protein activity: preparation, photoactivation, and spectroscopic characterization of caged G-actin conjugates, *Biochemistry*, 33, 31, 9092, 1994.
25. Marriott, G., Ottl, J., Heidecker, M., and Gabriel, D., Light-directed activation of protein activity from caged protein conjugates, *Methods Enzymol.*, 291, 95, 1998.
26. Self, C.H. and Thompson, S., Light activatable antibodies: models for remotely activatable proteins, *Nat. Med.*, 2, 7, 817, 1996.
27. Kossel, A.H., Cambridge, S.B., Wagner, U., and Bonhoeffer, T., A caged Ab reveals an immediate/instructive effect of BDNF during hippocampal synaptic potentiation, *Proc. Natl. Acad. Sci. USA*, 98, 25, 14702, 2001.
28. Minden, J., Namba, R., Mergliano, J., and Cambridge, S., Photoactivated gene expression for cell fate mapping and cell manipulation, *Sci. STKE 2000*, 62, L1, 2000.
29. Olejnik, J., Sonar, S., Krzymanska-Olejnik, E., and Rothschild, K.J., Photocleavable biotin derivatives: a versatile approach for the isolation of biomolecules, *Proc. Natl. Acad. Sci. USA*, 92, 7590, 1995.
30. Gite, S., Mamaev, S., Nuara, M., Chaley, S., Bayley, H., and Rothschild, K., Light-mediated activation of a-hemolysin, *Biophys. J.*, 76, A125, 1999.
31. Moritz, M., Braunfeld, M.B., Guenebaut, V., Heuser, J., and Agard, D.A., Structure of the gamma-tubulin ring complex: a template for microtubule nucleation, *Nat. Cell Biol.*, 2, 6, 365, 2000.
32. Pandori, M.W., Hobson, D.A., Olejnik, J., Krzymanska-Olejnik, E., Rothschild, K.J., Palmer, A.A., Phillips, T.J., and Sano, T., Photochemical control of the infectivity of adenoviral vectors using a novel photocleavable biotinylation reagent, *Chem. Biol.*, 9, 5, 567, 2002.
33. Chang, C.-Y., Niblack, B., Walker, B., and Bayley, H., A photogenerated pore-forming protein, *Chem. Biol.*, 2, 391, 1995.
34. Pan, P. and Bayley, H., Caged cysteine and triphosphoryl groups, *FEBS Lett.*, 405, 81, 1997.
35. Bayley, H., Chang, C.Y., Miller, W.T., Niblack, B., and Pan, P., Caged peptides and proteins by targeted chemical modification, *Methods Enzymol.*, 291, 117, 1998.
36. Zou, K., Cheley, S., Givens, R.S., and Bayley, H., Catalytic subunit of protein kinase A caged at the activating phosphothreonine, *J. Am. Chem. Soc.*, 124, 28, 8220, 2002.
37. Sreekumar, R., Ikebe, M., Fay, F.S., and Walker, J.W., Biologically active peptides caged on tyrosine, *Methods Enzymol.*, 291, 78, 1998.
38. Pirrung, M.C., Drabik, S.J., Ahamed, J., and Ali, H., Caged chemotactic peptides, *Bioconjug. Chem.*, 11, 5, 679, 2000.

39. Tatsu, Y., Nishigaki, T., Darszon, A., and Yumoto, N., A caged sperm-activating peptide that has a photocleavable protecting group on the backbone amide, *FEBS Lett.*, 525, 1–3, 20, 2002.
40. Hiraoka, T. and Hamachi, I., Caged RNase: photoactivation of the enzyme from perfect off-state by site-specific incorporation of 2-nitrobenzyl moiety, *Bioorg. Med. Chem. Lett.*, 13, 1, 13, 2003.
41. Ottl, J., Gabriel, D., and Marriott, G., Preparation and photoactivation of caged fluorophores and caged proteins using a new class of heterobifunctional, photocleavable cross-linking reagents, *Bioconjug. Chem.*, 9, 2, 143, 1998.
42. Politz, J.C., Use of caged fluorochromes to track macromolecular movement in living cells, *Trends Cell Biol.*, 9, 7, 284, 1999.
43. Okabe, S. and Hirokawa, N., Differential behavior of photoactivated microtubules in growing axons of mouse and frog neurons, *J. Cell Biol.*, 117, 1, 105, 1992.
44. Rodionov, V.I., Lim, S.S., Gelfand, V.I., and Borisy, G.G., Microtubule dynamics in fish melanophores, *J. Cell Biol.*, 126, 6, 1455, 1994.
45. Yvon, A.M., Gross, D.J., and Wadsworth, P., Antagonistic forces generated by myosin II and cytoplasmic dynein regulate microtubule turnover, movement, and organization in interphase cells, *Proc. Natl. Acad. Sci. USA*, 98, 15, 8656, 2001.
46. Spudich, J.L. and Bogomolni, R.A., Sensory rhodopsin I: receptor activation and signal relay, *J. Bioenerg. Biomembr.,* 24, 2, 193, 1992.
47. Bousché, O., Spudich, E.N., Spudich, J.L., and Rothschild, K.J., Conformational changes in sensory rhodopsin I: similarities and differences with bacteriorhodopsin, halorhodopsin, and rhodopsin, *Biochemistry*, 30, 22, 5395, 1991.
48. Porter, N.A., Bruhnke, J.D., and Koenigsm, P., Bioorganic photochemistry, Vol. 2, in *Biological Applications of Photochemical Switches*, Morrison, H., Ed., John Wiley & Sons, New York, 1993, pp. 197–241.
49. Arroyo, J.G., Jones, P.B., Porter, N.A., and Hatchell, D.L., *In vivo* photoactivation of caged-thrombin, *Thromb. Haemost.*, 78, 2, 791, 1997.
50. Harvey, A.J. and Abell, A.D., Alpha-ketoester-based photobiological switches: synthesis, peptide chain extension and assay against alpha-chymotrypsin, *Bioorg. Med. Chem. Lett.*, 11, 18, 2441, 2001.
51. James, D.A., Burns, D.C., and Woolley, G.A., Kinetic characterization of ribonuclease S mutants containing photoisomerizable phenylazophenylalanine residues, *Protein Eng.*, 14, 12, 983, 2001.
52. Muranaka, N., Hohsaka, T., and Sisido, M., Photoswitching of peroxidase activity by position-specific incorporation of a photoisomerizable non-natural amino acid into horseradish peroxidase, *FEBS Lett.*, 510, 1–2, 10, 2002.
53. Weston, D.G., Kirkham, J., and Cullen, D.C., Photo-modulation of horseradish peroxidase activity via covalent attachment of carboxylated-spiropyran dyes, *Biochim. Biophys. Acta*, 1428, 2–3, 463, 1999.
54. Ito, Y., Sugimura, N., Kwon, O.H., and Imanishi, Y., Enzyme modification by polymers with solubilities that change in response to photoirradiation in organic media, *Nat. Biotechnol.*, 17, 1, 73, 1999.
55. Shimoboji, T., Larenas, E., Fowler, T., Kulkarni, S., Hoffman, A.S., and Stayton, P.S., Photoresponsive polymer-enzyme switches, *Proc. Natl. Acad. Sci. USA,* 99, 16592, 2002.
56. Harada, M., Sisido, M., Hirose, J., and Nakanishi, M., Photoreversible antigen-antibody reactions, *FEBS Lett.*, 286, 1–2, 6, 1991.
57. Flint, D.G., Kumita, J.R., Smart, O.S., and Woolley, G.A., Using an azobenzene cross-linker to either increase or decrease peptide helix content upon trans-to-cis photoisomerization, *Chem. Biol.*, 9, 3, 391, 2002.
58. Renner, C., Behrendt, R., Sporlein, S., Wachtveitl, J., and Moroder, L., Photomodulation of conformational states. I. Mono- and bicyclic peptides with (4-amino)phenylazobenzoic acid as backbone constituent, *Biopolymers*, 54, 7, 489, 2000.
59. Renner, C., Cramer, J., Behrendt, R., and Moroder, L., Photomodulation of conformational states. II. Mono- and bicyclic peptides with (4-aminomethyl)phenylazobenzoic acid as backbone constituent, *Biopolymers*, 54, 7, 501, 2000.

60. Renner, C., Behrendt, R., Heim, N., and Moroder, L., Photomodulation of conformational states. III. Water-soluble bis- cysteinyl-peptides with (4-aminomethyl) phenylazobenzoic acid as backbone constituent, *Biopolymers*, 63, 6, 382, 2002.
61. Kumita, J.R., Flint, D.G., Smart, O.S., and Woolley, G.A., Photo-control of peptide helix content by an azobenzene cross-linker: steric interactions with underlying residues are not critical, *Protein Eng.*, 15, 7, 561, 2002.
62. Cattani-Scholz, A., Renner, C., Oesterhelt, D., and Moroder, L., Photoresponsive dendritic azobenzene peptides, *Chembiochem.*, 2, 7–8, 542, 2001.
63. Pieroni, O., Fissi, A., Angelini, N., and Lenci, F., Photoresponsive polypeptides, *Acc. Chem. Res.*, 34, 1, 9, 2001.
64. Griffin, B.A., Adams, S.R., and Tsien, R.Y., Specific covalent labeling of recombinant protein molecules inside live cells, *Science*, 281, 5374, 269, 1998.
65. Adams, S.R., Campbell, R.E., Gross, L.A., Martin, B.R., Walkup, G.K., Yao, Y., Llopis, J., and Tsien, R.Y., New biarsenical ligands and tetracysteine motifs for protein labeling *in vitro* and *in vivo*: synthesis and biological applications, *J. Am. Chem. Soc.*, 124, 21, 6063, 2002.
66. Gaietta, G., Deerinck, T.J., Adams, S.R., Bouwer, J., Tour, O., Laird, D.W., Sosinsky, G.E., Tsien, R.Y., and Ellisman, M.H., Multicolor and electron microscopic imaging of connexin trafficking, *Science*, 296, 5567, 503, 2002.
67. Nakanishi, J., Nakajima, T., Sato, M., Ozawa, T., Tohda, K., and Umezawa, Y., Imaging of conformational changes of proteins with a new environment-sensitive fluorescent probe designed for site-specific labeling of recombinant proteins in live cells, *Anal. Chem.*, 73, 13, 2920, 2001.
68. Marcaurelle, L.A.B. and Bertozzi, C.R., Direct incorporation of unprotected ketone groups into peptides during solid-phase synthesis: application to the one-step modification of peptides with two different biophysical probes for FRET, *Tetrahedron Lett.*, 39, 40, 7279, 1998.
69. Gaertner, H.F. and Offord, R.E., Site-specific attachment of functionalized poly(ethylene glycol) to the amino terminus of proteins, *Bioconjug. Chem.*, 7, 1, 38, 1996.
70. Kochendoerfer, G.G. and Kent, S.B., Chemical protein synthesis, *Curr. Opin. Chem. Biol.*, 3, 6, 665, 1999.
71. Perler, F.B. and Adam, E., Protein splicing and its applications, *Curr. Opin. Biotechnol.*, 11, 4, 377, 2000.
72. Hofmann, R.M. and Muir, T.W., Recent advances in the application of expressed protein ligation to protein engineering, *Curr. Opin. Biotechnol.*, 13, 4, 297, 2002.
73. Hofmann, R.M., Cotton, G.J., Chang, E.J., Vidal, E., Veach, D., Bornmann, W., and Muir, T.W., Fluorescent monitoring of kinase activity in real time: development of a robust fluorescence-based assay for Abl tyrosine kinase activity, *Bioorg. Med. Chem. Lett.*, 11, 24, 3091, 2001.
74. Sydor, J.R., Herrmann, C., Kent, S.B., Goody, R.S., and Engelhard, M., Design, total chemical synthesis, and binding properties of a [Leu-91-N1-methyl-7-azaTrp]Ras-binding domain of c-Raf-1, *Proc. Natl. Acad. Sci. USA*, 96, 14, 7865, 1999.
75. Becker, C.F., Hunter, C.L., Seidel, R.P., Kent, S.B., Goody, R.S., and Engelhard, M., A sensitive fluorescence monitor for the detection of activated Ras: total chemical synthesis of site-specifically labeled Ras binding domain of c-Raf1 immobilized on a surface, *Chem. Biol.*, 8, 3, 243, 2001.
76. Zhang, J., Campbell, R.E., Ting, A.Y., and Tsien, R.Y., Creating new fluorescent probes for cell biology, *Nat. Rev. Mol. Cell Biol.*, 3, 12, 906, 2002.
77. Gross, L.A., Baird, G.S., Hoffman, R.C., Baldridge, K.K., and Tsien, R.Y., The structure of the chromophore within DsRed, a red fluorescent protein from coral, *Proc. Natl. Acad. Sci. US A*, 97, 22, 11990, 2000.
78. Chan, F.K., Siegel, R.M., Zacharias, D., Swofford, R., Holmes, K.L., Tsien, R.Y., and Lenardo, M.J., Fluorescence resonance energy transfer analysis of cell surface receptor interactions and signaling using spectral variants of the green fluorescent protein, *Cytometry*, 44, 4, 361, 2001.
79. Rehm, M., Dussmann, H., Janicke, R.U., Tavare, J.M., Kogel, D., and Prehn, J.H., Single-cell fluorescence resonance energy transfer analysis demonstrates that caspase activation during apoptosis is a rapid process. Role of caspase-3, *J. Biol. Chem.*, 277, 27, 24506, 2002.

80. Tawa, P., Tam, J., Cassady, R., Nicholson, D.W., and Xanthoudakis, S., Quantitative analysis of fluorescent caspase substrate cleavage in intact cells and identification of novel inhibitors of apoptosis, *Cell Death Differ.*, 8, 1, 30, 2001.
81. Luo, K.Q., Yu, V.C., Pu, Y., and Chang, D.C., Application of the fluorescence resonance energy transfer method for studying the dynamics of caspase-3 activation during UV-induced apoptosis in living HeLa cells, *Biochem. Biophys. Res. Commun.*, 283, 5, 1054, 2001.
82. Majoul, I., Straub, M., Duden, R., Hell, S.W., and Soling, H.D., Fluorescence resonance energy transfer analysis of protein–protein interactions in single living cells by multifocal multiphoton microscopy, *J. Biotechnol.*, 82, 3, 267, 2002.
83. Truong, K. and Ikura, M., The use of FRET imaging microscopy to detect protein–protein interactions and protein conformational changes in vivo, *Curr. Opin. Struct. Biol.*, 11, 5, 573, 2001.
84. Kohl, T., Heinze, K.G., Kuhlemann, R., Koltermann, A., and Schwille, P., A protease assay for two-photon crosscorrelation and FRET analysis based solely on fluorescent proteins, *Proc. Natl. Acad. Sci. USA*, 99, 19, 12161, 2002.
85. Zhang, J., Ma, Y., Taylor, S.S., and Tsien, R.Y., Genetically encoded reporters of protein kinase A activity reveal impact of substrate tethering, *Proc. Natl. Acad. Sci. USA*, 98, 26, 14997, 2001.
86. Ting, A.Y., Kain, K.H., Klemke, R.L., and Tsien, R.Y., Genetically encoded fluorescent reporters of protein tyrosine kinase activities in living cells, *Proc. Natl. Acad. Sci. USA*, 98, 26, 15003, 2001.
87. Sato, M., Ozawa, T., Inukai, K., Asano, T., and Umezawa, Y., Fluorescent indicators for imaging protein phosphorylation in single living cells, *Nat. Biotechnol.*, 20, 3, 287, 2002.
88. Truong, K., Sawano, A., Mizuno, H., Hama, H., Tong, K.I., Mal, T.K., Miyawaki, A., and Ikura, M., FRET-based *in vivo* Ca^{2+} imaging by a new calmodulin-GFP fusion molecule, *Nat. Struct. Biol.*, 8, 12, 1069, 2001.
89. Batard, P., Szollosi, J., Luescher, I., Cerottini, J.C., MacDonald, R., and Romero, P., Use of phycoerythrin and allophycocyanin for fluorescence resonance energy transfer analyzed by flow cytometry: advantages and limitations, *Cytometry*, 48, 2, 97, 2002.
90. McCartney, L.J., Pickup, J.C., Rolinski, O.J., and Birch, D.J., Near-infrared fluorescence lifetime assay for serum glucose based on allophycocyanin-labeled concanavalin A, *Anal. Biochem.*, 292, 2, 216, 2001.
91. Rothschild, K.J. and Gite, S., tRNA-mediated protein engineering, *Curr. Opin. Biotechnol.*, 10, 1, 64, 1999.
92. Khorana, H.G., Nucleic acid synthesis in the study of the genetic code, in *Nobel Lectures in Molecular Biology*, Elsevier, Amsterdam; New York, 1977, pp. 303–333.
93. Nirenberg, M.W. and Leder, P., RNA codewords and protein synthesis, *Science*, 145, 1399, 1964.
94. Richmond, M.H., The effect of amino acid analogs on growth and protein synthesis in microorganisms, *Bacteriol.* Rev., 26, 398, 1962.
95. Krieg, U.C., Walter, P., and Johnson, A.E., Photocrosslinking of the signal sequence of nascent preprolactin to the 54-kilodalton polypeptide of the signal recognition particle, *Proc. Natl. Acad. Sci. USA*, 83, 22, 8604, 1986.
96. Krieg, U.C., Johnson, A.E., and Walter, P., Protein translocation across the endoplasmic reticulum membrane: identification by photocross-linking of a 39-kD integral membrane glycoprotein as part of a putative translocation tunnel, *J. Cell Biol.*, 109, 5, 2033, 1989.
97. Thrift, R.N., Andrews, D.W., Walter, P., and Johnson, A.E., A nascent membrane protein is located adjacent to ER membrane proteins throughout its integration and translation, *J. Cell Biol.*, 112, 5, 809, 1991.
98. Noren, C.J., Anthony-Cahill, S.J., Griffith, M.C., and Schultz, P.G., A general method for site-specific incorporation of unnatural amino acids into proteins, *Science*, 244, 182, 1989.
99. Anthony-Cahill, S.J., Griffith, M.C., Noren, C.J., Suich, D.J., and Schultz, P.G., Site-specific mutagenesis with unnatural amino acids, *TIBS*, 14, 10, 400, 1990.
100. Thorson, J.S., Cornish, V.W., Barrett, J.E., Cload, S.T., Yano, T., and Schultz, P.G., A biosynthetic approach for the incorporation of unnatural amino acids into proteins, *Methods Mol. Biol.*, 77, 43, 1998.

101. Furter, R., Expansion of the genetic code: site-directed p-fluoro-phenylalanine incorporation in *Escherichia coli*, *Protein Sci.*, 7, 2, 419, 1998.
102. Budisa, N., Minks, C., Medrano, F.J., Lutz, J., Huber, R., and Moroder, L., Residue-specific bioincorporation of non-natural, biologically active amino acids into proteins as possible drug carriers: structure and stability of the per-thiaproline mutant of annexin V, *Proc. Natl. Acad. Sci. USA*, 95, 2, 455, 1998.
103. Bessho, Y., Hodgson, D.R., and Suga, H., A tRNA aminoacylation system for non-natural amino acids based on a programmable ribozyme, *Nat. Biotechnol.*, 20, 7, 723, 2002.
104. Ma, C., Kudlicki, W., Odom, O.W., Kramer, G., and Hardesty, B., *In vitro* protein engineering using synthetic tRNA(Ala) with different anticodons, *Biochemistry*, 32, 31, 7939, 1993.
105. Kramer, G., Kudlicki, W., and Hardesty, B., *In vitro* engineering using synthetic tRNAs with altered anticodons including four-nucleotide anticodons, *Methods Mol. Biol.*, 77, 105, 1998.
106. Hohsaka, T.A., Murakami, H., and Sisido, M., Incorporation of nonnatural amino acids into streptavidin through *in vitro* frame-shift suppression, *J. Am. Chem. Soc.*, 118, 40, 9778, 1996.
107. Hohsaka, T., Ashizuka, Y., Taira, H., Murakami, H., and Sisido, M., Incorporation of nonnatural amino acids into proteins by using various four-base codons in an *Escherichia coli in vitro* translation system, *Biochemistry*, 40, 37, 11060., 2001.
108. Hohsaka, T., Ashizuka, Y., Murakami, H., and Sisido, M., Five-base codons for incorporation of nonnatural amino acids into proteins, *Nucleic Acids Res.*, 29, 17, 3646, 2001.
109. Magliery, T.J., Anderson, J.C., and Schultz, P.G., Expanding the genetic code: selection of efficient suppressors of four- base codons and identification of "shifty" four-base codons with a library approach in *Escherichia coli*, *J. Mol. Biol.*, 307, 3, 755, 2001.
110. Anderson, J.C., Magliery, T.J., and Schultz, P.G., Exploring the limits of codon and anticodon size, *Chem. Biol.*, 9, 2, 237, 2002.
111. Johnson, A.E., Protein translocation across the ER membrane: a fluorescent light at the end of the tunnel, *Trends Biochem. Sci.*, 18, 12, 456, 1993.
112. Cornish, V.W., Benson, D.R., Altenbach, C.A., Hideg, K., Hubbell, W.L., and Schultz, P.G., Site-specific incorporation of biophysical probes into proteins, *Proc. Natl. Acad. Sci. USA*, 91, 8, 2910, 1994.
113. Steward, L.E., Collins, C.S., Gilmore, M.A., Carlson, J.E., Ross, J.B.A., and Chamberlin, A.R., *In vitro* site-specific incorporation of fluorescent probes into beta-galactosidase, *J. Am. Chem. Soc.*, 119, 6, 1997.
114. Turcatti, G., Nemeth, K., Edgerton, M.D., Meseth, U., Talabot, F., Peitsch, M., Knowles, J., Vogel, H., and Chollet, A., Probing the structure and function of the tachykinin neurokinin-2 receptor through biosynthetic incorporation of fluorescent amino acids at specific sites, *J. Biol. Chem.*, 271, 33, 19991, 1996.
115. Turcatti, G., Nemeth, K., Edgerton, M.D., Knowles, J., Vogel, H., and Chollet, A., Fluorescent labeling of NK2 receptor at specific sites *in vivo* and fluorescence energy transfer analysis of NK2 ligand-receptor complexes, *Receptors Channels*, 5, 3–4, 201, 1997.
116. Cohen, B.E., McAnaney, T.B., Park, E.S., Jan, Y.N., Boxer, S.G., and Jan, L.Y., Probing protein electrostatics with a synthetic fluorescent amino acid, *Science*, 296, 5573, 1700, 2002.
117. Gite, S., Mamaev, S., Olejnik, J., and Rothschild, K., Ultrasensitive fluorescence-based detection of nascent proteins in gels, *Anal. Biochem.*, 279, 2, 218, 2000.
118. Nemoto, N., Miyamoto-Sato, E., and Yanagawa, H., Fluorescence labeling of the C-terminus of proteins with a puromycin analogue in cell-free translation systems, *FEBS Lett.*, 462, 1–2, 43, 1999.
119. Doi, N., Takashima, H., Kinjo, M., Sakata, K., Kawahashi, Y., Oishi, Y., Oyama, R., Miyamoto-Sato, E., Sawasaki, T., Endo, Y., and Yanagawa, H., Novel fluorescence labeling and high-throughput assay technologies for *in vitro* analysis of protein interactions, *Genome Res.*, 12, 3, 487, 2002.
120. Murakami, H., Hohsaka, T., Ashizuka, Y., Hashimoto, K., and Sisido, M., Site-directed incorporation of fluorescent nonnatural amino acids into streptavidin for highly sensitive detection of biotin, *Biomacromolecules*, 1, 1, 118, 2000.

121. Taki, M., Hohsaka, T., Murakami, H., Taira, K., and Sisido, M., Position-specific incorporation of a fluorophore-quencher pair into a single streptavidin through orthogonal four-base codon/anticodon pairs, *J. Am. Chem. Soc.*, 124, 49, 14586, 2002.
122. Hohsaka, T., Daisuke, K., Ashizuka, Y., Murakami, H., and Sisido, M., Efficient incorporation of nonnatural amino acids with large aromatic groups into streptavidin in *in vitro* protein synthesizing systems, *J. Am. Chem. Soc.*, 121, 34, 1999.
123. Taki, M., Hohsaka, T., Murakami, H., Taira, K., and Sisido, M., A non-natural amino acid for efficient incorporation into proteins as a sensitive fluorescent probe, *FEBS Lett.*, 507, 1, 35, 2001.
124. Anderson, R.D., III, Zhou, J., and Hecht, S.M., Fluorescence resonance energy transfer between unnatural amino acids in a structurally modified dihydrofolate reductase, *J. Am. Chem. Soc.*, 124, 33, 9674, 2002.
125. Mendel, D., Ellman, J.A., and Schultz, P.G., Construction of a light-activated protein by unnatural amino acid mutagenesis, *J. Am. Chem. Soc.*, 113, 2758, 1991.
126. England, P.M., Lester, H.A., Davidson, N., and Dougherty, D.A., Site-specific, photochemical proteolysis applied to ion channels *in vivo*, *Proc. Natl. Acad. Sci. USA*, 94, 20, 11025, 1997.
127. Philipson, K.D., Gallivan, J.P., Brandt, G.S., Dougherty, D.A., and Lester, H.A., Incorporation of caged cysteine and caged tyrosine into a transmembrane segment of the nicotinic ACh receptor, *Am. J. Physiol. Cell Physiol.*, 281, 1, C195, 2001.
128. Tong, Y., Brandt, G.S., Li, M., Shapovalov, G., Slimko, E., Karschin, A., Dougherty, D.A., and Lester, H.A., Tyrosine decaging leads to substantial membrane trafficking during modulation of an inward rectifier potassium channel, *J. Gen. Physiol.*, 117, 2, 103, 2001.
129. Mamaev, S., Olejnik, J., Krzymanska-Olejnik, E., and Rothschild, K.J., Efficient N-terminal labeling of proteins using amber suppresor initator tRNA in an *in vitro* system, *Protein Sci.*, 11, suppl. 1, 171, 2002.
130. Rothschild, K.J., Gite, S., and Olejnik, J., U.S. Patent 6,303,337, 2001, N-terminal and C-terminal markers in nascent proteins, October 16, 2001.
131. Gite, S., Lim, M., Carlson, R., Olejnik, J., Zehnbauer, B., and Rothschild, K., A high throughput non-isotopic protein truncation test, *Nat. Biotechnol.,* 21, 194, 2003.
132. Kobs, G., Hurst, R., Betz, N., and Godat, B., FluoroTect GreenLys in vitro translation labeling system, *Promega Notes*, 77, 23, 2001.
133. Beernink, P.T., Segelke, B.W., and Coleman, M.A., High-throughput, cell-free protein expression screening using the RTS 100 *E. coli* HY kit, *Biochemica* (Roche), 1, 4, 2003.
134. Iborra, F.J., Jackson, D.A., and Cook, P.R., Coupled transcription and translation within nuclei of mammalian cells, *Science*, 293, 5532, 1139, 2001.
135. Lien, L., Ananda, P., Seneviratne, K., Jaikaran, A.S., and Andrew Woolley, G., Site-specific biosynthetic incorporation of a fluorescent tag into proteins via Cysteine-tRNA(Cys), *Anal. Biochem.*, 307, 2, 252, 2002.
136. Den Dunnen, J.T. and Van Ommen, G.J., The protein truncation test: a review, *Hum. Mutat.*, 14, 2, 95, 1999.
137. Roest, P., Roberts, R., Sugino, S., van Ommen, G., and den Dunnen, J., Protein truncation test (PTT) for rapid detection of translation-terminating mutations, *Hum. Mol. Genet.*, 2, 10 (Oct.), 1719–1721, 1993.
138. Powell, S.M., Petersen, G.M., Krush, A.J., Booker, S., Jen, J., Giardiello, F.M., Hamilton, S.R., Vogelstein, B., and Kinzler, K.W., Molecular diagnosis of familial adenomatous polyposis [see comments], *N. Engl. J. Med.*, 329, 27, 1982, 1993.
139. DeGrado, W.F., Summa, C.M., Pavone, V., Nastri, F., and Lombardi, A., De novo design and structural characterization of proteins and metalloproteins, *Annu. Rev. Biochem.*, 68, 779, 1999.
140. Neidigh, J.W., Fesinmeyer, R.M., and Andersen, N.H., Designing a 20-residue protein, *Nat. Struct. Biol.*, 9, 6, 425, 2002.
141. Luque, I., Leavitt, S.A., and Freire, E., The linkage between protein folding and functional cooperativity: two sides of the same coin?, *Annu. Rev. Biophys. Biomol. Struct.*, 31, 235, 2002.

142. Luecke, H., Schobert, B., Cartailler, J.P., Richter, H.T., Rosengarth, A., Needleman, R., and Lanyi, J.K., Coupling photoisomerization of retinal to directional transport in bacteriorhodopsin, *J. Mol. Biol.*, 300, 5, 1237, 2000.
143. Subramaniam, S. and Henderson, R., Molecular mechanism of vectorial proton translocation by bacteriorhodopsin, *Nature*, 406, 6796, 653, 2000.
144. Luecke, H., Schobert, B., Lanyi, J.K., Spudich, E.N., and Spudich, J.L., Crystal structure of sensory rhodopsin II at 2.4 angstroms: insights into color tuning and transducer interaction, *Science*, 293, 5534, 1499, 2001.
145. Royant, A., Nollert, P., Edman, K., Neutze, R., Landau, E.M., Pebay-Peyroula, E., and Navarro, J., X-ray structure of sensory rhodopsin II at 2.1-A resolution, *Proc. Natl. Acad. Sci. USA*, 98, 18, 10131, 2001.
146. Gordeliy, V.I., Labahn, J., Moukhametzianov, R., Efremov, R., Granzin, J., Schlesinger, R., Bueldt, G., Savopol, T., Scheidig, A.J., Klare, J.P., and Engelhard, M., Molecular basis of transmembrane signalling by sensory rhodopsin II-transducer complex, in *Nature (London, United Kingdom)*, 2002, pp. 484–487.
147. Spudich, J.L., Spotlight on receptor/transducer interations, *Nature Struct.* Biol., 9, 11, 707, 2002.
148. Hunt, J.F., Rath, P., Rothschild, K.J., and Engelman, D.M., Spontaneous, pH-dependent membrane insertion of a transbilayer alpha- helix, *Biochemistry*, 36, 49, 15177, 1997.
149. Hunt, J.F., Earnest, T.N., Bousche, O., Kalghatgi, K., Reilly, K., Horvath, C., Rothschild, K.J., and Engelman, D.M., A biophysical study of integral membrane protein folding, *Biochemistry*, 36, 49, 15156, 1997.
150. Shen, Y., Safinya, C.R., Liang, K.S., Ruppert, A.F., and Rothschild, K.J., Stabilization of the membrane protein bacteriorhodopsin to 140 C in two dimensional films, *Nature*, 366, 48, 1993.
151. Bayley, H., Building a door into cells, *Sci. Am.*, 277 (September), 62, 1997.
152. Wang, H. and Branton, D., Nanopores with a spark for single-molecule detection, *Nat. Biotechnol.*, 19, 7, 622–623, 2001.
153. Vercoutere, W., Winters-Hilt, S., Olsen, H., Deamer, D., Haussler, D., and Akeson, M., Rapid discrimination among individual DNA hairpin molecules at single-nucleotide resolution using an ion channel, *Nat. Biotechnol.*, 19, 3, 248, 2001.
154. Howorka, S., Cheley, S., and Bayley, H., Sequence-specific detection of individual DNA strands using engineered nanopores, *Nat. Biotechnol.*, 19, 7, 636, 2001.
155. Yang, H. and Xie, X.S., Probing single molecule dynamics photon by photon, *J. Chem. Phys.*, 117, 10965, 2002.

134

Molecular Electronic Switches in Photobiology

Felix T. Hong
Wayne State University School of Medicine

134.1 Introduction

Light is used by bioorganisms for two major purposes: sensory perception and energy conversion. The functional requirements of molecular devices are drastically different for these two purposes. The former demands sensitivity and a wide dynamic range of photon energy detection, and the latter demands efficiency of photon energy conversion. Superficially, there seems to be a dichotomy of nature's choice of molecular materials for these two diverse functions: visual membranes utilize retinal as the chromophore, whereas photosynthetic membranes utilize magnesium porphyrin as the chromophore. Fundamentally, there are features in common to these two types of photobiological membranes. In Chapter 128, light-induced charge separation and the photoelectric effect are examined in detail. In this chapter, we will consider the molecular switching processes in these two diverse systems from a broad perspective.

The vertebrate rod is a highly sensitive photoreceptor. Hecht and coworkers[1] demonstrated that a single visible photon absorbed by a single molecule of rhodopsin is capable of eliciting an electrical response of the vertebrate rod photoreceptor. The energy required for the generation of a synaptic potential — the generator potential — is not provided by the absorbed photon alone. Rather, photon energy merely serves as the trigger for releasing previously stored energy in the form of transmembrane Na^+ gradient. The latter event constitutes the generator potential of a visual photoreceptor, which was identified with the *a* wave of the electroretinogram (ERG).[2] What transpires in the process of absorption–excitation coupling is an energy amplification of 100,000-fold. In this sense, rhodopsin is a light-sensitive molecular switch. In order for this switch to be reliable and useful, several requirements must be met in addition to an amplification mechanism. The rise time of the trigger signal must be fast. The

0-8493-1348-1/04/$0.00+$1.50

initial response must be localized and linear. In contrast, the generator potential is global and highly nonlinear. The wide dynamic range of photon sensing — nine orders of magnitude — is made possible partly by virtue of light–dark adaptation and partly by virtue of a logarithmic light-dependence of the generator potential. It was well established that the cyclic GMP cascade is the biochemical amplification process that converts the initial linear photoresponse to the logarithmic, nonlinear electrical response of the generate potential. Biochemically, molecular switching is accomplished by a sequence of conformational changes of several molecules of visual transduction: each step of switching contributes a significant factor of amplification.[3] Detailed knowledge of these conformational changes is now available because of elucidation of crystal structures of several key molecules, including rhodopsin. Of particular interest is the mechanistic aspect of molecular switching during the process of molecular recognition: molecular switching leads to enhanced recognition. As described in Chapter 128, the early receptor potential (ERP) appears to be a natural suspect of the initial mechanistic trigger, because it is linear and localized with an ultrafast rise time, and because it is in the right place at the right time. Lying between ERP and LRP is a gap of 1.5 to 1.7 ms of time delay. Previously, we speculated about its mechanistic role.[4,5] It is, therefore, of interest to reexamine the topic in light of the now-known detailed molecular events.

Photosynthesis, nature's other major photobiological function, is the conversion of the solar photon energy into chemical energy. Photosynthetic energy conversion starts as a light-induced vectorial charge separation across the photosynthetic membrane. These separated charges are stored on the membrane capacitor in the form of a transmembrane voltage and a transmembrane proton gradient. According to the chemiosmotic theory advanced by Mitchell[6] and by Williams,[7–9] the stored energy is then preferentially channeled to ATP synthase to drive the reaction of converting ADP and inorganic phosphate into ATP — the universal energy currency in the living world. Superficially, molecular switching function has little to do with photosynthetic energy conversion, because sensitivity is not the primary concern. In reality, switching function is important in bolstering the efficiency of energy conversion. In general, the efficiency of photon conversion is contingent on the relative fraction of separated charges that recombines through an external device so as to perform useful mechanical or chemical work. Any other route of charge recombination must be considered wasteful: short-circuiting, so to speak. Photosynthetic bacteria and higher plants evolved efficient photosynthetic apparatuses that manage to minimize such wasteful diversion of energy. Often, such improvement relies on well-orchestrated short-range noncovalent bond interactions, which include hydrogen bonding, electrostatic, hydrophobic, and van der Waals interactions.

Nature seldom adopted a single approach to improve physiological functions of a living organism. In addition, it is not uncommon that successful strategies in nature's repertoire are seen to repeat across the boundary between plants and animals, and, in particular, the boundary between vision and photosynthesis. The purple membrane of *Halobacterium salinarum*, a photosynthetic apparatus that utilizes a "visual" pigment, offers an unusual glimpse into common features in vision and photosynthesis.[10] This chapter begins with a general description of the role of noncovalent bond interactions in molecular recognition. Detailed molecular switching processes will be examined in two mobile electron carrier systems in photosynthesis (each residing on the opposite side of the photosynthetic membrane), three key molecules in visual transduction (rhodopsin, transducin, and arrestin), and bacteriorhodopsin.

An emerging interest in molecular electronic switches accompanies the advent of molecular electronics research — attempts to fabricate electronic devices based on organic materials. Computer scientist Michael Conrad[11] pointed out that the predominant feature of a biological information process is shape-based rather than switch-based. Absent a predominant role played by switches, Conrad found himself in a position to search for an explanation to reconcile how diffusion and random collisions of macromolecules can give rise to highly deterministic processes, such as decision making by human brains. Of course, there are switching processes in biology, as implied by visual transduction and, more generally, by phosphorylation as a major mechanism for enzyme activation. Even so, these switches are not as deterministic in operations as "gates" and "flip-flops" commonly used in computer technology. The intriguing question is: why did nature not make the processes less uncertain and more deterministic? Speculations will be presented to make some sense of nature's choice.

134.2 Short-Range Noncovalent Bond Interactions in Molecular Switching Processes

As Conrad[11] frequently emphasized, molecular recognition is primarily based on the lock–key principle of Emil Fischer. It is instructive to examine an example offered by cytochrome *c*.[12] Cytochrome *c*, a mobile electron carrier, shuttles between cytochrome b–c_1 complex and the cytochrome oxidase; it receives an electron from the former and passes it to the latter in the mitochondrial inner membrane. The recognition primarily involves a small number of matching ionic bonds (electrostatic interactions). Furthermore, the lock–key matching is not unique: cytochrome *c* utilizes two slightly different sets of ionic bonds to dock with the cytochrome b–c_1 complex and with cytochrome oxidase. Thus, shape fitting in macromolecular recognition is only approximate, and the geometric shapes of the two docking sites are not precisely complementary to each other. Apparently, perfect shape fitting in molecular recognition is neither desirable nor necessary. Perfect shape fitting would make molecular recognition an unacceptably slow process. Also, perfect shape fitting tends to make the complex much too stable to be able to come apart subsequently. In other words, perfect or near-perfect shape fitting confers an affinity (to the encountering partners) that is too high to make molecular recognition functionally useful.

Molecular recognition is determined in part by shape matching and in part by the matching of specifically aligned ionic bonds, hydrogen bonds, van der Waals contacts, and hydrophobic interactions. The docking process is achieved by minimizing the combined potential energy of all short-range noncovalent bond interactions. These noncovalent bonds are weaker than covalent bonds. However, depending on the total number of bonds, together they are sufficiently strong to overcome dislodging by thermal agitation.

The van der Waals forces, which are nonspecific, require close proximity of atoms (3 to 4 Å) for action. These forces contribute to the stability of complex formation but require close shape-match to exert effect. Hydrophobic forces are also nonspecific and confer no polarity of bonding. As we will see, a docking cavity is often lined with hydrophobic amino acid residues. Hydrogen and ionic bonds, however, exhibit "directionality" and require matching parts with opposite polarities, just like Velcro® fasteners' *loops* and *hooks*. These bonds thus confer some specificity on molecular recognition. However, as indicated by the action of cytochrome *c*, the specificity is not absolute and unique. Because these bonds are not highly specific, a "false" (imperfect or incorrect) match can occur with fewer, "accidentally" aligned, hydrogen or ionic bonds, thus settling in a *local* potential-energy minimum. However, a false match helps trap the encountering molecules and allows them to form a transient complex. As a result, the contact dwell time is significantly increased, and a three-dimensional searching process is converted into a two-dimensional one for the *global* potential-energy minimum. This trapping effect is known as the reduction-of-dimensionality principle.[13] Specificity of the correct docking position is provided by the *pattern* formed collectively by the geometric distribution of these bonds at the interface of the two complexing molecules. In other words, the complementary shape of the docking site, which often looks like a cavity in the larger one of the two partners, helps define the bond distribution pattern and, hence, its specificity. The shape of the docking site matters, because, with the exception of electrostatic interactions, the noncovalent bond interactions are extremely short-ranged (no more than a few Å) and, therefore, the shape of the docking site affects the distance between the matching recognition sites.

Is two-dimensional searching for the correct docking position purely random? Not necessarily. In operations research and human problem solving, approaching the task by trial and error and by examining every possible way is simply not realistic. This is because the number of possibilities rapidly increases beyond bound, as the complexity of the problem increases (a situation known as combinatorial explosion). A typical example is provided by the enormous number of possible moves, countermoves, countermoves against countermoves, etc., in a chess game, when a player tries to outsmart the opponent and searches for a strategic move by planning ahead at a search depth of several levels (or, rather, plies — half moves). Even IBM supercomputer Deep Blue, which defeated world chess champion Garry Kasparov in 1997, could not afford to explore the search space exhaustively.[14] Therefore, selective searching based

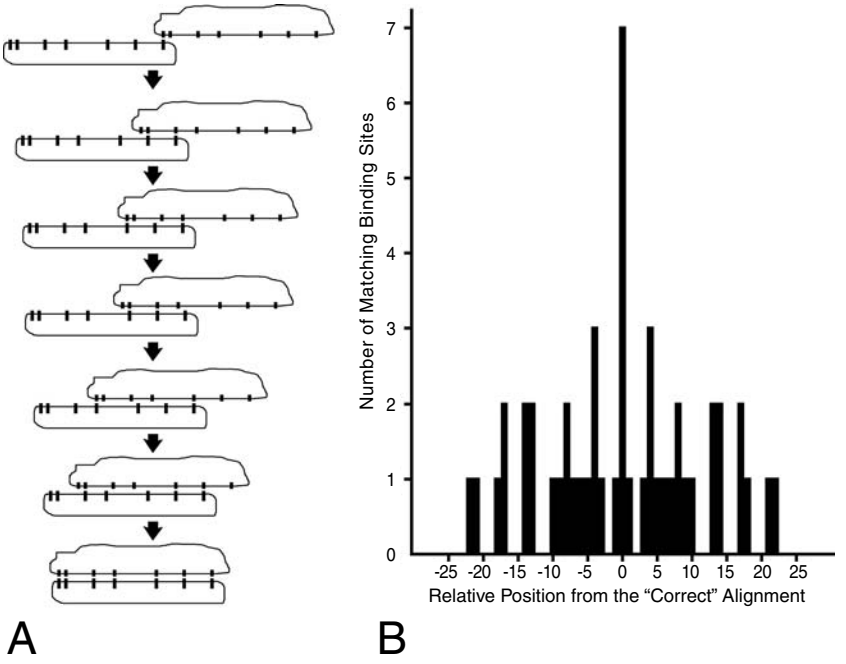

FIGURE 134.1 A gradient strategy of molecular recognition. (A) The schematic shows that any initial imperfect match between two encountering macromolecules locks them together, while a gradient of varying bonding strengths guides the two molecules to find the "intended match" by means of free energy minimization. Here, the shape factor is ignored, and the search for docking is restricted to one dimension for simplicity. Only one type of noncovalent bond interaction, such as ionic or hydrogen bonding, is considered, and the bond polarity is disregarded. The sequence shows unidirectional sliding, but in reality, the two encountering molecules slide against each other back and forth in Brownian motion. (B) The free energy landscape is, therefore, represented by a number of peaks that depict bonding at one, two, three, and seven sites. The initial search is conducted by means of two-dimensional random diffusion and collisions. When the two encountering parties slide along each other, some local peaks (i.e., local minima in the free energy landscape) of two- and three-site bonding are reached. If the two molecules overshoot the target and continue to slide in the same direction, the number of matching sites will decrease to three and two (separated by some one-site matches). If thermal agitation dislodges the two molecules from the global minimum, the gradient will "discourage" the two encountering molecules from sliding away from each other, thus prolonging the dwell-time of the encounter. On the other hand, thermal agitation prevents the encountering molecules from being trapped at any of the local minima.

on explicitly prescribed rules of thumb or *heuristics* often allows a problem to be solved in a reasonable length of time, whereas an undirected or trial-and-error search would require an enormous amount of time, and often could not be completed in a human lifetime. The approach is known as *heuristic searching* in cognitive science and operations research.[15]

Searching in molecular recognition and other biocomputing processes cannot be readily quantified as in chess games, but the implication of combinatorial explosion is no less alarming. As we shall see, nature was perfectly capable of evolving additional mechanisms, which are increasingly deterministic so as to avoid random searching. Variations in the number of hydrogen or ionic bonds permit fine-tuning of the overall bonding strength by evolution. Protein conformations offer virtually unlimited variations of the shape of contact surfaces. The variation in shape allows for variation in geometric distributions of noncovalent bonds. Thus, in principle, a *gradient* of bonding strengths could be evolutionarily arranged, and a *cascade* of local minima could be evolutionarily constructed to guide the two-dimensional searching process toward the global minimum instead of away from it (*biased* two-dimensional random searching or heuristic searching). Schematically, the gradient strategy can be implemented with a hypothetical

model, as shown in Figure 134.1, in which only electrostatic interactions in one dimension are considered. For simplicity, the bond polarity and the shape factor of the matching surfaces are ignored in the schematic diagram. When two (flat) matching surfaces slide over each other, down the potential-energy gradient, the initial match involves only one or two matching bonds, then three bonds, and finally all seven bonds. In reality, all of the noncovalent bond interactions are involved. Furthermore, the shape factor modulates the interactions, because noncovalent bond formation requires the proximity of matching sites.

The validity of the "gradient" strategy is supported by the following observations. A steering effect based on a two-step strategy was reported by Colson et al.[16] The reduction-of-dimensionality effect was observed in a Brownian dynamics simulation of cytochrome *c* and cytochrome *c* peroxidase complex formation.[17] A simulation of the free-energy landscape for two complexing proteins, reported by Camacho et al.,[18] showed that electrostatic interactions have a steering effect toward the correct mutual orientation in some cases, while desolvation energy (hydrophobic interaction) serves as an attracting and aligning force in other cases. Myosin globular heads were found to hop stochastically in steps from 5.5 to 27.5 nm (integral multiples of 5.5 nm) along an actin filament during muscle contraction.[19,20] Myosin globular heads sometimes even jumped backward instead of forward, but mostly forward. The existence of a gradient of varying binding constants along the actin filament is apparent; it was the thermal fluctuations that allowed the myosin globular heads to seek sites with higher binding constants.

An additional steering effect can take place at a greater distance than is possible to form ionic or hydrogen bonds, because the electrostatic force does not suddenly vanish but rather tapers off gradually, albeit at a rate that is still faster than that predicted by the inverse square law due to electrostatic charge screening. Two clusters of charges on two separate molecules can interact electrostatically at a considerably greater distance than is possible for other types of noncovalent bond interactions, because the collective magnitude of the clustered charges may be sufficiently large to make the force, though attenuated by distance and charge screening, still felt at a distance of more than just a few Å. However, the cluster of charges has to be regarded as a *point* source of charges under this circumstance. This is because the distance of separation between individual charges in the same cluster is small compared to the distance between the two macromolecules; every charge on a macromolecule is of about equal distance to any charge on another macromolecule at a distance. Thus, its docking partner at such a distance cannot recognize the detailed charge distribution pattern of the charged amino acid residues on the surface of a macromolecule. This type of electrostatic interaction shall be referred to as *global* electrostatics. In contrast, when the partners are within a few Å apart, each charged residue experiences mainly the attraction of another charged residue that is well-aligned to form a complementary pair together; attractions or repulsions due to other charged residues that are not aligned are weak by comparison (*charge pairing*). It is the pairing of complementary charges that helps define the specificity of the correct docking position. This type of electrostatic interaction shall be referred to as *local* electrostatics. Of course, other types of noncovalent bond interactions and the shape of the matching docking sites also contribute to the *local* specificity. In particular, hydrogen bonding provides another means of pairing for local specificity.

As we will see, mobile electron carriers often exhibit an asymmetry of charge distribution on their exposed surfaces so as to form a giant electric dipole. The interaction of two encountering electric dipoles thus helps align the two approaching partners for preferred mutual orientation prior to a collision. This type of interaction must be distinguished from interactions that form ionic bonds. The dipole–dipole interaction does not require charge pairing.

Thus, electrostatic interactions are invoked twice: for the purpose of homing (oriented collision) and for the purpose of defining the specificity of transient complex formation (docking). It is often referred to as long-range interactions in the biochemistry literature, even though it is mesoscopic in origin and it operates at a shorter range than prescribed by the inverse square law. The homing action during the first stage of activation of protein kinase C belongs to this type of steering effect.[21]

Electrostatic interactions are important mainly for the initial complex formation and crude alignment, but they are not the sole determinants for final orientation in an electron transfer reaction. Other types of interactions, such as hydrophobic interactions, are often called upon to finalize the docking process,

as was demonstrated in the interaction of the following redox partners: plastocyanin and cytochrome *f* complex[22] (of the cytochrome b_6–*f* complex), cytochrome c_6 and Photosystem I,[23] and ferredoxin and ferredoxin:NADP$^+$ reductase (FNR).[24,25] In fact, direct measurements of the ionic strength dependence of intracomplex electron transfer rate constants for several redox partners, such as yeast or horse cytochrome *c*–cytochrome *c* peroxidase, spinach ferredoxin–FNR, and bovine cytochrome *c*–cytochrome *c* oxidase, demonstrated that electrostatic forces are not the sole determinants of optimal electron transfer rates (reviewed by Tollin and Hazzard[26]). At low ionic strengths, the electrostatic interactions are enhanced, but the redox pairs are "frozen" into a nonoptimal electrostatically stabilized orientation. This is in part because charge pairing is not highly specific, and false matches are common. Excessive electrostatic interactions distort the delicate balance among various types of noncovalent bond interactions and increase the chance of trapping the redox partners in a local minimum, thus preventing them from reaching the global minimum in the free energy landscape. Additional experiments were performed to cross-link redox pairs at low ionic strengths and lock the pairs into electrostatically stabilized complexes. In all systems examined, which included cytochrome *c*–cytochrome *c* peroxidase, flavodoxin–FNR, and cytochrome *c*–cytochrome *c* oxidase, electron transfer rate constants were actually smaller for the covalent complex than for the transient complex formed upon collision at the optimum ionic strength. Apparently, a certain degree of flexibility of the docking process is required to allow for exploration of the optimal orientation. In other words, short-range interactions between the docking partners should be sufficiently strong to link them together so as to increase the contact dwell time but not so strong as to inhibit two-dimensional explorations for the optimal orientation.

134.3 Molecular Switching Processes in Major Photobiological Systems

Ferredoxin and Ferredoxin:NADP$^+$ Reductase

We will first consider the interactions between ferredoxin:NADP$^+$ reductase (FNR) and its redox partners: ferredoxin (Fd) and NADP$^+$. A ternary complex consisting of Fd, FNR, and NADP$^+$ was studied by Batie and Kamin.[27,28] It was proposed that a transient ternary complex involving Photosystem I, Fd, and FNR could be formed.[29] More recently, a complex of Fd and FNR was crystallized.[30] The complex is biologically relevant, because the structure agrees with what was inferred from studies in the solution phase. The two proteins can cocrystallize only with a molar excess of FNR over Fd, resulting in a ternary complex consisting of two reductases (named FNR1 and FNR2) and one Fd molecule. Fd is bound to a hydrophobic cavity provided by FNR1. The Fd [2Fe–2S] cluster is 7.4 Å apart from the exposed C8-isoalloxazine methyl group of the cofactor FAD of FNR1, which is sufficiently close to enable effective fast electron transfers. In contrast, Fd makes a contact with FNR2 at the site where NADP$^+$ is physiologically bound. The Fd iron cluster is too far from the FNR2-FAD (14.5 Å) to enable a fast electron transfer. Therefore, the complexation between Fd and FNR2 is probably a crystallographic artifact; the role of FNR2 could be to stabilize crystal packing by contacts with neighboring proteins. Morales et al.[30] pointed out that the interactions between Fd and FNR1 are far more specific than those between Fd and FNR2, as indicated by the following pairs of data: the number of hydrogen bonds and ion pairs (10 versus 3), van der Waals contacts (<4.1 Å) (54 versus 21), and buried area upon complex formation, i.e., cavity (1600 Å^2 versus 1100 Å^2). The molecular electric dipoles of Fd and FNR1 are nearly colinearly orientated, resulting in the negative pole of Fd being close to the positive pole of FNR1.[31] Additional arguments in support of the biological relevance of the Fd–FNR1 pair of the ternary crystal complex can be found in an important article by Gómez-Moreno and coworkers.[30]

Gómez-Moreno and coworkers extensively analyzed the effect of site-directed mutagenesis of FNR and its redox partners. Charged amino acids were replaced with neutral or amino acids with reversed charge polarity (and sometimes with concurrent side-chain elimination). These investigators found that some charged amino acids are absolutely critical for electron transfers, while replacements of other nearby

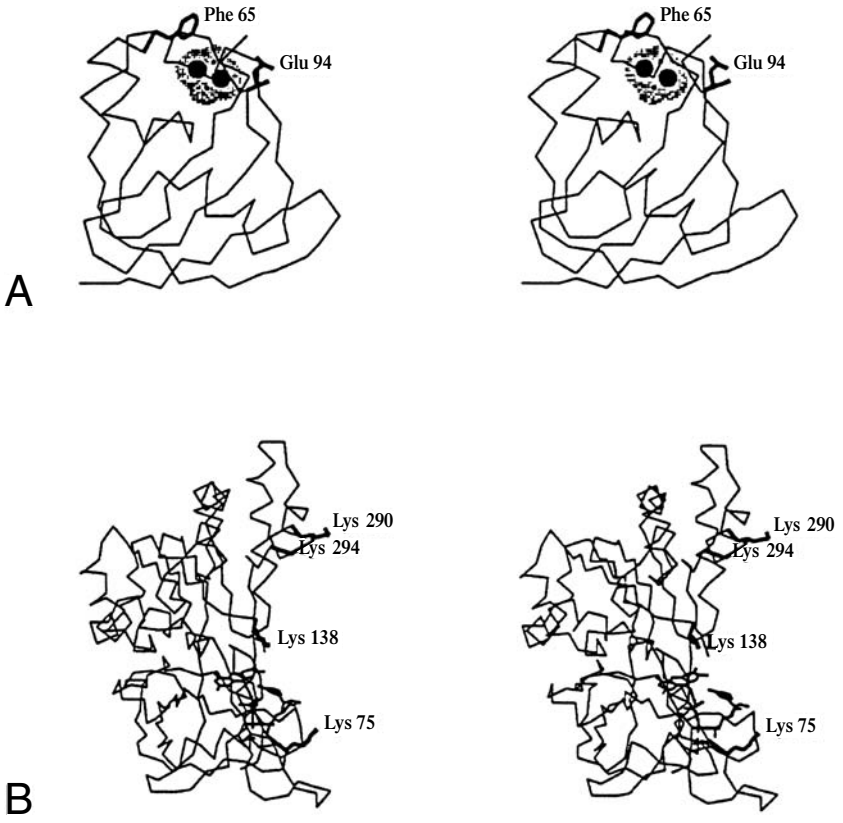

FIGURE 134.2 Stereoscopic views of ferredoxin (A) and FNR (B) of *Anabaena* PCC 7119 showing the positions of key amino acid residues that are critical for molecular recognition. (From Gómez-Moreno, C., Martínez-Júlvez, M., Fillat, M.F., Hurley, J.K., and Tollin, G., *Biochem. Soc. Trans.*, 24, 111, 1996. With permission.)

residues have moderate or no effect. For example, Phe65 and Glu94 on Fd are required for efficient electron transfers between Fd and FNR[32] [Figure 134.2(A)]. In contrast, nearby residues Glu95, Asp67, Asp68, and Asp69 play significant but less dominant roles in maintaining an appropriate protein–protein orientation (not shown; see Figure 1 of Hurley et al.[33]). These investigators suggested that charge pairing (ionic bonds) involving Glu94 is apparently important for maintaining a productive orientation — ionic bonds for docking — for electron transfers. The exact role of the aromatic residue Phe65 is not certain but is more likely involved in docking (hydrophobic interaction) than in the electron transfer pathway. Similarly, a cluster of hydrophobic residues (Leu76, Leu78, and Val136) on FNR was found to be critical for electron transfers between FNR and Fd but not between FNR and $NADP^+$.[25] Likewise, alterations of several basic residues on FNR that line the Fd-binding cavity (Lys75, Lys138, Lys290, and Lys294) also caused significant impairment of electron transfer between Fd and FNR, but the affinity of FNR for NADPH did not seem to change (NADPH binds to the opposite side of FNR) [see Figure 134.2(B)]. Viewing the stereoscopic structure of Fd and FNR on Figure 134.2 facilitates an appreciation of the spatial relationship of the two docking partners. A critical role was confirmed for Arg100 on FNR for the FNR–$NADP^+$ interaction, whereas Arg264 is not critical.[34] However, the mutant R264E (charge-reversal; positive Arg to negative Glu) showed an altered behavior in its interaction and electron transfer with Fd and flavodoxin. Here, it should be pointed out that Arg100 is near the binding pocket of FNR for $NADP^+$, whereas Arg264 is near the binding pocket of FNR for Fd (see Figures 1 and 6 of Martínez et al.[34], respectively).

In summary, there are two classes of amino acid residues: one involved in critical alignment of docking for electron transfers and the other involved in crude orientation or transient complex formation. Those involved in critical docking alignment tend to be different for the two substrates, Fd and those bound to opposite sides of FNR. Finally, hydrophobic clusters usually line the binding cavity and are critical for electron transfer. The situation with plastocyanin and cytochrome c_6 to be presented next is similar; the two independent sets of data demonstrate a common design scheme for redox partners of long-distance electron transfers.

Plastocyanin and Cytochrome c_6

We will now consider two mobile electron carriers that feed electrons from the cytochrome b_6–f complex to the oxidizing end of Photosystem I: plastocyanin and cytochrome c_6. In green plants, copper-containing plastocyanin is the sole mobile electron carrier between the cytochrome b_6–f complex and Photosystem I. Cyanobacteria and green algae, under the condition of a low copper concentration, can synthesize an alternate heme-containing mobile carrier, cytochrome c_6, to replace plastocyanin.[35,36] De la Rosa and coworkers[37] compared the structures and functions of these two electron carriers in two cyanobacteria (prokaryotes), *Synechocystis* and *Anabaena*, in a green alga (eukaryote) *Monoraphidium*, and in spinach chloroplast (eukaryote). These investigators found three different types of reaction mechanisms of the Photosystem I reduction: Type I (oriented collisional reaction mechanism), which involves an oriented collision between the two redox partners; Type II (a minimal two-step mechanism), which proceeds through the formation of a transient complex prior to electron transfer; and Type III, which requires an additional rearrangement step to make the redox centers orientate properly within the complex.

Cytochrome c_6 and plastocyanin are different in their basic structures. Their redox centers are heme and copper, respectively. The β-sheet structure of plastocyanin is absent in cytochrome c_6, which has several α-helices instead. However, there is analogous surface topology in these two mobile proteins. Both proteins feature a north hydrophobic pole around the redox center (Site 1) and an east face with charged groups (Site 2). The north pole is important in electron transfer, whereas the east face is important for orientation during the interaction of these proteins with Photosystem I but is not directly involved in electron transfer. As expected from their equivalent roles, the east face of plastocyanin and that of cytochrome c_6 are both acidic or both basic.

In cyanobacterium *Synechocystis*, both proteins contain an acidic patch at Site 2: the equivalent charges are Asp44 and Asp47 in plastocyanin and Asp70 and Asp72 in cytochrome c_6, respectively. When these charges were reversed by site-directed mutagenesis (e.g., plastocyanin mutants D44R and D47R, in which the respective negatively charged aspartate was changed to positively charged arginine), the electron transfer reaction was retarded but not abolished. The ionic strength dependence became the opposite of the wild type, i.e., the electron transfer rate was increased with increasing ionic strengths. Kinetic analysis revealed that the interactions followed the simple oriented collision (Type I). Apparently, these charged amino acids are not involved directly in the docking of the redox partners but are responsible for the generation of an electric dipole. This electric dipole helps orient the mobile electron carrier with the correct orientation toward the binding site on its redox partner. There was no evidence of transient complex formations in the interactions of Photosystem I and wild-type or mutant plastocyanin, such as D44R and D47R. The exception was the double mutant D44R/D47R .

The prokaryote *Anabaena* presents a different scenario. Site 2 of plastocyanin and cytochrome c_6 is positively charged. However, the function of Site 2 in plastocyanin is similar in *Anabaena* and *Synechocystis*. Alterations of these charges by site-directed mutagenesis (e.g., D49K, K58A, K58E) alter the surface potential distribution, thus allowing plastocyanin to modulate its kinetic rate of electron transfer: the more positively charged, the higher the rate constant.[38] Similar changes took place when the positively charged patch of cytochrome c_6 of *Anabaena* was altered by site-directed mutagenesis at Lys62 or Lys66.[23] Kinetic analysis by laser flash absorption spectroscopy indicated that these charges in plastocyanin and cytochrome c_6 are involved in the formation of a transient complex (Type III mechanism). Some mutations at the east face changed the kinetics to either Type I or Type II.

While alterations of charges in the east face modulate the electron transfer rate without completely abolishing electron transfer, alterations of charges at the north hydrophobic region are critical. Arg88 (adjacent to the copper ligand His87) in plastocyanin and Arg64 (close to the heme group) in cytochrome c_6 are required for efficient electron transfers.[23,38] These charges form part of the binding pocket and are critical for proper orientation of the redox partners.

In eukaryote green alga *Monoraphidium braunii*, plastocyanin and cytochrome c_6 contain acidic east faces, and both proteins exhibit a prominent electric dipole moment.[39] The reaction mechanism of electron transfer belongs to Type III: an additional arrangement is required after the formation of a transient complex. The postulated rearrangement can be a conformational change of the induced-fit type or elimination of water from the hydrophobic pocket (desolvation, involving reorganization energy, as stipulated by Marcus[40]), or a two-dimensional random walk, as stipulated in the reduction-of-dimensionality principle by Adam and Delbrück,[13] or both. As expected, cytochrome *f* (of the cytochrome b_6–*f* complex) also possesses an electric dipole moment; its docking surface with plastocyanin or cytochrome c_6 is negatively charged.[39]

In summary, studies of the structure–function relationships in the interactions of plastocyanin/cytochrome c_6 and their redox partners reveal the evolution of reaction mechanisms.[37] The north hydrophobic region is the *cavity* for lock–key style docking, whereas the east face is the site responsible for electrostatic interactions for mutual orientation and transient complex formation. In prokaryote *Synechocystis*, electrostatic interactions are invoked as a homing mechanism. The distribution of individual charges is not critical. The electron transfer process is made more deterministic by a proper orientation prior to collision (Type I). The overall electric dipole moment helps orient the mobile carrier via long-range electrostatic interactions. The Type II mechanism then evolved to increase the contact dwell time of the redox partners. In prokaryote *Anabaena*, eukaryote *Monoraphidium*, and higher plant, the reaction mechanism evolved to three steps: long-range electrostatic interactions for homing, a possible two-dimensional search or conformational rearrangement to refine the docking alignment, which requires shape fitting, and a final step of electron transfer. The mechanism of heuristic searching in molecular recognition is thus a product of evolution rather than an inherent feature of molecular interactions.

Rhodopsin, Transducin, and Arrestin

Three major proteins are involved in the initiation and termination of visual transduction: rhodopsin, transducin, and visual arrestin. Rhodopsin belongs to a large family of molecules known as the G-protein-coupled receptor superfamily[41] and is characterized by seven transmembrane α-helices. One of the partners, transducin (Gt), belongs to one of the most important classes of molecules in signal transduction: GTP-binding proteins (G proteins).[42,43] Visual arrestin is also a member of a large family of molecules involved in the deactivation of G proteins.

Like other G proteins, inactive transducin is a heterotrimer consisting of three subunits: Gα (which has a GTPase domain that binds a molecule of GDP, and two switch regions that initiate a major conformational change, once activated by its receptor), Gβ, and Gγ. Photoactivated rhodopsin — i.e., metarhodopsin II, or MII — binds the inactive transducin heterotrimer, triggers the switch regions, and causes the bound GDP to be released and a fresh GTP molecule to be bound to Gα. The GDP–GTP exchange then causes the three subunits of transducin to dissociate from metarhodopsin II and from one another, thus activating transducin and forming Gα-GTP and Gβγ. The activated Gα-GTP then triggers the cGMP cascade. Subsequent hydrolysis of the bound GTP in Gα then reassembles the three subunits into the inactive transducin heterotrimer.

The cGMP cascade is a nonlinear system that greatly amplifies the action of an absorbed photon on rhodopsin. Sitaramayya and Liebman[44] demonstrated that the termination of the cGMP cascade requires phosphorylation of rhodopsin. The phosphorylation of photoactivated rhodopsin is catalyzed by rhodopsin kinase[45] and takes place at the *C*-terminal region, where nine serine and threonine residues are phosphorylated.[46] Phosphorylation of rhodopsin reduces[47,48] or even blocks[49] Gt activation. This inhibitory effect is greatly enhanced by arrestin,[50] which binds specifically to phosphorylated MII.[48,51]

The investigations of molecular recognition between rhodopsin and its two reaction partners in the cGMP cascade were greatly facilitated by the elucidation of the crystal structures of rhodopsin,[52] transducin,[53–55] and arrestin.[56,57] More recently, using site-directed cysteine mutagenesis to place cross-linkers on rhodopsin, Khorana and coworkers[58,59] identified the contact sites of the photoactivated rhodopsin–transducin transient complex. Gα are cross-linked at residues 310 to 313 and 342 to 345 at the *C*-terminal region, which was previously known to be the receptor-binding domains,[60,61] and at residues 19 to 28 of the *N*-terminal region; both the *C*- and *N*-terminal regions are in contact with the third cytoplasmic loop of photoactivated rhodopsin, which was postulated to be the site that binds Gt.[62] The *N*-terminus of Gα and the *C*-terminus of Gγ are relatively close. Both are sites of lipid modification and are likely to be the sites of membrane attachment. The region around Glu134–Arg135–Tyr136 on Helix II of rhodopsin is surrounded by hydrophobic residues and is known to bind Gt.[52] However, this region is buried in the ground-state rhodopsin and is in no way to make contact with Gt. Therefore, this region must become exposed in the photoactivated rhodopsin via a conformational change. Definite conclusions regarding the docking of Gt with MII must await the elucidation of the crystal structure of photoactivated rhodopsin–transducin complex.

The *C*-terminal of MII is crucial for arrestin binding and rapid deactivation of the cGMP cascade, as could be demonstrated by abnormally prolonged responses in a rhodopsin mutant, of which 15 amino acid residues at the *C*-terminal region were truncated.[63] The truncated segment is apparently not needed for Gt binding and activation.[45,63,64] This *C*-terminal segment of rhodopsin is most likely the initial recognition site but not the ultimate binding site of arrestin, because excess Gt displaces arrestin from phosphorylated rhodopsin. Gt, which binds to phosphorylated and nonphosphorylated MII, apparently competes with arrestin for the same binding site.[48] Arrestin undergoes a conformational change after binding to the *C*-terminal of phosphorylated MII.[65–67] This change exposes a critical buried region of arrestin that enables it to bind to a second binding site on phosphorylated MII, which also binds Gt competitively. This interpretation is supported by an experiment with a synthetic peptide that mimics the *C*-terminal tail of phosphorylated MII. This synthetic peptide comprises the fully phosphorylated *C*-terminal phosphorylation region of bovine rhodopsin, residues 330 to 348 (known as 7P-peptide).[65] This peptide binds to arrestin, induces a conformational change that is similar to that induced by binding to phosphorylated MII, and activates it. Furthermore, this activated arrestin can then bind to photoactivated but *nonphosphorylated* rhodopsin, i.e., nonphosphorylated MII.

Thus, an electrostatic switching mechanism is implicated in at least the initial binding of arrestin to the phosphorylated *C*-terminal of MII. However, the multiple phosphate groups apparently do more than just provide negative charges, because synthetic peptides in which all potential phosphorylation sites were substituted with glutamic acid (7E-peptide) or with cysteic acid (7Cya-peptide) did not mimic the negative charge of phosphorylated amino acid residues.[68] Evidence of electrostatic effects came from kinetic analysis of the complexation between Gt and MII and between arrestin and MII. Investigations of the kinetics of rhodopsin–arrestin complexation were hampered by the similarity of the absorption spectra of free MII, MII–Gt complex, and MII–arrestin complex; they all have an absorption maximum at 390 nm and, therefore, the three forms of MII are not spectroscopically distinguishable. Because there exists an acid–base equilibrium between MI and MII, binding of Gt shifts the equilibrium to the right, by virtue of the law of mass action, thus stabilizing highly phosphorylated MII as a MII–Gt complex.[69,70] Similarly, binding of arrestin stabilizes phosphorylated MII as a MII–arrestin complex.[51] Both complexation processes increase absorption at 390 nm. The situation is further complicated by the finding that phosphorylation increases the MI–MII equilibrium constant.[71,72] Thus, the equilibrium of MI–MII is shifted to the right for two reasons: the change of the equilibrium constant and the effect of product removal. As a consequence, the relative proportions of free MII and its two complexed forms cannot be directly measured spectrophotometrically. These enhanced portions of MII formation are known as extra-metarhodopsin II.

Parkes et al.[73] subsequently developed a nonlinear least-square curve-fitting procedure (Simplex) to sort the three forms of MII amidst three concurrent equilibria. Using this approach, Gibson et al.[74] found

that the binding affinity of Gt to MII is dependent on ionic strengths, with maximum affinity at 200 m*M*. The affinity decreases toward higher and lower ionic strengths. Similar ionic strength dependence was found for the binding affinity of arrestin to MII, at various phosphorylation levels. The decrease of affinity at high ionic strengths is consistent with the effect of charge screening, but the decrease at lower ionic strengths is not. Gibson et al.[74] attributed the decrease to the possibility of two separate binding processes: binding to MII and to the photoreceptor membrane. However, similar decreases were observed in several mobile electron carriers in photosynthetic membranes; there is no compelling evidence to postulate an additional binding site on the photosynthetic membrane. In view of the ubiquity and possible universality of this type of ionic strength dependence among mobile electron carriers in photosynthetic membranes, we favor, instead, the interpretation, proposed by Tollin and Hazzard,[26] that excessive electrostatic stabilization of a docking complex hampers further interactions between the complexed partners by inhibiting exploration. This is especially relevant, because there appear to be two separate stages of arrestin binding to MII; an excessively stabilized complex of arrestin with the *C*-terminal binding site of phosphorylated MII would interfere with its binding to a second site. Tollin and Hazzard's interpretation is further justified by additional independent evidence suggesting that protein flexibility may be a universal necessity in macromolecular reactions. Garbers et al.[75] studied the electron transfer from negatively charged semiquinone $Q_A^{-\bullet}$ to oxidized quinone Q_B in Photosystem II. These investigators found that the extent of reoxidation of $Q_A^{-\bullet}$ starts to decrease below 275 K and is almost completely suppressed at 230 K. Detailed analyses of Mössbauer spectra measured at different temperatures in ^{57}Fe-enriched samples indicated that the onset of fluctuations between conformational subsets of the protein matrix occurs also at around 230 K. They suggested that the head group of plastoquinone-9 (a membrane-bound mobile electron carrier) bound to the Q_B-site in Photosystem II requires a structural reorientation for its reduction to the semiquinone.

The kinetic analysis of Gibson et al. also showed that Gt affinity for MII decreases with increasing phosphorylation, whereas arrestin affinity for MII increases almost linearly with increasing phosphorylation. The data were also consistent with the assumption of 1:1 binding stoichiometry for Gt–MII and for arrestin–MII. The reciprocal fashion of the phosphorylation dependence of Gt and arrestin-binding affinity is in keeping with their respective roles as the activator and the deactivator of the cGMP cascade, thus reflecting nature's way of optimization by means of simultaneous modulation of the two binding processes. The incremental change for each added phosphate indicates that the switches of visual transduction are not simple on–off switches but are similar to the kind of rotary switch (incremental switch) that allows for continuous adjustment of the brightness level of a lamp.[76]

Despite the similarity of affinity changes, the (second-order) binding rates of Gt and arrestin are different at equal concentrations. The kinetics of Gt binding to MII at 0.6 μ*M* Gt are exponential with a relaxation time constant near 1 s, whereas arrestin binding to MII at 0.6 μ*M* arrestin is much slower, with a relaxation time constant of more than 20 s.[74] This disparity of kinetics allows for a window of time for Gt to take action before deactivation prevails, thus avoiding shutting down the process prematurely.

Although phosphorylation does not cause global conformational changes of MII, local changes that include changes of the membrane surface potential and the membrane surface pH may affect the binding kinetics of Gt and arrestin.[72] The increased negativity of the membrane surface potential lowers the surface pH relative to the bulk pH. The ensuing lowering of pH can affect the protonation state (ionization state) of exposed charged amino acid residues in two possible ways: increasing reactant (proton) availability by virtue of the law of mass action and the direct effect of pH on the binding constant. The resulting change of the protonation state of charged amino acid residues at the membrane surface further changes the membrane surface potential. The interaction is therefore highly nonlinear. Using the nonlinear least-squares fitting scheme, Gibson et al.[74] determined the pH dependence of the respective binding affinity of Gt and of arrestin to MII at various levels of MII phosphorylation. They found a phosphorylation-dependent shift in the pH maximum for the binding affinity of Gt. While the Gt affinity for nonphosphorylated MII peaks at pH 8, the pH for the maximum binding affinity shifted to the alkaline values with increasing phosphorylation and became immeasurably high at 4.1 PO_4/rhodopsin or higher. This shift was more apparent than real, because

the shift disappeared if the binding affinity was plotted against the surface pH instead of the bulk pH. Thus, the Gt–MII interaction depends directly on the membrane surface pH. The maximum Gt affinity now peaks at the membrane surface pH of 7.5 at all levels of phosphorylation.

Gibson et al.[74] also determined the pH dependence of the binding affinity of arrestin to MII, at various levels of MII phosphorylation. The affinity of arrestin for MII increases more or less linearly with pH up to pH 8.5, beyond which no data were available because of technical difficulty. The arrestin-binding kinetics is also pH dependent. With increasing pH or decreasing phosphorylation levels, the speed of arrestin binding decreases, so that the reaction does not reach equilibrium in time between flashes of illumination. The effect of phosphorylation on the arrestin-binding kinetics is also mediated via its electrostatic effect on the membrane surface pH, according to the analysis of Gibson et al.

Considerably more specific local electrostatic interactions may be involved in arrestin action, as suggested by a recent model for the rhodopsin phosphorylation dependence of arrestin binding.[57,77,78] When analyzing the model, it can be suggested that the negative phosphate charges on the *C*-terminal tail of MII destabilize a series of salt bridges and hydrogen bonds in the polar core of arrestin (switch region), which has a strongly positive local electrostatic potential, thus causing the conformational change of arrestin upon its activation.

The recognition of MII by Gt and by arrestin apparently belongs to a Type III mechanism designated by Hervás et al.[37] (transient complex formation with molecular rearrangement). Gt and arrestin undergo major conformational changes after initial binding. Furthermore, arrestin eventually binds to a second site, which is close to or identical to the binding site of Gt. There are several sequences of contiguous cationic amino acids in arrestin, which can be identified as positively charged patches near the *N*-domain of arrestin,[56,57] the proposed rhodopsin binding site (see also Figure 11A of Gibson et al.[74]). The key residue Arg175 in the so-called polar core of arrestin allows arrestin to distinguish between phosphorylated and nonphosphorylated rhodopsin.[66,67] The complementarity of charge pairing is apparent. The putative binding surface of Gt is mostly negatively charged, with some small patches of positive potentials (Figure 11B of Gibson et al.[74]). Hamm[79] pointed out the overall charge complementarity between the cytoplasmic surface of rhodopsin (positively charged residues Lys248, Lys141, and Arg147) and the receptor-binding surface of Gα (negatively charged residues Asp311 and Glu212) (see Figure 2 of Hamm[79]). The charge distribution on the surfaces of Gt and that of arrestin do not suggest the presence of a sufficiently strong electric dipole moment to lead to oriented collisions. However, judging from the contrast of the overall negative surface of Gt and the patchy positive surface of arrestin, we suspect that the membrane surface potential may play an additional role in making the encounter of the partners more deterministic via long-range electrostatic interactions (homing mechanism). The largely positive cytoplasmic surface of rhodopsin favors attraction of Gt but not arrestin (see Figure 2 of Hamm[79]). The additional positive surface potential generated by the ERP (R2 component) probably adds little to the already positive potential. The electrostatic interactions caused by the ERP are probably local in nature. However, its role in triggering Gt binding cannot be completely ruled out. The membrane surface potential subsequently turns in favor of arrestin binding (homing mechanism); the dramatic buildup of negative surface charges brought about by phosphorylation is probably sufficient to overshadow the positive surface charges that were originally present on MII prior to phosphorylation. Of course, as suggested by Gibson et al.,[74] the opposite surface potentials can also influence the affinity of both proteins to MII (short-range electrostatic interactions). Their interpretation is supported by the data showing that the affinity of arrestin for MII increases linearly with pH between pH 7.0 and 8.5,[74] and that the negative photoreceptor membrane surface potential also increases linearly within this same pH range.[72]

In summary, the interactions between rhodopsin and its two partners, transducin and arrestin, echo the general scheme of interactions of mobile electron carriers, discussed earlier, despite the differences in terms of structures and functions. Again, nature deployed short-range noncovalent bond interactions to make collisions and reactions between encountering partners more deterministic than random processes. Nature also orchestrated the sequence of events with appropriate timing. When the interactions between Gt and MII need to be more deterministic, the interactions between arrestin and MII are made more random. Conversely, when the interactions between arrestin and MII need to be more deterministic,

the interactions between Gt and MII are made more random, all by means of the intricate interplays of the same set of fundamental forces. During visual transduction, electrostatic interactions are invoked in a number of different mechanisms: local and global, nonspecific and specific. Nature seemed to recruit whatever mechanisms were workable, in a highly flexible way, and did not stick to any particular "ideological" scheme. On the other hand, highly successful schemes were evolutionarily multiplied and perpetuated in different systems in the same organism and among different species of organisms, as exemplified by the huge family of G protein receptors and their partners, G proteins and arrestins.

Bacteriorhodopsin

Bacteriorhodopsin, like its sister molecule rhodopsin, is also a member of the G-protein-coupled receptor superfamily. As a one-molecule light-driven proton pump, bacteriorhodopsin essentially carries out the entire task of the photosynthetic reaction center of phototrophic purple bacteria — a far more complex chlorophyll–protein complex of several subunits. The mechanistic detail of its operation is of great interest in understanding photosynthesis. Bacteriorhodopsin is also a relevant model molecule for understanding electrogenic ion pumps; its light sensitivity provides an additional handle with which to probe its kinetic properties. In Chapter 128, we exploited its similarity to rhodopsin to enhance our understanding of ERP. In this section, we will examine the factors that enhance its efficiency of photon energy conversion.

At the molecular level, it is the light-induced *trans*-to-*cis* isomerization of the chromophore retinal that drives the vectorial proton transport. A detailed understanding of the molecular events leading to proton transport was greatly enhanced by elucidation of the crystal structures of ground-state bacteriorhodopsin and several intermediates of the photocycle. The detailed picture is gradually emerging but is still in a state of flux. Periodic reviews were provided by Lanyi.[80–84]

Like rhodopsin, photon absorbed by bacteriorhodopsin initiates isomerization of the chromophore. But unlike the open-ended photobleaching of rhodopsin, bacteriorhodopsin undergoes a cyclic sequence of reactions (photocycle). Photoisomerization causes the retinal Schiff base at lysine residue 216 (K216) to deprotonate. The primary acceptor of the Schiff base proton is aspartate 85 (D85). The remaining reactions of the photocycle are thermally driven. Transfer of a proton from the retinal Schiff base, first to D85 and then eventually to the extracellular aqueous phase, dominates the first half of the photocycle. The active site of this sequential transfer is the highly polarized bound water 402, which is coordinated by the protonated retinal Schiff base and two anionic aspartates, Asp212 and Asp85.[85] The release of proton from the deeply buried D85 to the extracellular space requires the participation of Arg82, Tyr57, Glu194, and Glu204 that, together with six bound water molecules, form a column of hydrogen-bonded network.[86] The second half of the photocycle is featured by reprotonation of the Schiff base from aspartate 96 (D96), which, in turn, accepts a proton from the cytoplasmic space via another hydrogen-bonded chain with four bound water molecules positioned in single file. Kinetically, the action of the protonation switch, from an extracellular access to an intracellular access, takes place during the $M_1 \rightarrow M_2$ step. The $M_1 \rightarrow M_2$ transition incurs a major conformational change and a large entropic change; the probability of charge recombination is greatly diminished by virtue of this protonation switch.[87] This transition is unidirectional under some conditions but reversible under others (summarized by Lanyi[81]).

Speaking about the unidirectionality or reversibility of the protonation switch, it is of interest to examine the macroscopic electrical behavior of the bacteriorhodopsin membrane. Despite the conventional practice of referring to bacteriorhodopsin as a photodiode,[88] direct evidence of rectification of proton conductance is lacking. An unequivocal experimental determination of the existence or absence of rectification is contingent on a clear-cut separation of the photovoltaic effect and the photoconductive effect. A detailed argument explaining why separation of these effects is important was presented elsewhere.[89,90] It suffices to say that the presence of photoemf renders classical electrophysiological methodology inadequate, because a voltage-clamp or a current-clamp measurement, together with Ohm's law, is insufficient to determine all four experimental variables: photoemf, membrane voltage, photoconductance, and photocurrent; an additional act of measurement is required. A null current method that combines the principle of potentiometry with the classical voltage-clamp method was specifically

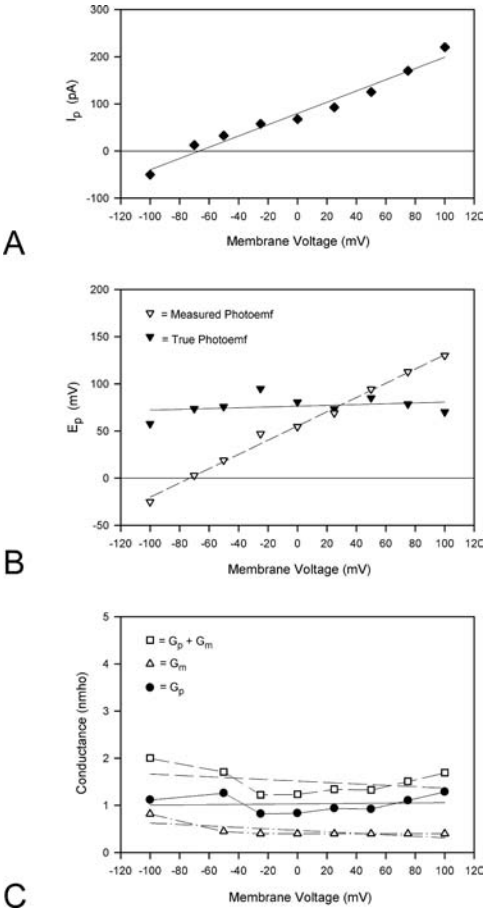

FIGURE 134.3 Steady-state photoelectric response of a bacteriorhodopsin-containing black lipid membrane. The aqueous solutions contained 0.1 *M* NaCl and 0.5 m*M* $CeCl_3$. Measurements were made at pH 6.9 and 24°C. (A) Measured photocurrent I_p is shown as a function of the transmembrane voltage. (B) Photoemf E_p, as determined by the null current method, is shown as a function of the membrane voltage. Apparent photoemf is shown as open inverted triangles, whereas true photoemf, corrected by eliminating voltage-driven photocurrent and shunting of G_m, is shown as filled inverted triangles. (C) Apparent photoconductance ($G_p + G_m$) (open squares), measured dark conductance (G_m) (open triangles), and true photoconductance (G_p) (filled circles), corrected for the shunting effect of G_m, are shown. All data were taken from the same membrane. (From Fuller, B.E., Okajima, T.L., and Hong, F.T., *Bioelectrochem. Bioenerg.*, 37, 109, 1995. With permission.)

designed for this purpose.[91] Determining the photoemf by invoking the principle of potentiometry constitutes the second act of measurement.

Drachev et al.[92,93] were the first to report that the photocurrent is linearly dependent on the transmembrane voltage. It was repeatedly observed by other investigators, and more than half a dozen interpretations were proposed. In view of Ohm's law, a voltage dependence of the photoemf and the photoconductance can both give rise to a voltage-dependent photocurrent. However, the result of null current analysis of photoelectric measurements made in reconstituted bacteriorhodopsin-containing black lipid membranes (BLM) indicates that the steady-state photoemf and photoconductance are not voltage dependent[89] (Figure 134.3). Furthermore, direct measurements of the conductance of the reconstituted BLM, during illumination and in the absence of illumination, together with a similar measurement using a "control" BLM without incorporated bacteriorhodopsin, showed that the proton conductance channel opens only during illumination. A reconstituted bacteriorhodopsin membrane in

the absence of illumination has the same low conductance as the "control." Essentially, it is a photon-gated conduction channel: it opens upon the onset of illumination but shuts off upon the cessation of illumination. Furthermore, the proton conduction channel created by illumination is available for the passage of the proton current driven by a transmembrane electrochemical potential difference. In other words, the measured photocurrent includes the light-driven current (generated by photochemical reactions) and the voltage-driven current (which merely takes advantage of the availability of a proton conduction channnel created by photoreactions). It is of interest to note that the light-driven portion constitutes an active transport of proton, capable of driving the current against an existing proton electrochemical gradient, whereas the voltage-driven current reflects a passive transport, similar to Na^+ and K^+ currents, commonly encountered in classical electrophysiology. Thus, a sufficiently intense transmembrane voltage or transmembrane pH difference can drive the proton current in the reverse direction. The voltage-driven current is, of course, voltage-dependent, but is counted as part of the measured photocurrent, because it exists only during illumination. In addition, the photoconductance is not rectified; the voltage-driven proton current encounters the same resistance in either direction during illumination. The photoconductance exhibits no voltage dependence. That is the reason the voltage-driven current is linearly dependent on the transmembrane voltage, in accordance with Ohm's law.

The generation of a transmembrane proton gradient is the intermediate step between photon energy conversion and bioenergetic synthesis of ATP. The formation of the transmembrane electrical gradient (i.e., the photovoltage) constitutes a situation similar to back-biasing of a photodiode. Back-biasing provides the driving force to drive protons back into the cell. In principle, there are several ways the electrochemical potential can drive protons from the extracellular space back into the cytoplasm:

1. Protons or other small ions reentering the cell via leakage through the phospholipid portion of the purple membrane, and thus dissipating the converted energy
2. Protons reentering the cell via a reverse proton flow through the same proton-translocating channel in bacteriorhodopsin (direct charge recombination)
3. Protons reentering the cell via the proton-transport channel of ATP synthase (in the reverse direction), thus synthesizing ATP
4. Protons reentering the cell via the flagella motor apparatus, and thus powering the motion of the flagellas
5. Protons reentering the cell to power a cotransport system (symport or antiport)

With the exception of the first two routes, all other routes of charge recombination do useful work for the bacterium. The wasteful dissipation of converted energy via leakage is minimized in the purple membrane by having a relatively small area of phospholipid portion in the two-dimensional crystalline structure of the purple membrane.[94,95] In the reconstituted bacteriorhodopsin BLM, G_p in the dark is considerably smaller than G_m. This property means that the insulation against a proton backflow, in the dark, via the proton-translocating channel, is more effective than the insulation of the phospholipid portion of the artificial BLM. During illumination, however, G_p of a reconstituted membrane is only comparable to G_m. Quantitative comparison of G_p and G_m in a native purple membrane is not available. But the ratio G_p/G_m should be much greater in the native purple membrane than in our experimental system, because reconstitution in our experimental system could not have achieved the same high density of bacteriorhodopsin packing as in the native purple membrane.

The direct charge recombination by a reversal of charge flow (Number 2 above) is the major problem to be overcome in artificial solar energy conversion. In the case of silicon photodiode, this problem is mitigated by rectification of the charge conduction channel; the resistance that the photocurrent encounters during (internal) charge recombination is much greater than the forward resistance encountered during charge separation. The null current analysis demonstrated that bacteriorhodopsin is a photocell but not a photodiode in the strict sense. As for achieving good energy conversion efficiency, bacteriorhodopsin apparently relies on a different strategy than rectification to prevent charge recombination. Let us take a close look at how bacteriorhodopsin and a photodiode differ in minimizing direct charge recombination.

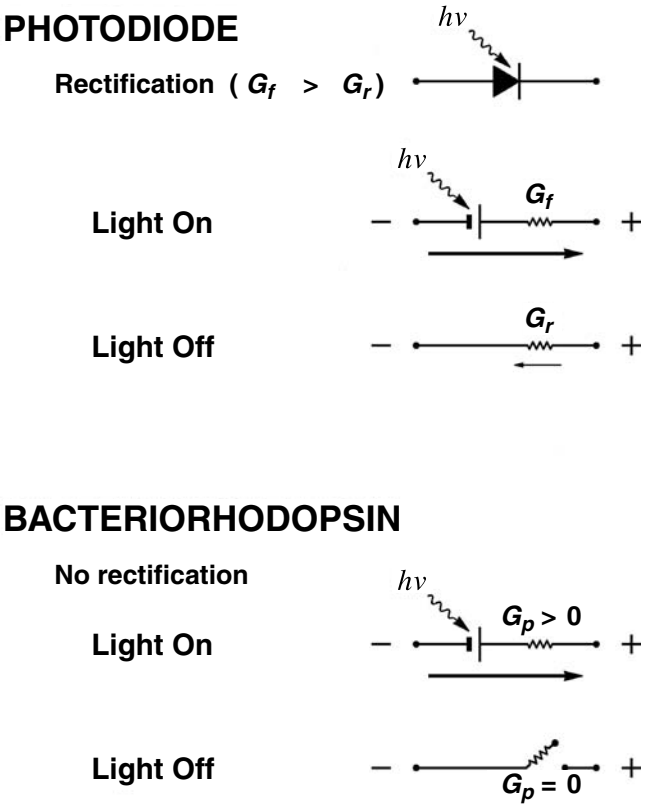

FIGURE 134.4 Comparison of rectification in a conventional photodiode and light-gated proton conduction in bacteriorhodopsin. Plus and minus signs indicate polarity of photovoltage under open-circuit conditions. G_f and G_r are forward conductance and reverse conductance of the photodiode, respectively. Photoactivation causes a photocurrent to flow in the forward direction, as indicated. Elicited photovoltage back-biases photodiode (under open-circuit conditions), and drives current in the reverse direction during illumination, thus canceling part of the (forward) photocurrent. But reverse current encounters much greater resistance than forward current (rectification: $G_f >> G_r$). In the photodiode, charge recombination in the dark is minimized because of rectification. There is no rectification in bacteriorhodopsin; forward photocurrent (driven by light and reverse current — driven by back-biasing voltage) encounters the same resistance ($1/G_p$). Note that externally observed photocurrent is actually the difference (algebraic sum) of voltage-independent light-driven current and voltage-driven (and, therefore, voltage-dependent) current. Constancy of the true photoemf, as membrane potential varies, indicates that illuminated bacteriorhodopsin's ability to maintain net "driving force" is not affected by back-biasing. In bacteriorhodopsin, charge recombination in dark is minimized because of closing of the proton conduction channel in the dark (G_p = 0 in dark). (From Hong, F.T., *Prog. Surface Sci.*, 62, 1, 1999. With permission.)

As shown in Figure 134.4, light-induced forward charge separation in a photodiode generates a photocurrent that encounters a resistance $1/G_f$. In contrast, charge recombination during illumination, as well as in the absence of illumination, encounters a much greater resistance $1/G_r$ (where $G_f >> G_r$). In this way, charge recombination is greatly minimized in a photodiode. Charge recombination in bacteriorhodopsin takes place by virtue of the ubiquitous reverse biochemical reactions. Although the $M_1 \rightarrow M_2$ transition is at times a one-way reaction, it does not make its presence evident as rectification. However, a one-way photochemical reaction is not an absolute requirement. As long as continuing input of photon energy is guaranteed, a photon-driven forward reaction continues to offset charge recombination caused by reverse reactions. As a consequence, a steady state is maintained, and an externally connected device can continue to drain energy to perform useful work. That a one-way reaction is not

required is experimentally demonstrated by an artificial magnesium porphyrin-containing BLM in which no provisions were instigated to minimize reverse electron transfer.[91]

From a mechanistic point of view, charge recombination in the dark is a more serious problem than charge recombination during illumination. While light-driven forward charge reaction continues to counterbalance charge recombination as long as illumination persists, charge recombination runs unopposed in the absence of illumination. A nonrectified conduction channel that remains open in the dark will eventually dissipate the entire amount of stored energy. The usefulness of a solar cell is contingent on its continuing operation in the absence of illumination. Bacteriorhodopsin's light-gated proton conduction channel thus meets this latter requirement. By completely shutting off the proton conduction channel, the peril of charge recombination in the dark is averted. Bacteriorhodopsin thus achieves the same goal (in the dark, at least), without rectification, as does a silicon photodiode with rectification. Regarding the photo-gating mechanism, a molecular interpretation is presently lacking. However, based on the crystal structure of dark-adapted bacteriorhodopsin and several photointermediates revealed by Lanyi's group, bound water and the associated hydrogen-bonded network are absent in the cytoplasmic half of the proton conduction channel, both in the absence of illumination and during the first half of the photocycle; bound water and the hydrogen-bonded network make their appearance only during the latter half of the photocycle as bacteriorhodopsin reprotonates its Schiff base from the cytoplasmic aqueous phase via Asp96.[86] These structural data imply that bacteriorhodopsin is an insulator in the dark and during the first half of the photocycle; photoconduction becomes activated during the latter half of the photocycle. But how the lack of rectification transpires in spite of the reprotonation switch remains unclear.

The null current analysis of proton conduction in bacteriorhodopsin also has important bearing on the fundamental bioenergetic principle. According to chemiosmotic theory, the converted energy by bacteriorhodopsin photoreactions is stored as a transmembrane voltage gradient (ΔV) and a transmembrane gradient of protons (ΔpH). The electrical and chemical components are equivalent and interconvertible, and both are available as sources of energy for ATP synthesis. The equivalence of the two types of gradients is made possible by the facts that the light-driven proton current and the voltage-driven proton current pass through the same conduction channel, and the proton current encounters the same resistance in either direction. In other words, by imposing a transmembrane voltage across the purple membrane, protons can be driven in either direction with equal ease, and a voltage gradient can be converted into an additional proton gradient to be added to or subtracted from an existing one. The lack of rectification guarantees the exchange between ΔV and ΔpH is conducted at an "equal exchange rate." Were there a rectification, the interconversion would not be equal, because the IR drop would be more in the back-biasing direction than in the forward-biasing direction (which is tantamount to a difference between buying and selling rates of currency exchange). Null current analysis thus furnished a quantitative demonstration that the two components of electrochemical energy are interchangeable.

The light-dependent gating mechanism of bacteriorhodopsin's proton conduction channel may also explain a long-standing puzzle. As shown in Figure 128.8(B), the equivalent circuit that contains chemical capacitance responds to a long square-wave light pulse by exhibiting a sharp spike of current upon the onset of illumination, and another spike with opposite polarity upon the cessation of illumination. This waveform is known as differential responsivity in the molecular sensor literature[96,97] [see, for example, that shown in Figure 128.2(B)]. It is the characteristic waveform of the output of a linear RC high-pass filter. The equivalent circuit shown in Figure 128.8(A) predicts such a waveform with two symmetric spikes (the RC circuit comprised of R_pC_p constitutes a high-pass filter). However, with few exceptions, the two spikes appeared asymmetric in many reconstituted pigment-containing membranes. The "on" spike is more prominent and decays faster than the "off" spike. The asymmetry is barely discernible in Figure 128.8(B) but is more prominently displayed in Figure 134.5. Note that by assuming $R_s = \infty$, the equivalent circuit predicts symmetric spikes. The asymmetric waveform can be explained, however, if the equivalent circuit is modified to reflect the presence of a light-gated proton conduction channel — i.e., R_s assumes a considerably smaller value during illumination than in the dark. Thus, the apparent decay time constant of a spike is shorter during illumination than in the dark. That the spikes are a manifestation of a capacitative response is reflected in the equality of the area enclosed by the spikes and

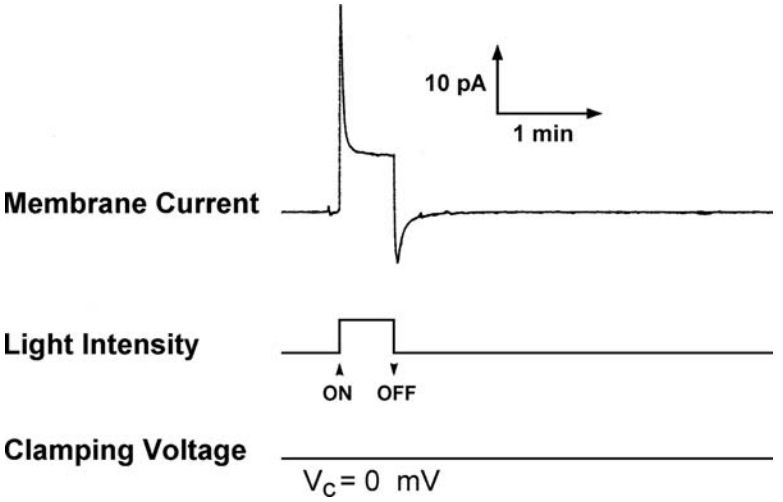

FIGURE 134.5 Photoelectric signals from a reconstituted bacteriorhodopsin black lipid membrane in response to a long square-wave light pulse (xenon arc lamp). The black lipid membrane permits steady-state photocurrent to pass through it. The photocurrent exhibits the characteristic "spikes" of a high-pass filter. See text for explanation. (From Fuller, B.E., Okajima, T.L., and Hong, F.T., *Bioelectrochem. Bioenerg.*, 37, 109, 1995. With permission.)

the baseline. Thus, the fast-decaying spike during illumination has a more prominent peak than the slower one, as is evident in Figure 134.5. It is also not difficult to understand why photogating of R_s is not apparent in measured ERP-like signals when a brief (δ-function) light pulse is used; the diminished source impedance (due to C_p) in the microsecond time range renders the change of R_s insignificant by comparison. The asymmetry of the two peaks appeared in many different types of reconstituted membranes (see Hong[98] for a summary) and is a constant feature rather than an artifact.

We further suspect that the photogating mechanism exhibited by bacteriorhodopsin may also be present in the electron-transfer channel of a chlorophyll-based photosynthetic membrane. As shown in Figure 134.6, asymmetry of the two transient spikes is evident in an *in vivo* voltage-clamp measurement of a giant chloroplast of *Peperomia metallica*.[99] Thus, the electron-conduction path in this giant chloroplast may also be activated only by light, thus preventing electron backflow in the dark. A direct determination of G_p (as compared to G_m) in *Peperomia metallica* is presently lacking. However, if this interpretation is correct, then it appears that nature implemented the same design principle by using completely different molecular constructs.

134.4 Lateral Mobility of Protons on the Membrane Surface

Although what is to be considered next is not a molecular switch, an omission of it makes the ongoing discussion incomplete. In addition to the energy loss due to charge recombination, there is yet another route of energy loss in photosynthesis. ATP synthase and the photosynthetic reaction center (or bacteriorhodopsin) are located side by side in the membrane. The transported protons must diffuse laterally in order to reach the site of ATP synthase, but they can also diffuse into the vast nearby aqueous solution, instead. Energetically speaking, this process of proton diffusion into the bulk solutions incurs an unacceptable loss of energy because of the dilution effect (known as the Pacific Ocean effect). It has long been a dispute between two camps of theoreticians — the localized[7–9,100] and the delocalized[6] version of chemiosmotic process (reviewed by Kell[101]). Somehow a switching function that allows protons to be diverted preferentially into the site of ATP synthase instead of the bulk aqueous solution would be advantageous. Without such a switch, photosynthesis would still work. However, advocates of the localized mechanism suspected that evolution could have eliminated this unnecessary energy loss. Kell speculated about the existence of some sort of barrier in the vicinity of the membrane surface, which converts the

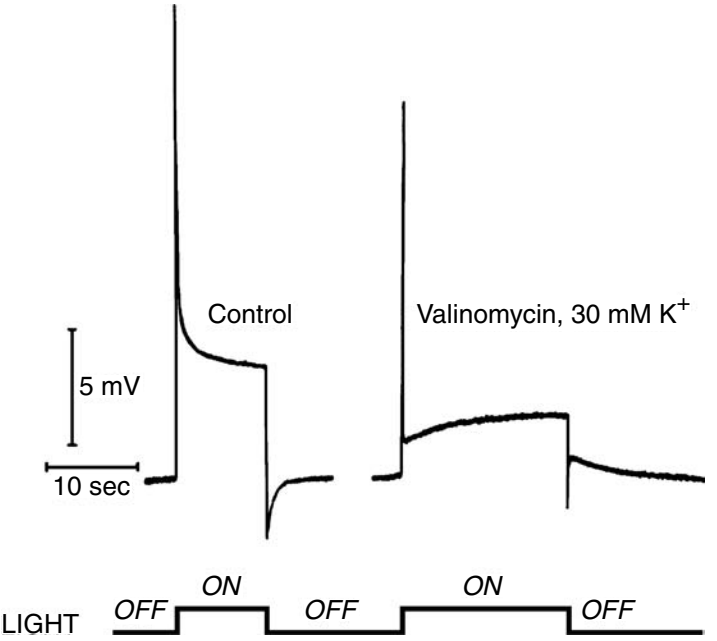

FIGURE 134.6 Photoelectric signals recorded *in vivo* from a photosynthetic membrane in response to a long square-wave light pulse. Open-circuit photovoltage was recorded intracellularly from an intact chloroplast of *Peperomia metallica*. Control signal, taken before addition of valinomycin, is shown at left, and effect of adding 1 μM valinomycin and 30 m*M* potassium ions in external medium is shown at right. See text for discussion. (From Vredenberg, W.J. and Bulychev, A.A., *Plant Sci. Lett.*, 7, 101, 1976. With permission.)

Pacific Ocean effect into a San Francisco Bay effect — an imperfect barrier that minimizes leakage of protons into the bulk solutions. Such a speculated barrier was realized by the discovery of Teissié and coworkers.[102,103] These investigators found that proton conduction is considerably faster on the membrane–water interface than in the bulk water. Subsequently, Alexiev et al.[104] found similar proton conduction on the surface of the purple membrane of *Halobacterium salinarum*.

Teissié and coworkers detected rapid lateral movement of protons on a phospholipid monolayer–water interface by a number of measurements: fluorescence from a pH indicator dye near the membrane surface, electrical surface conductance, and surface potential. These investigators found that the conduction of protons along the surface is considerably faster than proton conduction in the bulk phase (2 to 3 min versus 40 min for a comparable distance in their measurement setup). This novel conduction mechanism is proton-specific, as confirmed by a radioactive electrode measurement as well as by replacement with deuterated water. It is a consequence of cooperativity between neighboring phospholipid molecules; the conduction mechanism disappears when phospholipid molecules are not in contact with each other.

Teissié and coworkers indicated that the enhanced lateral proton movement occurs along a hydrogen-bonded network on the membrane surface in accordance with a mechanism previously proposed by Onsager[105] for proton conduction in ice crystals and by Nagle and Morowitz[106] for proton translocation in membranes. The hydrogen-bonded network is formed by the polar head-groups of phospholipid and the associated ordered water molecules at the membrane surface. Thus, a proton jumps from H_3O^+ to a neighboring H_2O. The newly formed H_3O^+ then rotates and becomes a new proton donor to its neighbor farther down the chain in the network. As a result, protons move considerably faster on the membrane surface than expected by classical diffusion. In fact, a similar mechanism was used to explain proton diffusion in the bulk phase, which is considerably faster than the diffusion of ions of comparable size in the same medium. Therefore, the "hop-and-turn" mechanism enhances proton movement at the interface and in the bulk phase. What makes the lateral proton movement on the membrane surface so much faster than proton diffusion in bulk water?

I think that there are at least two reasons. First, the proton movement at the membrane surface is two-dimensional, whereas the movement in bulk water is three-dimensional (reduction-of-dimensionality principle of Adam and Delbrück). It is true that simple diffusion in a two-dimensional space is faster than in a three-dimensional space according to the probability theory. It may also be true for the "hop-and-turn" mechanism. The second reason may be the increased surface concentration of protons as compared to the bulk concentration caused by a negative surface potential. The negative surface potential is primarily due to the net negative surface charges of the phospholipid polar head-groups. The increased concentration at the surface makes the "hop-and-turn" mechanism work better along the surface than in bulk water. Teissié's group showed that there is a steep gradient near the membrane surface (two pH units in less than 1.5 nm). However, these authors also observed similar facilitated lateral proton movement with monolayers formed from neutral and zwitterionic phospholipids. Therefore, the effect of a negative surface potential is probably secondary and supplementary but not essential.

134.5 Discussions and Conclusions

Webster's Third International Dictionary defines the verb "switch" as to change or shift things, places, methods, actions, or directions. This definition covers enzyme action at the molecular level, which helps channel branching reactions into a single pathway at the expense of other (side) reactions. This definition also covers shifting of attention or decision making of the whole organism at the systems level. An intriguing question that computer scientists and philosophers frequently ask is: how do seemingly random processes at the molecular level lead to decisive information processing at the systems level? A crude answer is that random molecular processes are punctuated by switching processes exemplified by enzyme or gene activation. A survey of major photobiological systems offers ample opportunity to probe this question, because light often serves as the trigger to activate switching processes. Included in the present discussion is the role played by noncovalent bond interactions in molecular recognition. These interactions help switch the processes from random diffusion and collisions to significantly more deterministic docking in molecular recognition.

Implied in the above definition are a sudden action, a threshold, a trigger, and an amplification mechanism. A switch falling short of these implied features is usually regarded as a bad switch, e.g., a "sticky" switch or hesitation. In visual photoreceptor membranes, the sudden, snapping action is implemented in terms of a sequence of the light-induced conformational changes of rhodopsin, which culminates in the formation of metarhodopsin II. In Chapter 128, the mechanistic events accompanying the appearance of the early receptor potential (ERP) are examined. The electrochemical aspect of ERP was amply discussed, while the molecular details remain unsettled. Some investigators attempted to make fairly definitive assignments of individual components of the ERP-like signal in reconstituted bacteriorhodopsin membranes. However, these assignments must be called into question, primarily because of the improper use of classical electrophysiological methodology and the indiscriminate use of multiexponential analysis. Although a major consensus — ERP plays no physiological role — was reached more than three decades ago, the mechanistic reinterpretation of ERP warrants a reexamination of the same old question: the possible physiological role, because absence of evidence is not evidence of absence. In light of the ever-increasing knowledge of the molecular detail of the cyclic GMP cascade, the time is ripe to launch a renewed inquiry. Our suspicion regarding a possible physiological role of ERP is reinforced rather than subdued in the intervening years: ERP still looks suspiciously like the mechanistic trigger prior to biochemical amplification, because ERP positions in the right place at the right time to serve as the mechanistic (electrostatic) trigger of visual transduction. Electrostatic interactions have the virtue of a snapping action — with a picosecond rise time and localized effect (limited to the diffuse double-layer region where light hits rhodopsin). However, correlation is, of course, no proof of causality. The present survey of visual and photosynthetic systems reveals that nature usually solved problems by recruiting and mobilizing every possible molecular interaction. As a result, the role played by each type of noncovalent bond interaction is obscured by the concurrent presence of various types of interactions. Although a survey of known structural and functional interactions between metarhodopsin, transducin, and

arrestin does not clarify the question, it seems promising to begin to dissect the event into separate contributions from various kinds of noncovalent bond interactions. At this moment, there is no compelling reason to sustain or overturn the old verdict.

The molecular switching processes in photosynthetic membranes serve the purpose of enhancing the efficiency of photon energy conversion rather than photon detection. The molecular switches are triggered directly or indirectly by absorbed photons. In the previous edition of this chapter,[5] photophosphorylation of light-harvesting chlorophyll-protein Complex II was cited to illustrate how nature utilized electrostatic interactions to dynamically allocate resources.[107] In the present article, the discussion is focused on mobile electron carrier systems that shuttle electrons from complex to complex in a photosynthetic membrane, as well as bacteriorhodopsin, which manages to perform almost the entire task of photosynthesis with a single molecule.

Because photon energy conversion in photobiological membranes involves light-induced charge separation, prevention of unproductive charge recombination enhances its efficiency. Charge recombination in bacteriorhodopsin and photosynthetic reaction centers takes place by virtue of the ubiquitous reverse biochemical reactions. Photochemical charge separation is not an equilibrium process but rather a steady state because of a continuing photon energy input during illumination. Strictly speaking, a one-way photochemical reaction is not an absolute requirement: as long as continuing input of photon energy is guaranteed, photon-driven forward reaction continues to offset charge recombination through reverse reactions. In practice, a molecular switch that minimizes reverse reactions is advantageous. In the case of a chlorophyll-based photosynthetic reaction center, Kuhn[108] proposed a molecular mechanism with which to minimize reverse electron transfer (see also Reference 5). In the case of bacteriorhodopsin, the major molecular switch is the protonation switch — conformational changes initiated by photoisomerization of the chromophore — that switches from an extracellular access during the first half of the photocycle to an intracellular access during the second half of the photocycle. The conformational changes minimize reverse proton transfer during illumination.

A conventional photodiode also converts energy by light-induced charge separation: the separation of electrons and holes over a barrier or an interface of different kinds of solid-state materials. Ideally, the separated charges recombine only through an external circuit that includes a lamp, an electric motor, or other electrically powered devices. Any charge recombination must be considered wasteful and unproductive and is usually referred to as short-circuiting. Short-circuiting via external circuits can readily be prevented by proper insulation and is usually not a serious technical problem. Internal short-circuiting due to direct charge recombination at the semiconductor junction is minimized by rectification. For quite some time, bacteriorhodopsin was regarded as a photodiode. Although rectification is quite common in ion channels, the same conclusion cannot be transferred to photosynthetic apparatus without the support of experimental evidence. Our experimental analysis of reconstituted bacteriorhodopsin membranes indicated that, contrary to common belief, the proton conduction channel of bacteriorhodopsin is not rectified. However, bacteriorhodopsin manages to minimize charge recombination in the absence of illumination by a different strategy: the proton conduction channel is gated by light and is completely shut off in the dark. Indirect evidence indicates that the same strategy might have been utilized in chlorophyll-based photosynthetic systems to minimize charge recombination in the dark.

Finally, we return to the question of why nature did not make molecular processes highly deterministic. It is noted that molecular recognition starts as exploration by means of random diffusion and collisions but switches to a more deterministic search once noncovalent bond interactions kick in. Why is this so? We can only speculate from what we know about the brain's higher function: cognition. Cognition, like molecular recognition, is a process of pattern recognition.[109] The brain's strategy of cognition is neither highly deterministic nor highly random. In other words, the brain solves novel problems not by preprogrammed, deterministic procedures or by trial and error but rather by heuristic searching — essentially an approach of the middle ground. This approach is reflected in cerebral lateralization, by means of which the brain uses the nondominant hemisphere (the right hemisphere in most individuals) for explorations and parallel processing of information, and the dominant hemisphere for decisive, focused sequential processing of information. In essence, cerebral lateralization makes heuristic searching feasible. This is the reason why the brain is fault tolerant, but a digital computer, which uses a deterministic

procedure for information processing, is not. Thus, when malfunctions occur, a digital computer degrades catastrophically, but the brain degrades gracefully.

Acknowledgments

The author thanks Janos Lanyi for a helpful discussion. The author also thanks Stephen DiCarlo for editorial help.

References

1. Hecht, S., Shlaer, S., and Pirenne, M.H., Energy, quanta, and vision, *J. Gen. Physiol.*, 25, 819, 1942.
2. Brown, K.T., The electroretinogram: its components and their origins, *Vision Res.*, 8, 633, 1968.
3. Stryer, L., Cyclic GMP cascade of vision, *Annu. Rev. Neurosci.*, 9, 87, 1986.
4. Hong, F.T., Relevance of light-induced charge displacements in molecular electronics: design principles at the supramolecular level, *J. Mol. Electron.*, 5, 163, 1989.
5. Hong, F.T., Molecular electronic switches in photobiology, in *Handbook of Organic Photochemistry and Photobiology*, Horspool, W. and Song, P.-S., Eds., CRC Press, Boca Raton, FL, 1995, p. 1557.
6. Mitchell, P., Chemiosmotic couling in oxidative and photosynthetic phosphorylation, *Biol. Rev.*, 41, 445, 1966.
7. Williams, R.J.P., Possible functions of chains of catalysts, *J. Theoret. Biol.*, 1, 1, 1961.
8. Williams, R.J.P., Possible functions of chains of catalysts II, *J. Theoret. Biol.*, 3, 209, 1962.
9. Williams, R.J.P., The multifarious couplings of energy transduction, *Biochim. Biophys. Acta*, 505, 1, 1978.
10. Hong, F.T., Does nature utilize a common design for photoactive transport and sensor proteins?, in *Molecular Electronics*, Lazarev, P.I., Ed., Kluwer, Dordrecht, 1991, p. 291.
11. Conrad, M., Molecular computing, in *Advances in Computers*, Vol. 31, Yovits, M.C., Ed., Academic Press, New York, 1990, p. 235.
12. Capaldi, R.A., Darley-Usmar, V., Fuller, S., and Millett, F., Structural and functional features of the interaction of cytochrome *c* with complex III and cytochrome *c* oxidase, *FEBS Lett.*, 138, 1, 1982.
13. Adam, G. and Delbrück, M., Reduction of dimensionality in biological diffusion processes, in *Structural Chemistry and Molecular Biology*, Rich, A. and Davidson, N., Eds., W.H. Freeman, San Francisco, 1968, p. 198.
14. Newborn, M., *Kasparov versus Deep Blue: Computer Chess Comes of Age*, Springer-Verlag, Heidelberg, 1997.
15. Simon, H.A. and Newell, A., Heuristic problem solving: the next advance in operations research, *Operations Research*, 6, 1, 1958. Reprinted in *Models of Bounded Rationality, Volume 1: Economic Analysis and Public Policy*, Simon, H.A., Ed., MIT Press, Cambridge, MA, 1982, p. 380.
16. Colson, A.-O., Perlman, J.H., Smolyar, A., Gershengorn, M.C., and Osman, R., Static and dynamic roles of extracellular loops in G-protein-coupled receptors: a mechanism for sequential binding of thyrotropin-releasing hormone to its receptor, *Biophys. J.*, 74, 1087, 1998.
17. Northrup, S.H., Boles, J.O., and Reynolds, J.C.L., Brownian dynamics of cytochrome c and cytochrome c peroxidase association, *Science*, 241, 67, 1988.
18. Camacho, C.J., Weng, Z., Vajda, S., and DeLisi, C., Free energy landscapes of encounter complexes in protein-protein association, *Biophys. J.*, 76, 1166, 1999.
19. Kitamura, K., Tokunaga, M., Iwane, A.H., and Yanagida, T., A single myosin head moves along an actin filament with regular steps of 5.3 nanometers, *Nature*, 397, 129, 1999.
20. Astumian, R.D., Making molecules into motors, *Sci. Am.*, 285(1), 56, 2001.
21. Newton, A.C., Interaction of proteins with lipid headgroups: lessons from protein kinase C, *Annu. Rev. Biophys. Biomol. Struct.*, 22, 1, 1993.
22. Ejdebäck, M., Bergkvist, A., Karlsson, B.G., and Ubbink, M., Side-chain interactions in the plastocyanin-cytochrome *f* complex, *Biochemistry*, 39, 5022, 2000.

23. Molina-Heredia, F.P., Díaz-Quintana, A., Hervás, M., Navarro, J.A., and De la Rosa, M.A., Site-directed mutagenesis of cytochrome c_6 from *Anabaena* species PCC 7119: identification of surface residues of the hemeprotein involved in photosystem I reduction, *J. Biol. Chem.*, 274, 33565, 1999.
24. Hurley, J.K., Hazzard, J.T., Martínez-Júlvez, M., Medina, M., Gómez-Moreno, C., and Tollin, G., Electrostatic forces involved in orienting *Anabaena* ferredoxin during binding to *Anabaena* ferredoxin:$NADP^+$ reductase: site-specific mutagenesis, transient kinetic measurements, and electrostatic surface potentials, *Protein Sci.*, 8, 1614, 1999.
25. Martínez-Júlvez, M., Nogués, I., Faro, M., Hurley, J.K., Brodie, T.B., Mayoral, T., Sanz-Aparicio, J., Hermoso, J.A., Stankovich, M.T., Medina, M., Tollin, G., and Gómez-Moreno, C., Role of a cluster of hydrophobic residues near the FAD cofactor in *Anabaena* PCC 7119 ferredoxin-$NADP^+$ reductase for optimal complex formation and electron transfer to ferredoxin, *J. Biol. Chem.*, 276, 27498, 2001.
26. Tollin, G. and Hazzard, J.T., Intra- and intermolecular electron transfer processes in redox proteins, *Arch. Biochem. Biophys.*, 287, 1, 1991.
27. Batie, C.J. and Kamin, H., Ferredoxin:$NADP^+$ oxidoreductase: equilibria in binary and ternary complexes with $NADP^+$ and ferredoxin, *J. Biol. Chem.*, 259, 8832, 1984.
28. Batie, C.J. and Kamin, H., Electron transfer by ferredoxin:$NADP^+$ reductase: rapid-reaction evidence for participation of a ternary complex. *J. Biol. Chem.*, 259, 11976, 1984.
29. van Thor, J.J., Geerlings, T.H., Matthijs, H.C.P., and Hellingwerf, K.J., Kinetic evidence for the PsaE-dependent transient ternary complex photosystem I/ferredoxin/ferredoxin:$NADP^+$ reductase in a cyanobacterium, *Biochemistry*, 38, 12735, 1999.
30. Morales, R., Charon, M.-H., Kachalova, G., Serre, L., Medina, M., Gómez-Moreno, C., and Frey, M., A redox-dependent interaction between two electron-transfer partners involved in photosynthesis, *EMBO Rep.*, 1, 271, 2000.
31. Nicholls, A., Sharp, K.A., and Honig, B., Protein folding and association: insights from the interfacial and thermodynamic properties of hydrocarbons, *Proteins: Struct., Function, and Genet.*, 11, 281, 1991.
32. Gómez-Moreno, C., Martínez-Júlvez, M., Fillat, M.F., Hurley, J.K., and Tollin, G., Molecular recognition in protein complexes involved in electron transfer, *Biochem. Soc. Trans.*, 24, 111, 1996.
33. Hurley, J.K., Fillat, M., Gómez-Moreno, C., and Tollin, G., Structure-function relationships in the ferredoxin/ferredoxin:$NADP^+$ reductase system from *Anabaena*, *Biochimie*, 77, 539, 1995.
34. Martínez-Júlvez, M., Hermoso, J., Hurley, J.K., Mayoral, T., Sanz-Aparicio, J., Tollin, G., Gómez-Moreno, C., and Medina, M., Role of Arg100 and Arg264 from *Anabaena* PCC 7119 ferredoxin-$NADP^+$ reductase for optimal $NADP^+$ binding and electron transfer, *Biochemistry*, 37, 17680, 1998.
35. Chitnis, P.R., Xu, Q., Chitnis, V.P., and Nechushtai, R., Function and organization of Photosystem I polypeptides, *Photosynth. Res.*, 44, 23, 1995.
36. Navarro, J.A., Hervás, M., and De la Rosa, M.A., Co-evolution of cytochrome c_6 and plastocyanin, mobile proteins transferring electrons from cytochrome b_6-f to photosystem I, *J. Biol. Inorg. Chem.*, 2, 11, 1997.
37. Hervás, M., Navarro, J.A., Díaz, A., Bottin, H., and De la Rosa, M.A., Laser-flash kinetic analysis of the fast electron transfer from plastocyanin and cytochrome c_6 to Photosystem I: experimental evidence on the evolution of the reaction mechanism, *Biochemistry*, 34, 11321, 1995.
38. Molina-Heredia, F.P., Hervás, M., Navarro, J.A., and De la Rosa, M.A., A single arginyl residue in plastocyanin and in cytochrome c_6 from the cyanobacterium *Anabaena* sp. PCC 7119 is required for efficient reduction of Photosystem I, *J. Biol. Chem.*, 276, 601, 2001.
39. Frazão, C., Soares, C.M., Carrondo, M.A., Pohl, E., Dauter, Z., Wilson, K.S., Hervás, M., Navarro, J.A., De la Rosa, M.A., and Sheldrick, G.M., *Ab initio* determination of the crystal structure of cytochrome c_6 and comparison with plastocyanin, *Structure*, 3, 1159, 1995.
40. Marcus, R.A. and Sutin, N., Electron transfers in chemistry and biology, *Biochim. Biophys. Acta*, 811, 265, 1985.
41. Dohlman, H.G., Thorner, J., Caron, M.G., and Lefkowitz, R.J., Model systems for the study of seven-transmembrane-segment receptors, *Annu. Rev. Biochem.*, 60, 653, 1991.

42. Gilman, A.G., G proteins and dual control of adenylate cyclase, *Cell*, 36, 577, 1984.
43. Clapham, D.E., The G-protein nanomachine, *Nature*, 379, 297, 1996.
44. Sitaramayya, A. and Liebman, P.A., Phosphorylation of rhodopsin and quenching of cyclic GMP phosphodiesterase activation by ATP at weak bleaches, *J. Biol. Chem.*, 258, 12106, 1983.
45. Sitaramayya, A. and Liebman, P.A., Mechanism of ATP quench of phosphodiesterase activation in rod disc membranes, *J. Biol. Chem.*, 258, 1205, 1983.
46. Wilden, U. and Kühn, H., Light-dependent phosphorylation of rhodopsin: number of phosphorylation sites, *Biochemistry*, 21, 3104, 1982.
47. Liebman, P.A. and Pugh, Jr., E.N., Gain, speed and sensitivity of GTP binding vs. PDE activation in visual excitation, *Vision Res.*, 22, 1475, 1982.
48. Kühn, H., Hall, S.W., and Wilden, U., Light-induced binding of 48-kDa protein to photoreceptor membranes is highly enhanced by phosphorylation of rhodopsin, *FEBS Lett.*, 176, 473, 1984.
49. Sitaramayya, A., Rhodopsin kinase prepared from bovine rod disk membranes quenches light activation of cGMP phosphodiesterase in a reconstituted system, *Biochemistry*, 25, 5460, 1986.
50. Bennett, N. and Sitaramayya, A., Inactivation of photoexcited rhodopsin in retinal rods: the roles of rhodopsin kinase and 48-kDa protein (arrestin), *Biochemistry*, 27, 1710, 1988.
51. Schleicher, A., Kühn, H., and Hofmann, K.P., Kinetics, binding constant, and activation energy of the 48-kDa protein-rhodopsin complex by extra-metarhodopsin II, *Biochemistry*, 28, 1770, 1989.
52. Palczewski, K., Kumasaka, T., Hori, T., Behnke, C.A., Motoshima, H., Fox, B.A., Trong, I.L., Teller, D.C., Okada, T., Stenkamp, R.E., Yamamoto, M., and Miyano, M., Crystal structure of rhodopsin: a G protein-coupled receptor, *Science*, 289, 739, 2000.
53. Noel, J.P., Hamm, H.E., and Sigler, P.B., The 2.2 Å crystal structure of transducin-α complexed with GTPγS, *Nature*, 366, 654, 1993.
54. Wall, M.A., Coleman, D.E., Lee, E., Iñiguez-Lluhi, J.A., Posner, B.A., Gilman, A.G., and Sprang, S.R., The structure of the G protein heterotrimer $G_{i\alpha1}\beta_1\gamma_2$, *Cell*, 83, 1047, 1995.
55. Lambright, D.G., Sondek, J., Bohm, A., Skiba, N.P., Hamm, H.E., and Sigler, P.B., The 2.0 Å crystal structure of a heterotrimeric G protein, *Nature*, 379, 311, 1996.
56. Granzin, J., Wilden, U., Choe, H.-W., Labahn, J., Kraft, B., and Büldt, G., X-ray crystal structure of arrestin from bovine rod outer segments, *Nature*, 391, 918, 1998.
57. Hirsch, J.A., Schubert, C., Gurevich, V.V., and Sigler, P.B., The 2.8 Å crystal structure of visual arrestin: a model for arrestin's regulation, *Cell*, 97, 257, 1999.
58. Cai, K., Itoh, Y., and Khorana, H.G., Mapping of contact sites in complex formation between transducin and light-activated rhodopsin by covalent crosslinking: use of a photoactivatable reagent, *Proc. Natl. Acad. Sci. USA*, 98, 4877, 2001.
59. Itoh, Y., Cai, K., and Khorana, H.G., Mapping of contact sites in complex formation between light-activated rhodopsin and transducin by covalent crosslinking: use of a chemically preactivated reagent, *Proc. Natl. Acad. Sci. USA*, 98, 4883, 2001.
60. Bourne, H.R., How receptors talk to trimeric G proteins, *Curr. Opin. Cell Biol.*, 9, 134, 1997.
61. Hamm, H.E., The many faces of G protein signaling, *J. Biol. Chem.*, 273, 669, 1998.
62. Franke, R.R., König, B., Sakmar, T.P., Khorana, H.G., and Hofmann, K.P., Rhodopsin mutants that bind but fail to activate transducin, *Science*, 250, 123, 1990.
63. Chen, J., Makino, C.L., Peachey, N.S., Baylor, D.A., and Simon, M.I., Mechanisms of rhodopsin inactivation *in vivo* as revealed by a COOH-terminal truncation mutant, *Science*, 267, 374, 1995.
64. Miller, J.L. and Dratz, E.A., Phosphorylation at sites near rhodopsin's carboxyl-terminus regulates light initiated cGMP hydrolysis, *Vision Res.*, 24, 1509, 1984.
65. Puig, J., Arendt, A., Tomson, F.L., Abdulaeva, G., Miller, R., Hargrave, P.A., and McDowell, J.H., Synthetic phosphopeptide from rhodopsin sequence induces retinal arrestin binding to photoactivated unphosphorylated rhodopsin, *FEBS Lett.*, 362, 185, 1995.
66. Gurevich, V.V. and Benkovic, J.L., Visual arrestin binding to rhodopsin: diverse functional roles of positively charged residues within the phosphorylation-recognition region of arrestin, *J. Biol. Chem.*, 270, 6010, 1995.

67. Gray-Keller, M.P., Detwiler, P.B., Benkovic, J.L., and Gurevich, V.V., Arrestin with a single amino acid substitution quenches light-activated rhodopsin in a phosphorylation-independent fashion, *Biochemistry*, 36, 7058, 1997.
68. McDowell, J.H., Robinson, P.R., Miller, R.L., Brannock, M.T., Arendt, A., Smith, W.C., and Hargrave, P.A., Activation of arrestin: requirement of phosphorylation as the negative charge on residues in synthetic peptides from the carboxyl-terminal region of rhodopsin, *Invest. Ophthal. Vis. Sci.*, 42, 1439, 2001.
69. Emeis, D. and Hofmann, K.P., Shift in the relation between flash-induced metarhodopsin I and metarhodopsin II within the first 10% rhodopsin bleaching in bovine disc membranes, *FEBS Lett.*, 136, 201, 1981.
70. Emeis, D., Kühn, H., Reichert, J., and Hofmann, K.P., Complex formation between metarhodopsin II and GTP-binding protein in bovine photoreceptor membranes leads to a shift of the photoproduct equilibrium, *FEBS Lett.*, 143, 29, 1982.
71. Gibson, S.K., Parkes, J.H., and Liebman, P.A., Phosphorylation stabilizes the active conformation of rhodopsin, *Biochemistry*, 37, 11393, 1998.
72. Gibson, S.K., Parkes, J.H., and Liebman, P.A., Phosphorylation alters the pH-dependent active state equilibrium of rhodopsin by modulating the membrane surface potential, *Biochemistry*, 38, 11103, 1999.
73. Parkes, J.H., Gibson, S.K., and Liebman, P.A., Temperature and pH dependence of the metarhodopsin I-metarhodopsin II equilibrium and the binding of metarhodopsin II to G protein in rod disk membranes, *Biochemistry*, 38, 6862, 1999.
74. Gibson, S.K., Parkes, J.H., and Liebman, P.A., Phosphorylation modulates the affinity of light-activated rhodopsin for G protein and arrestin, *Biochemistry*, 39, 5738, 2000.
75. Garbers, A., Reifarth, F., Kurreck, J., Renger, G., and Parak, F., Correlation between protein flexibility and electron transfer from $Q_A^{-\bullet}$ to Q_B in PSII membrane fragments from spinach, *Biochemistry*, 37, 11399, 1998.
76. Wilden, U., Duration and amplitude of the light-induced cGMP hydrolysis in vertebrate photoreceptors are regulated by multiple phosphorylation of rhodopsin and by arrestin binding, *Biochemistry*, 34, 1446, 1995.
77. Vishnivetskiy, S.A., Patz, C.L., Schubert, C., Hirsch, J.A., Sigler, P.B., and Gurevich, V.V., How does arrestin respond to the phosphorylated state of rhodopsin? *J. Biol. Chem.*, 274, 11451, 1999.
78. Vishnivetskiy, S.A., Schubert, C., Climaco, G.C., Gurevich, Y.V., Velez, M.-G., and Gurevich, V.V., An additional phosphate-binding element in arrestin molecule: implications for the mechanism of arrestin activation, *J. Biol. Chem.*, 275, 41049, 2000.
79. Hamm, H.E., How activated receptors couple to G proteins, *Proc. Natl. Acad. Sci. USA*, 98, 4819, 2001.
80. Lanyi, J.K., Proton translocation mechanism and energetics in the light-driven pump bacteriorhodopsin, *Biochim. Biophys. Acta*, 1183, 241, 1993.
81. Lanyi, J.K., Progress toward an explict mechanistic model for the light-driven pump, bacteriorhodopsin, *FEBS Lett.*, 363, 103, 1999.
82. Lanyi, J.K., Bacteriorhodopsin, *Biochim. Biophys. Acta*, 1460, 1, 2000.
83. Lanyi, J.K. and Pohorille, A., Proton pumps: mechanism of action and applications, *Trends Biotechnol.*, 19, 140, 2001.
84. Lanyi, J.K. and Luecke, H, Bacteriorhodopsin, *Curr. Opinion Struct. Biol.*, 11, 415, 2001.
85. Luecke, H., Richter, H.-T., and Lanyi, J.K., Proton transfer pathway in bacteriorhodopsin at 2.3 Angstrom resolution, *Science*, 280, 1934, 1998.
86. Luecke, H., Schobert, B., Richter, H.-T., Cartailler. J.-P., and Lanyi, J.K., Structure of bacteriorhodopsin at 1.55 Å resolution, *J. Mol. Biol.*, 291, 899, 1999.
87. Váró, G. and Lanyi, J.K., Thermodynamics and energy coupling in the bacteriorhodopsin photocycle, *Science*, 30, 5016, 1991.
88. Rayfield, G.W., Photodiodes based on bacteriorhodopsin, in *Molecular and Biomolecular Electronics* (Advances in Chemistry Series 240), Birge, R.R., Ed., American Chemical Society, Washington, DC, 1994, p. 561.

89. Fuller, B.E., Okajima, T.L., and Hong, F.T., Analysis of the d.c. photoelectric signal from model bacteriorhodopsin membranes: d.c. photoconductivity determination by means of the null current method and the effect of proton ionophores, *Bioelectrochem. Bioenerg.*, 37, 109, 1995.
90. Hong, F.T., Interfacial photochemistry of retinal proteins, *Prog. Surface Sci.*, 62, 1, 1999.
91. Hong, F.T. and Mauzerall, D., The separation of voltage-dependent photoemfs and conductances in Rudin-Mueller membranes containing magnesium porphyrins, *Biochim. Biophys. Acta*, 275, 479, 1972.
92. Drachev, L.A., Jasaitis, A.A., Kaulen, A.D., Kondrashin, A.A., Liberman, E.A., Nemecek, I.B., Ostroumov, S.A., Semenov, A.Yu., and Skulachev, V.P., Direct measurement of electric current generation by cytochrome oxidase, H-ATPase and bacteriorhodopsin, *Nature*, 249, 321, 1974.
93. Drachev, L.A., Frolov, V.N., Kaulen, A.D., Liberman, E.A., Ostroumov, S.A., Plakunova, V.G., Semenov, A.Yu., and Skulachev, V.P., Reconstitution of biological molecular generators of electric current, *J. Biol. Chem.*, 251, 7059, 1976.
94. Henderson, R. and Unwin, P.N.T., Three-dimensional model of purple membrane obtained by electron microscopy, *Nature*, 257, 28, 1975.
95. Balwin, J.M., Henderson, R., Beckman, E., and Zemlin, F., Images of purple membrane at 2.8 Å resolution obtained by cryo-electron microscopy, *J. Mol. Biol.*, 202, 585, 1988.
96. Miyasaka, T., Koyama, K., and Itoh, I., Quantum conversion and image detection by a bacteriorhodopsin-based artificial photoreceptor, *Science*, 255, 342, 1992.
97. Wang, J.P., Li, J.R., Tao, P.D., Li, X.C., and Jiang, L., Photoswitch based on bacteriorhodopsin Langmuir-Blodgett films, *Adv. Mater. Optics Electron.*, 4, 219, 1994.
98. Hong, F.T., Molecular sensors based on the photovoltaic effect of bacteriorhodopsin: origin of differential responsivity, *Mater. Sci. Eng. C*, 4, 267, 1997. Reprinted with corrections, *Mater. Sci. Eng. C*, 5, 61, 1997.
99. Vredenberg, W.J. and Bulychev, A.A., Changes in the electrical potential across the thylakoid membranes of illuminated intact chloroplasts in the presence of membrane-modifying agents, *Plant Sci. Lett.*, 7, 101, 1976.
100. Williams, R.J.P., The history and the hypotheses concerning ATP-formation by energised protons, *FEBS Lett.*, 85, 9, 1978.
101. Kell, D.B., On the functional proton current pathway of electron transport phosphorylation, *Biochim. Biophys. Acta*, 549, 55, 1979.
102. Teissié, J., Prats, M., Soucaille, P., and Tocanne, J.F., Evidence for conduction of protons along the interface between water and a polar lipid monolayer, *Proc. Natl. Acad. Sci. USA*, 82, 3217, 1985.
103. Gabriel, B. and Teissié, J., Proton long-range migration along protein monolayers and its consequences on membrane coupling, *Proc. Natl. Acad. Sci. USA*, 93, 14521, 1996.
104. Alexiev, U., Mollaaghababa, R., Scherrer, P., Khorana, H.G., and Heyn, M.P., Rapid long-range proton diffusion along the surface of the purple membrane and delayed proton transfer into the bulk, *Proc. Natl. Acad. Sci. USA*, 92, 372, 1995.
105. Onsager, L., The motion of ions: principles and concepts, *Science*, 166, 1359, 1969.
106. Nagle, J.F. and Morowitz, H.J., Molecular mechanisms for proton transport in membranes, *Proc. Natl. Acad. Sci. USA*, 75, 298, 1978.
107. Kyle, D.J. and Arntzen, C.J., Thylakoid membrane protein phosphorylation selectively alters the local membrane surface charge near the primary acceptor of Photosystem II, *Photochem. Photobiophys.*, 5, 11, 1983.
108. Kuhn, H., Electron transfer mechanism in the reaction center of photosynthetic bacteria, *Phys. Rev. A*, 34, 3409, 1986.
109. Hong, F.T., The enigma of creative problem solving, in *Molecular Electronics: Bio-sensors and Biocomputers*, Barsanti, L., Evangelista, V., Gualtieri, P., Passarelli, V., and Vestri, S., Eds., Kluwer, Dordrecht, 2003, p. 457.

135

Biomolecular Photonics Based on Bacteriorhodopsin

Kevin J. Wise
University of Connecticut

Robert R. Birge
University of Connecticut

135.1 Bacteriorhodopsin as a Photonic Material

Biomolecular electronics examines the use of biological molecules or biomimetic systems in electronic or photonic devices. The principal rationale for using biomolecular electronics is that natural selection already evolved materials with key properties desired for device applications. Organisms are required to continuously optimize the organic and inorganic components that are critical to their biological or survival functions. The assumption that biology cannot provide materials with sufficient stability or efficiency to compete with semiconductor technology is shortsighted. Many organisms generated materials capable of withstanding high thermal or photochemical stress while maintaining high efficiency, and the search for such materials in extremophiles (organisms that survive optimally under extreme variations in temperature, ion concentration, lack of oxygen, etc.) often yields successful results. Recent advances in molecular biology provide efficient methods of improving upon native materials through genetic engineering and directed evolution. Bacteriorhodopsin (BR) is a protein isolated from a halophilic organism that can be manipulated by genetic methods. The protein is synthesized by an archae extremophile to provide a source of photosynthetic energy for a salt-marsh bacterium that must survive in a

0-8493-1348-1/04/$0.00+$1.50

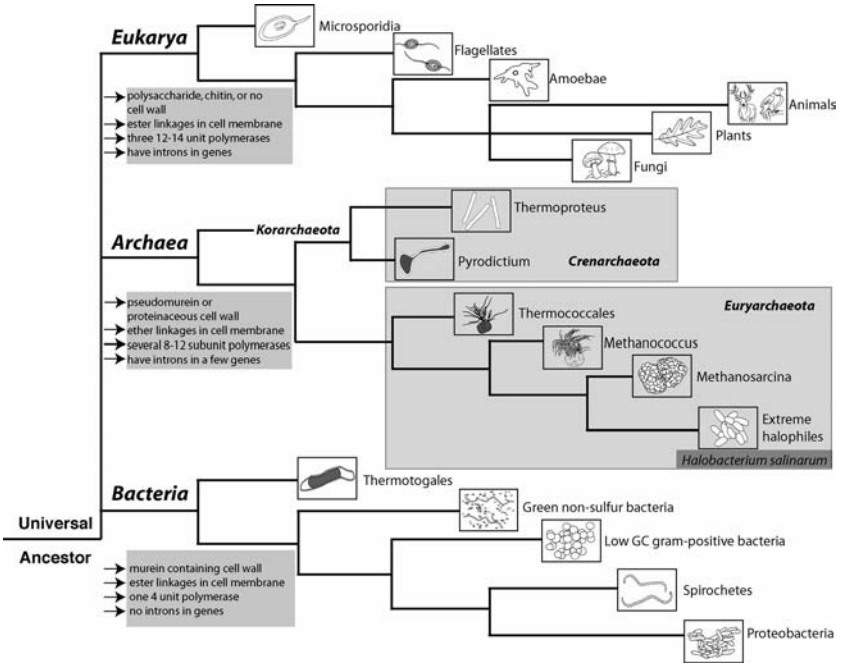

FIGURE 135.1 Phylogenetic tree showing selected representative organisms from major divisions. The three major kingdoms are the Eukarya, the Archaea, and the Bacteria. The Eukarya include microsporidia, flagellates, amoeba, fungi, plants, and animals. The Archaea include three phyla: Korarchaeota, Crenarchaeota, and Euryarchaeota. *Halobacterium salinarum*, which contains bacteriorhodopsin, is a member of the Euryarchaeota. Bacteria include Thermotogales, green non-sulfur bacteria, low GC content Gram-positive bacteria, spirochetes, and proteobacteria. Some key features of each kingdom are shown in boxes under the kingdom name.

hot, high solar flux environment.[1] The native protein is relatively stable and highly efficient in converting light into energy.[2–4] More recent work demonstrated that the properties of the protein can be improved dramatically for specific device applications through chemical modification or genetic engineering.[5–7]

Examined in this chapter is BR as a photonic material for a variety of device applications and materials. An introduction to the organism that produces this protein is provided. The structure and photocycle of the protein are discussed to provide a detailed explanation of the mechanism by which BR absorbs light. Three classes of BR-based devices are described: holographic memories, three-dimensional memories, and hybrid protein-semiconductors. Finally, current efforts and advances in optimization of BR via chemical and genetic methods are discussed.

The Salt Marsh Archaeon *Halobacterium salinarum* Generates a Photonic Material

Bacteriorhodopsin is the predominant protein found in the purple membrane of *Halobacterium salinarum* (also historically referred to as *Halobacterium halobium* or *Halobacterium salinarium*), a halophilic (e.g., "salt-loving") organism that functions in environments where native salt concentrations exceed 4 molar, or approximately six times that of seawater.[1,8] Introduced in this section are the phylogeny of the organism as well as the native environment of the organism.

Phylogeny of *Halobacterium salinarum*

Halobacterium salinarum is a member of the domain Archaea.[9,10] Some representative organisms of the modern kingdoms are shown in Figure 135.1. Based on sequence analysis of ribosomal RNA genes, life on earth was divided into three primary lineages (domains): Eukarya, Bacteria, and Archaea. Archaea is

a kingdom of prokaryotic single-celled organisms that share some of the common features of eukaryotes and prokaryotes and usually inhabit extreme environments. Based on sequence analysis of translation elongation factors, it was suggested that archaebacteria are more closely related to eukaryotes (organisms that contain a defined nucleus) than to bacteria. For this reason, the suffix "bacteria" was dropped from the domain name, yet the etymology of the word bacteriorhodopsin still contains reference to the older classification scheme.

The three major phyla of Archaea are the Crenarchaeota, the Euryarchaeota, and the Korarchaeota. The phylum Crenarchaeota includes thermophiles and hyperthermophiles; most of these organisms are anaerobes, but there are a few aerobic lineages. The Euryarchaeotes include all the methanogens, all the extreme halophiles, and some of the hyperthermophiles. Recently, new organisms were identified that possess ancestral characteristics of the other two lineages; these organisms are classified into the phylum Korarchaeota. Bacteriorhodopsin is found in the cell membrane of *Halobacterium salinarum* (*H. salinarum*), and these organisms are found in the phyla Euryarchaeota. A comparison of the main differences in the three domains of life is shown in Figure 135.1.

The Native Environment of a Halophile

The majority of the Euryarchaeotes adapted to survival under extreme environmental conditions. The thermophiles exist at extreme ranges in temperatures, while the halophiles exist at extremely high salt concentrations. *H. salinarum* grows maximally when sodium chloride (NaCl) concentrations are approximately 4 *M*; this concentration is equivalent to approximately 234 g of salt dissolved in 1 liter of water. This organism can be seen in salt marshes across the world (i.e., the Dead Sea, Owens Lake, California), and the formation of BR in the cell membrane can be associated with the purple hue characteristic of these briny marshes.

Evolution optimized BR for high photochemical efficiency, thermal stability, and cyclicity. The organism must be able to function in a hot, stagnant, and resource-limited environment. Under conditions of low oxygen availability and high light intensities, and under the coordinated regulation of other proteins, BR formation is induced. In the cell, formation of the protein and chromophore are controlled by other genes that are together referred to as the *bop* gene cluster, or regulon.[11,12] The bacterio-opsin (bop) regulon is not fully understood, but some of the key components were identified. Two upstream regulatory genes, *blh* and *brp*, were shown to respond to oxygen and light levels and are involved in regulating synthesis of the protein and chromophore. Abolishment of these regions results in no production of BR.[11] An overproducer strain was isolated that has a constitutive mutation in another upstream region, called *bat*. This strain (called S9 in the literature) synthesizes BR regardless of light intensity, making it an attractive candidate for growing large amounts of protein in the laboratory.

Structure of the Purple Membrane

Shown in Figure 135.2(A) and Figure 135.2(B) are cells of *H. salinarum*. The cells are rod-shaped and measure approximately 0.5 to 1 μM in diameter by 1 to 6 μM in length. The cells stain Gram negative, a feature characteristic of the Archaea that signifies that these organisms do not contain a high concentration of peptidoglycans in the cell membrane.

The purple membrane is comprised of a trimer of BR molecules arranged in a hexagonal two-dimensional lattice. Mature BR accounts for approximately 70 to 75% of the total membrane protein. The protein exists as a trimer in the organism, but trimers and monomers show no significant spectroscopic or kinetic differences in proton pumping ability.[13–15] Shown in Figure 135.2(C) are the lattice structure of BR and the surrounding phospholipid molecules. The importance of lipids on the stability, function, and photocycle of BR was demonstrated.[16–18] The major lipids in the membrane are the phospholipids PGP-Me, PG, and PGS, a sulfoglycolipid S-TGA-1, and squalene. The phospholipids and sulfoglycolipids contain an apolar archaeol moiety.[18]

The remarkable stability of BR is attributed to interactions between membrane lipids and the protein in the purple membrane. Removal of the protein or lipids by chemical means impacts the stability of the lattice. The purple membrane patches were shown to be stable up to 140°C and a wide range of pH

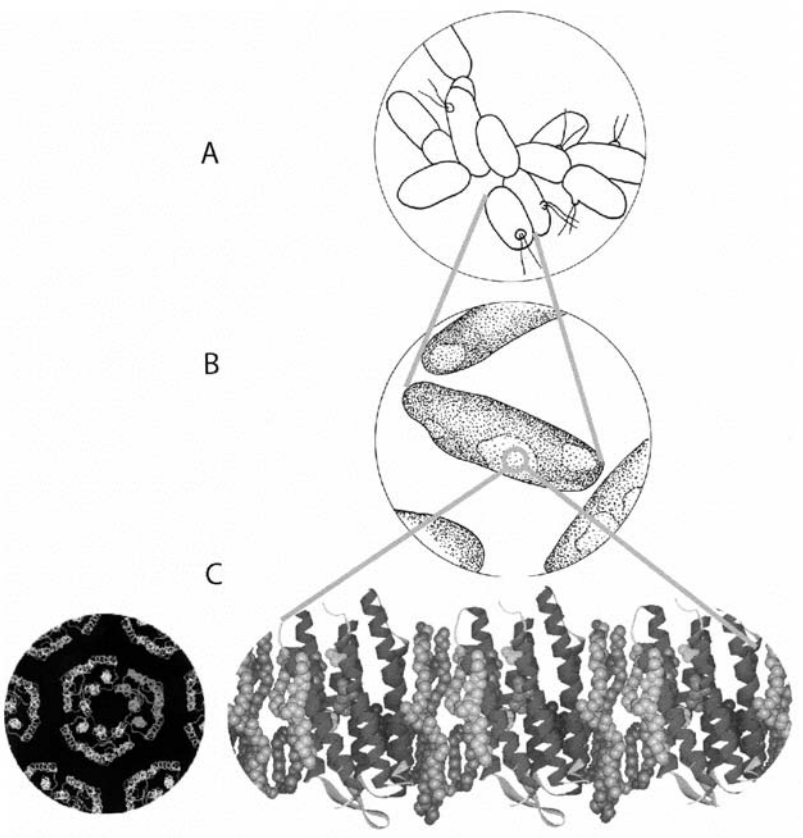

FIGURE 135.2 Magnification of *Halobacterium salinarum* from the native organism to the protein. (A) A rod-shaped cluster of H. salinarum. (B) A single cell of H. salinarum. (C) A top view and side view of the two-dimensional crystalline lattice from the cell membrane of H. salinarum. Bacteriorhodopsin forms a trimer within this lipid lattice.

values.[19,20] The high stability of BR under a wide range of conditions is a primary advantage for use of BR in device applications. It should be stressed, however, that the 140°C stability does not apply to most of the environments utilized for BR-based devices. In a majority of cases, photonic devices based on BR must operate at temperatures below 80°C.

The purple membrane is generated under conditions of low oxygen availability and is used for photosynthetic energy production. The BR photocycle results in the transport of protons from the intracellular to the extracellular surface of the membrane. This generates an electrochemical gradient that is used for energy production as protons enter the cell through ATP synthase channels. This process of nonphotosynthetic photophosphorylation is the only example found in nature. *H. salinarum* also respires by aerobic means when the concentration of oxygen is sufficient to sustain oxidative phosphorylation. The organism is quite harmless to humans and osmotically dissociates into harmless fragments when placed in low salt environments (<2 *M*). This property makes it easy to manipulate the organism in the laboratory without fear of contamination or generation of hazardous variants.

135.2 The Photocycle of Bacteriorhodopsin

Shown in Figure 135.3 is the molecular structure of BR, and highlighted are important residues involved in the photocycle. The BR monomer is a 26 kDa protein that contains seven membrane-spanning α-helices. A nonprotein moiety, retinal, is covalently linked to an internal lysine residue, Lys-216. This molecule is the light-absorbing molecule responsible for initiating photochemistry in the protein.

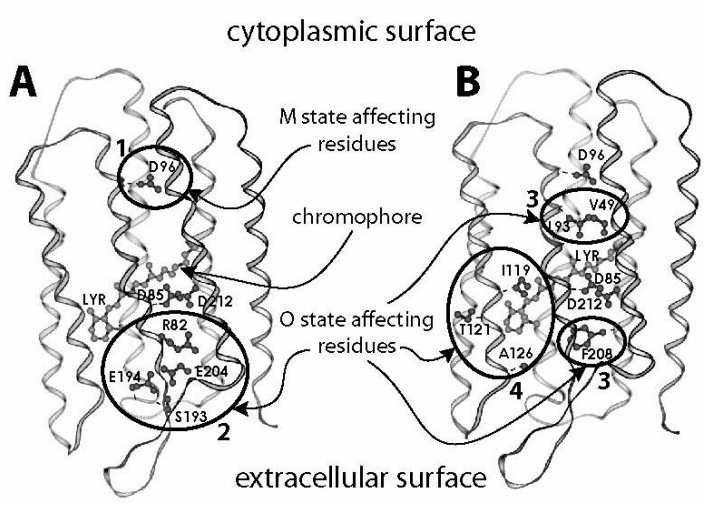

FIGURE 135.3 Bacteriorhodopsin, highlighting important residues and groups of mutation. (A) Group 1. Mutants to D96 affect the lifetime and yield of the M state. Group 2. Mutants to the proton release region consisting of R82, S193, E194, and E204 result in altered **O** state kinetics. (B) Group 3. Mutants that inhibit chromophore isomerization from 13-*cis* to all-*trans* can also affect the **O** state. Group 4. A novel semi-random mutant that has been found to lengthen the **O** state includes the residues I119, T121, and A126.

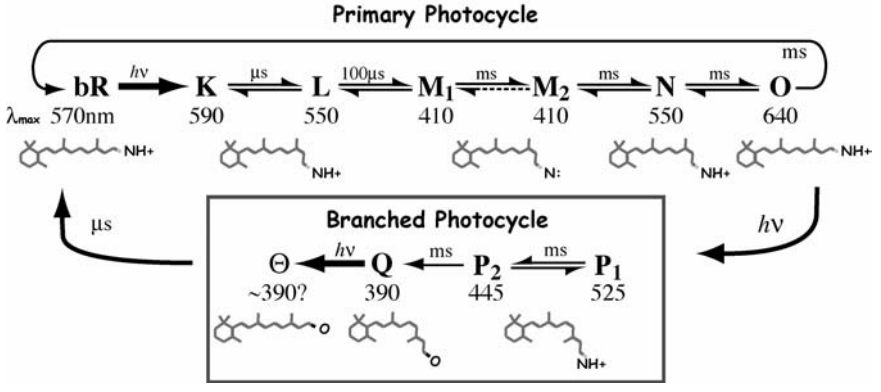

FIGURE 135.4 The main and branched photocycles of bacteriorhodopsin. The λ_{max} value for each intermediate is shown under the intermediate name. The chromophore conformation is shown for each intermediate: **bR**, **O**, and **Θ** have an all-*trans* chromophore; **K**, **L**, $\mathbf{M_1}$, $\mathbf{M_2}$, and **N** have a 13-*cis* chromophore; $\mathbf{P_1}$, $\mathbf{P_2}$, and **Q** have a 9-*cis* chromophore. $\mathbf{M_1}$ and $\mathbf{M_2}$ are the only intermediates which contain a deprotonated Schiff base. Q is characterized by a chromophore which has been detached from the Schiff base via a hydrolysis reaction.

The proton pumping process of bacteriorhodopsin commences when the protein-bound chromophore of the light-adapted form, the all-*trans* retinal Schiff base, absorbs light and undergoes the photocycle schematically shown in Figure 135.4. Although the complete proton pumping mechanism is not understood, many of the key amino acids participating in proton mobility were identified.[3,21] A photon of light is absorbed by the chromophore, inducing an isomerization from all-*trans* to 13-*cis*. This event produces the first trappable intermediate named K. The bR → K transition is the only light-dependent reaction. The remainder of the primary photocycle occurs via a series of thermal relaxations that form, in succession, the L, M, N, and O intermediates (see Figure 135.4).

TABLE 135.1 Protonation States of Key Residues during the Photocycle; Conformation of the Chromophore; pK_a Values for Selected Residues (in parentheses); Change in Protonation or Conformation State from the Previous Intermediate (Shown in Grey); Protonation States Not Assigned Experimentally [a]

	Intermediate						
Residue(s)	bR_{568}	M_{412}	N_{560}	O_{640}	P_{525}	P_{445}	Q_{390}
Retinal	all-*trans*	13-*cis*	13-*cis*	all-*trans*	9-*cis*	9-*cis*	9-*cis*
Asp-96 (10)	COOH	COOH	COO–	COOH	(COOH)	(COOH)	(COOH)
Schiff base (13)	NH+	N:	NH+	NH+	NH+	NH+	N/A
Asp-85 (2.5)	COO–	COOH	COOH	COOH	(COOH)	(COO–)	?
Leaving group (>9)	prot	unprot	unprot	unprot	?	?	?

[a] Those in parentheses are based on theory; those with a question mark are unexamined (Prot = protonated, Unprot = unprotonated).

Table 135.1 shows the protonation states of some of the key residues through the primary and branched photocycle intermediates in BR. Isomerization of the chromophore creates an electrostatic environment that destabilizes the protonated Schiff base. The Schiff base donates a proton to a nearby aspartic acid residue, Asp-85 (D85). Concomitant with the protonation of Asp-85 is a release of a proton from the proton release group, collectively referred to as "XH," because the process is still poorly understood. Deprotonation of "XH" involves the participation of Arg-82, Glu-194, Glu-204, and a hydrogen-bonded network of internal water molecules.[22,23] The proton movement from the Schiff base to Asp-85 generates the M state, which is blue-shifted, because the Schiff base is unprotonated. The O state is characterized by a deprotonated leaving group and an all-*trans* chromophore. The chromophore is reprotonated in the M → N transition by transfer of a proton from another nearby aspartic acid, Asp-96.

BR-based memory devices are primarily based on M-state or O-state photochemistry. Holographic devices are based on the blue-shifted M state, although a Q-state-based holography will be discussed. In three-dimensional memories, the write process is particularly dependent on O-state photochemistry.

Note in Figure 135.4 the presence of the branched photocycle intermediates P and Q. These intermediates will be discussed in more detail later in this section, but it should be pointed out that this branching reaction provides a potential "dead end" for the protein. Any protein that enters this branched photocycle will become unable to pump protons and is therefore considered functionally silent. As will be discussed in the section on BR-based three-dimensional memories, regeneration of the bR state from the Q state is possible and is responsible for resetting the memo bit. In the salt marsh, the P and Q states may serve as a photochemical sunscreen.[24]

Protonation State Changes Result in Altered Absorption Maxima

The absorption maxima listed in Figure 135.4 can be explained by differences in protonation states of key residues, chromophore isomerization, and by conformational changes in the protein. Other visual pigments such as rhodopsin and the cone pigments all vary one of more of these criteria to achieve a different maximal absorption in the resting state.[25–28] Protonation state changes in the vicinity of the Schiff base result in varied absorption maxima in BR. The bR resting state absorbs at 568 nm. During the course of the photocycle, it becomes as blue-shifted as 410 nm in the M state, and as red-shifted as 640 nm in the O state. Examined in this section are the molecular changes responsible for such disparate spectra, and their importance in the creation of BR-based biophotonic devices.

M-State Kinetics and Device Applications

The M state is the most blue-shifted of all intermediates in the primary BR photocycle, absorbing maximally at 410 nm (see Figure 135.4 and Table 135.1). Entry into the M state is characterized by a deprotonation of the Schiff base and a subsequent protonation of Asp-85. The deprotonated Schiff base

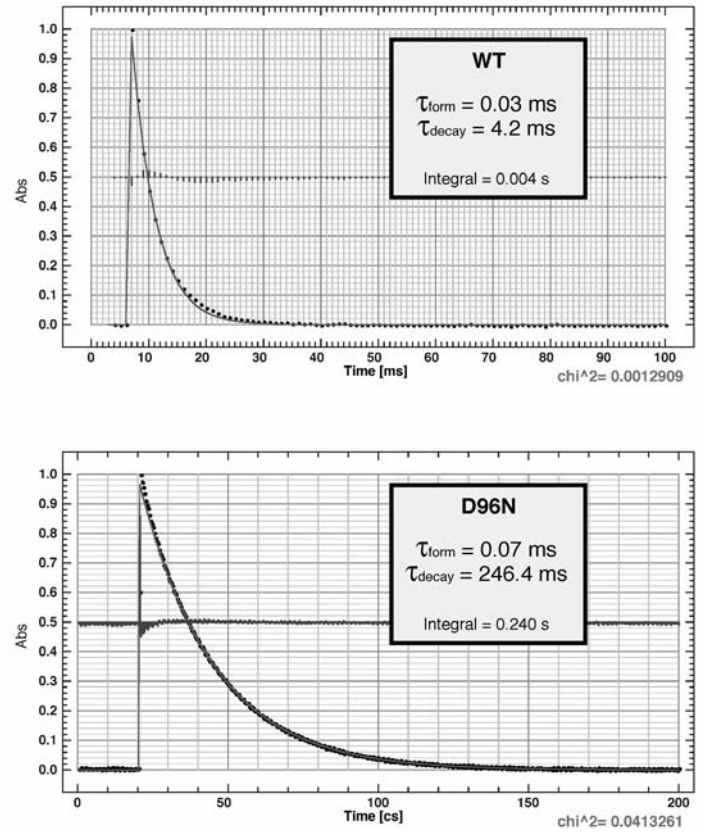

FIGURE 135.5 Normalized time-resolved spectra of wild-type (WT) and D96N protein, both obtained at pH 7. Formation and decay times are shown, as well as the integral under the curve. Note the time is registered in centiseconds for D96N, and milliseconds for WT.

is responsible for the blue shift of the protein. In wild-type BR, reprotonation of the Schiff base occurs from a protonated Asp-96. However, in the variant D96N, which contains no internal primary proton donor, the M-state lifetime increases significantly due to the absence of proton transfer from Asp-96 to the Schiff base [see Figure 135.3(A), Group 1). It is believed that the Schiff base is eventually reprotonated but from another source in the protein that requires significantly more time. Proton availability is the key step for exit from the M state. The D96N mutant can be chemically modified to produce lifetimes ranging from a few milliseconds to minutes. For this reason, and other reasons to be discussed, D96N has been the principle mutant used in holographic applications. A comparison of M-state kinetics for wild-type and D96N protein is shown in Figure 135.5.

O-State Kinetics and Device Applications

The O state is the most red-shifted of all the BR photocycle intermediates, having a maximum absorption of about 640 nm. The O-state intermediate is characterized by an all-*trans* chromophore and a protonated Asp-85. Exit from the O state (i.e., reformation of the resting state) requires proton transfer from Asp-85 to a deprotonated "XH" leaving group. Generation of the O-state intermediate is controlled by the protonation of numerous residues.[29,30] Inhibition of proton movement from Asp-85 to the leaving group was shown to lengthen the O state considerably.

Shown in Figure 135.3 are the main classes of residues for which mutants have been made that show altered photocycle kinetics. There are two classes of mutants that were shown to lengthen the O state. First, the O state can be lengthened by inhibiting chromophore isomerization from 13-*cis* to all-*trans*.

This was accomplished in the Val-49 and Leu-93 mutants, shown in Figure 135.3(B), Group 3.[31,32] However, these mutants are not optimal for use in BR-based three-dimensional memories, because the O → P transition requires all-*trans* to 9-*cis* photochemistry.[24,33] Thus, mutants that inhibit chromophore isomerization to all-*trans* will decrease the probability of entry into the branched photocycle.

The second class of mutants includes those that affect proton release in the Glu-194 and Glu-204 region, shown in Figure 135.3(A), Group 2. These mutants lengthen the O state by interfering with proton transfer from Asp-85, Arg-82, and a hydrogen-bonded network of water molecules to Glu-194 and Glu-204.[22,34–36] The O-state lifetime in WT is between 6 to 8 ms. The O-state lifetimes of E194Q and E204Q at neutral pH and ambient temperature are 70 ms and 125 ms, respectively. Progress in optimization of the O state using site-directed mutagenesis in the proton release region is discussed in Section 135.5.

The Branched Photocycle Intermediates P and Q

Shown in Figure 135.4 are the branched photocycle intermediates P and Q. The O state absorbs maximally at 640 nm; protein molecules that are in the O-state intermediate and absorb a photon enter the P state. The P state is actually a pair of distinct intermediates that will spontaneously form Q.[24] The P → Q transition is a hydrolysis reaction that results in detachment of the chromophore from the protein. Removal of water from the sample results in trapping of the P intermediate. The bR state can be regenerated from Q upon illumination with UV light. This bistable system is the basis for BR-based three-dimensional memories.

Biophotonics that Result from the Photocycle of Bacteriorhodopsin

A summary of BR-based processes and applications can be found in Hampp.[6] Most applications utilize the photochromic properties of BR. Two of these processes are discussed in this chapter: the two-dimensional holographic memory and the three-dimensional associative memory. However, other biomolecular photonic applications are currently being examined. BR is also being used in the process or formation of desalination of seawater, conversion of sunlight into electricity, artificial retinae, motion detection, optical filtering, neural networking, radiation detection, and biosensor applications.[6] The universal application of BR in many different biomaterials is testament to the flexibility and utility of the protein.

135.3 Holographic Applications

A few groups postulated the use of BR in photosensitive applications such as holographic devices.[37–39] A prototype system was established based on a genetic variant of the native protein, called D96N.[40,41] In this variant, the primary proton donor to the Schiff base, Asp-96, is replaced with asparagine, Asn.[42] This removes a functional charge from the molecule and removes an important proton channel participant [see Figure 135.3(A), Group 1]. In Figure 135.5, the kinetics of the M state in wild-type and D96N protein are shown.

D96N-Based Variant Systems

The lifetime of the M state in the D96N mutant is optimal for real-time holographic recording.[40,41,43,44] Oesterhelt, Brauchle, Hampp, and their coworkers exploited this mutant to make a number of holographic systems, some of which yielded commercial success.[6,41,43,45–47]

Real-time holographic recording relies on four attributes of the M state. First, the M state can be formed with high quantum efficiency (65%). Coupled with the broadband absorptivity and large oscillator strength of the 570 nm band of bR, the protein can be used to generate a high-sensitivity photochromic film. Second, the M state is shifted 158 nm to the blue to produce phase-based diffraction efficiencies of 3 to 8% or better. Third, the M state is a transient intermediate that decays back to the

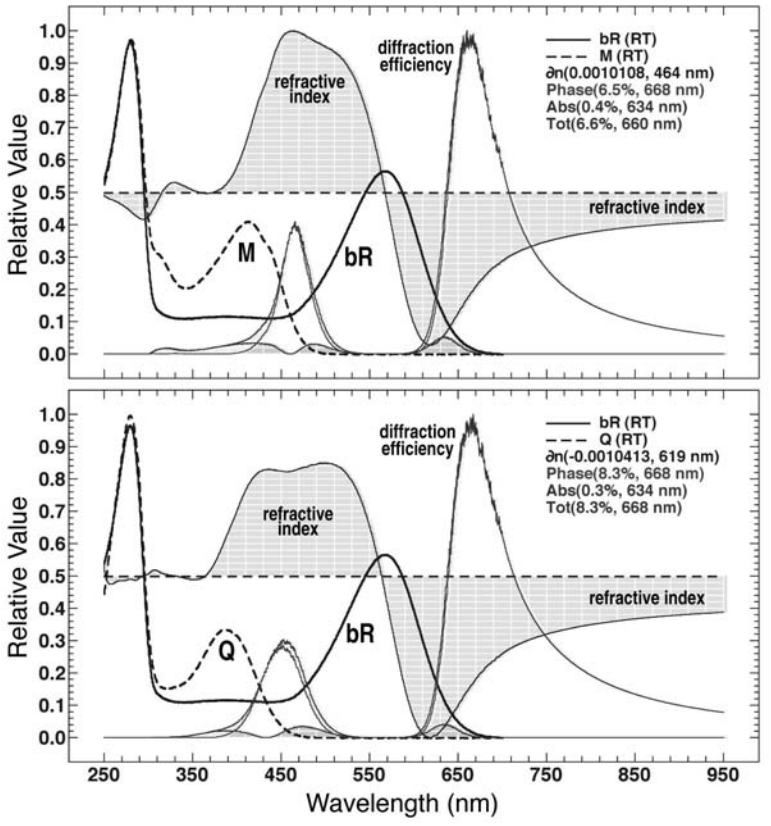

FIGURE 135.6 Comparison of the diffraction efficiency of an M-state photochromic system (top) versus a Q-state photochromic system (bottom). The diffraction efficiencies associated with phase and absorption are plotted as well as the total efficiency, and the maximum values and wavelength maxima are listed in the caption at the top right. The calculations assume 50% conversion using a write wavelength of 532 nm, a write angle of 10 degrees and a film thickness of 100 μm. The read angle was allowed to seek maximum diffraction.

resting state in roughly 100 ms. While this lifetime is far too short for long-term storage, it is optimal for real-time recording and storage of multiple holograms with temporal weighting. Fourth, the M state decay can be enhanced by using blue light or higher temperatures and can be slowed by lowering the temperature. Relatively long-term M state storage is possible at -30°C, a temperature well within the range of Peltier devices. The above attributes combine to make D96N one of the best real-time holographic materials known. In addition, D96N does not form observable amounts of the red-shifted O state, which can interfere with red light recording.

Q-Based Holographic Systems

The M state is not the optimal intermediate with which to create a hologram when using BR as a substrate. Despite many years of effort, methods to increase the stability of the M state have yet to achieve lifetimes of greater than a few months at ambient temperature.[5] It would appear that there are no intermediates within the main photocycle that are good candidates for long-term data storage, but as shown in Figure 135.6, the Q state provides a suitable candidate for long-term storage. To a first approximation, this state is stable for an indefinite period of time unless subjected to blue light. This Q state has a lifetime of many years at ambient temperature and can be formed in high yield under the appropriate conditions.[24] Most important, the Q state can be quantitatively erased under the appropriate conditions[24,44,48] despite earlier suggestions to the contrary.[49] Thus, holography can be based on the binary pair bR and Q instead

of bR and M photochemistry. There are advantages and disadvantages associated with the bR and Q binary pair. The advantages include long-term storage (7 years at 25°C) and increased holographic efficiency (8.3% versus 6.6% for a 5 OD, 100 μm film) (see Figure 135.6). The disadvantages include significantly lower sensitivity (the quantum yield for the O → Q photochemistry in the native protein is only 0.001) and the complexities of using a sequential two-photon write process. However, for volumetric layered holographic storage, the sequential two-photon requirement presents a significant advantage, leaving the problem of low quantum yield. Random mutagenesis is currently being used to find variants that provide higher quantum efficiencies for the O → P and Q photochemistry.

135.4 Three-Dimensional Bacteriorhodopsin-Based Memory Devices

Three-dimensional memory devices using BR as a substrate were demonstrated.[44,50,51] A schematic diagram of the optical system used to write, read, and erase information within a cuvette containing the protein is shown in Figure 135.7. The resting state (bR) is assigned to bit 0, and P and Q are assigned to bit 1 (bit 0 should not be confused with the O state):

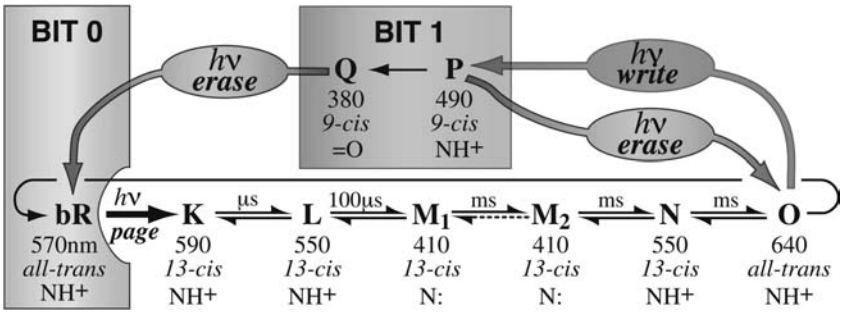

SCHEME 1

As noted in Section 135.2, the P state as shown in Scheme 1 is more properly represented as a pair of P states in dynamic equilibrium.[52] But for the purposes of this discussion, these two states are simplified to a single state called P. The details of reading, writing, and erasing information are summarized in the caption for Figure 135.7. There are a number of complications associated with volumetric data storage, and the interested reader is referred to the literature[44] for detailed discussion. In this chapter, concentration will be on the protein, rather than on the optics, and various methods of optimizing the protein for volumetric data storage are discussed in the sections below.

135.5 Optimizing Bacteriorhodopsin for Biophotonic Devices

Although the native protein can be used in the branched-photocycle architecture, it is ineffective and improvements are necessary. The quantum efficiency of the O → P photoconversion ($\sim 2 \times 10^{-4}$) is low, and the O state has a low yield (~1 to 3% under ambient conditions). Mutations directed at optimizing these two photophysical properties suggest that significant improvements can be made to enhance conversion into the branched photocycle intermediates. Site-directed mutants were created that enhance the yield of the O state and the quantum efficiency of the O → P photoreaction. However, site-directed mutants are restricted to knowledge of the protein based on modeling information. Because there are many aspects of the photocycle yet to be discovered, more randomized mutagenesis methods are necessary to complete the optimization process. A summary of optimization methods is shown in Table 135.2.

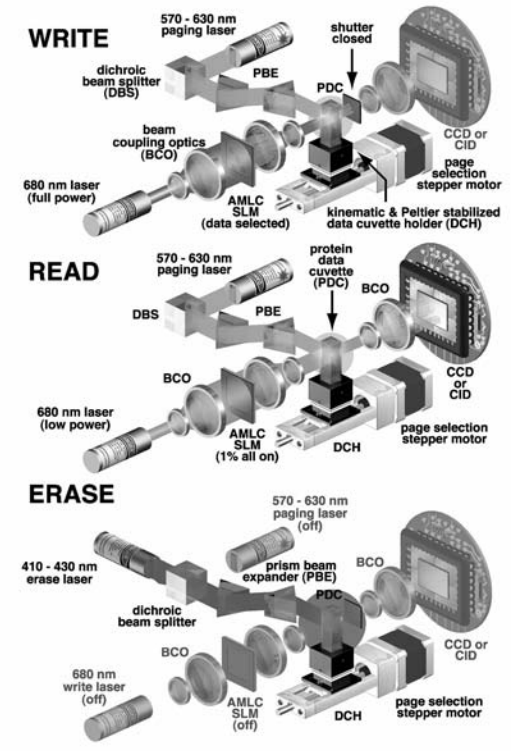

FIGURE 135.7 The write, read and erase operations of the bacteriorhodopsin-based branched-photocycle memory. The write and read operations are both initiated by using a paging beam to activate the photocycle in a thin region within the memory medium (green light). Upon formation of the **O** state in this page, a write beam is activated and the data imposed on the beam using a spatial light modulator (SLM). The read process is similar, but in this case the modulator is turned off so that just enough light gets through to image the page onto the CCD (or CID) array. Because the **O** state is the only species that absorbs the write beam, the read and write processes only involve interaction of the light beam with the **O** state in the paged regions. A blue laser erases an entire page. These processes are shown schematically in Scheme 1.

TABLE 135.2 Optimization Methods in BR; Genetic Mutagenesis Methods are Chosen Depending on Desired Specificity; Chemical Modification to the Protein can be Used to Alter Photocycle Intermediate Lifetimes

	Genetic					Chemical
Technique	Site-directed mutagenesis	Semirandomm utagenesis	Random mutagenesis	Directed Evolution 1	Directed Evolution 2	pH, additives, chromophore analogs
Specificity	Single amino acid	Local region of amino acids	Global *bop* gene	Individual colony or protein	Individual *H. salinarum* cell	Protein or membrane patch
Variability generated	Low	Medium	High	N/A	N/A	High
Primary use	Fine-tuning	Narrowing in on optimal mutation	New search	Colony/protein screening	Organism screening/ selection	Material optimization
Requires	Modeling, *a priori* knowledge	Manageable segments	No *a priori* knowledge	Medium-throughput screening	High-throughput screening	High-level characterization

Chemical Modification and Organic Cation Substitution

Chemical modification was used to stabilize BR photocycle intermediates, typically the M or O states. An increase in the lifetime of a particular intermediate is usually accompanied by a delay in proton mobility. The M-state lifetime can be enhanced by increasing pH, removing water, and adding amine compounds. Dried polymer films treated with organic amines can prolong the M state by several orders of magnitude (from microseconds to minutes).[44] The disadvantage of most chemicals added to BR is that they decrease the photochemical stability of the protein, which translates to a reduced cyclicity of the protein.

The yield and lifetime of the late photocycle intermediates are pH dependent.[29,53,54] The O-state yield increases and the lifetime decreases as the pH is dropped from 7 to 5. This is especially true for O-state mutants. The O-state lifetime can also be lengthened by adding glycerol and a slight decrease in pH, thereby inhibiting proton transfer.[33,55,56]

An alternative approach is to replace the native metal cations in the protein with synthetic organic cations known as "bolaforms" (see Birge et al.[44] for examples). Removal of native cations results in a purple to blue transition in the protein, caused by protonation of Asp-85. Cations are removed using EDTA (Sigma E 9884) or cation-exchange resins (BioRad AG MP-50 Resin).[57–59] Bolaforms are then added to the solution or the polymer matrix. Some bolaforms are capable of regenerating the purple form of BR and show an increased lifetime of the O-state intermediate. Glycerol and other poly-hydroxyl compounds may enhance the O $\rightarrow$ P transition (results not shown).

Genetic Modification is Used to Optimize Photocycle Properties

Site-directed mutagenesis was the traditional technique used to optimize BR for device application. However, this technique is dependent on information provided by protein modeling, x-ray crystallography, and other data. It is difficult to predict which mutations will have a desired photocycle effect, although some variants were created with successful results. In the development of the D96N mutant, currently used for holographic applications, a known participant in proton transfer from Asp-96 to the Schiff base was altered.[45,46] But for more complicated applications (i.e., BR-based three-dimensional memories), multiple variables must be optimized simultaneously. An optimal mutant must be one that optimizes the formation time of O state, the decay of O state, the quantum efficiency of the O $\rightarrow$ P photochemical transformation, the efficiency of the P $\rightarrow$ Q hydrolysis and the lifetime of the Q state. Current models are not sophisticated enough to predict which single or multiple mutations will accomplish these tasks simultaneously. Nevertheless, site-directed mutagenesis was successful in optimization of the O state.

Site-Directed Mutagenesis

Previous studies demonstrated that the Glu-194 and Glu-204 residues are actively involved in the proton release process. A series of mutations involving Glu-194 and Glu-204 residues were constructed, and all of these single and double mutations improved the yield and lengthened the lifetime of the O state. Shown in Figure 135.8 are kinetic spectra for the double mutant E194C/E204C. The double mutant E194C/E204C has an O-state lifetime of ~1 sec; this is the largest lifetime found for any O-state mutant, and it represents greater than a 100-fold increase in the O-state lifetime. The origin of this considerably lengthened O state is still unclear, but presumably involves formation of a covalent bond between two cysteine residues, thus removing any potential of these residues to participate in proton exchange.

Because there are so many variables to optimize, a quality value or "Q value" was developed to account for multiple parameters. It should be mentioned that the parameters of this value change depending on the characteristics being screened. An example of one Q value developed for mutant screens is shown below:

$$Q = \tau_0^{-1} \int_{t=0}^{t=\infty} [O] dt \tag{1}$$

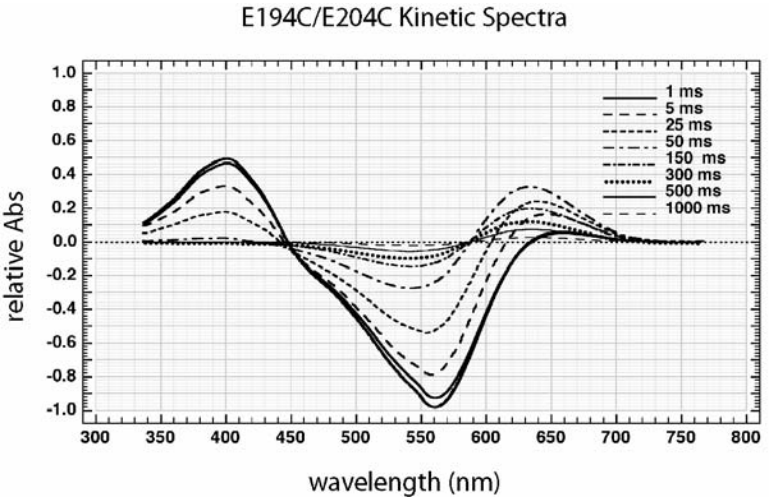

FIGURE 135.8 Standardized difference kinetic spectra of the double mutant E194C/E204C. A cuvette containing protein at OD 1.2 at λ_{max} was illuminated at 568 nm, and the resultant changes measured on an Olis rapid-scanning monochromator. Even after 1 second, the protein has yet to return to baseline.

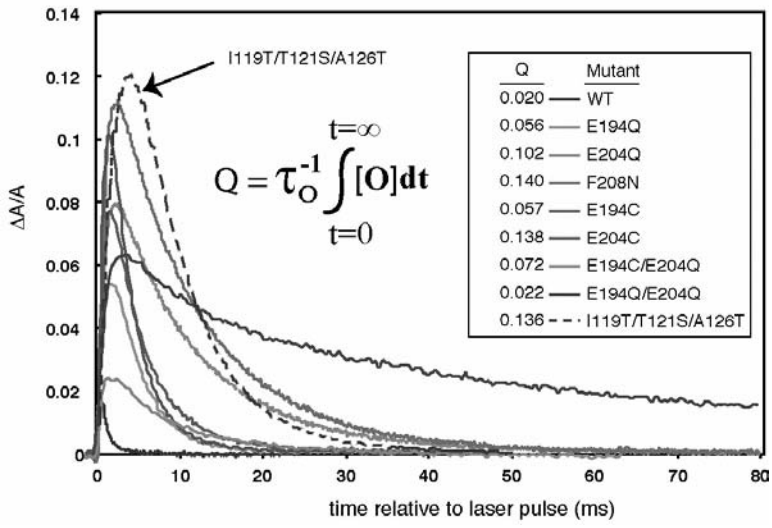

FIGURE 135.9 Single-wavelength spectra obtained for mutants proteins. The semi-random mutant, I119T/T121S/A126T yields more **O** state and has a higher Q value (see equation in text) than any site-directed mutant. Proteins were monitored at pH 6 at 650 nm following a laser pulse at 568 nm.

The Q stands for quality of mutation, and it is a coincidence that the higher the Q value, the more efficient is the Q-state formation process. A protein that produces a large amount of O state in the shortest time has the highest Q value. Despite E194C/E204C having the longest lifetime, other mutants have higher Q values, because they produce the largest amount of O state in the shortest time period. Note that the total lifetime is divided into the integral of the yield. Some Q values for a sample of mutants are shown in Figure 135.9. The wild type has the smallest integral and Q value of any of the proteins shown. This is not surprising, because *H. salinarum* optimized bacteriorhodopsin as a proton pump, not as a three-dimensional storage medium.

Random Mutagenesis

The next step in the genetic optimization process is to create random mutations. This process requires high-throughput screening of mutations, detection of optimized photophysical properties using spectroscopy, and determination of which mutants should be used as templates for further exploration. Random mutations are as likely to optimize or diminish photocycle intermediate lifetimes and yields as they are neutral in effect. The total number of unique mutations possible for a protein containing N amino acids for which M residues have been modified is:

$$\frac{19^M N!}{(N-M)!M!} \tag{2}$$

Because BR provides roughly 5000 single mutations and 11 million double mutations, it is clear that a single cycle is unlikely to produce an optimization. For this reason, a restriction of mutations to a local region (also know as "saturation mutagenesis") was used to generate controlled numbers of mutants in 10 to 15 amino acid regions, a process called semirandom mutagenesis.

SemiRandom Mutagenesis

Semirandom mutagenesis essentially combines site-directed and random mutagenesis techniques. In this technique, a narrow window of roughly 15 amino acids (this number can be varied) is mutated without disturbing the surrounding sequence. The complete BR protein sequence can be divided into 17 such segments that span the entire range of the protein. This method of mutagenesis is less specific than site-directed mutagenesis but grants the opportunity to partition the gene into 17 manageable segments. Details on how these mutants are created can be found in the literature.[7] This medium-throughput method can be used to generate and screen small amounts of proteins in 96-well plate format.

Results of a spectral scan and O-state lifetime screen for a 96-well plate of mutants are shown in Figure 135.10. Each well contained approximately 0.06 mg amount of protein. Photocycle lifetimes were collected for each mutant, and Q values were calculated (see Equation 135.1). One triple mutant, I119T/T121S/A126T showed a Q value that was higher than any other mutant yet discovered. The residues involved in this mutation are shown in Figure 135.3(B), Group 4.

Calculations suggest that this mutant is lengthening the O state in a functionally different way than other known O-state mutants. In the I119T/T121S/A126T mutant, an electrostatic field appears to be stabilizing Arg-82 farther away from the binding site than in wild type. Stabilizing Arg-82 in the "down" position presumably lengthens the O state by inhibiting reprotonation of the proton release group. Further kinetic studies are currently being conducted on this interesting mutant. This mutant endorses the use of semirandom mutagenesis to locate unpredictable mutants that result in optimized protein.

Directed Evolution

Combinatorial methods were used to optimize materials.[60–63] Some useful biophotonic materials have already been refined through evolution; in the case of BR, nature optimized a durable and efficient proton pump. This is evidenced by the fact that greater than 90% of mutants result in an increased lifetime of a photocycle intermediate, thereby decreasing the overall speed of the proton pump. However, some mutants were created that shorten a photocycle intermediate lifetime; this indicates that it is possible to improve BR for device applications given the proper mutagenesis techniques. The challenge in using directed evolution for materials optimization is establishing a selection method that focuses on the desired properties of the material generated by the host. In the case of BR, developing a screen to detect optimized proteins in the host *H. salinarum* is essential for development of high-throughput methods.

The directed evolution of BR is divided into two classes: Type I and Type II. These stages are not discrete but rather represent a continuum of procedures that start with a screening process and end with a selection process. The different optimization levels are shown in Table 135.2. Type I directed evolution includes screening of protein variants at the colony or protein level, whereas Type II includes screening/selection of BR in individual archaea. Each round consists of starting with those variants that were most

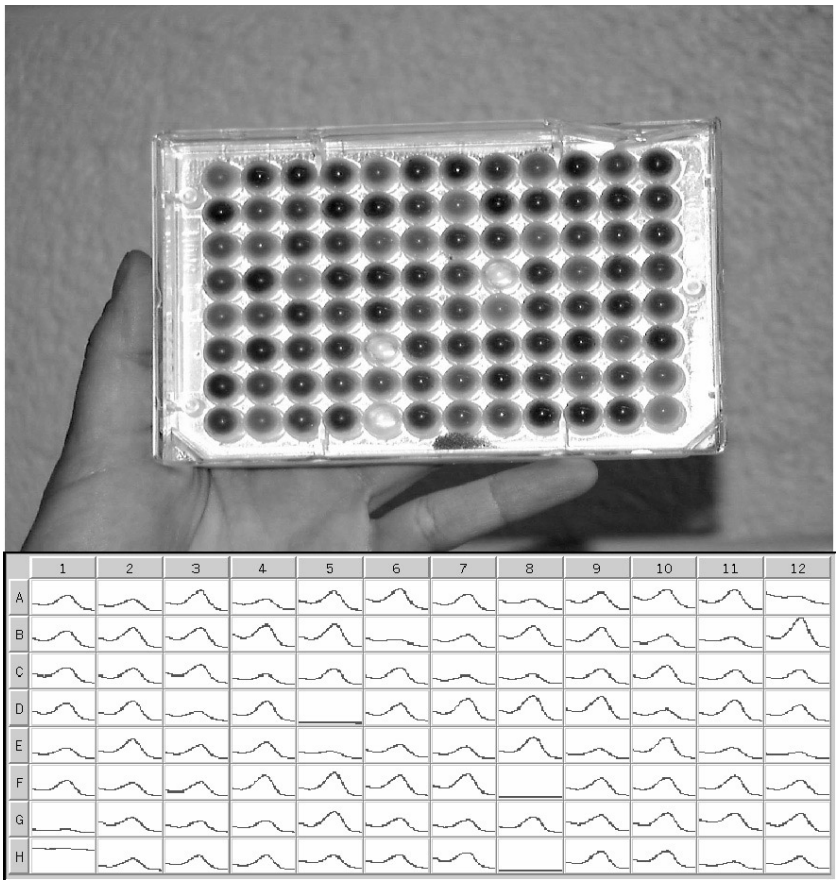

FIGURE 135.10 A 96-well plate containing 93 unique proteins created using semi-random mutagenesis (3 wells did not purify well and were not included in this plate). Corresponding UV-vis spectra were taken using a Bio-tek® μQuant 96-well plate reader. Each mutant was then studied by using time-resolved pump-probe spectroscopy to assign the formation and decay times of the **M** and **O** intermediates.

optimal from the previous round, as defined by the Q value of choice. The essence of directed evolution is that a determined subset of protein representatives is used as the starting point in the next mutational round. Each new round provides an iterative improvement and shifted distribution of characteristics from the previous round.

Type I directed evolution is a medium-throughput method that involves screening purified protein or colonies in 96-well plate, medium-throughput levels. Shown in Figure 135.10 are the results of a screen done on a Type I evolution process in 96-well plate format. Type II directed evolution is currently being developed and involves selecting individual archaea using a flow cytometer. Those organisms that meet a given photocycle optimization criteria are shunted to a collection vessel, while those that do not are discarded.

The choice of optimization method is dependent on the desired level of variation. To explore small changes, site-directed mutagenesis is used to mutate a single residue. To examine larger mutational effects, semirandom and random mutagenesis are used. Results from different optimization methods can be used in tandem; a favorable result from one technique can be combined with variants from another source. Proton release mutants developed from site-directed mutagenesis in the Glu-194 and Glu-204 regions are now being combined with the triple mutant I119T/T121S/A126T to test for synergistic optimization.

135.6 Hybrid Protein-Semiconductor Devices

The high quantum efficiency, large oscillator strength, broadband absorptivity, thermal stability, and fast photovoltaic response of BR make it an attractive material for the photoactive element in high-speed photodetectors.[38] Such applications include high-speed tracking, motion and edge detection, as well as high-resolution imaging.[38,64–67] The significant potential of BR as a light-transducing material was recently shown in a hybrid protein-semiconductor monolithically integrated transimpedance photoreceiver.[68] In this device, the photovoltage generated by the protein biases the gate of an amplifying field effect transistor (FET), creating a photocurrent signal further amplified as a current or voltage signal in subsequent transistor-based amplifying stages. The optoelectronic integrated circuit (OEIC) uses the protein as a photodetector, demonstrating performance characteristics comparable to, or better than, all-semiconductor OEIC photoreceivers.[69]

The utility of this protein in hybrid protein-semiconductor devices derives added value from the sensitivity of the protein to external molecular stimuli.[70–84] Thus, it is possible to use the photocycle kinetics[76,78,79] or photovoltaic responsivity[71,72,83] to monitor the concentration of volatile species. Most of the work to date concentrated on anesthetics, but these and other studies indicate that many organic compounds will directly bind to BR and alter the photophysical properties.[71,74,82] It can be concluded that the complexity of the photovoltaic signal and the sensitivity of this signal to external media combine to make BR a strong candidate for the design of hybrid protein-semiconductor sensors.

Before any of the above hybrid devices can be created reproducibly, the protein–metal and protein–semiconductor surfaces must be optimized. A few years ago, this was viewed as a fairly straightforward challenge upon the discovery that organic cations could be used to prevent protein–semiconductor cross contamination.[85] More recent work demonstrated that the homogeneity of the protein and the long-term stability of the protein, when attached to surfaces, is a complex variable dependent upon hydration, pH, surface charge, surface conditions, applied charge, preparation history, and genetic variation (results to be published). Of great interest and importance to the viability of protein-based sensors is the observation that some mutants produce a "Swiss-cheese" matrix with numerous ~50 to 100 nm diameter holes that extend through the entire membrane. The presence of these defects was not observed in purple membrane patches containing wild-type BR and deposited in the same way. The above observations are from research being done in Professor Ronald Reiffenberger's laboratory in the Department of Physics at Purdue University. The origin and solution for these problems remain to be discovered and are an area of active research.

135.7 Future Direction and Conclusions

Bacteriorhodopsin is an example of a biophotonic material that shows considerable promise as a template for a number of device applications. The above examples are illustrative but not exhaustive, and interest in the use of this protein for devices shows exponential growth. The enthusiasm stems not from the intrinsic characteristics of the native protein but rather the ability to modify the protein for specific applications with an efficiency that far exceeds that possible using organic chemistry. Current medium-throughput optimization screens of BR mutants resulted in significant alterations to photocycle lifetimes and yields. However, high-throughput optimization and directed evolution are necessary tools if BR is ever to reach full potential. The implementation of directed evolution and other systematic genetic methods might enhance the utility of BR an additional order of magnitude.

Acknowledgments

The authors would like to thank Virge Kask for her artistry in Figures 135.1 and 135.2. The authors would also like to thank Dr. Kenneth Noll at the University of Connecticut for his contribution to Figure 135.1.

References

1. Oesterhelt, D. and Stoeckenius, W., Rhodopsin-like protein from the purple membrane of *Halobacterium halobium*, *Nature (London), New Biol.* 233, 149–152, 1971.
2. Ebrey, T.G., Light energy transduction in bacteriorhodopsin, in *Thermodynamics of Membrane Receptors and Channels*, Jackson, M.B., CRC Press, Boca Raton, FL, 1993, pp. 353–387.
3. Lanyi, J. and Luecke, H., Bacteriorhodopsin, *Current Opinion in Struct. Biol.*, 11, 415–419, 2001.
4. El-Sayed, M.A., On the molecular mechanisms of the solar to electric energy conversion by the other photosynthetic system in nature, bacteriorhodopsin, *Accts. Chem. Res.*, 25, 7, 279–286, 1992.
5. Vsevolodov, N.N., *Biomolecular Electronics. An Introduction via Photosensitive Proteins*, Birkhauser, Boston, MA, 1998.
6. Hampp, N., Bacteriorhodopsin: mutating a biomaterial into an optoelectronic material, *Appl. Microbiol. Biotechnol.*, 53, 6, 633–639, 2000.
7. Wise, K.J., Gillespie, N.B., Stuart, J.A., Krebs, M.P., and Birge, R.R., Optimization of bacteriorhodopsin for bioelectronic devices, *Trends in Biotechnol.*, 20, 9, 387–394, 2002.
8. Stoeckenius, W., Lozier, R.H., and Bogomolni, R., Bacteriorhodopsin and the purple membrane of Halobacteria, *Biochem. Biophys. Acta,* 505, 215–278, 1979.
9. Ibawe, N., Kuma, K.-I., Hasegawa, M., Osawa, S., and Migata, T., Evolutionary relationships of archaebacteria, eubacteria, and eukaryotes inferred from phylogenetic trees of duplicated genes, *Proc. Natl. Acad. Sci. USA,* 86, 9355–9359, 1989.
10. Madigan, M.T., Martinko, J.M., and Parker, J.B., *Biology of Microorganisms*, 8th ed., Prentice Hall, New York, 1997.
11. Peck, R.F., Echavarri-Erasun, C., Johnson, E.A., Ng, W.V., Kennedy, S.P., Hood, L., DasSarma, S., and Krebs, M.P., *brp* and *blh* are required for synthesis of the retinal cofactor of bacteriorhodopsin in *Halobacterium salinarum*, *J. Biol. Chem.*, 276, 8, 5739–5744, 2001.
12. Baliga, N.S., Kennedy, S.P., Ng, W.V., Hood, L., and DasSarma, S., Genomic and genetic dissection of an archael regulon, *Proc. Natl. Acad. Sci. USA*, 98, 5, 2521–2525, 2001.
13. Dencher, N. and Heyn, M., Bacteriorhodopsin monomers pump protons, *FEBS Lett.*, 108, 2, 307–310, 1979.
14. Dencher, N.A. and Heyn, M.P., Preparation and properties of monomeric bacteriorhodopsin, *Methods Enzymol.,* 88, 5–10, 1982.
15. Wang, J., Link, S., Heyes, C., and El-Sayed, M., Comparison of the dynamics of the primary events of bacteriorhodopsin in its trimers and monomeric states, *Biophys. J.*, 83, 3, 1557–1566, 2002.
16. Heyes, C. and El-Sayed, M., The role of native lipids and lattice structure in bacteriorhodopsin protein conformation and stability as studied by temperature-dependent Fourier transform-infrared spectroscopy, *J. Biol. Chem.*, 277, 33, 29427–29443, 2002.
17. Hendler, R. and Dracheva, S., Importance of lipids for bacteriorhodopsin strcture, photocycle, and function, *Biochemistry, Biokhimiia,* 66, 11, 1311–1314, 2001.
18. Krebs, M. and Isenbarger, T., Structural determinants of purple membrane assembly, *Biochim. at Biophys. Acta*, 1460, 15–26, 2000.
19. Shen, Y., Safinya, C.R., Liang, K.S., Ruppert, A.F., and Rothschild, K.J., Stabilization of the membrane protein bacteriorhodopsin to 140°C in two-dimensional films, *Nature*, 366, 48–50, 1993.
20. Lukashev, E.P. and Robertson, B., Bacteriorhodopsin retains its light-induced proton-pumping function after being heated to 140°C, *Bioelectrochem. Bioenerg.*, 37, 157–160, 1995.
21. Lanyi, J. and Varo, G., The photocycles of bacteriorhodopsin, *Isr. J. Chem.*, 35, 365–385, 1995.
22. Rammelsberg, R., Huhn, G., Luebben, M., and Gerwert, K., Bacteriorhodopsin's intramolecular proton-release pathway consists of a hydrogen-bonded network, *Biochemistry*, 37, 14, 5001–5009, 1998.
23. Zscherp, C., Schlesinger, R., and Heberle, J., Time-resolved FT-IR spectroscopic investigation of the pH-dependent proton transfer reactions in the E194Q mutant of bacteriorhodopsin, *Biochem. Biophys. Res. Commun.*, 283, 57–63, 2001.

24. Gillespie, N.B., Wise, K.J., Ren, L., Stuart, J.A., Marcy, D.L., Hillebrecht, J., Li, Q., Ramos, L., Jordan, K., Fyvie, S., and Birge, R.R., Characterization of the branched-photocycle intermediates P and Q of bacteriorhodopsin, *J. Phys. Chem. B,* 106, 13352–13361, 2002.
25. Kochendoerfer, G.G., Lin, S.W., Sakmar, T.P., and Mathies, R.A., How color visual pigments are tuned, *Trends Biochem. Sci.*, 24, 8, 300–305, 1999.
26. Okada, T., Le Trong, I., Fox, B., Behnke, C., Stenkamp, R., and Palczewski, K., X-ray diffraction analysis of three-dimensional crystals of bovine rhodopsin obtained from mixed micelles, *J. Struct. Biol.*, 130, 73–80, 2000.
27. Kusnetzow, A., Dukkipati, A., Babu, K.R., Singh, D., Vought, B.W., Knox, B.E., and Birge, R.R., The photobleaching sequence of a short-wavelength visual pigment, *Biochemistry*, 40, 7832–7844, 2001.
28. Dukkipati, A., Kusnetzow, A., Babu, K.R., Ramos, L., Singh, D., Knox, B.E., and Birge, R.R., Phototransduction by vertebrate ultraviolet visual pigments: protonation of the retinylidene Schiff base following photobleaching, *Biochemistry,* 41(31), 9842–9851, 2002.
29. Bressler, S., Friedman, N., Li, Q., Ottolenghi, M., Saha, C., and Sheves, M., Generation of the O_{630} photointermediate of bacteriorhodopsin is controlled by the state of protonation of several protein residues, *Biochemistry*, 38, 2018–2025, 1999.
30. Váró, G. and Lanyi, J.K., Protonation and deprotonation of the M, N, and O intermediates during the bacteriorhodopsin photocycle, *Biochemistry*, 29, 6858–6865, 1990.
31. Kandori, H., Yamazaki, Y., Hatanaka, M., Needleman, R., Brown, L.S., Richter, H.-T., Lanyi, J.K., and Maeda, A., Time-resolved Fourier transform infrared study of structural changes in the last steps of the photocycles of Glu-204 and Leu-93 mutants of bacteriorhodopsin, *Biochemistry*, 36, 5134–5141, 1997.
32. Greenhalgh, D., Farrens, D., Subramaniam, S., and Khorana, H., Hydrophobic amino acids in the retinal-binding pocket of bacteriorhodopsin, *J. Biol. Chem.,* 268, 27, 20305–20311, 1993.
33. Popp, A., Wolperdinger, M., Hampp, N., Bräuchle, C., and Oesterhelt, D., Photochemical conversion of the O-intermediate to 9-*cis*-retinal-containing products in bacteriorhodopsin films, *Biophys. J.,* 65, 1449–1459, 1993.
34. Balashov, S., Imasheva, E., Ebrey, T., Chen, N., Menick, D., and Crouch, R., Glutamate 194 to cysteine mutation inhibits fast light-induced proton release in bacteriorhodopsin, *Biochemistry*, 36, 8671–8676, 1997.
35. Misra, S., Govindjee, R., Ebrey, T.G., Chen, N., Ma, J.X., and Crouch, R.K., Proton uptake and release are rate-limiting steps in the photocycle of the bacteriorhodopsin mutant E204Q, *Biochemistry*, 36, 16, 4875–4883, 1997.
36. Richter, H.-T., Brown, L.S., Needleman, R., and Lanyi, J.K., A linkage of the pKa's of asp-85 and glu-204 forms part of the reprotonation switch of bacteriorhodopsin, *Biochemistry*, 35, 13, 4054–4062, 1996.
37. Oesterhelt, D., Bräuchle, C., and Hampp, N., Bacteriorhodopsin: a biological material for information processing, *Quart. Rev. Biophys.*, 24, 425–478, 1991.
38. Birge, R.R., Photophysics and molecular electronic applications of the rhodopsins, *Annu. Rev. Phys. Chem.*, 41, 683–733, 1990.
39. Wherrett, B.S., Materials for optical computing, *Synth. Metals*, 76, 3–9, 1996.
40. Hampp, N., Bräuchle, C., and Oesterhelt, D., Bacteriorhodopsin wildtype and variant aspartate-96 to asparagine as reversible holographic media, *Biophys. J.*, 58, 83–93, 1990.
41. Hampp, N., Popp, A., Bräuchle, C., and Oesterhelt, D., Diffraction efficiency of bacteriorhodopsin films for holography containing bacteriorhodopsin wildtype BRwt and its variants BR_{D85E} and $BR_{D96N.}$, *J. Phys. Chem.*, 96, 4679–4685, 1992.
42. Otto, H., Marti, T., Holz, M., Lindau, M., Khorana, H.G., and Heyn, M.P., Aspartic acid-96 is the internal proton donor in the repronation of the Schiff base of bacteriorhodopsin, *Proc. Natl. Acad. Sci. USA*, 86, 23, 9228–9232, 1989.

43. Hampp, N., Thoma, R., Zeisel, D., and Bräuchle, C., Bacteriorhodopsin variants for holographic pattern recognition, *Adv. Chem.*, 240, 511–526, 1994.
44. Birge, R.R., Gillespie, N.B., Izaguirre, E.W., Kusnetzow, A., Lawrence, A.F., Singh, D., Song, Q.W., Schmidt, E., Stuart, J.A., Seetharaman, S., and Wise, K.J., Biomolecular electronics: protein-based associative processors and volumetric memories, *J. Phys. Chem. B.*, 103, 10746–10766, 1999.
45. Juchem, T. and Hampp, N., Interferometric system for non-destructive testing based on large diameter bacteriorhodopsin films, *Opt. Lasers in Eng.*, 34, 2, 87–100, 2000.
46. Hampp, N. and Juchem, T., Fringemaker — the first technical system based on bacteriorhodopsin, in *Bioelectronic Applications of Photochromic Pigments*, Keszthelyi, L., IOS Press, Szeged, Hungary, 2000, pp. 44–53.
47. Wolperdinger, M. and Hampp, N., Bacteriorhodopsin variants as versatile media in optical processing, *Biophys. Chem.*, 56, 1–2, 189–192, 1995.
48. Dancshazy, Z. and Tokaji, Z., Blue light regeneration of bacteriorhodopsin bleached by continuous light, *FEBS Lett.*, 476, 3, 171–173, 2000.
49. Dancshazy, Z., Tokaji, Z., and Der, A., Bleaching of bacteriorhodopsin by continuous light, *FEBS Lett.*, 450, 154–157, 1999.
50. Birge, R.R., Zhang, C.F., and Lawrence, A.F., Optical random access memory based on bacteriorhodopsin, in *Molecular Electronics*, Hong, F., Plenum Press, New York, 1989, pp. 369–379.
51. Birge, R.R., Three-dimensional optical memories, *Amer. Sci.*, 82, 349–355, 1994.
52. Gillespie, N.B., Wise, K.J., Ren, L., Stuart, J.A., Marcy, D.L., Hillebrecht, J., Li, Q., Ramos, L., Jordan, K., Fyvie, S., and Birge, R.R., Characterization of the branched-photocycle intermediates P and Q of bacteriorhodopsin, *J. Phys. Chem. B.*, 106, 13352–13361, 2002.
53. Balashov, S., Protonation reactions and their coupling in bacteriorhodopsin, *Biochim. at Biophys. Acta*, 1460, 75–94, 2000.
54. Balashov, S., Lu, M., Imasheva, E., Govindjee, R., Ebrey, T., Otherson III, B., Chen, Y., Crouch, R., and Menick, D., The proton release group of bacteriorhodopsin controls the rate of the final step of its photocycle at low pH, *Biochemistry*, 38, 2026–2039, 1999.
55. Váró, G., Duschl, A., and Lanyi, J.K., Interconversions of the M, N, and O intermediates in the bacteriorhodopsin photocycle, *Biochemistry*, 29, 15, 3798–3804, 1990.
56. Chizov, I., Englehard, M., Chernavskii, D.S., Zubov, B., and Hess, B., Temperature and pH sensitivity of the O_{640} intermediate of the bacteriorhodopsin photocycle, *Biophys. J.*, 61, 1001–1006, 1992.
57. Tallent, J.R., Stuart, J.A., Song, Q.W., Schmidt, E.J., Martin, C.H., and Birge, R.R., Photochemistry in dried polymer films incorporating the deionized blue membrane form of bacteriorhodopsin, *Biophys. J.*, 75, 1619–1634, 1998.
58. Tallent, J., Song, Q.W., Li, Z., Stuart, J., and Birge, R.R., Effective photochromic nonlinearity of dried blue-membrane bacteriorhodopsin films, *Optics Lett.*, 21, 1339–1341, 1996.
59. Chang, C.H., Chen, J.G., Govindjee, R., and Ebrey, T., Cation binding by bacteriorhodopsin, *Proc. Natl. Acad. Sci. USA*, 82, 396–400, 1985.
60. Whaley, S.R., English, D.S., Hu, E.L., Barbara, P.F., and Belcher, A.M., Selection of peptides with semiconductor binding specificity for directed nanocrystal assembly, *Nature*, 405, 6787, 665–668, 2000.
61. Anni, H., Nikolaeva, O., and Israel, Y., Selection of phage-display library peptides recognizing ethanol targets on proteins, *Alcohol*, 25, 3, 201–209, 2001.
62. Brust, M. and Kiley, C.J., Some recent advances in nanostructure preparation from gold and silver particles: a short topical review, *Colloids and Surf. A: Physicochem. Eng. Aspects*, 202, 2–3, 175–186, 2002.
63. Mulholland, S.E., Gibney, B.R., Rabatal, F., and Dutton, P.L., Determination of nonligand amino acids critical to [4Fe-4S]2+/+ assembly in ferredoxin maquettes, *Biochemistry*, 38, 32, 10442–10448, 1999.
64. Takei, H., Lewis, A., Chen, Z., and Nebenzahl, I., Implementing receptive fields with excitatory and inhibitory optoelectrical responses of bacteriorhodopsin films, *Appl. Opt.*, 30, 500–509, 1992.
65. Miyasaka, T., Koyama, K., and Itoh, I., Quantum conversion and image detection by a bacteriorhodopsin-based artifical photoreceptor, *Science*, 255, 342–344, 1992.

66. Chen, Z. and Birge, R.R., Protein based artificial retinas, *Trends Biotech.*, 11, 292–300, 1993.
67. Fukuzawa, K., Yanagisawa, K., and Kuwano, H., Photoelectrical cell utilizing bacteriorhodopsin on a hole array fabricated by micromachining techniques, *Sensors & Actuators B*, 30, 121–126, 1996.
68. Bhattacharya, P., Xu, J., Varo, G., Marcy, D.L., and Birge, R.R., Monolithically integrated bacteriorhodopsin-GaAs field-effect transistor photoreceiver, *Opt. Lett.*, 27, 839–841, 2002.
69. Xu, J., Bhattacharya, P., and Varo, G., A photoreceiver based on the monolithic integration of oriented bacteriorhodopsin and GaAs MODFET's, in *Lasers and Electro-Opt. Soc. 2001 14th Annual Meeting, IEEE Annual Meeting Conference Proceedings*, 2001, pp. 833–834.
70. Uruga, T., Hamanaka, T., Kito, Y., Uchida, I., Nishimura, S., and Mashimo, T., Effects of volatile anesthetics on bacteriorhodopsin in purple membrane, *Halobacterium halobium* cells and reconstituted vesicles, *Biophys. Chem.,* 41, 2, 157–168, 1991.
71. Hong, F.T., Molecular sensors based on the photoelectric effect of bacteriorhodopsin: origin of differential responsivity, *Mater. Sci. Eng.*, C 4, 267–385, 1997.
72. Boucher, F., Taneva, S.G., Elouatik, S., Dery, M., Messaoudi, S., Harvey-Girard, E., and Beaudoin, N., Reversible inhibition of proton release activity and the anesthetic-induced acid-base equilibrium between the 480 and 570 nm forms of bacteriorhodopsin, *Biophys. J.*, 70, 2, 948–961, 1996.
73. Gao, M.M. and Boucher, F., The uncoupling of bacteriorhodopsin by high temperature and anaesthetics, *Toxicol. Lett.*, 100–101, 393–396, 1998.
74. Hamanaka, T., Nakagawa, T., Kito, Y., Nishimura, S., Uchida, I., and Mashimo, T., Binding of volatile anesthetics to purple membranes studied by x-ray diffraction, *Toxicol. Lett.,* 100–101, 397–403, 1998.
75. Lee, K.H., McIntosh, A.R., and Boucher, F., The interaction between halogenated anaesthetics and bacteriorhodopsin in purple membranes as examined by intrinsic ultraviolet fluorescence, *Biochem. Cell Biol.*, 69, 2–3, 178–184, 1991.
76. Lin, C.T., Chyan, Y.G., Kresheck, G.C., Bitting, H.C., Jr., and El-Sayed, M.A., Interaction of dibucaine HCl local anesthetics with bacteriorhodopsin in purple membrane: a spectroscopic study, *Photochem. Photobiol.,* 49, 5, 641–648, 1989.
77. Lin, C.T., Mertz, C.J., Bitting, H.C., and El-Sayed, M.A., Fluorescence anisotropy studies of dibucaine HCl in micelles and bacteriorhodopsin, *J. Photochem. Photobiol. B*, 13, 2, 169–185, 1992.
78. Nakagawa, T., Hamanaka, T., Nishimura, S., Uruga, T., and Kito, Y., The specific binding site of the volatile anesthetic diiodomethane to purple membrane by x-ray diffraction, *J. Mol. Biol.,* 238, 3, 297–301, 1994.
79. Nakagawa, T., Hamanaka, T., Nishimura, S., Uchida, I., Mashimo, T., and Kito, Y., The quantitative analysis of three action modes of volatile anesthetics on purple membrane, *Biochim. Biophys. Acta,* 1468, 1–2, 139–149, 2000.
80. Nishimura, S., Mashimo, T., Hiraki, K., Hamanaka, T., Kito, Y., and Yoshiya, I., Volatile anesthetics cause conformational changes of bacteriorhodopsin in purple membrane, *Biochim. Biophys. Acta,* 818, 3, 421–424, 1985.
81. Perozo, E. and Hubbell, W.L., Voltage activation of reconstituted sodium channels: use of bacteriorhodopsin as a light-driven current source, *Biochemistry,* 32, 39, 10471–10478, 1993.
82. Renthal, R., Brogley, L., and Vila, J., Altered protein-chromophore interaction in dicyclohexylcarbodiimide-modified purple membrane sheets, *Biochim. Biophys. Acta*, 935, 2, 109–114, 1988.
83. Taneva, S.G., Caaveiro, J.M., Petkanchin, I.B., and Goni, F.M., Electrokinetic charge of the anesthetic-induced bR480 and bR380 spectral forms of bacteriorhodopsin, *Biochim. Biophys. Acta*, 1236, 2, 331–337, 1995.
84. Uchida, I., Mashimo, T., and Yoshiya, I., Pressure-anesthetic interaction on the molecular conformation of bacteriorhodopsin, *Ann. NY Acad. Sci.*, 625, 767–769, 1991.
85. Tan, E.H.L., Govender, D.S.K., and Birge, R.R., Large organic cations can replace Mg^{2+} and Ca^{2+} ions in bacteriorhodopsin and maintain proton pumping ability, *J. Am. Chem. Soc.*, 118, 2752–2753, 1996.

136

Bacterial Bioluminescence: Biochemistry

Shiao-Chun Tu
University of Houston

136.1 Introduction

Most photobiological processes are triggered by light absorption. A wide range of biochemical reactions and physiological functions can be initiated by the capture of photons at an appropriate energy level by specific sensing or receptor molecules. In contrast, bioluminescence is an unusual subfield of photobiology; energy derived from biochemical reactions is coupled to the generation of excited states and, in turn, emission of visible light with high quantum yields, usually in the range of 0.1 to near unity. Bioluminescent species are found in prokaryotes and eukaryotes. The underlying biological and chemical principles for the expression and regulation of bioluminescence were the subject for active basic and applied research for several decades. Among known bioluminescent systems, bacterial bioluminescence is one of the most extensively studied few with respect to biochemistry. A chapter by this author on the subject of biochemistry of bacterial bioluminescence was published in the 1995 edition of this book.[1] In order for the present chapter to be self-sustaining, some salient points from the previous chapter are again briefly summarized. Comprehensive coverage of all important aspects of the biochemistry of bacterial bioluminescence is not intended. The *lux* operon induction by the quorum-sensing autoinducer, mechanisms of luciferase protein folding, functions of bioluminescence-related fluorescent proteins, structures and mechanisms of aldehyde synthesizing enzymes and NAD(P)H-dependent flavin reductases, mechanisms of reduced flavin transfer to luciferase, and applications of luciferase and *lux* genes in basic research and technological development are notably among areas of omission.

Most known luminous bacteria are from the marine ecosystem. They are free living or symbionts. Among them, *Vibrio harveyi* (initially designated MAV or *Benekea harveyi*), *Vibrio fischeri* (formerly *Photobacterium fischeri*), and *Photobacterium phosphoreum* are the three most extensively studied strains. *Xenorhabdus* (later reclassified as *Photorhabdus*) *luminescens* is a notable exception, with strains isolated from human wounds or as nematode symbionts. Essential enzymes for bacterial bioluminescence *in vivo* are shown in Scheme 136.1. The light-emitting reaction is catalyzed by luciferase, a flavin-dependent

0-8493-1348-1/04/$0.00+$1.50

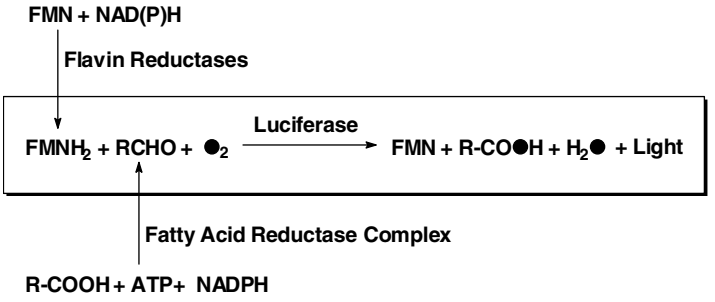

SCHEME 1

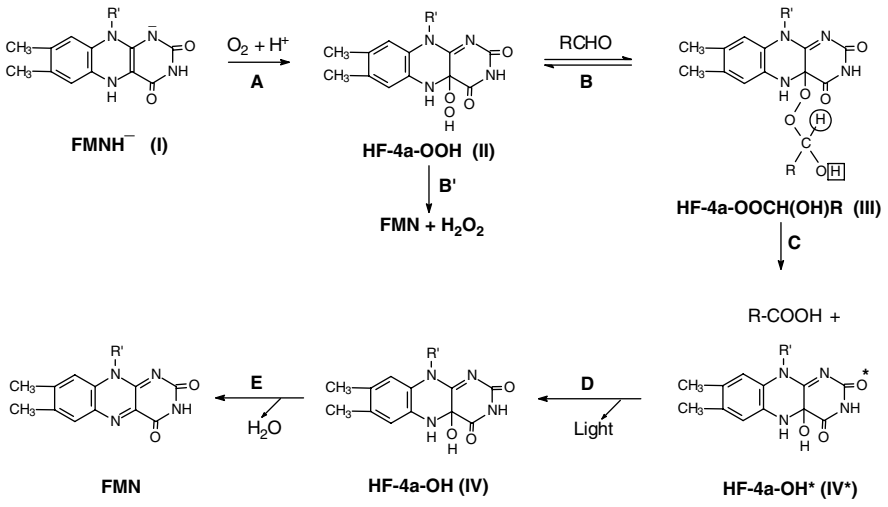

SCHEME 2

monooxygenase. The emission peak wavelength is around 490 nm, which could be shifted *in vitro* and *in vivo* to a shorter (~476 nm) or longer (~530 nm) wavelength in the presence of a lumazine- or flavin-containing fluorescence protein. The required substrate-reduced flavin mononucleotide ($FMNH_2$) is believed to be provided *in vivo* by flavin reductases using NADH or NADPH as a reductant. Structures and properties of flavin reductases and mechanisms of reduced flavin transfer to luciferase were recently reviewed.[2] The long-chain aliphatic aldehyde substrate can be obtained from reduction of fatty acid catalyzed by a reductase complex.

136.2 Luciferase Mechanism

Intermediates and Chemical Mechanism

The foundation for the chemical mechanism of bacterial luciferase is primarily laid by the work of Hastings and colleagues.[3–8] These studies and the work of others were the subjects of a number of reviews. Main features of the luciferase chemical mechanism are summarized in Scheme 136.2. The luciferase-bound N1-deprotonated $FMNH^-$ (Intermediate I) reacts with oxygen to generate the 4a-hydroperoxy-FMNH (HF-4a-OOH; Intermediate II), which undergoes a dark decay to form FMN and H_2O_2 in the absence of aldehyde or reacts with aldehyde to form the 4a-peroxyhemiacetalFMNH (Intermediate III).

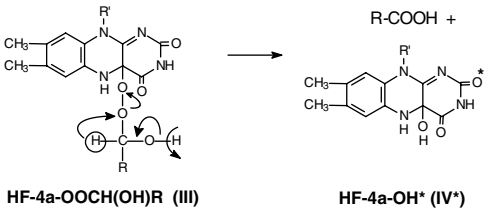

SCHEME 3

Intermediate III undergoes a still poorly understood reaction to generate 4a-hydroxyFMNH at the excited state (Intermediate IV*) and fatty acid. The relaxation of IV* is accompanied by light emission. The final decay of Ground State IV produces FMN and water and releases free luciferase.

An NMR study revealed that the luciferase-bound $FMNH_2$ is in the N1-deprotonated state.[9] In this connection, a computational analysis demonstrated that the N1-deprotonated $FMNH^-$ is significantly more active than $FMNH_2$, and the flavin 4a-position is the preferred site in reacting with oxygen to form II.[10] In a flavin model system, II is initially formed as HF-4a-OO^-, which undergoes an energy barrier-free conversion to HF-4a-OOH.[10] In the enzymatic reaction, which form of II is stabilized by luciferase is unclear. However, HF-4a-OO^- is expected to react with aldehyde to generate III. The substrate hydroxylation activities of flavoprotein monooxygenases in general and the bioluminescence activity of luciferase in particular depend on an efficient fission of the O–O bond over the C(4a)–O bond of flavin-4a-hydroperoxide or, in the case of luciferase, flavin-4a-peroxyhemiacetal. The energy of these reactions was studied using flavin models.[11–13] The O–O bond dissociation enthalpies for HO-OH, CH_3O-OH, CH_3O-OCH_3, $CH_3C(O)O$-$OC(O)CH_3$, and flavin-4a-O-OH were found to be, respectively, 51, 45, 38, 30, and <26 kcal/mol.[12] Clearly, flavin-4a-hydroperoxide is effective in activating the O–O bond. Furthermore, in flavin-4a-hydroperoxide, the free energies of the O–O bond and the C(4a)–O bond fission were determined to be 16 and 21 kcal/mol, respectively.[11,13] Hence, the O–O bond breakage is favored over that of the C(4a)–O bond. The O–O bond in flavin-4a-peroxyhemiacetal is even weaker than that in flavin-4a-hydroperoxide by 7 kcal/mol.[12] All of the cases mentioned above indicate that the O–O bond in flavin-4a-hydroperoxide and flavin-4a-peroxyhemiacetal is highly activated for the light-emitting reaction. The converse was also shown for the C(4a)–O bond fission. Using the wild-type luciferase and 18 mutants, we demonstrated an inverse linear correlation between the bioluminescence activity and the rate of Intermediate II dark decay involving the C(4a)–O bond fission.[14] By the use of fluorescent aldehyde substrates, it was also demonstrated that IV* instead of activated aliphatic carboxylic or carbonyl species is generated as the primary excited state.[15] As reviewed earlier,[1] a large body of studies provided supporting evidence for the existence of Intermediates II and IV and documentation of their spectral and chemical properties.

The most intriguing but also the least understood reaction in Scheme 136.2 is the formation of the excited 4a-hydroxyFMNH emitter (Step C). Thus far, two major types of mechanisms were postulated, namely, the Baeyer–Villiger (BV) mechanism and the Chemically Initiated Electron Exchange Luminescence (CIEEL) or Electron/Charge Transfer (ECT) mechanism. First, the BV mechanism[5] is depicted in Scheme 136.3. The abstraction of a proton from the OH in Intermediate III sets off the electron and hydride transfers as shown to generate IV* and carboxylic acid. The main attraction of this mechanism is that it is based on a well-established reaction mechanism. However, a potential major problem with this mechanism for luciferase is that energy released from multiple steps of bond rearrangement must be pooled together at the same time to elevate 4a–hydroxyFMNH to its excited state. Similar to luciferase, cyclohexanone monooxygenase is a member of flavin-dependent monooxygenases and was shown to follow the Baeyer–Villiger mechanism.[16] Boronic acids can be used by cyclohexanone monooxygenase as substrates to produce the corresponding boric acids as products. In contrast, such a mechanistic probe cannot be utilized by luciferase for boric acid formation or light emission.[17] The results obtained from a study using eight-substituted flavin analogs as mechanistic probes are also opposite to what is expected

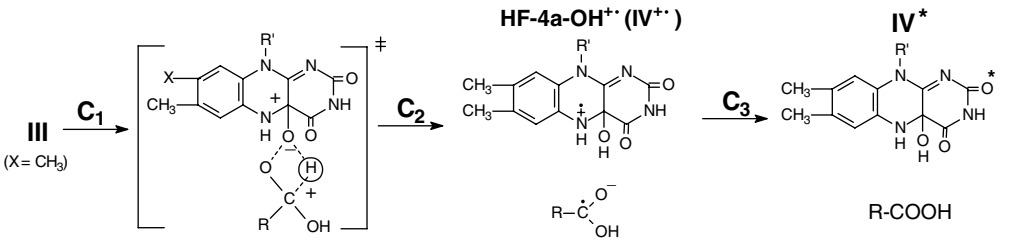

SCHEME 4

for a BV mechanism.[8] This will be discussed in more detail below. Since its original introduction in 1972,[5] the BV mechanism has not gained wide support, despite a formidable effort for its resurrection.[18]

Next, two versions of mechanisms following the principle of CIEEL[19] were proposed. In the original CIEEL mechanism formulated for bacterial luciferase,[8,20–23] a fission of the O–O bond in Intermediate III and transfers of electron and proton take place, resulting in the formation of a caged pair of one-electron-reduced carboxylic acid radical R-C(OH)$O^{-\bullet}$ and a novel 4a-hydroxyFMNH radical cation (HF-4a-OH)$^{+\bullet}$ (Intermediate $IV^{+\bullet}$). A subsequent electron transfer from the carboxylic acid radical to $IV^{+\bullet}$ generates the fatty acid and excited 4a-hydroxyFMNH (IV*). There are a few minor variations regarding how the caged radical pair of R-C(OH)$O^{-\bullet}$ and $IV^{+\bullet}$ are formed from III. Our updated version[13,24] is shown in Scheme 136.4. This scheme involves a full one-electron separation in the formation of the radical pair and a subsequent radical annihilation, but it can be modified to involve charge transfers instead.[1,25,26] Conceptually, it should be considered an ECT mechanism.[1]

Several major aspects of this mechanism are strongly supported by experimental results or theoretical consideration. The formation of the IV* emitter is proposed to occur in a single step of radical annihilation, an efficient process for generating an excited state. A key intermediate in this mechanism is the novel 4a-hydroxyFMNH radical cation ($IV^{+\bullet}$). The formation and characterization of this type of radicals from flavin models were achieved by electrochemical oxidation,[11] chemical comproportionation,[27] and pulse radiolysis.[13] The absorption spectra and redox potentials of several 4a-hydroxyflavin radical cations were determined.[11,13] Moreover, the annihilation between a 4a-hydroxyflavin radical and a one-electron-reduced carboxylic acid radical was calculated to release ~90 kcal/mol of energy,[13] in excess of the 67 kcal/mol required for generating the excited emitter IV*. In fact, chemical[28] and electrochemical[29] reduction of preformed 5-ethyl-4a-hydroxyflavin radical cations are found to emit chemiluminescence in model systems. Other important supporting evidence is a study to correlate the redox potentials of flavin analogs with the luciferase light decay rates.[8,30,31] By making different substitutions at Position 8 (marked as *X* in Scheme 136.4), redox potentials of a series of flavin analogs are varied. A lower one-electron oxidation potential of the flavin is expected to enhance its tendency to form the 4a-hydroxyflavin radical cation and, in turn, the luminescence reaction rate. Indeed, such a trend was observed in this study. This observation is consistent with the CIEEL/ECT mechanism but is opposite to what is expected for the BV mechanism. Also consistent with the CIEEL/ECT mechanism is the observation that superoxide anion is able to increase the rate of light decay, presumably by reacting with and removing the Intermediate III in competition with the productive Step C2 in Scheme 136.4.[32]

The same principle of CIEEL/ECT mechanism has also been adapted for a mechanism[33,34] (Scheme 136.5) involving dioxirane[35] as an intermediate. Key aspects of this dioxirane mechanism are similar to the CIEEL/ECT mechanism mentioned above. The exited emitter formation involves the same annihilation of radicals (Step C4). The same 4a-hydroxyFMNH radical cation proposed earlier in the CIEEL/ECT mechanism is again formulated as a key intermediate. Hence, the correlation of flavin redox potentials with the luciferase light decay rates also supports this dioxirane version of the CIEEL/ECT mechanism. One difference between the two mechanisms shown in Schemes 136.4 and 136.5 is that a dioxirane species is depicted as an intermediate in the latter. As a test, dimethyldioxirane was reacted

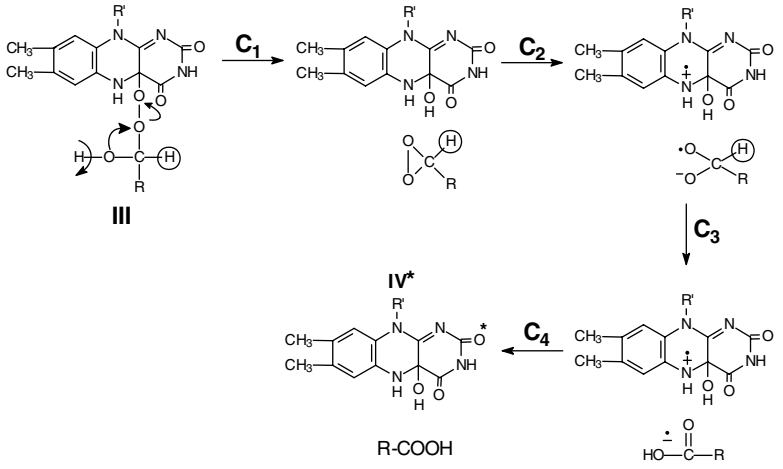

SCHEME 5 Adapted with permission from Francisco, W.A., Abu-Soud, H.M., DelMonte, A.J., Singleton, D.A., Baldwin, T.O., and Raushel, F.M., *Biochemistry,* 37, 2596, 1998.

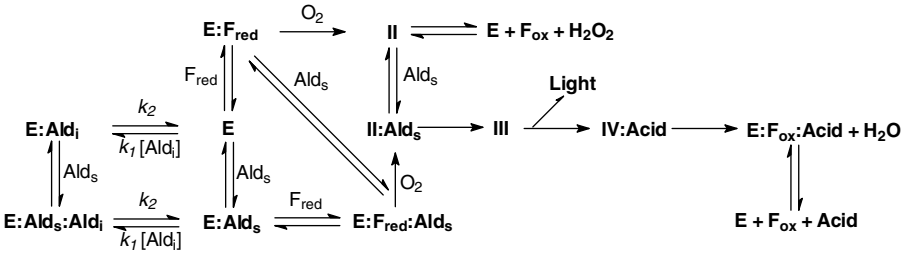

SCHEME 6

with 5-ethyl-4a-hydroxy-3-methyl-4a,5-dihydrolumiflavin. Only trace chemiluminescence was detectable, which cannot be enhanced by the addition of the highly fluorescent 3-methyllumiflavin as a sensitizer.[23] While this does not rule out the dioxirane mechanism as shown in Scheme 136.5, the observation certainly does not provide any support to this mechanism. Another difference is related to deuterium kinetic isotope effects arising from the substitution of the circled hydrogen in Intermediate III by deuterium by using [1-^{2}H]-labeled aldehyde substrate. This kinetic isotope effect will be discussed later. The dioxirane mechanism also requires that 4a-hydroxyFMNH is first formed at the ground state before the rate-limiting step of the generation of the corresponding radical cation.[34] In subsequent steps, 4a-hydroxyFMNH is again formed, in excited state and finally the ground state. The first appearance of 4a-hydroxyFMNH is proposed to be before the rate-limiting step and, hence, should be detectable before the light emission. Thus far, the luciferase-bound 4a-hydroxyFMNH intermediate was only detected as a ground state product of the emitter, not before the formation of the emitter.[7,36–39] These considerations should be incorporated into the evaluation of this dioxirane mechanism.

Kinetic Mechanism and Aldehyde Inhibition

The kinetic mechanism will be confined to *V. harveyi* luciferase, the most extensively studied bacterial luciferase to date. Our version of the kinetic scheme is shown in Scheme 136.6. Aside from the aldehyde

inhibition, most of this scheme should be of general relevance to other bacterial luciferase species. Intermediates II, III, and IV are the same as defined in Scheme 136.2. F_{red}, F_{ox}, Ald_s, and Ald_i are, respectively, reduced FMN, oxidized FMN, aldehyde substrate, and aldehyde inhibitor.

Luciferase follows a random binding of F_{red} and Ald_s to form the ternary complex of $E:F_{red}:Ald_s$. This complex reacts with oxygen to generate $II:Ald_s$ complex that is subsequently converted to III. In fact, Ald_s can also bind to II to form the same $II:Ald_s$ complex and, subsequently, III. The random binding of Ald_s and F_{red} to form a productive intermediate was first noted by Holzman and Baldwin,[40] but the same group later published another scheme in which prior binding of aldehyde to luciferase prevents the binding of $FMNH_2$ by luciferase (see below). Our more recent results are consistent with the random binding of Ald_s and F_{red}.[41] The reaction of bound F_{red} with oxygen to form II was documented first by kinetic evidence[3] and, later, most definitively by the isolation of this intermediate.[6] Using the isolated II, it was established that Ald_s can directly react with II for light production[6,42–44] in an oxygen-independent reaction.[45] In the absence of Ald_s, II undergoes a dark decay to yield equal molar F_{ox} and H_2O_2.[42,44] The addition of H_2O_2 to F_{ox} in the presence of luciferase can also generate II in a low-yield reaction.[46] Once III is formed, subsequent reactions take place to form the excited emitter (not shown in Scheme 136.6 for simplicity) and, in turn, light and ground state IV in complex with the carboxylic acid product. While the carboxylic acid is still bound, the decay of 4a-hydroxyFMNH gives rise to F_{ox} and water. Finally, F_{ox} and carboxylic acid are released as the final products, and luciferase is liberated for the next catalytic cycle. The carboxylic acid remains in the luciferase-bound form until the final step in the scheme. This was demonstrated for the *P. luminescens* luciferase,[47] and the same is assumed for the similar *V. harveyi* enzyme.

The *V. harveyi* luciferase was long known to be inhibited by high concentrations of aldehyde[48] when added to luciferase before $FMNH_2$.[49] The *P. luminescens* luciferase was also shown to be inhibited by high concentrations of aldehyde.[50] There are three schemes for aldehyde inhibition. The first mechanism[40] involves the sequential binding of two aldehydes, herein referred to as the "Two-Site Sequential" (TSS) mechanism. The first aldehyde is bound as a substrate. Subsequently, a second aldehyde, as an inhibitor, binds to the initial luciferase:aldehyde complex to trap the enzyme in an inactive $luciferase:(aldehyde)_2$ form. This scheme also depicts a random binding of the aldehyde and $FMNH_2$ substrates. The TSS scheme was later replaced by a second kinetic mechanism,[51] in which only one aldehyde is shown in luciferase-bound form. In this "One-Site" (OS) scheme, luciferase can bind $FMNH_2$ or aldehyde first. However, when aldehyde is bound first, the luciferase:aldehyde complex is incapable of binding $FMNH_2$. Moreover, the dissociation of the aldehyde from the inactive luciferase:aldehyde complex is slower than the autooxidation of $FMNH_2$, thus in a nonturnover assay, little or no free $FMNH_2$ would be available when enzyme is liberated from the luciferase:aldehyde complex. Hence, active enzyme intermediates can be formed only when $FMNH_2$ is bound to luciferase prior to aldehyde. We proposed a "Two-Site Random" (TSR) mechanism[41] (part of Scheme 136.6) for aldehyde inhibition with the following key features:

1. The binding of substrates F_{red} and Ald_s by luciferase is random.
2. Luciferase can bind one Ald_s and one Ald_i per $\alpha\beta$ dimer, at two presumably independent sites.
3. The Ald_s has a higher binding affinity than that of the Ald_i.
4. Ald_i is a competitive inhibitor against $FMNH_2$. While $E:Ald_s$ is active, both $E:Ald_i$ and $E:Ald_s:Ald_i$ are inactive.
5. The on and off constants for the Ald_i binding are substantially slower than not only those of the $FMNH_2$ binding but also those of the Ald_s binding.

Results of equilibrium binding, chemical relaxation analysis, and activity and inhibition kinetic measurements are all consistent with this scheme.[41]

The TSS and our TSR scheme share the common features of random binding of Ald_s and F_{red} substrates and two aldehyde sites per $\alpha\beta$ luciferase. However, TSS is based on a sequential binding, whereas our mechanism involves a random binding of the two aldehydes. Subsequent to the proposal of the TSS scheme,[40] a different OS scheme[51] was published involving a common author for both publications. Apparently, the latter OS scheme is favored by these researchers over the first mechanism. The OS and our TSR mechanisms are consistent with respect to two points:

1. Once an aldehyde inhibitor is bound to luciferase, the enzyme can no longer bind the F_{red} substrate.
2. The dissociation of the aldehyde inhibitor from luciferase is slower than the autooxidation of F_{red}.

However, the OS scheme differs from TSS and TSR in depicting the binding of only one aldehyde by luciferase. This is inconsistent with the binding of two aldehydes by luciferase measured under aldehyde concentrations suitable for inhibition.[41] Another questionable feature of the OS scheme is the report of $k_{19} = 9.1 \times 10^5\ M^{-1}s^{-1}$ and $k_{20} = 5.8\ s^{-1}$ for the on and off rate constants for the binding of decanal inhibitor to luciferase[51,52] Using decanal, the on and off rate constants for the binding of the aldehyde inhibitor to luciferase or to E:Ald_s complex are determined by us by chemical relaxation to be $k_1 = 3.5 \times 10^3\ M^{-1}s^{-1}$ and $k_2 = 0.038\ s^{-1}$, respectively (Scheme 136.6). In our study, a limiting amount of luciferase was equilibrated with aldehyde at several concentrations suitable for inhibition. The samples were each diluted with buffer for the dissociation of aldehyde until a new equilibrium was reached. The measured relaxation times are in the range of tens of seconds.[41] If the k_{19} and k_{20} of the OS scheme were used, the relaxation times would be ≤0.1 s, clearly inconsistent with our experimental observations. Interestingly, a similar dilution experiment was reported in the inset in Figure 1 in the paper for the TSS scheme,[40] and tens of seconds were required for the dissociation of the aldehyde inhibitor. Last, aldehyde inhibition was shown in our study to arise from the ability of Ald_i functioning as a competitive inhibitor against $FMNH_2$ substrate. This feature was not addressed or established for the TSS mechanism or the OS mechanism.

Deuterium Kinetic Isotope Effect of Aldehyde

Deuterium isotope effects of up to 1.7 of [1-^{2}H]-labeled aldehydes on the luciferase light decay were first noted more than 20 years ago.[53,54] Results of these earlier studies are likely complicated by aldehyde inhibition or flavin semiquinone formation. Nonetheless, these findings demonstrated that the excited emitter formation is coupled to the aldehyde oxidation and the abstraction of C1-H from aldehyde, presumably at a point after the formation of Intermediate III is at least partially rate limiting. Using an assay without the complication of aldehyde inhibition, Tu et al. determined the kinetic isotope effects of [1-^{2}H]-decanal on the light decay rate (^{D}k) and quantum yield (^{D}Q) of the *V. harveyi* luciferase reaction.[55] By allowing a light-emitting reaction (with k_1) and a competing dark decay (with k_2) branching out from II:Ald_s complex or III, the following relationships are obtained:

$$^Dk = (k_{1H} + k_2)/(k_{1D} + k_2) \quad (136.1)$$

$$^DQ = (k_{1H})(k_{1D} + k_2)/(k_{1D})(k_{1H} + k_2) \quad (136.2)$$

When light pathway is predominant (i.e., $k_1 >> k_2$), $^Dk \cong k_{1H}/k_{1D}$ and $^DQ \cong 1.0$. If $k_2 >> k_1$, $^DQ \cong k_{1H}/k_{1D}$ and $^Dk \cong 1.0$. When the light and the dark pathways are significant, then $^Dk < k_{1H}/k_{1D}$ and $^DQ > 1.0$. Using $FMNH_2$ and decanal as substrates in a low concentration (i.e., 0.02 *M*) phosphate buffer, light reaction is predominant as evident from $^Dk = 1.4$ and $^DQ = 1.1$. However, when reduced riboflavin or 2,3-diacetylFMN are used as the flavin substrate, the dark decay becomes dominating, as shown by $^Dk = 1.0$ and $^DQ = 1.4$. The dark decay is also enhanced at higher phosphate concentrations and, especially, in Tris buffers.

Macheroux et al. also examined the deuterium isotope effects of [1-^{2}H]-labeled octanal and dodecanal by reacting with isolated luciferase Intermediate II.[56] Three kinetic phases were detected, and isotope effects of 1.23 to 1.62 were observed for the second kinetic phase and the parallel light decay. Importantly, the first kinetic phase is free from deuterium isotope effect. This optically and kinetically definable phase is postulated to correspond to the luciferase flavin-4a-peroxyhemiacetal Intermediate III, detected for the first time in this work.

More recently, Francisco et al. carried out a detailed deuterium isotope effect study at pH 6 to 9 using different [1-^{2}H]-labeled aldehydes, flavin analogs, and wild-type and mutated luciferases.[34] An important conclusion from this work is that the observed deuterium isotope effects of aldehyde arise from the change of rate of a single kinetic step. It is also estimated that deuterium isotope effect of aldehyde after the formation of the Intermediate III is ~1.9.

TABLE 136.1 Compatibility of Subunits in Forming Active Heterodimeric Luciferase Hybrids[a]

	Vhβ	Vfβ	Pluβ	Pleβ	Ppβ
Vhα	++	+[61]	nd[b]	+[61]	+[58]
		−[60]		−[60]	−[60]
Vfα	−[60,61]	++	+[59]	+[60,61]	+[60]
Pluα	nd	+[59]	++	nd	nd
Pleα	−[60,61]	+[60,61]	nd	++	+[60]
Ppα	−[58,60]	−[60,61]	nd	+[60]	++

[a] Abbreviations for cell strains are as follows: Vh, *Vibrio harveyi*; Vf, *Vibrio fischeri*; Plu, *Photorhabdus luminescens*, Ple, *Photobacterium leiognathi*; Pp, *Photobacterium phosphoreum*. The bacterium strain is followed by the designation of the luciferase subunit. Active luciferase heterodimers are indicated by ++ for the native enzymes and + for the hybrid enzymes. Inactive hybrids are indicated by the negative sign.

[b] Not determined.

The observed deuterium isotope effects of aldehydes as mentioned above have important mechanistic implications. The Baeyer–Villiger mechanism (Scheme 136.3) and the CIEEL/ECT mechanism (Scheme 136.4) involve the transfer of the hydrogen or deuterium in the circled position. This could give rise to a primary kinetic isotope effect. The observed deuterium isotope effects of different aldehydes are in the range of 1.4 to 1.9, which are consistent with the usual sizes of primary deuterium isotope effects arising from a partially rate-limiting step. In contrast, the dioxirane mechanism depicts Reaction C2 in Scheme 136.5 as the isotope-sensitive rate-limiting step. This C2 step is associated with a secondary deuterium kinetic isotope effect that is usually much smaller than the 1.88 observed by Francisco et al.[34] Arguments were presented by these authors to account for this unusually large secondary isotope effect. Nonetheless, it is easier to account for the observed 1.4 to 1.9 isotope effects on the basis of a primary isotope effect on a partially rate-limiting reaction step.

136.3 Luciferase Structure

Subunits and Three-Dimensional Structure

All known bacterial luciferases are αβ heterodimers. The two subunits are bound tightly through non-covalent interactions. Luciferases from different luminous bacteria all have an α subunit (molecular weight 40,100 to 41,400) and a slightly smaller β subunit (molecular weight 36,400 to 37,700). Based on sequences of seven species of bacterial luciferase,[57] the α subunits are better conserved (54 to 88% identity) than the β subunits (45 to 77% identity). Also, α and β are believed to arise from gene duplication, consistent with the ≥30% sequence identity between the two subunits. Although there are considerable sequence identities among the α subunits and among the β subunits, interspecies hybrids of the two types of luciferase subunits do not always yield active enzyme[58–61] (Table 136.1). Some inconsistent results were reported for the hybrids consisting of the *V. harveyi* α and the β from *V. fischeri*, *P. phosphoreum*, and *Photobacterium leiognathi*. In general, the β subunit of the *V. harveyi* luciferase seems to be more specific for the counter-α subunit in forming an active enzyme. The signal for this higher degree of specificity was shown to come from the *N*-terminal segment of the *V. harveyi* β.[61]

The α and β subunits can be separated chromatographically under partial denaturing conditions and can be renatured after isolation. Alternatively, the two subunits can be expressed individually using recombinant plasmids harboring a single *luxA* or *luxB* gene. Individual α and β are reported to be active in bioluminescence, at levels about four to five orders of magnitude lower than that of the αβ dimer.[62] The active species were identified to be α monomer and β_2 dimer.[63] The existence of β_2 homodimer was observed more than 30 years ago for the *V. fischeri*[64] and *V. harveyi*[48] luciferases. In the latter case, the homodimer was initially referred to as α_2-based chromatographic behavior and was later reclassified as β_2 based on subunit size to be consistent with the now widely accepted criterion for luciferase subunit

classification. In the absence of α, the dissociation constant of β_2 was estimated to be 10^{-16} M at 18°C.[65] The αβ native luciferase requires one $FMNH_2$[66] and one aldehyde[40,67] as substrates. As mentioned above, *V. harveyi* αβ luciferase has a second aldehyde inhibitor site. It is highly intriguing that *V. harveyi* α and β_2 each also has one $FMNH_2$ site, one aldehyde substrate site, and one aldehyde inhibitor site.[63] How α and β_2 are able to maintain the same binding stoichiometry for substrates and aldehyde inhibitor as that of the native αβ, and why αβ is four to five orders of magnitude higher in bioluminescence activity than α and β_2 are important questions that remain to be answered. More recently, the *V. harveyi* α was also shown to undergo a dimerization with a dissociation constant of 15 μ*M* at 18°C.[68]

A major advancement is the elucidation of the structure of *V. harveyi* luciferase, at 2.4 Å[69] and 1.5 Å resolution,[70] with key structural features summarized and discussed.[71] Each subunit assumes a $(\beta/\alpha)_8$ barrel structure, originally shown for the structure of triosephosphate isomerase (TIM).[72] There are considerable structural similarities between the α and β subunits; the main chains of these two subunits show good superposition.[69] The structure of *V. harveyi* luciferase β_2 was also solved.[73,74] The four *C*-terminal residues (321–324) of β that are not resolved in the original αβ structure were determined. In general, the secondary and tertiary structures of β_2 are quite similar to those of αβ. The intersubunit areas for β_2 and αβ are also similar, except that the former is smaller. The two subunits in β_2 are highly homologous but not identical in structure; the root-mean-square difference between the main β chains in β_2 is 0.45 Å.[73] A possible FMN site in β_2 is discussed.[73]

In *P. leiognathi* and *P. phosphoreum*, a nonfluorescent protein (NFP) is coded by the *luxF* gene. NFP has 16 and 30% sequence identities with, respectively, the α and β subunits of the *P. leiognathi* luciferase. The function of NFP is still unknown, but the structure of NFP from *P. leiognathi* was determined.[75,76] It is a homodimer and is homologous to luciferase in folding. However, one β strand and three α helices are missing in comparison with a typical $(\beta/\alpha)_8$ barrel protein. Moreover, each monomer binds two molecules of an unusual FMN, in which the C6 of the flavin isoalloxazine ring is covalently linked to the C3′ of a myristic acid. It was cautioned that the mode of flavin binding by NFP is likely not representative of the flavin site in luciferase.[70] Other TIM barrel flavoproteins include old yellow enzyme,[77] glycolate oxidase,[78] flavocytochrome b_2,[79] trimethylamine oxidase,[80] and dihydroorotate dehydrogenase.[81] These enzymes all have a bound FMN cofactor. In contrast, bacterial luciferase does not contain any flavin cofactor. Instead, it utilizes $FMNH_2$ as a substrate. Luciferase also contains a nonprolyl *cis* peptide bond between A74 and A75.[70] Recently, methylenetetrahydromethanoprotein reductase (Mer) was shown to be most similar to luciferase in a three-dimensional structure.[82] Mer exists as a homodimer or tetramer consisting of two loosely associated dimers. Despite a relatively low sequence identity of 22%, the general folding of the Mer dimer is similar to luciferase αβ or β_2. The subunit interface of Mer is related to that of luciferase αβ. Mer does not have any bound flavin prosthetic group and requires a 5-deazaflavin (namely, F_{420}) as substrate. Moreover, Mer also has a nonprolyl *cis* peptide bond at a location equivalent to that in luciferase. However, the structure of the presumed active site in Mer is significantly different from the equivalent site in luciferase. This is the first example of a flavin-dependent enzyme that shows a high degree of structural similarity to luciferase. Thus far, in the family of proteins that contain a bound flavin prosthetic group or require flavin as a cofactor or substrate, bacterial luciferase remains unique in its ability to catalyze a light-emitting reaction.

Active Site and Structure–Function Relationships

Active Site

Luciferase structure was determined without any bound flavin or aldehyde substrate or specific inhibitor. Hence, the exact structural features of the active site remain to be established. However, the general location of the luciferase active site was postulated to be in a pocket next to the *C*-terminal end of the β barrel in the α subunit.[69,70] This postulation is based on three considerations. First, a phosphate or sulfate is bound to the α subunit. The position of the bound phosphate is proposed to correspond to the phosphate moiety of FMN.[69] Second, the proposed luciferase active site pocket is extrapolated from the fact that all $(\beta/\alpha)_8$ barrel enzymes have their active site at the *C*-terminal end of the β barrel. Third,

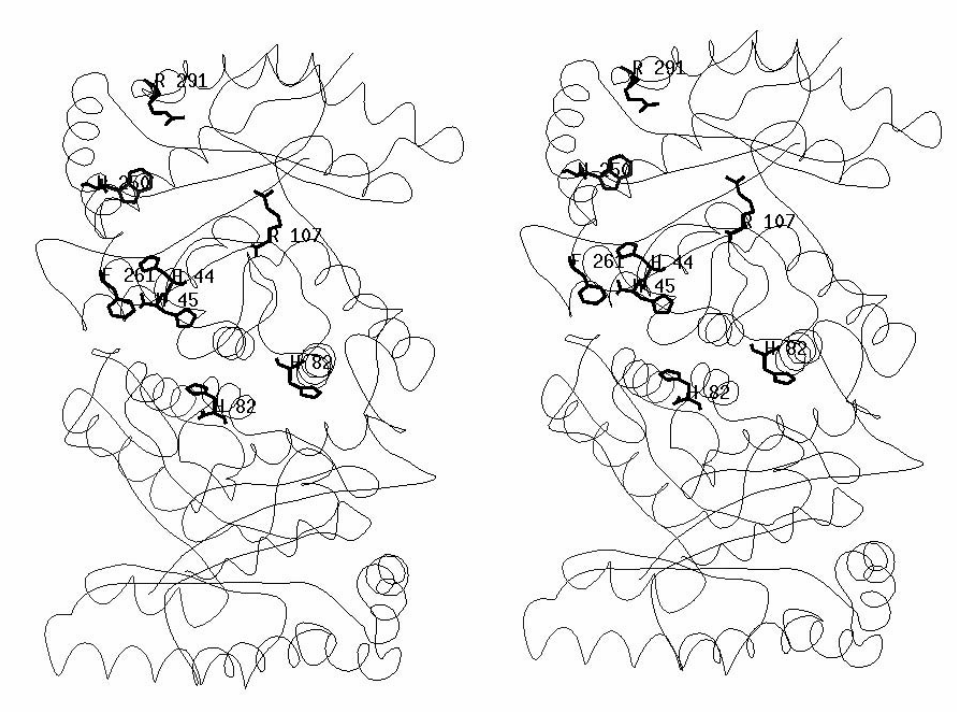

FIGURE 136.1 Proposed luciferase active site and some critical residues. The structure of luciferase is based on the coordinates from the Protein Data Bank file 1LUC.[70] The α subunit is at the top, and the β subunit is at the bottom.

a nonprolyl *cis* peptide bond connecting A74 and A75 is found in luciferase α subunit. The existence of nonprolyl *cis* peptide bond is generally rare, and such a bond is usually critical in positioning key residues required for ligand binding or catalysis. In the case of luciferase, this *cis* peptide bond is at the end of β_3 at the *C*-terminal end of the β barrel. This proposed luciferase active site location is generally supported by computational modeling and experimental results. Figure 136.1 shows a stereo view of this proposed active site pocket and some of the critical residues.

Critical Residues on α

On the same assumption that the bound phosphate or sulfate corresponds to the phosphate moiety of bound FMN, computer models for the FMN binding and aldehyde binding were recently reported.[83] The FMN site in this model is consistent with the active site pocket proposed earlier. It should be noted, however, that the modes of FMN and $FMNH_2$ binding are likely to have some differences. The α-bound phosphate or sulfate interacts with αR107 through a slat linkage.[69] This αR107 was mutated to alanine, serine, and glutamate, and the resulting luciferase variants were characterized with respect to K_m for decanal, $FMNH_2$, and reduced riboflavin in low (0.01 or 0.05 *M*) and high (0.3 *M*) phosphate buffers.[84] Results are consistent with a critical role of αR107 in interacting with the phosphate group of $FMNH_2$. The αW250 was also shown by mutagenesis study to be important in interactions with the flavin isoalloxazine ring and aldehyde.[85]

Chemical modifications of the αC106 (not shown in Figure 136.1) result in luciferase inactivation. This residue is believed to be at or near the aldehyde inhibitor site[41] but is not essential to the binding of $FMNH_2$ or decanal[67] or catalysis.[86,87]

Mutations of five conserved histidine residues (at Positions 44, 45, 82, 224, and 285) on the α were shown to result in markedly different degrees of luciferase inactivation.[88] Residues αH44 and αH45 are particularly critical; their mutations can individually result in four to six orders of magnitude of activity reduction. Although αH44 and αH45 are adjacent residues, they are associated with different functions.

TABLE 136.2 Relative Yields of Reaction Intermediates and Light Output by Luciferase Mutants in Comparison with Wild-Type *V. harveyi* Luciferase

	Relative Yield (= Mutant/Wild Type)								
Enzyme	Φ	=	Y_{II}	×	Y_{III}	×	$Y_{IV}+\bullet \times Y_{IV^*}$	×	Φ_{IV^*}
αF261D	1.0×10^{-5}		0.42		~1		0.1		$\sim 2 \times 10^{-4}$
αG275P	2.4×10^{-4}		0.73		~1		0.2		$\sim 2 \times 10^{-3}$

αH45 is important to the formation of the catalytically active 4a-hydroperoxyFMNH Intermediate II.[14] On the other hand, the extremely low activity of the luciferase αH44A variant can be rescued by exogenously added imidazole or simple amines. Hence, αH44 of luciferase was identified as a catalytic base.[89] Moreover, αH44 participates in the catalysis at a point subsequent to the formation of Intermediate II. Conceivably, αH44 could function in the abstraction of a proton from Intermediate III from the boxed or circled position (Scheme 136.2). In addition, theoretical calculation indicates that the conversion of HF-4a-OO^- to HF-4a-OOH is barrier free.[10] However, the former should be the active species in attacking aldehyde to form Intermediate III. αH44 could also be required to maintain Intermediate II in the HF-4a-OO^- form. Thus far, αH44 is the only case for which a catalytic residue was identified for bacterial luciferase.

Residues 257–291 of the luciferase α subunit are a highly conserved, protease labile, and disordered loop. In the 1.5 Å structure of luciferase, residues between αF261 and αR291 within this loop are not resolved (Figure 136.1). Also, the 29-residue segment from α258 to α286 is not found in the β sequence. This luciferase loop region is next to the opening of the proposed luciferase active site pocket and was postulated to act as a shield for catalytic intermediates.[71] This postulation is supported by a mutagenesis study using a luciferase variant in which the 29-residue disordered loop is deleted from the α subunit.[90] This mutant retains the ability to bind substrates and to catalyze the normal luciferase chemical reaction with an efficiency similar to that of the wild-type luciferase. However, the bioluminescence quantum yield is about two orders of magnitude lower. In a more thorough mutagenesis study,[91] conserved residues αG284 and, particularly, αF261 and αG275 in this loop were found to be critical to luciferase activity. Moreover, the 10^{-5} activity of αF261D can be gradually restored when the side chain increases in size and hydrophobicity as shown by αF261S, αF261A, and αF261Y. Also, the greatly reduced activity of αG275P can be compensated by changing the side chain to a smaller and more flexible residue, as shown by αG275F, αG275I, and αG275A.

The bioluminescence quantum yield (Φ) of luciferase can be expressed as in Equation 136.3:

$$\Phi = Y_{II}\, Y_{III}\, Y_{IV}+\bullet\, Y_{IV^*}\, \Phi_{IV^*} \tag{136.3}$$

where each *Y* is the yield of a particular intermediate (as designated by the subscript) from its immediate precursor intermediate and Φ_{IV^*} is the quantum yield of the excited emitter. Mutants αF261D and αG275P were examined in detail[91] according to Equation 136.3 on the basis of relative yield, defined as the ratio of the yield of mutant over that of the wild-type luciferase (Table 136.2). The quantum yield (Φ) is based on (bioluminescence peak intensity)/(light decay rate). Yields of Intermediate II were determined by stopped-flow measurements. Yields of Intermediate III are estimated as (light decay rate)/[(light decay rate) + (dark decay rate of II)]. The light decay rate is used in place of the true rate for III formation from II. The two rates should be the same if the III formation is rate limiting in the overall reaction of light emission. Otherwise, the III formation rate will be faster than the light decay rate. Hence, the yield of III determined as stated above is a lower limit of the true value. Individual $Y_{IV}+\bullet$ and Y_{IV^*} values cannot be determined, but the overall yield of these two intermediates can be estimated from the yield of carboxylic acid from aldehyde. An important finding from such analyses is that the predominant factor in the reduction of bioluminescence activities of αF261D and αG275P is the three to four orders of magnitude reductions of the emission quantum yields of the excited emitter (Φ_{IV^*}). In comparison with a $\Phi_{IV^*} = 0.18$ for the wild-type emitter,[44] the fluorescence quantum yields of free 4a-hydroxyflavin models are four orders of magnitude lower[29] but can be enhanced by freezing or a hydrophobic environment.[92]

Clearly, the emission quantum yield of excited 4a-hydroxyflavin is highly sensitive to binding by luciferase. As an important demonstration, the fluorescence quantum yield of a 5-decyl-4a-hydroxyFMN model was weak but could be enhanced to 0.08 with a λ_{max} at 440 nm upon binding to luciferase.[93] Our mutagenesis study indicates that a major function of αF261 is to maintain a high degree of hydrophobicity of the luciferase active site so that the bound emitter can undergo a highly efficient emission relaxation. We also propose that αG275 is important in keeping the α262-α290 loop mobile. Possibly, the loop assumes an open conformation in the resting state but will change to a closed conformation to block the opening of the active site pocket during catalysis. This closed conformation can conceivably retard the dark decay of II, enhance the yield of III, and, most importantly, enhance the emission quantum yield of IV*.

Critical Residues on β and Intersubunit Communication

Although αβ dimer is required for the high efficiency of bioluminescence of luciferase, the specific function of β is not clear. Earlier results indicate that β is important in keeping luciferase in a thermally stable form[94,95] or in involving substrate binding.[58,96] In a later site-specific mutagenesis study, mutations of the conserved βH81 and βH82 to several other residues resulted in decreases in V_{max} by about one to two orders of magnitude and decreases in $V_{max}/K_{m,flavin}$ by one to three orders of magnitude.[97] These decreased bioluminescence activities can be correlated with lower yields of II, lower yields of IV*, and enhanced quenching of the emitter IV*. This is the first demonstration that mutations of a specific single residue in β can substantially decrease the luciferase activity. Moreover, in comparison with the wild-type luciferase, αH82K and βH82K were associated with higher values of $K_{m,flavin}$ and increased rates of urea or thermal inactivation. Interestingly, these adverse effects of αH82K and βH82K mutations were compensated to various degrees by the double mutation of βH82D and αH82D, respectively. Hence, it was demonstrated[97] that communication exists between α and β subunits with respect to structural and functional information. The choice of αH82 and βH82 for such mutational studies was based on sequence analysis. The x-ray structure of luciferase[69,70] later revealed that βH82 and αH82 are close to the luciferase subunit interface (Figure 136.1). Recently, protein equilibrium unfolding studies were carried out using luciferase variants containing mutations of residues near the subunit interface.[98] Results obtained with βH81A, βH82A, and αA81H again show that β is able to communicate structural information to α.

Acknowledgments

The author wishes to thank his previous and present group members and collaborators. The author also acknowledges the support of Grant GM25953 from the National Institutes of Health and Grant E-1030 from the Robert A. Welch Foundation.

References

1. Tu, S.-C., Bacterial bioluminescence: biochemistry, in *CRC Handbook of Organic Photochemistry and Photobiology*, Horspool, W.M. and Song, P.-S., Eds., CRC Press, Boca Raton, FL, 1995, p. 1587.
2. Tu, S.-C., Reduced flavin: donor and acceptor enzymes and mechanisms of channeling, *Antioxid. Redox Signal.*, 3, 881, 2001.
3. Hastings, J.W. and Gibson, Q.H., Intermediates in the bioluminescent oxidation of reduced flavin mononucleotide, *J. Biol. Chem.*, 238, 2537, 1963.
4. Mitchell, G. and Hastings, J.W., The effect of flavin isomers and analogues upon the color of bacterial bioluminescence, *J. Biol. Chem.*, 244, 2572, 1969.
5. Eberhard, A. and Hastings, J.W., A postulated mechanism for the bioluminescent oxidation of reduced flavin mononucleotide, *Biochem. Biophys. Res. Commun.*, 47, 348, 1972.
6. Hastings, J.W., Balny, C., LePeuch, C., and Douzou, P., Spectral properties of an oxygenated luciferase-flavin intermediate isolated by low-temperature chromatography, *Proc. Natl. Acad. Sci. USA*, 70, 3468, 1973.

7. Kurfürst, M., Ghisla, S., and Hastings, J.W., Characterization and postulated structure of the primary emitter in the bacterial luciferase reaction, *Proc. Natl. Acad. Sci. USA*, 81, 2990, 1984.
8. Eckstein, J.W., Hastings, J.W., and Ghisla, S., Mechanism of bacterial bioluminescence: 4a,5-dihydroflavin analogs as models for luciferase hydroperoxide intermediates and the effect of substitutions at the 8-position of flavin on luciferase kinetics, *Biochemistry*, 32, 404, 1993.
9. Vervoort, J., Müller, F., O'Kane, D.J., Lee, J., and Bacher, A., Bacterial luciferase: a carbon-13, nitrogen-15, and phosphorus-31 nuclear magnetic resonance investigation, *Biochemistry*, 25, 8067, 1986.
10. Wada, N., Sugimoto, T., Watanabe, H., and Tu, S.-C., Computational analysis of the oxygen addition at the C_{4a} site of reduced flavin in the bacterial luciferase bioluminescence reaction, *Photochem. Photobiol.*, 70, 116, 1999.
11. Mager, H.I.X., Sazou, D., Liu, Y.H., Tu, S.-C., and Kadish, K.M., Reversible one-electron generation of 4a,5-substituted flavin radical cations: models for a postulated key intermediate in bacterial bioluminescence, *J. Am. Chem. Soc.*, 110, 3759, 1988.
12. Merényi, G. and Lind, J., Chemistry of peroxidic tetrahedral intermediates of flavin, *J. Am. Chem. Soc.*, 113, 3146, 1991.
13. Merényi, G., Lind, J., Mager, H.I.X., and Tu, S.-C., Properties of 4a-hydroxy-4a,5-dihydroflavin radicals in relation to bacterial bioluminescence, *J. Phys. Chem.*, 96, 10528, 1992.
14. Li, H., Ortego, B.C., Maillard, K.I., Willson, R.C., and Tu, S.-C., Effects of mutations of the αHis45 residue of *Vibrio harveyi* luciferase on the yield and reactivity of the flavin peroxide intermediate, *Biochemistry*, 38, 4409, 1999.
15. Cho, K.W., Tu, S.-C., and Shao, R., Fluorescent polyene aliphatics as spectroscopic and mechanistic probes for bacterial luciferase: evidence against carbonyl product from aldehyde as the primary excited species, *Photochem. Photobiol.*, 57, 396, 1993.
16. Branchaud, B.P. and Walsh, C.T., Functional group diversity in enzymatic oxygenation reactions catalyzed by bacterial flavin-containing cyclohexanone oxygenase, *J. Am. Chem. Soc.*, 107, 2153, 1985.
17. Ahrens, M., Macheroux, P., Eberhard, A., Ghisla, S., Branchaud, B.P., and Hastings, J.W., Boronic acids as mechanistic probes for the bacterial luciferase reaction, *Photochem. Photobiol.*, 54, 295, 1991.
18. McCapra, F., Mechanisms in chemiluminescence and bioluminescence — unfinished business, in *Bioluminescence and Chemiluminescence. Molecular Reporting with Photons*, Hastings, J.W., Kricka, L.J., and Stanley, P.E., Eds., John Wiley & Sons, New York, 1997, p. 7.
19. Schuster, G.B., Chemiluminescence of organic peroxides. Conversion of ground-state reactants to excited-state products by the chemically initiated electron-exchange luminescence mechanism, *Acc. Chem. Res.*, 12, 366, 1979.
20. Mager, H.I.X. and Addink, R., On the role of some flavin adducts as one-electron donors, in *Flavins and Flavoproteins*, Bray, R.C., Engel, P.C., and Mayhew, S.G., Eds., Walter deGruyter, Berlin, 1984, p. 37.
21. Macheroux, P., Ghisla, S., Kurfürst, M., and Hastings, J.W., Studies on the bacterial luciferase reaction: isotope effects on the light emission. Is a 'CIEEL' mechanism involved?, in *Flavins and Flavoproteins*, Bray, R.C., Engel, P.C., and Mayhew, S.G., Eds., Walter deGruyter, Berlin, 1984, p. 669.
22. Mager, H.I.X. and Tu, S.-C., One-electron transfers in flavin systems: relevance to the postulated CIEEL mechanism in bacterial bioluminescence, in *Flavins and Flavoproteins*, Edmondson, D.E. and McCormick, D.B., Eds., Walter deGruyter, Berlin, 1987, p. 583.
23. Tu, S.-C., Mager, H.I.X., Shao, R., Cho, K.W., and Xi, L., Mechanisms of bacterial luciferase and aromatic hydroxylases, in *Flavins and Flavoproteins*, Curti, B., Ronchi, S., and Zanetti, G., Eds., Walter deGruyter, Berlin, 1991, p. 253.
24. Mager, H.I.X. and Tu, S.-C., Chemical aspects of bioluminescence, *Photochem. Photobiol.*, 62, 607, 1995.
25. Catalani, L.H. and Wilson, T., Electron transfer and chemiluminescence. Two inefficient systems: 1,4-dimethoxy-9,10-diphenylanthracece peroxide and diphenoyl peroxide, *J. Am. Chem. Soc.*, 111, 2633, 1989.

26. Wilson, T., Comments on the mechanisms of chemi- abd bioluminescence, *Photochem. Photobiol.*, 62, 601, 1995.
27. Mager, H.I.X. and Tu, S.-C., Spontaneous formation of flavin radicals in aqueous solution by coproportionation of a flavinium cation and a flavin pseudobase, *Tetrahedron*, 44, 5669, 1988.
28. Tu, S.-C., Oxygenated flavin intermediates of bacterial luciferase and flavoprotein aromatic hydroxylases: enzymology and chemical models, in *Advances in Oxygenated Processes*, Vol. 3, Baumstark, A.L., Ed., Jai Press, Greenwich, 1991, p. 115.
29. Kaaret, T.W. and Bruice, T.C., Electrochemical luminescence with N(5)-ethyl-4a-hydroxy-3-methyl-4a,5-dihydrolumiflavin. The mechanism of bacterial luciferase, *Photochem. Photobiol.*, 51, 629, 1990.
30. Macheroux, P., Eckstein, J., and Ghisla, S., Studies on the mechanism of bacterial bioluminescence. Evidence compatible with a one electron transfer process and a CIEEL mechanism in the luciferase reaction, in *Flavins and Flavoproteins*, Edmondson, D.E. and McCormick, D.B., Eds., Walter deGruyter, Berlin, 1987, p. 613.
31. Eckstein, J.W. and Ghisla, S., On the mechanism of bacterial luciferase. 4a,5-Dihydroflavins as model compounds for reaction intermediates, in *Flavins and Flavoproteins*, Curti, B., Ronchi, S., and Zanetti, G., Eds., Walter deGruyter, Berlin, 1991, p. 269.
32. Wada, N., Hastings, J.W., and Watanabe, H., Superoxide anion reacts with enzyme intermediate in the bacterial luciferase reaction competitive with intramolecular electron transfer, *J. Biolumin. Chemilumin.*, 12, 15, 1997.
33. Raushel, F.M. and Baldwin, T.O., Proposed mechanism for the bacterial bioluminescence reaction involving a dioxirane intermediate, *Biochem. Biophys. Res. Commun.*, 164, 1137, 1989.
34. Francisco, W.A., Abu-Soud, H.M., DelMonte, A.J., Singleton, D.A., Baldwin, T.O., and Raushel, F.M., Deuterium kinetic isotope effects and the mechanism of the bacterial luciferase reaction, *Biochemistry*, 37, 2596, 1998.
35. Cho, K.-W. and Lee, H.-J., Nature of high energy intermediate involved in the bioluminescence reaction catalyzed by bacterial luciferase, *Korean Biochem. J.*, 17, 1, 1984.
36. Matheson, I.B.C., Lee, J., and Müller, F., Bacterial bioluminescence: spectral study of the emitters in the *in vitro* reaction, *Proc. Natl. Acad. Sci. USA*, 78, 948, 1981.
37. Kurfürst, M., Macheroux, P., Ghisla, S., and Hastings, J.W., Isolation and characterization of the transient, luciferase-bound flavin-4a-hydroxide in the bacterial luciferase reaction, *Biochim. Biophys. Acta*, 924, 104, 1987.
38. Lee, J., O'Kane, D.J., and Gibson, B.G., Bioluminescence spectral and fluorescence dynamics study of the interaction of lumazine protein with the intermediates of bacterial luciferase bioluminescence, *Biochemistry*, 28, 4263, 1989.
39. Lee, J., Wang, Y., and Gibson, B.G., Electronic excitation transfer in the complex of lumazine protein with bacterial bioluminescence intermediates, *Biochemistry*, 30, 6825, 1991.
40. Holzman, T.F. and Baldwin, T.O., Reversible inhibition of the bacterial luciferase catalyzed bioluminescence reaction by aldehyde substrate: kinetic mechanism and ligand effects, *Biochemistry*, 22, 2838, 1983.
41. Lei, B., Cho, K.W., and Tu, S.-C., Mechanism of aldehyde inhibition of *Vibrio harveyi* luciferase. Identification of two aldehyde sites and relationship between aldehyde and flavin binding, *J. Biol. Chem.*, 269, 5612, 1994.
42. Hastings, J.W. and Balny, C., The oxygenated bacterial luciferase-flavin intermediate. Reaction products via the light and dark pathways, *J. Biol. Chem.*, 250, 7288, 1975.
43. Tu, S.-C., Isolation and properties of bacterial luciferase-oxygenated flavin intermediate complexed with long-chain alcohols, *Biochemistry*, 18, 5940, 1979.
44. Tu, S.-C., Isolation and properties of bacterial luciferase intermediates containing different oxygenated flavins, *J. Biol. Chem.*, 257, 3719, 1982.
45. Becvar, J.E., Tu, S.-C., and Hastings, J.W., Activity and stability of the luciferase–flavin intermediate, *Biochemistry*, 17, 1807, 1978.

46. Hastings, J.W., Tu, S.-C., Becvar, J.E., and Presswood, R.P., Bioluminesce from the reaction of FMN, hydrogen peroxide, and long chain aldehyde with bacterial luciferase, *Photochem. Photobiol.*, 29, 383, 1979.
47. Li, Z. and Meighen, E.A., The turnover of bacterial luciferase is limited by a slow decomposition of the ternary enzyme-product complex of luciferase, FMN, and fatty acid, *J. Biol. Chem.*, 269, 6640, 1994.
48. Hastings, J.W., Weber, K., Friedland, J., Eberhard, A., Mitchell, G.W., and Gunsalus, A., Structurally distinct bacterial luciferases, *Biochemistry*, 8, 4681, 1969.
49. Meighen, E.A. and MacKenzie, R.E., Flavine specificity of enzyme-substrate intermediates in the bacterial bioluminescent reaction. Structural requirements of the flavine side chain, *Biochemistry*, 12, 1482, 1973.
50. Xi, L., Cho, K.W., and Tu, S.-C., Cloning and nucleotide sequences of *lux* genes and characterization of luciferase of *Xenorhabdus luminescens* from a human wound, *J. Bacteriol.*, 173, 1399, 1991.
51. Francisco, W.A., Abu-Soud, H.M., Baldwin, T.O., and Raushel, F.M., Interaction of bacterial luciferase with aldehyde substrates and inhibitors, *J. Biol. Chem.*, 268, 24734, 1993.
52. Abu-Soud, H.M., Clark, A.C., Francisco, W.A., Baldwin, T.O., and Raushel, F.M., Kinetic destabilization of the hydroperoxy flavin intermediate by site-directed modification of the reactive thiol in bacterial luciferase, *J. Biol. Chem.*, 268, 7699, 1993.
53. Shannon, P., Presswood, R.B., Spencer, R., Becvar, J.E., Hastings, J.W., and Walsh, C., A study of deuterium isotope effects on the bacterial bioluminescence reaction, in *Mechanisms of Oxidizing Enzymes*, Singer, T.P. and Ondarza, R.N., Eds., Elsevier/North Holland, Amsterdam, 1978, p. 69.
54. Presswood, R.P. and Hastings, J.W., Steps in the population of the emitter in the bacterial luciferase reaction, *Photochem. Photobiol.*, 30, 93, 1979.
55. Tu, S.-C., Wang, L.-H., and Yu, Y., Applications of deuterium and tritium isotope effects to the elucidation of kinetic mechanisms of flavoprotein hydroxylases, in *Flavins and Flavoproteins*, Edmondson, D.E. and McCormick, D.B., Eds., Walter deGruyter, Berlin, 1987, p. 539.
56. Macheroux, P., Ghisla, S., and Hastings, J.W., Spectral detection of an intermediate preceding the excited state in the bacterial luciferase reaction, *Biochemistry*, 32, 14183, 1993.
57. Meighen, E.A., Molecular biology of bacterial bioluminescence, *Microbiol. Rev.*, 55, 123, 1991.
58. Meighen, E.A. and Bartlet, I., Complementation of subunits from different bacterial luciferases. Evidence for the role of the β subunit in the bioluminescent mechanism, *J. Biol. Chem.*, 255, 11181, 1980.
59. Xi, L. and Tu, S.-C., Construction and characterization of hybrid luciferases coded by *lux* genes from *Xenorhabdus luminescens* and *Vibrio fischeri*, *Photochem. Photobiol.*, 57, 714, 1993.
60. Ruby, E.G., and Hastings, J.W., Formation of hybrid luciferases from subunits of different species of *Photobacterium*, *Biochemistry*, 19, 4989, 1980.
61. Almashanu, S., Gendler, I., Hadar, R., and Kuhn, J., Interspecific luciferase beta subunit hybrids between *Vibrio harveyi*, *Vibrio fischeri* and *Photobacterium leiognathi*, *Protein Eng.*, 9, 803, 1996.
62. Sinclair, J.F., Waddle, J.J., Waddill, E.F., and Baldwin, T.O., Purified native subunits of bacterial luciferase are active in the bioluminescence reaction but fail to assemble into the αβ structure, *Biochemistry*, 32, 5036, 1993.
63. Choi, H., Tang, C.-K., and Tu, S.-C., Catalytically active forms of the individual subunits of *Vibrio harveyi* luciferase and their kinetic and binding properties, *J. Biol. Chem.*, 270, 16813, 1995.
64. Friedland, J. and Hastings, J.W., Nonidentical subunits of bacterial luciferase: their isolation and recombination to form active enzyme, *Proc. Natl. Acad. Sci. USA*, 58, 2336, 1967.
65. Sinclair, J.F., Ziegler, M.M., and Baldwin, T.O., Kinetic partitioning during protein folding yields multiple native states, *Nature Struct. Biol.*, 1, 320, 1994.
66. Becvar, J.E. and Hastings, J.W., Bacterial luciferase requires one reduced flavin for light emission, *Proc. Natl. Acad. Sci. USA*, 72, 3374, 1975.
67. Paquatte, O. and Tu, S.-C., Chemical modification and characterization of the alpha cysteine 106 at the *Vibrio harveyi* luciferase active center, *Photochem. Photobiol.*, 50, 817, 1989.

68. Noland, B.W., Dangott, L.J., and Baldwin, T.O., Folding, stability, and physical properties of the α subunit of bacterial luciferase, *Biochemistry*, 38, 16136, 1999.
69. Fisher, A.J., Raushel, F.M., Baldwin, T.O., and Rayment, I., Three-dimensional structure of bacterial luciferase from *Vibrio harveyi* at 2.4 Å resolution, *Biochemistry*, 34, 6581, 1995.
70. Fisher, A.J., Thompson, T.B., Thoden, J.B., Baldwin, T.O., and Rayment, I., The 1.5-Å resolution crystal structure of bacterial luciferase in low salt conditions, *J. Biol. Chem.*, 271, 21956, 1996.
71. Baldwin, T.O., Christopher, J.A., Raushel, F.M., Sinclair, J.F., Ziegler, M.M., Fisher, A.J., and Rayment, I., Structure of bacterial luciferase, *Curr. Opin. Struct. Biol.*, 5, 798, 1995.
72. Banner, D.W., Bloomer, A.C., Petsko, G.A., Phillips, D.C., Pogson, C.I., Wilson, I.A., Corran, P.H., Furth, A.J., Milman, J.D., Offord, R.E., Priddle, J.D., and Waley, S.G., Structure of chicken muscle triose phosphate isomerase determined crystallographically at 2.5 angstrom resolution using amino acid sequence data, *Nature*, 255, 609, 1975.
73. Tanner, J.J., Miller, M.D., Wilson, K.S., Tu, S.-C., and Krause, K.L., Structure of bacterial luciferase β_2 homodimer: implications for flavin binding, *Biochemistry*, 36, 665, 1997.
74. Thoden, J.B., Holden, H.M., Fisher, A.J., Sinclair, J.F., Wesenberg, G., Baldwin, T.O., and Rayment, I., Structure of the β_2 homodimer of bacterial luciferase from *Vibrio harveyi*: x-ray analysis of a kinetic protein folding trap, *Protein Sci.*, 6, 13, 1997.
75. Moore, S.A., James, M.N.G., O'Kane, D.J., and Lee, J., Crystal structure of a flavoprotein related to the subunits of bacterial luciferase, *EMBO J.*, 12, 1767, 1993.
76. Moore, S.A. and James, M.N., Structural refinement of the non-fluorescent flavoprotein from *Photobacterium leiognathi* at 1.60 Å resolution, *J. Mol. Biol.*, 249, 195, 1995.
77. Fox, K.M. and Karplus, P.A., Old yellow enzyme at 2 Å resolution: overall structure, ligand binding, and comparison with related flavoproteins, *Structure*, 2, 1089, 1994.
78. Lindqvist, Y., Refined structure of spinach glycolate oxidase at 2 Å resolution, *J. Mol. Biol.*, 209, 151, 1989.
79. Xia, Z.X. and Mathews, F.S., Molecular structure of flavocytochrome b_2 at 2.4 Å resolution, *J. Mol. Biol.*, 212, 837, 1990.
80. Lim, L.W., Shamala, N., Mathews, F.S., Steenkamp, D.J., Hamlin, R., and Xuong, N.H., Three-dimensional structure of the iron-sulfur flavoprotein trimethylamine dehydrogenase at 2.4-Å resolution, *J. Biol. Chem.*, 261, 15140, 1986.
81. Rowland, P., Nielsen, F.S., Jensen, K.F., and Larsen, S., The crystal structure of the flavin containing enzyme dihydroorotate dehydrogenase A from *Lactococcus lactis*, *Structure*, 5, 239, 1997.
82. Shima, S., Warkentin, E., Grabarse, W., Sordel, M., Wicke, M., Thauer, R.K., and Ermler, U., Structure of coenzyme F_{420} dependent methylenetetrahydromethanopterin reductase from two methanogenic archaea, *J. Mol. Biol.*, 300, 935, 2000.
83. Lin, L.Y., Sulea, T., Szittner, R., Vassilyev, V., Purisima, E.O., and Meighen, E.A., Modeling of the bacterial luciferase-flavin mononucleotide complex combining flexible docking with structure-activity data, *Protein Sci.*, 10, 1563, 2001.
84. Moore, C., Lei, B., and Tu, S.-C., Relationship between the conserved α subunit arginine 107 and effects of phosphate on the activity and stability of *Vibrio harveyi* luciferase, *Arch. Biochem. Biophys.*, 370, 45, 1999.
85. Li, Z. and Meighen, E.A., Tryptophan 250 on the α subunit plays an important role in flavin and aldehyde binding to bacterial luciferase. Effects of W → Y mutations on catalytic function, *Biochemistry*, 34, 15084, 1995.
86. Baldwin, T.O., Chen, L.H., Chlumsky, L.J., Devine, J.H., and Ziegler, M.M., Site-directed mutagenesis of bacterial luciferase: analysis of the 'essential' thiol, *J. Biolumin. Chemilumin.*, 4, 40, 1989.
87. Xi, L., Cho, K.W., Herndon, M.E., and Tu, S.-C., Elicitation of an oxidase activity in bacterial luciferase by site- directed mutation of a noncatalytic residue, *J. Biol. Chem.*, 265, 4200, 1990.
88. Xin, X., Xi, L., and Tu, S.-C., Functional consequences of site-directed mutation of conserved histidyl residues of the bacterial luciferase α subunit, *Biochemistry*, 30, 11255, 1991.

89. Huang, S. and Tu, S.-C., Identification and characterization of a catalytic base in bacterial luciferase by chemical rescue of a dark mutant, *Biochemistry*, 36, 14609, 1997.
90. Sparks, J.M. and Baldwin, T.O., Functional implications of the unstructured loop in the $(\beta/\alpha)_8$ barrel structure of the bacterial luciferase α subunit, *Biochemistry*, 40, 15436, 2001.
91. Low, J.C. and Tu, S.-C., Functional roles of conserved residues in the unstructured loop of *Vibrio harveyi* bacterial luciferase, *Biochemistry*, 41, 1724, 2002.
92. Ghisla, S., Massey, V., Lhoste, J.-M., and Mayhew, S.G., Fluorescence and optical characteristics of reduced flavins and flavoproteins, *Biochemistry*, 14, 589, 1974.
93. Lei, B. and Tu, S.-C., Modeling the intermediate IV of the luciferase reaction: characterization of the complex of 5-decylFMN-4a-OH with *Vibrio harveyi* luciferase, in *Flavins and Flavoproteins*, Ghisla, S., Kroneck, P., Macheroux, P., and Sund, H., Eds., Agency for Scientific Publications, Berlin, 1999, p. 337.
94. Meighen, E.A., Nicoli, M.Z., and Hastings, J.W., Functional differences of the nonidentical subunits of bacterial luciferase. Properties of hybrids of native and chemically modified bacterial luciferase, *Biochemistry*, 10, 4069, 1971.
95. Cline, T.W. and Hastings, J.W., Mutationally altered bacterial luciferase. Implications for subunit functions, *Biochemistry*, 11, 3359, 1972.
96. Watanabe, H., Hastings, J.W., and Tu, S.-C., Activity and subunit functions of immobilized bacterial luciferase, *Arch. Biochem. Biophys.*, 215, 405, 1982.
97. Xin, X., Xi, L., and Tu, S.-C., Probing the *Vibrio harveyi* luciferase β subunit functionality and the intersubunit domain by site-directed mutagenesis, *Biochemistry*, 33, 12194, 1994.
98. Inlow, J.K. and Baldwin, T.O., Mutational analysis of the subunit interface of *Vibrio harveyi* bacterial luciferase, *Biochemistry*, 41, 3906, 2002.

137

Photobiology of Circadian Rhythms

David E. Somers
Ohio State University

137.1 Introduction

One consequence of the daily rotation of the earth was the evolution of a 24-h-based (circadian) timing mechanism in most organisms. A wide range of behavioral, physiological, and molecular processes is under the control of a circadian clock. In mammals, the wheel-running rhythm in mice and the familiar jet lag experienced by air travelers are both controlled by the circadian clock. Many aspects of human physiology, including core body temperature, oscillate with a near 24 h rhythm.[1] Similarly, *Drosophila* eclosion (emergence from the pupa) and locomotor activity are clock regulated, presumably to optimize survival and energy use under natural conditions. In plants, the circadian clock helps to coordinate the developmental switch from vegetative to reproductive growth that occurs in response to changes in day length. At the cellular level, stomatal cell expansion and contraction oscillates with a 24 h rhythm. The clock also regulates gene expression at the transcriptional and translational levels. These include key photosynthetic genes, which show peak expression near dawn, and entire biosynthetic pathways (e.g., phenylpropanoid biosynthesis), in which the gene expression level of all the key enzymes cycles with identical phase.[2] This phenomenon is seen in the extreme in cyanobacteria, in which the expression of the entire genome is under circadian control.[3] Overall, the circadian clock system can be viewed as having at least two functions. It can allow an organism to anticipate the regular daily changes of light and dark, and it can act as a buffer against random or transitory environmental fluctuations. The former role helps maximize use of predictable and favorable environmental conditions by preparing (through new syntheses or mobilizations) in advance of its actual occurrence. The latter function would guard against being too responsive to a short-lived environmental condition, where resources put into adjusting to the condition would be wasted.

The circadian clock is defined by a number of characteristics.[4] First, the endogenous period is approximately 24 h *(circa*dian). The period becomes exactly 24 h only when a 24 h environmental cycle is imposed on the organism. Within limits, a non-24 h environmental cycle (e.g., 10 h light:10 h dark) can constrain the clock to oscillate with an altered period length (i.e., 20 h). This occurs through a second characteristic, the process of entrainment, whereby the clock is synchronized to the outside world. The primary entraining stimuli are temperature and light. Diurnal oscillations in temperature (high/low) or

0-8493-1348-1/04/$0.00+$1.50

light (light/dark) are the cues (zeitgebers) that adjust the circadian system in each cycle by changing the phase of the oscillation.[4] In some organisms (e.g., *Drosophila*), a short 15 min light pulse can fully reset the phase of the clock, whereas plants often require 3 to 4 h of illumination.

A third, unique, characteristic of circadian rhythms is temperature compensation. Whereas a temperature shift up or down can reset the phase of the clock, this new temperature regime has little effect on endogenous period. Most biochemical processes are sensitive to temperature, with reaction rates doubling or tripling with each 10°C change in temperature ($Q_{10} = 2 - 3$).[5] The Q_{10}s of circadian rhythms lie between 0.8 to 1.4.[6]

The fourth feature, the persistence of rhythmicity in the absence of periodic input, is the most intriguing aspect of circadian biology. Most research focused on identifying clock components and the interactions that allow the maintenance of a self-sustained oscillation in a nonperiodic environment.[7–12]

The current, simplified, working model of the circadian system consists of three components. The input pathway is the signal transduction chain that links the environmental light or temperature variations to the second component, the central oscillator. Without some form of link between the environment and a pacemaker, there is no meaningful time-keeping function of a clock. Similarly, a link from the pacemaker to the overt output processes is the third component of the circadian system.[5,13] The changes in behavior, physiology, or gene expression that are actually being controlled by the clock are considered "outputs," and clearly without a connection between the oscillator and these processes, a clock has no influence.

Recently, molecular analyses of many of the circadian model systems are demonstrating that a simple linear flow from input to oscillator to output is not a realistic view. There is evidence that the oscillator can control the sensitivity of the input pathway, potentially through the circadian modulation of photoreceptor expression.[14–16] This review summarizes the current state of knowledge of circadian photoperception in the five model systems. What is becoming clear in many systems is the close molecular connection between the primary photoperception events and the central oscillator. Other recent reviews on this topic focus on different elements of the circadian photoperception field.[17–20]

137.2 Cyanobacteria

Investigation of the circadian clock in cyanobacteria (*Synechococcus* sp. PCC 7942) came relatively late for the field but then progressed rapidly at the molecular level. This came about largely through the use of promoter-luciferase reporters. It became quickly apparent that the promoters of nearly the entire genome are under circadian regulation, as all random promoterless-luciferase insertions showed robust rhythmic expression.[3] A mutagenic approach screening for period mutants using a clock-controlled promoter-luciferase reporter then identified a three-gene operon, *kai* (*kaiA*, *kaiB*, and *kaiC*) that is responsible for establishing rhythmicity and setting period length. The transcripts of all three cycle robustly in constant light, as do the protein levels of *kaiB* and *kaiC*. None are DNA-binding proteins, and the precise biochemical role for none has been identified. The three proteins can undergo homotypic and heterotypic dimerizations; one period mutation is due to an aberrant KaiA/KaiB interaction. KaiC can autophosphorylate and contains an ATP/GTP binding domain (P-loop motif), which was shown to bind these nucleotides and to cause arrhythmicity when mutated.[21] There are no apparent homologues between the *kai* genes and known clock-associated proteins in eukaryotes. An additional class of proteins, Group 2 σ-factors, is also involved in setting period and phase. Interestingly, expression from only certain promoters are affected when specific factors are knocked out or overexpressed, leading to the conclusion that these σ-factors act as a consortium, via independent timing circuits, to control circadian output as a whole.[22] All evidence suggests that, in comparison to eukaryotes, different genes are involved, and likely a different mechanism evolved in the development of circadian control in cyanobacteria.

Like eukaryotes, light is the primary entraining stimulus in cyanobacteria. Surprisingly, cyanobacteria possess no unequivocal circadian photoreceptors that correspond to the phytochromes, cryptochromes, or *white collar* genes that are part of the circadian signaling system in eukaryotes. However, two components that may be part of an input pathway were identified. SasA is a histidine protein kinase that was

identified as a KaiC interaction partner in a yeast two-hybrid screen. This protein has the primary structure of the sensory component of a two-component sensory kinase system, with the cognate response regulator still unknown. SasA contains a KaiB-like sensory domain, which is sufficient for interactions with KaiC and likely connects to the primary circadian elements through this interaction. Loss of SasA strongly reduces the amplitude of *kai* expression rhythms and shortens the period, whereas overexpression causes arrhythmicity, through suppression of *kaiBC* promoter activity.[23] Growth under light and dark cycles is severely disrupted in *sasA* mutants, suggesting that it may have a role outside of circadian regulation as well. Two models were proposed for the point of action for SasA. One places it acting on the input pathway as an amplifier of circadian phototransduction, because the amplitudes of the oscillations are more light sensitive in the mutant than in the wild type. Alternatively, SasA may act as one of the first elements of the output pathway that also feeds back on the expression of the *kai* gene cluster.[23] In either case, SasA is not an essential element of the central oscillator but a modulator of clock activity.

The second candidate, *cikA* (circadian input kinase), also affects circadian period and output amplitude but is more closely related to previously known phototransduction components. Like *sasA*, inactivation of *cikA* shortens the circadian period of gene expression rhythms (by approximately 2 h), and reduces the amplitude of cyclic gene expression. In addition, *cikA* mutations change the phasing of a subset of rhythms and nearly abolish phase resetting by dark pulses.[24] It is this loss of light-mediated phase resetting coupled with the protein sequence that strongly suggests a role for CikA in the input pathway. CikA is a divergent bacteriophytochrome with characteristic histidine protein kinase motifs and a carboxy terminal response regulator domain. However, it lacks the essential Cys to which the phytochromiblin chromophore normally covalently attaches in plant phytochromes, and an adjacent conserved His residue, to which bilins can bind in bacteriophytochromes.[24] Hence, either CikA does not bind a bilin or it does so in a manner different from that of known proteins. Similarly, the response regulator motif of CikA lacks the characteristic Asp that is the normal phosphotransfer site. Here too, either another residue receives the phosphate, or this motif plays a different, unknown role. Taken together, CikA appears to be a key component of phototransduction input to the circadian oscillator, but its precise function remains unclear.

137.3 Neurospora

The *Neurospora* circadian clock was extensively studied for more than 30 years. Three core elements necessary for sustained function of the system were identified and well characterized. *Frequency* (*frq*) was the first locus defined and proved to be an essential element for robust and sustained circadian cycling. The *frq* protein (FRQ) contains a nuclear localization signal (NLS), a putative helix-turn-helix DNA binding domain, and highly charged domains.[12] The precise biochemical function of FRQ is unclear, but it is involved in transcription activation and in transcription complex disruption, positioning it as a central element of two interlocked feedback loops that comprise the *Neurospora* circadian system.[12] The *white collar-1* (*wc-1*) and the *white collar-2* (*wc-2*) are equally essential, but unlike *frq*, they play important noncircadian roles as well. Both genes were initially identified in genetic screens for blue-light photoperception mutants, the only wavelengths to which *Neurospora* is known to respond. To date, these are still the only two loci that, when either is disrupted, confer photic insensitivity to a wide range of physiological responses. They have long been the best candidates for blue-light photoreceptors and as photoreceptor complexes for circadian entrainment. Loss-of-function mutations in either gene cause arrhythmicity under standard conditions. This suggests a close link between photoperception and clock function. Both proteins are putative transcription factors, containing GATA-type zinc fingers, and they are able to bind promoter regions of the light-inducible *al-3* and *frq* genes.[25,26]

The 54 kDa *wc-2* protein (WC-2) contains a nuclear-targeting domain and a PAS domain.[25,26] Both the mRNA and protein are constitutively expressed, and the polypeptide appears to undergo no circadian phase-dependent modifications,[26] though it is phosphorylated in response to light.[27] The WC-2 PAS domain dimerizes with itself and with WC-1 via its PAS domain, forming hetero- and homodimers *in vitro*[28] and *in vivo*.[26,29] Together, WC-1 and WC-2 form the white collar complex (WCC) in which both proteins appear in a 1:1 stoichiometry.[26,29] This differs from the cellular concentrations of the two

components, in which WC-2 is in significantly greater abundance than WC-1. While FRQ, WC-1, and WC-2 are normally found complexed together, FRQ and WC-1 are unable to associate in the absence of WC-2, leading to the view that WC-2 acts as a scaffold by which FRQ and WC-1 can interact.[30]

WC-1 is a 125 kDa protein that contains a glutamine-rich putative transcription activation domain and two PAS domains. One of the PAS domains is similar (ca. 40% amino acid identity) to the LOV/PAS domain found in the plant blue-light receptors phot1 and phot2.[31] Of these two proteins, phot1 is the best characterized, and purified protein can catalyze blue-light dependent autophosphorylation *in vitro*.[31] Although there is no evidence that WC-1 possesses kinase activity, *in vivo*, it is transiently and progressively phosphorylated in response to light, which appears to facilitate its degradation.[26,27] The LOV/PAS domain in phot1 binds flavin mononucleotide (FMN),[31] and crystallization of this domain showed that it folds to form an FMN binding pocket with a three-dimensional structure bearing strong similarity to previously crystallized PAS domains.[32] By virtue of the high degree of amino acid identity, WC-1 was expected to fold to form a similar structure and possibly bind a flavin as well. This was recently confirmed by two separate approaches. He and colleagues[10] removed the LOV domain from WC-1 and showed that all light responses are lost, including light entrainment of the circadian clock. They further purified the native WC-1/WC-2 (WCC) complex and showed that both molecules associate in a 1:1 stoichiometry and that flavin adenine dinucleotide (FAD) is noncovalently bound to the 200 kDa complex.[29] Interestingly, the WC-1 LOV domain contains an additional nine amino acid insertion, relative to the phototropin LOV domain, which is predicted to extend one region of the flavin-binding pocket. This may serve to accommodate the larger dinucleotide moiety of FAD not found in FMN. In a different study, Froehlich and colleagues[15] used gel mobility shift assays to show that the native WCC can bind specifically to the *frq* promoter. When *in vitro* translated, both components still bind, showing that additional factors are not necessary for the mobility shift. An additional blue-light-induced change in the mobility of the DNA–WCC complex required the presence of FAD, and its addition during the WC-1 translation reaction was sufficient to effect the shift.[25] Together, these two studies conclusively demonstrate that the WCC, specifically WC-1, binds FAD and is the primary blue-light photoreceptor for the circadian clock system in *Neurospora*. This does not exclude the presence of other photoreceptors. A recent report demonstrated residual photoresponses in the *wc-1*, *wc-2*, and the double mutants, suggesting the presence of one or more additional photoreceptors. These responses include the ability to synchronize conidiation in response to light and dark cycles and the light induction of *frq* mRNA.[33]

An additional protein, VIVID (VVD), plays a role in modifying the response of the *Neurospora* circadian clock to light.[34] Remarkably, 50% of the small (20 kDa) VVD polypeptide consists of a PAS/LOV domain, with a high degree of identity to the phototropin and WC-1 LOV domains.[35] The loss-of-function mutant phenotype is characterized by an increased sensitivity to light, and VVD's role appears to be as a clock-regulated repressor of light-regulated genes. The ability of the clock to modulate the effects of light on the clock, known as gating, is also affected by mutations in VVD. Light-induced induction of FRQ and VVD in *vvd* mutants is substantially increased over the circadian time course, and light-induced resetting of the clock, as assessed by changes in the phase-response curve, is significantly altered.[35] One model consistent with these data places VVD as a negative modulator of the WCC, possibly through a dimeric interaction with the WC-1 LOV domain. Given that light, via the WCC, induces VVD expression, this places VVD as a negative feedback regulator of its own expression and as a modulator of light input to the circadian system.[35]

Taken together, the accumulated evidence is that the WCC complex plays the role of the primary photoreceptor of the *Neurospora* circadian clock but is inextricably linked to the function of the clock. In light, the WCC upregulates FRQ, WC-1, and VVD transcription, while FRQ feeds back to block the transcriptional activity of the WCC, thereby downregulating its own transcription. However, FRQ also promotes WC-1 synthesis, indirectly contributing to increased WCC levels, because WC-1 is the limiting partner of the pair. VVD also acts to limit WCC complex activity. The interacting feedback loops of these complex interactions form the core of the clock. What remains to be added are the full temporal and spatial descriptions that sum to a 24 h cycle.

137.4 Plants

Most of the progress in identifying plant photoreceptors and understanding their signal transductions has come from genetic screens for mutations that alter development, such as stem elongation and bending. The best-characterized visible light photoreceptors in plants are the phytochromes, cryptochromes, and phototropins. The phytochromes are large (ca. 120 kDa) polypeptides that reversibly mediate red and far-red light photoperception. There are two empirically determined classes of phytochrome molecules; light-labile and light-stable forms. Phytochrome A (phyA) encodes the light-labile phytochrome, which is degraded rapidly in the presence of light. Four additional genes encode phyB, C, D, and E in *Arabidopsis* and are light-stable molecules. Most of the phytochrome in the plant is phyA and phyB, and mutant analyses confirm that phyC, D, and E are largely additive to the effects of phyB.[36,37]

The two cryptochrome proteins, cry1 and cry2, are related to DNA photolyases. These are blue-light-activated DNA repair enzymes that catalyze the repair of UV-induced thymine dimers in prokaryotes and eukaryotes. Like the photolyases, the cryptochromes have two chromophores, a light-harvesting folate or deazaflavin, and a catalytic flavin adenine dinucleotide (FAD), responsible for the blue-light absorbance and action spectra. The two *Arabidopsis* cry proteins are 51% identical and have distinct, but overlapping, roles in plant development.[38]

The role of the phytochromes and cryptochromes in circadian photoperception was effectively addressed by using null mutations in both classes of photoreceptors in *Arabidopsis*. Fluence-rate response tests in the different mutant backgrounds were used to define the range of light intensities over which each photoreceptor acts. This was possible, because the relationship between light intensity and period in *Arabidopsis* follows Aschoff's rule for diurnal organisms: free-running period increases with decreasing light intensity.[39,40] Relative to wild type, loss of phyB lengthens the period at high-red-light intensities (>5.0 μmol m^{-2} s^{-1}), but under blue light, there is no effect. Conversely, phyA mutants show period lengthening only under low-fluence-red (<1.5 μmol m^{-2} s^{-1}) or blue light (<5.0 μmol m^{-2} s^{-1}).[41] Both results are consistent with other studies showing that the role of phyB is primarily at higher-red-light fluences, and that of phyA is at low-red, far-red, and blue-light intensities.[37] The period of the *phyA phyB* double mutant is consistently 2 to 3 h longer than wild type over a 100-fold range of red-light intensity (1 to 150 μmol m^{-2} s^{-1}). These results demonstrate that the separate domains of high- and low-light intensity over which the two phytochromes operate are additive, and that over some fluence rates (1.5 to 10 μmol m^{-2} s^{-1}), they act redundantly.[42] Triple mutants (*phyA phyB phyD* and *phyA phyB phyE*) still show increased period shortening at high-red-light fluence rates, indicating an overlap with phyB function among the more minor forms of phytochrome.[42]

Parallel studies using *cry1* and *cry2* null mutants under blue and red light outlined the relationship between the two cryptochrome proteins and between the phys and crys, to some extent. A cry1 deficiency lengthens the period by 2 h over a 40-fold range of fluence rates, with the exception of a mid-range (between 4 and 10 μmol m^{-2} s^{-1}), where there is no effect.[41,42] The absence of cry2 has little to no affect on the free-running period in blue light, but the *cry1 cry2* double mutant causes a clear and consistent 3 to 4 h lengthening of period over the entire fluence range tested. The slope of the fluence-rate-response curve in blue light in wild-type plants is shallow, in some experiments it is zero, so the relative contribution of the cryptochromes is difficult to assess: are other blue-light receptors active in the absence of the crys? The *phyA cry1* double mutant tested in white light had period effects only over the same intensity range as the *cry1* mutant, suggesting that the two photoreceptors act in the same pathway. Other evidence showing a physical interaction between phyA and the crys, including a phyA-red-light-dependent phosphorylation of cry1,[19] is consistent with cry1 acting immediately downstream of phyA action. However, a triple *phyA cry1 cry2* mutant would be a desirable combination to further test in blue light. Of the other blue-light photoreceptors, such as the phototropins, only a deficiency in *phot1* (*nph1*) was shown to have no effect on free-running period (D.E. Somers, unpublished data). Although all evidence suggests that phototropins are involved exclusively in phototropisms,[31] multiple mutant combinations between the crys and phototropins might prove to be revealing.

The redundancy of plant photoreceptor input to the clock was also demonstrated using the *phyAphyBcry1cry2* quadruple mutant. In white light, robust leaf movement rhythms were evident, indicating that other photopigments, likely the remaining three phys, are able to sustain sufficient photic input to the oscillator.[43]

Although current evidence suggests that no single photoreceptor or photoreceptor class is an essential element of the plant circadian oscillator, more may be learned about their connection to the clock by examining whether the expressions of these receptors undergo circadian regulation and whether their intracellular localization changes over time. Using a firefly luciferase (luc) reporter, promoter-luc fusions were made with all five *Arabidopsis* phytochromes and both cryptochromes.[14] Most fusions showed a distinct circadian control of promoter activity, with different phases of peak promoter activity. All showed maximal expression during the subjective photoperiod, with the most light-labile of the receptors (phyA and cry2) peaking near subjective dusk. Only the phyC-luc reporter showed no sign of circadian regulation, although *phyC* mRNA was cyclic under LL, indicating circadian regulation at a posttranscriptional level.[14] Interestingly, although this study and others[44] demonstrate the clock-controlled regulation of photoreceptor promoters, there is still no evidence of cyclic changes in global phy or cry protein levels. However, temporal changes in intracellular localization were recently reported using GFP-phytochrome reporters. Under an 8/16 white light/dark cycle, there was a diurnal variation in the number of nuclear GFP speckles seen for four of the GFP–phy fusions. Importantly, there was a clear increase in the number of nuclear speckles in anticipation of lights-on, which increased throughout the light period and subsequently decreased during the dark.[45] This increase in anticipation of lights-on strongly suggests that circadian regulation of photoreceptor nuclear import may play a role in the spatial and temporal localizations of the phytochromes. One inconsistency between the promoter-luc studies and the GFP-phytochrome work lies in phasing. All GFP-phytochromes showed similar timing and kinetics with respect to nuclear import; nuclear accumulation was clearly beginning prior to lights-on. The five phy–luc fusions showed different phasing of maximum expression among them; some phased early in the day (e.g., phyC, D, and E) and others late in the day (e.g., phyA). Higher-resolution studies, conducted throughout the circadian cycle, will be necessary to resolve this discrepancy.

Apart from the photoreceptors, there were few other components implicated in the circadian phototransduction pathway. Most intriguing is the *ZEITLUPE* (*ZTL*) gene family.[46–49] These three closely related proteins (ZTL, FKF1, LKP2; also reported as *ADO* genes[50]) appear to be a special type of F-box protein, a class of polypeptides involved in proteasome-dependent proteolysis.[51] In most F-box proteins, the amino proximal 45 amino acid F-box domain targets the protein for association with an E3 ubiquitin ligase complex, by which ubiquitin moieties are then attached to the substrate associated with the carboxy terminal region of the F-box protein. In this way, F-box proteins act as the physical links between target substrates and ligase complexes. Many F-box proteins lack additional amino terminal domains to the F-box, but the ZTL family contains a LOV/PAS domain. The LOV motif was defined based on similarity to a number of prokaryotic and eukaryotic proteins involved in light, oxygen, and voltage sensing (*LOV*[31]) and is a distinct subgroup of the more general PAS domain.[46] The PAS superfamily can be divided into two fundamental classes: those involved in mediating protein–protein interactions and those primarily involved in environmental sensing.[52] In eukaryotes, the former class is a common motif in clock-related proteins, whereas the latter class, which includes the LOV domain, is found largely in photoreceptors. These include the phototropins in plants[31] and WC-1 in *Neurospora*.[29] The ZTL family LOV domains are 40% identical to the LOV domains of the phototropins and WC-1, strongly suggesting a phototransduction role for these proteins.

At least two of the family members affect circadian period. Loss of function mutations in *ZTL* lengthen the free-running period,[47,50] and overexpression of ZTL (Somers, unpublished) and LKP2[49] cause arrhythmicity. ZTL mutations also affect the response of free-running period to light. The significant increase in period with decreasing light intensity evident in WT plants is greatly accentuated in *ztl* mutants. At low-light intensities, *ztl* loss of function mutations causes a 7 to 8 h period lengthening, compared to a 3 h lengthening at high-light intensities.[47] This light-dependent effect coupled with a demonstrated interaction *in vitro* and in yeast between ZTL and phyB and cry1[50] suggests that this member of the ZTL

gene family may play a critical role in bridging the primary light absorption of the photoreceptors with downstream changes in clock protein abundance. One model of ZTL action would involve control of circadian period through a light-dependent proteolysis of key clock components. This could occur via activation of ZTL activity by direct signaling from the light-activated photoreceptors, or through direct blue-light absorption by ZTL via the LOV domain.

Another likely component of the phototransduction pathway is *ELF3*. Loss of function mutations in *ELF3* (*elf3–1*) result in arrhythmicity under all light conditions but have little effect on cycling in the dark.[53,54] Interestingly, although ELF3 promoter activity and mRNA and protein levels cycle, overexpression does not cause arrhythmicity but only lengthens the period.[53,55] This strongly suggests that ELF3 is not an oscillator component. Instead, evidence suggests that ELF3 acts to negatively modulate light input to the clock. Red- and blue-light phase-response curves (PRC) are altered in *ELF3* mutant and overexpression backgrounds. The *elf3–1* accentuates the amplitude of the phase-response curve (PRC), while ELF3 overexpression blunts the effectiveness of phase resetting relative to wild type. Similarly, rapid light-induced gene expression is increased in *elf3–1* and strongly reduced in the overexpressor.[53] These results, and others testing the circadian phase dependence of the effect of light pulses on weaker alleles of ELF3,[56] support ELF3 as an element of the light input pathway.

The ELF3 polypeptide is novel, giving little clue to its molecular function. However, *in vitro* and in yeast, ELF3 interacts specifically with the *C*-terminus of phyB.[55] This appears to link ELF3 directly to phyB signal transduction, and the phenotypes of the *elf3–1 phyB* double mutant and the *phyB* ELF3 OX plants show that *phyB* is largely epistatic to the ELF3 phenotype in both combinations. Although there have been no reports of cry interactions with ELF3, ELF3 overexpression is more effective in lengthening period under constant blue light, as compared to red light.[53] Together with the PRC results (see above), it is clear that blue-light signaling to the clock is also modulated by ELF3.

The photoperception pathway appears to be connected to the molecular components of the plant circadian oscillator by way of a direct binding of a phyB/PIF3 complex to the promoter of two likely oscillator components, *LHY* and *CCA1*. PIF3 is a basic helix-loop-helix transcription factor identified as a phyB and phyA interaction partner by way of a yeast-two hybrid screen. It binds specifically to a G-box DNA-sequence motif present in various light-regulated gene promoters, including the promoter of *CCA1*.[57] Together with the closely related family member, *LHY*, the CCA1 myb transcription factor is a likely oscillator component. Both genes cause arrhythmicity when overexpressed and shortened periods when knocked out or reduced in expression.[58,59] The double mutant displays poor rhythmicity in constant light (LL) and constant dark (DD), implying an additive and partially redundant function for the two genes.[59,60]. The light-dependent association of phyB with PIF3 at the G-box binding site present in the CCA1 and LHY promoters establishes a direct physical connection between a circadian photoreceptor and the transcriptional machinery driving the expression of a clock gene. The potential for rapid, light-induced changes in phase resetting appears great. However, much remains to be determined, as phase shifting in plants (including *Arabidopsis*) is remarkably recalcitrant to the effects of a brief pulse of light. More commonly, a pulse of light (or dark) on the order of an hour or more is required to obtain stable phase resetting.[53]

137.5 Drosophila

The molecular genetic approach to circadian biology began with a period mutant screen in *Drosophila*.[9] Because much of the research in the field was spearheaded using flies, much of the molecular and biochemical specifics of how the clock functions was worked out in this organism. Four core proteins were identified as essential to the function of the oscillator in flies. Loss of any one of the four genes causes arrhythmicity. The first two, CLOCK (CLK) and CYCLE (CYC), are PAS domain-containing bHLH transcription factors that form a heterodimer to activate the transcription of the other two essential genes, *period (per)* and *timeless (tim)*. Three of the four components cycle at the RNA and protein levels; *cycle* transcription is constitutive. PER and TIM proteins accumulate in the cytoplasm, where they dimerize to facilitate their own nuclear transport. In the nucleus, they act to disrupt the CLK-CYC dimer,

thus turning off their own transcription. Eventual nuclear degradation of PER and TIM releases this repression and CLK-CYC-mediated transcription of both genes begins again, renewing the cycle.[8,9] A second, interlocked loop is also part of the process. Here, CLK is cycling in antiphase with PER and TIM and (with CYC) negatively regulates its own transcription, which is derepressed by PER and TIM.[61]

Key steps in this process are the refining elements that help determine period length. These would be the synthesis and degradation rates of these players, as well as the rates of nuclear translocation. Mutant screens turned up three such modifiers of period. A casein kinase Iε (doubletime) is important in controlling the phosphorylation state and half-life of PER, thereby affecting period length. A second kinase (shaggy) regulates the nuclear translocation of the PER/TIM complex through its effect on TIM phosphorylation.[9]

A third modifier of clock function, cryptochrome (CRY), was also identified in a mutant screen, using a period-luciferase reporter in adult flies. Cryptochrome was identified first in plants many years before as a blue-light photoreceptor that mediates light control of stem elongation (see above).[38] As noted earlier, cryptochromes are structurally closely related to blue-light-activated DNA repair enzymes, the photolyases, but lack photolyase activity. Like the photolyases, they bind two blue-light absorbing chromophores, a flavin (usually FAD), and a pterin (methenyltetrahydrofolate), and may function via an intramolecular energy transfer. Photolyases absorb light via the pterin, which transfers the excitation energy to FAD, which in turn, transfers an electron to the DNA photoproduct, effecting pyrimidine restoration.[62] The *C*-terminal regions of the cryptochromes are the most divergent and are the domains most likely to confer specificity among the crys.[38]

Interestingly, although the cryptochrome mutant, cry^{baby} (cry^{b}), fails to entrain PER and TIM to light and dark cycles, locomotor rhythms are little affected.[63] This discrepancy was clarified when it was discovered that *per* and *tim* cycling persists in a subset of lateral neurons in the cry^{b} mutant. Why these cells remain rhythmic is still not clear, but apparently, their function is necessary to maintain whole fly activity rhythms. Entrainment to temperature cycles was also unaffected in this mutant, suggesting that CRY is not an essential component of the central oscillator. Phase resetting by light pulses was also eliminated in the cry^{b} background, though entrainment to 12/12 L/D cycles was normal. This suggested that light responsiveness was diminished but not eliminated. Further tests used the $norpA^{41}$ mutant, deficient in a phospholipase C (PLC) that functions downstream of the rhodopsin-based visual system, in combination with cry^{b}. These double mutant flies entrained poorly to full 12/12 L/D cycles, indicating that the two photoreceptor systems may work in parallel as part of the phototransduction input to the clock in flies.[63] However, unlike WT flies that become arrhythmic with increasing light intensity, cry^{b} flies allowed to free-run at high-light intensities maintain a period similar to WT flies in constant darkness. Entrainment of these flies might occur via the opsin-based visual system, where locomotor activity driven by light and dark cycles feeds back to reset phase nonphotically.[64]

The molecular role for cryptochrome in the phototransduction pathway appears to be direct. CRY protein interacts directly with TIM and PER in yeast two-hybrid assays and transiently transfected *Drosophila* cell culture (S2 cells).[65,66] CRY interaction with TIM is light dependent and appears to disrupt PER–TIM interactions, possibly by hastening the ubiquitination and degradation of TIM.[65,67] Similarly, CRY and PER interact in yeast two-hybrid assays and S2 cells, and as with its interaction with TIM, requires the *C*-terminus of CRY for nuclear localization.[9] The great proportion of CRY is found in the nucleus, independent of light conditions. PER and TIM appear necessary to effect CRY nuclear accumulation, although light is not required for this interaction. CRY is degraded by light, probably through an intramolecular conformational change that is redox dependent.[67] The cry cycles at the mRNA and protein levels in constant darkness, and in light and dark cycles, CRY cycles particularly robustly, with maximum accumulation during the night.[15] The phase of peak CRY accumulation is similar to TIM, making it likely that CRY mediates light-induced phase resetting through its effect on TIM protein levels. This model is consistent with the notion that CRY is not a component of the oscillator but is simply mediating photic input from the environment. One exception lies in a recent examination of rhythms in olfactory responses in fly antenna, which implies a more central role for CRY in this tissue. In this tissue, temperature entrainment in cryb flies failed in constant dark.[68] Hence, recruitment of molecules for clock function may vary among tissue types.

137.6 Mammals

Unsurprisingly, the mammalian clock is the most complex in terms of the number of molecules that were implicated in its composition. The task of sorting out the function of each player was made only slightly simpler in its basic molecular similarity to the *Drosophila* system. Using mouse as the model system, mammals were found to contain three *PER* genes and two *CRY* genes, in addition to *TIM*, *BMAL/MOP3* (fly *cycle*), and *CLK*. Casein kinase 1ε (*CK1ε*) and a BMAL-like protein, MOP9, were also implicated in mammalian clock function.[69,70,71] However, the functions of some of these proteins are surprisingly different from those in flies. The fundamental transcription-translation autoregulatory negative feedback loop is structured the same, but some roles were swapped. A CLK/BMAL bHLH transcription factor heterodimer drives rhythmic transcription of the *cry* and *per* genes, rather than of *timeless* and *per*, as in flies. The PER–TIM pairing, so essential to the *Drosophila* clock, is replaced by PER–CRY interactions in mouse. CRY acts to repress further CLK/BMAL activity, while PER (PER2) promotes BMAL1 transcription.[8–11] Numerous combinations of CRY/CRY, CRY/PER, and PER-PER dimers can form *in vitro*, but PER2 appears to be the critical PER family member, based on the mutant phenotype.[10,11] Unlike in flies, the apparent mammalian homologue to TIMELESS may have little role in the clock.[11] And unlike in flies, both *Cry* genes appear to encode key oscillator components and are less likely to be acting as photoreceptors. This became clear from the phenotypes of *Cry1* and *Cry2* single- and double-knockout mice. Loss of CRY2 lengthens the free-running period in constant darkness and causes an increased responsivity to light during the subjective night. Conversely, *Cry1* mutant mice have a shorter period. Surprisingly, the double mutant is arrhythmic in constant darkness, a result not to be expected from the elimination of components involved only in light perception.[10,11] Since the findings of the cry^b mutant left little doubt of the importance of CRY in circadian photoperception in flies, the *cry1cry2* double mutant put the mammalian field in a quandary over just what mediates phototransduction in mice.

This result came on the heels of a long debate over the role of opsins in mammalian circadian photoperception. Eyeless mice are unable to entrain, clearly localizing the site of primary photoperception to this organ.[17] Retinal degenerate, coneless (*rd/rd cl*) mice, which lack all rod and cone photoreceptors but develop otherwise normal eyes, entrain entirely normally, implying that known opsins, and the retinal-based vision system in general, play no significant role in circadian photoperception. However, the "opsin option" was recently revived through the discovery of a number of novel opsins in vertebrates.[17] Relevant to mammals, melanopsin has become the strongest candidate photopigment for circadian phototransduction. It is localized to a subset of retinal ganglion cells (RGC) that are anatomically distinct from the regions lost in *rd/rd cl* mice and reside in RGC that project into the SCN and can mediate entrainment.[72–76] Melanopsin knockout mice will be key to resolving the question of its role in photoentrainment.

The close association of cryptochromes with the molecular machinery of the mammalian oscillator does not preclude an additional role as photoreceptor. Loss of cycling in the *cry1cry2* double mutant eliminates circadian output, making it difficult to assess a photic role for these proteins. However, *cry1cry2* double-mutant mice still respond behaviorally to light and dark (LD) cycles and *Per2* expression cycles in LD and responds acutely to light pulses in this background.[77] These responses are also present in *rd* mice, but the triple-mutant (*rdcry1cry2*) mice were nearly behaviorally arrhythmic under LD cycles, and light-induced c-*fos* transcription in the suprachiasmatic nucleus (SCN) was also markedly reduced. These results suggest parallel, partially redundant roles for the two classes of molecules and indicate that cryptochrome may function in two anatomically distinct places: in the retina and in the SCN.[78]

137.7 Conclusions

The diversity of components involved in circadian photoperception across the five systems described here appears to reflect the degree of evolutionary distance among these organisms. To the extent that the molecular bases are known, there is no one element that is commonly used across all systems. Clearly, the metazoans (flies and mammals) share a great number of components, and the molecular construction

of the two systems is similar enough to have allowed each to benefit from the most recent discovery of the other. However, even here, the *cry*^{b} mutant in flies misled the field into assuming that *cry* would play the same role in mammals.

What is nearly common, and perhaps surprising, is the extremely close connection between photoperception and the molecular components of the oscillator. Signal transduction cascades do not appear to play a major role in circadian phototransduction. In three of the five systems, photoreceptors physically associate with clock proteins or with the promoters of these proteins. Both in plants and in *Neurospora*, the phyB/PIF3-*CCA1* promoter complex and the WCC-*frequency* promoter interaction, respectively, provide a direct link between light perception and the gene transcription of clock components. In the case of plants, the importance of this interaction to circadian entrainment was not fully tested. For example, does the loss of PIF3 affect circadian period? In addition, other phytochromes are known to affect period, and their ability to signal through PIF3 is unclear. Finally, a direct molecular link between the cryptochromes, the other class of plant circadian photoreceptor, and the clock is still absent. In contrast, the WCC in *Neurospora* appears to be the primary molecular connection between light and the circadian oscillator, despite recent evidence for an additional phototransduction pathway.[33]

In flies, cryptochrome is clearly involved in mediating light-induced disruption of the TIM/PER complex. However, the story may not end here. Interestingly, the recent suggestion that cryptochrome in peripheral oscillators (antenna) may play a nonphotic role in clock function in the fly, is analogous to the clear nonphotic role of CRY as a key oscillator component that normally associates with PER in mammals.

Interestingly, it is the two systems at the opposite ends of complexity, cyanobacteria and mammals, where a molecular bridge between phototransduction and the clock is still unknown. The phytochrome-related *cikA* is a strong candidate as the primary cyanobacterial photoreceptor, but a conclusive molecular partnership with the Kai proteins or other clock component is still absent. In mammals, the physical separation between the primary photoreceptor site, the eye, and the brain-localized central pacemaker in the SCN, dictates that a direct molecular interaction between photoreceptive molecules and the oscillator will not be found. However, the separation is likely based on the necessary consequences derived from the development of a large, highly specialized body plan, where direct light penetration to the master oscillator is not possible. The relative light transparency of the organisms of the other four systems still allows for a direct link between photoperception and the mechanism of the central oscillator. This and the fact that cryptochrome is involved in the molecular machinery of the circadian system in some way in all eukaryotes studied to date, also suggests that the progenitor molecule of circadian photoperception may have been a derivative of an early light-sensitive DNA repair molecule: the cry-like DNA photolyases.[15,79]

Acknowledgment

This work was supported by the NSF (MCB-0080090).

References

1. Moore-Ede, C.M., Sulzman, F.M., and Fuller, C.A., *The Clocks That Time Us*, Harvard University Press, Cambridge, MA, 1982.
2. Harmer, S.L., Hogenesch, J.B., Straume, M., Chang, H.S., Han, B., Zhu, T., Wang, X., Kreps, J.A., and Kay, S.A., Orchestrated transcription of key pathways in Arabidopsis by the circadian clock, *Science,* 290, 2110, 2000.
3. Liu, Y., Tsinoremas, N.F., Johnson, C.H., Lebedeva, N.V., Golden, S.S., Ishiura, M., and Kondo, T., Circadian orchestration of gene expression in bacteria, *Genes Dev.,* 9, 1469, 1995.
4. Edmunds, L.N., *Cellular and Molecular Bases of Biological Clocks*, Springer-Verlag, Heidelberg, 1988.

5. Johnson, C.H., Knight, M., Trewavas, A., and Kondo, T., A clockwork green: circadian programs in photosynthetic organisms, in *Biological Rhythms and Photoperiodism in Plants*. Lumsden, P.J. and Millar, A.J., Eds., Bios, Oxford, 1998, pp. 1–34.
6. Lakin-Thomas, P.L., Coté, G.G., and Brody, S., Circadian rhythms in *Neurospora crassa*: biochemistry and genetics, *CRC Crit. Rev. Microbiol.,* 17, 365, 1990.
7. Harmer, S.L., Panda, S., and Kay, S.A. Molecular bases of circadian rhythms, *Annu. Rev. Cell Dev. Biol.,* 17, 215, 2001.
8. Panda, S., Hogenesch, J.B., and Kay, S.A., Circadian rhythms from flies to human, *Nature,* 417, 329, 2002.
9. Young, M.W. and Kay, S.A., Time zones: a comparative genetics of circadian clocks, *Nat. Rev. Genet.,* 2, 702, 2001.
10. Reppert, S.M. and Weaver, D.R., Coordination of circadian timing in mammals, *Nature,* 418, 935, 2002.
11. Reppert, S.M. and Weaver, D.R., Molecular analysis of mammalian circadian rhythms, *Annu. Rev. Physiol.,* 63, 647, 2001.
12. Loros, J.J. and Dunlap, J.C., Genetic and molecular analysis of circadian rhythms in Neurospora, *Annu. Rev. Physiol.,* 63, 757, 2002.
13. Somers, D.E., The physiology and molecular bases of the plant circadian clock, *Plant Physiol.,* 121, 9, 1999.
14. Toth, R., Kevei, E., Hall, A., Millar, A.J., Nagy, F., and Kozma-Bognar, L., Circadian clock-regulated expression of phytochrome and cryptochrome genes in Arabidopsis, *Plant Physiol.,* 127, 1607, 2001.
15. Emery, P., So, W.V., Kaneko, M., Hall, J.C., and Rosbash, M., CRY, a *Drosophila* clock and light-regulated cryptochrome, is a major contributor to circadian rhythm resetting and photosensitivity, *Cell,* 95, 669, 1998.
16. Roenneberg, T. and Merrow, M., Circadian systems: different levels of complexity, *Philos. Trans. R. Soc. Lond. B Biol. Sci.,* 356, 1687, 2001.
17. Bellingham, J. and Foster, R.G., Opsins and mammalian photoentrainment, *Cell Tissue Res.,* 309, 57, 2002.
18. Devlin, P.F., Signs of the time: environmental input to the circadian clock, *J. Exp. Bot.,* 53, 1535, 2002.
19. Devlin, P.F. and Kay, S.A., Circadian photoperception, *Annu. Rev. Physiol.,* 63, 677, 2001.
20. Van Gelder, R.N., Tales from the crypt(ochromes), *J. Biol. Rhythms,* 17, 110, 2002.
21. Iwasaki, H. and Kondo, T., The current state and problems of circadian clock studies in cyanobacteria, *Plant Cell Physiol.,* 41, 1013, 2000.
22. Nair, U., Ditty, J.L., Min, H., and Golden, S.S., Roles for sigma factors in global circadian regulation of the cyanobacterial genome, *J. Bacteriol.,* 184, 3530, 2002.
23. Iwasaki, H., Williams, S.B., Kitayama, Y., Ishiura, M., Golden, S.S., and Kondo, T., A kaiC-interacting sensory histidine kinase, SasA, necessary to sustain robust circadian oscillation in cyanobacteria, *Cell,* 101, 223, 2000.
24. Schmitz, O., Katayama, M., Williams, S.B., Kondo, T., and Golden, S.S., CikA, a bacteriophytochrome that resets the cyanobacterial circadian clock, *Science,* 289, 765, 2000.
25. Froehlich, A.C., Liu, Y., Loros, J.J., and Dunlap, J.C., White Collar-1, a circadian blue light photoreceptor, binding to the frequency promoter, *Science,* 297, 815, 2002.
26. Talora, C., Franchi, L., Linden, H., Ballario, P., and Macino, G., Role of a white collar-1-white collar-2 complex in blue-light signal transduction, *EMBO J.,* 18, 4961, 1999.
27. Schwerdtfeger, C. and Linden, H., Localization and light-dependent phosphorylation of white collar 1 and 2, the two central components of blue light signaling in *Neurospora crassa*, *Eur. J. Biochem.,* 267, 414, 2000.
28. Ballario, P., Talora, C., Galli, D., Linden, H., and Macino, G., Roles in dimerization and blue light photoresponse of the PAS and LOV domains of *Neurospora crassa* white collar proteins, *Mol. Microbiol.,* 29, 719, 1998.

29. He, Q., Cheng, P., Yang, Y., Wang, L., Gardner, K.H., and Liu, Y., White Collar-1, a DNA binding transcription factor and a light sensor, *Science,* 297, 840, 2002.
30. Denault, D.L., Loros, J.J., and Dunlap, J.C., WC-2 mediates WC-1-FRQ interaction within the PAS protein-linked circadian feedback loop of Neurospora, *EMBO J.,* 20, 109, 2001.
31. Briggs, W.R. and Christie, J.M., Phototropins 1 and 2: versatile plant blue-light receptors, *Trends Plant Sci.,* 7, 204, 2002.
32. Crosson, S. and Moffat, K., Structure of a flavin-binding plant photoreceptor domain: insights into light-mediated signal transduction, *Proc. Natl. Acad. Sci. USA,* 98, 2995, 2001.
33. Dragovic, Z., Tan, Y., Gorl, M., Roenneberg, T., and Merrow, M., Light reception and circadian behavior in "blind" and "clock-less" mutants of *Neurospora crassa*, *EMBO J.,* 21, 3643, 2002.
34. Shrode, L.B., Lewis, Z.A., White, L.D., Bell-Pedersen, D., and Ebbole, D.J., vvd is required for light adaptation of conidiation-specific genes of *Neurospora crassa,* but not circadian conidiation, *Fungal Genet. Biol.,* 32, 169, 2001.
35. Heintzen, C., Loros, J.J., and Dunlap, J.C., The PAS protein VIVID defines a clock-associated feedback loop that represses light input, modulates gating, and regulates clock resetting, *Cell,* 104, 453, 2001.
36. Quail, P.H., The phytochrome family: dissection of functional roles and signalling pathways among family members, *Philos. Trans. R. Soc. Lond. [Biol.],* 353, 1399, 1998.
37. Neff, M.M., Fankhauser, C., and Chory, J., Light: an indicator of time and place, *Genes Dev.,* 14, 257, 2000.
38. Lin, C., Blue light receptors and signal transduction, *Plant Cell,* 14 Suppl, S207, 2002.
39. Aschoff, J., Circadian rhythms: influences of internal and external factors on the period measured in constant conditions, *Z. Tierpsychol.,* 49, 225, 1979.
40. Somers, D.E., Webb, A.A.R., Pearson, M., and Kay, S., The short-period mutant, *toc1–1*, alters circadian clock regulation of multiple outputs throughout development in *Arabidopsis thaliana*, *Development,* 125, 485, 1998.
41. Somers, D.E., Devlin, P.F., and Kay, S.A., Phytochromes and cryptochromes in the entrainment of the arabidopsis circadian clock, *Science,* 282, 1488, 1998.
42. Devlin, P.F. and Kay, S.A., Cryptochromes are required for phytochrome signaling to the circadian clock but not for rhythmicity, *Plant Cell,* 12, 2499, 2000.
43. Yanovsky, M.J., Mazzella, M.A., and Casal, J.J., A quadruple photoreceptor mutant still keeps track of time, *Curr. Biol.,* 10, 1013, 2000.
44. Bognar, L.K., Hall, A., Adam, E., Thain, S.C., Nagy, F., and Millar, A.J., The circadian clock controls the expression pattern of the circadian input photoreceptor, phytochrome B, *Proc. Natl. Acad. Sci. USA,* 96, 14652, 1999.
45. Kircher, S., Gil, P., Kozma-Bognar, L., Fejes, E., Speth, V., Husselstein-Muller, T., Bauer, D., Adam, E., Schafer, E., and Nagy, F., Nucleocytoplasmic partitioning of the plant photoreceptors phytochrome A, B, C, D, and E is regulated differentially by light and exhibits a diurnal rhythm, *Plant Cell,* 14, 1541, 2002.
46. Somers, D.E., Clock-associated genes in Arabidopsis: a family affair, *Philos. Trans. R. Soc. Lond. B Biol. Sci.,* 356, 1745, 2001.
47. Somers, D.E., Schultz, T.F., Milnamow, M., and Kay, S.A., *ZEITLUPE* encodes a novel clock-associated PAS protein from *Arabidopsis*, *Cell,* 101, 319, 2000.
48. Nelson, D.C., Lasswell, J., Rogg, L.E., Cohen, M.A., and Bartel, B., FKF1, a clock-controlled gene that regulates the transition to flowering in Arabidopsis, *Cell,* 101, 331, 2000.
49. Schultz, T.F., Kiyosue, T., Yanovsky, M., Wada, M., and Kay, S.A., A role for LKP2 in the circadian clock of Arabidopsis, *Plant Cell,* 13, 2659, 2001.
50. Jarillo, J.A., Capel, J., Tang, R.H., Yang, H.Q., Alonso, J.M., Ecker, J.R., and Cashmore, A.R., An Arabidopsis circadian clock component interacts with both CRY1 and phyB, *Nature,* 410, 487, 2001.
51. Deshaies, R.J., SCF and Cullin/Ring H2-based ubiquitin ligases, *Annu. Rev. Cell Dev. Biol.,* 15, 435, 1999.

52. Crews, S.T. and Fan, C.M., Remembrance of things PAS: regulation of development by bHLH-PAS proteins, *Curr. Opin. Genet. Dev.,* 9, 580, 1999.
53. Covington, M.F., Panda, S., Liu, X.L., Strayer, C.A., Wagner, D.R., and Kay, S.A., Elf3 modulates resetting of the circadian clock in Arabidopsis, *Plant Cell,* 13, 1305, 2001.
54. Hicks, K.A., Millar, A.J., Carré, I.A., Somers, D.E., Straume, M., Meeks-Wagner, R., and Kay, S.A., Conditional circadian dysfunction of the Arabidopsis early-flowering 3 mutant, *Science,* 274, 790, 1996.
55. Liu, X.L., Covington, M.F., Fankhauser, C., Chory, J., and Wagner, D.R., ELF3 encodes a circadian clock-regulated nuclear protein that functions in an Arabidopsis PHYB signal transduction pathway, *Plant Cell,* 13, 1293, 2001.
56. McWatters, H.G., Bastow, R.M., Hall, A., and Millar, A.J., The ELF3 zeitnehmer regulates light signalling to the circadian clock, *Nature,* 408, 716, 2000.
57. Martinez-Garcia, J.F., Huq, E., and Quail, P.H., Direct targeting of light signals to a promoter element-bound transcription factor, *Science,* 288, 859, 2000.
58. Alabadi, D., Oyama, T., Yanovsky, M.J., Harmon, F.G., Mas, P., and Kay, S.A., Reciprocal regulation between TOC1 and LHY/CCA1 within the Arabidopsis circadian clock, *Science,* 293, 880, 2001.
59. Mizoguchi, T., Wheatley, K., Hanzawa, Y., Wright, L., Mizoguchi, M., Song, H.R., Carre, I.A., and Coupland, G., LHY and CCA1 are partially redundant genes required to maintain circadian rhythms in Arabidopsis, *Dev. Cell,* 2, 629, 2002.
60. Alabadi, D., Yanovsky, M.J., Mas, P., Harmer, S.L., and Kay, S.A., Critical role for CCA1 and LHY in maintaining circadian rhythmicity in Arabidopsis, *Curr. Biol.,* 12, 757, 2002.
61. Glossop, N.R., Lyons, L.C., and Hardin, P.E., Interlocked feedback loops within the Drosophila circadian oscillator, *Science,* 286, 766, 1999.
62. Sancar, A. Cryptochrome: the second photoactive pigment in the eye and its role in circadian photoreception, *Annu. Rev. Biochem.,* 69, 31, 2000.
63. Stanewsky, R., Kaneko, M., Emery, P., Beretta, B., Wager-Smith, K., Kay, S.A., Rosbash, M., and Hall, J.C., The cryb mutation identifies cryptochrome as a circadian photoreceptor in Drosophila, *Cell,* 95, 681, 1998.
64. Emery, P., Stanewsky, R., Hall, J.C., and Rosbash, M., A unique circadian-rhythm photoreceptor, *Nature,* 404, 456, 2000.
65. Ceriani, M.F., Darlington, T.K., Staknis, D., Mas, P., Petti, A.A., Weitz, C.J., and Kay, S.A., Light-dependent sequestration of TIMELESS by CRYPTOCHROME, *Science,* 285, 553, 1999.
66. Rosato, E., Codd, V., Mazzotta, G., Piccin, A., Zordan, M., Costa, R., and Kyriacou, C.P., Light-dependent interaction between Drosophila CRY and the clock protein PER mediated by the carboxy terminus of CRY, *Curr. Biol.,* 11, 909, 2001.
67. Lin, F.J., Song, W., Meyer-Bernstein, E., Naidoo, N., and Sehgal, A., Photic signaling by cryptochrome in the Drosophila circadian system, *Mol. Cell Biol.,* 21, 7287, 2001.
68. Krishnan, B., Levine, J.D., Lynch, M.K., Dowse, H.B., Funes, P., Hall, J.C., Hardin, P.E., and Dryer, S.E., A new role for cryptochrome in a Drosophila circadian oscillator, *Nature,* 411, 313, 2001.
69. Lowrey, P.L., Shimomura, K., Antoch, M.P., Yamazaki, S., Zemenides, P.D., Ralph, M.R., Menaker, M., and Takahashi, J.S., Positional syntenic cloning and functional characterization of the mammalian circadian mutation tau, *Science,* 288, 483, 2000.
70. Eide, E.J., Vielhaber, E.L., Hinz, W.A., and Virshup, D.M., The circadian regulatory proteins BMAL1 and cryptochromes are substrates of casein kinase I epsilon, *J. Biol. Chem.,* 277, 17248, 2002.
71. Hogenesch, J.B., Gu, Y.Z., Moran, S.M., Shimomura, K., Radcliffe, L.A., Takahashi, J.S., and Bradfield, C.A., The basic helix-loop-helix-PAS protein MOP9 is a brain-specific heterodimeric partner of circadian and hypoxia factors, *J. Neurosci.,* 20, RC83, 2000.
72. Berson, D.M., Dunn, F.A., and Takao, M., Phototransduction by retinal ganglion cells that set the circadian clock, *Science,* 295, 1070, 2002.
73. Gooley, J.J., Lu, J., Chou, T.C., Scammell, T.E., and Saper, C.B., Melanopsin in cells of origin of the retinohypothalamic tract, *Nat. Neurosci.,* 4, 1165, 2001.

74. Hannibal, J., Hindersson, P., Knudsen, S.M., Georg, B., and Fahrenkrug, J., The photopigment melanopsin is exclusively present in pituitary adenylate cyclase-activating polypeptide-containing retinal ganglion cells of the retinohypothalamic tract, *J. Neurosci.,* 22, RC191, 2002.
75. Hattar, S., Liao, H.W., Takao, M., Berson, D.M., and Yau, K.W., Melanopsin-containing retinal ganglion cells: architecture, projections, and intrinsic photosensitivity, *Science,* 295, 1065, 2002.
76. Provencio, I., Rollag, M.D., and Castrucci, A.M., Photoreceptive net in the mammalian retina, *Nature,* 415, 493, 2002.
77. Okamura, H., Miyake, S., Sumi, Y., Yamaguchi, S., Yasui, A., Muijtjens, M., Hoeijmakers, J.H., and van der Horst, G.T., Photic induction of mPer1 and mPer2 in cry-deficient mice lacking a biological clock, *Science,* 286, 2531, 1999.
78. Selby, C.P., Thompson, C., Schmitz, T.M., Van Gelder, R.N., and Sancar, A., Functional redundancy of cryptochromes and classical photoreceptors for nonvisual ocular photoreception in mice, *Proc. Natl. Acad. Sci. USA,* 97, 14697, 2000.
79. Cashmore, A.R., Jarillo, J.A., Wu, Y.J., and Liu, D., Cryptochromes: blue light receptors for plants and animals, *Science*, 284, 760, 1999.

138

Cryptochrome: Discovery of a Circadian Photopigment

Carol L. Thompson
University of North Carolina School of Medicine

Aziz Sancar
University of North Carolina School of Medicine

138.1 Introduction

Most organisms, from fruit flies to humans, exhibit daily fluctuations in behavioral and molecular processes such as sleep–wake cycles and metabolic rate. These daily fluctuations are governed by an internal circadian clock, which is generated by a transcriptional feedback loop that exists in individual cells as well as in neural tissue, where it coordinates an organism's global rhythms. These rhythms can exist in the absence of light but are adjusted by light exposure in order to coordinate organismal behavior with the solar day. While circadian photoreception is not fully understood and may involve integration of multiple signals from different light input pathways, it appears that cryptochrome, a blue-light photoreceptor, is a major circadian photosensory pigment. Our understanding of the role of cryptochrome in mammalian circadian photoreception evolved from the merging of two distinct fields: plant blue-light photoreception and photoreactivation.

Blue-light responses in plants were first described by Charles Darwin in the 1800s and attributed to an unknown blue-light photoreceptor (cryptochrome). However, no progress was made toward identification of this pigment until 1980, when the HY4 gene locus in Arabidopsis was discovered to be responsible for conferring blue-light sensitivity.[1] When a gene was cloned and sequenced from the HY4 locus in 1993, it was found that the putative protein encoded by HY4 had high sequence homology to photolyase, a blue-light-activated DNA repair protein.[2] The level of sequence identity between the HY4 gene and photolyase was so high that it was unclear whether this protein was a photolyase or a new type of protein. By 1995, we and others demonstrated that this photolyase-homolog lacked DNA repair activity and appeared to represent a new class of blue-light photoreceptor that was called cryptochrome, a name previously used as a universal designation for plant blue-light photoreceptors of unknown (cryptic) identity.[3–6]

The study of photolyase began with the first description of photoreactivation in *S. griseus* in 1949.[7] Photoreactivation is the reversal of the harmful and mutagenic effects of ultraviolet irradiation by blue-light, and in 1958, the enzyme responsible for this phenomenon, photolyase, was discovered.[8] Photolyase uses blue-light energy to repair the two major UV photoproducts in DNA, cyclobutane pyrimidine dimers

0-8493-1348-1/04/$0.00+$1.50

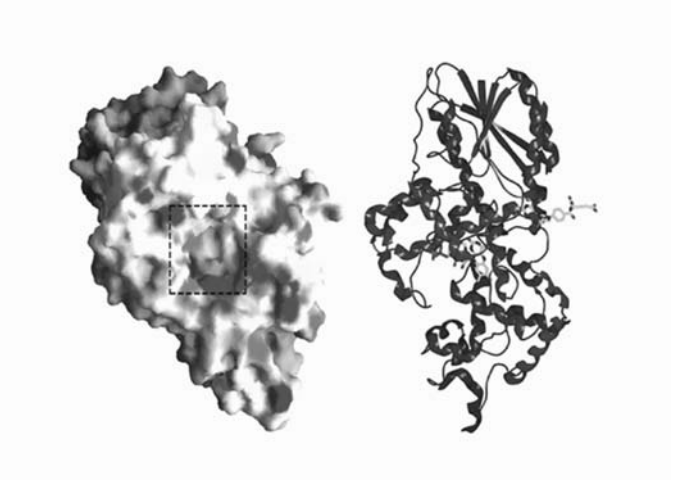

FIGURE 138.1 Crystal structure of *E. coli* photolyase. The surface potential representation (left) shows the positively charged DNA-binding groove and the pocket for UV photoproduct binding (dashed box). The ribbon diagram representation (right) shows the orientation of the two chromophores bound to the protein. (From Sancar, A., *Annu. Rev. Biochem.*, 69, 31, 2000. Used with permission by the Annual Review of Biochemistry, vol. 69, copyright 2000 by Annual Reviews.)

and pyrimidine-pyrimidone (6–4) photoproducts, via a cyclic electron transfer mechanism. Although photolyase was found in bacteria, yeast, fruit flies, fish, and even in rattlesnakes and opossums, in 1993, we determined by enzymatic assays that photolyase was absent in humans and all other placental mammals.[9] Therefore, the report of a photolyase-homolog as an EST in the human genome database in 1995 was puzzling.[10] Both this first homolog and a second human homolog we discovered were tested and found to lack photolyase activity, and so in the manner of the plant cryptochromes, we named these proteins CRY1 and CRY2 for Cryptochrome 1 and 2 and hypothesized that they might be circadian photopigments in mammals.[11,12] Later, five groups cloned the sole *Drosophila* homolog, *dCry*.[13–17]

Cryptochromes are 60 to 70 KD proteins that possess a high degree of sequence identity with photolyase throughout the chromophore and DNA-binding regions; therefore, clues to the function and mechanism of mammalian cryptochromes may be gained by modeling upon the α carbon backbone of *E. coli* photolyase crystal structure.[18] Photolyase possesses two main regions, an *N*-terminal α/β domain and a *C*-terminal helical domain. Photolyase family members noncovalently bind two cofactors, which absorb blue light: a pterin, in the form of methenyltetrahydrofolate, which binds along a shallow groove between the two domains; and a flavin, which is bound in a pocket in the α-helical domain. The phosphodiester backbone of DNA interacts with photolyase along a trace of positive electrostatic potential, and during binding, the UV photoproduct is flipped out of the DNA helix into a pocket in the protein (dashed box, Figure 138.1) in a light-independent manner, where it comes into van der Waals contact with the flavin. Photoreactivation is carried out by the following mechanism: the folate absorbs a photon of blue light and transfers energy to the flavin.[19,20] The excited singlet state flavin transfers an electron to the pyrimidine dimer (cyclobutane dimer or [6–4] photoproduct) and thus initiates a cyclic electron transfer, whereby the pyrimidine dimer is reversed to canonical dipyrimidines concomitant with back electron transfer to restore flavin to the catalytically active two-electron reduced form ($FADH^-$). At the end of the repair reaction, there is no net change in the oxidation state of the chromophores.

Molecular modeling of mammalian cryptochromes on the structure of photolyase indicates conservation of the chromophore-binding regions, the DNA binding groove, as well as the damage-binding pocket. However, the functional implications of these structural features for cryptochrome function in circadian photoreception are unknown. The major difference between cryptochrome and photolyase lies in the presence of an extended *C*-terminal tail in cryptochrome, which is absent in photolyase. Based on

evidence from cryptochromes in drosophila and arabidopsis, this tail is believed to be responsible for protein–protein interactions and signal phototransduction.[21,22]

To examine the role of cryptochrome as a photoreceptor in mammals, it is important to understand the anatomy of circadian photoreception. All mammalian photoreception occurs in the retina, including visual and circadian photoreception.[23] While vision is mediated by rod and cone photoreceptors in the outer retina, circadian photoreception does not require the visual photopigments; certain retinal degeneration diseases in mice that result in the loss of the outer retina but leave the inner retina intact do not eliminate circadian photoreception[24–26]; therefore, a circadian photopigment must reside in the inner retina. After a light signal is detected, signal phototransduction is initiated from the retina and transmitted through the optic nerve, and finally to the suprachiasmatic nucleus (SCN) in the hypothalamus, a structure that is located just above the optic chiasm and contains the master circadian clock. In mammals, every cell in the body houses an autonomous circadian clock, but the cellular clocks are coordinated within each organ, and the circadian rhythms of the entire animal are controlled by the master clock in the SCN.[27]

Experiments to determine the photoreceptive function of cryptochrome in mammals have thus far relied on molecular and genetic approaches. While significant strides were made recently in understanding the molecular clock mechanism and the role of cryptochrome in the clockworks, the molecular clock model is becoming ever more complicated and raises new questions. Similarly, while recent intriguing studies concerning circadian photoreception have not yet solved the actual mechanism of signal phototransduction, the genetic data strongly support a major role for cryptochrome in circadian photoreception as well as the integration of photic signals generated by opsins and cryptochromes. In this review, we will detail the current evidence for the role of cryptochrome in circadian photoreception as well as the apparent functional redundancy between the two classes of mammalian photoreceptors.

138.2 Evidence for Cryptochrome as a Circadian Photoreceptor

Historically, circadian photoreception in mammals was attributed to the vitamin A-based opsins, but the discovery of a blue-light absorbing flavoprotein, cryptochrome, introduced new possibilities in understanding clock-resetting by light. To determine whether cryptochrome could be a potential circadian photoreceptor, we examined whether it was expressed appropriately in the inner retina. As shown in Figure 138.2, *Cry2,* and to a lesser extent *Cry1,* were both expressed in the inner retina, specifically in the ganglion cell layer and the inner nuclear layer.[28] The presence of cryptochrome in the ganglion cell layer is especially intriguing in light of the recent discovery of a small subset of ganglion cells that are intrinsically photosensitive.[29] These cells contain a candidate photopigment, melanopsin, that has been postulated as the circadian photoreceptor[30,31]; however, cryptochrome expression in these cells supports a role for cryptochrome in this photoresponse.

Surprisingly, cryptochrome was not found solely in the retina. In addition to low levels found in all tissues, *Cry1* was also expressed in the SCN, and *Cry1* mRNA oscillated with circadian rhythmicity, which indicated an additional role for cryptochrome in circadian clock function.[28] Based on the mRNA expression pattern, we postulated a role for Cry2 in circadian photoreception in the retina as well as a light-independent role for Cry1 in the circadian clock mechanism in the SCN.

The generation of knockout mice for *Cry1* and *Cry2* indicated redundant functions between the two mammalian photolyase-homologs. Both the *Cry1*-/- mouse[32,33] and the *Cry2*-/- mouse[34] exhibited a change in period length, indicating a potential role in clock regulation, as well as a reduction in circadian photosensitivity as measured by circadian gene induction by light in the SCN.[32,34] Based on the hypothesis that the two cryptochromes were the sole circadian photoreceptors in mice, we expected the *Cry1*-/- *Cry2*-/- mice to be "circadian blind." Surprisingly, the double knockout mice responded behaviorally to light–dark cycles (Figure 138.3), and circadian oscillation of the circadian clock gene, *per2* (but not *per1*), as well as acute photoinduction of both *per2*, and *c-fos* was observed in the SCN.[32,33] Therefore, cryptochrome was not absolutely required for circadian responses to light. However, these mice entirely lost

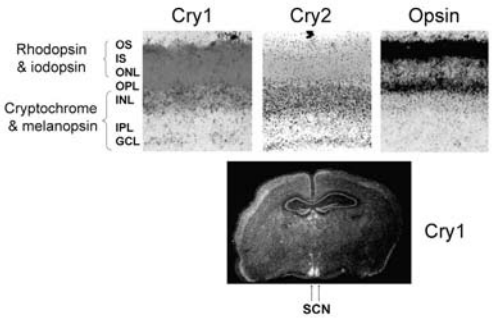

FIGURE 138.2 Expression of cryptochromes in mouse retina and SCN. In situ hybridization for *Cry1* and *Cry2* mRNA in the retina revealed a strong signal in the inner nuclear layer and ganglion cell layer (top, left, and middle). Opsin expression in the outer retina is shown for comparison (top, right). *Cry1* signal is shown in the SCN (bottom). Abbreviations: OS, outer segment; IS, inner segment; ONL, outer nuclear layer; OPL, outer plexiform layer; INL, inner nuclear layer; IPL, inner plexiform layer; GCL, ganglion cell layer. (From Miyamoto, Y. and Sancar, A., *Proc. Natl. Acad. Sci. USA*, 95, 6097, 1998. With permission.)

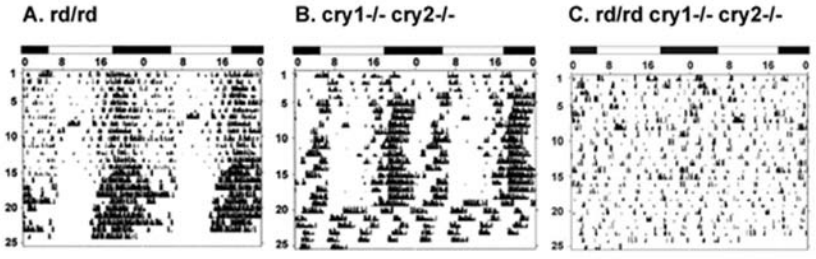

FIGURE 138.3 Wheel-running actograms of cryptochrome and *rd* mutants. Animals were entrained to 12 h light: 12 h dark cycles, followed by constant darkness at Day 19. Numbers on the Y-axis indicate days; numbers on the X-axis indicate time of day. White bars indicate light, black bars indicate dark (top). (From Selby, C.P., et al., *Proc. Natl. Acad. Sci. USA*, 97, 14697, 2000. With permission.)

circadian rhythmicity of behavior and of circadian gene oscillation in the absence of light cues, indicating that cryptochromes were required for circadian clock function.

The light-independent role of cryptochrome in the core circadian clock machinery is now known. Circadian rhythmicity is generated by a transcriptional feedback loop (Figure 138.4). Certain genes, such as circadian clock genes *per1*, *per2*, and *cry1*, as well as output genes like vasopressin, contain an E-box element in the promoter, which governs circadian transcription of these genes.[35–38] The transcriptional activators Bmal and Clock bind the E-box as a heterodimer to drive transcription,[36] and after Per and Cry proteins are made, they reenter the nucleus and negatively regulate transcription from the E-box.[39–41] After light signals are received and transmitted from the retina to the SCN, the clock is reset by activation of the CREB transcription factor, which binds the CRE element in the promoter of *per* genes resulting in acute induction of *per*.[42]

While cryptochrome's role in the circadian clock mechanism is clear, its light-dependent function remains to be elucidated. The evidence for cryptochrome as a blue-light circadian photoreceptor is the following:

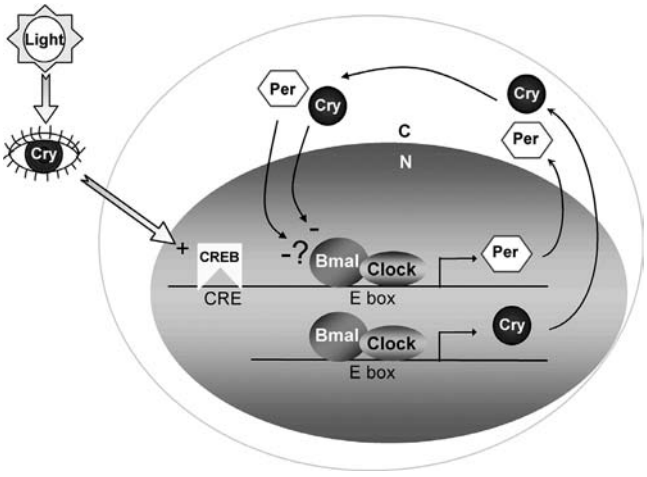

FIGURE 138.4 Molecular mechanism of circadian rhythm. Circadian rhythm is established by a negative feedback loop. This simplified model shows transcriptional activation by the Bmal-Clock heterodimer to drive transcription from E-box containing genes such as Per and Cry. Per and Cry then feed back to inhibit their own transcription. Light input resets the clock by rapid induction of the *per* transcript through the CRE element.

1. Cryptochrome has a high level of sequence identity to the blue-light activated enzyme, photolyase.
2. The homolog of cryptochrome in plants serves as a photoreceptor for a myriad of blue-light responses.[43]
3. Genetic evidence demonstrates that *cry1*-/-*cry2*-/- mice have impaired photoresponses, as shown by reduced gene induction by light in the SCN.[32]

There are two main arguments against cryptochrome as a circadian photoreceptor. The first argument is that the double knockout mice still retain responses to light, both behaviorally and molecularly, indicating the presence of other photoreceptors that can govern these responses. Although this evidence precludes an absolute requirement for cryptochrome in circadian photoreception, it would be consistent with a scenario in which multiple photoreceptors simultaneously contribute to circadian clock resetting, including cryptochromes and opsins.

The second major argument against cryptochrome as a circadian photoreceptor is that the action spectra of circadian photoresponses do not match the absorption spectrum of cryptochrome. Several action spectra were generated for a variety of circadian responses to light. Recently, two groups published similar action spectra for human melatonin suppression by light.[44,45] After testing wavelengths from 420 to 600 nm, they attempted to fit an opsin nomogram to the data (Figure 138.5). They concluded that the best fit of an opsin absorption spectrum to the data was an opsin with peak absorption at 464 nm; however, the peak of the action spectrum clearly did not coincide with the opsin nomogram. The peak of the action spectrum for melatonin suppression was not determined by these experiments, because the maximum effectiveness of light was at the lowest wavelength tested, 420, so it is unclear whether the peak was at 420 or at some even lower wavelength. The preliminary absorption spectrum of cryptochrome revealed a peak at 420 nm, which matches the peak of melatonin suppression, but the shape of the curve does not match.[46] The action spectra appear to indicate to a peak at 420 nm and perhaps a shoulder at 500 nm, but the resolution of the data is insufficient. Therefore, examination of the currently available action spectra support a model in which multiple photoreceptors, such as a cryptochrome and an opsin, contribute to circadian photoresponses.

Action spectra are notoriously difficult to generate, especially in whole animals. Ideally an action spectrum would be generated from a purified enzyme system; however, no such assay exists for cryptochrome or circadian photoreception. A cell-based assay would be a simpler and more favorable system for action spectrum generation. While no such system exists in mammalian cells, a system for circadian

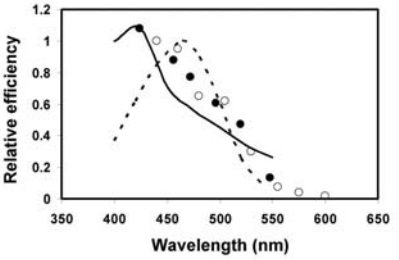

FIGURE 138.5 Combined action spectra of human melatonin suppression. Two separate studies examined the action spectra of melatonin suppression. Dashed line: opsin 464 nomogram. Solid line: hCry2 absorption spectrum (black circles: From Thapan, K., Arendt, J., and Skene, D.J., *J. Physiol.*, 535.1, 261, 2001; white circles: From Brainard, G.C., et al., *J. Neurosci.*, 21, 6405, 2001.)

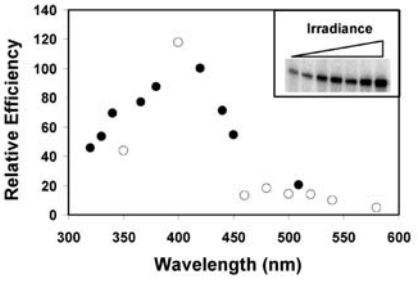

FIGURE 138.6 Action spectrum of photic induction of zebrafish *per2* mRNA. Induction of *per2* occurs in a dose-dependent manner, as shown by RNase protection assay (inset). Relative efficiency of induction was determined as the slope of the dose–response curve for each wavelength (data points from Cermakian et al.[47]).

photoreception was recently established in zebrafish cells. Sassone-Corsi and colleagues established a cell line (Z3) that expresses at least four different cryptochromes.[47] The Z3 cell line not only exhibits circadian oscillation of clock genes, it is the only cell line in which the circadian rhythm can be directly reset by light.[48] A good marker for circadian reception in this line is the acute induction of the *per2* gene by light in a dose-dependent manner (Figure 138.6). Therefore, we generated an action spectrum for *per2* induction by light in the Z3 line (Figure 138.6),[47]

We tested wavelengths of light ranging from 320 to 580 nm and found that wavelengths between 380 and 420 nm were the most effective wavelengths for *per2* induction, and wavelengths above 450 had little effect on *per2* induction. Photolyase family members with folate and FAD chromophores exhibit absorption peaks between 380 to 420 nm,[19,20] so this action spectrum is consistent with a cryptochrome-mediated response. However, zebrafish are known to contain a UV opsin that absorbs blue light as well, but these cells did not contain detectable levels of the opsin cofactor retinaldehyde,[47] so we concluded the response was due to cryptochrome.

138.3 Functional Redundancy of Opsins and Cryptochromes

Although the action spectrum for a circadian photoresponse in zebrafish points to cryptochrome as the responsible photoreceptor in a vertebrate animal, the lack of a similar assay in mammals made elucidation

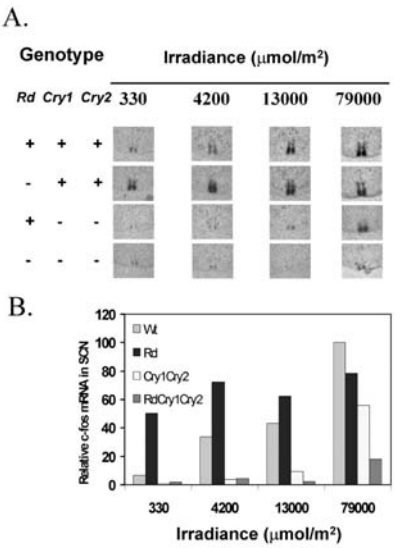

FIGURE 138.7 Acute induction of *fos* mRNA in the SCN by light. Mice lacking rods (*rd*), *Cry1,* or *Cry2* were exposed to four doses of light and examined for *fos* induction after 30 min. (A) Representative SCN images from peak sections. (B) Quantitation of data in A. (From Selby, C.P., et al., *Proc. Natl. Acad. Sci. USA*, 97, 14697, 2000. With permission.)

of mammalian circadian photoreception problematic. Simultaneous input from multiple photoreceptors made interpretation of action spectra in whole animals difficult. There appears to be only two classes of photoreceptors in mammals: cryptochromes and opsins. The contribution of cryptochromes to circadian photoreception can be examined genetically by use of *cry1-/- cry2-/-* mice. The opsin class encompasses the visual opsins (rod and cone opsins) as well as novel opsins, such as the recently discovered melanopsin, expressed in the ganglion cell layer. There are a variety of different genetic mutations in mice that have been used to measure the input of various opsins to this response: *rd/rd* mice, which undergo retinal degeneration and lose all rod photoreceptors as well as the majority of cone photoreceptors[49]; *rdta*/*rdta* mice, which have transgenic expression of a toxin targeted to rod cells, resulting in destruction of rod photoreceptors[50]; and *cl*/*cl* mice, which lack all cone cells.[51] Recently, melanopsin knockouts were also constructed. Thus far, none of these mutations that take out opsins had any significant effects on circadian photoreception. However, in order to examine the input of all opsins to the circadian clock by genetics, it would be necessary to combine at least three mutations to eliminate rods, cones, and melanopsin, and there may be additional novel opsins in the eye.

Cryptochrome knockout mice exhibit reduced circadian photosensitivity, and therefore, we set out to determine whether visual opsins were responsible for the remaining photoresponse. Initially, we compared the circadian responses of the *cry1-/-cry2-/-* mouse with a *rd/rd cry1-/- cry2-/-* mouse to see if the residual response remaining in the cryptochrome-free mouse was mediated by the most abundantly expressed opsin, the rod opsin. We found that most, but not all, of the triple mutant mice were arrhythmic under light–dark cycles, as compared to the *cry1-/- cry2-/-* mice, which responded to light–dark cycles (Figure 138.3).[52] This indicated that visual opsins were primarily responsible for behavioral photoresponses in the absence of cryptochromes. Using induction of *fos* mRNA in the SCN by light, we found that although wild-type and *rd* mice had robust *fos* induction by light, the *cry1-/-cry2-/-* mice had 10- to 100-fold reduced circadian photosensitivity at limiting light fluences and about twofold reduced sensitivity even at the highest light dose given (Figure 138.7). Strikingly, even at the highest light dose, the triple mutant mice had drastically reduced *fos* induction, exhibiting only 15% of wild-type induction

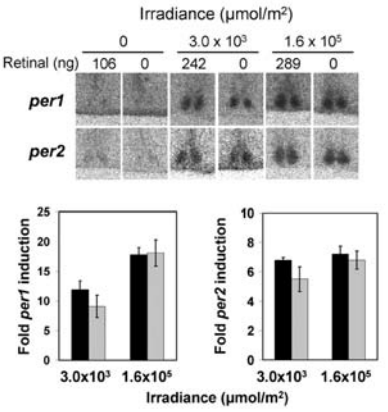

FIGURE 138.8 Opsin-free mice have normal *per* gene induction by light. Mice were exposed to two different doses of light during night phase and were sacrificed after 1.5 h. In situ hybridization for *per1* and *per2* mRNA in the SCN was performed. (A) Representative SCN images from peak sections. (B) Quantitation of data in A. (From Thompson, C.L., et al., *Proc. Natl. Acad. Sci. USA*, 98, 11708, 2001. With permission.)

levels. While this data indicated that visual opsins could allow the *cry1-/-cry2-/-* mice to coordinate their behavior to lighting conditions, the residual *fos* induction in the triple mutant mouse as well as the few triple mice that were not arrhythmic suggested that another photoreceptor may also play a role, and we postulated that a few surviving cone cells or melanopsin may be responsible.

Recently, a new mouse model was developed that allows us to examine photoresponses in an entirely opsin-free mouse model. Opsins require their chromophore, 11-*cis*-retinal, for function, and therefore, one obvious approach to create an opsin-free model would be to deprive mice of dietary vitamin A, rendering all opsins nonfunctional, including rod and cone opsins as well as known and yet to be discovered novel opsins. This approach is not feasible in normal mice, because vitamin A is required during development, and adult mice have stored sufficient vitamin A in their liver to last for the lifetime of the animals, even if they were put on a vitamin-A-free diet. The creation of the plasma retinol-binding protein mutant (*rbp*) enables us to deplete ocular retinal in mice.[53] The Rbp protein transports retinal from storage in the liver to peripheral tissues. With the Rbp mutation, peripheral tissues such as the eye can be vitamin A depleted in 6 to 8 months. Therefore, we used the vitamin-A-depleted *rbp* mouse as an opsin-free model for circadian photoreception.

In Rbp animals maintained on a vitamin-A-free diet and with no detectable retinal, phototransduction from the retina to the SCN was normal, as shown by acute photoinduction of *per* genes[54] (Figure 138.8) as well as *fos*[55] in the SCN. This result is somewhat surprising, because *rd* mice exhibit an increased response to light compared with wild-type mice. In the absence of opsins, the only remaining candidate photoreceptor is cryptochromes, and therefore, these data strongly suggest that cryptochromes are sufficient to mediate photoinduced gene expression in the SCN. Another marker of circadian photoreception is behavioral response to light as measured by wheel running. Because the gene induction by light is normal, we expected behavioral responses to light to be normal. We found that *rbp* -/- mice have circadian behavior coordinated to light–dark cycles and exhibit masking and phase shifting to light, although there are some interesting features of these animals that are consistent with input from opsins to circadian photoreception.[55] This aspect of the mutants remains to be explored.[55] Similarly, like the *rd/rd cry1 -/- cry2-/-* mice which become largely arrhythmic under light–dark cycles, the opsin-free and cryptochrome-free mice, which have lost rod opsins, cone opsins, novel opsins, and cryptochromes, were entirely arrhythmic.[55] This again corroborates that cryptochromes primarily and opsins secondarily contribute to mammalian circadian photoreception. Similar studies in drosophila showed that in that organism as well, cryptochrome and opsin function as redundant circadian photoreceptors.[56]

138.4 Conclusion

The mounting evidence in fruit flies and mammals indicates that circadian photoreception in animals evolved to allow several different light input pathways into resetting the circadian clock. The role of the clock in coordinating behavioral and molecular functions impacts feeding and evading predation, and evolving multiple redundant pathways to circadian photoreception would help ensure survival. The use of multiple photoreceptors, each with different chromophores and separate signaling mechanisms, might allow animals to control a variety of behavioral processes in response to a wide spectrum of light frequencies and intensities, and thereby, allow them to respond appropriately to changing light quality over the course of the day. In mammals, the redundant pathways include signaling by rod opsin and either cone opsin or melanopsin, as well as the blue-light photoreceptor cryptochrome, which appears to be the major contributor to circadian photoreception.

References

1. Koornneef, M., Rolff, E., and Spruitt, C.J.P., Genetic control of light-inhibited hypocotyl elongation in *Arabidopsis thaliana* (L) Heynh, *Z. Pflanzenphysiol.*, 100, 147, 1980.
2. Ahmad, M. and Cashmore, A.R., HY4 gene of *A. thaliana* encodes a protein with the characteristic of a blue-light photoreceptor, *Nature*, 366, 162, 1993.
3. Hoffman, P.D., Batschauer, A., and Hays, J.B., PHH1, a novel gene from *Arabidopsis thaliana* that encodes a protein similar to plant blue-light photoreceptors and microbial photolyases, *Mol. Gen. Genet.,* 253, 259, 1996.
4. Lin, C.T., Yang, H.Y., Guo, H.W., Mockler, T., Chen, J., and Cashmore, A.R., Enhancement of blue-light sensitivity of *Arabidopsis* seedlings by a blue-light receptor cryptochrome 2, *Proc. Natl. Acad. Sci. USA*, 95, 2686, 1998.
5. Malhotra, K., Kim, S.T., Batschauer, A., Dawut, L., and Sancar, A., Putative blue-light photoreceptors from *Arabidopsis thaliana* and *Sinapis alba* contain two photolyase cofactors but lack DNA repair activity, *Biochemistry*, 34, 6892, 1995.
6. Lin, C., Robertson, D.E., Ahmad, M., Raibekas, A.A., Jorns, M.S., and Cashmore, A.R., Association of flavin adenine dinucleotide with the *Arabidopsis* blue light receptor Cry1, *Science*, 269, 968, 1995.
7. Kelner, A., Effect of visible light on the recovery of *Streptomyces griseus* conidia from ultraviolet irradiation, *Proc. Natl. Acad. Sci. USA*, 35, 73, 1949.
8. Rupert, C.S., Goodgal, S., and Herriot, R.M., Photoreactivation of ultraviolet inactivated *Hemophila influenzae* transforming factor, *J. Gen. Physiol.*, 41, 451, 1958.
9. Li, Y.F., Kim, S.T., and Sancar, A., Evidence for lack of DNA photoreactivating enzyme in humans. *Proc. Natl. Acad. Sci. USA*, 90, 4389, 1993.
10. Adams, M.D., Kerlavage, A.R., Fleischmann, R.D., Fuldner, R.A., Bult, C.J., Lee, N.H., Kirkness, E.F., Weinstock, K.G., Gocayne, J.D., and White, O., et al., Initial assessment of human gene diversity and expression patterns based upon 83 million nucleotides of cDNA sequence, *Nature*, 377, 3, 1995.
11. Hsu, D.S., Zhao, X., Zhao, S., Kazantsev, A., Wang, R., Todo, T., Wei, Y., and Sancar, A., Putative human blue-light photoreceptors hCRY1 and hCRY2 are flavoproteins, *Biochemistry*, 35, 13871, 1996.
12. Todo, T., Tsuji, H., Otoshi, E., Hitomi, K., Kim, S.T., and Ikenaga, M., Characterization of a human homolog of (6–4) photolyase, *Mutat. Res.*, 384, 195, 1997.
13. Ishikawa, T., Matsumoto, A., Kato Jr., T., Togashi, S., Ryo, H., Ikenaga, M., Todo, T., Ueda, R., and Tanimura, T., DCRY is a *Drosophila* photoreceptor protein implicated in light entrainment of circadian rhythm, *Genes Cells,* 4, 57, 1999.
14. Egan, E.S., Franklin, T.M., Hilderbrand-Chae, M.J., McNeil, G.P., Roberts, M.A., Schroeder, A.J., Zhang, X., and Jackson, F.R., An extraretinally expressed insect cryptochrome with similarity to the blue light photoreceptors of mammals and plants, *J. Neurosci.,* 19, 3665, 1999.

15. Selby, C.P., Thompson, C., Schmitz, T.M., Van Gelder, R.N., and Sancar, A., Functional redundancy of cryptochromes and classical photoreceptors for nonvisual ocular photoreception in mice, *Proc. Natl. Acad. Sci. USA*, 97, 14697, 2000.
16. Emery, P., So, W.V., Kaneko, M., Hall, J.C., and Rosbash, M., CRY, a *Drosophila* clock and light-regulated cryptochrome, is a major contributor to circadian rhythm resetting and photosensitivity, *Cell*, 95, 669, 1998.
17. Okano, S., Kanno, S., Takao, M., Eker, A.P.M., Isono, Y., Tsukahara, Y., and Yasui, A., A putative blue-light receptor from *Drosophila melanogaster*, *Photochem. Photobiol.*, 69, 108, 1999.
18. Park, H.W., Kim, S.T., Sancar, A., and Deisenhofer, J., Crystal structure of DNA photolyase from *Escherichia coli*, *Science*, 268, 1866, 1995.
19. Sancar, A., Structure and function of DNA photolyase, *Biochemistry*, 33, 2, 1994.
20. Sancar, A., Cryptochrome: the second photoactive pigment in the eye and its role in circadian photoreception, *Annu. Rev. Biochem.*, 69, 31, 2000.
21. Rosato, E., Codd, V., Mazzotta, G., Piccin, A., Zordan, M., Costa, R., and Kyriacou, C.P., Light-dependent interaction between *Drosophila* CRY and the clock protein PER mediated by the carboxy terminus of CRY, *Curr. Biol.*, 11, 909, 2001.
22. Yang, H.-Q., Wu, Y., Tang, R., Liu, D., Liu, Y., and Cashmore, A.R., The C-termini of *Arabidopsis* cryptochromes mediate a constitutive light response, *Cell*, 103, 815, 2000.
23. Ibuka, N., Inouye, S.I., and Kawamura, H., Analysis of sleep-wakefulness rhythms in male rats after suprachiasmatic nucleus lesions and ocular enucleation, *Brain Res.*, 122, 33, 1977.
24. Foster, R.G., Provencio, I., Hudson, D., Fiske, S., De Grip, W., Menaker, M., Circadian photoreception in the retinally degenerate mouse (*rd/rd*), *J. Comp. Physiol. A,* 169, 39, 1991.
25. Masana, M.I., Benloucif, S., and Dubocovich, M.L., Light-induced *c-fos* mRNA expression in the suprachiasmatic nucleus and the retina of C3H/HeN mice, *Mol. Brain Res.*, 42, 193, 1996.
26. Yoshimura, T. and Ebihara, S., Decline of circadian photosensitivity associated with retinal degeneration in CBA/J-*rd/rd* mice, *Brain Res.*, 779, 188, 1998.
27. Balsalobre, A., Damiola, F., and Schibler, U., A serum shock induces circadian gene expression in mammalian tissue culture cells, *Cell*, 93, 929, 1998.
28. Miyamoto, Y. and Sancar, A., Vitamin B2-based blue-light photoreceptors in the retinohypothalamic tracts as the photoactive pigments for setting the circadian clock in mammals, *Proc. Natl. Acad. Sci. USA*, 95, 6097, 1998.
29. Hattar, S., Liao, H., Takao, M., Berson, D.M., and Yau, K., Melanopsin-containing retinal ganglion cells: architecture, projections, and intrinsic photosensitivity, *Science*, 295, 1065, 2002.
30. Provencio, I., Rollag, M.D., and Catrucci, A.M., Photoreceptive net in the mammalian retina, *Nature*, 415, 493, 2002.
31. Berson, D.M., Dunn, F.A., and Takao, M., Phototransduction by retinal ganglion cells that set the circadian clock, *Science*, 295, 1070, 2002.
32. Vitaterna, M.H., Selby, C.P., Todo, T., Niwa, H., Thompson, C., Fruechte, E.M., Hitomi, K., Thresher, R.J., Ishikawa, T., Miyazaki, J., Takahashi, J.S., and Sancar, A., Differential regulation of mammalian *Period* genes and circadian rhythmicity by cryptochromes 1 and 2, *Proc. Natl. Acad. Sci. USA*, 96, 12114, 1999.
33. van der Horst, G.T.J., Muijtjens, M., Kobayashi, K., Takano, R., Kanno, S., Takao, M., Wit, J., Verkerk, A., Eker, A.P.M., van Leenen, D., Buijs, R., Bootsma, D., Hoeijmakers, J.H.J., and Yasui, A., Mammalian Cry1 and Cry2 are essential for maintenance of circadian rhythms, *Nature*, 398, 627, 1999.
34. Thresher, R.J., Vitaterna, M.H., Miyamoto, Y., Kazantsev, A., Hsu, D.S., Petit, C., Selby, C.P., Dawut, L., Smithies, O., Takahashi, J.S., and Sancar, A., Role of mouse cryptochrome blue-light photoreceptor in circadian photoresponses, *Science*, 282, 1490, 1998.
35. Jin, X., Shearman, L.P., Weaver, D.R., Zylka, M.J., Vries, G.J.D., and Reppert, S.M., A molecular mechanism regulating rhythmic output from the suprachiasmatic circadian clock, *Cell*, 96, 57, 1999.

36. Gekakis, N., Staknis, D., Nguyen, H.B., Davis, F.C., Wilsbacher, L.D., King, D.P., Takahashi, J.S., and Weitz, C.J., Role of the CLOCK protein in the mammalian circadian clock, *Science*, 280, 1564, 1998.
37. Chaudhary, J. and Skinner, M.K., Basic helix-loop-helix proteins can act at the E-box within the serum response element of the c-fos promoter to influence hormone-induced promoter activation in Sertoli cells, *Mol. Endocrinol.,* 13, 774, 1999.
38. Metz, R. and Ziff, E., The helix-loop-helix protein rE12 and the C/EBP-related factor rNFIL-6 bind to neighboring sites within the c-fos serum response element, *Oncogene*, 6, 2165, 1991.
39. Griffin, E.A., Jr., Staknis, D., and Weitz, C.J., Light-independent role of CRY1 and CRY2 in the mammalian circadian clock, *Science*, 286, 768, 1999.
40. Kume, K., Zylka, M.J., Sriram, S., Shearman, L.P., Weaver, D.R., Jin, X., Maywood, W.S., Hastings, M.H., and Reppert, S.M., mCry1 and mCry2 are essential components of the negative limb of the circadian clock feedback loop, *Cell*, 98, 193, 1999.
41. Shearman, L.P., Sriram, S., Weaver, D.R., Maywood, W.S., Chaves, I., Zheng, B., Kume, K., Lee, C.C., van der Horst, G.T.J., Hastings, M.H., and Reppert, S.M., Interacting molecular loops in the mammalian circadian clock, *Science*, 288, 1013, 2000.
42. Travnickova-Bendova, Z., Cermakian, N., Reppert, S.M., and Sassone-Corsi, P., Bimodal regulation of *mPeriod* promoters by CREB-dependent signaling and CLOCK/BMAL1 activity, *Proc. Natl. Acad. Sci. USA*, 99, 7728, 2002.
43. Lin, C., Blue light receptors and signal transduction, *Plant Cell*, 14Suppl, S207, 2002.
44. Thapan, K., Arendt, J., and Skene, D.J., An action spectrum for melatonin suppression: evidence for a novel non-rod, non-cone photoreceptor system in humans, *J. Physiol.*, 535, 261, 2001.
45. Brainard, G.C., Hanifin, J.P., Greeson, J.M., Byrne, B., Glickman, G., Gerner, E., and Rollag, M.D., Action spectrum for melatonin regulation in humans: evidence for a novel circadian photoreceptor, *J. Neurosci.*, 21, 6405, 2001.
46. Zhao, S. and Sancar, A., Human blue-light photoreceptor hCRY2 specifically interacts with protein serine/threonine phosphatase 5 (PP5) and modulates its activity, *Photochem. Photobiol.*, 66, 727, 1997.
47. Cermakian, N., Pando, M.P., Thompson, C.L., Pinchak, A.B., Selby, C.P., Gutierrez, L., Wells, D.E., Cahill, G.M., and Sancar, A., Light induction of a vertebrate clock gene involves signaling through blue-light receptors and MAP kinases, *Curr. Biol.*, 12, 844, 2002.
48. Pando, M.P., Pinchak, A.B., Cermakian, N., and Sassone-Corsi, P., A cell-based system that recapitulates the dynamic light-dependent regulation of the vertebrate clock, *Proc. Natl. Acad. Sci. USA*, 98, 10178, 2001.
49. Carter-Dawson, L.D., LaVail, M.M., and Sidman, R.L., Differential effect of the *rd* mutation in rods and cones in the mouse retina, *Invest. Ophthalmol. Visual Sci.*, 17, 489, 1978.
50. McCall, M.A., Gregg, R.G., Merriman, K., Goto, N.S., Peachey, N.S., and Stanford, L.R., Morphological and physiological consequences of the selective elimination of rod photoreceptors in transgenic mice, *Exp. Eye Res.*, 63, 35, 1996.
51. Freedman, M.S., Lucas, R.J., Soni, B., von Schantz, M., Muñoz, M., David-Gray, Z., and Foster, R., Regulation of mammalian circadian behavior by non-rod, non-cone, ocular photoreceptors, *Science*, 284, 502, 1999.
52. Selby, C.P., Thompson, C., Schmitz, T.M., Van Gelder, R.N., and Sancar, A., Functional redundancy of cryptochromes and classical photoreceptors for nonvisual ocular photoreception in mice, *Proc. Natl. Acad. Sci. USA*, 97, 14697, 2000.
53. Quadro, L., Blaner, W.S., Salchow, D.J., Vogel, S., Piantedosi, R., Gouras, P., Freeman, S., Cosma, M.P., Colantuoni, V., and Gottesman, M.E., Impaired retinal function and vitamin A availability in mice lacking retinol-binding protein, *EMBO J.*, 18, 4633, 1999.
54. Thompson, C.L., Blaner, W.S., Van Gelder, R.N., Lai, K., Quadro, L., Colantuoni, V., Gottesman, M.E., and Sancar, A., Preservation of light signaling to the suprachiasmatic nucleus in vitamin A-deficient mice, *Proc. Natl. Acad. Sci. USA*, 98, 11708, 2001.

55. Thompson, C.L., Selby, C.P., and Sancar, A., unpublished data, 2002.
56. Helfrich-Forster, C., Winter, C., Hofbauer, A., Hall, J.C., and Stanewsky, R., The circadian clock of fruit flies is blind after elimination of all known photoreceptors, *Neuron*, 30, 249, 2001.

139

Green Fluorescent Proteins and Their Applications to Cell Biology and Bioelectronics

Valentina Tozzini
NEST-INFM Scuola Normale Superiore

Vittorio Pellegrini
NEST-INFM Scuola Normale Superiore

Fabio Beltram
NEST-INFM Scuola Normale Superiore

139.1 Introduction

The Green Fluorescent Protein (GFP) appeared on the scientific arena in 1962, when Shimomura et al.[1] first purified the companion protein of the chemiluminescent aequorin from the jellyfish *Aequorea Victoria* and observed its fluorescence in solution. The subsequent spectral characterization[2] showed that GFP absorbs blue light and emits green light, working as the converter of the blue chemoluminescence of aequorin in the greenish bioluminescence of the jellyfish. Evolution and natural selection produced an efficient, highly specialized nano-sized optical device that *Aequorea Victoria* and other organisms have been successfully using for millions of years. This "evolution-driven optimization" is probably at the basis of GFP success in biotechnology. Indeed, the amount of work and publications on GFPs exponentially increased from the 1960s and a vast literature was produced.[3] Cloning[4] and expression[5] of the GFP gene at the beginning of the 1990s were true breakthroughs. They opened the way for the use of GFPs in molecular and cell biology. Nowadays, GFPs are commonly used as markers of gene expression and, genetically fused to other proteins, as fluorescent tags to monitor protein trafficking, localization, and interactions in living cells and organisms.[6] Moreover, in the last decade, the number of available engineered GFP mutants exploded and yielded a whole range of artificial proteins with enhanced fluorescence, different colors, or peculiar sensitivity to external conditions (temperature, pH, etc.).

0-8493-1348-1/04/$0.00+$1.50

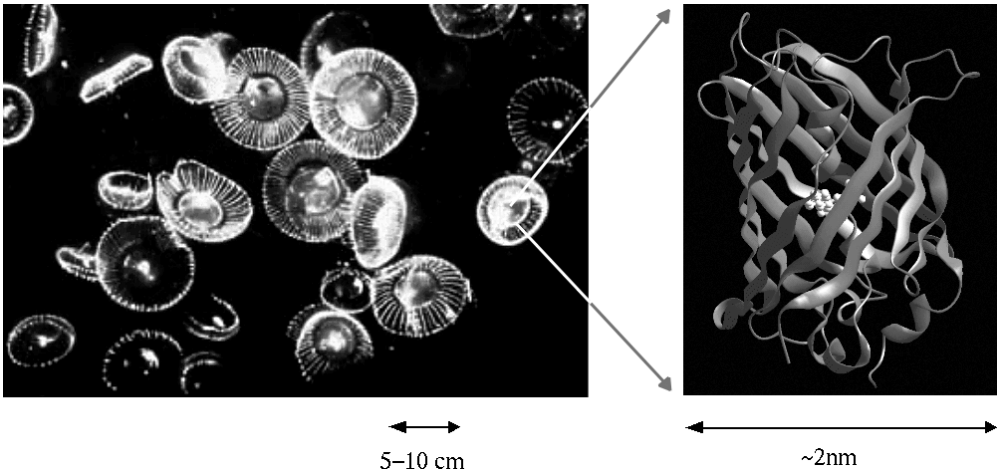

FIGURE 139.1 Specimens of *Aequorea Victoria* (left) and GFP fold (right). The tertiary structure of the protein (β-barrel) is represented in strand style, and the chromophore (represented in *ball and sticks* style) is highlighted in the center of the structure. The approximate size is indicated.

Applications of GFPs are not limited to molecular and cell biology, however. The recent discovery of multistable GFPs acting as optically controllable switches,[7,8] in fact, opens a wide field of new possibilities in bioelectronics. The relatively recent idea of using photoactive proteins to design optical memories was originally associated with another important photoactive protein: rhodopsin. The intrinsic fluorescence of GFPs, however, is a major advantage and allows its use for the implementation of single-molecule optical elements in optobioelectronics.

In this chapter, we review GFP properties and applications. Sections 139.1 through 139.4 are devoted to general and bulk properties, while in Sections 139.5 through 139.7, we focus on single-particle properties that led to the most recent and challenging applications. Other interesting review articles on GFP are listed in the literature.[9]

139.2 GFP Production, Folding, and Structure

Production

The jellyfish *Aequorea* (Figure 139.1), equally named *A. Victoria, A. Aequorea*, or *A. Forskalea*, was the first from which GFP was isolated[1] and the gene cloned[4] and expressed.[5] In the following, we refer to wild-type (WT-)GFP as the protein of *Aequorea*. GFPs with the same core chromophore and fold and similar spectral properties were extracted from other organisms, such as the sea pansy *Renilla* and the hydroid *Obelia*,[9,10] as well as from several other coelenterates of the classes of hydrozoa and anthozoa.[11] The red-fluorescent DsRed protein extracted from the *Discosoma* corallimorpharian and the nonfluorescent purple asCP extracted from *Anemonia sulcata* share the same fold of GFP but have a different chromophore.[12,13]

In the following, we will restrict our discussion to the *Aequorea* protein. We will refer to it simply by GFP. This was first sequenced and cloned in 1992[4] and expressed in heterologous systems in 1994.[14]

Fold and Chromophore Maturation

The WT-GFP was first crystallized and its atomic structure solved by Yang et al. in 1996.[15] The fold (see Figure 139.1) comprises 11 β-sheets arranged in a cylindrical shape. This cylinder is capped by short helical segments. This structure was named "β-can." The chromophore is located in the middle of the can and is bonded to the two α-helix fragments. Crystalline WT-GFP appears in dimeric form, although

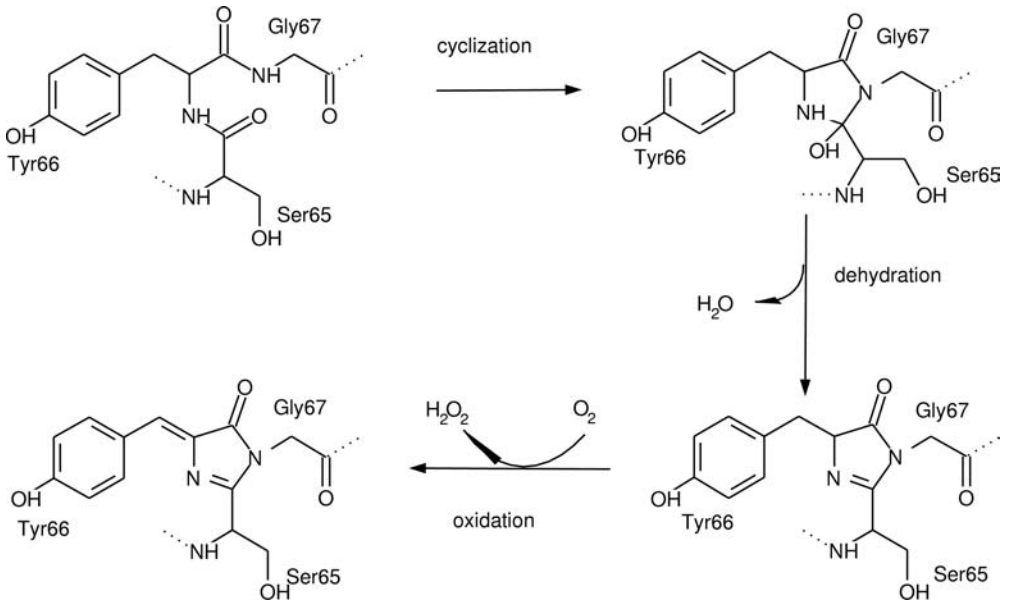

FIGURE 139.2 Chromophore formation, according to the currently accepted mechanism:[21–23] the cyclization occurs via the bonding of the carbonilic carbon of Ser65 to the nitrogen of Gly67; the subsequent dehydration of the C-N bond between Ser65 and Tyr66 with the release of a water molecule is then followed by the oxidation of the C–C bond of Tyr66. The last step is the bottleneck of the process, necessitating more than 1 h to occur. The first two steps occur in a few minutes after the folding of the protein (which necessitates about 10 min).

this characteristic depends on crystallization conditions and is lost in some of the engineered mutants.[16] The whole structure height is about 42 Å, and the diameter is about 24 Å. This unique motif with negligible variations is common to all proteins of the GFP family, including those from *Renilla* and DsRed, in spite of the relatively low sequence homology (about 23% between DsRed and Aequorea GFP).[12] The chromophore autocatalytically forms by the cyclization of the three consecutive amino acids 65, 66, and 67 (Ser, Tyr, and Gly in WT-GFP, see Figure 139.2). It is buried inside a compact, rigid, and chemically protective structure. The latter is thought to be responsible for the high stability and quantum yield of the fluorescence: classical fluorescence quenching agents, such as acrylamide and molecular oxygen, are almost ineffective on GFP fluorescence,[17] and denaturation by heating occurs only at 76°C.[18] Conversely, WT-GFP is sensitive to pH conditions, showing a dramatic decrease in the fluorescence passing from alkaline to acidic conditions.[18] Deletion experiments[19,20] showed that almost all the sequence is necessary for the protein to be functional, indicating a particularly efficient structural optimization of this protein with respect to its function. This, together with the fact that GFPs do not need any external cofactors for the fluorescence, makes these fluorescent proteins unique.

The chromophore formation is the bottleneck of protein folding and requires the presence of oxygen, releasing H_2O_2 at the end of the process. The currently accepted mechanism involving a cyclization followed by an oxidation-dehydration is shown in Figure 139.2 and is supported by the observed kinetics of the phases of the reaction and of the released intermediate by-products,[21–23] although an alternative mechanism, where the oxidation precedes the cyclization, was also proposed on the basis of a theoretical analysis.[24]

The correct folding and configuration of the residues around the chromophore are the main requisite for the fluorescence, because the isolated chromophore is not fluorescent in aqueous solution,[25] and denaturation produces a loss of fluorescence, which is recovered upon correct refolding.[26] Because WT-GFP folds better at temperatures lower than the physiological mammalian cell temperatures, "folding mutations" were designed in order to improve its use as marker in human cell biology. These are, for instance, F64L, F99S, M153T, and V163A, and they are often included in last-generation mutants. The

F64L mutation is widespread: it reduces the average distance between the carbonyl carbon of Ser65 and the amide nitrogen of Gly67 by changing a phenylalanine into the less bulky leucine in proximity of the chromophore. This favors the cyclization and results also in generally brighter mutants at the physiological temperature.[27] Analogously, any mutation of Gly67 produces nonfluorescent proteins,[28–30] indicating the crucial role of a small residue (actually, the smallest) in Position 67 in keeping Residue 65 near Residue 67 during protein maturation. More details on the other folding mutations can be found in the literature.[3,9]

139.3 Steady-State Optical Properties

Wild-Type Fluorescence Mechanism

The fluorescence mechanism of WT-GFP is prototypical of the GFP family. WT-GFP at thermal equilibrium displays two absorption peaks — at 398 nm and at 475 nm.[2,18] It emits at 503 to 509 nm when excited at 398 nm (with quantum yield ~0.7) and at 482 when excited at 475 nm.[21,31] The two absorption peaks were early attributed to structural substates of the protein, where the chromophore takes the phenolic-neutral (A state) form and the phenolate-anionic (B state) form, respectively.[32] The fluorescence mechanism was proposed on the basis of ultrafast excited-state dynamics measurements[31] and rationalized on the basis of the resolved atomic structure of A and B states[32] (Figure 139.3). A and B states are populated with a 3:1 ratio at equilibrium and differ not only in the protonation state of the chromophore but also for the different hydrogen-bond network conformation surrounding the chromophore. According to x-ray structures, a hydrogen-bond network connecting the phenol to E222 is present in the A state. It is interrupted in B state. Also, the T203 residue adopts a different conformation: it is H-bonded to the phenolate in the B state, while it is twisted in the opposite direction in the A state. When GFP is excited in the anionic state at 470 nm, it emits directly from the excited state (B*) at 482 nm and displays the typical Stokes shift and "mirror structure" in the absorption/emission spectra due to the excitation of different vibrational substates. When the neutral state is excited, an excited-state proton transfer (ESPT) occurs from the chromophore to Glu222 in a timescale of the order of picoseconds. ESPT leads to the I* form, which is attributed to an unrelaxed form of the B state. It is characterized by a deprotonated chromophore in an environment similar to that of A for what concerns the conformation of T203 and the H-bond network. The emission of I* peaks at 503 nm. Following radiative relaxation, the system goes back from I to A in the ground state. ESPT is one of the mechanisms competing with the direct fluorescence of A, occurring at 420–470 nm, which is weak in all mutants. The occasional relaxation from I* to B* in the excited state was proposed as the mechanism responsible for the observed A to B photoconversion process occurring on the timescale of minutes/hours when the GFP is excited in the UV,[31] the result of which is a depopulation of A in favor of B. A/B population equilibrium is recovered in 24 h in the dark. Recently, it was proposed that this process is paralleled by an oxidative decarboxilation of residue E222,[33] resulting in a release of CO_2.

This mechanism was supported by most of the subsequent studies. Some controversy was raised on the protonation of the imidazolinone nitrogen on the basis of quantum chemical studies of the absorption energies[34] leading to the cationic and zwitterionic forms (see Figure 139.4). However, up to now, no experimental study provided evidence for these forms in the emitting states of the proteins, as far as for forms protonated on the carbossilic oxygen (quinoid forms, see Figure 139.4). The latter are excluded by calculations in a vast range of pH around the physiological one.[35] Conversely, Raman studies confirm indirectly the attribution of A and B to neutral and anionic states, respectively.[36] The structural changes upon A↔B conversion were addressed by Fourier-transform infrared spectroscopy. No changes linked to a change in Glu protonation and in T203 conformation were observed in the vibrational spectrum.[37] These conclusions were superseded by a subsequent interpretation of the data on the basis of density functional theory (DFT) calculations.[38] We note, however, that the I state was observed also in T203 mutants, which cannot undergo the conformational T203 change.[39] This may indicate that the T203 conformational change is not a main requisite for GFP structural conversions.

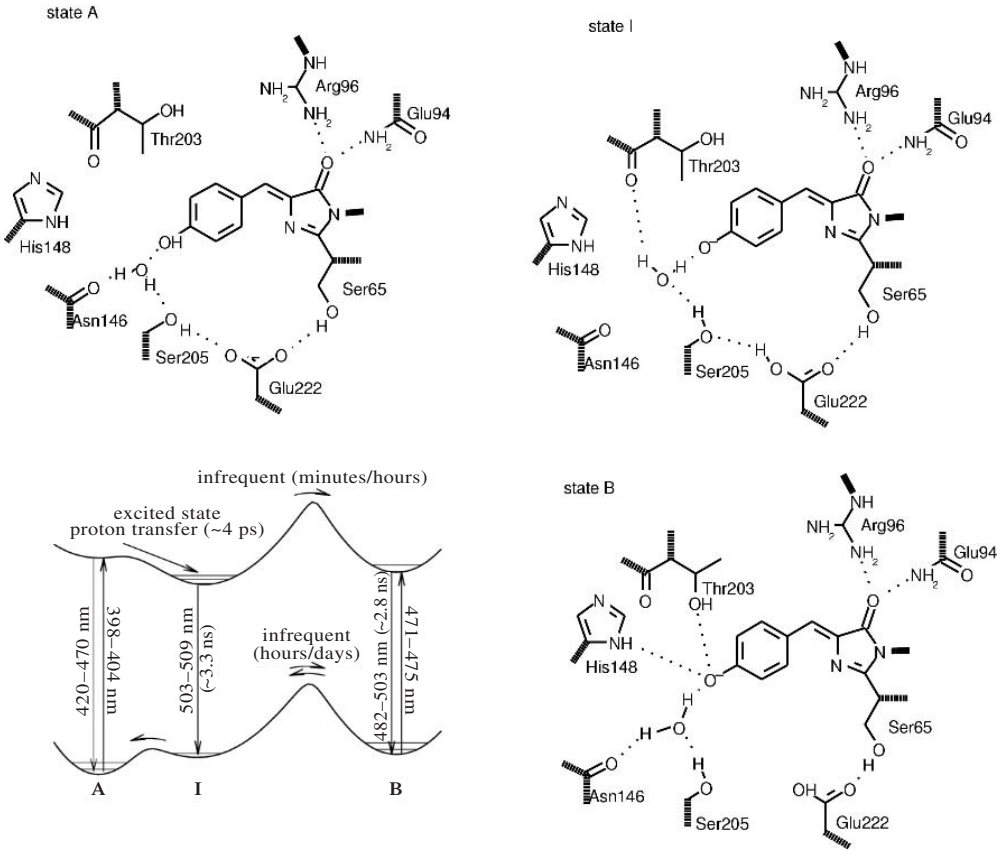

FIGURE 139.3 Structure of the active site of WT-GFP in the bright states and schematic representation of the fluorescence mechanism (bottom-left corner). A state absorbs at 398 to 404 nm (depending on the temperature). The weak direct emission at 420 to 470 nm is competitive with the more favored excited state proton transfer into the excited I state occurring in ~4 ps along the hydrogen bond network connecting the chromophore phenol with Glu222. After emission from I at 503 to 509 nm, the reprotonation of the chromophore occurs in the ground state back from Glu222 to the chromophore penolate along the same hydrogen bond network. State B absorbs at 471–475 nm and emits directly at 482 nm. B and I possess an anionic chromophore but differ in the hydrogen bond configuration, because the network from Glu222 to the chromophore is interrupted in B state.

Phenomenology and Taxonomy of the Mutants: Correlation between Structure and Optical Properties

With the exception of ineffective mutations (such as Q80R appearing in most of the mutants) and the already mentioned folding mutations, mutations occurring in the chromophore or in the chromophore environment can affect one or more steps of the above-described fluorescence mechanisms and change the absorption and emission wavelengths or the equilibrium between A/B/I states.

The large number of engineered mutants makes it necessary to begin this discussion with a classification. In 1998, Tsien[9] divided GFP mutants into seven classes based on the color (blue, cyan, green, and yellow). The green class was, in turn, subdivided into three classes based on the relative population of phenolic and phenolate states: prevalence of phenol (A), prevalence of phenolate (B), and phenol and phenolate mixtures. Here, we extend Tsien's classification also to yellow variants. This has become necessary due to the large amount of yellow mutants investigated in the last years. A list of mutants with some spectral characteristics is given in Table 139.1. For the mutants with atomic structures that are solved, the Protein Data Bank code[40] is also given.

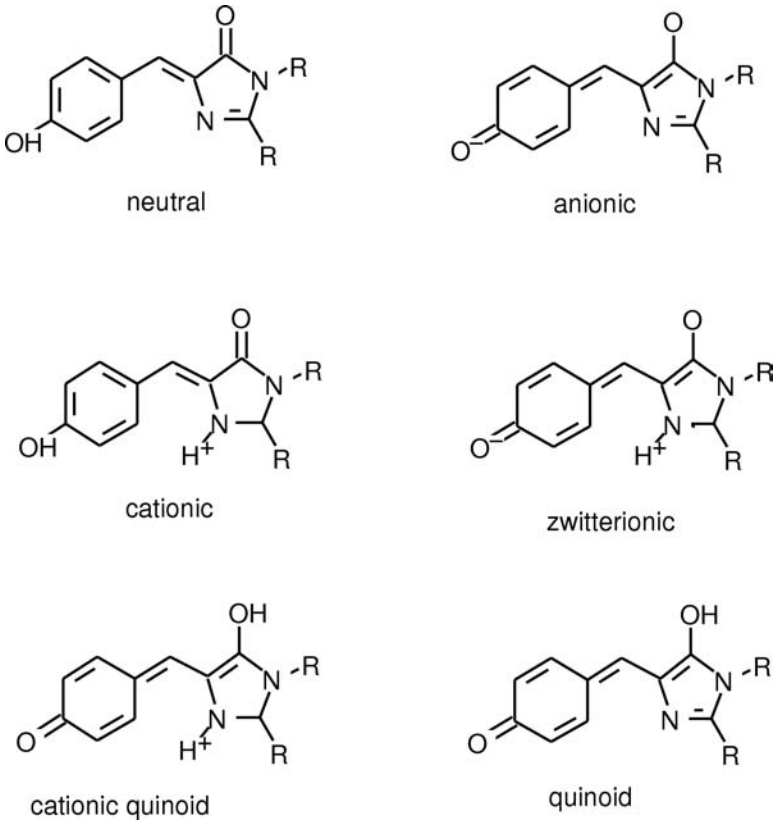

FIGURE 139.4 Possible protonation states of the chromophore. Only the neutral and the anionic forms are thought to be present in the normal state of the protein. The cationic and zwitterionic forms were proposed as candidates for the dark states, while the quinoid forms were proposed to exist in solutions at extremely low pH.[35]

Mutations involving Residues 56 and 66 in the chromophore change the chemical nature of the chromophore and lead to differently colored variants. Chromophore types are reported in Table 139.2. Y66F or Y66H produce blue mutants by reducing the extension of the aromatic system (Classes 6 and 7 in Tsien classification). The same mechanism, to a lesser extent, produces cyan variants for the case of the Y66W mutation (Tsien Class 5). Blue and cyan mutants display only one absorption peak that was associated with state A, because the chromophore is thought to be neutral.[41,43] There is no evidence for ESPT associated to the fluorescence,[44] which is thought to occur by direct A* decay. Even in the presence of folding and enhancing mutations (including Y145F, a specific enhancing mutation for blue variants), cyan and blue mutants present low brightness.

Green and yellow mutants are characterized by a T66 in the chromophore. As already mentioned, these classes are subdivided into three subclasses, i.e., GREEN, GREEN A, and GREEN B (analogous for YELLOW), displaying similar A/B population, prevalent A or B, respectively (see Table 139.1 — these correspond to Classes 1 through 4 in Tsien classification). According to this classification, sgBFP[45] belongs to class GREEN A, although it emits in the cyan.

S65T[32] is the prototype of GREEN B mutants. These are widely used for tagging applications due to their relatively high quantum yield and spectral simplicity (they present a single excitation peak, and ESPT is suppressed). The shift of thermal equilibrium toward B is achieved with different mechanisms. In S65T/C mutants, Thr65 (Cys65) adopts a different conformation with respect to Ser65, forming a less stable hydrogen bond with Glu222 and weakening the hydrogen bond network connecting Glu222 with the chromophore.[32,45] In S65G/A/L mutants, the same effect is produced by eliminating the H-bonding

TABLE 139.1 Classification of GFP Mutants

Class	Mutations	Ref. ([]), Year, Name	PDB Code and Oligomer	Chromophore Type	λ_{exA} (ε 103)	λ_{exB} (ε)	λ_{em} (Q)	A/B Population
BLUE	Y66F	[22] 1995		CSF	360		442	—
	F64L/S65T/Y66H/Y145F	[47] 1997		CTH	380 (31.0)		440 (0.17)	—
		[45] 2001 EBFP						
	Y66H/Y145F	[41] 1997	1BFP monomer	CSH	382(22.3)		446 (0.3)	—
		[42] 1998						
		[48] 1996 P4-3			381		445	
	F64L/Y66H/Y145F	[49] 1999 EBFP		CSH	383 (26.6)		447 (0.26)	—
	Y66H	[21] 1994 BFP, P4		CSH	382 (21)		448 (0.24)	—
	F645L/Y66H/Y145F/V163A	[49] 1999		CSH	384 (22.0)		448 (0.27)	—
	F64L/Y66H (A1[b] Q80R)	[43] 1997	2EMD, 2EMN dimer	CSH	384 (15.6)		450 (0.24)	—
	F64L/Y66H/V163A (A1[b] Q80R)	[50]1998 BFPsg50		CSH	387		450	—
		[43] 1997	1EMF, 2EMO, dimer		384 (16.5)		450 (0.25)	
	Y66H/F64M	[44] 1996 BFP11		CSH	387		451	—
CYAN	Y66W	[21] 1994 W		CSW	430–458		480–485	—
	Y66W/I123V/Y145H/H148R/ M153T/V163A/N212K	[48] 1996 W2		CSW	432		480	—
	F64L/S65T/Y66W/N146I/M153T/ V163A(/N121A)	[49] 1999 W1B		CTW	434–452 (32.5)		476–505 (0.4)	—
		[45] 2001 ECFP			434 (26.0)		477	
	K62R/N164I/N212K	[51] 1997 ECFP			434		474	
	S65A/Y66W/S72A/N146I/M153T/ V163A	[49] 1999 W1C		CAW	435 (21.2)		495 (0.39)	—
	Y66W/N146I/M153T/V163A	[49] 1999 W7		CSW	434–452 (32.5)		476–505 (0.42)	—
	Y66W/N146I/M153T/V163A/ N212K	[45] 2001			433 (18.0)		475–501	
		[48] 1996 W7			443		474	
CYAN/ GREEN A	F64L/S65C/I167T	[45] 2001 sgBFP		CCY	387		450	A >> B
GREEN	None or Q80R	[15] 1996 WT	1GFLdimer	CSY	395 (25–030)	475 (9–14)	509 (0.79)	A > B (4/1)
		[33] 2002	1HCJ dimer					
	F99S/M153T/V163A		Q222 decarboxilated 1B9C, dimer		397 (30)	475 (6.5–8.5)	506 (0.79)	
		[52] 2000 cycle3						
	F64L/I167T/K238N(/A1[b] Q80R)	[43] 1997	1EMC dimer/ monomer 1EME monomer 1EML dimer	CSY	395 (11.5)	468 (12.7)	506 (0.84)	A ~ B
	S65T/H148D	[53] 1999		CTY	415	487	510	A ~ B

TABLE 139.1 Classification of GFP Mutants (continued)

Class	Mutations	Ref. ([]), Year, Name	PDB Code and Oligomer	Chromophore Type	λ_{exA} (ε 103)	λ_{exB} (ε)	λ_{em} (Q)	A/B Population
GREEN A	F64L (A1[b] Q80R)	[43] 1997	1EMM dimer	CSY	393 (18.3)	473 (4.0)	508 (0.85)	A > B (~6/1)
	K238N				394			
	(S202F)T203I	[54] 2000		CSY	393 (18.3)		473 (4.0)	A >> B (~20/1)
		[48] 1994 H9						
	S72A/T203I/Y145F	[49] 1999 H9—40			399 (29.0)		511 (0.6)	
	T203V	[54] 2000		CSY	398		513	A >> B (~20/1)
GREEN B	I167V	[21] 1994 P9		CSY	396	471	502 (507)	A < B (~1/3)
	I167T	[21] 1994 P11		CSY	396	471	502 (507)	A < B
	E222Q	[55] 1998		CSY		478	506	A << B
	S65A	[22] 1995		CAY		471	504	A << B
	S65C	[22] 1995		CCY		478	507	A << B
	F64L/S65C/I167T/K238N	[43] 1997	1EMK dimer	CCY		474	506	A << B
		[50] 1998 rsGFP				473	509	
	S65T (Q80R)	[49] 1999		CSY	394	489 (52–48)	511 (0.64)	A << B
		[32] 1997	1EMA,1EMB monomer					
		[53] 1999	1C4F, 1EMG					
	S65G	[56] 2001		CGY		476	510	A << B
	S65L	[22] 1995		CLY		484	510	A << B
	T203V/E222Q	[56] 2001		CSY		496	513	A << B
	F64L/S65T/S72A/N149K/M153T/I167T/H231L	[45] 2001 Emerald		CTY		484 (36.0)	508	A << B
	S65T/S72A/V163/N149K/M153T/I167T	[49] 1997				487 (57.5)	509 (0.68)	
	F64L/S65T/V163A	[49] 1997		CTY		488 (42)	511 (0.58)	A << B
	F64L/S65T	[57] 1998		CTY	400	480	515	A < B (1/4)
		[49] 1997 EGFP				488 (55–57)	507–509 (0.60)	
	F64L/S65T/Y145T/H14V/V140A/I167V	[57] 1998		CTY	394	502	519	A < B (1/3)
	F64M/S65G/Q69L	[58] 2000 RSGFP		CGY		476–495	503–530	A << B(I)

YELLOW	T203F	[54] 2000		CSY	404	506	522	A ~ B (0.8/1)
YELLOW A	T203H	[54] 2000		CSY	403	506	517	A >> B (100/1)
	T203Y	[54] 2000		CSY	404	510	524–527	A > B (2/1)
	Q80R/S65G/V68L/S72A/H148G/ T203Y	[46] 1998 YFP/H148G	2YFP, monomer	CGY				A > B
		[53] 1999			397	512	528	
	Q80R/S65G/V68L/S72A/H148Q/ T203Y	[59] 2000 YFP H148Q	1F09 1F0B monomer	CGY				
	F64L/S65T/T203Y	[57] 1998		CTY	415	516	525	A > B (4/1)
		[60] 2001 E^2GFP						
YELLOW B	S65G/S72A/T203F	[49] 1999		CGY		512 (65.5)	522 (0.70)	A << B (1/20)
		[47] 1997						
	S65G/S72A/T203H	[49] 1999		CGY		508 (48.5)	518 (0.78)	A << B
	S65G/S72A/T203Y	[47] 1997		CGY		~515	~525	A << B (1/100)
		[45] 2001 EYFP				514 (84.0)	527	
	S65G/V68L/S72A/T203Y	[58] 2000 EYFP		CGY		520	525	A < B (1/5)
	Q80R/S65G/V68L/S72A/T203Y	[49] 1999 10C				514 (83.4)		
	S65G/S72A/T203Y/H231L	[46] 1998 YFP	1YFP, dimer		392	514	528	
		[61] 1998 YFP			392	514	528	
	S65G/V68L/Q69M/S72A/T203Y	[62] 2001 Citrine	1HUY, monomer	CGY		516 (77)	529 (0.76)	A < B
	S65G/V68L/Q69K/S72A/T203Y	[62] 2001 EYFP/ V68L/Q69K				516 (62)	529 (0.71)	
	S65G/V68L/S72A/T203Y/E222Q	[53] 1999		CGY	402	510	525	A < B
	S65G/S72A/K79R/T203Y(/H231L)	[49] 1999 Topaz		CGY		514 (94.5)	527 (0.60)	A << B
		[45] 2001				514 (48.0)		
	S65G/V68L/O69K/S72A/T203Y	[64]10C Q69K 2001		CGY		516 (62.0)	529 (0.71)	A << B
	C48V/S65A/V68L/S72A/Q80R/ N149C/M153V/S202C/T203Y/ D234H	[63] 2001	1H6R	CAY				

Note. The chromophore names are assigned as shown in Table 139.2. Q is the quantum yield of fluorescence, and ε is the extinction coefficient. Mutants that are spectrally indistinguishable are grouped in the same cell.

TABLE 139.2 Chromophore Types

6665	Phe (F)	His (H)	Trp (W)	Tyr (Y)
Gly (G)				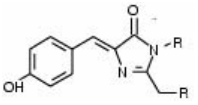 CGY 510-529 (green-yellow)
Ala (A)			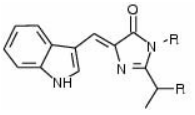 CAW (495, cyan)	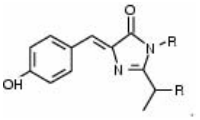 CAY (504, green)
Cys (C)		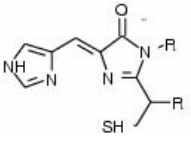 CCH (450, blue)		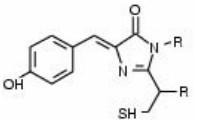 CCY 450-509, blue-green
Ser (S)	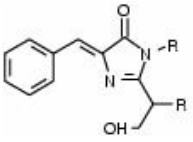 CSF (442, blue)	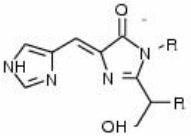 CSH (446–451,blue)	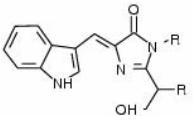 CSW(474–505,cyan)	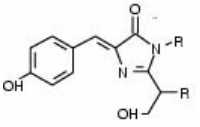 CSY (506–527, green-yellow)
Thr (T)		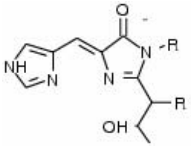 CTH (440, blue)	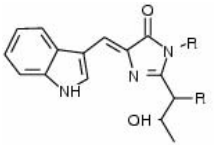 CTW(474–505,cyan)	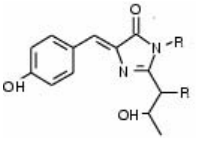 CTY (510–525, green yellow)
Leu (L)				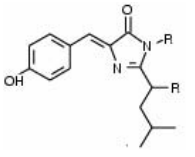 CLY (510,green)

Note. The names of the chromophore are assigned as follows: C (standing for chromophore) followed by the one-letter notation for amino acids 65 and 66. Residue 67 is always a Gly.

hydroxy group of Residue 65. Mutations of E222 in a residue with opposite polarity (i.e., E222Q) act by disrupting the possibility of donating the proton to the chromophore, again, resulting in a destabilization of A. Finally, I167T, which produces the particularly bright Emerald mutant, adds an additional hydrogen bond donor to the chromophore phenolate, producing additional stabilization of the B state.

Conversely, mutations eliminating a hydrogen donor on the phenolate chromophore, such as T203I and T203V, destabilize State B in favor of A and produce Class GREEN A. These variants emit by ESPT with a relatively high quantum yield and find applications due to their large Stokes shift between absorption and emission.

Mutations of T203 in aromatic residues (F, Y, or H) produce a red shift of 15 to 20 nm in the absorption/emission of State B and of 5 to 10 nm in the absorption of State A, which was attributed to the π-stacking interaction between the chromophore and the aromatic residue.[46] We must note, however, the smaller red shift in A with respect to B and the fact that a slight red shift in B absorption occurs also in the case of T203V. These facts indicate that the elimination of the T203 hydrogen bond in State B must play some role in the red shift of fluorescence. A probable source is the destabilization of the ground state and the consequent reduction of the absorption energy. Accordingly, when only T203Y/F mutations are present, State A tends to be more stable than B, producing the class YELLOW A. In contrast to GREEN A, YELLOW A mutants show relatively lower quantum yields and suppression of ESPT. They were shown to offer some interesting properties at the single molecule level (see next sections). When the typical mutations stabilizing the B state are added (for instance, S65G or the other mentioned above for the green variants), the equilibrium is again restored toward B, and the class YELLOW B is produced, which has similar properties to the class GREEN B.

Acid–Base Equilibria

GFP fluorescence is strongly affected by changes in pH. The chromophore tends to ionize from neutral to anionic in passing from acidic to basic conditions. The population or depopulation of the anionic state is paralleled by an enhancement or quenching of the fluorescence, and thus, the titration curve can be measured with optical techniques, displaying a first titration point (pKa) around pH = 5 (in WT), and a second pKa in basic conditions (around pH = 12[26]). This two-step titration mechanism was interpreted on the basis of force-field-based calculations.[65] In acidic conditions, only the neutral chromophore is present with Glu222 protonated, at basic–intermediate conditions, the protein displays an internal equilibrium between A and B states (shifted on A or B depending on the mutant, see previous section) involving a proton exchange with Glu222. Finally, in basic conditions, the anionic states can only be present with Glu222 deprotonated.

Yellow mutants present particularly high values of the first pKa (~7), which makes them particularly sensitive to pH conditions and not suitable for applications at physiological pH. Q69K reduces the pKa to 6.1, improving folding and thermostability.[62] Mutation Q69M produced the mutant Citrine (pKa = 5.7) that is both less sensitive to pH changes within physiological conditions and more resistant to halide attack.[62] This property stems from the occupation by the Met residue of the halide-binding cavity present in WT-GFP.[62] Conversely, mutation H148G[46] makes the protein more sensitive to the pH conditions (pKa = 8) by producing a "hole" in the β-barrel at position 148 and exposing the chromophore to the solvent. Acidic and halide sensitivity seem to be coupled in YFP-H148Q,[59] where the binding of a halide (I^-) raises the chromophore pKa value.

139.4 Applications to Live-Cell Imaging

Recent experimental results demonstrated that sophisticated optical approaches conjugated with the use of suitable optical tags make it possible to visualize biomolecular events at the surface and in the interior of a living cell, down to the single-molecule level.[6] The application of high-resolution optical spectroscopies to the visualization of proteins labeled with optical tags now offers a series of new tools for the investigation of protein trafficking and interactions inside different cellular compartments. Thanks to the realization of a large set of GFP variants with tunable optical properties, the use of GFPs for live-cell imaging has revolutionized this field in the last years. Particularly relevant is the development and use of suitable GFP markers for the identification of protein–protein interactions *in vivo*. To this end, one of the most powerful optical techniques is based on fluorescence resonant energy transfer (FRET).[66] The development of several pairs of GFP mutants with the required overlap between absorption and emission spectra provided a new arena of FRET applications *in vivo*. In this section, we will mainly concentrate on this application. Before that we recall that FRET exploits radiationless energy transfer driven by dipole–dipole interaction occurring from a fluorophore (the donor) in the excited state to

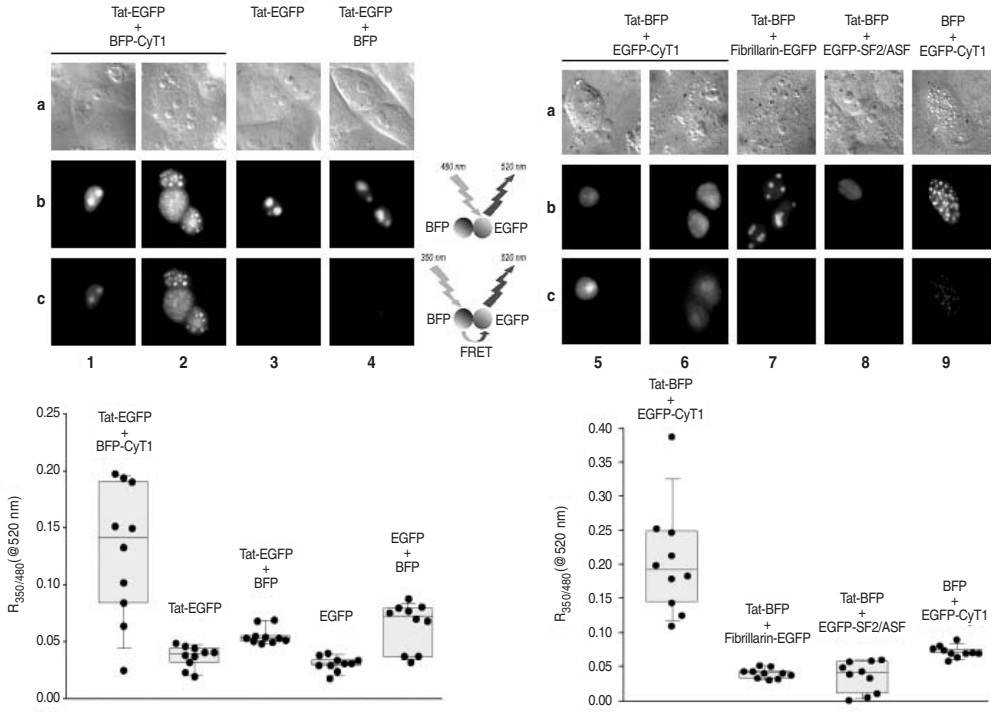

FIGURE 139.5 (Upper) Visualization of FRET in human HL3T1 cells. Transfected cells were visualized by transmitted light in Nomarski configuration (panels in Row a), by excitation at 480 nm, and collection at 520 nm, showing EGFP fluorescence after direct EGFP excitation (panels in Row b), and by excitation at 350 nm and collection at 520 nm, showing EGFP fluorescence after BFP excitation, indicating FRET (panels in Row c). EGFP-SF2/ASF and Fibrillarin-EGFP were generously provided by T. Misteli (National Institute of Health, Bethesda, MD, USA). (Lower left panel) Quantification of FRET between Tat-EGFP and BFP-Cyclin T1. Fluorescent emission at 520 nm from individual cells was recorded after excitation at 350 or 480 nm, and integrated intensities over the whole cell were evaluated. Plotted values (indicated by dots) represent the ratio between these two measurements: higher values indicate more efficient resonant energy transfer between BFP and EGFP. Ten consecutively analyzed cells were considered for each transfection; their individual fluorescence ratios and their percentile box plot distribution are shown. Horizontal lines from top to bottom mark the 10th, 25th, 75th, and 90th percentiles, respectively. (Lower right panel) Quantification of FRET between Tat-BFP and EGFP-Cyclin T1. Graphic representation of FRET is as in the lower left panel. (After Marcello, A., Cinelli, R.A., Ferrari, A., Signorelli, A., Tyagi, M., Pellegrini, V., Beltram, F., and Giacca, M., *J. Biol. Chem.*, 276, 42, 39220–39225, 2001.)

another fluorophore (the acceptor) when in close proximity; energy transfer is followed by acceptor fluorescence. Simple colocalization of two proteins is not sufficient to yield energy transfer. FRET efficiency, in fact, is proportional to $(R/R_o)^{-6}$, where R is the distance between the two fluorophores, and R_o is typically of the order of (or less than) 10 nm: the presence of FRET indicates actual protein–protein interaction at distances of the order of the nanometer for many pairs of optically matched fluorophores.

Shown in Figure 139.5 is an example of FRET observation of protein interaction in human HeLa (HL3T1) cells based on GFP-class tagging.[67] In this experiment, the interaction between two key proteins involved in HIV-1 transcriptional activation, HIV-1 Tat, and human CycT1, was monitored by fusing to them BFP and EGFP mutants. FRET analysis was performed in two steps. First, EGFP fluorescence at 520 nm (this represents the optimum wavelength for EGFP detection) was collected after direct excitation at 480 nm, resonant with EGFP absorption. Second, EGFP emission at 520 nm was measured after excitation at 360 nm, resonant with BFP absorption. In the latter case, EGFP emission mainly originates from the energy transfer. The ratio between the two EGFP emissions provides the FRET efficiency $R_{360/480}$(@520). FRET image analysis of cells transfected with Tat-EGFP and BFP-Cyclin T1 and

controls are shown in Figure 139.5 Panels a1 to c4. Panels (1 through 4) in Row b show the intracellular distribution of fluorescence around 520 nm under excitation at 480 nm. In these conditions, most cells transfected with Tat-EGFP (Panels b1 to b4) showed the characteristic pattern of overexpressed Tat, consisting of diffuse nucleoplasmic fluorescence and intense nucleolar staining. FRET analysis was performed by illuminating the same cells at 360 nm (to excite BFP) and recording at 520 nm (panels in Row c), thus allowing comparison of EGFP emission following BFP excitation with that following direct EGFP excitation. In these conditions, only samples expressing both Tat-EGFP and BFP-Cyclin T1 scored positive for fluorescence (Panels c1 and c2). This result provides strong evidence that the two proteins directly interact inside the cell. Detailed quantitative analysis of several cells transfected with the two proteins or with controls are presented in Figure 139.5(bottom), which shows the experimental FRET signal and its distribution. Most cells transfected with Tat-EGFP plus BFP-Cyclin T1 showed FRET values that were clearly higher than those detected in control transfections. For quantitative analysis based on FRET data, it is often important to eliminate possible artifacts due to different expression efficiencies and quantum yields of the two GFPs. This is particularly relevant for the case of BFP and also for many other EGFP companions in FRET applications. In order to overcome this limitation, one useful additional experiment is to visualize FRET with the reciprocal constructs. In the case of the experiment above described, FRET was analyzed in cells transfected with Tat-BFP and EGFP-Cyclin T1. Also, this protein pair showed intracellular FRET [Figure 139.5, Panels 5 to 9), with acceptor (EGFP) fluorescence in the nucleus (including the nucleolus) after excitation at 350 nm. In contrast, when Tat-BFP was cotransfected with Fibrillarin-EGFP [a protein that specifically localizes in nucleoli, see Figure 139.5, Panels 7] or with EGFP-SF2/ASF [Figure 139.5, Panels 8], which marks sites of mRNA splicing, no FRET was observed. The interaction was also quantitatively analyzed by observing fluorescence in a series of individual cells [see Figure 139.5(lower panels)]. Cells transfected with Tat-BFP plus EGFP-Cyclin T1 showed average FRET values of 0.20 ± 0.08, which were about five times higher than those expressing Tat-BFP and Fibrillarin-EGFP (0.040 ± 0.007) or Tat-BFP and EGFP-SF2/ASF (0.036 ± 0.023; $p < 0.001$ in both cases). FRET values can also be used to address the specific spatial configuration of the two fluorophores. In the case of Tat-CyT1, the observed high FRET signal values imply that the product $n_A \cdot E_T$ between the fraction of EGFPs coupled to a BFP and FRET efficiency is very close to unity.[67] In light of the fact that by definition the two factors have one as an upper bound, this indicates that $E_T \sim 1$. Given the peculiar β-can structure of GFPs, we are led to conclude that the interacting fluorophores are juxtaposed along the β-sheet outer shield with core-to-core distance of approximately 3 nm.

Real-time movement of proteins between different cellular compartments can also be visualized by exploiting GFP optical markers. In these experiments, GFP molecules in a defined area of a living cell are photobleached by an intense laser pulse. The recovery of GFP fluorescence in this area is recorded as a function of time. This technique is called fluorescence recovery after photobleaching (FRAP). Because this recovery is due to movement of GFP-fusion proteins into the bleached area, FRAP analysis allows us to carefully investigate the mobility of proteins in the target area within the cellular environment.[68] Other more sophisticated optical techniques can complement the spectroscopic information with radiative lifetime data, allowing for the development of accurate fingerprints of protein localization and interaction pattern. An important advantage of such lifetime imaging is that the absolute values of lifetimes are independent of the probe concentration, photobleaching, light scattering, and the amount of excitation intensity. Fluorescence lifetime imaging (FLIM) thus offers many additional opportunities for studies of dynamic events in living cells.[69]

139.5 Single-Molecule Photophysics and Applications

Molecular Basis of the ON–OFF Photodynamics

GFP applications are influenced by several photoinduced processes that can drive molecules into states that are dark or have altered fluorescence properties, such as, the already mentioned A → B photoconversion induced by UV illumination of WT-GFP. Another photoinduced process is the conversion to a

red-emitting (~600 nm) species occurring by illumination at 488 nm at low oxygen concentration.[70] However, the more problematic processes are those involving dark states. These affect bulk fluorescence properties but were directly observed and characterized only with the aid of single-molecule techniques. These processes were separated in at least three different classes, based on the different phenomenology: a fast ON–OFF blinking observed during illumination, a photobleaching leading to a long-lived dark state occurring after a certain number of normal photocycles, and, possibly, a recovery of the fluorescence after bleaching induced by illumination at specific wavelengths in the blue-UV range.

Phenomenology

Most of the single molecule experiments were performed on GREEN B and YELLOW class mutants. In general, GREEN B mutants are among the most resistant to photobleaching and blinking, while some yellow mutants revealed an interesting controllable ON–OFF switching behavior. Time-resolved single-molecule spectroscopy and fluorescence correlation experiments were performed on S65T, EGFP, and E222Q,[55,71,72] revealing a common phenomenology: the fluorescence trajectories undergo ON–OFF blinking events until a final long-lived dark state is reached (bleaching). The average ON time during blinking is inversely proportional to the illumination intensity,[71–72] being of the order of tens of ms to s for ordinary illumination intensities. This indicates that turning off is a photoinduced event with a transition yield calculated to be 0.5×10^{-5} in S65T.[73] The average OFF time is of the order of seconds (or tens of seconds[71]) and is not dependent on illumination intensity. Additionally, some experiments[55,71] indicate that more than one process with different timescales may be present in the blinking phenomenology. While single-molecule experiments showed that in EGFP[71] blinking time constants are independent of pH conditions, correlation fluorescence spectroscopy indicates that in EGFP and S65T,[71] the equilibrium time constant between emissive and nonemissive species has two components (both illumination-intensity dependent). One is pH dependent and one is pH independent and is characterized by a much shorter timescale (fraction of ms, *flickering*). Two-color fluorescence correlation spectroscopy on E222Q[72] also revealed a fast dynamics on the order of hundreds of μs. Single-molecule and correlation fluorescence spectroscopy experiments were performed on some YELLOW B class mutants[7,74] displaying almost the same blinking and flickering phenomenology.

In the two YELLOW B mutants S65G/S72A/T203Y(T203F),[7] a controllable switching behavior was observed for the first time. In this work, in addition to blinking (on the timescale of seconds) and photobleaching (after 5 min of illumination), a recovery of the fluorescence was reproducibly observed with 5 min of irradiation at 405 nm. Switching behavior and controllable fluorescence recovery were also observed to occur at a shorter timescale (seconds) in the YELLOW A mutant E^2GFP by illumination in the UV,[60] whereas no fluorescence recovery after bleaching was observed in the same conditions in EGFP.[60]

Photobleaching is usually attributed to a distinct phenomenon with respect to blinking, because it leads to a long-lived dark state after about 10^6 emissive cycles.[7] However, in the literature,[71] the photobleaching observed in bulk experiments for EGFP on timescales dependent on the intensities was associated with the same state transition of blinking, attributed to a bulk manifestation of the latter, and a common transition yield was calculated (3.6 to 8 10^{-6}).

Models

Most of the models for the bright-to-dark dynamics are based on the observation that only B-type states display a significant intrinsic fluorescence. Excitation of State A produces a low fluorescence at about 450 nm, even in mutants with a depressed ESPT. This implies the existence of a nonradiative decay channel for the neutral state, which was identified by some authors[57,70] with a chromophore torsion. According to quantum chemical calculations,[75] the electronic structure of the neutral state allows for the possibility of a nonadiabatic conversion (NAC) between excited and ground state occurring by a torsion of the two bonds connecting the rings. Conversely, owing to the different electronic structure, in anionic species, NAC is not allowed in the restricted volume of the active site, and thus B displays fluorescence. In aqueous

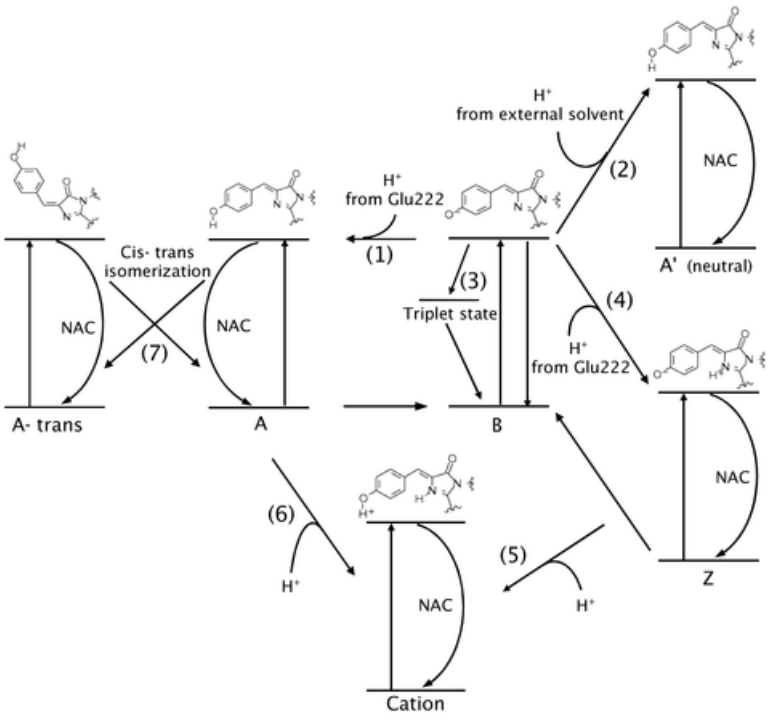

FIGURE 139.6 Hypothetical schemes for blinking, flickering, and photobleaching dynamics. Blinking was attributed to internal (1) or external (2) excited state deprotonation of the chromophore,[56,71–73] or to the zwitterion (Z) formation (4),[70] or the a transient formation to a triplet state (3).[70–71] Process (1) is considered responsible for the photobleaching in mutants where A state is almost dark.[75] The cationic state, reachable by processes (5) or (6) was never seriously considered. Process (7) involving a *cis-trans* isomerization was recently proposed by us as a possible process leading to a reactivable dark state.

solutions, thanks to the absence of the constraints imposed by the protein environment, NAC can always occur, and fluorescence is quenched. Theoretical calculations indicate that the zwitterionic[75] and cationic[76] species are also prone to NAC, and thus can be considered as candidates for the role of dark states.

Following these considerations, several different schemes were proposed to explain the observed phenomenology (Figure 139.6). Several authors[7,71,75] attributed the main blinking component to a B $\rightarrow$ A interconversion with the proton taken from Glu222 (Process 1 in Figure 139.6). The B $\rightarrow$ A process is thought to occur in the excited state, in agreement with the inverse linear dependence of the ON time on light intensity. The inverse process A $\rightarrow$ B is expected to occur in the ground state. The presence of a component dependent on pH in S65T and EGFP was attributed to a different process (Process 2 in Figure 139.6) involving a protonation from the external solvent, leading to a different state (A'), where chromophore and Glu222 are protonated.[71] The fast ms or sub-ms component observed in E222Q and EGFP[77,78] was attributed to a temporary population of the triplet excited state of B (Process 3 in Figure 139.7).

Alternatively, blinking was attributed to the zwitterionic state by several authors, following the scheme suggested in Weber et al.[75] (Process 4 of Figure 139.6). Within the framework proposed by these authors, the B $\rightarrow$ A conversion is responsible for the molecular switching OFF, leading to photobleaching at the bulk level, and lower photostability of yellow mutants reflects the presence of Y203, which yields a larger flexibility in the chromophore environment.

The cationic scheme was discussed by some authors but was not favorably accepted, probably because the two-step process necessary to pass from B to cation is not unique (Processes 5 and 6).

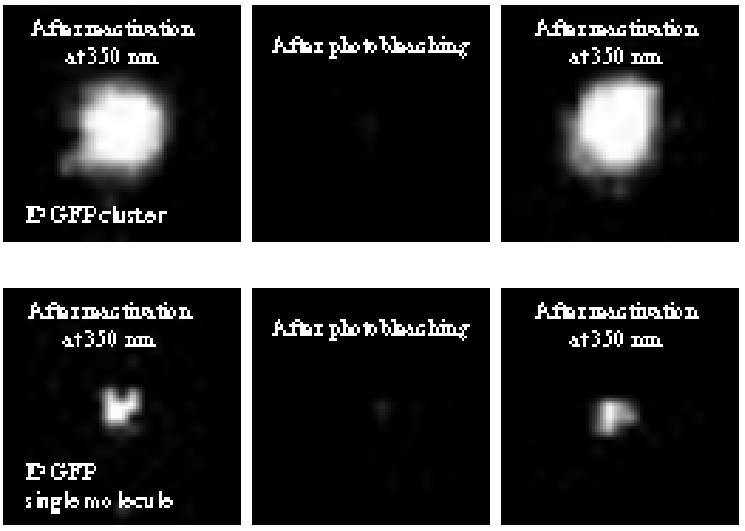

FIGURE 139.7 Typical images (from left to right) of an E²GFP cluster (upper row) and a single E²GFP molecule (lower row) in polyacrylamide (PAA) gels after alternate photobleaching by 10 s excitation at 476 nm and photoconversion by 2 s at 350 nm (0.2 kW/cm² at both wavelengths). Each frame size is 2 μm x μ2 m and integration time 100 ms (After Cinelli, R.A.G., Pellegrini, V., Ferrari, A., Faraci, P., Nifosì, R., Tyagi, M., Giacca, M., and Beltram, F., *Appl. Phys. Lett.*, 79, 3353–3356, 2001.)

As discussed in Section 139.5.1.1, a controllable ON–OFF switching dynamics was recently observed in two different yellow mutants, EYFP[7] and E²GFP.[60] Both of these variants can be reactivated by UV irradiation (400 nm for EYGFP and 350 nm for E²GFP) after bleaching. Notably, E²GFP was reported to require much shorter irradiation times and intensities. In E²GFP, photobleaching was shown to populate a distinct state absorbing at ~365 nm (State C in the following[79]). A theoretical analysis based on *ab initio* calculations indicates that interactions between a chromophore and its environment, such as hydrogen bonds or aromatic stacking, produce a red shift in the chromophore absorption.[34,45,79,80] Consequently, any model for the ON–OFF mechanism should include a neutral chromophore state embedded in an environment forming smaller numbers of or less-stable hydrogen bonds with the chromophore than normal A state. A possibility was suggested[79] for a process of Type 2 in Figure 139.6. Protonation should occur via His148 acting as a proton bridge between the chromophore phenol and the external buffer. At variance with respect to normal A state, Glu222 should be protonated, and this could destabilize some of the hydrogen bonds coordinating the chromophore. An alternative mechanism proposed is based on a *cis-trans* isomerization of the neutral chromophore (Part 7 in Figure 139.6). Nonadiabatic crossing could occasionally convert A* into A-*trans* instead of simply relaxing A* to its ground state. State A-*trans* is dark, because it is prone to NAC, as State A is, and has no possibility of ESPT. This mechanism was supported by Classical Molecular Dynamics simulations that showed that one of the hydrogen bonds on the carbonilic oxygen of the chromophore breaks in the *trans*-neutral state. In this model, the fluorescence recovery can be easily explained as the inverse *trans-cis* isomerization occurring by nonadiabatic crossing (as for the *cis-trans* transition).

The existence of an additional neutral state absorbing at almost the same wavelength as A was previously proposed[81] on the basis of time-resolved single-photon counting spectroscopy, although a role was not assigned to this state in the dark dynamics.

Applications to Bioelectronics

The availability of the distinct photoconvertible ground states in selected GFP variants discussed in the previous paragraph opens the way to the exploitation of these biomolecules for data storage and manipulation

at the single-molecule level, thus expanding the area of GFP applications beyond cell biology. The optical control of the molecular structure as obtained in EYFP and E^{2}GFP represents, in fact, a viable strategy for storing and manipulating data at high density. Among the most remarkable applications, we will mention volumetric memory devices.[82] Prototypes with extremely high capacities, high throughput rates, and fast access times were demonstrated. These concepts, using spectral, spatial, or temporal coordinates, offer attractive alternatives that are compatible with optical interconnection protocols. It is expected that terabits per cubic centimeter storage densities are possible in these volumetric optical memories, with data throughput rates in the range of gigabits/sec and access times of only a few nanoseconds.

Much of the research effort in this direction was directed toward the development of photonic components based on photochromic molecules.[83] Although a number of proteins were explored for device applications,[84] bacteriorhodopsin was the subject of the most intense research effort stimulated by the understanding of the nature of photocycle intermediates and the microscopic pathways connecting them.[85] Following these studies, bacteriorhodopsin-based volumetric optical memories were proposed that exploit photoisomerization between distinct chromophore states populated during the photochemical cycle, and they were shown to offer great improvement in data storage capacity.[86] Bacteriorhodopsin, however, photoisomerizes without fluorescing. This makes it unsuitable for single-molecule detection and use. This ultimate regime represents the most promising strategy toward electronic and photonic detection at the nanoscale level. To this respect, the photochromic GFP variants represent ideal candidates, because their fluorescence can be detected at the single-molecule level.

In the case of the yellow variant E^{2}GFP, in particular, States B and C can be used to encode a (0, 1) bit that can be stored and manipulated in the protein. One possible implementation for the basic operations of writing, reading, and erasing data of a memory device is the following: WRITE corresponds to photoconversion from C to B with irradiation at 350 nm, READ to fluorescence emission following weak excitation at 476 nm, and ERASE to photobleaching (B to C). The latter process can be induced by intense or prolonged excitation at 476 nm. Shown in Figure 139.7 (upper panels) is that controlled photoconversion after irradiation at 350 nm is achieved for a cluster of around 100 E^{2}GFP molecules trapped in polyacrylamide (PAA) gel films. As mentioned above, one important issue for advanced bioelectronic applications concerns the possibility of addressing the protein state at the single-molecule level. This limit was reached in the case of E^{2}GFP optical switching. Individual E^{2}GFP molecules in State B were imaged (Figure 139.7, lower panels) as bright spots at the resolution limit of the optical setup (~0.3 μm). The fluorescence intensity of single spots (~300 CCD counts) was similar to EGFP and displayed the characteristic signatures of single-molecule emission. Most of the molecules blinked and then photobleached within 10 s under excitation at 476 nm. In the lower panels of Figure 139.7, it is shown that the same molecule was repeatedly photobleached by excitation at 476 nm (ERASE), was photoconverted with 350 nm laser irradiation (WRITE), and its fluorescent emission was detected with 100 ms integration time (READ). More recent results demonstrated WRITE processes with irradiation times down to 250 ms.[79]

139.6 Conclusions and Perspectives

Green fluorescent proteins are flexible tools. Their uniqueness stems from the fact that their intrinsically fluorescent chromophore forms autocatalytically during folding, without the need of any external cofactor, and that they can be fused by standard genetic engineering techniques to other proteins. For these reasons, they are considered almost ideal fluorescent markers to monitor protein function and gene expression in living cells. The large quantity of mutants produced in these last decades covers almost all the visible spectrum and this allowed for significant advancements in biotechnology and favorably impacted molecular biology research. In spite of all this, however, the ideal markers do not yet exist. All available mutants suffer from photobleaching and blinking effects that limit their use in biotechnology.

The fluorescence mechanism is known in its general aspects, but the molecular mechanisms underlying the "dark dynamics" are still to be clarified. Detailed knowledge of GFP photophysics would have much impact on single-molecule studies. The development and application of suitable techniques able to probe

protein function down to the ultimate limit of the single-molecule resolution hold the potential to revolutionize modern molecular biology and biomolecular physics. By overcoming the limitation of ensemble averaging, these techniques can address questions that cannot be answered by conventional approaches and can give information on protein function and dynamics with vast impact on biomedicine, diagnostics, and molecular biology.

From another perspective, optical-memory elements that exploit the peculiar photophysics of these proteins show great promise. These molecules are photochemically stable at room temperature; offer photoconnected states addressable to the single-molecule level; and display optical control with wavelength, power, and dynamics suggestive of attractive technological implementations. To this end, further studies aimed at controlling blinking dynamics by appropriate mutant design and at addressing the impact of possible residual blinking events on the ultimate speed of operation of such devices must be carried out. E^2GFP and other mutants that display controllable photochromism can also find new applications in biology, where prolonged monitoring of protein function in living cells is required. Specific mutations that can fine-tune sensitivity to the environments of the optical properties seem to also be at reach. They will lead to highly specialized probes of the cellular milieu that would be of vast interest in cell biology.

Finally, another challenge is the tailoring of the spectral properties of GFP variants, particularly toward the ends of the visible spectrum. Blue variants still suffer from a low quantum yield with respect to green and yellow variants. Furthermore, they display slightly different fluorescence mechanisms, and modeling studies are also lacking for these variants. The other side of the spectrum, the red region, is not covered by GFP mutants, owing to the intrinsic limitations of the chromophore chemical structure. Naturally occurring red proteins have a different chromophore, either modified by a further chemical maturation with respect to the GFP chromophore (such as in DsRed) or produced by a different cyclization process (like in the AsCP). Investigation and tailoring of these variants are at their infancy, and much room for improvement in the photophysics of these molecules is available. It will result only from a detailed understanding and quantitative modeling of their properties.

Acknowledgments

We wish to thank Caterina Arcangeli, Riccardo Cinelli, Aldo Ferrari, Mauro Giacca, Alessandro Marcello, and Riccardo Nifosì, for useful discussions. This work was supported by grants from INFM/B/G (Istituto Nazionale per la Fisica della Materia, Sections B and G).

References

1. Shimomura, O., Johnson, F.H., and Saiga, Y., Extraction, purification and properties of aequorin, a bioluminescent protein from the luminous hydromedusan, Aequorea, *J. Cell. Comp.,* 59, 223–239, 1962.
2. Shimomura, O., Johnson, F.H., and Saiga, Y., Extraction, purification and properties of aequorin, a bioluminescent protein from the luminous hydromedusan, Aequorea, *J. Cell. Comp. Physiol.*, 59, 223–239, 1962; Morise, H., Shimomura, O., Johnson, F.H., and Winant, J., Intermolecular energy transfer in the bioluminescent system of Aequorea, *Biochemistry*, 13, 2656–2662, 1974.
3. Suggested lectures on GFPs: *Green Fluoresecent Proteins: Properties, Applications and Protocols*, Chalfie, M. and Chain, S., Eds, Wiley-Liss, New York, 1998; *Green Fluoresecent Protein*, Vol. 302, Conn, P.M., Ed., Academic Press, New York, 1999; *Green Fluorescent Protein*: *Methods in Cell Biology*, Vol, 58, Sullivan, K.F. and Kay, S.A., Eds., Academic Press, New York, 1998.
4. Prasher, D.C., Eckenrode, V.K., Ward, W.W., Prendergast, F.G., and Cormier, M.J., Primary structure of the Aequorea victoria green-fluorescent protein, *Gene*, 111, 229–233, 1992.
5. Chalfie, M., Tu, Y., Euskirchen, G., Ward, W.W., and Prasher, D.C., Green fluorescent protein as a marker for gene expression**,** *Science*, 263, 802–805, 1994.

6. See for instance: Harms, G.S., Cognet, L., Lommerse, P.H., Blab, G.A., and Schmidt, T., Autofluorescent proteins in single-molecule research: applications to live cell imaging microscopy, *Biophys. J.*, 80, 5, 2396–2408, 2001.
7. Dickson, R.M., Cubitt, A.B., Tsien, R.Y., and Moerner, W.E., On/Off blinking and switching behaviour of single molecules of green fluorescent protein, *Nature*, 388, 355–357, 1997.
8. Elowitz, M.B., Surette, M.G., Wolf, P.E., Stock, J., and Leibler, S., Photo-activation turns green fluorescent protein red, *Curr. Biol.*, 7, 809–812, 1997.
9. Zimmer, M., Green Fluorescent Protein (GFP): applications, structure, and related photophysical behavior, *Chem. Rev.*, 102, 759–782, 2002. Tsien, R.Y., The Green Fluorescent Protein, *Annu. Rev. Biochem.*, 67, 509–544, 1998. Zumbusch, A. and Jung, G., Single molecule spectroscopy of the Green Fluorescent Protein: a critical assessment, *Single Mol.*, 1, 261–270, 2000.
10. Ward, W.W. and Cormier, M.J., An energy transfer protein in coelenterate bioluminescence: characterization of the Renilla green-fluorescent protein (GFP), *J. Biol. Chem.*, 254, 781–788, 1979.
11. Morin, J.G., Coelenterate bioluminescence, in *Coelenterate Biology: Reviews and New Perspectives*, Muscatine, L. and Lenhoff, H., Eds., Academic Press, New York, 1974, pp. 397–438.
12. Labas, Y.A., Gurskaya, N.G., Yanushevich, Y.G., Fradkov, A.F., Lukyanov, K.A., Lukyanov, K.A., Matz, M.V., Diversity and evolution of the green fluorescent protein family, *Proc. Natl. Acad. Sci. USA*, 99, 4256–4261, 2002.
13. Baird, G.S., Zacharias, D.A., and Tsien, R.Y., Biochemistry, mutagenesis, and oligomerization of DsRed, a red fluorescent protein from coral, *Proc. Natl. Acad. Sci. USA*, 97**,** 11984–11989, 2000.
14. Wang, S. and Hazelrigg, T., Implications for bcd mRNA localization from spatial distribution of exu protein in Drosophila oogenesis, *Nature*, 369, 400–403, 1994.
15. Yang, F., Moss, L.G., and Phillips, G.N. Jr., The molecular structure of green fluorescent protein, *Nat. Biotechnol.*, 14, 1246–1251, 1996.
16. Phillips, G.N.J., Structure and dynamics of green fluorescent protein, *Curr. Opin. Struct. Biol.*, 7, 821–827, 1997.
17. Rao, B., Kemple, M., and Prendergast, F., Proton nuclear magnetic resonance and fluorescence spectroscopic studies of segmental mobility in aequorin and green fluorescent protein, *Photochem. Photobiol.*, 51, 92, 1980.
18. Ward, W.W. and Bokman, S.H., Reversible denaturation of Aequorea green-fluorescent protein: physical separation and characterization of the renatured protein, *Biochemistry*, 21, 4535–4540, 1982.
19. Dopf, J. and Horiagon, T.M., Deletion mapping of the Aequorea victoria green fluorescent protein, *Gene*, 173, 39–44, 1996.
20. Li, X., Zhang, G., Ngo, N., Zhao, X., Kain, S., and Huang, C.-C., Deletions of the Aequorea victoria green fluorescent protein define the minimal domain required for fluorescence, *J. Bio. Chem.*, 272, 28545–28549, 1997.
21. Heim, R., Prasher, D.C., and Tsien, R.Y., Wavelength mutations and posttranslational autoxidation of green fluorescent protein, *Proc. Natl. Acad. Sci. USA*, 91, 12501–12504, 1994; Sieghbahn, P.E.M., Wirstam, M., and Zimmer, M., Theoretical study of the mechanism of peptide ring formation in green fluorescent protein, 81, 169–186, 2001.
22. Cubitt, A.B., Heim, R., Adams, S.R., Boyd, A.E., Gross, L.A., and Tsien, R.Y., Understanding, improving and using green fluorescent proteins, *Trends Biochem. Sci.*, 20, 448–455, 1995.
23. Reid, B.G. and Flynn, G.C., Chromophore formation in green fluorescent protein, *Biochemistry*, 36, 6789–6791, 1997.
24. Donnelly, M., Fedeles, F., Wirstam, M., Siegmahn, P.E., and Zimmer, M.**,** Computational analysis of the autocatalytic posttranslational cyclisation observed in hystidine Ammonia Lyase. A comparison with Green Fluorescent Proteins, *J. Am. Chem. Soc.*, 123, 4679–4686, 2002.
25. Niva, H., Mattsuno, T., Kojima, T., Kubota, M., Hirano, T.L, Ohashi, M., Inoyuye, T., Omiya, Y., and Tsuji, F.I., Aequorea green fluorescent protein: structural elucidation of the chromophore, in

Bioluminescence and chemoluminescence, Hastings, J.W., Krocka, L.J., and Stanley, P.E., Eds., Wiley, New York, 1977, pp. 2395–2398.
26. Bokman, S.H. and Ward, W.W., Renaturation of Aequorea Green fluorescent protein, *Biochem. Biophys. Res. Commun.*, 101, 1372–1380, 1981.
27. Branchini, B.B., Nemser, A.R., and Zimmer, M., A computational analysis of the unique protein induced tight turn that results in posttranslational chromophore formation in green fluorescent protein, *J. Am. Chem. Soc.*, 120, 1–6, 1998.
28. Dellagrave, S., Hawtin, F.E., Silva, C.M., Yang, M.M., and Yoiuvan, D.C., Red shifted excitation mutants of the green fluorescent protein, *Biotechnology*, 13, 151–154, 1995.
29. Cormack, B.P., Valdivia, R.H., and Falkow, S., FACS-optimized mutants of the green fluorescent protein (GFP), *Gene*, 173, 33–38, 1995.
30. Heim, R., Cubitt, A.B., and Tsien, R.J.Y., Improved green fluorescence, *Nature,* 373, 663–664, 1995.
31. Chattoraj, M., King, B.A., Bublitz, G.U., and Boxer, S.G., Ultrafast excited state dynamics in green fluorescent protein: multiple states and proton transfer, *Proc. Natl. Acad. Sci. USA*, 93, 8362–8367, 1996.
32. Brejc, K., Sixma, T.K., Kitts, P.A., Kain, S.R., Tsien, R.Y., Ormö, M., and Remington, S.J., Structural basis for dual excitation and photoisomerization of the Aequorea victoria green fluorescent protein, *Proc. Natl. Acad. Sci. USA*, 94, 2306–2311, 1997.
33. van Thor, J.J., Gensch, T., Hellingwerf, K.J., and Johnson, L.N., Phototransformation of green fluorescent protein with UV and visible light leads to decarboxylation of glutamate 222, *Nature Str. Biol.*, 9, 37–41, 2002.
34. Voitiuk, A.A., Michel Beyerle, M.-E., and Rösch, N., Quantum chemical modeling of structure and absorption spectra of the chromophore in green fluorescent proteins, *Chem. Phys.*, 231, 13–25, 1998.
35. El Yazal, J., Prendergast, F.G., Shaw, D.E., and Pang, Y.-P., Protonation states of the chromophore of denaturated green fluorescent proteins predicted by *ab initio* calculations, *J. Am. Chem. Soc.*, 122, 11411–11415, 2000.
36. Bell, F.A., He, X., Wachter, R.M., and Tonge, P.J., Probing the ground state structure of the Green Fluorescent Protein chromophore using Raman spectroscopy, *Biochemistry*, 39, 4423–4431, 2000.
37. van Thor, J.J., Pierik, A.J., Nugteren Roodzant, I., Xie, A., and Hellingwerf, K.J., Characterization of the photoconversion of Green Fluorescent Protein with FTIR spectroscopy, *Biochemistry*, 37, 16915–16921, 1998.
38. Yoo, H.-Y., Boatz, J.A., Helms, V., McCammon, J.A., and Langhoff, P.W., Chromophore protonation states and the proton shuttle mechanism in green fluorescent protein: inferences drawn from *ab initio* theoretical studies of chemical structures and vibrational spectra. *J. Phys. Chem. B.*, 105, 2450–2457, 2001.
39. Creemers, T.M.H., Lock, A.J., Subramaniam, B., Jovin, T.M., and Völker, S., Red-shifted mutants of green fluorescent protein: reversible photoconversion studied by hole-burning and height resolution spectroscopy, *Chem. Phys.*, 275, 109–201, 2002.
40. http://www.rcsb.org/pdb/
41. Wachter, R.M., King, B.A., Heim, R., Kallio, D., Tsien, R.Y., Boxer, S.G., and Remington, S.J., Crystal structure and photodynamic behavior of the blue emission variant Y66H/Y145F of Green Fluorescent Protein, *Biochemistry*, 36, 9759–9765, 1997.
42. Yang, T.-T., Sinai, P., Green, G., Kitts, P.A., Chen, Y.-H., Lybarger, L., Chervenak, R., Patterson, G.H., Piston, D.W., and Kain, S.R., Improved fluorescence and dual color detection with enhanced blue and green variants of the green fluorescent protein, *J. Biol. Chem.*, 273, 8212–8216, 1998.
43. Palm, G.J., Zdanov, A., Gaitanaris, G.A., Stauber, R., Pavlakis, G.N., and Wlodawer, A., The structural basis for spectral variations in green fluorescent protein, *Nature Str. Biol.,* 4, 361–365, 1997.
44. Lossau, H., Kummer, A., Heinecke, R., Pollinger-Dammer, F., Kompa, C., Bieser, G., Jonsson, T., Silva, C.M., Yang, M.M., Houvan, D.C., and Michel-Beyerle, M.E., Time resolved spectroscopy of

wild-type and mutant Green Fluorescent Proteins reveals excited state deprotonation consistent with fluorophore–protein interaction, *Chem. Phys.*, 213, 1–16, 1996.

45. Tavaré, M.J., Fletcher, L.M., and Welsh, G.I., Using Green Fluorescent Proteins to study intracellular signaling, *J. Endocr.*, 170, 297–306, 2001.
46. Wachter, R.M., Elsliger, M.-A., Kallio, K., Hanson, G.T., and Remington, S.J., Structural basis of spectral shifts in the yellow-emission variants of green fluorescent protein, *Structure*, 6, 1267–1277, 1998.
47. Patterson, G.H., Knobel, S.M., Sharif, W.D., Kain, S.R., and Piston, D.W., Use of the Green Fluorescent Protein and its mutants in quantitative fluorescence microscopy, *Biophys. J.*, 73, 2782–2790, 1997.
48. Heim, R. and Tsien, R.Y., Engineering green fluorescent protein for improved brightness, longer wavelengths and fluorescence resonance energy transfer, *Curr. Biol.*, 6, 178–182, 1996.
49. Cubitt, A.B., Wooleenweber, L.A., Heim, R., Understanding structure-function relationships in the Aequorea victoria green fluorescent protein, *Methods Cell Biol.*, 58, 19–30, 1999.
50. Stauber, R.H., Horie, K., Carney, P., Hudson, E.A., Tarasova, N.I., Gaitanaris, G.A., and Pavlakis, G.N., Development and applications of enhanced green fluorescent protein mutants, *BioTechniques*, 24, 468–471, 1998.
51. Miyawaki, A., Llopis, J., Heim, R., McCaffery, J.M., Adams, J.A., Ikura, M., Tsien, R.Y., Fluorescent indicators for Ca^{2+} based on green fluorescent proteins and calmodulin, *Nature*, 338, 882–887, 1997.
52. Battistutta, R., Negro, A., and Zanotti, G., Crystal structure and refolding of the mutant F99S/M153T/V163A of the Green Fluorescent Protein, *Proteins,* 41, 429–437, 2000.
53. Elsliger, M.-A., Wachter, R.M., Hanson, G.T., Kallio, K., and Remington, S.J., Structural and spectral response of Green Fluorescent Protein variants to changes in pH, *Biochemistry*, 38, 5296–5301, 1999.
54. Kummer, A.D., Wiehler, J., Renhaber, H., Kompa, C., Steipe, B., and Michel-Beyerle, M.E., Effects of Threonine 203 replacements on excited-state dynamics and fluorescence properties of the Green Fluorescent Protein (GFP), *J. Phys. Chem. B.*, 104, 4791–4798, 2000.
55. Jung, G., Wiehler, J., Göhde, W., Tttel, J., Basché, T., Steipe, B., and Bräuchle, C., Confocal microscopy of single molecules of the green fluorescent protein, *Bioimaging*, 6, 54–61, 1998.
56. Jung, G., Wiehler, J., Steipe, B., Bräuchle, C., and Zumbush, A., Single-molecuele microscopy of the Green Fluorescent Protein using simultaneous two-color excitation, *Chem. Phys. Chem.,* 6, 392–396, 2001.
57. Kummer, A.D., Kompa, C., Lossau, H., Pöllinger-Dammer, F., Michel Beyerle, M.E., Silva, C.M., Bylina, E.J., Coleman, W.J., Yang, M.M., and Youvan, D.C., Dramatic reduction in fluorescence quantum yield in mutants of Green Fluorescent Proteins due to fast internal conversion, *Chem. Phys.*, 237, 183–193, 1998.
58. Creemers, T.M.H., Lock, A.J., Subramaniam, V., Jovin, T.M., and Völker, S., Photophysics and optical switching in green fluorescent protein mutants, *Proc. Natl. Acad. Sci. USA,* 87, 2974–2978, 2000.
59. Wachter, R.M., Yarbrought, D., Kallio, D., and Remington, S.J., Crystallographic and energetic analysis of binding of selected anions to the yellow variants of green fluorescent protein, *J. Mol. Biol.*, 301, 157–171, 2000.
60. Cinelli, R.A.G., Pellegrini, V., Ferrari, A., Faraci, P., Nifosì, R., Tyagi, M., Giacca, M., and Beltram, F., Green fluorescent proteins as optically controllable elements in bioelectronics, *Appl. Phys. Lett.*, 79, 3353–3356, 2001.
61. Llopis, J., McCaffery, J.M., Miyawaki, A., Farquhar, M.G., and Tsien, R.Y., Measurement of cytosolic, mitochondrial and Golgi pH in single living cells with green fluorescent proteins, *Proc. Natl. Acad. Sci. USA*, 95, 6803–6808, 1998.
62. Griesbeck, O., Baird, G.S., Capbell, R.E., Zacharias, D.A., and Tsien, R.Y., Reducing the environmental sensitivity of Yellow Fluorescent Protein, *J. Biol. Chem.*, 276, 29188–29194, 2001.

63. Østergaard, H., Hinriksen, A., Hansen, F.G., and Winther, J.R., Shedding light on disulfide bond formation: engineering a redox switch in green fluorescent protein, *EMBO J.*, 20, 5853–5862, 2001.
64. Matus, A., GFP moves on, *Trends Cell. Biol.*, 11, 183, 2001.
65. Scharnagl, C., Rapp-Kossmann, R., and Fischer, S.F., Molecular basis for pH sensitivity and proton transfer in green fluorescent protein: protonation and conformational substates from electrostatic calculations, *Biophys. J.*, 77, 1839–1857, 1999.
66. Selvin, P.R., The renaissance of fluorescence resonance energy transfer, *Nat. Struct. Biol.*, **7,** 730–734, 2000.
67. Marcello, A., Cinelli, R.A., Ferrari, A., Signorelli, A., Tyagi, M., Pellegrini, V., Beltram, F., and Giacca, M., Visualization of *in vivo* direct interaction between HIV-1 TAT and human cyclin T1 in specific subcellular compartments by fluorescence resonance energy transfer, *J. Biol. Chem.*, 276, 42, 39220–39225, 2001.
68. Phair, R.D. and Misteli, T., High mobility of proteins in the mammalian cell nucleus, *Nature*, 404, 6778, 604–609, 2000.
69. Periasamy, A., Elangovan, M., Elliott, E., and Brautigan, D.L., Fluorescence lifetime imaging (FLIM) of green fluorescent fusion proteins in living cells, *Methods Mol. Biol.*, 183, 89–100, 2002.
70. Patterson, H.G. and Lipppincott-Shwartz, J., A photoactivatable GFP for selective photolabeling of proteins and cells, *Science*, 297, 187, 2002.
71. Haupts, U., Maiti, S., Schwille, P., and Webb, W.W., Dynamics of fluorescence fluctuations in green fluorescent protein observed by fluorescence correlation spectroscopy, *Proc. Natl. Acad. Sci. USA*, 95, 13572–13578, 1998; Peterman, E.J.G., Brasselet, S., and Moerner, W.E., The fluorescence dynamics of single molecules of green fluorescent protein, *J. Phys. Chem. A*, 103, 10553–10560, 1999.
72. Jung, G., Bräuchle, C., and Zumbush, A., Two color fluorescence correlation spectroscopy of one chromophore: application to E222Q mutant of the green fluorescent protein, *J. Chem. Phys.*, 114, 3149–3156, 2001.
73. Garcia-Parajo, M.F., Segers-Nolten, G.M.J., Veerman, J.-A., Greve, J., and van Hlst, N.F., Real-time light driven dynamics of the fluorescence emission in single green fluorescent protein molecules, *Proc. Natl. Acad. Sci. USA*, 97, 7237–7242, 2000.
74. Schwille, P., Kummer, S., Heikal, A.A., Moerner, W.E., and Webb, W.W., Fluorescence correlation spectroscopy reveals fast optical excitation-driven intramolecular dynamics of yellow fluorescent proteins, *Proc. Natl. Acad. Sci. USA,* 97, 151–156, 2000.
75. Weber, W., Helms, V., McCammon, J.A., and Langhoff, P.W., Shedding light on the dark and weakly fluorescent states of green fluorescent proteins, *Proc. Natl. Acad. Sci. USA*, 96, 6177–6182, 1999.
76. Voityuk, A., Michel-Beyerle, M.-E., and Rosch, N., Structure and rotation barriers for ground and excited states of the isolated chromophore of the green fluorescent protein, *Chem. Phys. Lett.*, 296, 269–276, 1998.
77. Cotlet, M., Hofkens, J., Köhn, F., Jichiels, J., Dirix, G., Van Guyse, M., Vanderleyden, J., and De Schryer, F.C., Collective effects in individual oligomers of the red fluorescent coral proteins DsRed, *Chem. Phys. Lett.*, 336, 415–423, 2001.
78. Jung, G., Mais, S., Zumbush, A., and Bräuchle, C., The role of dark states in the photodynamics of the green fluorescent protein examined with two color fluorescence excitation spectroscopy, *J. Chem. Phys. A*, 104, 873–877, 2000.
79. Nifosì, R., Ferrari, A., Arcangeli, C., Tozzini, V., Pellegrini, V., and Beltram, F., Photoreversible dark state in a tristable green fluorescent protein variant, *J. Phys. Chem. B.,* 107, 1679–1684, 2003.
80. Nifosì, R. and Tozzini, V., Molecular dynamics simulations of enhanced Green Fluorescent Proteins: effects of F64L, S65T and T203Y mutations on the ground state proton equilibria, *Proteins,* 51, 378–389, 2003.
81. Cotlet, M., Hofkens, J., Maus, M., Gensch, T., Van der Auweraer, M., Michiels, J., Dirix, G., Van Guyse, M., Vanderleyden, J., Visser, A.J.W.G., and De Schriyever, F.C., Excited-state dynamics in the enhanced green fluorescent protein mutant probed by picosecond time resolved single photon counting spectroscopy, *J. Phys. Chem. B*, 105, 4999–5006, 2001.

82. Vsevolodov, N., Biomolecular Electronics: An Introduction via Photosensitive Proteins, Birkhauser, Boston, MA, 1998; Stuart, A. et al., *Proc. IEEE Nonvol. Mem. Tech.* (INVMTC), 6, 45–51, 1996.
83. Toriumi, A., Herrmann, J.M., and Kawata, S., Nondestructive readout of a three-dimensional photochromic optical memory with a near-infrared differential phase-contrast microscope, *Opt. Lett.,* 22, 555–557, 1997.
84. Tsujioka, T., Hamada, Y., Shibata, K., Taniguchi, A., and Fuyuki, T., Nondestructive readout of photochromic optical memory using photocurrent detection, *Appl. Phys. Lett.*, 78, 2282–2284, 2001.
85. Haupts, U., Tittor, J., and Oesterhelt, D., *Closing in on bacteriorhodopsin: progress in understanding the molecule, Annu. Rev. Biophys. Biomol. Struct., 28,* 367–399, 1999; *Kobayashi, T., Saito, T., and Ohtani, H., Real-time spectroscopy of transition states in bacteriorhodopsin during retinal isomerization, Nature, 414, 531–534, 2001;* Chizhov, I., *Chernavskii, D.S., Engelhard, M., Mueller, K.H., Zubov, B.V., and Hess,* B., Spectrally silent transitions in the bacteriorhodopsin photocycle, *Biophys. J., 71, 2329–2345,* 1996.
86. Birge, R.R., Gillespie, N.B., Izaguirre, E.W., Kunetzow, A., Lawrence, A.F., Sihgh, D., Song, W., Schmidt, E., Stuart, J.A., Seetharaman, S., and Wise, K.J., Biomolecular electronics: protein-based associative processors and volumetric memories, *J. Phys. Chem. B,* 103, 10746–10766, 1999.

140

DNA Damage and Repair

David L. Mitchell
M.D. Anderson Cancer Center

140.1 Introduction

Ultraviolet radiation (UVR) is a primordial and ubiquitous genotoxin. During the earliest stages of molecular evolution as the dynamics of DNA chemistry were being formulated, the surface of the planet was bombarded by extremely high levels of UVR. Any DNA exposed to sunlight during or soon after the genesis of life would require rapid and accurate repair of UVR damage for continued survival and procreation. Hence, it is probable that mechanisms of DNA repair evolved early in the Earth's history and, in fact, may have coevolved with DNA replication and transcription. Today, the amount of UV-B radiation reaching the earth's surface increased due to industrialization and chlorofluorocarbon pollution of the upper atmosphere. The consequences of stratospheric deozonation and increased UV-B exposure to the human population are difficult to predict, but research over the past 40 years suggests that accelerated rates of skin cancer and aging as well as deterioration of the natural environment and major food crops are probable outcomes.

Due to their strong absorbance within the UV-B region of the solar spectrum (290 to 320 nm), certain nucleic and amino acids are considered the primary chromophores of UVR. RNA and proteins are encoded by DNA and are readily replaced by the cellular machinery. DNA, on the other hand, requires an intact copy of itself for replication, and any mistakes made during the replication process can result in mutation, loss of fitness, and cell death. The absorption spectrum of DNA correlates well with photoproduct formation, cell killing, mutation induction, and carcinoma. UVR induces a plethora of structural lesions in DNA that can be detected and measured using a variety of analytical techniques. The sensitive and precise measurement of DNA damage and repair are essential for understanding the lethal and mutagenic effects of UV-induced photoproducts on individual cells and complex organisms. Indeed, over the past 30 years, these techniques were instrumental in revealing the many faces of DNA repair, ranging from the relatively simple photoenzymatic repair system to the elegant interactions of the nucleotide excision repair complex. Our current knowledge of DNA damage and repair derives from a broad range of scientific disciplines, including environmental, evolutionary, cellular, molecular, and structural biology. Indeed, connections between DNA repair and such fundamental cellular processes as transcription and the cell cycle attest to the importance of this ancient and essential biochemical process.

0-8493-1348-1/04/$0.00+$1.50

140.2 Biological Significance

The sun emits energies at wavelengths that range through 17 orders of magnitude, from 10^{-4} nm to 10^{12} nm.[1] The vast majority of this energy is biologically irrelevant; short wavelength radiation such as high-energy particles, x-rays, and gamma rays are expended by atomic collisions in the upper atmosphere, and long wavelength far infrared, microwaves, and radiowaves do not have sufficient energy to influence biochemical reactions. Although UVR comprises a minute portion of the total solar output of energy, its biological impact is, by comparison, immense. UVR is divided into three regions: UV-C (240 to 290 nm) is not present in ambient sunlight but is readily produced by low-pressure mercury sterilizing lamps. The peak wavelength of mercury excitation (254 nm) coincides with the peak of DNA absorption (260 nm), and this wavelength has been of major importance in experimental studies. Fortunately, wavelengths below -295 nm are catalytically absorbed by ozone molecules in the stratosphere (i.e., O_3: O_2 + O), and little light shorter than 300 nm reaches the earth's surface. UV-B (290 to 320 nm) overlaps the upper end of the DNA and protein absorption spectra and is the range mainly responsible for environmental and pathological effects through direct photochemical damage to DNA. UV-A (320 to 400 nm) is photocarcinogenic and involved in photoaging but is weakly absorbed in DNA and protein. The relevant chromophores for UV-A probably involve reactive oxygen species (ROS) that secondarily cause damage to DNA.

UV-B is a potent and ubiquitous carcinogen responsible for much of the skin cancer in the human population today.[2,3] Tumor incidence and mortality correlate with exposure: basal and squamous cell carcinomas are most prevalent on the faces and trunks of men and on the faces and legs of women; carcinomas increase with decreasing latitude; tumor incidence is increased in individuals working in occupations with high exposure, such as ranchers or fisherman; and the protective action of skin pigmentation results in lower cancer rates in dark-skinned populations compared to lighter-skinned populations. The importance of UV-B damage and its repair in humans is exemplified by genetic diseases that greatly increase the risk of sunlight-induced skin cancer. In one such disease, xeroderma pigmentosum, a failure in the DNA repair process is associated with a major increase in the rate of squamous and basal cell carcinoma and melanoma. Although UV-B is probably responsible for most of the biological effects of sunlight, lower-energy UV-A comprises the bulk of the solar UVR reaching the earth's surface and, hence, is not without biological importance.

There is now strong evidence that UVR is increasing over many locations on the earth's surface, with the most significant ozone depletion observed over Antarctica and parts of the Southern Ocean, Australia, and New Zealand.[4] Marine plankton comprise the base of oceanic food webs and are sensitive to UV-B stress. There is growing evidence that UV-B and UV-A radiations inhibit primary and heterotrophic production. Ozone thinning, particularly during the austral spring over Antarctica, selectively allows penetration of higher-energy UV-B wavelengths through the upper atmosphere, and the proportion of UV-B relative to UV-A increases. UV penetration in the water column is also selective and wavelength dependent. UV-B is attenuated by water to a greater degree than UV-A, hence, with increasing depth, the proportion of UV-A relative to UV-B increases. Marine organisms are exposed to significant amounts of solar UV-B, even under normal ozone conditions, but organisms living near the surface of the ocean under low ozone conditions are exposed to particularly high levels.

The biological effects of DNA photodamage depend on the type of lesion induced and its genomic location, as well as the nature of the target cell and its developmental state. If the photoproduct is repaired correctly, the DNA is restored to its original state, and after some delay, the cell proceeds with its normal activities. If the damage is not repaired, it may interfere with DNA replication or transcription. Should this occur, cell proliferation will cease or, if the block is situated in a gene required for an essential metabolic function, the cell will die. Alternatively, the damage may not block replication. Bypass of the lesion by a DNA polymerase may produce an incorrect complementary base (i.e., a mutation) that can have several possible outcomes:

1. It may not alter the genetic code and, hence, not affect normal metabolism.
2. It may produce a truncated or partial RNA transcript encoding a dysfunctional protein.
3. It may result in activation of an oncogene or inactivation of a tumor suppressor gene, thereby initiating the carcinogenic process.

140.3 DNA Photoproduct

Photon absorption rapidly converts a pyrimidine base to an excited state.[5] This event promotes an electron in a filled bonding orbital in the singlet ground state into a higher energy, empty * antibonding orbital, thus initiating photoproduct formation. Formation of an excited base occurs within 10^{-12} sec after photon absorption. Various pathways are then available for resolution of this unstable electronic configuration. The major pathway involves rapid dissipation of the energy of the excited singlet base to the ground state (10^{-9} sec) by nonradiative transition or by fluorescence, yielding heat or light in the process. Second, the excited base can react with other molecules to form unstable intermediates (i.e., free radicals) or stable photoproducts. Finally, there is a low probability that intersystem crossing, another nonradiative pathway, can transfer a base from the excited singlet state to the excited triplet state. The lifetime of the triplet state is several orders of magnitude longer than the excited singlet state (10^{-3} sec), increasing the chance of photoproduct formation. Formation of the triplet state can be greatly enhanced in the presence of ketone sensitizers.

Dimerizations between adjacent pyrimidine bases are by far the most prevalent photoreactions resulting from UVC or UV-B irradiation of DNA (Table 140.1), with the relative induction dependent on wavelength, DNA sequence, and protein–DNA interactions.[6] The major photoproducts in DNA are the cyclobutyl pyrimidine dimer (CPD), formed through the excited triplet state, and the pyrimidine-(6–4)pyrimidone dimer [(6–4)PD], formed from a Paterno–Büchi reaction. The (6–4) photoproduct undergoes further UV-B-dependent conversion with its valence photoisomer, the Dewar pyrimidinone. In addition to the major photoproducts, rare dimers may also form, such as the adenine-thymine heterodimer or the 2-imidazolone(5–4)pyrimidone product, another photoisomerization product of the (6–4)PD.

The yield of the individual types of dimers is dependent on the nucleotide composition in and around the potential lesion as well as the wavelengths of UVR used to induce the damage.[7] The induction of both CPDs and (6–4)PDs is greater in the presence of 5′ flanking pyrimidines compared to purines with guanine inhibiting induction more than adenine. UV-B irradiation increases the relative induction of cytosine-containing cyclobutane dimers compared to thymine homodimers.[8] The (6–4)PD is induced primarily at T-C and to a lesser extent at C-C dinucleotides, and its formation is not as wavelength-dependent as the CPD. Although the T-T (6–4)PD is refractory to piperidine digestion and is not detected using conventional sequencing techniques, it may occur at levels comparable to the T-C (6–4)PD in DNA.[6] Cytosine methylation significantly increases the yield of (6–4)PDs after irradiation with UV-C light and of cytosine-containing CPDs and (6–4)PDs after irradiation with UV-B light. The data suggest that CPDs and (6–4)PDs are preferentially induced at 5-methylcytosine bases in DNA of cells exposed to sunlight. And, they comprise a major component of the mutation spectrum leading to the initiation of sunlight-induced skin cancer.[9,10]

The organization of chromatin into nucleosomal particles connected by linker DNA influences sites of dimer induction.[11] Limited flexibility of the DNA helix resulting from histone–DNA interactions inhibits CPD formation and modulates their distribution along DNA with a periodicity of 10.3 bases. Whereas CPDs form with equal efficiencies in core and linker DNA, (6–4)PDs occur with sixfold greater frequency per nucleotide in linker DNA. The preferential formation of the (6–4)PD in "open" chromatin configurations (e.g., transcriptionally active genes and regulatory sequences) may enhance the biological impact of this lesion and partially explain its preferential repair (see below).

In contrast to the direct induction of DNA damage by UV-C and UV-B light, UV-A produces damage indirectly through highly reactive chemical intermediates.[6] Similar to ionizing radiation, UV-A generates

TABLE 140.1 Structures and Relative Induction Frequencies of the Major Photoproducts Induced by UVR

Photoproduct	Structure	Lesions/10^8 Da	J/m^2	% of total photoproducts	
		UV-C	UV-B	UV-C	UV-B
Cyclobutyl pyrimidine dimer	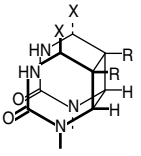	2.3	0.30	77	78
Pyrimidine pyrimidone [6-4]-photoproduct	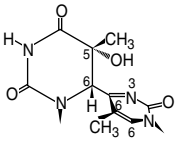	6 x 10-1	4 x 10-2	20	10
Dewar pyrmidinone	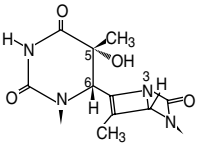	2.3 x 10-2	~4 x 10-2	0.8	10
Adenine-thymine heterodimer	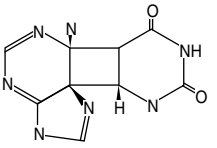	6 x 10-3	nd	0.2	nd
Pyrimidine pyrimidone [5-4]-photoproduct	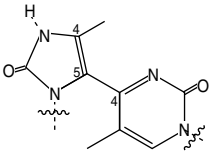	nd	nd	nd	nd
Cytosine photohydrate	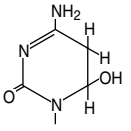	5 x 10-2	6.6 x 10-3	~2	~2
Thymine photohydrates	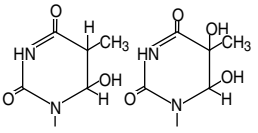	nd	nd	nd	nd
Single-strand break		~5 x 10-4	~4 x 10-6	<0.1	<0.1
DNA-protein crosslink	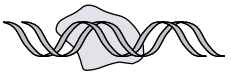	~3 x 10-4	~1 x 10-6	<0.1	<0.1

oxygen and hydroxyl radicals, which in turn, react with DNA to form monomeric photoproducts, such as cytosine and thymine photohydrates, photooxidation products (such as 8-oxodeoxyguanine), as well as strand breaks and DNA-protein cross-links (Table 140.1). The relationship between the frequencies of these photoproducts and their biological effects depends on the cytotoxic and mutagenic potentials of the individual lesion. Hence, even though a photoproduct may occur at a low frequency, its structure and location may elicit a potent biological effect.

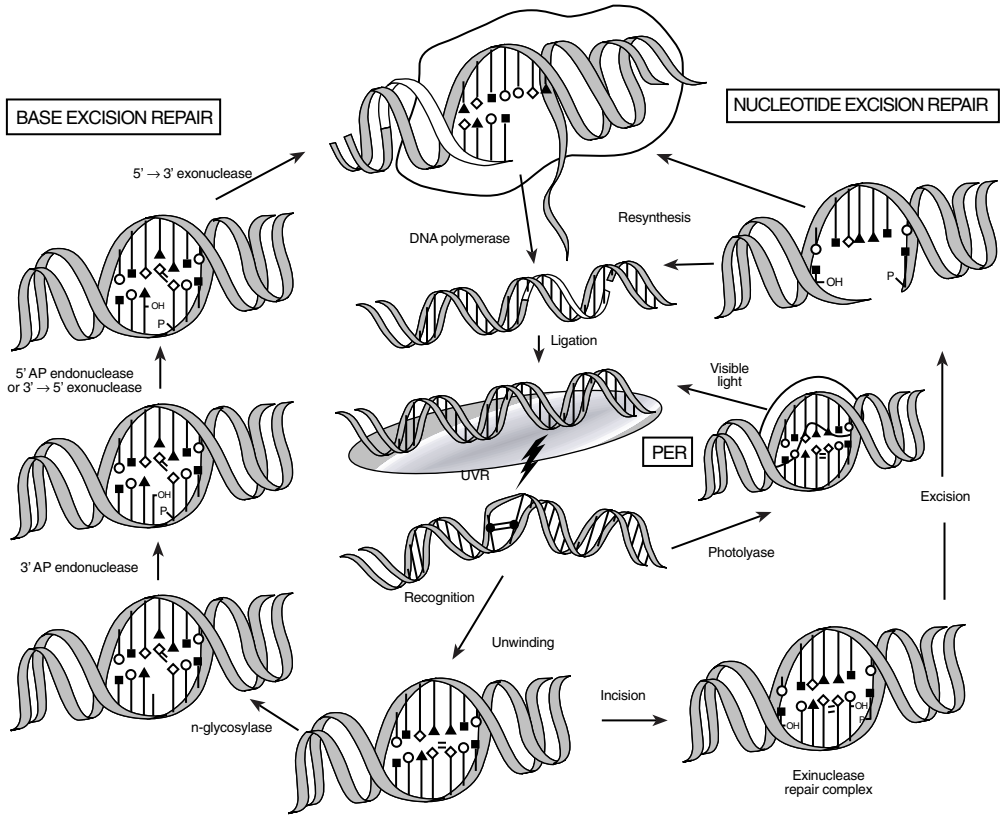

FIGURE 140.1 Enzymatic pathways for the repair of UVR damage in DNA. Shown are photoenzymatic repair (PER), base excision repair, and nucleotide excision repair.

140.4 Detection of DNA Damage

A variety of analytical procedures were developed to measure UVR damage and repair in DNA.[12–14] Many types of photoproducts have been identified and quantified by chromatographic techniques. Since the initial detection of the CPD by two-dimensional paper chromatography, thin-layer chromatography, and high-performance liquid chromatography were adapted to the analysis of this and other types of damage. All of these procedures require DNA that was prelabeled with a radioactive tracer (e.g., ^{3}H-thymidine) and hydrolyzed to free bases or nucleotides by enzymatic digestion or treatment in strong acid at high temperature. Development of ^{32}P-postlabeling procedures obviated the need for prelabeling and expanded the sample repertoire available to chromatographic techniques.

Many types of photodamage can be converted into single-strand breaks in DNA by enzymatic or biochemical treatment. Frank breaks induced directly in DNA by UV and breaks produced at sites of photoproducts by targeted enzymatic or biochemical procedures can be quantified by alkaline gradient centrifugation, alkaline elution, or agarose gel electrophoresis. The sensitivity of these procedures requires maintenance of high-molecular-weight DNA throughout the extraction and analytical procedures. *Uvr*ABC exinuclease, a partial excision repair complex purified from *Escherichia coli*, cleaves DNA on either side of a bulky adduct [e.g., CPD or (6–4)PD; see Figure 140.1, right side]. *Uvr*ABC and the yeast UV DNA damage endonuclease (UCDE) are used to cut sites of CPDs and (6–4)PDs prior to molecular weight analysis. *In vitro* repair by CPD or (6–4)PD photolyase prior to digestion with *uvr*ABC or UVDE focuses the analysis on one or the other photoproduct.

More specific cleavage was achieved by using purified glycosylase-endonucleases from various prokaryotic hosts, primarily *E. coli*. These enzymes combine a glycosylase that cuts the base from the sugar, leaving an apyrimidinic (AP) site, and an AP endonuclease that cleaves the phosphodiester backbone on either side of this site (Figure 140.1, left side). These enzymes range from the CPD-specific T4 phage endonuclease V and 8-oxodeoxyguanine-specific oxoguanine glycosylase (OGG) to more broad-spectrum reagents like endonuclease III (nth) and formamido glycosylase (fpg) that cut a variety of photohydrates and photooxidative products. Nonenzymatic cleavage of alkali-labile sites, such as AP sites or Dewar pyrimidinones, also produces quantifiable strand breaks for analysis of induction and repair.

These techniques were recently adapted to the analysis of UV photoproduct induction and repair at the gene and base sequence levels. Photodamage at the gene level can be mapped as strand breaks in DNA fragments irradiated with high doses of UV-C and UV-B light, and at the gene level using Southern blot hybridization of DNA fragments separated by denaturing agarose gel electrophoresis. Alternatively, gene damage can be measured using quantitative PCR, a technique dependent on the ability of a lesion to block progression of Taq polymerase. Highest resolution is obtained using ligation-mediated polymerase chain reaction, whereby the distribution of photoproducts at the sequence level can be quantified.

In addition to molecular biology techniques, various immunological procedures are available for DNA damage analyses. Polyclonal and monoclonal antibodies recognize and bind a variety of photoproducts, including the CPD, (6–4)PD, Dewar pyrimidinone, and 8-oxodeoxyguanine. Techniques such as immunoprecipitation, enzyme-linked immuoassays, dot and slot-blot assays, radioimmunoassays, quantitative immunofluorescence, and immunoelectron microscopy are powerful analytical tools; each with its own unique attributes and applications. Unlike chromatography, immunological assays do not require chemical or enzymatic degradation of DNA before analysis; unlike assays that require strand scission, sensitivity does not depend on the molecular weight or purity of sample DNA.

140.5 DNA Repair

The total number of photoproducts remaining in cellular DNA at any time depends on the amount of UVR absorbed and the amount of damage repaired. Damage tolerance strategies are complex and vary greatly among organisms and at different times during development.[15,16] Nearly all organisms have behaviors or natural features that mitigate exposure of DNA to solar UVR and reduce the amount of photodamage. In addition to habitat selection, avoidance responses, and physical morphologies that attenuate the transmission of UVR to sensitive, internal areas of cells, many organisms evolved biochemical mechanisms to protect themselves. UVR-absorbing compounds such as melanin and anthocyanin are produced in human skin and in plants; colorless UV-absorbing compounds, such as flavonoids in terrestrial plants, mycosporine amino acids in fungi, and mycosporine-like compounds in marine organisms, were also identified as possible UV-protective chemicals.

Once DNA damage is present, its removal may proceed in whole or in part by at least two well-studied mechanisms, photoenzymatic repair (PER)[17] or excision repair (Figure 140.1). PER involves specific recognition and binding of a small enzyme called a photolyase to a cyclobutane dimer. This enzyme catalyzes the direct reversal of the dimer upon absorption of a photon within the UV-A/visible range of light. Photoreactivation occurs widely throughout the plant and animal kingdoms.[15] Its presence and operation in placental mammals, particularly in human skin, are matters of some controversy.

Organisms that display reduced PER often have a greater capacity for excision repair. The excision repair mechanism utilized by the cell depends on the type of damage encountered and the location of the damage in chromatin. Two major pathways of NER are transcription-coupled repair (TCR) and global genome repair (GGR),[3,18] both of which remove CPDs and (6–4)PDs in DNA and replace the damaged site with a newly synthesized polynucleotide patch ~29 bases in length. TCR removes damage preferentially from transcribing strands.[19] GGR is targeted to nontranscribed regions and is regulated by p53 through expression of the XPE p48 protein. There is considerable difference in the rates of removal of CPDs and (6–4)PDs in the genome overall. In rodent and human fibroblasts, the half-life for (6–4)PD removal is 6 h; the half-life for CPD repair is 24 h in human cells and considerably longer (>72 h) in

rodent cells. The excision of CPDs may be partly delayed, because the strong affinity of the excision system for (6–4)PDs initially sequesters available enzymes. The different rates of excision may also reflect the fact that (6–4)PDs are considerably more distortive in DNA and are preferentially located in internucleosomal regions of DNA.

The differences in excision from active and inactive genes occur because the general transcription factor, TFIIH, regulates basal transcription by RNA polymerase II and plays a major role in repair. Many of the genes that regulate TCR are associated with the human disorders xeroderma pigmentosum (XP), Cockayne syndrome (CS), trichothiodystrophy (TTD), and other disorders.[3] Two of the helicases in TFIIH correspond to the *XPB* and *XPD* genes. TCR also involves the Cockayne syndrome genes, *CSA* and *CSB*, *XPG*, the mismatch repair gene *MLH2*, and the breast cancer susceptibility gene *BRCA1*. The XPC-hHR23B complex is involved in earliest damage recognition, initiates NER in nontranscribed DNA, acting before the XPA protein, and serves to stabilize XPA binding to the damaged site with a high affinity for the (6–4)PD. This complex is specifically involved in GGR but not TCR, where the arrest of RNA polymerase II at a damaged base may function in its place. The core protein factors include the XPA-RPA dimer, the 6 to 9 subunit TFIIH, the XPC-hHR23B complex, the XPG nuclease, and the ERCC1-XPF nuclease. After assembly, the XPC-hHR23B complex dissociates, the XPG protein cuts 3′ to the lesion, and the ERCC1-XPF heterodimer cuts 5′ to the CPD. The nuclease complex plus the 29 to 30 nt single-strand fragment is released by the action of transcription factor TFIIH. The XPG protein is also required for TCR of oxidative damage and is a cofactor for endonuclease III. Once this oligonucleotide is removed, the resulting gap is filled by DNA Pol D, proliferating cell nuclear antigen (PCNA), and single-strand-binding protein and ligase. These processes involve sequential steps of photoproduct recognition, assembly of the excision complex, displacement of the excised fragment, and polymerization of the replacement patch.

Base excision repair is initiated by enzymatic recognition of the lesion and scission of the bond between the damaged base and its associated deoxyribose sugar, a process called aglycosylation (Figure 140.1, left side). Examples of *n*-glycosylases include endonuclease III from *E. coli*, which repairs photohydrates, and endonuclease V from T4 phage, which recognizes CPDs (see above). In the latter case, cleavage of the *n*-glycosyl bond of the 5′ pyrimidine base leaves an abasic site that is subsequently recognized by an AP endonuclease that cleaves the phosphodiester bond 3′ to the abasic site. The remaining abasic site is digested with a 5′ AP endonuclease or 3′6 5′ exonuclease associated with DNA polymerase. The damaged strand is removed and resynthesized by a DNA polymerase complex, and the remaining gap is ligated.

140.6 Summary

The clinical effects of defective DNA repair can include increased risk of skin cancer and accelerated aging, as well as neurological and growth disorders. This phenotypic heterogeneity belies the complexity of the excision repair process and presents a formidable task in defining the functions of the various proteins involved in DNA repair. Advances in cloning the genes involved in DNA repair in mammals, yeast, and *Drosophila melanogaster* have greatly increased our understanding of the DNA repair process. In addition to defining the components of an ancient and essential molecular process, future studies in DNA repair may help direct the prevention and clinical treatment of sunlight-induced skin cancer and lessen the impact of stratospheric deozonation on the human population.

References

1. *The Science of Photobiology*, Smith, K.C., Ed., Plenum Press, New York, 1977.
2. Cleaver, J.E. and Kraemer, K.H., Xeroderma pigmentosum, in *The Metabolic Basis of Inherited Disease*, Vol. II, 6th ed., Scriver, C.R., Beaudet, A.L., Sly, W.S., and Valle, D., Eds., McGraw-Hill, New York, 1989, p. 2949.
3. Cleaver, J.E. and Mitchell D.L., Ultraviolet radiation carcinogenesis, in *CancerMedicine*, 5th ed., Holland, J.F., Frei, E. III, Bast, R.C. Jr., Kufe, D.W., Morton, D.L., and Weichselbaum, R.R., Eds., Williams and Wilkins, Baltimore, 2000, p. 219.

4. Calkins, J. and Thordardottir T., The ecological significance of solar UV radiation on aquatic organisms, *Nature*, 283, 563, 1980.
5. Wang, S.Y., Ed., *Photochemistry and Photobiology of Nucleic Acids*, Vols. I and II, Academic Press, New York, 1976.
6. Cadet, J. and Vigny, P., The photochemistry of nucleic acids, in *Bioorganic Photochemistry, Vol. 1: Photochemistry and the Nucleic Acids*, Morrison, H., Ed., John Wiley & Sons, New York, 1990, p. 1.
7. Pfeifer, G.P., Formation and processing of UV photoproducts: effects of DNA sequence and chromatin environment, *Photochem. Photobiol.*, 65, 270, 1997.
8. Mitchell, D.L., Jen, J., and Cleaver, J.E., Sequence specificity of cyclobutane pyrimidine dimers in DNA treated with solar (ultraviolet B) radiation, *Nucl. Acids Res.*, 20, 225, 1991.
9. Mitchell, D.L., Effects of cytosine methylation on pyrimidine dimer formation in DNA. *Photochem. Photobiol.,* 71, 162, 2000.
10. Tommasi, S., Denissenko, M.F., and Pfeifer, G.P., Sunlight induces pyrimidine dimers preferentially at 5-methylcytosine bases, *Cancer Res.*, 57, 4727, 1997.
11. Meijer, M. and Smerdon, M.J., Accessing DNA damage in chromatin: insights from transcription. *Bioessays* 21, 596, 1999.
12. Friedberg, E.C. and Hanawalt, P.C., Eds.,,*DNA Repair: A Laboratory Manual of Research Procedures*, Vols. 1A, 1B, 2, and 3, Marcel Dekker, Inc., New York, 1981–1987.
13. Pfeifer, G., Ed., *Technologies for Detection of DNA Damage and Mutations*, Plenum Press, New York, 1996, p. 73..
14. Henderson, D.S., Ed., *Methods in Molecular Biology, DNA Repair Protocols*, The Humana Press, Totowa, New Jersey, 165, 1999.
15. Mitchell, D.L. and Karentz, D. The induction and repair of DNA photodamage in the environment, in *Environmental UV Photobiology*, Young, A.R., Bjorn, L.O., Moan, J., and Nultsch, W., Eds., Plenum Press, New York, 1993, p. 345.
16. Mitchell, D.L. and Hartman, P.S., The regulation of DNA repair during development, *BioEssays*, 12, 74, 1990.
17. Sancar G.B., Enzymatic photoreactivation: 50 years and counting, *Mutat. Res.*, 451, 25, 2000.
18. Friedberg, E.C., Walker, G.C., and Siede, W., Eds., .*DNA Repair and Mutagenesis*, American Society for Microbiology Press, Washington, D.C., 1995.
19. Balajee, A.S. and Bohr, V.A., Genomic heterogeneity of nucleotide excision repair, *Gene*, 250, 15, 2000.

141

DNA Damage and Repair: Photochemistry

Marcus G. Friedel
Philipps Universität

Michaela K. Cichon
Philipps Universität

Thomas Carell
Philipps Universität

141.1 Biological Background

The harmful wavelengths of sunlight belong to the UV-B/C region between 260 and 320 nm. These wavelengths damage DNA and proteins. They are, to a great extent, filtered out of the solar radiation by the ozone layer, which forms an efficient UV-shield in the upper stratosphere.[1,2] Anthropogenous factors, however, have over the past decade severely reduced the amount of ozone.[3,4] This, in turn, led to a measurable increase in UV radiation, which now reaches the surface of our planet. It is estimated that UV radiation increased by about 10% in Western Europe.[5] The ozone hole, which appears every year during the Antarctic spring, is an area in which the ozone layer is almost completely diminished. It is the most prominent example of how anthropogenic emissions of nitric oxide and other ozone-degrading gases trigger the decrease of the ozone shield, leading to an increase in UV radiation.

UV radiation is harmful for all organisms that live exposed to sunlight. The energy-rich UV-C radiation damages particularly the genome of exposed cells, because the DNA bases exhibit absorption bands around 260 to 280 nm. The light absorption transfers the bases into their excited singlet and triplet states, out of which chemical reactions occur. These lead to severe base modifications[6,7] accompanied by a change of the base pairing properties, which in turn, causes mutations. Herein the most important UV-induced base modifications together with the light-dependent repair processes developed by nature to counteract the harmful effect of base lesions will be covered in this review.

The UV-induced base modifications, generally termed UV-induced DNA lesions, are the fundamental reasons for the development of skin cancer.[8–12] It is today known that every human being has an individual sunlight account. Too much sunlight, and hence too much UV irradiation, which induced too many DNA lesions, particularly during the early years of our life, triggers as the ultimate consequence the development of skin cancer. Skin cancer is today one of the most prevalent forms of cancer. The three most prominent forms are basal cell carcinoma, squamous cell carcinoma, and malignant melanoma. The first two variants contribute about 90 to 95% of all skin cancer incidents. Incidents of 5 to 10% are due to malignant melanoma, which is the most dangerous form of skin cancer because of the rapid

0-8493-1348-1/04/$0.00+$1.50

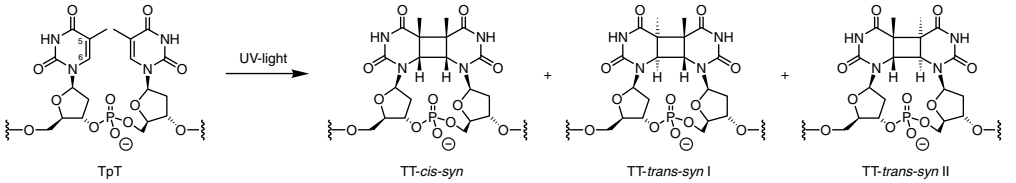

SCHEME 1 Three cyclobutane thymidine dimer DNA lesions (*cis-syn*, *trans-syn* I, *trans-syn* II) formed after UV irradiation of TT sequences in DNA.

formation of metastases.[13,14] In 1980, about 1600 people died from malignant melanoma in Germany. In the year 2000, the death toll rose to about 2100, which represents a 30% increase. Worldwide, the number of new skin cancer incidents was estimated by the World Health Organization (WHO) to be around 130,000 cases, with about 35,000 deaths directly linked to skin cancer.[15,16]

What is our key hint in linking these skin cancer cases to UV irradiation? Analysis of the *p53* tumor suppressor gene from basal and squamous cell carcinomas showed in more than 30% of all investigated cases deleterious mutations in this critical gene, which is the guardian of the cell.[17] Approximately 68% of the detected mutations are C → T transitions, which in over 90% of cases, are present at dipyrimidine sites.[18–20] Tandem-transition mutations CC → TT make up about 14% of all detected *p53* mutations.[13,14,21,22] These C to T transitions, particularly at dipyrimidine sites, are so-called fingerprint mutations. They are formed due to DNA replication mistakes made by the cell in the presence of UV-induced DNA lesions. The main mechanisms believed to be responsible for these mutations are also covered in this review.

141.2 The Chemistry of Lesion Formation

Cyclobutane Pyrimidine Dimers

Lesion Formation

Absorption of light around 260 nm by the DNA bases, particularly by the pyrimidine bases thymine and cytosine, results in the formation of cyclobutane pyrimidines dimers at dipyrimidine sites. The reaction depicted in Scheme 1 for thymidine is a [2π + 2π] cycloaddition reaction between the two C(5) = C(6) double bonds. The reaction furnishes three isomers: *cis-syn*, *trans-syn* I, and *trans-syn* II. Due to the constrains imposed by the DNA double strand, the *cis-syn* dimer is the major photoproduct.[18,23–25] It is formed when both pyrimidines adopt a *syn*-conformation around the glycosidic bond, which is the case in the double-strand environment. For both *trans-syn* photoproducts, one of the pyrimidines has to react out of the *anti*-conformation. This conformation is energetically more costly, and consequently, the reaction is less likely. Cyclobutane pyrimidine dimers are formed predominantly at TT sites, but cytosines can react as well (Scheme 2). The cyclobutane thymine dimer reaction products show only a weak absorption in the UV-C regime. Because the dimer formation is reversible (irradiation of cyclobutane pyrimidine dimers with UV light splits the dimer), this absorption characteristic drives the photostationary state toward dimer formation. The cyclobutane cytosine dimers feature residual absorption in the UV-C region and, therefore, give a photostationary state with a much smaller photoproduct content.[26] HPLC-MS/MS investigations provided detailed information about the relative yields of the various cyclobutane pyrimidine dimers after UV irradiation of DNA.[27] The relative ratios of all *cis-syn* dimer reaction products are: 5′-TT-3′, 5′-TC-3′, 5′-CT-3′, 5′-CC-3′ (2:1:0.4:0.1).

Structural Effects and Repair by the Nucleotide Excision Repair System

All of these cyclobutane pyrimidine dimers cause a structural distortion of the DNA double helix and a significant destabilization of the duplex around the lesion. The destabilizing effects are, however, different for the *cis-syn* and the *trans-syn* dimers. Detailed melting point studies,[28] theoretical calculations,[29–31]

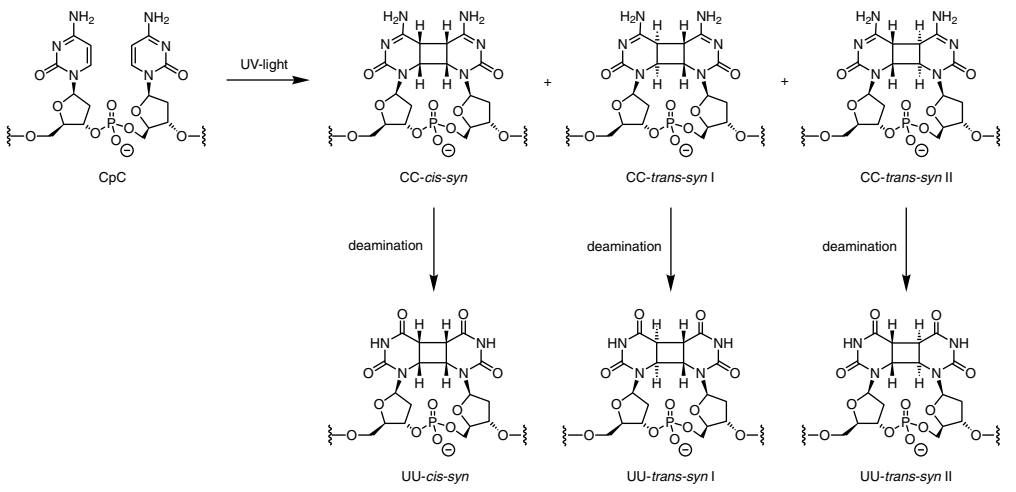

SCHEME 2 Formation of the cyclobutane cytosine dimers and of their deamination products, which are uridine-containing dimer lesions.

and NMR structural investigations[28,32–34] showed that the predominantly formed *cis-syn* lesions induce relatively small structural changes. The DNA double helix is bent by about 7 to 10°. The 3′-T of the T = T dimer remains well paired in the double strand, whereas almost no pairing occurs at the 5′-side of the DNA lesion. Overall, one T = T dimer destabilizes a DNA duplex approximately like one mismatch. Interestingly, the destabilization of a DNA:RNA double strand by a *cis-syn* dimer, which exists in the A conformation, is much less pronounced.[35,36] This could indicate that the dimer lesion is much better at accommodating in duplexes that have more A-like conformations. The destabilization effects of *trans-syn* dimers are significantly stronger, as are the structural distortions.[37] None of the two *trans-syn* dimers fit into a DNA double helix.

The amount of destabilization caused by a lesion is of paramount importance. All DNA lesions have to be removed from the genome in order to avoid cell death and mutagenesis. This is performed by a series of repair proteins and repair factors.[38] Some are believed to recognize DNA lesions based on their destabilization effect.[39,40] The UV lesions are generally repaired by the nucleotide excision repair pathway (NER), where a small piece of DNA around the lesion is excised.[38] It is known that this repair system recognizes DNA lesions predominantly based on their disturbing effect on the duplex structure. Based on our knowledge of how lesions destabilize the duplex, it can now be rationalized why repair of the *cis-syn* cyclobutane thymidine dimer is, in general, so sluggish, and in certain sequence contexts, almost not measurable.[18] These lesions cause simply only a small destabilization, which is readily overlooked by the nucleotide excision repair system. The large destabilization induced by the *trans-syn* dimers makes them, in contrast, excellent substrates for the nucleotide excision repair machinery.

The Mutagenic Potential of the Cyclobutane Cytosine Dimer Lesions

Particularly mutagenic are the cytosine-containing cyclobutane pyrimidine dimers depicted in Scheme 2.[41] The cytosine unit within a cyclobutane pyrimidine dimer rapidly hydrolyzes under physiological conditions.[42] In fact, the half-life time of a dihydrocytosine in a cyclobutane-type UV lesion was estimated to be just around 1.5 h for CpT *in vitro* and 5 h *in vivo*.[43,44] The hydrolysis furnishes uridine-containing lesions, as shown in Scheme 2 and Figure 141.1(a). These lesions instruct polymerases to incorporate an adenine as the counterbase if the polymerase reads over the lesion (Figure 141.1) upon copying the DNA strand.[41] This gives a U = U:AA double mismatch sequences which will subsequently force any repair system to replace the U = U lesion with two thymidines. This mechanism could be one main reason for the observed C → T and CC → TT transitions in the genes of skin cancer cells.[42] Another

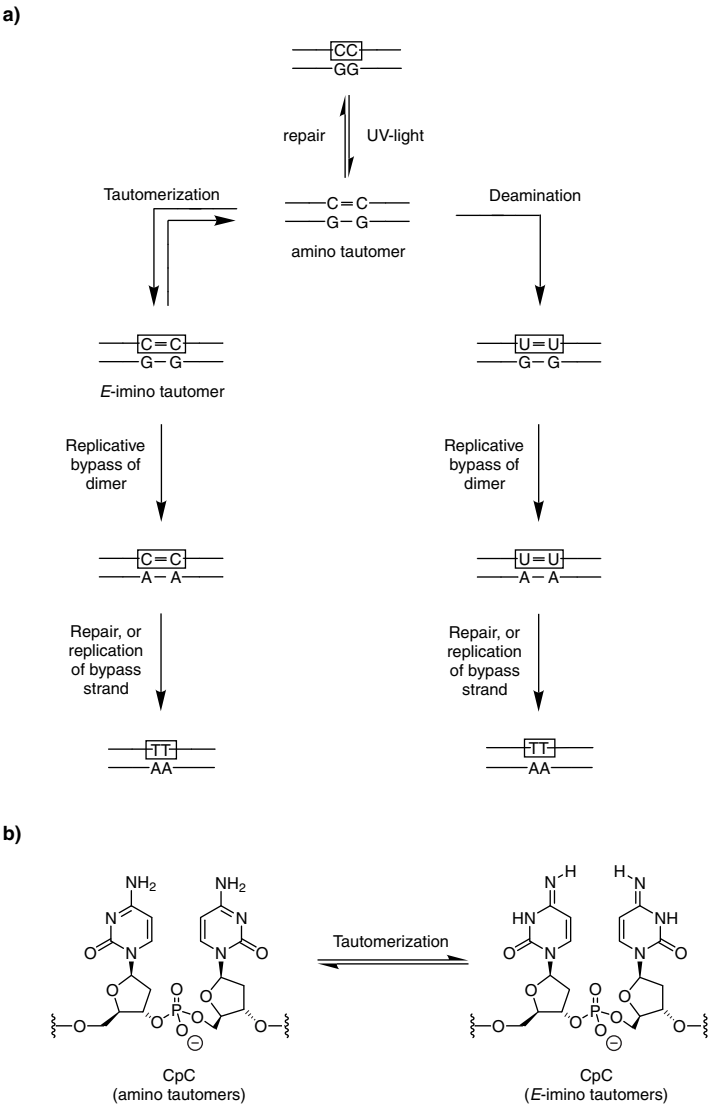

FIGURE 141.1 (a) The tautomer bypass and the deamination mechanism of CC-dimer mutagenicity, used to explain C → T transitions and CC → TT tandem transition mutations. (b) A cytidylyl–cytidine sequence and a situation in which both cytidins are present in their *E*-imino tautomeric forms.

explanation for the observed mutations invokes tautomerization of the cytosine in a cyclobutane pyrimidine dimer into the (*E*)-imino tautomeric form [Figure 141.1(b)]. This tautomeric form would also instruct polymerases to pair the lesion with one or two adenines. Both mechanisms provide plausible explanation for the observed UV-fingerprint mutations.[10]

⟨6–4⟩ Photolesions

Another main photoreaction that occurs upon UV-light absorption of pyrimidine bases is the Paternó–Büchi reaction between the C(5) = C(6) double bond of the first pyrimidine and the C(4) = O carbonyl group of the second base. This reaction furnishes initially an oxetane intermediate at TT dipyrimidine sites.[9] The cytosine can react out of its (*E*)-imino tautomeric form with its C(4) = NH. The formed reaction product is an azetidine intermediate.

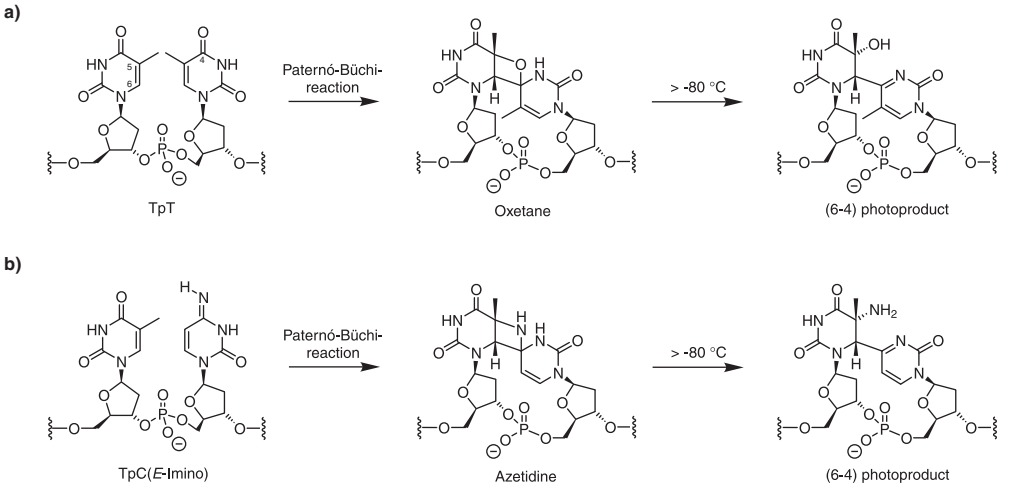

SCHEME 3 Reaction of a dipyrimidine site in a Paternó–Büchi reaction to give first an oxetane or azetidine reaction intermediate, which rearranges to give the stable (6–4) photolesions. (a) Reaction at a TT bis-pyrimidine site. (b) Reaction at a TC bis-pyrimidine sequence to give a cytidine-derived (6–4) photoproduct.

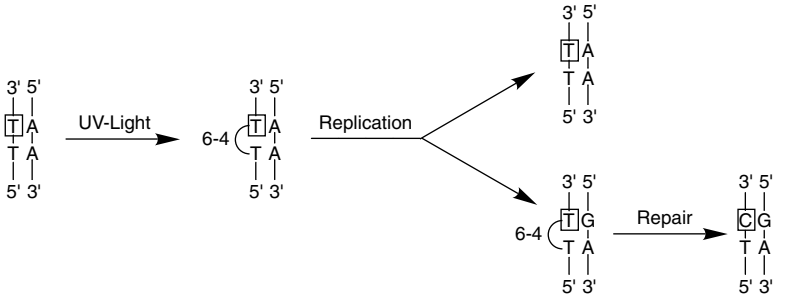

FIGURE 141.2 Modified pairing properties of the (6–4) lesion induce a T → C transition mutation. The mispairing 3′-T of the (6–4) lesion is shown in a box.

The oxetane and azetidine reaction products formed at 5′-TC-3′, 5′-CC-3′, 5′-TT-3′, and 5′-CT-3′ sites are not stable above -80°C. They rapidly undergo a ring-opening reaction to the corresponding (6–4) photolesions depicted in Scheme 3.[9,45,46] The stereochemistry of the pyrimidine–pyrimidine reaction products is again determined by the chiral DNA environment. The relative ratios of (6–4) lesions at different dipyrimidine sites were determined by HPLC-MS/MS[27] as follows: 5′-TC-3′ > 5′-TT-3′ > 5′-CC-3′ > 5′-CT-3′ (1:0.2:0.1:0.01).

Detailed NMR investigations show that the (6–4) lesions strongly change the B conformation of the DNA duplex.[47] The NMR studies suggest that the DNA duplex is bent at the lesion site by about 44°.[48,49] FRET experiments[50] and calculations,[31] however, point to a much smaller bend of just 5°. The 5′-T of a T-T (6–4) lesion is still paired in the Watson–Crick modus. The 3′-T, however, pairs preferentially with a guanine.[48,51,52] This observation offers an explanation for T → C transition mutations in UV-irradiated cells (depicted in Figure 141.2).[53,54]

The Dewar Valence Isomer

Irradiation of DNA containing the (6–4) photoadduct with wavelength above 300 nm induces a rearrangement of this (6–4) lesion into a Dewar valence isomer (Scheme 4).[55]

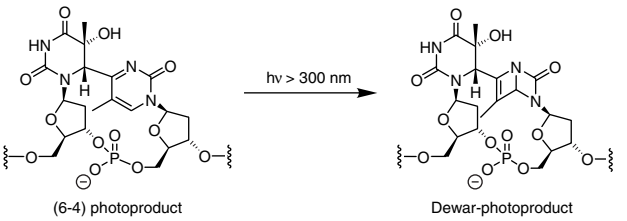

SCHEME 4 Rearrangement of the (6–4) photoproduct to the Dewar valence isomer upon irradiation with light >300 nm (UV-B).

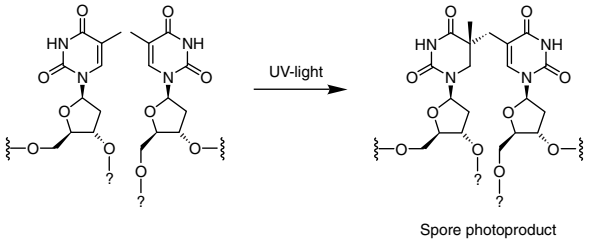

SCHEME 5 UV-light-induced formation of the spore photoproduct in spore DNA by an intrastrand or interstrand reaction of two thymidines.

J.-S. Taylor[46,56,57] could clarify that the pyrimidone substructure of the (6–4) lesion is the rearranging unit. So far, formation of this Dewar lesion was detected by HPLC-MS/MS only at CC-sites upon irradiation of isolated or cellular DNA with UV-B and UV-C light.[27] Our understanding of its biological impact is still rudimentary. Information of how this lesion influences the structure and stability of DNA duplexes is, at this point, consequently limited.[47] From the available information, however, one can conclude that the structural effect on the DNA duplex is substantially different compared to the (6–4) adduct.[47,58] DNA repair enzymes seem to recognize this lesion like an abasic site.[59] Whereas the cyclobutane pyrimidine dimers, and to a lesser extent, also the (6–4) adducts, can still instruct polymerases (misinstruction), the Dewar valence isomer seems to be fully noninstructional. Polymerases, however, which are forced to read through a noninstructional site preferentially incorporates an adenine. This feature of polymerases is known as the A rule. This A rule seems to govern the mutagenicity of the Dewar valence isomer.

To summarize, at our current level of understanding, the mutagenic effect of UV light is clearly dominated by the formation of the cyclobutane pyrimidine dimers and (6–4) photoadducts. Among them, the cytosine-containing lesions are the most mutagenic lesions due to their sensitivity to hydrolytic deamination.

The Spore Photoproduct

DNA in spores is densely packed and covered by small acid-soluble spore proteins.[60,61] The DNA is strongly dehydrated and exits in a more A-like conformation.[62] This dense packing enables spores to "survive" even extreme conditions like extreme cold and heat or severe dryness. Irradiation of spores with UV light causes formation of yet another photolesion, which is exclusively formed in spores, possibly due to the unusual A-like conformation of the DNA.[63,64] The formation of this lesion (Scheme 5) can be mimicked by irradiation of a thin film of dry thymine or of a frozen thymidine solution with a UV-C light source (254 nm), as depicted in Scheme 6(a).[65–68]

The mechanism of formation is still unclear. Attempts to simulate the formation of the spore lesion with thiophenyl substituted thymidine [Scheme 6(b)], which produces a 5-centered radical upon irradiation, failed.[69] This failure indicates that the lesion may not form via a 5-(2′-deoxyuridilyl)methyl

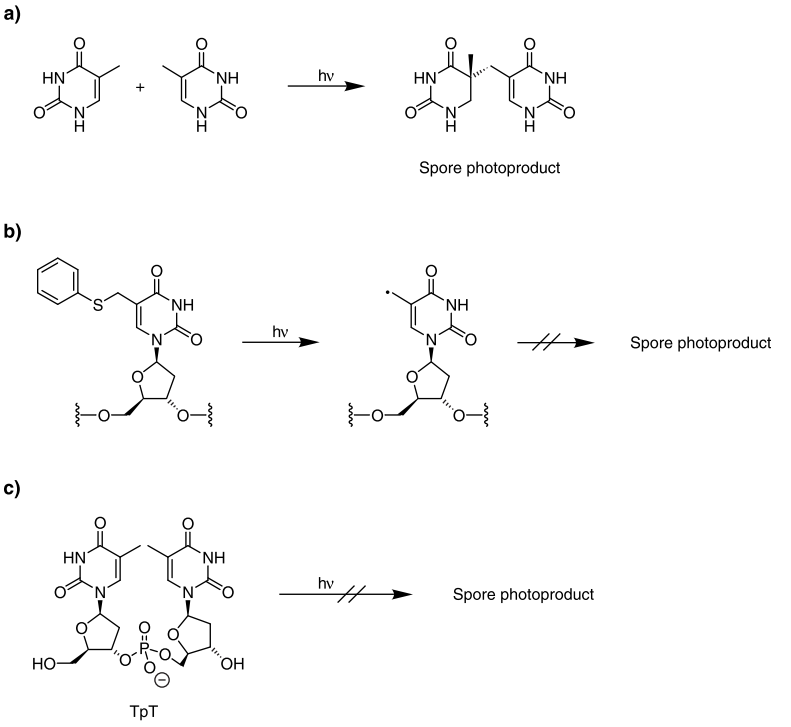

SCHEME 6 Attempt to prepare the spore photoproduct by irradiation of chemically synthesized precursors. (a) Irradiation of thymine in a thin dry film. (b) Irradiation of a thiophenyl-substituted thymidine, which yields an intermediate 5-(2′-deoxyuridilyl)methyl radical. (c) Irradiation of a thymidylyl-thymidine dinucleotide.

radical intermediate that could attack a second thymine. Alternatively, a precise geometrical rearrangement of the two involved thymines may be required, which is not accessible by the thymines if one bears the 5-thiophenyl modification. In our opinion, it is also unclear whether the lesion is formed in an intrastrand or in an interstrand reaction. So far, all attempts to create the lesion through irradiation of a TpT dinucleotide [Scheme 6(c)] failed,[70] which indicates that the lesion could be, in fact, an interstrand cross-link.

Other DNA Photoproducts

The described UV photolesions are the best-studied photoproducts so far. We can, however, be sure that many more UV-induced lesions exist, which await structural characterization. Recently, Clivio et al.[71] isolated a new photoproduct after UV irradiation of an amide-linked thymidyl-thymidine. The UV photoproduct is an interesting 2-imidazolone-(5–4)-pyrimidone adduct, shown in Scheme 7. It is yet unclear if similar photoproducts are also formed in DNA.

141.3 Photoinduced DNA Repair

DNA photorepair is one of the most fascinating enzymatic activities that nature invented to remove UV-induced DNA lesions from the cellular genome. In general, cells need to remove DNA lesions with high efficiency in order to avoid cell death or the development of mutations, which may result in carcinogenic cell growth. The UV lesions are prominent DNA alterations formed in DNA, because life exists in exposure to sunlight. Already, the earliest photosynthetic cyanobacteria, about 2 to 3 billion years ago, required an efficient repair pathway for UV lesions.[72] Due to the lack of any ozone shield, this must have been of paramount importance for survival. The fascinating creativity of nature is manifested in the development

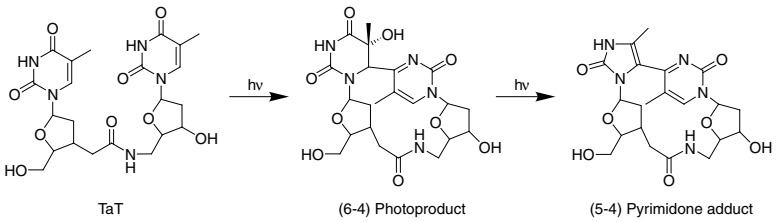

SCHEME 7 Irradiation of an amide-linked thymidylyl-thymidine (TaT) furnished a novel (5–4) photoproduct via the (6–4) photolesion.

of enzymes that use the harmless long-wavelength part of sunlight as an energy source to drive the repair of the UV-induced lesions. These enzymes are the DNA-photolyases.[73–75] Although repair of UV lesions in many higher organisms, like humans, is achieved by the nucleotide excision pathway (see above), photolyases still represent a major defense shield against UV-induced lesions in many plants, bacteria, reptiles, fish, and marsupials.

Cyclobutane Pyrimidine Dimer DNA Photolyases

Cyclobutane pyrimidine dimer DNA-photolyases (CPD-photolyases) are monomeric DNA repair proteins (~55 kDa) that directly repair cyclobutane containing UV-light-induced DNA lesions.[73,74] Another type of photolyases repairs (6–4) lesions. They will be discussed later. The CPD-photolyases are mechanistically the best understood, and three crystal structures of CPD-photolyases from *E. coli*,[76] *A. nidulans*,[77] and *T. thermophilus*[78] provide detailed information about the structural requirements for efficient genome repair.

Structures and Lesion Recognition

The crystal structures of all photolyases revealed a globular shape and the presence of two coenzymes at a distance of 16.8 Å and 17.5 Å to each other, respectively.[76,77] Every photolyase known today contains one FAD-cofactor bound in a cavity with the right dimension and polarity to also accommodate the DNA lesion. The architecture suggests that photolyases recognize the lesion substrate in a flipped out conformation. The second coenzyme, either a methenyltetrahydrofolate (MTHF) (Type-I photolyases) or a 5-deazaflavin (5-DF) (Type-II photolyase), depending on the type of photolyase, is bound in a shallow groove close to the surface of the protein (Figure 141.3).

In accordance with x-ray crystal structures obtained from other repair enzymes in complex with lesioned DNA,[79–82] photolyase seems to trigger, upon binding to damaged DNA, a major conformational rearrangement.[83] Atomic force microscopy studies suggest that photolyases induce upon binding to DNA a bend of about 36°, which possibly leads to the extrusion of the dimer lesion into the putative lesion binding site.[84,85] A recent crystal structure of the photolyase from *T. thermophilus*,[78] together with a thymine, shows the thymine inside this putative active site in close van der Waals contact to the isoalloxazine ring of the FAD coenzyme. Additional stacking interactions of the thymine with the Trp_{353} and van der Waals contacts with Trp_{247}, Met_{314}, and Gln_{349} fix the thymine in the active site. This "cocrystal" structure provides compelling evidence that the dimer is bound in a flipped-out conformation.

Although the enzyme binds to the DNA lesion in a light-independent process, it, however, requires long wavelength light (350 to 450 nm) as the energy source to repair the lesion. Photolyases are, hence, only operative in tissues exposed to daylight. Biochemical investigations and model compound studies showed that the light energy is initially absorbed by the second cofactor like the MTHF.[73] This antenna chromophore funnels the energy to the $FADH^-$ which must exist in the two-electron reduced and deprotonated state. The excited, fully reduced flavin subsequently injects one electron into the dimer, which undergoes spontaneous splitting into two thymidine monomers (Scheme 8).

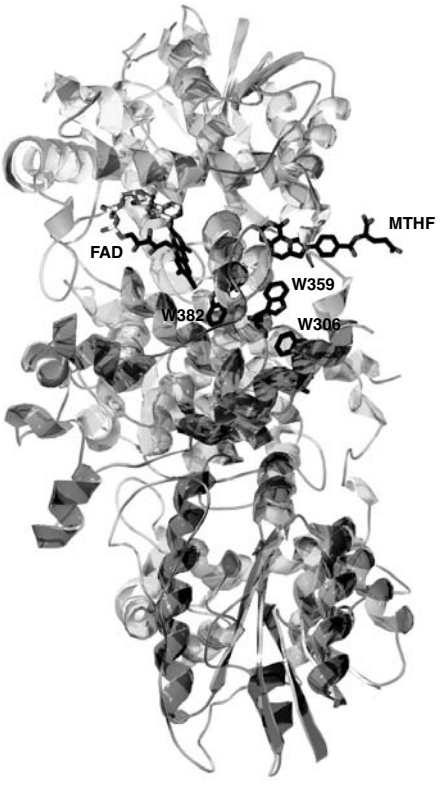

FIGURE 141.3 DNA photolyase from *E. coli*, with the two cofactors FAD and MTHF.

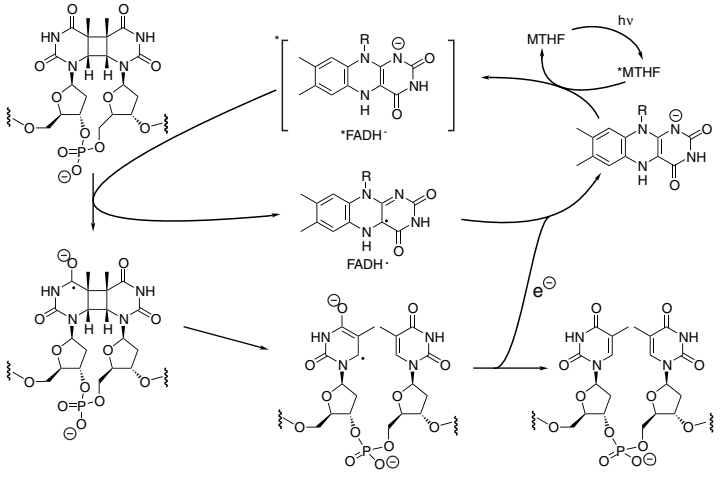

SCHEME 8 Reaction mechanism of CPD-photolyases (Type-I) with a methenyltetrahydrofolate (MTHF) as the second cofactor.

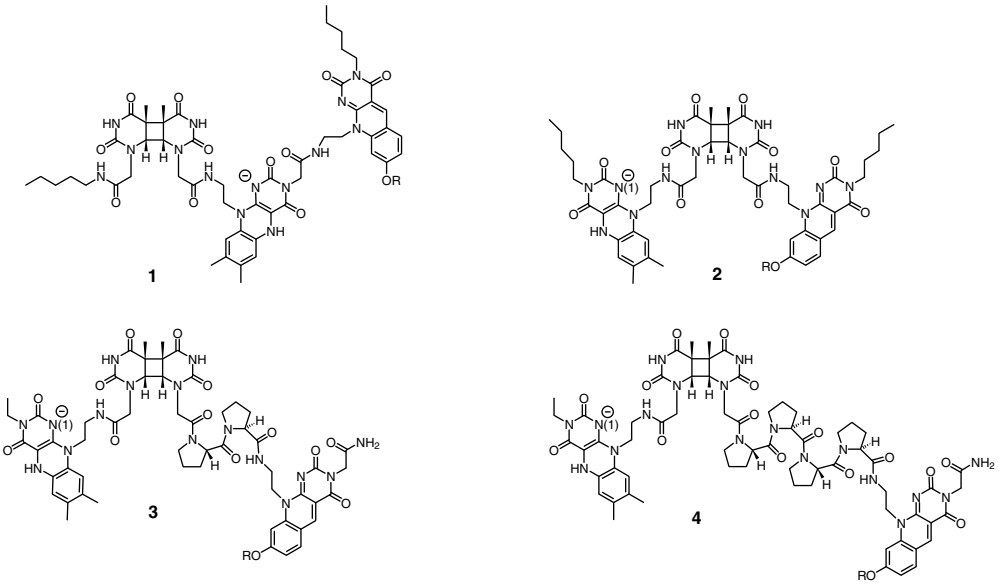

FIGURE 141.4 Covalent flavin-deazaflavin-thymine dimer model compounds **1** to **4** for the investigation of the photolyase-catalyzed repair reaction. The flavin-dimer distance is kept constant, while the distance between the deazaflavin and the dimer is systematically increased from **1** over **2** and **3** to **4**.

Electron Transfer to the Dimer Lesion in CPD-Photolyases

Recently, the structure of the DNA-lesion-photolyase complex and the electron-transfer pathway from the flavin to the dimer was investigated theoretically.[86,87] Applying the DOCK 4.0 program to model a hypothetical dimer–DNA complex, it was shown that the distance between the FAD and the dimer lesion could be around 3 Å. Other studies point, however, to a much larger distance.[88] Regardless of the distance, theory predicts that the electron is transferred indirectly from the $FADH^{\cdot}$ via the adenine to the dimer. The adenine moiety of the FAD closely approaches the dimer lesion due to the U-type conformation of the FAD (Figure 141.3). Model compound studies recently revealed further details about the critical electron transfer process.[75,89] Using model compounds like **1** to **4** (Figure 141.4), which contain a cyclobutane thymine dimer covalently connected to a flavin, it was shown that the deprotonation at N(1) (pK_a = 6.5) is critical for the repair reaction.[90] Protonation of N(1) stops the cleavage reaction immediately. The strict necessity of deprotonating the reduced flavin indicates that the system has to avoid a zwitterionic $FADH_2^{+}$-$Dimer^{-}$ state, which would form soon after electron transfer from the neutral $FADH_2$. Instead, photolyases seem to favor a charge shift reaction intermediate $FADH^{\cdot}$-$Dimer^{-}$, may be in order to reduce the rate of an unproductive charge recombination process, which competes with the dimer-splitting reaction ($k_{split} = 2 \cdot 10^6\ s^{-1}$). Protonation of the dimer radical anion or H-bonding was suggested to accelerate the cleavage process.[89,91]

Energy Transfer between the Two Coenzymes

Investigations of model compounds **1** to **4** also allowed us to get deeper insight into the energy transfer event from a deazaflavin, as the second cofactor in Type-II photolyases, to the flavin.[92,93] Of particular interest was to study how the cofactor–cofactor distance affects the dimer-splitting process. It was noted by Deisenhofer[76] that the large separation between the two cofactors in the protein structures is difficult to rationalize in light of the energy-transfer mechanism. The rate for such a dipole–dipole energy transfer (k_{EET}), as described by the Förster theory, depends strongly on the distance ($k_{EET} \propto r^{-6}$). This distance

dependence argues for a preferred short cofactor separation, in order to increase the light-transfer efficiency.

The model compounds **1** to **4** feature constant flavin–dimer arrangements and systematically increased flavin–deazaflavin separation. Monochromatic and selective irradiation of the deazaflavins in each model compound proved that fastest dimer cleavage occurs in Compound **4**. Model Compound **4** features, however, the largest cofactor–cofactor separation and, hence, the worst energy-transfer efficiency. A systematic decrease of the cofactor–cofactor distances from Compound **3** to model system **1**, furnished a surprisingly systematic decreased splitting rate, although increasing energy-transfer efficiencies were noted. Short cofactor distances, therefore, allow efficient energy transfer but inefficient dimer splitting. This unexpected result was explained with a "short-circuit" reaction, which interferes with the dimer-splitting process. We now believe that this short-circuit process is an alternative electron transfer from the reduced flavin FlH^- to the deazaflavin. The deazaflavin has the more positive reduction potential compared to the thymine dimer and should be the preferred electron acceptor. The large distance between the antenna-chromophore and the flavin reduces the rate for this short-circuit reaction, while the short $FADH^-$ dimer separation favors electron transfer to the lesion.

The Photoactivation Process

In the model Compounds **1** to **4**, an efficient energy transfer was observed from the deazaflavin to flavin, when both chromophores were present in their oxidized redox states. This energy transfer strongly accelerated any photoreduction of the flavin-chromophore in the presence of external photo reductants like EDTA. A similar photoreduction is also needed in photolyases in order to transform the semireduced $FADH^{\cdot}$ cofactor, present in the resting state of many enzymes, into the fully reduced $FADH^-$ redox state needed for catalysis. This one-electron photoreduction process was recently investigated by time-resolved absorption and EPR spectroscopy (Figure 141.5).[94,95] In the *A. nidulans* photolyase [Figure 141.5(a)], without the deazaflavin coenzyme, it was found that after a 7 ns laser flash pulse, which excitated the $FADH^{\cdot}$, a fast electron transfer from a nearby tryptophan occurs. This electron transfer leads to the formation of the fully reduced state $FADH^-$, and gives a tryptophanyl radical in less than 500 ns. Surprisingly, a tyrosine residue subsequently donates an electron to the tryptophanyl radical forming a deprotonated neutral tyrosyl radical ($TyrO^{\cdot}$) with $t_{1/2} = 50\ \mu s$. The $TyrO^{\cdot}$ is subsequently reduced by an external electron donor in a bimolecular reaction. Further evidence for the formation of the $TyrO^{\cdot}$ was obtained by time-resolved EPR spectroscopy.[95]

The photoactivation process in Type-I photolyases involves even more tryptophan units [Figure 141.5(b)]. Short time spectroscopic studies of the *E. coli* enzyme revealed an intraprotein multistep radical transfer cascade. Approximately 30 ps after the laser flash pulse exciting the FADH; formation of a first tryptophanyl radical ($Trp^{\cdot+}_{382}$) was observed, followed by two additional fast (<10 ns) electron-transfer events from Trp_{359} to $Trp^{\cdot+}_{382}$ and Trp_{306} to $Trp^{\cdot+}_{359}$, respectively. Final deprotonation of the radical $Trp_{306}^{\cdot+}$ to $Trp_{306}^{\cdot}$ in about 300 ns seems to trap the radical at Trp_{306}, which is located close to the surface of the protein. Here, reduction of $Trp_{306}^{\cdot}$ can occur by an external reducing agent. The energies for the individual electron-transfer steps in these cascades were recently calculated.[96] The first electron transfer between Trp_{359} and $Trp^{\cdot+}_{382}$ is almost isoenergetic. The second electron transfer from Trp_{306} to $Trp^{\cdot+}_{359}$ is, however, exothermic with 200 meV, which stabilizes the $Trp^{\cdot+}_{306}$ radical cation. Another 214 meV are gained by the deprotonation. All the tryptophan residues involved in this radical transfer cascade are precisely aligned. The distances between the tryptophan "stepping stones" are 4.2 Å, 5.2 Å, and 3.9 Å, which is optimal for electron transfer. The function of Trp_{306} as an essential partner in the photoactivation cascade was also supported by side-directed mutagenesis studies. Replacement of the Trp amino acids by alanine fully diminished the ability of the *E. coli* photolyase to activate the $FADH^{\cdot}$ cofactor.[73] From these studies, it became clear that photolyases use the transfer of radicals along amino acid side chains to photoreduce the FAD. Photolyases seem to share this property with class I ribonucleotide reductases, in which a radical transfer occurs over 35 Å from a tyrosyl radical to a cysteine in the active site.[97]

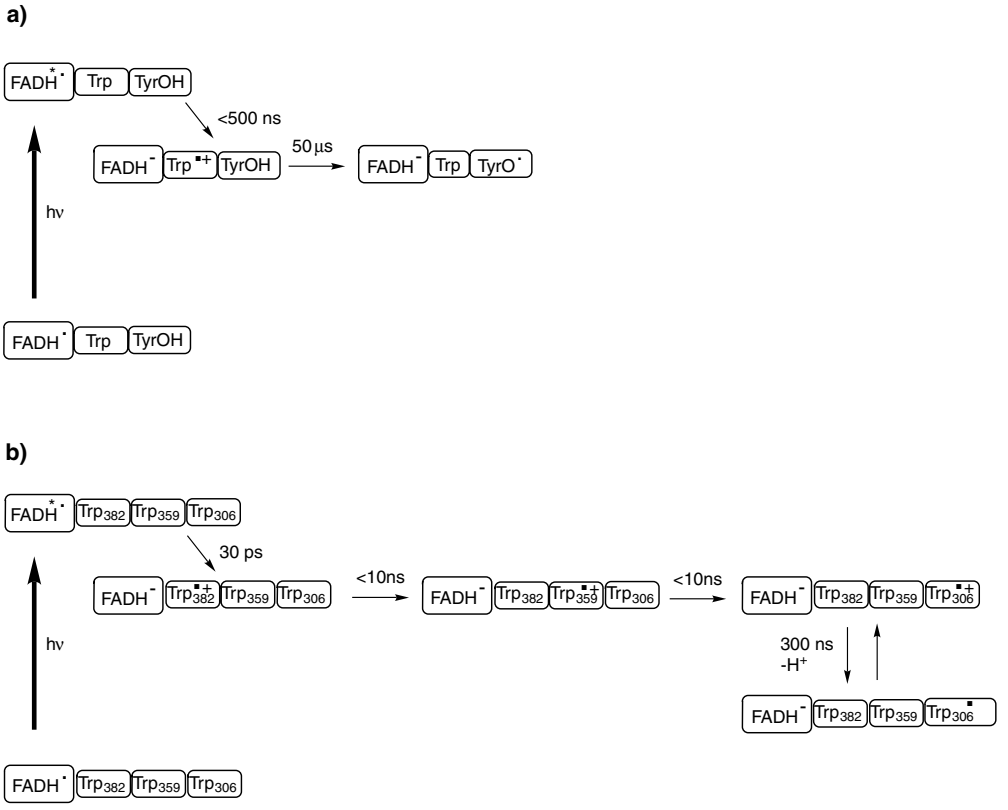

FIGURE 141.5 Trp- and Tyr-mediated electron-transfer cascades in Type-II DNA photolyases (a) and in Type-I DNA photolyases (b). The electron-transfer cascade is responsible for the photoreduction of the FAD-coenzyme to give the active $FADH^-$.

The Mechanism of Action of (6–4) Photolyase

Photoactivation of the Enzyme

The (6–4) photoadducts and the Dewar valence isomers are repaired by a special class of (6–4) photolyases.[98] The strong sequence homology between the (6–4) and the "classical" CPD-photolyases fuels the belief that both enzymes utilize a similar mechanism, which includes binding of the substrate, absorption of a photon, and restoration of the normal bases via electron transfer. Support for this assumption stems from the observation that (6–4) photolyases contain an FAD cofactor and presumably a folate as the second cofactor. The FAD is again needed in the two-electron reduced form ($FADH^-$). A recent EPR study of the (6–4) photolyase from *X. laevis* showed clearly that the FAD is reduced to the $FADH^-$ in two successive, light-induced electron-transfer steps via an intermediate that was assigned to be the neutral $FADH^•$ radical, formed after protonation of an initially formed $FAD^{•-}$.[99] Similar to CPD-photolyases, a Trp seems to function as the electron donor in question. Due to the lack of a crystal structure of a (6–4) photolyase, the structural requirements for this electron transfer are yet unclear. Based on the observed structural similarity between CPD and (6–4) photolyases, Kim et al.[100] suggested a repair mechanism for (6–4) photolyases shown in Figure 141.6. He proposed that the (6–4) lesion is first converted back into the oxetane within the active site of the enzyme. This rearrangement could be followed by a retro-Paternó–Büchi reaction, triggered by a single-electron donation from the reduced $FADH^-$ (Figure 141.6).

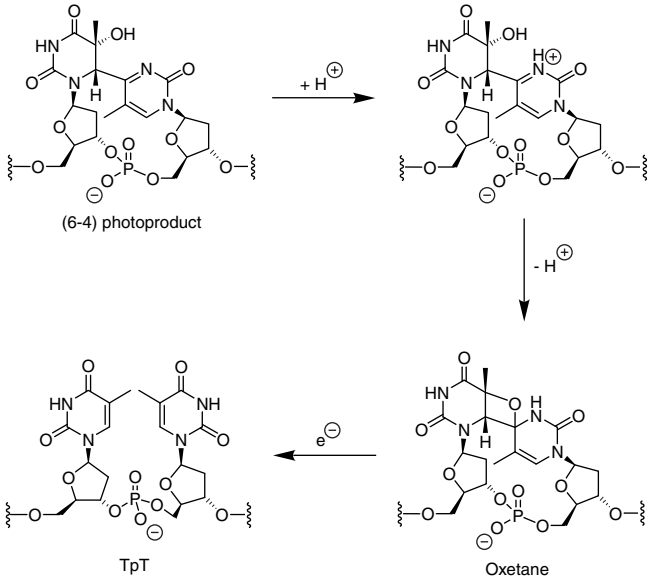

FIGURE 141.6 Proposed mechanism for the repair of (6–4) lesions by the (6–4) photolyase. Protonation gives an *N*-acyliminium ion, which is attacked by the *tert*-OH group to form the oxetane intermediate. This is split by single-electron reduction.

Enzymatic Studies with (6–4) Photolyases

Recent enzymatic investigation of the (6–4) photolyases from *D. melanogaster*[101] and *X. laevis*[102] provided the basis for our current understanding of the light-induced (6–4) repair process. (6–4) photolyases bind strongly ($K_D \approx 10^{-9}$ M – 10^{-10} M) and with high specificity to the (6–4) lesion. DNase I footprinting studies show that (6–4) photolyases protect an 11 (*X. laevis*) to 20 (*D. melanogaster*) base pair long patch around the lesion-containing site.

The quantum yield for the repair of the (6–4) lesion is smaller ($\phi = 0.1$) compared to the repair of cyclobutane pyrimidine dimer (CPD) lesions ($\phi = 0.7$) by CPD photolyases. (6–4) photolyases also bind and repair the Dewar photoproduct, although binding is not as tight ($K_D = 10^{-8}$ M – 10^{-9} M), and the relative quantum yield for repair $\phi_{rel} = 0.5$ is two orders of magnitude smaller compared to the (6–4) lesion ($\phi_{rel} = 100$).

Semiempirical AM1 and PM3 calculations suggest that a hypothetical oxetan intermediate would efficiently split after single-electron reduction or oxidation.[103] The reductive pathway was found to be more exothermic and should proceed over lower rate-determining barriers, which supports the assumption that the (6–4) repair is based on a reductive electron transfer from the $FADH^-$ to the lesion.[103] It was also calculated that the Dewar valence isomer could be transformed into the (6–4) lesion by a single-electron reduction, which could explain the ability of (6–4) photolyases to repair this lesion as well, although with much lower efficiency.[103]

Investigation of the (6–4) Repair Mechanism with Model Compounds

The key step in the proposed oxetane repair mechanism is the rapid fragmentation of the oxetane radical anion. This ring-opening reaction was recently studied with model compounds. Falvey and coworkers[104,105] prepared stable oxetane adducts from dimethylthymine and various benzaldehyde derivatives. Laser flash photolysis investigations in the presence of external electron donors like dimethyl aniline showed efficient oxetane splitting, which allowed investigation of the radical intermediates. The radical cations of the various sensitizers and the radical anions of the carbonyl products formed after

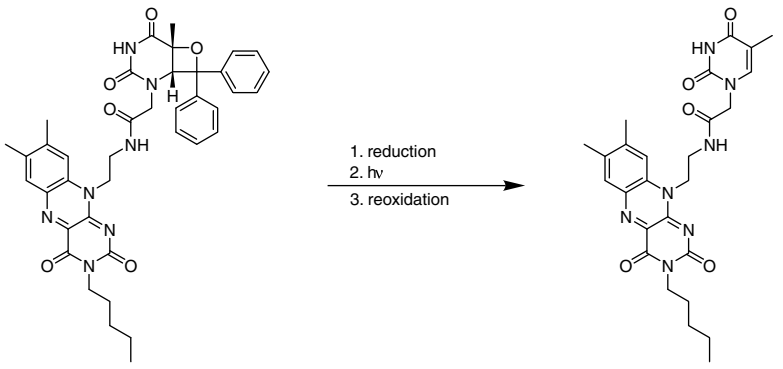

FIGURE 141.7 Model compound for the (6–4) photolyase, used to study the reductive flavin (FlH^-)-induced oxetane cleavage.

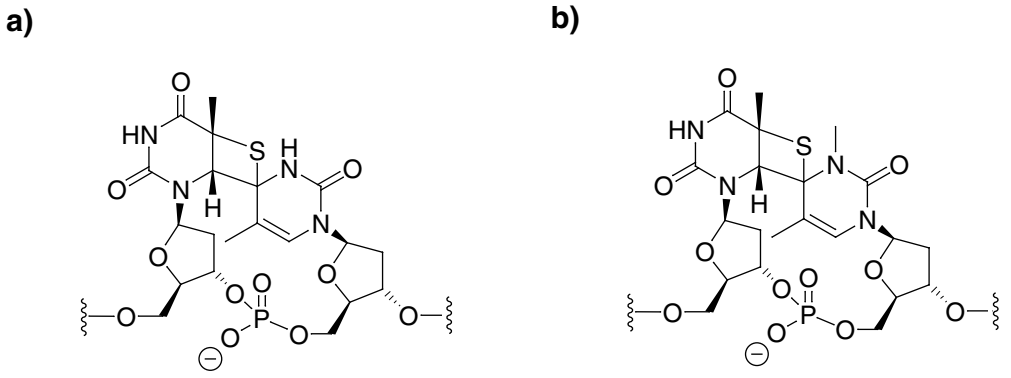

FIGURE 141.8 Two stable thietane analogs used to study the binding of the (6–4) photolyase to an assumed oxetane intermediate.

oxetane cleavage were both detected. Estimation of the oxetane–anion cleavage rate provided a value of $k_d \approx 5 \cdot 10^7\ s^{-1}$. This value is significantly larger than the rate measured for the splitting of cyclobutane pyrimidine dimers ($k_d \approx 2 \cdot 10^6\ s^{-1}$), indicating that the model oxetane anions, generated in this study, cleave about 10 times faster.[105] Recently, the first model compound containing a stable oxetane covalently connected to a flavin derivative was prepared.[106] With these compounds, it was shown that only the reduced and deprotonated flavin is able to cleave the oxetane. This result supports the assumption that the repair is triggered by an electron transfer from the $FADH^-$ to the dimer (Figure 141.7).

The alternative oxidative ring opening of oxetanes after electron abstraction is currently under intensive investigation in the Miranda group.[107,108] Although this process is, at this point, biologically not relevant, it provides currently, detailed information about the chemical properties of oxetanes.

Although reductive splitting of a hypothetical oxetane is now established as the most plausible biologically relevant mechanism, direct evidence for the formation of an oxetane intermediate during enzymatic (6–4) repair is yet to be determined. In this context, it was found that binding and repairing the thietane compounds [Figure 141.8(a,b)],[101,109–111] which closely resemble the structure of the hypothetical oxetane intermediate, by (6–4) DNA photolyases, failed. In addition, density functional calculations and semiempirical studies revealed free energy difference between 14.5 to 16.5 kcal/mol for the rearrangement of the (6–4) into the oxetane species.[112] This suggested that shifting the (6–4)/oxetane equilibrium toward the oxetane compound is energetically costly. Even though the calculated values might be too large, as recently speculated, the rearrangement of the (6–4) lesion to the oxetane intermediate is

difficult to explain, and it therefore remains an open question. The rearrangement would require reaction of the 5-OH group of the (6–4) adduct with the enamide substructure. This attack could be accelerated if the corresponding nitrogen is protonated to give an *N*-acyliminium ion (Figure 141.6). Recently, two histidine residues were identified by side-directed mutagenesis, which could be responsible for this protonation.[113] *N*-acyliminium ions possess a highly electrophilic reactivity. This high reactivity allows even weak nucleophiles to attack. The addition of oxygen nucleophiles to *N*-acyliminium ions was observed and yields *N,O*-acetals. The rate-determining step in this reaction is thought to be the formation of the *N*-acyliminium ion. The rearrangement of the (6–4) adduct to the oxetane could therefore depend on the efficiency of protonation in the lesion-binding pocket, which could explain the low quantum yield of the enzymatic (6–4) repair.

The Spore Photoproduct Lyase

Although the spore photoproduct lyase is not a light-dependent enzyme,[114] we are, nevertheless, covering the recently gained mechanistic insights, mainly because this enzyme repairs one of the major UV lesions. The spore photoproduct lyase is only able to repair the special UV-irradiation products in spores. Other UV lesions like the cyclobutane-containing photoproducts are not substrates for this unusual enzyme. The enzyme is only expressed during sporulation and then stored inside the spore. If the spore starts to develop (germination), the spore photoproduct lyase becomes active.[114–116] Today, it is known that the enzyme, e.g., from *Bacillus subtilis*, is made from 342 amino acid. The protein has a molecular weight of about 40 kDa and shows some sequence homology with the *C*-terminus of other photolyases.[116,117] The spore photoproduct lyase reverts the spore UV lesions directly back into the original thymine bases, similar to the other photolyases. Light, however, is not required. In contrast, the repair mechanism involves *C*-centered radicals. The enzyme contains four cysteins in close contact to a Fe in a [4Fe + 4S] cluster.[118,119] This cluster is oxygen sensitive, so that efficient repair requires anaerobic conditions. The enzyme also needs one molecule of *S*-adenosyl-methionine (SAM) as an additional cofactor. Strong sequence homology of the spore photoproduct lyase with other adenosyl methionine radical enzymes and recent mechanistic studies led to the formulation of the mechanism shown in Figure 141.9.[119–122] The initial step in the reaction mechanism could be the formation of an adenosyl radical, which abstracts an H-atom from the 6-position of the spore photoproduct. The formed lesion radical could then rearrange to give a thymine and a 5-(2′-deoxyuridilyl)methyl radical. Back transfer of the H-atom from adenosine would furnish a restored second thymine base under regeneration of the radical coenzyme. Our current understanding of the spore photoproduct lyase indicates therefore that the enzyme belongs to the family of SAM-dependent radical enzymes. The protein is the first DNA repair protein, which utilizes a radical mechanism for repair.

141.4 Conclusions

In the past decades, much knowledge was gained about UV-light-induced DNA lesions. The structures of the main lesions, e.g., the CPD lesions, the (6–4) lesions, and of the spore photoproduct, were elucidated. Plausible mechanisms of how these lesions induce mutations were proposed. Although still awaiting rigorous proof, these mechanisms explain why UV-induced lesions induce mutations and cancerogenous cell growth.

The repair of these lesions in higher organisms is performed mainly by nucleotide excision repair. However, light is also used as an energy source to remove these lesions from the genome in many organisms. DNA photolyases convert sunlight into DNA repair activity. They repair cyclobutane pyrimidine dimer lesions (CPD photolyases) and (6–4) lesions [(6–4)-photolyases] using a unique electron-transfer-driven mechanism. A similar mechanism is used by the spore photoproduct lyase to repair spore photoproducts. The spore photoproduct lyase is an interesting radical enzyme, which, however, operates light independently. The mechanism of action of CPD photolyase is well understood. For (6–4) photolyases,

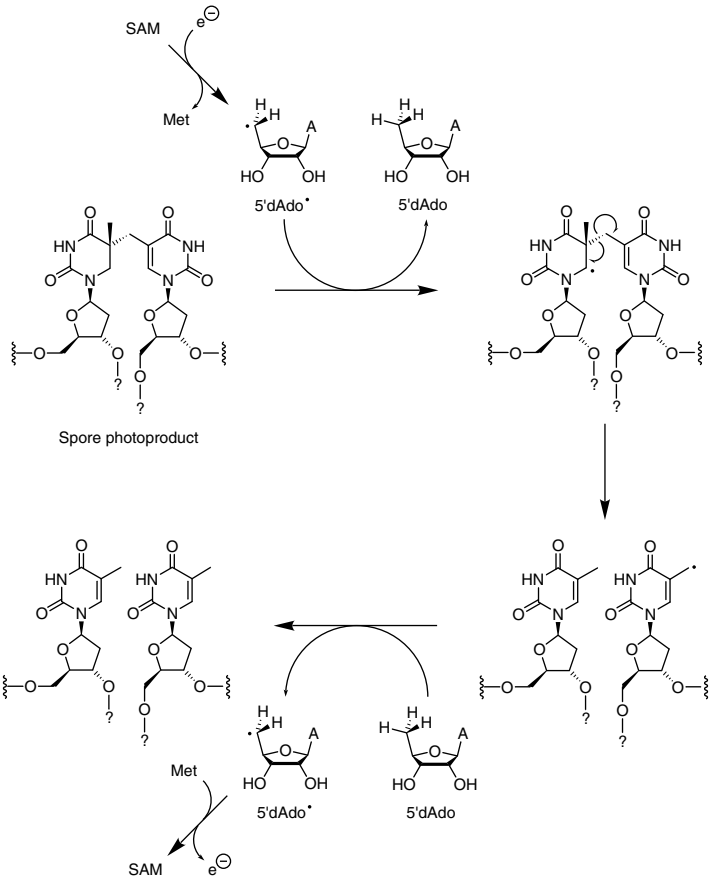

FIGURE 141.9 Proposed mechanism of action of the spore photoproduct lyase, which specifically repairs UV-induced spore DNA lesions.

a solid mechanistic theory was developed, but many steps still wait for scientific proof. The mechanism of action of the spore photoproduct lyase is still rather unknown.

Future developments must also address the question of what happens inside the cell. We clearly need a better understanding of how photolesions promote the development of cancer.

References

1. Prather, M., Midgley, P., Rowland, F.S., and Stolarski, R., The ozone layer: the road not taken, *Nature*, 381, 551, 1996.
2. Ravishankara, A.R., Hancock, G., Kawasaki, M., and Matsumi, Y., Photochemistry of ozone: surprises and recent lessons, *Science*, 280, 60, 1998.
3. Johnston, H., Reduction of stratospheric ozone by nitrogen oxide catalysts from supersonic transport exhaust, *Science*, 173, 517, 1971.
4. Molina, M.J. and Rowland, F.S., Stratospheric sink for chlorofluoromethanes: chlorine atom catalysed destruction of ozone, *Nature*, 249, 810, 1974.
5. Stolarski, R., Bojkov, R., Bishop, L., Zerefos, C., Staehelin, J., and Zawodny, J., Measured trends in stratospheric ozone, *Science*, 256, 342, 1992.
6. Cadet, J. and Vigny, P., The photochemistry of nucleic acids, in *Bioorganic Photochemistry*, vol. 1, chap. 1, Morrison, H., Ed., Wiley, New York, 1990.

7. Douki, T. and Cadet, J., UV and nucleic acids, in *Interface between Chemistry and Biochemistry*, Jollés, P. and Jörnvall, H., Eds., Birkhäuser Verlag, Basel, 1995, p. 173.
8. Ananthaswamy, H.N. and Pierceall, W.E., Molecular mechanisms of ultraviolet radiation carcinogenesis, *Photochem. Photobiol.*, 52, 1119, 1990.
9. Taylor, J.-S., DNA, sunlight and skin cancer, *J. Chem. Ed.*, 67, 835, 1990.
10. Taylor, J.-S., Unraveling the molecular pathway from sunlight to skin cancer, *Acc. Chem. Res.*, 27, 76, 1994.
11. Taylor, J.-S., DNA, sunlight and skin-cancer, *Pure Appl. Chem.*, 67, 183, 1995.
12. Black, H.S., de Gruijl, F.R., Forbes, P.D., Cleaver, J.E., Ananthaswamy, H.N., de Fabo, E.C., Ullrich, S.E., and Tyrrell, R.M., Photocarcinogenesis: an overview, *J. Photochem. Photobiol. B: Biol.*, 40, 29, 1997.
13. Brash, D.E., Rudolph, J.A., Simon, J.A., Lin, A., McKenna, G.J., Baden, H.P., Halperin, A.J., and Pontén, J., A role for sunlight in skin cancer: UV-induced *p53* mutations in squamous cell carcinoma, *Proc. Natl. Acad. Sci. USA*, 88, 10124, 1991.
14. Daya-Grosjean, L., Dumaz, N., and Sarasin, A., The specificity of *p53* mutation spectra in sunlight induced human cancers, *J. Photochem. Photobiol. B: Biol.*, 28, 115, 1995.
15. Globocan 2000: http://www-dep.iarc.fr/globocan/globocan.html.
16. WHO cancer mortality database: http://www-depdb.iarc.fr/who/menu.htm.
17. Ferbeyre, G. and Lowe, S.W., The prize of tumor suppression, *Nature*, 415, 26, 2002.
18. Tornaletti, S. and Pfeifer, G.P., Slow repair of pyrimidine dimers at *p53* mutation hotspots in skin cancer, *Science*, 163, 1436, 1994.
19. Natarja, A.J., Trent, J.C., II, and Ananthaswamy, H.N., *p53* gene mutations and photocarcinogenesis, *Photochem. Photobiol.*, 62, 218, 1995.
20. Pfeifer, G.P. and Holmquist, G.P., Mutagenesis in the *p53* gene, *Biochim. Biophys. Acta*, 1333, M1, 1997.
21. Ziegler, A., Leffell, D.J., Kunala, S., Sharma, H.W., Gailani, M., Simon, J.A., Halperin, A.J., Baden, H.P., Shapiro, P.E., Bale, A.E., and Brash, D.E., Mutation hotspots due to sunlight in the *p53* gene of non melanoma skin cancers, *Proc. Natl. Acad. Sci. USA*, 90, 4216, 1993.
22. Nakazawa, H., English, D., Randell, P.L., Nakazawa, K., Martel, N., Armstrong, B.K., and Yamasaki, H., UV and skin cancer: specific *p53* gene mutation in normal skin as a biologocally relevant exposure measurement, *Proc. Natl. Acad. Sci. USA*, 91, 360, 1994.
23. Kao, J.F.L., Nadji, S., and Taylor, J.-S., Identification and structure determination of a third cyclobutane photodimer of thymidylyl-(3′ → 5′)-thymidine: the *trans-syn*-II product, *Chem. Res. Toxicol.*, 6, 561, 1993.
24. Perdiz, D., Grof, P., Mezzina, M., Nikaido, O., Moustacchi, E., and Sage, E., Distribution and repair of bipyrimidine photoproducts in solar UV-irradiated mammalian cells — possible role of Dewar photoproducts in solar mutagenesis, *J. Biol. Chem.*, 275, 26732, 2000.
25. Yoon, J.H., Lee, C.S., O'Connor, T.R., Yasui, A., and Pfeifer, G.P., The DNA damage spectrum produced by simulated sunlight, *J. Mol. Biol.*, 299, 681, 2000.
26. Texter, J., Saturation photodimerization of thymines in DNA, *Biopolymers*, 30, 797, 1990.
27. Douki, T. and Cadet, J., Individual determination of the yield of the main UV-induced dimeric pyrimidine photoproducts in DNA suggests a high mutagenicity of CC photolesions, *Biochemistry*, 40, 2495, 2001.
28. Taylor, J.-S., Garett, D.S., Brockie, I.R., Svoboda, D.L., and Telser, J., ^{1}H-NMR assignment and melting temperature study of *cis-syn* and *trans-syn* thymine dimer containing duplexes of d(CGTATTATGC)·d(GCATAATACG), *Biochemistry*, 29, 8858, 1990.
29. Rao, S.N., Keepers, J.W., and Kollman, P., The structure of d(CGCGAAT[]TCGCG) ·d(CGCGAATTCGCG): the incorporation of a thymine photodimer into a B-DNA helix, *Nucl. Acids Res.*, 12, 4789, 1984.
30. Miaskiewicz, K., Miller, J., Cooney, M., and Osman, R., Computational simulations of DNA distortions by a *cis-syn*-cyclobutane thymine dimer lesion, *J. Am. Chem. Soc.*, 118, 9156, 1996.

31. Spector, T.I., Cheatham, T.E., III, and Kollman, P.A., Unrestrained molecular dynamics of photodamaged DNA in aqueous solution, *J. Am. Chem. Soc.*, 119, 7095, 1997.
32. Kemmink, J., Boelens, R., Koning, T.M.G., Kaptein, R., van der Marel, G.A., and van Boom, J.H., Conformational changes in the oligonucleotide duplex d(GCGTTGCG) ·d(CGCAACGC) induced by formation of a *cis-syn* thymine dimer, *Eur.J. Biochem.*, 162, 37, 1987.
33. Kemmink, J., Boelens, R., Koning, T., van der Marel, G.A., van Boom, J.H., and Kaptein, R., ^{1}H-NMR study of the exchangeable protons of the duplex d(GCGT<>TGCG) ·d(CGCAACGC) containing a thymine photodimer, *Nucl. Acids Res.*, 15, 4645, 1987.
34. McAteer, K., Jing, Y., Kao, J., Taylor, J.-S., and Kennedy, M.A., Solution-state structure of a DNA dodecamer duplex containing a *cis-syn* thymine cyclobutane dimer, the major UV photoproduct of DNA, *J. Mol. Biol.*, 282, 1013, 1998.
35. Butenandt, J., Eker, A.P.M., and Carell, T., Synthesis, crystal-structure and enzymatic evaluation of a DNA-photolesion isostere, *Chem. Eur.J.*, 4, 642, 1998.
36. Butenandt, J., Burgdorf, L.T., and Carell, T., "Base Flipping": photodamaged DNA-RNA duplexes are poor substrates for photoreactivating DNA-repair enzymes, *Angew. Chem. Int. Ed.*, 38, 708, 1999.
37. Wang, C.-I. and Taylor, J.-S., The *trans-syn*-I thymine dimer bends DNA by ~22° and unwinds DNA by ~15°, *Chem. Res. Toxicol.*, 6, 519, 1993.
38. Friedberg, E.C., Walker, G.C., and Siede, W., *DNA Repair and Mutagenesis*, ASM, Washington, DC, 1995.
39. Hess, M.T., Gunz, D., Luneva, N., Geacintov, N.E., and Naegeli, H., Base pair conformation-dependent excision of benzo[*a*]pyrene diol epoxideguanine adducts by human nucleotide excision repair enzymes, *Mol. Cell. Biol.*, 17, 7069, 1997.
40. Gunz, D., Hess, M.T., and Naegeli, H., Recognition of DNA adducts by human nucleotide excision repair — evidence for a thermodynamic probing mechanism, *J. Biol. Chem.*, 271, 41, 25089, 1996.
41. Jiang, N. and Taylor, J.-S., *In vivo* evidence that UV-induced C → T mutations at dipyrimidine sites could result from the replicative bypass of *cis-syn* cyclobutane dimers or their deamination products, *Biochemistry*, 32, 472, 1993.
42. Tu, Y., Dammann, R., and Pfeifer, G.P., Sequence and time-dependent deamination of cytosine bases in UVB-induced cyclobutane pyrimidine dimers *in vivo*, *J. Mol. Biol.*, 284, 297, 1998.
43. Fix, D. and Bockrath, R., Thermal resistance to photoreactivation of specific mutations potentiated in *E. coli* B/r *ung* by ultraviolet light, *Mol. Gen. Genet.*, 182, 7, 1981.
44. Taylor, J.-S. and Nadji, S., Unraveling the origin of the major mutation induced by ultraviolet light, the C → T transition at dTpdC sites. A DNA synthesis building block for the *cis-syn* cyclobutane dimer of dTpdU, *Tetrahedron*, 47, 2579, 1991.
45. Taylor, J.-S., Garett, D.S., and Wang, M.J., Models for the solution structure of the (6–4) photoproduct of thymidylyl-(3′ → 5′)-thymidine derived via a distance- and angle-constrained conformation search procedure, *Biopolymers*, 27, 1571, 1988.
46. Douki, T., Voituriez, L., and Cadet, J., Characterization of the (6–4) photoproduct of 2′-deoxycytidylyl-(3′ → 5′)-thymidine and of its Dewar valence isomer, *Photochem. Photobiol.*, 53, 293, 1991.
47. Hwang, G.S., Kim, J.-K., and Choi, B.S., NMR structural studies of DNA decamer duplex containing the Dewar photoproduct of thymidylyl(3′ → 5′)thymidine. Conformational changes of the oligonucleotide duplex by photoconversion of a (6–4) adduct to its Dewar valence isomer, *Eur. J. Biochem.*, 235, 359, 1996.
48. Kim, J.-K. and Choi, B.S., The solution structure of DNA duplex-decamer containing the (6–4) photoproduct of thymidylyl(3′ → 5′)thymidine by NMR and relaxation matrix refinement, *Eur. J. Biochem.*, 228, 849, 1995.
49. Kim, J.-K., Patel, D., and Choi, B.-S., Contrasting structural impacts induced by *cis-syn* cyclobutane dimer and (6–4) adduct in DNA duplex decamers: implication in mutagenesis and repair activity, *Photochem. Photobiol.*, 62, 44, 1995.

50. Mizukoshi, T., Kodama, T.S., Fujiwara, Y., Furuno, T., Nakanishi, M., and Iwai, S., Structural study of DNA duplexes containing the (6–4) photoproduct by fluorescence resonance energy transfer, *Nucl. Acids Res.*, 29, 4948, 2001.
51. Fujiwara, Y. and Iwai, S., Thermodynamic studies of the hybridization properties of photolesions in DNA, *Biochemistry*, 36, 11050, 1997.
52. Jing, Y.Q., Kao, J.F.L., and Taylor, J.-S., Thermodynamic and base-pairing studies of matched and mismatched DNA dodecamer duplexes containing *cis-syn*, (6–4) and Dewar photoproducts of TT, *Nucleic Acids Res.*, 26, 3845, 1998.
53. LeClerc, E.J., Borden, A., and Lawrence, C.W., The thymine-thymine pyrimidine-pyrimidone(6–4) ultraviolet light photoproduct is highly mutagenic and specifically induces 3′ thymine-to-cytosine transitions in *Escherichia coli*, *Proc. Natl. Acad. Sci. USA*, 88, 9685, 1991.
54. Lee, J.H., Hwang, G.S., and Choi, B.S., Solution structure of a DNA decamer duplex containing the stable 3′ T:G base pair of the pyrimidine(6–4)pyrimidone photoproduct [(6–4) adduct]: implications for the highly specific 3′ T → C transition of the (6–4) adduct, *Proc. Natl. Acad. Sci. USA*, 96, 6632, 1999.
55. Taylor, J.-S., Lu, H.-F., and Kotyk, J.J., Quantitative conversion of the (6–4) photoproduct of TpdC to its Dewar valence isomer upon exposure to simulated sunlight, *Photochem. Photobiol.*, 51, 161, 1990.
56. Taylor, J.-S. and Cohrs, M.P., DNA, light, and Dewar pyrimidones: the structure and biological significance of TpT3, *J. Am. Chem. Soc.*, 109, 2834, 1987.
57. Taylor, J.-S., Garett, D.S., and Cohrs, M.P., Solution-state structure of the Dewar pyrimidinone photoproduct of thymidylyl-(3′-5′)-thymidine, *Biochemistry*, 27, 7206, 1988.
58. Kan, L.-S., Voituriez, L., and Cadet, J., The Dewar valence isomer of the (6–4) photoadduct of thymidylyl-(3′-5′)-thymidine monophosphate: formation, alkaline lability and conformational properties, *J. Photochem. Photobiol. B: Biol.*, 12, 339, 1992.
59. Lee, J.H., Bae, S.H., and Choi, B.S., The Dewar photoproduct of thymidylyl(3′ → 5′)-thymidine (Dewar product) exhibits mutagenic behavior in accordance with the "A rule," *Proc. Natl. Acad. Sci. USA*, 97, 4591, 2000.
60. Setlow, P., Small, acid-soluble spore proteins of *Bacillus* species: Structure, synthesis, genetics, function and degradation, *Ann. Rev. Microbiol.*, 42, 319, 1988.
61. Mohr, S.C., Sokolov, N.V.H.A., He, C., and Setlow, P., Binding of small acid-soluble spore proteins from *Bacillus subtilis* changes the conformation of DNA from B to A, *Proc. Natl. Acad. Sci. USA*, 88, 77, 1991.
62. Setlow, P., DNA in dormant spores of *Bacillus* species is in an A-like conformation, *Mol. Microbiol.*, 6, 563, 1992.
63. Donnellan, J.E. and Setlow, R.B., Thymine photoproducts but not thymine dimers found in ultraviolet-irradiated bacterial spores, *Science*, 149, 308, 1965.
64. Varghese, A.J., 5-Thyminyl-5,6-dihydrothymine from DNA irradiated with ultraviolet light, *Biochem. Biophys. Res. Commun.*, 38, 484, 1970.
65. Rahn, R.O. and Hosszu, J.L., Photoproduct formation in DNA at low temperatures, *Photochem. Photobiol.*, 8, 53, 1968.
66. Rahn, R.O. and Hosszu, J.L., Influence of relative humidity on the photochemistry of DNA films, *Biochim. Biophys. Acta*, 190, 126, 1969.
67. Varghese, A.J., Photochemistry of thymidine in ice, *Biochemistry*, 9, 4781, 1970.
68. Varghese, A.J., Photochemistry of thymidine as a thin solid film, *Photochem. Photobiol.*, 13, 357, 1971.
69. Romieu, A., Bellon, S., Gasparutto, D., and Cadet, J., Synthesis and UV photolysis of oligodeoxynucleotides that contain 5-(phenylthiomethyl)-2′-deoxyuridine: a specific photolabile precursor of 5-(2 '-deoxyuridilyl)methyl radical, *Org. Lett.*, 2, 1085, 2000.
70. Douki, T., Court, M., and Cadet, J., Electrospray-mass spectrometry characterization and measurement of far-UV-induced thymine photoproducts, *J. Photochem. Photobiol. B: Biol.*, 54, 145, 2000.

71. Thomas, M., Guillaume, D., Fourrey, J.L., and Clivio, P., Further insight in the photochemistry of DNA: structure of a 2-imidazolone (5–4) pyrimidone adduct from the mutagenic pyrimidine (6–4) pyrimidone photolesion by UV irradiation, *J. Am. Chem. Soc.*, 124, 2400, 2002.
72. Kanai, S., Kikuna, R., Toh, H., Ryo, H., and Todo, T., Molecular evolution of the photolyase-blue light photoreceptor familiy, *J. Mol. Evol.*, 45, 535, 1997.
73. Sancar, A., Structure and function of DNA photolyase, *Biochemistry*, 33, 2, 1994.
74. Carell, T., Burgdorf, L.T., Kundu, L., and Cichon, M., The mechanism of action of DNA photolyases, *Curr. Opin. Chem. Biol.*, 5, 491, 2001.
75. Heelis, P.F., Hartman, R.F., and Rose, S.D., Photoenzymatic repair of UV-damaged DNA: a chemist's perspective, *Chem. Soc. Rev.*, 289, 1995.
76. Park, H.W., Kim, S.T., Sancar, A., and Deisenhofer, J., Crystal-structure of DNA photolyase from *Escherichia coli*, *Science*, 268, 1866, 1995.
77. Tamada, T., Kitadokoro, K., Higuchi, Y., Inaka, K., Yasui, A., de Ruiter, P.E., and Eker, A.P.M., Crystal structure of DNA photolyase from *Anacystis nidulans*, *Nat. Struct. Biol.*, 4, 887, 1997.
78. Komori, H., Masui, R., Kuramitsu, S., Yokoyama, S., Shibata, T., Inoue, Y., and Miki, K., Crystal structure of thermostable DNA photolyase: pyrimidine-dimer recognition mechanism, *Proc. Natl. Acad. Sci. USA*, 98, 13560, 2001.
79. Roberts, R.J., On base flipping, *Cell*, 82, 9, 1995.
80. Bruner, S.D., Norman, D.P.G., and Verdine, G.L., Structural basis for recognition and repair of the endogenous mutagen 8-oxoguanine in DNA, *Nature*, 403, 859, 2000.
81. Lloyd, R.S. and Cheng, X., Mechanistic link between DNA methyltransferases and DNA repair enzymes by base flipping, *Curr. Op. Chem. Biol.*, 4, 139, 1998.
82. Varnai, P. and Lavery, R., Base flipping in DNA: pathways and energetics studied with molecular dynamics simulations, *J. Am. Chem. Soc.*, 124, 7272, 2002.
83. van de Berg, B.J. and Sancar, G.B., Evidence for dinucleotide flipping by DNA photolyase, *J. Biol. Chem.*, 273, 20276, 1998.
84. van Noort, S.J.T., van der Werf, K.O., Eker, A.P.M., Wyman, C., de Grooth, B.G., van Hulst, N.F., and Greve, J., Direct visualization of dynamic protein-DNA interactions with a dedicated atomic force microscope, *Biophys.J.*, 74, 2840, 1998.
85. van Noort, J., Orsini, F., Eker, A., Wyman, C., de Grooth, B., and Greve, J., DNA bending by photolyase in specific and non-specific complexes studied by atomic force microscopy, *Nucl. Acids Res.*, 27, 3875, 1999.
86. Sanders, D.B. and Wiest, O., A model for the enzyme-substrate complex of DNA photolyase and photodamaged DNA, *J. Am. Chem. Soc.*, 121, 5127, 1999.
87. Antony, J., Medvedev, D.M., and Stuchebrukhov, A.A., Theoretical study of electron transfer between the photolyase catalytic cofactor $FADH^{\cdot}$ and DNA thymine dimer, *J. Am. Chem. Soc.*, 122, 1057, 2000.
88. Weber, S., Richter, G., Schleicher, E., Bacher, A., Möbius, K., and Kay, C.W.M., Substrate binding to DNA photolyase studied by electron paramagnetic resonance spectroscopy, *Biophys. J.*, 81, 1195, 2001.
89. Carell, T. and Epple, R., Repair of UV light induced DNA lesions: a comparative study with model compounds, *Eur. J. Org. Chem.*, 1245, 1998.
90. Epple, R., Wallenborn, E.-U., and Carell, T., Investigation of flavin-containing DNA-repair model compounds, *J. Am. Chem. Soc.*, 119, 7440, 1997.
91. Saettel, N.J. and Wiest, O., DFT study of the [2 + 2] cycloreversion of uracil dimer anion radical: waters matter, *J. Am. Chem. Soc.*, 123, 2693, 2001.
92. Epple, R. and Carell, T., Flavin and deazaflavin containing model compounds mimic the energy-transfer step in type II DNA-photolyases, *Angew. Chem. Int. Ed.*, 37, 938, 1998.
93. Epple, R. and Carell, T., Efficient light-dependent DNA repair requires a large cofactor separation, *J. Am. Chem. Soc.*, 121, 7318, 1999.

94. Aubert, C., Mathis, P., Eker, A.P.M., and Brettel, K., Intraprotein electron transfer between tyrosine and tryptophan in DNA photolyase from *Anacystis nidulans*, *Proc. Natl. Acad. Sci. USA*, 96, 5423, 1999.
95. Aubert, C., Brettel, K., Mathis, P., Eker, A.P.M., and Boussac, A., EPR detection of the transient tyrosyl radical in DNA photolyase from *Anacystis nidulans*, *J. Am. Chem. Soc.*, 121, 8659, 1999.
96. Popovic, D.M., Zmiric, A., Zaric, S.D., and Knapp, E.-W., Energetics of radical transfer in DNA photolyase, *J. Am. Chem. Soc.*, 124, 3775, 2002.
97. Stubbe, J. and van der Donk, W.A., Protein radicals in enzyme catalysis, *Chem. Rev.*, 98, 705, 1998.
98. Todo, T., A new photoreactivating enzyme that specifically repairs ultraviolet light-induced (6–4)photoproducts, *Nature*, 361, 371, 1993.
99. Weber, S., Kay, C.W.M., Mögling, H., Hitomi, K., and Todo, T., Photoreactivation of the flavin cofactor in *Xenopus laevis* (6–4) photolyase: observation of a transient tyrosyl radical by time-resolved electron paramagnetic resonance, *Proc. Natl. Acad. Sci. USA*, 99, 1319, 2002.
100. Kim, S.T., Malhotra, K., Smith, C.A., Taylor, J.-S., and Sancar, A., Characterization of (6–4)-photoproduct DNA photolyase, *J. Biol. Chem.*, 269, 8535, 1994.
101. Zhao, X.D., Liu, J.Q., Hsu, D.S., Zhao, S.Y., Taylor, J.-S., and Sancar, A., Reaction mechanism of (6–4) photolyase, *J. Biol. Chem.*, 272, 32580, 1997.
102. Hitomi, K., Kim, S.T., Iwai, S., Harima, N., Otoshi, E., Ikenaga, M., and Todo, T., Binding and catalytic properties of *Xenopus* (6–4) photolyase, *J. Biol. Chem.*, 272, 32591, 1997.
103. Wang, Y.S., Gaspar, P.P., and Taylor, J.-S., Quantum chemical study of the electron-transfer-catalyzed splitting of oxetane and azetidine intermediates proposed in the photoenzymatic repair of (6–4) photoproducts of DNA, *J. Am. Chem. Soc.*, 122, 5510, 2000.
104. Prakash, G. and Falvey, D.E., Model studies of the (6–4)-photoproduct DNA photolyase — synthesis and photosensitized splitting of a thymine-5,6-oxetane, *J. Am. Chem. Soc.*, 117, 11375, 1995.
105. Joseph, A., Prakash, G., and Falvey, D.E., Model studies of the (6–4) photoproduct photolyase enzyme: laser flash photolysis experiments confirm radical ion intermediates in the sensitized repair of thymine oxetane adducts, *J. Am. Chem. Soc.*, 122, 11219, 2000.
106. Cichon, M.K., Arnold, S., and Carell, T., A (6–4) photolyase model: repair of DNA (6–4) lesions requires a reduced and deprotonated flavin, *Angew. Chem. Int. Ed.*, 41, 767, 2002.
107. Miranda, M.A. and Izquierdo, M.A., Stepwise cycloreversion of oxetane radical cations with initial C-O bond cleavage, *J. Am. Chem. Soc.*, 124, 6532, 2002.
108. Miranda, M.A., Izquierdo, M.A., and Galindo, F., Involvement of triplet excited states and olefin radical cations in electron-transfer cycloreversion of four-membered ring compounds photosensitized by (thia)pyrylium salts, *J. Org. Chem.*, 67, 4138, 2002.
109. Clivio, P. and Fourrey, J.-L., DNA photodamage mechanistic studies: characterization of a thietane intermediate in a model reaction relevant to "(6–4) lesions," *J. Am. Chem. Soc.*, 113, 5481, 1991.
110. Clivio, P. and Fourrey, J.L., (6–4) photoproduct DNA photolyase mechanistic studies using s^5-(6–4) photoproducts, *Chem. Commun.*, 2203, 1996.
111. Liu, J.Q. and Taylor, J.-S., Remarkable photoreversal of a thio analog of the Dewar valence isomer of the (6–4) photoproduct of DNA to the parent nucleotides, *J. Am. Chem. Soc.*, 118, 3287, 1996.
112. Heelis, P.F. and Liu, S.B., Photoenzymic repair of the DNA (6–4) photoproduct — a density functional theory and semiempirical study, *J. Am. Chem. Soc.*, 119, 2936, 1997.
113. Hitomi, K., Nakamura, H., Kim, S.T., Mizukoshi, T., Ishikawa, T., Iwai, S., and Todo, T., Role of two histidines in the (6–4) photolyase reaction, *J. Biol. Chem.*, 276, 10103, 2001.
114. Setlow, P., Mechanisms for the prevention of damage to DNA in spores of *Bacillus* species, *Ann. Rev. Microbiol.*, 49, 29, 1995.
115. Pedraza-Reyes, M., Gutierrez-Corona, F., and Nicholson, W.L., Temporal regulation and forespore-specific expression of the spore photoproduct lyase gene by σ-G RNA-polymerase during *Bacillus subtilis* sporulation, *J. Bacteriol.*, 176, 3983, 1994.

116. Nicholson, W.L., Munakata, N., Horneck, G., Melosh, H.J., and Setlow, P., Resistance of *Bacillus* endospores to extreme terrestrial and extraterrestrial environments, *Microbiol. Mol. Biol. Rev.*, 64, 548, 2000.
117. Fajardo-Cavazos, P., Salazar, C., and Nicholson, W.L., Molecular cloning and characterization of the *Bacilllus subtilis* spore photoproduct lyase (*spl*) gene, which is involved in repair of UV radiation-induced DNA damage during spore germination, *J. Bacteriol.*, 175, 1735, 1993.
118. Rebeil, R., Sun, Y.B., Chooback, L., Pedraza-Reyes, M., Kinsland, C., Begley, T.P., and Nicholson, W.L., Spore photoproduct lyase from *Bacillus subtilis* spores is a novel iron-sulfur DNA repair enzyme which shares features with proteins such as class III anaerobic ribonucleotide reductases and pyruvate-formate lyases, *J. Bacteriol.*, 180, 4879, 1998.
119. Rebeil, R. and Nicholson, W.L., The subunit structure and catalytic mechanism of the *Bacillus subtilis* DNA repair enzyme spore photoproduct lyase, *Proc. Natl. Acad. Sci. USA*, 98, 9038, 2001.
120. Mehl, R.A. and Begley, T.P., Mechanistic studies on the repair of a novel DNA photolesion: the spore photoproduct, *Org. Lett.*, 1, 1065, 1999.
121. Cheek, J. and Broderick, J.B., Adenosylmethionine-dependent iron-sulfur enzymes: versatile clusters in a radical new role, *J. Biol. Inorg. Chem.*, 6, 209, 2001.
122. Cheek, J. and Broderick, J.B., Direct H atom abstraction from spore photoproduct C-6 initiates DNA repair in the reaction catalyzed by spore photoproduct lyase: evidence for a reversibly generated adenosyl radical intermediate, *J. Am. Chem. Soc.*, 124, 2860, 2002.

142

Molecular Basis of Psoralen Photochemotherapy

Francesco Dall'Acqua
University of Padova

Giampietro Viola
University of Padova

Daniela Vedaldi
University of Padova

142.1 Introduction

Psoralens, also known as furocoumarins, are naturally occurring or synthetic tricyclic aromatic compounds (Figure 142.1), deriving from the condensation of a coumarine nucleus with a furan ring. They exhibit interesting photobiological and phototherapeutical activities, such as skin photosensitization characterized by the onset of erythema followed by dark pigmentation. The related angular isomers, angelicins and allopsoralens, are also present in the vegetal world; namely, angelicin is present in *Angelica archangelica*, and a derivative of allopsoralen is present in *Mammea americana*.[1]

The ancient Hindus, Turks, Egyptians, and other Orientals exploited this property in popular medicine. In fact, the use of *Psoralea corylifolia* extracts to treat vitiligo is mentioned in the Indian sacred book "*Atharva Veda*" and in the old Buddhist Bower manuscript. Another plant, *Amni Majus* that grows in the Nile valley, was used for centuries as a cure for leukoderma.[1,2]

Psoralens have a toxic effect on the skin, which manifests itself in the summer as phytophotodermatitis. It results from contact with certain plants or herbs that contain psoralens and then from exposure to sunlight. However, it was also recognized that this may be a beneficial effect that, because it allows modulation of skin pigmentation, can be used for medicinal purposes or in cosmetics.[1,2]

An important application of psoralens and UV-A light (PUVA therapy) was introduced into clinical practice by Parrish et al.[3] A treatment consisting of the oral administration of 8-methoxypsoralen (8-MOP), followed by artificial ultraviolet illumination (UV-A) of patients' skin was used for the first time to cure psoriasis, a disease characterized by hyperproliferation of skin cells. It is now recognized that psoriasis is an autoimmune disorder, and hyperproliferation is only one aspect of its manifestation.

In 1982, an extracorporeal form of 8-MOP photochemotherapy (photopheresis) was developed by Edelson et al.[4] for the treatment of cutaneous T-cell lymphoma, a CD4-positive T-cell malignancy. Photopheresis was also found to be effective in a number of other T-cell-mediated diseases. Clinical trials demonstrated beneficial effects in *pemphigo vulgaris*,[5] severe atopic dermatitis,[6] AIDS-related complex,[7] rheumatoid arthritis,[8] and systemic lupus erythematosus.[9]

0-8493-1348-1/04/$0.00+$1.50

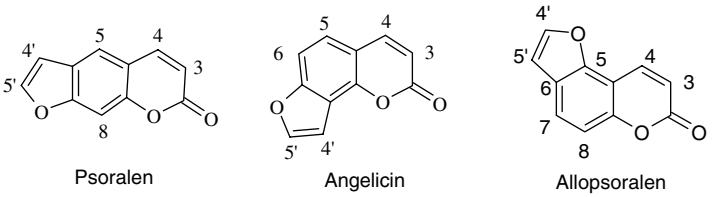

FIGURE 142.1 Molecular structures of psoralen, angelicin, and allopsoralen.

Some psoralens are also used in the photosterilization of blood products, in particular, platelet concentrate.[10] Different psoralen derivatives, such as 8-MOP and 4′-aminomethyl-4,5′,8-trimethylpsoralen (AMT) combined with UV-A are useful for sterilizing platelet concentrate, because of its capacity to target nucleic acids.[10,11] Lipid-enveloped viruses such as the model-virus vesicular stomatitis virus,[12] as well as immunodeficiency virus[13] and duck hepatitis B virus,[14] are sensitive to this photochemical treatment. On the other hand, platelets are well preserved, especially in the presence of rutin, which prevents damage to the platelet membrane by reactive oxygen species.[13] The newly synthesized psoralen derivative S-59, with a structure that is covered by patent, is claimed to have a high nucleic acid binding affinity and would, therefore, be an efficient inactivating agent, while preserving platelet quality. Interestingly, S-59 in combination with UV-A was shown to inactivate not only different lipid-enveloped viruses but also gram-positive and most gram-negative bacteria.[10] Non-lipid enveloped viruses are not inactivated, probably because their protein coating prevents the psoralen derivative from reaching the cellular target.

A completely different and unusual application of psoralens, without light activation, is to exploit the ability of some derivatives to interact with ionic channels. It was recently shown that 5-methoxypsoralen (5-MOP)[15] and 5,8-disubstituted psoralens,[16] can block voltage-dependent K^+ channels (K_v). In addition, they are able to alleviate functional deficits in certain multiple sclerosis patients in a manner similar to 4-aminopyridine.

Some new photobiological and pharmacological aspects of psoralen compounds are reported in this chapter.

142.2 Properties of Psoralens

Photophysical and Photochemical Properties of Psoralens

The absorption spectra of the most common psoralen derivatives exhibit two bands centered at about 250 and 300 nm and a shoulder at 330 to 340 nm, extending to about 400 nm. Absorption is due to two main transitions in the 320 to 400 nm (UV-A) range: an n,π^* transition resulting from the excitation of a nonbonding electron on the C_2 carbonyl group to the π^* orbital and a π,π^* transition occurring when a π^* electron in the psoralen ring system is excited to the π^* orbital. The lowest singlet and triplet states are the (π,π) states.[17] The intrinsic photoreactivity of psoralens is determined by the electronic structure of the lowest excited states (S_1 and T_1). Intersystem quantum yields for various psoralen derivatives fall within the range of 0.1 to 0.4, with the exception of 5-MOP, which has $\phi_t < 0.01$.[18] The UV-A absorption bands of all psoralen derivatives derive from their benzopyrone moiety. Their extinction coefficients, however, differ appreciably from one compound to another in the UV region.

The photosensitizing effects of psoralens may involve oxygen-dependent and oxygen-independent mechanisms that are summarized in Figure 142.2. Types I and II are oxygen dependent, whereas Type III is an anoxic pathway. Energy transfer to thymine bases was also shown to occur with pyridopsoralens leading to the formation of thymine dimer.[19,20]

In particular, the Type I mechanism may involve one-electron oxidation of targets like guanine[21] and the generation of reactive oxygen species ($O_2^{\cdot-}$ and ·OH), which may further react with substrates. The Type II mechanism implies generating singlet oxygen by energy transfer, which, in turn, may induce

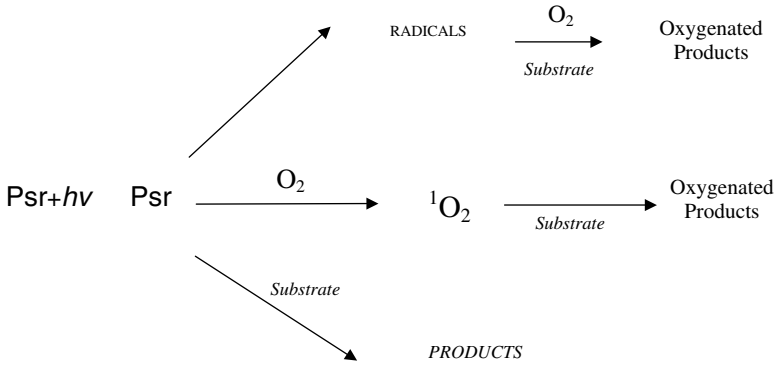

FIGURE 142.2 Pathways of the photosensitizing actions of psoralens.

oxidation of guanine,[22] histidine, cysteine, or tryptophan. The Type III mechanism consists of photoreactions between psoralens and a substrate that do not involve oxygen, which are favored by polar solvents. At the molecular level, the first photoreaction investigated concerning coumarins and furocoumarins was dimerization.[23]

Under the action of UV-A light, a [2 + 2] cycloaddition occurs between one of the double bonds of each monomer. In general, both double bonds of psoralen are potentially photoreactive, but which one is involved in a particular reaction depends on the reactivity of the excited states. In solution, only the pyrone 3,4-double bond is involved, showing that the triplet states make this site particularly reactive. In order to elicit the reactivity of the furan 4′,5′-double bond, the psoralen derivative has to be excited in the vicinity of the substrate, which may be achieved by freezing the solution.

Recently, detailed studies have thrown new light on these aspects, in particular the photophysical features of angelicins and methylated thioangelicins.[24,25] Lifetimes and quantum yields were measured for the different excited states of these compounds in different solvents, and the results were compared to semiempirical quantum mechanical calculations. It may be concluded that the polarity of the solvent in which the radiative excitation occurs, plays a major role in photoreactivity. In fact, methylthioangelicin derivatives show more singlet states at increasing energy, the most important being S_1 and S_2. The first excited state is a π,π^* transition, whereas the second is an n,π^* transition, known as a forbidden transition.

The deactivation of the excited molecule in hydrophobic solvents occurs almost totally by internal conversion. On the other hand, the internal conversion quantum yields decrease progressively in polar solvents, while the fluorescence and triplet quantum yields increase. In conclusion, polar solvents favor the triplet formation. This leads to an increase in its half-life, indicating that the photophysical properties are strongly solvent dependent.

The question remains whether the chemical reactivity of this class of compounds is correlated to biological activity.[26] For example, 1-thiopsoralen was studied, and it was calculated that the quantum yield of intersystem crossing and fluorescence of photoexcited 1-thiopsoralen is very low, and practically the only excited state is the triplet. It should be noted that 1-thiopsoralen undergoes intercalation into DNA. Subsequent UV-A irradiation of the latter complex is found to promote [2 + 2] photocycloaddition of the furan ring with the thymine. In this regard, it is interesting to note the different behavior manifested by visnagin and khellin,[27] two compounds with similar chemical structures but that exhibit different biological activities. The former is more active, and studies performed in dioxane–water mixtures demonstrate that the triplet quantum yields of visnagin are higher than khellin. These facts account for the greater photobiological activity of visnagin with respect to khellin in some biological models.[27]

Psoralen Photolysis

It is generally accepted that photosensitizing agents act toward biological substrates through the three main mechanisms mentioned above.

Some of these pathways are also useful for explaining photolysis of furocoumarins in solution. When a furocoumarin is UV-A-excited in solution in the absence of any substrate, its target may be another furocoumarin molecule (in its ground state) or a solvent molecule. In both cases, a Type III (oxygen-independent) addition reaction occurs. When the solution is aerated, the Type II pathway is also involved, and singlet oxygen may oxidize a psoralen molecule.[28]

[2 + 2] Photocycloadditions are the most common psoralen photoaddition reactions. Ciamician and Silber[23] first proposed a cyclobutane structure for a photodimer of coumarin. Von Wessely and Dinjaski[29] and von Wessely and Plaichinger[30] found that the same reaction occurs with UV-irradiated psoralens. They obtained dimers in which the pyrone rings of both monomers are joined through a cyclobutane ring (pyrone–pyrone dimer).

Von Wessely and Plaichinger[30] reported some data on pimpinellin (5,6-dimethoxyangelicin) and 8-MOP photodimers; however, the data concerning two isomeric compounds are not clear in terms of structure assignment. Successively, Krauch and Farid,[31] working with 8-MOP, reported that only a single pyrone–pyrone is formed, having a *trans-anti* configuration.

In any case, taking into account that both the double bonds of psoralens are photoreactive (furan side and pyrone side), cyclodimerization not only yields pyrone–pyrone dimers but also pyrone–furan dimers, as shown by Caffieri and Dall'Acqua.[32]

A third type of dimerization involving the furan ring of each monomer was observed, and a furan–furan dimer was found, although only in particular experimental conditions, such as with a thin layer of the solid compound.[32]

Oxidative processes were studied by Rodighiero et al.[33] and Musajo et al.[34] that showed that photolysis of psoralen and 5-methoxypsoralen (5-MOP), in water–methanol solution in the presence of flavin-mono nucleotide, leads to the formation of 6-formyl-7-hydroxycoumarin (from psoralen) and 6-formyl-7-hydroxy-5-methoxycoumarin, derived from 5-MOP. The corresponding aldehyde deriving from 8-methoxypsoralen (8-MOP) was isolated by Rodighiero et al.[35]

The same 6-formyl-7-hydroxy-8-methoxycoumarin was later characterized as a direct photolysis product of 8-MOP with the involvement of singlet oxygen, generated by the psoralen.[36]

The same hydroxyaldehyde was obtained from 8-methoxypsoralen (8-MOP) producing singlet oxygen with methylene blue and visible light.[37] On this basis, a mechanism in which an excited oxygen molecule binds to the furan side of 8-MOP giving rise to a dioxetane, was proposed. The C4′-C5′ bond of this intermediate is broken, followed by the loss of formic acid forming hydroxyaldehyde. Similar products were obtained as products of photolysis of 4,5′,8-trimethylpsoralen (TMP).[38]

The same mechanism should also lead to fission of the pyrone ring, according to Marley and Larson.[39] These authors for the first time isolated the unstable 5-formyl-6-hydroxybenzofuran by UV irradiation of 8-methoxypsoralen.

From the dioxetane intermediate described above, other compounds can be formed, which in turn, may have biological effects. Dioxetane intermediate may be opened by nucleophilic compounds (e.g., a solvent molecule) in a way different from that leading to the aldehyde; that is, it leaves the C–C bond unaffected, therefore avoiding fission of the furan ring.

This mechanism was further supported by Adam et al.,[40] who studied the chemical reaction of 2,3-dimethylbenzofuran dioxetane derivatives.

Biological Effects of Photolysis and Metabolic Products

It was shown that some products of photolysis of psoralen may exhibit interesting biological effects in the dark.[28]

In this connection, Potapenko et al.[41] suggested that the photobiological activity of psoralens derives from its photooxidized products formed during preirradiation (POP). These authors analyzed the efficacy of crude preirradiated solutions of psoralen in a variety of biological models. First, they proved that the solutions are active only when irradiation is carried out in the presence of oxygen, and they concluded that the activity should be ascribed to photooxidized psoralen species (POP).

POP is active in inducing hemolysis in erythrocytes, in oxidizing unsaturated fatty acids and altering cell membrane lipids. POP is generally stable at room temperature and in organic solvents, while heat and water decompose them, as do ferrous ions.[41]

It was found that POP induces hemolysis of erythrocyte,[42] modifies the "respiratory burst" of phagocytes, and increases the permeability of their membranes.[43] Chemically oxidized or photooxidized psoralens inhibit chemotactic activity of polymorphonucleate cells,[44] and induce mutagenic and lethal effects in the microorganism.[45]

The products of photooxidation of psoralens administered to mice were shown to induce modulation of the T-cell-mediated immune response and inhibit growth of grafted EL-4 lymphoma.[46] Administration of POP to eczema patients induced therapeutic effects with remission of more than 1 year.[47] The above-mentioned effects were produced in the dark.

A final remark concerns the immune-suppressive effects of psoralens. A possible mechanism of action concerns modulation of the major histocompatibility complex (MHC) located in antigen-presenting cells.[48]

The immune functions of these MHC peptides depend on the interaction of carbonyls and amino groups present on the surface of antigen-presenting cells and T-cells.

Small molecules able to form Shiff bases were proven to interfere with this mechanism and modulate the profile of cytokine release. The most potent among the set of molecules tested is tucaresol,[48] an *O*-hydroxybenzaldehyde, closely correlated chemically to various photoproducts deriving from psoralen photolysis. Thus, it is reasonable to expect that some photoproducts of psoralen, formed *in vivo*, may play a role in regulating the immune system.

Recently in this connection, Koenig and Trager[49] observed that psoralen and 8-MOP are potent inhibitors of P450 2A6 and 2B1 reductase activity in human hepatic microsomes in the dark. 5-MOP is also active, while trimethylpsoralen (TMP) is not. P450 inactivation, however, was induced not by intact psoralen but by its metabolite formed in liver microsomes. This metabolite is able to bind covalently to an amino acid of the active site of the enzyme, forming a product with molecular weight that corresponds to that of the enzyme plus 8-MPO plus one oxygen atom. Similar behavior was observed when exogenous nucleophiles were added (reduced glutatione, *N*-acethylcysteine, methoxamine), suggesting that the photobinding to the enzyme takes place at the nucleophilic site. Moreover, a dihydrodiol formed by the saturation of the furan ring, which is strictly similar to the dihydrodiols isolated from UV-A irradiation of khellin, was found in the medium. The occurrence of these metabolic products can be accounted for by hypothesizing the formation of an epoxide, as an instable intermediate, which is attacked by amines, thiols, or water to yield the observed dihydrodiols. These compounds were identified in the case of psoralens, 5-MOP, and 8-MOP, but not in the case of TMP.

To summarize, the mechanism of inactivation of this enzyme takes place through the initial oxidation of the furan ring to generate a furan epoxide that then reacts with a nucleophilic amino acid at the active site of P450 2A6, leading to the inactivation of the enzyme, or it reacts with H_2O to form dihydrodiol (Figure 142.3).

Photoadduct Formation with Biomolecules

According to the different mechanisms involved in photosensitization, psoralens may affect various cellular components and involve precise molecular targets. These are summarized in Table 142.1 and are discussed later in the text.

The main psoralen photosensitizing effect used in the treatment of certain skin diseases involves stimulating the pigmentation of melanocytes, increasing melanin synthesis on one hand and antiproliferative activity of psoriatic plaques on the other. The effects may, therefore, appear to be contradictory. However, recent findings explain that the two activities are likely to be connected to distinct cellular targets that are photomodified by psoralens in different ways.

TABLE 142.1 Target of Psoralen at Cellular Level

Membranes	C_4-cycloaddition to unsaturated fatty acids and phospholipids, lipid peroxidation, formation of cross-links in membrane proteins. Interaction of psoralen photolysis products with proteins
Receptors	Dark and photointeractions with membrane and cytoplasm receptors
Cytoplasm	Photoreactions with proteins, inactivation of enzymes, inactivation of ribosomes, etc.
Nucleus	Photoreaction with nucleic acids and chromatin, formation of DNA-protein cross-links
Mitochondria	Mitochondria alteration of pore opening that triggers apoptosis
Ionic Channels	Psoralen by blocking voltage-dependent K^+ channels (Kv), may alleviate functional deficits in certain multiple sclerosis patients

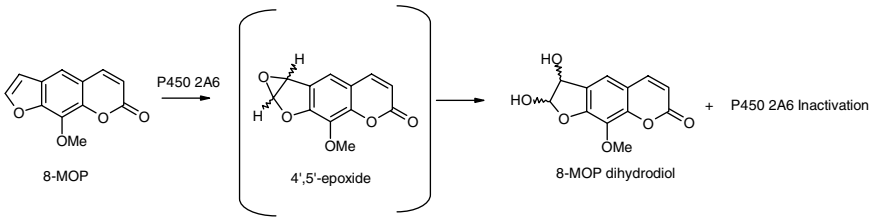

FIGURE 142.3 Metabolic inactivation of P450 2A6 enzyme by 8-MOP metabolite.

Photoreactions with DNA

The photochemical reactions of psoralens with DNA are well characterized, having been studied for a considerable amount of time.[50,51] The photoreaction between psoralens and DNA takes place in two steps:

1. A molecular complex is formed in the ground state, in which the psoralen derivative intercalates inside the nucleic acid duplex.[52] This step is critical for the subsequent reaction.
2. Upon photoactivation of the intercalated psoralen molecule, the excited molecule reacts with the 5,6-double bond of thymine, and to a lesser extent with those of cytosine, giving a C_4-cycloadduct.

A psoralen photoadduct to adenine was also isolated and characterized upon irradiation of a mixture of adenine and psoralen derivative,[53] however, the latter photoadduct does not appear to be generated in cellular DNA.[53] The psoralen adducts within nuclear DNA are formed primarily by a [2 + 2] photocycloaddition reaction between the 4′,5′-furan double bond of the psoralen molecule and the 5,6-double bond of thymine. Monoadducts involving the 3,4-pyrone double bond of the psoralen and the pyrimidine 5,6-double bond are also formed, but to a lesser extent (Figure 142.4). Photoisomerization can lead to 4′,5′-monoadducts being converted into 3,4-monoadducts, at least in isolated DNA.[54] Interstrand cross-links can be generated as the result of photoexcitation of the 4′,5′-monoadduct and its subsequent cycloaddition with the pyrone 3,4 double bond. The structures of the monoadducts and cross-links are shown in Figure 142.4. The cross-linking process depends on the structure of the psoralen derivative. Linear psoralens form cross-links efficiently with a yield, which may reach up to 50% of the overall adducts formed.

It is likely that substituting the psoralen molecule with alkyl groups like methyls, which increase lipophilicity of the compound and, within certain limits the intercalation capacity, can modify this picture. In particular, the photoreaction of 4-methyl psoralen derivatives with DNA yields a lower percentage of pyrone-side monoadducts.[55] This may be rationalized in terms of a hindering effect partly due to the methyl group of thymine, although the cross-linking capacity is not affected. The photoreactivity of one of the double bonds of the furan and pyrone moieties may be reduced or completely canceled if the substituting groups are bulkier or exhibit electron-withdrawing properties. This could also be achieved by introducing a fourth aromatic ring, fused at the 4′,5′ or 3,4 position. As a result, linear monofunctional compounds, including carbetoxy-, pyrido-, and benzopsoralen are available.[56,57,58]

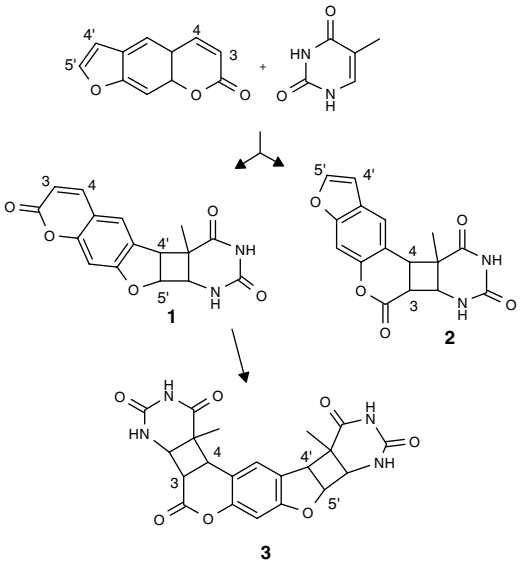

FIGURE 142.4 Molecular structure of mono- and diadducts between psoralen and thymidine. 1: furan-side monoadduct involving the 4′,5′ double bond of psoralen and the 5,6 double bond of thymidine; 2: Pyrone-side monoadduct involving the 3,4 double bond of psoralen and the 5,6 double bond of thymidine; 3: diadduct involving the cross-link by two thymidines by a psoralen molecule.

The regio- and stereochemistry of the resulting monoadducts formed in isolated DNA were found to exhibit a *cis-syn* configuration. This was recently confirmed by an x-ray diffraction analysis of the furan-side 4,6-dimethyl tetrahydrobenzoangelicin monocycloadduct to thymine generated within naked DNA.[59,60]

Angular psoralens, also called angelicins, are designed to obtain monofunctional agents toward DNA. In fact, both double bonds of the furan and pyrone moieties are photoreactive. However, the intercalation geometry within DNA base pairs does not favor cross-link formation, although some angelicins induce the generation number of cross-links. It was shown that photoexcited 4,6,4′-trimethylangelicin is able to induce cross-links.[61] Thus, the extent and nature of adduct formation, together with the distribution of monoadducts and cross-links, depends on the psoralen derivative and the DNA sequence.

Photoreactions with Proteins

Yoshikawa et al.[62] observed that adding a preirradiated solution of tritiated 8-MOP (POP) to an aqueous solution of serum albumin leads to covalent binding between the protein and psoralen. The structure of the product was not clarified, but the observation that photobinding proceeds faster in oxygen-saturated solution suggests that it should derive from an oxic pathway. Moreover, the higher photobinding rate in D_2O strongly suggests that singlet oxygen is involved in its formation in the protein-binding photoproduct. Other authors studied the photoreactions between 8-MOP and protein, evidencing the formation of a covalent binding between the two molecules.[63,64,65]

The structural basis of the chemical adducts between psoralen on the one hand, and proteins and amino acids on the other, was only recently elucidated, and not yet completely.

Interestingly, studies on the subcellular fractions of rat epidermis after treatment with 8-MOP and UV-A, showed that 17% of 8-MOP was bound to DNA, while a substantial amount was tethered to proteins (57%) and lipids (26%).[66]

Photobinding of 8-MOP was quantified, but no specific photoproduct could be isolated by Schmitt et al.[65] Nevertheless, there is evidence of photobinding to protein. Psoralen covalently photobinds *in vitro* to several proteins, such as bovine serum albumin[17] and lysozyme.[63] Inactivation of enzymes and cross-linking of their subunits were also observed. 8-MOP can photobind *in vivo* to proteins even more than to lipids and DNA of epidermal cells of rats; the more lipophilic 4,6,4′-trimethylangelicin has lipid as its

main target.[66] In addition, it was observed that lysozyme and ovalbumin exhibit different enzymatic processing patterns after *in vitro* treatment with 8-MOP and UV-A. The photomodification of these proteins also alters the ability of endopeptidases (trypsin and chymotrypsin) to recognize the usual sites of incision.[65] When PUVA effects on proteins were measured, it was commonly found that much greater doses of 8-MOP and UV-A are required, compared with the doses necessary to induce DNA damage. Recently, Sastry[67] characterized a photoadduct formed between 8-MOP and tyrosine from the acid hydrolysate of 8-MOP-treated T7RNA polymerase. Spectroscopic analyses suggest that the pyrone moiety of the original 8-MOP is modified in the isolated photoadduct, and that the adduct probably contains a benzofuran. Mass spectrometry analysis was consistent with the photoaddition of tyrosine to 8-MOP, although low yields of the adduct prevented confirmation of the proposed structure by NMR analysis.

Formation of DNA-Protein Cross-Links

It was shown that psoralen can photoinduce, in mammalian cells, a covalent linkage between a DNA molecule and a protein forming DNA-protein cross-links,[68] and this photodamage provokes evident biological effects. In particular, the formation of these photocompounds in mammalian cells by psoralen and UV-A light was evidenced by alkaline elution, protein precipitation, and isopycnic sedimentation.[68,69] It was observed that psoralens are more effective in inducing this photochemical event than are angular angelicins.[68] The induction of DNA-protein cross-links (DPC) was obtained by using the *double irradiation* method, previously used by Ashwood-Smith and Grant,[70] to study the formation of interstrands cross-links in DNA in *E. coli in vivo*. Psoralens form DNA-protein cross-links (DPC) by a two-step reaction that requires the sequential absorption of two photons.[69,71] This method was applied in whole mammalian cells and *in vitro* on a chromatin-like complex formed by mixing purified DNA and histones from calf thymus.[71,72] The results of these studies, together with similar data independently obtained by Sastry et al.,[73] suggest that in a first-step furan-side, monoadducts are formed, which in a second step, further react with proteins, forming DNA-protein cross-links (DPC). These data support that these lesions are bifunctional adducts, in which the psoralen moiety is a physical part of the bridge linking the two macromolecules; therewith, they must be defined DPC *at length greater than zero* ($DPC_{L>0}$), differently from DNA-protein cross-links induced by UVC light ($DPC_{L=0}$), in which DNA and proteins are connected without any intermediate molecule.[74] Some angelicin isosters [angular furoquinolinones (FQ)] induce DNA-protein cross-links, in a similar way as do psoralens, by means of the double irradiation method. Surprisingly, biological consequences produced by these compounds, in spite of their inability to cross-link DNA, are more pronounced than those induced by 4,5′,8-trimethylpsoralen (TMP).[72,75] To explain these results, and the difference emerging by the comparison with that obtained by TMP, Marzano et al.[76] suggested that DNA-protein cross-links induced by FQ could be repaired by topoisomerase II, which cuts DNA, but similar to what happens with topoisomerase poisons, cannot conclude its enzymatic functions, thus leading to an extensive DNA fragmentation and to cell death.

Photoreactions with Lipids

The possible photointeractions between psoralens and membrane constituents (phospholipids and unsaturated fatty acids) were suggested by Kittler and Lober.[84] Preliminary experimental evidence of the covalent photobinding between psoralen and unsaturated fatty acids was obtained by Caffieri et al.[85] and by Specht et al.,[86] and phospholipids by Antony et al.[87]

It was also shown that UV irradiation activates phospholipase A_2 in human skin and cultured human keratinocytes, thereby giving rise to the release of arachidonic acid, the fatty acid precursor of proinflammatory eicosanoids.[88]

Moreover, a further class of second messengers released from the plasma membrane, as illustrated by 1,2-diacylglycerols (DAG), may play major roles in melanogenesis. Gordon and Gilchrest[89] demonstrated that the exogenous addition of synthetic DAG 1-oleoyl-2-acetylglycerol to cultured human melanocytes increases the basal melanin content and the melanogenic responses of the cells to UV irradiation.

In this context, the formation of covalent adducts between unsaturated fatty acids of membrane phospholipids and psoralens may affect the regulation of some cell processes.

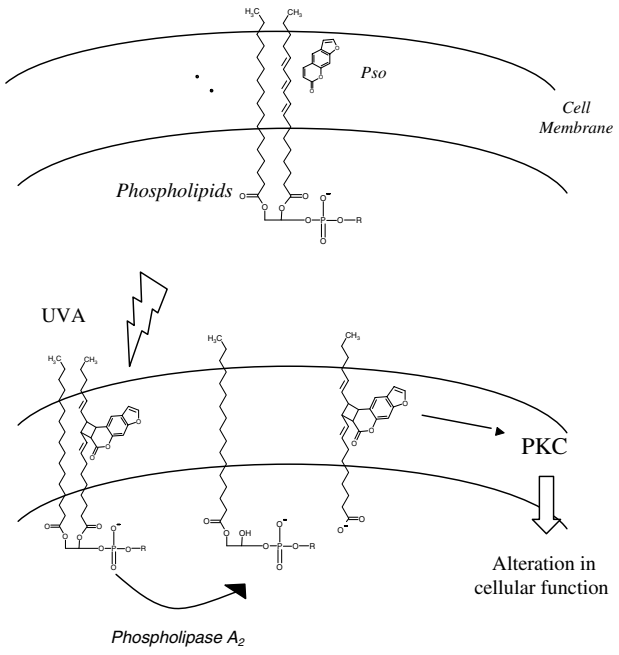

FIGURE 142.5 Proposed mechanism of psoralen-fatty-acid adduct action on protein kinase C (PKC). UV-A irradiation induces a covalent adduct between psoralen and phospholipids that stimulates phospholipase A_2. The enzyme hydrolizes the photocompound, producing psoralen-fatty-acid adduct, which in turn, activates protein kinase C. The activation of this phosphorylating enzyme can modulate cell function and metabolism, i.e., stimulating melanogenesis in melanocytes.

In fact, the cycloadducts between psoralen and unsaturated fatty acid of a phospholipid once formed inside the cell, undergo hydrolysis by phospholypases A_2, generating photocompounds that play the role of second messenger, exhibiting behavior similar to that of DAG (Figure 142.5). To study this photochemical event *in vitro*, studies of the photoreactions between unsaturated fatty acid and psoralen were carried out; it consists of a [2 + 2] photocycloaddition between the 3,4 double bond of the psoralen and one of the olefin bonds of the fatty acid. Some adducts were isolated and their structures elucidated. This concerned several psoralen derivatives and unsaturated fatty acids, including oleic, elaidic, linoleic, and linolenic acid and their methyl esters.[83,84] It was shown that the latter adducts are produced in the skin of rats[66] and in human lymphocytes.[85]

Recently, the structure of psoralen–oleic-acid adducts was assigned in detail.[83] The photocycloadducts were isolated, and it was shown that the photoreaction between psoralen and oleic acid gives rise to four main photoproducts: two exhibit a *cis,cis* structure, whereas the two others have a *trans,cis* stereochemistry (Figure 142.6).

On the other hand, Caffieri et al.[86] showed that fatty–fatty acids cycloadducts in platelets, stimulate the activity of protein kinase C, promoting, in particular, the process of melanogenesis in human epidermis.

The study was extended to a synthetic lecithin bearing an oleyl moiety esterified at position 2 of the glycerol backbone.[87] Structural analysis indicates the similarity of the isomeric forms of cycloadducts involving lecithin and those formed with oleic acid. Moreover, the four diastereomeric oleic–oleic acid photoadducts were tested for their ability to activate protein kinase C in platelets: all were active in a dose-dependent manner, but a significant difference between them could not be noted.

More recently, Anthony et al.[80] showed that 8-MOP-fatty-acid adduct plays the same role of DAG in terms of melanocyte protein kinase C activation. Interestingly, they showed that radiolabeled 8-MOP binds to cell phospholipids specifically in the PI/PS fraction. PI, which is a source of arachidonate, is the

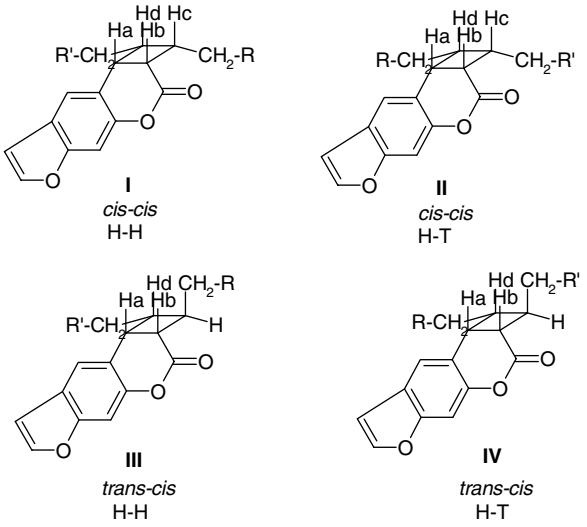

FIGURE 142.6 Molecular structure of isolated cycloadducts between psoralen and oleic acid. R' = $(CH_2)_6$-CH_3 and R = $(CH_2)_6$-COOH. (Adapted from Frank, S., Caffieri, S., Raffaelli, A., Vedaldi, D., and Dall'Acqua, F., *J. Photochem. Photobiol., B: Biol.*, 44, 39, 1998. With permission.)

principal substrate of phospholipase C.[88] In this regard, it was shown that the β-isoform of protein kinase C activates cytoplasmic tyrosinase directly by phosphorylating its serine residues in the melanocytes.[89]

Also, PUVA modulates nonmelanogenic cell functions; thus, 8-MOP fatty acid adducts may influence PKC-mediated pathways in other types of cells.[97] Interestingly, Zarebska et al.[98] showed that acid–fatty-acid adducts are able to induce apoptosis of human lymphocytes in culture.

Apoptosis

In the 1990s, some authors demonstrated that apoptosis was involved in PUVA and psoralen photopheresis treatments.[92] Early studies were carried out essentially by nick translation analysis of DNA fragmentation.[93] The literature of that time does not report indications concerning the action mechanism of apoptosis.[92,93] Only recently have some authors suggested a possible correlation between apoptosis and DNA damage.[94] A recent paper gives experimental evidence that DNA damage by extracorporeal photochemotherapy and psoralen induces apoptosis in mononuclear cells of patients suffering from Sezary syndrome, mycosis fungoides, systemic sclerosis, pemphigus vulgaris, and Hodgkin's disease.[94] Subcellular structures, moreover, other than nucleic acids, may be involved. In particular, considering that mitochondria[95,96] may play a vital role in terms of cell vitality, and that the role of these organelles in the apoptotic event was shown in photodynamic therapy, studies are now being developed to highlight a possible role of mitochondria damage in terms of psoralen apoptosis.[95,96] A recent study carried out on Jurkat cells gives experimental evidence that this is the prevailing form of cell death in Jurkat cells treated with PUVA. In particular, the apoptotic event is due to mitochondrial disfunction caused by mitochondrial alterations of the pore opening,[97] supporting that PUVA damage induced in mitochondria triggers the apoptotic event.[98]

142.3 Dark Effects of Psoralens

Psoralen Receptors

Laskin et al.[99] identified cellular protein as a target for the psoralen molecules linked to cell growth regulation. Subcellular fractionation studies revealed that this receptor is located in membranes and the cytoplasmic fractions of various cell types, in particular, melanocytes and keratinocytes.[99,100]

This receptor was characterized by SDS-PAGE electrophoresis and was found to be a protein with a molecular weight of 22.000. Psoralens bind reversibly to this receptor and with high affinity in a dark reaction.[99] Laskin et al. also found that a number of structurally related psoralen analogues that are active as cutaneous photosensitizers also bind to this receptor. However, 5-methyl angelicin, which is a poor photosensitizer, only binds weakly, indicating that the receptor can readily discriminate between structurally related analogues of psoralens. In addition, a psoralen binds specifically to its receptors, because structurally unrelated compounds fail to compete with psoralens in receptor-binding assay.

It is not necessary to expose a psoralen to UV light in order for the molecule to bind to its receptor. However, once bound to its receptor, the psoralen molecule is photoactivated, producing photoalkylation of the receptor.[99] This event appears to be necessary in order to initiate a biological response.[101] Extensive studies suggest that the ability of psoralens to induce sensitization reactions, including alteration of epidermal cell growth and differentiation, is highly specific and due to interaction with the epidermal growth factor receptor.[102]

Interestingly, the presence of a specific saturable high affinity [^{3}H]8-methoxypsoralen binding protein in cultured S-91 mouse melanoma cells is reported, similar to that mentioned above.[103]

Interaction with Ionic Channels

Recently, it was observed that psoralens, by blocking voltage-dependent K^+ channels (K_v), may alleviate functional deficits in certain multiple sclerosis patients in a manner similar to 4-aminopyridine.[15,16]

In voltage clamp experiments on amphibian nodes of Ranvier, 5-MOP was found to selectively block delayed rectifier K currents. In this line, single trials showed that 5-MOP can alleviate functional deficits in certain patients affected by multiple sclerosis.[104]

A series of psoralens and structurally related 5,7-disubstituted coumarins were synthesized and investigated for their K^+ channel-blocking activity and their phototoxicity. After screening the compounds on Ranvier nodes of the Xenopus Laevis toad, the affinities of the most promising compounds, which proved to be psoralens bearing alkoxy substituents in the 5-position or alkoxymethyl substituents in the neighboring 4- or 4′-positions, to a number of homomeric K^+ channels were characterized. All compounds exhibited the highest affinity to $K_v1.2$. 5,8-Diethoxypsoralen was found to be an equally potent inhibitor of $K_v1.2$ and $K_v1.3$, while lacking the phototoxicity normally inherent in psoralens. These compounds represent a novel series of nonpeptide blockers of Shaker-type K^+ channels that could be developed further into selective inhibitors of $K_v1.2$ or $K_v1.3$.

Because K_v channel blockers are known to inhibit T-cell-mediated immune responses *in vitro* and *in vivo*, subsequent studies investigated *in vivo* the effects of three psoralen derivatives, 5-methoxypsoralen, 8-methoxypsoralen, and 5,8-diethoxypsoralen, in Lewis rats challenged for experimental autoimmune encephalomyelitis (EAE). The derivatives examined exhibited suppressive effects on the parameters measured with the same sequence of efficacy: 5,8-diethoxypsoralen > 5-MOP > 8-MOP. The authors suggest that K_v channel-blocking psoralens interfere with voltage-controlled signal transduction in lymphocytes and might thereby suppress immune responses in autoimmune diseases of the central nervous system and probably also in other autoimmune disorders. These derivatives, especially the nonphototoxic 5,8-diethoxypsoralen, are, therefore, new candidates for further studies on K^+ channel-blocking immunosuppressive drugs. The agents may exert a dual beneficial effect on demyelinating diseases like multiple sclerosis, because they could attenuate the inflammatory process and improve axonal conductivity.

Another interesting report suggests that psoralens open cystic fibrosis transmembrane conductance regulator Cl^- channels in T84 cell monolayer. Similar results with psoralens in rat colon and primary cultures of murine tracheal epithelium were obtained. On the basis of these observations, it was suggested that psoralens represent a novel class of Cl^- channel openers that can be used to probe mechanisms underlying Ca^{2+}-mediated Cl^- secretion.

142.4 Future Perspectives

The basic mechanisms responsible for the photosensitizing effects of psoralens were clarified, although some aspects require additional research in order to be able to give a more complete picture of the various processes.

Demonstrating that fatty–fatty-acid adducts are formed in cells stimulated studies of the biological role of these adducts. In this regard, these photocompounds may play the role of second messenger that stimulates protein kinase C. This may lead to stimulation of melanin synthesis in melanocytes, thus explaining one of the mechanisms of the melanogenic effect of psoralen. A proposed mechanism is depicted in Figure 142.6. Because photoactivated psoralens have a wide range of biological effects, it is likely that their ability to generate signals, e.g., by modulating protein kinase C activity, is dependent on cell type.

Besides their application in PUVA therapy to treat diseases characterized by hyperproliferation or the lack of pigmenting ability of some regions of the skin, in the last years, psoralens were also used in photopheresis, a therapeutic approach useful in treating immune disorders.

An important application, recently developed, is represented by sterilizing blood components, in particular, platelet concentrate. Recently, clinical trials carried out with a novel psoralen S-59 derivative demonstrated the efficacy of the photochemical treatment, thus offering the potential to reduce transfusion-related viral and antibacterial diseases.

In the last decade, the involvement of apoptosis in PUVA and in photopheresis strongly stimulated research in this field. A recent paper reports that mitochondria represent an important target psoralen photoinduced apoptosis.[98]

The important finding that some psoralen molecules, in particular 5,8 disubstituted derivatives, have significant *in vitro* and *in vivo* activity as potassium channel blockers, although lacking the phototoxicity normally inherent in psoralen, opened a new field of research toward an innovative application of this class of molecule in many important diseases, such as multiple sclerosis, in which the capacity to block voltage-gated potassium channels improves conduction in demyelinated fibers. It is also important to point out that potassium channels are involved in the control of membrane potential, production of lymphokine, and proliferation of human T-lymphocytes. Therefore, 5,8 disubstituted psoralens represent a novel series of compounds able to block potassium channels that could be developed further into more selective inhibitors.

Acknowledgments

The authors thank Professor Franco Bordin for helpful discussion. This work was supported in part by funds of MIUR, Rome.

References

1. Dall'Acqua, F., Furocoumarins photochemistry and main biological implications, in *Current Problem in Photomedicine*, Hoenigsman, H., Ed., Karger, Basel, 1986, p. 137.
2. Musajo, L. and Rodighiero, G., Mode of photosensitizing action of furocoumarins, in *Photophysiology*, Vol. VII, Giese, A.C., Ed., Academic Press, New York, 1972, p. 115.
3. Parrish, J.A., Fitzpatrick, T.B., Tanembaum, L., and Pathak, M.A., Photochemotherapy of psoriasis with oral methoxsalen and long wave ultraviolet light, *New. Eng. J. Med.*, 291, 1207, 1974.
4. Edelson, R., Berger, C., Gasparro, F., Jegasothy, C.B., Heald, P., Wintroub, B., Vonderheid, E., Knobler, R., Wolff, K., Plewig, G., McKiernan, G., Christiansen, I., Oster, M., Honigsmann, H., Wilford, H., Koroska, E., Rehle, T., Stingl, G., and Laroche, L., Treatment of cutaneous T-cell lymphoma by extracorporeal photochemotherapy. Preliminary results, *N. Engl. J. Med.*, 316, 297, 1987.
5. Gollnick, H.P., Owsianowski, M., Taube, K.M., and Orfanos, C.E., Unresponsive and severe generalized pemphigo vulgaris successfully controlled by extracorporeal photopheresis, *J. Acad. Dermatol.*, 28, 122, 1993.
6. Prinz, B., Nachbar, F., and Plewig, G., Treatment of severe atopic dermatitis with extracorporeal photopheresis, *Arch. Dermatol. Res.*, 287, 48, 1994.
7. Bisaccia, E., Berger, C., Di Spaltro, F., and Klainer, A.S., Extracorporeal photopheresis in the treatment of AIDS-related complex: extended trial, *J. Acquir. Immune Defic. Syndr.*, 6, 386, 1993.

8. Malavista, S.H., Trock, D.H., and Edelson, R.L., Treatment of rheumatoid arthritis by extracorporeal photopheresis, *Arthritis Rheum.,* 34, 646, 1991.
9. Knobler, R.M., Extracorporeal photochemotherapy for the treatment of lupus erythematosus: preliminary observations, *Springer Semin. Immunopathol.*, 16, 323, 1994.
10. Lin, L., Cook, D.N., Wiesehahn, G.P., Alfonso, R., Behrman, B., Cimino, G.D., Corten, L., Damonte, R., Dikeman, P.B., Dupuis, K., Fang, Y.M., Hanson, C.V., Hearst, J.E., Lin, C.Y., Isaacs, H.T., Wollowitz, S., and Corash, L., Photochemical inactivation of viruses and bacteria in platelet concentrates by use of novel psoralen and long-wavelength ultraviolet light, *Transfusion*, 37*,* 423, 1997.
11. Ben-Hur, E. and Horowitz, B., Virus inactivation in blood, *AIDS*, 10, 1183, 1996.
12. Margolis-Nunno, H., Bardossy, L., Robinson, R., Ben-Hur, E., Horowitz, B., and Blajchman, M.A., Psoralen-mediated photodecontamination of platelet concentrates: inactivation of cell-free and cell-associated forms of human immunodeficiency virus and assessment of platelet function *in vivo*, *Transfusion*, 37*,* 889, 1997.
13. Margolis-Nunno, H., Robinson, R., Ben-Hur, E., and Horowitz, B., Quencher-enhanced specificity of psoralen photosensitized virus inactivation in platelet concentrates, *Transfusion*, 34, 802, 1994.
14. Eble, B.E. and Corash, L., Photochemical inactivation of duck hepatitis B virus in human platelet concentrates: a model of surrogate human hepatitis B virus infectivity, *Transfusion*, 36*,* 406, 1996.
15. Bohuslavisky, K.H., Hansel, W., Kneip, A., Koppenhofer, E., Niemoller, E., and Sanman, K., Mode of action of psoralens, benzofurans, acridinones and coumarins on the ionic currents in intact myelinated nerve fibres and its significance in demyelinating disease, *Gen. Physiol. Biophys.*, 13, 309, 1994.
16. Wulff, H., Rauer, H., During, T., Hanselmann, C., Ruff, K., Wrisch, A., Grissmer, S., and Hansel, W., Alkoxypsoralens, novel nonpeptide blockers of Shaker-Type K^+ channels: Synthesis and photoreactivity, *J. Med. Chem.*, 41, 4542, 1998.
17. Mantulin, W.W. and Song, P.S., Excited states of skin sensitizing coumarins and psoralens. Spectroscopic studies, *J. Am. Chem. Soc.*, 104, 7631, 1973.
18. Bensasson, R.V., Land, E.J., and Salet, C., Triplet excited states of furocoumarins: reaction with nucleic acid bases and amino acids, *Photochem. Photobiol.*, 27, 273, 1978.
19. Moysan, A., Viari, A., Vigny, P., Voituriez, L., Cadet, J., Moustacchi, E., and Sage, E., Formation of cyclobutane thymine dimers photosensitized by pyridopsoralens: quantitative and qualitative distribution within DNA, *Biochemistry*, 30, 7080, 1991.
20. Costalat, R., Blais, J., Ballini, J.-P., Moysan, A., Cadet, J., Chalvet, O., and Vigny, P., Formation of cyclobutyl thymine dimers photosensitized by pyridopsoralens: a triplet-triplet energy transfer mechanism, *Photochem. Photobiol.*, 51, 255, 1990.
21. Cadet, J., Berger, M., Douki, T., Morin, B., Raoul, S., Ravanat, J., and Spinelli, S., Effects of UV and visible radiation on DNA-final base damage, *Biol Chem.*, 378, 1275, 1997.
22. Cadet, J. and Vigny, P., The photochemistry of nucleic acids, in *Bioorganic Photochemistry*, Morrison, H., Ed., John Wiley & Sons, New York, 1990, p. 1.
23. Ciamician, G. and Siber, P., Chemische Lichtwwirkungen.V. Mitt., *Chem. Ber.*, 35, 4128, 1902.
24. Elisei, F., Aloisi, G.G., Lattarini, C., Latterini, L., Dall'Acqua, F., and Guiotto, A., Photophysical properties of some methyl-substituted angelicins: fluorimetric and flash photolytic studies, *Photochem. Photobiol.*, 64, 67, 1996.
25. Elisei, F., Aloisi, G.G., Dall'Acqua, F., Latterini, L., Masetti, F., and Rodighiero, P., Photophysical behaviour of angelicins and thioangelicins: semiempirical calculation and experimental studies, *Photochem. Photobiol.*, 68, 164, 1998.
26. Vedaldi, D., Piazza, G., Moro, S., Caffieri, S, Miolo, G., Aloisi, G.G., Elisei, F., and Dall'Acqua, F., 1-Thiopsoralen a new photobiologically active heteropsoralen: photophysical, photochemical and computer aided studies, *Il Farmaco*, 52, 645, 1997.
27. Borges, M.L., Latterini, L., Elisei, F., Silva, P.F., Borges, R.S., and Maçanita, A.L., Photophysical properties and photobiological activity of the furanochromones visnagin and khellin, *Photochem. Photobiol.*, 67, 184, 1998.

28. Caffieri, S., Furocoumarin photolysis: chemical and biological aspects, *Photochem. Photobiol. Sci.*, 1, 149, 2002.
29. von Wessely, F. and Dinjaski, K., Uber die Lichteinwirkung auf Stoffe von Typus der Furo-cumarine, *Monatsh. Chem.,* 131, 1934.
30. Von Wessely, F. and Plaickinger, I., Uber der komstitution der photodimerisate der coumarine und furocoumarine, *Chem. Ber.,* 75, 971, 1942.
31. Krauch, H., Farid, S., and Schenk, O., Photo-C_4-cyclodimerisation von coumarin, *Chem. Ber.,* 99, 625, 1966.
32. Caffieri, S. and Dall'Acqua, F., C_4-cyclodimers of psoralen engaging the 4′,5′ double bond, *Photochem. Photobiol.*, 45, 13, 1987.
33. Rodighiero, G., Musajo, L., Dall'Acqua, F., and Caporale, G., La fotoreazione fra psoralene e flavinmononucleotide, *Gazz. Chim. Ital.*, 94, 1073, 1964.
34. Musajo, L., Rodighiero, G., Caporale, G., Fornasiero, U., Malesani, G., Dall'Acqua, F., and Giacomelli, C., La fotoreazione fra bergaptene e flavinmononucleotide, *Gazz. Chim. Ital.*, 94, 1054, 1964.
35. Rodighiero, G., Musajo, L., Fornasiero, U., Caporale, G., Malesani, G., and Chiarelotto, G., La fotoreazione fra xantotossina e flavinmononucleotide, *Gazz. Chim. Ital.*, 94, 1084, 1964.
36. Logani, M.K., Austin, W.A., Shah, B., and Davies, R.E., Photooxidation of 8-MOP with singlet oxygen, *Photochem Photobiol.*, 35, 569, 1992.
37. Wasserman, H.H. and Berdahl, D.R., The photooxidation of 8-methoxypsoralen, *Photochem. Photobiol.*, 35, 565, 1982.
38. Caffieri, S. and Favretto, D., UV-A photolysis of khellin: products and reaction mechanism, *J. Org. Chem*, 58, 7059, 1993.
39. Marley, K.A. and Larson, R.A., A new photoproduct from furocoumarin photolysis in dilute aqueous solution: 5-formyl-6-hydroxybenzofuran, *Photochem. Photobiol.*, 59, 503, 1994.
40. Adam, W., Bialas, J., Hadjiarapoglou, L., and Sauter, M., Epoxidation of 2,3-dimethylbenzofurans by dimethyldioxirane, *Chem. Ber.*, 125, 231, 1992.
41. Potapenko, A.Ya., Mechanism of photodynamic effects of furocoumarins, *J. Photochem. Photobiol., B: Biol.*, 9, 1, 1991.
42. Lysenko, P.E., Melnikova, V.O., Andina, E.S., Wunderlich, S., Pliquett, F., and Potapenko, A.Ya., Effect of glutatione peroxidadase and catalase on hemolysis and methemoglobin modifications induced by photooxidized psoralen, *J. Photochem. Photobiol., B: Biol.*, 56, 187, 2000.
43. Mizuno, N., Esaki, K., Sakakibara, J., Murakami, N., and Nagai, S., Structural elucidation of the 8-methoxypsoralen oxidized product that inhibits the chemotactic activity of polymorphonuclear neutrophils toward anaphylatoxin C5a., *Photochem. Photobiol.*, 54, 697, 1991.
44. Esaki, K. and Mizuno, N., Effect of psoralens + ultraviolet-A on the chemotactic activity of polymorphonuclear neutrophils towards anaphylatoxin C5a des Ag, *Photochem. Photobiol.*, 55, 783, 1992.
45. Kyagova, A.A., Korkina, L.G., Snigireva, T.V., Lisenko, E.P., Tomashaeva, S.K., and Potapenko, A.Ya., Psoralen-photosensitised damage of rat peritoneal exudate cells, *Photochem. Photobiol.*, 53, 633, 1991.
46. Potapenko, A.Ya., Kyagova, A.A., Bezdetnaya, L.N., Lisenko, E.P., Chernyakhovskaya, I.Yu., Bekhalo, V.A., Nagurskaya, E.V., Nesterenko, V.A., Korotky, N.G., Akhtyamov, S.N., and Lanshchikova, T.M., Products of psoralen photooxidation possess immunomodulative and antileukemic effects, *Photochem. Photobiol.*, 60, 171, 1994.
47. Potapenko, A.Ya., Butov, Y.S., Levinzon, E.S., Mamedov, I.S., Kyagova, A.A., and Nikonenko, B.V., Psoralen photochemotherapy of eczema without UVA-irradiation of patients, presented at 13th International Congress on Photobiology, San Francisco, California, July 1–6, 2000, Abstract 508.
48. Rhodes, J., Chen, H., Hall, S.R., Beesley, J.E., Jenkings, D.C., and Zheng, B., Therapeutic potentiation of the immune system by costimulatory Schiff-base-forming, *Nature*, 337, 71, 1995.
49. Koenigs, L.L. and Trager, W.F., Mechanism-based inactivation of cytochrome P450 2B1 by 8-methoxypsoralen and several other furanocoumarins, *Biochemistry*, 37, 13184, 1998.

50. Dall'Acqua, F., Marciani, S., and Rodighiero, G., Inter-strand cross-linkages occurring in the photoreaction between psoralen and DNA, *FEBS Lett.,* 9, 121, 1970.
51. Cimino, G.D., Gamper, H.B., Isaacs, S.T., and Hearst, J.E., Psoralens as photoactive probes of nucleic acid structure and function: organic chemistry, photochemistry, and biochemistry, *Ann. Rev. Biochem.*, 54, 1151, 1985.
52. Dall'Acqua, F., Terbojevitch, M., Marciani, S., Vedaldi, D., and Recher, M., Investigation on the dark interaction between furocoumarins and DNA, *Chem. Biol. Intract.*, 21, 103, 1978.
53. Yun, M.H., Choi, S.J., and Shim, S.C., A novel photoadduct of 4,5′,8-trimethylpsoralen and adenosine, *Photochem. Photobiol.*, 55, 457, 1992.
54. Tessmann, J.W., Isaacs, S.T., and Hearst, J.E., Photochemistry of the furan-side 8-ethoxypsoralen-thymidine monoadduct inside the DNA helix. Conversion to diadduct and to pyrone-side monoadduct, *Biochemistry*, 24, 1669, 1985.
55. Kanne, D., Isolation and characterization of pyrimidine-psoralen-pyrimidine photodiadducts from DNA, *J. Am. Chem. Soc.*, 104, 6764, 1982.
56. Gaboriau, F., Vigny, P., Averbeck, D., and Bisagni, E., Spectroscopic study of the dark interaction and of the photoreaction between a new monofunctional psoralen: 3-carbethoxy psoralen, and DNA, *Biochimie*, 63, 899, 1981.
57. Blais, J., Vigny, P., Moron, J., and Bisagni, E., Spectroscopic properties and photoreactivity with DNA of new monofunctional pyridopsoralens, *Photochem. Photobiol.*, 39, 145, 1984.
58. Teran, C., Miranda, R., Santana, L., Tejiera, M., and Uriarte, E., Synthesis of linear and angular furocoumarins, *Synthesis, Stuttgard,* 12, 1384, 1997.
59. Miolo, G., Lucchini, V., Vedaldi, D., Guiotto, A., and Caffieri, S., Dark and photochemical interaction of dimethyltetrahydrobenzoangelicin with DNA, *Photochem. Photobiol.*, 67, 628, 1998.
60. Caffieri, S., Miolo, G., Dall'Acqua, F., Benetollo, F., and Bombieri, G., Photoaddition of 4,6-dimethyltetrahydrobenzoangelicin to thymine in DNA: x-ray studies and experiments with model oligonucleotides, *Photochem. Photobiol.*, 72, 23, 2000.
61. Bordin, F., Marzano, C., Gatto, C., Carlassare, F., Rodighiero, P., and Baccichetti, F., 4,6,4′-Trimethylangelicin induces interstrand cross-links in mammalian cell DNA, *J. Photochem. Photobiol. B: Biol.*, 26**,** 197, 1994.
62. Yoshikawa, K., Mori, N., Sakakibara, S.D., Mizuno, N., and Song, P.S., Photoconjugation of 8-methoxy-psoralen with proteins, *Photochem. Photobiol.*, 29, 1127, 1979.
63. Veronese, F., Schiavon, O., and Bevilacqua, R., Photoinactivation of enzymes by linear and angular furocoumarins, *Photochem. Photobiol.*, 36, 25, 1982.
64. Beijersbergen van Henegouwen, G.M.J., Wijn, E.T., Schoonderwoerd, S.A., and Dall'Acqua, F., Method for the determination of the *in vivo* irreversible binding of 8-methoxypsoralen (8-MOP) to epidermal lipids, proteins and DNA/RNA of rats after PUVA treatment, *J. Photochem. Photobiol., B: Biol.*, 3**,** 631, 1989.
65. Schmitt, I.M., Chimenti, S., and Gasparro, F.P., Psoralen-protein photochemistry: a forgotten field, *J. Photochem. Photobiol., B: Biol.*, 27**,** 101, 1995.
66. Schoonderwoerd, S.A., Beijersbergen van Hengouwen, G.M.J., Person, C.C.M., Caffieri, S., and Dall'Acqua, F., Photobinding of 8-methoxypsoralen, 4,6,4′-trimethylangelicin and chlorpromazine to Wistar rat epidermal biomacromolecules *in vivo*, *J. Photochem. Photobiol., B: Biol.*, 10, 257, 1991.
67. Sastry, S.S., Isolation and partial characterization of a novel psoralen-tyrosine photoconjugate from a photoreaction of psoralen with a natural protein, *Photochem. Photobiol.*, 65**,** 937, 1997.
68. Bordin, F., Carlassare, F., Busulin, L., and Baccichetti, F., Furocoumarin sensitization induces DNA-proteins cross-links, *Photochem. Photobiol.*, 58, 133, 1993.
69. *Bordin, F.*, Photochemical mechanism of DNA damage induced by furocoumarins, in *Advances in Biomedical Application of Photochemistry & Photobiology*, Vargas, F., Ed., Research Signpost Review, Kerala, India, 2002, p. 95.

70. Ashwood-Smith, M.J. and Grant, E., Conversion of psoralen monoadducts in *E. coli* to interstrand DNA crosslinks by new UV light (320–360 nm): inability of angelicin to form crosslinks *in vivo*, *Experientia*, 33, 384, 1977.
71. Bordin, F., Marzano, C., Carlassare, F., Rodighiero, P., Guiotto, A., and Caffieri, S., Photobiological properties of a new tetramethylfuroquinolinone, *J. Photochem. Photobiol., B:Biol.*, 34, 159, 1996.
72. Bordin, F., Baccichetti, F., Marzano, C., Carlassare, F., Miolo, G., Chilin, A., and Guiotto, A., DNA damage induced by 4,6,8,9-tetramethyl-2H-furo[2,3-h]quinolin-2-one, a new furocoumarin analog: photochemical mechanisms, *Photochem. Photobiol.*, 71, 254, 2000.
73. Sastry, S.S., Spielmann, H.P., Hoang, Q.S., Phillips, A.M., Sancar, A., and Hearst, J.E., Laser-induced protein-DNA cross-links via psoralen furanside monoadducts, *Biochemistry*, 32, 5526, 1993.
74. Shetlar, M.D., Cross-linking of proteins to nucleic acids by ultraviolet light, in *Photochemical and Photobiological Review*, Vol. 5, Smith, K.C., Ed., Plenum Press, New York, 1980, p. 105.
75. Marzano, C., Baccichetti, F., Carlassare, F., Miolo, G., Chilin, A., and Guiotto, A., DNA damage induced by 4,6,8,9-tetramethyl-2H-furo[2,3-h]quinolin-2-one, a new furocoumarin analog: biological consequences, *Photochem. Photobiol.*, 71, 263, 2000.
76. Marzano, C., Severin, E., and Bordin, F., Can a mixed damage interfere with DNA-protein cross-links repair?, *J. Cell. Mol. Med.*, 5, 171, 2001.
77. Kittler, L. and Lober, G., Photoreaction of furocoumarins with membrane constituents. Results with fatty acids and artificial bilayers, *Stud. Biophys.*, 101, 69, 1984.
78. Caffieri, S., Tamborrino, G., and Dall'Acqua, F., Formation of photoadducts between unsaturated fatty acids and furocoumarins, *Med. Biol. Environ.*, 15, 11, 1987.
79. Specht, K.G., Kittler, L., and Midden, W.R., The chemical structures of the trimethylpsoralen-oleic acid methyl ester adducts, *Photochem. Photobiol.*, 45s, 51S, 1987.
80. Anthony, F.A., Laboda, J.C., and Costlow, M.E., Psoralen-fatty acid adducts activate melanocyte protein kinase C: a proposed mechanism for melanogenesis induced by 8-methoxypsoralen and ultraviolet A light, *Photodermatol. Photoimmunol. Photomed.*, 13, 9, 1997.
81. Cohen, D., and De Leo, V.A., Ultraviolet radiation-induced phospholipase A_2 activation occurs in mammalian cell membrane preparations, *Photochem. Photobiol.*, 57, 383, 1993.
82. Gordon, P.R. and Gilchrest, B.A., Human melanogenesis is stimulated by diacylglycerol, *J. Invest Dermatol.*, 93, 700, 1989.
83. Frank, S., Caffieri, S., Raffaelli, A., Vedaldi, D., and Dall'Acqua, F., Characterization of psoralen oleic acid cycloadducts and their possible involvement in membrane photodamage, *J. Photochem. Photobiol., B: Biol.*, 44, 39, 1998.
84. Specht, K.G., Kittler, L., and Midden, W.R., A new biological target of furocoumarins: photochemical formation of covalent adducts with unsaturated fatty acids, *Photochem. Photobiol.*, 47, 537, 1988.
85. Caffieri, S., Zarebska, Z., and Dall'Acqua, F., Membrane lymphocyte damage by 8-methoxypsoralen and UVA radiation, *Med. Biol. Environ.*, 19, 45, 1991.
86. Caffieri, S., Ruzzene, M., Guerra, B., Frank, S., Vedaldi, D., and Dall'Acqua, F., Psoralen-fatty acid cycloadducts activate protein kinase C (PKC) in human platelets, *J. Photochem. Photobiol., B: Biol.*, 22, 253, 1994.
87. Zarebska, Z., Waszkowska, E., Caffieri, S., and Dall'Acqua, F., Photoreactions of psoralens with lecithins, *J. Photochem. Photobiol., B: Biol.*, 45, 122, 1998.
88. Berridge, M.J., Inositol triphosphate and diacylglycerol as second messengers, *Biochem. J.*, 220, 345, 1984.
89. Park, H.Y., Perez, J.M., Laursen, R., Hara, M., and Gilchrest, B.A., Protein kinase C-β activates tyrosinase by phosphorilating serine residues in its cytoplasmic domain, *J. Biol. Chem.*, 274, 16470, 1999.
90. Mermelstein, F.H., Abidi, T.F., and Laskin, J.D., Inhibition of epidermal growth factor receptor tyrosine kinase activity in A431 human epidermoid cells following psoralen/ultraviolet light treatment, *Mol. Pharmacol.*, 36, 848, 1989.

91. Zarebska, Z., Waszkowska, E., Caffieri, S., and Dall'Acqua, F., Photoreactions of psoralen with lecithins, presented at 13th International Congress on Photobiology, San Francisco, CA, July 1–6, 2000, Abstract 614.
92. Marks, D.I., Mechanism of photochemotherapy induced apoptotic cell death in lymphoid cells, *Biochem. Cell Biol.*, 69, 754, 1991.
93. Yoo, E.K., Rook, A.H., Elentsas, R., Gasparro, F.P., and Vowels, B.R., Apoptosis induction by ultraviolet light A and photochemotherapy in cutaneous T-cell lymphoma: relevance to mechanism of therapeutic action, *J. Investig. Dermatol.*, 107, 235, 1996.
94. Efferth, T., Fabry, U., and Osieka, R., Induction of apoptosis, depletion of glutatione, and damage by extracorporeal photochemotherapy and psoralen with exposure to UV light *in vitro*, *Anticancer Res.*, 21, 2777, 2001.
95. Lam, M., Oleinick, N.L., and Miemien, A.L., Photodynamic therapy-induced apoptosis in epidermoid carcinoma cells, *J. Biol. Chem.*, 276, 47373, 2001.
96. Oleinick, N.L., Morris, R.L., and Belichenko, I., The role of apoptosis in response to photodynamic therapy: what, where, why, and how, *Photochem. Photobiol. Sci.,* 1, 1, 2002.
97. Vousden, K.H., p53: death star, *Cell,* 103, 691, 2001.
98. Canton, M., Caffieri, S., Dall'Acqua, F., and Di Lisa, F., PUVA induced apoptosis involves mitochondrial dysfunction caused by opening of the permeability transition pore, *FEBS Lett.,* 522, 168, 2002.
99. Laskin, J.D., Lee, E., Yurkow, E.J., Laskin, D.L., and Gallo, M.A., A possible mechanism for psoralen phototoxicity not involving direct interaction with DNA, *Proc. Natl. Acad. Sci. USA*, 82, 6158, 1985.
100. Yurkow, E.J. and Laskin, J.D., Characterization of a photoalkylated receptor in HeLa cells, *J. Biol Chem.*, 262, 8439, 1987.
101. Laskin, J.D. and Lee, E., Psoralen binding and inhibition of epidermal growth factor binding by psoralen/ultraviolet light (PUVA) in human epithelial cells, *Biochem. Pharmacol.*, 41, 125, 1991.
102. Laskin, J.D., Lee, E., Laskin, D.L., and Gallo, M.A., Psoralens potentiate ultraviolet light-induced inhibition of epidermal growth factor binding, *Proc. Natl. Acad. Sci. USA,* 83, 8211, 1986.
103. Dowdy, J.C., Anthony, F.A., Sayre, R.M., and Stevens, S.E., Characterization of the 8-methoxypsoralen/22 KDA protein photoadduct in S-91 mouse melanoma cells, presented at 13th International Congress on Photobiology, San Francisco, CA, July 1–6, 2000, Abstract 512.
104. Bohuslavisky, K.H., Heink-Kneip, C., Kneip, A., Koppenhofer, E., and Reimers, A., Reduction of MS-related scotoma by a new class of potassium channel blockers from *Ruta graveolens*, *Neuro-ophthalmology*, 13, 191, 1993.

143

Photosensitization with Emphasis on the Cardiovascular System

Dennis Paul Valenzeno
University of Kansas Medical Center

John G. Wood
University of Kansas Medical Center

Norberto C. Gonzalez
University of Kansas Medical Center

Merrill Tarr
University of Kansas Medical Center

143.1 Introduction

As the field of photosensitization enters its second century of intensive scientific study, it has matured into an area of science that has broad applicability in a variety of settings, many of them health related.[1] Since the turn of the 20th century when Oscar Raab and his mentor Hermann von Tappeiner published their observations on the effects of dyes on paramecia,[2,3] photosensitization of molecules, organelles, cells, tissues, plants, and animals has been investigated using a wide array of photosensitizers, including xanthenes, porphyrins, phenothiazines, and flavins.

In contrast to the descriptive studies of photosensitization effects that were the subject of so many publications 100 years ago, current work capitalizes on a better understanding of the underlying mechanism of photosensitization. For example, therapeutic applications in photodynamic therapy currently in use to treat malignant tumors as well as other conditions, are increasingly exploring two-photon excitation processes to improve localization of the effects. Because two-photon excitation requires a high-energy density of illumination for activation of the photosensitizer, the intensity of a convergent beam can be adjusted so that this critical energy density is only reached near the focal point of the beam, providing excellent spatial resolution. This approach also allows control of the depth of the photodynamic effect (Figure 143.1). In two-photon excitation, each absorbed photon carries only half of the excitation energy, exciting the photosensitizer through a virtual excited state.[4] Planck's Law dictates that these lower-energy

0-8493-1348-1/04/$0.00+$1.50

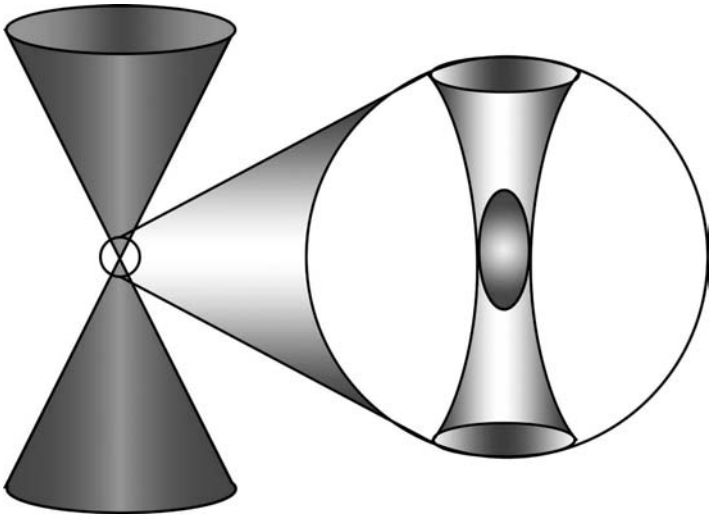

FIGURE 143.1 Two-photon excitation allows activation of photosensitizers at deeper tissue depths, because it uses longer wavelength illumination. In addition, the energy density required for near simultaneous absorption of two photons can be manipulated to restrict the volume of excitation to a small region near the focal point of a convergent beam.

photons will have a longer wavelength. Because longer wavelength illumination has much greater tissue penetration compared to shorter wavelengths, two-photon techniques can produce effects at much greater depths than previously possible. While the high-energy requirement is still a problem for clinical applications, this may well become less critical as laser technology improves.

Better understanding of the localization of different chemical species of photosensitizers allowed better targeting of photosensitization effects. For example, using aluminum phthalocyanine disulfonate as photosensitizer, Selbo et al.[5] demonstrated localization of the photosensitizer in endocytic vesicles in tumor-bearing mice. They subsequently administered a membrane-impermeable chemotherapeutic agent, gelonin, which is normally taken up by endocytic vesicles. Illumination of the tumors of these mice, reduced tumor cell survival while producing complete remission in six of nine treated animals.

Like the examples cited above, there are several current hot topics of research in photosensitization, including the use of photodynamic therapy for malignancies,[6] the use of photosensitizers as model systems for studying physiological and pathological processes involving reactive oxygen species,[7] the development of model systems to produce cerebral ischemia,[8] the use as antimicrobials and to treat blood and blood products,[9] and photosensitization in the cardiovascular system, the main topic area of this review.

143.2 Photosensitization of the Microcirculation

Reactive Oxygen Effects in the Microcirculation

Because photosensitization effects are thought to occur via the intermediacy of reactive oxygen species (ROS), an understanding of the considerable literature in this field of study is useful in understanding photosensitization effects in the microcirculation. ROS are molecules that have an unpaired electron in their outer orbit, and as a result, they are highly reactive.[10] Addition of an electron to molecular oxygen forms superoxide, with approximately 5% of oxygen converted to ROS under normal conditions. Cells contain several enzymatic free-radical scavengers (i.e., superoxide dismutase, catalase, and glutathione peroxidase) as well as antioxidants (i.e., glutathione, lipoic acid) that protect against ROS-induced damage under normal conditions. In situations associated with increased ROS production, however, the antioxidant defenses are not sufficient to detoxify ROS, with higher ROS levels resulting in irreversible changes in lipids and proteins.

ROS can be produced in a variety of cells, with endothelial cells and leukocytes of particular significance to the cardiovascular system. Endothelial cells form a single cell layer along the inner surface of all blood vessels and play a critical role in regulating microvascular function, the nature of which is dependent on the particular vascular segment:[11]

1. *Arterioles*: These vessels, consisting largely of vascular smooth muscle, regulate organ blood flow via changes in vessel diameter and, thereby, vascular resistance to blood flow. The endothelial cell layer produces a variety of vasoactive mediators that cause relaxation or constriction of vascular smooth muscle. One of these mediators, nitric oxide (NO), is of particular importance, as it is continuously produced under normal conditions and, therefore, plays an important role in regulating vascular tone. In addition, NO mediates the effects of certain vasoactive agents; for example, increased blood flow in response to acetylcholine is dependent on increased NO formation by endothelial cells.
2. *Capillaries*: These vessels consist of a single cell layer of endothelial cells. The absence of overlying vascular smooth muscle cells permits exchange of fluid and nutrients between blood and tissue. NO produced by capillary endothelial cells appears to maintain low vascular permeability under normal conditions.
3. *Venules*: Postcapillary venules play an important role in regulating leukocyte recruitment into tissues. Circulating leukocytes interact with venular endothelial cells through a highly coordinated process.[11] The first step involves a leukocyte rolling along the endothelium, which is mediated through interaction of specific adhesion molecules with their corresponding ligands. Leukocyte rolling reduces the forward velocity of leukocytes sufficiently to allow interaction between different types of adhesion molecules on each cell, leading to firm adherence of leukocytes within the venule. The final step, leukocyte emigration, involves movement of leukocytes out of the circulation into the tissue.

To illustrate the effects of ROS on microvascular function, ischemia–reperfusion (I/R) will be briefly discussed. A prolonged reduction or absence of blood flow (i.e., ischemia) results in a series of biochemical changes within endothelial cells that will initiate a microvascular inflammatory response upon reintroduction of blood flow to the tissue (i.e., reperfusion).[12,13] Clinical situations involving I/R-induced microvascular dysfunction include organ transplantation, coronary angioplasty, thrombolytic therapy, and cardiopulmonary bypass.[13]

During prolonged ischemia, calcium levels within endothelial cells rise, resulting in conversion of xanthine dehydrogenase to xanthine oxidase.[11,14] Upon reintroduction of oxygen to tissue upon reperfusion, a marked increase in ROS generation occurs primarily via xanthine oxidase. The resulting oxidant stress will have site-specific effects within the microcirculation:

1. *Arterioles*: The primary effect of I/R on arterioles is impaired endothelium-dependent relaxation of vascular smooth muscle. The net result is arteriolar constriction and reduced blood flow, which may promote organ injury. ROS generation during reperfusion appears to be the underlying cause of this response, as antioxidants attenuate I/R-induced arteriolar constriction. The specific oxidant involved is superoxide, which interacts with NO, such that levels of this endothelial-derived dilator are reduced during reperfusion.
2. *Capillaries*: I/R results in increased filtration of fluid across capillaries as well as a decrease in the number of perfused capillaries. The mechanisms underlying these responses are still not clearly defined but may be related to decreased NO levels in capillary endothelial cells as a result of oxidant stress, as described above. Lower NO levels may increase capillary permeability, and increase the rate of filtration of fluid into the tissue. The resulting edema was proposed to compress the capillaries sufficiently to impede blood flow through these vessels.
3. *Venules*: ROS generation during reperfusion has several effects on postcapillary venules: increased leukocyte adherence to venular endothelium, with subsequent emigration of some leukocytes into the tissue; platelet aggregation; and increased vascular permeability. These responses are dependent

on reduced levels of the anti-inflammatory agent NO within endothelial cells (via inactivation of NO by superoxide), generation of lipid inflammatory mediators (such as platelet activating factor and leukotriene B_4), and activation of perivascular mast cells, resulting in local release of proinflammatory mediators.

Microcirculatory Effects of Photodynamic Therapy for Tumors

Much of what is known about photosensitization effects on microcirculation comes from studies related to photodynamic therapy of tumors. Photodynamic therapy of tumors will be covered more fully in subsequent chapters. Nonetheless, a brief synopsis of the vascular effects is appropriate here to allow comparison with other results in the vasculature.[15]

It is now well established that, depending on the photosensitizer used and the route of administration, the effects on tumors can be predominantly at the cellular level, on the vasculature, or on both. Observations made on tumor microcirculation must be interpreted carefully, because it differs morphologically and functionally from normal microcirculation. Tumor microcirculation is characterized by spatial and temporal heterogeneity in structure and function. This includes increased leakiness, incomplete basement membranes, and overexpression of glycoproteins. There is an increased proliferative rate of endothelial cells. Tumors can have areas that are relatively hypoxic, such that its microcirculation is similar in many ways to embryonic vascular beds.

Photodynamic therapy of tumor microvasculature damages sensitive sites on endothelial cells, largely their surface membranes or mitochondria. Tight junctions between the cells separate, exposing basement membrane. The exposed basement membrane serves as a thrombogenic site causing platelet aggregation, release of vasoactive substances such as thromboxane and the leukotrienes, and leukocyte adhesion leading to increased vascular permeability and vessel constriction. Mediators such as VEGF/VPF and EDRF/NO are thought to be important intermediates, as are LDL receptors.

Because photodynamic therapy is an oxygen-dependent process, typically thought to occur via a Type II singlet oxygen mechanism, it is often combined with hyperbaric oxygen or hyperthermia to augment tumor destruction, particularly in hypoxic areas of the tumor.

Effects of Hypoxia on the Microcirculation

In the next section, we will briefly discuss the acute and chronic effects of hypoxia (i.e., reduced oxygen levels) on microcirculation. As indicated previously, the efficacy of photosensitizers in the treatment of cancer may be limited in part by the development of tissue hypoxia within rapidly growing tumors.

In contrast to ischemia–reperfusion, relatively few studies examined the effect of hypoxia on microvascular function, despite clinical evidence of a microvascular inflammatory response in this setting. For example, systemic hypoxia occurs in people at high altitudes and may result in high-altitude cerebral edema (HACE). Although the underlying cause of this serious condition is not yet known, microcirculatory alterations were proposed to play a major role. For example, increased leukocyte–endothelial interactions are frequently associated with the pathological features of environmental hypoxia.[16,17]

A growing body of evidence implicates ROS as an underlying cause of hypoxia-induced microvascular inflammatory responses. As described above, the initiating cause of microvascular injury following I/R is generation of reactive oxygen species (ROS) upon reintroduction of oxygen after prolonged ischemia.[11,12] It is now known that a reduction in the PO_2 of the culture media increases ROS levels within isolated endothelial cells, cardiomyocytes, and hepatocytes.[18,19] The view that hypoxia promotes ROS generation is also consistent with studies showing reduced antioxidant levels in cultured endothelial cells,[20] as well as in the liver *in vivo*.[21] Recent observations implicate alterations in the electron transport system within mitochondria as the major site of ROS formation during hypoxia.[22]

Under *in vivo* conditions, an acute reduction of the inspired PO_2 initiates a rapid microvascular response characterized by increased leukocyte–endothelial interactions,[23] followed by leukocyte emigration into the interstitium and increased vascular permeability.[24] An alteration in the balance between

ROS and NO appears to play a critical role in this phenomenon.[25] In support, microvascular ROS levels (as assessed using oxidant-sensitive fluorescent probes) increased during hypoxia.[26] Antioxidants attenuated the hypoxia-induced increase in ROS formation, leukocyte adherence, vascular permeability, and leukocyte emigration. Interventions designed to increase tissue levels of NO also attenuated these microvascular inflammatory responses during hypoxia.[23]

A potential consequence of oxidant stress during hypoxia due to alterations in the ROS/NO balance is local formation of lipid inflammatory mediators, such as platelet activating factor and leukotriene B_4.[27] These mediators promote leukocyte and platelet adhesiveness to venular endothelium and may contribute to enhanced thrombosis reported during hypoxia.[28,29]

If hypoxia is maintained, the initial microvascular responses described previously eventually resolve. In the mesenteric and cremasteric microcirculations of rats exposed to a hypoxic environment for 3 weeks, measurements of leukocyte adherence, leukocyte emigration, and vascular permeability are not significantly different from values obtained in animals maintained in a normal oxygen environment (i.e., normoxic animals). The mechanisms responsible for the acclimatization of vascular endothelial function during sustained hypoxia are not yet clear. However, it is well known that chronic hypoxia leads to an increase in red blood cell mass in response to increased erythropoietin secretion. It is possible that the elevated hemoglobin concentration resulting from the increased red blood cells could improve oxygen delivery to tissues and attenuate the severity of hypoxia at the venular level. However, systemic hypoxia did not result in leukocyte adherence to mesenteric venules of acclimatized rats, even after the red blood cell concentration was reduced to normal values.[23]

Because the initial microvascular inflammatory response to hypoxia is dependent on an increase in the ROS/NO balance, microvascular acclimatization may be associated with a restoration of this balance. Two observations support this possibility: microvascular ROS levels in the mesenteric microcirculation do not increase when acclimatized rats are exposed to hypoxia; and inhibition of inducible NO synthase (iNOS) results in an increase in leukocyte rolling and adherence, and in ROS generation, during hypoxia in acclimatized rats.

These effects of iNOS inhibition suggest that the microvascular acclimatization involves upregulation of iNOS. Under normal conditions, NO is formed by eNOS, an enzyme that is constitutively expressed in endothelial cells. However, the inducible form can be expressed in various situations, and it is capable of generating higher amounts of NO than eNOS. It is possible, therefore, that the rate of NO formation in the vascular endothelium of acclimatized rats is markedly increased over normal levels. Because NO is an anti-inflammatory agent, increased microvascular NO levels could inhibit leukocyte–endothelial interactions and may contribute to acclimatization of vascular endothelial function during sustained hypoxia.

The upregulation of iNOS in acclimatized animals may be secondary to induction of hypoxia-inducible factor-1 (HIF-1). Recent studies showed that increased intracellular ROS generation promotes HIF-1 expression.[30,31] HIF-1 activates gene transcription and results in multiple cellular changes, including expression of iNOS, vascular endothelial growth factor (VEGF), and heme oxygenase-1. The latter two factors may also contribute to microvascular acclimatization to hypoxia. Interestingly, VEGF is an important mediator of angiogenesis and appears to play a major role in sustaining tumor growth. It is possible that the increased ROS generation may participate in initiating the events that eventually lead to acclimatization of the vascular endothelium during sustained hypoxia. Further knowledge of the mechanisms underlying microvascular acclimatization to hypoxia may potentially be relevant to studies of the efficacy of photosensitizers in limiting tumor growth.

In summary, exposure to environmental hypoxia promotes increased leukocyte–endothelial interactions characterized by increased leukocyte rolling and adherence to the vascular endothelium, followed by leukocyte emigration and increased vascular permeability. This response is observed in several microcirculatory beds, suggesting that it represents a generalized response to systemic hypoxia. After 3 weeks of continuous hypoxic exposure, the microvascular inflammatory response resolves, and the vascular endothelium is resistant to even lower PO_2 levels. The initial microvascular response to hypoxia is

characterized by an increase in the ROS/NO balance, while the acclimatization process features a restoration of this balance, in part due to upregulation of iNOS.

Photodynamic Therapy for Macular Degeneration

Roughly 1.7 million Americans are afflicted with age-related macular degeneration (AMD). Although the form of the disease known as wet AMD accounts for only about 10% of these cases, it accounts for 90% of blindness from AMD. Approximately 100,000 people in the United States are blind from the disease. The major cause of visual problems in wet AMD is choroidal neovascularization, growth of new blood vessels in the choroidal layer beneath the macular region of the retina.[32]

Photodynamic occlusion of vessels was investigated in the 1980s using various photosensitizers, including Rose Bengal and aluminum sulfonated phthalocyanine, but the main focus gravitated to benzoporphyrin derivatives by the 1990s.[33,34] One such lipophilic derivative known as Vertoporfin with an absorption peak at 690 nm underwent a clinical trial involving more than 400 patients, with promising results.[35] In a single case report using the same photosensitizer, fluorescein angiography, 2 weeks posttreatment, revealed a 60% decrease in the area of neovascularization with evidence of endothelial cell degeneration, platelet aggregation, and thrombus formation. Macrophages were sometimes seen in the treated area. However, at 3 weeks posttreatment, the fluorescein leakage area returned to the same size as before treatment.[36] The changes induced by treatment are not permanent. In the larger case study, patients had an average of five treatments over the course of 24 months, and it was only during the last 12 months of the regimen that visual acuity began to differ significantly from sham-treated controls. In April 2000, the FDA (US) approved Vertoporfin for treatment of choroidal neovascularization from AMD,[37] and in August 2001, the approval was extended to include choroidal neovascularization from pathologic myopia and from presumed ocular histoplasmosis.[38]

143.3 Photosensitization of the Macrocirculation

Heart disease was the leading cause of death in the United States in 1999, and the preliminary data for 2000 are similar,[39] with atherosclerotic changes contributing to many of the categories included in this broad grouping. In the past, therapeutic protocols were aimed at enlarging narrowed vessels using interventions such as balloon angioplasty of stenotic (narrowed) regions of arteries. Restenosis often occurred, which limited the efficacy of such procedures and led to intensive efforts to minimize this process. An alternate treatment involves grafting a segment of vein to replace affected arterial segments. These grafts also show structural changes that often lead to their failure. Recent studies focused on arterial plaque development, aiming to intervene before stenosis recurs. Photosensitizers used in photoangioplasty are promising candidates for treatment of atherosclerosis and prevention of restenosis.[40]

Photodynamic Therapy for Vascular Plaques

Interest recently focused on so-called vulnerable plaque as an initiator of serious cardiac and vascular events. These plaques begin as cholesterol is deposited in fatty streaks within arterial walls. The intima, the inner layer of the arterial wall, thickens, and monocytes infiltrate, becoming tissue macrophages. In vulnerable plaque, macrophages release lytic enzymes, including colagenase and elastase.[41] These enzymes degrade the fibrous cap separating the plaque from the arterial lumen that can then rupture, exposing thrombogenic connective tissue and lipids. This event initiates a cascade of platelet and clotting factor activations producing intravascular thrombosis and occlusion. Such vulnerable plaque can contribute to myocardial ischemia, unstable angina, and myocardial infarction.[42]

Vulnerable plaque is often not easily detectable by angiography, because the luminal area may not be compromised until late in the disease process. Recently, fluorescent photosensitizers were used to localize vulnerable plaque.[43] Specific targeting of some photosensitizers to macrophages of vulnerable plaque may depend on scavenger receptors.[44,45] Photosensitizers were also used to treat vulnerable plaque and are

particularly valuable, because they are able to reduce the number of resident macrophages. Using Lu-Tex, a water-soluble, expanded porphyrin that absorbs at 732 nm, a wavelength in the red end of the visible spectrum with good tissue penetration, Hayase et al.[42] demonstrated a small but statistically significant reduction in plaque volume but a dramatic reduction in macrophages within the intima and the media. Lu-Tex was previously shown to localize within macrophages in plaque and to cause plaque regression over a period of days following endovascular illumination.

Photodynamic Therapy to Create Nonthrombogenic Vessel Grafts

Coronary artery bypass surgery, as well as bypass of other arteries, is often accomplished using a vein graft, most often, the saphenous vein. The major complication is occlusion of the graft, typically as a result of intimal hyperplasia.[46] Within 2 months of implantation, the transplanted vein becomes little more than a "stiff, fibrous-tissue conduit." Thickening of the intima of veins implanted into the arterial system was recognized since the early 1900s.[47] It is now recognized that vein grafts demonstrate rapid infiltration of inflammatory cells and development of a fibrous coating. As in arterial plaques, there is infiltration of macrophages. Within a month, there is subendothelial proliferation of smooth muscle cells and fibroblasts, producing intimal thickening. This is followed by gradual loss of smooth muscle cells and their replacement by fibrous tissue, as elastic tissue disappears.

In vitro treatment of excised segments of vein with chloroaluminum sulfonated phthalocyanine and light prior to their implantation as arterial grafts significantly reduced the processes that lead to graft occlusion.[46] When compared to untreated control arterial grafts, intimal and medial cross-sectional areas were reduced in the treated grafts. However, in this study, there was no difference in the intimal hyperplasia at the junctions between the carotid artery and its venous graft. This may reflect proliferation of untreated arterial cells adjacent to the graft and may indicate a problem associated with the *in vitro* graft treatment used here.

The photosensitizer Lu-Tex was shown to localize in smooth muscle cells of vein grafts and to produce apoptotic death of these cells following illumination. Intimal thickening was significantly reduced by treatment but was strongly dependent on the interval between graft implantation and treatment — 4 weeks was effective, while 12 weeks was not.[48] The authors interpreted this dependence to indicate an important role for macrophages in the process, because macrophages are strongly active at 4 weeks. Prevention of monocyte recruitment (the precursors of tissue macrophages) may prevent much of the venous remodeling that normally occurs in grafts.[49]

Similarly encouraging results were obtained in a rat heart transplant model. A second heart was transplanted into the abdomen to study graft coronary artery disease. Photosensitizer and light treatment significantly reduced the percent of vessels affected and reduced intimal hyperplasia in those that were.[50]

Photodynamic Inhibition of Restenosis

Restenosis following procedures such as balloon angioplasty was reported to occur in 30 to 50% of cases within 6 months.[51] Intimal hyperplasia from smooth muscle cell proliferation is a major cause of restenosis, but there are contributions from changes in elastic recoil, extracellular matrix, and constrictive arterial remodeling. The use of stents has obviated the problems associated with changes in elastic recoil but may actually augment intimal hyperplasia.[52,53]

Photosensitizers and light were shown to kill human vein endothelial cells and cultured vascular smooth muscle cells via apoptosis *in vitro*. Treatment of extracellular matrix results in reduced attachment of smooth muscle cells[54] and cross-linking of collagen that inhibits smooth muscle cell migration.[55]

In normal arteries, photosensitizers and light denude the endothelial cell lining and reduce smooth muscle cell numbers without generating an inflammatory response.[56,57] Endothelial repopulation occurs with time after treatment, and there are no problems with late thrombotic occlusion of treated vessels, as there are with radiation treatments to prevent restenosis.[58] Importantly, the mechanical responses of normal arteries are not altered by photosensitizers and light treatment.[59]

Reduction of arterial intimal hyperplasia following balloon injury was demonstrated a decade ago using chloraluminum sulfonated phthalocyanine.[60] A variety of photosensitizers are now known to produce similar effects, including Photofrin, texaphyrins, and the porphyrin precursor that is converted to an active form *in vivo*, 5-aminolevulinic acid. As seen in normal arteries, endothelial denudation occurs, but there is rapid repopulation. Medial smooth muscle cell repopulation is relatively delayed,[57,61] Injured pig femoral arteries treated with Photofrin and light showed a reduced media/intima thickness ratio 3 weeks after treatment compared to injured, untreated controls.[62] Another study using 5-ALA in pig arteries found improvement that could be attributed to inhibition of constrictive arterial remodeling in the treated arteries. Limited clinical results are promising,[51] but the number of patients treated is still small.

143.4 Cardiac Effects of Photosensitization

It is well established that not only is the ischemic myocardium susceptible to arrhythmias, the myocardium that is reperfused following ischemia (e.g., after successful angioplasty) is also susceptible,[63–65] Ventricular tachycardia, accelerated idioventricular rhythms, ventricular premature beats, and rate-dependent fibrillation occur within minutes of reperfusion after an ischemic episode. In a series of studies using isolated, aerobically perfused rat hearts, Hearse and colleagues[66–68] demonstrated that photosensitization leads to rapid development of electrocardiographic (ECG) abnormalities and arrhythmias similar to those that occur during reperfusion of the ischemic myocardium. To induce photosensitization, the perfusion fluid contained rose bengal, and the heart was uniformly illuminated with green light via 200 fiber optic cables placed in a manner that illuminated the entire heart surface. The initial ECG changes, induced within 12 sec of photosensitization onset, consisted of inversion of the terminal portion of the T wave and of an increase in the Q–T interval indicative of increased duration of the ventricular action potential. This was followed by production of ventricular premature beats (within 2 min), ventricular tachycardia (within 3 min), and complete atrioventricular block (within 6 min). Light intensity and rose bengal concentration affected the time to onset and severity of the arrhythmias. Arrhythmia production was attenuated by adding histidine (a $^1O_2$ quencher) to the perfusion fluid, but other antioxidants such as ascorbate, dimethylthiourea, glutathione, superoxide dismutase, and methionine did not provide protection. The ability of a $^1O_2$ quencher, but not other antioxidants, to protect the heart against photosensitization-induced arrhythmias implicates $^1O_2$ as the mediator of the electrophysiological events. This is of interest, because there is now a variety of evidence indicating that $^1O_2$ plays a role in cardiac ischemic–reperfusion (I/R) injury. For example, Kukreja et al.[69] demonstrated that histidine provided better protection against cardiac I/R injury than did a mixture of superoxide dismutase, catalase, and mannitol. Zhai and Ashraf[70] demonstrated that $^1O_2$ is detectable in postischemic reperfused isolated rat hearts. More recently, Lee et al.[71] demonstrated that improvement in functional recovery of ischemic rat hearts correlated with the effectiveness with which agents quenched $^1O_2$.

Photosensitization studies using isolated cardiac tissue (muscle fibers or the isolated single cell) provided insights into the mechanisms responsible for the ECG changes and arrhythmia production discussed above. Increased and decreased duration of the cardiac action potential were reported,[72–74] and duration and intensity of photosensitization can affect the outcome. Continuous, low-level photosensitization first prolongs the action potential and then shortens it.[72,73] However, brief (<10 s), high-intensity photosensitization can shorten the action potential without first prolonging it.[75] Accordingly, regional differences in the level of $^1O_2$ exposure could produce refractory period inhomogeneity; a condition that plays an important role in production of reentrant arrhythmias. These arrhythmias are also favored by a decrease in action potential duration. Shortening of the action potential favors reentrant conduction by reducing the length of tissue occupied by the action potential (a product of conduction velocity and action potential duration). It was demonstrated that reperfusion of ischemic myocardial tissue can transiently produce conditions that favor reentrant conduction.[63] In addition to modifying action potential duration, photosensitization can initiate abnormal spontaneous electrical activity and aftercontractions related to production of early and delayed afterdepolarizations.[74,76] Early afterdepolarizations

(EADs) occur during the plateau or rapid repolarization phase of the action potential, and these can lead to tachycardias independent of reentrant conduction. It was reported that about 75% of tachycardias initiated early during reperfusion are initiated by a nonreentrant mechanism.[65] It is also well established that fibrillation can be initiated by EADs. By comparison, delayed afterdepolarizations (DADs) occur following action potential repolarization, and these can trigger premature action potentials and contractions.

Photosensitization effects on cardiac ionic currents provided insights into mechanisms responsible for alterations in action potential waveform and conduction in different cardiac regions. A wide variety of cardiac voltage-gated ionic currents are suppressed or completely blocked by photosensitization.[72,73,77–80] These include the sodium current (I_{Na}), L-type calcium current (I_{CaL}), transient outward potassium current (I_{to}), slow-activating delayed rectifier potassium current (I_{Ks}), and inward rectifier potassium current (I_{K1}). Suppression of I_{Na} slows action potential conduction in atrial and ventricular tissue and enhances the probability of production of reentrant arrhythmias. Suppression of I_{CaL} would act to decrease action potential duration and reduce the probability of EAD production related to the so-called calcium window current. It would also suppress production of the calcium-dependent action potential in AV-node cells and produce AV-block. Suppression of I_{to} and I_{Ks} acts to prolong the action potential and enhance the probability of EAD production. Suppression of I_{K1} depolarizes the resting potential of atrial and ventricular cells, an event that occurs late during continuous photosensitization.

Calcium overload is a ubiquitous phenomena associated with cellular oxidant stress, including photosensitization-induced stress. Ver Donck et al.[81] were the first to demonstrate that photosensitization causes calcium overload-induced hypercontracture of the isolated cardiac cell. Subsequent studies provided evidence that a variety of mechanisms play a role in photosensitization-induced calcium overload. These include inhibition of the sodium-potassium pump,[82] the sodium–calcium exchanger,[83] and calcium uptake by the sarcoplasmic reticulum.[84] Inhibition of the sodium–potassium pump leads to increased intracellular sodium and subsequent reduction of calcium efflux via the sodium–calcium exchanger. Suppression of sodium–calcium exchange also reduces calcium efflux. Inhibition of calcium uptake by the sarcoplasmic reticulum increases free-ionized intracellular calcium concentration. Calcium influx also plays an important role in photosensitization-induced calcium overload. Photosensitization increases membrane permeability and produces an associated leak current.[85,86] The membrane conductance related to this leak current increases with time during photosensitization, does not require a rise in intracellular calcium for its activation, and provides a path for sodium and calcium influx and potassium efflux. Calcium influx via the membrane permeability pathway created by photosensitization produces a calcium-dependent hypercontracture of the isolated cardiac cell at membrane conductances indicative of an intact membrane.[87] It also plays a role in cell killing.[88,89]

It is well established that calcium overload can be arrhythmogenic by enhancing two calcium-sensitive, inward currents that play a role in DAD production. One is a nonselective cation current, and the other is the sodium–calcium exchange current. Matsuura and Shattock[73,78] presented evidence that photosensitization enhances both of these currents. In the mammalian cardiac cell, photosensitization-induced calcium overload produces oscillatory release of calcium from the sarcoplasmic reticulum that is arrhythmogenic via production of EADs.[76] This finding indicates that inward current via the sodium–calcium exchanger, rather than the L-type calcium channel, accounts for photosensitization-induced EAD production.

143.5 Other Photosensitization Effects in the Cardiovascular System

Sterilization of Blood and Blood Products

The risk of disease transmission through blood transfusion improved considerably thanks to donor counseling and much improved blood-screening procedures. Nonetheless, a risk remains that is thought to be primarily associated with a "window period," the interval of time between infection and development of detectable antigen, antibody, or nucleic acid.[90] Photosensitization was shown to inactivate a

broad range of pathogens. Its selectivity relative to photosensitization of normal blood components is the basis for the treatment of whole blood and blood products, such as plasma, platelets, or pack cells, by this means.

Phenothiazines, such as methylene blue, were used as virucidal agents for more than 70 years, and they were investigated as agents to prevent the transfusion-mediated spread of hepatitis during the Korean War.[9] In plasma, 5 to 6 log virus inactivation can be obtained. Further treatment inactivates clotting factors, particularly fibrinogen and C1 inactivator.

Successful treatment of packed red cells can be more difficult than plasma treatment because of the need to inactivate extracellular and intracellular viruses. The choice of photosensitizer is critical in this regard. For example, uncharged phenothiazines are more effective at inactivating intracellular virus than are charged species.[91] Other promising candidates include merocyanine-540, tetrasulfonated aluminum phthalocyanine,[92] and hypericin.[93] Manipulation of the composition and pH of the medium can shift the selectivity of the method for virus versus red cells. Strong treatment can damage red cell membranes, inducing potassium leakage and enhanced hemolysis.

Another interesting possibility in blood product treatment stems from the high sensitivity of T cells to photosensitized inactivation. T cells were shown to be more sensitive than viruses using phenothiazines as photosensitizers,[94] and this may provide a means by which to inhibit transfusion-associated graft-versus-host disease, because T cells play an important role in this disease process.

Inhibition of Clotting by $^1O_2$

Treatment of blood with photosensitizers and light *in vitro* does not produce the same effect as treatment *in vivo*. Due to the inhibition of clotting factors, treatment of blood inhibits clotting,[95–98] but *in vivo* treatment may produce thrombosis and vessel occlusion. The difference *in vivo* is the simultaneous treatment of the vasculature along with the blood. Effects on the vasculature, as described above, can initiate microvascular responses that lead to thrombogenic foci. This effect was often observed in studies related to photodynamic therapy for malignancies. With careful selection of the photosensitizer, its concentration, and its illumination intensity, thrombosis may be avoided, as discussed previously.

143.6 Summary and Conclusions

Clinical applications of photosensitization hold considerable promise. Unlike alternative therapies, such as ionizing radiation, photodynamic therapy can be repeated with no known limits. It poses considerably less risk to administering personnel. The photon energy is not sufficient to produce DNA damage directly, and most photosensitizers in use do not penetrate to the nucleus or interact with nuclear DNA, so mutation is not as significant a concern. With the current protocols, an apoptotic response appears to be dominant, with no inflammatory response at the treatment site.

References

1. Coohill, T.P. and Valenzeno, D.P., Eds., *Photobiology for the 21st Century*, Valdenmar Publ. Co., Overland Park, KS, 2001.
2. Raab, O. Uber die Wirkung fluoreszierender Stoffe auf Infusorien, *Z. Biol.*, 39, 524, 1900.
3. Von Tappeiner, H., Uber die Wirkung fluoreszierender Stoffe auf Infusorien nach Versuchen von O. Raab, *Munch. Med. Wochenschr.*, 47, 5, 1900.
4. Fisher, W.G., Partridge, W.P., Jr., Dees, E., and Wachter, E.A., Simultaneous two-photon activation of type-I photodynamic therapy agents, *Photochem. Photobiol.*, 66, 141, 1997.
5. Selbo, P.K., Sivam, G., Fodstad, O., Sandvig, K., and Berg, K., *In vivo* documentation of photochemical internalization, a novel approach to site specific cancer therapy, *Int. J. Cancer*, 92, 761, 2001.

6. Ackroyd, R., Kelty, C., Brown, N., and Reed, M., The history of photodetection and photodynamic therapy, *Photochem. Photobiol.*, 74, 656, 2001.
7. Peravaiz, S., Reactive oxygen-dependent production of novel photochemotherapeutic agents, *FASEB J.*, 15, 612, 2001.
8. Shimakura, A., Kamanaka, T., Ikeda, T., Kondo, K., Suzuki, Y., and Umemura, K., Neutrophil elastase inhibition reduces cerebral ischemic damage in the middle cerebral artery occlusion, *Brain Res.*, 858, 55, 2000.
9. Wagner, S.J., Virus inactivation in blood components by photoactive phenothiazine dyes, *Transfusion Med. Rev.*, 16, 61, 2002.
10. Grisham, M.B., Granger, D.N., and Lefer, D.J., Modulation of leukocyte-endothelial interactions by reactive metabolites of oxygen and nitrogen: relevance to ischemic heart disease, *Free Radic. Biol. Med.*, 25, 404, 1998.
11. Granger, D.N., Grisham, M.B., Levendag, P.C., and Seurruys, P.W., Mechanisms of microvascular injury, in *Physiology of the Gastrointestinal Tract*, 3rd ed., Johnson, L.R., Ed., Raven Press, New York, 1994, p. 1693.
12. Gute D.C., Ishida, T., Yarimizu, K., and Korthuis, R.J., Inflammatory responses to ischemia and reperfusion in skeletal muscle, *Mol. Cell. Biochem.*, 179, 169, 1998.
13. Carden, D.L. and Granger, D.N., Pathophysiology of ischaemia-reperfusion injury, *J. Pathol.*, 190, 255, 2000.
14. Lefer D.J. and Granger D.N., Oxidative stress and cardiac disease, *Am. J. Med.*, 109, 315, 2000.
15. Krammer, B., Vascular effects of photodynamic therapy, *Anticancer Res.*, 21, 4271, 2001.
16. Siegel, J. H., Physiologic, metabolic and mediator responses in post trauma ARDS and sepsis: is oxygen debt a critical initiating factor?, *J. Physiol. Pharmacol.*, 48, 559, 1997.
17. Hultgren, R.N., High altitude pulmonary edema: hemodynamic aspects, *Int. J. Sports Med.*, 18, 20, 1997.
18. Duranteau, J., Chandel, N.S., Kulisz, A., Shao, Z., and Schumacker, P.T., Intracellular signaling by reactive oxygen species during hypoxia in cardiomyocytes, *J. Biol. Chem.*, 273, 11619, 1998.
19. Park, Y., Kanekal, S., and Kehrer, J.P., Oxidative changes in hypoxic rat heart. *Am. J. Physiol.*, 260, H1395, 1991.
20. Plateel M., Dehouck, M.P., Torpier, G., Cecchelli, R., and Teissier, E., Hypoxia increases the susceptibility to oxidant stress of the blood-brain barrier endothelial cell monolayer, *J. Neurochem.*, 65, 2138, 1995.
21. El-Bassiouni, E.A., Abo-Ollo, M.M., Helmy, M.H., Ismail, S., and Ramadan, M.I., Changes in the defense against free radicals in the liver and plasma of the dog during hypoxia and/or halothane anaesthesia, *Toxicology*, 128, 25, 1998.
22. Chandel, N.S. and Schumacker, P.T., Cellular oxygen sensing by mitochondria: old questions, new insights, *J. Appl. Physiol.*, 88, 1880, 2000.
23. Wood, J.G., Mattioli, L.F., and Gonzalez, N.C., Hypoxia causes leukocyte adherence to mesenteric venules in nonacclimatized, but not in acclimatized, rats, *J. Appl. Physiol.*, 87, 873, 1999.
24. Wood, J.G., Johnson, J.S., Mattioli, L.F., and Gonzalez, N.C., Systemic hypoxia increases leukocyte emigration and vascular permeability in conscious rats, *J. Appl. Physiol.*, 89, 1561, 2000.
25. Steiner D.R.S., Gonzalez, N.C. and Wood, J.G. Interaction between reactive oxygen species and nitric oxide in the microvascular response to systemic hypoxia, *J. Appl. Physiol.*, 93, 1411, 2002.
26. Wood, J.G., Johnson, J.S., Mattioli, L.F., and Gonzalez, N.C., Systemic hypoxia promotes leukocyte-endothelial adherence via reactive oxidant generation, *J. Appl. Physiol.*, 87, 1734, 1999.
27. Steiner D.R., Gonzalez, N.C., and Wood J.G. Leukotriene B_4 promotes reactive oxidant generation and leukocyte adherence during acute hypoxia, *J. Appl. Physiol.*, 91, 1160, 2001.
28. Brundrett, G., Sickness at high altitude: a literature review, *J.R. Soc. Health*, 122, 14, 2002.
29. Yan, S.F., Mackman, N., Kisiel, W., Stern, D.M., and Pinsky, D.,J. Hypoxia/hypoxemia-induced activation of the procoagulant pathways and the pathogenesis of ischemia-associated thrombosis, *Arterioscler. Thromb. Vasc. Biol.*, 19, 2029, 1999.

30. Choi, A.M. and Alam, J., Heme oxygenase-1: function, regulation, and implication of a novel stress-inducible protein in oxidant-induced lung injury, *Am. J. Respir. Cell Mol. Biol.*, 15, 9, 1996.
31. Wang, G.L., Jiang, B.H., and Semenze, G.L., Effect of altered redox states on expression of DNA-binding activity of hypoxia-inducible factor 1, *Biochem. Biophys. Res. Commun.*, 21, 550, 1995.
32. Varmus, H., Age-related macular degeneartion: status of research, *National Eye Institute of the U.S. National Institutes of Health*, http://www.nei.nih.gov/news/statements/varmus.htm, 1997.
33. Lin, S.C., Lin, C.P., Feld, J.R., Duker, J.S., and Puliafito, C.A., The photodynamic occlusion of choroidal vessels using benzoporphyrin derivative, *Curr. Eye Res.*, 13, 513, 1994.
34. Kramer, M., Miller, J.W., Michaud, N., Moulton, R.S., Hasan, T., Flotte, T.J., and Gragoudas, E.S., Liposomal benzoporphyrin derivative verteporfin photodynamic therapy. Selective treatment of choroidal neovascularization in monkeys, *Ophthalmology*, 103, 427, 1996.
35. Bressler, N.M., Verteporfin therapy of subfoveal choroidal neovascularization in age-related macular degeneration: two-year results of a randomized clinical trial including lesions with occult with no classic choroidal neovascularization-verteporfin in photodynamic therapy report 2, *Am. J. Ophthalmol.*, 133, 168, 2002.
36. Ghazi, N.G., Clinicopathologic studies of age-related macular degeneration with classic subfoveal choroidal neovascularization treated with photodynamic therapy, *Retina*, 21, 478, 2001.
37. U.S. Deptartment of Health and Human Services, FDA approves treatment for wet macular degeneration. *HHS News*, http://www.fda.gov/bbs/topics/NEWS/NEW00724.html, 2000.
38. U.S. Food and Drug Administration, Center for Drug Evaluation and Research. CDER Report to the Nation: 2001. *CDER Report*: http://www.fda.gov/cder/reports/rtn/2001/rtn2001–1.htm, 2002.
39. Minino, A.M. and Smith, B.S., Deaths: Preliminary Data for 2000. *Nat'l Vital Stats. Repts.*, 49, 12, 1, 2001.
40. Rockson, S.G., Lorenz, D.P., Cheong, W.-F., and Woodburn, K.W., Photoangioplasty: an emerging clinical cardiovascular role for photodynamic therapy, *Circulation*, 102, 592, 2000.
41. Christov, A., Dai, E., Drangova, M., Liu, L., Abela, G.S., Nash, P., McFadden, G., and Lucas, A., Optical detection of triggered artherosclerotic plaque disruption by fluourescence emission analysis, *Photochem. Photobiol.*, 72, 242, 2000.
42. Hayase, M., Woodburn, K.W., Perlroth, J., Miller, R.A., Baumgardner, W., Yock, P.G., and Yeung, A., Photoangioplasty with local motexafin lutetium delivery reduces macrophages in a rabbit post-balloon injury model, *Cardiovasc. Res.*, 49, 449, 2001.
43. Machida, M., Kameyama, K., Asano, G., and Kumazaki, T., Fluorescence spectroscopic and histochemical analysis using hematoporphyrin as a microenvironmental probe for atherosclerotic change in the human aorta, *Lab. Invest.*, 79, 733, 1999.
44. DeVries, H.E., Moor, A.C., Dubbelman, T.M.A.R., van Berkel, T.J.C., and Kuiper, J., Oxidized low-density lipoprotein as a delivery system for photosensitizers: implications for photodynamic therapy of atherosclerosis, *J. Pharm. Exp. Ther.*, 289, 528, 1999.
45. Hamblin, M.R., Tawakol, A., Ahmadi, A., Zahra, T., Syed, S., Ortel, B., Fischman, A., and Miller, J., Scavenger receptor-targeted photodynamic therapy for diagnosis and treatment of vulnerable atherosclerotic plaques, *Abstr. Amer. Soc. Photobiol.*, 31, 2002.
46. LaMuraglia, G.M., Klyachkin, M.L., Adili, F., and Abbott, W.M., Photodynamic therapy of vein grafts: suppression of intimal hyperplasia of the vein graft but not the anastomosis, *J. Vasc. Surg.*, 21, 882, 1995.
47. Carrel, A. and Guthrie, C.C., Results of biterminal transplantation of veins, *Amer. J. Med. Sci.*, 132, 415, 1906.
48. Yamaguchi, A., Woodburn, K.W., Hayase, M., and Robbins, R.C., Reduction of vein graft disease using photodynamic therapy with motexafin lutetium in a rodent isograft model, *Circulation*, 102[suppl. III], III–275, 2000.
49. Ross, R., Atherosclerosis: an inflammatory disease, *N. Engl. J. Med,* 340,115 1999.

50. Yamaguchi, A., Woodburn, K.W., Hayase, M., Hoyt, G., and Robbins, R.C., Photodynamic therapy with motexafin lutetium (Lu-Tex) reduces experimental graft coronary artery disease, *Transplant*, 71, 1526, 2001.
51. Mansfield, R., Bown, S., and McEwan, J., Photodynamic therapy: shedding light on restenosis. *Heart*, 86, 612, 2001.
52. Dussaillant, G.R., Small stent size and intimal hyperplasia contribute to restenosis: a volumetric intravascular ultrasound analysis, *J. Am. Coll. Cardiol.,* 26, 720, 1995.
53. Post, M.J., Borst, C., and Kuntz, R.E., The relative importance of arterial remodeling compared with intimal hyperplasia in lumen renarrowing after balloon angioplasty. A study in the normal rabbit and the hypercholesterolimic Yucatan micropig, *Circulation*, 89, 2816, 1994.
54. Adili, F., Statius van Eps, R.G., Karp, S.J., Watkins, M.T., and LaMuraglia, G.M., Differential modulation of vascular endothelial and smooth muscle cell function by photodynamic therapy of extracellular matrix: novel insights into radical-mediated prevention of intimal hyperplasia, *J. Vasc. Surg.*, 23, 698, 1996.
55. Overhaus, M., Heckenkamp, J., Kossodo, S., Leszczynski, D., and LaMuraglia, G.M., Photodynamic therapy generates a matrix barrier to invasive vascular cell migration, *Circ. Res.*, 86, 334, 2000.
56. Grant, W.E., Speight, P.M., MacRobert, A.J., Hopper, A.J., and Bown, S.G., Photodynamic therapy of normal rat arteries after photosensitization using disulphonated aluminium phthalocyanine and 5-aminolaevulinic acid, *Br. J. Cancer*, 70, 72, 1994.
57. Nyamekye, I., Anglin, S., McEwan, J., MacRobert, A., Bown, S., and Bishop, C., Photodynamic therapy of normal and balloon-injured rat carotid arteries using 5-amino-levulinic acid, *Circulation*, 91, 417, 1995.
58. Costa, M.A., Sabat, M., van der Giessen, W.J., Kay, I.P., Cervinka, P., Ligthart, J. M., Serrano, P., Coen, V.L., Levendag, P.C., and Seurruys, P.W., Late coronary occlusion after intracoronary brachytherapy, *Circulation*, 100, 789, 1999.
59. Grant, W.E., Buonaccorsi, G., Speight, P.M., MacRobert, A.J., Hopper, C., and Bown, S.G., The effect of photodynamic therapy on the mechanical integrity of normal rabbit carotid arteries, *Laryngoscope*, 105, 867, 1995.
60. Ortu, P., LaMuraglia, G.M., Roberts, W.G., Flotte, T.,and Hasan, T., Photodynamic therapy of arteries. A novel approach for treatment of experimental intimal hyperplasia, *Circulation*, 85, 1189, 1992.
61. LaMuraglia, G.M., ChandraSekar, N.R., Flotte, T.J., Abbott, W.M., Michaud, N., and Hasan, T., Photodynamic therapy inhibition of experimental intimal hyperplasia: acute and chronic effects, *J. Vasc. Surg.*, 19, 321, 1994.
62. Gonschior, P., Gerheuser, F., Fleuchaus, M., Huehns, T.Y., Goetz, A.E., Welsch, U., Sroka, R., Dellian, M., Lehr, H.A., and Hofling, B., Local photodynamic therapy reduces tissue hyperplasia in an experimental restenosis model, *Photochem. Photobiol.*, 64, 758, 1996.
63. Murdock, D.K., Loeb, J.M., Euler, D.E., and Randall, W.C., Electrophysiology of coronary reperfusion, *Circulation*, 61, 175, 1980.
64. Manning, A.S. and Hearse, D.J. Reperfusion-induced arrhythmias: mechanisms of prevention, *J. Mol. Cell. Cardiol.*, 16, 497, 1984.
65. Pogwizd, S.M. and Corr, P.B., Electrophysiologic mechanisms underlying arrhythmias due to reperfusion of ischemic myocardium, *Circulation*, 76, 404, 1987.
66. Hearse, D.J., Kusama, Y., and Bernier, M., Rapid electrophysiological changes leading to arrhythmias in the aerobic rat heart, *Circ. Res.*, 65,146, 1989.
67. Kusama, Y., Bernier, M., and Hearse, D.J., Singlet oxygen-induced arrhythmias, *Circulation*, 80, 1432, 1989.
68. Bernier, M., Kusama, Y., Borgers, M., VerDonck, L., Valdes-Aguilera, O., Neckers, D.C., and Hearse, D.J., Pharmacological studies of arrhythmias induced by rose bengal photoactivation, *Free Radic. Biol. Med.*, 10, 287, 1991.

69. Kukreja, R.C., Loesser, K.E., Kearns, A.A., Naseem, S.A., and Hess, M.L., Protective effects of histidine during ischemia-reperfusion in isolated perfused rat hearts, *Am. J. Physiol.*, 264, H1370, 1993.
70. Zhai, X. and Ashraf, M., Direct detection and quantification of singlet oxygen during ischemia and reperfusion in rat hearts, *Am. J. Physiol.*, 269, H1229, 1995.
71. Lee, J.W., Miyawaki, H., Bobst, E.V., Hester, J.D., Ashraf, M., and Bobst, A.M., Improved functional recovery of ischemic rat hearts due to singlet oxygen scavengers histidine and carnosine, *J. Mol. Cell. Cardiol.*, 31, 113, 1999.
72. Tarr, M. and Valenzeno, D.P., Modification of cardiac action potential by photo-sensitizer-generated reactive oxygen, *J. Mol. Cell. Cardiol.*, 21, 539, 1989.
73. Matsuura, H. and Shattock, M.J., Effects of oxidant stress on steady-state background currents in isolated ventricular myocytes, *Am. J. Physiol.*, 261, H1358, 1991.
74. Satoh, H. and Matsui, K., Electrical and mechanical modulations by oxygen-derived free-radical generating systems in guinea-pig heart muscles, *J. Pharm. Phamacol.*, 49, 505, 1997.
75. Tarr, M. and Valenzeno, D.P., Modification of cardiac ionic currents by photosensitizer-generated reactive oxygen, *J. Mol. Cell. Cardiol.*, 23, 639, 1991.
76. Shattock, M.J., Matsuura, H., and Hearse, D.J., Functional and electrophysiological effects of oxidant stress on isolated ventricular muscle: a role for oscillatory calcium release from sarcoplasmic reticulum in arrhythmogenesis? *Cardiovasc. Res.*, 25, 645, 1991.
77. Valenzeno, D.P. and Tarr, M., Membrane photomodification of cardiac myocytes: potassium and leakage currents, *Photochem. Photobiol.*, 53, 195, 1991.
78. Matsuura, H. and Shattock, M.J., Membrane potential fluctuations and transient inward currents induced by reactive oxygen intermediates in isolated rabbit ventricular cells, *Circ. Res.*, 68, 319, 1991.
79. Tarr, M., Arriaga, E., and Valenzeno, D.P., Progression of cardiac delayed rectifier potassium current modification following brief reactive oxygen exposure, *J. Mol. Cell. Cardiol.*, 27, 1099, 1995.
80. Pike, G.K., Bretag, A.H., and Roberts, M.L., Modification of the transient outward current of rat atrial myocytes by metabolic inhibition and oxidant stress, *J. Physiol. (Lond.)*, 470, 365, 1993.
81. Ver Donk, L., Van Reempts, J., Vandeplassche, G., and Borgers, M., A new method to study activated oxygen species induced damage in cardiomyocytes and protection by Ca^{2+}- antagonists, *J. Mol. Cell. Cardiol.*, 20, 811, 1988.
82. Vinnikova, A.K., Kukreja, R.C., and Hess, M.L., Singlet oxygen-induced inhibition of cardiac sarcolemmal Na+K+-ATPase, *J. Mol. Cell. Cardiol.*, 24, 465, 1992.
83. Coetzee, W.A., Ichikawa, H., and Hearse, D.J., Oxidant stress inhibits Na-Ca-exchange current in cardiac myocytes: mediation by sulfhydryl groups?, *Am. J. Physiol.*, 266, H909, 1994.
84. Kujreja, R.C., Jesse, R.L., and Hess, M.L., Singlet oxygen: a potential culprit in myocardial injury?, *Mol. Cell. Biochem.*, 111, 17, 1992.
85. Tarr, M., Arriaga, E., Goertz, K.K., and Valenzeno, D.P., Properties of cardiac ILEAK induced by photosensitizer-generated reactive oxygen, *Free Rad. Biol. Med.*, 16, 477, 1994.
86. Tarr, M. and Valenzeno, D.P., Photomodification of cardiac membrane: chaotic currents and high conductance states in isolated patches, *Photochem. Photobiol.*, 68, 353, 1998.
87. Tarr, M., Frolov, A., and Valenzeno, D.P., Photosensitization-induced calcium overload in cardiac cells: direct link to membrane permeabilization and calcium influx, *Photochem. Photobiol.*, 73, 418, 2001.
88. Valenzeno, D.P. and Tarr, M., GH_3 cells, ionic currents and cell killing: photomodification by rose bengal, *Photochem. Photobiol.*, 68, 519, 1998.
89. Valenzeno, D.P. and Tarr, M., Calcium as a modulator of photosensitized killing of H9c2 cardiac cell, *Photochem. Photobiol.*, 74, 605, 2001.
90. Moor A.C.E., Dubbelman, T.M.A.R., VanSteveninck, J., and Brand, A., Transfusion-transmitted diseases: risks, prevention and perspectives, *Eur. J. Haematol.,* **62**, 1, 1999.
91. Skripchenko, A., Robinette, D., and Wagner, S.J., Comparison of methylene blue and methylene violet for photoinactivation of intracellular and extracellular virus in red cell suspensions, *Photochem. Photobiol.*, 65, 451, 1997.

92. Lagerberg, J.W.M., Überriegler, K.P., Krammer, B., VanSteveninck, J., and Dubbelman, T.M.A.R., Plasma membrane properties involved in the photodynamic efficacy of merocyanine 540 and tetrasulfonated aluminum phthalocyanine, *Photochem. Photobiol.*, 71, 341, 2000.
93. Prince, A.M., Strategies for evaluation of enveloped virus inactivation in red cell concentrates using hypericin, *Photochem. Photobiol.*, 71, 188, 2000.
94. Skripchenko, A. and Wagner, S.J., Photoinactivation of leukocytes in erythrocyte suspensions: comparison of methylene blue and dimethylmethylene blue, *Transfusion*, 40, 968, 2000.
95. Stief, T.W. and Fareed, J., The antithrombotic factor singlet oxygen/light ($^1O_2$/hν), *Clin. Appl. Thromb. Hemost.*, 6, 1, 2000.
96. Aznar, J.A., Bonanad, S., Montoro, J.M., Hurtado, C., Cid, A.R., Soler, M.A., and De Miguel, A., Influence of methylene blue photoinactivation treatment on coagulation factors from fresh frozen plasma, cryoprecipitates and cryosupernatants, *Vox Sang.*, 79, 156, 2000.
97. Aznar, J.A., Molina, R., and Montore, J.M., Factor VIII/von Willebrand factor complex in methylene blue-treated fresh plasma, *Transfusion*, 39, 748, 1999.
98. Zeiler, T., Riess, H., Wittmann, G., Hintz, G., Zimmermann, R., Muller, C., Heuft, H.G., and Huhn, D., The effect of methylene blue phototreatment on plasma proteins and *in vitro* coagulation capability of single-donor fresh-frozen plasma, *Transfusion*, 34, 685, 1994.

144

Synthetic Strategies in Designing Porphyrin-Based Photosensitizers for Photodynamic Therapy

Ravindra K. Pandey
Roswell Park Cancer Institute

144.1 Introduction

Photodynamic therapy (PDT) is a promising cancer treatment that involves the combination of visible light and a photosensitizer.[1] Each factor is harmless by itself, but when combined with oxygen, they can produce lethal cytotoxic agents, initially singlet oxygen, that inactivate tumor cells.[2] This enables greater selectivity toward diseased tissue, as only those cells that are simultaneously exposed to the photosensitizer, light, and oxygen are exposed to the cytotoxic effect. The dual selectivity of PDT is produced by a preferential uptake of the photosensitizer by the diseased tissue and the ability to confine activation of the photosensitizer to this diseased tissue by restricting illumination to the specific site.

The porphyrins and related tetrapyrrolic systems are among the most widely studied compounds for use as photosensitizers in PDT.[3] Porphyrins are 18π-electron aromatic macrocycles that exhibit characteristic optical spectra with a strong π–π^* transition around 400 nm (Soret band) and usually four Q

0-8493-1348-1/04/$0.00+$1.50

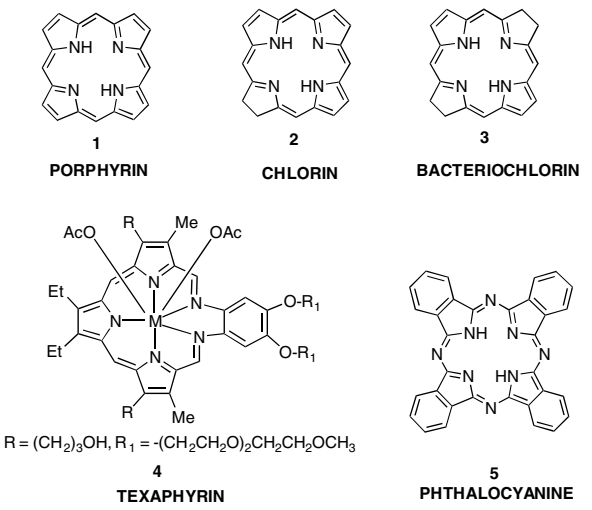

FIGURE 144.1

bands in the visible region. As can be seen in Figure 144.1, two of the peripheral double bonds in opposite pyrrolic rings are cross-conjugated and are not required to maintain aromaticity. Thus, reduction of one or both of these cross-conjugated double bonds (to give chlorins and bacteriochlorins, respectively) maintains much of the aromaticity, but the change in symmetry results in bathochromically shifted Q bands with high extinction coefficients.[4] Nature uses these optical properties of the reduced porphyrins to harvest solar energy for photosynthesis with chlorophylls and bacteriochlorophylls as both antenna and reaction-center pigments.[5] The long wavelength absorption of these natural chromophores led to explorations of their use as photosensitizers in PDT.

As indicated previously, PDT is based on the interaction of a photosensitizer retained in tumors with photons of visible light, resulting in the formation of singlet oxygen ($^1O_2$), the putative lethal agent.[6] To achieve an effective destruction of tumor cells, a high quantum yield of singlet oxygen is required. Even in the absence of heavy atom substitution and coordination of transition-metal ions, porphyrin systems generally satisfy these criteria, which is why most of the sensitizers currently under clinical evaluation for PDT are porphyrins or porphyrin-based molecules.

At present, Photofrin®* , a hematoporphyrin derivative,[7] is the only photosensitizer that has been approved worldwide for the treatment of various types of cancer by PDT. It fits some of the criteria for ideal photosensitizers, but it also suffers from several drawbacks. First, it is a complex mixture of various monomeric, dimeric, and oligomeric forms.[7b–d] Second, its long wavelength absorption falls at 630 nm, which lies well below the wavelength necessary for maximum tissue penetration. Finally, it induces prolonged cutaneous phototoxicity, a major adverse effect associated with most of the porphyrin-based photosensitizers.

It is well established that absorption and scattering of light by tissue increases as the wavelength decreases, and that most efficient sensitizers are those that have strong absorption bands from 700 to 800 nm.[8] Light transmission by tissues drops rapidly below 550 nm; however, it doubles from 550 to 630 nm and doubles again from 630 to 700 nm. This is followed by an additional 10% increase in tissue penetration as the wavelength increases toward 800 nm.[3] Another reason to set the ideal wavelength for PDT at 700 to 800 nm is due to the availability of easy-to-use diode lasers. Although diode lasers are now available at 630 nm (where clinically approved Photofrin absorbs), photosensitizers with absorptions between 700 to 800 nm, in conjunction with diode lasers, are still desirable for treating deeply seated

* Registered trademark of Axcan Scandipharm Inc., Birmingham, AL.

tumors. Therefore, in recent years, a variety of photosensitizers related to chlorins, bacteriochlorins, porphycenes, phthalocyanines, naphthalocyanines, and expanded porphyrins were synthesized and evaluated for PDT efficacy. However, for designing improved photosensitizers for PDT, it becomes necessary to consider several other factors, such as overall lipophilicity (i.e., a proper balance between hydrophobicity and hydrophibicity), pH, lymphatic drainage, and lipoprotein binding, which could influence the biodistribution and localization of sensitizers in tissue and tumors.[9]

The main focus of this chapter is to summarize the various synthetic strategies followed by several research groups in designing long-wavelength-absorbing photosensitizers related to chlorins, bacteriochlorins, expanded porphyrins, and phthalocyanines. An ongoing interest on developing target-specific photosensitizers is also briefly reviewed. The majority of chlorins and bacteriochlorins were generated through three different approaches. One method involves modification of a preformed porphyrin. The second approach utilizes the use of chlorophyll *a* as the starting material for the synthesis of other chlorins and bacteriochlorins. The third approach utilizes the unstable bacteriochlorophyll *a* as a substrate for the synthesis of stable bacteriochlorins. Each procedure was used successfully for preparing sensitizers that show promise in photodynamic therapy and is discussed in terms of synthetic methodology and biological significance.

144.2 Chlorins and Bacteriochlorins from Porphyrins

Chlorins and Bacteriochlorins by Diimide Reduction

Almost 30 years ago, Whitlock et al.[10] developed an efficient diimide reduction method for the synthesis of bacteriochlorins and isobacteriochlorins from porphyrins. Diimide reduction of metal-free tetraphenyl chlorin afforded tetraphenyl bacteriochlorin, while reduction of the corresponding zinc analog produced the related tetraphenylisobacteriochlorin. It is now accepted that the reduced double bond in chlorins induces a pathway for the delocalized π electrons that "isolates" the diagonal crossing-conjugated pyrrolic double bond, such that reduction of this double bond is favored due to minimal loss of π energy over the double bond present in the adjacent ring. The presence of a metal changes the delocalization of the π electrons, which makes the adjacent pyrrolic ring more reactive, and diimide reduction produces mainly the corresponding isobacteriochlorin. In order to avoid the formation of an isomeric mixture, this approach is useful only for reduction of symmetrical porphyrins. This diimide-reduction approach was later employed by Bonnett et al.[11] for preparing the *meso*-tetra (*m*-hydroxyphenyl)-chlorin (*m*-THPC) **7** (650 nm) and the bacteriochlorin (*m*-THPBC) **8**. The formation of these components was found to depend on the amount of reductant used.

Although the formation of a bacteriochlorin resulted in further red shift in the electronic absorption spectrum, with long-wavelength absorption near 750 nm, these molecules were generally found to be air sensitive. Among various chlorin analogs, *m*-THPC (Foscan®) 7 (Scheme 1) appears to be quite effective and is currently under Phase III human clinical trials (see Chapter 147).

Chlorins and Bacteriochlorins by Diels–Alder Reaction

Cycloaddition reactions are among the most powerful reactions available to organic chemists.[12] The ability to simultaneously form and break several bonds, with a wide variety of atomic substitution patterns, and often with high degree of stereocontrol, has made cycloaddition reactions the subject of intense study. In porphyrin chemistry, the [4 + 2] Diels–Alder reactions were used by various investigators for converting porphyrins into chlorin systems. Callot et al. were the first to show that protoporphyrin IX dimethyl ester 9 can undergo cycloaddition reactions with various dienophiles[13] (Scheme 2). A few years later, Dolphin and coworkers discovered the utility of one such analog named benzoporphyrin derivative monocarboxylic acid (BPDMA) 12a and 12b for treating age-related macular degeneration (AMD) when activated with light at 690 nm.[14] This treatment has already received approval worldwide. BPDMA has also been used for the treatment of cancer by photodynamic therapy (see Chapter 147). However, due

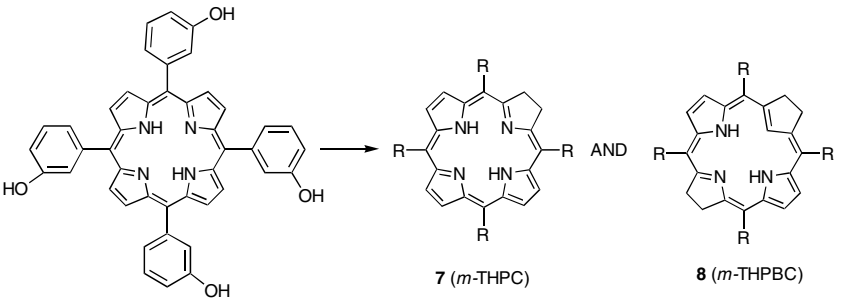

SCHEME 1

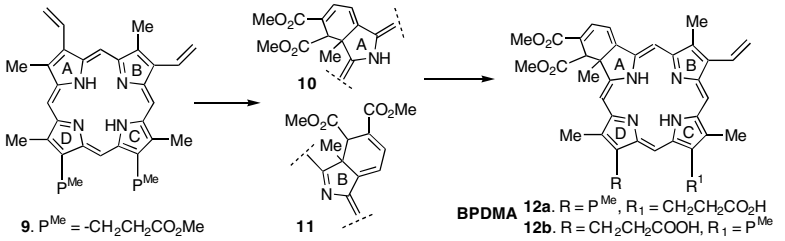

SCHEME 2

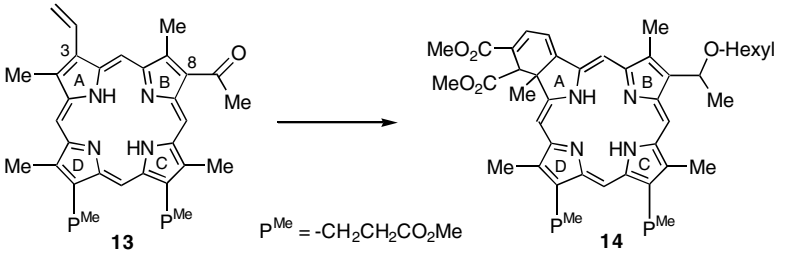

SCHEME 3

to its rapid clearance, it was found to be effective only if the tumors were treated with light at 3 h post injection of the drug. Pandey et al.[15] developed another approach for preparing these analogs, starting from 8-acetyl-3-vinyl deuteroporphyrin IX dimethyl ester (Scheme 3).

The vinyl group was replaced with various alkyl ether functionalities. Among these analogs, the related 8-(1-hexyloxy ethyl)-derivative 14 was found to be more effective than BPDMA in eradicating tumors in mice bearing SMT-F tumors.[15] This methodology was further extended independently by Pandey et al.[16] and Yon-Hin et al.[17] for the synthesis of novel bacteriochlorins, which involved a double Diels–Alder reaction on divinylporphyrins 15 and 17 (Scheme 4). These bacteriochlorins 16 and 18 exhibit long-wavelength absorption maxima near 800 nm with limited PDT efficacy.

Morgan et al.[18] showed that bacteriochlorin-like macrocycles can also be generated by cyclization of either 5,10- or 5,15-bis[(ethoxycarbonyl)vinyl]-porphyrins. However, the resulting products rapidly decomposed upon exposure to air, thus precluding their use as photosensitizers for PDT. For developing a general synthesis of stable bacteriochlorins, the same authors[19] followed the pinacol-pinacolone approach in preparing ketochlorins 22 and 23. In brief, dehydration of 19 produced a mixture of 20 and

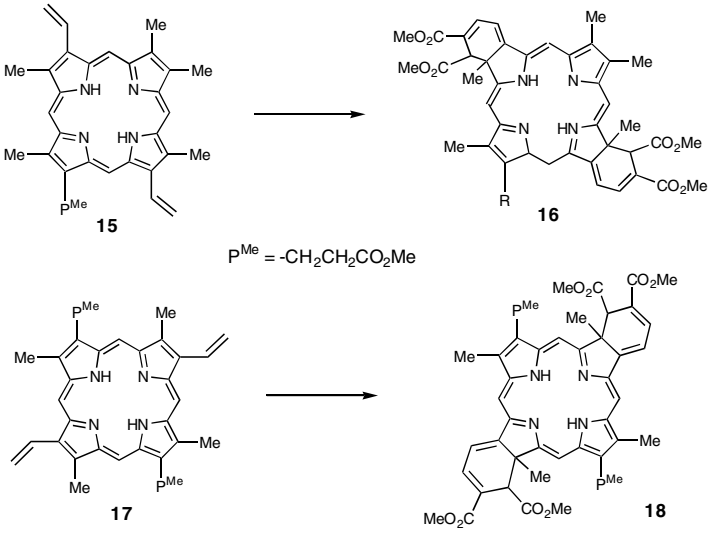

SCHEME 4

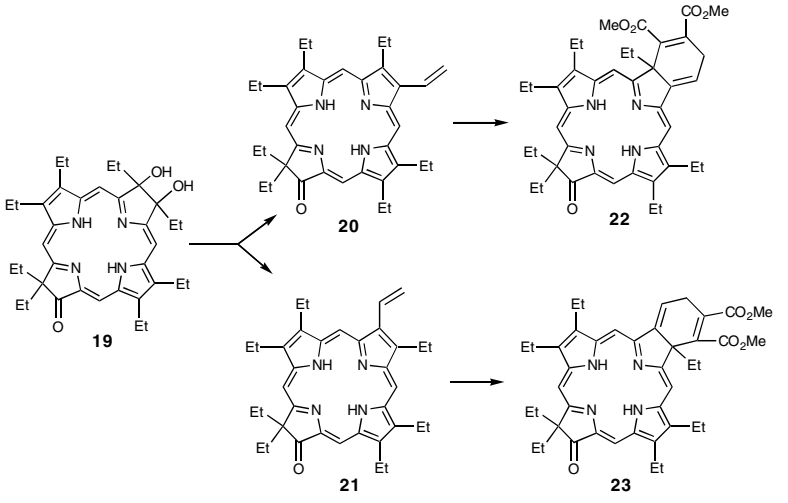

SCHEME 5

21, which on reaction with dimethylacetylenedicarboxylate (DMAD) produced the corresponding bacteriochlorins 22 and 23 as an isomeric mixture. This isomeric mixture showed some photodynamic activity in a mouse tumor model: 75% of the mice treated at a dose of 1 mg/kg were found to be free from palpable tumor 12 days after the light treatment. However, in this class of compounds, the spectroscopic properties of 22 and 23 resemble those of porphyrinones (long-wavelength absorption near 700 nm) rather than bacteriochlorins (Scheme 5).

Benzochlorins and Benzobacteriochlorins

Benzochlorin consists of a benzene ring fused between the *meso*- and the adjacent β-position of the pyrrole ring. In a sequence of reactions, this class of compounds was first reported by Arnold et al. from

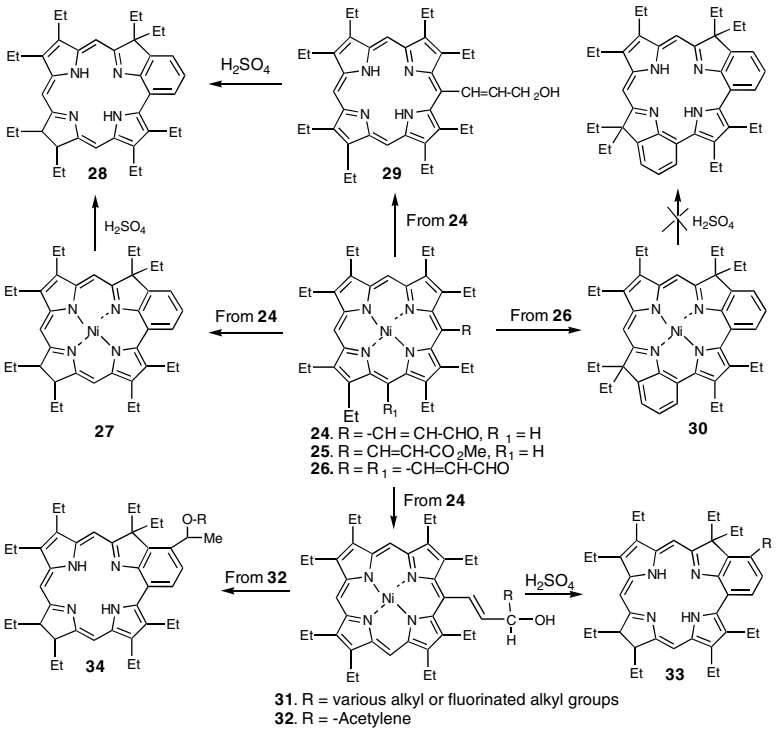

SCHEME 6

octaethylporphyrin.[20] Morgan et al.[21] were the first to demonstrate the photosensitizing efficacy of these analogs (e.g., 28). One of the major problems associated with this preparation is the difficulty in demetalation at the final step of the synthesis, and it is also difficult to chemically modify these benzochlorins. Therefore, this procedure has limited application in preparing a series of analogs with variable lipophilicity. This problem can be avoided by following the method recently reported by Li et al.[22,23] (Scheme 6). In their approach, Ni(II)meso-(2-formylvinyl)octaethylporphyrin 26 was reacted with the Grignard's reagent of various fluorinated or nonfluorinated alkyl halides or Ruppert's reagent. The corresponding intermediates via intramolecular cyclization under acidic conditions afforded the related free-base benzochlorins **34.** In this series of compounds, compared to the free-base analogs, the related Zn(II) complexes (671 to 677 nm) were found to be more effective both *in vitro* and *in vivo*. In preliminary screening, the fluorinated analogs showed better efficacy than the corresponding nonfluorinated derivatives.[22b]

This methodology was later extended by Vicente et al.[24] for the preparation of octaethylporphyrin-based benzochlorin 30 by intramolecular cyclization of Ni(II)5,10 bis-(2-formylvinyl) porphyrin 21 (Scheme 7). Unfortunately, attempts to remove the Ni(II) metal were unsuccessful. When Ni(II)5-(2-formyl-vinyl)-10-(2-ethoxycarbonyl-vinyl)octaethyl porphyrin was used as a substrate, the formation of the reaction product was found to depend on the strength of the acid used.[25] For example, reaction of **35** with sulfuric acid produced a chlorin containing six- and five-member rings fused at the same pyrrole unit **36**. Replacing sulfuric acid with trifluoroacetic acid (TFA) produced **37**, the Ni (II) complex of bacteriochlorin containing an ethylidine group at the peripheral position (λ_{max} 895 nm). Attempts to prepare the desired free-base analogs for investigating their application as photosensitizers were unsuccessful.

Purpurins (Tin Etiopurpurin Dichloride)

Purpurins have been known as degradation products of chlorophyll for quite some time.

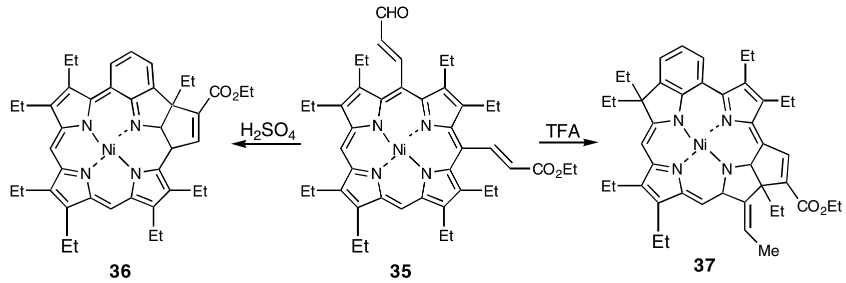

SCHEME 7

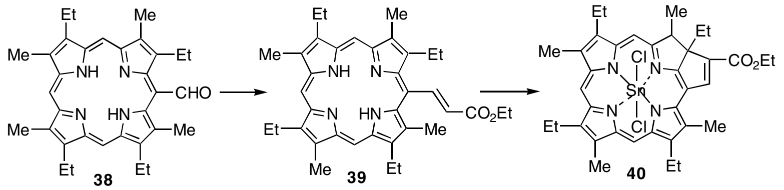

SCHEME 8

The first synthesis of this class of compounds was reported by Woodward[26] during the synthesis of chlorophyll *a* by intramolecular cyclization of a *meso*-acrylate functionality to a β-pyrrolic position. This methodology was later followed by Morgan et al.[27] and others[28] to synthesize a series of octaetylporphyrin, etioporphyrin, 5,10-diphenyl- and 5,10-dipyridylporphyrin-based purpurin analogs. Among all the purpurins evaluated for PDT efficacy, the Sn etiopurpurin ($SnEt_2$) 40 (Scheme 8) is considered to be the most effective *in vivo*.[27] Its long wavelength absorption falls at 650 nm and produces a high singlet oxygen quantum yield. This product is currently in Phase III clinical trials for the treatment of age-related macular degeneration (AMD), a major cause of blindness among people over 50 years of age.

144.3 Chlorins and Bacteriochlorins from Chlorophyll

Chlorophyll *a*, the green photosynthetic pigment, is one of the prototypes of the chlorin class of natural product. Because it is readily available, a large amount of work was done by several investigators to modify and to synthesize other chlorin-like chromophores. The photosensitizers derived from chlorophyll *a* can be divided into three categories in which the five-member isocyclic ring was cleaved or kept intact or was replaced with other ring systems. Some of the photosensitizers in these series attracted enormous attention; their description follows.

Aspartic Acid Derivative of Chlorin e_6 (Npe_6)

Chlorophyllin, a water-soluble degradation product of chlorophyll *a*, can be obtained by cleavage of the isocyclic ring of chlorophyll.[29] Removal of magnesium resulted in chlorin e_6 with limited *in vivo* photosensitizing efficacy. It was shown that replacing the vinyl group with alkyl ether groups of variable carbon units generally enhances the photosensitizing efficacy.[30] However, in this series, better results were obtained with the monoaspartyl derivative known as Npe_6.[31] This photosensitizer appears to clear rapidly from skin, and good tumor response was obtained only after irradiation within 3 to 4 h of sensitizer administration. Npe_6 is in human clinical trials in Japan for treatment of endobronchial lung cancer. The recent extensive NMR studies of Npe_6 confirmed that in Npe_6, the aspartic acid functionality is linked

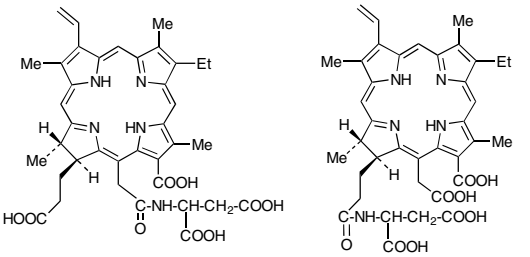

SCHEME 9

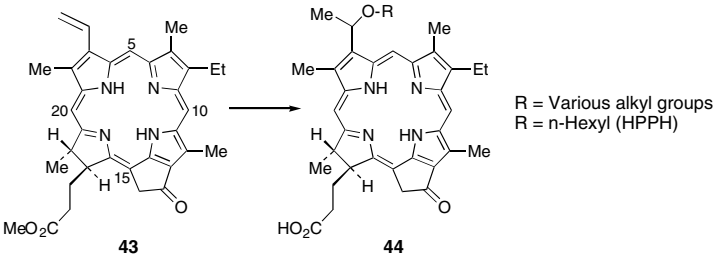

SCHEME 10

with an amide bond at Position-15 (41) of chlorin e_6,[32] instead of at Position-17 (42) as reported in several publications[33] (Scheme 9).

Alkyl Ether Derivatives of Pyropheophorbide *a*

To understand the effect of various substituents on photosensitizing efficacy, the Roswell Park group synthesized and evaluated a series of pyropheophorbide *a* analogs with variable lipophilicity. In their effort to establish a structure–activity relationship (QSAR), a congeneric series of the primary and secondary alkyl ether derivatives of pyropheophorbide *a* was synthesized (the isocyclic ring was kept intact). For the preparation of these analogs, methylpheophorbide *a* obtained from *Spirulina Pacifica* was converted into more stable pyropheophorbide *a* 43, which on reacting with HBr/AcOH and then the appropriate alcohol, produced the corresponding ether analogs in excellent yield[34] (Scheme 10). At the final step, the methyl ester functionality was hydrolyzed into the corresponding carboxylic acid 44 (HPPH: R = *n*-hexyl). These analogs exhibit long-wavelength absorption near 665 nm *(in vivo)* and show excellent singlet-oxygen-producing efficiency (45%). The results obtained from *in vivo* studies in mice demonstrated that the photodynamic efficacy of these photosensitizers increased by increasing the length of the carbon chain, reaching a maximum in compounds with *n*-hexyl and *n*-heptyl chains at Position-3. Interestingly, the PDT efficacy decreased by further increasing the length of alkylether carbon units. When compensated for differences in tumor photosensitizer concentration, the *n*-hexyl derivative (HPPH) (optimal lipophilicity) was fivefold more potent than the *n*-dodecyl derivative (more lipophilic) and threefold more potent than the *n*-pentyl analog (less lipophilic). Interestingly, the introduction of the hexyl ether side chain at other positions of the macrocycle (Position-8 or Position-20) significantly reduced the *in vivo* efficacy.[35] These data suggest that besides the lipophilicity, the presence and position of the substituent possibly play an important role in drug efficacy. HPPH is currently at Phase I/II human clinical trials for the treatment of a variety of cancers. Among the patients treated so far, no long-term skin phototoxicity was observed.[36]

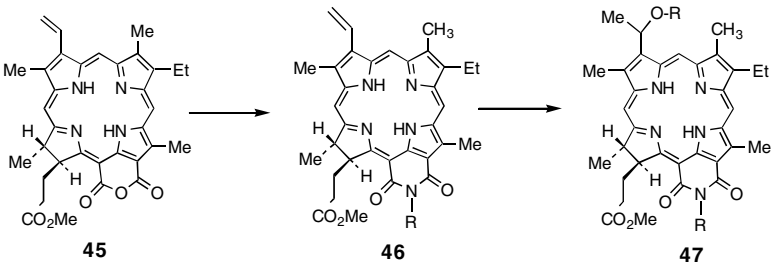

R = Various Alkyl groups

SCHEME 11

Alkyl Ether Analogs of Purpurinimides

Having developed a QSAR for the alkyl ether analogs of pyropheophorbide series, the Roswell Park group extended their approach to photosensitizers with longer wavelength absorption. For this study, the purpurin-18 methyl ester obtained from methylpheophorbide *a*[37] was converted into purpurin-18-*N*-alkyl imides **46**.[38] The vinyl group at Position-3 was then replaced with a variety of alkyl ether analogs **47** (Scheme 11) with variable carbon units with log *P* values ranging from 5.32 to 16.44 and exhibiting long-wavelength absorption near 700 nm.[39]

In animal studies, this class of compounds was found to be effective *in vivo*. The results obtained from a set of photosensitizers with similar lipophilicity (log *P* 10.68 to 10.88) indicate that similar to the pyropheophorbide series, in addition to the overall lipophilicity, the presence and position of the alkyl groups (*O*-alkyl versus *N*-alkyl) in a molecule also play an important role in tumor uptake, tumor selectivity, and *in vivo* PDT efficacy.[39,40]

Benzoporphyrin Derivatives from Pyropheophorbide *A* and Purpurinimides

One of the main synthetic problems associated with PP-IX-based benzoporphyrin derivatives is to isolate the most effective analog (ring-A reduced, monocarboxylic acid) from the complex reaction mixture. In order to solve this problem, the Roswell Park and Vancouver groups[41,42] reported the preparation of various BPD analogs (e.g., 49) from phylloerythrrin and methyl 9-deoxypyropheophorbide (Scheme 12). Among these compounds, the benzoporphyrin derivative (*cis*- isomer) obtained from rhodoporphyrin XV di-*tert*-butyl aspartate was found to have PDT efficacy similar to BPDMA. This methodology was also extended in the purpurinimide series, and the lipophilicity was altered by introducing *N*-alkyl groups with variable carbon units at the imide ring system 50.[43] In preliminary *in vivo* testing, the corresponding *N*-hexyl and *N*-dodecyl analogs were found to be effective at a dose of 0.5 μM/kg when treated with light (135 J/cm^2, 75 mW/cm^2) at 728 nm and 24 h postinjection. Under similar treatment conditions (treated with light at 690 nm), the BPDMA obtained from protoporphyrin IX dimethyl ester did not produce any photosensitizing efficacy.[44] Therefore, the Diels–Alder approach in a purpurinimide system provides a simple approach for generating effective photosensitizers with variable lipophilicity.

vic-Dihydroxy- and Ketobacteriochlorins

Osmium tetroxide was frequently used for the conversion of porphyrins to the corresponding *vic*-dihydroxy chlorins and tetrahydroxy bacteriochlorins as a mixture of isomers.[45] The overall lipophilicity of these analogs can be altered by subjecting them to pinacolpinacolone reaction conditions. The formation of the corresponding keto- analog is not straightforward and depends not only on the intrinsic nature of the migratory group but also of the electronic and steric factors elsewhere on the porphyrin nuclues.[46] Therefore, the concept of designing chlorin and bacteriochlorin analogs from porphyrins by following this approach was not successful. A few years ago, Chang et al.[47] showed that chlorins under

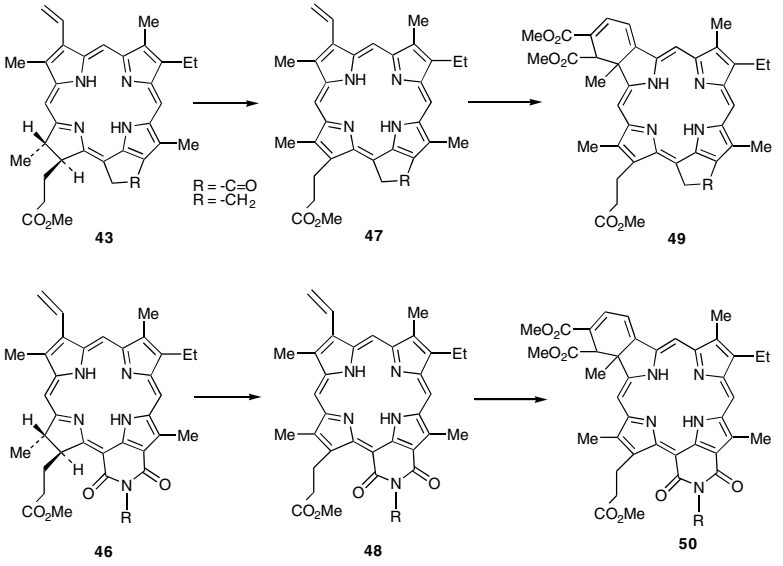

SCHEME 12

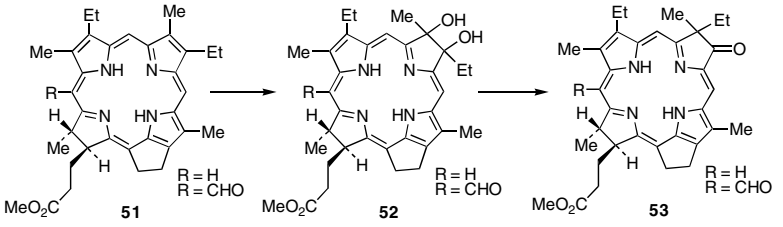

SCHEME 13

certain conditions can be converted into *vic*-dihydroxybacteriochlorins upon reaction with osmium tetroxide. The Roswell Park group extended this methodology to the pheophorbide, chlorin e_6, and a series of *vic*-hydroxy- and ketobacteriochlorins were synthesized. The stable ketobacteriochlorins had strong absorptions in the 710 to 760 nm region but did not show any significant photosensitizing activity in mice (DBA/2) transplanted with SMT-F tumors.[48] However, the ketobacteriochlorins obtained from 9-deoxypyropheophorbide *a* 51 and the related *meso*-formyl derivative with long-wavelength absorption showed long-wavelength absorptions at 734 and 758 nm, respectively (Scheme 13). Among these bacteriochlorins, the triplet states were quenched by ground-state molecular oxygen in a relatively similar manner, yielding comparative singlet oxygen quantum yields. In preliminary *in vivo* screening, the ketochlorins 53 (R = CHO) were found to be more photodynamically active than the related *vic*-dihydroxy analogs. Replacement of the methyl ester functionalities with di-*tert*-butylaspartic acids enhanced the *in vivo* efficacy.[49] It appears to be cleared rapidly from skin, and good tumor responses can be obtained after irradiation within 3 to 4 h of sensitizer administration.

Bacteriochlorins Derived from 8-Vinyl Chlorins

The Roswell Park group combined the use of osmium tetroxide and Diels–Alder approach to construct stable bacteriochlorins. In their approach, mesopurpurin-18 methyl ester 54, obtained from methylpheophorbide *a*, was reacted with osmium tetroxide. The resulting *vic*-dihydroxy bacteriochlorin on

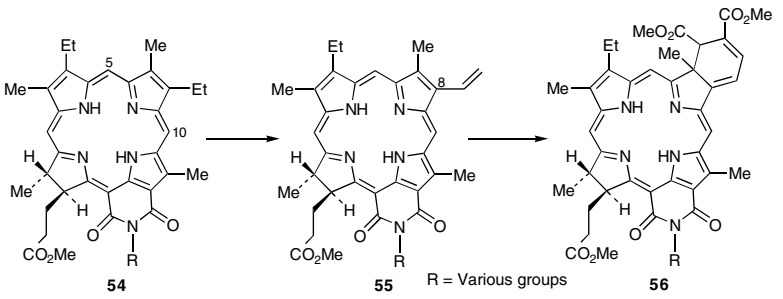

SCHEME 14

reacting with *p*-toluenesulfonic acid in refluxing benzene produced the 8-vinyl derivative 55, which on reacting with dimethylacetylene dicarboxylate (DMAD) under Diels–Alder reaction conditions produced bacteriochlorin 56 with long-wavelength absorption near 800 nm.[50] Unfortunately, the utility of this compound for use in PDT was diminished due to the unstable nature of the six-member anhydride ring system (Scheme 14). In their recent approach, the anhydride ring is replaced with an *N*-hexyl-imide ring system, and these compounds were found to be stable *in vivo*.[51] The preliminary *in vitro* photosensitizing results obtained from this compound are promising. This system also possesses a unique opportunity to prepare a series of *N*-alkyl ether derivatives with variable carbon units and to establish the structure and activity relationship in a particular series of compounds.

Bacteriochlorins from Bacteriochlorophyll

Most of the naturally occurring bacteriochlorins have absorptions between 760 to 780 nm and were studied by various investigators for their use as photosensitizers for PDT.[52] They were found to be extremely sensitive to oxidation, resulting in a rapid transformation into the chlorin state, which generally has an absorption maximum at or below 660 nm.[53] Furthermore, if a laser is used to excite the bacteriochlorin *in vivo*, oxidation may result in the formation of a new chromophore absorbing outside the laser window, reducing the photodynamic efficacy. Due to the desirable photophysical properties and promising *in vitro*/*in vivo* photosensitizing efficacy of bacteriochlorins, there is increasing interest in the synthesis of stable bacteriochlorins, either from bacteriochlorophyll *a* or from the other related tetrapyrrolic systems.

In general, for designing improved photosensitizers, overall lipophilicity was proven to be one of the important factors. For example, among porphyrin-based photosensitizers, the hydrophobic porphyrins are preferentially accumulated and partitioned into corresponding hydrophobic loci *in vivo*. Moan and coworkers[54] showed that among diether derivatives of hematoporphyrin, retention in cells increases with decreasing polarity. The Roswell Park group studied the uptake of a series of alkyl ether derivatives of pyropheophorbide *a* and found that a strong correlation exists between uptake and hydrophobicity, although each correlation cannot be extended to the *in vivo* PDT efficacy. On the other hand, photosensitizers with high partition coefficient values (increased hydrophobicity) induce sensitizer insolubility, thus preventing drugs from entering the circulation. Therefore, a proper balance between hydrophobicity and hydrophilicity is probably the most important factor that influences tumor localization of sensitizers.

A simple approach used by the Roswell Park group was to vary the overall lipophilicity of various types of photosensitizers, such as pyropheophorbide *a*, benzoporphyrin derivatives, benzochlorins, and purpurinimides by altering the length of carbon units in alkyl ether substituents; an approach that was successful. It was demonstrated that replacing an anhydride ring system in purpurin-18 (a chlorophyll *a* analog) with a six-member imide ring substantially enhanced its *in vivo* stability and retained effective *in vivo* photodynamic activity.[55] Therefore, in order to investigate the effect of such substitutions in the bacteriochlorin series, bacteriochlorophyll *a,* present in *Rb. Sphaeroides*, was first converted (*in situ*) into bacteriopurpurin-18 (**57**),[56] which in a sequence of reactions, was transformed into a series of related

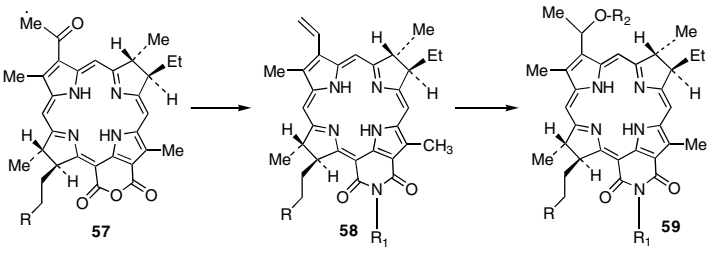

SCHEME 15

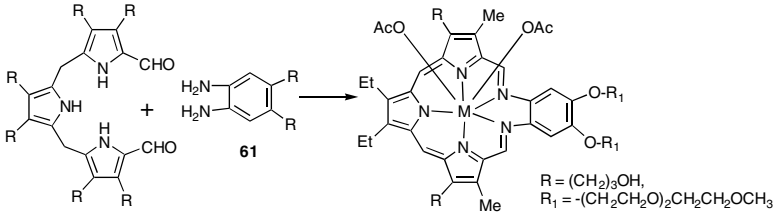

SCHEME 16

N-alkyl derivatives **58**[57] (Scheme 15). To determine the effect of the presence of these alkyl substituents with variable carbon units, the acetyl group was first reduced with sodium borohydride that on reacting with HBr gas and an appropriate alcohol produced the corresponding alkyl ether derivatives of bacteriochlorin **59** in high yield. These compounds are stable *in vitro* and *in vivo*, exhibit long-wavelength absorption near 790 nm, and show high tumor uptake. In preliminary *in vitro* and *in vivo* studies, some of these compounds were found to be effective at low injected doses.[58]

144.4 Expanded Porphyrins

The texaphyrins are aromatic tripyrrolic, pentaaza, Schiff-base macrocycles that bear a strong, but "expanded" resemblance to the porphyrins and other naturally occurring tetrapyrrolic prosthetic groups.[59] Similar to porphyrins, the texaphyrins are fully aromatic and colored compounds (Scheme 16). However, they are 22 π-electron electron systems rather than 18 π-electron ones. This class of compounds exhibits long-wavelength absorption >700 nm, depending on the nature of substituents present at the peripheral position. Also, in contrast to porphyrins, the texaphyrins are monoanionic ligands that contain five, rather than four, coordinating nitrogen atoms within the central core that is roughly 20% larger than that of the porphyrins. High-yield production of long-lived triplet states and their remarkable singlet-oxygen-producing efficiency are important features of this class of photosensitizers. Currently, two different water-solubilized lanthanide(III)texaphyrin complexes, namely, the gadolinium(III) (62)[60] and lutetium(III) (63)[61] derivatives (Gd-Tex and Lu-Tex, respectively), are being tested clinically. The first of these, XCYTRIN™, is in a pivotal Phase III clinical trial as a potential enhancer of radiation therapy for patients with metastatic cancers of the brain receiving whole-brain radiation therapy. The second, in various formulations, is being tested as a photosensitizer for use in the treatment of recurrent breast cancer (LUTRIN), in Phase II clinical trials; photoangioplastic reduction of atherosclerosis involving peripheral arteries (ANTRIN); and light-based treatment of age-related macular degeneration (OPRTIN), currently in Phase I clinical trials.[59]

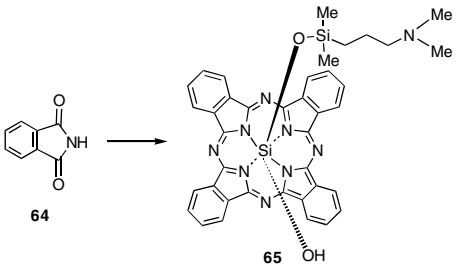

SCHEME 17

144.5 Phthalocyanines and Naphthalocyanines

Phthalocyanines (Pc) and naphthalocyanines (Nc) can be regarded as azaporphyrins containing four isoindoles linked by nitrogen atoms[62] (Scheme 17). Compared to porphyrins, Pc and Nc offer high molar-extinction coefficients and red shift maximums at 680 nm for Pc and 780 nm for Nc, resulting from the benzene or naphthalene rings condensed at the periphery of the porphyrin-like macrocycle. They possess high-singlet-oxygen-producing efficiency, and interestingly, chelation of metal ions such as zinc or aluminum increases the singlet-oxygen yield to nearly 100%. Therefore, metal complexes of the Pc and Nc attracted attention for their use as photosensitizers in PDT. In recent years, a large number of metalated or nonmetalated phthalocyanine-based photosensitizers were synthesized by introducing a variety of substituents at the peripheral positions. If the valency of the central metal is higher than two, it binds various axial ligands. All of these chemical changes of the Pc and Nc skeletons alter their PDT efficacy. Aggregated Pc and Nc are inactive photochemically because of a greatly enhanced rate of excited singlet-state deactivation by internal conversion of the ground state. In the phthalocyanine series, Olenick and coworkers in collaboration with Kenney[63] synthesized and evaluated four silicon analogs with variable lipophilicity to learn more about the structural features that silicon phthalocyanine must have in order to be a good PDT photosensitizer. All of these analogs produced similar photophysical properties; however, the photosensitizer denoted as Pc4, bearing a long-chain amino axial ligand 65, showed promising results *in vitro* and *in vivo* and is presently entering clinical trials.[64] Further, it was concluded that the presence of structural features leading to improvement in the association between photosensitizers and important cellular targets is more useful than the presence of those leading to improvements in their already acceptable photophysical and photochemical characteristics. A series of benzyl-substituted phthalonitriles, substituted at the 3,4 and 4,5 positions were converted into a series of Zn(II) hydroxyphthalocyanines phthalocyanine phenol analogs). Their efficacy as sensitizers for PDT was evaluated on the EMT-B mammary tumor cell line. The most active *in vitro* was the 2-hydroxy Zn Pc, followed by 2,3- and 2,9-dihydroxy ZnPc, with the 2,9,16-trihydroxy ZnPc exhibiting the least activity. In inducing tumor necrosis, *in vivo*, the monohydroxy derivative and the 2,3-dihydroxy analog were efficient, but complete tumor regression was poor even at high doses. In contrast, the 2,9-dihydroxy isomer at 2 μM/Kg induced tumor necrosis in all animals treated, with 75% complete regression. These results underline the importance of the position of the substituents on the Pc macrocycle to optimize tumor response and confirm the PDT potential of the unsymmetrical Pcs bearing functional groups on adjacent benzene rings.[65]

Rodgers et al. in collaboration with Kenney and collaborators[66] developed a new route to silicon-substituted phthalocyanines and phthalocyanines-like compounds that is robust and flexible. One of the siloxysilicon compounds, that with the ligand 5,9,12,16,23,28,32-octabutoxy-33H, 35H[b,g]dinaphtho[2,3–1:2′,3′-q]porphyrazine **69**, has a q band at a wavelength of 804 nm and an extinction coefficient of 1.9×10^5 M-1 cm^{-1} (Scheme 18). These compounds showed promising *in vitro* photosensitizing efficacy *in vitro*, however, in animal studies, compared to phthalocyanine (Pc 4) were found to be less effective. A first photophysical study of a member of the family of subnaphthalocyanones is described.[67] The cone-shaped unsubstituted subnaphthalocyanines, synthesized in 35% yield, showed distinctive photophysical

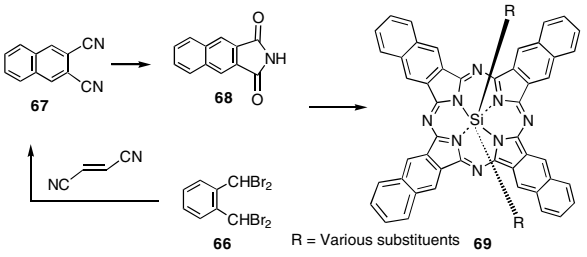

SCHEME 18

properties that are better than those of the related planar phthalo- and naphthalocyanines. SubNc absorbs in the red part of the spectrum and has substantial fluorescence. Triplet and singlet oxygen quantum yield are substantially higher than that of the related phthalo- and naphthalocyanines. These results, together with their synthetic availability, high solubility, and low tendency to aggregate, make this class of sensitizers interesting for further study, with a view to investigate their photodynamic therapy applications.

144.6 Target-Specific Photosensitizers

Since the introduction of the first PDT drug Photofrin, there has not been much success on improving the photosensitizer's tumor selectivity and specificity, because tumor cells in general have nonspecific affinity to porphyrins.[68] Although the mechanism of porphyrin retention by tumors is not well understood, the balance between lipophilicity and hydrophilicity is recognized as an important factor.[69] Some attempts were made to direct photosensitizers to known cellular targets by creating a photosensitizer conjugate, where the other molecule is a ligand that is specific for the target. For example, to improve localization to cell membranes, cholesterol[70] and antibody conjugates were also prepared to direct photosensitizers to specific tumor antigens.[71–73] Certain chemotherapeutic agents were also attached to porphyrin chromophores to increase the lethality of the PDT treatment.[74] Certain protein and microsphere conjugates were made to improve the pharmacology of the compounds.[75] These strategies seldom work well, because the pharmacological properties of both compounds are drastically altered.[76]

Recently, the bovine serum albumin conjugate of a sulfonated phthalocyanine (BSA-AlPcS_4) prepared by Brasseur et al. was shown to target the scavenger receptor of macrophages.[77] Relative photocytotoxicities were reported using a receptor-positive and a receptor-negative cell line, where their lethal effects correlated with its receptor affinity. Also, certain adenoviral proteins were employed to target lung cancer cells rich in the appropriate class integrin receptor.[78] Using the EMT-6 murine model, *in vivo* results were encouraging, with Pc-adenoviral protein conjugates. Further, AlPc and CoPc were covalently labeled with epidermal growth factor (EGF), and this conjugate produced a fivefold increase in photocytotoxicity as compared to nonconjugated phthalocyanine.[79]

Because oligosaccharides play essential roles in molecular recognition,[80] porphyrins with sugar moieties should not only have good aqueous solubility but also possible specific membrane interaction. In addition to providing the molecule with polar hydroxy groups, it is possible that the sugar moiety might lead the conjugate to a cell surface target through specific binding to its receptor. Oligosaccharides play essential roles in various cellular activities, as antigens, growth signals, targets of bacterial and viral infections, and glues in cell adhesion and metastasis, where the saccharide–receptor interactions are usually specific and multivalent.[81] This specificity suggests a potential utility of synthetic saccharide derivatives as carriers in directed drug delivery. Therefore, in recent years, a number of carbohydrate derivatives of various photosensitizers were synthesized. Hombrecher and Schell[82] reported the preparation of a galactopyranosyl-cholesteryloxy-substituted porphyrin by following the McDonald approach. Several tetra- and octaglycoconjugated tetraphenylporphyrins were also reported by Yano and coworkers,[83] Cornia et al.,[84]

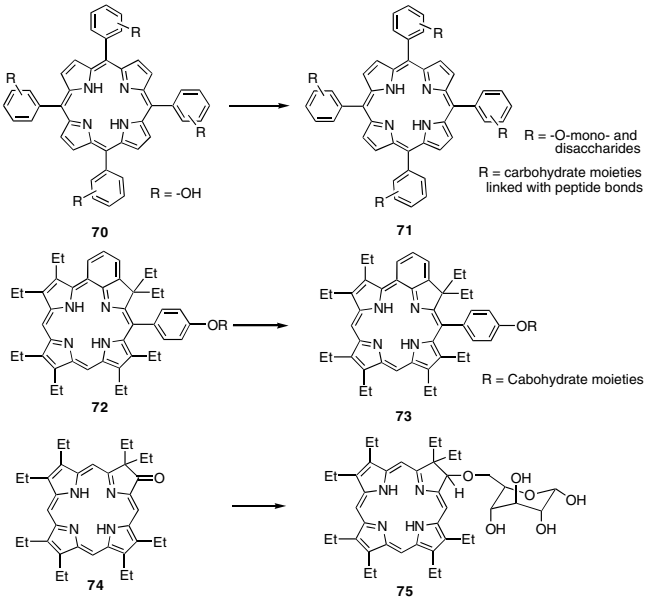

SCHEME 19

Momemteau and coworkers,[85] and Ono et al.[86] A glycosylated peptide porphyrin synthesized by Krausz and coworkers[87] showed promising *in vitro* PDT efficacy. Millard and Momemteau[88] reported the synthesis of a glycoconjugated *meso*- monoarylbenzochlorin (related to 71 and 73) (see Scheme 19). This compound displayed good *in vitro* PDT efficacy in tumor cell lines. A few years ago, Bonnett and coworkers[89] showed that compared to β-hydroxy-octaethylchlorin 75, the related glycosylated analog was more effective as a photosensitizing agent *in vitro* as well as *in vivo*. Montforts et al.[90] further explored this approach by attaching hydrophilic carbohydrate structural units to certain chlorins. Such conjugation increased the water solubility of the parent chlorins by introducing an estradiol with a diethyl spacer. The chlorin–estrogen conjugate was then prepared with the hope that it would bind to an estrogen receptor, which could induce destruction of a mammalian carcinoma. In a recent report, Aoyama and coworkers[91] reported the synthesis of certain tetraphenylporphyrin-based saccharide-functionalized porphyrins and demonstrated the importance of hydrophobicity masking for the saccharide-directed cell recognition. Because the saccharide–receptor interactions are ubiquitous, well-defined and well-designed synthetic saccharides clusters may serve as a new tool in glycoscience and glycotechnology.

It is known that galectins are involved in the modulation of cell adhesion, cell growth, immune response, and angiogenesis, therefore, there is a good possibility that their expression might have a critical role in tumor progression.[92] Gal-1 mRNA levels increase 20-fold in low tumorigenic and up to 100-fold in highly tumorigenic cells.[93] The Roswell Park group recently reported the synthesis and biological significance of certain β-galactose-conjugated purpurinimides (a class of chlorins containing a six-member fused imide ring system) **78–90** (Scheme 20) as Gal-1 recognized photosensitizer via enyne metathesis.[94] Molecular modeling analysis utilizing model photosensitizers and the available crystal structures of galectin-carbohydrate moiety indicates that when placed at an appropriate position, the photosensitizer does not interfere with the galectin-carbohydrate recognition. The intracellular studies with known cell surface counterstains confirmed the cell surface recognition of the conjugates. Under similar drug and light doses, compared to the free purpurinimide analog, the galactose and lactose conjugated analog showed a considerable increase in *in vitro* and *in vivo* photosensitizing efficacy. These results, therefore, indicate the possibility of development of a new class of tumor-specific photosensitizers for PDT based on recognition of a cellular receptor.[94]

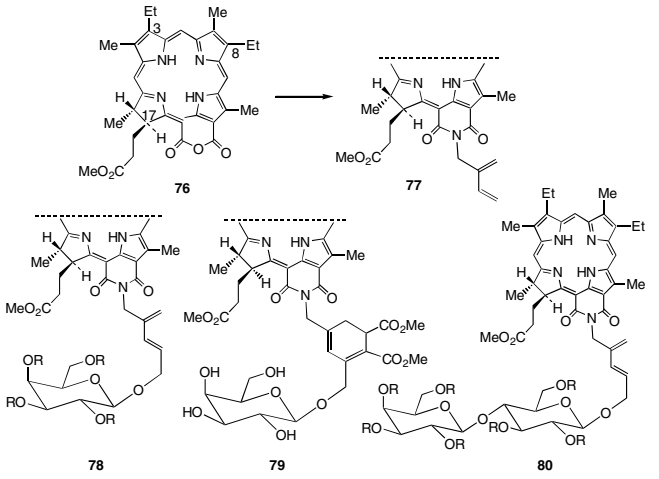

SCHEME 20

144.7 Summary

The focus in this chapter is largely on chemical rather than biological aspects of various porphyrin-based photosensitizers for their use in photodynamic therapy. It is important to note that porphyrin-based compounds, in addition to their use in cancer, also show potential for application in other areas: treatment of age-related macular degeneration (AMD), tumor imaging by MRI, psoriasis, bone marrow purging, and purification of blood infected with various viruses, including HIV. Since the discovery of Photofrin, enormous progress has been made in the development of various porphyrin-based compounds with improved photophysical characteristics. In recent years, a number of pharmaceutical companies, such as QLT Pharmaceuticals, Vancouver, B.C.; Miravant, California; Scotia Pharmaceuticals, U.K.; Ciba Vision, New Jersey; Pharmacia, Sweden; DUSA, New Jersey; Pharmacyclics, California; and Light Sciences Corp., Washington, have shown major interest in PDT. However, given the possible implications for the use of porphyrin-based compounds (porphyrins, chlorins, bacteriochlorins, expanded porphyrins, phthalocyanines) for the treatment of cancer by photodynamic therapy, future design strategies for new agents should be directed toward tumor-specific drug molecules. Such compounds might show greater tumor selectivity with reduced skin phototoxicity, a major problem associated with most of the porphyrin-based compounds.

References

1. Dougherty, T.J., Gomer, C., Henderson, B.W., Jori, G., Kessel, D., Korbelik, M., Moan, J., and Peng, Q., Photodynamic therapy, *J. Natl. Cancer Inst.*, 90, 889, 1998.
2. Weishaupt, K.R., Gomer, C.J., and Dougherty, T.J., Identification of singlet oxygen as the cytotoxic agent in photoinactivation of murine tumor, *Cancer Res.,* 36, 2326, 1976.
3. Pandey, R.K. and Zheng, G., Porphyrins as photosensitizers in photodynamic therapy, in *The Porphyrin Handbook*, Vol. 6, Kadish, K.M., Smith, K.M., and Guilard, R., Eds., Academic Press, New York, 2000, chap. 43.
4. Chang, C.K., Cation radicals of ferrous and free base isobacteriochlorins: models for siroheme and sirohydrochlorin, *Proc. Natl. Acad. Sci. USA*, 78, 2653, 1981.
5. Barkigia, K.M. and Fajer, J., *The Photosynthetic Reaction Center*, Vol. 2, Deisenhofer, H. and Norris, J.R., Eds. Academic Press, New York, 1993, p. 514.
6. Sherman, W.M., Allen, C.M., and van Lier, J.E., Role of activated oxygen species in photodynamic therapy, *Methods in Enzymol.*, 319, 376, 2000.

7. (a) Dougherty, T.J., Kaufman, J.H., Goldfrab, A., Weishaupt, K.R., Boyle, D., and Mittleman, A., Photoradiation therapy for the treatment of malignant tumors, *Cancer Res.*, 38, 2628, 1978; (b) Pandey, R.K., Marshall, M.S., Tsao, R., McReynolds, J.H., and Dougherty, T.J., Fast atom bombardment mass spectral analyses of Photofrin II and its synthetic analogs, *Biomed. Environ. Mass Spec.,* 19, 405, 1990 and references therein; (c) Pandey, R.K., Smith, K.M., and Dougherty, T.J., Porphyrin dimers as photosensitizers in photodynamic therapy, *J. Med. Chem.,* 33, 2032, 1990; (d) Pandey, R.K. and Dougherty, T.J., Syntheses and photosensitizing activity of porphyrins joined with ester linkages, *Cancer Res.,* 49, 2042, 1989; (e) Pandey, R.K., Shiau, F.-Y., Dougherty, T.J., and Smith, K.M., Regioselective syntheses of ether linked porphyrin dimers and trimers related to Photofrin II, *Tetrahedron*, 47, 9571, 1991 and references therein.
8. Dolphin, D., *Can. J. Chem*., 72, 1005, 1994, and references therein.
9. MacDonald, I. and Dougherty, T.J., Basic principles of photodynamic therapy, *J. Porphyrins Phthalocyanines*, 5, 105, 2001.
10. Whitlock, H.W., Hanaurer, R., Oester, M.Y., and Bower, B.K., Diimide reduction of porphyrins, *J. Am. Chem. Soc.,* 91, 7485, 1969.
11. Bonnett, R., Photosensitizers of the porphyrin and phthalocyanine series for photodynamic therapy, *Chem. Soc. Rev.*, 24, 19, 1995.
12. Hamata, M., in *Advances in Cycloaddition*, Vol. 4, Hamata, M., Ed., Jai Press, London, U.K., 1998.
13. Callot, H.L., Johnson, A.W., and Sweeney, A., Addition to porphyrins involving the formation of new carbon–carbon bonds, *J. Chem. Soc. Perkin Trans. I*, 1424, 1973.
14. Morgan, A.R., Pangka, V.S., and Dolphin, D., Ready syntheses of benzoporphyrins vis Diels–Alder reactions with protoporphyrin IX, *Chem. Commun*., 1047, 1984.
15. (a) Meunier, I., Pandey, R.K., Walker, M.M., Senge, M.O., Dougherty, T.J., and Smith, K.M., New syntheses of benzoporphyrin derivatives and analogs for use in photodynamic therapy, *Bioorg. Med. Chem. Lett*., 2, 1575, 1992; (b) Meunier, I., Pandey, R.K., Senge, M.O., Dougherty, T.J., and Smith, K.M., Benzoporphyrin derivatives: synthesis, structure and preliminary biological activity, *J. Chem. Soc. Perkin Trans. 1*, 961, 1994; (c) Pandey, R.K., Potter, W.R., Meunier, I., Sumlin, A.B., and Smith, K.M., Structure-activity relationships among benzoporphyrin derivatives, *Photochem. Photobiol*., 62, 764, 1995.
16. Pandey, R.K., Shiau, F.Y., Ramachandran, K., Dougherty, T.J., and Smith, K.M., Long wavelength photosensitizers related to chlorins and bacteriochlorins for the use in photodynamic therapy, *J. Chem. Soc. Perkin Trans. 1*, 1377, 1992.
17. Yon-Hin, P., Wijesekera, T.P., and Dolphin, D., A convenient synthetic route for the bacteriochlorin chromophore, *Tetrahedron Lett.,* 32, 2875, 1991.
18. Morgan, A.R., Skalkos, D., Garbo, G.M., Keck, R.W., and Selman, S.H., Synthesis and *in vivo* photodynamic activity of some bacteriochlorin derivatives against bladder tumors in rodents, *J. Med. Chem.,* 34, 2126, 1991.
19. Morgan, A.R., unpublished results.
20. Arnold, D.P., Johnson, A.W., and Williams, G.A., Wittig condensation products from nickel mesoformyl-octaethylporphyrin and aetioporphyrin-I and some cyclization reactions, *J. Chem. Soc. Perkin Trans. I,* 1660, 1978.
21. (a) Morgan, A.R., Garbo, G.M., Ranapersaud, A., Shalkos, D., Keck, R.W., and Selman, S.H., Photodynamic action of benzochlorins, *Proc. SPIE*, 146, 1065, 1989; (b) Morgan, A.R., Skalkos, D., Maguire, G., Ranpersaud, A., Garbo, G., Keck, K., and Selman, S.H., Observations of the synthesis and in vivo photodynamic activity of some benzochlorins, *Photochem. Photobiol*., 55, 133, 1992.
22. (a) Li, G., Graham, A., Potter, W.R., Grossman, Z.D., Oseroff, A., Dougherty, T.J., and Pandey, R.K., A simple and efficient approach for the synthesis of fluorinated and non-fluorinated octaethylporphyrin-based benzochlorins with variable lipophilicity. Their in vivo tumor uptake, and the preliminary *in vitro* photosensitizing efficacy, *J. Org. Chem.,* 66, 1316, 2001; (b) Li, G., Graham, A., Oseroff, A., Dougherty, T.J., and Pandey, R.K., unpublished results.

23. Li, G., Chen, Y., Missert, J.R., Rungta, A., Dougherty, T.J., and Pandey, R.K., Application of Ruppert's reagent in preparing novel perfluorinated porphyrins, chlorins and bacteriochlorins, *J. Chem. Soc. Perkin. Trans. 1*, 1785, 1999.
24. Vicente, M.G.H., Rezanno, I.N., and Smith, K.M., Efficient new syntheses of benzochlorins, isobacteriochlorins and bacteriochlorins, *Tetrahedron Lett.,* 31, 1365, 1990.
25. Morgan, A.R. and Gupta, S., Synthesis of benzopurpurins, isobacteriobenzopurpurins and bacteriobenzopurpurins, *Tetrahedron Lett.,* 35, 4291, 1994.
26. Woodward, R.B. et al., The total synthesis of chlorophyll-a, *J. Am. Chem. Soc.*, 82, 3800, 1960, and *Tetrahedron,* 46, 7599, 1990.
27. Morgan, A.R., Garbo, G.M., Keck, R.W., and Selman, S.H., New photosensitizers for photodynamic therapy: combined effect of metallopurpurin derivatives and light in transplantable bladder, *Cancer Res.,* 48, 194, 1988.
28. (a) Gunter, M.J. and Robinson, B.C., Purpurins bearing functionality at the 6,16 meso-positions: synthesis from 5,15-disubstituted meso-[β-(methoxycarbonyl)vinyl] porphyrins, *Aust. J. Chem.,* 43, 1839, 1990; (b) Forsyth, T.P., Nurco, D.J., Pandey R.K., and Smith, K.M., Syntheses and structure of 5,15-bis-(4-pyridyl)purpurins, *Tetrahedron Lett.*, 36, 9093, 1995.
29. Smith, K.M., Ed., *Porphyrins and Metalloporphyrins*, Elsevier, Amsterdam; New York, 1975.
30. Pandey, R.K., Bellnier, D.A., Smith, K.M., and Dougherty, T.J., Chlorin and porphyrin derivatives as potential photosensitizers in photodynamic therapy, *Photochem. Photobiol.,* 53, 65, 1991.
31. Bommer, J.C. and Burnham, B.F., Tetrapyrrole compounds, *Euero Patent* 169831, 1986.
32. Gomi, S., Nishizuka, T., Ushiroda, O., Uchida, N., Takahashi, H., and Sumi, S., The structures of mono-L-aspartyl chlorin e_6 and its related compounds, *Heterocycles*, 48, 2231, 1998.
33. (a) Nelson, J.S., Roberts, W.G., and Berns, M.W., *In vivo* studies on the utilization of mono-L-aspartyl chlorin (NPe_6) in photodynamic therapy, *Cancer Res.,* 47, 5681, 1987; (b) Roberts, W.G., Shiau, F.Y., Nelson, J.S., Smith, K.M., and Berns M.W., *In vitro* characterization of monoaspatyl chlorin e_6 and diaspartyl chlorin e_6 for photodynamic therapy, *J. Natl. Cancer Inst.*, 80, 330, 1988.
34. Pandey, R.K., Sumlin, A.B., Constantine, S., Potter, W.R., Bellnier, D.A., Henderson, B.W., Rodgers, M.A., Smith, K.M., and Dougherty, T.J., Alkyl ether analogs of chlorophyll-a derivatives. Synthesis, photophysical properties and photodynamic efficacy of chlorophyll-a derivatives, *Photochem. Photobiol.,* 64, 194, 1996.
35. Henderson, B.W., Bellnier, D.A., Greco, W.R., Sharma, A., Pandey, R.K., Vaughan, L.A., Weishaupt, K.R., and Dougherty, T.J., An *in vivo* quantitative structure-activity relationship for a congeneric series of pyropheophorbide derivatives as photosensitizers for photodynamic therapy, *Cancer Res.,* 57, 4000, 1997.
36. Dougherty, T.J., Pandey, R.K., Nava, H.R., Smith, J.A., Douglass, H..O., Edge, S.B., Bellnier, D.A., and Cooper, M., Preliminary clinical data on a new photodynamic therapy photosensitizer — HPPH, *Proc. SPIE*, 3909, 25, 2000.
37. Lee, S.H., Jagerovic, N., and Smith, K.M., Use of chlorophyll derivative purpurin-18 for syntheses of sensitizers for use in photodynamic therapy, *J. Chem. Soc. Perkin Trans. 1*, 2369, 1993.
38. Kozyrev, A.N., Zheng, G., Lazarou, E., Dougherty, T.J., Smith, K.M., and Pandey, R.K., Synthesis of emeraldin and purpurin-18 analogs as target-specific photosensitizers for photodynamic therapy, *Tetrahedron Lett.*, 38, 3335, 1997.
39. Zheng, G., Potter, W.R., Camacho, S.H., Missert, J.R., Wang, G., Bellnier, D.A., Henderson, B.W., Rodgers, M.A.J., Dougherty, T.J., and Pandey, R.K., Synthesis, photophysical properties, tumor uptake and preliminary *in vivo* photosensitizing efficacy of a homologous series of 3-(1-alkoloxy)ethyl-3-devinyl-purpurin-18-*N*-alkylimides with variable lipophilicity, *J. Med. Chem.*, 44, 1540, 2001.
40. (a) Zheng, G., Potter, W.R., Sumlin, A.B., Dougherty, T.J., and Pandey, R.K., Photosensitizers related to purpurin-18-*N*-alkylimides. A comparative *in vivo* tumoricidal ability of ester versus amide functionalities, *Bioorg. Med. Chem. Lett.*, 10, 123, 2000; (b) Rungta, A., Zheng, G., Missert, J.R., Potter, W.R., Dougherty, T.J., and Pandey, R.K., Purpurinimides as photosensitizers: effects of the

position and presence of the substituents in the *in vivo* photodynamic efficacy, *Bioorg. Med. Chem. Lett*., 10, 1463, 2000.
41. Pandey, R.K., Jagerovic, N., Ryan, J.M., Dougherty, T.J., and Smith, K.M., Syntheses and preliminary *in vivo* photodynamic efficacy of benzoporphyrin derivatives from phylloerythrin and rhodoporphyrin XV methyl ester and aspartyl amides, *Tetrahedron,* 52, 5349, 1996.
42. Ma, L. and Dolphin, D., Chemical modification of chlorophyll-a: synthesis of new regiochemically pure benzoporphyrin and dibenzoporphyrin derivatives, *Can. J. Chem*. 75, 262, 1997.
43. Mettath, S., Dougherty, T.J., and Pandey, R.K., Cycloaddition reaction of 2-vinylemeraldines: formation of unexpected porphyrins with seven member exocyclic ring systems, *Tetrahedron Lett*., 40, 6171, 1999.
44. Mettath, S., Synthesis of new photosensitizers and their biological significance, Ph.D. thesis, Roswell Park Graduate Division, SUNY, Buffalo, January 2000.
45. Chang, C.K. and Sotiriou, C.., Migratory aptitudes in pinacol-pinacolone rearrangement of *vic*-dihydroxychlorins, *J. Heterocyclic Chem*., 22, 1739, 1985, and references therein.
46. Pandey, R.K., Issac, M., MacDonald, I., Medforth, C.J., Senge, M.O., Dougherty, T.J., and Smith, K.M., Pinacol-pinacolone rearrangements in vc-dihydroxychlorins and bacteriochlorins. Effect of substituents at the peripheral positions, *J. Org. Chem*., 62, 1463, 1997.
47. Chang, C.K., Sotiriou, C., and Weishih, W., Differentiation of bacteriochlorin and isobacteriochlorin formation by metallation. High yield synthesis of porphyrindiones via OsO_4 oxidation, *Chem. Commun.*, 1213, 1986.
48. Kessel, D., Smith, K.M., Pandey, R.K., Shiau, F.Y., and Henderson, B.W., Photosensitization with bacteriochlorins, *Photochem. Photobiol.,* 58, 200, 1993.
49. Pandey, R.K., Tsuchida, T., Constantine, S., Zheng, G., Medforth, C., Kozyrev, A., Mohammad, A., Rodgers, M.A.J., Smith, K.M., and Dougherty, T.J., Synthesis, photophysical properties and *in vivo* photosensitizing activity of some novel bacteriochlorins, *J. Med. Chem.,* 40, 3770, 1997.
50. Zheng, G., Kozyrev, A.N., Dougherty, T.J., Smith, K.M., and Pandey, R.K., Synthesis of novel bacteriopurpurinimides by Diels-Alder cycloaddition, *Chem. Lett.,* 1119, 1996.
51. Li, G., Graham, A., Potter, W.R., Oseroff, A., Dougherty, T.J., and Pandey, R.K., unpublished results.
52. Beems, E.M., Dubbelman, T.M.A.R., Lugtenberg, J., Best, J.A.V., Smeets, M.F.M.A., and Boefheim, J.P.J., Photosensitizing properties of bacteriochlorophyll-a and bacteriochlorin-a, *Photochem. Photobiol.,* 46, 639, 1987.
53. Henderson, B.W., Sumlin, A.B., Owczarczak, B.L., and Dougherty, T.J., Bacteriochlorophyll-a as photosensitizer for photodynamic treatment of transplantable murine tumors, *J. Photochem. Photobiol.*, 10, 303, 1991.
54. Moan, J., Peng, Q., Evenson, J.F., Berg, K., Western, A., and Rimington, C., Photosensitizing efficacy, tumor and cellular uptake of different photosensitizing drugs for photodynamic therapy, *Photochem. Photobiol.*, 46, 713, 1987.
55. Pandey, R.K. and Herman, C., Shedding some light on tumors, *Chem. Ind.*, 739, 1998.
56. Kozyrev, A.N., Zheng, G., Dougherty, T.J., Smith, K.M., and Pandey, R.K. Syntheses of stable bacteriochlorophyll-a derivatives as potential photosensitizers for PDT, *Tetrahedron Lett.*, 37, 6431, 1996.
57. Chen, Y., Graham, A., Potter, W.R., Morgan, J., Vaughan, L., Bellnier, D.A., Henderson, B.W., Oseroff, A., Dougherty, T.J., and Pandey, R.K., Bacteriopurpurinimides: highly stable and potent photosensitizer for photodynamic therapy, *J. Med. Chem.*, 45, 255, 2002.
58. Chen, Y., Pandey, R.K. et al., unpublished results.
59. Mody, T.R. and Sessler, J.L., Texaphyrins: a new approach to drug development, *J. Porphyrins Phthalocyanines*, 5, 892, 1996.
60. Young, S.W., Woodburn, K.W., Wright, M., Modt, T.D., Fan, Q., Sessler, J.L., Dow, W.C., and Miller, R.A., Lutetium texaphyrin (PC-0123): a near-infrared water-soluble photosensitizer, *Photochem. Photobiol.,* 63, 692, 1996.

61. Young, S.W., Quing, F., Harriman, A., Sessler, J.L., Dow, W.C., Mody, T.D., Hemmi, G.W., Hao, Y., and Miller, A., Gadolinium(III) texaphyrin: a tumor selective radiation sensitizer that is detectable by MRI, *Proc. Natl. Acad. Sci. USA*, 93, 6610, 1996.
62. Allen, C.M., Sharman, W.M., and van Lier, J.E., Current status of phthalocyanines in the photodynamic therapy of cancer, *J. Porphyrins Phthalocyanines*, 5, 161, 2001.
63. Olenick, N.L., Antunez, A.R., Clay, M.E., Rihter, B.D., and Kenney, M.E., New phthalocyanine photosensitizers for photodynamic therapy, *Photochem. Photobiol.*, 57, 242, 1993.
64. Sherman, W.M., Allen, C.M., and van Lier, J.E., Photodynamic therapeutics: basic principles and clinical applications, *Current Trends*, Vol. 4, Elsevier Scientific, London, 1999, p. 507.
65. Hu, Ma, Brasseur, N., Yildiz, S.Z., van Lier, J.E., and Leznoff, C.C., Hydroxyphthalocyanines as potential photodynamic agents for cancer therapy, *J. Med. Chem*, 41, 1789, 1998.
66. Aoudia, M., Cheng, G.Z., Kennedy, V.O., Kenney, M.E., and Rodgers, M.A.J., Synthesis of a series of octabutoxy- and octabutoxybenzonaphthalocyanines and photophysical properties of two members of the series, *J. Am. Chem. Soc.,* 119, 6029, 1997.
67. He, J., Larkin, J.E., Li, Y.S., Rihter, B.D., Zaidi, S.I.A., Rodgers, M.A.J., Mukhtar, H., Kenney, M.E., and Oleinick, N.L., The synthesis, photophysical and photobiological properties and *in vitro* structure-activity relationships of a set of silicon-phthalocyanine PDT photosensitizers, *Photochem. Photobiol.*, 65, 581, 1997.
68. (a) Schmidt-Erfurth, U., Diddens, H., Birngruber, R., and Hasan, T., Photodynamic targeting of human retinoblastoma cells using covalent low density lipoprotein conjugates, *Br. Jr. Cancer*, 75, 54, 1997; (b) Finger, V.H., Guo, H.H., Lu, Z.H., and Peiper, S.C., Expression of chemokine receptors by endothelial cells: detection by intravital microscopy using chemokine-located fluorescent microspheres, *Methods in* Enzymol., 28, 148, 1997.
69. Pandey, R.K., Photosensitizers related to chlorins and bacteriochlorins, effect of lipophilicity in PDT efficacy, First international conference on porphyrins and phthalocyanines, Dijon, France, Abstract SYM 149, June 25–30, 2001.
70. Hombrecher, H.K., Schell, C., and Thiem, J., Synthesis and investigation of galactopyranosylcholesteryloxy substituted porphyrins, *Bioorg. Med. Chem. Lett.,* 6, 1199, 1999.
71. Donald, P.J., Cardiff, R.D., He, D., and Kendell, K., Monoclonal antibody-porphyrin conjugate for head and neck cancer, the possible magic bullet, *Head Neck Surg.*, 105, 781, 1991.
72. Hemming, A.W., Davis, N.L., Dubois, B. et al., Photodynamic therapy of squamous cell carcinoma. An evaluation of a new photosensitization agent, benzoporphyrin derivatives and new photoimmunoconjugate, *Surg. Oncol.*, 2, 187, 1993.
73. Vrouenraets, M.B., Visser, G.W.M., Stewart, F.A. et al., Development of *meta*-tetrahydroxyphenylchlorin-monoclonal antibody conjugate for photoimmunotherapy, *Cancer Res.,* 59, 1505, 1999.
74. Karagianis, G., Reiss, J.A., Marchesini, R. et al. Biophysical and biological evaluation of porphyrin-bisacridine conjugates, *Anti-Cancer Drug Design,* 11, 205, 1996.
75. Bachor, B.S., Shea, C.R., Gillies, R., and Hasan, T., Photosensitized destruction of human bladder carcinoma cells treated with chlorine e_6-conjugated microspheres, *Proc. Natl. Acad. Sci., USA*, 88, 1580, 1991.
76. Ali, H. and van Lier, J.E., Metal complexes as photo- and radiosensitizers, *Chem. Rev.*, 99, 2379, 1999.
77. Brasseur, N., Langlois, R., La Madeleine, C., Ouellet, R., and van Lier, J.E., Receptor-mediated targeting of phthalocyanines to macrophages via covalent coupling to native or maleylated bovine serum albumin, *Photochem. Photobiol.*, 69, 345, 1999.
78. Allen, C.M., Sharman, W.M., La Madeleine, C., Weber, J.M., Langlois, R., Guellet, R., and van Lier, J.E., Photodynamic therapy: tumor targeting with adenoviral proteins, *Photochem. Photobiol.,* 70, 512, 1999.
79. Lutsenko, S.V., Feldman, N.B., Finakova, G.V., Posypanova, G.A., Severin, S.E., Skryabin, K.G., Kirpichnikov, M.P., Lukyanets, E.A., and Vorozhtsov, G.N., Targeting phthalocyanines to tumor cells using epidermal growth factor conjugates, *Tumor Biol.,* 20, 218, 1999.

80. Sears, P. and Wong, C.H., Carbohydrate mimetics: a new strategy for tackling the problem of carbohydrate-mediated biological recognition, *Angew. Chem. Int. Ed. Eng.*, 38, 2301, 1999.
81. Lee, Y.C. and Lee, R.T., Carbohydrate-protein interactions: basis of glycobiology, *Acc. Chem. Res.*, 28, 321, 1995.
82. Schell, C. and Hombrecher, H.K., Synthesis and investigation of glycosylated mono- and diarylporphyrins for photodynamic therapy, *Bioorg. Med. Chem. Lett.*, 6, 1199, 1996.
83. Mikata, Y., Onchi, Y., Tabata, K., Ogure, S., Okura, I., Ono, H., and Yano, S., Sugar-dependent photocytotoxic property of tetra- and octa-glycoconjugated tetraphenyl porphyrins, *Tetrahedron Lett.,* 19, 4505, 1998.
84. Cornia, M., Valenti, C., Capacchi, S., and Cozzini, P., Synthesis, characterization and conformational studies of lipophilic, amphiphilic and water-soluble c-glyco-conjugated porphyrins, *Tetrahedron*, 54, 8091, 1998.
85. Millard, P., Guerquin-Kern, J.-L., Huel, C., and Momemteau, M., Glycoconjugated porphyrins: synthesis of sterically constructed polyglycosylated compounds derived from tetraphenylporphyrins, *J. Org. Chem*, 58, 2774, 1993.
86. Ono, N., Bougauchi, M., and Marutama, K., Water-soluble porphyrins with four sugar molecules, *Tetrahedron Lett.,* 33, 1629, 1992.
87. Sol, V., Blais, J.C., Bolbach, G., Carre, V., Granet, R., Guillonton, M., Spiro, M., and Krausz, P., Toward glycosylated peptide porphyrins: a new strategy for PDT, *Tetrahedron Lett.*, 38, 6391, 1997; Synthesis, spectroscopy, and phototoxicity of glycosylated amino acid porphyrin derivatives as promising molecules for cancer therapy, *J. Org. Chem.*, 64, 4431, 1999.
88. Millard, P., Hery, C., and Momemteau, M., Synthesis, characterization and phototoxicity of a glycoconjugated *meso*-monoarylbenzochlorin, *Tetrahedron Lett.*, 38, 3731, 1997.
89. Adams, K.R., Berenbaum, M.C., Bonnett, R., Nizhnik, A.N., Salgado, A., and Valles, M.A., Second generation tumour photosensitizers: the syntheses and biological activity of octaethyl chlorines and bacteriochlorins with graded amphiphilic character, *J. Chem. Soc. Perkin Trans. 1*, 1465, 1992.
90. Montforts, F.P., Gerlach, B., Haake, G., Hoper, F., Kusch, D., Meier, A., Scheurich, G., Brauer, H.D., Schiwon, K., and Schermann, G., Selective synthesis and photophysical properties of tailor-made chlorins for photodynamic therapy, *Proc. SPIE*, 29, 2325, 1994.
91. Fujimoto, K., Miyata, T., and Aoyama, Y., Saccharide-directed cell recognition using monocyclic saccharide clusters: masking of hydrophobicity to enhance specificity, *J. Am. Chem. Soc.*, 122, 3558, 2000.
92. Chiariotti, L., Berlingieri, M.T., De Rosa, P., Battaglia, C., Berger, N., Bruni, C.B., and Fusco, A., Increased expression of the negative growth factor, galactoside-binding gene in transformed thyroid cells and in human thyroid carcinoma, *Oncogene,* 7, 2507, 1992.
93. Chiariotti, L., Salvatore, P., Benvenuto, G., and Bruni, C.B., Control of galectin gene expression, *Biochimie*, 81, 381, 1999.
94. Zheng, G., Graham, A., Shibata, M., Missert, J.R., Oseroff, A.R., Dougherty, T.J., and Pandey, R.K., Synthesis of β-galactose conjugated chlorines by enyne metathesis as galectin-specific photosensitizers for photodynamic therapy, *J. Org. Chem.*, 66, 8709, 2001.

145

Mechanistic Principles of Photodynamic Therapy

Barbara W. Henderson
Roswell Park Cancer Institute

Sandra O. Gollnick
Roswell Park Cancer Institute

Abbreviations

ALA, 5-aminolevulinic acid
BPD-MA, benzoporphyrin derivative, monoacid ring A
CHS, contact hypersensitivity
HpD, hematoporphyrin derivative
HPPH, hexyl pyropheophorbide ether
Lutex, lutetium texaphyrin
mTHPC, meso-tetra-hydroxyphenyl-chlorin
NPe_6, mono-L-aspartyl chlorin e_6
Pc, phthalocyanine
PDT, photodynamic therapy
PpIX, protoporphyrin IX
$SnEt_2$, tin etiopurpurin
TPPS, sulfonated tetraphenyl porphines

0-8493-1348-1/04/$0.00+$1.50

145.1 Introduction

Photodynamic therapy (PDT) exploits the biological consequences of localized oxidative damage inflicted by photodynamic processes. Three critical elements are required for the initial photodynamic processes to occur: a drug that can be activated by light (a photosensitizer), light, and oxygen.[1] Interaction of light at the appropriate wavelength with a photosensitizer produces an excited triplet-state photosensitizer that can interact with ground-state oxygen via two different pathways, designated as Type I and Type II. The Type II reaction that gives rise to singlet oxygen ($^1O_2$) is believed to be the dominant pathway, because elimination of oxygen or scavenging of $^1O_2$ from the system essentially eliminates the cytocidal effects of PDT.[2–4] Type I reactions, however, may become important under hypoxic conditions or where photosensitizers are highly concentrated.[5] The highly reactive $^1O_2$ has a short lifetime (<0.04 μsec) in the biological milieu and, therefore, a short radius of action (<0.02 μm).[6] Consequently, $^1O_2$-mediated oxidative damage will occur in the immediate vicinity of the subcellular site of photosensitizer localization. Depending on photosensitizer pharmacokinetics, these sites can be varied and numerous, resulting in a large and complex array of cellular effects. Similarly, on a tissue level, tumor cells as well as various normal cells can take up photosensitizer, which, upon activation by light, can lead to effects upon such targets as the tumor cells proper, the tumor and normal microvasculature, and the inflammatory and immune host system. PDT effects on all of these targets may influence each other, producing a plethora of responses; the relative importance of each has yet to be fully defined. It seems clear, however, that the combination of all these components is required for long-term tumor control.

145.2 Subcellular Targets for Photosensitization

The cellular targets of PDT depend on the specific pharmacokinetic characteristics, such as lipophilicity, amphiphilicity, aggregation, and serum protein interactions (reviewed in MacDonald and Dougherty[1]) of the photosensitizer, but appear to be largely independent of cell type. Localization studies were generally carried out in *in vitro* cell systems, where exposure conditions to the photosensitizer can be easily controlled or varied. Such studies revealed that cellular photosensitizer distribution can be a dynamic process, influenced by such parameters as length of exposure and drug concentration.[7–9] Photosensitizers may even relocalize after photodamage to an initial site of accumulation, such as from lysosomes to other, possibly more sensitive, cellular locations, where they will then be available for activation.[10,11] That subcellular localization of a photosensitizer, and consequently the target of PDT, may influence *in vivo* treatment outcome was demonstrated in a series of studies that could relate structure and activity of a congeneric series of pyropheophorbide-*a* ether derivatives to their subcellular localization.[9,12] The most and least active compounds in the series revealed mitochondrial localization for the former and lysosomal localization for the latter. Nevertheless, such less-active compounds can be effective photosensitizers, because the lack of sensitivity can be compensated by higher dosing, given that treatment selectivity is maintained.

Mitochondria

Although the first-generation photosensitizer Photofrin®* and its forerunners are chemically heterogeneous and, therefore, exhibit heterogeneous subcellular distributions,[8] the major target also appears to be the mitochondria.[13–16] The development of chemically pure and well-defined photosensitizers, and the use of 5-aminolevulinic acid (ALA) for the intramitochondrial generation of photosensitizing protoporphyrin IX (PpIX),[17] allowed for the targeting of specific subcellular sites and the analysis of the relative sensitivity to photodamage of these sites.[18–21] Again, the mitochondria emerged as especially sensitive targets. Recent interest focused on the mitochondrial permeability transition pore, a protein complex consisting of hexokinase, the peripheral benzodiazepine receptor (PBR), the voltage-dependent

*Registered trademark of Axcan Scandipharm Inc., Birmingham, AL.

anion channel (VDAC), creatinin kinase, the adenine nucleotide translocator (ANT), and cyclophyllin D. Several of its components were implicated as PDT targets.[22–32]

Lysosomes

Hydrophilic or highly aggregated sensitizers may be taken up by pinocytosis and endocytosis and therefore accumulate in cytoplasmic vesicles.[9,10,18,33] While PDT-induced rupture of lysosomes and release of damaging hydrolytic enzymes into the cytoplasm were described,[33,34] it appears now that lysosomes per se are not effective targets for PDT.[9,18] In a recent study, selective lysosomal photodamage that was associated with release of cathepsin B was followed by a gradual loss of mitochondrial membrane potential, release of cytochrome *c* into the cytosol, caspase 3 activation, and a limited apoptotic response.[35] Thus, lysosomal damage may secondarily mediate mitochondrial damage. It was also suggested that lysosomes might serve as reservoirs, from which photosensitizers might be released after vesicle rupture and migrate to more sensitive sites.[10] All of these studies assume that initial sensitizer accumulation is restricted to the lysosomes, but the possibility cannot be entirely excluded that high lysosomal concentration may mask small but highly effective sensitizer accumulations at other sites.[9] An innovative approach to intracellular delivery of macromolecules from endocytic vesicles, such as, for example, immunotoxins or protein encoding DNA, to the cytosol uses lysosome-targeted PDT to rupture the vesicles that entrapped these agents.[36]

Nucleus

Photosensitizers used in PDT generally do not accumulate in the cell nucleus. Therefore, frank DNA damage, such as strand breaks, sister–chromatid exchanges, and chromatid aberrations, are much less frequently observed in PDT than in ionizing or UV irradiation.[37–39] Consistent with these findings, the mutation potential of PDT was found to be significantly less than that of ionizing radiation or UV.[40]

Plasma Membrane

The plasma membrane may become a target of PDT, especially if the sensitizer is highly lipophilic and the incubation time of cells *in vitro* is brief. Membrane damage manifests itself rapidly through blebbing,[20,41] as well as leakage of cytosolic enzymes[42,43] and chromium.[44] Leakage of lactate dehydrogenase (LDH) showed the same kinetics as generation of prostaglandin E_2 from tumor cells *in vitro*, directly relating membrane disruption to production of eicosanoids.[43] The biosynthesis of eicosanoids, which play an important role in mediating the PDT tissue response (discussed below), is set in motion when phospholipases catalyze the liberation of free fatty acids from membrane phospholipids. Unsaturated phospholipids and cholesterol are important membrane targets of photodamage, and lipid peroxidation by PDT was extensively studied and linked with cell lethality.[45,46] Oxidation of intrinsic membrane proteins[47] and protein cross-linking[48] was also observed. PDT can inhibit the plasma membrane enzymes Na^+K^+-adenosine triphosphate (ATPase) and Mg^{2+}-ATPase.[49] Ca^{2+} flux may be affected, and the plasma membrane may become depolarized.[50]

Certain membrane-localized photosensitizers, such as mesotetraphenylporphines (TPPS), can destroy microtubules in interphase cells and lead to arrest of cells in mitosis.[34,51]

145.3 Mode of Cell Death

PDT can induce cell death via the apoptotic or necrotic pathways.[52] Necrosis is metabolism independent and a result of massive insult. In contrast, the apoptotic pathway is an intrinsic physiological process dependent upon active cellular metabolism and characterized by chromatin condensation, DNA fragmentation, and the formation of apoptotic bodies.[53] The dominant mode of cell death is dependent upon the photosensitizer used, the localization of the photosensitizer, and the treatment protocol.[1] Dellinger[54] demonstrated that increasing the drug incubation time, prior to administration of light, altered the mode

of cell death induced by Photofrin-PDT; longer incubation times (1 day) resulted in apoptosis, while shorter incubation times (1 h) induced necrosis. The cellular localization of Photofrin changes with time of incubation, moving from the cell membrane to the intracellular sites as the incubation time increases.[9] Similar results were recently published for zinc II phthalocyanine (Pc).[55] Studies by Kessel and Luo[19] demonstrated that photosensitizers that localize to the mitochondria (porphycenes PcM and PcD) resulted in apoptotic cell death, while those that localize to the lysosome (chlorin LCP) or cell membrane (cationic porphyrin, MCP) do not. Kessel et al.[56] also demonstrated that photodamage of the cell membrane can inhibit the induction of apoptosis by photodamage to the mitochondria. These results were confirmed by Luo and Kessel,[57] and this study also demonstrated that the mode of cell death shifts in response to the photodynamic dose, such that high doses result in a necrotic cell death, while lower doses result in an apoptotic mode of death. Similar results were recently obtained for the photosensitizer hypericin.[58]

The kinetics and extent of PDT-induced apoptosis also varies with photosensitizer and cell type treated.[56,57,59–62] Photodynamic treatment of L5178Y murine lymphoma cells with ClAlPc resulted in apoptosis within 30 min of treatment.[62] Treatment of the lymphoma line P388 with ClAlPc or tin etiopurpurin ($SnEt_2$), which localize to the lysosome and the mitochondria, induced apoptotic nuclei within 1 h.[56,57] However, treatment of the same cell line with tin octaethylpurpurin amidine, which localizes to the mitochondria, the lysosome, and the cell membranes, did not result in apoptotic nuclei until 24 h after treatment.

The rapid induction of apoptosis suggests that PDT triggers late-stage apoptotic processes directly. Release of cytochrome *c* from the mitochondria triggers caspase 3 activation and results in initiation of apoptosis at a late stage in the pathway.[63] Cytochrome *c* release is associated with a loss of mitochondrial potential. PDT results in the loss of mitochondrial potential and the rapid release of cytochrome *c*.[64–71] Several studies demonstrated that PDT also induces rapid activation of caspases 3, 6, 7, and 8 and cleavage of poly(ADP-ribose) polymerase (PARP).[61,64] Kessel and Luo showed that PDT-induced release of cytochrome *c* is sufficient to directly initiate a caspase-dependent apoptotic cell death.[72] However, a recent study by Xue et al.[73,74] indicates that while caspase 3 is required for the late stages of apoptosis, it is not the critical lethal event in PDT-induced apoptosis.

Bcl-2 was shown to block the release of cytochrome *c* from the mitochondria and thus to prevent apoptosis.[63] Several groups altered the expression of bcl-2, through overexpression or antisense technology, and demonstrated that increasing the levels of bcl-2 enhances cellular resistance to PDT-induced apoptotic cell death.[75–78] Xue et al.[79] demonstrated that Pc 4-PDT results in photochemical destruction of bcl-2. Similar results were reported for AlPc-PDT.[80] Interestingly, a study by Kim et al.[80] reported that overexpression of bcl-2 enhanced the apoptotic response. In these studies, overexpression of bcl-2 was accompanied by an increase in bax, a proapoptotic member of the bcl-2 family. PDT resulted in the selective destruction of bcl-2 but had no effect on bax. The greater apoptotic response in the cells overexpressing bcl-2 was attributed to a higher bax:bcl-2 ratio after PDT. A PDT-induced shift in the bax:bcl-2 ratio toward apoptosis was also reported.[75,81] Bcl-2 was implicated in the release of Ca^{2+} from endoplasmic reticulum and mitochondrial stores during PDT-induced apoptosis.[82]

PDT also affects other proteins implicated in apoptosis. Phospholipases C and A2, which are involved in the transient increases in intracellular calcium levels and DNA fragmentation, are activated by Photofrin-PDT.[83] The apoptotic associated proto-oncogenes c-jun and c-fos are also activated by PII-PDT.[84] Ceramide, which was linked to apoptosis in several malignant cell lines, accumulates following PDT and was associated with PDT-induced apoptosis and cytotoxicity.[85] Gupta et al.[86] demonstrated that Pc 4-PDT induces expression of nitric oxide and suggested that it may be involved in PDT-induced apoptosis. The tumor necrosis factor-related apoptosis-inducing ligand (TRAIL) was implicated in apoptosis mediated by hypericin PDT of Jurkat cells.[87] The tumor suppressor gene p53, which is able to force damaged cells into the apoptotic pathway, was found to be associated with Photofrin-PDT resistance,[88,89] although there were dichotomous reports on the role of p53 in PDT sensitivity.[90] Finally, similarly diverse effects on apoptosis were described for IL-6, a cytokine strongly induced by PDT,[91,92] when it was transduced into cells *in vitro*. While one report described increased PDT-induced apoptosis in IL-6 overexpressing

cells due to an increased bax/bcl-2 ratio,[81] another reports enhanced resistance to PDT-induced apoptosis and tumorigenic potential.[93]

145.4 Molecular Mechanisms

Alterations in gene expression are generally due to changes in the molecular mediators present in the cell. PDT was shown to alter the expression of several molecular mediators, including the redox-regulated transcription factor, AP-1.[91,94] AP-1 is induced by changes in the redox potential[95–97] and hypoxia.[98] It is composed of homodimers of the products of the c-jun gene family or heterodimeric combinations of c-jun and c-fos family members. PDT induces prolonged expression of c-fos and c-jun as a result of oxidative stress.[84,99] Therefore, modulation of AP-1 activity by PDT might be mediated by changes in oxidative potential as a result of the generation of singlet oxygen or PDT-induced hypoxia.

NF-κB plays a critical role in the expression of immunomodulatory and proinflammatory genes.[100] Activated NF-κB is a heterodimeric protein most commonly comprised of the p50 and p65 (Rel A) species. It is also activated in response to cellular oxidative stress.[101] NF-κB is sequestered in the cytoplasm by IκB proteins; phosphorylation of IκB results in its proteosomal degradation and release of NF-κB.[102,103] NF-κB binding activity was found to be induced by PDT[104–106] and was proposed to play a role in determining the cellular response to PDT.[107] Granville et al.[104] demonstrated that cellular levels of IκB were transiently depressed following Verteporfrin®-PDT. Pyropheophorbide — a methyl ester — PDT also leads to IκB degradation.[106] In contrast to these studies, other groups failed to demonstrate NF-κB activation following Photofrin-PDT.[91,94] Thus, NF-κB activation may be photosensitizer specific. It was also suggested that activation is related to PDT dose in that higher doses do not result in decreases in IκB.[104]

In addition to AP-1 and NF-κB activation, PDT was been shown to stimulate stress kinase signaling pathways (SAPK/JNK, p38/HOG1)[108,109] and HS1 phosphorylation,[110] as well as stress response transcriptional activators. HIF-1 (hypoxia inducible factor-1) is a key regulator of the cellular response to hypoxia and is induced in response to PDT.[111,112] PDT also enhanced the expression of the HIF-1 target gene, vascular endothelial growth factor (VEGF),[112] and it was proposed that HIF-1 expression may act as a predictor of PDT responsiveness.[111] Cyclooxygenase (COX)-2 expression was found upregulated by PDT in preclinical tumor models, and combined PDT and COX-2 inhibitor treatment proved beneficial for tumor control.[113] Finally, PDT activates the heat shock protein (HSP) family promoters[114] and induces the expression of HSPs and the related glucose regulated proteins,[115–119] as well as heme oxygenase (HSP 32).[120] Luna et al.[121] used the PDT-induced activation of the GRP-78 promoter as a molecular switch to drive the expression of the herpes simplex virus-thymidine kinase (HSV-tk) suicide gene in murine tumor cells *in vitro* and *in vivo*. HSPs 27 and 60 were implicated in the resistance of cells to PDT-mediated oxidative damage.[122,123] Finally, Ahmad et al.[124] demonstrated that PDT can result in a downmodulation of the protein expression and phosphorylation of the epidermal growth factor receptor (EGFR) that may have important consequences for PDT surviving tumor cells.

145.5 Tissue Targets of Photosensitization

Tumor Cells

The capacity of PDT to eliminate tumor cells through direct photodamage was most effectively studied by *in vivo–in vitro* tumor explant methodology.[125] Such in-depth analysis revealed that the full potential of direct photodynamic tumor cell kill, provided by the gross tumor photosensitizer concentration and absorbed light dose, is generally not realized by *in vivo* PDT treatment.[126] Clonogenic assays carried out with a number of different photosensitizers and tumor systems immediately after potentially curative PDT exposures *in vivo* revealed that at most, 1 to 2 logs of direct tumor cell kill were achieved,[127–132] far less than the 7 to 8 logs required for tumor cure. Clearly, limitations to direct tumor cell kill exist *in vivo*, the most important of which may be the following:

1. Inhomogeneous photosensitizer distribution within the tumor, including a gradual decrease of photosensitizer concentration with distance from blood vessels.[133]
2. Insufficient light penetration through the tissue (light is attenuated exponentially with depth of tissue penetration).[134,135]
3. Insufficient oxygen availability (discussed below).

That intrinsic tumor cell sensitivity contributes to the overall PDT response was suggested by studies using tumor cells selected to be resistant to PDT.[136] Tumors of resistant phenotype were less responsive to PDT than sensitive tumors, while exhibiting equal vascular responses. The studies did not exclude the possibility, however, that tumor immunogenicity might have differed in the two tumor lines, thus affecting the response. On the other hand, tumors expressing a multidrug-resistance phenotype that prevented the uptake of a cationic photosensitizer were, nevertheless, found responsive to PDT carried out with that agent, the antitumor effect being attributed to vascular disruption.[137] Studies like these illustrate the capacity of PDT to exert its antitumor action through several different tissue targets.

Initial studies trying to establish a pattern of selectivity of photosensitizer uptake in malignant versus normal cells *in vitro* were largely unsuccessful.[138] *In vivo*, moderately favorable tumor-to-normal-tissue ratios can be found for almost all photosensitizers, with establishment of these ratios depending on the specific pharmacokinetics of the compound as well as the pathophysiology of the tumor (for detailed reviews see the literature[1,139,140]). Mechanisms invoked for this "selectivity" range from leaky vasculature and impaired lymphatic drainage in tumors, to low tumor pH and an increase in low-density lipoprotein and other membrane receptors on tumor cells.[141,142] Carrier systems, such as photosensitizer (immuno) conjugates, were designed to direct the photosensitizer directly to the tumor cells. Such conjugates were directed against epitopes on ovarian[143–145] and colon cancer cells,[146] as well as against the epidermal growth factor receptor (EGFR) that is overexpressed in oral precancer.[147]

Microvasculature

The microvasculature was one of the earliest tissue targets identified, because vascular PDT effects are rapid and dramatic, especially with the use of the sensitizer Photofrin and its forerunners. Reduction and cessation of tumor microcirculation following *in vivo* PDT exposure employing a variety of photosensitizers were demonstrated in preclinical models through numerous different techniques, including window chamber observation,[148,149] radiobiological assay,[150] tracers,[151,152] contrast-enhanced MRI,[153] oxygen microelectrodes,[151,154] laser Doppler,[155] and hypoxia markers.[156] Because the kinetics of vascular shutdown and tumor cell death coincide[128,157] and inhibition of shutdown retards tumor response,[158] it was argued that disruption of the tumor microcirculation is a major factor contributing to tumor control by PDT. Differences in response between tumor and normal microvasculature are subtle and difficult to discern.[159] Careful dose-ranging studies revealed that the tumor vasculature is slightly more susceptible to shutdown than its normal counterpart.[160,161] It was also demonstrated that Photofrin-PDT at high fluence rate can protect the normal skin microvasculature, but the same treatment fails to protect tumor vessels.[151,162] Occlusion of the tumor-surrounding vasculature can contribute to tumor control, at least in preclinical models, presumably by adding to the nutrient deprivation and retardation of vascular resupply of the tumor.[160,163] Another approach toward retardation of vessel regrowth after PDT is the use of antiangiogenic agents in combination with PDT, which was shown to enhance long-term tumor control.[112,164] PDT-mediated ischaemia may be transient, and the oxidative stress following tissue reperfusion may contribute to tumor control.[165,166]

The acute manifestations of PDT-induced vascular damage greatly depend on the type and dose of photosensitizer used. On the microscopic level, vascular changes in a rat cremaster muscle preparation after Photofrin PDT included vessel constriction, occlusive platelet thrombi in arteries, arterioles, veins and venules, edema, and neutrophil margination and migration.[148,167,168] Ultrastructural features included damage to numerous endothelial cell organelles, as well as perivascular changes, such as degranulation of perivascular mast cells and damage to myocytes.[167] Npe_6 (mono-L-aspartyl chlorin e_6)-PDT in a rat chondrosarcoma model resulted in obstructive platelet thrombi but no vasoconstriction.[169] PDT with

variously substituted zinc Pcs, tested in the same tumor model, showed a spectrum of effects, including vessel constriction and leakage, with one compound (disulfonated zinc Pc) exhibiting no apparent effects.[149]

Numerous vascular response mediators seem to be involved in these processes, including histamine,[170] serotonin,[171] clotting factors,[172] and most prominently, eicosanoids.[43,173,174] The latter are products of the release from the cell membrane of arachidonic acid that is subsequently metabolized by cyclooxygenase to generate prostaglandins and thromboxanes, and by lipoxygenase to form leukotrienes and hydroxy acids. The generation of a wide spectrum of arachidonic acid metabolites by PDT was described in mast cells, macrophages, endothelial cells, platelets and tumor cells, as well as in animals. Interestingly, *in vitro* PDT exposure of platelets blocks their capacity to aggregate,[175,176] and *in vitro* exposure of endothelial cells is dominated by the release of prostacyclin (PGI_2) that inhibits platelet aggregation.[176] These *in vitro* findings contradict the well-established, proaggregating mechanisms observed *in vivo* and demonstrate the difficulty of translating *in vitro* data to the *in vivo* situation. The latter represents a much more complex interplay of mechanistic components that likely involves platelets, endothelial cells, leukocytes, macrophages, and other stromal cells. Thromboxane appears to play a major role in mediating the observed vascular effects, at least in rat models.[174] Anti-inflammatory drugs, such as indomethacine or aspirin, can block the release of eicosanoids *in vitro*[43,176] and *in vivo*.[149,174,177,178] Rats made thrombocytopenic and thus deprived of a source for thromboxane generation also showed a diminished vascular response.[179] Eicosanoids, as well as serotonin, appear to also be involved in changes of tumor interstitial pressure observed after Photofrin-PDT, a consequence of fluid leakage from the vasculature, possibly contributing to occlusion of the tumor microvasculature.[180]

145.6 Tumor Oxygenation and PDT

Any restriction of tissue oxygen supply *during* PDT light delivery will reduce $^1O_2$ production and, therefore, have negative consequences for treatment outcome. Such restrictions can arise from numerous sources, including preexisting tumor hypoxia, acute vascular damage, and photochemical oxygen depletion. All of these can interact, and the dynamics of these interactions may determine treatment success.

Preexisting Tumor Hypoxia

Preexisting tumor hypoxia, a therapeutic problem still grappled with by radiation oncologists because of the oxygen dependence of sparsely ionizing radiation treatment, may limit the oxygen supply for PDT as well. Solid tumors are prone to develop hypoxic tumor regions due to deteriorating diffusion geometry, structural abnormalities of tumor microvessels, and disturbed microcirculation.[181] Hypoxic, but viable, tumor cells located in these areas may be protected from PDT-induced photodamage. In a preclinical study, Fingar et al.[182] manipulated tumors pharmacologically and physically to induce a wide range of hypoxic tumor fractions (~2% to ~40%) and followed this by aggressive Photofrin-PDT. It was found that hypoxic fractions below 5% did not adversely affect tumor control, hypoxic fractions of ~10% slightly diminished tumor control, and hypoxic fractions of ~40% totally blocked tumor control. Vascular shutdown and nutrient deprivation following PDT were believed to be responsible for the elimination of small numbers of initially surviving hypoxic tumor cells. Early preclinical attempts to raise tumor oxygenation prior to PDT through the administration of a perfluorochemical emulsion and carbogen breathing were highly successful in increasing tumor oxygen levels (~10-fold) up to 1 h after PDT. The intervention did not alter long-term tumor control,[183] probably because the vascular damage induced by the aggressive PDT regime overwhelmed any subtle improvement in treatment outcome that might have been attributed to increased tumor oxygenation. More recent studies, preclinical and clinical, demonstrated significantly improved PDT efficiency with adjuvant administration of hyperbaric oxygen or carbogen.[77,184,185]

The factor, however, that probably influences preexisting tumor hypoxia most profoundly is one that accompanies most PDT treatments, namely, changes in tumor temperature. Temperature increases due

to PDT light delivery were analyzed by Svaasand et al.[186] and recorded in preclinical models[187] and in patient's tumors.[188] Measurements of baseline intratumoral temperature and pO_2 in nodular basal cell carcinomas demonstrated a linear relationship between increasing tumor pO_2 and lesion temperature in the ranges between 0 to 20 mm Hg and 30 to 35°C.[188] Upon laser illumination during Photofrin-PDT, the temperature in these lesions increased further in a fluence-rate-dependent manner. Surprisingly, even low-fluence-rate light produced significant temperature rises (150 mW/cm^2: median temperature change +1.°9C [range 1.0 to 6.2], 30 mW/cm^2: median temperature change +1.5°C [range -1.3 to 3.6]), and these correlated with increased tumor pO_2. Whether these relationships hold true for tumors other than skin tumors remains to be seen.

Oxygen Limitation through Vascular Damage

With photosensitizers that can acutely constrict and occlude vessels, blood flow obstruction can be marked, rapidly limiting the oxygen supply to the tumor. Photofrin-PDT in mouse models, for example, rendered up to 10% of tumor cells hypoxic within a moderate light exposure (45 J/cm^2, 10 min).[126] This hypoxia was persistent and progressive with time, 50% of tumor cells being hypoxic within 1 h of such light exposure. Similar observations were reported for a rabbit skin tumor model, where a series of brief light exposures resulted in induction of irreversible tumor hypoxia that was cumulative with the number of exposures, i.e., fluence.[189] Hypoxia induction by PDT depends greatly on the vascular supply of a given tumor, and even on the site of tumor implantation in rodent models.[190] Transient reoxygenation may occur, depending on PDT dose.[190] With certain second-generation sensitizers, many of which exert less severe acute effects on the vasculature than Photofrin,[149] and a tendency toward the use of lower drug doses, such acute vascular effects are less likely to occur. As discussed above, the extent and timing of vascular damage, and therefore induction of tumor hypoxia, are of significant importance for treatment outcome. Vascular occlusion can be detrimental when occurring during treatment but beneficial when occurring *after* completion of the PDT tumor treatment.

Oxygen Limitation through Photochemical Oxygen Depletion

Photochemical oxygen depletion is roughly characterized by instantaneous or near instantaneous development of tumor hypoxia upon light exposure of a photosensitized tumor or tissue and equally rapid reoxygenation upon cessation of light. The theoretical basis for this phenomenon was provided through mathematical modeling of the dynamic changes to be expected in tissue when oxygen is consumed in the process of $^1O_2$ generation.[191,192] Photochemical oxygen depletion will occur in tissue if the rate of photodynamic oxygen consumption is faster than the rate of oxygen resupply from the vasculature. The major parameters that determine whether or not photochemical oxygen depletion will occur are as follows:

1. Absorption coefficient of the photosensitizer
2. Tissue concentration of the photosensitizer
3. Fluence rate of light
4. Vascular supply of the tissue.[191,193,194]

If the first three parameters are high, $^1O_2$ production will be rapid, and oxygen depletion will be favored; if the vascular supply of the tissue is poor, oxygen depletion will also be favored. The mathematical predictions were validated in tightly defined *in vitro* systems,[195,196] in tumor models,[151,156,189,197] and in humans.[188] Light fluence rate is the most easily controlled parameter, one that can be readily modulated during light delivery. Therefore, much attention is paid to the effects of fluence rate on PDT oxygen consumption. It is clear that lowering of the fluence rate can diminish or eliminate photochemical oxygen consumption through lowering the $^1O_2$ generation rate. However, the optimal fluence rate will depend on the other parameters listed above, and will therefore vary from situation to situation. In human tumors, the variability is great, among patients and among lesions in the same patient.[188]

The Role of Photobleaching in Photochemical Oxygen Depletion

Photobleaching is the destruction of the photosensitizer by light-mediated processes.[198–201] Because photosensitizer concentration is one of the major determinants for photochemical oxygen depletion, it stands to reason that the destruction of photosensitizer through photobleaching during PDT will reduce the likelihood that oxygen depletion will occur. The most detailed studies of photobleaching were carried out in an *in vitro* multicell tumor spheroid model.[202] It was shown that sustained illumination of Photofrin photosensitized spheroids led to a progressive decrease of photochemical oxygen depletion, implying reduction of photosensitizer levels, and being consistent with a theoretical model in which bleaching occurs via a self-sensitized singlet oxygen reaction with the photosensitizer ground state. Similarly, protoporphyrin IX was degraded by $^1O_2$-mediated mechanisms, while another photosensitizer (Nile blue selenium) was degraded by $^1O_2$-independent mechanisms.[203] Oxygen measurements in rodent tumor models and human basal cell carcinomas also implicated photobleaching in influencing photochemical oxygen depletion.[151,188] In these studies, significant oxygen depletion was observed during the early time periods of illumination at high fluence rates of Photofrin-photosensitized lesions, but less or no oxygen depletion was detected toward the end of illumination, implying that the Photofrin concentration was reduced through photobleaching below the threshold needed for oxygen depletion.

Enhancement of PDT Efficiency through Modified Light Delivery Schemes

It is evident that any means by which the well-oxygenated tumor volume can be increased during light exposure should have beneficial effects on treatment outcome. Downward adjustment of treatment fluence rate is one such means, fractionation of light delivery is another.[151,204–207] While the former allows for continuous maintenance of oxygen levels sufficient for $^1O_2$ production, the latter facilitates reoxygenation of the tissue between light exposures. Significant enhancements of tumor response were observed with these alternatives for PDT with Photofrin, ALA/protoporphyrin IX and mTHPC. In part, this may be due to a significant but moderate increase in direct photodamage to tumor cells. Direct tumor cell death increased with low fluence rate PDT by ~1/2–1 log in the RIF mouse model.[132] However, the microvasculature, especially the normal, tumor-surrounding microvasculature, can also be affected by modification of fluence rate.[162] One practical drawback of low-fluence-rate treatment, as compared to high fluence rate, is the increase in exposure time required to deliver a given fluence. Due to the higher treatment efficiency, this can be somewhat, but not entirely, compensated for by a reduction of the total fluence delivered. In fact, a reduction of the total fluence may be necessary with low-fluence-rate treatment, because the PDT efficiency for causing vascular and normal tissue effects will also increase, thus decreasing treatment selectivity.[162,207]

Enhanced responses to light dose fractionation in ALA-PDT of murine tumors and normal rat colon may involve relocalization or resupply of protoporphyrin IX during dark periods, in addition to reoxygenation.[208,209]

145.7 Immune Effects of PDT

Immune Suppression

The effect of PDT on the host immune system is dichotomous, resulting in immune suppression or immune activation. Although the mechanism leading to immune activation or suppression is unclear, recent studies indicated that the nature and extent of the tissue treated and the dose play a major role.[210,211] Cutaneous PDT suppresses allograft rejection[212–214] and contact hypersensitivity (CHS) reactions.[210,215–218] PDT suppression of CHS in murine models was demonstrated with a number of different photosensitizers[215–217,219–222] and is antigen specific.[215,216] The kinetics of CHS suppression is photosensitizer dependent.[216] $TPPS_4$ and HpD-PDT induce immediate CHS suppression, while *m*-THPC and Photofrin-PDT suppression require 72 h to develop. Kinetic differences were linked to photosensitizer

localization.[216] The mechanism of PDT-induced suppression appears to be associated with the induction of immunosuppressive cytokines. PDT induces tumor necrosis factor (TNF)-α,[218,223] which is involved in some aspects of UV-mediated immunosuppression.[224] However, it is not responsible for PDT-induced CHS suppression.[218] PDT also induces interleukin (IL)-10,[92,210,220] which was shown to inhibit cell-mediated immune responses, including CHS.[220,225,226] Gollnick et al.[210] showed that *in vitro* PDT induces IL-10 expression from keratinocytes as a result of activation of the IL-10 gene promoter by enhanced expression of AP-1 and prolonged IL-10 mRNA half-life. IL-10 is thought to mediate its suppressive activity through inhibition of the ability of antigen-presenting cells (APCs) to stimulate $CD4^+$ T-helper (Th) 1 cells.[225] Th1 cells, which secrete IL-2 and interferon (IFN)-γ, are necessary for induction of cell-mediated immune responses. The duration and strength of CHS reactions are increased in the presence of Th1 cells.[220] Th1 cells are dependent upon the presence of IL-12, secreted from APCs such as macrophages and dendritic cells, for their development.[227,228] Cytotoxic T-cell (Tc) 1 cells are the major effector cells in the CHS response[226] and are also dependent upon IL-12 for their development. IL-12 secretion from APCs is inhibited by IL-10.[225,226] Interestingly, Lynch et al.[217] demonstrated that adoptive transfer of macrophages from mice treated with peritoneal Photofrin-PDT, which involves treatment of the entire peritoneal cavity, suppressed the CHS response to dinitrofluorobenzene (DNFB) in the adoptively transferred animals, suggesting that this PDT regime altered the ability of the macrophages to induce Th1 and Tc1 cells. Direct mechanistic studies into the role of IL-10 in PDT-induced suppression of CHS yielded contradictory results that can be explained, at least in part, by the treatment regime and dose of PDT. Treatment with cutaneous PDT, using Photofrin and blue light centered at 430 nm, results in irradiation that is mostly limited to the skin. In contrast, transdermal PDT, with BPD-MA and illumination with 690 nm light, involves whole-body irradiation. Also, due to the greater depth of light penetration of this wavelength, some irradiation of internal sites may occur. Both transdermal and cutaneous PDT result in CHS suppression and induce IL-10 expression in the skin.[92,210,220] Simkin et al.[220] implicated IL-10 as the active mediator in transdermal PDT-induced suppression of CHS by demonstrating that IL-10 knockout (KO) mice did not undergo transdermal PDT-induced CHS suppression. In contrast, cutaneous PDT treatment of IL-10 KO mice induced CHS suppression.[210] The lack of involvement of IL-10 in suppression of CHS by cutaneous PDT was further confirmed when studies using neutralizing anti-IL-10 antibodies failed to inhibit cutaneous PDT-induced CHS suppression.[210,222] Thus, it appears as though the mechanism of PDT-induced suppression of CHS is dependent upon the treatment regime. Regimes that result in large treatment fields and internal exposure, i.e., transdermal and potentially peritoneal PDT, mediate CHS suppression via IL-10. PDT regimes that employ lower doses and superficial cutaneous exposure suppress CHS reactions via an IL-10 independent mechanism.

Interestingly, CHS suppression by transdermal and cutaneous PDT was reversed by administration of exogenous IL-12,[210,220] suggesting that these processes share a common regulatory point, perhaps in the development of Th1 or Tc1 cells. A second potential suppressor of Th1 and Tc1 development, and thus CHS, is IL-4. IL-4 was shown to directly inhibit Th1 cell proliferation[229] and to induce anergy in Tc1 cells.[230] Th2 cells, which are critical for the development of humoral immunity[229] and secrete IL-4, were shown to negatively regulate CHS responses.[89] Induction of systemic IL-4 by cutaneous PD may result in direct inhibition of Th1/Tc1 cells and suppression of CHS responses. Preliminary data from our group suggest that cutaneous PDT results in the induction of systemic IL-4 and a recent study demonstrated that cutaneous PDT suppression could be transferred by a $CD4^+$ T-cell population.[211]

In addition to the effects of cytokines on PDT-induced suppression of immune responses, it is important to consider the effect of PDT on the expression of immune molecules critical to immune system activation. Transdermal PDT was shown to inhibit the ability of Langerhans cells (LC) to stimulate alloreactive T-cells[212] and LC treated *ex vivo* expressed lower levels of major histocompatibility (MHC) antigens and CD80 and CD86 costimulatory molecules, which are needed for T-cell activation. Additionally, *in vitro* PDT-treated murine DC had a reduced ability to stimulate alloreactive T-cells and exhibited lower levels of MHC molecules, costimulatory molecules, and adhesion molecules.[231] Thus, in addition to altering the function of APCs, PDT has the ability to disrupt the APC-T-cell cognate, which is needed for T-cell activation.

Immune Potentiation

In contrast to the immunosuppressive effects of transdermal or cutaneous PDT, tumor-directed PDT was shown by a number of preclinical studies to trigger an inflammatory response and, depending on the treatment regimen, enhance a specific antitumor response.[140,232,233] PDT is characterized by the onset of an inflammatory reaction that is dominated by an influx of neutrophils.[92,234] The strength of the inflammatory response varies with photosensitizer; Photofrin-PDT induces a strong inflammatory response and a rapid influx of neutrophils, which appear to be critical to long-term tumor control.[235–240] HPPH-PDT induces a mild inflammatory response that is associated with reduced neutrophil infiltration,[241] which is not critical to long-term tumor control following HPPH-PDT.[241] The influx of neutrophils into the treatment site is preceded by an induction of chemokines and adhesion molecules critical to neutrophil migrations.[241] Neutrophil infiltration is followed by an influx of mast cells and macrophages.[92,234] PDT enhances macrophage tumoricidal activity[242–244] and stimulates macrophage release of TNF-α and tumor cell recognition.[84] It was suggested that nonspecific killing of tumor cells by inflammatory cells, potentially through the release of reactive oxygen species, contributes to the overall tumor kill by PDT.[237] This hypothesis is supported by studies showing that if the PDT-induced inflammatory response is further stimulated by addition of adjuvants or macrophage-activating factors, the overall tumor response to PDT is greater.[245–247] The role of the innate immune response in overall tumor kill by PDT was also shown to involve NK (natural killer) cells. Depletion of NK cells reduced the long-term tumor control by PDT,[232] and augmentation of NK activity enhanced PDT tumor control.[248]

PDT was also shown to enhance the adaptive or specific host antitumor response.[140,237] Tumor-draining lymph node cells isolated from PDT-treated mice are able to suppress subsequent tumor challenges when transferred to a naïve host.[249,250] Canti et al.[250] showed that PDT-treated mice that remain tumor free for 100 days post-PDT are resistant to subsequent tumor challenges, suggesting the presence of immune memory cells. The establishment of immune memory by PDT was recently confirmed by studies of Korbelik and Dougherty,[232] showing that immune cells isolated at protracted times post-PDT could transfer tumor immunity. The importance of the immune response in PDT was definitively shown by a series of experiments in *scid* (severe combined immunodeficient) and nude mice.[232,235] PDT treatment, at a dose that was curative in immunocompetent BALB/c mice, provided only short-term cures of EMT6 tumors in *scid* and nude mice. The ability to provide long-term cures was restored when immunodeficient animals were reconstituted with bone marrow cells from BALB/c mice. Depletion studies showed that the critical cells involved in the PDT-induced immune response were $CD8^+$ cells, although $CD4^+$ cells played a supportive role.[232,238] Interestingly, a recent clinical study demonstrated an infiltration of $CD8^+$ cells into PDT-treated tumor tissue.[251] These studies suggest that a functional immune system is necessary for long-term tumor control by PDT; however, the mechanism behind the potentiation of the immune response by PDT is unknown.

Several factors were postulated to contribute to the ability of PDT to enhance the host antitumor immune response, including release of tumor antigens and stimulation of various proinflammatory cytokines and other immunologically important genes via activation of stress response factors such as AP-1 and NF-κB.[92] PDT was shown to enhance the expression of a number of cytokines, including IL-6, TNF-α, IL-1β, IL-2, and granulocyte macrophage colony-stimulating factor (GM-CSF).[92,218,223,252,253] PDT modulation of IL-6 is the result of increased AP-1 activity.[91] The release of tumor antigens by PDT is also likely to play a role in the initiation of the antitumor immune response. The mechanism by which tumor cells are killed and the environment into which tumor antigens are released were shown to dictate the ensuing immune response.[254,255] Release of tumor antigens into an inflammatory milieu is thought to promote an effective antitumor immune response,[254] and the presence of apoptotic and necrotic tissue acts to stimulate dendritic cells,[255] which are necessary for initiation of the immune response.[256] Thus, PDT, by stimulating inflammation and by generating apoptotic and necrotic tissue, provides an ideal environment for initiation of an antitumor immune response. Preliminary evidence demonstrating that PDT-generated tumor cell lysates are able to activate DC in the absence of cofactors[257] supports this hypothesis. An understanding of the mechanisms leading to PDT enhancement of the host antitumor

immune response may allow for amplification of the response, thereby enhancing the effectiveness of PDT and potentially providing protection against metastases outside the treatment field. Information regarding the impact of PDT on metastasis formation is at present inconclusive. While several publications describe a reduction in metastases following PDT, invoking changes in adhesion molecule expression[244] or innate immune responses[258] as mechanisms for the observed effects, other work suggests that PDT enhances lung metastases in an orthotopic prostate tumor model.[259]

145.8 Conclusion

The scientific effort that supports this new cancer therapy led to numerous significant advances. The development of new photosensitizers is essentially eliminating the problem of prolonged cutaneous photosensitivity and is extending treatment depth, an issue dealt with in detail elsewhere in this volume. The complex dynamics of tumor oxygenation in response to PDT are now largely understood. The oxidative stress effects of PDT on redox-sensitive transcription factors and the genes they control are being uncovered. The complex interplay of biological mechanisms governing the PDT tumor response was realized. Given these accomplishments, it remains for them to be translated into actual patient benefit. Noninvasive probes need to be perfected that will allow for monitoring photosensitizer levels, oxygen status, or ideally, singlet oxygen, the cytotoxic agent. New light delivery regimes need to be devised for clinical use that will minimize oxygen limitations. The ways in which such regimes might influence redox-sensitive gene regulation and how these genes might affect treatment outcome need to be explored. Finally, our expanding understanding of the complex effects of PDT on host immunity needs to be exploited to modulate the PDT response.

References

1. MacDonald, I.J. and Dougherty, T.J., Basic principles of photodynamic therapy, *J. Porphyrins Phthalocyanines*, 5, 105, 2001.
2. Moan, J. and Sommer, S., Oxygen dependence of the photosensitizing effect of hematoporphyrin derivative in NHIK 3025 cells, *Cancer Res.*, 45, 1608, 1985.
3. Henderson, B.W. and Miller, A.C., Effects of scavengers of reactive oxygen and radical species on cell survival following photodynamic treatment *in vitro*: comparison to ionizing radiation, *Radiat. Res.*, 108, 196, 1986.
4. Delaey, E., Vandenbogaerde, A., Merlevede, W., and deWitte, P., Photocytotoxicity of hypericin in normoxic and hypoxic conditions, *J. Photochem. Photobiol. B: Biology*, 56, 19, 2002.
5. Foote, C.S., Mechanisms of photooxygenation, *Prog. Clin. Biol. Res.*, 170, 3, 1984.
6. Moan, J. and Berg, K., The photodegradation of porphyrins in cells can be used to estimate the lifetime of singlet oxygen, *Photochem. Photobiol.*, 53, 549, 1991.
7. Kessel, D., Chemical and biochemical determinants of porphyrin localization, *Prog. Clin. Biol. Res.*, 170, 405, 1984.
8. Kessel, D., Sites of photosensitization by derivatives of hematoporphyrin, *Photochem. Photobiol.*, 44, 489, 1986.
9. MacDonald, I.J., Morgan, J., Bellnier, D.A., Paszkiewicz, G., Whitaker, J.E., Litchfield, D.J., and Dougherty, T.J., Subcellular localization patterns and their relationship to photodynamic activity of pyropheophorbide-α derivatives, *Photochem. Photobiol.*, 70, 789, 1999.
10. Moan, J., Berg, K., Anholt, A., and Madslien, K., Sulfonated aluminum phthalocyanines as sensitizers for photochemotherapy. Effects of small doses on localization, dye fluorescence and photosensitivity in V79 cells, *Int. J. Cancer*, 58, 865, 1994.
11. Berg, K., Madslien, K., Bommer, J.C., Oftebro, R., Winkelman, J.W., and Moan, J., Light induced relocalization of sulfonated meso-tetraphenylporphines in NHIK 3025 cells and effects of dose fractionation, *Photochem. Photobiol.*, 53, 203, 1991.

12. Henderson, B.W., Bellnier, D.A., Greco, W.R., Sharma, A., Pandey, R.K., Vaughan, L.A., Weishaupt, K.R., and Dougherty, T.J., An *in vivo* quantitative structure-activity relationship for a congeneric series of pyropheophorbide derivatives as photosensitizers for photodynamic therapy, *Cancer Res.*, 57, 4000, 1997.
13. Murant, R.S., Gibson, S.L., and Hilf, R., Photosensitizing effects of Photofrin II on the site-selected mitochondrial enzymes adenylate kinase and monoamine oxidase, *Cancer Res.*, 47, 4323, 1987.
14. Gibson, S.L. and Hilf, R., Photosensitization of mitochondrial cytochrome c oxidase by hematoporphyrin derivative and related porphyrins *in vitro* and *in vivo*, *Cancer Res.*, 43, 4191, 1983.
15. Salet, C. and Moreno, G., Photosensitization of mitochondria. Molecular and cellular aspects, *J. Photochem. Photobiol. B.*, 5, 133, 1990.
16. Salet, C., Hematoporphyrin and hematoporphyrin-derivative photosensitization of mitochondria, *Biochimie*, 68, 865, 1986.
17. Peng, Q., Berg, K., Moan, J., Kongshaug, M., and Nesland, J.M., 5-aminolevulinic acid-based photodynamic therapy: principles and experimental research, *Photochem. Photobiol.*, 65, 235, 1997.
18. Kessel, D., Woodburn, K., Gomer, C.J., Jagerovic, N., and Smith, K.M., Photosensitization with derivatives of chlorin p6, *J. Photochem. Photobiol. B*, 28, 13, 1995.
19. Kessel, D. and Luo, Y., Mitochondrial photodamage and PDT-induced apoptosis, *J. Photochem. Photobiol. B*, 42, 89, 1998.
20. Kessel, D., Woodburn, K., Henderson, B.W., and Chang, C.K., Sites of photodamage *in vivo* and *in vitro* by a cationic porphyrin, *Photochem. Photobiol.*, 62, 5, 875, 1995.
21. Morgan, J., Potter, W.R., and Oseroff, A.R., Comparison of photodynamic targets in a carcinoma cell line and its mitochondrial DNA-deficient derivative, *Photochem. Photobiol.*, 71, 747, 2000.
22. Verma, A., Focchina, S.L., Hirsch, S., Dillahey, L., Williams, J., and Snyder, S.H., Photodynamic tumor therapy: mitochondrial benzodiazepine receptors as a therapeutic target, *Mol. Med.*, 4, 40, 1998.
23. Tsuchida, T., Zheng, G., Pandey, R.K., Potter, W.R., Bellnier, D.A., Henderson, B.W., Kato, H., and Dougherty, T.J., Correlation between Site II-specific human serum albumin (HSA) binding affinity and murine *in vivo* photosensitizing efficacy of some Photofrin® components, *Photochem. Photobiol.*, 66, 224, 1997.
24. Dubbelman, T.M.A.R., Prinsze, C., Penning, L.C., and Van Steveninck, J., Photodynamic therapy: membrane and enzyme photobiology, in *Photodynamic Therapy*, Henderson, B.W. and Dougherty, T.J., Eds., Marcel Dekker, New York, 1992, p. 37.
25. Miccoli, L., Beurdeley-Thomas, A., DePinieux, G., Sureau, F., Oudard, S., Dutrillaux, B., and Poupon, M.-F., Light induced photoactivation of hypericin affects the energy metabolism of human glioma cells by inhibiting hexokinase bound to mitochondria, *Cancer Res.*, 58, 5777, 1998.
26. Atlante, A., Moore, G., Passarella, S., and Salet, C., Hematoporphyrin derivative (Photofrin II): impairment of anion translocation, *Biochem. Biophys. Res. Commun.*, 141, 584, 1986.
27. Perlin, D.S., Murant, R.S., Gibson, S.L., and Hilf, R., Effects of photosensitization by hematoporphyrin derivative on mitochondrial adenosine triphosphatase-mediated proton transport and membrane integrity of R3230AC mammary adenocarcinoma, *Cancer Res.*, 45, 653, 1995.
28. Ratcliffe, S.L. and Matthews, E.K., Modification of the photodynamic action of δ-aminolaevulinic acid (ALA) on rat pancreatoma cells by mitochondrial benzodiazepine receptor ligands, *Br. J. Cancer*, 71, 300, 1995.
29. Morgan, J. and Oseroff, A.R., Mitochondria-based photodynamic anti-cancer therapy, *Adv. Drug Delivery Rev.*, 49, 71, 2001.
30. Kessel, D., Antolovich, M., and Smith, K.M., The role of the peripheral benzodiazepine receptor in the apoptotic response to photodynamic activity, *Photochem. Photobiol.*, 74, 346, 2001.
31. Morris, R.L., Varnes, M.E., Kenney, M.E., Li, Y.S., Azizuddin, K., McEnery, M.W., and Oleinick, N.L., The peripheral benzodiazepine receptor in photodynamic therapy with the phthalocyanine photosensitizer Pc4, *Photochem. Photobiol.*, 75, 652, 2002.

32. Dougherty, T.J., Sumlin, A.B., Greco, W.R., Weishaupt, K.R., Vaughan, L.A., and Pandey, R.K., The role of the peripheral benzodiazepine receptor in photodynamic activity of certain pyropheophorbide ether photosensitizers: albumin site II as a surrogate marker for activity, *Photochem. Photobiol.*, 76, 91, 2002.
33. Geze, M., Morliere, P., Maziere, J.C., Smith, K.M., and Santus, R., Lysomes, a key target of hydrophobic photosensitizers proposed for chemotherapeutic applications, *J. Photochem. Photobiol. B.*, 20, 23, 1993.
34. Berg, K. and Moan, J., Lysosomes and microtubules as targets for photochemotherapy of cancer, *Photochem. Photobiol.*, 65, 403, 1997.
35. Kessel, D., Luo, Y., Mathieu, P., and Reiners, J.J., Jr., Determinants of the apoptotic response to lysosomal photodamage, *Photochem. Photobiol.*, 71, 196, 2000.
36. Selbo, P.K., Hogset, A., Prasmickaite, L., and Berg, K., Photochemical internalisation: a novel drug delivery system, *Tumour Biol.*, 23, 103, 2002.
37. Gomer, C.J., Rucker, N., Banerjee, A., and Benedict, W.F., Comparison of mutagenicity and induction of sister chromatid exchange in Chinese hamster cells exposed to hematoporphyrin derivative photoradiation, ionizing radiation, or ultraviolet radiation, *Cancer Res.*, 43, 2622, 1983.
38. Evensen, J.F. and Moan, J., Photodynamic action and chromosomal damage: a comparison of haematoporphyrin derivative (HpD) and light with X-irradiation, *Br. J. Cancer*, 45, 456, 1982.
39. McNair, F.L., Marples, B., West, C.M.L., and Moore, J.V., A comet assay of DNA damage and repair in K562 cells after photodynamic therapy using hematoporphyrin derivative, methylene blue and *meso*-tetrahydroxyphenylchlorin, *Br. J. Cancer*, 75, 1721, 1997.
40. Evans, H.H., Horng, M.-F., Ricanati, M., Deahl, J.T., and Oleinick, N.L., Mutagenicity of photodynamic therapy as compared to UVC and ionizing radiation in human and murine lymphoblast cell lines, *Photochem. Photobiol.*, 66, 690, 1997.
41. Moan, J., Pettersen, E.O., and Christensen, T., The mechanism of photodynamic inactivation of human cells *in vitro* in the presence of haematoporphyrin, 82, 90, 1993.
42. Christensen, T., Volden, G., Moan, J., and Sandquist, T., Release of lysosomal enzymes and lactate dehydrogenase due to hematoporphyrin derivative and light irradiation of NHIK 3025 cells *in vitro*, *Ann. Clin. Res.*, 14, 46, 1982.
43. Henderson, B.W. and Donovan, J.M., Release of prostaglandin E2 from cells by photodynamic treatment *in vitro*, *Cancer Res.*, 49, 6896, 1989.
44. Bellnier, D.A. and Dougherty, T.J., Membrane lysis in Chinese hamster ovary cells treated with hematoporphyrin derivative plus light, *Photochem. Photobiol.*, 36, 43, 1982.
45. Thomas, J.P. and Girotti, A.W., Role of lipid peroxidation in hematoporphyrin derivative-sensitized photokilling of tumor cells: protective effects of glutathione peroxidase, *Cancer Res.*, 49, 1682, 1989.
46. Girotti, A.W., Photosensitized oxidation of membrane lipids: reaction pathways, cytotoxic effects, and cytoprotective mechanisms, *J. Photochem. Photobiol. B:Biol.*, 63, 103, 2001.
47. Deuticke, B., Henseleit, U., Haest, C.W., Heller, K.B., and Dubbelman, T.M., Enhancement of transbilayer mobility of a membrane lipid probe accompanies formation of membrane leaks during photodynamic treatment of erythrocytes, *Biochim. Biophys. Acta*, 982, 53, 1989.
48. Moan, J. and Vistnes, A.I., Porphyrin photosensitization of proteins in cell membranes as studied by spin-labelling and by quantification of DTNB-reactive SH-groups, *Photochem. Photobiol.*, 44, 15, 1986.
49. Gibson, S.L., Murant, R.S., and Hilf, R., Photosensitizing effects of hematoporphyrin derivative and photofrin II on the plasma membrane enzymes 5'-nucleotidase, Na^+K^+-ATPase, and Mg^{2+}-ATPase in R3230AC mammary adenocarcinomas, *Cancer Res.*, 48, 3360, 1988.
50. Specht, K.G. and Rodgers, M.A.J., Plasma membrane depolarization and calcium influx during cell injury by photodynamic action, *Biochim. Biophys. Acta*, 82, 519, 1993.
51. Berg, K., Steen, H.B., Winkelman, J.W., and Moan, J., Synergistic effects of photoactivated tetra(4-sulfonatophenyl)porphine and nocodazole on microtubule assembly, accumulation of cells in mitosis and cell survival, *J. Photochem. Photobiol. B*, 13, 59, 1992.

52. Oleinick, N.L. and Evans, H.H., The photobiology of photodynamic therapy: cellular targets and mechanisms, *Radiat. Res.*, 150(5 Suppl.), S146, 1998.
53. Henkel, T., Apoptosis: corralling the corpses, *Cell*, 104, 325, 2001.
54. Dellinger, M., Apoptosis or necrosis following photofrin photosensitizaton: influence of the incubation protocol, *Photochem. Photobiol.*, 64, 182, 1996.
55. Fabris, C., Valduga, G., Miotto, G., Borsetto, L., Jori, G., Garbisa, S., and Reddi, E., Photosensitization with zinc (II) phthalocyanine as a switch in the decision between apoptosis and necrosis, *Cancer Res.*, 61, 7495, 2001.
56. Kessel, D., Luo, Y., Deng, Y., and Chang, C.K., The role of subcellular localization in the initiation of apoptosis by photodynamic therapy, *Photochem. Photobiol.*, 65, 422, 1997.
57. Luo, Y. and Kessel, D., Initiation of apoptosis versus necrosis by photodynamic therapy with chloroaluminum phthalocyanine, *Photochem. Photobiol.*, 66, 479, 1997.
58. Agostinis, P., Vantieghem, A., Merlevede, W., and deWitte, P.A., Hypericin in cancer treatment: more light on the way, *Int. J. Biochem. Cell Biol.*, 34, 221, 2002.
59. He, X.-Y., Sikes, R.A., Thomsen, S., Chung, L.W.K., and Jaques, S.L., Photodynamic therapy with Photofrin II induces programmed cell death in carcinoma cell lines, *Photochem. Photobiol.*, 59, 468, 1994.
60. Luo, Y., Chang, C.K., and Kessel, D., Rapid initiation of apoptosis by photodynamic therapy, *Photochem. Photobiol.*, 63, 528, 1996.
61. Granville, D.J., Levy, J.G., and Hunt, D.W.C., Photodynamic therapy induces caspase-3 activation in HL-60 cells, *Cell Death & Differentiation*, 4, 623, 1997.
62. Agarwal, M.L., Clay, M.E., Harvey, E.J., Evans, H.H., Antunez, A.R., and Oleinick, N.L., Photodynamic therapy induces rapid cell death by apoptosis in L5178Y mouse lymphoma cells, *Cancer Res.*, 51, 5993, 1991.
63. Yang, J., Bhalla, K., Kim, C.N., Ibrado, A.M., Peng, T.I., Jones, D.P., and Wang, X., Prevention of apoptosis by Bcl-2: release of cytochrome c from mitochondria blocked, *Science*, 275, 1129, 1997.
64. Granville, D.J., Carthy, C.M., Jiang, H., Shore, G.C., McManus, B.M., and Hunt, D.W.C., Rapid cytochrome c release, activation of caspases 3, 6, 7 and 8 followed by Bap31 cleavage in HeLa cells treated with photodynamic therapy, *FEBS Lett.*, 437, 5, 1998.
65. Chiu, S.M., Evans, H.H., Lam, M., Nieminen, A., and Oleinick, N.L., Phthalocyanine 4 photodynamic therapy-induced apoptosis of mouse L5178Y-R cells results from a delayed but extensive release of cytochrome c from mitochondria, *Cancer Lett.*, 165, 51, 2001.
66. Granville, D.J., Cassidy, B.A., Ruehlmann, D.O., Choy, J.C., Brenner, C., Kroemer, G., van Breemen, C., Margaron, P., Hunt, D.W.C., and McManus, B.M., Mitochondrial release of apoptosis-inducing factor and cytochrome c during smooth muscle cell apoptosis, *Am. J. Pathol.*, 159, 305, 2001.
67. Chiu, S.M. and Oleinick, N.L., Dissociation of mitochondrial depolarization from cytochrome c release during apoptosis induced by photodynamic therapy, *Br. J. Cancer*, 84, 1099, 2001.
68. Varnes, M.E., Chiu, S.M., Xue, L.Y., and Oleinick, N.L., Photodynamic therapy-induced apoptosis in lymphoma cells: translocation of cytochrome c causes inhibition of respiration as well as caspase activation, *Biochem. Biophys. Res. Commun.*, 255, 679, 1999.
69. Vantieghem, A., Xu, Y., Declercq, W., Vandenabeele, P., Denecker, G., Vandenheede, J.R., Merlevede, W., de Witte, P.A., and Agostinis, P., Different pathways mediate cytochrome c release after photodynamic therapy with hypericin, *Photochem. Photobiol.*, 74, 133, 2001.
70. Lam, M., Oleinick, N.L., and Nieminen, A.L., Photodynamic therapy-induced apoptosis in epidermoid carcinoma cells. Reactive oxygen species and mitochondrial inner membrane permeabilization, *J. Biol. Chem.*, 276, 47379, 2001.
71. Vantieghem, A., Xu, Y., Declercq, W., Vandenabeele, P., Denecker, G., Vandenheede, J.R., Merlevede, W., deWitte, P.A., and Agostinis, P., Different pathways mediate cytochrome c release after photodynamic therapy with hypericin, *Photochem. Photobiol.*, 74, 133, 2001.
72. Kessel, D. and Luo, Y., Photodynamic therapy: a mitochondrial inducer of apoptosis., *Cell Death & Differentiation*, 6, 28, 1999.

73. Xue, L.Y., Chiu, S.M., and Oleinick, N.L., Photodynamic therapy-induced death of MCF-7 human breast cancer cells: a role for caspase-3 in the late steps of apoptosis but not for the critical lethal event, *Exper. Cell Res.*, 263, 145, 2001.
74. Whitacre, C.M., Satoh, T.H., Xue, L., Gordon, N.H., and Oleinick, N.L., Photodynamic therapy of human breast cancer xenografts lacking caspase-3, *Cancer Lett.*, 179, 43, 2002.
75. Srivastava, M., Ahmad, N., Gupta, S., and Mukhtar, H., Involvement of bcl-2 and bax in photodynamic therapy-mediated apoptosis, *J. Biol. Chem.*, 276, 15481, 2001.
76. Granville, D.J., Jiang, H., An, M.T., Levy, J.G., McManus, B.M., and Hunt, D.W.C., Bcl-2 overexpression blocks caspase activation and downstream apoptotic events instigated by photodynamic therapy, *Br. J. Cancer*, 79, 95, 1999.
77. Schouwink, H., Ruevekamp, M., Oppelaar, H., van Veen, R., Bass, P., and Stewart, F.A., Photodynamic therapy for malignant mesothelioma: preclinical studies for optimization of treatment protocols, *Photochem. Photobiol.*, 73, 410, 2001.
78. He, J., Agarwal, M.L., Larkin, H.E., Friedman, L.R., Xue, L.Y., and Oleinick, N.L., The induction of partial resistance to photodynamic therapy by the protooncogene bcl-2, *Photochem. Photobiol.*, 64, 845, 1996.
79. Xue, L.Y., Chiu, S.M., and Oleinick, N.L., Photochemical destruction of the Bcl-2 oncoprotein during photodynamic therapy with the phthalocyanine photosensitizer Pc 4, *Oncogene*, 20, 3420, 2001.
80. Kim, H., Luo, Y., Li, G., and Kessel, D., Enhanced apoptotic response to photodynamic therapy after bcl-2 transfection, *Cancer Res.*, 59, 3429, 1999.
81. Usuda, J., Okunaka, T., Furukawa, K., Tsuchida, T., Kuroiwa, Y., Ohe, Y., Saijo, N., Nishio, K., Konaka, C., and Kato, H., Increased cytotoxic effects of photodynamic therapy in IL-6 gene transfected cells via enhanced apoptosis, *Int. J. Cancer*, 93, 475, 2001.
82. Granville, D.J., Ruehlmann, D.O., Choy, J.C., Cassidy, B.A., Hunt, D.W.C., van Breemen, C., and McManus, B.M., Bcl-2 increases emptying of endoplasmic reticulum Ca^{2+} stores during photodynamic therapy-induced apoptosis, *Cell Calcium*, 5, 343, 2001.
83. Agarwal, M.L., Larkin, H.E., Zaidi, S.I.A., Mukhtar, H., and Oleinick, N.L., Phospholipase activation triggers apoptosis in photosensitized mouse lymphoma cells, *Cancer Res.*, 53, 5897, 1993.
84. Kick, G., Messer, G., Plewig, G., Kind, P., and Goetz, A.E., Strong and prolonged injuction of c-*jun* and c-*fos* proto-oncogenes by photodynamic therapy, *Br. J. Cancer*, 74, 30, 1996.
85. Separovic, D., Mann, K.J., and Oleinick, N.L., Association of ceramide accumulation with photodynamic treatment-induced cell death, *Photochem. Photobiol.*, 68, 101, 1998.
86. Gupta, S., Ahmad, N., and Mukhtar, H., Involvement of nitric oxide during phthalocyanine (Pc4) photodynamic therapy-mediated apoptosis, *Cancer Res.*, 58, 1785, 1998.
87. Schempp, C.M., Simon-Haarhaus, B., Termeer, C.C., and Simon, J.C., Hypericin photo-induced apoptosis involves the tumor necrosis factor-related apoptosis-inducing ligand (TRAIL) and activation of caspase-8, *FEBS Lett.*, 493, 26, 2001.
88. Fisher, A.M., Danenberg, K., Banerjee, D., Bertino, J.R., Danenberg, P., and Gomer, C.J., Increased photosensitivity in HL60 cells expressing wild-type p53, *Photochem. Photobiol.*, 66, 265, 1997.
89. Tong, Z., Singh, G., and Rainbow, A.J., The role of the p53 tumor suppressor in the response of human cells to photofrin-mediated photodynamic therapy, *Photochem. Photobiol.*, 71, 201, 2000.
90. Fisher, A.M., Ferrario, A., Rucker, N., Zhang, S., and Gomer, C.J., Photodynamic therapy sensitivity is not altered in human tumor cells after abrogation of p53 function, *Cancer Res.*, 59, 331, 1999.
91. Kick, G., Messer, G., Goetz, A., Plewig, G., and Kind, P., Photodynamic therapy induces expression of interleukin 6 by activation of AP-1 but not NF-kB DNA binding, *Cancer Res.*, 55, 2373, 1995.
92. Gollnick, S.O., Liu, X., Owczarczak, B., Musser, D.A., and Henderson, B.W., Altered expression of interleukin 6 and interleukin 10 as a result of photodynamic therapy *in vivo*, *Cancer Res.*, 57, 3904, 1997.
93. Jee, S.H., Shen, S.C., Chiu, H.C., Tsai, W.L., and Kuo, M.L., Overexpression of interleukin-6 in human basal cell carcinoma cell lines increases anti-apoptotic activity and tumorigenic potency, *Oncogene*, 20, 198, 2001.

94. Gollnick, S.O., Lee, B.Y., Vaughan, L., Owczarczak, B., and Henderson, B.W., Activation of the IL-10 gene promoter following photodynamic therapy of murine keratinocytes, *Photochem. Photobiol.*, 73, 170, 2001.
95. Abate, C., Patel, L., Rauscher, F.J., and Curran, T., Redox regulation of fos and jun DNA-binding activity *in vitro*, *Science*, 249, 1157, 1990.
96. Xanthoudakis, S., Miao, G., Wang, F., Pan, Y.-C.E., and Curran, T., Redox activation of Fos-Jun DNA binding activity is mediated by a DNA repair enzyme, *EMBO J.*, 11, 3323, 1992.
97. Meyer, M., Schreck, R., and Baeuerle, P.A., H_2O_2 and antioxidants have opposite effects on activation of NF-κB and AP-1 in intact cells: AP-1 as secondary antioxidant-responsive factor, *EMBO J.*, 12, 2005, 1993.
98. Yao, K.-S., Zanthoudakis, S., Curran, T., and O'Dwyer, P.J., Activation of AP-1 and of nuclear redox factor, Ref1, in the response of HT29 colon cancer cells to hypoxia, *Mol. Cell. Biol.*, 14, 5997, 1994.
99. Luna, M.C., Wong, S., and Gomer, C.J., Photodynamic therapy mediated induction of early response genes, *Cancer Res.*, 54, 1374, 1994.
100. Baeuerle, P.A. and Henkel, T., Function and activation of NF-B in the immune system., *Ann. Rev. Immunol.*, 12, 141, 1994.
101. Schreck, R., Albermann, K., and Baeuerle, P.A., Nuclear factor κB: an oxidative stress-responsive transcription factor of eukaryotic cells, *Rad. Res. Commun.*, 17, 221, 1992.
102. DiDonato, J.A., Mercurio, R., Rosette, C., Wu-Li, J., Suyang, H., Ghosh, S., and Karin, M., Mapping of the inducible IκB phosphorylation sites that signal its ubiquination and degradation, *Mol. Cell. Biol.*, 16, 1295, 1996.
103. DiDonato, J.A., Hayakawa, M., Rothwarf, D.M., Zandi, E., and Karin, M., A cytokine-responsive IκB kinase that activates the transcription factor NFκB, *Nature*, 388, 548, 1997.
104. Granville, D.J., Carthy, C.M., Jiang, H., Levy, J.G., McManus, B.M., Matroule, J.Y., Piette, J., and Hunt, D.W.C., Nuclear factor-κB activation by the photochemotherapeutic agent verteporfin, *Blood*, 95, 256, 2000.
105. Ryter, S.W. and Gomer, C.J., Nuclear factor κB binding activity in mouse L1210 cells following Photofrin II-mediated photosensitization, *Photochem. Photobiol.*, 58, 753, 1993.
106. Matroule, J.Y., Bonizzi, G., Morliere, P., Paillous, N., Santus, R., Bours, V., and Piette, J., Pyropheophorbide-a methyl ester-mediated photosensitization activates transcription factor NF-κB through the interleukin-1 receptor-dependent signaling pathway, *J. Biol. Chem.*, 270, 2899, 1999.
107. Legrand-Poels, S., Schoonbroodts, S., Matroule, J.Y., and Piette, J., NF-κB: an important transcription factor in photobiology, *J. Photochem. Photobiol. B*, 45, 1, 1998.
108. Tao, J.-S., Sanghera, S., Pelech, S.L., Wong, G., and Levy, J.G., Stimulation of stress-activated protein kinase and p38 HOG1 kinase in murine keratinocytes following photodynamic therapy with benzoporphyrin derivative, *J. Biol. Chem.*, 271, 27107, 1996.
109. Oleinick, N.L., He, J., Xue, L.Y., and Separovic, D., Stress-activated signalling responses leading to apoptosis following photodynamic therapy, in *Optical Methods for Tumor Treatment and Detection: Mechanisms and Techniques in Photodynamic Therapy VII*, Proc. SPIE, 3247, 82, 1998.
110. Xue, L.Y., He, J., and Oleinick, N.L., Rapid tyrosine phosphorylation of HS1 in the response of mouse lymphoma L5178Y-R cells to photodynamic treatment sensitized by the phthalocyanine Pc4, *Photochem. Photobiol.*, 66, 105, 1997.
111. Koukourakis, M.I., Giatromanolaki, A., Skarlatos, J., Corti, L., Blandamura, S., Piazza, M., Gatter, K.C., and Harris, A.L., Hypoxia inducible factor (HIF-1a and HIF-2a) expression in early esophageal cancer and response to photodynamic therapy and radiotherapy, *Cancer Res.*, 61, 1830, 2001.
112. Ferrario, A., von Tiehl, K.F., Rucker, N., Schwarz, M.A., Gill, P.S., and Gomer, C.J., Antiangiogenic treatment enhances photodynamic therapy responsiveness in a mouse mammary carcinoma, *Cancer Res.*, 60, 4066, 2000.
113. Ferrario, A., Von Tiehl, K., Wong, S., Luna, M., and Gomer, C.J., Cyclooxygenase-2 inhibitor treatment enhances photodynamic therapy-mediated tumor response, *Cancer Res.*, 62, 3956, 2002.

114. Luna, M.C., Ferrario, A., Wong, S., Fisher, A.M.R., and Gomer, C.J., Photodynamic therapy-mediated oxidative stress as a molecular switch for the temporal expression of genes ligated to the human heat shock promoter, *Cancer Res.*, 60, 1637, 2000.
115. Gomer, C.J., Ryter, S.W., Ferrario, A., Rucker, N., Wong, S., and Fisher, A.M.R., Photodynamic therapy-mediated oxidative stress can induce expression of heat shock proteins, *Cancer Res.*, 56, 2355, 1996.
116. Curry, P.M. and Levy, J.G., Stress protein expression in murine tumor cells following photodynamic therapy with benzoporphyrin derivative, *Photochem. Photobiol.*, 58, 374, 1993.
117. Gomer, C.J., Ferrario, A., Rucker, N., Wong, S., and Lee, A.S., Glucose regulated protein induction and cellular resistance to oxidative stress mediated by porphyrin photosensitization, *Cancer Res.*, 51, 6574, 1991.
118. Xue, L.Y., Agarwal, M.L., and Varnes, M.E., Elevation of GRP-78 and loss of HSP-70 following photodynamic treatment of V79 cells: sensitization by nigericin, *Photochem. Photobiol.*, 62, 135, 1995.
119. Morgan, J., Whitaker, J.E., and Oseroff, A.R., GRP-78 induction by calcium ionophore potentiates photodynamic therapy using the mitochondrial targeting dye Victoria Blue BO, *Photochem. Photobiol.*, 67, 155, 1998.
120. Gomer, C.J., Luna, M., Ferrario, A., and Rucker, N., Increased transcription and translation of heme oxygenase in Chinese hamster fibroblasts following photodynamic stress or Photofrin II incubation, *Photochem. Photobiol.*, 53, 275, 1991.
121. Luna, M.C., Chen, X., Wong, S., Tsui, J., Rucker, N., Lee, A.S., and Gomer, C.J., Enhanced photodynamic therapy efficacy with inducible suicide gene therapy controlled by the grp promoter, *Cancer Res.*, 62, 1458, 2002.
122. Hanlon, J.G., Adams, K., Rainbow, A.J., Gupta, R.S., and Singh, G., Induction of Hsp60 by Photofrin-mediated photodynamic therapy, *Photochem. Photobiol. B*, 64, 55, 2001.
123. Wang, H.P., Hanlon, J.G., Rainbow, A.J., Espiritu, M., and Singh, G., Up-regulation of Hsp27 plays a role in the resistance of human colon carcinoma HT29 cells to photooxidative stress, *Photochem. Photobiol.*, 76, 98, 2002.
124. Ahmad, N., Kalka, K., and Mukhtar, H., *In vitro* and *in vivo* inhibition of epidermal growth factor receptor-tyrosine kinase pathway by photodynamic therapy, *Oncogene*, 20, 2314, 2001.
125. Henderson, B.W., Probing the effects of photodynamic therapy through *in vivo–in vitro* methods, in *Photodynamic Therapy of Neoplastic Disease*, Vol 1, Kessel, D., Ed., CRC Press, Boca Raton, FL, 1990, p. 169.
126. Henderson, B.W. and Fingar, V.H., Oxygen limitation of direct tumor cell kill during photodynamic treatment of a murine tumor model, *Photochem. Photobiol.*, 49, 299, 1989.
127. Henderson, B.W., Waldow, S.M., Mang, T.S., Potter, W.R., Malone, P.B., and Dougherty, T.J., Tumor destruction and kinetics of tumor cell death in two experimental mouse tumors following photodynamic therapy, *Cancer Res.*, 45, 572, 1985.
128. Henderson, B.W., Sumlin, A.B., Owczarczak, B.L., and Dougherty, T.J., Bacteriochlorophyll-a as photosensitizer for photodynamic treatment of transplantable murine tumors, *J. Photochem. Photobiol. B: Biol.*, 10, 303, 1991.
129. Henderson, B.W., Vaughan, L., Bellnier, D.A., vanLeengoed, H., Johnson, P.G., and Oseroff, A.R., Photosensitization of murine tumor, vasculature and skin by 5-aminolevulinic acid-induced porphyrin, *Photochem. Photobiol.*, 62, 780, 1995.
130. Cincotta, L., Foley, J.W., MacEachern, T., Lampros, E., and Cincotta, A.H., Novel photodynamic effects of a benzophenothiazine on two different murine sarcomas, *Cancer Res.*, 54, 1249, 1994.
131. Chan, W.-S., Brasseur, N., La Madeleine, C., and van Lier, J.E., Evidence for different mechanisms of EMT-6 tumor necrosis by photodynamic therapy with disulfonated aluminum phthalocyanine or Photofrin: tumor cell survival and blood flow, *Anticancer Res.*, 16, 1887, 1996.
132. Sitnik, T.M. and Henderson, B.W., Effects of fluence rate on cytotoxicity during photodynamic therapy, in *Optical Methods for Tumor Treatment and Detection: Mechanisms and Techniques in Photodynamic Therapy VI*, Proc. SPIE, 2972, 95, 1997.

133. Korbelik, M. and Krosl, G., Cellular levels of photosensitisers in tumours: the role of proximity to the blood supply, *Br. J. Cancer*, 70, 604, 1994.
134. Svaasand, L.O., Optical dosimetry for direct and interstitial photoradiation therapy of malignant tumors, *Prog. Clin. Biol. Res.*, 170, 91, 1984.
135. Wilson, B.C., Jeeves, W.P., Lowe, D.M., and Adam, G., Light propagation in animal tissues in the wavelength range 375–825 nanometers, *Prog. Clin. Biol. Res.*, 170, 115, 1984.
136. Adams, K., Rainbow, A.J., Wilson, B.C., and Singh, G., *In vivo* resistance to Photofrin-mediated photodynamic therapy in radiation-induced fibrosarcoma cells resistant to *in vitro* Photofrin-mediated photodynamic therapy, *J. Photochem. Photobiol. B: Biol.*, 49, 136, 1999.
137. Kessel, D., Hampton, J., Fingar, V., and Morgan, A., Tumor versus vascular photodamage in a rat tumor model, *J. Photochem. Photobiol. B: Biol.*, 45, 25, 1998.
138. Pass, H.I., Evans, S., Matthews, W.A., Perry, R., Venzon, D., Roth, J.A., and Smith, P., Photodynamic therapy of oncogene-transformed cells, *J. Thorac. Cardiovasc. Surg.*, 101, 795, 1991.
139. Henderson, B.W. and Dougherty, T.J., How does photodynamic therapy work?, *Photochem. Photobiol.*, 55, 145, 1992.
140. Dougherty, T.J., Gomer, C.J., Henderson, B.W., Jori, G., Kessel, D., Korbelik, M., Moan, J., and Peng, Q., Photodynamic therapy, *J. Natl. Cancer Inst.*, 90, 889, 1998.
141. Hamblin, M.R. and Newman, E.L., Photosensitizer targeting inphotodynamic therapy II. Conjugates of hematoporphyrin with serum lipoproteins, *J. Photochem. Photobiol. B: Biol.*, 26, 147, 1994.
142. Hamblin, M.R. and Newman, E.L., Photosensitizer targeting in photodynamic therapy I. Conjugates of hematoporphyrin with albumin and transferrin, *J. Photochem. Photobiol. B: Biol.*, 26, 45, 1994.
143. Molpus, K.L., Hamblin, M.R., Rizvi, I., and Hasan, T., Intraperitoneal photoimmunotherapy of ovarian carcinoma xenografts in nude mice using charged photoimmunoconjugates, *Gynecol. Oncol.*, 76, 397, 2000.
144. Shiah, J.G., Sun, Y., Kopeckova, P., Peterson, C.M., Straight, R.C., and Kopecek, J., Combination chemotherapy and photodynamic therapy of targetable *N*-(2-hydroxypropyl) methacrylamide copolymer-doxorubicin/mesochlorin e(6)-OV-TL 16 antibody, *J. Controlled Release*, 74, 249, 2001.
145. Hamblin, M.R., Miller, J.L., Rizvi, I., Ortel, B., Maytin, E.V., and Hasan, T., Pegylation of a chlorin(e6) polymer conjugate increases tumor targeting of photosensitizer, *Cancer Res.*, 61, 7155, 2001.
146. DelGovernatore, M., Hamblin, M.R., Shea, C.R., Rizvi, I., and Hasan, T., Experimental photoimmunotherapy of hepatic metastases of colorectal cancer with a 17.1A chlorin (e6) immunoconjugate, *Cancer Res.*, 60, 4200, 2000.
147. Soukos, N.S., Hamblin, M.R., Keel, S., Fabian, R.L., Deutsch, T.F., and Hasan, T., Epidermal growth factor receptor-targeted immunophotodiagnosis and photoimmunotherapy of oral precancer *in vivo*, *Cancer Res.*, 61, 4490, 2001.
148. Fingar, V.H., Wieman, J., Wiehle, S.A., and Cerrito, P.B., The role of microvascular damage in photodynamic therapy: the effect of treatment on vessel constriction, permeability, and leukocyte adhesion, *Cancer Res.*, 53, 4914, 1992.
149. Fingar, V.H., Wieman, T.J., Karavolos, P.S., Doak, K.W., Ouellet, R., and van Lier, J.E., The effects of photodynamic therapy using differently substituted zinc phthalocyanines on vessel constriction, vessel leakage and tumor response, *Photochem. Photobiol.*, 58, 251, 1993.
150. Henderson, B.W. and Fingar, V.H., Relationship of tumor hypoxia and response to photodynamic treatment in an experimental mouse tumor, *Cancer Res.*, 47, 3110, 1987.
151. Sitnik, T.M., Hampton, J.A., and Henderson, B.W., Reduction of tumor oxygenation during and after photodynamic therapy *in vivo*: effects of fluence rate, *Br. J. Cancer*, 77, 1386, 1998.
152. Chen, B., Zupko, I., and deWitte, P.A., Photodynamic therapy with hypericin in a mouse P388 tumor model: vascular effects determine the efficacy, *Internat. J. Oncol.*, 18, 737, 2001.
153. Zilbertstein, J., Schreiber, S., Bloemers, M.C., Bendel, P., Neeman, M., Schechtman, E., Kohen, F., Scherz, A., and Salomon, Y., Antivascular treatment of solid melanoma tumors with bacteriochlorophyll-serine-based photodynamic therapy, *Photochem. Photobiol.*, 73, 257, 2001.

154. Pogue, B.W., Braun, R.D., Lanzen, J.L., Erickson, C., and Dewhirst, M.W., Analysis of the heterogeneity of pO2 dynamics during photodynamic therapy with verteporfin, *Photochem. Photobiol.*, 74, 700, 2002.
155. Engbrecht, B.W., Menon, C., Kachur, A.V., Hahn, S.M., and Fraker, D.L., Photofrin-mediated photodynamic therapy induces vascular occlusion and apoptosis in a human sarcoma xenograft model, *Cancer Res.*, 59, 4334, 2001.
156. Busch, T.M., Hahn, S.M., Evans, S.M., and Koch, C.J., Depletion of tumor oxygenation during photodynamic therapy: detection by the hypoxia marker EF3, *Cancer Res.*, 60, 2636, 2000.
157. Henderson, B.W., Dougherty, T.J., and Malone, P.B., Studies on the mechanism of tumor destruction by photoradiation therapy, *Prog. Clin. Biol. Res.*, 170, 601, 1984.
158. Fingar, V.H., Siegel, K.A., Wieman, T.J., and Doak, K.W., The effects of thromboxane inhibitors on the microvascular and tumor response to photodynamic therapy, *Photochem. Photobiol.*, 58, 393, 1993.
159. Reed, M.W.R., Wieman, T.J., Schuschke, D.A., Tseng, M.T., and Miller, F.N., A comparison of the effects of photodynamic therapy on normal and tumor blood vessels in the rat microcirculation, *Radiat. Res.*, 119, 542, 1989.
160. Fingar, V.H. and Henderson, B.W., Drug and light dose dependence of photodynamic therapy: a study of tumor and normal tissue response, *Photochem. Photobiol.*, 46, 837, 1987.
161. Fingar, V.H., Kik, P.K., Haydon, P.S., Cerrito, P.B., Tseng, M., Abang, E., and Wieman, T.J., Analysis of acute vascular damage after photodynamic therapy using benzoporphyrin derivative (BPD), *Br. J. Cancer*, 79, 1702, 1999.
162. Sitnik, T. and Henderson, B.W., The effect of fluence rate on tumor and normal tissue responses to photodynamic therapy, *Photochem. Photobiol.*, 67, 462, 1998.
163. Henderson, B.W., Sitnik-Busch, T.M., and Vaughan, L.A., Potentiation of PDT anti-tumor activity in mice by nitric oxide synthase inhibition is fluence rate dependent, *Photochem. Photobiol.*, 70, 64, 1999.
164. Dimitroff, C.J., Klohs, W., Sharma, A., Pera, P., Driscoll, D., Smith, J., Steinkampf, R., Schroeder, M., Klutchko, S., Sumlin, A., Henderson, B., Dougherty, T.J., and Bernacki, R.J., Anti-angiogenic activity of selected receptor tyrosine kinase inhibitors, PD166285 and PD173074: implications for combination treatment with photodynamic therapy, *Invest. New Drugs*, 17, 121, 1999.
165. Korbelik, M., Parkins, C.S., Shibuya, H., Cecic, I., Stratford, M.R., and Chaplin, D.J., Nitric oxide production by tumour tissue: impact on the response to photodynamic therapy, *Br. J. Cancer*, 82, 1835, 2000.
166. Curnow, A. and Bown, S.G., The role of reperfusion injury in photodynamic therapy with 5-aminolaevulinic acid — a study on normal rat colon, *Br. J. Cancer*, 86, 989, 2002.
167. Tseng, M.T., Reed, M.W., Ackermann, D.M., Schuschke, D.A., Wieman, T.J., and Miller, F.N., Photodynamic therapy induced ultrastructural alterations in microvasculature of the rat cremaster muscle, *Photochem. Photobiol.*, 48, 675, 1988.
168. Dolmans, D.E., Kadambi, A., Hill, J.S., Waters, C.A., Robinson, B.C., Walker, J.P., Fukumura, D., and Jain, R.K., Vascular accumulation of a novel photosensitizer, MV6401, causes selective thrombosis in tumor vessels after photodynamic therapy, *Cancer Res.*, 62, 2151, 2002.
169. McMahon, K.S., Wieman, T.J., Moore, P.H., and Fingar, V.H., Effects of photodynamic therapy using mono-L-aspartyl chlorin e_6 on vessel constriction, vessel leakage, and tumor response, *Cancer Res.*, 54, 5374, 1994.
170. Kerdel, F.A., Soter, N.A., and Lim, H.W., *In vivo* mediator release and degranulation of mast cells in hematoporphyrin derivative-induced phototoxicity in mice, *J. Invest. Derm.*, 88, 277, 1987.
171. Zieve, P.D. and Solomon, H.M., The effect of hematoporphyrin and light on human platelets. 3. Release of potassium and acid phosphatase, *J. Cell Physiol.*, 68, 109, 1966.
172. Ben-Hur, E., Heldman, E., Crane, S.W., and Rosenthal, I., Release of clotting factors from photosensitized endothelial cells: a possible trigger for blood vessel occlusion by photodynamic therapy, in *Selected Papers on Photodynamic Therapy*, Kessel, D., Ed., 82, 408, 1993.

173. Lim, H.W., Effects of porphyrins on skin, *Ciba Found. Symp.*, 146, 148, 1989.
174. Fingar, V.H., Wieman, T.J., and Doak, K.W., Role of thromboxane and prostacyclin release on photodynamic therapy-induced tumor destruction, *Cancer Res.*, 50, 2599, 1990.
175. Zieve, P.D., Solomon, H.M., and Krevans, J.R., The effect of hematoporphyrin and light on human platelets. I. Morphologic, functional, and biochemical changes, *J. Cell Physiol.*, 67, 271, 1966.
176. Henderson, B.W., Owczarczak, B., Sweeney, J., and Gessner, T., Effects of photodynamic treatment of platelets or endothelial cells *in vitro* on platelet aggregation, *Photochem. Photobiol.*, 56, 513, 1992.
177. Reed, M.W., Schuschke, D.A., and Miller, F.N., Prostanoid antagonists inhibit the response of the microcirculation to "early" photodynamic therapy, *Radiat. Res.*, 127, 292, 1991.
178. Taber, S.W., Wieman, T.J., and Fingar, V.H., The effects of aspirin on microvasculature after photodynamic therapy, *Photochem. Photobiol.*, 57, 856, 1993.
179. Fingar, V.H., Wieman, T.J., and Haydon, P.S., The effects of thrombocytopenia on vessel stasis and macromolecular leakage after photodynamic therapy using Photofrin, *Photochem. Photobiol.*, 66, 513, 1997.
180. Fingar, V.H., Wieman, T.J., and Doak, K.W., Changes in tumor interstitial pressure induced by photodynamic therapy, *Photochem. Photobiol.*, 53, 763, 1991.
181. Höckel, M. and Vaupel, P., Tumor hypoxia: definitions and current clinical, biologic, and molecular aspects, *J. Natl. Cancer Inst.*, 93, 266, 2001.
182. Fingar, V.H., Wieman, T.J., Park, Y.J., and Henderson, B.W., Implications of a pre-existing tumor hypoxic fraction on photodynamic therapy, *J. Surg. Res.*, 53, 524, 1992.
183. Fingar, V.H., Mang, T.S., and Henderson, B.W., Modification of photodynamic therapy-induced hypoxia by fluosol-DA (20%) and carbogen breathing in mice, *Cancer Res.*, 48, 3350, 1988.
184. Jirsa, M.J., Pouckova, P., Dolezal, J., Pospisil, J., and Jirsa, M., Hyperbaric oxygen and photodynamic therapy in tumour-bearing nude mice [letter], *Eur. J. Cancer*, 27, 109, 1991.
185. Maier, A., Tomaselli, F., Anegg, U., Rehak, P., Fell, B., Luznik, S., Pinter, H., and Smolle-Juttner, F.M., Combined photodynamic therapy and hyperbaric oxygenation in carcinoma of the esophagus and the esophago-gastric junction, *Europ. J. Cardio-Thor. Surg.*, 18, 649, 2001.
186. Svaasand, L.O., Doiron, D.R., and Dougherty, T.J., Temperature rise during photoradiation therapy of malignant tumors, *Med. Phys.*, 10, 10, 1983.
187. Mattiello, J., Hetzel, F., and Vandenheede, L., Intratumor temperature measurements during photodynamic therapy, *Photochem. Photobiol.*, 46, 873, 1987.
188. Henderson, B.W., Busch, T.M., Vaughan, L.A., Frawley, N.P., Babich, D., Sosa, T.A., Zolo, J.D., Dee, A.S., Cooper, M.T., Bellnier, D.A., Greco, W.R., and Oseroff, A.R., Photofrin photodynamic therapy can significantly deplete or preserve oxygenation in human basal cell carcinomas during treatment, depending on fluence rate, *Cancer Res.*, 60, 525, 2000.
189. Tromberg, B.J., Orenstein, A., Kimel, S., Barker, S.J., Hyatt, J., Nelson, J.S., and Berns, M.W., *In vivo* tumor oxygen tension measurements for the evaluation of the efficiency of photodynamic therapy, *Photochem. Photobiol.*, 52, 375, 1990.
190. Chen, Q., Chen, H., and Hetzel, F.W., Tumor oxygenation changes post-photodynamic therapy, *Photochem. Photobiol.*, 63, 128, 1996.
191. Foster, T.H., Murant, R.S., Bryant, R.G., Knox, R.S., Gibson, S.L., and Hilf, R., Oxygen consumption and diffusion effects in photodynamic therapy, *Radiat. Res.*, 126, 296, 1991.
192. Henning, J.P., Fournier, R.L., and Hampton, J.A., A transient mathematical model of oxygen depletion during photodynamic therapy, *Radiat. Res.*, 142, 221, 1995.
193. Foster, T.H. and Gao, L., Dosimetry in photodynamic therapy: oxygen and the critical importance of capillary density, *Radiat. Res.*, 130, 379, 1992.
194. Pogue, B.W. and Hasan, T., A theoretical study of light fractionation and dose-rate effects in photodynamic therapy, *Radiat. Res.*, 147, 551, 1997.
195. Foster, T.H., Hartley, D.F., Nichols, M.G., and Hilf, R., Fluence rate effects in photodynamic therapy of multicell tumor spheroids, *Cancer Res.*, 53, 1249, 1993.

196. Mitra, S., Finlay, J.C., McNeill, D., Conover, D.L., and Foster, T.H., Photochemical oxygen consumption, oxygen evolution and spectral changes during UVA irradiation of EMT6 spheroids, *Photochem. Photobiol.*, 73, 703, 2001.
197. Zilberstein, J., Bromberg, A., Frantz, A., Rosenbach-Belkin, V., Kritzmann, A., Pfefermann, R., Salomon, Y., and Scherz, A., Light-dependent oxygen consumption in bacteriochlorophyll-serine-treated melanoma tumors: on-line determination using a tissue-inserted oxygen microsensor, *Photochem. Photobiol.*, 65, 1012, 1997.
198. Mang, T.S., Dougherty, T.J., Potter, W.R., Boyle, D.G., Somer, S., and Moan, J., Photobleaching of porphyrins used in photodynamic therapy and implications for therapy, *Photochem. Photobiol.*, 45, 501, 1987.
199. Spikes, J.D., Quantum yields and kinetics of the photobleaching of hematoporphyrin, Photofrin II, tetra(4-sulfonatophenyl)porphine and uroporphyrin, *Photochem. Photobiol.*, 55, 797, 1992.
200. Coutier, S., Mitra, S., Bezdetnaya, L.N., Parache, R.M., Georgakoudi, I., Foster, T.H., and Guillemin, F., Effects of fluence rate on cell survival and photobleaching in meta-tetra-(hydroxyphenyl)chlorin-photosensitized Colo 26 multicell tumor spheroids, *Photochem. Photobiol.*, 73, 297, 2001.
201. Finlay, J.C., Conover, D.L., Hull, E.L., and Foster, T.H., Porphyrin bleaching and PDT-induced spectral changes are irradiance dependent in ALA-sensitized normal rat skin *in vivo*, *Photochem. Photobiol.*, 73, 54, 2001.
202. Georgakoudi, I., Nichols, M.G., and Foster, T.H., The mechanism of Photofrin photobleaching and its consequences for photodynamic dosimetry, *Photochem. Photobiol.*, 65, 135, 1997.
203. Georgakoudi, I. and Foster, T.H., Singlet oxygen- *versus* nonsinglet oxygen-mediated mechanisms of sensitizer photobleaching and their effects on photodynamic dosimetry, *Photochem. Photobiol.*, 67, 612, 1998.
204. Gibson, S.L., VanDerMeid, K.R., Murant, R.S., Raubertas, R.F., and Hilf, R., Effects of various photoradiation regimens on the antitumor efficacy of photodynamic therapy for R3230AC mammary carcinomas, *Cancer Res.*, 50, 7236, 1990.
205. Iinuma, S., Schomacker, K.T., Wagnieres, G., Rajadhyaksha, M., Bamberg, M., Momma, T., and Hasan, T., *In vivo* fluence rate and fractionation effects on tumor response and photobleaching: photodynamic therapy with two photosensitizers in an orthotopic rat tumor model, *Cancer Res.*, 59, 6164, 1999.
206. van Geel, I.P.J., Oppelaar, H., Marijnissen, J.P.A., and Stewart, F.A., Influence of fractionation and fluence rate in photodynamic therapy with Photofrin or mTHPC, *Radiat. Res.*, 145, 602, 1996.
207. Blant, S.A., Woodtli, A., Wagnieres, G., Fontolliet, C., Van den Bergh, H., and Monnier, P., *In vivo* fluence rate effect in photodynamic therapy of early cancers with tetra(*m*-hydroxyphenyl)chlorin, *Photochem. Photobiol.*, 64, 963, 1996.
208. Curnow, A., McIlroy, B.W., Postle-Hacon, M.J., MacRobert, A.J., and Bown, S.G., Light dose fractionation to enhance photodynamic therapy using 5-aminolevulinic acid in the normal rat colon, *Photochem. Photobiol.*, 69, 71, 1999.
209. DeBruijn, H.S., van der Veen, N., Robinson, D.J., and Star, W.M., Improvement of systemic 5-aminolevulinic acid-based photodynamic therapy *in vivo* using light fractionation with a 75-minute interval, *Cancer Res.*, 59, 901, 1999.
210. Gollnick, S.O., Musser, D.A., Oseroff, A.R., Vaughan, L.A., Owczarczak, B., and Henderson, B.W., IL-10 does not play a role in cutaneous Photofrin® photodynamic therapy-induced suppression of the contact hypersensitivity response, *Photochem. Photobiol.*, 74, 811, 2001.
211. Musser, D. and Oseroff, A.R., Characteristics of the immunosuppression induced by cutaneous photodynamic therapy: persistence, antigen specificity and cell type involved, *Photochem. Photobiol.*, 73, 518, 2001.
212. Obochi, M.O.K., Ratkay, L.G., and Levy, J.G., Prolonged skin allograft survival after photodynamic therapy associated with modification of donor skin antigenicity, *Transplantation*, 63, 810, 1997.

213. Gruner, S., Meffert, H., Volk, H.D., Grunow, R., and Jahn, S., The influence of haematoporphyrin derivative and visible light on murine skin graft survival, epidermal Langerhans cells and stimulation of the allogeneic mixed leucocyte reaction, *Scand. J. Immunol.*, 21, 267, 1985.
214. Qin, B., Selman, S.H., Payne, K.M., Keck, R.W., and Metzger, D.W., Enhanced allograft survival after photodynamic therapy: association with lymphocyte inactivation and macrophage stimulation, *Transplantation*, 56, 1481, 1993.
215. Elmets, C.A. and Bowen, K.D., Immunological suppression in mice treated with hematoporphyrin derivative photoradiation, *Cancer Res.*, 46, 1608, 1986.
216. Musser, D.A. and Fiel, R.J., Cutaneous photosensitizing and immunosuppressive effects of a series of tumor localizing porphyrins, *Photochem. Photobiol.*, 53, 119, 1991.
217. Lynch, D.H., Haddad, S., King, V.J., Ott, M.J., Straight, R.C., and Jolles, C.J., Systemic immunosuppression induced by photodynamic therapy (PDT) is adoptively transferred by macrophages, *Photochem. Photobiol.*, 49, 453, 1989.
218. Anderson, C., Hrabovsky, S., McKinley, Y., Tubesing, K., Tang, H.-P., Dunbar, R., Mukhtar, H., and Elmets, C.A., Phthalocyanine photodynamic therapy: disparate effects of pharmacologic inhibitors on cutaneous photosensitivity and on tumor regression, *Photochem. Photobiol.*, 65, 895, 1997.
219. Simkin, G., Obochi, M., Hunt, D.W.C., Chan, A.H., and Levy, J.G., Effect of photodynamic therapy using benzoporphyrin derivative on the cutaneous immune response, in *Optical Methods for Tumor Treatment and Detection: Mechanisms and Techniques in Photodynamic Therapy IV,* Proc. SPIE, 2392, 23, 1995.
220. Simkin, G., Tao, J.-S., Levy, J.G., and Hunt, D.W.C., IL-10 contributes to the inhibition of contact hypersensitivity in mice treated with photodynamic therapy, *J. Immunol.*, 164, 2457, 2000.
221. Musser, D.A., Gollnick, S.O., Oseroff, A.R., and Henderson, B.W., Photodynamic therapy (PDT) induces long term suppression of CHS which is correlated with systemic and localized expression of IL-10, *Photochem. Photobiol.*, 67S, 102S, 1998.
222. Reddan, J.C., Anderson, C., Xu, H., Hrabovsky, S., Freye, K., Fairchild, R., Tubesing, K.A., and Elmets, C.A., Immunosuppressive effects of silicon phthalocyanine photodynamic therapy, *Photochem. Photobiol.*, 70, 72, 1999.
223. Ziolkowski, P., Symonowicz, K., Milach, J., and Szkudlarek, T., *In vivo* tumor necrosis factor-α induction following chlorin e_6-photodynamic therapy in Buffalo rats, *Neoplasma*, 44, 192, 1996.
224. Rivas, J.M. and Ullrich, S.E., The role of IL-4, IL-10, and TNF–α in the immune suppression induced by ultraviolet radiation, *J. Leukoc. Biol.*, 56, 769, 1994.
225. Moore, K.W., de Waal Malefyt, R., Coffman, R.L., and O'Garra, A., Interleukin-10 and the interleukin-10 receptor, *Ann. Rev. Immunol.*, 19, 683, 2001.
226. Xu, H., DiIulio, N.A., and Fairchild, R.L., T cell populations primed by hapten sensitization in contact sensitivity are distinguished by polarized patterns of cytokine production: interferon γ-producing (Tc1) effector $CD8^+$ T cells and interleukin (Il)4/Il-10-producing (Th2) negative regulatory $CD4^+$ T cells, *J. Exp. Med.*, 183, 1012, 1996.
227. Macatonia, S.E., Hsieh, C.-S., Murphy, K.M., and O'Garra, A., Dendritic cells and macrophages are required for Th1 development of $CD4^+$ T cells from $\alpha\beta$ TCR trangenic mice: IL-12 substitution for macrophages to stimulate IFN-γ production is IFN-γ-dependent, *Int. Immunol.*, 5, 1119, 1993.
228. Macatonia, S.E., Hosken, N.A., Litton, M., Vieira, P., Hsieh, C.-S., Culpepper, J.A., Wysocka, M., Trinchieri, G., Murphy, K.M., and O'Garra, A., Dendritic cells produce IL-12 and direct the development of Th1 cells from naive $CD4^+$ T cells, *J. Immunol.*, 154, 5071, 1995.
229. O'Garra, A., Cytokines induce the development of functionally heterogeneous T helper cell subsets, *Immunity*, 8, 275, 1998.
230. Sad, S. and Mosmann, T.R., Interleukin (IL)-4, in the absence of antigen stimulation, induces an anergy-like state in differentiated CD8+ Tc1 cells: loss of IL-2 synthesis and autonomous proliferation but retention of cytotoxicity and synthesis of other cytokines, *J. Exp. Med.*, 182, 1505, 1995.

231. King, D.E., Jiang, H., Simkin, G., Obochi, M., Levy, J.G., and Hunt, D.W.C., Photodynamic alteration of the surface receptor expression pattern of murine splenic dendritic cells, *Scand. J. Immunol.*, 49, 184, 1999.
232. Korbelik, M. and Dougherty, G.J., Photodynamic therapy-mediated immune response against subcutaneous mouse tumors, *Cancer Res.*, 59, 1941, 1999.
233. Blank, M., Lavie, G., Mandel, M., and Keisari, Y., Effects of photodynamic therapy with hypericin in mice bearing highly invasive solid tumors, *Oncology Res.*, 12, 409, 2001.
234. Krosl, G., Korbelik, M., and Dougherty, G.J., Induction of immune cell infiltration into murine SCCVII tumour by Photofrin-based photodynamic therapy, *Br. J. Cancer*, 71, 549, 1995.
235. Korbelik, M., Krosl, G., Krosl, J., and Dougherty, G.J., The role of host lymphoid populations in the response of mouse EMT6 tumor to photodynamic therapy, *Cancer Res.*, 56, 5647, 1996.
236. deVree, W.J.A., Essers, M.C., DeBruijn, H.S., Star, W.M., Koster, J.F., and Sluiter, W., Evidence for an important role of neutrophils in the efficacy of photodynamic therapy *in vivo*, *Cancer Res.*, 56, 2908, 1996.
237. Korbelik, M., Induction of tumor immunity by photodynamic therapy, *J. Clin. Laser Med. Surg.*, 14, 329, 1996.
238. Korbelik, M. and Cecic, I., Contribution of myeloid and lymphoid host cells to the curative outcome of mouse sarcoma treatment by photodynamic therapy, *Cancer Lett.*, 137, 91, 1999.
239. Cecic, I., Parkins, C.S., and Korbelik, M., Induction of systemic neutrophil response in mice by photodynamic therapy of solid tumors, *Photochem. Photobiol.*, 74, 712, 2001.
240. Cecic, I. and Korbelik, M., Mediators of peripheral blood neutrophilia induced by photodynamic therapy of solid tumors, *Cancer Lett*, 2002.
241. Gollnick, S.O., Evans, S.E., Owczarczak, B., Maier, P., Vaughan, L.A., Wang, W.C., Unger, E., and Henderson, B.W., Role of chemokines in the long-term response to photodynamic therapy, *Br. J. Cancer*, 88, 1722, 2003.
242. Yamamoto, N., Hoober, J.K., and Yamamoto, S., Tumoricidal capacities of macrophages photodynamically activated with hematoporphyrin derivative, *Photochem. Photobiol.*, 56, 245, 1992.
243. Korbelik, M. and Krosl, G., Enhanced macrophage cytotoxicity against tumor cells treated with photodynamic therapy, *Photochem. Photobiol.*, 60, 497, 1994.
244. Rousset, N., Vonarx, V., Eléouet, E., Carré, J., Kerninon, E., Lajat, Y., and Patrice, T., Effects of photodynamic therapy on adhesion molecules and metastasis, *J. Photochem. Photobiol. B*, 52, 65, 1999.
245. Korbelik, M., Sun, J., and Posakony, J.J., Interaction between photodynamic therapy and BCG immunotherapy responsible for the reduced recurrence of treated mouse tumors, *Photochem. Photobiol.*, 73, 403, 2001.
246. Korbelik, M., Naraparaju, V.R., and Yamamoto, N., Macrophage-directed immunotherapy as adjuvant therapy, *Br. J. Cancer*, 75, 202, 1997.
247. Korbelik, M. and Cecic, I., Enhancement of tumour response to photodynamic therapy by adjuvant mycobacterium cell-wall treatment, *J. Photochem. Photobiol. B*, 44, 151, 1998.
248. Korbelik, M. and Sun, J., Cancer treatment by photodynamic therapy combined with adoptive immunotherapy using genetically altered natural killer cell line, *Int. J. Cancer*, 93, 269, 2001.
249. Curry, P.M. and Levy, J.G., Tumor inhibitory lymphocytes derived from the lymph nodes of mice treated with photodynamic therapy, *Photochem. Photobiol.*, 61S, 72S, 1995.
250. Canti, G., Lattuada, D., Nicolin, A., Taroni, P., Valentini, G., and Cubeddu, R., Immunopharmacology studies on photosensitizers used in photodynamic therapy (PDT), in *Photodynamic Therapy of Cancer*, Proc. SPIE, 2078, 268, 1994.
251. Abdel-Hady, E.S., Martin-Hirsch, P., Duggan-Keen, M., Stern, P.L., Moore, J.V., Corbitt, G., Kitchener, H.C., and Hampson, I.N., Immunological and viral factors associated with the response of vulval intraepithelial neoplasia to photodynamic therapy, *Cancer Res.*, 61, 192, 2001.

252. Nseyo, U.O., Whalen, R.K., Duncan, M.R., Berman, B., and Lundahl, S.L., Urinary cytokines following photodynamic therapy for bladder cancer. A preliminary report, *Urology*, 36, 167, 1990.
253. deVree, W.J.A., Essers, M.C., Koster, J.F., and Sluiter, W., Role of interleukin 1 and granulocyte colony-stimulating factor in Photofrin-based photodynamic therapy of rat rhabdomyosarcoma tumors, *Cancer Res.*, 57, 2555, 1997.
254. Matzinger, P., Tolerance, danger, and the extended family, *Annu. Rev. Immunol.*, 12, 991, 1994.
255. Sauter, B., Albert, M.L., Francisco, L.M., Larsson, M., Somersan, S., and Bhardwaj, N., Consequences of cell death: exposure to necrotic tumor cells, but not primary tissue cells or apoptotic cells, induces the maturation of immunostimulatory dendritic cells, *J. Exp. Med.*, 191, 423, 2000.
256. Lanzavecchi, A. and Sallusto, F., Regulation of T cell immunity by dendritic cells, *Cell*, 106, 263, 2001.
257. Gollnick, S.O., Vaughan, L.A., and Henderson, B.W., Generation of effective anti-tumor vaccines using photodynamic therapy, *Cancer Res.*, 62, 1604, 2002.
258. Schreiber, S., Gross, S., Brandis, A., Harmelin, A., Rosenbach-Belkin, V., Scherz, A., and Salomon, Y., Local photodynamic therapy (PDT) of rat C6 glioma xenografts with Pd-bacteriopheophorbide leads to decreased metastases and increase of animal cure compared with surgery, *Int. J. Cancer*, 99, 279, 2002.
259. Momma, T., Hamblin, M.R., Wu, H.C., and Hasan, T., Photodynamic therapy of orthotopic prostate cancer with benzoporphyrin derivative: local control and distant metastasis, *Cancer Res.*, 58, 5421, 1998.

146

Photodynamic Therapy: Basic and Preclinical Aspects

Giulio Jori
University of Padova

146.1 Introduction

Photodynamic therapy (PDT) represents an increasingly accepted modality for the curative or palliative treatment of cancer and some noncancerous conditions that are generally characterized by overgrowth of transformed cells.[1] Interest in this technique was promoted by the recent approval of PDT with Photofrin® (a complex mixture of hematoporphyrin derivatives[2]) by regulatory health authorities in several countries for the treatment of lung, gastric, esophageal, bladder, and cervical tumors, in addition to cervical dysplasia and actinic keratosis.[3] At the same time, a more detailed understanding of the mechanisms involved in the photosensitized damage of cells and tissues, as well as a definition of the correlation between chemical structure and photodynamic activity for various classes of porphyrin derivatives,[4] led to the development of second-generation photosensitizers with improved phototherapeutic properties and the extension of PDT outside the oncological field; a typical example is represented by the approval of PDT with benzoporphyrin derivative for the treatment of the wet form of age-related macular degeneration.[5] As known, the successful outcome of PDT depends on the optimal interaction among three elements: light, photosensitizer, and oxygen. In general, light wavelengths in the red/near-infrared region of the visible spectrum are endowed with good penetration power into most human tissues, ranging from 4 to 5 mm for the 630 nm wavelength (which is used to activate Photofrin *in vivo*) to about 1.5 cm for wavelengths around 800 nm.[6] As a consequence, porphyrins and their analogues (such as chlorins, bacteriochlorins, phthalocyanines) are most frequently used as PDT agents: such compounds exhibit absorption bands in selected intervals within the 600 to 800 nm range and show no detectable cytotoxicity at the doses that are photochemically active. Red light has an additional advantage in that it undergoes no appreciable absorption by the chromophores commonly present in mammalian tissues, with the exception of melanin; therefore, there is a minimal risk to initiate photoprocesses in areas different from those containing the exogenously introduced photosensitizer that might induce generalized and undesired side effects. Last, several noncoherent and coherent light sources specifically suitable for PDT applications for different diseases and different anatomical sites were developed in the

0-8493-1348-1/04/$0.00+$1.50

TABLE 146.1 Physicochemical Properties of an Efficient PDT Agent in the Ground and Electronically Excited States

Property	Typical Values	Related Features
Absorption range	700–800 nm	Large tissue transmittance; sufficient triplet energy to generate singlet oxygen
Molar extinction coefficient	$>10^5$ M^{-1} cm^{-1}	Extensive π electron delocalization; use of low photosensitizer dosages
Fluorescence quantum yield	≥0.2	Useful for diagnostic applications; not too large to compete with intersystem crossing to the triplet state
Triplet quantum yield	>0.7–0.8	Essential for efficient photosensitization
Triplet lifetime	Longer than 100 μs	Typical of monomeric photosensitizers, allows a major role in diffusion-controlled processes
Singlet oxygen quantum yield	>0.5	Easy accessibility to oxygen for the triplet photosensitizer
Photobleaching quantum yield	$<10^{-5}$	Prevents a decrease that is too fast in the photosensitizer concentration during irradiation

last few years.[7] Notable is the availability of typically low-cost and compact red-emitting diode lasers that can be efficiently coupled with optical fibers, thus allowing for irradiation of lesions in internal organs, which has been useful for broadening the utilization of this technique. Recent findings[8] also suggest that less tissue-penetrating light wavelengths (e.g., green or even blue light) might be preferable in specific cases to avoid the photoinduced damage of deeper tissue layers not involved in the disease (for example, the treatment of neoplastic lesions of the gastric mucosa) or the perforation of tissues (for example, in the removal of atherosclerotic plaques). Thus, it is likely that the final PDT protocol needs to be tailored to any given disease.

In general, the successful outcome of PDT largely depends on the choice of a photosensitizer with optimal properties for any specific application. Such properties can be subdivided into photophysical/photochemical, photobiological, and pharmacokinetic/phototherapeutic properties.

146.2 Photophysical and Photochemical Processes in PDT

A synthetic list of the photophysical and photochemical properties, which are typical of an efficient PDT photosensitizer, is shown in Table 146.1. Apparently, the first requirement is represented by the presence of intense absorption bands in the 700 to 800 nm wavelength region, which guarantees the uniform illumination of relatively large tissue volumes. To achieve this goal, selected modifications of the porphyrin-type tetrapyrrolic macrocycle were devised, [9] including the following:

1. Expansion of the macrocycle through condensation of a benzene or naphthalene moiety with each pyrrole ring — as a result, the 18 π electron cloud of porphyrins increases to 24 or 26 π electrons with a consequent shift of the longest wavelength absorption maximum to ca. 680 to 720 nm (phthalocyanines) and, respectively, 780 to 820 nm (naphthalocyanines); the latter wavelength is considered a kind of energy threshold for the triplet state of the photosensitizer to be phototherapeutically active[10]
2. Hydrogenation of a carbon–carbon double bond in one or two pyrrole rings to generate chlorins and, respectively, bacteriochlorins — this modification results in a shift of the red absorption to around 690 to 700 nm and around 780 nm, as well as in a marked increase in the molar extinction coefficient
3. Synthesis of a porphyrin isomer, the porphycene, differing from traditional porphyrins in the number of carbon–carbon bonds between the individual pyrrole rings — even though the total number of resonating π electrons is still 18, such an alteration of the overall molecular geometry is accompanied by an about 50 nm red shift of the lowest-energy absorption band and a simultaneous ca. 10-fold enhancement of the molar extinction coefficient; a similar pattern of structural changes is typical of texaphyrins, which also display a maximum absorption at 680 to 700 nm

TABLE 146.2 Main Targets of Photodynamic Processes in Biological Systems

Cell Constituent	Photosensitive Targets	Main Photoproduct	
		Type I	Type II
Proteins	Tryptophan	Hydroxy-indoles	Kynurenines
	Histidine	Keto derivatives	Keto derivatives
	Methionine	Methional	Methionine sulfoside
	Cysteine	Cysteic acid	Cystine
Unsaturated lipids	Oleic, linoleic, linolenic, arachidonic acids	Polymeric derivatives	Endoperoxides, hydroperoxides
Steroids	Cholesterol	5α-Hydroperoxide	7α-Hydroperoxide
Nucleosides	Guanosine	Various	Various

Further modifications of the absorbance properties of PDT photosensitizers, including a fine-tuning of the position and intensity of the absorption maxima, can be obtained by a careful choice of other structural elements, such as the following:

1. The nature of the substituents protruding from the peripheral positions of the macrocycle or appended to the meso-carbon or nitrogen atoms — Alkoxy-type substituents are particularly effective in bathochromically shifting the absorption.
2. The insertion of a metal ion at the center of the macrocycle, the ion being coordinated with the four pyrrole nitrogen atoms — Such ions should be diamagnetic or have filled *d* orbitals; paramagnetic ions are known to cause drastic shortening of the photosensitizer triplet lifetime, with a consequent inhibition of the PDT activity. Typical ions successfully introduced into the tetrapyrrolic macrocycle include Zn(II), Al(III), Pd(II), Si(IV), and Ge(IV) ions.[11]
3. The addition of axial ligands in the fifth or sixth coordinative position of the centrally located metal ion[12] — This approach offers large flexibility in the choice of the auxochromic or bathochromic functional groups, allowing for precise control of the photosensitizer physicochemical properties in both ground and electronically excited states.

In spite of the broad number of photosensitizers so far tested as PDT agents and the variety of their microenvironments in biological systems, the photophysical pathways involved in the early steps of photodynamic processes are of fairly general occurrence. Thus, it is now widely accepted[13,14] that the main cytotoxic intermediate is represented by singlet oxygen ($^1\Delta g\ O_2$) generated via electronic energy transfer from the photoexcited sensitizer in its long-lived (a few hundred microseconds) lowest triplet state. A minor contribution to the photoprocess is given by radical species originated through redox reactions that are based on electron–hydrogen transfer steps between the triplet photosensitizer and nearby substrates (including ground-state oxygen). The latter step may give rise to the superoxide anion ($O_2\cdot^-$), which is intrinsically characterized by a low reactivity; however, under specific circumstances, the superoxide anion can undergo the Fenton reaction originating the OH· radical, which is extremely reactive.

In any case, the photochemically produced transients are characterized by a high level of electrophilicity, hence, only electron-rich sites of molecules located in the immediate surroundings (a few nanometers) of the photosensitizer are modified, at least in the initial stages of the photoprocess. Therefore, the PDT action is most frequently characterized by a high spatial selectivity. As shown in Table 146.2, typical targets of photodynamic processes occurring in biological systems include aromatic and sulfur-containing amino acids, unsaturated lipids, steroids, and guanosine nucleotides.[15–17] In several cases, the end-products of the photoprocess are dependent on the prevailing mechanism; this circumstance can be utilized as a diagnostic tool between Type I and Type II photosensitization pathways.

One factor that strongly influences the photophysical properties of porphyrin derivatives is represented by the tendency of these compounds to undergo aggregation in aqueous media.[18] Dimers and higher oligomers are readily formed as a result of π–π and hydrophobic interactions between the flat tetrapyrrolic macrocycles with an aim to minimize the contact area with the polar milieu. In such aggregates, the excitation energy is largely dissipated through nonradiative channels, thus drastically shortening the

lifetime of the photosensitizer triplet state. As a consequence, oligomeric porphyrins are generally inefficient photodynamic agents.[18,19] The tendency to aggregate can be counteracted by various strategies, such as the presence of charged peripheral substituents (e.g., carboxylate or ammonium functions), the introduction of bulky axial substituents, or the localization of the porphyrin in hydrophobic niches of cells and tissues.

Last, it is important to underline that the energy–electron transfer process from the triplet photosensitizer is usually competitive with one or more photochemical reactions, causing an irreversible modification of the photosensitizer molecule. The latter process is also known as "photobleaching," because it is accompanied by a cleavage of the tetrapyrrolic macrocycle and a consequent disappearance of the visible absorption bands. The efficiency of the photoprocess is strongly dependent on the nature of the coordinated metal ion and the side chains attached to the macrocycle: quantum yields typically are in the 10^{-4} to 10^{-6} range.[20] From the point of view of phototherapeutic applications, the occurrence of photobleaching may have positive effects, because it avoids the persistence of significant photosensitizer concentrations in the irradiated site that could induce some long-lasting photosensitivity.

146.3 Photobiology of PDT

It is now established[21] that the photosensitizing agent must be bound to a cell for the photodynamic process to proceed with high efficiency. As a consequence, a large variety of mechanisms are involved in the response of cells to photodynamic action. Such responses usually vary with the cell type and its metabolic characteristics, such as the mitotic index, the presence of pigmented endocellular constituents, and the development of photoprotective factors. At the same time, cell responses are modulated by the interplay among several experimental variables,[22,23] including the following:

- Subcellular distribution of the photosensitizer (this is, in turn, influenced by the chemical structure of the photosensitizer and the cell-photosensitizer incubation time prior to irradiation)
- Photosensitizer concentration in the incubation medium
- Irradiation fluence-rate (mW/cm^2), which may particularly control the onset of repair processes
- Total delivered light dose (J/cm^2)

In general, porphyrins and their derivatives, which are most frequently used as PDT agents, localize at the level of cell membranes, including the cytoplasmic, mitochondrial and lysosomal membranes, the Golgi apparatus, and the rough endoplasmic reticulum.[18] Relative partitioning of the porphyrin-type photosensitizers among these subcellular compartments is at least partially dependent on the degree of hydrophilicity or hydrophobicity. Thus, highly water-soluble derivatives, such as tetrasulfonate or tetracarboxylate porphyrinoids, preferentially localize in lysosomes; on the other hand, appreciably lipophilic compounds (e.g., porphyrins having *n*-octanol/water partition coefficient greater than ca. 20) are almost exclusively associated with the lipid domains of the cytoplasmic membrane, at least for short incubation times, while binding to mitochondria is favored by the presence of positively charged functional groups in the porphyrin molecule.[24]

In spite of such a large variety of possible situations, three levels of cell response to PDT treatment can be identified (see Table 146.3). Thus, when mild irradiation regimes are used, cells are sublethally damaged. As a result, a variety of signaling pathways are activated that can counteract the photoinduced damage (e.g., expression of stress proteins) or promote the development of repair processes. Frequently, the action of photodynamic sensitizers causes a transient increase in the intracellular Ca^{2+} ions, due to an influx of extracellular Ca^{2+} and a release of Ca^{2+} from intracellular stores (e.g., the endoplasmic reticulum).[24] Photosensitization of cells by porphyrinoids often produces an oxidative stress that can lead to the upregulation of specific factors, such as tumor necrosis factor (TNF) and nuclear factor-kB (NF-kB), as well as the inactivation of sphingomyelinase with the consequent generation of ceramide.[25,26]

These processes may play an important stimulatory or inhibitory role in the photosensitized induction of apoptosis. There are several modes by which photodynamic reactions can promote the activation of processes eventually leading to programmed cell death (for an excellent review, see Oleinick et al.[27]). The

TABLE 146.3 Cell Response to Visible Light Irradiation in the Presence of Photodynamic Sensitizers

Response	Typical Features	Irradiation Protocol
Signaling events	Formation of cytokines; expression of surface receptors; increase in intracellular Ca^{2+}; activation of second messengers (e.g., ceramide)	**Mild** (low light and sensitizer doses; short incubation times)
Cell death via apoptotic pathways	Chromatin condensation; membrane blebbing; release of cytochrome *c* through the permeability transition pore complex; activation of caspases	**Intermediate** (fluence rates in the 10–20 mW/cm^2 range; short irradiation times; sensitizer binding mainly to mitochondria)
Cell death via random necrosis	Disruption of cytoplasmic membrane and other organelles (e.g., lysosomes, Golgi apparatus); drastic alteration of transmembrane transport processes; inhibition of protein synthesis	**Intensive** (prolonged irradiation at fluence rates as high as 50 $mW/cm;^2$ photosensitizer distribution in several membranous districts)

relative importance of the different mechanisms appears to be determined by a multiplicity of factors, such as the cell type, the nature of the photosensitizer, and the irradiation protocol. In any case, a central pathway for the induction of cell apoptosis by photosensitization involves the oxidative damage of mitochondrial components. In particular, photomodification of the Bcl-2 protein, which performs an important antiapoptotic role, certainly gives a major contribution to the promotion of apoptosis.[28,29] Other important targets of mitochondria-localized photosensitizers are represented by some constituents of the permeability transition pore complex; this results in the release of cytochrome *c* into the cytosol, where it binds to the so-called apoptosis-activating Factor-1 and activates the cascade of caspases, a family of proteins responsible for the final stages of apoptosis.[30] Recent findings suggest that apoptosis can also be initiated by photodynamic processes occurring at the level of the cytoplasmic membrane or lysosomes.[29]

Most often, when drastic irradiation regimes are adopted, apoptotic processes become less frequent (partly because of the irreversible photodamage of proapoptotic proteins), and cell death takes place mainly via a less-controlled mechanism, which is designated as random necrosis. This type of process is characterized by an early disruption of various membranous systems and is clearly favored by a heterogeneous distribution of the photosensitizer in the cell. As a consequence, multiple sites are almost simultaneously damaged.[29,31,32] Typical effects can be summarized as follows:

- *Plasma membrane*: Increased permeability, enzyme inactivation, extensive loss of membrane potential
- *Lysosomes*: Release of hydrolases into the cytosol, inactivation of specific enzymes, reduction of cytosolic pH
- *Mitochondria*: Inhibition of ATP production; inactivation of ATPase, the ADP/ATP translocator, and the enzymes associated with the inner membrane; uncoupling of oxidative phosphorylation
- *Endoplasmic reticulum (ER) and Golgi apparatus*: Inactivation of the ER-specific enzyme acyl coenzyme A; cholesterol-*O*-acyl transferase; extensive swelling; decreased synthesis and transport of plasma membrane proteins (which occurs in rough ER and Golgi apparatus)
- *Cytosol*: Damage of tubulin and other microtubule-associated proteins, increase in the intracellular concentration of free Ca^{2+}

Finally, it must be underlined that a photosensitizer can undergo an extensive relocalization within the cell owing to the disruption or modification of the initial binding sites, as documented by time-resolved fluorescence microscopic studies.[33] This can significantly amplify the overall photoinduced damage.

146.4 Experimental PDT of Tumors

As mentioned in Section 2, the most efficient and selective targeting of tumor tissues is achieved by using hydrophobic photosensitizers. The low water-solubility of such compounds requires the utilization of

TABLE 146.4 Delivery Systems Used for the *in vivo* Administration of Tumor Photosensitizer

Delivery System	Photosensitizer	Observed Behavior of the Photosensitizer
Liposomes made by		
DPPC	Hp, ZnPc, $SnET_2$	Highly preferential delivery to serum lipoproteins
DMPC	ZnPc, $SnET_2$	Delivery to albumin and lipoproteins
POPC, OOPS	ZnPc	Selective release to lipoproteins
Cremophor EL emulsions	$SnET_2$, ZnPc	Preferential delivery to serum LDL as compared to liposome-delivered photosensitizers
LDL	Hp, ZnPc, BPD	Fast redistribution among all members of the lipoprotein family
Albumin	Photofrin	Exchange with lipoproteins in serum; large amounts recovered in the vascular stroma
Epidermal growth factor (EGF)	Hp, Photofrin	Efficient binding to the EGF receptor
Monoclonal antibodies	Chlorin e_6, BPD	Highly selective targeting of tumor cells (encouraging results with cell cultures)

Note: Abbreviations are as follows: DPPC, diplamitoyl-phosphatidylcholine; DMPC, dimiristoyl-phosphatidylcholine; POPC, monooleyl-monopalmitoyl-phosphatidylcholine; OOPS, dioleyl-phosphatidylserine; LDL, low-density lipoproteins; Hp, hematoporphyrin; ZnPc, Zn(II)-phthalocyanine; $SnET_2$, Sn(IV)-etiopurpurin; and BPD, benzoporphyrin derivative.

suitable delivery systems for their intravenous administration. The main delivery systems, which have so far been tested in experimental or clinical PDT, are listed in Table 146.4 (see Jori and Reddi[34] for a more detailed discussion of this topic). In this connection, a few photosensitizers presently involved in clinical trials, such as $SnET_2$ and BPD, are formulated in liposomal vesicles. The choice of the delivery system affects the distribution of the incorporated photosensitizer among serum proteins, which are the actual carriers of the photosensitizer *in vivo*. As shown in Table 146.4, albumin-bound photosensitizers are largely released in the vascular stroma, whereas LDL-carried photosensitizers are preferentially released to malignant cells: it is well known that LDL express a specific interaction with rapidly proliferating cells through a process of receptor-mediated endocytosis.[35,36]

As a consequence, the use of delivery systems is useful for controlling the partitioning of the photosensitizer among the various compartments of the tumor tissue and enhancing the selectivity of tumor loading. Therefore, there are two possible targets of tumor PDT:

1. Direct killing of malignant cells — Three main parameters determine the efficiency of the phototoxic effect: the photosensitizer concentration (which in turn determines the dose of absorbed light), the subcellular distribution of the photosensitizer, and the oxygen level. The lack of vascular occlusion when the photoprocess is focused on tumor cells guarantees a steady supply of oxygen throughout the irradiation procedure, thereby reducing the risk of oxygen depletion that would limit the progress of the photoinduced damage. On the other hand, attempts at improving the oxygenation of the tumor tissue by using oxygen-rich prefluorochemical emulsions as blood substituents yielded no appreciable results.
2. Damage of blood vessels in the tumor leading to vascular occlusion — The consequent development of ischemia provokes the inactivation of neoplastic cells that are spared from direct killing. This process normally induces the onset of a strong inflammatory reaction, which typically triggers the appearance of gross edema and erythema. The release of powerful inflammatory mediators, induced by PDT, such as metabolites of arachidonic acid, histamine, components of the complement cascade clotting system, nitric oxide, and various cytokines, was repeatedly documented.[37,38]

The marked inflammatory reaction induced by PDT elicits an important additional consequence, namely, directing immune cells into the site of injury.[39–41] Massive invasion of neutrophils, mast cells, and macrophages provides a significant contribution to the photodestruction of cancerous cells. Furthermore, the PDT-induced tumor immune reaction may be important in attaining long-term tumor control. It was shown that tumor-associated macrophages can phagocytize cancer cells that were killed

TABLE 146.5 Main Pharmacological Properties of an Efficient Photodynamic Agent

Property	Related Structural and Biological Features
Efficient and selective targeting of the tumor tissue	Hydrophobic or amphiphilic properties; association with suitable delivery systems
Degree of hydrophobicity	Partition coefficient *n*-octanol/water greater than 10
Fast clearance from serum and healthy tissues	High affinity for serum proteins (e.g., high-density lipoproteins) responsible for transport of photosensitizers from peripheral tissues to liver
Low systemic toxicity	Lethal dose (LD-50) higher than ca. 100 mg/kg body weight

or extensively damaged by the photodynamic treatment, thus mediating the initial step of tumor-specific immune development. The mechanisms regulating this process were clearly discussed by Korbelik and Krosl.[42] The induction of immunity against a weakly immunogenic murine fibrosarcoma by PDT with Al(III)-phthalocyanine was detected by Canti et al.[41] These findings open challenging new perspectives for achieving long-term tumor control, e.g., by combining PDT with other immunotherapy protocols.

On the basis of the considerations developed so far, it is possible to outline at least some optimal pharmacological properties of an efficient PDT agent for tumors (see Table 146.5). The basically hydrophobic character imported by the flat aromatic macrocycle, which is present in porphyrinoid derivatives, can be adequately modulated by inserting suitable peripheral substituents; in particular, the presence of two polar moieties on two adjacent pyrrole rings generates an amphiphilic molecule with a lipophilic and a hydrophilic matrix. The need for fast clearance of the systemically injected photosensitizer from nontumor tissues is motivated by two aims: to obtain a high selectivity of tumor labeling, and to avoid the onset of a persistent cutaneous or ocular photosensitivity, which represents one main undesired side effect of PDT.[43] Because porphyrins and their analogues (with the exception of a few highly water-soluble derivatives, such as uroporphyrin) are eliminated from the organism via the bile–gut pathway, it is essential that the adopted photosensitizer display a high affinity for those serum proteins (e.g., high-density lipoproteins) that are deputed to the transport of lipophilic substances from peripheral tissues to liver. This circumstance further stresses the importance of hydrophobicity as a peculiar feature of PDT agents.

146.5 Novel Perspectives

A large variety of solid tumors were shown to be positively responsive to PDT, independent of their histological type or the nature of the anatomical site from which the tumor originates or into which the neoplastic lesion grows.[44,45] One notable exception is represented by malignant melanotic melanoma, where the large concentration of melanin-type pigments acts as an optical filter and prevents the in-depth penetration of sufficient light intensity. Because the absorption of UV and visible light by melanin decreases in an exponential fashion with increasing wavelength, the possibility exists to circumvent its optical filtering by using photosensitizers with intense absorbance above 800 nm.[46] However, such photosensitizers usually have no sufficient energy in their lowest triplet state to generate singlet oxygen. Recent findings[47–49] indicate that such a limitation can be overcome through photothermal sensitization, i.e., by using ns-pulsed laser sources emitting in the 800 to 1000 nm range to photoexcite phthalocyanine or naphthalocyanine complexes with paramagnetic metal ions, such as Ni(II), Fe(II), and Cu(II). These derivatives are characterized by short-lived triplet states and can efficiently convert electronic energy into heat. Under suitable irradiation conditions, temperature increases as large as 100°C are achieved in a sphere of a few nanometers diameter surrounding the photosensitizer binding site. Photothermal sensitization proved to be effective toward cultured neoplastic cells and subcutaneously transplanted tumors in mice.[48] Because the mechanisms of action of photothermal and photodynamic sensitization are substantially different, one can envisage a new phototherapeutic modality, named photothermal therapy (PTT), as well as a combination therapy involving the sequential application of PTT and PDT.

References

1. Dougherty, T.J., Gomer, C.J., Henderson, B.W., Jori, G., Kessel, D., Korbelik, M., Moan, J., and Peng, Q., Photodynamic therapy: a review, *J. Natl. Cancer Inst.*, 90, 889, 1998.
2. Boyle, R.W. and David, D., Structure and biodistribution relationships of photodynamic sensitizers, *Photochem. Photobiol.*, 64, 469, 1996.
3. Levy, J.G. and Obochi, M., New applications in photodynamic therapy, *Photochem. Photobiol.*, 64, 737, 1996.
4. Allen, C.M., Sharman, W.M., and van Lier, J.E., Current status of phthalocyanines in the photodynamic therapy of cancer, *J. Porphyrins Phthalocyanines*, 5, 161, 2001.
5. Schmidt-Erfurth, U. and Hasan, T., Mechanisms of action of photodynamic therapy with Verteporfin for the treatment of age-related macular degeneration, *Survey Ophthalmol.*, 45, 195, 2000.
6. Anderson, R.R. and Parrish, J.A., Optical properties of human skin, in *The Science of Photomedicine*, Regan, J.D. and Parrish, J.A., Eds., Plenum Press, New York, 1982, p. 174.
7. Brancaleon, L. and Moseley, H., Laser and non-laser light sources for photodynamic therapy, *Lasers Med. Sci.*, 17, 173, 2002.
8. Krishnadath, K.K., Feyes, D.K., Boothman, D., Mukhtar, H., and Sano, K., Persistent genetic abnormalities in Barrett's oesophagus after photodynamic therapy, *Gastroenterology*, 119, 624, 2000.
9. Jori, G., Tumour photosensitizers: approaches to enhance the selectivity and efficiency of photodynamic therapy, *J. Photochem. Photobiol., B: Biol.,* 36, 87, 1996.
10. Sounik, J.R., Schechtman, L.A., Rihter, B.D., Ford, W.E., Rodgers, M.A.J., and Kenney, M.E., Synthesis and characterization of naphthalocyanines and phthalocyanines of use in sensitizer studies, in *Photodynamic Therapy: Mechanisms II*, Vol. 1203, Dougherty, T.J. and Katzir, A., Eds., SPIE, Bellingham, 1990, p. 224.
11. Reddi, E. and Jori, G., Steady-state and time-resolved spectroscopic studies of photodynamic sensitizers: porphyrins and phthalocyanines, *Rev. Chem. Interm.*, 10, 241, 1998.
12. Soncin, M., Busetti, A., Biolo, R., Jori, G., Kwag, G., Li, Y.-S., Kenney, M.E., and Rodgers, M.A.J., Photoinactivation of amelanotic and melanotic melanoma cells sensitized by axially substituted Si-naphthalocyanines, *J. Photochem. Photobiol., B: Biol.*, 42, 202, 1998.
13. Dougherty, T.J., Photodynamic therapy, *Photochem. Photobiol.*, 58, 895, 1993.
14. Nonell, S. and Redmond, R.W., On the determination of quantum yields for singlet molecular oxygen photosensitization, *J. Photochem. Photobiol., B: Biol.,* 22, 171, 1994.
15. Oleinick, N.L. and Evans, H.H., The photobiology of photodynamic therapy: cellular targets and mechanisms, *Radiat. Res.*, 150, 146, 1998.
16. Girotti, A.W., Photosensitized oxidation of cholesterol in biological systems: reaction pathways, cytotoxic effects and defense mechanisms, *J. Photochem. Photobiol., B: Biol.*, 13, 105, 1992.
17. Spikes, J.D., Photobiology of porphyrins, in *Porphyrin Localization and Treatment of Tumours*, Doiron, D.R. and Gomer, C.J., Eds., Alan R. Liss, New York, 1994, p. 19.
18. Jori, G. and Spikes, J.D., Photobiochemistry of porphyrins, in *Topics in Photomedicine*, Smith, K.C., Ed., Plenum Press, New York, 1983, p. 183.
19. Jori, G., Molecular and cellular mechanisms in photomedicine, in *Primary Photoprocesses in Medicine and Biology*, Plenum Press, New York, 1985, p. 349.
20. Spikes, J.D., Quantum yield and kinetics of the photobleaching of haematoporphyrin, Photofrin II, tetra(4-sulfonatophenyl)porphine and uroporphyrin, *Photochem. Photobiol.*, 55, 797, 1992.
21. Henderson, B.W. and Dougherty, T.J., How does photodynamic therapy work?, *Photochem. Photobiol.*, 55, 145, 1992.
22. Jori, G. and Reddi, E., Second generation photosensitizers for the photodynamic therapy of tumours, in *Light in Biology and Medicine*, Vol. 2, Douglas, R.H., Moan, J., and Ronto G., Eds., Plenum Press, New York, 1991, p. 253.
23. Kessel, D., Subcellular localization of photosensitizing agents, *Photochem. Photobiol.*, 65, 387, 1997.

24. Berg, K., Mechanisms of cell damage in photodynamic therapy, in *The Fundamental Basis of Phototherapy*, Honigsmann, H., Jori, G., and Young, A.R., Eds., OEMF, Milan, 1996, p. 181.
25. Evans, S., Matthews, W., Perry, R., Fraker, D., Norton, J., and Pass, H.I., Effect of photodynamic therapy on tumour necrosis factor production by murine macrophages, *J. Natl. Cancer Inst.*, 82, 34, 1990.
26. Gomer, C.J., Luna, M., Ferrario, A., Wong, S., Fischer, A., and Rucker, N., Cellular targets and molecular responses associated with photodynamic therapy, *J. Clin. Laser Med. Surg.*, 14, 315, 1996.
27. Oleinick, N.L., Morris, R.L., and Belichencko, I., The role of apoptosis in response to photodynamic therapy: what, where, why and how, *Photochem. Photobiol. Sci.*, 1, 1, 2002.
28. Agarwal, M.L., Larkin, H.E., Zaidi, S.I., Antunez, A.R., and Oleinick, N.L., Photodynamic therapy induces rapid cell death by apoptosis in L5178Y mouse lymphoma cells, *Cancer Res.,* 51, 5993, 1991.
29. Fabris, C., Valduga, G., Miotto, G., Borsetto, L., Jori, G., Garbisa, S., and Reddi, E., Photosensitization with Zn(II)-phthalocyanine as a switch in the decision between apoptosis and necrosis, *Cancer Res.*, 61, 7495, 2001.
30. Kessel, D. and Luo, Y., Photodynamic therapy: a mitochondrial inducer of apoptosis, *Cell Death Differ.*, 6, 28, 1999.
31. Dellinger, M., Apoptosis or necrosis following Photofrin photosensitization: influence of the incubation protocol, *J. Photochem. Photobiol., B: Biol.*, 39, 19, 1997.
32. Ochsner, M., Photophysical and photobiological processes in the photodynamic therapy of tumours, *J. Photochem. Photobiol., B: Biol.*, 39, 1, 1997.
33. Ruck, A. and Diddens, H., Uptake and subcellular distribution of photosensitizing drugs in malignant cells, in *The Fundamental Bases of Phototherapy*, Honigsmann, H., Jori, G., and Young, A.R., Eds., OEMF, Milan, 1996, p. 209.
34. Jori, G. and Reddi, E., The role of lipoproteins in the delivery of tumour-targeting photosensitizers, *Int. J. Biochem.*, 25, 1369, 1993.
35. Allison, B.A., Warefield, E., Richter, A.M., and Levy, J.G., The effects of plasma lipoproteins on *in vitro* tumour cell killing and *in vivo* tumour photosensitization with benzoporphyrin derivative, *Photochem. Photobiol.*, 54, 709, 1991.
36. Kongshaug, M., Distribution of tetrapyrrole photosensitizers among human plasma proteins, *Int. J. Biochem.*, 24, 1239, 1992.
37. Fingar, V.H., Vascular effects of photodynamic therapy, *J. Clin. Laser Surg. Med.*, 14, 323, 1996.
38. Fingar, V.H., Kik, P.K., Haydon, P.S., Cerrito, P.B., Tseng, M., Abang, E., and Wieman, T.J., Analysis of acute vascular damage after photodynamic therapy using benzoporphyrin derivative, *Br. J. Cancer*, 79, 1702, 1999.
39. Korbelik, M., Induction of tumour immunity by photodynamic therapy, *J. Clin. Laser Surg. Med.*, 14, 329, 1996.
40. Canti, G., Lattuada, D., Nicolin, A., Taroni, A., Valentini, G., and Cubeddu, A., Antitumour immunity induced by photodynamic therapy with aluminum phthalocyanine and laser light, *Anticancer Drugs*, 5, 443, 1994.
41. Canti, G., De Simone, A., and Korbelik, M., Photodynamic therapy and the immune response system in experimental oncology, *Photochem. Photobiol. Sci.*, 1, 79, 2002.
42. Korbelik, M. and Krosl, G., Enhanced macrophage cytotoxicity against tumour cells treated with photodynamic therapy, *Photochem. Photobiol.*, 60, 497, 1994.
43. Hsi, R.A., Rosenthal, D.I., and Glatstein, E., Photodynamic therapy in the treatment of cancer, current state of the art, *Drug*, 57, 725, 1999.
44. Pass, H.I., Photodynamic therapy in oncology: mechanisms and clinical use, *J. Natl. Cancer Inst.*, 85, 443, 1993.
45. Ochsner, M., Photodynamic therapy: the clinical perspective. Review of applications for the control of diverse tumorous and non-tumorous diseases, *Arzneim. Forsch.*, 47, 1185, 1997.

46. Busetti, A., Soncin, M., Jori, G., and Rodgers, M.A.J., Treatment of malignant melanoma by high-peak-power 1064 nm irradiation followed by photodynamic therapy, *Br. J. Cancer,* 79, 821, 1999.
47. Jori, G. and Spikes, J.D., Photothermal sensitizers: possible use in tumour therapy, *J. Photochem. Photobiol., B: Biol.*, 6, 93, 1990.
48. Busetti, A., Soncin, M., Reddi, E., Rodgers, M.A.J., Kenney, M.E., and Jori, G., Photothermal sensitization of amelanotic melanoma cells by Ni(II)-octabutoxy-naphthalocyanine, *J. Photochem. Photobiol., B: Biol.*, 53, 103, 1999.
49. Soncin, M., Busetti, A., Fusi, F., Jori, G., and Rodgers, M.A.J., Irradiation of amelanotic and melanotic melanoma cells with 532 nm high peak power pulsed laser radiation in the presence of the photothermal sensitizer Cu(II)-haematoporphyrin: a new approach to cell photoinactivation, *Photochem. Photobiol.*, 69, 708, 1999.

147

Clinical Applications of Photodynamic Therapy

Thomas J. Dougherty
Roswell Park Cancer Institute

Julia G. Levy
QLT Inc.

147.1 Introduction: Photodynamic Therapy

Photodynamic therapy refers to photodynamic action *in vivo* to destroy or modify tissue. Originally developed for treatment of various solid cancers, applications of it expanded to include treatment of precancerous conditions, e.g., actinic keratoses, high-grade dysplasia in Barrett's esophagus, and noncancerous conditions, e.g., various eye diseases, including age-related macular degeneration (AMD).

Photodynamic therapy (PDT) is currently approved for commercialization worldwide for various cancers (lung, esophagus) and for AMD.

PDT requires a drug (photosensitizer), light corresponding to an absorption band of the photosensitizer, and endogenous oxygen. The absence of any of these agents precludes the photodynamic effect.

0-8493-1348-1/04/$0.00+$1.50

The putative cytotoxic agent is singlet oxygen,[1] an electronically excited state of ground-state triplet oxygen formed according to the Type II photochemical process, as follows:

$P + h\nu \rightarrow P^* (S)$	Absorption
$P^* (S) \rightarrow P^* (T)$	Intersystem crossing
$P^* (T) + O_2 \rightarrow {}^1O^*_2 + P$	Energy transfer

where P = photosensitizer; $P^*(S)$ = excited singlet state; $P^*(T)$ = excited triplet state; and ${}^1O^*_2$ = singlet excited state of oxygen.

The Photosensitizer

Only photosensitizers that undergo efficient intersystem crossing to the excited triplet state and that possess a triplet state that is relatively long lived (to allow time for collision with oxygen) and have few other competing pathways will produce high yields of singlet oxygen. Most photosensitizers in clinical use have triplet quantum yields in the range of 40 to 60%, with the singlet oxygen yield being slightly lower. Competing processes include loss of energy by deactivation to ground state by fluorescence or internal conversion (loss of energy to the environment). However, while a high yield of singlet oxygen is desirable, it is by no means sufficient for a photosensitizer to be clinically useful. Pharmacokinetics, pharmacodynamics, stability *in vivo*, and acceptable toxicity play critical roles as well. For example, it is desirable to have relatively selective uptake in the tumor or other tissue being treated relative to the normal tissue that necessarily will be exposed to the exciting light as well. Pharmacodynamic issues, such as the subcellular localization of the photosensitizer, may be important, as certain organelles appear to be more sensitive to PDT damage than others (e.g., the mitochondria). Toxicity can become an issue if high doses of photosensitizer are necessary in order to obtain a complete response to treatment. For example, although PDT is rarely carried out on the liver, dark toxicity to the liver is often the main limiting toxicity seen in animal toxicity studies. Along the same lines, lack of *in vivo* stability would be a further issue relating to toxicity, as the toxicity profile of the breakdown products may need to be evaluated as well. In spite of all these impediments, there are large numbers of photosensitizers potentially useful in PDT, several of which are currently in various stages of clinical trials for FDA approval. Additional information on photosensitizers and mechanisms involved in PDT is discussed in Chapter 145.

Light

A limiting factor in PDT is the penetration of the activating light into tissue. Visible light in the red region of the spectrum (the most penetrating) generally has a penetration depth ($1/\varepsilon$) in the range of 2 to 6 mm, depending on the wavelength and the tissue. However, the depth of the biological effect of PDT (necrosis, apoptosis, vascular collapse) is generally found to occur at approximately twice this depth, i.e., 4 to 12 mm, meaning that approximately 10% of the incident light, i.e., the intensity drop-off at two penetration depths, is sufficient to elicit the photodynamic effect in tissue. As would be expected, the liver is one of the most opaque of tissues (due to pigmentation) and the muscle one of the most transparent. Most solid cancers originate in epithelial tissue (carcinomas) and have optical penetration depths of 3 to 5 mm (at ~600 nm) to approximately 6 to 10 mm (at 800 nm, where an optical window exists between absorption by blood and that of water).

Light sources are generally gas vapor lasers, e.g., argon pumped, wavelength tunable dye lasers, or solid-state lasers, such as frequency doubled Nd-YAG pumped dye lasers, or, now more frequently being used, diode lasers. However, appropriate lamps can be used as well, as was the case in the early days of PDT and is currently the case for treatment of actinic keratoses. Light from the laser is generally coupled into quartz fibers of various configurations. For lesions involving the skin and in certain other instances, a lens fiber is used that has a microlens on the tip to produce a homogeneous spot. For treatment of esophageal and lung tumors as well as for interstitial placement, a fiber is used that has a diffuser on the

end of the fiber, allowing for scattering of the light laterally from the fiber over a distance of 1 to 5 cm generally. For bladder treatment, a bulb-type tip is used to produce isotropic distribution over the entire bladder wall. Details of the light dosimetry for particular types of treatments will be described below.

147.2 Methodology of Clinical PDT

The following refers to the photosensitizer Photofrin®* (as used in PDT, for which the most information is available, and with only some differences, applies to the use of most photosensitizers.

Photosensitizer Injection

Patients receive an intravenous bolus injection of Photofrin in doses ranging from 1 to 2 mg/kg body weight. With Photofrin as well as certain other photosensitizers taken up by the skin, this immediately renders the patient susceptible to severe burns from bright light exposure (sunlight being the most likely source), a condition which generally lasts 4 to 6 weeks and possibly longer. Therefore, the patient, family, and others are educated prior to injection to take appropriate precautions, e.g., wearing clothing to cover the body completely, wearing a broad-brimmed hat, etc. However, it is important to point out that patients should not remain in darkened rooms during the day, as photobleaching by low-level light enhances clearance of the drug from the skin. Patients are asked to expose a small area on the back of their hand to bright sunlight for 10 min beginning about 4 weeks after injection, before slowly beginning to go into the sun. Should a reaction occur, they are advised to wait an additional week and retest their sun sensitivity. While cutaneous photosensitivity is a bothersome side effect of certain photosensitizers, it is our experience that patients rarely refuse PDT treatment for this reason.

Injection-Light Treatment Time Interval

The amount of time between injection and light exposure varies considerably between photosensitizers, ranging from 1 to 2 days for Photofrin to 15 min for AMD treatment. In general for solid tumor treatment, it is best (but not always necessary) to allow for photosensitizer clearance from normal tissue that may also be exposed to the activating light during treatment in order to minimize damage as much as possible. Some photosensitizers, however, demonstrate little retention in tumors and are therefore generally activated shortly after injection. While this could present some risks to normal tissue, in some cases, the dosimetry can be adjusted to minimize the damage to normal tissue. Selectivity can also be increased by using a minimum amount of photosensitizer and increasing the light dose to compensate because photobleaching of the lower amount of photosensitizer generally found in the normal tissue can lead to protection. Interstitial placement of the fibers into the tumor also tends to protect surrounding normal tissue but is not always feasible or desirable, e.g., attempts to insert fibers into obstructing esophageal tumors can result in perforations; in this case they are generally placed within the lumen adjacent to the tumor, while in the case of endobronchial tumors, insertion into the tumor can often be done without risking perforation.

Light Dosimetry

This is probably the most difficult variable to define in PDT because the optimum light dose in one organ may be ineffective or toxic in another. Time-consuming light dose ranging protocols must be carried out to define this parameter for each indication. (Recently, it was recognized that the light dose rate may also be important, see Chapter 145.) Summarized in Table 147.1 is the general range of PDT variables used for various photosensitizers, showing the large range of time interval, drug doses, and

*Registered trademark of Axcan Scandipharm Inc., Birmingham, AL.

TABLE 147.1TABLE 147.1 Photosensitizers in Clinical Trials

Photosensitizer[a]	Photosensitizer Dose (mg/kg)	Interval (hours)	Energy Dose[b] J/cm^2(1) or J/cm (2)	Wavelength (nm)	Indications
Photofrin®	1–2	24–48	15–215 (1) 100–300 (2)	630	Esophageal, lung, skin, bladder, head and neck, brain, and certain other sites
ALA (Levulan)	Topical ALA (20% in vehicle)	14–18	10 (1)	Blue (peak at 417 nm)	Actinic keratosis
mTHPc (Foscan)	0.15	72–96	10–20 (1)	650	Oral (approved in Europe)
$SnET_2$* (Purlytin)	1.2	4	200 (1)	660	Breast metastases
Lutetium Texaphyrin*+	1.5–3	3	100–150	732	Prostate, photoangioplasty, AMD
BPD-MA (Visudyne)	6 mg/m^2 (~0.15 mg/kg)	0.25	50 (1)	699	AMD (also in Phase III trial for skin cancer)
HPPH (Photochlor)	3–6 mg/m^2 (~0.08–0.15 mg/kg)	24–48	50–150 (1) 150 (2)	665	Skin, lung, esophagus
PC4	—	—	—	—	Cutaneous cancers (no further information available)

[a] Chemical structures can be found in Chapter 144.

[b] J = Joules; J/cm^2 refers to surface dose; J/cm refers to the Joules delivered/cm from a diffusing fiber.

Note: Photosensitizers are as follows: Photofrin®, polyhematoporphyrin ethers; ALA, aminolevulinic acid; mTHPc, meta-tetetrahydroxyphenylchlorin; SnET2, tin etiopurpurin,; Lutetium Texaphyrin, a pendadentate aromatic metalloporphyrin; BPD-MA, benzoporphyrin derivative mono acid; HPPH, 2-[1-hexyloxyethyl]-devinylpyropheophorbide-a; PC4, a silicon phthalocyanine; AMD, age-related macular degeneration.

light fluence. However, even for a single photosensitizer, Photofrin, light doses range from 15 J/cm^2 in bladder to over 200 J/cm^2 for skin lesions.

PDT with Photofrin®

Photofrin® (polyhematoporphyrin ethers), the first and so far only photosensitizer approved by health agencies worldwide for treatment of cancer, remains the most widely used in routine clinical practice for treatment of esophageal and lung cancers (approved), as well as in a host of off-label indications (e.g., skin cancer, bladder cancer, brain tumors, head and neck cancers, etc.).

The following describes the methods of treatment and outcomes for the various indications, beginning with those approved by various health agencies worldwide.

147.3 Health Agency Approved Indications for Photofrin®-PDT

Obstructive Esophageal Cancer

This indication is for palliation of partially or totally obstructing tumors in the esophagus. Photofrin, obtained as lyophilized powder, is dissolved in 5% dextrose for injection shortly before a single bolus injection of 2 mg/kg body weight. Because this photosensitizer is accumulated and retained in the skin (as well as in most other tissues and tumors), patients are immediately rendered photosensitive and must take precautions against exposure to bright lights (e.g., in a dental office) and especially sunlight. While the supplier of Photofrin suggests that precautions continue for 90 days, it is our experience that clearance occurs within 30 to 60 days, although there are some reported cases of up to 90 days. We ask our patients to expose a small patch of skin on the hand to bright sunlight for 10 min at 30 days postinjection, and if redness and swelling occur, to continue to take precautions for another week, and continue this until reaction no longer occurs, at which time they can then slowly increase exposure. It should be noted that patients should not remain in the dark, as low-level light aids clearance by photobleaching the drug. It should also be noted that because Photofrin is activated by visible light, sunscreens and window glass are not protective. As a further precaution, we supply sunglasses to wear when outside. This cutaneous photosensitivity is an annoyance, but rarely has a patient refused treatment because of it.

Approximately 48 h postinjection, the photosensitizer localized to the tumor is activated by light at 630 nm (generally derived from a laser) that is directed via a single quartz fiber optic and delivered to the tumor through the biopsy channel of an endoscope. The distal end of the fiber is fitted with a diffusing surface, generally 2.5 to 5.0 cm in length, that allows the light to scatter laterally to the tumor on the wall of the esophagus. In some instances, the fiber may be inserted directly into the tumor, although care must be taken to avoid perforation of the esophageal wall. This can be problematical because obstructing tumors may cause distortion of the esophagus, making insertion of the fiber somewhat blind. In most instances, the fiber is placed in the remaining lumen adjacent to the tumor. Some physicians place patients under general anesthesia, but this is generally not necessary, and conscious sedation is used most often. The light dose is 300 J/cm of diffuser length, with a power density of 400 mW/cm diffuser length, requiring 12.5 min to deliver the prescribed dose. Patients will often experience mild to severe chest pain (due to edema induced by treatment) controlled with analgesics. Other adverse reactions include fever, abdominal pain, constipation, and substernal pain. Two days following treatment, patients are examined endoscopically to judge initial response, to obtain biopsies, and to remove necrotic debris (not generally necessary). Also, if necessary, a second light treatment can be administered at this time (an advantage of long tumor retention of Photofrin). The treated tumor becomes blanched, and noninvolved areas in the light field are generally found to be edematous and erythemic. Summarized in Table 147.2 is the outcome of the randomized clinical trial of PDT versus Nd-YAG laser thermal ablation, carried out for the FDA and other health agency approvals.[2]

Only at 1 month was the advantage of PDT evident, a similar outcome seen for PDT treatment of obstructive endobronchial tumors versus Nd-YAG ablation (see below). This may reflect the ability of

TABLE 147.2 Objective Tumor Response — PDT versus Nd-YAG Laser in Partially Obstructing Esophageal Cancer

	Week 1		Month 1	
	PDT	Nd-YAG	PDT	Nd-YAG
Complete + partial response	45	40	32[a]	20
Stable disease	24	22	15	14
Progressive disease	3	1	11	14

[a] Statistically different, $p < 0.05$; 118 patients in each arm.

TABLE 147.3 Objective Tumor Response of PDT versus Nd-YAG Laser for Obstructing Endobronchial Cancer (211 Patients)

	Week 1		Month 1	
	PDT	Nd-YAG	PDT	Nd-YAG
Complete and partial response	59	58	52	41

the light to reach more of the tumor than is possible with the Nd-YAG laser, which must be aimed at the tumor, where care must be taken to avoid perforation. (In the clinical trial noted above, there were seven perforations in the Nd-YAG group versus one in the PDT group.)

Obstructing Endobronchial Tumors (Nonsmall-Cell Lung Cancer)

Also approved by the U.S. FDA and other health agencies is the palliative treatment of obstructive endobronchial tumors. The treatment approach is similar to that for the obstructing esophageal tumors (2.0 mg/kg body weight Photofrin and 630 nm light treatment approximately 48 h later), with certain notable differences. The light dose is 200 J/cm diffuser (8.3 min), generally delivered interstitially, when feasible, with 1.0 or 2.5 cm diffuser fibers. Also, 2 days following treatment, patients are reendoscoped and all necrotic tumor debris and exudates must be removed because this can further obstruct the airway. This step is especially critical when the treatment is near the carina, and debris and exudates can extend into both main-stem bronchi, presenting a potentially life-threatening outcome.[3]

As in the esophageal study, patients in this multicenter Phase III trial were randomized to PDT or thermal ablation with the Nd-YAG laser. Also, as was seen in the esophageal trial, there was no statistical difference in outcome until after 1 week.[4] (See Table 147.3.)

For example, at 1 month, 40% of PDT-treated patients demonstrated improvement in symptoms (dyspnea, cough, hemoptysis) versus 27% of Nd-YAG patients. Adverse reactions included photosensitivity reaction (20% in PDT arm only), hemoptysis, cough, dyspnea, chest pain, and fever, which occurred with similar frequency in both arms.

Early-Stage Endobronchial Tumors

Treatment of microinvasive, nonsmall-cell endobronchial tumors using Photofrin-PDT is the only indication so far approved by the FDA and other health agencies, where the intent is not palliation but cure. Also, unlike the above palliative approval, this study was approved based on several studies not specifically designed and carried out by the sponsoring company but carried out independently in three noncomparative studies. Patients in this study included those with CIS (carcinoma-*in situ*) or microinvasive tumors. Also included were patients not considered candidates for surgery (or radiation therapy in some cases).

Patients received Photofrin, 2 mg/kg, and 2 days later were treated endoscopically using a diffuser fiber (usually 1 to 2.5 cm) delivering 200 J/cm diffuser length at 630 nm. As these lesions are very thin, the

TABLE 147.4 Outcome of Patients with Microinvasive Lung Cancer

	11 Patients	62 Patients
CR (3 month) (biopsy proven)	3/11	31/62
Recurrence	1	11
Median time to recurrence		>2.7 years
Median survival		2.9 years
Median disease-specific survival		4.1 years

fiber was held in the lumen adjacent to the lesion. Two days following treatment, patients were rescoped, and the treated area was debrided.

Results with 102 patients indicated biopsy-proven complete response in 79% of patients (initial follow-up) with more than half continuing to be complete responders, often more than 2 years posttreatment. The median survival was 3.5 years, and disease-specific survival was 5.7 years. In a smaller segment of this trial population with microinvasive lung cancer (the actual approved indication), 62 inoperable patients were treated, 11 of whom were considered not to be candidates for surgery or radiation therapy. Indicated in Table 147.4 are the outcomes in this group.[5,6]

Early-Stage Esophageal Cancer

Although not yet approved by the U.S. FDA, a Phase III randomized, controlled, multicenter trial of Photofrin-PDT in patients with high-grade dysplasia (HGD) in Barrett's esophagus was recently completed for filing with the FDA. This study randomized patients to receive an acid suppressor, Omeprazole (Prilosec) or PDT plus Omeprazole. Endoscopic PDT was applied using a specially designed balloon light applicator with windows of 3, 5, or 7 cm in lengths produced from diffuser fibers of 5, 7, or 9 cm in length. The last 1 cm on each end is blocked off because the power at the ends of the diffuser is less than that emitted in the center of these fibers. The balloon was inserted deflated and then inflated in place to an appropriate pressure to allow "unfolding" of the esophageal wall without shutting down the blood flow. The Photofrin dose was 2.0 mg/kg injected approximately 2 days prior to light delivery of 130 J/cm of diffuser length. A preliminary report[7] at 6 months follow-up indicated that HGD was eliminated in 72% of patients in the PDT group but only in 31% of patients in the control group (Omeprazole alone). Moreover, at 2 years, 70% of responders in the PDT group continued to be complete responders, while none of the patients in the Omeprazole alone group were without HGD. Significantly, only 10% of patients in the PDT group progressed from HGD to esophageal cancer, compared to 19% of patients receiving only Omeprazole.

Overholt et al. reported on 100 patients treated for this indication with Photofrin and the balloon light emitter. Fifty-six of 73 patients with HGD were complete responders, and 32 had complete elimination of the Barrett's.[8]

The current practice in patients with HGD is to subject them to an esophagectomy, a surgical procedure associated with high mortality (5 to 10%) and morbidity.

It should be noted that Barrett's esophagus also is eliminated by the PDT treatment to the extent of 70 to 100% in most patients, being replaced with normal squamous mucosa. While not a specific endpoint in the trial, PDT appears to be one of the few methods currently available to remove this acid-reflux-induced inflammatory process, a risk factor for developing esophageal cancer (from 0.5 to 1.9% of patients with Barrett's esophagus will progress to HGD, and up to 50% of patients with HGD will go on to esophageal cancer over a 3-year period.[9]

147.4 Other Indications for Photofrin®-PDT

In addition to the approved or soon-to-be-approved indications of PDT using Photofrin, numerous other types of cancers were treated, including those of the head and neck, especially early-stage,[10] skin,[11,12]

brain,[13,14] bladder,[15] intrathoracic cavity (especially as an adjunct to surgery for mesothelioma),[16,17] and intraperitoneal tumors, such as ovarian studding[18] and cholangiocarcinoma.[19] Several of these are discussed below.

Cholangiocarcinoma

A potentially useful application of PDT is in the treatment of cholangiocarcinoma cancer. These tumors are generally diagnosed late, when surgery is rarely curative. In nonresectable cases, drainage or biliary bypass is used for palliation. Radiation therapy and chemotherapy appear to be of little benefit. In a series of 21 patients reported by Ortner et al.,[19] nonresectable patients were treated with Photofrin (2 mg/kg) 2 days prior to endoscopic fiber placement in the lumen (630 nm, diffuser fibers, 2.5 or 4.0 cm of diffuser length delivering 180 J/cm at a constant power output of 800 mW total). There was a dramatic drop in bilirubin in the PDT group (69 μmol/L) compared to stenting alone (20 μmol/L) and the Karnofsky score improved from 49 to 73 in the PDT arm. Eight patients were alive at 82 to 739 days posttreatment, and median survival was about 1 year. A small randomized trial was reported[20] with 35 patients, 20 to PDT + endoprostheses insertion (EP) and 15 to EP alone. An additional 34 patients who refused randomization received compassionate PDT + EP and were analyzed separately. The PDT treatment was as above. The median survival for the PDT + ES was 493 days, compared to the EP alone group of 98 days. The compassionate PDT + EP group had median survival of 406 days. All patients in the control arm (EP alone) are dead; six are alive in the PDT + EP compassionate group and two in the PDT + EP group. Significant improvement in bilirubin levels was seen in both groups receiving PDT + ED, but none was seen in the EP alone group. The Karnofsky scale score improved only in the PDT + EP compassionate group. It was concluded that addition of PDT to EP was a valuable improvement in palliation treatment because of significantly increased survival and improvement in quality of life. Because of this outcome, the randomized trial was stopped for ethical considerations.

Head and Neck Cancers

Application of PDT to treatment of head and neck cancers was initially limited to treatment of patients with advanced disease who failed or recurred on standard therapy. These patients rarely benefited from PDT. However, more recently, Biel[10] showed a high success rate in PDT treatment of early-stage disease of the oral cavity and larynx. Twenty-five patients who failed radiation therapy for early laryngeal cancers (carcinoma-*in situ* or T1) received Photofrin (2 mg/kg) followed 2 days later by 630 nm light at an energy dose of 80 J/cm^2. All patients received a complete response and remain free of disease, with a mean follow-up of 27 months. An additional 23 patients with early carcinomas (carcinoma-*in situ*, T1, T2) of the oral cavity, nasal cavity, and nasopharynx were treated similarly, and all were initially complete responders, with a mean follow-up of 26 months. One patient with recurrent leukoplakia of the tongue recurred at 12 months, one with recurrent cancer of the tongue and floor of the mouth recurred at 8 months, one patient developed regional metastases at 2 months, and another patient with recurrent nasal ala cancer recurred at 3 months post-PDT.

Skin Cancers

At this institution, we completed an extensive dose ranging study of Photofrin-PDT in patients with basal cell carcinoma (BCC). This represents the largest dose ranging clinical trial of PDT ever undertaken (80 patients, over 2000 lesions, three different Photofrin doses). We found that 1.0 mg/kg (215 J/cm^2 48 h postinjection, 630 nm) was more effective than 0.75 or 0.875 mg/kg Photofrin. Some 20 of these patients had nevoid basal cell carcinoma syndrome (NBCCS), an autosomal dominant mutation with loss of function of one copy of the PTCH tumor suppressor gene, resulting in these patients having a high susceptibility to frequently develop large numbers of BCC lesions over their lifetime. Some NBCCS patients in the study presented with 50 or more lesions, no longer susceptible to surgery without extensive scarring. PDT was of particular benefit to these patients because 30 to 40 lesions could be treated in a

single day with high and long-lasting complete response rates (>92%, 1.0 mg/kg Photofrin, 215 J/cm^2 48 h postinjection). Several of these patients were treated 4 to 5 times over several years as new lesions appeared. Taking into account all patients (NBCCS and non-NBCCS patients), the overall complete response rate was over 90%, comparable to other methods for treatment of BCC. Within this group, we found that larger lesions (>2 cm) responded slightly less than smaller lesions, and that those on the scalp were somewhat less responsive to PDT.

Treatment was accomplished using a laser beam splitter system that allowed treatment of up to eight lesions simultaneously. The delivery fibers were directly attached to the patient with special tripod holders,[21] allowing for some movement of the patient without diverting the beam from the lesion. At 150 mW/cm^2, treatment time to deliver 215 J/cm^2 was 23.9 min. Thus, in four such sessions, 32 lesions could be treated. This was easily accomplished in a single day. Without this capability, adequate treatment of the NBCCS patients would have been impossible.

147.5 PDT as Adjuvant Treatment

Head and Neck Cancers

PDT has been used frequently as an adjuvant to surgery in an attempt to "clean up" the remaining cancer cells in the operative bed. Biel reported on five patients with recurrent infiltrating squamous cell carcinoma — all who had failed previous surgery, radiation therapy, and chemotherapy. Patients received 2 mg/kg Photofrin followed 2 days later by surgery and PDT at 50 J/cm^2. He reported no postoperative complications. With a follow-up of 18 to 30 months, only one patient had recurred in an area outside the surgical and PDT field.

Brain Tumors

Muller treated over 100 patients with surgery and PDT.[13] Most had glioblastoma or astrocytoma, newly diagnosed or recurrent. These tumors are rarely curable by surgery, radiation therapy, or chemotherapy. The adjuvant studies were undertaken to determine the safety and feasibility of adding PDT to the surgical resection. Photofrin (2 mg/kg) was injected 12 to 36 h prior to light treatment using a specially designed expandable balloon applicator that fit within the surgical cavity and was filled with a light scattering material (1:1000 dilution of lipid). The delivered light at 630 nm was measured using a "pick-up" fiber placed adjacent to the balloon. Total energy doses ranged from 440 to 4500 J, with an energy density of 8 to 110 J/cm^2. The mortality rate was 3%, with a combined serious mortality and morbidity rate of 8%. Eight patients with recurrent gliomas who received greater than 60 J/cm^2 had a median survival of 58 weeks, while 24 who received less than 60 J/cm^2 had a median survival of 29 weeks.

Twenty patients with all types of brain tumors who received PDT at first operation had median survival of 44 weeks, with a 1-year survival of 40% and 2-year survival of 15%. Again, a light dose effect was found, with those patients receiving less than a total light dose of 1200 J having a median survival of 39 weeks and those with light doses greater than 1200 J having a median survival of 52 weeks. Patient characteristics in the two groups were similar. Patients with high Karnofsky score (>70) and who received light doses over 1260 J had a median survival of 92 weeks, with 1- and 2-year survival rates of 83 and 33%, respectively. The authors conclude that PDT with Photofrin is safe and appears to increase survival, especially at higher light doses. There is currently a multicenter, randomized (high- or low-light dose) trial ongoing to verify this conclusion.

Mesothelioma

This asbestos-induced disease of the mesothelium can be advanced before becoming symptomatic, and like the brain tumors discussed above, it is rarely curable by surgery and radiation therapy or chemotherapy. Moskal et al. reported on a series of 40 patients treated by a combination of surgery and PDT.[17]

Patients received Photofrin, 2 mg/kg, and 2 days later, as much tumor was removed as possible or debulked to 5 mm or less. PDT was then carried out by delivering 630 nm light to the entire thoracic cavity via 4 to 6 diffuser-type delivery fibers (2.5 to 5.0 cm in diffuser length), placed so as to deliver 20 to 30 J/cm^2 as evenly as possible. This was done in two placements of the fibers, posteriorly and anteriorly. Because of the large area to be treated (estimated from the CT scans), total light treatment time can range up to 4 h at a power density of approximately 10 J/cm^2. Postoperative staging indicated 12 patients with Stage I disease, 10 being completely resected; 11 patients with Stage II disease, with complete resection; 25 patients with Stage III disease, only five of whom could be completely resected (three died); and two patients with Stage IV disease. Morbidity and mortality rates for patients with Stage I or II disease were 38 and 0%, respectively, and for Stage III or IV disease were 48 and 11%, respectively. Patients requiring extrapleural pneumonectomy did not benefit from the combined treatment, as 43% of these patients had a bronchopleural fistula, much higher than the 1 to 4% reported in the literature. However, patients with disease in Stages I and II not requiring pneumonectomy appear to have increased survival rates (41% at 2 years) compared to those receiving surgery alone.

147.6 Other Photosensitizers

Because of prolonged cutaneous photosensitivity induced by Photofrin (30 to 60 days) and less than optimum absorption in the red region of the spectrum, a host of newer photosensitizers are undergoing clinical trials.

ALA (δ-Aminolevulinic acid)

δ-Aminolevulinic acid (ALA) is involved in the heme pathway, in which the final metal insertion step can be obviated with a large excess of ALA, thus causing the buildup of protoporphyrin IX (PPIX), a porphyrin photosensitizer. Injectable PPIX is not a useful photosensitizer because it is not well retained by tumors or other tissues and clears the system rapidly. However, the intracellular accumulation of PPIX through excess ALA can be effective. In fact, topically applied ALA is approved by the U.S. FDA for the treatment of actinic keratosis, a precancerous lesion that can lead to squamous cell carcinoma. The sponsor also developed a special blue light source that can be fitted on the patient's head to allow treatment of the entire face for patients with numerous lesions. In the Phase III trials,[22] patients were treated topically with 20% ALA in a proprietary vehicle (Levulan®, registered trademark of DUSA Pharma Inc., Wilmington, MA), and the next day received the blue light treatment (approximately 15 min exposure). In one study of 117 patients, 80% of lesions had a complete response that increased to 94% with a second treatment, while in the placebo group (placebo + light), only 32% of lesions responded completely after two treatments. Adverse reactions included a stinging, burning sensation that was well tolerated.

Topical ALA was also applied to the treatment of superficial skin cancers with excellent results. It is less effective for nodular lesions.[12] In this treatment, the ALA (10 to 40%) was applied topically in leucerin cream for various periods (usually 4 or 24 h) and then activated at 635 nm derived from a dye laser delivering light doses up to 200 J/cm^2. In this treatment, the pain is sufficient to require local injection of an anesthetic prior to treatment. Most patients tolerate this well.

ALA is currently being investigated as a fluorescent localizing agent in bladder cancer (see below) and for treatment of low-grade dysplasia in Barrett's esophagus.[23]

mTHPc (Foscan)

This chlorin-type photosensitizer was approved in Europe for treatment of oral cancers. Fan et al. reported preliminary clinical results.[24] Nineteen patients with various stages of disease (eight with field change disease) were injected with mTHPc (0.15 mg/kg), and 72 to 96 h later were treated with varying light doses at 652 nm. Three patients with single T3 lesions received a complete response, as did three of six T4 tumors. Field change disease responded less well, with nine of 14 T1 and T2 lesions responding

completely. Adverse reactions included one patient with tongue tethering and necrosis of normal tissue in another. However, while approved in Europe for this indication, the U.S. FDA chose not to approve it for use in the United States, although as of this writing, this is under review.

SnET2 (Purlytin, Tin Etiopurpurin)

While trials were completed with this photosensitizer in cutaneous breast cancer metastasis, the sponsoring company chose not to file for approval for the indication. However, they completed two placebo-controlled clinical trials with 933 patients in 59 centers for AMD (age-related macular degeneration).[25] These trials concluded in December 2001 (a two-year follow-up period is required).

Lutetium Texaphrin (Lutex)

This is an example of so-called expanded metalloporphyrin system resulting in a strong shift in the red absorption band from near 620 nm to 732 nm, where nearly optimum tissue penetration occurs. Current clinical trials are in locally recurrent prostate cancer, and noncancerous indications, AMD and photoangioplasty.[26] Details are not available. Moderate to severe pain during treatment hampered studies of treatment of various cutaneous malignancies.

HPPH (Photochlor)

Three clinical trials (Phases I and II) of PDT with this new chlorin-type photosensitizer are underway at Roswell Park Cancer Institute: partially obstructing esophageal cancer, early-stage lung cancer, and basal cell carcinoma.

In obstructing esophageal cancer, eight patients were treated at 6 mg/m^2 (0.15 to 0.19 mg/kg body weight) and 150 J/cm of 665 nm light delivered at approximately 48 h postinfusion of HPPH. All patients achieved partial or complete opening of the esophageal obstruction, and most had improvement in dysphagia. In these trials, patients are tested daily for cutaneous photosensitivity for 3 to 4 days using a solar simulator (1 cm spot on the underside of the wrist) at doses up to 133 J/cm^2. Only two patients had a mild erythemic reaction. Although the in-house solar simulator indicates little cutaneous photosensitivity, patients are still advised to test their reaction to sunlight by exposing a small area on the back of their hand for 10 to 30 min daily until no HPPH-induced reaction is found before ceasing precautions.

PC4

This silicon phthalocyanine with two axial ligands on silicon, a hydroxy group, and a dimethylaminopropyl siloxy group, recently entered Phase I dose escalation clinical studies with cutaneous lesions. No information is available as of this writing.

147.7 Treatment of Age-Related Macular Degeneration by PDT with BPD-MA (Verteporfin)

Background

The macula constitutes a small, highly specialized region of the human retina. The central part is rich in photoreceptor cells and is the area responsible for high visual acuity in humans. The end result of macular degeneration is the ultimate destruction of photoreceptor cells in the macula as well as the underlying cells of the retinal pigmented epithelium (RPE). Macular degeneration is the leading cause of blindness in the developed world and is most prevalent in people over the age of 60. There are two principal forms of age-related macular degeneration (AMD), dry or nonexudative AMD and wet or exudative AMD. While wet AMD constitutes only about 10% of all cases of AMD, it is responsible for most of the vision loss associated with the disease. There are approximately 500,000 new cases of wet

AMD every year worldwide. As this is a disease predominantly of Caucasians, the main areas of disease incidence are North America and Europe. Wet AMD occurs when rapidly growing abnormal blood vessels develop under the macula in a process described as subretinal neovascularization. The newly formed vessels do not mature properly and leak into the subretinal space, effecting detachment of the RPE and the ultimate degeneration and destruction of the photoreceptor cells in the region of the lesion.

The underlying causes of wet or dry AMD are not well understood, but there is evidence for genetic tendencies because there are familial as well as racial propensities in disease occurrence. While there is strong circumstantial evidence for a genetic base for the disease, the genes relating to susceptibility are clearly complex and are not well understood at this time. Familial studies on patients with Stargardt's disease clearly identified a specific gene mutation associated with this severe macular disorder. The gene identified is a photoreceptor cell-specific ATP-binding cassette transporter gene (ABCA4), and patients with Stargardt's disease as well as a number of other disorders associated with the retina express mutations in this gene, which is polymorphic.[27] A recent study showed that patients who express particular mutations in at least one allele of this same gene are at a threefold or fivefold greater risk of developing wet AMD.[28] These studies support the genetic basis for susceptibility to AMD and demonstrate that the genetic basis is complex and no doubt involves additional gene loci. A functional role for the ABCA4 gene was suggested in the eye. Most ABC transporters act as "flippases," i.e., as transporters of the protonated complex of all-*trans* retinal and phosphatidylethanolamine (*N*-retinylidene-PE). In knockout mice lacking the ABCA4 gene, phosphatidylethanolamine accumulates with resulting deposition of a major lipofuscin fluorophore (A2-E or a pyridium *bis*-retinoid, which is derived from two molecules of vitamin A aldehyde and one molecule of ethanolamine) in the retina. Accumulation of lipofuscin in the macular region of aging eyes is characteristic of AMD.[29]

The exudative or wet form of AMD is diagnosed using standard fluorescein angiography. Serial fluorescent photography of the macular area can readily identify where areas of vessel leakage are occurring because fluorescein will pool in the area of neovasculature. Exudative AMD is subdivided into two categories on the basis of the speed of visible leakage on angiographs. The "classic" form of AMD is considered the most aggressive form of the disease, and leakage occurs rapidly during the angiography. This form of AMD is characterized by rapid progression and concurrent vision loss. Lesions that leak slowly and show up on angiograms late are defined as "occult" wet AMD. These lesions lead to vision loss at a slower rate than with the classic form.

Although the overwhelming majority of research and clinical testing with PDT addressed the application of this technology in the treatment of solid tumors, during the past decade and a half, possible applications in other disease areas were investigated. Because many photosensitizers accumulate or are retained somewhat selectively in rapidly dividing cells as well as neovascular endothelial cells, the PDT effect, at least on solid tumors, was elegantly demonstrated, using Photofrin, to effect the tumor cells and the neovascular bed underlying rapidly growing tumors.[30,31]

Ocular conditions involving neoplasias or hypervascularity lend themselves to PDT because of the accessibility to light of all parts of the eye. Early investigator-sponsored studies using Photofrin for the treatment of ocular tumors demonstrated the effectiveness of this therapy in destroying local tumors as well as the neovascular bed surrounding them. The Verteporfin molecule (also termed BPD-MA or Visudyne) is a hydrophobic photosensitizer with pharmacokinetic properties that make it a desirable drug to use in indications such as AMD. It is formulated as a liposome in order to render it soluble in water. However, once in association with plasma, the drug demonstrates an affinity for lipoproteins much greater than its affinity for the liposomal constituents. Consequently, it is almost instantaneously released from the liposome and transferred to LDL and HDL in blood. This somewhat unusual characteristic results in rapid uptake of the drug by neovascular endothelia and a treatment window for selective accumulation at between 15 and 30 min following intravenous administration. Therefore, unlike most photosensitizers, which rely on selective retention by target cells, Verteporfin achieves selectivity by differential uptake by target tissue.[32] Verteporfin has the additional advantage of having a very short half-life (4 to 5 h in humans). Thus, treatment at an early time interval permits use of relatively low drug doses, and with the rapid half life, patients are only photosensitive for 24 h.

Research was undertaken in 1992 to investigate the feasibility of using Verteporfin for the treatment of AMD. Initially, two models in the rabbit were used: induced corneal neovasculature and implanted ocular tumors. Results from these studies were encouraging and showed in both instances that the expected thrombotic closure of neovasculature was seen in PDT-treated eyes. These studies also suggested a window of selectivity in which normal vasculature might be preserved.[33] Final proof of concept work involved the primate model for AMD, in which thermal laser damage to the retina induces a neovascular lesion on the choroid. Although self-limiting, this model is considered the most reliable for testing treatments for AMD. Results from these studies were encouraging and continued to demonstrate effective closure of neovascular vessels at time intervals from 10 to 60 min following intravenous administration.[34]

AMD Clinical Trials

Clinical work with Verteporfin for Phases I and II was initiated in 1996, where patients with AMD received a single treatment with Verteporfin and were followed for 12 weeks by angiographic examination and visual acuity evaluation. A variety of regimens were tested, involving two different drug doses, five different light doses, and two different times of treatment. These studies revealed that at 7 days post-PDT, all lesions treated showed complete closure of neovasculature, with no accompanying vision loss or closure of normal retinal blood vessels, with the exception of two patients who received the highest light dose (150 J/cm^2 at 690 nm and 600 mW/cm). In these patients, closure of normal retinal vessels was observed, thus demonstrating the level at which selectivity was lost. It was of interest to note that while patients on average did not lose significant visual acuity at either 4 weeks or 12 weeks following treatment, a majority showed the presence of vascular leakage at the 12-week time point, indicating that repeat treatment would likely be necessary if a sustained benefit of PDT were to be maintained.[35]

These preliminary clinical trials in which approximately 150 patients participated, led to development of a protocol for two pivotal Phase III trials for treatment of patients with AMD with lesions that contained a classic component. The study design involved randomization of patients in a 2:1 ratio to Verteporfin treatment versus placebo. A total of 609 patients were accrued in the two trials — approximately 400 received treatment, while 200 received placebo. Patients were tested for baseline visual acuity and lesion assessment by angiography. They received Verteporfin intravenously at a dose of 6 mg/m^2 or placebo. At 15 min after drug administration, light treatment of 50 J/cm^2 at 600 mW/cm^2 was administered to the lesion using a diode laser emitting at 690 nm. Patients returned every 3 months, at which time, they were tested by angiography for evidence of vessel leakage. If leakage was present, they received another treatment. Visual acuity was tested at each visit. The primary endpoint was designated as showing a significant difference between treatment versus placebo in a loss of three lines of vision (approximately 15 letters on a standard eye chart) at 12 months. Secondary endpoints included serious vision loss (six lines), lesion size and progression, contrast sensitivity (a measure of reading ability), and actual visual acuity. Although the study was a 2-year study, agreement with regulatory bodies permitted filing for approval if the 12 month primary endpoint was achieved. All primary endpoints achieved significance at the 12 month time point.[36] These patients have now been followed for nearly 4 years. After 2 years, all patients, including placebo patients, have been receiving treatment if needed. Visual acuity in treated patients stabilized within the first year, and no loss of vision was observed in years two and three.[37]

Visudyne (Verteporfin) therapy was approved for wet, predominantly classic AMD in more than 50 countries, and over 50,000 patients have been treated.

Further clinical trials were carried out to test the ability of PDT to arrest progression of the occult form of AMD. A placebo-controlled study of similar design to that used for the classic containing lesions was carried out, with similar endpoints. In this study, significance of the primary endpoint was not reached at 12 months, but patients on treatment stabilized during the second year, and all endpoints were significant at 2 years. Because occult disease progresses slower than the classic form, it is not surprising that the difference between placebo and treatment arms took longer to show a significant difference.[38]

In addition to AMD, other ocular conditions were treated with Visudyne therapy. These diseases include conditions that cause choroidal neovasculature similar to that seen in AMD. Among these are pathologic

myopia, a complication of extreme nearsightedness, and ocular histoplasmosis syndrome, a complication of a parasitic infection. Regulatory approval for these conditions was also granted in North America and Europe.[39]

These studies established PDT as first-line therapy for AMD and other conditions. The safety of repeated treatments was established with few side effects noted. In the occult trial, it was noted that about 4% of patients experienced severe vision loss within the first week after treatment. A majority of these patients had recovery from this event, but further treatment is not recommended.

Two other photosensitizers were tested clinically for their effect on choroidal neovasculature. These are tin ethyl etiopurpurin (Purlytin) and texaphrin. Phases I and II studies with Purlytin showed similar vessel closure to that seen with Visudyne.[40] A Phase III placebo-controlled trial is almost completed, with 2 years of follow-up, and results should be made available early in 2002. Since this also is a hydrophobic photosensitizer, one would assume that vessel closure similar to that seen with Visudyne should be achieved. Texaphrin was tested in Phases I and II clinical trials in approximately 70 patients. These results, reported at various ophthalmology meetings, suggested that vessel closure was difficult to achieve, even at high drug doses. It is possible that the relative water solubility of this drug in comparison to Visudyne and Purlytin to some extent does not lend itself to rapid cell uptake.

PDT is now established as part of the ophthalmologist's armamentarium for the treatment of abnormal vascular conditions in the eye. The therapy is proven to be safe and efficacious. In addition to the diseases mentioned above, there are a number of other ocular conditions in which PDT could play a role. These include diabetic macular edema, diabetic retinopathy, corneal neovasculature, and ocular tumors. While there are alternative therapies for these conditions, unlike AMD where there was no treatment, it is possible that PDT may offer some advantages over existing therapies.

147.8 Photodetection

Photosensitizer fluorescence as a marker of early-stage cancers was studied in several indications. Protoporphyrin IX fluorescence derived *in situ* from ALA was shown to be capable of detecting lesions in the bladder not detectable by ordinary cystoscopy.[41] Riedl et al. recently demonstrated the clinical significance of this increased detection rate.[26] In a prospective, randomized study of 102 bladder cancer patients with tumors ranging from TaG1 to T1G3, 51 received transurethral resection under white light cystoscopy, and 51 received ALA-induced fluorescence-guided transurethral resection. Fluorescence detection was carried out by instilling into the bladder 1.5 g ALA in 50 cc sodium bicarbonate (to achieve a pH of 6.5) and left in place 1 to 4 h (the time did not appear to affect the outcome). A white light source coupled with a bandpass filter to produce blue light was used to excite the red fluorescence of protoporphyrin IX. Six weeks later, all patients underwent ALA-assisted transurethral resection. Tumor was detected in 39% (20/51) of patients who initially received the standard method and 16% (8/51) in the ALA group, a reduction in tumor recurrence of 59% ($p = 0.005$). The authors conclude that ALA-assisted transurethral resection is an inexpensive and effective method for significantly increased tumor detection in the bladder.

Detection of Early-Stage Lung Cancer

As is well known, early-stage lung cancer is difficult to detect, and earlier screening studies of high-risk patients, using chest x-ray and sputum cytology, show no survival benefit. Recently, however, spiral CT and fluorescence bronchoscopy were investigated for detection of early lung lesions: the former to detect peripheral lesions and the latter mainly for centrally located lesions. At this institution, we initiated a screening program of high-risk patients (previous history of lung cancer or head and neck cancers or exposure to asbestos) using an FDA-approved fluorescence endoscopic method, LIFE (Light-Induced Fluorescence Excitation), from Xillix Technologies Corp. (Richmond, British Columbia,
Canada), for examination of the central airways. This system was shown to be nearly three times as likely to detect an early lesion when used with white light bronchoscopy as white light bronchoscopy alone. It is based on the principle that even early dysplasia or carcinoma-*in situ* tend to accumulate endogenous

chromophores (e.g., porphyrins), thus presenting a reddish-brown fluorescence compared to normal bronchial mucosa, which is seen as greenish in color.[42] The suspicious areas are confirmed by biopsy. In addition, each patient will be screened using spiral CT for detection of peripheral lesions. Appropriate patients will be treated by PDT. While this is a relatively modest trial of 500 patients, the intention is not only to investigate these techniques for efficacy in detection of early lesions but also to determine the effect on survival after appropriate treatment, and not incidentally, to assist in convincing third-party payers to reimburse for screening.

147.9 Future Directions for Photodynamic Therapy

While PDT has mainly been used as a cancer therapy, it is clear that its applications are extending to many noncancerous conditions, as is evident from some of the foregoing. Other areas currently being investigated are prevention of restenosis after balloon angioplasty for cardiac artery disease, treatment of rheumatoid arthritis (inflammatory cells are particularly prone to photosensitizer uptake), and certain early detection indications.

References

1. Weishaupt, K.R., Gomer, C.J., and Dougherty, T.J., Identification of singlet oxygen as the cytotoxic agent in photoinactivation of a murine tumor, *Cancer Res.*, 36, 2326, 1976.
2. Lightdale, C.J., Heier, S.K., Marcon, N.E., McCaughan, J.S., Jr., Gerdes, H., Overholt, B.F., Sivak, M.V., Jr., Stiegmann, G.V., and Nava, H.R., Photodynamic therapy with porfimer sodium versus thermal ablation therapy with Nd:YAG laser for palliation of esophageal cancer: a multicenter randomized trial, *Gastrointest. Endosc.*, 42, 507, 1995.
3. Vincent, R.G., Dougherty, T.J., Rao, U., Boyle, D.G., and Potter, W.R., Photoradiation therapy in advanced carcinoma of the trachea and bronchus, *Chest*, 85, 29, 1984.
4. Package insert: Photofrin® (porfimer sodium) for injection, 1999.
5. Lam, S., Haussinger, K., Leroy, M., Sutedja, T., and Huber, R., Photodynamic therapy (PDT) with Photofrin®, a treatment with curative potential for early stage superficial lung cancer, *Proc. 34th Annu. Meet. Am. Soc. Clin. Oncol.*, 1998, Abstract 1781.
6. Sutedja, T., Lam, S., LeRiche, J., and Postmus, P., Response and pattern of failure after photodynamic therapy for intraluminal Stage I lung cancer, *J. Bronchology*, 1, 295, 1994.
7. Axcan Web site: www.axcan.com.
8. Overholt, B.F., Panjehpour, M., and Haydek, J.M., Photodynamic therapy for Barrett's esophagus: follow-up in 100 patients, *Gastrointest. Endosc.*, 49, 1, 1999.
9. Buttar, N., Wang, K., Sebo, T., Riehle, D., Krishnadath, K., Lutzke, L., Anderson, M., Petterson, T., and Burgart, L., Extent of high grade dysplasia in Barrett's esophagus correlates with risk of adenocarcinoma, *Gastroenterology*, 120, 1630, 2001.
10. Biel, M., Photodynamic therapy and the treatment of head and neck neoplasia, *Laryngoscope*, 108, 1259, 1998.
11. Schweitzer, V., Photofrin-mediated photodynamic therapy for treatment of aggressive head and neck non-melanomatous skin tumors in elderly patients, *Laryngoscope*, 111, 1091, 2001.
12. Oseroff, A., Shieh, S., Frawley, N., Blumenson, L., Parsons, J., Potter, W., Graham, A., Henderson, B., and Dougherty, T., PDT for skin cancer: what do we know about how to go, *29th Annu. Meet., Am. Soc. Photobiol.*, 2001, Abstract 146.
13. Muller, P. and Wilson, B., Photodynamic therapy for recurrent supratentorial gliomas, *Semin. Surg. Oncol.*, 11, 346, 1995.
14. Popovic, E., Kaye, A., and Hill, J., Photodynamic therapy for brain tumors, *J. Clin. Laser Med. & Surg.*, 14, 251, 1996.

15. Nseyo, U., Shumaker, B., Klein, E., and Sutherland, K., Photodynamic therapy using porfimer sodium as an alternative to cystectomy in patients with refractory transitional cell carcinoma-*in situ* of the bladder, *J. Urol.*, 160, 39, 1998.
16. Pass, H.I. and Donington, J.S., Use of photodynamic therapy for the management of pleural malignancies, *Sem. Surg. Oncol.*, 11, 360, 1995.
17. Moskal, T.L., Dougherty, T.J., Urschel, J.D., Antkowiak, J.G., Regal, A.-M., Driscoll, D.A., and Takita, H., Operation and photodynamic therapy for pleural mesothelioma: six year follow-up, *Ann. Thoracic Surg.*, 66, 1128, 1998.
18. Delaney, T.F., Sindelar, W.F., Tochner, Z.S., Friauf, W.S., Thomas, G., Dachowski, L., Cole, J.W., Steinberg, S.M., and Glatstein, E., Phase I study of debulking surgery and photodynamic therapy for disseminated intraperitoneal tumors, *Int. J. Radiat. Oncol. Biol. Phys.*, 25, 445, 1993.
19. Ortner, M., Photodynamic therapy of cholangiocarcinoma, *Cancer GI Endoscopy Clin. North Am.*, 10, 481, 2000.
20. Ortner, M., Photodynamic therapy for cholangiocarcinoma, *J. of Hepato-Biliary-Pancreatic Surg.*, 8, 137, 2001.
21. Bellnier, D.A., Wood, L.M., Potter, W.R., Weishaupt, K.R., and Oseroff, A.R., Design and construction of a light delivery system for photodynamic therapy, *Med. Phys. J.*, 26, 1552, 1999.
22. Jeffes, E., McCullogh, J., Weinstein, G., Kaplan, R., Glazer, S., and Taylor, R., Photodynamic therapy of actinic keratoses with topical aminolevulinic acid hydrochloride and fluorescent blue light, *J. Am. Acad. Dermatol.*, 45, 96, 2001.
23. DUSA Web site: www.dusapharma.com.
24. Fan, K., Hopper, C., Speight, P., Buonaccorsi, G., and Bown, S., Photodynamic therapy using mTHPC for malignant disease in the oral cavity, *Int. J. Cancer*, 73, 25, 1997.
25. Miravant Web site: www.miravant.com.
26. Sessler, J.L. and Miller, R.A., Texaphyrins: new drugs with diverse clinical applications in radiation and photodynamic therapy, *Biochem. Pharmacol.*, 59, 733, 2000.
27. Maugeri, A., Klevering, B.J., Rohrschneider, K., Blankenagel, A., Brunner, H.G., Deutman, A.F., Hoyng, C.B., and Cremers, F.P.M., Mutations in the ABCA4 (ABCR) gene are the major cause of autosomal recessive cone-rod dystrophy, *Am. J. Hum. Genet.*, 67, 960, 2000.
28. Allikmets, R.a.t.I.A.S.C., Further evidence for an association of ABCR alleles with age-related macular degeneration, *Am. J. Hum. Genet.*, 67, 487, 2000.
29. Allikmets, R., Simple and complex ABCR: genetic predisposition to retinal disease, *Am. J. Hum. Genet.*, 67, 791, 2000.
30. Fingar, V.H., Vascular effects of photodynamic therapy, *J. Clin. Laser Med. & Surg.*, 14, 323, 1996.
31. Henderson, B.W. and Dougherty, T.J., How does photodynamic therapy work?, *Photochem. Photobiol.*, 55, 145, 1992.
32. Richter, A.M., Waterfield, E., Jain, A.K., Canaan, A.J., Allison, B.A., and Levy, J.G., Liposomal delivery of a photosensitizer, benzoporphyrin derivative monoacid ring A (BPD) to tumor tissue in a mouse tumor model, *Photochem. Photobiol.*, 57, 1000, 1993.
33. Schmidt-Erfurth, U. and Hasan, T., Mechanisms of actions of photodynamic therapy with verteporfin for the treatment of age-related macular degeneration, *Surv. Ophthalmol.*, 45, 195, 2000.
34. Kramer, M., Miller, J.M., Michaud, N., Moulton, R.S., Hasan, T., Flotte, T.J., and Gragoudas, E.S., Liposomal benzoporphyrin derivative verteporfin photodynamic therapy. Selective treatment of choroidal neovascularization in monkeys, *Ophthalmology*, 103, 427, 1996.
35. Miller, J.W., Schmidt-Erfurth, U., Sickenburg, M. et al., Photodynamic therapy with verteporfin for choroidal neovascularization caused by age related macular degeneration: results of a single treatment in a Phase I and 2 study, *Arch. Ophthalmol.*, 117, 1161, 1999.
36. TAP Study Group, Treatment of age related macular degeneration with photodynamic therapy (TAP), photodynamic therapy of subfoveal choroidal neovascularization in age related macular degeneration with verteporfin: one year results of two randomized clinical trials - TAP report 1, *Arch. Ophthalmol.*, 117, 1329, 1999.

37. TAP Study Group, Treatment of age-related macular degeneration with photodynamic therapy (TAP). Photodynamic therapy of subfoveal choroidal neovascularization in age related macular degeneration with verteporfin: two year results of two randomized clinical trials - TAP report 2, *Arch. Ophthalmol.*, 119, 198, 2001.
38. Verteporfin in Photodynamic Study Group, Verteporfin therapy of subfoveal choroidal neovascularization in age-related macular degeneration: two year results of a randomized trial including lesions with occult with no classic choroidal neovascularization. Verteporfin in photodynamic therapy report 2, *Am. J. Ophthalmol.*, 131, 541, 2001.
39. Verteporfin in Photodynamic Study Group, Verteporfin therapy of subfoveal choroidal neovascularization in pathologic myopia. Twelve month results of a randomized trial, *Ophthalmology*, 108, 841, 2001.
40. El, T., Li, X.Y., and Paciotti, N.M., Fluorescein angiographic characteristics of subfoveal choroidal neovascular lesions secondary to age related maculopathy in pivotal Phase III trial for SnET2 PDT, Abstract, Association for Research in Vision and Opthamology, 2352, 2001.
41. Zaak, D., Kriegmair, M., Stepp, H., Baumgartner, R., Oberneder, R., Schneede, P., Corvin, S., Frimberger, D., Knuchel, R., and Hofstetter, A., Endoscopic detection of transitional cell carcinoma with 5-aminolevulinic acid: results of 1012 fluorescence endoscopies, *Urology*, 57, 690, 2001.
42. Lam, S., Kennedy, T., Unger, M., Miller-York, E., Gelmont, D., Rusch, V., Gipe, B., Howard, D., LeRiche, J.C., Coldman, A., and Gazdar, A.F., Localization of bronchial intraepithelial neoplastic lesions by fluorescence bronchoscopy, *Chest*, 113, 696, 1998.

Index

A

B

C

D

E

F

G

H

I

J

K

L

M

N

O

P

Q

R

S

T

U

V

W

X

Y

Z